ANGEWANDTE CHEMIE
International Edition in English
Volume 31 · Number 1
January 1992
Pages 1–110

Optically Anomalous Crystals

By Bart Kahr* and J. Michael McBride*

The optical symmetry of many crystals is lower than would be expected from their external form and X-ray diffraction data. Recently such *optical anomalies* have been attributed to nonequilibrium structures resulting from kinetically controlled crystal growth. Impurities are incorporated to different extents at various surface sites that would otherwise have become symmetry-related within the bulk crystal. After their discovery by Brewster in 1815, optically anomalous crystals were the subject of lively debate throughout the 19th century among some of the most distinguished contributors to the development of crystallography including Biot, Berzelius, Herschel, Mitscherlich, Frankenheim, Pasteur, Mallard, Klein, Groth, Wyrouboff, Barlow, Brauns, Rinne, Pockels, and Friedel. From a sea of wild speculation two conflicting postulates emerged: that the symmetric form resulted from accidental twinning of segments with lower symmetry, or that the optical peculiarities resulted from stress due to impurities or external perturbations. Neither postulate expresses the present view. Interest in this research waned at the turn of the century, and after 1917 no one pursued Tammann's alternative correct insight. The problem of anomalous double refraction attracted no attention for more than half a century until its recent solution. This review discusses both mineral and organic systems with particular emphasis on the phyllosilicate apophyllite and on 1,5-dichloro-2,3-dinitrobenzene. These nonequilibrium structures relate to questions of crystal order, crystal growth, molecular recognition, and the design of new materials. The review provides a reminder of the enduring value of the polarizing microscope as a research tool in chemistry.

1. Introduction

1.1. What is an Optically Anomalous Crystal?

In a literal sense any crystal whose optical properties deviate from expectation could be called optically anomalous. Descriptions of optical anomalies are scattered throughout the crystallographic literature. Examples from the work of David Brewster, a pioneer in crystal optics at the beginning of the 19th century, range from interference patterns associated with fluid inclusions in diamonds[1] to the variegated interference colors in some types of quartz.[2] However, a phenomenon that seems anomalous to one generation can seem commonplace to a succeeding generation with more sophisticated expectations. For example, some minerals were considered optically anomalous because their sequence of interference colors in convergent light does not follow Newton's scale of colors.[3] Such behavior is now assigned to variation of refractive index with wavelength in highly dispersive minerals.

The most common type of optical anomaly occurs when a crystal's optical symmetry is lower than its apparent structural symmetry, as established by measuring dimensions of the bulk crystal or by X-ray diffraction. Such cases have been

[*] Prof. Dr. B. Kahr
Department of Chemistry, Purdue University
West Lafayette, Indiana 47907 (USA)
Prof. Dr. J. M. McBride
Department of Chemistry, Yale University
New Haven, Connecticut 06511 (USA)

 © VCH Verlagsgesellschaft mbH, W-6940 Weinheim, 1992 0570-0833/92/0101-0001 $ 3.50+.25/0

recognized for 175 years but have remained mysterious until quite recently. In this paper we use *optically anomalous* or *anomalous* to refer only to this type of crystal.

The optical symmetry of a crystal can be determined by measuring its refractive index tensor, which depends on its electric polarizability. Most crystals are biaxial (Fig. 1a); they have one direction of maximum polarizability and refractive index (***M***), and a perpendicular direction of minimum polarizability (***m***). Within the plane defined by ***M*** and

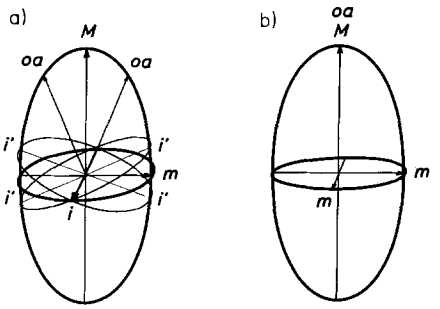

Fig. 1. Refractive index tensors (indicatrices) of a biaxial and a uniaxial crystal.

m there are four other directions (***i'***) whose intermediate polarizability matches that in the third orthogonal direction (***i***). Pairs of these directions together with ***i*** define a *circular section*, a plane within which the polarizability is constant in all directions. The normal to a circular section is called an *optic axis* (***oa***). Plane-polarized light can propagate along an optic axis without becoming elliptically polarized. A crystal is called biaxial when it has two circular sections and two optic axes.[4b]

Figure 1b shows an *axially symmetric* anisotropic crystal (a crystal with only one axis of three-, four-, or sixfold symmetry) in which one polarizability extremum (***M***) must lie along the axis, while the other two orthogonal axes are equivalent in polarizability (***m*** and ***m***). Such a crystal has a single optic axis, parallel to the symmetry axis, and is called *uniaxial*. Crystals with higher symmetry have the same polarizability in all directions and are called *isotropic*. By observing the passage of polarized light through a crystal with a polarizing microscope, or in favorable circumstances with the eye, it is possible to establish its symmetry as biaxial, uniaxial, or isotropic.[4a] When this symmetry is lower than that revealed by morphology or some other technique, the crystal is optically anomalous.

Anomalous crystals are usually twinned. They possess several distinct homogeneous regions, or *sectors*, whose number and relative orientation appear to be determined by the rotational symmetry of the crystal morphology. For example, a crystal with four- or sixfold symmetry should be uniaxial. Anomalous crystals with four- or sixfold morphological symmetry are typically composed of four or six biaxial segments, these being rotated from one another by 90° or 60°, respectively (see Fig. 2). Such twinning is called mimetic, because the composite crystal mimics a single crystal of higher symmetry and shows no reentrant angles between the constituent segments. Most of the hundreds of crystals described as optically anomalous in the literal sense fall into this specific class.

1.2. How Crystal Growth Causes Optical Anomalies

In 1988, while studying the growth of mixed crystals of fatty acid diacyl peroxides in this laboratory, Steven Bert-

Bart Kahr was born in New York City in 1961. He developed an interest in structural chemistry working with David Reingold at Middlebury College. At Princeton University he studied stereochemically unusual molecules with Kurt Mislow, obtaining a PhD degree in 1988. During graduate school he was fortunate to have shared a laboratory with Jeffrey Chance. After two years of crystallographic research in J. M. McBride's laboratory at Yale University, he joined the faculty of Purdue University as Assistant Professor of Chemistry.

Michael McBride was born in Lima, Ohio, in 1940. After undergraduate work at the College of Wooster and Harvard College, he earned the Ph.D. for research on free radical chemistry under Paul D. Bartlett at Harvard University. Since 1966 he has been on the faculty of Yale University. His research on organic solids has emphasized spectroscopic studies of free radical reactions in single crystals and the relationship among molecular structure, reactivity, and the mechanical properties of organic solids. He has an active interest in the history of organic chemistry. In 1987 he shared the Nobel Laureate Signature Award for Graduate Education with his student M. D. Hollingsworth. In 1990 he was Jacob and Erna Michael Visiting Professor at the Weizmann Institute of Science.

man recognized an optically anomalous crystal.[5] Square plates of pure di-11-bromoundecanoyl peroxide have true fourfold symmetry and are thus uniaxial. Inclusion of 5–15% of structurally analogous molecules of an impurity also gave square plates, but examination of these mixed crystals with the polarizing microscope showed that they were mimetic twins. Typical crystals were divided diagonally into four biaxial sectors interrelated by 90° rotation (Fig. 2). X-ray diffraction of single sectors showed that the fourfold symmetry had been broken. We attributed this desymmetrization to selective incorporation of impurity molecules among otherwise symmetry-related sites of the host lattice.

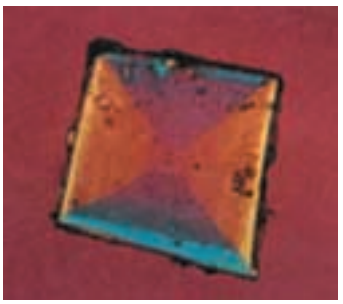

Fig. 2. Sectoring in a mixed crystal of di-11-bromoundecanoyl peroxide containing 15% of the analogue in which one terminal bromine atom is replaced by hydrogen; viewed along [001] between crossed polarizers with first-order red retarder (γ at 45°) [5]. Change in color from one growth sector to the next is due to a difference in orientation of the monobrominated compound caused by kinetic control of molecular addition to the lateral faces. (This same crystal was illustrated in [5], where the impurity was incorrectly identified as having one terminal bromine replaced by a *methyl* group. The effect of the impurity is nearly the same whether bromine is replaced by hydrogen or methyl.)

We were delighted by the prospect of using crystal optics to study this subtle aspect of crystal growth. But we were not surprised by the selectivity, because we had been attempting to apply to our crystals the elegant techniques of Addadi, Lahav, Leiserowitz, and their collaborators, whose comprehensive studies have revealed and exploited analogous selectivity in less symmetrical systems.[6]

It is easy to imagine that enantiomorphous lattice sites should be differently populated by a resolved chiral impurity, since the two kinds of defects must have different energies. It may at first seem surprising that impurity populations should also differ among sites related by a proper symmetry element, such as rotation. Such defects have identical energies, and thermodynamics requires their concentrations to be equivalent in a dilute solid solution at equilibrium. However most real crystals, especially those of solid solutions, are *not* at equilibrium. Once a molecule becomes incorporated into the crystal lattice, it is usually difficult for it to undergo a dramatic change in position or orientation. Thus many structural features of real crystals are controlled by the kinetics of growth rather than by equilibrium thermodynamics. To understand selective population one must recognize that growth occurs at the crystal surface and that most crystal faces lack the full symmetry of the three-dimensional lattice. For example, crystallographic axes are defined near a crystal face only when they are perpendicular to the surface; and even then the face must be flat and free of growth steps. Sites that should ultimately become equivalent by space group symmetry are thus different in structure and energy at the time impurities chose whether or not to occupy them.[7] Sectors of a crystal that have grown through different faces should have different impurity distributions and different optical properties, as illustrated in Section 2.3.2. When two crystal faces are related by symmetry, impurity distributions in the corresponding crystal sectors, resulting from growth through the two faces, should be related by the same symmetry.

After observing the optical anomaly in organic peroxides, we searched the literature for reports of analogous phenomena. We discovered that, although current texts give them little attention, descriptions were common in the 19th century when optical microscopy was the most powerful method of crystallographic analysis. Unsuccessful attempts to resolve these anomalies, which were observed in a wide variety of organic and inorganic crystals, form a consistent thread that parallels the development of crystallography generally. The present understanding of optical anomalies has emerged only over the last dozen years.

Section 2 of this paper outlines the history of the study of optically anomalous crystals within the context of the history of crystallography in the 19th and early 20th centuries. The mineral apophyllite is illustrated specifically. Section 3 discusses the present status of optical anomalies in inorganic and organic systems. Section 4 describes their relevance to current research on molecular recognition, on the kinetics and mechanism of crystal growth, and on rational approaches to designing crystalline materials for technical applications.

2. The History of Optical Anomalies

2.1. Crystal Classification according to Form

The mature development of any science requires a coherent classification of the objects under study. Thus progress in crystallography[8, 9] required classification of crystals. Crystals may be classified according to their external morphology, their physical and chemical properties, or their internal structure. All sorts of information may be relevant: shape, cleavage, chemical composition, color, hardness, density, refractive index, phase transition temperatures, space group symmetry, atomic positions, and many others.

Because the outstanding macroscopic feature of mineral samples is their polyhedral shape, attempts to classify crystals according to form trace back at least to the work of Nicolaus Steno (1638–1687),[10] who articulated a form of the Law of the Constancy of Interfacial Angles.[11] Maurice Cappeller (1685–1769) extended Steno's emphasis on form for the purpose of identification.[12] As in this botanical work, Carolus Linnaeus (1707–1778) sought to classify minerals within a system of genera.[13] Form was the most important organizing principle in his system. In an early attempt to approach the question of internal structure, A. G. Werner (1750–1817) sought a small group of *primary forms* to which the vast array of possible crystal shapes might be referred.[14]

Not everyone agreed that form should be the primary consideration in crystal classification. Romé de l'Isle (1736–1790) thought that form should be supplemented by chemi-

cal analysis, because shape alone was neither unique nor unambiguous. Not only can a single polymorph of a given chemical substance with a particular unit cell structure appear in many different shapes or *habits*, but also different substances can appear as isomorphs displaying the same form.[15] Through his Law of Rational Intercepts René Just Haüy (1743–1822) could relate the various shapes of a given polymorph by showing that crystal faces can be described by small integral indices when referred to three vectors. He further sought by successive cleavages to discover the unique building block, or *molécule intégrante*, for polymorphic crystals.[16] But Haüy sought idealized relationships among a crystal's dimensions and neglected precise goniometry (the quantitative measurement of form) when the results did not agree with his theory.[17] The limitations of his method were emphasized after Wollaston (1766–1828) invented the reflecting goniometer.[18] At the start of the 19th century it was clear that crystallography was in need of a physical method, independent of the measurement of form, that could assist in classification by confirming at least some of the qualitative aspects of crystal symmetry.[19]

2.2. Optical Classification of Crystals

The development of the science of crystal optics in the 19th century revealed the utility of birefringence in crystal classification. The first observation of birefringence or double refraction was reported by Erasmus Bartholinus (1625–1698), who noticed that within a crystal of calcite a single ray of light was split into two.[20] Christian Huygens (1629–1695) realized that one of these rays obeyed the ordinary law of refraction while the other did not and was always contained within a plane defined by the direction of incidence and a special axis, the direction of high rotational symmetry in the rhombohedral crystal.[21] Haüy, undoubtedly because of his own researches with calcite, undertook studies of double refraction and noticed that crystals of other substances with the form of a cube or octahedron lacked this property. Finally Johann Jacob Bernhardi (1774–1850) suggested explicitly that double refraction was directly related to a crystal's form.[22] However only two optical classes were distinguished at this time: crystals that were birefringent and those that were not. There was as yet no distinction between uniaxial and biaxial birefringent crystals.

In 1808 Etienne Malus (1775–1812), while examining a crystal of calcite in sunlight reflected from the windows of the Palais Luxembourg, noticed that the intensity of the two rays varied as a function of the crystal's orientation.[23, 24] He correctly recognized this as the phenomenon of polarization.[25] His discovery that the rays had different polarization greatly assisted studies of doubly refracting minerals, because researchers were no longer restricted to examining large, strongly birefringent crystals in which divergence of the two rays was readily visible.

In 1811 François Arago (1786–1853) discovered that brilliant colors sometimes are produced when a crystal is examined between two polarizers.[26] Immediately after Arago's discovery David Brewster (1781–1868)[27] and Jean-Baptiste Biot (1774–1862)[28] recognized the colors as a signature of *weak* birefringence and began systematic explorations of a wide variety of crystals and biological specimens.[29] Independently they distinguished between uniaxial and biaxial birefringent crystals. They also discerned the connection to morphology, since well formed uniaxial crystals always had three-, four-, or sixfold rotational symmetry.

This new method of analysis inspired Brewster to challenge Haüy's assignments of primive forms to eleven mineral substances[30] and to write:

> "If the physiology of mineral bodies shall ever attain the dignity of a science, its foundations must be laid upon optical results, and its progress directed by the unerring light of optical analysis."[31]

> "If we take a crystal... bounded by six equal square faces, the crystallographer will content himself with calling it a *cube*, but the optical mineralogist will only call it a *cube* when it has *no double refraction*."[30]

The optical classification of crystals as isotropic, biaxial, or uniaxial by Brewster[32] and Biot[33] in the second decade of the 19th century is still valid. One may further assign a biaxial crystal to one of three classes, where both, one, or neither of the directions of maximum and minimum polarizability are fixed by symmetry. This may be accomplished optically because principal directions that are not fixed by symmetry will in general differ for light of different wavelength.[34]

2.3. The First Observations of Optical Anomalies[35b]

2.3.1. *Brewster's Initial Report*

As Brewster was developing his optical classification scheme, he discovered several minerals that appeared to be exceptions and chose to treat them separately. In 1815 he announced to the Royal Society of Edinburgh:

> "Philosophers will no doubt be surprised to learn, that *muriate of soda, fluate of lime,*[*] *the Diamond, Alum* [despite their high symmetry][**] have actually the property of Double Refraction, but under circumstances of such a singular kind, as to entitle them to be regarded as a new class of doubly refracting crystals."[36]

He then described optically anomalous crystals of fluorspar (CaF_2, Fig. 3). To observe the indistinct low-order interference effects of a fluorspar crystal more clearly, he supplemented its birefringence by laying it on a plate of calcium sulfate which by itself between crossed calcite polarizers gave "a *brilliant blue* colour of the second order on Newton's scale." He was surprised to observe that

> "when the cube of fluor-spar remained stationary, there was one portion of it at *m*, which made the *blue* colour [of the $CaSO_4$] *red*... while another portion, at *n*, made the *blue* colour *green*."

[*] sodium chloride, calcium fluorosilicate

[**] Square brackets in quotations indicate interpolations by the authors.

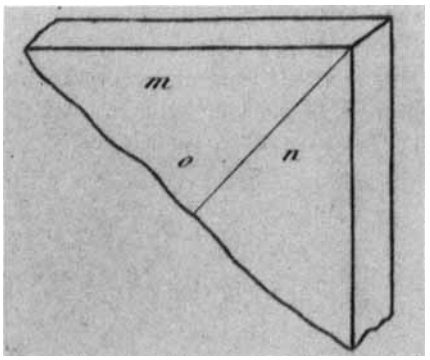

Fig. 3. Brewster's first illustration of an optically anomalous crystal (1815); when superimposed on a calcite crystal that gave a blue interference color, sectors *m* and *n* at the corner of the fluorspar crystal appear red and green, respectively [29].

In this first report of an optical anomaly, the cubic crystal was not only birefringent, it was not even homogeneous, but rather divided into sectors like those of the peroxide crystals (Fig. 2). Brewster speculated that the anomaly had probably originated during crystal growth:

> "If the laws which regulate the crystallisation of these minerals had been allowed an undisturbed operation, it is probable that the crystals would have had a perfect cube or an octahedron for their primitive form, and would have exhibited none of the phenomena of double refraction."

Brewster clearly understood that such optical properties imply a reduction from the symmetry of the crystal form. But he was in no position to identify the nature of the irregularities of growth which produce the deviations. During the next decade Brewster studied other optically anomalous minerals including chabazite,[37] garnet,[38] topaz,[39] and apophyllite.

2.3.2. *Apophyllite*

2.3.2.1. *The Structural Basis for the Optical Anomaly of Apophyllite*

It is worth interrupting the chronological narrative to describe apophyllite in greater detail, because its optical anomalies have been debated from Brewster's time until the present, and understanding these anomalies will help to focus the historical discussion.

Apophyllite is a silicate, empirical formula $KCa_4Si_8O_{20}F \cdot 8\,H_2O$, formed by hydrothermal recrystallization within cavities in rocks derived from lava.[40] The name (Greek: formed of leaves) reflects its ready cleavage perpendicular to the fourfold symmetry axis and its separation into layers on heating. The cleavage is consistent with the sheet structure revealed in 1931 by the X-ray study of Taylor and Náray-Szabó.[41, 42]

Silicate units form the covalent sheet shown in Figure 4. Each Si atom shares three oxygens with neighbors and is connected to a fourth, negatively charged oxygen by a bond that is roughly perpendicular to the sheet. Four silicate units make up a ring surrounding the crystallographic fourfold rotation axis that is perpendicular to the sheet, so that all four "axial" oxygens point toward the same side of the sheet. Axial oxygens of neighboring rings point toward the other side of the sheet.

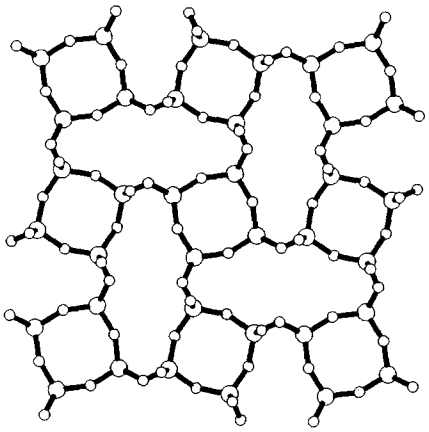

Fig. 4. Silicate units forming a covalent sheet in apophyllite, viewed along [001]. Axial oxygens of the rings in the center and corners of this figure point away from the viewer; those on the other four rings point toward the viewer.

Adjacent sheets are related by mirror symmetry (Fig. 5). Between silicate rings whose axial bonds point toward the mirror is a slightly flattened cube of negative oxygens; between those silicate rings whose axial oxygens point away from this mirror is a roughly spherical void with a diameter of about 8.5 Å. The void accommodates a potassium ion

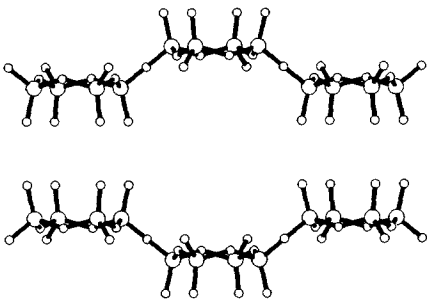

Fig. 5. Adjacent, mirror-related silicate sheets in apophyllite, viewed along [100].

solvated by eight waters, and each cube of negative oxygens holds a square of four calcium ions surrounding a fluoride ion (Fig. 6). Potassium, calcium, and fluoride all lie on the mirror plane between silicate sheets.

As an apophyllite crystal grows, impurities from the hydrothermal medium can be incorporated into its lattice. Some possible substitutions are OH^- for F^- (hydroxyapophyllite), Na^+ for K^+ (natroapophyllite), Mg^{2+} for Ca^{2+}, and Al^{3+} for Si^{4+}.[43] Substitution for F or K does not disturb the local fourfold symmetry, since each lies on a fourfold axis,[44] but substitution for Ca or Si breaks the local symmetry. If growth occurs through a crystal face where a bias consistently inhibits substitution in some of the "symmetry-related" silicon (or calcium) sites, the fourfold

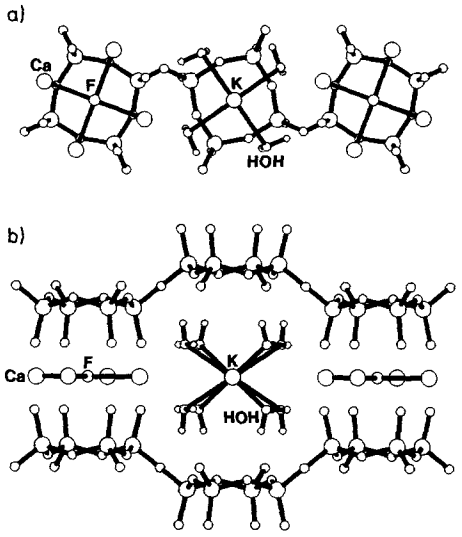

Fig. 6. View of the silicate sheets of apophyllite showing the positions of the water molecules and potassium, calcium, and fluoride ions between them: a) from the top along [001] and b) from the side along [100].

axis would disappear and the corresponding growth sector would be biaxial and optically anomalous.

Idealized patterns for thin sections cleaved perpendicular to the fourfold axis of optically anomalous apophyllite crystals are illustrated in Figure 7. They can be rationalized in

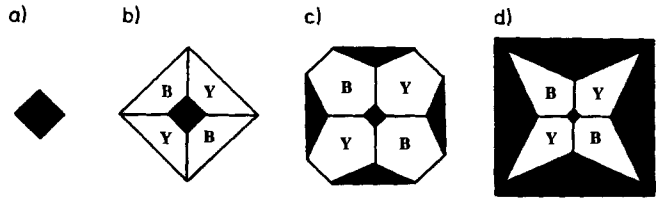

Fig. 7. Idealized patterns in thin sections of an apophyllite crystal (see Fig. 8) successively cleaved perpendicular to its fourfold axis and viewed with a first-order red retarder. Uniaxial sectors appear red (shown as black), biaxial sectors appear blue (B) or yellow (Y). For detailed explanation, see text.

terms of the growth of the crystal shown in Figure 8. The crystal displays three forms, or sets of symmetry related faces (Fig. 8a): two small square {001} or *basal* faces at the top and bottom, four hexagonal {110} or *prism* faces around the middle, and eight pentagonal {101} or *pyramid* faces between the basal and prism faces. Behind each face is a sector of the crystal that grew by deposition of material through that face. Figures 8b–d show the smaller crystal from which the crystal of Figure 8a grew, and the three classes of sectors that were involved in the growth. Figure 8b shows the two basal sectors, Figure 8c the four prism sectors, and Figure 8d the eight pyramid sectors. In indicating colors in Figure 7 we have assumed that when impurities are incorporated through the basal and prism faces they are not selectively ordered in a way that breaks the fourfold symmetry, but that those incorporated through a pyramid face are ordered so that the sector becomes biaxial, with axes oriented relative to the particular growth face. Thus when viewed through a polarizing microscope with a first-order red retarder, material from the uniaxial basal and prism sectors (Fig. 8b,c) appears red, while that from the biaxial pyramid sectors (Fig. 8d) is either yellow or blue.

The section of Figure 7a came from the very top of the crystal in Figure 8a, and thus includes only material from the uniaxial basal sector. Section 7b came lower in the crystal, so

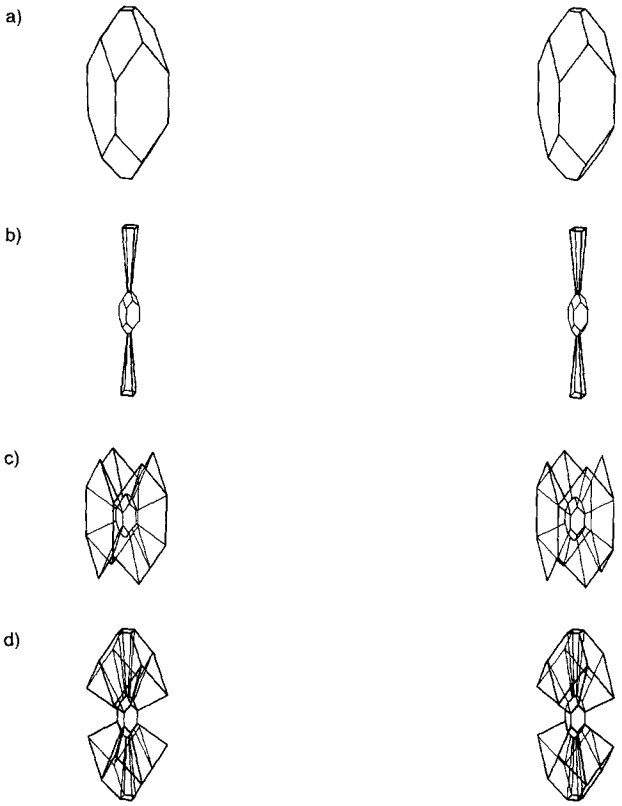

Fig. 8. Stereo views of a typical optically anomalous apophyllite crystal. a) The three sets of symmetry-related faces: two *basal* faces at the top and bottom, four *prism* faces around the middle, and eight *pyramid* faces between the basal and prism faces. b)–d) The smaller crystal from which the crystal of a) grew, and the three classes of sectors that were involved in the growth: b) basal sectors, c) prism sectors, d) pyramid sectors.

a somewhat smaller basal square is surrounded by trapezoidal portions from the four adjacent biaxial pyramid sectors. The octagonal section 7c came lower still so that it intersected both pyramid and prism faces. Thus the small central square is surrounded by hexagonal portions from pyramid sectors while the horizontal and vertical edges include triangular portions of uniaxial prism sectors. Section 7d originated so low in the crystal that it intersected only prism faces. The border is all material from uniaxial prism deposition. The center is a small square from the uniaxial basal sector which is surrounded by portions of four biaxial pyramid sectors.

2.3.2.2. *Brewster and Apophyllite*

Sir David Brewster (Fig. 9), whose name is recalled in Brewster's angle, made many contributions to mineralogy, crystallography, and physical optics.[45] Besides inventing the lenticular stereoscope and the kaleidoscope, he became the first to suggest that spectroscopy be used for chemical

Fig. 9. David Brewster (1781–1868), a pioneer in the development of optics [45], first observed anomalous birefringence in crystals and speculated with keen insight on its origin.

analysis when, after observing that certain lines are removed from the solar spectrum when the light passes through NO_2 gas, he wrote of

> "a general principle of chemical analysis in which simple and compound bodies might be characterized by their action on definite parts of the spectrum."[46]

Brewster, who made so many fundamental scientific contributions, underlined the importance he assigned to his work on the optical anomaly of apophyllite in a striking, if indirect way. Since he held no academic appointment until his 56th year, he was forced to rely on editing and voluminous writing to support his family. In 1819 he launched a new enterprise by founding *The Edinburgh Philosophical Journal*. For the very first paper in this journal Brewster chose his own contribution *On a New Optical and Mineralogical structure exhibited in certain specimens of Apophyllite and other minerals*.[47]

Upon examining slices of apophyllite crystals cut normal to the unique axis of a tetragonal prism Brewster observed figures resembling "tesselated pavements" in which the presumed uniaxial crystal was actually composed of discrete biaxial tiles (Fig. 10a). "The interior conformation of Apophyllite," he conjectured, "presents us with the new fact in crystallography, that a regular crystalline form arises from the union of smaller crystals whose homologous sides are not parallel to each other... The tessellated structure which is possessed by [these crystals] is a property so singular and so distinctive, that I would propose to mark it by the name of *Tesselite*."

In 1821 Brewster published a more detailed *Account of a Remarkable Structure in Apophyllite, with Observations on the Optical Peculiarities of that Mineral*,[48] in which he even used hand-colored plates to illustrate the sectoring. He described new specimens of anomalous apophyllite and drew remarkably prescient conclusions regarding the growth of these unusual objects. It seemed to him that crystal growth by orderly aggregation of identical minute particles must create a body that is

> "homogeneous throughout, possessing the same mechanical and physical properties in all parallel directions... The tessellated Apophyllite, however, could not have been formed by this process. It resembles more a work of art, in which the artist has varied, not only the materials, but the laws of their combination ... The boundaries of these corresponding, though distant zones, are marked with the greatest precision, and all their parts as nicely adjusted, as if some skilful workman had selected the materials, measured the spaces they were to occupy, and finally, combined them into the finest specimen of natural Mosaic."

He went further to emphasize that ordinary twinned crystals

> "...and those compound groups which arise from the mutual penetration of crystals, are merely accidental deviations from particular laws, which govern the crystalliza-

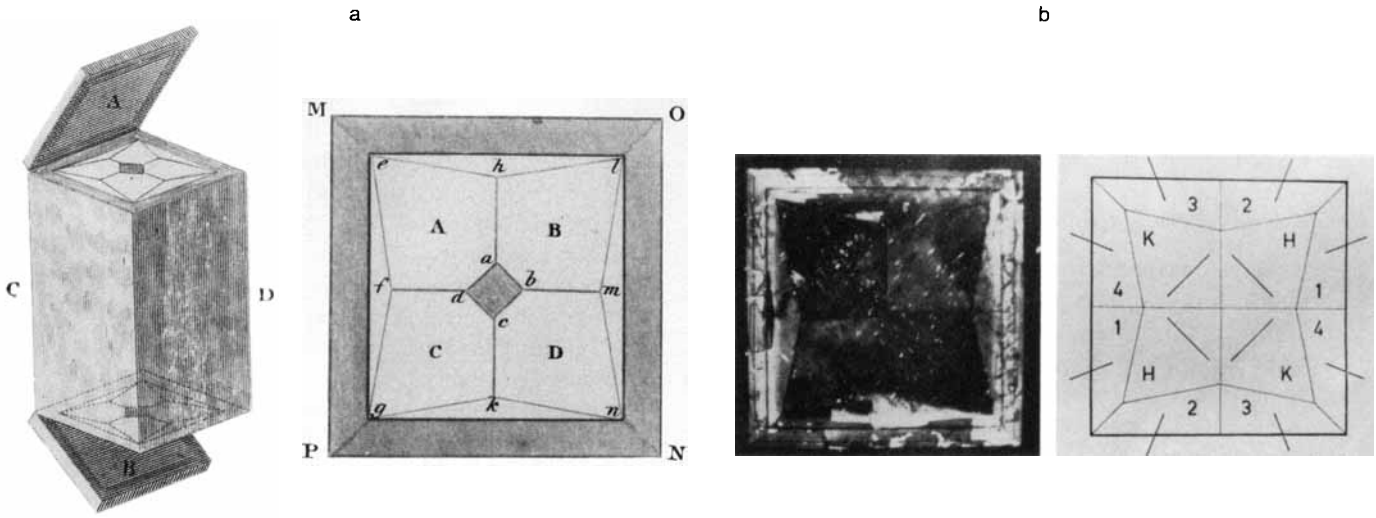

Fig. 10. a) The drawing of Brewster's apophyllite shows on the left a thin section being removed from a square prism, and on the right a projection of that slice revealing nine optically discrete tiles [48]. b) Photomicrograph and diagram of a similar apophyllite section reported in 1965 by Sahama, who attributed the optical inhomogeneities to "penetration twinning" [155].

tions in which they occur... The compound structure of the Apophyllite, however, cannot be referred to these capricious formations. It is itself the result of a general law, to which there are no exceptions, and when more deeply studied, and better understood, it must ultimately lead to the introduction of some new principle of organisation, of which crystallographers have at present no conception."

Brewster was almost correct when he supposed that tesselite must have been assembled in concentric stages (first a uniaxial core, then surrounding biaxial tiles, and finally a uniaxial border), but he was unable to suggest the "new principle of organisation" that could rationalize this sequence of events.

2.3.3. *Berzelius's Chemical Analysis*

Since there might have been a chemical difference between tesselites and other apophyllites, Brewster asked Jöns Jakob Berzelius (1779–1848) to compare their chemical compositions. Not only was Berzelius Europe's leading analytical chemist, he had also been the first scientist to propose a chemical classification of minerals.[49] He recognized silica as capable of forming a "negative" constituent and identified the Silicates, of which apophyllite was an example, as those minerals that contained it.[50] In 1822 Berzelius reported that analyses of anomalous and normal apophyllites agreed for every component within 0.3% (Fig. 11) and he added:[51]

"Differences of this kind, however great be the influence which they exercise upon light, can never constitute differences of species in mineralogy, differences which can only be founded on a real diversity of composition."

4 M. Berzelius *on the Chemical Composition of*

By reducing the Fluo-silicate of Lime into its elements, we obtain

	Tesselite.	Apophyllite of Uto.	Old Method.
Silex, - -	52.38	52.13	52.90
Lime, - -	24.98	24.71	25.21
Potash, - -	5.27	5.27	5.27
Fluoric Acid, -	0.84	0.82	...
Water, - -	16.20	16.20	16.20
	99.47	99.13	99.38

Fig. 11. Analyses by which Berzelius established the chemical identity of Tesselite with apophyllite, as published in Brewster's journal [51].

This assertion drew a stern retort from Brewster:[52]

"Of the three methods of analysis, we conceive the crystallographic method [measuring crystal dimensions] to be the least perfect; the chemical method next to it; and the optical method decidedly superior to both... When the chemist determines that two bodies have the same ingredients, he is ignorant of the manner in which these ingredients are combined. If the analysis of a quadruped and a bird indicated the same elements, he could not discover that these elements formed hair and horn in the one, while in the other they displayed themselves in the finest plumage. The chemist, indeed must fail in detecting structures, because he commences his process by destroying them."

Thus long before chemists spoke of structure Brewster criticized the analyst's neglect of possible isomerism. Berzelius was not to not coin the word "isomer" for another eight years.[53] Insisting on the uniqueness of tesselite Brewster continued:

"It would be a strange abridgment of the privileges of the optical observer, if he were not permitted to designate by a new name a body which possesses one of the most remarkable structures that has ever come under the notice of the mineralogist."

2.3.4. *Biot's Initial Interpretation*

Brewster's work on optical anomalies went largely unnoticed.[54] The only contemporary comments on his observations came from the two other authorities on crystal optics, J. F. W. Herschel (1792–1871)[55] and J.-B. Biot (Fig. 12), a leading French physicist and crystallographer, whose name is recalled in the Biot and Biot-Savart Laws of electromagnetism.

Fig. 12. Jean-Baptiste Biot (1774–1862) attempted the first comprehensive explanation of optical anomalies in crystals with his *Mémoire sur la polarisation lamellaire* (1841) [59, 61]. This theory of Lamellar Polarization was popular but not successful.

Biot and Brewster were rivals of a sort. They exchanged visits and correspondence, referred to one another in writing in the most respectful terms, and tried to collaborate, but they seem to have been fundamentally incompatible. Representatives of nations recently at war, they had a number of common interests which put them at loggerheads, including the mental health of Isaac Newton.[56] Biot took a deep interest in Brewster's "new class of doubly refracting crystals." He attributed the optical anomalies that Brewster had "accidentally" observed to stress caused by rapid cooling or evaporation during crystal growth.[57] For support Biot cited Brewster's own observation that pressure could generate analogous birefringence in animal gelatin and glass (Fig. 13).

Brewster was offended that the fruit of his systematic studies should be termed "accidental" and responded:[36]

"Had M. Biot repeated the experiments to which he alludes... and compared the results with those produced by

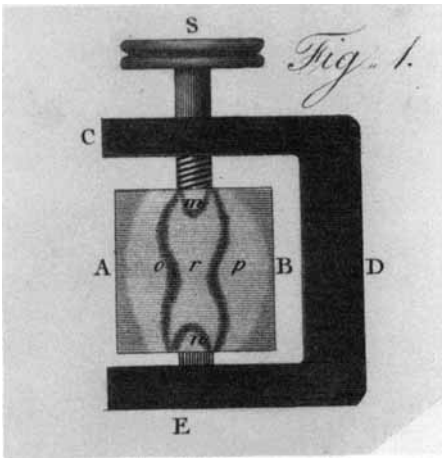

Fig. 13. A piece of glass rendered birefringent by pressure (Brewster, 1815) [81a]. The letters mark progressive changes in the interference colors between pressure points *m* and *n*. A, B = white; *o*, *p* = yellow; *r* is of higher order.

heat and rapid evaporation, he would have instantly seen that the two classes of phenomena are essentially distinct, and could not possibly have the same origin."

Brewster objected both because the birefringence was too strong to be explained plausibly by stress and because the sector boundaries were so regular. In his view some higher law must be at work. Much later Brewster wrote that he had convinced Biot, in a private communication, that the phenomenon was not due to extreme external conditions.[58]

2.4. Twinning Hypotheses

2.4.1. Biot's Lamellar Polarization

Biot undertook an extensive study of optical anomalies that culminated[59] in 1842 in what Brewster called an "elaborate Memoir peculiarly marked by the genius and sagacity of that distinguished philosopher."[60] Biot presented this theory of *polarisation lamellaire* in three lectures to the Academy of Sciences in Paris.[61] In fact lamellar polarization was not theory at all, but rather the hint of an analogy. He suggested that, if a stack of glass slides can impart plane polarization to transmitted light by repeated refraction, it would not be surprising if a stack of crystal lamellae could impart elliptical polarization. Thus a set of lamellae might possess birefringence that individual layers lacked. Biot's distinction between contributions due to the elementary molecular particles and contributions due to the macroscopic crystal structure was central to his theory.

The ready cleavage of apophyllite made it a natural candidate for Biot's analysis. He wrote:

"...aucune corps jusqu'ici connu ne s'est montré plus désespérant pour les cristallographes, ni plus riche en effects optiques pour les physiciens... Sans cette analyse intime et complète, le minéralogiste qui s'arrête aux formes ne connaît pas plus un cristal d'apophyllite, qu'on ne connaît une lettre par son enveloppe, un livre par sa couverture, un écrin par l'étui où il est renfermé... Tous les phénomènes optiques opérés par les diverses variétés de cristaux d'apophyllite résultent de la simultanéité des actions moléculaires... Les premiers dépendant de leur axe double réfraction unique... et les autres de l'existence des systèmes lamellaires..."[*]

Because of the optical complexity of some tesselite samples Biot began to invoke intricate systems of *hypothetical* lamellae, first in apophyllite and then in anomalous crystals of other minerals that showed no independent sign of layering. He proposed that the phenomenon provided a new structural tool:[62]

"Cette manière simple de pénétrer dans l'intime structure du cristal total, décèle une infinité d'accidents de pénétration que l'on ne soupçonnerait jamais par le seul aspect des faces externes."[**]

Biot observed that alum crystals containing ammonia were anomalous, and inferred from his theory that they must be layered. Brewster challenged this interpretation, because alum free of ammonia was optically normal. Since the two alums must be equally lamellar, Brewster reasoned, the double refraction must be due to an inherent property of ammonia and not to lamellar crystal structure.[63] Brewster asserted that despite Biot's ingenuity his lamellar structures were "scarcely to be reconciled with the principles of crystallography."[64]

During the 1820s neither Brewster nor Biot subscribed to the wave theory of light.[65b] Prior to its general acceptance sundry phenomena were explained by invoking new species of polarization.[25] Now defunct ideas of *chromatic polarization, alternate polarization,* and *proportionate polarization* proliferated in the early 19th century. *Mobile polarization* involving elaborate gyrations of the "luminous molecules" as they passed through crystals was another of Biot's bizarre inventions.[28, 66] Lamellar polarization was just such an ad hoc concept, and Biot made no attempt to put the analogy with polarization by a stack of glass slides on a theoretical foundation:[67]

"...je n'ai pas cru devoir taire ces analogies, si éloignées qu'elles pussent être... j'ai pensé qu'il n'était pas inutile d'indiquer les connexions... afin de les présenter aux théoriciens qui auraient l'habilete de les rendre plus intimes, si elles peuvent le devenir."[***]

No theoretician was equal to this challenge. Nevertheless, Biot's reputation and authority attracted the attention of many crystallographers to the problem of optically anomalous crystals. In 1846 a leading German crystallographer Eilhard Mitscherlich (1794–1863) assigned the optical

[*] ...no substance thus far known has been more exasperating for crystallographers, nor richer in optical effects for physicists... Without such an intimate and complete analysis the mineralogist who stops at forms would no more understand a crystal of apophyllite than one understands a letter by its envelope, a book by its cover, or a jewel by the box that contains it... All the optical phenomena... result from the simultaneity of molecular and nonmolecular effects... The former deriving from their unique axis of double refraction, and the others from the existence of lamellar systems...

[**] This simple way of penetrating into the intimate structure of a total crystal reveals an infinity of accidental penetrations that one would never suspect from the external aspect of the faces.

[***] I have not thought it appropriate to silence these analogies, however remote they might be [but rather to] present them to theoreticians who have the skill to make them closer, if possible.

anomaly of sodium chlorate to lamellar polarization and communicated his observations to Biot, who reported them to the French Academy of Sciences.[68] In 1848, the revolutionary year in which he demonstrated resolution of racemate salts in Biot's Collège de France laboratory, the young Louis Pasteur (1822–1895) published a note on sector twinning in crystals of potassium sulphate.[69] M. L. Frankenheim (1801–1869) in Breslau, an independent inventor of the theory of point lattices,[70] also adopted a version of Biot's theory.[71]

2.4.2. *Microscopic and Macroscopic Views*

Over the next thirty years most references to lamellar polarization were in the context of alternative explanations of optical anomalies. Most of the propositions were of two types, *stress theories* and *twinning theories*, each of them related in a way to Biot's thinking.[72]

Stress theories resembled Biot's theory in attributing birefringence to a macroscopic physical source, rather than to a molecular source, but they differed in assuming that the source was anisotropic mechanical stress in a solid continuum, rather than lamellar discontinuities. For example, in his 1855 Breslau habilitationsschrift Marbach suggested that whether or not a crystal was lamellar, its optical anomalies were due to tension as in stressed glass.[73] In a hybrid theory of 1852 Wertheim proposed that crystals without lamellar polarization can acquire it if pressure causes their irreversible separation into layers.[74]

Twinning theories resembled lamellar polarization in supposing that anomalous crystals were composed of many domains, but differed in attributing birefringence to reduced symmetry at the molecular level within each domain. The most successful of these, Mallard's theory of network twinning, is discussed in Section 2.4.3.

During the quarter century that followed Biot's hypothesis, optical anomalies were sometimes attributed to twinning, sometimes to stress. In the decade following the Franco–Prussian War, these views became doctrinaire and strongly polarized along national lines.

2.4.3. *Mallard's Network Twinning*

Perhaps no researcher in the 19th century did more to encourage the microscopic view of the internal structure of crystals than Auguste Bravais (1811–1863). His theory of the point lattices showed how crystals with different external forms might be composed of repetitively translated elemental units. This work inspired Ernest Mallard (1833–1894), Professor at the École supérieure des Mines (Fig. 14),[75] in his efforts to understand anomalous crystals.[76]

Mallard became spokesman for the French view of optical anomalies in 1876 by publishing a comprehensive theory in the *Annales des Mines* that relied heavily on the existence of Bravais lattices.[77] After rejecting lamellar polarization because it depended on a weak analogy and hypothetical crystal fissures,[78] he presented a theory based on a different kind of domain structure.

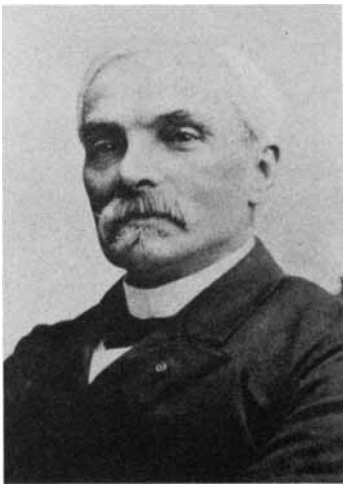

Fig. 14. Ernest Mallard (1833–1894) championed a "twinning model" in his 1876 treatise on anomalous birefringence [77]. Because it required the existence of hypothetical crystalline lamellae, it could be considered a successor to Biot's theory of Lamellar Polarization.

Mallard assumed that optical anomalies and a number of other peculiarities are due to isomorphism. When two different unsymmetrical "integrant molecules" accidentally have similar cell dimensions it is possible to mix them in a single lattice. In the same way, when a single unsymmetrical "integrant molecule" has dimensions that are close to those for a symmetrical cell, it is possible to align differently oriented biaxial domains into a twinned structure that mimics higher symmetry. In Mallard's view, symmetrical crystals can arise from the interpenetration of isomorphous space lattices which have little or nor symmetry. He applied his analysis to several dozen mineral substances with cubic, hexagonal, and tetragonal morphologies.

One of these minerals was apophyllite. More than half a century after Brewster's original report Mallard wrote:[79]

> "L'apophyllite est une des substances dont les propriétés optiques ont le plus excité l'étonnement. Signalées pour la première fois par Brewster, qui a particulièrement examiné les surprenantes figures... à la lumière polarisée parallèle... ces anomalies optiques n'ont reçu encore aucune explication satisfaisante."[*]

Mallard then argued that Brewster's tesselite was simply a twin made up of biaxial sectors. He rationalized the uniaxial regions of apophyllite in terms of accidental compensation of birefringence between interleaved submicroscopic lamellae in different orientations. Had Brewster still been living, he would surely have objected that this "explanation" avoided the fundamental problem: what kind of law determined the exquisite twinning pattern? The modern interpretation explains the pattern in terms of orientation at the crystal surfaces through which different sectors grew, and indeed Mallard noticed that differently oriented sectors in garnet were related to the external growth faces. But he provided no explanation for the mechanism of orientation, and no aspect of his theory endured.

[*] Apophyllite is one of the substances whose optical properties have aroused the most astonishment. Indicated first by Brewster, who examined particularly the surprising patterns... in parallel polarized light... these optical anomalies have still received no satisfactory explanation.

2.5. Stress Hypotheses

2.5.1. External Stress

Brewster had shown as early as 1814 that optically isotropic bodies, like glass and gelatin, become birefringent if stressed anisotropically by irregular heating[80] or compression.[81] A number of researchers assumed that stresses must account for the anomalous double refraction in regularly shaped crystals. Reusch, for example, proposed in 1867 that deposition on the surface of a growing crystal involved an intermediate state analogous to a colloid in that it would contract on solidification. This external stress from the crystal border could be the source of birefringence.[82]

From 1880 the various stress interpretations were dominant in Germany. Their principal exponents were Friedrich Klocke (1847–1884) and Carl Klein (1842–1907) (Fig. 15),[83] professors of mineralogy at the Universities of Marburg and Göttingen, respectively, and their students.

Fig. 15. Carl Klein (1842–1907) believed that external stresses resulting from catastrophic events in a crystal's history could account for anomalous birefringence.

Klocke followed the external stress interpretations of Marbach and Reusch[84] and showed the effects of anisotropic forces on the interference patterns of uniaxial crystals.[85] The stress hypothesis gained considerable impetus when Alfredo Ben-Saude, a student of Klein, allowed gelatins to dry rapidly in molds made in the shape of optically anomalous crystals (Fig. 16). Sections of the dried gelatins were birefringent and showed sectoring analogous to that of corresponding crystal sections.[86, 87] Ben-Saude assumed that rapid crystallization, like rapid drying of the gelatins, caused stress within the crystalline structure.

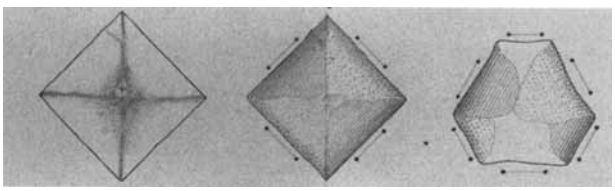

Fig. 16. Sections showing Ben-Saude's attempts to mimic anomalously birefringent crystals with rapidly dried, molded gelatin. Barbells in the center and right figures show indicatrix orientations in the different sectors as observed with crossed polarizers and a first-order red retarder [86].

Klein studied the effects of rapid heating and cooling on crystals, particularly the igneous minerals, boracite and leucite.[88] He subscribed to the theory that cataclysmic events in a crystal's history could account for the anomalies in many cases. As coeditor of the journal *Neues Jahrbuch für Mineralogie*, the principle forum for research on optical anomalies, Klein was an effective spokesman for this point of view, and was widely remembered as its leading proponent.[89]

Klocke, Klein, and Klein's student Friedrich Rinne (1863–1934) each studied and published on anomalous apophyllite. Like every predecessor except Brewster, each of them saw in apophyllite what he expected to see. Klocke[90] and Klein[91] both noted the relationship of the sectors to the external faces. The same relationship was used in Section 1.2 to support the modern view of sectoring by selective incorporation of impurities in apophyllite, but Klocke and Klein interpreted the relationship as evidence for stress exerted perpendicular to the growth faces. Rinne, noting that three different sectors participated in the same etch figure, inferred that they were not separated by the structural discontinuity that might have been expected from Mallard's twinning.[92]

2.5.2. Internal Stress Due to Impurities

Brewster's early speculation that the anomaly of apophyllite might be due to variation in its composition was refuted by the apophyllite analysis of Berzelius. In 1860 Leander Ditscheiner (1839–1903) revived interest in impurities when he suggested that optical properties could be adjusted over a wide range by averaging contributions from two isomorphous components in a mixed crystal.[93]

In 1882 Klocke encouraged his student Reinhard Brauns (1861–1931) (Fig. 17) to enter a university competition, which he won with a study of optically anomalous crystals.

Fig. 17. Reinhard Brauns (1861–1931) attributed anomalous birefringence to internal stress [112]. As a student in Marburg he launched his successful career in mineralogy by studying the role of impurities in this phenomenon.

Brauns continued this work and soon suggested that anomalous double refraction in some simple salts must be due to impurities.[94] Pure crystals of alum and barium nitrate were optically normal, but adding ammonium alum or lead nitrate, respectively, gave optically anomalous crystals. Since so many anomalous crystals were known to contain impurities, Brauns proposed that the cause of the anomalies could indeed be stress, but *internally* imposed stress resulting from a guest species acting upon the mismatched lattice of the host.

Klocke died suddenly in the summer of 1884 at the age of 37. Brauns continued the work in Marburg alone, developing his idea in a dissertation on optical anomalies in 1885,[95] and in a habilitationsschrift on the same subject two years later.[96] Although he focused on stress, in some ways Brauns's understanding of the relationship between impurities and optical anomalies by 1890 was quite similar to our present view:[97]

> "Die Spannungen entstehen durch den Eintritt der zwar isomorphen, aber doch chemisch und physikalisch etwas verschiedenen Substanz... Wenn wir uns vorstellen, dass bei dem Wachsen der Krystalle die Theilchen sich in Ebenen nach bestimmten Richtungen ablagern... so können wir hinzufügen: Die... auftretenden Kräfte ändern in den zu vorhandenen Krystallflächen gehörenden Anwachskegeln das optische Verhalten nach der geometrischen Symmetrie dieser Flächen."[*]

Our present view, like Ditscheiner's, assigns the optical effect to the direct contribution of an impurity rather than to its indirect mechanical influence on the host lattice. Ben-Saude, who showed that some mixed crystals with regular forms were optically normal, continued to favor the theory of external stress,[98] but Brauns faced a more serious challenge from France.

2.5.3. *Criticism of the Stress Hypothesis*

Stress as the explanation of crystal anomalies had been considered and rejected previously, when Brewster discounted Biot's suggestion in 1818.[36] Biot ultimately agreed and reported in his *Memoir on Lamellar Polarization*[59] that when he had shattered an anomalous crystal to relieve the hypothetical stress and reassembled the pieces, they produced the same anomalous effect on light as in the undamaged state.

Mallard published a rebuttal of the German interpretations in 1886.[99] He dismissed Klein's idea that anomalies are caused by rapid cooling, because the boundaries between sectors are sharp, and not gradual as in unannealed glass. He further contended that rapid cooling produces birefringence only in amorphous substances like glass and gelatin. Brauns quickly reported that birefringence is produced by sudden cooling of rock-salt crystals.[100] Mallard tried to dismiss Brauns's hypothesis involving isomorphous impurities by noting that many confirmed solid solutions are not optically anomalous.

Paul Groth (1843–1927) was atypical in Germany because he was inclined favorably toward Mallard's hypothesis.[101] His monumental *Physikalische Krystallographie* shows that he had a deeper appreciation of thermodynamic influence on crystal structure than his contemporaries.[102] Groth wondered how internal tensions could be the cause of the optical anomalies in simple salts grown from solution. He questioned the relevance of the gelatin experiments to crystalline materials because, in his view, any crystal must represent the most stable balance of forces among its constituent particles.[103]

Mallard's crowning achievement was his *Traité de cristallographie géométrique et physique*.[104] The first two volumes covered the geometrical and physical aspects of crystals. The third volume on crystalline assemblages would have addressed optical anomalies and answered his critics most fully. Although the manuscript had supposedly been completed, it was never found after the author's sudden death in 1894.[105]

2.6. The Golden Age of Optical Anomalies

2.6.1. *Explosion of Research on the Optical Anomalies*

The inauguration of Groth's *Zeitschrift für Krystallographie* in 1877 marked the emergence of crystallography as a mature science independent of geology.[106] Groth was concerned with the form and physical properties of all crystalline materials, mineral, organic, and synthetic, regardless of their origin. The *Mineralogical Magazine* was started by the Mineralogical Society of London in 1876. The *Bulletin de la Societé Minéralogique de France* first appeared in 1878, as did Gustav Tschermak's *Mineralogische und Petrographische Mittheilungen* from Vienna. These new journals were required to accommodate the rapid expansion in crystallographic research. Mallard's comprehensive theory was new and controversial, and the time was ripe to support or criticize his hypothesis. Reports of optical anomalies and speculations on their source blossomed about 1880. Figure 18

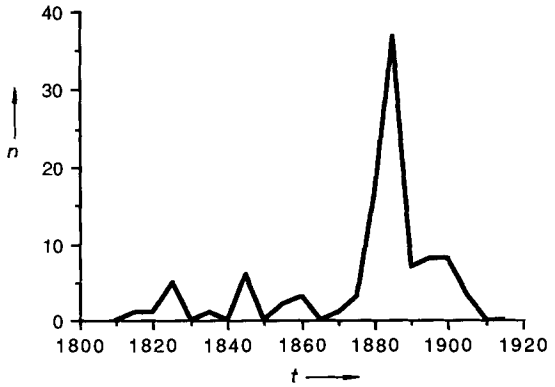

Fig. 18. The rise and fall of interst in research on optically anomalous crystals, based on the 99-reference bibliography of Johannsen (1919). n = number of citations, t = time in years.

[*] The stresses result from inclusion of a substance that is indeed isomorphous, but somewhat different chemically and physically... If we assume that during crystal growth the pieces are added in planes with given orientations... we can conclude [that the stresses will] alter the optical properties of growth sectors related to given crystal faces according to the geometrical symmetry of these faces.

plots the publication dates of the 99 significant papers on optical anomalies from 1815 to 1915 that were reviewed by Johannsen in 1918.[107] The steady stream of publication became a torrent in the 1880s, but it quickly shrank and disappeared about 1900.

The scientific significance of optical anomalies one hundred years ago is underlined by the professional stature of the principle researchers. From 1878 to 1892 six different active participants in the debate served as president of the French Mineralogical Society,[108] and all the principal crystallographic journals were edited by participants: Groth, Klein, Brauns, and Tschermak, as well as Rosenbusch, who edited *Neues Jahrbuch für Mineralogie, Geologie, und Paläontologie*.

2.6.2. Brauns's "Die Optischen Anomalien"

By 1890 the question of the cause and nature of optical anomalies had become so confused and contentious that, at the instance of Ferdinand Zirkel (1838–1912), professor of mineralogy at Leipzig,[109] the Fürstliche Jablonowski'schen Gesellschaft zu Leipzig[110] announced its competition[111] for

> "eine übersichtliche und kritische Zusammenstellung der auf die 'optischen Anomalien' der Krystalle bezüglichen bisherigen Forschungen, sowie die Ausführung neuer Untersuchungen, welche geeignet sind, die Ursachen jener anomalen Erscheinungen näher zu erläutern."[*]

The prize was awarded to Reinhard Brauns, now a privatdozent at Marburg, and his book, *Die Optischen Anomalien der Krystalle*, was published by the Society in 1891 (Fig. 19). This comprehensive 380-page monograph was an example of outstanding scholarship and served to launch Brauns's long and distinguished academic career that would include professorships in Karlsruhe, Kiel, Giessen, and Bonn.[112]

Although the book naturally represented Brauns's point of view, he discussed the contributions of others fully and for the most part fairly. For the title page he chose a motto from Goethe,[113] that evokes both the structure of anomalous crystals and the role he assumed as mediator:

> "Wo Parteien entstehen, hält Jeder sich hüben und drüben;
> Viele Jahre vergehn, eh' sie die Mitte vereint."[**]

He presented detailed discussions of some six dozen substances, most of which were anomalously birefringent crystals with optically discrete growth sectors (Fig. 20). In addition to apophyllite these included mixed crystals of barium nitrate and of alum as well as boracite, leucite, rock salt, garnet, analcime, chabasite, milarite, and pharmacosiderite. Brauns attributed most of these optical anomalies to internal stress resulting from inclusion of isomorphous impurities. But since many of the substances appeared to be pure, he did not insist that all optical anomalies conform to his model. He attributed many examples to external forces in the crystal's past history, such as mechanical compression, rapid cooling, or uneven heating. There were also categories for anomalies associated with solid–solid phase transitions, and for cases where no etiology could be identified.

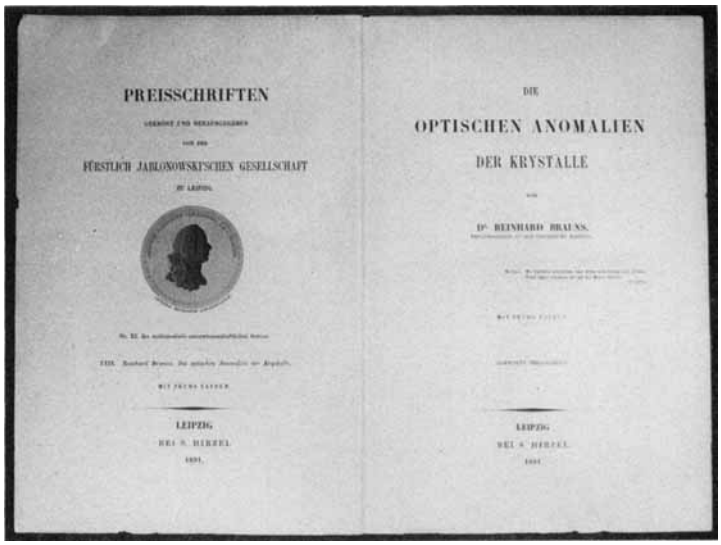

Fig. 19. Title page from Brauns's scholarly classic *Die Optische Anomalien der Krystalle* (1891). The book attempted, and for the most part succeeded, to present research on optically anomalous crystals as a closed subject [35a].

Notably absent was a category for network twinning. After discussing Mallard's hypothesis extensively, Brauns was emphatic in discarding it. He acknowledged that optical complexity could arise from differently oriented lamellae as in micas, but considered it fundamentally different from the sectoring produced by other mechanisms.[114] Despite this bias Brauns's book remains by far the most carefully reasoned, most objective, and most comprehensive source on the 19th century literature.

That Brauns had, for the first time, encapsulated all the experimental and theoretical observations on optical anomalies within a single volume may have given his work more authority than it merited. Subsequent writers frequently cited *Die Optischen Anomalien* as the definitive source,[115] and many of his assignments as to the cause of anomalous birefringence undoubtedly went unchallenged because of the impressive detail and scholarly excellence of the work.

2.6.3. Optically Anomalous Organic Crystals

Of all the anomalous crystals discussed by Brauns, only one was organic. This was strychnine sulfate hexahydrate, whose optical anomaly had been decribed in 1884 by Grigori Wyrouboff (1843–1913), a follower of Mallard in Paris,[116] then reinvestigated by Johannes Martin, a doctoral student of Klein[117] in Göttingen. Martin's dissertation was published in 1891,[118] the same year Brauns's text appeared. In addition to strychnine sulfate (Fig. 21) Martin described optical anomalies in pentaerythritol, benzil, and guanidinium carbonate. Two of these had also been discovered by Wyrouboff.

[*] a critical collection and overview of previous research related to the 'optical anomalies' of crystals as well as of the results of recent research which are appropriate to explain more fully the source of these anomalous phenomena.

[**] Where parties arise, each remains here or there;
Many years pass, before the middle unites them.

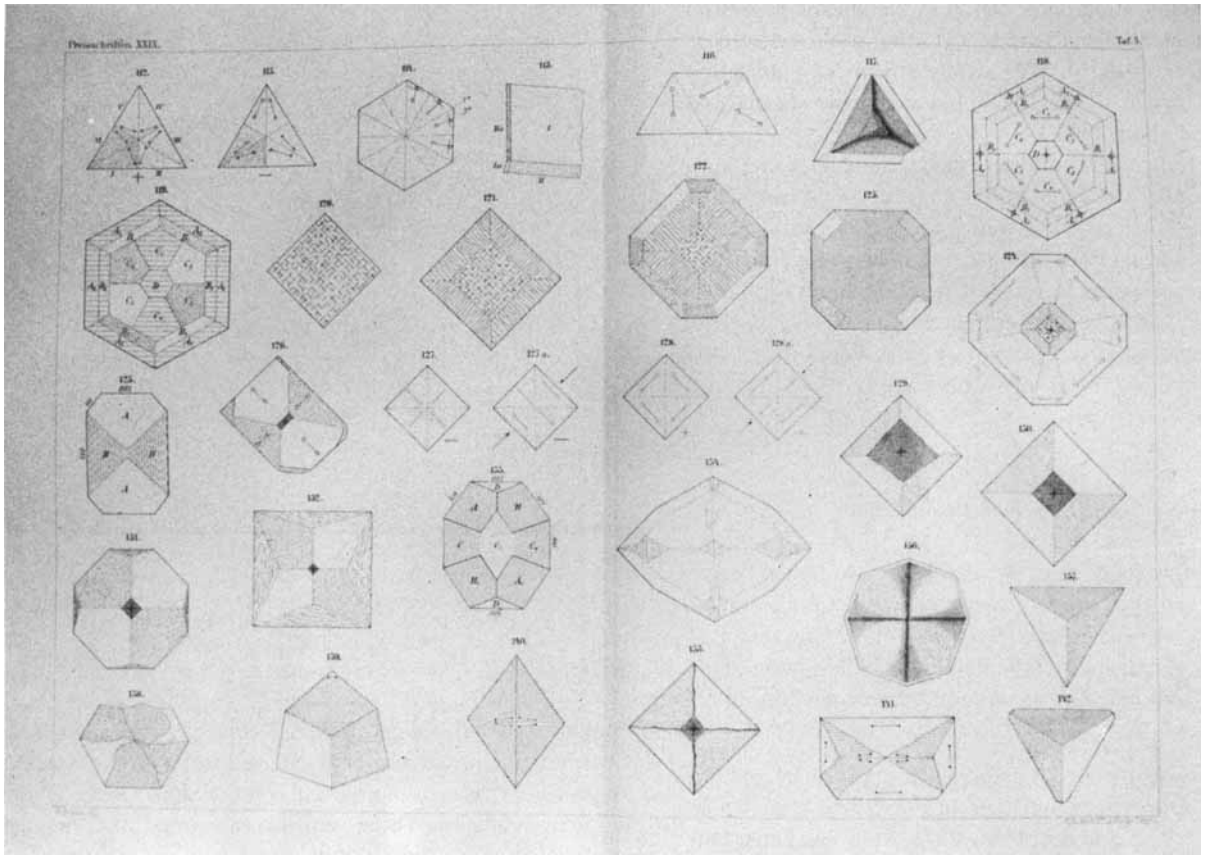

Fig. 20. Typical illustrations of optically anomalous minerals from Brauns's monograph [35a]. These figures, due among others to Mallard, Klein, and Brauns, show chabazite (112–115), apatite (116), diadelphite (117), corundum (118–119), vesuvianite (120–128a), apophyllite (129–132), an isomorphous solution of sodium ammonium sulfate and chromate (133), topaz (134), analcime (135–141), and eulytine (142).

Rejecting Mallard's theory, Martin was inclined toward the stress hypothesis, although he puzzled at how these ostensibly pure substances could give rise to the kind of optical anomaly that Brauns had attributed to solid solutions. To invoke external stress from drastic growth conditions seemed less appropriate for molecular crystals than for minerals. Martin suggested that the inherently isotropic particles were stressed by the "skeleton" of the crystal that had been previously laid down. Wyrouboff, who would later eulogize Mallard as the greatest philosopher of crystallography since Haüy,[106] excoriated Martin's dissertation, which he characterized as a stack of contradictory hypotheses.[119]

Other anomalous organic crystals were discovered at the end of the 19th century and will be discussed in Section 3.2.

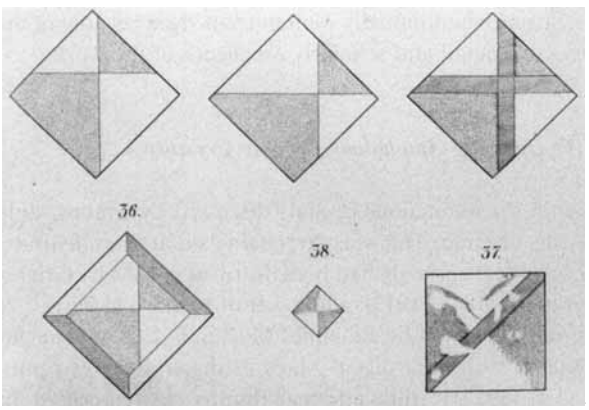

Fig. 21. Illustration from the dissertation of Johannes Martin showing sectored crystals of strychnine sulfate hexahydrate [118]. The complex pattern at the top right was interpreted as a superposition of the two layers with simple hour-glass figures on the left. The "picture-frame" pattern on the lower left has been observed for many substances (cf. Fig. 24c, 28c, d).

2.6.4. Why the Research Waned

By the early 20th century optical anomalies had ceased to be a field for active research, even though the simple modern interpretation described in Section 1.2 had not been considered. Crystallography and mineralogy texts continued to include a short section on optical anomalies, usually deferring to one or more of the accepted hypotheses. In the absence of active research, hypotheses became dogma, even though none of them really explained the facts.

There are at least four reasons for the demise of this line of research:

1. Mallard died in 1894, and his successors in France did not have the prestige or interest to continue the debate.
2. Brauns's monograph was seen as so authoritative that many researchers, particularly in Germany, incorrectly considered the question to be closed.
3. The scientific community became bored with the polemic. Already in 1887 a review had begun, "The never-failing discussion of the optical anomalies of crystals is contin-

ued by R. Brauns, who combats the assertion of Mallard ..."[120]

4. Interest in crystallographic research shifted away from bulk properties toward developing the kind of detailed structural model for crystals that had become so successful for molecules in organic chemistry.

2.7. Arrangement of Atoms within Crystals

Elaboration of the 230 space groups by Fedorov[121] and Schoenflies[122] in 1891 encouraged crystallographers to speculate in more detail about the internal structure of crystals. William Barlow (1845–1934), a self-taught crystallographer who would ultimately derive the space groups independently, tried to relate the external form of crystals to the symmetrical internal arrangement of their constituents.[123] Like other crystallographers since the days of Haüy, Barlow began by using spheres or other bodies to model crystal packing.[124] He ultimately realized that the variability of form reflected in the crystal kingdom could be more closely approximated by packing particles of different size. His close-packed models of dissimilar spheres agree remarkably well with modern models of simple binary salts.[125]

Barlow's 1897 treatment of the internal structure of crystals considered the problem of optical anomalies at length and relied heavily on the viewpoint of Brauns.[126] Like Brauns he believed that one class of optical anomalies derive somehow from solid–solid phase transitions that convert optically normal crystals into anomalous twins.[127] He also devised detailed geometric models that attempted to rationalize the contribution of isomorphous impurities to optical anomalies:[128]

> "Suppose that a linked group [of balls] has cubic symmetry, except that out of twenty-four outermost balls but twenty-two or twenty-three are similar and similarly situated, dissimilar balls making up the twenty-four and occupying places which are symmetrically situated, or nearly so; it is then conceivable that the closest-packing of a number of groups of this description may be one which disregards the slight irregularity and puts the groups together with their centres at the points of a cubic lattice, and with their predominating symmetrically arranged balls forming, as far as they go, a system in cubic symmetry.
>
> In a case of this kind the positions of the irregularities will not be symmetrically distributed; in other words the groups, when the deformities are taken into account, will be found variously orientated and the assemblage will not be strictly—i.e., mathematically—homogeneous, although, owing to the average effect of the deformities being the same in corresponding directions, the general symmetry will not be appreciably impaired."

Thus he visualized not only desymmetrization within each sector, but also the mimetic twinning of sectors that preserves the external morphology. He did not consider how the kinetics of crystal growth might make the desymmetrization systematic.

Writing in 1897 Barlow had little influence on the optical anomalies debate, which was already stale. However, optical anomalies were sufficiently common and considered sufficiently important that his new theory of the internal structure of crystals had to address them.

2.8. X-Ray Studies

X-rays, discovered in 1895, had been applied to crystal structure analysis by 1913. Speculation concerning the internal structure of crystals could now be tested directly. Within ten years optical crystallography had all but vanished as a subject for innovative research, and the problem of optical anomalies was swept aside by the rising tide of X-ray diffraction. In 1927 W. G. Burgers observed that because optical investigations "have led to different conceptions about the constitution [of certain anomalous samples], it is worthwhile to see how far X-rays are able to reveal the true nature of such crystals,"[129] suggesting that optical evidence may be ignored if it contradicts evidence from X-rays.

Apophyllite and other anomalous minerals were studied by X-rays in both Germany and France. By 1926 Friedrich Rinne, who as a student of Klein in Göttingen forty years earlier had studied apophyllite optically, was directing the Mineralogical Institute in Leipzig, where he transformed mineralogy "from a quaint determinative science to a modern branch of applied physics."[130] He was a pioneer in applying X-rays to mineralogy. His Laue photographs of apophyllite and other optically anomalous minerals showed no departure from the expected morphological symmetry (Fig. 22). For him this confirmed Klein's hypothesis that the anomalies were due to stress.[131]

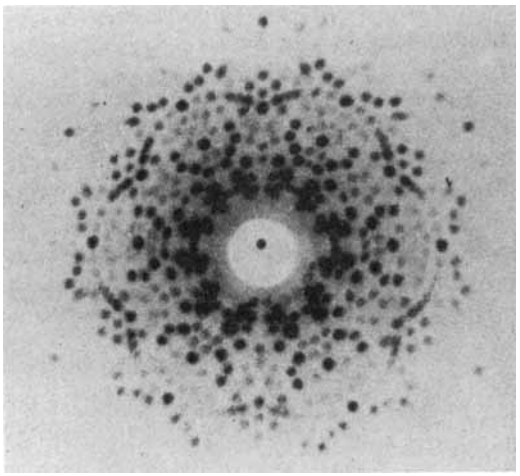

Fig. 22. Rinne's X-ray diffraction photograph of a single sector of optically anomalous milarite [131]. The density and resolution of such Laue photographs was inadequate to reveal small deviations from high symmetry.

In 1931, the year in which the atomic coordinates of apophyllite were first determined by X-ray diffraction,[41] Gossner and Kraus reported Laue photographs that seemed to confirm its tetragonal symmetry.[132] Gossner (1877–1937), a former student of Groth and his successor in Munich, surmised that because anomalous apophyllites have abnormal chemical composition, the substitution of impurities

such as hydroxide for fluoride must cause the anomalies by creating local stress, as Brauns had suggested.

In his 1934 dissertation Raymond Hocart in Strasbourg wrote the last word in a controversy that had lasted sixty years and would soon be forgotten.[133] His research on optically anomalous minerals had been suggested by his adviser, the late Georges Friedel (1865–1933). In addition to formulating Friedel's Law, Hocart's teacher had made his life's work the study of twinned crystals that he had begun in Paris as a student of Mallard. Hocart's historical survey recalled criticisms of stress theories, such as the incompatibility between the existence of distinct birefringent sectors and the continuity of internal stress (Mallard), and the observation of Friedrich Pockels (1865–1913) that certain crystals fracture under considerably less pressure than would be required to generate their observed birefringence.[134] Hocart also noted[135] that

> "Rinne s'efforce de justifier la sensibilité médiocre de cette méthode en rapportant l'altération des propriétés optiques à une déformation des atomes; cette déformation est inaccessible aux rayons X."[*]

After reporting his own much more precise X-ray work Hocart concluded,[136]

> "...la théorie du mimétisme proposée par Mallard s'applique à un certain nombre de cas; dans les mêmes cas la théorie dite des tensions intérieures n'est d'aucun secours pour expliquer les faits connus... Si le cas de l'apophyllite est insuffisamment élucidé, il n'en est pas moins établi que dans les autres exemples cités ici la symétrie du cristal simple est au plus égale à celle qu'on peut déduire des propriétés optiques. Cette symétrie est inférieure à la symétrie extérieure apparente qui est manifestée par le groupement de plusieurs individus en un même édifice."[**]

Although X-ray results confirmed what was seen optically in several anomalous crystals—that for some reason the symmetry of individual sectors was lower than apparent external symmetry of the crystal—they did not address the source of the desymmetrization and the precision of the tesselation. In most anomalous crystals, optical detection of the desymmetrization is more sensitive than X-ray detection, as well as faster and easier. In Hocart's words,[137]

> "...il est regrettable que par l'application des rayons X à l'étude des cristaux l'attention ait été détournée des résultats acquis par les méthodes classiques de la cristallographie."[***]

[*] Rinne is forced to justify the mediocre sensitivity of [his X-ray] method by attributing the alteration of optical properties to a deformation of the atoms which is inaccessible to X-rays.

[**] the mimesis theory proposed by Mallard is applicable in a certain number of cases; in the same cases the so called theory of internal strain is of no use in explaining the known facts... If the case of apophyllite is still unclear, it is at least established that like other examples cited here [boleite, pharmacosiderite, boracite, and senarmontite] the symmetry of the simple crystal is at most equal to that which one would deduce from the optical properties. This symmetry is lower than the apparent external symmetry which results from the grouping of a number of individuals into a single structure.

[***] It is regrettable that by applying X-rays to the study of crystals, attention has been diverted from results obtained by the classical methods of crystallography.

Until very recently the long unsettled debate on optically anomalous crystals seems to have been almost completely forgotten. In 1943 Alfred Neuhaus (1903–1975), Professor of Mineralogy in Darmstadt, reported an optically anomalous sectoring of 1,8-dihydroxyanthraquinone that was not reflected in its X-ray patterns.[138] He cited none of the earlier literature describing crystals with precisely the same optical form, although there had been dozens of references to them in the same journal before he was born. His report was of an isolated phenomenon. In 1951 Neuhaus assumed the Professorship of Mineralogy in Bonn that had formerly been occupied by Brauns.[139]

Between 1945 and 1984 Brauns's classic book on optical anomalies, which remains the most comprehensive source in the field, was cited in the scientific literature only four times, and then only peripherally.[140]

2.9. Tammann's Insight

The closest approach to our present understanding of the phenomenon of optical anomalies was the isolated insight of a physical chemist who made pioneering contributions to the study of heterogeneous systems, crystallization, solid state reactions, and metallurgy.[141] In connection with his interest in alloys, Gustav Tammann (1861–1938, Fig. 23) in Göttingen published a series of papers on mixed crystals.[142] These papers focused on the equilibrium and nonequilibrium distribution of constituents in solid solutions.

Fig. 23. Gustav Tammann (1861–1938) suggested that optically anomalous crystals might be metastable "isomers" of more symmetrical normal crystals, but his prescient ideas were not well regarded by the crystallographic community, nor was X-ray crystallography sufficiently well-developed to test his hypothesis [142].

In a 1917 paper, *Die anomale Molekülverteilung in Mischkristallen als Ursache ihrer anomalen Doppelbrechung*,[*] Tammann discussed the theory of Brauns on internal stress from isomorphous impurities.[143] He speculated that although internal stress should play a role, the ordering of

[*] *The Anomalous Molecular Arrangement in Mixed Crystals as a Cause of their Anomalous Birefringence*

components alone would suffice to cause birefringence. Going further than Barlow he clearly indicated that the arrangements resulted from kinetic, not thermodynamic, control of crystal growth:

> "Die optisch anomalen Mischkristalle können als Isomere der optisch normalen Mischkristalle aufgefaßt werden. Der Grund der Isomerie ist hier eine verschiedene Verteilung der Moleküle in demselben Raumgitter, während er bei der gewöhnlichen Isomerie eine verschiedene Verteilung der Atome im Molekül ist. Die Mischkristalle abnormer Molekül- oder atomverteilung im Gitter sind aus atomistischen Gründen total instabile Phasen, denen kein Zustandsfeld zukommt, in dem sie stabiler als ihre Gitterisomeren mit normaler Molekülverteilung sind."[*]

Tammann did not consider what sort of mechanism might generate the observed asymmetry. In reviewing this paper Brauns criticized[144] its neglect of "die Abhängigkeit der optischen Symmetrie von der geometrischen Symmetrie einer Fläche, in dem Bezirk dieser, wenn sie vorhanden ist."[**] Brauns was almost certainly thinking of the face as a source of stress, rather than as a source of the molecular orientation during crystal growth that would have made Tammann's views congruent with our present understanding. He asserted correctly that there was insufficient evidence to support Tammann's views and concluded that the question should still not be considered settled.

No one developed Tammann's ideas on this subject. As Garner pointed out forty years ago,[141b] numerous aspects of Tammann's work were unconventional and "appear to many of us to be disconnected flights of genius, probably because their point of origin lies beyond our ken." Belated recognition of the correctness of Tammann's insight on optically anomalous crystals may help address Garner's concern that

> "[since] the changing language of scientific thought makes it uneconomic to absorb work done ahead of the time, [it is] problematical whether the theoretical investigations of Tammann will have any better success with a future generation of scientists than they have had with his contemporaries."

3. Current Status

3.1. Mineral Crystals

3.1.1. New Evidence and Understanding

Two kinds of zoning in which chemical composition varies from region to region within a crystal are familiar in mineralogy. One of them involves bands that are analogous to the growth rings of trees and result from changes in the composition of the fluid during crystallization. The other involves differences in composition between sectors that grew through faces that were not related by symmetry.[145] A third, less familiar type of zoning involves symmetry-related sectors that have identical composition but different impurity orientation. Tammann's views on lattice isomers are closely related to the latter and to the "order–disorder" concept which concerns phase transitions between structures with different patterns or degrees of atomic ordering.[146] One difference is that many discussions of order–disorder transitions assume reversibility, which Tammann specifically excluded.[147] Until recently there was no recognition that selective incorporation of impurities, or of disordered host molecules, among differently oriented lattice sites at the crystal surface should play an important role in generating a nonequilibrium structure. Optically anomalous crystals continued to be considered, in terms that had not changed for almost a century, as resulting either from stress or from some unexplained twinning mechanism.[148] Research over the last dozen years has begun to change that perception.

A neutron diffraction study of topaz in 1980 demonstrated symmetry lowering due to orientation of OH bonds.[149] In 1986 Rossman and Aines used polarized FTIR spectroscopy to demonstrate that the optical anisotropy of grossular garnets was associated with a selective orientation of OH ions that was assumed to have been established during crystal growth.[150] In 1988 Allen and Buseck reported X-ray results on similar garnets showing that during growth selective incorporation of Fe^{+3} for Al^{+3} and of Fe^{+2} for Ca^{+2} had lowered the symmetry of individual sectors to "$I\bar{1}$" from $Ia3d$,[151] confirming earlier observations by Takéuchi et al.[152] Although sectoring was easily observed by optical microscopy, it was invisible to the transmission electron microscope.

The most comprehensive recent work on optically anomalous minerals is due to Akizuki et al. In 1978 he explained optical observations on the anomalous feldspar adularia in terms of proposed differences among nominally symmetry-related unit cell sites at growth surfaces.[153] This was the first of a series of impressive papers in which he and his collaborators have rationalized the optical anomalies of more than a dozen minerals, including garnet, apophyllite, and a sample from Strontian, Scotland, of brewsterite, a rare strontium-containing zeolite named for Sir David Brewster.[154]

3.1.2. Present State of the Apophyllite Riddle

Until Akizuki's work, fundamental understanding of the optical anomaly of apophyllite had progressed little since its discovery by Brewster 175 years ago. In 1965 Sahama described an apophyllite from Finland with tesselation almost identical to that described Brewster[155] (Fig. 10b). His conclusions, coming on the sesquicentennial of the first report on optical anomalies, were not significantly more sophisticated that Brewster's. Noting that the optical properties were too regular to be attributed to strain, Sahama went no further than to invoke "penetration twinning" of orthorhombic

[*] Optically anomalous mixed crystals can be understood as isomers of optically normal mixed crystals. Here the basis of the isomerism is a different arrangement of molecules in the same space lattice, while in normal isomerism it is a different arrangement of atoms in molecule. Mixed crystals with abnormal molecular or atomic arrangement in the lattice are on atomistic grounds totally unstable phases; there is no condition under which they are more stable than their lattice isomers with normal molecular arrangements.

[**] the dependence of the optical symmetry on the geometrical symmetry of a face, in the sector in which it occurs.

sectors whose "deviation from a strictly tetragonal symmetry must evidently be very slight." In his report of how growth conditions determine the morphology of apophyllite, Kostov mentioned the possible influence of impurities, but did not relate them to a mechanism of symmetry reduction.[156]

The paper of Akizuki and Konno, based on comprehensive, sophisticated optical observation of bulk and surface structures and on chemical analysis, presented a clear explanation of the way in which selective incorporation of impurities at growth sites on particular crystal facets could give rise to the tesselated structure.[157] Since substitution for K or F would not break the tetragonal symmetry, they favored selective substitution of Al for Si (or perhaps selective orientation of the O–H bond) as the source of desymmetrization. That neither of these orderings would have much influence on X-ray scattering is consistent with the failure of repeated efforts to detect the desymmetrization in apophyllite by X-ray diffraction. Although selective substitution of Al for Si seems plausible, there is still no direct evidence to confirm this explanation. We have recently studied growth banding in sectors associated with pyramid faces of an apophyllite from Bergen Hill, New Jersey. An electron microprobe analysis showed that in this sample the biaxial bands are actually *poorer* in aluminum than the uniaxial bands, although the opposite might be expected if biaxiality were due to inclusion of aluminum.[158] Thus Brewster's riddle is still not fully solved.

3.2. Organic Crystals

3.2.1. Literature Survey

Because of our desire to use optically anomalous organic crystals for studying molecular recognition during crystal growth,[5, 7] we surveyed the literature to identify promising systems. There must be a very large number of such crystals. Most axially symmetric organic crystals can probably be rendered optically anomalous by the presence of a suitable impurity. We searched crystal identification tables[159] for axially symmetric crystals that were not optically uniaxial.

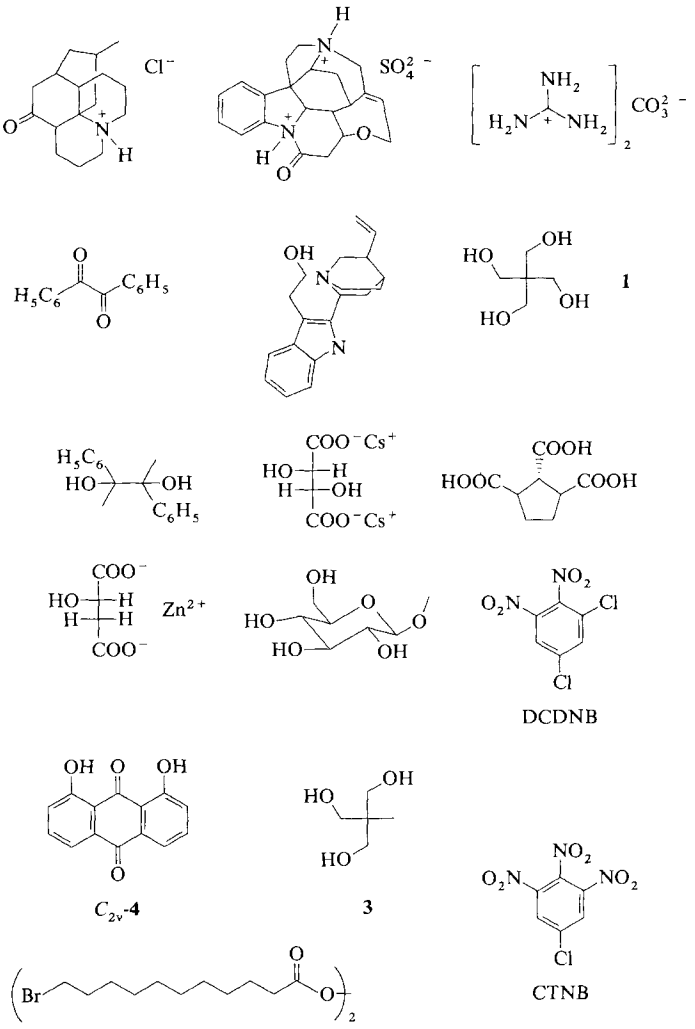

Scheme 1. Structural formulas of compounds in Table 1 (in order from left to right).

Since optical properties are no longer commonly reported for organic crystals, it is not surprising that almost all of the cases we found were included in Groth's 72-year-old compendium of crystal data.[160]

Table 1 presents 16 reports of optically anomalous organic crystals in chronological order. In a number of cases we have

Table 1. Optically anomalous organic crystals.

Compound (see Scheme 1 also)	Morphology	Possible Source of Anisotropy	Year	Ref.
lycopodine-hydrochloride · H_2O	trigonal	?	1883	[a]
strychnine sulfate · 6 H_2O	tetragonal	ordering of water of hydration	1884	[176]
guanidinium carbonate	tetragonal	?	1884	[161]
benzil	hexagonal	impurities	1884	[161]
cinchonamine	trigonal	?	1887	[b]
pentaerythritol **1**	tetragonal	isomorphous impurities	1890	[118]
3,4-dihydroxy-3,4-diphenylbutane	tetragonal	?	1894	[c]
cesium tartrate	trigonal	cation impurity	1895	[169]
trans, trans-cyclopentane-1,2,3-tricarboxylic acid	hexagonal	?	1896	[d]
zinc (or magnesium) malate	tetragonal	impure salt	1898	[170]
β-methyl-D-glucoside	tetragonal	inclusion of α-anomer	1899	[162]
1,5-dichloro-2,3-dinitrobenzene (DCDNB)	tetragonal	selective disorder	1907	[184]
1,8-dihydroxyanthraquinone **4**	tetragonal	?	1943	[138]
deoxypentaerythritol **3**	tetragonal	incomplete disorder	1983	[166]
di(11-bromoundecanoyl) peroxide	tetragonal	monodebrominated impurity	1988	[5]
5-chloro-1,2,3-trinitrobenzene (DTNB)	tetragonal	brominated impurities	1990	[186]

[a] H. Söffing, Dissertation, University of Göttingen, **1883**; *Z. Krystallogr.*, **1884**, *9*, 620. [b] C. Friedel, *C. R. Hebd. Seances Acad. Sci.*, **1887**, *105*, 985; *Z. Krystallogr.*, **1889**, *14*, 605. [c] C. Riva, *G. Min. Crist. Petr. Sansoni.*, **1894**, *5*, 303; *Z. Krystallogr.*, **1886**, *26*, 218. [d] W. J. Pope, *J. Chem. Soc.* **1896**, *69*, 971.

been able to confirm the anomalous phenomenon, and in some we can suggest its source on the basis of preliminary experiments described in this section. Section 3.2.2 summarizes the results from a more detailed study of one case.

For one compound of which we have obtained only uniaxial crystals and three others of which we have grown anomalous crystals, we suspect that the optical anomaly reported in the literature was due to selective incorporation of foreign or misordered molecules during crystallization. These substances are benzil, β-methyl-D-glucoside, pentaerythritol, and deoxypentaerythritol, respectively.

Our recrystallization of commercial benzil (Matheson) from carbon disulfide gave uniaxial hexagonal prisms, rather than the anomalous crystals reported by Martin[118] and by Wyrouboff.[161] His observations were probably due to an oriented impurity, although in our hands dissolving small amounts of benzoin or deoxybenzoin in the crystallizing solution did not give biaxial benzil crystals.

In 1899 Tietze[162] described optically anomalous β-methyl-D-glucoside crystals which he had obtained from Emil Fischer. The anomalous crystals were grown from mother liquors that remained after crystallization of the α isomer from the anomeric mixture of glucosides. The anomaly probably results from selective incorporation of residual α glucoside in the tetragonal lattice of the β anomer, since the α and β anomers of several carbohydrates cocrystallize.[163] We grew optically sectored crystals from an ethanol solution of β-methyl-D-glucoside (Sigma) in the presence of 17.5 mol% of the α anomer. The order of the interference colors in our crystals was considerably lower than in those described by Tietze, however.

Although Martin reported anomalous crystals of pentaerythritol (**1**),[118] pure crystals are genuinely tetragonal and uniaxial; molecules occupy sites of S_4 symmetry.[164] Pentaerythritol is difficult to obtain in pure form,[165] and crystals are almost invariably biaxial and sectored. Impurities of lower symmetry are probably oriented by selective incorporation on particular growth faces. R. L. Carter has grown anomalous crystals from pure pentaerythritol by adding 2-ethyl-2-(hydroxymethyl)butanol (**2**) as an impurity.[166]

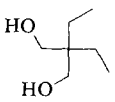

2

In 1983 Eilerman, Lippman, and Rudman reported that crystals of 2-(hydroxymethyl)-2-methyl-1,3-propanediol (deoxypentaerythritol, **3**) were isomorphous to pentaerythritol and appeared tetragonal by X-ray diffraction, suggesting that the methyl group was randomly disordered among the four hydroxymethyl sites.[167] However, by polarized microscopy they observed that the crystals were twinned, each plate being divided into four biaxial sectors. They inferred that each sector possessed a monoclinic *C*-centered cell containing four molecules. Together with Carter we have grown crystals from ethyl acetate and collected X-ray data from a single growth sector which shows a much more intricate structure.[168] Our triclinic supercell contains 32 independent molecules.

Traube described optically anomalous crystals of cesium tartrate[169] and of zinc malate.[170] For easy observation of deviation from axial symmetry, crystals should have well-developed faces perpendicular to the symmetry axis. We did not obtain appropriate crystals of these salts. A cation impurity, perhaps rubidium, is a likely source of Traube's observation. Crystals of cesium hydrogen tartrate, prepared from commercial purified CsCl in 1978, showed as much as 0.12% Rb by X-ray fluorescence.[171] Dicesium tartrate and dirubidium tartrate are isomorphous; a modern structure determination assigned the latter crystals to space group $P3_221$.[172]

We confirmed Wyrouboff's report that guanidinium carbonate is biaxial using crystals grown from the commercial salt (Aldrich). An ordered tetragonal structure of the salt in space group $P4_12_12$ has been reported with no mention of the optical anomaly.[173]

In the case of strychnine sulfate hexahydrate we have reproduced the reported anomaly, but we are again uncertain of its source. In 1857 this substance was used in the first demonstration that an organic crystal can rotate the plane of polarized light.[174, 175] Almost 30 years later Wyrouboff noted that the tetragonal crystals were optically anomalous and sectored,[176] an observation confirmed by Martin[118] and by Brauns[35a] (Fig. 21). Under conditions that apparently led to loss of an equivalent of water (heating, storage in desiccator, or long storage in air), the crystals became much more strongly birefringent. More remarkably, they often regained their original optical form on rehydration. We have confirmed these observations by growing crystals from cooled aqueous solution, exposing them to the air for dehydration, and returning them to the refrigerator for rehydration. X-ray data from a single growth sector of the hexahydrate crystal fit a tetragonal cell,[177] but the crystals diffracted poorly, and no further structural information was obtained. On standing at room temperature the crystals became so strongly birefringent that it was impossible to use a compensator to distinguish sectors with different directions of maximum polarizability.[178] The optical anomaly is certainly related to the state of hydration and perhaps to ordering of the waters of hydration. Brauns reported reversible changes in birefringence within a few minutes on transferring crystals between room air and a desiccator. Since a few minutes seems a short time to restore hydration and symmetry throughout a crystal, stress might play some role in this phenomenon.

We have reproduced the optical anomaly of 1,8-dihydroxyanthraquinone (**4**) but can offer no plausible explanation for the phenomenon. In 1943 Neuhaus reported optically sectored crystals.[138] These spectacular square, orange plates grow readily from acetone (Fig. 24). The solution ^1H NMR (500 MHz) spectrum from a single crystal of the quinone (Aldrich) showed no impurity peak larger than 0.5% of the hydroxyl signal from the pure compound. Previous structure determinations assigned the crystals to the space group $P4_1$.[179] Our structure, refined from X-ray intensities of one growth sector, showed no evidence of the desymmetrization that is implied optically.[180]

Rapid crystallization yields a metastable modification of 1,8-dihydroxyanthraquinone in the form of fine fibers. On the basis of vibrational spectroscopy Smulevich and Mar-

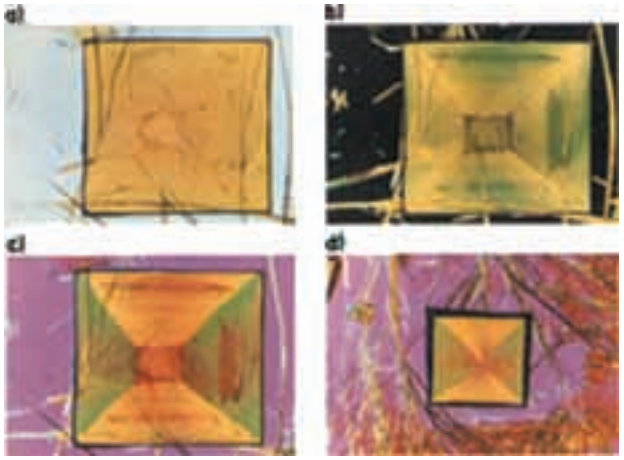

Fig. 24. Plate of 1,8-dihydroxyanthraquinone (**4**; $0.64 \times 0.57 \times 0.02$ mm) grown within 30 minutes from acetone. View along [001] a) directly, b) between crossed polarizers (at 45°), and c) with a first-order red retarder (γ vertical). d) A smaller plate from the same batch. The source of anomalous birefringence in these crystals remains mysterious. Also visible are fine needles, the metastable modification.

zocchi have argued that the predominant species in the two forms are the tautomers C_{2v}-**4** (see Scheme 1) and C_s-**4**.[181] The needles presumably contain the C_{2v} tautomer, while the plates have hydrogens bound to the oxygens at positions 1 and 9.[182] One might imagine that the minor species in the

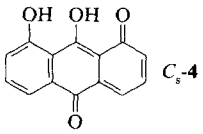

C_s-**4**

optically anomalous plates is the C_{2v} tautomer, selectively included in some of the four lattice sites, and that tautomerization, although rapid in solution, is frozen out in the solid state. However, not only did solid-state ^{1}H and ^{13}C NMR spectra fail to reveal a second species in the anomalous plates, the needles and plates gave identical spectra.[183] In neither case was the resolution of the spectra sufficient to draw definitive conclusions.

3.2.2. *1,5-Dichloro-2,3-dinitrobenzene and Its Derivatives*

After this preliminary survey of optically anomalous organic crystals, we studied the reported anomaly of 1,5-dichloro-2,3-dinitrobenzene (DCDNB) in much greater detail. DCDNB (see Scheme 1) is one of more than 70 substituted benzenes whose crystals were described by the mineralogist Ettore Artini (1866–1928) in a series of 10 papers between 1905 and 1918. Artini had undertaken this work in connection with the systematic investigation of aromatic compounds by the organic chemist Wilhelm Koerner (1839–1925), his colleague in Milan. Artini reported that although crystals of DCDNB from many solvents appeared to be tetragonal, microscopy of square (001) sections showed division along the diagonals into four distinctly biaxial sectors related to one another by rotation about [001], the apparent fourfold symmetry axis.[184] He also noted that departure from uniaxial character was small and variable "come spesso accade nelle sostanze otticamente anomale."[*]

We found that crystal plates from ether, chloroform, or benzene invariably showed the twinning described by Artini (Fig. 25). Refined lattice parameters from X-ray diffraction data on each of three of the sectors from a single plate showed an apparently orthorhombic cell with the principal axes in adjacent sectors rotated by 90° about c.[185] At a superficial level the absence of fourfold symmetry in this cell explains biaxiality and resolves the anomaly. That the crystals are multiply twinned may not be surprising, but why do they twin with precisely this pattern? Closer analysis reveals a novel mechanism for twinning that exemplifies the type of molecular recognition during crystal growth that we believe underlies most optical anomalies.

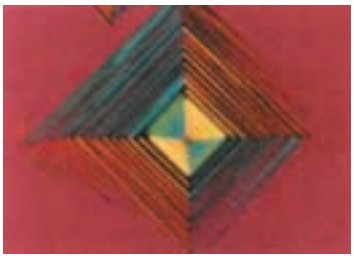

Fig. 25. Terraced plate of DCDNB (0.24 mm diagonal width, 0.024 mm thick at rim of central bright square) grown within 5 minutes by evaporation of $CHCl_3$ and viewed along [001] between crossed polarizers with a first-order red retarder (γ at 45°). In this pure crystal sectoring results from nonrandom disorder of a chloro and a nitro group.

An ordered crystal structure for DCDNB was refined to $R = 0.087$ in space group $P2_12_12_1$. This orthorhombic space group differs from the tetragonal group $P4_32_12$ by the absence of twofold rotational axes in locations close to the molecular C2–C5 axis. Thus 5-chloro-1,2,3-trinitrobenzene (CTNB, see Scheme 1), the analogue of DCDNB in which the chlorine at position 1 has been replaced by a nitro group to make a molecular twofold rotation axis possible, gives crystals in space group $P4_32_12$ that are isomorphous with DCDNB.[186] If the growing crystal of DCDNB were totally unable to distinguish between the 3-chloro and 1-nitro groups flanking the 2-nitro position, the molecule would be incorporated from solution with complete rotational disorder about the C2–C5 axis, and the additional effective molecular symmetry would make the crystal truly tetragonal.

Close inspection of residual electron density after refinement of the $P2_12_12_1$ structure showed peaks consistent with this kind of disorder. Since other crystals have shown disorder from interchange of nitro and chloro positions,[187] it is not surprising that DCDNB has difficulty ordering these two groups. We refined the amount of rotational disorder independently in each of the four molecular sites which are nominally related by symmetry in space group $P2_12_12_1$. This five-parameter model gave much improved agreement with X-ray data collected from an untwinned crystal fragment ($R = 0.065$). The model showed that the minor molecular

[*] as happens frequently in optically anomalous substances

orientation was present in substantial amounts that varied from site to site (32, 31, 15, and 18%, all ±1%).

These population differences that lower the crystal symmetry to $P1$ are due to differences in how molecules from solution were incorporated during growth into the different "symmetry-related" sites of this crystal fragment. The differences can be visualized by examining how molecules are oriented in one of the four molecular layers which stack along [001], the approximate fourfold screw axis of the unit cell. Figure 26a shows five molecules in one layer with the identity of the 1- and 3-substituents (Cl or NO_2) left ambiguous. The molecules are related by *a* and *b* translations. Figure 26b is a graph in which the central square symbolizes a growing crystal plate, and the four surrounding trapezoids represent the four growth sectors formed by adding molecules through the sides of the square to yield a final, larger crystal. Average orientation of the molecules within each sector is indicated by the shading of the circles standing for the 1- and 3-substituents. The ratio of dark to light area in a circle shows the ratio of NO_2 to Cl occupancy of the corresponding position. Ordering of the 1- and 3-substituents within the central square is irrelevant for the following argument, so they are shown as if fully disordered—half light for chloro and half dark for nitro.

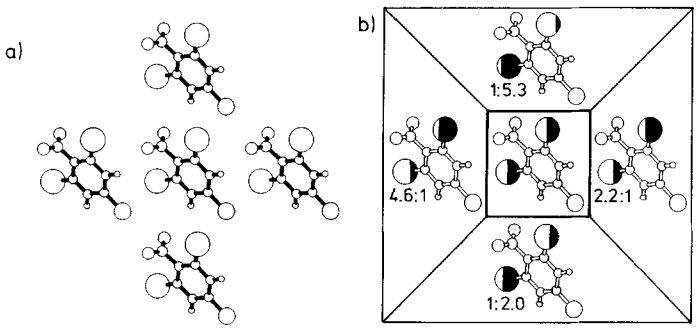

Fig. 26. a) Arrangement of neighboring molecules related by *a* and *b* translation within one layer of DCDNB. The approximate crystallographic fourfold screw axis is perpendicular to the paper, and the approximate molecular twofold symmetry axis joins the 2-nitro group at the upper left to the 5-chloro group at the lower right. The 1- and 3-substituents are indicated by large, nonspecified balls. b) Averaged molecular orientation in each trapezoidal growth sector of a macroscopic crystal. In real crystals the central square representing in the nucleus is much smaller. The average chloro:nitro population ratio at the 1-position is given explicitly for each sector.

In the bottom and right sectors orientation of chlorine to contact the growth surface of the central square is favored with a bias of ca. 2:1. At the top and left edges the bias is ca. 5:1 in the opposite direction, favoring contact of nitro with the growth surface. Apparently molecules from solution prefer to approach the bottom and right faces with their 1-chloro substituent toward the 5-chloro group of the surface molecules, and to approach the top and left faces with their 3-nitro group toward the 2-nitro group of the surface molecules. The bias favoring nitro–nitro contact (ca. 5:1) seems to be stronger than that favoring chloro–chloro contact (ca. 2:1). This naive picture ignores the role of molecules in adjacent layers and the specific structure of growth sites on the crystal surface (steps, kinks, etc.).[188] It also ignores the solvent. These additional factors will certainly be required to explain the small difference between top and left faces, and that between bottom and right faces.

Within the molecular layer of Figure 26 the resulting crystal is divided into four growth sectors surrounding the core. The division is along diagonal lines traced by corners of the expanding square plate. Each sector has a characteristic ratio of chlorine to nitro populations in position 1, as shown in Figure 26b. The same pattern arises by the same mechanism in the other three molecular layers of the unit cell, except that each is rotated by the fourfold screw axis that passes through the center of the original square. Thus under the 1:2.0 sector (top front in Fig. 27, bottom of Fig. 26) lies a 4.6:1 sector obtained by rotating the layer counterclockwise by 90° from the top layer. Next comes a 1:5.3 sector (180° rotation), and

Fig. 27. Perspective view of a stack of four successive layers of DCDNB showing the sequence of chloro:nitro population ratios in the 1-position of molecules in each sector and layer. Adjacent growth sectors of a macroscopic crystal are rotated by 90° from one another and offset by one layer. This corresponds to the presence of a fourfold screw axis passing through the middle of the square.

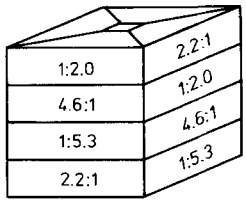

the cell is completed by a 2.2:1 sector (270° rotation). Each of the four sectors of the macroscopic 3-dimensional crystal is a stack of the same set of four different orientational populations in the same order, but from sector to sector the entire set is rotated by 90° and displaced by one layer (Fig. 27). The apparent rotation from sector to sector simply results from exchange of major and minor chloro:nitro populations among molecules with *identical framework orientation throughout the multiply twinned crystal.*

Selective incorporation of misordered molecules in pure DCDNB is analogous to many cases where selective incorporation of impurities gives optically anomalous solid solutions. To support this analogy S. H. Tolbert prepared mixed crystals consisting of about 15% of 5-bromo-1,2,3-trinitrobenzene or 1-bromo-5-chlor-2,3-dinitrobenzene in CTNB, the isomorph of DCDNB with genuine fourfold symmetry.[189] Both solid solutions were optically anomalous, and in both cases X-ray diffraction from single growth sectors showed unsymmetrical distribution of the bromine substituent that differentiates guest from host. Bromine occupancy in sites that would have been related by symmetry in the pure host crystal varied from 1% to 27%. As might be expected, the sites with high bromine occupancy were oriented away from the crystal face that was active in growth of the sector.

4. Current Scientific Relevance of Optical Anomalies

4.1. The Challenge of Crystal Synthesis

One of the most challenging problems for modern chemistry is to develop tools for designing and assembling supra-

molecular structures that involve association of many molecules. Molecular crystals are a familiar and important class of these structures. Since the nonbonded interactions that hold molecular crystals together are weaker and less specific than the bonding interactions among atoms and groups within a single molecule, it is not surprising that methods for controlled crystal synthesis lag far behind those for molecular synthesis. Developing reliable methods for crystal synthesis is an important task, because the external habit and unit cell structure of crystals often determine crucial chemical and physical properties of commercially important solids ranging from pharmaceuticals to explosives, and from devices for nonlinear optics and integrated microelectronics to photographic emulsions. Optically anomalous crystals will assist in this effort both by serving as cases where the mechanism of crystal growth is particularly easy to study and by demonstrating new possibilities for tailoring crystal microstructure both at the growth sector and at the unit cell levels.

Twenty years ago Schmidt began discussing "Crystal Engineering" as the solid-state analogue of synthesis design.[190] Many concepts from molecular synthesis in the fluid phase have their analogues in the controlled preparation of crystals. Table 2 lists some comparisons. Specific growth sites at which new molecules add to a crystal surface play a role in the construction of nonbonds that is analogous to the role of reactive intermediates in the construction of bonds. In particular, the formation of a crystal nucleus, or of a screw defect or kink site on a crystal surface, is analogous to initiation of a free radical chain reaction; addition of a molecule to a kink so as to generate a new kink is analogous to propagation. Determining the structure and properties of these sites will be a key element in learning to control crystal growth.

Table 2. Some analogies between molecular and crystal synthesis.

Molecular Synthesis	Crystal Synthesis
synthetic strategy	crystal engeneering
bond construction	nonbond construction
reactive intermediate	growth site
initiation	nucleation
propagation	growth
termination	poisoning
chemoselectivity	guest discrimination
regioselectivity	habit modification
stereoselectivity	defect orientation
optical activity	birefringence

The growth of pure crystals and solid solutions provides several analogues to the types of selectivity that are sought in molecular synthesis. The choice between host and one or several guests for incorporation in a growing crystal is analogous to chemoselectivity. Purification by recrystallization is a familiar and dramatic example of this kind of selectivity. Addition to selected faces, which dictates the crystal habit, is analogous to regioselectivity. Incorporation of a guest in one among several symmetry-related host sites, as in optically anomalous crystals, is analogous to stereoselectivity.[5, 7, 191]

As in the case of molecular synthesis, the development of new techniques for crystal preparation will profit from an improved understanding of mechanism based on careful studies of prototypical cases. For mechanistic studies the birefringence of solid solutions can play a role analogous to that of optical activity in classical studies of fluid chemistry—it provides a permanent optical record of the course of the reaction. Optically anomalous crystals provide an excellent tool for studying the mechanism of crystal growth because the birefringence of individual sectors presents their growth history in a form that is easily read with a polarizing microscope. For example, while the crystal of Figure 2 grew as a square expanding from the center, the crystal of Figure 28 a grew from a nucleus on the lower edge with molecules in the blue region adding through the right face and those in the yellow region through the top face, and the crystal of Figure 28 b grew in a very complex way with blue regions growing through horizontal faces and yellow regions through vertical faces. The crystal of Figure 28 c grew from at least five different nuclei at various times; four of the nuclei grew toward the front of the crystal and the one nearest the center, toward the rear. Enhanced birefringence in picture frames surrounding the crystals of Figure 28 d indicates some change in crystallization mechanism.

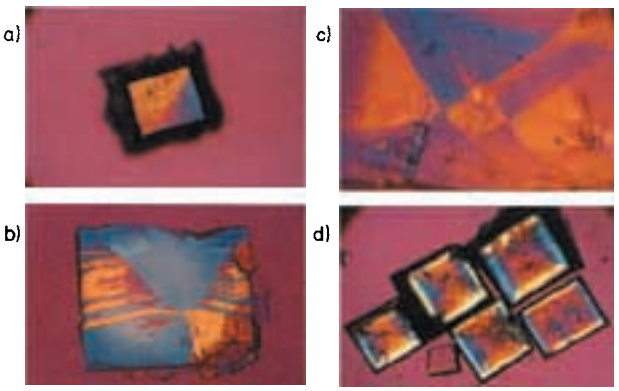

Fig. 28. Crystal plates with curious sectoring. a) Di-11-bromoundecanoyl peroxide containing 15% of the analogue in which one terminal bromine atom is replaced by a methyl group (11-bromoundecanoyl lauroyl peroxide). Although the shape of the rectangle may have been determined by a very thin crystal nucleated at the center, most of the thickening occurred from a nucleus near the left end of the lower edge. b) Pure 11-bromoundecanoyl lauroyl peroxide from acetone/$CHCl_3$. The bent stripes reveal a very complex pattern of crystal growth. c) The same peroxide mixture as in Figure 2. In this case growth occurred from at least five nuclei which occur at different depths in the crystal and thus were active at different times. d) Pure 11-bromoundecanoyl 11′-iodoundecanoyl peroxide. The source of the "picture frame" effect is not yet fully understood.

Birefringence shows not only which face was active during growth of a particular region, but also what kind of symmetry the growth site possessed and how effective it was at ordering the defects. For studies of dilute solid solutions the impurity may be thought of as an "indicator" whose incorporation reveals the growth history of the host. In principle, the same information is present in any solid solution, but strong intrinsic birefringence of the host lattice usually overwhelms the small contribution from unsymmetrically distributed defects. Isotropic or uniaxial hosts provide a blank background against which to view the effect of impurities.

4.2. Design of Desymmetrized Crystals

Optically anomalous crystals are common in both organic and inorganic materials and have even been observed in lunar samples.[192] They should be expected whenever growth kinetics can dictate a nonequilibrium distribution of defects in a high-symmetry crystal. The structure of solid solutions and disordered crystals should always be considered from this point of view. Even when a single crystal appears to have high symmetry, as in the case of DCDNB, single growth sectors can easily belong to the space group of lowest symmetry, $P1$. This realization relates to a general principle for designing crystalline materials: symmetry may be reduced selectively by the introduction of impurities. Symmetry reduction could be useful for developing new technological materials, especially for applications in nonlinear optics,[193] where high symmetry can be deleterious. With increased understanding of surface topography and the mechanisms of crystal growth, it should become possible to design and prepare mixed crystal with more finely tailored microstructures.

4.3. Study of Molecular Reorientation

In cases where a pure crystal is optically anomalous because of nonequilibrium orientation of disordered host molecules, there may be a temperature below the melting point at which the molecules can reorient to achieve the random, symmetrical orientation. The resulting change in birefringence could be used to follow the kinetics of molecular reorientation more easily and in smaller crystal regions than is possible with many spectroscopic techniques.

4.4. Mechanism of Crystal Twinning

The precise cause of crystal twinning is rarely understood.[194] Sometimes it has been attributed to growth of several crystals from a special seed with a higher symmetry than that of the individual crystallites.[194, 195] This cannot be the case for DCDNB because, when a seed cut from a single sector of a twinned crystal was placed in a supersaturated solution of DCDNB in chloroform, it grew into four sectors with the optical orientations predicted by the mechanism outlined in Section 3.2.2. In DCDNB twinning is a natural consequence of the growth kinetics and is not due to a special event or random mistake. The generality of this mechanism merits further study.

4.5. Molecular Recognition

There is great current interest in understanding the way in which weak intermolecular forces operate to allow the components of a supramolecular assembly to recognize one another. Since optical anomalies represent a breakdown of the recognition process during crystallization, investigating them carefully should yield valuable information on intermolecular forces and the mechanism of molecular recognition.

Information on molecular orientation from polarized microscopy is averaged over domains of at least micron dimensions. Standard X-ray diffraction results also represent spatial averages, as in the average Cl/NO_2 ratios depicted in Figure 26. Analysis of diffuse X-ray scattering can provide much more detailed information about molecular recognition by showing specific short-range pair correlations. For a given misordered molecule, diffuse scattering can provide the conditional probability that a particular neighbor is also misordered, rather than just the global probability that molecules in averaged sites are misordered. Following initial work by Flack and Glazer,[196] Welberry has made important theoretical and experimental contributions over the past fifteen years toward understanding short-range order in molecular crystals through diffuse scattering experiments.[197] He and his collaborators have found that local pair correlations can easily be two to four times larger than the average orientational preference revealed by normal Bragg scattering.[198] Optically anomalous, pure crystals like DCDNB, whose growth sectors are easily recognized and could be studied independently, should be particularly well suited for this type of study.

4.6. Value of the Polarizing Microscope

Current studies of optically anomalous crystals demonstrate the value of polarized light microscopy as clearly as investigations in the 19th century did.[199] Fifty years ago the microscope was still recognized as an important tool for chemistry, and students were routinely instructed in its proper use. Although microscopy persists in some areas, such as polymer, liquid crystal, and forensic chemistry, the rise of new analytical techniques and the concentration of academic chemistry on fluid phases have displaced microscopy from most chemistry curricula. McCrone has persistently advocated increased use of the polarizing microscope in analytical chemistry,[200] and growing interest in the solid state should favor a renaissance of this technique, particularly among organic chemists.

Although a microscope may cost 20 to 200 times less than newer tools for studying solids, it is unrivaled for rapid survey of transparent samples, particularly when they are inhomogeneous. Microscopy can be an indispensable adjunct for identifying regions in a solid that are worth more detailed study by other techniques. Without the help of the microscope to identify homogeneous growth sectors, X-ray diffraction can mislead by providing a crystal structure that is averaged over several domains. Microscopy can be as reliable as X-ray diffraction for determining the lattice orientation of a crystal being mounted for spectroscopic study, and it is much faster, but modern reports typically fail to provide relevant simple information on crystal birefringence.

Diffraction methods are unrivaled in providing quantitative structural detail at the atomic level. Still, it is instructive to note that many optical anomalies in mineral samples probably involve Al/Si ordering. These anomalies are easily seen with a microscope, but are nearly invisible to X-rays. Solid-state NMR or neutron diffraction could reveal Al/Si ordering, but both require samples some 10^7 times larger than those necessary for optical microscopy. Quantitative

applications of optical microscopy in organic solid state chemistry would be helped greatly by improvement in simple models for predicting the electric polarizability of molecules.[201]

We are particularly grateful for the contributions of Ms. Sarah Tolbert, Dr. Steven Bertman, and Mr. Randall Carter. This research also benefited greatly from the advice and assistance of Drs. Jay Ague, Fred Allen, Paul Bartholomew, Donald Bloss, Jack Dunitz, Angelo Gavezzotti, Richard Gilardi, Frank Herbstein, Meir Lahav, Antonio Lasaga, Leslie Leiserowitz, John Longhi, Paul Moore, George Rossman, Danny Rye, and Horace Winchell as well as of David Blocher, Ellen Faller, and John Toscano. The work was supported by grants from the Petroleum Research Fund of the American Chemical Society (22712-AC4.6), the National Science Foundation (DMR-8203662), and Merck, Sharp, and Dohme Research Laboratories. In addition J.M.M. was supported by the Office of Naval Research (N00014-89-K-0437) and by a Jacob and Erna Michael Visiting Professorship at the Weizmann Institute of Science.

Received: January 16, 1991 [A 850 IE]
German version: *Angew. Chem.* **1992**, *104*, 1

[1] D. Brewster, *Philos. Mag.* **1835**, *7*, 245.
[2] D. Brewster, *Trans. R. Soc. Edinburgh* **1823**, *9*, 139.
[3] D. Brewster, *Trans. R. Soc. Edinburgh* **1831**, *11*, 273.
[4] a) N. H. Hartshorne, A. Stuart, *Crystals and the Polarising Microscope*, 4th ed., Edward Arnold, London, **1970**; b) [4a], pp 122–124.
[5] J. M. McBride, S. B. Bertman, *Angew. Chem.* **1989**, *101*, 342; *Angew. Chem. Int. Ed. Engl.* **1989**, *28*, 330.
[6] L. Addadi, Z. Berkovitch-Yellin, I. Weissbuch, M. Lahav, L. Leiserowitz, *Top. Stereochem.* **1986**, *16*, 1; M. Vaida, L. J. W. Shimon, Y. Weisinger-Lewin, F. Frolow, M. Lahav, L. Leiserowitz, R. K. McMullan, *Science (Washington)* **1988**, *241*, 1475.
[7] J. M. McBride, *Angew. Chem.* **1989**, *101*, 391; *Angew. Chem. Int. Ed. Engl.* **1989**, *28*, 377.
[8] For the early history of crystallography see a) J. G. Burke, *Origins of The Science of Crystals*, University of California Press, Berkeley, **1966**; b) J. G. Burke in *Toward a History of Geology* (Ed.: C. J. Schneer), MIT Press, Cambridge, **1969**, pp 62–77.
[9] S. H. Mauskopf, *Trans. Am. Philos. Soc.* **1976**, *66*, 5.
[10] In later life Steno left natural science and took Holy Orders. He will probably remain the only crystallographer to have been beatified. C. C. Albritton, Jr., *The Abyss of Time*, Jeremy P. Tarcher, Los Angeles, **1986**, p 40.
[11] N. Steno, *The prodromus of Nicolaus Steno's dissertation concerning a solid body enclosed by process of nature within a solid body* (translated by J. G. Winter) Macmillan, London, **1916**.
[12] M. A. Cappeller, *Prodromus Crystallographie de Crystallis Improprie sic dictis Commentarium*, Heinrich Rennovard Wyssing, Lucerne, **1723** (translated by K. Mieleitner, Munich **1922**).
[13] C. Linnaeus, *Systema naturae*, L. Slavii, Holmiae, Sweden, **1768**.
[14] A. G. Werner, *On the External Character of Minerals* (translated by A. V. Carozzi), University of Illinois Press, Urbana, USA, **1962**.
[15] J. B. L. Romé de l'Isle, *Essai de crystallographie*, Didot Jeune, Paris, **1772**.
[16] R. J. Haüy, *Traité de Minéralogie*, C. Louis, Paris, **1801**.
[17] See [8a], pp 89–93.
[18] H. H. Wollaston, *Philos. Trans. Roy. Soc. London* **1809**, *99*, 253.
[19] In 1830 J. F. C. Hessel ultimately discovered that the external forms of crystals were consistent with the 32 modern point groups (*Krystallometrie oder Krystallonomie und Krystallographie*, Wilhelm Engelmann, Leipzig **1897**) but his work was overlooked until long after Bravais reported similar findings in the 1850s.
[20] E. Bartholinus, *Philos. Trans. R. Soc. London* **1670**, *5*, 2039.
[21] C. Huygens, *Treatise on Light* (translated by S. Thompson), Macmillan, Chicago, **1912**.
[22] J. J. Bernhardi, *J. Chem. Phys. Gehlen* **1807**, *4*, 230.
[23] E. Malus, *Mém. Phys. Chim. Soc. Arcueil.* **1809**, *2*, 143.
[24] An account of the discovery is given by F. Arago, in: *Biographies of Distinguished Men 2*, (translated by W. H. Smyth, B. Powell, R. Grant), Longman, Brown, Green, London, **1857**, pp 117–170.
[25] While Malus recognized the phenomenon of polarization, his conceptual framework, prior to the development of the wave theory of light, was that of the Selectionist. He believed that light was composed of bundles of individual rays each endowed with some polarity, and that polarization phenomena could be accounted for by an elaborate system of ray statistics. See: Jed Buchwald, *The Rise of the Wave Theory of Light*, The University of Chicago Press, Chicago, **1989**, pp 41–67.
[26] F. Arago, *Mém. Inst. Paris* **1811**, *11*, 93–134. We now know that this phenomenon is due to the difference in polarizability, refractive index, and velocity for perpendicularly polarized components of light within the crystal. When these two waves recombine on leaving the crystal, they have suffered an amount of dephasing that depends on their wavelength, so that different colors acquire different degrees of elliptical polarization.
[27] D. Brewster, *Trans. R. Soc. Edinburgh* **1812**, *6*, 184.
[28] J.-B. Biot, *Mém. Inst. Paris* **1812**, *13*, 1.
[29] D. Brewster, *Trans. R. Soc. Edinburgh* **1815**, *7*, 29.
[30] D. Brewster, *Ed. Phil. J.* **1823**, *9*, 361; See also: *ibid.* **1821**, *5*, 217, 218.
[31] D. Brewster, *Ed. Phil. J.* **1819**, *1*, 8.
[32] D. Brewster, *Phil. Trans. Roy Soc. London* **1818**, *108*, 199.
[33] J.-B. Biot, *Mém. Acad. Sci* **1818**, *3*, 177.
[34] A. V. Shubnikov, *Principles of Optical Crystallography*, Consultants Bureau, New York, **1960**, pp 54–61.
[35] a) R. Brauns, *Die Optischen Anomalien der Krystalle*, S. Hirzel, Leipzig, **1891**. b) A more detailed history of the optical anomalies between 1815 and 1891 is given in [35a], pp 5–56.
[36] D. Brewster, *Trans. R. Soc. Edinburgh.* **1818**, *8*, 155.
[37] D. Brewster, *Phil. Trans. Roy Soc. London* **1830**, *120*, 93.
[38] D. Brewster, *Phil. Mag. Ser. 4* **1853**, *6*, 371.
[39] D. Brewster, *Trans. Cam. Phil. Soc.* **1822**, *2*, 1.
[40] A. N. Winchell, *Elements of Optical Mineralogy*, 4th ed., Wiley, New York, **1951**, p. 394.
[41] W. H. Taylor, S. Náray-Szabó, *Z. Krist.* **1931**, *57*, 146.
[42] For refined parameters based on modern X-ray and neutron diffraction data see a) A. A. Colville, C. P. Anderson, *Am. Mineral* **1971**, *56*, 1222; b) G. Y. Chao, *Am. Mineral.* **1971**, *56*, 1234; c) E. Prince, *Am. Mineral.* **1971**, *56*, 1243.
[43] The last substitution requires additional changes for charge compensation. Substitution of AlO for CaF was suggested by M. R. Belsare, *Mineral. Mag.* **1969**, *37*, 288. See [155] and [157] for modern analytical data.
[44] The hydrogen atom of hydroxide also appears to lie on the tetrad axis. See [42c].
[45] A. D. Morrison-Low, J. R. R. Christie, *"Martyr of Science": Sir David Brewster 1781–1868*, Royal Scottish Museum, Edinburgh, **1984**.
[46] D. Brewster, *Trans. R. Soc. Edinburgh* **1834**, *12*, 519.
[47] D. Brewster, *Ed. Phil. J.* **1819**, *1*, 1.
[48] D. Brewster, *Trans. Roy. Soc. Edinburgh* **1823**, *9*, 317.
[49] J. J. Berzelius, *Nouveau Système de Minéralogie*, Méquignon-Marvis, Paris, **1819**.
[50] J. J. Berzelius, *An Attempt to Establish a Pure Scientific System of Mineralogy by the Application of the Electro-Chemical Theory and the Chemical Proportions* (translated by J. Black), Baldwin and Blackwood, London, **1814**.
[51] J. J. Berzelius, *Ed. Phil. J.* **1822**, *7*, 1.
[52] D. Brewster, *Ed. Phil. J.* **1822**, *7*, 12.
[53] J. J. Berzelius, *Poggendorf's Ann. Phys. Chem.* **1830**, *19*, 305.
[54] See [35a], p. 17.
[55] J. F. W. Herschel, *Vom Licht* (translated by E. Schmidt), J. G. Cotta, Stuttgart, **1831**, p. 630.
[56] a) Biot supported the notion that Newton had become insane when, late in life, he became seriously interested in theology. Brewster vigorously defended Newton against these assertions in the second volume of his *Memoirs of the Life, Writings and Discoveries of Sir Isaac Newton*, Edinburgh, **1855**. See [45], pp. 53–56. b) At the age of 72 Biot himself formally returned to the Catholic Church, an institution which Brewster had comdemned. See M. Crossland, *The Society of Arcueil*, Harvard University Press, Cambridge, **1967**, p. 93.
[57] J.-B. Biot, *Traité de Physique IV*, Ch. Deterville, Paris, **1816**, p. 573.
[58] a) D. Brewster, *A Treatise on Optics*, Longman, Brown, Green, and Longmans, London, **1853**, p. 280.
[59] J.-B. Biot, *Mémoire sur la polarisation lamellaire*, in: (*Mém. Acad. Sci. Inst. Fr., 2ème Ser.* **1842**, *18*; pp. 539–725).
[60] See [58a], p. 279.
[61] a) J.-B. Biot, *C. R. Hebd. Seances Acad. Sci.* **1841**, *12*, 967; b) **1841**, *13*, 391.
[62] See [61a], p. 973.
[63] See [58a], p. 279–283.
[64] See [58a], p. 346.
[65] a) V. Ronchi, *The Nature of Light*, Harvard University Press, Cambridge, **1970**; b) pp. 231–260.
[66] Cf. [61], pp. 99–107; See also E. Frankel, *Jean-Baptiste Biot: The Career of a Physicist in Nineteenth Century France* (*Dissertation*, Princeton University, **1972**, pp.234–256).
[67] See [61a], p. 979.
[68] J.-B. Biot, *C. R. Hebd. Seances Acad. Sci.* **1846**, *23*, 909.

[69] L. Pasteur, *C. R. Hebd. Seances Acad. Sci.* **1848**, *26*, 304.
[70] M. L. Frankenheim, *Die Lehre von der Kohäsion umfassend die Elastizität der Gase, die Elastizität und Kohärenz der flüssigen und festen Körper und die Kristallkunde*, August Schulz Breslau, **1835**.
[71] M. L. Frankenheim, *Ann. Phys. Chem.* **1860**, *111*, 31.
[72] See [35a], p. 22.
[73] H. Marbach, *Ann. Phys. Chem.* **1885**, *170*, 412.
[74] W. Wertheim, *Ann. Phys. Chem.* **1852**, *86*, 325; **1852**, *87*, 498.
[75] For biographical information see G. Wyrouboff, *Bull. Soc. Min. Fr.* **1894**, *17*, 241; A. de Lapperant, *Ann. Mines. Mem. 9ème Ser.* **1895**, *7*, 267.
[76] A. Bravais, *On the Systems Formed by Points Regularly Distributed on a Plane or in Space* (translated by A. J. Shaler), Crystallographic Society of America, **1949**.
[77] E. Mallard, *Ann. Mines. Mem. 7ème Ser.* **1876**, *10*, 60.
[78] See [77], pp. 65–66.
[79] See [77], pp. 121–122.
[80] D. Brewster, *Phil. Trans. Roy. Soc. London* **1814**, *104*, 397, 436; **1815**, *105*, 1.
[81] a) D. Brewster, *Phil. Trans. Roy. Soc. London* **1815**, *105*, 60; b) **1816**, *106*, 156; **1830**, *120*, 87, c) *Trans. Roy. Soc. Edinburgh.* **1818**, *8*, 218, 354.
[82] E. Reusch, *Ann. Phys. Chem.* **1867**, *208*, 618.
[83] For biographical information see F. von Wolff, *Centralblatt. Mineral. A* **1907**, 640.
[84] F. Klocke, *Neues Jahrb. Mineral. Geol. Paläontol.* **1880**, *I*, 53.
[85] F. Klocke, *Neues Jahrb. Mineral. Geol. Paläontol.* **1881**, *II*, 249.
[86] A. Ben-Saude: *Neues Jahrb. Mineral. Geol. Paläontol.* **1882**, *I*, 41.
[87] A. Ben-Saude, *Beitrag zu einer Theorie der Optischen Anomalien der Regulären Krystalle*, National Druckerei, Lissabon, **1894**.
[88] C. Klein, *Neues Jahrb. Mineral. Geol. Paläontol.* **1885**, *II*, 237; **1887**, *I*, 223.
[89] A. Fock, *An Introduction to Chemical Crystallography* (translated by W. J. Pope), Clarendon Press, Oxford, **1895**, pp. 164–165.
[90] F. Klocke, *Neues Jahrb. Mineral. Geol. Paläontol.* **1881**, *I*, 204; see also [85].
[91] C. Klein, *Neues Jahrb. Mineral. Geol. Paläontol.* **1884**, *I*, 253.
[92] F. Rinne, *Neues Jahrb. Mineral. Geol. Paläontol.* **1885**, *II*, 19.
[93] L. Ditscheiner, *Sitzungsb. Kaiser. Akad. Wiss. Wien*, **1860**, *43*, 229. Brauns later pointed out that it would be difficult to mimic high symmetry by this means, because simultaneous compensation at all wavelengths would be unlikely. See also [35a], p. 26.
[94] R. Brauns, *Neues Jahrb. Mineral. Geol. Paläontol.* **1883**, *II*, 102.
[95] R. Brauns, *Neues Jahrb. Mineral. Geol. Paläontol.* **1885**, *I*, 96; *Dissertation*, Marburg, **1885**.
[96] R. Brauns, *Was wissen wir über die Ursachen der optischen Anomalien?* Habilitacion, Verein der preussischen Rheinlande und Westfalen, **1887**, p. 510.
[97] See [35a], p. 257–258.
[98] A. Ben-Saude, *Die Wahrscheinlichen Ursachen der Anomalen Doppelbrechung der Krystalle*, National Druckerei, Lisbon, **1896**. For a review by R. Brauns see *Neues Jahrb. Mineral. Geol. Paläontol. Ref.* **1897**, *II*, 249. For an earlier critique see R. Brauns, *ibid*, **1895**, *I*, 1, **1895**, 133.
[99] E. Mallard, *Bull. Soc. Min. Fr.* **1886**, *9*, 54.
[100] R. Brauns, *Neues Jahrb. Mineral. Geol. Paläontol.* **1887**, *I*, 47.
[101] P. Groth reviewed Mallard's treatise. See: *Z. Kryst.* **1877**, *6*, 309.
[102] P. Groth, *Physikalische Krystallographie*, Wilhelm Engelmann, Leipzig, **1876**, (4th ed. 1905).
[103] See [35a], p. 55.
[104] E. Mallard, *Traité de cristallographie géométrique et physique*, Paris, **1879–1884**.
[105] F. Wallerant, *Cristallographie*, C. Béranger, Paris, **1909**, p. I. Wallerant's book was intended to address some of the concerns in the lost volume, but it did not contain the polemic against the German view that might have expected from Mallard.
[106] G. Wyrouboff, *Mineral. Mag.* **1894**, *10*, 828.
[107] A. Johannsen, *Manual of Petrographic Methods*, McGraw-Hill, New York, **1918**, pp. 510–514.
[108] Des Cloizeaux (1878, 1889), Mallard (1879, 1892), G. Friedel (1881), Bertrand (1886, 1901), Jannettaz (1887) and Wyrouboff (1891, 1902); also Wallerant (1899, 1905, 1916, 1930).
[109] See obituary notice of F. Zirkel, *Centralblatt Min.* **1912**, 513.
[110] The Society sponsored 14 other prize competitions in mathematics and the natural sciences between 1847 and 1911.
[111] See [35a], p. iv.
[112] For biographical information see *Festband Reinhard Brauns*: E. Kaiser, E. Lehmann, H. Schneiderhölm, O. Weigel, *Neues Jahrb. Mineral. Geol. Paläontol. Beilage-Band* **1931**, *64* iv-xxii.
[113] J. W. v. Goethe, *Vier Jahreszeiten*, Werkstätten der Stadt Halle, Burg Giebichstein, **1937**.
[114] See [35a], p. 57.
[115] C. M. Viola, *Grundzüge der Kristallographie*, Wilhelm Engelmann, Leipzig, **1904**, pp. 269–274; M. Bauer, *Lehrbuch der Mineralogie*, E. Schweizerbart, Stuttgart, **1904**, pp. 325–328; F. Pockels, *Lehrbuch der Kristalloptik*, B. G. Teubner, Stuttgart, **1906**, pp. 488–490; A. Johannsen, *Manual of Petrographic Methods*, McGraw-Hill, New York, **1918**, pp. 508–514; G. Tschermak, *Lehrbuch der Mineralogie*, Alfred Hölder, Wien, **1921**, pp. 256–260; E. S. Dana, *A Textbook of Mineralogy*, J. Wiley, New York, **1932**, pp. 329–332; P. Ramdohr, *Klockmanns Lehrbuch der Mineralogie*, Ferdinand Enke, Stuttgart, **1948**, pp. 179–181; *History of Science in the Nineteenth Century* (Ed..: R. Taton; translated by A. J. Pomerans), Basic Books, New York, **1961**, p. 313.
[116] For biographical information, see F. Wallerant, *Bull. Soc. Min. Fr.* **1914**, *37*, 44.
[117] At least three previous dissertations from the Göttingen Mineralogical Institute had also dealt with anomalous organic crystals. (J. Zingel, 1883; H. Söffing, 1883; and O. Heintze, 1884), but their nature, and sometimes even the molecular structures, are unclear. They include methylbenzylhydroxamic acid, a paradinitrotoluidine/$C_9H_{10}N_4O_6$ mixture, biphenyldodecachloride, and glucose sodium chloride (Traubenzuckerchlornatrium). See: C. Klein, *Neues Jahrb. Mineral. Geol. Paläontol.* **1885**, *II*, 237.
[118] J. Martin, *Beiträge zur Kenntniss der optischen Anomalien einaxiger Krystalle*, Dissertation, Universität Göttingen, **1890**; J. Martin, *Neues Jahrb. Mineral. Geol. Paläontol. Beilage-Band* **1891**, *7*, 1. Reviewed by J. Beckenkamp, *Z. Kryst.* **1892**, *21*, 138.
[119] G. Wyrouboff, *Bull. Soc. Min. Fr.* **1890**, *13*, 94.
[120] H. A. Miers, *Mineral. Mag. Abs.* **1887**, *7*, 177.
[121] E. S. Fedorov, *Zap. Ross. Mineral. Obshchestva. Ser. 2*, **1891**, *28*, 345.
[122] A. Schoenflies, *Kristallsysteme und Kristallstruktur*, Leipzig, **1891**.
[123] W. J. Pope, *J. Chem. Soc.* **1935**, 1328.
[124] W. Barlow, *Nature* **1883**, *29*, 186, 205. See also editor's comments: *Crystal Form and Structure* (Ed..: C. J. Schneer), Dowden, Hutchison and Ross, Stroudsburg, PA, **1976**, pp. 54–55.
[125] While Barlow was aware of the contributions of Federov and Schoenflies he refers his proposed structures to the incomplete space group symmetry theory of Leonhard Sohncke (*Entwicklung einer Theorie der Kristallstruktur*, Leipzig, **1879**).
[126] W. Barlow, *Scientific Proceedings of the Royal Society of Dublin, New Series* **1897**, *8*, 620–665.
[127] See [126], p. 624.
[128] See [126], p. 663.
[129] W. G. Burgers, *Proc. Roy. Soc. London* **1927**, *A 116*, 553.
[130] J. W. Gruner, *Am. Mineral.* **1934**, *19*, 112.
[131] F. Rinne, *Centralblatt Mineral. A* **1925**, 225; **1927**, 1; see also F. Rinne, *Z. Krist.* **1926**, *63*, 236.
[132] B. Gossner, O. Kraus, *Z. Krist.* **1928**, *68*, 595.
[133] a) R. Hocart, *Contribution à l'étude de quelques cristaux à anomalies optiques*. Thèse Univ. Strasbourg, Paris, **1934**; b) *Bull. Soc. Min. Fr.* **1934**, *57*, 5–125.
[134] F. Pockels, *Neues Jahrb. Mineral. Geol. Paläontol. Beilage-Band*, **1893**, *38*, 217.
[135] See [133b], pp. 18–19.
[136] See [133b], p. 125.
[137] See [133b], p. 7.
[138] A. Neuhaus, *Z. Kristallogr.* **1943**, *105*, 195.
[139] G. Will, *Fortschr. Miner.* **1977**, *54*, 1.
[140] *Science Citation Index*, Institute for Scientific Information.
[141] a) *Dictionary of Scientific Biography, Vol. 13*, (Ed.: C. C. Gillispie), Charles Scribner's, New York, **1970**, p. 242; b) W. E. Garner, *J. Chem. Soc. 1952*, 1961; c) G. Masing, *Ber. Dtsch. Chem. Ges.* **1940**, *73*, 25.
[142] Collected in G. Tammann, *Z. anorg. allg. Chem.* **1919**, *107*, 107ff, and in *Die chemischen und galvanischen Eigenschaften von Mischkristallreihen und ihre Atomverteilung*, L. Voss, Leipzig, **1919**. See comments in: W. Fraenkel, *Die Naturwissenschaften* **1920**, *8*, 161.
[143] G. Tammann, *Nachr. Ges. Wiss. Göttingen Math-Phys. Kl.* **1917**, *2*, 216.
[144] R. Brauns, *Neues Jahrb. Mineral. Geol. Paläontol. Ref.* **1919**, 262.
[145] L. S. Hollister, *Am. Mineral.* **1970**, *55*, 742; E. Dowty, *Am. Mineral.* **1976**, *61*, 460; J. Paquette, R. R. Reeder, *Geology* **1990**, *18*, 1244–1247.
[146] F. D. Bloss, *Crystallography and Crystal Chemistry*, Holt, Rinehart, and Winston, New York, **1971**, Chap. 10.
[147] M. A. Carpenter, *Phys. Chem. Miner.* **1986**, *13*, 119.
[148] See [4], pp. 321–322.
[149] J. B. Parise, C. Cuff, F. H. Moore, *Mineral. Mag.* **1980**, *43*, 943.
[150] G. R. Rossman, R. D. Aines, *Am. Mineral.* **1986**, *71*, 779.
[151] F. M. Allen, P. R. Buseck, *Am. Mineral.* **1988**, *73*, 568.
[152] Y. Takéuchi, N. Haga, S. Umizu, G. Sato, *Z. Krist.* **1982**, *158*, 53.
[153] M. Akizuki, I. Sunagawa, *Mineral. Mag.* **1978**, *42*, 453.
[154] M. Akizuki, *Am. Mineral.* **1987**, *72*, 645.
[155] T. G. Sahama, *Mineral. Mag.* **1965**, *34*, 406. Since Sahama's sample showed no basal planes, his layer lacked the central uniaxial sector.
[156] I. Kostov, *N. Jahrb. Min. Abh.* **1975**, *123*, 128.
[157] M. Akizuki, H. Konno, *N. Jahrb. Min. Abh.* **1985**, *151*, 99.
[158] The microprobe analysis was carried out by P. Bartholomew, Department of Geology and Geophysics, Yale University.
[159] J. H. Donnay, H. M. Ondik, *Crystal Data, Determinative Table*, 3rd ed., U.S. Department of Commerce, National Bureau of Standards, and Joint Committee on Powder Diffraction Standards, **1972, 1973**. M. W. Porter, R. C. Spiller, *The Barker Index of Crystals*, W. Heffer, Cambridge, **1956**.

[160] P. Groth, *Chemische Krystallographie*, Wilhelm Engelmann, Leipzig, **1906–1919**.
[161] The optical anomaly in benzil was first observed by Wyrouboff; see: G. Wyrouboff, *Bull. Soc. Min. Fr.* **1884**, *7*, 86. For a modern X-ray topographical study see: H. Klapper, *J. Cryst. Growth* **1971**, *10*, 13.
[162] O. Tietze, *Neues Jahrb. Mineral. Geol. Paläontol.* **1899**, *II*, 21.
[163] G. A. Jeffrey, R. A. Ward, P. E. Pfeffer, K. B. Hicks, *J. Am. Chem. Soc.* **1983**, *105*, 2128.
[164] Space group *I4*. For three generations of pentaerythritol diffraction studies see: F. J. Llewellyn, E. G. Cox, T. H. Goodwin, *J. Chem. Soc. London* **1937**, 883; J. Nitta, T. Watanabé, *Nature* **1937**, *140*, 365; J. Hvoslef, *Acta Cryst.* **1958**, *11*, 383; R. Shiono, D. W. J. Cruickshank, E. G. Cox, *ibid.* 389; D. Eilerman, R. Rudman, *Acta Cryst.* **1979**, *B35*, 2458; M. F. C. Ladd, *ibid.* 2375.
[165] For common impurities see: T. J. Simons, R. L. DeSilva, D. E. Creasy, *J. Chem. Tech. Biotechnol.* **1976**, *26*, 30; B. Clatworthy, S. Rehmatullah, A. B. A. Wahab; D. E. Creasy, *ibid.* **1982**, *32*, 518.
[166] R. L. Carter, unpublished.
[167] D. Eilerman, R. Lippman, R. Rudman, *Acta Crystallogr. Sect. B* **1983**, *B39*, 263.
[168] Space group $P1$, $a = 12.075$, $b = 27.054$, $c = 24.584$ Å, $\alpha = 131.22$, $\beta = 119.35$, $\gamma = 63.53°$. R. L. Carter, B. Kahr, J. M. McBride, unpublished.
[169] H. Traube, *Sitz. Akad. Wiss. Ber.* **1895**, *10*, 198; *Z. Kryst.* **1898**, *30*, 403.
[170] H. Traube, *Neues Jahrb. Mineral. Geol. Paläontol. Beilage-Band* **1897**, *11*, 624. There is some confusion as to which salt of malic acid gives optically anomalous tetragonal crystals. Traube's later publication (*Z. Krystallogr.* (**1898/1899**) 160) indicates that the interesting crystals are the magnesium salt..
[171] L. K. Tempelton, D. H. Tempelton, *Acta Crystallogr. A* **1978**, *34*, 368.
[172] L. Bohaty', R. Fröhlich, *Z. Kristallogr. B* **1978**, *164*, 291.
[173] J. M. Adams, R. W. H. Smith, *Acta Crystallogr.* **1974**, *30*, 2191.
[174] Rotation is difficult to observe in biaxial crystals because of the simultaneous transformation from plane to elliptical polarization. In uniaxial plates it is easier to arrange for measurement along the optic axis, in which direction light can remain plane polarized.
[175] A. Des Cloizeaux, *Ann. Phys.* **1857**, *102*, 474.
[176] G. Wyrouboff, *Bull. Soc. Mineral. Fr.* **1884**, *7*, 10.
[177] $a = b = 7.61$, $c = 62.0$ Å.
[178] A monoclinic pentahydrate from ethanol has been studied, but it may differ from the dehydration product. C. Bokhoven, J. C. Schoone, J. M. Bijvoet, *Acta Crystallogr.* **1951**, *4*, 275.
[179] A. V. Jagannadham, *Z. Kristallogr.* **1957**, *108*, 457; A. Prakash, *Z. Krist.* **1965**, *122*, 272.
[180] B. Kahr, unpublished.
[181] G. Smulevich, M. P. Marzocchi, *Stud. Biophys.* **1984**, *104*, 105; *Chem. Phys.* **1985**, *94*, 99; *ibid.* **1986**, *105*, 159.
[182] The site symmetry of molecules in the plates is $C1$; it is not known for the needles.
[183] We thank Dr. K. Valentine at Princeton University for obtaining the ^{13}C CPMAS-NMR spectra and Dr. Bruce Hawkins at the NSF Regional NMR Facility at Colorado State University for the ^{1}H CRAMPS-NMR spektra.
[184] E. Artini, *Rendiconti Ist. Lomb. Sc. Lett.* **1907**, *11*, 1024.
[185] $a = 6.775(8)$, $b = 6.805(7)$, $c = 19.06(3)$ Å, $\alpha = 90.08(8)$, $\beta = 90.05(6)$, $\gamma = 89.98(5)°$. B. Kahr, J. M. McBride, unpublished.
[186] $a = b = 6.7815(5)$, $c = 19.386(2)$ Å. However, 1,3,5-trichloro-2-nitrobenzene (space group $C2/c$) is not isomorphous with DCDNB and CTNB. B. Kahr, S. H. Tolbert, J. M. McBride, unpublished.
[187] Pentachloronitrobenzene: I. Tanaka, F. Iwasaki, A. Aihara, *Acta Crystallogr. Sect. B* **1974**, *30*, 1546; *p*-chloronitrobenzene: T. C. W. Mak, J. Trotter, *Acta Crystallogr.* **1962**, *15*, 1078.
[188] Other observations suggest that *inter*layer contacts between nitro groups not only establish the screw relationship between adjacent layers but also favor the pattern of *intra*layer contacts by an indirect mechanism.
[189] B. Kahr, J. M. McBride, S. H. Tolbert, unpublished.
[190] G. M. J. Schmidt, *Pure Appl. Chem.* **1971**, *27*, 647.
[191] H. E. Buckley, *Crystal Growth*, Wiley, New York, **1952**.
[192] U. B. Marvin, J. W. Carey, M. M. Lindstrom, *Science*. **1990**, *243*, 925.
[193] *Nonlinear Optical Properties of Organic Molecules and Crystals*, (Eds.: D. S. Chemla, J. Zyss), Academic Press, New York, **1987**; D. J. Williams, *Angew. Chem. Int. Ed. Eng.* **1984**, *23*, 690–703; I. Weissbuch, M. Lahav, L. Leiserowitz, G. R. Meredith, H. Vanherzeele, *Chem. Mater.* **1989**, *1*, 114.
[194] M. Senechal, *Comput. & Math. Appl.* **1986**, *12B*, 565.
[195] H. P. Zeck, *Nature, Physical Science* **1972**, *238*, 47.
[196] H. D. Flack, A. M. Glazer, *Philos. Trans. R. Soc. London* **1970**, *A266*, 559ff.
[197] T. R. Welberry, *Rep. Prog. Phys.* **1985**, *48*, 1543, and references cited therein.
[198] T. R. Welberry, J. Siripitayananon, *Acta Crystallogr. Sect. B* **1987**, *B43*, 97; T. R. Welberry, R. D. G. Jones, J. Epstein, *ibid* **1982**, *38*, 1518.
[199] For recent descriptions of the use of the polarizing microscope see: F. D. Bloss, *An Introduction to the Methods of Optical Crystallography*, Holt, Rinehart, and Winston, New York, **1961**; W. C. McCrone, L. B. McCrone, J. G. Delly, *Polarized Light Microscope*, 8th ed., Ann Arbor Science, Ann Arbor, MI, USA, **1978**; and [4a].
[200] W. McCrone, *Acc. Chem. Res.* **1990**, *23*, 77; F. W. McLafferty, *Acc. Chem. Res.* **1990**, *23*, 63.
[201] S. S. Batsanov, *Refractometry and Chemical Structure* (translated by P. P. Sutton), Consultants Bureau, New York, **1961**.

Cycloalkadiynes—From Bent Triple Bonds to Strained Cage Compounds

By Rolf Gleiter*

Dedicated to Professor Heinz A. Staab on the occasion of his 65th birthday

The synthesis of cycloalkadiynes with medium-sized rings may be accomplished by a number of ring-closing and elimination reactions. Information concerning the conformation of the rings as well as the extent of transannular interaction between the triple bonds is obtained by analysis of X-ray crystallographic data and by photoelectron spectroscopy. The diacetylene complexes of Ag^I and Cu^I show hardly any structural change compared to the uncomplexed compounds while the bis(hexacarbonyldicobalt) complexes differ significantly in their structural parameters. Reaction of cycloalkadiynes with dicarbonyl(η^5-cyclopentadienyl)cobalt yields inter- and intramolecular cyclobutadiene complexes. The superphane of cyclobutadiene formed by the intermolecular reaction can be transformed into a number of highly strained cage compounds in few steps. In addition, the variety of such cage compounds can be increased if the reaction of a cyclic diacetylene is carried out with dimethylacetylenedicarboxylate in the presence of aluminum chloride. The intermediate bridged Dewar benzenes eventually lead to propellaprismanes.

1. Introduction

Research carried out on dehydroannulenes in the 60s and 70s initiated chemists' interest in cyclic conjugated alkadiynes and oligoynes.[1] Among the first such compounds to be studied were 1,8-dehydrol[14]annulene (**1**)[2] and 5,6,11,12,17,18-hexadehydrotribenzo[*a*,*e*,*i*]cyclododecene (**2**).[3] Interest was focused on syntheses and properties of novel 4n and (4n + 2) π systems. The ultimate question was

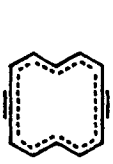

1

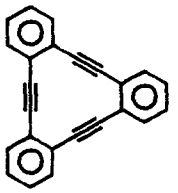

2

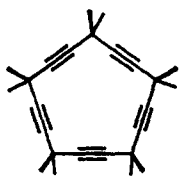

3

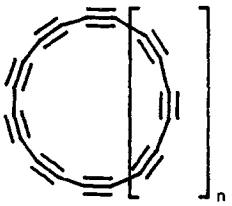

4

whether a triple bond could function as part of an aromatic polyene. Spectroscopic evidence as well as results from X-ray structures could unequivocally confirm this matter.[1] Closely related to the research on conjugated eneynes was the work carried out on pericyclynes,[4] in which the key point was the possible homoconjugation of triple bonds as is seen for example in [5]pericyclyne (**3**). Also related to the early research[1-3] are the attempts to synthesize cyclic polyacetylenes of the generic structure **4** with 18, 24, or 30 carbon atoms.[5] Besides the conjugative effects exhibited by these cycles in their neutral as well as ionic states these compounds are of interest due to their relationship to C_{60}-fullerene.[6]

Another group of compounds which should be mentioned at this point are the recently discovered enediynes with structures **5**–**7** (aglycons of the anticancer antibiotics neocarzinostatin, calicheamicin, and esperamicin).[7] In the decisive step

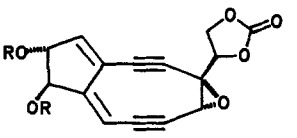

5

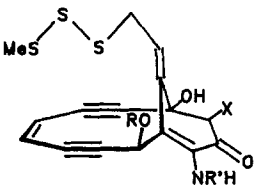

6 X = H
7 X = OH

responsible for the biological activity of this type of compound, a Bergman cyclization (**8** → **9**) is postulated, which yields a ring-contracted species.[8] The short-lived diradical **9** acts as a H atom scavenger and presumably is the primary cause of DNA scission.

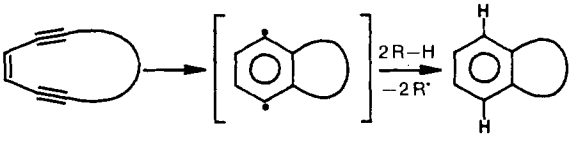

8 **9** **10**

The synthetic potential of open-chain α,ω-diynes and their exploitation as precursors for carbo- and heterocyclic compounds has been extensively reviewed elsewhere.[9]

Our initial interest in cyclic diacetylenes was stimulated by model calculations and spectroscopic measurements in the

[*] Prof. Dr. R. Gleiter
Organisch-Chemisches Institut der Universität Heidelberg
Im Neuenheimer Feld 270, D-W-6900 Heidelberg (FRG)

area of π/σ interactions.[10] Cyclic diacetylenes prove to be ideal model systems for studying such effects, as is evident from the following arguments: Consider the highest occupied molecular orbitals (HOMOs) of cisoid 1,5-hexadiyne (**11**) and 1,6-heptadiyne (**12**). The π molecular orbitals of the two triple bonds in **11** and **12** may be divided into two sets, those that lie in the plane of the molecule (π_i) and those that lie perpendicular to the latter (π_o). Each basis set leads to two

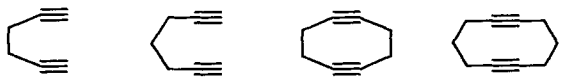

11 **12** **13** **14**

linear combinations, which are either symmetric (π_i^+, π_o^+) or antisymmetric (π_i^-, π_o^-) with respect to the x,z-plane (Fig. 1). Figure 2 shows the corresponding MO energy levels of **11** and **12** compared to those of two propyne molecules separated by distances of approximately 2.6 and 3.0 Å. The splitting

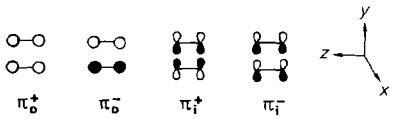

Fig. 1. Schematic representation of the four linear combinations π_o^+, π_o^-, π_i^+ and π_i^-.

of the π_o levels can be easily understood: The difference in energies between π_o^+ and π_o^- is larger for **11** than **12**, because the distance between the triple bonds ($r \approx 2.6$ Å) in **11** is smaller than in **12** ($r \approx 3$ Å). The splitting of the π_i levels, on the other hand, is much smaller in **11** than in **12**.

The reason for these large deviations can be traced back to the different extent of π/σ interaction. In **11** the π_i^+ MO is destabilized in comparison to the analogous MO in the two propyne molecules by interaction with a_1 (σ) of the ethano bridges while π_i^- remains unaffected. In **12** on the other hand π_i^- is mainly destabilized by interaction with the σ frame. The predictions made in Figure 2 can best be tested by examining two model compounds, 1,5-cyclooctadiyne (**13**) and 1,6-cyclodecadiyne (**14**). Photoelectron spectroscopy (PE) is the most appropriate method, since this procedure gives direct information about the energy levels in molecules within the limits of Koopmans' approximation.

These initial contemplations motivated us to synthesize **14** and a number of other cyclic diacetylenes with medium-sized

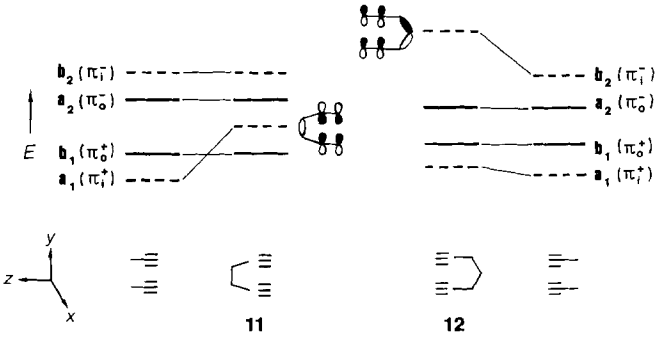

Fig. 2. Correlation between the HOMOs of two propyne units (left, right), 1,5-hexadiyne (**11**), and 1,6-heptadiyne (**12**).

rings.[11] To limit the extent of this review, we will only discuss those cyclic diynes which are generally unconjugated.

2. Synthesis of Cyclic Diacetylenes

Synthetic routes to cyclic acetylenes with medium-sized rings have been extensively reviewed in the literature.[12, 13] Therefore, these older methods will be referred to only in those cases where they are also relevant to the syntheses of cyclic diacetylenes.

2.1. Cycloalkadiynes from Nucleophilic Substitution Reactions (Ring-Closing Reactions)

Reaction of α,ω-dihaloalkanes with the dialkalimetal salt (Na, Li) of α,ω-diacetylenes yields cyclic diacetylenes, as is exemplified by the preparation of 1,8-cyclotetradecadiyne (**17**) from 1,5-dibromopentane (**15**) and 1,8-nonadiyne (**16**). Application of this method to the synthesis of 1,7-cyclododecadiyne (**18**) and other C_{13} to C_{16} rings furnishes these products in yields ranging from 10 to 57%.[14, 15] In an analogous fashion 1,6-dioxa-3,8-diyne (**21**)[16] and 1,6-dithia-3,8-diyne (**27c**)[17] may be prepared in one-pot reactions. As an illustration the multistep synthesis of the thia-3,8-diynes **27a–d** will be outlined.[18]

The starting metalated 1,6-heptadiyne derivatives **24a–d** are hydroxymethylated to **25a–d** and then transformed to the dibromides **26a–d**. Thiacyclization to **27a–e** is achieved with either tributyltinsulfide,[19] $NaS_2 \cdot 9H_2O$ (making use of the cesium effect[20]), or NaS_2 on Al_2O_3.[21] The latter method, originally described by Nicolaou and coworkers,

Rolf Gleiter studied chemistry at the University of Stuttgart, completing his Ph.D. in 1964 under F. Effenberger. After postdoctoral stays with P. von R. Schleyer at Princeton University (1966) and R. Hoffmann at Cornell University (1967–1968), he went to Basel and completed his habilitation under E. Heilbronner (1969–1972). In 1973 he accepted the position of Professor for Theoretical Organic Chemistry at the Technische Hochschule in Darmstadt. Since 1979 he has been Professor for Organic Chemistry at the University of Heidelberg. His areas of interest include the bonding relationships in inorganic and organic ring systems and the interactions in nonconjugated π systems as well as those between free electron-pairs in heterocycles and polyketones. In the last few years he has been involved mainly with the syntheses of model compounds, for example cyclic acetylenes, cage molecules, and polyketones.

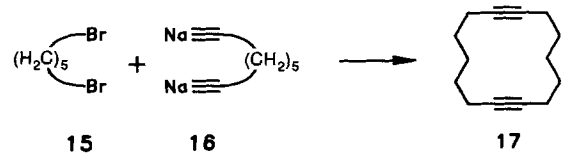

15 16 17

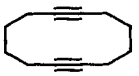

18

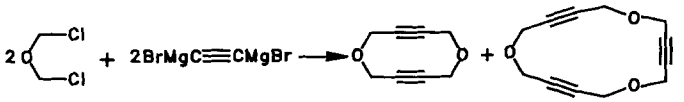

19 20 21 22

has been used successfully in the syntheses of cyclic enediynes of type **8**.[8, 21] The preparation of undec-3-ene-1,5-diyne (**31**) illustrates this method (Scheme 1) in which the

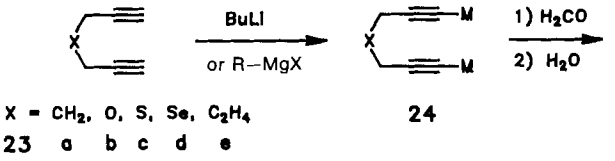

X = CH_2, O, S, Se, C_2H_4

23 a b c d e

24

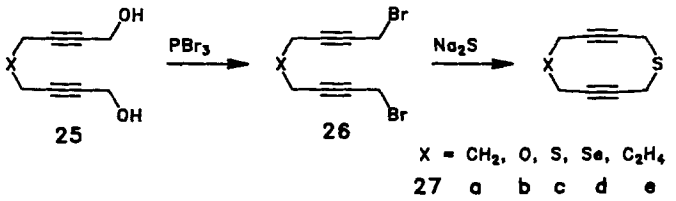

X = CH_2, O, S, Se, C_2H_4

25 26 27 a b c d e

decisive step is a Ramberg–Bäcklund ring contraction (**30** → **31**). A heterocyclic diyne, 1,6-diselena-3,8-cyclodecadiyne (**34**) was prepared by reductively coupling diselenacyanate **33** with dibromide **32** according to Misumi's method.[22] This reaction furnished **34** in up to 50% yield.[18b] The alkyl derivatives of 1,6-diazacyclodeca-3,8-diyne, for example **36**, have been prepared in one-pot reactions from the corresponding alkylamines and **32** in yields of 5%.[23a] In a procedure analogous to that used in the synthesis of **27** the 1-aza-6-thia-3,8-diynes of type **37** and **38** were prepared.[23b, 23c]

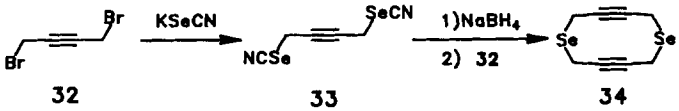

32 33 34

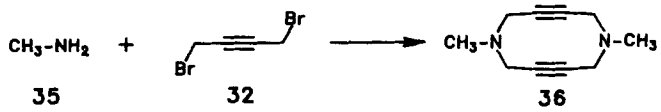

35 32 36

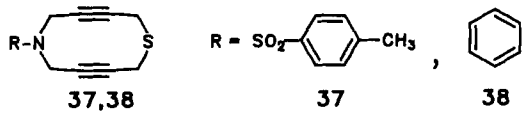

37,38 37 38

Recently nucleophilic substitution has also been used to obtain a number of homoconjugated enediynes with C_{10}–C_{12} rings.[24] Scheme 2 outlines this method in the preparation of **41**–**43**;[24b] diynes **39** and **40** were synthesized in an analogous manner. Although the last step of this route gives in some cases only 5% yield, this sequence still provides the easiest access to this type of structure. Earlier attempts at the synthesis of **41** and **42a** failed probably because the final step was carried out in the presence of Cu^I salts.[25, 26]

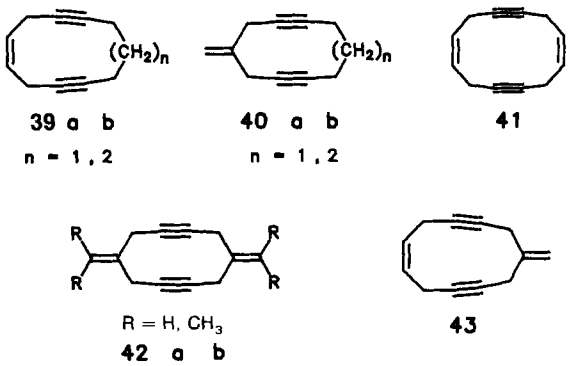

39 a b n = 1, 2

40 a b n = 1, 2

41

R = H, CH_3

42 a b

43

Scheme 2. Synthesis of compounds **41**–**43**.

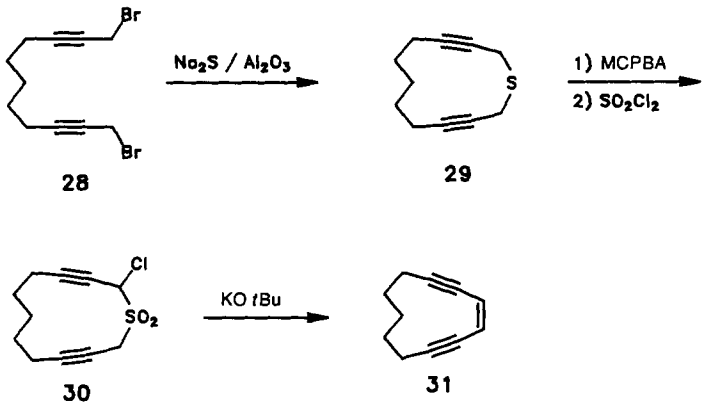

28 29 30 31

Scheme 1. MCPBA = *meta*-chloroperbenzoic acid.

Other cyclic dialkynes, such as conjugated **50**[27] and **53**,[28] were prepared by nucleophilic substitution reactions via the metalated intermediates **49** and **52**. A nice adaptation of this procedure is the intramolecular nucleophilic attack of a C-H acidic moiety on an electrophilic component as in **54**, leading to the synthesis of the 10–13-membered rings **55** (n = 1–4).[29] Unfortunately the ester groups in **55** can be cleaved only with difficulty or not at all.

Two methods employed more recently should be mentioned at this point, since they were used in the synthesis of the potential anticancer agents **59** and **62**.[30, 31] In the preparation of **59** the $[Co_2(CO)_6]$ fragment is used to stabilize an

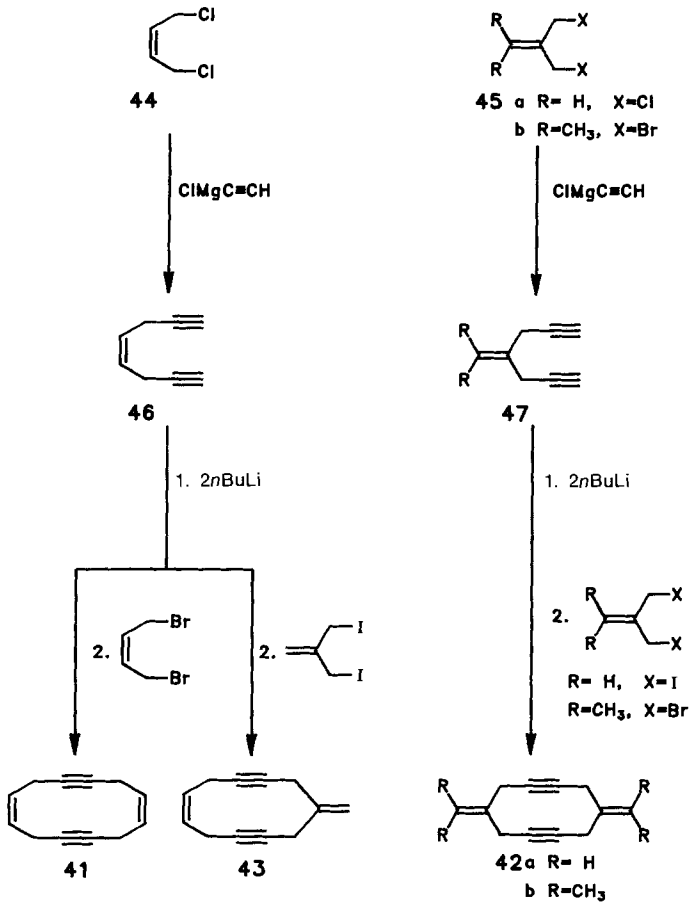

Scheme 3. Tos = $O_2SC_6H_4CH_3$.

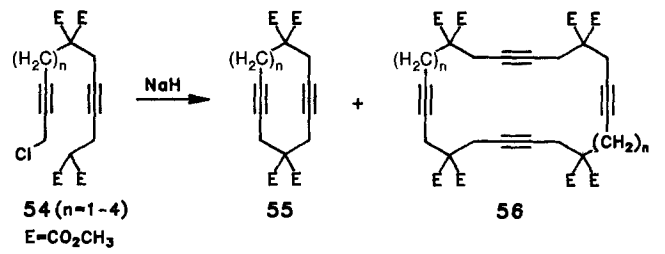

strated by the reaction of dichloroalkylsilanes **63** with alkynyl Grignard reagents furnishing diynes **64**.[32] Another extraordinary reaction is found in the synthesis of **67**–**69**.[33] Remarkably, the strained trisilacyclohepta-1,4-diyne **69** is produced on thermolysis of **68**,[33] thus implying that **67** and **68** are only slightly strained.

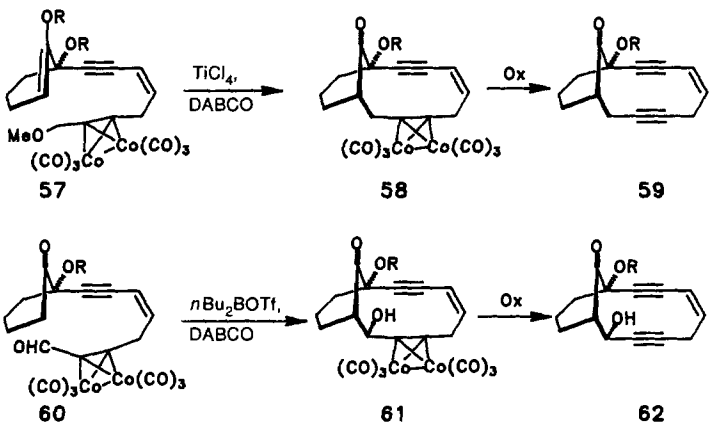

Scheme 4. DABCO = 1,4-diazabicyclo[2.2.2]octane, nBu$_2$BOTf = di-n-butylboron trifluoromethanesulfonate.

intermediate propargylic cationic species. In **60** complexation by $[Co_2(CO)_6]$ leads to activation of the aldehyde group, in this case by stabilizing a partial positive charge in the propargylic position.

Formation of cyclic diacetylenes by nucleophilic substitution is by no means restricted to hydrocarbons, as is demon-

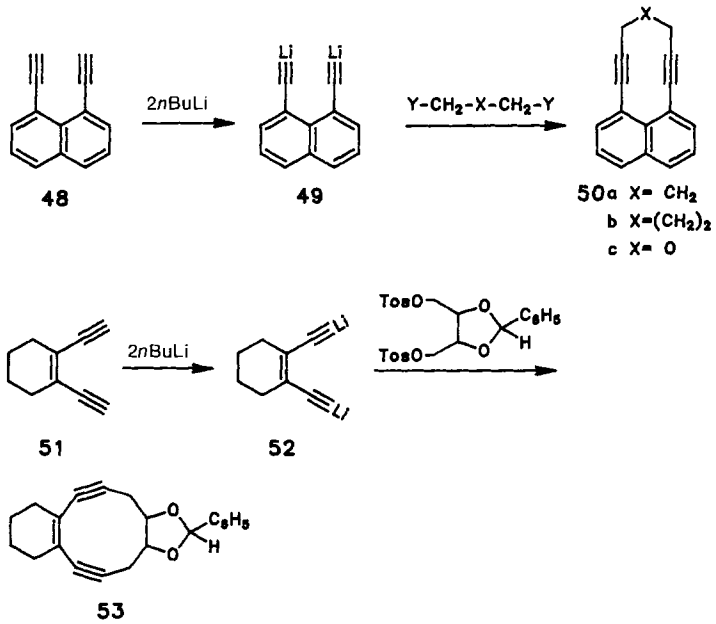

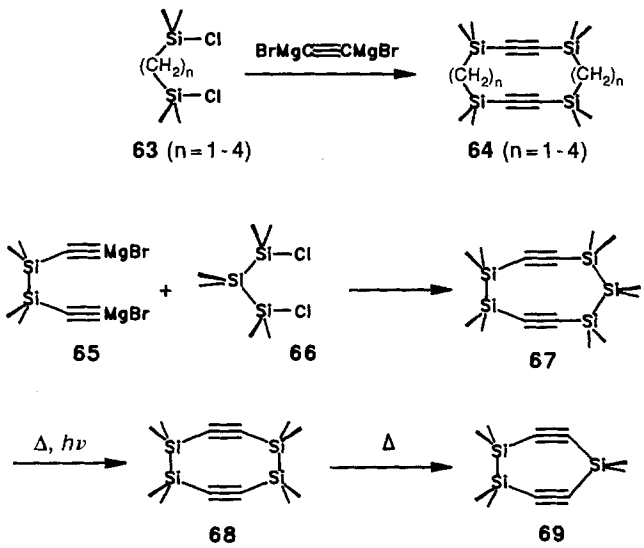

2.2. Cycloalkadiynes from Elimination Reactions

The synthesis of 5,6,11,12-tetradehydrodibenzo[*a*,*e*]cyclooctene (**72**) is illustrative of the elimination of HBr using a

strong base.[34] In an analogous manner **13**[12b] and the cyclic conjugated diynes **73** and **74** were also prepared.[35]

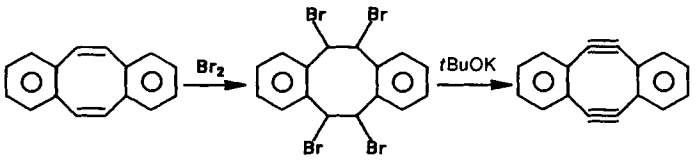

70 **71** **72**

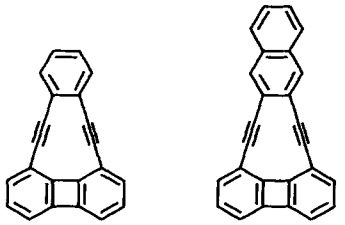

73 **74**

Another important elimination method is the reaction first described by Lalezari et al. in which a selenadiazole is thermolyzed.[12, 13, 36–38] This reaction is used effectively in the synthesis of 1,6-cyclodecadiyne (**14**).[39a] The bisselenadiazole **77** is prepared from 1,6-cyclodecadione (**75**) via the bissemicarbazone **76**. Thermolysis of **77** in the presence of

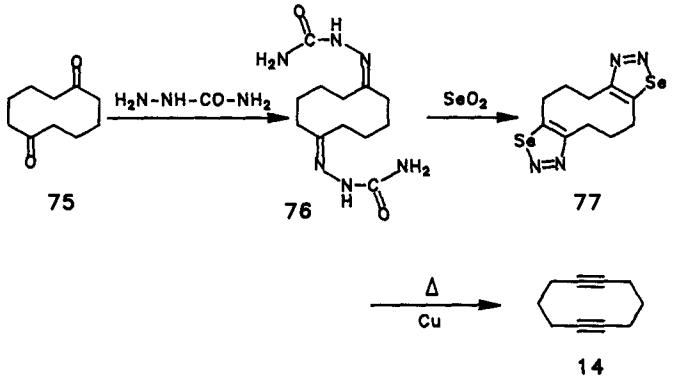

75 **76** **77** **14**

copper powder provides the desired product, 1,6-cyclodecadiyne (**14**). The depicted reaction sequence leads only to traces of bis(selenadiazole) **78**, the regioisomer of **77**. We attribute this to the fact that *cis,cis*-1,6-cyclodecadiene (**79**)[40] is more stable (ca. 8 kcal mol^{-1}) than the two other conformers of 1,5-cyclodecadiene, **80** and **81**, according to MM2 calculations. The thermolysis of selenadiazoles was used to obtain the diacetylenes **24** and **82**–**86** from the respective cyclic diones and cyclic yneones.

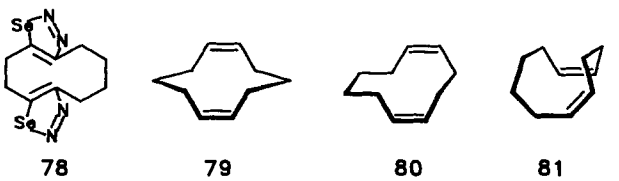

78 **79** **80** **81**

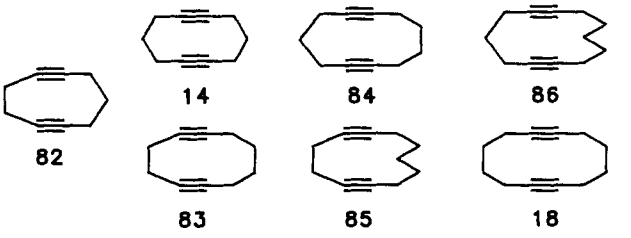

82 **14** **84** **86** **83** **85** **18**

2.3. Cycloalkadiynes from Special Methods

The first reported synthesis of 1,8-cyclooctadiyne (**13**) was achieved by the dimerization of butatriene (**87**).[41] A considerably higher yield is obtained when 1,5-dibromo-1,5-cyclooctadiene (**88**) serves as starting material.[12b] The con-

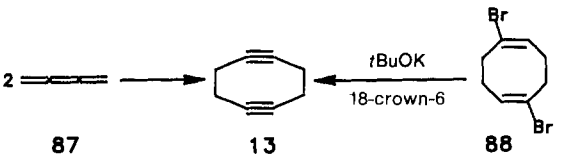

87 **13** **88**

struction of ten-membered rings similar to that of neocarzinostatin was accomplished with the Pd^0-catalyzed coupling reaction of an alkenylbromide fragment with an alkynylstannane.[42] Another interesting coupling reaction is the intramolecular reaction of an allylbromide with an aldehyde in the presence of $CrCl_2$.[43] Even the nine-membered ring of diyne **92** can be closed in this way. The acyloin con-

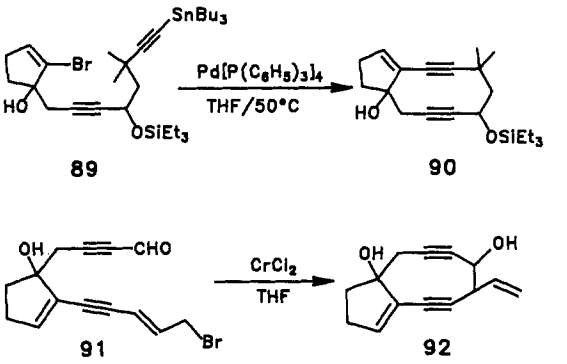

89 **90** **91** **92**

densation has also been used successfully to prepare 1,7-cyclododecadiyne (**18**) in good yields.[44] The attempt to close a ten-membered ring failed, but this ring size is generally not

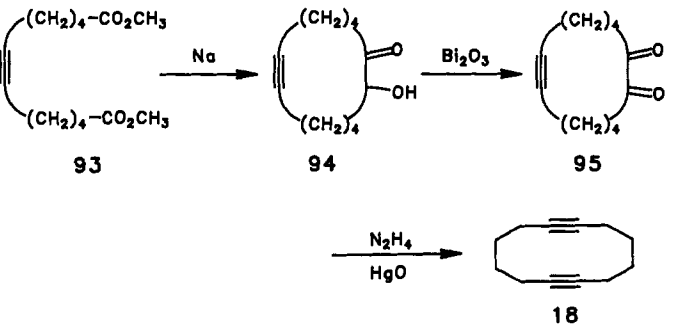

93 **94** **95** **18**

favored in this reaction. To synthesize the 14-membered ring in **97** the ten-membered ring in **96** was expanded by oxidation.[45] Astonishingly, the final product **97** is isolated in

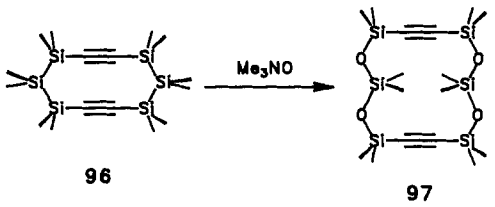

96 **97**

89% yield, even though this ring expansion probably proceeds through a number of steps.

3. Structures and Spectroscopic Properties of Cyclic Diacetylenes

3.1. Structures of Cyclic Diacetylenes

The most relevant structural parameters of cyclic diacetylenes have been collated in Tables 1–3. Of the diynes whose structures have been investigated 1,5-cyclooctadiyne (**13**) and 5,6,11,12-tetradehydrodibenzo[*a,e*]cyclooctene (**72**) are the most strained. Their structural parameters indicate a strong bending at the sp centers of the eight-membered rings of 20.7° in **13** and 24.3° in **72**. The transannular distances between the triple bonds are reported as 2.597 Å (**13**) and 2.617 Å (**72**). A further consequence of the imposed strain is an elongation of the bonds; the bonds between the two sp^2-hybridized C atoms in **72** are stretched to 1.431 Å, those between the two sp^3 centers in **13**, to 1.57 Å. In the tetrasila-compound **68**, on the other hand, most of the strain is relieved in the long Si–Si bonds. Consequently the bond angles at the sp centers deviate only 11–16° from linearity.

A somewhat smaller deviation from the linear arrangement (between 2 and 13°) is found in the ten-membered cyclic 1,6-diynes (Table 2). With the exception of diyne **64** all of these compounds are found in the chair conformation in the solid state. Depending on the heteroatom incorporated in the bridging unit, the transannular distance between the triple bonds varies between 2.91 Å and 3.5 Å. One should also note that the substituents on the nitrogen atom in **36**[23b] and **37**[23a] are in the axial position in the crystalline state. This also holds for the 1,6-diazacyclodeca-3,8-diyne ring even when it is substituted with bulky isopropyl or *tert*-butyl groups.[48] The 11- and 12-membered rings (Table 3) show deviations of 4 to 9° at the sp centers. The conformations of **17** and **21** have been discussed by J. Dale based on early investigations of their X-ray structures.[40]

Table 1. Comparison of selected bond lengths and bond angles in diacetylenes.

Compound	Distance [a]	Angle [b]	Deformation [c]	Lit.
13	2.597	159.3	20.7	[41]
72	2.617	155.7	24.3	[46]
68	3.223 3.269	168.6 164.1	11.4 15.9	[33]

[a] Transannular distances in [Å]. [b] Bond angles at sp centers in [°]. [c] Cisoid deformation in [°].

Table 2. Comparison of selected bond lengths and bond angles in diacetylenes with ten-membered rings.

Compound	Distance *a,b* [a]	Angle [b]	Deformation [c]	Distance *c* [d]	Lit.
14	2.991(2)	171.7(2)	8.3(2)	5.141(2)	[39a]
21	2.909(2)	169.6(1)	10.4(1)	4.935(2)	[47]
27b	3.014(4)	171.4(3)	8.6(3)	5.244(4)	[47]
27a	2.976(3) 3.068(3)	172.7(2) 173.9(2)	7.3(2) 6.1(2)	5.422(3)	[47]
27c	3.102(2)	174.2(2)	5.8(2)	5.623(2)	[47]
37	2.983(3) 3.072(2)	171.1(2) 171.9(2) 173.7(2) 173.7(2)	8.5(2) 6.3(2)	5.352(2)	[23a]
36	2.952(2)	170.8(1) 169.8(1)	9.2 10.2	5.137(2)	[23b]
42a	2.996(2)	172.8(2) 171.2(2)	7.2(2) 8.8(2)	5.106	[49]
98	3.488(1)	175.1(1) 173.8(1)	4.9(1) 6.2	5.622	[50]
50a	2.795(3) 2.917(3)	177.9(2) 170.4(2)	2.1(2) 9.6(2)	–	[51]
99	2.706 3.261	166.7 174.8	13.3 5.2	– –	[52]
64 (n = 1)	3.471(2) [e] 3.449(2) [e] 3.449(2) [f] 3.446(2) [f]	176.6 [e] 176.9 [f] 177.0 [e] 176.9 [f] 178.3 [e] 176.5 [f] 175.9 [e] 177.3 [f]	0 0	5.906 [e] 6.142 [f]	[53]

[a] Transannular distances *a,b* in [Å]. [b] Bond angles at sp centers in [°]. [c] Cisoid deformations in [°]. [d] Distances *c* between positions 1 and 6 in [Å]. [e] Distances in the boat conformation. [f] Distances in the chair conformation.

3.2. Photoelectron Spectra of Cyclic Diacetylenes

PE spectroscopy is the proper tool for investigating the influence of the length of the bridging units on the trans-

Table 3. Comparison of selected bond lengths in cyclic diacetylenes with 11- and 12-membered rings.

Compound		Distance *a,b* [a]	Angle deviation[b]	Angle [c]	Lit.
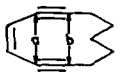	**31**	2.778(5) 3.661(5)	7.4(4) 6.8(4)	0	[54]
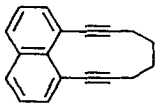	**50b**	2.824 3.291	5.2 4.7	25.6	[51]
	18	4.06	6.2(1)	24	[39a]
	41	3.356(1)	5.6(1) 6.8(1)	0	[49]
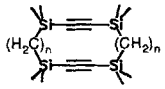	**64** (n = 2)	4.850(1)	6.2(1) 6.5	0	[53]
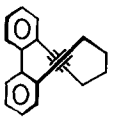	**100**	3.036 3.108	8.7	48	[55, 56]
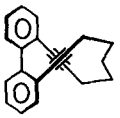	**101**	3.051 3.411	4.1 4.6	58	[55]
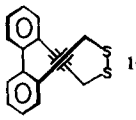	**102**	3.011 3.408	5.3	58	[55, 57]
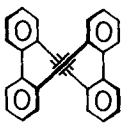	**103**	2.85	6.2	53	[58]

[a] Transannular distances *a*, *b* in [Å]. [b] Deviations from 180° at the sp centers in [°]. [c] Twist angle in [°].

annular interaction of the two triple bonds. This is best demonstrated by comparison of the PE spectra of **13**[59] and **14**[39] (Fig. 3). The predictions made in Section 1 and in Figure 2 are confirmed: For **13** (eight-membered ring) the peak attributed to the π_i^+ MO is at lower energy than that assigned to the π_i^-. Conversely, in **14** (ten-membered ring) the peak assigned to the π_i^- MO is lower in energy than that of π_i^+. In contrast to the small separation of the bands in **13**, a large splitting (1.5 eV) is observed in **14** between π_i^+ and π_i^-. An analogous relationship is observed in the comparison of the PE spectra of **50a** and **50b**.[60] In Figure 4 the energies of the first bands taken from the PE spectra of a series of cyclic diacetylenes are compared. Most noticable is that the

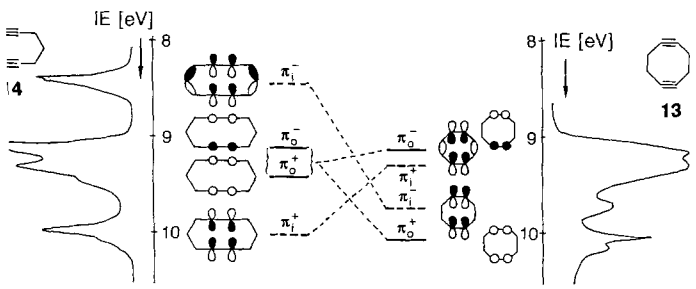

Fig. 3. Comparison of the first bands of the PE spectra of **13** and **14**.

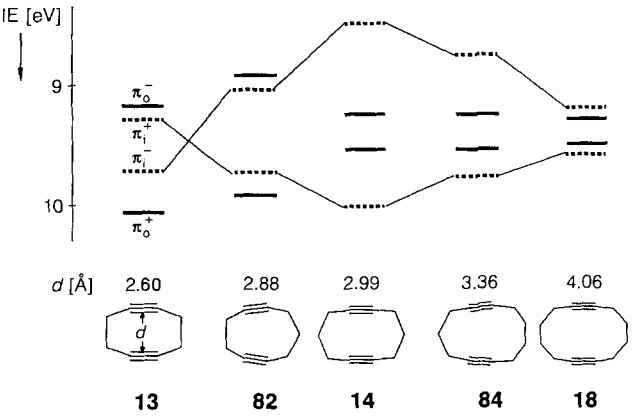

Fig. 4. Comparison of the first bands of the PE spectra of **13**, **14**, **18**, **82**, and **84**.

splitting of the π_i levels reaches its maximum at **14** (ten-membered ring) and then diminishes with increasing bridge length. The splitting observed for the π_o levels remains virtually constant for diynes with transannular distances greater than 3.0 Å between the triple bonds. In the PE spectra of the ten-membered heterocycles (Fig. 5) with the exception of **21**

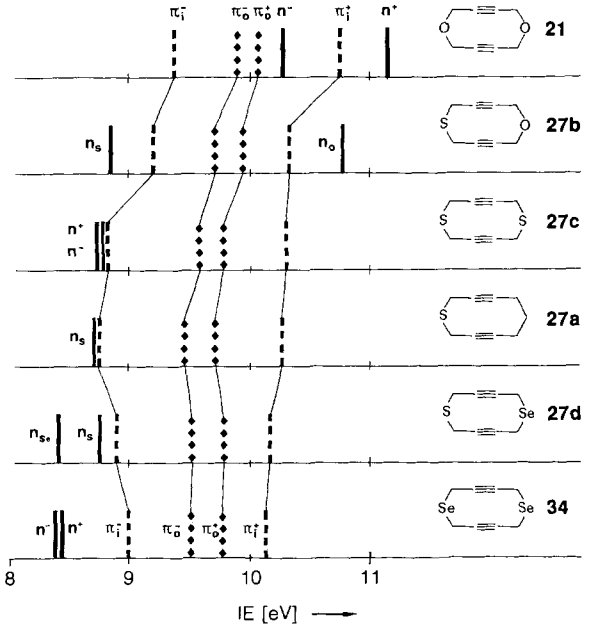

Fig. 5. Comparison of the first bands of the PE spectra of the heterodiynes **21**, **27a–d**, and **34**.

the peak attributed to the HOMO arises from the heteroatom (n) MO. The splitting of the in-plane (π_i) MO energy levels varies from 0.9 to 1.5 eV. The PE spectra of the enediynes **39** and **40** as well as dienediynes **41–43** indicate

that the π_i^+ and π_o^+ linear combinations of the triple bonds interact significantly with the π MOs of the double bonds (homoconjugation).[24]

4. Reactions with Metal Compounds

4.1. Complexation

Figure 3 shows that the highest occupied MO (π_i^-) of 1,6-cyclodecadiyne (**14**) lies in the molecular plane. It seems likely, therefore, that an electrophilic reagent will attack preferentially in this plane.[11] To verify this hypothesis we carried out experiments with the cyclic diacetylenes and a number of electrophilic transition-metal compounds, such as silver trifluorosulfonate [$Ag(SO_3CF_3)$] and copper trifluoromethanesulfonate [$Cu(SO_3CF_3)$].[61] The reaction of **14**, **17**, and **18** with [$Ag(SO_3CF_3)$] in THF yields a colorless, sparingly soluble 1:1 complex. Analogous results are obtained for the precipitates resulting from the reaction of **14** and **18** with [$Cu(SO_3CF_3)$][61]. The characteristic IR and NMR data of the uncomplexed acetylenes are not influenced to any significant amount by complexation with Ag^+ or Cu^+.

The complex $[(C_{10}H_{12})Ag(SO_3CF_3)]_n$ has a two-dimensional layered structure in the crystal. In each of these layers the Ag atoms lie in the molecular plane between two 1,6-cyclodecadiyne rings in chairlike conformations (Fig. 6). This

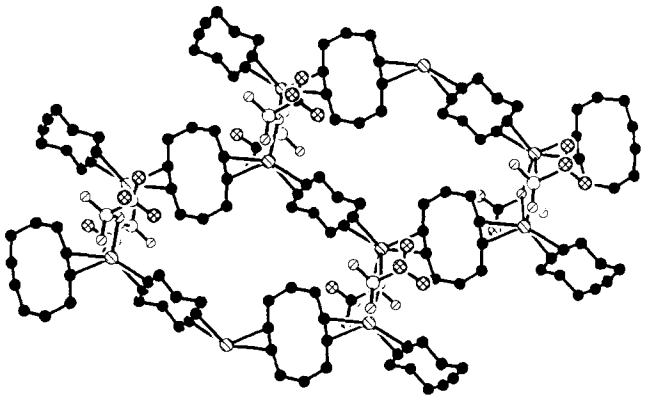

Fig. 6. A section of the polymer structure of $[(C_{10}H_{12})Ag(SO_3CF_3)]$ (view from the top). Carbon ●, silver ⊘, oxygen ⊗, sulfur ○, fluorine ⊘.

experiment supports the prediction mentioned above. The X-ray structures of $([C_{12}H_{16})Ag(SO_3CF_3)]_n$ and $[(C_{12}H_{16})Cu(SO_3CF_3)]_n$ show the 12-membered rings to be connected by respective silver and copper ions. In these complexes two of the three oxygen atoms of the triflate ligand are coordinated to different metal-centers giving rise to a three-dimensional network in the solid state. A similar three-dimensional polymeric structure is found for $[(C_{14}H_{20})Ag(SO_3CF_3)]_n$. In Figure 7 the most important structural parameters of cyclodecadiyne **14** in its uncomplexed and complexed states are compared. A slight elongation of the triple bonds and a small increase of the transannular distance occur upon complexation. Along with the spectroscopic results this implies that the metal cation is only loosely coordinated to the diacetylene.

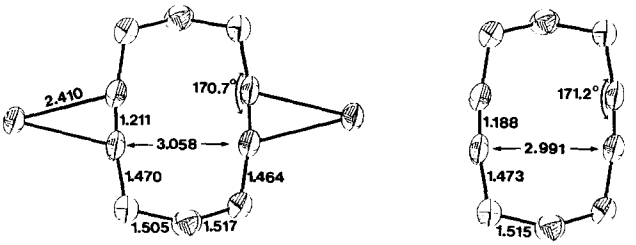

Fig. 7. Comparison of the uncomplexed (right) and complexed (left) structures of 1,6-cyclodecadiyne (**14**).

Cyclic diacetylenes with medium-sized rings react with $[Co_2(CO)_8]$ to form red bis(hexacarbonyldicobalt) complexes[62]. As expected, this type of complexation leads to a substantial change of the structural parameters of the cyclic diacetylene. An example is the complex of 1,6-cyclodecadiyne **14** depicted in Figure 8, in which the Co_2C_2 tetrahedral structure is easily discerned. The large increase in the

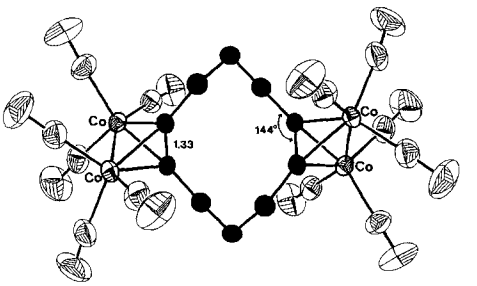

Fig. 8. Structure of $[(C_{10}H_{12})\{Co_2(CO)_6\}_2]$. The carbon atoms of 1,6-cyclodecadiyne ring are filled in for clarity.

distances between the originally sp-hybridized centers and the concomitant rehybridization at these carbon atoms changes the conformation of the ten-membered ring considerably. The bis(hexacarbonyldicobalt) complexes of **14**, **18**, and **82**–**86**[62] as well as those of **41** and **42** have been prepared. All of these are stable red compounds in the solid state. The formation of complexes with cyclic monoalkynes has already been reviewed.[63]

4.2. Reactions with Formation of Cyclobutadiene Complexes

The reactions of cyclic diacetylenes such as **17** and **18** with dicarbonyl(η^5-cyclopentadienyl)cobalt [$CpCo(CO)_2$], dicarbonyl(η^5-cyclopentadienyl)rhodium [$CpRh(CO)_2$], and pentacarbonyliron [$Fe(CO)_5$] have been studied by King and coworkers.[65–68] They reported the formation of tricyclic cyclobutadiene complexes in yields of 40–80% for Co and 15–70% for Rh. One example is the reaction of 1,7-cyclododecadiyne (**18**) with [$CpM(CO)_2$] (M = Co, Rh) leading to **104** and **105**.[64–65] The complexation of [$Fe(CO)_5$] or [$Fe_3(CO)_{12}$] with cyclic diacetylenes is more complicated: Besides tricyclic cyclobutadiene complexes such as **106**, Fe_2 complexes like **107** and **108** could be isolated.[67, 68]

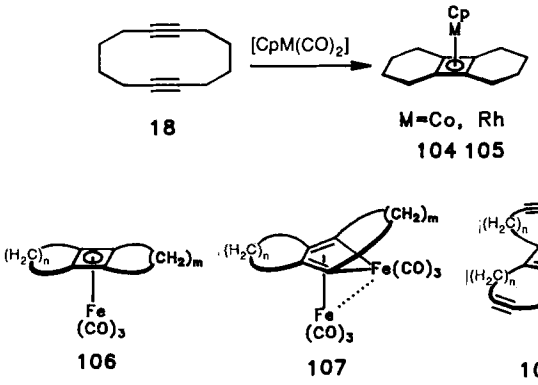

The complexation reactions of the two silaoxadiynes **97** and **98** take a different course. The reaction of **97** with $[Fe_2(CO)_9]$ provides complex **109** in 45% yield. This product may in fact be viewed as a $[Fe(CO)_3]$ complex of a methylenecyclopropene unit.[69] For **98** the same reaction leads to the trimethylenemethane complex **110** in a yield of 34%.[69]

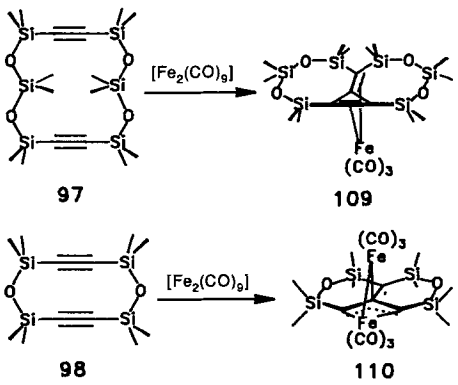

The mechanism of cyclobutadiene formation from two acetylene units in the presence of $[CpCoL_2]$ or $[Fe(CO)_5]$ is postulated to occur via a metallacycle such as **112**, which is formed from diacetylene complex **111**. Metallacycle **112** subsequently rearranges to the cyclobutadiene complex **113**.

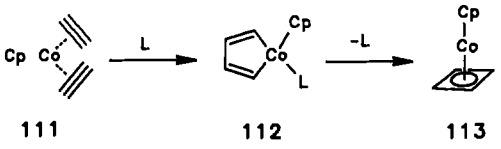

MO calculations lend support to this proposed mechanism, since they predict the direct transformation of **111** to **113** to be symmetry-forbidden. Such a conversion would require a considerable amount of electronic activation.[70, 71] Furthermore, this mechanism is supported by research carried out by Wakatsuki and Yamazaki,[72–75] in which they were able to isolate cobaltacycles of type **112** stabilized by a phosphine ligand.

The reaction path **111** → **112** → **113** may be transferred to cyclic diacetylenes (**B**) (Scheme 5). Obviously the intramolecular ring formation (**C** → **E** → **F**) may be hindered if

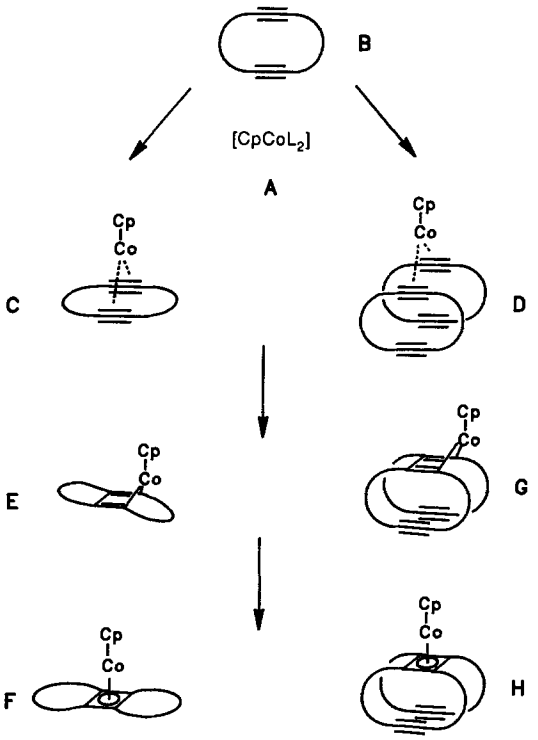

Scheme 5. Reaction of cyclic diacetylenes with $[CpCoL_2]$.

the bridges between the triple bonds are short (**E**, for instance, is an *anti*-Bredt structure). An alternative path is the intermolecular formation of cyclobutadienes (**D** → **G** → **H**).

To test these hypotheses we carried out a number of reactions with 1,6-cyclodecadiyne (**14**) and $[CpCo(CO)_2]$.[11] When the reaction is carried out in *n*-octane the main product (12% yield) is the superphane of cyclobutadiene (**115**) stabilized on both faces by [CpCo] units.[76] The tricyclic cyclobutadiene complex **116** (6%) and the mixed superphane **117** (0.7%)[76–78] were isolated as side prod-

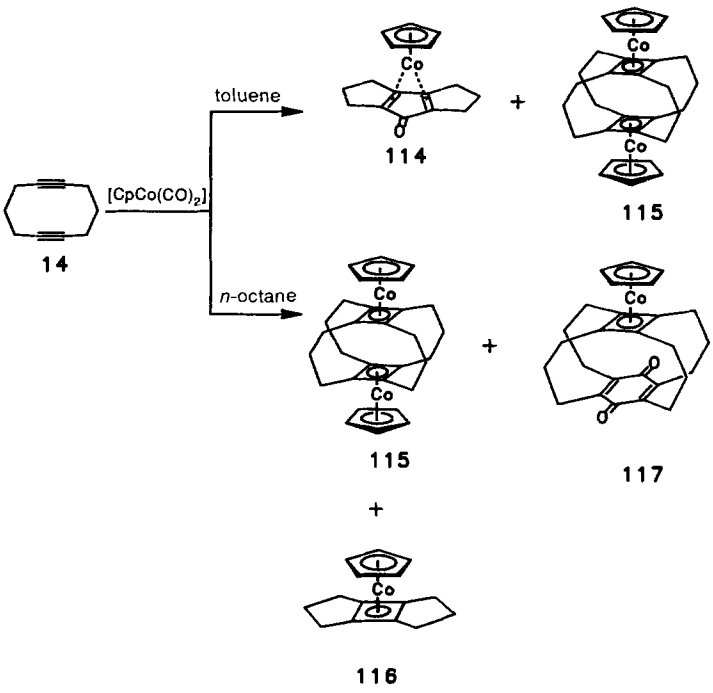

ucts. When the reaction is conducted in toluene, complex **114** (5%) is formed as well as **115** (2%).

The X-ray structures of all three Co complexes (**115**–**117**) are shown in Figures 9–11.[76–78] The cyclobutadiene rings in **115** and the connecting propano units show C_{4h} symmetry (Fig. 9). In fact, this local symmetry is observed in all the

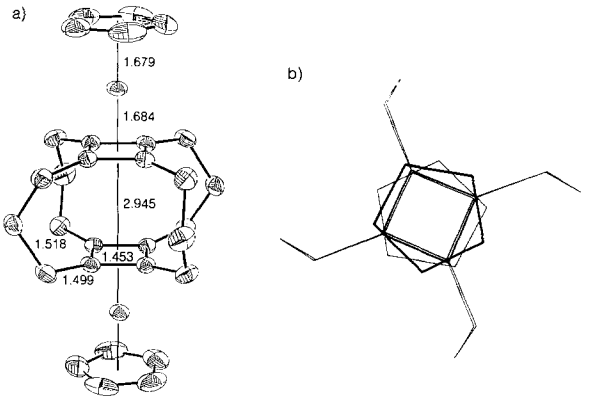

Fig. 9. Structure of **115**; a) side view b) top view.

superphanes prepared from **14** or **42b**. The two complexed cyclobutadiene moieties of **115** are not far apart (2.94 Å). In the structure of **116** the cyclobutadiene unit has distinctly alternating bond lengths caused by the strain from the fused five-membered rings. (Complexed cyclobutadienes usually

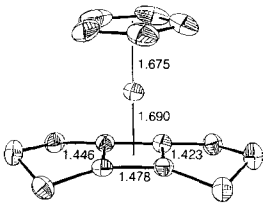

Fig. 10. Most relevant structural parameters of **116**.

have nearly square structures.[66]) The mixed superphane **117** shows a deformation of the quinone ring, in which the CO groups are twisted out of the plane of the double bonds by 27°. Of the seven possible conformations of the propano bridges (Scheme 6) structure **a** is the one observed in the solid state.

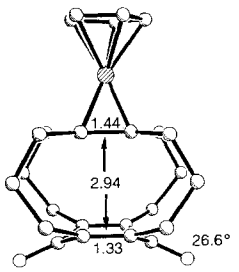

Fig. 11. Side view of the structure of **117**.

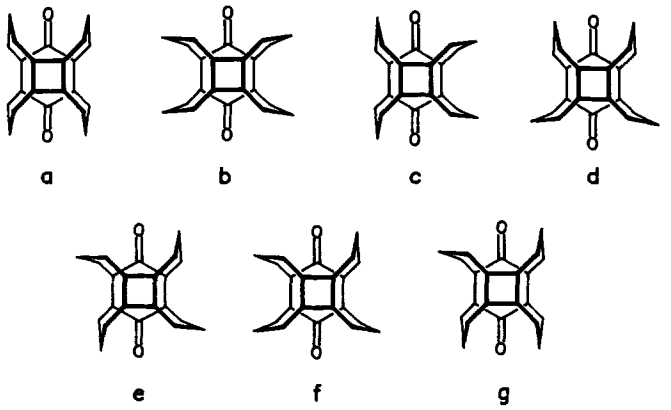

Scheme 6. Conformation of the propano bridges in Co complex **117**.

To determine the influence of a substituted cyclopentadienyl ligand on the Co atom on the reaction between **14** and [R-CpCo(cod)] we allowed **14** to react with the set of Co complexes **118**–**122** under reaction conditions similar to those described previously (refluxing *n*-octane).[79] The correlation between the observed yields of the superphane and the relative chemical shifts of the complexes as determined by ^{59}Co NMR spectroscopy is shown in Figure 12.[79] As a

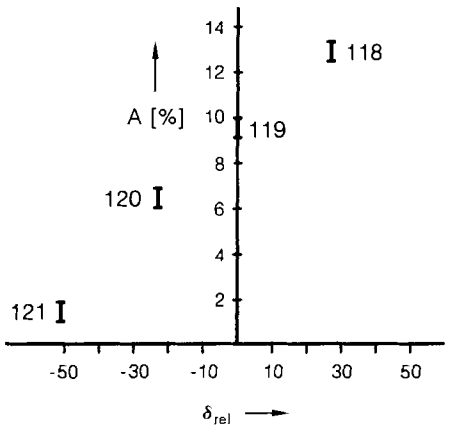

Fig. 12. Correlation between the yields obtained from the reaction of 1,6-cyclodecadiyne (**14**) with [(η^5-R-C_5H_4)Co(cod)]-complexes **118**–**121** and the products' relative chemical shifts, δ^{59}Co.

reference for the ^{59}Co shifts in the series of η^5-(cyclopentadienyl)Co(cod) complexes the value δ_{rel} (^{59}Co) of the unsubstituted compound (R = H) was set at zero. This type of correlation was first reported by Bönnemann.[9b] When the reaction was carried out with **123** and **14**, the corresponding cyclobutadiene superphane capped with two indenyl-Co fragments could be isolated in 25 to 30% yield.[79]

In order to find out more about the competition between the intra- and intermolecular pathways of cyclobutadiene formation and the dependence on the ring strain in the starting compound, two diynes with 11-membered rings, **84** and **85**, were treated with [$CpCo(CO)_2$]. Two intermolecularly formed products (**124**, **125**) were isolated[80] from complexation of **84**.[80] In contrast, if the slightly less strained diyne **85** is complexed, two compounds, **126** (32%) and **127** (2.5%),

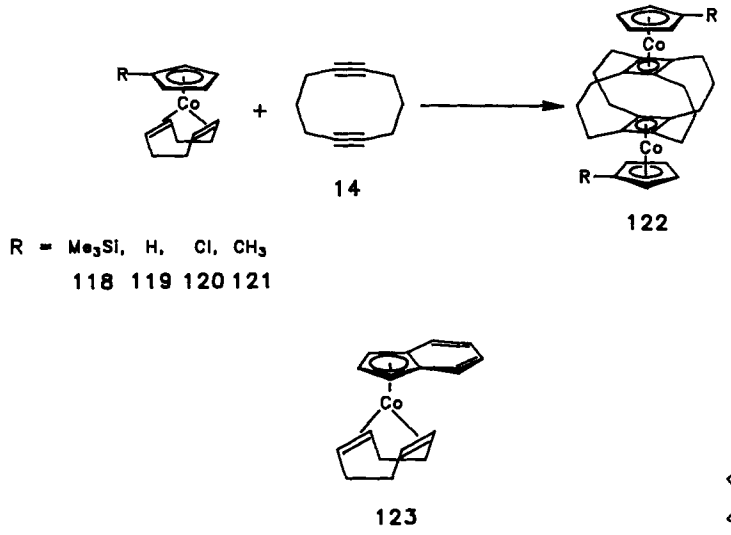

arising from intramolecular reaction are formed. The same applies for the dienediynes **41** and **42b**; the less strained compound **41** gives an intramolecular complex **128** (56%), while the reaction between **42b** and $[CpCo(CO)_2]$ leads to formation of the superphane **129** in 10% yield.[81] Yet there

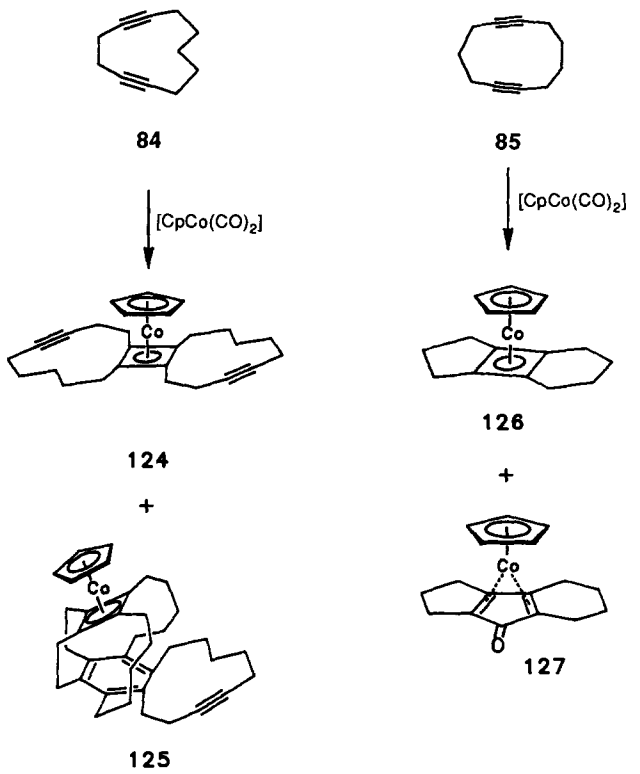

must be other (to date unknown) factors apart from ring strain that influence the outcome of this type of reaction. Even the unstrained starting compound 1,8-cyclotetradecadiyne (**17**) forms not only the intramolecular product **130** (17%)[64] but also superphane **131** (5%).[82] In this context it is of interest that the reaction between **18** and $[CpCo(CO)_2]$ leads only to the tricyclic product **104** (86% yield).[64]

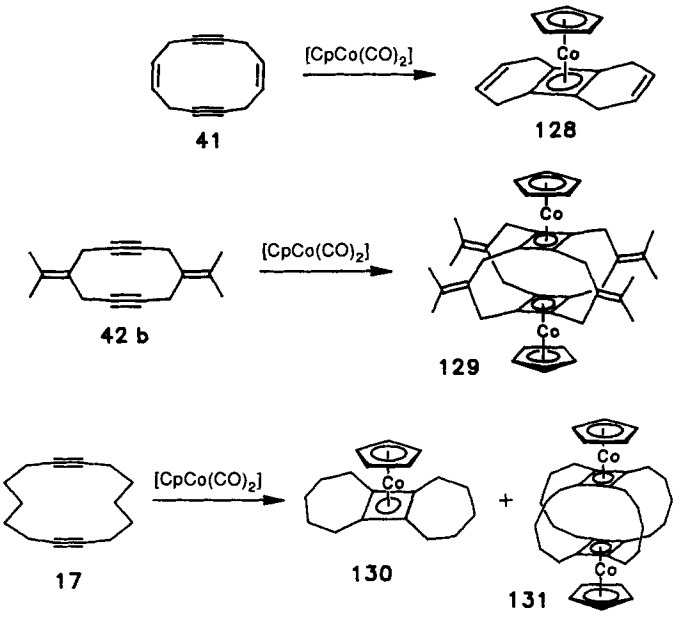

4.3. Reactions between $[CpCo(CO)_2]$ and Heterodiynes

Stimulated by the fascinating results that were observed in the reactions of carbocyclic diynes with ten-membered rings described above, we thought it logical to carry out similar experiments using heterodiynes. Our first attempts with the two components, **21** and $[CpCoL_2]$ ($L = C_2H_4$, CO), were disappointing since we were only able to detect polymeric material.[83] On the other hand, reactions with the sulfur-containing diynes **27a**, **27c**, and **27e** showed promising results. Even when only catalytic amounts of $[CpCo(CO)_2]$ were used, thiophenophane **132** could be isolated (12% for **27a** and **27c**).[18, 84] The configuration of thiophenophane **132b** was established by X-ray structural analysis.[84] We then proceeded in an analogous manner as described previously for the carbocyclic diynes, that is, we examined the influence of ring size on this reaction. In the complexation of **27e** the yield of thiophenophane **132e** is reduced to 6%; for

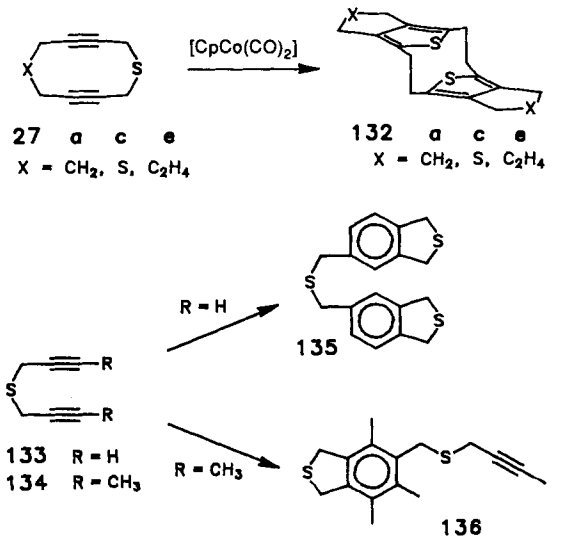

acyclic diynes exemplified by **133** and **134** [2 + 2 + 2]cycloaddition dominate, and products of constitution **135** or **136**[18] can be detected.

To interpret these results we propose the following mechanism: In the first step the CO or cod ligands of $[CpCo(CO)_2]$ or [CpCo(cod)] are replaced by the cyclic heterodiyne, thus forming **137** in which the two acetylene moieties are η^2-coordinated to cobalt. This complex is then postulated to undergo oxidative addition to **138**. To lead to thiophenophane **132** the next step must comprise a rearrangement of **138**, in which the sulfur and cobalt atoms exchange places. Two modes of reaction are feasible, either a double dyotropic rearrangement[85] or a coordination of sulfur at the metal. The resulting intermediate **139** finally dimerizes to give the desired [2.2](2,5)thiophenophane. In the transformation **138** → **139** the [CpCo] fragment is liberated and completes the catalytic cycle by reaction with further diacetylene to **137**. Therefore

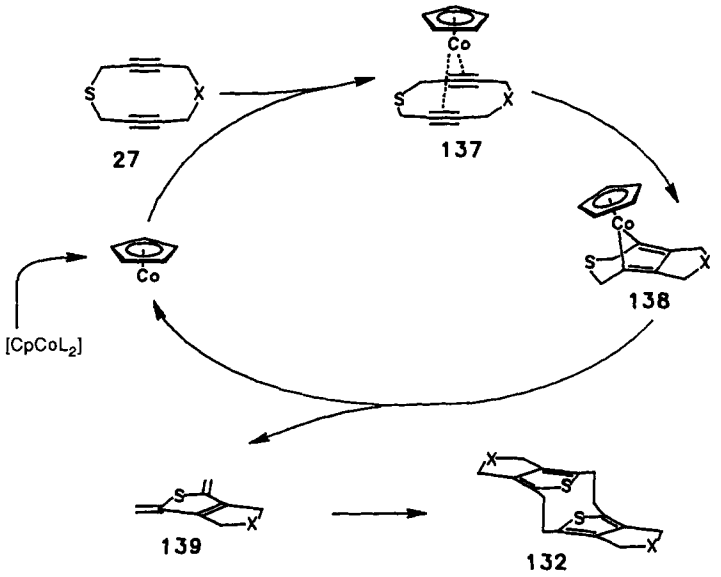

only catalytic amounts of $[CpCoL_2]$ are required for the reaction, which is also in line with the formation of [2 + 2 + 2] cycloadducts[18b] from larger diynyl rings.

5. Stepwise Synthesis of Superphanes

Up to this point our research has shown that a one-step synthesis of superphanes is especially facile with 1,6-cyclodecadiyne rings. Also, it seems that the only metal templates to achieve superphane formation are the $[CpCoL_2]$ complexes. A more general route to the superphane complexes

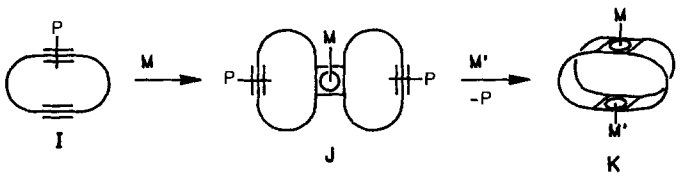

Scheme 7. P = protecting group, M = metal fragment.

should be possible, if a monoprotected diacetylene (**I** in Scheme 7) could first be dimerized and in a second step cyclized intramolecularly (**J** → **K**).

First attempts at dimerizing monosubstituted diacetylenes using $[Co_2(CO)_8]$ failed, and heating them with $[CpCo(CO)_2]$ led to disproportionation.[62] The main reaction of yneones and $[CpCo(CO)_2]$ is the formation of trimers with only a minimal amount of the desired dimerized product.[86]

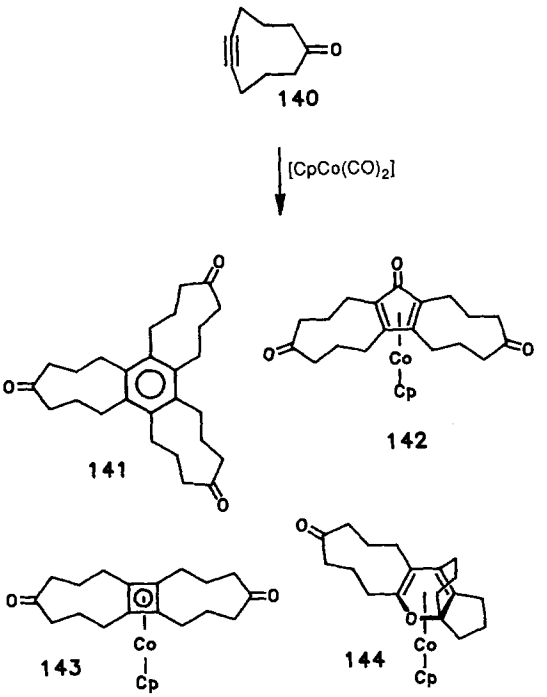

Scheme 8. Attempts at yneone dimerization.

This is demonstrated for 5-cyclononyneone **140** in Scheme 8. Surprisingly, a CO bond participates in a [2 + 2 + 2]cycloaddition to form **144**. We tested this unexpected reaction on a number of open-chain systems[86] and were able to prepare a variety of metal-complexed 2*H*-pyranes.[87]

The use of 5-cyclodecyneol **145** finally led to the stepwise synthesis of metal-stabilized cyclobutadiene superphanes.[88] Dimerization of cycloalkyne **145** to a mixture of isomeric alcohols **146** and **147** may readily be achieved with [CpCo(cod)] in about 40% yield. This mixture is oxidized to the ketones **148** and **149** by the Oppenauer oxidation; at this stage the mixture can be separated, though this is not necessary for the further reaction sequence. Treatment with semicarbazide and SeO_2 gives rise to good yields of only two of the possible four isomeric selenadiazoles. An explanation for the selective formation of **150** and **151** is provided by examination of the solid-state conformation of **148** (Fig. 13, right). The minimum energy conformation of 1,6-cyclodecadiene[40] (Fig. 13, left) has a very similar geometry to that of the ten-membered rings in **148**. We therefore conclude that the formation of the double bonds of the selenadiazole heterocycles occurs predominantly at the 6-position with respect to the cyclobutadiene ring in analogy to **79**. Fragmentation of the mixture with BuLi affords the desired diyne

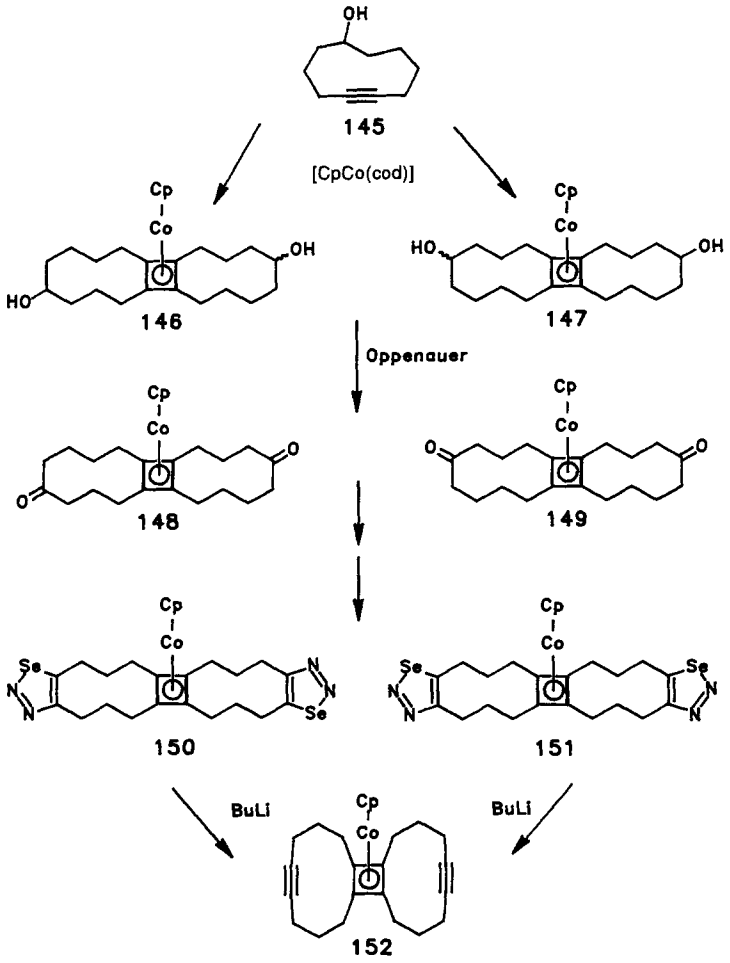

152. The X-ray structure of **152** (Fig. 14)[78] shows that the triple bonds are 6.3 Å apart, parallel to each other, and in the same region of space. Conformational calculations (AM1) performed on the hydrocarbon skeleton of **152** predict, besides the global minimum **A**, two local minima, **B** and **C**, which are 10.0 and 8.3 kcal mol^{-1} higher in energy. In **B** and **C** the distance between the triple bonds is estimated to be 3.9 and 4.6 Å, respectively.

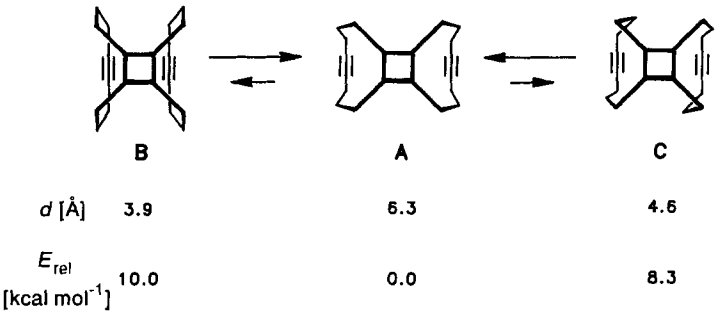

Scheme 9 shows that **152** may be transformed into a variety of metal-stabilized cyclobutadiene superphanes. Reaction with [CpCo(CO)$_2$] affords the superphane **115** in 80% yield. Remarkably, this reaction is much faster than the corresponding reaction starting with **14** (see Section 4.2.). This lends support to our hypothesis that **152** is an intermediate in the reaction of **114** with [CpCo(CO)$_2$] to **115**. Note also that reaction of **152** with [Cp*Co(CO)$_2$] (Cp* = C_5Me_5) provides good yields of **153**; however, the reaction of **152** with [Fe(CO)$_5$] furnishes the mixed superphane **155** in only 8% yield. The X-ray structure of **155** shows that the propano

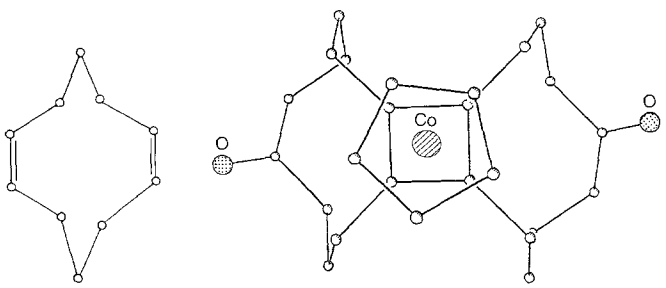

Fig. 13. Comparison of the conformations of **148** (right) and 1,6-cyclodecadiene (**79**) (left) obtained by X-ray structural analysis [78].

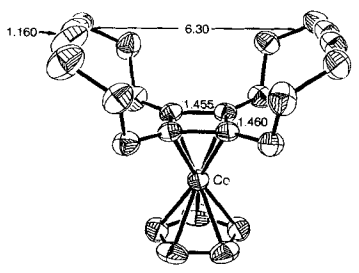

Fig. 14. Structure of **152** [78].

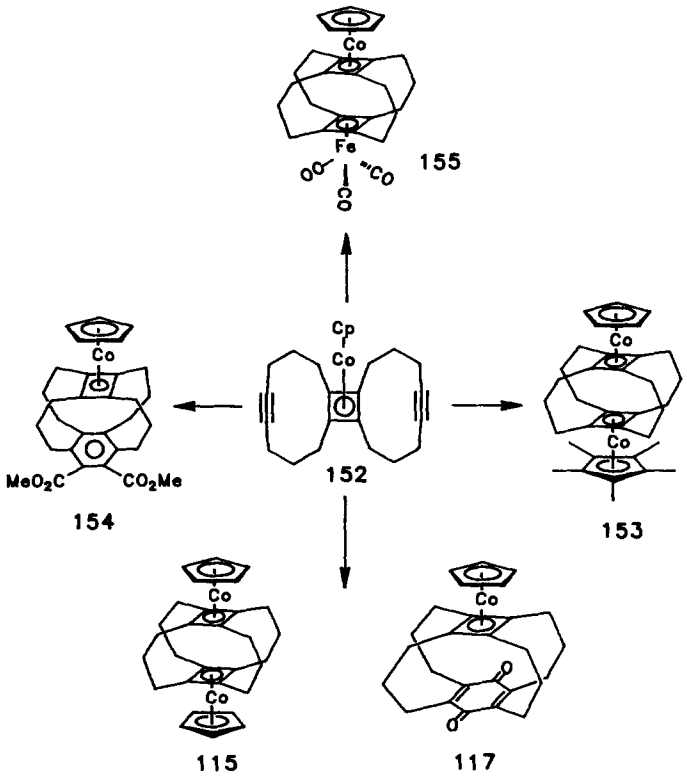

Scheme 9. Cyclization reactions of Co complex **152**.

bridges have the same conformation as that observed in **115**. The distance from the center of the cyclobutadiene ring to the Fe atom (1.77 Å) is identical to that measured for the recently synthesized [2.2](1,3)-cyclobutadienophane, in which both cyclobutadiene moieties are complexed by $[Fe(CO)_3]$ units.[89] The distance between the two cyclobutadiene rings in **155** is 2.98 Å, practically the same as that in **115**. Finally, when **152** is reacted with dimethylacetylenedicarboxylate in the presence of $[CpCo(CO)_2]$, a mixed cyclophane **154** (5%) can be isolated.

6. Reactions of Several Cyclobutadienecyclopentadienylcobalt Complexes

6.1. Reactions of "Rectangular" Cyclobutadiene Complexes

The pronounced alternation of the bond lengths in the cyclobutadiene moiety of $[CpCo(C_{10}H_{12})]$ **116**[76] is unusual considering that complexed cyclobutadienes normally have bonds of equal length.[66] This led us to the assumption that the reactivity of **116** should be enhanced as compared to that of complexes with a square-shaped cyclobutadiene unit. This proved to be true, since **116** is prone to expansion of the four-membered ring when heated with reagents containing triple bonds (Scheme 10) leading to the 6π systems **156** and **157**.[90] Even when the bonds of the four-membered ring are

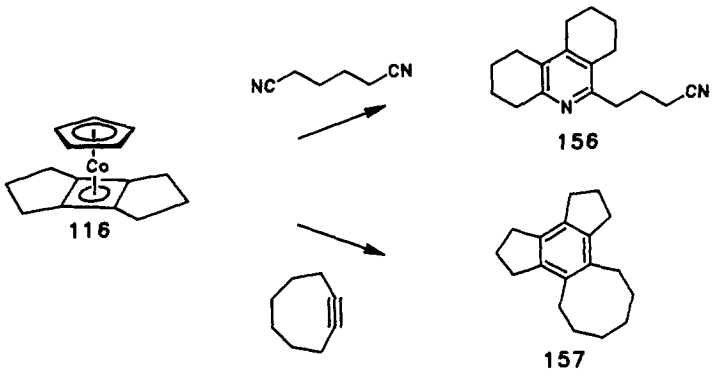

Scheme 10. Reactions of **116** with reagents containing triple bonds.

virtually equivalent as in the tricyclic cyclobutadiene complex **104** (see Section 4.2.), analogous ring expansions can be performed.[90]

In explanation of the reactivity of **116** and **104** we assume the cobalt complex **116** is in equilibrium with the cobaltacyclopentadiene derivatives **158** and **159**. Note that this step is equivalent to alkyne metathesis for which intermediates such as metal-stabilized cyclobutadienes have been proposed.[91] The cycloaddition of another triple bond then occurs either directly to **116** or to **159** with prior coordination at the cobalt center. The formation of cyclopentadienone derivatives (for example **114**, **117**, and **127**) in the reaction of cyclic diacetylenes and $[CpCo(CO)_2]$ is also accounted for by this proposed mechanism.

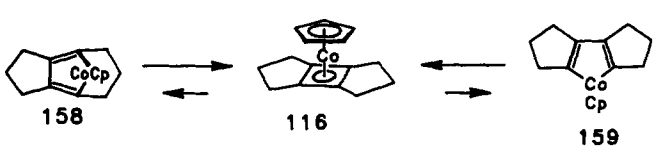

6.2. Reactions of the Cyclobutadiene–Quinone Superphane

On irradiation of $[CpCo\{C_4(C_3H_6)_4C_6O_2\}]$ **117** a colorless and an orange product are formed in equimolar amounts.[92] The colorless compound **160** exhibits a bishomocubane structure. The structure of the colored

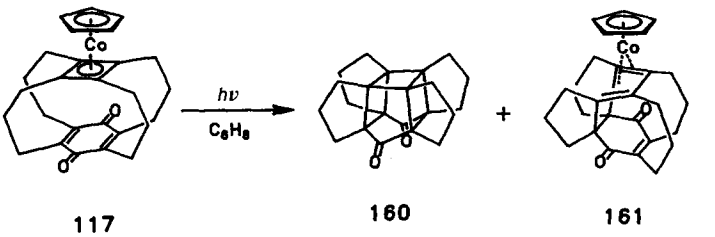

product **161**, which contains a [CpCo] fragment, has been confirmed by X-ray analysis.[92]

6.3. From Cyclobutadiene Superphane to Propella[3$_4$]prismane

The conversion of the complexed superphane **115** to the bridged *syn*-tricyclo[4.2.0.0^{2,5}]octa-3-7-diene derivative **162** may be achieved either by oxidation with Ce^{IV} or by irradiation.[93] Interestingly, the four propano units of compound

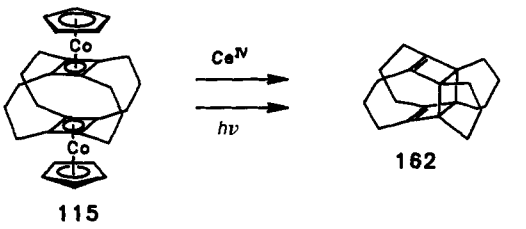

162 alter its properties significantly compared to those of the unsubstituted tricyclooctadiene **163**. On heating, **163** rearranges to cyclooctatetraene **165**.[94] The bridged derivative **162**, on the other hand, undergoes a degenerate Cope rearrangement with an activation energy of 73–75 kcal mol^{-1}.

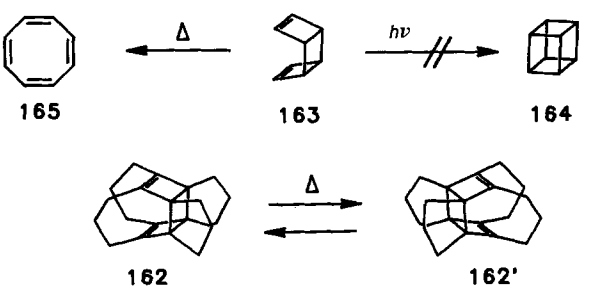

Because the first ionization potential of **162** lies at relatively low energy (7.6 eV), this compound should be prone to attack by electrophiles. This can be easily confirmed, and Scheme 11 shows that the expected products are formed. With *m*-chloroperbenzoic acid or diazomethane both the monoepoxide **166** as well as the bisepoxide and the propellanes **168** and **169** can be isolated, respectively[95].

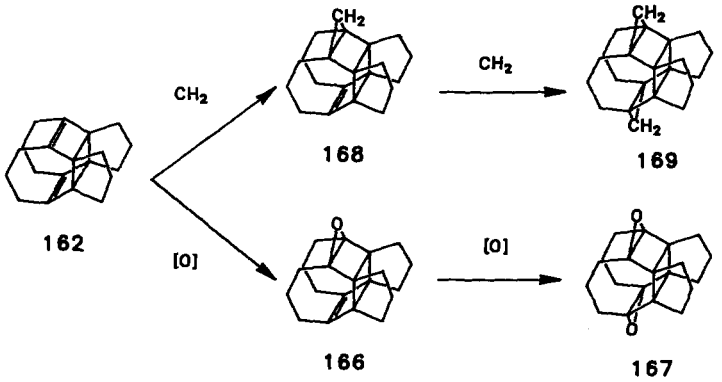

Scheme 11. Reactions of **162** with *meta*-chloroperbenzoic acid and diazomethane.

Before we continue the discussion of the photochemistry of **162**, it is worth considering why irradiation of **163** cannot lead to a cubane.[96, 97] The following two arguments can be invoked: 1) The increase in strain energy in the conversion of **163** to **164** is calculated to be about 72 kcal mol^{-1}.[98] 2) The light-induced [2 + 2]cycloaddition of **163** to **164** is only possible with a large amount of (electronic) activation energy.[11] We clarify this point in Figure 15. The orbital sequence of two cyclobutene molecules is depicted on the left, and it can be deduced that their photochemical [2 + 2]cycloaddition is an allowed process.[99] For both the occupied π MOs and the vacant π^* MOs the antisymmetric (with respect to the *x*,*z*-plane) linear combination π_- lies at higher energy than the bonding linear combination π_+. On excitation of an electron from the HOMO (π_-) to the LUMO (π^*_+) the bond order between carbon atoms 1 and 1′ as well as between 2 and 2′ is increased. That is, the reaction is "allowed".[99]

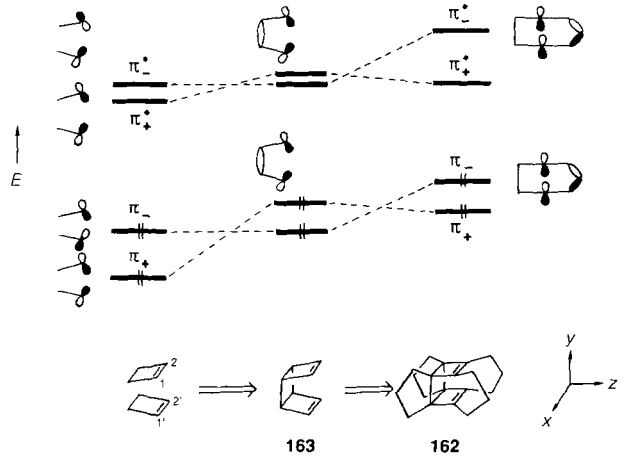

Fig. 15. Correlation between the occupied and unoccupied π MOs of two cyclobutene molecules (left), tricyclo[4.2.0.0^{2,5}]octadiene (**163**) (middle), and **162** (right).

When the two cyclobutene units are connected to *syn*-tricyclo[4.2.0.0^{2,5}]octa-3,7-diene (**163**) a strong through-bond interaction is possible and the orbital sequence is switched, so that π_+ and π^*_+ are now higher in energy than π_- and π^*_-.[100] Consequently the [2 + 2]cycloaddition reaction requires considerable (electronic) activation energy, making the reaction therefore "forbidden". To make the process an "allowed" one, the original orbital sequence (π_- above π_+) must be reinstated. One way of achieving this is by bringing the two olefinic sites closer together through the introduction of propano bridges. This has two effects: 1) The greater proximity of the double bonds (3.05 Å in **163** compared to 2.65 Å in **162**) decreases the energetic difference between π_+ and π_-. 2) The propano bridges destabilize π_- (see Figs. 2 and 3) so that an orbital sequence as shown on the right side of Figure 15 results. We can predict that as a result of the better electronic situation, a [2 + 2]cycloaddition is more likely to occur in **162** than in **163**. These qualitative arguments[11] can easily be substantiated by quantum mechanical calculations.[101]

On irradiation of **162** two products are observed,[93] one of which rearranges at room temperature. After purification one of the isolated products was shown to have a very simple ^{13}C NMR spectrum with only three resonances in the high-field region. According to the analytical data of the isolated hydrocarbons the reaction sequence depicted in Scheme 12 is most likely, in which the isolated propella[3$_4$]cubane **170** rearranges in the presence of trace amounts of acids or on heating to **162**. The strain energies calculated by an MM2 force field are as follows:[102] 164.31 kcal mol^{-1} for **162**, 229.20 kcal mol^{-1} for **170** and 181.96 kcal mol^{-1} for **171**. Interestingly the fourfold bridged cyclooctatetraene **172** cannot be obtained by thermolysis of **162**.

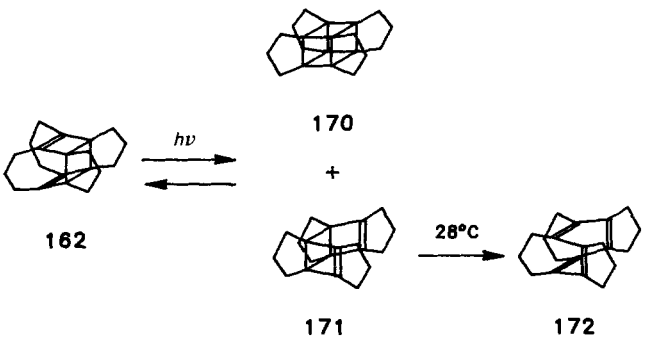

Scheme 12. Irradiation of **162**.

The cubane derivative **170** can be viewed as either a tetramer of cyclopentyne[13] or as the first representative of a new class of compounds termed the propella[n$_m$]prismanes.[11, 93] If the adjacent centers of an [m]prismane are connected by n equivalent atoms or groups of atoms, the isomers **173**–**179** are obtained for the series of [3] to [5]prismanes.

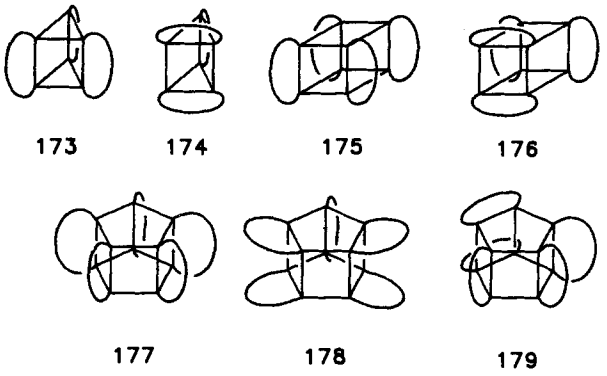

7. Other Propellaprismanes: Propella[n_3]prismanes

A prismane skeleton in which all adjacent centers are connected by methylene bridges, as for example in **173**, may be constructed starting from mono- or diacetylenes. This section briefly describes the preparation of two promising precursors, the doubly bridged prismane derivatives **180a, b**.

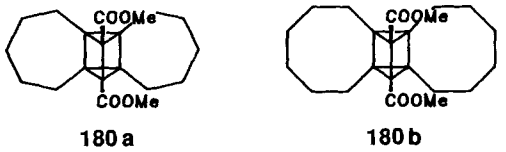

Ideal starting compounds for the synthesis of **180a, b** are 1,8-cyclotetradecadiyne (**17**) and cyclooctyne (**181**). The reaction of these two compounds with $AlCl_3$ in CH_2Cl_2 provides the two expected complexes **182** and **183**.[103-105] Addition of dimethylacetylenedicarboxylate (DMAD) leads to formation of the isomeric Dewar-benzene derivatives **184**–**187** (Scheme 13). The respective isomers **184**/**185** and **186**/**187** are formed in a ratio of 1:1.[106]

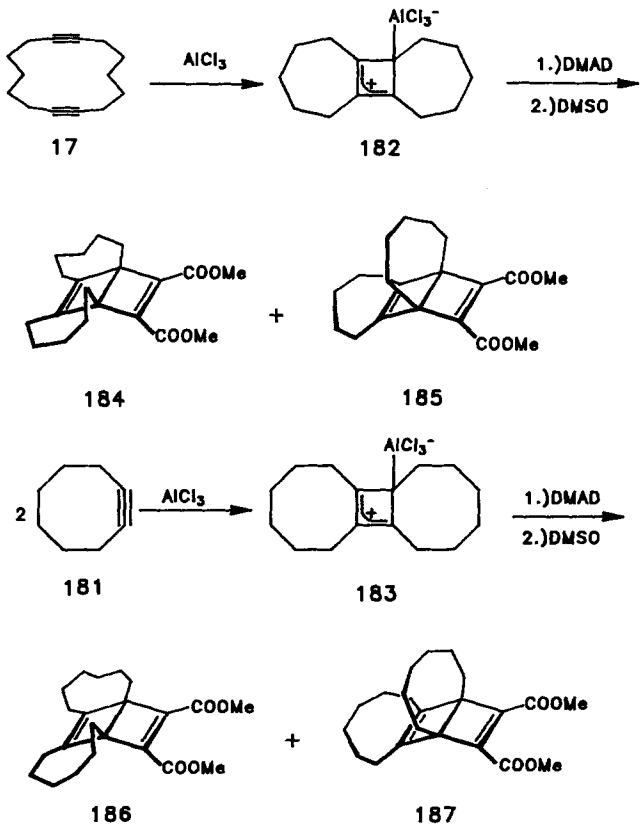

Scheme 13. Preparation of bridged Dewar-benzene derivatives from **17** and **181**, respectively.

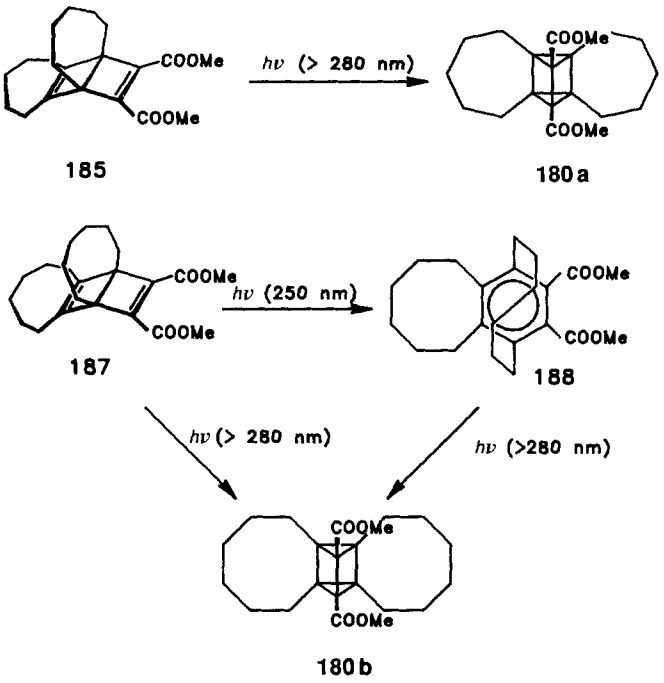

When **185** is irradiated at a wavelength of >280 nm the prismane **179** can be isolated in 15% yield. Irradiation of **187** at $\lambda = 250$ nm leads to the rapid formation of [6]cyclophane **188**. When the wavelength is increased to >280 nm the prismane **180b** is formed, which can also be obtained from **188**.

8. Outlook

Cyclic diacetylenes with medium-sized rings have been examined for the following two reasons: First, they are valuable model compounds for an extensive examination of transannular electronic effects. Second, they are ideal precursors for novel cyclophanes and strained cage compounds.

Further useful model compounds are the two bicyclic triacetylenes **189** and **190**. Not only are they fascinating structures for the study of transannular interactions, but also good candidates for further conversion with transition-metal fragments.

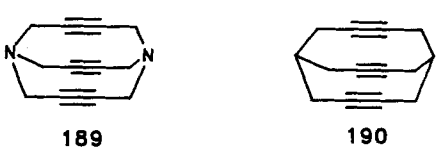

Of all the reactions described in this review the stepwise approach to cyclobutadiene superphanes stabilized by complex fragments shows the most synthetic potential, especially if one considers that up to now only the cobalt and iron

derivatives have been prepared. Closely related to this is an approach to a superphane of benzene[109] by means of a stepwise intermolecular trimerization. Unfortunately, experiments aimed at transforming **192** to **193** have been unsuccessful so far.[108]

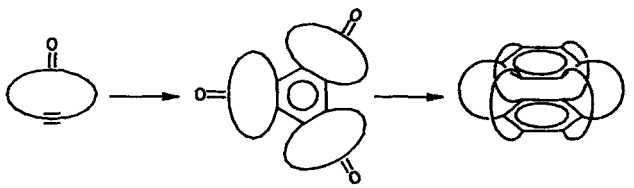

191 **192** **193**

It should be possible to rearrange the obtained highly strained and multiply bridged cage compounds (e.g. **166**–**169**, **170**, **180**, and **184**–**187**) either thermally, photochemically, or by reaction with transition-metal complexes. The bridging alkyl units should lead to unusual reaction paths.

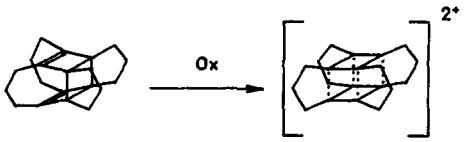

162 **194**

Considering the low ionization energy of **162**, its oxidation to **194** seems feasible. Like pagodane[109] the dication **194** is also a molecule of theoretical interest.[101b]

Most of the results described in this review are based on the experimental work of M. Karcher, D. Kratz, H. Langer, R. Merger, K.-H. Pfeifer, G. Pflästerer, J. Ritter, S. Rittinger, W. Schäfer, V. Schehlmann, and B. Treptow. Because of their dedication, creativity, and ability these results could be obtained in only a few years. My special thanks go to my colleagues H. Irngartinger, M. L. Ziegler, and B. Nuber for the numerous X-ray structures. Our work is funded by the state of Baden-Württemberg, the Volkswagen-Stiftung, the Deutsche Forschungsgemeinschaft (SFB 247), the BASF Aktiengesellschaft, and DEGUSSA. I am indebted to Mrs. P. Schlickenrieder for typing this manuscript.

Received: June 3, 1991 [A 849 IE]
German version: *Angew. Chem.* **1992**, *104*, 29.

[1] F. Sondheimer, *Acc. Chem. Res.* **1972**, *5*, 81–91; M. Nakagawa in *Topics in Nonbenzenoid Aromatic Chemistry, Vol. 1*, Hirokawa Publish. Co, Tokyo, **1973**, p. 191–219.
[2] F. Sondheimer, I. C. Calder, J. A. Elix, Y. Gaoni, P. J. Garratt, K. Grohmann, G. di Maio, J. Mayer, M. V. Sargent, R. Wolovsky, *Aromaticity (Spec. Publ. Chem. Soc.* **1967**, *21*, 75–109).
[3] H. A. Staab, F. Graf, *Tetrahedron Lett.* **1966**, 751–757.
[4] L. T. Scott, *Pure Appl. Chem.* **1986**, *58*, 105–110.
[5] Y. Rubin, M. Kahr, C. B. Knobler, F. Diederich, C. L. Wilkins, *J. Am. Chem. Soc.* **1991**, *113*, 495–500, and references therein.
[6] H. W. Kroto, J. R. Heath, S. C. O'Brien, R. F. Curl, R. E. Smalley, *Nature* **1985**, *318*, 162–163; W. Krätschmer, L. D. Lamb, K. Fostiropoulos, D. R. Huffman, *Nature* **1990**, *347*, 354–358; J. F. Stoddart, *Angew. Chem.* **1991**, *103*, 71–72; *Angew. Chem. Int. Ed. Engl.* **1991**, *30*, 70–71; F. Diederich, R. L. Whetten, *Angew. Chem.* **1991**, *103*, 695–697; *Angew. Chem. Int. Ed. Engl.* **1991**, *30*, 678–680.
[7] K. C. Nicolaou, W. M. Dai, *Angew. Chem.* **1991**, *103*, 1453–1481; *Angew. Chem. Int. Ed. Engl.* **1991**, *30*, 1387–1416; H. Waldmann, *Nachr. Chem. Techn. Lab.* **1991**, *39*, 211–217, and references therein.
[8] R. G. Bergman, *Acc. Chem. Res.* **1973**, *6*, 25–31; J. P. Snyder, *J. Am. Chem. Soc.* **1990**, *112*, 5367–5369; I. H. Goldberg, *Acc. Chem. Res.* **1991**, *24*, 191–198, and references therein; see also lit. [42] and [54].
[9] a) K. P. C. Vollhardt, *Angew. Chem.* **1984**, *96*, 525–541; *Angew. Chem. Int. Ed. Engl.* **1984**, *23*, 539–556; b) H. Bönnemann, *Angew. Chem.* **1978**, *90*, 517–526; *Angew. Chem. Int. Ed. Engl.* **1978**, *17*, 505–515; c) N. E. Schore, *Chem. Rev.* **1988**, *88*, 1081–1119, and references therein; see also lit. [109].
[10] R. Gleiter, *Pure Appl. Chem.* **1987**, *59*, 1585–1594; R. Gleiter, W. Schäfer, *Acc. Chem. Res.* **1990**, *23*, 369–375.
[11] R. Gleiter, M. Karcher, D. Kratz, S. Rittinger, V. Schehlmann, *Organomet. Org. Synth. Proc. Sympo. Org. Synth. Organomet. 2nd.* **1989**, 109–125.
[12] a) H. Meier, *Synthesis* **1972**, 235–253; b) H. Meier in *Advances in Strain in Organic Chemistry* (Ed.: B. Halton), JAI-Press, **1991**.
[13] a) A. Krebs in *Chemistry of Acetylenes* (Ed.: H. G. Viehe), Dekker, New York, **1969**, pp. 987–1062; b) A. Krebs, J. Wilke, *Top. Curr. Chem.* **1983**, *109*, 189–233; c) V. Jäger, *Methoden Org. Chem. (Houben-Weyl) 4th ed.* **1977**, Bd. V, 2a, pp. 33–637.
[14] J. H. Wotiz, R. F. Adams, C. G. Parsons, *J. Am. Chem.* **1961**, *83*, 373–376; J. Dale, A. J. Hubert, G. S. D. King, *J. Chem. Soc.* **1963**, 73–86; A. J. Hubert, *J. Chem. Soc. C* **1967**, 6–10.
[15] G. Schill, U. Keller, *Synthesis* **1972**, 621–627; G. Schill, E. Logemann, H. Fritz, *Chem. Ber.* **1976**, *109*, 497–502.
[16] M. Lespieau, *Compt. rend. Acad. Sci.* **1929**, *188*, 502–503; F. Sondheimer, Y. Gaoni, J. Bregman, *Tetrahedron Lett.* **1960**, *26*, 25–29.
[17] G. Eglinton, I. A. Lardy, R. A. Raphael, G. A. Sim, *J. Chem. Soc.* **1964**, 1154–1158.
[18] a) R. Gleiter, S. Rittinger, *Tetrahedron Lett.* **1988**, *29*, 4529–4532; b) R. Gleiter, S. Rittinger, H. Langer, *Chem. Ber.* **1991**, *124*, 357–363.
[19] D. N. Harpp, M. Gingras, T. Aida, T. H. Chan, *Synthesis* **1987**, 1122–1124; D. N. Harpp, M. Gingras, *Tetrahedron Lett.* **1987**, *28*, 4373–4376.
[20] G. Dijkstra, W. H. Kruizinga, R. M. Kellogg, *J. Org. Chem.* **1987**, *52*, 4230–4234.
[21] K. C. Nicolaou, G. Skokotas, P. Maligres, G. Zuccarello, E. J. Schweiger, K. Toshima, S. Wendeborn, *Angew. Chem.* **1989**, *101*, 1255–1257; *Angew. Chem. Int. Ed. Engl.* **1989**, *28*, 1272–1274.
[22] H. Higuchi, K. Tani, T. Otsubo, Y. Sakata, S. Misumi, *Bull. Chem. Soc. Jpn.* **1987**, *60*, 4027–4036.
[23] a) R. Gleiter, J. Ritter, H. Irngartinger, J. Lichtenthäler, *Tetrahedron Lett.* **1991**, *32*, 2883–2886; b) *ibid.* **1991**, *32*, 2887–2890; c) B. S. Thyagarajan, T. Traugott, T. Takahashi, *J. Indian Chem. Soc.* **1978**, *55*, 1228–1231.
[24] a) R. Gleiter, R. Merger, *Tetrahedron Lett.* **1989**, *30*, 7183–7186; b) *ibid.* **1990**, *31*, 1845–1848.
[25] M. Brudermüller, H. Musso, *Chem. Ber.* **1988**, *121*, 2255–2256; M. Brudermüller, H. Musso, A. Wagner, *ibid.* **1988**, *121*, 2239–2244.
[26] B. E. Looker, F. Sondheimer, *Tetrahedron* **1971**, *27*, 2567–2571.
[27] A. Nissen, H. A. Staab, *Chem. Ber.* **1971**, *104*, 1191–1198.
[28] N. Darby, C. U. Kim, J. A. Salaün, K. W. Shelton, S. Takada, S. Masamune, *J. Chem. Soc. Chem. Commun.* **1971**, 1516–1517; see also H. N. C. Wong, F. Sondheimer, *Tetrahedron Lett.* **1980**, *21*, 217–220; R. Singh, G. Just, *ibid.* **1990**, *31*, 185–188.
[29] A. Etournaud, H. Wyler, *Helv. Chim. Acta* **1973**, *56*, 625–630; P. Deslongchamps, S. Lamothe, H. S. Lin, *Can. J. Chem.* **1984**, *62*, 2395–2398; D. Brillon, P. Deslongchamps, *Tetrahedron Lett.* **1986**, *27*, 1131–1134.
[30] P. Magnus, R. T. Lewis, J. C. Huffman, *J. Am. Chem. Soc.* **1988**, *110*, 6921–6923; K. Tomioka, H. Fujita, K. Koga, *Tetrahedron Lett.* **1989**, *30*, 851–854.
[31] P. Magnus, H. Annoura, J. Harling, *J. Org. Chem.* **1990**, *55*, 1709–1711.
[32] E. Kloster-Jensen, G. A. Eliassen, *Angew. Chem.* **1985**, *97*, 587–588; *Angew. Chem. Int. Ed. Engl.* **1985**, *24*, 565–567.
[33] H. Sakurai, Y. Nakadaira, A. Hosomi, Y. Eriyama, C. Kabuto, *J. Am. Chem. Soc.* **1983**, *105*, 3359–3360.
[34] H. N. C. Wong, P. J. Garratt, F. Sondheimer, *J. Am. Chem. Soc.* **1974**, *96*, 5604–5605.
[35] C. F. Wilcox, Jr., K. A. Weber, *J. Org. Chem.* **1986**, *51*, 1088–1094.
[36] I. Lalezari, A. Shafiee, M. Yalpani, *Tetrahedron Lett.* **1969**, *10*, 5105–5106; *Angew. Chem.* **1970**, *82*, 484; *Angew. Chem. Int. Ed. Engl.* **1970**, *9*, 464–465.
[37] H. Meier, H. Petersen, *Synthesis* **1978**, 596–598.
[38] H. Bühl, H. Gugel, H. Kolshorn, H. Meier, *Synthesis* **1978**, 536–537.
[39] a) R. Gleiter, M. Karcher, R. Jahn, H. Irngartinger, *Chem. Ber.* **1988**, *121*, 735–740; b) R. Gleiter, D. Kratz, V. Schehlmann, *Tetrahedron Lett.* **1988**, *29*, 2813–2816.
[40] a) J. Dale, *Angew. Chem.* **1966**, *78*, 1070–1093; *Angew. Chem. Int. Ed. Engl.* **1966**, *5*, 1000–1021; b) J. Dale in *Chemistry of Acetylenes* (Ed.: H. G. Viehe), Dekker, New York, **1969**, pp. 3–96.
[41] E. Kloster-Jensen, J. Wirz, *Helv. Chim. Acta* **1975**, *58*, 162–177; *Angew. Chem.* **1973**, *85*, 723; *Angew. Chem. Int. Ed. Engl.* **1973**, *12*, 671.

[42] M. Hirama, K. Fujiwara, K. Shigematu, Y. Fukazawa, *J. Am. Chem. Soc.* **1989**, *111*, 4120–4122.
[43] P. A. Wender, J. A. McKinney, C. Mukai, *J. Am. Chem. Soc.* **1990**, *112*, 5369–5370.
[44] D. J. Cram, N. L. Allinger, *J. Am. Chem. Soc.* **1956**, *78*, 2518–2524.
[45] H. Sakurai, M. Kira, M. Kumada, *Bull. Chem. Soc. Jpn.* **1971**, *44*, 1167–1167; see also ref. [69].
[46] R. Destro, T. Pilati, M. Simonetta, *Acta Crystallogr. Sect. B* **1977**, *33*, 447–456.
[47] R. Gleiter, S. Rittinger, H. Irngartinger, *Chem. Ber.* **1991**, *124*, 365–369.
[48] H. Irngartinger, J. Ritter, R. Gleiter, unpublished.
[49] H. Irngartinger, R. Merger, R. Gleiter, unpublished.
[50] E. Kloster-Jensen, C. Römming, *Acta Chem. Scand. Ser. B* **1986**, *40*, 604–605.
[51] H. Irngartinger, A. E. Jungk, *Chem. Ber.* **1977**, *110*, 749–759.
[52] M. J. Bennett, R. A. Smith, *Acta Crystallogr. Sect. B* **1977**, *33*, 1123–1126.
[53] G. A. Eliassen, E. Kloster-Jensen, C. Römming, *Acta Chem. Scand. Ser. B* **1986**, *40*, 574–582.
[54] K. C. Nicolaou, G. Zuccarello, Y. Ogawa, E. J. Schweiger, T. Kumazawa, *J. Am. Chem. Soc.* **1988**, *110*, 4866–4868.
[55] H. Irngartinger, *Chem. Ber.* **1977**, *110*, 744–748.
[56] H. Irngartinger, *Chem. Ber.* **1972**, *105*, 1184–1202.
[57] H. Irngartinger, *Chem. Ber.* **1973**, *106*, 751–760.
[58] H. Irngartinger, *Chem. Ber.* **1973**, *106*, 761–772.
[59] G. Bieri, E. Heilbronner, E. Kloster-Jensen, A. Schmelzer, J. Wirz, *Helv. Chim. Acta* **1974**, *57*, 1265–1283.
[60] R. Gleiter, W. Schäfer, A. Flatow, *J. Org. Chem.* **1984**, *49*, 372–374.
[61] R. Gleiter, M. Karcher, D. Kratz, M. L. Ziegler, B. Nuber, *Chem. Ber.* **1990**, *123*, 1461–1468.
[62] V. Schehlmann, *Ph.D. Thesis*, Heidelberg, **1990**; D. Kratz, *Ph.D. Thesis*, Heidelberg, **1991**.
[63] S. L. Buchwald, R. B. Nielsen, *Chem. Rev.* **1988**, *88*, 1047–1058; M. A. Bennett, H. P. Schwemlein, *Angew. Chem.* **1989**, *101*, 1349–1373; *Angew. Chem. Int. Ed. Engl.* **1989**, *28*, 1296–1320.
[64] R. B. King, A. Efraty, *J. Am. Chem. Soc.* **1972**, *94*, 3021–3025; R. B. King, *J. Ind. Chem. Soc.* **1977**, *55*, 169–175.
[65] R. B. King, M. N. Ackermann, *J. Organomet. Chem.* **1974**, *67*, 431–441.
[66] A. Efraty, *Chem. Rev.* **1977**, *77*, 691–744.
[67] R. B. King, I. Haiduc, *J. Am. Chem. Soc.* **1972**, *94*, 4044–4046.
[68] R. B. King, I. Haiduc, C. W. Eavenson, *J. Am. Chem. Soc.* **1973**, *95*, 2508–2516.
[69] a) H. Sakurai, K. Hirama, Y. Nakadaira, C. Kabuto, *Chem. Lett.* **1988**, 485–486; b) *J. Am. Chem. Soc.* **1987**, *109*, 6880–6881.
[70] F. D. Mango, J. H. Schachtschneider, *J. Am. Chem. Soc.* **1969**, *91*, 1030–1031.
[71] Y. Wakatsuki, O. Nomura, K. Kitaura, K. Morokuma, H. Yamazaki, *J. Am. Chem. Soc.* **1983**, *105*, 1907–1912.
[72] L. P. McDonnell Bushnell, E. R. Evitt, R. G. Bergman, *J. Organomet. Chem.* **1978**, *157*, 445–456.
[73] K. Yasufuku, A. Hamada, K. Aoki, H. Yamazaki, *J. Am. Chem. Soc.* **1980**, *102*, 4363–4372.
[74] Y. Wakatsuki, K. Aoki, H. Yamazaki, *J. Chem. Soc. Dalton Trans.* **1982**, 89–94.
[75] Y. Wakatsuki, S. Miya, S. Ikuta, H. Yamazaki, *J. Chem. Soc. Chem. Commun.* **1985**, 35–37, and references therein.
[76] R. Gleiter, M. Karcher, M. L. Ziegler, B. Nuber, *Tetrahedron Lett.* **1987**, *28*, 195–198.
[77] R. Gleiter, D. Kratz, *Tetrahedron Lett.* **1990**, *31*, 5893–5896.
[78] M. L. Ziegler, B. Nuber, unpublished.
[79] G. Pflästerer, unpublished.
[80] R. Gleiter, D. Kratz, M. L. Ziegler, B. Nuber, *Tetrahedron Lett.* **1990**, *31*, 6175–6178.
[81] R. Gleiter, R. Merger, unpublished.
[82] R. Gleiter, B. Treptow, unpublished.
[83] S. Rittinger, *Ph.D. Thesis*, Heidelberg, **1990**.
[84] R. Gleiter, M. Karcher, B. Nuber, M. L. Ziegler, *Angew. Chem.* **1987**, *99*, 805–806; *Angew. Chem. Int. Ed. Engl.* **1987**, *26*, 763–764.
[85] M. T. Reetz, *Angew. Chem.* **1972**, *84*, 161–162, 163; *Angew. Chem. Int. Ed. Engl.* **1972**, *11*, 129–130, 130; *Adv. Organomet. Chem.* **1977**, *16*, 33–65; G. Erker, K. Kropp, *Chem. Ber.* **1982**, *115*, 2437–2446.
[86] R. Gleiter, V. Schehlmann, *Tetrahedron Lett.* **1989**, *30*, 2893–2896.
[87] D. F. Harvey, B. M. Johnson, C. S. King, K. P. C. Vollhardt, *Synlett* **1989**, *1*, 15–18.
[88] R. Gleiter, V. Schehlmann, *Angew. Chem.* **1990**, *102*, 1450–1452; *Angew. Chem. Int. Ed. Engl.* **1990**, *29*, 1426–1427.
[89] C. M. Adams, E. M. Holt, *Organometallics* **1990**, *9*, 980–986.
[90] R. Gleiter, D. Kratz, *Angew. Chem.* **1990**, *102*, 304–307; *Angew. Chem. Int. Ed. Engl.* **1990**, *29*, 276–279.
[91] J. R. Fritch, K. P. C. Vollhardt, *Angew. Chem.* **1979**, *91*, 439–440; *Angew. Chem. Int. Ed. Engl.* **1979**, *18*, 409–410; G. Ville, K. P. C. Vollhardt, M. J. Winter, *J. Am. Chem. Soc.* **1981**, *103*, 5267–5269; *Organometallics* **1984**, *3*, 1177–1187.
[92] R. Gleiter, D. Kratz, M. L. Ziegler, B. Nuber, unpublished.
[93] R. Gleiter, M. Karcher, *Angew. Chem.* **1988**, *100*, 851–852; *Angew. Chem. Int. Ed. Engl.* **1988**, *27*, 840–841.
[94] H. M. Frey, H. D. Martin, M. Hekman, *J. Chem. Soc. Chem. Commun.* **1975**, 204–205; R. S. Case, M. J. S. Dewar, S. Kirschner, R. Pettit, W. Slegeir, *J. Am. Chem. Soc.* **1974**, *96*, 7581–7582.
[95] R. Gleiter, G. Pflästerer, unpublished.
[96] R. Criegee, *Angew. Chem.* **1962**, *74*, 703–712; *Angew. Chem. Int. Ed. Engl.* **1962**, *1*, 519–527; H. Iwamura, K. Morio, H. Kihara, *Chem. Lett.* **1973**, 457–460.
[97] The photolysis of *syn*- und *anti*-perfluoroctamethyltricyclo[4.2.0.$0^{2,5}$]-octa-3,7-diyne gives perfluoroctamethylcubane: L. F. Pelosi, W. T. Miller, *J. Am. Chem. Soc.* **1976**, *98*, 4311–4312.
[98] E. Osawa, K. Aigami, Y. Inamoto, *J. Org. Chem.* **1977**, *42*, 2621–2626.
[99] R. B. Woodward, R. Hoffmann, *Angew. Chem.* **1969**, *81*, 797–869; *Angew. Chem. Int. Ed. Engl.* **1969**, *8*, 781–853.
[100] R. Gleiter, E. Heilbronner, M. Hekman, H.-D. Martin, *Chem. Ber.* **1973**, *106*, 28–34.
[101] a) E. Osawa, J. M. Rudzinski, Y.-M. Xun, *Struct. Chem.* **1990**, *1*, 333–344; b) R. Gleiter, K.-H. Pfeifer, W. Koch, unpublished.
[102] W. Schäfer, Böhringer, Mannheim, private communication.
[103] W. Schäfer, H. Hellmann, *Angew. Chem.* **1967**, *79*, 566–573; *Angew. Chem. Int. Ed. Engl.* **1967**, *6*, 518–525.
[104] J. B. Koster, G. J. Timmermans, H. van Bekkum, *Synthesis* **1971**, 139–140.
[105] H. Hogeveen, D. M. Kok in *Chemistry of Triple-Bonded Functional Groups, Supplement C, Part 2* (Ed.: S. Patai, Z. Rappoport), Wiley, New York, **1983**, p. 981–1013, and references therein.
[106] R. Gleiter, B. Treptow, *Angew. Chem.* **1990**, *102*, 1452–1454; *Angew. Chem. Int. Ed. Engl.* **1990**, *29*, 1427–1429.
[107] Y. Sekine, M. Brown, V. Boekelheide, *J. Am. Chem. Soc.* **1979**, *101*, 3126–3127; H. Hopf in *Cyclophanes, Vol. II* (Ed.: P. M. Keehn, S. M. Rosenfeld), Academic, New York, **1983**, pp. 521–572.
[108] A. J. Hubert, *J. Chem. Soc. C* **1967**, 13–14; R. D. Stephens, *J. Org. Chem.* **1973**, *38*, 2260–2262; J. A. Gladysz, J. G. Fulcher, S. J. Lee, A. B. Bocarsley, *Tetrahedron Lett.* **1977**, *39*, 3421–3424.
[109] G. K. S. Prakash, V. V. Krishnamurthy, R. Herges, R. Bau, H. Yuan, G. A. Olah, W.-D. Fessner, H. Prinzbach, *J. Am. Chem. Soc.* **1986**, *108*, 836–838; *ibid.* **1988**, *110*, 7764–7772.

Field-Effect Transistors as Sensors of Neural Systems

By *Hans-Joachim Galla* *

The active components of the nervous system are the individual nerve cells, the neurons. The human brain contains some 10^{11}–10^{12} of these cells, which communicate with each other and with the target organs. To do this, they must receive input signals from other neurons through the synapses, via chemical transmitters and electrical signals. The excitatory and inhibitory impulses from up to 10^4 synapses are integrated in the cell body of the neuron and are then passed on to the target cell as an electrical signal. The signal itself contains very little information. Rather, this information is found in the coupling of the origin and the target of the signal, that is, in the connections between the nerve cells, in the neural network. To understand how this network functions, we must understand how the many input signals are processed to give one inner signal and how this in turn determines the output signal. It is therefore necessary to measure local electrical voltages on defined neural structures in a noninvasive manner and with high spatial and temporal resolution.

Neurons in cell cultures are the most suitable objects for these studies. Fromherz et al.[1] have succeeded in growing leech neurons on preformed protein paths, about 10 μm in breadth and with defined geometry. The protein was obtained from the extracellular matrix of the leech, mixed with bovine serum albumin, and applied to a microscope slide as an air-dried protein layer. Suitable patterns were produced by UV-lithography, using masks made previously. Although the neurite trees grow with irregular branchings on a homogeneous layer of protein, neurons with linear structures are obtained on linear protein paths, and branched neurons are generated by branched paths. The use of these cell-culture systems allows the study of signal conduction in the neurite tree. The aim of this work is to construct networks with synapses at defined positions.

Membrane potentials may be measured by spectroscopic and electrical methods. Fluorescence techniques[2] may be used: The conduction velocity of the action potential can be followed spectroscopically with "voltage-dependent dyes", which change their fluorescence intensity in the nerve cell membrane with changes in potential. Fromherz and Vetter have shown that the conduction of the action potential by cultivated cells corresponds to the situation in vivo, that is, action potentials that are induced in the region outside the soma are transmitted to the soma and to the periphery with conduction velocities similar to those observed in vivo. The relative changes in fluorescence intensity are small, however, and the sensitivity is regiodependent. Although a resolution of up to 1 μm can be attained by optimization of the chemical structure of the dyes, the method's disadvantages are that it is not possible to stain and measure individual neurons in the network selectively, and that most of the dyes are strongly phototoxic.

These problems can be overcome by establishing a direct electrical contact with the cell. The aim of this more interesting and progressive technique is the construction of a bidirectional connection between semiconductors and neurons, a sort of artificial "silicon–neuron synapse".

The most simple, classical method of making an electrical contact with a cell is to pierce the cell body with a capillary electrode, or insert the electrode lengthwise into the axon, if this has a large enough diameter. The patch-clamp method developed by Neher and Sakmann[3] in the so-called whole-cell mode is more elegant. In this technique, the cell surface is sucked onto a pipette by reduced pressure. When the pressure is reduced further, a membrane fragment is broken out of the cell membrane, creating a connection with low electrical resistance between the pipette and the cell interior. In the study of neural networks, however, both methods have the disadvantage of being invasive, and it is also difficult to maintain the connection for several hours or days. In addition, attaching several electrodes to a cell simultaneously is not easy.

Extracellular electrodes have brought a distinct improvement here. The cells are grown in specially prepared culture dishes on a planar array of electrodes. Microelectrodes about 10×10 μm in size can record action potentials from individual neurons at a distance of 40 μm from the center of the electrode. Using an array of 32 microelectrodes per culture plate, J. Pine[4] could show that action potentials can be detected for individual neurons, and that action potentials may be generated simultaneously by stimulation of the cell body or the neural processes. This method is noninvasive, and the contact between cell and electrode can be maintained for weeks. It is not possible, however, to record synaptic potentials below the threshold level. There is also the danger that signals from several cells may be measured at the same time, and that a current pulse from the electrode may stimulate more than one cell simultaneously.

A further improvement was attained by the so-called loose-patch method,[5] which does not break the membrane

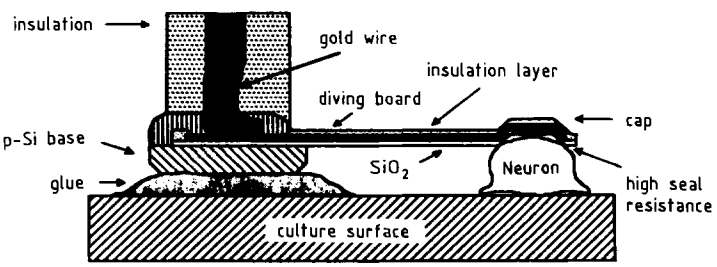

Fig. 1. System for recording and inducing action potentials with a "diving-board electrode". The metal surface forms a cap on top of the neuron with high seal resistance. This set-up corresponds to the loose-patch electrode. The signal obtained is capacitive in nature (from ref.[6]).

[*] Prof. Dr. H.-J. Galla
Institut für Biochemie
Wilhelm-Klemm-Strasse 2, D-W-4400 Münster (FRG)

and is hence noninvasive. This method was significantly improved by the use of the "diving-board electrode", depicted in Figure 1, which creates a permanent connection between the electrode and the cell body. The microelectrode consists of a p-silicon base, which is fixed to the bottom of the culture dish. Contact to the cell surface is made by a long, flexible arm (the "diving board"), which has a gold conductor embedded between two insulating layers. The diving-board electrode can be positioned on several neurons in culture and can be used for long-term multielectrode measurements and stimulations. Action potentials can be recorded with a good signal-to-noise ratio, though here, too, signals below the threshold level are not detected. One major goal remains: measuring an induced action-potential with the same diving-board electrode used to stimulate the cell.

The introduction of field-effect transistors (FETs) as potential probes was a clear step forward in the analysis of signal processing in small neural networks. Fromherz et al.[7] have grown neurons directly on a thin, insulating layer of the gate oxide on n-silicon. The voltage changes in the cell during an action potential affect the source–drain current by capacitative coupling, like potential changes on a metal gate.

Figure 2 shows the object under investigation, a leech neuron, the Retzius cell. The cell body, to which a short piece of

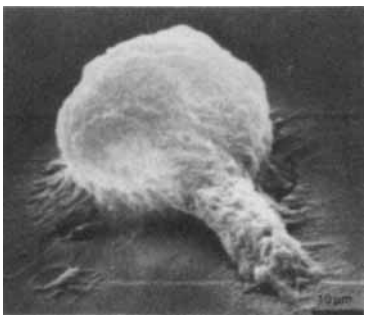

Fig. 2. Raster electron-micrograph of a Retzius cell on a field-effect transistor. The cell covers the poly-L-lysine coated gate. The contours of source and drain are visible. The bar represents 10 μm (from ref.[7]).

the neurite is attached and can still be seen, is in direct contact with the metal-free gate of a p-channel field-effect transistor. In freshly isolated cells, the action potentials are 40–60 mV. The FET was constructed on the surface of n-silicon by diffusion of boron into source and drain. The 1 μm thick insulating SiO_2 layer is opened in the middle, and the channel is filled with a layer of the gate oxide 20 nm thick (Fig. 3 right). The gate was coated with polylysine for improved

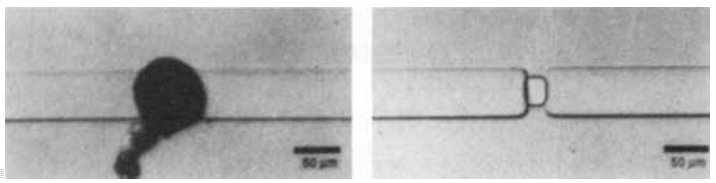

Fig. 3. Left: Top view of the FET with a neuron. Right: Top view of the FET. The distance between source and drain is 16 μm. The insulating layer (1 μm SiO_2) is opened in the middle and filled with a layer of gate oxide 20 nm thick (from ref. [7]).

adhesion, and the neuron was positioned on it with a glass pipette (Fig. 3 left). Figure 4 (top) shows the construction schematically. By capacitive coupling, the cell modulates the source–drain current in a manner analogous to the voltage change at a metal gate. The neuron–Si contact zone is an FET; the change in voltage during an action potential lifts the surface potential of the Si by reducing the density of defect electrons. A clear reduction in the source–drain current is observed (Fig. 4 bottom). The voltage change at the

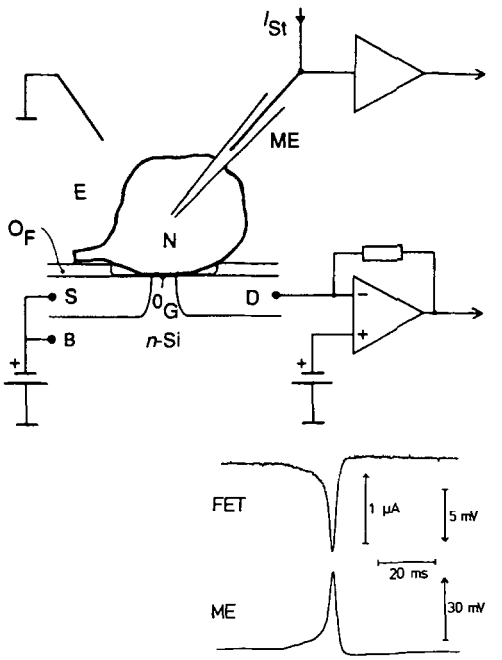

Fig. 4. Top: Schematic diagram of the apparatus. The neuron N is attached directly to the thin gate-oxide layer O_G of a field- effect transistor. Source S and drain D are insulated by a thicker SiO_2 layer O_F. The electrolyte solution E is at ground potential, and the source is held at a positive bias voltage so that a p-channel FET is created. Changes in the membrane potential have a capacitive effect on the insulating layer and modulate the measured source–drain current. The inserted microelectrode ME is only present for stimulation and for comparative measurements of the action potential. I_{st} = stimulation current, B = bulk silicon. Bottom: Measurement of the action potential. The membrane potential measured by the inserted microelectrode (ME) is compared with the source–drain current at the FET (from ref.[7]).

gate amounts to about 25% of the intracellular change in membrane potential (up to 40 mV). The shape of the action potential is retained in the response of the FET. This procedure is suitable for measurement of spontaneous or stimulated action potentials. Fromherz et al. applied a series of stimuli at intervals of 30 ms and observed perfect agreement between the induction signal and the FET response. Signals below the threshold level can also be detected.

There are still problems with this technique. Reproducible coupling between the neuron and the insulating layer is not achieved in all experiments, nor is it always possible to isolate the neurons without damaging them. However, it can already be seen that the direct coupling between neuron and silicon is much superior to metallic microelectrodes (cf. Fig. 1), with extracellular voltage amplitudes of under 1 mV. Whether this method offers advantages over the use of po-

tential-dependent dyes, which can affect cell function, will doubtless soon be reported by the Fromherz group. The goal of measuring electrical potentials in neuron cultures using an array of transistors on a chip with resolutions of 1 μm or less has come within reach. The assumption that bidirectional neuron–silicon synapses could already provide an "on-line" connection to the brain is definitely premature. However, it may be possible in the foreseeable future to interface the nervous system to stimulate paralyzed muscles, for example, or to couple an artificial limb directly to the nervous system of the remaining stump, and hence control it from the brain.[8,9] The establishment of the neuron–silicon synapse is a major requirement in achieving this goal.

German version: *Angew. Chem.* **1992**, *104*, 47

[1] P. Fromherz, H. Schaden, T. Vetter, *Neurosci. Lett.* **1991**, *129*, 77.
[2] P. Fromherz, T. Vetter, *Z. Naturforsch. C* **1991**, *46*, 687.
[3] E. Neher, B. Sakmann, *Nature* **1976**, *260*, 799.
[4] J. Pine, *J. Neurosci. Methods* **1980**, *2*, 19.
[5] W. Stuhmer, W. M. Roberts, W. Almers in *Single-Channel Recording* (Eds.: B. Sakmann, E. Neher), Plenum, New York, **1983**, p. 123.
[6] W. G. Regehr, J. Pine, D. Rutledge, *IEEE Trans. Biomed. Eng.* **1988**, *35*, 1023.
[7] P. Fromherz, A. Offenhäusser, T. Vetter, J. Weis, *Science* **1991**, *252*, 1290.
[8] S. Williams, *Science* **1990**, *248*, 555.
[9] I. Amato, *Science* **1991**, *253*, 34.

Synthesis of Optically Active Macromolecules Using Metallocene Catalysts

By *Jun Okuda**

Although nature is capable of efficiently producing monodisperse macromolecules in optically pure form, the rational synthesis of organic polymers having a well-defined microstructure and a narrow molecular-weight distribution remains a significant challenge. One of the goals in synthetic chemistry, therefore, is the development of well-characterized subtances which can catalyze the polymerization of unsaturated monomers in a living fashion and, in the case of prochiral monomers, in a stereoselective manner.

Some years ago the cocatalyst methylalumoxane was found to increase the activity of Ziegler–Natta catalysts derived from Group 4 metallocenes considerably.[1] Shortly thereafter the fundamental control of the tacticity of polypropylene through the molecular structure of the transition metal catalyst was reported.[2] Since the pioneering work by Turner et al.[3a], Jordan,[3b] and others it has been established that the cationic 14-electron alkyl $[Cp_2MR]^+$ ($Cp = \eta^5$-C_5H_5) is the active site for chain propagation.[3] Elegant kinetic studies performed recently by the teams of Brintzinger et al.[4a] and of Bercaw et al.[4b] have proved the decisive role of α-agostic interaction of the growing chain with the transition metal center. At present intense effort worldwide[5] is concentrating on evaluating the critical parameters for the stereoregularity of α-olefin polymerization[5a] and finding an explicit relationship between ligand properties of the catalyst and polymer structure.[5b] Thus the use of racemic C_2-symmetrical zircononcene (*R,S*)-[1,1′-ethylenebis(4,5,6,7-tetrahydro-1-indenyl)]zirconium dichloride (**1**) developed by Brintzinger leads to highly isotactic polypropylene. Here an enantiomorphic site control is proposed on the basis of defects within the polymer chain.[2b] On the other hand, the achiral titanocene derivative $[Cp_2TiPh_2]$ gives an isotactic block polymer that is formed by chain-end control. Finally the C_s-symmetrical hafnocene complex **2** with a bridged cyclopentadienyl–fluorenyl ligand system yields syndiotactic polypropylene.[6]

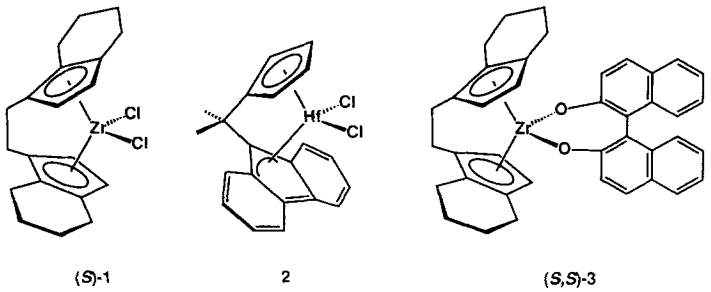

(*S*)-1 2 (*S,S*)-3

Recently Waymouth of Stanford University has demonstrated that it is also possible to produce an optically active polymer using a chiral metallocene catalyst of the Brintzinger type.[7] Although optically active oligomers can be obtained in the presence of a resolved metallocene complex according to the above mentioned procedure,[8] high molecular weight isotactic and syndiotactic polypropylenes generally contain mirror planes and are therefore achiral ("cryptochiral").[9]

Waymouth employed the homogeneously catalyzed cyclopolymerization of 1,5-hexadiene to poly(methylene-1,3-cyclopentane) developed in his group in order to utilize the stereoselectivity of the monomer insertion for the construction of a polymer with main-chain chirality. The cyclopolymerization is a remarkable chain-growth reaction during which a conventional insertion of a vinylic function into the transition-metal–carbon bond is followed by an intramolecular insertion resulting in a cyclization.[10] Thus from 1,5-hexadiene, a polymer chain is obtained in which methylene and 1,3-cyclopentanediyl fragments are arranged in a strictly alternating sequence (Scheme 1). By modifying the catalyst's ligand, control over the diastereoselectivity could be achieved ($[Cp_2ZrCl_2]$ leads to *trans*, $[Cp^*_2ZrCl_2]$ ($Cp^* = \eta^5$-

[*] Dr. J. Okuda
Anorganisch-chemisches Institut der Technischen Universität München
Lichtenbergstrasse 4, D-W-8046 Garching (FRG)

C_5Me_5) to *cis* connection of the cyclopentane fragments). Of the four possible structures of maximum order all but the *racemo*-diisotactic polymer are achiral. The latter does not contain a mirror plane and is chiral due to the main-chain stereochemistry determined by the configuration. Waymouth recognized that by using a chiral catalyst the enantioselective cyclopolymerization of 1,5-hexadiene would be possible. The catalyst used by Waymouth was chiral [1,1'-ethylenebis(4,5,6,7-tetrahydro-1-indenyl)]zirconium 1,1'-binaphtholate (**3**), which had been prepared according to Brintzinger[11] by reacting the racemic dichloro derivative **1** with optically active (*R*)- or (*S*)-1,1'-binaphthol.

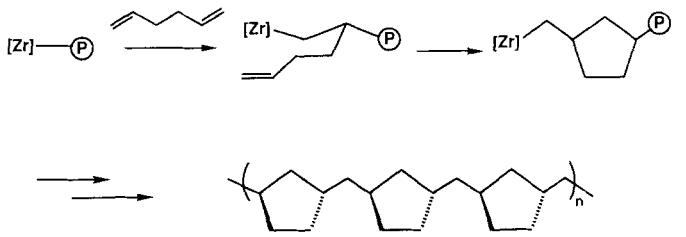

Scheme 1. [Zr] = Zr complex fragment, —Ⓟ = polymer chain.

Poly(methylene-1,3-cyclopentane) synthesized in the presence of (−)-(*R,R*)-**3** and methylalumoxane revealed a molar optical rotation of $[\Phi]_{405}^{28} = +50.1°$, whereas the polymer analogously prepared using the enantiomer (+)-(*S,S*)-**3** showed a value of $[\Phi]_{405}^{28} = -49.3°$. These findings are consistent with the formation of polymers with main-chain chirality.[9a]

In summary, Waymouth has for the first time realized the enantioselective synthesis of an optically active polymer starting with an achiral monomer by using an optically active, structurally well-defined metallocene catalyst. His results are promising, since the synthesis of organic polymers in a more rational way through modification of the transition-metal catalyst seems within reach. In addition, Waymouth's study emphasizes that knowledge of well-characterized organotransition-metal complexes offers an unprecedented opportunity for the design of novel polymerization reactions.

German version: *Angew. Chem.* **1992**, *104*, 49

[1] H. Sinn, W. Kaminsky, *Adv. Organomet. Chem.* **1980**, *18*, 99.

[2] a) J. A. Ewen, *J. Am. Chem. Soc.* **1984**, *106*, 6355; b) W. Kaminsky, K. Kulper, H. H. Brintzinger, F. R. W. P. Wild, *Angew. Chem.* **1985**, *97*, 507; *Angew. Chem. Int. Ed. Engl.* **1985**, *24*, 507; c) P. G. Gassman, M. R. Callstrom, *J. Am. Chem. Soc.* **1987**, *109*, 7875; d) M. Bochmann, A. J. Jaggar, J. C. Nicholls, *Angew. Chem.* **1990**, *102*, 830; *Angew. Chem. Int. Ed. Engl.* **1990**, *29*, 780.

[3] a) G. G. Hlatky, H. W. Turner, R. R. Eckman, *J. Am. Chem. Soc.* **1989**, *111*, 2728; b) R. Jordan, *J. Chem. Educ.* **1988**, *65*, 285.

[4] a) H. Krauledat, H. H. Brintzinger, *Angew. Chem.* **1990**, *102*, 1459; *Angew. Chem. Int. Ed. Engl.* **1990**, *29*, 1412; H. H. Brintzinger in *Organic Synthesis via Organometallics* (Eds.: K. H. Dötz, R. W. Hoffmann), Vieweg, Braunschweig, **1991**, p. 33; b) W. E. Piers, J. E. Bercaw, *J. Am. Chem. Soc.* **1990**, *112*, 9406.

[5] a) G. Erker, R. Nolte, Y.-H. Tsay, C. Krüger, *Angew. Chem.* **1989**, *101*, 642; *Angew. Chem. Int. Ed. Engl.* **1989**, *28*, 628; G. Erker, *Pure Appl. Chem.* **1991**, *63*, 797; G. Erker, C. Fritze, *Angew. Chem.*, in press; b) W. Röll, H. H. Brintzinger, B. Rieger, R. Zolk, *Angew. Chem.* **1990**, *102*, 339; *Angew. Chem. Int. Ed. Engl.* **1990**, *29*, 279; c) W. A. Herrmann, J. Rohrmann, E. Herdtweck, W. Spaleck, A. Winter, *Angew. Chem.* **1989**, *101*, 1536; *Angew. Chem. Int. Ed. Engl.* **1989**, *28*, 1511; W. Spaleck, M. Antberg, V. Dolle, R. Klein, J. Rohrmann, A. Winter, *New. J. Chem.* **1990**, *14*, 499; d) T. Mise, S. Miya, H. Yamazaki, *Chem. Lett.* **1989**, 1853; e) J. A. Bandy, M. L. H. Green, I. M. Gardiner, K. Prout, *J. Chem. Soc., Dalton Trans.* **1991**, 2207.

[6] J. A. Ewen, R. L. Jones, A. Razavi, J. D. Ferrara, *J. Am Chem. Soc.* **1988**, *110*, 6255.

[7] G. W. Coates, R. M. Waymouth, *J. Am. Chem. Soc.* **1991**, *113*, 6270.

[8] P. Pino, P. Cioni, J. Wei, *J. Am. Chem. Soc.* **1987**, *109*, 6189; W. Kaminsky, A. Ahlers, N. Möller-Lindenhof, *Angew. Chem.* **1989**, *101*, 1304; *Angew. Chem. Int. Ed. Engl.* **1989**, *28*, 1216.

[9] a) G. Wulff, *Angew. Chem.* **1989**, *101*, 22; *Angew. Chem. Int. Ed. Engl.* **1989**, *28*, 21; b) M. Farina, *Top. Stereochem.* **1987**, *17*, 1.

[10] a) L. Resconi, R. M. Waymouth, *J. Am. Chem. Soc.* **1990**, *112*, 4953; b) G. B. Butler, *Acc. Chem. Res.* **1982**, *15*, 370.

[11] F. R. W. P. Wild, M. Wasiucionek, G. Huttner, H. H. Brintzinger, *J. Organomet. Chem.* **1985**, *288*, 63.

New Directions in Polyvanadate Chemistry: From Cages and Clusters to Baskets, Belts, Bowls, and Barrels

By *Walter G. Klemperer,* Todd A. Marquart,* and *Omar M. Yaghi*

Like other early transition-metal polyoxoanions, large polyvanadates are known to adopt complex cage/cluster structures.[1] The Keggin structure observed in the anion of **1**[2] is typical. Here, the $[V_{14}O_{38}]^{6-}$ cage **A**[**] encapsulates a PO_4^{3-} anion. This cage is defined by 24 bridging oxygen atoms, and 14 of its 18 square faces are occupied by vanadium atoms, each of which is bonded to a terminal oxygen atom. The closely related Schlemper structure was first observed in **2**.[3] Here, the $[V_{18}O_{42}]^{12-}$ cage **B** encapsulates a water molecule. This cage is also defined by 24 bridging oxygen atoms, but all 18 of its square faces are occupied by V=O groups. The Keggin and Schlemper structures are very similar since they are both based on O_{24} cage frameworks. They differ in that the 24 bridging oxygens define the vertices of the O_h rhombicuboctahedron in Keggin structures and the D_{4d} elongated square gyrobicupola in Schlemper structures.[4]

$[(CN_3H_6)_8H][PV_{14}O_{42}] \cdot 7\,H_2O$ **1**

$K_{12}[V_{18}O_{42}] \cdot 16\,H_2O$ **2**

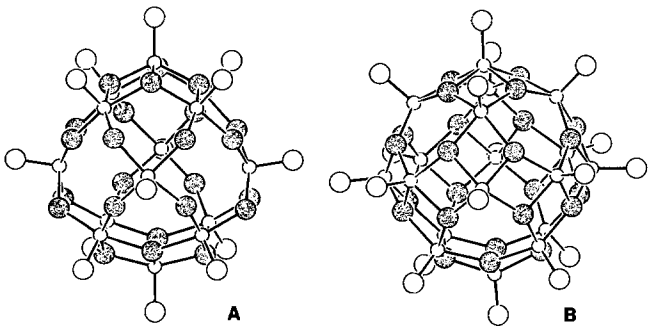

Research in polyvanadate chemistry has very recently expanded beyond classical cage/cluster structures to include hitherto unknown basket, belt, bowl, and barrel structures shown in **C**–**H**. The $[V_{12}O_{32}]^{4-}$ basket **C** contains an acetonitrile molecule in crystalline **3**.[4] The belt-shaped $[V_8O_{24}]^{16-}$ anion **D** is found in **4**,[5] where it encircles an oxalate ion. Two vanadate bowl strutures are also shown: One (**E**) is observed in **5**,[6] where the $[V_4O_{16}]^{12-}$ bowl contains a nitrate ion, and in **6**,[7] where the $[V_4O_{16}]^{12-}$ ion contains a potassium ion. The second, the $[V_5O_{17}]^{13-}$ bowl **F**, contains a Cl^- ion in **7**.[6] In **8**, $V_4O_{14}^{11-/12-}$ units **G** are joined together by CH_3P^{4+} groups to form $[(CH_3P)_8V_{16}O_{56}]^{14-}$ barrels **H** that contain tetramethylammonium cations.

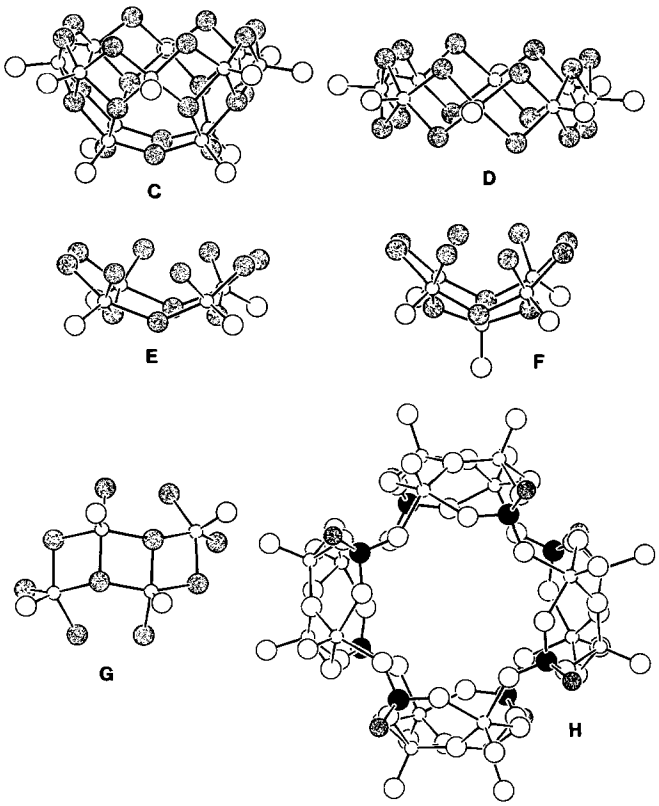

$(NEt_4)_2[V_4O_8(NO_3)(tca)_4] \cdot H_2O$ **5**, tca = thiophene-2-carboxylate

$[K\{V_4O_4(\mu\text{-}O)_4(\mu\text{-}O_2CCH_2t\text{Bu})_4][O_2CCH_2t\text{Bu}] \cdot 2\,t\text{BuCH}_2\text{COOH}$ **6**

$(PhCH_2NEt_2)_2[V_5O_9Cl(tca)_4] \cdot CH_3CN$ **7**

$(NMe_4)_8[H_6(MeP)_8V_{16}O_{56}] \cdot 11\,H_2O$ **8**

These recent developments in polyvanadate chemistry raise interesting questions regarding structural principles. Clearly, the new structures **C**–**F** can be viewed as fragments of classical Keggin and Schlemper cages **A** and **B**, but what about the barrel fragment **G** or the recently reported $[V_{30}O_{74}]^{10-}$,[9] $[V_{22}O_{54}]^{6-}$,[10] and $[V_{18}O_{44}]^{6-}$[10] cages in **9**, **10**, and **11**? What about larger cages that are yet to be

$K_{10}[V_{34}O_{82}] \cdot 20\,H_2O$ **9**

$(NEt_4)_6[HV_{22}O_{54}(ClO_4)]$ **10**

$(NEt_4)_5[H_2V_{18}O_{44}(N_3)]$ **11**

[*] Prof. W. G. Klemperer, T. A. Marquart, O. M. Yaghi
Department of Chemistry and
Beckman Insitute for Advanced Science and Technology
University of Illinois
Urbana, IL 61801 (USA)

[**] In structures **A**–**G** bridging oxygens are represented by large shaded spheres, terminal oxygens by large open spheres, and vanadium atoms by small open spheres. For the sake of clarity, the CH_3P^{4+} groups in **H** are shaded, and vanadium and oxygen atoms are represented by small and large open spheres, respectively. In the structures **I**–**L** the vanadium atoms are represented by small black spheres and oxygen atoms by large open spheres.

discovered? An answer to these questions is to be found in the infinite sheet (Fig. 1) observed in the V_2O_5 layer structure.[11] Consider first the $[V_4O_{16}]^{13-}$ bowl structure **E**. When flattened out into a sheet, this structure becomes the fragment of the V_2O_5 sheet labeled in orange (Fig. 1) after terminal oxygen atoms have been removed. The barrel fragment **G** is similarly displayed as the green V_2O_5 sheet fragment. In other cases, structures can be flattened into V_2O_5 sheet fragments only after cleaving selected V—O bonds. In the $[V_{12}O_{32}]^{4-}$ basket, for example, eight V—O bonds must be cleaved as in **I**, where terminal oxygen atoms have been omitted for clarity. Only then can the basket be flattened (see **J**) into the red V_2O_5 fragment of Figure 1. Large cage structures can be reduced to V_2O_5 layer fragments in the same way. The $[V_{30}O_{74}]^{10-}$ cage in **9**[9] is reduced to the yellow V_2O_5 fragment at the bottom of Figure 1 after cleaving 15 V—O bonds, as shown in **K** and **L**. The $[V_{22}O_{54}]^{6-}$ (**10**[10]) and $[V_{18}O_{44}]^{6-}$ (**11**[11]) cages both reduce to V_2O_5 fragments that are subfragments of this yellow fragment after 14 bonds are broken. The purpose of the exercise is now clear: by reversing the procedure, it is possible to cut out V_2O_5 sheet fragments, fold them up, and stitch them together to generate new polyvanadate structures. The recently discovered metastable γ'-V_2O_5 polymorph[12] can be derived from the V_2O_5 structure in an analogous fashion by first removing the terminal oxygen atoms, then corrugating the infinite sheet structure, and finally reintroducing the terminal oxygen atoms in new positions.

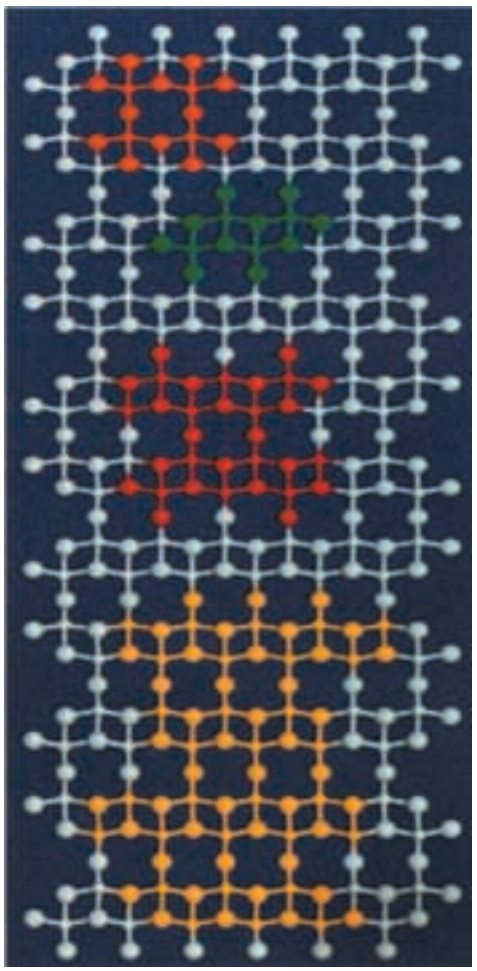

Fig. 1. Fragment of the V_2O_5 layer structure (small spheres represent vanadium; large spheres oxygen; for clarity the terminal oxygen atoms at the square-pyramidal vanadium centers have been omitted). The colored V—O units are observed in new, molecular polyvanadate structures. For details, see text.

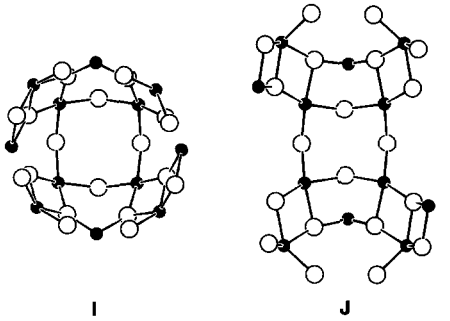

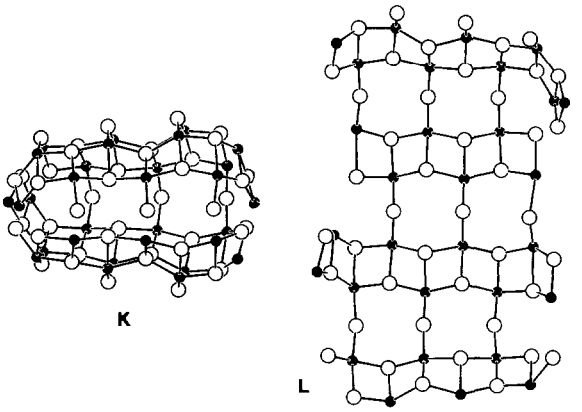

The relationship between V_2O_5 sheets and polyvanadate baskets, belts, bowls, and barrels extends beyond topology into chemistry. The sheets of VO_5 square pyramids found in V_2O_5 and related vanadates such as α-$VOPO_4$[13] are bonded together by weak V—O bonds, 2.8 Å long. As a result, the layers are easily separated to form intercalation complexes.[11, 14] In classical vanadate cages, a similar structural situation is observed. The cage of VO_5 square pyramids in the anion of **2**,[3] for example, is bonded to an encapsulated water molecule by very weak V—O bonds. "Intercalation" chemistry is impossible, however, since the cage framework blocks access to the vanadium coordination sites. Such is not the case with the new structures **C**—**F** and **H**, where access to square-pyramidal vanadium centers is relatively unrestricted, and guest–host chemistry becomes a real possibility. To date, only the $[L \subset (V_{12}O_{32}^{4-})]$ system has been investigated from this point of view,[4, 15] but a rich chemistry can be anticipated given the analogy with the solid oxide guest–host chemistry of zeolites.

German version: Angew. Chem. **1992**, *104*, 51

 © VCH Verlagsgesellschaft mbH, W-6940 Weinheim, 1992 0570-0833/92/0101-0050 $ 3.50+.25/0

[1] M. T. Pope, A. Müller, *Angew. Chem.* **1991**, *103*, 56; *Angew. Chem. Int. Ed. Engl.* **1991**, *30*, 34.
[2] R. Kato, A. Kobayashi, Y. Sasaki, *J. Am. Chem. Soc.* **1980**, *102*, 6571; *Inorg. Chem.* **1982**, *21*, 240.
[3] G. K. Johnson, E. O. Schlemper, *J. Am. Chem. Soc.* **1978**, *100*, 3645.
[4] V. W. Day, W.G. Klemperer, O. M. Yaghi, *J. Am. Chem. Soc.* **1989**, *111*, 5959.
[5] Q. Chen, S. Liu, J. Zubieta, *Inorg. Chem.* **1989**, *28*, 4433.
[6] D. D. Heinrich, K. Folting, W. E. Streib, J. C. Huffman, G. Christou, *J. Chem. Soc. Chem. Commun.* **1989**, 1411.
[7] W. Priebsch, D. Rehder, M. von Oeynhausen, *Chem. Ber.* **1991**, *124*, 761.
[8] G. Huan, A. J. Jacobsen, V. W. Day, *Angew. Chem.* **1991**, *103*, 426; *Angew. Chem. Int. Ed. Engl.* **1991**, *30*, 422.
[9] A. Müller, R. Rohlfing, J. Döring, M. Penk, *Angew. Chem.* **1991**, *103*, 575; *Angew. Chem. Int. Ed. Engl.* **1991**, *30*, 588.
[10] A. Müller, E. Krickemeyer, M. Penk, R. Rohlfing, A. Armatage, H. Bogge, *Angew. Chem.* **1991**, *103*, 1720; *Angew. Chem. Int. Ed. Engl.* **1991**, *30*, 1674.
[11] R. Enjalbert, J. Galy, *Acta Crystallogr. Sect. C* **1986**, *42*, 1467.
[12] J. M. Cocciantelli, P. Graverean, J. P. Doumerc, M. Pouchard, P. Hagenmüller, *J. Solid State Chem.* **1991**, *93*, 497.
[13] B. Jordan, C. Calvo, *Can. J. Chem.* **1973**, *51*, 2621.
[14] J. W. Johnson, A. J. Jacobson, J. F. Brody, S. M. Rich, *Inorg. Chem.* **1982**, *21*, 3820.
[15] W. G. Klemperer, T. A. Marquart, O. M. Yaghi, *Mater. Chem. Phys.*, **1991**, *29*, 97.

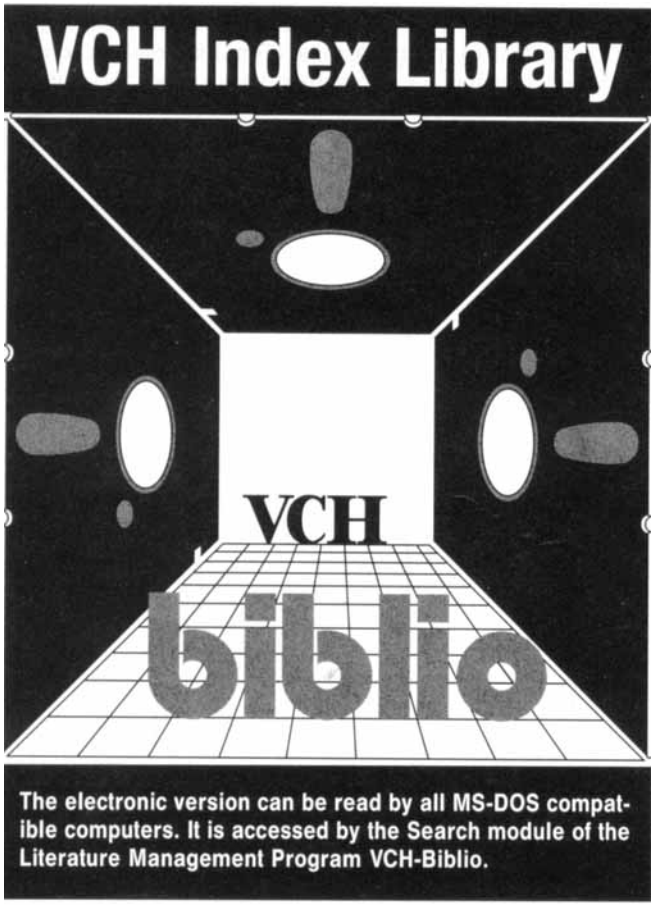

ANGEWANDTE CHEMIE
A Journal of the Gesellschaft Deutscher Chemiker
International Edition in English

30 Year Index of Reviews
– in print or on diskette –

The reviews in Angewandte Chemie are amongst the most often cited chemical publications of each year. Many have become classics of the chemical literature. For thirty years they have been available in English as well as German. The 30 year review index now celebrates this anniversary by facilitating access to these important documents of the rapid development of our discipline. The index—both a chemical dictionary and a history book—offers you:

1. A list of all authors, indicating the main author and the title of the review.
2. A subject index giving the main author.
3. Both indexes provide complete information on date of issue and first and last page numbers of the German and English editions.

The electronic version of the index is available on 5¼" and 3½" diskettes.

The price of the index is DM 98.00, $ 64.00 or £ 37.00. Please order by telephone or in writing to **VCH, Software und Datenbanken, Postfach 10 11 61, D-W-6940 Weinheim, Tel. 0 62 01/6 02-2 71, Telefax 0 62 01/6 02-3 28.**

Communications may be submitted in English *or* in German. Further details regarding the submission of communications can be found in the "Notice to Authors" reproduced in the January issue of the journal. Copies thereof may be obtained from the editorial office upon request.

Structure of the Tunichrome of Tunicates and its Role in Concentrating Vanadium

By *Ernst Bayer,* Gerhard Schiefer, Dietmar Waidelich, Silvia Scippa,* and *Mario de Vicentiis*

Dedicated to Professor Michael Hanack on the occasion of his 60th birthday

Tunicates (Urochorda) concentrate vanadium in their blood cells to a million times the concentration in sea water.[1–3] Although the vanadium compound in tunicates was discovered 80 years ago, its structure is still not known. A proven fact is that in *Phallusia mammillata* and *Ascidia nigra* vanadium is predominantly trivalent.[4,5] Apart from the vanadium-containing signet-ring and compartment cells, vanadium-free blood cells (morula cells) are found in *P. mammillata*[6] and *A. nigra*.[7] Nakanishi et al.[8–11] have used a laborious process with low recovery to isolate peptides[12] (which they named tunichromes) from the morula cells of *A. nigra*. The major component was assigned a dipeptide structure incorporating a β-(3,4,5-trihydroxyphenyl)-alanine and a β-(3,4,5-trihydroxyphenyl)dehydroalanine containing a *C*-terminal 3,4,5-trihydroxystyrylamide unit.

Because the peptides of the blood cells are exceptionally unstable and sensitive to oxidation, we have developed a very simple isolation involving few losses for the peptides from *P. mammillata*. The tunichromes were extracted with methanol quite selectively from lyophilized cells and purified by HPLC on polystyrene phases with a recovery rate 80–90% or by capillary electrophoresis, or introduced on-line from HPLC into an ion spray tandem mass spectrometer. In contrast, the separation on reversed phases based on silica gel caused large losses. All operations were performed in an inert atmosphere.

Figure 1 depicts the HPLC separation of the methanol extract. Besides three minor components, a major component was obtained, which was studied by ion spray MS, tandem MS, ^1H and ^{13}C NMR, UV/VIS, and IR spectroscopy. The separation of the methanol extract by capillary zone electrophoresis also proved valuable, as it also provided a major component.

[*] Prof. E. Bayer, Dr. G. Schiefer, Dipl.-Chem. D. Waidelich
Institut für Organische Chemie der Universität
Auf der Morgenstelle 18, D-W-7400 Tübingen 1 (FRG)
Prof. Dr. S. Scippa, Prof. Dr. M. de Vincentiis
II Cattedra di Istologia e Embriologia
Facolta di Scienze Fisiche Matematiche e Naturali
Universita di Napoli
Via Mezzocannone 8, I-80134 Napoli (Italy)

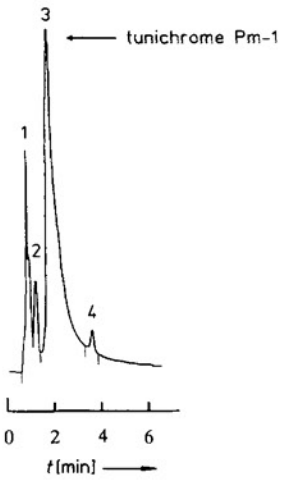

Fig. 1. HPLC of the methanol extract from blood cells of *Phallusia mammillata*. Column: 125 × 4.6 mm, 5 μm Hamilton PRP-1; UV detection at 210 nm; elution with CH_3CN/H_2O (50:50), 1 mL min^{-1}; p = 36 bar.
Fractions: 1, *p*-aminobenzoic acid; 2, sugar derivative; 3, tunichrome Pm-1; 4, tunichrome Pm-2 and Pm-3.

The UV spectrum of the major component shows a maximum at 301 nm and not the maximum at 340 nm found by Nakanishi et al.[9–11] for the tunichrome An-1 isolated from *A. nigra*. Moreover, the tunichrome from *P. mammillata* (Pm-1) has a molecular ion peak of $(M + H)^+ = 558.4$, two Daltons higher than the tunichrome from *A. nigra*, as seen in the ion spray mass spectrum (IMS). The MS–MS spectrum of molecular ion 558 of the IMS spectrum gives the fragmentation scheme illustrated in Figure 2 (top). It shows that tunichrome Pm-1 is dipeptide **1**, constructed from two β-(3,4,5-trihydroxyphenyl)alanine (Topa) molecules and a *C*-terminally bound 3,4,5-trihydroxystyrylamine. The only difference between Pm-1 and the tunichrome from *A. nigra* An-1 lies in the one double bond instead of conjugation between two trihydroxyphenyl residues, but it results in a

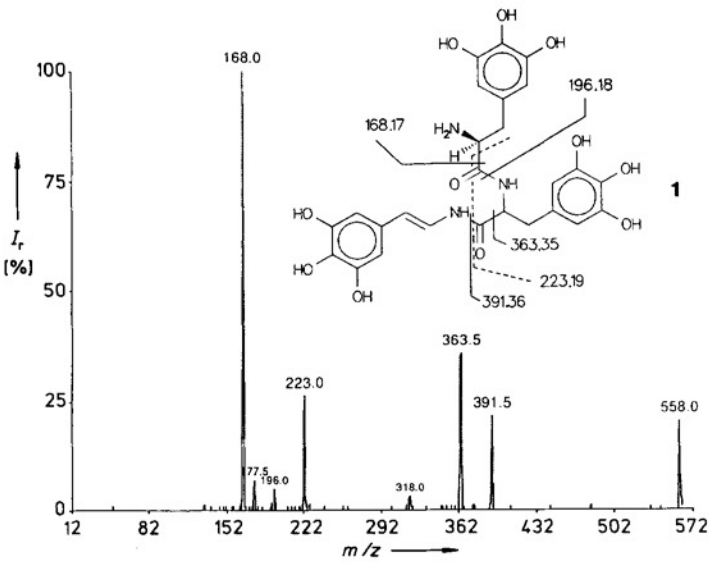

Fig. 2. Top: Ion spray MS (SCIEX mass spectrometer): daughter-ion mass spectrum of molecular ion peak 558 of the methanol extract from blood cells of *P. mammillata*. Bottom: structure and fragmentation scheme of tunichrome Pm-1 (**1**), derived from the ion spray mass spectrum.

 © VCH Verlagsgesellschaft mbH, W-6940 Weinheim, 1992 0570-0833/92/0101-0052 $ 3.50+.25/0

dramatic change in conformation and complex formation behavior with vanadium.

The ^1H and ^{13}C NMR spectra of the free tunichrome Pm-1 (**1**) and the peracylated derivative confirm the structural assignment. To determine the stereochemistry of the two asymmetric centers, Pm-1 was hydrolyzed with 5 N HCL at 110 °C, and the 3,4,5-trihydroxyphenylalanine formed was isolated by chromatography and characterized by mass spectrometry. The absolute configuration was established by the positive Cotton effect of the carbonyl band at 215 nm in the circular dichroism (CD) spectrum and confirmed by enantiomer separation on a chiral, thin-layer chromatography plate (Macherey & Nagel). Both chiral centers were shown to have an L-configuration. The stereochemistry of the styrylamide group in the third, dehydrogenated, and decarboxylated Topa was deduced from the ^1H NMR spectrum. The signals of the two vinyl protons at $\delta = 7.12$ and 6.01 show a coupling constant of 14.6 typical for *trans*-olefins. The position of the substituents on the phenyl ring was determined by ^{13}C and ^1H NMR spectroscopy, as well as IR spectroscopy. Topa and synthetic Topa tripeptide served as comparison.

The question whether the tunichrome occurs as complex in the blood cells was answered by a comparison between the NMR spectra of the free tunichrome Pm-1 (**1**) in solution and the ^{13}C CP-MAS NMR spectrum of the lyophilized blood cells in the solid state. As Table 1 shows, the positions of the major signals are in good agreement. Thus the native tunichrome in the blood cells is present as free peptide, and not bound to vanadium.

Table 1. Comparison of the ^{13}C NMR signals from tunichrome Pm-1 (**1**) in CD_3OD with those in the CP-MAS ^{13}C NMR spectrum of freeze-dried cells.

^{13}C NMR (CD_3OD) Chemical Shift	CP MAS ^{13}C NMR	Assignment	
168.5	173.3	amide	CONH
146.2–144.3	145.7		C-3, C-5
132.3–131.6	131.7	arene	C-1
127.3–124.8			C-4
120.5	120.7	styrylamide	C-β
113.2	110.4		C-α
108.3–108.1		arene	C-2, C-6 Topa
104.3	103.5		C-2, C-6 Tosa [a]
55.0	57.3	aliphatic	$CHNH_2$
53.7			CHNHR
37.2	38.9		CH_2CHNH_2
36.8			CH_2CHNHR

[a] Tosa = 3,4,5-trihydroxystyrylamide.

After the major peak of the tunichrome Pm-1 (**1**) a smaller peak appeared in the chromatogram of the methanol extract of the blood cells (Fig. 1). With on-line HPLC–ion spray MS–MS, separation and structure assignment is possible in one step. In the ion spray mass spectrum, apart from the peaks of the tunichrome Pm-1 (**1**) at 558 and Pm-1 adducts at 580 $(M + Na)^+$, 596 $(M + K)^+$, and 638 $(M + H + SO_3)^+$, a peak at $(M + H)^+ = 542$ is observed. A molecular ion peak of 542 is 16 Da lower than that of tunichrome **1**, corresponding to one hydroxyl group less. The molecular ion peak 542 in Figure 3 has an analogous fragmentation pattern to that seen for tunichrome **1**. In addition pairs of fragments are observed, which suggests that two isomeric tunichromes Pm-2 and Pm-3 of molecular mass 542 are involved. These were attributed the sequence isomers with structures **2** and **3** (Fig. 3, bottom). In **2** the *N*-terminal trihydroxyphenylalanine residue is replaced by a 3,4-dihydroxyphenylalanine substituent, while in **3** the *C*-terminal 3,4-dihydroxystyrylamine is replaced by 3,4-dihydroxystyrylamine.

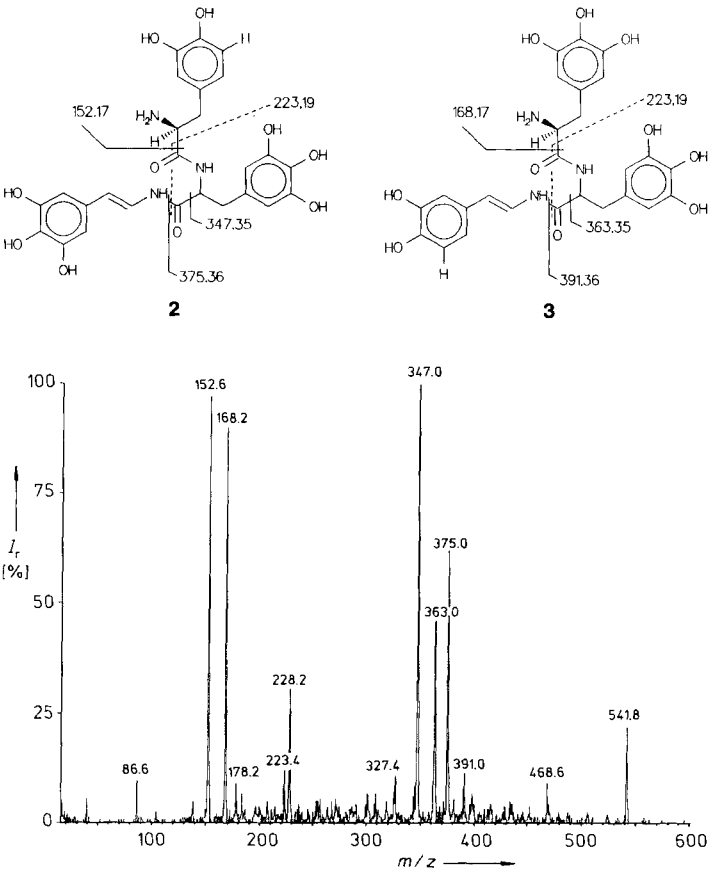

Fig. 3. Top: Ion spray MS: daughter-ion mass spectrum of molecular ion peak 542 of the methanol extract from blood cells of *P. mammillata*. Bottom: structure and fragmentation schemes of tunichrome Pm-2 (**2**) and tunichrome Pm-3 (**3**), derived from the ion spray mass spectrum.

These investigations show that the tunichromes of *P. mammillata* have a lower oxidation state than those of *A. nigra*. In no case could we detect the tunichromes described by Nakashani et al.[9–11] in extracts from fresh blood cells of *P. mammillata*. However, these tunichromes appeared as artifacts during intensive chromatography on silica gel phases or when long reaction times were required for the formation of derivatives, for example, in complete methylation with diazomethane.

Ion spray tandem mass spectrometry[13] of the methanol extracts represents a simple process for testing whether tunichromes are present. We analyzed the blood cells of different tunicates for the presence of tunichromes and found them only in *P. mammillata*, which concentrates vanadium strongly, but not in *Ciona intestinalis*, which concentrates vanadium only weakly, or in the iron-concentrating *Halocynthia papillosa* and *Microcosmus sulcatus*. This suggests that tunichromes are involved in vanadium-concentrating processes. The semiquantitative comparison of the tunichrom content (determined by HPLC) with the sulfate and vanadium content reveals approximately equivalent amounts of the vanadium compound in the vanadium-containing blood cells and tunichrome in the morula cells.

Characteristic for tunichromes is the styrylamide structure, which is possibly formed biogenetically by decarboxylation and dehydrogenation of a tripeptide with three trihydroxyphenylalanines. It is thus possible that vanadium enrichment in the blood cells takes place according to the scheme in Figure 4, in which at first a sulfoconjugate of this tripeptide without the styrylamide structure is present. Such

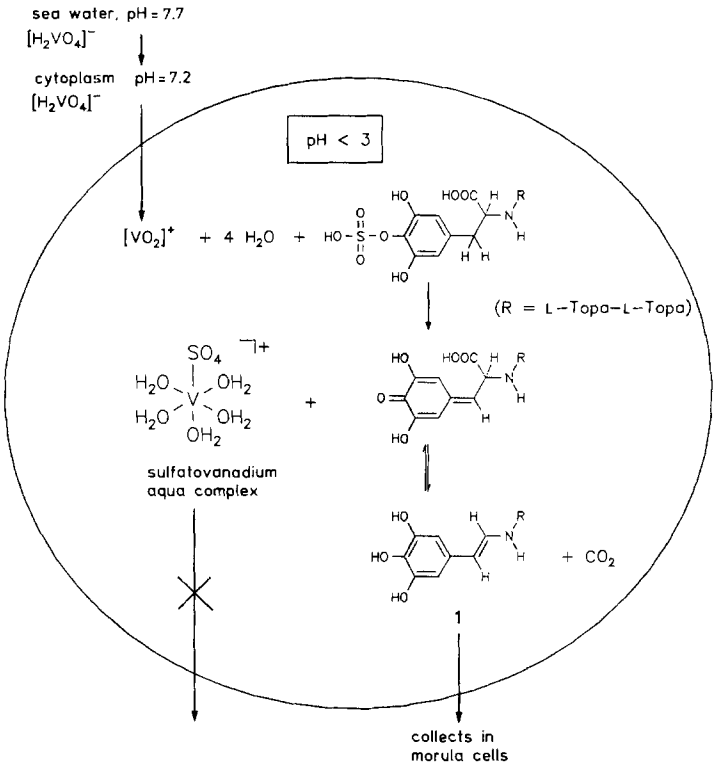

Fig. 4. Proposed scheme for vanadium concentration in blood cells of *P. mammillata*.

a conjugate with **1** has been identified by mass spectrometry. $[H_2VO_4]^-$ from sea water passes into the vanadocytes through the anionic channels of the lipid membrane. In the strongly acidic milieu there, it is present as the $[VO_2]^+$ ion, which can attack the sulfur while itself being reduced to the trivalent sulfatovanadium aqua complex. At the same time the peptide is oxidized to quinone, which undergoes decarboxylation to form styrylamide **1**. Whereas the positively charged sulfatovanadium complex cannot pass through the anionic channels, the tunichrome can leave the now vanadium-containing blood cells and collects in the morula cells.

Received: June 4, 1991 [Z4675 IE]
German version: *Angew. Chem.* **1992**, *104*, 102

CAS Registry numbers:
tunichrome Pm-1, 137824-58-9; tunichrome Pm-2, 137824-59-0; tunichrome Pm-3, 137844-92-4; vanadium, 7440-62-2.

[1] H. J. Bielig, E. Bayer, L. Califano, L. Wirth, *Pubbl. Stn. Zool. Napoli* **1954**, *25*, 26.
[2] H. J. Bielig, E. Bayer, *Justus Liebigs Ann. Chem.* **1953**, *580*, 135.
[3] A. L. Dingley, K. Kustin, I. G. Macara, G. C. McLeod, *Biochem. Biophys. Acta* **1981**, *649*, 493.
[4] H. J. Bielig, E. Bayer, *Pubbl. Stn. Zool. Napoli* **1957**, *29*, 109.
[5] S. Lee, K. Kustin, W. E. Robinson, R. B. Frankel, K. Spartalian, *J. Inorg. Biochem.* **1988**, *33*, 183.
[6] S. Scippa, L. Botte, M. de Vincentiis, *Cell Tissue Res.* **1985**, *239*, 459.
[7] E. M. Oltz, S. Pollack, T. Delohery, M. J. Smith, M. Ojika, S. Lee, K. Kustin, K. Nakanishi, *Experientia* **1989**, *45*, 186.
[8] I. G. Macara, G. C. McLeod, K. Kustin, *Biochem. J.* **1979**, *181*, 457.
[9] R. C. Bruening, E. M. Oltz, J. Furukawa, K. Nakanishi, K. Kustin, *J. Am. Chem. Soc.* **1985**, *107*, 5298.
[10] E. M. Oltz, R. C. Bruening, M. J. Smith, K. Kustin, K. Nakanishi, *J. Am. Chem. Soc.* **1988**, *110*, 6162.
[11] R. C. Bruening, E. M. Oltz, J. Furukawa, K. Nakanishi, *J. Nat. Prod.* **1986**, *49*, 193.
[12] a) K. Kustin, W. E. Robinson, M. J. Smith, *Invertebr. Reprod. Dev.* **1990**, *17*, 129. b) From 1000 *A. nigra* animals, 1 g tunichrome crude product was obtained. A further purification in three steps yielded pure tunichrome in only 1.5% yield.
[13] E. Bayer in *Modern Methods in Protein and Nucleic Acid Research* (Ed.: H. Tscheche), de Gruyter, Berlin, **1990**, p. 133.

$[Ni_4(SC_3H_7)_8Br]$ and $[Ni_4(SC_3H_7)_8I]$: Mixed Valent Nickel Thiolates with Integral and Nonintegral Metal Oxidation States**

By *Thomas Krüger, Bernt Krebs,** and *Gerald Henkel**

Dedicated to Professor Peter Sartori on the occasion of his 60th birthday

The thiolato and sulfidothiolato complexes of divalent nickel are of great interest due to their unusual structures and properties. The discovery of nickel-containing enzymes with partial coordination of sulfur to nickel has given the investigation of thiolates new impetus.[1-3]

Although not much is known about the architecture of the nickel sites in enzymes, X-ray absorption spectra of the nickel-containing hydrogenases and the CO-dehydrogenases show that the nickel atom has a planar coordination with up to four cysteine sulfur atoms. Both of these classes of enzymes catalyze redox processes, in which the nickel atoms are proposed to be in oxidation states between 0 and +IV.[1-3] Thus the investigation of electrochemical properties of nickel–sulfur complexes is important in the understanding of these enzymes' mode of action.

We reported recently the preparation and structure of the mixed-valent sulfidothiolatonickel complex $[Ni_8S(SC_4H_9)_9]^-$ in which the nickel has the intermediate oxidation state of +1.25.[4] We could prove for the first time that saturated alkanethiolato ligands are able to reduce nickel under mild conditions and stabilize the metal in low oxidation states.

The reversible oxidation of polynuclear thiolatonickel complexes is also possible if they are cyclic molecules of the general type $[Ni_n(SR)_{2n}]$ ($n = 4-6$).[5,6] In contrast to the open-chain complex anions with the composition $[Ni_n(SR)_{2n+2}]^{2-}$ ($n = 2$, 3, and 6) the cyclic complexes have no terminally bound thiolato ligands which can be irreversibly oxidized at potentials in the range of −200 to −400 mV.[5-7]

We report here the syntheses and X-ray structural analyses of compounds **1** and **2**, which can be obtained from the direct reaction of $[Ni_4(SiC_3H_7)_8]$ with the corresponding halogen.

$[Ni_4(SiC_3H_7)_8Br]$ **1** $[Ni_4(SiC_3H_7)_8I]$ **2**

[*] Prof. Dr. G. Henkel
Fachgebiet Anorganische Chemie/Festkörperchemie der Universität
Lotharstrasse 1, D-W-4100 Duisberg 1 (FRG)
Prof. Dr. B. Krebs, Dr. T. Krüger
Anorganisch-chemisches Institut der Universität
Wilhelm-Klemm-Strasse 8, D-W-4400 Münster (FRG)

[**] This work was supported by the Deutsche Forschungsgemeinschaft, the Bundesminister für Forschung und Technologie, and the Fonds der Chemischen Industrie.

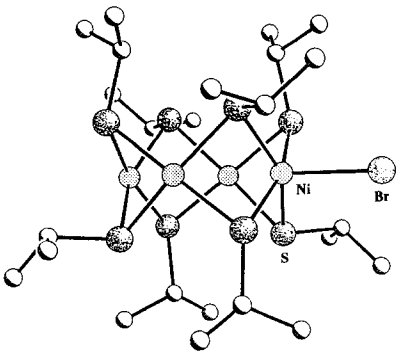

Fig. 1. Molecular structure of **1** (without H atoms). White circles = C atoms, regularly dotted circles = Ni atoms, circles with a heavy random dot pattern = S atoms, circle with a light random dot pattern = Br atom.

According to X-ray structural studies, crystalline **1** and **2** contain one-dimensional infinite chains, consisting of individual $[Ni_4(SiC_3H_7)_8X]$ molecules threaded along their Ni–X axes.[8] Their structures are related to those of the known tetranuclear neutral complexes $[Ni_4(SiC_3H_7)_8]$,[4] $[Ni_4(SC_6H_{11})_8]$,[9] and $[Ni_4(SC_5H_9NMe)_8]$[10] with crystallographic C_2 symmetry (idealized D_{2d}) in which the Ni atoms form a distorted square and thus occupy the centers of the side faces of a tetragonal prism of S atoms. This leads to square-planar Ni–S coordination centers, which are somewhat distorted due to a slight compression of the prism and repulsive Ni ··· Ni interactions. Upon chemical oxidation of $[Ni_4(SiC_3H_7)_8]$ to **1** or **2** the Ni–S frame and the arrangement of the thiolato ligands are basically retained. This reaction is formally an oxidative addition of a halogen radical to one of the four nickel atoms, which can then be considered Ni^{3+} with an axial bond to the halogen atom. As a result the twofold axis in the starting complex is retained (Fig. 1).

The electronic spectrum of $[Ni_4(SiC_3H_7)_8]$ in dichloromethane displays absorptions at 264, 340, and 427 nm. These absorptions are also observed as shoulders in the spectra of **1** and **2**, perhaps as a result of decomposition. An intense band at 292 (**1**) or 296 nm (**2**) is characteristic for the halogenated derivatives and also dominates the spectra of the electrochemically oxidized complex.

Upon crystallization of the bromine derivative the molecules organize in one-dimensional infinite chains along the twofold axes of the space group $C2/c$, resulting in secondary bonding between the halogen and formally divalent nickel atoms of neighboring molecules. The Ni^{3+}–Br ··· Ni^{2+} bridges are unsymmetrical (Ni–Br 2.530(3), Ni ··· Br 3.018(3) Å) and do not support a model with nonintegral oxidation states of the nickel atoms involved.

In contrast, crystalline **2** displays (almost) equivalent bond lengths in the halogen bridges. Apparently there is a bonding mechanism here which makes the two nickel atoms participating in the halogen bridge practically identical. One electron is completely delocalized between the two centers (Fig. 2). In the $Ni^{2.5+}$–I–$Ni^{2.5+}$ bridge of **2** the Ni–I bond lengths of 2.878(3) and 2.824(3) Å are indicative of nonintegral oxidation states of the nickel atoms. A possible disorder of the iodine atoms can be discounted, since all the atoms in the bridge oscillate with similar amplitudes in the bonding direction (Ni3: 0.203 Å; Ni2: 0.216 Å; I: 0.212 Å).

The chainlike arrangement of the molecules in the crystal is apparently stabilized if a small percentage of the oxidized molecules is replaced by the halogen-free species. In crystalline **1** statistically every eighth molecule is exchanged; in **2**, every seventh.[8]

According to our knowledge, the mixed valent dithioacetato complex $[Ni_2(S_2CCH_3)_4I]$[12] is the only other known nickel–sulfur compound with similar symmetric, though somewhat longer Ni–I–Ni bridges (2.928 and 2.940 Å) in the crystal. In this case the two nickel atoms in the almost parallel NiS_4 planes are only 2.514 Å apart, supporting direct electronic interactions by overlap of d_{z^2} orbitals. Comparable metal–metal interactions are not possible in **1** and **2** since the distances between the relevant nickel atoms are prohibitively long (4.121 Å in **1**; 4.111 Å in **2**).

The unusual relationships in these two complexes allow for the first time a comparison between the bonding geometries of mixed valent systems with localized Ni^{2+}/Ni^{3+} centers on one hand and delocalized $Ni^{2.5+}/Ni^{2.5+}$ centers on the other.

The oxidation of $[Ni_4(SiC_3H_7)_8]$ to **1** and **2** has a characteristic effect on the Ni–S framework. The square of Ni atoms in the starting material is stretched along the twofold axes to a rhombus, which is more distorted in **1** due to the localized oxidation states. Simultaneously, the edges are lengthened by roughly 0.06 Å to an average of 2.731 (**1**) and 2.728 Å (**2**).

Interestingly, the average nickel–sulfur bond length depends on oxidation state in a simple fashion. The average Ni–S bond length is 2.210 Å for Ni^{2+} (in **1** and **2**); 2.236 Å for $Ni^{2.5+}$ (in **2**); and 2.255 Å for Ni^{3+} (in **1**). For divalent nickel one thus finds the same values as in the starting molecule.[4] We attribute the observed increase in the nickel–sulfur bond lengths with increasing oxidation, which at first appears unusual, to the gradual strengthening of the bond of an additional axial ligand.

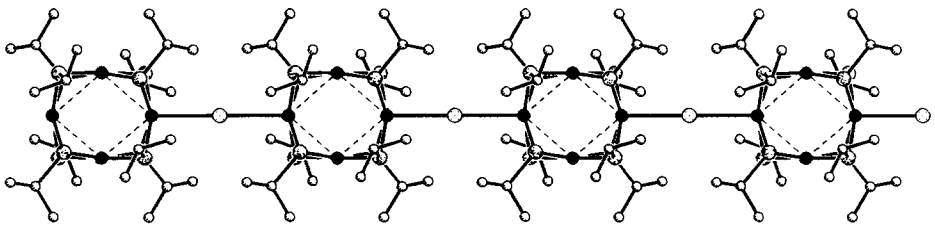

Fig. 2. Structure of crystalline **2** (without H atoms). Regularly dotted circles = I atoms, white circles = C atoms, black circles = Ni atoms, randomly dotted circles = S atoms.

Experimental Procedure

1 and **2**: To a solution of $[Ni_4(SiC_3H_7)_8]$ (0.84 g, 1 mmol) in 20 mL of CH_2Cl_2 was slowly added a solution of Br_2 (0.20 g) or I_2 (0.32 g, 2.5 mmol) in 5 mL of CH_2Cl_2 with vigorous stirring. After the addition was complete the resulting brown-violet (Br_2) or green-brown (I_2) solution was filtered and evaporated to dryness over 2–3 days. In both cases a conglomerate of $[Ni_4(SiC_3H_7)_8]$ crystals

(black, tetragonal needles) and $[Ni_4(SiC_3H_7)_8X]$ (X = Br, I; black hexagonal plates) were obtained.

Received: August 10, 1991 [Z4861 IE]
German version: *Angew. Chem.* **1992**, *104*, 71

CAS Registry numbers:
1, 137594-54-8; **2**, 137594-55-9; $[Ni_4(SiC_3H_7)_8]$, 118458-91-6; $[Ni_4(SC_6H_{11})_8]$, 115707-92-1; $[Ni_5(SC_2H_5)_{10}]$, 115707-94-3; $[Ni_6(SnC_3H_7)_{12}]$, 137594-56-0; $[Ni_2(SC_2H_5)_6]^{2-}$, 97316-44-4; $[Ni_6(SC_3H_6S)_7]^{2-}$, 116663-38-8; $[Ni_4(SiC_3H_7)_8X]$, 15941-30-7; $[Ni_4(SC_6H_{11})_8X]$, 115817-74-8; $[Ni_5(SC_2H_5)_{10}X]$, 10327-49-8; $[Ni_6(SnC_3H_7)_{12}X]$, 15941-29-4.

[1] *The Bioinorganic Chemistry of Nickel*, (Ed.: J. R. Lancaster, Jr.), VCH, Weinheim, **1988.**
[2] C. T. Walsh, W. H. Orme-Johnson, *Biochemistry* **1987**, *26*, 4901, and references therein.
[3] R. Cammack, *Adv. Inorg. Chem.* **1988**, *32*, 297.
[4] T. Krüger, B. Krebs, G. Henkel, *Angew. Chem.* **1989**, *101*, 54; *Angew. Chem. Int. Ed. Engl.* **1989**, *28*, 61.
[5] B. Krebs, G. Henkel, *Angew. Chem.* **1991**, *103*, 785; *Angew. Chem. Int. Ed. Engl.* **1991**, *30*, 769, and references therein.
[6] Cyclic voltammetry (CH_2Cl_2, Pt electrode vs. SCE, 0.05 M $[Bu_4N][ClO_4]$): $[Ni_4(SiC_3H_7)_8]$, $E_{1/2} = 0.64$ V, $E_{pa} - E_{pc} = 160$ mV, $I_{pa}/I_{pc} = 0.96$; $[Ni_4(SC_6H_{11})_8]$, $E_{1/2} = 0.53$ V, $E_{pa} - E_{pc} = 140$ mV, $I_{pa}/I_{pc} = 1.03$; $[Ni_5(SC_2H_5)_{10}]$, $E_{1/2} = 0.62$ V, $E_{pa} - E_{pc} = 110$ mV, $I_{pa}/I_{pc} = 1.59$; $[Ni_6(SnC_3H_7)_{12}]$, $E_{1/2} = 0.63$ V, $E_{pa} - E_{pc} = 230$ mV, $I_{pa}/I_{pc} = 1.25$.
[7] Cyclic voltammetry (CH_3CN, Pt electrode vs. SCE, 0.05 M $[Bu_4N][ClO_4]$): $[Ni_2(SC_2H_5)_6]^{2-}$, $E_{ox,irr} = -0.37$ V; $[Ni_6(SC_3H_6S)_7]^{2-}$, $E_{ox,irr} = -0.24$ V.
[8] Crystal structure analyses: Siemens P3 four-circle diffractometer, $Mo_{K\alpha}$ radiation, graphite monochromator, scintillation counter, 290 K, empirical absorption corrections, SHELXTL-PLUS program, direct methods, least-squares fit. – **1**: monoclinic, space group $C2/c$, $a = 24.195(8)$, $b = 9.668(4)$, $c = 19.923(7)$ Å, $\beta = 123.30(3)°$, $V = 3895.1$ Å^3, $Z = 4$, $\rho_{calc} = 1.562$ g cm^{-3}, $\mu(Mo_{K\alpha}) = 3.36$ mm^{-1}, crystal dimensions $0.03 \times 0.30 \times 0.30$ mm^3, ω-2θ scan, $2\theta_{max} = 48°$, 3061 independent reflections, R (R_w) = 0.0542 (0.0632) for 1941 observed reflections ($F_o > 3.92\sigma(F_o)$), 170 variables. All nonhydrogen atoms were refined with anisotropic temperature factors; hydrogen atoms were calculated at idealized positions (U(H) = 0.08); occupation factor for Br free (0.88), one scaling factor. – **2**: monoclinic, space group $C2/c$, $a = 24.383(6)$, $b = 9.812(3)$, $c = 19.897(6)$ Å, $\beta = 123.67(2)°$, $V = 3962.0$ Å^3, $Z = 4$, $\rho_{calc} = 1.614$ g cm^{-3}, $\mu(Mo_{K\alpha}) = 3.08$ mm^{-1}, crystal dimensions $0.04 \times 0.28 \times 0.28$ mm^3, ω-scan, $2\theta_{max} = 48°$, 3101 independent reflections, R (R_w) = 0.0726 (0.0698) for 2115 observed reflections ($F_o > 3.92\sigma(F_o)$), 170 variables. All nonhydrogen atoms were refined with anisotropic temperature factors; hydrogen atoms were calculated at idealized positions (U(H) = 0.08); occupation factor for I free (0.85), one scaling factor. Further details of the crystal structure investigation may be obtained from the Fachinformationszentrum Karlsruhe, Gesellschaft für wissenschaftlich-technische Information mbH, D-W-7514 Eggenstein-Leopoldshafen 2 (FRG) on quoting the depository number CSD-55830, the names of the authors, and the journal citation.
[9] M. Kriege, G. Henkel, *Z. Naturforsch. B* **1987**, *42*, 1121.
[10] W. Gaete, J. Ros, X. Solans, M. Font-Altaba, J. L. Brianso, *Inorg. Chem.* **1984**, *23*, 39.
[11] C. Bellitto, G. Dessy, V. Fares, *Inorg. Chem.* **1985**, *24*, 2815.

One-Pot Synthesis of Tagatose 1,6-Bisphosphate by Diastereoselective Enzymatic Aldol Addition**

By *Wolf-Dieter Fessner** and *Oliver Eyrisch*

Enzyme-catalyzed C–C bond formations[1] hold much promise for use in asymmetric synthesis because of the potentially high level of asymmetric induction achievable at two stereocenters, the applicability of a convergent synthetic strategy, and the fact that in general no protecting groups are required. A building block scheme[2] for the production of each of four possible diastereomeric dihydroxyacetone phosphate (DHAP) aldol adducts is based on a tetrad of complementary DHAP lyases. So far a broad substrate acceptance and high enantio- and diastereoselectivity have been demonstrated for the D-fructose 1,6-bisphosphate (FruA),[3] L-fuculose (FucA),[2,4] and L-rhamnulose 1-phosphate aldolases (RhuA).[2] The fourth enzyme of this series, a D-tagatose 1,6-bisphosphate aldolase (TagA) involved in the galactose metabolism of cocci, has previously been described to be stereochemically completely nonselective.[5] We report here the isolation and characterization of a highly diastereoselective TagA from *Escherichia coli* and on first results concerning its suitability for asymmetric synthesis.

Based on our experience with other DHAP aldolases of class II (Zn^{2+} dependent) from *E. coli*, we were expecting that galactitol-metabolizing strains of this organism would produce a TagA of the same type. In the crude extract of cells of strain JWL183,[6] which had been grown on this carbon source, an enzyme was indeed detectable, which in the presence of Zn^{2+} ions was able to cleave chemically synthesized[7] D-tagatose 1,6-bisphosphate **1** (ca. 1500 U in 90 g of wet cells from a 10 L culture).[8] The constitutive FruA, which is expressed at a similar level of activity (ca. 1000 U), can be separated quantitatively by anion-exchange chromatography due to its distinct isoelectric points (p*I* TagA 4.4, FruA 5.1). The TagA is obtained free from contaminating side-activities by further application of standard methods of protein purification in about 35% total yield.

The TagA catalyzes the reversible cleavage of **1** to D-glyceraldehyde 3-phosphate **2** and DHAP **3**. The enzyme shows a high substrate-specificity in the cleavage direction; relative to the natural substrate **1** the 4-epimeric D-fructose 1,6-bisphosphate **4** is converted at only 1% of the maximum rate.

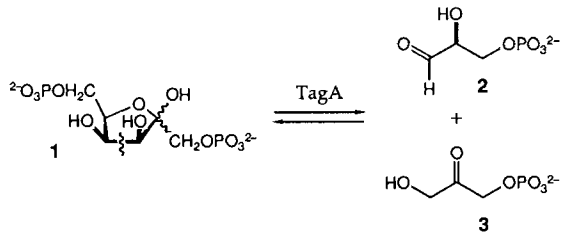

Because of comparably strong binding constants ($K_m = 3.3 \times 10^{-4}$ M) **4** acts as a competitive inhibitor for the cleavage of **1**. Although the TagA has a relatively narrow pH profile around an optimum at about 7.5, it still displays sufficient activity (≥40%) within the range of pH 6.5–7.0, most suitable for synthetic applications. The molecular weight is roughly 110 kDa according to the mobility during gel permeation chromatography; a single band at about 28 kDa in the denaturing SDS polyacrylamide gel electrophoresis suggests the presence of a homotetramer, quite like that established for RhuA and FucA.[2]

Priority was given to the development of a novel access to **1**, which was previously available only by a low yielding (ca. 2%), multistep synthesis from D-galacturonic acid.[7] A coupled enzymatic synthesis (Scheme 1) offered the possibility to prepare **1** directly from dihydroxyacetone **5**: After enzymatic phosphorylation of **5** using ATP and glycerol kinase, combined with an economical cofactor regeneration scheme based on phosphoenolpyruvate (PEP),[9] the **3** generated can be partially isomerized in situ into the aldehyde **2** and subsequently added to the latter stereoselectively by the TagA with formation of **1**.

[*] Dr. W.-D. Fessner, Dipl.-Chem. O. Eyrisch
Institut für Organische Chemie und Biochemie der Universität
Albertstraße 21, D-W-7800 Freiburg (FRG)

[**] Enzymes in Organic Synthesis, Part 2. This research was supported by the Deutsche Forschungsgemeinschaft (Grant Fe 244/2-1), the Wissenschaftliche Gesellschaft Freiburg, and the Fonds der Chemischen Industrie. We thank Prof. Dr. J. W. Lengeler, University of Osnabrück for the gift of bacterial strains and Dipl.-Chem. G. Sinerius for chemically [7] synthesized **1**.—Part 1: [2].

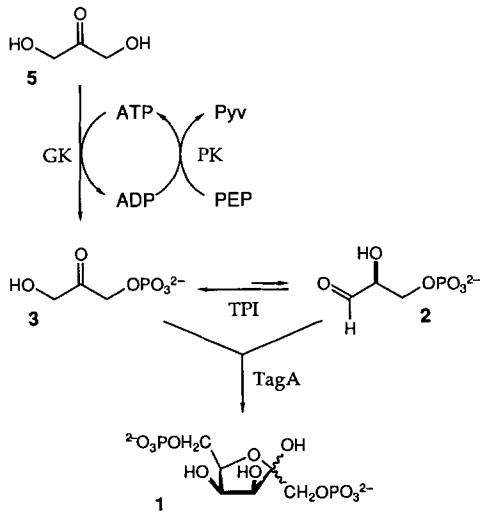

Scheme 1. Enzymatic one-pot synthesis of D-tagatose 1,6-bisphosphate **1**. Abbreviations: ADP, ATP = adenosine di(tri)phosphate; Pyv = pyruvate; PEP = phosphoenolpyruvate. Enzymes involved are: GK = glycerokinase, PK = pyruvate kinase, TPI = triosephosphate isomerase, TagA = tagatose 1,6-bisphosphate aldolase.

For this route to become preparatively useful the compatibility of each of the catalysts and reactants and also a high equilibrium concentration of **1** is prerequisite. The latter depends not only on the thermodynamic relation to the cleavage products **2** and **3**, but also on their interrelation.[10] Starting from either **1** or **3** we could unequivocally determine the equilibrium constant for addition to be $K_{eq} = [\mathbf{2}][\mathbf{3}]/[\mathbf{1}] = 10^{-3}$ M. As a consequence of the all-*cis* substitution of the furanose forms present in aqueous solution, the adduct is barely favored in the equilibrium. For this reason the yield of **1** cannot significantly exceed a level of 80%, even with reaction parameters optimized. During these investigations we also found that, in addition to the known components, an increasing fraction of **4** is produced rather unexpectedly (Fig. 1). This implies that the TagA in the (reversible) synthesis of **1** also forms a small percentage of the 4-epimer which itself is cleaved only at a significantly lower rate.[10] However, timely termination of the reaction (after formation of 60–65% of **1**) guarantees that the fraction of **4** in the product mixture remains small ($\leq 10\%$).

The separation of **4** would obviously be facilitated by its selective transformation into derivatives of lower charge density. We have checked the following alternatives (Scheme 2): 1) Fructose 1,6-bisphosphatase dephosphorylates **4** selectively in the presence of **1** to provide fructose 6-phosphate **7**; in contrast to the specific enzyme from yeast, the one from rabbit muscle concurrently also converts **1** very slowly into tagatose 6-phosphate **6** ($K_2/K_1 = 5\%$).[10] Although this process can thus be combined with the previously described one-pot procedure, the relatively high price of the phosphatases becomes prohibitive. 2) Preferably after separation of all enzymes, for example by ultrafiltration, FruA cleaves the diastereomer **4** highly selectively; the liberated **3** (in the presence of triosephosphate isomerase) is then recombined with another arbitrarily added, neutral aldehyde (e.g. DL-glyceraldehyde) for quantitative formation of the corresponding ketose 1-phosphates (e.g. the fructose/sorbose derivatives **8**/**9**).[3] After preparation according to either variants, **1** was easily separated by ion-exchange chromatography using $NEt_3H(HCO_3)$ buffer and was isolated in satisfactory overall yield (40% relative to limiting PEP) in 10 mmol quantity as the crystalline tetrakis(cyclohexylammonium) salt of analytical purity. Unequivocal structural proof was obtained by quantitative dephosphorylation of **1** using acid phosphatase for the liberation of authentic D-tagatose.

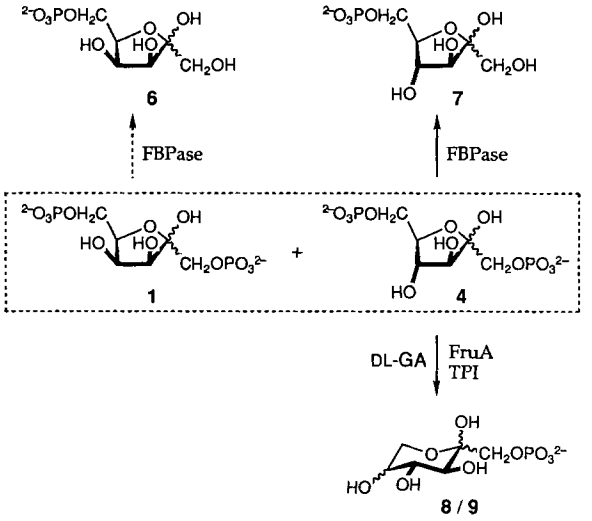

Scheme 2. Enzymatic differentiation of D-fructose 1,6-bisphosphate **4** in the presence of D-tagatose 1,6-bisphosphate **1**. Abbreviations: DL-GA = DL-glyceraldehyde, FBPase = fructose 1,6-bisphosphatase, FruA = fructose 1,6-bisphosphate aldolase, TPI = triosephosphate isomerase.

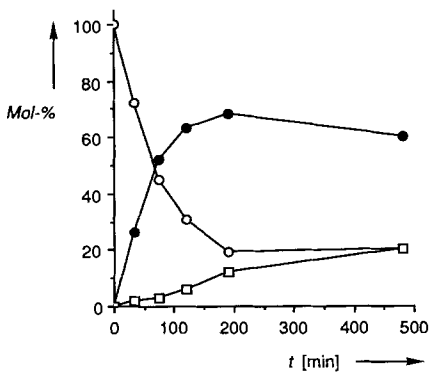

Fig. 1. Product composition during enzymatic synthesis of **1** starting from **3** (200 mM; 50 U mL^{-1} TPI, 8 U mL^{-1} TagA; pH 7.0, 25°C). ○ The sum of triosephosphates **2** and **3**; ● D-tagatose 1,6-bisphosphate **1**; □ D-fructose 1,6-bisphosphate **4**; data refer to mol% of bisphosphates[10].

though this process can thus be combined with the previously described one-pot procedure, the relatively high price of the phosphatases becomes prohibitive. 2) Preferably after separation of all enzymes, for example by ultrafiltration, FruA cleaves the diastereomer **4** highly selectively; the liberated **3** (in the presence of triosephosphate isomerase) is then recombined with another arbitrarily added, neutral aldehyde (e.g. DL-glyceraldehyde) for quantitative formation of the corresponding ketose 1-phosphates (e.g. the fructose/sorbose derivatives **8**/**9**).[3] After preparation according to either variants, **1** was easily separated by ion-exchange chromatography using $NEt_3H(HCO_3)$ buffer and was isolated in satisfactory overall yield (40% relative to limiting PEP) in 10 mmol quantity as the crystalline tetrakis(cyclohexylammonium) salt of analytical purity. Unequivocal structural proof was obtained by quantitative dephosphorylation of **1** using acid phosphatase for the liberation of authentic D-tagatose.

The substrate tolerance of the TagA was evaluated by additional preparative reactions. Like the complementary DHAP aldolases, the TagA accepts a variety of different aldehydes as substrate analogues (e.g. glycolaldehyde, D- or L-glyceraldehyde, acetaldehyde, isobutyraldehyde). In each case investigated so far, product analysis indicated the formation of diastereomer mixtures. Surprisingly, however, instead of the expected products with tagatose configuration at C-3/C-4 (L-*erythro*; $\leq 10\%$) those of the fructose type (D-*threo*; $\geq 90\%$) predominated.

The comparatively high diastereoselectivity of the TagA from *E. coli* thus allows the simple preparative synthesis of the valuable metabolic intermediate **1** and the rare ketosugar D-tagatose. Although the enzyme does not seem to be directly suitable for the proposed building block scheme,[2] its optimization by protein engineering, based on structural motifs of complementary aldolases,[2, 11] presents a rewarding perspective.

Received: July 8, 1991 [Z 4781 IE]
German version: *Angew. Chem.* **1992**, *104*, 76

CAS Registry numbers:
1, 55529-38-9; **2**, 591-57-1; **3**, 57-04-5; **4**, 488-69-7; D-tagatose-1,6-bisphosphate aldase, 39433-95-9.

[1] a) G. M. Whitesides, C.-H. Wong, *Angew. Chem.* **1985**, *97*, 617–638; *Angew. Chem. Int. Ed. Engl.* **1985**, *24*, 617–638; b) E. J. Toone, E. S. Simon, M. D. Bednarski, G. M. Whitesides, *Tetrahedron* **1989**, *45*, 5365–5422; c) W.-D. Fessner in *Methoden Org. Chem. (Houben-Weyl) 4th Ed.* **1952**, Band E22 ["Stereoselective Synthesis of Organic Compounds." (Eds.: G. Helmchen, R. W. Hoffmann, J. Mulzer, E. Schaumann)], in print.

[2] W.-D. Fessner, G. Sinerius, A. Schneider, M. Dreyer, G. E. Schulz, J. Badia, J. Aguilar, *Angew. Chem.* **1991**, *103*, 596–599; *Angew. Chem. Int. Ed. Engl.* **1991**, *30*, 555-558.

[3] a) M. D. Bednarski, E. S. Simon, N. Bischofberger, W.-D. Fessner, M.-J. Kim, W. Lees, T. Saito, H. Waldmann, G. M. Whitesides, *J. Am. Chem. Soc.* **1989**, *111*, 627–635; b) J. R. Durrwachter, D. G. Drueckhammer, K. Nozaki, H. M. Sweers, C.-H. Wong, *ibid.* **1986**, *108*, 7812–7818; c) C. H. von der Osten, A. J. Sinskey, C. F. Barbas, R. L. Pederson, Y.-F. Wang, C.-H. Wong, *ibid.* **1989**, *111*, 3924–3927; d) A. Straub, F. Effenberger, P. Fischer, *J. Org. Chem.* **1990**, *55*, 3926–3932; e) M. Schultz, H. Waldmann, H. Kunz, W. Vogt, *Liebigs Ann. Chem.* **1990**, 1019–1024; f) H. P. Brockamp, M. R. Kula, *Tetrahedron Lett.* **1990**, *31*, 7123–7126.

[4] A. Ozaki, E. J. Toone, C. H. von der Osten, A. J. Sinskey, G. M. Whitesides, *J. Am. Chem. Soc.* **1990**, *112*, 4970–4971.

[5] a) *Streptococcus* sp.: V. L. Crow, T. D. Thomas, *J. Bacteriol.* **1982**, *151*, 600–608; b) *Staphylococcus aureus*: D. L. Bissett, R. L. Anderson, *J. Biol. Chem.* **1980**, *255*, 8750–8755. The simultaneous formation of *all four* possible diastereomers as reported here, however, can hardly be due to a single DHAP aldolase since enantiospecificity has to be assumed for mechanistic reasons regarding the configuration at C-3: D. J. Hupe in *Enzyme Mechanisms* (Eds.: M. I. Page, A. Williams), The Royal Society of Chemistry, London, **1987**, p. 324–332.

[6] J. Lengeler, *MGG Mol. Gen. Genet.* **1977**, *152*, 83–91. In this paper, strain JWL183 is referred to as L153 and TagA as "ketose-bis-phosphate aldolase".

[7] a) R. L. Anderson, W. C. Wenger, D. L. Bissett, *Methods Enzymol.* **1982**, *89*, 93–98; b) E. L. Totton, H. A. Lardy, *ibid.* **1957**, *3*, 174–176.

[8] Classification of the enzyme [EC 4.1.2.n] is pending. 1 Unit catalyzes the cleavage of 1 μmol of **1** per minute at 25 °C; assayed photometrically by coupling to glycerophosphate dehydrogenase-catalyzed NADH oxidation. Activity was completely inhibited upon addition of EDTA and could be restored upon addition of Zn^{2+} ions (class II; reactivation can also be achieved with Co^{2+} (>100%), Mn^{2+} (≥100%) and Ca^{2+} ions (60%)), while a control test for covalent fixation of **3** as a Schiff base by $NaBH_4$ reduction (class I) proved negative.

[9] a) D. C. Crans, G. M. Whitesides, *J. Am. Chem. Soc.* **1985**, *107*, 7019–7027; b) B. L. Hirschbein, F. P. Mazenod, G. M. Whitesides, *J. Org. Chem.* **1982**, *47*, 3765–3766.

[10] K_{eq}[3]/[2] = 22; P. Oesper, O. Meyerhof, *Arch. Biochem. Biophys.* **1950**, *27*, 223–225. K_{eq}[3][2]/[4] = 1.2×10^{-4} M; A. L. Lehninger, J. Sice, E. V. Jensen, *Biochim. Biophys. Acta* **1955**, *17*, 286–287. Concentration of sugar phosphates was determined enzymically according to [8] or by standard protocols; see: A. U. Bergmeyer, *Methods of Enzymatic Analysis 3rd Ed. Vol. 6*, Verlag Chemie, Weinheim, **1984**, p. 342–350.

[11] X-ray structure determinations of other DHAP aldolases are being conducted in cooperation with Prof. Dr. *G. E. Schulz*, Universität Freiburg.

The Structures of Thiosulfuric Acid $H_2S_2O_3$ and Its Monoanion $HS_2O_3^-$ **

By *Karol Miaskiewicz** and *Ralf Steudel**

Inorganic chemistry textbooks present the structure of thiosulfuric acid by either formula **1**[1] or **2**.[2] Both structures have been of speculative nature so far since the molecule $H_2S_2O_3$ has never been observed directly, and consequently structural information is not available. The existence of thiosulfuric acid in strongly acidic aqueous thiosulfate solutions is, however, beyond any doubt[3] and the preparation of nonaqueous $H_2S_2O_3$ solutions has been reported.[4]

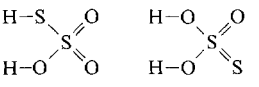

The monoanion of thiosulfuric acid may have either the structure $HOS(S)O_2^-$ **3** or $HSSO_3^-$ **4**, derived from **1** and **2**, respectively. Recently, the first hydrogenthiosulfate, $NH_4HS_2O_3$, was prepared and shown by Raman spectroscopy to contain the anion **4**.[5] To establish the equilibrium structures of the free molecules $H_2S_2O_3$ and $HS_2O_3^-$ we have performed ab initio molecular orbital calculations of the species **1** to **4** using a 6-311 G** basis set for geometry optimization and single-step energy calculations according to the 2nd to 4th order of Moeller–Plesset perturbation theory. Zero-point energies have been calculated from 6-311 G** wave numbers scaled by 0.89.[6] The results are shown in Figure 1, and Tables 1 and 2.

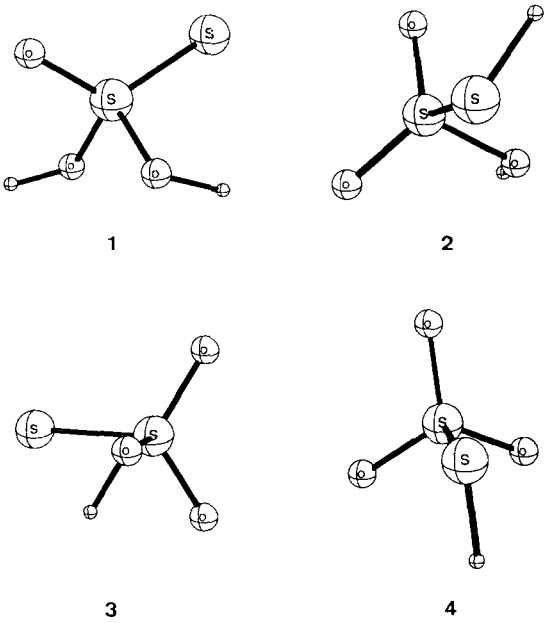

Fig. 1. Calculated structures of two isomers each of thiosulfuric acid, $H_2S_2O_3$ (**1** and **2**), and its monoanion, $HS_2O_3^-$ (**3** and **4**).

$H_2S_2O_3$ and $HS_2O_3^-$ are most stable as the H-S bonded isomers **2** and **4**; however, the energy differences between **2** and **4** and the most stable H-O bonded forms, **1** and **3**, are small (41 and 20 kJ mol^{-1}; Table 1). Isomer **2** which has C_1 symmetry contains an SS bond of length 205.7 pm. The orientation of the OH and SH groups of **1** and **2** is staggered with respect to the neighboring SO and SS bonds. The most stable conformer of **1** has C_1 symmetry[7] with nonequivalent OH groups and an SS bond of distance 198.2 pm, which is about halfway between the established single (205 pm) and double (188 pm) bond distances.[8] The geometries of other rotational isomers of **1** were also optimized; their energies were higher than that of **1** at all levels of calculation mentioned in Table 1.

[*] Dr. K. Miaskiewicz
The Mount Sinai Medical Center
Department of Physiology and Biophysics
New York, NY 10029-6574 (USA)
Prof. Dr. R. Steudel
Institut für Anorganische und Analytische Chemie der
Technischen Universität, Sekt. C 2,
Straße des 17. Juni 135, D-W-1000 Berlin 12, (FRG)

[**] Sulfur Compounds, Part 147; Part 146: R. Steudel, M. Papavassiliou, F. Baumgart, *Z. Naturforsch. B*, **1991**, *46*, 1674–1678.

Table 1. Absolute and relative energies of two isomers each of thiosulfuric acid, $H_2S_2O_3$, and of its monoanion, $HS_2O_3^-$, as calculated with the 6-311G** basic set.

Isomer	Symmetry	E_{tot} [Hartree] [a]	ΔE_{rel} [kJ mol^{-1}] [b] HF	MP 2	MP 3	MP 4	MP 4 + ZPE [c]
$H_2S_2O_3$							
1	C_1	−1020.774507	18	30	27	34	41
2	C_1	−1020.781246	0	0	0	0	0
$HS_2O_3^-$							
3	C_1	−1020.280137	0	11	5	13	20
4	C_s	−1020.276758	9	0	0	0	0

[a] The total energies (E_{tot}) apply to the Hartree–Fock (HF) level. [b] The relative energies E_{rel} of the most stable isomers have been set equal to zero; ΔE_{rel} is the difference in energy at the corresponding level of calculation. [c] The zero-point energies (ZPE) are based on calculated wavenumbers scaled by a factor of 0.89.

The anion **3** has C_1 symmetry and an SS bond length of 200.1 pm, slightly longer than in the parent compound **1**. The isomeric anion **4** has C_s symmetry and is less stable than **3** at the Hartree–Fock level. If electron correlation is taken into account, **4** is considerably more stable than **3**. The zero-point energies also favor the isomers **2** and **4** (see Table 1). The reliability of the present calculations can be vouched for by the fact that the harmonic vibrational wavenumbers calculated for **4**[9] correlate in a linear fashion with the 11 observed fundamental wavenumbers of the anion of $NH_4HS_2O_3$[5] (correlation coefficient 0.999).

Table 2. Selected bond distances d [pm], bond angles α [°] [a], torsion angles τ [°], and dipole moments μ [D] of **1** through **4**.

	$H_2S_2O_3$ (**1**)	$H_2S_2O_3$ (**2**)	$HS_2O_3^-$ (**3**)	$HS_2O_3^-$ (**4**)
d(S–H)	–	133.0	–	133.0
d(O–H)	94.9	94.9	94.3	–
d(S–S)	191.4	205.7	200.1	215.5
d(S–OH)	156.8	157.7	161.3	–
d(S=O)	141.1	141.2	143.1	143.5
α(S-O-H)	111.3	111.1	107.9	–
α(S-S-H)	–	93.3	–	95.5
τ(S-S-O-H)	156.9	178.8	62.0	–
τ(O-S-S-H)	–	78.6	–	60.0
μ	3.60	3.00	3.24	3.03

[a] The bond angles at the central sulfur atoms of all four species are in the range 99.5–122.4°.

Expectedly, the negative charge of the anion destabilizes the SS bond of **4** compared to **2** as can be seen from the rather large SS bond distance of 215.5 pm. In this respect **4** resembles other sulfur oxyanions like $S_2O_4^{2-}$ (d_{ss} = 239 pm), $S_2O_5^{2-}$ (d_{ss} = 221 pm), and $S_2O_6^{2-}$ (d_{ss} = 215 pm).[8] All these species dissociate at the SS bond on heating. Anion **4** is the key intermediate in the acid decomposition of thiosulfate[10] which starts according to Equation (a).

$$HSSO_3^- + SSO_3^{2-} \rightleftharpoons HSSSO_3^- + SO_3^{2-} \quad (a)$$

The weak SS bond of **4** expedites the transfer of the SH unit to the attacking nucleophilic thiosulfate anion.[11] Reaction (a) is followed by similar sulfur-transfer steps until the chain length of the sulfanemonosulfonate ion ($HS_xSO_3^-$) has sufficiently grown to allow the splitting off of S_6, S_7, or S_8 [Eq. (b)].[12]

$$H{-}S_x{-}SO_3^- \rightleftharpoons S_x + HSO_3^- \quad (b)$$

$x = 6,7,8$

It therefore seems that the instability of thiosulfuric acid in aqueous solution is mainly caused by the high reactivity of its two anions. This explains why the decomposition rate has a maximum at pH 2–4 and why strongly acidic solutions of $Na_2S_2O_3$ decompose only slowly.[3] Nonaqueous solutions of $H_2S_2O_3$ which do not contain the $S_2O_3^{2-}$ or $HS_2O_3^-$ anions should therefore be more stable, which has in fact been observed.[4, 13]

Received: July 25, 1991 [Z 4823 IE]
German version: *Angew. Chem.* **1992**, *104*, 87

CAS Registry numbers:
1, 13686-28-7; **4**, 20386-50-9.

[1] F. A. Cotton, G. Wilkinson, *Advanced Inorganic Chemistry*, 5th ed., Wiley, New York, **1988**, p. 520; *Anorganische Chemie*, 4th ed., VCH, Weinheim, **1985**, p. 543; A. G. Massey, *Main Group Chemistry*, Horwood, New York, **1990**, p. 332; N. N. Greenwood, A. Earnshaw, *Chemistry of the Elements*, Pergamon, Oxford, **1984**, p. 835; *Chemie der Elemente*, VCH, Weinheim, **1988**, p. 925.

[2] A. F. Holleman, E. Wiberg: *Lehrbuch der Anorganischen Chemie*, 91st–100th ed., de Gruyter, Berlin, **1985**, p. 520; R. Steudel: *Chemistry of the Non-Metals*, de Gruyter, Berlin, **1977**, p. 221.

[3] J. C. Gil, J. Beato, *Ber. Dtsch. Chem. Ges.* **1923**, *56*, 2451–2453; J. Janickis, *Z. Anorg. Allg. Chem.* **1937**, *234*, 193–223.

[4] M. Schmidt, *Z. Anorg. Allg. Chem.* **1957**, *289*, 141–157; M. Schmidt, G. Talsky, *Chem. Ber.* **1959**, *92*, 1526–1538; M. Schmidt, M. Wieber, *Z. Anorg. Allg. Chem.* **1963**, *326*, 174–181.

[5] R. Steudel, A. Prenzel, *Z. Naturforsch. B* **1989**, *44*, 1499–1502.

[6] For details of the calculations which were conducted with the GAUSSIAN 86 and 88 programs see: K. Miaskiewicz, R. Steudel, *J. Chem. Soc. Dalton Trans.* **1991**, 2395–2399; this work describes the analogous treatment of the molecule $H_2S_2O_2$ (7 isomers).

[7] Gaseous H_2SO_4 adopts the analogous structure which is, however, of C_2 symmetry: R. L. Kuczkowski, R. D. Suenram, F. J. Lovas, *J. Am. Chem. Soc.* **1981**, *103*, 2561–2566.

[8] R. Steudel, *Angew. Chem.* **1975**, *87*, 683–692; *Angew. Chem. Int. Ed. Engl.* **1975**, *14*, 655–664.

[9] Harmonic unscaled fundamental wavenumbers of **4**: 194, 293, 335, 384, 579, 586, 693, 884, 1121, 1361, 1373, 2869 cm^{-1}.

[10] R. E. Davis, *J. Am. Chem. Soc.* **1958**, *80*, 3565–3569.

[11] The Mulliken atomic charge on the sulfane -S- atom of **4** is −0.29, while the terminal sulfur atom of $S_2O_3^{2-}$ bears a considerably higher negative charge.

[12] R. Steudel, H.-J. Mäusle, *Z. Anorg. Allg. Chem.* **1979**, *457*, 165–173; R. Steudel, T. Göbel, G. Holdt, *Z. Naturfosch. B.* **1988**, *43*, 203–218.

[13] The formation of gaseous $H_2S_2O_3$ (**2**) from H_2S and SO_3 is exothermic by 68 kJ mol^{-1} which follows from the energies of the three compounds calculated at the HF/6-311G** level (H_2S: −398.701237, SO_3: −622.054076 Hartree).

A Germanium Sesquisulfide, $(t\text{BuGe})_4S_6$, without Adamantane Structure

By *Wataru Ando,* Tetsuji Kadowaki, Yoshio Kabe,* and *Motohiko Ishii*

Organo-substituted sesquichalcogenides with Group IV elements $(RE)_{2n}Y_{3n}$ (E = Si, Ge, Sn; Y = O, S, Se) have attracted theoretical and practical interest for a long time.[1–3] These molecules have polyhedral cagelike frameworks: The structure for n = 2 is an adamantane (or tetrahedrane) type **Ia**,[2] for n = 3, a prismane type **II**,[3d, e] for

[*] Prof. Dr. W. Ando, T. Kadowaki, Dr. Y. Kabe
Department of Chemistry, The University of Tsukuba
Tsukuba, Ibaraki 305 (Japan)
Dr. M. Ishii
National Institute for Research in Inorganic Materials
Tsukuba, Ibaraki 305 (Japan)

[**] This work was supported by a Grant-in-Aid for Scientific Research from the Ministry of Education, Science and Culture of Japan. The authors are grateful to the Asai Germanium Institute for the gift of tetrachlorogermane.

n = 4, a cubane type **III**,[3a] for n = 5, a pentagonal prismane type **IV**,[3a] and for n = 6, a hexagonal prismane type **Va**. The known sesquisulfides and selenides (E = Si, Ge, Sn) have been restricted to those with adamantane-type structures

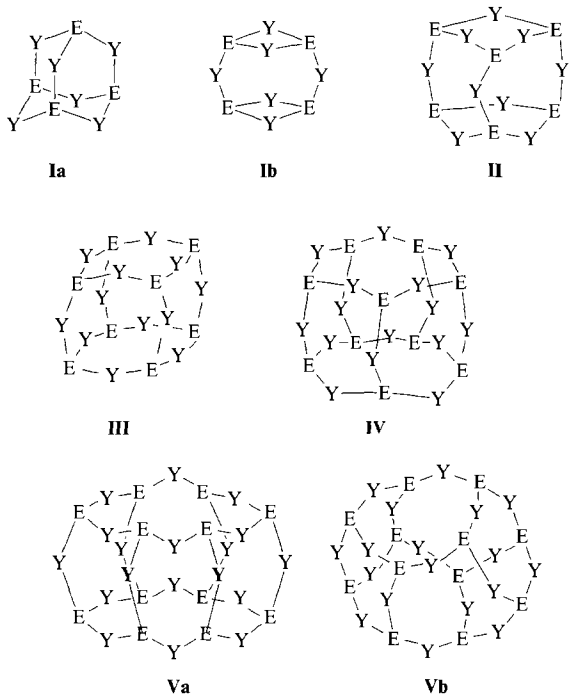

(**Ia**), while the sesquioxide compounds may display the higher homologous structures (**II**, E = Ge; **III**, **IV**, E = Si). An attempted synthesis of **Va** failed and resulted in the formation of structural alternative **Vb**.[3a-c] The "double decker"-type isomer **Ib**[4] isomeric to **Ia** is regarded as another polyhedral sesquichalcogenide because of the equivalence of its four vertices; however, its existence has never been confirmed.[2b-d,f,i] We describe here the synthesis and X-ray crystal structure of the first germanium sesquicalcogenide of type **Ib**.

Treatment of *tert*-butylgermanium trichloride (**1**) with 2 equivalents of ammonium pentasulfide at room temperature provided sesquisulfide **2** with the stoichiometry $(t\mathrm{BuGe})_4S_6$ in 30% yield after preparative HPLC and fractional recrystallization. Unfortunately neither the ^1H nor the ^{13}C NMR spectra of **2**[5] permit one to distinguish between "double decker" and adamantane-type structures. The adamantane-type isomer **3**, prepared by the reported procedure[2b,e] (heating **1** in benzene at reflux with H_2S/pyridine), showed singlets in its NMR spectrum at the same chemical shifts as those in **2**. On the other hand, the Raman spectrum of **2** exhibits six bands in the range expected for Ge–S framework vibrations (200–650 cm^{-1}), whereas that of **3** shows only two bands.[5] This observation not only distinguishes two isomers but also reveals that the molecular symmetry of **2** (D_{2h}) is lower than that of **3** (T_d).[6] When **2** is heated above 200 °C the five Raman bands (308, 337, 364, 398, and 429 cm^{-1}) fade and one strong band (348 cm^{-1}) appears, which is consistent with the spectrum of **3**. Since compound **2** is thought to be an intermediate in the formation of **3** even in reactions with the H_2S/pyridine reagent system, the reaction was carried out at room temperature under our set of conditions. After preparative HPLC of the reaction mixture bisgermanethiol **4** was isolated in 43% yield; **4** releases one mole of H_2S upon heating to afford **3**. The bisgermanethiol **4** exists as two isomers which could not be separated; the spectral data[5] correspond to two isomers (**4**-*syn* and **4**-*anti*). On one occasion isomerically pure crystals were successfully grown and an X-ray structure[7] of the **4**-*syn* isomer was obtained. On the basis of this structure and 2D-NMR experiments on **4**, we believe that the other isomer is the **4**-*anti* compound shown, which differs from **4**-*syn* by the inversion of one germanium atom bearing an SH group. Therefore the reaction proceeds via completely different intermediates depending on the sulfurization reagents. A milder reagent such as $(NH_4)_2S_5$ might make a kinetically-controlled reaction possible, affording the four-membered cage compound **2**.

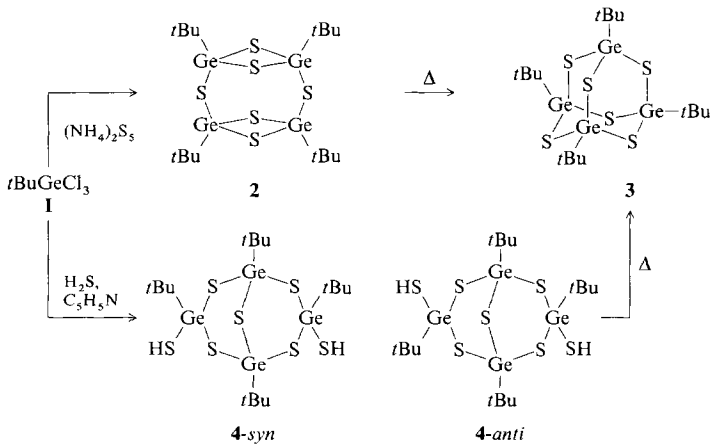

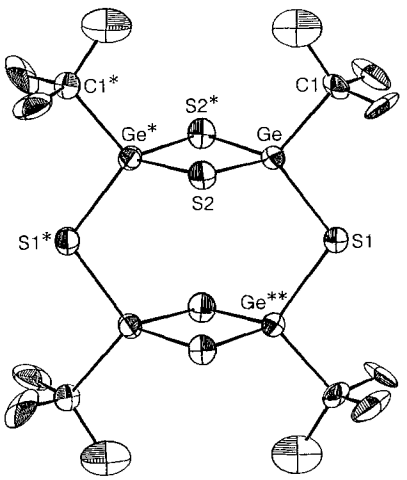

Fig. 1. Crystal structure of **2** (ORTEP). Selected bond lengths [Å] and angles [°]: Ge-S1 2.216(3), Ge-S2 2.243(8), Ge-C1 2.00(1); S1-Ge-S2 114.2(2), S2-Ge-S2* 96.7, Ge-S1-Ge** 108.5, Ge-S2-Ge* 83.2, S1-Ge-C1 103.8(3), S2-Ge-C1 114.9(7).

According to the X-ray structure analysis of **2**,[7] the compound crystallizes in the cubic space group *I*23 and possesses three orthogonal twofold crystallographic axes. The Ge atoms and S atoms form two four-membered and two eight-membered rings; the four-membered rings are perpendicular to the common plane of the two eight-membered rings (Fig. 1). The Ge_2S_2 rings are almost planar. Two twofold axes pass through the midpoints of the four-membered and eight-membered rings. The remaining axes bisect the eight-membered rings through S1 and S1*. Thus the entire molecular structure can be generated by symmetry operations on

one-fourth of the molecule. The packing of the molecules in the unit cell is shown in Figure 2. It is noteworthy that the highly symmetric isomer **3** with an adamantane structure has lower crystal symmetry ($C2/c$)[2f] than **2**. The molecules lie

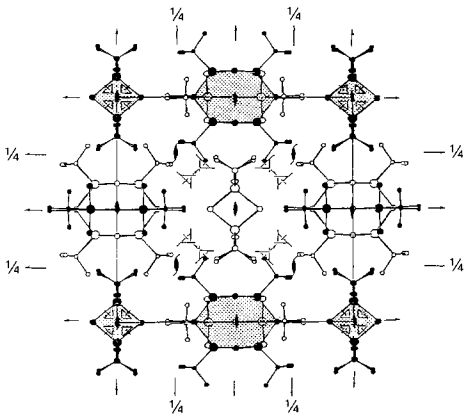

Fig. 2. The crystal packing of **2**. The lower half of the cubic unit cell is shown. Atoms and molecules in the (001) plane are white or without dots, those in the (001/2) plane are black or dotted.

on the twelve edges and the six faces of a cube ($Z = 6$). The eight vertices and the center of the cube are unoccupied to afford a body-centered lattice.

Received: July 29, 1991 [Z 4833 IE]
German version: *Angew. Chem.* **1992**, *104*, 84.

CAS Registry numbers:
1, 1184-92-5; **2**, 137915-99-2; **3**, 137916-02-0; **4**-*syn*, 137916-00-8; **4**-*anti*, 138124-02-4; $(NH_4)_2S_5$, 12135-77-2.

[1] Another branch of our research on the lowest homologous (n = 1) sesquichalcogenides: H. Yoshida, Y. Kabe, W. Ando, *Organometallics* **1991**, *10*, 27.

[2] Sesquisulfides and -selenides of type **Ia**: a) J. A. Forstner, E. L. Muetterties, *Inorg. Chem.* **1966**, *5*, 552; b) K. Moedritzer, *ibid.* **1967**, *6*, 1248; c) V. D. Kobelt, E. F. Paulus, H. Scherer, *Acta Crystallogr. Sect. B28*, **1972**, 2323; d) R. H. Benno, C. J. Fritchie, *J. Chem. Soc. Dalton Trans.* **1973**, 543; e) A. Müller, P. Christophliemk, H. P. Ritter, *Z. Naturforsch. B28*, **1973**, 519; f) J. C. J. Bart, J. J. Daly, *J. Chem. Soc. Dalton Trans.* **1975**, 2063; g) A. Müller, W. Nolff, S. J. Cyrin, B. N. Cyrin, A. J. P. Alix, *Spectrochim. Acta, Part A34*, **1978**, 386; h) A. Blecher, M. Drager, B. Mathiasch, *Z. Naturforsch. B36*, **1981**, 1361; i) H. Berwe, A. Haas, *Chem. Ber.* **1987**, *120*, 1175.

[3] Sesquioxides of types **II**, **III**, **IV**, and **Va**: a) M. G. Voronkov, V. I. Lavrent'yev, *Top. Curr. Chem.* **1982**, *102*, 199; b) W. Clegg, G. M. Sheldrick, N. Vater, *Acta Crystallogr. Sect. B36*, **1980**, 3162; c) F. J. Feher, T. A. Budzichowski, *J. Organomet. Chem.* **1989**, *373*, 153; d) H. Puff, S. Franken, W. Schuh, *ibid.* **1983**, *256*, 23; e) H. Puff, K. Braun, S. Franken, T. R. Kok, W. Schuh, *ibid.* **1988**, *349*, 293.

[4] Another "double decker" molecule whose ring consists of P and N, $P_4(NiPr)_6$: O. J. Scherer, K. Andres, C. Krüger, Y.-H. Tsay, G. Wolmerhäuser, *Angew. Chem.* **1980**, *92*, 563; *Angew. Chem. Int. Ed. Engl.* **1980**, *19*, 571.

[5] **2**: Decomposition > 200 °C; ^{1}H NMR (500 MHz, $CDCl_3$): $\delta = 1.29$ (s); ^{13}C NMR (125 MHz, $CDCl_3$): $\delta = 25.8$ (q), 37.5 (s); Raman (50–1050 cm^{-1}): $\tilde{\nu}$[cm^{-1}] = 79, 106, 111, 153, 159, 308, 337, 364, 398, 429, 543, 806; EI-MS: *m/z* 706–716 (M^+); correct C,H analysis. – **3**: m.p. > 300 °C; ^{1}H NMR (90 MHz, $CDCl_3$): $\delta = 1.29$ (s); ^{13}C NMR (22.4 MHz, $CDCl_3$): $\delta = 25.8$ (q), 37.5 (s); Raman (50–1050 cm^{-1}): $\tilde{\nu}$[cm^{-1}] = 80, 107, 133, 164, 348, 541, 788, 803; EI-MS: 706–716 (M^+); correct C,H analysis. – **4**-*syn*: ^{1}H NMR (500 MHz, $CDCl_3$): $\delta = 1.26$ (s, 18H), 1.32 (s, 18H), 1.13 (S, 2H); ^{13}C NMR (125 MHz, $CDCl_3$): $\delta = 26.4$ (q), 26.7 (q), 36.6 (s), 38.0 (s). – **4**-*anti*: ^{1}H NMR (500 MHz, $CDCl_3$): $\delta = 1.25$ (s, 9H), 1.29 (s, 18H), 1.30 (S, 9H), 1.51 (s, 1H), 2.50 (s, 1H); ^{13}C NMR (125 MHz, $CDCl_3$): $\delta = 25.9$ (q), 26.1 (q), 26.9 (q), 36.0 (s), 36.8 (s), 38.0 (s). The product ratio of **4**-*syn*/**4**-*anti* varied with experimental conditions. In the C-H COSY and COLOC spectra of **4**-*syn*/**4**-*anti*, the signals of the methyl and quaternary carbons correspond to those of the methyl protons of the appropriate isomer. In both the EI and FAB mass spectra of **4**-*syn*/**4**-*anti* the most intense peak is $[M - H_2S]^+$.

[6] According to group theoretical considerations for $(RGe)_4S_6$, the vibrational modes of molecules with D_{2h} and T_d symmetries are distributed among the following fundamental vibrations: $\Gamma(D_{2h}) = 7A_g(R) + 3A_u(-) + 5B_{1g}(R) + 4B_{1u}(ir) + 3B_{2g}(R) + 5B_{2u}(ir) + 3B_{3g}(R) + 6B_{3u}(ir)$; $\Gamma(T_d) = 3A_1(R) + 3E(R) + 3F_1(-) + 6F_2(ir,R)$.

[7] **2**: $C_{16}H_{36}Ge_4S_6$, $M = 711.21$, cubic, $a = b = c = 16.164(1)$ Å, $V = 4223.0$ Å^3, space group *I23*, $Z = 6$, $\mu(Mo_{K\alpha}) = 46.1$ cm^{-1}, $\rho_{calcd.} = 1.68$ g cm^{-3}, 693 reflections, $R = 0.051$ ($R_w = 0.061$). – **4**-*syn*: $C_{16}H_{38}Ge_4S_7$, $M = 745.29$, orthorombic, $a = 13.904(4)$, $b = 16.340(6)$, $c = 13.438(3)$ Å, $V = 3053.0$ Å^3, space group *Pbcn*, $Z = 4$, $\mu(Mo_{K\alpha}) = 43.2$ cm^{-1}, $\rho_{calcd.} = 1.62$ g cm^{-3}, 993 reflections, $R = 0.070$ ($R_w = 0.082$). The independent reflections [$2\theta \leq 50°$; $|F_0^2| > 3\sigma|F_0^2|$] were measured on an Enraf-Nonius CAD4 diffractometer using $Mo_{K\alpha}$ irradiation and ω-2θ (or ω) scans. An empirical absorption correction based on a series of Ψ-scans were applied to the data (0.934/1.00 for **2**; 0.465/0.999 for **4**-*syn*). The structures were solved by direct methods and all nonhydrogen atoms were refined anisotropically. The hydrogen atoms were not located. Further details of the crystal structure investigation may be obtained from the Fachinformationszentrum Karlsruhe, Gesellschaft für wissenschaftlich-technische Information mbH, D-W-7514 Eggenstein-Leopoldshafen 2 (FRG), on quoting the depository number CDS-55660 the names of the authors, and the journal citation.

A Synthetic Receptor for Cyclic Adenosine Monophosphate**

By *Ghislain Deslongchamps, Amalia Galán, Javier de Mendoza,** and *Julius Rebek, Jr.**

Molecular recognition plays a central role in biological processes, and the synthesis of receptors for biorelevant molecules is a rapidly maturing branch of bioorganic chemistry. A number of synthetic receptors for heterocyclic bases,[1–4] carbohydrates,[5, 6] and phosphates[7, 8] employ multiple contact sites on concave surfaces. Those with a cleft-like shape offer particular advantages for molecular recognition since optimal hydrogen bonds can be formed between the concave surface of the receptor and the convex surface of the substrate. Here we report the binding of cyclic adenosine monophosphates (cAMPs) by this type of receptor.

For complexation of the purine nucleus, compound **1** with a molecular cleft featuring two hydrophobic imide functions was developed for simultaneous Watson–Crick and Hoogsteen base-pairing in a triple-helix motif. A 3,6-disubstituted carbazole spacer in **1** poises the two imide functions at an ideal distance and orientation, and the carbazole nucleus allows arene stacking interactions with the complexed guest. The carbazole nitrogen was elaborated to a phosphate-binding site. The bicyclic guanidinium unit, derived from L-asparagine[7, 9, 10] and outfitted with the lipophilic naphthoyl residue, was connected to the carbazole unit with the short two-carbon spacer shown. The receptor was assembled without difficulty (Figure 2) from the tripropylimide acid chloride **4**[11] and diamine **5**; the final coupling reaction of the guanidine derivative to **6** was performed with carbonyldiimidazole (CDI) in dimethylformamide (DMF).[12]

The affinity of receptor **1** toward nucleotide derivatives was determined by liquid–liquid extraction experiments, in which aqueous solutions of cAMP salts (0.11 M) were ex-

[*] Prof. J. Rebek, Jr., Dr. G. Deslongchamps
Department of Chemistry, Massachusetts Institute of Technology
Cambridge, Massachusetts 02139 (USA)
Prof. J. de Mendoza and Dr. A. Galán
Departamento de Química, Universidad Autonoma de Madrid
Cantoblanco, E-28049 Madrid (Spain)

[**] We are grateful to the U. S. National Institutes of Health for support of this work. G. D. thanks the Natural Sciences and Engineering Research Council of Canada for a postdoctoral fellowship. We are indebted to Dr. Marta Bruix (C. S. I. C, Madrid) for the ROESY experiments.

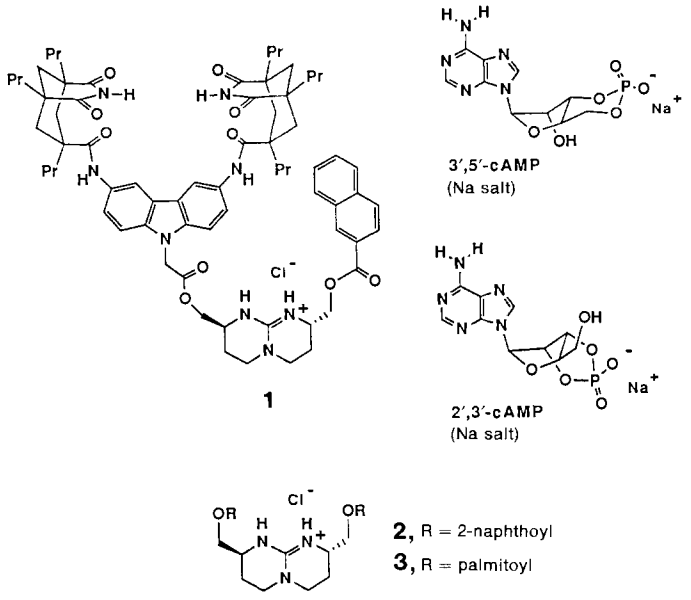

tracted into CH_2Cl_2 solutions of the receptor (2.75 mM). The extraction efficiency (i.e. fraction of receptor molecules occupied by substrate) in the organic phase was determined by NMR integration. Reference extraction experiments were also carried out with the methyl ester **6**, which lacks the phosphate binding site, and with the bis-2-naphthoylguanidinium derivative **2** and the bispalmitoylguanidinium derivative **3**,[9, 10] both of which lack the adenine recognition module.

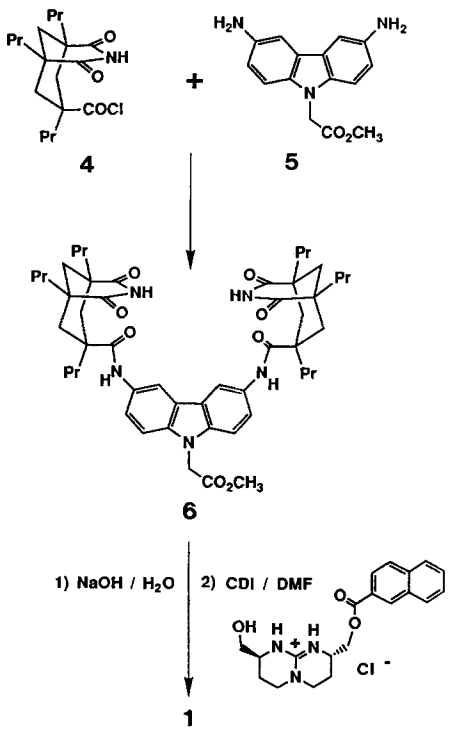

Receptor **1** displays high affinity for cAMP derivatives (Table 1); it extracts one equivalent of either 2′,3′-cAMP or 3′,5′-cAMP into the organic layer! The extraction ratios are consistent with a 1:1 stoichiometry for the complex, and spectroscopic data support the binding model illustrated in Figure 1. The 600 MHz NMR ROESY spectrum of the complex

Table 1. Liquid–liquid extraction of cAMP and cGMP with abiotic receptors **1**–**3** and **6**. The numbers refer to the percentage of the receptor molecules occupied by substrate in the extraction. A solution of receptor (5.5×10^{-3} mmol) in dichloromethane (2 mL) was shaken for two minutes with a solution of nucleotide (5.5×10^{-2} mmol) in water (0.5 mL). The mixture was centrifuged and the organic layer was removed and evaporated. The residue was redissolved in 4:1 $CDCl_3$:CD_3OD (or in [D_6] DMSO) and analyzed by ^1H NMR spectroscopy.

Receptor	Nucleotide extracted [%]			
	2′,3′-cAMP	3′,5′-cAMP	2,3′-cGMP	3′,5′-cGMP
6	<5	<5	<5	<5
2	50	20	8	<5
3	27	13	<5	<5
1	100	100	60	34

of **1** with 3′,5′-cAMP (in [D_6]DMSO showed (among others) interactions between the spacer NCH_2CO and the carbazole H-1, H-8 signals to H-2′ and H-3′ in the ribose of the guest.

The selectivity, however, is modest: 60% extraction was observed in parallel experiments with 2′,3′-cGMP and 34% with 3′,5′-cGMP. Guanine can undergo only "wobble" base-pairing[13] to the imide functions of the receptor, and the diminished binding strength is consistent with the loss of a single hydrogen bond.[14] In addition, the lower solubility of cGMP in CH_2Cl_2 may also contribute to its lower extraction efficiency.

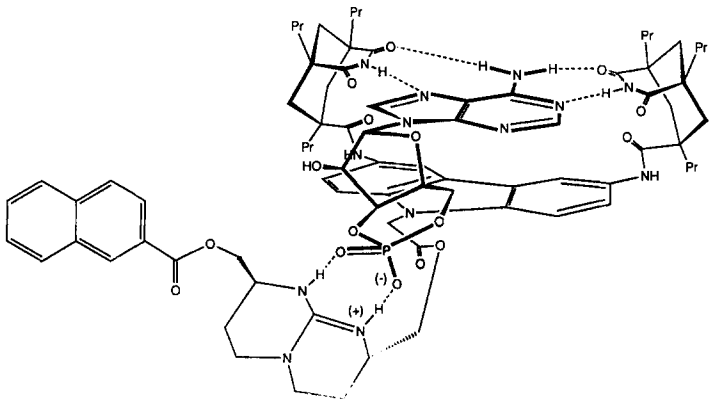

Fig. 1. Proposed binding in the complex of **1** and 3′,5′-cAMP based on NMR spectroscopic data.

Despite its high affinity for the aminopurine nucleus the cleft module of **1** alone did not suffice for the extraction of cAMP (**6** in Table 1). For example, the association constant for the binding of 9-ethyladenine with **6** in $CDCl_3$ is $\approx 50000\ M^{-1}$, and **6** also extracts adenosine (0.3 equiv) and 2′-deoxyadenosine (0.8 equiv) from their aqueous solutions. The esterified guanidinium receptors **2** and **3** are capable of extracting considerable amounts of cAMP into the organic layer, suggesting effective binding of the phosphate ion by the guanidinium function. However, **2**, **3** and **6** were unable to extract significant amounts of cGMP out of water (in the best case, a ca. 8% extraction of 2′,3′-cGMP was detected with **2**).

We have recently developed receptor **1** for the binding of dinucleotides.[15] Transport of nucleotides across membranes[16] should be possible with such receptors.

Received: August 12, 1991 [Z 4867 IE]
German version: *Angew. Chem.* **1992**, *104*, 58

[1] J. Rebek, Jr., *Angew. Chem.* **1990**, *102*, 261–272; *Angew. Chem. Int. Ed. Engl.* **1990**, *29*, 245–255, and references therein.
[2] A. D. Hamilton, D. van Engen, *J. Am. Chem. Soc.* **1987**, *109*, 5035–5036.
[3] T. R. Kelly, M. P. Maguire, *J. Am. Chem. Soc.* **1987**, *109*, 6549–6551.
[4] J. C. Medina, C. Li, S. G. Bott, J. L. Atwood, G. W. Gokel, *J. Am. Chem. Soc.* **1991**, *113*, 366–367.
[5] Y. Kikuchi, Y. Kato, Y. Tanaka, H. Toi, Y. Aoyama, *J. Am. Chem. Soc.* **1991**, *113*, 1349–1354.
[6] R. P. Bonar-Law, A. P. Davis, B. A. Murray, *Angew. Chem.* **1990**, *102*, 1497–1499; *Angew. Chem. Int. Ed. Engl.* **1990**, *29*, 1407–1408.
[7] F. P. Schmidtchen, *Tetrahedron Lett.* **1989**, *30*, 4493–4496; H. Kurzmeier, F. P. Schmidtchen, *J. Org. Chem.* **1990**, *55*, 3749.
[8] W. Hosseini, A. J. Blacker, J.-M. Lehn, *J. Am. Chem. Soc.* **1990**, *112*, 3896–3904.
[9] A. Galán, E. Pueyo, A. Salmerón, J. de Mendoza, *Tetrahedron Lett.* **1991**, *32*, 1827–1830.
[10] A. Echavarren, A. Galán, J.-M. Lehn, J. de Mendoza, *J. Am. Chem. Soc.* **1989**, *111*, 4994–4995.
[11] K. S. Jeong, T. Tjivikua, A. Muehldorf, G. Deslongchamps, M. Famulok, J. Rebek, Jr., *J. Am. Chem. Soc.* **1991**, *113*, 201–209.
[12] All new compounds were characterized by a full complement of high resolution spectra. The receptor exhibited no tendencies toward intermolecular aggregation in deuterated dimethyl sulfoxide ([D_6]DMSO) at the concentrations (10^{-2} to 10^{-5} M) used in the experiments.
[13] W. Saenger, *Principles of Nucleic Acid Structure*, Springer, New York, 1984, Chapter 6.
[14] A. R. Fersht, J.-P. Shi, J. Knill-Jones, D. M. Lowe, A. J. Wilkinson, D. M. Blow, P. Brick, P. Carter, M. M. Waye, G. Winter, *Nature* **1985**, *314*, 235–239.
[15] A. Galán, J. de Mendoza, C. Toiron, M. Bruix, G. Deslongchamps, J. Rebek, Jr., *J. Am. Chem. Soc.* **1991**, *113*, 9424–9425.
[16] For progress on nucleoside and nucleotide transport see: H. Furuta, K. Furuta, J. L. Sessler, *J. Am. Chem. Soc.* **1991**, *113*, 4706–4707; H. Furuta, M. J. Cyr, J. L. Sessler, *ibid.* **1991**, *113*, 6677–6678.

The Stability of Buckminsterfullerene (C_{60}): Experimental Determination of the Heat of Formation

By *Hans-Dieter Beckhaus, Christoph Rüchardt,* Michelle Kao, François Diederich,** and *Christopher S. Foote**

In 1990, Krätschmer and Huffman et al. reported the preparation of macroscopic quantities of buckminsterfullerene (C_{60}), the third allotropic and first molecular form of carbon, by resistive heating of graphite under an inert atmosphere.[1] In the subsequent burgeoning worldwide developments, the cagelike truncated icosahedral structure of C_{60} has been firmly established.[2] This structure was predicted in 1985 by Kroto and Smalley et al. to account for the exceptional stability of the C_{60} species in carbon cluster beams produced by laser vaporization of graphite.[3] Solid C_{60} is indeed of remarkable stability and can be sublimed without decomposition at 400 °C under reduced pressure. The initial exploration of the material properties of this unique molecular structure led to alkali-metal-doped high-temperature superconductors[4] and to a doped organic ferromagnet.[5] Early investigations into the chemistry of C_{60} demonstrated its high oxidation potential[6] and its efficiency in the sensitization of singlet oxygen.[7] Functionalization of the carbon ball is best achieved by nucleophilic[8] and carbene attack[9] at its reactive "pyracyclene double bonds". Osmium and platinum complexes of C_{60}, obtained by bridging these electron-deficient C–C bonds, have been structurally characterized by X-ray crystallography.[10]

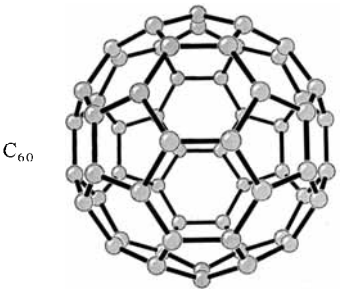

Many of the physical properties of buckminsterfullerene including its thermochemical stability was predicted in theoretical calculations initiated by the work of Kroto and Smalley in 1988.[11] The computational assessement of the thermostability of C_{60} by a variety of quantum mechanical and molecular mechanics methods produced greatly diverging results: the calculated heats of formation ΔH_f° at 298 K vary between 973 kcal mol^{-1} (16.2 kcal mol^{-1} per C atom) and 286 kcal mol^{-1} (4.8 kcal mol^{-1} per C atom) (Table 1). The large discrepancy in the theoretical predictions underlines the importance of determining this fundamental thermodynamic quantity by an accurate experimental thermochemical analysis. Here, we report the results of such a study, which was undertaken with 300 mg of C_{60} of highest purity.

Table 1. Computed heats of formation ΔH_f° at 298 K for C_{60} compared to the experimental value ΔH_f° (c) determined for the crystalline state.

ΔH_f° [kcal mol^{-1}]	ΔH_f° per C atom [kcal mol^{-1}]	Method	Ref.
973	16.2	AM1	[13]
869	14.5	MNDO	[14]
672	11.2	6-31G*//STO-3G[a]	[15]
570	9.6	MM3	[16]
286	4.8	MMP2	[13]
545 (ΔH_f^0) (c)	9.1	combustion	this work

[a] 6-31G* SCF energy at STO-3G geometry.

To isolate pure C_{60}, the toluene extract of the soot prepared by resistive heating of graphite under a helium atmosphere was chromatographed on neutral alumina with hexane/toluene (95:5 v/v) as previously described.[6, 12] After evaporation of the solvent, the material was digested in a small amount of hexane and collected by filtration. HPLC analysis (C-18 reversed-phase column, CH_2Cl_2/toluene (70:30 v/v) as eluent) indicated complete separation of C_{60} from C_{70} and the higher fullerenes. For further purification, the material was recrystallized from toluene and subsequently dried at 80 °C/10^{-3} Torr for 5 hours. Final HPLC, MS and ^{1}H NMR analysis showed that all residual traces of solvent had been removed and that the sample of C_{60} was more than 99.9% pure. A toluene-methyl resonance could not be detected in the 360 MHz ^{1}H NMR spectrum recorded in [D_6]benzene, even at the highest signal amplification.

The heat of combustion of C_{60} was measured by oxygen bomb calorimetry. The isoperibolic aneroid microcalorimeter and the experimental procedures have been described previously.[17] Pellets of C_{60} were used with and without

[*] Professor Dr. C. Rüchardt, Dr. H.-D. Beckhaus
Institut für Organische Chemie und Biochemie der Universität
Albertstrasse 21, D-W-7800 Freiburg (FRG)
Professor F. Diederich, Prof. C. S. Foote, M. Kao
Department of Chemistry and Biochemistry
University of California, Los Angeles, CA 90024-1569 (USA)

[*] Support by the Deutsche Forschungsgemeinschaft, and the Fonds der Chemischen Industrie is gratefully acknowledged.

Table 2. Summary of the combustion experiments of C_{60} [a].

	Run number					
	1	2	3	4	5	6
m (C_{60}) [g]	0.026708	0.039313	0.041660	0.033739	0.035587	0.035655
m_{oil} [g]	0.014340	–	–	–	–	–
m_{fuse} [g]	0.000434	0.000433	0.000563	0.000484	0.000523	0.000463
ΔT_c [K] [b]	1.14208	0.99691	1.05819	0.85808	0.90449	0.90482
ε_{calor} ($-T_c$) [cal] [c]	−388.57	−339.18	−360.03	−291.95	−307.74	−307.85
ε_{cont} ($-\Delta T_c$) [cal] [d]	−0.97	−0.85	−0.90	−0.73	−0.77	−0.77
ΔE_{corr} [cal] [e]	0.22	0.27	0.28	0.23	0.24	0.24
$-m_{oil}\Delta u_c^i$ [cal]	157.61	–	–	–	–	–
$-m_{fuse}\Delta u_c^o$ [cal]	1.76	1.75	2.28	1.96	2.12	1.88
Δu_c (C_{60}) [cal g^{-1}]	−8589.4	−8584.0	−8589.0	−8593.5	−8587.3	−8580.9
ΔH_c (C_{60}) [kcal mol^{-1}] [f]	−6189.54	−6185.61	−6189.23	−6192.51	−6188.02	−6183.43

[a] $T_h = 25\,^{\circ}C$; $V_{bomb} = 0.0820$ L; $p^i_{gas} = 30.00$ atm (30.40 bar); $m^i_{water} = 0.23$ g; $E_{ign} = 0.55$ cal; $T_i = 23.720\,^{\circ}C - 24.017\,^{\circ}C$; $m_{platin} = 1.159$ g. [b] $\Delta T_c = T_f - T_i + \Delta T_{corr}$. [c] $\varepsilon_{calor} = 340.234 \pm 0.020$ cal K^{-1} ($\pm 0.0058\%$) calibration with benzoic acid. [d] $\varepsilon_{cont}(-T_c) = \varepsilon^i_{cont}(T^i - 25\,^{\circ}C) + \varepsilon^f_{cont}(25\,^{\circ}C - T^f + \Delta T_{corr})$. [e] ΔE_{corr}: sum of the items 81–85, 87–90, 93 and 94 in ref. [18]. [f] Mean value: ΔH_c (1) = −6188.06 kcal mol^{-1} ±1.30 (0.021%).

auxiliary paraffin oil. No trace of soot was detectable in any experiment and the auxiliary material showed no effect on the results (Table 2).

The density of C_{60} ($\rho = 1.78$ g cm^{-3}) was measured to calculate its mass in vacuum. The specific heat (c_p = 0.151 cal g^{-1} at 298 K) was determined by differential scanning calorimetry to calculate the isothermal bomb process. The reduction to standard state was performed in the usual manner.[18] A mean value of ΔH_c° (c) = −6188.06 kcal mol^{-1} for the standard heat of combustion was calculated from six calorimetric runs; the standard deviation of ±1.35 kcal mol^{-1} accounts for all experimental uncertainties. Thus a standard heat of formation ΔH_f° (c) = 544.99 kcal mol^{-1} is obtained for crystalline C_{60}. This corresponds to 9.08 ± 0.02 kcal mol^{-1} per C atom which compares with zero for graphite and 0.4 kcal mol^{-1} per C atom for diamond.

Of all the computational predictions (Table 1), the standard heat of formation calculated with the MM3 force field[19] shows by far the best agreement with the experimental value determined for crystalline C_{60}.[20, 21] It is notable that MM3 calculations, performed on the five possible isomers of the higher fullerene C_{78} that satisfy the isolated pentagon rule, also correctly found the two isomers which are the most stable and can be isolated. Apparently, the parameters of this force field account particularly well for the strain caused by the curvature in fullerene π systems and should therefore be very useful for predicting the entirely unexplored properties of the many higher members in the fullerene family of all-carbon molecules.

Received: October 29, 19991 [Z 4994 IE]
German version: *Angew. Chem.* **1992**, *104*, 69

CAS Registry number: C_{60}, 99685-96-8.

[1] W. Krätschmer, L. D. Lamb, K. Fostiropoulos, D. R. Huffmann, *Nature (London)* **1990**, *347*, 354.
[2] Reviews of the early work: a) J. F. Stoddart, *Angew. Chem.* **1991**, *103*, 71; *Angew. Chem. Int. Ed. Engl.* **1991**, *30*, 70; b) F. Diederich, R. L. Whetten, *ibid.* **1991**, *103*, 695 and **1991**, *30*, 678.
[3] H. W. Kroto, J. R. Heath, S. C. O'Brien, R. F. Curl, R. E. Smalley, *Nature (London)* **1985**, *318*, 162.
[4] a) A. F. Hebard, M. J. Rosseinsky, R. C. Haddon, D. W. Murphy, S. H. Glarum, T. T. M. Palstra, A. P. Ramirez, A. R. Kortan, *Nature (London)* **1991**, *350*, 350; b) K. Holczer, O. Klein, S.-M. Huang, R. B. Kanar, K.-J. Fu, R. L. Whetten, F. Diederich, *Science (Washington DC)* **1991**, *252*, 1154.
[5] P. M. Allemand, K. C. Khemani, A. Koch, F. Wudl, K. Holczer, S. Donovan, G. Grüner, J. D. Thompson, *Science (Washington DC)* **1991**, *253*, 301.
[6] P. M. Allemand, A. Koch, F. Wudl, Y. Rubin, F. Diederich, M. M. Alvarez, S. J. Anz, R. L. Whetten, *J. Am. Chem. Soc.* **1991**, *113*, 1050.
[7] J. W. Arbogast, A. P. Darmanyan, C. S. Foote, Y. Rubin, F. Diederich, M. M. Alvarez, S. J. Anz, R. L. Whetten, *J. Phys. Chem.* **1991**, *95*, 11.
[8] a) J. W. Bausch, G. K. Surya Prakash, G. A. Olah, D. S. Tse, D. C. Lorents, Y. K. Bae, R. Malhotra, *J. Am. Chem. Soc.* **1991**, *113*, 3205; b) F. Wudl, A. Hirsch, K. C. Khemani, T. Suzuki, P.-M. Allemand, A. Koch, G. Srdanov, *ACS Monograph Atlanta ACS Meeting*, **1991**, in press.
[9] T. Suzuki, Q. Li, Ö. Almarsson, K. C. Khemani, F. Wudl, *Science (Washington DC)*, in press.
[10] a) J. M. Hawkins, A. Meyer, T. A. Lewis, S. D. Loren, F. J. Hollander, *Science (Washington DC)* **1991**, *252*, 312; b) P. J. Fagan, J. C. Calabrese, B. Malone, *ibid.* **1991**, *252*, 1160.
[11] R. F. Curl, R. E. Smalley, *Science (Washington DC)* **1988**, *242*, 1017.
[12] R. L. Whetten, M. M. Alvarez, S. J. Anz, K. E. Schriver, R. D. Beck, F. Diederich, Y. Rubin, R. Ettl, C. S. Foote, A. P. Darmanyan, J. W. Arbogast, *Mater. Res. Soc. Symp. Proc.* **1991**, *206*, 639.
[13] J. M. Rudzinski, Z. Slanina, M. Togasi, E. Osawa, T. Iizuka, *Thermochim. Acta* **1988**, *125*, 155.
[14] M. D. Newton, R. E. Stanton, *J. Am. Chem. Soc.* **1986**, *108*, 2469.
[15] J. M. Schulman, R. L. Disch, *J. Chem. Soc. Chem. Commun.* **1991**, 411.
[16] F. Diederich, R. L. Whetten, C. Thilgen, R. Ettl, I. Chao, M. M. Alvarez, *Science (Washington DC)*, submitted.
[17] H.-D. Beckhaus, C. Rüchardt, M. Smisek, *Thermochim. Acta* **1984**, *79*, 149.
[18] W. N. Hubbard, D. W. Scott, G. Waddington, in *Experimental Thermochemistry Vol. 1*, (Ed.: F. D. Rossini), Interscience, New York, **1956**, Chap. 5.
[19] N. L. Allinger, Y. H. Yuh, J.-H. Lii, *J. Am. Chem. Soc.* **1989**, *111*, 8551.
[20] It is hardly possible to make a precise estimation of the heat of sublimation of C_{60} for a proper comparison of ΔH_f (g) values obtained by experiment with the results of calculations. Considering the heats of sublimation of a series of polycyclic aromatic hydrocarbons (J. D. Cox, G. Pilcher, *Thermochemistry of Organic and Organometallic Compounds*, Academic Press, London/New York, **1970**) we suggest that the heat of sublimation per carbon atom should in principle be lower for C_{60} than for arenes like pyrene (1.41 kcal mol^{-1}), triphenylene (1.57), 3,4-benzphenanthrene (1.41), chrysene (1.56), tetracene (1.66) or perylene (1.50), because in the crystal the C atoms of the arenes can interact with two layers of adjacent molecules, but those of C_{60} with only one.
[21] *Note added in proof* (December 18, 1991): Recently a value for $\Delta H_{subl.}$ of 40.1 ± 1.3 kcal mol^{-1} for C_{60} at 707 °C was reported by C. Pan, M. P. Sampson, Y. Chai, R. H. Hauge, J. L. Margrave, *J. Phys. Chem.* **1991**, *95*, 2944.

1-*O*-(2-Acetoxyhexadec-1-enyl)choline Iodide, a New Anticancer Agent

By *Werner Kern, Arnulf Lutz, Gerhard Spiteller,** and *W. Jens Zeller**

Recently we proved the presence of α-hydroxyaldehydes **1** (Scheme 1) in a masked form in bovine and swine tissue

[*] Prof. Dr. G. Spiteller, W. Kern, Dr. A. Lutz
Organische Chemie I der Universität
Postfach 101251 D-W-8580 Bayreuth (FRG)

[*] Prof. Dr. W. J. Zeller
Institut für Toxikologie und Chemotherapie
Deutsches Krebsforschungszentrum
Im Neuenheimer Feld 280, D-W-6900 Heidelberg (FRG)

lipids.[1-4] Model studies showed that the α-acyloxyplasmalogens **2** could be precursors to α-hydroxyaldehydes **1**. It is also possible that **1** arises from plasmalogens by means of biological oxidation processes, since our model studies demonstrated that epoxidation of enolethers could produce α-hydroxyaldehydes.[4]

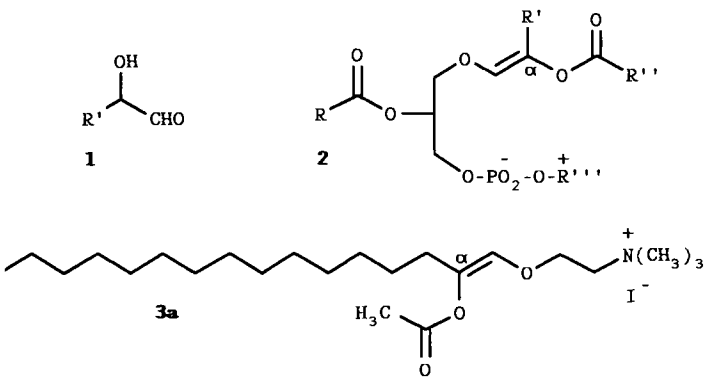

Scheme 1. R,R',R'' = alkyl, R = $CH_2CH_2N(CH_3)_3I$, $CH_3CH_2NH_2$.

Aldehydes have cytotoxic properties, which can be augmented by increasing the carbonyl reactivity.[5-7] However, attempts at combating tumors with unsaturated aldehydes and hydroxyalkenals[6,7] were unsuccessful due to their poor bioavailibility.[6,7] Using the fact that the pH value in tumor tissue drastically decreases upon supply of glucose,[8,13-16] Tietze et al.[8-12] synthesized "prodrugs" in the form of masked aldehydes. These acetalglucosides, stable under physiological conditions, should provide the reactive aldehyde at the place of action when the pH value is lowered.[8-12]

We suspect that the masked α-hydroxyaldehydes, which either are found in the tested cells or arise in them, are natural "prodrugs" along the same lines as those synthesized by Tietze et al.[8-12] As such, masked α-hydroxyaldehydes should display similar cytotoxic properties. To prove our assumption we synthesized the simple model compound **3a**, which has an active enolether–enolacetate structural unit, that is, a masked α-hydroxyaldehyde moiety. In addition a choline residue was built in to ensure the water solubility of **3a**.

First 1,2-epoxyhexadecane (**4**) was treated with the sodium salt of 2-*N*,*N*-dimethylaminoethanol (**5**) following the method of Parker and Isaacs[17] to furnish 1-*O*-(2-hydroxyhexadecyl)-2-*N*,*N*-dimethylaminoethanol (**6**). Ether **6** was converted to 1-*O*-(2-oxohexadecyl)-2-*N*,*N*-dimethylaminoethanol (**7**) with pyridinium chlorochromate (PCC) according to the procedure developed by Corey et al.[18] and Piancatelli et al.[19] Compound **7** underwent reaction with acetic anhydride/K_2CO_3 under the conditions of Barbier et al. [20] providing 1-*O*-(2-acetoxyhexadec-1-enyl)-2-*N*,*N*-dimethylaminoethanol **3** [(*Z*)/(*E*)-isomers].[21] This reaction was unfortunately not regiospecific; besides enolacetate **3** the isomeric compound **8** [(*Z*)/(*E*)-isomers] also arose. This mixture of **3** and **8** was quaternized with methyl iodide and purified by repeated recrystallizations from ethyl acetate. The product mixture, designated C16-AC, consisting of approximately 70% **3a** and 30% **8a** (each with both (*Z*)- and (*E*)-isomers), was tested for inhibition of tumor growth. The results are summarized in Table 1.

The tumor cell lines (ovarian tumors O-342 and O-342/DPP as well as Gliom T 406) with an initial concentration of

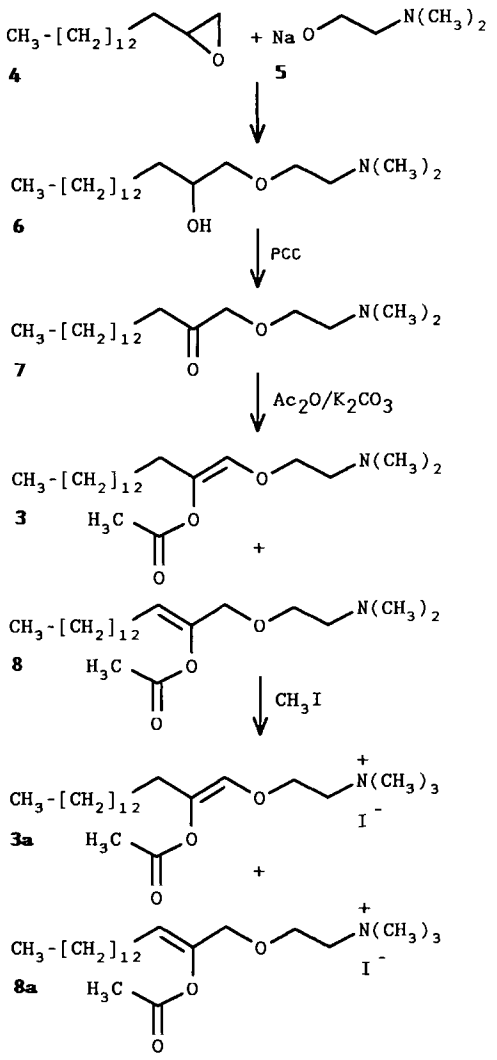

1×10^5 cells per mL medium were incubated seven days with C16-AC (70% (*Z*)/(*E*)-isomers of **3a** and 30% **8a**) in the concentrations 0.1, 1.0, 10, and 100 $\mu g\,mL^{-1}$. The cell count was determined after one, four, and seven days from the average counts of three tissue culture dishes. The regression lines for the percentile growth inhibition was determined from the cell counts from day four. Finally the ID_{10}, ID_{50}, and ID_{90} values (ID_x = dose which inhibits growth by x% relative to the untreated control) were determined graphically.

Table 1. Inhibition of growth for the tumor cells lines O-342, O-342/DPP, and T 406 by C16-AC (see text) in vivo [a].

Tumor cell line	Inhibition dose [$\mu g\,mL^{-1}$]		
	ID_{10}	ID_{50}	ID_{90}
O-342	<0.05[b]	0.7	20
	<0.2[b]	1.9	25
O-342/DPP	<0.2	1.8	25
	<0.3	3	30
T-406	<0.05	0.6	25
	<0.05	1.0	25

[a] O-342 is a malignant granulosa cell rat tumor; O-342/DPP is the related subline which is resistent to cisplatin; T 406 is a gliom cell line of human origin. [b] Two independent experiments were conducted per tumor cell type; the results of the individual experiments are presented here.

The results of the chemotherapeutic investigation show ID_{50} values between 0.6 and 1.9 $\mu g\,mL^{-1}$ for all three tumor cell types examined. This proves a significant therapeutic activity for C16-AC in vitro. Comparison of the antitumor effects of C16-AC with those of alkylphosphocholine HePc proved the latter to be ten times less effective.

Received: July 27, 1991 [Z 4831IE]
German version: *Angew. Chem.* **1992**, *104*, 54

CAS Registry numbers:
(*E*)-**3**, 137569-13-2; (*Z*)-**3**, 137569-18-7; (*E*)-**3a**, 137569-11-0; (*Z*)-**3a**, 137569-12-1; **4**, 7320-37-8; **5**, 37616-36-7; **6**, 137569-14-3; **7**, 137569-15-4; (*E*)-**8**, 137569-16-5; (*Z*)-**8**, 137569-17-6; (*E*)-**8a**, 137569-19-8; (*Z*)-**8a**, 137569-26-1.

[1] W. Knörr, *Ph.D.Thesis*, Universität Bayreuth, **1989**.
[2] A. Lutz, G. Spiteller, *Liebigs Ann. Chem.* **1991**, 563.
[3] A. Lutz, G. Spiteller, W. Knörr, *Liebigs Ann. Chem.* **1991**, in press.
[4] A. Lutz, *Ph.D.Thesis*, Universität Bayreuth, **1991**.
[5] E. Schauenstein, H. Esterbauer, H. Zoller, *Aldehydes in Biological Systems*, Pion Limited, London, **1977**.
[6] E. Schauenstein, H. Esterbauer in *Submolecular Biology and Cancer* (Ciba Found. Symp. 67), Elsevier/North Holland, Amsterdam, **1979**, pp. 225–244.
[7] A. Perin, A. Sessa, G. Scalabrino, A. Arnaboldi, E. Ciarauf, *Eur. J. Cancer* **1979**, *8*, 111.
[8] L. F. Tietze, *Nachr. Chem. Tech. Lab.* **1988**, *36*, 728.
[9] L. F. Tietze, R. Fischer, M. Beller, R. Seele, *Liebigs Ann. Chem.* **1990**, 151.
[10] L. F. Tietze, A. Gorlach, M. Beller, *Liebigs Ann. Chem.* **1988**, 565.
[11] L. F. Tietze, A. Gorlach, M. Beller, *Liebigs Ann. Chem.* **1988**, 559.
[12] L. F. Tietze, R. Fischer, H. J. Guder, M. Neumann, *Liebigs Ann. Chem.* **1987**, 847.
[13] M. von Ardenne, P. G. Reitnauer, *Acta Biol. Med. Ger.* **1970**, *25*, 483.
[14] E. Jähde, M. F. Rajewsky, H. Baumgärtl, *Cancer Res.* **1983**, *42*, 1498.
[15] S. Osinsky, L. Bubnovskaya, T. Sergienko, *Anticancer Res.* **1987**, *7*, 199.
[16] J. L. Wike-Hooley, J. Haveman, H. S. Reinhold, *Radiother. Oncol.* **1984**, *2*, 343.
[17] R. E. Parker, N. S. Isaacs, *Chem. Rev.* **1959**, *59*, 737.
[18] E. J. Corey, J. W. Suggs, *Tetrahedron Lett.* **1975**, 2647.
[19] G. Piancatelli, A. Scettri, M. D'Auria, *Synthesis* **1982**, 245.
[20] P. Barbier, C. Benezra, *J. Org. Chem.* **1983**, *48*, 2705.
[21] **6**: Yield 86 g (87%), almost colorless liquid; thin layer chromatography (TLC) (cyclohexane/diethylamine, 10:1): $R_F = 0.29$; M.p. = 27–30 °C; (TLC) (cyclohexane/diethylamine, 10:1): $R_F = 0.29$; gas chromatography (GC) (OV 101): $R_t = 2333$; MS (70 eV): *m/z* 329 (M^+, 1%), 328 ($M - H^+$, 1), 58 (100), 72 (11), 43 (8), 59 (6), 45 (5), 73 (3), 132 (2). – **7**: Yield 53.4 g (66.5%), yellow oil; B.p. (0.4 Torr) = 164–168 °C; TLC (cyclohexane/diethylamine, 10:1): $R_F = 0.41$; GC (OV 101): $R_t = 2314$; MS (70 eV): *m/z* 327 (M^+, 1%), 326 ($M - H^+$, 1), 58 (100), 43 (38), 72 (31), 59 (25), 86 (5), 145 (1), 158 (1). – **3**/**8**: Mixture of (*Z*)- and (*E*)-isomers, pale yellow oil; B.p. (0.4 Torr) = 175–178 °C; DC (cyclohexane/diethylamine, 10:1) $R_F = 0.46$; GC (OV 101): $R_t = 2410/2435$; MS (70 eV): *m/z* 369 (M^+, 1%), 58 (100), 72 (76), 73 (24), 45 (23), 43 (20), 87 (2), 100 (2), 145 (1), 283 (2), 326 (2), 327 (2); ^{1}H NMR (500 MHz C_6D_6): $\delta = 0.90$ (t, $^3J = 7.0$ Hz, 3H), 1.22–1.34 (m, 22H), 1.42–1.48 (m, 2H), 1.81 (s, 3H), 1.83 (s, 3H), 2.05 (s, 3H), 2.06–2.09 (m, 2H), 2.15 (s, 3H), 2.44–2.47 (m, 2H), 3.63–3.66 (m, 2H), 5.63 (s, 1H). – **3a**/**8a** (C16-AC): Yield 1.45 g (28.4%) yellow solid; M.p. (mixture of isomers) = 88–93 °C.

Unprecedented Stereospecific Ligand Exchange at a W≡W Template**

By *Steven D. Dietz, Nancy W. Eilerts,* and *Joseph A. Heppert**

The stereochemistry of molecules is important in determining their chemical reactivity.[1, 2] The development of novel and more efficient chiral reagents and catalysts for asymmetric synthesis has become the rationale for a wide range of investigations of chiral transition-metal coordination complexes, covering the breadth of the transition elements.[3–5] Unfortunately, it is still difficult to predict the stereochemical outcome of some exchange reactions involving chiral ligands at early transition-metal templates. Our interests have recently focused on the development of 1,1′-bi-2-naphtholate derivatives[6] as chiral auxiliary ligands for early transition-metal complexes.[7] During these studies, we have discovered some unique aspects of the coordination chemistry of this multifaceted bidentate alcoholato ligand.[7] In this communication, we report the first examples of highly stereospecific coordination by a chiral bidentate alcoholato ligand at a d^3-d^3 $[W_2(OR)_6]$ template. Our studies indicate that the stereochemical courses of these reactions are controlled by thermodynamics, producing diastereomeric products in nonstatistical distributions.

The addition of two equivalents of racemic 1,1′-bi-2-naphthol (*rac*-H_2bino) to a solution of $[W_2(OtBu)_6]$[8] in toluene at 0 °C results in the formation of an analytically pure pale-yellow precipitate of empirical formula $[W_2(bino)_2(OtBu)_2]$ (**1a**).[9] The ^{1}H and ^{13}C NMR spectra of the product are invariant over a wide range of temperatures and are consistent with the magnetic equivalence of both the *t*BuO and the naphtholate units. The chemical shift of the *t*BuO ligands (Fig. 1 above), $\delta = 0.1$, is unusual by comparison with the typical value $\delta = 1.6$ for the *t*BuO ligands in $[W_2(OtBu)_6]$.[8] The *gauche* *t*BuO ligands of $[W_2(3,3'\text{-}R_2bino)(OtBu)_4]$ (R = H or Me), which are shielded by a single naphtholate ring, appear at $\delta = 0.70$.[7a] This dramatic upfield shift, $\Delta\delta = 1.15$, indicates that the *t*BuO ligands of **1a** probably lie in the

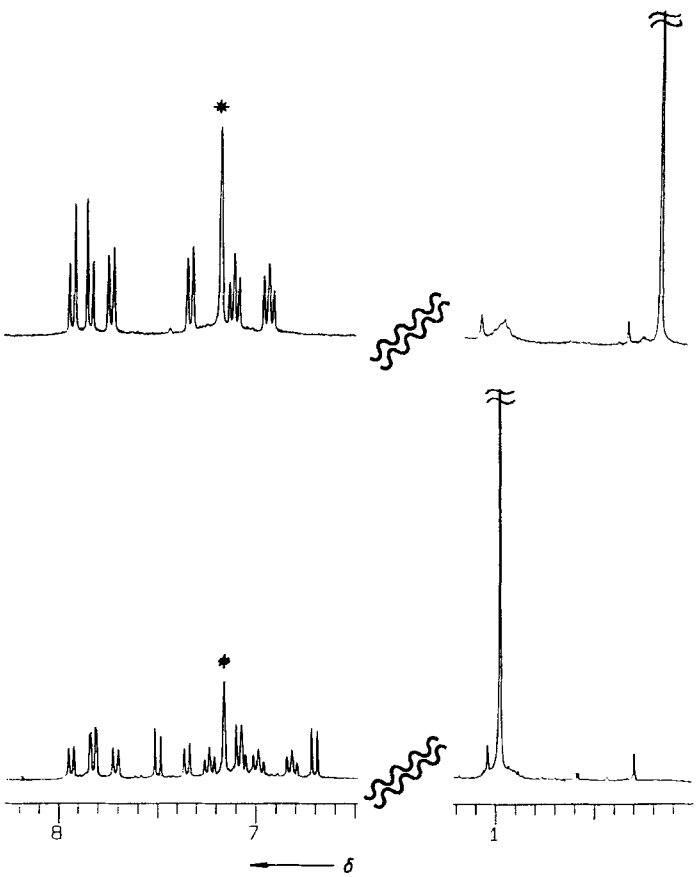

Fig. 1. 300 MHz ^{1}H NMR spectra of the $[W_2(bino)_2(OtBu)_2]$ diastereomers **1a** (above) and **2b** (below). * = C_6D_5H.

[*] Prof. J. A. Heppert, S. D. Dietz, N. W. Eilerts
Department of Chemistry, University of Kansas
Lawrence, KS 66045 (USA)

[**] We thank the University of Kansas Research Fund and donors of the Petroleum Research Fund of the American Chemical Society for financial support of this study.

shielding cones of two naphtholato ligands. The symmetry and NMR data allow the assignment of this product as the C_{2h} symmetric *anti*-(*R*,*S*) isomer **1a**. All of the alternative disubstituted isomers, including the *gauche*-(*R*,*S*) complex **1b** and both of the $[W_2(S^*,S^*)\text{-(bino)}_2(O\textit{t}Bu)_2]$ isomers **2a** and **2b**, can be eliminated on the basis of symmetry considerations. Two minor products ($\leq 10\%$ each) are found in the soluble residues of the reaction. One of these products, a highly symmetric compound whose spectrum consists of a single set of naphtholate signals, was later unequivocally identified as tris(bino)complex **3** (vide infra). The second minor product exhibits a single O*t*Bu resonance and signals for two nonequivalent naphtholate units. This could attributed to either the C_2 symmetric *anti*-(S^*,S^*) isomer **1b** or the *gauche*-(S^*,S^*) isomer **2b** of $[(\text{bino})_2W_2(O\textit{t}Bu)_2]$. This minor product was finally assigned as **1b** after **2b** was prepared by an independent synthesis.

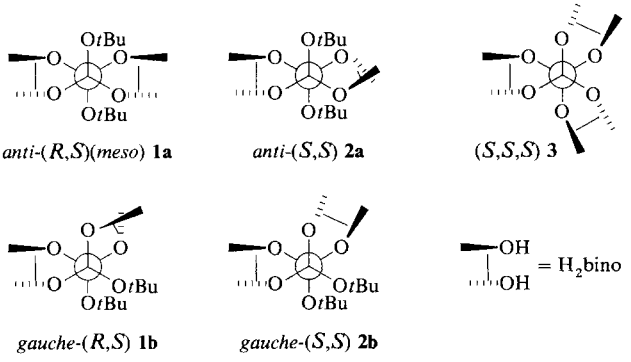

gauche-$[W_2(R,R)\text{-(bino)}_2(O\textit{t}Bu)_2]$ (**2b**) was the only observable product of the reaction of $[W_2(O\textit{t}Bu)_6]$ with two equivalents of optically pure (*R*)-H_2bino. The resonance associated with the *t*BuO ligands at $\delta = 1.0$ (Fig. 1 below) is consistent with a single *gauche* interaction between the *t*BuO and naphtholato ligands. The relative instability of $[W_2(R,R)\text{-(bino)}_2(O\textit{t}Bu)_2]$ provides some circumstantial evidence in support of the *gauche* orientation of the *t*BuO ligands. The molecule decomposes in solution at 20 °C with a half-life of thirty minutes, producing isobutene, *tert*-butanol, and significant quantities of the unidentified minor product **3**, originally observed in the synthesis of **1a**. The *gauche* arrangement of the *t*BuO ligands in **2b** may provide an optimal geometry for intramolecular proton transfer in the rearrangement of the two *t*BuO ligands to yield isobutene and *tert*-butanol.

The highly symmetrical "by-product" noted in each of the reactions above is the yellow "homostereoleptic"[9] tris(binaphtholato) complex, $[W_2(S^*,S^*,S^*)\text{-(bino)}_3]$ (**3**). An enantiomerically pure form can be produced in improved yields by reaction of $[W_2(O\textit{t}Bu)_6]$ with three equivalents of (*R*)-H_2 bino. A related product from the reaction of *rac*-H_2-bino and $[W_2(O\textit{t}Bu)_6]$ provides an uninterpretable ^{1}H NMR spectrum, in which traces of **3** can be identified. The formation of **3** through the decomposition of **2b** implies that facile intermolecular ligand exchange is occurring under the conditions of synthesis of **2b**.

Direct evidence of intermolecular ligand migration was obtained by mixing solutions of (*R*,*R*)-**2b** and (*S*,*S*)-**2b** in the presence of *t*BuOH at 0 °C. After several hours at ambient temperature **1a** was the major identifiable product of the reaction, although trace quantities of **3** were also observed. This study confirms that intermolecular ligand migration can occur under the conditions of $[W_2(\text{bino})_2(O\textit{t}Bu)_2]$ synthesis, and that **1a** is thermodynamically more stable than the corresponding *gauche* complex **2b**. Some amount of **2b** is formed during this synthesis of **1a**, since traces of **3**, a decomposition product of **2b**, are found. Based on the results of this crossover study most of (S^*,S^*)-**2b** formed in the initial exchange process is probably converted to **1a**, suggesting that the production of **1a** from *rac*-H_2bino is a result of thermodynamic control.

While these studies serve to rationalize the evident stability of **1a** over **2b**, they do not account for the observed preference for isomers **1a** and **2b** over their *gauche*-(*R*,*S*) and *anti*-(*S*,*S*) counterparts, **1b** and **2a**. We believe that these latter differences in stability originate in the diastereoisomerism of bino bridges across the W-W bond. Figure 2 emphasizes that a bino unit generates two skew axes: 1) the natural skew axis of the chiral bino ligand, which in the case of an (*S*)-bino ligand is always δ configured and 2) the skew axis defined by the chelating O ··· O unit across the W-W axis, which can be either λ or δ. It is clear that an (*S*)-bino

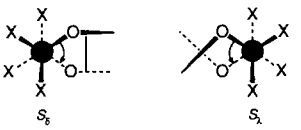

Fig. 2. Structures of diastereomeric chelate complexes of the $[W_2X_4]$ template and the bridging (*S*)-binaphtholato ligand.

ligand produces significantly different linkage geometries, depending on whether its chelating O ··· O unit bridges the ditungsten unit to give a product with a λ or δ configuration. Attaching the stereochemistry of this structural element as a subscript on the stereochemical description of the chiral bino unit unequivocally specifies the bonding mode; consequently, an (*S*)-bino unit can be linked S_δ or S_λ to the W_2 unit, leading to diastereomeric complexes. Because we have observed a nonstatistical distribution of these bonding modes in the ditungsten products, it seems that there are significant differences in the stabilities of the two bridging structures. The degree of selectivity observed in these exchange processes probably stems from the relative rigidity of the bino ligand, reinforced by the π-donor effects of the binaphtholato ligands. In confirmation of this hypothesis, recent work on bridge formation across the Mo-Mo bond in dinuclear molybdenum complexes containing more flexible chiral diphosphine ligands reports substantially lower diastereoselectivity[10] (approximately 3:1 in the solid state and 2:1 in solution).[10a]

One of the characteristic reactions of the $[W_2(OR)_6]$ template is the formation of stable organometallic complexes derived from the addition of one, two, or three equivalents of acetylene to the ditungsten unit.[11] Reactions between three equivalents of acetylene and **1a** immediately generate a tris(acetylene) complex **4**.

$[W_2(R,S)\text{-(bino)}_2(O\textit{t}Bu)_2(\mu_2\text{-}C_4H_4)(\eta\text{-}C_2H_2)]$ **4**

Although the product has thus far defied attempts at crystallization, features common to other(tris)acetylene ditungsten complexes have been identified by ^{1}H and ^{13}C NMR spectroscopy, including resonances characteristic of the μ_2-C_4H_4 and η^2-C_2H_2 units. The spectroscopic studies also indicate that two diastereomers of the (tris)acetylene complex are formed in a ratio of 2:1. The diastereomers are distinguished by significantly different chemical shifts (at -50 °C)

for the static η^2-C_2H_2 unit ($\delta = 11.59$ and 10.96 for the major product, and 11.32 and 10.76 for the minor diastereomer). The formation of the diastereoisomeric complexes of **4** is readily explained by the presence of chelating chiral ligands in the coordination spheres of the tungsten centers. This leads to the further differentiation of the ordinarily enantiomeric (tris)acetylene skeletons of **5a** and **5b**. These

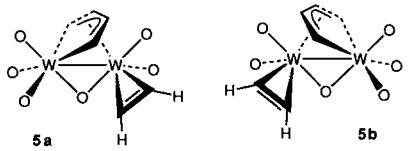

5a **5b**

acetylene complexes are, to the best of our knowledge, the first examples of diastereomeric derivatives generated on the synthetically versatile $[W_2(OR)_6]$ template.

Experimental Procedure

1a: In a Schlenk flask (25 mL) $[W_2(OtBu)_6]$ (0.70 g, 0.87 mmol) was dissolved in toluene (12 mL), and then racemic binaphthol (0.50 g, 1.7 mmol) was slowly added. The solution was stirred for 12 h; a yellow powder precipitated after about 45 min. The solution was removed by syringe and the yellow powder was washed with cold toluene then dried (0.47 g, 50% yield). ^{1}H NMR (C_6D_6, 20 °C) δ = 7.91 (d, 4H, J = 9.9 Hz), 7.81 (d, 4H, J = 9.6 Hz), 7.71 (d, 4H, J = 7.8 Hz), 7.31 (d, 4H, J = 7.2 Hz), 7.08 (t, 4H, J = 5.7 Hz), 6.91 (t, 4H, J = 6.3 Hz; bino), 0.13 (s, 18H; OtBu). ^{13}C NMR (C_6D_6, 20 °C) δ = 168.2 (C(2,2); bino), 135.2, 131.0, 129.6, 126.9, 126.3, 124.4, 122.0, 121.0, 110.4 (bino), 76.1 ($OC(CH_3)_3$), 31.8 ($OC(CH_3)_3$). Correct C, H analysis.

2b: In a Schlenk flask (25 mL), $[W_2(OtBu)_6]$ (0.70 g, 0.87 mmol) was dissolved in toluene (12 mL), and then (*R*)-binaphthol (0.50 g, 1.7 mmol) was added. The solution was stirred for 16 h and the solvent was removed in vacuo. Redissolving the solid in toluene followed by reduction of the solution volume and refrigeration at −20 °C for 12 h provided a yellow powder (0.51 g, 54% yield). ^{1}H NMR (C_6D_6, 20 °C) δ = 7.94 (d, 2H, J = 7.8 Hz), 7.82 (d, 2H, J = 8.8 Hz), 7.71 (d, 2H, J = 7.9 Hz), 7.49 (d, 2H, J = 8.8 Hz), 7.34 (d, 2H, J = 8.3 Hz), 7.24 (t, 2H, J = 7.5 Hz), 7.15–6.96 (m, 8H), 6.83 (t, 2H, J = 6.6 Hz), 6.69 (d, 2H, J = 8.8 Hz; bino), 0.97 (s, 18H, OtBu). ^{13}C NMR ($C_6D_5CD_3$, 20 °C) δ = 167.8, 167.2 (C(2,2); bino), 135.6, 135.4, 131.0, 130.6, 129.9, 128.2, 127.1, 126.9, 126.8, 126.7, 124.5, 123.4, 122.3, 121.5, 121.4, 121.0 (bino), 80.4 ($OC(CH_3)_3$), 32.5 ($OC(CH_3)_3$). Correct C,H analysis.

3: In a Schlenk flask (100 mL), $[W_2(OtBu)_6]$ (0.374 g, 0.463 mmol) was dissolved in toluene (20 mL), and then (*R*)-binaphthol (0.400 g, 1.397 mmol) was added. The solution was stirred for 20 h and the solvent was removed in vacuo. The residue was taken up in toluene and filtered through a glass frit. The toluene was removed in vacuo and the resulting brown powder was washed with hexane then dried in vacuo. Dichloromethane was added to precipitate a yellow powder (18% yield). ^{1}H NMR (C_6D_6, 20 °C) δ = 7.85, 7.08 (d, 1H, J = 8.3 Hz; H(3,4)), 7.56, 6.18 (d, 1H, J = 8.7 Hz; H(8,5)), 7.21, 6.90 (t, 1H, J = 9.0 Hz; H(6,7)). ^{13}C NMR (C_6D_6, 20 °C), δ = 166.4 (C(2)), 135.4 (C(1)), 130.9 (C(10)), 128.0, 124.8 (C(7,8)), 127.1, 127.0 (C(4,6)), 121.4 (C(9)), 121.3 (C(5)). Correct C,H analysis.

4: $[W_2(bino)_2(OtBu)_2]$ (0.40 g, 0.50 mmol) was dissolved toluene (20 mL) in a small Schlenk flask (50 mL). After the flask was cooled to 77 K, excess acetylene (6 equiv) was condensed onto the frozen solution. The reaction mixture was warmed to room temperature and stirred for 30 min before the solvent was removed in vacuo. The residue was redissolved in hexane, filtered to remove polyacetylene, and the volume of the solution was reduced. During refrigeration at −20 °C, a brown powder was deposited. The ^{1}H NMR spectrum of the powder, which proved to be representative of the bulk sample, was consistent with the presence of two diastereoisomers of **4** in a ratio of approximately 2:1. ^{1}H NMR ($C_6D_5CD_3$, −50 °C), major diastereomer: δ = 11.53, 10.94 (s, 1H; η^2-C_2H_2), 9.82, 9.24 (d, 1H, μ_2-W-CH=CH-CH=CH, J(HH) = 5.0 Hz), 0.98, 0.53 (s, 9H, OtBu); minor diastereomer: δ = 11.30, 10.68 (s, 1H; η^2-C_2H_2), 10.21, 8.09 (d, 1H; W-CH=CH-CH=CH), J(HH) = 5.0 Hz), 1.04, 0.96 (s, 9H; OtBu). ^{13}C NMR ($C_6D_5CD_3$, −50 °C), major diastereomer: δ = 193.5, 179.1 (η^2-C_2H_2), 200.6, 188.0 (W-CH=CH-CH=CH), 87.3, 86.9 ($OC(CH_3)_3$), 30.5, 29.5 ($OC(CH_3)_3$); minor diastereomer: δ = 194.8, 189.5 (η^2-C_2H_2), 198.0, 173.9 (W-CH=CH-CH=CH), 86.8, 85.8 ($OC(CH_3)_3$), 30.6, 29.7 ($OC(CH_3)_3$).

Received: August 8, 1991 [Z 4858 IE]
German version: *Angew. Chem.* **1992**, *104*, 67

CAS Registry numbers:
1a, 137698-10-3; **2b**, 137698-11-4; **3**, 137698-12-5; *rac*-bino, 41024-90-2; (*R*)-bino, 18531-94-7; $[W_2(OtBu)_6]$, 57125-20-9.

[1] C. J. Hawkins, *Absolute Configuration of Metal Complexes*, Wiley, New York, **1971**.
[2] *Asymmetric Synthesis: Chiral Catalysis, Vol. 5*, (Ed.: J. D. Morrison) Academic Press, New York, **1985**.
[3] D. A. Evans, *Science* **1988**, *240*, 420–425.
[4] a) M. Kitamure, S. Okada, S. Suga, R. Noyori, *J. Am. Chem. Soc.* **1989**, *111*, 4028–4036; b) J. S. M. Wai, I. Marko, J. S. Svendsen, M. G. Finn, E. N. Jacobsen, K. B. Sharpless, *ibid.* **1989**, *111*, 1123–1125; c) K. Mikani, M. Terada, T. Nakai, *ibid.* **1990**, *112*, 3949–3954.
[5] a) A. Togni, S. D. Pastor, *J. Org. Chem.* **1990**, *55*, 1649–1664; b) M. Riediker, R. O. Duthaler, *Angew. Chem.* **1989**, *101*, 488–490; *Angew. Chem. Int. Ed. Engl.* **1989**, *28*, 494–495; c) J. A. Gladysz, G. S. Bodner, T. S. Peng, A. M. Arif, *Organometallics* **1990**, *9*, 1191–1205; d) J. Blagg, S. G. Davies, C. L. Goodfellow, K. H. Sutton, *J. Chem. Soc. Perkin Trans. 1* **1990**, 1133–1144.
[6] R. Noyori, S. Suga, K. Kanai, S. Okada, M. Kitamura, *Pure Appl. Chem.* **1988**, *60*, 1597–1606.
[7] a) J. A. Heppert, S. D. Dietz, T. J. Boyle, F. Takusagawa: *J. Am. Chem. Soc.* **1989**, *111*, 1503–1505; b) J. A. Heppert, T. J. Boyle, D. Barnes, L. Morales, F. Takusagawa, *Organometallics*, in press.
[8] M. H. Chisholm, M. Akiyama, F. A. Cotton, M. W. Extine, D. A. Haitko, D. Little, P. E. Fanwick, *Inorg. Chem.* **1979**, *18*, 2266–2270.
[9] The term homostereoleptic, derived from homoleptic, indicates that all of the ligands in the complex are identical and that each ligand bridges the W_2 unit with identical stereochemistry.
[10] a) J. D. Chen, F. A. Cotton, C. R. Favello, *J. Am. Chem. Soc.* **1990**, *112*, 1076–1082; b) J. D. Chen, F. A. Cotton, *Inorg. Chem.* **1991**, *30*, 6–7.
[11] a) M. H. Chisholm, K. Folting, D. M. Hoffman, J. C. Hoffman, *J. Am. Chem. Soc.* **1984**, *106*, 6794–6805; b) M. H. Chisholm, D. M. Hoffman, J. C. Hoffman, *ibid.* **1984**, *106*, 6806–6815.

Formation of a Toxic Dimerization Product of 3,4-Dichloroaniline by Lignin Peroxidase from *Phanerochaete chrysosporium***

By *Dietmar Helmut Pieper, Reinhard Winkler,* and *Heinrich Sandermann, Jr.**

Six years ago it was discovered that the white rot fungus, *Phanerochaete chrysosporium*, specialized in breaking down lignin, has the unusual capability to metabolize free chlorinated hydrocarbons and free as well as lignin-bound chlorinated anilines, degrading substantial amounts completely to CO_2.[1] Since then a number of research groups have been working on the possible application of this fungus in biological decontaminations.[2] The extracellular lignin peroxidases (ligninase complex) are often assumed to participate in the degradation of foreign substances. Experimental support for this hypothesis has been found in studies with benzo[*a*]pyrene and chlorinated phenols,[3] but not in the case of the mineralization of DDT (1,1,1-trichloro-2,2-bis(4-chlorophenyl)ethane) or chlorinated anilines.[4] To complement our earlier in vivo experiments[1b,5] we have now tested the in vitro conversion of 3,4-dichloroaniline (**1**) by lignin peroxidase obtained from *P. chrysosporium*. A major product formed was identified as 3,4,3',4'-tetrachloroazobenzene (**3**), a substance comparable to 2,3,7,8-tetrachloro-*p*-dibenzodioxin in structure and toxicity.[6]

A lignin peroxidase preparation was obtained from the supernatant of *P. chrysosporium* mycelium grown under carbon-limited conditions.[7] The enzyme was purified by ultrafiltration and repeated washings with tartrate buffer in order

[*] Prof. Dr. H. Sandermann, Dr. D. H. Pieper, Dr. R. Winkler
GSF-Forschungszentrum für Umwelt und Gesundheit GmbH
Institut für Biochemische Pflanzenpathologie
Ingolstädter Landstrasse 1, D-W-8042 Neuherberg (FRG)

[**] This research was supported by the Deutsche Forschungsgemeinschaft (Sa 180/15-5), the Bundesministerium für Forschung und Technologie (PBE 038657), and the Fonds der Chemischen Industrie.

to remove remaining components of the culture medium.[8] The conversion rate of **1** by this crude enzyme in tartrate buffer (50 mM, pH 3.2) was about 30% of that of the standard substrate veratryl alcohol.[8]

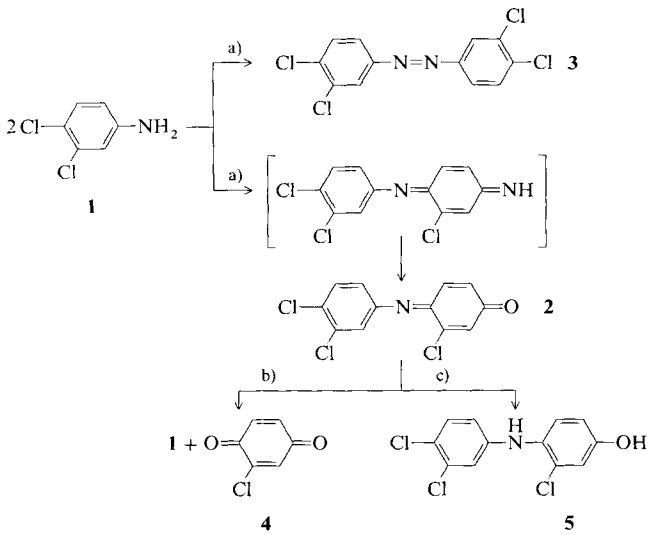

Scheme 1. Conversion of 3,4-dichloroaniline **1** to the toxic 3,4,3',4'-tetrachloroazobenzene **3** and 2,3',4'-trichloro-4-hydroxydiphenylamine **5**. a) Ligninase, b) acid catalysis, c) ascorbic acid.

After complete conversion of **1** (1 mL of a 100 mM solution incubated 20 min with 0.02 U lignin peroxidase) the product mixture was analyzed by reversed phase HPLC on an analytical column using an elution gradient. The samples were applied directly to the column in order to prevent artifacts.[9] The analysis showed that a number of nonpolar products were formed (net retention volume of **1**: 2.9 mL; net retention volume of the products > 6 mL). This indicated the occurrence of oligomerization reactions. In order to quantify the reaction by means of radioactivity detection, [^{14}C]-3,4-dichloroaniline was employed as substrate. The subsequent HPLC eluates could account for 95% of the initial radioactivity; 60% was present in the main product **2** (net retention volume 7.6 mL) and 15% in product **3** (net retention volume 14.3 mL). No polar products were formed, in contrast to the results of in vitro experiments with benzo[*a*]pyrene and chlorophenols.[3]

The conversion of **1** on a preparative scale (1 mmol) was performed in phosphate buffer (500 mM, pH 3.2) despite its low buffer capacity. The tartrate buffer system was not used in order to avoid overloading the HPLC column by application of the extractable buffer. Thus 1 L of a 1 mM solution of **1** was allowed to react with lignin peroxidase corresponding to a total activity of 18 U (relative to the conversion of veratryl alcohol). The reaction was initiated by the addition of H_2O_2 in concentration increments of 40 μM. After complete consumption of **1** the reaction mixture was extracted with ethyl acetate. The extract was concentrated, taken up in acetonitrile, and passed through a preparative HPLC column[10] for the separation and purification of products **2** and **3**. By means of UV/VIS and ^{1}H NMR spectroscopy **3** was unequivocally identified as 3,4,3',4'-tetrachloroazobenzene.[11] Product **2** was relatively unstable; acid-catalyzed cleavage (addition of HCl to a final concentration of 0.5 M) led to **1** and 2-chloro-*p*-benzoquinone **4**.

The addition of ascorbic acid to **2** caused a quantitative transformation to **5** (net retention volume under analytical HPLC conditions[9] 6.6 min). This transformation also occurred as a spontaneous reaction. The mass spectrum and the high resolution mass spectrum of **5**, purified by preparative HPLC, verified the molecular formula $C_{12}H_8OCl_3N$.[12] The ^{1}H NMR spectrum indicates that **5** is 2,3',4'-trichloro-4-hydroxydiphenylamine, a compound not previously described in the literature.[13] Its toxicological properties are not known.

The reaction steps leading to the formation of **5** may be deduced from related studies in the literature. The radicals formed from **1** by lignin peroxidase should react by an *N-para*-coupling to *N*-(3',4'-dichlorophenyl)-*p*-2-chlorobenzoquinone diimine. An analogous dimer has been described as a metabolite in the peroxidase-catalyzed conversion of 4-chloroaniline.[14] In this case the corresponding quinone imine was formed by spontaneous hydrolysis. The classification of compound **2** as a quinone monoimine is chemically supported by its spontaneous dissociation to **1** and **4** under acidic conditions.[15] Consistent with this, the reduction of **2** by ascorbic acid led to the formation of **5** (Scheme 1).

The present results show that the enzymatic activity of lignin peroxidase towards **1** leads to its conversion to the highly toxic compound **3** in good yield. Yields between 10 and 15% were obtained in experiments conducted at various pH values (2.5–4.5), with different concentrations of **1** (10–200 μM), and with three buffer systems (tartrate, dimethylsuccinate, and citrate buffers). The production of **3** from **1** with peroxidases was already detected qualitatively.[16] In addition the formation of chlorinated dibenzodioxins and dibenzofurans from chlorophenyls was catalyzed by peroxidases in low yield.[17]

In earlier investigations[1b,5] the in vivo production of **3** from **1** could not be detected under the culture conditions used. It has now been proved that this was a result of rapid conjugate formation, which removed **1** from lignin peroxidase attack. The simultaneous existence of competing toxifying and detoxifying reactions requires an exact control of the reaction conditions for biotechnological applications of *P. chrysosporium*.

Received: August 7, 1991 [Z 4857 IE]
German version: *Angew. Chem.* **1992**, *104*, 60

CAS Registry numbers:
1, 95-76-1; **1**, ^{13}C-labeled, 80333-59-1; **2**, ^{13}C-labeled, 137768-48-0; **3**, 14047-09-7; **5**, 137768-49-1; lignin peroxidase, 42613-30-9.

[1] a) J. A. Bumpus, M. Tien, D. Wright, S. D. Aust, *Science* **1985**, *228*, 1434–1436; D. C. Eaton, *Enzyme Microb. Technol.* **1985**, *7*, 194–196; b) M. Arjmand, H. Sandermann, Jr., *J. Agric. Food. Chem.* **1985**, *33*, 1055–1060.

[2] J. A. Bumpus, *Appl. Environ. Microbiol.* **1989**, *56*, 154–158; R. T. Lamar, M. J. Larsen, T. K. Kirk, *ibid.* **1990**, *56*, 3519–3526.

[3] S. D. Haemmerli, M. S. A. Leisola, D. Sanglard, A. Fiechter, *J. Biol. Chem.* **1986**, *261*, 6900–6903; K. E. Hammel, P. J. Tardone, *Biochemistry* **1988**, *27*, 6563–6568; K. Valli, M. H. Gold, *J. Bacteriol.* **1991**, *173*, 345–352.

[4] a) A. Köhler, A. Jäger, H. Willershausen, H. Graf, *Appl. Microbiol. Biotechnol.* **1988**, *29*, 618–620; b) R. Winkler, H. Sandermann, *Int. Congr. Pestic. Chem.* IUPAC, Hamburg, Abstract Volume **1990**, Abstract No. 06C–03.

[5] M. Arjmand, H. Sandermann, *Z. Naturforsch. C* **1986**, *41*, 206–214.

[6] A. Poland, J. C. Knutson, *Annu. Rev. Pharmacol. Toxicol.* **1982**, *22*, 517–554; J. V. Pothuluri, J. A. Hinson, C. E. Cerniglia, *J. Environ. Qual.* **1991**, *20*, 330–347.

[7] The propagation/growth of the enzyme was conducted under carbon-limited conditions with agitation according to A. Jaeger, S. Croan, T. K. Kirk, *Appl. Environ. Microbiol.* **1985**, *50*, 1274–1278.

[8] Enzyme isolation and enzyme assays with veratryl alcohol as the test substrate were conducted according to [4a] and as described by M. Tien, T. K. Kirk, *Proc. Nat. Acad. Sci. USA* **1984**, *81*, 2280–2284. For the determination of the conversion rate of **1**: 1 mL of a 50–200 μM solution was allowed to react with 5×10^{-3}–2×10^{-2} U ligninase and 40 μM H_2O_2. The conversion of the substrate was followed by reversed phase HPLC on an analyt-

ical column (Lichrosphere RP8, 5 μm, 4 × 125 mm, UV detection at 210 nm). Isocratic elution with acidic (0.1% phosphoric acid) aqueous acetonitrile (54%) gave a net retention volume of 2.9 mL.

[9] Column Lichrosphere RP8, 5 μm, 4 × 125 mm, UV detection at 210 and 254 nm. Elution (flow rate 1 mL per min) proceeded with acidic (0.1% phosphoric acid) aqueous eluent (54% acetronitrile) 3 min isocratically with a subsequent linear gradient over 7 min to 90% acetonitrile and finally isocratic elution with 90% aqueous acetonitrile.

[10] Column Lichrosphere RP8, 5 μM, 16 × 250 mm, UV detection at 340 nm. Eluent: acidic (0.1% phosphoric acid) aqueous solvent; linear gradient from 45 to 55% acetonitrile over 5 min followed by gradient elution from 55 to 90% acetonitrile over 10 min and finally isocratic elution with 90% aqueous acetonitrile; flow rate 7 mL per min.

[11] UV/VIS (methanol): λ_{max} [nm] (log ε) = 239 (4.28), 330 (4.36), see H. A. B. Linke, D. Pramer, *Z. Naturforschung. B* **1969**, *24*, 997–999. ^{1}H NMR ([D$_6$]acetone): δ = 7.97 (dd, 2H, *J* = 2.2, 8.6 Hz), 8.12 (d, 2H, *J* = 2.2 Hz), 18.85 (d, 2H, *J* = 8.6 Hz) see also M. T. S. Hsia, C. F. Burant, *J. Assoc. Off. Anal. Chem.* **1979**, *62*, 746–750. These data agree with those of the *trans* isomer.

[12] HRMS: *m/z* 286.9675 (calculated for $^{12}C_{12}{}^1H_8{}^{35}Cl_3{}^{14}N^{16}O$: *m/z* 286.9671) MS (70 eV): *m/z* (%) 294 (2), 293 (7), 292 (18), 291 (38), 290 (53), 289 (100), 288 (59), 287 (96), 255 (1), 254 (2), 253 (5), 252 (4), 251 (6), 220 (15), 219 (33), 218 (46), 217 (75).

[13] ^{1}H NMR ([D$_6$]acetone): δ = 6.76 (dd, 1H, *J* = 2.7, 8.8 Hz), 6.86 (dd, 1H, *J* = 2.7, 8.8 Hz), 6.90 (d, 1H, *J* = 2.7 Hz), 7.00 (d, 1H, *J* = 2.7 Hz), 7.25 (d, 1H, *J* = 8.6 Hz), 7.30 (d, 1H, *J* = 8.6 Hz); UV/VIS (methanol): λ_{max} [nm] (log ε) = 212 (4.82), 281 (4.52), 493 (1.90).

[14] K. E. Simmons, R. D. Minard, A. J. Freyer, J.-M. Bollag, *Int. J. Environ. Anal. Chem.* **1986**, *26*, 209–227; K. E. Simmons, R. D. Minard, J.-M. Bollag, *Environ. Sci. Technol.* **1987**, *21*, 999–1003.

[15] B. C. Saunders, A. G. Holmes-Siedle, B. P. Stark, *Peroxidase*, Butterworth, Washington D. C., **1964**, p. 14.

[16] H. B. Lieb, C. C. Still, *Plant Physiol.* **1969**, *44*, 1672–1673; L. M. Bordeleau, R. Bartha, *Can. J. Microbiol.* **1972**, *18*, 1873–1882.

[17] A. Svenson, L.-O. Kjeller, C. Rappe, *Environ. Sci. Technol.* **1989**, *23*, 900–902; L. G. Öberg, B. Glas, S. E. Swanson, C. Rappe, K. G. Paul, *Arch. Environ. Contam. Toxicol.* **1990**, *19*, 930–938; H.-C. Wagner, K.-W. Schramm, O. Hutzinger, *Z. Umweltchem. Ökotoxicol.* **1990**, *2*, 63–65.

First Example of a Chlorophin from an Unexpected Oxidative Ring-Opening of an (Octadehydrocorrinato)nickel(II) Salt **

By *Chi K. Chang,* Weishih Wu, Shuenn-Shing Chern,* and *Shie-Ming Peng**

The presence of *vic*-dihydroxychlorin or its lactone as the heme prosthetic group in d-type cytochromes has recently been elucidated.[1] The diol structure raises the possibility that these green heme compounds might be derived biosynthetically from epoxidation of the porphyrin β–β double bond. In pursuit of such an epoxychlorin, we examined the green compound **1** first reported by Johnson and co-workers,[2] who obtained it from air oxidation of (1,19-dimethyloctadehydrocorrinato)nickel(II) chloride (**2**). Until very recently[3] this was the only known example of epoxychlorin. We discovered that structure **1** is nonexistent; this compound is in fact a totally unexpected and unprecedented tetraaza macrocycle consisting of only three pyrrole units with the fourth pyrrole torn apart and reassembled into an exocyclic furan ring. This structure is so unusual that it represents a new member in the porphyrin family.

Following Johnson's procedure,[2] **2** was stirred in *o*-dichlorobenzene at 150–160 °C in air for about 20 minutes to give a green pigment as the major product (34%) along with a nickel porphyrin **3** (15%). Although the mass spectrum (*m/z* 536) of the green product[4] showed the addition of one oxygen atom to **2**, and its absorption spectrum resembled those of metallochlorins, the chemical reactivities were incompatible with the suggested epoxide structure. For example, it failed to react with methyllithium and could not be reduced by $LiAlH_4$. Since NMR analyses were unable to determine where the oxygen atom had attached, we turned to X-ray diffraction. Crystallization of this compound from a series of solvent systems almost always gave twinned crystals unsuitable for X-ray study. A single crystal was finally obtained from diethyl ether. From its structure (Fig. 1[5]) one can readily appreciate what complicated rearrangements have taken place: The corrin frame has expanded and one angular methyl group has become a methine bridge. The pyrrole α–β bond adjacent to the other angular methyl group was broken, and the vinylic appendage of the broken pyrrole turned through 180° to reattach itself to the macrocycle via an oxide. The resultant structure is a fully conjugat-

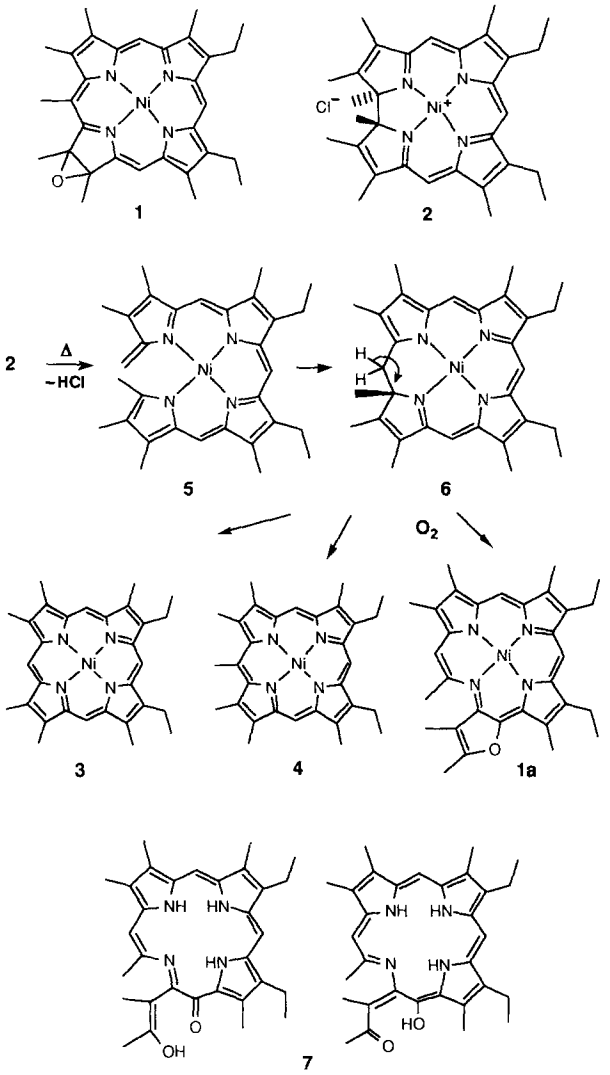

[*] Prof. C. K. Chang, Dr. W. Wu
Department of Chemistry
Michigan State University
East Lansing, MI 48824 (USA)
Prof. S.-M. Peng, S.-S. Chern
Department of Chemistry
National Taiwan University
Taipei (Taiwan)

[**] This research was supported by the National Institutes of Health (GM 34468 and GM 36520) at Michigan State University and by the National Science Council of the Republic of China (NSC80-0208-M002-58). CKC thanks the NSC and National Taiwan University for a Visiting Professorship.

ed 18 π chlorin-like skeleton with only three pyrrolic components. In order to highlight the relationship with the parent chlorin we propose the name "furochlorophin" for the new compound, since "chlorophin" has been suggested[6] for the hitherto unknown tripyrryltetraaza macrocycle. The crystal structure showed normal carbon–carbon and metal–nitrogen bond lengths typical of nickel porphyrinoids.[7] The nickel ion is essentially coplanar with the four nitrogens but the molecule deviates noticeably from planarity, for example, by 0.86 Å at C15, 0.57 Å at C16 and particularly for the furan ring by −0.74 Å at C17, −1.58 Å at C18, −1.93 Å at C19, and −1.38 Å at O. The contracted core of Ni porphyrins caused by short N–Ni bonds often results in a warped ring, but nonplanarity in this molecule is additionally attributed to the repulsion between C29 and C30 methyl groups.

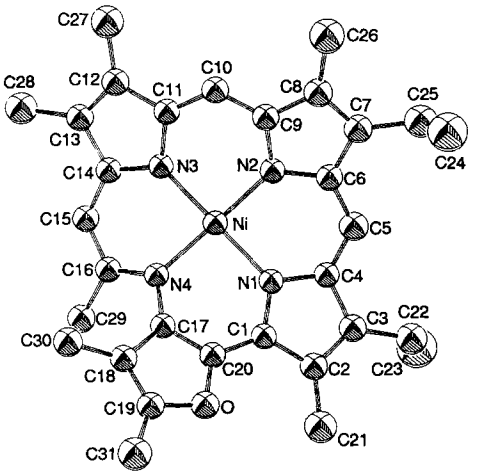

Fig. 1. Structure of **1a** in the crystal. Selected bond distances [Å]: Ni-N(1) 1.945, Ni-N(2) 1.902, Ni-N(3) 1.901, Ni-N(4) 1.908, N(1)-C(1) 1.355, N(4)-C(17) 1.377, N(4)-C(16) 1.372, C(17)-C(20) 1.372, C(17)-C(18) 1.432, C(20)-O 1.377, C(19)-O 1.381.

The initial step proposed for the thermolysis of **2**[2] is a proton abstraction from one of the angular methyl groups by the anion to give the ring fission product **5**, which then cyclizes to **6**. The oxidation of **6** could give rise to porphyrin **3** and **4**, depending on the nature of the original anion. In the present case the fission of the pyrrole α–β bond competes favorably with the cleavage of the angular methyl group. As often the case, the reaction mechanism associated with air oxidation is difficult to establish. No concrete mechanism can be offered at this time for the formation of the furan ring. Possibly an oxophlorin-like intermediate is formed first at C20, as this *meso* position is particularly susceptible to oxidation.[8]

Treatment of **1a** with concentrated sulfuric acid yielded two metal-free derivatives. As deduced by mass spectra and NMR, the major component (60% yield) is the free base furochlorophin (**1b**).[9] In the minor component (20%) the furan ring has opened with the addition of H_2O (most likely structure **7** or its tautomers).[10] The structure of furochlorophin has been confirmed by X-ray diffraction (Fig. 2).[11] The macrocycle is visibly more planar than the Ni complex due to the absence of the short-bond doming effect; the core size of **1b** is also enlarged. This new macrocyclic ligand is easily converted into its Cu^{II}, Zn^{II}, as well as back to the Ni^{II} complex under mild conditions (metal acetate in $CHCl_3$/MeOH). The UV/VIS spectrum of the free base is shown in Figure 3. While the overall features are chlorin-like, there are two notable differences. First, the

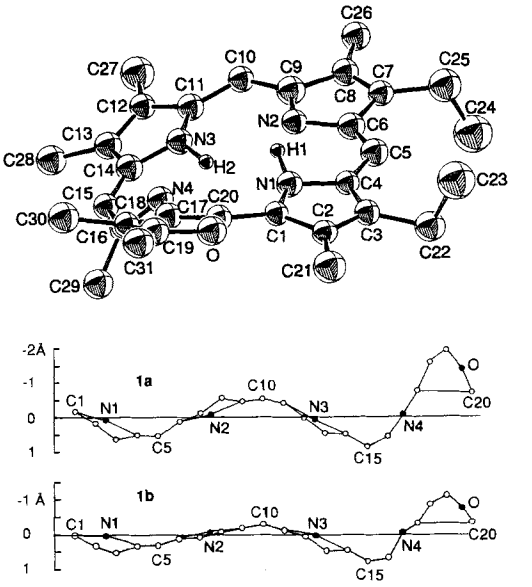

Fig. 2. Structure of **1b** in the crystal. The deviation of the core atoms of **1a** and **1b** from the nitrogen plane is shown by the cylindrical projection plots. The horizontal axis is not to scale.

Soret band as well as the long-wavelength band of **1b** are significantly red shifted (22 nm and 55 nm, respectively, from those of a typical chlorin). Large bathochromic shifts

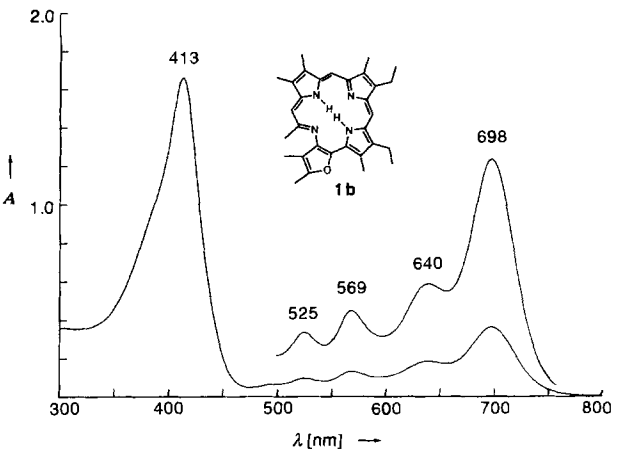

Fig. 3. UV/VIS spectrum of free base **1b** in CH_2Cl_2. A = absorbance.

are also observed in the spectra of metal complexes **1a**, **1c**, and **1d** (Table 1). Second, the extinction coefficients of this series of compounds are relatively small (only about 1/3 of those of corresponding chlorins). The bathochromic shift is probably brought about by an extension of the conjugation by the furan ring. The diminishing HOMO–LUMO gap is

Table 1. UV/VIS data (CH_2Cl_2) for furochlorophin and its metal complexes.

Compound	λ max (ε) [nm ($M^{-1}cm^{-1}$)]				
1b (M = 2H)	413(60700)	526(4900)	569(5800)	641(7200)	699(13000)
1a (M = Ni)	422(41600)	523(3800)	580(4200)		685(18200)
1c (M = Cu)	414(37200) 433(38700)	522(4600)			682(11400)
1d (M = Zn)	440(50300)	513(4500)	583(2800)	638(6300)	683(11800)

also reflected in redox potentials. The furochlorophin **1b** oxidizes to its π cation radical at 0.47 V and reduces at -1.25 V to the anion radical (determined by cyclic voltammetry, versus Ag/AgCl, in CH_2Cl_2). In comparison with etiochlorin I,[12] **1b** is easier to oxidize as well as to reduce by about 180 mV. This smaller redox span correlates well with the observed first absorption band shift. Although the absorption bands of the furochlorophin derivatives have lower extinction coefficients, their bandwidths are broader than those found in chlorins; thus the difference in total oscillator strength between the two systems is less drastic. The decrease in absorption extinction coefficient may be attributable to the reduced rigidity of a macrocycle missing some of the peripheral carbons. Previously Flitsch reported the synthesis of "isobacteriophin", which has two pyrrolic β–β bonds removed; that chromophore also exhibits reduced absorption intensity as compared to isobacteriochlorins.[13]

To our knowledge **1a**–**1d** are the first porphyrinoids that possess a chlorophin core structure. A previous attempt to prepare such compound was not successful.[14] The inherent simplicity of this serendipitous synthesis not only enriches the chemistry of corrinoids[15] but may have potential applications in the emerging photodynamic cancer therapy because of the desirable long-wavelength absorption characteristics of these pigments.

Received: August 21, 1991 [Z 4880 IE]
German version: Angew. Chem. **1992**, *104*, 61

CAS Registry numbers:
1, 36544-38-4; **1a**, 137869-29-5; **1b**, 137869-28-4; **1c**, 137869-30-8; **1d**, 137869-31-9; **2**, 14319-82-5; **7** (tautomer 1), 137895-20-6; **7** (tautomer 2), 137895-21-7.

[1] a) R. Timkovich, M. S. Cork, R. B. Gennis, P. Y. Johnson, *J. Am. Chem. Soc.* **1985**, *107*, 6069–6075; b) C. Sotiriou, C. K. Chang, *ibid.* **1988**, *110*, 2264–2270; c) J. T. Chiu, P. C. Lowen, J. Switala, R. B. Gennis, R. Timkovich, *ibid.* **1989**, *111*, 7046–7051.

[2] a) R. Grigg, A. W. Johnson, K. Richardson, K. W. Shelton, *J. Chem. Soc. C* **1969**, 655–666; b) A. Hamilton, A. W. Johnson, *ibid.* **1971**, 3879–3882.

[3] P. Iakovides, K. M. Smith, *Tetrahedron Lett.* **1990**, *31*, 3853–3856.

[4] **1a**: ^{1}H NMR (300 MHz, [D$_6$]acetone, TMS): δ = 8.83, 8.62, 7.29 (s, 1H each; H-5, 10, 15), 3.47 (m, 4H; Et), 3.08, 2.95, 2.94, 2.85, 2.81, 2.46, 2.17 (s, 3H each; Me), 1.53, 1.49 (t, 3H each; Et); ^{13}C NMR [D$_6$]acetone: δ = 148.18, 146.63, 146.58, 146.26, 145.21, 141.92, 141.73, 139.51, 139.35, 137.80, 137.27, 136.94, 136.36, 134.54, 134.25, 132.22, 128.01, 113.03, 105.16 (*meso*), 100.68 (*meso*), 95.07 (*meso*), 24.54, 24.48, 18.55, 16.63, 16.55, 11.50, 10.99, 9.84, 9.63, 8.23.

[5] **1a**: $C_{31}H_{34}N_4NiO$, M_r = 537.35, monoclinic, space group $P2_1/c$, a = 9.329(6), b = 21.733(5), c = 13.630(7) Å, β = 104.14(5)°, V = 2679.7(22) Å^3, Z = 4, ϱ_{calcd} = 1.332 gcm^{-3}, $F(000)$ = 1135.76, λ = 0.70930 Å, $\mu(Mo_{K\alpha})$ = 0.76 mm^{-1}, crystal dimensions 0.03 × 0.50 × 0.60 mm. A total of 3489 unique reflections and 2287 reflections with $[I > 2.0\sigma(I)]$ were collected on a Nonius diffractometer ($\theta/2\theta$ mode) to $2\theta < 44.8°$. Final model involved anisotropic refinement of all non-hydrogen atoms, R = 0.051 (R_w = 0.053). Assignment of the O atom was based on satisfactory temperature factors and R value during refinement with O at that position. See also [11b].

[6] W. Flitsch, *Pure & Appl. Chem.* **1986**, *58*, 153–160.

[7] A. Eschenmoser, *Ann. N. Y. Acad. Sci.* **1986**, *471*, 108–129.

[8] a) When a CH_2Cl_2 solution of **2**, containing a few drops of triethylamine, was allowed to stand in air for 4 days, (8,12-diethyl-1,2,3,7,17,18,19-octamethyl-5-oxooctadehydrocorrinato)nickel(II) was obtained in 15% yield. This structure was originally proposed by Johnson et al. [2b] and has been verified recently by X-ray crystal structure [8b]. b) C. K. Chang, W. Wu, S.-S. Chern, G.-H. Lee, S.-M. Peng, *Acta Crystallogr.* submitted.

[9] **1b**: MS: m/z 480 (M^+). ^{1}H NMR (300 MHz, $CDCl_3$, TMS): δ = 8.86, 8.37, 7.33 (s, 1H each; H-5, 10, 15), 3.62, 3.49 (q, 2H each; Et), 3.27, 3.05, 3.01, 2.99, 2.93, 2.63, 2.48 (s, 3H each; Me groups), 2.08, 1.98 (br s, 1H each; NH) 1.60, 1.57 (t, 3H each; Et); ^{13}C NMR ($CDCl_3$): δ = 161.65 (C-20), 154.46 (C-19), 143.75, 143.45, 143.07, 139.85, 139.52, 139.09, 136.35, 134.92, 132.68, 131.38, 130.07, 128.25, 123.35, 113.92, 104.73 (*meso*), 98.29 (*meso*), 94.27 (*meso*), 25.43, 19.25, 18.94, 17.35, 17.15, 12.60, 12.11, 10.90, 10.83, 10.78, 10.63. The two signals above 150 ppm, distinct in **1b**, were not observed in **1a**.

[10] **7**: MS: m/z 498 (M^+). ^{1}H NMR (300 MHz, $CDCl_3$, TMS): δ = 11.29 (s, 1H; OH), 6.79, 6.18, 5.48 (s, 1H each; H-5, 10, 15), 4.21 (br s, ≥2H; NH), 2.67, 2.66 (q, 2H each; Et), 2.26, 2.23, 2.13, 2.12, 1.99, 1.84, 1.71 (s, 3H each; Me), 1.18, 1.16 (t, 3H each; Et). The ratio of **1b**/**7** could be increased by shortening the time **1a** was exposed to acid.

[11] a) **1b** (crystallized from CH_2Cl_2/methanol): $C_{31}H_{36}N_4O$, M_r = 480.65, monoclinic, space group $P2_1/n$, a = 13.859(9), b = 14.479(6), c = 14.506(9) Å, β = 116.940(5)°, V = 2595(4) Å^3, Z = 4, ϱ_{calcd} = 1.230 gcm^{-3}, $F(000)$ = 1032, λ = 0.71069 Å, $\mu(Mo_{K\alpha})$ = 0.70 cm^{-1}, crystal dimensions 0.06 × 0.09 × 0.14 mm. A total of 2436 unique reflections and 933 reflections with $[I > 3.0\sigma(I)]$ were collected on a Rigaku diffractometer using $\omega - 2\theta$ scan mode ($2\theta < 40.1°$). Due to the low reflection/parameter ratio, all non-H atoms were refined isotropically, including H1 and H2 which were located from the difference Fourier map. Final R value is 0.102 (Rw = 0.117). b) Further details of the crystal structure investigation are available on request from the Director of the Cambridge Crystallographic Data Center, University Chemical Laboratory, Lensfield Road, GB-Cambridge CB2 1EW (UK), on quoting the full journal citation.

[12] C. K. Chang, J. Fajer, *J. Am. Chem. Soc.* **1980**, *102*, 848–850.

[13] W. Flitsch, D. Schulz, H.-G. Kneip, *Liebigs Ann. Chem.* **1985**, 1004–1011.

[14] M. J. Crossley, L. G. King, *J. Chem. Soc. Chem. Commun.* **1984**, 920–922.

[15] a) R. Grigg in *The Porphyrins, Vol. 2*, (Ed.: D. Dolphin), Academic Press, New York, **1978**, Chapter 10; b) T. A. Melent'eva, *Usp. Khim.* **1983**, *52*, 1136–1172; *Russ. Chem. Rev. (Engl. Transl.)* **1983**, *52*, 641–661.

The Synthesis and Structure of an Unusual Uranium Pentachloride Derivative**

By *Michael Wedler, Mathias Noltemeyer,* and *Frank T. Edelmann**

Dedicated to Professor Oskar Glemser on the occasion of his 80th birthday

Uranium pentachloride $(UCl_5)_2$ is a highly reactive compound which is reduced even by aliphatic hydrocarbons to uranium(IV) complexes in a vigorous reaction.[1,2] A selective exchange of one or more chlorine atoms has not yet been possible. We report here the unexpected formation of a uranium pentachloride derivative as well as its structural characterization.

According to investigations by Dehnicke et al.,[3] fully silylated benzamidines $RC_6H_4C(=NSiMe_3)N(SiMe_3)_2$ react with various metal halides with cleavage of $SiMe_3X$ (X = halide) to give metal complexes with benzamidinato ligands L. The reaction of benzamides L-$SiMe_3$ with UCl_4

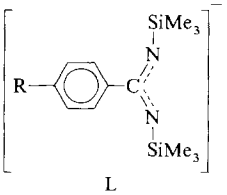

L

L^1, R = H
L^2, R = Me
L^3, R = OMe
L^4, R = CF_3
L^5, R = Ph

provides the green bis(benzamidinato)dichlorouranium(IV) complexes $[L_2UCl_2]$, which we have previously described.[4,5] In addition, well-formed black single crystals were isolated from the reaction of $MeC_6H_4C(=NSiMe_3)N(SiMe_3)_2$ with UCl_4. This side product apparently arose from the unintentional introduction of air to the reaction mixture. This black compound could be obtained cleanly and reproduceably by controlled oxidation of the reaction

[*] Dr. F. T. Edelmann, Dr. M. Wedler, Dr. M. Noltemeyer
Institut für Anorganische Chemie der Universität
Tammannstrasse 4, D-W-3400 Göttingen (FRG)

[**] We thank Prof. Dr. H. W. Roesky for his generous support. This research was funded by the Deutsche Forschungsgemeinschaft and the Fonds der Chemischen Industrie (habilitation fellowships for F. T. E.).

mixture with dry air. According to the X-ray crystallographic data, this compound is $[L^2_2UCl_3]$ **1**, a stable substitution product of uranium pentachloride. The unexpected formation of **1** can be explained only qualitatively.

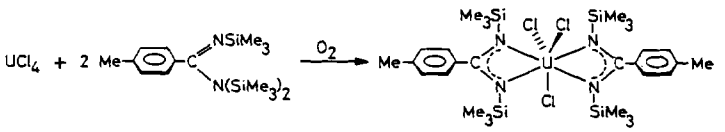

1

The driving force of the reaction may be the formation of hexamethyldisiloxane. The yield of **1** is about 11% and is limited by the heterogeneity of the reaction, which is conducted as a suspension in hexane. The hexane-insoluble portion consists of a mixture of $[L^2_2UCl_2]$ and $[L^2UCl_3(THF)]$ (^{1}H NMR). According to the IR spectroscopic measurements, further oxidation to a benzamidinatodioxouranium(VI) complex $[L^2_2UO_2]$ does not occur. Only oxidation with molecular oxygen can provide uranium(V) complex **1**. When $AgAsF_6$ is used as oxidant only UF_4 results. The synthesis of **1** from $[L^2_2UCl_2]$ and Cl_2 appears rational on first glance, but is not possible due to the labile N–Si bonds in the ligand system, resulting in the formation of $SiMe_3Cl$.

The reactivity of uranium pentachloride is decreased dramatically by the introduction of the bulky benzamidinato chelating ligands. Complex **1** is noticeably sensitive to moisture, but can be dissolved without decomposition in organic solvents like hexane, toluene, and THF. In dry air **1** is not prone to further oxidation. In the EI-mass spectrum the peak corresponding to the molecular ion appears with low intensity. The coordination geometry of the formally seven-coordinate uranium atom can be described as distorted pentagonal-bipyramidal (Fig. 1.). The U–Cl distances of 252.7(4)

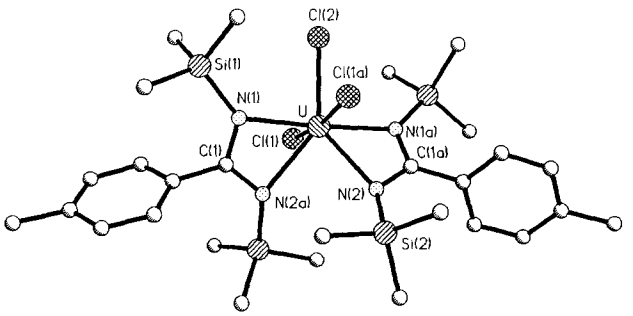

Fig. 1. Structure of **1** in the crystal [6, 7]. Selected bond lengths [pm] and angles [°]: U-Cl(1) 256.8(5), U-Cl(2) 252.7(5), U-N(1) 226.5(8), U-N(2) 237.2(5), C(1)-N(2) 132.3(11), C(1)-N(2a) 131.9(11); N(1)-U-N(2a) 57.5(2), N(1)-U-N(1a) 176.4(3), N(1)-C(1)-N(2a) 115.3(6), Cl(1)-U-Cl(1a) 170.7(2).

and 256.8(5) pm are significantly shorter than that of the benzamidinatouranium(IV) complex $[L^1_3UCl]$ (266.0(9) pm[5]). The same is true for the U–N distances of **1** (226.5(8) and 237.2(5) pm) compared to those of $[L^1_3UCl]$ (241.3(5) and 244.9(19) pm). Two almost linear axes in the molecule are quite noticeable: The C1(1)-U-Cl(1a) and N(1)-U-N(1a) units form angles of 170.7(2) and 176.4(3)°.

Finally we would like to point out an interesting parallel to the organometallic chemistry of uranium. According to our investigations, the steric demands of *N*-silylated benzamidinato ligands L are about the same as those of cyclopentadienyl ligands. Thus the benzamidinato complexes $[L_2UCl_2]$ and $[L_3UCl]$[4,5] correspond to the cyclopentadienyl complexes $[Cp^*_2UCl_2]$ ($Cp^* = \eta^5$-C_5Me_5)[8] and $[Cp_3UCl]$.[9] A Cp or Cp* complex analogous to **1** is not known. The preparation of organometallic complexes of uranium in high oxidation states, for example $Cp^*_2UCl_3$ or $Cp^*_2UO_2$, remains a synthetic goal. The unexpected formation **1** could point the way in that direction.

Experimental Procedure

UCl_4[10] (1.00 g, 2.6 mmol) and $MeC_6H_4C(=NSiMe_3)N(SiMe_3)$[11] (1.85 g, 5.3 mmol) in THF (80 mL) was stirred for 24 h at room temperature under N_2. After the solvent was removed the green precipitate (mainly $[L^2_2UCl_2]$[5]) was suspended in hexane (100 mL). A $CaCl_2$ drying tube was attached to the flask and the reaction mixture was allowed to stir at room temperature for another 5 d, during which time it turned black. The reaction mixture was filtered through a thin layer of Celite and the volume of the filtrate was reduced to about 20 mL. Cooling to −25° provided black crystals (0.25 g, 11%). M.p. = 120° (decomp); IR (Nujol): $\tilde{\nu}$[cm^{-1}] = 1608m, 1242vs ($SiMe_3$), 1180m, 1155m, 975vs, 841vs ($SiMe_3$), 759s, 710s, 641m, 628m; MS: *m/z* 897 (M^+, 9%), 862 (M^+ − Cl, 2%), 827 (M^+ − 2Cl, 100%), 812 (M^+ − 2Cl − CH_3, 51%); ^{1}H NMR (80 MHz, C_6D_6, 32°): δ = 6.72 (m, 8H, C_6H_4), 1.75 (s, 6H, Me), 0.08 (s, 36H, $SiMe_3$); Correct C,H,N analyses.

Received: July 25, 1991 [Z 4822 IE]
German version: *Angew. Chem.* **1992**, *104*, 64
CAS Registry numbers:
$[L^2_2UCl_3]$, 137516-00-8; 4-$MeC_6H_4C(=NSiMe_3)N(SiMe_3)_2$, 117057-77-4.

[1] *Gmelin Handbuch der Anorganischen Chemie*, Springer, Berlin, **1979**, Band C9 „Uranium", p. 29.
[2] W. Kolitsch, U. Müller, *Z. Anorg. Allg. Chem.* **1974**, *410*, 21.
[3] K. Dehnicke, *Chem.-Ztg.* **90**, *114*, 295.
[4] M. Wedler, H. W. Roesky, F. Edelmann, *J. Organomet. Chem.* **1988**, *345*, C1.
[5] M. Wedler, F. Knösel, M. Noltemeyer, F. T. Edelmann, U. Behrens, *J. Organomet. Chem.* **1990**, *388*, 21.
[6] **1** (M_r = 899.5): Monoclinic, space group *C*2/*c*, *a* = 2387.5(8), *b* = 1044.1(3), *c* = 2031.9(5) pm, β = 127.77(1)°, *V* = 4.0004 nm^3, *Z* = 4, ϱ_{calc} = 1.49 g cm^{-3}, crystal size 0.5 × 0.6 × 0.7 mm^3, Siemens-Stoe-AED2 four-circle diffractometer, $2\theta_{max}$ = 45°, 2594 symmetry-independent reflections, of these 2290 with $F > 3\sigma F$ used in the refinement (SHELXS-86, SHELX-76); 182 refined parameters, R = 0.044, R_w = 0.054, $w^{-1} = \sigma^2(F) + 0.0008\,F^2$.
[7] Further details of the crystal structure investigation may be obtained from the Fachinformationszentrum Karlsruhe, Gesellschaft für wissenschaftlich-technische Information mbH, D-W-7514 Eggenstein-Leopoldshafen 2 (FRG) on quoting the depository number CSD-55846, the names of the authors, and the journal citation.
[8] P. J. Fagan, J. M. Manriquez, E. A. Maatta, A. M. Seyam, T. J. Marks, *J. Am. Chem. Soc.* **1981**, *103*, 6650.
[9] T. J. Marks, A. M. Seyam, W. A. Wachter, *Inorg. Synth.* **1976**, *16*, 147.
[10] J. A. Herrmann, J. F. Suttle, *Inorg. Synth.* **1957**, *5*, 143.
[11] R. T. Boeré, R. T. Oakley, R. W. Reed, *J. Organomet. Chem.* **1987**, *331*, 161.

The Photochemistry of *N*-Phthaloyl α-Amino Acid Esters: A New Approach to β,γ-Unsaturated α-Amino Acids and Dihydrobenzazepinediones**

By *Axel G. Griesbeck** and *Harald Mauder*

N-Substituted phthalimides have occupied an important place in synthetic organic photochemistry for quite some time. By means of hydrogen abstraction from the appropriate positions (γ or δ to the carbonyl group) and cyclization of the resulting 1,4- or 1,5-diradical, heteropolycycles may be

[*] Priv.-Doz. Dr. A. G. Griesbeck, Dipl.-Chem. H. Mauder
Institut für Organische Chemie der Universität
Am Hubland, D-W-8700 Würzburg (FRG)

[**] This research was supported by the Deutsche Forschungsgemeinschaft, the Fonds der Chemischen Industrie, and the Universitätsbund Würzburg. We thank Degussa AG for their gift of chemicals and Dr. K. Drauz, Degussa AG, for helpful discussions.

assembled.[1] The irradiation of α-amino acids with a phthaloyl protecting group on the amino function leads exclusively to decarboxylation.[2] We report here the photochemical transformation of the related methyl ester to a palette of highly interesting products.

The *N*-phthaloyl amino acid methyl esters **1**–**5** of (*S*)-2-aminobutanoic acid, (*S*)-valine, (*S*)-norvaline, (2*S*,3*S*)-isoleucine, and (*S*)-*tert*-leucine were synthesized according to a modified literature method[3] by reaction of *N*-ethoxycarbonylphthalimide with the corresponding methyl ester hydrochloride (Scheme 1, Method A). Except for **1** and **5**, these compounds could also be prepared by esterification of the free *N*-phthaloyl amino acid (Method B).

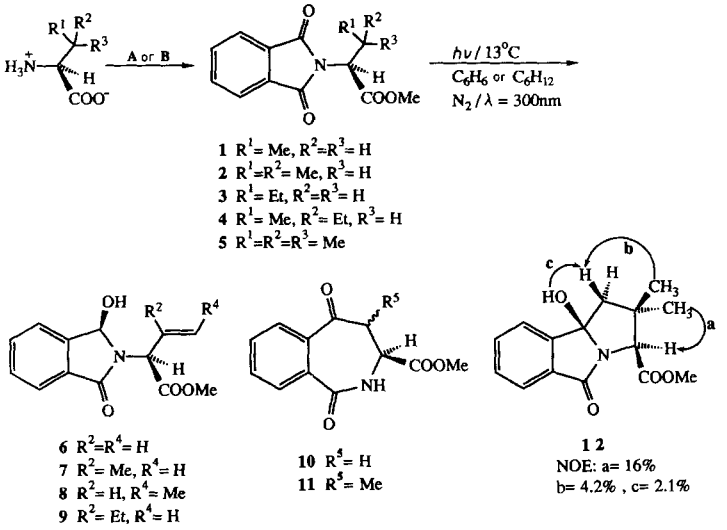

Scheme 1. Synthesis and photochemical reactions of the *N*-phthaloyl α-amino acid methyl esters **1**–**5**. Method A: a) MeOH/HCl, room temperature (RT) (> 98%); b) carboethoxyphthalimide/H_2O/Na_2CO_3 (45–55%). Method B: a) phthalic anhydride, 135° (100%); b) MeOH/HCl, 10° (> 98%).

The irradiation of these compounds in benzene with $\lambda = 300$ nm (Rayonet photoreactor, RPR 3000 Å lamps, 13°, 0.02–0.1 M solutions, 24–75 h until complete conversion of starting material) leads to three types of products: a) photoisomerization products **6**–**9**, b) dihydrobenzazepinedione esters **10** and **11**, and c) the pyrrolizidinone derivative **12**. The photoreaction of compounds **2** and **5** proceeds with high chemoselectivity; the isomerization product **7** (85% yield) and the benzannelated pyrrolizidinone **12** (90% yield) are the only respective detectable products. Both compounds are formed diasteromerically pure (^{1}H and ^{13}C NMR, Scheme 1).

Nuclear Overhauser Enhancement (NOE) measurements of **12** prove that the methoxycarbonyl group is *cis* to the hydroxy group. Saturation of the H atom α to the ester led to the unequivocal assignment of the neighboring diastereotopic methyl groups and H atoms in the methylene group. Analogous experiments showed the olefinic product **7** to have a related configuration, that is the new chiral center arises from two H-transfers to the phthalimidocarbonyl group with the second occurring on the *Si* side (*lk* topicity). In the photoreaction of **5** the transfer of a second hydrogen atom is not possible, thus the radical centers recombine.

A more complex spectrum of products results from the irradiation of *N*-phthaloyl methyl esters **1**, **3**, and **4**. In all cases the products of isomerization as well as ring expansion are generated. All the new compounds could be separated by column chromatography. The product distribution is summarized in Table 1; the physical and spectroscopic data are listed in Table 2.

Table 1. Products of the photoreactions of *N*-phthaloyl α-amino acid methyl esters **1**–**4** [a,b].

Substrate	Product type (a)	Product type (b)	Total yield [%]	Irradiation time [h]
1	**6** (25%)[c]	**11** (75%)[d]	80	75
2	**7** (100%)	–	85	24
3	**8** (20%)	**10** (80%)	75	50
4[e]	**9** (89%)	**11** (11%)[f]	84	50

[a] 0.04 M solution in benzene or cyclohexane, 15°, N_2. [b] If not specified *d.r.* > 95:5. [c] *d.r.* = 70:30. [d] *d.r.* = 67:33 (*trans*:*cis*). [e] See text for the experiment with *allo*-**4**. [f] Exclusively the *cis* diastereomer.

Table 2. Selected physical and spectroscopic data for **7**, *cis*-**11**, and **12**[a].

7: Colorless oil; ^{1}H NMR: δ = 1.79 (s, 3H; CH_3), 3.79 (s, 3H; OCH_3), 4.72 (br.s, 1H; OH), 5.03 (s, 1H; C=CH_2), 5.25 (s, 1H; C=CH_2), 5.59 (s, 1H; NCHCOOMe), 5.82 (s, 1H; NCHOH), 7.55 (dd, J = 4.1, 7.6 Hz, 1H; aromat. H), 7.59 (d, J = 3.9 Hz, 2H; aromat. H), 7.78 (d, J = 7.1 Hz, 1H; aromat. H); ^{13}C NMR: δ = 21.4 (q, C_qCH_3), 52.9 (q, OCH_3), 59.2 (d, NCHCOOMe), 80.3 (d, NCHOH), 117.4 (t, C=CH_2), 123.3 (d), 123.6 (d), 129.5 (d), 129.9 (d), 132.8 (d), 137.5 (s), 144.5 (s, C=CH_2), 168.1 (s, COOMe), 172.8 (NCO); IR (neat): $\tilde{\nu}$ [cm^{-1}] = 3350, 2900, 1670, 1520, 1415, 1340.

cis-**11**: Colorless oil; ^{1}H NMR: δ = 1.26 (d, J = 7.2 Hz, 3H; $CHCH_3$), 3.15 (dq, J = 2.7, 7.2 Hz, 1H; $CHCH_3$), 3.78 (s, 3H; OCH_3), 4.78 (dd, J = 2.7, 5.4 Hz, 1H; CHCOOMe), 6.86 (d, J = 5.4 Hz, 1H; NH), 7.53–7.86 (m, 4H; aromat. H); ^{13}C NMR: δ = 10.6 (q, $CHCH_3$), 51.8 (d, $CHCH_3$), 53.8 (q, OCH_3), 55.4 (d, CHCOOMe), 129.0 (d), 130.4 (d), 131.9 (s), 132.7 (d), 133.2 (d), 147.6 (s), 168.5 (s), 169.7 (s), 202.4 (s); IR (neat): $\tilde{\nu}$[cm^{-1}] = 3385, 2955, 1750, 1678, 1270, 1180.

12: Colorless oil; ^{1}H NMR: δ = 0.99 (s, 3H; C_qMe_2), 1.19 (s, 3H; C_qMe_2), 1.88 (d, J = 13.7 Hz, 1H; C_qCH_2), 2.24 (d, J = 13.7 Hz, 1H; C_qCH_2), 3.72 (s, 3H; OCH_3), 4.30 (s, 1H; NCHOH), 4.58 (br.s, 1H; OH), 7.36–7.65 (m, 4H; aromat. H); ^{13}C NMR: δ = 24.1 (q, $C_q(CH_3)_2$), 29.0 (q,$C_q(CH_3)_2$), 47.6 (s, C_q), 49.0 (t, C_qCH_2), 51.3 (q, $COOCH_3$), 66.6 (d, NCHCOOMe), 95.7 (s, NCOH), 121.6 (d), 123.0 (d), 128.6 (d), 129.4 (s), 132.4 (s), 147.5 (s), 169.9 (s), 171.7 (s); IR (neat): $\tilde{\nu}$[cm^{-1}] = 3350, 2880, 1670, 1520, 1230, 990.

[a] All new compounds provided correct elemental analyses.

The relative configuration of **11** (from the photoreaction of **1**) could be determined by comparison of $J_{H,H}$ coupling constants. The main diastereomer of the dihydrobenzazepinedione, isolated in 50% yield, was identified as the *trans* diastereomer, *trans*-**11** ($^3J_{H,H}$ = 8.5 Hz). *cis*-**11** ($^3J_{H,H}$ = 2.7 Hz) and a mixture of **6a**/**6b** were both collected in 25% yield (Table 1). The formation of this type of product can be explained by the following reaction sequence: γ-hydrogen abstraction (the position is relative to the phthalimidocarbonyl group), cyclization of the 1,4-diradical **i** to the N/O-hemiacetal with a four-membered ring, and ring opening to the benzannelated seven-membered ring **ii** (Scheme 2). This sequence was already postulated by Kanoaka et al. for the formation of the related achiral *N*-alkylphthalimides.[4] In this context it is worth mentioning that amino acid derivatives without H atoms in the δ or ε positions, for example *N*-phthaloyl derivatives of alanine or phenylalanine, do not react even after 100 h irradiation. If the dihydrobenzazepinedione intermediate **ii** in the previous mechanism has an ethyl substitutuent α to the keto group, a second Norrish Type II reaction takes place and ethylene is eliminated. (This is illustrated in Scheme 2 for the isoleucine derivative **4**.) The tautomerization to the final product is highly stereoselective, leading to **11** (from **4**); only the product with a *cis* configuration was isolated.

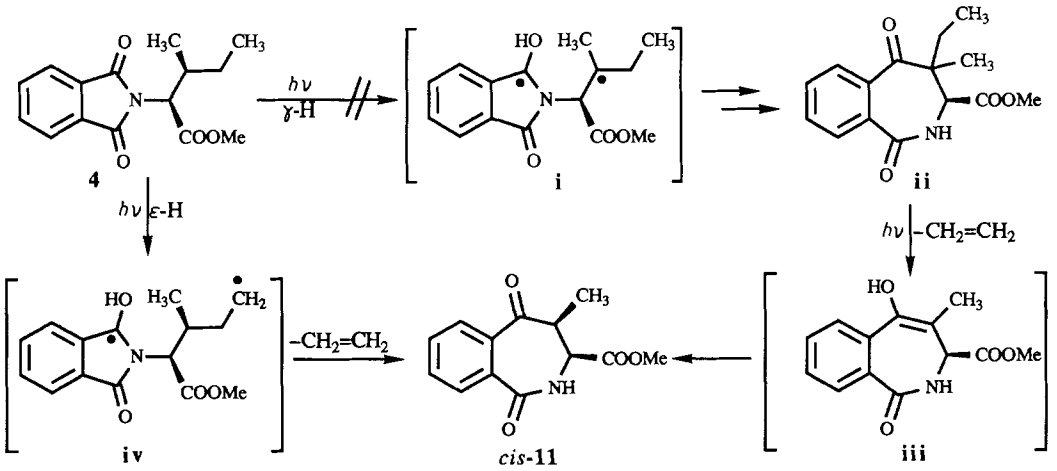

Scheme 2. Formation of *cis*-**11** by photochemical reaction of (2*S*,3*S*)-*N*-phthaloylisoleucine methyl ester **4**.

An alternative to this mechanism is an ε abstraction[5] from **4** and subsequent S_H2 reaction on the 1,6-diradical **iv** (Scheme 2). This would also explain why the ethyl-substituted benzazepinediones **ii** presumed to be intermediates were never observed. This reaction should proceed stereospecifically with configurational conversion, which is also in accord with the relative configuration of product **11**. After irradiation of a 60:40 mixture of the isoleucine derivative **4** and the related *allo*-isoleucine derivative (2*S*,3*S*), 88% of the isomerization product **9** and 12% of a 60:40 mixture of *cis*-**11** and *trans*-**11** were isolated. Analysis of the mass balance indicates that *trans*-**11** arises exclusively from *allo*-**4**. Thus the reaction via a common intermediate like **iii** can be ruled out.

To be certain that epimerization of the α center did not occur during the irradiation of the *N*-phthaloyl amino acid esters, we converted the dehydrogenation product **7** back to **2**. After treatment of **7** with pyridinium chlorochromate (PCC) on alumina[6] for 50–60 h, the *N*-phthaloyl-protected isodehydrovaline methyl ester could be isolated quantitatively. Subsequent hydrogenation with Pd/C provided **2**. Comparison of the optical rotation of **2** to that of the compound from (*S*)-valine indicated a retention of absolute configuration > 95% (Scheme 3). We assume the absolute configuration of the α chirality center is also retained during the irradiation of the other amino acid derivatives.

What is the reason for the remarkably high diastereoselectivity in the formation of products **7**–**9** and **12** from **2**–**5**, a selectivity which was not observed in the photoreaction of the 2-aminobutanoic acid derivative **1**? An analysis of the temperature dependence of the ^{13}C NMR spectrum of compound **5** shows that rotation about the N–C_α single bond has an activation barrier of roughly 12 kcal mol^{-1}. (Two sets of signals are observed in the ^{13}C NMR spectra measured at temperatures below $T_{coal.} = -35\,^{\circ}C$.) The photochemical transformations of *N*-substituted phthalimides proceed via

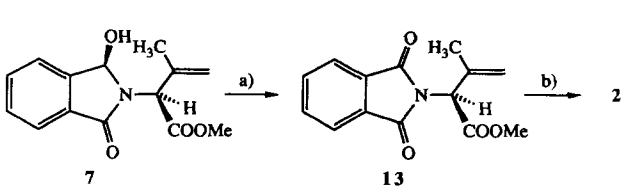

Scheme 3. Transformation of **7** {$[\alpha]_D$ 6.1 (MeOH, $c = 1.0$)} into **2**: a) pyridinium chlorochromate (PCC) on alumina/CH_2Cl_2 {80%, $[\alpha]_D$ −70.1 (MeOH, $c = 1.0$)}; b) H_2, Pd/C {98%, $[\alpha]_D$ −62.4 (MeOH, $c = 1.5$)}. **2**: $[\alpha]_D$ −66.7 (MeOH, $c = 1.2$)}.

the first excited singlet state.[7] The diradical formed after the abstraction of the first hydrogen atom (in the γ or δ position)[8] in the $^1[n\pi^*]$ excited state of the carbonyl function should therefore be a 1,4- or 1,5-*singlet* biradical. This short-lived intermediate can undergo transfer of the second H atom faster than the rotation about the sterically encumbered N–C_α single bond, thus explaining the high diastereoselectivity in the formation of the second chiral center. The rotational barrier of 2-butanoic acid derivative **1** could not be determined (valine derivative **2** $\Delta G^{\neq}$ ca. 9 kcal mol^{-1}) and accordingly its photoreaction is not stereoselective.

β,γ-Unsaturated α-amino acids are often proposed as enzyme inhibitors[9] (especially isodehydrovaline[10] and vinylglycine[11]). Our synthetic approach to these compounds is much simpler than the previously known procedures and can compete with elegant synthetic routes, for example that reported recently by Duthaler proceeding via *N*-acylthiazolidines.[12]

Received: July 10, 1991 [Z 4787IE]
German version: *Angew. Chem.* **1992**, *104*, 97

CAS Registry numbers:
1, 69043-98-7; **2**, 124729-87-9; **3**, 137649-34-4; **4**, 137649-35-5; **5**, 137649-36-6; **6** (isomer 1), 137649-37-7; **6** (isomer 2), 137649-45-7; **7**, 137649-38-8; **8**, 137649-39-9; **9**, 137649-40-2; **10**, 137649-41-3; *cis*-**11**, 137649-42-4; *trans*-**11**, 137764-48-8; **12**, 137649-43-5; **13**, 137649-44-6; (*S*)-2-aminobutanoic acid, 1492-24-6; (*S*)-valine, 72-18-4; (*S*)-norvaline, 6600-40-4; (2*S*,3*S*)-isoleucine, 73-32-5; (*S*)-*tert*-leucine, 20859-02-3; carboethoxyphthalimide, 22509-74-6; phthalic anhydride, 85-44-9

[1] a) J. D. Coyle in *Synthetic Organic Photochemistry* (Ed.: W. A. Horspool), Plenum Press, New York, 1984, p. 259; b) P. H. Mazzocchi, *Org. Photochem.* **1981**, *5*, 421–471.
[2] Y. Sato, H. Nakai, T. Mizoguchi, M. Kawanishi, Y. Hatanaka, Y. Kanaoka, *Chem. Pharm. Bull.* **1982**, *30*, 1263–1270.
[3] G. H. L. Nefkens, *Nature* **1960**, *185*, 309.
[4] Y. Kanaoka, Y. Migata, K. Koyama, *Tetrahedron Lett.* **1973**, 1193–1196.
[5] ε-Hydrogen abstractions are known see: a) M. A. Meador, P. J. Wagner, *J. Org. Chem.* **1985**, *50*, 419–420; b) H. A. J. Carless, G. K. Fekarurhobo, *Tetrahedron Lett.* **1984**, *25*, 5943–5946.
[6] Y.-S. Cheng, W.-L. Liu, S. Chen, *Synthesis* **1980**, 223–224.
[7] Numerous examples of δ-hydrogen abstractions have been reported. See: a) M. A. Meador, P. J. Wagner, *J. Am. Chem. Soc.* **1983**, *105*, 4484–4486; b) P. J. Wagner, M. A. Meador, B. P. Giri, J. C. Scaiano, *ibid. Soc.* **1985**, *107*, 1087–1088; c) P. J. Wagner, *Acc. Chem. Res.* **1989**, *22*, 83–91.
[8] J. D. Coyle, A. Harriman, G. L. Newport, *J. Chem. Soc. Perkin Trans. 2* **1979**, 799–802.
[9] R. R. Rando, *Acc. Chem. Res.* **1975**, *8*, 281–288.
[10] J. E. Baldwin, S. B. Haber, C. Hoskins, L. I. Kruse, *J. Org. Chem.* **1977**, *42*, 1239–1241.
[11] A. Afzali-Ardakani, H. Rapoport, *J. Org. Chem.* **1980**, *45*, 4817–4820.
[12] R. O. Duthaler, *Angew. Chem.* **1991**, *103*, 729–731; *Angew. Chem. Int. Ed. Engl.* **1991**, *30*, 705.

Stable Intermediates in the Addition and Elimination of $SnBuCl_3$ at Molybdenum Centers by Cleavage or Formation of an Sn–Cl Bond: Crystal Structure of $[Mo(CO)_2(PCy_3)(\mu\text{-}Cl)(\mu\text{-}S_2CPCy_3)(BuSnCl_2)] \cdot CH_2Cl_2$ **

By *Daniel Miguel, Julio A. Pérez-Martinez, Victor Riera,** and *Santiago García-Granda*

We recently reported the preparation of homo-[1,2] and heterodinuclear[3] complexes of Mn and Re containing S_2CPR_3 ligands acting as $\eta^2(S,S')$ and $\eta^3(S,C,S')$ bridges across a metal–metal bond. In a systematic exploration of the coordination properties of the S_2CPR_3 ligands, we focused on the molybdenum complex **1**,[4] attempting to exploit both the facile displacement of the two acetonitrile ligands and the ability of the metal center to coordinate S_2CPR_3 ligands in an $\eta^3(S,C,S')$ pseudoallylic fashion.[5,6] Our goal was to obtain MoSn compounds containing S_2CPR_3 bridges.

$[Mo(CO)_3(SnBuCl_2)(Cl)(NCMe)_2]$ **1**

$[Mo(CO)_2(PR_3)(\mu\text{-}Cl)(\mu\text{-}S_2CPR_3)(SnBuCl_2)]$ **3**

Here we wish to report the reactions leading to compounds of type **3** in which an S_2CPR_3 group acts as an $\eta^3(S,C,S')$ pseudoallylic ligand toward Mo, and as an $\eta^2(S,S')$ chelate toward Sn. To our knowledge compounds of type **3** are the first examples of complexes containing S_2CPR_3 ligands serving as bridges between a transition and main group metal. Both the structural features and the reactions leading to their formation suggest that these complexes can be considered as intermediates in the oxidative addition/reductive elimination of $SnBuCl_3$ at molybdenum centers.

Complex **1** reacts with two mole equivalents of S_2CPR_3 in CH_2Cl_2 at room temperature to give compounds **3a–c** (Scheme 1) which have been characterized by analytical and spectroscopic methods.[7] An X-ray structure determination[8] of a crystal of **3a** (R = *cyclo*-C_6H_{11}, Cy) (Fig. 1) reveals that the molecule can be described as consisting of a $SnBuCl_2$ unit attached to $Mo(CO)_2(PCy_3)$ by a chlorine bridge and an S_2CPCy_3 bridging ligand bonded as an $\eta^2(S,S')$ chelate ligand to Sn and as an $\eta^3(S,C,S')$ pseudoallyl ligand to Mo. The long Mo–Sn distance (3.636(2) Å) precludes the existence of any significant bonding between the two metals. The Mo atom lies in a highly unsymmetrical seven-coordinate environment; the Sn atom is surrounded by six atoms in an octahedral disposition, an unusual coordination for Sn in transition metal–tin complexes.[9] The bridging chlorine atom, Cl(1), is not positioned symmetrically between the two metals but rather much closer to Mo than to Sn. The Mo–Cl(1) distance (2.560(4) Å) is similar to that observed for Mo–Cl (terminal) (2.525(4) Å) in $[Mo(SnCl_2Bu)(CO)_2(Cl)\{P(OMe)_3\}_3]$,[4] while the Sn–Cl(1) distance (2.762(4) Å) is significantly longer than that observed for the Sn–Cl (terminal) bonds (2.407(4) and 2.421(5) Å).

[*] Prof. Dr. V. Riera, Dr. D. Miguel, J. A. Pérez-Martinez
Departamento de Química Organometálica
Universidad de Oviedo
E-33071 Oviedo (Spain)
Dr. S. García-Granda
Departamento de Química Física y Analítica
Universidad de Oviedo

[**] This work was supported by the Spanish Dirección General de Investigación Científica y Técnica (DGICYT) (Project PB88-0467), Metalúrgica del Nalón S. A., and the Fundación de Investigación Científica y Técnica (FICYT). J. A. P.-M. wishes to thank the FICYT for a grant. Cy = cyclohexyl.

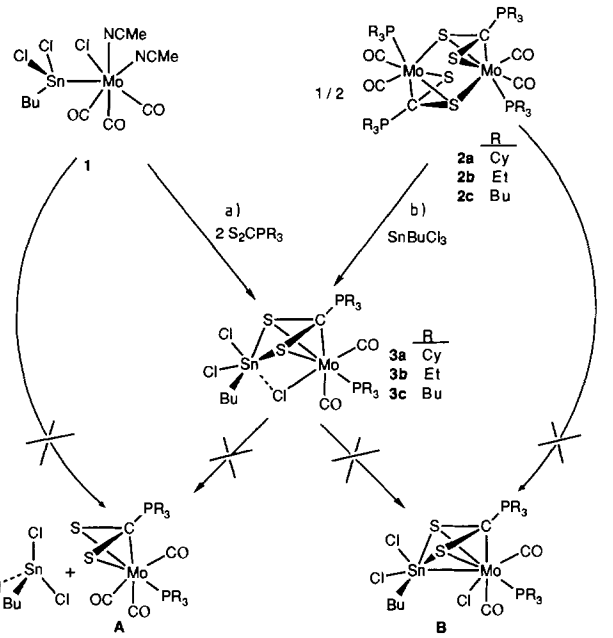

Scheme 1. Synthesis of **3** from **1** or **2**. The reaction of **1** to **A** is the complete reductive elimination of $SnBuCl_3$; that of **2** to **B**, the complete oxidative addition.

This suggests that the Mo–Cl(1) bond is normal and the Sn–Cl(1) bond is weak. A similar bonding relation is found in $[Mo(CO)_3(SnMeCl_2)(bipy)(Cl)]$[10] (bipy = 2,2′-bipyridine), which unlike **3a** contains a Sn–Mo single bond.

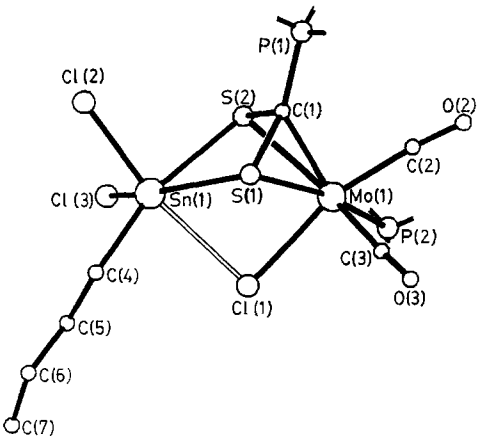

Fig. 1. Structure of **3a** in the crystal. (Hydrogen atoms and cyclohexyl substituents have been omitted for clarity.) Selected bond lengths [Å] and angles [°]: Mo(1)-S(1) 2.496(4), Mo(1)-S(2) 2.579(4), Mo(1)-C(1) 2.16(1), Sn(1)-S(1) 2.720(4), Sn(1)-S(2) 2.538(4), Mo(1)-P(2) 2.562(4), Mo(1)-C(2) 1.93(2), Mo(1)-C(3) 1.95(2), Sn(1)-C(4) 2.13(2); C(2)-Mo(1)-Cl(1) 164.1(5), C(3)-Mo(1)-Cl(1) 96.7(5), C(1)-Mo(1)-Cl(1) 109.7(4), P(2)-Mo(1)-Cl(1) 84.0(1), C(1)-Mo(1)-C(3) 118.2(6), C(1)-Mo(1)-P(2) 136.2(4), S(1)-Mo(1)-Cl(1) 82.5(1), S(1)-Mo(1)-C(2) 110.8(5), S(1)-Mo(1)-P(2) 164.3(1), S(2)-Mo(1)-Cl(1) 83.8(1), S(2)-Mo(1)-C(2) 108.5(5), S(2)-Mo(1)-C(3) 159.1(5), S(2)-Mo(1)-P(2) 100.6(1), C(3)-Mo(1)-P(2) 100.2(5), C(4)-Sn(1)-Cl(1) 87.6(7), C(4)-Sn(1)-Cl(2) 97.6(7), C(4)-Sn(1)-Cl(3) 102.4(6), Cl(2)-Sn(1)-Cl(1) 168.9(2), S(2)-Sn(1)-C(4) 164.1(6), S(1)-Sn(1)-Cl(3) 153.5(1).

Alternatively, the structure of **3a** can be viewed as consisting of a $SnBuCl_3$ group attached to a $Mo(CO)_2(PR_3)(S_2CPR_3)$ fragment similar to that existing in the dinuclear Mo(0) complex **2b** (R = ethyl). As a matter of fact, fresh

$[Mo(CO)_2(PR_3)(S_2CPR_3)]_2$ **2**

solutions of **2** (prepared as reported for **2b** in reference[5]) react with $SnBuCl_3$ in CH_2Cl_2 at room temperature (Reaction b in Scheme 1) to give the heterodinuclear complexes **3** in good yields.

The conversion of **1** to **3** (Reaction a in Scheme 1) involves the total cleavage of the Mo–Sn bond while a weak Sn ··· Cl bond is created; the Mo–Cl bond remains unaltered. Thus the reaction can be considered as an "incomplete" reductive elimination of $SnBuCl_3$ from the coordination sphere of molybdenum. The complete reductive elimination would lead to the formation of $SnBuCl_3$ and the Mo^0 complex **A** as found for the reaction of $[Mo(CO)_3(t\text{Bu-dab})(SnCl_3)(Cl)]$ (tBu-dab = tBuN=CH–CH=NtBu) with an isocyanide CNR′ to give $[Mo(CO)_3(t\text{Bu-dab})(CNR')]$.[11]

On the other hand, the complete oxidative addition of $SnBuCl_3$ to **2** (Reaction b) would give compound **B**. In this reaction one Mo–Sn bond and one Mo–Cl bond are formed while one Sn–Cl bond is cleaved. Instead, we found the reaction product to be complex **3** in which the Sn–Cl bond is relaxed, and one Mo–Cl (but not a Mo–Sn) bond is formed. Compound **3** appears to be, therefore, an intermediate in both the oxidative addition and the reductive elimination of $SnBuCl_3$ at molybdenum(0) centers and more stable than the expected final products **A** and **B**.

Since there is not a direct Mo–Sn bond in **3** and the Mo–Cl ··· Sn bridge is weak, we assume that the two metals are held together by the bridging S_2CPR_3 ligand which precludes the complete reductive elimination of the $SnBuCl_3$ group. We have already discussed the strong interaction between the η^2,η^3-S_2CPR_3 bridges and fragments of dinuclear complexes having a direct metal–metal bond in Mn–Mn and Mn–Re complexes. The metal-metal distances were 2.737(1) Å in $[Mn_2(CO)_6(S_2CPCy_3)]$,[1] 2.830(1) Å in $[MnRe(CO)_6(S_2CPCy_3)]$,[3] and 2.855(1) Å in $[Mn_2(CO)_4(S_2CPCy_3)(dppm)]$ (dppm = bis(diphenylphosphino)methane.[2] In the case of **3a**, the S_2CPR_3 adduct forms a fairly stable bridge between two different metals separated by 3.636(2) Å, showing a remarkable structural flexibility when coordinated in an $\eta^2(S,S')$, $\eta^3(S,C,S')$ fashion. It can be expected, therefore, that these S_2CPR_3 adducts could behave as ligands in other homo- or heterodinuclear systems with or without metal–metal bonds.

Experimental Procedure

Reaction a: To a solution of **1**[4] (0.2 g, 0.37 mmol) in CH_2Cl_2 (20 mL) were added CS_2 (3 mL, excess), and PCy_3 (0.177 g, 0.74 mmol) and the mixture was stirred for 30 min. After evaporation of the solvent in vacuo, the residue was extracted with a mixture of CH_2Cl_2/hexane (1:4). The combined extracts were filtered and concentrated in vacuo to afford **3a** as a dark red microcrystalline solid which was washed with hexane and dried. Yield 54%.

Reaction b: To a stirred solution of $[Mo(CO)_3(C_7H_8)]$ (0.2 g, 0.83 mmol) in CH_2Cl_2 (20 mL) were added CS_2 (4 mL, excess) and PCy_3 (0.397 g, 1.66 mmol). After 10 min $SnBuCl_3$ (0.138 mL, 0.83 mmol) was added and the mixture was stirred again for 15 min. The solvents were then evaporated and the residue was treated as described above. Yield 69%. **3b** and **3c** were prepared analogously.

Received: June 27, 1991 [Z 4751 IE]
German version: *Angew. Chem.* **1992**, *104*, 81

CAS Registry numbers:
1, 137400-33-0; **2a**, 137669-97-7; **2b**, 80137-00-4; **2c**, 137669-98-8; **3a**, 137669-99-9; **3a** · CH_2Cl_2, 137765-90-3; **3b**, 137670-00-9; **3c**, 137670-01-0; $[Mo(CO)_3(C_7H_8)]$, 12125-77-8; PCy_3, 2622-14-2; PEt_3, 554-70-1; PBu_3, 998-40-3; $SnBuCl_3$, 1118-46-3; CS_2, 75-15-0.

[1] D. Miguel, V. Riera, J. A. Miguel, X. Soláns, M. Font-Altaba, *J. Chem. Soc. Chem. Commun.* **1987**, 472.
[2] D. Miguel, V. Riera, J. A. Miguel, M. Gómez, X. Soláns, *Organometallics* **1991**, *10*, 1683.
[3] B. Alvarez, D. Miguel, V. Riera, J. A. Miguel, S. Garcia-Granda, *Organometallics* **1991**, *10*, 384.
[4] D. Miguel, J. A. Perez-Martinez, V. Riera, S. Garcia-Granda, *Polyhedron* **1991**, *10*, 1717.
[5] C. Bianchini, C. A. Ghilardi, A. Meli, S. Midollini, A. Orlandini, *Organometallics* **1982**, *1*, 778.
[6] E. Carmona, E. Gutiérrez-Puebla, A. Monge, P. J. Pérez, L. J. Sánchez, *Inorg. Chem.* **1989**, *28*, 2120.
[7] Correct elemental analysis for **3a–c**. Selected spectroscopic data (Conditions: IR in CH_2Cl_2; ^{31}P NMR: 121.5 MHz, $CDCl_3$, 85% H_3PO_4 external; $^{13}C\{^1H\}$ NMR: 75.5 MHz, $CDCl_3$, 25 °C, TMS; $^{119}Sn\{^1H\}$ NMR: 112 MHz, $CDCl_3$, 25 °C, $SnMe_4$); **3a**: IR: $\tilde{\nu}$ [cm^{-1}] = 1919 s, 1818 s (CO). $^{31}P\{^1H\}$ NMR: δ = 45.34 (s; $MoPCy_3$), 40.58 (s, J(P,Sn) = 57 Hz; S_2CPCy_3); $^{13}C\{^1H\}$ NMR: δ = 251.9 (dd, J(P,C) = 18 and 4 Hz; CO), 234.9 (d, J(P,C) = 6 Hz; CO), 65.3 (dd, J(P,C) = 47 and 3 Hz; S_2CP), 51.7 (s, J(C,Sn) = 699.6 Hz; C-1 (Bu)). – **3b**: IR: $\tilde{\nu}$ (cm^{-1}) = 1930 s, 1822 s. $^{31}P\{^1H\}$ NMR: δ = 48.48 (s, J(P,Sn): 54 Hz; S_2CPEt_3), 35.03 (s; $MoPEt_3$); $^{13}C\{^1H\}$ NMR; δ = 248.7 (dd, J(P,C) = 21 and 7 Hz: CO), 233.9 (d, J(P,C) = 6 Hz; CO), 69.1 (dd, J(P,C) = 67 and 4 Hz; S_2CP), 51.5 (s, J(C,^{119}Sn) = 832 Hz, J(C,^{117}Sn) = 794 Hz, C-1 (nBu)); $^{119}Sn\{^1H\}$ NMR: δ = 343.12 (d, J(^{119}Sn,P) = 55 Hz). – **3c**: IR: $\tilde{\nu}$ [cm^{-1}] = 1929 s, 1820 s (CO), $^{31}P\{^1H\}$ NMR: δ = 43.52 (s, J(P,Sn) = 52 Hz; S_2CPnBu_3), 28.30 (s; $MoPnBu_3$); $^{13}C\{^1H\}$ NMR: δ = 249.4 (dd, J(P,C) = 21 and 7 Hz; CO), 233.6 (d, J(P,C) = 6 Hz, CO), 69.6 (dd, J(P,C) = 67 and 5 Hz, S_2CP), 51.6 (s, J(C,Sn) = 816 Hz, C-1 (Snn′Bu).
[8] Crystal data for **3a**: $C_{43}H_{75}Cl_3MoO_2P_2S_2Sn \cdot CH_2Cl_2$, M_r = 1156.05, triclinic, space group $P\bar{1}$, a = 10.648(2), b = 14.483(3), c = 18.982(3) Å, α = 88.72(2), β = 79.55(1), γ = 80.15(2)°, V = 2845.7(9) Å^3, Z = 2, $\varrho_{calc.}$ = 1.35 g cm^{-3}, $F(000)$ = 1192, $\lambda(Mo_{K_\alpha})$ = 0.71073 Å, μ = 10.49 cm^{-1}, room temperature. Dark red prismatic crystal (0.4 × 0.4 × 0.25 mm) from CH_2Cl_2/hexane. Enraf–Nonius CAD4 diffractometer, ω-2θ scan technique. Of 10382 reflections measured ($0 \le \theta \le 25°$), 7500 used in the refinement ($I \ge 3\sigma(I)$). Mo and Sn atoms obtained from a Patterson synthesis, remaining nonhydrogen atoms by DIRDIF[11]. An absorption correction was applied with DIFABS[12]. Full-matrix least-squares refinement was made with SHELX-76[13]. All nonhydrogen atoms in the molecule of **3a** were refined anisotropically. Several peaks were found to correspond to disordered CH_2Cl_2 molecules. These were refined as rigid models in four positions (occupation factors 0.35, 0.35, 0.18, and 0.12); fixed overall isotropic temperature factor 0.15 Å^2. The hydrogen atoms were placed in calculated positions. Final R = 0.084. No weights applied. Total number of parameters 512. Further details of the crystal structure investigation are available on request from the Director of the Cambridge Crystallographic Data Centre, University Chemical Laboratory, Lensfield Road, GB-Cambridge CB2 1EW (UK), on quoting the full journal citation.
[9] M. S. Holt, W. L. Wilson, J. H. Nelson, *Chem. Rev.* **1989**, *89*, 11.
[10] M. Elder, D. Hall, *Inorg. Chem.* **1969**, *8*, 1268.
[11] A. Bell, R. Walton, *J. Organomet. Chem.* **1985**, *290*, 341.
[12] P. T. Beurskens, W. P. Bosman, H. M. Doesburg, T. E. M. van der Hark, P. A. Prick, J. H. Noordik, G. Beurskens, R. O. Gould, V. Parthasarathi, in *Conformation in Biology* (Eds.: R. Srinivasan, R. H. Sarma), Adenine Press, New York, **1982**, p. 389–406.
[13] N. Walker, D. Stuart, *Acta Crystallogr. Sect.* **1983**, *A39*, 158.
[14] G. M. Sheldrick, *SHELX-76. Program for Crystal Structure Determinations*, University of Cambridge, **1976**.

A Water-Complexed Organolithium Compound: $[LiCH(CN)_2 \cdot H_2O \cdot TMEDA]_\infty$ **

By *Christoph Lambert, Paul von Ragué Schleyer,* Ursula Pieper,* and *Dietmar Stalke*

Lithiated organic compounds are notoriously sensitive to hydrolysis. A dramatic exception, [OxLi · H_2O · TMEDA] (OxH = 2-mercaptobenzoxazole), was reported recently.[1a]

[*] Prof. Dr. P. v. R. Schleyer, Dipl.-Chem. C. Lambert
Institut für Organische Chemie der Universität Erlangen-Nürnberg, Henkestraße 42, D-W-8520 Erlangen (FRG)
Dipl.-Chem. U. Pieper, Dr. D. Stalke
Institut für Anorganische Chemie der Universität Göttingen, Tammannstrasse 4, D-W-3400 Göttingen (FRG)

[**] This work was supported by the Deutsche Forschungsgemeinschaft, and the Fonds der Chemischen Industrie. We thank Dr. R. Snaith, Dr. D. S. Wright, and D. Hoffmann for their interest and stimulation as well as Dr. W. Bauer in particular for determining the HOESY spectrum. (TMEDA = N,N,N′,N′-Tetramethylethylenediamine).

First prepared fortuitously, this complex has stimulated the development of synthetic strategies for obtaining other polar metalated organic compounds with aqua ligands.[1b,c] We now report the first structural characterization of an H_2O-containing complex of the lithium salt of a CH- (rather than a NH-) acid: $[LiCH(CN)_2 \cdot H_2O \cdot TMEDA]_\infty$ **1**. The X-ray structure shows several remarkable features: TMEDA is incorporated but $R(CH_3)_2N\cdots Li$ contacts are not evident; a three-dimensional H-bridged network is preferred instead.

Only a few nitriles are found among the many structurally characterized organolithium compounds.[2] Perhaps this is due to the tendency of metal salts with nitrile anions to polymerize.[3] Nevertheless, the relatively low pK_a of malononitrile (pK_a of $CH_2(CN)_2$ in dimethyl sulfoxide (DMSO) $=11$, in $H_2O=11$; pK_a (H_2O) in DMSO $=32$, in $H_2O=15.75$[4]) prompted our attempt to prepare a lithiated organic compound with aqua ligands. The lithiation of $CH_2(CN)_2$ with *n*BuLi in tetrahydrofuran (THF) resulted in the precipitation of an amorphous solid, which did not dissolve upon addition of TMEDA; however, the precipitate did dissolve when a small amount of water was added. The water molecules evidently were incorporated into a less highly aggregated lithiomalononitrile complex.[5] Recrystallization of the isolated product from a 2:1 mixture of THF and diethyl ether gave crystals of **1** suitable for X-ray analysis.[6]

As shown in Figure 1, **1** exhibits a three-dimensional polymeric structure comprising lithiomalonodinitrile, TMEDA, and water in a 1:1:1 molar ratio. The topology of the repeating $(H_2O \cdot LiNCCHCN)_n$ unit is remarkably similar to that in $[LiCH(CN)_2 \cdot HMPA]_\infty$ (HMPA = hexamethylphosphoric triamide) reported by Weiss et al.[2a] Both show the same connectivity of the malonodinitrile anion, the lithium cation, and the hetero atom of the ligand (HMPA in the structure of Weiss et al., water in ours). Our structure is elaborated further by remarkably short intermolecular hydrogen bonds between each of the water hydrogens and a TMEDA nitrogen (the N3···H1 and the N4···H2 separations are 185.4 and 186.0 pm, respectively; the O1···H1 and the O1···H2 distances are 87.4 and 90.4 pm). The electron density distribution shows two maxima of electron density along the N–O vectors. One maximum was refined to give 80% probability of occupation, the other, 20%. Therefore we reasoned that 80% of the molecular units comprise TMEDA-complexed water molecules $[(C_4H_{10}N)NMe_2\cdots HOH\cdots Li\cdots(C_3HN_2)]_n$, while the other 20% resulted from hydrolysis $[(C_4H_{10}N)NMe_2H^+\cdots OH^-\cdots Li^+\cdots(C_3HN_2)]_n$. Support for this partial hydrolysis is provided by an IR spectrum (KBr) which exhibits a small, but sharp OH^- stretching band at 3540 cm^{-1} and a very broad and intense H_2O stretching band at 3600–2600 cm^{-1}. These values are similar to those reported by Jones for $LiOH \cdot H_2O$.[7] In addition we found a split R_3N^+–H stretching vibration at 2370 cm^{-1}.[8]

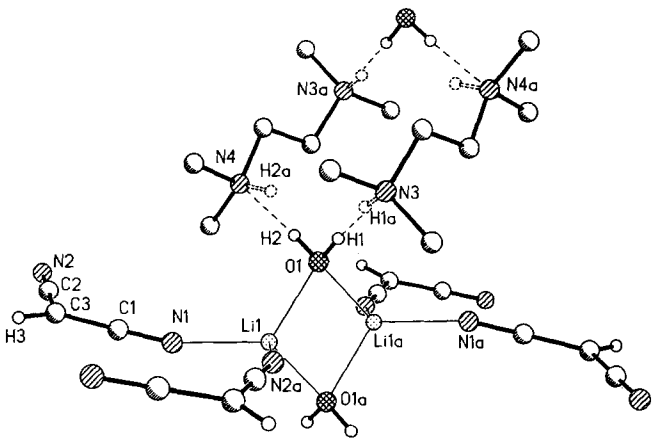

Fig. 1. Structure of **1** in the solid state. Selected bond distances [pm] and angles [°]: Li1-O1 201.8(3), Li1-O1a 197.6(3), Li1-N1 202.1(3), Li1-N2a 202.0(3), O1-H1 87.4(21), O1-H2 90.4(26), O1···N3 272.7(2), O1···N4 276.0(2), O1···H1a 190.5(22), O1···H2a 202.8(26), N3···H1 185.4(21), N4···H2 186.0(22), C1-N1 116.1(2), C1-C3 138.5(2), C2-N2 115.6(2), C2-C3 139.0(3), C3-H3 90.4(24); N1-Li1-N2a 105.7(1), O1-Li1-O1a 90.1(1), Li1-O1-Li1a 89.9(1), N1-C1-C3 178.9(2), N2-C2-C3 179.2(2), C2-C3-H3 118.4(15), C1-C3-H3 121.1(15), C1-C3-C2 120.4(2), Li1-N1-C1 166.7(2), H1-O1-H2 109.0(21).

These features contribute to the binding in the remarkable three-dimensional lattice structure of **1**. In contrast, the HMPA derivative of Weiss et al. has an essentially two-dimensional layer arrangement. Both structures exhibit $-CN\cdots Li^+\cdots NC-$ contacts between different malononitrile anions. The H_2O planes in **1** are approximately perpendicular to the nearly square-planar Li_2O_2 four-membered rings. The lack of TMEDA–Li interactions is unprecedented and is the second remarkable feature of the structure of **1**. Since TMEDA is a bidentate ligand, its complexation to lithium should be favored over that of water.[9] Innumerable solid-state structures of lithium compounds exhibit TMEDA ligand complexation.[10] But the structural preference in **1** results from the ability of water to function simultaneously as donor and acceptor. Each water molecule hydrogen-bonds to two TMEDA molecules and *each* binds two lithium atoms. TMEDA cannot function in this manner. The synergistic binding characteristics of the water molecules result in the preferred coordination in **1**. This emphasizes the point made by Snaith et al.[1c] that pK_a considerations alone are insufficient to determine whether water will be incorporated into lithiated organic solid-state structures.

The structural parameters of the lithiomalonodinitrile unit are in good agreement with those reported by Weiss et al.[2a] We found a planar malonodinitrile anion with an angle sum of 359.9° at C3 and a C1-C3-C2 angle of 120.4(2)° indicating the trigonal planar geometry of the central carbon atom. The average C–C and C–N distances are 138.8 pm and 115.9 pm, respectively. While the C–N distance in **1** is 0.8 pm less than that in malononitrile (116.7 pm),[11] the C–C distance is 8.0 pm less. Similar values are found in other lithionitriles.[2] The Li–N distances (202 pm) are slightly shorter than those in dimeric lithionitriles with a square-planar Li_2N_2 arrangement which exhibit two Li–N contacts per nitrile group (Li–N distances: 204–211 pm).[2b,c] The Li–O distances are 201.8 and 197.6 pm, respectively. Bridging water ligands are rare in solid-state lithium structures. They are present, however, in $LiOH \cdot H_2O$ and in $LiClO_4 \cdot 3H_2O$; the Li–O distances are 197.4 and 212.4 pm, respectively.[12]

While the structure and aggregation state of **1** in solution is of interest, colligative measurements[13] unfortunately are not applicable. A ^6Li, ^1H HOESY spectrum (HOESY = *H*eteronuclear *O*verhauser *E*ffect *S*pectroscopy)[14] of **1** in THF shows one lithium signal and cross peaks with all the signals of the hydrogen atoms (methylene-H, H_2O, TMEDA). This indicates that in THF solution a) lithium is coordinated by water and/or by TMEDA, and b) at least one species with an –HCLi– unit is involved. The observed cross peak between H3 and Li indicating the proximity between these atoms can only be rationalized by a close Li–C3 contact as supported by MNDO and *ab initio* calculations.[15] In the ^1H NMR spectrum at -100 °C in THF, no splitting of

the H_2O signal is detected. This suggests that the proton exchange between the TMEDA nitrogen and the H_2O oxygen atoms is rapid in solution.

Experimental Procedure

To a solution of 428 mg (6.48 mmol) malonodinitrile in 15 mL THF at −78 °C was added dropwise 4.06 mL (6.5 mmol) 1.6 M *n*BuLi in hexane. While the mixture was warmed to −50 °C and stirred for ca. 2 h, a precipitate (occasionally a brownish oil) formed. This dissolved on further addition of 10 mL THF, 4 mL (26.5 mmol) TMEDA, and (in particular) 0.6 mL (33 mmol) water. After stirring for 12 h at room temperature the mixture was filtered. The filtrate was concentrated under reduced pressure to one-third of its original volume. This solution was filtered and cooled to −18 °C. Colorless needles of **1** formed, were washed with ether, and dried in vacuo. Yield: 500 mg (37%). Single crystals were obtained by recrystallization in a 2:1 THF/diethyl ether mixture at 5 °C. Correct C, H, N analyses.

^{1}H NMR (400 MHz, [D_8]-THF, 25 °C): δ = 3.92 (s, 2H, H_2O), 2.33 (s, 4H, CH_2 (TMEDA)), 2.17 (s, 12H, CH_3, (TMEDA)), 1.35 (s, 1H, CH). ^{13}C NMR (100.6 MHz, [D_8]-THF, 25 °C): δ = 131.7 (CN), 58.5 (CH_2 (TMEDA)), 46.1 (CH_3 (TMEDA)), −1.5 (CH). IR(KBr) $\tilde{\nu}$[cm^{-1}] = 2190 m, 2130 m, 2100 m (CN).

Received: July 24, 1991 [Z 4821 IE]
German version: *Angew Chem.* **1992**, *104*, 78

CAS Registry numbers:
1, 137516-88-2; $[LiCH(CN)_2 \cdot H_2O]_2$, 137516-87-1; $CH_2(CN)_2$, 109-77-3.

[1] a) D. Barr, P. R. Raithby, P. von R. Schleyer, R. Snaith, D. S. Wright, *J. Chem. Soc. Chem. Commun.* **1990**, 643; b) D. R. Armstrong, D. Barr, P. R. Raithby, P. von R. Schleyer, R. Snaith, D. S. Wright, *Inorg. Chim. Acta* **1991**, *185*, 163; c) P. Mukulcik, P. R. Raithby, R. Snaith, D. S. Wright, *Angew. Chem.* **1991**, *103*, 452; *Angew. Chem. Int. Ed. Engl.* **1991**, *30*, 428; d) An example of an ethanol-complexed Li-nitronate: K. Klebe, K. H. Böhn, M. Marsch, G. Boche, *ibid.* **1987**, *99*, 62 and **1987**, *26*, 78.

[2] a) K. Jens, J. Kopf, N. P. Lorenzen, E. Weiss, *Chem. Ber.* **1988**, *121*, 1201; b) G. Boche, M. Marsch, K. Harms, *Angew. Chem.* **1986**, *98*, 373; *Angew. Chem. Int. Ed. Engl.* **1986**, *25*, 373; c) W. Zarges, M. Marsch, K. Harms, G. Boche, *ibid.* **1989**, *101*, 1424; d) G. Boche, K. Harms, M. Marsch, *J. Am. Chem. Soc.* **1988**, *110*, 6925; e) W. Zarges, M. Marsch, K. Harms, G. Boche, *Chem. Ber.* **1989**, *122*, 1307; f) G. Boche, *Angew. Chem.* **1989**, *101*, 286; *Angew. Chem. Int. Ed. Engl.* **1989**, *28*, 277; g) W. Hiller, G. Boche, W. Zarges, K. Harms, M. Marsch, R. Wollert, K. Dehnicke, *Chem. Ber.*, in press.

[3] J. Fatiadi, *Synthesis* **1978**, *165*, 241.

[4] F. G. Bordwell, *Acc. Chem. Res.* **1988**, *21*, 456.

[5] An aggregation state of less than 10 monomer units of **1** in solution is supported by spin lattice relaxation time measurements made by ^{13}C NMR spectroscopy.

[6] Crystal data: $C_9H_{19}LiN_4O$, M = 206.2, monoclinic, space group $P2_1/c$, a = 8.292(2), b = 14.086(3), c = 11.315(2) Å, β = 104.55(3)°, V = 1279.2(5) Å^3, Z = 4, $\varrho_{calc.}$ = 1.071 Mgm^{-3}, 4393 collected (8.0° < 2θ < 55.0°), 2925 independent, and 2094 observed reflections ($F \geq 3.0\sigma$ (F)), 212 refined parameters, R = 0.053, wR = 0.045; all data were collected on a Siemens-Stoe AED diffractometer at 153 K with $Mo_{K\alpha}$ (λ = 0.71073 Å) radiation. The structure was solved by direct methods (SHELXTL PLUS). All nonhydrogen atoms were refined anisotropically, the hydrogen atoms isotropically except H 1a and H 2a which were refined with fixed isotropic U values and restrained N–H distanees (85.0 pm). Further details of the crystal structure investigation are available on request from the Fachinformationszentrum Karlsruhe, Gesellschaft für wissenschaftlich-technische Information mbH, D-W-7514 Eggenstein-Leopoldshafen 2 (FRG), on quoting the depository number CSD-55645, the names of the authors, and the journal citation.

[7] L. H. Jones, *J. Chem. Phys.* **1954**, *22*, 217.

[8] N. B. Colthup, L. H. Daly, S. E. Wiberly, *Introduction to Infrared and Raman Spectroscopy*, Academic Press, New York, **1964**, p. 281–282.

[9] a) E. Kaufmann, J. Gose, P. von R. Schleyer, *Organometallics* **1989**, *8*, 2577; b) C. Lambert, P. von R. Schleyer, unpublished.

[10] a) W. N. Setzer, P. von R. Schleyer, *Adv. Organomet. Chem.* **1985**, *24*, 353; b) K. Gregory, P. von R. Schleyer, R. Snaith, *Adv. Inorg. Chem.*, in press.

[11] E. Hirota, Y. Morino, *Bull. Chem. Soc. Jpn.* **1960**, *33*, 705.

[12] a) N. W. Alcock, *Acta Crystallogr. Sect. B* **1971**, *27*, 1682; b) S. Chomnilpan, R. Liminga, R. Tellgren, *ibid.* **1977**, *33*, 3954.

[13] W. Bauer, D. Seebach, *Helv. Chim. Acta* **1984**, *67*, 1972.

[14] For descriptions of ^{6}Li, ^{1}H HOESY see e.g.: a) W. Bauer, T. Clark, P. von R. Schleyer, *J. Am. Chem. Soc.* **1987**, *109*, 970; b) W. Bauer, P. von R. Schleyer, *Magn. Reson. Chem.* **1988**, *26*, 827.

[15] C. Lambert, P. von R. Schleyer, unpublished.

Lithiodiphenylmethylisocyanide-(−)-sparteine-bis(tetrahydrofuran): Crystal Structure of a Lithiated Isocyanide**

By *Burkhard Ledig, Michael Marsch, Klaus Harms,* and *Gernot Boche**

Dedicated to Professor Ulrich Schöllkopf

Although lithiated isocyanides have not been systematically investigated for very long[1]—the isomeric lithiated cyanides were discovered one hundred years earlier[2]—their versatility in preparative chemistry is well documented.[3] Experiments aimed at stabilizing a negative charge with an isocyanide group showed that this stabilization is a result of the inductive effect (field effect) of the strongly electronegative sp-hybridized N atom. A conjugative interaction is thus negligible.[4] Further verification was found in quantum mechanical[5,6] and photoelectron spectroscopical[6] investigations of the H_2C^-–NC anion and the metalated isocyanides Li(Na,MgH)CH_2–NC. These studies predicted that in the transition from H_3C–NC to H_2C^-–NC the C–N and N=C bond lengths change only insignificantly (Table 1) and that the anionic C atom remains pyramidal (though with a low inversion barrier of 2.8 kcal mol^{-1}).

Table 1. Structural parameters of H_3C–N=C (experimental) [7] and H_2C^-–N=C (calculated) [5d]; r [pm], ∢ [°].

	r(C–N)	r(N=C)	∢ HCH	∢ HCN	∢ CNC
H_3C–NC	142.4	116.6	109.8	109.1	180
H_2C^-–NC	143.1	115.4	109.9	107.4	175.8

We report here the first structural determination of an isocyanide "anion": lithiodiphenylmethylisocyanide-(−)-sparteine-bis(tetrahydrofuran) (**1** · sparteine · 2 THF). In the crystal **1** · sparteine · 2 THF is monomeric (Fig. 1). The Li atom is bound to C1 of the isocyanide group, to N2 and N3 of the (−)-sparteine ligand, and to O1 of one THF molecule. The second THF molecule is not coordinated to Li.[8] The N1–C1 bond of the isocyanide group (116.2(1) pm) is almost as long as the related bond in the neutral H_3C–NC (116.6 pm, see Table 1) and somewhat longer than the average N–C bond in $C_{sp^2(sp^3)}$-bonded isocyanides (114.6(114.5) pm[13]) as well as the calculated bond length in H_2C^-–NC (115.4 pm, see Table 1). The C2–N1 bond (137.8(9) pm) is roughly as long as the related bond in C_{sp^2}-bonded neutral isocyanides; the mean value calculated from eight compounds is 139.0 pm.[13,14] The sp^2 hybridization of C2, which is deduced from the angle sum of C2 (360°), is due to the conjugation of the negative charge on C2 with the two phenyl rings. The torsion angles are accordingly small (N1-C2-C9-C14 −6(1) and N1-C2-C3-C4 −8(1)°). The C1-N1-C2 angle (178.4(6)°) shows that this unit is almost linear. Thus, the bond lengths and angles in the C^-–NC moiety of **1** · sparteine · 2 THF agree well with the theoretical predictions of $H_2C_2^-$–NC, and the inductive stabilization of the negative charge is structurally proven. The pyramidal geometry about the anionic C atom and the predicted aggregation to a dimer with a Li-C-N-C-Li-C-N-C eight-membered

[*] Prof. Dr. G. Boche, Dipl.-Chem. B. Ledig, M. Marsch, Dr. K. Harms
Fachbereich Chemie der Universität
Hans-Meerwein-Strasse, D-W-3550 Marburg (FRG)

[**] This research was supported by the Fonds der Chemischen Industrie and the Deutsche Forschungsgemeinschaft (SFB 260).

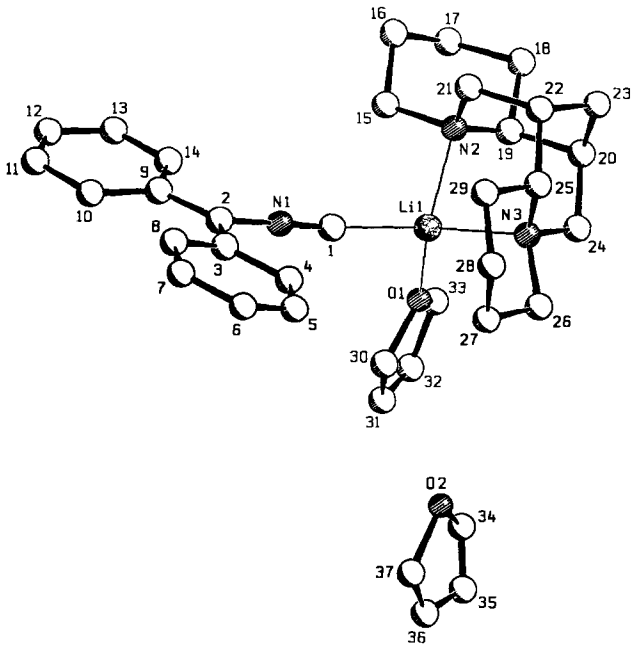

Fig. 1. Crystal structure of **1** · sparteine · 2 THF [8, 12]. Important bond lengths [pm] and angles [°]. (In the numbering of the carbon atoms in the graphic representation the element symbol was omitted.) C2-N1 137.8(9), N1-C1 116.2(10), C1-Li1 210(2); Li1-N2 206.5(13), Li1-N3 210.3(12), Li1-O1 194(2); Li1-C1-N1 176.8(8), C1-N1-C2 178.4(6), N1-C2-C9 113.6(6), N1-C2-C3 116.0(6), C3-C2-C9 130.4(7).

ring is not observed, however, in the case of **1** · sparteine · 2 THF . This is undoubtably due to the influence of the two phenyl substituents (instead of two H atoms) on the anionic C atom. **1** · Sparteine · 2 THF, as the only structurally characterized metalated isocyanide, contrasts dramatically with the large number of structurally characterized transition metal complexes with neutral isocyanide ligands.[15] Most of these contain an almost linear N=C–metal arrangement, the same as that in **1** · sparteine · 2 THF; here the N1-C1-Li1 angle is 176.8(8)°. Remarkably, the short distance between Li1 and the (nonionic!) C1 in the title molecule is only 210(2) pm.

Received: August 16, 1991 [Z 4873 IE]
German version: *Angew. Chem.* **1992**, *104*, 80

CAS Registry numbers:
1 · sparteine · THF, 137595-29-0; **1** · sparteine · 2 THF, 137595-28-9; diphenylmethylisocyanide, 3128-85-6; (−)-sparteine, 90-39-1.

[1] U. Schöllkopf, F. Gerhart, *Angew. Chem.* **1968**, *80*, 842–843; *Angew. Chem. Int. Ed. Engl.* **1968**, *7*, 805, and references therein.
[2] P. Kurtz, *Methoden Org. Chem. (Houben-Weyl) 4th Ed.* **1952**, Band 8, p. 349.
[3] a) U. Schöllkopf, *Angew. Chem.* **1970**, *82*, 795–805; *Angew. Chem. Int. Ed. Engl.* **1970**, *9*, 763; b) U. Schöllkopf, *Methoden Org. Chem. (Houben-Weyl) 4th Ed.* **1970**, Band 13/1, p. 234; c) D. Hoppe, *Angew. Chem.* **1974**, *86*, 878–893; *Angew. Chem. Int. Ed. Engl.* **1974**, *13*, 795; d) U. Schöllkopf, *ibid.* **1977**, *89*, 351–360 and **1977**, *16*, 339; e) U. Schöllkopf, *Pure Appl. Chem.* **1979**, *51*, 1347–1355; f) Syntheses with *p*-toluene sulfonyl methyl isocyanide: A. M. van Leusen, *Heterocycl. Chem.* **1980**, *5*, 111.
[4] M. P. Periasamy, H. M. Walborsky, *J. Am. Chem. Soc.* **1977**, *99*, 2631–2638.
[5] a) M. H. Lien, A. C. Hopkinson, M. A. McKinney, *J. Mol. Struct. THEOCHEM* **1983**, *105*, 37–47; b) A. C. Hopkinson, M. A. McKinney, M. H. Lien, *J. Comput. Chem.* **1983**, *4*, 513; c) D. J. Swanton, G. B. Backskay, G. D. Willett, N. S. Hush, *J. Mol. Struct. THEOCHEM* **1983**, *91*, 313–323; d) J. Kaneti, P. von R. Schleyer, T. Clark, A. J. Kos, G. W. Spitznagel, J. G. Andrade, J. B. Moffat, *J. Am. Chem. Soc.* **1986**, *108*, 1481–1492.
[6] S. Moran, H. B. Ellis, Jr., D. J. DeFrees, A. D. McLean, S. E. Paulson, G. B. Ellison, *J. Am. Chem. Soc.* **1987**, *109*, 6004–6010.
[7] M. Kessler, H. Ring, R. Trambornio, W. Gordy, *Phys. Rev.* **1950**, *79*, 54.
[8] **1** · Sparteine · 2 THF crystallizes in the monoclinic space group $P2_1$, $a = 921.6(10)$, $b = 1766.7(10)$, $c = 1098(2)$ pm, $\beta = 107.65(7)°$, $V = 1703(4)$ Å^3, $Z = 2$, $\rho_{calc} = 1.127$ g cm^{-3} for $M = 577.8$, $\mu = 0.498$ mm^{-1}. A crystal (0.6 × 0.4 × 0.3 mm) was measured at 163 K on an Enraf-Nonius four-circle diffractometer with a graphite monochromator using $Cu_{K\alpha}$ radiation. Of the 4606 measured reflections 4279 were unique ($R_{int} = 0.0533$) and 3467 observed ($F > 4\sigma(F)$). Solution (PATSEE)[9] and refinement with the SHELXTL PLUS (VMS) program,[10] $R = 0.0837$, $wR = 0.0764$; nonhydrogen atoms, anisotropic; H atoms with set isotropic temperature factors at calculated positions, 387 parameters. The high temperature factors and unusual geometry parameters arise from the disorder of the single THF molecule, which could not be resolved. The data were corrected with the DIFABS program.[11] Further details of the crystal structure investigation may be obtained from the Fachinformationszentrum Karlsruhe, Gesellschaft für wissenschaftlich-technische Information mbH, D-W-7514 Eggenstein-Leopoldshafen 2 (FRG) on quoting the depository number CSD-320245, the names of the authors, and the journal citation.
[9] E. Egert, *PATTSEE Fragment Research by Integrated Patterson and Direct Methods*, Universität Göttingen **1985**.
[10] G. M. Sheldrick, *SHELXTL-Plus: Siemens Analytical X-Ray Instruments*, Madison (USA).
[11] N. Walker, D. Stuart, *Acta Crystallogr. Sect. A* **1983**, *39*, 158–166.
[12] Preparation of **1** · sparteine · 2 THF: Diphenylmethylisocyanide (100 mg, 0.52 mmol) was dissolved in 1.5 mL tetrahydrofuran and treated with (−)-sparteine (143.3 mg, 0.62 mmol). The deprotonation was accomplished at −78° with *n*-butyllithium in *n*-hexane (0.62 mmol of a 1.6 M solution). The reaction mixture was kept at −28° for 12 h, after which time crystals suitable for structural analysis were removed from the solution.
[13] Cambridge Structural Data Base, Version 4.5, July **1991**. F. H. Allen, O. Kennard, R. Taylor, *Acc. Chem. Res.* **1983**, *16*, 146–153.
[14] The corresponding mean obtained from 23 sp^2-bound isocyanides is 145.6 pm[13].
[15] a) E. Singleton, H. E. Oosthuizen, *Adv. Organomet. Chem.* **1983**, *22*, 209–310, with references to other review articles and many original reports; b) a more recent report: F. E. Hahn, M. Tamm, *Angew. Chem.* **1991**, *103*, 213–215; *Angew. Chem. Int. Ed. Engl.* **1991**, *30*, 203.

Concave Wrapped Protons: Reagents for Contra-Thermodynamic Protonations**

By *Ulrich Lüning** and *Michael Müller*

Dedicated to Professor Horst Prinzbach on the occasion of his 60th birthday

No widely applicable reagent for selective, and in particular stereoselective, protonations is known.[1] A very promising solution to this problem is offered by concave reagents, which are standard reagents of organic chemistry built into concave structural units.[2] The class of compounds that contains pyridine rings in a concave arrangement (concave

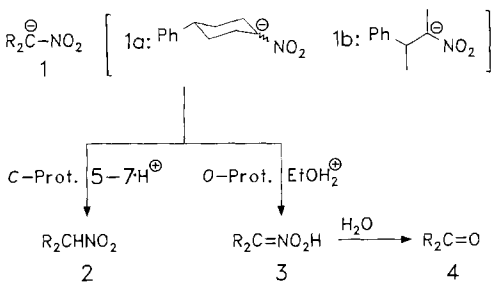

Scheme 1. Protonation reactions with nitronate ions **1**.

[*] Priv.-Doz. Dr. U. Lüning, Dipl.-Chem. M. Müller
Chemisches Laboratorium der Universität
Albertstrasse 21, D-W-7800 Freiburg (FRG)

[**] Concave Reagents, Part 10. This work was supported by the Fonds der Chemischen Industrie and the Deutsche Forschungsgemeinschaft. We thank Prof. C. Rüchardt for his generous support. Part 9: U. Lüning, R. Baumstark, W. Schyja, *Liebigs Ann. Chem.* **1991**, 999.

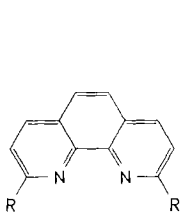

5

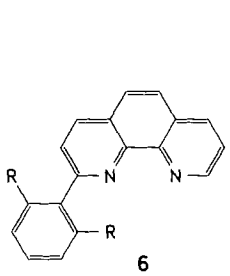

6

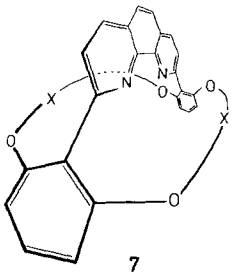

7

Table 1. Substituents R of compounds **5** and **6** and bridging units X of compounds **7**.

	R		R		–X–
5a	H	**6a**	H	**7a**	$-CH_2(CH_2OCH_2)_2CH_2-$
5b	Me	**6b**	Me		
5c	Ph	**6c**	OMe	**7b**	$-CH_2(CH_2OCH_2)_3CH_2-$
		6d	OAc		
		6e	$OCOtBu$	**7c**	$-(CH_2)_{10}-$
5d	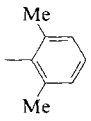	**6f**	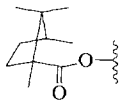		
5e	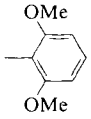	**6g**	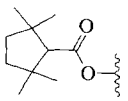		
5f	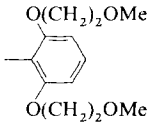	**6h**	OH		

pyridines) has already been studied in connection with their substrate-[3] and chemoselectivity[4] in protonation reactions of "nitronate" ions (Scheme 1). Competition between the *C*-protonation of the nitronate ions **1** by protonated, concave pyridines yielding **2** and the Nef reaction[5] affording the carbonyl compounds **4** (soft Nef reaction[4]) is observed in these buffers.

On the other hand, the stereoselectivity of the nitronate ion reprotonation by buffers of concave macrocyclic pyridines (and also by concave 1,10-phenanthrolines **7**, see Table 1) was minimal.[4] But with buffers of 2-aryl-1,10-phenanthrolines **6**, which are not as sterically hindered as a concave pyridine[4] or a concave 1,10-phenanthroline **7**, good stereoselectivities are observed for the reprotonation of the nitronate ions **1**. Table 2 lists these selectivities, as well as the proportion of the (soft) Nef reaction products **4**, for the transformation of anions **1** with buffers of different bases under standard conditions.[6] Using as example the protonation of **1a** by **6c**, we could show that the stereoselectivity depended little on the concentration[7] of the buffer, but strongly on the solvent.[8] Alcohols were the media that provided the largest selectivities.

A comparison of the stereoselectivities in Table 2 reveals three facts: a) Compounds **2** are produced with high stereoselectivity only when bis-*ortho*-substituted 2-aryl-1,10-phenanthrolines **6** are the proton source. b) More reagents react stereoselectively with the cyclic anion **1a** than with the more flexible acyclic anion **1b**. c) In both cases the thermodynamically *less stable* product is favored (*cis*-**2a**, *threo*-**2b**).

How can one explain that the bis-*ortho*-substituted arylphenanthrolines **6**, in particular, react so selectively and that thermodynamically *less stable* products are formed preferentially? The data in Table 2 for 2-phenyl-1,10-phenanthroline (**6a**) and the bis-*ortho*-substituted 2-aryl-1,10-phenanthrolines **6** show a distinct increase in selectivity on the introduction of *ortho* substituents. A possible explanation is that the *ortho* substituents cause a twisting of the molecule. The steric consequence is that the concave (arched) form of the 2-phenyl-1,10-phenanthroline **6a** is supplemented by a similar arched expansion into the third dimension (Fig. 1). In protonated form the proton to be transferred is more strongly shielded in this domed form and the reagent is therefore more selective.

Table 2. Product distribution for the reprotonation of the nitronate ions **1** by substituted 1,10-phenanthrolines **5** and **6** and bimacrocyclic 1,10-phenanthrolines **7**.

Proton Source [13]	**4a** [%]	**1a → 2a** **2a** [%]	*cis*-**2a**/ *trans*-**2a**	**4b** [%]	**1b → 2b** **2b** [%]	*threo*-**2b**/ *erythro*-**2b** [a]
thermodynamic equilibrium [17]			0.2–0.25			<1
5a [b]	17	84	3.4	20	80	0.9
5b [b]	67	33	0.7	72	28	1.2
5c [c]	>99	–	–	–	–	–
5d [c]	95	5	1.5	–	–	–
5e [c]	86	14	1.0	–	–	–
5f [c]	17	83	0.8	–	–	–
6a [c]	45	55	1.5	–	–	–
6b [b]	55	45	8.0	–	–	–
6c [c]	3	97	8.7	10	90	1.0
6d [c]	30	70	2.7	22	78	10.4
6e [b]	25	75	16.1	37	63	1.1
6f [b]	10	90	13.3	4	96 [d]	27.4 [d]
6g [b]	17	83	12.6	39	61	0.9
7a [c]	4	96	0.7	–	–	–
7b [c]	6	94	0.7	–	–	–
7c [c]	–	100	0.7	–	–	–

[a] The assignment of the diastereoisomers **2b** was achieved by catalytic reduction (Pd/C, $NH_4^+HCOO^-$, MeOH) [18] of one of the isomers to the amine, which was isolated as the hydrochloride in 86% yield. M.p.(crude product) = 193 °C, m.p. (from benzene) = 210 °C. (Lit.: *erythro*-**2b**: 212–212.5 °C [19], 218.1–218.5 °C [20], *threo*-**2b**: 137–138 °C [19]). [b] Homogeneous reaction mixture. [c] Inhomogeneous reaction mixture. [d] The chiral reagent **6f** did not lead to enantioselectivity in the case of **1b**, because the anion mixture **1b** was racemic and formed the *threo* product (*RS*/*RS*, 96%); that is, the intramolecular asymmetric 1,2-induction dominated. The selectivity of **6f** is thus determined only by the steric and not by the chiral properties of the acyl substituent.

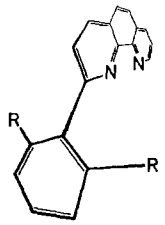

Fig. 1. A twist of the 2,6-disubstituted phenyl ring against the 1,10-phenanthroline unit extends the concave shielding of the proton-binding region of 1,10-phenanthroline into another dimension.

On consideration of the conformation of **6** shown in Figure 1, an equatorial protonation of **1a** appears easier because axial protonation involves interactions with the H atoms in the 3- and 5-position (1,3-diaxial interaction, see ref. [9]). For a discussion of the protonation of **1b**, however, various conformations for the anion must be considered. For steric reasons an *anti* attack with respect to the phenyl ring in **1b** by the protonated concave 1,10-phenanthroline **6** · H^+ is most likely. Since in this orientation the phenyl residue interacts strongly with the (solvated) nitro group, a twisting is probable. In this twisted form the major difference between the two diastereoisomeric transition states **8** is the **6** · H^+/Me or **6** · H^+/H interaction (Fig. 2). Transition state

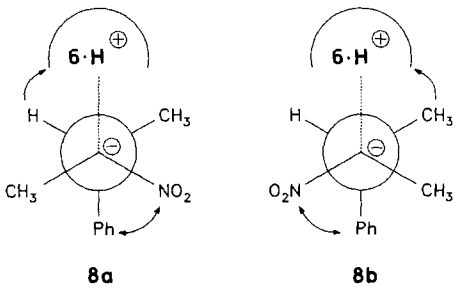

8a **8b**

Fig. 2. Diastereomeric transition states **8** for the attack of a proton "wrapped" in a concave 2-aryl-1,10-phenanthroline (**6**) on the nitronate ion **1b**.

8a is thus more favorable and leads to the thermodynamically less stable *threo* product.

Thus for protonation of both anions **1a** and **1b** with concave 1,10-phenanthrolines **6** · H^+, the more favorable transition state affords the thermodynamically less stable product. In each case the largest pseudosubstituent in the transition state leads to the smallest substituent, a H atom, in the product. The secret of forming the thermodynamically less stable stereoisomer stereoselectively in protonation reactions lies in "wrapping" the protons[10] in a way that ensures that they will be the larger substituents in the transition state. This is undoubtedly not only true for the protonation of the nitronate ions shown here, but should apply to most other anions too.[11] Moreover, a concave wrapping for hydride ions (H^-) and hydrogen atoms ($H^·$) should also lead to high stereoselectivity, as investigations of reduction reactions of cyclohexanones[9] and stereoselective H-capture by radicals[12] suggest.

Experimental Procedure

For experimental details, see [13]. A solution of potassium-*tert*-butoxide (19 mg, 0.17 mmol), the nitro compounds **2a** or **2b** (0.11 mmol) and [18]crown-6 (51 mg, 0.19 mmol) in 2 mL of dry ethanol was stirred for 15 h [14]. For each reprotonation experiment, 40 µL of this solution was added to mixtures of base (0.22 mmol) and *p*-toluenesulfonic acid monohydrate (11.4 mg, 0.06 mmol) in 1 mL dry ethanol. The reaction mixture was stirred for 16 h at room temperature, whereupon 2 N HCl (0.5–1.0 mL), water (2 mL), and diethyl ether (4 mL) was added and the phases were separated. The aqueous phase was extracted with 4 mL of diethyl ether, and the combined organic phase was washed with ca. 2 mL of water, and dried over $MgSO_4$. The sample was concentrated, and analyzed by gas chromatography (Carlo-Erba 4130, Carlo-Erba GC 6000 Vega or Carlo-Erba HRGC 5300 Mega; column: SE 30/25 m (from the company J&W [15]); 180 °C isothermally or OV 17/15 m temperature program: 160 °C for 5 min and heating at 5 °C per min to 240 °C.

Received: July 17, 1991
Revised: October 4, 1991 [Z 4798 IE]
German version: *Angew. Chem.* **1992**, *104*, 99

CAS Registry numbers:
1a, 29916-50-5; **1b**, 128575-88-2; **5a**, 66-71-7; **5b**, 484-11-7; **5c**, 25677-69-4; **5d**, 124318-71-4; **5e**, 124318-69-0; **5f**, 137572-10-2; **6a**, 109559-47-9; **6b**, 124318-72-5; **6c**, 124318-70-3; **6d**, 137572-11-3; **6e**, 137572-12-4; **6f**, 137572-13-5; **6g**, 137594-03-7; **6h**, 137572-14-6; **7a**, 137572-15-7; **7b**, 137572-16-8; **7c**, 137572-17-9.

[1] Some examples of stereo- and enantioselective protonations: a) S. Hünig, N. Klaunzer, R. Schlund, *Angew. Chem.* **1987**, *99*, 1322; *Angew. Chem. Int. Ed. Engl.* **1987**, *26*, 1281; b) U. Gerlach, S. Hünig, *ibid.* **1987**, *99*, 1323 and **1987**, *26*, 1283; c) D. Potin, K. Williams, J. Rebek, Jr., *ibid.* **1990**, *102*, 1485 and **1990**, *29*, 1420; d) H. E. Zimmermann, *Acc. Chem. Res.* **1987**, *20*, 263; e) C. Fehr, J. Galindo, *J. Am. Chem. Soc.* **1988**, *110*, 6909; f) L. Duhamel, P. Duhamel, S. Fouquay, J. J. Eddine, O. Peschard, J.-C. Plaquevent, A. Ravard, R. Solliard, J.-Y. Valnot, H. Vincens, *Tetrahedron* **1988**, *44*, 5495, and references cited therein; g) J. Jähme, C. Rüchardt, *Angew. Chem.* **1981**, *93*, 919; *Angew. Chem. Int. Ed. Engl.* **1981**, *20*, 885; h) H. Pracejus, G. Pohl, *Liebigs Ann. Chem.* **1969**, *722*, 1; i) R. D. Larsen, E. G. Corley, P. Davis, P. J. Reider, E. J. Grabowski, *J. Am. Chem. Soc.* **1989**, *111*, 7650; j) G. Coutois, L. Miginiac, *J. Organomet. Chem.* **1974**, *69*, 1; k) J. Tanaka, M. Nojima, S. Kusabayashi, S. Nagase, *J. Chem. Soc. Perkin Trans. 2* **1987**, 673; l) Review: H. Waldmann, *Nachr. Chem. Tech. Lab.* **1991**, *39*, 413.
[2] Concave Reagents 8: U. Lüning, R. Baumstark, M. Müller, *Liebigs Ann. Chem.* **1991**, 987, and references cited therein.
[3] Concave Reagents 6: U. Lüning, F. Schillinger, *Chem. Ber.* **1990**, *123*, 2073.
[4] Concave Reagents 4: U. Lüning, R. Baumstark, M. Müller, C. Wangnick, F. Schillinger, *Chem. Ber.* **1990**, *123*, 221.
[5] Review: H. W. Pinnick, *Organic Reactions* **1990**, *38*, 655.
[6] By changing the concentration of the buffer solution, the ratio of *O*- to *C*-protonation can be varied over a wide range [4].
[7] The concentration of the buffer ([**6c**] + [**6c** · H^+]) was varied between 55 and 220 mM. Although the mixture was heterogeneous above 126 mM, the *cis*/*trans* stereoselectivity of the protonation changed only slightly over the whole concentration range (on average 9:1).
[8] The solvent for the buffer solution **6c**/**6c** · H^+ was varied from nonpolar and aprotic solvents such as ethers to polar, protic solvents such as alcohols. Only mixtures in acetonitrile, DMF, and DMSO were homogeneous.
[9] For example, E. C. Ashby, J. T. Laemmle, *Chem. Rev.* **1975**, *75*, 521.
[10] The "wrapping" must still allow sufficiently fast reaction rates for the protonation and deprotonation. For a kinetically extremely hindered, protonated polymacrocycle, see H. Takemura, T. Shinmyozu, T. Inazu, *J. Am. Chem. Soc.* **1991**, *113*, 1323.
[11] Also the α/γ-selectivity of the protonation of the triphenylsilylallyl anion may be varied from 2:1 (water/acetic acid) to 1:10 by the use of 2,6-bis(2,6-dimethylphenyl)benzoic acid! C. Wangnick, *Dissertation*, Universität Freiburg **1991**.
[12] For the stereoselective generation of thermodynamically unstable products by $H^·$ transfer to 2,3-disubstituted succinic acid anhydride 2-yl radicals, see a) B. Giese, J. Meixner, *Tetrahedron Lett.* **1977**, 2783; b) B. Giese, G. Kretzschmar, *Chem. Ber.* **1984**, *117*, 3175; c) B. Giese, *Angew. Chem.* **1989**, *101*, 993; *Angew. Chem. Int. Ed. Engl.* **1989**, *28*, 969. For stereoselective formation of *cis* alkenes by hydrogen transfer to 2-substituted vinyl radicals, see c) and d) S. Lachhein, *Dissertation*, Technische Hochschule Darmstadt **1982**.
[13] For experimental details see also [3] and [4]. The aryl-1,10-phenanthrolines **5** and **6**, and the bimacrocyclic 1,10-phenanthrolines **7** were synthesized analogous to [16]. The dihydroxy compound **6h** can be prepared analogously to 2,9-bis(2,6-dihydroxyphenyl)-1,10-phenanthroline.
[14] The deprotonation to form the nitronate ions is already complete after 2 h.
[15] Isomerization of the stereoisomers of **2a** was observed on a GC column from Macherey & Nagel (SE 30/50 m).
[16] Concave Reagents 5: U. Lüning, M. Müller, *Chem. Ber.* **1990**, *123*, 643.
[17] When distinctly more basic buffers (e.g. NaOPh/PhOH) were used, the stereoisomers formed under kinetic control isomerized in a protonation/deprotonation equilibrium.
[18] a) S. Ram, R. E. Ehrenkaufer, *Synthesis* **1986**, 133; b) A. G. M. Barrett, C. D. Spilling, *Tetrahedron Lett.* **1988**, *29*, 5733.
[19] F. Y. Rachinskii, N. M. Vinokurova, *Zhur. Obshch. Khim.* **1954**, *24*, 272; [*Chem. Abstr.* **1955**, *49*, 4553c].
[20] D. J. Cram, J. E. McCarty, *J. Am. Chem. Soc.* **1954**, *76*, 5740.

(Isocyanide)ruthenate Analogues of Tetracarbonylferrate**

By *Joseph A. Corella II, Robert L. Thompson,* and *N. John Cooper**

We recently reported the synthesis of K[Co(CNPh*)$_4$] (K-**1**) (CNPh* = 2,6-$Me_2C_6H_3NC$), the first isocyanide transition-metalate.[1] The low frequencies (1890 (sh) and 1815 (vs) cm^{-1}) of the $\nu_{C\equiv N}$ absorptions of K-**1** are consistent with bent rather than linear isocyanide ligands,[1, 2] and we speculated that the ligands bend as a consequence of back-donation from the electron-rich metal into the isocyanide π^* orbitals.[1, 3] Calculations indicate that the π-acceptor character of $CNCH_3$ increases markedly as the CNC angle decreases.[6] The $\nu_{C\equiv N}$ frequencies of $\mathbf{1}^-$ are similar to those of the bent isocyanide ligands in [Fe(CN*t*Bu)$_5$],[4b, c] but well above C=N stretching frequencies. This raised the intriguing possibility that even stronger π backbonding might allow isocyanides to stabilize even lower oxidation states than Co^{-I}. This, and the obvious analogy to the rich chemistry of the tetracarbonylferrate dianion,[7] led us to explore the synthesis of tetraisocyanide complexes of the Group 8 metals in the $-II$ oxidation state. We now report that (isocyanide)-ruthenates $[Ru(CNR)_4]^{2-}$ are accessible as reactive intermediates, and that they undergo oxidative addition reactions with a range of electrophiles (Scheme 1).

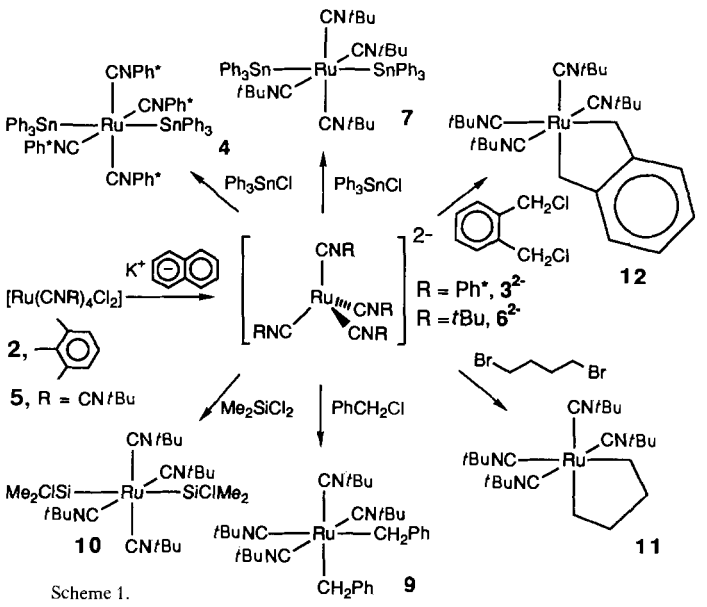

Scheme 1.

We synthesized $[Ru(CNR)_4]^{2-}$ complexes by reduction of the Ru^{II} isonitrile complexes $[Ru(CNR)_4X_2]$ **2** and **5**[8] with potassium–naphthalene in tetrahydrofuran (THF). In a typical experiment, K[$C_{10}H_8$] (4 equiv) readily reduced *trans*-[Ru(CNPh*)$_4$Cl$_2$] (**2**) to give a clear, burgundy-red solution. The $\nu_{C\equiv N}$ absorption of **2** at 2140 (s) cm^{-1} had been replaced by bands at 1670 (vs br) and 1580 (s) cm^{-1}, indicative of the formation of a highly reduced (isocyanide)ruthenate, formulated as K_2[Ru(CNPh*)$_4$] (K_2-**3**).[9] Attempts to isolate a salt of $\mathbf{3}^{2-}$ have been unsuccessful to date, but we have been able to chemically derivatize K_2-**3** by oxidative addition of 2 equiv of Ph_3SnCl[1, 10] to give [Ru(CNPh*)$_4$(SnPh$_3$)$_2$] (**4**) in 75% yield. The solubility of **4** in hexane, together with the ^{1}H NMR equivalence of all the CNPh* ligands, strongly suggests exclusive formation of the *trans* isomer.

Our inability to characterize a salt of $\mathbf{3}^{2-}$ by crystallography raises the question whether $\mathbf{3}^{2-}$ contains discrete isocyanide ligands or (*N,N'*-dialkyldiamino)acetylene ligands, which could be formed by a coupling reaction analogous to that observed by Lippard et al. in the reduction of some early transition-metal isocyanide complexes.[11] The IR data fail to distinguish between these possibilities, but three arguments suggest that $\mathbf{3}^{2-}$ contains discrete isocyanide ligands: 1) this is not a sterically crowded environment of the type which favors reductive coupling;[11] 2) the derivative **4** contains discrete isocyanide ligands; 3) we have established crystallographically that the isoelectronic anion in [K(dme)]-[Co(CNPh*)$_4$] is tetrahedral and contains discrete, bent isocyaniide ligands.[12]

The synthesis of dianionic isocyanide complexes of ruthenium is not limited to aryl isocyanides and *trans*-[Ru(CN-*t*Bu)$_4$Cl$_2$][8] (**5**) underwent similar potassium–naphthalene reduction at $-78\,^\circ C$. IR spectra indicated consumption of the starting material, but the highly reduced product was too thermally unstable to be observed spectroscopically. We have, however, provided chemical evidence for the formation of a dianionic isocyanide complex, K_2[Ru(CN*t*Bu)$_4$] (K_2-**6**), since the addition of Ph_3SnCl furnished *trans*-[Ru(CN*t*Bu)$_4$-(SnPh$_3$)$_2$] (**7**) following a workup similar to that used to isolate *trans*-**4**.

Si- and C-centered electrophiles also undergo oxidative addition to K_2-**6**. IR monitoring of the reaction of fresh solutions of K_2-**6** with 2 equiv of $PhCH_2Cl$, CH_3I, or Me_2SiCl_2 at $-78\,^\circ C$ suggested that bisadducts are formed. The presumed dimethyl derivative [Ru(CN*t*Bu)$_4$Me$_2$] (**8**) was too unstable to isolate, but the dibenzyl derivative

Table 1. Spectroscopic data for compounds **4**, **7**, and **9**–**12**. (All compounds provided correct C,H,N analyses.)

4: IR (THF): ν(C≡N) = 2085 cm^{-1}; ^{1}H NMR (C_6D_6, 500 MHz): δ = 7.94 (m, 12H, *ortho*-H of $SnPh_3$), 6.95 (m, 18H, *meta*- and *para*-H of $SnPh_3$), 6.70 (t, J = 7.6 Hz, 4H, *para*-H of $C_6H_3Me_2$), 6.63 (d, J = 7.8 Hz, 8H, *meta*-H of $C_6H_3Me_2$), 1.99 (s, 24H, Me); ^{13}C NMR (CD_2Cl_2, 75 MHz): δ = 167.0 (C≡N), 148.1 (*ipso*, $SnPh_3$), 137.4 (*ortho*, $SnPh_3$), 134.0 (*ortho*, Ph*), 128.6 (*ipso*, Ph*), 127.3 (*meta*, Ph*), 127.1 (*meta*, $SnPh_3$), 126.9 (*para*, $SnPh_3$), 126.3 (*para*, Ph*), 18.5 (CH_3).

7: IR (hexane): ν(C≡N) = 2119 (s), 2085 (m, sh) cm^{-1}; ^{1}H NMR (CD_2Cl_2, 500 MHz): δ = 7.66 (m, 12H, *ortho*-H of $SnPh_3$), 7.20 (m, 18H, *meta*- and *para*-H of $SnPh_3$), 0.97 (s, 36H, Me).

9: IR (THF): ν(C≡N) = 2110 (s, br), 2050 (s, br) cm^{-1}; ^{1}H NMR ([D_6]acetone, 500 MHz): δ = 7.00 (d, J = 6.8 Hz, 4H, *ortho*-H of Ph), 6.90 (t, J = 7.6 Hz, 4H, *meta*-H of Ph), 6.53 (t, J = 7.2 Hz, 2H, *para*-H of Ph), 1.89 (s, 4H, CH_2), 1.40 (s, 18H, Me), 1.25 (s, 18H, Me).

10: IR (THF): ν(C≡N) = 2130 (s), 2090 (m, sh) cm^{-1}; ^{1}H NMR (C_6D_6, 300 MHz): δ = 1.42 (s, 36H, CMe_3), 0.60 (s, 12H, $SiMe_2$).

11: IR (hexane): ν(C≡N) = 2108 (m), 2070 (s), 2020 (m, sh) cm^{-1}; ^{1}H NMR (C_6D_6, 500 MHz): δ = 2.46 (m, 4H, $RuCH_2$), 1.81 (m, 4H, $RuCH_2CH_2$), 1.15 (s, 18H, CH_3), 1.12 (s, 18H, CH_3); ^{13}C NMR (C_6D_6, 125 MHz): δ = 167.2 (s, C≡N), 166.9 (s, C≡N), 54.8 (s, CMe_3), 38.9 (t, $^1J_{CH}$ = 122 Hz, $RuCH_2CH_2$), 31.5 (qm, $^1J_{CH}$ = 122 Hz, CH_3), 31.2 (qm, $^1J_{CH}$ = 122 Hz, CH_3), 14.4 (t, $^1J_{CH}$ = 125 Hz, $RuCH_2$).

12: IR (hexane): ν(C≡N) = 2115 (m, sh), 2072 (s), 2040 (m, sh) cm^{-1}; ^{1}H NMR (CD_2Cl_2, 500 MHz): δ = 6.92 (m, 2H, $C_6H_2H_2$), 6.61 (m, 2H, $C_6H_2H_2$), 2.07 (s, 4H, CH_2), 1.44 (s, 18H, CH_3), 1.20 (s, 18H, CH_3); ^{13}C NMR (CD_2Cl_2, 125 MHz): δ = 164.0 (s, C≡N), 163.2 (s, C≡N), 158.0 (s, *ipso*-C_{arom}), 128.8 (dd, $^1J_{CH}$ = 150 Hz, $^3J_{CH}$ = 8 Hz, C_{arom}), 121.1 (dd, $^1J_{CH}$ = 154 Hz, $^3J_{CH}$ = 8 Hz, C_{arom}), 55.8 (s, CMe_3), 55.6 (s, CMe_3), 31.7 (q, $^1J_{CH}$ = 127 Hz, CH_3), 31.1 (q, $^1J_{CH}$ = 127 Hz, CH_3), 15.0 (td, $^1J_{CH}$ = 124 Hz, $^3J_{CH}$ = 3 Hz, CH_2).

[*] Prof. Dr. N. J. Cooper, J. A. Corella II, R. L. Thompson
Department of Chemistry, University of Pittsburgh
Pittsburgh, PA 15260 (USA)

[**] We thank the U.S. National Science Foundation for generous financial support through Grant 8722424 and Dr. Garry Warnock and Patricia Leach for stimulating discussions.

$[Ru(CNtBu)_4(CH_2Ph)_2]$ (**9**) and $[Ru(CNtBu)_4(SiMe_2Cl)_2]$ (**10**) were both isolated in good yield (78% and 71%, respectively). NMR spectra indicate that **10**, like **4** and **7**, is formed as the *trans* isomer, while **9**, surprisingly, is formed as the *cis*.

Extensions of these reactions to more complex alkyls have already, for example, led to the preparation of five-membered metallacycles. Stoichiometric quantities of α,ω-dihaloalkyls such as 1,4-dibromobutane and α,α'-dichloro-*o*-xylene were added to freshly prepared solutions of K_2-**6** to give the respective complexes **11** and **12** in reasonable yield (40% each).

The accessibility of K_2-**3** and K_2-**6** as reactive intermediates supports our previous suggestion that the ability of isocyanides to stabilize metals in negative oxidation states has been severely underestimated. The chemistry of the (isocyanide)metalates appears as rich and diverse as that of carbonylmetalates. The successful preparation of a range of Sn, Si, and C-centered derivatives of K_2-**3** and K_2-**6** more specifically supports the analogy between these complexes and tetracarbonylferrate. Thus the path to other (isocyanide)-ruthenates with other functional groups has been paved.

Experimental Procedure

4: A solution of **2** (0.35 g, 0.5 mmol) in THF (25 mL) was reduced by dropwise addition of 4.2 molar equiv of a 0.47 M solution of $K[C_{10}H_8]$ in THF (4.25 mL) at $-78\,^{\circ}C$ to give a clear, burgundy-red solution. Dropwise addition of Ph_3SnCl (0.39 g, 1 mmol) in THF (10 mL) gave a clear tan solution, which was warmed to room temperature, and the solvent was removed under reduced pressure. The product **4** was extracted into warm hexane. When the solution was slowly cooled to $-78\,^{\circ}C$, white needles (0.49 g, 0.3 mmol) formed. **7**, **9**, **10**, **11**, and **12** were prepared by procedures similar to those used to prepare **4**.

Received: July 30, 1991 [Z 4837 IE]
German version: *Angew. Chem.* **1992**, *104*, 55

CAS Registry numbers:
2, 128507-02-8; K_2-**3**, 137822-91-4; **4**, 137822-92-5; **5**, 64315-53-3; K_2-**6**, 137822-93-6; **7**, 137822-94-7; **9**, 137822-95-8; **10**, 137822-96-9; **11**, 137822-97-0; **12**, 137822-98-1; $K[C_{10}H_8]$, 4216-48-2; Ph_3SnCl, 639-58-7; Me_2SiCl_2, 75-78-5; 1,4-dibromobutane, 110-52-1; α,α'-dichloro-*o*-xylene, 612-12-4.

[1] G. F. Warnock, N. J. Cooper, *Organometallics* **1989**, *8*, 1826.
[2] For a review of transition-metal isocyanide complexes see: a) L. Malatesta, *Prog. Inorg. Chem.* **1959**, *1*, 283; b) L. Malatesta, F. Bonanti, *Isocyanide Complexes of Transition Metals*, Wiley, New York, 1969; c) P. M. Treichel, *Adv. Organomet. Chem.* **1973**, *11*, 21; d) Y. Yamamoto, *Coord. Chem. Rev.* **1980**, *32*, 193; e) E. Singleton, M. E. Oosthuizen, *Adv. Organomet. Chem.* **1983**, *22*, 209.
[3] Similar explanations have been advanced to account for the bending of isocyanide ligands in the few cases for which this has been crystallographically established [4, 5].
[4] a) G. K. Barker, A. M. R. Galas, M. Green, J. A. K. Howard, F. G. A. Stone, T. W. Turney, A. J. Welch, P. Woodward, *J. Chem. Soc. Chem. Commun.* **1977**, 256; b) J.-M. Bassett, M. Green, J. A. K. Howard, F. G. A. Stone, *ibid.* **1977**, 853; c) J.-M. Bassett, D. E. Berry, G. K. Barker, M. Green, J. A. K. Howard, F. G. A. Stone, *J. Chem. Soc. Dalton Trans.* **1979**, 1003.
[5] a) J. Chatt, C. M. Elson, A. J. L. Pombeiro, R. L. Richards, G. H. D. Royston, *J. Chem. Soc. Dalton Trans.* **1978**, 165; b) A. J. L. Pombeiro, J. Chatt, R. L. Richards, *J. Organomet. Chem.* **1980**, *190*, 297.
[6] J. A. S. Howell, J.-Y. Saillard, A. LeBeuze, G. Jaouen, *J. Chem. Soc. Dalton Trans* **1982**, 2533.
[7] a) J. P. Collman, *Acc. Chem. Res.* **1975**, *8*, 342; b) J. P. Collman, L. S. Hegedus, J. R. Norton, R. G. Finke, *Principles and Applications of Organotransition Metal Chemistry*, University Science Books, Mill Valley, CA, USA, 1987, p. 755.
[8] L. Malatesta, G. A. Padoa, A. Sonz, *Gazz. Chim. Ital.* **1955**, *85*, 1111.
[9] The 1670 cm^{-1} absorption does not have a Lorentzian line shape and is tentatively assigned to C≡N stretching absorptions of an isocyanide complex which exists as multiple ion pairs, while the narrower 1580 cm^{-1} absorption is assigned to ring-breathing modes of the 2,6-$Me_2C_6H_3NC$ ligand.
[10] For leading references see: V. S. Leong, N. J. Cooper, *Organometallics* **1987**, *6*, 2000.
[11] a) C. T. Lam, P. W. R. Corfield, S. J. Lippard, *J. Am. Chem. Soc.* **1977**, *99*, 617; b) C. M. Giandomenico, C. T. Lam, S. J. Lippard, *ibid.* **1982**, *104*, 1263; c) S. Warner, S. J. Lippard, *Organometallics* **1986**, *5*, 1716.
[12] P. A. Leach, J. A. Corella II, S. J. Geib, N. J. Cooper, unpublished.

Enantiomerically Pure Tertiary Alcohols by TADDOL-Assisted Additions to Ketones—or How to Make a Grignard Reagent Enantioselective**

By *Beat Weber* and *Dieter Seebach**

Tertiary stereogenic centers are generally more difficult to generate selectively than secondary ones, as evidenced by the few examples of C–C bond formation with enantio- and diastereoselective nucleophilic addition to ketones.[1] Thus, we were very happy to see that primary alkyl Grignard reagents in the presence of TADDOL (**1**) magnesium alkoxide (TADDOL: $\alpha,\alpha,\alpha',\alpha'$-tetraaryl-2,2-dimethyl-1,3-dioxolane-4,5-dimethanol) add to aryl, vinyl, and alkynyl ketones with enantioselectivities up to >99:1.

The general procedure, which was optimized for acetophenone (products **2**–**8**), is quite straightforward: TADDOL[2] is doubly deprotonated with 2 equivalents of Grignard reagent, and to the resulting solution in THF is added another equivalent of RMgBr (resulting in an approximately 0.1 M diolate and RMgBr solution). The reaction mixture is cooled to $-100\,^{\circ}C$ and a ketone is added to the resulting suspension. After stirring at $-100\,^{\circ}C$ for 9 h, the reaction mixture is given an aqueous workup [Eq. (a)]. The results summarized

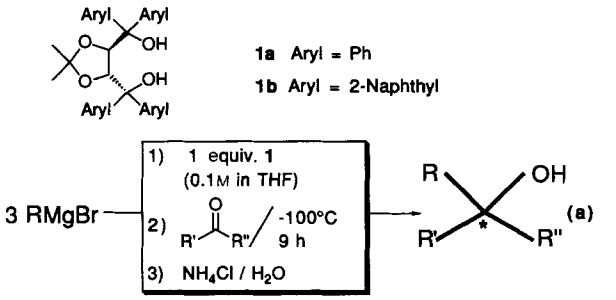

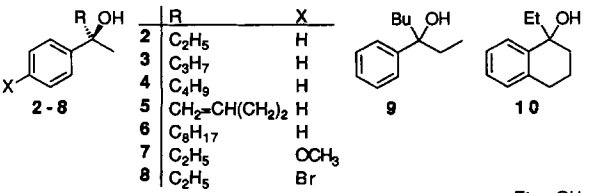

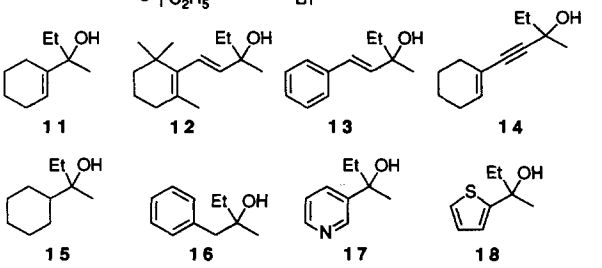

in Table 1 were obtained with 0.5 mmol runs, but larger scale reactions are also possible (see the Experimental Procedure).

The following reaction characteristics have been observed to date:

[*] Prof. Dr. D. Seebach, Dipl. Chem. B. Weber
Laboratorium für Organische Chemie der
Eidgenössischen Technischen Hochschule
ETH-Zentrum, Universitätstrasse 16, CH-8092 Zürich (Switzerland)

[**] The results described herein are part of the projected dissertation of B. Weber; first presented at the ESOC-7 Symposium, Namur (July 17, 1991).

Table 1. Addition of Grignard reagents to ketones in the presence of $(BrMg)_2$ diolates of **1** [Eq. (a)]. Ratios of enantiomers were determined by GC analyses on cyclodextrin capillary columns; >99:1 means that the second enantiomer cannot be detected. The optical rotations are given for $[\alpha]_D^{rt}$ values in methanol.

R in RMgBr and in **2**–**8**	TADDOL	Ketone	No.	Product yield [%]	Ratio of Enantiomers (Rotation)
C_2H_5	**1a**	$C_6H_5COCH_3$ [a]	**2** (X = H)	62	99:1 (+)
C_3H_7	**1a**	$C_6H_5COCH_3$	**3** (X = H)	84	>99:1 (+)
C_4H_9	**1a**	$C_6H_5COCH_3$ [b]	**4** (X = H)	75	>99:1 (+)
$(CH_2)_2CH{=}CH_2$	**1a**	$C_6H_5COCH_3$	**5** (X = H)	60	>99:1 (−)
C_6H_{17}	**1a**	$C_6H_5COCH_3$	**6** (X = H)	58	>99:1 (+)
C_2H_5	**1a**	$4\text{-}(CH_3O)C_6H_4COCH_3$	**7** (X = OCH_3)	76	96:4 (+)
C_2H_5	**1a**	$4\text{-}BrC_6H_4COCH_3$	**8** (X = H)	90	97:3 (+)
C_4H_9	**1a**	$C_6H_5COC_2H_5$	**9**	7	95:5 (−)
C_2H_5	**1a**	α-tetralone	**10**	28	95:5 (+)
C_2H_5	**1b**	α-tetralone	**10**	12	97:3 (+)
C_2H_5	**1a**	1-cyclohexenyl methyl ketone	**11**	56	85:15 (−)
C_2H_5	**1a**	β-ionone	**12**	64	92:8 (−)
C_2H_5	**1a**	(*E*)-4-(phenyl-3-buten-2-one	**13**	40 [c]	85:15
C_2H_5	**1a**	4-(1-cyclohexenyl)-3-butyn-2-one	**14**	88	88:12
C_4H_9	**1a**	cyclohexyl methyl ketone	**15**	trace	62:38
C_2H_5	**1a**	benzyl methyl ketone	**16**	22	75:25
C_2H_5	**1a**	3-acetylpyridine	**17**	50	98:2 (+)
C_2H_5	**1a**	2-acetylthiophene	**18**	43	98:2 (+)

[a] This reaction was run 3 times (0.5–10 mmol scale) yielding **2** with 97.7–98.3% *ee*; 10 mmol scale run see below. [b] At −78 °C: 69% yield, ratio of enantiomers 94:6. [c] In addition to **13** the 1,4-adduct $PhCH(Et)CH_2COCH_3$ was also formed (40% yield, ratio of enantiomers 70:30).

a) Addition of ethyl- and propylmagnesium bromide to acetophenone occurs from the *Re*-face (determined by comparison of the optical rotation of **2** and **3** with literature data[3a]). For this reason all compounds of the same type (**2**–**8**) are shown with (*R*)-configuration.

b) Even with only 0.25 equivalents of the **1a** Mg alkoxide the (+)-enantiomer of **4** was formed preferentially (92:8).[3b]

c) Steric hindrance (especially from iC_3H_7 and tC_4H_9 Grignard reagents, higher aryl ketones, or *ortho*-tolyl methyl ketone) decreases the rate of reaction drastically (products **9** and **10**).

d) With the tetra-β-naphthyl-TADDOL **1b**[2a] the enantioselectivity may be somewhat greater than with the tetraphenyl analogue (product **10**).[3c]

e) Aliphatic methyl ketones do not react as well as aromatic ones (products **11**–**16**).

f) The heteroaromatic methyl ketones 3-acetylpyridine and 2-acetylthiophene give good results (products **17** and **18**).

g) If the solvent is changed from THF to Et_2O (under otherwise identical conditions) stereoselectivity is lost.

h) Stereoselectivity is much lower for reactions with benzaldehyde than with aromatic methyl ketones. However, a reversal of the stereochemical course is observed in this case when the solvent is changed from THF to Et_2O [Eq. (b)].[3d]

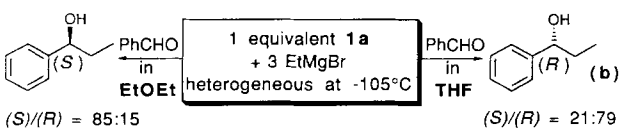

The effect caused by the addition of chiral alkoxides to polar organometallic compounds has been thoroughly investigated for Li compounds (LiX effect)[4] and can be rationalized by assuming either aggregate formation $[(metal\text{-}R)_m(metal\text{-}X^*)_n]$ (here RMgOR* as well), or by chiral Lewis acid (R*OMgBr) activation of the ketone in the rate-determining step. Whatever the mechanism of this reaction is (heterogeneous reaction mixture!), the high degree of enantioselectivity obtained in a nucleophilic alkyl-transfer to a keto carbonyl group is unprecedented.

Experimental Procedure

2: In a 250 mL Schlenk tube equipped with magnetic stirring bar and PT100 thermometer, 10 mmol (4.66 g) TADDOL **1a** was dissolved in 40 mL of THF (distilled from K) under argon atmosphere and cooled to −70 °C. To the colorless solution was added 31 mmol (8.9 mL 3.5 M in ether) EtMgBr. The cooling bath was removed, another 70 mL THF added, and the reaction mixture allowed to warm to room temperature. The colorless solution was then cooled to −105 °C[5] resulting in the formation of a colorless precipitate. Under vigorous stirring 9.4 mmol (1.13 g) acetophenone was added. Stirring was continued for 9 h at −105° to −100 °C. Afterwards the reaction mixture was quenched with 40 mL of a saturated NH_4Cl solution and ether was added. The organic layer was separated, washed with brine, and dried over anhydrous Na_2SO_4. The solvent was removed under reduced pressure and the product was freed from TADDOL by distillation in a kugelrohr apparatus (0.1 Torr, 150 °C). Crude **2** (1.17 g, ratio of enantiomers 99:1) was obtained, containing 20% acetophenone. Pure **2** was isolated after flash chromatography (solvent: pentane/ether 10:1) and distillation. Yield: 0.88 g (62%), ratio of enantiomers 99:1, $[\alpha]_D^{rt} = +17.3$ (neat).

Received: August 26, 1991 [Z 4890 IE]
German version: *Angew. Chem.* **1992**, *104*, 96.

CAS Registry numbers:
1a, 93379-48-7; **1b**, 137365-09-4; **2**, 1006-06-0; **3**, 52992-90-2; **4***R*, 73464-88-7; **4***S*, 19641-54-4; **5**, 137628-36-5; **6**, 137628-37-6; **7***R*, 137628-38-7; **7***S*, 137628-39-8; **8***R*, 137628-40-1; **8***S*, 137628-41-2; **9***R*, 137628-42-3; **9***S*, 137524-67-5; **10***R*, 137628-43-4; **10***S*, 137628-44-5; **11***R*, 137628-45-6; **11***S*, 137628-46-7; **12***R*, 137694-58-7; **12***S*, 137694-59-8; **13***R*, 137694-60-1; **13***S*, 137694-61-2; **14***R*, 137628-47-8; **14***S*, 137647-80-4; **15***R*, 115921-18-1; **15***S*, 33204-54-5; **16***R*, 55016-95-0; **16***S*, 56640-51-8; **17***R*, 137628-48-9; **18***R*, 137628-49-0; EtMgBr, 925-90-6; PrMgBr, 927-77-5; BuMgBr, 693-03-8; 4-(1-cyclohexenyl)-3-butyn-2-one, 13757-03-4; (*R*)-4-phenylhexan-2-one, 115651-75-7; (*S*)-4-phenylhexan-2-one, 16460-85-8; (*S*)-α-ethylbenzenemethanol, 613-87-6; (*R*)-α-ethylbenzenemethanol, 1565-74-8; bromo-3-butenylmagnesium, 7103-09-5; bromooctylmagnesium, 17049-49-9; acetophenone, 98-86-2; 4-methoxyacetophenone, 100-06-1; 4-bromoacetophenone, 99-90-1; propiophenone, 93-55-0; α-tetralone, 529-34-0; 1-cyclohexenyl methyl ketone, 932-66-1; β-ionone, 79-77-6; (*E*)-4-phenyl-3-buten-2-one, 1896-62-4; cyclohexyl methyl ketone, 823-76-7; benzyl methyl ketone, 103-79-7; 3-acetylpyridine, 350-03-8; 2-acetylthiophene, 88-15-3; benzaldehyde, 100-52-7.

[1] For some diastereoselective syntheses of β-hydroxycarbonyl derivatives (aldols) which are *formally* derived from ketones (*tert*-hydroxy groups) see: D. Seebach, L. Widler, *Helv. Chim. Acta* **1982**, *65*, 1972–1981; D. A. Evans, M. D. Ennis, T. Le, N. Mandel, G. Mandel, *J. Am. Chem. Soc.* **1984**, *106*, 1154–1156; D. Seebach, U. Gysel, J. N. Kinkel, *Chimia* **1991**, *45*, 114–117 and literature cited therein.

[2] Syntheses of TADDOLs and their application in Ti-catalyzed enantioselective additions of R_2Zn to aldehydes are described in: a) A. K. Beck, B. Bastani, D. A. Plattner, W. Petter, D. Seebach, H. Braunschweiger, P. Gysi, L. LaVeccia, *Chimia* **1991**, *45*, 238–244; b) B. Schmidt, D. Seebach, *Angew. Chem.* **1991**, *103*, 100–101; *Angew. Chem. Int. Ed. Engl.* **1991**, *30*, 99–101; c) D. Seebach, L. Behrendt, D. Felix, *ibid.* **1991**, *103*, 991–992; and **1991**, *30*, 1008–1009; d) B. Schmidt, D. Seebach, *ibid.* **1991**, *103*, 1383; and **1991**, *30*, 1321.

[3] a) (*R*)-(+)-2-Phenyl-2-butanol and -pentanol: for determination of the configuration see: D. J. Cram, J. Allinger, *J. Am. Chem. Soc.* **1954**, *76*, 4516–4522 and M. Tramontini, L. Angiolini, C. Fouquey, J. Jacques, *Tetrahedron* **1973**, *29*, 4183–4187; b) Under the same conditions as in the 1:1 run the yield drops to 20%. c) With α-naphthyl-TADDOL [2a] only traces of **10** are formed, with 11% *ee*; cf. the results for R_2Zn addition [2d]. d) Analysis and correlation see [2b–d].

[4] For discussions see the following review articles and literature cited therein: D. Seebach, *Proc. R. A. Welch Foundation Conf. Chem. Res. XXXVII*, (Stereospecificity in Chemistry and Biochemistry) **1984**, 93–145; D. Seebach, *Angew. Chem.* **1988**, *100*, 1685–1715; *Angew. Chem. Int. Ed. Engl.* **1988**, *27*, 1624–1654 (there especially Table 9). Structure of $[(BuLi)_4\cdot(t\text{BuOLi})_4]$: M. Marsch, K. Harms, L. Lochmann, G. Boche, *ibid.* **1990**, *102*, 334–336; and **1990**, *29*, 308–309. Newer applications of the LiX* effect: M. Murakata, M. Nakajima, K. Koga, *J. Chem. Soc., Chem. Commun.* **1990**, 1657–1658. Cf. discussion on autocatalysis and asymmetric amplification for reactions of polar metal derivatives: H. Wynberg, *Chimia* **1989**, *43*, 150–152; A. H. Alberts, H. Wynberg, *J. Am. Chem. Soc.* **1989**, *111*, 7265–7266; R. Noyori, M. Kitamura, *Angew. Chem.* **1991**, *103*, 34–55; *Angew. Chem. Int. Ed. Engl.* **1991**, *30*, 49–69.

[5] For a description of a suitable low-temperature apparatus see D. Seebach, A. Hidber, *Chimia* **1983**, *37*, 449–462.

The Phosphorus Ylide CH_2PH_3 is Stable in the Gas Phase**

By *Helmut Keck, Wilhelm Kuchen,* Peter Tommes, Johan K. Terlouw,* and *Thomas Wong*

Dedicated to Professor John L. Holmes on the occasion of his 60th birthday

The phosphorus ylide CH_2PH_3 **1** (methylenephosphorane) is one of the most often discussed hypothetical molecules in the chemistry of organophosphorus compounds. This is because it is the simplest member of the class of phosphorus ylides which have a great synthetic potential in the Wittig reaction.[1] A great number of theoretical studies deal with predictions of the structure, reactivity, and bonding properties of this molecule and its ionized conterpart.[2] According to these reports **1** can formally be represented as a methylene–phosphane adduct in which the C–P bond has partial double-bond character.

$$\underset{\mathbf{1}}{H_3\overset{\oplus}{P}-\overset{\ominus}{\ddot{C}}H_2} \longleftrightarrow \underset{\mathbf{2}}{H_3P{=}CH_2} \qquad CH_3PH_2$$

Although the phosphorus ylide **1** is 237 kJ mol^{-1} higher in energy than its isomer methylphosphane, CH_3PH_2, **2**, the two isomers are separated by a high energy barrier (**2** → **1**: 378 kJ mol^{-1}).[3] The ionized ylide $[\mathbf{1}]^{+\cdot}$ is also less stable than the radical cation $[\mathbf{2}]^{+\cdot}$ but the difference in their energies, $\Delta E = 40$ kJ mol^{-1}, is less than that between their neutral counterparts. Both ions lie in deep potential wells with significant barriers towards dissociation or isomerisation ($[\mathbf{2}]^{+\cdot} \rightarrow [\mathbf{1}]^{+\cdot}$: 220 kJ mol^{-1}).[3]

These theoretical predictions led to the suggestion[3] that the technique of neutralization–reionization mass spectrometry (NRMS)[4] be used to generate **1** by reduction of its radical cation $[\mathbf{1}]^{+\cdot}$. After we first established the structure of the ion $[\mathbf{1}]^{+\cdot}$ using collisional activation (CA) mass spectrometry,[5] we were able to show that its reduction in an NRMS experiment indeed leads to the formation of the elusive neutral ylide **1** as a stable species in the rarefied gas phase. Our experimental findings provide a gratifying confirmation of the theoretical predictions.

Dissociative ionization (electron impact, 70 eV)[6] of *n*-hexylphosphane ($C_6H_{13}PH_2$)[7] abundantly provides ions (*m/z* 48) whose structure was identified[8] as the ylide ion $[CH_2PH_3]^{+\cdot}$, $[\mathbf{1}]^{+\cdot}$. Mass selection of this ion and subsequent collisional activation (collision gas O_2, 80% transmission, *T*) afforded the collisional activation (CA) mass spectrum shown in Figure 1a which features peaks diagnostic for $[\mathbf{1}]^{+\cdot}$ at *m/z* 34 ($[PH_3]^{+\cdot}$) and *m/z* 14 ($[CH_2]$)$^{+\cdot}$. In agreement with the earlier study[8] this CA mass spectrum is significantly different from that of the isomeric radical cation $[CH_3PH_2]^{+\cdot}$, $[\mathbf{2}]^{+\cdot}$, (Fig. 1b).[9] Note that this spectrum does not contain the *m/z* 34 peak characteristic of $[\mathbf{1}]^{+\cdot}$ and that its low-mass region is dominated by the signal at *m/z* 15, characteristic for an intact methyl group.

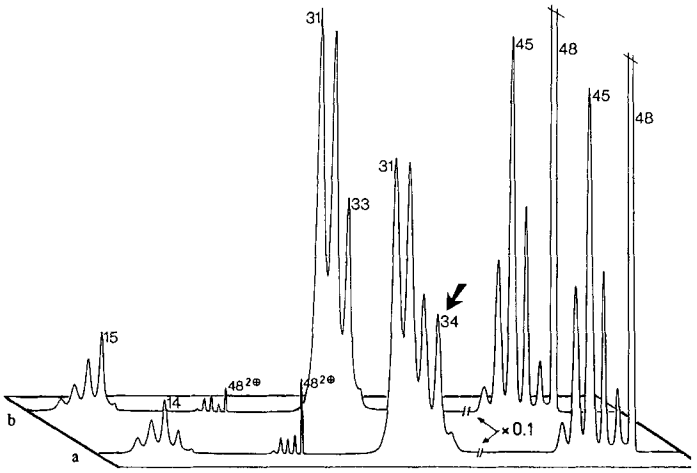

Fig. 1. CA mass spectra of (a) $[\mathbf{1}]^{+\cdot}$ (*m/z* 48) and (b) $[\mathbf{2}]^{+\cdot}$ (*m/z* 48).

A neutralization–reionization (NR) experiment on $[\mathbf{1}]^{+\cdot}$ involving neutralization by electron transfer to cyclopropane (80% *T*,[10]) followed after roughly 1 μs by reionization with O_2 (80% *T*) yields the NR mass spectrum which features an intense "recovery signal" at *m/z* 48 (Fig. 2). Quite likely this reflects the stability of the ylide **1** and may point to relatively favorable Franck–Condon factors in the vertical electron-transfer processes $[\mathbf{1}]^{+\cdot} \rightarrow \mathbf{1} \rightarrow [\mathbf{1}]^{+\cdot}$. Note, however, that the intensity distribution of the peaks in the NR

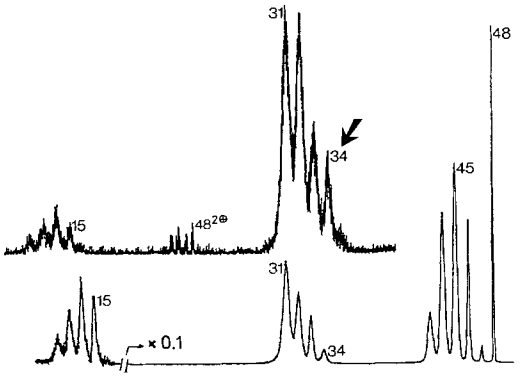

Fig. 2. NR mass spectrum of $[\mathbf{1}]^{+\cdot}$ (*m/z* 48); insert (upper spectrum): the interference-free NR mass spectrum of ions $[\mathbf{1}]^{+\cdot}$ resulting from the sequence $[\mathbf{1}]^{+\cdot} \rightarrow \mathbf{1} \rightarrow [\mathbf{1}]^{+\cdot}$.

[*] Prof. Dr. W. Kuchen, Dr. H. Keck, Dipl.-Chem. P. Tommes
Institut für Anorganische Chemie und Strukturchemie der Universität
Universitätsstrasse 1, D-W-4000 Düsseldorf 1 (FRG)
Prof. Dr. J. K. Terlouw, T. Wong
McMaster University, Department of Chemistry
1280 Main Street West, Hamilton, Ontario L8S 4M1 (Canada)

[**] This work was supported by the Fonds der Chemischen Industrie and the National Sciences and Engineering Research Council of Canada (NSERC).

spectrum of $[1]^{+\cdot}$ differs considerably from that displayed in its conventional CA mass spectrum (Fig. 1a). In particular, the structure-diagnostic peak-intensity ratios m/z 34: m/z 33 ($[PH_3]^{+\cdot}$ vs. $[PH_2]^+$) and m/z 14: m/z 15 ($[CH_2]^{+\cdot}$ vs. $[CH_3]^+$) have become lower, which may indicate that **1** has isomerized to **2** to a significant extent (NR mass spectrum of **2** in Fig. 3). Alternatively, one may argue that the discrepancies between the two spectra originate from contributions to the NR mass spectrum by dissociation products of **1** which are reionized and recorded as well.[4d-f, 11] Proof of this may be found in the substantial increase in the cluster of peaks m/z 31–34.

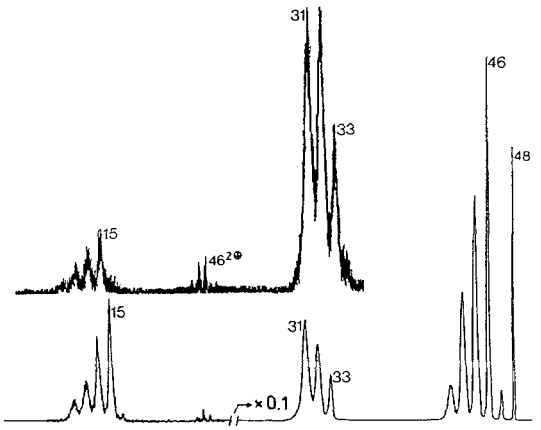

Fig. 3. NR mass spectrum of $[CH_3PH_2]^{+\cdot}$, $[2]^{+\cdot}$ (m/z 48); insert (upper spectrum): the interference-free NR mass spectrum of ions $[2]^{+\cdot}$ resulting from the sequence $[2]^{+\cdot} \rightarrow 2 \rightarrow [2]^{+\cdot}$.

Compelling evidence that the "recovery signal" in the NR mass spectrum of **1** is indeed that of the reionized stable neutral ylide **1** and not its counterpart **2** comes from a multistep collision experiment in which the reionized species **1** and **2** are mass-selected with the third sector (E_2) and then subjected to a CA experiment.[4d-f] These "survivor" CA mass spectra of interference-free reionized **1** and **2**—see inserts in Figures 2 and 3—are almost identical to their characteristic conventional CA mass spectra (Fig. 1).[12] These observations clearly show that upon neutralization of the radical cations both the ylide **1** and its isomer **2** retain their structural identities. The smallest possible phosphorus ylide, CH_2PH_3, has been detected experimentally and shown to be a stable species in the rarefield gas phase.

Received: July 31, 1991 [Z 4844 IE]
German version: *Angew. Chem.* **1992**, *104*, 65

CAS Registry numbers:
1, 36429-11-5; $[1]^{+\cdot}$, 56898-66-9; **2**, 593-54-4; $[2]^{+\cdot}$, 91391-14-9.

[1] U. Schöllkopf, *Angew. Chem.* **1959**, *71*, 260; A. Maercker, *Org. React.* **1965**, *14*, 270; E. Zbiral, *Synthesis* **1974**, 775.
[2] J. R. van Wazer, *J. Am. Chem. Soc.* **1972**, *94*, 2382; H. Lischka, *ibid.* **1977**, *99*, 353; G. Trinquier, J. P. Malreu, *ibid.* **1979**, *101*, 7169; R. Höller, H. Lischka, *ibid.* **1980**, *102*, 4632; J. Absar, D. J. Mitchell, S. Wolfe, H. B. Schlegel, *Can. J. Chem.* **1981**, *59*, 3280; R. A Eades, P. G. Gassmann, D. A. Dixon, *J. Am. Chem. Soc.* **1981**, *103*, 1066; D. A. Dixon, T. H. Dunning, R. A. Eades, P. G. Gassmann, *ibid.* **1983**, *105*, 7011; H. J. Bestmann, A. J. Kos, K. Witzgall, P. von R. Schleyer, *Chem. Ber.* **1986**, *119*, 1331; B. F. Yates, W. J. Bouma, L. Radom, *J. Am. Chem. Soc.* **1987**, *109*, 2250.
[3] B. F. Yates, W. J. Bouma, L. Radom, *J. Am. Chem. Soc.* **1984**, *106*, 5805.
[4] Reviews of NRMS: a) C. Wesdemiotis, F. W. McLafferty, *Chem. Rev.* **1987**, *87*, 485; b) J. K. Terlouw, H. Schwarz, *Angew. Chem.* **1987**, *99*, 829; *Angew. Chem. Int. Ed. Engl.* **1987**, *26*, 805; c) H. Schwarz, *Pure Appl. Chem.* **1989**, *61*, 685; d) J. K. Terlouw, *Adv. Mass Spectrom.* **1989**, *11*, 984; e) J. L. Holmes, *Mass Spectrom. Rev.* **1989**, *8*, 513; f) F. W. McLafferty, *Science (Washington DC)* **1990**, *247*, 925.
[5] Reviews of CA mass spectrometry: K. Levsen, H. Schwarz, *Angew. Chem.* **1976**, *88*, 589; *Angew. Chem. Int. Ed. Engl.* **1976**, *15*, 509; *Mass. Spectrom. Rev.* **1983**, *2*, 77; J. L. Holmes, *Org. Mass Spectrom.* **1985**, *20*, 169.
[6] All experiments were carried out with a VG Analytical ZAB-R mass spectrometer with BE_1E_2 geometry (B: magnetic sector; E: electric sector).
[7] Synthesis of *n*-hexyl phosphane: F. Pass, H. Schindelbauer, *Monatsh. Chem.* **1959**, *90*, 148.
[8] E. Weger, K. Levsen, I. Ruppert, P. C. Burgers, J. K. Terlouw, *Org. Mass Spectrom.* **1983**, *18*, 327.
[9] Synthesis of **2**: J. E. Bissey, H. Goldwhite, D. G. Rowsell, *J. Org. Chem.* **1967**, *32*, 1542. Compound **2** was introduced into the mass spectrometer as **2** · HI.
[10] C. E. C. A. Hop, J. L. Holmes, *Org. Mass Spectrom.* **1991**, *26*, 476.
[11] Contributions like the isomeric purity of the ion flux prior to neutralization and cross sections for the neutralization–reionization process, which may differ widely with mass and structure, may severly hamper the interpretation of the NR spectrum. A case in point is the identification of the chlorine ylide, CH_2ClH: a) P. C. Burgers, J. K. Terlouw in: *Mass. Spectrom.* **1988**, *10*, Chap. 2; b) J. C. Lorquet, B. Leyh-Nihant, F. W. McLafferty, *Int. J. Mass Spectrom. Ion Processes* **1990**, *100*, 465. For the $[CH_3PH_2]^{+\cdot}/[CH_2PH_3]^{+\cdot}$ system the neutralization–reionization cross sections appear to be similar. The results of the multistep collision experiment show that the ylide ion flux is quite pure.
[12] The intensity distributions of the "charge stripping" (CS) peaks (45^{2+}–48^{2+}) in the CA spectra of the reionized isomeric ions are quite different. However, the patterns do not correspond with those of the conventional CA mass spectra. This is not unexpected since collisional reionization may produce ions with different internal energy distributions.

$[Et_4N]_2[\{MO(S_2)_2\}_2(\mu_2\text{-}S_7)(\mu_2\text{-}H_2NNH_2)]$ (M = Mo, W)—Doubly Bridged Complexes with S_7^{2-} and Doubly End-On-Bound H_2NNH_2 Bridging Ligands

By *Zhu Nianyong, Du Shaowu, Wu Xintao,* and Lu Jiaxi*

The chemistry of transition-metal–polysulfido complexes[1, 2] is of broad interest, especially that of the polysulfido–molybdenum complexes in connection with the hydrodesulfurization (HDS) catalysts. These complexes often have surprising structures. Complexes with dinitrogen ligands bridging two metal-centers are also of interest, and the reduction of the N_2 ligand has a number of proposed reaction mechanisms.[3, 4] The feasibility of introducing nitrogenase substrates bonded in a doubly end-on mode as additional bridges between two cubane subunits already bound by a μ_2-S bridge has been demonstrated.[5] Very few doubly bridged complexes with bridging S_7^{2-} ligands[6] or bridging NH_2NH_2 ligands[5, 7] have been reported. The title complexes **1** (M = Mo) and **2** (M = W) contain not only the almost planar zig-zag $[M^{VI}\text{-}H_2N\text{-}NH_2\text{-}M^{VI}]$ unit, but also a doubly bridging S_7^{2-} ligand. In fact **1** and **2** have the longest polysulfide chains of all polysulfido–molybdenum (or tungsten) complexes. Complexes **1** and **2** were obtained from the new reaction system of $MO_2S_2^{2-}/S_x/H_2NNH_2 \cdot 2HCl$ (M = Mo, W), in which the biologically relevant H_2NNH_2 ligand may be introduced. Both complexes, $[Et_4N]_2[\{MO(S_2)_2\}_2(\mu_2\text{-}S_7)(\mu_2\text{-}H_2NNH_2)]$, were characterized by elemental analysis, IR and UV/VIS spectroscopy, cyclic voltammetry[8], and

[*] Prof. X. T. Wu, N. Y. Zhu, S. W. Du, Prof. Dr. J. X. Lu
Fuzhou Laboratory of Structural Chemistry
Fujian Institute of Research on Structure of Matter
Chinese Academy of Sciences
Fuzhou, Fujian 350002 (People's Republic of China)

[**] This research was supported by grants from the Structural Chemistry Research Laboratory of the Fujian Institute of Research on Structure of Matter, the Chinese Academy of Sciences, and the National Science Foundation of China.

X-ray structural analysis.[9] Since **1** and **2** are isomorphous, only the structure of complex **1** will be discussed.

In the anion of complex **1**, the two Mo^{VI} centers, which are each coordinated by two disulfide ligands and one double-bonded terminal oxo ligand, are linked by an S_7^{2-} bridge and an H_2NNH_2 bridge (Fig. 1; the S_7^{2-} ligand is statistically disordered at S6 and S7 with an equivalent degree of occupancy of 0.5 for S6′ and S7′. The two S_2^{2-} ligands on Mo2 are also disordered.) The coordination polyhedron of the

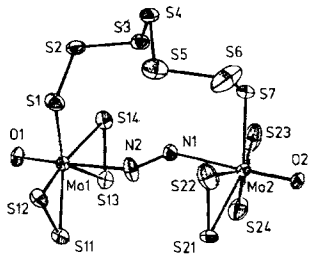

Fig. 1. The structure of the anion $[\{MoO(S_2)_2\}_2(\mu_2\text{-}S_7)(\mu_2\text{-}H_2NNH_2)]^{2-}$ (for clarity only one disordered anion is drawn). Selected bond lengths [Å] and bond angles [°]: Mo1-S1 2.473(1), Mo1-S11 2.386(4), Mo1-S12 2.410(3), Mo1-S13 2.383(3), Mo1-S14 2.380(3), Mo1-O1 1.668(6), Mo2-S7 2.44(2), Mo2-S21 2.46(2), Mo2-S22 2.39(2), Mo2-S23 2.37(1), Mo2-S24 2.47(2), Mo2-O2 1.671(6), Mo1-N2 2.486(8), Mo2-N1 2.491(8), S1-S2 2.030(5), S2-S3 2.031(5), S3-S4 2.046(5), S4-S5 2.015(5), S5-S6 2.24(1), S6-S7 1.93(2), N1-N2 1.40(1), S11-S12 2.029(5), S13-S14 2.047(5), S21-S22 1.95(2), S23-S24 1.94(2); O1-Mo1-N2 175.3(4), O2-Mo2-N1 175.9(3), N2-N1-Mo2 126.7(7), N1-N2-Mo1 125.7(6).

Mo^{VI} centers is a pentagonal bipyramid, whose two apexes are formed by the terminal oxo atom and the coordinating atom of H_2NNH_2 ligand. This type of coordination with a pentagonal-bipyramidal environment around each Mo(VI) atom is often found in other oxodisulfido-molybdate complexes.[10] The five equatorial sulfur atoms of each pentagonal bipyramid are planar to within 0.07 Å, and the S2 and S6 (and S6′) atoms are in a least-squares plane with deviations of 0.08 and 0.1 Å (0.1 Å), respectively. The average Mo–N bond length of 2.489(8) Å is relatively long, due to the *trans* influence[10b] of the Mo=O bond opposite the N atom (average O-Mo-N angle 175.6(4)°). The N–N bond length of 1.40(1) Å is much shorter than that found in free hydrazine which has a staggered conformation. The [Mo(μ_2-H_2NNH_2)Mo] fragment is planar to within 0.11 Å, and the Mo substituents approach an ideal *trans* configuration.

Experimental Procedure

1: Sulfur (0.675 g, 21.04 mmol) was added to a solution of $(NH_4)_2MoO_2S_2$ (1.2 g, 5.26 mmol) in DMF (30 mL) and stirred for 1.5 h. Afterwards, $H_2NNH_2 \cdot 2HCl$ (0.3 g, 2.86 mmol) and Et_4NBr (1.5 g, 7.14 mmol) were added to the solution which was stirred another 4.5 h. The solution was filtered, and the filtrate was layered with 50 mL isopropanol, then left undisturbed at −15 °C for several days. The dark orange precipitate was filtered and recrystallized from MeCN/ether. Dark orange analytically pure crystals were obtained; 1.15 g, yield 44%. Correct analyses were obtained.

2: Following the procedure for **1** $(NH_4)_2WO_2S_2$ (2.0 g, 6.3 mmol), sulfur (0.81 g, 25 mmol), $H_2NNH_2 \cdot 2HCl$ (0.50 g, 4.8 mmol), and Et_4NBr (2.0 g, 9.5 mmol) provided orange-red analytically pure crystals; 0.81 g, yield 22%. Correct analyses were obtained.

Received: July 3, 1991 [Z 4770 IE]
German version: *Angew. Chem.* **1992**, *104*, 83

CAS Registry numbers:
1, 137648-06-7; **2**, 137648-08-9; $(NH_4)_2MoO_2S_2$, 16150-60-0; $(NH_4)_2WO_2S_2$, 16150-61-1; S, 7704-34-9.

[1] M. Draganjac, T. B. Rauchfuss, *Angew. Chem.* **1985**, *97*, 745; *Angew. Chem. Int. Ed. Engl.* **1985**, *24*, 742.
[2] A. Müller, E. Diemann, *Adv. Inorg. Chem.* **1987**, *31*, 89.
[3] L. A. Nikonova, A. E. Shilov in *Recent Developments in Nitrogen Fixation* (Eds.: W. E. Newton, J. R. Postgate, C. Rodriguez-Barrueco), Academic, New York, **1977**, pp. 41–52.
[4] G. I. Likhtenstein in *Nitrogen Fixation, Vol. 1* (Eds.: W. E. Newton, W. H. Orme-Johnson), University Park Press, Baltimore, **1980**, pp. 195–209.
[5] P. R. Challen, Sang-Man Koo, C. G. Kim, W. R. Dunham, D. Coucouvanis, *J. Am. Chem. Soc.* **1990**, *112*, 8606.
[6] A. Müller, K. Schmitz, E. Krickemeyer, M. Penk, H. Bögge, *Angew. Chem.* **1986**, *98*, 470; *Angew. Chem. Int. Ed. Engl.* **1986**, *25*, 453.
[7] a) L. Blum, I. D. Williams, R. R. Schrock, *J. Am. Chem. Soc.* **1984**, *106*, 8316; b) D. Sellmann, *Z. Naturforsch.* **1971**, *B*, *26*, 1070; c) D. Sellmann, P. Kreutzer, G. Huttner, A. Frank, *ibid.* **1978**, *33*, 1341; d) D. Sellmann, A. Brandl, R. Endell, *J. Organomet. Chem.* **1976**, *111*, 303.
[8] Complex **1**: IR (KBr): $\tilde{\nu}[cm^{-1}] = 3290(w), 3210(w), 1120(s), 925(vs), 532(s), 485(w, sh), 470(w), 344(s)$; UV/VIS (MeCN): $\lambda_{max}[nm]$ (ε) = 530 (2430), 452 (4000), 317 (14900), 248 (25000). Cyclic voltammogram (in MeCN vs. SCE with a Pt electrode): two irreversible reduction waves at −0.69 and −0.92 V and one irreversible oxidation wave at +0.78 V. Complex **2**: IR (KBr): $\tilde{\nu}[cm^{-1}] = 3280(w), 3210(w), 1126(s), 930(vs), 518(s), 466(w), 455(w, sh), 325(s), 315(s), 300(w, sh)$; UV/VIS (MeCN): $\lambda_{max}[nm]$ (ε) = 350 (11000), 236 (29500). Cyclic voltammogram (in MeCN vs. SCE with a Pt electrode): one irreversible reduction wave at −1.21 V and one irreversible oxidation wave at +0.82 V.
[9] Crystal data: Complex **1**: $P2_1/c$, $a = 14.912(8)$, $b = 17.066(7)$, $c = 17.81(1)$ Å, $\beta = 113.87(4)°$, $V = 4144(4)$ Å^3, $Z = 4$, $\lambda(Mo_{K\alpha}) = 0.71069$ Å, Rigaku AFC 5R Diffractometer. Lorentz and polarization corrections as well as absorption correction (empirical). The structure was solved by direct methods and fourier synthesis using the TEXSAN program package. $R = 0.060$ for 4358 reflections [$I > 3\sigma(I)$]. Complex **2**: $P2_1/c$, $a = 14.86(1)$, $b = 17.14(2)$, $c = 17.81(3)$ Å, $\beta = 114.04(8)°$, $U = 4145(9)$ Å^3; $Z = 4$; $\lambda(Mo_{K\alpha}) = 0.71069$ Å, Rigaku AFC 5R Diffractometer, Lorentz and polarization corrections as well as absorption correction (empirical). The structure was solved by direct methods and fourier synthesis using the TEXSAN program package. $R = 0.049$ for 3962 reflections [$I > 3\sigma(I)$]. Further details of the crystal structure determination are available on request from the Fachinformationszentrum Karlsruhe, Gesellschaft für wissenschaftlich-technische Information mbH, D-W-7514 Eggenstein-Leopoldshafen (FRG) on quoting the depository number CSD-55788, the names of the authors, and the journal citation.
[10] a) Wu Xintao, Lu Shaofang, Zu Lianyong, Wu Quangjin, Lu Jiaxi, *Inorg. Chem. Acta* **1987**, *133*, 43; b) A. I. Hadjikyriacou, D. Coucouvanis, *Inorg. Chem.* **1989**, *28*, 2169.

An Unusual Interplay Between Macromolecular and Supramolecular Helicity in Polyisocyanates Dissolved in a Chiral Liquid Crystal

By *Mark M. Green,* Dexi Weng, Wen Shang,* and *M. M. Labes*

The stiff and wormlike nature of the widely studied poly(alkyl isocyanates) arises from their stable helical conformations, of which both helical senses are equally populated.[1] In this report we show that the observed change of pitch caused by the dissolution of small amounts of an optically inactive poly(alkyl isocyanate) in a doped, cholesteric liquid crystal can be explained by the surprising induced excess of one helical sense in the polymer caused by the chiral arrangement of the liquid crystal.

[*] Prof. M. M. Green, D. Weng
Department of Chemistry and Polymer Research Institute
Polytechnic University, Six MetroTech Center
Brooklyn, NY 11201 (USA)
Prof. M. M. Labes, W. Shang
Department of Chemistry, Temple University
Philadelphia, PA 19122 (USA)

[**] We are grateful to the U.S. National Science Foundation for financial support for the work at Temple University and the Polytechnic University under grants DMR 89-17833 and CHE 90-02536 respectively. Efforts at the Polytechnic University were also aided by financial support from IBM corporation (Almaden Laboratory) and by the Petroleum Research Foundation administered by the American Chemical Society.

The thermotropic nematic *N*-(4-methoxybenzylidene)-4-*n*-butylaniline (**1**) is known to form cholesteric phases with left- or right-handedness upon addition of cholesteryl propionate or cholesteryl chloride respectively.[2] At low concentrations the pitch of the cholesteric array, defined as the vertical distance over which the molecular axis precesses by 360°, is inversely proportional to the concentration of chiral dopant. Scheme 1 shows the effect of the addition of polymeric solutes on the pitch of such cholesteric phases. Small

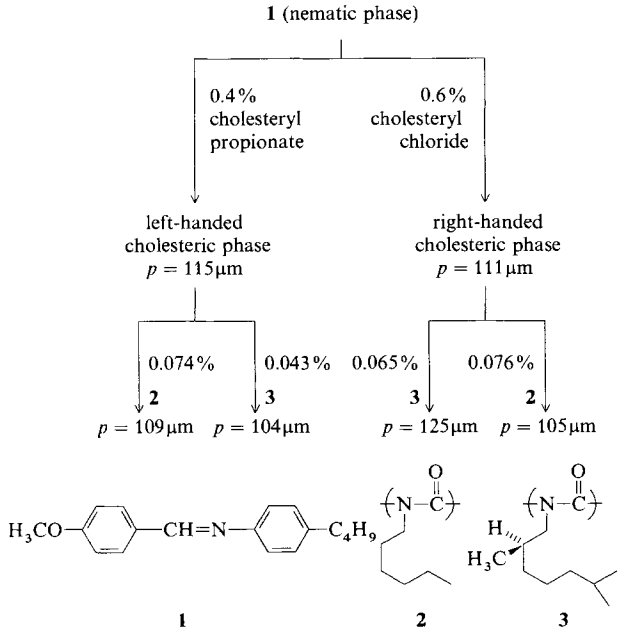

Scheme 1. Influence of polyisocyanates **2** and **3** on the pitch of doped cholesteric **1**; added quantities in wt%.

amounts of either poly(*n*-hexyl isocyanate) (**2**) or poly((*R*)-2,6-dimethylheptyl isocyanate) (**3**) were added. The data presented in Scheme 1 demonstrate that addition of the optically inactive polymer **2** causes a large decrease in the pitch of both the right- and left-handed cholesteric phases. Addition of the optically active polymer **3** has opposite effects in the oppositely handed cholesteric phases. Varying the concentrations of all the polyisocyanate dopants causes an approximately linear response in the inverse pitch of the cholesteric phases in accord with theory (Fig. 1). Hardly any change in pitch can be detected on addition of atactic polystyrene of two molecular weights (Fig. 1).

The effect of the optically active polyisocyanate **3** on the pitch characteristics of the cholesteric phase of **1** follows from the stereocenter in the side chain, which causes the polymer backbone to adopt a uniform left-handed helical conformation.[3, 4] Chiral nonracemic molecular additives, of which **3** is a rare polymeric example,[5] are known to both alter the pitch of cholesteric phases and to convert nematic to cholesteric phases.[6] Our experiments illustrate this effect; the handedness of **3** is either compatible or incompatible with the left- and right-handed cholesteric phases (Fig. 1).

To be consistent with the effect of the left-handed macromolecular helix of **3**, poly(*n*-hexyl isocyanate) (**2**) should maintain an excess of helices with the opposite handedness in their macromolecular backbones in the two cholesteric phases, i.e. left- and right-handed macromolecular helices for **1** doped with cholesteryl propionate and cholesteryl chloride, respectively (Scheme 1). This would require the cholesteric phase to break the energetic degeneracy of the left- and right-handed

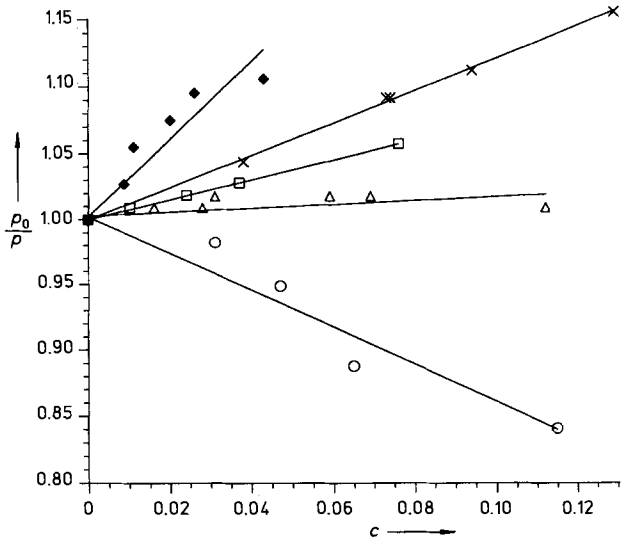

Fig. 1. Relationship between pitch p and concentration c [wt%] of the dissolved polymer in right-handed **1** (doped with 0.6% cholesteryl chloride, CC) and in left-handed **1** (with 0.4% cholesteryl propionate, CP). p_0 = pitch at $c = 0$. ○ = CC/**1**/**3**; □ = CC/**1**/**2**; • CP/**1**/**3**; × CP/**1**/**2**; △ = CP/**1**/polystyrene.

helical conformations of the added **2**, thereby favoring the macromolecular helical state which "fits" best into the supramolecular helix of the cholesteric phase.

In principle this result is not surprising, since one could expect the interaction of the chiral cholesteric phase with the enantiomeric helices of poly(*n*-hexyl isocyanate) to enforce the prerequisite diastereomeric relationship. Nevertheless the sensitivity of the polyisocyanate to the macroscopic chirality of the cholesteric phase is astonishing. For a pitch of a thermotropic cholesteric phase of about 100 μm, as we have here, the twist between contiguous molecules along the cholesteric helical axis is roughly 0.001°. Even if the polymer chain were extended fully along the helical axis of the cholesteric liquid crystal it would only traverse approximately 500 Å (molecular weight 35000),[1] which would correspond to only about a 0.2° turn of the director of the molecules **1** along the cholesteric helical axis. Although the local arrangements of the mesogenic molecules can therefore hardly be distinguished from the achiral nematic state, this is apparently adequate to change the ratio of the left- and right-handed helical states of the poly(*n*-hexyl isocyanate) (**2**). Moreover the displacement of this ratio of macromolecular helical senses must be considerable when one compares the effect of **2** on the pitch to that of the optically active polyisocyanate **3**, which is fully left-handed (Fig. 1).[3, 4]

Since the monomer units between the rarely occurring helix reversals in a poly(*n*-hexyl isocyanate) must take the same helical sense, cooperative interactions arise,[4] which amplify the tiny chiral perturbations per monometer unit. Such cooperativity is responsible for the large disproportionate displacement in the ratio of the helical senses which has been observed experimentally for unusually small chiral influences built into the side chains of these polymers. Although this phenomenon[4, 7] must be at work here it is not the only factor, since analogous pitch changes are observed in oligophenyls, including substituted biphenyls,[8] which share the dynamic racemic quality though not the cooperativity of poly(*n*-hexyl isocyanate).

Although the chiral enforcement of the twist necessary to convert the nematic to the cholesteric phase has been treated theoretically,[9] to our knowledge there is no work on the chiral forces inherent in the cholesteric phase, or for that mat-

ter in the chiral smectic C phase, which could explain the phenomenon reported here.

The observation of these effects in both the substituted oligophenyls[8] and in the polyisocyanates suggests that a wide structural range of dynamically racemic materials may be subject to, and in turn affect, the chiral properties of cholesteric or other twisted liquid crystal states.[8, 10–12]

Experimental Procedure

Poly(*n*-hexyl isocyanate) (**2**) has an average molecular weight of 35000 determined by viscosity and a polydispersity of 1.31 determined by gel permeation chromatography. Poly((*R*)-2,6-dimethylheptyl isocyanate) (**3**) was determined by light scattering to have an average molecular weight of 250000 with unknown polydispersity. Both polyisocyanates were judged soluble in mesogenic **1** by careful inspection of samples under the optical microscope. The solubility of **3** was further confirmed on filtered samples subjected to quantitative analysis by gel permeation chromatography. The two samples of polystyrene had molecular weights of 3050 and 9200.

In the procedure for determining pitch the "fingerprint texture" of aligned cholesteric liquid crystals was observed and measured between crossed polars on a polarization microscope. The thin samples were treated so that the helix axis was parallel to the glass slides. Cholesteryl chloride, cholesteryl propionate, and **1** were obtained from Aldrich or Eastman Kodak, The measurement technique is described in reference [8].

Received: June 11, 1991 [Z 4694 IE]
German version: *Angew. Chem.* **1992**, *104*, 86

CAS Registry numbers:
1, 26227-73-6; **2** (homopolymer), 26746-07-6; **3** (homopolymer), 122093-50-9; polystyrene, 9003-53-6; cholesteryl propionate, 633-31-8; cholesteryl chloride, 910-31-6.

[1] For leading references see: R. Cook, R. D. Johnson, C. G. Wade, D. J. O'Leary, B. Muñoz, M. M. Green, *Macromolecules* **1990**, *28*, 3454; T. Itou, H. Chikiri, A. Teramoto, S. M. Aharoni, *Polym. J. (Tokyo)* **1988**, *20*, 143.

[2] H. Baessler, M. M. Labes, *J. Chem. Phys.* **1970**, *52*, 631; W. Elser, R. D. Ennulat in *Advances in Liquid Crystals Vol. 2*, (Ed.: G. H. Brown), Academic, New York, **1976**, p. 73.

[3] The assumption of a left-handed helix for **3** follows from force field calculations [4], which are also in agreement with an assignment from the temperature dependence of the pitch of the lyotropic cholesteric phase of **3** (T. Sato, A. Teramoto, M. M, Green, unpublished).

[4] S. Lifson, C. Andreola, N. C. Peterson, M. M. Green, *J. Am. Chem. Soc.*, **1989**, *111*, 8850.

[5] R. S. Kumar, H. Lee, R. B. Blumstein, A. Blumstein, *Polym. Prepr. (Am. Chem. Soc. Div. Polym. Chem.)* **1987**, *28*, 185.

[6] G. Friedel, *Ann. Phys. (Paris)*, **1922**, *18*, 273; I. G. Chistyakow, *Kristallografiya*, **1962**, *7*, 746; R. Cano, P. Chatelain, *C. R. Hebd. Seances Acad. Sci.* **1961**, *253*, 1815; A. D. Buckingham, G. P. Caesar, M. B. Dunn, *Chem. Phys. Lett.* **1969**, *3*, 540; G. Solladié, R. G. Zimmermann, *Angew. Chem.* **1984**, *96*, 335; *Angew. Chem. Int. Ed. Engl.* **1984**, *23*, 348; C. S. Bak, M. M. Labes, *J. Chem. Phys.* **1975**, *62*, 3066; *ibid.* **1975**, *63*, 805.

[7] M. M. Green, C. Andreola, B. Muñoz, M. P. Reidy, K. Zero, *J. Am. Chem. Soc.*, **1988**, *110*, 4063; M. M. Green, M. P. Reidy, R. D. Johnson, G. Darling, D. J. O'Leary, G. Willson, *ibid.* **1989**, *111*, 6452.

[8] M. M. Labes, W. Shang, *ibid.* **1991**, *113*, 2773.

[9] For leading reviews and references to original work see: H. Schröder and B. W. van der Meer, G. Vertogen in *The Molecular Physics of Liquid Crystals* (Ed.: G. R. Luckhurst, G. W. Gray), Academic Press, New York, **1979**, Chapters 5 and 6; P. G. de Gennes, *The Physics of Liquid Crystals*, Clarendon Press, Oxford, **1974**, Chapter 6. See also specifically: W. J. A. Goossens, *Mol. Cryst. Liq. Cryst.* **1971**, *12*, 237; J. P. Straley, *Phys. Rev.* **1976**, *14*, 1835; H. Kimura, M. Hosino, H. Nakano, *J. Phys. Soc. Jpn.*, *51*, 1584, M. A. Osipov, *Nuovo Cimento Soc. Ital. Fis. D* **1988**, *10*, 1249. See also A. B. Buda, K. Mislow *J. Mol. Struct.* **1991**, *232*, 1.

[10] Transfer of conformational chiral information between neighboring molecules may be of importance. See: J. Naciri, G. P. Spada, G. Gottarelli, R. G. Weiss, *J. Am. Chem. Soc.* **1987**, *109*, 4352; G. Gottarelli, M. A. Osipov, G. P. Spada, *J. Phys. Chem.* **1991**, *95*, 3897. For a general review see: R. G. Weiss *Tetrahedron* **1988**, *44*, 3413.

[11] M. M. Green, B. Christiani, C. Andreola, T. Sato, Y. Nagamura, J. Wagner, Y. Okamoto, A. Teramoto, *Polym. Prepr. (Am. Chem. Soc. Div. Polym. Chem.)* **1991**, *32*, 453.

[12] The unusual dependence of pitch on temperature in doped mesogens might be related to these effects. G. Heppke, D. Lotzsch, F. Ostreicher, *Z. Naturforsch. A* **1987**, *42*, 279; B. Kirste, G. Scherowsky, *Liq. Cryst.* **1989**, *6*, 17. See also: L. N. Lisetski, A. I. V. Tolmachev, *ibid.* **1989**, *5*, 877.

Synthesis and Reactions of Isothiocyanate-Substituted Allenes and 1,3-Butadienes**

By *Klaus Banert,** *Holger Hückstädt,* and *Kai Vrobel*

Dedicated to Professor Adalbert Maercker on the occasion of his 60th birthday

The isomerization of allyl thiocyanate (**1**) to allyl isothiocyanate (**2**) has been thoroughly investigated[1] and is interpreted as a [3,3]-sigmatropic rearrangement.[2] Attempts to transform propargyl thiocyanates of type **3**[3,4] into isothiocyanates analogously by heating gave only decomposition and polymerization products.[3] We now report an isomerization reaction that for the first time provides access to the highly reactive allenyl isothiocyanates **4** and the isothiocyanate-substituted 1,3-butadienes **18**, **22**, and **25**.

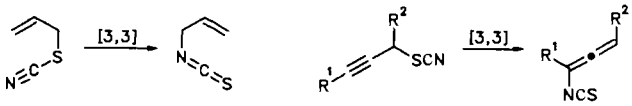

1 **2** **3** **4**

Scheme 1. **3a**, **4a**: $R^1 = R^2 = H$; **3b**, **4b**: $R^1 = H$, $R^2 = Me$; **3c**, **4c**: $R^1 = Me$, $R^2 = H$.

Table 1. Selected physical data of compounds **4ac**, **18a,b**, **22**, and **25a–c** [a].

4a: colorless, lacrimatory liquid; ^1H NMR: $\delta = 5.39$ (d, $^4J = 6.3$, 2 H; H-3), 6.16 (t, $^4J = 6.3$, 1 H; H-1); ^{13}C NMR: $\delta = 85.5$ (t, $^1J \approx 170$; C-3), 90.35 (d, $^1J \approx 200$; C-1), 135.4 (s; NCS), 210.0 (s; C-2); IR: $\tilde{\nu}$[cm^{-1}] = 2095 (NCS), 1334; GC-MS: *m/z* 97 (M^+, 100 %), 70 (42)

4b: ^1H NMR: $\delta = 1.79$ (dd, $^3J = 7.5$, $^5J = 2.7$, 3 H; H-4), 5.77 (qd, $^3J = 7.5$, $^4J \approx 6$, 1 H; H-3), 6.01 (dq, $^4J \approx 6$, $^5J = 2.7$, 1 H; H-1); IR: $\tilde{\nu}$[cm^{-1}] = 2092 (NCS), 2035 (NCS); GC-MS: *m/z* 111 (M^+, 33 %), 53 (M^+ – NCS, 100)

4c: ^1H NMR: $\delta = 2.00$ (t, $^5J = 3.2$, 3 H; H-4), 5.21 (q, $^5J = 3.2$, 2 H; H-1); ^{13}C NMR: $\delta = 19.8$ (q; C-4), 83.25 (t; C-1), 100.2 (s; C-3), 136.0 (s; NCS), 207.85 (s; C-2); IR: $\tilde{\nu}$[cm^{-1}] = 2104 (NCS), 1280, 1018

18a: ^1H NMR: $\delta = 5.08$ (s, 1 H; H-1), 5.20 (s, 1 H; H-1), 5.33 (d, $^3J = 10.4$, 1 H; H-4), 5.60 (d, $^3J = 16.9$, 1 H; H-4), 6.29 (dd, $^3J = 16.9$, $^3J = 10.4$, 1 H; H-3); IR (CCl_4): $\tilde{\nu}$[cm^{-1}] = 2122, 2090, 2060; UV/VIS: λ_{max} [nm] (ε) = 271 (9950); GC-MS: *m/z* 111 (M^+, 77 %), 53 (M^+ – NCS, 100)

18b: colorless oil; ^1H NMR: $\delta = 1.93$ (s, 3 H; CH_3), 5.19 (s, 1 H), 5.21 (s, 1 H), 5.24 (s, 1 H), 5.42 (s, 1 H); ^{13}C NMR: $\delta = 19.25$ (q; CH_3), 111.0 (t), 116.0 (t), 133.45 (br, s; NCS), 136.6 (s), 137.2 (s); IR (CCl_4): $\tilde{\nu}$[cm^{-1}] = 2090 (NCS); UV/VIS: λ_{max} [nm] (ε) = 275 (7700); GC-MS: *m/z* 125 (M^+, 66 %), 67 (M^+ – NCS, 50), 41 (100)

22: ^1H NMR: $\delta = 5.43$ (d, $^2J = 1.0$, 2 H), 5.61 (d, $^2J = 1.0$, 2 H); ^{13}C NMR: $\delta = 113.1$ (t, $^1J = 165$; C-1, C-4), 130.75 (s; C-2, C-3), 136.45 (s; NCS); IR: $\tilde{\nu}$[cm^{-1}] = 2089 (NCS), 2038 (NCS), 1581

25a: ^1H NMR: $\delta = 1.93$ (d, $^3J = 6.5$, 6 H; H-1, H-6), 5.99 (q, $^3J = 6.5$, 2 H; H-2, H-5); ^{13}C NMR: $\delta = 13.8$ (q; C-1, C-6), 123.6 (d; C-2, C-5), 125.4 (s; C-3, C-4), 136.7 (s; NCS); UV/VIS: λ_{max} [nm] (ε) = 269 (68000)

25b: ^1H NMR: $\delta = 1.83$ (d, $^3J = 7.6$, 3 H; CH_3), 1.92 (d, $^3J = 7.0$, 3 H; CH_3), 5.73 (q, $^3J = 7.0$, 1 H; CH), 5.80 (q, $^3J = 7.6$, 1 H; CH); ^{13}C NMR: $\delta = 13.7$ (q; CH_3), 14.0 (q; CH_3), 123.4 (s; C-4), 125.7 (s; C-3), 125.85 (d; CH), 128.25 (d; CH), 134.9 (s; NCS), 137.35 (s; NCS)

25c: ^1H NMR: $\delta = 1.70$ (d, $^3J = 7.3$, 6 H; H-1, H-6), 5.88 (q, $^3J = 7.3$, 2 H; H-2, H-5); ^{13}C NMR: $\delta = 13.9$ (q; C-1, C-6), 123.6 (s; C-3, C-4), 127.2 (d; C-2, C-5), 135.8 (s; NCS)

[a] NMR and IR spectra in $CDCl_3$ (if not stated otherwise), UV spectra in cyclohexane; ^1H NMR at 80 and 400 MHz, ^{13}C NMR at 100.6 MHz; GC-MS at 70 eV; *J* in Hz.

[*] Dr. K. Banert, Dipl.-Chem. H. Hückstädt, Dipl.-Chem. K. Vrobel
Fachbereich 8, Organische Chemie II der Universität-Gesamthochschule Adolf-Reichwein-Strasse, D-W-5900 Siegen (FRG)

[**] Rearrangement Reactions, Part 1. This work was supported by the Deutsche Forschungsgemeinschaft and the Fonds der Chemischen Industrie. We thank Mrs. E. Reissaus for her cooperation.

If compounds **3** are warmed to 60–100 °C not as isolated substances,[3] but in dilute solution, they undergo [3,3]-sigmatropic rearrangement to afford the cumulenes **4**. The yields are limited to 7–20% by subsequent polymerization reactions. A much more effective synthesis strategy for **4** is gas-phase thermolysis;[5] for example, **4a** can be obtained in 95–100% yield from **3a** (98% conversion) in a maximum daily yield of 1 mol (for characterization, see Table 1).

In spite of their pronounced tendency to polymerize, the isothiocyanates **4** react with oxygen-, nitrogen-, or sulfur-containing nucleophiles to afford good yields of thiazoles (Scheme 2).[6] In some cases the transformations are highly

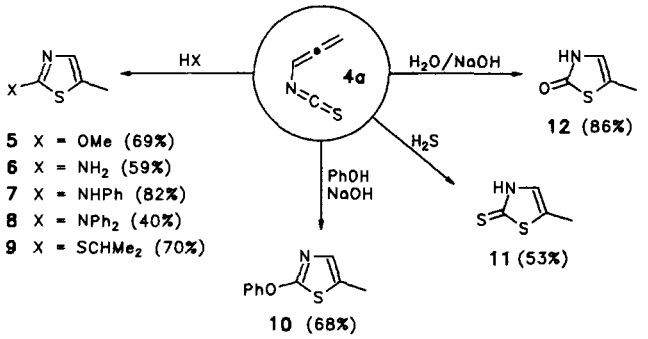

Scheme 2. Conversion of **4a** into thiazoles with nucleophiles.

exothermic. Compound **4a** is extremely reactive, as is exemplified by its conversion into **8** with diphenylamine at room temperature. Phenyl isothiocyanate is attacked by this weak nitrogen nucleophile only at 280 °C.[7] Whereas normal isothiocyanates react so slowly with water that they can be purified by steam-distillation, **4a** forms the heterocycles **12**, **14**, and **15** in water/THF (1:2) at room temperature already (Scheme 3). These products are possibly derived from the

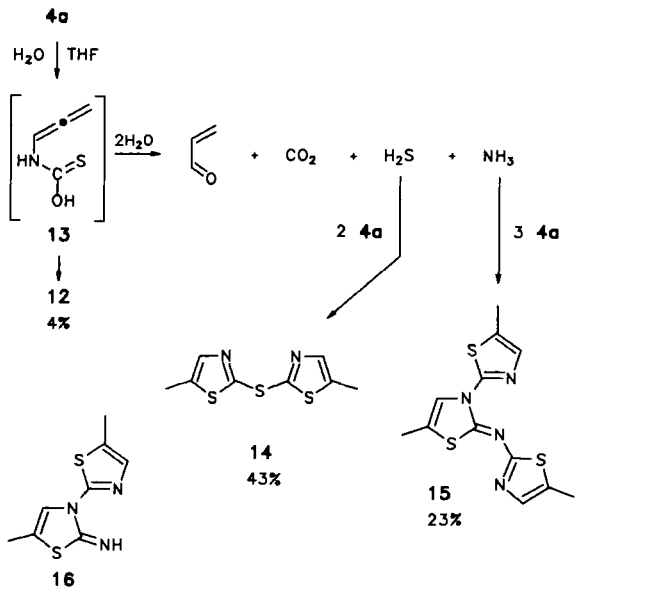

Scheme 3. Conversion of **4a** into **12**, **14**, and **15**.

intermediate **13**, which can not only cyclize to afford **12**, but as a labile thiocarbamic acid can also decompose to acrolein, carbon dioxide, hydrogen sulfide, and ammonia. The latter two compounds are more nucleophilic than water and subsequently react with **4a** to afford the major products **14** and **15**.

In accord with this reaction pathway, **14** may be prepared in higher yields (77%) from **4a** and H_2S/H_2O or in 99.6% yield from **4a** and **11**. Similarly, the synthesis of **15** takes place from **4a** and less than stoichiometric quantities of aqueous ammonia (88% yield) or from **4a** and **6** (90%). The intermediate for these reactions (**16**) can be isolated.

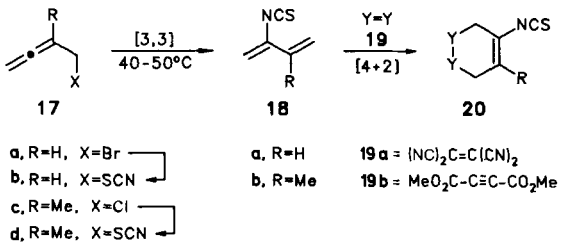

Scheme 4. Yields: **17b**, 80%; **17d**, quantitative; **18b**, 69% based on **17c**; **20**, 70% based on **17b** and **19a**, 80% on **18b** and **19a**, and 88% on **18b** and **19b**.

Not only propargyl thiocyanates, but also the 2,3-butadienyl thiocyanates **17b** and **17d**, easily accessible from the respective precursors **17a**[8] or **17c**[9] and ammonium thiocyanate, are suitable reactants for rearrangements that direct the isothiocyanate function to a vinylic position. The products are 1,3-dienes (**18**), which undergo [4 + 2]-cycloadditions with the reactive dienophiles **19** (Scheme 4).

Heating of a dilute solution of **21**[10] causes a double [3,3]-sigmatropic isomerization to give **22**, whose yield is limited by subsequent, very rapid polymerization. The instability of the rearrangement product **22** may be the reason why only decomposition occurred on attempts to distill **21**.[10] The chromatographically separable hexadienes **25** are simpler to handle, and their precursor **23b** is easily accessible from ammonium thiocyanate and **23a**.[11] Already on distillation

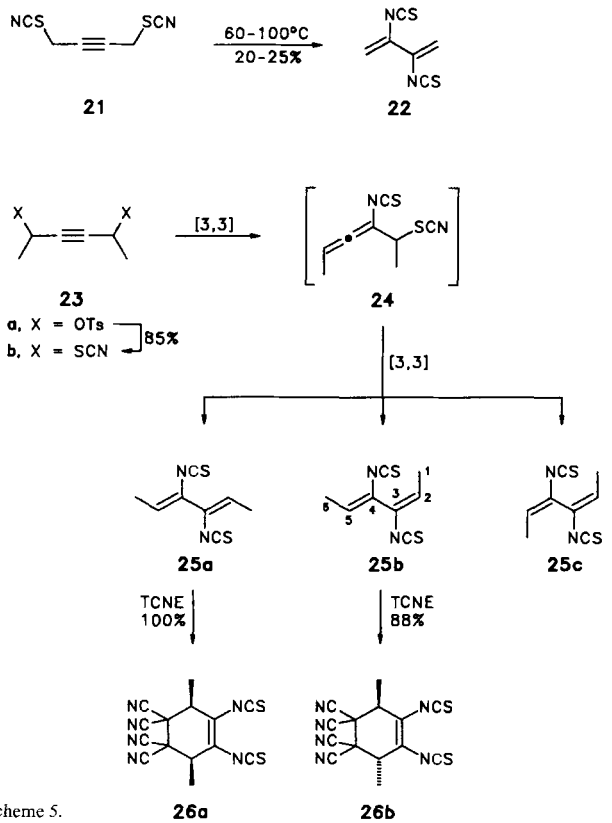

Scheme 5.

(90 °C/0.001 Torr) **23b** affords the products **25a–c** in almost statistical 1:2:1 distribution (67% yield). If the distillation is conducted at 180 °C/26 mbar, the thermodynamically favored *Z,Z* isomer **25a** predominates (56% yield of **25**, 8:1:1 distribution). Apparently at least the second rearrangement step, **24** → **25**, is reversible at higher temperatures.

As anticipated, on treatment with tetracyanoethylene (TCNE) **25a** reacts considerably faster to **26a** than its stereoisomer **25b** to the cycloadduct **26b**.

Isothiocyanate-substituted 1,3-butadienes can be used as well as the allenes **4** for the synthesis of thiazoles, but also for the preparation of other heterocycles.

Received: August 3, 1991 [Z 4852 IE]
German version: *Angew. Chem.* **1992**, *104*, 72

CAS Registry numbers:
3a, 24309-48-6; **3b**, 113079-35-9; **3c**, 52423-16-2; **4a**, 137768-73-1; **4b**, 137768-92-4; **4c**, 137768-93-5; **5**, 79307-66-7; **6**, 7305-71-7; **7**, 52829-93-3; **8**, 137768-76-4; **9**, 137768-77-5; **10**, 137768-78-6; **11**, 17626-82-3; **12**, 79307-64-5; **14**, 137768-79-7; **15**, 137768-80-0; **16**, 137768-81-1; **17a**, 18668-68-3; **17b**, 137708-74-2; **17c**, 76397-24-5; **17d**, 137768-75-3; **18a**, 137768-82-2; **18b**, 137768-83-3; **19a**, 670-54-2; **19b**, 762-42-5; **20a**, 137768-84-4; **20b**, 137768-85-5; **21**, 98141-73-2; **22**, 137768-86-6; **23a**, 26494-11-1; **23b**, 137768-87-7; **25a**, 137768-88-8; **25b**, 137768-89-9; **25c**, 137768-90-2; **26a**, 137792-29-1; **26b**, 137768-91-3.

[1] P. A. S. Smith, D. W. Emerson, *J. Am. Chem. Soc.* **1960**, *82*, 3076–3082, and references cited therein; A. Iliceto, A. Fava, U. Mazzucato, *Tetrahedron Lett.* **1960**, *11*, 27–35; A. Fava, *Chem. Org. Sulfur Compd.* **1966**, *2*, 73–91.
[2] R. J. Ferrier, N. Vethaviyaser, *J. Chem. Soc. C* **1971**, 1907–1913.
[3] L. Henry, *Ber. Dtsch. Chem. Ges.* **1873**, *6*, 728–730; T. Midtgaard, G. Gundersen, C. J. Nielsen, *J. Mol. Struct.* **1988**, *176*, 159–179.
[4] P. W. Austin (Imperial Chemical Industries) EP 244962, **1987**; *Chem. Abstr.* **1988**, *108*, P 89483d.
[5] Compound **3a** was passed at about 0.75 Torr without carrier gas through a glass tube (ca. 45 × 1.5 cm) filled with Raschig rings and heated to 400 °C. The product **4a** was collected in a cold trap. Large quantities should already be diluted in an inert solvent before thawing to prevent spontaneous, strongly exothermic polymerization.
[6] Alternative syntheses for thiazoles **5–7**, **11**, and **12**: S. P. Cornwell, P. T. Kaye, A. G. Kent, G. D. Meakins, *J. Chem. Soc. Perkin Trans. 1* **1981**, 2340–2343; H. Nagazawa, *Yakugaku Zasshi* **1940**, *60*, 433–441; *Chem. Abstr.* **1941**, *35*, 458[8]; F. Eloy, A. Deryckere, *Chim. Ther.* **1973**, *8*, 437–446; M. O. Kolosova, *Zh. Obshch. Khim.* **1963**, *33*, 3667–3671.
[7] W. Gebhardt, *Ber. Dtsch. Chem. Ges.* **1884**, *17*, 2088–2095.
[8] J. Pornet, B. Randrianoelina, L. Miginiac, *J. Organomet. Chem.* **1979**, *174*, 1–13.
[9] E. D. Bergmann, D. Herrman, *J. Am. Chem. Soc.* **1951**, *73*, 4013–4015.
[10] A. W. Johnson, *J. Chem. Soc.* **1946**, 1009–1014.
[11] G. A. M. Van den Ouweland, H. G. Peer (Unilever) DE-1932800, **1970**; *Chem. Abstr.* **1970**, *72*, P 90265d.

Zinc Pyrazolylborate Complexes Relevant to the Biological Function of Carbonic Anhydrase**

By *Adrian Looney, Gerard Parkin,* Ralf Alsfasser, Michael Ruf,* and *Heinrich Vahrenkamp**

The zinc enzyme carbonic anhydrase, which is present in red blood cells, is a biological counterpart of hemoglobin, since it provides for efficient removal of the respiratory product CO_2 by catalyzing the equilibrium between carbon dioxide and bicarbonate [Eq. (a)].[1]

$$CO_2 + H_2O \rightleftharpoons HCO_3^- + H^+ \qquad (a)$$

Numerous studies have revealed the molecular structure and function of the enzyme, its modification, and inhibition.[2] Although details of the active site of the enzyme, consisting of a tetrahedral zinc center coordinated to three histidine imidazole groups and a water molecule $[His_3Zn(OH_2)]^{2+}$, have been determined by X-ray diffraction, it has not proven possible to crystallographically characterize either the enzyme–substrate (i.e. CO_2) complex or other intermediates of the catalytic cycle. As such, mechanistic suggestions concerning the catalytic pathway, which have invoked species with zinc-bound H_2O, OH^-, and HCO_3^- as reactive intermediates, have been guided by kinetic, spectroscopic, and theoretical studies only.[3]

Model studies with simple zinc compounds have been hampered by the difficulty of obtaining low-coordinate aqua- or hydroxozinc complexes;[4] Kimura's recent work is a notable exception.[5] However, using the highly substituted pyrazolylborato ligand HBL_3^- (L = 3-*tert*-butyl-5-methylpyrazolyl), we have recently been able to prepare and structurally characterize the first mononuclear tetrahedral hydroxozinc complex **1**.[6] This complex structurally mimics the $[His_3Zn–OH]^+$ moiety, which has been suggested as the active state of carbonic anhydrase. The hydroxide **1** appears to be well-suited for model reactivity studies related to the function of the enzyme, as borne out by our observations reported here.

Solutions of **1** in benzene react instantaneously with CO_2 resulting in an equilibrium mixture of **1** and a compound tentatively assigned as the hydrogencarbonato complex **2**, which is characterized by ν(CO) absorptions at 1675 and 1302 cm^{-1} in the IR spectrum. The reversibility of this reaction has been confirmed; removal of the CO_2 atmosphere results in rapid regeneration of the hydroxide **1**. In view of this facile interconversion, attempts to isolate the complex **2** as a crystalline solid were performed under CO_2 atmosphere. However, due to its lower solubility, the crystalline product that was isolated under these conditions was the dinuclear carbonato complex **3**. Complex **3** contains a bridging carbonato ligand and is characterized by ν(CO) absorptions at 1587 and 1311 cm^{-1} in the IR spectrum, which differ significantly from those observed for **2**, and a resonance at $\delta = 164.0$ in the ^{13}C NMR spectrum in C_6D_6. The molecular structure of **3** has been confirmed by X-ray diffraction.[7] While it is not unusual for hydroxo complexes to react with CO_2 to form carbonato complexes,[8] this is the first report of a carbonatozinc complex prepared by such a method. Furthermore, the role of the carbonate ion as a bis(unidentate) bridging ligand is also unprecedented.[8, 9]

In view of the lability of the hydrogencarbonato complex **2**, we have explored other methods to isolate a stable analogue. Thus, the methylcarbonato complex **4** was successfully obtained by treatment of the hydroxo complex **1** with dimethylpyrocarbonate as reagent and solvent. The molecular structure of the complex **4** was also determined by X-ray diffraction.[7] Five- and six-coordinate alkylcarbonatozinc complexes have been described previously,[10] but **4** is the first example with tetrahedral coordination and also an excellent structural model for the hydrogencarbonato complex **2**. The structural details of the [Zn-OCO_2] moiety close-

[*] Prof. G. Parkin, A. Looney
Department of Chemistry
Columbia University, New York, NY 10027 (USA)
Prof. Dr. H. Vahrenkamp, Dipl.-Chem. R. Alsfasser, M. Ruf
Institut für Anorganische und Analytische Chemie der Universität
Albertstrasse 21, D-W-7800 Freiburg (FRG)

[**] This work was supported by the National Science Foundation and the Deutsche Forschungsgemeinschaft. G. P. is the recipient of an A. P. Sloan Research Fellowship (1991–1993) and a Camille and Henry Dreyfus Teacher–Scholar Award (1991–1996). We thank S. Trofimenko, Du Pont, for making the synthesis of the tris(pyrazolyl)borato ligand accessible to us.

ly resemble those of both the dinuclear carbonato complex **3** and the related acetatozinc complex $[\{\eta^3\text{-}HBL_3\}Zn(\eta^1\text{-}OCOCH_3)]$ (L = 3-*tert*-butylpyrazolyl).[11] Furthermore, the similarity of the IR stretching frequencies of **2** (1675 and 1302 cm^{-1}) and **4** (1689 and 1297/1280 cm^{-1}) furnishes good evidence for an analogous coordination mode.

The hydrogencarbonato complex **2**, carbonato complex **3**, and methylcarbonato complex **4** are rapidly hydrolyzed by water in organic solvents to the hydroxo complex **1**. This observation is particularly significant since facile displacement of bicarbonate and the regeneration of the hydroxozinc species is a critical step in the proposed catalytic cycle for carbonic anhydrase.

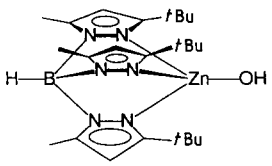

1

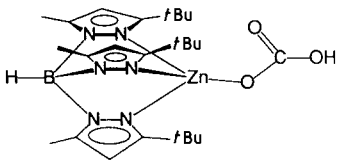

2

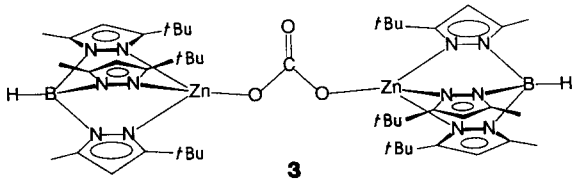

3

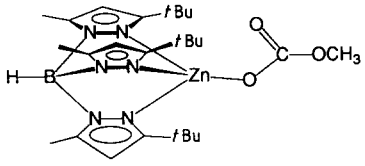

4

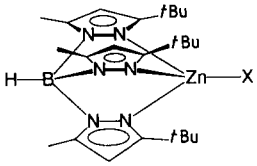

5a: X = Cl
5b: X = N_3
5c: X = CN

The pyrazolylboratozinc system in **2**, **3**, and **4** models the proposed action of carbonic anhydrase and also imitates the inhibition of carbonic anhydrase activity that is observed in the presence of small anions. Thus, methanol solutions of the hydroxo complex **1** react rapidly with chloride, azide, and cyanide salts, resulting in displacement of the hydroxo ligand and formation of the neutral complexes **5a–c**, which were characterized by spectra and analyses. However, the most well-known inhibitor of carbonic anhydrase, acetazolamide,[12] did not react with **1**.

These experiments indicate the close structural and chemical similarity that exists between the pyrazolylboratozinc system and the carbonic anhydrase enzyme system. In particular, the zinc-bound hydroxo ligand in **1** is observed to be both an efficient nucleophile and good leaving group, and the hydrogencarbonato ligand in **2** is labile, thereby fulfilling the prerequisites for catalytic turnover. The facile interconversions between these complexes provide the first functional model of carbonic anhydrase activity.

Received: August 19, 1991 [Z 4878 IE]
German version: *Angew. Chem.* **1992**, *104*, 57

CAS Registry numbers:
1, 136379-29-8; **2**, 137596-09-9; **3**, 137596-10-2; **3** · $2(C_6H_6)$, 137596-15-7; **4**, 137596-11-3; **5a**, 137596-12-4; **5b**, 137596-13-5; **5c**, 137596-14-6; CO_2, 124-38-9; pyrocarbonic acid dimethyl ester, 4525-33-1; carboanhydrase, 9001-03-0.

[1] B. L. Vallee in *Zinc Enzymes* (Ed.: T. G. Spiro), Wiley, New York, **1983**, p. 1; Y. Pocker, S. Sarkanen, *Adv. Enzymol.*, **1978**, *47*, 149–274.
[2] For recent reviews see: a) *Zinc Enzymes* (Eds.: I. Bertini, C. Luchinat, W. Maret, M. Zeppezauer), Birkhäuser, Boston, **1986**; b) S. Lindskog in [2a], p. 307, c) E. A. Eriksson, T. A. Jones, A. Liljas in [2a], p. 317; d) A. Galdes, B. L. Vallee in *Zinc and its Role in Biology and Nutrition* (Ed.: H. Sigel), Dekker, New York, **1983**, p. 1.
[3] For recent reviews see: J.-Y. Liang, W. Lipscomb, *Proc. Natl. Acad. Sci. USA*, **1990**, *87*, 3675–3679; B. L. Vallee, D. S. Auld, *ibid.* **1990**, *87*, 220–224. For recent theoretical studies see: O. Jacob, R. Cardenas, O. Tapia, *J. Am. Chem. Soc.* **1990**, *112*, 8692–8705; M. Sola, A. Lledos, M. Duran, J. Bertran, *Inorg. Chem.* **1991**, *30*, 2523–2527.
[4] See: R. S. Brown, J. Huguet, N. J. Curtis in [2d], p. 55; R. H. Prince in *Comprehensive Coordination Chemistry Vol. 5*, (Eds.: G. Wilkinson, R. D. Gillard, J. A. McCleverty), Pergamon, Oxford, **1987**, p. 925.
[5] E. Kimura, T. Shiota, T. Koike, M. Shiro, M. Kodama, *J. Am. Chem. Soc.* **1990**, *112*, 5805–5811.
[6] R. Alsfasser, S. Trofimenko, A. Looney, G. Parkin, H. Vahrenkamp, *Inorg. Chem.*, **1991**, *30*, 4098–4100.
[7] Crystal data: **3** · $2(C_6H_6)$: monoclinic, $C2/m$, $a = 20.475(5)$, $b = 12.831(2)$, $c = 17.360(4)$ Å, $\beta = 132.78(1)°$, $Z = 2$, 1579 reflections, $R = 0.042$. **4**: monoclinic, $P2_1/n$, $a = 10.698(2)$, $b = 18.244(4)$, $c = 15.657(3)$ Å, $\beta = 90.08(3)°$, $Z = 4$, 3163 reflections, $R = 0.045$ Details of the structure determinations will be given with the full publication.
[8] D. A. Palmer, R. van Eldik, *Chem. Rev.* **1983**, *83*, 651–731.
[9] See: N. Kitajima, K. Fujisawa, T. Koda, S. Hikichi, Y. Moro-oka, *J. Chem. Soc. Chem. Commun.* **1990**, 1357–1358; I. Murase, G. Vuckovic, M. Kodera, H. Harada, N. Matsumoto, S. Kida, *Inorg. Chem.* **1991**, *30*, 728–733, and references cited in these papers.
[10] M. Kato, T. Ito, *Inorg. Chem.* **1985**, *24*, 509–514.
[11] R. Han, I. B. Gorell, A. G. Looney, G. Parkin, *J. Chem. Soc. Chem. Commun.* **1991**, 717–719.
[12] A. E. Eriksson, P. M. Kylsten, T. A. Jones, A. Liljas, *Proteins* **1988**, *4*, 283–293; J. E. Coleman, *Annu. Rev. Pharmacol.* **1975**, *15*, 221–242; J. L. Evelhoch, D. F. Bocian, J. L. Sudmeier, *Biochemistry* **1981**, *20*, 4951–4954.

Crystal and Solution Structures of the Novel Complex of Sodium Ketimide with Two Ketimine Ligands $[(tBu_2C{=}NNa)_4(HN{=}CtBu_2)_2]$: Stacking of Complexed and Uncomplexed $(NNa)_2$ Rings to give a Highly Distorted $(NNa)_4$ Cubane**

By *William Clegg, Murray MacGregor, Robert E. Mulvey,** and *Paul A. O'Neil*

Lithium ketimides $(R^1R^2C{=}NLi)_n$ have proved to be valuable compounds in two respects. Firstly, they provide a convenient source of free ketimine anions $(R^1R^2C{=}N)^-$ for transfer to other metal and metalloid centers in metathetical reactions.[1] Secondly, their crystal structures serve as models for the ring stacking in lithium structural chemistry.[2] The XLi compounds (X = e.g., alkyl, aryl, enolate, halide) form small, single $(XLi)_n$ ring units which maximize their electrostatic (attractive) contacts in face-to-face stacking arrangements. Hexameric lithium ketimides form stacks of two trimeric $(R^1R^2C{=}NLi)_3$ rings.[3] Prior to the work described

[*] Dr. R. E. Mulvey, M. MacGregor
Department of Pure and Applied Chemistry
University of Strathclyde
GB-Glasgow, G1 1XL (UK)
Dr. W. Clegg, P. A. O'Neil
Department of Chemistry
The University
GB-Newcastle upon Tyne, NE1 7RU (UK)

[**] This work was supported by the U. K. Science and Engineering Research Council and by the Royal Society. We thank Dr. P. R. Dennison (University of Strathclyde) for running the NMR spectra.

here, monometallic sodium ketimide chemistry[4] was represented by a single report from 1934 on ammonia-contaminated $(Ph_2C{=}NNa)_n$ characterized by N, Na-microanalysis;[5] this preempted the first lithium ketimide study[6] by over thirty years. We investigated the metallation reaction of the ketimine $tBu_2C{=}NH$ with nBuM (M = Li, Na) [Eq. (a)].

$$n\text{BuM} + t\text{Bu}_2\text{C}{=}\text{NH} \rightarrow {}^1/_n\,(t\text{Bu}_2\text{C}{=}\text{NM})_n + n\text{BuH} \qquad \text{(a)}$$

For M = Li the metallation proceeds as expected giving crystalline $(tBu_2C{=}NLi)_6$ in nearly quantitative yield.[7] Reaction mixtures having excess ketimine afford the same solid product. In contrast, when M = Na, two products are detectable: a yellow amorphous material (the major product) which is still under investigation[8] and a few crystals of **1**, an unexpected complex of ketimide and nonmetalated

$[(tBu_2C{=}NNa)_4(HN{=}CtBu_2)_2]$ **1**

ketimine. We suspect the reaction stoichiometry was not exactly 1.0:1.0, since the purity of the nBuNa reactant, freshly prepared from nBuLi and tBuONa,[9] though high, fell short of 100%. Hence, a trace excess of ketimine is available to complex two Na^+ cations in **1**. On deliberately increasing the nBuNa:$tBu_2C{=}NH$ ratio to 1.0:1.5, consistent with the metal:ligand ratio in **1** (4:6), no amorphous material is produced and the yield of **1** (first batch, 46%) is greatly enhanced.

The crystal structure of **1** (Fig. 1)[10] displays a cubane-like (imido-N-Na)$_4$ core. This structure is made up of a stack of complexed and uncomplexed $(NNa)_2$ rings with tetra-

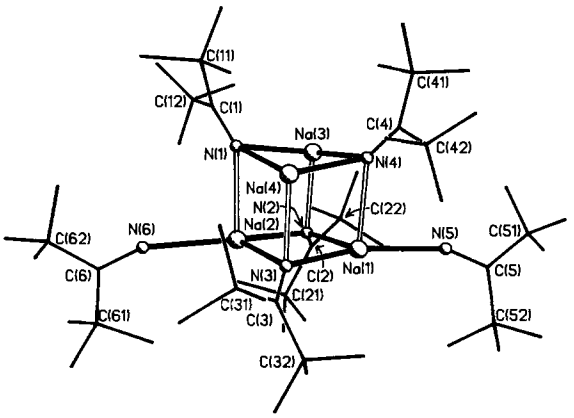

Fig. 1. Crystal structure of **1** (without hydrogen atoms). Important distances [Å] and angles [°]: Na(1)-N(2) 2.449(6), Na(1)-N(3) 2.478(4), Na(2)-N(2) 2.462(4), Na(2)-N(3) 2.425(6), Na(3)-N(1) 2.351(4), Na(3)-N(4) 2.311(7), Na(4)-N(1) 2.287(7), Na(4)-N(4) 2.275(4), Na(1)-N(4) 2.450(5), Na(2)-N(1) 2.476(5), Na(3)-N(2) 2.326(5), Na(4)-N(3) 2.291(5), Na(1)-N(5) 2.475(5), Na(2)-N(6) 2.465(5), Na···Na 3.021(4)–3.183(3), N(1)-C(1) 1.241(8), N(2)-C(2) 1.253(8), N(3)-C(3) 1.255(8), N(4)-C(4) 1.254(7), N(5)-C(5) 1.266(7), N(6)-C(6) 1.256(7); N(2)-Na(1)-N(3) 98.3(2), N(2)-Na(1)-N(4) 92.0(1), N(3)-Na(1)-N(4) 91.2(1), N(2)-Na(2)-N(3) 99.4(2), N(2)-Na(2)-N(1) 93.6(1), N(3)-Na(2)-N(1) 95.9(2), N(1)-Na(3)-N(4) 94.2(2), N(1)-Na(3)-N(2) 100.7(2), N(4)-Na(3)-N(2) 104.2(2), N(1)-Na(4)-N(4) 96.9(2), N(1)-Na(4)-N(3) 105.3(2), N(4)-Na(4)-N(3) 100.9(2), Na(3)-N(1)-Na(4) 82.1(2), Na(3)-N(1)-Na(2) 81.4(1), Na(4)-N(1)-Na(2) 78.6(2), Na(3)-N(4)-Na(4) 83.2(2), Na(3)-N(4)-Na(1) 79.6(2), Na(4)-N(4)-Na(1) 83.3(2), Na(1)-N(2)-Na(2) 80.8(2), Na(1)-N(2)-Na(3) 79.3(2), Na(2)-N(2)-Na(3) 82.2(1), Na(1)-N(3)-Na(2) 81.0(2), Na(1)-N(3)-Na(4) 82.3(1), Na(2)-N(3)-Na(4) 79.6(2), N(5)-Na(1)-N(2) 103.5, N(5)-Na(1)-N(3) 157.6(2), N(5)-Na(1)-N(4) 91.4(2), N(6)-Na(2)-N(2) 151.6(2), N(6)-Na(2)-N(3) 107.8(2), N(6)-Na(2)-N(1) 91.8(2), N(1)-C(1)-C(11) 121.0(6), N(1)-C(1)-C(12) 119.9(5), C(11)-C(1)-C(12) 119.1(5), N(2)-C(2)-C(21) 118.4(5), N(2)-C(2)-C(22) 123.2(5), C(21)-C(2)-C(22) 118.4(5), N(3)-C(3)-C(31) 121.5(5), N(3)-C(3)-C(32) 120.1(4), C(31)-C(3)-C(32) 118.4(5), N(4)-C(4)-C(41) 120.7(7), N(4)-C(4)-C(42) 119.5(5), C(41)-C(4)-C(42) 119.7(6), N(5)-C(5)-C(51) 121.3(6), N(5)-C(5)-C(52) 115.9(5), C(51)-C(5)-C(52) 122.8(5), N(6)-C(6)-C(61) 116.3(4), N(6)-C(6)-C(62) 120.9(5), C(61)-C(6)-C(62) 122.7(5).

(Na(1),(Na(2)) and tricoordinate (Na(3),Na(4)) sodium, respectively. To optimize stacking the ketimine nitrogens (N(5),N(6)) lie approximately in the same plane as the complexed ring; the N(4)Na(1)N(5) and N(1)Na(2)N(6) bond angles are close to 90°. Complexation weakens the intramolecular ring bonding, expanding the Na(1)N(2)Na(2)N(3) face (perimeter 9.814 Å; cf. 9.224 Å for the uncomplexed Na(3)N(1)Na(4)N(4) face). The deviation from an ideal cube is most pronounced at the Na(4) corner resulting in the shortest N-Na edge lengths for those bonds with Na(4) (sum, 6.853 Å, cf. 6.988 Å for the related Na(3) corner). This strong distortion brings Na(4) into close proximity with a tBu hydrogen atom. Without independently refined hydrogen positions we cannot comment on the significance of this feature except to note that assuming normal tBu C-H geometries, the calculated H···Na length would be remarkably short (2.186 Å). Triply bridged by Na atoms, each imido N center exhibits pseudotetrahedral coordination. The remaining N centers (N(5),N(6)) belonging to nonmetalated ketimine molecules (i.e., retaining acidic N-H bonds) act as monodentate, terminal Lewis bases to two of the four Na^+ ions (Na(1),Na(2)). This is the first example of ketimine → alkali-metal dative bonding. The structure most similar to **1** is the pinacolone-solvated sodium enolate of pinacolone, but even here its $(ONa)_4$ cubane core is solvated by four rather than two molecules which could potentially be metalated.[11]

Evidence that **1** remains intact in [D_8]toluene solution over the wide temperature range examined (193–298 K) comes from ^{1}H NMR spectroscopic studies. The spectrum at 193 K shows the two ketimine (NH) protons downfield (δ = 9.09) and four distinct types of tBu resonances (δ = 1.39, 1.35, 1.03, 0.81) with intensity ratios (36:36:18:18) in agreement with the crystal structure. The first two tBu signals which overlap can be assigned to ketimido ligands associated with N(2),N(3) in the complexed ring (36H) and with N(1),N(4) in the uncomplexed ring (36H). The remaining signals are attributed to the two magnetically nonequivalent tBu groups (18H + 18H) on each (identical) ketimine molecule and are a result of the rigid attachment of the C=N(5)H and C=N(6)H units to the Na(1)N(2)Na(2)N(3) ring. The spectrum at 298 K similarly shows four tBu resonances. Thus both X-ray crystallographic studies and ^{1}H NMR spectroscopic studies confirm the presence of (ketimine)-N–Na donor–acceptor contacts. This is an important distinction from the structural chemistry of organolithium compounds, since Li^+ cations in $(tBu_2C{=}NLi)_6$ resist complexation by stronger donors.[7]

Experimental Procedure

1: An equimolar amount of $tBu_2C{=}NH$ added to a chilled heptane suspension of nBuNa under argon gave an insoluble yellow solid and a yellow solution. The solution was refrigerated (−30 °C) and large yellow crystals identified as **1** formed; 4% yield of first batch (based on ketimine consumption). From the reaction with the 1.0:1.5 molar ratio a 46% yield of **1** was obtained. M.p. = 91–93 °C; satisfactory C,H,N,Na-analyses. Compound **1** decomposes in contact with moisture or oxygen but is nonpyrophoric. Single crystals suitable for X-ray crystallography were sealed under argon in Lindemann capillary tubes prior to data collection.

Received: July 26, 1991 [Z 4830 IE]
German version: *Angew. Chem.* **1991**, *104*, 74

CAS Registry numbers:
1, 137695-99-9; nBuNa, 3525-44-8; $tBu_2C{=}NH$, 29097-52-7.

[1] Such reports were usually published by Wade et al. For a detailed list of examples see ref. [2], p. 168.
[2] R. E. Mulvey, *Chem. Soc. Rev.* **1991**, *20*, 167. This review focuses on the ring stacking of organonitrogen lithium compounds.

[3] D. R. Armstrong, D. Barr, R. Snaith, W. Clegg, R. E. Mulvey, K. Wade, D. Reed, *J. Chem. Soc. Dalton Trans.* **1987**, 1071.
[4] Two mixed lithium–sodium ketimides have been described: W. Clegg, R. E. Mulvey, R. Snaith, G. E. Toogood, K. Wade, *J. Chem. Soc. Chem. Commun.* **1986**, 1740; D. Barr, W. Clegg, R. E. Mulvey, R. Snaith, *ibid.* **1989**, 57.
[5] G. E. P. Smith, F. W. Bergstrom, *J. Am. Chem. Soc.* **1934**, *56*, 2095.
[6] L.-H. Chan, E. G. Rochow, *J. Organomet. Chem.* **1967**, *9*, 231.
[7] Ether, pentamethyldiethylenetriamine (PMDETA), pyridine, tetramethylethylenediamine (TMEDA), and triethylamine fail to give solid adducts, though a 1:1 adduct is formed with the exceptionally strong donor hexamethylphosphoramide (HMPA). D. Barr, R. Snaith, W. Clegg, R. E. Mulvey, K. Wade, *J. Chem. Soc. Dalton Trans.* **1987**, 2141.
[8] A strong IR band at 1600 cm^{-1} characteristic of a C=N bond and an ^1H NMR spectrum in [D_8]toluene consisting of a singlet at $\delta = 1.19$ characteristic of a *t*Bu group suggest this product is uncomplexed $(tBu_2C{=}NNa)_n$. M.p. 178–180 °C (decomp.).
[9] L. Lochmann, J. Pospíšil, D. Lím, *Tetrahedron Lett.* **1966**, 257.
[10] **1**: $M_r = 935.5$, triclinic, space group $P\bar{1}$, $a = 13.072(5)$, $b = 13.469(5)$, $c = 20.613(8)$ Å, $\alpha = 78.74(2)$, $\beta = 74.68(2)$, $\gamma = 64.67(2)°$, $V = 3149.7$ Å^3, $Z = 2$, $\varrho_{calcd} = 0.984$ g cm^{-3}, $F(000) = 1036$, $Mo_{K\alpha}$ radiation, $\lambda = 0.71073$ Å, $\mu = 0.08$ mm^{-1}. The structure was determined by direct methods and refined from 4864 unique observed reflections measured at 240 K with a Stoe-Siemens diffractometer ($2\theta_{max} = 45°$), with anisotropic thermal parameters and with isotropic H atoms in calculated positions: $R = 0.103$, $R_w = 0.116$, $S = 1.16$ for 577 parameters. Further details of the crystal structure investigation can be obtained from the Director of the Cambridge Crystallographic Data Centre, University Chemical Laboratory, Lensfield Road, Cambridge, CB2 1EW (U. K.), on quoting the full journal citation.
[11] P. G. Williard, G. B. Carpenter, *J. Am. Chem. Soc.* **1986**, *108*, 462.

Unusual Coordination of the 1,3-Diphosphacyclobutadiene Derivative $(i\mathrm{Pr_2NCP})_2$ to Two $[Ni(CO)_3]$ Fragments**

By *Joseph Grobe,* Duc Le Van, Marianne Hegemann, Bernt Krebs,* and *Mechtild Läge*

The chemistry of the phosphaalkynes RC≡P contains many surprises, as the investigations of recent years have shown.[1] In particular, studies on reactivity of *tert*-butylphosphaethyne have uncovered many new aspects in organophosphorus and complex chemistry.[2] Yet phosphaalkyne derivatives with donor or acceptor substituents have hardly received any attention.[1,3] We report here an unexpected reaction of the only recently synthesized di(isopropyl)aminophosphaethyne $i\mathrm{Pr_2NC{\equiv}P}$ (**1**)[4] with tetracarbonylnickel.

On dropwise addition of **1** to a solution of $[Ni(CO)_4]$ in ether, CO evolution is observed, and complex **2**, which contains two $[Ni(CO)_3]$ groups on one of the phosphorus atoms of the 1,3-diphosphacyclobutadiene ring, is formed as exclusive product (monitoring by IR during the reaction and by NMR afterwards).

$$2\ i\mathrm{Pr_2N\text{-}C{\equiv}P} + 2\ [Ni(CO)_4] \xrightarrow[-2CO]{20\,^\circ C} [(CO)_3Ni\{\eta^1\text{-}\mu_2\text{-}(i\mathrm{Pr_2NCP})_2\}Ni(CO)_3]$$
1 **2**

The composition and constitution of the ruby-red crystals of compound **2** were established by elemental analysis, IR and NMR (^1H, ^{13}C, ^{31}P) spectroscopy, and by X-ray structure analysis. The isopropyl groups are shown to be nonequivalent in the ^1H and ^{13}C NMR spectra, which suggests restricted rotation of the R_2N group about the PC–N bond. The sp^2-hybridized C atoms of the cyclic phosphorus ligand are magnetically equivalent; one of the $^1J(P, sp^2\text{-}C)$ couplings is only 3.8 Hz. Two signals of equal intensity are observed in the ^{31}P NMR spectrum ($\delta = 106.3$ and 94.2), and the $^2J(P,P)$ is remarkably small (9.0 Hz). The frequencies of the CO valence bands are ca. 30 cm^{-1} higher than those of the phosphanido-bridged carbonylnickel complexes $[(CO)_3Ni(\eta^1\text{-}\mu_2\text{-}PR_2)Ni(CO)_3]^-$ [5] and are best compared with the CO absorptions of a tricarbonylnickel–phosphaallene compound.[6]

The most important information on the unusual compound **2** is found in the crystal structure analysis.[7] In accord with the NMR and IR data, it shows that both $[Ni(CO)_3]$ fragments are bound to only one P atom (Fig. 1). In the heart

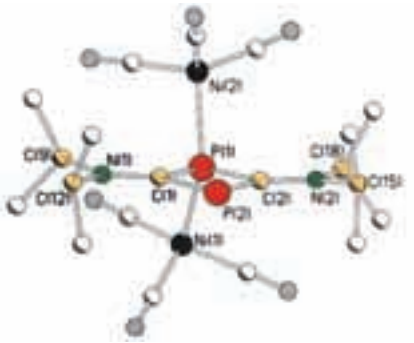

Fig. 1. Molecular structure of **2** in the crystal; important bond lengths [Å] and angles [°]: P(1)-C(1) 1.850(4), P(1)-C(2) 1.855(3), P(1)-Ni(1) 2.271(1), P(1)-Ni(2) 2.271(1), P(2)-C(1) 1.784(3), P(2)-C(2) 1.783(4), C(1)-N(1) 1.304(4), C(2)-N(2) 1.308(4); C(1)-P(1)-C(2) 77.8(2), Ni(1)-P(1)-C(1) 107.2(1), Ni(2)-P(1)-C(1) 109.0(1), Ni(1)-P(1)-C(2) 114.7(1), Ni(2)-P(1)-C(2) 111.3(1), Ni(1)-P(1)-Ni(2) 125.8(1), C(1)-P(2)-C(2) 81.4(2), P(1)-C(1)-P(2) 100.4(2), P(1)-C(2)-P(2) 100.3(2), N(1)-C(1)-P(1) 128.0(3), N(1)-C(1)-P(2) 131.6(3), N(2)-C(2)-P(1) 128.2(3), N(2)-C(2)-P(2) 131.4(3), C(1)-N(1)-C(9) 121.2(3), C(9)-N(1)-C(12) 116.2(3), C(1)-N(1)-C(12) 122.5(3), C(2)-N(2)-C(15) 122.2(3), C(2)-N(2)-C(18) 121.3(3), C(15)-N(2)-C(18) 116.4(3).

of the molecule all ten skeletal atoms of $-[C_2NCP]_2-$ lie in one plane (average deviation: 0.059 Å). This result indicates an extensively delocalized electronic system. The distances P1–C1 and P1–C2 are virtually the same and correspond to the length of a P–C single bond (1.85 Å). In contrast, the practically identical P2–C1 and P2–C2 distances (1.784 and 1.783 Å, respectively) result from a bond order greater than 1. The participation of the lone pairs of the $i\mathrm{Pr_2N}$ substituents in the resonance formulas is confirmed by both the planar environment and the marked shortening of the C1–N1 and C2–N2 bonds (1.304 and 1.308 Å, respectively). The Ni1–P1 and Ni2–P1 distances are equal (2.271 Å) and lie within the range expected for phosphanenickel complexes.

This interesting structure, and likewise the spectroscopic data, prove the presence of a delocalized π electron system. The bonding relationships are approximately represented by

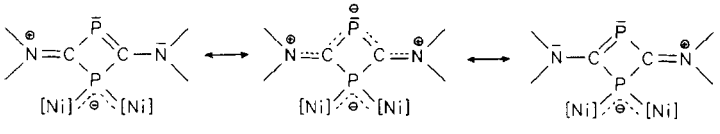

2A **2B** **2C**

[*] Prof. Dr. J. Grobe, Dr. D. Le Van, Dipl.-Chem. M. Hegemann, Prof. Dr. B. Krebs, M. Läge
Anorganisch-Chemisches Institut der Universität
Wilhelm-Klemm-Strasse 8, D-W-4400 Münster (FRG)

[**] Reactive E=C(p–p)π Systems, Part 29. This work was supported by the Deutsche Forschungsgemeinschaft and the Fonds der Chemischen Industrie. Part 28: J. Grobe, D. Le Van, T. Grosspietsch, *Z. Naturforsch. B*, **1991**, *46*, 978–984.

the zwitterionic resonance formulas **2A** and **2C** and best described by formula **2B** ([Ni] = [Ni(CO)$_3$]).

This type of coordination of a 1,3-diphosphacyclobutadiene to complex fragments is hitherto unparalleled and documents the influence of the donor substituents NR_2 on the coordinating properties of phosphaalkyne **1**. Complex **2** forms so rapidly that not even IR and NMR spectroscopy can detect intermediates. Thus in principle several reaction paths are possible. Scheme 1 depicts the most probable

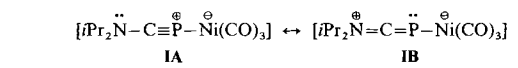

routes. Along route a, the mononuclear complex **I** postulated as primary product undergoes a [2 + 2]-cycloaddition with another molecule of **1** to form the 1,3-diphosphacyclobutadiene derivative **II**, which reacts with additional [Ni(CO)$_4$] to give the end product **2**. We favor route b in which the zwitterion **IB** that best represents the bonding situation in **I** forms intermediate **III** with [Ni(CO)$_4$]. This intermediate reacts with another molecule of **1** to yield the complex **2**. These proposals take account of the following

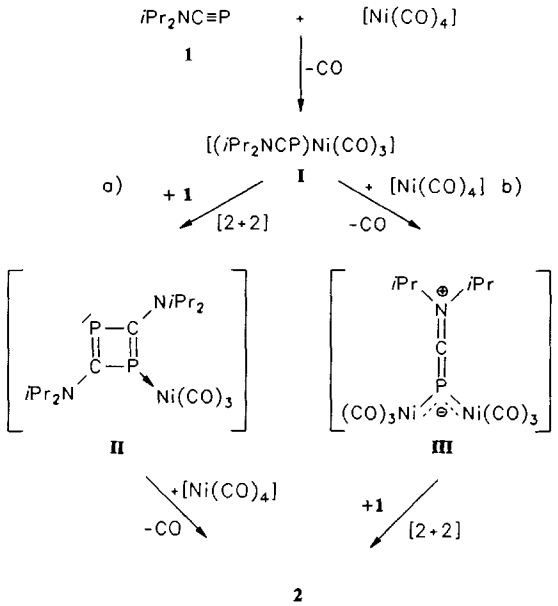

Scheme 1. Proposed routes for the formation of 2.

facts: a) Di(isopropyl)aminophosphaethyne (**1**) shows no tendency to cyclodimerize without activation.[4] b) The coordination of phosphaalkynes and alkynes to transition-metal complexes makes a [2 + 2]-cycloaddition possible.[8] c) *C*-amino substituted phosphaalkenes like $F_3CP{=}C(X)NR_2$ (X = F, OR) react with [Cr(CO)$_5$(thf)] via the isolable mononuclear complexes [(CO)$_5$CrP(CF$_3$)C(X)NR$_2$] to yield the dinuclear complexes [{(CO)$_5$Cr}$_2${P(CF$_3$)C(X)NR$_2$}] containing a 4e donor η^1-μ_2 bridge.[9, 10]

Experimental Procedure

To a solution of [Ni(CO)$_4$] (0.26 g, 1.5 mmol) in 10 mL diethylether was added dropwise at 20 °C in an argon atmosphere a solution of *i*Pr$_2$N–C≡P (**1**, 0.15 g, 1.0 mmol, in 10 mL ether). The reaction mixture was then stirred for 2 h at room temperature, the solvent removed under vacuum, and the residue taken up in ca. 20 mL *n*-pentane. The finely divided nickel which separated was removed in an inert atmosphere on a frit sealed with a 1 cm layer of silanized silica gel. The deep red filtrate was concentrated to 5 mL and stored at −30 °C. After three days the ruby red crystals of complex **2** were isolated. NMR studies of the reaction mixture showed that **2** was the only product of the quantitative reaction of **1**, but workup introduced considerable losses. The isolable yield was only 46%.

Spectroscopic data of **2**: IR (KBr), pentane: $\tilde{\nu}$ (CO) = 2063 (w), 2046 (s), 1991 (vs, br.), 1986 (vs, br.); ^{1}H NMR (300 MHz, CDCl$_3$, 25 °C, TMS): δ = 1.09 (d, ^3J(H,H) = 6.50 Hz, 6H; CH$_3$), 1.33 (d, ^3J(H,H) = 6.94 Hz, 6H; CH$_3$), 3.29 (sept, ^3J(H,H) = 6.94 Hz, 1H; CH), 4.45 (dsept, ^3J(H,H) = 6.50 Hz, ^4J(P,H) = 2.68 Hz, 1H; CH); ^{31}P NMR (36.44 MHz, CDCl$_3$, 25 °C, 85% H$_3$PO$_4$): δ = 106.3 (d, ^2J(P,P) = 9.0 Hz), 94.2 (d, ^2J(P,P) = 9.0 Hz); ^{13}C NMR (75.43 MHz, CDCl$_3$, 25 °C, TMS): δ = 19.9 (s; CH$_3$), 20.4 (d, ^4J(P,C) = 14.8 Hz; CH$_3$), 51.6 (s; CH), 56.7 (d, ^3J(P,C) = 18.2 Hz; CH), 197.7 (d, ^2J(P,C) = 3.4 Hz; CO), 210.2 (dd, ^1J(P,C) = 3.8 and 56.1 Hz, sp^2-C).

Received: August 2, 1991 [Z 4850 IE]
German version: *Angew. Chem.* **1992**, *104*, 94

CAS Registry numbers:
1, 128871-10-3; **2**, 137494-45-2; Ni(CO)$_4$, 13463-39-3.

[1] M. Regitz, *Chem. Rev.* **1990**, *90*, 191–213.
[2] M. Regitz, P. Binger, *Angew. Chem.* **1988**, *100*, 1541–1565; *Angew. Chem. Int. Ed. Engl.* **1988**, *27*, 1484–1508; J. F. Nixon, *Chem. Rev.* **1988**, *88*, 1327–1362.
[3] R. Appel, M. Poppe, *Angew. Chem.* **1989**, *101*, 70–71; *Angew. Chem. Int. Ed. Engl.* **1989**, *28*, 53–54; E. Niecke, R. Streubel, M. Nieger, D. Stalke, *ibid.* **1989**, *101*, 1708–1710 and **1989**, *28*, 1673–1674.
[4] J. Grobe, D. Le Van, B. Lüth, M. Hegemann, *Chem. Ber.* **1990**, *123*, 2317–2320.
[5] K. Jonas, L. Schieferstein, *Angew. Chem.* **1976**, *88*, 682–683; *Angew. Chem. Int. Ed. Engl.* **1976**, *15*, 622.
[6] R. Appel, F. Knoch, V. Winkhaus, *J. Organomet. Chem.* **1986**, *307*, 93–95.
[7] Crystal structure analysis of **2** at 170 K: $C_{20}H_{28}N_2O_6P_2Ni_2$, space group $P2_1/n$, a = 11.226(2), b = 17.734(4), c = 13.658(3) Å, β = 98.48(2)°, Z = 4, ϱ_{calcd} = 1.41 gcm^{-3}; $Mo_{K\alpha}$ radiation (λ = 0.71069 Å), Siemens P3 four-circle diffractometer, number of independent reflections: 5917, number of reflections with $I > 2\sigma(I)$: 4222, R_1 = 0.0428, R_2 = 0.0369, solution by Patterson methods (SHELXTL-plus). Further details of the crystal structure investigation may be obtained from the Fachinformationszentrum Karlsruhe, Gesellschaft für wissenschaftlich-technische Information mbH, D-W-7514 Eggenstein-Leopoldshafen 2 (FRG) on quoting the depository number CSD-55661, the names of the authors, and the journal citation.
[8] P. Binger, J. Haas, A. T. Herrmann, F. Langhauser, C. Krüger, *Angew. Chem.* **1991**, *103*, 316–318; *Angew. Chem. Int. Ed. Engl.* **1991**, *30*, 310–312.
[9] J. Grobe, D. Le Van, B. Krebs, R. Fröhlich, A. Schiemann, *J. Organomet. Chem.* **1990**, *389*, C29–C33; J. Grobe, D. Le Van, U. Althoff, B. Krebs, M. Dartmann, R. Gleiter, *Heteroat. Chem.* **1991**, *2*, 385–394.
[10] Note added in proof (November 8, 1991): E. Niecke and co-workers (Universität Bonn) have obtained an analogous complex by the reaction of (Me$_3$Si)*i*PrNC≡P with Ni(CO)$_4$. Personal communication; *Chem. Ber.* **1992**, submitted.

Bicyclocalix[4]arenes**

By *Bettina Berger, Volker Böhmer,* Erich Paulus, Amado Rodriguez,* and *Walter Vogt*

Dedicated to Professor Hermann Kämmerer on the occasion of his 80th birthday

Exciting molecules have always caught the interest of chemists.[1] The ever-increasing attention that the calixarenes[2] are receiving[3] over and above the already realized practical applications is probably largely due to fascination caused by the structure of these compounds. Questions related to the conformation,[4–7] the mechanism of conforma-

[*] Dr. V. Böhmer, Dipl.-Ing. B. Berger, Dr. A. Rodriguez, Prof. Dr. W. Vogt
Institut für Organische Chemie der Universität
J.-J. Becherweg 34, SB1, D-W-6500 Mainz (FRG)
Dr. E. F. Paulus
Hoechst AG
D-W-6230 Frankfurt (FRG)

[**] This work was supported by the Deutsche Forschungsgemeinschaft and the European Community.

tional interconversion,[7-13] and the fixing of particular conformations by suitable derivatives[14,15] are main topics of experimental[7-9,12,13] and theoretical studies.[11]

If two *para* positions of opposite arene rings in calix[4]arenes are linked by an aliphatic chain,[16] the calix[4]arene system is fixed in the cone conformation. At least temperature-dependent ^{1}H NMR spectra give no indication of conversion to the partial cone or 1,3-alternate conformations, which are in principle still possible. Reinhoudt et al. synthesized similar compounds in which opposite *para* positions were linked by an oligoethyleneglycol chain.[10] In order to prepare these compounds and to increase their stability, the phenolic hydroxy groups were methylated, which increased the flexibility of this calixarene system in comparison to those with free hydroxy groups.[7,9] Here a mixture of the partial cone and cone conformations were found at lower temperatures. For the first time detailed information about the mechanism of conformational interconversion could be obtained from 2D-EXSY NMR spectroscopy (EXSY = chemical *ex*change *s*pectroscop*y*). The limited conformational possibilities (no 1,2-alternate conformation) were helpful in this case.[10]

We were interested in compounds like **3** in which two opposite *para* positions were linked by a methylene-1,3-(2-hydroxyphenylene)-methylene bridge. The additional macrocyclic system formed by the bridge is also a calix[4]arene; thus, molecules of this type can be classified as macrobicyclo- or simply as bicyclocalix[4]arenes.[17] We report here the first examples of such compounds.

Condensation of 1,5-bis(4-hydroxyphenyl)pentan-3-one (obtained by aldol condensation of *p*-methoxybenzaldehyde followed by catalytic hydrogenation of the double bond and ether cleavage) yields, analogously to the known synthesis of bridged calixarenes,[16] compounds with a keto group in the bridge (Scheme 1). The yields of the purified compounds **1**

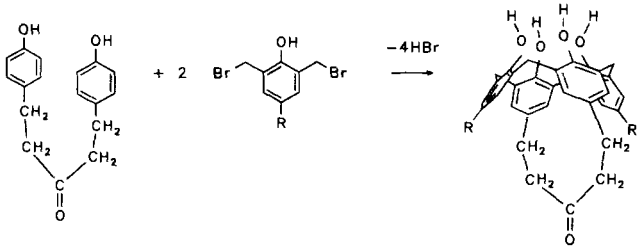

Scheme 1. **a**: R = CH_3, **b**: R = $C(CH_3)_3$, **c**: R = *cyclo*-C_6H_{11}, **d**: R = C_8H_{17}

(not optimized for particular cases) previously lay between 5 (**1d**, R = *n*-C_8H_{17}) and 37% (**1b**, R = $C(CH_3)_3$). The cone conformation observed for the calixarene part of **1** was not necessarily anticipated, since a partial-cone conformation with intramolecular hydrogen bonds to the keto group is also conceivable. In solution this is deduced from the ^{1}H NMR spectra, which show two doublets for the protons of the methylene bridge independent of temperature, and in the crystalline state from the X-ray structure analysis of **1c** (R = *cyclo*-C_6H_{11}, Fig. 1a).[18] The short bridge orients the two connected phenol units almost parallel to each other. They form angles of 91.2 and 93.5° with the best plane through the carbon atoms of the methylene groups. The corresponding angles for the other phenol units are 137.5 and 157.9°. As Figure 1a shows, the carbonyl group of the bridge points to the side of the phenol group that bends further outward, and forms an angle of 30° with the other phenol unit. The very strong distortion of the cone conformation directs the OH groups of the bridged phenol units outward and those of the two other phenol units inward. Thus, in contrast to free calix[4]arenes, the OH region becomes so polar that layers are formed in the crystal lattice with OH regions directed toward each other. The hydroxy groups are arranged in such a way that besides the intramolecular hydrogen bonds, intermolecular hydrogen bonds cannot be entirely excluded. The weakening of the intramolecular hydrogen bonds (O–O distances 2.88, 3.11, 2.93, and 2.76 Å) relative to those in the nonbridged calix[4]arenes is reflected in their OH stretching frequencies, which lie between 3420 and 3480 cm^{-1}, clearly higher than usually found for calix[4]arenes (about 3150 cm^{-1}).[3]

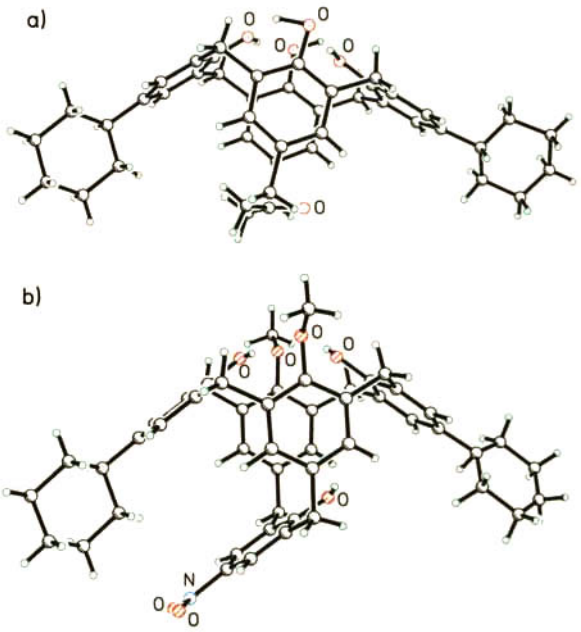

Fig. 1. a) Conformation of **1c** and b) **3b** in the crystal.

Whereas 1,5-bis(4-hydroxyphenyl)pentan-3-one (like other compounds with the same structural element) reacts smoothly with nitromalonaldehyde under alkaline conditions in a double aldol condensation to yield 2,6-bis(4-hydroxybenzyl)-4-nitrophenol,[19] the construction of a *p*-nitrophenol unit by the same reaction with compounds of type **1** is not possible. We suppose that under these strongly alkaline conditions **1** is present as tetraanion, in which the CH_2 group in α-position to the keto group is no longer CH-acidic enough. Methylation of **1** under mild conditions, even with an excess of methyl iodide, affords only the dimethyl ether **2** (a symmetric compound according to the ^{1}H NMR spectrum). However, this methylation of two hydroxyl groups is sufficient to permit the aldol condensation of **2** with nitro-

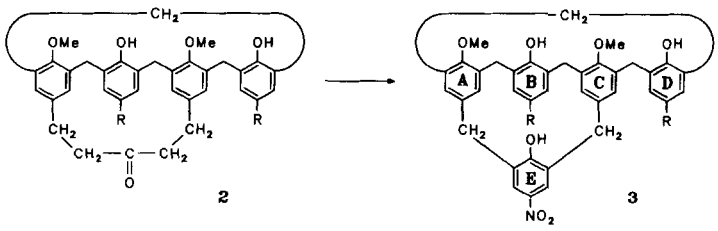

Scheme 2. **a** R = $C(CH_3)_3$, **b**: R = *cyclo*-C_6H_{11}.

malonaldehyde. The calixarenes **3** were prepared by this route with 60–70% yield of the purified compounds (Scheme 2).

The compound with R = *cyclo*-C_6H_{11} (**3b**) was characterized by X-ray structure analysis (Fig. 1b).[18] This showed that the methylation of **2** occurred at the two exposed hydroxyl groups of the bridged phenol units. Again, the original calix[4]arene system A-B-C-D is in the cone conformation. The relatively weak hydrogen bonds (O–O distances 3.00, 3.09, 2.96,and 3.12 Å) between the "*endo*" hydroxyl and methoxy groups are apparently sufficient to stabilize this conformation. The newly formed nitrophenol unit E is virtually parallel (7.3°) to one of the nonbridged phenol units, which shows that the CH_2–CO–CH_2 group hardly changed position or orientation on incorporation into the nitrophenol unit. The calix[4]arene systems with "*endo*" hydroxyl and "*exo*" methoxy groups (A-B-C-E and A-E-C-D) thus assume the 1,3-alternate or partial-cone conformation.

However, from the ^{1}H NMR spectrum of **3** in solution a conformation with (on average) C_{2v} symmetry may be deduced. The calix[4]arene part A-B-C-D is present in the cone conformation, which follows from the two doublets at about $\delta = 4.2$ and 3.25 for the Ar–CH_2–Ar methylene groups. The methylene groups on the nitrophenol unit give rise to a singlet ($\delta = 3.45$). One signal each is observed for the aromatic protons of the units D (nitrophenol), A/C (anisol), and B/D (phenol), for the methoxy and *tert*-butyl groups, and the OH groups of the B/D units (overlapping with the signal from the methoxy groups). Apparently the nitrophenol unit is mobile at room temperature and swings through the cavity of the calixarene like the clapper of a bell. As Figure 2 shows, this movement begins to freeze between −50 and −70 °C. At −90 °C two singlets are found for the aromatic protons of each of the units A/C (the *meta* coupling cannot be recognized because of line broadening) and B/D, for the OH groups on B/D, and for the *tert*-butyl groups. In the region between $\delta = 3$ and 4.4 six doublets for the three different (paired) methylene groups are expected in addition to the singlets for the methoxy and hydroxyl groups. Of these 14 signals, 12 are observed in the 200 MHz spectrum (Fig. 2).

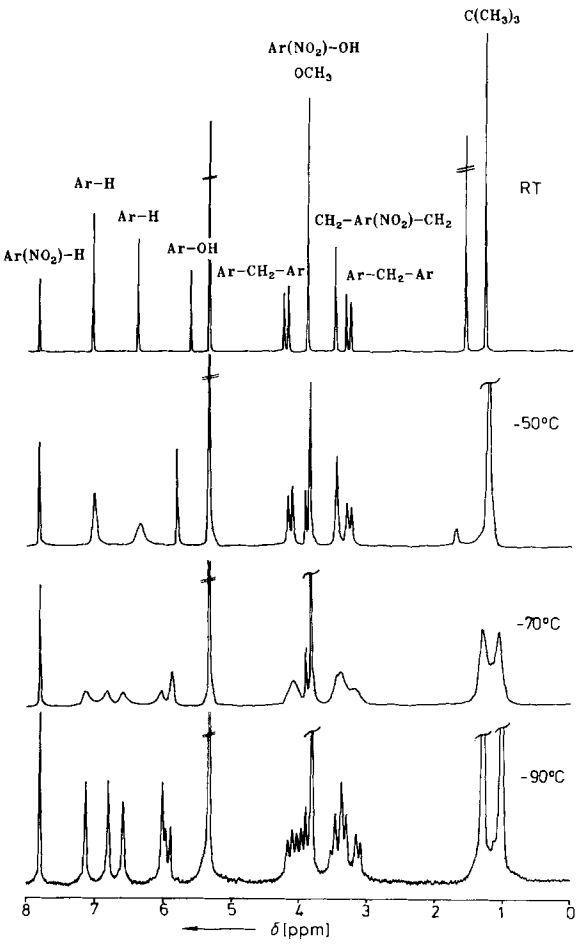

Fig. 2. Temperature dependence of the ^{1}H NMR spectra of **3a**, showing the different flexibilities of the calix[4]arene subunits (the signals for CH_2Cl_2 and H_2O are crossed through). RT = room temperature.

Due to the special situation in molecule **3**, differences in reactivity are expected for the OH groups of the *p*-nitrophenol unit in **3** and in the model compound, 2,6-(4-methoxybenzyl)-4-nitrophenol (**4**). In dioxane the absorption maximum of **4** undergoes a bathochromic shift from 312 to 332 nm on addition of triethylamine, which can be explained by a hydrogen bond between **4** and the amine.[20] On the other hand, the absorption maximum of **3a** at 318 nm (indicating perhaps a weakening of the OH group compared to **4**) is not shifted on addition of triethylamine in concentrations up to 2 M. Apparently the OH group is not accessible to the amine.

However, the cleavage of the proton from the nitrophenol unit is possible with alkali-metal hydroxides in dioxane/methanol (1:1). In the case of **4** the absorption maximum shifts from 322 nm to 425 nm in the presence of small concentrations of LiOH, but nothing else changes significantly if the LiOH concentration is increased to 0.1–0.2 M. The absorption maximum of **3a** ($\lambda_{max} = 322$ nm) also undergoes a strong bathochromic shift ($\lambda_{max} = 446$ nm) at low LiOH concentrations (2×10^{-4}–5×10^{-2} M), but in contrast to the behavior of **4**, an increase in LiOH concentration causes the opposite shift, to shorter wavelengths ($\lambda_{max} = 426$ nm, at [LiOH] = 0.1–0.2 M). In principle the same behavior is observed in the presence of KOH. Smaller differences in the changes in absorption coefficient, resulting perhaps from the size of the cation, should not be overemphasized. The spectroscopic findings thus show that a nitrophenolate ion also forms in the case of **3a**, but that it is less solvated than in **4**, a result which agrees with the molecular structure of **3a**. We are continuing to prepare other compounds of the type **3** in which the building blocks A and C, in particular, are replaced by resorcinol or phloroglucin, in order to make possible a ring of intramolecular hydrogen bonds in the calix[4]arene systems A-B-C-E and A-E-C-D as well.

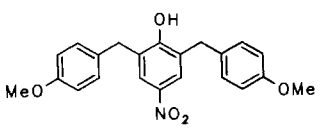

4

Experimental Procedure

General procedure for the synthesis of **1**: 1,5-bis(4-hydroxyphenyl)pentan-3-one (5 mmol) and the appropriate *p*-alkyl-2,6-bis(bromomethyl)phenol (10 mmol) were dissolved in dry dioxane, $TiCl_4$ (25 mmol) was added, and the volume was increased to 500 mL. The mixture was heated at reflux for 100–140 h under an inert atmosphere (argon). The solvent was then removed in vacuum, and the red-brown residue was dissolved in CH_2Cl_2. Silica gel (50 g) was added to the solution, which was once again evaporated to dryness. The silica gel thus impregnated was extracted in a Soxhlet apparatus (this procedure was repeated once). Thereafter **1** could easily be isolated by flash chromatography without the column becoming clogged.

Physical data for **1b**: Colorless crystals (37%) from *n*-hexane, m.p. = 264–266 °C. ^{1}H NMR (200 MHz, $CDCl_3$): δ = 7.16 (s, 4H; ArH), 6.51 (s, 2H; ArOH), 6.45 (s, 2H; ArOH), 6.37 (s, 4H; ArH), 4.07 (d, J = 14.4 Hz, 4H; Ar-CH_2-Ar), 3.34 (d, J = 14.4 Hz, 4H; Ar-CH_2-Ar), 2.38 (m, 4H; Ar-CH_2-CH_2), 2.02 (m, 4H; CH_2-CO), 1.41 (s, 18H; *t*Bu); MS: *m/z* 618 (M^+, 100%), 561 (14).

Methylation: The bridged calixarene **1** (0.3 mmol) was heated with CH_3I (0.25 g, 1.8 mmol) and K_2CO_3 (0.25 g, 1.8 mmol) in dry acetonitrile (25 mL) for 24 h at reflux. The solution was cooled, acidified with dilute HCl, and shaken with $CHCl_3$. The organic phase was dried over $MgSO_4$, the solvent removed in vacuum, and the residue purified by flash chromatography (CH_2Cl_2).

Physical data for **2b**: Colorless crystals (80%), m.p. = 272–274 °C. ^{1}H NMR (200 MHz, $CDCl_3$): δ = 6.96 (s, 4H; ArH), 6.35 (s, 4H; ArH), 5.52 (s, 2H; ArOH), 4.23 (d, J = 13.7 Hz, 4H; Ar-CH_2-Ar), 3.84 (s, 6H; OCH_3), 3.26 (d, J = 13.7 Hz, 4H; Ar-CH_2-Ar), 2.5 (m, 2H; C_6H_{11}), 2.38 (m, 4H; Ar-CH_2-CH_2), 2.03 (m, 4H; CH_2-CO), 1.85 (m, 10H; C_6H_{11}), 1.35 (m, 10H; C_6H_{11}); MS: *m/z* 698 (M^+, 100%), 684 (47).

Reaction with nitromalonaldehyde: Dimethyl ether **2** (0.1 mmol) and sodium nitromalonaldehyde [21] (80 mg, 0.6 mmol) were suspended in ethanol (15 mL), and a solution of Na (20 mg) in ethanol (1 mL) was added at reflux. After some time the mixture became homogeneous. Forty-eight hours later more of the aldehyde (80 mg) was added, and after another 72 h, a further 40 mg. After a total of 120 h the solution was filtered hot, and the filtrate added dropwise to dilute HCl. The precipitate was purified by flash chromatography (silica gel 60/CH_2Cl_2) and finally recrystallized from hexane.

Physical data for **3b**: Colorless crystals (70%), m.p. = 220 °C. ^{1}H NMR (400 MHz, $CDCl_3$): δ = 7.82 (s, 2H; ArH), 6.83 (s, 4H; ArH), 6.35 (s, 4H; ArH), 5.57 (s, 2H; ArOH), 4.19 (d, J = 13.6 Hz, 4H; Ar-CH_2-Ar), 3.85 (s, 6H; OCH_3), 3.83 (s, 1H; ArOH), 3.44 (s, 4H; Ar-CH_2-Ar), 3.23 (d, J = 13.6 Hz, 4H; Ar-CH_2-Ar), 2.33 (m, 2H; C_6H_{11}), 1.77 (m, 10H; C_6H_{11}), 1.31 (m, 10H; C_6H_{11}); MS: *m/z* 779 (M^+, 74%), 761 (27).

Received: July 26, 1991 [Z 4826 IE]
German version: *Angew. Chem.* **1992**, *104*, 89

CAS Registry numbers:
1b, 137569-06-3; **1c**, 137569-07-4; **1c** · CH_2Cl_2, 137624-54-5; **1d**, 137569-08-5; **2b**, 137569-09-6; **3b**, 137569-10-9; **3b** · *n*-C_6H_{14}, 137624-55-6; 1,5-bis(4-hydroxyphenyl)pentan-3-one, 93652-23-4; 2,6-bis(bromomethyl)-*p*-*tert*-butylphenol, 5011-36-9; 2,6-bis(bromomethyl)-*p*-cyclohexylphenol, 108817-19-2; 2,6-bis(bromomethyl)-*p*-octylphenol, 112921-43-4; sodium nitromalonaldehyde, 34461-00-2.

[1] F. Vögtle, *Reizvolle Moleküle der Organischen Chemie*, Teubner, Stuttgart **1989**.
[2] In a narrow sense calix[n]arenes are cyclic compounds in which n = 4 or more monovalent phenolic units coupled by methylene bridges *ortho* to the phenolic hydroxyl groups. The n OH groups are in *endo* positions. We use the name here generally for [1$_n$]-metacyclophanes with *exo* hydroxyl groups (cf. D. W. Chasar, *J. Org. Chem.* **1985**, *50*, 545–546), that is, also for cyclic tetramers obtained from resorcinol and aldehydes.[3] This is justifiable because lately calixarenes containing both *exo* and *endo* hydroxyl groups have been obtained. (M. Tabatabai, W. Vogt, V. Böhmer, *Tetrahedron Lett.* **1990**, *31*, 3295–3298.)
[3] C. D. Gutsche, *Calixarenes*, The Royal Chemical Society, Cambridge, **1990**; *Calixarenes, A Versatile Class of Macrocyclic Compounds*, (Eds.: J. Vicens, V. Böhmer), Kluwer, Dordrecht, **1991**.
[4] Four conformations can be distinguished for calix[4]arenes (and their derivatives). Gutsche named them the cone, partial-cone, 1,2-alternate, and 1,3-alternate conformations.
[5] S. Shinkai, K. Araki, M. Kubota, T. Arimura, T. Matsuda, *J. Org. Chem.* **1991**, *56*, 295–300.
[6] T. Arimura, M. Kubota, K. Araki, S. Shinkai, T. Matsuda, *Tetrahedron Lett.* **1989**, *30*, 2563–2566.
[7] L. C. Groenen, J.-D. van Loon, W. Verboom, S. Harkema, A. Casnati, R. Ungaro, A. Pochini, F. Ugozzoli, D. N. Reinhoudt, *J. Am. Chem. Soc.* **1991**, *113*, 2385–2392.
[8] K. Araki, S. Shinkai, T. Matsuda, *Chem. Lett.* **1989**, 581–584.
[9] S. Shinkai, K. Iwamoto, K. Araki, T. Matsuda, *Chem. Lett.* **1990**, 1263–1266.
[10] J.-D. van Loon, L. C. Groenen, S. S. Wijmenga, W. Verboom, D. N. Reinhoudt, *J. Am. Chem. Soc.* **1991**, *113*, 2378–2384.
[11] P. D. J. Grootenhuis, P. A. Kollman, L. C. Groenen, D. N. Reinhoudt, G. J. van Hummel, F. Ugozzoli, G. D. Andreetti, *J. Am. Chem. Soc.* **1990**, *112*, 4165–4176.
[12] L. Abis, E. Dalcanale, A. Du vosel, S. Spera, *J. Org. Chem.* **1988**, *53*, 5475–5479.
[13] L. Abis, E. Dalcanale, A. Du vosel, S. Spera, *J. Chem. Soc. Perkin Trans. 2*, **1990**, 2075–2080.
[14] K. Iwamoto, K. Fujimoto, T. Matsuda, S. Shinkai, *Tetrahedron Lett.* **1990**, *31*, 7169–7172.
[15] K. Iwamoto, A. Yanagi, K. Araki, S. Shinkai, *Chem. Lett.* **1991**, 473–476.
[16] H. Goldmann, W. Vogt, E. Paulus, V. Böhmer, *J. Am. Chem. Soc.* **1988**, *110*, 6811–6817.
[17] The name makes clear that *all* macrocyclic ring systems in **3** have a calix[4]arene structure. A "bicyclophane" in which two 1,3,5-substituted benzene rings are linked, not by three 1,3-xylylene bridges as in **3**, but by three ethylene(1,4-phenylene)ethylene bridges was described for the first time byH.-E. Högberg, B. Thulin, O. Wennerström, *Tetrahedron Lett.* **1977**, *11*, 931–934.
[18] **1c**: Single crystals from CH_2Cl_2; $C_{45}H_{50}O_5 \cdot 2\,CH_2Cl_2$, M_r = 840.8, triclinic, $P\bar{1}$, a = 13.276(3), b = 13.615(1), c = 13.673(2) Å, α = 84.85(2), β = 63.51(1), γ = 82.33(2)°, V = 2190.9 Å^3, Z = 2, $F(000)$ = 888, ϱ_{calcd} = 1.274 Mg m^{-3}, μ = 2.85 min^{-1}, T = 293 K, R = 0.100, R_w = 0.0968 [4507 ($>1\,\sigma(I)$) of 4512 independent reflections], $w = 1/\sigma^2(|F|)$ according to the counting statistics, S = 5.53; $-13 \le h \le 13$, $-13 \le k \le 13$, $-13 \le l \le 13$, R_{int} = 0.066. **3b**: Single crystals from *n*-Hexan; $C_{50}H_{53}NO_{70}$ 1/4 C_6H_{14}, M_r = 801.5, tetragonal, $P4/n$, a = 22.239(5), c = 17.453(1) Å, V = 8631.8 Å, Z = 8, $F(000)$ = 3428, ϱ_{calcd} = 1.233 Mg m^{-3}, μ = 0.074 min^{-1}, T = 293 K, R = 0.22, R_w = 0.058 [7244 ($>1\,\sigma(I)$) of 7626 independent reflections], $w = 1/\sigma^2(|F|)$ according to the counting statistics, S = 1.30; $-26 \le h \le 18$, $-26 \le k \le 0$, $-20 \le l \le 0$, R_{int} = 0.0688. The coordinates of only the hydroxyl-hydrogen atoms were determined experimentally. The positions of the remaining hydrogen atoms were calculated and their isotropic temperature coefficients estimated according to the relevant sites. For all other atoms, coefficients of anisotropic temperature factors were used and subjected to refinement. In the last refinement cycle the largest parameter change was smaller than 3(1)% of the standard deviation, and the ten largest maxima of the final difference Fourier synthesis of the electron density lay between 0.28 (0.50) and 0.55 (0.55) e Å^{-3}. The reason for the large difference between R and R_w is that reflections down to 1σ were taken into account in the calculation. Further details of the crystal structure investigation may be obtained from the Fachinformationszentrum Karlsruhe, Gesellschaft für wissenschaftlich-technische Information mbH, W-7514 Eggenstein-Leopoldshafen 2 (FRG) on quoting the depository number CSD-55724, the names of the authors, and the journal citation.
[19] See, for example, P. J. Dijkstra, M. Skowronska-Ptasinska, D. N. Reinhoudt, H. J. den Hertog, J. van Erden, S. Harkema, D. de Zeeuw, *J. Org. Chem.* **1987**, *52*, 4913–4921.
[20] In general, the absorption maximum of the longest wavelength band of *p*-nitrophenol undergoes a stronger bathochromic shift, the weaker the OH bond. Compare for example P. C. Dwivedi, A. K. Banga, N. Sharm, *Spectrochim. Acta Part A* **1986**, *42*, 623–629, zit. Lit.
[21] P. E. Fanta, *Organic Syntheses. Collective Volume 4* (Ed.: E. Rabjohn), Wiley-Interscience, New York, **1963**, S. 844–845.

Three Independent Molecules in the Unit Cell of a Phosphorus Ylide; Changes in the Molecular Geometry on Rotation about the Phosphorus–Carbon Ylide Bond**

By *Hansjörg Grützmacher** and *Hans Pritzkow*

The π interaction between the phosphorus atom and the ylide carbon atom of a phosphorus ylide is described as negative hyperconjugation.[1] This interaction transfers electron density from the occupied p orbital on the carbon atom to the unoccupied σ* orbitals of the phosphorus–ligand (L,X) bonds (Scheme 1); d orbitals on phosphorus fulfill only a polarizing function.[2] The phosphorus–ligand bond in an eclipsed position to the p orbital (P–X) becomes weaker and therefore longer, while the corresponding X-P-C angle opens. The ylidic carbon atom has a pyramidal configuration and the substituents in the x,y plane at phosphorus and carbon assume a *trans*-bent conformation with respect to the P–C(ylide) bond.[3] These theoretical characteristics are

[*] Dr. H. Grützmacher, H. Pritzkow
Anorganisch-chemisches Institut der Universität
Im Neuenheimer Feld 270, D-W-6900 Heidelberg (FRG)

[**] This work was supported by Prof. W. Sundermeyer, Prof. G. Huttner, the Deutsche Forschungsgemeinschaft, the Fonds der Chemischen Industrie and the Dr.-Otto-Röhm-Gedächtnisstiftung.

found in the molecular structures of ylides **1**,[4] **2**,[5] and **6**[6] reported in the pioneering work of Schmidbaur et al. (Scheme 1).

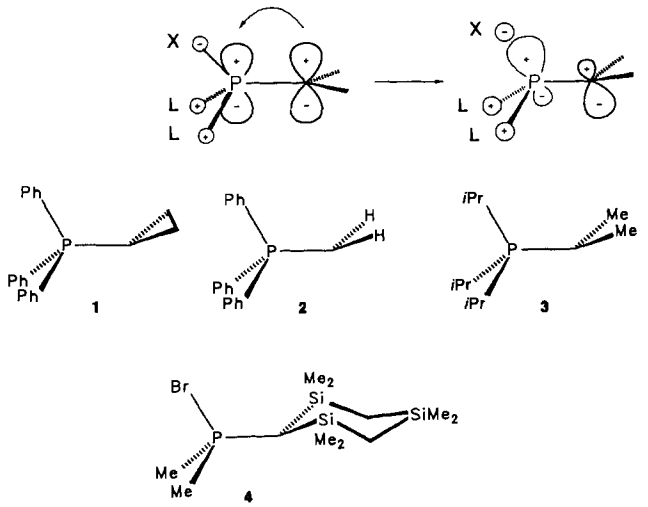

Scheme 1.

The phosphorus ylides of the type $R_2XP^+-CR'_2{}^-$ (X = halogen; R, R′ = alkyl, aryl)[7] should be excellent examples in which the above-mentioned characteristics can be studied, because the σ* orbital of the P–halogen bond is energetically low-lying and can accept electron density from the ylidic carbon atom particularly well. Indeed, Fritz, von Schnering et al. detected a dramatic lowering of the bond order of the P–Br bond (0.63) in brominated phosphorus ylide **4**.[8] We now report unambiguous, experimental findings that can be explained by negative hyperconjugation in phosphorus ylides.

The chlorinated phosphorus ylide **5**[9] precipitates from *n*-hexane in the form of yellow crystals. These crystals have three independent molecules, **5a**, **5b**, and **5c**, in the unit cell.[10] The essential difference between them lies in two directly related parameters: torsion about the P–C(ylide) bond and the P–Cl bond length (Fig. 1). In **5c** the p orbital at C1, which is perpendicular to the C4–C1–C5 plane, almost eclipses the P–Cl bond (deviation 7.2°). The P–Cl bond of the three molecules **5a–c** is longest in **5c** (2.235 Å; Table 1) and corresponds to a bond order of only 0.58 calculated by Donnay and Allmann's method.[11] In **5a** the deviation from an ecliptic arrangement is the largest (21.4°) and the P–Cl distance the shortest. The *trans*-bent orientation of the substituents at P1 and C1 becomes more pronounced as the P–Cl distance increases and as the p orbital of C1 and the

Table 1. Selected bond distances and angles of **5a**, **b**, **c** und **6b**.

	5a	5b	5c	6b
P1-Cl1 [a]	2.195(2)	2.228(2)	2.235(2)	–
P1-C1	1.673(5)	1.667(5)	1.668(5)	1.683(11)
P1-C2	1.883(5)	1.874(5)	1.886(5)	1.836(13)
P3-C3	1.881(5)	1.870(5)	1.884(5)	1.896(13)
Cl1-P1-C1	116.5(1)	115.9(1)	117.5(1)	–
Cl1-P1-C1-C4	60.1	70.3	72.2	–
Cl1-P1-C1-C5	−102.9	−92.1	−86.7	–
X[b]	−0.45	−0.45	−0.45	0.03
Y[c]	0.12	0.13	0.15	0.02

[a] In no molecule were the temperature factors for P1 and C1 unusual or of a different order of magnitude. [b] Distance of P1 from the plane defined by C1-C2-C3. [c] Distance of C1 from the plane defined by P1-C4-C5.

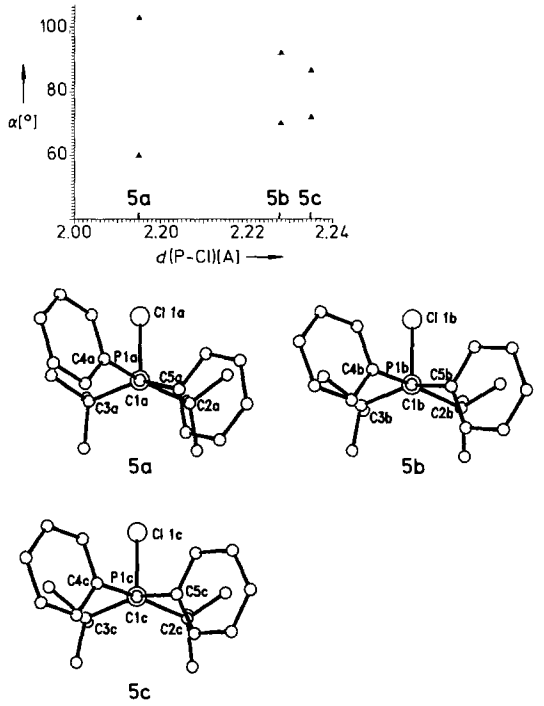

Fig. 1. Top: Plot of the torsion angles Cl1-P1-C1-C4 and Cl1-P1-C1-C5 (α, [°]) vs. the Cl1-P1 distance (*d*, [Å]); below: molecular structures of **5a**, **5b**, and **5c** viewed along the C1–P1 bond; selected bond distances and angles in Table 1.

P–Cl bond approach an eclipsed conformation. The molecules **5a–c** correspond to rotamers about the P–C ylide bond on the energy surface. Their experimentally determined bonding parameters provide insights into the changes in molecular geometry in the course of this dynamic process and are in accord with the concept of negative hyperconjugation.

The weakening of the P–Cl bond allows even a relatively weak Lewis acid like tin dichloride to abstract a chloride ion from phosphorus ylide **5**. The methylenephosphonium ion **6a** that contains only hydrocarbon substituents can be isolated as a yellow solid by rapid workup of the reaction solution (Scheme 2). Compound **6b** was isolated with $AlCl_4^-$ as counter-ion in an analytically pure state and characterized

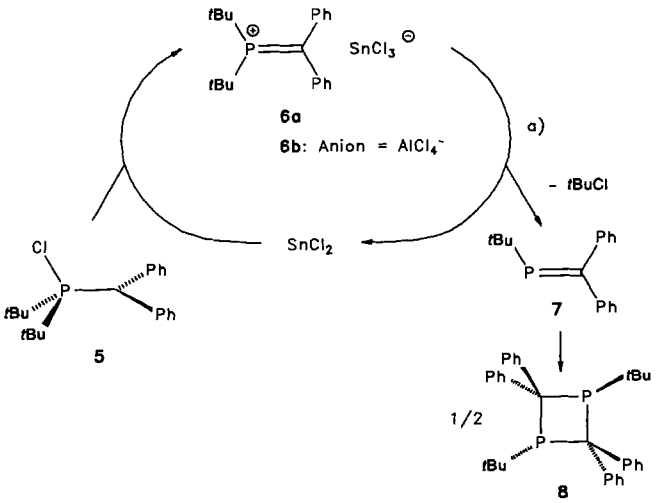

Scheme 2. a) $k = 7.3 \times 10^{-4}\ s^{-1}$, $t_{\frac{1}{2}} = 16$ min.

by NMR spectroscopy and a single-crystal X-ray structure analysis (Fig. 2).[10] The P1–Cl1 distance in **6b** (1.683 Å) is close to that in ylide **5** (1.666 Å) and comparable with the P–C distances in methylenephosphanes RP = CR'_2.[13] The longer P1–C1 distance in **6b** relative to the theoretically calculated 1.624 Å[14] may be attributed to steric hindrance, which is also responsible for the torsion angle of 20° about the P1–C1 bond. Both the carbon atom C1 and the phosphorus atom P1 have a nearly trigonal planar configuration [$\Sigma°$(C1) = 359.6°; $\Sigma°$(P1) = 359°]. The methylenephosphonium salt **6a** is not stable in solution (Scheme 2). It decomposes quantitatively according to a first-order rate law ($k = 7.3 \times 10^{-4}\ s^{-1}$; $t_{1/2} = 16$ min) to methylenephosphane **7** (to the best of our knowledge this compound has not yet been described), *t*BuCl, and $SnCl_2$.

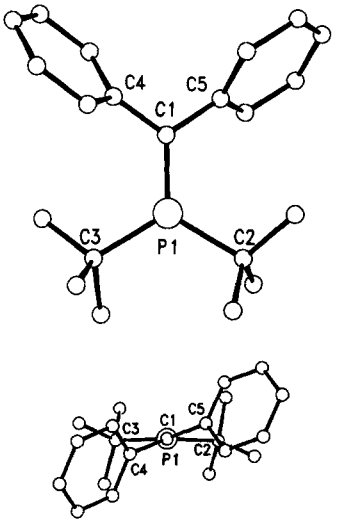

Fig. 2. Molecular structure of the methylenephosphonium cation **6b** in the crystal; selected bond distances and angles in Table 1.

The methylenephosphane **7** may be stored for some time at low temperatures as yellow oil. It was characterized by NMR spectroscopy. At room temperature the oil **7**—pure or in solution—dimerizes to 1,3-diphosphetane **8**. This novel reaction between **5** and $SnCl_2$ represents the first *catalytic* synthesis of methylenephosphanes, and is of preparative interest because the *P*-halogen phosphorus ylides are easily accessible. Studies on the scope of this reaction and its mechanism, in which methylenephosphonium ions[15] play a key role, are under way.

Experimental Procedure

A solution of compound **5** (1.73 g, 5 mmol) in dried and degassed CH_2Cl_2 (15 mL) was added dropwise from a syringe to a suspension of $AlCl_3$ (0.8 g, 6 mmol) in 10 mL CH_2Cl_2, at −78 °C. The resulting yellow solution was filtered immediately without warming and evaporated to dryness in vacuum. The yellow solid residue was suspended in 20 mL hexane and dissolved by adding CH_2Cl_2 (≈ 20 mL). At −30 °C long yellow needles of **6b** crystallize out. Compound **6b** is exceptionally sensitive in solution! **6b**: M.p. = 108–109 °C; $^{31}P\{^1H\}$ NMR (CD_2Cl_2): δ = 183.5; ^1H NMR (CD_2Cl_2): δ = 1.52 (d, $^3J(^{31}P, ^1H)$ = 19.1 Hz, 18H, CH_3), 7.24–7.64 (m, 10H, aromat. H); ^{13}C NMR (CD_2Cl_2): δ = 31.5 (s, CH_3), 49.9 (d, $^1J(^{31}P, ^{13}C)$ = 9.0 Hz, CCH_3), 129.5 (s, *meta*-C), 131.5 (d, $^3J(^{31}P, ^{13}C)$ = 15.1 Hz, *ortho*-C), 134.9 (s, *para*-C), 139.4 (d, $^2J(^{31}P, ^{13}C)$ = 7.4 Hz, *ipso*-C), 178.1 (d, $^1J(^{31}P, ^{13}C)$ = 73.6 Hz, P=C). **7**: $^{31}P\{^1H\}$ NMR (CD_2Cl_2): δ = 289.6; ^1H NMR ($CDCl_3$): δ = 1.01 (d, $^3J(^{31}P, ^1H)$ = 10.7 Hz, 9H, CH_3), 7.02–7.44 (m, 10H, aromat. H); ^{13}C NMR (CD_2Cl_2): δ = 30.6 (d, $^2J(^{31}P, ^{13}C)$ = 12.5 Hz, CH_3), 35.8 (d, $^1J(^{31}P, ^{13}C)$ = 42.2 Hz, CCH_3), 126.6–130.5 (m, aromat. C), 143.7 (d, $^2J(^{31}P, ^{13}C)$ = 13.1 Hz, *ipso*-C), 145.5 (d, $^2J(^{31}P, ^{13}C)$ = 22.6 Hz, *ipso*-C), 192.8 (d, $^1J(^{31}P, ^{13}C)$ = 51.1 Hz, P=C). – **8**: Fp = 137–138 °C; $^{31}P\{^1H\}$ NMR (CD_2Cl_2): δ = 30.1; ^1H NMR (CD_2Cl_2): δ = 0.99 (d, $^3J(^{31}P, ^1H)$ = 7.1 Hz, 9H, CH_3), 1.03 (d, $^3J(^{31}P, ^1H)$ = 6.8 Hz, 9H, CH_3), 6.59–8.22 (m, 10H, aromat. H); ^{13}C NMR (CD_2Cl_2): δ = 30.5 (d, $^2J(^{31}P, ^{13}C)$ = 9.9 Hz, CH_3), 30.7 (d, $^2J(^{31}P, ^{13}C)$ = 9.9 Hz, CH_3), 33.2 (d, $^1J(^{31}P, ^{13}C)$ = 15.1 Hz, CCH_3), 33.5 (d, $^1J(^{31}P, ^{13}C)$ = 14.6 Hz, CCH_3), 67.4 (t, $^1J(^{31}P, ^{13}C)$ = 8.3 Hz, C_{ring}), 125.8 (d, $^3J(^{31}P, ^{13}C)$ = 19.2 Hz, *ortho*-C), 126.4 (br., aromat. C), 127.5 (d, $^3J(^{31}P, ^{13}C)$ = 34.6 Hz, *ortho*-C), 131.2 (m, aromat. C), 132.5 (s, br.), aromat. C), 142.3 (s, aromat. C), 146.6 (d, $^2J(^{31}P, ^{13C})$ = 11.4 Hz, *ipso*-C), 146.9 (d, $^2J(^{31}P, ^{13}C)$ = 13.2 Hz, *ipso*-C).

Received: July 30, 1991 [Z4838 IE]
German version: *Angew. Chem.* **1992**, *104*, 92

CAS Registry numbers:
5, 81176-00-3; **6a**, 137516-86-0; **6b**, 137516-85-9; **7**, 126118-33-0; **8**, 137516-83-7.

[1] a) P. von Ragué Schleyer, A. J. Kos, *Tetrahedron* **1983**, *39*, 1141, and references cited therein; b) H.-J. Bestmann, A. J. Kos, K. Witzgall, P. von Ragué Schleyer, *Chem. Ber.* **1986**, *119*, 1331; c) K. A. Ostoja Starzewski, H. Bock, *J. Am. Chem. Soc.* **1976**, *98*, 8486; d) M. A. Vincent, H. F. Schaefer III, A. Schier, H. Schmidbaur, *J. Am. Chem. Soc.* **1983**, *105*, 3806; e) W. W. Schoeller, J. Niemann, *J. Am. Chem. Soc.* **1986**, *108*, 22; for negative hyperconjugation in silicon compounds, see for example, f) Y. Apeloig in S. Patai, Z. Rappoport (Eds.): *The Chemistry of Organic Silicon Compounds* (Eds.: S. Patai, Z. Rappoport), Wiley, Chichester, 1989, p. 57; g) S. Shambayati, J. F. Blake, S. G. Wierschke, W. L. Jorgensen, S. L. Schreiber, *J. Am. Chem. Soc.* **1990**, *112*, 697; the anomeric effect in compounds with elements of the second period is discussed, for example, in h) A. J. Kirby, *Pure Appl. Chem.* **1987**, *59*, 1605, zit. Lit.; i) A. J. Kirby, *Acc. Chem. Res.*, **1984**, *17*, 305; cf. also the discussion on phosphane complexes: j) B. J. Dunne, R. B. Morris, A. G. Orpen, *J. Chem. Soc. Dalton Trans.* **1991**, 653, and references cited therein.

[2] The chemical bond in hypervalent molecules is discussed in: A. L. Reed, P. von Ragué Schleyer, *J. Am. Chem. Soc.* **1990**, *112*, 1434, zit. Lit.

[3] a) J.-P. Malrieu, G. Trinquier, *J. Am. Chem. Soc.* **1989**, *111*, 5916; b) G. Trinquier, J.-P. Malrieu, *J. Am. Chem. Soc.* **1987**, *109*, 5303.

[4] H. Schmidbaur, A. Schier, B. Marla-Milewski, U. Schubert, *Chem. Ber.* **1982**, *115*, 722.

[5] H. Schmidbaur, J. Jeong, A. Schier, W. Graf, D. L. Wilkinson, G. Müller, C. Krüger, *New J. Chem.* **1989**, *13*, 341.

[6] H. Schmidbaur, A. Schier, C. M.F. Frazão, G. Müller, *J. Am. Chem. Soc.* **1986**, *108*, 976.

[7] O. I. Kolodiazhnyi, *Z. Chem.* **1989**, *29*, 396, and references cited therein.

[8] a) G. Fritz, W. Schick, W. Hönle, H. G. von Schnering, *Z. Anorg. Allg. Chem.* **1984**, *511*, 95; b) Fritz, U. Braun, W. Schick, W. Hönle, H. G. von Schnering, *ibid.* **1981**, *472*, 45.

[9] O. I. Kolodiazhnyi, *Zh. Obshch. Khim.* **1981**, *51*, 2466.

[10] **5**: Space group *Pbca*, a = 16.234(3), b = 17.521(4), c = 41.853(10) Å, V = 11904 Å^3, Z = 24, 8894 measured reflections ($Mo_{K\alpha}$, ω scan), 5175 observed ($I > 2\sigma(I)$). P, Cl, C anisotropic, phenyl and methyl groups refined as rigid groups, 616 parameters; R = 0.064, R_w = 0.068. **6b**: Space group $P2_1/n$, a = 11.045(8), b = 14.203(9), c = 16.52(1) Å, β = 97.75(6)°, V = 2668 Å^3, Z = 4. Crystal twinned, 3744 measured reflections ($Mo_{K\alpha}$, ω scan), 1722 observed reflections ($I > 2\sigma(I)$), of which 1111 were used for the structure determination (P, Al, Cl anisotropic, phenyl and methyl groups isotropic as rigid groups, 135 parameters); $R = R_w$ = 0.086. Further details of the crystal structure investigation may be obtained from the Fachinformationszentrum Karlsruhe, Gesellschaft für wissenschaftlich-technische Information mbH, W-7514 Eggenstein-Leopoldshafen 2 (FRG) on quoting the depository number CSD-55647, the names of the authors, and the journal citation.

[11] R. Allmann, *Monatsh. Chem.* **1975**, *106*, 779, and references cited therein. The bond order is obtained from the relationship: $n_i = (d^*/d_i)^5$ where d^* is the reduced bond length for a single bond. A bond length of d^*(P–Cl) = 2.01 Å, calculated by von Schnering and Hönle [8, 12] was used.

[12] W. Hönle, H. G. von Schnering, *Z. Anorg. Allg. Chem.* **1980**, *464*, 139.

[13] a) R. Appel, in *Multiple Bonds and Low Coordination in Phosphorus Chemistry*, (Eds.: M. Regitz, O. J. Scherer) Thieme, Stuttgart, **1990**, p. 367.

[14] a) M. Ehrig, H. Horn, C. Kölmel, R. Ahlrichs, *J. Am. Chem. Soc.* **1991**, *113*, 3701; b) L. L. Lohr, H. B. Schlegel, K. Morokuma, *J. Phys. Chem.* **1984**, *88*, 1981.

[15] a) H. Grützmacher, H. Pritzkow, *Angew. Chem.* **1991**, *103*, 721; *Angew. Chem. Int. Ed. Engl.* **1991**, *30*, 709; b) A. Igau, A. Bacereido, H. Grützmacher, H. Pritzkow, G. Bertrand, *J. Am. Chem. Soc.* **1989**, *111*, 6853.

Book Reviews are written by invitation from the editor. Suggestions for books to be reviewed and for book reviewers are welcome. Publishers should send brochures or (better) books to the following address: Redaktion Angewandte Chemie, Postfach 101161, W-6940 Weinheim, Federal Republic of Germany. The editor reserves the right of selecting which books will be reviewed. Uninvited books not chosen for review will not be returned.

Metals and Their Compounds in the Environment: Occurrence, Analysis and Biological Relevance. Edited by E. Merian. VCH Verlagsgesellschaft, Weinheim/VCH Publishers, New York, 1991. xxiii, 1438 pp., hardcover DM 380.00.—ISBN 3-527-26521-X

A person unaware of the problems associated with shortages of essential elements and with excesses of toxic elements is difficult to find. Even newspapers and magazines discuss (not always in the spirit of providing scientifically sound information) the effects of metals and metalloids (or more generally of trace elements) on the environment and on the health of man, animals, and plants. No one, not the common person, not the experts in medical, scientific and technical disciplines, and especially not the servants of the public at all levels of government, can afford not to be informed about these important issues. Unfortunately these issues are in most cases not clear-cut. Rarely was all the information necessary for a decision at the disposal of even the experts, and hardly ever was the available information easily accessible from a single source. This situation has changed: one handy, although rather heavy, volume provides a wealth of information about metals and their compounds in the environment. Should the information presented prove not to be detailed enough, more can be gleaned from the publications given in the references.

"Metals and Their Compounds in the Environment" consists of two parts. The first part (700 pages) covers general aspects in 20 chapters including cycles of metals in nature; production and processing of metals; chemical processes in the environment; relevance of chemical speciation; analytical chemistry; metal concentrations in human samples; bioindicators for monitoring metals; metals and their compounds in water, in the atmosphere, in soils, in sludges and wastes, as well as in the indoor environment; mobilization from sediments; metals in and their effects on plants, animals, and humans; metals in feed and food; essentiality of metals; interactions between metals; cell biochemistry of metals; metallothionines; acute and chronic toxicity, immunotoxicology, mutagenicity, carcinogenicity, teratogenicity, ecogenetics of metals; standard setting, risk assessment, and legislative regulations concerning metals. Environmental radioactivity is not discussed, with the exception of radioactivity associated with uranium, thorium, and their decay products.

The second part (700 pages) provides information about the following elements: Al, As, Au, Be, Bi, Cd, Co, Cu, Cr, Fe, Ga, Ge, In, the lanthanides, Hg, Li, Mg, Mn, Mo, Nb, Ni, Pb, platinum-group metals, Ag, Se, Sn, Ta, Te, Ti, Tl, W, U and its decay products, Th and its decay products, V, Y, Zn, and Zr. Each of these chapters has sections on physical and chemical properties of an element and its environmentally important compounds; analytical methods for their determination; sources, production, important compounds, uses, waste products, and recycling; their distribution in the environment, in foods, and in living organisms; uptake, absorption, transport and distribution, metabolism and elimination in plants, animals, and humans; effects on plants, animals, and humans; hazard evaluation and limiting concentrations; a list of review articles and original publications arranged alphabetically according to authors; and a list of additional recommended literature. A very useful 22-page glossary and a 65-page subject index close this volume.

The editor stated in the preface: "The book aims to provide... a balanced presentation of the topic 'Metals in the Environment' based on up-to-date international scientific knowledge. For this purpose it was necessary to compile, examine, and critically evaluate the most recent comprehensive and widely distributed literature, and present the results in a unified and well-structured form. In addition the conclusions reached at many symposia have been included... Eighty-six scientific experts carried out an interdisciplinary evaluation, incorporating important results from all five continents; previous publications very often only concentrated either on North American or on European literature... An attempt has been made to assess the ecological and toxicological risks on the basis of national and international requirements, for example, recommended exposure limits. In addition to environmental evidence, the discussion is also based on experience from allied fields, such as industrial medicine and clinical chemistry. In controversial cases, in which certain questions have not yet been resolved, diverging opinions have been equally considered as far as possible." What the editor and his co-workers set out to do, they have accomplished. I know of no other book about metals in the environment that presents information in such an up-to-date, compact, and well-structured manner. Whenever summaries and overviews are written, the compression of information leads to losses in details. Experts working on the frontiers of research will certainly find statements in these chapters with which they cannot agree. They might consider formulations to be too general, perhaps somewhat misleading. As a chemist, I found the sections on the physical and chemical properties of the elements and their compounds of nonuniform coverage and quality. Frequently, information is given which does not aid in understanding the connection between the chemistry of an element and its environmental impact; often chemical facts of great importance are not presented; and on occasion incorrect statements are uncritically taken from the literature.

Random examples illustrate this criticism: Aluminum hydroxide with its pH-dependent solubility is not mentioned. Frequently confusion reigns about oxidation number, valency, and ionic charge. The myth about a cationic chemistry of arsenic in the +3 oxidation state in aqueous solution is presented as a fact. To claim that arsenic in trimethylarsine oxide has one of the lowest oxidation states is pushing the oxidation state concept beyond acceptable limits. Incorrect formulas occur infrequently ($NaBiO_6$, AsO_5, As_2Se). The statement that lithium and the other alkali metals do not form stable complexes is much too general. Dimethyl derivatives of selenium and tellurium—important in biological sys-

 © VCH Verlagsgesellschaft mbH, W-6940 Weinheim, 1992 0570-0833/92/0101-0102 $ 3.50+.25/0

tems—are not mentioned, whereas rather exotic compounds ($TeOCl_2$, TeF_6) are included.

These irritating details as well as some halting sentences could (and should) have been corrected during the editing process. A few typing errors also slipped through. Elements that should have been included are barium, silicon, and perhaps fluorine and iodine.

These minor criticisms must not, however, distract from the great value of this volume. I heartily recommend that all who are interested in metals in the environment buy a copy. These include the scientists from numerous fields concerned with effects of metal compounds listed in the preface of this book (geologists, metallurgists, material scientists, chemists, analytical chemists, environmental engineers, security experts, waste disposal engineers, biochemists, biologists, toxicologists, ecotoxicologists, veterinarians, industrial hygienists, physicians, teachers, administrators, and decision-makers) and interested lay people and all those who already own the much shorter first edition of this book in German.

Kurt J. Irgolic
Institut für Analytische Chemie
der Universität Graz (Austria)

Contrasts in Scientific Style. Research Groups in the Chemical and Biochemical Sciences. By *J. S. Fruton*. American Philosophical Society, Philadelphia PA (USA), 1990. ix, 473 pp., hardcover $ 40.00. – ISBN 0-87169-191-4

This is a thought-provoking book. J. S. Fruton was involved in the pioneering days of classical biochemistry, and writes with a keen awareness of his origins—he dedicated his basic textbook of general biochemistry to Max Bergmann, Leonor Michaelis, Rudolf Schoenheimer and Gerty T. Cori, and the book certainly lived up to these standards. Here he examines the interplay between organization and success in research, taking as examples the outstanding research groups active in organic and medicinal chemistry in Germany between 1830 (Justus Liebig) and 1914 (Emil Fischer), a period that provided clear evidence of the value of basic research for the chemical and pharmaceutical industries. One finds here a remarkably complex interplay between opportunity and initiative, or between different forms of giving and taking. Fruton regards these matters with the detachment of the historian; nevertheless, one senses that his sympathies do not lie with the powerful and forceful team managers and single-minded achievers, but rather with those research groups in which, while certainly a main focus of attention was not lacking, there was also scientific tolerance and a liberal attitude, which made it possible to take up a wide range of topics and to initiate discussion that stimulated new ideas. This occurred, for example, in the groups led by Felix Hoppe-Seyler and Franz Hofmeister (both of whom, interestingly, worked at Straßburg, the German empire's new showpiece university), and also, in a more centralist but nevertheless thoroughly liberal style, in Adolf von Baeyer's group. Here we have the question that is debated time and time again: how does one achieve a "critical mass"? Through a systematic bringing together of talented and compatible scientists, or by a process of generating ideas through the multicolored interests of different individuals? Is success best achieved by a frontal attack with massive forces, or by "minelaying" at the critical spot?—should one opt for a chemists' pile in the manner of Liebig, or aim at the drudgery of making molecules according to the Fischer rules but in the nimbus of the "master", or the less glamorous training of the independent searching mind in a variety of current problem areas—the Hofmeister series—which, although less immediately spectacular, is more enduring and fruitful in the long term? The answer is that one must decide whether the aim is to apply the knowledge gained quickly, or to invest for the future. Here one is concerned with style that makes the man rather than with the idea that is often put forward of a tree of learning branching out from the grand masters of chemistry and forgers of Nobel laurels, which mostly only illustrate the old maxim that eminent teachers tend to gather around them able and well-motivated students.

This is how it was in the days of the old-style professors: they were never far away from the laboratory; they were as much concerned with the novices as with the post-graduate students, and with the "post-docs" who were in many cases only in the laboratory for a few months as visiting colleagues, and they gave practical advice to all of these. Of course, the "bosses" differed widely in their characters. Justus Liebig wanted to force nature to follow his rules, and to that end he set up an almost military organization (it was no accident that chemistry at Gießen had started life in a former guard-room); in the end, however, this only made him, the Chief of General Staff and PR man, severely ill, as evidenced by the less Olympian the daguerrotypes. In a similar way, Emil Fischer, almost systematically staking one claim after another, became prematurely burned out by the grind of chemistry and family problems, yet he led his loyal team, firmly kept in their subordinate roles, to a string of successes along paths known only to him. Again, a size smaller, there was A. Kossel who, although his horizons were more limited, kept on resolutely towards his objectives. In contrast to these is Baeyer, who lived a self-contented and well-balanced life of idiosyncratic professorial grandeur, whose charisma left no room for self-doubt, and whose integrity, even when authoring his colleagues' work, could therefore not be doubted. The fastidious and assertive character Hoppe-Seyler, imbued with the sheer positivism of his time, impressed his contemporaries. Then there was the critically aggressive and highly imaginative W. Kühne, and the impressively relaxed Hofmeister, whose Bohemian poetic streak enabled him to build a successful team—here one finds the roots of the sort of biochemistry that the organic chemists were never able to understand, rhyming "Biochemie" with "Schmierchemie" ("slime chemistry"), even though this was the origin of the crystals that they came to love so much that they shunned all other forms. This situation persisted into the middle of the present century, when the much-vaunted German school of chemistry failed to link up with the emerging field of molecular biology, whereas the British and American chemists turned out to be more adaptable for a number of reasons, partly but not entirely through having no "Schule", and thereby profiting from the biochemical expertise that fled from Germany.

It is very instructive to examine the styles of working that prevailed in different groups. On the one hand are those that are committed to using just a few methods, from which they extract the maximum possible, while on the other hand are the developers of methods, who often are unable themselves to derive the optimum benefit from them. Here one can see many parallels with the present-day development of biochemistry into molecular biology, and there is a sense of déjà vu about this area. An older chemist recalls with amusement the time when the biologists transformed the university faculties against the resistance of the narrow-minded chemist slave-drivers. With hindsight things look different; it is opportunity that determines character, and as results have developed into patentables, personality and

style have become identical—an ironic twist in the social history of science. Only the list of coauthors now looks different—on this, however, one should read Professor Djerassi who has more to say on this subject...

The appendices, in which the subsequent life histories of the members of these seven classic examples of important research groups have been thoroughly investigated and detailed, are impressive, and quantify the theories put forward. Whereas groups of one type have mainly produced scientists useful to industry, and have therefore appeared as an attractive proposition for the market, those of another type can proudly point to an output of academic scientists that is well above average, both in quantity and quality – though many of these were lost to Germany as victims of persecution in the Nazi era. In passing it is interesting to note that although the number of women was still small in those days (we are talking here of the years before 1914!), there were some nevertheless, even though few of them succeeded in rising beyond the level of head of a clinical laboratory (or, with luck, a teacher of Greek after having emigrated).

The contents of the book have been collected together from many sources. However, readers who are already familiar to some extent with the main threads of the development of biochemistry in Germany will not find much information here that is fundamentally new. On the other hand, the particular appeal of this account, which makes it especially interesting for us in Germany, is in the critical discussion that comes from the author's more detached perspective, seen from the viewpoint of the Angloamerican scientific tradition. Also the descriptions of the characters of the protagonists, which are mainly taken not from the anecdotal folklore of chemistry but from correspondence and scientific publications, add a more human side to the facts. Which of us will eventually have a Fruton to write about us?

Finally, this volume provides comforting evidence for those who love books that it is still possible nowadays, if the will is there, to make a book with care: with clear and attractive printing, on good paper with a generous margin, with sewn pages and a substantial binding, and, last but not least, with the characteristic smell of a book. It is satisfying to find here that a substantial content and a durable quality of production each enhance the other.

Lothar Jaenicke
Institut für Biochemie
der Universität Köln (FRG)

Supramolecular Photochemistry. By *V. Balzani* and *F. Scandola*. Ellis Horwood, New York, 1991. 427 pp., hardcover $ 121.00.—ISBN 0-13-877531-1

In the authors' own words, "Supramolecular chemistry is the chemistry of systems (supermolecules) made up of molecular components in the same way as molecules are made up of atoms... Supramolecular photochemistry concerns the control and tuning of the excited state properties of these molecular components and the study of their intercomponent processes... It can be profitably used to make progress towards the understanding of photobiological processes and the design of artificial systems capable of performing useful light-induced functions." Their stated goal is to illustrate the fundamental concepts of this field and to review and discuss some important results and possible applications.

The book is divided into 12 chapters. After an introduction (1. Scope and Limitations) the chapters 2. Principles of Molecular Photochemistry, 3. Supramolecular Properties, and 4. Control and Tuning of Excited-State Properties of Molecular Components provide a basic but sufficient knowledge of the photophysical concepts needed later. Among the topics are a discussion of potential energy surfaces and a concise introduction to the Marcus theory of electron transfer. They are no substitute for one of the more comprehensive monographs on photochemistry but no such attempt is made.

The following chapters are based on the way in which the molecular components are held together and/or interact with one another: 5. Covalently-Linked Systems: Photoinduced Electron Transfer, and 6. Covalently-Linked Systems: Electronic Energy Transfer. These recapitulate and give further details of the underlying physics, as well as numerous experimental examples. The section on electron transfer is very informative, whereas some aspects of electronic energy transfer remain somewhat sketchy. In both chapters figures with experimental data on the distance dependence of each process would be helpful.

Chapter 7. Structural Changes in Photoflexible Systems deals with photoinduced isomerizations of TICT-compounds, stilbenes, spiropyrans and azobenzene-containing molecules. Incorporation of these functional units in crown ethers and other multidentate ligands enables light-induced changes of the complexating properties of these systems. Chapters 8. Ion Pairs, and 9. Electron Donor-Acceptor Complexes and Exciplexes give short introductions to charge-transfer absorption and emission properties and their relationship to thermal charge transfer processes, as well as dynamic and static quenching in these systems.

The following chapters 10. Host-Guest Systems (comprising crown ethers, macrocycles and cyclodextrin inclusion compounds), and 11. Other Systems (cage ligands, catenanes, and related systems) again deal predominantly with complexation of metal ions by these structures for the control of their excited state properties.

Chapter 12. Photochemical Molecular Devices finally develops a very illustrative, conceptual framework of how the systems in earlier chapters can be utilized to design more complex structures with specific photochemical functions and proposes possible experimental realizations.

In style and content the book is partly textbook and partly review article of recent work up to early 1990. Organic systems and systems based on metal complexes are extensively discussed, with the latter in considerably more detail, probably reflecting the authors' own predilection and very extensive work in this field. Occasionally too great an effort is made to present variety and structural differences of many systems instead of focusing on common mechanisms and concepts. The emphasis is on systems with a small number of discrete molecular components. More complex materials such as polymers, liquid crystals, semiconductors, micelles, and films are explicitly omitted. In fact, much of the material would not necessarily be classified as supramolecular, but as building blocks of larger supramolecular systems. The photochemistry is almost exclusively reversible; irreversible chemical change in general constitutes undesirable photochemical degradation. In this sense, the book deals predominantly with what one might call elementary processes of supramolecular photophysics.

Taken as a whole the selection of the material is a sensible one and the discussion comes to the point. It emphasizes the interdisciplinary nature of the subject, linking organic, inorganic, and physical chemistry, and the close relationship between molecular structure and photophysical function.

Great effort seems to have been made to make the text comprehensible for the nonspecialist. Readability is facilitat-

 © VCH Verlagsgesellschaft mbH, W-6940 Weinheim, 1992 0570-0833/92/0101-0104 $ 3.50+.25/0

ed by a large number of illustrative figures, energy-level diagrams, numerous references and cross references, and extensive author and subject indexes. The book presents basic physical concepts in simple terms with little formalism and numerous experimental examples not easily found elsewhere in such breadth. As such, it provides an interesting and comprehensible introduction for the newcomer to this fascinating field and a valuable source of information for the specialist. However, the readership the book deserves could be limited by its prohibitive price.

Hans Heitele
Institut für Physikalische und Theoretische Chemie
der Technischen Universität München,
Garching (FRG)

The Chemistry of Enols. (Series: The Chemistry of Functional Groups; Series editor: *S. Patai*). Volume editor: *Z. Rappoport*. Wiley, Chichester, 1990. xvi, 823 pp., hardcover £ 195.00.—ISBN 0-471-91720-6

The addition to the Patai series of a volume treating enols as a functional group in its own right is clearly warranted by the revolutionary recent advances achieved in the direct investigation of enol chemistry. The editor of this volume has succeeded in engaging leading proponents of recent developments, thus providing a highly competent and informative account of all the aspects usually covered in the series, namely preparation, structure, and reactivity. Personal views given by the individual authors provide a vivid presentation of a lively research area from different standpoints. As a consequence, there is some reiteration of material in different chapters, but, overall, the editor and authors have achieved a consistent and comprehensive presentation of the chemistry of enols. Literature coverage is up to 1988 (in part 1989) and contains nearly 2500 references as well as extensive author and subject indexes providing easy access to up-to-date information. A majority of the references cited are from the last decade, but important early work starting from Erlenmeyer's first contribution to enol chemistry in 1875 is also included. The chemistry of enolates and enol ethers is deliberately excluded.

Chapter 1 on "Theoretical Calculations" by Y. Apeloig provides an exemplary description of the fruitful interactions between state-of-the-art theoretical methods and current experimental research. In Chapter 2 J. P. Guthrie derives increments for the Benson group additivity scheme from the presently available data, and shows how reliably these allow one to estimate thermodynamic parameters of enols. Chapter 3, "The Chemistry of Ionized Enols in the Gas Phase" by F. Tureček, discusses the reversal of keto–enol equilibria in radical cations. In Chapter 4 on "NMR, IR, Conformation and Hydrogen Bonding" by B. Floris the emphasis is on systems with substantial equilibrium concentrations of two or more tautomers; the chapter includes a comprehensive compilation of spectral data as well as studies of the effects of solvent, substituents and temperature on equilibria. In Chapter 5 methods for generating unstable enols in pure form or in higher than equilibrium concentrations are presented by B. Capon. In Chapter 6 reliable keto–enol equilibrium constants are compiled by J. Toullec, and the merits and limitations of various methods for determining these data are critically reviewed. Old and new insight into the kinetics and mechanism of enolization and ketonization is reviewed by J. R. Keefe and A. J. Kresge (Chapter 7). Emphasis is laid on new developments in monitoring ketonization reactions in aqueous solution, general-acid and general-base catalysis, isotope effects, and the pathways of the "uncatalyzed" reactions in protic solvents. Isolable and relatively stable simple enols are discussed by H. Hart, Z. Rappoport and S. E. Biali in Chapter 8. As "simple" enols they consider those lacking stabilizing functional groups such as CO in the β-position, in particular the kinetically stabilized aryl-substituted enols of the type studied by Fuson in the early forties. Chapter 9 on "Photochemical Reactions Involving Enols" by A. C. Weedon covers the numerous reactions which lead to the formation of enols as primary products, as well as the photoreactions of enols themselves. In Chapter 10 the scarce experimental data on enols of carboxylic acids and esters are reviewed by A. F. Hegarty and P. O'Neill. In "The Biochemistry of Enols" (Chapter 11) J. P. Richard focusses on the biochemical reactions of carbonyl compounds which proceed through enol or enolate reaction intermediates, excluding reactions of the stable enol Vitamin C. Unstable tautomers can sometimes be stabilized by complexation; the properties of transition metal–enol complexes are covered by D. Milstein in Chapter 12 "Organometallic Chemistry of Enols". Experimental data on "Structural Chemistry", mainly from single crystal X-ray measurements on isolable enols, are compiled and discussed by G. Gilli and V. Bertolasi in Chapter 13.

The Patai series needs no recommendation as an indispensable source of comprehensive, critical and up-to-date information. It is clearly a must for any chemical library. Unfortunately this situation is being exploited by the publishers: the astronomical price of this volume will discourage most researchers from purchasing their own copy.

Jakob Wirz
Institut für Physikalische Chemie
der Universität Basel (Switzerland)

Synthesis of Lanthanide and Actinide Compounds. Edited by *G. Meyer* and *L. R. Morss*. Kluwer Academic Publishers, Dordrecht, 1991. xvi, 367 pp., hardcover HFl 220.00.–ISBN 0-7923-1018-7

This compendium of invited reviews is the second in a series of "Topics in *f*-Element Chemistry" edited by Shyama P. Shinha, the first having appeared some six years ago, entitled "Americium and Curium Chemistry and Technology", edited by Edelstein, Navratil, and Schulz. Meyer and Morss have assembled an outstanding array of contributions from several of the more noteworthy contemporaries in the area of synthesis of *f*-element compounds. As they observe in their Preface, "The history of the rare earths has entered its third century; transuranium elements are now a half century old", so we cannot expect contributions from all of the major players in *f*-element chemistry. The fourteen contributions do, however, contain over 1400 citations that do well to encompass much of the previous work. The goal of the editors and authors to compile a review of "tried and true" synthetic techniques has been achieved. Since no single volume of synthetic reviews can ever be complete, we should anxiously await the next volume. What follows are some brief comments on each of the fourteen sections.

John Haschke of Rockwell International presents a very detailed synopsis of *Actinide Hydride* synthesis in which he includes an extensive review of kinetics. An additional section concerning the safe handling of hydrides and reduced actinides was a welcome sight. So often in the literature we neglect the "obvious" safety concerns. A very detailed sec-

tion describing the synthesis of hydrides follows, with only a few noticeable printing errors such as "10 bar" where the author meant "10 μbar", presenting a minor technical problem if one is concerned with storing An–H compounds. Overall, this section provides a very thorough synopsis of current synthetic techniques.

Bernd Müller remarks "...only such routes have been selected that lead to the purest samples of fluorides", in the beginning of his section on *Lanthanide Fluorides*. This review, although perhaps not as detailed in background material as others, emphasizes the cleanest routes to a variety of lanthanide fluorides. Müller has certainly provided the reader with a number of quality synthetic techniques.

The very thoroughly researched review of *Actinide Fluorides* coauthored by Nigel Freestone and John Holloway of Northampton and Leicester, Great Britain, respectively, sports a host of citations numbering well over 400. This review contains not only synthetic techniques but most of the crystallographic data gathered over the lifespan of actinide fluorides research. In the seventeen sections, containing twenty-eight tables, a gallant attempt has been made to include all of the available examples of each of the oxidation states of the actinides and the plethora of compounds therein. It should be noted that this volume has been limited to actinide fluorides; Meyer and Morss would have us wait until the next volume for the other actinide halides together with the lanthanide hydrides.

Gerd Meyer contributes three sections describing the synthesis of lanthanide halides: *Binary Lanthanide(III) Halides, MX_3 (X = Cl, Br, I); Complex Lanthanide(III) Chlorides, Bromides, and Iodides*; and *Action of Alkali Metals on Lanthanide(III) Halides*, the last being coauthored by Thomas Schleid. These sections are a very comprehensive review of this chemistry, a field that has been pioneered by these authors, along with Corbett, Seifert and others. They have included detailed illustrations of their own reaction apparatus as well as a variety of useful phase diagrams and tables.

John Corbett of Iowa State University nicely complements the halide discussion in his section *Conproportionation Routes to Reduced Lanthanide Halides*. Through conproportionation, Corbett, as well as Gerd Meyer and Arndt Simon, has explored the solid state redox chemistry of the lanthanides and scandium. The highly reactive nature of the reduced metal halides, although desirable for novel chemistry, presents several synthetic problems that Corbett has addressed using a special tantalum containment system. Corbett also remarks on the frustrating role of adventitious elements in a variety of reactions, not yielding the reduced binary metal halides, but rather a host of new centered metal clusters—another story for another day.

The second half of the book is devoted to the synthesis of *f*-element oxides, chalcogenides and pnictides. LeRoy Eyring presents a well written review: *The Binary Lanthanide Oxides: Synthesis and Identification*. His review identifies a variety of synthetic means to achieve the desired end. Eyring addresses each element and its achievable oxides by including numerous phase diagrams and stability plots. This section nicely condenses many years of oxide chemistry into one convenient package, and will be an asset to any scientist with a desire to study rare earth oxides.

Rudolf Hoppe and Stephan Voigt coauthor the next chapter entitled *Polynary Alkali-Metal Lanthanide Oxides*, beginning with a synopsis of seven synthetic caveats. They proceed to address these points within several thorough, albeit brief, sections that include much of their own work together with citations from Bärnighausen. Nine tables summarize major sections of this research, and are quite detailed in reaction conditions and references. They conclude this chapter with a glimpse into the most current and future problems in research, perhaps encouraging us to dream of new synthetic schemes.

"This chapter describes the most appropriate synthesis...on the laboratory scale", begins Lester Morss in his contribution *Synthesis of Actinide Oxides*. Morss ascends through the oxidation states of each of the actinide oxides, directing the reader to the most appropriate sources for further review. A section describing the ultramicroscale chemistry required for handling the transplutonics introduces the reader to the complex nature of this chemistry. Although much of this research has been buried in obscure reports, by citing papers that are available in most good collections Morss has delivered a chapter that affords the reader an opportunity to explore this chemistry in detail.

Reginald Gruehn, Giessen, coauthors two chapters concerning *Chemical (Vapor Phase) Transport in Lanthanide and Actinide Oxide and Oxychloride Chemistry*. Uwe Schlaffrath coauthors the first chapter with Gruehn, dealing with the tantalates, oxychlorotantalates and niobates of the lanthanides. This first chapter concentrates on crystal growth techniques perfected in their Giessen laboratory. Utilizing the vapor phase above their reaction mixtures at high temperatures, they discovered that materials of X-ray quality could be grown in the absence of the often interfering salt fluxes. The second chapter, coauthored by Gerhard Schmidt, examines the thorium tantalates and niobates. The theme of vapor phase transport prevails throughout this review, although the cited examples are limited to Cl_2 and NH_4Cl as transport agents. The reader is left wondering why they have limited themselves to these two systems (aluminum halides have been used successfully in zirconium halide systems). In retrospect, this was a well drafted review.

C. E. Bamberger of Oak Ridge National Laboratory has made a valiant attempt to describe the *Synthesis of Phosphates, Carbonates, Titanates and Other Metallates of the Lanthanide and Actinide Elements*, that would have needed four separate chapters to be comprehensive. Bamberger does warn us that this chapter is but a brief summary of current synthetic methods, and offers citations for specific preparative routes. This section represents an updated version of the author's chapter in Freeman and Keller's "Handbook on the Physics and Chemistry of the Actinides" (Elsevier, 1985). It is not clear whether the broad subject matter was an editorial choice, but that is this reviewer's only complaint.

M. Guittard and J. Flahaut of CRNS, Paris, coauthor a well documented chapter on the *Preparation of Rare Earth Sulfides and Selenides*. They provide a variety of historical and contemporary preparative routes, including seven detailed schematic diagrams of reaction vessels. They address the preparation of monosulfides and selenides as well as the polychalcogenide phases. A variety of crystal growing techniques are also introduced. They do not, however, clearly distinguish the best synthetic methods from those that simply "work".

The last chapter describes the synthesis of an important class of compounds. J. C. Spirlet of the Institute for Transuranium Elements, Karlsruhe, discusses the *Synthesis of f-Element Pnictides*. These compounds have afforded physicists and chemists alike an opportunity to probe a variety of unusual physical phenomena. They also present an enormous synthetic challenge owing to the high temperatures employed and, in the case of the actinides, the obvious safety constraints. The author provides a table of known compounds and a variety of detailed synthetic methods. This section is worth reading if only for the ingenious crystal growing techniques.

A section of the scientific community has waited too long for such a collection to be published. This chemistry has developed dramatically since Brown's review "Halides of the Lanthanides and Actinides" (Wiley, 1969), which had been one of only a very few resources for much of this chemistry. Katz, Seaborg and Morss updated their comprehensive series on the "Chemistry of the Actinide Elements" (2nd ed., Chapman and Hall, 1986), but this does not contain detailed synthetic methods for the lanthanide compounds. The Meyer and Morss collection provides a much needed condensed review of current chemical techniques. Aside from only a few inconsequential proofreading errors and the other minor complaints listed above, this book is highly recommended and belongs on the shelf of every chemist studying lanthanides and/or actinides.

Peter K. Dorhout
Department of Chemistry
Colorado State University
Fort Collins, CO (USA)

Sulphur-Containing Drugs and Related Organic Compounds. Chemistry, Biochemistry and Toxicology. In 6 parts (Volumes 1–3, each with Parts A and B). (Ellis Horwood Series in Biochemical Pharmacy). Edited by *L. A. Damani*. Ellis Horwood, Chichester, 1989. Hardcover. Prices: £ 35.00 each for Vol. 1, Pt. A; Vol. 2, Pts. A and B; Vol. 3, Pts. A and B; £ 45.00 for Vol. 1, Pt. B. Vol. 1, Pt. A: 167 pp., ISBN 0-7458-0215-X; Pt. B: 324 pp., ISBN 0-7458-0216-8; Vol. 2, Pt. A: 163 pp., ISBN 0-7458-0217-6; Pt. B: 175 pp., ISBN 0-7458-0218-4; Vol. 3. Pt. A: 204 pp., ISBN 0-7458-0573-6; Pt. B: 280 pp., ISBN 0-7458-0574-4

The outstanding importance of organosulfur compounds in many different areas of application, and especially in modern chemical synthesis, is sufficiently well known to need no explanation. However, the importance of such compounds in the biological field is an aspect in which the chemist should be no less interested, when one takes into consideration that sulfur plays an essential role in many biochemical processes, that it is estimated to have an average concentration in the biosphere of about 600 ppm, that most microorganisms and plants are capable of reducing its oxidized forms (e.g. sulfate ion), and that sulfur is incorporated into amino acids (usually as cysteine) and into the catalytic centers of many enzymes, and has a functional role in these.

Accordingly, there have been many monographs and books, even some quite early ones, describing the biochemistry of *endogenous* organosulfur compounds (for example, L. Young, G. A. Maw: *The Metabolism of Sulphur Compounds*, Methuen, London 1958; D. M. Greenberg (ed.): *Metabolism of Sulfur Compounds*, Academic Press, New York 1975; J. W. Anderson: *Sulphur in Biology*, Arnold, London 1978; W. B. Jakoby, O. W. Griffith (eds.): *Sulfur and Sulfur Amino Acids* in *Methods in Enzymology, Vol. 143*, Academic Press, New York 1987). On the other hand much less attention was given in earlier publications to the sulfur biochemistry of *exogenous* synthesis products, which have only recently come into greater prominence, and are clearly important from an ecological standpoint. The work reviewed here is aimed specifically at covering this currently important topic, thereby filling a noticeable gap. An attempt has been made to bring together the widely scattered information on the biochemistry of sulfur-containing xenobiotics, i.e. synthetic agents that are used in a wide variety of applications as agrochemicals, pharmaceuticals or other products made on an industrial scale.

This has resulted in a collection of 46 chapters, which are essays rather than encyclopedically arranged compilations, in accordance with the principle that "he who has much to offer will bring benefits to many". The ground covered is remarkably extensive, touching on nearly every aspect of metabolism, of toxicity, and in general of the biochemical fate and mode of action of synthetically produced organosulfur compounds used in many different areas of application. All this is covered in three volumes, each of which is subdivided into Parts A and B. Volume 1 is devoted to the metabolism of sulfur-containing functional groups (with an excellent introduction by the editor to the topic as a whole, namely "Aspects of Sulphur Chemistry, Biochemistry and Xenobiochemistry"). In Volume 2 the analytical, biochemical and toxicological aspects of sulfur xenobiochemistry are described in detail. Lastly, Volume 3 deals specifically with the metabolism and pharmacokinetics of sulfur-containing drugs.

The work has involved a whole team of experts, although it must be added that this has resulted in a lack of uniformity of quality and in some overlapping of subject matter (admittedly with occasional cross-references). However, this does not detract from the work as a whole—on the contrary, the reader can benefit from the different points of view that are presented, and must approach the reading of the work in a comprehensive way. A wealth of literature references is provided, extending from the early years to the latest state of knowledge. Readers familiar with the subject as well as those seeking an introduction to it will get good value from the work and will find that it fulfills their expectations. There is a wealth of information and stimulating ideas, and also much material for teaching purposes. The standard of production, paper quality, typographical layout and printing convey an excellent impression. In brief: the work can be confidently recommended for all libraries concerned with chemistry, biochemistry, pharmacology and pharmaceutical chemistry, and for the corresponding industrial establishments, and not least for reading by individual scientists.

Werner Schroth
Sektion Chemie
der Universität Halle-Wittenberg (FRG)

Plants for Medicines. A Chemical and Pharmacological Survey of Plants in the Australian Region. Edited by *D. J. Collins, C. C. J. Culvenor, J. A. Lamberton, J. W. Loder* and *J. R. Price*. CSIRO Publications, Melbourne, 1990. 320 pp., hardcover $ 70.00.—ISBN 0-643-04992-7

This book presents an overview of the pharmacologically interesting plants of an entire continent. It summarizes the results of a search for new drugs undertaken from 1939 to the end of the 1980s. The motivation for this survey and for the intensification of research in this area was the outbreak of the Second World War. The results were initially reported in a number of different journals and a summary of these reports was begun in 1984. Attention focused on alkaloids and tumor inhibitors with pharmacological studies being carried out not only in Australia but also in America in collaboration with Smith, Kline and French (SKF) and the National Institutes of Health (NIH). The work with the NIH involved the investigation of the antitumor properties of about 1500 species, 122 of which exhibited reproducible activities.

Another focus of interest was the investigation of plants that are poisonous to animals. Particularly noteworthy is the work on pyrrolizidine-containing plants. One result of the work was the cultivation of *Datura myoporoides* and *D. leichardii* for the production of hyoscyamine. In addition to the above-mentioned effects, the plant extracts or their isolated constituents were tested for the following pharmacological activities: effects on the heart and circulation, in particular high blood pressure, spasmolysis, suppression of inflammation, antimicrobial and antiparasitic activity. The comprehensive tables list the results according to plant families. Not only flowering plants but, to a lesser extent, ferns, algae, fungi, and lichens were included in the investigations. A total of 64 plants are pictured on color plates and the book contains 2152 references to the literature. The extensive index is arranged according to plant families, species, authors, and substances.

Although the book only deals with Australian flora, many species and genera occur in other regions of the world and, therefore, it is of general interest to all scientists working with plants of pharmacological importance. In terms of its length, high-quality layout, and color tables, the book is very inexpensive (the price includes airmail delivery). It can be recommended without hesitation.

Hans Becker
Pharmakognosie und Analytische Phytochemie
der Universität des Saarlandes
Saarbrücken (FRG)

NMR, NQR, EPR, and Mössbauer Spectroscopy in Inorganic Chemistry. (Series: Inorganic Chemistry; Series Editor: *J. Burgess*). By *R. V. Parish*. Ellis Horwood, Chichester, 1990. 223 pp., hardcover $ 50.95.—ISBN 0-13-625518-3

"NMR, NQR, EPR and Mössbauer Spectroscopy in Inorganic Chemistry" presents fundamentals and applications of these techniques with the aim of helping the inorganic chemist understand and interpret spectra. To the extent that the intended readership stems from the inorganic community, this text is somewhat unique. The book opens with nuclear magnetic resonance methods and considers problems associated with organometallic, phosphorus, and transition-metal hydride chemistry. There is a brief excursion into multinuclear NMR with comments on ^{31}P, ^{13}C, $^{14,15}N$, ^{19}F, ^{27}Al, ^{29}Si and some transition metals. This is followed by a section on special methods, e.g. INDOR, DEPT, INEPT, DANTE, and a few words on two-dimensional spectroscopy. The NMR portion encompasses ca. 110 of the book's 223 pages. A short section on NQR contains comments and data on the halogens, Group 4 elements, and several transition metals, and is followed by a chapter on Mössbauer spectroscopy with emphasis on ^{57}Fe, ^{119}Sn, ^{121}Sb, $^{127,129}I$, ^{193}Ir, and ^{197}Au. The book closes with a discussion of EPR spectra, mainly of transition metal complexes.

Even allowing for the restriction of the subject matter to inorganic systems, it is, of course, impossible to cover any of these subjects in depth. Indeed the author clearly states that this work should not be considered as either a spectroscopic or theoretical treatise, but rather should provide an introduction to these subjects and, presumably, assist the practicing inorganic chemist in his day-to-day contacts with these methods.

The text is easy to read, well illustrated and contains many practical examples which are certain to be of value to a beginning graduate student. There are problems and answers at the end of each section and these will be useful for both students wishing to practice, as well as teachers seeking material for upper-level undergraduate or preliminary graduate courses. Still, there are some problems in presentation and language which might have been avoided: p. 27, it is not likely that the ^{13}C spectra of 2.I and 2.III will yield the same information, as suggested; p. 29, resolution does not necessarily increase with increasing spectrometer frequency (does the author refer to dispersion?); p. 48, it is not at all clear whether the relatively large value for $^{2}J(P,P)_{trans}$ is at all related to the *trans* influence concept; p. 59, for "normal hydrides" T_1 is *not* usually several seconds or more. On a more subjective note, I would have been pleased to see ranges of chemical shift for both ^{13}C and ^{31}P, including the more interesting types of complexes found in the last decade or so, for example, the extremely low field shifts for carbenes and carbynes as well as the very low field resonance positions associated with bridging phosphide ligands. Furthermore, in view of the blossoming literature associated with the NMR of transition metals, more time could have been devoted to this subject. It might have been interesting to bridge the gap between the liquid state (NMR) and the solid state measurements which follow (NQR, Mössbauer) by a few examples of solid-state NMR spectroscopy; however, it is likely that such an excursion would lead to an unreasonable balance. Despite these and other minor problems I feel that, in general, the book will prove useful for students and teachers of inorganic chemistry.

P. S. Pregosin
Laboratorium für Anorganische Chemie
der Eidgenössischen Technischen Hochschule
Zürich (Switzerland)

Particle Beam Microanalysis. Fundamentals, Methods and Applications. By *E. Fuchs, H. Oppholzer* and *H. Rehme*. VCH Verlagsgesellschaft, Weinheim/VCH Publishers, New York, 1990. xv, 507 pp., hardcover DM 215.00.—ISBN 3-527-26884-7/0-89573-505-9

To make effective use of modern instrumental methods in microanalysis requires a considerable knowledge of the fundamentals of these techniques, and a thorough appreciation of their limitations. This book aims to equip the reader with that information. The methods chosen are those that yield structural and chemical information by means of lateral resolution, are commercially available, and are suitable for use in any (well equipped) industrial laboratory. All three authors are internationally recognized scientists active in the area of microelectronics. For this reason the book is confined to those methods that are relevant to applications in the field of semiconductor and thin-film technology. The book succeeds in giving a comprehensive treatment within this limited area.

The standard of production is excellent (printed on acid-free paper), and the book is plentifully illustrated by diagrams and photographs. A clearly set out list of contents and a useful index make it easy for the reader to locate specific topics. The methods whose applications are covered in the book are the various forms of electron microscopy (scanning, transmission and high-resolution transmission electron microscopies, i.e. SEM, TEM, and HRTEM, respectively), those of electron-induced X-ray emission spectrometry (energy- and wavelength-dispersive spectrometries, EDS and WDS respectively, and also electron beam microprobe anal-

ysis), Auger electron spectroscopy (AES), secondary ion mass spectrometry (SIMS), and the testing of complex semiconductor structures using low-energy electron beams. A further chapter giving detailed descriptions of case studies in the microelectronics field completes the book. References to recent monographs afford access to the extensive original literature; additional references to special and company reports are of less value to most readers.

The first part of the book describes the basic principles of the techniques. The reader is given a mixture of detailed information, varying from the highly relevant and interesting to the trivial. This part is difficult to appreciate without a basic knowledge of solid state physics. However, the discussions of the properties of the individual particles used as probes (electrons and positively charged ions) are very useful from the standpoint of the nonspecialist. For those working in this area, the thorough treatment of the interactions of the particles with the sample material will be especially useful; this applies especially to the section on sputtering effects and depth profiles.

Each of the chapters that follow is devoted to a single technique. In each case the experimental principles of the method are first explained, and the latest instruments are described. This is followed by a very useful section on sampling and sample preparation. In these sections, and in those that follow dealing with the interpretation of data, the practical experience of the authors comes clearly to the fore.

The chapter on scanning electron microscopy contains an excellent discussion of contrast mechanisms, and also includes information on channeling and cathode luminescence effects, which many other monographs do not cover. The chapter on tramsmission electron microscopy will not be understandable to readers without any previous knowledge; in particular it does not provide an introduction to geometrical crystallography. Electron diffraction techniques are treated in a similarly inadequate manner. The chapter on X-ray spectroscopy is impressive for its very good description of the operational features of the latest commercial instruments and data processing software, which have now become highly sophisticated. The critical discussion of the quantitative aspects of X-ray spectroscopy is also useful. However, in this chapter, even if not earlier, one becomes aware of a serious shortcoming of the book: there are no tables of numerical data such as scattering cross-sections and other quantities that one needs to know in practice for calculating results from spectra. Giving references to such tables is no substitute for the experimentalist. Through this regrettable omission the book misses the opportunity to be a working tool used alongside the instrument, a role that it would otherwise have filled admirably by virtue of the rest of its contents and their orderly arrangement.

The chapter on Auger spectroscopy again includes an excellent introduction to the technique, and describes how the results are affected by instrumental variables and settings, followed by a detailed treatment of spatially-resolved quantitative Auger analysis. Unfortunately the section on qualitative "spectroscopy" is very brief, which is likely to disappoint readers whose interests lie outside the silicon-chip field, since in these areas quantification is intrinsically more difficult and questionable, whereas qualitative analysis is more important than in the semiconductor field.

The chapter on applications begins with a section on "Analysis Strategy", but unfortunately the reader is only presented with statements of the obvious. Here one would have expected to find a comparative evaluation of the different methods. The examples of applications that follow are well chosen to illustrate the general principles described in the earlier parts of the book. It is here especially that the reader benefits from the practical experience of the authors, who give lively and interesting accounts of work in their own field. An additional useful feature is the inclusion of experimental conditions in some of the figure captions.

On the whole the most impressive aspect of the book lies in the excellent practically-orientated descriptions of the chosen techniques. However, this is not a laboratory handbook, as it does not contain the tables of data that are essential in everyday practice. The book can be recommended for everyone involved in experimental research on semiconductors, whether in industry or universities. With regard to the interpretation of results, as applied to the everyday work of an industrial laboratory, it provides excellent guidance and stimulation for the critical application of these methods. The same is true to a certain extent for the related fields of thin films, surface coatings and information storage. As a general introduction to the techniques the book is only of limited value. Moreover, users with interests in particulate samples, oxide powders or materials that are predominantly organic will find the book less useful.

The book should be useful for preparing advanced lecture courses on instrumental analysis methods, especially as it brings together in a concise form information on physical aspects that would be laborious to extract from other monographs. It should be included in every collection of works on analytical methods, since it instructs the reader, by means of examples, in the interpretation of experimental results.

Robert Schlögl
Institut für Anorganische Chemie
der Universität Frankfurt/Main (FRG)

Chemical Oscillations and Instabilities. Non-Linear Chemical Kinetics. (International Series of Monographs on Chemistry, Vol. 21). By *P. Gray* and *S. K. Scott*. Clarendon Press, Oxford, 1990. xvi, 453 pp., hardcover £ 50.00.—ISBN 0-19-855646-2

Nonlinear chemical reactions under conditions far removed from chemical equilibrium have become a focus of attention during the last few years, and can involve fascinating phenomena such as chemical oscillations, multiple stabilities and chaos on both the time and the spatial axes. The properties of such systems, described by Prigogine as dissipative structures, confer on them the ability for self-organization. The two authors of this book have been involved for several years in fruitful studies of nonlinear processes in the gas phase. This has resulted in a book which shows some of the classical features that characterized the early Russian publications in the area of combustion processes. The authors have included in their overview of the subject their own numerous publications. The lively personality of one of the two permeates the whole book: its aim is to inform, to teach, and to correct inaccuracies—it is never boring.

Taking as an example the cases of quadratic and cubic autocatalysis with a wide variety of boundary conditions, the authors derive numerous analytical solutions to the problem. The topics treated include oscillations in closed isothermal and thermokinetic systems, Hopf bifurcations, relaxation oscillations, the excitability of stationary states, autocatalysis and oscillations in isothermal and nonisothermal continuous flow stirred tank reactors (CSTRs), reaction-diffusion equations for pattern formation (Turing processes), chemical waves, heterogeneous catalytic systems and chemical chaos. Local stability analysis methods using the

Jacobian matrix and its eigenvalues are applied to all these processes. The analytical solutions are illustrated by numerous figures, such as highly informative flow diagrams and phase portraits. In the interests of generality the differential equations are given in dimensionless form. The lucid treatments of Hopf bifurcation and of the excitability of stationary states via nullclines are especially worth mentioning. In the analysis of bistability in a CSTR and the accompanying flow diagrams it is found, interestingly, that recognizable patterns having the appearance of islands (isolas) or mold growths appear.

The second part of the book deals with real chemical systems, with particular emphasis on the well known Belousov–Zhabotinsky reaction and the analysis of the Oregonator model. As examples of gas phase reactions the hydrogen-oxygen reaction, the $CO/H_2/O_2$ reaction and the oxidation of acetaldehyde (also in the CSTR) are discussed, together with models developed for these. The authors are able to show that the understanding of these gas phase reactions has now reached a level similar to that for the Belousov–Zhabotinsky reaction in the liquid state.

Looked at from a teaching standpoint the structure of each individual chapter is in the style of a lecture, and consequently it is sometimes difficult to enter the text at an arbitrary point. On the other hand, a systematic reading proves to be very fruitful. However, the book does not describe the numerical methods that are of such great importance to the practical user, such as the attractor constructions, Poincaré sections, Lyapunov exponents and the dimensionality of an attractor. For these one needs to refer to other textbooks. Also the examples of chemical reactions are rather few, and no biological examples or gas-solid reactions related to technical catalytic processes are given.

This interesting and well written book is intended, as the title indicates, for the chemist with mathematical inclinations who is interested in analytical solutions of simple nonlinear reaction steps. It can be thoroughly recommended.

Friedemann W. Schneider
Institut für Physikalische Chemie
der Universität Würzburg (FRG)

Registered names, trademarks, etc. used in this journal, even when not marked as such, are not to be considered unprotected by law.

© VCH Verlagsgesellschaft mbH, W-6940 Weinheim, 1992. – Printed in the Federal Republic of Germany by Konrad Triltsch Druck- und Verlagsanstalt Würzburg.

All rights reserved (including those of translation into foreign languages). No part of this issue may be reproduced in any form — by photoprint, microfilm, or any other means — nor transmitted or translated into a machine language without written permission from the publishers. Only single copies of contributions, or parts thereof, may be made for personal use. This journal was carefully produced in all its parts. Nevertheless, authors, editors and publisher do not warrant the information contained therein to be free of errors. Readers are advised to keep in mind that statements, data, illustrations, procedural details or other items may inadvertently be inaccurate.

Valid for users in the USA: The appearance of the code at the bottom of the first page of an article (serial) indicates the copyright owner's consent that copies of the article may be made for personal or internal use, or for the personal or internal use of specific clients. This consent is given on the condition, however, that the copier pay stated per-copy fee through the Coypright Clearance Center, Inc. (CCC), for copying beyond that permitted by Sections 107 or 108 of the U.S. Copyright Law. This consent does not extend to other kinds of copying, such as copying, for general distribution, for advertising or promotional purposes, for creating new collective works, or for resale. For copying from back volumes of this journal see 'Permissions to Photo-Copy: Publisher's Fee List' of the CCC.

Editorial office: Postfach 10 11 61, W-6490 Weinheim, Federal Republic of Germany, Telephone (06201) 60 23 15, Telex 465 516 vchwh d, Telefax (06201) 602 328, E-Mail Z16@DHDURZ2 in Earn Bitnet.

Editor: *Peter Gölitz*

Associate editors: *D. I. Loewus, K. J. Schneider, A. Stimson.* **Editorial assistant:** *E. Schweikart*

Publishers: VCH Verlagsgesellschaft mbH. (Managing Director: *Hans Dirk Köhler.*), Pappelallee 3, W-6940 Weinheim, Federal Republic of Germany.

Advertising office (Advertising Manager *R. J. Roth*): Postfach 10 11 61, W-6940 Weinheim, Federal Republic of Germany, Telephone (0 62 01) 60 61 36, Telex 4 67 155, Telefax (0 62 01) 606 156.

ANGEWANDTE CHEMIE
International Edition in English
Volume 31 · Number 2
February 1992
Pages 111–246

C_{60}: Buckminsterfullerene, The Celestial Sphere that Fell to Earth

By Harold W. Kroto*

In 1975–1978 the long-chained polyynylcyanides, HC_5N, HC_7N, and HC_9N were surprisingly discovered in the cold dark clouds of interstellar space by radioastronomy. The subsequent quest for their source indicated that they were being blown out of red giant, carbon stars. In 1985 carbon-cluster experiments aimed at simulating the chemistry in such stars confirmed these objects as likely sources. During these cluster studies a serendipitous discovery was made; a stable pure-carbon species, C_{60}, formed spontaneously in a chaotic plasma produced by a laser focused on a graphite target. A closed spheroidal cage structure was proposed for this molecule, which was to become the third well-characterized allotrope of carbon and was named buckminsterfullerene. It has taken five years to produce sufficient material to prove the correctness of this conjecture. There may be a timely object lesson in the fact that exciting new and strategically important fields of chemistry and materials science have been discovered overnight due to fundamental research, much of which was unable to attract financial support, and all of which was stimulated by a fascination with the role of carbon in space and stars. In this account, interesting aspects of this discovery, its origins, and its sequel are presented. The story has many facets, some of which relate to the way scientific discoveries are made.

Molecules with Unsaturated Carbon Bonds

In the early 1970s, the chemistry of carbon in unsaturated configurations became the prime research focus for my group at the University of Sussex.[1] We were interested in free unstable species and reaction intermediates containing C-S, C-P, C-Si, or even C-C multiple bonds. The work originated from an abortive attempt to produce thioformaldehyde ($H_2C{=}S$) by photolysis. However, we switched immediately to thermolytic activation after I heard a lecture in which Don Johnson (from the U.S. National Bureau of Standards in Washington, D.C.) described how he and Powell had made this compound[2] by passing MeSSMe vapor through a quartz tube heated simply by a bunsen burner! This approach worked beautifully; we produced numerous other new compounds containing the C=S moiety such as thioethanal and thioketene by thermolysis of specially synthesised precursors, and characterized them mainly by microwave and photoelectron spectroscopy.[1] These sulfur species possessed a distinctive odor, and I for one have sympathy with the citizens of Freiburg who, according to Noller,[3] forced Baumann and Fromm to abandon their work on these compounds. We gave up our work on seleno analogues for similar reasons after detecting selenopropanal! After success with sulfur/carbon compounds we jumped, in the spirit of Mendeleev, to the next element in the second row of the periodic table, phosphorus. The first phosphaalkenes, $CH_2{=}PH$ and $CH_2{=}PCl$,[4] were produced in 1976 in a joint project with John Nixon; several more followed.[1] Simultaneously, Becker in Germany made $PhP{=}C(t\text{Bu})OSiMe_3$.[5] At this stage I envisaged a simple possible solution to the problem which had been on my mind

[*] Prof. Dr. H. W. Kroto
School of Chemistry and Molecular Sciences
University of Sussex
Brighton BN1 9QJ (UK)

 © VCH Verlagsgesellschaft mbH, W-6940 Weinheim, 1992 0570-0833/92/0202-0111 $ 3.50+.25/0

since 1964, namely to ascertain whether derivatives of Gier's beautiful molecule HC≡P[6] could be made. I had been fascinated with HC≡P since the day I arrived as a postdoc at the National Research Council (NRC) laboratory in Ottawa and heard Takeshi Oka (who was then also an NRC postdoc) enthuse over a spectrum of this molecule which Kelvin Tyler (another NRC postdoc) had just obtained.[7] It seemed to me that the chemistry of HC≡P and its analogues must parallel that of the nitriles. Transition-metal complexes could probably be prepared, and cycloadditions to generate phosphorus-containing rings would be feasible.[8, 9] The simple approach worked very well, and we produced the first phosphaacetylene derivative, $CH_3C{\equiv}P$,[10] by thermolysis of $EtPCl_2$ (provided by R. Schmutzler). We followed this breakthrough with the syntheses of other XC≡P species (X = Hal, Ph, N≡C, N≡C−C≡C, etc.[11]). It is most satisfying that, as I had originally conjectured in 1964, the phosphaalkynes (and the phosphaalkenes) have subsequently been exploited by ourselves and other groups as synthetic building blocks.

In parallel with our studies of compounds made up of second-row elements and carbon we probed molecules containing chains with C−C multiple bonds. My fascination with such chains developed very early on in a study of the peculiar molecule, carbon suboxide O=C=C=C=O (one subject of my Ph.D. work at Sheffield in the early 1960s with my supervisor Richard Dixon). This stimulated my curiosity in extended carbon chains and the unusual flexibility which they often exhibited; a preoccupation with such molecules has continued to this day. When I flash-photolyzed C_3O_2 a year or two later at the NRC, I ended up with a cell full of black soot and a magnificent spectrum of the C_3 molecule, whose enigmatic patterns had finally been deciphered by Gausset et al.[11] Almost everything about these carbon chains seemed idiosyncratic, and I stored such observations up for the future. These memories were reawakened in the early 1970s by David Walton's work on polyynes at the University of Sussex. David had developed elegant methods for synthesizing long-chain polyynes, based upon silyl-protection techniques which he pioneered in acetylene chemistry.[12–14] He and his students had made the parent 24 carbon-atom species in minute quantities in solution and

H−C≡C−C≡C−C≡C−C≡C−C≡C−C≡C−C≡C−C≡C−C≡C−C≡C−C≡C−C≡C−C≡C−C≡C−C≡C−H

even a 32 carbon-atom (silyl-protected) polyyne.[13] These chains were precisely what was needed for a study of vibration–rotation dynamics—a topic which had attracted my interest. In my mind they conjured up an image of a microscopic quantum-mechanical cheerleader tossing a very bendy bamboo baton high into the air—and then attempting to catch the violently flexing and turning baton it as it descended. The obvious first compound for microwave study was the cyanopolyyne, HC_5N, because of its expected enormous dipole moment. Walton devised a synthetic route; Anthony Alexander, a "Chemistry by Thesis" student (editorial comment: for an explanation see the acknowledgements at the end of the review), successfully prepared it and measured its microwave spectrum in 1974.[15] This was a wonderful achievement for an undergraduate and a very important one for me, since it was the first molecule to be characterized on our newly acquired microwave spectrometer.

Fig. 1. The dark clouds in Taurus from Barnards 1927 survey, *Atlas of Selected Regions of the Milky Way*, (Ed.: E. B. Frost, R. Calvert), Carnegie Institute, Washington, D.C., 1927. Heiles's Cloud 2 is in the left-hand bottom corner as indicated by coordinate markers.

At about this time spectacular advances were being made in molecular radioastronomy. The black clouds which are smeared across our Milky Way galaxy (Fig. 1) were found to possess long-hidden dark secrets. Townes and co-workers[16] opened the Pandora's box in 1968 and revealed that the clouds are full of identifiable molecules. Astronomers suddenly realized what a key role molecules played in the

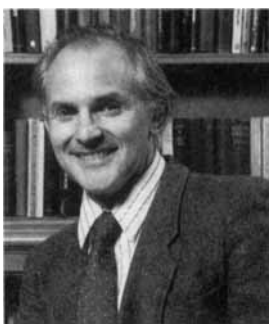

Harold Kroto, born in 1939, studied in Sheffield from 1958 to 1964 and received his Ph.D. for his research in the electronic spectroscopy of free radicals with R. N. Dixon. After three years of postdoctoral research at the National Research Council in Ottawa and Bell Laboratories, he started his academic career in 1967 at the University of Sussex in Brighton, where he became full professor in 1985. The most recent distinction Kroto has received is a Royal Society Research Professorship (1991). Since 1990 he has been chairman of the editorial board of the Chemical Society Reviews. His research interests include the spectroscopy of unstable species, carbon and metal clusters and microparticles, as well as interstellar molecules and circumstellar dust. Graphic design is his other passion.

intimate gas dynamics involved in the birth of stars and planets. Apart from well-known species such as ammonia, water, and ethanol—enough for 10^{28} bottles of schnapps in Orion alone—Bill Klemperer ingeniously identified the HCO^+ ion (protonated CO)[17] which had not previously been detected in the laboratory. Thus space served not only as a playground reserved for astronomers, but it now presented chemists with a novel piece of apparatus, indeed a colossal new spectroscopic sample cell, containing a plethora of exotic molecules in a wide range of physico–chemical environments.[18] Shortly after Turner[19] had detected HC_3N by microwave frequencies, I wrote to Takeshi Oka at the NRC; my group had recorded the analogous frequencies of HC_5N, and I wanted to search for the molecule in space. Takeshi and I had worked (1964–1966) in the same laboratory at the NRC during the golden years of that research organization.[*] He replied saying that he was "very, very, very, very, very much interested".

In November 1975 the search for radio waves of HC_5N (with Canadian astronomers Lorne Avery, Norm Broten, and John MacLeod) resulted in the successful detection of a signal from Sgr B_2, a giant cloud of molecules near the center of the galaxy.[20] Although we had been hopeful, we were surprised by our discovery since it had seemed such a long shot. In 1975 molecules with more than three or four heavy (C, N, or O) atoms were assumed to be far too rare to be detectable. However, having found HC_5N in space, we thought that HC_7N might also be present. Walton devised a synthesis of HC_7N, and graduate student Colin Kirby managed the very difficult problem of making it and measuring its spectrum.[21]. By the time Colin (in England) finally succeeded in recording the vital frequency, we were actually working on the radio telescope, since our allotted observing session had already started. Colin telephoned my wife, who wrote the value on an envelope (Fig. 2 left). She then telephoned Fokke Creutzberg, a friend in Ottawa, who also noted it carefully (Fig. 2 right) and transmitted it to us at the telescope site in Algonquin park (Fig. 3). The next few hours were high drama. We dashed out to the telescope and tuned the receiver to the predicted frequency range as Taurus

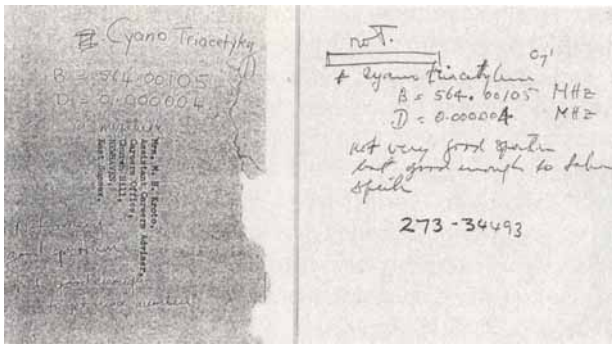

Fig. 2. The envelope (left) and intermediate note (right) with the precious experimental data from which the frequency of HC_7N in space was determined.

[*] Under the guidance of Gerhard Herzberg the NRC had become the Mecca for spectroscopists, and it was here that Cec Costain introduced me to the delights of microwave spectroscopy.

Fig. 3. The 46 m radiotelescope in Algonquin Park, Ontario, Canada with which the long-chain carbon molecules in space were detected.

(Fig. 1) rose above the horizon (perfect timing). We tracked the extremely weak signals from the cold dark cloud throughout the evening. The computer drove the telescope and stored incoming data, but to our frustration we could not process the data on-line while the telescope was running. The system did, however, display individual ten-minute integrations, and as the run progressed we watched the oscilloscope for the slightest trace of the predicted signal in the receiver's central channel. During the course of these ten-minute snapshots, we gradually concluded that the central channel signal was possibly higher on the average than nearby ones. Desperate for even the faintest scent of success, we carried out a simple statistical analysis in order to determine whether the signal level of the channel was greater than the noise. As the night wore on we became more and more excited, convinced that the signal was significantly more often high than low; we could hardly wait for Taurus to set. By 1:00 a.m. we were too excited and impatient to wait any longer, and shortly before the cloud vanished completely, Avery stopped the run and processed the data. The moment when the trace in Figure 4 appeared on the oscilloscope was one of those that scientists dream about and which, at a stroke, compensate for all the hard work and the disappointments which are endemic in life. The circumstances of this discovery—the arrival of the value of the microwave fre-

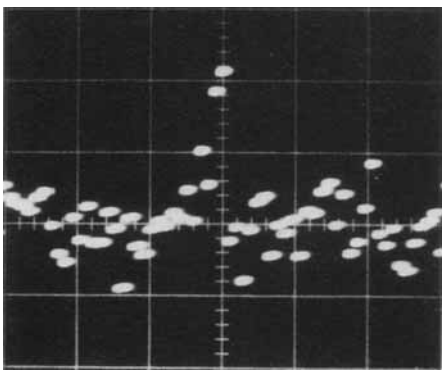

Fig. 4. The first oscilloscope trace of the radio signal emitted by interstellar HC_7N in Heiles's Cloud 2 in the constellation of Taurus (see the coordination markers in Fig. 1).

quency from the UK just in the nick of time, the gradual growth of the conviction that there might be a signal in that central channel of the receiver, and then finally the revelation that we (Fig. 5) had detected an enormous molecule in space[22]—made for a truly cathartic scientific experience. (Modern on-line data processing would have diminished the experience). Obviously, the next candidate was HC_9N, but

Fig. 5. The team at the NRC laboratory just after the detection of HC_7N in space (from left): Avery, Oka, Broten, MacLeod, and Kroto.

its synthesis was a daunting task. Fortunately, Oka developed a beautifully simple extrapolation technique with which he predicted the radio frequencies of HC_9N. Almost unbelievably, we detected this molecule as well![23] Bell et al. later detected even $HC_{11}N$.[24]

The Search for the Source of Carbon Chains in Space

It is not so obvious today, but in 1975–1978 such long-chain molecules were a totally new and unexpected component of the interstellar medium. How such species came to be present was not at all clear. I felt that it was not sufficient just to have co-discovered them; I really wanted to solve the puzzle of how they got there in the first place, and indeed what they were doing there anyway. After all, everything in nature seems to have some role to play. The search for the source of these compounds became something of a preoccupation (even an obsession). By the early 1980s I was convinced that the ion–molecule reactions which Eric Herbst and Bill Klemperer,[25] and Alex Dalgarno and John Black[26] had devised, and which accounted beautifully for almost all other interstellar molecules, really could not explain the origins of chain molecules.[1,18] It gradually became clear to me that red giant, carbon stars must hold the key. Particularly interesting was the spectacular infrared object IRC+10216, discovered by Eric Becklin and his colleagues,[27] which pumps vast quantities of chains and grains out into space. I wondered about this red giant and the fact that it was shrouded in grains and chains, which were formed at roughly the same time,[1,18] and whether "the long chains may be an intermediate form of carbon, between atoms and small molecules such as C, C_2, and C_3, which are well known, and particles with high carbon content such as soot".[1] Perhaps some symbiotic chain/dust chemistry was involved.

The First Visit to Rice University (Easter 1984)

The foregoing account sets out the background for my thoughts about the role of carbon in space prior to my trip to Rice University in Texas during Easter 1984 to visit Bob Curl. Almost the first thing that Curl told me was that I should visit his colleague, Rick Smalley. He enthused over a very recent result obtained by Smalley and his co-workers, who had analyzed the spectrum of the SiC_2 and had shown the molecule not to be linear, as some might have expected, but triangular.[28] (The analogous C_3 species is linear, although only just.[11]) I visited Smalley's laboratory and saw the laser vaporization cluster-beam apparatus which he and his co-workers had recently developed. This powerful technique enabled the mass-spectrometric study of stable clusters formed in a helium-entrained plasma, produced by a pulsed laser focused on a solid target. In this particular experiment silicon carbide was vaporized and the electronic spectrum of SiC_2 observed.[28] I was much impressed by the result but even more by the experimental technique.[29] This method was clearly a major breakthrough in cluster science, since it made refractory clusters accessible for detailed study for the first time. I had already heard of it, but to see the apparatus in operation was quite fascinating. The result of the SiC_2 experiment was particularly interesting to me, because it was consistent with some unusual theoretical results for >Si=C< species[30] obtained at Sussex in collaboration with John Murrell some years earlier. What excited me most, however, was the thought that by simply replacing silicon carbide with graphite, it should be possible to simulate the type of chemistry which takes place in the atmosphere of a carbon star and produce the long carbon chains. As the day wore on I became more and more convinced that the technique was perfect for this purpose and that evening discussed it with Curl. Because of his interest in microwave spectroscopy, he was immediately enthusiastic, and we made plans for a joint project in the hope that Smalley would also be interested. Perhaps we could detect chains with as many as 24–32 carbon atoms related to Walton's polyynes or Hintenberger's equally amazing pure-carbon species (C_{33} etc.), which were detected by mass spectrometry in the early 1960s in a carbon arc.[31] I dreamt that one day it might be possible to detect a chain molecule such as $HC_{33}N$ (which is as long as the chains that Walton had made in a test tube) in space. Curl was particularly excited by the prospect that we could check out an interesting idea of the late Alec Douglas,[32] namely, that carbon chains might be carriers of the famous Diffuse Interstellar Bands—a set of absorption features[33] which have puzzled astronomers and spectroscopists for more than six decades. Because the project was not considered a priority by the cluster group at Rice University at that stage, it had to await a convenient slot in their program.

In the interim, a group at Exxon carried out the basic graphite-vaporization experiment. In the summer of that year (1984) they published a fascinating result: the discovery of a totally new family of carbon clusters C_{30}–C_{190}[34]—

much larger species than those prepared by Walton et al.[12-14] or observed by Hintenberger.[31] This exciting discovery was peculiar because only even-numbered clusters were detected. It is important to note that at this juncture no specific cluster was perceived to be special. In August 1985 (almost 18 months after my visit) Curl telephoned to say that carbon experiments were at long last imminent. He asked whether I wanted to come to Houston to participate or if they should carry out the experiments and send the data to me. One thing was certain in my mind: I had not waited this long to have my experiments carried out by others in my absence; I wanted to do them myself and to direct the operation personally. Therefore I packed my bags and at my wife Marg's expense arrived at Rice University within days.

Second Visit to Rice University— The Discovery of C_{60}

Silicon and germanium cluster studies were on the Rice plate in August 1985 because of their implications for semiconductors. Such experiments were considered to be important because the results might have useful applications (!) The carbon project, on the other hand, was thought to have no possible application (other than for astronomy) and was to be completed quickly, causing as little delay to the semiconductor study as possible. Preliminary measurents on carbon had already been carried out, and the Exxon spectra had been reproduced; nothing untoward was noticed. As soon as I arrived (August 28th) I presented a lengthy informal seminar on everything I knew about carbon in space, stars, and soot. My experiments started on Sunday, September 1st, 1985. I worked in the laboratory alongside two research students, Jim Heath and Sean O'Brien—an exhilarating experience; Yuan Liu was also involved. We toiled late into the night, varying the clustering conditions and monitoring the reactions of the carbon clusters with hydrogen, oxygen, and ammonia—gases which I thought would give rise to polyynylcyanides and other chain molecules. They did! The experiments thus immediately confirmed that the chemistry in red giant stars could be responsible for interstellar carbon chains. Curl and Smalley paid frequent visits to the laboratory. As the experiments progressed it gradually became clear that something quite remarkable was taking place: As we varied the conditions from one run to the next, we noticed that a peak at 720 amu[*] (corresponding to a C_{60} species) behaved in a most peculiar fashion. Sometimes it was completely off-scale; at other times it was quite unassuming. The spectrum recorded on Wednesday, September 4th, 1985 was astounding (Fig. 6). Our reactions were noted in the laboratory record book (Fig. 7a), and I annotated my copy of the printout (Fig. 6). From that point onwards the idiosyncratic behavior of this peak was followed very, very closely (Fig. 7b). When this result appeared, the carbon project—

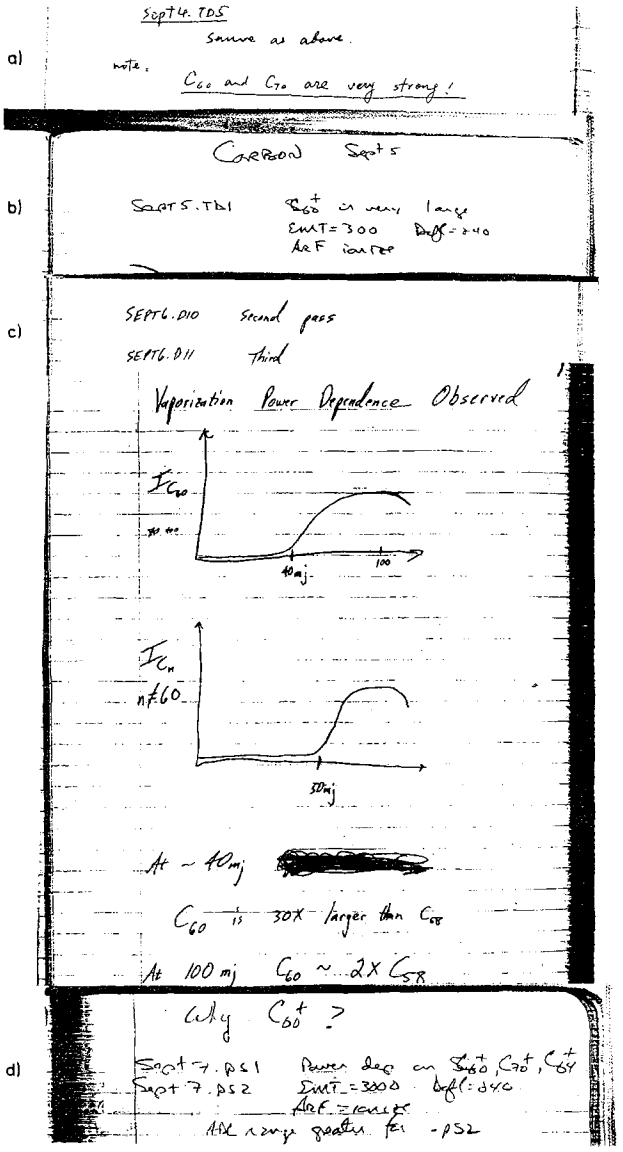

Fig. 7. Entries by Heath, Liu, and O'Brien in the Cluster Laboratory Notebook from the period September 4–7, 1985 when key experiments were carried out at Rice University. a) September 4th: First recorded note that C_{60} and C_{70} were very strong (see also Fig. 6). b) September 5th: C_{60} signal again very strong. c) September 6th: Record of first experiments which specifically aimed at optimization of the conditions for production of a dominant C_{60} signal ("C_{60} is 30 × larger than C_{58}."). d) September 7th: Further power-dependence studies.

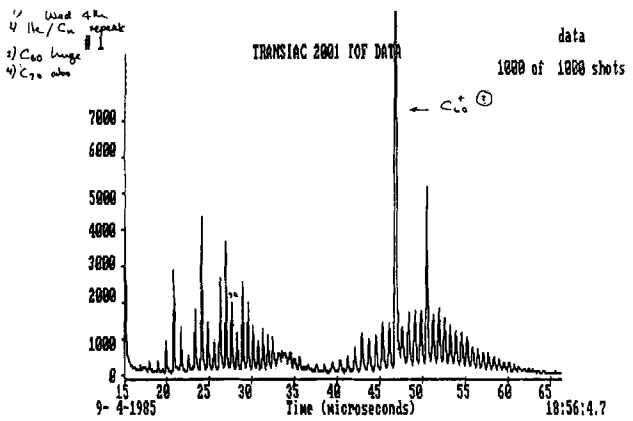

Fig. 6. Annotated time-of-flight (TOF) mass spectrum of carbon clusters produced on Wednesday, September 4th, 1985, the day on which the dominance of the C_{60} signal was first recorded (see also Fig. 7a).

[*] Editorial note: amu = atomic mass unit. According to *Quantities, Units and Symbols in Physical Chemistry* (Ed.: Int. Union of Pure and Applied Chemistry), Blackwell, Oxford, **1989** (Chapter 2.10), amu is the symbol for the unified atomic mass unit m_u and the unit u. In this review the unit amu which is still encountered frequently is used.

for the first time—engendered general interest, and by mutual agreement continuation of the semiconductor program was delayed so that we could concentrate on the remarkable phenomenon which we had uncovered. As the weekend approached our actions, thoughts, and conversations turned more and more to the phenomenon. What might this special "wadge" of carbon be? Smalley had never come across this British term for a cluster and liked it so much that he started to refer to C_{60} as the "Mother Wadge"; the omnipresence of the cluster led me to call it the "Godwadge". On Friday, September 6 during a group meeting, Curl suggested that we should concentrate on identifying the conditions under which the 720 amu peak was most prominent. O'Brien and Heath agreed to work shifts during the weekend. Experiments aimed specifically at optimizing the signal were carried out that same evening, and conditions were immediately found under which C_{60} peak was 30 times stronger than the adjacent C_{58} signal (Fig. 7c). After further optimization (Fig. 7d) the striking spectrum (Fig. 8) was finally obtained. C_{70} is also prominent!

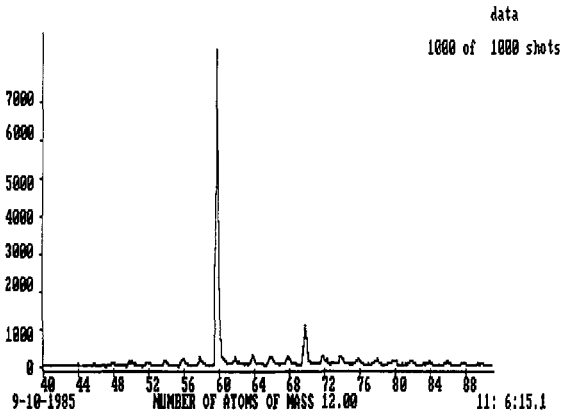

Fig. 8. TOF mass spectrum of carbon clusters under the optimum conditions for the observation of a dominant C_{60} signal.

The Structure of C_{60}(?)

What on earth could C_{60}(?) be? In the days following our discovery of C_{60} (Fig. 6), the signal began gradually to dominate our results as well as our thoughts and conversation. The quest for a structure which could account for this precocious wadge of carbon led to numerous, synergistic [Editorial comment: R. Buckminster Fuller's architectural constructions were based on a vectoral geometry which he called energetic—synergetic geometry. This was founded on a natural philosophy, according to which nature constructs systems of forces such that the maximal strength can be obtained from the minimum effort in construction.] discussions among all five members of the team during those days. The deliberations were particularly intense on Monday, September 9th. As this day wore on and all the ideas which had surfaced during the period were assessed and reassessed, a consensus grew that C_{60} might be some sort of spheroid. One possibility we considered was that the laser had blasted flakes of hexagonal carbon from the graphite surface, and that these hot graphite-like networks had somehow wrapped themselves up into closed cages, thus eliminating the dangling edge bonds and making the cage unreactive. This idea had instant appeal for all. For me this concept brought back vivid memories of Buckminster Fuller's geodesic dome at EXPO '67 in Montreal (Figs. 9 and 10). I had actually

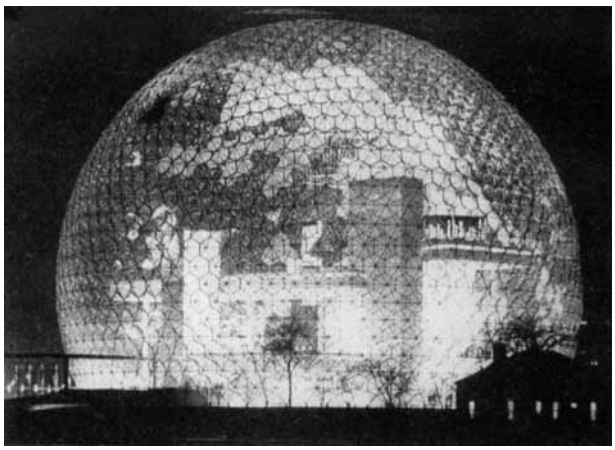

Fig. 9. Photograph (by Michel Proulx) of the geodesic dome designed by Buckminster Fuller for the U.S. exhibit at EXPO '67 in Montreal (taken from *Graphis* **1967**, *132* 379). One of the pentagons necessary for closure is discernable in this photograph.

been inside this remarkable structure at that time and remembered pushing my small son in his pram along the ramps and up the escalators, high up among the exhibition stands and close to the delicate network of struts from which the edifice was primarily constructed. This experience had left an image in my mind which could never be erased. I had collected numerous photographs of the dome from magazines over

Fig. 10. Photograph (by Robin Whyman) of the inside of the EXPO '67 dome in Montreal. One of the pentagons necessary for closure is clearly visible in the middle section, as is the way in which the strut lengths have been adjusted to achieve a smooth round shape.

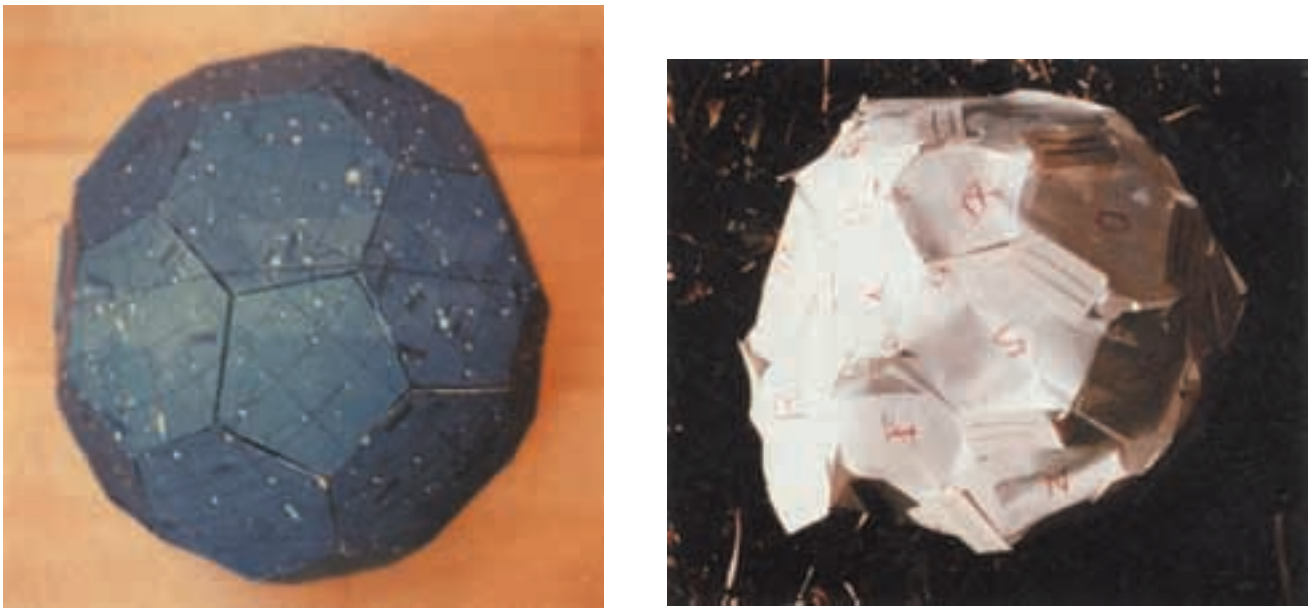

Fig. 11. The two cardboard polyhedra which played key roles in our search for the structure of C_{60} (see text). Left) stardome map of the sky (Buckminster Fuller patented t-icosahedral and other polyhedral world-map projections); right) Smalley's model with 60 vertices and 12 pentagonal and 20 hexagonal faces.

the years from Life, Paris Match, and Graphis. Particularly striking were those in my favorite graphic art and design magazine, Graphis, to which I had subscribed since my university days. As I remembered it, the Graphis pictures (Fig. 9) showed that the dome consisted of a plethora of hexagonally interconnected struts. Indeed, the dome had actually initiated my interest in some of Buckminster Fuller's other projects; I had even been in the process of writing to him with a view to working with him on the organized growth of massive urban structures. However, I did not pursue this, because I was offered a permanent academic position at Sussex at just that time.

As far as C_{60} was concerned, I wondered whether Buckminster Fuller's domes might provide some clue. Smalley also strongly favored some sort of spheroidal structure and suggested that we borrow a book from the Rice University library. We obtained a book by Marks[35] in which geodesic domes of all kinds were described. In addition I had one or two other structural proposals which intrigued me: One was a four-deck model 6:24:24:6 (two coronene-like sheets sandwiched between two benzenoid ones) with a roughly spheroidal shape. It contained 60 atoms, and its symmetry suggested that the dangling bonds might be somewhat deactivated. However, I really could see no reason why this species would be as unreactive as C_{60} appeared to be; a closed-cage solution would certainly be more stable. A second image came to mind several times, most vividly on this particular Monday. This was of a polyhedral cardboard stardome (Fig. 11 left) which I had constructed many years before when my children were young. This map of the stars in the sky was tucked away in a cardboard box (that universal quantum of storage) downstairs in my home far away in England. I itched to get my hands on it and even described its features to Curl at lunch time. I remembered cutting out not only hexagons but also pentagons. I wondered whether I should telephone my wife to ask her to count the vertices in order to ascertain whether, as I half-suspected, they totaled sixty.

The Mexican Restaurant

I was due to return to the UK the next day, so that evening (Monday, September 9th) I thought we should celebrate our extraordinary discovery. I invited the group out to dinner at what had become our favorite Mexican restaurant. During the meal the conversation was naturally dominated by C_{60}(?). We again considered all the ideas which had come up in our deliberations during the days that had passed since the signal had first been noticed. We agreed unanimously on a *closed cage* structure. We talked about Buckminster Fuller's domes, Smalley, about chicken-wire cages, and I reiterated the essentials of the stardome—its spheroidal shape, hexagonal faces, and, in particular, the pentagonal faces. Smalley expressed an interest. After the meal other members of the group went home; I returned to the laboratory in order to study the Marks' book on Buckminster Fuller, but I could not find it. I again considered telephoning home about the number of vertices in the stardome. But it was now far too late since it was well after midnight in the UK.

Very early the next morning Curl telephoned to say that Smalley had experimented with paper models based on the stardome characteristics I had mentioned the previous day. Smalley had come up with something bigger than anything he (Curl) had ever been involved with before. When I got to the laboratory and saw the paper model (Fig. 11 right) which Smalley had constructed during the night I was ecstatic and overtaken by its beauty. It seemed identical to the stardome as I remembered it, and I was quietly pleased that my conjecture had been right all along. Heath and his wife Carmen had also experimented with a geodesic structure modeled out of jelly beans and toothpicks; it was not quite so convincing.[36]

In summary, the quest for a rational explanation of the dominant line in the mass spectrum had reached a climax on Monday, September 9th. Ideas were suggested, refined, or critized in earnest throughout that final day. Buckminster Fuller's domes were invoked, Marks' book was consulted, and the stardome's pentagonal faces introduced at midday

and again in the evening; Smalley and the Heaths experimented further with models during the night after our meal. All this took place in a matter of hours, leaving no time for anything important—other than perhaps Marks' book—to "slip through the cracks".[37] It was most satisfying that synergistic (a Fullerism) teamwork had been involved in the experimental observation as well as in the positing of the structure.

I delayed my flight home for one extra day (until Wednesday, September 11th) in order to help to write the publication. At one point Heath was sitting at Smalley's desk when the telephone rang. A mathematician, whom Smalley had consulted earlier to ask about the structure, informed Heath, "Tell Rick—it's a soccerball!" Almost unbelievably, until that moment, none of us had realized that the C_{60} structure we were proposing had the same symmetry as the modern soccer-(USA) or football (rest of the world). I do not know how I could have been so blind—my only (feeble) excuse was that the modern football was introduced after I ended my serious soccer-playing days. The other members of the team could be excused, since a structure related to the American football really was an unlikely contender, at least at that stage. We immediately purchased a real football and our five-a-side team posed for a photograph (Fig. 12). I also

Fig. 12. The five-a-side Rice/Sussex football team (from left): O'Brien, Smalley, Curl, Kroto, and Heath.

photographed Smalley's paper ball (Fig. 11 right), but when I queried the whereabouts of the Heath model in order to photograph it for posterity, I was informed that it no longer existed because Mary-Joe (another Rice graduate student) had eaten it. So all tangible record of a truly remarkable edifice was lost for all time.

Since the geodesic dome concepts had played such an important part in helping us to arrive at the solution (at least as far as I was concerned), I suggested that we name the compound buckminsterfullerene. Smalley and Curl fortunately agreed, accepting that though the name was long, it did indeed roll smoothly off the tongue. Thus we avoided the fearful international conflict over terminology which would have raged had we named it after a certain well-known ball game. Smalley could not resist putting some alternative suggestions for names at the end of the publication. The name engendered the occasional mild criticism[38] which was dispatched with a little help from Shakespeare.[39] Now that some time has passed, it is satisfying to note how instructive (about geodesy) others have found the name and how flexible it has turned out to be. The whole family of closed cages can be appropriately named—fullerenes.[40] The paper[41] was dispatched by Federal Express to the journal *Nature* on the afternoon of Wednesday, September 11th, 1985.

Five Long Years in the Desert

The ten-hour nonstop flight home to England was a physical and psychological high for me. My first action upon entering the house was to open the cardboard box and take out the stardome which had influenced my deliberations during the search for the structure of C_{60}. It had always looked beautiful; now it positively glowed. When the news of our result spread, Martyn Poliakoff at Nottingham wrote that his friend, David Jones, had already thought of hollow carbon cages. In 1966 Jones had written a delightful article under the pseudonym Daedalus in the journal *New Scientist*[42, 43] in which he had suggested that the high-temperature process in the production of graphite might be modified to generate graphite balloons. This was a typical example of the presciently "crazy" ideas of Jones. I thus learned about the Euler principle, which says that 12 pentagons are needed to close a network and that hexagons alone just will not do. I was introduced to D'Arcy Thompson's elegant book[44] and learned that one could close an even-numbered carbon cage with any number of hexagons (except one, I subsequently learned) provided 12 pentagons were included in the network. The beautiful Aulonia (Fig. 13 photograph from Tibor Tarnai) already knew more than we about these simple (pentagonal) facets of (its) life. This was all fun and truly

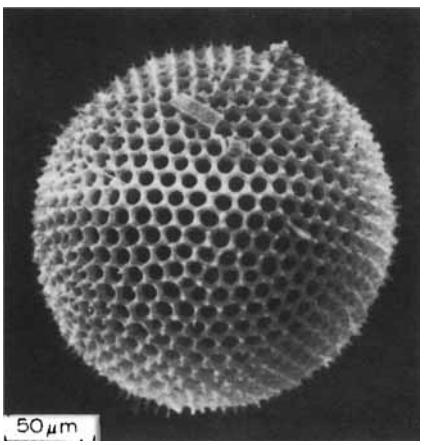

Fig. 13. A siliceous sea creature, *Aulonia hexagona*, appears at first glance to possess a skeleton composed completely of hexagons. Pentagonal structural elements are discernable, however (photograph supplied by Tibor Tarnai).

fascinating, because it became clear that there might even be other (even-numbered) carbon cages—there were certainly other (even-numbered) peaks (Fig. 6), in particular C_{70}. O'Brien and Smalley reached the same conclusions independently. Particularly important were a series of reactivity ex-

periments carried out by O'Brien, which showed that all the even-numbered carbon species were totally unreactive, a result neatly commensurate with closed structures for all the even-numbered cages.[45]

I met David Jones, a most fascinating individual, who epitomizes so much of what the spirit of science should be about. We also learned that Osawa and Yoshida had already thought of C_{60} in 1970 and had even suggested that it might be superaromatic.[46,47] In 1973 Bochvar and Gal'pern[48] also published a theoretical paper on the molecule. Thus it transpired that although there were some most imaginative scientists around, few—other than Orville Chapman at the University of California at Los Angeles (UCLA)[49]—had noticed these pioneering flights of imagination.

Circumstantial Evidence for the Identity of the "Third Man"

The first question stimulated by the realization that we might have found a "third form of carbon" with a hollow, cage structure was obvious: is it possible to trap an atom inside the cage? My early Sheffield background led me to wonder whether iron might form an intriguing ferrocene-like analogue. The day I left, Heath tried to encapsulate iron without success, but the next day he succeeded in detecting a stable $C_{60}La$ complex.[50] This experiment provided the first convincing piece of evidence to support our proposal of the cage structure. Then began what was to become a truly exhausting schedule for me: Every four to six weeks I flew to Houston, and after two to three weeks' work with the group at Rice I returned to the UK and my commitments in Sussex. As soon as I arrived in Houston I would present a group seminar based on ideas which I had developed while in the UK. This schedule continued until April 1987. From the outset the joint Rice/Sussex follow-up program had two clear objectives. First, to make enough C_{60} to prove beyond doubt that our structure was correct and second, to measure the optical spectrum of C_{60} which we had surmised might in some way be responsible for the Diffuse Interstellar Bands.[41] These astronomical features had of course been partly responsible for the carbon-cluster experiment in the first place. These goals were all-consuming and we often talked about "the little yellow (Smalley's guess) or pink (my guess) vial" of C_{60}.

During the late 70s and early 80s I felt that it was simply not enough just to detect the carbon chains; the source must be tracked down. This obsession with the source led ultimately to the discovery of C_{60}. After 1985 I developed a similar attitude to C_{60}. Our discovery of a species which probably had a truncated icosahedral structure was "not enough", and as months and then years passed, confirmation of the structure and its identification in space also became somewhat of an obsession. We (the Rice group and myself) were convinced from the outset that our proposed structure was correct; surely it was too beautiful and perfect to be wrong. However, if for once aesthetics were misleading us, it would be much better if we proved our model wrong ourselves. It is certainly fair to say that the proposed structure was greeted with scepticism by some, though many loved C_{60} and were convinced that we were right from the start. During this period (1985–1990) I examined the problem independently at Sussex, as well as in collaboration with the Rice group, who also made independent studies. In time all these efforts resulted in a mass of convincing evidence in support of our proposal.

From the moment we discovered that C_{60} was stable I had one all-consuming dream: I wanted so solve the molecule's structure by NMR spectroscopy. Because all 60 carbon atoms in buckminsterfullerene are equivalent, the ^{13}C NMR spectrum should consist of a single line. Proof of our radical proposal in such an exquisitely simple manner was to remain elusive for some five years; this goal was almost like a holy grail—far, far beyond reach. I was quite convinced that a clever young organic chemist would accomplish this task. I had one consoling thought, namely that we had been rather successful in the past with a series of molecules whose identifications were based on spectra consisting of single lines: Phosphaethene, $CH_2{=}PH$ (the first phosphaalkene made) had been assigned by its $J = 1 - 0$ microwave line[1,4] and HC_5N and also HC_7N had both been originally single radioline detections in space.[20,22] Then there was, of course, the 720 amu peak in the mass spectrum of C_{60}.[41] How fitting it would be to round it all off by *proving* by another *single* line that C_{60} was buckminsterfullerene.

C_{70} and the Fullerene Family

It is fair to say that I (and perhaps also my colleagues at Rice University) occasionally woke up in the middle of the night and wondered whether I should have to commit suicide if our idea turned out to be wrong. Had we stuck our necks out too far? These thoughts only lasted seconds. I would reassess all the evidence, realize that everything fitted, and go back to sleep convinced more than ever that C_{60} had to be a geodesic cage. Time pased, we made several advances,[51,52] and each time the cage concept clarified our observations. That was important. I remembered hearing Richard Feynman on BBC radio say that it seemed to him that if a radical new theory were right, it would allow the solution of previously unsolved puzzles. I quantified this: If an idea fitted 80–90% of the observations, it was almost certainly right; if more than 10–20% of the details had to be bent to fit, it was almost certainly wrong. Buckminsterfullerene was well up in the first category.

I remember vividly the day on which all my lingering doubts vanished. I was sitting at my desk thinking about the reasons why C_{60} might be stable. The missing piece of evidence in this personal jigsaw puzzle turned out to be so simple, it was almost child's play; indeed it evolved from my playing with molecular models of various conceivable cages. The solution was related to the C_{70} signal which always popped up prominently when C_{60} was strong. I used to call the two species "the Lone Ranger and Tonto"[*] because

[*] The Lone Ranger und Tonto were a famous cowboy and Indian duo from the movies. As a child I saw them every week fighting crime in the Wild West. Bob Dylan immortalized them in the following blues text:
Well the Lone Ranger and Tonto
They are ridin' down the line
Fixin' ev'rybody's troubles
Ev'rybody's 'cept mine.
Somebody must a tol' 'em that I was doin' fine.

they were so inseparable and because C_{60} was always dominant (Figs. 6 and 8). As far as C_{60} was concerned, it seemed no accident that the modern soccerball with the same layout is one of the most, if not *the* most, resilient of constructs, able to survive being kicked around the world (and perhaps around the galaxy). Maybe the football held a simple clue. When I looked carefully at a football, I was struck by the fact that all the (black) pentagons are isolated, whereas all the (white) hexagons are linked. It is known that unsaturated compounds composed of abutting pentagons (the pentalene configuration, Type **II**, Fig. 14), without substituents which allow extended conjugation, tend to be unstable. Curiously, a compound with just such a structure appeared on the cover of *Angewandte Chemie* (July 1987) that very week.

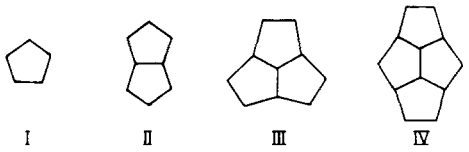

Fig. 14. Isolated and abutting pentagons: **I**, isolated; **II**, fused pair (pentalene configuration); **III**, symmetrically fused triplet (triquinacene configuration); **IV**, directly fused quartet [53].

Since Euler's law requires 12 pentagons for closure, it was also clear that C_{60} was the smallest carbon cage for which all the pentagons could be isolated. O'Brien's reactivity experiments had convinced us that closure was possible, even probable, for all the even clusters. I conjectured that a *pentagon isolation rule* could be formulated to account for the stability[53]; then I began to wonder which was the next cage for which pentagon isolation was feasible.

By playing with the models I saw immediately that it was not C_{62}, and as I added more atoms, try as I would, I could not find cage structures for C_{64}, C_{66}, or C_{68} without abutting pentagons. We had already proposed a structure for C_{70},[50] after Smalley had shown that by splitting C_{60} into two C_{30} hemispheres a ring of ten extra carbons could be neatly inserted, producing a most elegant, symmetric, egg-shaped structure (Fig. 15 right). Suddenly I realized that perhaps this C_{70} cage was the next structure after C_{60} which could close and which also had *isolated* pentagons (Fig. 15). This surprised me. Perhaps closure *necessitated* that 70 be the second magic number! We had stuck our necks out with the C_{60} hypothesis on the basis of a single peak in the mass spectrum, but it now seemed that the cage concept positively insisted that C_{70} *as well as* C_{60} are special.[53] That would be wonderful. A second solution which required both of these particular magic numbers was impossible to conceive, especially since 70 would be an unusual number to be deduced as magic at all, let alone the second in order. I knew that nature would not be that perverse, and thus for first time my conviction that our structure was corrrect became absolute, and I never again doubted that one day we would be vindicated. Indeed in my opinion this result meant that we were home and dry.

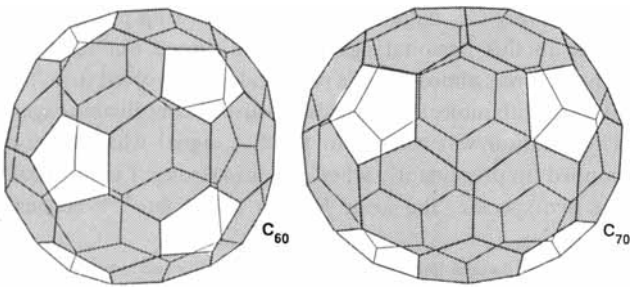

Fig. 15. For species with less than 72 atoms these two structures are the only ones which can be constructed without abutting pentagons. Thus on the basis of the *pentagon isolation principle* and geodesic considerations C_{60} and C_{70} are predicted to be the first and second magic fullerenes. This result together with Figure 8 provided the simplest and strongest circumstantial evidence supporting the closed-cage concept.

I was elated by this line of reasoning, but I really needed proof. I remembered that Tom Schmalz and his colleagues, Klein and Hite, in nearby Galveston had published some elegant graph-theoretical studies on the fullerenes. I contacted him and asked him what he thought about my idea. I was amazed and delighted when he told me that they had been looking at this same problem and had proven that cages composed of 62, 64, 66, and 68 atoms cannot be constructed without abutting pentgagons.[54] So it was true! I told him that I wondered whether the semimagic C_{50} might be the smallest cage able to avoid abutting triplets of pentagons (Type **III**, Fig. 14, Lit.[53]). Schmalz et al. subsequently showed this also to be correct.[54] One Sunday afternoon, sitting in front of the molecular models strewn all over our coffee table at home, I decided to investigate other semimagic numbers. I wondered about C_{32} which had been shown by the group at Rice University to be the first cage relatively stable towards photolysis. I toyed with the idea that it might be the smallest cage able to avoid fused quartets of pentagons (Type **IV**, Fig. 14). I tried to make the smallest model containing such a structure, and as I counted up the atoms I suddenly realized, that it was not C_{32} but a delightfully symmetric C_{28} cage (Fig. 16). I became excited because I knew, that during the Rice/Sussex collaboration period we had occasionally obtained mass spectra in which C_{28} was almost as dominant as C_{60}. At this point it seemed that essentially all the magic numbers would fall into place if these clusters were *all* cages. In particular, I found that I could explain the fascinating spectrum (Fig. 17) published by the Exxon group.[55] Here was all the proof I needed to convince myself that a whole family of cage molecules was sitting around waiting to be discovered. The first somewhat

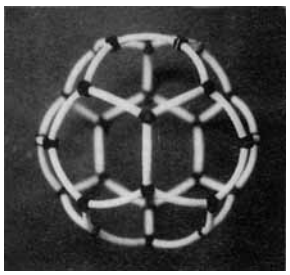

Fig. 16. Molecular model of C_{28}, one of several fullerenes (with 24, 28, 32, 50, and 70 atoms) predicted to be stable on the basis of geodesic and chemical considerations [53]. These magic-number predictions fitted almost perfectly the observations made under certain clustering conditions [51, 55] (see Fig. 17).

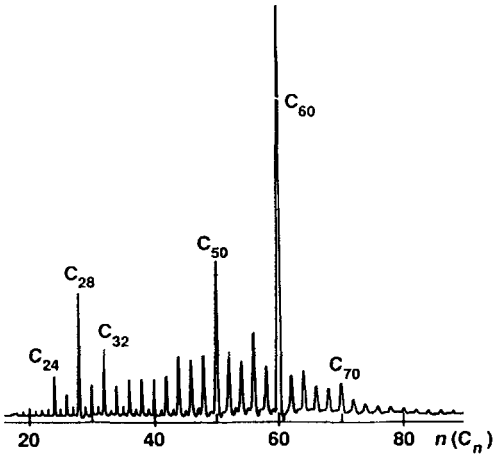

Fig. 17. The particularly interesting mass spectrum of C_n clusters obtained by Cox et al. [55]. The correspondence with the magic fullerene sequence 24, 28, 32, 50, 60, and 70 [53] was the most convincing evidence for the existence of the fullerene *family* prior to the extraction breakthrough. The sharp cut-off at 24 is articularly convincing, since no C_{22} fullerene can exist.

stable member of the family appeared to be C_{24}. This can be explained by the fact that C_{22} cannot exist (I am indebted to Patrick Fowler for pointing out this fact to me) and that C_{20} is the smallest cage and as it has no hexagons at all, almost certainly the least stable. To some extent C_{28} (Fig. 16) became my own personal favorite, because regardless of which of the four threefold axes one views this tetrahedral molecule along, it looks uncannily like Gomberg's famous free radical, triphenylmethyl; this also just had to be right. I knew about Moses Gomberg's discovery from my favorite organic text (Fieser and Fieser[56] which Harry Heaney, my chemistry teacher in school, had encouraged me to buy and read so long ago). It had always amused me to think that on attempting to make the rather mundane compound hexaphenylethane, Gomberg failed (miserably), produced the triphenylmethyl radical, and had to be consoled with becoming known as the father of free radical chemistry instead. This was the sort of "failure" that really appealed to me. If C_{28} is relatively stable, then $C_{28}H_4$ should be a fairly stable hydrofullerene. This seemed not at all farfetched; after all, dodecahedrane which Paquette and co-workers first made[57] is basically the perhydrofullerene of dodecahedrene (fullerene-20), the simplest and probably the least stable of all the fullerenes since it contains no hexagons. At this time I had a telephone conversation about nomenclature with Alex Nickon in which we came to the conclusion that the name "fullerenes" would work well for the family of carbon cages.[40, 53] I gained much satisfaction from the refined concept which was even more appropriate, because Buckminster Fuller had patented constructs of all shapes and sized based on the 5/6 ring principle;[58] some were very similar to the elongated framework of C_{70}. Nickon was just finishing his entertaining book with Silversmith on the origins of the trivial names of compounds.[40]

In Houston a particularly important series of experiments was carried out by Curl, Smalley, and their co-workers which offered further overwhelming evidence for closed cages.[52] One of these was a photofragmentation experiment which provided even-numbered products. Curl had worked out a neat way of explaining how the cages might "spit out" even-numbered (2, 4, 6, ...) carbon chains and then reseal. Another most convincing study showed that when the encapsulation of atoms of various sizes appeared to be successful, the smallest caged species detectable had diameters commensurate with the known sizes of the encapsulated atoms.

C_{60} and Soot

During one of my eight visits to Rice University between August 1985 and April 1987 we considered carefully the reactivity results and developed a hypothetical mechanism for the formation of C_{60}.[45] Heath, O'Brien, and I spent hours in the library digging through an excellent selection of books and journals on carbon. The final version of the mechanism grew out of intense synergistic group discussion. It was also clear that the mechanism might explain soot formation as well. After all in a review on soot, Harris and Weiner[59] had pointed out the complete absence of knowledge of the chemistry involved in soot formation. Thus a fresh idea probably would be welcome. Our mechanism implied C_{60} should be a by-product of soot formation. Curl was apprehensive about introducing the word soot, especially in the title. How prescient were his worries! However, Smalley and I decided to throw caution to the wind—after all, when you have gone as far as you can go (in postulating C_{60} formation in a chaotic plasma), you might as well go further. Our paper met with some criticism.[60] To our delight, however, in 1987 we heard that Klaus Homann's group in Darmstadt discovered that C_{60} was a dominant ion in a sooting flame.[61] (Note: Very recently, a careful study by Howard's group at the Massachusetts Institute of Technology has shown that up to 7% of the soot from a benzene flame consists of fullerenes.[62])

The Giant Fullerenes

One day I decided to spend £300 on ten-thousand sp^2 carbon atoms (molecular models!) The odd eyebrow was raised at Sussex when I said that I was buying them just because I wanted to see what giant fullerenes such as C_{6000} (with a diameter ten times that of C_{60}) looked like. Ken McKay (a graduate student) obtained Coxeter's book[63] and Goldberg's paper[64] and set to work. When he came into my room with models of C_{240} and C_{540} (Fig. 18), I was delighted but perplexed—they were beautiful, but not at all what I had expected. C_{540}, in particular, was not round like Buckminster Fuller's domes, but in fact much more interesting: It was essentially a monosurface which swept between cusps in the vicinity of the pentagons; it had icosahedral symmetry, but was not an icosahedron.[65] Then we realized that its shape might explain[65] the polyhedral patterns in graphite microparticle electron microscope pictures published by Iijima (Fig. 19).[66] The structure of these microparticles could be nicely explained as concentric shells of graphitic carbon in which the shells had giant fullerene shapes. Few of our discoveries have delighted me more than these objects, partly because they are so elegant, but also because the exercise, which was started *purely* for fun and with no serious aim, had yielded such an apparently important result. It was also an object lesson, since I had assumed

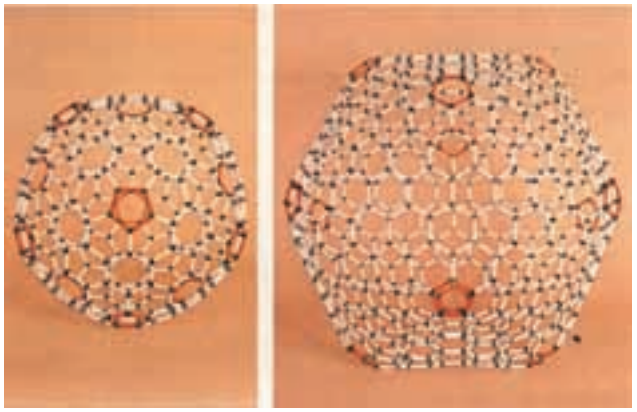

Fig. 18. Molecular models of the giant fullerenes C_{240} (left) and C_{560} (right). The models possess icosahedral shapes rather than perfectly spheroidal ones similar to the geodesic domes. Each of these structures can be considered as an initially flat hexagonal network which has warped into a closed monosurface (of icosahedral symmetry) by 12 pentagonal disclinations giving rise to the cusps.

that the giant fullerenes would be spherical like Buckminster Fuller's domes and had not looked carefully at Iijima's images. Even the most spheroidal giant fullerene (Fig. 19a) was clearly polyhedral (Fig. 19b). To see what one wants to see

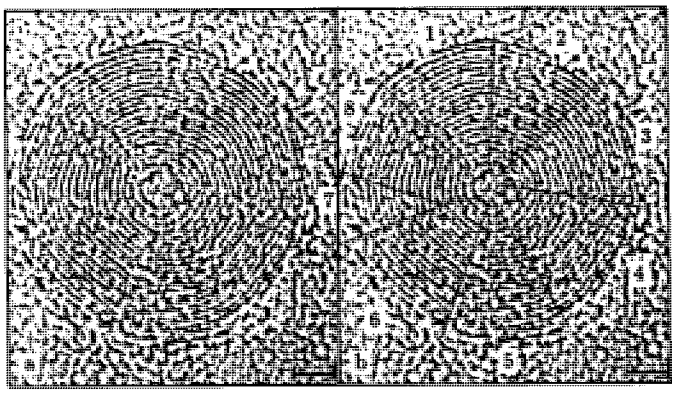

Fig. 19. The image obtained by electron microscopy of an onionlike graphite microparticle observed by Iijima [66] which appears superficially to be spheroidal (a). Careful scrutiny of this image, however, indicates that the object has a polygonal outline consistent with a set of concentric quasi-icosahedral fullerene-like shells (b) [65]. The marker indicates a scale of 20 Å.

rather than what is, is a cardinal sin for a scientist and the temptation is to be resisted at all costs.

The Quest for C_{60}

Until late 1989 the evidence in support of our structure proposal was, to my mind, very convincing, but it could not be deemed anything other than circumstantial. Clearly a macroscopic sample of C_{60} was needed—not just a whisper in a supersonic helium wind, detectable only by that ultrasensitive sensor, the mass spectrometer. At Sussex we sought more tangible evidence. The Science and Engineering Research Council (SERC) funded the construction of a cluster-beam apparatus, which was assembled with Tony Stace; Steve Wood helped us to obtain financial support from British Gas in the form of Collaborative Award in Science and Engineering (CASE) studentship for combustion-related studies. It was this assistance which was ultimately our salvation (vide infra). In a third project conducted with Ken McKay, we probed (by electron microscopy) the films produced by a carbon arc under helium in an old bell jar evaporator. We found that the film microstructure changed as the helium pressure was increased (to ca. 50 mmHg). The quadrupole mass spectrometer, with which I sought to monitor whether C_{60} was produced in this experiment, was the integral part of a modest carbon materials research project which failed to attract support from any funding source (including chemical companies). Because Stace and I had been quite generously funded by the SERC solely for the cluster-beam studies, another application (and indeed a rather applied one) to that source was difficult. Time slipped by and this program faltered even though I had put a great deal of effort into trying to obtain financial support.

The First Paper by Krätschmer, Fostiropoulos, and Huffman

In September 1989 Michael Jura (UCLA Astronomy Department) sent me a copy of a thought-provoking paper[67] (Fig. 20) presented by Krätschmer, Fostiropoulos, and Huffman at a symposium on interstellar dust. This research group from Heidelberg and Tucson had observed four weak but distinct infrared absorptions in a film of arc-processed graphite, which were tantalizingly consistent with the expected spectrum of buckminsterfullerene. From theoretical studies[68] it was known that C_{60} should exhibit only four lines. What was more, the observed frequencies agreed quite well with those predicted. I had long followed the work of this group and knew that they had developed great expertise in studying carbon by spectroscopy. We had occasionally tried related studies, and I was only too aware of how tricky they were. I was sceptical about their result and also rather cha-

SEARCH FOR THE UV AND IR SPECTRA OF C_{60} IN LABORATORY-PRODUCED CARBON DUST

W.Krätschmer, K. Fostiropoulos *Max-Planck-Institut für Kernphysik, Heidelberg, W.-Germany*
and
D.R. Huffman *University of Arizona, Tucson, Arizona, USA*

Carbon dust samples were prepared by evaporating graphite in an atmosphere of an inert quenching gas (Ar or He). Changes of the spectral features of the carbon dust were observed when the pressure of the quenching gas was increased. At low pressures (order 10 torr), the spectra show the familiar broad continua. At high pressures (order 100 torr), narrow lines in the IR and two broad features in the UV emerge. The four strongest IR features are located in the vicinity of the lines predicted for the C_{60} molecule. One of the observed UV features may be related to the known 368 nm transition of C_{60}. It thus appears that at high quenching gas pressures C_{60} is produced along with the carbon dust.

Fig. 20. Annotated copy of the key paper presented by Krätschmer, Fostiropoulos, and Huffman at the conference *Dusty Objects in the Universe* in Capri (1989) [67]. This paper with the appended query was sent to me by Michael Jura (UCLA) who attended this conference.

grined, for had not Ken McKay and I made soot in a bell jar in exactly the same way three years before during the project, which we were forced to abandon through lack of funds?

I decided to resurrect the old and decrepit bell jar and with Jonathan Hare (holder of the British Gas CASE graduate studentship) tried to reproduce the infrared features obtained by Krätschmer et al. Michael Jura's missive arrived around September 1989, just before the start of the Sussex academic year, a time when third year undergraduate projects are needed. It does not matter whether these projects yield results; they should imbue the student with the flavor and excitement of genuine research, that is, the experience of working in the dark, not—as all too often happens—the frantic scramble for results at all costs! I had often initiated the most speculative of projects in this way, and my experience had shown time and time again that important and exciting studies could often start from such inauspicious beginnings. It seemed perfect for Amit Sarkar's third-year project, and he joined Hare on this wildly speculative project. Fairly soon these students succeeded in obtaining the IR bands (Fig. 21), which, although always very weak and highly irreproducible, confirmed the observations of the group from Heidelberg and Tucson. The obsolete apparatus then

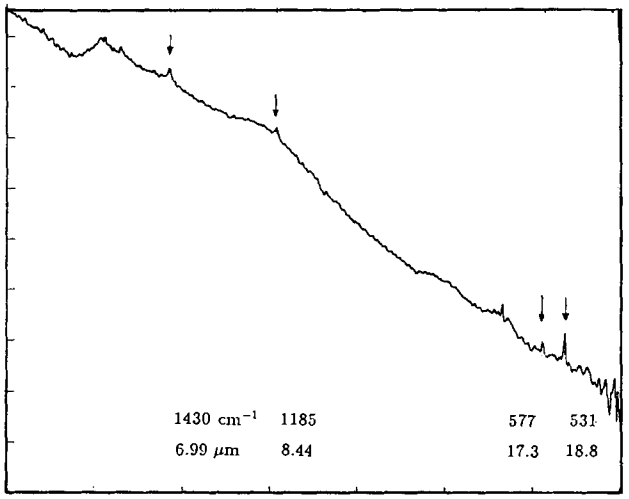

Fig. 21. Infrared spectrum of a film of arc-processed carbon obtained by Hare and Sarkar at Sussex which shows weak but clear (and confirmatory) evidence that the features first observed by Krätschmer et al. [67] (see Fig. 20) and tentatively assigned to C_{60} were real and repeatable.

promptly fell to pieces! After rebuilding it almost completely from scratch, Hare tried to repeat the earlier observations, but consistent results eluded him. Sometimes he obtained the characteristic spectral features, sometimes they disappeared for days or weeks at a time. In retrospect, I suspect that the original discovery of the IR features by Krätschmer et al. could have been made by few other groups. Hare carefully varied every experimental parameter he could think of and finally developed the expertise to produce films which exhibited the telltale infrared features consistently. He wrote to Krätschmer about his efforts and received an encouraging reply containing useful advice. This certainly helped, because it was quite difficult to make films amenable to analysis.

The Dimerization of C_{30}

I spent about one month in the UCLA Astronomy Department around Easter 1990. One day, Mark Morris brought François Diederich from the Chemistry Department to see me. Diederich appeared excited and exhorted me to come to his office because he had something to show me. In response to his manner I somewhat disdainfully quipped, "You've not made C_{60}?" When he replied, "How do you know?". I was startled and suddenly became apprehensive since there was genuine surprise in his voice. When we arrived at his office he showed me an astonishing mass spectrum. In their attempts to make a pure carbon ring of 30 atoms Diederich, Rubin, Whetton, and their co-workers, had found that the molecule spontaneously dimerized to form C_{60} with almost unbelievable efficiency.[69] This staggering result seemed to answer, almost at a stroke, many puzzling questions that had been on my mind for years about carbon chains, their relationship with C_{60}, and soot. But I became even more apprehensive when I comprehended that the UCLA group might be on the verge of obtaining the coveted C_{60} NMR line. Subsequent discussions with David Walton, with whom I had probed aspects of the C_{60} formation mechanism,[70] alleviated my worries; he convinced me that scaling up the UCLA experiment so as to produce sufficient C_{60} for the key NMR measurement presented an anormous challenge.

Mass Spectrometry

I returned to Sussex and by early summer 1990 started to believe for the first time that C_{60} really might be in our sooty deposit. We therefore decided to probe the material by solid-state magic-angle-spinning (MAS) NMR. Indeed Ken Seddon (a Sussex colleague) had encouraged me to do this some years before. Perhaps the single ^{13}C NMR line was close at hand in the black soot, which at least we could now touch. I considered buying the most isotopically pure ^{13}C graphite, but that would have been very expensive, and we had no

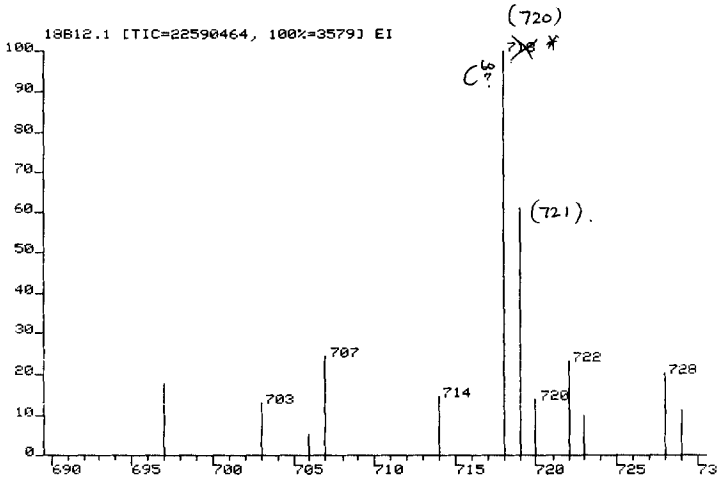

Fig. 22. Part of the FAB mass spectrum of a deposit of arc-processed soot obtained by Abdul-Sada on July 23rd, 1990 at Sussex. The calibration was off by 2 amu; however, the isotope pattern was convincing since the peaks are close to the intensity ratio 1.0/0.66/0.44 expected for $^{12}C_{60}/^{12}C_{59}/^{12}C_{58}\ ^{13}C_2$.

money anyway. The problem of generating enough material for solid-state NMR from the scrapings of thin sooty films, seemed insurmountable, especially since it was so difficult to produce the films in the first place, let alone analyze them. We really needed another way to monitor the samples, so we tried Fast Atom Bombardment (FAB) mass spectrometry. Ala'a Abdul-Sada helped us, and finally we obtained the mass spectrum shown in Figure 22. The signal containing the ^{13}C satellites was really quite convincing, but I wanted the result confirmed. The entry in Jonathan Hare's laboratory notebook on July 26th, 1990 (Fig. 23 top, second sentence) epitomizes many of our problems and requires little further comment.

The Red Solution

During this period we had considered the properties of C_{60}. What form would the compound take? Would it be a high-melting solid or a liquid? Would it be soluble? Benzene was an obvious solvent, since C_{60} should look like benzene from every side (or at least from 20 sides). I remembered the little pink (or yellow) vial of liquid we used to talk about and wondered if the compound might even be volatile. In addition I had often discussed (with Smalley, Rohlfing, and others) how much C_{60} was being made in our experiments. The rough proportion which always seemed to arise was $<1/10000$ of the total amount of carbon. At this level, given the amount of soot available, only a supreme optimist would attempt solvent extraction. Fortunately Hare is one—perhaps partly because he is a physicist working among chemists. On Friday, August 3rd Hare made up a mixture of the soot and benzene in a small vial, which he set aside over the weekend (Fig. 23, second entry). When he came in on Monday morning (August 6th) he noted (Fig. 23, third entry) that the solution looked "slightly red(d)ish" (Fig. 24). The generation of a red solution from pure carbon was scarcely believable. Hare made more material during the next few days and attempted mass spectrometric measurements on extracted material for the first time on Thursday, August 9th (Fig. 23, fourth entry).

possible use of FAB Mass Spect. 26/7/90.

Came back from Scotland Walk to find Fab Mass Spec had been done with exciting results. unfortunately the machine has broken down so we can't repeat.

Results so far.

Seen decent signal @ (12x60) = 720amu !

also ^{13}C is ~1% of natural carbon so calculations show that for C_{60} one 60% sould have One 5%

3/8/90

1) Made approx ½ a (30ml) tube of C_{60}^{6} + Carbon Powder, Actual Volume would be much smaller than this bcos powder is so uncompact.

2) added about 25ml of Benzene and shook mixture

3) allowed to stand for Weekend.

6/8/90

Solution looks slightly reddish, tried to pipet liquid out from top but mixed up.

9/8/90

Vacume lined sample to about 5th of Volume could go lower (ie more concentrated) but we need about this Volume if we want to use IR liquid cell, so will keep to this.

Continued evaporation down to about 4-5 drops (Final ?). FAB showed No C_{60} (720).

Fig. 23. Entries by Hare in his laboratory notebook: July 26th, 1990; August 3rd, 1990; August 6th, 1990; August 9th, 1990.

Fig. 24. Original reddish extract obtained on Monday, September 6th, 1990 (see Fig. 23).

About 10 o'clock the next morning (Friday, August 10th) I received a telephone request from the journal *Nature* to referee a paper by the Heidelberg/Tucson group which I accepted. I was totally unprepared for the bombshell which arrived minutes later by telefax. Following up their own earlier work, Krätschmer, Lamb, Fostiropoulos, and Huffman had successfully sublimed from their carbon deposit a volatile brown material, which dissolved in benzene to give a RED SOLUTION (!!!!!).[71] Crystals obtained from this solution yielded X-ray and electron-diffraction data commensurate with material composed of arrays of spheroidal molecules 7 Å in diameter separated by 3 Å, just as expected for buckminsterfullerene. This beautiful paper even contained photographs of crystals. I was convinced that they had isolated C_{60}, and we had been pipped at the post. Somewhat stunned, I pondered our demise and faxed my report back to *Nature* after lunch. I recommended that the paper be published without delay and requested the editor to convey my sincere congratulations to Krätschmer and his associates.

This was what the British call a difficult moment, but as I slowly surveyed the damage I realized that all was not quite lost. It gradually dawned on me that there was not a single(!) NMR line to be seen in the manuscript (nor was there a mass spectrum. We later learned that they had the mass spectrum, but certain problems had arisen which precluded its inclu-

sion in the manuscript.) At this point we had spent nearly a year struggling independently learning how to make the arc-processed material; we had made our own soot, we had confirmed the presence of C_{60} mass spectrometrically, and we had solvent-extracted the red materal—and all this *before* the manuscript arrived. I decided that we were not going to abandon our efforts now after we had achieved all this. We still had a lot going for us, and I thought we might be able to obtain the desired NMR result. However, now that the Heidelberg/Tucson study was essentially in the public domain it would be transmitted around the world by telefax within hours. I had studiously tried to avoid such situations in science—competition—all my life; my philosophy is to probe areas in which few others, preferably no one, work. That is where, it seems to me, the most unexpected discoveries are likely to be made.

We had to act very quickly if five years of effort were not to be completely in vain. A race must be on because the material was now so easy to make, and it could not be long before other groups, far better equipped than we, recognized that there was one last exquisite prize remaining in the story of the discovery of C_{60}—the NMR line. Our one priceless advantage was that Hare had already made a reasonable quantity of material, and that, at that moment, only the Heidelberg/Tucson group had any at all. We needed help and fast. Roger Taylor, an organic chemist, provided the desperately needed expertise; he separated the material quickly and efficiently. Since our mass spectrometer had broken down again, Hare rushed by train to Manchester with a sample of the precious extract. Numerous frantic telephone calls passed between Sussex and Manchester, because the sample refused to respond to analysis. Then with a key piece of

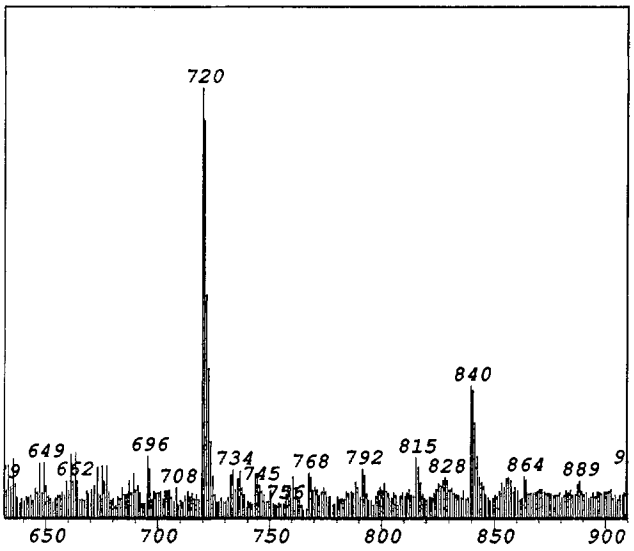

Fig. 25. Part of the FAB mass spectrum of the red extract which confirmed that it consisted mainly of C_{60} and C_{70}. The spectrum also indicates the presence of other fullerenes [72].

advice from Taylor about solubility, the Manchester operators (at Kratos) managed to dissolve the material in the FAB matrix and obtained the FABulous mass spectrum shown in Figure 25. It was hard to believe, but besides C_{60} other fullerenes with 56 to 72 atoms were detected; in particular, C_{70} was abundant. The whole family of fullerenes appeared to be present in the soot, not just C_{60}!

C_{60} is Magenta (Pink?) in Solution

Taylor noted that the extract was soluble in hexane and recognized that he might be able to separate the fullerenes chromatographically. To his delight he found that on an alumina column resolution into two bands, one red, the other magenta, could be achieved. The magenta fraction, (Fig. 26) was a delight to the eye in the delicacy of its color.

Fig. 26. Chromatographic separation of the red extract by Taylor resulted in a magenta C_{60} fraction (left) and a red C_{70} fraction (right).

Its mass spectrum showed a peak at 720 amu, and we sent the sample to Tony Avent for NMR analysis. We were summoned to see our single line (Fig. 27), which Avent assured

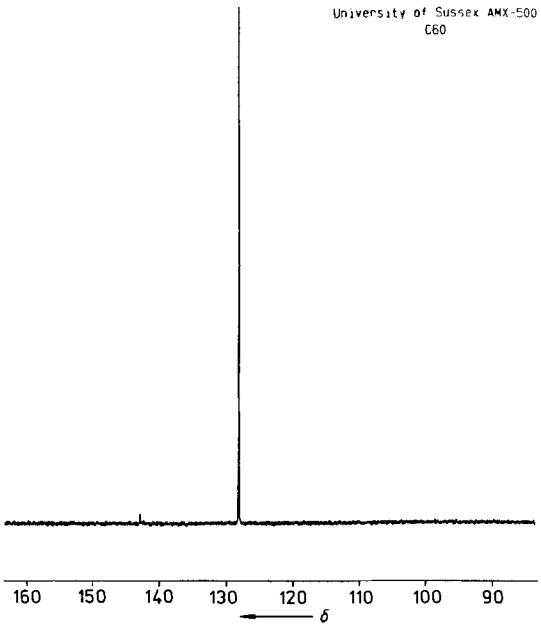

Fig. 27. The first NMR spectrum in which the C_{60} resonance (at $\delta = 143$ ppm) was first identified (barely). The strong line at $\delta = 128$ ppm is (rather appropriately) the resonance of benzene.

us was present. So this was it: a line so small I needed a microscope to see it! Could this insignificant little blip really be the line I had dreamed about for five years? Further work confirmed beautifully that this was the result which we had sought for so long.[72] The joy alleviated almost all the despair I had first felt on reading the paper by Krätschmer et al. One might have thought, as some said, that I should have been pleased to have been proven right when so many had been sceptical. That was not my feeling, probably because I had known ever since the recognition of C_{70} as the second magic fullerene[51] that our structure could not possibly be wrong. I know that my colleagues at Rice University also had no doubts.

What about C_{70}? It turned out to be the icing on the cake, although not without attendent trauma. The wine-red fraction which had masked the pale magenta of C_{60} yielded a mass spectral peak at 840 amu and was clearly C_{70}. According to the expected structure (Fig. 15 right) this compound should exhibit a ^{13}C NMR spectrum with five lines. On Sunday, September 2nd, 1990 I entered the laboratory at the same time as Avent who told me the C_{70} measurement should have just been completed. The spectrum we plotted was sensational—or almost so. There were indeed five lines, but one was in the same position as the C_{60} peak. Could it be that one line was underneath the C_{60} signal? After repeated chromatography to remove the last vestiges of C_{60}, further NMR studies showed the fifth line to be rather different from the others. The resonance of the ten atoms in the waist (Fig. 28c) is more "benzenoid" than the other four resonances.[72] Indeed this line lies dangerously close to the benzene solvent line; had it been a little closer to the benzene signal it would have been swamped and missed altogether. In many ways the five lines of C_{70} are (arguably) more important and significant than the C_{60} singlet. For one thing, they confirm that fullerene carbon atoms are not fluxional; for another, they show that the atoms are not on the perimeter of a monocyclic ring. Both of these cases would lead to a spectrum with a single resonance. Even more important was the fact that the NMR results confirmed the family concept for fullerene cages. It was now clear that a host of stable fullerenes were just waiting to be discovered, as we had long suspected.[53]

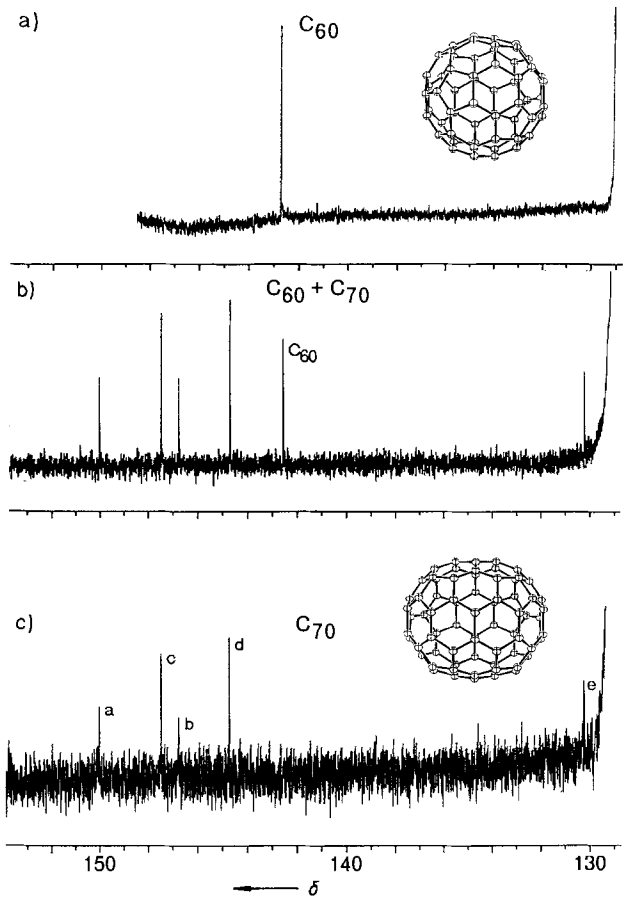

Fig. 28. ^{13}C NMR spectra obtained from chromatographed samples of soluble material extracted from arc-processed graphite: a) spectrum of purified C_{60} (magenta fraction); b) mixed C_{60}/C_{70} sample; c) spectrum of purified C_{70} (red fraction) showing five lines as expected for the symmetric egg-shaped molecule (see Fig. 15).

"The Third Man" is as Elusive as Ever in Space

The elusiveness of C_{60} and my belief that it has been lurking in that blackest of black materials, soot, since time immemorial often reminded me of the role played by Orson Welles in the film "The Third Man". The spirit of this antihero pervades the whole movie although he is seldom seen. Indeed he makes his first appearance late on in the movie in the black shadows of a dark street in Vienna when his face is suddenly illuminated by a light being switched on. For five years C_{60} played a very similar shadowy role—at least as far as I was concerned. My part in the buckminsterfullerene story really started out in space, and this celestial sphere has come down to earth with more of a bounce than a bump; but will it bound back up into space? Is this third form of carbon distributed ubiquitously in space as we surmised the day we found it in the laboratory?[41] Now that we know something about fullerene-60, we should be able to study all its optical properties. It is clear that the UV radiation density in the optically observable interstellar medium is such that the species will be ionized.[73] The possible existence of encapsulated complex ions[73, 74] is quite interesting. However, even with buckminsterfullerene in our hands, we find that this "third man" is as elusive as he ever was in the space between the stars. Perhaps the interstellar form is related to protonated carbon monoxide (HCO^+), which Bill Klemperer identified about 20 years ago.[17] If there are any C_{60} molecules in space there can be little doubt that most will have a proton or some other atom adhering to their surface.[74] $C_{60}H^+$ could probably survive for eons. Other abundant elements, particularly alkali and alkaline-earth metals, must also stick to the surface. Such species will have fascinating optical spectra. For instance, the energy and wavelength of the charge-transfer transition $(C_{60}^+)X \rightarrow (C_{60})X^+$ can be estimated to a first approximation as simply the difference between the ionization potentials of the separated species. For $(C_{60}H)^+$ this transition lies at about 2200 Å. For $(C_{60}Na)^+$ and $(C_{60}K)^+$ the transitions lie in the region of the Diffuse Interstellar Bands[33] and for $(C_{60}Mg)^+$ near zero frequency(!) These observations imply that this and related species will have unusual electrical properties. These processes are probably related to the recently observed superconductivity

of metal-doped fullerene-60 materials.[75] This conjecture is supported by an important new result which comes not from work with bulk material but from cluster-beam studies by McElvaney and Callahan.[76] They found that the gas-phase proton affinity of C_{60} is similar to that of ammonia—a remarkable result! I like to put my trust in intuition; when all else fails it is, after all, our only guide: It is curious to note that some important spectral features of space (the Diffuse Bands) have been visible for decades, yet we do not know what causes them. Now we have discovered that an unexpected molecule, C_{60}, has been under our noses on earth since time immemorial and was invisible until now. It seems to me highly likely that these two observations will turn out to be connected.

Epilogue

Since the time that graphite balloons and C_{60} were twinkles in the eyes of David Jones, Eiji Osawa, and a few other imaginative scientists,[42, 43, 46–48] there have been many significant contributions, both experimental and theoretical, to the first chapter of the buckminsterfullerene story which has just been completed. These have recently been comprehensively reviewed.[77] Figure 12 shows the Rice/Sussex team and Figure 29, the Sussex Buckaneers. These two teams together with the Heidelberg/Tucson team scored many of the goals in the football match which has just ended. Many new teams have now started to play an exciting, but different, ball game. The important difference is that the players can now see what they are kicking.

Fig. 29. The Sussex Buckaneers football team. From left: Kroto, Abdul-Sada, Taylor, Hare, and Walton.

Apart from the successful observation of the "lone" NMR line, two other matters give me a sense of deep pleasure: one was the beautiful color of C_{60} and, furthermore, that it was seen first at Sussex. The second was that apparently no one else appeared to have followed up the early IR results obtained by the group from Heidelberg and Tucson (September 1989). In retrospect I find this astounding; perhaps it was because the work appeared in the astronomy literature, but more likely it was because research today is carried out under such pressure, and our fear of failure is so great (and exacerbated by funding procedures). Few groups enjoy the luxury of working in the dark—a condition which I feel lies at the heart of true scientific endeavor. I have a videotape of a marvellous BBC documentary on Richard Feynman (the greatest lecturer I had ever heard) from the series "Horizon". In one part he talks on essentially this topic. This 50 minute program had the most profound effect on me. At one point Feynmann described how, when he was hired at Cornell, Bob Wilson had told him that it was the university's responsibility whether he accomplished anything—it was their risk(!) It was not for Feynman to worry about, he should amuse himself. In this way he was freed from the psychological burden of doing anything "important", and he was able to relax and do what he most enjoyed—physics and mathematics—just for the fun of it. How lucky he was. I know of few professional scientists today, certainly no young ones, who are in such a utopian scientific environment. What a sad reflection on today's research, especially since we know in our hearts that human beings achieve most when they are free of pressure. We know that small children learn and discover the joys of nature most efficiently during their play.

News of the breakthroughs spread like wildfire during September 1990, and the method of production developed by the Heidelberg/Tucson group was immediately improved upon[78] at Rice University. As soon as it was known that fullerenes are chromatographically separable and that solution NMR is feasible, other groups confirmed these measurements.[79, 80] Don Huffman remarked laconically at a recent symposium, "Everyone is able to repeat these experiments".

A new postbuckminsterfullerene world of round organic chemistry and materials science has been discovered overnight. Almost every day a new paper appears on some novel aspect of fullerene behavior. The group from Rice University has shown that C_{60} forms species such as $C_{60}H_{36}$.[78] Hawkins et al. have made an osmium complex in which the spinning of the fullerene ball is stopped and has enabled accurate bond lengths to be determined.[81] NMR studies by Yannoni et al. have also yielded accurate bond lengths.[82] The radical anion has been polymethylated by Olah's group;[83] platinum complexes have been prepared at DuPont.[84] At AT&T it has been found that the metal-doped material now holds the temperature record for molecular superconductivity.[75] Fascinating differences in the crystal structure of C_{60} have been found which depend upon how the crystals are produced.[77] Foote and co-workers at UCLA have shown that C_{60} transfers light energy efficiently to generate singlet oxygen.[85] Diederich, Whetten, and co-workers have evidence for oxides such as $C_{70}O$.[86] C_{60} is decomposed by light under circumstances which still need to be fully identified.[87] Also interesting is the fact that more fullerenes, such as C_{76} and C_{84}, are being extracted and characterized.[86] The fullerene family has arrived in force, and there are balls of all shapes and sizes for everyone to play with.

This advance is an achievement of fundamental science, not applied science, and serves as a timely reminder that fundamental science can achieve results of importance for strategic and applied areas. The origin of the whole program lay in an interest in aspects of molecular dynamics, allied

with the quest for an understanding of the origin of the carbon chains in space and their possible relationship to circumstellar and interstellar grains as well as soot.[1] These ideas welded together beautifully with the major advance in cluster science brought about by the experimental techniques developed by Smalley and co-workers at Rice University. Krätschmer and Huffman and co-workers were originally motivated by an interest in space dust and, in their recent breakthrough, by astrophysical implications of C_{60}. The C_{60} story has many facets, but more than anything else it is yet another archetypal lesson on the benefits to be gained by supporting pure fundamental science. The field has exploded, and its applications in chemistry and the science of materials are only just starting to be explored. Finally it is worth noting that C_{60} might have been detected 20–40 years ago, perhaps in a sooting flame; one wonders why it took so long.

Another lesson may be learned from these acknowledgements. Important contributions were made in research programs at the University of Sussex (Brighton, UK), the National Research Council (Ottawa, Canada), Rice University (Houston, Texas, USA), the Max-Planck-Institut für Kernphysik (Heidelberg, Germany) and the University of Arizona (Tucson, USA). The discovery of C_{60} is a tribute to not only the international nature of science but also the necessity of interdisciplinary cooperation. The contribution from the University of Sussex to the story started as a consequence of the "Chemistry by Thesis" degree course initiated by Colin Eaborn, which enabled undergraduates (such as Anthony Alexander) to carry out research with supervisors from more than one field. It could only have been successful in the interdisciplinary scientific research and teaching environment which the university pioneered when Sussex was founded in the "optimistic 60s". Sadly this and other courses have been "regulated" out of existence by bureaucrats who have little understanding of how student research expertise is brought to maturity and no awareness of the dire consequences for our future scientific capability. The first part the story could also not have been achieved had chemistry at Sussex been divided into those traditional subsections of organic, inorganic, and physical chemistry. I also had close contacts with astronomers at Sussex, particularly Bill McCrea and Robert Smith. The carbon discoveries resulted from a free-wheeling research program which started with synthetic chemistry (with David Walton, Anthony Alexander, and Colin Kirby) and moved via spectroscopy and quantum mechanics to radioastronomy (with Takeshi Oka, Lorne Avery, Norm Broten, and John MacLeod at the NRC). It moved back to the laboratory and chemical physics (with Jim Heath, Sean O'Brien, Bob Curl, and Rick Smalley at Rice University). In the last phase, key advice came from Michael Jura (an astronomer) which initiated some basic chemistry (with Jonathan Hare, Amit Sarkar, Ala'a Abdul Sada, Roger Taylor, and David Walton). Apart from those mentioned in the text who played direct (and sometimes crucial parts) such as Steve Wood of British Gas, I also acknowledge greatly the help of many others who played indirect parts, particularly graduate students and post-doctoral fellows as well as colleagues such as Tony Stace, Roger Suffolk, and Mike Lappert. Finally I wish to thank Ed Wasserman for some invaluable advice and David Walton in particular for his unfailing help throughout the period of this story and his painstaking assistance in preparing this account.

Received: June 26, 1991 [A 853 IE]
German version: *Angew. Chem.* **1992**, *104*, 113

[1] H. W. Kroto, *Chem. Soc. Rev.* **1982**, *11*, 435.
[2] D. R. Johnson, F. X. Powell, *Science* **1970**, *169*, 679.
[3] C. R. Noller, *Chemistry of Organic Compounds*, Saunders, Philadelphia, **1957**, p. 282.
[4] M. J. Hopkinson, H. W. Kroto, J. F. Nixon, N. P. C. Simmons, *J. Chem. Soc. Chem. Commun.* **1976**, 513.
[5] G. Becker, *Z. Anorg. Allg. Chem.* **1976**, *423*, 242.
[6] T. E. Gier, *J. Am. Chem. Soc.* **1961**, *83*, 1769.
[7] J. K. Tyler, *J. Chem. Phys.* **1964**, *40*, 1170.
[8] W. Rösch, M. Regitz, *Angew. Chem.* **1984**, *96*, 898; *Angew. Chem. Int. Ed. Engl.* **1984**, *23*, 900.
[9] M. Regitz, P. Binger, *Angew. Chem.* **1988**, *100*, 1541; *Angew. Chem. Int. Ed. Engl.* **1988**, *27*, 1484; M. Regitz, *Chem. Rev.* **1990**, *90*, 191.
[10] M. J. Hopkinson, H. W. Kroto, J. F. Nixon, N. P. C. Simmons, *Chem. Phys. Lett.* **1976**, *42*, 460.
[11] L. Gausset, G. Herzberg, A. Lagerqvist, B. Rosen, *Discuss. Faraday Soc.* **1963**, *35*, 113.
[12] R. Eastmond, D. R. M. Walton, *Chem. Commun.* **1968**, 204.
[13] R. Eastmond, T. R. Johnson, D. R. M. Walton, *Tetrahedron* **1972**, *28*, 4601.
[14] T. R. Johnson, D. R. M. Walton, *Tetrahedron* **1972**, *28*, 5221.
[15] A. J. Alexander, H. W. Kroto, D. R. M. Walton, *J. Mol. Spectrosc.* **1976**, *62*, 175.
[16] A. C. Cheung, D. M. Rank, C. H. Townes, D. D. Thornton, W. J. Welch, *Phys. Rev. Lett.* **1968**, *21*, 1701.
[17] W. Klemperer, *Nature (London)* **1970**, *227*, 267.
[18] H. W. Kroto, *Int. Rev. Phys. Chem.* **1981**, *1*, 309.
[19] B. E. Turner, *Astrophys. J.* **1971**, *163*, L35.
[20] L. W. Avery, L. W. Broten, J. M. MacLeod, T. Oka, H. W. Kroto, *Astrophys. J.* **1976**, *205*, L173.
[21] C. Kirby, H. W. Kroto, D. R. M. Walton, *J. Mol. Spectrosc.* **1980**, *83*, 261.
[22] H. W. Kroto, C. Kirby, D. R. M. Walton, L. W. Avery, N. W. Broten, J. M. MacLeod, T. Oka, *Astrophys. J.* **1978**, *219*, L133.
[23] N. W. Broten, T. Oka, L. W. Avery, J. M. MacLeod, H. W. Kroto, *Astrophys. J.* **1978**, *223*, L105.
[24] M. B. Bell, P. A. Feldman, S. Kwok, H. E. Matthews, *Nature (London)* **1982**, *295*, 389.
[25] E. Herbst, W. Klemperer, *Astrophys. J.* **1973**, *185*, 505.
[26] A. Dalgarno, J. H. Black, *Rep. Prog. Phys.* **1976**, *39*, 573.
[27] E. E. Becklin, J. A. Frogel, A. R. Hyland, J. Kristian, G. Neugebauer, *Astrophys. J.* **1969**, *158*, L133.
[28] D. L. Michalopoulos, M. E. Geusic, P. R. Langridge-Smith, R. E. Smalley, *J. Chem. Phys.* **1984**, *80*, 3556.
[29] T. G. Dietz, M. A. Duncan, D. E. Powers, R. E. Smalley, *J. Chem. Phys.*, **1981**, *74*, 6511.
[30] J. N. Murrell, H. W. Kroto, M. F. Guest, *J. Chem. Soc. Chem. Comm.*, **1977**, 619.
[31] H. Hintenberger, J. Franzen, K. D. Schüy, *Z. Naturforsch. A*, **1963**, *18*, 1236.
[32] A. E. Douglas, *Nature (London)*, **1977**, *269*, 130.
[33] G. H. Herbig, *Astrophys. J.* **1975**, *196*, 129.
[34] E. A. Rohlfing, D. M. Cox, A. Kaldor, *J. Chem. Phys.* **1984**, *81*, 3322.
[35] R. W. Marks, *The Dymaxion World of Buckminster Fuller*, Reinhold, New York, **1960**.
[36] H. W. Kroto, *Proc. R. Inst. G.B.* **1986**, *58*, 45.
[37] R. E. Smalley, *Sciences (N.Y.)* **1991**, *31*(2), 22; see also: R. F. Curl, R. E. Smalley, *Sci. Am.* **1991** (10), 32.
[38] P. J. Stewart, *Nature (London)* **1986**, *319*, 444.
[39] H. W. Kroto, *Nature (London)* **1986**, *322*, 766.
[40] A. Nickon, E. F. Silversmith, *Organic Chemistry: The Name Game: Modern Coined Terms and Their Origins*, Pergamon, New York, **1987**.
[41] H. W. Kroto, J. R. Heath, S. C. O'Brien, R. F. Curl, R. E. Smalley, *Nature (London)* **1985**, *318*, 162.
[42] D. E. H. Jones, *New. Sci.* **1966**, *32* (November 3rd), p. 245.
[43] D. E. H. Jones, *The Inventions of Daedalus*, Freeman, Oxford, **1982**, pp. 118–119.
[44] D. W. Thompson, *On Growth and Form*, Cambridge University Press, **1942**.
[45] Q. L. Zhang, S. C. O'Brien, J. R. Heath, Y. Liu, R. F. Curl, H. W. Kroto, R. E. Smalley, *J. Phys. Chem.* **1986**, *90*, 525.
[46] E. Osawa, *Kagaku (Kyoto)* **1970**, *25*, 854 (in Japanese), *Chem. Abstr.* **1971**, *74*, 75698v.
[47] Z. Yoshida, E. Osawa, *Aromaticity*, Kagakudojin, Kyoto **1971** (in Japanese).
[48] D. A. Bochvar, E. G. Gal'pern, *Dokl. Akad. Nauk SSSR* **1973**, *209*, 610 (English translation *Proc. Acad. Sci. USSR* **1973**, *209*, 239).
[49] O. Chapman, private communication.
[50] J. R. Heath, S. C. O'Brien, Q. Zhang, Y. Liu, R. F. Curl, H. W. Kroto, F. K. Tittel, R. E. Smalley, *J. Am. Chem. Soc.* **1985**, *107*, 7779.
[51] H. W. Kroto, *Science* **1988**, *242*, 1139.
[52] R. F. Curl, R. E. Smalley, *Science* **1988**, *242*, 1017.
[53] H. W. Kroto, *Nature (London)* **1987**, *329*, 529.

[54] T. G. Schmalz, W. A. Seitz, D. J. Klein, G. E. Hite, *J. Am. Chem. Soc.* **1988**, *110*, 1113.
[55] D. M. Cox, K. C. Reichmann, A. Kaldor, *J. Chem. Phys.* **1988**, *88*, 1588.
[56] L. F. Fieser, M. Fieser, *Organic Chemistry*, Reinhold, New York, **1956**.
[57] L. A. Paquette, R. J. Ternansky, D. W. Balogh, G. Kentgen, *J. Am. Chem. Soc.* **1983**, *105*, 5446.
[58] R. B. Fuller, *Inventions – The Patented Works of Buckminster Fuller*, St. Martin's Press, New York, **1983**.
[59] S. J. Harris, A. M. Weiner, *Annu. Rev. Phys. Chem.* **1985**, *36*, 31.
[60] M. Frenklach, L. B. Ebert *J. Phys. Chem.* **1988**, *92*, 561.
[61] P. Gerhardt, S. Loeffler, K. Homann, *Chem. Phys. Lett.* **1987**, *137*, 306.
[62] J. B. Howard, J. T. McKinnon, Y. Makarovsky, A. L. Lafleur, M. E. Johnson, *Nature (London)* **1991**, *352*, 139.
[63] H. S. M. Coxeter, *Regular Polytopes*, Macmillan, New York, **1963**.
[64] M. Goldberg, *Tohoku Math. J.* **1937**, *43*, 104.
[65] H. W. Kroto, K. G. McKay, *Nature (London)* **1988**, *331*, 328.
[66] S. Iijima, *J. Cryst. Growth* **1980**, *5*, 675.
[67] W. Krätschmer, K. Fostiropoulos, D. R. Huffman in *Dusty Objects in the Universe* (Eds.: E. Bussoletti, A. A. Vittone), Kluwer, Dordrecht, **1990**.
[68] Z. C. Wu, D. A. Jelski, T. F. George *Chem. Phys. Lett.* **1987**, *137*, 291.
[69] Y. Rubin, M. Kahr, C. B. Knobler, F. Diederich, C. L. Wilkins, *J. Am. Chem. Soc.*, in press.
[70] H. W. Kroto, D. R. M. Walton, in press.
[71] W. Krätschmer, L. D. Lamb, K. Fostiropoulos, D. R. Huffman, *Nature (London)* **1990**, *347*, 354.
[72] R. Taylor, J. P. Hare, A. K. Abdul-Sada, H. W. Kroto, *J. Chem. Soc. Chem. Commun.* **1990**, 1423.
[73] H. W. Kroto in *Polycyclic Aromatic Hydrocarbons and Astrophysics* (Eds.: A. Leger, L. B. d'Hendecourt), Reidel, Dordrecht, **1987**, p.197.
[74] H. W. Kroto, M. Jura, in preparation.
[75] R. C. Haddon, L. F. Schneemeyer, J. V. Waszczak, S. H. Glarum, R. Tyko, G. Dabbagh, A. R. Kortan, A. J. Muller, A. M. Mujsce, M. J. Rosseinsky, S. M. Zahurak, A. V. Makhija, F. A. Thiel, K. Raghavachari, E. Cockayne, V. Elser, *Nature (London)* **1991**, *350*, 46.
[76] S. W. McElvany, J. H. Callahan, *J. Phys. Chem.* **1991**, *95*, 166.
[77] H. W. Kroto, A. W. Allaf, S. P. Balm *Chem. Rev.* **1991**, *91*, 1213—Editorial comment: See also the highlight by H. Schwarz in the March issue. A critical overview by R. N. Thomas on the synthesis, properties, and reactions of C_{60} will be published shortly in *Angewandte Chemie*.
[78] E. E. Haufler, J. Conceicao, L. P. F. Chibante, Y. Chai, N. E. Byrne, S. Flanagan, M. M. Haley, S. C. O'Brien, C. Pan, Z. Xiao, W. E. Billups, M. A. Ciufolini, R. H. Hauge, J. L. Margrave, L. J. Wilson, R. F. Curl, R. E. Smalley, *J. Phys. Chem.* **1990**, *94*, 8634.
[79] R. D. Johnson, G. Meijer, D. S. Bethune, *J. Am. Chem. Soc.* **1990**, *112*, 8983.
[80] H. Ajie, M. M. Alvarez, S. J. Anz, R. D. Beck, F. Diederich, K. Fostiropoulos, D. R. Huffman, W. Krätschmer, Y. Rubin, K. E. Schriver, D. Sensharma, R. L. Whetten, *J. Phys. Chem.* **1990**, *94*, 8630.
[81] J. M. Hawkins, A. Meyer, T. A. Lewis, S. D. Loren, F. J. Hollander, *Science* **1991**, *252*, 312.
[82] C. S. Yannoni, P. P. Bernier, D. S. Bethune, G. Meijer, J. R. Salem, *J. Am. Chem. Soc.* **1991**, *113*, 3190.
[83] J. W. Bausch, G. K. Surya Prakash, G. A. Olah, *J. Am. Chem. Soc.* **1991**, *113*, 3205.
[84] P. J. Fagan, J. C. Calabrese, B. Malone, *Science* **1991**, *252*, 1160.
[85] J. W. Arbogast, A. P. Darmanyan, C. S. Foote, Y. Rubin, F. Diederich, M. M. Alvarez, S. J. Anz, R. L. Whetten, *J. Phys. Chem.* **1991**, *95*, 11.
[86] F. Diederich, R. Ettl, Y. Rubin, R. L. Whetten, R. Beck, M. Alvarez, S. Anz, D. Sensharma, F. Wudl, K. C. Khemani, A. Koch, *Science* **1991**, *252*, 548.
[87] R. Taylor, J. P. Parsons, A. G. Avent, S. P. Rannard, T. J. Dennis, J. P. Hare, H. W. Kroto, D. R. M. Walton, *Nature (London)* **1991**, *351*, 277.

Two-Dimensional Crystallography of Amphiphilic Molecules at the Air–Water Interface

By Didier Jacquemain, Sharon Grayer Wolf, Franck Leveiller, Moshe Deutsch, Kristian Kjaer,* Jens Als-Nielsen,* Meir Lahav,* and Leslie Leiserowitz*

The advent of well-collimated, high-intensity synchrotron X-ray sources and the consequent development of surface-specific X-ray diffraction and fluorescence techniques have recently revolutionized the study of Langmuir monolayers at the air–liquid interface. These methods allowed for the first time the determination of the in-plane and vertical structure of such monolayers with a resolution approaching the atomic level. We briefly describe these methods, including grazing incidence X-ray diffraction, specular reflectivity, Bragg rods, standing waves, and surface fluorescence techniques, and review recent results obtained from them for Langmuir films. The methods have been successfully applied in the elucidation of the structure of crystalline aggregates of amphiphilic molecules such as alcohols, carboxylic acids and their salts, α-amino acids, and phospholipids at the water surface. In addition, it became possible to monitor by diffraction the growth and dissolution of the crystalline self-aggregates as well as structural changes occurring by phase transitions. Furthermore, the surface X-ray methods shed new light on the structure of the underlying ionic layer of attached solvent or solute species. Examples are given where singly or doubly charged ions bound to the two-dimensional (2D) crystal form either an ordered or diffuse counterionic layer. Finally, the surface diffraction methods provide data on transfer of structural information from 2D clusters to 3D single crystals, which had been successfully accomplished by epitaxial-like crystallization both in organic and inorganic crystals.

1. Introduction

Early in the century, Langmuir demonstrated in a series of elegant experiments that amphiphilic molecules composed of a hydrophobic tail and a hydrophilic head group accumulate at the air–water interface.[1] These films still elicit wide interest because of their importance in the pure and applied sciences. For instance, Langmuir monolayers serve as useful models for elucidating structure and function of biological membranes in their interactions with lipids, steroids, sugars, proteins, and ions.[2] They may also be designed to induce nucleation of organic or inorganic three-dimensional (3D) crystals from molecules or ions present in the subphase by a form of epitaxial growth.[3] In this respect they may be used as models for the study of biological mineralization which involves the use of two-dimensional (2D) surfaces of biological macromolecules to induce the mineral crystallization.[4] The design of monolayers with interfaces which mimic the surfaces of 3D crystals also provides a means of examining crystal surface–solvent interactions in order to understand the effect of the solvent on crystal growth. Furthermore, a knowledge of the characteristics of compressed and uncompressed Langmuir monolayers of water-insoluble amphiphiles should help to unravel the packing characteristics at the air–water interface of water-soluble amphiphiles, where even less is known about their 2D arrangements.[5] In addition Langmuir films are easily transferred to solid supports for the formation of multilayer (Langmuir–Blodgett) films,[6] for potential use as piezoelectric sensors,[7] soft X-ray monochromators, nonlinear optical devices,[8] and in molecular electronics.[9]

Despite the widespread interest in Langmuir films, many of the methods used to characterize their properties do not give direct information on their crystalline packing arrangements. These methods include measurements of surface pressure versus average molecular area,[10] surface potential data,[10] nonlinear optics from surfaces,[11] and IR spectroscopy.[12] Epifluorescence microscopy does furnish some information on crystallinity and morphology on the micron level, but is limited to films of dyes or films containing dye probes.[13] Thus, knowledge on the molecular level of two-dimensional monolayers has been achieved, in the main, from three-dimensional crystals. Indeed, M. Lundquist wrote[14] in a review from 1978: "...there still remains much to be learned especially about the detailed structure of condensed monolayers and regarding the mechanism of molecular rearrangement in monolayer phase transitions. As there are no methods available for direct structure analysis of a monolayer on a water substrate, knowledge of the monolayer structure has, for the most part, been achieved by a sort of translation and application of the knowledge gained from the study of the ordinary three-dimensional state." Only recently, with the advent of intense and well-collimated X-ray beams of variable wavelength from synchrotron sources, has it became possible to obtain direct structural information on the packing of these films by X-ray surface methods.

Here we shall describe some of these new techniques, the information they provide, and review some of the structural results obtained. Emphasis will be placed on monolayer packing arrangements, particularly in terms of the polar head

[*] Dr. M. Lahav, Dr. L. Leiserowitz, D. Jacquemain, Dr. S. Grayer Wolf, F. Leveiller
Department of Materials and Interfaces
Weizmann Institute of Science
Rehovot 76100 (Israel)
Dr. M. Deutsch
Physics Department, Bar-Ilan University
Ramat-Gan 52100 (Israel)
Dr. K. Kjaer, Dr. J. Als-Nielsen
Physics Department, Risø National Laboratory
DK 4000 Roskilde (Denmark)

 © VCH Verlagsgesellschaft mbH, W-6940 Weinheim, 1992 0570-0833/92/0202-0130 $ 3.50+.25/0

groups. We shall examine self-aggregation, growth and domain size of 2D crystallites, surface pressure- and temperature-driven phase transitions, and the effect of pH, ions and solute molecules in the aqueous subphase on molecular packing and crystallinity. We shall discuss the role played by electrostatic interactions and structural complementarity in the induction of 3D crystal nucleation at the monolayer–solution interface.

The results obtained so far already necessitate a revision of our basic concepts on properties such as crystallinity, phase assignment, and diffuse and nondiffuse counterionic layers.

2. Surface Sensitive X-ray Methods

The intensity measured in a conventional X-ray scattering experiment is proportional to the number of scatterers, i.e., the irradiated sample volume. This, in turn, is proportional to the penetration depth of the radiation in a sample. For X-rays of about 1 Å wavelength, this penetration ranges from a few micrometers for highly absorbing material to a few millimeters for low absorbing materials. By contrast, the depth to which surface effects persist rarely extends beyond 100 Å. Consequently, scattering from the surface region is so weak compared to that from the bulk that it is completely swamped. A method restricting the penetration depth to the surface region is therefore a prerequisite for all surface diffraction/scattering experiments. This can be achieved by using grazing angles of incidence and employing the phenomenon of total external reflection from the surface.

The refractive index n of matter for X-rays in the 1 Å wavelength range is given by Equation (1),[15] where $\delta = 2\pi\rho r_0/k^2$ ($k = 2\pi/\lambda$ is the X-ray wavenumber and λ is the wavelength). ρ is the electron density and $r_0 = 2.82 \times 10^{-13}$ cm is the classical electron radius. Typically δ is of the order of 10^{-5}. The term β is equal to $-\mu/(2k)$ where μ is the linear absorption coefficient. For X-rays of wavelength $\lambda \approx 1$ Å, absorption is small and $\beta \ll \delta$.

$$n = 1 - \delta - i\beta \tag{1}$$

Consider now a plane wave with wavevector $\boldsymbol{k}_i$ incident at an angle α_i on a planar interface separating a homogeneous medium from the vacuum, as shown in Figure 1. The wave will be partially reflected into the vacuum in the direction given by $\alpha_r = \alpha_i$ and partially refracted into the lower medium in the direction given by α_r'. Snell's law for this case yields Equation (2).

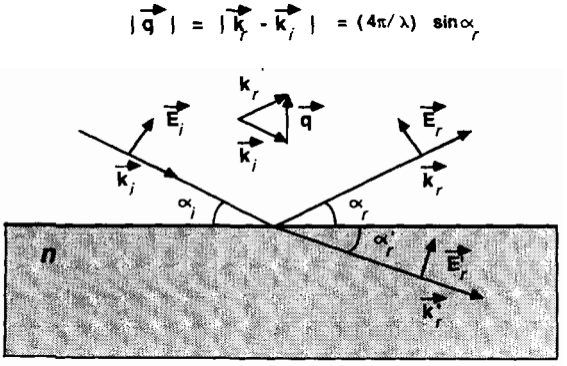

Fig. 1. Refracted (E_t') and reflected (E_r) waves resulting from an incident plane wave with amplitude $|E_i|$ upon an interface between air and a material of refractive index n. Electric fields E are illustrated for one polarization only. The symbol q is the scattering vector, with k_i and k_r the incident and reflected wave vectors of magnitude $2\pi/\lambda$. Note that for $n \lesssim 1$, $\alpha_t' < \alpha_i = \alpha_r$. This provides for total reflection at angles $\alpha_r < \alpha_c$, where α_c is the critical angle for total external reflection.

$$n \cos \alpha_t' = \cos \alpha_i \tag{2}$$

As $n < 1$, for angles of incidence α_i less than or equal to an angle α_c, which is defined as $\alpha_c = \cos^{-1}(n) = (2\delta)^{1/2}$, the well-known phenomenon of total reflection occurs:[16] the incident wave is totally reflected, while the refracted wave becomes evanescent traveling along the surface. The amplitude of the evanescent wave decays exponentially with depth. Figure 2 shows the penetration depth Λ of the X-rays in water versus angle of incidence α_i. For $\alpha_i < 0.5\alpha_c$, the penetration depth is 46 Å independent of the X-ray wavelength. The evanescent wave may therefore be diffracted by crystalline material in a surface layer of that thickness and provides information on its in-plane structure. Such diffraction is called grazing incidence diffraction (GID).[17]

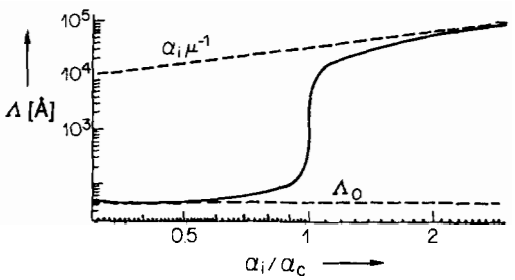

Fig. 2. X-ray beam penetration depth Λ in water at $\lambda = 1.38$ Å versus incidence angle α_i/α_c. The limiting value Λ_0 of the penetration depth for $\alpha_i/\alpha_c \ll 1$ is a characteristic materials constant, ($\Lambda_0 = (\pi r_0 \rho)^{-1/2}/4$), independent of the X-ray wavelength λ. For $\alpha_i/\alpha_c \gg 1$ the penetration depth is $\alpha_i\mu^{-1}$; the linear absorption coefficient μ *does* depend on λ.

In 3D crystals, diffraction from a set of crystal planes with an interplanar spacing d occurs only when the Bragg law is obeyed; namely when, firstly, the scattering vector length $|\boldsymbol{q}|$ (given by $|\boldsymbol{k}_f - \boldsymbol{k}_i| = 4\pi \sin\theta/\lambda$) is equal to $2\pi d^*$, where d^* is the reciprocal of the interplanar spacing d, and, secondly, the normal to the planes bisects the angle between the incident and outgoing beam. This condition may be mathematically expressed in terms of the reciprocal lattice vectors $\boldsymbol{d}^* = h\boldsymbol{a}^* + k\boldsymbol{b}^* + l\boldsymbol{c}^*$ where $\boldsymbol{a}^*$, $\boldsymbol{b}^*$, $\boldsymbol{c}^*$ are the reciprocal vectors of the unit-cell vectors $\boldsymbol{a}$, $\boldsymbol{b}$, $\boldsymbol{c}$, and h, k, l are integers that represent the Miller indices of planes with a spacing d_{hkl}. Diffraction therefore only takes place in 3D crystals when the scattering vector $\boldsymbol{q}$ coincides with (h,k,l) points of the reciprocal 3D lattice (Fig. 3c).

For a 2D crystal there is no selection rule or restriction on the scattering vector component $\boldsymbol{q}_z$ along the film normal. Thus the Bragg scattering extends as continuous rods (BR) through the 2D reciprocal lattice points[18] (Fig. 3b). The finite thickness of the 2D crystal causes the BR to extend over finite $\boldsymbol{q}_z$ intervals. The intensity distribution along these intervals is determined by the vertical electron density distribution in the molecules and is expressed as the Fourier transform of the resulting electron density along the film normal.

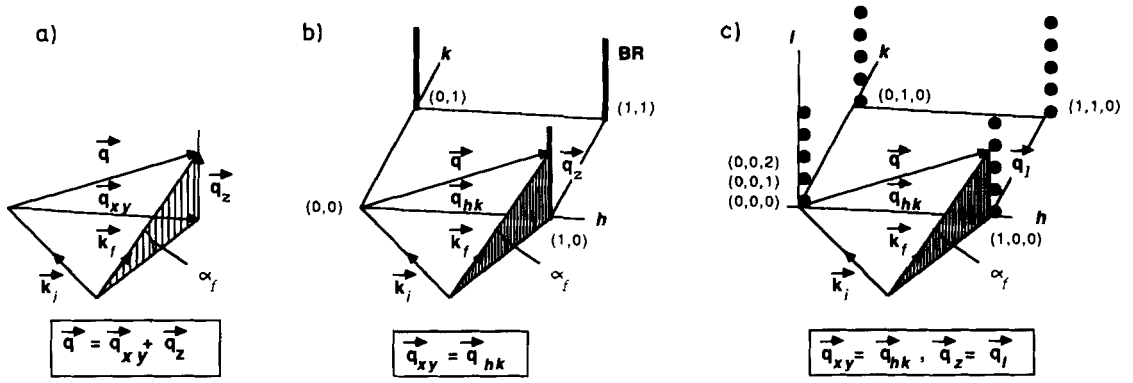

Fig. 3. a) General scattering geometry k_i and k_f are the wavevectors of the incident and diffracted beams respectively. The scattering vector $q = k_f - k_i$ has components q_{xy} parallel to the monolayer plane and q_z perpendicular to it. b) The scattering from a 2D crystalline material in reciprocal space extends in rods (Bragg rods) in the q_z direction, perpendicular to the plane of the monolayer and of its reciprocal 2D net. The scattering vector q must end on an (h,k) Bragg rod for Bragg diffraction. c) The scattering from a 3D crystal in a given orientation lies in reciprocal or q space at the reciprocal lattice points (h,k,l). Diffraction takes place when q coincides with a specific reciprocal lattice point [(1,0,3) in this particular case].

This intensity modulation can now be analyzed to obtain information, for example, on the direction and magnitude of the molecular tilt in the crystalline part of Langmuir monolayers.[19, 20] In addition, detailed information on the electron density distribution in the vertical direction, laterally averaged over both the ordered and disordered parts of the monolayer can be obtained from the deviation of the measured X-ray reflectivity[19, 21] (XR) from the Fresnel law.[16] By combining the methods of GID and XR, the structure of Langmuir films can be accurately characterized. Finally, grazing incidence X-ray excited fluorescence[22] and X-ray standing wave[23, 24] measurements yield information on the location and concentration of ions bound to the monolayer at the liquid interface. We now discuss these methods in some detail.

2.1. Specular Reflectivity (XR)

Specular reflection means that the reflected ray measured is in the plane spanned by k_i and the vector normal to the surface and that $\alpha_i = \alpha_r$ (see Fig. 1). The specular reflectivity of an ideal surface is given by the well-known Fresnel law of optics.[16] In the limit of small angle of incidence,[19, 21] applicable here, it reduces to Equation (3), where $q_z = (4\pi/\lambda)\sin\alpha_i$ is the z component of the momentum transfer and $q_c = (4\pi/\lambda)\sin\alpha_c$ is the critical value of q_z for total external reflection. The complex term arises from absorption effects (see Section 2). Neglecting absorption ($q_z < q_c$) Equation (3) yields $R_F = 1$, that is, total reflection. As q_z is increased beyond q_c, however, R_F decreases and, for $q_z \geq 4q_c$, approaches $R_F(q_z) \approx (q_c/2q_z)^4$. As the range of interest may extend to $q_z/q_c \approx 30$ or more,[19, 21] reflectivities down to 10^{-8} have to be measured. Hence the importance of high-intensity synchrotron sources or high-power rotating anode X-ray generators for XR measurements. Equation (3) is valid only for an ideally flat surface across which the electron density $\rho(z)$ varies steplike between two constant values. If $\rho(z)$ is not a step function, but varies continuously in the surface region, the reflectivity is modified,[19, 21] yielding Equation (4), where ϕ is defined as in Equation (5) and ρ_∞ is the constant electron density in the subphase bulk. Thus, by measuring $R(q_z)$ it is possible in principle to determine $\rho(z)$, the variation of the electron density normal to the surface, and, in particular, that of a monolayer floating on it. The function ϕ is complex, and only its modulus can be derived from the measured reflectivity but not its phase. Thus one is faced with the usual phase problem of X-ray crystallography and therefore to date virtually all specular reflectivity data has been analyzed by fitting a parametrized model density $\rho(z)$ to the measured data applying Equations (3), (4) and (5).

$$R_F(q_z) = \left[\frac{q_z - [q_z^2 - q_c^2 + i(4\pi\mu/\lambda)]^{1/2}}{q_z + [q_z^2 - q_c^2 + i(4\pi\mu/\lambda)]^{1/2}}\right]^2 \quad (3)$$

$$R(q_z) = R_F(q_z)|\phi(q_z)|^2 \quad (4)$$

$$\phi(q_z) = \frac{1}{\rho_\infty}\int \frac{d\rho(z)}{dz} e^{iq_z z} dz \quad (5)$$

One strategy has been to generate $\rho(z)$ as the sum of densities $\rho_i(z)$ from individual atoms at height $z = z_i$ and refine this *atomic model* of the monolayer molecules under suitable constraints.[25, 26] A typical constraint would be that, say, the hydrophobic moiety must tilt as a rigid body, that is, without distorting the a priori assumed internal bond lengths and angles. Adjustable parameters, then, would be the tilt angle of each molecular segment, the height of the molecule above the interface, and the area per molecule.

A computationally slightly simpler strategy presents the monolayer as a stack of slabs,[27] each with a constant density ρ_i and thickness l_i. Two such slabs would be needed for representing a simple fatty alcohol or acid monolayer.[28] When refining such a *slab model*, possible fit parameters would be the densities ρ_i and thicknesses l_i of the slabs.

For either representation of the monolayer, the constant density of the semi-infinite subphase has to be added below the interface. Finally, either model density must be smeared out in the z direction to account for the vertical roughness or diffuseness of the interface. The root-mean-square roughness, σ, is of order of 3 Å and stems mainly from thermally excited capillary waves on the water surface.[19, 21b, 21c] It leads to a Debye–Waller factor $\exp(-q_z^2\sigma^2)$ in $|\phi(q_z)|^2$ (Eq. 5)).

The rather large value of $\sigma \approx 3$ Å (equivalent in normal crystallographic parlance to $B = 8\pi^2\sigma^2 \approx 225$ Å^2) makes it unnecessary to use accurate charge densities for the atoms in the atomic model of $\rho(z)$, so long as each atom contributes its proper charge Z_i, the description will be adequate. Replacing groups of atoms by pseudoatoms is also feasible. Furthermore, since the value of σ is large, the monolayer may be adequately represented by the slab model. This is illustrated in Figure 4, which shows that the density $\rho(z)$ of a fatty acid monolayer may be represented by either model.

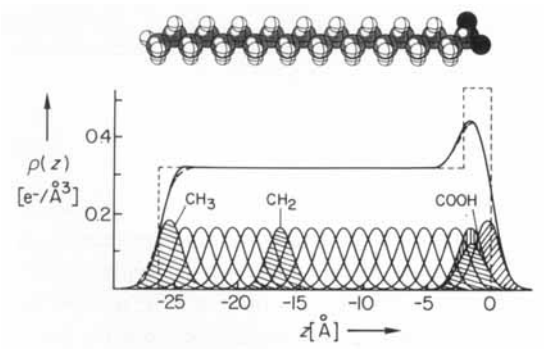

Fig. 4. Top: Space-filling model of a $C_{19}H_{39}CO_2H$ molecule. Bottom: Model electron densities $\rho(z)$. The dashed lines refer to a slab model and a smoothed slab model. The full lines refer to an atomic model using CH_3 and CH_2 as pseudoatoms. The contribution of each pseudoatom (or atom at the CO_2H head group) to the electron density is indicated by Gaussian curves. The two models agree nearly exactly even though drawn for display purposes with an unrealistically small smearing parameter σ of 1 Å.

2.2. Grazing Incidence Diffraction (GID) and Bragg Rods

In the GID geometry (Fig. 5) the angle of incidence α_i of the X-ray beam is kept below the critical angle α_c, limiting the penetration depth of the beam to that of the evanescent wave. Scattering due to the subphase is efficiently eliminated, which allows an accurate measurement of the weak diffraction signal originating from the crystalline monolayer. For all the diffraction patterns measured so far, the monolayers were found to be composed of 2D crystallites randomly oriented on the water surface, that is a 2D "powder". Hence

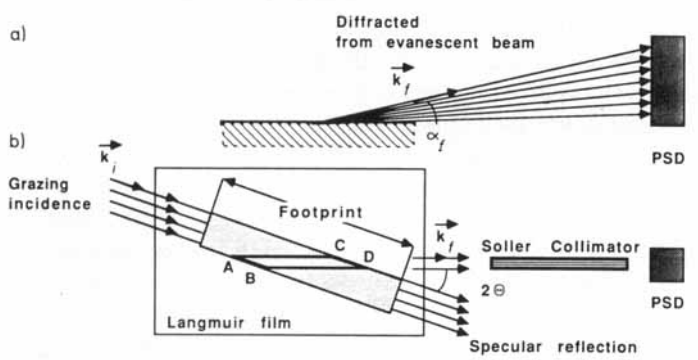

Fig. 5. a) Side and b) top view of the grazing incidence X-ray diffraction geometry. The footprint of the grazing incident beam is indicated by the shaded area. The position sensitive detector (PSD) has its axis along the vertical. Only the cross-beam area ABCD contributes to the measured scattering. The Soller collimator consists of thin vertical absorbing foils stacked together to define the horizontal resolution of the detector.

only a 2θ or q_{xy} scan in the monolayer plane is required to measure the diffraction pattern. The analysis is similar to that of a conventional 3D powder pattern; the reflections can be indexed by two Miller indices, h and k. Their angular positions $2\theta_{hk}$ corresponding to $q_{hk} = (4\pi/\lambda)\sin\theta_{hk}$ yield the repeat distances $d_{hk} = 2\pi/q_{hk}$ of the 2D lattice structure. Their resolution-corrected 2θ-line width (FWHM) Δ yields the 2D crystalline coherence length L through the well-known Scherrer formula [Equation (6)].[29]

$$L = \frac{0.9\,\lambda}{\cos\theta_{hk}\,\Delta} \tag{6}$$

Finally, the square of the molecular structure factor $|F_{hk}|^2$ integrated along the Bragg rod over the window of q_z seen by the detector determines the integrated intensity in the peak.[15] The structure factor F_{hk} is given by Equation (7),[18-20, 30a] where f_j is the scattering factor of the atom j, $\boldsymbol{r}_{x_j y_j}$ is the vector specifying the (x,y) position of the atom j in the unit cell and z_j is the atomic coordinate along the vertical direction.

$$F_{hk}(q_z) = \sum_j f_j e^{i(\boldsymbol{q}_{hk}\boldsymbol{r}_{x_j y_j} + q_z z_j)} \tag{7}$$

More information can be obtained by resolving the variation with q_z along the Bragg rod of the intensity $I_{hk}(q_z)$, given by Equation (8).[18-20, 30a]

$$I_{hk}(q_z) = |V(q_z)F_{hk}(q_z)|^2 e^{-q_z^2\sigma^2} \tag{8}$$

The observed BR intensity I is actually a sum over those (h,k) reflections whose Bragg rods coincide at a particular horizontal 2θ-angle or q_{xy} position.[18-20, 30a] In Equation (8), the most important variation is due to the molecular structure factor $|F_{hk}(q_z)|$. For the simple linear surfactant molecules considered here, the square of the structure factor $|F(\boldsymbol{q})|^2$ is a bell-shaped function which reaches its maximum when the scattering vector $\boldsymbol{q} = (\boldsymbol{q}_{hk}, \boldsymbol{q}_z)$ is orthogonal to the molecular axis. Thus, when the molecules are vertical or tilted in a plane perpendicular to $\boldsymbol{q}_{hk}$, the maximum intensity along the Bragg rod will occur at the horizon, for $q_z = 0$ Å^{-1}. For molecules tilted otherwise, we expect the Bragg rod maximum at a finite q_z, dependent upon both the magnitude and direction of the tilt relative to the in-plane scattering vector $\boldsymbol{q}_{hk}$. The width of the bell-shaped Bragg rod profile measured in a direction parallel to the molecular axis is inversely proportional to the length of the molecule.[19, 20]

The simple description of $F(\boldsymbol{q})$ alluded to above may be improved on by calculating $F(\boldsymbol{q})$ according to an atomic model of the molecule[20, 30a] [Eq. (7) and (8)]. For linear molecules, qualitatively similar results are obtained with both models.[20] The exponential factor [the vertical Debye–Waller factor, Eq. (8)] accounts for the internal thermal motion of the atoms in the molecule, as well as for ripples on the water surface, which lead to roughness of the interface.[19, 21b, 21c] The factor $V(q_z)$ describes the interference of rays diffracted upwards with rays diffracted down and subsequently reflected back up by the interface.[18a] $V(q_z)$ differs from 1 only in the vicinity of $q_z = 1/2\,q_c$, where it contributes a sharp peak to I (cf. Fig. 8 and the related discussion).

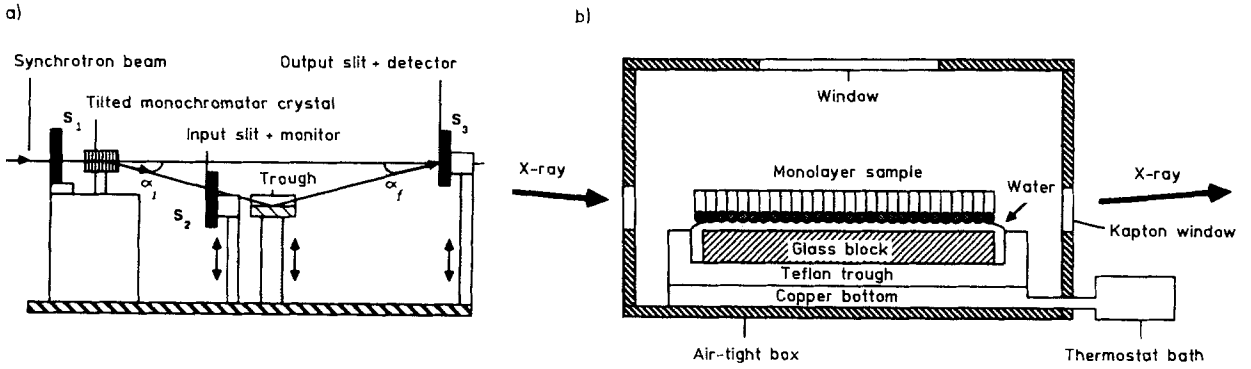

Fig. 6. Example of an experimental setup of a diffractometer for studying liquid surfaces (beamline D4, X-ray synchrotron source at Hasylab, Hamburg). a) Side view of the vertical scattering plane. Beam directions are defined by slits. The monochromatic beam is bent down towards the sample by tilting the monochromator crystal. The incident beam intensity is monitored beyond slit S_2. b) Enlarged view of the trough showing the monolayer sample spread on a thin film of water. The glass block guarantees a thin liquid film (about 0.3 mm thick) and thus effectively reduces surface capillary waves.

While both BR and XR data provide information on the vertical variation of the electron density, there are important differences between the two methods. The BR recorded at a given GID peak position originates solely from crystalline material. This is in contrast with XR, where the reflected signal is an average over *all* of the illuminated area regardless of coverage and in-plane structure. Furthermore, as the molecules in the contributing crystallites have a well-defined orientation relative to $\boldsymbol{q}_{hk}$, the BR profile depends very sensitively on the azimuthal direction of the molecular tilt. XR, on the other hand, averages over all azimuthal angles and hence provides no information on the molecular azimuthal orientation.

We now describe briefly a possible experimental setup (Fig. 6) for the diffraction geometry[31–33] shown in Figure 5. A suitable aperture S_1 is placed in the horizontal synchrotron radiation beam incident from the left (Fig. 6a). A monochromatic beam is selected from the "white" spectrum by Bragg reflection from a monochromator crystal, typically a perfect Ge crystal in the (111) orientation. By tilting the normal to the reflecting planes out of horizontal plane, the monochromatic beam can be bent down to yield a glancing angle with the horizontal liquid surface. The sample is mounted on an elevator so that the liquid surface always intersects the monochromatic beam. A narrow slit S_2 in front of the sample defines a suitable footprint of the beam on the liquid surface. The slit S_3 excludes diffuse scattered background around the reflected beam. This slit together with a scintillation detector is mounted on an elevator situated on a diffractometer arm which is pivoted around a vertical axis through the sample center. For in-plane diffraction measurements the slit S_3 is replaced by a Soller collimator giving 1 or 2 mrad collimation and the scintillation counter by a position-sensitive detector allowing Bragg rod measurements to be made (Fig. 5).

2.3. X-ray Fluorescence Methods

Atoms illuminated by X-rays of energy higher than that of their absorption edges will emit characteristic secondary radiation, the intensity of which is proportional to the number of excited atoms. Thus, by employing monochromatic X-rays of energy higher than, for example, the energy of the K absorption edge of a given ion dissolved in the subphase, it is possible to study the depth dependence of the concentration of that ion in the subphase. From Figure 2, we see that by varying α_i in the vicinity of α_c we can fine-tune the penetration depth of the primary radiation, and hence the depth to which we excite the ions dissolved in the subphase. Roughly speaking, the intensity variation of the secondary radiation will therefore follow the concentration variation with depth of the emitting ions.[34]

The method of near-total external fluorescence (NTEF) presented above provides information on the *vertical* concentration variation of the fluorescing probe ion. A variation on this method involves surface-EXAFS (Surface Extended X-ray Absorption Fine Structure, SEXAFS), where the fluorescence intensity variation is measured while varying the energy of the exciting radiation across the absorption edge of the probe atoms.[22] By keeping the angle of incidence α_i smaller than α_c, the penetration depth is kept to a few tens of Ångstroms. The short-range atom–atom correlation function in the surface layer (which gives a measure of interatomic distances) can be extracted by conventional EXAFS data analysis methods. By observing changes in this function induced by surface pressure variation in a deposited monolayer on the surface of the subphase, the interatomic distances in a layer of ions adsorbed from the subphase at its interface with the monolayer can be determined.[22] Thus a combination of NTEF and SEXAFS can be employed to provide information on both the vertical and horizontal structure of the probe ion near the surface. However, in contrast to GID, the in-plane information provided by SEXAFS is short range only and extends up to second nearest neighbors at most. On the other hand, GID is applicable only if reasonably long-range order exists (≥ 100 Å), while SEXAFS will provide average nearest-neighbor distances even for completely disordered systems.

2.4. X-ray Standing Waves

Standing waves are created when two coherent plane traveling waves are superimposed in the same region of space.[23] This is schematically depicted in Figure 7a, which shows the

resulting standing wave created by interference between an incident plane wave of vector $\boldsymbol{k}_i$ and its reflection from a mirror surface with a wavevector $\boldsymbol{k}_r$.

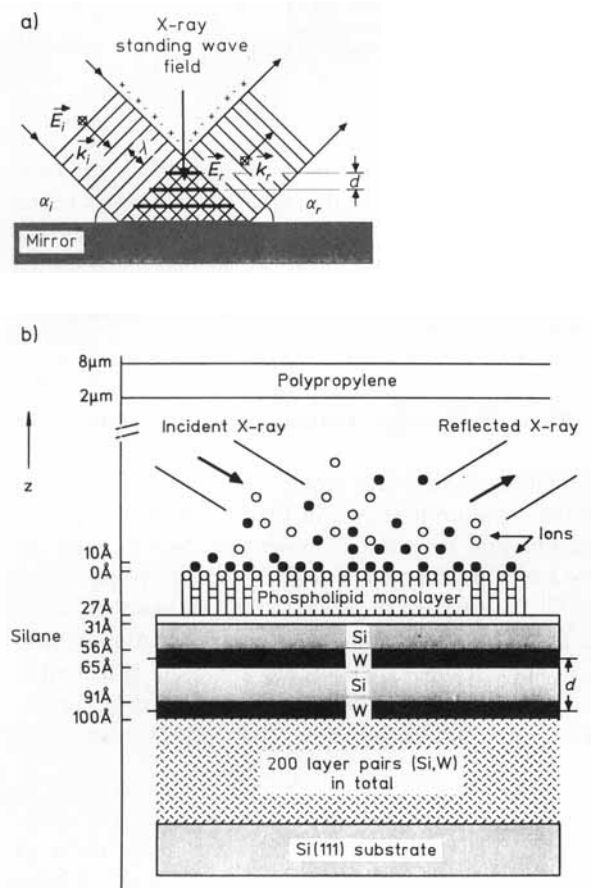

Fig. 7. a) Illustration of the X-ray standing wave field formed by the interference between the incident (E_i) and specular-reflected (E_r) plane waves above a mirror surface. By locating the intersections of the crests (labeled + lines) and troughs (labeled – lines) of the two plane waves, one can easily show that the antinodes of the standing wave are parallel to the mirror surface. Since total external reflection of X-rays (wavelength in Å range) occurs at incident angles α_i smaller than 0.5°, the spacing d typically varies between 100 Å and 1000 Å. b) Scheme showing a phospholipid monolayer deposited on a silanated Si/W layered synthetic microstructure (LSM). In the experiment depicted here [24b], the head group of the phospholipid containing an anionic phosphate group is exposed to solution and attracts zinc ions from a 0.1 mM $ZnCl_2$ aqueous solution. The polypropylene film traps a 2 μm thick water layer.

Conventionally, dynamical Bragg diffraction from perfect single crystals is used to generate an X-ray standing wave, whose period d is exactly commensurate with the diffracting planes of the crystal. For films adsorbed onto the crystal surface, with a thickness of say 20 to 100 Å, one requires long-period X-ray standing waves[24] which may be generated by Bragg diffraction from layered synthetic microstructures (LSM, Fig. 7b). For Bragg diffraction purposes a LSM is fabricated as a periodic layered structure consisting of 10 to 200 layer pairs of alternating high and low electron density materials (such as tungsten and silicon) to yield a diffraction plane spacing varying from 20 to 200 Å (Fig. 7b). Long period X-ray standing waves are also generated by total external reflection when the incident angle is less than the critical angle α_c (Fig. 7a). The period of the standing waves is $d = \lambda/2 \sin\alpha_i$.

To measure the effect of standing waves, an energy-dispersive detector is positioned above the surface and picks up the X-ray fluorescence from atoms adsorbed at the crystal surface or close to it. The fluorescence radiation of these atoms will depend on their positions as the period and phase of the standing wave changes with the angle of incidence of the primary beam. Figure 7b depicts an interesting application of the technique to ion–surfactant interactions: the study of interfaces between adsorbed charged monolayers and the distribution of the counterions in solution.[24b]

3. General Packing Characteristics of Langmuir Monolayers on Water

Before the development of surface X-ray diffraction techniques, knowledge of molecular arrangement in the three-dimensional state was used to increase understanding of the structure and behavior of molecules in the monolayer state, as already mentioned in Section 2. Analogous packing is not always possible however, because of environmental differences between the two- and three-dimensional states. Phase diagrams constructed from surface pressure–area (π–A) measurements for such compounds revealed phase boundaries, depending upon pressure, temperature, and chain length, but could provide little information on the structure of these phases. Now, with recently acquired information from surface-sensitive X-ray techniques, the packing of such Langmuir films can be determined almost at atomic level. Although GID measurements have been carried out on several Langmuir monolayer systems, the monolayer structures corresponding to the complete phase diagrams have been elucidated by GID only for the acids $C_{20}H_{41}CO_2H$ and $C_{21}H_{43}CO_2H$, discussed in Section 3.2. In Section 3.1 we describe one or two examples from each chemical class studied to date: alcohols, amides, carboxylic acids, divalent salts of the latter, α-amino acids, and phospholipids (see Table 1 for their chemical formulas and abbreviations). The latter two classes of compounds possess an asymmetric carbon atom whose chirality is specified by the symbol (*R*) or (*S*).

Table 1. Abbreviations for monolayer compounds discussed here and their chemical formulae

Abbreviation	Full Name	Chemical Formula
C_nOH	aliphatic primary alcohols	$C_nH_{2n+1}OH$
C_nCO_2H	aliphatic primary acids	$C_nH_{2n+1}COOH$
C_nCONH_2	aliphatic primary amides	$C_nH_{2n+1}CONH_2$
$C_{19}CONHC_2H_4CO_2H$	*N*-arachidoyl-β-alanine	$C_{19}H_{39}CONHC_2H_4CO_2H$
DMPE	dimyristoyl-phosphatidylethanolamine	$C_{13}H_{27}COOCH_2CH(OOCC_{13}H_{27})$-$CH_2PO_4^-$, $C_2H_4NH_3^+$
PL	palmitoyl-lysine	$C_{15}H_{31}CONHC_4H_8CHNH_3^+CO_2^-$
PFA	"perfluoro"dodecyl-aspartate	$C_{10}F_{21}C_2H_4OCOCH_2CHNH_3^+CO_2^-$

It is useful at this stage to describe how unit cell dimensions and molecular orientation may be determined from GID data for simple cases. We consider the molecule as a freely rotating alkane chain; in other words, it has cylindrical symmetry. These molecules may pack in three different cell types: hexagonal ($a = b$, $\gamma = 120°$), distorted hexagonal ($a =$

b, $\gamma \neq 120°$) which may be more properly described as centered rectangular ($a' = |\boldsymbol{a} + \boldsymbol{b}|$, $b' = |\boldsymbol{a} - \boldsymbol{b}|$), and oblique ($a \neq b \neq |\boldsymbol{a} + \boldsymbol{b}|$) (Fig. 8). The molecules in a hexagonal cell are aligned vertically relative to the plane of the film, while in the distorted hexagonal cell they are tilted along a symmetry direction and in the oblique cell along an arbitrary direction. As mentioned earlier, all Langmuir monolayers studied

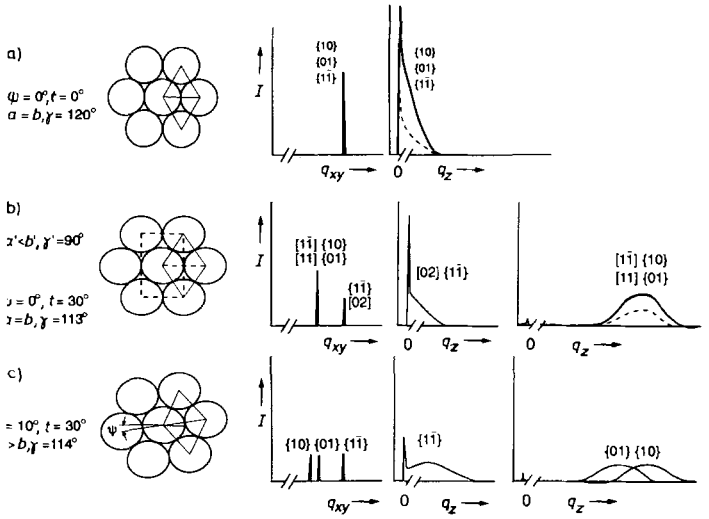

Fig. 8. Three possible structures and diffraction from a monolayer of close-packed, freely rotating alkyl chains. The left column shows schematic top views of the molecular packing in hexagonal, distorted hexagonal, and oblique unit cells. The second column shows the q_{xy}-pattern integrated over the vertical wavevector component q_z, and the last two columns show the Bragg rods integrated over the corresponding q_{xy}. When more than one reflection coincide, the dashed lines represent the intensity from individual reflections as indicated by the Miller indices. The solid line represents the intensity from a two-dimensional powder sample; that is, the sum of the intensities indicated by dashed lines. When the molecular axis is perpendicular to the water surface the lattice is hexagonal [a)], and the $\{1,0\}$, $\{0,1\}$ and $\{1,\bar{1}\}$ reflections are degenerate. The Bragg rod obtained from the single in-plane diffraction peak has its maximum at $q_z = 0\,\text{Å}^{-1}$. When the molecular axis is tilted towards nearest neighbors [b)], the hexagonal structure is distorted to a centered rectangular structure (rectangular notation at the top, distorted hexagonal notation at the bottom). The degeneracy of the three reflections is partially lifted resulting in two peaks. The Bragg rod of the two degenerate reflections $\{1,0\}$ and $\{0,1\}$ ([1,1], $[1,\bar{1}]$ in the rectangular notation) is centered at $q_z \geq 0\,\text{Å}^{-1}$. The Bragg rod of the $\{1,\bar{1}\}$ reflection ([0,2] in the rectangular notation) is still centered around $q_z = 0\,\text{Å}^{-1}$. Finally, when the molecular axis is tilted in a non-symmetry direction, the intersection between the close-packed circular chains and the water surface forms an oblique 2D lattice [c)]. The degeneracy is completely lifted and the peak positions of the three Bragg rods determine the tilt angle as well as the azimuthal angle Ψ unambiguously.

to date by GID consist of "powders" of randomly ordered 2D crystallites on the water surface so that the GID measurements are not made on single crystals. Thus, the diffraction spectra consist of coinciding Bragg rods of reflections (h,k,q_z) and $(\bar{h},\bar{k},q_z)$, the notation $\{h,k,q_z\}$ designating both reflections. In general, the intensity distribution along their two coinciding Bragg rods will be different unless the monolayer structure has twofold symmetry along the vertical axis.

The hexagonal cell has three equivalent lattice spacings d_{hk}: d_{10}, d_{01}, and $d_{1\bar{1}}$. The GID spectrum from these three reflections will appear as a single signal with all corresponding Bragg rods peaking at $q_z = 0\,\text{Å}^{-1}$ (Fig. 8a). The corresponding GID spectrum for the distorted hexagonal cell will comprise two peaks; one a superimposed doublet arising from the coinciding $\{1,0\}$ and $\{0,1\}$ reflections, and the other the remaining $\{1,\bar{1}\}$ peak (Fig. 8b). The separation between

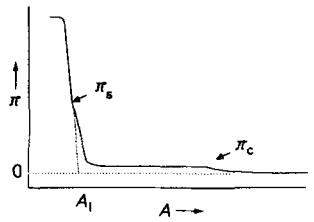

Fig. 9. General shape of a surface-pressure versus area isotherm (π–A isotherm) of a Langmuir monolayer. A_l is defined as the limiting area (i.e., the close-packed area for the molecules at zero pressure). π_s and π_c define transition pressures between phases.

the two peaks depends upon the deviation of the angle γ from 120°. In the oblique cell the degree to which the three reflections $\{1,0\}$, $\{0,1\}$, and $\{1,\bar{1}\}$ are resolved (Fig. 8c), depends upon the deviation from centered rectangular (i.e. distorted hexagonal) cell symmetry.

3.1. Phase Changes Induced by Surface Pressure

A typical pressure–area isotherm of Langmuir films at room temperature is shown in Figure 9. It has long been realised that the kinks in the isotherm (the surface pressures at the kinks are denoted π_c and π_s) indicate phase transitions.[10] The shape of the isotherm and the positions of the kinks are characteristics of a given monolayer. At room temperature the alcohol $C_{21}OH$ and acid $C_{20}CO_2H$ as well as the α-amino acid PFA exhibit isotherms with only one distinct kink at π_s (in the range 15–30 mN m^{-1}), whereas the

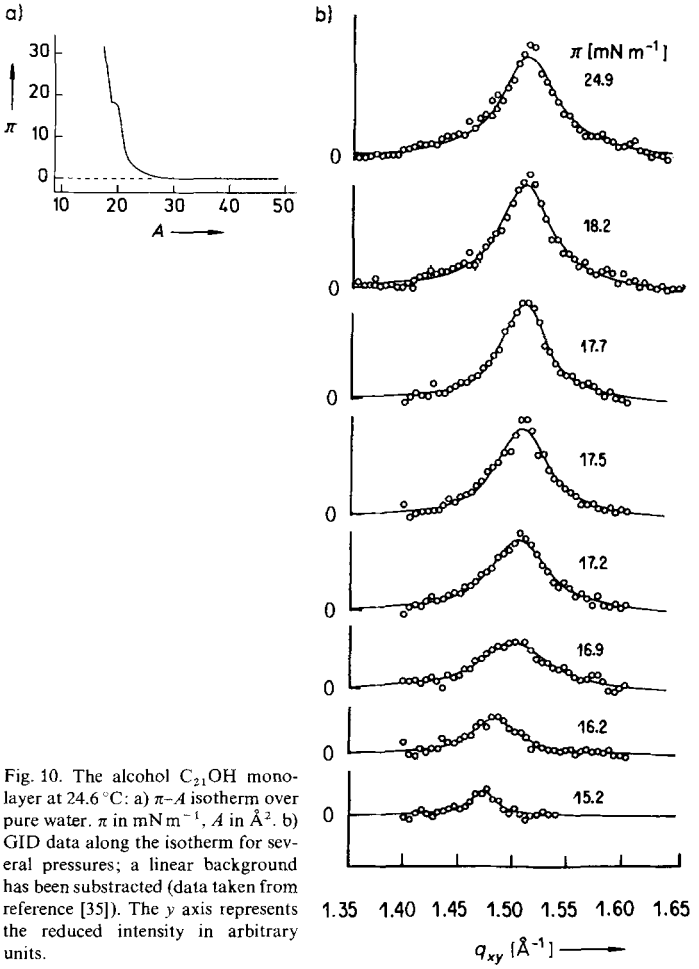

Fig. 10. The alcohol $C_{21}OH$ monolayer at 24.6 °C: a) π–A isotherm over pure water. π in mN m^{-1}, A in Å^2. b) GID data along the isotherm for several pressures; a linear background has been substracted (data taken from reference [35]). The y axis represents the reduced intensity in arbitrary units.

phospholipid compound DMPE has an isotherm with two kinks (π_c in the range 5–10 mN m^{-1} and π_s in the range 20–30 mN m^{-1}). The α-amino acid PL shows no observable kink. It has generally been assumed that a decrease in molecular area induces transitions from gaseous through "liquid-expanded" and "liquid-condensed" to the solid crystalline phases.[10] But the GID data on some systems reveal high crystallinity in the uncompressed state and a tendency towards a reduction of crystallinity with increased pressure. Thus, GID and XR results provide a more accurate description of the phases.

3.1.1. *Fatty Acids and Alcohols*

GID data for henicosanol[35] $C_{21}OH$ shows a single peak in the surface pressure range 15–30 mN m^{-1} and temperature range 15–30 °C (Fig. 10b). The changes in the peak with pressure observed at 24.6 °C (Fig. 10b) are typical of the isotherms measured (Fig. 10a). The gradual loss of intensity below π_s was interpreted[35] as being due to the appearance of *gauche* defects in the hydrocarbon chain. The kink then represents the lowest pressure at which the last of the gauche configurations are squeezed out. At higher pressures all the molecules stand straight with their hydrophobic tails in all-*trans* conformation.

Combined GID, Bragg rod, and XR room temperature measurements on arachidic acid[19, 28] $C_{19}CO_2H$ along the isotherm (Fig. 11) have been interpreted differently; the drop in GID intensity as a function of decreasing surface pressure was accounted for by a continuous change in tilt of rigid parallel molecules.

The low pressure structure was assigned to a distorted hexagonal cell, where molecules tilt toward nearest neighbors. Such a cell yields two diffraction peaks, one corresponding to the $\{1,\bar{1}\}$ reflection and the other to $\{1,0\}$ and $\{0,1\}$. The results reported[35] for $C_{21}OH$ could possibly be interpreted in a similar manner. A definitive answer would require BR and XR measurements of that system.

The GID and XR results for $C_{19}CO_2H$ on pure water allows us to deduce some information on the packing of the carboxyl groups in the compressed ordered state at room

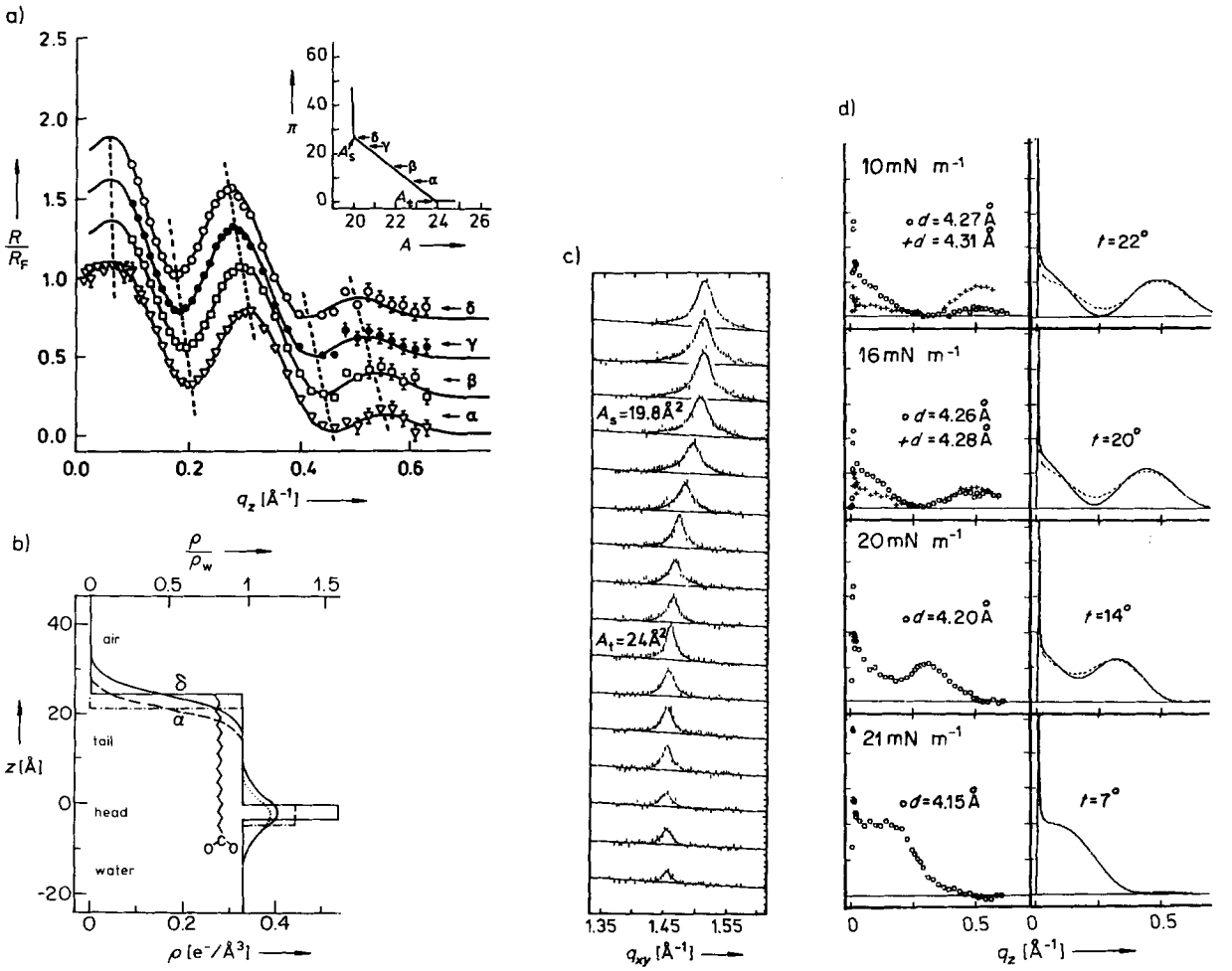

Fig. 11. Arachidic acid $C_{19}CO_2H$ monolayer at room temperature and over pure water: a) Normalized X-ray reflectivity (XR) data for increasing surface pressure (α–δ). The insert shows the π–A isotherm (π in mN m^{-1} and A in Å^2) of the monolayer and indicates the points where the XR measurements were performed. b) Fitted model of the vertical electron density $\rho(z)$. On compression, the monolayer thickness increases while the density remains constant in the tail region as shown by the change from the dashed lines to the full lines. $\rho_w = \rho_{water}$. c) GID data for decreasing mean molecular area; A_s and A_t correspond to the areas marked on the π–A diagram. d) Left: 2D powder Bragg rods observed at surface pressure of 10, 16, 20, and 21 mN m^{-1}. At 20 and 21 mN m^{-1}, the optimal q_{xy} settings for the merging peaks at $q_z = 0$ Å^{-1} and $q_z > 0$ Å^{-1} coincide, but for lower surface pressures they split as indicated by open circles (optimum q_{xy} for $q_z = 0$ Å^{-1}) and crosses (optimum q_{xy} for $q_z = 0.5$ Å^{-1}). Right: Calculated Bragg rod profiles from a slab model in which the molecules tilt towards next nearest neighbors by an angle t. The model parameters were determined essentially from the reflectivity data. The dashed line represents a perturbation of this model: the molecules were tilted in a direction 8° from the symmetry direction.

temperature. The hexagonal cell may at first sight imply complete rotational disorder about the chain axis. Indeed such structural disorder may be assumed for the alcohol $C_{21}OH$. However aliphatic carboxylic acids can hardly support such disorder for it could lead to a short contact $d_{O\cdots O}$ of about 1.5 Å between two adjacent oxygen atoms with their lone-pair electrons directed at each other (Fig. 12). Numerous studies[36] have demonstrated that two such adjacent oxygen atoms have a preferred separation of 3.5 Å. Whether hindered rotation of the acid molecules precludes a hexagonal symmetry (but not a hexagonal cell) is therefore a moot point.

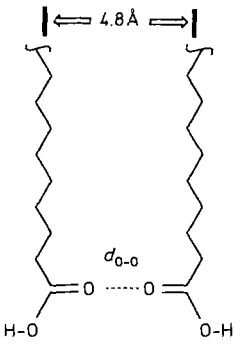

Fig. 12. Close contact ($d_{O\cdots O}$ spacing) between adjacent oxygen atoms of two fatty acid molecules separated by 4.8 Å and related by twofold symmetry.

3.1.2. *Phospholipids*

The extensive surface X-ray studies on phospholipid monolayers have been reviewed in detail in terms of structural changes along the π–A isotherm.[32, 37] We therefore confine this discussion to a brief review of some aspects of the condensed monolayer of α-dimyristoyl phosphatidylethanolamine (DMPE, see Table 1) from the view point of molecular packing (the isotherm is shown in Fig. 13a).

GID measurements[32] yielded a single peak in the pressure range between 10 and 38 mN m^{-1}. The variation with surface pressure of the diffraction peak characteristics is depicted in Figure 13b. The diffraction data for $\pi_c < \pi < \pi_s$ is consistent with coexistence between a nondiffracting liquid phase and a gel phase where the coherence length L increases with pressure. In the condensed phase (above π_s) the coherence length is no more than about 50 lattice distances, so the monolayer forms some crystalline solid phase, but with many defects. For the condensed phase region, the results of the X-ray reflectivity data (Fig. 13c) may indicate an ordering of the head groups.

Although little is known on the packing arrangement of hydrophobic chains and the hydrophilic head group PO_4^--CH_2-CH_2-NH_3^+ moieties, information thereon may be gleaned from the three-dimensional crystal structure of the racemic dilauryl derivative (*rac*-DLPE) whose packing arrangement[38] is shown in Figure 14. The most intense reflection from the layer structure of *rac*-DLPE has a spacing of 4.2 Å, which is the same value as that of the single GID peak observed from the chiral resolved compressed monolayer of DMPE (Fig. 13b, bottom), indicating a similarity in packing of their hydrophobic chains. In the 3D crystal the molecules

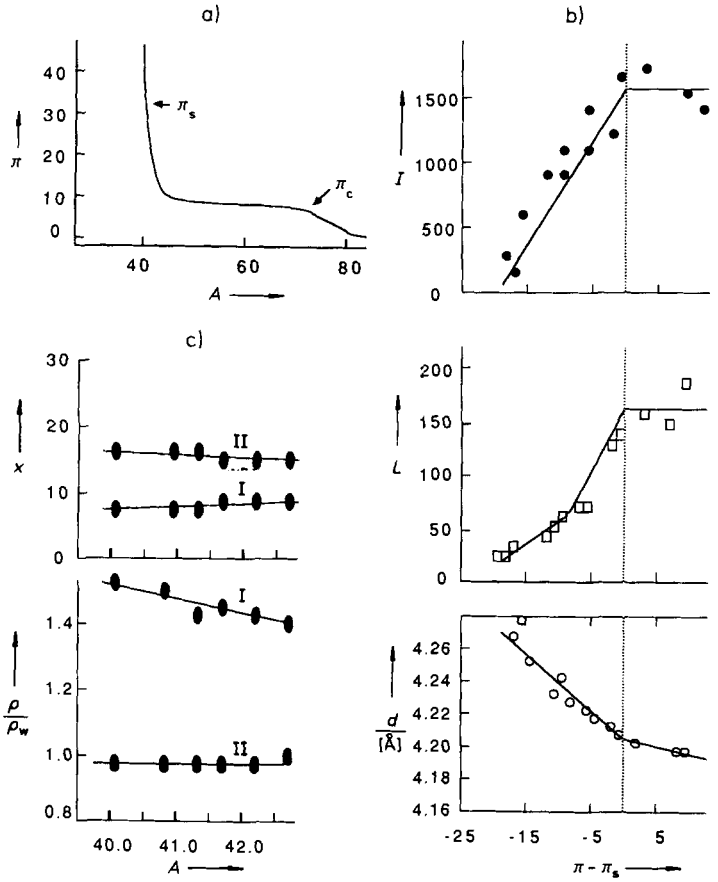

Fig. 13. Phospholipid DMPE monolayer over pure water at room temperature: a) π-A isotherm of DMPE; π in mN m^{-1}, A in Å^2. b) Three parameters extracted from the GID data as a function of surface pressure; the intensity of the integrated GID peak (I in arbitrary units), the coherence length L, and the lattice spacing d. c) Model parameters for the head (I) and tail (II) slabs [thickness x [Å] and electron densities $\rho(z)$ relative to that of water (ρ_w)] used in XR data fitting.

form a bilayer; within each layer the head groups are interlinked by NH···O hydrogen bonds by translation and glide symmetry. This head group packing is also observed in the crystal structure of (2-aminoethyl)phosphate $HO\text{–}PO_3^-$–

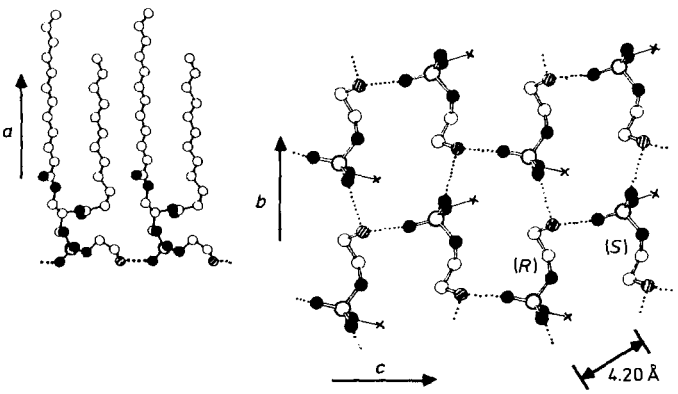

Fig. 14. The layer structure of *rac*-DLPE in its 3D crystal. The hydrogen atoms are omitted. Left: View down the c axis. Right: View down the a axis. For clarity each hydrocarbon chains are represented by a small cross. The molecules are interlinked by NH···O hydrogen bonds (dashed lines) by translation symmetry along the b axis (molecules of the same configuration) and by glide symmetry along the c axis (molecules of the opposite configuration). Note the characteristic 4.20 Å spacing imposed by the molecular packing. ● = O, ⊗ = N, ○ = C,P.

CH_2–CH_2–NH_3^+.[39] It is tempting to think that the head groups of chiral resolved monolayers of DMPE and DLPE would also pack in a pseudoglide arrangement. However, the monolayer study of DLPE and DMPE was performed on the resolved naturally occurring (*S*) enantiomer. Furthermore, the thickness of the layer of the head groups in the 3D crystal structure is 5.5 Å, but in the range of 7.15 to 9.5 Å in the monolayer structures according to the XR data.

3.1.3. α-Amino Acids

The α-amino acid surfactants were used for the oriented crystallization of the α-polymorph of glycine and of NaCl at the monolayer–solution interface (see Section 5). GID and XR measurements were performed on two of these monolayers in order to establish independently the similarity or complementarity of the head-group arrangement of the monolayer molecule and the layer arrangement of the crystal face attached to the monolayer.[25, 26, 30] Here we describe the packing characteristics of two α-amino acid surfactants, PL and PFA (see Table 1).

Palmitoyl-lysine (PL): The NH···O hydrogen bonding arrangement of the α-amino acid head groups NH_3^+-CH-CO_2^- and of the amide groups CO-NH in the chain essentially fixed the monolayer packing. The π–*A* isotherm of the monolayer of PL is shown in Figure 15a. A compressed (about 25 mN m^{-1}) monolayer of PL was found by GID to form crystalline domains with a coherence length of about 500 Å. The diffraction pattern[25] shows two Bragg peaks (Fig. 15c). The calculated GID positions and intensities for the model structure[25, 40] are also shown. Analysis of observed XR data (Fig. 15b) yields a tilt angle of the molecular chain axis of about 30° from the vertical. The deduced cell axes and packing arrangement of PL is shown in Figure 16. The α-amino acid head groups NH_3^+-CH-CO_2^- are arranged in a manner similar to that of crystalline α-glycine or other naturally occurring hydrophobic α-amino acids.[41–43] The linear NH···O hydrogen bonds between amide groups in the chain linking neighboring molecules along the (***a*** + ***b***) director (Fig. 16b) require a 30° tilt of the chain axes, as was independently deduced from the XR analysis.

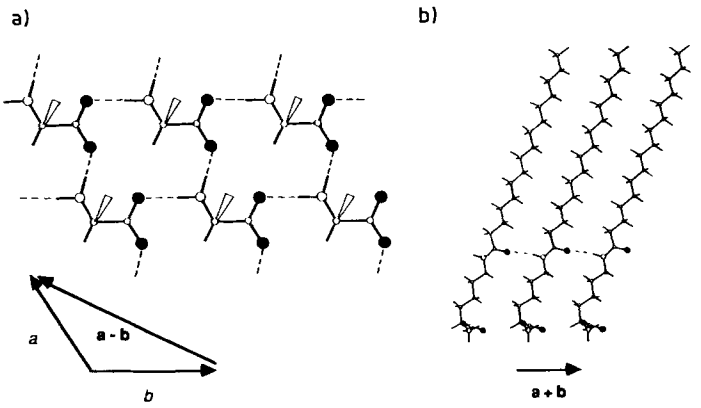

Fig. 16. Views of the model packing arrangement of (*R*)-PL monolayers over pure water; π = 25 mN m^{-1}. a) Perpendicular to the monolayer plane, the hydrophobic chain is represented by a wedge. The NH···O=C(acid) hydrogen bonds are symbolized by dashed lines. b) View along the ***a*** − ***b*** axis showing molecules in a row parallel to the ***a*** + ***b*** direction, interlinked by NH···O=C (amide) hydrogen bonds. ● = O.

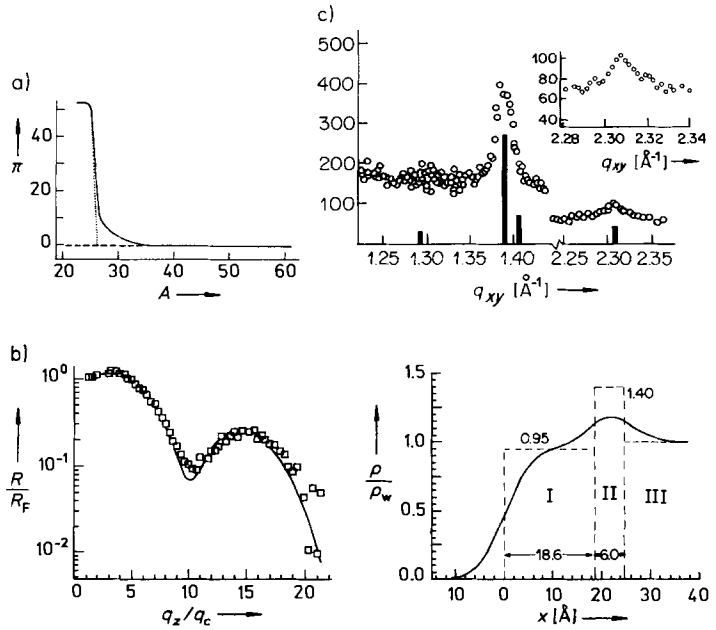

Fig. 15. (*R*)-PL monolayers over pure water at room temperature. a) π-*A* isotherms (π in mN m^{-1} and A in Å^2). b) Left: The measured, normalized *R* values and the theoretical model obtained by curve-fitting. Right: The refined model electron density $\rho(z)$ relative to that of water ρ_w. The PL molecules are modeled by two slabs, one corresponding to the head group (region II) and the other to the hydrocarbon tail (region I). Region III corresponds to the water subphase and z represents the height coordinate. The smoothed model shown as a solid line is obtained with a smoothing factor σ of 3 Å. c) GID of a compressed PL monolayer. The calculated relative intensities of the model (Fig. 16) drawn underneath the peaks are without adjustable parameters except for scale and Debye–Waller factors.

"Perfluoro"dodecylaspartate (PFA): The behavior of PFA upon compression is similar to that of arachidic acid in that the molecular tilt angle is continuously reduced with increasing surface pressure.[30a] However, the system revealed some original features. At low surface coverage (points α, β, γ on the isotherm in Fig. 17a), molecules of PFA self-assemble in large crystalline domains, in which they are arranged in an oblique cell and tilted by about 22° from the surface normal towards nearest neighbors (Fig. 18), as deduced from the three observed reflections in Figure 17d. Upon compression the three peaks first merge into a doublet (Fig. 17c) and then into a singlet (Fig. 17b), indicating that the symmetry of the cell, but not of the monolayer structure, goes from oblique (Fig. 17d), through distorted hexagonal (Fig. 17c), to hexagonal (Fig. 17b; see also Fig. 8 and the related discussion).

The molecular behavior of monolayers of PFA during a compression–decompression cycle can be explained with a knowledge of the head-group packing before compression.[30a] The hydrogen-bonding pattern of the α-amino acid head groups of uncompressed PFA was constructed from the known motifs of the 3D crystal structures of neopentylglycine,[5b] (*S*)-alanine,[44] and *rac*-alanine.[45] The major feature of this motif is the participation of intercalated, ordered water molecules interlinking adjacent hydrogen-bonded ribbons of PFA molecules (Fig. 18). The molecular area, which is dictated by the head group, is 30.9 Å^2 as compared with the cross-sectional area of the fluorocarbon chain

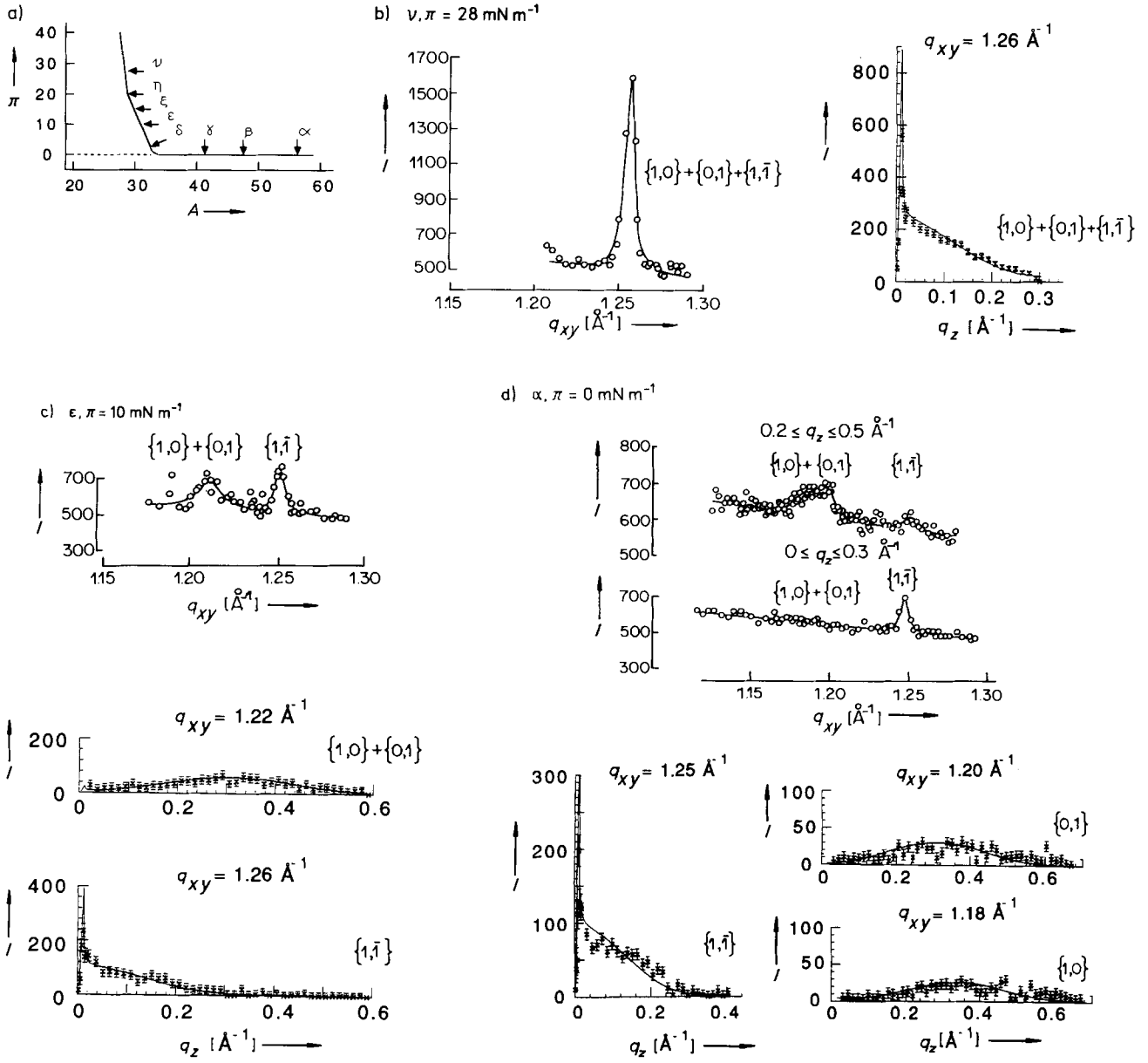

Fig. 17. PFA monolayers over pure water at room temperature. a) π-A isotherm (π in mN m^{-1} and A in Å^2). The points (α–ν) indicate where GID measurements were made. (b–d) A selection of GID measurements positions, ν, ε, and α) confirming the three observed 2D crystal symmetries (see also Fig. 8) when increasing the surface pressure. Left (b) or top (c,d): GID peaks. The Miller indices are indicated. Bottom: Bragg rod profiles measured on the GID peaks. Reflection positions and indices are given. Note that for position α in d) the GID peaks were measured for two different q_z intervals; furthermore, the Bragg rod intensity profiles have a different scale than in b) and c). In all cases, the solid line is the model fitted to the data. I = intensity in counts.

(28.5 Å^2). Upon increasing the pressure the molecular area is reduced and the water molecules are probably partially squeezed out of the hydrogen-bonded layer. At high pressure, hexagonal cell dimensions are imposed by the close contact between the fluorocarbon chains. Release of the surface pressure causes a dramatic decrease in coherence length L, an increased tilting of the molecules, and finally the disappearance of any observable diffraction, which is probably linked to the dynamics of the building process of a new bonding layer akin to the original one.

3.1.4. *Enantiomeric Mixtures of α-amino Acid Monolayers*

A little of the opposite enantiomer present in the chiral resolved monolayer of PL causes the GID peak to disappear (Fig. 19a). This indicates that the lattice of the monolayer becomes sufficiently distorted to reduce the crystalline coherence length drastically. The effect was explained by the inclusion of say an (*S*) molecule in a lattice of (*R*) molecules. Figure 19b shows that to reduce the resulting bad intermolecular contacts, the structure becomes distorted. Thus an appreciable fraction of the molecules in the monolayer are misaligned when even as little as 3% of the opposite enantiomer is added. The pure racemate also did not give a diffraction pattern at room temperature. Here we might have expected an arrangement in which the (*R*) and (*S*) molecules are interlinked in a layer by glide symmetry as observed in the crystal structure of hydrophobic *rac*-α-amino acids.[15, 45] We cannot rule out small ordered domains of this type in the solid solution of a pure PL racemate.

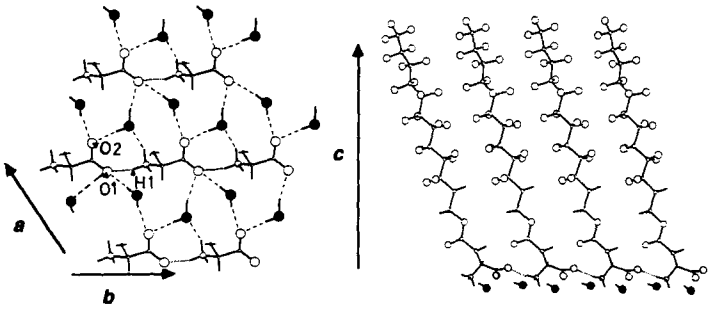

Fig. 18. Model of the arrangement of the self-assembled crystallites of a PFA monolayer over water at $\pi = 0\,mN\,m^{-1}$. Left: View perpendicular to the monolayer (i.e., along the c axis), showing hydrogen bonding of head groups and water molecules. O1 and O2 are oxygen atoms of the carboxylate groups; each forms hydrogen bonds with two water molecules. O1 forms a hydrogen bond with H1 of the NH_3^+ moiety of the neighboring molecule. The molecular chains are omitted for clarity. Right: View along the a axis showing the attached layer of water molecules and the projection of the chain tilt in the $(1,\bar{1})$ plane. • = oxygen atoms of the water molecules.

In contrast, the molecular area of compressed PFA monolayers (28.5 Å^2) imposed by the perfluorinated chain is larger than the molecular area observed in compressed monolayers of PL (24.3 Å^2) or in the crystal structure of glycine (25.5 Å^2). Therefore the more open head group arrangement of PFA is in keeping with the observation that racemic mixtures of compressed PFA display a very intense diffraction peak.[40b]

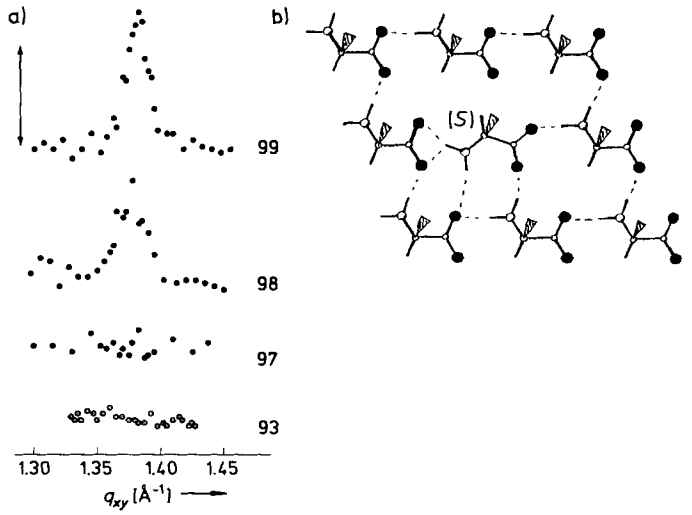

Fig. 19. a) GID data of mixed chiral monolayers of PL. The percentage of the (*S*)-enantiomer in the mixture is indicated on the right. The length of the double-sided arrow represents 200 counts. b) A PL molecule of (*S*) configuration surrounded by PL molecules of the opposite (*R*) configuration in a possible packing arrangement. All the chains are assumed to be related by translation and are indicated by wedges, so that the distortion of the hydrogen bonding (- - -) around the (*S*) isomer is visible. • = O.

Addition of the opposite enantiomer does not affect the crystal packing of PFA as it does for PL, since the distortion introduced in the hydrogen-bonding at the head group does not play a decisive role in the molecular packing of the compressed PFA monolayers.

3.2. Phase Changes Induced by Temperature

There is a wealth of macroscopic data available on temperature-induced phase transitions in Langmuir films, yet little reliable structural information on the molecular level. Only recently is such information becoming available from GID data. For example, the results on monolayers of fatty acids and fatty alcohols indicate a reduction in rotational disorder when the temperature decreases. Indeed, the diffraction pattern at high surface pressures (30 $mN\,m^{-1}$) for Langmuir films of the alcohol $C_{21}OH$ and the carboxylic acid $C_{20}CO_2H$ upon cooling from 30 °C to 0 °C shows additional peaks (Fig. 20a,b), indicative of a change from hexagonal to a centered rectangular cell.[46] The change was attributed to a pronounced reduction of librational motion of the molecule about its chain axis. Diffraction data on the acid monolayers $C_{21}CO_2H$[47] and $C_{29}CO_2H$,[48] and on the alcohols $C_{23}OH$, $C_{30}OH$, and $C_{31}OH$[48] at a temperature of 5 °C in the compressed state showed that the molecules of the film are vertically aligned.

The phase diagrams of the homologous series of long-chain fatty acids C_nCO_2H have been studied by means of pressure–area isotherms.[49] The phase diagrams of the series seem to be almost identical, provided that the temperature scale is shifted by 5–10 °C for each additional CH_2 moiety: extending the chain length has the effect of lowering the temperature. The available GID data,[19, 28, 47, 50, 51] taken as a whole, seem to confirm this conjecture. The phase diagram of docosanoic acid ($n = 21$) is reproduced in Figure 21. The acid $C_{21}CO_2H$ is convenient because nearly all the phases are observable at temperatures between 5 and 30 °C. Two independent synchrotron GID studies determined the structure of all the phases of docosanoic acid[47] and henicosanoic ($n = 20$) acid.[50] As the diffraction results were similar, we report here only those observed with docosanoic acid monolayers.

In each phase, the molecules are oriented with their long axes parallel and form a 2D crystal structure (Fig. 21), albeit with positional coherence lengths ranging from 50 Å at high temperature to more than 1000 Å at lower temperatures. The higher temperature structures may be similar to the mesophases found in liquid crystals. The L_2 phase has molecules tilted towards nearest-neighbors on a centered-rectangular net. On compression, at temperatures above ca. 25 °C one enters through a second-order phase transition into the hexagonal phase LS with vertical molecules. At these temperatures, indirect evidence suggests that the molecules are free rotators. At lower temperatures, compression leads from the L_2 phase through a first-order phase transition to the L_2' phase, again with tilted molecules on a centered-rectangular net, but with the molecules inclined towards next-nearest neighbors. Further compression leads to the phase S with vertical molecules on a centered-rectangular net. We note that lowering the temperature has the effect of reducing the symmetry of the high pressure phase from hexagonal (LS phase) to distorted hexagonal (S phase). One may speculate that the symmetry is reduced because the molecules have become hindered rotators. Below ca. 10 °C at high pressure, one observes the CS phase which has the same symmetry as the S phase. The CS phase, however, has long positional coherence lengths (> 1000 Å), a small area per molecule (18.6 Å^2), and a very low compressibility. It may be compared to 3D crystalline structures of alkanes well below their melting points, in which the molecular backbones are locked in a herringbone pattern.[52]

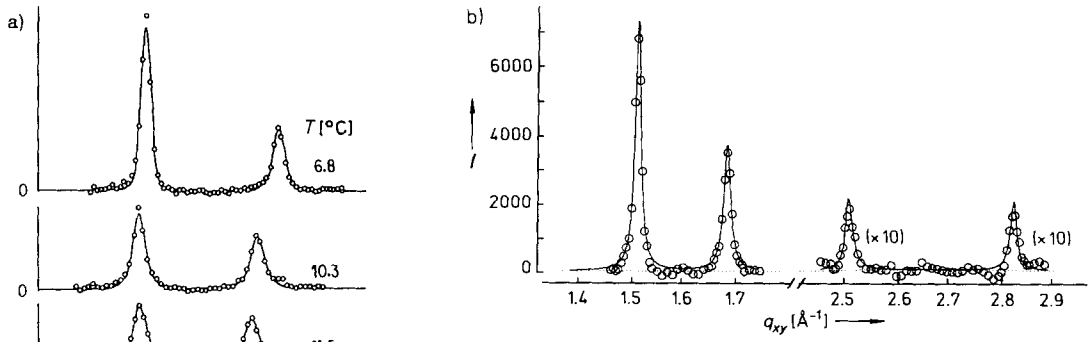

Fig. 20. a) GID data for a monolayer of the alcohol $C_{21}OH$ over pure water (from reference [35]) taken along the isobar at 30 mN m^{-1}. The peak intensity increases with decreasing temperature. The peak splitting is due to the transition from a hexagonal to a distorted hexagonal net. A linear background has been substracted. b) GID data for a monolayer of the acid $C_{20}CO_2H$ over pure water (from reference [46]) at 5 °C and $\pi \approx 35$ mN m^{-1}. Under these conditions the diffraction spectra of the alcohol and the acid are identical. A linear background has been subtracted. In addition to the two reflections observed in a) for 6.8 °C, two higher order reflections are shown here with 10 × magnification.

3.3. Crystalline Self-Assembly of Noncompressed Monolayers

The degree of crystalline order in biological lipid membranes in solution is probably low. But we may expect a high degree of order in self-aggregated clusters of amphiphilic molecules at the water surface because of the constraints imposed: a "flat" surface and solvent in contact only from the hydrophilic side. Direct evidence is now available from GID, but only for water-insoluble species. For soluble species, characterization by X-ray diffraction has not yet been achieved, possibly because of the low scattering power of these molecules. In addition, the range of crystallinity of the clusters may be very small. Nevertheless, evidence for aggregation comes from specular reflectivity data;[53] evidence for some degree of ordering comes from oriented epitaxial crystallization in the subphase at the solution surface.[5] More recently a remarkable observation was made by fluorescence microscopy:[54] two-dimensional faceted crystals of sodium dodecyl sulfate with sides of the facets as long as 50 μm could be seen on the water surface for a concentration of 0.055% by weight, which is far below the critical micelle concentration (0.25% by weight). For water-soluble surfactants, only reflectivity measurements yield structural information on the molecular level, which we now describe in some detail.

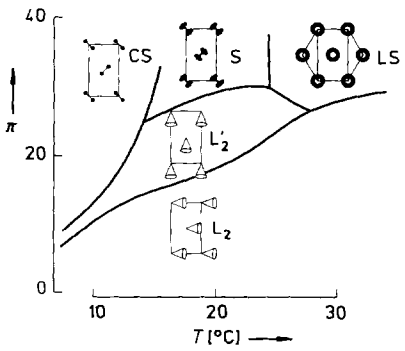

Fig. 21. π–T phase diagram of docosanoic acid ($C_{21}CO_2H$, also called behenic acid) monolayers over pure water. See text for an explanation of the structures.

Neutron reflectivity measurements (Fig. 22a) performed on a soluble surfactant, decyltrimethyl ammonium bromide (DTAB) at the air–solution interface[53] provide some information on the self-organization of the system. They indicate a vertical alignment of DTAB molecules, yielding a layer thickness of about 16 Å for concentrations varying from 0.002 to 0.01 M. Since the extended chain plus head group is about 17 Å thick, the molecules are assumed to lie in one layer as shown in Figure 22b. At a concentration of 0.05 M, where the monolayer is essentially complete, the reflectivity measurements yielded a film thickness of about 21 Å. This was explained in terms of a staggered arrangement reducing the electrostatic repulsion (Fig. 22b, bottom).

X-ray reflectivity measurements of norleucine solutions and surface tension measurements of several hydrophobic α-amino acids (for example, leucine, valine, isovaline, phenylalanine) and α-amino octanoic acid suggested accumulation of the molecules at the air–water interface.[5] Concrete evidence for organized 2D clusters of these molecules at the air–water interface was obtained by crystallization experiments:[5] they promote formation of α-glycine crystals at the water surface and growth through specific faces. The occurrence of these faces can be controlled by choosing the additive; thus a direct correlation is established between organized aggregates of the hydrophobic α-amino acid at the surface and the face of α-glycine through which the crystal grows.

If these short-chain hydrophobic α-amino acids spontaneously aggregate at the interface, Langmuir monolayers such as palmitoyl-lysine (PL) and "perfluoro"aspartate (PFA), which also induce α-glycine crystallization, should behave similarly. PL in the uncompressed state at room tem-

perature did not yield any diffraction signal.[25] But uncompressed PL with an average molecular area 10–15 times greater than its molecular area in the compressed state induced oriented crystallization of α-glycine, suggesting ordered monolayer domains.[3b, 3c] Apparently these domains at room temperature are too low in coherence length to be detected by surface diffraction. In contrast, as mentioned earlier, self-assembled crystalline domains of PFA were detected by GID with only 50% surface coverage. The fluorine

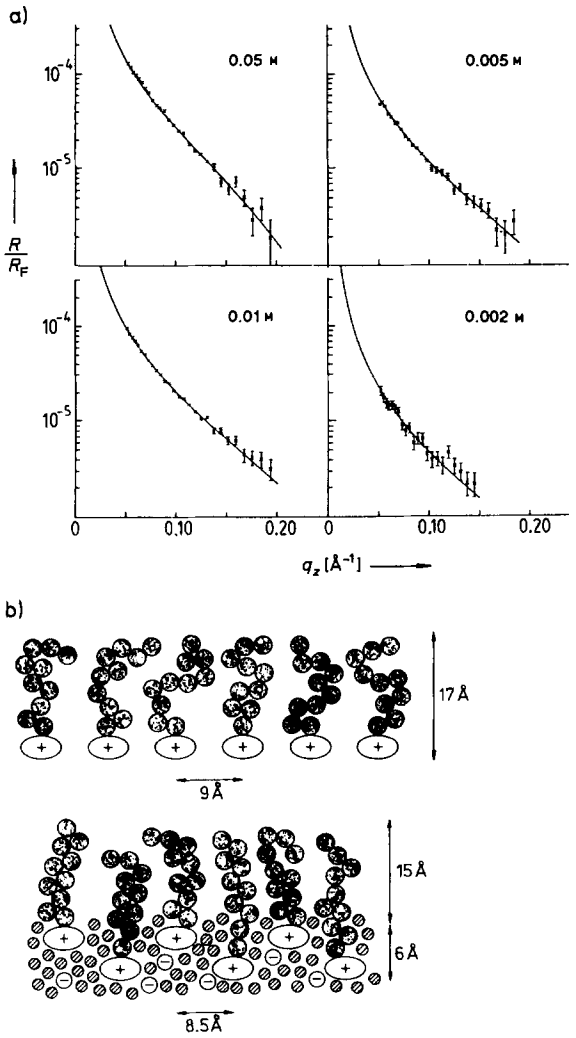

Fig. 22. a) Observed neutron specular reflectivity profiles of fully deuteriated DTAB in contrast matched water, for different concentrations, and the theoretical model fitted thereto ([53a]). b) Model for the distribution of water and DTAB ions at the air–solution interface. Top: Configuration of the molecules within the adsorbed layer at concentrations of 0.01 M or less. Bottom: The surface layer at 0.05 M, deduced from isotopic substitution neutron measurements ([53a]). ◉ = CH_2 and CH_3 of the carbon chain, ◎ = water molecules, ⊕ = head group $+N^+-CH_3$).

atoms, which induce a helical conformation in long fluorocarbon chains,[55] render these chains stiffer than aliphatic hydrocarbon chains and lower the possibility for conformational disorder. Hence, Langmuir monolayers of fluorinated molecules were characterized by a higher crystallinity than their hydrocarbon counterpart. GID data of fluorinated monolayers of PFA[30a] and $C_{10}F_{21}CH_2CO_2H$[56] suggested the coexistence of crystalline and dilute disordered phases; in dilute phases the PFA molecules have a molecular area of about 100 Å^2 and $C_{10}F_{21}CH_2CO_2H$ molecules an area of 2000 Å^2, indicating a gaseous state. This result may be compared with results obtained for arachidic acid monolayers ($C_{19}CO_2H$) at room temperature and at low surface pressure[47] where in the tilted solid phase the molecular area is 24 Å^2; this phase coexists with a fluid phase of molecular area 31 Å^2.

Lowering the temperature has considerably enhanced the tendency for high crystalline order in the uncompressed state, presumably by reducing molecular motion and so enabling effective intermolecular interactions. Low temperature GID studies were performed on several monolayers C_nX with different head groups X, such as $C_{23}OH$, $C_{30}OH$, $C_{31}OH$, $C_{29}CO_2H$, $C_{19}CONH_2$, and $C_{19}CONHC_2H_4CO_2H$. The probable packing characteristics of these spontaneously formed crystallites were extracted from the GID data.[48] We present here a brief description of the packing arrangements of the alcohols (X = OH), the acid (X = CO_2H) and the amide (X = $CONH_2$) monolayer. These packings were deduced by taking advantage of the known 3D crystal structures of molecules with long hydrocarbon chains. This strategy is meaningful since these 3D structures can be described as stacks of layers of molecules; thus the molecular arrangement in a single layer may well resemble that of the monolayer.

Long-chain alcohols and acids possess layered 3D crystal structures. In each layer the molecules are related by a glide so that neighboring hydrocarbon chains have parallel mean axes, but are in a mutually perpendicular orientation when viewed down the mean axis; the arrangement is described as orthorhombic orthogonal.[52] Common to all these structures are the parameters of the orthorhombic subcell, which is a projection of the unit cell onto a plane perpendicular to the molecular axis.[52] The subcell may be regarded as rectangular with dimensions $a_s = 4.98$, $b_s = 7.42$ Å, corresponding to a cross-sectional area of 18.48 Å^2. Remarkably, the calculated 2D cells of the monolayers projected onto a plane perpendicular to the molecular axis perfectly match the orthorhombic subcell of the 3D crystal structures. Following this observation and the diffraction data analysis, it was deduced that the alcohol and the acid monolayer molecules appear in the orthorhombic orthogonal packing, that is, they are related by a glide in a primitive rectangular cell as shown in Figure 23a and 23b. In this arrangement, the hydrogen atoms of adjacent hydrocarbon chains intermesh, thus ensuring close packing of the chains.[52] Further, the molecular chain axis is parallel to the glide plane so that intermolecular contacts between methylene CH_2 groups of the glide-related molecules are the same along the chains.

In 3D crystal structures of long-chain primary amides,[57] the interactions between the molecules are controlled by a network of hydrogen bonds at the $CONH_2$ head groups. The same feature applies to the motif proposed for the monolayer crystallites. The chains are stacked by translation with the molecular axis tilted at an angle of 18° to the normal to the *ab* plane (which is parallel to the water surface) in the direction of the 4.69 Å translation axis (Fig. 23c). The molecules are related by translation in a *c* centered rectangular cell. Thus, the monolayer space group is *c*1. The exact molecular orientation is determined by the fact that the $CONH_2$ amide

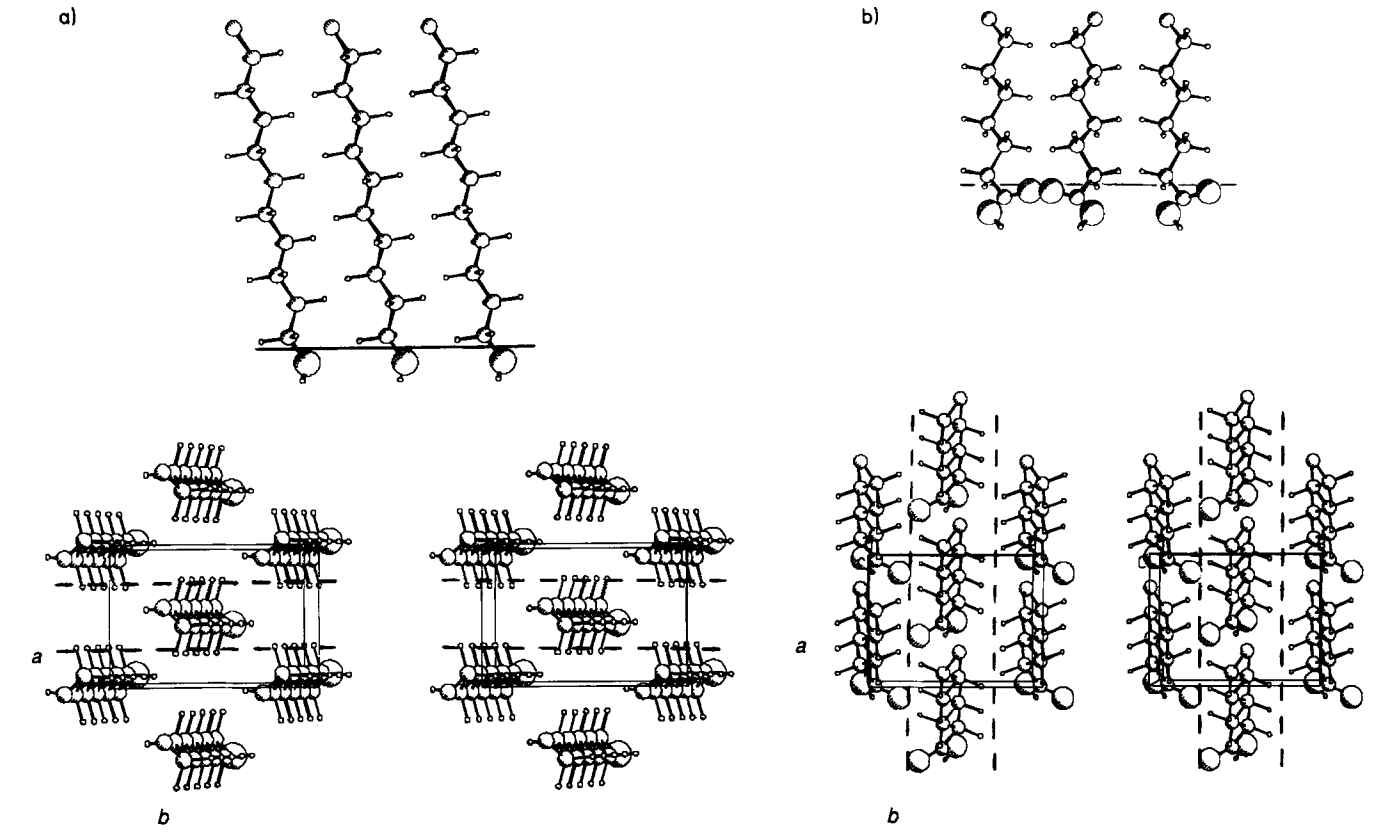

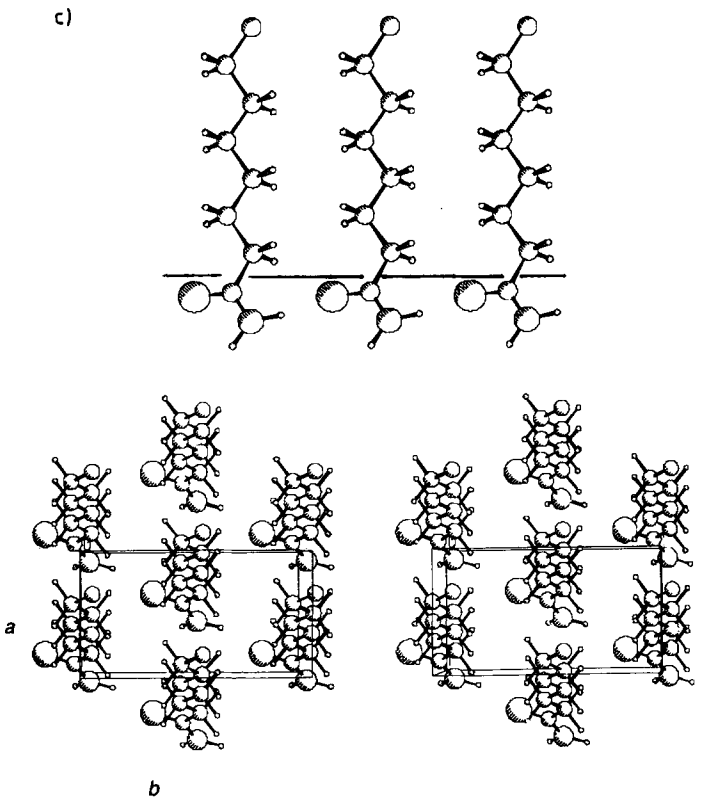

Fig. 23. Models of the hydrocarbon chain packing in the alcohol, carboxylic acid, and amide crystallites formed at 5 °C over pure water. Bottom: Stereoscopic view of the packing arrangement, seen perpendicular to the water surface; top: a side view along a direction parallel to the water surface (indicated by a solid line). For clarity only the head group and maximally eleven methylene groups CH_2 of each molecule are shown. On the last carbon atom drawn the hydrogen atoms are omitted. The rectangular cell (a,b) is indicated. The glide symmetry elements, when present, are shown as dashed lines. For convenience the origin of the unit cell is placed halfway between adjacent glide planes. a) Alcohol monolayers ($n = 23, 30, 31$). Since the molecules are tilted along the b axis ($t = 9.5°$), the projected cell down the mean molecular axis onto the water surface is given by $a_s = 4.99$ Å, $b_s = 7.53$ Å $\cos 9.5° \approx 7.43$ Å. b) Triacontanoic acid monolayer C_nCO_2H ($n = 29$). Since the molecules are tilted along the a axis ($t = 26.8°$), the projected cell down the mean molecular axis onto the water surface is given by $a_s = 5.53$ Å $\cos 26.8° \approx 4.94$ Å, $b_s = 7.44$ Å. c) Arachidamide monolayer ($n = 19$). Here $t = 18°$, $a = 4.69$, $b = 8.69$ Å.

groups form NH $\cdots$ O hydrogen bonds parallel to the diagonal (**a** $\pm$ **b**) (Fig. 23c).

The positional correlation lengths of all the crystallites were found to be anisotropic;[48] they extend over only 35 to 95 spacings parallel to the molecular tilt direction, but over 135 to 270 spacings perpendicular to it. These results suggest that the monolayer crystallites are strips elongated perpendicular to the molecular tilt direction. The same observation was made in the L_2 phase of behenic acid[47] (cf. Fig. 21 and the related discussion). It would be interesting at this point to understand the relationship between the amphiphilic structure and the monolayer crystal morphology.

4. Influence of Ions and Solutes on Monolayer Organization

4.1. Solute Binding and Its Effect on Growth and Dissolution of Monolayers

The binding of solute molecules to hydrophilic groups of monolayers allows us not only to probe the solutes effect on the growth, stability, and dissolution of 2D crystals, but also

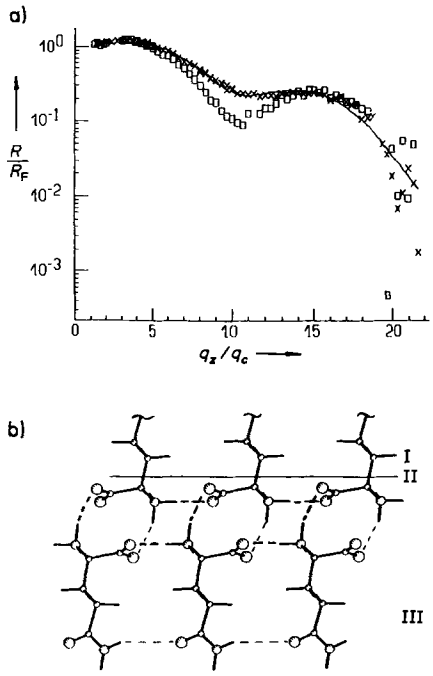

Fig. 24. a) Reflectivity data of compressed monolayers of (*R*)-PL over water (□) and over an unsaturated solution of (*S*)-glutamine (0.137 M, ×). b) A model of surface enrichment of glutamine at the interface (II). Only a short segment of the hydrophobic chains (I) are represented. Hydrogen bonding (– – –) between amide groups of neighboring glutamine molecules, and between the glutamine layer (III) and the monolayer is shown.

to simulate interactions between the surface of a 3D crystal and solvent or solute molecules.

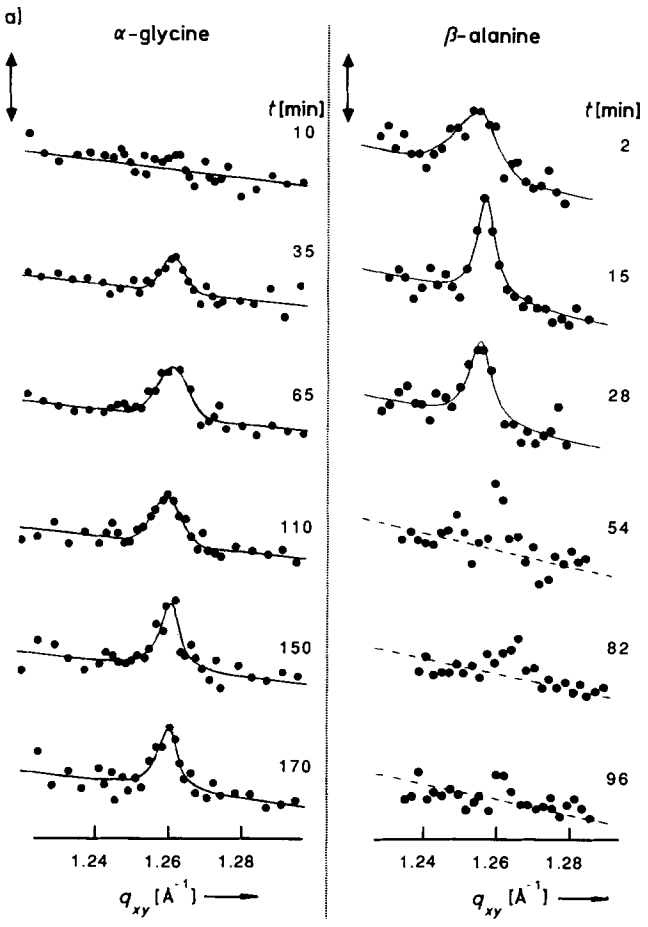

To date it has not been possible to monitor the process of nucleation and crystallization of layered 3D structures such as α-glycine or other amino acids from the air–water interface. But it is possible, with unsaturated solutions of these compounds, to show that the solute binds to the monolayer in a way that mimics the formation of the nucleating crystal's first layer. Indeed, XR studies showed that even in unsaturated solutions of amino acids, the solute molecules bind to the interface. Reflectivity measurements were made on monolayers of PL over a dilute aqueous solution of glutamine $NH_2COC_2H_4CH(NH_3^+)CO_2^-$.[40] Advantage was taken of the possibility that glutamine may bind to the monolayer through NH···O bonds as well as to neighboring glutamine molecules by NH···O (carboxylate) and NH···O=C (amide) hydrogen bonds (Fig. 24b). The reflectivities of a monolayer of palmitoyl-(*R*)-lysine over the solution or over pure water are quite different (Fig. 24a). Analysis of the two data sets shows that as many as a quarter of the sites below the head groups are occupied by glutamine. The result is in qualitative agreement with the model shown in Figure 24b.

Addition of a solute to the subphase can deter crystalline self-aggregation of monolayers, allowing its growth to be monitored as a function of time. The left part of Figure 25a shows that 10 minutes after a PFA monolayer was deposited over an unsaturated solution of α-glycine, no diffraction peak was observed. This is in contrast to the observation made when PFA was deposited over a pure water subphase.[30] It took around 30 minutes before crystalline domains could be detected. This inhibition can be understood from the top part of Figure 25b, which shows how one glycine molecule can bind to two neighboring molecules of the α-amino acid monolayer with very strong hydrogen bonds, hindering their assembly. The formation of this complex is in kinetic competition with that of the crystalline

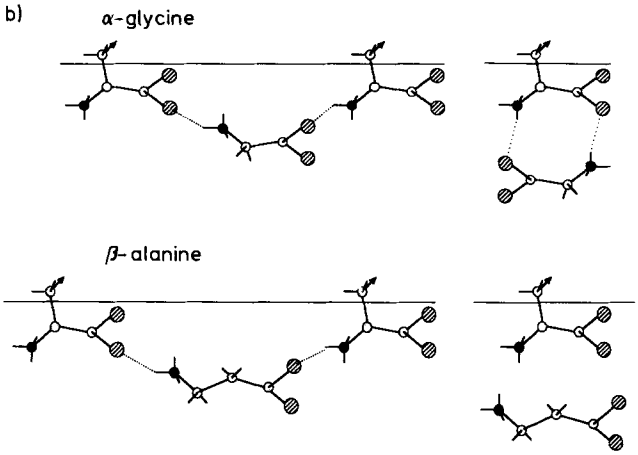

Fig. 25. Uncompressed monolayer ($\pi = 0\ mN\,m^{-1}$) of PFA with an average molecular area of 45 Å^2 over various solutions. a) GID measurements as a function of time after spreading. Left: Over α-glycine solution (0.015 M). Right: Over β-alanine solution (0.005 M). Note the increase in crystallinity in the former, and the decrease in the latter as indicated by the different time evolution of the peak. The length of the double-sided arrow represents 200 counts. b) Left: Schematic drawings of "bridging complexes" between PFA monolayer molecules and the solute molecules for α-glycine (top) and β-alanine (bottom). Right: A potential quasidimer is illustrated for α-glycine, while the mismatch is depicted for β-alanine. ◍ = O, ○ = C, ● = N, – – – = hydrogen bonds, → = hydrophobic chains.

hydrogen-bonded bilayer which is composed of quasi-cyclic dimers of PFA and α-glycine (Fig. 25b, top right). That this bilayer is eventually formed is deduced from the following observations: firstly, glycine forms oriented crystals attached to monolayers of PFA, denoting formation of a bilayer at the onset of crystallization;[3] secondly, monolayers of PFA over glycine solutions maintain their crystallinity after compression and decompression, unlike PFA over pure water;[30b] finally X-ray reflectivity measurements of monolayers of PL over glycine solutions showed that the glycine molecules accumulate at the interface,[40c] which is indirect evidence for the formation of an incomplete bilayer, as in the experiment with glutamine.

Use of β-alanine NH_3^+-CH_2CH_2-CO_2^- instead of glycine as a solute molecule had an entirely different effect on the 2D crystals of uncompressed PFA; this amino acid did not strongly inhibit growth, but caused a complete dissolution of the PFA crystals within two hours as shown by GID measurements (Fig. 25a, right). This dissolution can be rationalized in terms of a strong interaction of β-alanine with the amino acid head groups of adjacent surfactant molecules leading to a disruption of the 2D crystal (Fig. 25b, bottom). It is noteworthy that because of a molecular mismatch, β-alanine can hardly form a hydrogen-bonded cyclic dimer with the amino acid head group of the monolayer and certainly not a hydrogen-bonded counterlayer commensurate with the monolayer, as can glycine (Fig. 25b, bottom).

4.2. Ion Binding from Solution

The interfacial region between a charged surface and an electrolyte is central to many processes such as those occurring during electrodeposition, ion transport through biological membranes, preparation of Langmuir–Blodgett films,[6] biomineralization,[4] and induced oriented nucleation of inorganic systems[3c, 3d] under Langmuir monolayers. X-ray reflectivity measurements demonstrated that metal ions in the solution interact closely with the charged monolayer head groups at the interface.[28, 58] However, it was still an open question whether the ion distribution near such charged, ordered surfaces was crystalline. In a recent study,[24b] the interface between a phospholipid monolayer and a $ZnCl_2$ aqueous solution was measured with X-ray standing waves. The technique, described in Section 2 is sensitive to the ion distribution normal to the surface and allows the distinction between a vertically nondiffuse ionic layer (Helmholtz model) and diffuse ionic layers (Gouy–Chapman and Stern models). It was concluded that the double layer at the phospholipid membrane–aqueous interface is diffuse along the

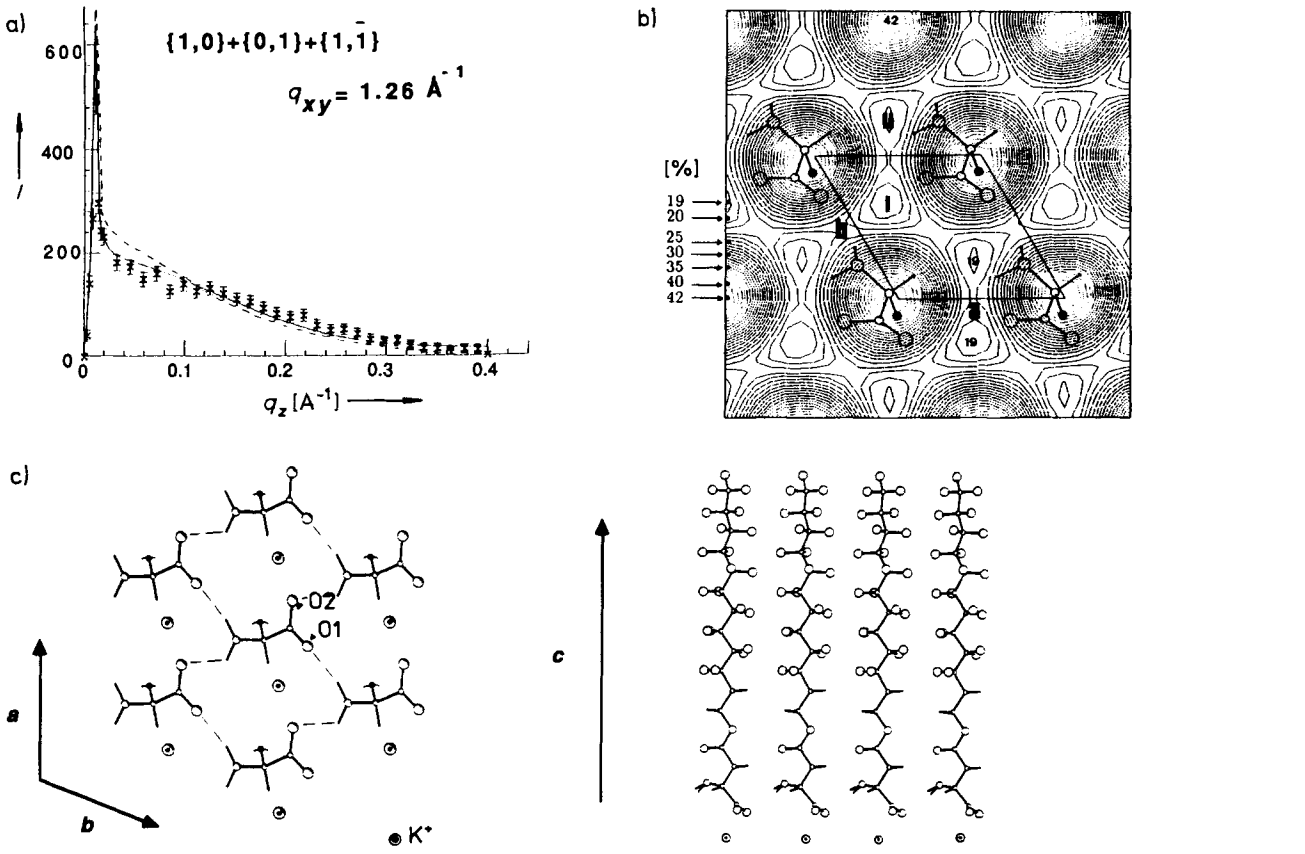

Fig. 26. Uncompressed PFA monolayers over KOH subphases (pH = 11.5; room temperature; π = 0 mN m^{-1}). a) Bragg rod scan measured on the GID peak (whose reflection assignment and position is indicated) with a calculated fit including (solid line) and excluding (dashed line) the contribution of K^+ ions. b) *R*-factor contour map (interval 1%), which expresses the fit between the calculated and observed data, obtained from BR fits as a function of the lateral position of the K^+ ion in the PFA hexagonal unit cell at a fixed *z* coordinate. The two sites with the lowest *R* factors (19%) labeled I and II are potential sites for the K^+ ion. The model (Fig. 26c) favors site I for the K^+ ion. c) Model of the uncompressed monolayer of PFA over K^+ ions. Left: View along the *c* axis (perpendicular to the monolayer) showing the hexagonal net of K^+ ions bridging the oxygen atoms O1 and O2 of two neighboring molecules. Right: View along the *a* axis showing the attached layer of K^+ ions (water molecules possibly interleaved in the ionic layer are not shown here).

normal to the film. GID measurements of lead–arachidate[59] monolayers at room temperature did not demonstrate the existence of laterally ordered or nondiffuse layers of Pb^{2+} counterions. Liquid surface EXAFS experiments on manganese–stearate films[22] at room temperature yielded a Mn–Mn nearest neighbor distance at the surface in the compressed phase only, indicating at least short-range order.

A weak indication of lateral order of ions is provided by GID data of uncompressed monolayers of PFA over a HCl solution[30a] at a pH of 1.5. A model was proposed in which the Cl^- ions were partially intercalated between neighboring NH_3^+-CHR-CO_2H sites, participating in attractive $NH^+ \cdots Cl^-$ and $COH \cdots Cl^-$ interactions. This model also explains the high molecular area of 31.6 Å^2, compared to the value of 28.5 Å^2 over basic subphases (discussed below), which imposes a tilt of the molecule of 25° from the vertical according to the GID data. The model is also in keeping with the observation that in 3D crystals of glycine · HCl, the molecules appear in a layered arrangement with intercalated Cl^- ions.[60]

PFA monolayers on highly basic KOH subphases (pH = 11.5) yielded results favoring a laterally ordered bilayer.[30a] The presence of the K^+ ions induces all molecules to be assembled into crystals even in the uncompressed state, with the molecules aligned vertically in a hexagonal cell. According to an analysis of the GID data (Fig. 26a,b), the K^+ ions occupy ordered sites bridging oxygen atoms of adjacent molecules (Fig. 26c). The XR measurements on compressed monolayers at high pH over KOH indicate excess electron density just below the head group. This excess density is consistent with one K^+ ion and one H_2O molecule per head group. Upon compression, lateral pressure introduces defects in the randomly oriented islands, causing a reduction in crystallinity. It is possible that the distortion occurs at the periphery of the crystallites due to strong electrostatic interperipheral forces between anion–cation bilayers of neighboring crystallites. It is noteworthy that in both systems, PFA over acidic and basic subphases, the counterions retain the original molecular packing and a long-range crystalline order is maintained after decompression. This is in contrast with results for films over pure water.[30a]

As mentioned earlier, lowering the temperature has the effect of reducing molecular rotational disorder and enhancing crystalline self-aggregation. Indeed, a GID study of uncompressed cadmium arachidate monolayers over a subphase with its pH adjusted to 8.8 with ammonia demonstrated the presence of an ordered Cd^{2+} layer[61] with a coherence length of 1000 Å at temperatures lower than 9 °C. The diffraction spectrum showed ten distinct peaks (Fig. 27), seven of which were attributed to the Cd^{2+} layer. The remaining three peaks were deduced to stem from the arachidate layer, on the basis of their Bragg rod profiles and q_{xy} positions. The diffraction peaks of the Cd^{2+} lattice, whose BR profiles were flat and extended, indicative of a thin monoatomic layer, could be indexed according to a 2 × 3 supercell of the arachidate cell. Such a supercell demands three cadmium ions, given a 1:2 molar ratio of cadmium ions to acid molecules. The two lattices are shown in Figure 27c. The calculated diffraction peaks due to the refined positions of three Cd^{2+} ions in the supercell are shown in Figure 27b. In contrast to films of cadmium arachidate, a film of calcium arachidate

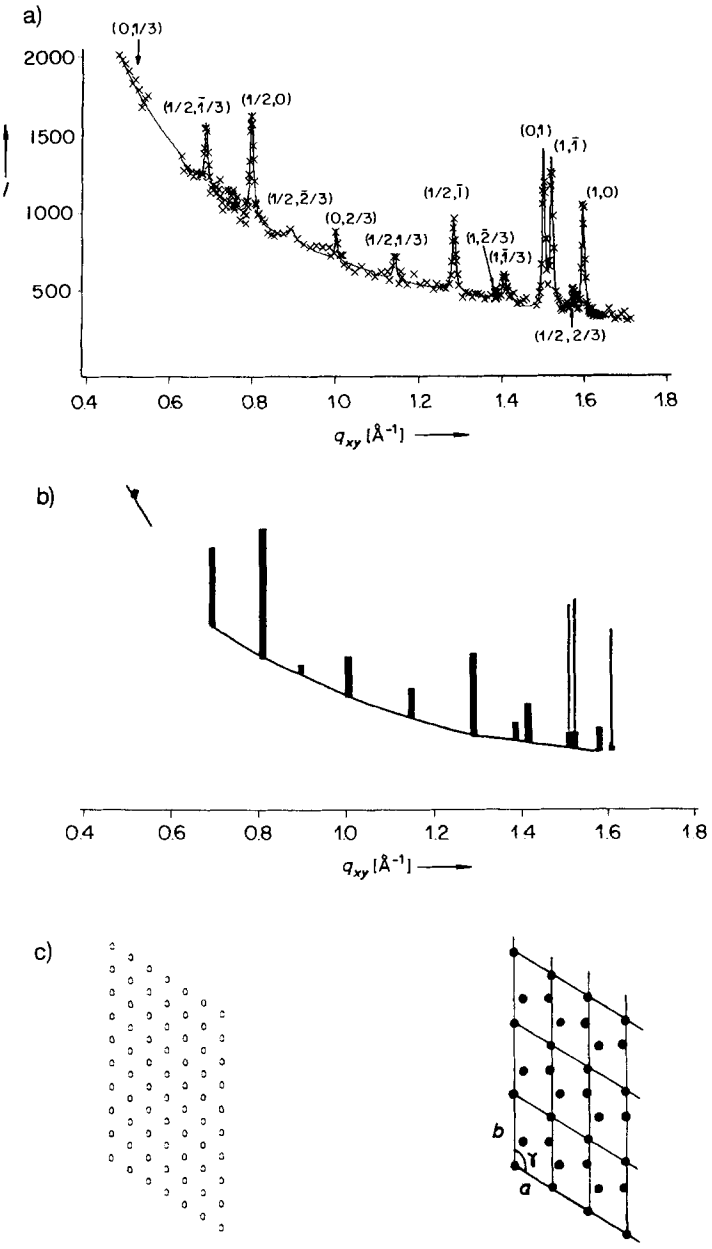

Fig. 27. Arachidic acid monolayer ($C_{19}CO_2H$) over a 10^{-3} M $CdCl_2$ subphase (pH = 8.8) in the uncompressed state ($\pi = 0$ mN m^{-1}) and at low temperature (9 °C). a) GID peaks and assignment of reflections. Reflections with integer indices correspond to scattering arising from arachidate moities, and those with fractional indices to scattering from a 2D layer of Cd^{2+} ions. b) Calculated powder pattern for the cadmium net superimposed on background scattering. The peaks labeled with thin lines are the arachidic triplet. c) Two-dimensional lattices of arachidate (left) and cadmium ions (right). The cadmium cell is a 2 × 3 supercell of the arachidate cell. The positions of the Cd^{2+} ions in the cell are marked as filled circles.

over water at low temperatures did not provide direct evidence for an ordered Ca^{2+} layer.[62] Nevertheless, the Ca^{2+} ions did induce high crystallinity of the uncompressed phase at high pH; the molecules were aligned vertically. These results agree with the conclusions of a recent surface-potential and surface-pressure study of ionic interactions with fatty acid monolayers:[63] whereas monolayer ordering is induced by covalent binding between carboxylate (CO_2^-) and metal ions in the case of Cd^{2+}, Ca^{2+} ions do not exhibit such an ordering effect because their interactions with carboxylates are mainly ionic in nature. The adsorption of ions at the

monolayer molecules and the resulting structural variations in the monolayer were also studied recently by GID.[64] The structural changes in henicosanoic acid monolayers induced by the introduction of Cu^{2+} or Ca^{2+} ions into the subphase were investigated.

5. Transfer of Structural Information from Langmuir Monolayers to Crystals

Langmuir monolayers have been shown to induce oriented crystallization from solution of proteins[65, 66] and other organic and inorganic compounds.[3] As mentioned in the introduction, these studies were motivated by their revelance to crystal nucleation, to two-dimensional ordering at the water surface of soluble hydrophobic molecules, and to biomineralization. The crystal systems studied to date include α-glycine,[3a] sodium chloride,[3c, 3d] calcium carbonate,[4a-d] parahydroxybenzoic acid,[67], hexagonal ice,[68] barium sulphate,[69] and silver propionate.[70] Mechanisms for crystallization through particular faces (oriented crystallization) involve structural fits and electrostatic attractions. Information on the monolayers used and the type of crystal face nucleated are listed in Table 2 for some of these crystal systems.

5.1. Inorganic Crystals and Biomineralization

Electrostatic interactions between Langmuir monolayers and crystals have been invoked to account for the oriented growth of inorganic salts. A first example is given by the oriented nucleation of NaCl crystals under α-amino acid monolayers such as PFA. NaCl precipitates from aqueous solution in a cubic cell ($a = 5.64$ Å) exhibiting six (100) faces. But when crystallized under α-amino acid monolayers at pH ≈ 7, crystals were found to be attached to the monolayer by the less stable (110) face (Fig. 28a).[3d, 30] This face is composed of alternating rows of Na^+ and Cl^- ions, separated by 2.82 Å. This distance is very close to the separation of 2.8 Å between rows of NH_3^+ and CO_2^- moieties in PFA. Thus we envisage an electrostatic attraction between small domains of a (110) surface layer of NaCl and the zwitterionic α-amino acid head groups of PFA at pH ≈ 7. At high pH (>10), PFA monolayers induce crystallization of NaCl from the metastable (111) face. A pure (111) face of NaCl exposes a singly charged layer consisting entirely of either Na^+ or Cl^- ions (Fig. 28b). This selectivity was explained in terms

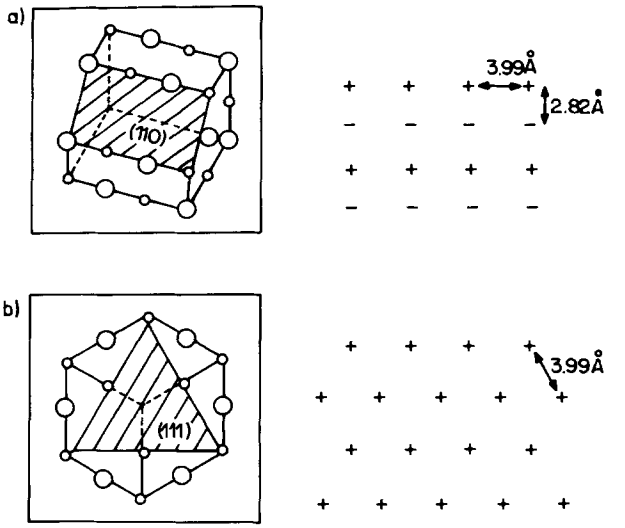

Fig. 28. Schematic representation (left) and point charge distribution (right) of faces of a NaCl crystal. a) The (110) face. b) The (111) face. o = Na^+, ○ = Cl^-.

of a simple electrostatic interaction between the CO_2^- charged monolayer surface and an underlying layer of Na^+ ions which induces a homogeneous surface potential for (111) nucleation. The lattices of the PFA monolayer and the (111) layer are not similar. There is a possibility of interleaving ordered water in the first attached layer of Na^+ ions, which could play a role in inducing oriented nucleation of the (111) face since OH groups can form OH···Cl^- hydrogen bonds with Cl^- ions in the second layer.[60]

As mentioned earlier, GID results on PFA monolayers over HCl solution at low pH was interpreted in terms of a partial intercalation of Cl^- ions within the head-group layer.[30] Thus, rows of positive (NH_3^+) and negative (Cl^-) charges are created at the surface, simulating the repeat mo-

Table 2. 3D crystals induced by monolayers at the air–water interface

3D Crystal	Monolayer[a]	Nature of Binding	Crystal Face	Ref.
NaCl	acids and α-amino acids			
High pH	RCO_2^- H_2N-CHR-CO_2^-	electrostatic binding, no match	(111) metastable charged face	[3c–d], [30a]
Neutral pH	$H_3\overset{+}{N}$-CHR-CO_2^-	electrostatic binding, partial match	(110) face, less stable than normal (100)	
$CaCO_3$	acids RCO_2H amines RNH_2	electrostatic binding, partial match for calcite	Calcite: (1$\bar{1}$0) face, vaterite: (0001) face Vaterite: (0001) and (110) faces	[4a–d]
α-Glycine $H_3\overset{+}{N}$-CH_2-CO_2^-	α-amino acids $H_3\overset{+}{N}$-$\overset{*}{C}$HR-CO_2^-	NH···O hydrogen bonds, structural match	(010) chiral face, not well developed in H_2O	[3]
Para-hydroxybenzoic acid monohydrate HO_2C-C_6H_4-OH + H_2O	alkoxybenzoic acid HO_2C-C_6H_4-OR	interlayer contacts induce a structural match	(401) face, not well developed in H_2O	[67]
Ice	alcohols ROH	OH···O hydrogen bonds, lattice plus structural match	(0001) hexagonal face	[68]

[a] R is a long chain alkyl group of general formula C_nH_{2n+1}.

tif of the charge distribution in the (110) face. Indeed, at low pH, NaCl crystallizes from its (110) face attached to the PFA monolayer.[30]

The influence of structured organic surfaces on oriented growth has a strong bearing on biomineralization.[*] Addadi, Weiner, and co-workers[4e] have studied the effect of β-pleated sheet proteins on crystallization of calcite. They demonstrated oriented calcite nucleation probably arising from a combination of electrostatic and structural requirements. To elucidate this result on a molecular level, Mann and co-workers studied the induced oriented crystallization of $CaCO_3$ under monolayers of stearic acid[4a, 4b] and other amphiphiles such as amines.[4c, 4d] Whereas crystallization of $CaCO_3$ in the absence of a monolayer of acid or amine results in rhombohedral calcite crystals, the stearic acid monolayers give rise to oriented nucleation of the less stable hexagonal polymorph of vaterite from the (001) face. We present here a model for the interface, based on the crystallization results of NaCl below a monolayer and the structural data of cadmium arachidate and calcium arachidate monolayers. The double layer comprising the stearic acid molecules and the calcium ions must be neutral, implying a 2:1 stochiometry as confirmed by X-ray and neutron reflectivity studies of the fatty acids over $CaCl_2$ and $CdCl_2$ solutions.[28, 58] Thus the repeat area per Ca^{2+} ion must be twice that of the stearic acid molecule. As mentioned earlier there is as yet no direct evidence of order in a layer of Ca^{2+} counterions. The density of such a Ca^{2+} layer is low and we may assume at least one to two interleaving water molecules per Ca^{2+} ion, which is consistent with X-ray reflectivity data.[28, 62] The water molecules would screen neighboring Ca^{2+} ions and form $OH\cdots O$ hydrogen bonds with the monolayer carboxylate groups CO_2^- above and carbonate ions CO_3^{2-} below the Ca^{2+} layer (Fig. 29a). According to GID data of calcium arachidate,[62] the arachidate molecules stand up straight even in the uncompressed state. Thus, the orientation of the CO_2^- groups is similar to that of the CO_3^{2-} groups in vaterite.

The hydrogen-bonded $OH\cdots OCO_2^{2-}$ system tends to be coplanar as in the crystal structure of $Na_2CO_3 \cdot 3/2\ H_2O_2$.[80] This preference would promote bound carbonate molecules oriented perpendicular to the Ca^{2+} layer. Vaterite has a crystal structure with carbonates oriented in this way (Fig. 29b), while the orientation of the carbonates in the calcite structure is different. This may account for the preferred nucleation of vaterite.

An alternative model for the preferential formation of vaterite involving an epitaxial relationship between the (001) face of vaterite and the 2D lattice of calcium stearate appears to be plausible since the *a* and *b* axes of vaterite are 7.15 Å, approximately 1.5 times the length of the *a* and *b* axes of the calcium arachidate monolayer. On such a basis, one may envisage a supercell common to both layers which is a 2×2 reconstruction of the vaterite lattice and a 3×3 reconstruction of the arachidate lattice. In such a cell, although the net charge brought in by the nine carboxylate groups is -9, the net charge brought in by the twelve calcium ions is $(+\ 24/2) = +12$ since each calcium ion contributes one charge to the neutralization of the carboxylate layer and one charge to the neutralization of the carbonate layer. There is no simple way to reconcile this charge difference.

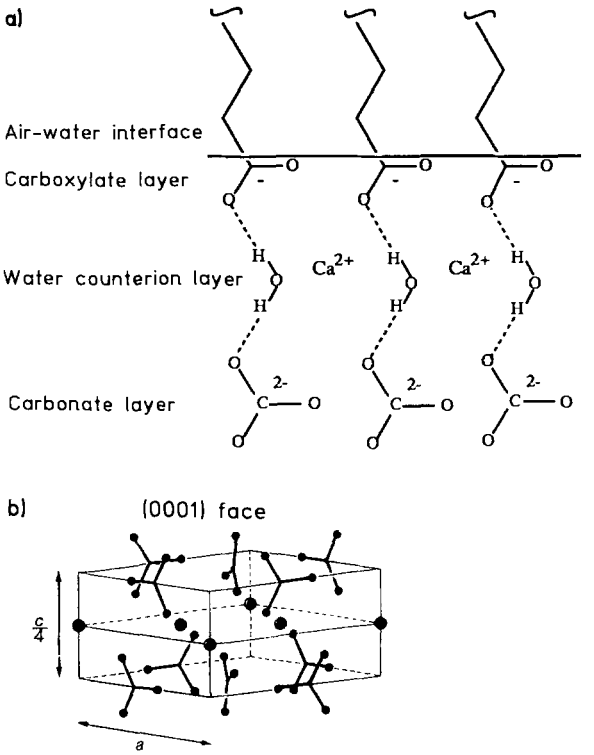

Fig. 29. a) Schematic representation of a calcium stearate monolayer, showing interleaved water molecules in the low density cationic layer which form hydrogen bonds with the carboxylate layer at the interface and with a carbonate layer in the subphase. In this layer the carbonate ions are oriented as in the (0001) layer structure of vaterite. b) Vaterite subcell showing the stereochemical arrangement of the carbonate ions perpendicular to the (0001) face (from [4a]). $a = 7.15$, $c = 17.00$ Å. ● = O atom, ● = Ca^{2+} ion.

5.2. Crystallization of Molecules under Monolayers with a Similar Head Group

An excellent structural fit between the head groups of the monolayer and the attached crystal layer is illustrated by the α-amino acid monolayer/glycine crystal system (Table 2). Glycine crystallizes in a bipyramidal habit (Fig. 30a) from aqueous solution in a monoclinic centrosymmetric arrangement. The glycine molecules form hydrogen-bonded layers (Fig. 30b). Such a layer may be easily replaced by a monolayer of resolved, chiral α-amino acid surfactant molecules provided the cross-sectional area of its hydrophobic chain is not larger than that of glycine (25.5 Å^2). Indeed glycine crystals grow stereospecifically from several α-amino acid Langmuir monolayers whose hydrophobic chains meet the above criterion.[3a, 3b] For example, the packing arrangement of the glycine head groups of the monolayer of PL, whose GID pattern[25] is shown in Figure 15, agrees very well with the layer structure of glycine.

The epitaxial crystallization of *para*-hydroxybenzoic acid (Table 2) under monolayers of *para*-alkoxybenzoic acid provides an example of how molecules in solution impose a change of monolayer structure probably at the onset of crystal nucleation. The *para*-hydroxybenzoic acid head groups of the monolayer change their orientation with respect to the

[*] Editorial comment: also in this issue is a review by L. Addadi and S. Weiner on "Control and Design Principles in Biological Mineralization".

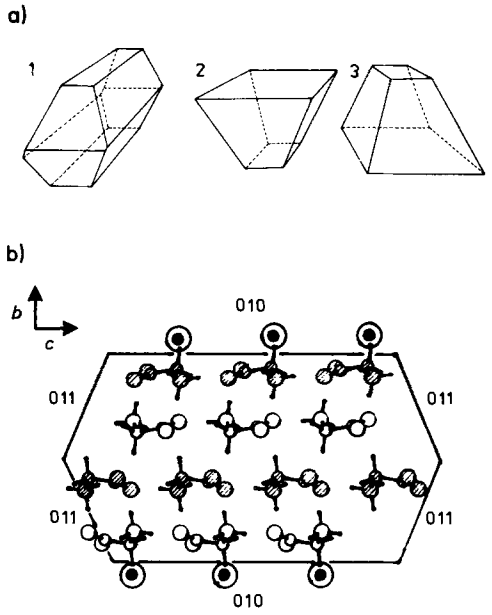

Fig. 30. a) Morphology of the pure α-glycine crystal grown from aqueous solutions (1) and at the monolayer solution interface (2 and 3). b) Crystal structure of α-glycine. An (*R*) α-amino acid monolayer induces the (010) face. An (*S*) α-amino acid monolayer induces the (0$\bar{1}$0) face. The hydrogen atoms of both faces are circled.

hydrocarbon chains so as to lie flat on the water surface, thus mimicking the (401) surface layer of the *para*-hydroxybenzoic acid crystal. It is noteworthy, as in the case of the α-glycine/monolayer system, that the crystals do not exhibit well-developed (401) faces in solution.

5.3. Nucleation of Ice by Monolayers

Pure water can be supercooled to temperatures as low as −40 °C. Therefore the induction or inhibition of the nucleation of ice, in particular through the role of auxiliaries such as membranes or proteins, has far-reaching ramifications for both the living and nonliving world. Promotion of ice nucleation has been exploited for the induced precipitation of rain by clouds seeded with silver iodide.[71] On the other hand, the promotion of ice nucleation by frost bacteria in crops can result in wide scale damage.[72]

Several mechanisms have been proposed to explain the promotion of ice nucleation such as a lattice or structural match between substrate and nucleated ice crystal[73] or an electric field present in the substrate, which orients the water molecules.[74] Experiments were conducted to design two-dimensional surfaces that raise the ice nucleation temperature. These experiments involved freezing of drops of water covered with monolayers of aliphatic alcohols (C_nOH) or carboxylic acids (C_nCO_2H). The structure of hexagonal ice[75] may be described for the oxygen atoms in terms of layers parallel to the *ab* plane where $a = b = 4.5$ Å, $\gamma = 120°$ (Fig. 31). Advantage was taken of the observation that at 5 °C uncompressed Langmuir monolayers of $C_{23}OH$, $C_{30}OH$ and $C_{31}OH$ over water pack in a distorted hexagonal net[48] ($a = b = 4.48$ Å, $\gamma = 113°$) that is similar in dimension to the *ab* lattice of hexagonal ice at 0 °C. The largest mismatch between the two lattices is 10% along the $a + b$ diagonal. The uncompressed monolayer of the carboxylic acid $C_{29}CO_2H$ has axial dimensions[48] $a = b = 4.6$ Å, $\gamma = 107°$. For this system the largest mismatch with ice is, once again, in the $a + b$ direction, but with a value of 27%. A structural similarity can be proposed for the OH head groups of the alcohol monolayer and the *ab* layer structure of ice; however, no such similarity exists for the corresponding carboxyl head groups of the fatty acid monolayer.

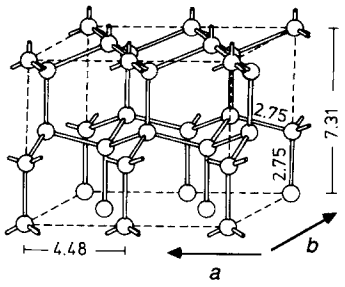

Fig. 31. Crystal structure of hexagonal ice (from [79]). The oxygen atoms of the water molecules are denoted by spheres and the disordered OH···O hydrogen bonds by rods. The hexagonal *a* and *c* axes are specified ($a = b = 4.48$, $c = 7.31$ Å).

The results of the ice nucleation temperature ("freezing point") measurements (Fig. 32) show that aliphatic chain alcohols are more efficient ice nucleators than the corresponding carboxylic acids.[68] Moreover, the freezing point

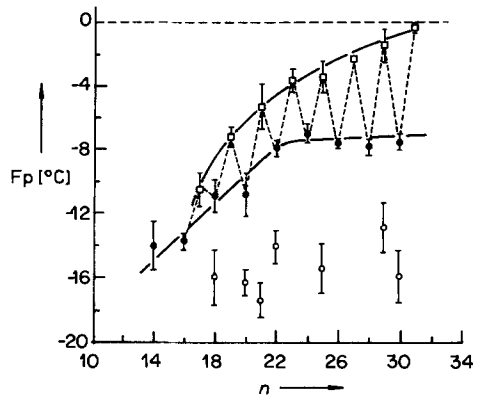

Fig. 32. Freezing points Fp of drops of supercooled water covered by monolayers of alcohols C_nOH (● = *n* even, and □ = *n* odd) and carboxylic acids C_nCO_2H (○). Freezing point curves are drawn separately for alcohols with *n* odd and *n* even. The error bars for each point were derived from 10 to 20 freezing point measurements.

is sensitive not only to chain length but also to chain parity (i.e., *n* odd or even) of the alcohol $C_nH_{2n+1}OH$ (Fig. 32). This trend suggests that at the temperature of ice nucleation the orientations of the alcohol OH groups in the odd and even analogues are not the same.

6. Outlook

The study of structures at interfaces has received an enormous boost with the recent development of surface X-ray diffraction methods using synchrotron radiation. Research in the crystallography of thin organic films should encompass a variety of exotic projects. For example, so far all the studies have been directed towards amphiphilic molecules bearing long hydrocarbon or fluorocarbon chains. With the

present advances in synchrotron techniques, it may soon be possible to obtain diffraction spectra from water-soluble amphiphilic molecules. Experimental results from oriented crystallization, chemical reactivity, and spectroscopic measurements suggest that molecules such as short chain α-amino acids, benzoic acids, or cinnamic acids form ordered clusters at the air–water interface.[5, 76]

The X-ray methods should allow one to test for the presence of lateral crystalline order in monolayers consisting of a collection of molecules engineered to construct a designed and well-defined lattice. Thus, these methods are intimately linked to the development of techniques to control and perfect the structure of Langmuir films on the molecular level. Perhaps we shall obtain a deeper insight into chemical transformation at the air–water interface by correlating the packing structure of reactant and product. An example of the latter is the topochemical photopolymerization of diacetylenes in monomolecular layers as studied by Göbel and Möhwald.[77] Another natural extension of these studies is the investigation of packing arrangements of amphiphilic molecules at organic solvent–water interfaces, as in emulsions. In such a system, the surface created by terminal groups of the hydrophobic chains makes van der Waals contacts with the organic solvent similar to those found for an alkane in a bilayer membrane.

The X-ray methods should in principle also be applicable to complex biological systems at interfaces which may involve enzymatic transformations or antigen–antibody interactions and where periodic order is present. Here we mention the elegant studies by Kornberg,[65] Ringsdorf,[66] and others, who monitored by electron-microscopic and fluorescence methods the dynamics of these interactions. We hope that deeper insight into some of these systems may be obtained by diffraction studies.

So far, most of the experiments had been carried out with "2D powders" at the smooth air–water interface. It is also possible to study the structure of thin organic films deposited on smooth solid supports.[78a] Recently, the structure of self-assembled monolayers on smooth mica coated with gold were determined in great detail.[78b] One may also anticipate, in the not too distant future, obtaining diffraction spectra from single crystals of these amphiphilic molecules and so providing structural information almost at the level of atomic resolution.

We thank Isabella Weissbuch, Ronit Popovitz-Biro, and Susan Weinbach for fruitful discussions. We acknowledge financial support from the German Israeli Foundation, the U.S.A.–Israel Binational Fundation, Jerusalem, the Petroleum Research Fund, the American Chemical Society, the Israel Academy of Sciences, the Danish Foundation for Natural Sciences, and HASYLAB, DESY, Hamburg, FRG for beam time.

Received: January 2, 1991 [A 851 IE]
German version: *Angew. Chem.* **1992**, *104*, 154

[1] I. Langmuir, *J. Am. Chem. Soc.* **1917**, *39*, 1848.
[2] J. D. Swalen, D. L. Allara, J. D. Andrade, E. A. Chandross, S. Garrof, J. Israelachvili, T. J. McCarthy, R. Munray, R. F. Pease, J. F. Rabolt, K. J. Wynne, H. Yu, *Langmuir* **1987**, *3*, 932.
[3] a) E. M. Landau, M. Levanon, L. Leiserowitz, M. Lahav, J. Sagiv, *Nature* **1985**, *318*, 353; b) E. M. Landau, S. Grayer Wolf, M. Levanon, L. Leiserowitz, M. Lahav, J. Sagiv, *J. Am. Chem. Soc.* **1989**, *111*, 1436; c) E. M. Landau, S. Grayer Wolf, J. Sagiv, M. Deutsch, K. Kjaer, J. Als-Nielsen, L. Leiserowitz, M. Lahav, *Pure Appl. Chem.* **1989**, *61*, 673; d) E. M. Landau, R. Popovitz-Biro, M. Levanon, L. Leiserowitz, M. Lahav, *Mol. Cryst. Liq. Cryst.* **1986**, *134*, 323; e) R. Popovitz-Biro, I. Weissbuch, D. Jacquemain, F. Leveiller, L. Leiserowitz, M. Lahav in *Advances in Industrial Crystallization* (Eds.: J. Garside, R. J. Davey, A. G. Jones), Butterworth-Heinemann, Oxford, **1991**, p. 3.
[4] a) S. Mann, B. R. Heywood, S. Rajam, J. D. Birchall, *Nature* **1988**, *334*, 692; b) S. Mann, *ibid.* **1988**, *332*, 119; c) S. Rajam, B. R. Heywood, J. B. A. Walker, S. Mann, R. J. Davey, J. D. Birchall, *J. Chem. Soc. Faraday Trans.* **1991**, *87*, 727; d) B. R. Heywood, S. Rajam, S. Mann, *ibid.* **1991**, *87*, 735; e) L. Addadi, J. Moradian, E. Shay, N. G. Maroudas, S. Weiner, *Proc. Natl. Acad. Sci. USA* **1987**, *84*, 2732.
[5] a) I. Weissbuch, L. Addadi, Z. Berkovitch-Yellin, E. Gati, M. Lahav, L. Leiserowitz, *Nature* **1984**, *310*, 161; b) I. Weissbuch, L. Addadi, L. Leiserowitz, M. Lahav, *J. Am. Chem. Soc.* **1988**, *110*, 561; c) I. Weissbuch, F. Frolow, L. Addadi, M. Lahav, L. Leiserowitz, *ibid.* **1990**, *112*, 7718.
[6] H. Kuhn, D. Möbius, *Angew. Chem.* **1971**, *83*, 672; *Angew. Chem. Int. Ed. Engl.* **1971**, *10*, 620.
[7] a) L. M. Blinov, N. V. Dubinin, L. V. Mikhnev, S. G. Yudin, *Thin Solid Films* **1984**, *120*, 161; b) T. Richardson, G. G. Roberts, M. E. C. Polywka, S. G. Davies, *ibid.* **1988**, *160*, 231; c) G. G. Roberts, B. Holcroft, A. Barraud, J. Richard, *ibid.* **1988**, *160*, 53.
[8] a) I. R. Girling, P. V. Kolinsky, N. A. Cade, J. D. Earls, I. R. Peterson, *Opt. Commun.* **1985**, *55*, 289; b) J. D. Swalen, *Thin Solid Films* **1988**, *160*, 197; c) W. Groh, D. Lupo, H. Sixl, *Angew. Chem. Adv. Mater.* **1989**, *101*, 1580; *Angew. Chem. Int. Ed. Engl. Adv. Mater.* **1989**, *28*, 1548; *Adv. Mater.* **1989**, 366; d) Y. R. Shen in *New Laser and Optical Investigations of Chemistry and Structure at Interfaces* (Eds.: R. B. Hall, A. B. Ellis), VCH, Weinheim, **1986**, p. 151; e) H. Fuchs, H. Ohst, W. Prass, *Adv. Mater.* **1991**, *3*, 10.
[9] a) G. G. Roberts, K. P. Paude, W. A. Barlow, *Proc. Inst. Electr. Eng.* **1978**, *125*, 169; b) T. Morizumi, *Thin Solid Films* **1988**, *160*, 413.
[10] G. Gaines, *Insoluble Monolayers at the Liquid-Gas Interface*, Interscience, New York, **1966**.
[11] a) T. F. Heinz, C. K. Chen, D. Ricard, Y. R. Shen, *Phys. Rev. Lett.* **1982**, *48*, 478; b) T. Rasing, Y. R. Shen, H. W. Kim, S. Grubb, *ibid.* **1985**, *55*, 2903; c) T. Rasing, G. Berkovic, Y. R. Shen, S. G. Grubb, M. W. Kim, *Chem. Phys. Lett.* **1986**, *130*, 1.
[12] a) D. L. Allara, R. G. Nuzzo, *Langmuir* **1985**, *1*, 52; b) J. Gun, R. Iscovici, J. Sagiv, *J. Colloid Interface Sci.* **1984**, *101*, 201.
[13] a) R. M. Weis, H. M. McConnell, *Nature* **1984**, *310*, 47; b) V. T. Moy, D. J. Keller, H. E. Graub, H. M. McConnell, *J. Phys. Chem.* **1986**, *90*, 3198; c) M. Lösche, E. Sachmann, H. Möhwald, *Ber. Bunsenges. Phys. Chem.* **1983**, *87*, 848; d) C. A. Helm, H. Möhwald, *J. Phys. Chem.* **1988**, *92*, 1262; e) C. M. Knobler, *Science* **1990**, *249*, 870.
[14] M. Lundquist, *Prog. Chem. Fats Other Lipids* **1978**, *16*, 101.
[15] R. W. James, *The Optical Principles of the Diffraction of X-Rays*, Ox Bow, Woodbridge, CT, USA, **1982**.
[16] M. Born, E. Wolf, *Principles of Optics*, MacMillan, New York, **1959**.
[17] a) W. C. Marra, P. Eisenberger, A. Y. Cho, *J. Appl. Phys.* **1979**, *50*, 6927; b) P. Eisenberger, W. C. Marra, *Phys. Rev. Lett.* **1981**, *46*, 1081.
[18] a) G. Vineyard, *Phys. Rev. B* **1982**, *26*, 4146; b) R. Feidenhans'l, *Surf. Sci. Rep.* **1989**, *10*, 105.
[19] J. Als-Nielsen, K. Kjaer, *NATO Adv. Study Inst. Ser., Ser. B* **1989**, *211*, 113.
[20] D. Jacquemain, S. Grayer Wolf, F. Leveiller, M. Lahav, L. Leiserowitz, M. Deutsch, K. Kjaer, J. Als-Nielsen, *J. Phys. Colloq.* **1989**, C7, p. 29.
[21] a) A. Braslau, M. Deutsch, P. S. Pershan, A. H. Weiss, J. Als-Nielsen, J. Bohr, *Phys. Rev. Lett.* **1985**, *54*, 114; b) A. Braslau, P. S. Pershan, G. Swislow, B. M. Ocko, J. Als-Nielsen, *Phys. Rev. A* **1988**, *38*, 2457; c) P. S. Pershan, *J. Phys. Colloq.* **1989**, C7, p. 1.
[22] a) J. M. Bloch, P. Eisenberger, *Nucl. Instrum. Methods Phys. Res. Sect. B* **1988**, *31*, 468; b) J. M. Bloch, *Phys. Rev. Lett.* **1988**, *61*, 2941.
[23] a) B. W. Batterman, *Phys. Rev.* **1964**, *133*, 1759; b) *Phys. Rev. Letts.* **1969**, *22*, 703.
[24] a) M. J. Bedzyk, D. H. Bilderback, G. M. Bommarito, M. Caffrey, J. S. Schildkraut, *Science* **1988**, *241*, 1788; b) M. J. Bedzyk, G. M. Bommarito, M. Caffrey, T. L. Penner, *ibid.* **1990**, *248*, 52; c) H. D. Abruñña, G. M. Bommarito, D. Acevedo, *ibid.* **1990**, *250*, 69; d) A. Ilda, T. Matsushita, T. Ishikawa, *Jpn. J. Appl. Phys.* **1985**, *24*, L 675; e) A. Y. Kazimirov, M. V. Kovalchuk, V. G. Kohn, Acta Crystallogr. Sect. A **1990**, *46*, 649.
[25] S. Grayer Wolf, L. Leiserowitz, M. Lahav, M. Deutsch, K. Kjaer, J. Als-Nielsen, *Nature* **1987**, *328*, 63.
[26] S. Grayer Wolf, M. Deutsch, E. M. Landau, M. Lahav, L. Leiserowitz, K. Kjaer, J. Als-Nielsen, *Science* **1988**, *242*, 1286.
[27] L. G. Parrat, *Phys. Rev.* **1954**, *95*, 359.
[28] K. Kjaer, J. Als-Nielsen, C. A. Helm, P. Tippman-Krayer, H. Möhwald, *J. Phys. Chem.* **1989**, *93*, 3200.
[29] A. Guinier, *X-Ray Diffraction*, Freeman, San Francisco, **1968**, Chap. 5.1.
[30] a) D. Jacquemain, S. Grayer Wolf, F. Leveiller, M. Lahav, L. Leiserowitz, M. Deutsch, K. Kjaer, J. Als-Nielsen, *J. Am. Chem. Soc.* **1990**, *112*, 7724; b) D. Jacquemain, unpublished.

[31] a) J. Als-Nielsen, F. Christensen, P. S. Pershan, *Phys. Rev. Lett.* **1982**, *48*, 1107; b) J. Als-Nielsen, P. S. Pershan, *Nucl. Instrum. Methods Phys. Res.* **1983**, *208*, 545.
[32] J. Als-Nielsen, H. Möhwald in *Handbook of Synchrotron Radiation Vol. IV* (Eds.: S. Ebashi, E. Rubenstein, M. Koch), North Holland, Amsterdam, in press.
[33] J. Als-Nielsen in *Handbook of Synchrotron Radiation Vol. III* (Eds.: S. Ebashi, E. Rubenstein, M. Koch), North Holland, Amsterdam, in press.
[34] J. M. Bloch, M. Sansome, F. Rondelez, D. G. Pfeiffer, P. Pincus, M. W. Kim, P. M. Eisenberger, *Phys. Rev. Lett.* **1985**, *54*, 1039.
[35] S. W. Barton, B. N. Thomas, E. B. Flom, S. Rice, B. Lin, J. B. Peng, J. B. Ketterson, P. Dutta, *J. Chem. Phys.* **1988**, *89*, 2257.
[36] Z. Berkovitch-Yellin, L. Leiserowitz, *J. Am. Chem. Soc.* **1982**, *104*, 4052.
[37] a) C. A. Helm, H. Möhwald, K. Kjaer, J. Als-Nielsen, *Biophys. J.* **1987**, *52*, 381; b) K. Kjaer, J. Als-Nielsen, C. A. Helm, L. A. Laxhuber, H. Möhwald, *Phys. Rev. Lett.* **1987**, *58*, 2224; c) C. A. Helm, H. Möhwald, K. Kjaer, J. Als-Nielsen, *Europhys. Lett.* **1987**, *4*, 697; d) P. Tippman-Krayer, C. A. Helm, H. Möhwald, J. Als-Nielsen, K. Kjaer, *Biophys. J.* **1991**, submitted.
[38] M. Elder, P. Hitchcock, R. Mason, G. G. Shipley, *Proc. R. Soc. London A* **1977**, *354*, 157.
[39] H.-P. Weber, R. K. McMullan, S. Swaminathan, B. M. Craven, *Acta Crystallogr. Sect. B* **1984**, *40*, 506.
[40] a) S. Grayer Wolf, E. M. Landau, M. Lahav, L. Leiserowitz, M. Deutsch, K. Kjaer, J. Als-Nielsen, *Thin Solid Films* **1988**, *159*, 29; b) S. Grayer Wolf, Ph.D. Thesis, The Weizmann Institute of Science, **1991**; c) S. Grayer Wolf, unpublished.
[41] B. Di Blasio, C. Pedone, A. Sirigu, *Acta Crystallogr. Sect. B* **1975**, *31*, 601.
[42] E. Benedetti, C. Pedone, A. Sirigu, *Acta Crystallogr. Sect. B* **1973**, *29*, 730.
[43] M. Mallikarjunan, S. Thyagarajarao, *Acta Crystallogr. Sect. B* **1969**, *25*, 296.
[44] M. S. Lehmann, T. F. Koetzle, W. C. Hamilton, *J. Am. Chem. Soc.* **1972**, *94*, 2657.
[45] J. Donohue, *J. Am. Chem. Soc.* **1950**, *72*, 949.
[46] T. M. Bohanon, B. Lin, M. C. Shish, G. E. Ice, P. Dutta, *Phys. Rev. B* **1990**, *41*, 4846.
[47] R. M. Kenn, C. Böhm, A. M. Bibo, I. R. Peterson, H. Möhwald, K. Kjaer, J. Als-Nielsen, *J. Phys. Chem.* **1991**, *95*, 2092.
[48] D. Jacquemain, F. Leveiller, S. P. Weinbach, M. Lahav, L. Leiserowitz, K. Kjaer, J. Als-Nielsen, *J. Am. Chem. Soc.* **1991**, *113*, 7684.
[49] a) S. Ställberg-Stenhagen, E. Stenhagen, *Nature* **1945**, *156*, 239; b) E. Stenhagen in *Determination of Organic Structures by Physical Methods* (Eds.: E. A. Braude, F. C. Nachod), Academic Press, New York, **1955**; c) A. M. Bibo, I. R. Peterson, *Adv. Mater.* **1990**, *2*, 309.
[50] B. Lin, M. C. Shih, T. M. Bohanon, G. E. Ice, P. Dutta, *Phys. Rev. Lett.* **1990**, *65*, 191.
[51] M. L. Schlossmann, D. K. Schwartz, P. S. Pershan, E. H. Kawamoto, G. J. Kellog, S. Lee, *Phys. Rev. Lett.* **1991**, *66*, 1599.
[52] D. M. Small, *The Physical Chemistry of Lipids, Handbook of Lipid Research Vol. 4*, Plenum, New York, **1986**.
[53] a) E. M. Lee, R. K. Thomas, J. Penfold, R. C. Ward, *J. Phys. Chem.* **1989**, *93*, 381; b) J. E. Bradley, E. M. Lee, R. K. Thomas, A. J. Willat, D. P. Gregory, J. Penfold, R. C. Ward, A. Waschkosky, *Langmuir* **1988**, *4*, 821.
[54] B. Berge, L. Faucheux, K. Schwab, A. Libehaber, *Nature* **1991**, *350*, 322.
[55] D. A. Dixon, F. A. van Catledge, B. E. Smart, *9th IUPAC Conf. Phys. Org. Chem.* **1988**, Abstr. p. A15.
[56] S. W. Barton, F. Rondeley, B. Lin, S. A. Rice, unpublished.
[57] a) J. D. Turner, E. C. Lingafelter, *Acta Crystallogr.* **1955**, *8*, 551; b) L. Leiserowitz, A. T. Hagler, *Proc. R. Soc. London A* **1983**, *388*, 133.
[58] a) R. M. Richardson, S. J. Roser, *Liq. Crysta.* **1987**, *2*, 797; b) M. J. Grundy, R. M. Richardson, S. J. Roser, J. Penfold, R. C. Ward, *Thin Solid Films* **1988**, *159*, 43; c) J. Daillant, L. Bosio, J. J. Benattar, J. Meunier, *Europhys. Lett.* **1989**, *8*, 453.
[59] P. Dutta, J. B. Peng, B. Lin, J. B. Ketterson, M. Prakash, *Phys. Rev. Lett.* **1987**, *58*, 2228.
[60] B. Di Blasio, V. Pavone, C. Pedone, *Cryst. Struct. Commun.* **1977**, *6*, 745.
[61] F. Leveiller, D. Jacquemain, M. Lahav, L. Leiserowitz, M. Deutsch, K. Kjaer, J. Als-Nielsen, *Science* **1991**, *252*, 1532.
[62] F. Leveiller et al., unpublished.
[63] M. Yazdanian, H. Yu, G. Zografi, *Langmuir* **1990**, *6*, 1093.
[64] B. Lin, T. M. Bohanon, M. C. Shih, P. Dutta, *Langmuir* **1990**, *6*, 1665.
[65] E. E. Uzgiris, R. D. Kornberg, *Nature* **1983**, *301*, 125.
[66] a) D. W. Grainger, A. Reichert, H. Ringsdorf, C. Salesse, *FEBS Lett.* **1989**, *252*, 73; b) M. Ahlers, R. Blankenburg, D. W. Grainger, H. Ringsdorf, C. Salesse, *Thin Solid Films* **1989**, *180*, 93; c) M. Ahlers, R. Blankenburg, H. Haas, D. Möbius, H. Möhwald, W. Müller, H. Ringsdorf, H.-U. Siegmund, *Adv. Mater.* **1991**, *3*, 39.
[67] I. Weissbuch, G. Berkovic, M. Lahav, L. Leiserowitz, *J. Am. Chem. Soc.* **1990**, *112*, 5874.
[68] M. Gavish, R. Popovitz-Biro, M. Lahav, L. Leiserowitz, *Science* **1990**, *250*, 973.
[69] S. Mann et al., unpublished.
[70] I. Weissbuch et al., unpublished.
[71] a) B. Vonnegut, *J. Appl. Phys.* **1947**, *18*, 593; b) M. L. Corrin, J. A. Nelson, *J. Phys. Chem.* **1968**, 643.
[72] a) R. C. Schnell, C. Vali, *Nature* **1972**, *263*, 163; b) L. R. Maki, E. L. Galyon, M. Chang Chien, D. R. Colwell, *Appl. Microbiol.* **1974**, *28*, 456; c) S. E. Lindow, D. C. Arny, C. D. Upper, *Phytopathology* **1978**, *68*, 523.
[73] N. Y. Fletcher, *The Chemical Physics of Ice*, Cambridge University Press, Cambridge, **1970**, p. 73.
[74] H. R. Prappacher, *Z. Angew. Math. Phys.* **1963**, *14*, 590.
[75] L. Pauling, *J. Am. Chem. Soc.* **1935**, *57*, 2680.
[76] I. Weissbuch, L. Leiserowitz, M. Lahav, *J. Am. Chem. Soc.* **1991**, *113*, 8491.
[77] H. D. Göbel, H. Möhwald, *Thin Solid Films* **1988**, *159*, 63.
[78] a) M. Seul, P. Eisenberger, H. M. McConnell, *Proc. Natl. Acad. Sci. USA* **1983**, *80*, 5795; b) M. G. Samant, C. A. Brown, J. G. Gordon, *Langmuir* **1991**, *7*, 437.
[79] B. Kamb, *Ice Polymorphism and the Structure of Water* (*Struct. Chem. Mol. Biol.* **1968**, 507).
[80] K. V. Titova, E. I. Kolmakova, V. Y. Rosolovskii, *Russ. J. Inorg. Chem. (Engl. Transl.)* **1982**, *27*, 347.

Control and Design Principles in Biological Mineralization

By Lia Addadi* and Stephen Weiner*

The control of crystal formation has been developed to a remarkable degree by many organisms. Oriented nucleation, control over crystal morphology, formation of unique composites of proteins and single crystals, and the production of ordered multicrystal arrays, are all well within the realm of biological capability. Understanding the control and design principles in biomineralization is a fascinating subject that may well contribute to the improved fabrication of synthetic materials on the one hand, and to the solution of many serious pathological problems involving mineralization, on the other.

1. Introduction

Organisms have been using minerals in one way or another for at least 3500 million years. Evidence of this earliest form of mineral manipulation is preserved in the form of fossil stromatolites found in sedimentary rocks. Stromatolites were communities of bacterialike prokaryotic organisms that both trapped and indirectly induced minerals to form around themselves. Since this time organisms slowly improved their ability to control mineral formation, until some 540 million years ago when within a period of "only" a few million years a multitude of primarily multicellular organisms began to produce mineralized skeletal structures. During this crucial period in the evolution of biomineralization, the basic structural patterns for skeletal formation were fixed, although it has been postulated that some of the underlying principles used for mineralization itself were acquired from ancestral organisms.[1]

Today the phenomenon of biomineralization is widespread; members of all five kingdoms of organisms are able to produce minerals that serve a wide variety of functions. The sheer volume of calcium carbonate and amorphous silica produced by marine organisms dominates important aspects of the chemistry of the oceans and, indirectly, that of the atmosphere as well. These minerals have accumulated in huge quantities at the bottom of the oceans and over time have contributed substantially to the record of sedimentary rocks on earth.

The enormous diversity of this phenomenon among living organisms, as well as the fact that the processes used possibly reflect eons of evolutionary adaptation, implies that much can be learned about mineral formation from these organisms, in particular, control of crystal formation. Furthermore, many of the mineralized tissues formed by organisms have advantageous mechanical properties. This in turn raises the possibility that some of the design principles used could be applied in the fabrication of superior synthetic materials. It is with these futuristic ideas in mind, that we have chosen to focus this review on the underlying principles used by organisms in controlling both amorphous and crystalline mineralization, as well as on the manner in which ordered crystalline arrays may be formed.

To accomodate readers with little or no knowledge of biomineralization, we begin with short overviews of the minerals and macromolecules involved in these processes. We have also integrated a number of short reviews or excursuses which elaborate on aspects of the biology discussed in the main text. This biology in itself emphasizes the solid-state structures involved and neglects many very important topics related to the activities of the cells that direct all these processes; the hormones and other molecules that communicate between the mineralizing cells and the remainder of the organism; and the elaborate and sophisticated processes involved in ion uptake and transport to the sites of deposition. Good sources of information on these topics are provided by Simkiss and Wilbur[2] and Evered and Harnett.[3]

The current understanding of biomineralization in vivo is of a descriptive nature. The underlying principles invoked are for the most part derived from observations in vitro. Understanding how a whole ordered array of macromolecules and crystals that make up a biological material are produced is well beyond our current knowledge. We can, as always, speculate about this, and indeed we do. The body of this review therefore describes control over specific aspects of mineralization. At the end we try to bring different concepts together and focus on how ordered crystal arrays may be formed in vivo.

2. The Minerals Formed by Organisms

More than sixty different minerals are known to be formed by living organisms. These include amorphous minerals, inorganic crystals, and organic crystals.[1] Calcium minerals represent some 50% of all known biogenic minerals, presumably reflecting in one way or another calcium's abundance in the ocean as well as its widespread use in cells as a messenger. The latter function requires very low intracellular concentrations of calcium and its efficient removal to the cell exterior by membrane pumps.[4] The fact that two of the three major skeleton-reinforcing minerals, calcium carbonate (calcite and aragonite) and calcium phosphate (dahllite), are calcium minerals may reflect the exploitation of the calcium ions pumped out.

Only a few of the amorphous minerals fulfill skeletal functions, the major exception being amorphous silica. Silica skeletons are formed in huge quantities by photosynthetic marine plants called diatoms, the single-celled marine protozoans, radiolarians, certain sponges, and many terrestrial plants (Fig. 1).[5, 6] Amorphous minerals, in particular amorphous calcium carbonate and phosphate, are often used as temporary storage depots for ions essential for cellular

[*] Prof. L. Addadi, Prof. S. Weiner
Department of Structural Biology
Weizmann Institute of Science
Rehovot 76100 (Israel)

metabolism. A host or organisms, many of which form no other mineralized deposits, have such special storage cells.[7] A fairly common and somewhat unusual use of amorphous minerals is as a repository for embedding toxic metals, which are then removed together with the host mineral by release from the cell. The most common host mineral is amorphous calcium pyrophosphate.[8]

Crystals are used by organisms in many different ways. One very common use, mostly by mobile organisms, is in gravity perception. Mineral deposits located in cavities surrounded by sensory cells are able to move around much like plumb bobs, and their relative movements are tracked by the sensory cells.[1] Single crystals of the magnetic iron oxide, magnetite, are used by bacteria, algae, and many animals to monitor the earth's magnetic field, usually for navigational purposes.[9] The size of these crystals is generally constrained to around 100 nm to assure that they function as single magnetic domains.[10] The most common use of crystals is in the form of multicrystalline arrays, primarily to form elaborate skeletal structures. The order of the crystals in these arrays can be quite extraordinary, a property we will address in this review.

3. The Macromolecules Used by Organisms for Controlling Mineralization

In 1967 Veis and Perry[11] discovered a most unusual protein in the dentin of vertebrate teeth. It is composed of about 40 mole percent aspartic acid and 40 mole percent phosphoserine. This unusually acidic polymer is closely associated with the mineralization process, but its precise function is still not known.[12] Since then, acidic proteins and glycoproteins, usually rich in aspartic acid and often containing glutamic acid, phosphorylated amino acids, and acidic sulfated polysaccharides have been found in the mineralized tissues of many organisms.[1] Their widespread distribution among organisms from different kingdoms is one of the reasons why Weiner et al.[13] proposed that their use in controlling mineralization evolved long before the advent of skeletal formation some 540 million years ago. These macromolecules are now considered to be key components in the mineralization process.

No really acidic macromolecules have been fully characterized in terms of primary and secondary structures, let alone tertiary structures. Many technical problems are associated with the manipulation of these highly charged polymers. Several partial sequences of amino acids have been reported, consisting of runs of poly-Asp[14] and alternating sequences with Asp at every second residue.[15] The proteins, and in some cases their associated sulfated polysaccharides, interact with calcium,[16] and in fact calcium appears to facilitate the formation of β-sheet structures in these macromolecules.[17] It should be noted that many proteins from mineralized tissues have been sequenced, including those of vertebrates[18] and to a lesser extent those of the spicules of larval sea urchins.[19] Many of these do not have unusually acidic compositions, although some do display repeating sequences, which could conceivably interact with a regular crystal lattice. It is also interesting to note that in bone, the most studied of all mineralized tissues, no highly acidic proteins comparable to those found in abundance in dentin and nonvertebrate mineralized tissues have yet been found.

The acidic macromolecules are often intimately associated with more hydrophobic macromolecules, which generally form extensive three-dimensional structures. These framework macromolecules vary from tissue to tissue and hence presumably also fulfill specific mechanical or other functions. Common examples of such framework molecules are type I collagen in bone and dentin, α-chitin–protein complexes in arthropods, and β-chitin–protein complexes in the shells of mollusks and brachiopods.[1, 13]

Lia Addadi, born in Padua (Italy) in 1950, studied organic chemistry at the Università degli Studi di Padova from 1968 to 1973. She then transferred to the Weizmann Institute of Science (Israel) where she completed her Ph.D. in 1979. After her postdoctoral stay with J. R. Knowles at Harvard (1981–1982) she returned to the Weizmann Institute and became Associate Professor in 1988. She received the Kennedy Award of the Weizmann Institute for Ph.D. students (1978), the G. M. J. Schmidt Prize for her Ph.D. thesis (1981), the Ernst David Bergmann Prize in Chemistry (1986), and the Annual Award of the Israel Chemical Society (1989). Her research interests include the mechanisms of biomineralization, pathological crystallizations, solid-state stereochemistry, and the interactions of proteins with crystal surfaces.

Stephen Weiner was born in 1948 in Pretoria (South Africa) and studied geology and chemistry from 1966 to 1972 at the University of Cape Town (South Africa) as well as geochemistry at the Hebrew University in Jerusalem. He completed his Ph.D. in the area of biomineralization and geobiology at the California Institute of Technology in Pasadena (California) in 1976. After a two-year postdoctoral stay at the Weizmann Institute of Science, Weiner stayed on and became Associate Professor in 1985 and Professor for Biomineralization and Archeological Chemistry in 1990. He received the Shmuel Jaroslavsky Prize in 1980 for his studies on the biogeochemistry of mineralized tissues and the Ernst David Bergmann Prize for Chemistry in 1984. Weiner co-authored a book on biomineralization.

4. Filling Space with Mineral: Amorphous versus Crystalline Materials

A key step in the control of mineralization employed by almost all organisms is the initial isolation of a space. Then under controlled conditions minerals are induced to form within the space.[20] The space is usually delineated by cellular membranes, vesicles, or predeposited macromolecular matrix frameworks. Filling up these spaces with amorphous minerals would appear to require a quite different strategy as compared to filling space with crystalline material.

The definition of an amorphous material is equivocal. From a theoretical point of view, amorphous materials are those that lack any structural regularity beyond the first coordination-sphere. From the practical point of view, however, the definition of amorphous depends on the technique used to detect crystallinity or the lack thereof, whether X-ray, infrared, or extended X-ray absorption fine structure (EXAFS). The distinction between an amorphous and a crystalline material with short-range order is thus not well defined. For space-filling purposes the problem is not too relevant, since the presence of short-range order at the molecular level does not influence the overall isotropic behavior of the solid phase. Hence the long-range interactions inside the bulk of the material are on the average the same in all directions. A consequence is that amorphous materials as well as materials with short-range order can easily be molded into desired shapes. The difference between these two types of materials is relevant, however, when one considers amorphous-to-crystalline phase transitions. The presence of very small, ordered domains may well play a dominant role in the transformation pathway and thus determine the nature of the mature phase. This question will be addressed in Section 8 concerning polymorphism.

A single crystal is characterized by the regular three-dimensional repetition of a basic structure which optimizes molecular interactions in a typically anisotropic fashion. The anisotropy of the unit cell is reflected in the anisotropic growth of the crystal. In other words, where interactions between molecules or ions are weaker, growth is slower.[2a] This in turn gives rise to a characteristic morphology for each crystal.[21] The development of particular crystal faces, ignoring interactions with the environment, is the result of a slower rate of deposition of crystal planes in these particular directions as compared to other directions. A similar observation, in a very intuitive way, can be made for the cleavage of a crystal. A single crystal will fracture more easily along crystallographic planes which are held together by relatively weak interactions. The fracture will follow the path of least resistance and propagate smoothly along flat surfaces.

Amorphous and crystalline materials thus present very different properties in terms of filling space. The absence of long-range repetitive structure in amorphous materials is associated with a number of possibly advantageous properties: the absence of a preferred direction of growth, the absence of preferred fracture planes, and the absence of well-defined faces. Possible mechanical advantages of crystalline phases, on the other hand, include lower solubility, higher density, and ordered surface and bulk structures, all of which may be associated with desired physical properties.

There are very few known cases in biomineralization where the intrinsic properties of crystals are directly exploited. The classic example is magnetite in magnetotactic bacteria. Here the magnetic properties of the single crystals and their size, which corresponds to that of a single magnetic domain, are used for the passive orientation of the bacteria in the earth's magnetic field. The optical properties of crystals may also be exploited by organisms for special purposes. Single crystals of calcite functioned as lenses in the eyes of the extinct trilobites;[22] uric acid crystals act as reflectors in the cuticles (shells) of certain scarab beetles, giving them a fantastic gold color.[23] These examples are, however, more the exception than the rule. Most crystalline phases are used for mechanical purposes, where the crystallinity is manipulated for controlling the growth of the mineral phase rather than exploited for its intrinsic properties. In view of this, the problem of the choice of amorphous or crystalline mineral phases in biomineralization may be reformulated in a way which is admittedly extreme, but serves the purpose of clarifying the above points.

1. For minerals that are stable in the amorphous state under normal conditions, the amorphous phase may be preferable for mechanical and space-filling purposes.

2. For minerals that are metastable in the amorphous state and spontaneously transform into crystalline materials, two options exist. Either the amorphous phase is stabilized, or special mechanisms are used to control the growth and properties of the crystalline phase and, if necessary, overcome its disadvantages.

The best example of the first class of compounds is amorphous silica and of the second class, calcium carbonates and phosphates.

4.1. Filling Space with Amorphous Materials

Amorphous materials have also been described as frozen liquids. Amorphous solids are generally formed spontaneously by oxide elements with intermediate electronegativity, where the bond character can be described as a mixture of ionic and covalent. The elements of common glass-forming oxides are found mostly in groups III, IV, and V of the periodic table. This particular type of bonding allows these oxides to form structures that can be regarded as three-dimensional polymers built of polyhedra joined at the corners.[24] The polymeric structure also accounts for the high viscosity and low solubility of the material, and both characteristics contribute to its kinetic stability. Amorphous silica is a classic representative of this class of compounds. The small coordination-number of the atoms and the linkage of the polyhedra at their corners, and not edges or faces, allow the formation of open structures in which the Si-O-Si angles can vary without distorting the SiO_4 tetrahedra themselves. Silicon is transported in the body fluids in the soluble form of silicic acid and is polymerized in situ by formation of Si-O-Si bonds and the partial loss of water. Silica dissolution thus involves a true hydrolysis reaction.[5, 25] These factors allow silica to be deposited and shaped into the often fantastically sculpted structures of diatoms (Fig. 1 above) and radiolarians, or to be woven into delicate basketlike structures in the choanoflagellates.[26] In many land plants, in particular

the grasses, portions of the plants are filled with silica[6] (Fig. 1 below). The silica acts as an abrasive, discouraging herbivores from feeding freely upon the grasses. Simpson[27] observed that when the grasses evolved the ability to silicify in the Miocene epoch, the structure of horses' teeth changed in order to adapt to this new reality.

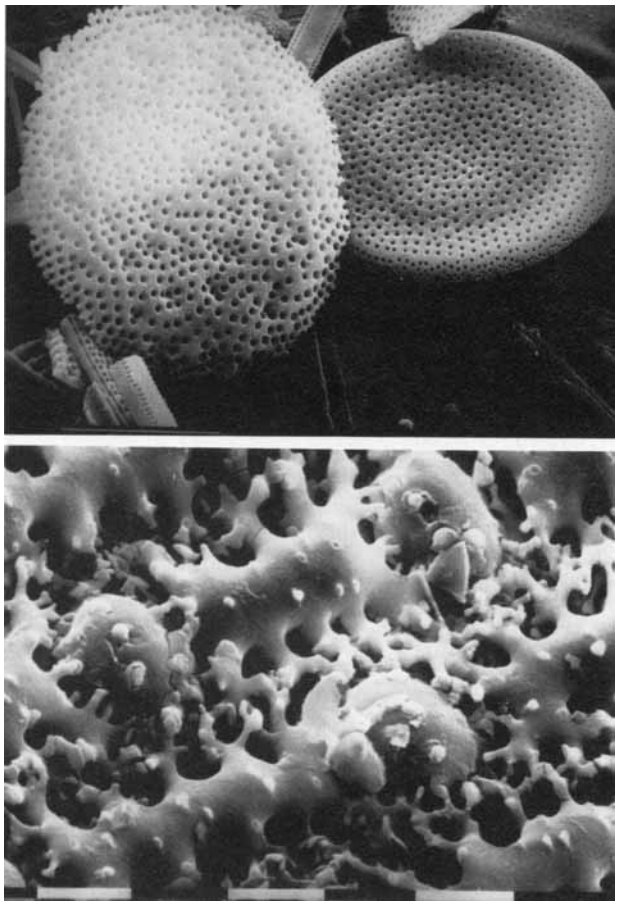

Fig. 1. Amorphous silica deposition by the marine diatom *Thalassiosira lentiginosa* (obtained from a deep-sea core; above) and by a wheat plant *Triticum aestivum* (below). The silica impregnates the cell walls, the organic material has been totally removed, and only the mineralized outlines of the cells are observed. In the upper photograph the line along the bottom edge represents 20 μm; in the lower photograph the scale bar is marked in 10 μm intervals.

Amorphous calcium carbonate and phosphate present a variety of most intriguing problems. These materials crystallize easily in a number of polymorphic crystalline forms, and their transformation from the amorphous to the crystalline phase under close to physiological conditions is not only thermodynamically favored, but kinetically fast.[28] The presence of these amorphous minerals as "stable" phases in organisms is not a manifestation of poor control over mineralization, but rather the result of deliberate inhibition of crystallization. The organism must invest energy to prevent these phases from crystallizing. The reason for the use of amorphous calcium phosphate or carbonate in intra- or extracellular temporary storage sites is probably because of its higher solubility (relative to the crystalline form) which makes it readily available for reuse. In the case of the chiton (a class of mollusks) teeth, the amorphous calcium phosphate is stabilized for some ten days, and only then does it transform into dahllite[29] (Excursus 1). This implies that there is a precise control over the rate and timing of the transformation. A number of examples are known in which amorphous materials are used for the construction of hard parts. The gill supports of the bivalve *Neotrigonia*[30] or the stylets of nemerteans (ribbon worms),[31] used like a harpoon for capturing prey, are both composed of amorphous calcium phosphate. The question of how these organisms prevent the material from crystallizing remains unanswered, although many inhibitors are known to be able to perform this task in a more or less specific way. This point will be discussed further in Section 8. Why organisms use a relatively soft amorphous material for such purely structural functions in the first place is a complete mystery.

Excursus 1: The Chiton Radula: A Natural Laboratory for the Study of Mineralization Dynamics

The chiton, a primitive member of the mollusk phylum, is found on rocky ocean shores all over the the world. It has a tonguelike tooth plate, called the radula (Fig. A, upper left), which it uses for scraping the surfaces of rock for food. In 1962 Lowenstam discovered that these teeth are capped by a layer of the hard magnetic iron-oxide mineral, magnetite.[88] Magnetite has subsequently been found in many organisms, in particular in those which are migratory. The crystals are part of a navigation system and are used to detect the orientation of the earth's magnetic field.[9]

The chiton wears down its teeth at a rate of roughly one to two rows per day.[89] New teeth are formed at the same rate, and the entire radula, containing about 100 rows of teeth, is in effect an assembly line for teeth. The radula of the chiton offers an ideal subject for the study of the dynamics of the mineralization process, because each row represents about a day's worth of tooth construction.[90] The basic stages are described here for the *Chitonida*,[89] since the details differ in different taxa. An individual tooth is essentially composed of three layers (Fig. A, upper and lower right) each of which differs mineralogically. At the first stage of tooth formation, cells form a capsulelike structure with a central cavity. The matrix framework is constructed in this extracellular space. After the construction of about ten rows of teeth the cells introduce iron atoms into the framework which precipitate in the outer tooth layer as the hydrated iron-oxide mineral, ferrihydrite. Within two or three rows, the ferrihydrite converts to magnetite. This process continues until the whole outer layer is filled with magnetite. Around the thirtieth row of teeth another iron-oxide mineral, called lepidocrocite, precipitates in a thin zone beneath the magnetite layer. Finally the core of the tooth begins to fill in with amorphous calcium phosphate, which is somehow stabilized for about ten rows, then begins crystallizing within a single row of teeth. The crystals continue to grow and/or the lattice becomes more ordered (infrared spectra cannot differentiate between these two possibilities) until the mature teeth are used and discarded. The most curious observation is that the crystals of dahllite are more or less aligned with the matrix sheet, suggesting that the structured matrix surface induces and controls the transformation process.[29]

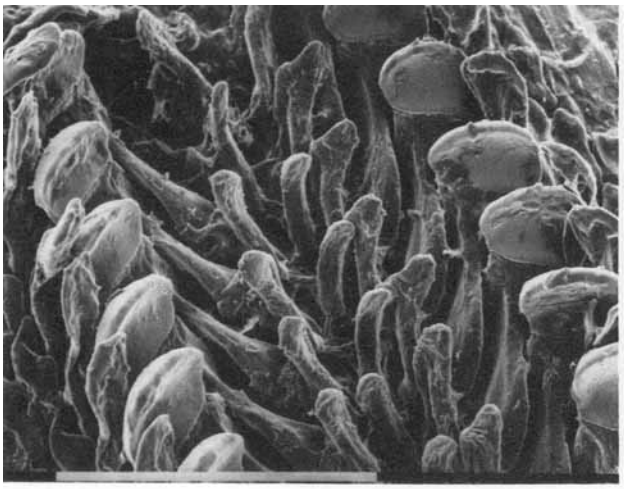

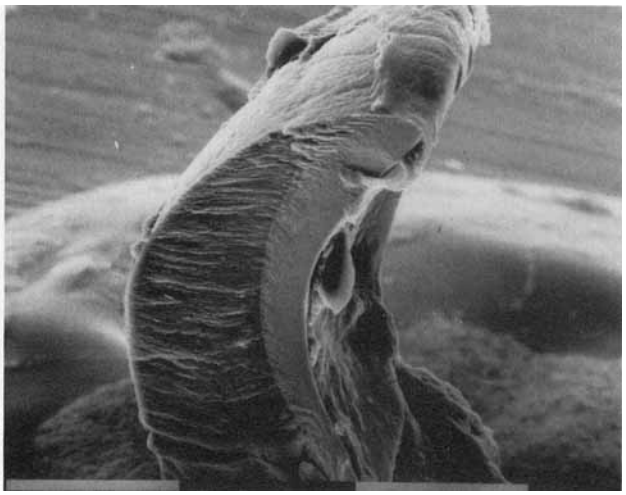

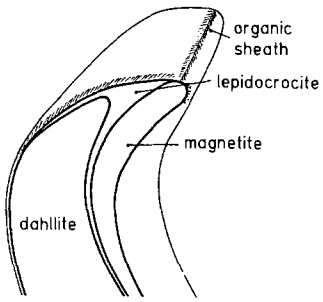

Fig. A. Upper left: View of the mature portion of the radula of the chiton, *Acanthopleura haddoni* showing five rows of teeth. Only the spoon-shaped objects are mineralized. Upper right: The fractured cross section of an individual mineralized tooth. The scale bars are marked in intervals of 1 mm (left) and 0.1 mm (right). Lower right: Schematic illustration of the three different layers of the tooth and their mineralogical compositions (compare with photograph upper right).

The chiton radula has proved to be a gold mine of information in biomineralization, and many of the most basic concepts now widely accepted for mineralization in most other tissues have their origin in the studies of this most interesting mollusk. Radula mineralization processes are still not completely understood, and many fundamental questions remain to be answered.

4.2. Filling Space with Crystalline Materials

Notwithstanding the possible advantages of using amorphous materials, the large majority of mineralized tissues contain a crystalline material. The simplest way to fill a space with crystals is to create as high a local supersaturation as possible, and then induce nucleation, or let the system spontaneously reach a state of lower energy by crystallization, while at the same time removing the excess solvent. If the concentration of metastable solute is high, and if crystallization is rapid and the crystals formed are small, then the resultant mineral phase, although crystalline, may not be too different from that of an amorphous material. This situation is observed in spherulites of calcium carbonate which spontaneously form in metastable supersaturated solutions. "Droplets" of calcium carbonate and water separate from the solution and with time, or upon drying, crystallize to give rise to spherulites of one of the three polymorphic modifications of calcium carbonate—calcite, aragonite, or vaterite.[32] The organization of the crystals in the spherulite is sometimes surprisingly ordered, and the overall shape, though variable, is typically round, as predicted by the requirement of liquid drops to reach minimal surface energy (Excursus 2). The problem with this type of crystallization is that it is not easy to control and is difficult to reproduce. Furthermore, if the crystals formed are larger, then their packing is progressively less compact. The presence of pores reduces the mechanical integrity. Control of the physical characteristics requires slow crystallization. Two main pathways are used in nature to improve control over crystal formation: the use of single crystals and the formation of ordered crystal arrays.

Excursus 2: Spherulitic Crystallization in Biology

Spherulites are crystal aggregates formed from rapidly crystallizing solutions. They are easily formed in vitro from highly supersaturated solutions of $CaCO_3$, and the crystal aggregates may develop remarkably ordered structures (Fig. B, lower left). The polymorph of $CaCO_3$ often formed is the very metastable form, vaterite. Spherulitic structures are produced by many different mineralizing organisms, including red calcareous algae, pennatulid sea fans, scleractinian (stony) corals, and birds (in egg shells).[1] It is of interest to note that the formation of avian egg shells and scleractinian coral skeletons are both among the most rapid mineralization processes known.

Probably the most common form of spherulitic mineralization occurs inside small spherical intracellular vesicles where the crystals function as temporary storage sites for ions important in the organism's metabolism. Such specialized cells, often referred to as calcium cells, are found in many different animals, most of which do not have any other form of mineralized deposit.[7] The crystals nucleate at a central point and grow out radially. The vesicle membrane presumably inhibits further crystal growth. Note that in the

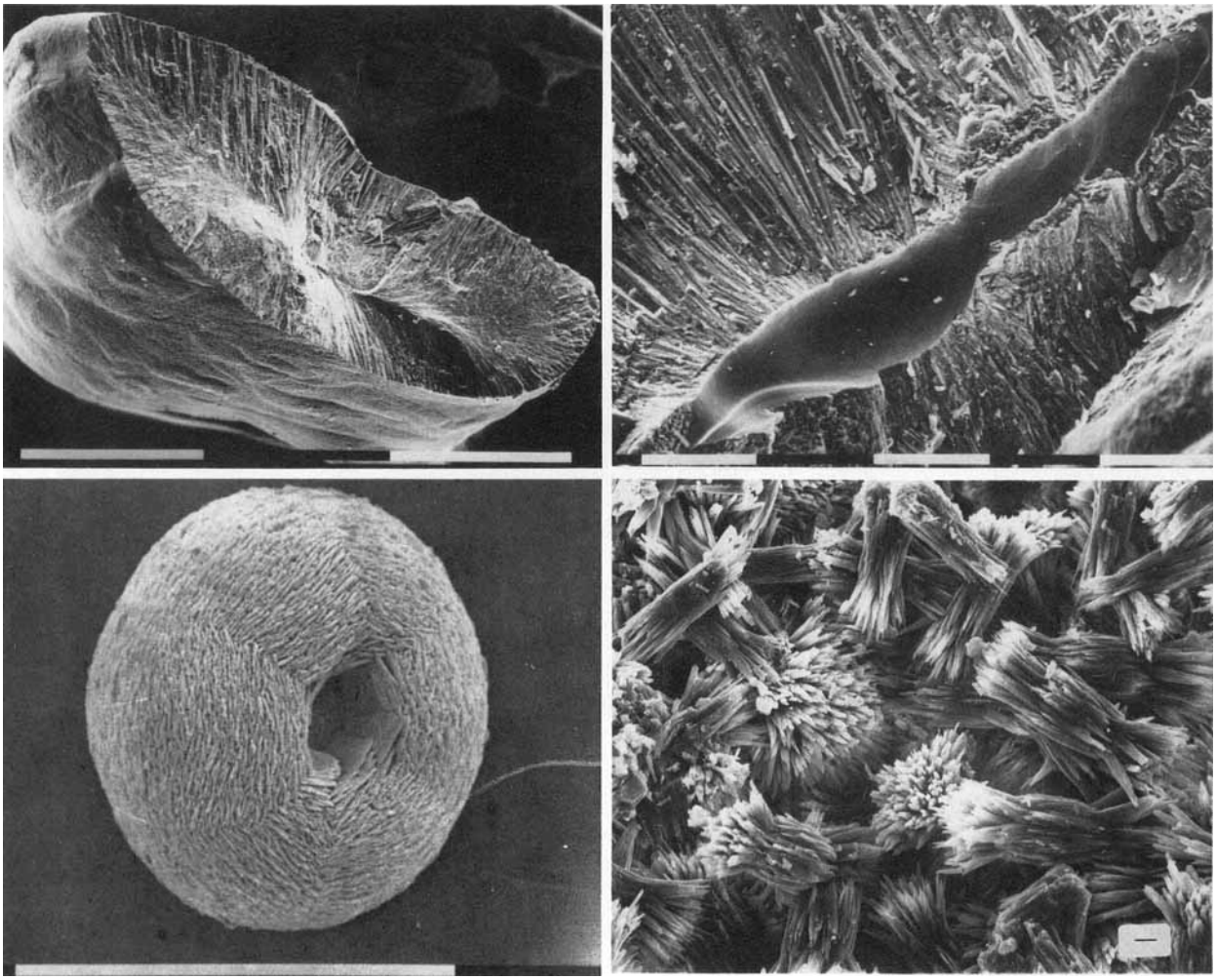

Fig. B. Upper left: Aragonitic otolith (sagitta) from the bony fish, *Seriphus politus*. The otolith is fractured revealing the central surface from which the aragonitic crystals nucleate. (The scale bar is marked in 1 mm intervals.) Upper right: The fracture surface and the radiating aragonitic crystals at higher magnification. Lower left: Spherulite formed in vitro composed of vaterite crystals. (The scale bars are marked in intervals of 0.1 mm in the photographs at the upper right and lower left.) Lower right: The aragonitic spherulites precipitated in the chamber of the cephalopod mollusk, *Nautilus pompilius*. Field width: 135 μm.

small extracellular matrix-vesicles of mineralizing cartilage, the carbonate apatite crystals rupture the membrane and continue growing outside the vesicle.[91]

This type of spherulite formation from only one nucleation site has been modified by a variety of organisms, such that spherulitic growth is induced by nucleation sites distributed on a surface. The otoliths of fish are good examples (Fig. B, left and upper right).[78] Otoliths are millimeter-sized, flat bodies in the inner ear. They are usually composed of aragonite or vaterite and function in sound reception, as well in the sensing of gravity and acceleration.[92] The crystals nucleate on an organic surface and grow with their *c* axes more or less ($\pm 10^\circ$) perpendicular to the surface.[78] A similar phenomenon occurs in egg shells, composed of calcite, and scleractinian corals, composed of aragonite.

A most interesting case of spherulitic mineralization occurs in the well-known mollusk, the pearly *Nautilus*. Its aragonitic shell is produced under very well-controlled conditions. In contrast, spherulitic aragonitic crystals precipitate out of the fluid present inside the shell chambers. (Fig. B, lower right).[76] These chambers are part of the buoyancy system and contain gas which is pumped in or out. Some of the extinct relatives of the modern *Nautilus*, the ammonites, partially or totally filled their chambers with spherulitic crystals to control their specific gravity and orientation in the water column.[93] Spherulitic mineralization in biology thus appears to provide a means of rapidly filling relatively large volumes with minerals.

5. Single Crystals

The formation of an entire object from a single crystal has the advantages of maximal packing, excellent order, and homogeneity. Only one major taxonomic group, the echinoderms have opted for this solution (Excursus 3). By definition, a single crystal is characterized by a unit cell, the smallest building block that incorporates all the basic spatial and symmetry relations between atoms and molecules. The unit cell is repeated in space by translation along the main crystal axes, giving rise to a perfect three-dimensional lattice, which ends abruptly at the boundaries of the crystal faces. In such an ideal crystal the faces are macroscopically and microscopically parallel to the planes with lowest surface energy. A real crystal differs, however, from this ideal description. The surface of a crystal growing in solution is in active

contact with its environment, including solvent, solute, and impurity molecules. The surface layer is thus probably never as ordered as the bulk. Even within the crystal the perfect translation between unit cells exists only over a short distance, called the coherence length, after which it is perturbed by mistakes or dislocations. A real crystal has thus a characteristic coherence length and mosaic spread, parameters which describe the deviation from perfect order in terms of frequency of mistakes and overall misalignment between perfect domains.

Domains separated by domain boundaries can be defined at a microscopic level inside each real crystal. The definition of a single crystal presents a problem similar to that encountered in the definition of an amorphous material, namely that the definition depends on the technique used to measure the property in question. This is not a semantic issue. Some organisms have acquired the ability to manipulate these properties of single crystals.

The echinoderms form most of their skeletal elements, namely spines, plates, ossicles, and other structures, from calcite (Excursus 3). Each skeletal element diffracts X-rays as a good single crystal.[33] In the case of the sea-urchin spine the average misalignment between unit cells over the whole skeletal element is as low as 0.15°.[34] The fenestrated and convoluted morphology of the element, as well as the smooth curved surfaces are certainly not reminiscent of a single crystal. Observations of the in vivo growth of the spicules of sea-urchin larvae[35a] and electron microscopic studies of test (external shell) formation in adult sea urchins,[35b] indicate that each skeletal element is the product of a single nucleation event. This is quite remarkable when one considers that many of these elements are centimeters in size. Shimizu and Yamada[36] proposed an alternative multinucleation process for the regeneration of a spine, which would require nucleation sites to be aligned to within 0.2° over enormous distances. Towe[37] has suggested that skeletal elements undergo recrystallization to form the macroscopic "single" crystal. Well-aligned nucleation sites are known to occur in biology (e.g. nacreous layers of certain bivalves), but their degree of misalignment is much greater[38] (roughly 10°) than in the echinoderm calcitic elements. This dilemma highlights an important aspect in understanding this single-crystal phenomenon, namely determining both the sequence of events that occur in the formation of a skeletal element and the nature of its final state.

Excursus 3: Crystals that Form in Vesicles—*Echinodermata* and *Coccolithophoridae*

Vesicles are widely used by organisms to delineate a space for mineral formation. The vesicles can be located within the cell or less commonly outside the cell, and their sizes range from submicrons to centimeters! Both amorphous and crystalline minerals are formed in vesicles, and in the case of the latter they can be either single crystals or multicrystalline. Two of the most fascinating examples of crystal growth in vesicles occur in the *Echinodermata*—the sea urchins, brittle

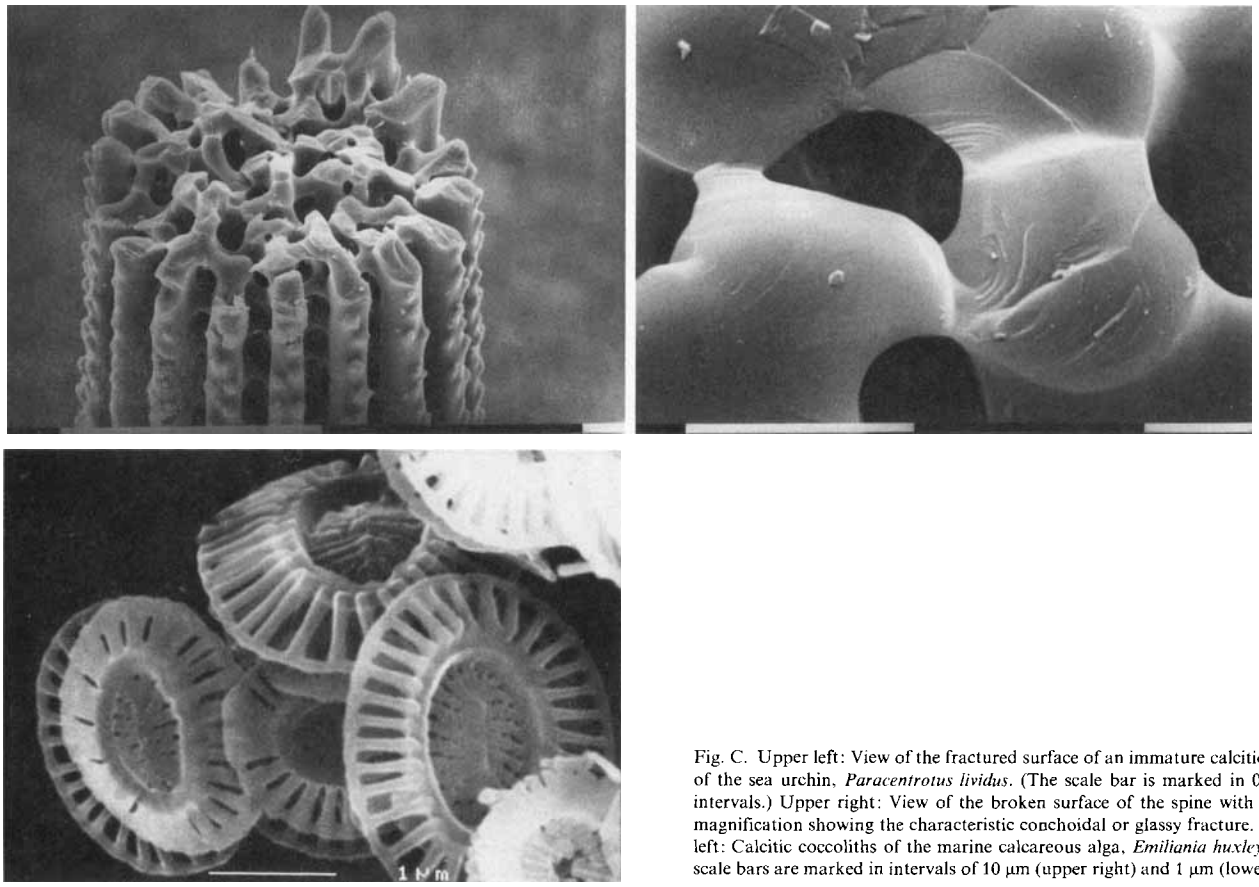

Fig. C. Upper left: View of the fractured surface of an immature calcitic spine of the sea urchin, *Paracentrotus lividus*. (The scale bar is marked in 0.1 mm intervals.) Upper right: View of the broken surface of the spine with higher magnification showing the characteristic conchoidal or glassy fracture. Lower left: Calcitic coccoliths of the marine calcareous alga, *Emiliania huxleyi*. The scale bars are marked in intervals of 10 µm (upper right) and 1 µm (lower left).

stars, and sea cucumbers—and the *Coccolithophoridae*, calcareous marine algae extremely abundant in the world's oceans.

The echinoderms form large single crystals of calcite intracellularly within very large vesicles (Fig. C, upper left). This is achieved by many cells fusing their cell-wall membranes together to create a large vacuole, inside which the mineralizing vesicle forms.[35] The stages of crystal formation are best described for the sea-urchin larvae, since these can be grown in laboratory cultures. The calcite crystal is nucleated inside the vesicle and has a triangular shape. The crystal then begins to grow in three different directions, each of which is along the *a* crystallographic axis, and forms a so-called triradiate spicule (see Section 9). Then quite amazingly, the spicule is rotated into a specific orientation after its initial formation.[94] At a later stage one of the arms changes its growth direction by 90° to continue growing along the *c* axis direction. Presumably the vesicle shape determines the direction of crystal growth but still "takes into account" crystallographic considerations—a delicate interplay between biology and crystallography.

Each skeletal plate of the adult sea urchin also has its origin most probably in a single nucleation event[95a] and then grows intracellularly to sizes of up to a centimeter or so. The spines are basically similar in structure to the plates but can reach sizes of up to 25 cm, and yet each one is still a single crystal.[95b] The crystal has a highly convoluted shape (Fig. C, upper left) with all its surfaces being smooth and curved, features never normally associated with a single crystal. Even more puzzling is the fact that the fracture surfaces of the calcite of the spine do not resemble the smooth and straight cleavage planes of inorganic calcite; they are curved and stepped and are very similar to the conchoidal fracture surfaces of amorphous glasses[37] (Fig. C, upper right). The sea urchin also has a set of five continuously growing teeth. These teeth are composed of calcite, but in their cores the magnesium content reaches more than 40 mole percent. The cores still retain the structure of calcite and not that of dolomite [$(Ca,Mg)CO_3$].[64] Despite the fact that the tooth has a highly complex fine-structure and is the product of many nucleation events, X-ray diffraction shows that all its crystals are well aligned.[64, 96]

The *Coccolithophoridae* are single-celled photosynthesizing algae which cover their outer cell-wall with layers of calcitic coccoliths (Fig. C, lower left). Each coccolith is formed intracellularly in a specialized vesicle, and upon completion is transported through the cell membrane to the outer surface.[97] An individual coccolith is in itself a highly complex structure. Its overall shape is that of a flat spherical scale, but the detailed morphology is intricate and highly species-specific.[98] A scale is in fact composed of some 20 or more individual elements, each of which is a single crystal of calcite.[99] The crystals nucleate on the rim of an organic base plate. A highly acidic polysaccharide containing both carboxylate and sulfate groups, which is able to bind calcium, is located within the mineral phase and possibly in the membrane itself.[100] Coccolith formation is thus an example of a highly ordered array of crystals being formed in association with a structural framework and acidic macromolecules. All this takes place within a vesicle inside a single cell.

5.1. Reinforcing Single Crystals Against Fracture

Sea-urchin skeletal elements demonstrate yet another challenging paradox. A single crystal of inorganic calcite cleaves easily along the hexagonal (104) planes. Sea-urchin skeletal elements do not cleave in this way, despite the fact that they are most respectable single crystals (Excursus 3). Instead they fracture with difficulty (relative to pure calcite), producing what is described as a conchoidal fracture normally found in amorphous glasses.[37] Acidic proteins are present inside the elements in the amount of 0.02 wt %.[39, 40] Significantly, the proteins are occluded inside the mineral phase and can be liberated only by dissolution. They are all soluble in water and do not form continuous sheaths of material as in the organic matrices of mollusk shells, for example. Experiments on crystal growth in vitro, as well as synchrotron X-ray measurements of crystal texture, show that the acidic proteins reside at the boundaries of crystal domains; the average coherence lengths (about 1500 Å) are significantly smaller than those of pure calcite crystals (about 4500 Å).[34] During crystal growth the proteins preferentially adsorb on defined crystallographic planes parallel to the *c* crystallographic axis of the crystal (Fig. 2).[40] The resulting synthetic crystals also cleave with a conchoidal fracture very similar to that of the spines themselves. Interestingly, acidic proteins extracted from a mollusk shell do not adsorb preferentially on the same crystallographic planes of calcite and do not affect single-crystal cleavage in the same fashion.[40] In this latter case the artificial crystals are more fragile, and their cleavage follows the set of regular {104} cleavage planes.

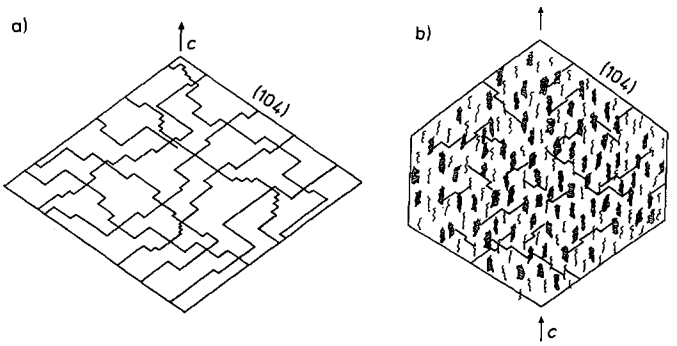

Fig. 2. Schematic representation of cleavage patterns in a) a pure calcite crystal; b) a calcite crystal with intercalated sea-urchin proteins. The cleavage planes are always parallel to the (104) faces. The protein is occluded on the three symmetry-related sets of {110} planes parallel to the *c* axis.

Although we do not yet have sufficient information on the compositions and structures of mollusk and sea-urchin acidic proteins, differences in the manner in which the proteins influence crystal growth may well reflect the functions they fulfill. We proposed that the sea-urchin proteins reinforce the crystalline material against fracture (Fig. 2) by controlled intercalation on planes oblique to the cleavage planes. Whether the mechanical reinforcement is due to direct intervention of the protein in deviating or absorbing a progressing fracture, or is limited to the modification of crystal texture induced during growth, is as yet unknown. This

solution adopted by nature to circumvent a problem intrinsic to the material used for construction is both new and surprising. It will be interesting to check whether it is unique.

6. Control Over Crystal Morphology

Biogenic minerals are perhaps best known and appreciated for their almost endless variety of shapes, many of which bear no resemblance to their inorganic counterparts (Excursus 4). Almost nothing is known about the manner in which this is achieved in vivo, except that it is likely to involve charged polymers such as proteins, polysaccharides, or a combination of both.

Interactions between charged polymers and growing crystals may or may not be specific. We define a nonspecific interaction as one in which the charged polymer interacts with all surfaces of a given crystal; in a specific interaction, on the other hand, one surface is favored over the others. Specific interactions are most likely to occur when relatively weak interactions are involved, since even slight differences in recognition will tend to be amplified. As the ionic character of the crystal and polymer surfaces increases and the interaction strengths are enhanced, particularly by the cooperative action of many charged groups on the macromolecule, the effect on crystal growth becomes less and less specific. This phenomenon has been observed in vitro for polyelectrolytes such as polyaspartate and polyacrylate on growing calcite crystals,[41] for acidic polysaccharides on sodium chloride,[42] and for chondroitin sulfate on hydroxyapaptite[43] and sodium urate.[44] The inhibition mechanism can be envisaged as a blanket-blocking or -poisoning of crystal steps and kinks over the entire surface of the growing crystal.

When the macromolecule is part of a flexible vesicle, physical contact with the external envelope is probably not sufficient to arrest growth because of the strong tendency of crystals to complete lattice layers having a minimal surface energy. For example, the single magnetite crystals of magnetotactic bacteria develop well-defined faces,[45] even though they are presumably in contact with the inner surface of the vesicle in which they form.[46] A chemical interaction is probably required to stop crystal growth inside a flexible envelope at any stage of layer completion. If an inhibitor is immobilized in a membrane structure, physical contact can cause chemical inhibition. Inhibition can also conceivably be achieved by the cooperative effect of the many carboxylate and phosphate groups of the lipids composing the membrane itself. This type of inhibition by immobilized molecules has the additional advantage of being active only when the crystal touches the membrane and not interfering with growth prior to that. It may account for the smooth and curved mineral skeleton of echinoderms and some coccolithophores (Excursus 3).

Crystal morphology can also be modified by the adsorption of impurities from solution onto specific crystal surfaces. This was known even before X-rays became the conventional tool for determining crystal structure.[47] Mechanisms of inhibition involved in the control of crystal morphology have been elucidated at the molecular level in a systematic series of studies on organic crystals and tailor-made inhibitors, performed by the solid-state group at the Weizmann Institute.[48] It was shown that such inhibitors are adsorbed selectively on specific crystal planes at lattice sites where a part of the molecule, identical to the substrate molecule, can fit into the regular arrangement of the surface layer. The remainder of the inhibitor molecule, which does not match the crystal structure, emerges from the surface and perturbs the regular deposition of the next layers, thus slowing growth in this direction. Crystal morphology is determined by the relative rates of growth of the crystal in different directions. It can thus be controlled at will by engineering the appropriate inhibitors.[49] Conversely, information about the crystal planes specifically interacting with inhibitor molecules can be deduced by analysis of the morphological modifications caused by the inhibitor upon crystal growth. This morphological tool can thus be exploited to obtain information on the interactions between crystal surfaces and biological macromolecules present in solution. This is independent of the possible function of the morphological modification itself.

The "impurities" thought to be active in changing the morphology of biological crystals are the acidic macromolecules or a subset thereof. In a series of experiments crystals were grown in vitro in solutions containing small quantities of the proteins.[50] The results showed that some but not all acidic proteins interact specifically with certain faces of growing crystals and alter their morphology. For this to occur the proteins must have, at least in part, regular β-sheet structures. Furthermore, it has been observed that acidic proteins from a variety of mineralized tissues often interact preferentially with crystal faces containing a certain structural motif, be they crystals of dicarboxylic acid salts,[50] calcite,[40] phosphate esters,[51] or the calcium phosphate minerals octacalcium phosphate[52] and dahllite.[53] The common feature of these motifs is that the anionic groups of the crystal form chains with alternating calcium ions, and their oxygen atoms are oriented more or less in the plane of the face, with their backbone perpendicular to it. In vivo the proteins could also act from solution in a similar way. The fact that similar stereochemical features were identified on the interacting faces in different systems is a hint that general rules of interaction between crystals and acidic macromolecules may exist.[54]

Excursus 4: Biological Control of Crystal Morphology

One of the hallmarks of biomineralization is the control of crystal morphology. The vast majority of organisms produce crystals of one specific mineral type and a uniform morphology at a particular tissue site. The same organism may produce the same mineral but with different morphologies at different tissue sites. An excellent example is the shell of a fresh-water bivalve (Fig. D, upper left), which is composed of two layers with differently shaped aragonitic crystals. Neither of the crystal shapes resemble aragonite crystals formed inorganically in the magnesium-rich Dead Sea (Fig. D, upper right). Many marine calcareous algae form aragonite under poorly controlled conditions, and their crystals (Fig. D, lower left) indeed resemble the inorganic aragonitic crystals (Fig. D, upper right).

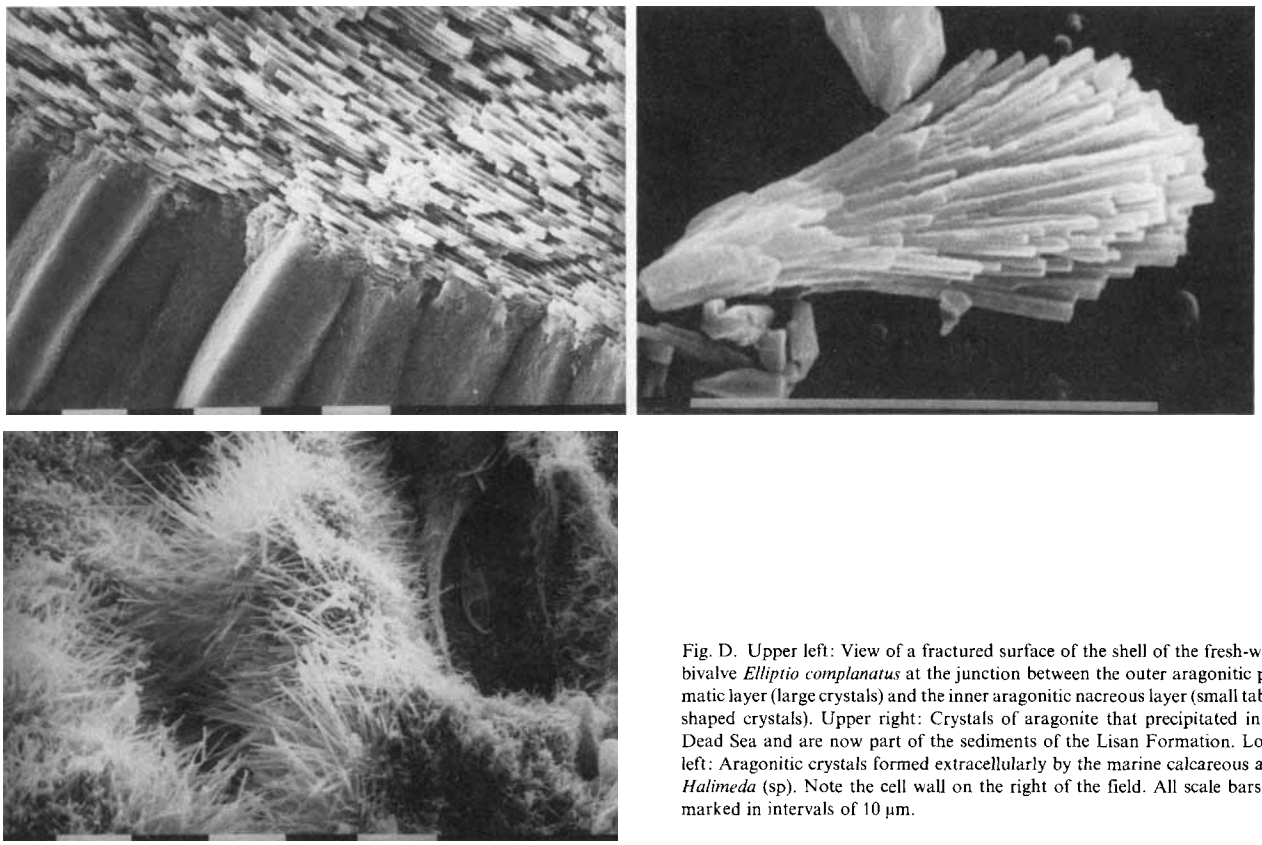

Fig. D. Upper left: View of a fractured surface of the shell of the fresh-water bivalve *Elliptio complanatus* at the junction between the outer aragonitic prismatic layer (large crystals) and the inner aragonitic nacreous layer (small tablet-shaped crystals). Upper right: Crystals of aragonite that precipitated in the Dead Sea and are now part of the sediments of the Lisan Formation. Lower left: Aragonitic crystals formed extracellularly by the marine calcareous alga, *Halimeda* (sp). Note the cell wall on the right of the field. All scale bars are marked in intervals of 10 μm.

Examples of species-specific crystal morphologies abound in biology. These include the magnetic crystals of magnetotactic bacteria,[101] which generally have well-defined crystal faces but in different proportions and hence difference morphologies. Some species, however, form bullet-shaped crystals with rounded surfaces.[45] Both types of crystals form in membrane-bound vesicles.[46] Different plants produce crystals of calcium oxalate monohydrate (whewellite) and dihydrate (weddelite) with species-specific morphologies.[102] Single-celled marine animals called *Acantharia* produce beautifully symmetrical (20fold symmetry!) skeletons composed of strontium sulfate (celestite). Three different spicule shapes are used to assemble the structure. Even though the main shaft of the spicule is curved, the ends that fit together at the hub of the complex have straight faces which correspond to well-defined crystal planes.[63] These spicules also form inside vesicles.

Crystal morphology is almost always a genetically defined property of a mineralized tissue. Little is known about the advantages of one morphology over another. Except for very basic observations about crystals forming in spaces delineated by lipid bilayers or macromolecular assemblies with well-defined shapes, almost nothing is known about the in vivo methods used by organisms to control crystal morphology. Almost all our knowledge to date is based on in vitro experiments.

7. Control Over Nucleation

The key to the formation of many mineralized tissues is control of nucleation. Crystals grown at specific locations and with well-defined orientations can best be exploited for producing optimal materials. The control of nucleation is sometimes fairly easily demonstrated by inspection of tissue ultrastructure, but how it is achieved is certainly one of the most fundamental questions to be addressed in biomineralization.

7.1. Specially Designed Nucleating Proteins

Conceptually the use of specific proteins adsorbed on a rigid substrate is a good strategy for nucleation, because nucleation will not occur until the nucleating macromolecule is in the correct place. This in turn requires that the nucleator is not only able to induce crystal nucleation but also able to also locate itself at a specific site on the framework scaffold. In the case of the nacreous layer (Excursus 5) the driving force of this process might be due to an alternating sequence within the acidic proteins.[113] When the chain adopts a β-sheet structure, the more hydrophobic residues form a surface which is adsorbed onto the scaffolding protein. The scaffolding matrix, also a β-sheet structure, holds and probably partly governs the folding of the soluble protein (Fig. 3). The acidic residues point towards the solution and form the nucleation site. They bind calcium ions in a layer, which constitutes the interface with the about-to-be-formed crystal. The formation of this initial two-dimensional calcium layer dictates that the nascent crystal will form with its *c* axis perpendicular to the nucleating surface. In vitro experiments using acidic macromolecules from mollusk shells show that when bound to a rigid substrate, some but not all of these proteins are able to induce the nucleation of calcite

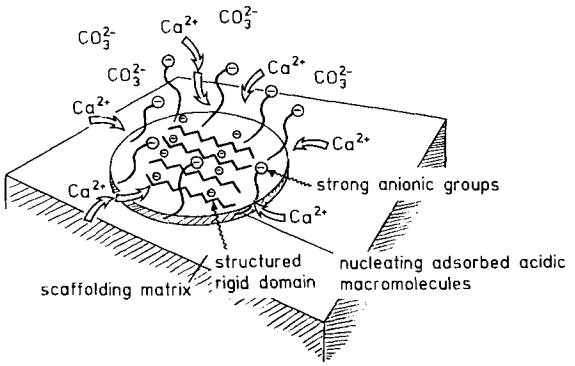

Fig. 3. Schematic representation of a nucleation site in the nacreous layer of a mollusk shell. The soluble acidic protein is immobilized by adsorption on the scaffolding matrix. Nucleation ensues by the cooperative action of flexible concentrating groups and structuring rigid domains.

crystals with their c axes perpendicular to the plane of the nucleating substrate[50] (Fig. 4). This is the most common orientation in vivo for calcite as well as aragonite. In both structures the c axis is perpendicular to layers of calcium and carbonate[54] (Fig. 5).

There is evidence, albeit indirect, for specific nucleating proteins in the nacreous layer (Excursus 5), but for almost all other tissues their existence is still hypothetical. In bone, for example, the crystals are located in spaces within the collagen fibril. Unless they are nucleated on the fibril surface and then grow into the fibril, there is little or no space available within the fibril for a nucleating molecule. At this stage, we limit ourselves to a description of the properties that contribute to controlled nucleation, based on in vitro studies of mollusk acidic glycoproteins.

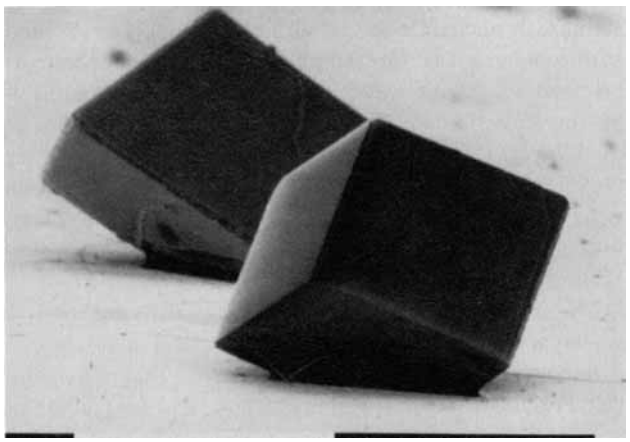

Fig. 4. Synthetic crystals of calcite nucleated from mollusk-shell acidic proteins adsorbed on an artificial substrate. The crystals are oriented with their c axes perpendicular to the substrate and assume the typical cleavage rhombohedron morphology of nonbiogenic calcite. (The scale bar is marked in 0.1 mm intervals.)

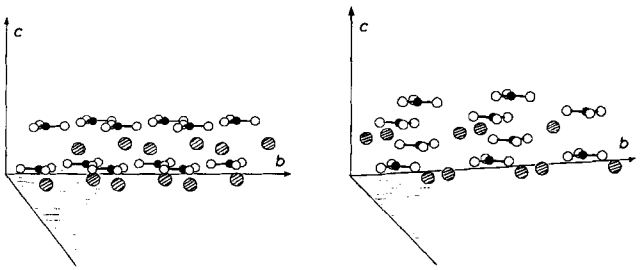

Fig. 5. Partial structures of calcite (left) and aragonite (right). The (001) layers in contact with the nucleating surface are represented. The calcium layers are practically identical; The difference between the two structures is reflected in the positions of the carbonate ions. Hatched circles are Ca ions; black circles, C atoms; and white circles, O atoms.

7.2. Conformation and Rigidity

Acidic soluble proteins can be nucleating in the adsorbed state but inhibit crystallization when present in solution. This ensures that crystallization will not take place in the wrong place and at the wrong time. Inhibition of crystallization from solution is guaranteed by the flexibility of the polypeptide chain in solution. We proposed that nucleation on the substrate is catalyzed by an array of carboxylate groups of aspartic acid residues locked in an ordered and rigid conformation.[55] In solution an extended sheet is not stable and rigid enough to be a good substrate for formation and stabilization of crystal nuclei. This hypothesis is supported by data from diverse fields. Flexible polyelectrolytes are well-known inhibitors of crystal nucleation and growth.[56] On the other hand, it has been observed that the same groups immobilized in a monolayer are selective nucleators of crystals[57, 58] from planes matching the monolayer surface structure. In experiments with tailor-made polymeric inhibitors, it has also been shown that an array of side chains, which match the structure of a mature crystal, selectively inhibit its nucleation when they are present in solution.[59]

In an attempt to understand the mechanism of oriented nucleation we have studied some model systems, including polycarboxylates in various conformations.[41] We observed that polyaspartate, which was adsorbed with partial β-sheet structure onto sulfonated polystyrene films, induces nucleation of calcite from the calcium (001) plane. Adsorbed polyacrylate with a random conformation, does not have the same effect, and polyglutamate with a small proportion of β-sheet structure relative to polyaspartate has an intermediate effect. All three polymers are strong inhibitors of calcite nucleation and growth from solution, because they adsorb onto the surface of the calcite crystallites or nuclei and retard and/or disrupt their growth.

It is interesting that the behaviour of these relatively small polymers and surface-active proteins is opposite to that of large globular proteins, yet the basic mechanisms involved are the same. Human serum albumin acts in vitro from solution as a nucleator of crystals of sodium urate monohydrate,[60] with the involvement of a number of carboxylate groups on its surface. The protein is large and stable enough to produce rigid domains on its surface even in solution. These stabilize the crystal's nuclei by interaction with their cation layer. On the other hand, adsorption of the protein on polystyrene films results in the total loss of this nucleating power. The adsorbed protein undergoes partial denaturation upon adsorption,[44] probably concomitant with disruption of the integrity of the nucleating domains.

7.3. Cooperative Interactions

An additional element that has been identified in the nucleation mechanism is the cooperativity between the array of structured, rigid carboxylates mentioned above and anionic sulfate groups attached to flexible oligosaccharide chains. Sulfated polysaccharides linked to polypeptide chains (proteoglycans) are present in cartilage and are involved in the osmotic equilibrium of the tissue through cation concentration. In the nucleation of calcium carbonate crystals the same effect has been postulated;[61] calcium ions are directed to the fixed carboxylate positions, where crystallization ensues by further carbonate binding[55] (see Fig. 3). The feasibility of such a process has been demonstrated in model systems of flexible polystyrene sulfonate chains and adsorbed polyaspartate with β-sheet structure. Again, the same process cannot occur in solution because of the lack of organization created by the restriction of mobility in the absorbed state.

Sodium cations are abundant in sea water and in the fluid found between the mantle and the shell (extrapallial fluid) of mollusks. Their concentration (0.5 M) is much higher than that of calcium, and as a result they interfere with the interactions between calcium and acidic proteins in solutions.[62] The composition of the actual fluid in contact with the matrix before crystal nucleation is, however, unknown. One may speculate on the existence of an additional possible mechanism which would ensure that crystallization occurs only when desired; this could be achieved by selective removal or supply of disturbing cations like sodium at the nucleation site. It is well known that ion separation can be accomplished by biological membranes. The marine protozoans *Acantharia* filter strontium from sea water against an enormous concentration gradient to build their strontium sulfate skeletons. They are capable of discriminating Sr from Ca ions, which are similar to Sr ions but much more abundant.[63] Sea urchins build their skeletons out of magnesium-containing calcite, parts of which contain as much as 40 mole percent Mg.[64] The calcite of mollusk shells generally contains very little magnesium. Clearly Mg contents are also well controlled.[65] It is therefore conceivable that sodium may be selectively removed, in order to activate certain proteins at the nucleation site by allowing them to interact more strongly with calcium.

8. Control Over Polymorph Type

Many organisms exert total control over the type of polymorph precipitated, and biology abounds with examples of organisms crystallizing a compound with a certain structure at one site and with a second structure at a different, often adjacent site.[1, 2] We do not understand how this is achieved, nor what advantages one polymorphic material offers over another.

According to the rules of thermodynamics, crystallization is favored when the absolute value of the bulk energy of the crystal nucleus is equal to or greater than the energy of interaction with the environment (surface energy). A solution, which is supersaturated with respect to the stable but not the metastable polymorph of a certain material, can yield crystals of the stable polymorph only. On the other hand, if the solution is supersaturated with respect to more than one crystalline form, all of them can precipitate. The equilibrium condition of lowest energy is obtained when all the less stable polymorphic forms transform into the most stable one. These considerations are only thermodynamic. It is known, however, that both the formation of a particular polymorph and the transformation of one phase into another can be kinetically controlled.[66]

In principle, crystallization of a metastable polymorph can be achieved by two opposing mechanisms: inhibition of nucleation of the stable form or preferred nucleation of the metastable form. There are many examples involving organic molecules of the former[59] and very few, if any, of the latter method of control.[58]

It is most convenient to study these processes using organic molecules, because they are easier to manipulate stereochemically. A tailor-made additive, resembling the mature crystal structure of the stable form and not the metastable form, can delay nucleation of the former sufficiently to allow crystallization of the less stable phase.[59] These experiments also support the notion that supersaturated solutions contain aggregates with a variety of different structures, some of which at least resemble the different mature crystal forms. When the crystallization of some of these is selectively inhibited, the growth of the others is kinetically favored. In an analogous manner, organized surfaces matching one polymorph on a certain crystal plane can in principle selectively stabilize its nuclei. Organized surfaces of monolayers[67] and surface aggregates[68] of amphiphilic molecules operate as crystal nucleators and can influence polymorph choice following this mechanism. It has been shown that stearate monolayers induce the nucleation of vaterite, an unstable polymorph of calcium carbonate. The induction mechanism is not completely understood, but a dependence on the orientation of the carbonate ions to the (001) nucleating plane has been proposed.[58]

The most widespread examples of the determination of crystal polymorphs in biomineralization occur in the calcium carbonates, calcite, aragonite, and vaterite. Thermodynamically, calcite is the most stable polymorph at normal atmospheric temperatures. Aragonite is less stable than calcite, and the most unstable polymorph is vaterite. The stabilities of calcite and aragonite in water are very similar, yet organisms are able to manipulate them with the highest precision. The presence of other doubly charged ions, such as magnesium and strontium, favor the formation of aragonite and calcite respectively.[69] Aragonite has a denser structure, which probably cannot accommodate the smaller magnesium ion, because of the larger hydration sphere associated with the ion during adsorption at the growing crystal sites. Magnesium can, however, be accomodated inside calcite, where it acts as an inhibitor of crystal growth. Sea water has high concentrations of Mg, and aragonite is indeed the polymorph formed spontaneously from sea water. Polymorphism may thus be regulated at the chemical level by adjusting the foreign ion composition and by kinetically preventing growth of the stable polymorph. On the other hand, control can also be envisaged at the nucleation level. We note, however, that the (001) layers of calcite and aragonite from which the crystals are most often nucleated, are practically

identical in terms of the positions of their calcium ions. Selective nucleation of one of the two polymorphs would probably have to include specification of the position of the carbonate anions as well (see Fig. 5).

The calcium phosphate minerals present another classic dilemma in our understanding of biomineralization. The dahllite (carbonate apatite) crystals of bone display a whole series of inconsistencies. They are not stoichiometric compounds,[70] their crystal dimensions ($\sim 200 \times 500 \times 30$ Å^3)[71] imply a very high surface/bulk ratio, and their crystal morphology, namely irregularly shaped, thin plates[71] elongated in the direction of the *c* axis,[71] does not reflect the symmetry of the hexagonal structure. The persistence of a "memory effect" of precursor phases has been proposed in order to explain some of these phenomena.[72] Indeed the phase diagram of calcium phosphate shows a wealth of different forms, whose formation and transformations are functions of pH, temperature, concentration, and presence of foreign inorganic and organic components.[73] The most likely precursor of apatite, octacalcium phosphate, has a structure almost identical to that of hydroxyapatite in one layer in the (100) plane[72] (Fig. 6). However, the hydroxyapatite layers are intercalated by hydrated layers also parallel to (100). These must be removed for the ions to assemble into the apatite structure. Although much is known about the behaviour of these systems in vitro, little is known yet about the nature and history of the nucleating crystals in bone.

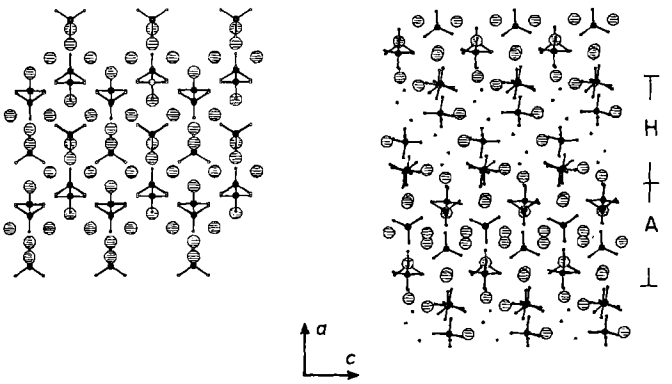

Fig. 6. Packing arrangements of hydroxyapatite (left) and octacalcium phosphate (right) in the (010) plane. In the structure of octacalcium phosphate the hydrated layer H is intercalated between "apatite layers" A in the (100) plane. Hatched circles are Ca ions; black circles, P atoms; and small white circles, O atoms. The *a* and *c* axes apply for both structures.

The concept of the transformation of one phase into another with a possible memory effect raises interesting possibilities regarding the transformation of amorphous phases into crystalline ones. Such transformations are known to occur in biology;[1] One of the best documented examples concerns chiton teeth (Excursus 1). Can the presence of very small domains of short-range order within an amorphous structure govern its transformation to a mature crystalline phase?[74] If this is possible, then the conditions of precipitation of the original amorphous phase or the presence of trace constituents may influence the short-range order domains and consequently the nature of the mature phase long before the final transformation. Removal of inhibitors or a change in the environmental conditions can then trigger crystallization allowing these prenuclei to grow.

9. Filling Space with Crystal Arrays: The Design of Biological Materials

The formation of mechanically sound mineralized tissues by organisms requires sophistication, and in fact it took nature thousands of millions of years to acquire this ability. Depending upon the degree of sophistication involved, it requires confining a space, controlling ion input, constructing a nucleation site, and controlling crystal morphology and orientation—processes which we have discussed individually. Here we conclude this review by surveying some of the products of these combined activities, namely the mineralized biological materials themselves.

Perhaps the simplest approach of all for organisms to form a material involves confining a space, pumping ions into it, and inducing crystals to form around nonspecific, randomly located nucleation sites. The product is a mineralized mass of spherulites. Examples of such materials are the spicules protruding from the mantle girdle of the chiton[75] (Fig. 7 upper left), the cameral deposits of the *Nautilus*[76] (Excursus 2), and the reinforced walls of the calcareous alga, *Halimeda*[77] (Excursus 4). The end-product is rather porous, has little or no internal organization, and in many ways resembles a synthetic ceramic.

By controlling the nucleation sites, and in particular by distributing them in some sort of regular manner, a significantly more ordered tissue can be formed, still on the basis of spherulites. Examples in which this strategy is used are fish otoliths[78] (Excursus 2) and avian eggshells[79] (Fig. 7 upper right). In the eggshell the nucleation site is controlled by organic molecules, including sulfated polysaccharides that form rounded structures. The calcite crystals nucleate with their *c* axes more or less perpendicular to the surface. Because the nucleation site is very close to the inner membrane, the crystals are prevented from growing in this direction. Crystals oriented in other directions stop growing upon contact with crystals from a neighboring nucleation site, or when they reach the distantly located outer membrane. Thus many of the crystals show a pseudo-preferred orientation simply because of the geometry of the available space. The packing density of this product is most certainly improved.

The previous examples involve the formation of multiple crystals at a single nucleation site. Much more control can be achieved when only one crystal is produced from a single nucleation site. In biology this phenomenon tends to occur concomitantly with the isolation of the local space around the nucleation site, such that an individual crystal forms in its own predefined space. The ideal example of this is the mollusk prismatic layer (Fig. 7 lower left), in which individual crystals of calcite, or less frequently aragonite, form in their own framework.[80] Mollusk mineralized tissues formed in this way generally comprise more than 95% mineral, less than 5% matrix,[81] and have a high density and excellent order. The crystal size is usually in the range of microns or submicrons.

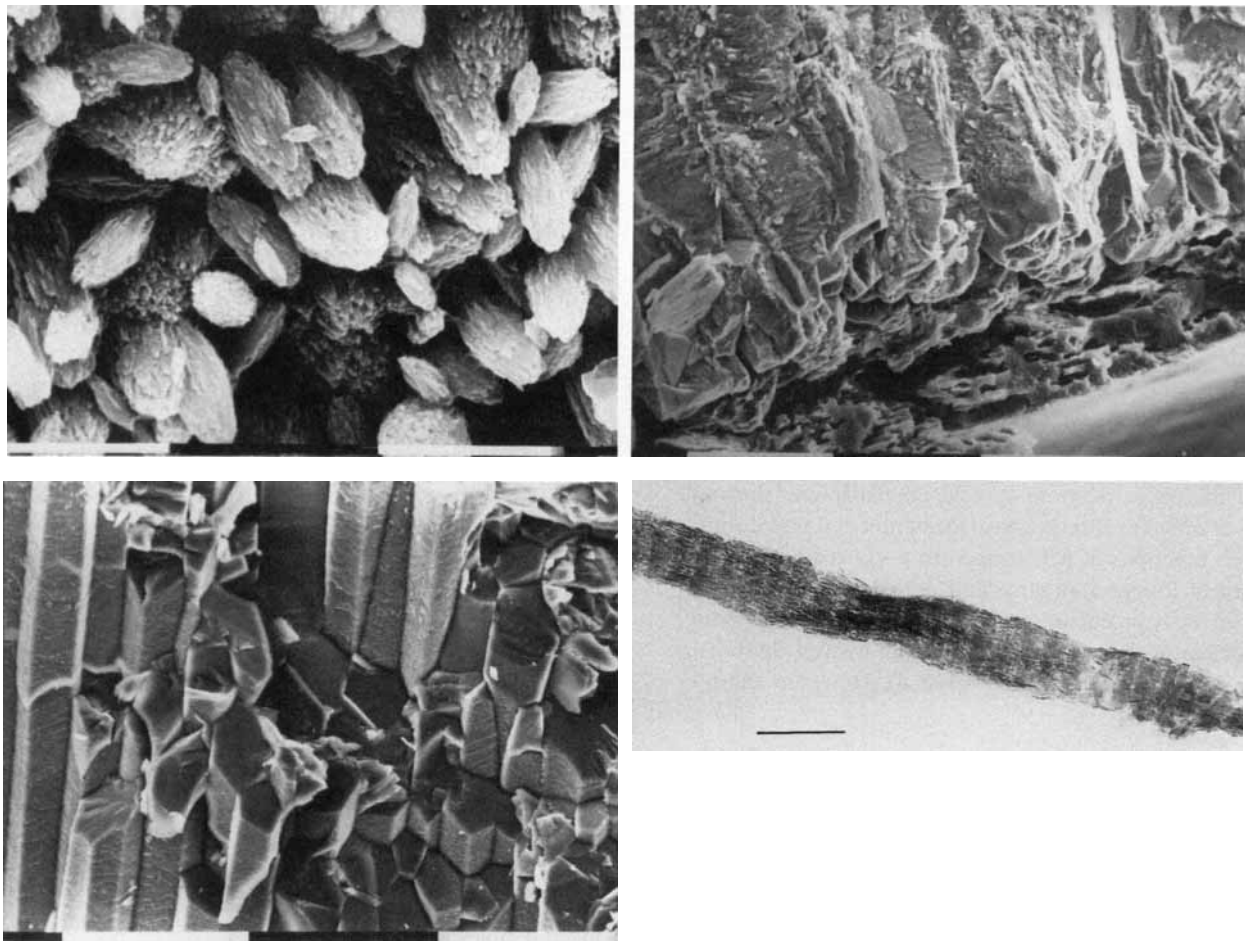

Fig. 7. Examples of four different approaches used by organisms for filling space with crystal arrays. Upper left: Aragonitic spherulites that make up the girdle spicules of the chiton *Acanthopleura haddoni* (Mollusca). The spherulites show no preferred orientation and are loosely packed (the scale bar is marked in 10 μm intervals). Upper right: View of the cross section and inner surface of the shell of a domestic hen's egg. In the lower part the nucleation centers of the calcite crystals can be seen, and in the upper part, the fusing of the crystals into columnar structures. (The scale bar is marked in 0.1 μm intervals.) Lower left: The calcitic prismatic outer layer of the shell of the bivalve, *Atrina serrata*. Each calcitic crystal nucleates from a single site and grows inside an organic matrix framework (not seen). (The scale bar is marked in 0.1 mm intervals.) Lower right: View from a transmission electron microscope of an individual lyophilized, but unstained mineralized collagen fibril from a turkey leg tendon. The electron density observed is due to the presence of the thin plate-shaped dahllite crystals located preferentially in the gap regions of the collagen fibril, thus revealing the characteristic banding pattern. The fibril is twisted such that in one region the crystals are viewed edge-on, and in other areas, face-on. The collagenous framework in which the crystals grow is not seen. (The line corresponds to 2.00 nm.)

In the formation of mineralized collagen fibrils, the building block of bone, dentin, and mineralized tendons, similar processes are involved, but the scale of the product is very different. Individual plate-shaped crystals of dahllite, just a few hundred Å in length and width and only 20 to 30 Å thick[71] are nucleated at specific sites on or within the collagen fibril. They grow into a preformed space within the fibril, which has the shape of a thin groove or channel.[82] These grooves do prevent the crystals from growing, but only momentarily.[83] The crystals continue to push their way into the overlap zone of the fibril.[84] The collagen framework apparently yields and the crystals essentially create their own space (Fig. 7 lower right). This was demonstrated by neutron-diffraction studies which showed that as the crystals grow the triple-helical collagen molecules come closer together; the average separation distances between collagen molecules is thereby reduced from about 15 to 12 Å.[85] Bone is a highly ordered composite material; the matrix comprises some 20% of the tissue by weight, mineral, 60 to 70%, and water, the rest.[86] The mechanical properties of bone—such as Young's modulus (the modulus of elasticity), bending strength, and work of fracture—are all directly related to the proportion of mineral present,[87] a parameter which is under strict biological control.

Another highly ordered tissue useful for illustrating design principles is the mollusk nacreous layer (Excursus 5). Here, too, nucleation involves the induction of a single crystal per nucleation site, but unlike many other tissues, the orientation of the crystal is completely controlled in all three dimensions relative to the structure of the matrix substrate. The crystals rapidly grow with their *c* axes perpendicular to the nucleating surface and adopt the normal acicular (needle-like) morphology of aragonite (Excursus 5). They stop growing in this direction when they meet the next prepositioned matrix layer and then only grow laterally. They stop growing altogether either when adjacent crystals touch each other or when they meet a matrix surface—as yet an unresolved issue. A most curious property of nacre results from the fact that some mollusks, such as the gastropods, do not control the relative orientations of neighboring crystals, except in the direction of the *c* axes. Individual crystals are, however, still specifically oriented with respect to the matrix substrate. In

contrast many bivalves and the cephalopod *Nautilus* do orient neighboring crystals such that their *a* and *b* axes are preferably aligned, in addition to the orientation of the *c* axes. Two bivalve species, *Neotrigonia margaritacea* and *Pinctada margaritifera*, are known to control the orientation of their *a* and *b* axes remarkably well.[38] It would be most interesting to determine whether the order of these crystal arrays offers any advantages, mechanical or other.

The more sophisticated space-filling strategies used by organisms rely heavily on the intervention and abilities of the cells themselves over and above the presumably exquisite structural design properties of the associated matrix macromolecules. These are properties which are well-nigh impossible to mimic in synthetic systems.

Excursus 5: The Mollusk Shell Nacreous Layer

The nacreous layer is responsible for the pearly luster of the inner surfaces of many mollusk shells and, of course, for the much admired pearl itself. The luster arises from the interference patterns of light passing through the alternating layers of uniformly thick aragonite crystals and organic matrices (Fig. E, upper left). The shell layer is formed by mantle cells which first assemble an organic matrix framework within the extracellular space composed primarily of layers parallel to the shell surface.[103] Each layer is in itself composed of no less than five sublayers (Fig. E, lower left).[104] The core is a highly ordered β-chitin–protein complex, whose proteins are rich in glycine and alanine and have a β-sheet structure similar to that of silk fibroin. The chitin polymers and the protein polypeptide-chains are orthogonally aligned forming a plywoodlike construction.[105] The surfaces of this core are coated with a layer of proteins rich in aspartic acid, possibly also with β-sheet structure.[106] Nucleation of the aragonite crystals takes place at a specific site on the surface which is known to have unique calcium-binding properties and to be rich in sulfur, presumably in the form of sulfate.[107] The nascent crystals grow rapidly in the direction of their *c* axes, initially appearing to have the normal acicular morphology of aragonite (Fig. E, upper right). When the crystals reach the surface of the next matrix layer they stop growing in the *c* axis direction, but continue growing laterally. The shape of the laterally growing crystals in the bivalve *Neotrigonia* are spherical (Fig. E, upper right), suggesting a nonspecific interaction with additives in solution. The growing crystals exhibit different shapes depending upon the species involved, implying more specific or less specific interactions.

The mollusk nacreous layer was the first mineralized tissue in which the spatial relations between crystal and organic matrix substrate were determined in three dimensions.[105, 108] It was shown that the *a* axis of the aragonite is aligned with the direction of the chitin polymer, and the *b* axis, with the protein polypeptide-chains of the core. It is assumed that the acidic surface proteins at the nucleation site are also aligned in a regular manner vis-a-vis the crystal, and that they are responsible for the observed spatial relation. Even though this is certainly a case of the oriented growth of a crystal on a substrate, actually proving that this is indeed true epitaxy requires more information on the structure of the nucleation site itself—one of the most challenging goals in the field of biomineralization.

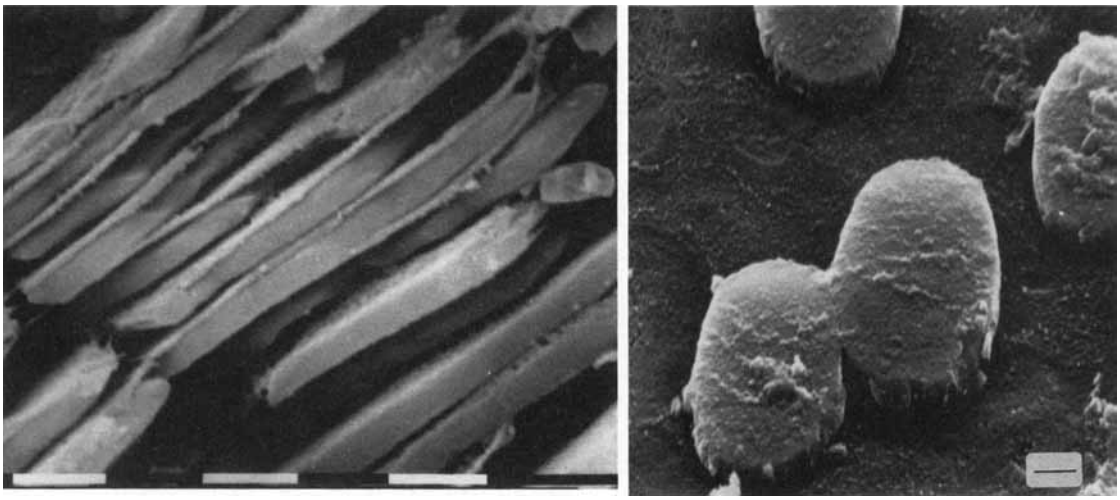

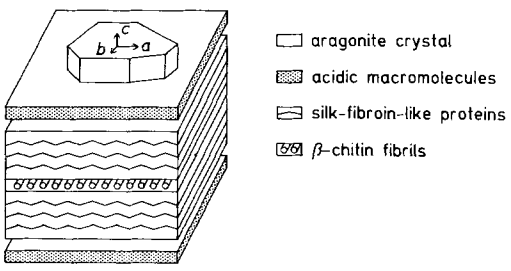

Fig. E. Upper left: Fractured surface of the aragonitic nacreous layer of the cephalopod, *Nautilus pompilius*. The surface was fixed and then etched for about a minute in EDTA to reveal the thin organic matrix-layers between the thicker aragonitic tablets. (The scale bar is marked in intervals of 1 μm.) Lower left: Schematic illustration of the structure of an individual matrix layer with its associated crystal. It can be seen that the crystallographic *a* and *b* axes of the aragonite are aligned with the macromolecular matrix constituents (printed with permission from Oxford University Press). Upper right: The surface of the growing nacreous layer of the bivalve *Neotrigonia margaratifera*. The oval-shaped aragonitic tablets growing laterally can be recognized. The rough texture on the tablet surfaces may represent the initial stages of formation of the next layer. The organic matrix is not distinctly seen in this preparation. (The line on the lower right of the picture represents 1 μm.)

10. Concluding Comments

The diversity in texture, composition, and scale of mineralized biological materials is enormous. These materials are adapted to a wide variety of functions. They may not, however, necessarily represent the "perfect" solution to each specific functional requirement; evolutionary limitations exist that restrict the extent to which mineralized materials can be optimally designed. Understanding the principles involved in their construction and modes of function is a fascinating subject in its own right. Furthermore, identifying the underlying mechanisms common to the formation processes of different mineralized materials provides insight into key underlying biological phenomena. The results of such investigations may well be a rich source of ideas for improving our ability to fabricate synthetic materials.

We thank the U.S.-Israel Binational Science Foundation and the U.S. Public Health Service (Grant DE 06954) for their support.

Received: April 3, 1991 [A 852 IE]
German version: *Angew. Chem.* **1992**, *104*, 159

[1] H. A. Lowenstam, S. Weiner, *On Biomineralization*, Oxford University Press, New York, **1989**.
[2] a) K. Simkiss, K. M. Wilbur, *Biomineralization*, Academic, San Diego, **1989**; b) *Biomineralization. Chemical and Biochemical Perspectives* (Eds.: S. Mann, J. Webb, R. J. P. Williams), VCH, Weinheim, **1989**.
[3] *Cell and Molecular Biology of Vertebrate Hard Tissues* (Eds.: D. Evered, S. Harnett, Ciba Foundation Symposium 136), Wiley, Chichester, **1988**.
[4] a) *Biomineralization and Biological Metal Accumulation* (Eds.: P. Westbroek, E. W. de Jong), Reidel, Dordrecht, **1983**; b) R. H. Kretsinger in [4a], pp. 123–131.
[5] *Silicon and Siliceous Structures in Biological Systems* (Eds.: T. L. Simpson, B. E. Volcani), Springer, New York, **1981**, p. 587.
[6] D. R. Piperno, *Phytolith Analysis*, Academic, San Diego, **1988**.
[7] B. E. Brown, *Biol. Rev.* **1982**, *57*, 621–667; K. Simkiss, *Symp. Soc. Exp. Biol.* **1976**, *30*, 423-444.
[8] B. Howard, P. C. H. Mitchell, A. Ritchie, K. Simkiss, M. G. Taylor, *Biochem. J.* **1981**, *194*, 507–511; M.G. Taylor, K. Simkiss in [2b], pp. 427-460.
[9] *Magnetite Biomineralization and Magnetoreception in Organisms* (Eds.: J. L. Kirschvink, D. S. Jones, B. J. McFadden), Plenum, New York, **1985**.
[10] J. L. Kirschvink, M. M. Walker in [9], pp. 243–254.
[11] A. Veis, A. Perry, *Biochemistry* **1967**, *6*, 2409–2416.
[12] a) *Surface Reactive Peptides and Polymers* (Eds.: C. S. Sikes, A. P. Wheeler), (*ACS Symp. Ser.* **1991**, *444*); b) A. Veis, B. Sabsay, C. B. Wu in [2a], pp. 1–12.
[13] S. Weiner, W. Traub, H. A. Lowenstam in [4a], pp. 205–224.
[14] A. P. Wheeler, C. S. Sikes in [2b], pp. 95–131.
[15] S. Weiner, L. Hood, *Science* **1975**, *190*, 987–989.
[16] S. L. Lee, A. Veis, T. Glonek, *Biochemistry* **1977**, *16*, 2971–2979.
[17] D. Worms, S. Weiner, *J. Exp. Zool.* **1986**, *237*, 11–20.
[18] J. D. Termine in [3], pp. 178–190.
[19] H. Sucov, S. Benson, J. J. Robinson, R. J. Britten, F. Wilt, E. H. Davidson, *Dev. Biol.* **1987**, *120*, 507–519.
[20] K. Simkiss in [26], pp. 19–37.
[21] J. D. H. Donnay, D. Harker, *Am. Mineral.* **1937**, *22*, 446–467; P. Hartman, W. G. Perdok, *Acta Crystallogr.* **1955**, *8*, 49–52; *ibid.* **1955**, *8*, 521–524.
[22] E. N. K. Clarkson, *Paleontology* **1973**, *16*, 425–444; E. N. K. Clarkson, R. Levi-Setti, *Nature* **1975**, *254*, 663–667.
[23] S. Caveney, *Proc. R. Soc. London B* **1971**, *178*, 205–225.
[24] W. H. Zachariasen, *J. Am. Chem. Soc.* **1932**, *54*, 3841–3852.
[25] C. C. Perry, S. Mann, in *Evolution and Modern Aspects of Biomineralization in Plants and Animals* (Eds.: R. E. Crick), Elsevier, Amsterdam, **1988**.
[26] *Biomineralization in Lower Plants and Animals* (Eds.: B. S. C. Leadbeater, R. Riding), Clarendon, Oxford, **1986**.
[27] G. G. Simpson, *Horses*, Oxford University Press, New York, **1951**.
[28] G. H. Nancollas, in [2b], pp. 157–187.
[29] H. A. Lowenstam, S. Weiner, *Science* **1985**, *227*, 51–53.
[30] H. A. Lowenstam, *Chem. Geol.* **1972**, *9*, 153–166.
[31] S. A. Stricker, S. Weiner, *Experientia* **1985**, *41*, 1557–1559.
[32] E. V. Lengyel, *Z. Kristallogr.* **1937**, *97*, 67–87; J. Dedek, *Le carbonate de Chaux*, Librarie Universitaire, Louvain, **1966**, pp. 19–20.
[33] M. Prenant, *Arch. Zool. Exp. Gen. Note Rev.* **1926**, *65*, 25–38.
[34] A. Berman, L. Addadi, A. Kvick, L. Leiserowitz, M. Nelson, S. Weiner, *Science* **1990**, *250*, 664–667.
[35] a) K. Okazaki, *Embryologia* **1960**, *5*, 283–320; K. Märkel, U. Röser, M. Stauber, *Zoomorphology* **1989**, *109*, 79–87; b) K. Märkel, Universität Bochum, private communication.
[36] M. Shimizu, J. Yamada in: *The Mechanisms of Biomineralization in Animals and Plants* (Eds.: M. Omori, N. Watabe), Tokai University Press, Tokyo, **1980**, pp. 169–178.
[37] K. M. Towe, *Science* **1967**, *157*, 1048–1050.
[38] S. W. Wise, *Ecolgae Geol. Helv.* **1970**, *63*, 775–797; S. Weiner, W. Traub in *Structural Aspects of Recognition and Assembly in Biological Macromolecules* (Eds.: M. Balaban, J. L. Sussman, W. Traub, A. Yonath), Balaban ISS, Rehovot, **1981**, pp. 467–482.
[39] S. Weiner, *J. Exp. Zool.* **1985**, *234*, 7–15.
[40] A. Berman, L. Addadi, S. Weiner, *Nature* **1988**, *333*, 546–548.
[41] L. Addadi, J. Moradian-Oldak, S. Weiner in [12a], pp. 13–27.
[42] J. D. Birchall, R. J. Davey, *J. Cryst. Growth* **1981**, *54*, 323–329.
[43] C. C. Chen, A. L. Boskey, *Calcif. Tissue Int.* **1985**, *37*, 935.
[44] D. Hanein, *M.Sc. Thesis*, Feinberg Graduate School, Weizmann Institute, Rehovot, Israel, **1989**.
[45] S. Mann, N. H. C. Sparks, R. P. Blakemore, *Proc. R. Soc. London B* **1987**, *231*, 469–476; T. Matsuda, T. Endo, N. Osakabe, A. Tonomura, T. Arii, *Nature* **1983**, *302*, 411–412.
[46] Y. A. Garby, T. J. Beveridge, R. P. Blakemore, *J. Bacteriol.* **1988**, *170*, 834–841.
[47] H. E. Buckley, *Z. Kristallogr.* **1935**, *91*, 375–401; A. F. Wells, *Philos. Mag.* **1946**, *37*, 184–199; *ibid.* **1946**, *37*, 217–236; *ibid.* **1946**, *37*, 605–630.
[48] L. Addadi, Z. Berkovitch-Yellin, I. Weissbuch, J. van Mil, L. J. W. Shimon, M. Lahav, L. Leiserowitz, *Angew. Chem.* **1985**, *97*, 476–496; *Angew. Chem. Int. Ed. Engl.* **1985**, *24*, 466–485; L. Addadi, Z. Berkovitch-Yellin, I. Weissbuch, M. Lahav, L. Leiserowitz, *Top. Stereochem.* **1986**, *16*, 1–80.
[49] Z. Berkovitch-Yellin, J. van Mil, L. Addadi, M. Idelson, M. Lahav, L. Leiserowitz, *J. Am. Chem. Soc.* **1985**, *107*, 3111–3122.
[50] L. Addadi, S. Weiner, *Proc. Natl. Acad. Sci. USA* **1985**, *82*, 4110–4114.
[51] L. Addadi, A. Berman, J. Moradian-Oldak, S. Weiner, *Connect. Tissue Res.* **1989**, *24*, 127–135; J. Moradian-Oldak, F. Frolow, L. Addadi, S. Weiner, *Proc. R. Soc. London B*, **1992**, in press.
[52] H. Furedi-Milhofer, L. Addadi, S. Weiner, unpublished results.
[53] J. Moradian-Oldak, *Ph.D. Thesis*, Feinberg Graduate School, Weizmann Institute, Rehovot, Israel, **1992**.
[54] L. Addadi, S. Weiner, in [2b], pp. 133–156.
[55] L. Addadi, J. Moradian, E. Shai, N. Maroudas, S. Weiner, *Proc. Natl. Acad. Sci. USA* **1987**, *84*, 2732–2736.
[56] S. Sarig, F. Kahana, R. Leshem, *Desalination* **1975**, *17*, 215.
[57] E. Landau, R. Popovitz-Biro, M. Levanon, L. Leiserowitz, M. Lahav, J. Sagiv, *Mol. Cryst. Liq. Cryst.* **1986**, *134*, 323–335.
[58] S. Mann, B. R. Heywood, S. Rajam, J. D. Birchall, *Nature* **1988**, *334*, 692–695; S. Mann, B. R. Heywood, S. Rajam, J. D. Birchall, *Proc. R. Soc. London A* **1989**, *423*, 457–471.
[59] I.Weissbuch, D. Zbaida, L. Addadi, L. Leiserowitz, M. Lahav, *J. Am. Chem. Soc.* **1987**, *109*, 1869; E. Staab, L. Addadi, L. Leiserowitz, M. Lahav, *Adv. Mater.* **1990**, *2*, 40–43.
[60] D. Perl-Treves, L. Addadi, *Proc. R. Soc. London B* **1988**, *235*, 145–159; *Mol. Cryst. Liq. Cryst.* **1990**, *187*, 1–16.
[61] M. Thiele, A. Awad, *J. Biomed. Mater. Res.* **1969**, *3*, 431–444; M. A. Crenshaw, M. Ristedt, *Biomineralisation* **1975**, *8*, 1–8.
[62] A. P. Wheeler, K. W. Rusenko, J. W. George, C. S. Sykes, *Comp. Biochem. Physiol. B* **1987**, *87*, 953–960.
[63] C. C. Perry, J. R. Wilcock, R. J. P. Williams, *Experimentia* **1988**, *44*, 638.
[64] J. H. Schroeder, E. J. Dwornik, J. J. Papike, *Geol. Soc. Am. Bull.* **1969**, *80*, 1613–1616.
[65] H. A. Lowenstam in *Recent Researches in the Field of Hydrosphere, Atmosphere and Nuclear Chemistry* (Eds.: Y. Miyake, T. Koyama), Maruzen, Tokyo, **1964**, pp. 373–404.
[66] J. Garside in *Biological Mineralization and Demineralization* (Eds.: G. H. Nancollas), Springer, Berlin, **1982**, pp. 23–36.
[67] E. M. Landau, M. Levanon, J. Leiserowitz, M. Lahav, J. Sagiv, *Nature* **1985**, *318*, 353–356.
[68] I. Weissbuch, F. Frolow, L. Addadi, M. Lahav, L. Leiserowitz, *J. Am. Chem. Soc.* **1990**, *112*, 7718–7724.
[69] Y. Kitano, *Bull. Chem. Soc. Jpn.* **1962**, *35*, 1873–1980.
[70] S. Morgulis, *J. Biol. Chem.* **1931**, *31*, 455–466; D. McConnell, *Clin. Orthop.* **1962**, *23*, 253–268.
[71] R. A. Robinson, *J. Bone Jt. Surg.* **1952**, *34*, 389–434; S. Weiner, P. A. Price, *Calcif. Tissue Int.* **1986**, *39*, 365–375; J. Moradian-Oldak, S. Weiner, L. Addadi, W. J. Landis, W. Traub, *Conn. Tissue Res.* **1990**, *25*, 1–10.
[72] W. E. Brown, *Nature* **1962**, *196*, 1048–1055; *Clin. Orthop. Relat. Res.* **1966**, *44*, 205–220.

[73] H. Füredi-Milhofer, B. Purgaric, L. Brecevic, N. Pavkovic, *Calcif. Tissue Res.* **1971**, *8*, 142-153.
[74] H. A. Lowenstam, *Chem. Geol.* **1972**, *9*, 153–166.
[75] a) *The Mechanisms of Mineralization in the Invertebrates and Plants* (Eds.: N. Watabe, K. M. Wilbur), Univ. South Carolina Press, Columbia, **1976**; b) W. Haas in [75 a], pp. 389–402.
[76] H. Mutvei, *Bull. Geol. Inst. Univ. Uppsala* **1972**, *8*, 237–261.
[77] K. M. Wilbur, L. H. Colinvaux, N. Watabe, *Phycologia* **1969**, *8*, 27–35.
[78] E. T. Degens, W. G. Deuser, R. L. Haedrich, *Mar. Biol. Berlin* **1969**, *2*, 105–113; R. W. Gauldie, D. G. A. Nelson, *Comp. Biochem. Physiol. A* **1988**, *90*, 501–509.
[79] K. Simkiss in *Egg Quality: A Study of the Hen's Egg* (Eds.: T. C. Carter), Oliver and Boyd, Edinburgh, **1968**, pp. 3–25; H. Silyn-Boberts, R. M. Sharp, *Proc. R. Soc. London B* **1986**, *227*, 303–324.
[80] H. Nakahara, G. Bevelander *Calcif. Tissue Res.* **1971**, *7*, 31–45.
[81] P. E. Hare, P. H. Abelson, *Year Book Carnegie Inst. Washington* **1965**, *64*, 223–234.
[82] E. P. Katz, E. Wachtel, M. Yamauchi, G. L. Mechanic, *Conn. Tissue Res.* **1989**, *21*, 149–158; W. Traub, T. Arad, S. Weiner, *Proc. Natl. Acad. Sci USA* **1989**, *86*, 9822–9826.
[83] W. Traub, T. Arad, S. Weiner, *Conn. Tissue Res.*, **1992**, in press.
[84] A. L. Arsenault, *Calcif. Tissue Int.* **1988**, *43*, 202–212; S. Weiner, W. Traub, *Conn. Tissue Res.* **1989**, *21*, 259–265.
[85] L. C. Bonar, M. D. Grynpas, J. E. Roberts, R. G. Griffen, M. J. Glimcher in *The Chemistry and Biology of Mineralized Tissues* (Ed.: W. T. Butler), EBSCO Media, Birmingham, AL, USA, **1985**, pp. 226–233.
[86] S. Doty, R. A. Robinson, B. Schofield in *Handbook of Physiology* (Ed.: G. D. Aurbach), Am. Physiol. Soc. Washington, **1976**, pp. 3–23.
[87] J. D. Currey, *Philos. Trans. R. Soc. London B* **1984**, *304*, 509–518.
[88] H. A. Lowenstam, *Geol. Soc. Am. Bull.* **1962**, *73*, 435–438.
[89] J. L. Kirschvink, H. A. Lowenstam, *Earth Planet. Sci. Lett.* **1979**, *44*, 193–204.
[90] M. H. Nesson, H. A. Lowenstam in [9], pp. 333–363.
[91] D. C. Morris, H. K. Väänänen, H. C. Anderson, *Metab. Bone Dis. Relat. Res.* **1983**, *5*, 131–137.
[92] R. W. Morris, L. R. Kittleman, *Science* **1967**, *158*, 368–370; O. Sand, *J. Exp. Biol.* **1974**, *60*, 881–899.
[93] G. E. G. Westermann, *Paleobiology* **1977**, *3*, 300–321.
[94] L. Wolpert, T. Gustafson, *Exp. Cell Res.* **1961**, *25*, 311–325.
[95] a) K. Märkel, Universität Bochum, private communication, **1991**; b) A. Burkhardt, W. Hansmann, K. Märkel, H. Niemann *Zoomorphology* **1983**, *102*, 189–203.
[96] K. Märkel, *Ann. Zool. Jpn.* **1970**, *43*, 188–199.
[97] H. H. Dixon, *Proc. R. Soc. (Biol.)* **1900**, *68*, 305–315.
[98] M. Black, *Proc. Linn. Soc. London* **1963**, *174*, 41–46.
[99] N. Watabe, *Calcif. Tissue Res.* **1967**, *1*, 114–121.
[100] P. Westbroek, E. W. de Jong, P. van der Wal, A. H. Borman, J. P. M. de Vrind, D. Kok, W. C. de Bruijn, S. B. Parker, *Philos. Trans. R. Soc. London B*, **1984**, *304*, 435–444.
[101] R. P. Blakemore, *Science* **1975**, *190*, 377–379.
[102] A. Frey-Wyssling, *Am. J. Bot.* **1981**, *68*, 130–141.
[103] G. Bevelander, H. Nakahara, *Calc. Tissue Res.* **1969**, *3*, 84–92.
[104] H. Nakahara in [4 a], pp. 225–230.
[105] S. Weiner, W. Traub, *Philos. Trans. R. Soc. London B* **1984**, *304*, 425–434.
[106] H. Nakahara, *Bull. Josai Dental Univ. II* **1982**, 209–215; D. Worms, S. Weiner, *J. Exp. Zool.* **1986**, *237*, 11–20.
[107] M. A. Crenshaw, H. Ristedt in [75 a], pp. 355–367.
[108] S. Weiner, W. Traub, *FEBS Lett.* **1980**, *111*, 311–316.

Phosphorus Nitrides—the Cinderella of Phosphorus Chemistry?

By *Otto J. Scherer**

In the latest edition of the monograph on phosphorus compounds by D. E. C. Corbridge,[1] which contains over a thousand pages, the chapter on molecules comprising only phosphorus and nitrogen atoms is merely three pages long. Besides the explosive azides[2] $P(N_3)_3$ and $P(N_3)_5$ characterized in solution by ^{31}P NMR and IR spectroscopy, only a few phosphorus nitrides of tri- and pentavalent phosphorus were described in a more or less complete manner (Scheme 1).

$$:P{\equiv}N: \qquad \dagger P{=}N\dagger_n \ (n = 2,3,\infty) \qquad P_3N_5$$
$$\mathbf{A} \qquad\qquad \mathbf{B} \qquad\qquad\qquad \mathbf{C}$$

Scheme 1. The phosphorus(III) nitrides **A** and **B**, and the phosphorus(V) nitride **C**.

In the thoroughly investigated, monomeric, gaseous phosphorus(III) nitride (**1**), synthesized according to Equation (a),[3] the P≡N bond length (1.49 Å) has been determined by

$$P_3N_5(s) \xrightarrow[-N_2(g)]{1050\,K} 3\,PN(g) \quad \mathbf{1} \qquad (a)$$
$$(Cl_2PN)_3(g) \xrightarrow[-6\,AgCl(g)]{6\,Ag(l)/1300\,K}$$

microwave spectroscopy and differs only slightly from the calculated value of 1.462 Å.[4]

The dimer $(PN)_2$ has not yet been detected experimentally, but SCF calculations predict as most stable form a molecular structure with D_{2h} symmetry.[5] Distinctly more stable than *cyclo*-$(PN)_2$ is the trimer $(PN)_3$, which forms by trimerization of **1** on warming the krypton matrix from 10 K to 40 K.[6a] Both the IR spectrum[6a] and theoretical studies[3] indicate a planar six-membered ring structure with D_{3h} symmetry.

The reaction of **1** with metal atoms of the copper group yields complexes **2** and **3**, characterized as yet only by IR spectroscopy and displaying η^1-P and μ-P coordination respectively[6b] [Eq. (b) and (c)]. An alternative interpretation of the IR data of **3** suggests a *cyclo*-$(PN)_2$ molecule containing an η^4-coordinated silver atom.[3]

$$:P{\equiv}N: \xrightarrow[10\,K,\,Krypton]{M=Cu,\,Au} :N{\equiv}P: \rightarrow M \leftarrow :P\ N: \quad \mathbf{2} \qquad (b)$$
$$:P{\equiv}N: \xrightarrow[10\,K,\,Krypton]{M=Ag} \mathbf{3} \qquad (c)$$

The molecule PNO was prepared by cocondensation of PN and O_3, also in a noble gas matrix. IR studies and ab initio calculations show that PNO is surprisingly more stable than NPO.[4]

Although Stock and Hoffmann synthesized phosphorus(V) nitride P_3N_5 (**C**) as early as 1903 by ammonolysis of tetraphosphorus decasulfide P_4S_{10},[7] its structure is still unknown. The same applies for polymeric phosphorus nitride $(PN)_n$, which forms from monomeric PN as well as from a reaction of PH_3 and N_2 or PCl_3 and NH_3.[1]

Starting with the preparation and refinement of the crystal structure of $LiPN_2$ (**4**),[8a] a lithium phosphorus(V) nitride whose PN_2^- substructure is isoelectronic with SiO_2 (isosteric to β-cristobalite) and which forms a three-dimensional network of corner-sharing PN_4 tetrahedrons (P–N = 1.65 Å), W. Schnick and co-workers have just achieved two breakthroughs in the field of ternary phosphorus(V) nitrides:

They allowed the binary nitrides P_3N_5 and Li_3N to react with each other and obtained $Li_{10}P_4N_{10}$ (**6**),[8c] as well as **4**[8a] and the compound Li_7PN_4 (**5**), whose PN_4^{7-} substructure is isoelectronic with PO_4^{3-} and affords "isolated" tetrahedral PN_4 anions ($\bar{d}$(P–N) = 1.71 Å). Compound **6** can also be synthesized from $LiPN_2/Li_3N$ or Li_7PN_4/P_3N_5 in a high-temperature solid-state reaction (700–720 °C, 5 days). $Zn_7[P_{12}N_{24}]Cl_2$ (**7**), a sodalite with a phosphorus–nitrogen framework, is also surprisingly simple to prepare[8d] [Eq. (d)].

$$7\,ZnCl_2 + 12\,NH_4Cl + 4(NPCl_2)_3 \xrightarrow[-48\,HCl]{700\,°C,\,2d} Zn_7[P_{12}N_{24}]Cl_2 \qquad (d)$$

The $P_4N_{10}^{10-}$ ion of **6** illustrates the principle of isoelectronic molecules in a simple but fascinating way (Fig. 1). The pendant of molecular phosphorus(V) oxide P_4O_{10} has ideal T_d symmetry in the solid state. The terminal P–N bonds (P1–N2 = 1.58 Å) are clearly shorter than the bridging bonds (P1–N1 = 1.68 Å). In the solid state the $P_4N_{10}^{10-}$ ions are arranged similarly to a zinc blende structure, result-

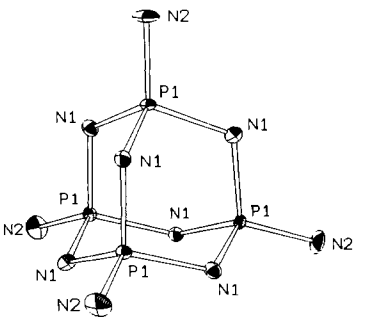

Fig. 1. Structure of the $P_4N_{10}^{10-}$ ion in the solid state.

[*] Prof. Dr. O. J. Scherer
Fachbereich Chemie der Universität
Erwin-Schrödinger-Strasse, D-W-6750 Kaiserslautern (FRG)

 © VCH Verlagsgesellschaft mbH, W-6940 Weinheim, 1992 0570-0833/92/0202-0170 $ 3.50+.25/0

ing in a considerably more favorable packing than in P_4O_{10}.[8c]

The $[P_{12}N_{24}]$ framework of **7**, analogous to sodalite $Na_8[Al_6Si_6O_{24}]Cl_2$, is constructed from $[P_4N_4]$ and $[P_6N_6]$ rings (P–N = 1.64 Å), which in turn resemble the typical capped octahedrons of the sodalite type's secondary construction feature—the so-called β cages. A chloride ion surrounded tetrahedrally by Zn^{2+} ions is found in the center of each cage.

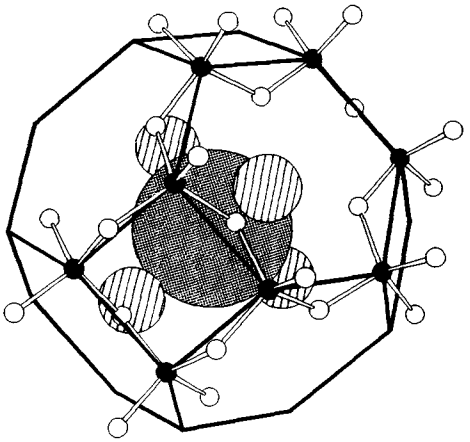

Fig. 2. Section of the crystal structure of $Zn_7[P_{12}N_{24}]Cl_2$ (**7**). The spheres are represented as follows: P = black, N = white, Cl = shaded, Zn = hatched.

As a result of their varied applications, for example, as ion-exchange resins, components of detergents, molecular sieves, and particularly as catalysts,[9a] zeolites still enjoy today an unrestricted interest shown to almost no other class of substances in inorganic chemistry. Their scientific importance is impressively documented by many up-to-date monographs, review articles on their topology and geometry,[9b] as well as the theoretical aspects,[9c] and not least by the ten-year old journal "Zeolites".

Against this background the nitrido sodalite **7**, a zeolite in which for the first time the ubiquitous oxygen in the anionic substructure is replaced by nitrogen, opens fascinating perspectives. With this new class of phosphorus(v) nitrides, the phosphorus nitrides that have been treated so shabbily in the past have become equals with their "sister" compounds in phosphorus chemistry and are expected to thrive. Strong indications for this are already to be seen in the lithium-ion conductivity[10] of $LiPN_2$ (**4**) and Li_7PN_4 (**5**).

German version: *Angew. Chem.* **1992**, *104*, 177

[1] D. E. C. Corbidge, *Phosphorus: An Outline of its Chemistry, Biochemistry and Technology*, 4th ed., Elsevier, Amsterdam, **1990**.

[2] W. Buder, A. Schmidt, *Z. Anorg. Allg. Chem.* **1975**, *415*, 263–267; K. B. Dillon, A. W. G. Platt, T. C. Waddington, *Inorg. Nucl. Chem. Lett.* **1978**, *14*, 511–513.

[3] R. Ahlrichs, M. Bär, H. S. Plitt, H. Schnöckel, *Chem. Phys. Lett.* **1989**, *161*, 179–184.

[4] R. Ahlrichs, S. Schunck, H. Schnöckel, *Angew. Chem.* **1988**, *100*, 418–420; *Angew. Chem. Int. Ed. Engl.* **1988**, *27*, 421–423.

[5] H. Schnöckel, T. Mehner, H. S. Plitt, S. Schunck, *J. Am. Chem. Soc.* **1989**, *111*, 4578–4582.

[6] a) R. M. Atkins, P. L. Timms, *Spectrochim. Acta Part A* **1977**, *33*, 853–857; b) *Inorg. Nucl. Chem. Lett.* **1978**, *14*, 113–115.

[7] A. Stock, B. Hoffmann, *Ber. Dtsch. Chem. Ges.* **1903**, *36*, 314–319.

[8] a) W. Schnick, J. Lücke, *Z. Anorg. Allg. Chem.* **1990**, *588*, 19–25; b) *J. Solid State Chem.* **1990**, *87*, 101–106; c) W. Schnick, U. Berger, *Angew. Chem.* **1991**, *103*, 857–858; *Angew. Chem. Int. Ed. Engl.* **1991**, *30*, 830–831; d) W. Schnick, J. Lücke, *ibid.* **1992**, *104*, 208 and **1992**, *31*, 213.

[9] a) W. Hölderlich, M. Hesse, F. Näumann, *Angew. Chem.* **1988**, *100*, 232–251; *Angew. Chem. Int. Ed. Engl.* **1988**, *27*, 226–246; b) J. V. Smith, *Chem. Rev.* **1988**, *88*, 149–182; see also: S. Andersson, *Angew. Chem.* **1983**, *95*, 67–80; *Angew. Chem. Int. Ed. Engl.* **1983**, *22*, 69–81; c) J. Sauer, *Chem. Rev.* **1989**, *89*, 199–255; see also: G. J. Kramer, A. J. M. de Man, R. A. van Santen, *J. Am. Chem. Soc.* **1991**, *113*, 6435–6441.

[10] W. Schnick, J. Lücke, *Solid State Ionics* **1990**, *38*, 271–273.

Structure and Reactivity of Silicon Clusters in the Gas Phase

By *Thomas Lange** and *T. Patrick Martin**

The rich variety of properties found for clusters – that is, small aggregates consisting of three to some hundreds of atoms – has attracted the attention of chemists and physicists alike. It is hoped that some of these properties can be incorporated into new solid materials composed of clusters. The recently available fullerenes are a first example. The continually diminishing size of semiconductor structures in microelectronics gives silicon clusters a special interest. Because the structure of clusters cannot at this time be determined directly from diffraction experiments, indirect methods must be used, for example, the observation of the chemical behavior of the Si_n clusters.

Reactions of Si_n clusters can be examined by allowing previously mass-selected Si_n^+ ions to interact with a reaction gas under controlled pressure and temperature conditions for a certain period of time. Figure 1 illustrates this method for the reaction of Si_n^+ ions with ethylene.[1, 2] Analysis of the products reveals how many and which types of reaction steps have taken place. From the clusters produced by laser evaporation (A), Si_{40}^+ ions were "extracted" with a quadrupole mass spectrometer (B). After the Si_{40}^+ clusters passed through the ethylene-filled chamber, the reaction products show up in the mass spectrum as $Si_{40}^+(C_2H_4)_m$ clusters with $m = 0,1,2$

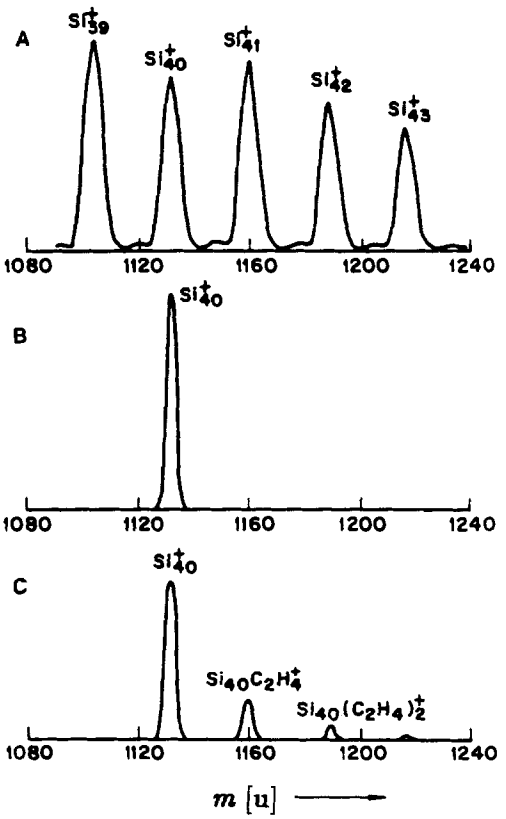

Fig. 1. Method for the determination of the reactivity of Si clusters, demonstrated for Si_{40}^+. A: Part of a Si_n^+ mass spectrum. B: Mass spectrum after the selection of Si_{40}^+ clusters. C: Mass spectrum after reaction of Si_{40}^+ clusters with ethylene. The reactivity of Si_{40}^+ towards ethylene can be calculated from the ratio of the Si_{40}^+ and $Si_{40}^+(C_2H_4)$ intensities.

[*] Dipl.-Chem. T. Lange, Dr. T. P. Martin
Max-Planck-Institut für Festkörperforschung
Heisenbergstrasse 1, D-W-7000 Stuttgart 80 (FRG)

(C). The reactivity of the Si_{40}^+ cluster with ethylene could be determined from the ratio of the Si_{40}^+ and $Si_{40}^+(C_2H_4)$ intensities.

Reactions of Si_n^+ clusters with C_2H_4, CO, O_2, NH_3, and H_2O show that the surface of Si clusters is far less reactive than the surface of the solids.[2, 3] While dangling bonds on the solid surface play an important role, it must be assumed that the cluster surface has a lower dangling-bond density. The example of Si_{10}^+ shows that this assumption is plausible:[4] A ten-atom bulk fragment from the silicon lattice is shown on the left of Figure 2. The atoms have a maximum of three binding partners, indicating at least one dangling bond. In the middle and on the right are two structures that represent, according to calculations, two (almost equal) minima of the total energy. In both structures the number of Si bonds have increased considerably. The structures of larger clusters have not until now been calculated with the same degree of reliability. However, their inertness may probably be attributed to an analogous reconstruction of the cluster surface accompanied by a corresponding reduction of the number of dangling bonds. In this way, the chemical behavior of these clusters allow qualitative conclusions about the structure of small Si_n clusters. At what size a silicon cluster takes on the crystal structure of a solid is presently not known.

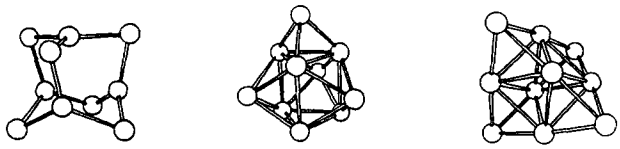

Fig. 2. Left: Bulk fragment of 10 Si atoms. Middle and right: Two structures of Si_{10} with minimal total energy. They are both approximately 5 eV more stable than the bulk fragment.

The determination of the structure of silicon clusters is made more difficult by the fact that Si_n clusters with a fixed number of atoms need not always have the same structure. After attaining a certain size, a continual reconstruction of the cluster's surface to the most favorable configuration during the growth process is no longer possible. This leads to the occurrence of structural isomers. Smalley et al.[5] and Jarrold et al.[6] have shown that such isomers can be distinguished from one another in spite of their mass equality. Both groups took advantage of the different chemical characteristics of isomers. Jarrold et al. observed that most of the Si_n^+ clusters in the size range $11 \leq n \leq 50$ show (at least) two distinct reaction rates with C_2H_4. Smalley et al. found a similar behavior for the reaction of Si_{39}^+ clusters. Both groups succeeded in showing that some of the less stable isomers could be converted thermally into the stable forms. This heat treatment was achieved either by laser annealing (Smalley et al.) or by melting the clusters with energy-rich collisions with noble gas atoms (Jarrold et al.). In some cases the more stable isomer even has a higher reactivity than the isomer from which it is produced. For instance, the more stable isomer of Si_{26}^+ shows enhanced reactivity, whereas in the case of Si_{39}^+, it proved to be less reactive.

In a few cases, it is even possible to predict the structure of a cluster based on these chemical experiments. Jarrold et al. discovered that the reactivity of small Si_n^+ ions towards a series of reactant gases showed strong irregularities as a function of n. Clusters that consist of 13, 14, and 23 atoms show a 10–100 times smaller reactivity towards C_2H_4 than the other clusters.[1] When H_2O is chosen as reactant,[7] clusters with $n = 11$, 13, 14, 19, and 23 prove to be particularly inert. The same is valid for the reaction of clusters containing 13 and 14 atoms with O_2.[8] It is assumed that this behavior of the clusters is caused by special structures that have very few dangling bonds. Exactly 13 atoms are needed for an icosahedral structure. Structures with $n = 19$ and $n = 23$ are obtained by adding caps on faces of this icosahedron. This icosahedral growth sequence provides a plausible explanation for the inertness of the corresponding clusters. However, the structure responsible for the inertness of the Si_{14}^+ cluster is still not known. For larger Si_n clusters, Smalley et al. observed an analogous series of particularly unreactive clusters ($n = 21, 25, 33, 39, 45$).[9] In this size range, however, the prediction of specific structures is even more speculative (see the following Highlight.)

These results for silicon reflect the present state of cluster research in general. The goal is to examine and understand the physical and chemical characteristics of smallest particles of condensed matter. Technological application of these results with silicon is not to be expected in the near future. Nevertheless, first experimental attempts in this direction have already been made: Jarrold et al. succeeded recently in depositing mass-selected Si_{10} clusters on surfaces and in characterizing them chemically[10] and electronically.[11] The day may yet come when silicon clusters will play an important role in microelectronics.

German version: *Angew. Chem.* **1992**, *104*, 179

[1] M. F. Jarrold, J. E. Bower, K. M. Creegan, *J. Chem. Phys.* **1989**, *90*, 3615.
[2] M. F. Jarrold, *Science (Washington D. C.)* **1991**, *252*, 1085.
[3] M. L. Mandich, V. E. Bondybey, W. D. Reents, Jr., *J. Chem. Phys.* **1987**, *86*, 4245.
[4] K. Raghavachari, *Phase Transitions* **1990**, *24–26*, 61.
[5] S. Maruyama, L. R. Anderson, R. E. Smalley, *J. Chem. Phys.* **1990**, *93*, 5349.
[6] K. M. Creegan, M. F. Jarrold, *J. Am. Chem. Soc.* **1990**, *112*, 3768.
[7] U. Ray, M. F. Jarrold, *J. Chem. Phys.* **1991**, *94*, 2631.
[8] M. F. Jarrold, U. Ray, K. M. Creegan, *J. Chem. Phys.* **1990**, *93*, 224.
[9] J. M. Alford, R. T. Laaksonen, R. E. Smalley, *J. Chem. Phys.* **1991**, *94*, 2618.
[10] J. E. Bower, M. F. Jarrold, unpublished.
[11] Y. Kuk, M. F. Jarrold, P. J. Silverman, J. E. Bower, W. L. Brown, *Phys. Rev. B* **1989**, *39*, 11168.

Si_{60}, an Analogue of C_{60}?

By *Christian Zybill**

The isolation of semiconductor clusters is an elusive goal, which could contribute to the understanding of quantum size effects (the size dependent variation of optical or magnetic properties of cluster molecules). Particularly silicon clusters Si_n with $n \leq 100$ formed by either laser vaporization of elemental silicon or ion-sputtering techniques have been investigated intensively in the gas phase by mass spectrometry or FT-ICR-spectroscopy (FT-ICR = Fourier Transform Ion Cyclotron Resonance). The applied methods include photofragmentation and collision-induced dissociation studies, photoelectron spectroscopy of negative ions, and chemical techniques such as ion–molecular reactions of both positive and negative ions and kinetic studies. The stability of the observed cluster ions depends on the cluster size;[1] particularly for the "magic number" clusters[2] Si_4^+, Si_6^+, Si_{13}^+, Si_{19}^+, Si_{21}^+, Si_{25}^+, Si_{33}^+, Si_{39}^+, Si_{45}^+ and Si_{60}^+ a significantly reduced reactivity is found.

Researchers in the fields of cluster chemistry and main-group chemistry avidly follow the advances in the understanding of structures of silicon clusters. Ab-initio calculations on HF- and UHF-level reveal the ground-state geometries (Fig. 1).[3,4] Si_3 is bent, Si_4 has a rhombohedral ground state geometry, Si_5 is trigonal bipyramidal, and Si_6 distorted (C_{2v}) octahedral. Si_7 has a pentagonal-bipyramidal form as ground state, similar to Li_7, Na_7, or Ag_7.[5] The most probable structure for Si_8 is a bicapped octahedron with two additional silicon atoms capping two opposite faces. However such a D_{3d} form has a triplet ground state and undergoes a Jahn–Teller distortion to give a geometry with C_{2h} symmetry. A similar Jahn-Teller effect occurs for the tricapped octahedron of Si_9 and results in symmetry reduction of the cluster from C_{3v} to C_s. Finally, Si_{10} is described by a tetracapped octahedron with T_d symmetry.

All clusters with more than five silicon atoms form (three-dimensional) cages constructed by consecutively adding face-bridging silicon atoms. In contrast, the analogous carbon clusters have two-dimensional linear or cyclic structures.

The structures of silicon clusters differ significantly from the cubic diamond type structure of elemental silicon and do not represent sections of the bulk crystal lattice. Thus for instance, a bulklike adamantane structure for Si_{10} is energetically about 100 kcal mol^{-1} less stable than the given compact C_s structure, because of too many undercoordinated surface atoms (dangling bonds). The calculated structures of "naked" silicon clusters are relatively closed and allow max-

[*] Dr. C. Zybill
Anorganisch-chemisches Institut der
Technischen Universität München
Lichtenbergstrasse 4
D-W-8046 Garching (FRG)

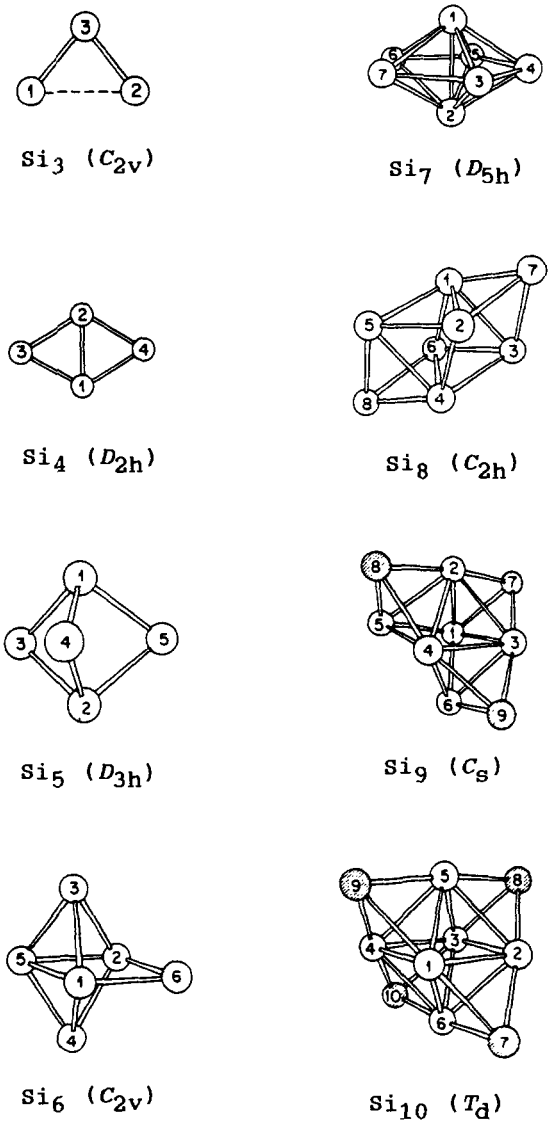

Fig. 1. Calculated structures for Si_3–Si_{10}.

imum coordination numbers of six, which are known to occur in the high-pressure phase of silicon (β-tin structure; approximately octahedral coordination[6]).

Semiempirical calculations also allow a description of the structures of larger stable clusters like Si_{39}^+ and Si_{60}^+.[7–10] The prediction for Si_{39}^+ is a toruslike structure with a stack of six planar Si_6 rings and three additional face-capping silicon atoms forming the top of the torus (Fig. 2). The calculations suggest that the angular strain energy (90° bond angles) can be partially compensated by charge delocalization in the planar rings.[11]

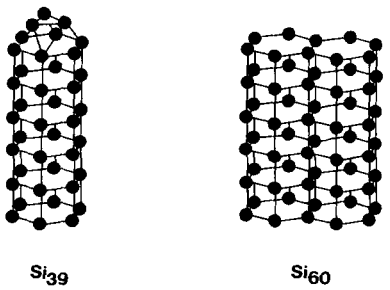

Fig. 2. Proposed structures of Si_{39}^+ and Si_{60}^+ (from [11] and [13], respectively).

In contrast to the structure of buckminsterfullerene (C_{60}),[12] the proposal for Si_{60}^+ is a stack of six planar bicyclic (silanaphthalene) units [d_{Si-Si} 2.356 Å (intraplanar), d_{Si-Si} 2.439 Å (interplanar distance)]. A variety of arguments are given in favor of this structural model:

1. The proposed Si_{60} polyhedron explains the observed selective fragmentation pattern of the Si_{60} cluster into unstable Si_{20} units and subsequently into Si_{10} fragments. The Si_{10} fragment ions (base peak of the mass spectrum) rearrange to the known C_s structure of Si_{10}.
2. The Si_{60} cluster is significantly stabilized by electronic conjugation within the Si_{10} planes.
3. All silicon atoms with the exception of the atoms at both faces on top and bottom of the cluster are four-coordinate.[13]

Gas-phase reactions of silicon clusters have been studied by several research groups (Bondybey, Jarrold, Bower, and Smalley; see the preceeding Highlight). Depending on the size of the cluster and the reagent applied, either cluster degradation (etching with O_2, WF_6, XeF_2, NO_2, ClF_3, NH_3[14]), cluster construction (reaction with CH_3SiH_3[15]), or chemisorption (e.g. ethylene or methane on Si_{25}^+)[16] have been observed. The rate constants and activation parameters are unique, differing significantly from the known parameters for the [111] silicon surface; for instance Si_{25}^+ is much less reactive toward C_2H_4 and O_2 (high activation barrier) than bulk silicon.

Recently some rare and distinct examples of thermodynamically stable Si_8 clusters have been synthesized in the laboratories of Masamune et al. and unequivocally characterized by single-crystal structure determination in the solid state as well as by ^{29}Si-(COSY)-NMR in solution. Similar germanium cluster compounds have been introduced by Weidenbruch et al.[17] Furthermore, Sekiguchi, Kabuto, and Sakurai have isolated stable derivatives of hexagermaprismane.[18] However, these cluster compounds are not directly comparable with the "naked" silicon clusters in the gas phase, since all silicon atoms at the vertices of a polyhedron are four-coordinate, and the bonds are satisfied by bulky substituents.[19]

In the case of C_{60}, the first evidence for the existence of this unique and fascinating molecule was obtained in 1985 by mass spectrometry by Smalley and Kroto.[20a] The isolation of substantial amounts of C_{60} followed shortly thereafter in 1990 by Krätschmer et al.[20b] However, the isolation of Si_{60} still seems rather unlikely.

German version: *Angew. Chem.* **1992**, *104*, 180

[1] J. C. Phillips, *J. Chem. Phys.* **1988**, *88*, 2090.
[2] According to a suggestion of Bondybey, magic numbers should only be applied to systems that have been formed under thermodynamically controlled reaction conditions [14b].
[3] K. Raghavachari, C. McMichael Rohlfing, *J. Chem. Phys.* **1988**, *89*, 2219.
[4] Calculations using the tight-binding method: D. Tomanek, M. A. Schlüter, *Phys. Rev. B* **1987**, *36*, 1208; *Phys. Rev. Lett.* **1986**, *56*, 1055.
[5] G. A. Thompson, F. Tischler, D. M. Lindsay, *J. Chem. Phys.* **1983**, *78*, 5946.
[6] a) J. C. Phillips, *Bonds and Bands in Semiconductors*, Academic Press, New York, **1973**; b) M. T. Yin, M. L. Cohen, *Phys. Rev. Lett.* **1980**, *45*, 1004.
[7] a) Y. Liu, Q. L. Zhang, F. K. Tittel, R. F. Curl, R. E. Smalley, *J. Chem.*

Phys. **1986**, *85*, 7434; b) Q. L. Zhang, Y. Liu, R. F. Curl, F. K. Tittel, R. E. Smalley, *ibid.* **1988**, *88*, 1670.
[8] J. L. Elkind, J. M. Alford, F. D. Weiss, R. T. Laaksonen, R. E. Smalley, *J. Chem. Phys.* **1987**, *87*, 2397.
[9] H. Kupka, K. Jug, *Chem. Phys.* **1989**, *130*, 23.
[10] J. R. Chelikowsky, J. C. Phillips, *Phys. Rev. Lett.* **1989**, *63*, 1653.
[11] J. C. Phillips, *J. Chem. Phys.* **1985**, *83*, 3330.
[12] See the "Highlights" in this journal: a) J. F. Stoddart, *Angew. Chem.* **1991**, *103*, 73; *Angew. Chem. Int. Ed. Engl.* **1991**, *30*, 70; b) F. Diederich, *ibid.* **1991**, *103*, 695 and **1991**, *30*, 678.
[13] D. A. Jelski, Z. C. Wu, T. F. George, *J. Cluster Sci.* **1990**, *1*, 143.
[14] a) W. D. Reents, M. L. Mandich, V. E. Bondybey, *Chem. Phys. Lett.* **1986**, *131*, 1; b) M. L. Mandich, V. E. Bondybey, W. D. Reents, *J. Chem. Phys.* **1987**, *96*, 4245; c) W. D. Reents, A. M. Mujsce, V. E. Bondybey, M. L. Mandich, *ibid.* **1987**, *86*, 5568.
[15] M. L. Mandich, W. D. Reents, V. E. Bondybey, *J. Phys. Chem.* **1986**, *90*, 2315.
[16] a) M. F. Jarrold, J. E. Bower, *J. Am. Chem. Soc.* **1989**, *111*, 1979; b) K. M. Creegan, M. F. Jarrold, *ibid.* **1990**, *112*, 3768.
[17] a) Y. Kabe, M. Kuroda, Y. Honda, O. Yamashita, T. Kawase, S. Masamune, *Angew. Chem.* **1988**, *100*, 1793; *Angew. Chem. Int. Ed. Engl.* **1988**, *27*, 1725; b) for a review see T. Tsumuroya, S. A. Botcheller, S. Masamune, *ibid.* **1991**, *103*, 916; and **1991**, *30*, 902; c) M. Weidenbruch, F. T. Grimm, S. Pohl, W. Saak, *ibid.* **1989**, *101*, 201; or **1989**, *28*, 198.
[18] A. Sekiguchi, C. Kabuto, H. Sakurai, *Angew. Chem.* **1989**, *101*, 97; *Angew. Chem. Int. Ed. Engl.* **1989**, *28*, 55.
[19] Silicon cluster compounds have lower strain energies than their C analogues: S. Nagase, T. Kudo, M. Aoki, *J. Chem. Soc. Chem. Commun.* **1985**, 1121.
[20] First experimental evidence for C_{60}: a) H. Kroto, J. R. Heath, S. C. O'Brien, R. F. Curl, R. E. Smalley, *Nature* **1985**, *318*, 162; isolation of macroscopic amounts of C_{60}: b) W. Krätschmer, L. D. Lamb, K. Fostiropoulos, D. R. Hufman, *ibid.* **1990**, *347*, 354.

Inhibition of Fruit Ripening by Antisense-RNA Technology

By *Peter Eckes**

The goal of plant breeding is the improvement of plants or plant products. Among the criteria of quality are the resistance of plants to pests, crop yield, and the taste of plant products. Because these characteristics are determined primarily by genetics, plant breeders attempt to bring about new traits by altering the genetic information of a plant. Until recently this was done by crossbreeding with other varieties or closely related species, followed by selection of the desired trait. This is a tedious and lengthy procedure, because in the mixing of all the genetic information of two plants, undesired traits may also be carried on to the next generation. The undesired traits must then be eliminated by several other crossbreedings with the mother plant. A more direct approach to the improvement of plants would be a great advantage.

Molecular biology offers new vantage points: the channeling of a specific gene in the plant genome has already led to plants with new characteristics, for example tolerance to herbicides or resistance to insects. It is also conceivable to develop plants of improved quality by the targeted activation or inactivation of specific metabolic pathways.

The so-called antisense-RNA technology is one biological method which can prevent the expression of a specific gene. The principle of this method is based on the formation of an antisense ribonucleic acid (antisense RNA), which is complementary to the RNA (sense RNA) of the protein to be inhibited. The translation of the sense RNA is blocked by its complement, and thus the expression of a certain trait is prevented (Fig 1).

In principle there are two methods of introducing antisense RNA into the cell. Attempts at channeling short oligonucleotides complementary to the target RNA directly into eukaryotic cells have been made in the medical field.[1] In another method used especially in plants, an antisense gene is built into the genome from which the antisense RNA is then transcribed. In the first method the correctly targeted supply of sufficient quantities of oligonucleotides and their instability in the cell pose great difficulties. The insertion of antisense genes into the genome, at least in humans, involves ethical problems besides the technical. Within the plant domain, however, this method is desirable and is already practiced.

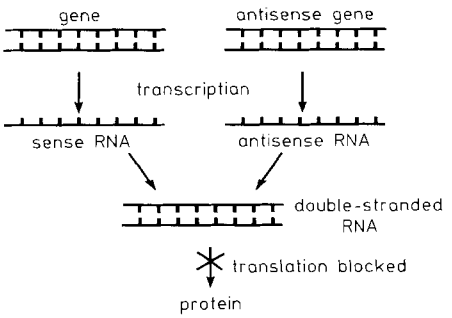

Fig. 1. Mechanism of the inactivation of a trait by antisense RNA.

The regulation of gene expression by antisense RNA also occurs in nature in prokaryotes.[2] In the bacterium *Escherichia coli*, for example, replication of plasmids is regulated by the interaction of sense and antisense RNA. The first proof that the antisense-RNA principle could also be applied in the inactivation of gene expression in eukaryotes was furnished in 1984. Izant and Weintraub[3] showed that the expression of a thymidine-kinase gene, which had been injected in cultivated mouse cells, could be significantly reduced when a plasmid, which produced the antisense RNA of that same gene, was coinjected. This experiment led to the idea of blocking the expression of a naturally occuring gene in higher organisms with antisense RNA and thus change the phenotype (observable characteristics) of the organism. The results of this strategy in plants were first published in

[*] Dr. Peter Eckes
Biologische Forschung C, H 872
Hoechst AG
D-W-6230 Frankfurt 80 (FRG)

1988.[4] The chalcone-synthase gene of a petunia, whose product is involved in the production of flower pigments, was "turned off" by the introduction of a chalcone-synthase antisense gene. The resulting petunias displayed varying amounts of flower pigmentation depending on the degree of gene inactivation (Fig 2).

Fig. 2. Flowers of petunia plants with varying degrees of inactivation of the synthesis of chalcone synthase caused by antisense RNA.

An American group has recently succeeded in suppressing the ripening process in tomato fruits with antisense-RNA technology.[5] Ripeness is an important factor in the storage and transportation of fruits like bananas, peaches, oranges, and tomatoes. These fruits are harvested unripe, they ripen during transportation, and they must then be delivered to the consumer immediately. If the transportation takes too long or refrigeration is insufficient, the fruit delivered to the stores may be overripe or even rotten and not marketable. Especially in warmer climates this results in large crop losses.

The ripening process of the tomato is induced by the signal compound ethylene. In the tomato plant, ethylene is produced from methionine via many intermediates. The rate-determining step in the biosynthesis of ethylene is catalyzed by the enzyme aminocyclopropanoic acid synthase (ACC synthase). This enzyme brings about the transformation of *S*-adenosylmethione to 1-aminocyclopropane-1-carboxylic acid, the direct precursor of ethylene. The American research group succeeded in inhibiting the formation of ACC synthase in genetically altered tomato plants so that the amount of ethylene in the fruit was reduced by 99.5%, and thus the fruit did not ripen.

The authors conducted their experiment in the following manner: The cDNA of an isolated ACC-synthase gene from a tomato was fused in inverted orientation to a promoter, which leads to constitutive expression in plants (35S-transcript promoter of the cauliflower mosaic virus). The gene was then integrated with molecular biological methods in the genome of tomato plants where it was to produce the antisense RNA of ACC synthase.

Of the 43 genetically altered plants produced in this procedure three showed a marked reduction of the C_2H_4 synthesis and a delay in fruit-ripening. Molecular biological analyses were conducted on the homozygotic (genetically identical) offspring of the plant which displayed the greatest inhibition of C_2H_4 biosynthesis. DNA investigations with the so-called Southern Blot method proved that ten copies of the antisense gene of ACC synthase were integrated in the genome of these transgenic plants. The naturally occurring ACC-synthase gene is known to occur only once in the genome. In contrast to the fruits of the unaltered control plants, transgenic fruits produced ACC-synthase antisense-RNA as expected. In the transgenic tomatoes the analogous sense-RNA could be detected in only minute amounts relative to that in the control plants. The RNA of a polygalacturonase gene, whose genetic product also contributes to fruit-ripening, was not affected.

The ethylene production in the tomato fruit starts 48–50 days after fertilization. After another ten days the fruits are red and ripe. In the fruits with antisense RNA, the C_2H_4 production was decreased by 99.5%, and the fruits were not ripe even 120 days after fertilization. The ripening process of the transgenic fruit could be initiated by exposure to ethylene or propylene (10 μL per L air) for a number of days. One- or two-day exposure did not provide the desired result; after exposure for seven days, however, the fruits were red and soft and had developed their natural aroma. The expression of the antisense RNA and inhibition of the sense RNA was not affected by the exposure to the gas. This reversal of the effect produced by the antisense RNA by the exposure to C_2H_4 shows that ethylene triggers fruit-ripening and is not merely a by-product.

These experiments illustrate how the synthesis of a metabolic product in plants can be blocked efficiently by means of antisense-RNA technology. ACC synthase is well suited for this method; because of its short half-life of roughly 25 minutes, new enzyme must be constantly produced. Inhibiting its translation (protein biosynthesis) thus leads quickly to an enzyme deficit.

An inhibition comparable to that described previously was accomplished by Hamilton et al.[6] by blocking the synthesis of ACC oxidase, the enzyme responsible for the conversion of ACC to ethylene. This was also achieved with antisense-RNA technology. The fact that the ripening process halted by antisense RNA can be activated by exposure to ethylene makes this system commercially attractive. The ripening can be timed exactly, and the losses due to fruit rotting from extended transportation times or insufficient refrigeration can be reduced.

Antisense-RNA technology is theoretically applicable to a broad range of organisms for shutting off undesired activities controlled by genes. Corresponding experiments have been conducted in many areas of molecular biology. For example, it was attempted to block the genes of viruses pathogenic to humans or plants with the analogous antisense molecules and thus prevent the spread of the virus. Antisense molecules may also lead to the switching off of oncogenes (genes capable of converting a normal cell into a cancerous cell) and thereby become relevant in cancer therapy. These experiments are far from commercial application, since the degree of effectiveness can not be predicted with reliability. This leads to the general problem connected with antisense technology, namely that the mechanisms in higher organisms are not yet well understood. According to the current

model, the sense RNA binds to the complementary antisense RNA; the resulting double-stranded molecule is then rapidly broken down by nucleases. Unlike in bacterial systems the existence of a double-stranded RNA consisting of sense and antisense strands has not been proved unequivocally. It was recently discovered that the introduction of additional sense-genes into the genome of plants can also lead to an inactivation of gene expression. Thus the principles controlling antisense effects appear to be even more complex.

Nevertheless, the example of the inhibition of fruit-ripening by antisense-RNA technology shows that after modifications with molecular biological methods, principles found in nature (e.g. control of plasmid replication in bacteria by antisense RNA) can be applied to other systems (e.g. plants), resulting in improved properties of a crop.

German version: *Angew. Chem.* **1992**, *104*, 182

[1] U. Englisch, D. H. Gauss, *Angew. Chem.* **1991**, *103*, 629; *Angew. Chem. Int. Ed. Engl.* **1991**, *30*, 613.
[2] P. J. Green, O. Pines, M. Inouye, *Annu. Rev. Biochem.* **1986**, *55*, 569.
[3] J. G. Izant, H. Weintraub, *Cell* **1984**, *36*, 1007.
[4] A. R. van der Krol, P. E. Lenting, J. Veenstra, I. M. van der Meer, R. E. Koes, A. G. M. Gerats, J. N. M. Mol, A. R. Stutje, *Nature* **1988**, *333*, 866.
[5] P. W. Oeller, L. M. Wong, L. P. Taylor, D. A. Pike, A. Theologis, *Science* **1991**, *254*, 437.
[6] A. J. Hamilton, G. W. Lycett, D. Grierson, *Nature* **1990**, *346*, 284.
[7] A. R. van der Krol, L. A. Mur, P. de Lange, J. M. N. Mol, A. R. Stuitje, *Plant Mol. Biol.* **1990**, *14*, 457.

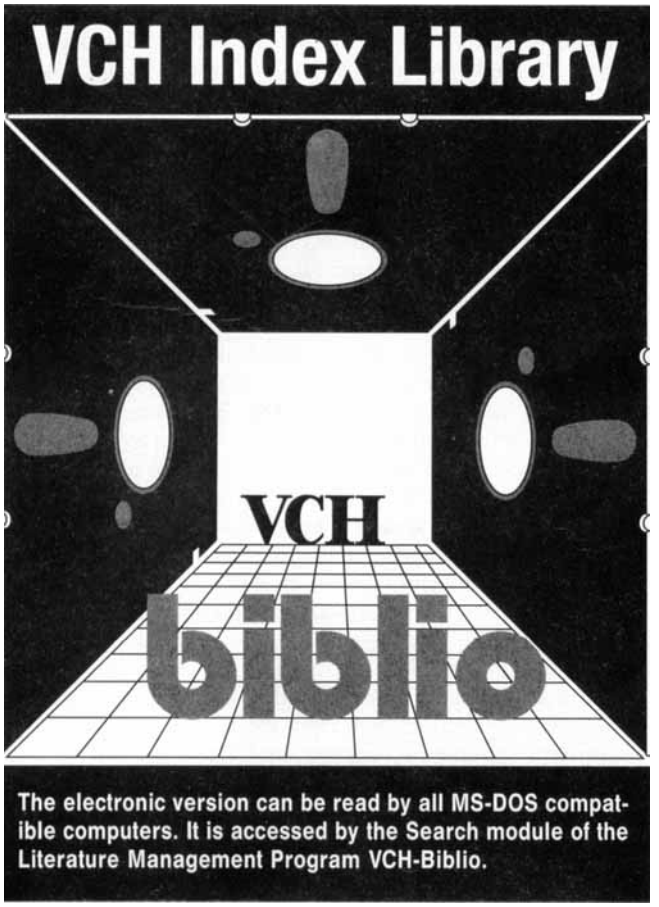

The electronic version can be read by all MS-DOS compatible computers. It is accessed by the Search module of the Literature Management Program VCH-Biblio.

ANGEWANDTE CHEMIE
A Journal of the Gesellschaft Deutscher Chemiker
International Edition in English

30 Year Index of Reviews
– in print or on diskette –

The reviews in Angewandte Chemie are amongst the most often cited chemical publications of each year. Many have become classics of the chemical literature. For thirty years they have been available in English as well as German. The 30 year review index now celebrates this anniversary by facilitating access to these important documents of the rapid development of our discipline. The index—both a chemical dictionary and a history book—offers you:

1. A list of all authors, indicating the main author and the title of the review.
2. A subject index giving the main author.
3. Both indexes provide complete information on date of issue and first and last page numbers of the German and English editions.

The electronic version of the index is available on 5¼" and 3½" diskettes.

The price of the index is DM 98.00, $ 64.00 or £ 37.00. Please order by telephone or in writing to **VCH, Software und Datenbanken, Postfach 10 11 61, D-W-6940 Weinheim, Tel. 0 62 01/6 02-2 71, Telefax 0 62 01/6 02-3 28.**

Communications may be submitted in English *or* in German. Further details regarding the submission of communications can be found in the "Notice to Authors" reproduced in the January issue of the journal. Copies thereof may be obtained from the editorial office upon request.

Microcalorimetry of the Spin-Transition Systems $[Fe(bts)_2(NCS)_2]$ and $[Fe(2\text{-}pic)_3]Cl_2 \cdot EtOH$ in the Range $15\,K < T < 300\,K$ **

By *Ralf Jakobi, Harald Romstedt, Hartmut Spiering,* and *Philipp Gütlich**

Dedicated to Professor Joseph Grobe on the occasion of his 60th birthday

Thermodynamic investigations of solid-state phase transitions of any type require exact measurements of heat capacity as a function of temperature. In such investigations of organic and inorganic solids with poor thermal conductivity substantial difficulties may arise, especially when only small amounts of material are available and when the phase transition should be followed over a wide temperature range, for example from 300 to 4 K.

The thermal spin transition in iron(II) complexes, High Spin (HS)⇌Low Spin (LS),[1] occurs in solids frequently below room temperature, in many cases even below the temperature of liquid nitrogen.[2] Measurements of the heat capacity $C_p(T)$ of spin-crossover compounds were first conducted by Sorai and Seki on $[Fe(phen)_2(NCS)_2]$ and $[Fe(phen)_2(NCSe)_2]$ (phen = 1,10-phenanthrolene).[3] The Nernst calorimeter employed required 15–20 g samples. Both compounds displayed a pronounced anomaly in the $C_p(T)$ curve at the temperature of the spin transition. The increase in entropy responsible for the spin transition was explained by the increased spin-multiplicity relative to that of the LS state and the changes in the molecular vibrations in the HS state. The anomaly in the heat capacity of $[Fe([D_2]2\text{-}pic)_3]Cl_2 \cdot EtOD$ ([D$_2$]2-pic = 2-picolylamine with a deuterated amino group) could be accounted for almost quantitatively by the spin transition.[4] Calorimetric measurements (according to the DSC method in the range of 150 to 300 K) have been reported for a few other spin-crossover systems,[5] but the authors discussed only the qualitative aspects of the transformation enthalpy and entropy. We have investigated the iron complexes **1** and **2** with a new microcalorimeter, which we introduce here.[6] It enables us to contribute to the understanding of the thermodynamics of the spin transition.

The sample chamber of the calorimeter is built into a cryostat (CryoVac, Troisdorf) and can reach temperatures between 4.2 and 300 K. The construction of the calorimeter

$[Fe(bts)_2(NCS)_2]$ bts = 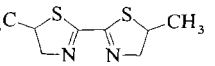

1

$[Fe(2\text{-}pic)_3]Cl_2 \cdot EtOH$ 2-pic = 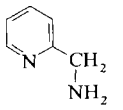

2

allows the simultaneous measurements of a sample and a reference. Both compounds are placed on sapphire sample holders, which are supplied with coated electrical heating units and thermocouples for temperature measurement. By exact measurement of the thermopotential the temperature can be determined with a resolution of up to 0.001 K.

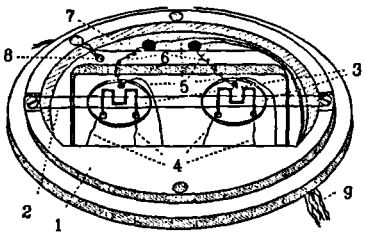

Fig. 1. The sample chamber of the calorimeter. 1 – Gold-plated copper baseplate, 2 – cotton thread, 3 – sapphire sample-holder with coated heating elements, 4 – gold wires for the heater, 5 – thermocouple wires, Chromel, 6 – thermocouple wires, Au/0.03% Fe, 7 – Mylar foil, 8 – silicon diode, 9 – electrical leads (inner diameter of the chamber ca. 10 cm).

Blueprints for the basic construction of the microcalorimeter were kindly provided by E. Gmelin (Max-Planck-Institut für Festkörperforschung, Stuttgart (FRG)). However, this version of the apparatus is best suited for measurements of heat capacities for substances with good heat conductance, but not for measurements on poorly conducting compounds like organometallic and coordination compounds. We have extended the preparation and measurement techniques beyond the original instrument design by E. Gmelin[7–9] and have developed a new method of data reduction and interpretation.

The entire measurement was controlled by use of an Atari ST computer (operating system RTOS, program language PEARL). In the measurement of the heat capacity the temperature of the sample/holder system is raised by a short heat pulse, and the thermal relaxation is observed until the temperature difference ΔT between the holder and sample reaches zero. Since the system is under vacuum during the measurement, the energetic contact between the sample holder and the environment is made by electrical leads and by the radiation of heat. Problems arise for poorly conducting samples, since the sample temperature deviates significantly from that measured for the holder. The decay curves $\Delta T(t)$ are then no longer simple exponential functions. We could take this into account with a new measurement technique, an improved sample preparation, and a new method of data analysis. In our procedure single crystals are wrapped in aluminum foil which has been coated with a mixture of powdered graphite and Apiezon-N grease. This way heat contact with the entire crystal surface is established and the radiation of heat is also independent of the radiation properties of the

[*] Prof. Dr. P. Gütlich, R. Jakobi, H. Romstedt, H. Spiering
Institut für Anorganische und Analytische Chemie der Universität
Staudinger Weg 9, D-W-6500 Mainz (FRG)

[**] bts = 2,2'-bis(4,5-dihydro-5-methyl-1,3-thiazole; 2-pic = 2-picolylamine

 © VCH Verlagsgesellschaft mbH, W-6940 Weinheim, 1992 0570-0833/92/0202-0178 $ 3.50+.25/0

sample. Polycrystalline samples are mixed with powdered graphite and sealed in aluminum pans, similar to the sample preparation for DSC measurements.

A complication in the measurement of poorly heat-conducting samples is that after the heat pulse the temperature of the sample/holder system is a function of location and time. Thus the decay curves depend on the thermal conductivity λ, that is on the given sample, its geometry, and also the temperature (due to the temperature dependence of λ). If the thermal relaxation in the sample is not taken into account, errors of up to 50% of the true value of the heat capacity may occur for one sample.

For this reason the data analysis was developed so that the total thermal relaxation of the sample and its holder could be accounted for. The sample is formally divided into layers of constant (or only time-dependent) temperature. The solution of the related system of differential equations is the temperature decay of the sample holder as a function of the specific heat C_p and the specific thermal conductivity λ of the sample. Fitting this expression to the measured temperature-decay curves by the least-squares method provides C_p and λ. The error in C_p was found empirically to be in the range of 2–4%. The accuracy is comparable to that of the DSC method; however, we can approach temperatures as low as 10 K, whereas measurements on commercially available DSC instruments have a lower temperature limit of roughly 110 K. All of the software for the regulation of the measurement and the data manipulation techniques briefly described here were developed in our laboratory. The calorimeter was calibrated with copper, silicon, and benzoic acid.

In the first test measurements on 22 mg of polycrystalline NH_4Cl, which shows an order–disorder transition at $T = 256$ K, the literature values[10] (obtained from measurements on 21 g NH_4Cl by the Nernst method) were reproduced quite well.

After that we started the first measurements on spin-crossover compounds. Complex **1** (coarse crystalline sample, ca. 20 mg) shows a noticeable anomaly in the $C_p(T)$ curve in the spin-transition range (roughly 210 K) (Fig. 2), as is expected from thermodynamic considerations.[4] Thus we refute the report by Kulshreshta et al. in which DSC measurements on the same compounds did not show a peak.[12]

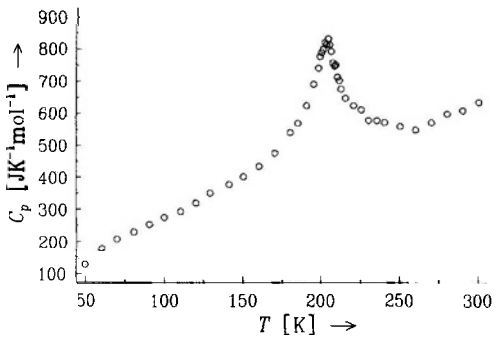

Fig. 2. Specific heat C_p of **1** as a function of temperature (coarse crystalline sample, ca. 20 mg).

We conducted measurements on a single crystal (21 mg) of the spin-crossover system **2** in the temperature range of 15 to 300 K. This system is of special interest because the thermal spin transition occurs with a plateau (step) between 113 and 121 K;[13] its cause has been a matter of speculation so far. Heat capacity measurements of complex **2** were already conducted by Sorai and Kaji[14] with a Nernst calorimeter on a sample almost 1000 times larger (15 g, polycrystalline) than ours. In Figure 3 the two sets of results are compared. Our experiment on the small sample shows a greater amount of scattering of the data points relative to that of Sorai and Kaji; however, the overall curves are in impressively good agreement. As is shown in the expanded region between 100 and 150 K, the resolution measured with our microcalorimeter in the region of the double peak resulting from the step of the spin transition is higher than that recorded with the Nernst calorimeter. This satisfying result demonstrates that the microcalorimeter introduced here can be used for thermodynamic investigations of solids, even if the samples conduct heat poorly, if limited amounts of the sample are available, or if single-crystal measurements are desired. Measurements may also be conducted at temperatures as low as 10 K, as we have shown here.

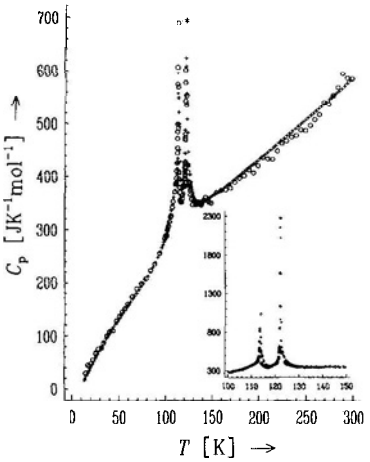

Fig. 3. Specific heat C_p of **2** as a function of temperature. +: Measurement made by Sorai and Kaji (coarse crystalline sample, ca. 15 g); o: our measurement on a single crystal (ca. 21 mg). The inset shows an expansion of the region of the spin transition between 114 and 121 K.

The heat-capacity measurements on system **2** have enabled us to perform a thermodynamic treatment of the spin transition.[15] Of special note is the indication that the step in the spin transition may be caused by cluster formation or the formation of a sublattice. This can be concluded from the observation that the entropy of mixing is markedly smaller in the temperature range of the step than would be expected for a statistical distribution of HS and LS molecules.

For the first time the specific thermal conductivity $\lambda(T)$ of a spin-crossover system could also be determined from the same calorimetric measurements. Figure 4 shows $\lambda(T)$ for **2** and also for the related zinc complex. For the latter, λ is quite

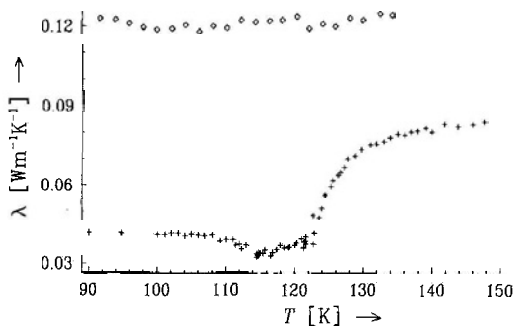

Fig. 4. Specific thermal conductivity λ of **2** (+) and $[Zn(2\text{-pic})_3Cl_2 \cdot EtOH$ (◇) (single crystals). Since reference measurements do not exist, the absolute values are not certain. However, the change of λ in the iron complex is significant.

temperature-independent in the temperature range shown. The iron complex **2** displays a change in the thermal conductivity by a factor of two at the spin transition.

Received: August 28, 1991 [Z 4892 IE]
German version: *Angew. Chem.* **1992**, *104*, 214

CAS Registry numbers:
1, 138433-12-2; **2**, 18433-69-7.

[1] In the context of the ligand field theory the transition $^5T_2(O_h) \rightleftharpoons {}^1A_1(O_h)$ pertains to system approaching O_h symmetry.
[2] P.Gütlich, *Struct. Bonding (Berlin)* **1981**, *44*, 83.
[3] M. Sorai, S. Seki, *J. Phys. Chem. Solids* **1974**, *35*, 555.
[4] R. Jakobi, H. Spiering, L. Wiehl, E. Gmelin, P. Gütlich, *Inorg. Chem.* **1988**, *27*, 1823.
[5] S. K. Kulshreshta, R. M. Iyer, *Chem. Phys. Lett.* **1987**, *134*, 239.
[6] A detailed description is found in the Ph.D. dissertation of R. Jakobi (Universität Mainz, Fachbereich Chemie und Pharmazie, **1990**) and will be repeated in a later publication.
[7] E. Gmelin, *Thermochim. Acta* **1987**, *110*, 183.
[8] W. Brill, E. Gmelin, *J. Therm. Anal.* **1988**, *33*, 365.
[9] We thank Prof. E. Gmelin and his co-workers for their help in the construction of our microcalorimeter.
[11] S. K. Kulshreshta, R. M. Iyer, E. König, G. Ritter, *Chem. Phys. Lett.* **1984**, *110*, 201.
[12] A detailed discussion of the investigation by H. Romstedt, R. Jakobi, H. Spiering, and P. Gütlich is planned in a separate paper.
[13] H. Köppen, E. W. Müller, C. P. Köhler, H. Spiering, E. Meißner, P. Gütlich, *Chem. Phys. Lett.* **1982**, *91*, 348.
[14] K. Kaji, M. Sorai, *Thermochim. Acta* **1985**, *88*, 185.
[15] R. Jakobi, H. Spiering, P. Gütlich, *J. Phys. Chem. Solids*, in press.

Stable *N,N'*-Di-*tert*-butyl-*meta*-phenylene-bisnitroxides—Unexpected Ground-State Singlets**

By *Maya Dvolaitzky, Robert Chiarelli, André Rassat**

m-Xylylene and related compounds have been predicted and shown[1, 2] to be ground-state triplets. A related bisnitroxide **1** behaves similarly, but unfortunately it undergoes spontaneous decomposition.[3] In order to obtain a more stable diradical, we have prepared the trimethyl derivative **2**. Steric hindrance is expected to prevent the reaction between two diradicals **2** and to twist the *t*BuNO groups, which should lead to atropoisomerism.[4] As described below, two isomers of **2** were isolated. Both were found to have a singlet ground-state in contrast to the unsubstituted bisnitroxide **1**[3] and other *m*-xylylene-related compounds.[1, 2]

N,N'-di-*tert*-butyl-2,4,6-trimethyl-*m*-phenylenediamine (**4**) was obtained from the commercially available diamine **3**, by the adaptation of a procedure used for the synthesis of *tert*-butyl ethers and *tert*-butyl esters[5] (Scheme 1). Under various experimental conditions, *tert*-butylation of **3** gave a mixture of unreacted diamine **3**, mono-*tert*-butylamine **5**, and the di-*tert*-butylamine **4** in roughly a 2:7:1 ratio. Although its yield was always very low (2%), pure **4** was easily isolated by thin layer chromatography (TLC) on silica gel. Product **4** was characterized by ^{1}H NMR and mass spectroscopy. Oxidation of **4** smoothly gave **2** in 55% yield.

TLC of an ethereal solution of **2** on silica gel (*n*-hexane/ethyl acetate 3:1, two elutions) gave two products, **2A** and **2B** (R_f = 0.29 and 0.34) isolated in a ratio of about 2:1. Eluted first, **2B** is an amorphous solid; eluted next, **2A** is crystalline and may be recrystallized as fine needles from *n*-hexane. The interconversion of the two isomers is rapid in solution (TLC detection). Without solvent, even at −20 °C, pure amorphous **2B** gave crystalline **2A** within a few days. Crystalline **2A** remains unchanged.[6]

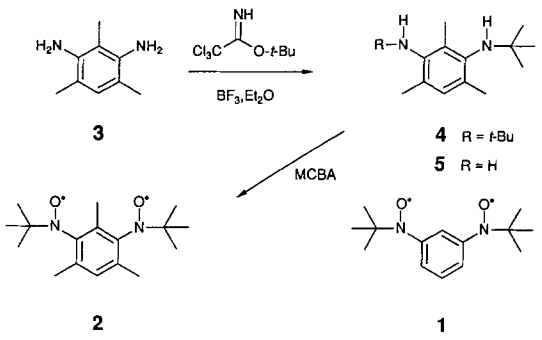

Scheme 1. MCPBA = *m*-chloroperbenzoic acid.

Frozen solutions of either diradical display the characteristic $\Delta m = 1$ and $\Delta m = 2$ spectra with hyperfine structures[7] (Fig. 1). A weak invariable signal of a monoradical can be seen in the central part of the $\Delta m = 1$ spectra, especially at 10 K; this implies that both diradicals are more than 99% pure. From 100 to 10 K the signal/noise ratio decreases dramatically with temperature, and below 5 K no triplet signal could be detected for either isomer—primary evidence of their singlet ground-states. Figure 2 shows the temperature-dependence of $2D$, the larger component of the dipolar tensor (in millitesla) and of the corresponding average interelectronic distance d (in Angstrom), ($D = 27810\, d^{-3}$)[8], for **2A** and **2B**. These values differ slightly from those of **1** ($2D$ = 36.6 mT; d = 5.34 Å)[3] and of a related bisnitroxide ($2D$ = 24.0 mT; d = 5.83 Å).[9]

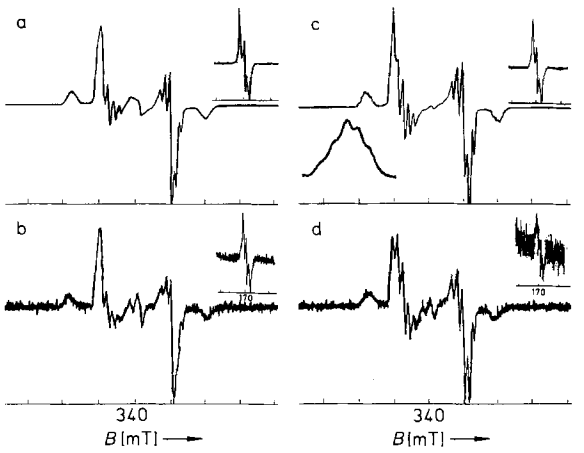

Fig. 1. ESR $\Delta m = 1$ spectra of isomer **2A** at a) 100 K and b) 10 K, and of isomer **2B** at c) 100 K and d) 10 K. The insets in the upper right of a)–d) shows the corresponding $\Delta m = 2$ signals; inset lower left in c) shows an enlargement of the first line with hyperfine structure. Solvent: ethanol.

In order to determine the ground-state multiplicity and the singlet–triplet separation $2J$, the classical method of investigation, the determination of the temperature-dependence of the intensity of the $\Delta m = 2$ transitions,[3] was conducted. Since both biradicals were pure in this study, the $\Delta m = 1$ transition was also considered. Using a dual-sample cavity

[*] Prof. Dr. A. Rassat, Dr. M. Dvolaitzky, Dr. R. Chiarelli
Laboratoire de Chimie, Ecole Normale Supérieure
24, Rue Lhomond, F-75231 Paris Cedex 05 (France)

[**] This research was supported by the Centre National de la Recherche Scientifique (Project CNRS URA 1110).

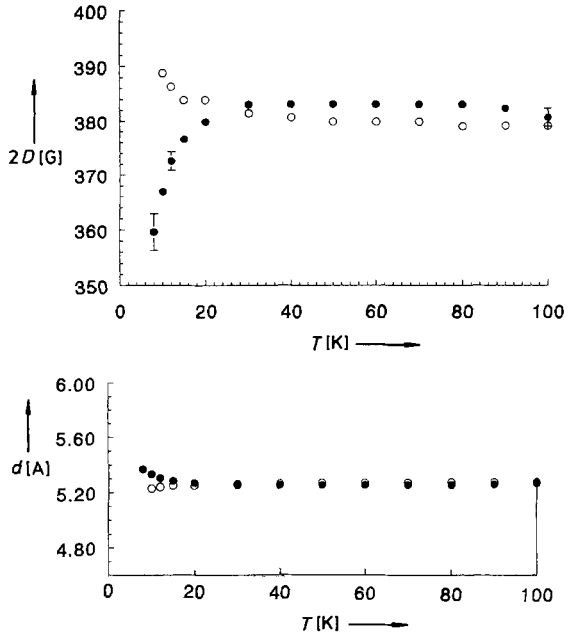

Fig. 2. Dependence of $2D$ (top) and d (bottom) on T for isomers **2A** (○) and **2B** (●).

with a reference, we measured the intensities (obtained by double integration of the ESR signal) I of the sample in ethanol (at temperature T) and I_{ref} of the reference (at room temperature). Figure 3 shows IT/I_{ref} and I_{ref}/I versus T for **2A** and **2B** at $\Delta m = 2$ and $\Delta m = 1$. The experimental curves were fitted to the Curie–Weiss law $I^{-1} = C_1^{-1}(T - \theta)$ ($40\ K < T < 100\ K$ for **2A** and $50\ K < T < 100\ K$ for **2B**), and to the Bleaney–Bowers expression, $I^{-1} = T(3 + e^{-2J/kT})C_2^{-1}$,[3,10] ($10\ K < T < 100\ K$, for both isomers)

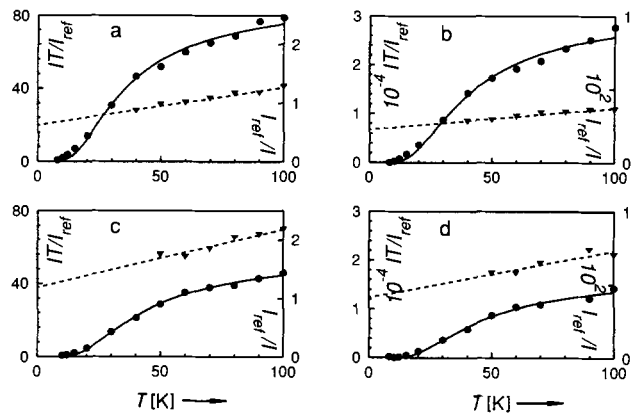

Fig. 3. Temperature-dependence of IT/I_{ref} (left axis, ●) and I_{ref}/I (right axis, ▼) in arbitrary units for isomer **2A** a) $\Delta m = 2$, b) $\Delta m = 1$, and isomer **2B** c) $\Delta m = 2$ and d) $\Delta m = 1$. Solid and dashed lines are the theoretical curves for the Bleaney–Bowers expression and the Curie–Weiss law, respectively.

Table 1. Best-fit parameters of the Curie–Weiss and Bleaney–Bowers expressions:

	2A		**2B**	
	$\Delta m = 2$	$\Delta m = 1$	$\Delta m = 2$	$\Delta m = 1$
θ [K]	−96	−156	−118	−129
C_1 [a]	154	69186	100	31358
$2J/k$ [K]	−66	−75.5	−81	−86
C_2 [a]	371	131809	235	72217

[a] C_1 and C_2 are the constants of the Curie–Weiss law and the Bleaney–Bowers expression, respectively (arbitrary units).

(Table 1). Since the Curie–Weiss approximation is valid for $T \gg |\theta|$ or $T \gg |2J|/k$, a condition not satisfied here, it only gives a qualitative indication of the sign of θ.

These results clearly show that both isomers are ground-state singlets. This is rather surprising for an *m*-xylylene derivative. In our case, conjugation in both isomers is probably prevented by steric hindrance, that is the electrons are localized on oxygen. However, the conjugation in the two perchloro isomers studied by Veciana et al.[2] is also prevented by steric hindrance, and the two compounds are ground-state triplets. One may wonder if antiferromagnetic superexchange[11] may take place by hyperconjugation of the methyl groups, or in valence-bond language if the contribution of structure **I**, although nonplanar, may stabilize the singlet state relative to the triplet.

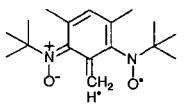

I

Experimental Procedure

General methods: ^1H NMR spectra were recorded on a Bruker instrument at 200 MHz (TMS standard). ESR spectra were obtained on a E 300 Bruker spectrometer equipped with a variable-temperature accessory (Oxford Instrument) and a data acquisition system. Measurements were performed using a dual-sample cavity with 4-hydroxy-2,2,6,6-tetramethylpiperidine-1-oxyl as reference. The spectra were obtained at a microwave power of 20 mW ($\Delta m = 2$) or 10 mW ($\Delta m = 1$). Absence of saturation was checked, especially at low temperature. The solution samples were degassed by a freeze-pump-thaw cycle and sealed under vacuo.

4: $BF_3 \cdot Et_2O$ (40 μL) was slowly added by syringe over 1 h to a stirred solution of **3** (0.15 g, 1 mmol) and *tert*-butyl-2,2,2-trichloroacetimidate (0.4 mL, 2.2 mmol) in dry C_6H_{12}/CH_2Cl_2 2:1 (6 mL). Stirring was continued for 18 h. TLC on silica gel (*n*-hexane/AcOEt 3:1) showed three spots ($R_f = 0.64$, 0.30, 0.06). Solid sodium hydrogencarbonate was then added to the reaction mixture, and the mixture was filtered. The solid was washed with C_6H_{12}/CH_2Cl_2 (2:1). The filtrate was concentrated to dryness providing about 0.3 g of a yellow waxy solid. In order to remove the trichloroacetamide, the product was suspended in *n*-hexane. After filtration, the solid fraction was resuspended in C_6H_{12}/CH_2Cl_2 (2:1) and filtered again. Evaporation of both filtrates in vacuo gave 0.194 g crude product, which after preparative TLC on silica gel (*n*-hexane/AcOEt 3:1) provided 5 mg of noncrystalline diamine **4** (2%); $R_f = 0.61$; CI-MS m/z 263 ($M^{\oplus} + H$); ^1H NMR ($CDCl_3$): $\delta = 1.17$ (s, 18 H; *t*Bu), 2.21 (s, 6 H; 4,6-CH_3), 2.31 (s, 3 H; 2-CH_3), 6.83 (s, 1 H; 5-H).

2: To a stirred solution of diamine **4** (4.4 mg, 0.017 mmol) in ether (1 mL) was added dropwise a solution of *m*-chloroperbenzoic acid (0.572 g, 3.3 mmol) in ether (3 mL). After the reaction mixture had been stirred 28 h at room temperature, dilute aqueous sodium carbonate was added. The orange-pink ether fraction was washed to neutrality with water and dried over sodium sulfate. TLC on silica gel (0.25 mm thickness, on aluminum foil) with *n*-hexane/AcOEt (3:1) (two elutions) gave crystalline **2A** (1.8 mg) and amorphous **2B** (0.9 mg); $R_f = 0.29$ and 0.34, respectively. CI-MS: m/z 293 ($M^{\oplus} + H$); Total yield 55%. **2A** was recrystallized from *n*-hexane to give fine needles. Because of the lack of material, microanalysis and melting point were not carried out.

Received: September 9, 1991 [Z 4906 IE]
German version: *Angew. Chem.* **1992**, *104*, 220

[1] For a recent review: H. Iwamura, *Adv. Phys. Org. Chem.* **1990**, *26*, 179–253 (p. 189).
[2] J. Veciana, C. Rovira, M. Crespo, O. Armet, V. M. Domingo, F. Palacio, *J. Am. Chem. Soc.* **1991**, *113*, 2552–2561.
[3] A. Calder, A. R. Forrester, P. G. James, G. R. Luckhurst, *J. Am. Chem. Soc.* **1969**, *91*, 3724–3727.
[4] M. Oki, *Top. Stereochem.* **1983**, *14*, 1–81.
[5] A. Armstrong, I. Brackenbridge, R. F. W. Jackson, J. M. Kirk, *Tetrahedron Lett.* **1988**, *29*, 2483–2486.
[6] An X-ray crystal analysis of isomer **2A** is in progress.
[7] E. Wassermann, L. C. Snyder, W. A. Yager, *J. Chem. Phys.* **1964**, *41*, 1763–1772.
[8] N. Hirota, S. I. Weissman, *J. Am. Chem. Soc.* **1964**, *86*, 2538–2545.
[9] A. Rassat, H. U. Sieveking, *Angew. Chem.* **1972**, *84*, 353–354; *Angew. Chem. Int. Ed. Engl.* **1972**, *11*, 303–304.
[10] B. Bleany, D. K. Bowers, *Proc. R. Soc. London A.* **1952**, *214*, 451–465.
[11] P. W. Anderson, *Phys. Rev.* **1950**, *79*, 350–356.

Activation Parameters and Stereochemistry of an Antibody-Catalyzed Claisen Rearrangement**

By *David Y. Jackson, Michael N. Liang, Paul A. Bartlett,* and *Peter G. Schultz**

The formal [3,3]sigmatropic rearrangement of chorismate **1** to prephenate **3** (Scheme 1), a key step in the biosynthesis of aromatic amino acids in bacteria and plants, is catalyzed by the well-studied enzyme chorismate mutase from *Escherichia coli*.[1-4] The rate of the enzymatic reaction, which has been demonstrated to proceed through a chairlike transition-state,[5] is approximately 3×10^6 times faster than that of the uncatalyzed reaction.[1] The thermal rearrangement also proceeds through a chairlike transition state in which the carbon–oxygen bond is broken substantially before the carbon–carbon bond begins to form; this rearrangement is characterized by an enthalpy ($\Delta H^{\neq}$) and entropy ($\Delta S^{\neq}$) of activation of 20.5 kcal mol^{-1} and -12.9 cal mol^{-1} K^{-1}, respectively.[6-8]

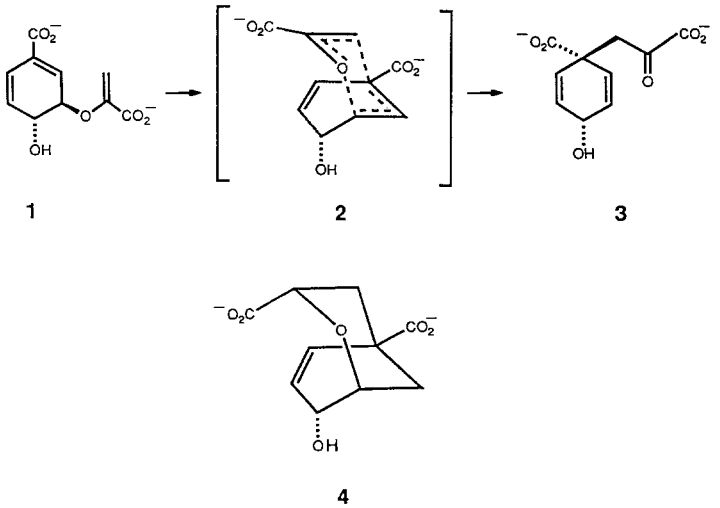

1 **2** **3**

4

Scheme 1. Claisen rearrangement of chorismate **1** to prephenate **3** and structure of the transition-state analogue hapten **4**.

Recently we[9] and others[10,11] demonstrated that antibodies raised against the bicyclic transition-state analogue **4**[12] also catalyzed the Claisen rearrangement of chorismate to prephenate. One antibody, 1F7, catalyzed the stereospecific conversion of the (−)-isomer with a rate acceleration of 250 over the uncatalyzed reaction. The activation parameters ($\Delta H^{\neq} = 15$ kcal mol^{-1} and $\Delta S^{\neq} = -22$ cal mol^{-1} K^{-1}) indicate that the antibody functions by reducing $\Delta H^{\neq}$ for the reaction with a counterproductive decrease in $\Delta S^{\neq}$.[10,11] A second antibody, 11F1-2E11, accelerated the rearrangement 10^4 fold over the uncatalyzed process.[9] For this antibody, mechanisms involving a cationic substituent effect or general acid catalysis were ruled out. We now report that this second antibody, 11F1-2E11, stereospecifically catalyzes the Claisen rearrangement of (−)-chorismate with an entropy of activation of nearly zero, supporting the notion that conformational restriction plays an important role in this antibody-catalyzed reaction.

[*] Prof. P. G. Schultz, D. Y. Jackson, M. N. Liang, Prof. P. A. Bartlett
Department of Chemistry, University of California
Berkeley CA 94720 (USA)

[**] This work was supported by grants from the National Institutes of Health (AI 24695-02 and GM 08352-01).

We anticipated that an antibody generated against hapten **4**, which mimics the conformationally restricted chairlike transition-state configuration[12], should act as an entropy trap by restricting the rotational degrees of freedom required to form the transition state. In order to define the entropic contribution to catalysis by the catalytic antibody 11F1-2E11, the temperature dependence of k_{cat} was determined (Lineweaver–Burk analysis, Fig. 1). The rate of the rearrangement was measured spectrophotometrically (absorption at $\lambda = 270$ nm) at pH 7 (5 mM NaCl, 50 mM Na_2HPO_4) at six temperatures from 5 °C to 41 °C and corrected for the uncatalyzed rate.[9] The values of $\Delta H^{\neq}$ and $\Delta S^{\neq}$ were calculated from the Arrhenius equation ($k_{cat} = Ae^{-E_a/RT}$) to be 18.3 kcal mol^{-1} and -1.2 cal mol^{-1} K^{-1}, respectively ($\Delta G^{\neq} = 18.7$ kcal mol^{-1}). Interestingly, monoclonal antibody 11F1-2E11 reduces $\Delta H^{\neq}$ by 2.2 kcal mol^{-1} and increases $\Delta S^{\neq}$ by 11.7 cal mol^{-1} K^{-1} ($\Delta\Delta G^{\neq} = 3.3$ kcal mol^{-1} at 10 °C) relative to the uncatalyzed process. The observation that the antibody–substrate complex proceeds to product with an entropic barrier of nearly zero argues that the antibody constrains the substrate in a favorable conformation for the rearrangement.[13] The fact that the antibody also lowers the $\Delta H^{\neq}$ might reflect the use of antibody binding energy to induce strain in the substrate,[14] or perhaps electrostatic stabilization of the transition state. A comparison of the activation parameters for the uncatalyzed, antibody-catalyzed, and enzyme-catalyzed processes is shown in Table 1. Both the enzyme and antibody 11F1-2E11 increase the $\Delta S^{\neq}$ to nearly zero. The enzyme reduces $\Delta H^{\neq}$ an additional 2.4 kcal mol^{-1} relative to antibody 11F1-2E11. An interesting question is whether a similar reduction in $\Delta H^{\neq}$

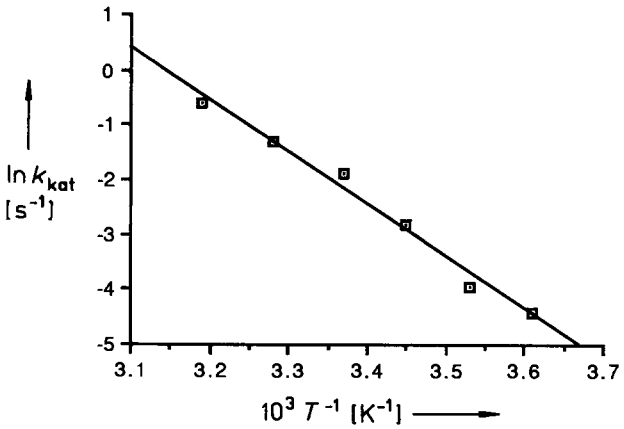

Fig. 1. Arrhenius plot of the temperature dependence of k_{cat}.

Table 1. Kinetic parameters for the uncatalyzed, antibody-catalyzed, and chorismate mutase-catalyzed Claisen rearrangements of chorismate **1** to prephenate **3**.

Parameter	Uncatalyzed [1]	Antibody 1F7 [11]	Antibody 11F1-2E11 [9]	Chorismate mutase [2]
k_{cat} [min^{-1}]		0.072	2.7	810
K_m [μM]		51	260	290
K_i [μM]		0.6	9	0.15
k_{cat}/k_{uncat}		250	10^4	3×10^6
$\Delta G^{\neq}$ [kcal mol^{-1}]	24.2	21.3	18.7	15.9
$\Delta H^{\neq}$ [kcal mol^{-1}]	20.5	15	18.3	15.9
$\Delta S^{\neq}$ [cal mol^{-1} K^{-1}]	−12.9	−22	−1.2	0.0

can be achieved for the antibody-catalyzed process by genetic selection and screening experiments.

If the antibody binding site is complementary to the bicyclic chair-shaped hapten **4**, then the reaction should be stereospecific. In order to test this notion racemic chorismate was synthesized by a previously described procedure.[15] A sample of (+)-chorismate was obtained by kinetic resolution of (±)-chorismate using the enzyme chorismate mutase.[10, 16] Unreacted (+)-chorismate was isolated by preparative HPLC and coeluted with authentic (−)-chorismate. The optical purity of the (+)-chorismate was determined to be 94% by optical rotation. The relative rates of conversion of (+)-chorismate, (±)-chorismate, and the natural (−)-chorismate were measured at 10 °C in the presence of catalytic antibody 11F1-2E11 (Fig. 2). The preference of antibody 11F1-2E11 for the natural (−)-chorismate to the synthetic (+)-chorismate is greater than 40:1 (after correction for enantiomeric purity), similar to the results of Hilvert and coworkers for antibody 1 F 7.[10]

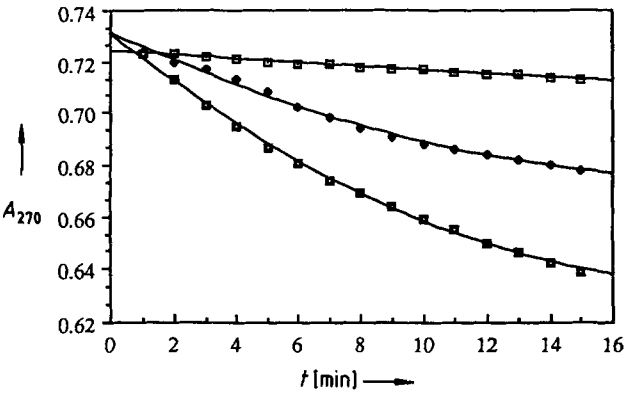

Fig. 2. Antibody-catalyzed conversion of (−)-chorismate (□), (+)-chorismate (○), and (±)-chorismate (◆). A_{270} = absorption at λ = 270 nm. The curvature is due to substrate depletion. Approximately 25% of the substrate is consumed in 15 min.

These results suggest that the diversity of the immune response may provide a number of mechanistic alternatives for a particular antibody-catalyzed reaction and consequently increased insight into the nature of biological catalysis. X-ray crystallographic analysis and genetic cloning and sequencing experiments will further define the mechanism of this catalytic antibody.

Received: September 9, 1991 [Z 4907 IE]
German version: *Angew. Chem.* **1992**, *104*, 196

[1] P. R. Andrews, G. D. Smith, I. G. Young, *Biochemistry* **1973**, *12*, 3492.
[2] H. Gorisch, *Biochemistry* **1978**, *17*, 3700.
[3] E. Haslam, *The Shikimate Pathway*, Wiley, New York, **1974**.
[4] W. J. Guilford, S. D. Copley, J. R. Knowles, *J. Am. Chem. Soc.* **1987**, *109*, 5013.
[5] S. G. Sogo, T. S. Widlanski, J. H. Hoare, C. E. Grimshaw, G. A. Berchtold, J. R. Knowles, *J. Am. Chem. Soc.* **1984**, *106*, 2701.
[6] S. D. Copley, J. R. Knowles, *J. Am. Chem. Soc.* **1985**, *107*, 5306.
[7] R. M. Coates, B. D. Rogers, S. J. Hobbs, D. R. Peck, D. P. Curran, *J. Am. Chem. Soc.* **1987**, *109*, 1160.
[8] J. J. Gajewski, J. Jurayi, D. Kimbrough, M. E. Gande, B. Ganem, B. K. Carpenter, *J. Am. Chem. Soc.* **1987**, *109*, 1170.
[9] D. Y. Jackson, J. W. Jacobs, R. Sugasawara, S. H. Reich, P. A. Bartlett, P. G. Schultz, *J. Am. Chem. Soc.* **1988**, *110*, 4841.
[10] D. Hilvert, K. D. Nared, *J. Am. Chem. Soc.* **1988**, *110*, 5593.
[11] D. Hilvert, S. H. Carpenter, K. D. Nared, M. M. Auditor, *Proc. Natl. Acad. Sci.* **1988**, *85*, 4953.
[12] P. A. Bartlett, C. R. Johnson, *J. Am. Chem. Soc.* **1985**, *107*, 7792.
[13] F. H. Westheimer, *Adv. Enzymol. Relat. Areas Mol. Biol.* **1962**, *24*, 441.
[14] W. P. Jencks, *Adv. Enzymol. Relat. Areas Mol. Biol.* **1975**, *43*, 219.
[15] J. H. Hoare, P. P. Policastro, G. A. Berchtold, *J. Am. Chem. Soc.* **1983**, *105*, 6264.
[16] To a solution of 2 mL (±)-chorismate (25 mM) in 100 mM *N*-ethyl morpholine-2-(*N*-morpholino)ethanesulfonate buffer, pH 7.5, at 25 °C was added chorismate mutase (10 units). A small aliquot (50 μL) was removed and diluted 1:10 with the same buffer. The reaction was monitored spectrophotometrically at 270 nm until no further increase in absorbance was detected (after ca. 10 min). Unreacted (+)-chorismate was isolated by preparative HPLC (50 mM triethyl ammonium acetate, pH 5/CH_3CN) and the structure confirmed by NMR spectroscopy.

The Neutralization of $HeC_{60}^{\bullet+}$ in the Gas Phase: Compelling Evidence for the Existence of an Endohedral Structure for $He@C_{60}$**

By *Thomas Weiske, Thomas Wong, Wolfgang Krätschmer, Johan K. Terlouw,* and *Helmut Schwarz**

Dedicated to Professor Fred W. McLafferty

One of the most interesting features of buckminsterfullerene, C_{60},[1] is its 7 Å diameter internal cavity[2] which could act as a "molecular container"[3] for atoms and provides a potential environment for *endohedral* chemistry[4] (chemistry inside the cage). Indeed, fullerene–metal complexes of the type MC_{60} (M = La, Ni, Na, K, Rb, Cs) and LaC_x (x = 60, 70, 74, 82) have been generated by Smalley and co-workers[5] in laser vaporization experiments on graphite doped with metal salts. Initially there was some debate about the location of the metal atom[6] (*endo* vs. *exo* complex). However, comparison with the characteristics of exohedral fullerene complexes of the type MC_{60}^+ (M = Fe, Co, Ni, Cu, La, VO), the exclusive products of ion/molecule reactions at thermal energy,[7] convincingly shows that in the experiments of Smalley et al.[5] the metal atom becomes incorporated during the cluster formation process and endohedral fullerene–metal complexes are obtained. For these endohedral complexes the symbol $M@C_x$ has been recommended.[5c]

Mass spectrometric studies using the techniques of collisional-induced dissociation or laser-induced photodissociation revealed that complexes of the type $M@C_{60}^{\bullet+}$ (and also complexes with higher fullerenes) lose C_2 and multiple units thereof while the loss of M is not observed (Scheme 1). In contrast, the *exohedral* complexes lose the metal upon activation, and C_m losses are not observed.

In a fundamentally different experiment we[8] and later other groups[9] showed that the noble gas atoms He and Ne can also be incorporated into $C_{60}^{\bullet+}$ and $C_{70}^{\bullet+}$, respectively.[10] This occurs when molecular beams of highly accelerated $C_x^{\bullet+}$ ions are fired through a stationary noble gas. The resulting

[*] Prof. Dr. H. Schwarz, Dr. T. Weiske
Institut für Organische Chemie der Technischen Universität
Straße des 17. Juni 135, D-W-1000 Berlin 12 (FRG)
Prof. Dr. J. K. Terlouw, T. Wong
Department of Chemistry
McMaster University
Hamilton, Ontario, L8S 4M1 (Canada)
Dr. W. Krätschmer
Max-Planck-Institut für Kernphysik
Postfach 103980, D-W-6900 Heidelberg (FRG)

[**] This research was supported by the Deutsche Forschungsgemeinschaft, the Fonds der Chemischen Industrie, and the Natural Sciences and Engineering Research Council of Canada (NSERC). Valuable discussions with Prof. D. K. Böhme and Dr. J. Hrušák are gratefully acknowledged.

$MC_x^{\bullet+}$ complexes (M = He, Ne) fragment upon excitation to produce C_m and not M (Scheme 1), which would be expected only for an endohedral association complex. In addition, theoretical arguments favor this structure in which the noble gas is located inside the cage and is prevented from leaving its prison by a barrier of more than 8 eV.[8, 9] However, the

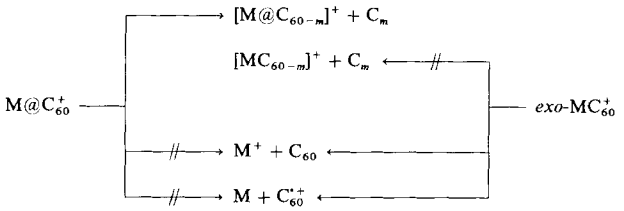

Scheme 1. Typical reactions of fullerene–metal complexes. m = 2, 4, 6...

staunchest critics may only be convinced that the noble gas–fullerene complex ion has an endohedral structure when the corresponding neutral species can be shown to exist. Experimental evidence that neutral noble gas–fullerene complexes have a finite lifespan would leave no doubt that the noble gas atom is physically trapped inside the cavity.

We report here a gas-phase experiment with the technique of neutralization–reionization mass spectrometry (NRMS)[11] in which a beam of $C_{60}He^{\bullet+}$ ions was successfully neutralized and subsequently reionized. The experimental conditions impose a minimum lifespan of about 90 μs on the neutral $C_{60}He$ complex, and the results show definitely that both the neutral complex and the precursor ion must possess the endohedral structure, represented as $He@C_{60}$ and $He@C_{60}^{\bullet+}$, respectively.[12]

All experiments were carried out on the four-sector mass spectrometer[13] schematically shown in Figure 1. The experimental evidence summarized in the spectra shown in Figure 2a–d was obtained from the following experiments. A mixture of C_{60} and C_{70} (containing > 90% C_{60}) was evaporated by heating the sample of 550 °C, and the vapor ionized by

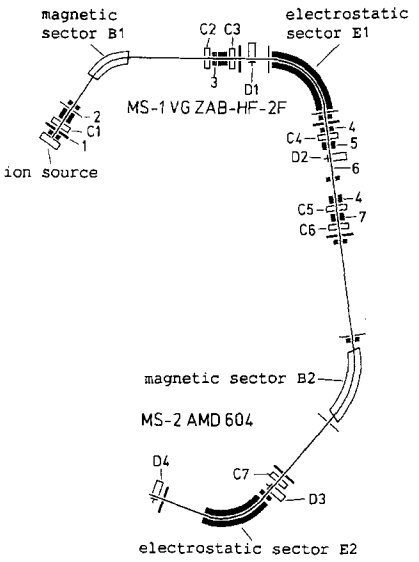

Fig. 1. Schematic diagram of the BEBE Tandem mass spectrometer at the TU Berlin [13]. Collision chambers C1–C7, ion detectors D1–D4, variable slit 1, fixed slit 2, beam deflection lens 3, focusing/deceleration lenses 4, focusing/acceleration lens 5, end of MS1 6, beam deflection/acceleration lenses 7.

electron impact (70 eV). The resulting ions were accelerated to 5000 eV, and magnet B1 was scanned (at constant E1) over the m/z range 714–734 under conditions of double focusing ($m/\Delta m$ = 1000, ion detection at D2). This yielded the partial mass spectrum displaying the molecular ion region of $C_{60}^{\bullet+}$ shown in Figure 2a.

The $C_{60}He^{\bullet+}$ were generated by collisions of the high energy $C_{60}^{\bullet+}$ ions (E_{kin} = 5000 eV) with quasi-stationary ^4He target atoms in collision cell C3 (transmission 40%). The center-of-mass collision energy of the C_{60}/He complex[8, 9] made this reaction endothermic by about 27 eV. Thus the accelerating voltage of the source-generated $C_{60}^{\bullet+}$ ions used for the synthesis of $C_{60}He^{\bullet+}$ was raised to 5027 eV so that $C_{60}He^{\bullet+}$ ions produced by collision with ^4He in C3 passed through electric sector E1 which remained set for the transmission of 5000 eV ions.

With ^4He in collision cell C3 and the concomitant raised accelerating voltage but otherwise identical conditions, a scan of B1 yielded the partial spectrum shown in Figure 2b: as in the first experiment, B1 transmitted the various isotopomers of $C_{60}^{\bullet+}$, but because of the kinetic energy constraint imposed by E1, this sector primarily transmitted the $C_{60}He^{\bullet+}$ particles generated in C3 to detector D2. (The diffuse background in Figure 2b arises from ions that lost kinetic energy in inelastic collisions between $C_{60}^{\bullet+}$ and He but did not incorporate helium).

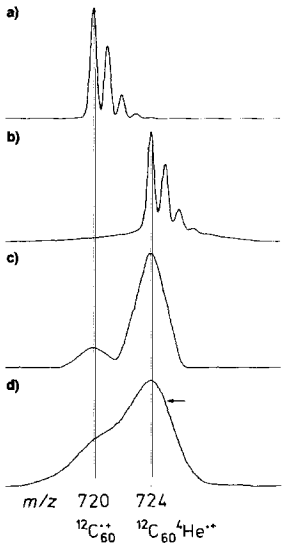

Fig. 2. Sequence of experiments (details in text): a) molecular ion region of $^{12}C_{60-x}{}^{13}C_x^{\bullet+}$ (x = 0 – 4), b) generation of $^{12}C_{60}He^{\bullet+}$, c) "purification" of m/z 724, d) NR experiment on $C_{60}^{\bullet+}$ and $C_{60}He^{\bullet+}$. Figure 2d represents an accumulation of about 400 spectra; for each spectrum approximately 6.3 ions were detected. The ratio of the number of ions in Fig. 2c to Fig. 2d is calculated as 6×10^4:1. The arrow indicates the recovery signal for $^{12}C_{60}{}^4He$.

This is demonstrated by the spectrum shown in Figure 2c: Under the conditions which lead to the spectrum shown in Figure 2b, B1 was set for optimal transmission of $^{12}C_{60}^{\bullet+}$ ions (m/z 724 in Fig. 2b). Then B2 was scanned over the appropriate mass range to separate $C_{60}{}^4He^{\bullet+}$ from the mixture of $C_{60}{}^4He^{\bullet+}$ (85%) and $^{12}C_{60}^{\bullet+}$ (15%) ions transmitted by E2. The voltages applied to sectors E1 and E2 were such that optimal transmission occurred for ions of 5000 eV translational energy and the signals were measured at D4.

The presence of the doublet signal (Fig. 2c) is an enormous advantage for the NR experiment since the $C_{60}^{\bullet+}$ component

acts as a mass marker. This avoids the problem of imprecise mass assignment that occasionally arises when using the "linked-scan" method. For the neutralization of the $C_{60}^{\bullet+}$ and $C_{60}He^{\bullet+}$ ions (Fig. 2d) an experiment analogous to that described for the spectrum in Figure 2c was performed as follows: To obtain the highest possible yield of neutral species in the electron transfer processes, a neutralization gas was used whose ionization energy (IE) lies close to the IE of C_{60} (7.6 eV)[14] (condition of near resonant electron transfer). From a great many neutralization experiments on $C_x^{\bullet+}$ clusters[15] $(CH_3)_3N$ (IE = 7.8 eV)[16] proved to be of the best reducing agents for $C_{60}^{\bullet+}$. Thus collision cell C5 was charged with $(CH_3)_3N$ at a pressure that reduced the beam transmission to approximately 10%. All unreacted ions were removed from the beam by maintaining the deflector electrode at 1000 eV so that only the beam of neutral species entered collision cell C6. In this cell a fraction of the neutral species was reionized by collision-induced ionization with $(CH_3)_3N$ as a target gas. Since the energy required for the collision-induced reionization was taken from the translational energy of the m/z 724 ion beam, the voltage applied to sector E2 was reduced slightly so that the $C_{60}He^{\bullet+}$ signal was detected at optimal transmission.

As shown in Figure 2d, the recovery signal for $C_{60}He$ shows up very clearly. This demonstrates unequivocally the existence of a species with the composition $C_{60}He$ for which the endohedral structure $He@C_{60}$ is the only conceivable physical arrangement. This result makes neutral $He@C_{60}$ the first identified noble gas–carbon compound.[17]

Considering the vertical nature of the electron transfer processes in neutralization–reionization experiments,[18] we conclude that the $He@C_{60}^{\bullet+}$ ionic complex also has the endohedral structure. In addition, the noble gas–fullerene complexes $MC_x^{\bullet+}$ (M = He, Ne; $x = C_{52}$–C_{70}) exhibit the same characteristics as $He@C_{60}^{\bullet+}$ in gas phase experiments [see Eqn. (a)] and must thus also have the endohedral structure.[19]

Received: December 6, 1991 [Z 5059 IE]
German version: *Angew. Chem.* **1992**, *104*, 242

CAS Registry numbers:
$C_{60}He^{\bullet+}$, 138855-72-8; $He@C_{60}$, 138855-73-9.

[1] Recent reviews: a) H. W. Kroto, *Science* **1988**, *242*, 1139; b) W. Weltner, Jr., R. J. Van Zee, *Chem. Rev.* **1989**, *89*, 1713; c) R. E. Smalley, in *Atomic and Molecular Clusters*, (Ed.: E. R. Bernstein), Elsevier, Amsterdam **1990**, Chapter 1; d) J. S. Miller, *Adv. Mater.* **1991**, *3*, 262; e) H. W. Kroto, A. W. Allaf, S. P. Balm, *Chem. Rev.* **1991**, *91*, 1213; f) R. F. Curl, R. E. Smalley, *Scientific American* **1991**, 32; g) R. E. Smalley, *Large Carbon Clusters*, (Eds.: C. Hammond, V. Kuck), (ACS Symp. Ser., in press); h) H. W. Kroto, *Angew. Chem.*, in press.

[2] J. M. Hawkins, A. Meyer, T. A. Lewis, S. Loren, F. J. Hollander, *Science* **1991**, *252*, 312.

[3] H. Hopf, *Angew. Chem.* **1991**, *103*, 1137; *Angew. Chem. Int. Ed. Engl.* **1991**, *30*, 1117.

[4] For theoretical work see: a) A. Rosen, B. Wästberg, *J. Am. Chem. Soc.* **1988**, *110*, 8701; b) J. Cioslowski, *ibid.* **1991**, *113*, 4139; c) J. Cioslowski, E. D. Fleischmann, *J. Chem. Phys.* **1991**, *94*, 3730; d) A. H. H. Chang, W. C. Ermler, R. M. Pitzer, *J. Chem. Phys.* **1991**, *94*, 5004; e) D. Bakewies, W. Thiel, *J. Am. Chem. Soc.* **1991**, *113*, 3704; f) B. Wästberg, A. Rosen, *Phys. Scr.* **1991**, *44*, 276; g) P. P. Schmidt, B. I. Dunlap, C. I. White, *J. Phys. Chem.*, submitted.

[5] a) J. R. Heath, S. C. O'Brien, Q. Zhang, Y. Lin, R. F. Curl, H. W. Kroto, F. K. Tittel, R. E. Smalley, *J. Am. Chem. Soc.* **1985**, *107*, 7779; b) F. D. Weiss, J. L. Elkind, S. C. O'Brien, R. F. Curl, R. E. Smalley, *ibid.* **1988**, *110*, 4464; c) Y. Chai, T. Guo, C. Jin, R. E. Haufler, L. P. F. Chibante, J. Fure, L. Wang, J. M. Alford, R. E. Smalley, *J. Phys. Chem.* **1991**, *95*, 7564; d) J. H. Weaver, Y. Chai, G. H. Kroll, C. Jin, T. R. Ohno, R. E. Haufler, T. Guo, J. M. Alford, J. Conceicao, L. P. F. Chibante, A. Jain, G. Palmer, R. E. Smalley, *Chem. Phys. Lett.*, submitted.

[6] D. M. Cox, D. J. Trevor, K. C. Reckmann, A. Kaldor, *J. Am. Chem. Soc.* **1986**, *108*, 2457.

[7] a) L. M. Roth, Y. Huang, J. T. Schwedler, C. J. Cassaday, D. Ben-Amotz, B. Kahn, B. S. Freiser, *J. Am. Chem. Soc.* **1991**, *113*, 6298; b) Y. Huang, B. S. Freiser, *ibid.* **1991**, *113*, 9418.

[8] a) T. Weiske, D. K. Böhme, J. Hrušák, W. Krätschmer, *Angew. Chem.* **1991**, *103*, 898; *Angew. Chem. Int. Ed. Engl.* **1991**, *30*, 884; b) T. Weiske, J. Hrušák, D. K. Böhme, H. Schwarz, *Helv. Chim. Acta*, in press.

[9] a) M. M. Ross, J. H. Callahan, *J. Phys. Chem.* **1991**, *95*, 5720; b) K. A. Caldwell, D. E. Giblin, C. S. Hsu, D. Cox, M. L. Gross, *J. Am. Chem. Soc.* **1991**, *113*, 8519; c) Z. Wan, J. F. Christian, S. C. Anderson, *J. Phys. Chem.*, submitted; d) K. A. Caldwell, D. E. Giblin, M. L. Gross, *J. Am. Chem. Soc.*, in press; e) E. E. B. Campbell, R. Ehrlich, A. Hielscher, J. M. A. Frazav, I. V. Hertel, *Z. Phys. D.*, in press; f) R. C. Mowrey, M. M. Ross, J. H. Callahan, *J. Phys. Chem.*, submitted.

[10] For experiments in which doubly and triply charged fullerene–noble gas complexes are generated, see: a) T. Weiske, J. Hrušák, D. K. Bohme, H. Schwarz, *Chem. Phys. Lett.* **1991**, *186*, 459; b) T. Weiske, D. K. Bohme, H. Schwarz, *J. Phys. Chem.* **1991**, *95*, 8451.

[11] Reviews: a) C. Wesdemiotis, F. W. McLafferty, *Chem. Rev.* **1987**, *87*, 485; b) J. K. Terlouw, H. Schwarz, *Angew. Chem.* **1987**, *99*, 829; *Angew. Chem. Int. Ed. Engl.* **1987**, *26*, 805; c) H. Schwarz, *Pure Appl. Chem.* **1989**, *61*, 685; d) J. L. Holmes, *Adv. Mass Spectrom.* **1989**, *11*, 53; e) J. K. Terlouw, *Adv. Mass Spectrom.* **1989**, *11*, 984; f) J. L. Holmes, *Mass Spectrom. Rev.* **1989**, *8*, 513; g) F. W. McLafferty, *Science* **1990**, *247*, 990; h) F. W. McLafferty, *Adv. Mass Spectrom.* **1992**, *12*, in press.

[12] For speculations and "experiments" regarding carbon clusters of unspecified structure as containers for noble gas atoms and their presence in interstellar space: a) R. S. Lewis, B. Srinivasan, E. Anders, *Science* **1975**, *190*, 1251; b) S. Niemeyer, K. Marti, *Proc. Lunar Planet Sci.* **1981**, *12B*, 1177; c) D. Heymann, *J. Geophys. Res.* **1986**, *B91*, E135.

[13] For a detailed description see: a) R. Srinivas, D. Sülzle, T. Weiske, H. Schwarz, *Int. J. Mass Spectrom. Ion Processes* **1991**, *107*, 369; b) R. Srinivas, D. Sülzle, W. Koch, C. H. DePuy, H. Schwarz, *J. Am. Chem. Soc.* **1991**, *113*, 5970.

[14] a) D. L. Lichtenberger, K. W. Nebesny, C. D. Ray, *Chem. Phys. Lett.* **1991**, *176*, 203; b) J. A. Zimmermann, J. R. Eyler, S. B. H. Bach, S. W. McElvany, *J. Chem. Phys.* **1991**, *94*, 3556.

[15] T. Wong, T. Weiske, J. K. Terlouw and H. Schwarz, *Int. J. Mass Spectrom. Ion Processes*, in press.

[16] S. G. Lias, J. E. Bartmess, J. F. Liebman, J. L. Holmes, R. D. Levin, W. G. Mallard, *J. Phys. Chem. Ref. Data* **1988**, Supplement 1.

[17] G. Frenking, D. Cremer, *Structure and Bonding* **1990**, *73*, 17, and references cited therein.

[18] a) P. Fournier, J. Appell, F. C. Fehsenfeld, J. Durup, *J. Phys. B* **1972**, *5*, L58; b) F. C. Fehsenfeld, J. Appell, P. Fournier, J. Durup, *J. Phys. B* **1973**, *6*, L268; c) J. C. Lorquet, B. Ley-Nihant, F. W. McLafferty, *Int. Mass Spectrom. Ion Processes* **1990**, *100*, 465.

[19] Initial communication: H. Schwarz, *Workshop on Fullerene Clusters*, Riso National Laboratory, Roskilde (Denmark), December 6–7, 1991.

On the Bonding in Carbosilanes**

By *Andreas Savin,* Heinz-Jürgen Flad, Jürgen Flad, Heinzwerner Preuss,* and *Hans Georg von Schnering*

Two problems among the variety of studies on the structural chemistry of the carbosilanes have attracted particular attention:

1. Does a through-space Si–Si bond exist in 1,3-disilacyclobutane? For example, in octachlorohexasilaasterane $Si_6C_6H_8Cl_8$ the bond lengths d(Si–C) = 189, d(Si–Si) = 261 pm and bond angles Si-C-Si = 87.2, C-Si-C = 92.7° are observed, in a hexadecamethyloctasiladispiro[5.1.5.1]tetradecane $Si_8C_{22}H_{56}$, d(Si–C) = 192, d(Si–Si) = 262 pm and Si-C-Si = 85.9°.[1] The Si–Si distances in these compounds are respectively 26 and 27 pm larger (11%) than a single bond (235 pm in silicon).

[*] Priv.-Doz. Dr. A. Savin, Dipl.-Chem. H.-J. Flad, Dr. J. Flad, Prof. Dr. H. Preuss
Institut für Theoretische Chemie der Universität
Pfaffenwaldring 55, D-W-7000 Stuttgart 80 (FRG)
Prof. Dr. H. G. von Schnering
Max-Planck-Institut für Festkörperforschung
Heisenbergstrasse 1, D-W-7000 Stuttgart 80 (FRG)

[**] This work was supported by the Fonds der Chemischen Industrie.

2. Does the very large C–C distance of 178 pm in 1,1,3,3-tetramethyl-2,4-bis(trimethylsilyl)-1,3-disilabicyclo[1.1.0]-butane represent a C–C bond?[2] Here d(C–C) is 24 pm (16%) longer than a single bond.

To answer these questions we applied the electron localization function (ELF)[3] to pure carbosilanes **1** and **2**.

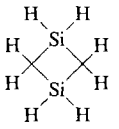

1

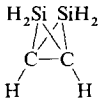

2a

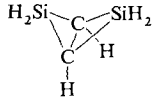

2b

The distribution of the electron pairs is influenced by the antisymmetry of the wave-function: the presence of one electron at position r lowers the probability of finding another electron with parallel spin in its vicinity (Pauli repulsion). A measure of this probability is the electron localization function. The value of the function approaches 1 when the wave-function allows the electrons to avoid each other and tends toward 0 when the electrons are forced to remain there in the same neighborhood around r. The regions of space in which the ELF values are high can be associated with the concepts bond, lone pair, or inner electronic shell.[3,4]

Technical details: The ELF was calculated at the Hartree–Fock level. The Hartree–Fock calculations themselves were performed with the program MOLPRO[5] using pseudopotentials.[6] The structural optimization did not yield a planar structure for **1**; instead the molecule was shown to be slightly folded. Nevertheless, since the energy difference between the planar and folded structure is small, the planar structure will be discussed. The calculated structural parameters of disilacyclobutane **1** (d(Si–C) = 189, d(Si–Si) = 264 pm, Si-C-Si = 88.7, C-Si-C = 91.3°) agree well with experimental parameters.[1]

The structural optimization of **2** shows that the Hartree–Fock calculation yields too small a C–C distance (166 pm). If the configurational space is extended to include another orbital, the bond energy sinks to 49 kJ mol^{-1} and d(C–C) lengthens to 179 pm. The structure is virtually identical from a CASSCF or a MCSCF calculation, which takes into account only promotion from the localized C–C bonding orbital into the C–C antibonding orbital. This arises from the C–C antibonding character of the included orbital. We wish to emphasize that this orbital was determined by energy optimization. Furthermore, in the improved calculation the following parameters are obtained: d(Si–C) = 181 pm, C-Si-C = 59.1, Si-C-C 60.5°, and 51.0° for the angle between the silacyclopropane planes (for comparison the experimental values:[2] 184 pm, 58, 61, 58°).

For the graphical representation[7] of the ELF in selected planes a published convention[2] was used. The electron density appears as "cloud" against a black background. The color of the points corresponds to the ELF value: analogous to the representation of altitudes in maps, high values are white, low values blue, and intermediate values are brown and green. The pictures do not show the inner shells; only the valence electron density is depicted.

In disilacyclobutane $C_2Si_2H_8$ (**1**) the angle Si-C-Si (88.7°) is smaller than C-Si-C (91.3°). According to the ELF, however, this effect is not attributable to a directly bonding Si–Si interaction, since a blue-green region of low ELF values lies between the Si atoms (Fig. 1a). But ELF provides an alternative explanation for the small Si-C-Si angle. The ELF

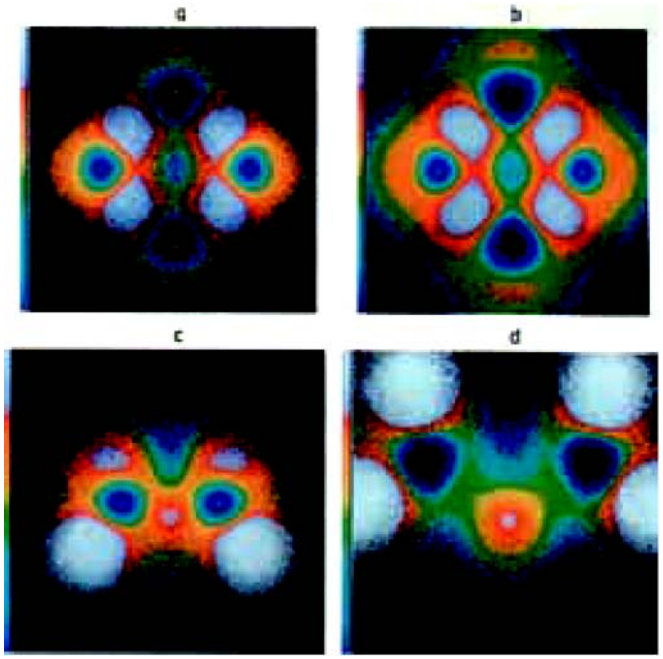

Fig. 1. Electron density ρ (as "cloud") and ELF (shown by color; scale at the left of the frames) in selected planes of the molecules **1** and **2**. a) and b) The plane containing the four-membered ring in **1**; to emphasize the structure of ELF the adjacent value-ranges in b) are depicted alternately bright and dark. The positions of the C and Si stoms are marked by white crosses: C left and right, Si top and bottom. The region between the Si atoms is characterized by a blue-green "valley". This implies that there is no direct Si–Si bond. The ELF maximum lies distinctly off the topological connecting lines of the C_2Si_2 ring (see Fig. 2). c) and d) The two mirror planes of **2** (the views correspond to **2a** and **2b**, respectively). The plane in c) contains the two C atoms and the H atoms bound to them; the SiH_2 wings lie above and below the illustrated plane. The small white region in the middle corresponds to the weak (bent) C–C bond, the large white regions at lower left and right to the C–H bonds, and the smaller white regions above the (blue) C atoms to fragments of the C–Si bonds. The plane in d) contains both Si atoms and the H atoms bound to them. No white region lies between the Si atoms. In the middle below the Si atoms, the plane intersects the C–C bond (small white region below the line joining the C atoms, which is perpendicular to the plane illustrated).

maxima (M and M′) lie outside the C_2Si_2 ring (Fig. 1b). As the calculation shows (Fig. 2), the Si–M and C–M distances differ and the M-C-M′ and M-Si-M′ angles are approximately 109.5°. These different lengths correspond to the different sizes of Si and C. The topological angles formed by the lines joining the Si and C nuclei (C-Si-C = 91.3° > 90° and Si-C-Si = 88.7° < 90°) arise naturally from *combining atoms of varying size and local bond angles of about 109.5° to form an "eight-membered ring" C-M-Si-M′-C-M-Si-M′*. One can

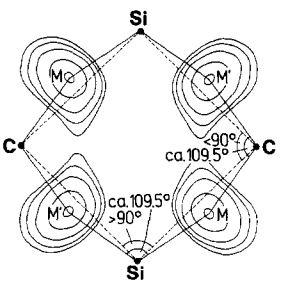

Fig. 2. ELF of **1** as contour diagram. Only the values 0.80, 0.84, 0.88, 0.92, and 0.96 are depicted. The dotted lines of the topological connections between the atoms represent the classical bonds with bond angles close to 90°. The solid lines join the C and Si nuclei with the ELF maxima M and M′. The resulting angles are indicated (see text).

easily verify this result half quantitatively using a model kit as analog computer. The different sizes of C and Si are simulated with tetrahedral joints whose arm lengths differ[8] and the atoms are joined by flexible bonds (bent bonds).

In disilabicyclo[1.1.0]butane $C_2Si_2H_6$ (**2**) the region between the two C atoms does have a high ELF value (Fig. 1c and 1d). This confirms the previously described bond.[2] The relatively small region of high ELF values implies a weak bond, in agreement with the long bond length. The white ELF maximum is also clearly off the straight topological C–C connecting line. Its position is remarkably close to that of the bent bond derived from the simple structural model.[2] As expected, there is no bond between the Si atoms (Fig. 1d).

Received: August 12, 1991 [Z4863 IE]
German version: *Angew. Chem.* **1992**, *104*, 185

CAS Registry numbers:
1, 287-55-8; **2**, 79647-93-1.

[1] G. Sawitzki, H. G. von Schnering, *Z. Anorg. Allg. Chem.* **1973**, *399*, 257–262; K. Peters, E.-M. Peters, H. G. von Schnering, *ibisd.* **1983**, *502*, 61–65; $C_2Si_2H_8$ was studied theoretically by, for example, M. O'Keeffe, G. V. Gibbs, *J. Phys. Chem.* **1985**, *89*, 4574–4577; the Si–Si bond was discussed by, for example R. S. Grey, H. F. Schaeffer III, *J. Am. Chem. Soc.* **1987**, *109*, 6577–6585.

[2] G. Fritz, S. Wartanessian, E. Matern, W. Hönle, H. G. von Schnering, *Z. Anorg. Allg. Chem.* **1981**, *475*, 87–108; P. von R. Schleyer, A. F. Sax, J. Kalcher, R. Janoschek, *Angew. Chem.* **1987**, *99*, 374–377; *Angew. Chem. Int. Ed. Engl.* **1987**, *26*, 364.

[3] A. D. Becke, K. E. Edgecombe, *J. Chem. Phys.* **1990**, *92*, 5397–5403.

[4] A. Savin, A. D. Becke, J. Flad, R. Nesper, H. Preuss, H. G. von Schnering, *Angew. Chem.* **1991**, *103*, 421–424; *Angew. Chem. Int. Ed. Engl.* **1991**, *30*, 409–412.

[5] Program MOLPRO: SCF part by W. Meyer, H. J. Werner; MC-SCF part by H. J. Werner, P. J. Knowles, (*J. Chem. Phys.* **1985**, *82*, 5053–5063; *Chem. Phys. Lett.* **1985**, *115*, 259–267); kindly made available by Prof. Dr. H. J. Werner and installed by Prof. H. Stoll on the Cray-2 in Stuttgart. Mr. M. Kohout (Universität Stuttgart) contributed to the development of the program MEROP (for the calculation of the electron density and of ELF) and wrote the program MPLOT (for drawing the contour lines of Fig. 2).

[6] G. Igel-Mann, H. Stoll, H. Preuss, *Mol. Phys.* **1988**, *65*, 1321–1328; basis sets: [4s, 4p] to (2s,2p) stipulated according to H.-J. Poppe (personal communication, **1988**). Polarization functions: see P. L. Harihan, J. A. Pople, *Theor. Chim. Acta* **1973**, *28*, 213–222; M. M. Francl, W. J. Pietro, W. J. Hehre, J. S. Binkley, M. S. Gordon, D. J. De Frees, J. A. Pople, *J. Chem. Phys.* **1982**, *77*, 3654–3665. The exponents of the Gauss functions are for C: s: 2.581190, 1.596882, 0.408595, 0.138945; p: 8.257547, 1.960285, 0.551454, 0.155007; d: 0.8, for Si: s: 3.513432, 1.503285, 0.408595, 0.089488; p: 1.462293, 0.939390, 0.152439, 0.058065; d: 0.45. H basis of R. Ditchfield, W. J. Hehre, J. A. Pople, *J. Chem. Phys.* **1971**, *54*, 724–728 (with polarization function p: 1.1).

[7] J. Flad, F. X. Fraschio, B. Miehlich, *Program GRAPA*, Institut für Theoretische Chemie der Universität Stuttgart, **1989**.

[8] C atom from the Prentice Hall Model Kit; Si atom as Dreiding model.

Electron Localization in Solid-State Structures of the Elements: the Diamond Structure**

By *Andreas Savin,* Ove Jepsen, Jürgen Flad, Ole Krogh Andersen, Heinzwerner Preuss,* and *Hans Georg von Schnering*

The methods for obtaining localized orbitals—often used in the chemistry of molecules to describe bonding—can be used in principle for solids as well (in methane and in diamond, for example). They can lead, however, to several equivalent sets of orbitals for a given structure and are nonunique in this case. This ambiguity occurs, for example, in monomeric monocycles such as benzene, or in an infinite polyene chain.[1] In solids ambiguity often arises on account of the higher coordination, and localized orbitals are therefore used only rarely. An analysis in positional space can nevertheless be performed when instead of the equivocal localized orbitals, the electron localization function (ELF) is used. In this work we have calculated ELF for crystalline solids for the first time.

The electron localization function was introduced by Becke and Edgecombe as a measure of the probability of finding an electron in the neighborhood of another electron with the same spin.[2] ELF is thus a measure of the Pauli repulsion. The explicit formulation is given in Equation (a)

$$\mathrm{ELF} = [1 + [K(r)/K_h(\varrho(r))]^2]^{-1} \qquad \text{(a)}$$

The parameter K is the curvature of the electron pair density for electrons of identical spin, $\varrho(r)$ the density at (r), and K_h the value of K in a homogeneous electron gas with density ϱ. The ELF values lie by definition between zero and one. Values are close to 1 when in the vicinity of one electron, no other with the same spin may be found, for instance as occurs in bonding pairs or lone pairs. Small values are typical for the region between two electron shells (Pauli principle). In a homogeneous electron gas, ELF = 0.5.

The method of local density functionals (LDF)[3,4] has proved exceptionally reliable for studies on solids. But in LDF the pair density and its curvature K are not explicitly defined. ELF may, however, be interpreted differently from (a), in order that the determination of its value is compatible with the LDF method. In this method (Kohn and Sham[6]) the single particle density matrix γ [Eq. (b)] is determined by energy minimization for a given electron density $\varrho(r)$ [φ are

$$\gamma(r,r') = \sum_i^N \varphi_i(r)\ \varphi_i(r') \qquad \text{(b)}$$

orbitals, N is the number of electrons; $\gamma(r,r') = \varrho(r)$]. Because $\gamma(r,r')$ occurs only in the expression for the kinetic energy T [Eq. (c), ∇ is the Nabla operator], the pertinent information

$$T = \tfrac{1}{2}\int \nabla_r\, \nabla_{r'}\gamma(r,r')|_{r=r'} \mathrm{d}^3r \qquad \text{(c)}$$

is contained in the three-dimensional kinetic energy density $t(r,r')$ [Eq. (d)] and the six-dimensional function $\gamma(r,r')$ is not required.

$$t(r) = \tfrac{1}{2}\nabla_r\, \nabla_{r'}\gamma(r,r')|_{r=r'} \qquad \text{(d)}$$

The function $t(r)$ cannot exceed a certain threshhold,[7] which is defined by Equation (e). This minimum value occurs

$$t(r) \geq \frac{1}{8}\frac{|\nabla\varrho|^2}{\varrho} \qquad \text{(e)}$$

when the orbitals are proportional to $\sqrt{\varrho}$. According to the Pauli principle this is possible for at most two orbitals, one

[*] Priv.-Doz. Dr. A. Savin, Dr. J. Flad, Prof. Dr. H. Preuss
Institut für Theoretische Chemie der Universität
Pfaffenwaldring 55, D-W-7000 Stuttgart 80 (FRG)
Dr. O. Jepsen, Prof. Dr. O. Krogh Andersen,
Prof. Dr. H. G. von Schnering
Max-Planck-Institut für Festkörperforschung
Heisenbergstrasse 1, D-W-7000 Stuttgart 80 (FRG)

[**] This work was supported by the Fonds der Chemischen Industrie. We thank Dr. O. Gunnarsson, Stuttgart, for valuable suggestions.

with α and one with β spin. Thus in general the deviation is positive [Eq. (f)]. We shall call it the Pauli kinetic energy

$$t_P(r) = t(r) - \frac{1}{8}\frac{|\nabla\varrho|^2}{\varrho} \qquad \text{(f)}$$

density.[8] In some regions of space t_P tends toward zero, and we say that here the electron pairs are localized. Using t_P we can find a well-defined measure which corresponds to the ELF calculated from the Hartree–Fock approximation [Eq. (g)]. The parameter $t_{P,h}$ represents the value of t_P for a homogeneous electron gas with density $\varrho(r)$.

$$\mathrm{ELF} = [1 + [t_P(r)/t_{P,h}(\varrho(r))]^2]^{-1} \qquad \text{(g)}$$

For the graphical representation we used, as we did previously for molecules, a program[10] that depicts the electron density and ELF values by the density of the points and their color, respectively. As in a map the colors range from blue (small ELF values) through green, yellow, and brown, to white (high ELF peaks). The background is black. Of the calculated electron density, only the valence electron density is illustrated. For this reason the (white) regions arising from the inner shells around the nuclei are missing in Figure 1. Instead each nucleus is surrounded by a blue-violet bubble.

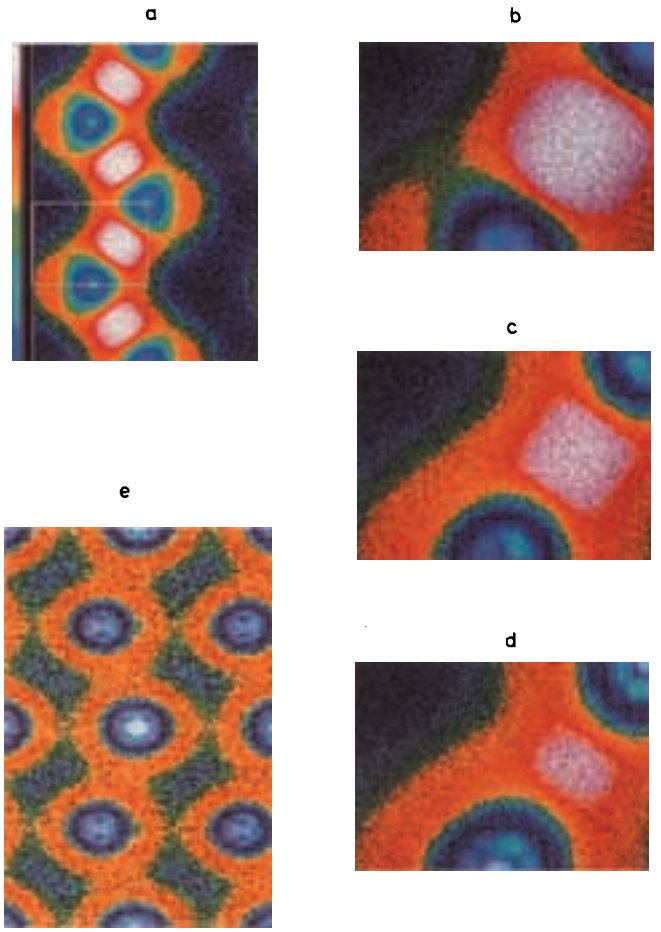

Fig. 1. Valence electron density ϱ (as "cloud") and ELF (depicted by color) for elements with diamond-type structures and for β-Sn. (Increasing ELF scale: blue, green, yellow, brown, white; background black; the blue regions around the nuclei arise from the missing inner shells) a) Diamond: the white regions represent C–C bonds; the small framed exerpt shows the section for the frames b) to d). b) Silicon. c) Germanium. d) α-Sn. e) β-tin; the white regions are no longer visible, and the chains show only a moderately high localization (orange-yellow). Interactions exist between the chains.

In this first report on ELF for solids, the diamond structure is investigated. Figure 1 shows the electron density and the ELF in the (110) plane. This plane contains the zig-zag chains of directly connected atoms and the essential details of the three-dimensional structure. In Figure 1 a (diamond) regions of high localization (white) are seen on the lines joining the C atoms—the electron pair of the C–C bond. The framed exerpt serves to illustrate the differences when the atoms are Si, Ge, and α-Sn (Figs. 1 b–d). Along this series the white regions of the covalent bonds become smaller, and the green waist (Si, Fig. 1 b) gives way to a brown area. The effect is to create channels of evenly distributed localization analogous to an electron gas. Here we should point out that the topology of the wavy, three-dimensional, blue-green region corresponds completely to that of the space-dividing periodic nodal surface D*, which in turn is determined by the three-dimensional symmetry alone.[11] Thus there exists a three-dimensional periodic surface of the same electron density[11] as well as a corresponding surface of identical ELF values that has nothing to do with the contours of the atoms, but is defined only by the symmetry of the translational group.

The tetragonal structure of metallic tin (β-Sn) is related to the diamond structure. Also present are the essential details of the (110) plane. The zig-zag chains of the diamond structure meet in this plane. Figure 1 e shows that in metallic β-Sn, the (white) regions of high localization have disappeared, and joining the chains are found (yellow) regions of localization similar to an electron gas. The change in the electron localization function along the series from carbon to tin thus shows spatially the characteristic transition from covalent to metallic bonding.

Received: August 12, 1991 [Z4864 IE]
German version: *Angew. Chem.* **1992**, *104*, 186

CAS Registry numbers:
C, 7440-21-3; Ge, 7440-56-4; Sn, 7440-31-5.

[1] W. England, *Int. J. Quantum Chem.* **1971**, *5*, 683.
[2] A. D. Becke, K. E. Edgecombe, *J. Chem. Phys.* **1990**, *92*, 5397.
[3] See for example O. K. Andersen, O. Jepsen, M. Sob in *Electronic Band Structure and its Applications* (Ed.: M. Yusouff), Springer, Berlin, **1987**, p. 1. Electron densities for elements with a diamond-type structure may be found in the following papers: O. K. Andersen, Z. Pawlowska, O. Jepsen, *Phys. Rev. B* **1986**, *34*, 5253; N. E. Christensen, S. Satpathy, Z. Pawlowska, *ibid.* **1987**, *36*, 1032.
[4] M. van Schilfgaarde, T. A. Paxton, O. Jepsen, O. K. Andersen, Program TB-LMTO. The exchange correlation potential used in this work is from U. Barth, L. Hedin, *J. Phys. C* **1972**, *5*, 1629. In the calculations for the diamond structure, we placed spheres of identical size at atomic and lattice positions to form a body-centered cubic structure.
[5] J. F. Dobson, *J. Chem. Phys.* **1991**, *94*, 4328; see also W. L. Luken, J. C. Culberson, *Theoret. Chim. Acta* **1984**, *66*, 279.
[6] W. Kohn, L. J. Sham, *Phys. Rev.* **1965**, *140*, 1133; see also J. P. Perdew, A. Zunger, *Phys. Rev. B* **1981**, *23*, 5048.
[7] Y. Tal, R. F. W. Bader, *Int. J. Quantum Chem. Quantum Chem. Symp.* **1978**, *12*, 153.
[8] The integral $\int t(r)\mathrm{d}^3r$ is called the Pauli kinetic energy, and the potential arising therefrom the Pauli potential (see N. H. March, *Phys. Lett. A* **1986**, *113*, 476; M. Levy, H. Ou-Yang, *Phys. Rev. A* **1988**, *38*, 625). The relation between K and $t(r)$ has been described previously by E. Ludena, *J. Chem. Phys.* **1982**, *76*, 3157. It is valid for the Hartree–Fock approximation used till now [2, 9] for the calculation of ELF.
[9] A. Savin, A. D. Becke, J. Flad, R. Nesper, H. Preuss, H. G. von Schnering, *Angew. Chem.* **1991**, *103*, 421; *Angew. Chem. Int. Ed. Engl.* **1991**, *30*, 409.
[10] J. Flad, F. X. Fraschio, B. Miehlich, *Programm GRAPA*, Institut für Theoretische Chemie der Universität Stuttgart, **1989**.
[11] H. G. von Schnering, R. Nesper, *Angew. Chem.* **1987**, *99*, 1097; *Angew. Chem. Int. Ed. Engl.* **1987**, *26*, 1059; *Z. Phys. B* **1991**, *83*, 407.

Molecular Imaging of Alkanol Monolayers on Graphite**

By *Stefan Buchholz* and *Jürgen P. Rabe**

The adsorption behavior of long-chain alkanes and alkyl derivatives on the basal plane of graphite has been of considerable interest as a model for molecular adsorption. Measurements of the adsorption isotherms have shown that alkanes, alkanols, and fatty acids adsorb from nonpolar solvents as densely packed monolayers with the molecules parallel to the basal plane of graphite. The monolayers are stable against further adsorption over a broad concentration range.[1-3] With scanning tunneling microscopy (STM) the direct in situ structure characterization of such[4-8] and similar[9-10] monolayers has become possible recently (see the review on STM investigations of molecular systems).[11] We report here on the structure and dynamics of monomolecular adsorbate layers of long-chain alkanols on graphite.

Figure 1 displays highly ordered areas in monolayers of octadecanol ($C_{18}H_{37}OH$), tetracosanol ($C_{24}H_{49}OH$), and 1,12-dodecanediol ($HOC_{12}H_{24}OH$). The molecules are packed parallel to each other in lamellae. From the width of the lamellae it can be deduced that they exhibit all-*trans* conformations. At the lamellae boundaries a displacement of half the molecular width is observed. The comparison of STM images before and after the adsorption of the monolayers shows that both the long axes of the molecules and the lamallae boundaries are oriented parallel to basis vectors of the graphite lattice. The angle of 60° between the molecular axes and the lamellae boundaries corresponds very well to a displacement of neighboring alkyl chains by two methylene units. Since the plane containing the carbon backbone is almost perpendicular to the substrate[7] only every second methylene unit is in direct contact with the graphite surface. The repeating unit of two methylenes amounts to 254 pm and agrees well with the periodicity observed along the alkyl chains by STM. In the octadecanol and the dodecanediol (Fig. 1a,c) predominantly herringbone structures are observed, while for the longer chain alkanols tetracosanol (Fig. 1b) and triacontanol ($C_{30}H_{61}OH$, Fig. 4) the long axes of the molecules in neighboring lamellae are parallel to each other. The fact that the shorter chain alkanol and the alkanediol exhibit the herringbone structure indicates that the tilted arrangement favors hydrogen bonding whereas the parallel arrangement allows a stable packing of the alkyl chains. In addition, small differences in the interaction energy of the monolayer with the substrate may influence the packing behavior.

In the case of the tetracosanol (Fig. 1b) in particular, neighboring lamellae boundaries clearly exhibit different image contrast, indicating a bilamellar structure. This difference is less obvious in the case of octadecanol but the bilamellar structure is also likely there, since only in that case can all hydroxyl groups partcipate in hydrogen bonds. In general hydroxyl groups and oxygen functionalities (e.g. carboxyl groups) do not produce a distinctly different image contrast from alkyl chains.

The monolayers of the monofunctional alkanols exhibit many defects—the areas shown in Figure 1a,b are the largest defect-free domains that have been observed. The reason is the tilted arrangement of the molecules in the lamellae, which allows a dense packing also at the domain boundaries. Hence, the line tensions at the domain boundaries are relatively small, similar to the case of 1,4-didodecylbenzene.[6] Figure 2a,b shows a domain boundary of a monolayer of tetracosanol and octadecanol, respectively. At the domain boundary of the tetracosanol, the direction of the displacement of neighboring molecules parallel to each other is reversed. In the octadecanol case shown here every second lamella encounters the lamella of a different domain at an obtuse angle, due to the herringbone structure. The CPK model displayed in Figure 3 shows that also in this case the molecules are able to pack densely without breaking hydrogen bonds. 1,12-Dodecanediol also exhibits a herringbone pattern, but in this case such a domain boundary would involve a loss of hydrogen bonds. Therefore such defects would be highly energetic and should occur rarely, if the development of the defects is not kinetically controlled. Indeed in the case of the diol, whose packing is highly stabilized

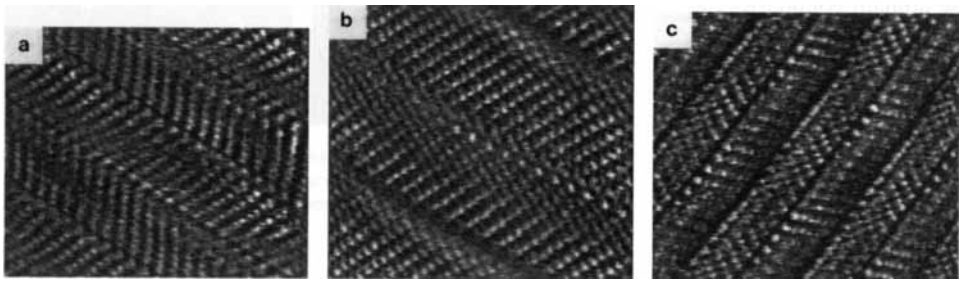

Fig. 1. STM images of alkanol monolayers on graphite: a) octadecanol (image size: 9.7 nm × 7.8 nm); b) tetracosanol (image size: 8.1 nm × 7.6 nm); c) 1,12-dodecanediol (image size: 8.8 nm × 7.4 nm).

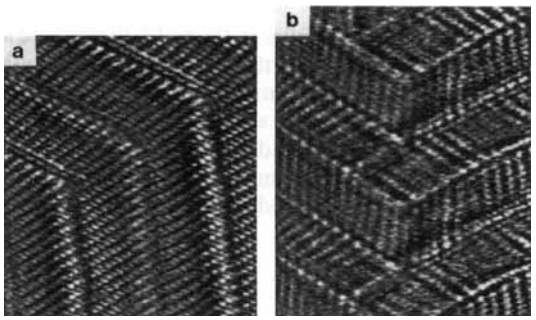

Fig. 2. STM images of domain boundaries in a a) tetracosanol and b) octadecanol monolayer (image sizes: a) 10.4 nm × 7.8 nm; b) 10.6 nm × 12.9 nm).

[*] Dr. J. P. Rabe, Dr. S. Buchholz
Max-Planck-Institut für Polymerforschung
Postfach 3148, D-W-6500 Mainz (FRG)

[**] This work was supported by the European Science Foundation (Additional Activity: "Chemistry and Physics of Polymer Surfaces and Interfaces") and the Fonds der Chemischen Industrie (Kekulé scholarship for S. B).

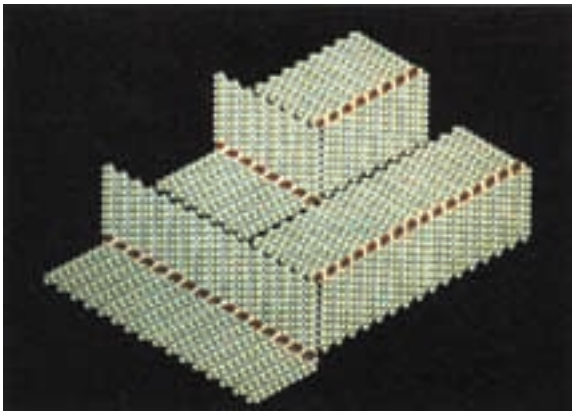

Fig. 3. CPK model of the domain boundary of the octadecanol monolayer shown in Figure 2b.

through the hydrogen bonds, not a single domain boundary has been observed on an area of several μm^2.

Another type of domain boundary often observed is shown in Figure 4a, which displays the STM image of a monolayer of triacontanol. At these domain boundaries the lamellae of one domain encounter those of another at an obtuse angle. Here also a dense packing of the molecules is observed. Corresponding to the lamella boundaries in the

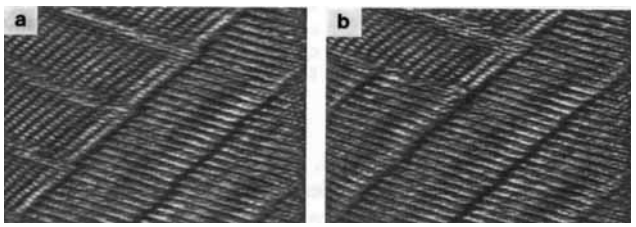

Fig. 4. STM images of domain boundaries in a triacontanol monolayer (image size: 13.9 nm × 10.3 nm).

left domain, the molecules in the right domain are shifted by one graphite repeat unit, thereby allowing adaptation to the contour of the left domain. This displacement in the right domain is extended over a few lamellae. Figure 5 shows an enlargement of such a displacement within the domain. Close to the region shown in Figure 4a a corner of the left domain could be recorded (Fig. 4b).

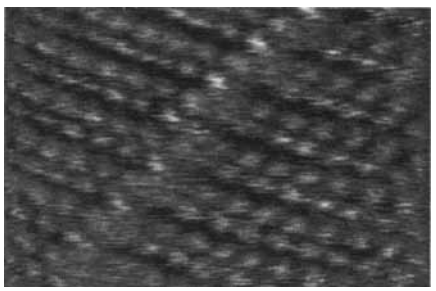

Fig. 5. STM image of a displacement at a lamella boundary in a triacontanol monolayer. The image has been recorded close to the domain boundary shown in Figure 4a (image size: 2.9 nm × 2.3 nm).

Often the domain boundaries described above are observed in combination with each other resulting in very complicated defect patterns. As an example, Figure 6a shows an image of a tetracosanol monolayer with a domain that consists of only two lamellae in one and probably seven molecules in the other direction. In such defect-rich areas of the monolayers reorientations occur very often, resulting in noisy pictures. Occasionally we succeeded in imaging the metastable states with high resolution before (Fig. 6a) and after (Fig. 6b) the reorientation (see also Ref. [6, 7]). Such reorganizations of the monolayers are probably combined with a desorption of at least part of the affected molecules. The reorientation processes are too fast to allow their details to be followed.

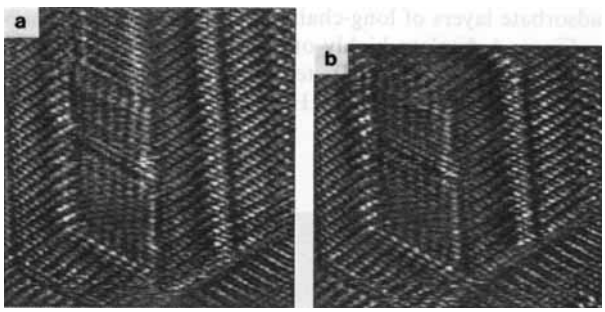

Fig. 6. STM images of a defect-rich area in a tetracosanol monolayer. Image b) was recorded only a few seconds after image a). In this time the monolayer was reorganized in the upper part of the image. (Image sizes: a) 11.5 nm × 12.3 nm; b) 11.5 nm × 10.9 nm).

Long-chain alkyl derivatives are often contaminated with homologous impurities, if no extensive purification is performed. As shown in Figure 7 such impurities can be included in the monolayers. Above one lamella (A) of triacontanol

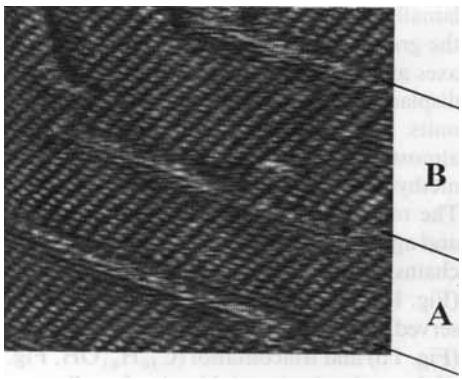

Fig. 7. STM image of a triacontanol monolayer containing a longer chain impurity. Whereas the width of lamella A is as expected for triacontanol, lamella B is significantly broader. The molecules in lamella B have a length of 40 methylene units. Furthermore, imbedded in lamella A are two longer molecules. Adjacent to them in lamella B are two shorter triacontanol molecules allowing a dense packing despite the defect (image size: 10.5 nm × 9.3 nm).

molecules there is a broader lamella (B), in which the impurities are enriched. Whereas in lamella A 15 repeat units are observed along the molecules, corresponding to the length of the triacontanol molecules, in lamella B the molecules con-

sist of 20 repeating units corresponding to a length of 40 methylene units. In addition, one can recognize that two molecules of the longer chain impurity are included in lamella A. Adjacent to them in lamella B are two triacontanol molecules allowing a regular packing in the following lamellae.

The present investigation has shown what detailed information on structure and dynamics of monomolecular alkanol adsorbate layers can be obtained by scanning tunneling microscopy. The packing pattern in monodomains as well as at domain boundaries indicate the importance of hydroxyl end groups for the packing of primary alkanols with up to 30 carbon atoms. In particular the patterns at the many domain boundaries are consistent with a tendency to form as many hydrogen bonds as possible. Reorganizations of the domain structure could be followed on a millisecond timescale, and finally the inclusion of single molecules of an impurity into the monolayer could be observed for the first time.

Experimental

For the basics of scanning tunneling microscopy see [11–13] and for technical details of the instrument used here, [14]. All images were recorded in the variable current mode with a tunneling current of 1 nA and a bias of 1 +/− 0.5 V (tip positive). In this regime no pronounced dependence of the image contrast on the bias was observed. Tunneling currents higher than 1 nA resulted generally in images with higher noise levels, whereas with lower currents only poor image contrast was obtained. The scanning frequencies in x and y direction were 200 and 0.3 Hz, respectively, equivalent to 1.5 s per image at a resolution of about 200 × 200 pixels. The data was recorded continuously on video tape [14]. Tunneling tips were mechanically formed from platinum/iridium wire. Only those allowing atomic resolution on graphite were used for the studies of the monolayers.

Imaging of the monolayers was performed at the interface of graphite with a solution of the appropriate alkanol in 1-phenyloctane. The alkanol solutions were prepared from concentrated solutions after removing undissolved material by filtration and subsequent dilution by 10% with pure solvent.

1-octadecanol (99%), 1-tetracosanol (99%), 1-triacontanol (96%), 1,12-dodecanediol (99%) were purchased from Aldrich and used without further purification.

Received: July 16, 1991 [Z 4797 IE]
German version: *Angew. Chem.* **1992**, *104*, 188

CAS Registry numbers:
$C_{18}H_{37}OH$, 112-92-5; $C_{24}H_{49}OH$, 506-51-4; $HOC_{12}H_{24}OH$, 5675-51-4; $C_{30}H_{61}OH$, 593-50-0; grahite, 7782-42-5.

[1] A. J. Groszek, *Nature* **1962**, *196*, 531–533; *ibid.* **1964**, *204*, 680; *Proc. R. Soc. London Ser. A* **1970**, *314*, 473–498.
[2] G. H. Findenegg, M. Liphard, *Carbon* **1987**, *25*, 119–128.
[3] U. Bien-Vogelsang, G. H. Findenegg, *Colloids Surf.* **1986**, *21*, 469–481.
[4] G. C. McGonigal, R. H. Bernhardt, D. J. Thomson, *Appl. Phys. Lett.* **1990**, *57*, 28–30.
[5] G. C. McGonigal, R. H. Bernhardt, Y. H. Yeo, D. J. Thomson, *J. Vac. Sci. Technol. B* **1991**, *9*, 1107–1110.
[6] J. P. Rabe, S. Buchholz, *Phys. Rev. Lett.* **1991**, *66*, 2096–2099.
[7] J. P. Rabe, S. Buchholz, *Science* **1991**, *253*, 424–427.
[8] J. P. Rabe, S. Buchholz, *Makromol. Chem. Macromol. Symp.* **1991**, *50*, 261–268.
[9] D. P. E. Smith, J. K. H. Hörber, G. Binnig, H. Nejoh, *Nature* **1990**, *344*, 641–644.
[10] R. Kuroda, E. Kishi, A. Yamano, K. Hatanaka, H. Matsuda, K. Egushi, T. Nakagiri, *J. Vac. Sci. Technol. B* **1991**, *9*, 1180–1183.
[11] J. P. Rabe, *Ultramicroscopy* **1992**, in press.
[12] G. Binnig, H. Rohrer, *Angew. Chem.* **1987**, *99*, 622–631; *Angew. Chem. Int. Ed. Engl.* **1987**, *26*, 606–615.
[13] H. Rohrer, *Scanning Tunneling Microscopy and Related Methods* (Eds.: R. J. Behm, N. Garcia, H. Rohrer), *NATO ASI Ser., Ser. E: Appl. Sci., Vol. 184*, Dordrecht, **1990**, p. 1–25.
[14] J. P. Rabe, M. Sano, D. Batchelder, A. A. Kalatchev, *J. Microsc. (Oxford)*, **1988**, *152*, 573–583.

The Trapping of Iron Hydroxide Units by the Ligand "heidi": Two New Hydroxo(oxo)iron Clusters Containing 19 and 17 Iron Atoms

By *Sarah L. Heath* and *Anne K. Powell**

Compounds containing extended arrays of iron centers linked by oxide and hydroxide ions are common in nature. Examples include the core of the iron-storage protein ferritin, which can accommodate up to 4500 iron atoms and a variety of iron minerals as well as rust. The importance of such materials has fueled efforts to synthesize and characterize smaller hydroxo(oxo)polyiron complexes to serve as models. Although a variety of interesting polyiron complexes has resulted, including structures with eight,[1] ten,[2] and eleven[3] iron centers, as well as the heterometal cluster $[Fe_{16}MO_{10}(OH)_{10}(O_2CPh)_{20}]$, M = Mn or Co,[4] none has exhibited the known features of the naturally occurring compounds.

We describe here the synthesis and characterization of three iron complexes with the ligand heidi (H_3heidi = $N(CH_2COOH)_2(CH_2CH_2OH)$); two of these complexes are examples of a new type of hydroxo(oxo)iron cluster, in which the close-packed cluster core is enclosed in a shell of ligands which are complexed to further iron atoms. X-ray crystallography[5] reveals these clusters to contain 19 and 17 iron atoms; thus **1** and **2** are the largest polyiron complexes of this type characterized to date (Fig. 1).[6]

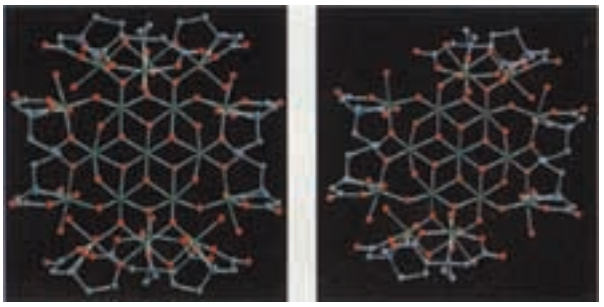

Fig. 1. The crystal structures of **1** (left) and **2** (right); Fe shown in green, O in red.

$[Fe_{19}(\mu_3\text{-}O)_6(\mu_3\text{-}OH)_6(\mu_2\text{-}OH)_8(heidi)_{10}(H_2O)_{12}]^+$ **1**
(FW = 3352.78)

$[Fe_{17}(\mu_3\text{-}O)_4(\mu_3\text{-}OH)_6(\mu_2\text{-}OH)_{10}(heidi)_8(H_2O)_{12}]^{3+}$ **2**
(FW = 2894.82)

The number of iron atoms in clusters **1** and **2** is determined by the arrangement of Fe/heidi units around the core structure common to both compounds. This cluster core consists of an $[Fe_7(\mu_3\text{-}OH)_6(\mu_2\text{-}OH)_4\{(\mu_3\text{-}O)Fe\}_2]^{13+}$ unit. In **1** this is surrounded by ten iron heidi units linked to the core by μ_3-O, μ_2-OH, and alkoxo bridge units from the heidi ligands. This shell, formulated as $[Fe_{10}(heidi)_{10}(H_2O)_{12}(\mu_3\text{-}O)_4(\mu_2\text{-}OH)_4]^{12-}$, gives an overall charge of 1+ to **1**. The vacant sites on the peripheral iron centers are taken up with water molecules so that each iron atom is octahedrally coordinat-

[*] Dr A. K. Powell, S. L. Heath
School of Chemical Sciences
University of East Anglia
Norwich NR4 7TJ (UK)

symmetry-related Fe/heidi units are absent and consequently two μ_2-OH units replace two of the μ_3-O units in **1**. The formula of the cluster shell is $[Fe_8(heidi)_8(H_2O)_{12}(\mu_3\text{-}O)_2(\mu_2\text{-}OH)_6]^{10-}$, giving **2** an overall charge of 3+. The heidi ligand coordinates in a tetradentate fashion but never associates with one Fe exclusively. Instead its alcohol function

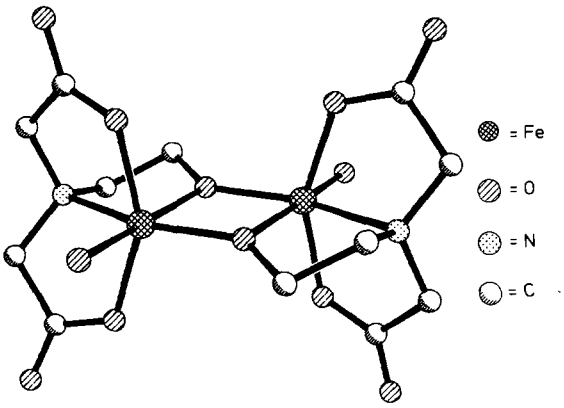

Fig. 2. The crystal structure of the alkoxo-bridged dinuclear complex **3**.

forms a μ_2-alkoxo bridge to a neighboring iron center. This behaviour is also demonstrated by the dinuclear iron complex **3** as illustrated in Figure 2.

$[Fe(heidi)(H_2O)]_2$ **3** (FW = 495.99)

The cluster core common to **1** and **2** (Fig. 3) derives from $\{(Fe(OH)_2)^+\}_n$. This can be visualized by the replacement of the iron atoms of the two $[(\mu_3\text{-}O)Fe]^+$ units of the cluster core by protons to give the structure $[Fe_7(\mu_3\text{-}OH)_6(\mu_2\text{-}OH)_6]^{9+}$. If the six outer μ_2-OH ions are then thought of as

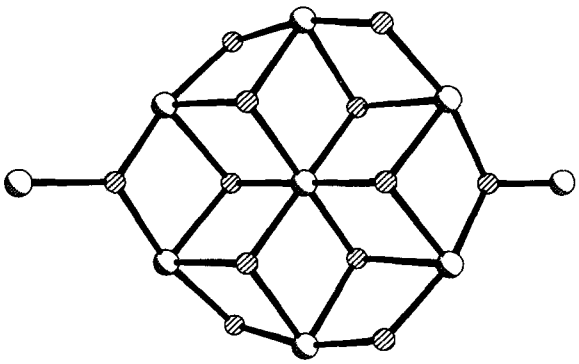

Fig. 3. The core unit common to **1** and **2**. Open circles represent Fe atoms.

extending this as a network by binding to further $\{FeOH\}^{2+}$ units, an infinite two-dimensional array of $\{Fe(OH)_2\}^+$ units results in which the Fe ions occupy octahedral holes in a hexagonal close-packed array of OH ions; this is equivalent to the AX_2 structural type found in CdI_2 or $Mg(OH)_2$.

The relationhip of the cluster core to the AX_2 structural type is illustrated in Figure 4. Normally the final hydrolysis product of Fe(III) salts is goethite, $\{Fe(O)OH\}_n$, whose structure is related to that of the cluster core by the replacement of half of the μ_3-OH bridges with μ_3-O bridges; these,

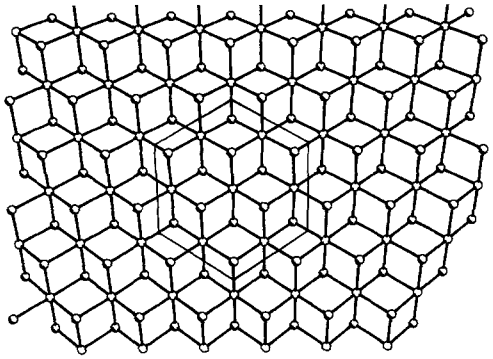

Fig. 4. The central core of **1** and **2** shown in the context of the AX_2 structural type.

in turn are hydrogen-bonded to the protons of the hydroxide ions in the next layer. The use of the charge, denticity, and bite-angles of the encapsulating ligands to dictate structural type probably finds parallels in biology in biomineralization processes. The transition-metal compound $[Mn_{10}O_{14}(tren)_6]^{8+}$ (tren = $N(CH_2CH_2NH_2)_3$) also possesses an AX_2 core-structure, although here the metal is in the III and IV oxidation states.[7]

EXAFS measurements of the Fe/O core of ferritin have been interpreted in terms of a hydroxo(oxo)polyiron compound in which the Fe centers are surrounded by six O atoms (Fe–O distance 1.9 Å) and a further six Fe centers (average Fe–Fe distance 3.1 Å).[8] More recent analyses of this Fe shell have indicated interactions with iron atoms roughly 2.9 and 3.5 Å distant.[9, 10] In **1** and **2** the average Fe–Fe distance is 3.1 Å, with the shortest being 2.95 Å, and the longest, 3.46 Å. Although the ferritin core is often likened to the mineral ferrihydrite, there is some controversy about the exact nature of the iron sites in this mineral.[11–14] Therefore compounds such as **1** and **2** whose construction models biomineralization processes should help in understanding the formation and constitution of naturally occuring hydroxo(oxo)polyiron compounds.

Experimental Procedure

Clusters **1** and **2** were prepared by adding H_3heidi (1 equiv, 2.5 mmol) to a solution of $Fe(NO_3)_3 \cdot 9H_2O$ (2 equiv, 5 mmol) in water (30–40 mL). The resulting solution was treated with pyridine (6 equiv, 15 mmol) and left to crystallize. Elemental analysis: found, C 16.9, H 4.4, N 4.3, Fe 26.5%; calculated for $C_{108}H_{332}Fe_{36}N_{22}O_{226}$, C 17.1, H 4.4, 4.1, Fe 26.6%.

Adjustment of the heidi: Fe ratio to 1:1 yields **3** exclusively. Elemental analysis: found, C 28.87, H 4.02, N 5.54, Fe 21.72%; calculated for $C_{12}H_{20}N_2O_{12}Fe_2$, C 29.41, H 4.53, N 5.72, and Fe 22.79%).

Received: August 16, 1991 [Z 4876]
German version: *Angew. Chem.* **1992**, *104*, 191

[1] K. Wieghardt, K. Pohl, I. Jibril, G. Huttner, *Angew. Chem.* **1984**, *96*, 66; *Angew. Chem. Int. Ed. Engl.* **1984**, *23*, 77–78.
[2] K. L. Taft, S. J. Lippard, *J. Am. Chem. Soc.* **1990**, *112*, 9629–9630.
[3] S. M. Gorun, G. C. Papaefthymiou, R. B. Frankel, S. J. Lippard, *J. Am. Chem. Soc.* **1987**, *109*, 3337.
[4] W. Micklitz, S. J. Lippard, *J. Am. Chem. Soc.* **1989**, *111*, 6856, and references cited therein.
[5] Crystal structure analyses: **1** and **2** crystallize within the same triclinic unit cell along with sixty waters of crystallization and four NO_3^- ions. $C_{54}H_{166}N_{11}O_{113}Fe_{18}$; $P\bar{1}$ (No. 2), $Z = 2$; $a = 12.693(13)$, $b = 18.061(17)$, $c = 28.784(15)$ Å, $\alpha = 93.66(6)$, $\beta = 94.95(6)$, $\gamma = 89.88(8)$; $V = 6561$ Å^3 ($T = 22$ °C); ϱ_{calc} 1.92 g cm^{-3} $Mo_{K\alpha}$, $\lambda = 0.71073$ Å, $2° < 2\theta < 50°$; 19119 reflections (8252 with $F > 4\sigma(F)$); direct methods (SHELXTL). The central iron atoms of both clusters are located at inversion centers at 0,0,0 and 0.5,0.5,0.5. For 878 parameters $R = 0.1345$ and $R_w = 0.1424$. These relatively high R-values reflect the high degree of disorder of the lattice water

and also the fact that only very small weakly diffracting single crystals of these materials have been obtained so far. We are currently optimizing the crystallization of this and related materials. **3**: $C_6H_{10}NO_6Fe$; $P\bar{1}$, $Z = 2$; $a = 6.838(1)$, $b = 7.058(1)$, $c = 9.676(2)$ Å, $\alpha = 103.29(1)$, $\beta = 93.58(1)$, $\gamma = 97.83(1)^\circ$, $V = 448.1$ Å^3 ($T = 22\,^\circ$C); $\varrho_{calc} = 1.84$ g cm^{-3}, $Mo_{K\alpha}$, $\lambda = 0.71073$ Å, $2^\circ < 2\theta < 52^\circ$; 1748 reflections (1659 with $F > 6\sigma(F)$); Patterson synthesis (SHELXTL). An inversion center relates the two halves of the molecule. For 157 parameters $R = 0.0351$ and $R_w = 0.0394$. Further details of the crystal structure investigations are available on request from the Fachinformationszentrum Karlsruhe, Gesellschaft für wissenschaftlich-technische Information mbH, D-W-7514 Eggenstein-Leopoldshafen 2, on quoting the following number CSD-55936, the names of the authors, and the journal citation.

[6] The assignment of the oxo and hydroxo bridges was made based on consideration of the geometry at each oxygen atom, and their number was confirmed by the results of the C,H,N,Fe-analysis. The elemental analysis is also consistent with the presence of four nitrate anions and sixty waters of crystallization in a unit cell containing one molecule of each of both **1** and **2**.

[7] K. S. Hagen, W. H. Armstrong, *J. Am. Chem. Soc.* **1989**, *111*, 774–775.

[8] S. M. Heald, E. A. Stern, B. Bunker, E. M. Holt, S. L. Holt, *J. Am. Chem. Soc.* **1979**, *101*, 67.

[9] Q. T. Islam, D. E. Sayers, S. M. Gorun, E. C. Theil, *J. Inorg. Biochem.* **1989**, *36*, 51–62

[10] J. S. Rohrer, Q. T. Islam, G. D. Watt, D. E. Sayers, E. C. Theil, *Biochemistry* **1990**, *29*, 259–264.

[11] K. M. Towe, W. F. Bradley, *J. Colloid Interface Sci.* **1967**, *24*, 384–392.

[12] R. A. Eggleton, R. W. Fitzpatrick, *Clays Clay Miner.* **1988**, *36*, 111–124.

[13] A. Manceau, J. M. Combes, G. Calas, *Clays Clay Miner.* **1990**, *38*, 331–334.

[14] R. A. Eggleton, R. W. Fitzpatrick, *Clays Clay Miner.* **1990**, *38*, 335–336.

synthesized by the method of Brunner and Schmidt,[2] but an efficient procedure for their preparation is not yet available.

We were interested in the enantiomerically pure α-benzyloxyacryliron(II) complex (**1b**), because Michael addition and subsequent alkylation of the intermediate enolate leads to α,α-dialkyl-α-hydroxycarbonyl derivatives, a class of compounds that are difficult to prepare in optically active form. We therefore developed a process that yielded the two optical antipodes (*R*)-**1b** and (*S*)-**1b** in gram quantities from inexpensive starting materials in good yield (Scheme 1).

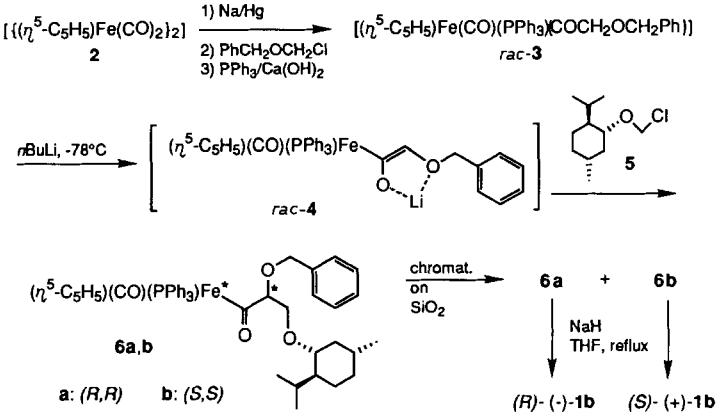

Scheme 1. Synthesis of α-benzyloxyacryliron(II) complexes (*R*)-**1b** and (*S*)-**1b**.

New Chiral α-Benzyloxyacryliron(II) Complex for Asymmetric Synthesis of α,α-Dialkyl-α-hydroxycarbonyl Compounds**

By *Felix Stolz, Peter Strazewski, Christoph Tamm,* Markus Neuburger,* and *Margareta Zehnder*

Davies et al. have shown[1] that a series of diastereoselective alkylations of carbonyl compounds can be performed with high selectivity by using an iron(II) complex of type **1** as chiral auxiliary. To our knowledge, in the past the only accessible enantiomerically pure starting materials for the preparation of derivatives was the acetyliron complex [(η^5-C_5H_5)CO(PPh_3)Fe($COCH_3$)] (**1a**). Both the (*S*)-(+) and the (*R*)-(−) forms are commercially available, but when their high molecular weight and the difficulty of regenerating the auxiliary in optically active form are taken in to account, they are rather expensive. Both configurations can also be

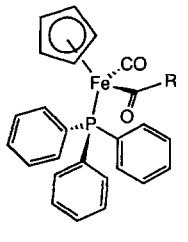

(*R*)-**1**

a: R = CH_3

b: R = $C(OCH_2Ph)=CH_2$

c: R = $HC=CHCH_3$

Compound *rac*-**3** was prepared by a known procedure from [{(η^5-C_5H_5)Fe($CO)_2$}$_2$] (**2**) in 42% overall yield.[1b,3] Deprotonation with *n*-butyllithium followed by a highly stereoselective alkylation of the intermediate enolate *rac*-**4** with chloromethyl (−)-menthyl ether (**5**) afforded **6a** (less polar) and **6b** (more polar). The relative configuration of the centers Fe* and α-C* were assumed to be (*R**,*R**) or *l* (like) on the grounds of the presumed configuration of the (*E*) lithium enolate **4** (cf. Davies et al.[1b–c]). The *u*-diastereomers [(*R**, *S**) or unlike)] are in principle also possible, but were not observed in the ^{1}H NMR spectrum of the product mixture. A single flash-chromatographic separation on silica gel (toluene/ether/pentane 90:5:5) furnished the virtually enantiomerically pure products in 43 (**6a**) and 42% (**6b**) yield. The elimination of (−)-menthol from **6a** and **6b** was achieved with sodium hydride under retention of configuration at the iron atom. After filtration over a short column (neutral Al_2O_3), precipitation of the only iron complex

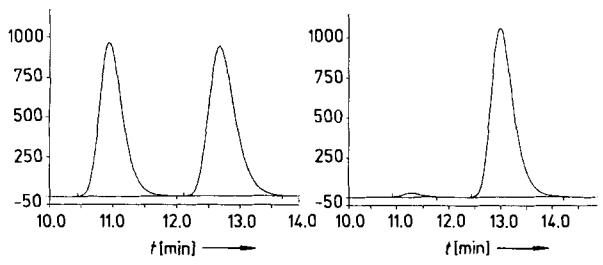

Fig. 1. Resolution of *rac*-**1b** and (*S*)-(+)-**1b** by HPLC on a chiral stationary phase. The *y* axis represents the UV absorption at $\lambda = 277$ nm [mV]. Mobile phase: 2-propanol/*n*-hexane 1.5:98.5. Derivatization of the stationary phase: cellulose carbamate (Chiralcel OD® by Daicel). Enantiomeric excess of (*S*)-(+)-**1b**: 96.1% *ee*. Enantiomeric excess of the (−)-menthol (Fluka) used for the synthesis of (*R*)-(−)-**1b** and (*S*)-(+)-**1b**: 98.75% *ee* (determined by gas chromatography with (−)-menthyl acetate on permethylated β-cyclodextrin.)

[*] Prof. Dr. C. Tamm, F. Stolz, Dr. P. Strazewski
Institut für Organische Chemie der Universität
St. Johanns-Ring 19, CH-4056 Basel (Switzerland)
Priv.-Doz. Dr. M. Zehnder, M. Neuburger
Institut für Anorganische Chemie der Universität
Spitalstrasse 51, CH-4056 Basel (Switzerland)

[**] This work was supported by the Swiss National Science Foundation. We thank Ms. Gisela Umbricht and Dr. C. Bolm, Institut für Organische Chemie der Universität Basel for the GC and HPLC separations.

present with *n*-pentane yielded (*R*)-(−)-**1b** or (*S*)-(+)-**1b** (from **6a** and **6b** respectively) in preparative amounts as amorphous, air- and moisture-insensitive solids in 87–92% yield (Fig. 1).[4]

The crystal structure of racemic **1b** has been solved (Fig. 2). As in the corresponding (*E*)-crotyliron complex **1c**,[1d] it reveals that the β carbon atom is oriented *s-cis* to the carbonyl oxygen atom of the same ligand. The *anti* arrangement of the two carbonyl oxygen atoms is the only possible one for steric reasons.[1d–e]

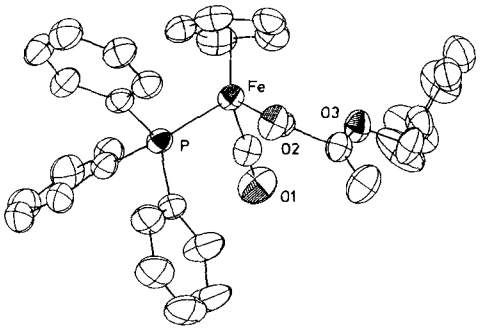

Fig. 2. Structure of (*R*)-**1b** in the solid state. Thermal ellipsoids represent 30% probability. Carbon atoms are complete ellipsoids; heteroatoms have a sector removed.

Compound **1b** was butylated in β position with *n*BuLi (two equivalents are required for complete conversion—cf. Davies et al.[1f]), and the resulting lithium enolate **7** trapped in situ with water, methyl iodide, or ethyl iodide (Scheme 2). The reaction mixture was filtered over a short column (neutral Al_2O_3), and the alkylation products precipited on addition of *n*-pentane. The yields determined at this stage lay between 76 (**10a,b**) and 88% (**8a, b**). The diastereoselectivity of the reactions was estimated from ^1H NMR spectroscopy and the preparative separation of the product mixture. The enolizable acyl derivatives **8**, like **6a,b**, were stable on silica gel, but **9** and **10** required separation on neutral Al_2O_3. The selectivity lay between 80 and 95% *ds*. In the case of **9a** and **b** (prepared from (*R*)-(−)-**1b**) the exact ratio (17:83) could be established by gas chromatography on permethylated β-cyclodextrin of the final product **14** formed on removal of the chiral auxiliary and the benzyl function. The ratio of **8a**:**8b** (7:93) was determined by HPLC (Si-60, 0.3% ether in hexane).

The racemic major product **9b** could also be crystallized. The crystal structure (Fig. 3b) shows that the *l* diastereomer was formed preferentially, as expected from the structure of **1b**. After methylation the acyl ligand rotated approximately 180° around the (OC)–(α-C) bond, allowing the smallest α substituent, the methyl group to point in the direction of the triphenylphosphane ligand. Additional noteworthy features of the crystal structure are the changes in some angles ($O{\equiv}C{-}Fe{-}COR$ is wider and $O{\equiv}C{-}Fe{-}PPh_3$ narrower than in **1b**) and the remarkable rigidity of the pentyl side chain.[5] The chirality of the propeller geometry of the triphenylphosphane ligand follows the general rule in both crystal structures:[1e] the screw in the (*R*) complex is clockwise and in the (*S*) complex counterclockwise.

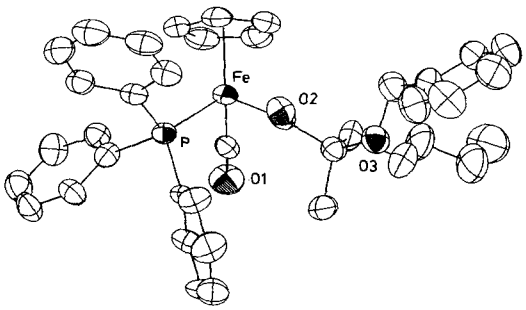

Fig. 3. Structure of (*R*)-**9b** in the solid state. The thermal ellipsoids represent 30% probability. Carbon atoms are complete ellipsoids; heteroatoms have a sector removed.

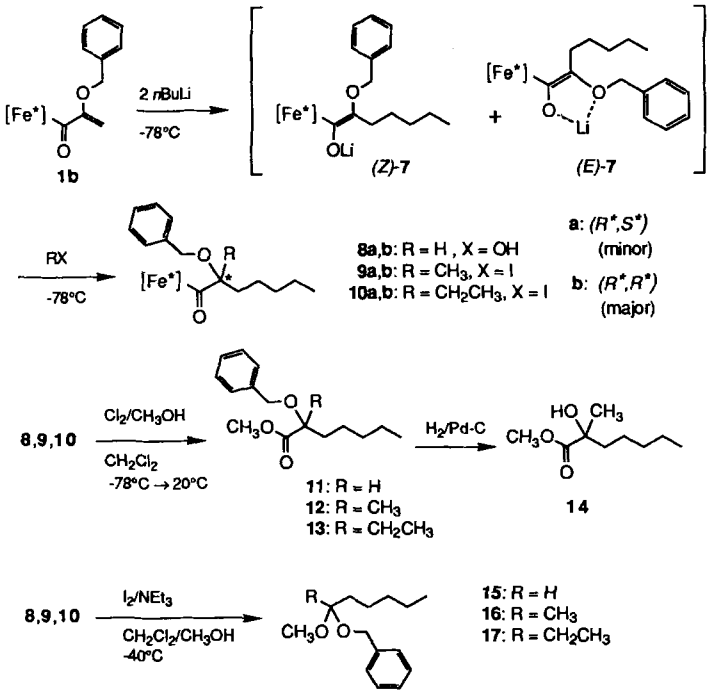

Scheme 2. Alkylation of (*R*)- or (*S*)-**1b**, followed by cleavage of the acyl ligands from iron. ([Fe*] = [(η^5-C_5H_5)CO(PPh_3)Fe]).

Both the extremely high diastereomeric selectivity of the alkylation of *rac*-**3** and the usually absolutely selective alkylations and protonations of comparable substrates[1d,g] show that in complexes **1** the chiral auxiliary does not even permit sterically nondiscriminating electrophiles to attack from the triphenylphosphane side. The diminished stereoselectivity of the alkylation of **1b** thus requires a different explanation. The ^1H NMR spectrum of **1b** suggests that in solution even at room temperature the complex exists virtually exclusively in the cisoid conformation, as in the solid state. Addition of *n*BuLi forces the enolate **7** into the (*Z*) configuration (Scheme 2). Then (**Z**)-**7** is alkylated stereospecifically to the *l* diastereomer. However chelation of the two oxygen atoms by a lithium ion in the (*E*) enolate **7** (as in enolate **4**) must lead specifically to the *u* diastereomer. Since two equivalents of *n*BuLi are required for complete conversion, it seems that the first equivalent of *n*BuLi merely coordinates to **1b**. The delayed onset of the red coloration typical of enolate formation supports this hypothesis. Apparently this type of activation is a prerequisite for the *n*-butylation of **1b** in β position. It is feasible that the presence of lithium ions simultaneously causes a partial isomerization to the transoid isomer of **1b**, which in turn reacts with the second equivalent of *n*BuLi to yield (*E*)-**7**. A greatly enhanced reactivity to *n*BuLi of the

mere traces of transoid conformer present would be another, but unlikely explanation.

The diastereoselectivity of the reaction presents no problem for synthesis, because the less polar side products **8a**–**10a** are separable by chromatography with minimum losses. Absolute diastereomeric purity of the products is attainable, and after cleavage of the acyl ligands enantiomerically pure α-benzyloxy-α,α-dialkylcarbonyl compounds are obtained.

The oxidative cleavage of the α-benzyloxyacyl ligands from the iron complex with bromine and methanol proved to be problematic at first. As Davies et al.[1c] had reported earlier, the bond between C(acyl) and α-C tends to break instead of the Fe-C(acyl) bond, forming not the desired methyl esters **11**–**13**, but the benzyl methyl acetal **15** or the ketals **16**, **17** that are shortened by one carbon atom. We therefore studied various cleavage conditions in order to bias the product composition. The most common cleavage reagent, bromine, yields varying mixtures of esters and acetals or ketals depending on the added mole equivalents of reagent and the reaction time. *N*-bromosuccinimide affords almost exclusively the acetal or ketal, but in poor yield. Iodine or bromine with added triethylamine furnishes exclusively the acetal or ketal (82% for **16**). However, with chlorine gas in dichloromethane the ester forms exclusively (54% for **12**).

Received: September 23, 1991 [Z4926 IE]
German version: *Angew. Chem.* **1991**, *104*, 225

CAS Registry numbers:
(*R*)-**1b**, 138061-03-7; (*S*)-**1b**, 138230-57-6; *rac*-**1b**, 138230-58-7; *rac*-**3**, 111618-46-3; **5**, 26127-08-2; (*R*,*R*)-**6a**, 138061-04-8; (*S*,*S*)-**6b**, 138230-59-8; (*R**,*S**)-**8a**, 138061-05-9; (*R**,*R**)-**8b**, 138230-60-1; *rac*-**9a**(*R**,*S**), 138061-06-0; (*R*,*S*)-**9a**, 138230-61-2; *rac*-**9b**(*R**,*R**), 138230-62-3; (*R*,*R*)-**9b**, 138230-63-4; (*R**,*S**)-**10a**, 138061-07-1; (*R**,*S**)-**10b**, 138230-64-5; **12**, 138061-00-4; **14**, 138061-01-5; **1b**, 138061-02-6.

[1] a) G. J. Baird, J. A. Bandy, S. G. Davies, K. Prout, *J. Chem. Soc. Chem. Commun.* **1983**, 1202–1203; b) S. G. Davies, M. Wills, *J. Organomet. Chem.* **1987**, *328*, C29–C33; c) S. G. Davies, D. Middlemiss, A. Naylor, M. Wills, *J. Chem. Soc. Chem. Commun.* **1990**, 797–799; d) S. G. Davies, I. M. Dordor-Hedgecock, K. H. Sutton, J. C. Walker, R. H. Jones, K. Prout, *Tetrahedron* **1986**, *42*, 5123–5137; e) S. G. Davies, A. E. Derome, J. P. McNally, *J. Am. Chem. Soc.* **1991**, *113*, 2854–2861; f) S. G. Davies, O. Ichihara, *J. Chem. Soc. Chem. Commun.* **1990**, 1554–1555; g) S. G. Davies, J. C. Walker, *ibid.* **1986**, 495–496.

[2] H. Brunner, E. Schmidt, *J. Organomet. Chem.* **1972**, *36*, C18–C22.

[3] E. J. Crawford, C. Lambert, K. P. Menard, A. R. Cutler, *J. Am. Chem. Soc.* **1985**, *107*, 3130–3139.

[4] The same absolute configuration as that of **1a** was assigned on the assumption that the α-benzyloxyacryl ligand does not reverse the optical rotation. (*R*)-(−)-**1b**: $[\alpha]_{546}^{20} = -294$; $[\alpha]_{D}^{20} \approx -191$ ($c = 0.4$, C_6H_6). (*S*)-(+)-**1b**: $[\alpha]_{546}^{20} = +300$; $[\alpha]_{D}^{20} = +192$ ($c = 0.4$, C_6H_6).

[5] *rac*-**1b** was crystallized from pentane at −20 °C. $C_{34}H_{29}FeO_3P$, triclinic space group space group *P*1 (no. 2), $Z = 4$ (2 independent molecules/asymmetric unit), $a = 10.713(3)$, $b = 15.395(8)$, $c = 18.200(7)$ Å, $\alpha = 83.17(6)$, $\beta = 92.06(4)$, $\gamma = 103.95(4)°$, $V = 2895.5(3)$ Å^3, $\varrho_{calcd} = 1.315$ g cm^{-3}, $F(000) = 1192$. Collection of data at room temperature, CAD4 diffractometer, graphite monochromator, $Mo_{K\alpha}$ ($\lambda = 0.71069$ Å), ω–2θ *scan*, $\theta_{max} = 28°$, 11973 independent reflections, 9235 of which with $(F) > 2\sigma(F)$. Solution by Patterson methods with subsequent weighted difference Fourier syntheses. Refinement: block matrix, least-squares method (SHELX-76) with anisotropic thermal parameters for all non-hydrogen atoms, $R = 0.0590$, $R_w = 0.0596$ for 704 parameters. *rac*-**9b** was crystallized in the dark from diethyl ether under a light stream of nitrogen at room temperature. $C_{39}H_{41}FeO_3P$, triclinic, space group (no. 2), $Z = 2$, $a = 8.126(4)$, $b = 12.234(5)$, $c = 16.465(9)$ Å, $\alpha = 96.11(4)$, $\beta = 93.48(5)$, $\gamma = 92.85(3)°$, $V = 1622.0(3)$ Å^3, $\varrho_{calcd} = 1.320$ g cm^{-3}, $F(000) = 680$. Data collection and structure determination as above, 5807 independent reflections, 3733 of which with $(F) > 2\sigma(F)$. $R = 0.0749$, $R_w = 0.0631$ for 403 parameters. Further details of the crystal structure investigation may be obtained from the Director of the Cambridge Crystallographic Data Centre, University Chemical Laboratory, Lensfield Road, GB-Cambridge CB2 1EW on quoting the full journal citation.

[6] The experimental details of the syntheses for all compounds and their physical and spectroscopic characterization will be published later. They are part of the proposed dissertation of F.S.

Enzymatic Preparation of Enantiomerically Pure *N*-alkyl Amino Acids**

By *Ulrich Groeger*,* *Karlheinz Drauz*, and *Herbert Klenk*

N-alkyl-L-amino acids L-**3**, and more particularly *N*-methyl-L-amino acids, are important building blocks of peptide and depsipeptide antibiotics.[1] They also occur free in biological material, as for instance, *N*-methyl-L-tryptophan in the seeds of *Abrus precatorius*.[2] Although preparation of optically inactive or racemic compounds **3** presents no problem, synthesis of the enantiomerically pure compounds L-**3** is laborious and sometimes provides unsatisfactory yields.[3]

One possible route to enantiomerically pure amino acids is the enantioselective hydrolysis of appropriate racemic *N*-acetylamino acids catalyzed by an aminoacylase from *Aspergillus oryzae* or from porcine kidney (acylase I, EC 3.5.1.14), as for instance is used in an industrial process to prepare L-methionine or L-valine.[4] Although acylase I displays high selectivity for a wide spectrum of substrates, this system has limitations. Replacement of the hydrogen on the amine nitrogen atom by an alkyl group causes loss of enzymatic activity. Thus *N*-acylated secondary amines such as *N*-acylated proline (**1a**) or *N*-acylated *N*-alkylamino acids cannot be hydrolyzed by this method.[5]

Recently we isolated and characterized a new bacterial *N*-acyl-L-proline-acylase, whose high enantioselectivity (*ee* > 99.8%) makes it suitable for preparing L-proline from **1a**.[6] This enzyme also hydrolyses only the L-enantiomer of *N*-acetyl and *N*-chloroacetyl derivatives of azetidine-2-carboxylic acid (**1b**) and pipecolic acid (**1c**), thus enabling the enzyme-catalyzed resolution of these compounds.[7]

Compounds **1a**–**c** are *N*-acylated cyclic secondary amines. Ring-opening leads to the corresponding *N*-acylated, straight-chain secondary amines **2**. The precursors **2** can be prepared as racemates in good yield from **3** in a modified Strecker synthesis via *N*-alkylaminonitriles **4** (Scheme 1, Table 1).

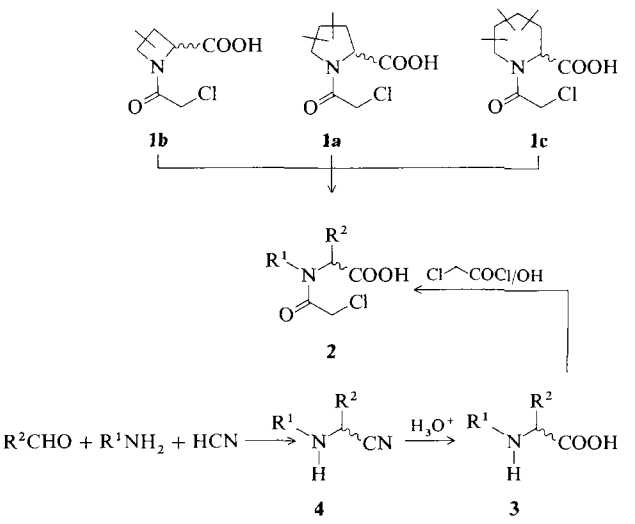

Scheme 1. For R^1, R^2 see Table 1.

[*] Dr. U. Groeger, Dr. K. Drauz, Dr. H. Klenk
Degussa AG
Fachbereich Forschung Organische und Biologische Chemie
Postfach 1345, D-W-6450 Hanau 1 (FRG)

[**] Amino Acid Transformation, Part 8. This work was supported by the Bundesminister für Forschung und Technologie (0319007 A3). Part 7: K. Drauz, M. Kottenhahn, K. Makryaleas, H. Klenk, M. Bernd, *Angew. Chem.* **1991**, *103*, 704–706; *Angew. Chem. Int. Ed. Engl.* **1991**, *30*, 712–714.

Table 1. *N*-alkyl-*N*-chloroacetyl-DL-amino acids synthesized according to Scheme 1 from the appropriate *N*-alkyl-DL-aminonitriles **4** via the *N*-alkylamino acids **3**.

Compounds **2–4**	R^1	R^2	Yields **2**	**3**	**4**
L-**a** [a]	CH_3	CH_3	47	–	–
a [a]	CH_3	CH_3	73	–	–
b	C_2H_5	CH_3	32	50	59
c	C_3H_7	CH_3	25	39	59
d	CH_3	C_2H_5	30	63	77
e	C_2H_5	C_2H_5	10	52	82
f	CH_3	C_3H_7	30	43	79
g	C_2H_5	C_3H_7	20	62	89
h	CH_3	C_4H_9	35	47	84
j [a, b]	CH_3	CH_3	98	–	–
L-**k** [a]	CH_3	$CH(CH_3)_2$	57	–	–
L-**l** [a]	CH_3	$C_2H_3(CH_3)_2$	94	–	–

[a] These compounds were synthesized from the appropriate *N*-methylamino acids. [b] α-H replaced by CH_3.

To our knowledge an acylase-catalyzed resolution of **3** was unknown and impossible in the past with aminoacylases from bacteria, moulds, or porcine kidneys because of their substrate specificity.[8] In order to prepare enantiomerically

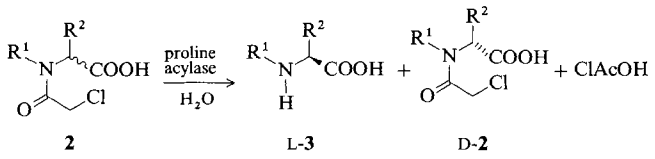

2 L-**3** D-**2**

Scheme 2. For R^1, R^2 see Table 1.

pure L-**3**, we therefore subjected *N*-chloroacetyl-*N*-methyl-DL-alanine **2a** to cleavage by *N*-acyl-L-proline-acylase (Scheme 2). Figure 1 shows the progress of the acylase-catalyzed hydrolysis of **2a** and its corresponding L-enantiomer L-**2a**. After 1 h L-**2a** was completely hydrolyzed, whereas **2a** was hydrolyzed to an extent of 48%. Prolonging the reaction time did not improve the conversion (49% after 2 h), indicating that, as with **1a–c**, only the L enantiomer of **2a** was hydrolyzed.[6,7] This was confirmed by gas chromatography on the chiral phase Lipodex D of a doubly derivatized *N*-methylalanine (*N*-methyl-*N*-trifluoroacetylalanine methyl ester) obtained from **2a**. The reaction product was identified as *N*-methyl-L-alanine (L-**3a**, *ee* ≥ 89%). We therefore synthesized further precursors **2** to test their reaction with this acylase.

The enzyme hydrolyzes **2a–c** with high activity (Table 2); for instance, **2a** is converted faster than **1a**, which is considered to be one of the best substrates.[6,7] With increasing length of the *N*-alkyl residue (**2a–c**), and of the alkyl residue of the amino acid side chain at the α-carbon atom (see **2a**, **d**, **f** and **2b**, **e**, **g**), the activity decreases. Alkyl substituents in α position of a chain length of more than two C atoms (**2f–h**) or branched residues (L-**2k**, **l**) cause a total loss of activity. In these cases the substituents apparently block access to the active site of the enzyme. The crucial influence on activity stems from the substituents on the α carbon: a proton, an alkyl group, and a carboxy group are essential substituents, since *N*-acetyl-*N*-methylglycine **2i** and **2j** are not hydrolyzed; the necessity for a free carboxy group in α-position has already been shown[6,7] and confirmed.[9]

Table 2. Substrate specificity of the *N*-acyl-L-proline-acylase relative to *N*-acyl-*N*-alkylamino acids **2**. The reaction conditions are described in the legend of Figure 1.

Substrate (20 mM)	Relative Activity	Conversion [%]
L-**1a** [b]	100	100
L-**2a**	175	100
2a	115	49
2b [c]	82	–
2c [c]	27	–
2d	10	50
2e [c]	2	–

[a] **2f-2j**, L-**2k**, and L-**2l** were not hydrolyzed. [b] L-**1a**: relative activity ≡ 100. [c] These compounds were also hydrolyzed chemically under the same reaction conditions. For this reason the conversion for the enzymatic reactions could not be determined. The enzyme activity was determined by the difference between runs with and without enzyme.

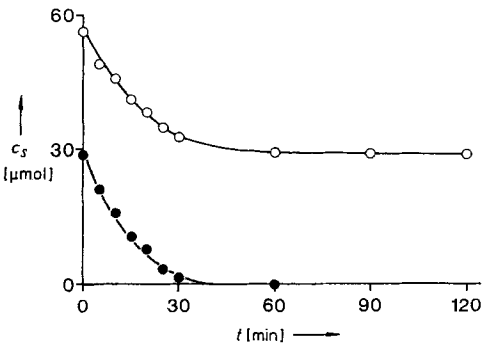

Fig. 1. Kinetics of the hydrolysis of L-**2a** (●) and **2a** (○). The reaction mixture (3 mL) contained 0.3 mmol of Tris-HCl (pH = 7), 30 or 60 μmol respectively of substrate, and 0.23 U of purified *N*-acyl-L-proline-acylase from *Comamonas testosteroni* DSM 5416. The specific activity of the purified enzyme with *N*-acetyl-L-proline as substrate was 115 U mg^{-1} at 30 °C and pH = 7.0. The unit U represents the amount of enzyme that catalyzes 1 μmol of L-proline per minute, and was determined by ninhydrin detection of the product L-proline according to Yaron and Mlynar [10]. The samples were incubated at 30 °C and the reaction stopped at predetermined times by the addition of an aliquot of 2 N HCl. The precipitated protein was separated by centrifugation at 11 000 rpm for 10 min, the supernatant diluted 1:50 with HPLC eluent (7% (v/v) acetonitrile in 0.01 M sodium heptanesulfonate/phosphoric acid, pH = 2.2), and L-**2a** and **2a** were determined quantitatively by HPLC over an RP-8 column with the same eluent at a flowrate of 1 mL min^{-1} at λ = 210 nm. c_s = substrate concentration.

These compounds were also hydrolyzed chemically under the same reaction conditions. For this reason the conversion for the enzymatic reactions could not be determined. The enzyme activity was determined by the difference between runs with and without enzyme.

Because of the substrate specificity of the hitherto known aminoacylases,[5,8] a gap existed in the acylase-catalyzed synthesis of enantiomerically pure *N*-alkyl-L-amino acids L-**3** from the appropriate *N*-acylated racemic precursors **2**, which we are able for the first time to close with this reaction. The substrate spectrum of the enzyme is restricted, but it should be possible by microbiological screening to isolate similar aminoacylases with a broader substrate spectrum, thereby opening the door to enzyme-catalyzed preparation of *N*-alkylamino acids **3** even wider.

Received: September 2, 1991 [Z4897 IE]
German version: *Angew. Chem.* **1992**, *104*, 222

CAS Registry numbers:
2a, 138062-74-5; (L)-**2a**, 138062-73-4; **2b**, 138062-75-6; **2c**, 138062-76-7; **2d**, 138062-77-8; **2e**, 138062-78-9; **2f**, 138062-79-0; **2g**, 138062-80-3; **2h**, 138062-81-4; **2i**, 5888-91-5; **2j**, 138062-82-5; (L)-**2k**, 56346-69-1; (L)-**2l**, 138062-83-6; **3a**, 600-21-5; (L)-**3a**, 3913-67-5; **3b**, 64991-30-6; (L)-**3b**, 65278-03-7; **3c**, 138062-69-8; (L)-**3c**, 13013-28-0; **3d**, 70606-05-2; (L)-**3d**, 88930-11-4; **3e**, 138062-70-1; (L)-**3e**, 138230-85-0; **3f**, 138062-71-2; **3g**, 138062-72-3; **3h**, 74530-78-2; **3j**, 2566-34-9; (L)-**3k**, 2480-23-1; (L)-**3l**, 3060-46-6; **4b**, 138062-62-

1; **4c**, 138062-63-2; **4d**, 138062-64-3; **4e**, 138062-65-4; **4f**, 138062-66-5; **4g**, 138062-67-6; **4h**, 138062-68-7; $ClCH_2COCl$, 79-04-9; CH_3CHO, 75-07-0; C_2H_5CHO, 123-38-6; C_3H_7CHO, 123-72-8; C_4H_9CHO, 110-62-3; CH_3NH_2, 74-89-5; $C_2H_5NH_2$, 75-04-7; $C_3H_7NH_2$, 107-10-8; proline acylase, 86352-21-8.

[1] P. A. Plattner, U. Nager, *Helv. Chim. Acta* **1948**, *31*, 665–671; J. C. Sheehan, H. G. Zachau, W. B. Lawson, *J. Am. Chem. Soc.* **1957**, *79*, 3933–3934; *ibid.* **1958**, *80*, 3349–3355; H. Vanderhaeghe, G. Parmentier, *ibid.* **1960**, *82*, 4414–4422; F. W. Eastwood, B. K. Snell, A. Todd, *J. Chem. Soc.* **1960**, 2286–2292; H. Brockmann, *Angew. Chem.* **1960**, *72*, 939–947; J.-I. Shoji, K. Tori, H. Otsuka, *J. Org. Chem.* **1965**, *30*, 2772–2776; H. Kleinkauf, H. von Döhren in *Regulation of Secondary Metabolite Formation* (Eds.: H. Kleinkauf, H. von Döhren, H. Dornauer, G. Nesemann), VCH, Weinheim, **1986**, p. 173–207, and references cited therein.

[2] T. Hoshino, *Justus Liebigs Ann. Chem.* **1935**, *520*, 31–34.

[3] K. A. Schellenberg, *J. Org. Chem.* **1963**, *28*, 3259–3261; P. Quitt, J. Hellerbach, K. Vogler, *Helv. Chim. Acta* **1963**, *46*, 327–333; M. Ebata, Y. Takahashi, H. Otsuka, *Bull. Chem. Soc. Jpn.* **1966**, *39*, 2535–2538.

[4] W. Leuchtenberger, U. Plöcker, *Ullmanns Encykl. Ind. Chem. 5. Aufl.* **1985–1990**, Band A 9, p. 423–429, and references cited therein; W. Leuchtenberger, U. Plöcker, *Chem. Ing. Tech.* **1988**, *60*, 16–23, and references cited therein.

[5] J. Kamphuis, W. H. J. Boesten, Q. B. Broxterman, H. F. M. Hermes, J. A. M. van Balken, E. M. Meijer, H. E. Shoemaker, *Adv. Biochem. Eng. Biotechnol.* **1990**, *42*, 133–186, and references cited therein.

[6] U. Groeger, K. Drauz, H. Klenk, *Angew. Chem.* **1990**, *102*, 428–429; *Angew. Chem. Int. Ed. Engl.* **1990**, *29*, 417–419, and references cited therein.

[7] K. Drauz, U. Groeger, M. Schäfer, H. Klenk, *Chem.-Ztg.* **1991**, *115*, 97–101.

[8] S. M. Birnbaum, L. Levintow, R. B. Kingsley, J. P. Greenstein, *J. Biol. Chem.* **1952**, *194*, 455–470; S.-C. J. Fu, S. M. Birnbaum, *J. Am. Chem. Soc.* **1953**, *75*, 918–920; H. K. Chenault, J. Dahmer, G. M. Whitesides, *ibid.* **1989**, *111*, 6354–6364; M. Sugie, H. Suzuki, *Agric. Biol. Chem.* **1980**, *44*, 1089–1095; S. Kang, Y. Minematsu, Y. Shimohigashi, M. Waki, N. Izumiya, *Mem. Fac. Sci. Kyushu Univ. Ser. C 16* **1987**, 61–68.

[9] Whereas *N*-ClAc-L-piperidine-2-carboxylic acid (*N*-ClAc-L-pipecolic acid) is a good substrate, *N*-ClAc-piperidine, *N*-ClAc-piperidine-3-carboxylic acid, and *N*-ClAc-piperidine-4-carboxylic acid are not hydrolyzed.

[10] A. Yaron, D. Mlynar, *Biochem. Biophys. Res. Commun.* **1968**, *32*, 658–663.

Threading Cyclodextrin Rings on Polymer Chains**

By *Gerhard Wenz** and *Bruno Keller*

The ability of cyclodextrins like α-cyclodextrin (**1a**) and β-cyclodextrin (**1b**) to include smaller guest molecules has been the subject of numerous investigations[1] since Cramer's extensive work in this area.[2] Depending on its ring size, a cyclodextrin molecule has room for one or two guest molecules;[3] if the guest is long enough, one or two cyclodextrin rings may be threaded along it.[4] The stringing of *many* cyclodextrin rings on a polymer chain has never been unequivocally proven.

We report here the first threading of cyclodextrin rings on poly(iminooligomethylene)s. Since the resulting polymeric inclusion compounds are highly soluble in water, the kinetics of the threading and unthreading could be examined for the first time. The structure of these polymeric inclusion compounds could be clearly proven by their conversion to polyrotaxanes.[5]

Poly(iminoundecamethylene) **2a** and poly(iminotrimethylene-iminodecamethylene) **2b** were obtained in almost quantitative yields by reductions of poly(11-undecaneamide) and poly(trimethylenedecanediamide) with $BH_3 \cdot Me_2S$.[6] Polymers **2a** and **2b** are soluble in water at pH values < 6. No indication of aggregation was observed for solutions with sufficient ion strength.[7] The degree of polymerization for **2a** was $P_n = 43 \pm 5$ (number average); for **2b**, $P_n = 23 \pm 2$ and $P_w = 60 \pm 12$ (weight average).[8]

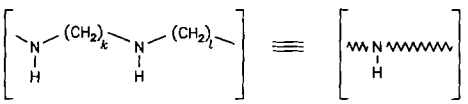

2a $k=l=11$
2b $k=10$, $l=3$

The reactions of the polymeric guest molecules **2a** and **2b** with hosts **1a** and heptakis(2,6-di-*O*-methyl)-β-cyclodextrin (**1c**) were conducted under homogeneous conditions[7] and could thus be followed by ^1H NMR spectroscopy and viscometry. The ^1H NMR spectrum of a mixture of **1a** and **2a**[7] differs distinctly from the spectra of the individual components (Fig. 1a–c). The signal at $\delta = 3.95$ attributed to

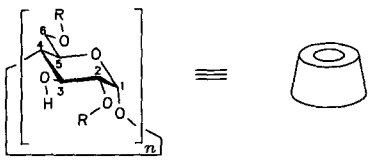

1a $n=6$, R=H
1b $n=7$, R=H
1c $n=7$, R=Me

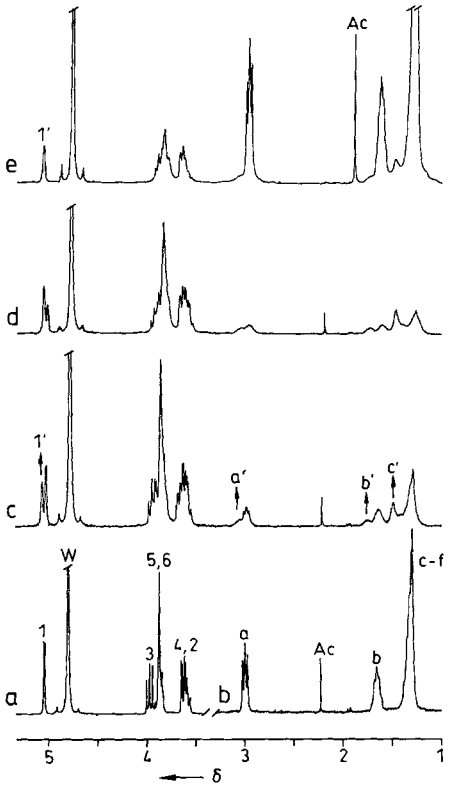

Fig. 1. Part of the ^1H NMR spectra at 20° for a) **1a**, b) **2a**, c) 45 mM **1a** + 45 mM **2a** after 5 min, d) 45 mM **1a** + 45 mM **2a** after 3.5 h, e) **4a**[7]; W = water, Ac = acetate.

[*] Dr. G. Wenz, Dipl.-Chem. B. Keller
Max-Planck-Institut für Polymerforschung
Ackermannweg 10, D-W-6500 Mainz 1 (FRG)

[**] This research was supported by the Bundesminister für Forschung und Technologie (BEO 0319055A), Henkel KGaA, and Wacker-Chemie GmbH. We thank B. Müller for the light-scattering measurements, A. Kühn for GPC measurements, and Prof. Dr. G. Wegner for helpful discussions.

a hydrogen in the cavity (H-3) vanishes, while a new signal at $\delta = 3.85$ arises. Similarly the signal of H-1 is shifted from $\delta = 5.04$ to $\delta = 5.08$. This shift could be attributed to conformational changes in **1a** upon inclusion. In addition, new signals at $\delta = 3.10, 1.75$, and 1.50 show up and are attributed to included **2a** (H-a', H-b', and H-c', respectively).

The observed downfield shifts of ^{1}H NMR signals of the guest molecule upon inclusion are not unusual.[9] It is more surprising that the chemical shifts of these new signals do not depend on the concentrations of **1a** and **2a**. In general the inclusion of low-molecular-weight guests is revealed by the continuous shift of the signals of one component upon variation of the concentration of the other due to signal averaging.[10] Since this averaged signal is not seen in the reaction of **1a** with **2a**, the individual inclusion steps must be slow on the NMR time scale. Averaged NMR signals were also not observed for the inclusion of α,ω-bis(1-pyridinium)alkanes in **1a**. This was attributed to the steric hindrance of the bulky cationic end-groups.[9] In our case the cationic ammonium groups (at pH 4.6) apparently also present steric barriers for the host molecules. Even more surprising is the change in the ^{1}H NMR spectra of **1a** with **2a** or **2b** over time. The spectrum of the system **1a** + **2a** is stable after 1.5 h (Fig. 1d);[11] that of **1a** + **2b**, after 170 h.

Viscosity measurements[7] also provide support for the slow equilibration (Fig. 2). System **1a** + **2a** has a constant viscosity after 2 h;[11] **1a** + **2b**, after 210 h. In comparison, the reaction of the larger host **1c** with **2a** or **2b** is complete after the mere mixing of the components.

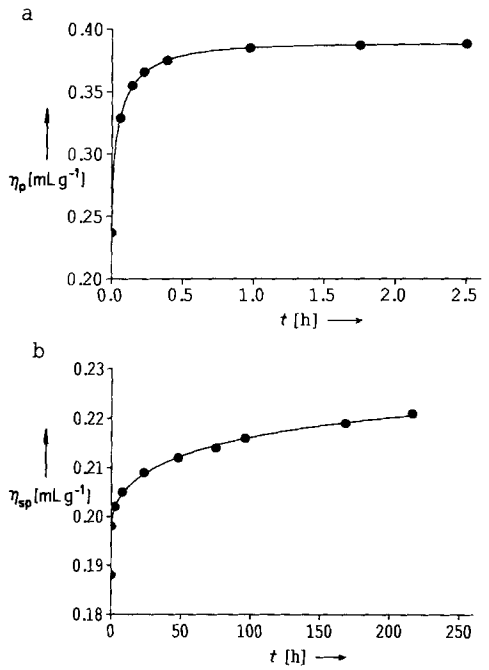

Fig. 2. Specific viscosity η_{sp} at 25° for a) 11.8 mM **1a** + 11.8 mM **2a** and b) 9.5 mM **1a** + 9.5 mM **2b** as a function of time t.

The extremely long reaction times of **1a** with **2a** and **2b** implies a mode of inclusion in which the rings are strung on the polymer chain, since each individual ring molecule must find a chain end in order to be threaded. Once strung along the polymer chain the rings must move towards the middle of the chain to make room for the next rings.

The formation of the polymeric inclusion compounds **1a** · **2a** and **1a** · **2b** according to Scheme 1 should be an

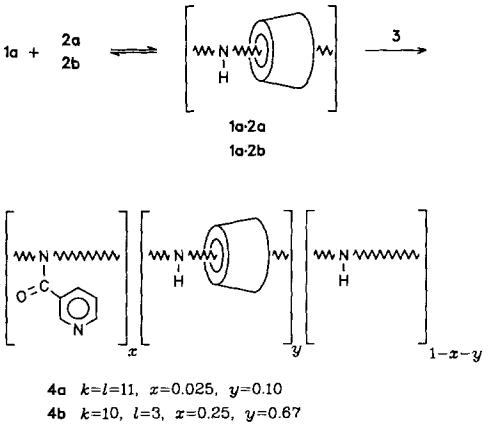

4a $k=l=11$, $x=0.025$, $y=0.10$
4b $k=10$, $l=3$, $x=0.25$, $y=0.67$

Scheme 1.

equilibrium reaction analogous to the formation of monomeric ones. Thus the continuous removal of **1a** from the equilibrium mixture should lead to the dissociation of **1a** · **2a** and **1a** · **2b**. In order to observe this dissociation we removed **1a** from the equilibrium mixture by dialysis.[12] The total concentration of cyclodextrin was determined by optical rotation measurements (Fig. 3). Although the dialysis of free **1a** was complete after 1.3 h,[13] the dialysis of the equilibrium mixture of **1a** · **2a** proceeded much more slowly after a fast initial period. This fast rate at the onset is due to excess **1a**, the slow progression thereafter, due to the slow dissociation of **1a** · **2a**. The unthreading of all the rings takes 15 h for **1a** · **2a**;[13] this process is far from complete after two weeks for **1a** · **2b**.

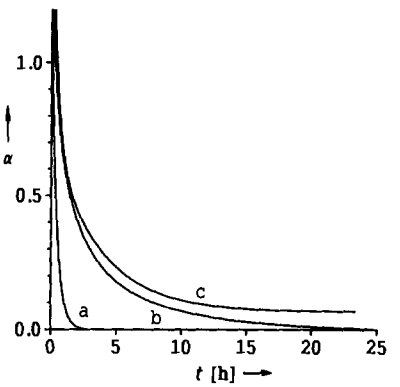

Fig. 3. Dialysis experiments[12]: Optical rotation α as a function of time t for a) 11.8 mM **1a**, b) the polymeric inclusion compound **1a** · **2a** from 23 mM **1a** and 15.4 mM **2a**, and c) the crude polyrotaxane **4a** from 23 mM **1a** and 15.4 mM **2a** after reaction with nicotinoyl chloride.

The low rates of formation and dissociation of these polymeric inclusion compounds and the marked dependence on the structures of the host and guest molecules may be indications for the threading but do not provide conclusive proof. Complex equilibria could also exist for nonspecific aggregates of host and guest molecules. By closing the polymer chain, however, one should be able to differentiate between the threaded and aggregated host molecules. Threaded rings become permanently bound upon closure of the chain; rings simply attached along the chain do not.

To completely close a polymeric inclusion compound, two bulky substituents must be attached to the ends of the chain. The attachment of at least two "blocking groups" at arbitrary positions on the chain would prevent unthreading

along a part of the chain and would be much easier to carry out. The nicotinoyl group was chosen as a blocking group since it is sufficiently hydrophilic. After the reaction of nicotinoyl chloride · HCl **3** with **1a** · **2b** the reaction mixture was dialyzed. The optical rotation of the mixture did not approach zero but rather stabilized at 0.065° (Fig. 3). Thus permanently bound α-cyclodextrin is present in product **4a**. The integration of the signals of the ^{1}H NMR spectrum of **4a** (Fig. 1d) indicates a concentration of 10 mol% cyclodextrin and 2.5 mol% nicotinoyl groups. The absence of the signal at $\delta = 5.04$ indicates that all the α-cyclodextrin units are threaded. All the cyclodextrin signals are sharp and identical to those of **1a** · **2a**. Since the structure of these rings is retained and since the rings are bound permanently, we believe that **4a** is a polyrotaxane.

Only those rings on the chain between the two blocking groups remain threaded. The probability of finding at least two blocking groups on *one* chain increases with the conversion x of the blocking reaction. Thus the relative amount y of permanently bound rings should increase with x. This is the case. From the reaction of **1a** · **2b** with **3** polyrotaxane **4b** is obtained in 43% yield with $x = 25$ mol% blocking groups and $y = 67$ mol% cyclodextrin rings per basic unit. The molecular mass of **4b**[7] $M_w = 55000 \pm 5000$ g mol^{-1} was found by light scattering; this corresponds to a degree of polymerization $P_w = 55 \pm 5$, in good agreement with that of **2b** ($P_w = 60 \pm 12$). Thus 37 cyclodextrin rings are permanently threaded in **4b**. By this synthesis of polyrotaxanes **4a** and **4b** we demonstrate not only the threading of rings **1a** on the chains **2a** and **2b** but also a promising new approach to polyrotaxanes.

Experimental Procedure

2a: Reprecipitated[6] Nylon 11 (6.0 g, 32.8 mmol, Aldrich) was suspended in dry THF (100 mL) and heated to reflux under inert gas. A 2 M solution of $BH_3 \cdot Me_2S$ in THF (55 mL, 110 mmol, Aldrich) was added dropwise over 1 h. The reaction mixture was heated 1 d at reflux. The THF was distilled off, water (100 mL) added, and the mixture heated at reflux 1 h. The reaction mixture was allowed to cool to 20° and glacial acetic acid (60 mL) was added. The mixture was stirred 1 h at room temperature and heated 3 h at reflux. The cooled solution was added dropwise to a 10% NaOH solution (2 L). The precipitate was removed by filtration, washed with water, dried in vacuum, and extracted with $CHCl_3$ in a Soxhlet apparatus. The extract was added dropwise to diethyl ether (1 L). Polymer **2a** precipitated and was filtered and dried in vacuum. Yield 5.2 g (94%), white powder, m.p. = 108°; Elemental analysis: C 78.03, H 13.56, N 8.38; calculated for $C_{11}H_{23}N$: C 78.03, H 13.69, N 8.27; Viscometry[7] (using Huggins' plot of the specific viscosity): $[\eta] = 91.7$ mL g^{-1}, $k_H = 0.28$; ^{1}H NMR (300 MHz, HOD)[7]: $\delta = 1.29$ (m, 14H; H-c to H-f), 1.65 (m, 4H; H-b), 3.00 (t, ^3J(H,H) = 7.8 Hz, 4H; H-a); ^{13}C NMR (75.46 MHz, $CDCl_3$, TMS): $\delta = 27.4$ (C-c), 29.6 (C-d, e, f), 30.2 (C-b), 50.2 (C-a); IR ($CHCl_3$-film): $\tilde{\nu}$ [cm^{-1}] = 3273 (N-H), 2920 (C-H), 1463 (C-H), 1128 (C-N).

2b: Poly(trimethylenedecanediamide)[14] (6.0 g) was converted to **2b** in an analogous manner to the preparation of **2a** from Nylon 11. Yield 5.04 g (95%), white powder, m.p. = 86 °C; Elemental analysis C 73.40, H 13.05, N 12.91, calculated for $C_{13}H_{28}N$: C 73.52, H 13.29, N 13.19; Viscometry (see **2a**): $[\eta] = 81.8$ mL g^{-1}, $k_H = 0.18$; ^{1}H NMR (HOD)[7]: $\delta = 1.30$ (m, 12H; H-c bis H-e), 1.66 (m, 4H; H-b), 2.09 (m, 2H; H-B), 3.03 (t, ^3J(H,H) = 7.7 Hz, 4H; H-a), 3.11 (t, ^3J(H,H) = 7.9 Hz, 4H; H-A); ^{13}C NMR ($CDCl_3$, TMS): $\delta = 27.4$ (C-c), 29.6 (C-d, e), 30.2 (C-b), 30.5 (C-B), 48.6 (C-A), 50.2 (C-a); IR ($CHCl_3$ film): $\tilde{\nu}$ [cm^{-1}] = 3260 (N-H), 2919 (C-H), 1467 (C-H), 1129 (C-N).

4a: Polymer **2a** (0.13 g, 0.77 mmol) and **1a** (1.12 g, 1.16 mmol) were dissolved in buffer[7] (20 mL). The solution was stirred at 20° for 24 h. The pH of the solution was adjusted to 6.3 with $NaHCO_3$, and **3** (0.286 g, 1.6 mmol, Aldrich) was added in small portions. During this addition the pH of the solution was held between 5.7 and 6.4 by further addition of $NaHCO_3$. After 16 h the solution was diluted to 50 mL and dialyzed with 2% acetic acid (24 h) until the optical rotation remained constant and with water (2 h) [12]. The product was then freeze-dried. Yield: 0.148 g (71%), white solid; Elemental analysis: C 63.23, H 10.38, N 4.99, calculated for $(C_{11}H_{23}N)_1(C_{36}H_{60}O_{30})_{0.1}$-$(C_6H_4NO)_{0.025}(C_2H_4O)_{0.5}$: C 63.21, H 10.47, N 4.80; 1H NMR (HOD)[7]: $\delta = 1.30$ (m, 13.6H; H-c to H-f), 1.50 (m, 0.4H; H-c'), 1.65 (m, 3.6H; H-b), 1.75 (m, 0.4H; H-b'), 1.95 (s, 1.5H; acetate), 3.00 (t, ^3J(H,H) = 7.7 Hz, 3.6 H; H-a), 3.10 (m, 0.4 H; H-a'), 3.67 (m, 1.2H; H-2', H-4'), 3.85 (m, 1.8H; H-3', H-5', H-6'), 5.09 (m, 0.6H; H-1'), 7.6, 8.0, 8.6 (3m, 0.1H; nic.).

4b: Polymer **2b** (0.29 g, 1.37 mmol) and cyclodextrin **1a** (4 g, 4.1 mmol) were added to a buffer solution[7] (20 mL) and stirred at 20° for 14 d. Compound **3** (0.79 g, 4.4 mmol) was added in small portions and the pH of the solution was maintained between 5 and 7 by addition of 5 M KOH. After 16 h the reaction was worked up analogously to that leading to **4a**. Yield: 0.565 g (43%), white solid; Elemental analysis C 48.94, H 7.43, N 3.11, calculated for $(C_{13}H_{28}N_2)_1$-$(C_{36}H_{60}O_{30})_{0.67}(C_6H_4NO)_{0.25}(C_6H_4O)_2$: C 50.65%, H 7.70%, N 3.12%; ^{1}H NMR (HOD)[7]: $\delta = 1.29$, 1.50, 1.65, 1.75 (4m, 16H; H-b', H-c', H-b to H-e), 1.95 (s, 6H; acetat), 2.08 (m, 2H; H-B), 3.00, 3.10 (2m, 5.6H; H-a, H-A, H-a'), 3.2–3.5 (m, 2H; $-CH_2-NR-C=O$), 3.67 (m, 8H; H-2', H-4'), 3.86 (m, 12H; H-3', H-5', H-6'), 5.09 (m, 4H; H-1'), 7.60 (m, 0.25H; nic.), 7.95 (m, 0.25H; nic.), 8.62 (m, 0.5H; nic.). nic. = nicotinoyl.

Received: August 14, 1991 [Z4872IE]
German version: *Angew. Chem.* **1992**, *104*, 201

[1] Review: J. Szejtli, *Cyclodextrin Technology* in *Topics in Inclusion Science* (Ed.: J. E. D. Davies), Kluwer, Dordrecht, **1988**.
[2] F. Cramer, *Chem. Ber.* **1951**, *84*, 851–854; F. Cramer, F. M. Henglein, *ibid.* **1957**, *90*, 2567–71; F. Cramer, *Einschlußverbindungen*, 1st ed., Springer, Heidelberg, **1954**, pp. 1–113.
[3] O. S. Tee, M. Bozzi, *J. Am. Chem. Soc.* **1990**, *112*, 7815–7816; H.-J. Schneider, N. K. Sangwan, *Angew. Chem.* **1987**, *99*, 924–925; *Angew. Chem. Int. Ed. Engl.* **1987**, *26*, 896.
[4] R. I. Gelb, L. M. Schwartz, D. A. Laufer, *J. Am. Chem. Soc.* **1978**, *100*, 5875–5879; B. Klingert, G. Rihs, *Organometallics* **1990**, *9*, 1135–1141.
[5] Several syntheses of rotaxanes: First synthesis of a rotaxane: I. T. Harrison, S. Harrison, *J. Am. Chem. Soc.* **1967**, *89*, 5723–5724. Main-chain polyrotaxanes: N. Ogata, K. Sanui, J. Wada, *J. Polym. Sci. Polym. Lett. Ed.* **1976**, *14*, 459–62; H. W. Gibson, P. Engen, P. Lecavalier, *Polym. Prepr. (Am. Chem. Soc. Div. Polym. Chem.)* **1988**, *29*, 248–9. Side-chain polyrotaxanes: M. Born, H. Ritter, *Makromol. Chem. Rapid. Commun.* **1991**, *12*, 471–476.
[6] Analogous to T. Perner, R. C. Schulz, *Br. Polym. J.* **1987**, *19*, 181–188.
[7] Solvent: 0.1 M sodium acetate buffer, pH = 4.6.
[8] P_n was determined by vapor pressure osmometry (Knauer) in $CHCl_3$, P_w by gel permeation chromatography (columns: TSKGPW from Toyo Soda) with 0.5 M sodium acetate buffer/acetonitrile 80/20 (v/v).
[9] H. Saito, H. Yonemura, H. Nakamura, T. Matsuo, *Chem. Lett.* **1990**, 535–538.
[10] D. J. Wood, F. E. Hruska, W. Saenger, *J. Am. Chem. Soc.* **1977**, *99*, 1735–40.
[11] The height of the signal reached >95% of the final height.
[12] The dialysis was carried out at 20° in 2% acetic acid with a hollow fiber membrane module (Reichelt, Thomapor LD-0C02). The polymer solution (50 mL) was circulated with a peristaltic pump (flow rate 8.5 mL min^{-1}). The optical rotation was measured continuously with a polarimeter (Polarmonitor IBZ-Messtechnik, Braunschweig); drift <0.002° per day.
[13] The cyclodextrin concentration is reduced to <5% of the starting concentration.
[14] Synthesis analogous to W. R. Sørenson, *J. Chem. Educ.* **1965**, *42*, 8–12.

Selectivity Control By Temperature Variation in the Formation of Isotactic vs. Syndiotactic Polypropylene with a Titanocene/Alumoxane Catalyst**

By *Gerhard Erker** and *Cornelia Fritze*

The syndioselective polymerization of α-olefins with vanadium catalysts probably proceeds by a different mechanism (2-1 insertion) than with Ziegler catalysts.[1] A few homogeneous catalyst systems based on the group 4 metallocenes, which direct the usual mode of polymerization (1-2 insertion), have led to the production of syndiotactic polypropylene as well.[2] In the past the few exceptional cases of syn-

[*] Prof. Dr. G. Erker, Dipl.-Chem. C. Fritze
Organisch-Chemisches Institut der Universität
Corrensstrasse 40, D-W-4400 Münster (FRG)

[**] This work was supported by the Fonds der Chemischen Insdustrie, the Alfred-Krupp-von-Bohlen-und-Halbach Stiftung, and the Bundesminister für Forschung und Technologie.

dioselective propylene-polymerizations by catalysts that usually deliver isotactic polypropylene have been explained by special structure/selectivity relationships. However, it was often not adequately considered that the selectivity of two competing processes may be temperature-dependent. Only when the influence of the reaction temperature has been determined is the discussion of the relationship between the structure of the catalyst system and the resulting selectivities meaningful.

For this study we have used homogeneous titanocene/alumoxane propylene-polymerization catalysts derived from achiral bent-metallocene complexes. The stereocontrol of the C–C bond formation is controlled here by the chiral end of the growing polymer-chain at the active metal-center alone (chain-end control).[3] We have found an example in which the change of the dominant mode of block polymerization from isotactic to syndiotactic can be accomplished by simply varying the reaction temperature.

We treated isopropylcyclopentadienyllithium with 0.5 mole equivalents of $TiCl_4$ to obtain $[(C_5H_4iPr)_2TiCl_2]$ **1**. The reaction of **1** with two mole equivalents of PhLi in ether provided $[(C_5H_4iPr)_2TiPh_2]$ **2**. The activation of **2** with a large excess of methylalumoxane **3** in toluene/propylene (5:1) at −50 °C furnished an active homogeneous Ziegler catalyst for propylene polymerization (Scheme 1).[4] The isotactic block-polymer obtained was similar to the product of propylene polymerization with $[Cp_2TiPh_2]$/**3** according to Ewen.[3] Polymerization with the system **2**/**3** at −50 °C provided a polypropylene PP1 ($\bar{M}_\eta \approx 16000$), which was stereochemically characterized by a statistical analysis of the ^{13}C NMR methyl signals (pentade analysis). In addition to the dominant isotactic *mmmm* pentade signal, resonances arising from *mmmr* and *mmrm* units in a 1:1 intensity ratio were found (Fig. 1). This characterizes the structural defects of the stereoregular polymer (isotactic block-polymer, see Scheme 1) as resulting from chain-end control. A randomly occuring mistake was not corrected, but rather propagated until another "erroneous" insertion of the prochiral olefin into the growing chain occurred.

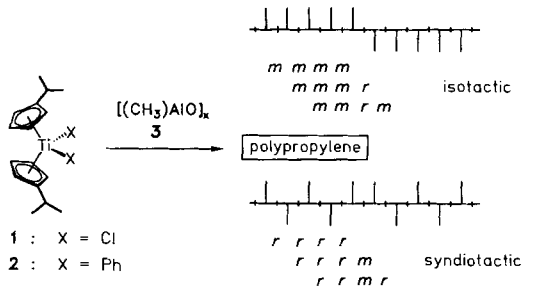

Scheme 1.

The intensity distribution of the ten ^{13}C pentade signals of PP1 can be described satisfactorily by Bernoulli statistics. The decisive statistical factor σ describes the probability of the formation of a *meso*-type dyad (*m*) upon the incorporation of a propylene monomer by formal insertion in the metal–carbon bond at the active catalytic center. For pure chain-end control the three possible limiting situations can be correctly described by this single statistical parameter (isotactic: $\sigma = 1$; atactic: $\sigma = 0.5$; syndiotactic: $\sigma = 0$). The polypropylene PP1 formed by **2**/**3** at −50 °C has $\sigma = 0.80$; this corresponds to an average isotactic block length $[\langle m \rangle_{n,\sigma} = (1-\sigma)^{-1}]$ of about five monomer units.[5]

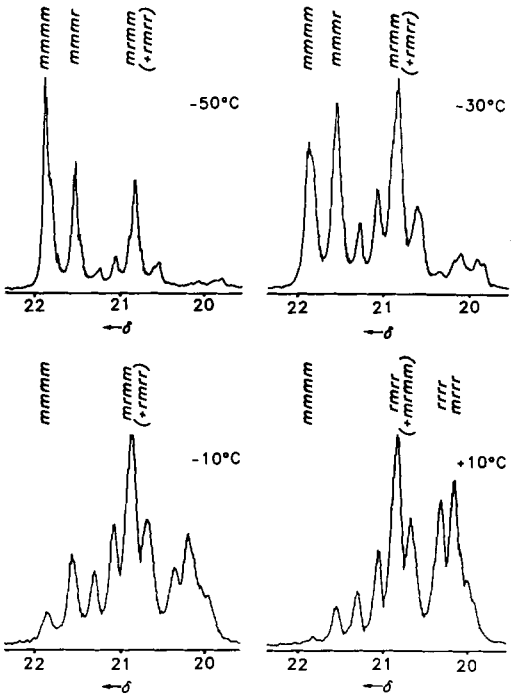

Fig. 1. ^{13}C NMR spectra (methylpentades) of polypropylenes (PP1–PP4) obtained from the **2**/**3** catalyst system at −50, −30, −10, and +10 °C.

As expected, polymerization with the catalyst system **2**/**3** at −30 °C provided a less isotactic polypropylene (PP2: $\sigma = 0.69$, see Table 1). At −10 °C an almost atactic polymer was obtained (PP3: $\sigma = 0.48$). This trend towards smaller σ values continued with increasing temperature. At +10 °C slightly syndiotactic polypropylene was produced (PP4: $\sigma = 0.39$, $\bar{M}_\eta \approx 12000$). This became further evident by the almost complete absence of the *mmmm* resonance signal in the methyl region of the ^{13}C NMR spectrum (Fig. 1). Moreover, the intensity of the *rrrr* signal is markedly increased. The ratio of the intensities of the *rrrm* and *rrmr* signals is nearly 1:1 as is expected for an appreciably syndiotactic block-polymer (Scheme 1). The average syndiotactic block-length of PP4 is estimated at about three monomer units.

In the temperature-dependent crossover from the production of isotactic to syndiotactic polypropylene the overall reaction mechanism does not basically change. The mechanistic uniformity of this reaction system becomes apparent upon plotting the logarithm of the quotient of σ ($\triangleq$ probabilty of the formation of the "isotactic" *m* dyad) and $(1-\sigma)$ ($\triangleq$ probability of the formation of the "syndiotactic" *r* dyad) versus T^{-1}. For the experimentally accessible range of

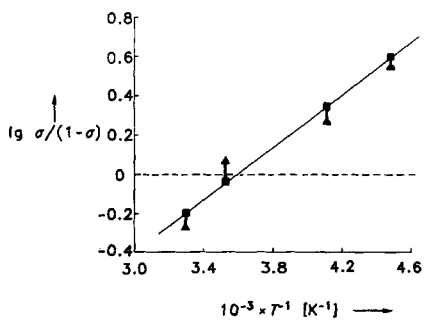

Fig. 2. Arrhenius plot of the stereoselective production of polypropylene. Catalysts: ■ **2**/**3**, ▲ **1**/**3**.

temperatures (-50 to $+10\,^{\circ}C$) the Arrhenius plot provides a straight line (Fig 2).[6]

We have tested the competition constants $\sigma(1-s)^{-1}$ obtained at these four temperatures independently by means of a second access to the same catalytically active species. An active propylene-polymerization catalyst is obtained from **1** and excess **3**. Although the activities of this system differ from those of the catalyst system **2/3**, the selectivities are almost the same (Table 1). The good agreement of the results of the two independent measurements (**1/3** and **2/3**) (Fig. 2) shows that the temperature-dependent competition constants $k_{isotact} \times (k_{syndiotact})^{-1}$ determined by this necessarily indirect procedure are quite reliable.

Table 1. Comparison of selected parameters of the propylene polymerization with the metallocene/methylalumoxane catalysts from **1** (PP1–PP4) and **2** (PP1′–PP4′).

PP	1	1′	2	2′	3	3′	4	4′
T (°C)	−50	−50	−30	−30	−10	−10	+10	+10
[Al]/[Ti]	500	240	360	230	500	270	290	270
a[a]	110	160	180	510	230	240	180	250
σ	0.80	0.78	0.69	0.65	0.48	0.46	0.39	0.35

[a] Activity in g[PP] g[titanium complex]$^{-1}$ h^{-1}.

How can one explain the temperature-dependent change in the formation of isotactic and syndiotactic polypropylene in a reasonably simple uniform mechanistic picture? According to the widely accepted mechanistic description of the stereoselective propylene-polymerization with homogeneous metallocene/alumoxane catalysts,[7] the α-olefin adds to a catalytically active alkylmetallocenyl cation[8] in such a way that the alkyl group of the α-olefin (CH_3) and the α substituent of the alkyl group (P = polymer chain) α-bound to the metallocene are oriented *trans* to each other (intermediate **4** in Scheme 2). (An α-agostic interaction[7a,d] could induce an effective transfer of chirality from the polymer chain to the reactive center). If the 1-2 insertion at the titanocenyl cation follows the usual rules for nucleophilic additions to prochiral sp^2 carbon centers, then it can be assumed that the olefin will rotate to minimize the steric interactions during the C–C bond formation.[9] Competing intermediates **5** (*anti* orientation of CH_3 and P) and **6** (CH_3 and P *gauche* to each other) may thus arise. From **5** C–C bond formation with concomitant switching of the coordination site of the σ-bound hydrocarbon ligand at $[(RCp)_2Ti]^+$ leads to a conformer to which the next addition of olefin can occur with the same relative topicity as in the formation of **4** (*re*, *re* in Scheme 2). This leads to isotactic polypropylene. In contrast the analogous process starting from **6** leads directly to a conformer to which the addition of the olefin proceeds with opposite topicity (*si* following *re* in Scheme 2), thus now favoring the formation of the syndiotactic polymer.[10]

The formal mathematical analysis of the Arrhenius plot of this reaction system (Fig. 2) yields differences in the activation parameters of the two competing pathways of $\Delta\Delta H^{\ddagger} = 2.9 \pm 0.1$ kcal mol^{-1} and $\Delta\Delta S^{\ddagger} = -11 \pm 1$ cal mol^{-1}K^{-1}. The polymerization of propylene with the bis(isopropylcyclopentadienyl)titanium/alumoxane catalyst system is thus probably another example of the counteracting influences of the activation enthalpy and entropy sometimes observed for very fast reactions. In this case the competing pathway exhibiting the less negative activation entropy can dominate over the enthalpically favored alternative at sufficiently elevated temperature.[6]

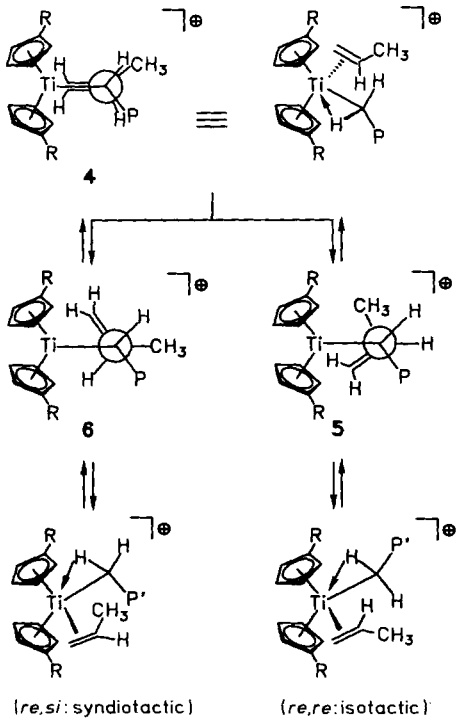

Scheme 2.

Received: August 28, 1991 [Z 4893 IE]
German version: *Angew. Chem.* **1992**, *104*, 204

[1] See for example: G. Natta, I. Pasquon, A. Zambelli, *J. Am. Chem. Soc.* **1962**, *84*, 1488; Y. Takegami, T. Suzuki, *Bull. Chem. Soc. Jpn.* **1969**, *42*, 848; *ibid.* **1970**, *43*, 1484; A. Zambelli, C. Tosi, C. Sacchi, *Macromolecules* **1972**, *5*, 649; Y. Doi, *ibid.* **1979**, *12*, 1012; A. Zambelli, G. Allegra, *ibid.* **1980**, *13*, 42; A. Zambelli, P. Locatelli, A. Provasoli, D. R. Ferro, *ibid.* **1980**, *13*, 267; P. Locatelli, M. C. Sacchi, E. Rigamonti, A. Zambelli, *ibid.* **1984**, *17*, 123; Y. Doi, F. Nazawa, K. Soga, *Makromol. Chem.* **1985**, *186*, 2539; P. Ammendola, X. Shijing, *Gazz. Chim. Ital.* **1988**, *118*, 769, and references therein.

[2] J. A. Ewen, R. L. Jones, A. Razavi, J. D. Ferrara, *J. Am. Chem. Soc.* **1988**, *110*, 6255; J. A. Ewen, M. J. Elder, R. L. Jones, S. Curtis, H. N. Cheng, *Stud. Surf. Sci. Catal.* **1990**, *56*, 439; V. Busico, P. Corradini, L. DeMartino, *Makromol. Chem. Rapid Commun.* **1990**, *11*, 49; T. Asanuma, Y. Nishimori, M. Ito, N. Uchikawa, T. Shiomura, *Polym. Bull. (Berlin)* **1991**, *25*, 567; L. Cavallo, G. Guerra, M. Vacatello, P Corradini, *Macromolecules* **1991**, *24*, 1784, and references therein.

[3] a) J. A. Ewen, *J. Am. Chem. Soc.* **1984**, *106*, 6355; J. A. Ewen in *Catalytic Polymerization of Olefins* (Eds.: T. Keii, K. Soga), Kodansha/Elsevier, Tokyo, **1986**, p. 271; b) Compare to B. Rieger, X. Mu, D. T. Mallin, M. D. Rausch, J. C. W. Chien, *Macromolecules* **1990**, *23*, 3559; J. C. W. Chien, B. Rieger, R. Sugimoto, D. T. Mallin, M. D. Rausch, *Stud. Surf. Sci. Catal.* **1990**, *56*, 535; G. Erker, R. Nolte, Y.-H. Tsay, C. Krüger, *Angew. Chem.* **1989**, *101*, *642*; *Angew. Chem. Int. Ed. Engl.* **1989**, *28*, 628; G. Erker, R. Nolte, R. Aul, S. Wilker, C. Krüger, R. Noe, *J. Am. Chem. Soc.* **1991**, *113*, 7594.

[4] H. Sinn, W. Kaminsky, *Adv. Organomet. Chem.* **1980**, *18*, 99.

[5] Details of the NMR analysis and the statistical evaluation: M. Farina, *Top. Stereochem.* **1987**, *17*, 1, and references therein; R. A. Sheldon, T. Fueno, T. Tsuntsugu, J. Kurukawa, *J. Polym. Sci. Part B: Polym. Lett.* **1965**, *3*, 23; F. A. Bovey, G. V. D. Tiers, *J. Polym. Sci.* **1960**, *44*, 173; Y. Inoue, Y. Itabashi, R. Chujo, Y. Doi, *Polymer*, **1984**, *25*, 1640.

[6] a) B. Giese, *Acc. Chem. Res.* **1984**, *17*, 438, and references therein; see also: O. Exner, B. Giese, *Angew. Chem.* **1978**, *90*, 816; *Angew. Chem. Int. Ed. Engl.* **1978**, *17*, 775; W. Linert, R. F. Jameson, *Chem. Soc. Rev.* **1989**, *18*, 477; O. Exner, *Prog. Phys. Org. Chem.* **1990**, *18*, 129; a recent example: N. A. Porter, D. M. Scott, I. J. Rosenstein, B. Giese, A. Veit, H. G. Zeitz, *J. Am. Chem. Soc.* **1991**, *113*, 1791; b) H. Pracejus, G. Kohl, *Justus Liebigs Ann. Chem.* **1969**, *722*, 1; H. Pracejus, *Fortschr. Chem. Forsch.* **1967**, *8*,

493; H. Buschmann, H.-D. Scharf, N. Hoffmann, P. Esser, *Angew. Chem.* **1991**, *103*, 480; *Angew. Chem. Int. Ed. Engl.* **1991**, *30*, 477.

[7] a) K. J. Ivin, J. J. Rooney, C. D. Stewart, M. L. H. Green, J. R. Mahtab, *J. Chem. Soc. Chem. Commun.* **1978**, 604; b) L. Clawson, J. Soto, S. L. Buchwald, M. L. Steigerwald, R. H. Grubbs, *J. Am. Chem. Soc.* **1985**, *107*, 3377; c) P. Pino, P. Cioni, J. Wei, *ibid.* **1987**, *109*, 6189; P. Pino, M. Galimberti, *J. Organomet. Chem.* **1989**, *370*, 1; P. Corradini, G. Guerra, M. Vacatello, V. Villani, *Gazz. Chim. Ital.* **1988**, *118*, 173; R. Waymouth, P. Pino, *J. Am. Chem. Soc.* **1990**, *112*, 4911; L. Resconi, R. M. Waymouth, *ibid.* **1990**, *112*, 4953; W. Kaminsky, A. Ahlers, N. Möller-Lindenhof, *Angew. Chem.* **1989**, *101*, 1304; *Angew. Chem. Int. Ed. Engl.* **1989**, *28*, 1216; d) H. Krauledat, H. H.Brintzinger, *ibid.* **1990**, *102*, 1459 and **1990**, *29*, 1412; H. H. Brintzinger in *Organic Synthesis via Organometallics* (Eds.: K. H. Dötz, R. W. Hoffmann), Vieweg, Braunschweig, **1991**, p. 33; W. E. Piers, J. E. Bercaw, *J. Am. Chem. Soc.* **1990**, *112*, 9406.

[8] D. S. Breslow, N. R. Newburg, *J. Am. Chem. Soc.* **1959**, *81*, 81; W. P. Long, D. S. Breslow, *ibid.* **1960**, *82*, 1953; J. J. Eisch, A. M. Piotrowski, S. K. Brownstein, E. J. Gabe, F. L. Lee, *ibid.* **1985**, *107*, 7219; P. G. Gassman, M. R. Callstrom, *ibid.* **1987**, *109*, 7875; R. F. Jordan, R. E. LaPointe, C. S. Bajgur, p. F. Echols, R. Willett, *ibid.* **1987**, *109*, 4111; M. Bochmann, A. J. Jaggar, J. C. Nicholls, *Angew. Chem.* **1990**, *102*, 830; *Angew. Chem. Int. Ed. Engl.* **1990**, *29*, 780; G. G. Hlatky, H. W. Turner, R. R. Eckman, *J. Am. Chem. Soc.* **1989**, *111*, 2728, and references therein.

[9] See for example: D. Seebach, R. Imwinkelried, T. Weber in *Modern Synthetic Methods, Vol. 4* (Ed.: R. Scheffold), Springer, Berlin, **1986**, p. 125; M. A. Brook, D. Seebach, *Can. J. Chem.* **1987**, *65*, 836, and references therein.

[10] In preliminary experiments the corresponding Arrhenius plots were determined for the polypropylene production with metallocene/alumoxane catalysts based on $[Cp_2TiCl_2]/[Cp_2TiPh_2]$; $[(C_5H_4Me)_2TiCl_2]/[(C_5H_4Me)_2TiPh_2]$; and $[(C_5H_4tBu)_2TiCl_2]/[C_5H_4tBu)_2TiPh_2]$. In all cases a more complicated picture emerged. Plots of $\lg \sigma(1-\sigma)^{-1}$ versus T^{-1} yields in each case two linear regions with differing slopes. According to Scharf and Pracejus[6] one can assume that a second level of stereoselection is kinetically significant here. In the proposed reaction (Scheme 2) this could be the primary step, i.e. the (reversible) addition of the prochiral olefin to the electrophilic metal center.

Observation and Properties of a Hydrogen Bond to Carbon in a Short-Lived, Gas-Phase Complex of Methyl Isocyanide and Hydrogen Fluoride**

By *A. C. Legon,* D. G. Lister*, and *H. E. Warner*

We report here the rotational spectrum of a short-lived $CH_3NC\cdots HF$ complex with C_{3v} symmetry frozen on the 10 μs timescale in a coaxial, pulsed supersonic expansion of CH_3NC/Ar and HF/Ar mixtures. This is the first characterization of a hydrogen bond to an isocyanide group in the gas phase.

Hydrogen bonds can form either by interaction with a nonbonding (n) electron pair on a terminal atom of a proton acceptor B or with a π-bonding electron pair on B. Such bonds involving the π-electron density between carbon atoms have been characterized extensively, first in solution[1, 2] through shifts $\Delta\nu_{OH}$ in the OH stretching frequencies of $\pi\cdots HO$ and pseudo-$\pi\cdots HO$ systems and then in the gas phase in ethyne$\cdots$HCl,[3] ethene$\cdots$HCl,[4] and cyclopropane$\cdots$HCl[5] by rotational spectroscopy. Hydrogen bonds to n electron pairs on terminal carbon atoms are less common. Isocyanides were first shown to form hydrogen bonds with suitable donors by infrared and NMR spectroscopy in solution.[6, 7] Consideration of the electronic structure $-\overset{+}{N}\equiv\overset{-}{C}$ of the isocyanide group[6, 7] suggested that bonding to carbon rather than nitrogen is favored, but the solution-phase work did not provide information regarding geometry. Some recently proposed empirical rules,[8] successful in rationalizing the angular geometries of a wide range of hydrogen-bonded dimers $B\cdots HX$, predict that the hydrogen bond in, for example, methyl isocyanide–hydrogen fluoride (**1**) should be to the nonbonding (n) electron pair localized on the C atom rather than to one of the π-electron pairs in the NC triple bond, and that at equilibrium the HF molecule should lie along the axis of the n electron pair as envisaged in the conventional model (**1**). Indeed, in a corollary to the rules,[9] it is proposed that the molecular axis of HF in dimers $B\cdots HF$ may be used as a probe of the direction of the n electron pair. The rules are based on investigations by rotational spectroscopy which normally provide[10] unequivocal answers to the question of the binding site and yield the angular geometries and further quantitative properties of hydrogen-bonded dimers in effective isolation.

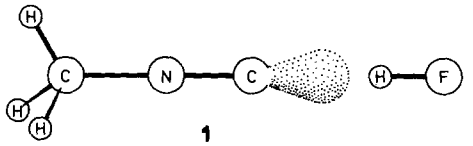

1

A difficulty arises when one attempts to apply these rules to complexes of isocyanides with acids HX, the obvious model systems for a hydrogen bond to carbon. Rapid addition reactions of anhydrous hydrogen halides (X = Cl, Br, I) to isocyanides have been reported.[11] The rapid reaction of CH_3NC with HF was demonstrated by monitoring the gas mixture with infrared spectroscopy,[12] and we have confirmed recently that on mixing gaseous CH_3NC and HF there is a virtually instantaneous precipitation on the vessel walls. The problem of high reactivity can be overcome, however, by using a fast mixing nozzle in conjunction with Fourier-transform microwave spectroscopy.[13] The essence of the method is to keep the components separate until they expand into the Fabry–Pérot cavity of the spectrometer. Any short-lived complexes of CH_3NC and HF formed on mixing are frozen on the ca. 10 μs timescale in the collisionless phase of the supersonic expansion. These species can then be probed, identified, and their properties obtained from the rotational spectrum.

The complex $CH_3NC\cdots HF$ was formed by coaxially mixing a pulsed jet of CH_3NC/Ar with a continuous jet of HF/Ar. Frequencies of transitions attributed to the ground-state rotational spectrum of $CH_3NC\cdots HF$ accurately obeyed the symmetric-top expression [Eq.(a)]. The observed frequencies, the residuals of their least-squares fit by Equation (a), and the rotational constant B_0 and the centrifugal distortion constants D_J and D_{JK} determined from this expression are recorded in Table 1 together with the corresponding data for the isotopomer $CH_3NC\cdots DF$. Transitions from levels with $K \geq 2$ had an unobservable intensity because of the low effective temperature of the expansion. In $K = 0$ transitions there was little evidence of hyperfine splitting due to ^{14}N nuclear quadrupole and H,F nuclear spin–nuclear spin coupling, and only a suggestion of these effects was seen in $K = 1$ transitions (Fig. 1). Model calculations made by assuming unchanged ^{14}N nuclear quadrupole[14] and H,F spin–spin

$$\nu = 2B_0(J+1) - 4D_J(J+1)^3 - 2D_{JK}K^2(J+1) \qquad \text{(a)}$$

[*] Prof. A. C. Legon, Prof. D. G. Lister[+], Dr. H. E. Warner
Department of Chemistry, University of Exeter
Stocker Road, GB-Exeter EX4 4QD (UK)

[+] Permanent address:
Dipartimento di Chimica Industriale
Casella Postale 29, I-98166 Sant' Agata di Messina (Italy)

[**] This work was supported by grants from the Science and Engineering Research Council and MURST.

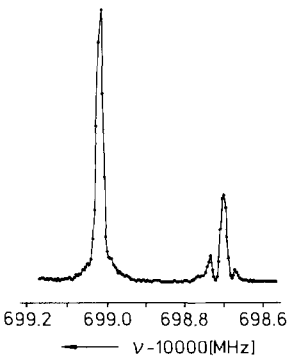

Fig. 1. Frequency spectrum of the $J = 3 \leftarrow 2\, K = 0$ and $K = 1$ transitions of $CH_3NC \cdots HF$ in the range of 10698.6 to 1069 MHz. This power spectrum was obtained by averaging 1003 gas pulses over a period of eight minutes. The data points are separated by 3.90625 kHz and have been joined by straight lines. No Doppler doubling effect is seen when the fast mixing nozzle is used. Partial resolution of hyperfine structure is apparent on the $K = 1$ transition centerd at 10698.71 MHz (see text).

coupling[15] constants from the free molecules CH_3NC and HF predict a very complicated hyperfine structure for the $J = 3 \leftarrow 2$, $K = 0$ transition, for example, with two-thirds of the intensity of the many components falling within ± 10 kHz of the unperturbed frequency. This is consistent with the observed full width at half height of approximately 20 kHz (see Fig. 1). The partial resolution for the $K = 1$ component seen in the spectrum is also as predicted but is too complicated to analyse.

The spectrum is characteristic of a symmetric top and establishes that the complex has C_{3v} symmetry. The magnitude of the change ΔB_0 in B_0 on D/H substitution is consistent only with the order of the nuclei $CNC \cdots HF$ along the symmetry axis and establishes that the intermolecular link is through a hydrogen bond to carbon as in **1**. The model geometry $CH_3NC \cdots HF$ with $r(C \cdots F) = 2.840$ Å proposed below predicts a value $\Delta B_{calc} = 22.5$ MHz, in excellent agreement with $\Delta B_0 = 22.6$ MHz. The other possible C_{3v} complex, $CH_3NC \cdots FH$, would require $r(C \cdots F) = 2.828$ Å and $\Delta B_{calc} = 77.9$ MHz, however. Quantitative properties of $CH_3NC \cdots HF$ are also available from the spectroscopic constants in Table 1.

Table 1. Observed and calculated rotational transition frequencies and spectroscopic constants of $CH_3NC \cdots H(D)F$ in the ground state.

		$CH_3NC \cdots HF$		$CH_3NC \cdots DF$	
$J+1 \leftarrow J$	K	ν_{obs} [MHz]	$\Delta\nu$ [kHz] [a]	ν_{obs} [MHz]	$\Delta\nu$ [kHz] [a]
$2 \leftarrow 1$	0	7132.7013	−1.6	7042.2509	−0.2
	1	7132.5025	0.5	–	–
$3 \leftarrow 2$	0	10699.0043	−0.6	10563.3268	−2.1
	1	10698.7054	1.9	10563.0430	2.3
$4 \leftarrow 3$	0	14265.2488	1.3	14084.3512	1.7
	1	14264.8440	−1.7	14083.9635	−1.7
		B_0 [MHz] [b]	1783.1823(4)		1760.5691(6)
		D_J [kHz] [b]	0.825(14)		0.795(24)
		D_{JK} [kHz] [b]	50.2(3)		48.0(4)

[a] $\Delta\nu = \nu_{obs} - \nu_{calc}$. [b] Standard errors in units of the least significant digit.

First, the distances $r(C \cdots F) = 2.840$ Å can be obtained by fitting the rotational constant of either $CH_3NC \cdots HF$ or $CH_3NC \cdots DF$. A familiar model[16] is used to allow for the zero-point oscillations of the CH_3NC and HF subunits, assuming the same oscillation amplitudes as those of the isomeric complex $CH_3CN \cdots HF$[16] and the same geometries as those of the monomers.[17–19] The $C \cdots F$ distances obtained should be compared with 2.752 Å ($CH_3CN \cdots HF$) and 2.750 Å ($CH_3CN \cdots DF$).[16] The difference Δr between $r(C \cdots F)$ and $r(N \cdots F)$ of $CH_3NC \cdots HF$ and $CH_3CN \cdots HF$ is apparently a measure of the difference of the van der Waals radii of C and N atoms.[20] The accepted value 1.4 Å for the van der Waals radius of the N atom then allows the estimate of 1.5 Å for the radius of the C atom. Secondly, the hydrogen-bond stretching force constant k_σ can be determined from D_J by Equation (b)[21]

$$k_\sigma = (16\pi^2\mu B^3/D_J)(1 - B/B^{CH_3NC} - B/B^{HF}) \qquad (b)$$

where $\mu = m^{CH_3NC}m^{HF}/(m^{CH_3NC} + m^{HF})$. When ground-state rotational constants B^{CH_3NC}, B^{HF}, and B^{DF} of the monomers are employed[17–19, 22] the resulting values are $k_\sigma = 19.9(3)$ and $20.5(6)$ Nm^{-1} for $CH_3NC \cdots HF$ and $CH_3NC \cdots DF$, virtually the same as for $CH_3CN \cdots H(D)F$.[16] The wavenumbers $\tilde{\nu}_\sigma = (2\pi c)^{-1}(k_\sigma/\mu)^{1/2}$ for the stretching mode σ are correspondingly 158(1) and 158(2) cm^{-1}.

It is possible that the short-lived, hydrogen-bonded C_{3v} complex $CH_3NC \cdots HF$ characterized in this work is the intermediate first formed in the addition reaction of HF to CH_3NC.

Experimental Procedure

Rotational spectra were observed with a Balle–Flygare Fourier-transform microwave spectrometer with a pulsed nozzle.[23, 24] The fast mixing nozzle consisted of a pair of coterminal concentric tubes attached to the outlet of a Series Nine (General Valve Corp.) solenoid valve, as described in detail elsewhere.[13] A mixture of roughly 3% CH_3NC in Ar was pulsed into the outer tube at a rate of about 3 Hz from a pressure of 2 atm and mixed with a continuous flow of 30% HF (Argot International plc) in Ar at a pressure of 1 atm issuing from the exit of the inner tube. Methyl isocyanide was prepared by dehydration of *N*-methylformamide[25] and purified by distillation under reduced pressure. DF was prepared in situ by exchange of HF with D_2O on the walls of the stainless-steel mixing tank.

Received: September 17, 1991 [Z 4916 IE]
German version: *Angew. Chem.* **1992**, *104*, 233

CAS Registry numbers:
CH_3NC, 593-75-9; HF, 7664-39-3; DF, 14333-26-7.

[1] P. von R. Schleyer, D. S. Trifan, R. Bacskai, *J. Am. Chem. Soc.* **1955**, *80*, 6691–6692.
[2] L. Joris, P. von R. Schleyer, R. Gleiter, *J. Am. Chem. Soc.* **1968**, *90*, 327–336.
[3] A. C. Legon, P. D. Aldrich, W. H. Flygare, *J. Chem. Phys.* **1981**, *75*, 625–630.
[4] P. D. Aldrich, A. C. Legon, W. H. Flygare, *J. Chem. Phys.* **1981**, *75*, 2126–2134.
[5] A. C. Legon, P. D. Aldrich, W. H. Flygare, *J. Am. Chem. Soc.* **1982**, *104*, 1486–1490.
[6] A. Allerhand, P. von R. Schleyer, *J. Am. Chem. Soc.* **1962**, *84*, 1322–1323; *ibid.* **1963**, *85*, 866–870.
[7] L. F. Ferstandig, *J. Am. Chem. Soc.* **1962**, *84*, 1323–1324; *ibid.* **1962**, *84*, 3553–3557.
[8] A. C. Legon, D. J. Millen, *Faraday Discuss. Chem. Soc.* **1982**, *73*, 71–87.
[9] A. C. Legon, D. J. Millen, *Chem. Soc. Rev.* **1987**, *16*, 467–498.
[10] A. C. Legon, *Chem. Soc. Rev.* **1990**, *19*, 197–237.
[11] G. Tennant, *Comprehensive Organic Chemistry*, (Ed.: I. O. Sutherland), Pergamon, Oxford, **1979**, Chapter 8, pp. 570–571.
[12] A. S. Georgiou, Ph.D. Thesis, University of London, **1979**, 77.
[13] C. A. Rego, A. C. Legon, *J. Chem. Soc. Faraday Trans.* **1990**, *86*, 1915–1921.
[14] S. G. Kukolich, *Chem. Phys. Lett.* **1971**, *10*, 52–55.
[15] J.S. Muenter, W. Klemperer, *J. Chem. Phys.* **1970**, *52*, 6033–6037; *ibid.* **1972**, *56*, 5409–5412.
[16] P. Cope, D. J. Millen, A. C. Legon, *J. Chem. Soc. Faraday Trans. 2* **1986**, *82*, 1197–1206.
[17] G. Guelachvili, *Opt. Commun.* **1976**, *19*, 150–154.
[18] F. J. Lovas, E. Tiemann, *J. Phys. Chem. Ref. Data* **1974**, *3*, 609–769.
[19] L. Halonen, I. M. Mills, *J. Mol. Spectrosc.* **1978**, *73*, 494–502.
[20] A. D. Buckingham, P. W. Fowler, *Can. J. Chem.* **1985**, *63*, 2018–2025.
[21] D. J. Millen, *Can. J. Chem.* **1985**, *63*, 1477–1479.
[22] A. Bauer, M. Bogey, *C.R. Acad. Sci.* **1970**, *271 B*, 892–893 for B_0 (A_0 was estimated from the CH_3NC geometry in ref. [19]).
[23] T. J. Balle and W. H. Flygare, *Rev. Sci. Instrum.* **1981**, *52*, 33–45.
[24] A. C. Legon, *Ann. Rev. Phys. Chem.* **1983**, *34*, 275–300.
[25] J. Casanova Jr., R. E. Schuster and N. D. Werner, *J. Chem. Soc.* **1963**, 4280–4281.

New Thermo-Response Dyes: Coloration by the Claisen Rearrangement and Intramolecular Acid–Base Reaction

By *Masahiko Inouye,* Kikuo Tsuchiya*, and *Teijiro Kitao*

Fluoran dyes have been widely used as pressure- and heat-sensitive dyes for carbonless paper and paper for fax systems, for example.[1] The coloration occurs when the dyes react with acid, normally phenolic compounds, upon heating (Scheme 1). To retain the colorless form before heating, the dyes must be protected from contact with acid. Indeed, this often causes technical problems and restricts the use of organic mediums such as polymer films. Here we introduce a class of purely thermally activated dyes, which color only upon heating without the addition of any other component. Our strategy utilizes the fact that upon heating, neutral allyl aryl ethers generate acidic phenol groups by the Claisen rearrangement.[2] Phenol groups thus generated undergo intramolecular acid–base reaction, which in turn causes the ring-opening of the lactone groups and the coloration (Scheme 2).

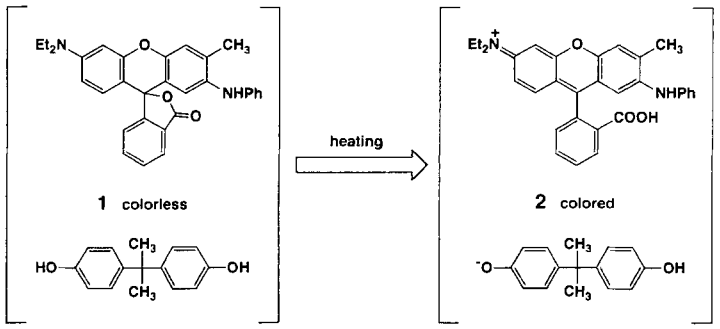

Scheme 1.

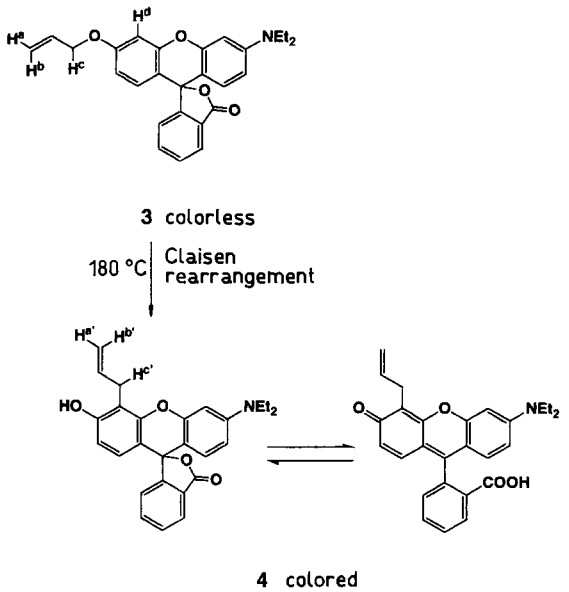

Scheme 2.

These new of dyes (**3**, **13**, and **14**), possessing both allyloxy and amino groups, were made in several steps from commercially available starting materials (Scheme 3).

The dyes thus prepared did not absorb above 400 nm in several solvents, indicative of the closed lactone forms. Heating the solutions (ca. 180 °C), however, caused changes in their absorption spectra, and new absorption bands above 400 nm appeared (Fig. 1a). These new absorption bands were attributed to the products of the Claisen rearrangement on the basis of the following NMR and isolation experiments: A solution of **3** in [D_6]dimethyl sulfoxide (DMSO) was heated (ca. 180 °C), and ^{1}H NMR spectra were measured as a function of time. New resonances appeared $\delta = 3.0$ to 5.8, which were attributed to *C*-allyl groups because of their high-field shifts relative to those of *O*-allyl groups (Fig. 1c). In the aromatic region the signal for H^d decreased, showing that the Claisen rearrangement occurred at the position depicted in Scheme 2. Furthermore, after purification by silica-gel column chromatography, the colored product **4** displayed an intense stretching band at 3300–3700 cm^{-1} in the infrared spectrum characteristic of the phenolic OH group.

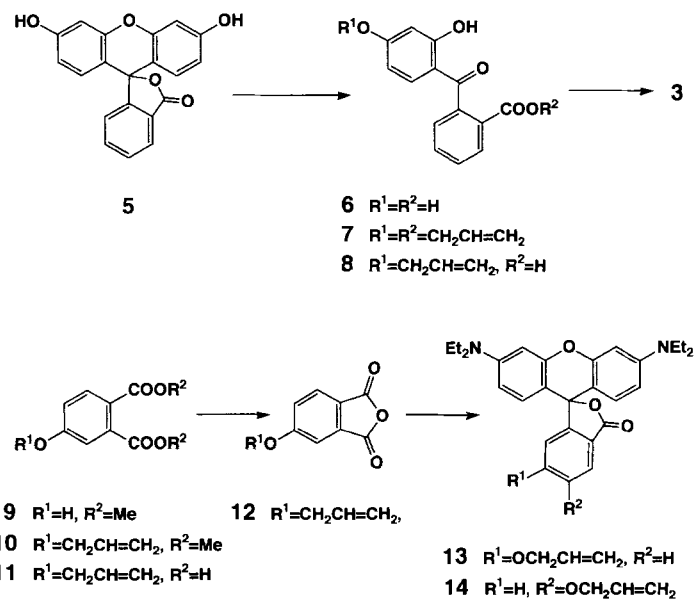

Scheme 3.

On the other hand, the absorption spectra (DMSO) of **3** and even the conventional acid-sensitive dyes such as **1**, which is a so-called one-dye black, showed no changes in the presence of a large excess of phenolic compound (intermolecular acid–base reaction), because of competitive proton capture with the highly polar solvent. In such cases a strong acid, for example trifluoroacetic acid (CF_3COOH), was needed for coloration.

Our method enabled the use of synthetic resins as solvating mediums for the dyes. Thus a composite film consisting of polymethylmethacrylate (PMMA) (50 wt%) and **3** (50 wt%) was prepared from a toluene/THF (1:1) solution on glass substrates. When the colorless film was heated, a change in the absorption spectra similar to that observed for

[*] Dr. M. Inouye, Prof. Dr. T. Kitao
Department of Applied Chemistry
University of Osaka Prefecture
Sakai, Osaka 591 (Japan)
K. Tsuchiya
Special Compounds & Colorants Division
Dainippon Ink & Chemicals, Inc.
Suita, Osaka 564 (Japan)

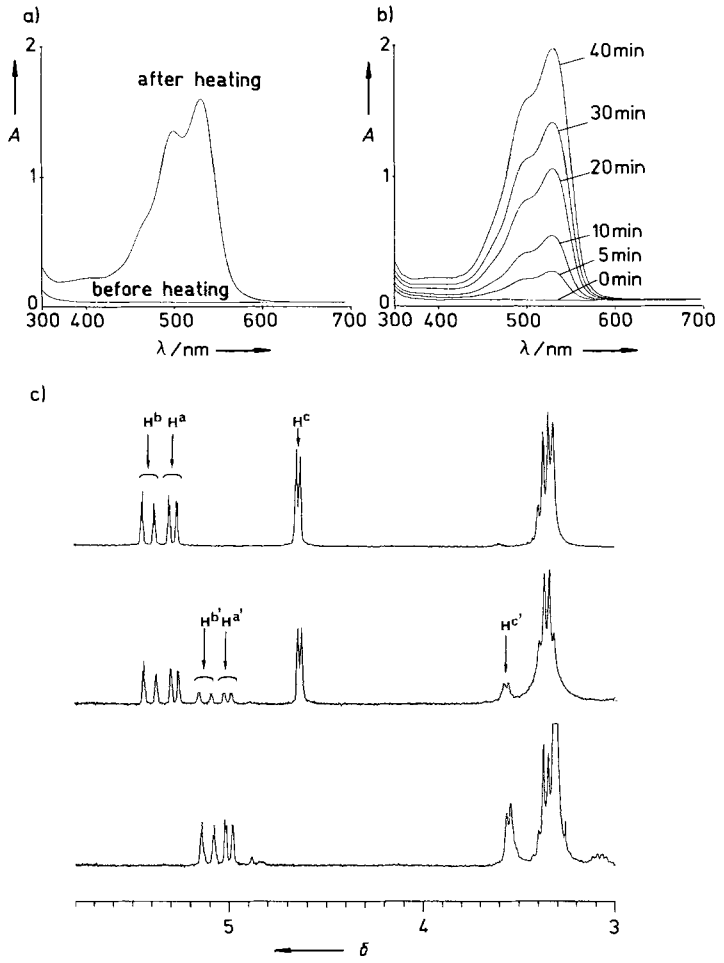

Fig. 1. The electronic absorption spectra of **3** before and after heating a) in DMSO and b) in the PMMA film. The spectra of **13** and **14** in DMSO were similar to that of **3**. **3**: λ_{max} = 530 nm, (ε = 3400) and 500 (ε = 2900); **13**: λ_{max} = 565 nm (ε = 6500); **14**: λ_{max} = 563 nm (ε = 9700). c) ^{1}H NMR spectra of **3** (270 MHz, [D$_6$]DMSO) δ = 3.0–5.8 before heating (top) and after heating for 4 h (middle), and of the isolated product **4** (bottom).

the solution was observed (Fig. 1 b). This colored film (red) is stable; even after more than 7 months in the presence of air its absorption bands did not change.

This new type of thermo-response dye may find several new applications in information-storage and thermally activated recording systems. The design of molecules which possess a lower temperature-response and/or different absorption bands in the colored forms (color variation) has great practical value.

Experimental Procedure

3: A solution of **5** (20 mmol) and KOH (400 mmol) in water (30 mL) was heated at reflux for 5 h. The reaction mixture was cooled to 0 °C, acidified with concentrated HCl, and extracted with ether. The ether extract was concentrated to dryness, and the product crystallized from CH_2Cl_2 (ca. 50 mL) to give **6** (86%). A suspension of **6** (10 mmol), allyl bromide (20 mmol), and K_2CO_3 (20 mmol) in acetone (100 mL) was heated at reflux for 6 h. After the solvent was removed, the reaction mixture was suspended in water. Extractive workup with ether followed by column chromatography (silica gel; eluent: hexane/ethyl acetate, 10:1) gave **7** (51%). A solution of **7** (10 mmol) and KOH (75 mmol) in ethanol (95%, 100 mL) was heated at reflux for 2 h. After the solvent was removed, the reaction mixture was dissolved in water and acidified with 6 N HCl. Extractive workup with ether gave **8** (100%). A suspension of **8** (0.5 mmol), *N*,*N*-diethyl-*m*-aminophenol (0.5 mmol), and $K_2S_2O_7$ (2.5 mmol) in xylene (2.5 mL) was heated at reflux for 6 h. The solvent was removed, and the reaction mixture was basified to pH 11 with aqueous NaOH solution. Extractive workup with ether followed by column chromatography (silica gel; eluent: hexane/ethyl acetate, 4:1) gave **3** (49%); m.p. = 108–110 °C; IR (KBr), ν = 2970, 1760, 1630, 1610, 1550, 1515, 1500, 1425, 1245, 1210, 1100 cm^{-1}; ^{1}H NMR (270 MHz, $CDCl_3$): δ = 1.17 (t, J = 7.3 Hz, 6 H), 3.36 (q, J = 7.3 Hz, 4 H), 4.56 (ddd, J = 1.2, 1.8, 5.5 Hz, 2 H), 5.31 (ddd, J = 1.2, 3.0, 10.4 Hz, 1 H), 5.42 (ddd, J = 1.8, 3.0, 17.1 Hz, 1 H), 6.04 (ddd, J = 5.5, 10.4, 17.1 Hz, 1 H), 6.35 (dd, J = 2.4, 8.5 Hz, 1 H), 6.45 (d, J = 2.4 Hz, 1 H), 6.56 (d, J = 8.5 Hz, 1 H), 6.59 (dd, J = 2.4, 8.6 Hz, 1 H), 6.66 (d, J = 8.6 Hz, 1 H), 6.76 (d, J = 2.4 Hz, 1 H), 7.19 (d, J = 6.1 Hz, 1 H), 7.59 (ddd, J = 1.2, 6.1, 7.3 Hz, 1 H), 7.65 (dt, J = 1.2, 7.3 Hz, 1 H), 8.01 (dd, J = 1.2, 7.3 Hz, 1 H). **4**: M.p. 138–141 °C; IR (KBr): ν = 3400, 2970, 1755, 1640, 1590, 1520, 1450, 1430, 1400, 1350, 1280, 1215, 1125 cm^{-1}; ^{1}H NMR (270 MHz, $CDCl_3$): δ = 1.19 (t, J = 6.7 Hz, 6 H), 3.39 (q, J = 6.7 Hz, 4 H), 3.66 (d, J = 6.1 Hz, 2 H), 5.10 (dd, J = 1.8, 10.4 Hz, 1 H), 5.19 (ddd, J = 1.2, 1.8, 17.1 Hz, 1 H), 5.96–6.10 (m, 1 H), 6.40 (dd, J = 1.2, 9.2 Hz, 1 H), 6.48 (d, J = 1.2 Hz, 1 H), 6.52 (d, J = 8.6 Hz, 1 H), 6.58 (d, J = 8.6 Hz, 1 H), 6.67 (d, J = 9.2 Hz, 1 H), 7.18 (dd, J = 1.2, 6.1 Hz, 1 H), 7.55–7.66 (m, 2 H), 8.04 (dd, J = 1.2, 6.1 Hz, 1 H).

13/**14**: A solution of **9** (100 mmol) in acetone (150 mL) was added dropwise to a suspension of allyl bromide (120 mmol) and K_2CO_3 (120 mmol) in acetone (150 mL) at 50 °C. The reaction mixture was heated 4 h, then filtered and concentrated to give **10** in quantitative yield. A solution of **10** (17.7 mmol) and KOH (40 mmol) in ethanol (50 mL) was heated at reflux for 2 h. After the solvent was removed, the reaction mixture was dissolved in water. This aqueous solution was washed with ether and acidified with 1 N HCl (pH < 4). Extractive workup with ether afforded **11** (99%). 4-Allyloxyphthalic anhydride (**12**) was prepared by the dehydration of **11** in toluene with the Dean-Stark apparatus (67%). A mixture of **12** (1.0 mmol) and *N*,*N*-diethyl-*m*-aminophenol (6.0 mmol) was heated (ca. 140 °C) for 24 h. Cooling followed by column chromatography (silica gel; eluent: ethyl acetate) gave **13** (10%) and **14** (14%). **13**: M.p. = 83–87 °C; IR (KBr): ν = 2960, 1750, 1610, 1540, 1515, 1425, 1330, 1260, 1215, 1115, 1100 cm^{-1}; ^{1}H NMR (270 MHz, $CDCl_3$): δ = 1.17 (t, J = 7.3 Hz, 12 H), 3.36 (q, J = 7.3 Hz, 8 H), 4.47 (dd, J = 1.2, 5.5 Hz, 2 H), 5.25 (dd, J = 1.2, 10.4 Hz, 1 H), 5.35 (dd, J = 1.2, 17.1 Hz, 1 H), 5.89–6.02 (m, 1 H), 6.34 (dd, J = 2.4, 8.6 Hz, 2 H), 6.43 (d, J = 2.4 Hz, 2 H), 6.61 (d, J = 8.6 Hz, 2 H), 6.62 (d, J = 2.4 Hz, 1 H), 7.09 (dd, J = 2.4, 8.6 Hz, 1 H), 7.88 (d, J = 8.6 Hz, 1 H). **14**: M.p. = 197–199 °C; IR (KBr): ν = 2960, 1750, 1610, 1540, 1515, 1485, 1425, 1350, 1330, 1305, 1270, 1230, 1200, 1120, 1070, 1010 cm^{-1}; ^{1}H NMR (270 MHz, $CDCl_3$): δ = 1.17 (t, J = 7.3 Hz, 12 H), 3.35 (q, J = 7.3 Hz, 8 H), 4.65 (ddd, J = 1.2, 1.8, 5.5 Hz, 1 H), 5.35 (td, J = 1.2, 10.4 Hz, 1 H), 5.48 (ddd, J = 1.2, 1.8, 15.9 Hz, 1 H), 6.09 (ddd, J = 5.5, 10.4, 15.9 Hz, 1 H), 6.33 (dd, J = 2.4, 8.6 Hz, 2 H), 6.43 (d, J = 2.4 Hz, 2 H), 6.61 (d, J = 8.6 Hz, 2 H), 7.09 (d, J = 8.6 Hz, 1 H), 7.21 (dd, J = 2.4, 8.6 Hz, 1 H), 7.42 (d, J = 2.4 Hz, 1 H).

All other new compounds provided spectra (^{1}H, ^{13}C NMR, IR) and elemental analyses in agreement with their structures.

Received: September 9, 1991 [Z 4905 IE]
German version: *Angew. Chem.* **1992**, *104*, 198

CAS Registry numbers:
3, 138518-26-0; **5**, 2321-07-5; **6**, 2513-33-9; **7**, 138518-27-1; **8**, 138518-28-2; **9**, 22479-95-4; **10**, 138518-29-3; **11**, 138518-30-6; **12**, 138518-31-7; **13**, 138518-32-8; **14**, 138518-33-9; PMMA, 9011-14-7; allyl bromide, 106-95-6; *N*,*N*-diethyl-*m*-aminophenol, 91-68-9.

[1] *Chemistry of Functional Dyes* (Eds.: Z. Yoshida, T. Kitao), Mita Press, Tokyo **1989**; H. Zollinger, *Color Chemistry*, VCH, Weinheim, **1987**, pp. 301–303.

[2] D. S. Tarbell, *Organic Reactions* **1944**, *2*, 1–48; S. J. Rhoads, N. R. Raulins, *ibid.* **1975**, *22*, 1–252.

Molecular Mechanisms of the Reduction of NO to NH_2OH at Mo–S Centers**

By *Dieter Sellmann** and *Bernd Seubert*

The enzymatic conversion of NO_3^- to NH_3 is catalyzed by various metal-oxidoreductases,[1] of which several nitrate[2] and nitrite reductases[3] have been more precisely characterized. With certainty, molybdenum and iron centers

[*] Prof. Dr. D. Sellmann, Dr. B. Seubert
Institut für Anorganische Chemie der Universität Erlangen-Nürnberg
Egerlandstrasse 1, D-W-8520 Erlangen (FRG)

[**] Transition-Metal Complexes with Sulfur Ligands, Part 83. This research was supported by the Deutsche Forschungsgemeinschaft and the Fonds der Chemischen Industrie. –Part 82: D. Sellmann, P. Lechner, F. Knoch, M. Moll *J. Am. Chem. Soc.*, in press.

in sulfur-dominated coordination spheres have been proven in these enzymes, and in nitrite reductases iron isobacteriochlorin and iron–heme groups have also been shown to occur.[4]

The 8e reduction of NO_3^- to NH_3 is postulated to proceed by 2e steps via NO_2^-, NO, and NH_2OH. These intermediates are assumed to function as ligands of the enzyme metal-centers, but almost nothing is known at present about the molecular processes of the individual steps.

Previous investigations showed that in complexes ML (M = Fe, Ru, Os; L = amine ligand) NO ligands can be reduced electrochemically to NH_3,[5] and a series of one-electron-transfer steps were discussed for these reductions. NH_2OH was established as an intermediate in the NO reduction; however, intermediates with complexed NH_2OH could not be isolated. For thermodynamic reasons it can be assumed that in the conversion of NO_3^- to NH_3 the $3e-3H^+$ reduction of NO to NH_2OH is a key step, since in this step the formation of the energetically favored N_2 must be avoided.

In order to gain a more detailed insight into the enzymatic mechanism, nitrosyl complexes are needed as model systems that allow a stepwise reduction of the NO ligands and the complete characterization of all intermediates. With the complex fragment [Mo(NO)('S_4')] ('S_4'$^{2-}$ = 2,2'-(ethylenedithio)dibenzenethiolate) we have now succeeded in achieving a stepwise and, in principle, catalytic reduction of NO to NH_2OH.

As recently reported, [Mo(NO)$_2$('S_4')] can be converted to [Mo(η^2-NH_2O)(NO)('S_4')] **1** in a $2e-2H^+$ reduction in which the NO ligand is hydrogenated to an η^2-hydroxylaminyl ligand *without* participation of the metal's electrons.[6] This η^2-NH_2O ligand could now be released with concomitant formation of the Mo^{III} complex [Mo(Cl)(NO)('S_4')] **2** according to Equation (a). $[N_2H_5]Cl$ and NH_4Cl are formed as by-products.

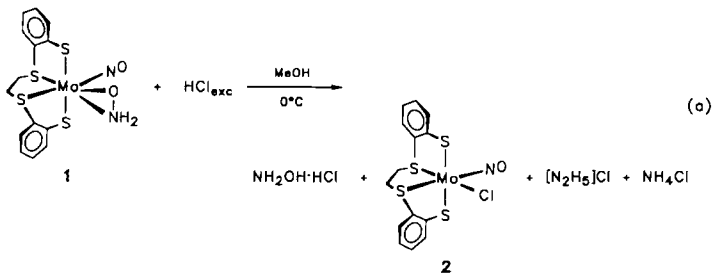

(a)

Complex **1** thus characteristically differs from the acid-stable NH_xO complexes (x = 1,2) that arise upon the protonation of NO complexes.[7]

Since **1** possesses a Mo^{II} center,[6] **2**, however, a Mo^{III} center, the formation of NH_2OH is an H^+-coupled 1e reduction of the NH_2O ligand as outlined in Equations (b) and (c); in this case, the electron comes from the metal center. (In assigning the oxidation states of the Mo centers, NO was regarded as a neutral 3e donor and the 'S_4' ligand as a dianion. The assignment of the oxidation states of Mo in **1**, **2**, and [Mo(NO)$_2$('S_4')] **3** is supported by ^{95}Mo NMR chemical shifts.[6,8])

$$NH_2O^{\bullet} + H^+ \xrightarrow{+e^-} NH_2OH \qquad (b)$$

$$Mo^{II} \xrightarrow{-e^-} Mo^{III} \qquad (c)$$

For the reaction mechanism, protonation of **1** to give [Mo(NH_2OH)(NO)('S_4')]$^+$ can be discussed as the primary step. Subsequent 1e transfer and release of the NH_2OH ligand yield the complex fragment [Mo(NO)('S_4')]$^+$, which is stabilized by coordination of Cl^- and formation of **2**. Primary protonation of **1** is further indicated by the observation that **1** reacts quickly with the strong acids HBr and HI, very slowly with the weaker acid HF, and not at all with the weak acid HCN.

The by-products NH_4Cl and $[N_2H_5]Cl$ may arise from subsequent reactions of the liberated NH_2OH according to Equations (d) and (e).[9] Identification of these products was

$$3\,NH_2OH \xrightarrow{[H_2O]} NH_3 + N_2 \xrightarrow{[HCl]} NH_4Cl \qquad (d)$$

$$NH_2OH + NH_3 \xrightarrow{[H_2O]} N_2H_4 \xrightarrow{[HCl]} [N_2H_5]Cl \qquad (e)$$

achieved by ^{1}H NMR spectroscopy and by specific color reactions.[10] For this purpose, the product mixture obtained from the reaction according to Equation (a) was concentrated to dryness and extracted with D_2O. The ^{14}N NMR spectrum of the D_2O extract (Fig. 1) showed $[NH_3OH]Cl$ to be the major product, while $[N_2H_5]Cl$ and NH_4Cl were detected in only minor amounts.

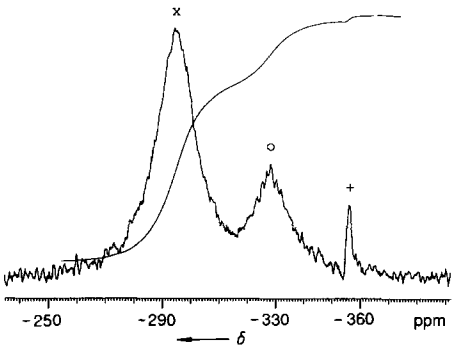

Fig. 1. ^{14}N NMR spectrum of the D_2O extract of the products of reaction (a) (× = $[NH_3OH]Cl$, o = $[N_2H_5]Cl$, + = NH_4Cl).

The reaction according to Equation (a) is thus the final step in the reduction of an NO ligand in **3** to free NH_2OH. Ultimately, this reduction could be conducted catalytically, since **2** was converted into **3** by reductive nitrosylation [Eq. (f)].

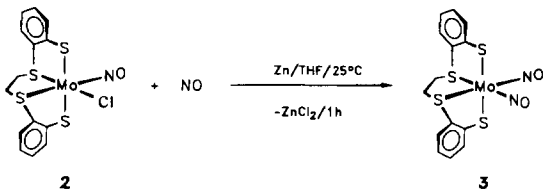

(f)

Accordingly, the cycle in Scheme 1 provides a model for the molecular course of the $3e-3H^+$ reduction of NO to NH_2OH in oxidoreductases with metal–sulfur centers. Two steps can be clearly distinguished: the $2e-2H^+$ reduction which bypasses the stage of the energetically favored N_2 and the $1e-1H^+$ reduction yielding free NH_2OH.

 © VCH Verlagsgesellschaft mbH, W-6940 Weinheim, 1992 0570-0833/92/0202-0206 $ 3.50+.25/0

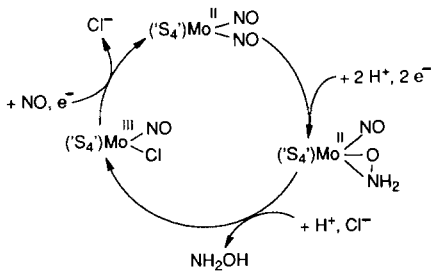

Scheme 1. Reduction of NO on the complex fragment [Mo(NO)('S_4')]; exc = excess.

Our results show that in the reduction of NO to NH_2OH at the [Mo(NO)('S_4')] fragment, intermediates may be obtained in preparative amounts and completely characterized, and that the enzymatic reduction of NO to NH_2OH should be favored at coordinatively flexible and redox-active molybdenum centers in sulfur-dominated coordination spheres.

Experimental Procedure

All procedures were carried out under N_2 and with dry, N_2-saturated solvents. **2**, NH_2OH: A yellow suspension of **1** · THF (1.035 g, 1.92 mmol) in MeOH (65 mL) was cooled to 0° and HCl gas was bubbled through the mixture for 15 min. The color changed immediately to red-violet. The suspension was stirred for 1.5 h at room temperature before N_2 gas was bubbled through in order to remove dissolved HCl. Complex **2** was filtered off as a dark-brown powder, washed with MeOH (50 mL) and Et_2O (20 mL), and recrystallized from boiling THF. 840 mg (93%) black-violet crystals. IR (KBr): $\tilde{\nu}$[cm^{-1}] = 1670 (NO); ^{14}N NMR (CD_2Cl_2) : δ = 44 (NO); FD/EI-MS: *m/z* 471 (M^+). Correct elemental analysis.

The filtrate of the reaction mixture was concentrated to dryness. Extraction of the residue with 5 mL of H_2O or D_2O provided a mixture of the salts $[NH_3OH]Cl$, $[N_2H_5]Cl$, and NH_4Cl, which were characterized by their IR, mass, and ^{14}N NMR spectra. ^{14}N NMR (D_2O): δ = −295.5 ($[NH_3OH]Cl$), −329.0 ($[N_2H_5]Cl$), −355.4 (NH_4Cl). $[NH_3OH]Cl$ in the aqueous extract was also identified by its reaction with a solution of Fe^{III}/HCHO.[10] Relative yields (estimated from NMR spectra): $[NH_3OH]Cl$ 68, $[N_2H_5]Cl$ 29, and NH_4Cl 3%.

3 from **2**: NO gas was bubbled through a suspension of **2** (745 mg, 1.59 mmol) and Zn (52 mg, 0.80 mmol) in THF (50 mL) for about 1 h until the color of the suspension had changed from violet to orange-brown. If no change in color occurred, some fresh Zn powder was added. The reaction mixture was then filtered, the filtrate evaporated to dryness, the residue taken up in CH_2Cl_2 (30 mL), and **3** precipitated by the addition of Et_2O (70 mL). Yield 220 mg (30%); IR (THF): $\tilde{\nu}$[cm^{-1}] = 1770, 1680 (NO); IR (KBr): $\tilde{\nu}$[cm^{-1}] = 1760, 1665 (NO); FD/EI-MS: *m/z* 464 (M^+).

Received: September 23, 1991 [Z4925 IE]
German version: *Angew. Chem.* **1992**, *104*, 200

CAS Registry numbers:
1, 116077-87-3; **2**, 121230-37-3; **3**, 97775-39-8; $[NH_3OH]Cl$, 5470-11-1; $[N_2H_5]Cl$, 2644-70-4; NH_2OH, 7803-49-8; NO, 10102-43-9; nitrate reductase, 901303-0; nitrite reductase, 9080-03-9.

[1] M. N. Hughes, *The Inorganic Chemistry of Biological Processes*, 2nd ed., Wiley, New York, **1981**, p. 188ff.
[2] M. W. W. Adams, L. E. Mortenson in *Metal Ions in Biology, Vol. 7, Molybdenum Enzymes* (Ed.: T. G. Spiro), Wiley, New York, **1985**, p. 519.
[3] R. J. Lancaster, J. M. Vega, H. Kamin, N. R. Orme-Johnson, W. H. Orme-Johnson, R. J. Krueger, L. M. Siegel, *J. Biol. Chem.* **1979**, *254*, 1268; D. W. Feng, M. D. Ryan, *Inorg. Chem.* **1987**, *26*, 2480.
[4] M. Losada, *J. Mol. Catal.* **1975**, *1*, 245; H. Scheer in *The Porphyrins, Vol. II* (Ed.: D. Dolphin), Academic Press, New York, **1979**, Chapter 1; C. Costa, J. J. G. Moura, I. Moura, M. Y. Liu, H. D. Peck, Jr., J. LeGall, Y. Wang, B. H. Huynh, *J. Biol. Chem.* **1990**, *265*, 14382; A. J. Pierik, W. R. Hagen, *Eur. J. Biochem.* **1991**, *195*, 505.
[5] M. H. Barley, K. Takeuchi, T. J. Meyer, *J. Am. Chem. Soc.* **1986**, *108*, 5876; F. T. Bonner, K. A. Pearsall, *Inorg. Chem.* **1982**, *21*, 1973; O. Kotaro, I. Hiroshi, *J. Chem. Soc. Faraday Trans.* **1984**, *80*, 2243.
[6] D. Sellmann, B. Seubert, M. Moll, F. Knoch, *Angew. Chem.* **1988**, *100*, 1221; *Angew. Chem. Int. Ed. Engl.* **1988**, *27*, 1164; D. Sellmann, *J. Organomet. Chem.* **1989**, *372*, 99; D. Sellmann, B. Seubert, F. Knoch, M. Moll, *Z. Naturforsch. B* **1991**, *46*, 1449.
[7] J. P. Collman, N. W. Hoffman, D. E. Morris, *J. Am. Chem. Soc.* **1969**, *91*, 5659; K. R. Grundy, C. A. Reed, W. R. Roper, *Chem. Commun.* **1970**, 1501; G. La Monica, M. Freni, S. Cenini, *J. Organomet. Chem.* **1974**, *71*, 57; K. Wieghardt, U. Quilitsch, *Z. Naturforsch. B.* **1981**, *36*, 683.
[8] D. Sellmann, G. Pöhlmann, F. Knoch, M. Moll, *Z. Naturforsch. B.* **1989**, *44*, 312.
[9] R. Nast, I. Föppl, *Z. Anorg. Allg. Chem.* **1950**, *263*, 310; G. Stedman, *Adv. Inorg. Chem. Radiochem.* **1979**, *22*, 113; K. Wieghardt, *Adv. Inorg. Bioinorg. Mech.* **1984**, *3*, 213.
[10] F. Feigel, V. Anger, *Spot Tests in Inorganic Chemistry*, Elsevier, New York, **1972**, p. 343.

En Route to Synthetic Phosphodiesterases: Supramolecular Phosphoryl-Transfer Mediated by Amidinium–Phosphate Contact Ion-Pairs**

By *Michael W. Göbel,* Jan W. Bats,* and *Gerd Dürner*

Dedicated to Professor Gerhard Quinkert on the occasion of his 65th birthday

Amidinium and guanidinium ions associate with carboxylates and phosphates forming hydrogen-bonded contact ion-pairs with well-defined structures. In the crystalline state[1,2] the cation and the O=P–O fragment are arranged almost in a coplanar fashion with symmetrical N–O distances (ca. 2.9 Å). The stability of the ion pairs in solution is dependent on the polarity of the solvent and its ability to form hydrogen bonds. Thus, in water the ion-pair stability is low;[3] however, in aprotic media association constants up to $1.4 \times 10^5\ M^{-1}$ have been recorded.[2]

Contact ion-pairs involving arginine side-chains play an important role in biochemistry.[4,5] In the active site of staphylococcal nuclease, for instance, the phosphodiester to be cleaved interacts with two arginine cations; because of their positive charges these residues not only bind the substrate but also facilitate the nucleophilic attack of water:[6,7] electrophilic catalysis.

Inspired by this example we are trying to design simple "synthetic phosphodiesterases"[8] on the basis of amidinium–phosphate ion-pair complexes (Scheme 1). As a first step we studied the reaction of amidinium alcohol **1**[9] with **2** to give **4**. This reaction proceeds via ion pair **3** and is markedly faster than the control reaction of **2** with **5**.

On addition of associating anions to **1** one observes a concentration-dependent downfield shift of the ^1H NMR

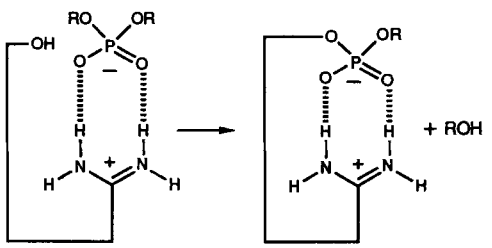

Scheme 1. Principle of supramolecular transesterification within an ion-pair complex.

[*] Dr. M. W. Göbel, Dr. J. W. Bats, Dr. G. Dürner
Institut für Organische Chemie der Universität
Niederurseler Hang, D-W-6000 Frankfurt am Main 50 (FRG)

[**] This research was supported by the Fonds der Chemischen Industrie, the Deutsche Forschungsgemeinschaft (Go 545/1-1), and the Bundesministerium für Forschung und Technologie. M. G. thanks Prof. Dr. G. Quinkert for his generous support.

signal of those amidinium hydrogens parallel to the biaryl axis ("axial"). Thus, the association constant K_a of ion pair **3** could be determined by NMR titration of **1** with the tetramethylguanidinium (TMG^+) salt **2**. In [D_7]DMF the value of K_a is 200($\pm$ 30) M^{-1} but is reduced to only 14 M^{-1} in [D_6]DMSO (both values 30 °). In contrast, the substantial downfield shift of the NH_{ax} signal of product **4** is independent of concentration. Compound **4** is thus assumed to be an inner ion-pair in solution.

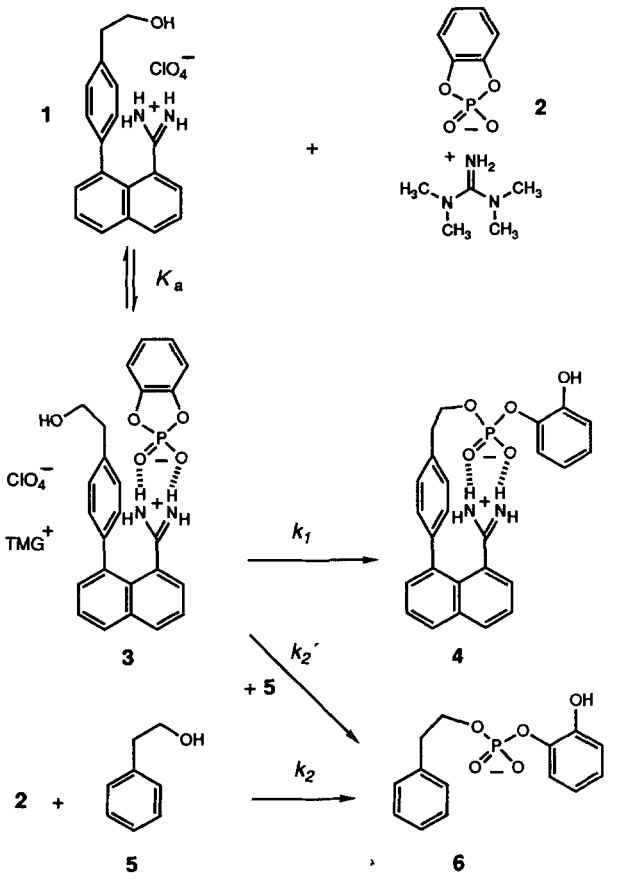

The crystal structure analysis of **4** provides further details[10] (Fig. 1). Due to the close proximity of the phenyl and amidinium groups these substituents are forced apart and the naphthalene frame is twisted. The torsion angle between the phenyl and naphthalene planes is 58°. In the barely disturbed ion-pair substructure, the unsubstituted oxygen centers of the phosphate group form hydrogen bonds with the cation 2.86 and 2.92 Å in length.

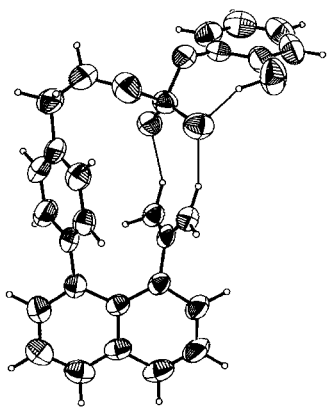

Fig. 1. Crystal structure of **4** [10].

Due to ring strain **2** is one of the most reactive phosphodiesters;[11] yet in its reaction with phenylethanol **5** and diisopropylethylamine in DMF, **2** opens very slowly to **6** ($k_2 = 2.2(\pm 0.2) \times 10^{-7}$ M^{-1} min^{-1}, 30°, 0.25 M base, analysis by HPLC). The reaction of **2** with amidinium alcohol **1** (30°, 0.25 M base in DMF) is much faster and follows a Michaelis–Menten-type saturation kinetics when the phosphate concentration exceeds the amidinium concentration (Fig. 2). This demonstrates that the phosphorylation of **1** is not an intermolecular but rather a supramolecular (quasi-intramolecular) process within ion pair **3**. Accordingly, the saturation curve (Fig. 2) can be predicted satisfactorily from the association constant K_a. If **1** is employed as an acetate instead of a perchlorate—the acetate counterion has a higher affinity to the amidinium group than the cyclophosphate in **2**—the reaction is strongly inhibited as expected.

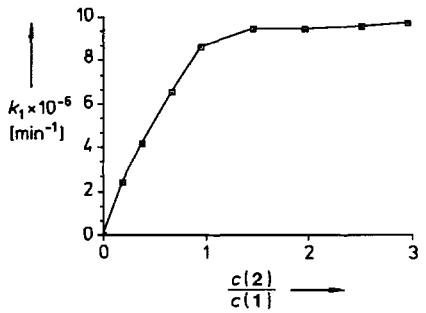

Fig. 2. Rate of the phosphorylation of **1** versus the concentration relationship $c(2)/c(1)$

The first-order rate constant measured at complete saturation for the quasi-intramolecular reaction of **3** was determined to be $9.9(\pm 0.4) \times 10^{-6}$ min^{-1}. To allow a comparison with k_2 of the control reaction the product $K_a k_1 = 1.98 \times 10^{-3}$ $M^{-1} min^{-1}$ can be used, which describes the second-order rate constant for the reaction of **1** and **2** at high dilution. $K_a k_1$ corresponds to the expression $k_{cat} K_M^{-1}$, well known in enzyme kinetics. The data show that **1** has a 9000-fold rate advantage over uncharged alcohol **5**. The effective molarity of the hydroxy group of **3** as expressed by $k_1 k_2^{-1}$ is 45 M.

The substantial acceleration of the phosphorylation reaction is due not only to the spatial proximity of the reacting groups in complex **3** but also to electrophilic activation of the phosphodiester by the coordinating amidinium ion (see staphylococcal nuclease). This coordination accelerates both the conversion of **3** to **4** and the intermolecular reaction of **3** with phenylethanol **5** and is comparable to electrophilic catalysis by coordinated metal-ions. As a result, the phosphorylation of **5** in the presence of amidinium salt **1** again shows a saturation effect when the phosphate concentration exceeds the amidinium concentration. For the reaction of **5** with ion pair **3** the constant k_2' is roughly 25 times greater than the constant k_2 for the free cyclophosphate **2**[12] (each measured at 30 °C, 0.25 M base in DMF). The addition of

one equivalent (relative to **2**) of bis(guanidinium) salt **7** accelerates the control reaction even more than 2000-fold. In the next step on the way to "synthetic phosphodiesterases" ke-

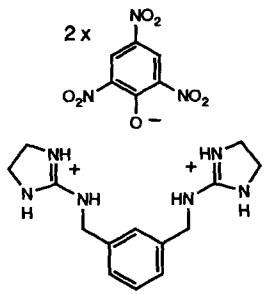

7

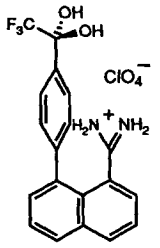

8

tone hydrates of type **8** will be used for the reversible binding of H_2O.

Received: September 30, 1991 [Z 4942 IE]
German version: *Angew. Chem.* **1992**, *104*, 217

CAS Registry numbers:
1, 137966-19-9; **2**, 137966-20-2; **3**, 137966-22-4; **4**, 137966-24-6; **4** · CH_3OH, 137966-25-7; **5**, 60-12-8; **6**, 137966-23-5.

[1] F. A. Cotton, V. W. Day, E. E. Hazen, Jr., S. Larsen, *J. Am. Chem. Soc.* **1973**, *95*, 4834–4840.
[2] G. Müller, J. Riede, F. P. Schmidtchen, *Angew. Chem.* **1988**, *100*, 1574–1575; *Angew. Chem. Int. Ed. Engl.* **1988**, *27*, 1516.
[3] B. Springs, P. Haake, *Bioorg. Chem.* **1977**, *6*, 181–190.
[4] J. F. Riordan, *Mol. Cell. Biochem.* **1979**, *26*, 71–92.
[5] B. J. Calnan, B. Tidor, S. Biancalana, D. Hudson, A. D. Frankel, *Science* **1991**, *252*, 1167–1171.
[6] F. A. Cotton, E. E. Hazen, Jr., M. J. Legg, *Proc. Natl. Acad. Sci. USA* **1979**, *76*, 2551–2555.
[7] J. Åqvist, A. Warshel, *Biochemistry* **1989**, *28*, 4680–4689.
[8] ATP hydrolysis mediated by macrocyclic polyammonium compounds: a) M. W. Hosseini, J.-M. Lehn, L. Maggiora, K. Bowman Mertes, M. P. Mertes, *J. Am. Chem. Soc.* **1987**, *109*, 537–544; cleavage of phosphodiesters: b) A. C. Hengge, W. W. Cleland, *J. Org. Chem.* **1991**, *56*, 1972–1974; (see also [8f]); metal-catalyzed: c) F. M. Menger, L. H. Gan, E. Johnson, D. H. Durst, *J. Am. Chem. Soc.* **1987**, *109*, 2800–2803; d) J. R. Morrow, W. C. Trogler, *Inorg. Chem.* **1988**, *27*, 3387–3394; e) J. Chin, *Acc. Chem. Res.* **1991**, *24*, 145–152; RNA hydrolysis: f) R. Breslow, E. Anslyn, D.-L. Huang, *Tetrahedron* **1991**, *47*, 2365–2376; g) B. Barbier, A. Brack, *J. Am. Chem. Soc.* **1988**, *110*, 6880–6882; h) A. S. Modak, J. K. Gard, M. C. Merriman, K. A. Winkeler, J. K. Bashkin, M. K. Stern, *ibid.* **1991**, *113*, 283–291; i) K. Yoshinari, K. Yamazaki, M. Komiyama, *ibid.* **1991**, *113*, 5899–5901; DNA hydrolysis: j) L. A. Basile, A. L. Raphael, J. K. Barton, *ibid.* **1987**, *109*, 7550–7551.
[9] We will report the synthesis of **1** in a later publication. All new compounds were characterized by the standard spectroscopic methods and provided correct elemental analyses.
[10] X-ray structure analysis of **4**: Enraf-Nonius-CAD4 diffractometer, $Cu_{K\alpha}$ radiation, $2\theta = 124°$, empirical absorption correction based on Ψ-scans; structure determination with direct methods with SHELX-86; the hydrogen atoms were not refined; the positions of the hydrogens at O and N were obtained from a difference Fourier synthesis: $C_{25}H_{23}N_2O_5P \cdot CH_3OH$, orthorhombic, space group $P2_12_12_1$, $a = 7.760(2)$, $b = 11.7190(8)$, $c = 27.577(2)$ Å, $V = 2507.9(9)$ Å^3, $Z = 4$, $\rho_{calc} = 1.310$ g cm^{-3}; of 3946 independent reflections 3906 with $I > 0$ were used; $R = 0.046$, $R_w = 0.045$. The residual density was less than 0.24 e Å^{-3}. Further details of the crystal structure investigation may be obtained from the Fachinformationszentrum Karlsruhe, Gesellschaft für wissenschaftlich-technische Information mbH, D-W-7514 Eggenstein-Leopoldshafen 2 (FRG) on quoting the depository number CSD-55686, the names of the authors, and the journal citation.
[11] a) E. T. Kaiser, K. Kudo, *J. Am. Chem. Soc.* **1967**, *89*, 6725–6728; b) L. Atwood, P. Haake, *Bioorg. Chem.* **1976**, *5*, 373–382; see also [8f].
[12] A similar effect was observed with guanidinium salts in aqueous solution: B. Springs, P. Haake, *Tetrahedron Lett.* **1977**, 3223–3226.

A New Synthesis for Imidazolo- and Pyrrolophanes by [3 + 2]Cycloaddition with Azaallenyl Radical Cations**

By *Felix Müller* and *Jochen Mattay**

Since the development of supramolecular chemistry the interest in cyclophanes and heterocyclophanes has grown steadily because of their possible use as receptor models and their application in phase-transfer catalysis.[1] Our recently published method, the [3 + 2]cycloaddition of azirines with olefins and imines by means of Photoinduced Electron Transfer (PET),[2] provides a new approach for the synthesis of heterocyclophanes.

The reaction is conducted under PET reaction conditions:[3] the electron acceptor 1,4-naphthalenedicarbonitrile (DCN) is excited by irradiation with light $\lambda = 350$ nm in the presence of azirine **1**, leading to the DCN radical anion and a reactive azirine radical cation. This latter species opens to the linear 2-azaallenyl radical cation **2**.[4] In a two-step process **2** adds to double bonds and their equivalents. Addition of **2** to the C=N bond of an imine under these conditions leads via a dihydroimidazole to an imidazole.[2, 5] Bicyclic azirines **1a–c** react with imines **3** to give [n](2,4)imidazolophanes (Scheme 1, Table 1).

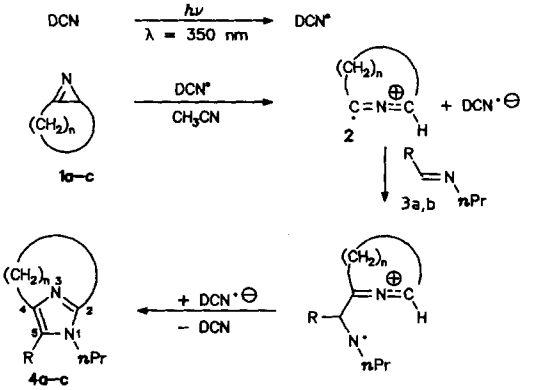

Scheme 1. **1a**, n = 4; **1b**, n = 5; **1c**, n = 6; **3a**, R = *n*-propyl; **3b**, R = phenyl. **4a–c** see Table 1.

Table 1. Isolated imidazolophanes.

Compd.	n	R	Yield
	4	*n*-propyl	no reaction
4a	5	*n*-propyl	2%
4b	6	*n*-propyl	27%
4c	6	phenyl	2%

The bridge must comprise at least five methylene units for the reaction to succeed. Reasonable yields may be obtained for products with bridges of at least six methylene units and appropriate substituents next to the N atom, as in **4b**. The

[*] Prof. Dr. J. Mattay, Dipl.-Chem. F. Müller
Organisch-chemisches Institut der Universität
Orléansring 23, D-W-4400 Münster (FRG)

[**] Radical Ions and Photochemical Charge-Transfer Phenomena (Series A), Part 33, and Cycloadditions (Series B), part 37. This work was supported by the Deutschen Forschungsgemeinschaft, the Fonds der Chemischen Industrie, and the state of Nordrhein-Westfalen. We also thank Bayer AG, Philips Bildröhrenwerke AG, and Heraeus AG for generous gifts of chemicals and equipment. – Series A, Part 32: E. Bischof, J. Mattay, *J. Photochem. Photobiol. A.* **1992**, *63*, 249–251; Series B, Part 36: K. Langer, J. Mattay, A. Heidbreder, M. Möller, *Liebigs Ann. Chem.* **1992**, in press.

preparation of imidazolophanes using the classic approach, 1,3-dipolar cycloaddition, is not possible.[6] The PET-catalyzed cycloaddition is therefore the first method allowing access to imidazolophanes with short bridges.[7]

Short-bridged [n](2,5)pyrrolophanes have been known for a long time and are readily available, for example by the Paal–Knorr synthesis.[8] The PET-promoted method, on the other hand, enables the preparation of 3,4-substituted pyrrolophanes in acceptable yields. The reaction of 2-azaallenyl radical ions with acetylenes leads to pyrroles. The azirines **1a–c** react with dimethyl 2-butynedioate **5** to give pyrrolophanes **6a–b** (Scheme 2).

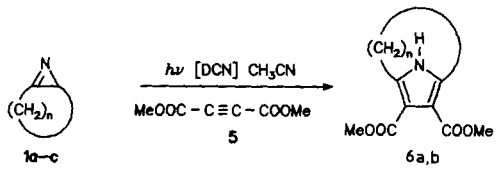

Scheme 2. n = 4: no reaction; **6a**, n = 5: 9% yield; **6b**, n = 6: 56% yield.

The trend in yields here resembles that of **4a–b**. Compounds with very short bridges could not be obtained. However, for the preparation of [6](2,5)pyrrolophanes this reaction is satisfactory. In order to obtain a [2,2](2,5)pyrrolophane in an analoguous fashion we prepared the tricyclic bisazirine **7**. Reaction under the standard PET-conditions leads not to the expected pyrrolophane but rather to the 3,4,7,8-tetrahydro-8b,8c-diazacyclopent[*f,g*]acenaphthylene **8** (15% yield).[9] A product arising from the annelation of only one azirine was not found in the reaction mixture. The mechanism of this reaction is not yet known.

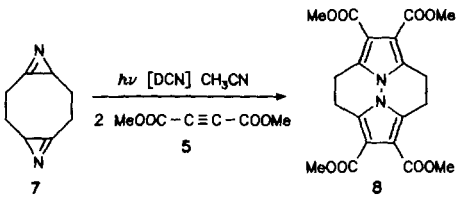

These examples show that new target molecules in heterocyclic chemistry may be obtained by PET-catalyzed [3 + 2]cycloadditions of azirines.

Experimental Procedure

The azirines **1a–c** and **7** were prepared according to ref.,[10], the imines according to ref.[11]. Azirines cooled at −18 °C are stable for 4–6 weeks. DCN was prepared as described in ref.[12]. Compound **7** was obtained as a mixture of two diastereomers, which were not separated before subsequent experiments. Dimethyl 2-butynedioate was obtained from Merck.

A solution of the azirine (0.3 mmol) and the imine or dimethyl 2-butynedioate (1.0 mmol) in acetonitrile (10 mL) was poured into a Duran tube. 1,4-Naphthalenedicarbonitrile (0.1 mmol, 18 mg) was added. The reaction solution was deoxygenated by argon bubbling, the tube was sealed, and the solution was irradiated with a Rayonet photochemical reactor (λ = 350 nm) for 16 hours. The solvent was evaporated and the residue separated by flash chromatography on alumina (Merck Neutral Act. 1) using diethyl ether as eluent. In the case of **7** 0.15 mmol azirine were employed.

4b: ^{1}H NMR (300, $CDCl_3$): δ = 0.9 (m, 6H; 2 CH_3), 1.5 (m, 12H; 6 CH_2), 1.9 (m, 6H; 3 CH_2), 2.9 (t, 2H, ^3J = 6.6 Hz; NCH_2); ^{13}C NMR (75.5 MHz, $CDCl_3$): δ = 11.78, 13.79 (CH_3), 21.63, 22.42, 23.92, 24.34, 25.38, 25.66 (CH_2), 31.17 (C2-CH_2), 33.51 (C3-CH_2), 35.07 (C5-CH_2), 126.45 (C2), 128.50 (C3), 145.16 (C5); MS (70 eV): *m/z* 234 (M^+, 18%), 219 (46), 205 (70), 191 (100), 164 (59); IR (film): $\tilde{\nu}$ [cm^{-1}] = 2920, 1650, 1510, 1450, 1280, UV (CH_3CN): λ_{max} [nm] (lg ε) = 284.2 (3.2), 221.0 (4.6), 196.5 (4.7); yellow oil.

6b: ^{1}H NMR (300 MHz, $CDCl_3$): δ = 1.3–1.5 (m, 8H; CH_2), 2.8 (m, 4H; CH_2-C2), 3.50 (s, 6H; OCH_3); ^{13}C NMR (75.5 MHz, $CDCl_3$): δ = 19.48, 24.38, 32.65 (CH_2), 52.05 (OCH_3), 111.52 (C3), 116.51 (C2), 167.25 (C=O); MS (70 eV): *m/z* 265 (M^+, 6%), 234 (39), 166 (24), 122 (8), 59 (100); IR (film): $\tilde{\nu}$ [cm^{-1}] = 3440, 3100, 3000, 1845, 1740, 1535; UV (CH_3CN): λ_{max} [nm] (lg ε) = 260 (3.3), 196 (4.8); brown oil.

8: ^{1}H NMR (300 MHz, $CDCl_3$): δ = 3.52 (s, 12H; OCH_3), 4.70 (s, 8H; CH_2); ^{13}C NMR (75.5 MHz, $CDCl_3$): δ = 35.89 (CH_2), 53.06 (OCH_3), 112.15 (C2), 118.42 (C1) 169.24 (C=O); MS (70 eV): *m/z* 416 (M^+, 0.1%), 264 (1.4), 208 (2), 206 (78), 109 (34), 67 (100); IR (film): $\tilde{\nu}$ [cm^{-1}] = 3050, 3020, 1810, 1745, 1480; UV (CH_3CN): λ_{max} [nm] (lg ε) = 281 (4.4), 209 (4.9); brown oil.

Received: October 8, 1991 [Z 4958 IE]
German version: *Angew. Chem.* **1992**, *104*, 207

[1] F. Vögtle, *Cyclophan-Chemie*, Teubner, Stuttgart, **1991**, pp. 30–32; S. M. Rosenfeld, K. A. Choe in *Cyclophanes, Vol. I* (Eds.: P. M. Keehn, S. M. Rosenfeld), Academic Press, New York/London, **1983**, pp. 311-357; W. W. Paudler, M. D. Bezoari in *Cyclophanes*, Vol. II (Eds.: P. M. Keehn, S. M. Rosenfeld), Academic Press, New York/London, **1983**, 359–440.

[2] F. Müller, J. Mattay, *Angew. Chem.* **1991**, *103*, 1352–1353; *Angew. Chem. Int. Ed. Engl.* **1991**, *30*, 1336–1337.

[3] J. Mattay, *Synthesis* **1989**, 233–252; H. Tomioka, D. Kobayashi, A. Hashimoto, S. Murata, *Tetrahedron Lett.* **1989**, *30*, 4685–4688; P. Clawson, P. M. Lunn, D. A. Whiting, *J. Chem. Soc. Perkin Trans. I*, **1990**, 153–157, *ibid.* **1990**, 159–162.

[4] Azirine- and 2-azaallenyl radical cations were calculated with ab-initio techniques (UMP 2/6-31G* basis set) by Prof. Dr. E. U. Würthwein, to whom we are very grateful. According to these calculations azirine radical cations are unstable and open spontaneously to linear 2-azaallenyl radical cations.

[5] K. Bunge, R. Huisgen, R. Raab, H. J. Sturm, *Chem. Ber.* **1972**, *105*, 1307–1323.

[6] Direct irradiation of the weak absorption band of the azirine leads primarily to tbe excitation of the reaction partner: A. Orahovats, H. Heimgartner, H. Schmid, W. Heinzelmann, *Helv. Chim. Acta* **1974**, *57*, 2626–2633.

[7] E. M. Beccalli, L. Majori, A. Marchesini, C. Torricelli, *Chem. Lett.* **1980**, 659–662.

[8] S. Fujita, T. Kawaguti, H. Nozaki, *Tetrahedron Lett.* **1971**, 1119-1120; J. F. Haley, Jr., S. M. Rosenfeld, P. M. Keehn, *J. Org. Chem.* **1977**, *42*, 1379–1386; W. Flitsch, H.-G. Kneip, *Liebigs Ann. Chem.* **1985**, 1895–1903.

[9] W. W. Paudler, E. A. Stephan, *J. Am. Chem. Soc.* **1970**, *92*, 4468–4470.

[10] G. Smolinsky, *J. Org. Chem.* **1962**, *27*, 3557–3559; F. W. Fowler, A. Hassner, L. A. Levy, *J. Am. Chem. Soc.* **1967**, *89*, 2077–2082; A. Hassner, F. W. Fowler, *ibid.* **1968**, *90*, 2869–2875.

[11] L. F. Tietze, T. Eicher: *Reaktionen und Synthesen*, Thieme, Stuttgart **1981**, pp. 69–70.

[12] A. Albini, D. R. Arnold, *Can. J. Chem.* **1978**, *56*, 2985–2993.

Calculation of Molecular Dynamics for Peptides in Dimethyl Sulfoxide: Elimination of Vacuum Effects**

By *Michael Kurz, Dale F. Mierke*, and *Horst Kessler**

Modern NMR techniques used to determine structurally relevant parameters[1] and subsequent molecular dynamics (MD) simulations[2] are the most important means of determining molecular conformation in solution. Until recently most MD simulations were performed without the inclusion of the solvent (in vacuo). For many peptides these types of simulations yield hydrogen bonds for which there is no experimental evidence. For example simulated cyclic hexapeptides often contain γ turns. Normally only two β turns would be expected in these peptides. The additional γ turns form along the length of the peptide and cause a strong kink in the

[*] Prof. Dr. H. Kessler, Dipl.-Chem. M. Kurz, Dr. D. F. Mierke
Organisch-chemisches Institut der Technischen Universität München
Lichtenbergstrasse 4, D-W-8046 Garching (FRG)

[**] This research was supported by the Deutsche Forschungsgemeinschaft and the Fonds der Chemischen Industrie.

molecule. But such a structure has never been observed in X-ray structural analysis.[3] In our calculations of the C_2-symmetric model compound *cyclo*-(D-Ala^1-Ala^2-Ala^3-D-Ala^4-Ala^5-Ala^6-) we show that additional γ turns are caused by vacuum effects, which can be eliminated by MD simulations including solvent.

All MD simulations were performed with the GROMOS program package.[4] The parameters for dimethyl sulfoxide (DMSO) were taken from an X-ray structure[5] and a microwave spectroscopic study.[6] Further details are described in ref. [7] The application of these parameters in the MD simulations results in hydrogen bonds between DMSO and the peptide, which are in agreement with the X-ray structural data of a cyclic peptide reported by Karle et al.[8]

Restrained MD simulation of the model compound *cyclo*-(-D-Ala^1-Ala^2-Ala^3-D-Ala^4-Ala^5-Ala^6-) was first carried out for a 100 ps trajectory. 30 distances obtained from a 500 MHz ROESY NMR spectrum (150 ms mixing time) were used. Only the last 60 ps were used for the analysis. A C_2-symmetric conformation with two βII' turns was obtained in which the D-amino acids occupy the position i + 1 (Fig. 1a). In addition two γ turns with hydrogen bonds between D-Ala^1-NH and Ala^5-O as well as D-Ala^4-NH and Ala^2-O respectively were also populated; these lead to the molecular kink mentioned above (Table 1).

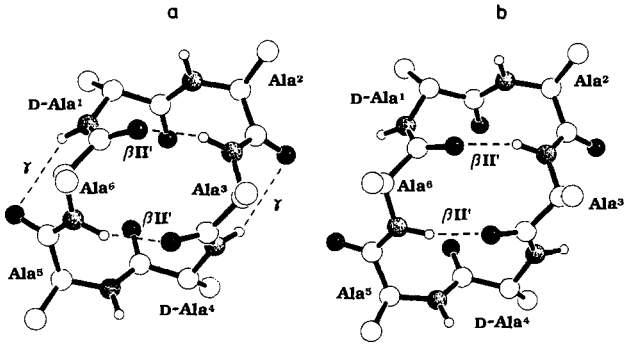

Fig. 1. Structure of *cyclo*-(-D-Ala^1-Ala^2-Ala^3-D-Ala^4-Ala^5-Ala^6-) after 100 ps MD simulation a) in vacuum, b) in DMSO.

Table 1. Intramolecular hydrogen-bonds obtained during the MD simulations in vacuum and in DMSO [a].

H bond between	and	Turn type	Distance [b] [pm]	Angle [°]	Population [%]
Vacuum					
Ala^3-NH	Ala^6-O	βII'	303	153	97
Ala^6-NH	Ala^3-O	βII'	303	153	97
D-Ala^1-NH	Ala^5-O	γ	335	135	58
D-Ala^4-NH	Ala^2-O	γ	335	135	54
DMSO					
Ala^3-NH	Ala^6-O	βII'	291	165	91
Ala^6-NH	Ala^3-O	βII'	297	160	90

[a] The criterion for a hydrogen bond is a donor–acceptor distance < 350 pm and an N-H-O angle > 120°; [b] N-O distance.

A restrained MD simulation including the solvent DMSO was performed using the "vacuum structure" as the starting conformation. The molecule was placed in a solvent box containing 116 DMSO molecules. This corresponds to a concentration of 100 mmol L^{-1}, which is comparable to the experimental conditions (roughly 50 mmol L^{-1}). A step size of 2 fs using the SHAKE algorithm was applied. First we calculated 10 ps at 300 K with a force constant of 2500 kJ mol^{-1} nm^{-2} for the restraints and a strong coupling to the heat bath (the temperature relaxation time was 0.01 ps). Then an additional 40 ps were simulated with the same force constant but weaker coupling to the heat bath (temperature relaxation time 0.1 ps). Finally the force constant was reduced to 1000 kJ mol^{-1} nm^{-2} and another 50 ps were used for the analysis.

During this simulation in DMSO the two γ turns disappeared (see Table 1) and the molecule flattened (Fig. 1b and Fig. 2). The intermolecular hydrogen bonds which appeared between the peptide and solvent during the MD simulation are listed in Table 2.

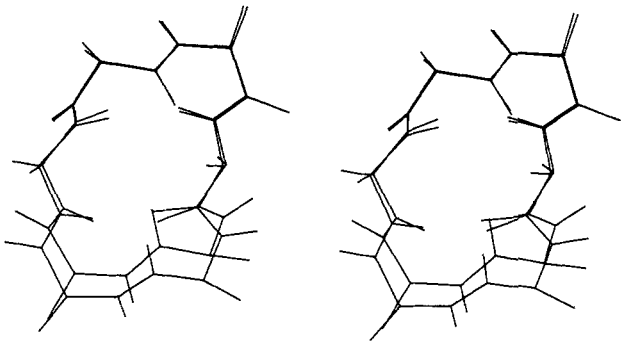

Fig. 2. Superimposed stereoplots of the structures of the cyclohexapeptide in vacuum and in DMSO. The two structures are superimposed so that amino acids 1 and 2 are overlayed.

Table 2. Intermolecular hydrogen bonds between peptide and DMSO(solv) during the MD simulation in DMSO [a].

H bond between	and	Distance [pm]	Angle [°]	Population [%]
D-Ala^1-NH	solv^{55}-O	288	152	72
D-Ala^4-NH	solv^3-O	282	169	86
Ala^2-NH	solv^{26}-O	281	168	85
Ala^5-NH	solv^{45}-O	284	169	86

[a] The criterion for a hydrogen bond is a donor–acceptor distance < 350 pm and an N-H-O angle > 120°.

Free MD simulation (without restraints) was continued for another 50 ps in solvent to prove the stability of the obtained structure. Essentially no structural change was observed. Finally an additional restrained MD simulation of the molecule in vacuo was performed resulting in a reappearance of the γ turns.

The distances in both structures, in vacuo as well as in DMSO, are in good agreement with the distances obtained from the ROESY spectrum. However, the temperature coefficients for the amide protons indicate only two intramolecular hydrogen bonds (Ala^3-NH/Ala^6-NH: $\Delta\delta/\Delta T = -1.3 \times 10^{-9}$ K^{-1}, D-Ala^1-NH/D-Ala^4-NH: $\Delta\delta/\Delta T = -8.7 \times 10^{-9}$ K^{-1}, Ala^2-NH/Ala^5-NH: $\Delta\delta/\Delta T = -8.0 \times 10^{-9}$ K^{-1}). These results indicate that the amide protons which are involved in the γ turns in the "vacuum structure" are exposed to the solvent. This latter fact is much better represented by that calculation including the solvent.

We observed the same effect for numerous other cyclic hexapeptides. The differences between the structures in vacuo and in DMSO increase with decreasing size of the amino acid side-chains in position i. Obviously larger substituents are better able to shield the charges of the polar groups.

Our experience shows the following general approach to be most advantageous in the determination of the preferred conformation in solution:

1. As a first approximation restrained MD-simulation in vacuo is performed. To search a larger conformational space it is recommended to use different starting structures and to calculate also at higher temperatures using different force constants for the restraints. In our experience MD simulation in vacuo without any restrictions yield structures which disagree with the experimental data. For peptides it is advisable to reduce the vacuum effects by reducing the charge on amide protons exposed to the solvent (information obtained from the temperature gradients of the NMR chemical shift of the amide protons) and by fixing the side chains in the dominant rotamer population (information obtained from homo- and heteronuclear coupling constants).[9]

2. The structure thus obtained is used for restrained MD simulation including the solvent. The solvent should not be represented merely by a hypothetical dielectric constant but should rather be included explicitly in the molecular dynamics.

3. An MD simulation in solution without restraints may then follow. This calculation proves if the structure is stable or moves to a structure quite different from the conformation obtained using experimental data.

In all of these calculations one must bear in mind that a static picture as shown in Figure 1 is only a crude approximation of reality, because it is obtained from an average of a constantly changing conformation (trajectory). In the case discussed here the observed vacuum effects are significant for the entire trajectory. MD simulations for small and polar molecules should therefore always be performed including solvent.

Received: September 5, 1991 [Z 4899 IE]
German version: *Angew. Chem.* **1992**, *104*, 213

[1] H. Kessler, M. Gehrke, C. Griesinger, *Angew. Chem.* **1988**, *100*, 507–554; *Angew. Chem. Int. Ed. Engl.* **1988**, *27*, 490–536.
[2] W. F. van Gunsteren, H. J. C. Berendensen, *Angew. Chem.* **1990**, *102*, 1020–1055; *Angew. Chem. Int. Ed. Engl.* **1990**, *29*, 992–1023.
[3] G. D. Rose, L. G. Gierasch, J. A. Smith, *Adv. Protein Chem.* **1985**, *37*, 1–109, and references therein.
[4] W. F. van Gunsteren, H. J. C. Berendsen, *Groningen Molecular Simulation (GROMOS) Library Manual*, Biomos B.V., Nijenborgh 16, NL 9747 AG Groningen, pp. 1–229.
[5] S. Itoh, H. Ohtaki, *Z. Naturforsch. A* **1987**, *42*, 858–862.
[6] W. Feder, H. Creizler, H. D. Rudolf, V. Typke, *Z. Naturforsch. A* **1969**, *24*, 266–272.
[7] D. F. Mierke, H. Kessler, *J. Am. Chem. Soc.* **1991**, *113*, 9466–9470; calculations for molecules in DMSO have already been published: B. G. Rao. U. C. Singh, *ibid.* **1990**, *112*, 3803–3811.
[8] I. L. Karle, J. L. Flippen-Anderson, R. Kishore, P. Balaram, *Int. J. Pept. Protein Res.* **1989**, *34*, 37–41.
[9] H. Kessler, J. W. Bats, C. Griesinger, S. Koll, M. Will, K. Wagner, *J. Am. Chem. Soc.* **1988**, *110*, 1033–1049.

$BaNb_7O_9$, a New Oxoniobate with Double Layers of Corner-Sharing Nb_6 Octahedra**

By *Gunnar Svensson,** *Jürgen Köhler,** and *Arndt Simon*

We recently reported on the compound $K_4Al_2Nb_{11}O_{21}$[1] whose structure consists of two condensed Nb_6O_{12} clusters connected by a common apex atom of the two Nb_6 octahedra. This structure represents the first step to building chains, sheets, and, ultimately, the three-dimensional NbO structure in which the octahedra share all apices with their neighbors. In the meantime, the cluster condensation concept[2] has been illustrated by many examples, especially within certain reduced oxide systems, such as structures with edge-sharing Mo_6 octahedra[3–5] and with corner-sharing Nb_6 octahedra.[6–8] We report here the new compound $BaNb_7O_9$, which holds a special intermediate position in the path to higher dimensionality in reduced oxoniobates, since in it the first structural step towards the transition from two- to three-dimensional systems is attained.

Electron microscope investigations on the Ba-Nb-O system[9] have shown that a "phasoid"[10, 11] exists containing a large variety of different structural assemblies with corner-sharing condensed Nb_6 octahedra, for example chains made up of four units and double layers. It was therefore of interest to attempt to develop such structural variants in compounds of stoichiometric composition. After extensive efforts the formation of $BaNb_7O_9$ was achieved at temperatures above 1800 K by additional use of $BaCl_2$ flux.[12] The size of the crystals formed under these conditions were just large enough (diameter < 0.01 mm) for a single-crystal structure determination.[13]

The structure of $BaNb_7O_9$ is made up of double layers of corner-sharing Nb_6 octahedra of composition Nb_7O_8 sandwiched between BaO layers (Fig. 1). The structure can be

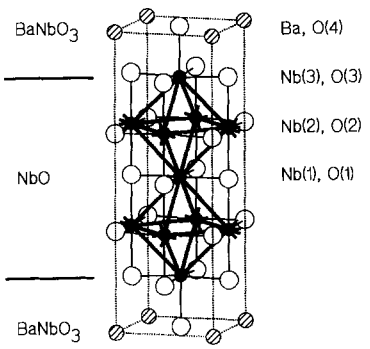

Fig. 1. Projection of the crystal structure of $BaNb_7O_9$ with its double layer of corner-sharing Nb_6 octahedra (the further connection of the Nb atoms is indicated).

envisioned as "intergrowths" of BaO and NbO or perovskite $BaNbO_3$ and NbO. The former description is simpler but does not account for the interconnection of the BaO layers with the NbO layers. In the latter description one can easily understand the interrelations between $BaNb_7O_9$, $BaNb_4O_6$, and $Ba_2Nb_5O_9$ which along with NbO and $BaNbO_3$ all belong to the homologous series $Ba_nNb_{n+3m}O_{3n+3m}$ (n = number of perovskite layers, m = number of NbO layers with complete octahedra).

The Ba atoms in $BaNb_7O_9$ are surrounded by a cuboctahedron of 12 O atoms, as in the known $Ba_{0.95}NbO_3$,[14] and the average Ba–O distance of 292 pm is only slightly longer than the respective Ba–O distance of 289 pm in $Ba_{0.95}NbO_3$. The distance from the central Nb(1) atom to the eight neighboring Nb(2) atoms is 298 pm and thus longer than both the Nb(2)–Nb(2) and Nb(2)–Nb(3) distances (297 pm and 290 pm respectively). These are all comparable to the Nb–Nb distances found in NbO (297 pm). The Nb–O distances are between 209 and 212 pm as in the other members of the homologous series.

[*] Dr. G. Svensson[+], Dr. J. Köhler, Prof. Dr. A. Simon
Max-Planck-Institut für Festkörperforschung
Heisenbergstrasse 1, D-W-7000 Stuttgart 80 (FRG)
[+] Permanent address: Department of Inorganic Chemistry
Stockholm University
S-10691 Stockholm (Sweden)

[**] We thank the Alexander-von-Humboldt Foundation for support (fellowship for G. S.)

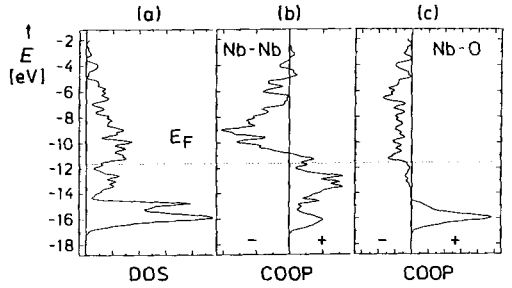

Fig. 2. a) Density of states (DOS), b) COOP diagram for Nb-Nb interactions, and c) COOP diagram for Nb-O interactions in $BaNb_7O_9$.

According to the charge balance for the ionic borderline case, 19 electrons occupy Nb–Nb bonding states (per Nb_7O_8 double-layer unit). Band-structure calculations (Extended-Hückel approximation,[15] parameters for Nb,[16] Sr parameters[17] were used for Ba) lead to the results illustrated in Figure 2. The density of states (DOS) at the Fermi level E_F shows the compound to be metallic (Fig. 2a). As the COOP (crystal orbital-overlap population) curves show, the bands with Nb–Nb bonding character are nearly full (Fig. 2b); this is at the cost of partial occupation of bands with Nb–O antibonding character (Fig. 2c). The Nb–O bonding states lie at −16 eV. The small band at −14.8 eV is of purely (nonbonding) O 2p-character and typical for perovskites[18] as well as evident in the band structure of NbO.[19] The occupation of all Nb–Nb bonding states and partial occupation of Nb–O antibonding states in $BaNb_7O_9$ reflects the situation found in isolated Nb_6O_{12} clusters possessing the maximum of 16 valence electrons in Nb–Nb bonding states.[20] Usually one finds that the magic number of 14 valence electrons[21–23] will completely fill just the purely bonding states. Likewise, in NbO,[19] $BaNb_4O_6$, and $K_4Al_2Nb_{11}O_{21}$[1, 24] not all of the Nb–Nb bonding states are occupied, and strongly Nb–O antibonding states are found directly above the Fermi level. Further reduction of the Nb_7O_8 layer in $BaNb_7O_9$, for example through substitution of Ba by La, should not be possible, because this would necessitate not only the occupation of Nb–Nb bonding but also strongly Nb–O antibonding states.

An entire series of structures with isolated Nb_6O_{12} clusters is now known.[21–23, 25–27] The first step in the condensation of Nb_6 octahedra through shared corners in $K_4Al_2Nb_{11}O_{21}$[1] has been mentioned already. Hypothetical oligomers of the general composition $Nb_{5n+1}O_{8n+4}$ for $n > 2$ (n = number of octahedra) are still unknown; however, the infinite chain of corner-sharing Nb_6 octahedra in $BaNb_5O_8$ was recently found.[7] Quadruple chains of octahedral units are obviously present in $Ba_4Nb_{17}O_{26}$[28] although a refinement of this crystal structure must still be performed. The Nb_6 clusters are connected by four shared corners into single layers in $BaNb_4O_6$, $Ba_2Nb_5O_9$,[6] and $Sr_2Nb_5O_9$[29]. In the structure of $BaNb_7O_9$ presented here, the Nb_6 clusters are connected by five shared corners into a cluster double-layer. Certainly further intermediate stages between the two extremes of isolated Nb_6O_{12} clusters on the one side, and the NbO structure with completely corner-sharing Nb_6 octahedra on the other, are forseeable.

Received: September 9, 1991 [Z 4908 IE]
German version: *Angew. Chem.* **1992**, *104*, 192

CAS Registry numbers:
$BaNb_7O_9$ 12291-80-4; NbO_2, 12034-59-2; $Ba_5Nb_4O_{15}$, 12291-80-4; Nb, 7440-03-1.

[1] A. Simon, J. Köhler, R. Tischtau, G. Miller, *Angew. Chem.* **1989**, *101*, 1695; *Angew. Chem. Int. Ed. Engl.* **1989**, *28*, 1662.
[2] A. Simon, *Angew. Chem.* **1981**, *93*, 23; *Angew. Chem. Int. Ed. Engl.* **1981**, *20*, 1; *ibid.* **1988**, *100*, 163 and **1988**, *27*, 159.
[3] C. C. Torardi, R. E. McCarley, *J. Am. Chem. Soc.* **1979**, *101*, 3963.
[4] J. D. Corbett, R. E. McCarley in *Crystal Chemistry and Properties of Materials with Quasi-One-Dimensional Structures* (Ed.: J. Rouxel), Reidel, Dordrecht, Netherlands, **1986**, p. 179.
[5] R. Dronskowski, A. Simon, *Angew. Chem.* **1989**, *101*, 775; *Angew. Chem. Int. Ed. Engl.* **1989**, *28*, 758.
[6] G. Svensson, J. Köhler, A. Simon, *J. Less-Common Met.* **1991**, *176*, 129.
[7] S. A. Davydov, B. N. Goschchitskii, E. A. Karkin, A. V. Mirmelstein, V. I. Voronin, V. D. Parkhomenko, V. G. Zubkov, V. A. Perelyayev, I. F Berger, I. A. Kontzevaya, *Int. J. Mod. Phys. B* **1990**, *4*, 1531.
[8] V. G. Zubkov, V. A. Perelyayev, I. F. Berger, I. A. Kontzevaya, O. B. Makarova, S. A. Turshevskii, V. A. Gubanov, V. I. Voronin, A. V. Mirmelstein, A. E. Karkin, Sverkhprovodimost': *Fiz. Khim. Tekhnol.* **1990**, *3(9)*, 2121.
[9] G. Svensson, *Microsc. Microanal. Microstruct.* **1990**, *1*, 343.
[10] A. Magneli, *Chem. Scr.* **1986**, *16*, 535.
[11] A. Magneli, *Microsc. Microanal. Microstruct.* **1990**, *1*, 299.
[12] Dried NbO_2, $Ba_5Nb_4O_{15}$, and Nb in a ratio of 3.75:1:4 together with 10 wt% $BaCl_2$ were pressed into a pellet and heated under Ar in a sealed Nb ampule at 1640 °C for 1 d. The product contained small black cuboid crystals (up to 0.01 mm) of $BaNb_7O_9$ besides larger crystals of $BaNb_4O_6$. The refinement of the lattice constants (tetragonal metrics) from a Guinier diagram resulted in $a = 419.5(1)$ and $c = 1242.6(2)$ pm.
[13] Space group $P4/mmm$ (No. 138), $Z = 1$, (CAD4 diffractometer); $Mo_{K\alpha}$; 240 Reflections, 207 with $F_0 \geq 4.0\sigma(F_0)$ $R = 0.095$, $R_w = 0.066$ $\rho_{calc} = 7.07\ g\,cm^{-3}$. Positional parameters: Ba 1a, Nb(1) 1d, Nb(2) 4i with $z = 0.3291(2)$, Nb(3) 2h with $z = 0.1681(2)$, O(1) 2e, O(2) 2g with $z = 0.335(2)$, O(3) 4i with $z = 0.160(1)$, O(4) 1c. Due to the extreme smallness of the crystal the intensity of the weak reflections could not be measured very accurately, which might explain the relatively high R value. Further details of the crystal structure investigation may be obtained from the Fachinformationszentrum Karlsruhe, Gesellschaft für wissenschaftlich-technische Information, D-W-7514 Eggenstein-Leopoldshafen (FRG), on quoting the depository number CSD-55880, the names of the authors, and the journal citation.
[14] B. Hessen, S. A. Sunshine, T. Siegrist, R. Jimenez, *Mater. Res. Bull.* **1991**, *26*, 85.
[15] Extended-Hückel approximation: R. Hoffmann, *J. Chem. Phys.* **1963**, *39*, 1397. H_{ij} matrixelements: J. H. Ammeter, H.-B. Bürgi, J. C. Thibeault, R. Hoffmann, *J. Am. Chem. Soc.* **1978**, *100*, 3686; tight-binding modification: M.-H. Whangbo, R. Hoffmann, *ibid.* **1978**, *100*, 6093; special k points: R. Ramirez, M. C. Böhm, *Int. J. Quantum Chem.* **1986**, *30*, 391.
[16] R. H. Summerville, R. Hofmann, *J. Am. Chem. Soc.* **1976**, *98*, 7240.
[17] J. Hinze, H. H. Jaffe, *J. Phys. Chem.* **1963**, *67*, 1501.
[18] R. A. Wheeler, J. K. Burdett, M. H. Whangbo, T. Hughbanks, R. Hoffmann, T. A. Allbright, *J. Am. Chem. Soc.* **1986**, *108*, 2222.
[19] J. K. Burdett, T. Hughbanks, *J. Am. Chem. Soc.* **1984**, *106*, 3101.
[20] F. A. Cotton, T. E. Haas, *Inorg. Chem.* **1964**, *3*, 10.
[21] B. O. Marinder, *Chem. Scr.* **1977**, *11*, 97.
[22] J. Köhler, A. Simon, *Z. Anorg. Allg. Chem.* **1987**, *553*, 106.
[23] J. Köhler, A. Simon, S. J. Hibble, A. K. Cheetham, *J. Less-Common Met.* **1988**, *142*, 123.
[24] J. Köhler, G. Svensson, A. Simon, unpublished results.
[25] D. M. Evans, L. Katz, *J. Solid State Chem.* **1973**, *6*, 459.
[26] J. Köhler, G. Miller, A. Simon, *Z. Anorg. Allg. Chem.* **1989**, *568*, 8.
[27] K. B. Kersting, W. Jeitschko, *J. Solid State Chem.* **1991**, *93*, 350.
[28] V. G. Zubkov, V. A. Perelyayev, G. P. Shveikin, unpublished results.
[29] G. Svensson, J. Köhler, A. Simon, *Acta Chem. Scand.*, in press.

$Zn_7[P_{12}N_{24}]Cl_2$—A Sodalite with a Phosphorus–Nitrogen Framework**

By *Wolfgang Schnick** and *Jan Lücke*

Dedicated to Professor Karl-Heinz Büchel on the occasion of his 60th birthday

Zeolites have increasingly found application as catalysts, molecular sieves, adsorbents, or ion exchangers in recent

[*] Dr. W. Schnick, Dipl.-Chem. J. Lücke
Institut für Anorganische Chemie der Universität
Gerhard-Domagk-Strasse 1, D-W-5300 Bonn 1 (FRG)

[**] This work was supported by the Minister für Wissenschaft und Forschung des Landes Nordrhein-Westfalen, the Deutsche Forschungsgemeinschaft, and the Fonds der Chemischen Industrie.

years. The useful properties of these aluminosilicates are based particularly on the characteristic topology of the tetrahedral skeletal structures, which have the general composition TO_2 (T = Al, Si).[1] Instead of aluminum and silicon, many other elements such as B, P, Fe, Cr, Sb, As, Ga, Ge, Ti, Zr, and Hf can be incorporated as central atoms of the tetrahedrons in the zeolite lattice.[1, 2] These modifications succeed in tailoring the catalytic properties of zeolites for certain reactions.[2] However, hardly any proven facts on the exchange of elements of the anionic part of the lattice are known. Yet the replacement of oxygen by other electronegative elements such as nitrogen should be a promising method of modifying the properties and potential applications of this class of substances.

Recently we prepared pure, crystalline HPN_2 through the ammonolysis of P_3N_5 in thick-walled quartz ampules under pressure [Eq. (a)]. The required NH_3 was formed in situ in another compartment of the apparatus by treatment of Mg_3N_2 with NH_4Cl [Eq. (b)].[3]

$$P_3N_5 + NH_3 \xrightarrow[6d,\ 30\ bar]{580\,^\circ C} 3\,HPN_2 \qquad (a)$$

$$Mg_3N_2 + 6\,NH_4Cl \xrightarrow{400\,^\circ C} 3\,MgCl_2 + 8\,NH_3 \qquad (b)$$

The structural investigation [3] shows a $[PN_2^-]$ skeleton isosteric with β-cristobalite, as has been found in $LiPN_2$.[4] Since these phosphorus(v) nitrides have structural similarities with silicates, the possibility of constructing zeolite-like P–N structures occurred to us. In fact, we succeeded in replacing Mg_3N_2 by Zn_3N_2 in the HPN_2 preparation and we obtained a new compound with composition $Zn_5H_4[P_{12}N_{24}]Cl_2$ in quantitative yield[5]. Analogously to HPN_2, a phosphorus(v) nitride had formed with molar ratio P:N = 1:2, while zinc from $ZnCl_2$, which is volatile under the given conditions, was incorporated into the solid while it forms. A complete exchange of the hydrogen atoms in the product was achieved afterwards through treatment with $ZnCl_2$ accompanied by evolution of HCl [Eq. (c)].

$$Zn_5H_4[P_{12}N_{24}]Cl_2 + 2\,ZnCl_2 \xrightarrow{700\,^\circ C,\ 3d} Zn_7[P_{12}N_{24}]Cl_2 + 4\,HCl \qquad (c)$$

Surprisingly however, the title compound $Zn_7[P_{12}N_{24}]Cl_2$ can also be prepared by reaction of the inexpensive starting materials NH_4Cl, $ZnCl_2$, and $(PNCl_2)_3$ [Eq. (d)].

$$7\,ZnCl_2 + 12\,NH_4Cl + 4(PNCl_2)_3 \xrightarrow{700\,^\circ C,\ 3d} Zn_7[P_{12}N_{24}]Cl_2 + 48\,HCl \qquad (d)$$

In all preparations $Zn_7[P_{12}N_{24}]Cl_2$ forms as a fine crystalline and colorless powder insoluble in water and acid. Only in a special autoclave system[6] does $Zn_7[P_{12}N_{24}]Cl_2$ decompose in dilute sulfuric acid (190 °C, 10 bar, 2 d; the phosphorus(v) nitride hydrolyses to ammonium hydrogen phosphate).

The powder diagram of the title compound indicates a cubic structure; the similarity to the powder diagram of sodalite $Na_8[Al_6Si_6O_{24}]Cl_2$ is evident.[7] The Rietveld refinement of the crystal structure of $Zn_7[P_{12}N_{24}]Cl_2$ on the basis of the powder diffraction data[8] confirmed the suspected analogy.[9] It shows that phosphorus and nitrogen form a sodalite-like framework of corner-sharing PN_4 tetrahedrons (Fig. 1). The P–N distance of 163.6(7) pm is comparable with that in $LiPN_2$ (164.5(7) pm).[4] Also the experimentally determined P-N-P bond angle (125.8(4)°) agrees with the corresponding angle in $LiPN_2$ (123.6(8)°).[4] This result is in

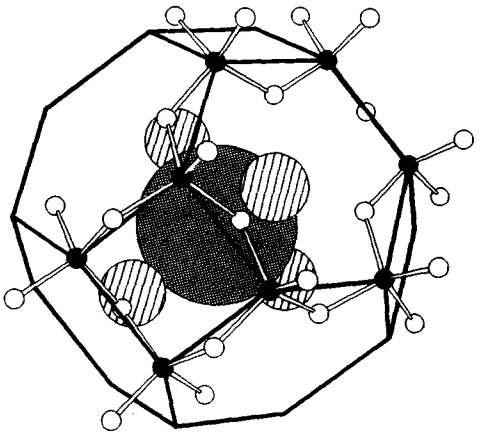

Fig. 1. Section of the crystal structure of $Zn_7[P_{12}N_{24}]Cl_2$. The $[P_{12}N_{24}]$ framework of the sodalite type is constructed from $[P_4N_4]$ and $[P_6N_6]$ rings (P–N 163.6(7) pm). In the center of each β cage is a Cl^- ion, surrounded by tetrahedrally arranged Zn^{2+} ions (Zn–Cl 259.6(2) pm). The Zn^{2+} ions are coordinated in a distorted tetrahedral manner by one Cl^- ion and three N atoms (Zn–N 196.0(8) pm). Size of Zn and Cl correspond to the respective ionic radii. P: black, N: white, Cl: gray, Zn: striped.

accord with the topological similarity between the P–N part of the structure in $LiPN_2$ (analogous to β-cristobalite) and the P–N structure found here: in both cases the network skeletons include PN_4 tetrahedrons linked through all four apexes by corner-sharing. However, whereas three-dimensionally bonded $[P_6N_6]$ rings occur exclusively in the β-cristobalite variant ($LiPN_2$), in the sodalite framework $[P_4N_4]$ rings are also found. The two types of rings together form capped octahedrons (β cages), which are typical building units of the sodalite type structure (Fig. 1). Situated at the center of each β cage is a Cl^- ion, in a tetrahedral environment of Zn^{2+} ions. Every metal cation has, besides the Zn–Cl contact (259.6(2) pm), three contacts to nitrogen atoms of the P–N framework (Z–N 196.0(8) pm) forming a distorted tetrahedron. In each case the contact distances correspond to the sum of the ionic radii.[10] Comparison of the composition of $Zn_7[P_{12}N_{24}]Cl_2$[5] with that of $Na_8[Si_6Al_6O_{24}]Cl_2$ reveals a statistical occupation of the Zn positions (occupancy factor 7/8). However, a part of the Zn^{2+} ions may be replaced by two protons each. The P–N sodalite described here has a phase width of $Zn_{(7-x)}H_{2x}[P_{12}N_{24}]Cl_2$ ($0 \le x \le 2$). A continuous increase in the lattice constant is observed with increasing zinc content. Other metals such as Co, Ni, and Yb were also built into the P–N sodalite in place of zinc, as described by Equation (d).

Received: July 11, 1991 [Z4789 IE]
Publication delayed at the authors' request
German version: *Angew. Chem.* **1992**, *104*, 208

CAS Registry numbers:
P_3N_5, 12136-91-3; NH_4Cl, 12125-02-9; Zn_3N_2, 128579-03-3; $Zn_5H_4[P_{12}N_{24}]Cl_2$, 136952-78-8; $ZnCl_2$, 7646-85-7; $Zn_7[P_{12}N_{24}]Cl_2$, 136952-79-9; $(PNCl_2)_3$, 940-71-6.

[1] J. V. Smith, *Chem. Rev.* **1988**, *8*, 149.
[2] W. Hölderich, M. Hesse, F. Näumann, *Angew. Chem.* **1988**, *100*, 232; *Angew. Chem. Int. Ed. Engl.* **1988**, *27*, 226.

[3] W. Schnick, J. Lücke, *Z. Anorg. Allg. Chem.*, in press.
[4] W. Schnick, J. Lücke, *Z. Anorg. Allg. Chem.* **1990**, *588*, 19.
[5] For the elemental analyses the products were hydrolyzed. Zinc was then determined complexometrically with EDTA, phosphorus photometrically as molybdovanadatophosphate, nitrogen photometrically as indophenol, and chloride argentometrically. In a parallel study the composition in the solid was checked by energy and wavelength dispersive X-ray microanalysis (EDX: Zn, P, Cl; WDX: absence of O). The presence of hydrogen (as N–H groups) was ascertained by IR spectroscopy.
[6] Cf. O. Buresch, H. G. von Schnering, *Fresenius Z. Anal. Chem.* **1984**, *319*, 418.
[7] I. Hassan, H. D. Grundy, *Acta Crystallogr. Sect. B* **1984**, *40*, 6.
[8] $Zn_7[P_{12}N_{24}]Cl_2$: $I\bar{4}3m$, $a = 824.21(1)$ pm, $Z = 1$, Stoe-Stadi-P transmission powder diffractometer, $Cu_{K\alpha 1}$ radiation, germanium monochromator, linear position-sensitive counter (Stoe Mini-PSD), Lindemann capillary, 5451 data points, measurement range $10° \leq 2\theta \leq 119°$, duration of measurement 12 h, 57 observed reflections, 3 refined site parameters, 4 temperature parameters. Rietveld refinement: $R_{wp} = 0.0848$, $R_I = 0.076$, GOF = 4.0. Further details of the crystal structure investigation may be obtained from the Fachinformationszentrum Karlsruhe, Gesellschaft für wissenschaftlich-technische Information mbH, D-W-7514 Eggenstein-Leopoldshafen 2 (FRG) on quoting the depository number CSD-55611, the names of the authors, and the journal citation.
[9] The P atoms in $Zn_7[P_{12}N_{24}]Cl_2$ occupy positions identical to those of Al and Si in $Na_8[Al_6Si_6O_{24}]Cl_2$. The structure of the P–N sodalite described in the space group $I\bar{4}3m$, a Klassengleich supergroup ($k2$) of $P\bar{4}3n$, which is the space group of Na sodalite. $Zn_7[P_{12}N_{24}]Cl_2$ thus crystallizes in a defect variant of the $Ca_8[Al_6Si_6O_{24}]O_2$ type; cf. V. I. Ponomarev, D. M. Kheiker, N. V. Belov, *Kristallografiya* **1970**, *15*, 918.
[10] a) W. H. Baur, *Crystallogr. Rev.* **1987**, *1*, 59; b) A. F. Wells: *Structural Inorganic Chemistry*, 5. ed., Clarendon, Oxford 1987, p. 313.

Radical Intermediates in the Coenzyme B_{12} Dependent Methylmalonyl-CoA Mutase Reaction Shown by ESR Spectroscopy**

By *Ymin Zhao, Peter Such,* and *János Rétey**

Methylmalonyl-CoA mutase catalyzes the reversible rearrangement of (2*R*)-methylmalonyl-CoA to succinyl-CoA by migration of the COSCoA group [Eq. (a)].[1] Both the proposed reaction mechanisms and the role of coenzyme B_{12} are still controversial. Some experiments with model compounds suggest a radical mechanism,[2] and others a nonradical mechanism.[3] The crucial initial step, the abstraction of a hydrogen atom from the nonactivated methyl group, could not yet be detected in any model reaction. From the chemical point of view a radical mechanism for this step is the more plausible.

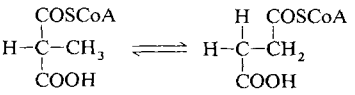

(a)

In some coenzyme B_{12} dependent enzyme reactions, a radical intermediate has been detected by ESR spectroscopy,[4–9] but the enzymes involved, ethanolamine ammonia lyase, diol dehydratase, and nucleoside triphosphate reductase, unlike methylmalonyl-CoA mutase and several other coenzyme B_{12} dependent mutases, do not catalyze rearrangements of the carbon skeleton. The only report[10] on an ESR study of the methylmalonyl-CoA mutase contains negative results. Since extremely pure methylmalonyl-CoA mutase is available in appropriate quantities, we again attempted to detect radicals in the enzymatic system.

Methylmalonyl-CoA mutase (5.3 mg, 35 nmol, 120 U) and coenzyme B_{12} (adenosylcobalamin, 0.1 mg, 63 nmol) in 15 mL of potassium phosphate buffer (0.1 M, pH 6.8) was incubated in a quartz ESR tube ($d = 2$ mm) for 5 min at 25 °C under argon. After addition of (*R,S*)-methylmalonyl-CoA (1.5 mg, 1.7 μmol) the samples were incubated for a further minute and then placed in liquid nitrogen. To avoid any possible photolysis, the samples were protected from light.[11]

Figure 1 A shows the ESR spectrum of methylmalonyl-CoA mutase coenzyme B_{12} holoenzyme. There is no clear signal visible above the noise level. Only in the presence of substrate does a distinct ESR signal appear at 320 mT (Fig. 1 B). The width and complexity of the signal makes the exact *g*-factor difficult to determine. Peaks are present between $g = 2.16$ and 1.86, the point of inflection is at $g = 2.06$. The assignment of the signals to definite paramagnetic species is not yet possible. Reported values for the *g*-factor of vitamin $B_{12r}(Co^{II})$ are 2.00 and 2.30[12] while that of a free alkyl radical is 2.002. We assume that in the enzyme-bound state a hitherto unknown interaction between such paramagnetic species exists. Besides the dependence of the ESR spectrum on the substrate, two further factors speak against the effect being an artifact. With synthetic substrate analogues we obtained similar ESR signals, though different in detail.[13] Comparable spectra, broad and difficult to interpret, were observed for a ternary complex of ribonucleotide reductase, coenzyme B_{12}, and guanosine-5′-triphosphate (GTP).[9]

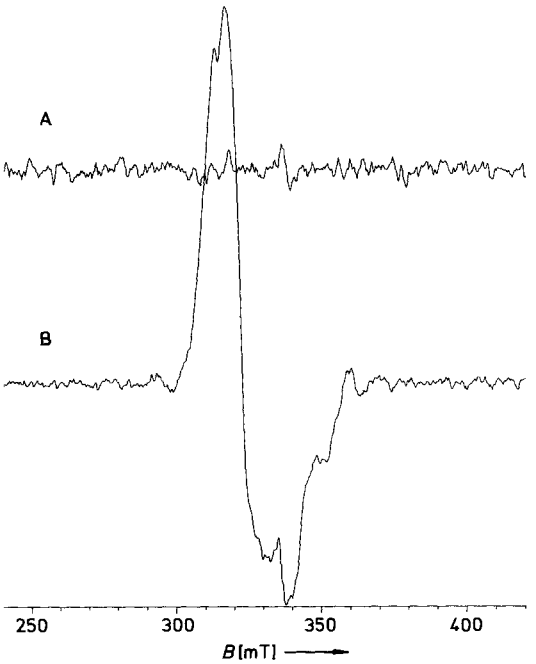

Fig. 1. A: ESR spectrum of the methylmalonyl-CoA mutase coenzyme B_{12} holoenzyme. B: ESR spectrum of the methylmalonyl-CoA mutase coenzyme B_{12} holoenzyme after addition of substrate (methylmalonyl-CoA)

Our experiments confirm that the homolysis of the cobalt–carbon bond of the coenzyme takes place only after addition

[*] Prof. Dr. J. Rétey, Dipl.-Chem. Y. Zhao
Lehrstuhl für Biochemie im Institut
für Organische Chemie der Universität
Richard-Willstätter-Allee, D-W-7500 Karlsruhe 1 (FRG)
Dr. P. Such
Bruker Analytische Messtechnik GmbH
Am Silberstreifen, D-W-7512 Rheinstetten 4 (FRG)

[**] This work was supported by the Deutsche Forschungsgemeinschaft and the Fonds der Chemischen Industrie (Y.Z. and J.R.)

of the substrate. The homolysis must therefore be induced by a change in conformation of the enzyme protein. Probably an equilibrium between substrate and product (succinyl-CoA), or the enzyme-bound intermediate, is immediately established at the active site. The position of this "internal" equilibrium is unknown and can differ considerably from the equilibrium of the free substrates. To our knowledge this communication reports the first direct proof of radicals in a coenzyme B_{12} dependent rearrangement of the carbon skeleton.

Received: August 23, 1991 [Z4885 IE]
German version: *Angew. Chem.* **1992**, *104*, 212

CAS Registry numbers:
Methylmalonyl-CoA mutase, 9023-90-9; coenzyme B_{12}, 13870-90-1.

[1] Review: J. Rétey in *Vitamin B_{12}*, *Vol. 2* (Ed.: D. Dolphin), Wiley, New York **1982**, p. 357–379.
[2] S. Wollowitz, J. Halpern, *J. Am. Chem. Soc.* **1984**, *106*, 8319–8321; *ibid.* **1988**, *110*, 3112–3120.
[3] G. Choi, S.-C. Choi, A. Galan, B. Wilk, P. Dowd, *Proc. Natl. Acad. Sci. USA* **1990**, *87* 3174–3176.
[4] B. M. Babior, T. H. Moss, D. C. Gould, *J. Biol. Chem.* **1972**, *247*, 4389–4392.
[5] B. M. Barior, T. H. Moss, W. H. Orme-Johnson, H. Beinert, *J. Biol. Chem.* **1974**, *249*, 4537–4544.
[6] S. A. Cockle, H. A. O. Hill, R. J. P. Williams, S. P. Davies, M. A. Foster, *J. Am. Chem. Soc.* **1972**, *94*, 275–277.
[7] T. H. Finlay, J. Valinsky, A. S. Mildvan, R. H. Abeles, *J. Biol. Chem.* **1973**, *248*, 1285–1290.
[8] K. L. Schepler, W. R. Dunham, R. H. Sauds, J. A. Fee, R. H. Abeles, *Biochim. Biophys. Acta* **1975**, *397*, 510–518.
[9] W. H. Orme-Johnson, H. Beinert, R. L. Blakley, *J. Biol. Chem.* **1974**, *249*, 2338–2343.
[10] J. D. Brodie, A. D. Woodams, B. M. Babior, *Fed. Proc.* **1972**, *31*, 1578.
[11] The ESR spectrum was recorded on an ESP 300 E 10/12 ESR spectrometer (Bruker Analytische Messtechnik) at a microwave frequency of 9.5 GHz and microwave power of 5 mW. An NMR Gauss meter and a frequency counter (model HP 5350B) was used to calibrate the magnetic field. A cylindrical TM resonator served as sample head. The ESR spectra were obtained at 77 K.
[12] J. R. Pilbrow in *Vitamin B_{12}* (Eds.: B. Zagalak, W. Friedrich), de Gruyter, Berlin, **1979**, p. 505–510.
[13] J. Rétey, P. Such, Y. Zhao, unpublished.

Electrostatic Activation of Nucleofuges: Cationic Leaving Groups**

By *Robert Weiss** and *Stefan Engel*

We have shown that the redox potentials of quinonoid oxidizing agents can be shifted dramatically to positive values by cationic substituents.[1] The nature of the dependence of this phenomenon on the number and spatial arrangement of the positive poles revealed that it was dominated by an F effect.[2] This effect causes a stabilization of the dianionic (reduced) form of the quinones by the cationic substituents. The electrostatic nature of the effect suggests that it can be used to stabilize any anionic system, which could have a direct bearing on the electrostatic activation of anionic nucleofuges.

We now report on poly-onio-substituted phosphorus compounds among which cationic leaving groups are found for the first time. Our experience with quinonoid systems[3] led us to conduct the poly-onio substitutions with 4-dimethylaminopyridine (DMAP, symbolized by L in the reaction equations).[4]

The reaction of PCl_3 with two equivalents of DMAP in ethyl acetate (EE) according to Equation (a) yielded the bis(onio)-substituted phosphane **1a** as isolable, hygroscopic salt. (The spectroscopic data of this and all other new compounds are given in Table 1.) The dicationic structure of **1a** follows from its quantitative transformation into the analytically pure bis(trifluoromethanesulfonate) (abbreviated bis(triflate), **1b**) with Me_3SiOTf ($OTf = O_3SCF_3$).

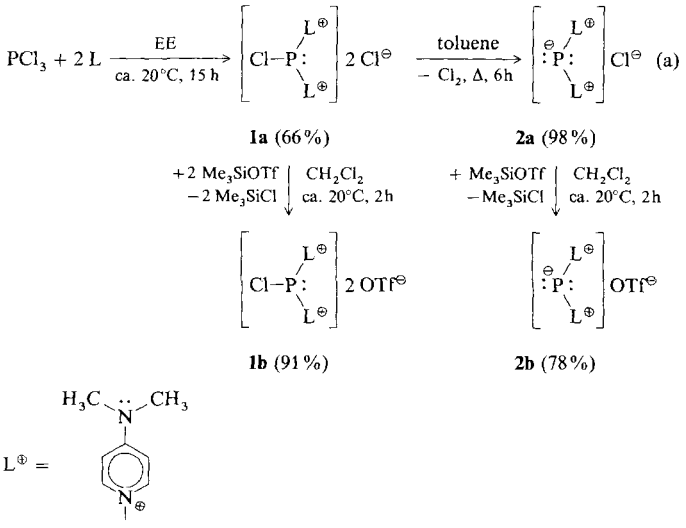

Both in the solid state and in solution, the salt **1a** loses one equivalent of chlorine slowly at room temperature and fast when heated. The novel bis(onio)phosphide **2a** results and can be transformed into the corresponding triflate **2b** by anion exchange with Me_3SiOTf. The spontaneous chlorine loss is interpreted as an S_N2 (Cl) reaction with redox character, in which the bis(onio)phosphide functions as a potent *cationic* nucleofuge. If all the ionically and covalently bound chlo-

Table 1. Spectroscopic data of the compounds **1**–**7** [a].

1a: IR: $\tilde{\nu}$[cm^{-1}] = 3100 (w), 1645 (ss), 1570 (s), 1410 (w), 1220 (w), 830 (m); ^{1}H NMR: δ = 3.17 (s, 12H), 7.47 (AA'BB', 8H)

1b: IR: $\tilde{\nu}$[cm^{-1}] = 3100 (w), 1650 (s), 1570 (s); 1405 (w), 1280 (s), 1215 (ss); ^{1}H NMR: δ = 3.31 (s, 12H), 7.67 (AA'BB', 8H); 830 (w)

2a: IR: $\tilde{\nu}$[cm^{-1}] = 3050 (w), 1640 (ss), 1560 (ss), 1400 (s), 1210 (s), 825 (s); ^{1}H NMR: δ = 3.23 (s, 12H), 7.56 (AA'BB', 8H)

2b: IR: $\tilde{\nu}$[cm^{-1}] = 3080 (w), 1650 (ss), 1550 (ss), 1405 (m), 1270 (ss), 1220 (s), 835 (w); ^{1}H NMR: δ = 3.17 (s, 12H), 7.41 (AA'BB', 8H); ^{31}P NMR (400 MHz, CD_3NO_2, 26 °C, H_3PO_4): δ = −20.06

2c: IR: $\tilde{\nu}$[cm^{-1}] = 3060 (w), 1630 (ss), 1550 (ss), 1400 (m), 1200 (s), 800 (s); ^{1}H NMR: δ = 3.17 (s, 12H), 7.49 (AA'BB', 8H); UV/VIS (CH_3CN): λ[nm] = 215, 275

2d: IR: $\tilde{\nu}$[cm^{-1}] = 3050 (w), 1640 (ss), 1560 (ss), 1200 (s), 785 (m); ^{1}H NMR: δ = 3.21 (s, 12H), 7.50 (AA'BB', 8H); UV/VIS (CH_3CN): λ[nm] = 278, 362

4b: IR: $\tilde{\nu}$[cm^{-1}] = 3060 (w), 1640 (s), 1560 (s), 1400 (m), 1270 (ss), 1210 (ss), 1025 (s), 830 (w); ^{1}H NMR: δ = 3.20 (s, 12H), 4.00 (d, ^2J(P, H) = 14 Hz, 3H), 7.47 (AA'BB', 8H)

5: IR: $\tilde{\nu}$[cm^{-1}] = 3060 (w), 1640 (ss), 1560 (ss), 1210 (w), 1030 (m), 810 (m); ^{1}H NMR: δ = 3.25 (s, 12H), 7.50 (AA'BB', 8H)

7: IR: $\tilde{\nu}$[cm^{-1}] = 3090 (w), 1630 (ss), 1560 (ss), 1400 (m), 1270 (ss), 1205 (ss), 1110 (m), 820 (m); ^{1}H NMR: δ = 3.21 (d, 12H), 7.47 (AA'BB', 8H); ^{31}P NMR (400 MHz, CD_3NO_2, 26 °C, H_3PO_4): δ = −19.08

[a] All IR spectra were recorded in Nujol; all NMR spectra were measured at 60 MHz and 25 °C in CD_3CN against TMS as standard.

[*] Prof. Dr. R. Weiss, Dr. S. Engel
Institut für Organische Chemie
der Universität Erlangen-Nürnberg
Henkestrasse 42
D-W-8520 Erlangen (FRG)

[**] This work was supported by the Fonds der Chemischen Industrie.

rine in **1a** is exchanged for bromine or iodine [Eq. (b)], the stable trihalogenides **2c, d** form spontaneously in high yields via the nonisolable dicationic salts **1c,d** in an analogous S_N2 (Hal) reaction at room temperature.

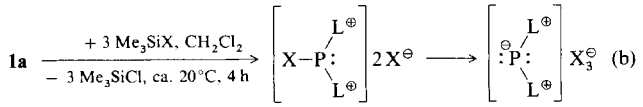

1c, $X^{\ominus} = Br^{\ominus}$ **2c** (77%)
1d, $X^{\ominus} = I^{\ominus}$ **2d** (82%)

The reduction $P^{III} \rightarrow P^{I}$ summarized in Equations (a) and (b) is without precedent. The driving force is the optimal stabilization of the phosphide center in salts **2** by the F and I effects of the cationic substituents. An increase in the oxidation state of phosphorus should increase the nucleofugality of the novel leaving groups **2**. The idea was pursued with derivatives of phosphoric and phosphorus acid analogous to **2**. The attempt to synthesize the methoxy-substituted dication salt **4** (analogous to **1**) from methyl dichlorophosphite **3** and two equivalents of DMAP at room temperature again yielded a structurally novel, stable salt, bis(onio)phosphite **5**, as the only product [Eq. (c)]. Under the activating influence

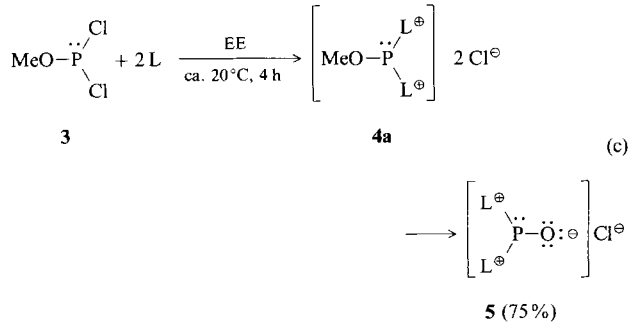

3 **4a** (c)

5 (75%)

of the onio substituents, a demethylation similar to the Arbuzov reaction occurs, but already at the stage of the trivalent P(III) derivative. That the site of the cleavage in this S_N reaction is the C–O and not the P–O bond of **4a** is controlled by the relative polarities and bond strengths of these bonds. If the same reaction is performed in the presence of two mole equivalents of Me_3SiOTf according to Equation (d), good yields of the corresponding dicationic salt **4b** are obtained.

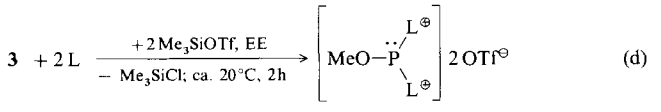

4b (86%)

The viability of this bis(triflate) confirms that the cationic leaving group in **4** is better as nucleofuge than Cl^-, but worse than OTf^-. A reaction of **6**, the phosphorus(v) derivative corresponding to **3**, with DMAP according to Equation (e)[5,6] yields as exclusive product the bis(onio)phosphate triflate **7**[7] besides one mol equivalent of methyl triflate, which is detectable in solution (CH_2Cl_2) and can be trapped quantitatively. The latter is formed in an "Arbuzov reaction" in which the triflate ion functions as nucleophile and the bis(onio)phosphate ion in **7** as *cationic leaving group*.

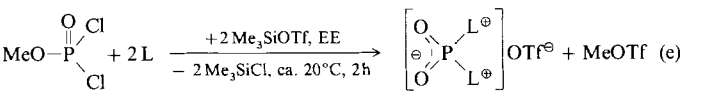

6 **7** (88%)

In this remarkable dealkylation reaction, the cation in salt **7** is a better leaving group than the triflate ion. Our results show that the electrostatic stabilization of the electron density of a nucleofuge by two adjacent onio substituents is exceptionally effective. We anticipate that the method can be extended to other element combinations and charged states, increasing the nucleofugality even further.

Experimental Procedure

All manipulations were performed in an inert nitrogen atmosphere in dried solvents. No melting points were determined on account of the extreme hygroscopic nature of the samples. All reported compounds gave correct elemental analyses.

General method to prepare the chloride salts: DMAP (20 mmol) was dissolved in EE or CH_2Cl_2 (100 mL) and treated with the appropriate P–Cl compound (10 mmol). The precipitate was filtered off and dried at 0.01 Torr.

2 is obtained by gradual dropwise addition of a solution of DMAP (10 mmol) in EE (75 mL) to a solution of PCl_3 in EE (5 mL). The triflates are prepared by dissolving DMAP with the corresponding amount of Me_3SiOTf.

Received: April 24, 1991 [Z4590 IE]
German version: *Angew. Chem.* **1991**, *104*, 239

CAS Registry numbers:
1a, 138784-98-2; **1b**, 138823-23-7; **1c**, 138785-02-1; **1d**, 138785-03-2; **2a**, 138784-99-3; **2b**, 138785-01-0; **2c**, 138785-04-3; **2d**, 138785-05-4; **3**, 3279-26-3; **4a**, 138785-06-5; **4b**, 138785-09-8; **5**, 138785-07-6; **6**, 677-24-7; 7, 138785-11-2; DMAP, 1122-58-3; PCl_3, 7719-12-2; Me_3SiOTf, 27607-77-8.

[1] R. Weiss, N. J. Salomon, G. E. Miess, R. Roth, *Angew. Chem.* **1986**, *98*, 925; *Angew. Chem. Int. Ed. Engl.* **1986**, *25*, 917.
[2] R. König, Diplomarbeit, Universität Erlangen-Nürnberg, **1989**. "Field" is used here in terms of a through-space interaction.
[3] S. Engel, Diplomarbeit, Universität Erlangen-Nürnberg, **1988**.
[4] G. Höfle, W. Steglich, H. Vorbrüggen, *Angew. Chem.* **1978**, *90*, 602; *Angew. Chem. Int. Ed. Engl.* **1978**, *17*, 569.
[5] D. R. Cowsar, D. H. Lewis, G. W. Whitehead, *Gov. Rep. Announce Index (U.S.)* **1978**, *18*, 265; *Chem. Abstr.* **1978**, *90*, P 109 134 f.
[6] M. Wakselman, E. Guibe-Jampel, *Tetrahedron Lett.* **1970**, *11*, 1521.
[7] H. P. Daskalov, M. Sekine, T. Hata, *Tetrahedron Lett.* **1980**, *21*, 3899.

$TaNi_2Te_2$, A Novel Layered Telluride, and $TaCo_2Te_2$, a Structural Variant with Peierls Distortion**

By *Wolfgang Tremel**

Dedicated to Professor Joseph Grobe on the occasion of his 60th birthday

Early-transition-metal chalcogenides are—as evident from their structural chemistry and their physical properties—textbook examples of the inadequacy of simplified

[*] Prof. Dr. Wolfgang Tremel[+]
Anorganisch-chemisches Institut der Universität
Wilhelm-Klemm-Strasse 8, D-W-4400 Münster (FRG)
[+] New address:
Institut für Anorganische und Analytische Chemie der Universität
J. J.-Becherweg 24, D-W-6500 Mainz

[**] This research was supported by a grant from the Bundesministerium für Forschung und Technologie under contract No. 05339 GAB/3 and the Fonds der Chemischen Industrie. I am grateful to Prof. Dr. B. Krebs for further support and to the Starck Company (Dr. Peters) for a Ta donation.

bonding descriptions. This is documented by the multitude of seemingly simple compounds such as TaS_2,[1] $NbSe_2$,[1] and $NbSe_3$[2]. The observed phase transitions and structure changes of even the simplest possible chalcogenides of the MS type (e.g. $V_{1-x}S$, $Nb_{1-x}S$)[3,4] are not yet completely understood.

The above examples show that almost all research on early-transition-metal chalcogenides has been restricted to sulfides and selenides, whereas tellurides have been mostly neglected. This may have historical reasons[5]—many minerals and traditionally investigated materials are of sulfidic origin—but may as well have resulted from the assumption that there are no significant differences between sulfides, selenides, and tellurides. Recent findings, however, indicate that the chemistry of the tellurides is significantly different from that of its lighter homologues.[6] The chemical uniqueness of the tellurides is indicated even by a formal comparison of the binary chalcogenides. The trichalcogenides MQ_3 (M = Nb,Ta)[2,7] exist only for Q = S and Se; the tetratellurides MTe_4 (M = Nb,Te),[8] on the other hand, have no counterparts among the sulfides and selenides. Reports on the chain compound Ta_4SiTe_4 give some indication of the structural variety that may be expected.[9] The examples, however, are not restricted to the area of solid-state research. Among the soluble sulfides and selenides we find no analogues for the polytelluride anion $NbTe_{10}^{3-}$;[10] and no Te analogues for textbook classics such as $Mo_3S_{13}^{2-}$ are known.[11]

Attempts to reduce MTe_2 with 3d metals lead to the layer compounds $TaFe_{1+x}Te_3$ ($x \approx 0.15$),[12] M_2FeTe_4 (M = Nb, Ta),[13] $M_2M'Te_4$ (M = Nb, Ta; M' = Fe, Co, Ni),[13,14,15] $Ta_2M_3Te_5$ (M = Ni, Pd)[13a,b,16], and $TaCo_2Te_2$.[17] An unexpected finding in these investigations was that Peierls-type distortions which dominate the structures of many low-dimensional chalcogenides[1c] were rarely observed. The structure of the title compound $TaNi_2Te_2$, however, shows that Peierls distortions[18] occur in metal-rich tellurides as well. The structure of $TaNi_2Te_2$ corresponds to the undistorted type, the structure of $TaCo_2Te_2$, to the distorted one.

$TaNi_2Te_2$ is synthesized at 950 °C from the elements.[19,20] A striking feature is the layer character of the structure. This is particularly surprising, since the metal:tellurium ratio is 3:2, and the compound has to be considered metal-rich. The shortest Te–Te distance between the layers is 3.795 Å; the layers are held together by Van der Waals forces only. Each unit cell contains two $TaNi_2Te_2$ layers, which are stacked along the *c* axis and related by an *n* glide plane. In Figure 1 a projection of the structure along *b* is shown above; a central projection of a single layer along *c* is shown below.

The layer character of the compound accompanies an anisotropy of its properties. This is immediately clear from the crystal structure and is supported by the results of tight-binding band structure calculations.[21] The energy bands along special lines of the Brillouin zone corresponding to space directions within a $TaNi_2Te_2$ layer, cross the Fermi level, but the bands in directions perpendicular to the layers are dispersionless and do not cross the Fermi level. Thus $TaNi_2Te_2$ can be regarded a two-dimensional metal.[22]

One possible description of the structure of $TaNi_2Te_2$ starts with the identification of *cis-trans* chains of Ni atoms running parallel to the crystallographic *a* axis. The Ni–Ni distances within the chain are 2.407(2) Å and 2.524(2) Å (see Fig. 1 below) and are thus comparable with Ni–Ni distances in Ni metal[23] and in several related compounds such as $Ta_2Ni_2Te_4$[13,14,15] and $Ta_2Ni_3Te_5$.[13] However, even in closed-shell molecular clusters such as $[Ni_8S(SC_4H_9)_9]^-$[24] and $[Ni_8Hg(PPh)_6(PPh_3)_4][Ni_8(PPh)_6(PPh_3)_4]$[25] comparable Ni–Ni distances are observed. The *cis-trans* Ni chains are connected by Ta atoms which are attached to six Ni–Ni bonds in a side-on fashion. Thereby each Ta atom obtains eight Ni neighbors; Ta–Ta separations of 3.370(1) Å and 3.566(1) Å allow significant Ta–Ta interactions. Each Ni atom has four Ta and two Ni neighbors. The tellurium atoms are situated above and below the $TaNi_2$ layers in such a way that every two Ni and two Ta atoms (μ_4-Te) or four Ni atoms and one Ta atom are bridged by tellurium (μ_5-Te).

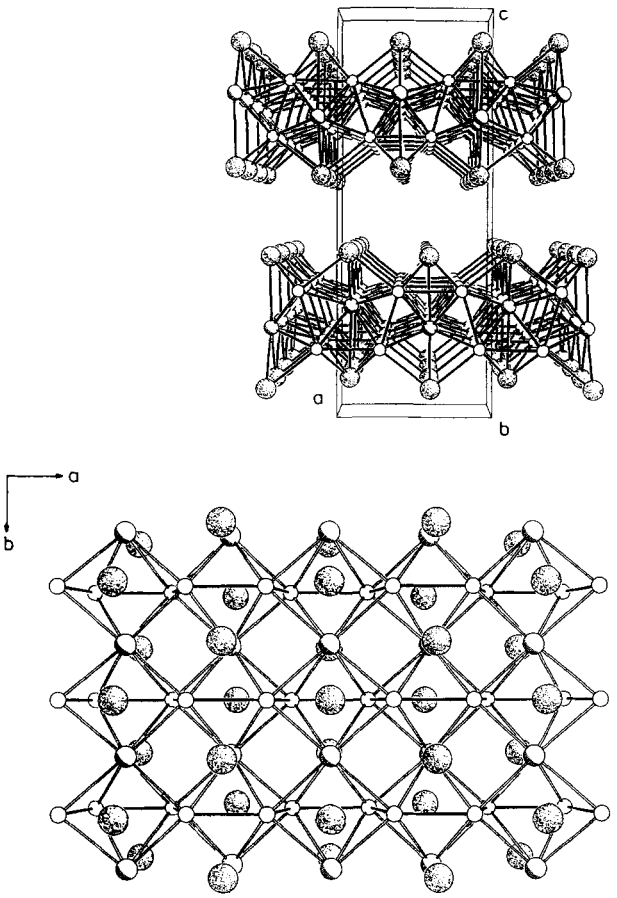

Fig. 1. $TaNi_2Te_2$: Above: Perspective view of the structure along [010]. Below: Projection of a single layer along [001]; large dotted circles: Te; medium-size hatched circles: Ta; small circles: Ni.

A possible alternative description starts with pinpointing a square (4^4) net of Ni_2 dumbbells which span a plane parallel to the crystallographic *a,b* plane. The $d_{Ni\text{-}Ni}$ distance within the dumbbells is 2.407(2) Å; the Ni–Ni distance between the dumbbells is $\approx$ 3.5 Å; the main axis of each dumbbell is oriented parallel to the crystallographic *c* axis. A 30° or −30° tilt of the Ni_2 dumbbells with respect to an axis parallel to *b* leads to alternation of the Ni–Ni distances along *a* ($d_{Ni\text{-}Ni}$: 2.524(2) and 3.952(2) Å). Distorted in this way the Ni_2 net is interpenetrated by an (idealized) square-planar net of Ta atoms ($d_{Ta\text{-}Ta}$: 3.566(1) Å). The $TaNi_2$ metal layer is capped top and bottom by Te layers.

Because of the high coordination numbers of the metal atoms and the many short metal–metal contacts we do not expect a crystal field splitting of the d orbitals which can be described easily. In addition, we encounter difficulties in assigning formal oxidation numbers. If one assumes tellurium to be Te^{-II}, then four formal charges have to be distributed

over one Ta and four Ni atoms. Figure 2 shows the computed density of states (DOS) for $TaNi_2Te_2$ and the contributions of Ta, Ni, and Te. The Ta- and Te-centered energy bands have a high dispersion, the Ni-centered bands, much less. The majority of the states around the Fermi level is centered on the metal atoms. A Mulliken population analysis shows that (except for the Ta–Te bonds) the Ta–Ni and Ta–Ta bonds are strong. In contrast, the computed Ni–Ni overlap populations are almost zero.[26]

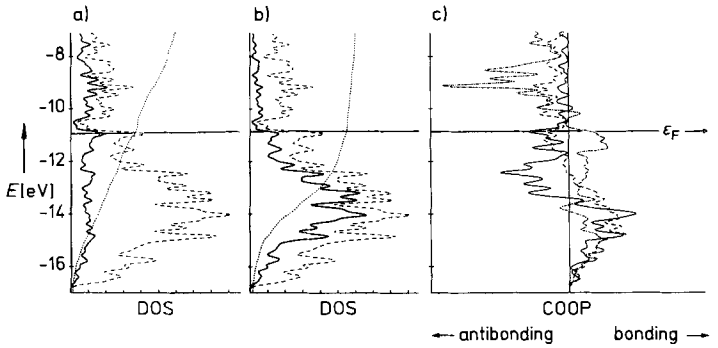

Fig. 2. Density of states (DOS) for $TaNi_2Te_2$: a) total DOS (broken line) and Ta contribution. b) Total DOS (broken line) and Ni contribution. The dotted lines represent integrations over the occupation of the orbital in question. c) COOP (Crystal *O*rbital *O*verlap *P*opulation) curve (average Ta-Ta, Ta-Ni and Ni-Ni overlap populations); solid line: Ni-Ni, dashed line: Ta-Ni; dashed-dotted line: Ta-Ta. The Fermi level is marked by a horizontal bar.

A better understanding of the $TaNi_2Te_2$ structure and the governing electronic factors can be obtained by a comparison with the closely related structure of $TaCo_2Te_2$ (Fig. 1 below and Fig. 3). Whereas in $TaNi_2Te_2$ the Ni atoms are

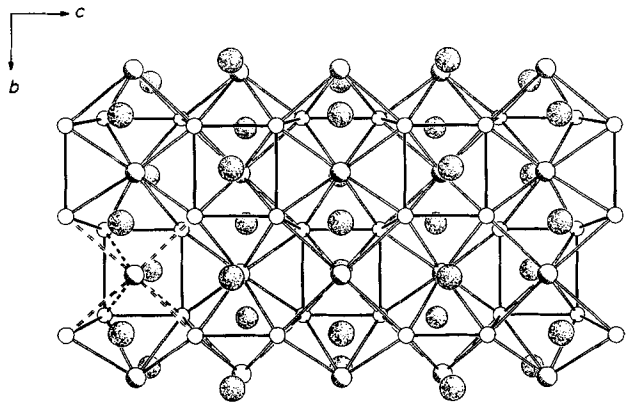

Fig. 3. $TaCo_2Te_2$: Projection of a single layer along [001]; large dotted circles: Te, medium hatched circles: Ta, small circles: Co.

equidistant along b ($d_{Ni\text{-}Ni}$: 3.566 Å), the $TaCo_2Te_2$ structure is distorted in such a way that Co atoms of two neighboring *cis-trans* chains pair up: one observes alternating short and long Co–Co distances between the *cis-trans* chains ($d_{Co\text{-}Co}$: 2.852(2) and 3.756(2) Å). The structural distortion is reflected in the Ta–M′ distances as well: in $TaCo_2Te_2$ the Ta–M′ distances which were uniform in $TaNi_2Te_2$ ($\bar{d}_{Ta\text{-}Ni}$: 2.733 Å) are derived into groups of shorter ($\bar{d}_{Ta\text{-}Co}$: 2.582 Å, bold dashed lines around Ta in Fig. 3) and longer ($\bar{d}_{Ta\text{-}Co}$: 2.843 Å, open dashed lines around Ta in Fig. 3) Ta–Co distances.

The pairing distortion in $TaCo_2Te_2$ can be viewed in a simple manner as a consequence of a Peierls instability. This interpretation is based on the idea that in spite of metal–metal bonding and the high coordination number of M in the TaM_2Te_2 layers, a fraction of the valence electrons (depending on M) is used to form quasilocalized M–M bonds. In this simple picture Ni–Ni bonding and antibonding states should be occupied in $TaNi_2Te_2$ (see Fig. 2c). Therefore no bonding Ni–Ni contacts are observed along b. Moving on to $TaCo_2Te_2$ we formally remove electrons from M–M antibonding states, and M–M (i.e. Co–Co) bonding interactions can develop in the corresponding spatial direction.

A more specific picture of the electronic factors which are responsible for the distortion can be obtained from the computed band structure.[27] Figure 4a shows the energy bands of $TaNi_2Te_2$ along the symmetry lines $X-\Gamma-Y$ of the Brillouin zone. Because the Fermi level crosses several bands, metallic properties are expected for this material. Note the high dispersion of several bands in the energy range between -10 eV and -11 eV and the distinct energy gap above -11 eV at X. Since one of the unit-cell translations is doubled as a consequence of the pairing distortion when we move from the $TaNi_2Te_2$ to the $TaCo_2Te_2$ structure, the corresponding reciprocal lattice-translation is halved, and the energy bands are "backfolded" along this line ($\Gamma-Y$, Fig. 4b).[18b,c] The representations in Figure 4a, 4b are therefore equivalent; the only difference is a doubling of the unit cell. Figure 4c shows the energy bands of $TaCo_2Te_2$ along the corresponding symmetry line ($\Gamma-Y$).

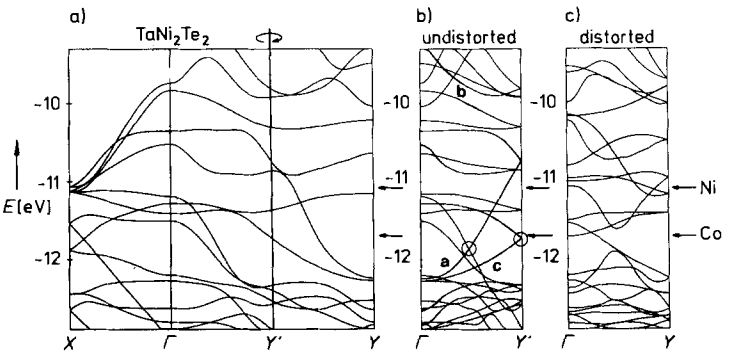

Fig. 4. Band structure of TaM_2Te_2. The Fermi level for $TaNi_2Te_2$ and $TaCo_2Te_2$ is indicated by an arrow. Energy bands for a) the undistorted $TaNi_2Te_2$ structure along the symmetry lines $X-\Gamma-Y$ of the Brillouin zone (2D); b) the undistorted structure, but with a unit cell which is doubled along the b direction; one obtains the backfolded band structure along $\Gamma-Y$; c) the distorted structure ($TaCo_2Te_2$).

The band structures of the undistorted and distorted structures (Fig. 4b and 4c) differ in the following points: 1) The band crossing close to the Fermi level which was possible in the undistorted structure for symmetry reasons is avoided in the distorted $TaCo_2Te_2$ structure. 2) One of the bands which is located around -12 eV in the $TaNi_2Te_2$ structure is higher in energy in the $TaCo_2Te_2$ structure type and is located just above the Fermi level. A better description of the electronic driving force for the observed structural change can be given by an analysis of the crystal orbitals at the zone center. In simplified form **A** and **B** show the composition of the bands labeled **a** and **b**, which cover the energy range from -12 eV to -10 eV and undergo several avoided crossings. At the zone center (Γ, ($k=0$)), band **a** has a Ni–Ta bonding maximum and runs "uphill"; at Γ, band **b** has a Ni–Ta antibonding maximum and runs "downhill". Upon relieving the translational symmetry which is present in the undistorted structure, mixing of these two bands (and sever-

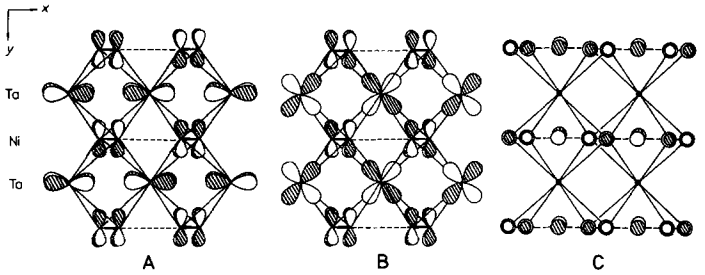

al others) leads to an electronic stabilization through Ta–M interactions.[28] This interpretation is consistent with the appearance of two different groups of Ta–M′ distances in the $TaCo_2Te_2$ structure and the computed increase in the corresponding Ta–M′ overlap populations.[26] **C** shows the composition of the bands labeled **c**. At Γ the $5p_z$ orbitals of the Te atoms are located in the nodal plane of the $3d_{z^2}$ orbitals of the Ni atoms. Their mixing with $5p_y$ orbitals of Te as a consequence of the reduction in symmetry leads to an increase of antibonding Ni–Te interactions and increases the energy of the corresponding band.

Based on total energies the distorted structure type is more stable by 0.26 eV for M = Fe; for M = Co and Ni the undistorted structure is preferred by 0.69 and 2.34 eV, respectively. The computed energies indicate the correct trend, although the numerical values are not correct. $TaFe_2Te_2$ is predicted to adopt the distorted structure type.

Received: July 18, 1991 [Z 4801 IE]
German version: *Angew. Chem.* **1992**, *104*, 230

CAS Registry numbers:
$TaNi_2Te_2$; 138008-36-3; $TaCo_2Te_2$, 137752-17-1; Ta, 7440-25-7; Ni, 7440-02-0; Te, 13494-80-9.

[1] a) J. A. Wilson, F. J. DiSalvo, S. Mahajan, *Adv. Phys.* **1975**, *24*, 117; b) *Electronic Properties of Inorganic Quasi One-Dimensional Compounds, Vol. 1 and Vol. 2* (Ed.: P. Monceau), Reidel, Dordrecht, **1985**; c) *Crystal Chemistry and Properties of Materials with Quasi One-Dimensional Structures* (Ed.: J. Rouxel), Reidel, Dordrecht, **1986**.

[2] a) *Physics and Chemistry of Materials with Layered Structures, Vol. 3: Electrons and Phonons in Layered Structures* (Eds.: T. J. Wieting, M. Schlüter), Reidel, Dordrecht, **1979**; b) *Physics and Chemistry of Materials with Layered Structures, Vol. 4: Optical and Electrical Properties* (Ed.: P. A. Lee), Reidel, Dordrecht, **1976**; c) F. Hulliger, *Physics and Chemistry of Materials with Layered Structures, Vol. 5: Structural Chemistry of Layer-Type Phases* (Ed.: F. Lévy), Reidel, Dordrecht, **1976**.

[3] a) A. Meerschaut, J. Rouxel, *J. Less Common Met.* **1975**, *24*, 117; b) J. L. Hodeau, M. Marezio, C. Rouceau, R. Ayroles, A. Meerschaut, J. Rouxel, P. Monceau, *J. Phys. C: Solid State Phys.* **1978**, *11*, 4117; c) A short summary is found in S. Kagoshima, H. Nagasawa, T. Sambongi, *One-Dimensional Conductors*, Springer, Berlin, **1988**, Chapter 4.

[4] a) H. F. Franzen, S. Westman, *Acta Chem. Scand.* **1963**, *17*, 2353; b) H. F. Franzen, T. J. Buerger, *J. Chem. Phys.* **1968**, *49*, 2268; c) H. F. Franzen, C. Haas, F. Jellinek, *Phys. Rev. B* **1974**, *10*, 1248; d) S. H. Liu, W. B. England, W. H. Myron, *Solid State Commun.* **1974**, *14*, 1003; e) J. Silvestre, W. Tremel, R. Hoffmann, *J. Less Common Met.* **1986**, *116*, 113; f) C. Haas, *J. Solid State Chem.* **1985**, *57*, 82; g) W. Tremel, unpublished results.

[5] P. Böttcher, *Angew. Chem.* **1988**, *100*, 781; *Angew. Chem. Int. Ed. Engl.* **1988**, *27*, 759.

[6] a) L. Bragg, G. F. Claringbull, W. H. Taylor, *Crystal Structures of Minerals*, Cornell University Press, Ithaca, New York, **1965**; b) L. Pauling. *The Nature of the Chemical Bond*, Cornell University Press, Ithaca, New York, **1960**; *Die Natur der chemischen Bindung*, Verlag Chemie, Weinheim, **1976**.

[7] A. Meerschaut, L. Guemas, J. Rouxel, *J. Solid State Chem.* **1981**, *36*, 118.

[8] E. Bjerkelund, A. Kjekshus, *J. Less Common Met.* **1964**, *7*, 231.

[9] a) M. E. Badding, F. J. DiSalvo, *Inorg. Chem.* **1990**, *29*, 3952; b) J. Li, R. Hoffmann, M. E. Badding, F. J. DiSalvo, *ibid.* **1990**, *29*, 3943.

[10] W. A. Flomer, J. W. Kolis, *J. Am. Chem. Soc.* **1988**, *110*, 3682.

[11] A. Müller, S. Pohl, M. Dartmann, J. P. Cohen, J. M. Bennett, R. M. Kirschner, *Z. Naturforsch. B.* **1979**, *34*, 434.

[12] a) W. Tremel, E. Potthoff, unpublished results; b) E. Potthoff, Diplomarbeit, Universität Münster, **1991**.

[13] a) W. Tremel, *Habilitationsschrift*, Universität Münster, **1991**; b) W. Tremel, *Angew. Chem.* **1991**, *103*, 900; *Angew. Chem. Int. Ed. Engl.* **1991**, *30*, 840.

[14] B. Huang, J. Huang, L. Shixiong, *Jiegou Huaxue* **1989**, *8*, 146. J. Huang, B. Huang, *ibid.* **1988**, *7*, 215.

[15] J. Li, F. J. DiSalvo, personal communication, **1991**.

[16] W. Tremel, *Chem. Ber.*, submitted for publication.

[17] W. Tremel, *J. Chem. Soc. Chem. Commun.* **1991**, 1405.

[18] a) R. E. Peierls, *Quantum Theory of Solids*, University Press, Oxford, **1955**; b) R. Hoffmann, *Angew. Chem.* **1987**, *99*, 871; *Angew. Chem. Int. Ed. Engl.* **1987**, *26*, 846; c) T. A. Albright, J. K. Burdett, M. H. Whangbo, *Orbital Interactions in Chemistry*, Wiley, New York, **1985**.

[19] $TaNi_2Te_2$ was synthesized by heating the elements in the appropriate molar ratio at 950 °C 14 d in a quartz tube sealed under vacuum with the addition of iodine as mineralizer. The reaction product (EDAX: Ta, Ni, Te) consisted of compact needles with a metallic luster.

[20] Space group *Pnma* (No. 62), $Z = 4$, $a = 6.488(1)$, $b = 3566(1)$, $c = 17.014(3)$ Å (Siemens R3), $Mo_{K\alpha}$ ($\mu = 51.30\ mm^{-1}$); crystal dimensions: $0.015 \times 0.015 \times 0.18$ mm; θ-2θ-Scan, $2\theta_{max} = 70°$, 2231 reflections ($h,k \pm l$, empirical absorption correction, 1376 symmetry independent reflections, 1193 of which were considered "observed" with $I > 2\sigma(I)$, $R(R_w) = 0.038$ (0.033). Further details concerning the crystal structure analysis can be obtained from the Fachinformationszentrum Karlsruhe, Gesellschaft für wissenschaftlich-technische Information mbH, D-W-7514 Eggenstein-Leopoldshafen 2, on quoting the depository number CSD-55889, the author, and the journal citation.

[21] a) Extended Hückel approximation: R. Hoffmann, *J. Chem. Phys.* **1963**, *39*, 1397; H_{ij}-matrix elements: J. H. Ammeter, H.-B. Bürgi, J. C. Thibeault, R. Hoffmann, *J. Am. Chem. Soc.* **1978**, *100*, 3686; b) Tight-binding approach: M.-H. Whangbo, R. Hoffmann, *J. Am. Chem. Soc.* **1978**, *100*, 6093; M.-H. Whangbo, R. Hoffmann, R. B. Woodward, *Proc. R. Soc. London A* **1979**, *366*, 23; c) Ta, Ni Parameters: M. J. Calhorda, R. Hoffmann, *Inorg. Chem.* **1988**, *27*, 3943; d) Te Parameters: E. Canadell, Y. Mathey, M.-H. Whangbo, *J. Am. Chem. Soc.* **1988**, *110*, 104; e) Special k points: R. Ramirez, M. C. Böhm, *Int. J. Quantum Chem.* **1986**, *30*, 391.

[22] This hypothesis is supported by the results of conductivity measurements: W. Tremel, R. Kremer, unpublished results, **1991**.

[23] *CRC Handbook of Chemistry and Physics*, 60th ed., CRC Press, Boca Raton, FL, USA, **1980**.

[24] T. Krüger, B. Krebs, G. Henkel, *Angew. Chem.* **1989**, *101*, 54; *Angew. Chem. Int. Ed. Engl.* **1989**, *28*, 61.

[25] D. Fenske, J. Magull, *Z. Naturforsch. B* **1990**, *45*, 121.

[26] 3D calculation for $TaNi_2Te_2$ (experimental geometry). Computed overlap populations: Ta-Ta (3.370 Å) 0.215; Ta-Ta (3.566 Å) 0.106; Ta-Ni (2.704 Å) 0.183; Ta-Ni (2.717 Å) 0.181; Ta-Ni (2.744 Å) 0.149; Ta-Ni (2.765 Å) 0.147; Ni-Ni (2.407 Å) 0.043; Ni-Ni (2.524 Å) −0.006.

[27] The band structures shown in the figures were calculated for 2D layers of $TaNi_2Te_2$ and $TaCo_2Te_2$ (experimental geometry) with parameters of Ta, Ni, and Te (see ref. [21]).

[28] Because of the large number of energy levels a pictorial representation is not given here.

A Dramatic Difference in the Reactivities of Alkoxido- and Aryloxidorhenium Complexes in Insertion Reactions**

By *Robert D. Simpson* and *Robert G. Bergman**

Due to the increasing recognition of their importance as intermediates in the metal-catalyzed functionalization of olefins and the hydrogenation of organic carbonyl groups, systematic studies of the synthesis and chemistry of complexes with metal–oxygen single bonds are beginning to appear.[1] We report here the synthesis and reactions of several new octahedral low-valent aryloxido- and alkoxidorhenium complexes, whose M–O bonds display profoundly different reac-

[*] Prof. R. G. Bergman, R. D. Simpson
Department of Chemistry
University of California
Berkeley, CA 94720 (USA)

[**] We are grateful for financial support of this work from the United States National Institutes of Health (Grant No. GM-25459). R. D. S. expresses his gratitude for a Squibb Fellowship (1990–1991). We wish to thank Prof. Milton Orchin for his willingness to disclose results before publication.

tivities. Unlike their anionic tungsten relatives, our neutral *aryl*oxidorhenium complexes react only very slowly with CS_2 and other electrophiles, and then only when the first step involves dissociation of another ligand. In contrast, analogous reactions of neutral (unfluorinated) *alk*oxide complexes apparently do not require the generation of a site of coordinative unsaturation at the metal center. CO_2 and CS_2 react exceedingly rapidly at temperatures as low as $-40\,^{\circ}C$, and kinetic experiments indicate that these transformations take place by attack of the electrophile directly at the oxygen atom of the alkoxido ligand.

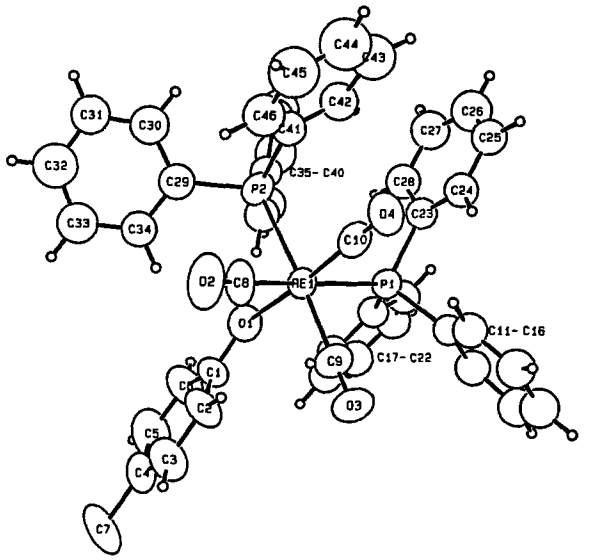

Fig. 1. Crystal structure of **2a**. Important bond lengths [Å] and angles [°]: Re-O1 2.143(9), O1-C1 1.341(20), Re-C8 1.963(12), Re-C9 1.954 (16), Re-C10 1.913(15); Re-O1-C1 131.5(11), O1-Re-C10 175.5(4), O1-Re-C9 94.6, P1-Re-P2 96.9.

Treatment of *fac,cis*-$[Re(CH_3)(CO)_3(PPh_3)_2]$ **1** with 1.5 equivalents of *p*-cresol in benzene at 45 °C affords the cresolato complex **2a** (74% yield, Fig. 1[12]) and methane (Scheme 1). The triphenylphosphine ligands of **2a** may be readily displaced by sterically less demanding ligands such as PMe_3 or *o*-phenylenebis(dimethylarsine) (diars). This approach cannot be employed for the synthesis of the corresponding alkoxido complexes; complex **1** reacts with alcohols (including trifluoroethanol) to give complicated mixtures of products (analysis by $^{31}P\{^1H\}$ NMR spectroscopy). However, the alkoxido complexes **6** may be prepared in 75–86% yield by treatment of the trifluoromethanesulfonato complexes **5** with an excess of sodium methoxide in a mixed benzene/methanol solvent system.[13] Attempts to use this method to prepare alkoxido complexes without chelating ligands failed except for the case of the bis(trimethylphosphine) complex **6b**. The *fac,cis* geometries of these complexes were established by their characteristic infrared and ^1H and ^{13}C NMR spectra.

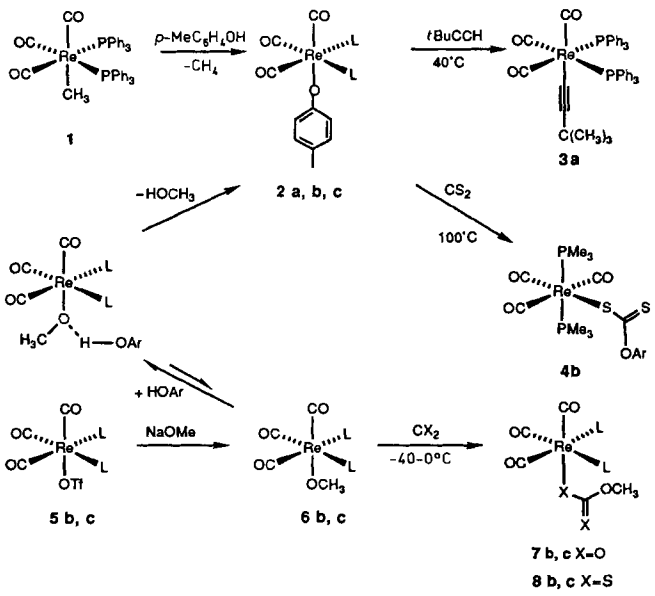

Scheme 1. **a**: L = PPh_3; **b**: L = PMe_3; **c**: L,L = diars. OTf = O_3SCF_3.

The cresolato and alkoxido complexes show similar behavior in protonolysis reactions. The metal–oxygen bonds may be cleaved by strong electrophiles such as HCl and acetyl chloride to yield the corresponding metal chloride and the free or acetylated alcohol. Alcohol exchange reactions also occur quite readily, but here the observed behavior is more sensitive to the nature of the complex, and leads to the following observations: a) Treatment of **6a** with 1.5 equivalents of isopropanol in benzene leads rapidly to a (presumably equilibrium) mixture of **6c** and the corresponding isopropoxido complex. b) In contrast, treatment of **6b** or **6c** with *p*-cresol in $[D_6]$benzene leads to the formation of hydrogen-bonded complexes which are temporarily stable in this medium.[14] Heating these complexes to 45 °C releases methanol and the exchanged aryloxido complexes **2b** or **2c** (observed by NMR spectroscopy). c) Product **2c** may be recovered unchanged after dissolving in methanol, establishing that the **2c**/**6c** equilibrium lies strongly on the side of the aryloxido complex.

Despite the fact that in some of these experiments hydrogen-bound species are directly observed, and in some they are not, it seems likely that all the reactions proceed by initial hydrogen-bonding. However, in order for these intermediates to be stabilized and characterized, the metal-bound alkoxido ligand apparently must be relatively basic (e.g., methoxide) and the proton donor relatively acidic (e.g., *p*-cresol).

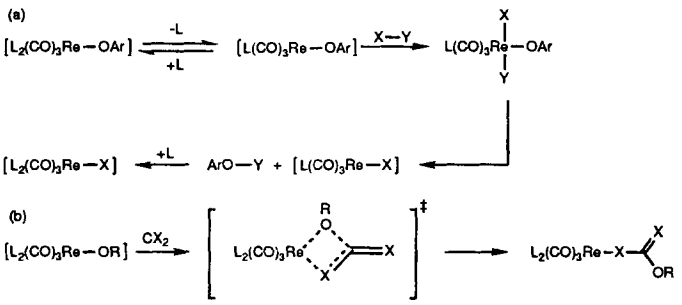

Scheme 2.

Other reactions of the aryloxido complexes proceed more slowly. For example, the PMe_3 and diars complexes **2b** and **2c** do not react readily with terminal alkynes such as $tBuC{\equiv}CH$. The bis(triphenylphosphine) complex **2a** reacts at 40 °C to form the σ-acetylide complex **3a** and *p*-cresol. Under pseudo-first-order conditions with respect to **2a** saturation kinetics are observed: a plot of $1/k_{obs}$ versus $[tBuC{\equiv}CH]/[PPh_3]$ is linear. This kinetic behavior is consistent with reversible loss of phosphine, followed by alkyne C-H activation, and then O-H reductive elimination (mechanism (a) in Scheme 2).[15, 6] A similar reaction of **2a** with trimethylsilane is observed, yielding the hydride complex

$[Re(CO)_3(H)(PPh_3)_2]$ and the silylated cresol. None of the cresolato complexes inserts CO_2. Carbon disulfide insertion occurs only very slowly with **2b** (7 d at 100 °C) to afford the *trans* product **4b** in 52% yield. Although the mechanism of this insertion reaction has not been investigated, the vigorous reaction conditions required and formation of the isomerized product strongly suggest that ligand loss is again required to initiate the transformation.[7]

Table 1. Spectroscopic and analytical data for representative compounds **2b**, **6b**, **7b**, and **8b** [a].

2b: ^{1}H NMR ($CDCl_3$): $\delta = 7.15$ (d, $J = 8.39$ Hz, 2H; $OC_6H_4CH_3$), 6.01 (d, $J = 8.39$ Hz, 2H; $OC_6H_4CH_3$), 2.29 (s, 3H; $OC_6H_4CH_3$), 1.22 ($A_9A_9'XX'$, "J" = 8.22 Hz, 18H; PMe_3); $^{13}C\{^1H\}$ NMR (CD_2Cl_2): $\delta = 197.4$ (br, Re(-CO)$_3$), 168.9 (t, $J = 2.74$ Hz, $OC_6H_4CH_3$(*ipso*-C), 130.2 (s, $OC_6H_4CH_3$), 122.5 (s, $OC_6H_4CH_3$(*ipso*-C), 119.6 (s, $OC_6H_4CH_3$), 20.65 (s, $OC_6H_4CH_3$), 15.77 (AXX', "J" = 30.09 Hz; PMe_3). IR (KBr): $\tilde{\nu}$ [cm^{-1}] = 2010, 1921, 1888 (ν, CO). – Correct C,H-analysis.

6b: ^{1}H NMR (C_7D_8, −70 °C): $\delta = 4.60$ (s, 1H; $ReOCH_3$), 0.90 ($A_9A_9'XX'$, "J" = 8.06 Hz; PMe_3); $^{13}C\{^1H\}$-NMR (C_7D_8, −70 °C): $\delta = 193.8$ (br, Re(-CO)$_3$), 69.7 (t, $J = 4.90$ Hz; $ReOCH_3$), 16.6 (AXX', "J" = 30.63 Hz; PMe_3). IR (KBr): $\tilde{\nu}$ [cm^{-1}] = 2012, 1921, 1876 (ν CO). – The instability of this complex in solution precluded attempts at recrystallization and further purification.

7b: ^{1}H NMR ($CDCl_3$): $\delta = 3.57$ (s, 1H; $ReO(CO)CH_3$), 1.58 ($A_9A_9'XX'$, "J" = 7.43 Hz, 6H; PMe_3); $^{13}C\{^1H\}$ NMR ($CDCl_3$): $\delta = 193.8$ (t, $J = 7.12$ Hz; CO *trans* to $O(CO)OCH_3$), 191.6 (AXX', "J" = 51.7 Hz; CO *cis* to $O(CO)OCH_3$), 159.8 (t, $J = 2.75$ Hz; $ReO(CO)OCH_3$), 53.9 (s, $O(CO)CH_3$), 17.11 (AXX', "J" = 31.9 Hz; PMe_3). IR (KBr) $\tilde{\nu}$ [cm^{-1}] = 2027, 1979, 1905 (ν CO), 1670 (ν C = O). – Correct C,H-analysis.

8b: ^{1}H NMR (C_6D_6): $\delta = 4.04$ (s, 1H; $ReS(CS)CH_3$), 0.90 ($A_9A_9'XX'$, "J" = 8.06 Hz, 6H; PMe_3); $^{13}C\{^1H\}$ NMR ($CDCl_3$): $\delta = 223.2$ (t, $J = 6.0$ Hz; $ReS(CS)OCH_3$), 192.1 (br. CO *trans* to $S(CS)OCH_3$), 191.7 (br, CO *cis* to $S(CS)OCH_3$), 59.6 (s, $S(CS)OCH_3$), 17.18 (AXX', "J" = 33.03; PME_3). IR (KBr) $\tilde{\nu}$ [cm^{-1}] = 2019, 1950, 1894 (ν CO), 1425 (ν CS). – Correct C,H-analysis.

[a] The ^{1}H NMR spectra were recorded at 400 MHz; the $^{13}C\{^1H\}$ NMR spectra, at 100 MHz.

In striking contrast, the corresponding methoxido complexes **6b** and **6c** react with both CO_2 and CS_2 to form the insertion products **7b**, **c** and **8b**, **c**, which exhibit C–O and C–S stretching absorptions at 1665 and 1417 cm^{-1}, respectively.[8] These reactions all occur very rapidly: In a sealed NMR tube, a 0.0244 M solution of **6c** reacts with 10 equivalents of CO_2 at −40 °C in less than 5 min. At higher dilution, the reaction of **6c** with CS_2 could be monitored by UV/VIS spectroscopy.[9] The rate of the reaction at 0 °C was found to be proportional to the concentration of CS_2. This suggests a simple bimolecular mechanism such as pathway (b) in Scheme 2, but the observation could also result from the failure to reach a limiting rate corresponding to saturation. This situation could arise from an initial rapidly reversible unimolecular reaction of **6c**, such as ionization of the methoxido ligand followed by slower attack of MeO^- on CS_2, or rapidly reversible loss of one of the other ligands.[10] An ionization mechanism should exhibit a large solvent effect, but the rate constant for the reaction varied only slightly: $k_2 = 8.0 \times 10^{-2}$ M^{-1}s^{-1} in THF, 6.3×10^{-2} M^{-1}s^{-1} in acetonitrile, and 2.4×10^{-2} M^{-1}s^{-1} in toluene.[11] Activation parameters of $\Delta H^{\neq} = 8.9$ kcal mol^{-1} and $\Delta S^{\neq} = -31$ cal K^{-1} mol^{-1} obtained for the insertion reaction in THF are characteristic of a bimolecular reaction. Loss of another ligand to provide an open coordination site was discounted by our failure to observe incorporation of $[D_9]PMe_3$ or ^{13}CO into **6b** (the instability of this compound precluded a full kinetic study). These observations and the activation parameters suggest that ligand dissociation is substantially slower than insertion.[12]

The lack of reactivity of the cresolato complex stands in marked contrast to Darensbourg's anionic aryloxido and fluoroalkoxido complexes which readily insert CO_2.[1b] We conclude that the actual insertion of CO_2 between the oxygen atom of the alkoxido ligand and the metal is a rapid bimolecular reaction, and that two factors are capable of promoting this process: a) negative charge on the complex, and b) the presence of a relatively electron-donating alkyl group attached to oxygen. Unfluorinated anionic alkoxido complexes, if they could be made, would combine these factors and should have exceptionally high reactivity toward carbon dioxide and other electrophilic species.

Received: July 26, 1991
Revised: September 2, 1991 [Z 4828 IE]
German version: *Angew. Chem.* **1992**, *104*, 209

CAS Registry numbers:
1, 138810-00-1; **2a**, 138695-26-8; **3a**, 138695-31-5; **4b**, 138695-32-6; **5b**, 138695-27-9; **5c**, 138695-30-4; **6b**, 138695-28-0; **6c**, 138695-29-1; **7b**, 138695-33-7; **7c**, 138695-34-8; **8b**, 138695-35-9; **8c**, 138722-00-6; CS_2, 75-15-0; p-$MeC_6H_4O^-$, 22113-51-5; MeO^-, 3315-60-4; CO_2, 124-38-9.

[1] For a review article on alkoxido and amido complexes of the late transition-metals (groups 8–10): a) H. E. Bryndza, W. Tam, *Chem. Rev.* **1988**, *88*, 1163. Recent examples of aryloxido and alkoxido complexes of metals from groups 6 and 7 in low oxidation states: Tungsten: b) D. J. Darensbourg, B. L. Mueller, J. H. Reibenspies, C. J. Bischoff *Inorg. Chem* **1990**, *29*, 1789; c) D. J. Darensbourg, K. M. Sanchez, J. H. Reibenspies, A. L. Rheingold, *J. Am. Chem. Soc.* **1989**, *111*, 7094; d) P. Kundel, H. Berke, *J. Organomet. Chem.* **1988**, *339*, 103; Rhenium: e) T. S. Cameron, K. R. Grundy, K. N. Robertson, *Inorg. Chem.* **1982**, *21*, 4149; f) K. R. Grundy, K. N. Robertson, *ibid.* **1985**, *24*, 3898; g) J. M. Fernandez, K. Emerson, R. D. Larsen, J. A. Gladysz, *J. Chem. Soc. Chem. Commun.* **1988**, 37; h) T. K. G. Erikson, J. C. Bryan, J. M. Mayer, *Organometallics* **1988**, *7*, 1930; i) While this work was in progress the synthesis of Mn and Re complexes similar to the ones described here were reported: S. K. Mandal, D. M. Ho, M. Orchin, *Inorg. Chem.* **1991**, *30*, 2244.

[2] X-ray structure of **2a** ($C_{46}H_{37}O_4P_2Re$): $M_r = 902.0$; clear crystals (0.15 × 0.33 × 0.44 mm); space group $Pbc2_1$ (No. 29); $a = 19.0169(16)$, $b = 20.6117(25)$, $c = 20.4698(22)$ Å, $\alpha = 90.0°$, $\beta = 90.0°$, $\gamma = 90°$; $V = 8023.6(25)$ Å^3; $Z = 8$; $\varrho_{calcd} = 1.49$ g cm^{-1}; $\mu_{calcd} = 31.9$ cm^{-1}. The structure was solved by Patterson methods and refined by standard least-squares and Fourier techniques. Because there were too few data to refine all atoms with anisotropic thermal parameters, only the Re, P, and the atoms of the carbonyl and cresol ligands refined anisotropically. Hydrogen atoms were included (except for those of the cresol methyl group) in idealized locations (values of B_{iso} were approximately 1.2 times the B_{eqv} of the atoms to which they were attached). Hydrogen atoms were included in the structure calculations but not refined. The final residuals for 494 variables refined against the 4286 reflections for which $F_2 > 3\sigma(F^2)$ were $R = 0.0307$, $R_w = 0.0355$, and GOF = 1.57. The R value for all 5417 reflections was $R = 0.0680$. Further details of the crystal structure investigation are available on request from the Director of the Cambridge Crystallographic Data Centre, University Chemical Laboratory, Lensfield Road, GB-Cambridge CB2 1EW (UK), on quoting the full journal citation.

[3] Typical experimental procedure: In an inert-atmosphere box, a Schlenk flask was charged with 50 mg of freshly cut sodium metal, stoppered, and removed from the box. Benzene (10 mL) and methanol (4 mL) were added via syringe. The resulting mixture was allowed to stir until effervescence had stopped. This solution was transferred via cannula to a rapidly stirred slurry of trifluoromethanesulfonate **5c** (625 mg, 0.877 mmol) in benzene (20 mL). The resulting mixture was allowed to stir under Ar for 12 h, after which time it was homogeneous. After this time the solvents were removed in vacuo and the resulting residue extracted with toluene (2 × 20 mL). The solvent was removed in vacuo to yield **6c** as a pale yellow powder (381 mg, 76%).

[4] Hydrogen bonds have been shown to form between metal-bound alkoxido ligands and free alcohols, for example: a) S. E. Kegley, C. J. Schaverien, J. H. Freudenberger, R. G. Bergman, S. P. Nolan, C. D. Hoff, *J. Am. Chem. Soc.* **1987**, *109*, 6563; b) C. Di Bugno, M. Pasquali, P. Leoni, P. Sabatino, D. Braga, *Inorg. Chem.* **1989**, *28*, 1390; c) Y.-J. Kim, K. Osakada, A. Takenaka, A. Yamamoto, *J. Am. Chem. Soc.* **1990**, *112*, 1096; d) K. Osakada, K. Ohshiro, A. Yamamoto, *Organometallics* **1991**, *10*, 404.

[5] The complexes $[(CH_3)Pt(dppe)(OCH_3)]$ and $[Ru(C_5Me_5)(OH)(PMe_3)_2]$ react with terminal alkynes to form σ-acetylide complexes without loss of ligands: a) H. E. Bryndza, L. K. Fong, R. A. Paciello, W. Tam, J. E. Bercaw, *J. Am. Chem. Soc.* **1987**, *109*, 1444; b) T. G. Appleton, M. A. Bennett, *J. Organomet. Chem.* **1973**, *55*, C88.

[6] An analogous reaction has been shown to occur with alkylrhenium complexes: J. G. Stack, R. D. Simpson, F. J. Hollander, R. G. Bergman, C. H. Heathcock, *J. Am. Chem. Soc.* **1990**, *112*, 2716.

[7] The complex **2a** also reacts with CS_2 at 45 °C, liberating triphenylphosphine and leading to a complex which was too insoluble to be characterized. Presumably this material is a dimer or higher oligomer. Complex **2c** does not react with CS_2.

[8] Experimental Procedure: In an inert-atmosphere box a glass vessel fitted with a Kontes vacuum-stopcock was charged with 50 mg (0.085 mmol) of **6c** and 3 mL of benzene, and transferred to a vacuum line. The vessel was frozen in liquid nitrogen and 0.255 mmol CO_2 was condensed into the vessel. As the reaction mixture thawed, the pale yellow solution quickly became colorless. After 1 h at room temperature the benzene was removed in vacuo to yield a white powder. This was returned to the inert-atmosphere box and washed with hexane (3 × 5 ml). The product was dissolved in CH_2Cl_2, hexane was layered on top of the solution, and the recrystallization mixture was cooled to −40 °C for 3 d. Complex **7c** was obtained as white crystals, 51 mg (98%).

[9] Further investigations of CS_2 and CO_2 insertions in metal–heteroatom bonds: ref. [1c] and a) B. P. Sullivan, M. R. M. Bruce, T. R. O'Toole, C. M. Bolinger, E. Megehee, H. Thorp, T. J. Meyer, *Catalytic Activation of Carbon Dioxide* (Ed.: W. M. Ayers), *ACS Symp. Ser. 363*, **1988**, pp. 52–90; b) A. Shaver, B. S. Lum, P. Bird, K. Arnold, *Inorg. Chem.* **1989**, *28*, 1900; c) L. J. Newman, R. G. Bergman, *J. Am. Chem. Soc.* **1985**, *107*, 5314.

[10] An ionization mechanism has been shown to be operative for the insertion of CO into the Ir–O bond of *trans*-[Ir(CO)(OR)$(PPh_3)_2$]: W. M. Rees, M. R. Churchill, J. C. Fettinger, J. D. Atwood, *Organometallics* **1985**, *4*, 2179.

[11] A large solvent effect observed for CO_2 insertion into a Re–O bond has been rationalized as resulting from metal-to-ligand charge transfer (see ref. [1c]).

[12] Photoinduced CS_2 insertion into a W–CH_3 bond has been reported: D. J. Darensbourg, H. P. Wiegreffe, J. H. Reibenspies, *Organometallics* **1991**, *10*, 6. In our experiment the rates of CS_2 insertion were unchanged when stray light was rigorously excluded.

A New Fullerene Synthesis**

By *Gregor Peters* and *Martin Jansen**

The fullerenes,[1] pure carbon molecules C_n with $n = 28–94$,[2] are a third allotropic form of carbon, or rather a family of allotropes, after graphite and diamond.[3] They offer fascinating perspectives for basic as well as applied research. Potential topics range from application in unaltered forms as materials or catalysts, to investigations of their solid-state reactions with metals and nonmetals, conversions to three-dimensional porous materials, and the numerous imaginable electrocyclic reactions of the olefinlike fullerene system.[4] Until now progress in this research has been hampered by the poor availability of the fullerenes.

The laser vaporization technique developed by Smalley and Kroto[1a,5] and the isolation of fullerenes from the soot produced by optimized flames[6] are not useful methods for the preparation of significant amounts of fullerenes. Both methods have been outstripped by the process developed by Krätschmer and Huffman in which graphite is evaporated in an electric arc by resistive heating.[7] The conditions necessary for the spontaneous formation of fullerenes are for the most part not known. Important parameters include the composition of the gas phase with respect to the type and pressure of the cooling gas as well as the temperature, which reaches up to 6000 °C in the arc. In our search for other methods of production (continuous if possible) with an optimizable space–time yield we first considered the thermal evaporation of carbon at significantly lower temperatures.

Cylindrical bodies made of carbon of various quality (isotactically pressed purest graphite, pyrolytic graphite, and glassy carbon containing residual hydrogen obtained from polymeric precursors) were heated inductively and evaporated. The apparatus employed is sketched in Figure 1. Graphite evaporates noticeably at temperatures above 2500 °C[8] under a helium atmosphere (150 hPa).[9] But the soot collected on the cooled quartz surface of the reaction tube is still free of fullerenes at vaporization temperatures between 2500 and 2600 °C. If the vaporization is conducted at 2700 °C, however, good yields of fullerenes can be obtained from the collected soot. The surprisingly low temperature of formation and the possibility of adapting this method for continuous production (by moving the graphite cylinder or the inductor) could be options in the production of larger amounts of fullerenes.

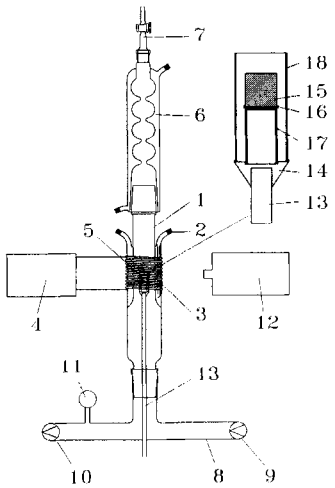

Fig. 1. Cross section of the high-frequency apparatus for the preparation of fullerenes (actual dimensions of the quartz tube: 70 mm diameter, 500 mm height). Quartz tube (1) with water jacket (2), inductor (3), HF generator (4), inductive heating zone (5), condensor (6) with vent (7), T-joint (8), gas-inlet valve (9), valve to vacuum pump (10), manometer (11), pyrometer (12), water-cooled copper tube (13), copper block (14), carbon body (15), graphite or boron nitride platform (16), boron nitride platform support (17), boron nitride insulation tube (18).

The fullerene content of the toluene extracts was determined by mass spectrometry.[10] We found that the percentage of fullerenes of higher molecular-weight (> 720 includ-

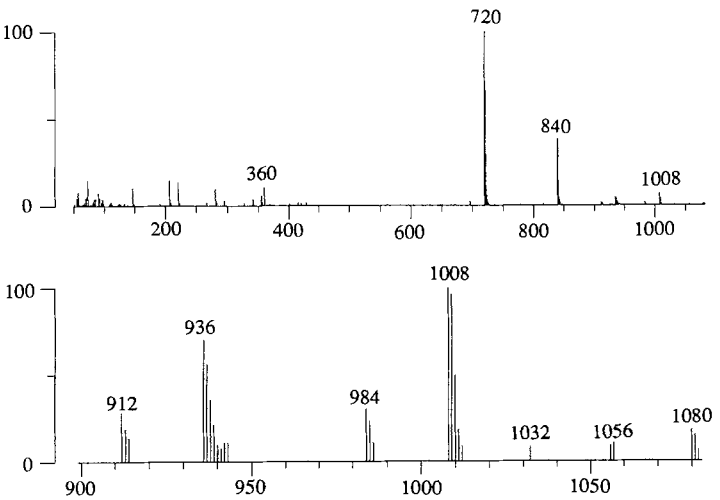

Fig. 2. Mass spectrum (above) of the toluene extract of the soot and an enlargement (below) of one portion. The relative frequency in % is plotted against m/z.

[*] Prof. Dr. M. Jansen, Dipl.-Chem. G. Peters
Institut für Anorganische Chemie der Universität
Gerhard-Domagk-Strasse 1, D-W-Bonn 1 (FRG)

[**] This research was supported by the Deutsche Forschungsgemeinschaft (Leibniz-Programm) and the Fonds der Chemischen Industrie.

ing C_{60}) is greater here than that observed in the crude fullerene mixture obtained from the electric arc.[7] A typical mass spectrum is shown in Figure 2. This indicates a fullerene composition (in decreasing amounts) of C_{60} (m/z 720), C_{70} (840), C_{84} (1008), C_{78} (936), C_{82} (984), C_{76} (912), C_{90} (1080), C_{88} (1056), C_{86} (1032).

Experimental Procedure

In the evaporation of graphite in a high-frequency furnace (Hüttinger IG 15/400, high-resistance version of a Hartley switch, 15 kW terminal power, 500 kHz) the following parameters were varied: a) graphite quality: purest graphite (EK 966, Ringsdorff, Bonn), pyrolytic graphite (Ringsdorff, Bonn), glassy carbon (Sigri, Meitingen); b) shape of the graphite bodies: tubes, cylinders, some slitted or laminated, some with cone-shaped cavities; c) thermal isolation by one or two additional boron nitride tubes between the graphite body and the water-cooled glass tube; d) water-cooling and inductor; e) type of cooling gas (Ar, He) and the pressure of the cooling gas.
These investigations led to the following optimized procedure: The apparatus (Fig. 1) was evacuated (10^{-3} hPa) and flushed a number of times and finally heated in vacuum and then under a stream of inert gas (each heating lasted 20 min). The graphite body was heated quickly (over several min) to 2700 °C and evaporated at this temperature under a weak helium stream (150 hPa). The soot deposited on the inside of the PBN insulation tube never contained fullerenes. Most of the soot collected on the wall of the quartz tube and had a large proportion of fullerene products. This soot was removed from the quartz tube with a brush. The fullerenes were extracted from the soot with toluene yielding a deep-red solution. The evaporation of 1 g of graphite in 10 min provided 80–120 mg of crude fullerenes.

Received: November 29, 1991 [Z 5044 IE]
German version: *Angew. Chem.* **1992**, *104*, 240

CAS Registry numbers:
Fullerenes, 99685-96-8; graphite, 7782-42-5; He, 7440-59-7.

[1] a) H. W. Kroto, J. R. Heath, S. C. O'Brien, R. F. Curl, R. E. Smalley, *Nature* **1985**, *318*, 162–163; b) R. F. Curl, R. E. Smalley, *Science* **1988**, *242*, 1017–1022.
[2] H. W. Kroto, *Pure Appl. Chem.* **1990**, *62*, 407–415; R. Ettl, J. Chao, F. Diederich, L. Whetten, *Nature* **1991**, *353*, 149–153; F. Diederich, R. Ettl, Y. Rubin, R. L. Whetten, R. Beck, M. Alvarez, S. Anz, D. Sensharma, F. Wudl, K. C. Khemani, A. Koch, *Science* **1991**, *252*, 548–551; D. H. Parker, P. Wurz, K. Chatterjee, K. R. Lykke, J. E. Hunt, M. J. Pellin, J. C. Hemminger, D. M. Gruen, L. M. Stock, *J. Am. Chem. Soc.* **1991**, *113*, 7499–7503.
[3] J. F. Stoddart, *Angew. Chem.* **1991**, *103*, 71–72; *Angew. Chem. Int. Ed. Engl.* **1991**, *30*, 70; H. W. Kroto, A. W. Allaf, S. P. Balm, *Chem. Rev.* **1991**, *91*, 1213–1235.
[4] J. S. Miller, *Adv. Mater.* **1991**, *3*, 262–265; F. Diederich, R. L. Whetten, *Angew. Chem.* **1991**, *103*, 695–697; Angew. Chem. Int. Ed. Engl. **1991**, *30*, 678–680.
[5] T. G. Dietz, M. A. Duncan, D. E. Powers, R. E. Smalley, *J. Chem. Phys.* **1981**, *74*, 6511–6512; R. E. Haufler, Y. Chai, L. P. F. Chibante, J. Conceicao, C. Jin, L. S. Wang, S. Maruyama, R. E. Smalley, *Mater. Res. Soc. Symp. Proc.* **1991**, *206*, 627–637.
[6] J. B. Howard, J. McKinnon, Y. Makarovsky, L. Laflleur, M. Elaine Johnson, *Nature* **1991**, *352*, 139–141.
[7] W. Krätschmer, K. Fostiropoulos, D. R. Huffman, *Chem. Phys. Lett.* **1990**, *170*, 167–170; W. Krätschmer, L. D. Lamb, K. Fostiropoulos, D. R. Huffman, *Nature* **1990**, *347*, 354–358; A. S. Koch, K. C. Khemani, F. Wudl, *J. Org. Chem.* **1991**, *56*, 4543–4545.
[8] The temperature could be measured pyrometrically on the graphite surface until soot formation started. Then the temperature was determined by extrapolation based on the power data of the generator.
[9] The necessary inert conditions can be best obtained by the use of a water-cooled quartz reaction tube, which is connected by a ground metal joint to a gas-inlet valve and a valve to a vacuum pump. A balance must be made between the power supplied to the inductor of the HF generator and the power lost by the cooling water. The heat loss can be reduced substantially by the use of a single- or double-walled insulation tube made of pyrolytic boron nitride (PBN) which increases the temperature at the location of the graphite body and reduces the temperature of the quartz surface. An additional effect of the PBN tube is seen in the creation of a larger hot reaction zone (possible gas-phase deposition of fullerene on soot particles) and in a chimney effect.
[10] The mass spectra were recorded with a Concept 1H spectrometer (Kratos, Manchester). Ionization method: EI.

New Route to α-[(1*E*,3*E*)-dienyl]allenes via Butadiene-tricarbonyliron Complexes**

By *Kurt Nunn, Paul Mosset, René Grée,* Rolf W. Saalfrank,* Karl Peters,* and *Hans Georg von Schnering*

Allenes are readily accessible from propargyl derivatives through reactions with organocopper(I) reagents.[1] The stereochemistry of this transformation results from an SN2′ process, which usually favors *anti*-configurated products.[1m, 1n, 2, 3] Organocopper(I) reagents of the type [RCuX)M] (X = halogen, M = Li, MgX) are preferable in this reaction since diorganocuprates [R_2Cu)M] are known to racemize chiral allenes.[4, 1k, 1n]

Here, we report on our successful synthesis of acyclic α-dienylallenes **7**, starting from complex **1**.[5] The introduction of planar chirality by the $Fe(CO)_3$-organometallic moiety enables us to verify the stereochemical course of the propargyl–allene transformation, since a partial epimerization of the allene part would generate two easily distinguishable diastereoisomeric α-(allenylbutadiene)tricarbonyliron complexes.

Reaction of butadienetricarbonyliron complex **1**[5] with 1-lithioalkynes **2** in the presence of lithium bromide (THF, −78 °C, 3 h) afforded ψ-*exo* and ψ-*endo* alcohols **3** and **4**[6] in 73–82 and 10–18% yield, respectively, after easy separation by chromatography on silica gel (Scheme 1). Due to the

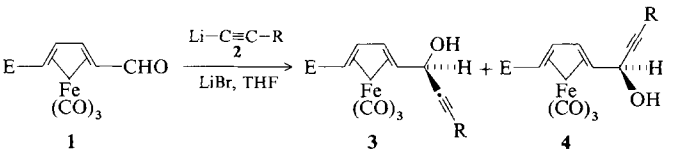

Scheme 1. E = CO_2Me. Reaction at −78 °C for 3 h.

stereoelectronic effects of the $Fe(CO)_3$ moiety of **3**, the choice of an appropriate nucleofugal group was rather difficult. Among numerous experiments, treatment of the alcohols **3** with phenyl chloroformate in the presence of pyridine in THF, and in situ[7] reaction of the resulting crude carbonates with six equivalents of (EtCuBr)MgBr · LiBr or (*t*Bu-

Table 1. Substituents R for compounds **2**–**5** and **7** and the yields of **3**–**5** and **7**.

2–5, 7	**a**	**b**	**c**	**d**	**e**
R	Ph	CH_2Ph	*n*Bu	*t*Bu	$SiMe_3$
Yield of **3** [%]	82	82	80	76	73
Yield of **4** [%]	13	13	12	10	18
Yield of **5** [%]	81	75	55 [a]	23	[b]
Yield of **7** [%]	88	72	77	–	–

[a] The reaction of **3c** with (*t*BuCuBr)MgBr · LiBr furnished **5f** in 77% yield.
[b] The reaction of **3e** with (*t*BuCuBr)MgBr · LiBr yielded a complex mixture.

[*] Dr. R. Grée, Dr. P. Mosset
Laboratoire de Chimie Organique Biologique, CNRS URA 1467, ENSCR
Avenue du Gal Leclerc
35700 Rennes-Beaulieu (France)
Prof. Dr. R. W. Saalfrank, K. Nunn
Institut für Organische Chemie der Universität Erlangen-Nürnberg
Henkestrasse 42, W-8520 Erlangen (FRG)
Dr. K. Peters, Prof. Dr. H.-G. von Schnering
Max-Planck-Institut für Festkörperforschung,
Heisenbergstrasse 1, W-7000 Stuttgart 80 (FRG).

[**] This work was supported by the Ministère des Affaires Etrangères Deutschen Akademischen Austauschdienst (MAE/DAAD) within the framework of project-oriented promotion of the scientific exchange between France and Germany (PROCOPE). K. N. thanks the Freistaat Bayern for a study grant.

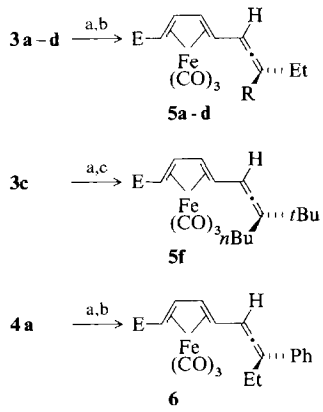

Scheme 2. E = CO_2Me. a) $ClCO_2Ph$, pyridine, THF, 25 °C, 10 min; b) (EtCuBr)MgBr · LiBr, ether, −65 °C, 15 min; c) (*t*BuCuBr)MgBr · LiBr.

CuBr)MgBr · LiBr gave the highest yields for the α-(allenylbutadiene)tricarbonyliron complexes **5a–c** or **5f** (81, 75, 55, and 77%)[8] (Scheme 2). Each of the allenes was formed as a single isomer as judged by NMR ($ds \geq 95\%$).

Starting from **3a** or **4a**, respectively, and (EtCuBr)MgBr · LiBr, the α-allenylbutadienetricarbonyliron complexes **5a** and **6** are formed (81 and 61%, Scheme 2). Complexes **5a** and **6** are clearly different by NMR. The relative stereochemistry of the allene and organometallic moieties was unequivocally established by X-ray crystallography (Fig. 1).[9]

These results strongly support a formal 1,3-*anti*-substitution mechanism for the formation of acyclic allenes from propargylic esters and organocopper(I) reagents.[1n]

Table 2. Physical data for **5a**, **6**, and **7a**.

5a: M.p. = 86 °C (light petroleum ether); IR (KBr): $\tilde{\nu}$ [cm^{-1}] = 2050, 1995, 1970, 1935 (sh), 1705; ^1H NMR (400 MHz, $CDCl_3$): δ = 1.17 (dd, 1 H, J = 8.2, 0.6 Hz, H-C_2), 1.21 (t, 3 H, J = 7.3 Hz, H-C_{10}), 2.14 (ddd, 1 H, J = 10.0, 8.9, 1.0 Hz, H-C_5), 2.47 (dqd, 1 H, J = 15.7, 7.3, 3.5 Hz, H-C_9), 2.55 (dqd, 1 H, J = 15.7, 7.3, 3.5 Hz, H-C_9), 3.66 (s, 3 H, OCH_3), 5.42 (ddd, 1 H, J = 8.9, 5.2, 0.6 Hz, H-C_4), 5.66 (dt, 1 H, J = 10.0, 3.5 Hz, H-C_6), 5.84 (ddd, 1 H, J = 8.2, 5.2, 1.0 Hz, H-C_3), 7.21 (ddt, 1 H, *para*, arom., J = 8.0, 6.0, 1.5 Hz), 7.28–7.38 (m, 4 H arom.); ^{13}C NMR (100 MHz, $CDCl_3$): δ = 12.08 (C10), 23.10 (C9), 45.38 (C2), 51.68 (OCH_3), 60.11 (C5), 83.21, 84.54 (C3, C4), 98.66 (C6), 110.67 (C8), 126.15 (2 arom. CH), 127.14 (*para*-CH), 128.40 (2 arom. CH), 135.82 (C arom.), 172.61 (C1), 206.37 (C7), 209.6 (CO-Fe); UV (MeCN): λ_{max} [nm] (ε) = 255 (41000), 305 (sh, 9700); MS, EI: *m/z* of major fragments: 394 ($M^{\oplus}$, 10%), 366 ($M^{\oplus}$-CO, 9), 363 ($M^{\oplus}$-OMe, 2), 338 ($M^{\oplus}$-2 CO, 0.5), 310 ($M^{\oplus}$-3 CO, 100), 278 (19), 250 (59), 236 (26), 165 (40), 115 (24), 91 (21), 56 (55).

6: M.p. 72 °C (*n*-pentane); IR (Nujol): $\tilde{\nu}$ [cm^{-1}] = 2060, 2000, 1980, 1700; ^1H NMR (400 MHz, $CDCl_3$): δ = 1.115 (t, 3 H, J = 7.3 Hz, H-C10), 1.19 (dd, 1 H, J = 8.2, 0.8 Hz, H-C2), 2.07 (ddd, 1 H, J = 9.6, 8.9, 1.0 Hz, H-C5), 2.465 (dq, 2 H, J = 7.3, 3.1 Hz, H-C9), 3.65 (s, 3 H, OCH_3), 5.43 (ddd, 1 H, J = 8.9, 5.1, 0.8 Hz, H-C4), 5.67 (dt, 1 H, J = 9.6, 3.1 Hz, H-C6), 5.84 (ddd, 1 H, J = 8.2, 5.1, 1.0 Hz, H-C3), 7.30 (ddt, 1 H, *para*, arom., J = 8.0, 6.0, 1.5 Hz), 7.30–7.48 (m, 4 H arom.); ^{13}C NMR (100 MHz, $CDCl_3$): δ = 12.72 (C10), 22.96 (C9), 45.47 (C2), 51.71 (OCH_3), 59.86 (C5), 83.25, 84.28 (C3, C4), 98.19 (C6), 110.76 (C8), 126.18 (2 arom. CH), 127.18 (*para*, CH), 128.52 (2 arom. CH), 135.70 (C arom.), 172.66 (C1), 206.32 (C7); MS, EI, the same main fragments as those for **5a** with very similar relative intensities.

7a: M.p. 74 °C (ether/petroleum ether 4:1); IR (Nujol): $\tilde{\nu}$ [cm^{-1}] = 1925, 1715, 1620; ^1H NMR (400 MHz, $CDCl_3$): δ = 1.14 (t, 3 H, J = 7.3 Hz, H-C10), 2.49 (dqd, 1 H, J = 15.5, 7.3, 3.3 Hz, H-C9), 2.52 (dqd, 1 H, J = 15.5, 7.3, 3.3 Hz, H-C9), 3.74 (s, 3 H, OCH_3), 5.875 (d, 1 H, J = 15.3 Hz, H-C2), 6.32 (dt, 1 H, J = 10.5, 3.3 Hz, H-C6), 6.36 (dd, 1 H, J = 14.8, 11.0 Hz, H-C4), 6.48 (dd, 1 H, J = 14.8, 10.5 Hz, H-C5), 7.22 (ddt, 1 H, *para*, arom., J = 7.5, 6.6, 1.4 Hz), 7.28–7.40 (m, 4 H arom. and H-C3, dd, δ = 7.325, J = 15.3, 11.0 Hz); ^{13}C NMR (100 MHz, $CDCl_3$): δ = 12.48 (C10), 23.10 (C9), 51.50 (OCH_3), 98.16 (C6), 109.85 (C8), 119.96 (C4), 126.23 (2 arom. CH), 127.23 (*para*, CH), 128.51 (2 arom. CH), 128.61 (C2), 135.60 (C arom.), 137.14 (C5), 144.46 (C3), 167.53 (C1), 211.14 (C7); UV (MeCN): λ_{max} [nm] (ε) = 255 (11000), 300 (49000); MS, EI: *m/z* of major fragments: 254 ($M^{\oplus}$, 65%) 239 ($M^{\oplus}$-Me, 6), 225 ($M^{\oplus}$-Et, 9), 223 ($M^{\oplus}$-OMe, 16), 207 (19), 195 (81), 179 (62), 165 (100), 117 (62), 91 (95), 77 (28).

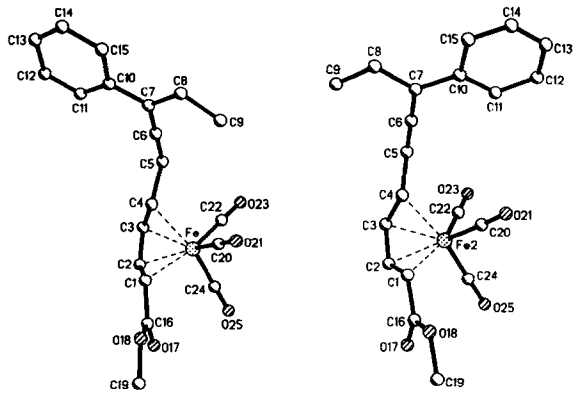

Fig. 1. Molecular structures of **5a** (left) and **6** (right) in the solid state.

Decomplexation of **5a–c** with ceric ammonium nitrate removed the organometallic moiety to afford the air-sensitive colorless α-dienylallenes **7a–c** (Scheme 3). The *E,E* stereochemistry of the diene unit was established by ^1H NMR ($J_{2,3}$ = 15.3 Hz, $J_{4,5}$ = 14.8–15.0 Hz). Starting from enantiomerically pure **5a–c** should lead to chiral non-racemic α-dienylallenes **7a–c** provided that the decomplexation step is accomplished without racemization.

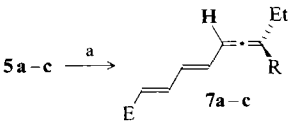

Scheme 3. E = CO_2Me. a) 3.5 equiv ceric ammonium nitrate, MeOH, 0 °C

To the best of our knowledge, this is the first example where allenes are obtained in the presence of a butadienetricarbonyliron organometallic moiety. The excellent reactivity of the carbonate leaving group compared to that of acetates and benzoates must be emphasized. Furthermore, these α-dienylallenes may be good substrates for sigmatropic rearrangements as shown by some studies in the retinoid field[1j, 10] or provide an entry to natural products[11] such as the antibiotic mycomicin[12] and its analogues.

Experimental Procedure

5a: To a solution of $LiCuBr_2$ cooled at −65° [6 equiv; prepared from lithium bromide (410 mg, 4.7 mmol) and cuprous bromide (680 mg, 4.7 mmol)] in THF (10 mL) was added an solution (8 mL) of ethylmagnesium bromide in ether [prepared from magnesium turnings (125 mg, 5.1 mmol) and bromoethane (0.35 mL, 4.7 mmol)]. After 30 min at −65 °C, a solution of propargylic carbonate was added. This was prepared by sequential addition of pyridine (0.165 mL, 2.05 mmol, 2.6 equiv) and phenyl chloroformate (0.13 mL, 1.01 mmol, 1.3 equiv) to a stirred THF solution (5 mL) of propargylic alcohol **3a** (300 mg, 0.78 mmol) followed by 10 min reaction at room temperature. After 15 min reaction at −65 °C between the carbonate and (EtCuBr)MgBr · LiBr, the reaction mixture was poured onto 25% aqueous ammonium chloride (100 mL) containing sodium cyanide (3 g). The resulting mixture was extracted twice with ether, and the combined organic extracts were dried with $MgSO_4$ and concentrated. Flash-chromatography of the remaining oily residue on silica gel (45 g) with ether/petroleum ether (1:19) as eluent afforded the allene **5a** as an orange oil which solidified on cooling.

7a: To a solution of complex **5a** (93 mg, 0.24 mmol) cooled to 0 °C in anhydrous methanol (5 mL) was added portionswise over 15 min ceric ammonium nitrate (448 mg, 0.82 mmol, 3.5 equiv). After stirring for a further 10 minutes at 0 °C, the reaction mixture was diluted with ether and water. The aqueous phase was extracted with ether and combined organic extracts were washed with brine. Drying ($MgSO_4$), concentration, and flash-chromatography of the remaining residue with ether/petroleum ether (1:9 and then 1:4) as eluents yielded **7a** (53 mg, 88%) as a white solid which gradually turned yellow upon exposure to air.

The physical data of compounds **5a**, **6**, and **7a** are listed in Table 2.

Received: July 5, 1991 [Z 4772 IE]
German version: *Angew. Chem.* **1992**, *104*, 228

[1] a) P. Ortiz de Montellano, *J. Chem. Soc. Chem. Commun.* **1973**, 709; b) P. Vermeer, J. Meijer, C. De Graaf, H. Schreurs, *Rec. Trav. Chim. Pays-Bas* **1974**, *93*, 46; c) A. Alexakis, J. F. Normant, J. Villieras, *J. Molecular Catalysis* **1975/1976**, *1*, 43; d) G. Tadema, P. Vermeer, J. Meijer, L. Brandsma, *Rec. Trav. Chim. Pays-Bas* **1976**, *95*, 66; e) A. Alexakis, A. Commercon, J. Villieras, J. F. Normant, *Tetrahedron Lett.* **1976**, 2313; f) *The Chemistry of Allenes, Vol. 1–3*, (Ed.: S. R. Landor), Academic, London, **1982**; g) A. C. Oehlshlager, E. Czyzewska, *Tetrahedron Lett.* **1983**, *24*, 5587; h) H. F. Schuster, G. M. Coppola: *Allenes in Organic Synthesis*, Wiley, New York, **1984**; i) C. Sahlberg, A. Claesson, *J. Org. Chem.* **1984**, *49*, 4120, and references cited therein; j) T. C. Norman, A. R. de Lara, W. H. Okamura, *Tetrahedron Lett.* **1988**, *29*, 1251; k) C. J. Elsevier, P. Vermeer, *J. Org. Chem.* **1989**, *54*, 3726, and references cited therein; l) K. M. Wu, M. M. Midland, W. H. Okamura, *ibid.* **1990**, *55*, 4381, and references cited therein; m) A. Alexakis, I. Marek, P. Mangeney, J. F. Normant, *J. Am. Chem. Soc.* **1990**, *112*, 8042; n) O. W. Gooding, C. C. Beard, D. Y. Jackson, D. L. Wren, G. F. Cooper, *J. Org. Chem.* **1991**, *56*, 1083, and references cited therein; o) A. Alexakis, I. Marek, P. Mangeney, J. F. Normant, *Tetrahedron* **1991**, *47*, 1677.

[2] C. J. Elsevier, J. Meijer, H. Westmijze, P. Vermeer, L. A. van Dijck, *J. Chem. Soc. Chem. Commun.* **1982**, 84.

[3] For examples where both *syn* and *anti* processes occur see [1m,o].

[4] A. Claesson, L.-I. Olsson, *J. Chem. Soc. Chem. Commun.* **1979**, 524.

[5] Although we worked with racemic compounds, all the representations are made for clarity as if this study was performed starting with (R,S)-**1**. Furthermore, the complex **1** can be easily resolved, see A. Monpert, J. Martelli, R. Grée, R. Carrié, *Tetrahedron Lett.* **1981**, *22*, 1961.

[6] For this terminology see N. A. Clinton, C. P. Lillya, *J. Am. Chem. Soc.* **1970**, *92*, 3058.

[7] The intermediate carbonates could not be isolated since they were quickly oxidized by air contact and had therefore to be used in situ.

[8] A limitation of this reaction was observed since **5d** was obtained in 23% yield and was moreover the only allenic compound of this study which was not enough pure for microanalysis. The reaction of **3e** with (EtCuBr)MgBr · LiBr yielded a complex mixture.

[9] Crystal data for **5a**: monoclinic, space group: $P2_1/c$, $a = 9.495(4)$, $b = 18.705(7)$, $c = 11.262(3)$ Å, $\beta = 107.70(3)°$, $M = 394.21$, $V = 1906.(1)$ Å^3, $Z = 4$, $\rho_{calcd} = 1.347$ g cm^{-3}, $Mo_{K\alpha}$ radiation. 4795 measured reflections, 4405 unique reflections, 3745 reflections with $F > 3\sigma(F)$. Full-matrix least-squares refinement gave $R = 0.042$, $R_w = 0.040$. Crystal data for **6a**: orthorhombic, space group: $Pna2_1$, $a = 19.610(5)$, $b = 13.566(6)$, $c = 14.777(6)$ Å, $M = 394.21$, $V = 3931.(3)$ Å^3, $Z = 8$, $\rho_{calcd} = 1.332$ g cm^{-3}, $Mo_{K\alpha}$ radiation. 5062 measured reflections, 4721 unique reflections, 3774 reflections with $F > 3\sigma(F)$. Full-matrix least-squares refinement gave $R = 0.048$, $R_w = 0.042$. Program used: Siemens SHELXTL PLUS (Micro Vax II). Further details may be obtained from the Fachinformationszentrum Karlsruhe, Gesellschaft für wissenschaftlich-technische Information mbH, W-7514 Eggenstein-Leopoldshafen 2 (FRG), on quoting the depository number CSD-55335, the names of the authors, and the journal citation.

[10] a) J. Sueiras, W. H. Okamura, *J. Am. Chem. Soc.* **1980**, *102*, 6255; b) W. H. Okamura, M. L. Curtin, *Synlett* **1990**, 1 and references cited therein.

[11] G. Balme, M. Malacria, J. Goré, *J. Chem. Res.* **1981**, (M) 2869; (S) 244.

[12] W. D. Celmer, I. A. Solomons, *J. Am. Chem. Soc.* **1952** *74*, 1870, 2245, 3838; *ibid.* **1953**, *75*, 1372, 3430. For a clinical use of mycomycin, see F. Fraschini et al. *Drugs Exp. Clin. Res.* **1988**, *14*, 253.

Ion-Spray Mass Spectrometry of Lipopeptide Vaccines**

By *Jörg W. Metzger, Werner Beck,* and *Günther Jung**

Dedicated to Professor Michael Hanack on the occasion of his 60th birthday

Ion spray (IS) is a soft ionization method in which a solution of the analyte is sprayed with compressed air through a capillary that is held at several kilovolts.[1] The high electric field and nebulization causes the formation of highly charged droplets from which predissolved ions are emitted directly into the gas phase. Two models for the mechanism of ion production from charged droplets are at present under discussion: ion evaporation[2] and Rayleigh disintegration.[3] The pneumatic nebulization assists droplet formation effecting a more stable ion current and therefore allows higher flow rates[1] than the closely related electrospray[4] technique. IS ionization takes place at atmospheric pressure (atmospheric pressure ionization mass spectrometry, API–MS). After ejection from the liquid the ions are sampled through a small orifice into the mass spectrometer. As no heat is applied, ion spray mass spectrometry (IS–MS) provides a highly sensitive method for molecular mass determination of thermolabile molecules like peptides and proteins.[5]

For routine analysis of a polypeptide or a protein the sample is dissolved and continuously introduced into the IS source at flow rates up to 200 μL min^{-1}. Sensitivity increases with decreasing flow rate. IS mass spectra of peptides or a protein consist of a series of peaks arising from singly and multiply charged, protonated molecular ions $[M + n\mathrm{H}]^{n+}$. For most peptides and proteins the multiplicity is related to the number of basic lysine, arginine, and histidine residues in addition to the *N*-terminal α-amino group.[5, 6] Each peak in the spectrum constitutes an independent measure of the mass of the parent species; from each pair of adjacent peaks the molecular mass can be calculated.[7] Therefore mass assignment can be made with greater precision and more confidence than is possible with singly charged ions. The effective mass range of any analyzer is increased by a factor equal to the number of charges on an ion. This opens the intriguing possibility to determine molecular masses of biomolecules in the kD range with quadrupole analyzers.

The increasing importance of synthetic lipopeptide vaccines for immunological screening[8] and the lack of a simple and reliable routine method for the characterization of these compounds were the reasons for this study. The synthetic vaccines investigated consist of the three-chain lipoamino acid *N*-palmitoyl-*S*-[2,3-bis(palmitoyloxy)-propyl]-(*R*)-cysteine (tripalmitoyl-*S*-glycerylcysteine, Pam_3Cys-OH; molecular mass 910.5 u)[9] and selected partial sequences (B- and T-cell epitopes containing 15–25 amino acids) of viral proteins.[8] We found IS–MS to be an extremely valuable tool for characterizing these compounds and their precursors. As common aqueous solvent mixtures cannot be used for the analysis of these highly lipophilic, water-insoluble compounds, we evaluated the possibility of using organic solvent mixtures for IS–MS.[10] Smaller lipopeptides of this kind, for example, the amphiphilic lipohexapeptide Pam_3Cys-Ser-$(Lys)_4$[11] or related lipoids[12] we could analyze by field-desorption mass spectrometry and plasma desorption mass spectrometry. Matrix-assisted laser desorption[13] has also be proven to be a powerful method for the mass determination of large lipophilic compounds.

Lipopeptide vaccines[8] are usually built up by solid-phase peptide synthesis (Merrifield synthesis). The lipoamino acid Pam_3Cys-OH is attached to the antigenic determinant either *N*-terminally in the last coupling step[8] or *C*-terminally beginning the synthesis with Pam_3Cys-Lys(Fmoc)-OH (Fmoc = 9-fluorenylmethoxycarbonyl) as a resin-bound building block.[14] A third possibility is to introduce *O,O'*-dipalmitoyl-*S*-glyceryl-cysteine within a peptide chain using an N_α-Fmoc protected derivative.[15] Thus, the partial sequence 135–154 of O_1K foot-and-mouth disease virus VP1[8], an icosapeptide, was built up on an acid-labile resin using Fmoc/*t*Bu strategy. This epitope contains three arginine residues, which were introduced by using Fmoc-Ar-

[*] Prof. Dr. G. Jung, Dr. J. W. Metzger, Dipl. Chem. W. Beck
Institut für Organische Chemie der Universität
Auf der Morgenstelle 18, D-W-7400 Tübingen (FRG).

[**] This work was supported by the Deutsche Forschungsgemeinschaft (SFB 323).

g(Mtr)-OH (Mtr = 4-methoxy-2,3,5-trimethylbenzenesulfonyl). Especially in longer sequences the quantitative removal of Mtr with trifluoroacetic acid can be problematic, even with elevated temperatures and prolonged reaction times. For controlling the synthesis of this epitope a small amount of the synthesized resin-bound peptide (the antigenic determinant) was split off the resin prior to the coupling of lipoamino acid Pam_3Cys-OH. The resultant crude peptide VP1 (135–154) was investigated by IS-MS. The mass spectrum showed the doubly, triply, and quadruply charged quasimolecular ions of three different peptides: the expected free peptide VP1 (135–154) (molecular mass 2325.7 u) and two partially deprotected peptides containing one and two Mtr protecting groups at the arginyl side chain (molecular masses 2537.9 and 2750.2 u; Fig. 1a). Optimized coupling and deprotection conditions afforded pure VP1 (135–154) (Fig. 1b).

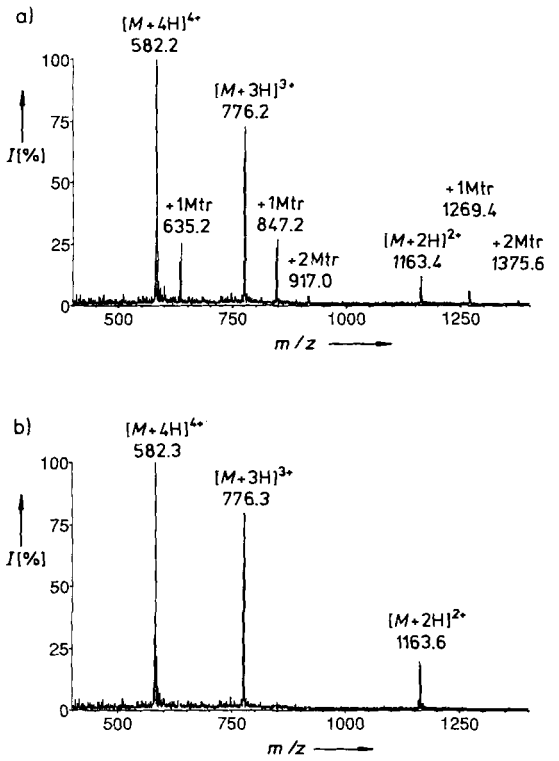

Fig. 1. a) IS mass spectrum of a peptide mixture obtained by solid phase peptide synthesis of the icosapeptide VP1 (135–154). Three series of doubly, triply, and quadruply charged ions indicate the presence of the free peptide (calculated molecular mass 2325.7) and two partially deprotected peptides (calculated molecular masses 2537.9 and 2750.2). b) the icosapeptide VP1 (135–154) (molecular mass 2325.7) obtained after optimizing coupling and cleavage conditions. The mass values annotated above the (not centroided) peaks correspond to the observed peak apices.

N-terminal coupling of the lipoamino acid Pam_3Cys-OH to the resin-bound peptide and subsequent cleavage from the resin with trifluoroacetic acid resulted in a conjugate,[8] which was only sparingly soluble in water or water/methanol mixtures.

We tried different mixtures of organic solvents including chloroform, dichloromethane, dimethylformamide, methanol, acetonitrile, 2-propanol, and *tert*-butyl alcohol for investigating such lipopeptides. Optimal results were obtained when the synthetic vaccine was pre-dissolved in chloroform (two parts by volume) followed by addition of methanol (three parts by volume) and 10% aqueous formic acid or 1% ammonium acetate (one part by volume). Chloroform/methanol mixtures not containing any acid or salt, which have been reported to give good ion yields with the atmospheric pressure spray method,[16] did not lead to satisfying results with the IS technique. The solution was introduced into the IS source at a flow rate of 5 $\mu L\,min^{-1}$. The IS mass spectra of Pam_3Cys-Ser-Ser-[VP1 (135–154)] (calcd. 3392 u; Fig. 2a) and Pam_3Cys-Lys([VP1 (135–154)])-Ala (calcd. 3417 u; Fig. 2b), a conjugate where the lipoamino acid was

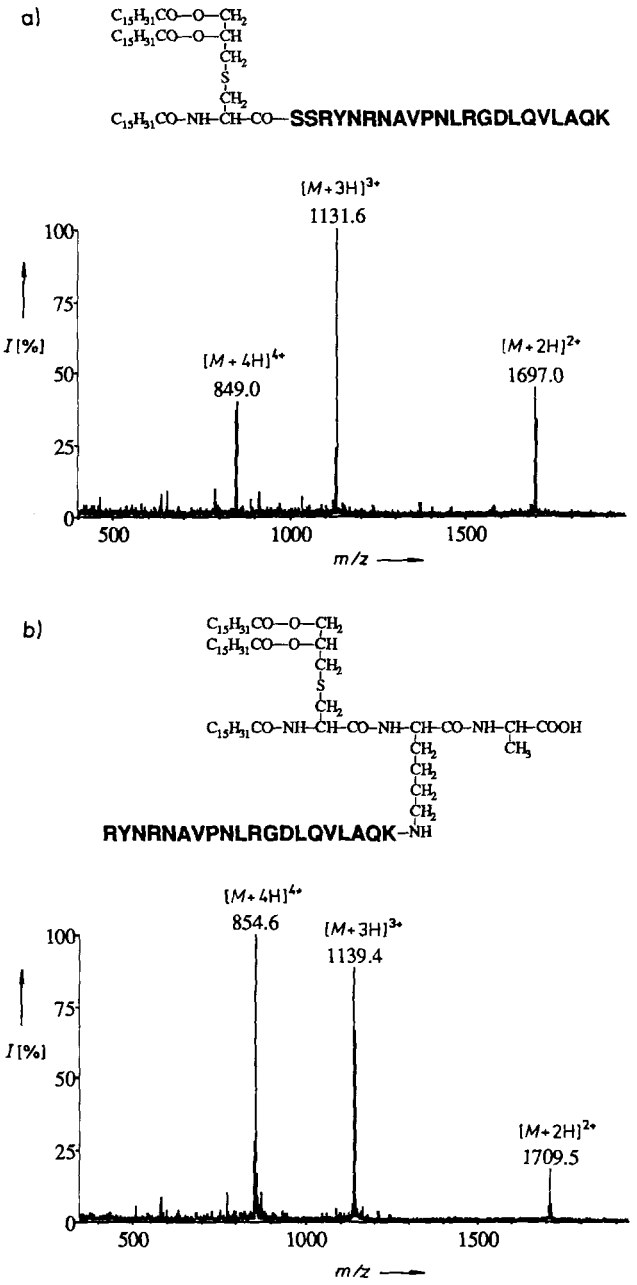

Fig. 2. Structural formulas and IS mass spectra of the lipopeptide vaccines. a) Pam_3Cys-Ser-Ser-[VP1 (135–154)] with *N*-terminally attached Pam_3Cys (calculated molecular mass 3392.3 u) and b) Pam_3Cys-Lys[VP1 (135–154)]-Ala with *C*-terminally attached Pam_3Cys (calculated molecular mass 3417.4 u).

placed at the *C*-terminus of the partial sequence, showed the doubly, triply, and quadruply charged quasi-molecular ions from which the molecular mass was determined with an ac-

curacy of ±1 u. Optimized cleavage conditions afforded pure and fully deprotected lipopeptides according to the IS mass spectra. The IS mass spectra showed the quasi-molecular peaks in high abundance; fragment peaks above 400 u were not found (Fig. 1 and 2). However, fragments can usually be observed together with solvent signals below 400 u (data not shown). The degree of fragmentation during IS ionization is influenced by the applied orifice potential and is also dependent on the structure of the lipopeptide; in the ion-spray mass spectrum of a lipopeptide constituting the synthetic *N*-terminus of the cytochrome subunit from a bacterial photoreaction center, for example, we observed two fragment peaks in high abundance, which resulted from cleavages at proline residues in the peptide chain during ionization.[17]

IS–MS proved to be a convenient method for the characterization of lipopeptide vaccines: it is fast and sensitive, and the sample preparation is very simple. Accuracies of better than ±1 u were achieved routinely for mass determinations up to 6000. The use of solvent mixtures containing chloroform in IS–MS not only allowed investigation of lipopeptides, but also of other lipophilic compound classes such as modified cyclodextrins.[18]

Received: July 17, 1991 [Z 4799 IE]
German version: *Angew. Chem.* **1992**, *104*, 235

CAS Registry numbers:
Pam_3Cys-Ser-Ser-[VP1(135–154)], 128820-63-3; Pam_3Cys-Lys-[VP1(135–154)], 138128-52-6.

[1] A. P. Bruins, T. R. Covey, J. D. Henion, *Anal. Chem.* **1987**, *59*, 2642.
[2] J. V. Iribarne, B. A. Thomson, *J. Chem. Phys.* **1976**, *64*, 2287.
[3] G. Schmelzeisen-Redeker, L. Bütfering, F. W. Röllgen, *Int. J. Mass Spectrom. Ion Processes* **1989**, *90*, 139; F. W. Röllgen, E. Bramer-Wegner, L. Bütfering, *J. Phys.* **1987**, *48*, C6-253.
[4] a) M. Dole, L. L. Mack, R. L. Hines, R. C. Mobley, L. D. Ferguson, M. B. Alice, *J. Chem. Phys.* **1968**, *49*, 2240; b) J. Gieniec, L. L. Mack, K. Nakamae, C. Gupta, V. Kumar, M. Dole, *Biomed. Mass Spectrom.* **1984**, *11*, 259; c) C. M. Whitehouse, R. N. Dreyer, M. Yamashita, J. B. Fenn, *Anal. Chem.* **1985**, *57*, 675.
[5] T. R. Covey, R. F. Bonner, B. I. Shushan, J. Henion, *Rapid Commun. Mass. Spectrom.* **1988**, *2*, 249.
[6] R. D. Smith, J. A. Loo, C. G. Edmonds, C. J. Baringa, H. R. Udseth, *Anal. Chem.* **1990**, *62*, 882.
[7] M. Mann, C. K. Meng, J. B. Fenn, *Anal. Chem.* **1989**, *61*, 1702.
[8] K.-H. Wiesmüller, G. Jung, G. Hess, G. *Vaccine* **1989**, *7*, 29; M. Krug, G. Folkers, B. Haas, K.-H. Wiesmüller, S. Freund, G. Jung, *Biopolymers* **1989**, *28*, 499; K. Deres, H. Schild, K.-H. Wiesmüller, G. Jung, H. G. Rammensee, *Nature* **1989**, *342*, 561.
[9] K.-H. Wiesmüller, W. Bessler, G. Jung, *Hoppe Seyler's Z. Physiol. Chem.* **1983**, *364*, 593.
[10] Ion spray mass spectra were recorded with a triple-quadrupole mass spectrometer API III (*Sciex*, Thornhill, Ontario, Canada) equipped with an IonSpray™ source. Lipopeptides (ca. 200 μg) were dissolved in chloroform/methanol/10% aqueous formic acid or 1% ammonium acetate (2:3:1, v:v:v; 1 mL), free peptides (ca. 200 μg) in methanol/1% formic acid (1:1 v:v; 1 mL). The solutions were introduced into the IS source at a flow rate between 2–10 μL min^{-1} using a medical syringe infusion pump (Model 22, *Harvard Apparatus*, USA).
[11] J. Metzger, K.-H. Wiesmüller, R. Schaude, W. G. Bessler, G. Jung, *Int. J. Peptide Protein Res.* **1991**, *37*, 46.
[12] J. Metzger, G. Jung, *Angew. Chem.* **1987**, *99*, 343; *Angew. Chem. Int. Ed. Engl.* **1987**, *26*, 336.
[13] F. Hillenkamp, *Proc. 38th ASMS Conf. Mass Spectrom. Allied Topics (Tucson, AZ,* **1990**), p. 8.
[14] W. Beck, J. W. Metzger, K.-H. Wiesmüller, A. Surovoy, B. Haas, G. Jung in *Innovation & Perspectives in Solid Phase Synthesis & Related Technologies (Proc. 2nd Int. Symp. Canterbury, England, 1991)* (Ed.: R. Epton) Intercept, Andover, **1992**, in press.
[15] J. Metzger, K.-H. Wiesmüller, G. Jung, *Int. J. Pept. Protein Res.* **1991**, in press.
[16] M. Sakairi, H. Kambara, *Anal. Chem.* **1989**, *61*, 1159.
[17] A. G. Beck-Sickinger, J. W. Metzger in *Peptides: Chemistry and Biology (Proc. 12th Am. Peptide Symp., Boston, MA, 1991)* (Eds.: J. A. Smith, J. E. Rivier), Escom, Leiden, **1992**, in press.
[18] J. W. Metzger, M. Jung, D. Schmalzing, E. Bayer, V. Schurig, *Carbohydr. Res.* **1991**, *222*, 23.

Asymmetric Ligands for Transition-Metal-Catalyzed Reactions: 2-Diphenylphosphinobenzoyl Derivatives of C_2-Symmetric Diols and Diamines**

By *Barry M. Trost** and *David L. Van Vranken*

The realization of transition-metal-catalyzed asymmetric hydrogenation[1, 2] and oxidation[1, 3] stimulates the search for chiral ligands for other types of transition-metal-catalyzed reactions. Allylic alkylation catalyzed by palladium complexes has proved to be particularly recalcitrant in responding to asymmetric induction, since both bond breaking and bond making occur on the face opposite palladium and its attendant ligands.[4–7] Of the various scenarios for asymmetric induction in allylic alkylation, differentiating between prochiral leaving groups as formulated in Equation (a) represents a generally useful strategy and coincides with our program directed towards the synthesis of glycosidase inhibitors.[8] We took the transformation of the diol **2** to the oxazolidinone **3** as our model reaction [Eq. (b)] for the general problem. This cyclization seemed to be a stringent test because a rather low enantiomeric excess (*ee*) was observed using BINAPO,[9] an asymmetric ligand that has proven to be rather successful in a related case.[7, 8]

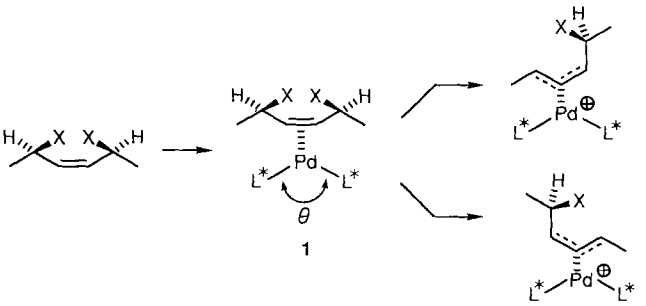

In designing ligands, ease of accessibility is a major criterion. The ready availability of 2-diphenylphosphinobenzoic acid (**4**) by Wurtz coupling of sodium 2-chlorobenzoate and sodium diphenylphosphide (from sodium and triphenylphosphane)[10] and of chiral alcohols and amides makes the

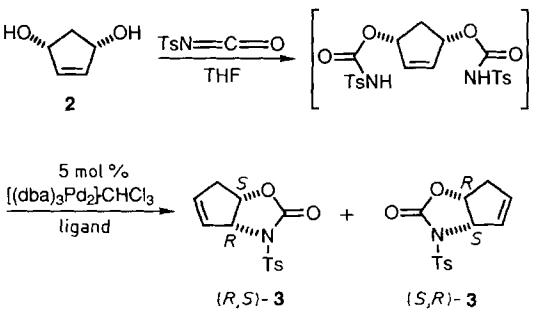

[*] Prof. B. M. Trost, D. L. Van Vranken
Department of Chemistry
Stanford University
Stanford, CA 94305 (USA)

[**] We thank the National Science Foundation (Graduate fellowship for DLvV) and the General Medical Sciences Institute of the National Institutes of Health (NIH) for their generous support of our programs. Mass spectra were provided by the Mass Spectrometry Facility, University of California-San Francisco, supported by the NIH Division of Research Resources.

corresponding esters and amines attractive potential ligands. Furthermore, by varying the length of the tether in bidentate-type ligands, the "bite angle" θ in **1** [Eq. (a)] can be modified. Opening this angle pushes the chiral environment of the ligands towards the reacting allyl system and could enhance asymmetric induction.[7]

The importance of ligands possessing C_2 symmetry for many asymmetric reactions[11] led to the synthesis of a series of potential bidentate diesters from C_2-symmetric diols. Diamides from C_2-symmetric diamines were also particularly desirable as ligands because the amide linkage makes them more rigid than esters. The availability of the corresponding diols and diamines in enantiomerically pure form provided

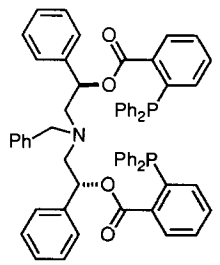

5

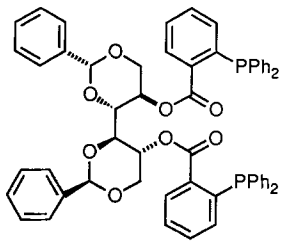

6

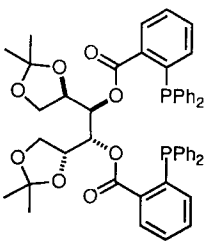

7

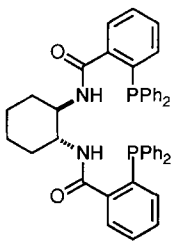

8

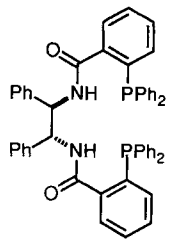

9

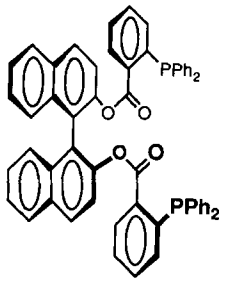

10

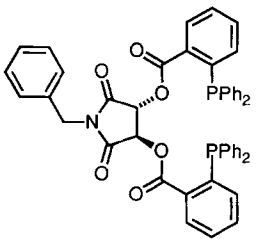

11

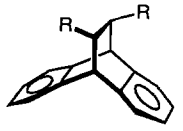

12a, R = CO_2H
12b, R = NH_2
12c, R =

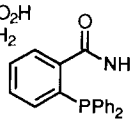

ready access to ligands **5**–**11** and **12c**[12] by dicyclohexylcarbodiimide (DCC) coupling (catalytic amounts of 4-dimethylaminopyridine (DMAP), THF, room temperature) with the acid **4**. We performed our selected reaction [Eq. (b)] with this diverse array of chiral ligands and $[(dba)_3Pd_2]\cdot CHCl_3$ (dba = dibenzylideneacetonate) (see Table 1). Several noteworthy trends appear. The good to excellent *ee*'s contrast with *ee*'s of 5–15% obtained with monodentate and non-C_2-symmetric polydentate ligands. Curiously, changing

Table 1. Catalysis using chiral 2-(diphenylphosphino)benzoyl esters and amides as ligands[a].

Ligand	t [h]	T [°C]	Yield [%]	$[\alpha]_D$	c (CH_2Cl_2)	*ee* [b] [%]
5	1	0	100	+ 83.9 (±.3)	3.90	60
6	8	0 to 20	98	+ 86.2 (±.3)	2.40	61
7	9	−8 to 20	100	+ 90.7 (±.1)	2.49	64
8	1.5	0 to 5	97	+110.0 (±.7)	0.99	78
9	1	0	97	+112.6 (±.3)	3.12	80
10	5	20	87	− 56.9 (±.2)	3.05	40
11	2	0 to 5	68	−105.9 (±.3)	2.82	75
12c	0.33	0	94	−124.2 (±.1)	3.41	88

[a] All reactions were run with 0.05 equiv Pd(0) in THF. [b] $[\alpha]_D$ = **141** (c = 2.52, CH_2Cl_2) for enantiomerically pure oxazolidinone; *ee* determined by ^1H NMR of the (+)-*O*-methylmandelate esters of the hydrolyzed product.

the distance between the two esters by modifying the precursors from a 1,2 (**7**) to a 1,4 (**6**) or a 1,5 diol (**5**) showed little variation in *ee*. On the other hand, increasing conformational rigidity by going to the flat tartrimide **11** or the less flexible amides **8** and **9** provides excellent yields of oxazolidin-2-one with high asymmetric induction at reasonable operating temperatures. Part of the increased *ee* observed with the tartrimide **11** may derive from increasing θ in **1** by an enlarged dihedral angle between the acyloxy substituents imposed by the flat ring.

Applying these arguments on the influence of conformation to the amides, which offer higher rigidity, led to the design of the bisamide **12c**. It is synthesized by the standard acylation of optically pure diamine **12b** which, in turn, derives from a Curtius rearrangement[13] of the known optically active diacid **12a**.[14] Indeed, cyclization proceeded in excellent yield with the highest *ee* obtained so far in this cyclization.

The absolute configuration of the product was determined from the *O*-methylmandelate ester[15] of the hydrolyzed hydroxytosylamide, as was the enantiomeric purity. The configurations were established as (*R,S*) for the levorotatory isomer of **3** and (*S,R*) for the dextrorotatory isomer. Ligands **5**–**9** all produced (*S,R*)-**3** and ligands **10**–**12** all produced (*R,S*)-**3**. If one views the ligands along the principal axis between the two stereogenic centers as drawn, the phosphine substituents are arranged in a clockwise (CW) helical sense as in **13** for ligands **10**–**12** and in a counterclockwise (CCW) helical sense for ligands **5**–**9**. The clockwise arrangement of the ligand induces ionization of the prochiral leaving group by a clockwise rotation of the palladium in **15** and vice versa.

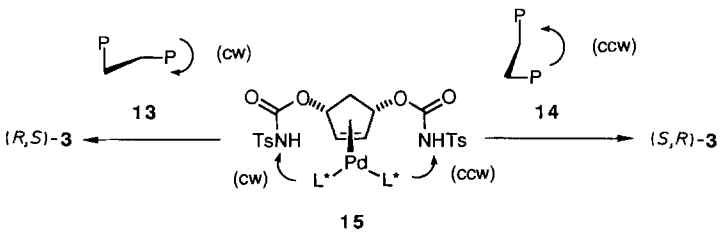

15

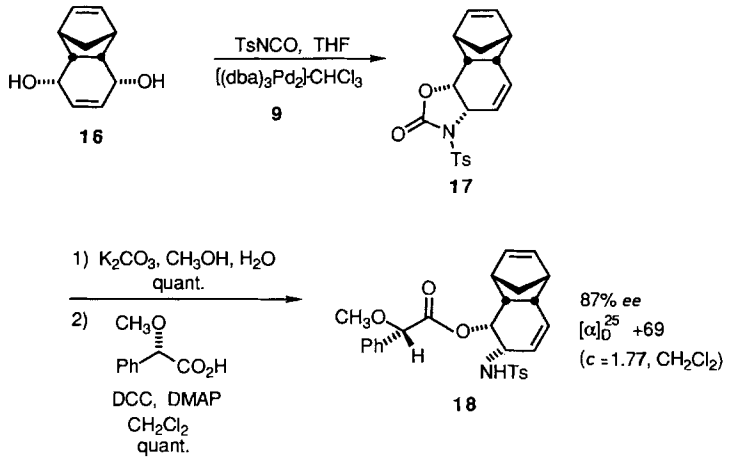

The high asymmetric induction observed with these new classes of ligands appears to be more general. The conversion of the diol **16**[16] to its oxazolidin-2-one **17** using diamide **9** provides 87% *ee* of the enantiomer depicted (determined by conversion to the mandelate **22**). The high *ee* observed here compared to that of the cyclization of **2** with the same ligand may arise because a six-membered ring is more inflexible than a five membered ring.

The strategy described herein offers wide scope in the design of asymmetric ligands for transition-metal-catalyzed reactions. In palladium-catalyzed allylic alkylation, a reaction in which asymmetric induction previously proved difficult to achieve, these ligands are highly effective. Many questions remain—the most prominent is whether these ligands are serving as chelating ligands. Two facts support a bidentate coordination. Firstly, a high *ee* is obtained when virtually equimolar quantities of ligand and palladium are used. Secondly, a C_2-symmetric ligand from isomannide which for steric reasons can act as a bidentate ligand only with difficulty effects cyclization with only low ee. An advantage of these ligands is the versatility for rational modification in the chiral scaffold independent of the phosphine substituents. Indeed, the ethanoanthracene ligand **16** was developed after identification of some of the structural parameters that appeared important for asymmetric induction in our allylic alkylations.

Received: September 12, 1991 [Z 4912 IE]
German version: *Angew. Chem.* **1992**, *104*, 194

CAS Registry numbers:
2, 29783-26-4; (*R*, *S*)-**3**, 138604-23-6; (*S*,*R*)-**3**, 138604-24-7; **5**, 138517-58-5; **6**, 138517-59-6; **7**, 138517-60-9; **8**, 138517-61-0; **9**, 138517-62-1; **10**, 138517-63-2; **11**, 138517-64-3; **12a**, 33216-00-1; **12b**, 138517-66-5; **12c**, 138517-65-4; **16**, 101312-33-8; **17**, 238540-73-5; **18**, 138517-67-6; TsN=C=O, 4083-64-1; (*S*)-PhCH(CH_3O)CO_2H, 26164-26-1; $(dba)_3Pd_2$, 51364-51-3.

[1] For most recent general reviews, see K. Tomioka, *Synthesis* **1990**, 541; R. Noyori; M. Kitamura, *Modern Syn. Methods* **1989**, *5*, 115; I. Ojima, N. Clos, C. Bastos, *Tetrahedron* **1989**, *45*, 6901; S. L. Blystone, *Chem. Rev.* **1989**, *89*, 1663; H. Kagan, *Bull. Soc. Chim. France* **1988**, 846; H. Brunner, *Synthesis* **1988**, 645.

[2] For some recent reviews, see R. Noyori; H. Takaya, *Acc. Chem. Res.* **1990**, *23*, 345; J. M. Brown, *Angew. Chem. Int. Ed. Engl.* **1987**, *26*, 190; V. Caplar, G. Comiso, V. Sunjic, *Synthesis* **1981**, 85.

[3] For some recent reviews, see K. A. Jorgensen *Chem. Rev.* **1989**, *89*, 431; A. Pfenninger, *Synthesis* **1986**, 89. See also B. H. McKee, D. G. Gilheany, B. K. Blackburn, K. B. Sharpless, *Tetrahedron Lett.* **1990**, *31*, 3817; H. L. Kwong, C. Sorato, Y. Ogino, H. Chen, K. B. Sharpless, *Tetrahedron Lett.* **1990**, *31*, 2999 and earlier papers in this series.

[4] G. Consiglio, R. M. Waymouth, *Chem. Rev.* **1989**, *89*, 257.

[5] T. Hayashi, A. Yamamoto, Y. Ito, *Tetrahedron Lett.* **1988**, *29*, 669; T. Hayashi; A. Yamamoto; Y. Ito, *Tetrahedron Lett.* **1988**, *29*, 99; T. Hayashi; A. Yamamoto; Y. Ito, *Chem. Lett.* **1987**, 177; T. Hayashi; A. Yamamoto; T. Hagihara; Y. Ito, *Tetrahedron Lett.* **1986**, *27*, 191.

[6] D. Müller, G. Umbrieht, B. Weber, A. Pfaltz, *Helv. Chim. Acta.* **1991**, *74*, 232; M. Yamaguchi, T. Shima, T. Yamagishi, M. Hida, *Tetrahedron Lett.* **1990**, *31*, 5049; R. L. Halterman; H. L. Nimmons, *Organometallics* **1990**, *9*, 273; P. B. Mackenzie, J. Whelan, B. Bosnich, *J. Am. Chem. Soc.* **1985**, *107*, 2046; P.R. Auburn, P. B. Mackenzie, B. Bosnich, *J. Am. Chem. Soc.* **1985**, *107*, 2033.

[7] B. M. Trost, D. J. Murphy, *Organometallics* **1985**, *4*, 1143; B. M. Trost, P. E. Strege, *J. Am. Chem. Soc.* **1977**, *99*, 1649.

[8] B. M. Trost, D. L. Van Vranken, *J. Am. Chem. Soc.* **1990**, *112*, 1261; B.M. Trost, D. L. Van Vranken, *J. Am. Chem. Soc.* **1991**, *113*, 6317.

[9] R. H. Grubbs, R. A. DeVries, *Tetrahedron Lett.* **1977**, *26*, 1879.

[10] J. E. Hoots, T. B. Rauchfuss, D. A. Wrobleski, *Inorg. Syn.* **1982**, *21*, 178.

[11] J. K. Whitesell, *Chem. Rev.* **1989**, *89*, 1581.

[12] For the diol precursors of **6**: N. Baggett, P. Stribblehill, *J. Chem. Soc. Perkin* **1977**, 1123; of **10**: M. Kawashima, A. Hirayama, *Chem. Lett.* **1990**, 2299; of **14**: C. M. Wong, J. Buccini, J. Tekaa, *Can. J. Chem.* **1986**, *46*, 3091. For the diamine precursor of **9**: P. Manganey, T. Tejero, A. Alexakis, F. Grosjean, J. Normant, *Synthesis* **1988**, 255; K. Saigo, N. Kubota, S. Takebayashi, M. Hasegawa, *Bull. Chem. Soc. Jpn.* **1986**, *59*, 931; E. J. Corey, R. Imwinkelried, S. Pikul, Y. B. Xiang, *J. Am. Chem. Soc.* **1989**, *111*, 5493. The diol precursor of 5 was obtained by heating commercially available, optically pure styrene epoxide (6 equiv) with 1 equiv of benzylamine at 120 °.

[13] See D. E. Horning, J. M. Muchowski, *Can. J. Chem.* **1967**, *45*, 1247.

[14] W. E. Bachmann, C. B. Scott, *J. Am. Chem. Soc.* **1948**, *70*, 1458; M.-J. Brienne, J. Jacques, *Bull Soc. Chim. France* **1973**, 190; S. Hagashita, K. Kuriyama, *Tetrahedron* **1972**, *28*, 1435.

[15] B. M. Trost, J. M. Belletire, S. Godleski, P. G. McDougal, . M. Balkovec, J. J. Baldwin, M. E. Christy, G. S. Ponticello, S.L. Varga, J. P. Springer, *J. Org. Chem.* **1986**, *512*, 370.

[16] A. P. Marchand, R. W. Allen, *J. Org. Chem.* **1974**, *39*, 1596; A. P. Marchand, W. D. LaRoe, G. V. Madhava Sharma, S. Chander Suoi, D. Sivakumar Reddy, *J. Org. Chem.* **1986**, *51*, 1622.

Spontaneous Self-Assembly of a Dinickel(II) Double Helicate Containing a 1,3-Benzenediyl Spacer Group

By *Edwin C. Constable,* Michael J. Hannon,* and *Derek A. Tocher*

Molecular species exhibiting a double-helical topology attract the chemist because of their inherent beauty and the synthetic challenge of controlling the twisting of the component strands.[1] There has been considerable recent interest in the utilization of the specific coordination requirements of metal ions to control the assembly of such species.[1-3] Simply mixing suitable ligands with compatible metal ions results in the spontaneous self-assembly of polynuclear double-helical arrays. A helicating ligand must contain two or more separate polydentate metal-binding sites which are either directly linked or are connected by a suitable spacer group.[3] We have been particularly interested in developing ligands in which the twisting of molecular threads occurs about interannular C–C bonds between aromatic rings (Scheme 1).[4] We now describe a new class of helicating ligand (**1**) containing a 1,3-benzenediyl spacer group.

[*] Dr. E. C. Constable, M. J. Hannon
Cambridge Centre for Molecular Recognition
University Chemical Laboratory
Lensfield Road, GB-Cambridge, CB2 1EW (UK)
Dr. Derek A. Tocher
Department of Chemistry
University College London
20 Gordon Street, GB-London WC1H 0AJ (UK)

[**] This work was supported by the U.K. Science and Engineering Research Council, Ciba-Geigy AG (studentship for MJH), and the Royal Society of Great Britain.

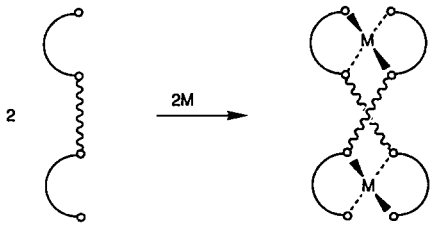

Scheme 1. Formation of a double-helical complex. The ligand has two bidentate coordination sites separated by a spacer group.

The new ligands are readily prepared as off-white solids[5] by routes involving the synthesis of rings B and D (Scheme 2). Compound **1a** is obtained in low and variable

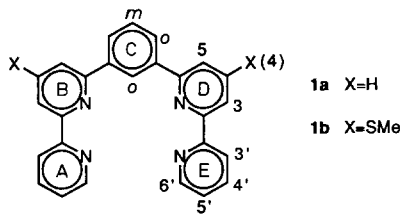

Scheme 2. The new ligands for the synthesis of double helical complexes, showing the ring designations used in the text.

yield from a Kröhnke synthesis[6] or 60% yield from the dethiomethylation of **1b** with $NiCl_2$/Na[BH_4].[7] The derivatized compound **1b** was prepared in 60% yield from a double Potts reaction.[7, 8]

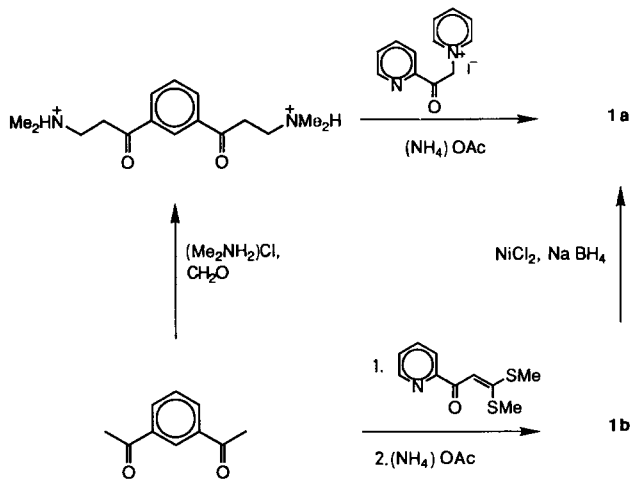

Scheme 3. Synthesis of the ligands **1a** and **1b**.

The reaction of **1a** or **1b** with solutions of either [Cu(MeCN)$_4$](BF$_4$) or [Cu(MeCN)$_4$](PF$_6$) in acetonitrile, or [{Cu(OAc)$_2$(H$_2$O)}$_2$] in methanol followed by the addition of methanolic $(NH_4)PF_6$ or $NaBF_4$, resulted in the formation of red-brown solutions from which deep red crystals of $[Cu_2L_2]X_2$ (L = **1a**,**1b**; X = PF_6,BF_4) separated.[9] Molecular modeling studies suggested that strain would make the formation of 1:1 complexes impossible and that binuclear double-helical complexes should result. Direct evidence for this comes from the FAB mass spectra. Similar compounds of 2:2 stoichiometry, $[Ag_2L_2]X_2$ (L = **1a**,**1b**; X = PF_6,BF_4) are obtained as colorless crystals from the reactions of ligands **1** with silver(I) salts.[10] Although these silver(I) and copper(I) complexes give well-formed crystals, these are invariably twinned and none suitable for X-ray structural analysis were obtained.

The reaction of **1a** or **1b** with Ni(OAc)$_2 \cdot 4H_2O$ in methanolic solution results in the formation of deep emerald green solutions, from which well-formed crystals of the blue-green salts $[Ni_2(OAc)_2L_2](PF_6)_2$ (L = **1a**,**1b**) could be obtained directly from the reaction mixture by the addition of methanolic $(NH_4)PF_6$ solution. We have determined the

$[Ni_2(OAc)_2(\mathbf{1b})_2][PF_6]_2$ **2**

crystal and molecular structure of **2**[11] and the structure of one of the two enantiomers of the cation is shown in Figure 1a.

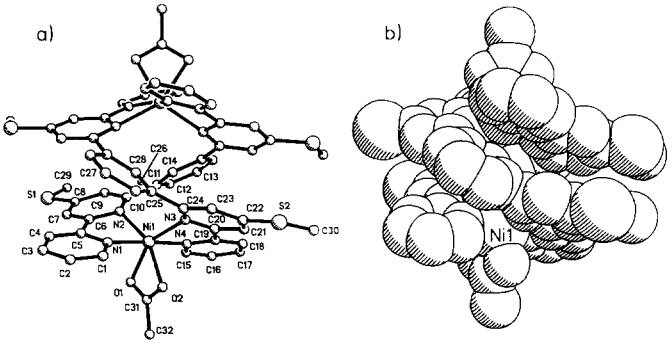

Fig. 1. The crystal structure of the $[Ni_2(\mathbf{1b})_2(OAc)_2]^{2+}$ cation in **2** showing the numbering scheme adopted. Important bond lengths [pm] and angles [°]: Ni1-N1 201.4(7), Ni1-N2 214.6(6), Ni1-N3 215.4(5), Ni1-N4 203.6(7), Ni1-O1 214.8(6), Ni1-O2 208.5(7), N1-Ni1-N2 78.9(3), N1-Ni1-N3 105.0(3), N2-Ni1-N3 116.8(2), N1-Ni1-N4 175.4(3), N2-Ni1-N4 100.2(3), N3-Ni1-N4 79.4(2), N1-Ni1-O1 86.8(3), N2-Ni1-O1 92.2(2), N3-Ni1-O1 150.0(2), N4-Ni1-O1 88.7(2), N1-Ni1-O2 91.6(3), N2-Ni1-O2 153.4(2), N3-Ni1-O2 89.6(2), N4-Ni1-O2 87.3(3)

The cation is double-helical with each nickel(II) center coordinated to a 2,2′-bipyridyl moiety from each of two **1b** ligands. Each nickel atom is in a distorted N_4O_2 octahedral environment with a bidentate acetate ligand completing the donor set. The Ni–N (2.014–2.154 Å) and Ni–O (2.085–2.148 Å) distances are unremarkable. Each 2,2′-bipyridyl–metal interaction is associated with a typical "bite-angle" of 79 ± 0.5°.[12] The helical structure is achieved by interannular twisting; the 2,2′-bipyridyl moieties are slightly nonplanar (13.9 and 14.9° interplanar angles for the two crystallographically unique 2,2′-bipyridyls) but the major twisting occurs between the 2,2′-bipyridyls and the 1,3-benzenediyl rings (38 and 35°). The two benzenediyl spacers are mutually skewed (62.8° with respect to one another).

Unlike other double helicates that we have studied, **2** does not exhibit any short face-to-face stacking interactions between near-coplanar aromatic rings.[4] A space-filling representation of **2** is shown in Figure 1b. The closest approaches between aromatic rings are those between the terminal pyridyl rings of one ligand and the central benzene spacer of the other (3.79 and 3.67 Å), although these rings are not coplanar (interplanar angles for the two crystallographically unique interactions, 28.1 and 24.7°). The two nickel(II) centers show no direct metal–metal bonding interactions and are 5.87(1) Å apart in the cation.

Experimental Procedure

1b: (3,3-bis(methylthio)-1-oxoprop-2-enyl)pyridine (14.0 g, 61.6 mmol) was added to a suspension of 1,3-diacetylbenzene (5.0 g, 30 mmol) and *t*BuDK (14.0 g, 126 mmol) in THF (200 mL) under an atmosphere of dinitrogen, and the mixture stirred at room temperature for 4 h. Then acetic acid (50 mL) and $(NH_4)OAc$ (10.0 g) were added, an air condensor fitted to the flask, and the suspension boiled for 3 h. After cooling, the reaction mixture was treated with H_2O (100 mL), and the solid precipitate recrystallized from EtOH/DMF in the presence of activated charcoal to yield relatively clean **1b** (8.6 g, 60%).

1a from **1b**: **1b** (2.17 g, 0.45 mmol) and $[Ni(H_2O)_6]Cl_2$ (21.61 g) were dissolved in EtOH (100 mL), and a solution of $NaBH_4$ (10.30 g) in 40% aqueous NaOH (100 mL) was added dropwise over 4 h while keeping the reaction mixture between 0° and 5 °C under an atmosphere of N_2. The reaction mixture was then heated at reflux for 24 h, filtered hot, and the filtrate evaporated to dryness and washed well with water to give an off-white residue. The precipitate was recrystallized from EtOH in the presence of activated charcoal to yield **1a** (1.03 g, 59%).

2: A solution of **1b** (0.05 g, 0.1 mmol) and $Ni(OAc)_2 \cdot 4H_2O$ (0.026 g, 0.1 mmol) in methanol (10 mL) was heated at reflux for 5 h to give a clear emerald-green solution. The solution was filtered hot, and the filtrate treated with methanolic $(NH_4)PF_6$ (0.1 g). On cooling, emerald-green crystals of $[Ni_2(OAc)_2(\mathbf{1b})_2](PF_6)_2$ separated. Yield 0.061 g, 79%; correct C, H, N analysis; FAB mass spectrum (3-nitrobenzyl alcohol matrix) *m/z* 535 [Ni(**1b**)], 593 [Ni(**1b**)(OAc)], 1191 $[Ni_2(\mathbf{1b})_2(OAc)_2]$, 1337 $]Ni_2(\mathbf{1b})_2(OAc)_2(PF_6)]$.

Received: September 25, 1991 [Z 4929 IE]
German version: *Angew. Chem.* **1992**, *104*, 218

CAS Registry numbers:
1a, 138336-94-4; **1b**, 138336-93-3; **2**, 138336-96-6; $(NH_4)OAc$, 631-61-8; $[Cu(MeCN)_4(BF_4)]$, 15418-29-8; $[Cu(MeCN)_4(PF_6)]$, 64443-05-6; $[\{Cu(OAc)_2(H_2O)\}_2]$, 15523-07-6; $[Cu_2(\mathbf{1a})_2](PF_6)_2$, 138353-47-6; $[Cu_2(\mathbf{1a})_2](BF_4)_2$, 138337-00-5; $[Cu_2(\mathbf{1b})_2](PF_6)_2$, 138337-02-7; $[Cu_2(\mathbf{1b})_2](BF_4)_2$, 138337-03-8; $[Ag_2(\mathbf{1a})_2](PF_6)_2$, 138337-05-0; $[Ag_2(\mathbf{1a})_2](BF_4)_2$, 138337-06-1; $[Ag(\mathbf{1b})_2](PF_6)_2$, 138337-08-3; $[Ag(\mathbf{1b})_2](BF_4)_2$, 138337-09-4; $[Ni_2(OAc)_2(\mathbf{1b})_2](PF_6)_2$, 138336-98-8; (3,3-bismethylthio)-1-oxoprop-2-enyl)-pyridine; 78570-34-0; 1,3-diacetylbenzene, 6781-42-6.

[1] See for example, E. C. Constable, *Angew. Chem.* **1991**, *103*, 1482; *Angew. Chem. Int. Ed. Engl.* **1991**, *30*, 1451; E. C. Constable, *Nature (London)* **1990**, *346*, 319.

[2] A full review of this topic is shortly to be published (E. C. Constable, *Tetrahedron*, in press). For an entry into the literature the most recent key references for various groups involved are given here: G. C. van Stein, G. van Koten, K. Vrieze, A. L. Spek, E. A. Klop, C. Brevard, *Inorg. Chem.* **1985**, *24*, 1367; J. F. Modder, G. van Koten, K. Vrieze, A. L. Spek, *Angew. Chem.* **1989**, *101*, 1723; *Angew. Chem. Int. Ed. Engl.* **1989**, *28*, 1698; D. Dolphin, R. L. N. Harris, J. L. Huppatz, A. W. Johnson, I. T. Kay, J. Leng, *J. Chem. Soc. C* **1966**, 98; W. S. Sheldrick, J. Engel, *J. Chem. Soc. Chem. Commun.* **1980**, 5; *Acta Crystallogr. Sect. B* **1981**, *37*, 250; D. Wester, G. J. Palenik, *J. Chem. Soc. Chem. Commun.* **1975**, 74; *Inorg. Chem.* **1976**, *15*, 755; M. G. B. Drew, A. Lavery, V. McKee, S. M. Nelson, *J. Chem. Soc. Dalton Trans.* **1985**, 1771; G. Struckmeier, U. Thewalt, J.-H. Fuhrhop, *J. Am. Chem. Soc.* **1976**, *98*, 278; C. Piguet, G. Bernardinelli, A. F. Williams, *Inorg. Chem.* **1989**, *28*, 2920; J.-P. Sauvage, *Acc. Chem. Res.* **1990**, *23*, 319; C. O. Dietrich-Buchecker, J. Guilhem, C. Pascard, J.-P. Sauvage, *Angew. Chem.* **1990**, *102*, 1202; *Angew. Chem. Int. Ed. Engl.* **1990**, *29*, 1154; C. O. Dietrich-Buchecker, J.-P. Sauvage, *ibid.* **1989**, *101*, 192 and **1989**, *28*, 189; J. F. Modder, J.-M. Ernsting, K. Vrieze, M. de Wit, C. H. Stam, G. van Koten, *Inorg. Chem.* **1991**, *30*, 1208.

[3] T. M. Garrett, U. Koert, J.-M. Lehn, A. Rigault, D. Meyer, J. Fischer, *J. Chem. Soc. Chem. Commun.* **1990**, 557; J.-P. Gisselbrecht, M. Gross, J.-M. Lehn, J.-P. Sauvage, R. Ziessel, C. Piccinni-Leopardi, J. M. Arrieta, G. Germain, M. van Meerssche, *Nouv. J. Chim.* **1984**, *8*, 661; M. M. Harding, U. Koert, J.-M. Lehn, A. Marquis-Rigault, C. Piguet, J. Siegel, *Helv. Chim. Acta* **1991**, *74*, 594; U. Koert, M. M. Harding, J.-M. Lehn, *Nature (London)* **1990**, *346*, 339; J.-M. Lehn, J.-P. Sauvage, J. Simon, R. Ziessel, C. Piccinni-Leopardi, G. Germain, J.-P. Declercq, M. van Meerssche, *Nouv. J. Chim.* **1983**, *7*, 413; J.-M. Lehn, A. Rigault, J. Siegel, J. Harrowfield, B. Chevrier, D. Moras, *Proc. Natl. Acad. Sci. USA* **1987**, *84*, 2565; J.-M. Lehn, *Angew. Chem.* **1988**, *100*, 91; *Angew. Chem. Int. Ed. Engl.* **1988**, *27*, 89; J.-M. Lehn, A. Rigault, *ibid.* **1988**, *27*, 1121 and **1988**, *27*, 1095; M. T. Youinou, R. Ziessel, J.-M. Lehn, *Inorg. Chem.* **1991**, *30*, 2144.

[4] M. Barley, E. C. Constable, S. A. Corr, R. C. S. McQueen, M. D. Ward, M. G. B. Drew, *J. Chem. Soc. Dalton Trans.* **1988**, 2655; E. C. Constable, J. M. Holmes, *Inorg. Chim. Acta* **1987**, *126*, 187; E. C. Constable, M. G. B. Drew, M. D. Ward, *J. Chem. Soc. Chem. Commun.* **1987**, 1600; E. C. Constable, M. G. B. Drew, G. A. Forsyth, M. D. Ward, *ibid.* **1988**, 1450; E. C. Constable, M. D. Ward, M. G. B. Drew, G. A. Forsyth, *Polyhedron* **1989**, *8*, 2551; E. C. Constable, S. M. Elder, J. Healy, M. D. Ward, D. A. Tocher, *J. Am. Chem. Soc.* **1990**, *112*, 4590; E. C. Constable, M. D. Ward, D. A. Tocher, *ibid.* **1990**, *112*, 1256; E. C. Constable, S. M. Elder, P. R. Raithby, M. D. Ward, *Polyhedron* **1991**, *10*, 1395; E. C. Constable, M. D. Ward, D. A. Tocher, *J. Chem. Soc. Dalton Trans.* **1991**, 1675; E. C. Constable, J. M. Holmes, P. R. Raithby, *Polyhedron* **1991**, *10*, 127.

[5] **1a**: ^1H NMR (CD_3SOCD_3): $\delta = 8.74$ (br, d; H6'), 7.51 (ddd; H5'), 8.02 (td; H4'), 8.66 (dd; H3'), 8.22 (dd; H3/5), 8.10 (t; H4), 8.41 (dd; H5/3), 9.07 (t; *o*H), 8.35 (dd; *o*H'), 7.72 (t; *m*H'); FAB-MS (3-nitrobenzylalcohol matrix): *m/z* 387, 307, 289; EI-MS: *m/z* 386, 308, 231, 159. **1b**: ^1H NMR (CD_3SOCD_3): $\delta = 8.74$ (br, d; H6'), 7.51 (ddd; H5'), 8.01 (td; H4'), 8.65 (dd; H3'), 8.01 (d; H3/5), 3.23 (s; SMe), 8.23 (d; H5/3), 9.04 (t; *o*Hø), 8.35 (dd; *o*H'), 7.70 (t; *m*H); FAB-MS (3-nitrobenzylalcohol matrix): *m/z* 479; EI-MS: *m/z* 478, 464, 433, 418. Coupling constants [Hz]: ^4J(*o*-H, *o*-H') 1.6, ^3J(*o*-H', *m*-H) 7.8, ^3J(H4, H5) 7.7, ^4J(H3, H5) 1.5, ^3J(H3'/H4') 7.9, ^4J(H3', H5') 1.5, ^3J(H4', H5') 7.7, ^3J(H5', H6') 4.8.

[6] F. Kröhnke, *Synthesis* **1976**, 1.

[7] K. T. Potts, *Org. Synth.* **1985**, *64*, 189.

[8] K. T. Potts, M. J. Cipullo, P. Ralli, G. Theodoridis, *J. Org. Chem.* **1982**, *47*, 3027; K. T. Potts, D. Konwar, *ibid.* **1991**, *56*, 4815; K. T. Potts, *Bull. Soc. Chim. Belg.* **1990**, *99*, 741; K. T. Potts, D. A. Usifer, A. Guadalupe, H. D. Abruna, *J. Am. Chem. Soc.* **1987**, *109*, 3961.

[9] $[Cu_2(\mathbf{1a})_2](PF_6)_2$: ^1H NMR (CD_3CN): $\delta = 7.65$ (br, d; H6'), 6.98 (dd; H5'), 7.80 (t; H4'), 7.98 (br, d; H3'), 7.55 (d; H3/5), 7.95 (H4), 7.95 (H5/3), 9.6 (s; *o*H), 7.4 (d; *o*H'), 7.10 (t; *m*H). FAB-MS (3-nitrobenzylalcohol matrix): *m/z* 449 [Cu(**1a**)], 835 $[Cu(\mathbf{1a})_2]$, 900 $[Cu_2(\mathbf{1a})_2]$, 1046 $[Cu_2(\mathbf{1a})_2(PF_6)]$.

[10] $[Ag_2(\mathbf{1a})_2](PF_6)_2$: ^1H NMR (CD_3CN): $\delta = 7.65$ (v, br, d; H6'), 7.05 (ddd; H5'), 7.81 (t; H4'), 7.87 (br, d; H3'), 7.48 (d, H3/5), 7.95 (t, H4), 7.88 (d; H5/3), 9.7 (s; *o*H), 7.52 (d; *o*H'), 7.28 (t; *m*H). FAB-MS (3-nitrobenzylalcohol matrix): *m/z* 495 [Ag(**1a**)], 880 $[Ag(\mathbf{1a})_2]$, 989 $[Ag_2(\mathbf{1a})_2]$, 1133 $[Ag_2(\mathbf{1a})_2(PF_6)]$.

[11] Crystal data for **2**: $C_{60}H_{50}F_{12}N_8Ni_2O_4P_2S_4$, monoclinic, $C2/c$, $a = 16.157(5)$, $b = 23.640(7)$, $c = 18.806(3)$ Å, $\beta = 97.66(2)°$, $V = 7119(3)$ Å^3, $M_r = 1482.7$, $Z = 4$, $\varrho_{ber} = 1.38$ g cm^{-1}, $F(000) = 3024$, $Mo_{K\alpha}$ radiation, $\lambda = 0.71073$ Å, $\mu(Mo_{K\alpha}) = 0.763$ mm^{-1}. The structure was solved by direct methods and refined by alternating cycles of least squares refinement and difference-Fourier synthesis. All non-hydrogen atoms anisotropic: H-atoms riding on appropriate carbon atom with fixed isotropic U. 6611 reflections measured ($5 < 2\theta < 50°$), corrected for absorption, 3616 unique observed reflections with $I > 6\sigma(I)$, $R = 0.0773$, $R_w = 0.0793$. Further details of the crystal structure investigation may be obtained from the Director of the Cambridge Crystallographic Data Centre, University Chemical Laboratory, Lensfield Road, Cambridge CB2 1EW (UK). Any request should be accompanied by the full literature citation for this communication.

[12] E. C. Constable, *Adv. Inorg. Chem.* **1989**, *34*, 1.

The Hydroxyl-Directed Hydrogenation of Vinylstannanes and Silanes: A Highly Diastereoselective Route to β-Stannyl and β-Silyl Alcohols

By *Mark Lautens,* ChunHao Zhang,* and *Cathleen M. Crudden*

Reactions in which an existing functional group directs a reagent to a nearby site represent an important strategy for the diastereo- and enantioselective construction of complex molecules. The directed hydrogenation of an olefin by an allylic or homoallylic alcohol in the presence of a soluble transition-metal catalyst is a powerful method for controlling the relative stereochemistry of alkyl and hydroxyl groups.[1, 2] All studies reported thus far have been limited to olefins bearing carbon substituents including alkyl, aryl, and acyl groups. We report a highly diastereoselective hydrogenation of olefins bearing silicon and tin substituents cata-

[*] Professor M. Lautens, Dr. C. H. Zhang, C. M. Crudden
Department of Chemistry
University of Toronto
Toronto, Ontario M5S 1A1 (Canada)

[**] The A. P. Sloan Foundation, the Natural Science and Engineering Research Council (NSERC) of Canada, the Merck Frosst Centre for Therapeutc Research, Bio-Mega Inc., and the University of Toronto are thanked for financial support.

lyzed by the cationic rhodium complex **1**.[3] Prior to these studies, they were regarded as unreactive towards typical hydrogenation conditions.[4]

(dppb)Rh(nbd)BF_4 **1**

The vinylstannanes for this study were prepared by our hydrometalation–stannylation sequence.[5] Vinylsilanes were prepared by known routes.[6]

Table 1. Directed hydrogenation of Γ-hydroxyvinylstannanes. The substrate is treated with catalyst **1** in CH_2Cl_2 for 24–48 h.

Substrate	Reaction Conditions	Product	Yield [%] [a] (*syn*:*anti* ratio)
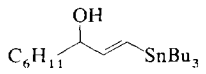 **2**	[b]	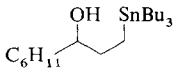 **3**	67 [c]
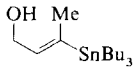 **4**	[d]	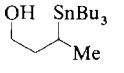 **5**	59
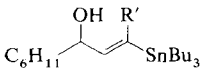 **6**, R′ = *n*Bu	[b]	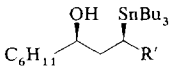 **7**, R′ = *n*Bu	70 (>100:1) 85 (>100:1)
10, R′ = *i*Pr	[b]	**11**, R′ = *i*Pr	83 (>200:1)
12, R′ = *t*Bu	[d]	**13**, R′ = *t*Bu	70
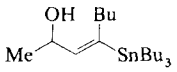 **14**	[b]	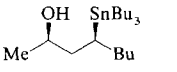 **15**	95
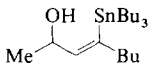 **16**	[e]	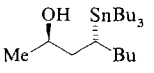 **17**	51
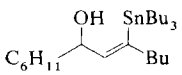 **18**	[f]	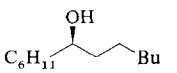 **19**	

[a] Yield refers to pure product after flash chromatography. [b] 5 mol % of **1** at 103×10^5 Pa. [c] 17% of the starting material was recovered. [d] 17 mol % of **1** at 96×10^5 Pa. [e] 20 mol % at 103×10^5 Pa. [f] 5–20 mol % at 103×10^5 Pa.

Hydrogenation of vinylstannanes **2** and **4** (Table 1) was examined first to determine the conditions necessary to achieve reaction without the additional complication of determining the diastereoselectivity. Treatment of **2** or **4** with 5 mol % of catalyst **1** in dichloromethane under ca. 1500 psi (103×10^5 Pa) of hydrogen for 24–36 h gave the saturated products **3** and **5** in 67% and 59% yields, respectively. The hydrogenation is therefore significantly more facile than destannylation by insertion into the C–Sn bond.[7]

The diastereofacial selectivity was probed by hydrogenation of vinylstannane **6**. By using 17 mol % of catalyst **1** at 1400 psi (96×10^5 Pa) for 36 h, alkylstannane **7** was isolated in 70% yield along with an additional product **8** in which hydrogenolysis of the vinylstannane and hydrogenation of the olefin had occurred [ca. 13%, Eq. (a)]. By reducing the amount of catalyst to 5 mol % and increasing the pressure to 103×10^5 Pa the yield of **7** improved to 85% and of **8** decreased to only 3%. The diastereoselectivity was found to be greater than 100:1 by HPLC following preparation of an authentic mixture of both diastereomers.

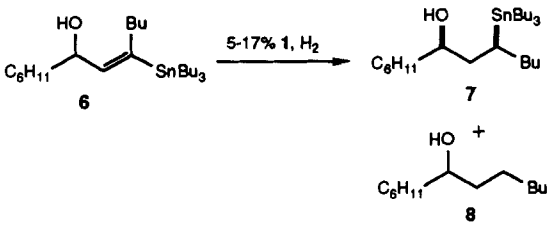

(a)

The relative stereochemistry of the hydroxyl and stannyl groups was determined to be *syn* by oxidation of the carbon–tin bond to a carbon–oxygen bond with retention of stereochemistry[8] and comparison with an authentic sample prepared by an independent route.

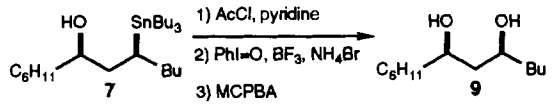

(b)

Selective formation of the 1,3-*syn* product is predicted by analysis of the Newman projections designated **A** and **B** (Scheme 1) representing the two most likely reactive conformers. The controlling element which determines the facial

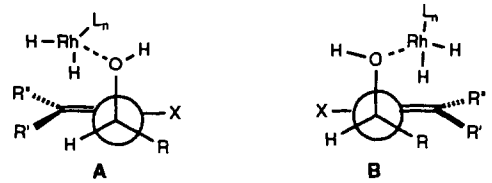

Scheme 1. X = H

selectivity of the hydrogenation is the nonbonded steric interaction between R′ and R which disfavors conformer **B**; **A** leads to the observed product.[9] In accord with this analysis, substrates **10** and **12** (Table 1) bearing increasingly bulky substituents R′ also undergo facile and highly diastereoselective hydrogenation with catalyst **1**. The diastereoselectivity exceeded 200:1 for **11**, and only one isomer was detected for **13**. In contrast, Evans has shown that the hydrogenation of 1,1-disubstituted allylic alcohols (X = alkyl group and R′,R″ = H) leads to the 1,2-*anti* diastereomers, indicating that conformer **B** is favored over **A**.[1g]

The stereochemistry of the vinylstannane and the size of R group on the carbon containing the hydroxy group were also found to play a significant role in determining the course of the reaction. Whereas the *E* and *Z* isomers **14** and **16** undergo hydrogenation to give the diastereomeric hydroxystannanes **15** and **17**, the *Z* isomer of **6** (**18**) led primarily to the destannylated alcohol **19**. Control experiments proved that destannylation precedes hydrogenation.

γ-Hydroxyvinylsilanes also undergo hydrogenation (Table 2). Treatment of **20a**, **b**, **22**, and **24** with catalyst **1** for

48 h gave the saturated silanes **21**, **23**, and **25** in greater than 90% yields. Exceptionally high diastereoselectivities (>500:1) were noted in all cases. No desilylation was observed under these conditions.

Table 2. Directed hydrogenation of γ-hydroxyvinylsilanes. The substrate was treated with 5 mol % of the catalyst **1** in CH_2Cl_2 for 24–48 h at 103×10^5 Pa.

Substrate	Product	Yield [%] [a] (*syn*:*anti* ratio)
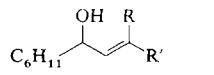	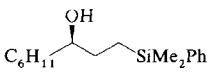	
20a, R = H, R′ = $PhMe_2Si$	**21**	99
b, R = $PhMe_2Si$, R′ = H		90
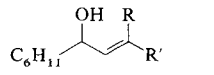	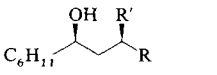	
22a, R = Me, R′ = $PhMe_2Si$	**23a**, R = Me, R′ = $PhMe_2Si$	99 (>500:1)
24, R = $PhMe_2Si$, R′ = Me	**25**, R = $PhMe_2Si$, R′ = Me	95 (1:>500)
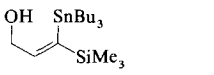	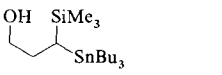	99
27	**28**	
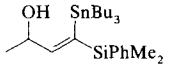	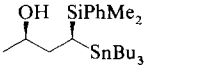	89 (60:1)
29	**30**	

[a] Yield of pure product.

The significance of these results lies in the ease of conversion of a carbon–silicon σ bond to a carbon–oxygen bond under very mild conditions with retention of stereochemistry.[10] Oxidation of **23a** under the conditions described by Fleming gives the *syn* diol **26a** in 68% yield [Eq. (c)]. Differentially protected diols are readily prepared by protection of the hydroxyl group prior to the oxidation step. Thus treatment of **23b** gives **26b** in 71% yield as a single diastereomer.

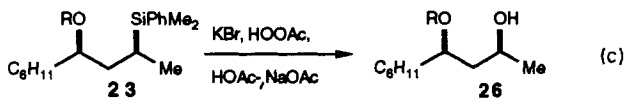

23 **26** (c)

a, R = H; **b**, R = Me

Olefins bearing both tin and silicon moieties also undergo hydrogenation (Table 2). Thus compounds **27** and **29** were formed in good yield, the latter with 60:1 diastereoselectivity. The sense of diastereoselection was assumed to be identical to that previously observed for the silanes and stannanes.

In conclusion, we have shown that vinylsilanes and stannanes can be readily hydrogenated by a cationic rhodium catalyst, that the hydroxyl group directs the addition to one face of the olefin with very high diastereoselectivities, and that a subsequent oxidation provides a route to 1,3-diols. The reactivity of diastereomerically enriched 1,1-dimetalated compounds such as **30** is currently under investigation.

Experimental Procedure

A high-pressure hydrogenation bomb (Parr instrument Co) containing a glass sleeve insert was charged with the substrate, the rhodium catalyst **1** (5 mol%), and dry, distilled, deaerated dichloromethane. The system was pressurized to 1500 psi (103×10^5 Pa), and the reaction stirred for 36–48 h. After the reaction was complete, the catalyst was precipitated by the addition of hexanes, the suspension was filtered through a plug of Na_2SO_4, and the volatiles removed in vacuo. Flash chromatography gave the pure product. ^1H NMR of **7**: (400 MHz, $CDCl_3$, 25 °C, TMS) δ = 3.4 (sb, 1H; *H*C-OH), 1.56–1.8 (m, 8H; HO-CH-CH_2, $(CH_2)_3$, Cy), 1.55 (m, 4H; -CH_2-CH-CH_2-), 1.4–1.45 (m, 7H; Sn-$(CH_2)_2$-CH_2-CH_3, O-*H*), 0.98–1.3 (m, 17H; Sn-CH_2-CH_2-CH_2-CH_3, Sn-*CH*-$(CH_2)_3$-CH_3, *CH*-CH-OH), 0.87, (t, ^3J(H,H) = 7.29 Hz., 9H; Sn-$(CH_2)_3$-CH_3), 0.79 (m, 6H; Sn-CH_2-$(CH_2)_2$-CH_3). ^{13}C NMR (50 MHz, $CDCl_3$, 25 °C, TMS) δ = 74.3, 43.8, 37.3, 32.3; 32.1, 29.3, 26.4, 26.3; 26.1, 29.2, 27.4, 22.9, 22.2, 13.9, 13.5, 8.8. ^{119}Sn NMR (25 MHz, $CDCl_3$, 25 °C, Me_4Sn) δ = −5.2. IR (neat) $\tilde{\nu}$ [cm^{-1}] = 3631, 2926, 1464, 1457, 1451, 1376, 1101. Correct C,H analysis for $C_{25}H_{52}OSn$.

Received: September 25, 1991 [Z 4930 IE]
German version: *Angew. Chem.* **1992**, *104*, 237

CAS Registry numbers:
1, 82499-43-2; **2**, 126531-28-0; **3**, 138407-97-3; **4**, 124607-17-6; **5**, 104108-22-7; **6**, 130708-13-3; **7**, 138407-98-4; **8** (≡ **19**), 4436-87-7; **9**, 138408-07-8; **10**, 138407-89-3; **11**, 138407-99-5; **12**, 138407-90-6; **13**, 138408-09-0; **14**, 138153-98-7; **15**, 138408-00-1; **16**, 138407-91-7; **17**, 138408-01-2; **18**, 138154-01-5; **20a**, 138407-92-8; **20b**, 138407-93-9; **21**, 138408-02-3; **22**, 138407-94-0; **23a**, 138408-03-4; **23b**, 138408-11-4; **24**, 138407-95-1; **25**, 138408-04-5; **26a**, 138408-10-3; **26b**, 138408-08-9; **27**, 138407-96-2; **28**, 138408-05-6; **29**, 131343-40-3; **30**, 138408-06-7.

[1] a) J. M. Brown, *Angew. Chem.* **1987**, *99*, 169; *Angew. Chem. Int. Ed. Engl.* **1987**, *26*, 190; b) J. M. Brown, R. G. Naik, *J. Chem. Soc. Chem. Commun.* **1982**, 348; c) J. M. Brown, S. A. Hall, *J. Organomet. Chem.* **1985**, *285*, 333; d) R. H. Crabtree, M. W. Davis, *Organometallics* **1983**, *2*, 681; e) R. H. Crabtree, M. W. Davis, *J. Org. Chem.* **1986**, *51*, 2655; f) G. Stork, D. E. Kahne, *J. Am. Chem. Soc.* **1983**, *105*, 1072; g) D. A. Evans, M. M. Morrissey, *ibid.* **1984**, *106*, 3866; h) *Tetrahedron Lett.* **1984**, *25*, 4637; i) D. A. Evans, M. DiMare, *J. Am. Chem. Soc.* **1986**, *108*, 2476.
[2] R. Noyori, H. Takaya, *Acc. Chem. Res.* **1990**, *23*, 345. b) H. Takaya, T. Ohta, N. Sayo, H. Kumobayashi, S. Akutagawa, S. Inoue, I. Kasahara, R. Noyori, *J. Am. Chem. Soc.* **1987**, *109*, 1596, 4129. c) M. Kitamura, K. Nagai, Y. Hsiao, R. Noyori, *Tetrahedron Lett.* **1990**, *31*, 549.
[3] Abbreviations: dppb = 1,4-bis(diphenylphosphino)butane, PDC = pyridinium dichromate, NBD = norbornadiene.
[4] Vinylstannanes are reported to be unreactive toward typical metal hydrogenation catalysts: a) T. N. Mitchell, *J. Organomet. Chem.* **1986**, *304*, 1. b) B. Joussequme, *J. Chem. Soc. Chem. Commun.* **1984**, 1452. For the reaction with diimide, see: A. Rahm, J. Grimeau, M. Petraud, B. Barbe, *J. Organomet. Chem.* **1985**, *286*, 297.
[5] M. Lautens, A. H. Huboux, *Tetrahedron Lett.* **1990**, *31*, 3105.
[6] a) F. Sato, *J. Organomet. Chem.* **1985**, *285*, 53. b) F. Sato, H. Watanabe, Y. Tanaka, M. Sato, *J. Chem. Soc. Chem. Commun.* **1982**, 1126. c) F. Sato, Y. Kobayashi, *Org. Syn.* **1990**, *69*, 106.
[7] J. K. Stille, *Angew. Chem. Int. Ed. Engl.* **1986**, *25*, 508.
[8] a) M. Ochiai, S. Iwaki, T. Ukita, Y. Matsuura, M. Shiro, Y. Nagao, *J. Am. Chem. Soc.* **1988**, *110*, 4606. b) J. W. Herndon, C. Wu, *Tetrahedron Lett.* **1989**, *30*, 6461.
[9] The formation of the 1,3-*syn* product in the hydrogenation of a *homoallylic alcohol* has been previously noted: D. H. Birtwistle, J. M. Brown, R. H. Herbert, A. P. James, K.-F. Lee, R. J. Taylor, *J. Chem. Soc. Chem. Commun.* **1989**, 194.
[10] I. Fleming, P. E. J. Sanderson, *Tetrahedron Lett.* **1987**, *28*, 4229.

Nucleophilic Attack at the Central Carbon Atom of (π-Allyl)palladium Complexes: Formation of α-Cyclopropyl Esters**

By *H. Martin R. Hoffmann*,* *Andreas R. Otte*, and *Andreas Wilde*

(π-Allyl)palladium complexes are key intermediates in organopalladium chemistry[1] and the structural formula of

[*] Prof. H. M. R. Hoffmann, A. R. Otte, A. Wilde
Institut für Organische Chemie der Universität
Schneiderberg 1B, D-W-3000 Hannover (FRG)

[**] This work was supported by the Fonds der Chemischen Industrie (PhD fellowship to A. Wilde) and Degussa AG (generous gift of palladium salts). We thank Dr. Victor Wray for kindly providing the 600 MHz NMR spectra.

the bridged dimer **1** has featured prominently as logo of a recent international symposium.[2] The reaction of (π-allyl)palladium complexes with various carbanions results in allylic alkylation (Tsuji–Trost reaction).[1] In these reactions, regiochemistry plays a decisive role. Although many studies have addressed the question of switching the site of terminal nucleophilic attack (C1 versus C3) for a given nucleophile,[1] only two isolated examples of C2 attack are known.[3, 4] More than a decade ago Hegedus and his coworkers observed attack at the central carbon (C2) of the allyl moiety with concomitant formation of a substituted cyclopropane ring.[3, 5] Recently, Santi reported that Pd complexes of bulky chelating phosphanes may catalyze the coupling of allyl acetates and ketene silyl acetates to produce cyclopropane derivatives in low yields.[4, 6]

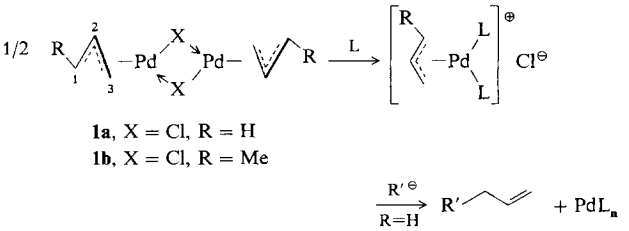

1a, X = Cl, R = H
1b, X = Cl, R = Me

We now show that proper choice of the coordination environment affords functionalized cyclopropane in high yield. Specifically, addition of 1,2-bis(dimethylamino)ethane (TMEDA) followed by carbon monoxide to the (π-allyl)-palladium solution gave the cyclopropanation products in large excess as Equation (a) and Table 1 show.[8] Separation of **2** and **3** by column chromatography proved difficult. However, pure cyclopropane derivatives were obtained after treatment with OsO_4/H_2O_2 and chromatographic separation of the resulting diol.[7] The yields of allylic alkylation products were determined by NMR and GC analysis and the *trans* configuration of the cyclopropanation products **2** and **4** by difference NOE NMR measurements.

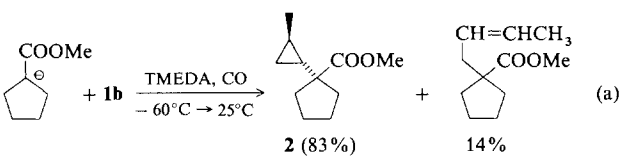

2 (83%) 14% (a)

In all cases the added ligand proved to be a crucial factor. TMEDA gave the highest yields, bis(dimethylamino)-methane and 1,3-bis(dimethylamino)-propane failed to deliver any cyclopropanation product, and sparteine provided moderate yields. According to calculations by Curtis and Eisenstein[9] published four years after the original paper by Hegedus,[3] the observed cyclopropanations should not be energetically accessible. As yet, theory has not dealt satisfactorily with these reactions.

Under the conditions we employed, lithium enolates of ketones and of less substituted esters (e.g., cyclohexanone, isobutyrophenone, methyl phenylacetate, and methyl 3,3-dimethylbutyrate) did not work. The scope and limitations of the reported transformations are under investigation.

Table 1. Cyclopropanes from (π-allyl)palladium complexes.

Entry	Nucleophile	π-Allylpalladium Complex	T [°C]	Added Ligand	Product	Yield [%]
1	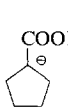	**1a**	−60	TMEDA, CO	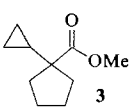 **3**	72
2	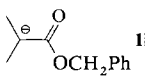	**1b**	−60	TMEDA, CO	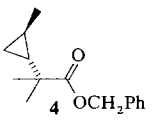 **4**	70
3	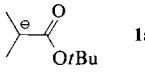	**1a**	−60	TMEDA, CO	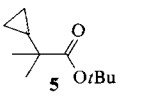 **5**	60
4	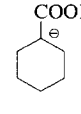		−78	HMPA/ [a] Et_3N	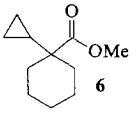 **6**	5
5		**1a**	−60	HMPA/ Et_3N		41
6			−60	TMEDA, CO		84 [b]

[a] HMPA = hexamethylphosphoric triamide. [b] Without CO the yield was smaller.

Experimental Procedure

Preparation of ester enolates: Diisopropyl amine (0.15 mL, 1.1 mmol) in dry THF (5 mL) was placed in an oven dried flask under N_2. After cooling the mixture to 0 °C, *n*BuLi (0.7 mL, 1.1 mmol, 1.6 M solution in hexane) was added. The solution was stirred for 5 min and cooled to −78 °C before the ester (1.1 mmol) was added. The reaction mixture was then stirred at 0 °C for 10 min, after which it was cooled to −78 °C and TMEDA (0.17 mL, 1.1 mmol) was added. The solution was stirred at −78 °C until required (about 30 min).

Cyclopropanation reaction: A dimeric (π-allyl)palladium chloride complex (0.275 mmol) in dry THF (5 mL) was placed in an oven dried flask under N_2. The solution was cooled to −78 °C and TMEDA (0.17 mL, 1.1 mmol) was added. After warming the mixture to −60 °C, the carbanion solution (see above) was added dropwise through a double tipped needle. Attachment of a CO balloon caused the reaction mixture to turn black and palladium to precipitate. After stirring for 1 h, the solvent was removed and ether (100 mL) was added. The mixture was filtered and the filtrate washed with water. The aqueous layer was back extracted with ether and the combined organic layers were washed with brine (20 mL), dried ($MgSO_4$), and concentrated. The resulting oil was purified by flash chromatography (silica gel, cyclohexane/ether, 10:1) to give the product as a colorless oil.

Received: September 20, 1991 [Z 4914 IE]
German version: *Angew. Chem.* **1992**, *104*, 224

CAS Registry numbers:
1a, 12012-95-2; **1b**, 12081-22-0; **2**, 138052-84-3; **3**, 138052-81-0; **4**, 138052-82-1; **5**, 138052-83-2; **6**, 75266-48-7; methyl cyclopentanecarboxylate, 4630-80-2; benzyl isobutyrate, 103-28-6; *tert*-butyl isobutyrate, 16889-72-8; methyl cyclohexanecarboxylate, 4630-82-4.

[1] a) B. M. Trost, *Angew. Chem.* **1989**, *101*, 1199; *Angew. Chem. Int. Ed. Engl.* **1989**, *28*, 1173; b) B. M. Trost, T. R. Verhoeven, *Comprehensive Organometallic Chemistry, Vol. 8* (Eds: G. Wilkinson, F. G. A. Stone, E. W. Abel), Pergamon, Oxford, **1982**, 799; c) J. Tsuji, *Organic Synthesis with Palladium Compounds*, Springer, Berlin, **1980**, p. 45–51; J. Tsuji, *Tetrahedron* **1986**, *42*, 4361.

[2] International Symposium on Palladium in Organic Synthesis, Sigtuna, Sweden, August 20–24, **1990**.

[3] L. S. Hegedus, W. H. Darlington, C. E. Russell, *J. Org. Chem.* **1980**, *45*, 5193.

[4] C. Carfagna, L. Mariani, A. Musco, G. Sallese, R. Santi, *J. Org. Chem.* **1991**, *56*, 3924.

[5] We observed that the procedure reported by Hegedus will work provided that the reaction temperature is kept at −60 °C instead of −78 °C as reported by him. However, reproducible yields of substituted cyclopropane are still well below our results with TMEDA (see Table 1, entries 4–6).

[6] Formation of metallacyclobutane complexes other than those of palladium by nucleophilic attack at the central carbon atom of the allyl ligand has been observed in a few reactions. See E. B. Tjaden, J. M. Stryker, *J. Am. Chem. Soc.* **1990**, *112*, 6420 and references therein.
[7] N. A. Milas, S. Sussman, *J. Am. Chem. Soc. 1936*, **58**, 1302.
[8] Selected NMR data: **2**: ^{1}H NMR (200 MHz, $CDCl_3$): $\delta = 3.67$ (s, 3 H), 2.1–1.25 (m, 8 H), 1.02 (d, 3 H), 0.78 (m, 1 H), 0.64 (m, 1 H), 0.40 (m, 1 H), 0.13 (m, 1 H); ^{13}C NMR ($CDCl_3$): δ = 178.4, 53.8, 51.7, 33.9, 33.7, 26.5, 24.8, 24.8, 18.8, 9.8, 9.5. **5**: ^{1}H NMR (200 MHz, $CDCl_3$): $\delta = 1.44$ (s, 9 H), 1.01 (s, 6 H), 0.94–1.08 (m, 1 H), 0.23–0.40 (m, 4 H); ^{13}C NMR ($CDCl_3$): δ = 177.2, 77.7, 41.6, 28.1, 23.0, 19.6, 0.7.
[9] M. D. Curtis, O. Eisenstein, *Organometallics* **1984**, *3*, 887. See also Davies-Green-Mingos rules: S. G. Davies, M. L. H. Green, D. M. P. Mingos, *Tetrahedron* **1978**, *34*, 3047; S. G. Davies, M. L. H. Green, D. M. P. Mingos in *Reactions of Coordinated Ligands* (Ed.: P. S. Braterman), Vol. 1, Plenum, New York, **1986**, p. 897.

BOOK REVIEWS

Book Reviews are written by invitation from the editor. Suggestions for books to be reviewed and for book reviewers are welcome. Publishers should send brochures or (better) books to the following address: Redaktion Angewandte Chemie, Postfach 101161, W-6940 Weinheim, Federal Republic of Germany. The editor reserves the right of selecting which books will be reviewed. Uninvited books not chosen for review will not be returned.

Atomic Spectroscopy. By *J. W. Robinson*. Marcel Dekker, New York, 1990. vi, 299 pp., hardcover $ 119.50.—ISBN 0-8247-8311-5

Atomic spectroscopy methods are nowadays the most important of the tools used in the analytical chemistry of the elements. Their great variety, which one can now barely keep track of, and the remarkably rapid pace of instrument developments in this field, already make it difficult for competent users to evaluate these with regard to such criteria as detection capability, reliability and value for money, so as to be able to solve analytical problems that are nowadays becoming ever more complicated.

The task of teaching young scientists the basic knowledge required is especially difficult. In principle, therefore, any attempt to make this easier by providing an up-to-date introduction to atomic spectroscopy, limited to the basic essentials, is appropriate and welcome.

The author of this book is an experienced spectroscopist and analyst who has been involved in the rapid developments that have occurred in this area of applied analysis since the 1950s, has made a name for himself through many original contributions, and now teaches analytical chemistry as a professor at the University of Louisiana, USA. He has previously written several monographs on the subject and chapters in handbooks, and is the editor of two specialist journals.

This monograph provides further evidence of his competence. He has set out to provide, in about 300 informative and richly illustrated pages, a picture of modern atomic spectroscopy, including the necessary basic physical background and the analytical capabilities and limitations of the methods.

A compressed introduction to such a broad subject obviously requires tight restrictions on the choice of methods and literature references. The textbook-style treatment is therefore limited to those methods of optical atomic spectroscopy that are currently most important and are in routine analytical use, such as atomic absorption, emission and fluorescence spectroscopies and their most important excitation sources, both classical and modern (radiofrequency plasmas).

However, this reviewer was disappointed at not finding at least some references to the most recent, highly interesting, developments in laser spectroscopy, which will revolutionize atomic spectroscopy in the future. Also there should have been some mention of microwave-induced plasmas (MIP) and glow discharges (GD), which are very powerful modern excitation sources for optical emission spectroscopy and mass spectrometry.

Unfortunately, too, not enough detail is given of the many different ways of reducing possible sources of error and improving detection capabilities by combining with appropriate chemical and physical methods of separation and enrichment, which are indispensable techniques in elemental trace analysis.

On the other hand, one could easily have done without the extensive tables of wavelengths (20 pages) used for the determination of elements by flame AAS, since practitioners already have access to adequate published tables, whereas newcomers to the field are unlikely to find them interesting. Also flame photometry is treated in too much detail in relation to its present importance.

Reading this book has again reminded the reviewer how difficult it is to give, in a limited space, a balanced treatment for teaching purposes of such an extensive and important field as atomic spectroscopy has now become in modern elemental analysis. Even more difficult is the undertaking of providing already practising analysts with anything more than just a condensed overview of the tools of the method and the basic physical principles on which they depend.

Just as providing a lump of marble, a hammer and a chisel does not at once result in a sculpture, so one finds that a description of the analytical techniques falls far short of enabling one to approach problems of analytical chemistry in the most effective way. To achieve this difficult task, which also involves teaching strategies, requires a more concentrated effort on the part of authors. Until that occurs we must be content with partial solutions; even this book has failed to achieve more than that.

With that reservation, however, I can recommend the book especially to students and analytical chemists wishing to make a start in atomic spectroscopy, provided that they

are not put off by its high price, which is not justifiable for a "textbook", despite the high standard of production and the clear and carefully prepared contents.

Günther Tölg
Institut für Spektrochemie und angewandte Spektroskopie
Dortmund (FRG)

Houben-Weyl. Methods of Organic Chemistry. Additional and supplementary volumes to the 4th Edition. Vol. E12b. Organotellurium Compounds. Edited by *D. Klamann*. Thieme, Stuttgart, 1990, xli, 1004 pp., hardcover DM 1340.00—ISBN 3-13-219904-4.

The series "Methoden der Organischen Chemie" was established in 1909 by Theodor Weyl and continued in 1913 by Heinrich Houben. At that time, publishing a handbook in organic chemistry in German seemed most appropriate. Today, more than eighty years later, changing the "official" language of Houben-Weyl from German to English seems just as well motivated. I am sure the change will increase the international character of the series even more and I would like to congratulate the editors on their decision.

Organotellurium compounds were previously described by Houben-Weyl in 1955 (Vol IX), together with organosulfur and organoselenium compounds. At that time Rheinboldt used 292 pages for the description of the surprisingly old but little explored fields of organoselenium and organotellurium chemistry. A few years ago, organosulfur chemistry was updated in two volumes of Houben-Weyl, while the work with the organoselenium volume(s) is presently ongoing.

The last twenty-five years have seen a steady increase in the number of publications in the field of organotellurium chemistry. Recently, a number of useful organic transformations brought about by organotellurium reactions and reagents has focused the attention of synthetic organic chemists on the area. Thus, organotellurium chemistry, viewed by many as rather odd and peculiar, has now developed into an almost respectable field of research close to the mainstream of organic chemistry.

The author, Kurt Irgolic, was very well prepared for the gigantic work of putting together a volume of Houben-Weyl. In 1972 he summarized all previous work in the field in "The Organic Chemistry of Tellurium" which has since been frequently used as reference by all involved in organotellurium research. For many years thereafter he also published annual reports on the chemistry of organic tellurium compounds in the *Journal of Organometallic Chemistry*. Unfortunately, this work was disrupted in 1980. Since that time organotellurium chemistry has been treated in depth only in the Patai series, "The Chemistry of Organic Selenium and Tellurium Compounds", Vol. 1 1986; Vol. 2 1987. Due to the organization of the Patai series, which focuses attention on a number of diverse aspects of the field, these volumes are complementary to, rather than overlapping with, the Houben-Weyl volume.

The contents of the present volume are logically organized in a way similar to the one used by the author in his previous writing. Thus, the organic tellurium compounds are classified according to the number (1–6) of carbon–tellurium bonds in the molecule, and their reactions subdivided according to the traditional Houben-Weyl scheme of presentation (i.e., A. Preparation; B. Transformations). Polymeric tellurium compounds as well as heterocyclic (3–7-membered) organic tellurium compounds are treated in separate sections. In addition, a chapter (150 pages) is devoted to organic tellurium compounds without a carbon–tellurium bond in the molecule. Compounds described in this section include molecules where the organic moiety is separated from tellurium by another heteroatom such as oxygen, sulfur, selenium, silicon, or phosphorus. These compounds were traditionally not classified as organotellurium compounds but left in a no-man's-land between inorganic and organic chemistry.

The classification of chemical reactions as "Preparations" or "Transformations" in the treatment of various classes of compounds is not always consistent. For example, the reaction of a diorganyltellurium(II) species with a halogen, to give the corresponding diorganyltellurium(IV) dihalide is sometimes treated as a method of preparation, sometimes as a transformation of the class of diorganyltellurium(II) compounds. The latter treatment is the preferred one. The formation of complexes of organotellurium compounds with transition metals or electron-deficient organic molecules is usually found under "Preparations". However, in some cases these compounds are also treated under "Transformations". In my opinion the latter classification is more logical and should be used consistently.

A third category of classification is introduced for diorganotellurium dihalides on p. 577: "C. Diorganotellurium dihalides as synthetic intermediates". However, when the similar use of diorganotellurium compounds is discussed earlier on p. 480, the material is presented as a transformation.

The present supplementary volume of Houben-Weyl contains a respectable number of references and examples from the period (1840–1955) covered by volume IX. The old results are often presented in the light of new findings and contribute to a feeling of complete understanding and coverage of a certain class of compounds or reactions. In other cases the old material was too sparsely treated in the previous version and was in need of an expansion.

The overall impression of the present volume of Houben-Weyl is that of a complete coverage of the field. The number of papers not included can probably be counted on your fingers. This completeness will of course make the book invaluable for all involved in organotellurium research and those in other areas in need of information concerning organotellurium chemistry. However, the philosophy on which Houben-Weyl was established requires not only a complete description of preparative methods but also their critical evaluation. While going through the representative examples of the present volume, I sometimes got the impression that the author should have been more selective/critical in his choice. There are too many full-detail preparations where the yields do not exceed 10%. For example, nobody "skilled in the art" would ever consider trying to execute the 1% yield synthesis of diphenyl ditelluride described on p. 270, when there are so many better methods available. Similarly, on p. 2 the existence of tellurium(II) dihalides is discussed, and it is concluded that they probably do not exist as molecular entities in the solid state. Nevertheless, on p. 37 an example is presented where $TeCl_2$ is used as one of the reactants for the preparation of a ferrocene derivative. Likewise, on p. 841 TeI_2 appears in an example describing the synthesis of a heterocyclic tellurium compound.

An index of authors and a compound index is included at the end of the book. The compound index is very good if you are looking for a particular compound; however, it is of little help if you are searching for something else. I think a book of this size could afford also a subject index.

The number of printing errors is kept to a minimum throughout this volume of Houben-Weyl. Less than 50 errors (and only very few serious ones) were noted while going through the material. Except for p. XXXVII (where a terrible 20% of the references contain minor errors or are incomplete) the citation is comparable in quality with that found in the best journals.

In conclusion, the updated Houben-Weyl volume on organotellurium compounds is a masterpiece which will be enthusiastically received by all readers with an interest in tellurium chemistry.

Lars Engman
Department of Organic Chemistry
Royal Institute of Technology
Stockholm (Sweden)

Electrochemical Interfaces. Modern Techniques for in-situ Interface Characterization. Edited by *H. D. Abruna*. VCH Publishers, New York/VCH Verlagsgesellschaft, Weinheim, 1991. xviii, 589 pp., hardcover DM 182.00.—ISBN 0-89573-715-9/3-527-27840-0

In seeking to describe and understand electrochemical processes that occur in the solid/liquid transition region, experimental data obtained by in-situ measurements are especially valuable. A classic example where this applies is the technique of cyclovoltammetry (CV). In this the flow of charge is recorded as a function of the potential, but the method is intrinsically incapable of yielding information of a highly specific kind. For this reason other techniques that can be used in combination with CV have recently been developed to complement it. Particularly interesting results can be obtained by carrying out in-situ measurements simultaneously with CV studies. This rapidly developing field is the subject of the specialist book edited by H. D. Abruna (Cornell University) which is reviewed here.

The book, with nearly 600 pages, contains ten chapters following an introduction by the editor, and there is a 22-page subject index at the end.

The individual chapters deal with X-ray absorption spectroscopy, surface X-ray scattering, X-ray standing waves, measurements of surface forces, surface-enhanced Raman scattering, nonlinear optical methods, surface infrared spectroscopy, in-situ Mössbauer spectroscopy, radioactive labeling, and measurements with vibrating quartz crystals. The contributions have been printed by the camera-ready method, and all except one are written by American authors.

Apart from the fact that several of the figures in Chapter 1 have been interchanged (see the comments of the editorial office), the contributions are impressively well prepared: they are logically set out, illustrated by clear figures, and packed with information. In each chapter the main emphasis is firmly on the description of the experimental techniques, but this is supported by informative examples of applications. In the description of the standing wave X-ray technique for characterizing the phase boundary region, it would have been desirable to have examples of a wider range of applications. Unfortunately the chapter on in-situ measurements with vibrating quartz crystals includes only two examples of applications, namely to coverages deposited in the under-potential range, and (in more detail) to studies of mass transport during redox processes in polymer films.

The selection of topics covered by the chapters is not exhaustive, nor can one expect it to be. However, it is noticeable that some important methods are not mentioned, for example UV/VIS reflectance spectroscopy, ellipsometry and photocurrent spectroscopy. It is also regrettable that in-situ topographic methods such as scanning tunneling microscopy (STM) and atomic force microscopy (AFM), which give a microscopic image of the surface, in some cases with atomic resolution, are not included. Furthermore, there seems to be no logical connection between the individual chapters. The fact that articles on optically based techniques alternate with others on non-optical methods prevents a systematic presentation of the subject matter. Consequently it is hardly surprising that the book lacks a final summary linking the various methods and results and evaluating them.

The book has a binding of appropriately high quality. Considered as a whole it provides a good insight into the progress that has been made in the development of various in-situ techniques. However, one cannot overlook the shortcomings in the choice of topics and their relative emphasis, and the lack of a logical arrangement of subject matter, with the result that the reader fails to get a deeper understanding of the progress made. The book is unquestionably of considerable importance to scientists with interests in interfacial electrochemistry, and it should therefore be in every relevant library, especially since the price of DM 182.00 will prevent students from buying it.

Rolf Schumacher
Schering AG, Forschungsabteilung GT
Berlin (FRG)

Chemistry of Organosulfur Compounds. General Problems. (Ellis Horwood Series in Organic Chemistry). Edited by *L. I. Belen'kii*. Ellis Horwood, New York, 1990. 378 pp., hardcover $ 129.95.—ISBN 0-13-132051-3

Organosulfur chemistry traditionally occupies a position of considerable importance in Soviet research, and there is even a special scientific committee to promote it. The monograph reviewed here is based on a status report on work in this field that was prepared in 1986 by various authors, mainly from Moscow and Irkutsk. For this English version the Russian text has been rearranged and updated (but, as becomes apparent, only in parts). The 15 chapters of this version deal with the preparation of organosulfur compounds, their transformations, and the methods used to study them. Details of the chapters are as follows: Modern Principles of the Synthesis of Organosulfur Compounds (M. G. Voronkov et al., 14 pp., 25 references); Radical Reactions of Some Thiocarbonyl Derivatives in Solutions (R. Kh. Freidlina et al., 21 pp., 64 references); Thermal Reactions and High Temperature Syntheses of Organosulfur Compounds (M. G. Voronkov et al., 20 pp., 56 references); Photochemical Synthesis and Transformations of Organosulfur Compounds (N. N. Vlasova, 22 pp., 65 references); Radiochemical Synthesis and Transformations of Organosulfur Compounds (E. M. Nanobashvili, 8 pp., 11 references); Sulfur-stabilized Carbanions and their Synthetic Use (F. M. Stoyanovich, 43 pp., 267 references); Formation of C–C Bonds Using Sulfur-containing Electrophilic Reagents (W. A. Smit et al., 32 pp., 99 references); Catalytic Synthesis of Organosulfur Compounds (A. V. Mashkina, 20 pp., 40 references); Methods of Desulfurization and their Use in Organic Synthesis (L. I. Belen'kii, 36 pp., 189 references); Investigation of Organic Reactions by the Use of Radioactive Sulfur (V. M. Fedeseev, 15 pp., 49 references); Mass

Spectrometry of Organosulfur Compounds (A. A. Polyakova, 11 pp., 10 references); Electronic and Vibrational Spectroscopy of Organosulfur Compounds (Yu. L. Frolov, 11 pp., 30 references); ^{33}S NMR Spectroscopy (V. M. Bzhezovsky et al., 21 pp., 49 references); X-Ray Fluorescence Spectroscopy of Sulfur Compounds (G. N. Dolenko, 76 pp., 199 references); Quantum Chemical Calculations of Organosulfur Compounds (Yu. L. Frolov, 11 pp., 66 references).

The intention of the book is to concentrate on reporting the work of Soviet authors, and the high proportion of references to Soviet publications makes this clearly apparent. In contrast, published work in this field from the West is incompletely represented. Consequently, although the breadth and potency of organosulfur chemistry become clearly evident, some of the newer and particularly elegant synthetic applications of sulfur-containing functions, such as those introduced by Vedejs and by Warren, are dismissed too briefly or even omitted altogether. Also the usefuless of the book is reduced by the inadequacy of the rather meager subject index. For example, there is no entry for thioaldehydes, despite the fact that this class of compounds is mentioned at several places in the text. It therefore comes as welcome news to learn from the preface that a further monograph dealing with the most important classes of organosulfur compounds is planned.

The book is visually pleasing, thanks to the clear and attractive typography. The incidence of printing errors is as low as can reasonably be expected. There is an unfortunate mistake on page 84, where thiofenchone is shown instead of thiocamphor. The book fills a gap by reporting in detail on Soviet work in organosulfur chemistry, but for newcomers to this field it fails to provide a comprehensive critical overview.

Ernst Schaumann
Institut für Organische Chemie
der Technischen Universität Clausthal (FRG)

Chemical Kinetics. By *K. A. Connors*. VCH Publishers, Cambridge, New York/VCH Verlagsgesellschaft, Weinheim, 1990. xiii, 480 pp., hardcover DM 168.00.—ISBN 1-56081-006-8/3-527-28037-5

Spectacular successes were achieved during the sixties using the techniques of "fast kinetics", and this led to the publication of numerous monographs dealing with this important area of physical chemistry. As an example of these one may mention particularly the classic work "Fast Reactions in Solution" by E. F. Caldin. Since then these methods have become widely used in chemistry, and therefore the publication now of an up-to-date and comprehensive work on kinetics, which will make it easier for those interested in the topic to become involved, is greatly to be welcomed.

This book by K. A. Connors deals in eight chapters with the important field of kinetics in solutions, with an emphasis on the chemical aspects. Chapter 1 begins with a discussion of the significance of time as a variable in chemistry, followed by an explanation of fundamental concepts involved in kinetics, such as transition states, reaction intermediates and the rate of a reaction. The second chapter then deals with the integration of simple rate equations, the determination of the order of a reaction, and the calculation of the corresponding rate constants. The numerical problems associated with error limits are discussed in great detail at this stage. Chapter 3 deals with systems described by more complex equations, and here the application of Laplace transforms is introduced. Classical examples such as microreversibility and the condition for a stationary state are discussed, as well as more innovative methods such as Monte-Carlo simulations.

Following these discussions of basic principles, Chapter 4 is concerned specifically with fast kinetics. After dealing with diffusion-controlled reactions, the chapter goes on to consider periodic and aperiodic relaxation processes. Next some fundamental aspects of nuclear magnetic resonance spectroscopy as applied to kinetic studies are discussed. The chapter ends with descriptions of flow techniques, fluorescence quenching, and a brief reference to electrochemical methods.

Chapter 5 takes the discussion of fundamental kinetic theories a stage further. Starting from the Arrhenius equation, the author deals with simple collision theory, potential energy surfaces, and quantum-mechanical aspects of the reaction between H_2 and H and of the transition state based on partition functions. Next some examples from actual kinetic studies are described, and the relationship between free activation enthalpies and free reaction enthalpies is discussed. Here the Hammond, Brønsted, and Marcus representations are discussed. Chapter 6 describes examples of some important kinetic phenomena. In the catalytic field the influence of acids and bases on chemical reactions and the pH-dependence of rate constants are discussed. The chapter concludes with a discussion of isotope effects, which are very interesting from a mechanistic standpoint.

For organic chemists the most interesting part of the book is likely to be Chapter 7 on structure–reactivity relationships. The chapter begins with a discussion of linear free energy relationships, by which activation data are related to reaction parameters. As an example, these considerations are applied to substituent effects in arenes, including a detailed discussion of the Hammett equation and its limitations. Next the theory is extended to nonlinear phenomena, including electronegativity, polarizability and resonance effects. Substituent effects in aliphatic compounds are also treated and discussed in relation to the Taft constants for alkaline and acidic hydrolysis reactions; here steric effects are also taken into consideration. In addition the "hard–soft" concept and isokinetic relationships are discussed. It is pleasing to find that the potentially troublesome problem of propagation of errors in determining activation parameters is taken into account here, so as to avoid the risk that numerical errors could lead to wrong conclusions about isokinetic relationships.

The book ends with a chapter on the influence of the medium. It is shown that, in the determination of rate constants, differences as great as a factor of 10^{15} compared with the gas phase can arise. Theories of the effects of a dielectric continuum are discussed, including the early suggestions by Born and also the Hughes–Ingold theory. The effects of intermolecular interactions with solvents are discussed, including molar refraction, polarization, Coulomb potentials, charge transfer effects and hydrogen bonding. In this connection the empirical solvent scales based on thermodynamic and spectroscopic data, such as those proposed by Gutmann, Kosower, or Reichardt, are especially important.

The range of topics covered in this book extends considerably beyond the treatments of kinetics found in comprehensive textbooks of physical chemistry. The numerous examples give an excellent overview of the many different types of phenomena and reactions that have been studied. For the

practising chemist the details of the many methods that are described for determining rate constants are especially useful, since they give particular attention to considerations of error limits. The book is easy to read and should also be of great value to students; it can be recommended unreservedly.

Franz L. Dickert
Institut für Physikalische Chemie
der Universität Erlangen-Nürnberg (FRG)

Cycloaddition Reactions in Organic Synthesis. By *W. Carruthers*. Pergamon, Oxford, 1990. viii, 373 pp., paperback $ 30.00.—ISBN 0-08-034712-6

In this book, published as the eighth volume of the very successful "Tetrahedron Organic Chemistry Series", William Carruthers has set out to show why cycloaddition reactions are so important in organic synthesis. The author, who sadly died shortly after the completion of the manuscript, has succeeded very convincingly in this aim.

The first three of the seven chapters begin by dealing with general aspects of the Diels–Alder reaction and its applications in both its inter- and intramolecular forms. The most useful types of dienes and dienophiles for this reaction are described (including heterofunctionalized species), and the effects of aqueous solvent systems, high pressures, and the use of Lewis acids as catalysts are discussed, illustrated by examples taken mainly from recently published work. Regio- and stereochemical aspects, asymmetrical syntheses using chiral auxiliary groups, and the importance of the retroreaction are also discussed. A considerable amount of space is devoted to the analogous reactions of heterodienes and heterodienophiles, followed by general applications of Diels–Alder reactions to the synthesis of arenes and quinones. Lastly the author makes a special point of emphasizing the effectiveness of intramolecular Diels–Alder reactions for synthesizing terpenoids, alkaloids and other nitrogen-containing heterocycles, cannabinoids, steroids, and lignans.

Chapter 4 is concerned with other types of [4 + 2] cycloaddition reactions. Those described include reactions using allylic anions and cations, and also oxyallyl and pentadienyl cations. Palladium(0)-catalyzed reactions using trimethylenemethane, together with other related reactions, and cobalt-catalyzed acetylene trimerizations are also described. Chapter 5 treats various aspects of inter- and intramolecular ene-reactions. Here the main emphasis is on reactions involving heteroatom species, for example with carbonyl compounds as enophiles or with allylic Grignard reagents as metalloenes. Chapter 6 is concerned with 1,3-dipolar cycloadditions. Here the author introduces the azomethine ylides, the nitrile oxides and the nitrones as the most important 1,3-dipolar molecules for synthetic purposes. The preparation of these intermediates and their use for synthesizing a variety of classes of compounds are discussed with a thoroughness that befits their importance for preparative chemistry. The seventh and last chapter deals with [2 + 2] cycloadditions. Particular emphasis is placed on reactions of ketenes and keteniminium salts with olefins and imines, and on the de Mayo and Paternò–Büchi reactions.

In his treatment Carruthers places special importance on describing and illustrating the synthetic potential of the many different types of cycloadditions. Mechanistic details are included only where they are essential for understanding the synthesis under discussion or for clarifying the stereochemistry of the reaction stages. In this book, in contrast to student textbooks, considerations of the frontier orbitals involved in the reactions are avoided entirely. This policy is followed in all seven chapters, each of which is a self-contained article that can be read independently of the rest, and has its own detailed bibliography (extending up to 1988). A short explanation of the basic principles is followed in each case by an account emphasizing recent developments and applications to building up complex structures; occasionally certain types of reactions are overrepresented (for example, the use of electron-rich siloxydienes as developed by Danishefsky et al.). In some sections the discussion of asymmetric cycloadditions is too brief in relation to their importance, or is omitted entirely. Also it has not been possible to include the development of efficient chiral catalysts, e.g. for Diels–Alder reactions, which has only recently attained full maturity. Nevertheless, in every chapter the author has succeeded convincingly in summarizing the most important developments that have occurred in the area of cycloadditions during the last three decades. The presentations are always lucid and comprehensible, and the numerous reaction schemes are clearly drawn. This ensures that one can quickly extract the most important information, and can then go into topics in greater depth with the help of the detailed bibliographies.

Carruther's book succeeds well in its aims. It contains a wealth of elegant and well-chosen examples, which are very well-suited for illustrating lectures to advanced students. At the same time it provides the interested synthetic chemist, whether in a university or industry, with an excellent overview of the current state of research (up to 1988). Thus the monograph fits well into the scheme of the other volumes in this "Organic Chemistry" series. Since no other comparable work exists at present, and this volume is also very attractively priced, its purchase can be recommended unreservedly.

Herbert Waldmann
Institut für Organische Chemie
der Universität Mainz (FRG)

Polymer Solutions. By *H. Fujita*. (Series: Studies in Polymer Science, Vol. 9). Elsevier, Amsterdam, 1990. xviii, 370 pp., hardcover HFl 285.00.—ISBN 0-444-88339-8

It is always something of a special occasion when one of the great old men of polymer physics makes use of the well-deserved, but not always welcome, leisure of retirement to write a monograph or textbook. *Hirosha Fujita*'s book belongs to this category of works.

On the one hand the book discusses the progress achieved in the study of polymer solutions, while at the same time indicating, with an unusual degree of openness and clarity, the unanswered questions and unsolved problems that remain. It is a critical stocktaking, with the emphasis on *Fujita*'s life's work, which recurs as a central theme throughout the ten chapters of the book. The broad scope of *Fujita*'s research interests prevents the treatment of the subject from becoming too narrow.

The two parts of the book deal with the properties of dilute and concentrated solutions respectively, in the equilibrium state. Time-dependent nonequilibrium processes are not covered, apart from a few exceptions, and indeed to do so would certainly have exceeded the planned size of this book. *Fujita* begins by developing theoretical concepts, which he then compares critically with the relevant experimental observations. In the first part, on dilute solutions, the

 © VCH Verlagsgesellschaft mbH, W-6940 Weinheim, 1992 0570-0833/92/0202-0240 $ 3.50+.25/0

important chain models for macromolecules are introduced, then different approaches to the problem of the excluded volume are described, the contributions of renormalization group theory to the understanding of solution properties are discussed, a separate chapter is devoted to the problems of describing semiflexible polymers, and a few selected topics of current research, such as computer simulations, coil collapse, dynamic light scattering, and polyelectrolytes, are described.

The second part, dealing with concentrated solutions, again begins with an introduction to the underlying theoretical concepts, which is then followed by a chapter on semidilute solutions. The dynamic properties of semiconcentrated solutions are discussed in detail from both theoretical and experimental standpoints, as also is the classical treatment of phase equilibria, although this is the only chapter that fails to mention some important new theoretical physics studies on the topic.

This book is certainly not intended as a textbook for students of macromolecular chemistry, although it contains extensive sections that could provide stimulating reading for advanced students. It is, on the other hand, a comprehensive evaluation of progress achieved in the understanding of polymer solutions, and is suitable for reading by researchers with interests in this field, whether in industry or academia.

Manfred Schmidt
Max-Planck-Institut für Polymerforschung
Mainz (FRG)

Cyclopropane Derived Reactive Intermediates. By *G. Boche* and *H. M. Walborsky*. Wiley, Chichester, 1990. V, 256 pp., hardcover £ 57.00.—ISBN 0-471-92748-1

As indicated on the front cover, this monograph is intended to be an updated version of the two volumes on cyclopropane derivatives that appeared in 1987 in the successful series *The Chemistry of Functional Groups*, by Patai and Rappoport. However, on the back cover it becomes apparent that the first chapter, "Cyclopropyl Radicals, Anion Radicals and Anions", is simply a reprint of the same authors' 1987 chapter with the same title. This at first strikes one as annoying, since after all, what reader wishes to pay a handsome price for something of which 45% (!) already exists on his or her bookshelf? The fact that it is almost an exact reprint is shown by the printing errors, all of which reappear, and are compounded by incorrect cross-references that were in the original and have not been put right. References to publications that were still in press in 1987 have, however, been given in full.

The subject matter of the first chapter has been augmented by an eight-page appendix with 22 references, which is introduced as Chapter 2. This is dominated by two X-ray structure analyses of cyclopropyllithium compounds carried out by one of the authors, and includes (on pages 114–115) a quite unnecessary speculation regarding the mechanism of an intramolecular nucleophilic substitution at a cyclopropane unit. The facts that the reactions reported by Seebach et al. that are cited here are stereospecific, that Bickelhaupt et al. observed an intramolecular substitution into a cyclopropane derivative with inversion, and that Banert has recently also described *intermolecular* substitutions with inversion, rule out any mechanism other than one of the S_N2 type.

Apart from these criticisms the contents of these first two chapters are of a very high quality. The criteria for deciding whether or not cyclopropyl radicals, anion radicals, and anions are likely to be formed as intermediates in any given reaction are clearly set out. This is especially valuable in view of the fact that the mechanistic situation is generally quite complicated. The task of reviewing the widely scattered results is one that only top-class experts in this field can undertake successfully.

Chapters 3–5 are entitled "Cyclopropyl Cations", "Cyclopropyl Carbenoids", and "Cyclopropyl Cation Radicals" respectively. There was a real need for a review of these topics, since the Patai–Rappoport series mentioned above does not contain chapters dealing specifically with these reactive intermediates, and consequently there are only a few isolated instances where such species are treated in adequate depth. Authoritative reports are now available which, although they do not cover the field comprehensively as this series aims to do, nevertheless deal with the main features in an appropriately concise way.

In the case of the cyclopropyl cations, the classification of substituent effects according to the nature of the leaving group and α- and β-substituents is sufficient to characterize some of the preconditions that determine whether a true three-membered ring cation or a partly ring-opened species is formed, or whether ring opening occurs immediately on departure of the leaving group.

Much space is devoted to the conversion of cyclopropyl carbenoids to allenes and insertion products. Explanations are offered as to why one or the other mode of reaction occurs preferentially in any given case, and why in bicyclic systems with more than seven atoms in the rings there is an overwhelming preference for the formation of cycloallenes, whereas with only seven ring atoms one obtains not 1,2-cycloheptadiene but predominantly tricyclo[4.1.0.$0^{2,7}$]-heptane. However, the discussion fails to mention that when the bicyclic system is further reduced in size, the preferred behavior alters yet again. Thus, the formation of 1,2-cyclohexadiene and its derivatives from 6-bicyclo[3.1.0]hexyl-carbenoids is not mentioned, even though these extremely short-lived cycloallenes are of preparative interest.

The chapter on cyclopropane cation radicals is especially topical. The conditions for the one-electron transfer process are now beginning to be understood, and it now seems likely that observations hitherto regarded as isolated curiosities can be fitted into an orderly scheme.

The relatively large frequency of printing errors is typical for these days, a situation that one has to get used to as time goes on. A possible cause of this is the time pressure under which the authors and those responsible for the final production have to work. Electronic information processing has not, in general, improved this unsatisfactory situation. On the contrary, one sometimes gets the impression that the number of mistakes is actually increased through trusting in the supposed infallibility of the computer.

A few examples: on page 65 the text belonging to the formula of *trans*-**145** is missing from above the bottom formula line; in formula **359** on page 98 and formula **101a** on page 145 substituents are missing; incorrect element or group symbols occur in the formulas of $Pb(OAc)_4$ on page 17, **357** on page 96, and **365** on page 98; double bonds are missing from formulas **46** on page 129 and **169** on page 159; the seven-membered rings in formulas **92** on page 143 and **55** on page 190 should be eight-membered rings; formula **67** on page 159 contains one CH_2 group too many, and formula **190** on page 165 contains an extra OH group; in Equation (10) on page 194 each of the formulas has an extra six-membered ring; reference 41b which appears on pages 228 and 233 is not in the bibliography; refer-

ence 207b on page 106 is incorrect; the name K. Rühlmann is spelt throughout with a "u" instead of "ü"; it was in fact possible to print the Umlaut, as is shown by the name L. Skattebøl, in which "ö" has consistently been used instead of "ø" to represent the Norwegian vowel sound œ; "ø" was actually available in the character set, as shown by the name Møller-Plesset on page 208; R. R. Squires has had a particularly raw deal, as his name only appears wrongly as Sguires (p. 68) or as Sguites (pp. 105, 248).

On the whole this monograph succeeds very well as regards its content. The properties of cyclopropane-derived reactive intermediates are treated collectively here in one convenient volume, which may well justify the reprinting of the first chapter. As considerable portions of the topic are not covered in any other comparable survey, this book will certainly be found to be indispensable for everyone concerned with cyclopropanes and their derived intermediates.

Manfred Christl
Institut für Organische Chemie
der Universität Würzburg (FRG)

Electronic Aspects of Organic Photochemistry. By *J. Michl* and *V. Bonačić-Koutecký*. Wiley, Chichester, 1990. XIII, 475 pp., hardcover £ 51.30. – ISBN 0-471-89626-8

The key to understanding photochemical reactions lies in the analysis of the electronic states that are involved and their interactions with each other. Although an exact calculation of the total potential energy hypersurface for a multicomponent reaction is not (at present) possible, that is not necessary for an understanding of the nature and rates of the conversion processes occuring. These concepts have, of course, already become familiar even to those photochemists who have only a limited interest in the quantum-theoretical fundamentals. Up to now the main activation barrier in the way of getting to grips with the electronic fundamentals of organic photochemistry has been the highly mathematical nature of the available textbooks. That situation has been remedied in the book reviewed here.

Two authors of international repute (J. Michl, University of Texas, and V. Bonačić-Koutecký, Freie Universität Berlin) have achieved the trick of providing, even for the reader with only a rudimentary knowledge of quantum theory, a convincing and lively presentation of the theory of (mainly organic) photochemical reactions. To ease the path for beginners, the first chapter (50 pp.) contains a description of electronic states, potential energy hypersurfaces, and wave functions. Chapter 2 (59 pp.) on photophysical and photochemical processes seems to me especially successful. These processes (excitation, rapid and slow events) are described in terms of a complex potential energy hypersurface, in relation to which each of the processes in turn is discussed in detail. Here one becomes especially aware of the high standard of diagrammatic presentation that the authors maintain. Most of the figures are outstandingly well thought out, and in all their complexity they are also aesthetically pleasing. Of course, this expensive artwork further increases the price, and thus makes the book unaffordable for many students.

Part A ("Background") ends with a short chapter on minima, funnels, and barriers, and leads into the consideration of elementary photochemical processes. However, readers looking for a detailed description of reactions from the synthetic chemist's viewpoint will need to resort to other books, with which this work is not intended to compete.

Part B ("Elementary Photochemical Steps") begins by discussing the electronic structure of diradicals and diradicaloids, which often occur as reaction intermediates. This leads on to a description of the transition to chemical bonding. The effects of spin-orbit coupling and of C-pyramidalization on the probability of the transition to the closed-shell product are discussed in a very lucid and informative way. The following chapters 5–7 (192 pp.) are devoted to the theoretical description of a wide variety of organic photoreactions, including electrocyclic and sigmatropic reactions, cycloadditions and cycloreversions (Chapter 5), reactions involving the transfer of atoms, ions or charges (Chapter 6), and isomerizations, bond dissociations (Norrish type I reactions, peroxides, azo compounds), the Paternò–Büchi reaction, tautomerizations, Norrish type II reactions, three-membered ring-opening reaction, and fragmentations (Chapter 7). For most of these reaction types the authors compare simple MO correlation diagrams with the results of complex ab initio calculations. Such an extensive comparison of simple easily understood models with sophisticated quantum-chemical calculations is unique, and it provides an outstandingly useful source of information to help in understanding photochemical reactions.

These latter chapters are especially useful for those wishing to apply photochemical methods, as the analysis of elementary photochemical processes given here offers a rich source of ideas. For a book that is excellent in every respect the high price is justified, and it is to be hoped that it will not be kept in professors' offices to gather dust, but will instead be available also to students for frequent use.

Axel G. Griesbeck
Institut für Organische Chemie
der Universität Würzburg (FRG)

The Biochemistry and Uses of Pesticides. Structure, Metabolism, Mode of Action and Uses in Crop Protection. 2nd Edition. By *K. A. Hassall*. VCH Verlagsgesellschaft, Weinheim/VCH Publishers, New York, 1990. xviii, 536 pp., hardcover DM 128.00.—ISBN 3-527-28151-7/0-89573-976-3

This is a new edition of the book originally published in 1982 with the main title "The Chemistry of Pesticides". In the preface to this second edition, and also in the epilogue, the author emphasizes the enormous advances that have been made during the last ten years in the understanding of the modes of action of pesticides, a development that is reflected in the altered title "The Biochemistry and Uses of Pesticides". This second edition consists of 16 chapters, each ending with a short list of references. Three chapters of a general nature (general biological aspects, formulation and use, metabolism) are followed by six dealing with insecticides, three with fungicides, and four with herbicides. The greatest emphasis in this monograph is on insecticides, both as regards numbers of pages and of chapters. The author states that the book is intended for a wide range of readers involved in the science and practice of pesticides, and its purpose is to contribute to a greater understanding of the biochemistry of pesticides.

Nevertheless, it is not clear to these reviewers which group of readers the book is primarily aimed at. Does it set out to provide a background of science and theory for the pesticides practitioner, or is it mainly concerned with the biochemical aspects of pesticides, as the title of the second edition suggests? In fact, it does not meet either of these

objectives. For the technologist it would have been sensible to limit the treatment to the most important points and to elucidating the main principles, while on the other hand a book dealing generally with the biochemistry of pesticides would be expected to give a full and accurate account of the current state of knowledge. One would expect that a book published in 1990 should include an appropriate coverage of the literature on pesticide mechanisms and other recent developments, some aspects of which are treated in numerous publications, including some good reviews. This task has not been adequately addressed here.

Of the six chapters on insecticides the first three are devoted to organophosphates, carbamates and organochlorine compounds. These groups are dealt with clearly and comprehensively, with the emphasis on applications. Each of these chapters includes a list of compounds compiled with the practitioner in mind (although consisting only of selected examples); the lists for the organophosphates and carbamates are arranged according to the crop plants to be protected, whereas that for the organochlorine compounds concentrates on the harmful insect species (why the difference?). The next chapter is a detailed treatment of the pyrethroids. Whereas much space is devoted to the older classical insecticides, more recent developments are only treated marginally, even though some of these have already joined the "classical" category; it is exactly here that some sound information should have been provided for the novice practitioner. Whereas at least eight pages have been devoted to the benzoylphenylureas, the growth regulators are given only a single page. Thus, these sections, which appear under the title "Other Insecticides and Similar Compounds", are unsatisfactory as regards their content. The delta-endotoxin from *Bacillus thuringiensis* is only briefly mentioned in the epilogue, even though it is a chemical rather than a biological agent; even the author himself refers to this as "unfortunate". The chapters on insecticides conclude with a discussion of resistance. The current trend towards integrated pest management (IPM) would undoubtedly have justified being given a chapter to itself, especially since this monograph is intended also for newcomers to the area of modern insect control methods.

The three chapters on fungicides cover the subject in a very general way. The older products are over-represented at the expense of more recent ones. For example, mercury compounds are treated exhaustively, whereas the melanin biosynthesis inhibitors, which have the interesting property of preventing the fungal hypha from penetrating into the leaves, are omitted entirely. The information on the chemistry, metabolism, and mode of action of fungicides is well presented. In contrast the biological information is of such a general nature that there is a risk of misunderstandings. In Table 10.1, which lists the molds according to the manner in which they exist on the host plant, it is wrongly stated, for example, that true honeydew molds live under the leaf cuticle. In the same table the phenylamides are not listed against the *Oomycetes* in Group 1A. In the chapter on systemic fungicides the comments on resistance need to be treated with some caution, and should be qualified by noting that saturation treatments are not recommended as a way of overcoming resistance to fungicides, and that mixtures of phenylamides with carbendazim have no anti-resistance effect. The discussion of negatively correlated cross-resistance fails to mention the only example of commercial importance, namely the benzimidazoles and the phenylcarbamates, which are used to combat *Botrytis*.

In the part on herbicides the introductory chapter is concerned with definitions of relevant terms, such as uptake and transport in the plant, selectivity, persistence, methods of application, and herbicide mixtures. Some of the newer techniques, such as the use of herbicide safeners, should have been mentioned in this introductory chapter. In Table 13.1 the herbicides are classified from the standpoints of agronomy (for Group 1) and of biochemical mechanisms (for Groups 2 and 3). Here a uniform method of classification was desirable; this could have been achieved by integrating Table 14.1 with Table 13.1. The general biological aspects are treated comprehensively in three chapters, one on leaf herbicides and two on soil herbicides. The author also covers a few of the more recent developments from the applications standpoint, such as the introduction of the sulfonylureas. However, for many of the classes of herbicides the treatment of mechanisms is inadequate. For some products, such as photosynthesis inhibitors of the PS-II type (Fig. 14.2), the mode of action has now been clarified, and the basic principle should have been described in this book, also listing a few of the most important literature references. The mechanism of resistance to triazines (p. 454) is also known. It is also known that herbicide safeners (not "antidotes") essentially function by activating enzymes that metabolize the herbicides (pp. 468, 483). On page 395 the structure of phosphoenolpyruvate is shown incorrectly.

The literature citations are complete for the period up to about ten years ago. While it is true that some more recent original papers are also listed, the selection does not seem to be representative. Instead of citing original papers it would have been more useful to give references to recent review articles or more advanced reading, even to the extent of excluding all but these; this applies especially to students, who are regarded by the author as an important section of the potential readership.

Included as an appendix is a list of some of the pesticides mentioned in the book, including a few of their trade names. No claims are made regarding the completeness of the list. What is the use of a list that is incomplete in every respect? It is of equally little value to all types of readers, whether practitioners or academic researchers.

In summary, the book cannot be recommended in its present from. It is not a textbook, but neither is it an up-to-date review of the biochemistry of pesticides. The structure of the book is not systematic enough for students, and the material is not adequately presented from a teaching standpoint. It does not represent the current state of knowledge. Recent developments in the pesticides area receive too little attention, or are even omitted altogether.

Edith Ebert, Hartmut Kayser, Theodor Staub
Ciba-Geigy AG
Basel (Switzerland)

Modern Pulsed and Continuous-Wave Electron Spin Resonance. Edited by *L. Kevan* and *M. K. Bowman*. Wiley, Chichester, 1990. 435 pp., hardcover £ 74.35.—ISBN 0-471-50274-X

The introduction of pulsed Fourier transform (FT) techniques, the trend towards using very high external magnetic fields, and the development of multidimensional methods (2D, 3D etc.) have brought about an enormous upsurge of activity in NMR spectroscopy during the past decade. Electron spin resonance (ESR) is a technique closely related to NMR, and it was evident from the start that its development must follow a similar course. However, it has taken a long time for this to happen, mainly due to problems of a techni-

cal nature. Nevertheless, Kevan and Schwartz edited an initial monograph on this theme as early as 1979 (*Time Domain Electron Spin Resonance*, Wiley). In recent years great strides have been made in this area, with regard to both instrumentation and technique. The most striking evidence of this is that since 1988 a commercial FT-ESR spectrometer has been on the market. Although several review articles dealing with this area have appeared, there has not until now been a monograph devoted especially to the techniques and instrumentation of pulsed ESR. The work reviewed here fills that gap.

The book contains six chapters dealing with particular aspects of pulsed ESR; a further three chapters are concerned with novel CW-ESR techniques, in which the microwave power is not pulsed (CW = continuous-wave). In the first chapter M. K. Bowman gives a good introduction to electron spin-echo (ESE) and FT-ESR spectroscopy and the historical development of these techniques. The resemblances to NMR and the differences are clearly pointed out, and the technical problems are discussed. As well as the instrumentation and data processing, some applications that are essentially inaccessible to CW-ESR are indicated. In Chapter 2 A. Schweiger reports on methodology and instrumentation of pulsed ESR, in particular with regard to the nuclear modulation effect observed in the electron spin-echo (ESEEM) for solids. An excellent introduction to the basic principles of this method is followed by an account of various special techniques for simplifying and interpreting spectra, most of which have been developed in the author's laboratory. A fairly long section is again devoted to the instrumentation, with a description of the important task of developing the probe-heads for pulsed ESR measurements. In Chapter 5 L. Kevan looks at the ESEEM effect from a different standpoint. He does not go into so much detail regarding the technique and instrumentation, emphasizing instead the methods for analyzing data in the time and frequency domains, and he draws attention to several new types of chemical applications. The two chapters devoted to ESEEM (Chapters 2 and 5) thus complement each other very nicely, and they show the importance of the method for measuring the electron-nuclear hyperfine couplings in solids, a technique which is complementary to the ENDOR (electron-nuclear double resonance) method. The latter method, which is already well-known from its use in CW spectroscopy, is the subject of Chapter 4, in which A. Grupp and M. Mehring give an excellent introduction to pulsed ENDOR (in which both the microwave and the radiofrequency power are pulsed). As well as the "classical" methods of Mims and Davies, some newer pulse sequences that have been developed by these authors or by Schweiger et al. are also described. Applications up to now have been confined to studies of solids. Chapter 3, by J. Gorcester, G. Millhauser, and J. Freed, is devoted to studies of molecular motions in condensed phases, especially in liquids, for which it appears that pulsed ESR is eminently suitable. The majority of the fascinating new methods described by these authors are two-dimensional ESE or FT-ESR techniques, some of which will already be familiar to the reader from NMR (e.g. spin–spin double resonance, COSY, SECSY etc.). Besides theory and the technique a considerable amount of space is also given (in an appendix) to the instrumentation needed to carry out such experiments and to the analysis of data. Chapter 6, by J. Allgeier et al., shows that pulsed ESR measurements are also now being carried out at high fields; here the authors describe their W-band spectrometer, which operates at a microwave frequency of 95 GHz, about ten times higher than that of a conventional X-band instrument (ca. 10 GHz). However, the evident advantages of this higher frequency band as regards spectral resolution and sensitivity are gained at the cost of more complex and expensive instrumentation.

A welcome feature of the book is that it also deals with those modern CW-ESR techniques that are related to the pulsed methods. Thus, in Chapter 7 K. McLauchlan reports on methods for detecting transient free radicals using CW-ESR. After a very good introduction to the theory and the experimental techniques the author discusses chemically induced dynamic electron spin polarization (CIDEP) and its application to studies of rate processes in solution, illustrated by various examples. In Chapter 8 Ya. Lebedev, one of the pioneers in the area of high-field ESR, describes CW-ESR techniques using microwave frequencies of 100 GHz and above. In addition to the physical principles he discusses technical aspects of all the high-field instruments of this kind that exist up to now. A considerable amount of space is devoted to chemical applications of such measurements, especially those that are inaccessible to ESR spectroscopy in the conventional frequency bands. In view of the great importance of imaging techniques in NMR one could hardly fail to include, in a book on modern ESR techniques, a contribution on ESR imaging. This topic is covered in Chapter 9 by S. and G. Eaton, who give a good survey of the current state of the art in this field. Here pulse techniques are beginning to play an increasingly important role. Applications to radiation chemistry, to polymer chemistry, and in the area of biological materials are described.

This book is intended for readers who wish to learn mainly about methods, techniques, instrumentation, and the sometimes difficult problems of data analysis in both pulsed and continuous-wave ESR. The reader must already have a solid background knowledge of magnetic resonance and of the analogous NMR techniques. Thus the book is addressed to the specialist rather than the novice. A recent review article by A. Schweiger[*] can be recommended as an introduction to the field of pulsed ESR.

Most of the authors in the book use application examples only to illustrate the techniques, and some of the chapters contain too little of this kind of material for my taste. One reason for this is that up to now very few applications-orientated research groups have adopted pulsed ESR methods, and consequently only a few systems of relevance to chemistry have been studied. In future these methods will become especially important in situations where they can yield information obtainable only with difficulty, if at all, by conventional ESR. Using pulsed ESR one can follow the time-dependent development of species such as photoinduced free radicals or triplet state molecules on time-scales from a few nanoseconds to milliseconds, so as to give information about the mechanisms of radical formation and conversion. For paramagnetic species with lifetimes longer than a few microseconds one can also use pulsed ENDOR to obtain valuable information about the electron distribution (via the hyperfine couplings). Time-resolved ESR techniques also make it possible to directly follow rate processes (by means of relaxation time measurements), thereby providing an insight into the motional processes of the molecules being studied. Certain CW and pulsed methods yield complementary information, for example ENDOR and ESEEM. For readers whose interests lie mainly in the biochemical and biological applications of the techniques discussed here, the recently published book *Advanced EPR—Applications in Biology and*

[*] *Angew. Chem.* **1991**, *103*, 223–251; *Angew. Chem. Int. Ed. Engl.* **1991**, *30*, 265–292.

Biochemistry, edited by A. J. Hoff (Elsevier), can be recommended.

Pulsed ESR methods are now at the beginning of a development that could follow a course analogous to the enormous qualitative improvement of NMR techniques that has occurred in recent years. However, it remains to be seen whether microwave pulses will "exorcize the evil from ESR"—as has happened in the case of NMR—thereby opening a new "Golden Age" for ESR spectroscopy. Everyone who wishes to get to grips with these new and fascinating techniques, or who even foresees possible applications in his or her own research, is strongly recommended to read this book. Regrettably, however, the very high price—which has now become the rule rather than the exception for books of this sort—will limit the potential readership.

Wolfgang Lubitz
Max-Volmer-Institut für Biophysikalische
und Physikalische Chemie
der Technischen Universität Berlin (FRG)

One Dimensional and Two Dimensional NMR Spectra by Modern Pulse Techniques. Edited by *K. Nakanishi*. University Science Books, Mill Valley (USA), 1990. XII, 234 pp., paperback $ 29.95. – ISBN 0-935702-63-6

Yet another book on NMR methods has been published; in this the aim is to convey a knowledge of NMR by means of a catalogue of 92 experiments, rather than by a systematic form of presentation. In accordance with the book's title, the examples are arranged in two groups consisting of 31 one-dimensional (1D) and 61 two-dimensional (2D) experiments. Each experiment is described in about half a page of text with a few literature references (in which the name Bodenhausen has been wrongly spelled in nearly every case), together with a diagram showing the pulse sequence and the structural formula of the compound. The spectrum is reproduced on the opposite page, edited in a form which corresponds to the structural formula, so that the assignments are directly apparent. A set of parameter values is also shown alongside the spectrum in most cases, although unfortunately these are often too small to be read clearly and are insufficient to enable one to do further work on the problem; moreover, the accompanying text seldom includes experimental details.

The selection of experiments covers nearly all the standard types of problems nowadays encountered in organic chemistry. Thus the 1D part includes examples of techniques such as NOE difference measurements, SPT, DEPT, selective decoupling, and suppression of water signals, while in the 2D part one finds, in addition to the expected variants of COSY and NOESY, examples of HOHAHA, ROESY, and 2D-INADEQUATE experiments.

There are a few key molecules, such as β-ionone or strychnine, that are used again and again as examples in the book, thus enabling the reader to progress comfortably from simple types of spectra to more complicated types as applied to the same molecule; this is undoubtedly one of the book's main strengths. On the other hand the examples chosen are sometimes unnecessarily complicated, as in the cases of brevetoxin (No. 56), cyanoviridin (No. 84), or dictyotalide (No. 81), which tend to obscure the merits of the techniques under discussion rather than to clarify them. Nevertheless, the book as a whole offers a wealth of stimulating ideas taken from all the main research themes of organic chemistry, thus conveying to the reader some of the pleasure evoked by the power of modern NMR spectroscopy. The spectra that are reproduced, which are certainly the main substance of the book, are of better than average quality. However, there are a few criticisms that must be mentioned. For example: the convention of having the f_2 axis as the horizontal one is not applied consistently; for inversely recorded spectra (such as some of the examples of HMBC and HMQC experiments), the f_1 projection appears sometimes at the left-hand and sometimes at the right-hand border of the spectrum; too often some of the peaks of the projection are allowed to protrude into the 2D spectrum, which to me appears rather inelegant. Here it becomes evident that the book is not a unified whole but a collection of contributions from a number of spectroscopists using different spectrometers with different software.

There is a 40-page appendix entitled "Principles of FT-NMR", in which an attempt is made to explain the theory behind the experiments that are included. Everyone is likely to appreciate that a meaningful summary of the theory of modern 1D and 2D multipulse NMR spectroscopy is not possible within such a limited space, and consequently the reader is unlikely to derive anything useful from this account.

In summary it can be said that this book offers, at a reasonable price, a stimulating survey of the NMR methods nowadays used in organic chemistry. It can certainly be recommended for libraries and textbook collections, and for serious organic chemists who wish to learn what their NMR section should be capable of; it is less suitable for NMR specialists, who need a more detailed knowledge of the subject than can be conveyed within the space of this book.

Stefan Berger
Fachbereich Chemie
der Universität Marburg (FRG)

Modern Methods in Protein- and Nucleic Acid Research. Edited by *H. Tschesche*. de Gruyter, Berlin, 1990. ix, 446 pp., hardcover DM 330.00.—ISBN 3-11-012275-8

This book can be regarded as a continuation of the series "Modern Methods in Protein Chemistry", previous volumes of which appeared in 1983, 1985, and 1988. The latest developments in analytical and preparative methods are here described in 20 review articles by well-known authors belonging mostly to German research groups. This volume is the first to cover molecular biological methods. After a brief introduction to the techniques, the methods are described in turn using examples from each author's own field of research, sometimes including an experimental section giving practical details. Each article provides an up-to-date list of references, including review articles and monographs. The book is convenient to use and sturdily bound. However, the authors' typescripts have been directly reproduced, and the resulting lack of uniformity in type style and line spacing is rather distracting.

The first three articles are devoted to nucleic acids chemistry and molecular biology. H. Tschesche et al. describe the use of digoxigenin-11-dUTP as a realistic alternative to radioactive labeling. W. Kramer and H.-J. Fritz discuss the advantages and disadvantages of the various methods for preparing mutants using oligonucleotide techniques. B. S. Reckmann then describes new analytical procedures in DNA diagnostics. H. Wagner and J. Heinrich kindle interest in free flow electrophoresis, an elegant preparative electrophoretic method for purifying peptides, proteins, and whole cells. Other innovations in the purification and isolation of proteins

are the use of new types of polymers that give improved yields in ion-exchange chromatography (C. Jansen and W. Müller), and the use of immobilized nickel for affinity chromatography applied to poly-His fusion proteins (E. Hochuli). Problems of chain folding are addressed by R. Rudolph using in-vitro redox reactions, and by P. Flecker using activation chromatography; in the examples described here both methods give highly active proteins. Advances in *C*-terminal sequencing offer a method for the identification of biomolecules, which is here critically compared with *N*-terminal sequencing (B. Wittmann-Liebold et al.). The introduction of cyclodextrin phases for the enantioselective analysis of amino-acids by gas chromatography can greatly improve the separation achieved (W. A. König). New opportunities and capabilities in the use of mass spectrometry to investigate biomolecules are described by E. Bayer. Soft ion-spray mass spectrometry allows characterization of proteins up to 120000 Dalton and sequencing of segments at picomolar concentrations. The technique also has impressive capabilities when combined on-line with capillary zone electrophoresis or HPLC. Next W. Voelter et al. describe what can be achieved by immunological characterization. D. M. Doran gives an excellent review and comparison of current methods for predicting epitopes in proteins. Three articles deal with modifications of nucleic acids and proteins. In the first, R. I. Zhadanov reports on ESR studies of spin-labeled Ca-ATPase. H. Fasold et al. describe interactions of proteins with modified nucleotides. D. Brandenburg et al. give a thorough account of the use of photoaffinity-labeling in combination with radioactive or biotin labeling for isolating and characterizing receptors and for studying their interactions; this comprehensive chapter includes practical advice, information on typical reagents and their areas of application, and a list of common abbreviations. The last group of articles are concerned with methods for studying the structures of proteins. "How do you get large protein crystals?" is the title of the chapter by G. Wiegand, in which the crucial factors in the various crystallization techniques are discussed from a practical standpoint, illustrated by useful figures. J. Reed gives a good review of circular dichroism measurements, their areas of application, the types of information yielded, and the methods used to interpret the data. S. Suhai describes the theoretically orientated approach of molecular dynamics stimulation; unfortunately some of the diagrams in this chapter are illegible. H. Rüterjans et al. complete the treatment of protein structural studies by describing the application of 2D-NMR spectroscopy to ribonuclease-T_1.

It is certainly not possible to describe the whole of protein and nucleic acids research in 446 pages, but the editor has neither attempted nor claimed to do that. Instead the book is intended to give an insight into the latest developments. In this it has succeeded outstandingly well. The choice of topics represents the most significant trends in protein chemistry, the main emphasis throughout being on the techniques. The subject matter is logically arranged, and corresponds to the many stages that are needed to express, isolate, and characterize a protein. As it is not possible for a single research group to be completely knowledgeable in all these areas and equipped to carry out the experimental work needed, progress can only be achieved through the interdisciplinary collaboration of many specialists. This book helps to overcome trepidation about making the necessary contacts and to remove obstacles of technical language. Thus, for example, the molecular biologist is introduced to expressions such as NOESY and COSY, and the physical chemist learns to understand the problems of PCR methods. The book is of value to everyone who wishes to look out beyond the limited confines of his or her own research. Furthermore, it should help the reader to apply new methods without repeating familiar mistakes.

Annette Beck-Sickinger
Laboratorium für Biochemie
der Eidgenössischen Technischen Hochschule
Zürich (Switzerland)

Registered names, trademarks, etc. used in this journal, even when not marked as such, are not to be considered unprotected by law.

© VCH Verlagsgesellschaft mbH, D-W-6940 Weinheim, 1992. - Printed in the Federal Republic of Germany by Konrad Triltsch Druck- und Verlagsanstalt Würzburg.

All rights reserved (including those of translation into foreign languages). No part of this issue may be reproduced in any form — by photoprint, microfilm, or any other means — nor transmitted or translated into a machine language without written permission from the publishers. Only single copies of contributions, or parts thereof, may be made for personal use. This journal was carefully produced in all its parts. Nevertheless, authors, editors, and publisher do not warrant the information contained therein to be free of errors. Readers are advised to keep in mind that statements, data, illustrations, procedural details, or other items may inadvertently be inaccurate.

Valid for users in the USA: The appearance of the code at the bottom of the first page of an article (serial) indicates the copyright owner's consent that copies of the article may be made for personal or internal use, or for the personal or internal use of specific clients. This consent is given on the condition, however, that the copier pay stated per-copy fee through the Copyright Clearance Center, Inc. (CCC), for copying beyond that permitted by Sections 107 or 108 of the U.S. Copyright Law. This consent does not extend to other kinds of copying, such as copying, for general distribution, for advertising or promotional purposes, for creating new collective works, or for resale. For copying from back volumes of this journal see 'Permissions to Photo-Copy: Publisher's Fee List' of the CCC.

Editorial office: Postfach 10 11 61, D-W-6490 Weinheim, Federal Republic of Germany, Telephone (06201) 60 23 15, Telex 465 516 vchwh d, Telefax (06201) 602 328, E-Mail Z16@DHDURZ2 in Earn Bitnet.

Editor: *Peter Gölitz*

Associate editors: *R. H. Schmidt-Radde, K. J. Schneider, A. Stimson.* **Editorial assistant:** *E. Schweikart*

Publishers: VCH Verlagsgesellschaft mbH. (Managing Directors: *Hans Dirk Köhler, Dr. Karlheinz Köpfer*), Pappelallee 3, W-6940 Weinheim, Federal Republic of Germany.

Advertising office (Advertising Manager: *R. J. Roth*): Postfach 10 11 61, D-W-6940 Weinheim, Federal Republic of Germany, Telephone (0 62 01) 60 61 36, Telex 4 67 155, Telefax (0 62 01) 606 156.

ANGEWANDTE CHEMIE
International Edition in English
Volume 31 · Number 3
March 1992
Pages 247–366

Benzene and Its Derivatives as Bridging Ligands in Transition-Metal Complexes

By Hubert Wadepohl*

Transition-metal complexes in which two or more metal atoms are bridged by one or more arene ligands led a shadowy existence in comparison to the extensive class of mononuclear arene complexes. Arene bridges can occur in a variety of coordination modes and with almost all of the transition-metal elements of the periodic table. Nowhere else are found so many forms of distorted and bent arene rings. The binuclear compounds can be divided into two classes: adducts which show relatively weak metal–arene bonding and complexes which show strong arene–metal interaction. Most of the adducts are in equilibrium with mononuclear complexes in solution or are only stable in the solid state (often as polymers). In both classes *syn* and *anti* coordination occurs; their geometries show a wide variation between the extreme cases of $\eta^1:\eta^1$-bridge and $\eta^6:\eta^6$-triple-decker structure. Metal surfaces with chemisorbed arenes can be seen as a form of multinuclear arene–metal complexes. On transition-metal surfaces, benzene can be bonded to one, two, or four surface atoms. Molecular clusters with face-capping arene ligands that are bonded to three metal atoms have until now mainly been limited to two classes. The arenes bound to $\{(CO)_3M\}_3$ (M = Ru, Os) or $(CpCo)_3$ clusters as μ_3-$\eta^2:\eta^2:\eta^2$ ligands show only a weak trigonal distortion towards a Kekulé structure. Detailed investigations of the molecular structure and ligand dynamics of $[(CpCo)_3(\mu_3\text{-arene})]$ complexes considerably help the understanding of the bonding of arenes to metal clusters and to metal surfaces.

1. Introduction

Metal–arene complexes[1] are true classics among the transition-metal complexes. As early as 1919 F. Hein[2] isolated his "phenyl–chromium compounds" from $CrCl_3$ and PhMgBr [Eq. (a)], which, however, were not identified until much later by H.H. Zeiss[3] as (η^6-benzene)(η^6-arene)-chromium(I) complex cations (**1**, arene = benzene, biphenyl).

The ability of Ag^+ ions to form complex compounds with arenes was also known in the 1920s. However, it was not until 1955 when E.O. Fischer and W. Hafner,[4] using the "reducing Friedel–Crafts method", found a rational synthesis for bis(η^6-benzene)chromium **2** [Eq. (b)] and with it laid the foundations for a rapidly expanding chemistry of bis(arene)metal complexes. These were soon joined by metal–arene carbonyls [5] and other "mixed" derivatives.

Today, a large number of arene complexes exists for almost all the transition metals.[6] Although the overwhelming

$$CrCl_3 + PhMgBr \xrightarrow[2.\ H_2O]{1.\ Et_2O} \underset{\mathbf{1}}{[Cr(\eta^6\text{-}C_6H_6)(\eta^6\text{-arene})]^+} \qquad (a)$$

$$3\ CrCl_3 + 6\ C_6H_6 + 2\ Al \xrightarrow[2.\ H_2O]{1.\ AlCl_3} 3\ [Cr(\eta^6\text{-}C_6H_6)_2]^+ + 2\ Al^{III} \xrightarrow[KOH]{Na_2S_2O_4} \underset{\mathbf{2}}{[Cr(\eta^6\text{-}C_6H_6)_2]} \qquad (b)$$

[*] Priv.-Doz. Dr. H. Wadepohl
Anorganisch-chemisches Institut der Universität
Im Neuenheimer Feld 270, D-W-6900 Heidelberg (FRG)

 © VCH Verlagsgesellschaft mbH, W-6940 Weinheim, 1992 0570-0833/92/0303-0247 $ 3.50+.25/0

majority of these complexes have η^6-bonded arene ligands, examples are also known with η^1-, η^2-, η^3-, and η^4-bonded arenes. Until a few years ago, compounds in which two or more metal atoms are bonded to the same arene ring were overshadowed by the large class of mononuclear arene complexes. However, today we know of a considerable number of such multinuclear complexes. Some of the most interesting aspects of these complexes are:

- Arene bridges occur in a large variety of coordination modes (μ_2- and μ_3-bridges, *syn* and *anti* coordination geometry, varying hapticity of the μ-arene ligands).
- Nowhere else are found so many types of distorted and bent arene rings.
- Arene bridges are found in complexes with almost all of the transition metals of the periodic table. Although the majority of syntheses take different routes, the characteristic chemical properties of complexes with the different metals are reflected in the reactions forming these substances.
- Multinuclear arene complexes are important model compounds for intermediate steps in arene-exchange reactions and for adsorbates on metal surfaces.

2. Binuclear Complexes with Arene Bridges

Binuclear complexes with arene bridges can be roughly divided into two classes. In complexes of the first class, relatively weak bonds from the metal atoms to the bridging ligands are formed. These *adducts* are frequently in equilibrium with mononuclear complexes in solution or are only stable in the solid state (often as polymers). In the second class, there are molecular arene-bridged binuclear *complexes* with metal–ligand bonds which are as strong as those in mononuclear arene complexes. Between these two extremes intermediate forms exist, for example, complexes which only exist in the solid state and decompose in solution, but nevertheless show relatively strong bonds between the arene and metal atoms.

2.1. Adducts with Weak Metal–Arene Interactions

Adducts of arenes with Ag^I compounds have a long history. The composition and structure of such complexes is strongly dependent on the counterion. Already in the 1920s it was known that as a precipitate complex **3** is in equilibrium with the saturated solution of $AgClO_4$ in benzene and benzene/H_2O.[7] By 1950 R.E. Rundle had succeeded in proving the existence of benzene bridges between the silver atoms in crystals of **3**.[8]

$[Ag(C_6H_6)ClO_4]$ **3**

The X-ray structural analysis of this compound, which is only stable in a benzene atmosphere, shows infinite zigzag chains of [Ag-benzene-Ag-benzene]$_n$. These run along an axis of the orthorhombic unit cell and are linked to one another through weaker Ag–O interactions via perchlorate ions (Fig. 1).[8] The benzene ligand is *anti*-(μ-1,2-η^2:4,5-η^2)

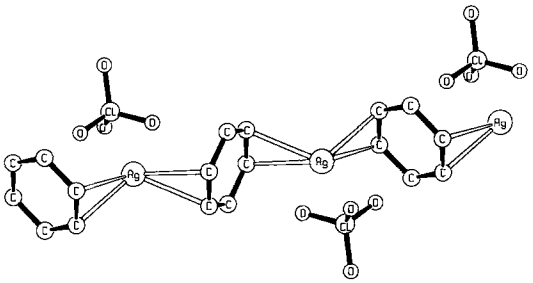

Fig. 1. Structure of [Ag(benzene)]$_n$ chains in a crystal of $[Ag(C_6H_6)]ClO_4$ (**3**).

coordinated. The silver atoms are bonded asymmetrically to the two opposite edges of the benzene rings [d_{Ag-C} = 2.496(6), 2.634(8) Å], so that the interaction of Ag with one carbon atom of each benzene ring predominates, as in the complex cations bridged only by anions, such as $[(arene)Ag]^+$ (arene = benzene,[9] for example) and $[(arene)_2Ag]^+$ (where (arene) = *m*-xylene[10a] or cyclohexylbenzene[10b] for instance). The metal-coordinated C–C bonds in the μ-benzene ligands are 1.354(17) Å, significantly shorter than the four other C–C bonds (1.427(10) Å). The results of solid-state ^1H NMR spectroscopic investigations[11] indicate that at 77 K the benzene molecules in **3** are rigidly held in the lattice whereas at 298 K they are more or less free to rotate about the sixfold axis. In contradiction of this assumption of a free or almost free rotation of the benzene rings at room temperature, the X-ray crystallographic

Hubert Wadepohl was born in 1954 and studied at first Chemistry and Mineralogy and then Chemistry from 1973–1980 at the University of Tübingen and in Bristol, England (1977/78). His research for his Diplom under F. G. A. Stone and J. A. K. Howard dealt with multinuclear platinum–alkyne complexes. In 1982 he obtained his doctorate with a thesis on double-, triple-, and quadruple-decker sandwich complexes of 1,3-diborolene. under W. Siebert in Marburg. He then spent a year and a half as post-doc with E. L. Muetterties at the University of California, Berkeley, initially as NATO Research Fellow and subsequently as Research Associate. From 1984 to 1990 he was Hochschulassistent at the Anorganisch-chemisches Institut der Universität Heidelberg where he habilitated in 1989 with a dissertation on cyclopentadienylcobalt fragments as building blocks for multinuclear complexes. He has been Privatdozent for inorganic chemistry and Heisenberg Fellow since 1990. His research interests include organometallic chemistry, multinuclear complexes containing bridging ligands, cluster complexes, and the structural chemistry of organometallic complexes in the solid and dissolved states.

electron-density synthesis has well-defined maxima and reveals distorted benzene rings.[12]

A further example of a silver complex with a bridging benzene ligand is **4**,[13] in which a *syn*-[Ag_2(benzene)] bridge

$[\{Ag(CF_3COO)\}_2(C_6H_6)]$ **4**

is observed. E.L. Amma et al. report only that a 1-η^1:4-η^1 coordinated benzene molecule is bonded to every second $Ag_2(\mu\text{-}CF_3COO)_2$ unit (Fig. 2). The Ag_2 units are part of polymeric chains bridged via the trifluoroacetate ions. Another benzene molecule is present per $Ag_2(CF_3COO)_2$ unit as solvent of crystallization. The distance of 2.851(3) Å between the silver atoms bridged by benzene was not considered to indicate Ag–Ag bonding.[13] Unfortunately no further information about the geometry of μ_2-benzene in **4** was given.

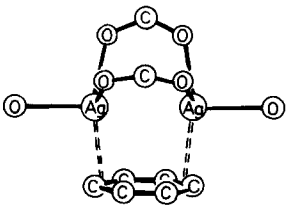

Fig. 2. Coordination of μ-benzene ligands on silver atoms in crystalline $[\{Ag(CF_3COO)\}_2(C_6H_6)]$ (**4**).

Apart from these complexes whose benzene bridges were established by structural analyses in the solid state, the existence of complexes such as $[(arene)Ag_n]^{n+}$ ($n = 1, 2$) have been proven by the measurement of the complex-formation constants in solution for several arenes.[14] As early as 1949 the (incorrect) [(η^6-arene)Ag]$^+$ half-sandwich structure for $n = 1$ was proposed. The dication $[(arene)Ag_2]^{2+}$, which for monocyclic arenes has a ten times smaller formation constant than the mononuclear complex, was assigned a symmetric triple-decker structure with a μ-η^6:η^6-arene bridge. Even though these proposed structures are incorrect, they were for this period—before the discovery of ferrocene!—a remarkable concept. The first triple-decker sandwich complexes $[Cp_3Fe_2]^+$ and $[Cp_3Ni_2]^+$ were observed by E. Schumacher und R. Taubenest[15] in 1964 when they examined the mass spectra of ferrocene and nickelocene. But it was not until 1972 that a triple-decker sandwich complex $[Cp_3Ni_2]^+$ was actually synthesized by H. Werner and A. Salzer.[16]

Benzene does not only bridge two silver(I) ions but also two cations of the lighter homologue, copper, in the solid state. The benzene bridges in polymeric **5**[17] show a less symmetrical *anti*-(μ-1,2-η^2:3,4-η^2) coordination than those in **3** or **4**. In **5**, infinite double chains of $Cu(CF_3SO_3)$ units are

$[\{Cu(CF_3SO_3)\}_2(C_6H_6)]_n$ **5**

bridged by the benzene molecules (Fig. 3). However, the structural analysis by M.B. Dines and P.H. Bird [17b] gave no precise information on the C–C bond lengths in the bridging ligands. The material, in contrast to the less stable silver complexes, liberates benzene under vacuum only above 120 °C.

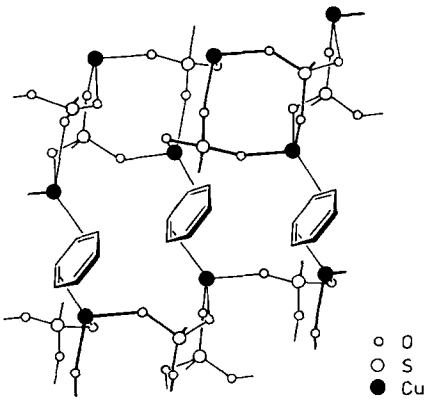

Fig. 3. Coordination of μ-benzene ligands on copper atoms in crystalline **5** (CF_3 groups are only shown as lines).

Through the exchange reaction of **5** with alkylbenzenes, the relative stability constants $K_{eq.}$ of the corresponding complexes were determined, yielding the series for $K_{eq.}$, benzene ≈ toluene ≈ *o*-xylene ≫ ethylbenzene ≈ *n*-butylbenzene ≈ isopropylbenzene ≈ mesitylene and *p*-xylene ≫ *o*-xylene > *m*-xylene. This sequence shows considerable shape selectivity, which cannot be correlated with the π basicity of the arenes.[17b]

The crystalline complex **6** reported by F.A. Cotton et al. can also be included among the coordination compounds with relatively weak bonding from benzene to two metal atoms.[18] In the crystal, $Cr_2(O_2CCPh_3)_4$ units are linked

$[Cr_2(O_2CCPh_3)_4(C_6H_6)]$ **6**

along the colinear Cr–Cr axes through benzene molecules to form infinite chains (Fig. 4). The benzene bridges are *anti*-(η^6:η^6) coordinated. From the Cr–benzene ring distance (3.299 Å) it follows that only a very loose bond exists in the $Cr_2 \cdots$ benzene $\cdots Cr_2$ "triple-decker" units. The μ-benzene ligands are trigonally distorted [alternating long (1.43(2) Å)

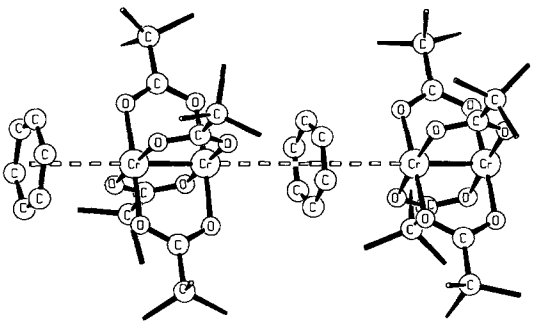

Fig. 4. Structure of $[Cr_2(O_2CCPh_3)_4(C_6H_6)]_n$ chains in crystalline **6** (of the phenyl rings only the *ipso*-C atoms are drawn).

and short (1.35(2) Å) C–C distances). According to MO calculations on the model system (C_6H_6)-$[Cr_2(O_2CH)_4]$-(C_6H_6), benzene functions as a π donor to the Cr_2 unit and thereby weakens the π component of the Cr–Cr quadruple bond.[18]

2.2. Molecular Complexes with μ_2-*Arene Bridges*

In this section, μ-arene binuclear complexes that in the solid state and almost without exception in solution, contain discrete [(μ-arene)M_2] molecular units with strong bonding of the metal atoms to the briding ligand will be summarized. Here, as for the adducts described previously, many modes of coordination of the arene bridge are known.

In general, it is possible to distinguish between *syn*-(μ-η^n:η^m)-arene and *anti*-(μ-η^n:η^m)-arene complexes. In both classes the hapticities η^n, η^m of the arene vary over a wide range. The *syn* bonding mode of two metal-complex fragments to an arene is always accompanied by a metal–metal bond which can be bridged by other ligands.

In each of the V_2 and Fe_2 complexes **7** [19,21] and **8**[20,21] (Cp = η^5-C_5H_5) described by K. Jonas et al., all the ring-carbon atoms of the arene are bonded to a M_2 unit. However, this is almost the only common feature of these two highly interesting complexes. In the synthesis of **7** from [K(Cp_2V)] and 1,3-cyclohexadiene, the "preformed" C_6 ring of the cyclohexadiene is dehydrogenated to benzene (Scheme 1). The

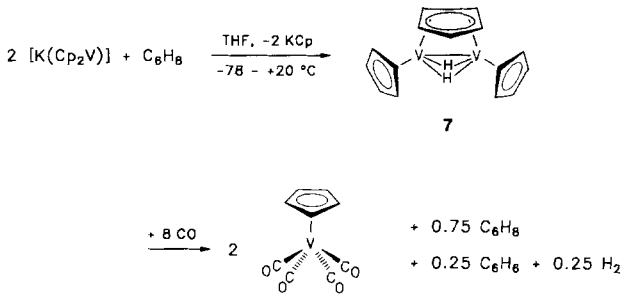

Scheme 1.

vanadium complex **7** reacts with CO to give [$CpV(CO)_4$]. In this reaction only a quarter of the expected amount of μ-benzene is eliminated intact, together with the equivalent amount of H_2. The dominant reaction pathway involves the migration of the hydridic H atoms to the benzene ring; in a sort of reversal of the formation reaction, cyclohexadiene is reformed (Scheme 1).[19] The hexaalkylbenzene in **8a** and **8b** is formed by the cyclotrimerization of 2-butyne and 3-hexyne, respectively. The mononuclear complex [CpFe(cod)] (cod = 1,5-cyclooctadiene), serving as a source for the CpFe fragments, reacts even at 0 °C with the alkynes affording **8** in approximately 90% yields.[20]

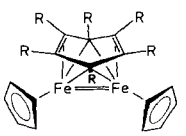

8a, R = CH_3
8b, R = C_2H_5

Complexes **7** and **8** have *syn*-(μ_2-1-4-η^4:4-6,1-η^4) coordinated arene bridges which are folded along the vectors C1···C4. In the divanadium complex **7** the fold-angle is approximately 20° and all the C–C distances within the benzene ring are equal (1.43(1) Å). In contrast, the folding of the hexamethylbenzene ligand in **8a** is much more pronounced (dihedral angle 43°). Both the C–C "double bonds" C2/5–C3/6, which are each coordinated to only one iron atom, are significantly shorter [1.38(1), 1.43(1) Å] than the other C–C bonds in the μ-hexamethylbenzene ligand (1.48(1) Å). For these reasons the notation with "aromatic" benzene was proposed for **7** and with a localized dienediyl structure for **8**. The assignment of valence electrons (VE) for these compounds is problematic; thus, **7** was formulated with a V–V single bond (corresponding to 16 VE per vanadium atom) in contrast to **8** which was formulated with a Fe–Fe double bond (18 VE on each iron atom). However, the authors pointed out that an assignment of the bond order from the lengths of bridged metal–metal bonds is problematic. The V–V bond order calculated from an ab initio CI–MO study[22] (CI = *c*onfiguration *i*nteraction) of **7** is 1.45; this relatively large value can be explained by the contribution of metal–metal bonding orbitals to the most stabilized ligand orbitals.

Complexes **7** and **8** are fluxional. A rotation of the arene rings above the M_2 units has been deduced from investigations by NMR spectroscopy. The dynamic process can be frozen on the NMR time scale at low temperatures. In addition, **8** shows an equilibrium between a diamagnetic low-temperature form and paramagnetic high-temperature form, which leads to antiferromagnetic behavior.

According to J. Müller et al.[23] the complexes **10**, **11**, and **12** were formed in 3, 5, and 1% yields following irradiation of a solution of **9** and benzene in hexane for 5 h (Scheme 2). On longer irradiation of the reaction mixture the concentrations of **10** and **11** decrease in favor of the trinuclear complex **12** (see Section 3).

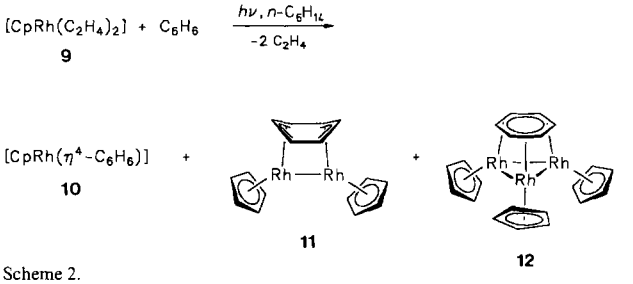

Scheme 2.

The *syn*-(1-3-η:4-6-η) bonded μ_2-benzene ligand in the crystal of the binuclear complex **11** can be described in a first approximation as a bis(enyl) ligand system showing a boat conformation. The angle between the two η^3-enyl planes ($\bar{d}_{C-C}$ = 1.42 Å), which indicates the extent of deviation of the benzene bridge from planarity to boat conformation is 125°. The ^1H NMR spectrum at room temperature shows a triplet (J_{RhH} = 1.1 Hz) for the μ_2-benzene ligands. Hence it can be supposed that the ligand can freely rotate above the metal framework in solution (identical coupling of the six

isochronous protons of the μ-benzene with both ^{103}Rh nuclei).

H. Suzuki et al.[24] investigated the reaction of triphenylphosphane with the tetrahydridodiruthenium complex $[(Cp^*Ru)_2(\mu\text{-}H)_4]$ ($Cp^* = \eta_5\text{-}C_5Me_5$) which affords the μ_2-benzene complex **13** [Eq. (c)]. A proposed mechanism for the formation is the oxidative addition of PPh_3 to a Ru center with breakage of a P–C bond (formation of μ_2-PPh_2 and σ phenyl units). Benzene can be reductively eliminated from the intermediate and then retained as a π bridging ligand in the complex.

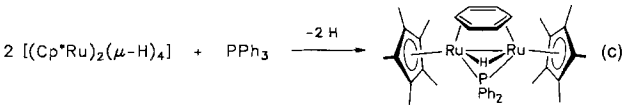

(c)

13

The μ-benzene ligand in **13** is replaced slowly in solution (ca. 1 h at 60 °C) by the solvent toluene. With C_6D_6, [D$_7$]**13** is formed quantitively [Eq. (d)]. This arene/arene exchange occurs much more quickly than the exchange Ru_2H/Ru_2D, which possibly implies that the reaction **13** → [D$_7$]**13** occurs by C–H activation of the μ-benzene ligand.

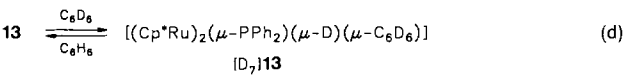

(d)

On the NMR time scale **13** is rigid up to 60 °C. The X-ray structural analysis[24] shows a *syn*-(μ-1,2-η^2:3,4-η^2) bonding mode of the nonplanar μ_2-benzene ligand. The C–C bond lengths in the metal-bonded planar "diene system" C1–C4 compare favorably with the values of olefin complexes despite the relatively large standard deviations. The benzene molecule is folded by 12° about C1 ··· C4, which causes the noncoordinated double bond C5–C6 (1.33(2) Å) to bend away from the Ru_2 unit.

Formally, the structure of the Ru_2 complex **13** can be related to that of the electronically unsaturated diiron complex **8** by oxidative addition of a secondary phosphane to the M_2 unit. After oxidation of the metal centers (formally Fe^I in **8**) the electronic situation in the Ru_2 complex is unambiguous; consequently the benzene now only uses four of its six π electrons for complex formation.

A similar coordination of benzene as in **13** was proven by G. Allegra et al.[25] from the X-ray structural analysis of the Pd_2 complex **14**. This and the analogous complex **15**[26] are products of the reaction of $PdCl_2$, $AlCl_3$, and Al in benzene. Both complexes are insoluble in hot benzene and decompose in polar solvents such as THF. Hence structural information was only obtainable for the crystalline solid. These were the first structurally characterized molecular complexes with bridging arenes. Despite their very similar composition, **14** and **15** show at first glance different coordination geometries for the μ-benzene ligands.

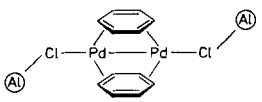

14, (Al) = $AlCl_3$
15, (Al) = Al_2Cl_6

The low-temperature X-ray structural analysis (−100 °C) of **15**[27] shows almost planar benzene ligands bound to the Pd_2 unit in a very unsymmetrical *syn*-(μ-1,2-η^2:3,4-η^2) coordination mode (Pd–C bond lengths 2.26(2)...2.63(2) Å). At room temperature the benzene rings are disordered.[25] In contrast, in **14** a more symmetrical *syn*-(1,2-η^2:3,4-η^2) coordination (d_{Pd-C} = 2.26(2), 2.37(2) Å) at room temperature was proven by X-ray crystallography (Fig. 5). In this case the arene rings are folded about C1 ··· C4 such that the uncoordinated formal double bond (1.37(4) Å) of each benzene ligand is bent towards the Pd_2 group (dihedral angle 7°). The observed C–C bond lengths in the μ_2-benzene ligands (1.37–1.45 Å in **14**, 1.36–1.49 Å in **15**) are difficult to interpret because of large standard deviations (0.04, 0.03 Å respectively) and systematic errors caused by the molecular dynamics in the solid.

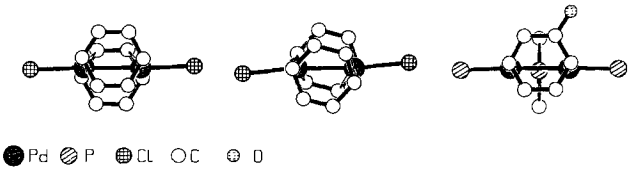

Fig. 5. Coordination geometry of the benzene ligands in **14** (left), **15** (center), and **16** (right).

The results of the X-ray structural analyses and solid state ^{1}H NMR spectroscopy[28] indicate that the barriers to the rotation of the μ_2-arene ligands about the (pseudo)C_6 axis in the crystalline dipalladium complexes **14** and **15** are only very low. The upper limit for the activation energy of this process in **15** of approximately 2 kJ mol^{-1} was determined from the X-ray crystallographic results.[27] From the temperature dependence of the ^{1}H spin-lattice relaxation a value of 5.9 kJ mol^{-1} is found for **14**.[28]

Isoelectronic to **14** and **15** is the zwitterion **16** formed as a minor product from the photolysis of [Pd(tBu$_3$P)$_2$] **17a** in the presence of phenol.[29] Remarkable in the formation of **16** is the breaking of P–C bonds of the phosphane ligands in the starting material **17a**, which was not observed for [Pd(Cy$_3$P)$_2$] **17b** (Cy = cyclohexyl). The latter forms only the mononuclear hydrido complexes *trans*-[(Cy$_3$P)$_2$Pd(H)(OAr)] · ArOH.[30] Zwitterion **16** crystallizes as an adduct in which three phenol molecules are linked together by hydrogen bonds and the first is similarly linked with the oxygen atom of the phenolate ligand. The almost planar six-membered ring of the phenolate ligand is bonded through *syn*-μ-2,3-η^2:4,5-η^2 coordination to the Pd_2 unit. The Pd–C bonds to the outer C atoms of the Pd-coordinated "diene unit"

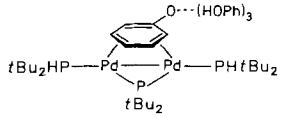

16

(2.3 Å) are shorter than those to the inner C atoms (2.5 Å) (Fig. 5). The distribution of C–C bond lengths (metal-coordinated C–C bonds 1.39(1) Å, free "double bond" 1.424(8) Å, others 1.41(1)–1.427(8) Å) in the μ-arene ligand indicates considerable bond delocalization. The ^{1}H NMR spectra of **16** point to a more symmetrical (dynamic?) structure, with respect to the NMR time scale in solution at $-50\,^{\circ}C$ (for the phenolate ligands only three signals occur for the five protons in the *ortho*, *meta*, and *para* positions relative to oxygen). Apparently at room temperature the complex-bound phenolate rapidly exchanges with the free phenol molecules (upfield shift for the signals of the ring protons on the phenolate ligand on decreasing the temperature).

As a MO study[31] of the hypothetical complexes $[(LPd)_2(\mu\text{-}C_6H_6)(\mu\text{-}A)]$ ($L = Cl^-$, NH_3; $A = \eta\text{-}C_3H_5^-$, $\eta\text{-}C_4H_6$, $\eta^4\text{-}C_6H_6$) shows, the stability of the corresponding μ-benzene complexes is due to a donor/acceptor interaction between the HOMOs of the benzene and the Pd_2 unit. Since the $Pd_2(\mu\text{-}A)$ group has only two low-lying empty orbitals with suitable symmetry at its disposal, the benzene can only function as a four-electron donor. However, the experimentally observed bending of the arene in **14** cannot be satisfactorily explained from the calculations.

The catalytic properties of the binuclear Pd^I complexes **14** and **15** have been examined in some organic reactions. Under mild conditions, **14** and **15** catalyze the dimerization of ethene to butenes.[32] Some alkynes were cyclotrimerized to fulvenes or polymerized in the presence of **14** or **15**.[33]

Binuclear complexes with *anti*-coordinated arene bridges include both "true" (that is, with (pseudo)axial symmetry) triple-decker sandwich complexes with $\mu\text{-}\eta^6\text{:}\eta^6$-coordination of the arene and less symmetrical molecules in which only some ring carbon atoms are bonded to the metals.

Among the many novel organovanadium compounds, which K. Jonas[34] showed to be either directly or indirectly accessible by the reductive disintegration of vanadocene, are also triple-decker complexes of the type $[L_nM(\mu\text{-}\eta^6\text{:}\eta^6\text{-arene})VCp]$. Thus, the complexes ***18a*** and ***18b*** are available from one-pot reactions of vanadocene, alkyllithium, and 1,3-cyclohexadiene.[35] The sandwich complex **18a** is still stable

18a, L = thf, n = 2
18b, L = tmeda, n = 1

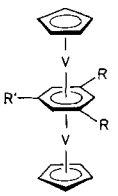

20a, R, R' = H
20b, R = H, R' = CH_3
20c, R = H, R' = n-C_3H_7
20d, R = R' = CH_3

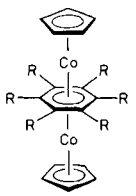

22, R = $COOCH_3$

in toluene at 100 °C. The triple-decker structure of **18b** is confirmed by a X-ray structural analysis.[35] The alcoholysis of **18** affords $[CpV(\eta^6\text{-}C_6H_6)]$, which reacts with Mg in THF to give the trinuclear complex **19**.[35] The structure of **19** is unknown; it is assumed that here too $\mu\text{-}\eta^6\text{:}\eta^6$-benzene bridges between vanadium and magnesium exist.[35]

$[(thf)_2Mg\{(C_6H_6)VCp\}_2]$ **19**

The reaction of $[CpV(allyl)_2]$ with 1,3-cyclohexadiene in n-heptane at 100 °C leads to a 50% yield of **20a**, the first triple-decker sandwich complex with complexed benzene as the "middle-deck" [Eq. (e)].[36] By-products of the reaction are **20c**, $[CpV(\mu\text{-}C_6H_6)]$, and H_2, besides aromatic and non-aromatic hydrocarbons. By heating **20a** in toluene or mesitylene it is converted into the toluene and mesitylene derivatives **20b** and **d**.[36] With lithium cyclopentadienide the VLi complex **18** is formed.[35]

$$[CpV(C_3H_5)_2] + 1,3\text{-}C_6H_8 \xrightarrow[100\,^{\circ}C]{n\text{-}C_7H_{16}} \underset{\textbf{20a}}{[(CpV)_2(\mu\text{-}C_6H_6)]} \quad \text{(e)}$$

$$[(CpV)_2(\mu\text{-}C_6H_5nPr)] + [CpV(C_6H_5)] + \ldots$$
20c

The X-ray structural analyses of **20a** and **20d** show planar Cp and arene rings parallel to one another. The C–C bond lengths in the arene bridges are 1.439(8) (**20a**) and 1.443(5) Å (**20d**).[36] For **20a**, X–X and X–N electron density deformations have been determined which indicate an approximate octahedral distribution around the vanadium atoms.[37]

The paramagnetic complexes **20** with 26 valence electrons do not correspond to the 30/34 VE rule of R. Hoffmann et al. for triple-decker complexes.[38] In more recent theoretical investigations,[39,40] it was proven that this rule is actually not applicable for complexes of the electron-poor early transition metals.

The cocondensation of arenes with metal vapors is a successful method for the preparation of bis(arene)metal complexes.[41] In noble gas matrices half-sandwich complexes $[(\eta^6\text{-arene})M]$ were formed along with $[(\eta^6\text{-arene})_2M]$.[42] By increasing the metal atom concentrations in the matrix, G.A. Ozin et al. could prove the existence of the species $[(arene)_nM_2]$ (M = V, Cr, Mo; n probably 2) using kinetic and spectroscopic investigations.[43] Similar molecules can be produced in the gas phase in different ways (e.g. $[(arene)_2Cr_2]^+$, by the molecule–ion reaction during the disintegration of $[(arene)Cr(CO)_3]$ in the mass spectrometer;[44] $[(C_6H_6)VFe]^+$ and $[(C_6H_6)_2VFe]^+$ as products from the reaction of $[VFe]^+$ with cyclohexene;[45] $[(C_6H_6)_2Pt_n]$ ($n = 2$–6) from benzene and beams of Pt_n clusters[46]). Although the structures of such multinuclear complexes have not been completely verified, there are arguments for formulating them as arene-bridged $(metal)_n$ clusters.[43]

W. M. Lamanna[47] was able to isolate along with the well-known $[Cr(C_6H_3Me_3)_2]$, a binuclear complex $[Cr_2(C_6H_3Me_3)_3]$ (**21**) from the cocondensation product of

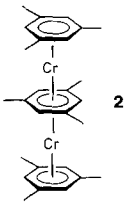

21

chromium vapor and mesitylene. The red, very air-sensitive complex has a triple-decker sandwich structure. In the solid the three planar mesitylene rings are parallel and eclipsed.[48] All three arene rings are expanded with respect to the free ligand, resulting in not significantly longer C–C bonds in the bridging ligand coordinated to both metals than in the terminal ligands (1.417(4) Å as opposed to 1.402(2) and 1.413(2) Å). The chromium–ligand distances are somewhat shorter for the terminal ligands (1.600(1) Å) than for the bridging ligand (1.669(1) Å).

As anticipated for a triple-decker complex with 30 VE, **21** is diamagnetic. In the ^{1}H NMR spectrum the ring protons of the bridging mesitylene ligands show a strong upfield shift ($\delta(^1H_{\text{bridging ring}}) = 2.9$, $\delta(^1H_{\text{terminal ring}}) = 3.4$).

Earlier, triple-decker sandwich complexes with an (η^6:η^6-arene)-bridge were postulated as intermediates in the exchange of arene ligands between mononuclear complexes such as $[(CO)_3Cr(\eta\text{-}C_6H_6)]$.[49] However, since the resulting "inversion" of the arene–metal bond could not be proven such an associative mechanism is rather unlikely.[50]

A triple-decker sandwich complex with 34 VE and a μ-η^6:η^6-arene ligand **22** was also prepared by the group of K. Jonas in Mülheim.[51] The diamagnetic compound is probably a stop-complex of the catalytic cyclotrimerization of dimethyl acetylenedicarboxylate with the bis(ethene) complex **23**. It melts without decomposition just under

$[(Cp(Co)_2\{\mu\text{-}C_6(COOMe)_6\}]$ **22** $[CpCo(C_2H_4)_2]$ **23**

200 °C. The highly symmetrical NMR spectra, even at −100 °C, practically exclude the alternative structures for **22** (e.g. with *syn* orientation of the CpCo groups).

A wide variety of structures are known for less symmetrical *anti*-(μ-arene) binuclear complexes, that is, complexes in which not all the ring-carbon atoms are simultaneously bonded to both metal atoms.

The sterically hindered strong Lewis acid $[Ta(silox)_3]$ (silox = $OSitBu_3$) reacts with pyridine affording the mononuclear complex $[Ta(silox)_3\{\eta^2\text{-(N,C)-pyridine}\}]$.[52] P. T. Wolczanski et al. obtained from a benzene solution of this compound after 10–14 days the crystalline diamagnetic Ta_2 complex **24** in 7% yield. The existence of the likely mononuclear precursor $[(silox)_3Ta(\eta^2\text{-}C_6H_6)]$ could not be proven.[52] Due to the bulky $Ta(silox)_3$ fragments, *anti*-(1,2-

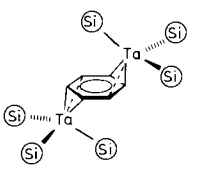

24, Si = $OSitBu_3$

η^2:4,5-η^2) coordination of the bridging benzene is observed in the crystal. Each tantalum atom is bound very unsymmetrically to one C–C bond of the benzene ($d_{Ta-C} = 2.11(1)$, 2.33(1) Å). Since a weaker interaction ($d_{Ta-C} = 2.71(1)$ Å) exists between each Ta and another C atom, the coordination type can also be described as distorted (η^3-enyl) bonding. Unfortunately, the geometry of the μ-benzene ligand could not be precisely determined in the X-ray structural analysis.[52]

The alternative *anti*-(μ_2-1,2-η^2:3,4-η^2) coordination of the benzene ligand is observed in the binuclear Re complex **25** reported by P. Pasman et al.[53] It is formed in 5% yield along with **26** and **27** during the photolysis of **28** in benzene (Scheme 3). A key intermediate in the formation of **25** is the

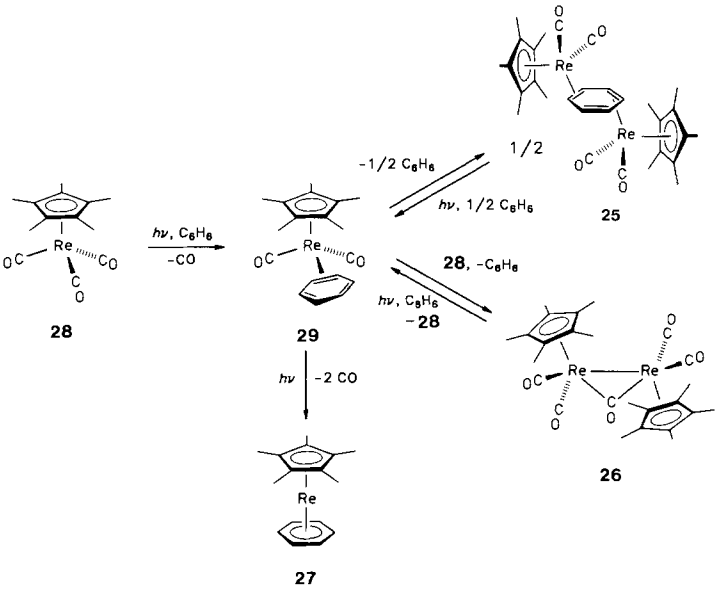

Scheme 3.

initially formed mononuclear complex **29**. This reacts in a dark reaction with the starting material **28** to give **26** or undergoes selfcondensation with the loss of a benzene ligand affording **25**. The complex **25** is photolabile and on longer irradiation reacts back to the η^2-benzene complex **29** which in turn forms the photolysis end product **27** with η^6-bound benzene through loss of CO (Scheme 3).

In the crystal, **25** has C_2 symmetry.[53] The planar bridging ligand can be well described as η^2:η^2-coordinated cyclohexatriene. The free C–C bond of 1.31(2) Å is considerably shorter than the C–C bonds (1.40(1) Å) which are coordinated to the rhenium atoms. The other C–C bond lengths are 1.46(1) and 1.47(2) Å, respectively. The NMR data (three ^{13}C NMR signals at δ = 40.9, 50.6, and 127.3) shows that in solution **25** had the same nonfluxional structure, at least at room temperature.

A series of binuclear complexes of benzene with $[Os(NH_3)_5]^{2+}$ and $[Ru(NH_3)_5]^{2+}$ metal-complex fragments was prepared by H. Taube et al.[54–56] In inert solvents the dication **30** loses benzene at room temperature and undergoes selfcondensation, affording the tetracation **31**.[54] This reaction also occurs in the presence of an excess of benzene. Cation **31** can also be prepared from **30** and $[Os(NH_3)_5(dme)]^{2+}$.[55] When **31** is heated in a vacuum to 90 °C, NH_3 is driven off and **32** is formed.[55] Tetracation **32** reacts with acetone to give the mononuclear complexes **30** and $[Os(NH_3)_5(\eta^2\text{-acetone})]^{2+}$ (Scheme 4).[55] The mixed-metal complex **33**, which is labile in solution, is accessible from **30** and $[Ru(NH_3)_5(MeOH)]^{2+}$.[56]

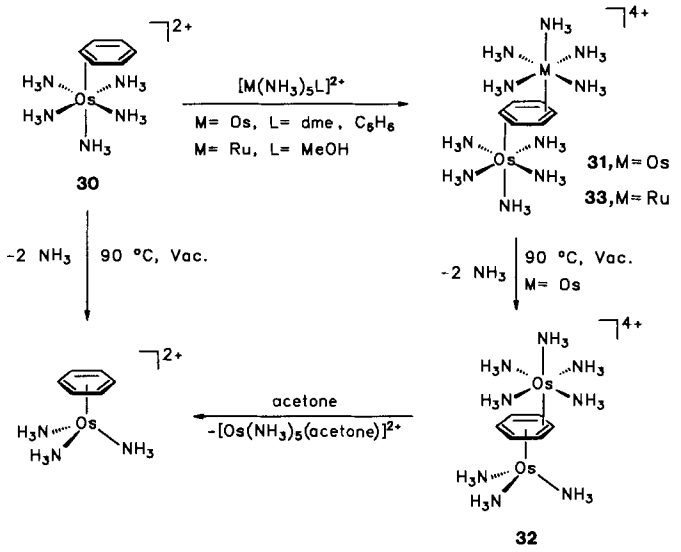

Scheme 4. dme = 1,2-dimethoxyethane, Vac. = vacuum.

The X-ray structural analysis[55] proves the *anti*-(μ-1,2-η^2:3,4-η^2) coordination of the benzene bridge for crystalline **31**-$(CF_3SO_3)_4$, which had been derived previously from the spectroscopic data of the salt in solution. The planar μ-benzene ligand has a similar ring geometry to that in **25**, within experimental error (lengths of the metal-coordinated C–C bonds 1.43(2), 1.49(2) Å, free double bond 1.32(2) Å, other C–C bonds 1.44(2) to 1.54(2) Å). Also the ^{13}C NMR shifts of the bridging ligands in **25** and **31** (δ = 49.6, 53.1, 127.6) are very similar despite the different charges of the complexes. The free C–C double bond in **31** is remarkably chemically inert. It is not attacked by $[Os(NH_3)_5]^{2+}$ fragments,[55] peroxo acids,[55] and H_2/Pd[57], probably due to steric effects.

Electrochemical oxidation of **31** furnishes the mixed-valent pentacation $[\{Os(NH_3)_5\}_2(\mu\text{-}C_6H_6)]^{5+}$, which has a delocalized electronic structure.[54] Based on the spectroscopic data the pyrolysis product **32** is assigned the very unusual *anti*-$[(NH_3)_5Os(\mu\text{-}\eta^2\text{:}\eta^6\text{-}C_6H_6)Os(NH_3)_3]^{4+}$ structure. Magnetization-transfer experiments show that the $[Os(NH_3)_5]^{2+}$ group bonded to only two ring carbon atoms moves slowly around the ring ($k \approx 1\ sec^{-1}$ at 20 °C). This tautomerization in **32** is approximately 10^4 times slower than in the mononuclear **30**.[55]

p-Xylene as a bis(enyl)-bound ligand is observed in the Co_2 complex **34a**. This complex prepared originally by K. Jonas et al.[20,21] is the "decomposition product" of the 1,4-dimethylcyclohexadienyl complex **35**, which is available via the hydrocobaltation of *p*-xylene with $[\{Cy_2P(CH_2)_2PCy_2\}$-Co(η-allyl)]/H_2 [Eq. (f)].

$$[\{Cy_2P(CH_2)_2PCy_2\}Co(\eta\text{-}C_3H_5)] + 2\,H_2 + p\text{-}(CH_3)_2C_6H_4 \longrightarrow$$

$$[\{Cy_2P(CH_2)_2PCy_2\}Co(1\text{-}5\text{-}\eta\text{-}(CH_3)_2C_6H_5)] + C_3H_8 \longrightarrow \quad \text{(f)}$$

35

$$1/2\ [\{(Cy_2P(CH_2)_2PCy_2)Co\}_2(\mu\text{-}1,4\text{-}(CH_3)_2C_6H_4)] + 1/2\ p\text{-}(CH_3)_2C_6H_4$$

34a

As in the starting complex $[\{Cy_2P(CH_2)_2PCy_2\}Co(\eta$-allyl)] each cobalt atom in **34** achieves only a 16 VE configuration (d^8-Co^I with pseudo-square-planar coordination) by bonding to three C atoms of the *p*-xylene. A symmetrical triple-decker structure (which would have 32 VE) is not formed. The structure containing a *syn*-(μ_2-η^4:η^4-arene) bridge and Co–Co multiple bond analogous to the isovalent $[(CpFe)_2(\mu\text{-}C_6R_6)]$ **8** would be improbable already on steric grounds. In the crystal the μ-(1-3-η^3:4-6-η^3-*p*-xylene) ligand shows a geometry typical for η^3-methallyl groups. Since the η^3-enyl planes are bent away from the planar xylene structure by 22.6°, the bridging ligand takes the form of a flattened chair. The same bonding situation as in **34a** was recently also proved for the benzene bridge in **34b** by X-ray crystallography.[21]

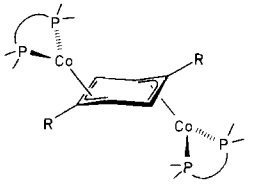

34a, P⌒P = $Cy_2P(CH_2)_2PCy_2$, R = CH_3

34b, P⌒P = $iPr_2P(CH_2)_2PiPr_2$, R = H

The major product (approximately 60%) of the reaction of hexafluorobut-2-yne with $[Ni(cod)_2]$ is the binuclear hexakis(trifluoromethyl)benzene complex **36a**, which can be converted into **36b** or **36c** with phosphites.[58] On the basis of ^{19}F and ^{31}P NMR data, F.G.A. Stone et al. had initially proposed dynamic structures with *syn*-(μ-η^3:η^3)-bound arene bridges for **36a–c**.[58] Later the same authors decided that an *anti*-$[(NiL_2)_2\{\mu\text{-}1,2\text{-}\eta^2\text{:}3\text{-}4\text{-}\eta^2\text{-}C_6(CF_3)_6\}]$ structure was more likely.[59]

$[(NiL_2)_2\{C_6(CF_3)_6\}]$ **36**

a, L = cod; **b**, L = $P(OMe)_3$; **c**, L = $P[(OCH_2)_3CMe]$

3. Chemisorbed Arenes on Metal Surfaces and Arene-Capped Cluster Compounds

From the point of view of the chemist, molecules chemisorbed on metal surfaces often do not greatly differ from the corresponding ligands in molecular metal complexes.[60] In many cases chemisorption can be described as being localized, that is, through a "cluster-like" bonding of the substrate to the surface.[61] In this respect, chemisorbed arenes on transition-metal surfaces are particularly interesting varieties of arene–metal multinuclear complexes.

The adsorption of benzene on transition-metal surfaces has been well studied.[62] Most investigations were carried out on single-crystal surfaces with low Miller indices. In almost all cases benzene is adsorbed as a molecule (i.e., no dissociation takes place). The plane of the adsorbed benzene ring lies parallel to the metal surface; nevertheless, different adsorption sites for different metals have been proposed. Benzene can be bonded to one or more surface atoms. For the simple case of benzene on a close packed, atomically flat metal surface (e.g., the (111) face of a metal with cubic closest packing) there are at least four different sites for the

chemisorbed benzene (Fig. 6): one with sixfold local symmetry (highest symmetry C_{6v}), e.g. Rh(111)/C_6H_6,[64] Pd(111)/C_6H_6[65]); with threefold local symmetry [$C_{3v}(\sigma_v)$ or $C_{3v}(\sigma_d)$, e.g. Os(0001)/C_6H_6,[66] Rh(111)/C_6H_6/Na,[67] Pd(111)/C_6H_6/2CO,[68] and Pt(111)/C_6H_6[69]]; and with twofold local symmetry (C_{2v}, e.g. Pt(111)/2C_6H_6/4CO[70]).

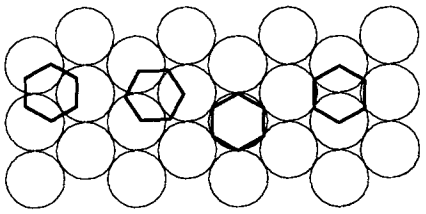

$C_{3v}(\sigma_d)$ $C_{3v}(\sigma_v)$ C_{6v} C_{2v}

Fig. 6. Adsorption sites of benzene on a densely packed transition-metal surface. The local symmetry at each site is given.

Once chemisorbed, benzene cannot be completely thermally desorbed from metal surfaces.[71] From all investigated metal/benzene adsorbates, both benzene and dihydrogen are desorbed by warming; the desorption:dehydrogenation ratio for benzene depends on the metal and the surface coverage.

Due to great experimental difficulties associated with the structural analysis of adsorbates on surfaces, only very little structural data is available for adsorbed arenes.[72] According to electron diffraction (*l*ow *e*nergy *e*lectron *d*iffraction, LEED) investigations by M.A. van Hove, G.A. Somorjai et al., the benzene rings in the Rh(111)/C_6H_6/CO coadsorbate[73] were found to be trigonally distorted (d_{C-C} = 1.33(15) and 1.81(15) Å for the alternating shorter C–C "double bonds" and the longer C–C "single bonds"). In Rh(111)/C_6H_6/2CO[70] and Pd(111)/C_6H_6/2CO[68] the distortion of the chemisorbed benzene is not significant (d_{C-C} = 1.46(15) and 1.58(15) Å, 1.40(10) and 1.46(10) Å, respectively). The same is true for benzene adsorbed at a C_{2v} site in Pt(111)/2C_6H_6/4CO[70] (two C–C bonds with d_{C-C} = 1.65(15) Å, four C–C bonds with d_{C-C} = 1.76(15) Å).

F.P. Netzer et al.[74] deduced from the angle-resolved photoelectron spectra (ARUPS, *a*ngle-*r*esolved *U*V *p*hotoemission *s*pectroscopy) C_{6v} symmetry for benzene in Rh(111)/C_6H_6/CO. This excludes a significant Kekulé distortion of the chemisorbed benzene. The obvious contradiction of the results from the electron diffraction studies has not yet been resolved.

If alkyl benzenes are adsorbed with the plane of the arene ring parallel to the metal surface, the C–H bonds of the side chains are close to the surface atoms. This leads to dissociative adsorption with the cleavage of C–H bonds.[71] In the case of the adsorption of toluene on a Pt(111) surface, the product of such a selective dehydrogenation, a $(\pi + \sigma)$-bound η^7-benzyl species, could be observed by spectroscopy at 350 K.[75]

Molecular cluster complexes [{L_mM}$_n$(μ-arene)] with $n \geq 3$, in which an arene ligand is bonded to three or more metal atoms, are of some significance as possible model substances for the metal-surface/arene chemisorbates.[63] The first syntheses of such molecules were successfully carried out by J. Lewis et al. in 1985.[76] In the octahedral Ru_6 cluster compound **37**,[76] obtained from [$Ru_6C(CO)_{12}(\eta^6$-$C_6H_6)]^{2-}$ and [$(PhCN)_3Ru(\eta^6$-$C_6H_6)]^{2+}$, one of the benzene rings is bonded as an η^6 ligand to a ruthenium atom. The second benzene molecule takes a position parallel to a triangular face of the Ru_6 octahedron and interacts with three metal atoms.

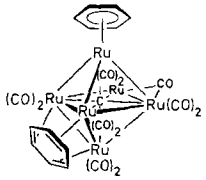

37

For the synthesis of the Os_3 cluster **38**, [$Os_3(CO)_{12}$], or the more reactive [$Os_3(CO)_{10}(NCMe)_2$] (**39a**) cannot simply be treated with benzene. In such a reaction benzene oxidatively adds to the metal cluster forming **40**, a complex of dehydrobenzene.[77] The method used by J. Lewis et al. for the preparation of **38** starts with **41** and 1,3-cyclohexadiene which are converted into the μ_3-benzene on the metal complex via **42**,[78] an intermediate containing the μ_3-cyclohexadienyl ligand (Scheme 5). In a similar way **44**, the Ru_3 homologue of **38**, is prepared from **43**.[79] With Me_3NO/MeCN **38** reacts to form the activated **45a**, from which the further monosubstituted products **45b–e** and the disubstituted [$Os_3(CO)_7(C_2H_4)$(MeCN)(μ_3-η-$C_6H_6)$] are accessible.[80,81] The latter reacts with alkynes C_2R_2 to give [$Os_3(CO)_7(\eta^6$-$C_6H_6)(\mu_3$-η^1:η^2:η^1-$C_2R_2)$]. In this reaction the benzene is transferred from the Os_3-face-capping position into a η^6-coordination at only one osmium atom.[81]

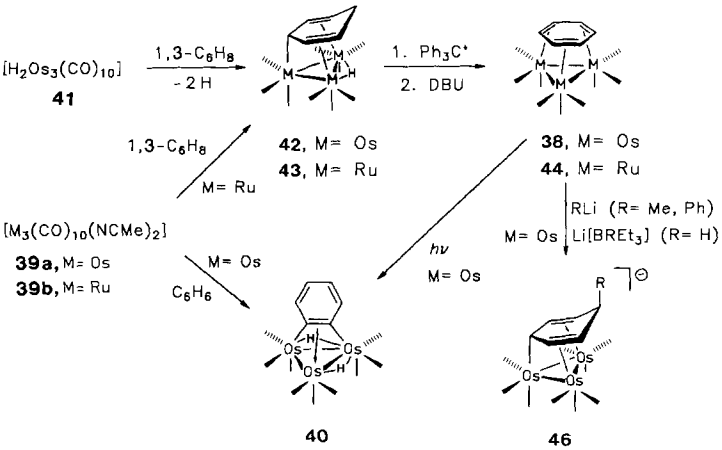

Scheme 5. DBU = 1,8-diazobicyclo[5.4.0]undec-7-ene. The CO ligands in the formulas for **38**, **40**, **42–44**, and **45** are indicated by dashes.

[$Os_3(CO)_8L(\mu_3$-η-$C_6H_6)$] **45**

a, L = MeCN; **b**, L = PPh_3; **c**, L = $P(OMe)_3$; **d**, L = C_2H_4; **e**, L = H_2C=CHPh)

Strong nucleophiles such as H^- and RLi (R = Me, Ph) add to the μ_3-arene ring of **38** in the *exo* position. The prod-

ucts are the anionic clusters **46** with substituted (μ_3-η^2:η^1:η^2-cyclohexadienyl) ligands.[82] In contrast, HBF_4 attacks **38** at the metal framework forming $[Os_3(CO)_9(\mu_2\text{-}H)(\mu_3\text{-}\eta^6\text{-}C_6H_6)]^+$[82]). On irradiation ($\lambda > 290$ nm) **38** isomerizes quantitatively by oxidative addition of the μ_3-benzene to the Os_3 cluster to form the μ-η^1:η^2:η^1-dehydrobenzene(dihydrido)cluster **40**.[83] In inert matrices at 12–20 K the photolysis probably occurs in two steps and without dissociation of CO.[83] The conversion of **38** into **40** is irreversible and can also be accomplished by prolonged heating of **38**. All these results indicate that **40** is the thermodynamically more stable isomer.

A few years ago a method of synthesis for tricobalt clusters with face-capping arene ligands $[(CpCo)_3(\mu_3\text{-arene})]$ **47–58** (Table 1) was developed in our research group.[63,84] Our method does not generate a benzene molecule on the metal cluster as in the case of the Os_3 clusters but a metal cluster is assembled on the arene. To achieve this, substituted

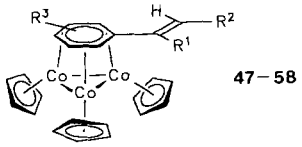

47–58

Table 1. Complexes of the type $[(CpCo)_3(\mu_3\text{-}\eta^2\text{:}\eta^2\text{:}\eta^2\text{-arene})]$ **47–58**.

Complex	R^1	R^2	R^3	Ref.
[(CpCo)$_3$(α-methylstyrene)] **47a**	Me	H	H	[63]
[(CpCo)$_3$(β-methylstyrene)] **47b**	H	Me	H	[84]
[(CpCo)$_3$(*p*-methylstyrene)] **48**	H	H	4-Me	[63]
[(CpCo)$_3$](*p*-ethylstyrene)] **49**	H	H	4-Et	[86]
[(CpCo)$_3$(*p*-methoxystyrene)] **50**	H	H	4-OMe	[63]
[(CpCo)$_3$(*o*-methyl-β-methylstyrene)] **51a**	H	Me	2-Me	[87]
[(CpCo)$_3$(*m*-methyl-β-methylstyrene)] **51b**	H	Me	3-Me	[87]
[(CpCo)$_3$(*p*-methyl-β-methylstyrene)] **51c**	H	Me	4-Me	[87]
[(CpCo)$_3$(β-ethylstyrene)] **52**	H	Et	H	[63]
[(CpCo)$_3$(1,1-diphenylethene)] **53a**	Ph	H	H	[63]
[(CpCo)$_3$(stilbene)] **53b**	H	Ph	H	[63]
[(CpCo)$_3$(*p*-methoxystilbene)] **54a**	H	4-anisyl	H	[63]
54b	H	Ph	4-OMe	[63]
[(CpCo)$_3$(*p*-distyrylbenzene)] **55**	H	Ph	4-styryl	[86]
[(CpCo)$_3$(1,1-diphenylpropene)] **56**	Ph	Me	H	[63]
[(CpCo)$_3${1-(*p*-anisyl)propene}] **57**	H	Me	4-OMe	[63]
[(CpCo)$_3$(2-phenyl-2-butene)] **58**	Me	Me	H	[86]

styrene derivatives are treated with Jonas reagent [CpCo(C_2H_4)$_2$] (**23**) or **59**, both excellent sources of CpCo complex fragments.[85] The yields of these one-pot reactions are

$[CpCo(\eta^6\text{-}C_6Me_6)]$ **59**

often very high, and are determined by the degree of substitution at the arene ring and at the side chain.[63] Allylarenes and 4-phenyl-1-butene can also be used. In these arenes, the double bond of the side chain is catalytically shifted into the α position to the arene ring in a preequilibrium.[63,84] Benzene and alkylarenes do not react.

The 1-alkenyl group on the arene ring serves as a "landing-strip" for the first complex fragment, which is probably initially coordinated to the double bond of the side chain, and then, aided by the chelate effect, attacks the aromatic π system (Scheme 6). The mononuclear primary product **60** is

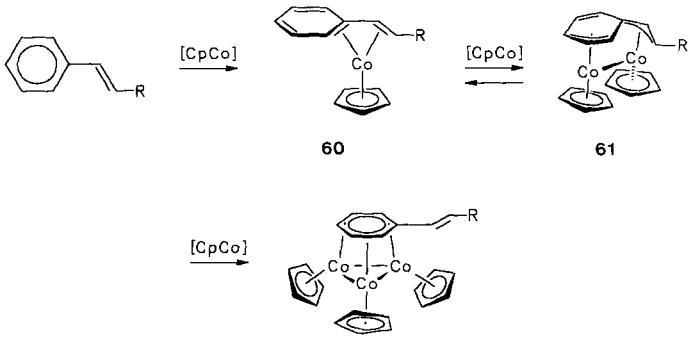

60 **61** **47–58**

Scheme 6.

activated for further reaction since the six π electrons of the arene are disturbed by the complexation of two carbon atoms. A Co_3 cluster can only be formed if further CpCo complex fragments attack in a *syn* position to the cobalt atom in **60**. Therefore, we proposed the complex **61** with a (β,α,1-η^3:2-4-η^3-alkenylbenzene) ligand as a binuclear intermediate[88] in which the cobalt atoms (each formally Co^{II}) are linked by a metal–metal bond and thus can be retained on the same side of the alkenylbenzene ligand. The third CpCo complex fragment can now be added to the uncoordinated C–C double bond in **61** to form the metal cluster. Simultaneously the alkenyl group is decomplexed. So far, however, there have only been indirect indications for the participation of such mono- and binuclear intermediates in the formation of the clusters **47–58**.

A good indication that complexes of the type **60** are intermediates is the formation of **62**, along with the μ_3-arene complex **55**, from *p*-distyrylbenzene and Jonas reagent **23** or **59** (Scheme 7).[86,87,89] In the mononuclear complex **63**, which has not yet been detected but is surely initially formed, the π system of the central arene ring is activated in comparison to the free ligand. The addition of two more CpCo com-

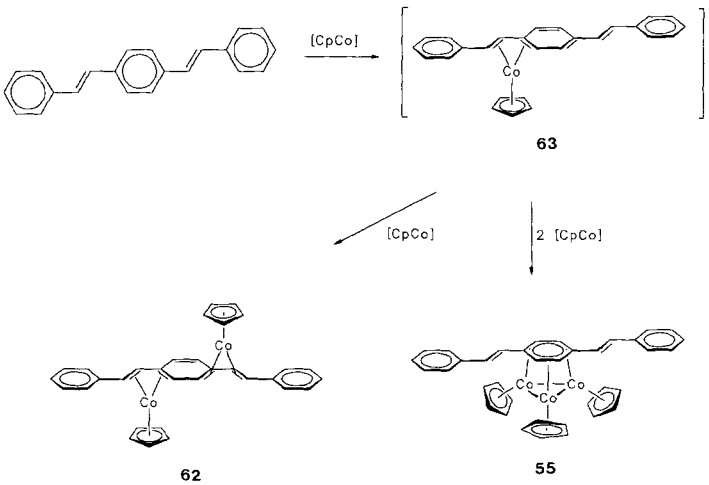

63 **62** **55**

Scheme 7.

plex fragments to the coordinated arene ring finally leads to the μ_3-arene cluster **55**. But the diene system formed from only two carbons of the inner six-membered ring and the second styryl group can also be coordinated. This forms the "trapped product" **62**. With *m*-distyrylbenzene as a ligand the binuclear complex analogous to **62** could be isolated.[87]

CpCo complexes with α- and β-vinylnaphthalene or α-styrylnaphthalene as ligands are the most similar to the postulated intermediates **60** containing β,α,1,2-η^4-alkenylarene ligands. In these crystalline solids, as in **60**, two carbon atoms of the aromatic ring and two of the 1-alkenyl side chain are bonded to the cobalt atom.[88,90] These substances are unstable already at room temperature and cannot be subjected to further reactions to form [$(CpCo)_3$(μ_3-alkenylnaphthalene)] clusters. A model compound for the binuclear intermediate **61** is **64**. The *syn*-(μ-η^3:η^3) coordination of a hexatriene unit postulated for **61** has been shown by X-ray crystallography[88] to occur in the (open-chain) 1,3,5-hexatriene ligand of **64**.

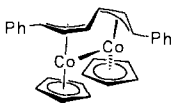

64

At this point attention should be drawn to the strikingly different reaction behavior of 1-alkenylbenzenes with the $(CO)_3Fe$ complex fragment, which is isolobal and isoelectronic with CpCo. Many stable complexes of the type [$(CO)_3$Fe(β,α,1,2-η-1-alkenylbenzene)] are known, which often react with further [$(CO)_3$Fe] affording binuclear complexes.[89] However, these have an *anti*-[{$(CO)_3Fe$}$_2$(β,α,1,2-η^4:3-6-η^4-1-alkenylbenzene)] structure, and they do not react any further to form the hypothetical clusters [{$(CO)_3Fe$}$_3$(μ_3-arene)].

As mentioned in Section 2.2, J. Müller et al.[23] recently obtained the trirhodium complex [$(CpRh)_3$(μ_3-η-C_6H_6)] (**12**) by the photolysis of [$CpRh(C_2H_4)_2$] (**9**) in the presence of benzene (Scheme 2). The complexes [$CpRh(\eta^4$-C_6H_6)] (**10**) and *syn*-[$(CpRh)_2$(μ-η^3:η^3-C_6H_6)] (**11**), isolable after several hours of irradiation, are probably direct precursors of **12**, since after longer reaction times only **12** is formed. Even a long reaction time affords **12** in very small quantities (approximately 2.5% yield after 7.5 h); this clearly illustrates the crucial role of the alkenyl substituents on the formation of the tricobalt cluster complexes [$(CpCo)_3$(μ_3-alkenylarene)], where in some cases an almost quantitative yield is obtained.[63]

In all the cluster compounds with arene bridges which have been structurally characterized so far, the (μ_3-η^2:η^2:η^2)-bonding mode of the arene ligand to an M_3 unit was found in the solid (Table 2). M_3-triangle and arene-hexagon are parallel to each other and adopt a staggered orientation. The μ_3-benzene ligands of the Ru and Os complexes **37** and **38** were at first described as M_3-face-capping cyclohexatrienes[76] because of the alternating long and short C–C bond lengths determined by X-ray crystallography. However, the X-ray structure analyses of five [$(CpCo)_3$-(μ_3-arene)] derivatives show that only a small (although crystallographically significant) alternation of the C–C bond lengths (average difference 0.03 Å) occurs, at least in the complexes of this type (Table 2).[63,84,92–94] The probability that this is also true for the previously mentioned (μ_3-benzene) clusters with metals of the 2nd and 3rd transition-metal series, for which the C–C distances show much larger experimental errors, is supported by the recently published structure of [$Ru_3(CO)_9$(μ_3-η-C_6H_6)] (**44**).[79] Although only small, the trigonal distortion of the μ_3-arenes towards a Kekulé structure is induced by a mixing of HOMO and LUMO of the arene, according to a theoretical MO analysis.[93] This occurs in such a way that the three C–C bonds which lie above the metal atoms are shortened, whereas the others are lengthened. This is made possible by the threefold symmetry enforced upon the arene by the M_3 cluster. There exists an interesting parallel to the mononuclear complexes [$(CO)_3M(\eta^6$-C_6H_6)] (M = Cr, Mo, W) which also show a weak alternation of the C–C bond lengths in the complex-bound benzene ligand.[95] The bending of the arene C–H bonds away from the metal cluster observed by crystallography can also be well understood from MO theory.[93]

Table 2. C–C bond lengths in several μ_3-η^2:η^2:η^2-arene ligands (standard deviations of single values in parentheses; for each complex, first line: the average value of the alternating long and short bonds [a], second line: difference between the longest and shortest single value).

Complex	*d*(C-C) [Å]		Ref.
[$(CpCo)_3$(β-methylstyrene)] **47b**	1.420(5)	1.446(5)	[63, 84]
	0.020	0.031	
[$(CpCo)_3$(1,1-diphenylethene)] **53a**	1.418(5)	1.449(5)	[63]
	0.014	0.006	
[$(CpCo)_3$(1,1-diphenylethane)] **66a**	1.414(6)	1.439(6)	[92]
	0.019	0.015	
[$(CpCo)_3$(1,2-diphenylethane)] **66b**	1.417(5)	1.442(5)	[92]
	0.017	0.023	
[$(CpCo)_3$(2-phenyl-2-butene)] **58**	1.41(1)	1.46(1)	[92]
	0.05	0.05	
[(μ_3-H)$(CpCo)_3$(1,1-diphenylethane)]$^+$ **68**	1.41(2)	1.46(2)	[92]
	0.02	0.01	
[$(CpCo)_3$(α-methylstyrene)]$^+$ **47a**$^+$	1.445(8)	1.419(8)	[92]
	0.11	0.014	
[$(CpRh)_3$(benzene)] **12**	1.453	1.424	[23]
	0.02	0.04	
[$Ru_3(CO)_9$(benzene)] **44**(295 K)	1.40(1)	1.45(1)	[79]
	0.04	0.01	
[$Ru_3(CO)_9$(benzene)] **44**(193 K)	1.41(1)	1.45(1)	[79b]
	0.01	0.01	
[$Ru_6C(CO)_{11}$(benzene)$_2$] **37**	1.39(2)	1.48(2)	[76]
	0.05	0.04	
[$Os_3(CO)_9$(benzene)] **38**	1.41(3)	1.51(3)	[76]
	0.08	0.11	
[$Os_3(CO)_8(C_2H_4)$(benzene)] **45d**	1.41(3)	1.47(3)	[80]
	0.06	0.06	

[a] Exception: **47a**$^+$ in which the order of shorter and longer C-C bonds is irregular.

In solution rotation of the M_3-triangle with respect to the arene ring is hindered. For the clusters **45d** and **45e**, this dynamic process is coupled with the rotation around its bonding axis of the alkene bound to one osmium atom. For this reason **45** was quite aptly named "organometallic helicopter".[80] In Rh_3 cluster **12** the ^{1}H NMR signal of the benzene protons at room temperature is a quartet (J_{RhH} = 0.7 Hz),[23] so that here, too, a rapid rotation of the arene can be assumed.

With 2D EXSY NMR spectroscopy (EXSY = *Ex*change *s*pectroscop*y*) successive [1,2]-shifts of the cobalt atoms at

the μ_3-arene (i.e. 60° rotation of the arene above the Co_3 cluster as the elementary step, Scheme 8) can be proven directly for the clusters $[(CpCo)_3(\mu_3\text{-}C_6H_5R)]$ (see below).[86] In the one-dimensional ^1H and ^{13}C NMR spectra the hindered ligand movement causes the singlet for the three CpCo groups (which at room temperature is often already broadened) to split into three separate signals at low temperature. The slow rotation has interesting stereochemical consequences.[86,89]

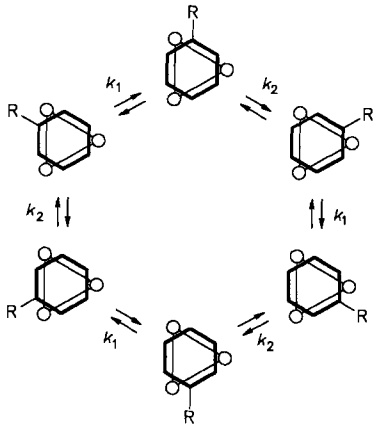

Scheme 8.

A cluster $[(CpCo)_3(\mu_3\text{-}\eta^2\text{:}\eta^2\text{:}\eta^2\text{-}C_6H_5R)]$ with a monosubstituted arene (e.g. **65** and **66** in Table 3), which when rigid is asymmetrical, is converted by a 60° rotation of the μ_3-arene ligand into its enantiomer. However, in **65a**, if the arene rotation is slow the methyl groups of the prochiral isopropyl substituent become diastereotopic. Thus on lowering the temperature, the ^1H NMR spectrum does not only show three CpCo resonances but also two methyl doublets. The same effect makes all methylene protons in **66b** nonequivalent at low temperature.

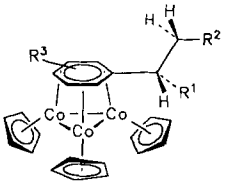

65–67

Table 3. Complexes of the type $[(CpCo)_3(\mu_3\text{-}\eta^2\text{:}\eta^2\text{:}\eta^2\text{-arene})]$ **65–67**.

Complex	R^1	R^2	R^3	Ref.
[(CpCo)$_3$(*iso*-propylbenzene)] **65a**	Me	H	H	[86]
[(CpCo)$_3$(*n*-propylbenzene)] **65b**	H	Me	H	[63]
[(CpCo)$_3$(1,1-diphenylethane)] **66a**	Ph	H	H	[86]
[(CpCo)$_3$(1,2-diphenylethane)] **66b**	H	Ph	H	[86]
[(CpCo)$_3$(*p*-diethylbenzene)] **67**	H	H	4-Et	[86]

In contrast, the arene rotation in **66a**, which has an asymmetrical C atom in α position to the μ_3-phenyl ring, converts the two chiral diastereomers **A** and **B** into each other (Fig. 7). At low temperature the equilibrium lies completely on one side: in solution at −70 °C only one diastereomer is observ-

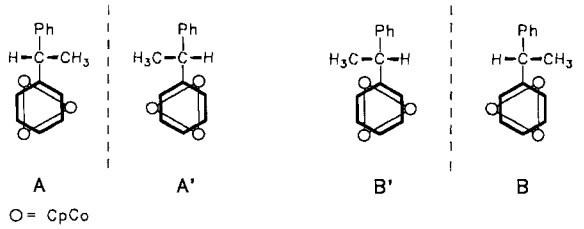

Fig. 7. Schematic representation of the diastereomeric pairs of enantiomers (**A**, **A'** and **B**, **B'**) of **66a**. In the crystal **A** and **A'** are observed.

able (three singlets in the region for Cp resonances in the ^1H (Fig. 8) and ^{13}C NMR spectra). Although not directly observable, the presence of the other diastereomer in the dynamic equilibrium becomes apparent in a characteristic way from temperature-dependent ^1H NMR spectra.[86,96] This can be particularly well observed from the signal for the methyl group ($\delta = 1.1$), which is sharp at high and low temperatures but is broadened at intermediate temperatures (Fig. 8). In the crystal also, only the two enantiomers of the

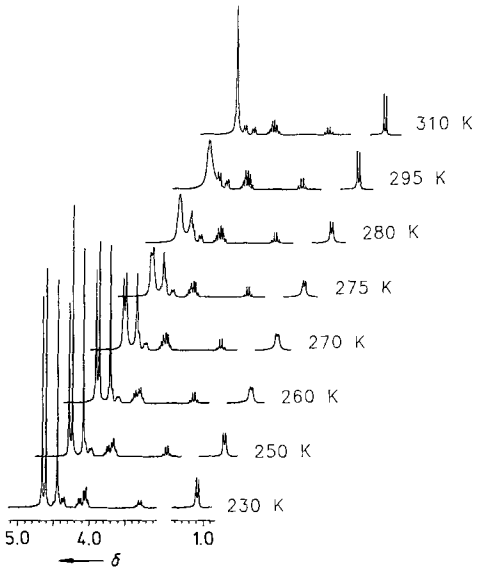

Fig. 8. Temperature-dependent ^1H NMR spectra of **66a** (200 MHz, in $[D_8]$toluene).

sterically more favorable diastereomer are observed.[92] A stereochemically similar situation exists for **51b**. However, in this case the two diastereomeric rotamers can be detected simultaneously at −90 °C in solution by NMR spectrocopy (two sets of three singlets each in the region for the Cp resonances, Fig. 9).[87]

A quantitative analysis of the temperature-dependent NMR spectra for the general case of a monosubstituted μ_3-arene ligand is difficult. In most cases only the Cp resonances can be analyzed. The mechanism of the arene rotation (60° rotation of μ_3-arene ligand and $(CpCo)_3$ cluster relative to one another) shown in Scheme 8 generates a complicated exchange matrix for the CpCo groups, since with each elementary step only two of the three chemical shifts are exchanged with one another (no simple cyclic permutation).[97] Furthermore, two different rotation barriers have to be con-

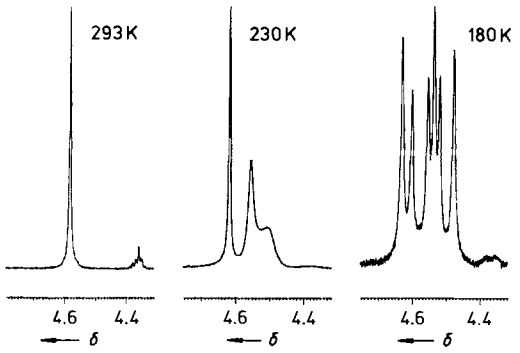

Fig. 9. Section of the temperature-dependent 200 MHz ^{1}H NMR spectrum of [(CpCo)$_3$(μ_3-(*m*-methyl)-β-methylstyrene)] **51b** (region of Cp signals). The spectrum at 180 K was folded with a Gaussian function. Signals at $\delta = 4.35$ stem from the protons on the μ_3-arene ring.

sidered a priori, depending on whether the substituent moves across a CpCo group (rate constant k_1) or between two such groups (k_2). Qualitatively it can easily be shown that the two activation barriers are indeed different. This is shown in Figure 10 with two ^{1}H EXSY NMR spectra of **47b** as illustration. With a short mixing time in the EXSY experiment[98] only the quicker exchange process is observed. In the 2D matrix, cross-signals occur between only two of the three Cp resonance signals (Fig. 10a). With longer mixing times the slower process also becomes apparent; now one of the Cp resonance signals is connected with *both* the others by cross-signals (Fig. 10b). This corresponds exactly with the mechanism of Scheme 8. Simulations of the exchange-broadened one-dimensional ^{1}H NMR spectra show the same result. Unfortunately neither method can be used to determine the activation barriers very precisely.

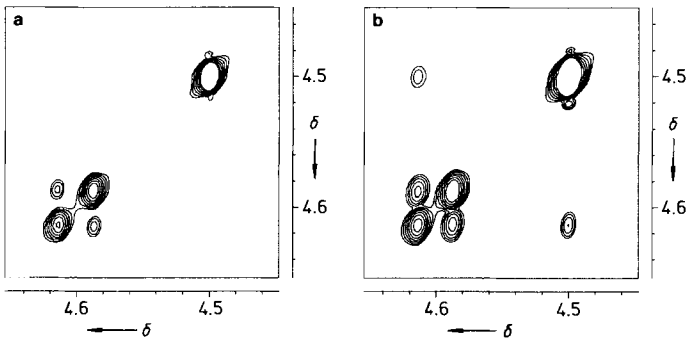

Fig. 10. Section of the 200 MHz ^{1}H EXSY NMR spectra of [(CpCo)$_3$(μ_3-β-methylstyrene)] **47b** at 230 K (region of the Cp resonance signals). Mixing times: 60 ms (a) and 150 ms (b); echo detection. In the phase sensitive 2D spectrum the diagonal and cross-signals have the same phase.

The temperature dependence of the methyl resonance signals in **65a** can be better analyzed (two exchanging doublets that are not coupled to each other in the ^{1}H NMR spectrum); however, it only gives the weighted mean of the two barriers ($\Delta G^{\neq}_{290K} = 57$ kJ mol^{-1}). Symmetrically *para*-disubstituted derivatives such as *p*-distyrylbenzene complex **55** or [(CpCo)$_3$(μ_3-*p*-diethylbenzene)] (**67**) offer better prospects. The latter is only accessible indirectly through the catalytic hydrogenation of the side chain in *p*-ethylstyrene complex **49**.[86] Complexes **55** and **67** have C_s symmetry and therefore only one rotation barrier. For both the ^{1}H resonance signal of the CpCo groups is split into two (ratio of intensities of 2:1) on lowering the temperature. Additionally, the methylene protons of the ethyl groups in **67** become diastereotopic, forming an exchanging spin system of the type $ABM_3 \rightleftarrows C_2M_3$. This now fulfils all the prerequisites for an iterative line shape analysis,[99] from which the values $\Delta H^{\neq} = 59 \pm 1$ kJ mol^{-1} and $\Delta S^{\neq} = 37 \pm 5$ J mol^{-1} K^{-1} can be obtained. From the coalescence of the Cp and μ-arene-CH signals, approximate values for $\Delta G^{\neq}_{235K} = 50$ kJ mol^{-1} and $\Delta G^{\neq}_{240K} = 49$ kJ mol^{-1} respectively, are obtained. These values are consistent with the free energies of activation calculated from $\Delta H^{\neq}$ and $\Delta S^{\neq}$. Taken together, all the data available up to now indicate that the energy barriers of the arene rotation ($\Delta G^{\neq}$) in clusters of the type [(CpCo)$_3$(μ_3-η-arene)], and the difference of the free energy (ΔG^0) of the diastereomeric conformers of **51b** and **66a** are due to steric hindrance by the substituents at the μ_3-arene rings and not by a localization of double and single bonds in the μ_3-arene rings.

Clusters of the type [(CpCo)$_3$(μ_3-arene)] are chemically more stable than the [(CO)$_3$Ru]$_3$ and [(CO)$_3$Os]$_3$ analogues.[63] The μ_3-arenes cannot be substituted by other arenes or two-electron ligands such as CO, PMe$_3$, and P(OMe)$_3$. Strong Lewis acids like AlCl$_3$ or BF$_3$, which could catalyze the arene exchange, lead to a decomposition of the substances. [(CpCo)$_3$(μ_3-stilbene)] (**53b**) catalyzes the cyclooligomerization of propargyl alcohol. The product mixture obtained after 5h at 114 °C consists of cyclotrimer and cyclotetramer in the approximate ratio 1:4.[100] Such a high proportion of the cyclotetramer is very unusual for cobalt catalysts (e.g. with [CpCo(C$_2$H$_4$)$_2$] (**23**) as catalyst under similar reaction conditions a typical product ratio of cyclotrimer:cyclotetramer $\approx$ 1:1 is obtained[100]).

The 1-alkenyl side chains are apparently deactivated by the bonding of the arene to the metal cluster. In contrast to the free ligands, they no longer react with diazomethane or diazoethylacetate, for instance. A bromination at the allyl position with *N*-bromosuccinimide is also no longer possible. However, as mentioned above, the hydrogenation of the 1-alkenyl groups can be accomplished at room temperature and atmospheric pressure on a Pd/charcoal catalyst. In this way derivatives with saturated side chains are accessible (see Table 3). This reaction convincingly shows that the 1-alkenyl side chain, although a prerequisite for the formation of the complexes, has little significance for the stability of an already formed [(CpCo)$_3$(μ_3-arene)] cluster.

[(CpCo)$_3$(μ_3-arene)] clusters with alkyl or phenylalkyl side chains are protonated at the metal framework by strong Brønstedt acids. According to a X-ray structural analysis of crystalline **68**-(CF$_3$COO), a μ_3-hydrido ligand caps the face of the Co$_3$ triangle which is not hindered by the arene.[86,92] This structure is retained in solution.

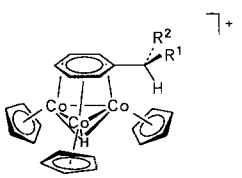

68, R^1 = CH$_3$, R^2 = Ph

If a C–C double bond is present in an α position to the μ_3-arene ring, a proton is added to the carbon atom in the β position on reaction with acid. The products **69** and **70**, which in the widest sense can be considered α-[$(CpCo)_3(\mu_3$-η-phenyl)]-substituted carbenium ions, are strongly stabilized by the interaction with the metal cluster. So far we have not

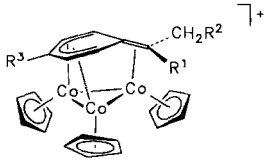

69a, $R^1 = CH_3$, $R^2 = R^3 = H$
69b, $R^1 = R^3 = H$, $R^2 = CH_3$
70, $R^1 = R^2 = H$, $R^3 = OCH_3$

been able to obtain these salts as single crystals. The temperature-independent ^1H and ^{13}C NMR spectra are consistent with a structure in which all the carbon atoms of the arene ring as well as the (formally positively charged) α-C atom of the side chain are bonded to the tricobalt cluster. Our proposed structure is similar to that of α-[(nonacarbonyltricobalt)carbynyl]-substituted carbenium ions **C**,[101,102] which show a similarly high stabilization.

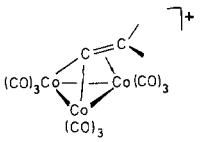

C

4. Outlook

Multinuclear complexes with arene bridges are no longer exotic! On the contrary, benzene and its derivatives have proven to be very flexible ligands that are capable of adapting to the needs of different metal-complex fragments. However, almost all of the μ-arene complexes reported in this review have been obtained fortuitously, often only as by-products. A systematic approach to the synthesis of such complexes has been attempted only for a very few cases. Consequently most of these complexes have not been investigated beyond their synthesis and characterization, so that almost nothing is known about the reactivity of the μ-arenes. This is even more amazing when one considers the significance of mononuclear arene–metal complexes in organic synthetic chemisty.[105]

The analogy between chemisorbates on metal surfaces and molecular cluster complexes, propagated in particular by E.L. Muetterties[60c], has in the recent past proven useful, especially for the understanding of chemisorbates,[106] but is still under discussion.[107] Cluster compounds with face-capping arenes are the simplest model compounds for adsorption states of benzene on metal surfaces. The interpretation of the data obtained by a multitude of sophisticated surface-analytical methods still encounters many difficulties. The knowledge about the structure, dynamics, and reactivity of the arene bridges obtained from the molecular (μ-arene)–metal cluster complexes should be invaluable for the interpretation of these data. For example, the structures of the molecular systems show that the local threefold symmetry of the cluster does not necessarily enforce a large Kekulé distortion on the μ_3-arene.

The theoretician finds himself confronted by challenging problems concerning arene-bridged multinuclear complexes. The geometrical distortion and thus probably also the electronic structure of the μ-arenes are very different in complexes which appear to be similar—a problem not yet theoretically addressed. The field is open for the synthetic chemist, spectroscopist, crystallographer, and theoretician. What is certain is that also in the future much will be heard about the arene complexes that are already considered classical.

I would like to thank my graduate students for their enthusiasm and commitment; their names appear in the literature citations. I am especially grateful to Dr. Hans Pritzkow for many X-ray structural analyses and his never-failing willingness to discuss the work. I also thank Prof. Dr. Walter Siebert for his continual support. Further thanks go to my colleagues Prof. Dr. Jörn Müller, Prof. Dr. Piera Sabatino, and Doz. Dr. Dirk Walther for informing me of their unpublished results. Our research has been financially supported by the Deutsche Forschungsgemeinschaft, the Fonds der Chemischen Industrie and the companies BASF AG and Degussa AG (donations of chemicals); I would like to thank these institutions for their help. Furthermore, I thank the Deutsche Forschungsgemeinschaft for a Heisenberg scholarship.

Received August 2, 1991 [A856 IE]
German version: *Angew. Chem.* **1992**, *104*, 253
Translated by Dr. N. A. Compton, Frankfurt am Main (FRG)

[1] A. Kekulé defined aromatic compounds as derivatives of benzene. (A. Kekulé, *Liebigs Ann. Chem.* **1866**, *137*, 129–196.) Later this term was used for similar (e.g. polycylic) hydrocarbons (see for example, W. Hückel, *Theoretische Grundlagen der organischen Chemie*, *1. Band*, 6. Aufl., Akademische Verlagsgesellschaft, Leipzig, **1949**, 2. Buch, Chapter 9.) Following IUPAC rule A-12.4, arene is the generic name for mono- and polycylic hydrocarbons. In this review, the term arene is used in Kekuléan sense, i.e. as benzenoid arene. See also: D. Lloyd, D. R. Marshall, *Angew. Chem.* **1972**, *84*, 447–451, *Angew. Chem. Int. Ed. Engl.* **1972**, *11*, 404.
[2] F. Hein, *Chem. Ber.* **1919**, *52*, 195–196; *ibid.* **1921**, *54*, 1905–1938.
[3] H. H. Zeiss, M. Tsutsui, *126th Meet. Am. Chem. Soc.* **1954**; *J. Am. Chem. Soc.* **1957**, *79*, 3062–3066; H. H. Zeiss, W. Herwig, *Justus Liebigs Ann. Chem.* **1957**, *606*, 209–215; W. Herwig, H. Zeiss, *J. Am. Chem. Soc.* **1957**, *79*, 6561, **1959**, *81*, 4798–4801.
[4] E. O. Fischer, W. Hafner, *Z. Naturforsch. B* **1955**, *10*, 665–668.
[5] a) E. O. Fischer, K. Öfele, *Chem. Ber.* **1957**, *90*, 2532–2535; *Z. Naturforsch. B.* **1958**, *13*, 458; b) G. Natta, R. Ercoli, F. Calderazzo, E. Santambrogio, *Chim. Ind. (Milan)* **1958**, *40*, 1003–1007. c) B. Nicholls, M. C. Whiting, *Proc. Chem. Soc.* **1958**, 152.
[6] More recent reviews: E. L. Muetterties, J. R. Bleeke, E. J. Wucherer, T. A. Albright, *Chem. Rev.* **1982**, *82*, 499–525; W. E. Silverthorn, *Adv. Organomet. Chem.* **1975**, *13*, 47–137; R. G. Gastinger, K. J. Klabunde, *Transition Met. Chem.* **1979**, *4*, 1–13; R. B. King in *The Organic Chemistry of Iron Vol. 2* (Eds.: E. A. Koerner von Gustorf, F.-W. Grevels, I. Fischler), Academic Press, New York, **1981**, p. 155ff.
[7] A. E. Hill, *J. Am. Chem. Soc.* **1921**, *43*, 254–268, 263–266; *ibid.* **1922**, *44*, 1163–1193.
[8] R. E. Rundle, J. H. Goring, *J. Am. Chem. Soc.* **1950**, *72*, 5337; H. G. Smith, R. E. Rundle, *ibid.* **1958**, *80*, 5075–5080.
[9] R. W. Turner, E. L. Amma, J. Am. Chem. Soc. **1966**, *88*, 320–344.
[10] a) I. F. Taylor, E. A. Hall, E. L. Amma, *J. Am. Chem. Soc.* **1969**, *91*, 5745–5749; b) E. L. Amma, E. A. Griffith, *J. Am. Chem. Soc.* **1971**, *93*, 3167–3172.
[11] D. F. R. Gilson, C. A. McDowell, *J. Chem. Phys.* **1963**, *39*, 1825–1826; *ibid.* **1964**, *40*, 2413.
[12] H. G. Smith, *J. Chem. Phys.* **1964**, *40*, 2412–2413.
[13] G. W. Hunt, T. C. Lee, E. L. Amma, *Inorg. Nucl. Chem. Lett.* **1974**, *10*, 909–913.

[14] a) L. J. Andrews, R. M. Keefer, *J. Am. Chem. Soc.* **1949**, *71*, 3644–3647; b) M. I. Foreman, J. Gorton, R. Foster, *Trans. Faraday Soc.* **1970**, *66*, 2120–2123.
[15] E. Schumacher, R. Taubenest, *Helv. Chim. Acta* **1964**, *47*, 1525–1529.
[16] H. Werner, A. Salzer, *Synth. React. Inorg. Metal-Org. Chem.* **1972**, *2*, 239–248.
[17] a) R. G. Solomon, J. K. Kochi, *J. Chem. Soc. Chem. Commun.* **1972**, 559–560; b) M. B. Dines, P. H. Bird, *ibid.* **1973**, 12.
[18] F. A. Cotton, X. Feng, P. A. Kibala, M. Matusz, *J. Am. Chem. Soc.* **1988**, *110*, 2807–2815.
[19] K. Jonas, V. Wiskamp, Y.-H. Tsay, C. Krüger, *J. Am. Chem. Soc.* **1983**, *105*, 5480–5481.
[20] K. Jonas, G. Koepe, L. Schieferstein, R. Mynott, C. Krüger, Y.-H. Tsay, *Angew. Chem.* **1983**, *95*, 637–638; *Angew. Chem. Int. Ed. Engl.* **1983**, *22*, 620–621; *Angew. Chem. Suppl.* **1983**, 920–928.
[21] K. Jonas, *J. Organomet. Chem.* **1990**, *400*, 165–184.
[22] C. Poumbga, C. Daniel, M. Bénard, *J. Am. Chem. Soc.* **1991**, *113*, 1090–1102.
[23] J. Müller, P. Escarpa Gaede, A. Guo, K. Qiao, unpublished; J. Müller (Technische Universität Berlin), personal communication.
[24] H. Omori, H. Suzuki, Y. Take, Y. Moro-oka, *Organometallics* **1989**, *8*, 2270–2272.
[25] G. Allegra, G. Tettamanti Casagrande, A. Immirzi, L. Porri, G. Vitulli, *J. Am. Chem. Soc.* **1970**, *92*, 289–293.
[26] G. Allegra, A. Immirzi, L. Porri, *J. Am. Chem. Soc.* **1965**, *87*, 1394–1395.
[27] G. Nardin, P. Delise, G. Allegra, *Gazz. Chim. Ital.* **1975**, *105*, 1047–1053.
[28] E. R. Mognaschi, A. Chierico, *J. Phys. Chem.* **1985**, *18*, 3815–3818.
[29] a) M. Sommovigo, M. Pasquali, P. Leoni, D. Braga, P. Sabatino, *Chem. Ber.* **1991**, *124*, 97–99. b). P. Sabatino (Università di Bologna), personal communication.
[30] C. Di Bugno, M. Pasquali, P. Leoni, P. Sabatino, D. Braga, *Inorg. Chem.* **1989**, *28*, 1390–1394.
[31] L. Zhu, N. M. Kostic, *Organometallics* **1988**, *7*, 665–669.
[32] P. Pertici, G. Vitulli, *Tetrahedron Lett.* **1979**, *21*, 1897–1900.
[33] G. A. Chukhadzhyan, Zh. I. Abramyan, G. M. Tonyan, N. A. Balyushina, *Arm. Khim. Zh.* **1975**, *28*, 348–349; G. A. Chukhadzhyan, Zh. I. Abramyan, G. M. Tonyan, L. Sagradyan, T. S. Elbakyan, *Zh. Org. Khim.* **1981**, *17*, 1831–1837.
[34] K. Jonas, *Pure Appl. Chem.* **1984**, *56*, 63–80; *Angew. Chem.* **1985**, *97*, 292–307, *Angew. Chem. Int. Ed. Engl.* **1985**, *24*, 295; *Pure Appl. Chem.* **1990**, *62*, 1169–1174.
[35] K. Jonas, W. Rüsseler, K. Angermund, C. Krüger, *Angew. Chem.* **1986**, *98*, 904–905; *Angew. Chem. Int. Ed. Engl.* **1986**, *25*, 927.
[36] A. W. Duff, K. Jonas, R. Goddard, H.-J. Kraus, C. Krüger, *J. Am. Chem. Soc.* **1983**, *105*, 5479–5480.
[37] K. Angermund, K. H. Claus, R. Goddard, C. Krüger, *Angew. Chem.* **1985**, *97*, 241–252; *Angew. Chem. Int. Ed. Engl.* **1985**, *24*, 241.
[38] J. W. Lauher, M. Elian, R. H. Summerville, R. Hoffmann, *J. Am. Chem. Soc.* **1976**, *98*, 3219–3224.
[39] P. T. Chesky, M. B. Hall, *J. Am. Chem. Soc.* **1984**, *106*, 5186–5188.
[40] E. D. Jemmis, A. C. Reddy, *Organometallics* **1988**, *7*, 1561–1564.
[41] a) F. W. S. Benfield, M. L. H. Green, J. S. Ogden, D. Young, *J. Chem. Soc. Chem. Commun.* **1973**, 866–867; b) R. Middleton, J. R. Hull, S. R. Simpson, C. H. Tomlinson, P. L. Timms, *J. Chem. Soc. Dalton Trans.* **1973**, 120–124.
[42] M. P. Andrews, H. X. Huber, S. M. Mattar, D. F. McIntosh, G. A. Ozin, *J. Am. Chem. Soc.* **1983**, *105*, 6170–6172.
[43] G. A. Ozin, M. P. Andrews in *Metal Clusters in Catalysis, Studies in Surface Science and Catalysis Vol. 29* (Eds.: B. C. Gates, L. Guczi, H. Knözinger), Elsevier, Amsterdam, **1986**, Chapter 7, and references cited therein.
[44] J. R. Gilbert, W. P. Leach, J. R. Miller, *J. Organomet. Chem.* **1973**, *56*, 295–301.
[45] R. L. Hettich, B. S. Freiser, *J. Am. Chem. Soc.* **1985**, *107*, 6222–6226.
[46] R. L. Whetten, D. M. Cox, D. J. Trevor, A. Kaldor, *Surf. Sci.* **1985**, *156*, 8.
[47] W. M. Lamanna, *J. Am. Chem. Soc.* **1986**, *108*, 2096–2097.
[48] W. M. Lamanna, W. B. Gleason, D. Britton, *Organometallics* **1987**, *6*, 1583–1584.
[49] W. Strohmeier, H. Mittnacht, *Z. Phys. Chem. (Munich)* **1961**, *29*, 339–346; W. Strohmeier, E. H. Starico, *ibid.* **1963**, *38*, 315–325; W. Strohmeier, H. Müller, *ibid.* **1964**, *40*, 85–95.
[50] E. L. Muetterties, J. R. Bleeke, A. C. Sievert, *J. Organomet. Chem.* **1979**, *178*, 197–216, and references cited therein.
[51] K. Cibura, Dissertation, Universität Bochum, **1985**.
[52] D. R. Neithamer, L. Párkányi, J. F. Mitchell, P. T. Wolczanski, *J. Am. Chem. Soc.* **1988**, *110*, 4421–4423.
[53] H. van der Heijden, A. G. Orpen, P. Pasman, *J. Chem. Soc. Chem. Commun.* **1985**, 1576–1578.
[54] W. D. Harman, H. Taube, *J. Am. Chem. Soc.* **1987**, *109*, 1883–1885.
[55] W. D. Harman, M. Gebhard, H. Taube, *Inorg. Chem.* **1990**, *29*, 567–569.
[56] W. D. Harman, H. Taube, *J. Am. Chem. Soc.* **1988**, *110*, 7555–7557.
[57] W. D. Harman, H. Taube, *J. Am. Chem. Soc.* **1988**, *110*, 7906–7907.
[58] F. G. A. Stone, J. Browning, C. S. Cundy, M. Green, *J. Chem. Soc. A* **1971**, 448–452.
[59] J. Browning, M. Green, J. L. Spencer, F. G. A. Stone, *J. Chem. Soc. Dalton Trans.* **1974**, 97–101.
[60] a) R. L. Burwell, J. B. Peri, *Annu. Rev. Phys. Chem.* **1964**, *15*, 131–154; b) P. Chini, *Inorg. Chim. Acta. Rev.* **1968**, *2*, 31–51; *J. Organomet. Chem.* **1968**, *200*, 37–61; c) E. L. Muetterties, *Science (Washington D.C.)* **1977**, *196*, 839–848; E. L. Muetterties, T. N. Rhodin, E. Band, C. F. Brucker, W. R. Pretzer, *Chem. Rev.*, **1979**, *79*, 91–137, and references cited therein.
[61] G. A. Somorjai, *J. Phys. Chem.* **1990**, *94*, 1013–1023, and references cited therein.
[62] Short reviews on the relevant work can be found for example in H.-P. Steinrück, W. Huber, T. Pache, D. Menzel, *Surf. Sci.* **1989**, *218*, 293–316; H.-P. Steinrück, P. Heimann, W. Huber, P. Jakob, T. Pache, D. Menzel, *J. Electron Spectrosc. Relat. Phenom.* **1990**, *52*, 91–102 and Ref. [63].
[63] H. Wadepohl, K. Büchner, M. Herrmann, H. Pritzkow, *Organometallics* **1991**, *10*, 861–871.
[64] M. Neumann, J. U. Mack, E. Bertel, F. P. Netzer, *Surf. Sci.* **1985**, *155*, 629–638; F. P. Netzer, G. Rosina, E. Bertel, H. Saalfeld, *ibid.* **1987**, *184*, L397–L403.
[65] F. P. Netzer, J. U. Mack, *J. Chem. Phys.* **1983**, *79*, 1017.
[66] F. P. Netzer, H. H. Graen, H. Kuhlenbeck, M. Neumann, *Chem. Phys. Lett.* **1987**, *133*, 49–53.
[67] G. Rosina, G. Rangelov, E. Bertel, H. Saalfeld, F. P. Netzer, *Chem. Phys. Lett.* **1987**, *140*, 200–204.
[68] G. A. Somorjai, *Pure Appl. Chem.* **1988**, *60*, 1499–1516, and references cited therein.
[69] J. Somers, M. E. Bridge, D. R. Lloyd, T. McCabe, *Surf. Sci.* **1987**, *181*, L167.
[70] R. F. Lin, G. S. Blackman, M. A. van Hove, G. A. Somorjai, *Acta Crystallogr. Sect. B* **1987**, *43*, 368–376.
[71] E. L. Muetterties, *Pure Appl. Chem.* **1982**, *54*, 83–96, and references cited therein.
[72] R. Hoffmann (*Rev. Mod. Physics* **1988**, *60*, 601–628) found that "In fact, a chemist who relaxes a little about the impressive surface probes will find an amusing phenomenological resemblance between current surface science studies and organic structure determinations by physical methods in the early days of the application of these methods, say the forties. Great stories, many of them true, are constructed about structures and reactions on the basis of a few evanescent bumps in an often hard-to-come-by spectrum.".
[73] M. A. van Hove, R. F. Lin, G. A. Somorjai, *J. Am. Chem. Soc.* **1986**, *108*, 2532–2537.
[74] E. Bertel, G. Rosina, F. P. Netzer, *Surf. Sci.* **1986**, *172*, L515.
[75] N. R. Avery, *J. Chem. Soc. Chem. Commun.* **1988**, 153–154.
[76] M. P. Gomez-Sal, B. F. G. Johnson, J. Lewis, P. R. Raithby, A. H. Wright, *J. Chem. Soc. Chem. Commun.* **1985**, 1682–1684.
[77] a) A. J. Deeming, M. Underhill, *J. Organomet. Chem.* **1972**, *42*, C60–C62; *J. Chem. Soc. Dalton Trans.* **1974**, 1415–1419; b) R. J. Goudsmit, B. F. G. Johnson, J. Lewis, P. R. Raithby, M. J. Rosales, *ibid.* **1983**, 2257–2261.
[78] E. G. Bryan, B. F. G. Johnson, J. W. Kelland, J. Lewis, M. McPartlin, *J. Chem. Soc. Chem. Commun.* **1976**, 254–256.
[79] a) B. F. G. Johnson, J. Lewis, M. Martinelli, A. H. Wright, D. Braga, F. Grepioni, *J. Chem. Soc. Chem. Commun.* **1990**, 364–366. b) D. Braga, F. Grepioni, B. F. G. Johnson, J. Lewis, C. E. Housecroft, M. Martinelli, *Organometallics* **1991**, *10*, 1260–1268.
[80] a) M. A. Gallop, B. F. G. Johnson, J. Lewis, P. R. Raithby, *J. Chem. Soc. Chem. Commun.* **1987**, 1809–1811; b) D. Braga, F. Grepioni, B. F. G. Johnson, J. Lewis, M. Martinelli, *J. Chem. Soc. Dalton Trans.* **1990**, 1847–1852.
[81] D. Braga, F. Grepioni, B. F. G. Johnson, J. Lewis, M. Martinelli, M. A. Gallop, *J. Chem. Soc. Chem. Commun.* **1990**, 53–55.
[82] M. A. Gallop, B. F. G. Johnson, J. Lewis, A. H. Wright, *J. Chem. Soc. Dalton Trans.* **1989**, 481–487.
[83] M. A. Gallop, B. F. G. Johnson, J. Lewis, A. McCamley, R. N. Perutz, *J. Chem. Soc. Chem. Commun.* **1988**, 1071–1073.
[84] H. Wadepohl, K. Büchner, H. Pritzkow, *Angew. Chem.* **1987**, *99*, 1294–1295; *Angew. Chem. Int. Ed. Engl.* **1987**, *26*, 1259.
[85] K. Jonas, C. Krüger, *Angew. Chem.* **1980**, *92*, 513–531; *Angew. Chem. Int. Ed. Engl.* **1980**, *19*, 520; K. Jonas, E. Deffense, D. Habermann, *ibid.* **1983**, *95*, 729 bzw. **1983**, *22*, 716; *Angew. Chem. Suppl.* **1983**, 1005–1016.
[86] H. Wadepohl, M. Herrmann, unpublished; M. Herrmann, Dissertation, Universität Heidelberg, **1991**.
[87] H. Wadepohl, K. Büchner, unpublished; K. Büchner, Dissertation, Universität Heidelberg, **1989**.
[88] H. Wadepohl, K. Büchner, H. Pritzkow, *Organometallics* **1989**, *8*, 2745–2748.
[89] H. Wadepohl, K. Büchner, M. Herrmann, H. Pritzkow, unpublished.
[90] H. Wadepohl, F.-J. Paffen, unpublished.
[91] R. Victor, R. Ben-Shoshan, S. Sarel, *J. Chem. Soc. Chem. Commun.* **1970**, 1680–1681; *J. Org. Chem.* **1972**, *37*, 1930–1937.
[92] H. Wadepohl, M. Herrmann, H. Pritzkow, unpublished.

[93] H. Wadepohl, L. Zhu, *J. Organomet. Chem.* **1989**, *376*, 115–121.
[94] H. Wadepohl, K. Büchner, H. Pritzkow, unpublished.
[95] a) B. Rees, P. Coppens, *Acta Crystallogr. Sect. B* **1973**, *29*, 2516–2528; b) T. A. Albright, P. Hofmann, R. Hoffmann, *J. Am. Chem. Soc.* **1977**, *99*, 7546–7557; c) R. A. Kok, M. B. Hall, *J. Am. Chem. Soc.* **1985**, *107*, 2599–2604; d) K. P. Angermund, Dissertation, Universität Wuppertal, **1986**, Y. Wang, K. Angermund, R. Goddard, C. Krüger, *J. Am. Chem. Soc.* **1987**, *109*, 587–589.
[96] For the problem of the line shape of an exchanging system with very different populations see: F. A. L. Anet, V. J. Basus, *J. Magn. Reson.* **1978**, *32*, 339–343.
[97] For the six different (diastereo-, enantiotopic) positions of the CpCo groups of both enantiomers in Scheme 8, there are only three different spin-Hamilton operators because of mirror symmetry. The ratio (determined by the chemical exchange) of two sites with identical spin-Hamilton operators to any third site need not necessarily be the same. See also: M. H. Levitt, K. Beshah, *J. Magn. Reson.* **1987**, *75*, 222–228.
[98] J. Jeener, B. H. Meier, P. Bachmann, R. R. Ernst, *J. Chem. Phys.* **1979**, *71*, 4546–4553.
[99] For the line shape analysis, NMR spectra with differential exchange broadening are particularly suitable. This occurs for example in the presence of "excessive" spins (here the nuclei M of the ABM_3 spin system): G. Binsch, H. Kessler, *Angew. Chem.* **1980**, *92*, 445–463; *Angew. Chem. Int. Ed. Engl.* **1980**, *19*, 411.
[100] D. Walther (Universität Jena), personal communication.
[101] a) D. Seyferth, G. H. Williams, C. S. Eschbach, M. O. Nestle, J. S. Merola, J. E. Hallgren, *J. Am. Chem. Soc.* **1979**, *101*, 4867–4878; b) D. Seyferth, C. S. Eschbach, G. H. Williams, P. L. K. Hung, *J. Organomet. Chem.* **1977**, *134*, 67–83.
[102] No X-ray structural analysis of an α-[$\{(CO)_3Co\}_3(\mu_3$-η-phenyl)] substituted carbenium ion exists. The NMR data in solution are in accordance with the nonrigid μ_3-vinylidene structure **C**.
[103] R. T. Edidin, J. R. Norton, K. Mislow, *Organometallics* **1982**, *1*, 561–562.
[104] B. E. Schilling, R. Hoffmann, *J. Am. Chem. Soc.* **1978**, *100*, 6274; *ibid.* **1979**, *101*, 3456–3467.
[105] J. Falbe, *Methoden Org. Chem. (Houben-Weyl) 4th ed.* **1986**, Vol. E18 I, II.
[106] Newer summary: G. Ertl in *Metal Clusters in Catalysis, Studies in Surface Science and Catalysis Vol. 29* (Eds.: B. C. Gates, L. Guczi, H. Knözinger), Elsevier, Amsterdam, **1986**, Chapter 11.
[107] See for example M. Moskovits, *Acc. Chem. Res.* **1979**, *12*, 229–236.

High Resolution Spectroscopy below the Doppler Width

By Hans Jürgen Neusser* and Edward William Schlag

Microscopic insights into elementary molecular processes are only feasible through the observation of unique quantum states and the study of their couplings and time-dependent behavior. In the case of larger chemically relevant molecules, the corresponding transitions lie so close that they mostly overlap and lead to band structures. For example, electronic band spectra of large molecules cannot be resolved into single lines even by high resolution UV-spectrometers. The reason for this is the Doppler broadening, arising from the random velocity of the molecules in the gas phase. In this article, we want to demonstrate that modern laser spectroscopic methods make it possible to overcome this "Doppler barrier" and to resolve the line structure in band spectra. The selective excitation of unique quantum states yields precise information on the mechanisms responsible for energy redistribution in molecules. Energy redistribution processes represent a crucial first step preceding chemical reactions, which they influence decisively. Very high resolution spectroscopy elucidates the influence of molecular rotation on the energy redistribution. Through Coriolis forces in rotating molecules, vibrations can couple, causing a flow of energy from the selectively excited vibrations to the many other vibrational degrees of freedom. Weak interactions, namely van der Waals interactions and hydrogen bonding, determine the structure of large molecules (biomolecules) and supermolecular systems. Weak intermolecular interactions, given their selectively resolved quantum states, can be analyzed and understood at the microscopic level. "Doppler-free spectroscopy" with its resulting line spectra furnishes information on the structure, including bond lengths, of van der Waals complexes. With this information, Doppler-free spectroscopy provides the model parameters indispensable for the quantitative description of complex systems.

1. Introduction

The general goal of chemical spectroscopy is the investigation of the positions of the quantum states of microscopic systems, such as atoms or molecules. On the one hand, the exact energetic position of these states when collated with predictions of theoretical models pins down the electronic arrangement, the bond strengths, and the structure of the nuclear frame in molecules. On the other hand, the line widths of the transitions yield information on the lifetimes of the excited states and thus about dynamical processes in the molecule. In this way spectroscopy has, up to now provided the key information for an understanding of the physical and chemical properties and the reactivity of elements and compounds.

In ultraviolet spectroscopy the absorbed photons excite electrons of the molecule. Typically, this electronic excitation proceeds according to the Franck-Condon principle, exciting, in addition, vibrations of the molecule. Furthermore, before the excitation, the molecules are in various rotational and vibrational states, as given by the Boltzmann distribution at the appropriate gas temperature. This rotational state distribution is preserved or changed insignificantly in the excitation. Unambiguous spectroscopic information can be expected only if unique quantum states can be excited, i.e. states for which all of the quantum numbers are fixed. This means that along with the electronic and the vibrational quantum number, the rotational quantum number must also be distinctly defined.

[*] Prof. Dr. H. J. Neusser, Prof. Dr. E. W. Schlag
Institut für Physikalische und Theoretische Chemie
der Technischen Universität München
Lichtenbergstrasse 4, D-W-8046 Garching (FRG)

In the case of large polyatomic molecules, single rotational lines in electronic or vibrational-electronic transitions (vibronic transitions) are so densely packed that they can no longer be resolved by conventional spectroscopic methods. This explains the broad band spectra with no line structure typically reported for large molecules. The culprit is the Doppler broadening of the transition, caused by the random velocity of the molecules in the gas phase. A typical value for the Doppler width of a molecule of the rough size of benzene (C_6H_6) is in the case of the $S_1 \leftarrow S_0$ transition at about 40000 cm^{-1}, 1.7 GHz or 0.05 cm^{-1} at room temperature.

Before discussing the possible methods of overcoming the Doppler barrier in order to achieve line structure in spectra, we enter briefly into the chemically relevant problems whose clarifications demand the separation of single rotational transitions in electronic or vibronic spectra. These are namely inquiries of the precise structure of molecules and extremely unstable weakly-bound van der Waals complexes (treated in the second half of this article). Using Doppler-free spectroscopy, quantities such as van der Waals bond lengths and potential parameters can be experimentally obtained which lead to a quantitative understanding of the weak intermolecular interactions inherent in complex systems.

Essential for an understanding of elementary chemical reactions are insights into the reaction dynamics, or the study of the course of reactions at the microscopic level. The study of reaction mechanisms is not only essential for an understanding of chemical processes, but could have a tremendous practical use if successfully applied to block, accelerate, or initiate selective chemical reactions.

For an understanding of the reactions of polyatomic molecules at the microscopic level, statistical theories, in particular the Rice-Ramsperger-Kassel-Marcus (RRKM) theory[1]

or Quasi-Equilibriums theory,[2] are at present very popular and useful. For many chemical reactions occurring along bound potential curves, these theories are able to explain the observed reaction course and its rate constant. The crucial assumption of these theoretical models is that the total energy of the molecule before the reaction is statistically distributed over all of the degrees of freedom of the molecule. In many cases a good agreement with experimental results is achieved with this hypothesis. Consequently, over the last decade and at present, the focus of studies in reaction dynamics is: How does a statistical distribution of energy in a molecule come about? Is the distribution complete or limited to certain vibrational states?

The process responsible for the redistribution of energy is the intramolecular vibrational redistribution (IVR) occurring within a molecule.[3] Precise information on the IVR process can only be obtained if distinct quantum states of the molecule are prepared and the intramolecular vibrational redistribution observed.

The states of polyatomic molecules lie so dense that state-selective excitation demands Doppler-free studies. Initiating such studies, the dye laser[4] with its very sharp frequency width, can be finely tuned over the molecular transitions. This in turn has led in the last decade to the development of various experimental methods such as saturation spectroscopy, optical double-resonance spectroscopy and two-photon absorption spectroscopy, which in principle serve to reduce or to eliminate the Doppler width of an optical transition.[5] These methods therefore hurdle a natural barrier to the spectral resolution. The use of collimated atomic or molecular beams should be included here, as this technique also reduces the Doppler width, in this case through geometric selection of molecules of the same velocity. However, application of the molecular beam technique for high resolution spectroscopy first became possible through the use of extremely narrow-band tunable lasers; examples of high resolution UV-spectroscopy on van der Waals complexes is presented in the second half of this article.

The various methods mentioned above were mainly developed for studying fine structure in atomic spectra. Extension to large molecules is not possible for every one of these methods. In a series of studies, our group has established that two-photon spectroscopy represents a practical method of obtaining Doppler-free high resolution spectra of large molecules.[6, 7]

2. Doppler-free Two-Photon Spectroscopy of Molecules and Intramolecular Energy Redistribution

2.1. Concepts of Doppler-free Two-Photon Absorption

At the microscopic level, energy is transferred to atoms and molecules in the smallest energy units, called photons. As early as 1930, Maria Göppert-Mayer postulated that not only one photon could be transferred, but rather that two photons could also participate in one elementary absorption step.[8] Not until 1960, through the discovery of the laser with its very high light intensity, could two-photon absorption be experimentally proved.[9] In two-photon absorption, absorption of two photons excites the molecule to a state whose energy is given by the summed photon energy. In this manner, it is possible for example to excite UV absorption bands of benzene with visible blue light. Moreover, as the selection rules for one- and two-photon absorption differ,[10] spectroscopic information on previously unknown vibrational[11, 12] and electronic states[13] is collected.[14] These selection rules complement each other in a way analogous to those of infrared and Raman spectroscopy, both of which

Edward W. Schlag was born in 1932 in Los Angeles. He studied chemistry at the Occidental College, Los Angeles. He gained his doctorate at the University of Washington in Seattle in 1958 under the supervision of Professor B. S. Rabinovitch for work on the unimolecular isomerization of cyclopropanes. Since 1971 Edward Schlag has held a professorial chair for Physical Chemistry at the Technical University of Munich. Several honors have been conferred on him for his diverse research activities, which have been reported on in more than 250 original papers and books: Since 1978 Schlag has been a full member of the Bavarian Academy of Sciences, and since 1984 a fellow of the American Physical Society. In 1988 he was made an honorary Doctor of the Hebrew University in Jerusalem. His main interests currently focus on the investigation of the structure and dynamics of molecules and molecular complexes using high-resolution spectroscopic methods.

Hans Jürgen Neusser was born in 1943 in Troppau (Czechoslovakia). He studied physics at the Technical University (TU) in Munich, where he was awarded his doctorate in 1971 for work with Professor W. Kaiser. Subsequently, he worked for seven years with W. E. Schlag and gained his habilitation in Physical Chemistry for work on the two-photon spectroscopy of molecules in the gas phase. In 1979 Neusser was appointed Professor of Physical Chemistry at the TU Munich. In 1983 he was awarded the Chemistry Prize of the Academy of Sciences, Göttingen, for his work in the field of Two-Photon Spectroscopy, Multiphoton Ionization and Doppler-free High-Resolution Molecular Spectroscopy. At present his main interests focus on the laser spectroscopy of molecules and molecular complexes, intramolecular dynamics, and the kinetics of ionic decomposition.

supplement spectroscopic information on the electronic ground state.

If both absorbed photons stem from one light bundle or from two different light bundles traveling in the same direction, then the spectral resolution of the two-photon absorption is limited, as that in one-photon absorption, by the Doppler broadening. The Doppler width of a specific transition arises from the individual molecular absorption lines from molecules with differing velocities; the shifts of their absorption frequencies, depending on their speed and velocity vector, vary in accordance with the first order Doppler effect. In the above absorption case, the resultant shift is the sum of that from light frequencies ν_1 and ν_2. The averaging over the differing Doppler shifts yields an inhomogenously-broadened Gaussian-shaped absorption line, as illustrated in Figure 1 (top).

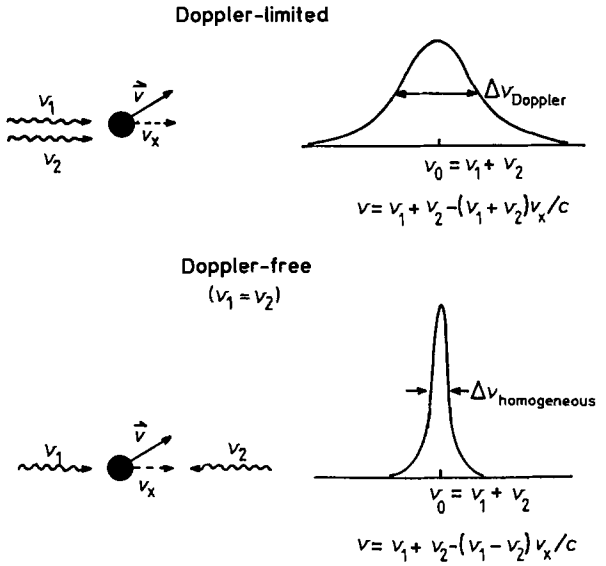

Fig. 1. Schematic representation of Doppler-limited (above) and Doppler-free (below) two-photon absorption processes. If both photons approach the absorbing molecule from the same direction, their Doppler shifts are added, resulting in a broadened transition with a Gaussian line shape. If, however, the two photons approach the absorbing molecule from opposite directions, the Doppler shifts are subtracted and thus compensate each other; this eliminates the Doppler broadening and reveals the sharp homogeneous line shape of the transition (after [14]).

In 1970, Chebotayev et al.[15] suggested the application of two-photon absorption of two antiparallel light bundles of an extreme monochromatic laser to avoid Doppler broadening. The principle of this method is illustrated schematically in Figure 1 (bottom). Note that now the Doppler shifts of the two light frequencies are subtracted. Whereas the light wave approaching from the left experiences a red shift, the frequency of the light wave approaching from the right is blue-shifted. If the two antiparallel light bundles have the same frequency, the two shifts compensate each other exactly, eliminating the Doppler shift for each and every velocity component, so that the transition is free from any Doppler broadening. Naturally, the transition frequency can then be determined with considerably higher accuracy, and transitions which were perhaps concealed under the Doppler broadening can be resolved. Furthermore, it is now possible to observe a transition's homogeneous line width. As we will see later, the homogeneous line width is of special significance in studies of intramolecular relaxation processes, as it supplies very important additional information on the dynamic behavior of the molecule. To summarize, Doppler-free two-photon absorption should enable, even for large molecules with very densely packed absorption lines, the excitation of unique rotational states in vibronic quantum states (unique rovibronic states), and consequently the precise monitoring of relaxation processes.

2.2. The Experimental Technique of Doppler-free Two-Photon Absorption

Doppler-free two-photon absorption was first realized in 1974 on atoms.[16] Attempts at extending this technique to large polyatomic molecules faced nontrivial experimental difficulties. Firstly, in molecules the oscillator strength of the two-photon transition is divided among many vibronic transitions. Secondly, about 10^3–10^4 rotational states are populated, as if having to work with an effective low molecular number density. And, in addition to these difficulties, two-photon absorption is inherently a weak higher order effect, whose observation requires high light intensities.[14]

A possible experimental setup to achieve sufficient signal strengths to observe the weak two-photon absorption is illustrated in Figure 2.[17] A continuous-wave single-mode

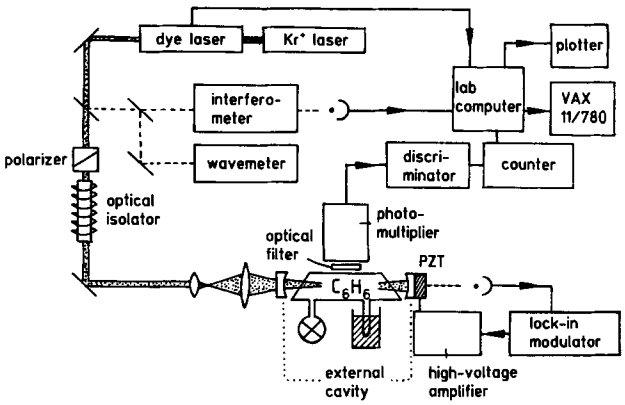

Fig. 2. Schematic diagram of the experimental setup for measurement of Doppler-free molecular spectra with high resolution. Elimination of the Doppler broadening proceeds by absorption of two photons, traveling in opposite directions, from the narrow-band standing light waves in the external resonator. PZT is a piezoelectric transducer.

ring dye laser, pumped by a Kr^+ laser, supplies very narrrow-band light ($\Delta\nu = 1$ MHz $= 3 \times 10^{-5}$ cm^{-1}). A "wavemeter" measures the absolute laser frequency, while an interferometer records very precisely the relative frequency. The molecular gas under study is contained in a fluorescence cell at the low pressure of less than 1 Torr so as to avoid molecular interactions through collisions. This cell is placed in an external resonator, so that the Doppler-free two-photon absorption occurs through a standing light wave composed of two antiparallel light bundles. If now a molecule absorbs one photon from each of the oppositely-traveling light bundles, the Doppler shift of the transition frequency for each mole-

cule, regardless of its velocity, will be compensated, and a Doppler-free spectrum at the sum of the two photons' energies will be observed. The use of the external resonator is crucial, as this can immensely amplify the light intensity, which in turn increases the two-photon signal intensity with its quadratic dependence on the light intensity by several orders of magnitude.

The resulting two-photon absorption is detected through the emitted UV fluorescence with the help of a photomultiplier tube. Scanning the laser light frequency requires synchronous fine tuning of the external resonator using a piezoelectric transducer (PZT); this ensures that the resonance conditions in the external cavity for the particular wavelength in question are constantly fulfilled. A data processing system facilitates the signal storage and the plotting of the Doppler-free two-photon spectrum on the desired scale.

2.3. Doppler-free Two-Photon Spectra of Benzene

To illustrate the potential of Doppler-free spectroscopy, Figure 3 displays a part of the $S_1 \leftarrow S_0$ spectrum of benzene at various spectral resolutions. The topmost trace shows the

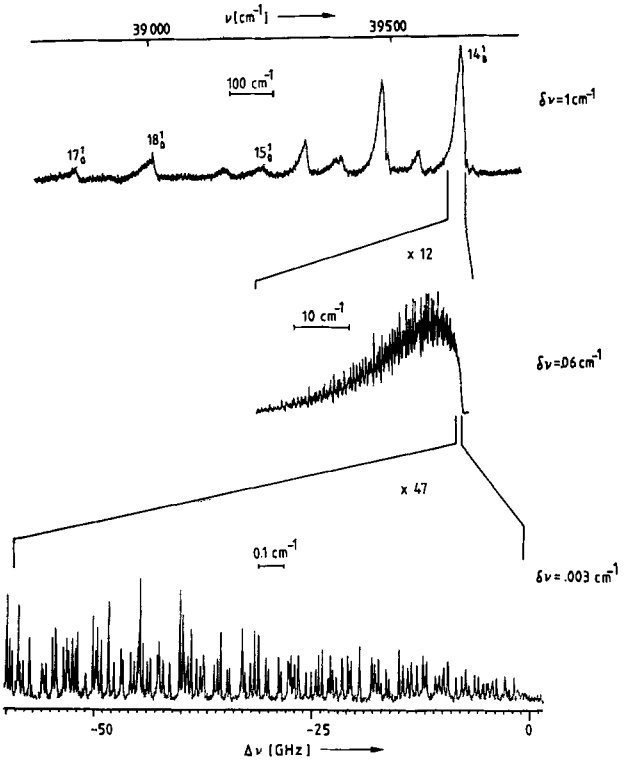

Fig. 3. The two-photon spectrum of the electronic $S_1 \leftarrow S_0$ transition in benzene at various spectral resolutions (after [14]). Top: Vibrational structure of the $S_1 \leftarrow S_0$ transition. Center: Q-branch of the strongest (14^1_0) band at Doppler-limited resolution. Bottom: After elimination of the Doppler broadening, single rotational lines appear which were hiding under the Doppler width. $\delta\nu$ gives the resolution.

two-photon spectrum at a spectral resolution of 1 cm^{-1}. (The structure of the one-photon spectrum of benzene is in principle similar, although due to the differing selection rules, different vibrational bands are observed.) The middle spectrum shows the central portion of the strongest vibrational band (14^1_0)[*] at a resolution limited by the Doppler broadening. This represents the highest resolution achievable through conventional one-photon spectroscopy, even with the help of a high-resolution spectrometer. The observed structure represents the overlapping of many rotational lines. The individual rotational lines become visible only after the introduction of a technique of elimination of the Doppler broadening and an increase in the resolution by a factor of 50. The lowermost spectrum, recorded using Doppler-free two-photon spectroscopy, displays single rotational lines. The frequency scale is now given in GHz instead of cm^{-1}, since the interferometer which measures the exact relative frequency is calibrated in GHz (1 $cm^{-1} \approx 30$ GHz). This spectrum represents the blue edge and thus only a small fraction of the complete vibrational band. Evidently thousands of rotational lines, hidden under the Doppler broadened vibrational band, first manifest themselves after elimination of the Doppler broadening.

The resulting rotational line spectrum can be unambiguously analyzed to yield extremely precise rotational and centrifugal distortion constants of the molecule in its electronic ground state (S_0) and in its electronic excited state (S_1). The accuracy is a factor of 100 larger than in conventional high-resolution (Doppler-limited) UV spectroscopy. A typical result for the rotational constants of the S_1 state with accompanying excitement of one quantum of C-C ring vibration ν_{14} of b_{2u} symmetry is[18] $B'_{14} = 0.181284$ and $C'_{14} = 0.090711$ cm^{-1}, accurate to 10^{-6} cm^{-1}. The rotational constants B and C are given by the rotational energy level formula for an oblate symmetric top molecule [Eq. (a)].[19]

$$E_{Rot} = BJ(J+1) - (B - C)K^2 \qquad (a)$$

J is here the quantum number of the total rotational angular momentum. K is also a good quantum number for a symmetric top molecule and describes the projection of the total angular momentum on the spinning top axis.

The accurately determined rotational constants and measurements on isotopomers (e.g. C_6D_6) allow exact determination of the bond lengths in the molecule and the changes in bond length upon electronic excitation. For benzene in its electronic ground state, an average C–C bond length of 1.397 Å and an average C–H bond length of 1.079 Å are determined. In the S_1 excited electronic state, the C–C bond length increases to 1.432 Å, whereas the C–H bond length decreases slightly to 1.075 Å. As anticipated, promotion of a π electron to an antibonding π^* state is accompanied by a decrease in binding energy, evoking an expansion of the benzene ring.

The accurately determined rotational and centrifugal distortion constants suffice to reproduce the measured rotational line structure with respect to the line positions and heights. A good agreement between the reproduced and measured line positions implies in this case that the excited rovibronic states are not coupled to other vibrational states, so that no energy transfer to other vibrational modes can take place.

[*] The superscript denotes the number of excited quanta of a particular vibration (here No. 14) in the final state of the transition (here S_1 state), while the subscript denotes the number of quanta of this vibration in the initial state (here S_0 state).

2.4. The Model of Intramolecular Energy Redistribution: a Primer

Before evidence of intramolecular energy redistribution in a Doppler-free spectrum is discussed, an introduction to the theoretical model of this process should be presented.

In the description of molecules, one assumes that electronic, vibrational, and rotational states can be considered as separated in the Born-Oppenheimer approximation. Theory designates such states as zeroth-order states. In reality, zeroth-order states are not isolated from each other, but are often coupled to other zeroth-order states of the molecule. This coupling can occur, e.g., between states of the same or differing multiplicities, resulting in internal conversion (IC) or intersystem crossing (ISC), two well-known processes of radiationless decay. In the case of intramolecular energy redistribution preceding a chemical reaction, the pertinent coupling is between different vibrational states of the same electronic potential (intramolecular vibrational redistribution, IVR).

A more precise formulation of intramolecular coupling is possible with the help of the theory of nonradiative processes.[20] The two limiting cases depicted in Figures 4 and 5 are the most intuitively clear. Figure 4 shows the situation

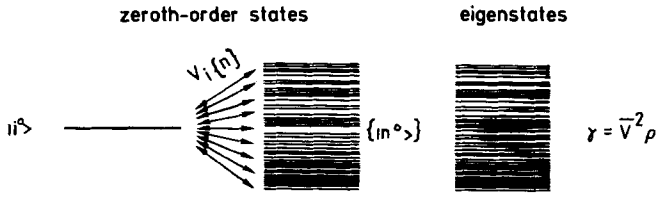

Fig. 4. Schematic representation of a nonradiative process at the statistical limit. The coupling of a molecular state $|i^0\rangle$ to a quasicontinuum of densely-packed states $\{|n^0\rangle\}$ leads to a broadened Lorentzian-shaped line.

present at the "statistical limit." Here a large number of states $|n^0\rangle$ lie within the width of the coupling matrix element $V_{i\{n\}}$ of a zeroth-order state $|i^0\rangle$. The manifold of states $\{|n^0\rangle\}$ form a quasicontinuum to which the zeroth-order state $|i^0\rangle$ is coupled. The case of coupling to a continuum is of course well-known for ionization and dissociation processes, but can also arise as a limiting case for the process of intramolecular vibrational redistribution in large molecules, due to the strongly increasing density ρ of vibrational states with increasing excess energy in the electronic state. In the simplest case, only state $|i^0\rangle$ carries oscillator strength and therefore can be optically populated or is, in spectroscopy jargon, "light", whereas the manifold of states $\{|n^0\rangle\}$ is "dark". If we now carry out an experiment with a low coherence width (such as with continuous-wave narrow-band laser light), we can expect for this coupling limit, a Lorentzian-broadened line shape of width $\gamma = \bar{V}^2\,\rho$, arising from the projection of the fragmented oscillator strengths or "light"

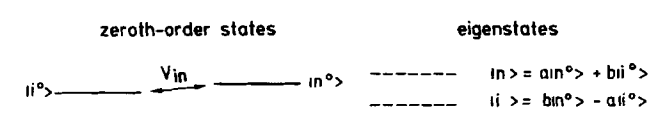

Fig. 5. Schematic representation of the coupling of two zeroth-order states, $|i^0\rangle$ and $|n^0\rangle$, yielding a mixing and repulsion of the eigenstates $|i\rangle$ and $|n\rangle$.

fractions on the eigenstates. On the other hand, using a large coherence width, such as short-time pulsed laser excitation, it is feasible to excite the "light" zeroth-order state $|i^0\rangle$, which due to the high state density evolves exponentially and irreversibly with time. Under these conditions, we are dealing with what we call "dynamics".

The situation is entirely different when the density of states is so low that the only coupling is between the two zeroth-order states $|i^0\rangle$ and $|n^0\rangle$ (Fig. 5). This is the natural case for small molecules or for very low excess energies in the electronic states of large molecules. As is well known in spectroscopy, such a coupling leads to repulsion of the states and mixing of the wave functions of the two states. The repulsion of the zeroth-order states leads to an "avoided crossing" of the energy level curves of the eigenstates, which is observable in the spectrum (static perturbation).

This short introduction to the theoretical description of nonradiative processes demonstrates that the intramolecular dynamics can reduce to the case of static coupling well known in spectroscopy at the low density of states typical for low excess energies. Unresolved questions and thus topics of current research are the following points:

- When does the statistical limit begin? What is the nature of the transitional region from static perturbations to dynamics at the statistical limit?
- Which coupling mechanisms are responsible for IVR? Are only the anharmonic couplings between the vibrational states of importance, or does the molecule's rotation in the form of rotational-vibrational coupling also play a role?
- Is the coupling selective? Does the redistribution occur only within a particular group of states?

With the example benzene, we are able to study a molecule at increasing total excitation energy and so to analyze diverse regions of the spectrum exhibiting strongly differing densities of vibrational states: as will be demonstrated below, the benzene molecule with its 30 vibrational degrees of freedom is especially suitable. Both limiting cases described above can be reached if, on the one hand, one excites a low excess energy up to 2000 cm^{-1}, and on the other, the excess energy within the optically-accessible region of the S_1 state is increased to about 4000 cm^{-1}; additionally, the excitation of unique states can be guaranteed by the Doppler-free two-photon spectroscopy. Concrete studies of the 14_0^1 vibrational band and the $14_0^1 1_0^1$ and $14_0^1 1_0^2$ progressions of this band at higher excess energies were carried out. These vibrational bands correspond to totally symmetric two-photon transitions originating in the ground state,[21] with one quantum each of the ν_{14} (b_{2u}) vibration with 1570 cm^{-1} of energy excited in the S_1 state. The progressions arise from addition of quanta of the totally symmetric C-C stretching vibration ν_1 (a_{1g}) amounting to excess energies of 2492 ($14^1 1^1$) and 3412 cm^{-1} ($14^1 1^2$). With regards to Figures 4 and 5, the final states of these three transitions correspond to "light" zeroth-order states in the S_1 state. The density of zeroth-order states increases from 1.2 (14^1) to 17 ($14^1 1^1$) to 165 ($14^1 1^2$) per cm^{-1}. These background states are not, however, directly visible in the spectrum, as they carry negligible oscillator strength for the two-photon transition. Nevertheless, through their interaction with the 14^1, $14^1 1^1$ and $14^1 1^2$ excited states, they have a characteristic influence on the spectrum as described below. Around 3000 cm^{-1}, the electronic

relaxation behavior of the molecule changes, as concluded by early measurements from the abrupt drop in the fluorescence quantum yield.[22] The cause of this behavior was tentatively attributed to a fast nonradiative relaxation channel ("Channel Three") whose origin was at the time unknown.

Using several selected examples, we shall explain in the following section the spectral effects of a strongly increasing density of background states with increasing excess energy and how these observations fit into the theory of intramolecular vibrational redistribution. With such information, a clarification of the mechanism of "Channel Three" is possible.

2.5. Information on the Mechanism of Intramolecular Energy Redistribution

A careful examination of the spectrum of Figure 3 (bottom) at higher rotational energies reveals irregular, seemingly unsystematic deviations between the measured and predicted (using the experimentally determined rotational constants) rotational structure, which cannot be consistently clarified by a new set of rotational or centrifugal distortion constants.[18, 23] This is a signature of perturbations in the spectrum, denoting interaction with a "dark" background state.

Figure 6 demonstrates such isolated perturbations in two sections of the spectrum. Below are two calculated sections of the spectrum of the 14_0^1 band: above, for collation, are the corresponding measured spectral sections. A collation of the calculated and measured spectra for each section yields good agreement for the majority of rotational lines. Nevertheless, there are lines (marked by an arrow) in the experimental

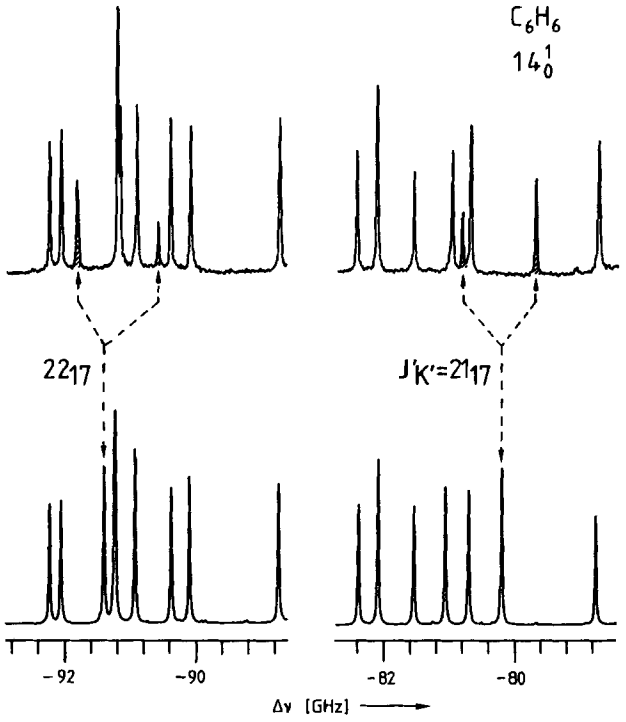

Fig. 6. Comparison of a section of the experimental (above) and calculated (below) spectrum of the 14_0^1 vibrational band; low excess energy in the S_1 electronic state of benzene. The lines tagged in the theoretical spectrum are absent in the experimental spectrum: instead, two nearly symmetrically shifted lines appear, analogous to the coupling case described in Figure 5 (after [23]).

spectrum with no direct match in the calculated spectrum and vice versa. Instead two smaller lines appear in the experimental spectrum which are nearly symmetrically shifted about the calculated line position. We are obviously witnessing here the coupling case described by Figure 5, namely the coupling of two states, leading to a repulsion of the two resulting eigenstates and to a mixing of the two coupled zeroth-order states. This coupling is selective since an energy resonance between a "light" and a "dark" state is rare with the low density of states of 1.2 states/cm^{-1} at the excess energy of 1570 cm^{-1}. The mixing of states results in two observable eigenstates (rather than the one anticipated "light" state) which share the oscillator strength of the one "light" state. These eigenstates are direct proof of the coupling of two normal vibrational states, which finally leads to an energy redistribution in the molecule.

A closer analysis of such perturbations in the spectrum indicates a value of the coupling matrix element of the order of a few 100 MHz. Moreover, a dependence of the coupling matrix element on the rotational quantum numbers J and K is found. This result can in no way be clarified through an anharmonic interaction of the coupled vibrations, rather it must follow that Coriolis coupling plays a crucial role. Coriolis forces appear in rotating molecules and can cause the coupling of vibrational states through the rotation of the molecule.

This result, fundamental to the understanding of intramolecular energy redistribution, was obtained for the spectral region of low excess energy, but can just as well be confirmed at high excess energies. The region of high excess energy is particularly interesting since the reactive region of the potential of an electronic state is in general first reached at high energies. Figure 7 displays results from the high resolution spectroscopy of the $14_0^1 1_0^2$ vibrational band at an excess energy of 3412 cm^{-1}. Here the line shapes (under extremely high resolution) of the three rotational lines $J_K = 2_0$, 6_0, and 14_0 of the $14_0^1 1_0^2$ vibrational band are presented.[24] For clarification, we emphasize that this spectral structure lies well below the Doppler width; the Doppler width of the transition in Figure 7 is namely 1.6 GHz or four times larger than the complete frequency range displayed in Figure 7. It is obvious here that the measured line width increases strongly with J, namely from 12.7 to 53.2 MHz as J increases from 2 to 14. In addition, the measured line shape corresponds with high accuracy to a Lorentzian line. (The solid lines represent Lorentzian lines fitted to the data points.) In contrast to the results at low excess energies, here the line widths rather than the positions depend strongly on the molecule's rotation. This rotational dependence cannot be attributed to an electronic relaxation process but rather must arise from coupling within S_1. The Lorentzian shape of the lines indicates moreover an irreversible vibrational relaxation at the statistical limit as given in Figure 4. A quantitative analysis of these results[24] establishes that even at these high excess energies, or even in the "Channel Three" region, Coriolis coupling produces an interaction of vibrational states within S_1 and decisively influences the IVR process. the rotationally-dependent line broadening directly demonstrates that Coriolis coupling to particular "dark" vibrational states represents the primary process of "Channel Three". These results, with respect to the intramolecular en-

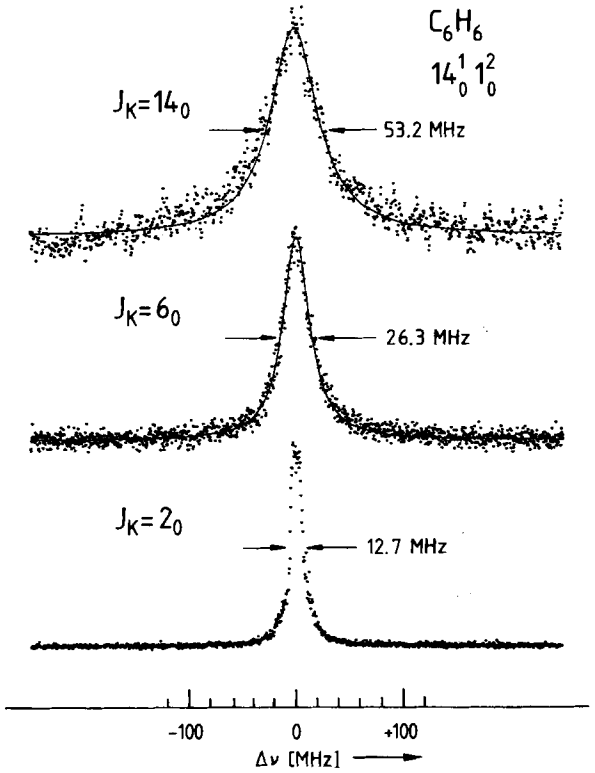

Fig. 7. Three rotational lines from the $14^1_0 1^2_0$ vibrational band; high excess energy in the S_1 electronic state of benzene. The Lorentzian line shapes and the strong increase in line width with increasing rotational quantum number J indicate that the rotation of the molecule plays a crucial role in the intramolecular vibrational relaxation via Coriolis coupling (after [24]).

ergy redistribution and the coupling mechanism, should in principle be transferable to the electronic ground state, since the S_1 and S_0 states behave similarly with respect to couplings and density of states.

Using selected examples from the spectrum of benzene, we have shown in this section that Doppler-free spectroscopy enables the excitation of uniquely defined quantum states even for large molecules with densely-lying transitions. Line splittings and homogeneous line widths present below the Doppler width have proven that rotation plays a decisive role in the energy redistribution in molecules. Couplings between individual normal vibrations of a molecule are not only generated through anharmonicities, but also through Coriolis forces in a rotating molecule. Selection rules apply to this coupling which determine the nature and symmetry of the coupled "dark" state. In such a way, we have gained an understanding of microscopic physical processes fundamental to energy redistribution. In conclusion, the basic mechanics of the energy redistribution process in a chemically relevant molecule has been presented for the first time.

3. Doppler-free Ultraviolet Spectroscopy of Weakly Bound van der Waals Complexes

3.1. Introduction

Interest in the spectroscopy of weakly-bound complexes has grown immensely in the last ten years. Such complexes or clusters result from clustering of molecules or atoms, made possible by long-range, but weak electrostatic forces, such as dipole-dipole interaction or induced dipole-dipole interaction.[25] With weak binding energies of the order of a few kJ/mol, these complexes are generally unstable at room temperature. The increasing number of cluster studies can be attributed to the convenient method of producing isolated gas phase atomic and molecular clusters in cooled supersonic beams.[26] The general goal of these studies is the quantitative microscopic understanding of van der Waals bonding, intrinsic to solvation processes and the structure and properties of the liquid phase and thus critically influencing chemical processes in the liquid phase. This goal in turn necessitates investigation of the exact structure of the complex, its binding energy, the shape of the van der Waals potential, and its dynamic behavior, i.e. the examination of its energy redistribution and its dissociation.

For complexes involving large organic molecules, the discussion of the previous section on polyatomics molecules applies to an even larger extent: the desired information can first be obtained when the spectral resolution is high enough to resolve individual rotational lines within the Doppler width. Particularly instructive are studies on complexes involving spectroscopically well-studied molecules. It is therefore natural to produce complexes containing the benzene molecule. Moreover, with the distinct planar ring structure of benzene, one expects a complexation behavior typical for the large class of aromatic molecules, thus acquiring important basic information for the description of solvation processes at the microscopic level. In the simplest case, noble gas atoms or small molecules are complexed with benzene. Here we can expect relatively minor changes in the well-known spectrum of benzene as the complexation entails no new chemical bonds, thus minimally influencing the molecular electronic structure.

This section presents results of the Doppler-free spectroscopy of complexes of benzene with noble gas atoms or small molecules such as N_2. As in the case of benzene itself, Doppler-free spectroscopy provides a resolution of the rotational structure below the Doppler width, enabling precise statements to be made on the structures and dynamic behavior of these clusters.

3.2. Experimental Techniques for the Preparation and Spectroscopy of van der Waals Complexes

Due to their small binding energies, isolated van der Waals complexes are not stable at room temperature. Such complexes are thus frequently prepared in cooled supersonic molecular beams.[26] Hereby a gas at a high pressure of a few atmospheres is expanded into a vacuum through a small orifice.[27] During the expansion process, the thermal energy of the gas particles is converted into translational expansion energy, resulting in a gas beam with a highly directed velocity and a low temperature of translational, rotational and vibrational degrees of freedom. In the cooling process, condensation of the gas can occur, leading to formation of van der Waals complexes of various sizes.

Figure 8 shows the experimental setup for the high resolution spectroscopy of van der Waals complexes. The core of the setup is the cooled molecular beam. Benzene at its natu-

rally-occurring vapor pressure of about 60 mTorr is mixed with a noble gas (e.g. Ar) at the high pressure of about 5 atm and then expanded through a small orifice ca. 0.3 mm in diameter into the first vacuum chamber. The gas throughput is limited by the short pulsed opening of a valve, which proceeds synchronously with the arrival of the laser light pulses. Due to the cooling upon expansion, various homo- and heteroclusters of benzene and Ar are formed. A conical-shaped skimmer peels away the outer shell of the molecular beam, enabling the expansion of the central part into a second vacuum chamber with a lower background pressure where the interaction with the light occurs. The skimmer contributes substantially to the realization of a Doppler-free spectrum, as its small opening selects exactly the molecules that have the smallest velocity components perpendicular to the direction of propagation of the molecular beam. Thereby the Doppler broadening amounting to ca. 0.05 cm^{-1} in a bulk gas is reduced to 0.001 cm^{-1}. This suffices for the resolution of rotational lines in the UV spectrum, so that the method of Doppler-free two-photon spectroscopy becomes superfluous here and, moreover, would not lead to a better resolution due to the limiting frequency width (ca. 0.0025 cm^{-1}) of the exciting laser light.

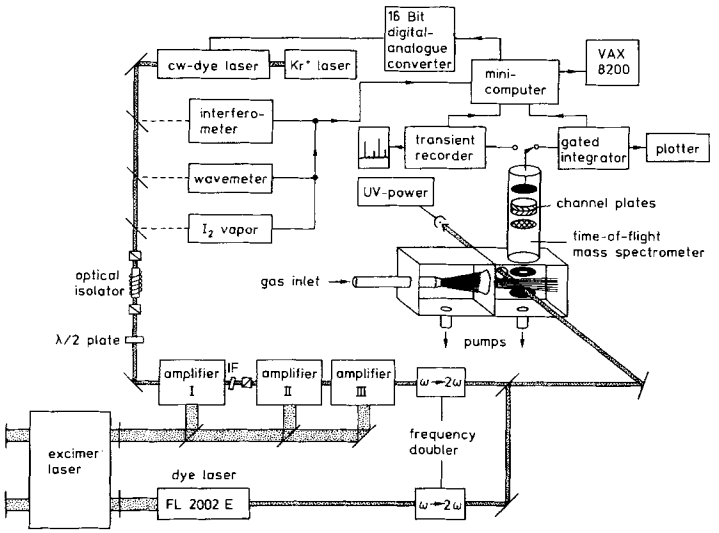

Fig. 8. Schematic diagram of the experimental setup for obtaining high resolution Doppler-free UV spectra of van der Waals complexes (after [31]). Van der Waals complexes of benzene and Ar are produced by expanding a gaseous mixture of benzene and Ar at high pressure through an orifice into vacuum. After a skimmer selects the central portion of the molecular beam, reducing the Doppler broadening, the complexes are excited to the S_1 state by a pulsed, narrow-band laser light and finally ionized by a second pulsed laser. The nascent ions are mass-analyzed in a time-of-flight mass spectrometer. To obtain spectra of the particular complex, free from obscuring overlaps with spectra of other species, only the current from ions of a selected mass is observed and integrated.

In the present experiments, the narrow-band light of the single-mode ring dye laser already described in Section 2.2 is pulsed-amplified to a high peak power in a three-stage excimer-laser-pumped amplifier setup. The generated visible blue-green light pulses have for their pulse length of 10 ns the best possible frequency sharpness of 80 MHz. In this case, the pulse length and the frequency width are linked to each other by a Fourier transform. The amplification and the use of pulsed laser light with its high peak intensities enable

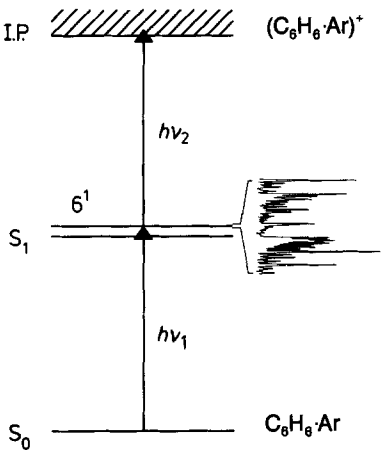

Fig. 9. Energy level scheme for resonance-enhanced two-photon ionization of molecules or van der Waals complexes. The efficiency of the ionization process is extremely enhanced when the energy of the first photon is resonant with a rovibronic transition in the complex (resonance-enhancement). As the frequency ν_1 of the narrow-band laser light is continuously scanned, the signal (ion current) is modulated due to the spectrum of the intermediate state. In this manner, Doppler-free rotationally-resolved spectra of mass-selected van der Waals complexes can be measured. I.P. = ionization potential.

frequency-doubling of the blue-green light into the ultraviolet spectral region, which in turn allows excitation of the $S_1 \leftarrow S_0$ transitions in the benzene-containing van der Waals complex through the absorption of one photon of energy $h\nu_1$ as depicted in the energy scheme of Figure 9. The subsequent absorption of a further UV photon ($h\nu_2$) stemming from a relatively broad-band dye laser, simultaneously pumped by the excimer laser, brings the excited (to S_1 state) complexes into the ionization continuum. The total excitation process corresponds to a two-photon ionization which is enhanced by the resonant state at the energy of the first absorbed narrow-band photon $h\nu_1$: each time the energy of the narrow-band photon agrees with a rovibronic transition of the cluster, the probability of a two-photon ionization is drastically enhanced. If the frequency of the narrow-band light $h\nu_1$ is tuned while monitoring the ion current, this will be modulated according to the spectrum of the intermediate state and consequently reflects this spectrum. The principal advantage of resonant two-photon ionization is that the created ions can be registered separately according to their mass in a mass spectrometer. This property of resonance-enhanced two-photon ionization was recognized at an early date[28] and is quite essential to the spectroscopy of van der Waals complexes. This was first demonstrated in several experiments with relatively low resolution just sufficient to resolve the vibrational structure in the spectra,[29] and is also essential for the high-resolution spectroscopy of the van der Waals complexes described here. Namely, a mixture of complexes of different composition and size whose spectra often overlap is produced in a cooled supersonic beam, as mentioned above. The mass-selective recording of the spectra facilitates the measurement of the spectrum of a selected complex in the mixture without interference by the presence of complexes of a different mass. In the experiment the mass separation proceeds in a simple time-of-flight mass spectrometer in which all cluster ions are accelerated to the same kinetic energy and subsequently separated in time in a field-free flight tube due to their mass-dependent flight times. Channel plates at the

end of the flight tube serve as the ion detector, delivering an ion current each time an ion bundle of the chosen mass arrives. The remaining units of the experimental setup facilitate the monitoring of the exact frequency of the exciting laser light and the recording and processing of the ion signal.

3.3. Structure and van der Waals Bond Lengths of Benzene–Noble Gas Dimers

Using the experimental method described in the previous section, the rotational lines of vibronic transitions in benzene–noble gas dimers were successfully resolved. In this section, we will show that analysis of the high-resolution spectrum allows the determination of the structure and van der Waals bond length to a high precision. The vibrational structure of the transition in benzene is only minimally perturbed by the weakly-bound Ar atom. Accordingly, the 6_0^1 band of the benzene–Ar complex is shifted by only 21 cm^{-1} to longer wavelength relative to the corresponding band in pure benzene.[30] This red shift denotes that the complex is more strongly bound in the S_1 state than in its electronic ground state. Whereas the vibrational structure of the $S_1 \leftarrow S_0$ transition changes negligibly through complexation, the rotational structures of the 6_0^1 band of benzene and the benzene–Ar complex, which were resolved by Doppler-free spectroscopy, no longer show any similarities. This can be traced back to the fact that two inertial moments of the system are altered by the addition of a noble gas atom. Figure 10 unequivocally demonstrates the high sensitivity of the rotational line positions to changes in the mass and structure. The high-resolution spectrum of the 6_0^1 band of the benzene–Ar complex is here contrasted with the corresponding band of benzene.[31] The spectral analysis proves that the complex, despite its completely altered moments of inertia, is to high accuracy, like benzene itself, a symmetric top. Moreover a temperature distribution of the rotational degrees of freedom of ca. 1.5 K can be derived and the rotational constants can be determined (by a procedure similiar to that described in Section 2.3) to the hitherto unattainable high accuracy of 10^{-5} cm^{-1}.

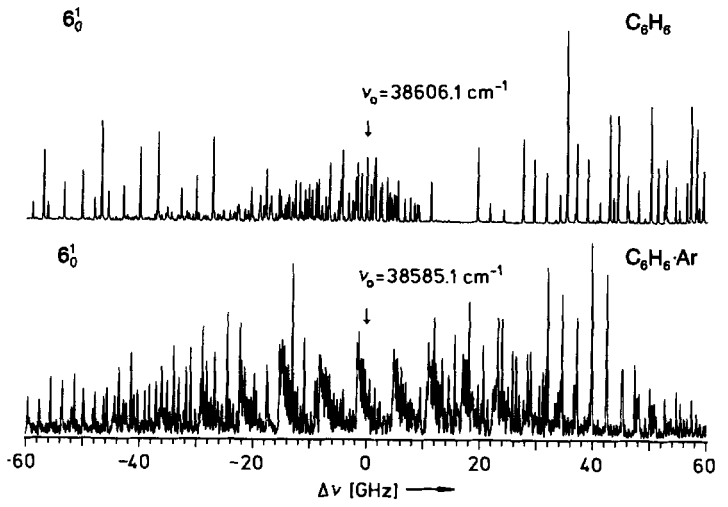

Fig. 10. Measured rotational structure of the 6_0^1 vibronic bands in the UV spectrum of benzene (above) and the benzene–Ar complex (below). The arrangement of the rotational lines differs completely, and indeed allows a precise determination of the structure of the complex by means of its inertial moments [31].

This spectral information is transposable into structural information. From the fact that the observed spectrum is that of a symmetric top, it follows that the sixfold rotational axis of the benzene is preserved even after complexation; consequently the Ar atom must sit on this axis (see Fig. 11).

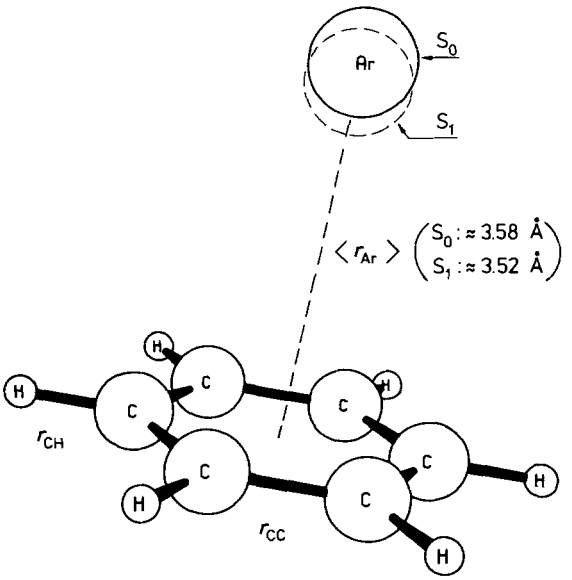

Fig. 11. The average structure of the benzene–Ar complex resulting from the high-resolution spectrum displayed in Figure 10. The Ar atom sits on the sixfold axis of benzene at a distance of 3.58 Å from the benzene ring. This distance decreases to 3.52 Å when the benzene is excited to the S_1 state (see text) [31].

The average van der Waals distance (Ar from the benzene plane) follows from the rotational constants. It is 3.58 Å in the ground state and *decreases* by 60 mÅ upon electronic excitation to the S_1 state. This behavior, in contrast to normal chemical bonds which typically expand upon electronic excitation, is thereby characteristic for van der Waals bonding. Since benzene and obviously the Ar atom as well have no permanent dipole moment, the induced dipole moments and hence the polarizabilities of each unit constitute the attractive van der Waals forces. The electron cloud expansion, in particular that of the π-orbital of benzene after an electronic excitation into the S_1 ($\pi\pi^*$) state, increases the polarizability and thus the attractive forces. The resulting decrease in the van der Waals bond distance is in addition supported by the expansion of the benzene ring accompanying electronic excitation (see Section 2.3); owing to the stronger attractive forces, the Ar atom can approach the expanded benzene ring more closely before the repulsion through overlap of the electron clouds dominates.

Similar results have been found for other benzene–noble gas complexes[32]: the van der Waals bond distance in the electronic ground state for the Ne atom complexed with benzene is 3.46 Å and increases gradually from Ar (3.58 Å) to Kr (3.68 Å) to Xe (3.81 Å). This moderate increase in the van der Waals bond distance is caused by the increase in atomic radius with increasing mass number along the row of noble gases. This effect, responsible for the repulsive part of the potential, is partially compensated by the strong increase in polarizability and hence attractive interaction from Ne to

Xe. Experimental values of comparable accuracy on the benzene–He complex have not yet been obtained, as the complexation process is so inefficient that, for example, no detectable concentration of complexes is observed in the present experiment. Values for the van der Waals bond distance of benzene–He are at present only known from experiments with lower spectral resolution,[33] and, due to their lower accuracy, cannot be instructively compared with the data presented in this work.

3.4. The Structure of a Larger Benzene–Noble Gas Cluster

After the exact position of the first clustered noble gas atom is known, a natural question concerns the subsequent complexation behavior, i.e. at which positions do further noble gas atoms attach. With the help of the technique described in Section 3.2 it is also possible to mass-selectively measure the spectra of such larger complexes, despite their lower concentrations and hence reduced signal strengths. In addition, however, the moments of inertia become larger and consequently the rotational lines in the spectrum become denser, making their resolution more difficult. Furthermore, it is not definite that further noble gas atoms are strongly enough bound to exclude isomerization processes, i.e. fast migration of the Ar atom about the benzene ring, at the vibrational temperature achieved in the cooled supersonic beam.

The first actual experiments yielded a rotationally resolved spectrum at mass 158 a.m.u., i.e. for the C_6H_6–Ar_2 complex.[34] Analysis of this spectrum yields a structure in which the Ar atoms are located on the sixfold axis, one on each side of the benzene ring (see Fig.12). From the precise experimental rotational constants, a bond distance of 3.58 Å is derived, exactly that in the benzene–Ar complex (with one Ar atom). This implies that the benzene ring completely screens any possible van der Waals interactions between the two Ar atoms. Such a behavior is typical for complexation processes in planar aromatic molecules.

At this point we must ask if the structure in Figure 12 is the only existing structure or do other stable structures of the benzene–Ar_2 complex also exist. Recent experiments with lower resolution[35] point to the stability of at least one additional structural isomer in which both Ar atoms lie on the same side of the benzene ring. Only the rotationally resolved Doppler-free spectrum can provide an unambiguous clarification of this problem. Such experiments will be possible in the near future.

3.5. Benzene–Molecule Complexes

The two previous sections were concerned with complexes formed by the absorption of noble gas atoms with isotropic polarizabilities to the benzene molecule. The next step is the absorption of simple diatomic molecules with anisotropic polarizabilites to the benzene surface. The benzene–N_2 complex has been studied by Doppler-free spectroscopy.[36]. The rotationally resolved spectrum yields the structure shown in Figure 13, in which the N_2 molecule is adsorbed parallel to the benzene surface. Besides the transitions which correspond to a symmetric rotor structure, there appear lines which can only be accounted for in terms of the internal rotation of the N_2 molecule about the C_6 axis of benzene. The distance of the center of mass of the N_2 molecule from the benzene plane is 3.50 Å and decreases by 45 mÅ upon electronic excitation of the benzene to the S_1 state. Despite the spectroscopic complexity presented by the internal rotation of the N_2 molecule, this phenomenon is nevertheless of particular interest for future studies. Namely, this internal rotation serves as a probe of the anisotropy and wavelike

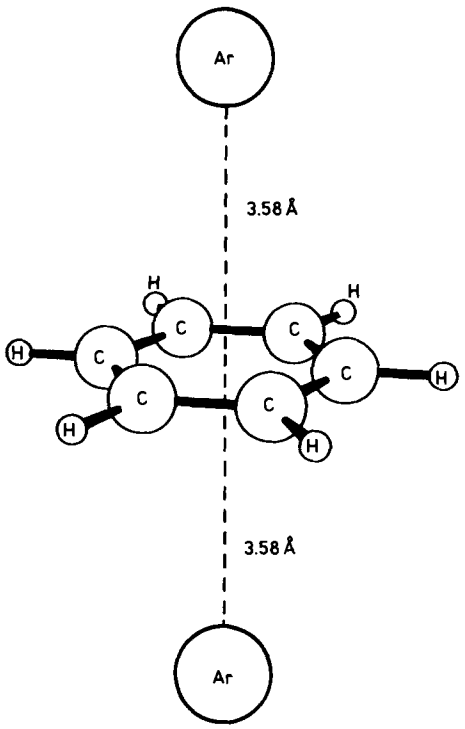

Fig. 12. The experimentally determined structure of the benzene–Ar_2 complex. The Ar atoms sit 3.58 Å from the benzene plane; a distance identical with that found for benzene–Ar (see Fig. 11). This signifies that the benzene ring effectively screens the long-range van der Waals interactions between the two Ar atoms.

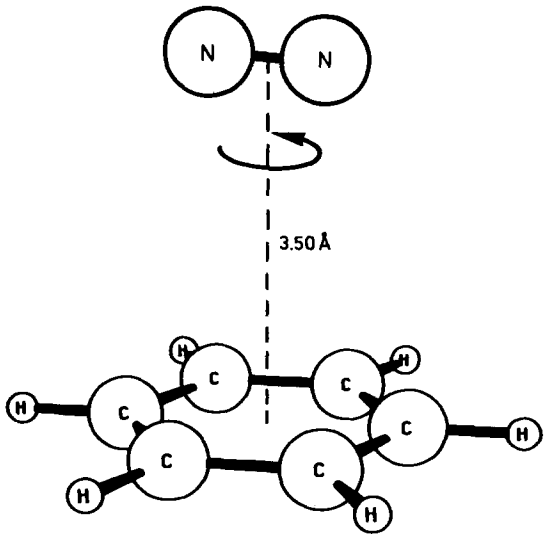

Fig. 13. The experimentally determined structure of the benzene–N_2 complex. Lying in the plane parallel to the benzene ring at a distance of 3.50 Å, the nitrogen molecule internally rotates about the sixfold rotational axis of the benzene.

curvature of the van der Waals binding potential with respect to rotation about the sixfold axis, which is caused by the periodic change in electron density along the benzene ring.

4. Summary and Outlook

Through the rapid development of new methods in laser spectroscopy it is possible, even for large molecular systems, to observe spectroscopic fine structures which are hidden by Doppler broadening in conventional high resolution spectroscopy. Elimination of the Doppler broadening allows the spectroscopic study of such systems with a precision previously possible only for atoms or small molecules; thus, access is provided to the domain of high resolution spectroscopy within the Doppler width. In this manner, more and more chemically relevant issues which are typical for large systems can be addressed.

Intramolecular energy redistribution, as the primary process preceding chemical reactions, is of fundamental importance in reaction kinetics. With a detailed understanding of this process, the influence or even control of chemical reactions should be possible. For this reason it is understandable that there has been substantial activity in the last two decades in the field of intramolecular vibrational redistribution. Whereas a general theoretical understanding of intramolecular vibrational redistribution through the theory of radiationless processes is available, precise experimental results to serve as critical tests of the theoretical models are seemingly scarce. In this article, using a test molecule we have proven the power of high resolution spectroscopy in this respect. Resolution of the band structure of the benzene spectrum into many individual rotational lines enables monitoring of the development of vibrational redistribution from the situation typical for small molecules to that for large molecules with their high level densities. Analysis of these initial results furnishes the surprising new finding that not only anharmonic coupling must be considered as the coupling mechanism, but rather that rotational-vibrational interaction in the form of Coriolis coupling also plays an essential role. The results thus obtained also permit a quantitative comparison with theoretical models and give a deeper insight into the coupling mechanisms.

The second part of this article demonstrated that Doppler-free spectroscopy furnishes detailed spectroscopic information on the large field of weakly-bound van der Waals complexes. The rotational line spectrum of selected complexes in the mixture of many clusters produced in the cooled molecular beam can be measured by the combination of Doppler-free excitation with mass-selective two-photon ionization. Initial experiments have yielded the structures and precise van der Waals bond distances for benzene–noble gas dimers and trimers and complexes of benzene with small molecules. These results demonstrate the precision and unambiguity of the statements regarding structure made possible by Doppler-free spectroscopy.

Doppler-free spectroscopy of van der Waals complexes is a very young field of research. For this reason Doppler-free spectra currently exist for only a few prototype systems. These few examples nevertheless outline the full scope of applications of this new spectroscopic method. Studies of larger and differently bound complexes will lead in the near future to a deeper understanding (at the microscopic level) of intermolecular bonds, such as the hydrogen bond, and of complexation and solvation processes integral to chemical and biological processes in the liquid phase.

The authors would like to thank the Deutsche Forschungsgemeinschaft and the Fonds der Chemischen Industrie for financial support of this research. We thank Drs. Riedle, Schubert, Sieber and Weber for invaluable collaboration with the experiments and interpretation of the results. We also wish to thank Dr. Alice M. Smith for the English translation of this article.

Received: December 3, 1991 [A 857 IE]
German version: *Angew. Chem.* **1992**, *104*, 269

[1] D. W. Noid, M. L. Koszykowski, R. A. Marcus, *Annu. Rev. Phys. Chem.* **1981**, *32*, 162.
[2] H. M. Rosenstock, M. B. Wallenstein, A. L. Wahrhaftig, H. Eyring, *Proc. Natl. Acad. Sci. U.S.A.* **1952**, *38*, 667.
[3] For a review see: C. S. Parmenter, *Faraday Discuss. Chem. Soc.* **1983**, *75*, 7.
[4] P. P. Sorokin, J. R. Lankard, *IBM J. Res. Dev.* **1966**, *10*, 162; F. P. Schäfer, W. Schmidt, J. Volze, *Appl. Phys. Lett.* **1966**, *9*, 306.
[5] For a review see: W. Demtröder, *Laser Spectroscopy*, Corrected Third Printing, Springer Series in Chemical Physics, Vol. 5, Springer, Berlin, 1988; W. Demtröder, Laser Spektroskopie, 2nd Edit. Springer, Berlin 1991.
[6] E. Riedle, H. J. Neusser, E. W. Schlag, *J. Chem. Phys.* **1981**, *75*, 4231.
[7] H. J. Neusser, E. Riedle, *Comments At. Mol. Phys.* **1987**, *19*, 331.
[8] M. Göppert-Mayer, *Ann. Phys.* **1931**, *9*, 273.
[9] W. Kaiser, C. G. B. Garrett, *Phys. Rev. Lett.* **1961**, *7*, 220.
[10] W. M. McClain, *J. Chem. Phys.* **1971**, *55*, 2789.
[11] R. M. Hochstrasser, J. E. Wessel, H. N. Sung, *J. Chem. Phys.* **1974**, *60*, 317.
[12] L. Wunsch, H. J. Neusser, E. W. Schlag, *Chem. Phys. Lett.* **1975**, *31*, 433.
[13] P. M. Johnson, *J. Chem. Phys.* **1976**, *64*, 4143.
[14] S. H. Lin, Y. Fujimura, H. J. Neusser, E. W. Schlag, *Multiphoton Spectroscopy of Molecules, Academic, New York*, **1984**.
[15] L. S. Vasilenko, V. P. Chebotayev, A. V. Shishaev, *JETP Lett.* **1970**, *12*, 113.
[16] F. Biraben, B. Cagnac, G. Grynberg, *Phys. Rev. Lett.* **1974**, *32*, 643; M. D. Levenson, N. Bloembergen, *ibid.* **1974**, *32*, 645; T. W. Hänsch, K. Harven, G. Meisel, A. L. Schawlow, *Opt. Commun.* **1974**, *11*, 50.
[17] E. Riedle, H. Stepp, H. J. Neusser in *Laser Spectroscopy VI (Springer Ser. Opt. Sci. 40)* (Eds.: H. P. Weber, W. Lüthy), Springer, Berlin, **1983**, p. 144.
[18] H. Sieber, E. Riedle, H. J. Neusser, *J. Chem. Phys.* **1988**, *89*, 4620.
[19] G. Herzberg, *Molecular Spectra and Molecular Structure, III. Electronic Spectra and Electronic Structure of Polyatomic Molecules*, van Nostrand Reinhold, New York **1966**.
[20] G. W. Robinson, *J. Chem. Phys.* **1967**, *47*, 1967; M. Bixon, J. Jortner, *ibid.* **1968**, *48*, 715.
[21] L. Wunsch, F. Metz, H. J. Neusser, E. W. Schlag, *J. Chem. Phys.* **1977**, *66*, 386.
[22] J. H. Callomon, J. E. Parkin, R. Lopez-Delgado, *Chem. Phys. Lett.* **1972**, *13*, 125; L. Wunsch, H. J. Neusser, E. W. Schlag, *Z. Naturforsch. A*, **1981**, *36*, 1340. For a review on radiationless processes in benzene see: C. S. Parmenter, *Adv. Chem. Phys.* **1972**, *22*, 365.
[23] E. Riedle, H. Stepp, H. J. Neusser, *Chem. Phys. Lett.* **1984**, *110*, 452.
[24] E. Riedle, H. J. Neusser, *J. Chem. Phys.* **1984**, *80*, 4686.
[25] J. O. Hirschfelder, C. F. Curtiss, R. B. Bird, *Molecular Theory of Gases and Liquids*, Wiley, New York **1954**.
[26] D. H. Levy, *Annu. Rev. Phys. Chem.* **1980**, *31*, 197.
[27] *Atomic and Molecular Beam Methods, Vol. 1*, (Ed.: G. Scoles), Oxford Univ. Press, New York **1988**.
[28] U. Boesl, H. J. Neusser, E. W. Schlag, *Z. Naturforsch. A*, **1978**, *33*, 1546.
[29] J. B. Hopkins, D. E. Powers, R. E. Smalley, *J. Phys. Chem.* **1981**, *85*, 3739; K. H. Fung, H. L. Selzle, E. W. Schlag, *J. Phys. Chem.* **1983**, *87*, 5113; S. Leutwyler, U. Even, J. Jortner, *Chem. Phys. Lett.* **1982**, *86*, 439; K. S. Law, M. Schauer, E. R. Bernstein, *J. Chem. Phys.* **1984**, *81*, 4871.
[30] K. H. Fung, H. L. Selzle, E. W. Schlag, *Z. Naturforsch. A*, **1981**, *36*, 1338.
[31] T. Weber, A. von Bargen, E. Riedle, H. J. Neusser, *J. Chem. Phys.* **1990**, *92*, 90.
[32] T. Weber, E. Riedle, H. J. Neusser, E. W. Schlag, *Chem. Phys. Lett.* **1991**, *183*, 77.
[33] S. M. Beck, M. G. Liverman, D. L. Monts, R. E. Smalley, *J. Chem. Phys.* **1979**, *70*, 232.
[34] T. Weber, H. J. Neusser, *J. Chem. Phys.* **1991**, *94*, 7689.
[35] M. Schmidt, M. Mons, J. LeCalvé, *Chem. Phys. Lett.* **1991**, *177*, 371.
[36] T. Weber, A. M. Smith, E. Riedle, H. J. Neusser, E. W. Schlag, *Chem. Phys. Lett.* **1990**, *175*, 79.

Alkynyl- and Alkenyl(phenyl)iodonium Compounds

New Synthetic Methods (86)

By Peter J. Stang*

Compounds with highly coordinated, polyvalent main-group elements represent an interesting alternative to the many well-known transition-metal complexes. Among the oldest and best known stable examples of such organic molecules are the iodine(III) compounds. Diaryliodonium species, Ar_2IX, for example, have been known for over a hundred years and play an important role in lithography. Likewise, acetylenes and olefins are among the oldest, most important, and most valuable compounds in chemistry. Besides simple hydrocarbon alkenes and alkynes, numerous functionalized derivatives are also known and widely employed in organic chemistry. Despite the ubiquity and prominance of both I^{III} species and olefins and acetylenes, the combination of these two types of functional groups in a single molecular unit, namely compounds with polyvalent iodine and at least one alkyne or olefin residue, was unknown until recently. The successful preparations of simple alkynyl- and alkenyl(phenyl)iodonium species during the 1980s has resulted in a renaissance in both acetylene and I^{III} chemistry. These alkynyliodonium compounds readily undergo nucleophilic substitution on the alkyne moiety (S_N-A reactions) which are difficult with other substrates. The application of a wide variety of nucleophiles in this reaction resulted in diverse functionalized alkynes including previously unknown acetylenic carboxylates, sulfonates, and phosphates. These are excellent substrates for cycloaddition reactions as well as numerous other interesting chemical transformations.

1. Introduction

Iodine was discovered in 1811, and although it is relatively uncommon in nature it plays an important role in biological organisms, including humans, for whom it is essential for the proper functioning of the thyroid gland. It is found most often as monovalent compounds and forms relatively weak bonds with first-row elements including carbon. However, because it is the most polarizable and largest element among the common halogens, it is also capable of forming stable polycoordinate, multivalent compounds.

Just over a hundred years ago, in 1886, the German chemist C. Willgerodt reported the preparation of (dichloroiodo)-benzene (**1**), the first compound with tricoordinate iodine(III) and at least one carbon substituent, by the simple chlorination of iodobenzene.[1] This was rapidly followed by the preparation of (diacetoxyiodo)benzene (**2**),[2] diaryliodonium bisulfate (**3**),[3] the first iodonium salt, and numerous other organic compounds with tri- and multicoordinate iodine. In 1914 when Willgerodt published his comprehensive treatise on these types of compounds[4] nearly 500 were known; the most intensely studied representatives were the diaryliodonium salts **4**.

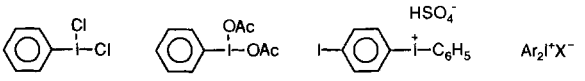

1 **2** **3** **4**

In the century since the publication of Willgerodt's synthesis of **1**, interest in organic tri- and multicoordinate iodine species waxed and waned until the 1980s.[5] Since the early 1980s the chemistry of organic compounds with multicoordinate (hypervalent) iodine has undergone a renaissance.[6] This rebirth of interest is generally attributed to several factors:[7] First, the recognition of the similarities (ligand exchange, reductive elimination, etc.) between compounds with I^{III} and other polyvalent main-group and transition-metal coordination compounds.[8] Second, the chemical behavior and reactivity of iodine(III) species are similar to those of compounds with Hg^{II}, Tl^{III}, and Pb^{IV}, but without the toxic and concomitant environmental problems of these heavy-metal analogues. Third, attention was focused on these unique compounds by the publication of a number of surveys[6] including two outstanding *comprehensive* reviews by G. F. Koser.[9, 10] Finally, numerous iodine(III) compounds such as **1**, **2**, PhIO (**16**), and $PhI(O_2CCF_3)_2$ (**9**) have become useful, commercially available, organic reagents.[11]

Despite this long and distinguished history and considerable current interest in iodine(III) compounds, alkynyl- and simple alkenyliodonium species **5** and **6** were conspicuously absent until recently from the family of compounds with tricoordinate iodine with at least one carbon substituent.

5 **6**

Such compounds are of interest from the perspective of tricoordinate iodine as well as from the aspect of acetylene[12] and olefin chemistry,[13] since they represent a new, unusual class of iodine(III) species with carbon ligands and are also uniquely functionalized alkynes and olefins. Hence, it is the purpose of this article to provide a comprehensive and critical review of the preparation, characterization, and chemistry of these two relatively new classes of organic iodine(III) species, with emphasis on the more recent and widely used alkynyl species.

[*] Prof. Dr. P. J. Stang
Department of Chemistry
The University of Utah
Salt Lake City, UT 84112 (USA)

 © VCH Verlagsgesellschaft mbH, W-6940 Weinheim, 1992 0570-0833/92/0303-0274 $ 3.50+.25/0

2. Synthesis of Organic Iodine(III) Compounds

2.1. Preparation of Alkynyl(phenyl)iodonium Compounds

The first preparation of an acetylenic iodonium species involved the reaction of phenylacetylide and Willgerodt's (dichloroiodo)benzene **1** [Eq. (1)] as reported by Beringer and Galton in 1965.[14] However, the yield of phenyl(β-

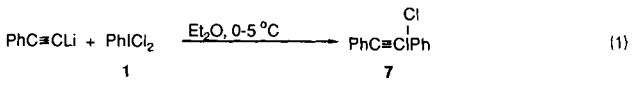

1 7 (1)

phenylethynyl)iodonium chloride (**7**) was only 12–20%. Moreover, **7** decomposed to chlorophenylacetylene and iodobenzene in a 1:1 ratio after a few hours at room temperature. As we shall see, this decomposition could be expected, at least in retrospect, since alkynyliodonium compounds are salts and must have a nonnucleophic counterion in order to be stable. The next reported synthesis of an alkynyliodonium species from the interaction of *para*-diethynylbenzene (**8**) with **9** in chloroform was reported by Merkushev and coworkers.[15] Iodonium salt **10** was isolated in 64% yield as a crystalline compound but was characterized only by IR spectroscopy and its ready "hydrolysis" to the bis(ketoester) **11**.

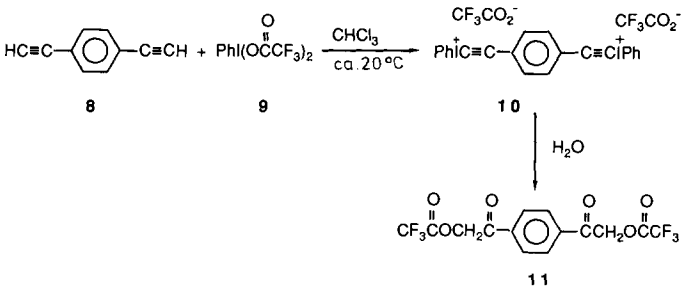

A more general approach to stable alkynyl(phenyl)-iodonium compounds as tosylates was developed by Koser et al. in the early 1980s.[16] According to this method terminal acetylenes are allowed to react with (hydroxy(tosyloxy)-iodo)benzene (**12**)[17,18] in refluxing chloroform [Eq. (2)]. Unfortunately, the product mixture consists of the desired iodonium species **13** and the related vinyl species **14**, resulting in purification problems and greatly diminished yields.

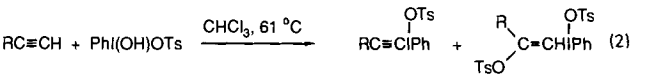

Nevertheless, the discovery of this relatively simple procedure, by Koser et al. was an impetus for the subsequent rapid developments in the synthesis and chemistry of this new class of phenyliodonium species. A number of modifications and improvements for the ready preparation of alkynyl(phenyl)-iodonium tosylates **13**[19,20] were developed by my group, such that these compounds are now routinely available in pure form in 60–90% yield. Parallel to our work Fujita et al.[21] synthesized a variety of alkynyl(phenyl)iodonium tetrafluoroborates **17** in 50–85% yield by the reaction of trimethylsilylacetylenes **15** with iodosobenzene **16** and $Et_2O \cdot BF_3$ in dichloromethane, followed by treatment with aqueous $NaBF_4$.

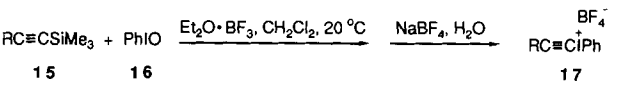

Most recently we developed two new efficient methods for the preparation of alkynyl(phenyl)iodonium trifluoromethanesulfonates (triflates). In the first procedure a trimethylsilyl- or stannylalkyne is treated with Zefirov's reagent **18** generated in situ[22,23] [Eq. (3)]. A variety of alkynyliodonium triflates **19** are obtained in good to excellent yields (45–95%) as stable, microcrystalline solids.[24]

Peter J. Stang was born in November 1941, in Nürnberg, Germany and raised in Hungary until 1956. He received a B. S. in Chemistry in 1963 from DePaul University, Chicago and a Ph.D. in 1966 from U. C. Berkeley under the direction of A. Streitwieser, Jr. After postdoctoral experience with P. von R. Schleyer and a year as instructor at Princeton University, he joined the faculty at the University of Utah in 1969, where he is currently Professor and Chairman of the Department of Chemistry. In 1977 he received a Senior US Scientist Award from the Alexander von Humboldt Stiftung and spent a year in Tübingen, Germany. Subsequent honors abroad included visits to Japan in 1985, the Technion in Haifa in 1986, Zagreb, Yugoslavia in 1988, and the Soviet Union in 1989. In 1992 he is in Kaiserslautern, Germany as a BASF Visiting Professor. He was elected a Fellow of the American Association for the Advancement of Science in 1986 and since 1982 has been an associate editor for the Journal of the American Chemical Society. In February 1992 he was awarded an honorary Doctorate of Science by the Russian Academy of Sciences and Moscow State University. His main research interests are reactive intermediates (vinyl cations and unsaturated carbenes), organometallic chemistry (mechanism of cross-coupling reactions between unsaturated compounds), alkynyliodonium and alkynyl ester chemistry, and strained ring compounds (alkylidenecycloproparenes). He has published over 200 papers and coauthored a text on the spectroscopy of organic compounds and a monograph on vinyl cations.

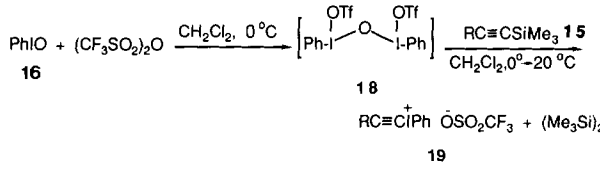

If a stannyl instead of a silyl substituent is used to stabilize[25] the intermediate vinyl cation (vide infra), this procedure even affords the parent ethynyl(phenyl)iodonium triflate in 56% isolated yield (see Section 3.3).[26] The analogous tetrafluoroborate **21** has been prepared by desilylation of **20** with HF/H_2O [Eq. (4)].[27]

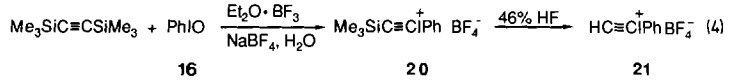

The second method involves the use of stannylalkynes and iodonium triflate **22**[28] for the preparation of a wide variety of β-alkyl- and β-arylethynyl(phenyl)iodonium triflates **19**. The previously inaccessible β-functionalized ethynyl(phenyl)iodonium triflates **23** may also be synthesized in this way.[29]

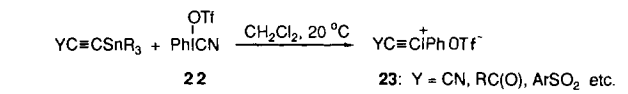

Likewise this procedure allowed us to prepare[30] the novel bis(iodonium)acetylenes **24** [Eq. (5)], diynes **25** [Eq. (6)], and related bis(iodonium) compounds **26**–**28**.[31] This reaction of **22**, an iodonium transfer, is the most general and simplest method to date for the preparation of alkynyliodonium species.[29, 30] This method can also be used for the syntheses of buta-1,3-diynyl(phenyl)iodonium triflates **29**.[32]

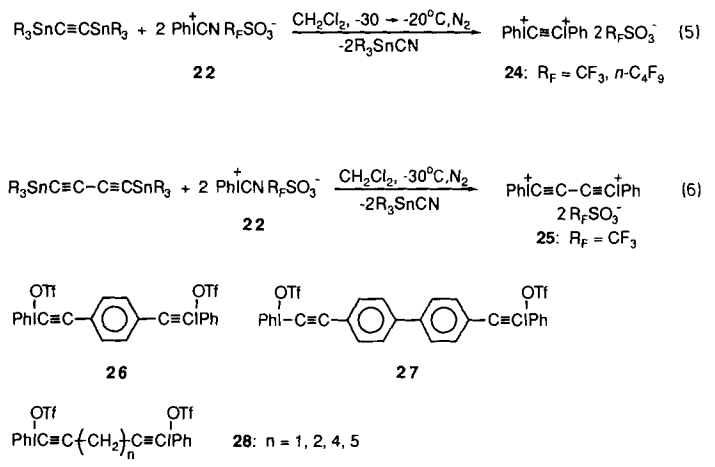

It is evident from the foregoing discussion that alkynyl(phenyl)iodonium species have become readily available in the past few years[20, 21, 24, 26, 29, 30] and represent a new member of the family of compounds with polycoordinate iodine and carbon substituents.

Although little direct mechanistic work has been reported concerning the formation of these alkynyliodonium species, indirect evidence provides a reasonable hypothesis. With the exception of Beringer's synthesis of **7** all methods employ some type of an electrophilic iodonium reagent such as **9**, **12**, **18**, and **22**. Hence, in the first step an iodonium species **30** must add electrophilically to an alkyne with formation of a vinyl cation[33] and/or cyclic iodonium species **31**. Subsequent loss of R'Y results in the alkynyl(phenyl)iodonium species [Eq. (7)]. In support of this mechanism[20] is the observed acceleration of the reaction in polar solvents, the regiochemistry of addition, and above all the stabilization of carbocations, particularly vinyl cations,[34, 35] by β-silyl and β-stannyl substituents.[25, 34]

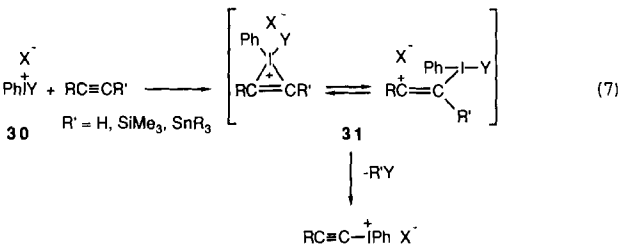

2.2. Preparation of Alkenyl(phenyl)iodonium Compounds

Although a few β-halogenvinyliodonium species have been reported[4, 5, 9] since the days of Willgerodt, their methods of preparation were rather inefficient and limited. More recent procedures[36] afford β-substituted alkenyl(phenyl)iodonium compounds **34** in low yields (5–10%) from the reaction of the related alkenylmercuric bromides **32** or alkenylstannanes **33** with Willgerodt's (dichloroiodo)benzene (**1**). A more general, simpler procedure[16] provides phenyl(β-tosyloxyalkenyl)iodonium tosylates **35** in yields of 40–60% from the reaction of alkynes with the iodonium compound **12** [Eq. (8)]. In a similar fashion the highly stereoselective electrophilic *anti* addition of PhIO CF_3SO_3H to acetylene derivatives furnishes ((*E*)-β-trifluoromethanesulfonyloxyalkenyl)iodonium triflates **36** in yields of 87–100% [Eq. (9)].[37]

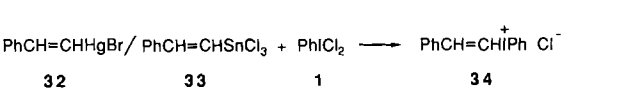

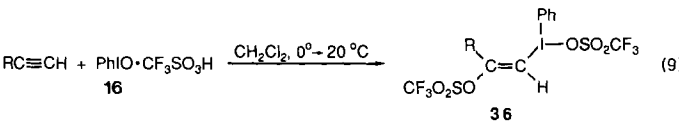

The best and most general procedure for the preparation of alkenyliodonium compounds was developed by Fujita, Ochiai et al.[38] Here readily available alkenylsilanes **37**[39] react stereospecifically with PhIO and $Et_3O^+BF_4^-$ with retention of olefin geometry. A wide variety of acyclic as well as cyclic alkenyl(phenyl)iodonium tetrafluoroborates **38**

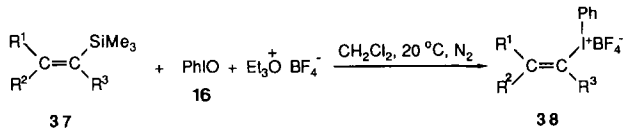

37 38

were obtained in 60–94% yields, [38] thereby encouraging the exploration and application of these alkenyl I^{III} reagents.

3. Characterization and Properties of Iodine(III) Compounds

3.1. Physical Properties

The great majority of alkynyl- and alkenyl(phenyl)-iodonium compounds are microcrystalline solids. Their stability depends both upon the substituents on the alkyne or alkene and on the counterion. The less nucleophilic the counterion, the more stable the resulting iodonium species. Hence, the most commonly used counterions are BF_4^- and $CF_3SO_3^-$ and to a lesser extent ClO_4^-. Tosylates, *p*-$CH_3C_6H_4SO_3^-$, and mesylates, $CH_3SO_3^-$, may also be stable but are usually less stable than those species previously mentioned. In general, the simple alkyl-substituted alkynyl-(phenyl)iodonium compounds such as **13**, **17**, and **19** (with R = alkyl or H) are indefinitely stable as solids when refrigerated. Substituted compounds such as **23** and the bis(iodonium) species **24** and **25** tend to be somewhat less stable.

Although explosions have been reported[40] with both $(Ph^+I{-}O{-}^+IPh)2BF_4^-$ [41] and the perchlorate analogue of **40** we have not experienced any problems with either alkynyl(phenyl)iodonium triflates or tosylates. Nevertheless, it is prudent to exercise caution in the handling of all iodonium species.

3.2. Spectral Properties

Both alkynyl- and alkenyl(phenyl)iodonium compounds have highly characteristic spectral properties. Their Fast Atom Bombardment (FAB) mass spectra generally show abundant peaks for the intact cations, $RC{\equiv}C^+IPh$ and $(M{-}OTf)^+$, and $R_2C{=}CR^+IPh$ and $(M{-}BF_4)^+$, respectively. These peaks are quite useful for the identification of the individual salts.

The infrared spectra display strong absorptions characteristic of the anions: for BF_4^-, intense broad bands between 1000–1100 cm^{-1} and for $CF_3SO_3^-$, two strong signals around 1270 and 1000 cm^{-1}. Moreover, the C≡C absorption of the alkynyl compounds, although generally weak, is usually discernible between 2120 and 2190 cm^{-1}.

Most diagnostic are the ^1H and ^{13}C NMR spectra. All alkynyl- and alkenyl(phenyl)iodonium species have ^1H NMR spectra with three signals between $\delta = 7.50$ and 8.25 in a 2:1:2 ratio for the hydrogens of the phenyl group (Fig. 1). The relatively low-field position of these signals is in accord with the strong electron-withdrawing effect of the iodonium moiety and its deshielding. The σ_I of ICl_2, for example, is 1.17 and for $I(OAc)_2$, 0.85 compared to only 0.45 for iodine itself.[42] Likewise, in alkenyl(phenyl)iodonium species **38** both H_α and H_β are considerably deshielded with $\delta = 6.8$–7.8.[38]

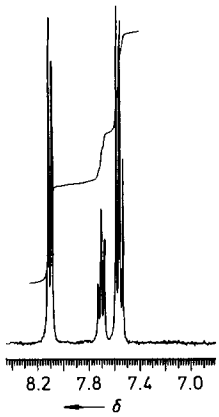

Fig. 1. Characteristic pattern in the aromatic region of the ^1H NMR spectra of alkynyl- and alkenyl(phenyl) iodonium compounds.

The most characteristic features of the ^{13}C NMR spectra of the alkynyl and alkenyl species **5** and **6** are the signals of the acetylenic and olefinic carbon atoms. The C_α and C_β signals in **5** are generally found at $\delta = 20$–40 and 110–120, respectively. The low-field resonance of the β carbon is due to the contribution of resonance from **5'**, the electronic distribution in the alkynyliodonium compound, and spin-orbital effects of the iodine atom.[43] For example, the β carbon in parent compound **39** resonates at $\delta = 98.3$ and C_α, at $\delta = 27.3$, whereas the signal for acetylene itself is at $\delta = 71.9$.[26] Interestingly, the ^{13}C NMR signal of **24** ($R_F = CF_3$) is found at $\delta = 51.8$, between the C_α and C_β signals of **5** and *upfield* from the ^{13}C NMR signal of acetylene.[30] For alkynyl(phenyl)iodonium triflates there is

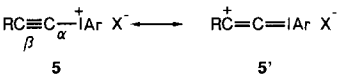

5 5'

a further signal generally centered at $\delta = 121$ (q, $J_{F,C} \approx 319$ Hz) arising from the triflate group. The alkenyliodonium species **6** display similar spectra. The C_α signal is found between $\delta = 75$–118, that of C_β at $\delta = 146$–159.[38] Finally, both iodonium triflates and tetrafluoroborates display highly characteristic signals in their ^{19}F NMR spectra: for $CF_3SO_3^-$ at $\delta = -77.5$ to -79.0 and for BF_4^- at $\delta \approx -150$.

3.3. X-Ray Structural Analyses

To date X-ray structural analyses have been reported for three alkynyl(phenyl)iodonium species: **39**,[26] **40**,[19b] and **41**.[44] The ORTEP representation and relevant structural

39 40 41

data of the simplest species, ethynyl(phenyl)iodonium triflate (**39**), are shown in Figure 2.

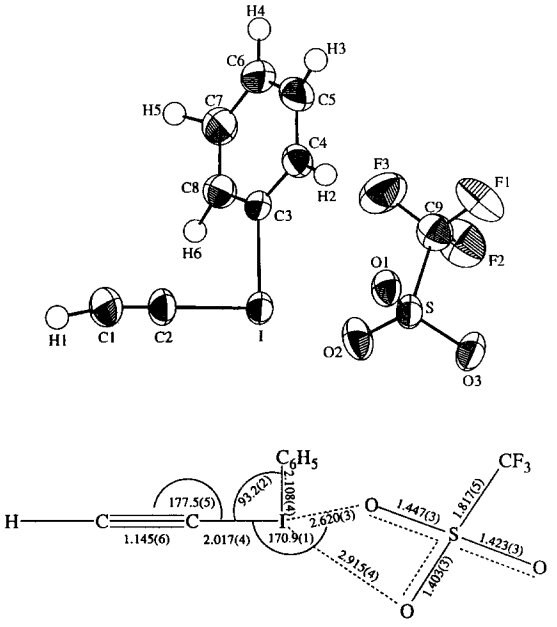

Fig. 2. Top: Crystal structure of **39** (ORTEP). Bottom: Important bond lengths [Å] and angles [°].

In all three compounds the geometry about the iodine can be described as distorted trigonal pseudobipyramidal or T-shaped (**42**). This is in accord with the hypervalent nature of these salts (10-I-3).[8a] In other words the central atom,

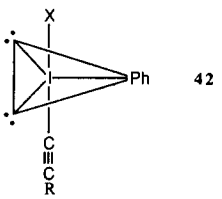

42

iodine, is surrounded by three ligands and has ten electrons in its valence shell. The equatorial positions are occupied by the phenyl group and two sets of lone-pair electrons; the axial positions are taken up by the alkyne and the anion. As expected the most electronegative groups occupy axial positions, and the least electronegative phenyl group resides in an equatorial position. Similar structures are observed for the related (10-I-3) iodine compounds $PhICl_2$,[45] PhI(OH)OTs (**12**),[46] and $PhI(OAc)_2$ (**2**).[47]

The most noteworthy features of the structure of **39** (and also of **40** and **41**) are the I–O distances of 2.620 and 2.915 Å, well outside both the sum of the theoretical covalent radii of I and O and the I–O single-bond length of 1.99 Å. This along with the three nearly identical S–O bond lengths of 1.424 ± 0.023 Å clearly indicate the ionic nature of these species, even in the solid state. These structural effects are in accord with the results of recent theoretical calculations on the nature of the bonding, and in particular the dominance of ionic bonding and negative hyperconjugation over d-orbital participation in hypervalent molecules.[48]

X-ray structural determinations have been carried out on the alkenyl(phenyl)iodonium species **43**–**49** to date. Again the common structural feature for all these iodonium compounds is a trigonal bipyramidal geometry analogous to that of **42**. The phenyl group occupies an equatorial position and

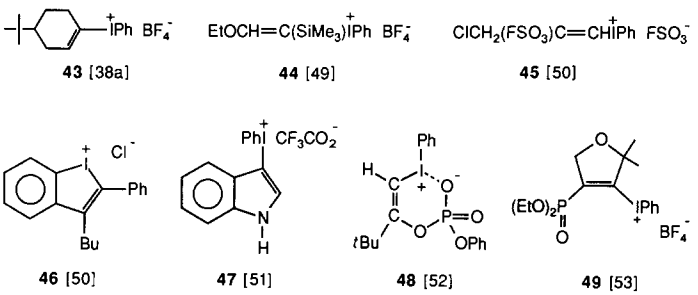

43 [38a] **44** [49] **45** [50]

46 [50] **47** [51] **48** [52] **49** [53]

the alkene and anion, the axial positions. Secondary interactions and geometries distorted from trigonal bipyramidal are observed in many I^{III} species including **5** and **6**. A typical

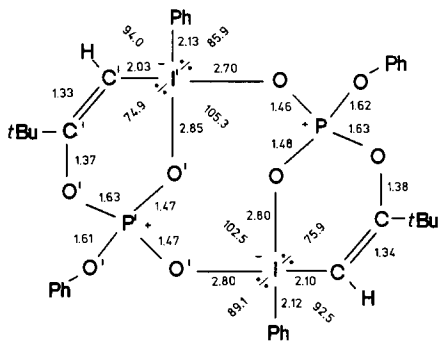

Fig. 3. Important bond lengths (Å) and structural features of the (12-I-4)-alkenyliodonium dimer $(\mathbf{48})_2$.

example is the novel zwitterionic alkenyl species **48** that is actually dimeric in the solid state (Fig. 3).[52]

4. Chemistry of the Iodine(III) Compounds

4.1. Chemistry of Alkynyl(phenyl)iodonium Compounds

Nucleophilic acetylenic substitutions (S_N-A), although known, are generally unfavorable.[54] However, iodonium groups are excellent leaving groups,[55] and loss of neutral iodobenzene from phenyliodonium salts, analogous to the loss of neutral nitrogen from diazonium salts, should facilitate S_N-A processes. Furthermore, alkynyl(phenyl)-iodonium species **5** may serve formally as masked alkynyl cations $RC{\equiv}C^+$. This amounts to an umpolung of the normal acetylene reactivity. Reactions with nucleophiles are possible in contrast to the better known reaction of acetylides $RC{\equiv}C^-$ with electrophiles. Hence, at least in principle, it is possible to think in terms of "alkynylations"

using **5** as the alkynylating agent, in analogy to the well-established alkylation reactions using saturated substrates RX.

4.1.1. Alkynylations

The first alkynylation reaction with an alkynyliodonium species was reported by Beringer and Galton.[14] Reaction of iodonium salt **7** with the anion of indandione **50** in refluxing *t*BuOH gave phenylethynylindandione **51** in 73% isolated

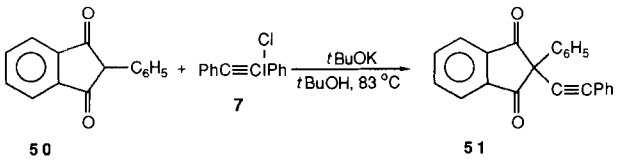

50 **7** **51**

yield. Ochiai et al.[27] demonstrated that **21** reacts with a variety of β-dicarbonyl enolates **52**–**54** resulting in the corresponding ethynyl products **55**–**57**. Similarly, Bachi, Stang

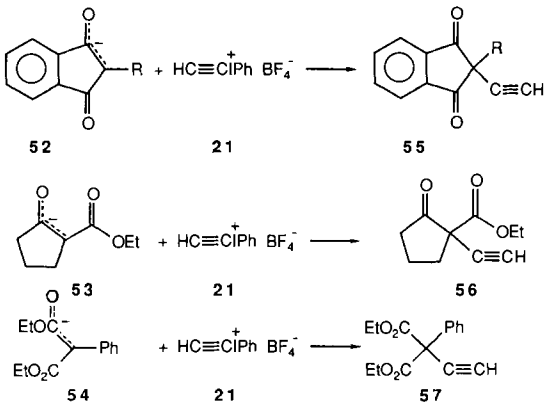

52 **21** **55**

53 **21** **56**

54 **21** **57**

et al.[24] established that alkynyl(phenyl)iodonium triflates **19** react with aminomalonate **58** providing the corresponding alkynylmalonates **59** in 30–95% yield. Unfortunately, this reaction only works with soft nucleophiles such as the anions of dicarbonyl compounds just mentioned. Alkynylation of simple enolates does *not* occur.

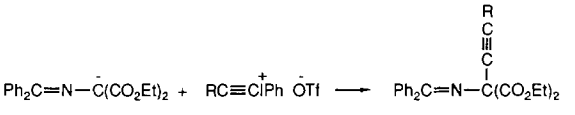

58 **19**: R = Ph, *n*Bu, *t*Bu, Me_3Si **59**

However, alkynylation is possible for soft inorganic nucleophiles such as trialkyl phosphites[56] [Eq. (10)], Ph_3P[57] [Eq. (11)], and even organometallic nucleophiles[58] [Eq. (12)]. Reaction (12) amounts to an oxidative addition to a metal center and is one of the best ways of introducing a terminal σ acetylide ligand into a metal complex.[58]

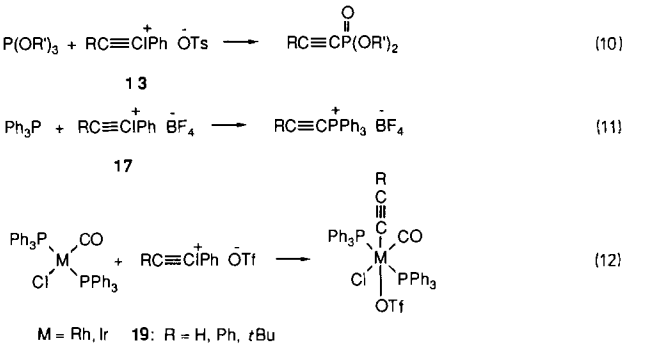

Similarly, the bis(iodonium) species **26** and **28** react with excess Ph_3P to furnish the corresponding bis(phosphonium)salts **60** and **61** in excellent yields.[31]

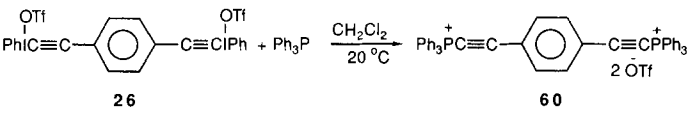

26 **60**

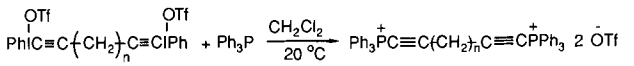

28 **61**

4.1.2. Acetylenic Ester Formation

Esters of all types, sulfonates **62**, carboxylates **63**, and phosphates **64**, are ubiquitous and play important roles in organic as well as biochemistry.[59] Likewise, their unsaturated congeners, enol esters **65**–**67**, are well known and widely used. The corresponding acetylenic esters **68**–**70**, on the other hand, were unknown until recently. This is all the more surprising, since a large number of functionalized acetylenes with diverse substituents are known to be generally stable.[12]

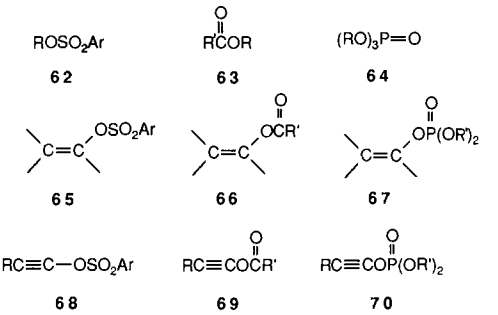

62 **63** **64**

65 **66** **67**

68 **69** **70**

Conventional methods of either ester or acetylene synthesis did not work for the preparation of these novel alkynyl esters **68**–**70**, which combine two of the most common and useful organic functional groups in a single molecule.[19b] The problem was solved by the use of alkynyl(phenyl)-iodonium species as progenitors. Treatment of alkynyl-(phenyl)iodonium sulfonates **13** with CuOTf in CH_3CN yielded the hitherto unknown but stable alkynyl sul-

fonates **68** [Eq. (13)]. (The reaction may also be conducted with the mesyl rather than tosyl derivative.) Likewise, treatment of **19** or related compounds with polyvalent iodine with $PhCO_2Na$ gave the corresponding alkynyl benzoates[60] [Eq. (14)]. The reaction of either **13** or **19** with $NaO_2P(OR')_2$ gave the corresponding alkynyl dialkyl phosphates **70**[61] [Eq. (15)]. These alkynyl esters derived from alkynyl-

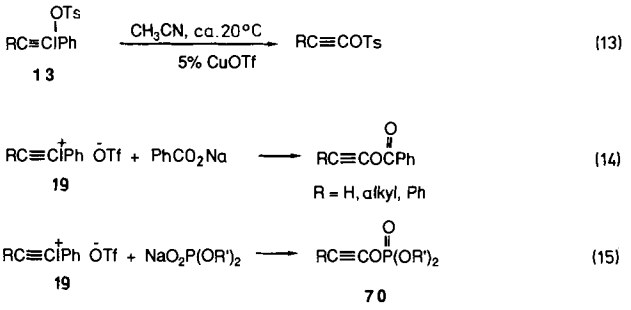

(phenyl)iodonium compounds have been the subject of numerous interesting studies[66] including the generation of ynolates,[62] novel hydrolyses,[63] enzyme inhibition,[64] and cycloadditions.[65]

4.1.3. Mechanism of the S_N-A Reaction

Formally both the alkynylations discussed in Section 4.1.1. and the acetylenic ester formations (Section 4.1.2.) are S_N-A processes. However, the actual reaction mechanism is more complex. There is increasing evidence that these reactions occur by Michael addition, formation of an unsaturated carbene, and rearrangement to the alkyne (Scheme 1). Specifically, Michael addition of the nucleophile to the alkynyl(phenyl)iodonium species results in ylide **71**.

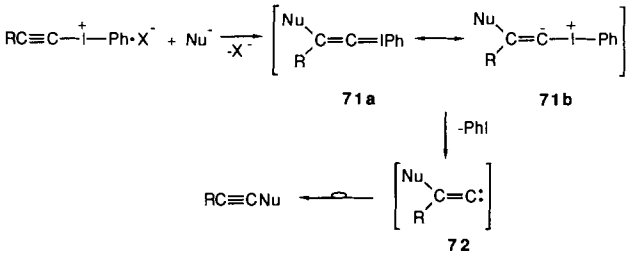

Scheme 1. Mechanism of the S_N-A reaction of alkynyl(phenyl)iodonium compounds.

Loss of iodobenzene from **71** gives the known unsaturated carbene **72**,[67] which in the absence of external traps rearranges to the alkyne. Evidence for this process includes the following: When **17** is treated with Me_3SiN_3 in *wet* CH_2Cl_2, (β-azidoalkenyl)phenyliodonium tetrafluoroborates **73** are isolated in yields of 50–90%.[68] This is the result of ylide **71b** being trapped by protons from water. If the reaction is carried out with NaN_3 in CH_3OH or in the presence of Et_3SiH, products **74** and **75** are obtained;[69] These result from the well-known insertion of unsaturated carbenes (**72**, Nu = N_3) into the CH_3O–H and Et_3Si–H bonds, respectively.[67] Moreover, carbene **72** (Nu = N_3) may also be trapped intramolecularly by insertion into a C–H bond;[69] intermediate **76** then gives the cyclic alkenyl azide **77**.

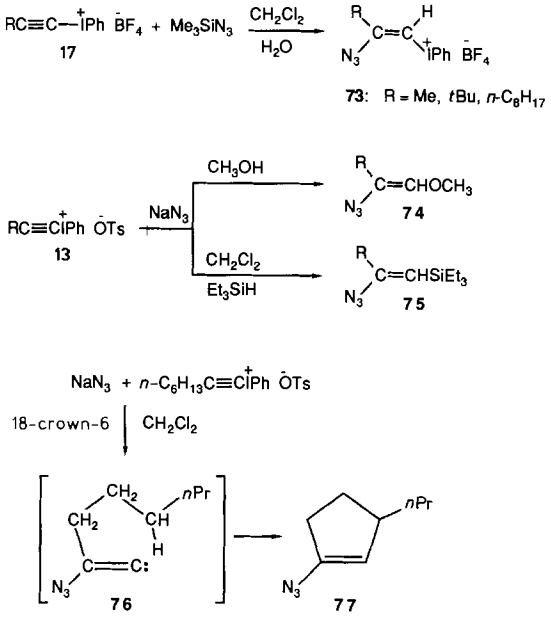

More recently we have isolated both the rearranged alkyne (major product) and the trapped product (a cyclopentene derivative) from the same reaction [Eq. (16)].[70] In fact, Ochi-

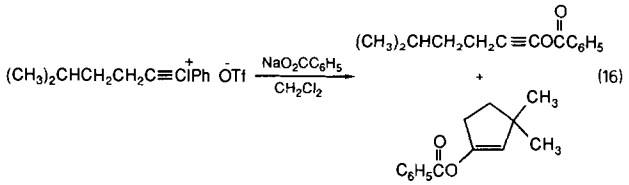

ai et al.[71] have taken advantage of these tandem Michael carbene-insertion reactions of alkynyliodonium compounds in an elegant, very efficient synthesis of cyclopentene derivatives

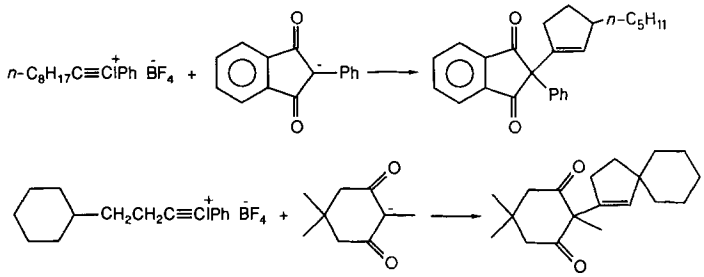

Scheme 2. Cyclopentene synthesis with alkynyliodonium compounds.

(Scheme 2). Likewise, addition of $PhSO_2H$ to alkynyliodonium compounds furnishes the β-(phenylsulfonyl)alkenyliodonium species **78**.[72] Treatment of **78** with Et_3N gives a mixture of the cyclopentene **79** (major product) and alkyne **80**.

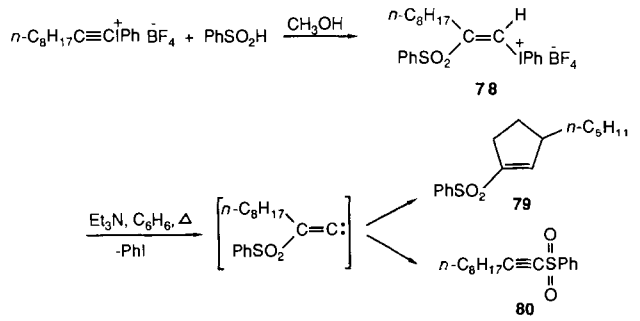

4.1.4. C_2- and C_4-Transfer Reactions

Interaction of **24**, $R_F = CF_3$, with a variety of nucleophiles results in novel difunctionalized acetylenes **81**–**84**. This corresponds formally to a C_2-transfer.[30] Analogously, **25** reacts with NaSPh by a C_4-transfer to give **85**.[30] Compounds **26**–**28** react with excess Ph_3P, as well as with other nucleophiles, resulting in the corresponding diphosphonium salts (analogous to **83**) and difunctionalized alkadiynes, respectively.[31]

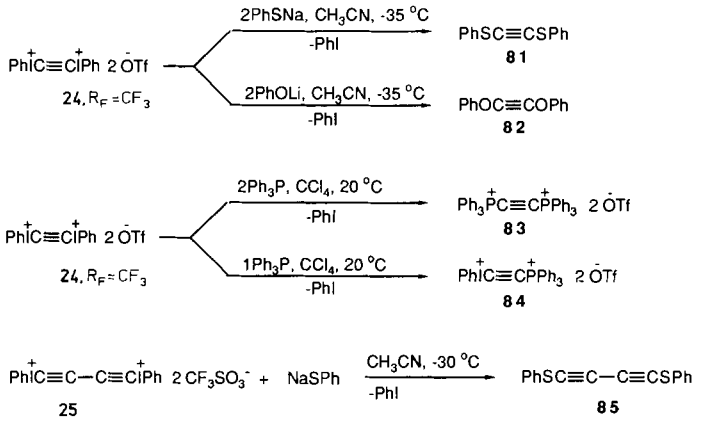

4.1.5. Cycloadditions

As highly electron-deficient acetylenes, alkynyliodonium compounds should be excellent cycloaddition partners. Indeed **19** and in particular the substituted systems **23** readily react with cyclopentadiene and furan resulting in cycloadducts **86** and **87**, $R_F = CF_3$.[73] Similarly, **24**, $R_F = CF_3$, reacts with a variety of dienes under very mild conditions providing the cycloadducts **88**–**90** in good yields.[30b] These adducts are versatile cyclic products suitable for further synthetic elaboration by virtue of the remaining iodonium functionality.

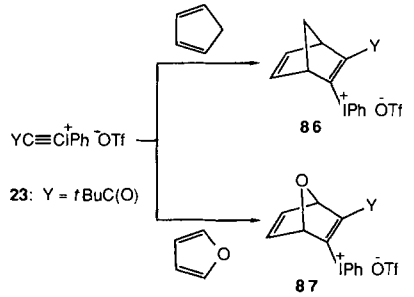

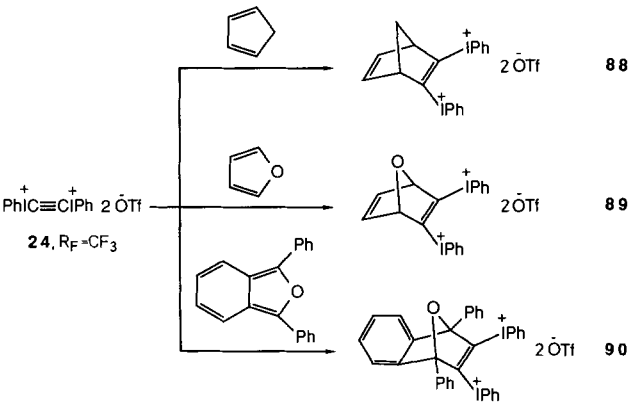

Alkynyliodonium salts have also been reported to react as 1,3-dipolarophiles towards nitrile oxides.[74] Thus reaction of **91** and **92** gave the isoxazole iodonium compound **93** as product. If **91** had Ar = *p*-$CH_3OC_6H_4$, a different regioisomer was formed.[74]

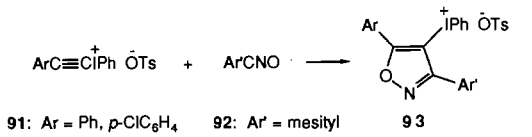

4.1.6. Other Reactions

Conjugated enynes **95** were obtained in 40–60% yield from the coupling of alkynyl(phenyl)iodonium tosylates **13** with vinylcopper reagents **94**.[75] In this reaction the configuration of the C–C double bond can be controlled by simply changing the order of the substituents in the individual components (Scheme 3). The method very nicely complements the recent Pd-catalyzed processes[76] for the formation of these useful aliphatic compounds.

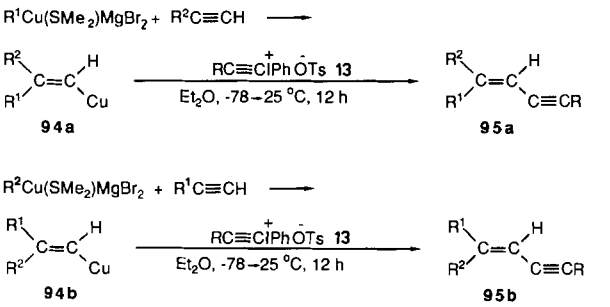

Scheme 3. Coupling reactions of alkynyliodonium compounds with vinylcopper reagents.

Pd-catalyzed carbonylation of **13** gave alkyne carboxylates **96** in 60–80% yield.[77] Reaction of **97** with 2-lithiofuran (**98**) gave the corresponding aryl(2-furyl)iodonium

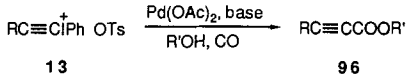

13 96

tosylates **99** by an exchange of carbon ligands.[78] In a similar reaction 2-lithiothiophene **100** gave the corresponding 2-thionyliodonium species **101**. Alkynyl(phenyl)iodonium compounds have been employed in the conversion of α-hydroxyketo groups to α-γ-dihydroxy-β-keto groups,[79] and alkynyl(phenyl)iodonium tosylates **13** have been used in the oxidative rearrangement of alkynes to carboxylic acid esters.[80]

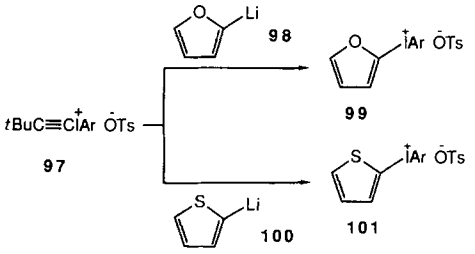

97 98 99 100 101

Finally, the reaction of **17** with sodium carboxylates in the presence of H_2O affords β-(oxoalkyl)carboxylates **102**.[81]

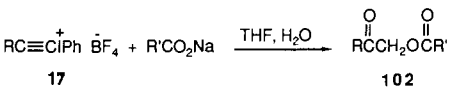

17 102

A mechanism involving a β-(alkoxycarbonyloxy)vinyliodonium intermediate **103** and a β-(oxoalkyl)iodonium species **104** has been invoked to explain these results (Scheme 4 top).[81] However, in light of the ready hydrolyses of alkynyl carboxylates **69** to (oxoalkyl)carboxylates via the cyclic

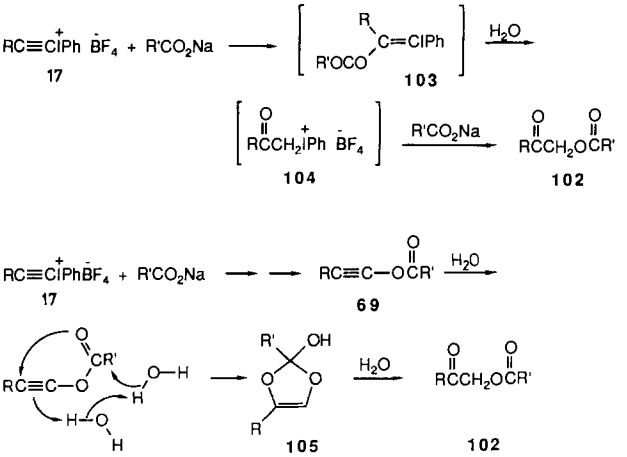

Scheme 4. Two possible mechanisms for the formation of **102**.

intermediate **105**,[63] another equally or more likely mechanism may be invoked for the formation of **102** (Scheme 4 bottom).

4.2. Chemistry of Alkenyl(phenyl)iodonium Compounds

Just as the alkynyl(aryl)iodonium species **5** serve as highly reactive functionalized acetylene derivatives, the analogous alkenyl species **6** serve as highly reactive functionalized alkenes. More specifically, alkenyl(phenyl)iodonium compounds **6** may be considered masked vinyl cations[33] and highly reactive substrates for nucleophilic vinylic substitutions (S_N-V).[82] The few reactions reported for the previously known alkenyl(phenyl)iodonium salts have been reviewed.[9] The modern chemistry of these species may be placed in three categories: substitution reactions, alkylidenecarbene formation, and other reactions.

4.2.1. Substitution Reactions

The many useful substitution reactions of alkenyl(phenyl)iodonium species, elegantly carried out by Ochiai, Fujita et al.,[38] are best summarized and illustrated by the examples in Scheme 5.

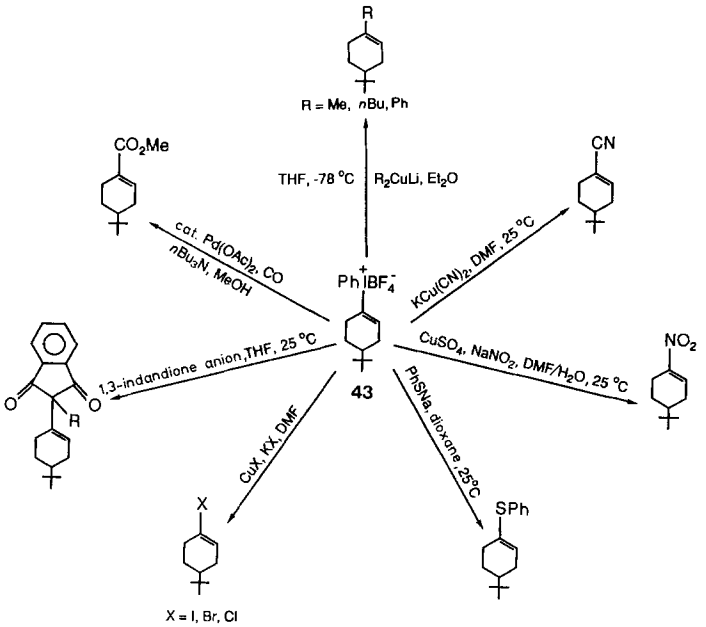

Scheme 5. Substitution reactions with alkenyl(phenyl)iodonium compounds. DMF = dimethylformamide.

4.2.2. Alkylidenecarbene Formation

Alkylidenecarbenes **106** are well-established reactive intermediates,[67] which were previously most often generated from alkenyl halides **107** and triflates **108** by base-initated α-eliminations. More recently, 1-alkenyl(phenyl)iodonium species have been employed as progenitors for **106**.

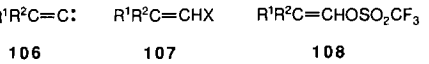

106 107 108

Ochiai et al.[83] have demonstrated that reaction of 1-alkenyl(phenyl)iodonium tetrafluoroborates such as **109**

with bases like *t*BuOK or Et_3N in THF gives **110**, which may undergo insertion to **111** and rearrangement to **112**. The related reaction of the β-sulfonylalkenyliodonium salt **78** to **79** and **80** has already been discussed in Section 4.1.3. Treatment of **113** with *t*BuOK in dimethoxyethane provides **115** via the carbene intermediate **114**.[69]

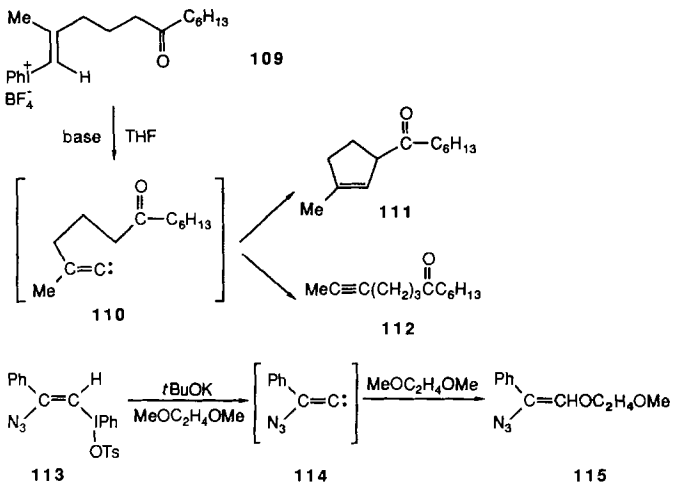

4.2.3. Other Reactions

(Arylalkenyl)phenyliodonium species **116** underwent intramolecular cyclization to **117** upon heating in various solvents between 40–60 °C.[84] Treatment of **118** with D_2O in THF gave the deuterated product **120** presumably via the ylide **119**.[49] A similar iodonium ylide was proposed as an intermediate in the H/D exchange of **48** [Eq. (17)].[52]

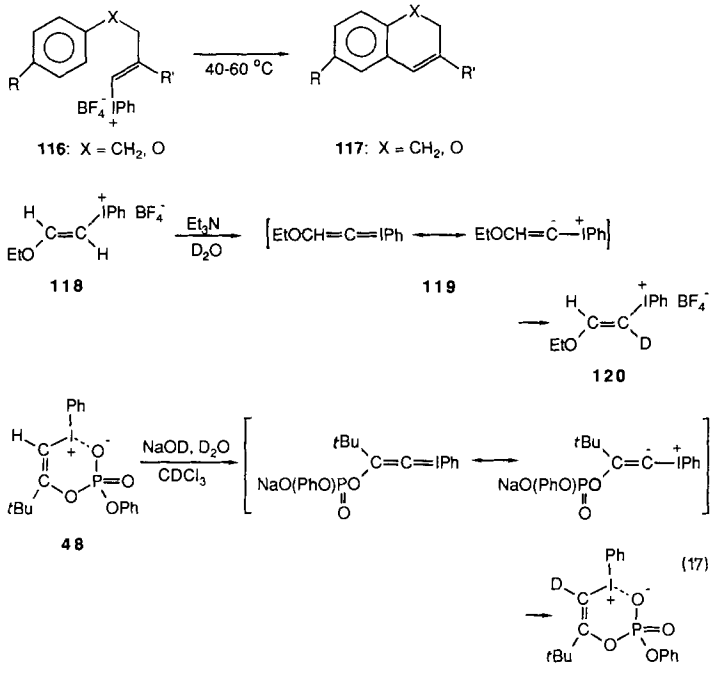

Finally, ethenyl(phenyl)iodonium triflate **121** is an excellent vinyl cation equivalent and precursor to the hitherto unknown parent vinyl triflate **122**.[85] In addition, **121** can vinylate organometallic complexes providing compounds like **123**.[86]

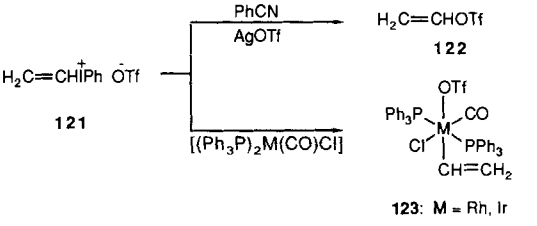

5. Conclusions and Prognostications

This review shows that a wide variety of both alkynyl- and alkenyl(phenyl)iodonium compounds are now readily available by simple, general, preparative procedures in good to excellent isolated yields. They are stable crystalline solids, which—with a few exceptions—can be easily stored for long periods. These newest members of the family of compounds with polyvalent iodine are revitalizing and revolutionizing the chemistry of alkynes and alkenes. They serve as highly reactive substrates for nucleophilic acetylenic, S_N-A, and vinylic, S_N-V, substitution reactions and allow the synthesis of hitherto unknown or not readily available functionalized acetylenes and olefins. Moreover, these compounds, as masked alkynyl and alkenyl cations or in other words through their *electrophilic* rather than nucleophilic character, allow an umpolung of the chemistry of the alkynes and, to a lesser extent, the alkenes. To date they have served, for example, as novel alkynylating and vinylating agents. Alkynyl(phenyl)iodonium compounds in particular have been used in the synthesis of previously unknown alkynyl esters, as novel C_2- and C_4-transfer agents, and as cycloaddition partners.

This is just the beginning of the many potential applications of these I^{III}-functionalized alkynes (and alkenes) since their first successful preparation only a decado ago. Considering the rich chemistry of the much longer and better known diaryliodonium compounds **4** and that of related species like **1**, **2**, **16**, etc., one may expect many more new developments in the chemistry of **5** and **6**. New synthetic procedures using **5** and **6**, polymers based upon or related to **5** or **6**, potential applications in biochemistry, and unique materials such as $[L_nMC{\equiv}CML_n]$ derived from alkynyl(phenyl)iodonium species are just a few examples of the nearly limitless possibilities opened up by these new I^{III} species. Moreover, such obvious congeners as **124** and **125** are yet to be discovered and reported.

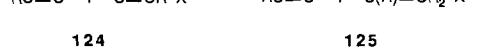

We thank the National Cancer Institute of the National Institutes of Health for the support of our own work described here (Grant number ROCA16903).

Received: June 5, 1991 [A 855 IE]
German version: *Angew. Chem.* **1992**, *104*, 281

[1] C. Willgerodt, *J. Prakt. Chem.* **1886**, *33*, 155.
[2] C. Willgerodt, *Chem. Ber.* **1892**, *25*, 3494.
[3] C. Hartmann, V. Meyer, *Chem. Ber.* **1894**, *27*, 426.
[4] C. Willgerodt, *Die Organischen Verbindungen mit Mehrwertigem Iod*, Enke, Stuttgart, **1914**.
[5] For early reviews see: R. B. Sandin, *Chem. Rev.* **1943**, *32*, 249–275; D. F. Banks, *ibid.* **1966**, *66*, 243–266; F. M. Berginger, E. M. Gindler, *Iodine Abstr. Rev.* **1956**, *3*, 1–62; G. A. Olah, *Halonium Ions*, Wiley, New York, **1975**.
[6] For recent reviews see: A. Varvoglis, *Chem. Soc. Rev.* **1981**, *10*, 377–407; A. Varvoglis, *Synthesis* **1984**, 709–726; R. M. Moriarty, O. Prakash, *Acc. Chem. Res.* **1986**, *19*, 244–250; E. B. Merkushev, *Russ. Chem. Rev.* (*Engl. Transl.*) **1987**, *56*, 826–845; M. Ochiai, *Rev. Heteroat. Chem.* **1989**, *2*, 92–111; I. I. Maletina, V. V. Orda, L. M. Yagupolskii, *Russ. Chem. Rev.* (*Engl. Transl.*) **1989**, *58*, 544–558.
[7] R. M. Moriarty, R. K. Vaid, *Synthesis* **1990**, 431–447.
[8] a) J. C. Martin, *Science* **1983**, *221*, 509–514; b) J. I. Musher, *Angew. Chem.* **1969**, *81*, 68–83; *Angew. Chem. Int. Ed. Engl.* **1969**, *8*, 65–68.
[9] a) *The Chemistry of Functional Groups, Supplement D* (Eds.: S. Patai, Z. Rappoport), Wiley, Chichester, **1983**; b) G. F. Koser in [9a], Chapter 25, pp. 1265–1351.
[10] G. F. Koser in [9a], Chapter 18, pp. 721–811.
[11] L. F. Fieser, M. Fieser, *Reagents for Organic Synthesis, Vol. 1–8*, Wiley, New York, **1967–1979**; Aldrich Catalog of Fine Chemicals, **1990/1991**.
[12] For reviews see: W. D. Huntsman in *The Chemistry of the Carbon Carbon Triple Bond* (Ed.: S. Patai), Wiley-Interscience, London, **1978**, pp. 553–620; *Methoden Org. Chem.* (*Houben-Weyl*), *4th ed. 1952–*, Vol. 5/2a; H. G. Viehe, *Chemistry of Acetylenes*, Dekker, New York, **1969**.
[13] *The Chemistry of Alkenes* (Ed.: S. Patai), Wiley-Interscience, London, **1964**.
[14] F. M. Beringer, S. A. Galton, *J. Org. Chem.* **1965**, *30*, 1930–1934.
[15] E. B. Merkushev, L. G. Karpitskaya, G. I. Novosel'tseva, *Dokl. Akad. Nauk SSSR* **1979**, *245*, 607–610.
[16] G. F. Koser, L. Rebrovic, R. H. Wettach, *J. Org. Chem.* **1981**, *46*, 4324–4326; L. Rebrovic, G. F. Koser, *ibid.* **1984**, *49*, 4700–4702.
[17] For a review of **12** and its chemistry see: R. M. Moriarty, R. K. Vaid, G. F. Koser, *Synlett* **1990**, 365–383.
[18] O. Neiland, B. Karele, *J. Org. Chem. USSR* (*Engl. Transl.*) **1970**, *6*, 889; G. F. Koser, R. H. Wettach, *J. Org. Chem.* **1977**, *42*, 1476–1478; *ibid.* **1980**, *45*, 1542–1543.
[19] a) P. J. Stang, B. W. Surber, *J. Am. Chem. Soc.* **1985**, *107*, 1452–1453; b) P. J. Stang, B. W. Surber, Z. C. Chen, K. A. Roberts, A. G. Anderson, *ibid.* **1987**, *109*, 228–235.
[20] T. Kitamura, P. J. Stang, *J. Org. Chem.* **1988**, *53*, 4105–4106.
[21] M. Ochiai, M. Kunishima, K. Sumi, Y. Nagao, E. Fujita, M. Arimoto, H. Yamaguchi, *Tetrahedron Lett.* **1985**, *26*, 4501–4504.
[22] N. S. Zefirov, V. V. Zhdankin, A. S. Koz'min, *Izv. Akad. Nauk SSSR Ser. Khim.* **1983**, 1682–1683; N. S. Zefirov, V. V. Zhdankin, Y. V. Dan'kov, A. S. Koz'min, *Zh. Org. Khim.* **1984**, *20*, 446–447.
[23] J. Gallos, A. Varvoglis, N. W. Alcock, *J. Chem. Soc. Perkin Trans. 1* **1985**, 757–763; T. R. Hembre, C. P. Scott, J. R. Norton, *J. Org. Chem.* **1987**, *52*, 3650–3654.
[24] M. D. Bachi, N. Bar-Ner, C. M. Crittell, P. J. Stang, B. L. Williamson, *J. Org. Chem.* **1991**, *56*, 3912–3915.
[25] J. B. Lambert, G. T. Wang, *Tetrahedron Lett.* **1988**, *29*, 2551–2554; J. B. Lambert, G. T. Wang, D. H. Teramura, *J. Org. Chem.* **1988**, *53*, 5422–5428.
[26] P. J. Stang, A. M. Arif, C. M. Crittell, *Angew. Chem.* **1990**, 307–308; *Angew. Chem. Int. Ed. Engl.* **1990**, *29*, 287–288.
[27] M. Ochiai, T. Ho, Y. Takaoka, Y. Masaki, M. Kunishima, S. Tani, Y. Nagao, *J. Chem. Soc. Chem. Commun.* **1990**, 118–119.
[28] V. V. Zhdankin, C. M. Crittell, P. J. Stang, N. S. Zefirov, *Tetrahedron Lett.* **1990**, *31*, 4828–4831.
[29] P. J. Stang, B. L. Williamson, V. V. Zhdankin, *J. Am. Chem. Soc.* **1991**, *113*, 5870–5871.
[30] a) P. J. Stang, V. V. Zhdankin, *J. Am. Chem. Soc.* **1990**, *112*, 6437–6438; b) *ibid.* **1991**, *113*, 4571–4576.
[31] P. J. Stang, V. V. Zhdankin, R. Tykwinski, *J. Org. Chem.* **1992**, *57*, in press.
[32] P. J. Stang, J. Ullmann, *Synthesis* **1991**, 1073–1076.
[33] P. J. Stang, Z. Rappoport, M. Hanack, L. R. Subramanian, *Vinyl Cations*, Academic Press, New York, **1979**.
[34] M. D. Schiavelli, D. M. Jung, A. K. Vaden, P. J. Stang, T. E. Fisk, D. S. Morrison, *J. Org. Chem.* **1981**, *46*, 92–95.
[35] C. Dallaire, M. A. Brook, *Organometallics* **1990**, *9*, 2873–2876.
[36] F. M. Beringer, R. A. Nathan, *J. Org. Chem.* **1970**, *35*, 2095–2096; A. N. Nesmeyanov, T. P. Tolstaya, N. F. Sokolova, V. N. Varfolomeera, A. V. Petrakov, *Dokl. Akad. Nauk SSR* **1971**, *198*, 115–117; A. N. Nesmeyanov, T. P. Tolstaya, A. V. Petrakov, A. N. Goltsev, *ibid.* **1977**, *235*, 591–594; A. N. Nesmeyanov, T. P. Tolstaya, A. V. Petrakov, I. F. Leshcheva, *ibid.* **1978**, *238*, 1109–1112.
[37] T. Kitamura, R. Furuki, H. Taniguchi, P. J. Stang, *Tetrahedron Lett.* **1990**, *31*, 703–706.
[38] a) M. Ochiai, K. Sumi, Y. Takaoka, M. Kunishima, Y. Nagao, M. Shiro, E. Fujita, *Tetrahedron* **1988**, *44*, 4095–4112; b). M. Ochiai, K. Sumi, Y. Nagao, E. Fujita, *Tetrahedron Lett.* **1985**, *26*, 2351–2354.
[39] For reviews see: E. W. Colvin, *Silicon in Organic Synthesis*, Butterworths, London, **1981**; W. P. Weber, *Silicon Reagents for Organic Synthesis*, Springer, Berlin, **1983**.
[40] G. van Look, *Chem. Eng. News* **1989**, *67*(30), 2; P. J. Stang, *ibid.* **1989**, *67*(34), 4.
[41] V. V. Zhdankin, R. Tykwinski, R. Caple, B. Berglund, A. S. Koz'min, N. S. Zefirov, *Tetrahedron Lett.* **1988**, *29*, 3717–3720; V. V. Zhdankin, R. Tykwinski, B. Berglund, M. Mullikin, R. Caple, N. S. Zefirov, A. S. Koz'min, *J. Org. Chem.* **1989**, *54*, 2609–2612.
[42] A. A. Mironova, I. I. Maletina, S. V. Iksanova, V. V. Orda, L. M. Yagupolskii, *Zh. Org. Khim.* **1989**, *25*, 306–308.
[43] P. Pyykkö, A. Görling, N. Rösch, *Mol. Phys.* **1987**, *61*, 195; Y. Nomura, Y. Takeuchi, N. Nakawa, *Tetrahedron Lett.* **1969**, 639–642; A. A. Cheremisin, P. Schastnev, *J. Magn. Reson.* **1980**, *40*, 459–462.
[44] M. Ochiai, M. Kunishima, K. Fuji, Y. Nagao, M. Shiro, *Chem. Pharm. Bull.* **1989**, *37*, 1948–1950.
[45] C. K. Lee, T. C. W. Mak, W. K. Li, J. F. Kirner, *Acta Crystallogr.* **1974**, *39*, 2812–2816.
[46] G. F. Koser, R. H. Wettach, J. M. Troup, B. A. Frenz, *J. Org. Chem.* **1976**, *41*, 3609–3611.
[47] N. W. Alcock, R. M. Countryman, S. Esperas, J. F. Sawyer, *J. Chem. Soc. Dalton Trans.* **1979**, 854–860.
[48] A. E. Reed, P. von R. Schleyer, *J. Am. Chem. Soc.* **1990**, *112*, 1434–1445.
[49] M. Ochiai, M. Kunishima, K. Fuji, M. Shiro, Y. Nagao, *J. Chem. Soc. Chem. Commun.* **1988**, 1076–1077.
[50] A. N. Chekhlov, R. G. Gafurov, I. A. Pomytkin, I. V. Martynov, N. N. Aleinikov, S. A. Kashtanov, F. I. Dubovitskii, *Dokl. Akad. Nauk SSSR* **1986**, *291*, 414–417.
[51] V. N. Petrov, S. V. Lindeman, Y. T. Struchkov, F. A. Chugtai, V. A. Budylin, Y. G. Bundel, *Dokl. Akad. Nauk SSSR* **1983**, *269*, 614–616.
[52] P. J. Stang, H. Wingert, A. M. Arif, *J. Am. Chem. Soc.* **1987**, *109*, 7235–7236.
[53] N. S. Zefirov, A. S. Koz'min, V. D. Sorokin, V. K. Brel, E. V. Abramkin, K. A. Potekhin, Y. T. Struchkov, V. V. Zhdankin, P. J. Stang, *J. Org. Chem.*, **1992**, *57*, in press.
[54] J. I. Dickstein, S. I. Miller in *The Chemistry of the Carbon Carbon Triple Bond* (Ed.: S. Patai), Wiley-Interscience, London, **1978**, Chapter 19, pp. 813–955.
[55] K. B. Wiberg, W. E. Pratt, M. G. Matturro, *J. Org. Chem.* **1982**, *47*, 2720–2722.
[56] J. S. Lodaya, G. F. Koser, *J. Org. Chem.* **1990**, *55*, 1513–1516.
[57] M. Ochiai, M. Kunishima, Y. Nagao, F. Fuji, E. Fujita, *J. Chem. Soc. Chem. Commun.* **1987**, 1708–1709.
[58] P. J. Stang, C. M. Crittell, *Organometallics* **1990**, *9*, 3191–3193.
[59] J. March, *Advanced Organic Chemistry: Reactions, Mechanisms and Structure*, 2nd ed., McGraw-Hill, New York, **1977**; H. O. House, *Modern Synthetic Reactions*, 2nd ed., W. A. Benjamin, Menlo Park, CA, USA, **1972**; T. H. Lowry, K. S. Richardson, *Mechanism and Theory in Organic Chemistry*, 2nd ed., Harper and Row, New York, **1981**; C. Walsh, *Enzymatic Reaction Mechanisms*, Freeman, San Francisco, **1979**.
[60] P. J. Stang, M. Boehshar, H. Wingert, T. Kitamura, *J. Am. Chem. Soc.* **1988**, *110*, 3272–3278.
[61] P. J. Stang, T. Kitamura, M. Boehshar, H. Wingert, *J. Am. Chem. Soc.* **1989**, *111*, 2225–2330.
[62] P. J. Stang, K. A. Roberts, *J. Am. Chem. Soc.* **1986**, *108*, 7125–7127.
[63] A. D. Allen, T. Kitamura, R. A. McClelland, P. J. Stang, T. T. Tidwell, *J. Am. Chem. Soc.* **1990**, *112*, 8873–8878; A. D. Allen, K. A. Roberts, T. Kitamura, P. J. Stang, T. T. Tidwell, *ibid.* **1988**, *110*, 622–624.
[64] D. Segal, Y. Shalitin, H. Wingert, T. Kitamura, P. J. Stang, *FEBS Lett* **1989**, *247*, 217–220; J. N. Blankenship, H. Abu-Soud, W. A. Francisco, F. M. Raushel, D. R. Fischer, P. J. Stang, *J. Am. Chem. Soc.* **1991**, *113*, 8560–8561.
[65] G. Maas, M. Regitz, R. Rahm, H. Wingert, J. Schneider, P. J. Stang, C. M. Crittell, *J. Chem. Soc. Chem. Commun.* **1990**, 1456–1457; G. Maas, R. Rahm, F. Krebs, M. Regitz, P. J. Stang, C. M. Crittell, *Chem. Ber.* **1991**, *124*, 1661–1665.
[66] For a review see: P. J. Stang, *Acc. Chem. Res.* **1991**, *24*, 304–310; P. J. Stang, K. A. Roberts, *J. Org. Chem.* **1987**, *52*, 5213–5217; P. J. Stang, T. Kitamura, A. M. Arif, M. Karni, Y. Apeloig, *J. Am. Chem. Soc.* **1990**, *112*, 374–381; P. J. Stang, C. M. Crittell, A. M. Arif, M. Karni, Y. Apeloig, *ibid.* **1991**, *113*, 7461–7470.
[67] P. J. Stang, *Methoden Org. Chem.* (*Houben-Weyl*) *4th ed. 1952–*, Vol. E19b, Part I, pp. 84–165; *Acc. Chem. Res.* **1982**, *15*, 348–354; *Chem. Rev.* **1978**, *78*, 383–405.
[68] M. Ochiai, M. Kunishima, K. Fuji, Y. Nagao, *J. Org. Chem.* **1988**, *53*, 6144–6145.
[69] T. Kitamura, P. J. Stang, *Tetrahedron Lett.* **1988**, *29*, 1887–1890.
[70] D. Fischer, P. J. Stang, unpublished results.
[71] M. Ochiai, M. Kunishima, Y. Nagao, K. Fuji, M. Shiro, E. Fujita, *J. Am. Chem. Soc.* **1986**, *108*, 8281–8283.
[72] M. Ochiai, M. Kunishima, S. Tani, Y. Nagao, *J. Am. Chem. Soc.* **1991**, *113*, 3135–3142.

[73] C. Crittell, B. L. Williamson, P. J. Stang, unpublished results.
[74] E. Kotali, A. Varvoglis, A. Bozopoulos, *J. Chem. Soc. Perkin Trans. 1* **1988**, 1–6.
[75] P. J. Stang, T. Kitamura, *J. Am. Chem. Soc.* **1987**, *109*, 7561–7563.
[76] Reviews: W. J. Scott, J. E. McMurry, *Acc. Chem. Res.* **1988**, *21*, 47–54; E. Negishi, *ibid.* **1982**, *15*, 340–348; A. Suzuki, *ibid.* **1982**, *15*, 178–184; J. K. Stille, *Angew. Chem.* **1986**, *98*, 504–519; *Angew. Chem. Int. Ed. Engl.* **1986**, *25*, 508–524; *Pure Appl. Chem.* **1985**, *57*, 1771–1780; A. Suzuki, *ibid.* **1985**, *57*, 1749–1758.
[77] T. Kitamura, I. Mihara, H. Taniguchi, P. J. Stang, *J. Chem. Soc. Chem. Commun.* **1990**, 614–615.
[78] A. J. Margida, G. F. Koser, *J. Org. Chem.* **1984**, *49*, 4703–4706.
[79] Y. Tamura, T. Yakura, J. Haruta, Y. Kita, *Tetrahedron Lett.* **1985**, *26*, 3837–3840.
[80] R. M. Moriarty, R. K. Vaid, M. P. Duncan, B. K. Vaid, *Tetrahedron Lett.* **1987**, *28*, 2845–2848.
[81] M. Ochiai, M. Kunishima, K. Fuji, Y. Nagao, *J. Org. Chem.* **1989**, *54*, 4038–4041.
[82] Z. Rappoport, *Recl. Trav. Chim. Pays-Bas* **1985**, *104*, 309–349; *Acc. Chem. Res.* **1981**, *14*, 7–15; G. Modena, *ibid.* **1971**, *4*, 73–80.
[83] M. Ochiai, Y. Takaoka, Y. Nagao, *J. Am. Chem. Soc.* **1988**, *110*, 6565–6566.
[84] M. Ochiai, Y. Takaoka, K. Sumi, Y. Nagao, *J. Chem. Soc. Chem. Commun.* **1986**, 1382–1384.
[85] P. J. Stang, M. Hanack, L. R. Subramanian, *Synthesis* **1982**, 85–126.
[86] P. J. Stang, J. Ullmann, *Angew. Chem.* **1991**, *103*, 1549–1550; *Angew. Chem. Int. Ed. Engl.* **1991**, *30*, 1469–1470.

Bond-Stretch Isomers: Fact or Artifact?

By *James M. Mayer**

Isomerism—the idea that a set of atoms can have more than one stable structure—is a fundamental concept in chemistry. The observation of isomers spurred the study of stereochemistry in both inorganic and organic chemistry well before the advent of modern tools for structure elucidation. Isomers can be broadly classified as constitutional isomers, with different connectivity between the atoms (e.g., 1-butene vs. 2-butene) or configurational (or conformational) isomers, with the same connectivity but different shape (*cis*- vs. *trans*-2-butene). In the early 1970s, a new kind of isomerism was independently proposed by Chatt et al.[1] and by Hoffmann et al.,[2] in which the isomers differ only in their bond lengths.

Chatt et al. performed X-ray structural studies of blue and green forms of the molybdenum oxo complexes $[Mo(O)Cl_2(PR_3)_3]$ ($PR_3 = PMe_2Ph$, PEt_2Ph) and found that both adopted a *cis-mer* arrangement of the ligands (**A**) but appeared to have very different molybdenum–oxygen bond lengths: 167.6(7) pm in the blue form (a normal length for Mo=O[3]) but 180.1(9) pm in the green form.[1] They termed these compounds "distortional isomers". Stohrer and Hoffmann proposed the more precise term "bond-stretch isomers" in their theoretical study of possible isomers of $(CH)_5^+$ (**B**) and related species.[2]

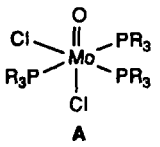

A

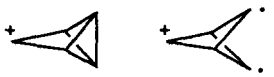

B

Bond-stretch isomers are defined theoretically by the presence of a double minimum in the potential energy surface along the coordinate of a vibrational bond stretch with enough of a barrier between the minima to allow observation of the isomers. In 1988 Jean, Lledos, Burdett, and Hoffmann examined Chatt's compounds using extended Hückel calculations[4] and proposed that bond-stretch isomerism could arise from electronic mechanisms described as Jahn–Teller distortions, which can be described in this case as the competition between the chloro and oxo ligands for π bonding to the metal. But Jahn–Teller minima typically have very small barriers between them, and observed structures are thought to be strongly affected by crystal-packing forces.[5] Two minima are more commonly found when two different potential energy surfaces are involved. There are a number of examples of transition-metal complexes with different spin states, for instance iron(III) tris(dithiocarbamate) complexes with high spin/low spin equilibria.[6] Kölle has recently reported an interesting example in this journal: The dimeric ruthenium complex $[\{Cp^*RuCl(\mu\text{-}Cl)\}_2]$ ($Cp^* = \eta\text{-}C_5Me_5$) appears to have two isomers, one diamagnetic with a metal–metal bond (Ru–Ru = 293.0(1) pm) (**C**) and the other paramagnetic without strong Ru–Ru bonding (375.2(1) pm) (**D**).[7] Kölle has also given a brief discussion of such bistable systems in a recent Highlight in this journal.[8]

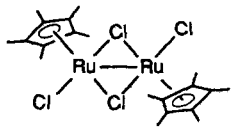

C

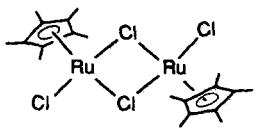

D

But bond-stretch isomers have the same bonding arrangement and yet two minima on the same energy surface. If unequivocally proven this would be an important new kind of isomerism.

However, the conclusion that there are isomeric forms of Chatt's molybdenum complex **A** has been recently shown to be in error. Yoon, Parkin, and Rheingold have re-examined $[Mo(O)Cl_2(PR_3)_3]$ ($PR_3 = PMe_3$, PMe_2Ph) by X-ray crystallography and found a variety of Mo="O" bond lengths, from 167.5(3) pm to more than 200 pm, depending on the specific crystal chosen.[9] Elemental analysis and spectroscopic investigation of the crystals, particularly by NMR, showed that the green crystals with the long Mo="O" bonds are actually solid solutions (mixtures) of $[Mo(O)Cl_2(PR_3)_3]$ (**1**) and $[MoCl_3(PR_3)_3]$ (**2**). Similar conclusions have been reached by Enemark et al. using a number of spectroscopic and analytical techniques.[10]

The critical feature is that **1** and **2** co-crystallize, because the crystal packing is determined by the bulky phosphine ligands. Therefore in the X-ray experiment one "sees" a mixture of O and Cl in the position of the oxygen atom, and measures a distance between the true M=O and Mo–Cl distances of 167.5(3) and 240.0(1) pm. In Yoon, Parkin and Rheingold's study each crystal had a different ratio of oxygen to chlorine and exhibited a different Mo–"O" distance. This crystallographic disorder had not been previously noticed, because the structures with Mo–O/Cl distances up to 187.1(3) pm were refined quite nicely as containing simply an oxygen atom (although at this distance the thermal ellipsoid of the "oxygen" atom begins to look a little elongated).[9b] Remarkably, the crystal that showed an apparent bond length of 187.1(3) pm, 20 pm longer than the true Mo=O distance, was obtained from a sample of composition 96% **1** and only 4% **2**. A small amount of **2** can cause a large change in the apparent bond length because the heavier chlorine atom scatters X-rays much more effectively than oxygen does.

Since the original report by Chatt, a dozen or more metal complexes have been suggested to be distortional or bond-stretch isomers.[11] Given that Chatt's compounds are not isomers, these claims must be called into question as well. Many of them appear to fit Parkin's explanation, that the

[*] Prof. J. M. Mayer
Department of Chemistry, University of Washington
Seattle WA 98195 (USA)

 © VCH Verlagsgesellschaft mbH, W-6940 Weinheim, 1992 0570-0833/92/0303-0286 $ 3.50+.25/0

"isomer" with the long bond is actually a mixture, in which the site in question may be occupied by either O or Cl (typically). For instance, Wieghardt now believes that the green "isomer" of $[(Me_3tacn)W(O)Cl_2]^+$ with the long W–O bond is likely a mixture of this type, with $[(Me_3tacn)W(O)_2Cl]^+$ as the impurity (Me_3tacn = *N*,*N*′,*N*″-trimethyltriazacyclononane).[12] In addition, recent ab initio calculations by Hall et al.[13] on the molybdenum–oxo complexes and related systems have failed to provide any evidence for bond-stretch isomers. This calls into question the earlier theoretical study based on more approximate calculational methods.

New reports of bond-stretch isomers thus bear a heavy burden to prove that the apparent isomers are not mixtures. A recent report in this journal by Bashall, Gibson, McPartlin, et al.[14] provides a good example. Yellow and green bond-stretch isomers of the niobium–oxo complex $[Nb(O)Cl_3(PMe_3)_3]$ (**3a, b**) and orange and green isomers of the thio analogue, $[Nb(S)Cl_3(PMe_3)_3]$ (**4a, b**), were proposed; the green forms in each case are reported to have unusually long M–E multiple bonds (E = O, S). If this case resembles that of **1** and **2**, the green isomers would contain $[NbCl_4(PMe_3)_3]$ (**5**), a known material[15] which is green and essentially isostructural with **3** and **4**. Indeed, the crystal of the green

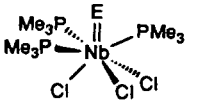

3: E = O; **3a**, *d*(Nb=O) = 178.1 (6) pm; **3b**, *d*(Nb=O) = 192.9 (6) pm

4: E = S; **4a**, *d*(Nb=S) = 219.6 (2) pm; **4b**, *d*(Nb=S) = 229.6 (2) pm

oxo complex **3b** was found to contain ca. 20% **5** by X-ray crystallography.[14] The fact that complex **5** is an impurity in this system can be explained easily, because PMe_3 is a good reducing agent and Nb^V is somewhat oxidizing—**3a** converts to **3b** on standing in toluene. According to Yoon, Parkin, and Rheingold,[9] as little as a few percent of **5** in a crystal of **3b** would be sufficient to increase the Nb="O" bond length by 14 pm. Bashall, Gibson, McPartlin et al. claim to have successfully modeled the compositional disorder in their crystal of **3b**, although the Nb–Cl bond length they obtain for the $NbCl_4(PMe_3)_3$ impurity in **3b** is 8 pm longer than the distance in crystals of pure **5** (see note 12 in ref. [14]). It is also troubling that while the X-ray data show 20% of paramagnetic (d^1) **5** in the crystals of **3b**, magnetic measurements show **3b** to be diamagnetic (note 11 in ref. [14]). Clearly, it is important in these cases that all measurements be done on samples from the same batch of material, preferably on the same crystal.

It is more difficult to prove that the green thio complex **4b** is a mixture. Sulfur and chlorine are next to each other in the periodic table and therefore have very similar X-ray scattering power. Thus a much higher level of impurity would be required for the observed bond lengths to be obtained. Assuming the same scattering from S and Cl, this argument would suggest that **4b** is a mixture of about 55% **4a** and 45% **5** based on the Nb="S" bond length of 229.6(2) pm, roughly halfway between the Nb=S and Nb–Cl bond lengths of **4a** and **5** (219.6(2) and 240.9(4) pm).

It is not clear that Gibson and McPartlin's results can be explained simply by the assumption that the green isomers are mixtures. The most difficult observation to explain are the different Nb=O and Nb=S stretching frequencies in the isomers, particularly in the case of the thio complex, for which different $\nu_{Nb=S}$ bands could be observed in IR spectra of solutions. (Although it is strange that **4b** has a *longer* Nb–S bond and a *higher* stretching frequency.) But given that there are no clear examples of bond-stretch isomers, more work is required—and more studies will certainly follow their brief and interesting communication—to demonstrate that these materials are truly isomers. One approach would be to show that there is very little **5** in both the single crystals and bulk samples of the green materials by EPR or optical spectroscopy, magnetic susceptibility measurements, elemental analysis for Cl, electrochemistry, or some other combination of techniques. Comparison of the properties of the green isomers with intentionally made mixtures of **3a** or **4a** with **5** in defined proportions could also be informative. Perhaps the most definitive results would be obtained from other X-ray structures. Parkin and Rheingold found that each batch of crystals had a different composition and therefore showed a different apparent bond length. If a number of structural analyses all yielded the bond lengths found for the **a** and **b** isomers, this would be good (though not conclusive) evidence for two discrete isomers.

The possible existence of bond-stretch isomers will likely continue to fascinate chemists for some time. However, because the early reports of bond-stretch isomers have been shown to be incorrect, there are now no established examples. Thus in new reports of bond-stretch isomers, chemists would be prudent to take the approach that they are proving a new, and challenging, form of isomerism.

German version: *Angew. Chem.* **1992**, *102*, 293

[1] J. Chatt, L. Manojlović-Muir, K. W. Muir, *Chem. Commun.* **1971**, 655–666; L. Manojlović-Muir, *J. Chem. Soc. A* **1971**, 2796; L. Manojlović-Muir, K. W. Muir, *J. Chem. Soc. Dalton Trans.* **1972**, 686–690; B. L. Haymore, W. A. Goddard III, J. N. Allison, *Proc. Int. Conf. Coord. Chem. 23rd.*, **1984**, 535.

[2] W.-D. Stohrer, R. Hoffmann, *J. Am. Chem. Soc.* **1972**, *94*, 1661.

[3] J. M. Mayer, *Inorg. Chem.* **1988**, *27*, 3899–3903.

[4] Y. Jean, A. Lledos, J. K. Burdett, R. Hoffmann, *J. Am. Chem. Soc.* **1988**, *110*, 4506.

[5] Ref. [4] contains a discussion of Jahn–Teller distortions in this context.

[6] E. König, *Prog. Inorg. Chem.* **1987**, *35*, 527; M. Bacci, *Coord. Chem. Rev.* **1988**, *86*, 245; J. K. Beattie, *Adv. Inorg. Chem.* **1988**, *32*, 1; P. Gütlich, *Struct. Bonding (Berlin)* **1981**, *44*, 83.

[7] U. Kölle, J. Kossakowski, N. Klaff, L. Wesemann, U. Englert, G. E. Herberich, *Angew. Chem.* **1991**, *103*, 732; *Angew. Chem. Int. Ed. Engl.* **1991**, *30*, 690. A related example is the observation that $[\{Cp^*Re(O)(\mu\text{-}O)\}_2]$ does not have a metal–metal bond while the isoelectronic $[\{(tacn)Re(O)(\mu\text{-}O)\}_2]$ has a Re–Re double bond: W. A. Herrmann, M. Flöel, J. Kulpe, J. K. Felixberger, E. Herdtweck, *J. Organomet. Chem.* **1988**, *355*, 297; G. Böhm, K. Wieghardt, B. Nuber, J. Weiss, *Angew. Chem.* **1990**, *102*, 832; *Angew. Chem. Int. Ed. Engl.* **1990**, *29*, 787.

[8] U. Kölle, *Angew. Chem.* **1991**, *103*, 970; *Angew. Chem. Int. Ed. Engl.* **1991**, *30*, 956.

[9] a) K. Yoon, G. Parkin, A. L. Rheingold, *J. Am. Chem. Soc.* **1991**, *113*, 1437; b) K. Yoon, G. Parkin, A. L. Rheingold, *J. Am. Chem. Soc.*, submitted.

[10] P. J. Desrochers, K. W. Nebesny, M. J. LaBarre, S. E. Lincoln, T. M. Loehr, J. H. Enemark, *J. Am. Chem. Soc.* **1991**, *113*, 9193.

[11] For a summary, see refs. [9b], [10] and W. A. Nugent, J. M. Mayer, *Metal-Ligand Multiple Bonds*, Wiley, New York, **1988**, pp. 152–154.

[12] K. Wieghardt, G. Backes-Dahmann, B. Nuber, J. Weiss, *Angew. Chem.* **1985**, *97*, 773; *Angew. Chem. Int. Ed. Engl.* **1985**, *24*, 777; K. Wieghardt, personal communication, **1991**.

[13] J. Song, M. B. Hall, *Inorg. Chem.*, **1991**, *30*, 4433.

[14] A. Bashall, V. C. Gibson, T. P. Kee, M. McPartlin, O. B. Robinson, A. Shaw, *Angew. Chem.* **1991**, *103*, 1021; *Angew. Chem. Int. Ed. Engl.* **1991**, *30*, 980.

[15] F. A. Cotton, M. P. Diebold, W. J. Roth, *Polyhedron* **1985**, *4*, 1103.

Sugars as Chiral Auxiliaries for the Synthesis of Enantiomerically Pure Compounds

By *Hans-Ulrich Reissig**

Practical solutions for the preparation of enantiomerically pure compounds by asymmetric synthesis have been found for most important reactions. An often recurring feature is the use of derivatives of amino acids or terpenes as inducing auxiliaries. Although economical and available in a large structural variety, sugar derivatives play a far smaller role in this respect, which is certainly attributable to their large number of functional groups that makes the interpretation of the reaction path difficult. This complexity apparently frightens off most chemists. But the rapidly increasing number of publications proves that the use of sugar derivatives can achieve an impressive asymmetric induction in many reactions.

As several papers by Duthaler et al.[1] show, the organotitanium compounds **2** and **3** may be prepared from [Cp-Ti(OR*)$_2$Cl] (**1**), which is easily accessible from "diacetoneglucose" and cyclopentadienyltitanium trichloride. These organotitanium complexes transfer their nucleophilic allyl or enolate component to aldehydes with high enantioselectivity. The resulting alcohols and aldol adducts are formed usually in more than 90% *ee*.

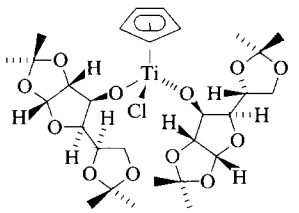

1

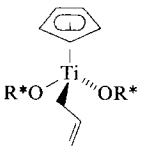

2

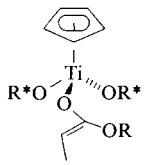

3, R = Alkyl, Aryl

As electrophilic reagents one can employ imines **4**, derived from D-galactosylamine. They react—mostly supported by Lewis acids—with several nucleophiles to form amines. The research group of Kunz, which studies the potential of carbohydrates as chiral matrixes, discovered that D-α-amino acids may be prepared in this way in a Strecker synthesis.[2] Although the asymmetric induction is seldom complete, the primary addition product may be obtained diastereomerically pure by simple recrystallization. They hydrolyze to the enantiomerically pure D-amino acids and tetra-*O*-pivaloyl-D-galactose, which can be converted back to imines.

The β-amino acids[3] are obtained analogously from mono-*O*-silylated ketene acetals, Mannich bases[4] (which may be cyclized to form piperidones) from 1-methoxy-3-trimethylsiloxybutadiene, and finally homoallylamines in high optical yields[5] from allyltrimethylsilane. No mechanistic interpretations of these reactions will be discussed because as yet they remain speculative. L-Fucose is a quasi-enantiomer to D-galactose and therefore the imines derived therefrom should undergo similar reactions to yield the antipodes of the above-mentioned compounds. This was verified for the homoallylamines at least.[6] Asymmetric 1,4-additions of cuprates to enones with a carbohydrate auxiliary have

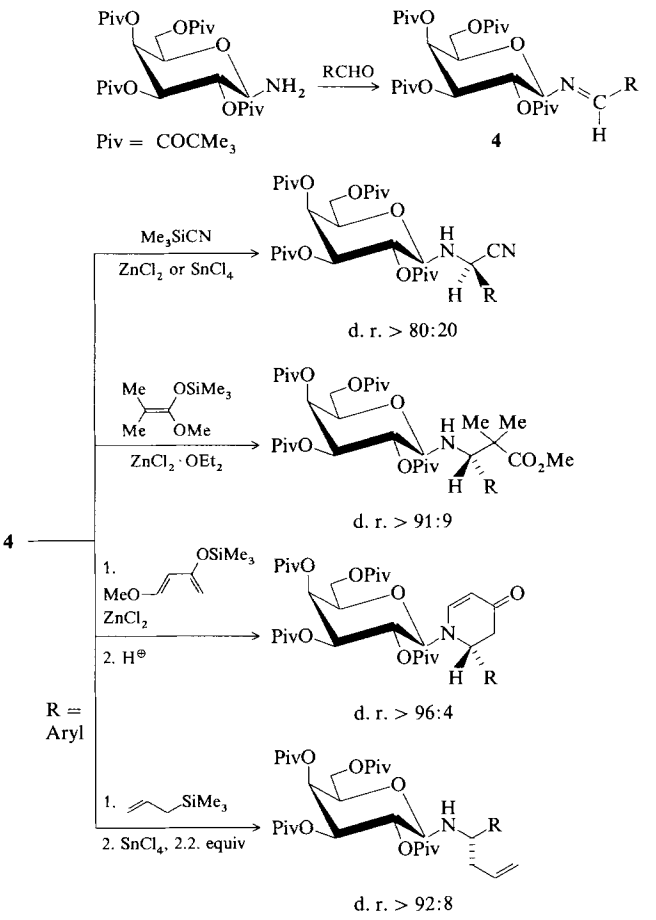

also been described recently.[7] Cuprates generated from Grignard reagents attack the D-xylofuranose derivative **5** with a strong preference for the front side and yield the corresponding adducts in a diastereomeric ratio of mostly more than 95:5.

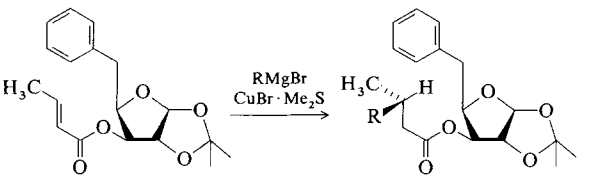

5

d. r. > 94:6

Certainly, sugar derivatives were also employed as auxiliaries for cycloaddition reactions. Often the selectivity may be improved by fixing the conformation of the carbohydrate component with Lewis acid catalysts or reagents like those in the examples already described. This is clearly fulfilled in the asymmetric cyclopropanation of allyl ethers of type **6**, which are easily accessible as pure β-anomers from tri-*O*-benzyl-D-glucal and allyl alcohols. Their reaction with an excess of diethylzinc/diiodomethane proceeds with diastereoselectivities of greater than 50:1 in favor of the front-side attack, effectively directed by a prior complexation of the carbenoid

[*] Prof. Dr. H.-U. Reissig
Institut für Organische Chemie der Technischen Hochschule
Petersenstrasse 22, D-W-6100 Darmstadt (FRG)

at the free hydroxyl group (Scheme 1).[8] Without the free 2-hydroxyl group, the preorientation of the reagent is very much less effective, and the selectivity falls to 2–3.5:1. The amount of cyclopropanation reagent (more than 2 equiv) is also crucial for success.

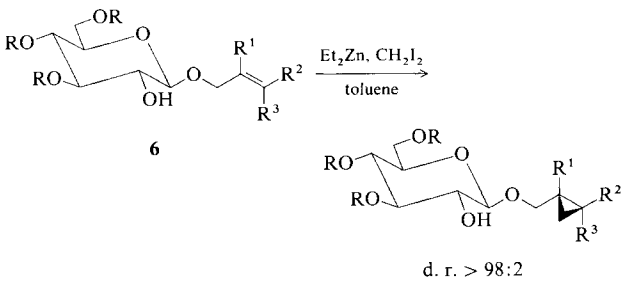

Scheme 1. R = $CH_2C_6H_5$; R^1 = H, alkyl; R^2 = alkyl, C_6H_5; R^3 = H, alkyl.

In this way several optically active, functionalized cyclopropane derivatives are available in high enantiomeric purity after the removal of the sugar auxilary. Interestingly, the use of the α anomer induces the opposite configuration at the cyclopropane ring! Thus, both enantiomers of a cyclopropane derivative are accessible through one auxiliary.

Kunz et al.[9] also thoroughly investigated Diels–Alder reactions of acrylates with carbohydrate auxiliaries. By correct choice of Lewis acids [4 + 2] cycloadditions are possible with many 1,3-dienes with excellent diastereoselectivities. The reactions of acrylates **7** and **8**, synthesized from D-glucose and L-rhamnose, respectively, with cyclopentadiene, which lead to stereochemically complementary cycloadducts, serve as representative examples.

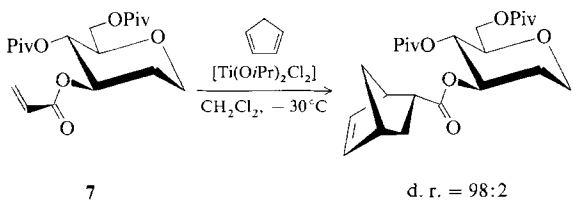

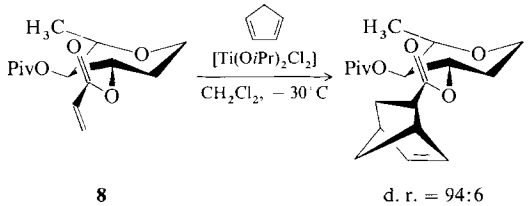

In addition, 1,3-dienes[10] and nitrones[11] with carbohydrate auxiliaries have already been employed in cycloadditions but with varied success. In these reactions the conformational fixation by metal-complex fragments is lacking, and the asymmetric induction is not always high. Kresze et al.[12] performed hetero-Diels–Alder and ene reactions with the nitroso compound **9** and obtained interesting hydroxylamine derivatives in high enantiomeric purity.

Moreover, for Diels–Alder reactions with inverse electronic demand, enol ethers with diacetoneglucose as inducing chiral auxiliary have proved to be quite effective

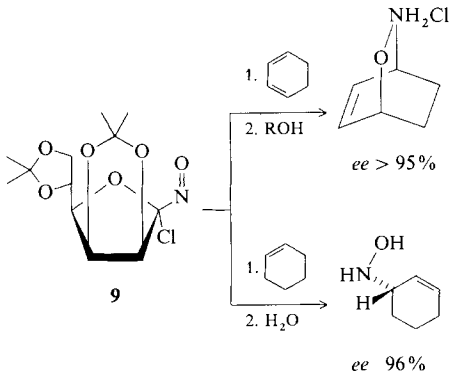

dienophiles.[13] Allene **10** or (*E*)-enol ether **11** react with nitrosoalkenes generated in situ to form 1,2-oxazines with high diastereoselectivities (Scheme 2). In particular the rapid and economical synthesis of diacetoneglucose distinguishes this auxiliary from others. The examples quoted emphasize that chelate effects for fixing conformations are not a prerequisite for successful asymmetric syntheses with sugar derivatives if suitable auxiliaries are chosen.

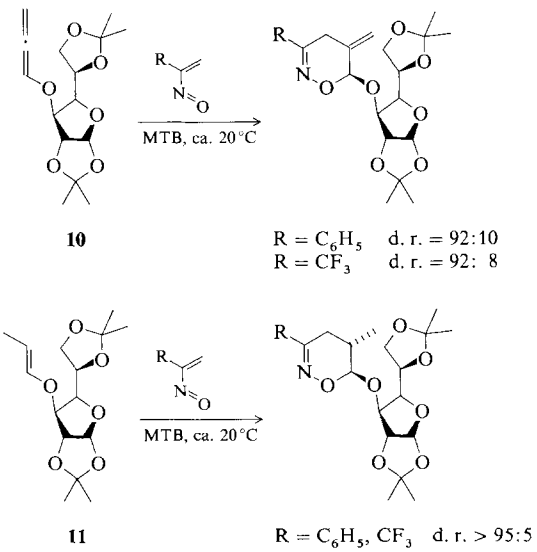

Scheme 2. MTB = *tert*-butyl methyl ether.

The intention of this (incomplete) summary is to demonstrate that carbohydrates are also securing their place as optically active chiral auxiliaries in organic synthesis, and that in this hitherto little explored area further successes can be anticipated.[14] These inexpensive compounds can be harnessed as willing workhorses for asymmetric syntheses. This method should stand beside with the more or less elegant dissection of carbohydrates, which makes use of only the stereochemically required fragment as building block for enantiomerically pure compounds.[15]

German version: *Angew. Chem.* **1992**, *104*, 295

[1] Reviews: R. O. Duthaler, A. Hafner, M. Riediker, *Pure Appl. Chem.* **1990**, *62*, 631–642; K. H. Dötz, *Nachr. Chem. Tech. Lab.* **1990**, *38*, 1244–1247.
[2] H. Kunz, W. Sager, D. Schanzenbach, M. Decker, *Liebigs Ann. Chem.* **1991**, 649–654. For Ugi's four component synthesis of amino acid deriva-

tives, see H. Kunz, W. Pfrengle, *J. Am. Chem. Soc.* **1988**, *110*, 651–652 and M. Goebel, I. Ugi, *Synthesis* **1991**, 1095–1098.
[3] H. Kunz, D. Schanzenbach, *Angew. Chem.* **1989**, *101*, 1042–1043; *Angew. Chem. Int. Ed. Engl.* **1989**, *28*, 1068.
[4] H. Kunz, W. Pfrengle, *Angew. Chem.* **1989**, *101*, 1041–1042; *Angew. Chem. Int. Ed. Engl.* **1989**, *28*, 1067.
[5] S. Laschat, H. Kunz, *Synlett* **1990**, 51–52.
[6] S. Laschat, H. Kunz, *Synlett* **1990**, 629–630. See also H. Kunz, W. Pfrengle, K. Rück, W. Sager, *Synthesis* **1991**, 1039–1042.
[7] Y.-S. Hon, F.-L. Chen, Y.-P. Huang, T.-J. Lu, *Tetrahedron: Asymmetry* **1991**, *2*, 879–882.
[8] A. B. Charette, B. Cote, J.-F. Marcoux, *J. Am. Chem. Soc.* **1991**, *113*, 8166–8167.
[9] H. Kunz, B. Müller, D. Schwanzenbach, *Angew. Chem.* **1987**, *99*, 269–271; *Angew. Chem. Int. Ed. Engl.* **1987**, *26*, 267; W. Stähle, H. Kunz, *Synlett* **1991**, 260–262; see also R. Nougier, J.-L. Gras, B. Giraud, A. Virgili, *Tetrahedron Lett.* **1991**, *32*, 5529–5530.
[10] S. A. David, A. Lubineau, A. Thieffry, *Tetrahedron* **1978**, *34*, 299–304; D. S. Larsen, R. J. Stoodley, *J. Chem. Soc. Perkin Trans. 1* **1989**, 1841–1852; S. W. Bird, A. Lewis, *Tetrahedron Lett.* **1989**, *30*, 6227–6228.
[11] R. Huber, A. Knieringer, J.-P. Obrecht, A. Vasella, *Helv. Chim. Acta* **1985**, *68*, 1730–1747, and literature cited therein.
[12] H. Felber, G. Kresze, R. Rewo, A. Vasella, *Helv. Chim. Acta* **1986**, *69*, 1137–1146; H. Braun, H. Felber, G. Kresze, A. Ritter, F. P. Schmidtchen, A. Schneider, *Tetrahedron* **1991**, *47*, 3312–3328.
[13] T. Arnold, B. Orschel, H.-U. Reissig, unpublished; *Angew. Chem.* submitted. For cycloadditions of vinyl ethers with sugar auxiliaries to isoquinolinium salts, see A. Choudhury, R. W. Franck, R. B. Gupta, *Tetrahedron Lett.* **1989**, *30*, 4921–4924.
[14] L. Duhamel, P. Angibaud, J. R. Desmurs, J. Y. Valnot, *Synlett.* **1991**, 807–808.
[15] See K. Krohn *Chiral Building Blocks from Carbohydrates* in J. Mulzer, H.-J. Altenbach, M. Braun, K. Krohn, H.-U. Reissig, *Organic Synthesis Highlights*, VCH, Weinheim, **1991**, p. 251–260, and literature cited therein.

Structures, Structures, and Structures

By *Rudolf Janoschek**

The production of new compounds has always been the main concern of chemistry. But what has changed in the course of time is the documentation of the corresponding molecules. For a long time the representation of empirical formulae was seen as sufficient. The phenomenon of isomerism then forced the chemist to write molecules in such a way that their atom connectivity could be seen. This notation not only made it possible to write two chemically different compounds also in a different way, but furthermore, made it possible that today for a given empirical formula using a topological algorithm the complete set of all possible constitutional isomers can be written down from which it can be realized just how few of all the possible compounds are known up to now. For example, there are 217 constitution isomers for the empirical formula C_6H_6, of which up to now only a small fraction is known.

However, the atom connectivity, too, from today's viewpoint is only an insufficient fact file. The times in which methane was drawn as a planar cross and benzene as an elongated hexagon have long since passed. This was the result of the arrival of new methods in chemistry for the determination of molecular structures. Here, above all, X-ray diffraction should be mentioned which led to bond lengths, bond angles, and dihedral angles now being seen as binding numerical data. The sign of recognition of a molecule today is a ball-and-stick model shown in perspective. For further details concerning the development of the chemical symbol terminology see an amusing essay of R. Hoffmann and P. Laszlo.[1]

As useful and successful as X-ray diffraction is to determine *the* structure for *one* molecule, it might nevertheless keep something significant from us. Apart from constitutional isomerism there are also other forms of isomerism as well, among them one for which the isomers do not differ in the atom connectivity, hardly differ in bond lengths and angles, however, they do differ in the dihedral angles. These isomers are called conformers. One example is the chair- and boat-forms of cyclohexane. Isomers which only differ in dihedral angles generally are energetically very similar. Of course, only those isomers which actually exist can be investigated by X-ray crystallography. In contrast, there are no limits for the quantum chemical structure determination if, on the basis of the energy hypersurface, it wants to break structurally new ground.

The concept of a calculated structure determination led to the realization that for a chemical compound one should no longer ask for *the* structure but should expect structures about structures. Quantum chemistry provides a precise differential geometric definition for the structure term: A structure corresponds to a point on the energy hypersurface at which the first derivatives of the energy to all inner degrees of freedom are zero (stationarity) and all second derivatives (force constants) are positive. The reader might be surprised to find such banalities under the heading "highlights". However, he is referred to last year's editions of some chemical journals to see how many declared structures have never been adequately identified as minima. This rebuke is not only directed at the authors. Where the calculated structures were correctly characterized by first and second derivatives of the energy, the author usually liked to point out that an interesting goal for the synthesis had been calculated. However, such prognoses, too, are premature because in the differential geometric structure definition the kinetic stability necessary for an experimentally relevant structure is not taken into consideration. For this a deterring example is described below.

The molecule of elemental phosphorus is the tetrahedral P_4; an N_4 homologue to this has so far not been proven. The study of the electronic structure of the calculated N_4 did not provide any indications concerning instability. There are sufficient bonding orbitals as for P_4. Thus, naive chemical bond theory in its innermost core shows a fatal inability, which

[*] Prof. Dr. R. Janoschek
Institut für Theoretische Chemie der Universität
Mozartgasse 14, A-8010 Graz (Austria)

manifests itself when the attempt is made to derive statements on stability from molecular orbitals. The reason for the instability of N_4 has to be searched for somewhere completely different: Tetrahedral N_4 corresponds to a minimum on the energy hypersurface but the activation energy for the decomposition of N_4 into $2\,N_2$ is only 1 kcal mol^{-1}. Not only that, on the other side of the transition structure an extreme energetic drop of 230 kcal mol^{-1} takes place to $2\,N_2$ (according to semiempirical PM3 calculations). Thus, it is the particular stability of N_2 which makes N_4 so unstable. It seems that a minimum on the energy hypersurface is only a necessary condition for an experimentally relevant structure. Additionally, it has to be made sure that all activation "barriers" which are directly reachable from this minimum have a certain energetic minimum height.

After this self-examination, we now want to turn to the "highlight". The authors T. Head-Gordon, M. Head-Gordon, M. J. Frisch, C. L. Brooks, and J. A. Pople had made it their objective to calculate all the conformers relative to the dihedral angles ϕ = C1-N1-C_α-C2 and ψ = N1-C_α-C2-N2 for two model compounds—the analogues **1** and **2** of glycinedipeptide and alaninedipeptide respectively—by ab initio methods.[2]

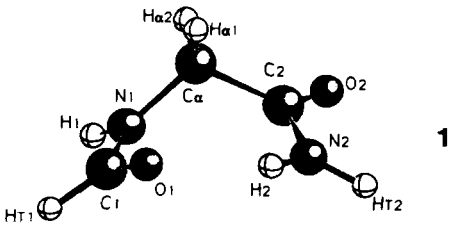

1

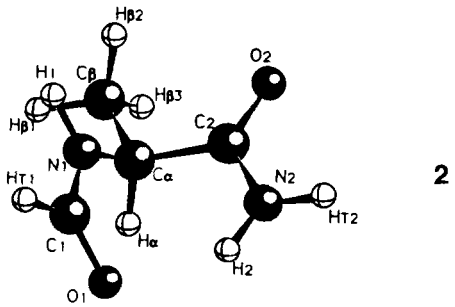

2

They proceeded as follows. At first an energy point-lattice was produced via the definition area of the dihedral angle pair. For each lattice point all remaining inner degrees of freedom were optimized. All in all, a total of 576 optimizations were carried out per molecule. From the energy point-lattice the approximate localization of all stationary points can be read off. In a second step these were numerically precisely recorded through total optimizations. In a third step the stationary points were characterized via the second derivatives of the energy. Apart from the structures of the conformers (minima) all transition structures between them could be recorded. The latter, too, correspond to stationary points but to those with one negative force constant. For **1** two minima and three transition structures were found, for **2** six minima and ten transition structures.

Figure 1 shows the (ϕ, ψ)-surface for **1**, which is symmetrical relative to the inversion center $\phi = \psi = 0°$. If improved calculations (HF/6-31+G*) for the stationary points are carried out, then the minimum 3 and the transition structures 4, 7, and 8 disappear. Via the saddle point 5 (activation

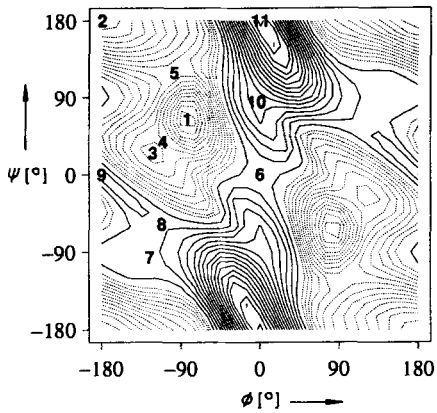

Fig. 1. The (ϕ,ψ)-surface of **1**, calculated at the HF/3-21G level. The zero of energy lies in the minimum 1 (the corresponding structure is **1**). The dashed energy contours are drawn every 0.5 kcal mol^{-1}, the solid contours every 1 kcal mol^{-1}, and the stationary points are numbered in ascending order of energy. (From [2])

energy 1.8 kcal mol^{-1}) the minimum 2 (1 kcal mol^{-1}) is thermally easily reached from the most stable minimum 1 (0 kcal mol^{-1}), whereas a transition via 6 (9.1 kcal mol^{-1}) is less favorable. The most stable minimum 1 corresponds to the NHO-bridged structure **1**. From this it can be concluded that the secondary structure of longer protein chains in solution, which is due to intermolecular H bridges, is most likely caused by interactions with solvent molecules and not by intramolecular interactions within the dipeptide unit. Thus, earlier traditional explanations for the formation of the secondary structure are disproved.[3]

Figure 2 shows the (ϕ, ψ)-surface for **2** which as a result of a lack of symmetry looks rather more complicated than that for **1**. Here, improved calculations (HF/6-31+G*) cause the minimum 7 and the transition structures 11 and 19 to disappear. Structure **2** corresponds to the most stable minimum 1

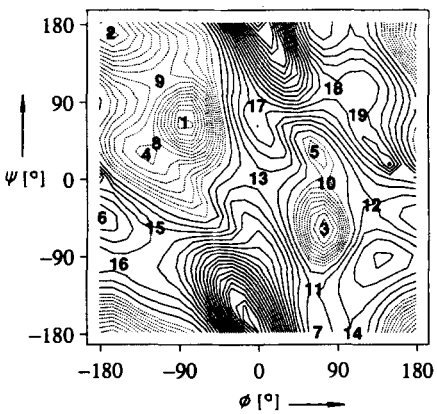

Fig. 2. The (ϕ,ψ)-surface of **2**, calculated at the HF/3-21G level (from [2]). For further annotations see Figure 1.

(0 kcal mol^{-1}). Via the saddle point 9 (activation energy 1.8 kcal mol^{-1}) the minimum 2 (1 kcal mol^{-1}) is, quite similar to that for compound **1**, thermally easily achieved. The other transition structures 13 (9.7 kcal mol^{-1}), 15 (8.0 kcal mol^{-1}), and 17 (9.3 kcal mol^{-1}) which all border onto the minimum 1 lie energetically significantly higher. The inclusion of the electron correlation via MP2/6-31 + G** single-point calculations on all found stationary points only changed the relative energies by 1 kcal mol^{-1} at most.

These results exceed earlier representations, in which the mere energetic arrangement of the conformers was deemed sufficient. The energetic positions of the transition structures make an alternative arrangement of more static to more dynamic structures possible. Complete conformer dynamics takes place in an energy interval of ca. 10 kcal mol^{-1}. The described procedure of the authors stands out because the information contained in the energy hypersurface is completely evaluated which creates a basis for the structure dynamics.

Received: September 26, 1991
German version: *Angew. Chem.* **1992**, *104*, 297

[1] R. Hoffmann, P. Laszlo, *Angew. Chem.* **1991**, *103*, 1; *Angew. Chem. Int. Ed. Engl.* **1991**, *30*, 1.
[2] T. Head-Gordon, M. Head-Gordon, M. J. Frisch, C. L. Brooks III, J. A. Pople, *J. Am. Chem. Soc.* **1991**, *113*, 5989.
[3] L. Pauling, The Nature of the Chemical Bond, 3rd ed., Cornell University Press, Ithaca, NY, (USA), 1960; Die Natur der chemischen Bindung, Verlag Chemie, Weinheim, 1973, p. 463.

Does the Naked Fluoride Ion Exist?

By *Konrad Seppelt**

Of course the naked fluoride ion does not exist in a chemical environment, just as no free proton is stable in a chemical environment. The potential usefulness of a naked fluoride ion is apparent: whereas H^+ or the closest to it, the magic acids, are extremely acidic, F^- would be extremely basic with immense catalytic properties.

To approximate a naked fluoride ion, CsF is often used. The "cesium effect" is here a result of the inverse (in the sense of ionic size) NaCl structure, that is, the F^- ion strives to increase its coordination number. However, in aprotic solvents the reactions take place on the surface of solid CsF only. Crown ethers or phase-transfer reagents can partly remove this difficulty.

A better approximation of the naked F^- would be achieved if, for example, tetrabutylammoniumfluoride could be prepared solvent-free. The commercially available material is always a hydrate. The solvent molecule strongly diminishes the fluoride activity. Attempts at complete thermal dehydration result in decomposition by Hofmann degradation. In THF solutions of $(C_4H_9)_4N^+F^-$ the water can at least be partly removed by reaction with $(CH_3)_3SiSi(CH_3)_3$.[1] The resulting F^- solution is substantially more reactive, but unstable, and the exact nature of the "active principle" is still unknown.

Only a short time ago two florides that can easily be prepared in every laboratory became accessible. Even more important, the chemical properties of the cations of these fluorides are complementary. K. O. Christie et al. published a detailed description of the preparation of pure $(CH_3)_4N^+F^-$ [Eq. (a)].[2] The synthesis of this compound in pure state has often been attempted in the past. Without doubt the methyl groups can no longer undergo Hofmann degradation, making this fluoride stable to about 150 °C. The cation is still rather small for a naked fluoride ion, resulting in unsatisfactory solubility. The most suitable solvent is acetonitrile, which is, however, itself slowly decomposed by F^- to its dimer. But the striking advantage of the tetramethylammonium ion is its stability against oxidative attack. One must assume that the positive charge is distributed over twelve hydrogen ions, which protects them to a large extent from oxidative attack.[3] It is thus not surprising that inorganic fluoro anions such as $[XeF_5]^-$, $[ClF_6]^-$, $[BrF_6]^-$, $[IF_6]^-$, $[IF_8]^-$, $[IOF_6]^-$, and $[TeF_7]^-$ could be synthesized with this fluoride, in some cases from extremely oxidizing fluorides.[4] This sparked off a renaissance in studies on coordination numbers larger than six, which is still only in its initial stages. A second disadvantage should, however, be mentioned: the high symmetry of the cation often results in strongly disordered crystals in compounds with almost spherical anions. A nonuniformly substituted tetraalkylammonium fluoride would be the ideal solution, but an essential feature must still be the lack of β hydrogen atoms.

$$(CH_3)_4N^+OH^- + HF \xrightarrow{H_2O} (CH_3)_4N^+F^- \cdot xH_2O \qquad \text{(a)}$$

$$\xrightarrow[2.\ 150\,^\circ C,\ \text{vacuum}]{1.\ \text{recryst. } (CH_3)_2CHOH} (CH_3)_4N^+F^-$$

1

The cation–anion distance of about 420 pm in $(CH_3)_4N^+F^-$ is not at all large when compared with that in cesium fluoride. Therefore a much higher reactivity is anticipated for the phosphazenium fluoride **2** of R. Schwesinger et al., which has a cation–anion distance of 630 pm.[5] Even though **2** is probably not as stable as **1** toward oxidation, it is just as readily accessible [Eq. (b)]—and anhydrous! Since **2** is al-

$$3PCl_5 + NH_4Cl \xrightarrow[CH_3NO_2]{-4HCl} [Cl_3P{=}\overset{+}{N}{=}PCl_3]PCl_6^- \xrightarrow[2)\ Na^+BF_4]{1)\ (CH_3)_2NH}$$

$$\longrightarrow [\{(CH_3)_2N\}_3P{=}\overset{+}{N}{=}P\{N(CH_3)_2\}_3]BF_4^- \xrightarrow[2)\ 120\,^\circ C,\ \text{vacuum}]{1)\ KF,\ CH_3OH} \qquad \text{(b)}$$

$$\longrightarrow [\{(CH_3)_2N\}_3P{=}\overset{+}{N}{=}P\{N(CH_3)_2\}_3]F^-$$

2

[*] Prof. Dr. K. Seppelt
Institut für Anorganische und Analytische Chemie
der Freien Universität Berlin
Fabeckstrasse 34-36, D-W-1000 Berlin 33 (FRG)

ready soluble in THF, it is ideal for use in organic chemistry. Elimination and halogen-exchange reactions have already been observed under the mildest of conditions;[5] Equation (c) gives an example.

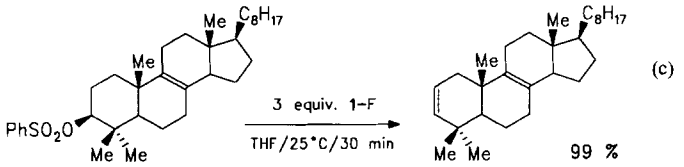

(c)

The field is now wide open—studies on C–C bond formation, formation of carbanions, elimination and condensation reactions, silylation and desilylation, and cyclization, each with stoichiometric or catalytic amounts of F^-, is possible.[6] Finally it must be noted that many physicochemical properties of F^- need to be redetermined, since without doubt the almost naked F^- ion differs substantially from the hydrated F^- ion.

German version: *Angew. Chem.* **1992**, *104*, 299

CAS Registry number:
F^-, 16984-48-8.

[1] H. Vorbrüggen, K. Krolikiewicz, *Tetrahedron Lett.* **1983**, *24*, 5337–5338; *ibid.* **1984**, *25*, 1259–1262.

[2] K. O. Christe, W. W. Wilson, R. D. Wilson, R. Bau, J. Feng, *J. Am. Chem. Soc.* **1990**, *112*, 7619–7625. This reference also contains an overview of earlier attempts to prepare pure $(CH_3)_4N^+F^-$.

[3] The formulation $(CH_3)_4N^+$ is only formally correct. Naturally the positive charge is localized least of all on the electronegative nitrogen atom.

[4] K. O. Christe, E. C. Curtis, D. A. Dixon, H. P. Mercier, J. C. P. Sanders, G. J. Schrobilgen, *J. Am. Chem. Soc.* **1991**, *113*, 3359–3361; K. O. Christe, W. W. Wilson, R. V. Chirakal, J. C. P. Sanders, G. J. Schrobilgen, *Inorg. Chem.* **1990**, *29*, 3506–3511; K. O. Christe, W. W. Wilson, *ibid.* **1989**, *28*, 3275–3277; A.-R. Mahjoub, K. Seppelt, *Angew. Chem.* **1991**, *103*, 309–311 and 844–845; *Angew. Chem. Int. Ed. Engl.* **1991**, *30*, 323–324 and 876–878; K. O. Christe, J. C. P. Sanders, G. J. Schrobilgen, W. W. Wilson, *J. Chem. Soc. Chem. Commun.* **1991**, 837–840; A.-R. Mahjoub, K. Seppelt, *ibid.* **1991**, 840–841.

[5] R. Schwesinger, R. Link, G. Thiele, H. Rotter, D. Honert, H.-H. Limbach, F. Männle, *Angew. Chem.* **1991**, *103*, 1376–1378; *Angew. Chem. Int. Ed. Engl.* **1991**, *30*, 1372–1375.

[6] The only newer summary appeared in Russian: S. G. Yacobson, V. V. Bardin in *Ftorid-Ion v Organitscheskoi Chimie* (Ed.: I. L. Knunyantz) Izdatelstvo Nauka, Novosibirsk, **1986** ("The Fluoride Ion in Organic Chemistry", Novosibirsk, Scientific Edition, **1986**).

C_{60}-Fullerene—A Playground for Chemical Manipulations on Curved Surfaces and in Cavities**

By *Helmut Schwarz**

Fullerenes are currently sparking the imaginations of not only journalists[1] and managers,[2] interest in this third allotrope of carbon is also reflected in the rapidly increasing number of reviews,[3] highlights,[4] semiscientific articles,[5] and the almost unbelievable rate of manuscript submission of one or two per day.[6] This boom was sparked by Krätschmer's and Huffman's[7] ingenious method, which has been improved on since then[8] by several other research groups,[8,9] allowing almost anyone to produce C_{60} and its fullerene analogues in macroscopic quantities.[10] As a result, C_{60}-fullerene is structurally and spectroscopically probably one of the best characterized molecules.[3,7] The disturbing discrepancies in the calculated values of the enthalpy of formation ΔH_f^0 (from 286 to 973 kcal mol^{-1}) were recently resolved by Rüchardt et al.[11] by their combustion studies of highly pure C_{60} which provided $\Delta H_f^0 = 545$ kcal mol^{-1}.

This article gives a summary of the many facets of the chemistry of C_{60}. A critical review of the current understanding of the fullerenes will appear shortly.[3h]

1. Organometallic Derivatives of C_{60}: The goal of the first attempts at derivatizing C_{60} was to break the I_h symmetry of the fullerene and provide ordered crystals. The successful preparation of crystalline $[C_{60}(OsO_4)(4\text{-}tert\text{-butylpyridine})_2]$ by Hawkins et al.[12] revealed new interesting questions: For example, are the electronic differences in the two types of C–C bonds in C_{60} reflected in its reactions with transition metals as predicted by theory?[13] Does C_{60} act as an electron-poor ligand as suggested by MO calculations?[14] Can C_{60} undergo multiple additions of organometallic fragments, and if so, are there geometrical preferences? Satisfying answers to these questions have been found in the last few months,[12,15] and the following generalizations may be drawn:

1) Only the six-ring/six-ring double bonds are attacked in η^2 coordination. Reactions on the longer six-ring/five-ring double bonds do not occur. This is also true for the complex $[(\eta^2\text{-}C_{70})Ir(CO)Cl(PPh_3)_2]$.[16]

2) The ready complexation with electron-rich Pt and Ir fragments and the structural analyses of the resulting C_{60} adducts indicate that C_{60} functions as an electron-poor olefin. The electron distribution in these complexes is similar to that in $[O_2Ir(CO)Cl(PPh_3)_2]$, and it is assumed[15b] that transition-metal complexes which bind O_2 relatively easily also react with C_{60}.

3) The recently described[15d] sixfold platinum-substituted derivative $[\{(Et_3P)_2Pt\}_6C_{60}]$ (Fig. 1) is remarkable in a number of respects: a) Its indisputable structural characterization is the first for multiply substituted fullerenes. b) The X-ray structural analysis proves that the six platinum complex fragments are added to C_{60} in an octahedral fashion; this results in the rare point group T_h. c) Again the complexation occurs exclusively on the six-ring/six-ring double bonds. Because there are 30 such bonds in C_{60}, and a com-

[*] Prof. Dr. H. Schwarz
Institut für Organische Chemie der Technischen Universität
Strasse des 17. Juni 135, D-W-1000 Berlin 12 (FRG)

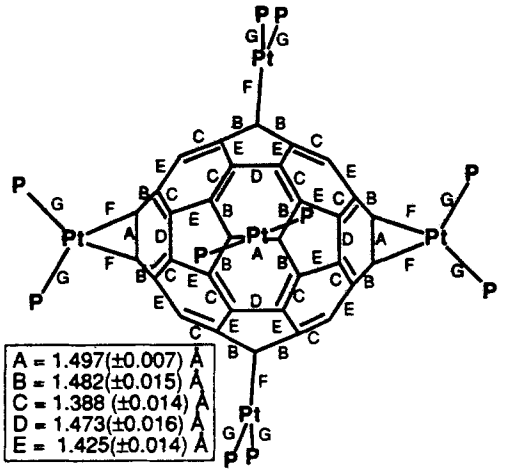

Fig. 1. Crystal structure of the complex $[\{(Et_3P)_2Pt\}_6C_{60}]$ (from [15d]).

plexed $(Et_3P)_2Pt$ fragment blocks the four adjacent C=C bonds, a maximum of six such fragments may add to C_{60}.

"Naked" transition-metal ions M^+ (M = Fe, Co, Ni, Cu, Cu, Rh, La, VO) were "glued" on the outer skin of C_{60} by Freiser et al. recently.[17] In gas-phase experiments M^+ was induced to react with C_{60} at thermal energies, and the resulting complex MC_{60}^+ was characterized by mass spectrometry. For M = Ni the preparation of a complex analogous to the metallocenes, $[Ni(C_{60})_2]^+$, was possible.[17c] As is expected for exohedral complexes (see Section 3), the excitation of MC_{60}^+ results in the loss of the metal; the C_{60} cluster itself remains intact (Scheme 1).

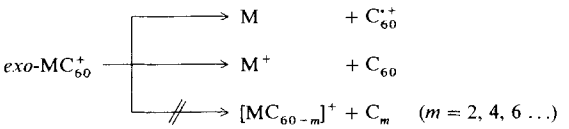

Scheme 1. Fragmentation of an exohedral complex MC_{60}^+ in the mass spectrometer.

2. Organic Chemistry on the Surface of C_{60}: The classification of the reactions of C_{60} as either redox or addition reactions is reasonable, although mechanistically these alternatives are not always clearly differentiated. As was already mentioned, C_{60} is electron-poor, that is its electron affinity (EA) is high,[14] and ab initio calculations predict that both $C_{60}^{\bullet-}$ and C_{60}^{2-} correspond to bonding states.[14] In fact Marshall et al. were able to prepare both ions by addition of electrons to C_{60} in the gas phase.[18]

This result is remarkable since *free* dianions (i.e. without stabilizing interactions with counterions) rarely have a finite lifetime. Stabilization is usually achieved either by "anchoring" the two charges to functional groups which are held a certain distance apart, or by solvation effects, which help reduce the intrinsic instability related to the loss of an electron $M^{2-} \rightarrow M^{\bullet-} + e^-$. C_{60}^{2-} does not need these tricks, because even with the additional electrons in the C_{60} framework the molecule has an overall bonding character. For C_{60}^{3-}, however, the Coulombic repulsions are great enough to cause the loss of an electron.[14d] In solution the environmental effects expected for ions play a role. Thus it is hardly surprising that the complete series of polyanions up to C_{60}^{5-} was generated by cyclic voltammetry.[19] A crystalline (tpp)-chromium(III) complex (tpp = tetraphenylporphyrinato) with $C_{60}^{\bullet-}$ as counterion was also reported recently.[20] It is worth mentioning that the position of the equilibrium in this system can be influenced dramatically by the solvent [Eq. (a)].

$$Cr^{II}(tpp) + C_{60} \underset{\text{toluene}}{\overset{\text{THF}}{\rightleftharpoons}} Cr^{III}(tpp)^+ C_{60}^{\bullet-} \quad \text{(a)}$$

Initial spectroscopic data indicate that $Al^{III}(tpp^{\bullet-})$ also reacts with C_{60} by electron transfer, producing $C_{60}^{\bullet-}$. Furthermore, investigations have shown that $C_{60}^{\bullet-}$ appears to be an extremely weakly coordinating counterion.[20]

Investigations on the reactivity of $C_{60}^{\bullet-}$ in the gas phase[21] have demonstrated that *no* proton transfer takes place in its reactions with H_2O, Me_2CHOH, CF_3CH_2OH, $EtCO_2H$, and CF_3CO_2H [Eq. (b)]. This means that $C_{60}H$ is either an

$$C_{60}^{\bullet-} + RH \not\longrightarrow C_{60}H^{\bullet} + R^- \quad \text{(b)}$$

extraordinarily strong acid ($\Delta G_{acid} \leq 317\ kcal\,mol^{-1}$) or that proton transfer is hampered by a large kinetic barrier. Both explanations are consistent with the notion that the charge in $C_{60}^{\bullet-}$ is highly delocalized.

On the other hand, $C_{60}^{\bullet-}$ reacts with NO_2 by association [Eq. (c)]. The fact that the addition of a second molecule of

$$C_{60}^{\bullet-} \xrightarrow[\text{fast}]{NO_2} C_{60}NO_2^- \xrightarrow[\text{slow}]{NO_2} C_{60}(NO_2)_2^{\bullet-} \quad \text{(c)}$$

NO_2 is three orders of magnitude slower than that of the first could be related to the doublet character of $C_{60}^{\bullet-}$. This spin argument may not necessarily hold, because even the association of the first molecule of O_2 or NO proceeds too slowly to be followed.

Because no electron transfer from $C_{60}^{\bullet-}$ takes place in Reaction (c), $EA(C_{60}) > EA(NO_2) = 2.27$ eV. This result agrees qualitatively with that obtained by PE spectroscopy ($EA(C_{60}) = 2.6-2.8$ eV).[22]

The reduction of C_{60} with Li/THF/ultrasound provides diamagnetic polyanions whose ^{13}C NMR signals are shifted 14 ppm *down*field—an unusual finding for carbanions.[23] Methylation of the C_{60} polyanions with an excess of MeI gave polymethylated C_{60}-fullerenes [Eq. (d)], which contained up to 24 methyl groups and were dominated by products with even numbers of methyl groups. The reaction of the

$$C_{60} \xrightarrow[\text{2) MeI}]{\text{1) Li/THF}} C_{60}Me_n\ (n \leq 24) \quad \text{(d)}$$

polyanions with Me_3SiCl succeeded, but quenching with D_2O did not.[23]

One of the first derivatizations of C_{60} was achieved with the Birch reduction,[8b] which furnished colorless $C_{60}H_{36}$. Because oxidation of this hydrogenation product with dichlorodicyanoquinone (DDQ) regenerates C_{60} [Eq. (e)], the reduction is assumed to proceed without structural

changes in the C_{60} cluster. The authors offer a simple explanation of the incorporation of up to 36 hydrogen atoms based primarily on the general experience that only conju-

$$C_{60} \underset{DDQ}{\overset{Li/NH_3/tBuOH}{\rightleftharpoons}} C_{60}H_{36} \qquad (e)$$

gated double bonds are attacked in the Birch reduction. The hydrogenation product $C_{60}H_{36}$ must therefore contain twelve isolated double bonds (one per five-membered ring), that is at most $(60 - 2 \times 12) = 36$ C atoms of C_{60} are hydrogenated.

The calculations of the stability of the dodecahedrane analogue, $C_{60}H_{60}$, carried out by Saunders[24] still await experimental verification. According to MM3 calculations, the stereoisomer with 60 *exo* hydrogen atoms is extremely strained (strain energy (SE) = 836(!) kcal mol^{-1}). The isomeric $C_{60}H_{60}$ with just *one endo* hydrogen atom is 53 kcal mol^{-1} more stable, and the global minimum correlates to a C_1 symmetric structure in which ten hydrogen atoms occupy *inner* positions. No doubt the "cage builders" among the organic chemists will be challenged to provide explanations and macroscopic amounts of samples.

Two groups have reported successful fluorination experiments. Selig et al.[25] produced partially fluorinated fullerenes $C_{60}F_n$ $(30 < n < 50)$ with a maximum for $n = 36$. In an experiment on a 10 mg scale Taylor et al.[26] obtained $C_{60}F_{60}$ after reaction over twelve days. The fact that the ^{19}F NMR spectrum of $C_{60}F_{60}$ consists of one single line does not necessarily prove the product to be I_h symmetric. The equivalence of the 60 fluorine and carbon atoms would also be retained in the less symmetric *I* structure, with the consequence, however, that such a $C_{60}F_{60}$ would be a chiral molecule.[27]

The chlorination and bromination of fullerenes combined with the nucleophilic methoxylation and an $AlCl_3$-mediated Friedel–Crafts reaction of the polychlorofullerenes were recently described by Olah et al.[28] The reaction of C_{60} with Br_2 at intermediate temperatures furnishes $C_{60}Br_2$ and $C_{60}Br_4$, which both lose the halogen quantitatively at 150 °C. Chlorination, however, affords fullerenes containing an average of 24 chlorine atoms. Complete dehalogenation of these chlorinated products could be achieved at temperatures greater than 400 °C and under mass spectrometric conditions. Remarkably, in the reaction of the polychlorofullerenes $C_{60}Cl_n$ with MeOH/KOH (in excess) at reflux, all of the chlorine atoms were replaced by methoxy groups. According to the FAB mass spectrum, the product mixture contains compounds with up to 26 MeO groups. Because methoxy groups do not add to C_{60} under the same conditions,[46] it appears that this Cl → OMe exchange occurs by a front-side substitution on the surface of the cluster. Of

$$C_{60}Cl_n \xrightarrow[\Delta]{MeOH/KOH} C_{60}(OMe)_n \xleftarrow[\Delta]{MeOH/KOH} C_{60} \qquad (f)$$
$$n \leq 26$$

course this need not be the unprecedented S_N2 reaction proceeding with retention, since an addition/elimination mechanism would easily explain the observation.

Polychlorofullerenes also undergo Friedel–Crafts ractions [Eq. (g)]. Thus $C_{60}Cl_n$ reacts with benzene or toluene in the presence of trace amounts of $AlCl_3$ providing polyarylfullerenes.

$$C_{60}Cl_n \xrightarrow[AlCl_3]{ArH} C_{60}(Ar)_n + n\,HCl \qquad (g)$$

The acid-catalyzed addition of fullerenes to arenes (fullerination) is also possible.[29] In the presence of $AlCl_3$, C_{60} reacts with benzene to give $C_{60}(HC_6H_5)_{12}$ as the major product and with toluene to the *para*-substituted C_{60}-$(HC_6H_4CH_3)_{12}$-fullerene. Whether this reaction proceeds by an SET mechanism or better yet by the electrophilic fullerination to arenes as illustrated in Equation (h) remains open. The fact that mixtures of C_{60}/C_{70} and polystyrene react with $AlCl_3$ in CS_2 to form highly cross-linked polymers may excite some materials scientists.

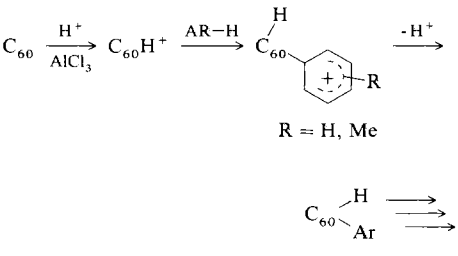

(h)

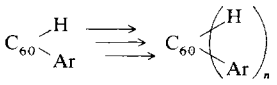

Electrophilic additions to C_{60} were also studied in the gas phase.[30] The proton affinity (PA) of C_{60} was found to be unusually high for an "arene" with a value of 204–207 kcal mol^{-1}. The ease with which $C_{60}H^+$ forms and the considerable resistance of $C_{60}H^+$ to charge transfer and fragmentation lend credence to the suggestion made by Kroto et al.[3c] that the diffuse absorption bands in interstellar space[3a] could be caused by this species.

Reactions of C_{60} with electrophiles E^+ (E = Me, Et, Bu) proceed readily in the gas phase.[30] One interesting observation is that in single-collision experiments on the adduct $C_{60}(t\text{-}C_4H_9)^+$, C_4H_8 is the main cleavage product. This could indicate that in the formation of the adduct no C–C bonds are formed, and that the adduct $C_{60}(t\text{-}C_4H_9)^+$ is better described as a proton-bound complex of the type $C_{60} \cdots H^+ \cdots C_4H_8$. Since it is true that $PA(C_{60}) > PA(C_4H_8)$, it is not surprising that the proton stays with the C_{60} cluster in the fragmentation caused by collisional excitation.

The addition of anions to C_{60} provides water-soluble fullerenes. The reaction of C_{60} with morpholine leads (presumably induced by an SET step) to the product $C_{60}H_6(N(CH_2CH_2)_2O)_6$.[31] ^1H NMR analysis of the adduct gives evidence of a reversible, rapid H-migration ($\Delta H^{\neq} \leq 10$ kcal mol^{-1}), and the degenerate [1,5]-sigmatropic rearrangement causes the H atoms to be "globe trotters" on the outer surface of the fullerene [Eq. (i)].

The fact that radicals and carbenes are also added to C_{60} does not justify the statement that C_{60} is not "choosy" in its choice of partners. Rather this completes the picture of the

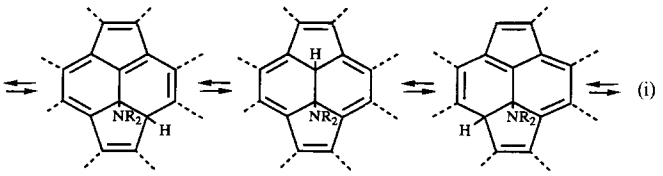

(i)

very stable molecule which is also capable of unusual reactions. For example, Krusic et al.[32] report the addition of up to 15 photochemically generated benzyl radicals to C_{60}. ESR investigations of derivatives with three or five benzyl groups indicate that the radical centers on the C_{60} surface are primarily localized within the substituted five-membered rings. O and CH_2 adducts of C_{60} were identified by Cooks et al. by mass spectrometry.[33a] Presumably these are formed in the course of photochemical processes. According to mass spectrometry, both the O atom and the CH_2 group can be cleaved from these adducts only at considerable energies, implying that these units are covalently bound. The speculation that these compounds and $C_{70}O$ described by Diederich et al.[34] are fullerene analogues of Vogel's oxa- and methano[10]-annulenes [Eq. (j)] is quite tempting. Preparation of a C_{60}

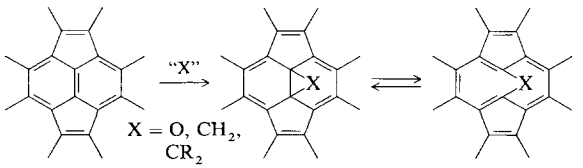

(j)

epoxide photochemically[33b] and by reaction of C_{60} with dimethyldioxirane have both been described.[33c] In the reaction with dimethyldioxirane the adduct C_{60}(1.3-dioxolane) was also isolated and identified.[33c] As proof of the insertion of a C_1 unit into the C_{60} framework, Wudl et al.[35] obtained X-ray data for the product of the reaction of C_{60} with diphenyldiazomethane. The product is assigned as Ph_2C_{61} and not as the diphenylcarbene adduct, Ph_2CC_{60}.

3. Endohedral C_{60} complexes: The perfect emptiness of the cavity of C_{60} (approximately 7 Å across) inevitably provokes questions, for example, if something could be placed inside and if fullerenes in general could serve as molecular containers and thereby offer the potential of endohedral chemistry[36]—chemistry inside of the cage. In the realization of these types of compounds two fundamentally differing concepts were applied: 1) Atoms M coincidentally present on the "inner" surface could be enclosed during the process of the formation of the fullerene clusters by "evaporation" of graphite. 2) Atoms M could penetrate the fullerene envelope in a bimolecular high-energy collision. Once the atoms are physically encaged they would be prevented from leaving their prison by high barriers. Both concepts were translated into reality, and a few examples serve to emphasize the fascinating aspects of endohedral fullerene complexes, for which the symbol $M@C_x$ has been suggested.[37c]

Smalley et al.[37] were able to prepare metal-containing fullerenes MC_{60} (M = La, Ni, Na, K, Rb, Cs) and LaC_x (x = 60, 70, 74, 82) by laser vaporization of doped graphite. The cluster ions MC_x^+ do not react with O_2, NH_3, or H_2O—the metal atom is protected from reactions by the carbon shell. Excitation with intense laser-light causes fragmentation. Unlike the typical fragmentation of the exohedral complexes (Scheme 1), the metal in the endohedral complex is not cleaved, but rather the cage shrinks with the loss of C_2 or several units of C_2 (Scheme 2). The complete destruction of the cluster occurs upon further excitation when the enclosed metal does not have enough room inside the cage.

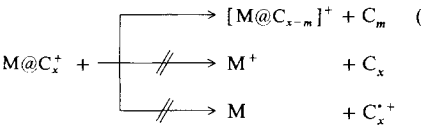

Scheme 2. Fragmentation of an endohedral complex $M@C_x^+$ in the mass spectrometer.

Recently macroscopic amounts of endohedral metal–fullerenes were produced and used in subsequent experiments.[37c,d] The results for $La@C_{82}$ are worth mentioning: According to investigations with X-ray photoelectron spectroscopy, the central La atom has a formal charge of +3 (two electrons are donated to the C_{82} cage in the formation of C_{82}^{2-}, which is presumed to be especially stable; the third electron is delocalized inside the cavity). The compound could be extracted with boiling toluene, and the carbon cluster defied decomposition in the humid August climate in Houston. Similar results were reported for the yttrium complex. A doubly doped $Y_2@C_{82}$ cluster as well as a soluble La_2C_{80}[37e] have also been made. Do these molecules point the way to superconducting metallofullerenes? Who knows; this hope is certainly harbored by the authors.[37d]

The second variation, the penetration of an intact fullerene, was first carried out at the Technische Universität in Berlin[38] and later in other laboratories.[39] It could be shown that noble-gas atoms He and Ne could be incorporated into $C_{60}^{\bullet+}$, if highly accelerated $C_{60}^{\bullet+}$ ions were shot through a stationary noble-gas atmosphere in a molecular-beam experiment.[40] The resulting $MC_{60}^{\bullet+}$ complexes (M = He, Ne) disintegrate upon further excitation giving the fragmentation pattern typical for endohedral compounds with retention of M and elimination of C_m (Scheme 2).

Definitive proof that the noble gas is physically trapped inside the cavity of C_{60} was recently provided;[41] $HeC_{60}^{\bullet+}$ was reduced, and the resulting neutral compound was shown to have a finite lifetime of >90 μs. $He@C_{60}$ is the first "noble gas–carbon compound", and the proof that such inclusion compounds exist substantiates earlier speculations and experiments based on the premise that carbon clusters (without further specified structure) could function as containers for noble gases—presumably in interstellar space as well.[42]

Two research groups recently reported inverse endohedral C_{60} complexes: O. Wennerström from Göteborg prepared a water-soluble C_{60} supermolecule, in which C_{60} is enclosed in γ-cyclodextrin. The (current) highlight in this area is the synthesis and structural characterization of a 3:1 complex of hydroquinone and C_{60} reported by O. Ermer in Cologne.[44] In this case, a C_{60} molecule is enclosed in a net made of the three hydroquinone molecules stabilized by hydrogen bonds. Although charge-transfer interactions between host and guest occur, the orientation of the C_{60}-fullerene remains disordered. The complex is one of those rare cases in which the

guest throws his weight around more than the host: C_{60} is 2.2 times heavier than the three hydroquinone molecules together and takes up 50% of the crystal volume.

Admittedly, we are still miles away from fulfilling the promises pinned to the "wonder molecule" by the popular- and pseudoscientific media.[1, 2, 5] But the potential and uniqueness of C_{60} illustrated in this report may have whetted the appetite of some readers. Unfortunately, indigestion may result, since in the normal daylight C_{60} is one of the most efficient producers of singlet oxygen.[4, 5]

German version: *Angew. Chem.* **1992**, *104*, 301

[1] For example see *Der Spiegel* **1991**, *48*, 284, in which an article entitled "Ships in the Bottle" credits the fullerenes with a "totally new chemistry".

[2] In *Capital* **1991**, *91*, 247 C_{60} is declared to be "the material of materials". The authors venture that this molecule could change the world as much as nuclear fission did.

[3] Recent reviews: a) H. W. Kroto, *Science* **1988**, *242*, 1139; b) W. Weltner, Jr., R. J. Van Zee, *Chem. Rev.* **1989**, *89*, 1713; c) R. E. Smalley in *Atomic and Molecular Clusters* (Ed.: E. R. Bernstein), Elsevier, Amsterdam, **1990**, Chapter 1; d) J. S. Miller, *Adv. Mater.* **1991**, *3*, 262; e) H. W. Kroto, A. W. Allafs, S. P. Balm, *Chem. Rev.* **1991**, *91*, 1213; f) H. W. Kroto, *Angew. Chem.* **1992**, *104*, 113; *Angew. Chem. Int. Ed. Engl.* **1992**, *31*, 111; g) S. W. McElvany, M. M. Ross, *J. Am. Soc. Mass Spectrom.* **1992**, in press; h) R. N. Thomas, *Angew. Chem.*, in press. i) The March edition of *Acc. Chem. Res.* will be dedicated completely to fullerene chemistry.

[4] a) J. F. Stoddart, *Angew. Chem.* **1991**, *103*, 71; *Angew. Chem. Int. Ed. Engl.* **1991**, *30*, 70; b) F. Diederich, R. L. Whetten, *ibid.* **1991**, *103*, 695 and **1991**, *30*, 678; c) H. Hopf, *ibid.* **1991**, *103*, 1137 and **1991**, *30*, 1117; d) H. W. Kroto, *J. Chem. Soc. Faraday Trans.* **1991**, *87*, 2871; e) R. E. Smalley, *Sciences (NY)* **1991**, *31*, 22; f) R. F. Curl, R. E. Smalley, *Sci. Am.* **1991**, *265*(4), 32; *Spektrum Wiss.* **1991** (12), 88.

[5] a) R. M. Baum, *Chem. Eng. News* **1990**, *68*(44), 22; b) R. Baum, *ibid.* **1991**, *69* (15), 4; c) E. Pennisi, *Sci. News* (Washington) **1991**, *140*, 120; d) J. Baggott, *New Sci.* **1991**, *131* (1776), 34.

[6] Bucky News Service provides a nearly complete overview of (almost) all aspects of the fullerenes. Interested parties are served by E-mail through bucky @sol1.Irsm.upenn.edu.

[7] a) W. Krätschmer, L. D. Lamb, K. Fostiropoulos, D. R. Huffman, *Nature (London)*, **1990**, *347*, 354; b) W. Krätschmer, K. Fostiropoulos, D. R. Huffman, *Chem. Phys. Lett.* **1990**, *170*, 167.

[8] The original yield of 1% extractable fullerene material [7] has been increased substantially: a) 8% (R. Taylor, J. P. Hare, A. Abdul-Sada, H. Kroto, *J. Chem. Soc. Chem. Commun.* **1990**, 1423); b) 10% (R. E. Haufler, J. Conceicao, L. P. F. Chibante, Y. Chai, N. E. Byrne, S. Flanagan, M. M. Haley, S. C. O'Brien, C. Pan, Z. Xiao, W. E. Billups, M. A. Ciufolini, R. N. Hauge, J. L. Margrave, L. J. Wilson, R. F. Curl, R. E. Smalley, *J. Phys. Chem.* **1990**, *94*, 8634); c) 14% (H. Ajie, M. M. Alvarez, S. J. Anz, R. D. Beck, F. Diederich, K. Fostiropoulos, D. R. Huffman, W. Krätschmer, Y. Rubin, K. E. Schriver, D. Sensharma, R. L. Whetten, *ibid.* **1990**, *94*, 8630); d) 25–35% (F. Diederich, R. Ettl, Y. Rubin, R. L. Whetten, R. Beck, M. M. Alvarez, S. J. Anz, D. Sensharma, F. Wudl, K. C. Khemani, A. Kuch, *Science* **1991**, *252*, 548); e) 44% (D. H. Parker, P. Wurz, K. Chatterjee, K. R. Lykke, J. E. Hurst, M. J. Pellin, J. C. Hemminger, D. M. Gruen, L. M. Stock, *J. Am. Chem. Soc.* **1991**, *113*, 7499).

[9] A new synthetic procedure conducted at significantly lower temperatures (evaporation of carbon in a high-frequency furnace instead of by the electric-arc method) is described by G. Peters, M. Jansen, *Angew. Chem.* **1992**, *104*, 240; *Angew. Chem. Int. Ed. Engl.* **1992**, *31*, 223.

[10] a) A model of fullerene formation aiming at a *quantitative* description is presented by A. Goeres, E. Sedlmayer, *Chem. Phys. Lett.* **1991**, *184*, 310. b) An interesting result with regard to the mechanism of fullerene formation (*statistical* incorporation of C_2 units in C_{60}) is found in J. M. Hawkins, A. Meyer, S. Loren, R. Nunlist, *J. Am. Chem. Soc.* **1991**, *113*, 9394. c) The exclusive isolation of one C_{2v} and one D_3 symmetric isomer of C_{78} probably has significant implications for the generation of fullerenes: F. Diederich, R. L. Whetten, C. Thilgen, R. Ettl, I. Chao, M. M. Alvarez, *Science* **1991**, *254*, 1768.

[11] H. D. Beckhaus, C. Rüchardt, M. Kao, F. Diederich, C. S. Foote, *Angew. Chem.* **1992**, *104*, 69; *Angew. Chem. Int. Ed. Engl.* **1992**, *31*, 63, and literature cited therein.

[12] a) J. M. Hawkins, T. A. Lewis, S. D. Loren, A. Meyer, J. R. Heath, Y. Shibato, R. J. Saykally, *J. Org. Chem.* **1990**, *55*, 6250; b) J. M. Hawkins, A. Meyer, T. A. Lewis, S. D. Loren, F. J. Hollander, *Science* **1991**, *252*, 312.

[13] D. Arnic, N. J. Trinajstic, *J. Chem. Soc. Perkin Trans. 2* **1990**, 1595.

[14] a) R. C. Haddon, L. E. Brus, K. Raghavachari, *Chem. Phys. Lett.* **1986**, *125*, 459; b) R. F. Curl, R. E. Smalley, *Science* **1988**, *242*, 1017; c) D. E. Weaks, W. G. Harter, *J. Chem. Phys.* **1989**, *90*, 4744; d) A. H. H. Chang, W. C. Ermler, R. M. Pitzer, *J. Phys. Chem.* **1991**, *95*, 9288; e) R. L. Hettich, R. N. Compton, R. H. Ritchie, *Phys. Rev. Lett.* **1991**, *67*, 1242.

[15] a) P. J. Fagan, J. C. Calabrese, B. Malone, *Science* **1991**, *252*, 1160; b) A. L. Balch, V. J. Catalano, J. W. Lee, *Inorg. Chem.* **1991**, *30*, 3980; c) R. S. Koefod, M. F. Hudgens, J. R. Shapley, *J. Am. Chem. Soc.* **1991**, *113*, 8957; d) P. J. Fagan, J. C. Calabrese, B. Malone, *ibid.* **1991**, *113*, 9408.

[16] A. L. Balch, V. J. Catalano, J. W. Lee, M. M. Olmstead, S. R. Parkin, *J. Am. Chem. Soc.* **1991**, *113*, 8953.

[17] a) L. M. Roth, Y. Huang, J. T. Schwedler, C. J. Cassady, D. Ben-Amotz, B. Kahr, B. S. Freiser, *J. Am. Chem. Soc.* **1991**, *113*, 6298; b) Y. Huang, B. S. Freiser, *ibid.* **1991**, *113*, 9418; c) *ibid.* **1991**, *113*, 8186.

[18] P. A. Limbach, L. Schweikhard, K. A. Cowen, M. T. McDermott, A. G. Marshall, J. V. Coe, *J. Am. Chem. Soc.* **1991**, *113*, 6795.

[19] Recent literature: a) D. Dubois, K. M. Kadish, S. Flanagan, R. E. Haufler, L. P. F. Chibante, L. J. Wilson, *J. Am. Chem. Soc.* **1991**, *113*, 4364; b) P.-M. Allemand, A. Koch, F. Wudl, Y. Rubin, F. Diederich, M. M. Alvarez, S. J. Anz, R. L. Whetten, *ibid.* **1991**, *113*, 1050; c) D. Dubois, K. M. Kadish, S. Flanagan, L. J. Wilson, *ibid.* **1991**, *113*, 7773.

[20] A. Pénicaud, J. Hsu, C. A. Reed, A. Koch, K. C. Khemani, P.-M. Allemand, F. Wudl, *J. Am. Chem. Soc.* **1991**, *113*, 6698.

[21] L. S. Sunderlin, J. A. Paulino, J. Chow, B. Kahr, D. Ben-Amotz, R. R. Squires, *J. Am. Chem. Soc.* **1991**, *113*, 5489.

[22] S. H. Yang, C. L. Pelliette, J. Conceicao, O. Chesnovsky, R. E. Smalley, *Chem. Phys. Lett.* **1987**, *139*, 233.

[23] J. W. Bausch, G. K. Surya Prakash, G. A. Olah, D. S. Tse, D. C. Lorents, Y. K. Bae, R. Malhotra, *J. Am. Chem. Soc.* **1991**, *113*, 3205.

[24] M. Saunders, *Science* **1991**, *253*, 330.

[25] H. Selig, C. Lifshitz, T. Peres, J. E. Fischer, A. R. McGie, W. J. Romanow, J. P. McCanley, Jr., A. B. Smith III, *J. Am. Chem. Soc.* **1991**, *113*, 5475.

[26] J. H. Holloway, E. G. Hope, R. Taylor, G. J. Langley, A. G. Avent, T. J. Dennis, J. P. Hare, H. W. Kroto, D. R. M. Walton, *J. Chem. Soc. Chem. Commun.* **1991**, 966.

[27] a) G. E. Scuseria, *Chem. Phys. Lett.* **1991**, *176*, 423; b) P. W. Fowler, H. W. Kroto, R. Taylor, D. R. M. Walton, *J. Chem. Soc. Faraday Trans.* **1991**, *87*, 2685.

[28] G. A. Olah, K. Bucsi, C. Lambert, R. Aniszfeld, N. J. Trivedi, D. I. Sensharma, G. K. Surya Prakash, *J. Am. Chem. Soc.* **1991**, *113*, 9385.

[29] G. A. Olah, K. Bucsi, C. Lambert, R. Aniszfeld, N. J. Trivedi, D. K. Sensharma, G. K. Surya Prakash, *J. Am. Chem. Soc.* **1991**, *113*, 9387.

[30] S. W. McElvany, J. H. Callahan, *J. Phys. Chem.* **1991**, *95*, 6186.

[31] A. Hirsch, Q. Li, F. Wudl, *Angew. Chem.* **1991**, *103*, 1339; *Angew. Chem. Int. Ed. Engl.* **1991**, *30*, 1309.

[32] P. J. Krusic, E. Wasserman, K. F. Preston, J. R. Morton, P. N. Keizer, *Science* **1991**, *254*, 1183.

[33] a) J. M. Wood, B. Kahr, S. H. Hoke II, L. Dejarme, R. G. Cooks, D. Ben-Amotz, *J. Am. Chem. Soc.* **1991**, *113*, 5907; b) K. M. Creegan, J. L. Robbins, W. K. Robbins, J. M. Millar, R. D. Sherwood, P. J. Tindall, D. M. Cox, J. P. McCaulry, Jr., D. R. Jones, T. T. Gallagher, A. M. Smith III, *J. Am. Chem. Soc.*, in press; c) Y. Elemes, S. Silverman, C. Sheu, M. Kao, C. S. Foote, M. M. Alvarez, R. L. Whetten, *Angew. Chem.*, submitted.

[34] F. Diederich, R. Ettl, Y. Rubin, R. L. Whetten, R. Beck, M. M. Alvarez, S. J. Anz, D. Sensharma, F. Wudl, K. C. Khemani, A. Koch, *Science* **1991**, *252*, 548.

[35] T. Suzuki, Q. Li, K. C. Khemani, F. Wudl, Ö. Almarson, *Science* **1991**, *254*, 1186.

[36] For theoretical work on endohedral complexes see a) A. Rosen, B. Wästberg, *J. Am. Chem. Soc.* **1988**, *110*, 8701; b) J. Cioslowski, *ibid.* **1991**, *113*, 4139; c) J. Cioslowski, E. D. Fleischmann, *J. Chem. Phys.* **1991**, *94*, 3730; d) A. H. H. Chang, W. C. Ermler, R. M. Pitzer, *ibid.* **1991**, *94*, 5004; e) D. Bakewies, W. Thiel, *J. Am. Chem. Soc.* **1991**, *113*, 3704; f) B. Wästberg, A. Rosen, *Phys. Scr.* **1991**, *44*, 276.

[37] a) J. R. Heath, S. C. O'Brien, Q. Zhang, Y. Lin, R. F. Curl, H. W. Kroto, F. K. Tittel, R. E. Smalley, *J. Am. Chem. Soc.* **1985**, *107*, 7779; b) F. D. Weiss, J. L. Elkind, S. C. O'Brien, R. F. Curl, R. E. Smalley, *ibid.* **1988**, *110*, 4464; c) Y. Chai, T. Guo, C. Jin, R. E. Haufler, L. P. F. Chibante, J. Fure, L. Wang, J. M. Alford, R. E. Smalley, *J. Phys. Chem.* **1991**, *95*, 7564; d) J. H. Weaver, Y. Chai, G. H. Kroll, C. Jin, T. P. Ohno, R. E. Haufler, T. Guo, J. M. Alford, J. Conceicao, L. P. F. Chibante, A. Jain, G. Palmer, R. E. Smalley, *Chem. Phys. Lett.*, submitted; e) M. M. Alvarez, E. G. Gillan, K. Holczer, R. B. Kaner, K. S. Min, R. L. Whetten *J. Phys. Chem.* **1991**, *95*, 10561.

[38] a) T. Weiske, D. K. Böhme, J. Hrušák, W. Krätschmer, *Angew. Chem.* **1991**, *103*, 898; *Angew. Chem. Int. Ed. Engl.* **1991**, *30*, 884; b) T. Weiske, J. Hrušák, D. K. Bohme, H. Schwarz, *Helv. Chim. Acta* **1992**, *75*, 79.

[39] a) M. M. Ross, J. H. Callahan, *J. Phys. Chem.* **1991**, *95*, 5720; b) K. A. Caldwell, D. E. Giblin, C. S. Hsu, D. Cox, M. L. Gross, *J. Am. Chem. Soc.* **1991**, *113*, 8519; c) Z. Wan, J. F. Christian, S. C. Anderson, *J. Phys. Chem.*, submitted; d) K. A. Caldwell, D. E. Giblin, M. L. Gross, *J. Am. Chem. Soc.*, in press; e) E. E. B. Campbell, R. Ehrlich, A. Hielscher, J. M. A.

Frazav, I. V. Hertel, *Z. Phys. D.*, in press; f) R. C. Mowrey, M. M. Ross, J. H. Callahan, *J. Phys. Chem.*, in press; g) S. W. McElvany, M. M. Ross, J. H. Callahan, *Acc. Chem. Res.*, in press.
[40] For experiments on the generation of doubly and triply charged fullerene–noble gas complexes see a) T. Weiske, J. Hrušák, D. K. Bohme, H. Schwarz, *Chem. Phys. Lett.* **1991**, *186*, 459; b) T. Weiske, D. K. Bohme, H. Schwarz, *J. Phys. Chem.* **1991**, *95*, 8451.
[41] T. Weiske, T. Wong, W. Krätschmer, J. K. Terlouw, H. Schwarz, *Angew. Chem.* **1992**, *104*, 242; *Angew. Chem. Int. Ed. Engl.* **1992**, *31*, 183.
[42] a) R. S. Lewis, B. Srinivasan, E. Anders, *Science* **1975**, *190*, 1251; b) S. Niemeyer, K. Marti, *Proc. Lunar Planet Sci B* **1981**, *12*, 1177; c) D. Heymann, *J. Geophys. Res. B* **1986**, *91*, E 135.
[43] O. Wennerström, *Interdisciplinary Workshop on C_{60}*, 6.–7. December 1991, Roskilde, Denmark.
[44] O. Ermer, *Helv. Chim. Acta* **1991**, *74*, 1339.
[45] a) R. R. Hung, J. J. Grabowski, *J. Phys. Chem.* **1991**, *95*, 6073, and literature cited therein.; b) M. Terazima, N. Hirota, H. Shinohara, Y. Saito, *ibid.* **1991**, *95*, 9080.
[46] This observation has not been confirmed. R. Taylor, Brighton (UK), January 21, 1992, personal communication.

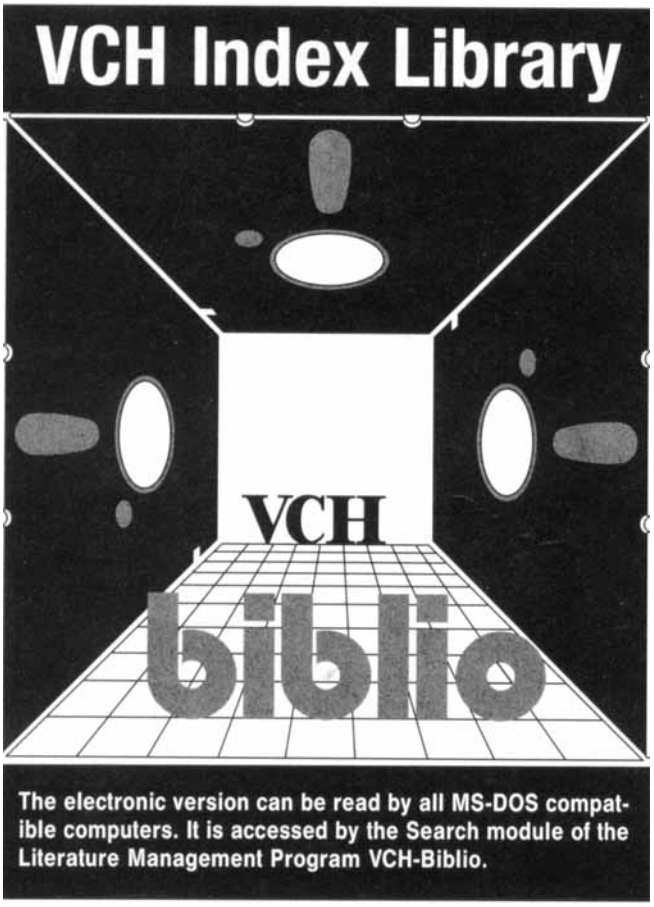

ANGEWANDTE CHEMIE
A Journal of the Gesellschaft Deutscher Chemiker
International Edition in English

30 Year Index of Reviews
– in print or on diskette –

The reviews in Angewandte Chemie are amongst the most often cited chemical publications of each year. Many have become classics of the chemical literature. For thirty years they have been available in English as well as German. The 30 year review index now celebrates this anniversary by facilitating access to these important documents of the rapid development of our discipline. The index—both a chemical dictionary and a history book—offers you:

1. A list of all authors, indicating the main author and the title of the review.
2. A subject index giving the main author.
3. Both indexes provide complete information on date of issue and first and last page numbers of the German and English editions.

The electronic version of the index is available on 5¼″ and 3½″ diskettes.

The price of the index is DM 98.00, $ 64.00 or £ 37.00. Please order by telephone or in writing to VCH, Software und Datenbanken, Postfach 10 11 61, D-W-6940 Weinheim, Tel. 0 62 01/6 02-2 71, Telefax 0 62 01/6 02-3 28.

Communications may be submitted in English *or* in German. Further details regarding the submission of communications can be found in the "Notice to Authors" reproduced in the January issue of the journal. Copies thereof may be obtained from the editorial office upon request.

Diprotonated Tetra(2-pyridyl)pyrazine and its Chemical Mimesis*** due to Different Hydrogen Bridges**

By *Hans Bock,* Thorsten Vaupel, Christian Näther, Klaus Ruppert*, and *Zdenek Havlas*

Dedicated to Professor Gerhard Quinkert on the occasion of his 65th birthday

Tetra(2-pyridyl)pyrazine, according to cyclovoltammetric measurements,[1] exhibits proton-sponge[2, 3] properties. This is of interest because the title compound contains four pyridine rings connected to a central pyrazine ring by four C–C axes; therefore, the altogether 132 degrees of freedom in the 40 center molecule $C_{24}H_{16}N_6$ are predominantly reduced to four rotations. Motivated by this dynamic aspect, we have determined the solid-state structures of the neutral compound[4] (Fig. 1 top) as well as of its diprotonated salts with either the "naked" or the "hydrocarbon-surrounded" counteranions Cl^-[5] (Fig. 1 middle) and $(C_6H_5)_4B^-$[6] (Fig. 1 bottom), respectively.

In the solid-state structure of tetra(2-pyridyl)pyrazine[4] (Fig. 1 top), the two pyridine rings on either side of the central pyrazine ring are twisted out of its plane by 50° either up or down. For this inversion-symmetric molecule with adjacent pyridine rings twisted in opposite directions an N ··· N distance of 324 pm results; this value exceeds the sum of two N-interference radii of 155 pm[7b] each and, therefore the repulsive nitrogen lone-pair interactions are reduced.

In the reaction of the title compound with HCl two diagonally opposing pyridine rings are protonated; hydrogen bridges N^+–H ··· Cl^- are formed to the two electron-rich

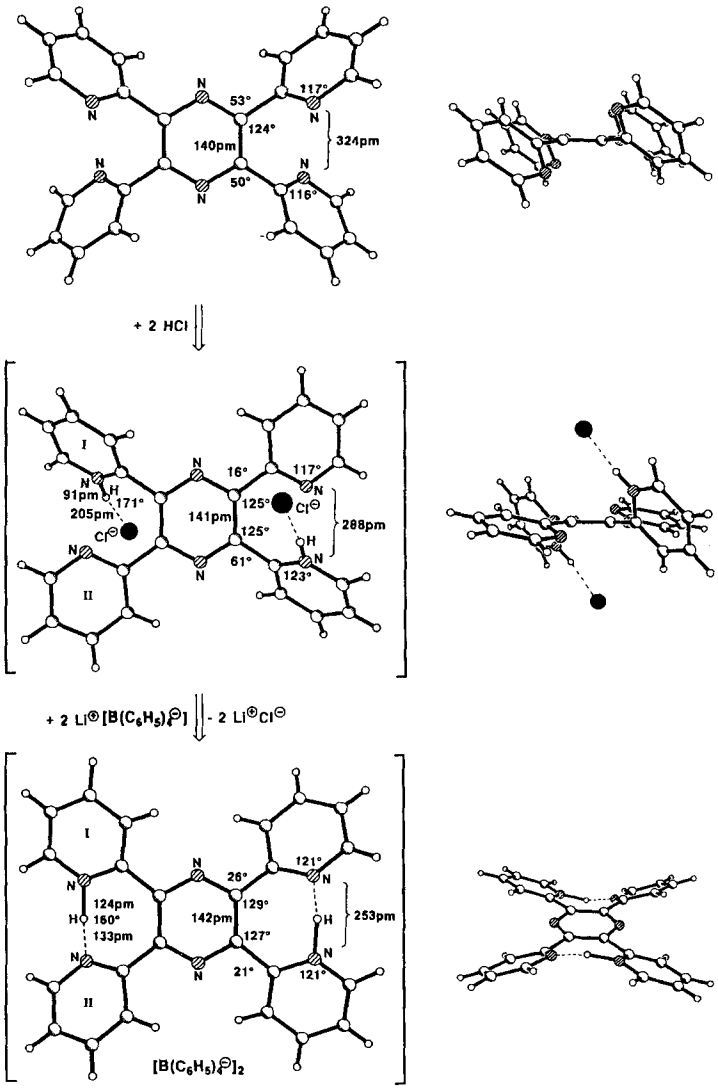

Fig. 1. Structures of tetra(2-pyridyl)pyrazine (top) and its diprotonated salts with chloride (middle) and tetraphenylborate anions (bottom). All six-membered ring skeletons exhibit inversion centers. Essential bond lengths [pm] (±1 pm) and angles [°] (±1°) are given; for further structural details see [4–6].

chloride anions (r_{Cl^-} = 180 pm),[7a] and distances between proton-donor and proton-acceptor centers of 295 pm are exhibited. Simultaneously, the unprotonated pyridine rings rotate into planarity with the pyrazine ring ($\varphi = 50° \rightarrow 16°$) causing the (H)$N^+$ ··· N distances to shorten to 288 pm, a distance less than the sum of two N interference radii (310 pm)[5] (Fig. 1 middle). The N^+–H bond lengths of 91 pm as determined by X-ray structural analysis must be corrected to about 104 pm, based on neutron-diffraction structural data. Concomitantly and in agreement with literature data,[7b] the distances H^+ ··· Cl^- must be corrected to about 185 to 190 pm. However, the angles $\sphericalangle N^+HCl^- = 171°$ can presumably be accepted without any correction.[7c]

Exchange of the electron-rich and therefore, preferred proton-acceptor center chloride ion for the phenyl surrounded one, tetraphenylborate, which under the reaction conditions is not protonated, can be achieved by anion exchange of tetra(2-pyridine)pyrazine dihydrochloride in acetonitrile

[*] Prof. Dr. H. Bock, T. Vaupel, Dipl.-Chem. C. Näther, Dipl.-Chem. K. Ruppert
Institut für Anorganische Chemie der Universität
Niederurseler Hang, D-W-6000 Frankfurt am Main 50 (FRG)
Dr. Z. Havlas
Institute of Organic Chemistry and Biochemistry
of the Czechoslovakian Academy of Sciences
Flemingova Nam 2, CS-16610 Prague 6 (Czechoslovakia)

[**] Structures of Charge-Perturbed and Sterically Overcrowded Molecules, Part 13. The research project has been supported by the Deutsche Forschungsgemeinschaft, the Fonds der Chemischen Industrie, and the State of Hesse. – Part 12: H. Bock, N. Borrmann, Z. Havlas, H. Oberhammer, K. Ruppert, A. Simon, *Angew. Chem.* **1991**, *109*, 1733; *Angew. Chem. Int. Ed. Engl.* **1991**, *30*, 1678.

[***] Mimesis = close external resemblance between one animal and another animal or inanimate object: (Greek: imitation); *The Concise Oxford Dictionary of Current English* (Eds.: H. W. Fowler and F. G. Fowler), Clarendon Press, Oxford, **1961**.

with $Li[B(C_6H_5)_4]$, on addition of which a yellow color is observed.[6] Structure determination of the yellow crystals proves drastic changes (Fig. 1 bottom). Thus, the torsion angles of the pyridine rings relative to the pyrazine ring are reduced to 21° and 26°, yielding a flattened molecular skeleton, which allows a rationalization of the color. This is essentially due to the formation of two intramolecular hydrogen bridges N^+–H···N between the N centers of adjacent pyridine rings, which are only 253 pm apart. The uncorrected distances N^+–H = 124 pm and H···N = 133 pm on both sides of the bending angle $\sphericalangle$ N^+-H-N = 160° differ by only 9 pm. These intramolecular N^+–H···N bridges are rather short even for proton sponges (N^+–(H)···N = 265–254 pm[3]) as well as almost symmetrical ($\Delta(N^+$–H/H···N) = 16–17 pm[3]) and change, in addition, other structural parameters of tetra(2-pyridyl)pyrazine (Fig. 1 top). Thus the external C-C-C angles of the pyrazine ring are expanded to 129°(!) and the differing pyridine *ipso* angles of 123° and 117° in the dihydrochloride (Fig. 1 middle) expectedly[2] equalize at 121°.

Additional information on the problem of different hydrogen bridges in one compound[7e,f] is provided by extensive quantum chemical calculations:[8]

1) The preferred conformation of tetra(2-pyridyl)pyrazine in the crystal (Fig. 1 top) is reproduced by a complete AM1 geometry optimization starting from standard structural parameters.[8a] The alternative arrangement, which would contain triazachelate pincers and could be constructed by rotation of all pyridine rings, proves to be energetically less favorable, presumably due to the resulting N···N distances of about 290 pm, which are less then the sum of interference radii.

2) For the diprotonation and the conversion of the two external H^+ bridges to intramolecular ones, enthalpy of formation contributions of +91 kJ mol^{-1} and +443 kJ mol^{-1} are predicted.[8b] However, these gas-phase values must be corrected for the unknown solvation and lattice energies.

3) The AM1 charge distributions for tetra(2-pyridyl)-pyrazine *M* and for its different diprotonation products $[MH_2^+Cl_2^-]$ and $[MH_2^+]$ calculated from the crystal structure data, exhibit significant differences: Thus for the H^+ bridge centers, residual charges of +0.33 ($[MH_2^+Cl_2^-]$) and of +0.38 ($[MH_2^+]$) are estimated as well as −0.82 for the chloride anion. The partial charges at the pyridine N centers change from −0.12 (*M*) to −0.05 and −0.16 ($[MH_2^+Cl_2^-]$) and to −0.16 and −0.19 ($[MH_2^+]$), predicting $\Delta q_N = 0.11$ for the dichloride with one-sided NH^+ bridges and only $\Delta q_N = 0.03$ for the bis(tetraphenylborate) with almost symmetrical intramolecular bridges. As expected, the positive charges introduced by diprotonation are partially distributed to the peripheral pyridine hydrogens.

4) For a simulation of the H^+ bridge potentials, which depend strongly on the N···N distance,[8c] the structure of the 4-aminopyridine semiperchlorate provides an appropriate starting point (Scheme 1).[9] This structure has been determined by neutron diffraction and shows an N···N distance of 270 pm between the two perpendicular pyridine rings as well as an unsymmetrical hydrogen bridge (N^+–H 117 pm, H···N 152 pm). Variation of the distance $d_{N\cdots N}$ between 280 pm and 240 pm and stepwise movement of the bridge proton along the N–N axis by Δr yield different potential curves after each total geometry optimization of the pyridine rings (Scheme 1).

Double minima are calculated for structures with N···N distances between 280 pm and 250 pm; the height of the barrier decreases from 35 to 2 kJ mol^{-1}, and the difference in the N–H bond lengths is reduced from 70 pm to 22 pm. For

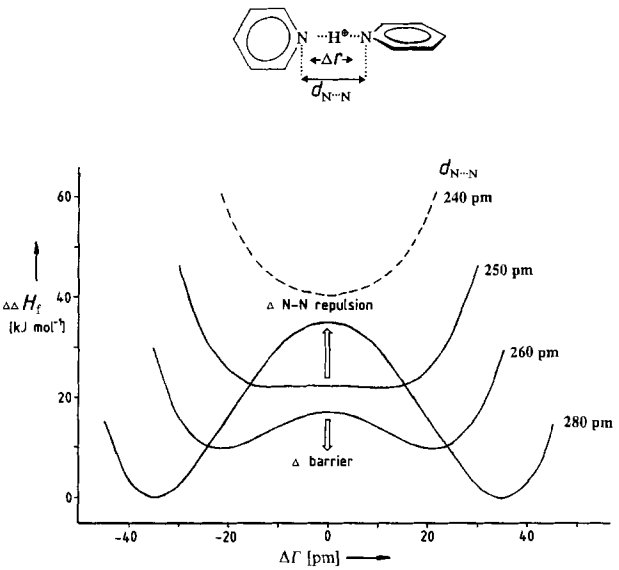

Scheme 1. Potential curves for pyridinium pyridine [8c] (see text).

the optimum N···N distance of about 270 pm, an N^+–H···N bond energy of 54 kJ mol^{-1} results. On shortening the N···N distance from 260 pm to 250 pm, the AM1 calculations predict an increase in energy due to increasing N–N repulsion, and for $d_{N\cdots N}$ = 245 pm a single minimum with equal distances N–H^+ of 122.5 pm is found. All other calculated properties exhibit only small changes: The pyridine *ipso* angles vary between 118° (H···N 197 pm) and 120° (N^+–H 103 pm) and the charges q_{H^+}, between +0.34 (N···N 280 pm) and +0.36 (N···N 250 pm).

5) In the diprotonated tetra(2-pyridyl)pyrazine containing two intramolecular hydrogen bridges (Fig. 1 bottom), the proton movement might be coupled to a "flip-flop" molecular dynamics: The adjacent pyridine rings are twisted by 26° and 21° out of the pyrazine plane. If their differing twisting angles are not caused by the crystal packing, the transition from one into the other double minimum should cause a change of ±5°. Therefore, in additional AM1 model calculations[8d] the proton was shifted in ten steps with Δd_{NH} = 9 pm along the experimentally determined structure with $d_{N\cdots N}$ = 253 pm. The following data are obtained for the barrier of the double minimum: height $\Delta\Delta H_f$ = 4 kJ mol^{-1}, d_{N-H^+} = 128 pm, bonding angle $\sphericalangle$ N(H^+)N = 170°, pyridine *ipso* angles of 121°, and a proton charge q_{H^+} = +0.38.

According to the approximate quantum chemical calculations, both tetra(2-pyridyl)pyrazine dihydrochloride and bis(tetraphenylborate) also differ in the type of their hydrogen bridge: With the electron-rich chloride ion as the proton acceptor, due to the rather long N···N distance of 288 pm, a simple potential minimum is approximated, in which the energetically favorably located proton vibrates only around its equilibrium position. The N^+–H···N bridges in the "naked" dication, on the other hand, are among the shortest known[3, 7, 19] with the smallest difference in the bond lengths N^+–H and H···N.[3, 7, 9, 10] Their formation causes the N···N distance to shorten by 35 pm (!) (Fig. 1 middle and 1 bottom), corresponding to a structure represented by a shallow double-minimum with a low barrier. The movement of the proton coupled with molecular dynamics, however, seems to be largely frozen in the crystal at 100 K[6] according to the center of inversion formed.

The mimetic behavior observed for tetra(2-pyridyl)-pyrazine upon exchange of the anions of the dichloride in

acetonitrile by addition of lithium tetraphenylborate presumably occurs in other protonatable nitrogen bases as well and is potentially of biological importance. In ongoing investigations the preparation of single crystals of metal-cation chelate complexes[11] of tetra(2'-pyridyl)pyrazine will be attempted.

Received: November 14, 1991 [Z 5019 IE]
German Version: *Angew. Chem.* **1992**, *104*, 348

CAS Registry numbers:
tetra(2-pyridyl)pyrazine dihydrochloride, 138901-51-6; tetra(2-pyridyl)-pyrazine bis(tetraphenylborate), 138901-52-7; tetra(2-pyridyl)pyrazine 25005-97-4.

[1] H. Bock, D. Jaculi, *Z. Naturforsch. B* **1991**, *46*, 1091.

[2] See: H. Bock, K. Ruppert, C. Näther, Z. Havlas, H.-F. Herrmann, C. Arad, I. Göbel, A. John, J. Meuret, S. Nick, A. Rauschenbach, W. Seitz, T. Vaupel, B. Solouki, *Angew. Chem.* **1992**, *104*, in press; *Angew. Chem. Int. Ed. Engl.* **1992**, *31*, in press (May issue) and literature cited therein.

[3] H. A. Staab, T. Saupe, *Angew. Chem.* **1988**, *100*, 895; *Angew. Chem. Int. Ed. Engl.* **1988**, *27*, 865; T. Barth, C. Krieger, F. A. Neugebauer, H. A. Staab, *ibid.* **1991**, *103*, 1006 and **1991**, *30*, 1030 and literature cited therein.

[4] Tetra(2-pyridyl)pyrazine (Alpha): 100 mg were recrystallized from 3 mL dry $HCCl_3$ under an atmosphere of *n*-hexane. Colorless plates; for the crystal structure analysis we are grateful to Dr. J. W. Bats (Universität Frankfurt); see T. Vaupel, *Diplomarbeit*, Universität Frankfurt, **1992**. The molecule is arranged around a crystallographic inversion center. Angle sum of all six-membered rings 720°, bond lengths C–N 134 pm, C–C (ring) 138–139 pm, C–C 149 pm.

[5] Tetra(2-pyridyl)pyrazine dihydrochloride: 520 mg (1.3 mmol) tetra(2-pyridyl)pyrazine were stirred in 60 mL aqueous 1 *N* HCl at room temperature for 2 h. The water was then removed under reduced pressure and the dried residue recrystallized from 200 mL acetonitrile. Single crystals: 70 mg were dissolved in 100 mL boiling acetonitrile and slowly cooled to room temperature; after 2 d colorless polyhedra had grown. Crystal structure analysis: $C_{24}H_{18}Cl_2N_6$ (461.23) $a = 940.5(2)$, $b = 771.8(2)$, $c = 1563.2(6)$ pm, $\beta = 105.13(3)°$, $V = 1095.3 \times 10^6$ pm^3 (100 K), $Z = 2$, $\rho_{calc.} = 1.399$ g cm^{-3}, $\mu(Mo_{K\alpha}) = 0.32$ mm^{-1}, monoclinic, space group $P2_1/n$, Siemens-AED II four-circle diffractometer, 6843 measured reflections $3° \le 2\theta \le 60°$, of which 2493 are independent with $I > 2\sigma(I)$. Structure resolution by direct methods and difference Fourier techniques (SHELXTL-Plus), N = 2943, NP = 182, $R = 0.033$, $R_w = 0.037$, $w = 1/\sigma^2(F) + 0.00008\,F^2$, GOOF = 2.864, Shift/Err ≤ 0.001, residual electron density +0.43/−0.30 e$_o$Å^{-3}. Empirical absorption correction, extinction correction, all C, N, and Cl atoms were anisotropically refined; H atoms (from difference Fourier analysis) isotropically refined. The dihydrochloride is arranged around a crystallographic inversion center. Angle sums of all rings 720°, bond lengths C–N 134 pm, C–C (ring) 139 pm, C–C 149 pm. b) Further details of the crystal structure determination are available on request from the Fachinformationszentrum Karlsruhe, Gesellschaft für wissenschaftlich-technische Information mbH, D-W-7514 Eggenstein-Leopoldshafen 2, on quoting the deposit number CSD-56020, the authors, and the literature citation.

[6] Tetraphenylborate salt of diprotonated tetra(2-pyridyl)pyrazine: A suspension of 200 mg (0.04 mmol) dihydrochloride in 20 mL acetonitrile was dissolved in methanol. On addition of 800 mg (2.5 mmol) lithium tetraphenylborate in 5 mL acetonitrile a yellow color appeared; after 3 h yellow cubes had grown. Crystal structure analysis: $C_{72}H_{58}B_2N_6$ (1028.7); $a = 11.082(6)$, $b = 11.160(7)$, $c = 12.366(6)$ pm; $\alpha = 80.98(5)$, $\beta = 84.87(4)$, $\gamma = 63.68(4)°$, $V = 1353 \times 46\ 10^6$ pm^3 (100 K), $Z = 1$, $\rho_{calc.} = 1.263$ g cm^{-3}, $\mu(Mo_{K\alpha}) = 0.07$ mm^{-1}, triclinic, space group $P\bar{1}$, Siemens-AED-II four-circle diffractometer, 5461 measured reflections between $3° \le 2\theta \le 55°$, of which 3833 are independent with $I > 1\sigma(I)$. Structure resolution by direct methods and difference Fourier technique (SHELXTL-Plus), N = 3833, NP = 478, $R = 0.054$, $R_w = 0.040$, $w = 1/\sigma^2(F) + 0.0002\,F^2$, GOOF = 1.3660, Shift/Err ≤ 0.001, residual electron density +0.40/−0.26 e$_o$Å^{-3}. Empirical absorption correction, extinction correction, B, C, and N atoms were anisotropically refined; H atoms (from difference Fourier analysis), isotropically refined. The dication is arranged around a crystallographic inversion center. Angle sums of all rings 720°, bond lengths C–N 134 pm, C–C (ring) 139 pm, C–C 150 pm. For further details of the crystal structure see [5b].

[7] Selected reviews on hydrogen-bridge bonds: a) A. F. Wells, *Structural Inorganic Chemistry*, 5th ed., Clarendon Press, Oxford, **1987**, pp. 355–376; b) J. Elmsley, *Chem. Soc. Rev.* **1980**, *9*, 91–24; c) R. Taylor, O. Kennard, *Acc. Chem. Res.* **1984**, *17*, 320; d) G. R. Desiraju, *Acc. Chem. Res.* **1991**, *24*, 290. e) Among the examples for different hydrogen bridges within one compound, the yellow and white polymorphic modifications of 3,6-dichloro-2,5-dihydroxyterephthalic acid dimethyl ester which have different intramolecular bridges O–H···O and O–H···Cl, are pointed out (Q.-C. Yang, M. F. Richardson, J. D. Dunitz, *Acta Crystallogr. Sect. B*, **1988**, *45*, 312). f) For mono- and diprotonation see for example R. Schwesinger, M. Missfeldt, K. Peters, H. G. von Schnering, *Angew. Chem.* **1987**, *99*, 210; *Angew. Chem. Int. Ed. Engl.* **1987**, *26*, 1165.

[8] All quantum chemical calculations were performed at the AM1 level (M. J. S. Dewar, E. G. Zoebisch, E. F. Healy, J. J. P. Stewart, *J. Am. Chem. Soc.* **1985**, *107*, 3902; program version SCAMP 4.0, T. Clark, Universität Erlangen). a) For the neutral molecule, a complete geometry optimization starting from standard structural parameters yields $\Delta H_f = 984$ kJ mol^{-1}, C–N 135 pm, C–C (ring) 140 pm, C–C 149 pm, *ipso* angle in pyridine 117°, twisting angle 54°, nonbonding distance N···N 320 pm; $\varepsilon_1 = 9.06$ eV (exp. $IE_1^V = 8.1$ eV; T. Vaupel, *Diplomarbeit*, Universität Frankfurt, **1992**). b) The calculations for the diprotonated compounds were based on the crystal structure data. Dichloride N^+–H distance corrected according to [7c] to 104 pm): $\Delta H_f = 1132$ kJ mol^{-1} ($[MH_2^+Cl_2^-]$) and 2314 kJ mol^{-1} (MH_2^+) as well as bis(tetraphenylborate) $\Delta H_f = 2411$ kJ mol^{-1} ($[MH_2^+]$). c) For the model calculations of $H_5C_5N^+$–H···NC_5H_5, the starting point was the structure determined by neutron diffraction [9] with the six-membered rings perpendicular to each other and the N···N distance varied between 280 pm and 240 pm. For the individual potential curves $\Delta\Delta H_f/\Delta r$ (Scheme 1), the bridge proton is moved in 5 pm steps along the N–N axis and the geometry of the complete system including both pyridine rings was optimized. Additional calculations for coplanar pyridine rings yield similar potential curves, the $\Delta\Delta H_f$ values of which are higher by 2–3 kJ mol^{-1}. It has been pointed out that semiempirical calculation procedures often exaggerate N/N repulsion relative to the H^+-bridge attraction due to insufficient N^+–H···N parametrization. d) For the calculations of diprotonated tetra(2-pyridyl)pyrazine with two intramolecular H^+ bridges, the simulation of the "flip-flop" molecular dynamics started with the cartesian coordinates of the experimental structure (Fig. 1 bottom), transforming the latter structure in ten equally weighted steps into that of its mirror image. In the fifth step the enthalpy of formation increased from 2410 kJ mol^{-1} to 2414 kJ mol^{-1}. The structural parameters given correspond to interpolation values.

[9] J. Roziere, J. M. Williams, E. Grech, Z. Malarski, L. Sobzyzk, *J. Chem. Phys.* **1980**, *72*, 6117; see also P. Tenlon, R. G. Delaplane, I. Olovson, J. Reziere, *Acta Crystallogr. Sect.* **1985**, *C41*, 479.

[10] An extensive literature search, although still incomplete with respect to the multitude of publications [7c], yields a comparably short N^+–H···N bridge of 252.6 pm for 1,6-diazabicyclo[4.4.4]tetradecane hydrochloride (R. W. Alder, A. G. Orpen, R. B. Sessions, *J. Chem. Soc. Chem. Commun.* **1983**, 999); the position of the H^+ center is not reported. The shortest N···N distance found so far (247 pm) is found in *syn*-1,6:8,13-diimino[14]annulene perchlorate (R. Sestro, T. Pilati, M. Simonetta, E. Vogel, *J. Am. Chem. Soc.* **1985**, *107*, 3185).

[11] See for example: S. Hünig, H. Quast, *Neuere Farbige Systeme* (Abstr. II. Int. Farbensymposium, Elmau, 1964), Verlag Chemie, Weinheim, **1964**, pp. 17–19 and 35–43; T. Vaupel, *Diplomarbeit*, Universität Frankfurt **1992**; see also H. A. Goodwin, F. Lions, *J. Am. Chem. Soc.* **1959**, *81*, 6415.

Crystalline Nitrogen Oxides—Crystal Structure of N_2O_3 and a Remark Concerning the Crystal Structure of N_2O_5

By *Arndt Simon,* Jörg Horakh, Axel Obermeyer,* and *Horst Borrmann*

Our knowledge of the crystal structures of nitrogen oxides, N_2O, N_2O_2, N_2O_3, N_2O_4, and N_2O_5, is still rather incomplete. The structure determinations of N_2O[1] and N_2O_2[2] were complicated by the static disorder of the molecules. Raman spectra[3] contradict the linearity of the NO_2^+ ion in $NO_2^+NO_3^-$ as determined in the crystal structure of N_2O_5.[4] In the course of a structure determination of N_2O_3 only a possible unit cell could be proposed.[5]

Our results on the structure of the stable cubic and the metastable monoclinic forms of N_2O_4 have already been published.[6] Here we report on phase transformations in crystalline N_2O_3/N_2O_4 samples, a single-crystal structure determination of N_2O_3, and indications of the existence of

[*] Prof. Dr. A. Simon, J. Horakh, A. Obermeyer, H. Borrmann
Max-Planck-Institut für Festkörperforschung
Heisenbergstrasse 1, D-W-7000 Stuttgart 80 (FRG)

hitherto unknown nitrogen oxides. In addition, we describe preliminary results, which prove that the crystal structure of N_2O_5 needs to be revised.

Indigo-blue N_2O_3 exists in its pure form only in the solid state, melting at about $-100\,^{\circ}C$.[7] Reed and Lipscomb discovered that single crystals become polycrystalline due to a phase transformation when cooled below $-125\,^{\circ}C$.[5] Therefore we first performed extensive powder diffraction experiments, using the modified Guinier technique,[8] in order to optimize conditions for crystal growth. The samples, prepared from NO_2 and NO,[9] showed a very complex behavior (Fig. 1). Depending on temperature and thermal treatment we were able to identify six different diffraction patterns besides those of N_2O_4.[10]

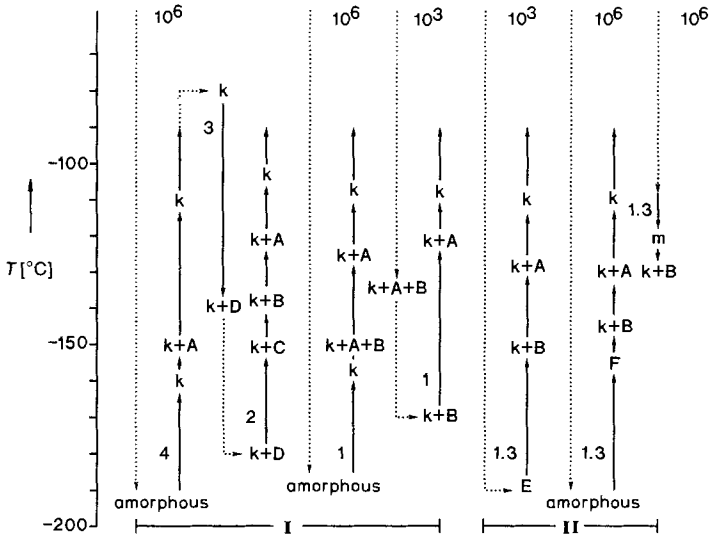

Fig. 1. Results of the investigation with the modified Guinier technique [8] of samples of N_2O_3 which were sealed in X-ray capillaries under vacuum (**I**) and 1 bar NO (**II**), respectively [9]. Arrows indicate directions of temperature changes (values in [$^{\circ}C\,h^{-1}$], dotted lines for temperature changes without X-ray observations, full lines for temperature changes with simultaneous X-ray diffraction). Cooling always began at room temperature with cooling rates of approximately 10^6 or $10^3\,^{\circ}C\,h^{-1}$. The diagrams of cubic and monoclinic N_2O_4 are denoted with k and m, respectively. Diagrams A through D were observed together with those of N_2O_4 in contrast to diagrams E and F[10].

Above approximately $-150\,^{\circ}C$ the intense lines of the cubic diagram k of N_2O_4 are observed with all samples. After being shock-cooled to $-190\,^{\circ}C$ the amorphous sample **I** was slowly heated up; at $-160\,^{\circ}C$ diagram k was observed first. At slightly higher temperature, diagram A of N_2O_3 was also observed. Obviously, N_2O_4 crystallizes more readily than N_2O_3. Therefore it is very surprising that after crystallization of the amorphous phase from either a shock-cooled or a slowly cooled sample **II**, the diagrams E and F did not show any lines for N_2O_4. At $-150\,^{\circ}C$ in both cases the cubic line pattern of N_2O_4 together with diagram B of N_2O_3 developed. These results are best explained with the existence of at least one new oxide below $-150\,^{\circ}C$, the composition of which must be between N_2O_3 and N_2O_4. We believe that diagrams A through D belong to distinctly different modifications of N_2O_3.

A single crystal of N_2O_3 was grown after the compound had been enriched locally in the sample by zone melting. Probably this is the reason why a crystal of phase B grew, in spite of the fact that in powder diagrams phase A was reproducibly observed in the same temperature range.[11, 12] Figure 2 shows a projection of the structure onto (100) of the orthorhombic unit cell.[13] As was proposed in 1920[14] and supported later by IR,[15] Raman,[16] and NMR experiments,[17] N_2O_3 must be described as a "nitroso-nitro" compound. There are only slight changes in geometric details

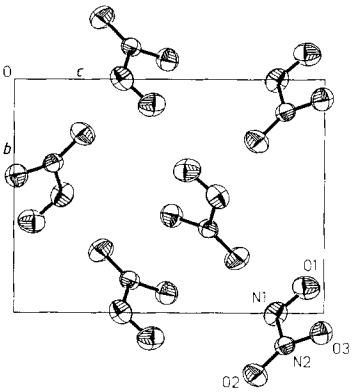

Fig. 2. Projection of the orthorhombic unit cell of N_2O_3 (phase B). The distances [pm] and angles [°] are: N1-N2 189.06(6), N1-O1 111.96(6), N2-O2 120.87(6), N2-O3 120.57(5); O1-N1-N2 105.12(4), O2-N2-O3 128.61(5), O2-N2-N1 119.55(4), O3-N2-N1 111.84(3).

determined in the solid state compared to the molecular shape as revealed from microwave spectra in the gas phase.[18] Especially the very long N–N distance (189.1 pm) is rather close to the value (186.4 pm) in the gas phase and represents a Pauling bond-order of about 0.2. A formal description as nitrosyl nitrite is also supported by the N–O distances and the O-N-O angle (N1–O1 112 pm compared to 115 pm in NO[19] and 106.5 pm in NO^+,[20] N2-O $\approx$ 121 pm and O-N-O 128.6° in comparison with 118 pm and 134.3° in N_2O_4[6] or 124 pm and 115° in NO_2^-[21]). The N_2O_3 molecule is almost planar; on the average the atoms deviate only 1.5 pm from the least-squares plane. However, because the angles around N2 add up to exactly 360.0°, this deviation is mainly due to the position of O1, which lies 7.8 pm above the plane through N1, N2, O2, and O3 (mean deviation 0.3 pm). The nitrosyl group and the nitrite unit are therefore twisted 3.7° about the N–N bond. The planarity of N_2O_4 was explained as a consequence of bonding interaction between the a_1 orbitals of the NO_2 fragments. These orbitals have significant oxygen character.[22] A similar explanation seems also reasonable for N_2O_3, since the O–O distance in N_2O_3 is even shorter than that in N_2O_4, despite the longer N–N distance. This particular geometry is also reflected in the smaller N1-N2-O3 angle relative to that of N1-N2-O2 and in the small O1-N1-N2 angle. Recently published ab initio calculations of the electronic structure of N_2O_3 were obviously performed only for the planar geometry without further explanation.[23] The calculated N–N distances are 10–15% shorter than the experimental value for all basis sets tested.

The redetermination of the structure of N_2O_5[4] from diffractometer data [24, 25] led to a surprising result. The (pseudo-)hexagonal structure was confirmed in the first instance, and the refinement converged at $R = 0.028$. The N–O distance in the NO_2^+ ion is 3.6 pm shorter and in the NO_3^- ion 1.5 pm longer than the values obtained from the earlier structure refinement. Refinements with data sets collected at different temperatures between 0 °C and $-168\,^{\circ}C$ did not give any hint for disorder or an erroneous description of the structure. However, a careful inspection of Guinier photo-

graphs showed very slight but systematic line splittings. Therefore the symmetry needs to be reduced from hexagonal to orthorhombic,[26] resulting in a very small deviation of 0.3% from the ideal $a:b$ ratio of the (ortho-)hexagonal system ($1:\sqrt{3}$). The structural consequences of this result are under investigation.

Received: October 8, 1991 [Z 49591E]
German version: *Angew. Chem.* **1992**, *104*, 325

[1] W. C. Hamilton, M. Petrie, *J. Phys. Chem.* **1961**, *65*, 1453.
[2] W. J. Dulmage, F. A. Meyers, W. N. Lipscomb, *J. Chem. Phys.* **1951**, *19*, 1432; *Acta Crystallogr.* **1953**, *6*, 760; W. N. Lipscomb, F. E. Wang, W. R. May, E. L. Lippert, *Acta Crystallogr.* **1961**, *14*, 1100.
[3] W. W. Wilson, K. O. Christe, *Inorg. Chem.* **1987**, *26*, 1631.
[4] E. Grison, K. Erics, J. L. De Vries, *Acta Crystallogr.* **1950**, *3*, 290.
[5] T. B. Reed, W. N. Lipscomb, *Acta Crystallogr.* **1953**, *6*, 781.
[6] A. Obermeyer, H. Borrmann, A. Simon, *Z. Kristallogr.* **1991**, *196*, 129.
[7] I. R. Beattie, S. W. Bell, A. J. Vosper, *J. Chem. Soc.* **1960**, 4796.
[8] A. Simon, *J. Appl. Crystallogr.* **1970**, *3*, 11; *ibid.* **1971**, *4*, 138.
[9] **I**: N_2O_4 was condensed at $-78\,^{\circ}C$ and allowed to react with gaseous NO by slowly raising the temperature. At approximately $-50\,^{\circ}C$ a deep blue liquid separated from the N_2O_4. An X-ray capillary ($\varnothing = 0.2$ mm) was filled to a height of 2 cm, cooled to roughly $-100\,^{\circ}C$ (ethanol/N_2(liq)), evacuated, and sealed. **II**: A gaseous mixture of NO_2 and NO was condensed into an X-ray capillary at $-78\,^{\circ}C$. The NO pressure in the apparatus was kept at about 1 bar to maximize the amount of N_2O_3 in the reaction product. After "annealing" at $-50\,^{\circ}C$ for several hours with intermittant warming to room temperature, the sample had changed color from greenish blue to dark blue. The capillary was sealed at approximately $-100\,^{\circ}C$ under 1 bar NO.
[10] The different powder diagrams in Figure 1 are characterized by the following d values [pm]: A ($-110\,^{\circ}C$): 557, 406, 401, 360, 349, 299, 290, 286, 281, 272, 258, 257, 236, 235, 198.1, 194.1, 185.2. B ($-130\,^{\circ}C$): 523, 440, 402, 362, 331, 295, 275, 262, 261, 255, 252, 238, 235, 233, 209, 182.6. C ($-145\,^{\circ}C$): 599, 461, 351, 336, 280, 269. D ($-180\,^{\circ}C$): 420, 378, 347, 322, 297, 286, 274, 273, 258, 251, 249, 242, 231, 226, 213, 211, 197.6, 189.1, 178.5, 173.5. E ($-155\,^{\circ}C$): 511, 479, 408, 349, 348, 312, 282, 277, 264, 257, 256, 242, 229, 225, 193.1. F ($-150\,^{\circ}C$): 600, 426, 407, 404, 369, 353, 348, 300, 275, 256, 254. k ($-170\,^{\circ}C$): 548.3, 387.7, 316.6, 245.2, 207.3, 182.8, 173.4, 152.1, 133.0, 129.2. m ($-112\,^{\circ}C$): 517, 362, 351, 322, 285, 266, 259, 244, 235, 217, 194.7, 192.6, 181.5, 149.7, 148.0, 131.0.
[11] From the structure factors given by Reed and Lipscomb [5] a powder diagram can be calculated which is very similar to diagram A.
[12] Sample **II** completely crystallized at $-115\,^{\circ}C$ to form a light blue solid. A small part of the sample was kept solid and the rest was melted. At $-106\,^{\circ}C$ a crystal started growing from the solid and became deeper in color as was observed with the microscope. Rotation photographs showed the crystal to be mainly cubic N_2O_4. At the end of the solid column a separated section (0.5 mm length) remained; this was very dark blue and solidified at $-108\,^{\circ}C$. It was almost completely melted at $-104.5\,^{\circ}C$ and recrystallized when cooled at a rate of $1\,^{\circ}C$ per h. According to rotation and oscillation photographs, few crystallites of different sizes formed at $-106.5\,^{\circ}C$. During the two days measurements of a data set, a perfect single crystal formed which could be cooled to $-160\,^{\circ}C$ without destruction. [13]
[13] a) Crystal data of N_2O_3: $a = 506.86(4)$, $b = 647.96(5)$, $c = 863.26(6)$ pm at $-160\,^{\circ}C$; $\rho_{X\text{-}ray} = 1.781\ g\,cm^{-3}$, $Z = 4$, space group $P\,2_12_12_1$ (No. 19), $R = 0.022$ and $wR = 0.021$ for 1352 reflections and 47 refined parameters. b) Further details of the crystal structure investigation are available on request from the Fachinformationszentrum Karlsruhe, Gesellschaft für wissenschaftlich-technische Information mbH, D-W-7514 Eggenstein-Leopoldshafen 2 (FRG) on quoting the depository number CSD-55934, the names of the authors, and the journal citation.
[14] H. Wieland, *Berichte* **1921**, *54*, 1781.
[15] W. A. Yeranos, M. J. Joncich, *Mol. Phys.* **1967**, *13*, 263.
[16] I. C. Hisatsune, J. P. Devlin, *Spectrochim. Acta* **1960**, *16*, 401.
[17] H. Schultheiss, E. Fluck, *Z. Naturforsch. B* **1977**, *32*, 257; L. O. Andersson, J. Mason, *Chem. Commun.* **1968**, 99.
[18] A. H. Brittain, A. P. Cox, R. L. Kuczkowski, *Trans. Faraday Soc.* **1969**, *65*, 1963.
[19] D. B. Keck, C. D. Hause, *J. Mol. Spectroscopy* **1968**, *26*, 163.
[20] J. Laane, J. R. Ohlsen, *Prog. Inorg. Chem.* **1980**, *27*, 473.
[21] M. I. Kay, B. C. Frazer, *Acta Crystallogr.* **1961**, *14*, 56.
[22] R. Ahlrichs, F. Keil, *J. Am. Chem. Soc.* **1974**, *96*, 7615; B. M. Gimarc, S. A. Khan, M. C. Kohn, *J. Am. Chem. Soc.* **1978**, *100*, 1996.
[23] S. A. Maluendes, A. H. Jubert, E. A. Castro, *J. Mol. Struct. (Theochem)* **1990**, *204*, 145.
[24] NO_2 was purified by repeated sublimation of (colorless) N_2O_4, diluted with argon, and allowed to react with ozone (approx. 20% O_3 in O_2) in an apparatus based on the principle of Daniell's burner. The ratio was such that the gas phase was colorless. The product, N_2O_5, was condensed at $-78\,^{\circ}C$ in a trap and further purified by sublimation in ozone containing O_2. The X-ray capillary was filled at $-78\,^{\circ}C$ and sealed under vacuum. At $-25\,^{\circ}C$ the sample slowly recrystallized, and at slightly higher temperature one of the crystallites grew to a size sufficient for measurement.
[25] Crystal structure of N_2O_5: Measurements and calculations were performed based on the (pseudo-)hexagonal cell (see text). $a = b = 540.19(9)$, $c = 652.68(13)$ pm at $-168\,^{\circ}C$, $\rho_{X\ ray} = 2.175\ g\,cm^{-3}$, $Z = 2$, space group $P\,6_3/m\,m\,c$ (No. 194), 3674 measured reflections averaged to 189 independent ones ($R_{int.} = 0.042$), $R = 0.028$ and $wR = 0.029$ for all 189 reflections and 12 refined parameters [13b].
[26] Least-squares refinement with 34 reflections of the completely indexed diagram leads to the lattice constants ($-179\,^{\circ}C$) $a = 541.07(6)$, $b = 934.20(8)$ and $c = 653.22(8)$ pm.

Regioselectivity Control in the Palladium-Catalyzed Copolymerization of Propylene with Carbon Monoxide**

By *Antonio Batistini, Giambattista Consiglio,** and *Ulrich W. Suter*

The control of regioselectivity is exceedingly important in the carbonylation of olefins.[1, 2] The archetype of this reaction is the hydroformylation of propylene. Even 50 years after the discovery of the reaction, the control of regioselectivity is still a problem.[3] Better results have been obtained in the carbonylation of aromatic or functionalized olefinic substrates.[4–8] For instance in the hydroalkoxycarbonylation of styrene catalyzed by L_2PdCl_2[9] the use of monophosphine or chelating diphosphine ligands results in a very good control of the regioselectivity, yielding the branched or the straight-chain ester.[4–7] For aliphatic olefins such as propylene such regiochemical control has never been achieved.

In the copolymerization of olefins with carbon monoxide control of the regioselectivity is even more important. The regioselective linkage of the olefinic monomer is a general prerequisite for the production of stereoregular polymers.[10] The copolymerization of styrene with carbon monoxide catalyzed by $[Pd(p\text{-}CH_3C_6H_4SO_3)_2(phen)]$ (phen = 1,10-phenanthroline) provides poly(1-oxo-2-phenyltrimethylene)[11–13] with considerable stereochemical control: The content of racemic dyads is higher than 90%, and the stereochemistry is probably controlled by the end of the growing chain. The related catalyst precursor $[Pd(CF_3COO)_2(dppp)]$ (dppp = 1,3-propanediylbis(diphenylphosphine)) is able to promote not only the strictly alternating copolymerization of ethylene but also that of aliphatic α-olefins like propylene.[14–16] However, a sample of the propylene–carbon monoxide copolymer prepared under conditions similar to those reported in the patent literature[14, 15] and recovered by precipitation with methanol shows poor constitutional regularity. In fact, the ^{13}C NMR spectrum of the recovered material exhibits three broad groups of signals in the carbonyl region ($\delta = 217–207$) which are centered at about $\delta = 215.5$, 212.0, and 207.8 and have an intensity ratio of

[*] Prof. Dr. G. Consiglio
Eidgenössische Technische Hochschule
Laboratorium für Technische Chemie, ETH-Zentrum
Universitätstrasse 6, CH-8092 Zürich (Switzerland)
Dr. A. Batistini, Prof. Dr. U. W. Suter
Eidgenössische Technische Hochschule, Institut für Polymere
ETH Zürich (Switzerland)

[**] We thank Prof. Dr. D. Milstein (The Weizman Institute of Science, Rehovot, Israel) for the ligand 1,3-propanediylbis(diisopropylphosphine) as well as for suggestions related to its synthesis.

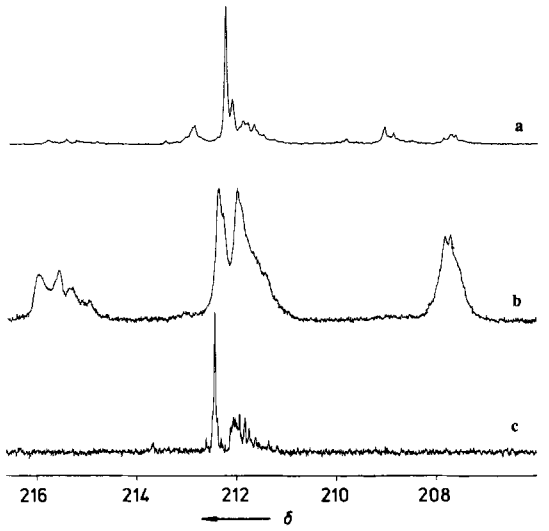

Fig. 1. The carbonyl region of the ^{13}C NMR spectra (125.8 MHz, $CDCl_3$) of propylene–carbon monoxide copolymers obtained with palladium catalysts modified by various ligands (bdpp (a), dppp (b), and dippp (c)).

roughly 1:2.4:1 (Fig. 1, spectrum b). On the basis of the chemical shifts[17] and comparisons with model compounds, the signals can be assigned to carbonyl groups with different types of linkage to the neighboring propylene units (Scheme 1). From the relative intensities of the signals it can be deduced that the ratio of the two insertion modes is about 77:23. No apparent control of the stereoselectivity can be recognized from this spectrum. The lack of a melting point is consistent with the irregular structure of this material ($T_g = 22\,^{\circ}C$).

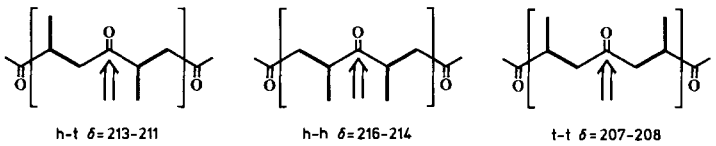

Scheme 1. Possible arrangements of the C_3 unit (regiosequences) in a propylene–carbon monoxide copolymer and the ^{13}C NMR chemical shifts for the inner carbonyl groups. h = head, t = tail.

In principle there are two possible approaches to improve the regularity of the polymer: 1. The use of chiral ligands, for example [(2,2-dimethyl-1,3-dioxolane-4,5-diyl)bis(methylene)]bis(diphenylphosphine),[18] to bring about enantiofacial selectivity,[19] thereby influencing the stereochemistry of the copolymer. 2. The use of ligands having different steric and electronic requirements, for example 1,3-propanediylbis(di-*n*-butylphosphine),[20, 21] to increase the amount of regular head-to-tail linkage. Regioselectivities over 90%[20] were obtained for a copolymer (melting point of 165 °C) defined as regio- and stereoregular.[18]

Following the same type of reasoning but emphasizing steric factors in the regulation of regioselectivity, we were able to obtain a considerable improvement in the stereoregularity of this copolymer and synthesized the first regioregular poly(1-oxo-2-methyltrimethylene). Figure 1 shows region of the ^{13}C NMR spectra of the most "regular" copolymers produced according to the two aforementioned approaches. The first copolymer (Fig. 1, spectrum a) was obtained with the modified catalytic system with (*R,R*)-2,4-pentanediylbis(diphenylphosphine) (bdpp)[22] under the same reactions conditions used for system with the achiral dppe ligand. The ^{13}C NMR spectrum reveals a remarkable improvement of both regio- and stereoselectivity. The intensity ratio of the signals centered at $\delta = 215.5$, 212.0, and 207.8 is about 1:9.9:1 in this case. The origin of the new signals at $\delta \approx 209$ and 213 is not yet clear. The high regularity of this material is reflected by the presence of (at least) two thermal transitions (at 130 and 200 °C), the higher of which is probably the melting point. The modification of the catalytic system with 1,3-propanediylbis(diisopropylphosphine) (dippp)[23] gives a polymer whose ^{13}C NMR spectrum (Fig. 1, spectrum c) gives evidence of the complete regioselectivity and good stereoselectivity of the polymerization. The same characteristics of regioregularity were observed for the polymer fraction which remained in solution after the addition of methanol. The less soluble material shows thermal transitions at 95 and 260 °C. The improved stereochemical control is also apparent from the narrow linewidth of the signals in the methyl region (Fig. 2). However, the ligands used to increase constitutional and configurational regularity caused a decrease in the molecular weight: $M_n = 25100$ (dppp), 4420 (bdpp), 2100 (dippp); the higher concentrations of terminal methyl groups are probably responsible for the signals at $\delta \approx 13$.

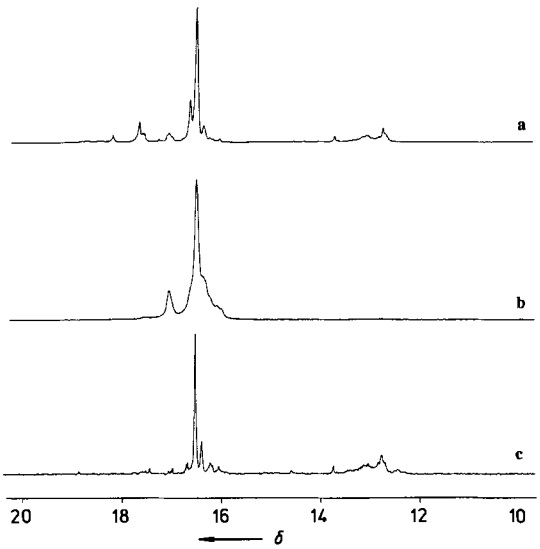

Fig. 2. The methyl region of the ^{13}C NMR spectra (125.8 MHz, $CDCl_3$) of propylene–carbon monoxide copolymers obtained with palladium catalysts modified by various ligands (bdpp (a), dppp (b), and dippp (c)).

These results clearly show the interconnection between enantiofacial selection and regioselectivity which was discussed previously for other addition reactions to olefins.[24] The regioselectivity can be, in fact, different on the two faces in reactions with enantiofacial discrimination. But complete regioselectivity can make the chain-end control of the entering olefin unit more effective. These results suggest possible ways to improve further the microstructure of this and related copolymers with other α-olefins.

Received: October 1, 1991 [Z 4947 IE]
German version: *Angew. Chem.* **1992**, *104*, 306

CAS Registry numbers:
[(dppp)Pd($CF_3COO)_2$], 138488-62-7; bdpp, 96183-46-9; dippp, 138459-85-5; propylene–carbon monoxide copolymer, 29612-55-3.

[1] P. Pino, F. Piacenti, M. Bianchi in *Organic Synthesis via Metal Carbonyls Vol. II* (Eds.: I. Wender, P. Pino), Wiley, New York, **1977**, pp. 43–296.
[2] B. Cornils in *New Syntheses with Carbon Monoxide* (Ed.: J. Falbe), Springer, New York, **1980**, pp. 1–225.
[3] L. Markó, *J. Organomet. Chem.* **1991**, *404*, 325; and references therein.
[4] G. Consiglio, M. Marchetti, *Chimia* **1976**, *30*, 26.
[5] G. Consiglio, *J. Organomet. Chem.* **1977**, *132*, C26.
[6] Y. Sugi, K. Bando, S. Shin, *Chem. Ind. (London)* **1975**, 397.
[7] K. Bando, Y. Sugi, *Chem. Lett.* **1976**, 727.
[8] G. Consiglio, S. C. A. Nefkens, C. Pisano, F. Wenzinger, *Helv. Chim. Acta* **1991**, *74*, 323.
[9] K. Bittler, N. von Kutepov, D. Neubauer, H. Reis, *Angew. Chem.* **1968**, *80*, 352; *Angew. Chem. Int. Ed. Engl.* **1968**, *7*, 329.
[10] For related considerations in another field of insertion polymerization, i.e. in Ziegler–Natta catalysis, see: P. Pino, R. Mühlhaupt, *Angew. Chem.* **1980**, *92*, 869; *Angew. Chem. Int. Ed. Engl.* **1980**, *19*, 857.
[11] E. Drent, *Eur. Pat. Appl.* **1986**, 229408 [*Chem. Abstr.* **1988**, *108*, 6617].
[12] P. Corradini, C. De Rosa, A. Panunzi, G. Petrucci, P. Pino, *Chimia* **1990**, *44*, 52.
[13] M. Barsacchi, G. Consiglio, L. Medici, G. Petrucci, U. W. Suter, *Angew. Chem.* **1991**, *103*, 992; *Angew. Chem. Int. Ed. Engl.* **1991**, *30*, 989.
[14] E. Drent, R. L. Wife, *Eur. Pat. Appl.* **1985**, 181014; see also *Neth. Appl.* NL 8403035 [*Chem. Abstr.* **1985**, *105*, 98172].
[15] E. Drent, *Eur. Pat. Appl.* **1988**, 322018 [*Chem. Abstr.* **1988**, *111*, 221150].
[16] E. Drent, J. A. M. van Broekhoven, M. J. Doyle, *J. Organomet. Chem.* **1991**, *417*, 235.
[17] E. Pretsch, T. Clerc, J. Seibl, W. Simon, *Strukturaufklärung organischer Verbindungen*, 3rd ed., Springer, Berlin, **1986**.
[18] P. K. Wong, *Eur. Pat. Appl.* **1989**, 384517 [*Chem. Abstr.* **1991**, *114*, 103079].
[19] For enantiofacial selection in the carbonylation of olefins see: G. Consiglio, P. Pino, *Top. Curr. Chem.* **1982**, *105*, 77; G. Consiglio, P. Pino, *Adv. Chem. Ser.* **1982**, *77*, 371.
[20] J. A. Van Doorn, P. K. Wong, O. Sudmeier, *Eur. Pat. Appl.* **1989**, 376364 [*Chem. Abstr.* **1991**, *114*, 24797].
[21] P. W. N. M. van Leeuwen, C. F. Roobeek, P. K. Wong, *Eur. Pat. Appl.* **1989**, 393790 [*Chem. Abstr.* **1991**, *114*, 103034].
[22] P. A. MacNeil, N. K. Roberts, B. Bosnich, *J. Am. Chem. Soc.* **1981**, *103*, 2273.
[23] K. Tani, E. Tanigawa, Y. Tatsuno, S. Otsuka, *J. Organomet. Chem.* **1985**, *279*, 87.
[24] P. Pino, A. Stefani, G. Consiglio in *Catalysis in Chemistry and Biochemistry, Theory and Experiments* (Ed.: B. Pullman), Reidel, Dordrecht, **1979**, p. 347.

Enantioselective Syntheses of Cyclopentanoid Compounds from Isoprene and *trans*-1,3-Pentadiene**

By *Kai.-U. Baldenius, Heindirk tom Dieck,* Wilfried A. König, Detlef Icheln,* and *Torsten Runge*

Dedicated to Professor Carl Heinrich Krauch on the occasion of his 60th birthday

Iron complexes with 1,4-diaza-1,3-diene (DAD) ligands catalyze the cyclodimerization of simples dienes.[1] A 1:1 mixture of *trans*-1,3-pentadiene and isoprene, for example, can be dimerized by **1a** activated with organomagnesium compounds[2] providing racemic 1,7-dimethyl-1,5-cyclooctadiene **2** in 88% yield (Scheme 1). We have found that reactions with precatalyst **1b** obtained from the C_2 symmetric (1*R*)-menthyl-DAD[3] deliver optically active (−)-1,7-dimethyl-1,5-cyclooctadiene (−)-**2** in 89% yield with up to 61% *ee*.

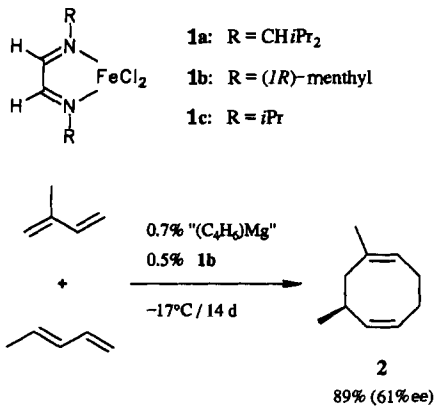

Scheme 1. Enantioselective codimerization of isoprene and *trans*-1,3-pentadiene.

Dimethylcyclooctadiene (DMCOD) **2** isomerizes readily under acidic conditions to derivatives of bicyclo[3.3.0]octane (Scheme 2). The cationic intermediate may be captured stereoselectively by a nucleophile resulting in the *endo* product (**3**–**5**). Alternatively, elimination or rearrangement/elimination may provide olefins like **7**–**9**. This elimination is always a side reaction and the cause for lowered yields of the addition product. Inspection of molecular models suggests that the cationic intermediate has a saddle conformation, in which the methyl group on the sp^3 C atom has a stereodirecting effect due to its preference for the *exo* position. Diastereomeric side products and racemization do not occur. In the reaction of **2** with acetic anhydride/$BF_3 \cdot Et_2O$, the electrophilic action of the acylium ion leads selectively to the *endo*-acetyl-*endo*-acetoxy product **4**.

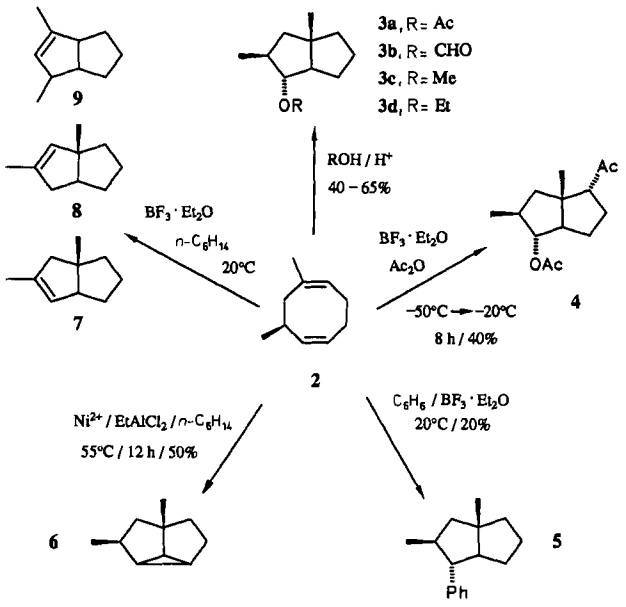

Scheme 2. Acid-catalyzed reactions of **2**.

[*] Prof. Dr. H. tom Dieck,[+] Dipl.-Chem. K.-U. Baldenius
Institut für Anorganische und Angewandte Chemie der Universität
Martin-Luther-King-Platz 6, D-W-2000 Hamburg 13 (FRG)
Prof. Dr. W. A. König, Dipl.-Chem. D. Icheln, Dipl.-Chem. T. Runge
Institut für Organische Chemie der Universität Hamburg
[+] New address:
Gesellschaft Deutscher Chemiker
Postfach 900440, D-W-6000 Frankfurt am Main 60

[**] This research was supported by the Volkswagen-Stiftung, the Deutsche Forschungsgemeinschaft, and the Fonds der Chemischen Industrie. We thank Hoechst AG for their gift of chemicals.

The reaction of (−)-**2** (61% *ee*) with $EtAlCl_2$ (20 mol%) in the presence of bis(2-ethylhexanoato)nickel (1.5 mol%) in hexane at 60 °C furnishes (−)-**6** in 50% yield (Scheme 2). Nickel plays a different role in this isomerization than that which we had originally assumed:[1b] The electron-rich Ni species present under these reaction conditions probably acts as a nucleophile; an alkylnickel compound is formed which undergoes a sterically favorable γ elimination leading to the tricyclic product.

1,2,4-Trimethyl-1,5-cyclooctadiene (**10**), in analogy to **2**, is converted to **11** by treatment with acetic acid/cat. H_2SO_4/20 °C and to **12** with acetic anhydride (Scheme 3); but in contrast to **2** its reaction with catalytic $Ni^{2+}/EtAlCl_2$ leads to C–C bond cleavage and product **13**. A Wagner–Meerwein

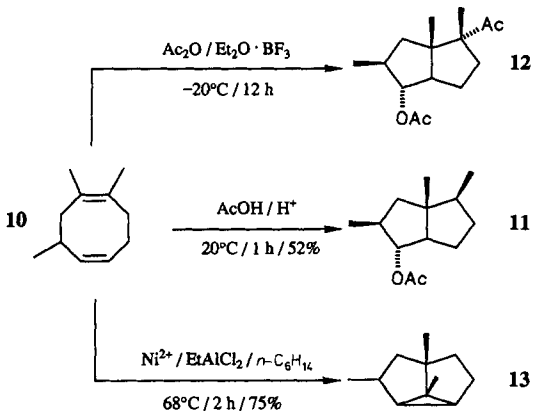

Scheme 3. Isomerizations of 1,2,4-trimethyl-1,5-cyclooctadiene (**10**).

rearrangement could precede the addition of the Ni nucleophile present in relatively low concentration here, as well in the reaction to **6**. A similar mechanism dependent on the presence of a nucleophile was formulated by Whitesell et al.[4] and Haufe et al.[5a] for the acid-catalyzed isomerization of 1,5-DMCOD **14**. The product of the rearrangement/elimination described by Whitesell et al. (**15**, Scheme 4) is also accessible from 1,6-DMCOD **16** and in better yields. Diene **16**, in turn, may be obtained with high selectivity from the dimerization of isoprene with DAD–iron catalysis.[1a]

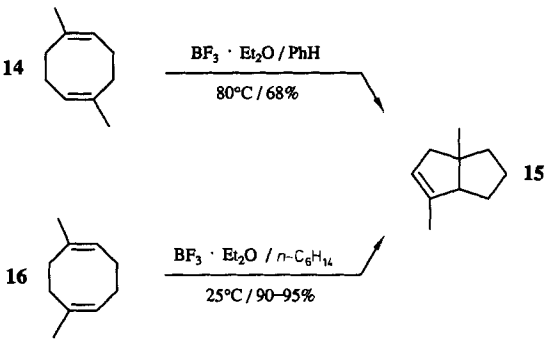

Scheme 4. Acid-catalyzed isomerizations of **14** and **16**.

The very simple approach to differently functionalized optically active bicyclo[3.3.0]octanes described here should provide new impetus for the synthesis of cyclopentanoid compounds. Mehta et al.[6] and Pattenden et al.[7] have already pointed out the importance 1,5-DMCOD **14** and its derivatives could have in the synthesis of several naturally occurring triquinanes. Closer examination of the substructures of some of these synthetic targets as well as biologically interesting compounds with intact eight-membered rings make 1,7-DMCOD **2** appear to be an attractive starting material with an already respectable enantiomeric excess.[8] Other COD derivatives, some demonstrating fascinating isomerizations, are accessible by iron catalysis.[9, 10]

In addition our results emphasize the value of derivatized cyclodextrins (CDs) as stationary GC phases for the analytical control of asymmetric syntheses.[11, 12] All the chiral reaction products in this report could be separated completely into their enantiomers on selectively *O*-alkylated β- and γ-CD derivatives[13] in glass or fused silica capillaries.

Experimental Procedure

(−)-**2**: Isoprene and *trans*-1,3-pentadiene (dried over $LiAlH_4$ and distilled under N_2; 11.2 g, 165 mmol of each) were cooled to −40 °C under N_2. Butadienemagnesium-bis(tetrahydrofuran) (260 mg, 1.2 mmol) was then added followed by **1b** (380 mg, 0.8 mmol). The reaction mixture was stirred at least 2 h at −20 °C. The deep red-brown solution was held at −17 °C for 14 d. The product mixture was distilled off at room temperature (RT) under vacuum (≤ 0.05 Torr): 22.1 g condensate contained (GC): 90% 1,7-DMCOD **2**, <2% 1,4-DMCOD. <1% **14** and **16**. Product **2** was purified by spinning-band distillation to >95%. $[\alpha]_D$ − 4 (c = 4.5, $CHCl_3$), *ee* = 61%. Higher reaction temperatures accelerate the reaction but with resulting loss in *ee*.

(−)-**3a**: Acetic acid (8 mL) was allowed to react with conc. sulfuric acid (0.1 mL) and (−)-**2** (1.55 g, 95% purity, 11 mmol, 56% *ee*). The reaction mixture was stirred 15 h at RT, then taken up in 2 M NaOH, extracted with hexane, and dried over sodium sulfate. After the solvent was removed, the product was distilled (ca. 0.08 Torr, 42 °C). Yield: 1.3 g colorless liquid (6.6 mmol, 61%, 54% *ee*. $[\alpha]_D$ − 82 (c = 1.6, $CDCl_3$)). According to GC, four isomeric side products were also present (each less than 2%). The preparations of **3b–d** and **11** proceeded analogously. Treatment with formic acid did not require additional catalysis. Reactions with alcohols require higher temperatures (55 °C) and yield products of lower purity.

(−)-**4**: A solution of (−)-**2** (0.87 g, 90% purity, 5.7 mmol, 56% *ee*) in acetic anhydride (7 mL) at −50 °C was stirred vigorously and $BF_3 \cdot Et_2O$ (7.7 mmol) was added. The reaction mixture was allowed to stand 10 h at −20 °C before workup with hexane/$NaHCO_3$. Chromatography (silica gel, hexane/ethyl acetate) provided 0.55 g colorless oil (40%, $[\alpha]_D$ − 30 (c = 1.7, $CDCl_3$)). The preparation of **12** proceeded analogously.

Received: August 19, 1991 [Z4877IE]
German version: *Angew. Chem.* **1992**, *104*, 338

CAS Registry numbers:
1b, 87226-78-6; **2**, 138541-38-5; **3a**, 138541-39-6; **3b**, 138541-40-9; **3c**, 138541-41-0; **3d**, 138541-42-1; **4**, 138541-43-2; **5**, 138541-44-3; **6**, 138661-25-3; **7**, 35408-34-5; **8**, 35408-33-4; **9**, 138541-45-4; **10**, 115679-01-1; **11**, 138541-46-5; **12**, 138541-47-6; **13**, 115679-05-5; **14**, 3760-14-3; **15**, 60329-18-2; **16**, 3760-13-2; 1,4-DMCOD, 19435-33-7; isoprene, 78-79-5; *trans*-1,3-pentadiene, 2004-70-8.

[1] a) H. tom Dieck, J. Dietrich, *Angew. Chem.* **1985**, *97*, 795; *Angew. Chem. Int. Ed. Engl.* **1985**, *24*, 781; b) M. Mallien, E. T. K. Haupt, H. tom Dieck, *ibid.* **1988**, *100*, 1091 and **1988**, *27*, 1062.
[2] Butadienemagnesium has proven to be an effective activator: U. M. Dzhemilev, A. G. Ibragimov, G. A. Tolstikov, *J. Organomet. Chem.* **1991**, *406*, 1. Preparation see K. Fujita, Y. Ohnuma, H. Yasuda, H. Tani, *ibid.* **1976**, *113*, 201.
[3] Preparation from (1*R*)-menthylamine (see O. Wallach, M. Kuthe, *Ann. Chem. Pharm.* **1893**, *276*, 296) and glyoxal in $CH_2Cl_2/NaSO_4$/cat. HCOOH at 20 °C (see H. tom Dieck, J. Dietrich, *Chem. Ber.* **1984**, *117*, 694). Recrystallization from cold methanol gives colorless crystals, m.p. = 78 °C, $[\alpha]_D$ −163 (c = 1, $CDCl_3$).
[4] J. K. Whitesell, R. S. Matthews, P. A. Solomon, *Tetrahedron Lett.* **1976**, 1549.
[5] a) G. Haufe, A. Wolf, K. Schulze, *Tetrahedron* **1986**, *42*, 1549. b) The acid-catalyzed cyclization with addition of solvent is known: A. C. Cope, M. M. Martin, M. A. Kervey, *Q. Rev. Chem. Soc.* **1966**, *20*, 119.
[6] G. Mehta, S. K. Rao, *J. Am. Chem. Soc.* **1986**, *42*, 1549, and literature cited therein.
[7] G. Pattenden, S. J. Teague, *Tetrahedron Lett.* **1984**, *25*, 3021.

[8] L. A. Paquette, H.-J. Kang, *J. Am. Chem. Soc.* **1991**, *113*, 2610, and literature cited therein; L. A. Paquette, *Top. Curr. Chem.* **1984**, *119*, 1; *ibid.* **1979**, *79*, 41; M. Vaudewalle, P. DeClercq, *Tetrahedron*, **1985**, *41*, 1767; M. Braun, *Nachr. Chem. Tech. Lab.* **1985**, *33*, 803.

[9] H. tom Dieck, C. Munz, J. Ehlers in *Organometallics in Organic Synthesis, Vol. 2* (Eds.: H. Werner, G. Erker), Springer, Heidelberg, **1989**, pp. 21–43.

[10] The iron catalysts employed are as sensitive as they are selective and usually do not tolerate dienes with heteroatom substituents. Other products than the desired ones with eight-membered rings are often produced due to steric reasons. For example, the reaction of 1-vinylcyclopentene with an excess of isoprene and **1c** does not lead to the anticipated bicyclo[6.3.0]undecadiene but rather to 4-(1-cyclopentenyl)-2-methylcyclohexene.

[11] a) W. A. König, *Nachr. Chem. Tech. Lab.* **1989**, *37*, 471; b) V. Schurig, H.-P. Nowotny, *Angew. Chem.* **1990**, *102*, 969; *Angew. Chem. Int. Ed. Engl.* **1990**, *29*, 939.

[12] J. Ehlers, W. A. König, S. Lutz, G. Wenz, H. tom Dieck, *Angew. Chem.* **1988**, *100*, 1614; *Angew. Chem. Int. Ed. Engl.* **1988**, *27*, 1556.

[13] W. A. König, D. Icheln, T. Runge, I. Pforr, A. Krebs, *J. High Res. Chromatogr.* **1990**, *13*, 702.

Selective Ketone Pyrolysis: New Synthetic Method for Mono- and Polycyclic Hydrocarbons**

By *Jörg Breitenbach, Frank Ott,* and *Fritz Vögtle**

The interest in polycyclic almost spherical molecular frameworks has increased, not least, through the results from the dodecahedrane[1] and fullerene area.[2] Our goals are large-cavity cage compounds, which could be isomerized and dehydrogenated to fullerene-like polycycles and those which retain guest molecules indefinitely.[3] In this context, we searched for synthetic methods for the preparation of macropolycyclic hydrocarbons. These can be obtained from the corresponding cyclic sulfones via the loss of sulfur dioxide.[4] However, sparing solubility, high melting points, and the insufficient volatility of sulfones as well as the sensitivity of some thiols and sulfides provide difficulties. Also the elimination of heteroatoms from aza-[5] and selenocyclophanes[6] does not occur readily. We have now found that cyclic ketones, via CO loss and C–C bond formation, can be preparatively ring contracted. As substrates for the development of the synthetic method, we chose cyclophanes which permit comparisons with the sulfone pyrolysis. The simple experimental design used there (horizontal, evacuated quartz tube, two tubular furnaces) also proved to be suitable here.

Optimization of the pyrolysis of the 12-membered ring diketone **1**[7] showed that the conditions (heat and pyrolysis temperature, vacuum) can be set to obtain the desired product (monoketone **2**, 23% yield; hydrocarbon **3**, 22% yield from **1**[8]).[9] Also [3.3.3]cyclophanetrione **4**, synthesized here for the first time, could be transformed selectively into the hitherto unknown ketones **5** (25% yield) and **6** (20% yield from **4**)[10] and then finally into the hydrocarbon **7** (31% yield in relation to **4**).[11]

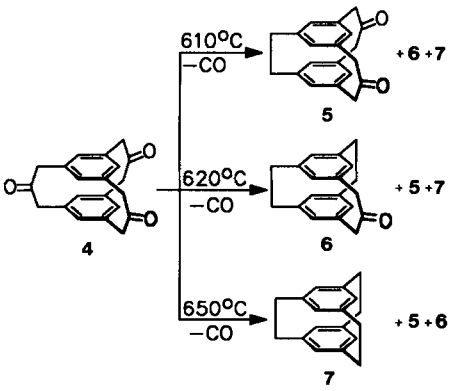

In the paracyclophane series this pyrolysis, which only requires a few minutes, was achieved as before without problems: the [2.2]paracyclophane was obtained from [3.3]paracyclophane-2,12-dione[12] at 625 °C in 30% yield; the intermediate monoketone ([3.2]paracyclophane-2-one) could be obtained in 32% yield at 614 °C.[13]

Table 1. Physical and spectroscopic data as well as yields of the new compounds **2**–**6** and **8**. NMR spectra at 250 MHz (^{1}H) and 50.3 MHz (^{13}C) measured in $CDCl_3$.

2: Yield 23% [8]; m.p. = 115–116 °C; ^{1}H NMR: δ = 1.32 (s, 18H; CH_3), 2.20 (AA′, 2H; CH_2), 3.04 (XX′, 2H; CH_2), 3.39–3.55 [$(AB)_2$, 4H; CH_2], 4.98 (s, 2H; CH_{arom}), 7.10 (s, 4H; CH_{arom}); MS (70 eV): *m/z* 348.2447 [M^+], calc. 348.2453.

3: Yield 22% [8]; m.p. = 176–178 °C; ^{1}H NMR: δ = 1.35 (s, 18H; CH_3), 2.09 (AA′; 4H; CH_2), 3.05 (XX′, 4H; CH_2), 4.08 (s, 2H; CH_{arom}), 7.05 (s, 4H; CH_{arom}); MS (70 eV): *m/z* 320.2510 [M^+], calc. 320.2504.

4: Yield 7%; FP = 289–291 °C; ^{1}H NMR: δ = 3.77 (s, 12H; CH_2), 6.87 (s, 6H; CH_{arom}); MS (70 eV): *m/z* 318.1256 [M^+], calc. 318.1386.

5: Yield 25% [10]; m.p. = 261 °C; ^{1}H NMR: δ = 3.11 (s, 4H; CH_2), 3.68 (s, 8H; CH_2), 6.39 (s, br, 4H; CH_{arom}), 7.00 (s, br, 2H; CH_{arom}); MS (70 eV): *m/z* 290.1308 [M^+], calc. 290.1310.

6: Yield 20% [10]; m.p. = 210 °C; ^{1}H NMR: δ = 2.88–3.08 (AA′BB′, 8H; CH_2), 3.54 (s, 4H; CH_2), 5.61 (s, br, 2H; CH_{arom}), 6.51 (s, br, 4H; CH_{arom}); MS (70 eV): *m/z* 262.1351 [M^+], calc. 262.1357.

8: Yield 10%; m.p. = > 250 °C (decomp.); ^{1}H NMR: δ = 3.82 (s, 12H; CH_2), 6.90 (AA′, 12H; CH_{arom}), 7.08 (BB′, 12H; CH_{arom}), 7.29 (s, 6H; CH_{arom}); MS (FAB$^+$): *m/z* 775.3 [M^+ + H].

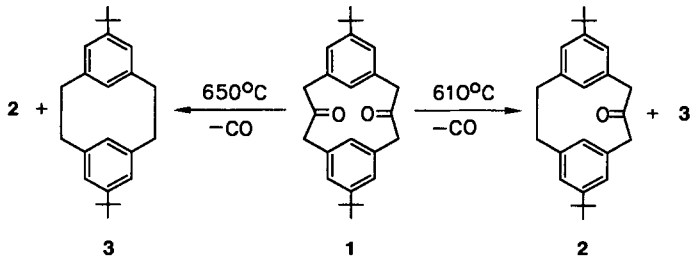

Thus, the ketone pyrolysis offers, besides a method for the production of the hydrocarbons, the possibility to obtain hitherto unknown, not easily accessible macrocyclic ketones. From the available examples, we conclude that the bond formation, as with the sulfone pyrolysis, occurs to a large extent intramolecularly. Even though the pyrolysis is a consecutive reaction, in which the intermediate products do not arise separately, the preferred formation of one of the products can nevertheless be achieved by the selection of the temperature.

For the preparation of the ketones, the TosMIC cyclization proved advantageous:[12,14] apart from the good accessibility of the building blocks, the simple procedure, and the good yields, the ketones obtained can be isolated without problems and are readily soluble. Starting from the tris(bromomethyl) compounds **9**[15] and **10**,[16] and toluene-4-sul-

[*] Prof. Dr. F. Vögtle, Dipl.-Chem. J. Breitenbach, F. Ott
Institut für Organische Chemie und Biochemie der Universität
Gerhard-Domagk-Strasse 1, D-W-5300 Bonn 1 (FRG)

[**] This work was supported by the Deutsche Forschungsgemeinschaft (SFB 334).

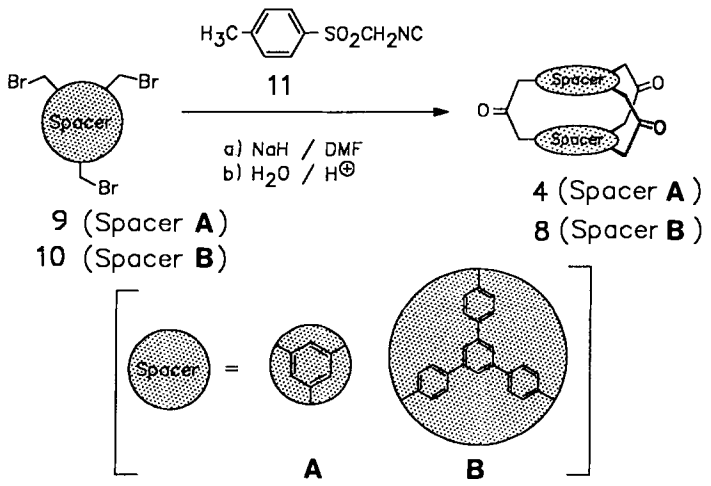

fonylmethyl isocyanide (TosMIC) **11**,[17] we obtained the cyclophanes **4** and **8** in one step in yields of 7% and 10%, respectively.

In contrast to the previously reported cyclizations with TosMIC **11** under dilute conditions[19] and in solvent mixtures,[20] we carried out the cyclizations in dimethylformamide (DMF). The amount of solvent can thus be reduced so that the concentration of the reactants favors the selective formation of the desired macrocycles.[21]

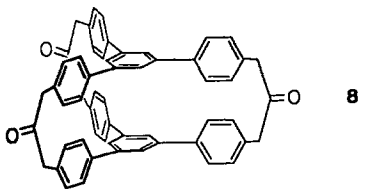

8

Investigations showed that, as with the sulfone pyrolysis, also non-benzylic and alicyclic ketones[22] can be preparatively ring contracted by this method. Even benzophenones afford biphenyls under analogous conditions.[23] The selectivity of the method as a function of the pyrolysis temperature and reaction time, therefore, brings new synthetic goals in many fields within reach. With this method, in contrast to the sulfone pyrolysis, oxidizable groups are not limiting factors.

Experimental Procedure

Ketone pyrolysis: With the help of a tubular furnace **4** (20 mg, 0.06 mmol) was evaporated at 10^{-5} Torr in a quartz tube filled with quartz wool and sealed at one end (diameter 0.3 cm, length 22 cm) . The tube had been preheated to 610-650 °C in the region of the quartz wool (pyrolysis zone) with a second tubular furnace along a length of 10 cm. After withdrawal from the pyrolysis zone, the product condensed in the quartz tube as a yellow solid. From the pyrolysate, the compounds **5** ($R_f = 0.58$, pyrolysis temperature 610 °C), **6** ($R_f = 0.84$, pyrolysis temperature 620 °C), and **7** ($R_f = 1.0$, pyrolysis temperature 650 °C) were obtained through preparative thick-layer chromatography with dichloromethane/methanol (100:1, v/v). Reactions using up to 100 mg were conducted analogously.

Preparation of oligoketones with TosMIC (e.g. **4** and **8**): To a solution of the trisbromide **9** or **10** respectively (26.35 mmol) and TosMIC **11** (39.52 mmol) in DMF (200 mL, dried over molecular sieves (4 Å)), a suspension of sodium hydride (2.84 g, 118 mmol) in dry DMF (50 mL) was added over a 45 min period. The reaction mixture was stirred at room temperature for 5 h, then hydrolyzed by the addition of ice (200 g), and the organic phase was separated off by the addition of dichloromethane (100 mL). After the organic phase was concentrated to approximately 30 mL, concentrated HCl (15 mL) was added and the mixture was stirred for 15 min. Again, the organic phase was separated, washed with water (50 mL), dried over magnesium sulfate, concentrated, and chromatographed on silica gel (60-100 μm) [gradient elution, dichloromethane, dichloromethane/methanol (20:1, v/v)]. Compounds **4** (281 mg, 7%) and **8** (1.07 g, 10%) were obtained respectively.

Received: September 17, 1991 [Z 4919 IE]
German version: *Angew. Chem.* **1992**, *104*, 360

CAS Registry numbers:
1, 138513-50-5; **2**, 138435-61-7; **3**, 69080-01-9; **4**, 127395-53-3; **5**, 138435-62-8; **6**, 138435-63-9; **7**, 27165-88-4; **8**, 138458-93-2; **9**, 18226-42-1; **10**, 42837-44-5; **11**, 36635-61-7.

[1] P. von R. Schleyer in *Cage Hydrocarbons* (Ed.: G. A. Olah), Wiley, New York, **1990**, pp. 1–38.
[2] W. Krätschmer, L. D. Lamb, K. Fostiropoulos, D. R. Huffman, *Nature (London)* **1990**, *347*, 354–358; F. Diederich, R. L. Whetten, *Science* **1991**, *252*, 548–556.
[3] Cf. D. J. Cram, M. E. Tanner, R. Thomas, *Angew. Chem.* **1991**, *103*, 1048–1051; *Angew. Chem. Int. Ed. Engl.*, **30**, 1024–1027.
[4] Reviews: F. Vögtle, L. Rossa, *Top. Curr. Chem.* **1983**, *113*, 1–86; F. Vögtle, J. Dohm, *ibid.* **1991**, *161*, 68–106.
[5] H. Takemura, T. Shinmyozu, T. Inazu, *Tetrahedron Lett.* **1988**, *29*, 1031–1032.
[6] Preparation of 7 by photodeselenation. H. Higuchi, K. Tani, T. Otsubo, Y. Sakata, S. Misumi, *Bull. Chem. Soc. Jpn.* **1987**, *60*, 4027–4036.
[7] Preparation: J. Breitenbach, R. Hoss, M. Nieger, K. Rissanen, F. Vögtle, *Chem. Ber.* **1992**, in press.
[8] From the pyrolysis, 55% of the starting material can be recovered. The yields from the pyrolysis of **1**, **2** (51%) and **3** (49%) are based on the reaction of all the starting material.
[9] For the optimization of the yield of sulfone pyrolyses see: H. A. Staab, W. R. K. Reibel, C. Krieger, *Chem. Ber.* **1985**, *118*, 1230-1253; G. Bodwell, L. Ernst, M. W. Haenel, H. Hopf, *Angew. Chem.* **1989**, *101*, 509-510; *Angew. Chem. Int Ed. Engl.* **1989**, *28*, 455-456.
[10] If the recovered starting material is included, yields of **5** (40%) and **6** (31%) are obtained.
[11] The sulfone pyrolysis, from which usually no starting material is recovered, afforded only the hydrocarbon **7** with only 20% yield: V. Boekelheide, R. A. Hollins, *J. Am. Chem. Soc.* **1973**, *95*, 3201-3208; N. Nakazaki, K. Yamamoto, Y. Miura, *J. Chem. Soc., Chem. Commun.* **1977**, 206-207.
[12] Preparation: Dilute conditions, phase transfer catalysis: K. Kurosawa, M. Suenaga, T. Inazu, T. Yoshino, *Tetrahedron Lett.* **1982**, *23*, 5335-5338.
[13] The sulfone pyrolysis afforded only the hydrocarbon (70-80% yield): V. Boekelheide, *Top. Curr. Chem.* **1983**, *113*, 87–143. 30% Conversion of 2,12-dione provided a total yield of [2.2]paracyclophane of 45%. If larger quantities of [3.3]paracyclophanedione are pyrolyzed at 650 °C, then a polymer film is formed on the inner wall of the tube, which shows no carbonyl bands in the IR spectrum and may correspond to "parylene" (poly-*para*-xylylene). Under these conditions the border between intra- and intermolecular C–C bond formation for the *para*-substitution is crossed.
[14] J. Breitenbach, F. Vögtle, *Synthesis* **1992**, in press.
[15] F. Vögtle, M. Zuber, R. G. Lichtenthaler, *Chem. Ber.* **1973**, *106*, 717–719.
[16] N. Sendhoff, W. Kißener, F. Vögtle, S. Franken, H. Puff, *Chem. Ber.* **1988**, *121*, 2179–2185.
[17] A. M. van Leusen, G. J. M. Boerna, R. B. Helmholdt, H. Siderius, J. Strating, *Tetrahedron Lett.* **1972**, 2367–2368.
[18] We could characterize the compounds **1**, **4**, and **8** by X-ray structural analyses.
[19] A. M. van Leusen, R. J. Bouma, O. Possel, *Tetrahedron Lett.* **1975**, 3487–3488; T. Shinmyozu, Y. Hirai, T. Inazu, *J. Org. Chem.* **1986**, *51*, 1551–1555.
[20] D. Hoppe, *Angew. Chem.* **1974**, *86*, 878–893; *Angew. Chem. Int. Ed. Engl.* **1974**, *13*, 789–840. H. Siderius, B. E. Hoogenboom, D. van Leusen, A. M. van Leusen, *Tetrahedron Lett.* **1972**, 5337–5340.
[21] C.-O. Dietrich-Buchecker, J. Guilhem, A. K. Khemiss, J.-P. Kitzinger, C. Pascard, J. P. Sauvage, *Angew. Chem.* **1987**, *99*, 711–714; *Angew. Chem. Int. Ed. Engl.* **1987**, *26*, 661–664; N. Sendhoff, K. H. Weissbarth, F. Vögtle, *ibid.* **1987**, *99*, 794–795 and **1987**, *26*, 777–778, respectively; J.-C. Rodriguez-Ubis, B. Alpha, D. Plancherel, J.-M. Lehn, *Helv. Chim. Acta* **1984**, *67*, 2264–2269.
[22] Pyrolytic loss of CO from chrysen-6,12-dione and several other quinones: G. Schaden, *Angew. Chem.* **1977**, *89*, 50–51; *Angew. Chem. Int. Ed. Engl.* **1977**, *16*, 50–51; See also: G. Seybold, *ibid.* **1977**, *89*, 377–385 and **1977**, *16*, 365–373, respectively; P. Schiess, S. Rutschmann, *Chimia*, **1985**, *39*, 213–224; U. E. Wiersum, *Recl. Trav. Chim. Pays-Bas*, **1982**, *101*, 317–332.
[23] From the pyrolysis of cyclododecanone at 600 °C, we could isolate cycloundecane (9% yield); from the pyrolysis of benzophenone at 700 °C, biphenyl (9% yield) was isolated; see also G. R. Newkome, H. C. R. Taylor, *J. Org. Chem.* **1979**, *44*, 1362-1363. Also from these reactions unused starting material can be reclaimed whereby yields of 40 and 35% are achieved.

A Donor Cage with Two Tetrathiafulvene Units**

By *Martin Adam, Volker Enkelmann, Hans-Joachim Räder, Jörg Röhrich*, and *Klaus Müllen**

The treatment of the bis-1,3-dithiol-2-thione derivative **1** with phosphoric acid esters affords the tetrathiafulvalene (TTF) cage molecule **2** (Scheme 1).[1] As a result of the strong bending within the TTF unit, **2** shows a significantly different behavior from planar tetrathiafulvalenes in charge-transfer reactions. We have now determined that a surprising metathesis-like dimerization with the formation of the "expanded" cyclophane **3** results from the anodic oxidation of **2**. The cage of the easily accessible macrocycle **3** consists of two hydroquinone, and two TTF units, and thus is formed from four good donors.

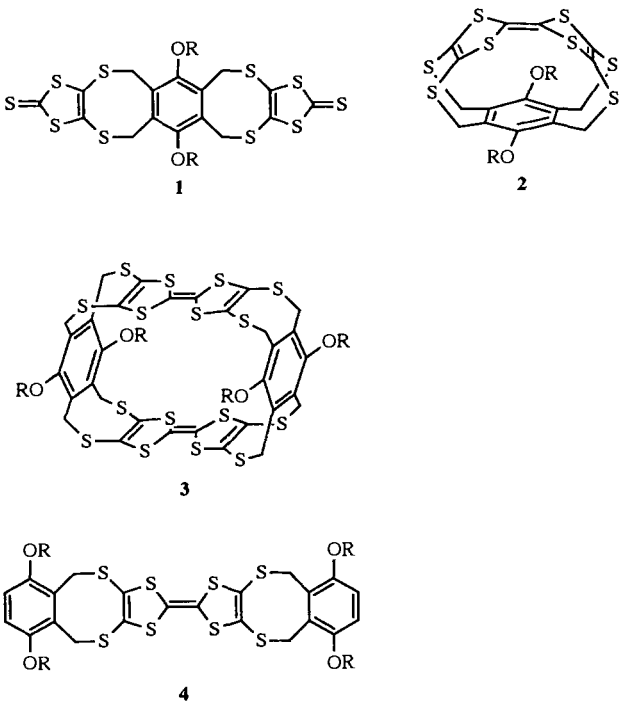
OR
S
S
S

The crystal structure by no means excludes conformations in solution, which can allow the inclusion of guest molecules.

The cyclic voltammetric investigation of **3**[12] shows three ideal reversible oxidations at $E^1_{1/2} = 0.36$ V (2e), $E^2_{1/2} = 1.01$ V (1e), and $E^3_{1/2} = 1.06$ V (1e). The first oxidation corresponds to a simultaneous loss of electrons from both TFF units, whereas the following oxidation waves correspond to the third and fourth charge. The electronic interaction of both donor units is apparently low because between the first and second oxidation no peak separation, and between the third and fourth oxidation only a very weak peak separation of 0.05 V is observed.

In the cyclic voltammogram of the monomeric cage **2** (Fig. 2), an irreversible oxidation wave at 0.93 V is observed, immediately followed by the oxidation waves corresponding to the formation of the tri- and tetracations of **3**. The first oxidation wave of **3** in the second scan of the cyclic voltammogram of **2** is observed even when the first scan is only carried out up to 0.93 V. Both results show that the

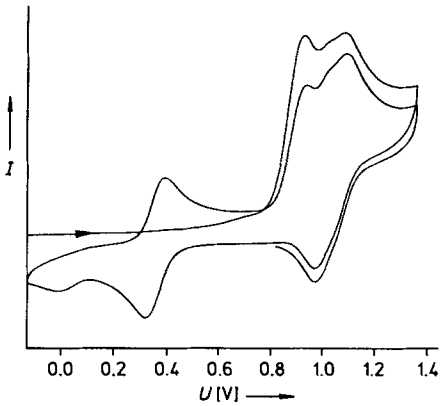

Fig. 2. Cyclic voltammogram of **2a** (potentials vs. SCE, dichloromethane, tetrabutylammonium hexafluorophosphate, 0 °C, 100 mVs^{-1}).

formation of **3** is already complete at a potential of 0.93 V. Therefore, the structure of the bisradical cation of **3** is attributed to the paramagnetic product of the preparative electrolysis of **2**, which as a result of the significantly higher concentrations, in contrast to the cyclic voltammetric experiment, is precipitated as the hexafluorophosphate salt.[13] Thus, the formation of **3** during the dissolution of the electrolysis product in dimethyl sulfoxide can be understood as a reverse reduction of the bisradical cationic salt to the neutral compound. The decomposition of charge-transfer (CT) complexes in solution via reformation of the neutral starting components has also been observed previously.[14]

The breakdown of ring strain during the transformation of **2** to **3** can be considered as the driving force for the ring-enlarging dimerization. So far, it is still unclear at which level of charge of **2** (radical-monocation or -dication) the primary C–C bond formation occurs and how the subsequent bond rearrangement within the four-center system of the fulvalene carbons takes place.

The macrocycle **3** forms CT complexes with iodine, 2,3-dichloro-5,6-dicyano-*p*-benzoquinone (DDQ), and 2,3,5,6-tetrafluorotetracyanoquinodimethane ($TCNQF_4$). No such CT complexes were observed with tetracyanoquinodimethane (TCNQ) or tetracyanoethylene (TCNE). The powder conductivity at room temperature of $\mathbf{3a}(I_3)_{1.8}$ is $\sigma_{RT} = 6.1 \times 10^{-4}$ Scm^{-1} and $\sigma_{RT} = 1.2 \times 10^{-3}$ Scm^{-1} for $\mathbf{3a}(PF_6)_{1.7}$.[15] The requirement for the existence of electronic conductivity in TTF radical cationic salts is the formation of short S–S contacts in donor stacks or two-dimensional networks. Therefore, the measured σ-values show that in radical cationic salts of **3** both short intra- and intermolecular TTF contacts are possible. Attempts to obtain single-crystal charge-transfer complexes of **3** are in progress.

Received: September 18, 1991 [Z 4921 IE]
German version: Angew. Chem. **1992**, *104*, 331

CAS Registry numbers:
2a, 117408-79-4; **2b**, 138572-23-3; **2c**, 117408-80-7; **3a**, 138572-19-7; **3a**(I_3^-), 138572-25-5; **3a**(PF_6^-), 138572-26-6; **3b**, 138572-20-0; **3c**, 138572-21-1; **4**, 138572-22-2.

[1] J. Röhrich, P. Wolf, V. Enkelmann, K. Müllen, *Angew. Chem.* **1988**, *100*, 1429–1430; *Angew. Chem. Int. Ed. Engl.* **1988**, *27*, 1377–1378.

[2] Potential given vs. SCE; electrolysis time: 30 minutes, temperature: 20 °C, supporting electrolyte: tetrabutylammonium hexafluorophosphate.

[3] Spectrum of a solution in dimethylacetamide (line width 1.1 Gauss). In the solid-state spectrum, a drastic line broadening to 19.0 Gauss is observed.

[4] F. Wudl, G. M. Smith, E. J. Hufnagel, *J. Chem. Soc. Chem. Commun.* **1970**, 1453–1454.

[5] No ^{13}C NMR spectra could be obtained due to the low solubility of **3a–c**. Nevertheless, the recording of a ^1H NMR spectrum of **3c** was successfully achieved (400 MHz, [D_3]1,2,4-trichlorobenzene, 60 °C): $\delta = 1.16$ (t, 12H, $OCH_2CH_2CH_2CH_2CH_2CH_3$), 1.55 (m, 16H, $OCH_2CH_2CH_2CH_2CH_2CH_3$), 1.73 (m, 8H, $OCH_2CH_2CH_2CH_2CH_2CH_3$), 2.06 (m, 8H, $OCH_2CH_2CH_2CH_2CH_2CH_3$), 4.43 (t, 8H, $OCH_2CH_2CH_2CH_2CH_2CH_3$), 4.45 (s, 16H, SCH_2).

[6] Indications of oligomeric or polymeric condensation products of **2** are not present. As by-products compounds of low molecular weight are found whose formation can be explained by the opening of the 1,4-dithiacyclooctane rings.

[7] Correct elemental analyses have been obtained for **3a** and **3b**. A high-resolution mass spectroscopic determination with peak matching under FAB-ionization conditions confirms the expected elemental consistency of **3c** (found: $m/z = 1316.058401$, calc.: $m/z = 1316.064910$).

[8] The preparation of **4** is achieved analogous to the synthesis of bisxylylene-dithio-tetrathiafulvalene (L. M. Gol'denberg, R. N. Lyubovskaya, *Khim. Geterotsikl. Soedin.* **1986**, *6*, 855-856) starting from 2,3-bisbromomethyl-1,4-bishexyloxybenzene, which is accessible by Williamson etherification of 2,3-dimethyl-*p*-hydroquinone and subsequent NBS bromination.

[9] The growth of single crystals suitable for crystallographic analysis was achieved via the crystallization of **3b** in 1,2-dichlorobenzene on slow cooling (rate of cooling: 2 °C/h; starting temperature 180 °C). The crystals contain a molecule of 1,2-dichlorobenzene per molecule of **3**. Enraf-Nonius-CAD-4 diffractometer ($Cu_{K\alpha}$ radiation, $\lambda = 1.5404$ Å, graphite monochromator). $C_{50}H_{48}Cl_2O_4S_{16}$, monoclinic, space group $P2_1/n$; $a = 12.840$, $b = 13.816$, $c = 18.748$ Å, $\beta = 107.35°$, $V = 3174.5$ Å^3, $Z = 2$, $\rho_{calc} = 1.35$ gcm^{-3}, $\mu = 61.175$ cm^{-1}, 3766 reflections of which 2585 were observed ($I > 3\sigma(I)$; $F_0 > 4$). On cooling to temperatures below 0 °C the crystals experience irreversible damage due to a phase transition. Therefore, data collection was carried out at room temperature. The solution of the structure was achieved by Patterson search methods with the help of the donor fragment in its known bonding geometry. The 1,2-dichlorobenzene disordered in the crystal was "rigid body" refined. One of the two butyl side groups also shows a disorder due to two statistically equivalently occupied orientations. In Figure 1, only one of the two disorders is shown to allow a better overview of the structure. In the final refinement cycle the calculated H atoms in the "riding mode" were assigned isotropic temperature coefficients and C, Cl, O, and S with anisotropic temperature coefficients ($R = 0.066$, $R_w = 0.069$ and $w = 1$ for 346 parameters). Further details of the crystal structure investigation may be obtained from the Fachinformationszentrum Karlsruhe, Gesellschaft für wissenschaftlich-technische Information mbH, D-W-7514 Eggenstein-Leopoldshafen 2 (FRG) on quoting the depository number CSD-55737, the names of the authors, and the journal citation.

[10] J.-Y. Ortholand, A. M. Z. Slawin, N. Spencer, J. F. Stoddart, D. J. Williams, *Angew. Chem.* **1989**, *101*, 1402–1404; *Angew. Chem. Int. Ed. Engl.* **1989**, *28*, 1394–1396.

[11] Calculations carried out with MMX 89.0 show that the energies of the conformers **B**, **C**, and **D** lie above those of the conformation **A** found in the solid state. We thank H. Kolshorn, Universität Mainz, for performing the calculations.

[12] Potentials vs. SCE with ferrocene calibration ($E_{1/2} = 0.31$ V), dichloromethane, tetrabutylammonium hexafluorophosphate, 100 mVs^{-1}.

[13] The elemental consistency of the product of the electrolysis of **2a** corresponds to the formula $\mathbf{3a}(PF_6)_{1.7}$.

[14] D. L. Coffen, J. Q. Chambers, D. R. Williams, P. E. Garrett, N. D. Canfield, *J. Am. Chem. Soc.* **1971**, *93*, 2258–2268.

[15] The determination of the conductivity was achieved on compressed pellets with a two-point measurement.

A New Structure–Magnetism Relationship for Face-Sharing Transition-Metal Complexes with d^3–d^3 Electronic Configuration**

By *Andrea Niemann, Ursula Bossek, Karl Wieghardt,* Christian Butzlaff, Alfred X. Trautwein,* and *Bernhard Nuber*

In dinuclear transition-metal complexes the connection of the coordination polyhedra of two metal ions with octahedral geometry by face-sharing is a commonly observed structural feature. Metal $\cdots$ metal distances can range from 2.3 to 4.0 Å depending on the type of the three bridging ligands, which are often composed of one atom or coordinate only with one atom, for example O^{2-}, OH^-, RO^-, Cl^-, Br^-, and I^- (Table 1). If both metal ions possess unpaired electrons

Table 1. Metal–metal distances and spin exchange coupling constants for dinuclear face-sharing octahedral complexes with d^3-d^3 electronic configuration [9].

Compound number	Formula	M $\cdots$ M, [Å]	$-2J$ [cm^{-1}]
1	$[L_2Mn_2^{IV}(\mu\text{-}O)_3](PF_6)_2 \cdot H_2O$ [a]	2.296(2)	780
2	$[L_2Mn_2^{IV}(\mu\text{-}O)_2(\mu\text{-}OH)](ClO_4)_3$	2.408(5)	512
3	$[L_2Cr_2^{III}(\mu\text{-}O)(\mu\text{-}OH)_2](ClO_4)_2 \cdot 2H_2O$	2.518(5)	250
4	$[(NH_3)_6Cr_2^{III}(\mu\text{-}OH)_3](ClO_4)_{3-x}I_x$	2.631(1)	119
5	$[L_2Cr_2^{III}(\mu\text{-}OH)_3]I_3 \cdot 3H_2O$	2.642(2)	132
6	$[L_2Cr_2^{III}(\mu\text{-}OH)_3](ClO_4)_3 \cdot 3H_2O$	2.664	128
7	$[L'_2Cr_2^{III}(\mu\text{-}OH)_3]Br_3 \cdot 2H_2O$ [b]	2.666(3)	96
8	$(NEt_4)[Cr_2^{III}(\mu\text{-}OEt)_3\{H_2B(pz)_2\}_2(NCS)_2]$	2.683(2)	87
9	$[V_2^{II}(\mu\text{-}Cl)_3(thf)_6]_2[Zn_2Cl_6]$	2.973(1)	75 [c]
10	$K_3[Cr_2^{III}(\mu\text{-}Cl)_3Cl_6]$	3.048	32
11	$Rb_3[Cr_2^{III}(\mu\text{-}Cl)_3Cl_6]$	3.07	26.6
12	$Cs_3[Cr_2^{III}(\mu\text{-}Cl_3)Cl_6]$	3.12	16.9
13	$Cs_3[Cr_2^{III}(\mu\text{-}Br)_3Br_6]$	3.30	10.3
14	$Cs_3[Cr_2^{III}(\mu\text{-}I)_3I_6]$	3.40	9.2
15	$(NEt_4)_3[Cr_2^{III}(\mu\text{-}Cl)_3Cl_6]$	3.89	3.3 [c]
16	$(NEt_4)_3[Cr_2^{III}(\mu\text{-}Br)_3Br_6]$	4.00	0

[a] L = *N,N',N''*-trimethyl-1,4,7-triazacyclononane. [b] L' = 1,5,9-triazacyclododecane. $H_2B(pz)_2^-$ = dihydrobis(1-pyrazolyl)borate. [c] Corrected value [10].

then intramolecular spin-exchange interactions and ferromagnetic or antiferromagnetic coupling results. This exchange interaction can be satisfactorily described for metals of the first transition-series by the isotropic Heisenberg–Dirac–van Vleck model with the spin-Hamiltonion operator $\boldsymbol{H} = -2J\boldsymbol{S}_1 \cdot \boldsymbol{S}_2$; here $\boldsymbol{S}_1$ and $\boldsymbol{S}_2$ are the total spins on ions 1 and 2, and J is the spin-exchange coupling constant in cm^{-1}.[11] The value of J can be obtained from the temperature-dependence of the magnetic susceptibility of a complex. Antiferromagnetic coupling arises for homodinuclear complexes in which the two metals have d^3–d^3 electronic configurations; at low temperatures these complexes are diamagnetic ($\boldsymbol{S} = 0$, ground state). The energy difference between the singlet state ($\boldsymbol{S} = 0$) and the first excited triplet-state ($\boldsymbol{S} = 1$) is expressed by $2J$.

[*] Prof. Dr. K. Wieghardt, Dipl.-Chem. A. Niemann, U. Bossek
Lehrstuhl für Anorganische Chemie I der Universität
Universitätsstrasse 150, D-W-4630 Bochum 1 (FRG)
Dipl.-Phys. C. Butzlaff, Prof. Dr. A. X. Trautwein
Institut für Physik der Medizinischen Universität Lübeck
Dr. B. Nuber [+]
Anorganisch-chemisches Institut der Universität Heidelberg

[+] X-ray structure analysis

[**] This research was supported by the Fonds der Chemischen Industrie and Deutsche Forschungsgemeinschaft under the auspices of the Schwerpunktsprogramm "Bioanorganische Chemie".

Although many face-sharing d^3–d^3 dinuclear complexes have been structurally characterized, and temperature-dependent susceptibility measurements have been carried out, no correlation has been found to date between structural parameters and the magnitude of J.[1c] We demonstrate here that the only relevant structural parameter that correlates with the value of J is the distance between the two metal ions.

We obtained **2** by protonation of an oxo bridge in **1**[2] (L = *N,N',N''*-trimethyl-1,4,7-triazacyclononane) with conc.

$[L_2Mn_2^{IV}(\mu\text{-}O)_3](PF_6)_2 \cdot H_2O$ **1** $[L_2Mn_2^{IV}(\mu\text{-}O)_2(\mu\text{-}OH)](ClO_4)_3$ **2**

$HClO_4$. The X-ray structure determination (Fig. 1, top)[3] shows the $Mn^{IV} \cdots Mn^{IV}$ distance in **2** to be 0.11 Å longer than in **1** (Table 1). Measurements of the temperature-dependent magnetic susceptibility of **2** in the range of 4–298 K[4] (Fig. 2) provides a J value of $-256\ cm^{-1}$ ($\boldsymbol{H} = -2J\boldsymbol{S}_1 \cdot \boldsymbol{S}_2$; $\boldsymbol{S}_1 = \boldsymbol{S}_2 = 3/2$; $g = 1.98$), which points to a markedly smaller antiferromagnetic coupling in **2** than in **1** ($J = -390\ cm^{-1}$).

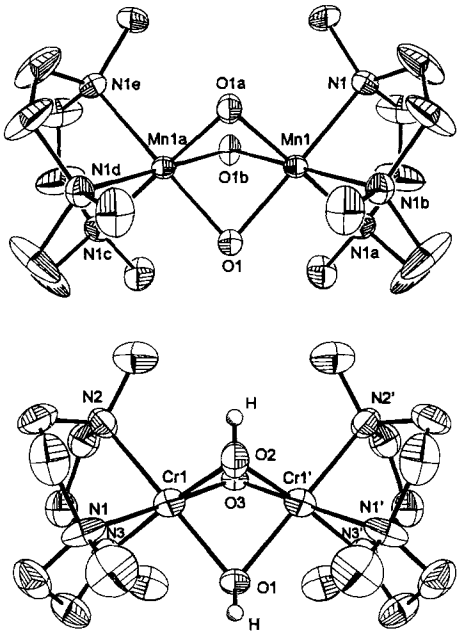

Fig. 1. Above: Structure of the trication in crystals of **2**. Important distances [Å] and angles [°]: Mn1-O1 1.858(7), Mn1-N1 2.086(8), Mn1 $\cdots$ Mn1a 2.408(5); Mn1-O1-Mn1a 80.7(4), O1-Mn1-O1a 82.6(1), N1-Mn1-N1a 84.3(3), O1-Mn1-N1 96.5. Below: Structure of the dication in crystals of **3**. Important distances [Å] and angles [°]: Cr1-Cr1' 2.518(5), Cr1-O1 1.983(8), Cr1-O2 1.961(10), Cr1-O3 1.869(8), Cr1-N1 2.148(11), Cr1-N2 2.085(10), Cr1-N3 2.093(12), Cr1-O1-Cr1' 78.8(4), Cr1-O2-Cr1' 79.9(5), Cr1-O3-Cr1' 84.7(5).

Complex **6**[5] can be deprotonated in alkaline[6, 7] solution to **3**. The Cr $\cdots$ Cr distance in **3** is shown by X-ray structure analysis (Fig. 1, bottom) to be 0.14 Å shorter than that in **6**.

$[L_2Cr_2^{III}(\mu\text{-}O)(\mu\text{-}OH)_2](ClO_4)_2 \cdot 2H_2O$ **3** $[L_2Cr_2^{III}(\mu\text{-}OH)_3](ClO_4)_3 \cdot 3H_2O$ **6**

A J value of $-125\ cm^{-1}$ was obtained from the temperature-dependent susceptibility measurements of complex **3**

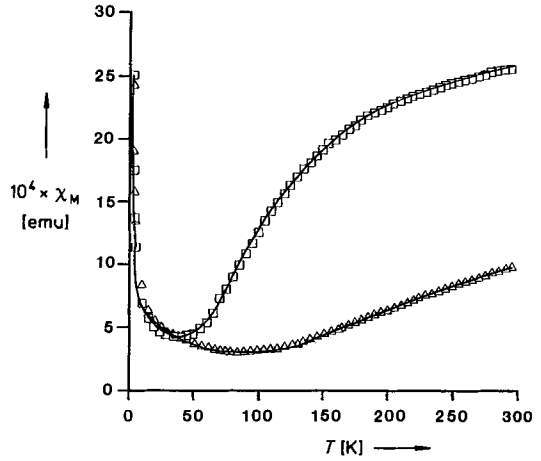

Fig. 2. Plot of χ_M versus temperature for complexes **2** (△) and **3** (□). The solid lines resulted from a fit of the data using the equation $\boldsymbol{H} = -2J\boldsymbol{S}_1 \cdot \boldsymbol{S}_2$; $\boldsymbol{S}_1 = \boldsymbol{S}_2 = 3/2$.

($\boldsymbol{H} = -2J\boldsymbol{S}_1 \cdot \boldsymbol{S}_2$; $\boldsymbol{S}_1 = \boldsymbol{S}_2 = 3/2$, $g = 2.00$); this value is roughly twice that of the value obtained for **6**, $-66\ cm^{-1}$.[5b]

Fifteen dinuclear octahedral face-sharing complexes whose structure and J values have been determined are listed in Table 1.[9] Complexes **1–8** each possess three oxygen atoms as O^{2-}, OH^-, or EtO^- bridging ligands; the central atoms are $Mn^{IV}(d^3)$ or $Cr^{III}(d^3)$. As is evident in Figure 3, the plot of $\ln|-2J|$ versus the metal–metal distance is linear. In complexes **9–12** and **15**, two metal ions, $Cr^{III}(d^3)$ or $V^{II}(d^3)$ are linked by three chloro bridges in each case. Remarkably

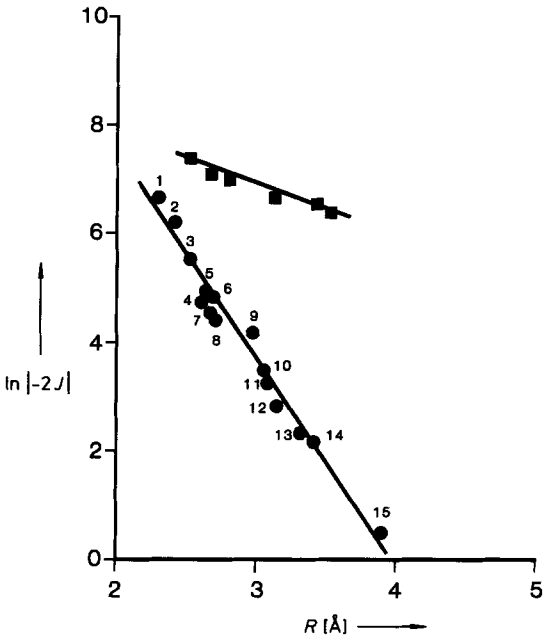

Fig. 3. Plot of $\ln|-2J|$ versus the metal–metal distance R for complexes **1–15** (●) and for complexes of the type $A_3[X_3Mo^{III}(\mu\text{-}X)_3Mo^{III}X_3]$ (A = K^+, Cs^+, NMe_4^+, NEt_4^+; X = Cl, Br) (■) [15].

the J values correlate with the M···M distances in the same way. Previous attempts at drawing correlation relationships for complexes **10–15** failed because of the application of the wrong J values.[9, 13] The values of the analogous tri-μ-bromodichromium(III) and tri-μ-iododichromium(III) complexes **13** and **14** also fit on the line in Figure 3. The correlation coefficient, 0.9935, shows how amazingly well this empirical correlation applies to so many different complexes. The plot of $\lg|-2J|$ versus $\lg|M\cdots M|$ is also linear[15] and with an equally good correlation coefficient (0.994). It is not possible to differentiate experimentally between the two relationships (a) and (b). The numerical values of the constant **A** is 7.52×10^6 with $n = 11.2$; of **B**, 7.50×10^6 with $\varepsilon = 4.0$ if J is given in cm^{-1} and the metal–metal distance R, in Å.

$$J = A R^{-n} \quad (a)$$

$$J = B\exp(-\varepsilon R) \quad (b)$$

Equation (b) is preferred,[11–13] because the spin-exchange interaction correlates with the extent of overlap of the magnetically relevant orbitals. The resonance integral β_{ii} (Hückel theory[12]) decreases *exponentially* with the increase in the distance between the two atoms. The antiferromagnetic coupling constant J^{AF} is dependent on β_{ii}, as shown in Equation (c).[12] The energy necessary for the transfer of one electron from metal 1 to metal 2 is described by U.

$$J_{ii}^{AF} = -4\beta_{ii}^2/U \quad (c)$$

The most important result is the observation that the spin-exchange interaction in face-sharing dinuclear complexes is *independent* of the type of a) bridging ligands and—amazingly—b) the metal centers,[13] as long as the electronic configuration is d^3–d^3. The metal–metal distance is the only relevant structural parameter. Thus it must be concluded that in face-sharing octahedral complexes with d^3–d^3 configurations *no* magnetic superexchange occurs through the bridging ligands, but rather a *direct* metal–metal interaction takes place. This can also be expressed as the existence of a very weak metal–metal bond. These results are in good agreement with the results of Extended-Hückel MO calculations conducted by Leuenberger and Güdel[14] for $[Cr_2X_9]^{3-}$ complexes (X = Cl, Br, I), which show that the main contribution to the exchange interaction arises from the interaction of the a_1 orbitals. On the other hand, in edge-sharing octahedral complexes with $Cr_2(\mu\text{-}OH)_2$ structural elements, the contribution to the exchange interaction through the bridging ligands is well documented (Glerup–Hodgson–Pederson model).[1c]

Equation (b) and the numerical values for the constants B and ε given here predict that no intramolecular antiferromagnetic coupling ($J \approx 0$) should be observed in complexes with metal–metal distances >4.0 Å. This is experimentally confirmed by complex **16**, which shows Curie paramagnetism (temperature-independent magnetic moment of 3.89 μ_B/Cr).[9]

Grey and Smith[15] found a similar structure–magnetism relationship for six complexes of type $A_3[X_3Mo^{III}(\mu\text{-}X)_3Mo^{III}X_3]$ (A = K^+, Cs^+, NMe_4^+, NEt_4^+; X = Cl, Br) (Fig. 3). The constants $B = 1.33 \times 10^4$ and $\varepsilon = 0.88$ [Eq.(b)] were determined when the Mo–Mo distance was expressed in Å and J, in cm^{-1} (correlation coefficient: 0.985). Because 4d valence orbitals are larger and more diffuse than 3d orbitals, the direct d–d orbital overlap is more effective than in 3d transition metals. Thus the exponential decrease in metal–metal interaction with increasing distance is not as dramatic. It remains to be seen if any, and if so what, physical meaning is related to the empirical terms B and ε in Equation (b).

Experimental Procedure

2: Complex **1** [2] (0.70 g) was dissolved in 60% $HClO_4$ solution (30 mL). Within a few days red-brown hexagonal crystals of **2** precipitated (yield: 0.52 g, 65%).

3: Solid NaOH (1.0 g) was added to an aqueous solution (30 mL) of **6** [5a] (0.80 g), and the color of the solution changed from red-orange to violet. After several days violet **3** precipitated (yield: 0.49 g, 70%). Both complexes provided correct elemental analyses (C,H,N,Cl).

Received: October 28, 1991 [Z 4991 IE]
German version: *Angew. Chem.* **1992**, *104*, 345

CAS Registry numbers:
1, 138694-58-3; **2**, 138721-98-9; **3**, 138694-61-8; **6**, 138694-63-0.

[1] a) C. J. O'Connor, *Prog. Inorg. Chem.* **1982**, *29*, 303; b) *Theory and Applications of Molecular Paramagnetism* (Eds.: E. A. Boudreaux, L. N. Mulay), Wiley, New York, **1976**; c) *Magneto-Structural Correlations in Exchange Coupled systems* (Eds.: O. Kahn, R. D. Willet, D. Gatteschi) *NATO ASI Ser. Ser. C* **1983**, *140*.

[2] K. Wieghardt, U. Bossek, B. Nuber, J. Weiss, J. Bonvoisin, M. Corbella, S. E. Vitols, J. J. Girerd, *J. Am. Chem. Soc.* **1988**, *110*, 7398.

[3] Crystal data for **2**: $C_{18}H_{43}Cl_3Mn_2N_6O_{15}$, hexagonal, $a = 8.810(4)$, $c = 22.65(1)$ Å, $V = 1522.5$ Å^3, $Z = 2$. Space group $P6_3/mmc$ (D_{6h}^4, No. 194). The cation lies on a crystallographic C_3 axis, thus the OH and O^{2-} groups cannot he distinguished from each other; $\mu(Mo_{K\alpha}) = 1.14$ mm^{-1}, 623 observed independent reflections with $I > 2.5\sigma(I)$, $R = 0.069$; $R_w = 0.062$. Further details of the crystal structure investigation may be obtained from the Fachinformationszentrum Karlsruhe, Gesellschaft für wissenschaftlich-technische Information mbH, D-W-7514 Eggenstein-Leopoldshafen 2 (FRG) on quoting the depository number CSD-56011, the names of the authors, and the journal citation.

[4] Measurements of the temperature-dependent magnetic susceptibilities (4–298 K) were conducted with a SQUID magnetometer (MPMS, Quantum Design) on powdered samples; correction for diamagnetism with Pascal's constants. In the fit of the data a paramagnetic impurity (monomeric complex with $S = 3/2$ ground state) was taken into account; for **2** with 0.15% impurity and for **3** with 0.2%.

[5] a) K. Wieghardt, P. Chaudhuri, B. Nuber, J. Weiss, *Inorg. Chem.* **1982**, *21*, 3086; b) D. E. Bolster, P. Gütlich, W. E. Hatfield, S. Kremer, E. W. Müller, K. Wieghardt, *ibid.* **1983**, *22*, 1725.

[6] K. Wieghardt, M. Guttmann, D. Ventur, W. Gebert, *Z. Anorg. allg. Chem.* **1985**, *527*, 33.

[7] We thank Dr. Glerup (University of Copenhagen) for providing us with single crystals of **3**.

[8] Crystal data for **3**: $C_{18}H_{48}Cl_2Cr_2N_6O_{17}$, monoclinic, $a = 8.610(3)$, $b = 12.889(7)$, $c = 14.859(9)$ Å, $\beta = 102.91(4)°$, $V = 1607.28$, $Z = 2$, space group $P2_1/m$ (C_{2h}^2, No. 11), $\mu(Mo_{K\alpha}) = 0.89$ mm^{-1}, 1004 observed independent reflections ($I > 2.0\sigma(I)$), $R = 0.087$; $R_w = 0.059$.

[9] References for the structure and magnetism of complexes **1**–**16** (Table 1) **1**: ref. [2]; **2**: this work; **3**: this work; **4**: P. Andersen, A. Dossing, E. Larsen, E. Pedersen, *Acta Chem. Scand. Ser. A* **1987**, *41*, 381; **5**: ref. [5] and S. Kremer, *Inorg. Chem.* **1985**, *24*, 887; **6**: D. J. Hodgson in [1c], p. 517; **7**: ref. [6]; **8**: A. Bencini, M. DiVaira, F. Mani, *J. Chem. Soc. Dalton Trans.* **1991**, 41; **9**: R. Bouma, J. H. Teuben, W. R. Beukema, R. L. Bansemer, J. C. Huffman, K. G. Caulton, *Inorg. Chem.* **1984**, *23*, 2715; **10**–**16**: I. E. Grey, P. W. Smith, *Aust. J. Chem.* **1971**, *24*, 73; B. Leuenberger, H. Güdel, P. Fischer, *J. Solid State Chem.* **1986**, *64*, 90; O. Kahn, B. Briat, *Chem. Phys. Lett.* **1975**, *32*, 376; B. Leuenberger, H. U. Güdel, J. K. Kjems, D. Petitgrand, *Inorg. Chem.* **1985**, *24*, 1035; A. Earnshaw, J. Lewis, *J. Chem. Soc.* **1961**, 396; R. Saillant, R. B. Jackson, W. E. Streib, K. Folting, R. A. D. Wentworth, *Inorg. Chem.* **1971**, *10*, 1453.

[10] The J value for complex **9** in ref. [9] was calculated too large by a factor of 2, because the formula given there for the calculation does not hold for χ_M but for χ/V. The J value for **15** reported by Earnshaw and Lewis [9] is miscalculated. A new evaluation of the published χ_M data for **15** [9] and also our new susceptibility measurements provided $J = -1.67$ cm^{-1}.

[11] R. E. Coffman, G. R. Buettner, *J. Phys. Chem.* **1979**, *83*, 2387.

[12] P. J. Hay, J. C. Thibeault, R. Hoffmann, *J. Am. Chem. Soc.* **1975**, *97*, 4884.

[13] The fact that the data of the face-sharing Mn_2^{IV}, Cr_2^{III}, and V_2^{II} complexes correlate well with Equation (b) implies that two opposing factors compensate for each other: the 3d metal-orbitals of Mn^{IV} ions are more strongly contracted than those of the Cr^{III} and V^{II} ions; thus the Mn–X bonds are shorter than the analogous Cr–X and V–X bonds (X = bridging atom). In analogous $M(\mu\text{-}X)_3M$ compounds ($M = Mn^{IV}$, Cr^{III}, V^{II}) this leads to $M\cdots M$ distances $Mn_2^{IV} > Cr_2^{III} > V_2^{II}$, which compensates for the contraction effect.

[14] B. Leuenberger, H. U. Güdel, *Inorg. Chem.* **1986**, *25*, 181.

[15] I. E. Grey, P. W. Smith, *Aust. J. Chem.* **1971**, *24*, 73.

Allylation of Quinones with Allylsilane in the Presence of Lithium Perchlorate in Ether**

By *Junes Ipaktschi** and *Akbar Heydari*

Dedicated to Professor Günther Maier on the occasion of his 60th birthday

A recent publication[1,2] concerning the dramatic acceleration of a Diels–Alder reaction by a 5 M solution of lithium perchlorate in diethyl ether (LPDE) has revived a great interest in this reaction medium which often has been compared to a molten salt.[2c] Apart from the internal pressure of the 5 M LPDE solution,[1a] the Lewis acidity of the lithium ions has also been given as the reason for the increase in the reactivity.[3] The LPDE solution is preparatively very useful, for example, it can be shown that in this medium allyl vinyl ether undergoes a smooth [1,3] sigmatropic shift.[4]

A surprising reaction of *p*-benzoquinone with furan in an LPDE solution which led to 2-furyl-*p*-benzoquinone (**1**)[5,6] caused us to investigate the allylation of quinones with allyltrimethylsilane (**3**) also in this medium. The allylation of quinones is an important reaction for the preparation of biologically active isoprenoid quinones such as vitamin E,[7] vitamin K,[8] coenzyme Q_1,[9] and plastoquinones,[10] for which a series of synthetic methods already exists.[11]

We have now found that the reaction of **2a**–**d** with allyltrimethylsilane (**3**) in a 5 M LPDE solution leads to the allylhydroquinones **4a**–**e**. If **2a** is warmed with **3** in a 5 M LPDE solution for 15 hours at 40 °C, the allylhydroquinone **4a** is obtained in 73% yield, together with the non-allylated hydroquinone **5a** (12%).

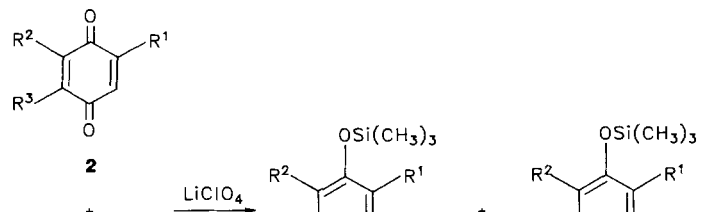

Scheme 1. **a**: $R^1 = R^2 = R^3 = H$; **b**: $R^1 = R^3 = H$, $R^2 = CH_3$; **c**: $R^1 = CH_3$, $R^2 = R^3 = OCH_3$; **d**: $R^1 = H$, $R^2R^3 = -CH{=}CH{-}CH{=}CH-$; **e**: $R^1 = R^2 = H$, $R^3 = CH_3$; **f**: $R^1 = R^3 = C(CH_3)_3$, $R^2 = H$.

The reaction of **2b** with **3** showed no selectivity. Here, **4e** (41%) and **4b** (20%) were formed together with **5b** (10%). From the very slow reaction (10 days) of coenzyme Q_0 (**2c**) was obtained **4c** (22%), **5c** (18%), and interestingly, the indane derivative **6** (10%). The reaction of naphthoquinone **2d** produces a substantial amount of the reduction product; thus, in addition to the allylation product **4d** (44%), 42% of **5d** was also formed. Analogously, the allylation of **2a** with the allylsilane **7** afforded **8** (75%). Here, the reduction product **5a** (12.5%) was also obtained as a by-product.

Obviously the Lewis acidity and the very high polarity of the LPDE solution facilitate the formation of the polar com-

[*] Prof. Dr. J. Ipaktschi, Dipl.-Chem. A. Heydari
Institut für Organische Chemie Universität
Heinrich-Buff-Ring 58, D-W-6300 Giessen (FRG)

[**] This work was supported by the Fonds der Chemischen Industrie. A. H. thanks the Science Ministry, Tehran, Iran for a doctorate research grant.

Table 1. Selected spectroscopic data for **1**, **4**, **6**, **8** and **9**.

1: IR: $\tilde{\nu}$ [cm^{-1}] = 1720, 1370, 910; ^{1}H NMR: δ = 7.6 (s, 1 H), 7.5 (d, 1 H), 7.08 (s, 1 H), 6.78 (s, 2 H), 6.6 (d, 1 H); ^{13}C NMR: δ = 187.31, 185.29, 146.19, 145.43, 136.54, 136.5, 133.56, 125.56, 118.58, 114.43
4a: ^{1}H NMR: δ = 6.64–6.55 (m, 2 H), 6.56–6.52 (m, 1 H), 5.96–5.85 (m, 1 H), 5.05 (m, 1 H), 5.0 (m, 1 H), 3.25–3.2 (d, 2 H), 0.23 (s, 9 H), 0.21 (s, 9 H); ^{13}C NMR: δ = 148.95, 147.37, 136.71, 131.29, 121.30, 119.02, 117.75, 115.38, 34.33, 0.26, 0.00
4b: ^{1}H NMR: δ = 6.55 (s, 1 H), 6.52 (s, 1 H), 5.9 (m, 1 H), 5.05–5.00 (m, 2 H), 3.22–3.24 (d, 2 H), 2.1 (s, 3 H), 0.24 (s, 9 H), 0.22 (s, 9 H); ^{13}C NMR: δ = 147.58, 147.04, 137.25, 128.26, 126.95, 121.03, 120.43, 115.26, 34.15, 16.38, 0.48, 0.41
4c: ^{1}H NMR: δ = 5.9–5.8 (m, 1 H), 4.97–4.9 (m, 1 H), 4.8–4.74 (m, 1 H), 3.77 (s, 3 H), 3.74 (s, 3 H), 3.3 (m, 2 H), 2.02 (s, 3 H), 0.2 (s, 9 H), 0.18 (s, 9 H); ^{13}C NMR: δ = 142.84, 142.10, 141.51, 136.35, 124.52, 123.80, 114.32, 60.49, 60.33, 31.01, 12.52, 0.40
4d: ^{1}H NMR: δ = 7.97–7.94 (m, 1 H), 7.88–7.9 (m, 1 H), 7.3–7.4 (m, 2 H), 6.68 (s, 1 H), 6.0–5.9 (m, 1 H), 5.12–5.05 (m, 2 H), 3.49–3.47 (m, 2 H), 0.3 (s, 9 H), 0.28 (s, 9 H); ^{13}C NMR: δ = 145.56, 142.75, 137.04, 129.07, 127.52, 125.46, 124.59, 124.31, 122.61, 122.55, 115.87, 114.86, 34.59, 0.89, 0.35
4e: ^{1}H NMR: δ = 6.5–6.46 (m, 2 H), 5.9 (m, 1 H), 5.0–5.1 (m, 2 H), 3.26–3.3 (d, 2 H), 2.15 (s, 3 H), 0.23 (s, 9 H), 0.22 (s, 9 H); ^{13}C NMR: δ = 148.70, 146.12, 136.73, 130.75, 129.04, 119.74, 118.45, 115.56, 34.41, 17.78, 0.67, 0.00
6: ^{1}H NMR: δ = 4.02 (s, 3 H), 4.01 (s, 3 H), 2.78 (dd, 1 H), 2.55 (dd, 1 H), 2.05 (dd, 2 H), 1.34 (s, 3 H), 1.28 (t, 1 H), 1.19–1.08 (m, 1 H), 0.0 (s, 9 H); ^{13}C NMR: δ = 198.6, 196.01, 148.51, 148.35, 60.58, 58.36, 56.74, 40.33, 33.21, 24.83, 24.50, −3.28
8: ^{1}H NMR: δ = 6.65–6.54 (m, 3 H), 5.4 (s, 2 H), 3.6 (s, 2 H), 0.2 (s, 9 H), 0.18 (s, 9 H); ^{13}C NMR: δ = 148.86, 147.80, 132.05, 128.40, 121.96, 119.04, 117.40, 41.99
9: ^{1}H NMR: δ = 6.7 (s, 1 H), 6.5 (s, 1 H), 4.46 (br.s, 1 H), 2.95 (s, 2 H), 1.45 (s, 6 H), 1.4 (s, 9 H); ^{13}C NMR: δ = 152.93, 147.93, 135.90, 124.59, 113.57, 107.74, 86.30, 43.09, 34.64, 29.7, 28.26

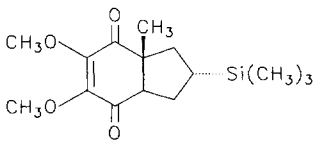

6

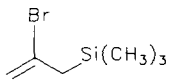

7

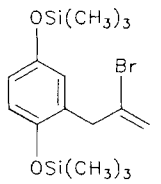

8

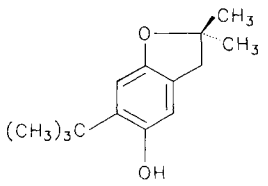

9

plex **B** and the ion pair **C** by an electron-transfer step from the quinone/allylsilane charge-transfer complex **A** (Scheme 2).[12] The subsequent C–C bond formation reaction and silylation of the resulting hydroquinone derivative with a further molecule of **3** then leads to the products **4** and **8**, respectively. Examples for the formation of **6** by the Sakurai reaction are already known.[13]

A **B** **C**

Scheme 2. D = donor, A = acceptor.

If the C–C bond formation step is prevented by a bulky substituent such as in 2,5-di-*tert*-butylbenzoquinone (**2f**), then in the presence of **3** as an electron donor in the step of **B** or **C**, the rearrangement to benzofuran **9** (45%) takes place, catalyzed by an electron-transfer reaction.

Experimental Procedure

4a: To a solution of **2a** (0.270 g, 2.5 mmol) in a 5 M solution of $LiClO_4$ (5 mL) in absolute diethyl ether, **3** (1.2 mL, 7.5 mmol) was added. The mixture was stirred for 15 h at 40 °C and subsequently diluted with pentane and washed with water. The GC analysis of the crude product showed that an almost quantitative reaction took place affording **4a** (73%) and **5a** (12%). Analytically pure **4a** and **5a** were isolated by fractional sublimation or gas chromatography

Received: October 15, 1991 [Z 4970 IE]
German version: *Angew. Chem.* **1992**, *104*, 335

CAS Registry numbers:
1, 138786-02-4; **2a**, 106-51-4; **2b**, 55-97-9; **2c**, 605-94-7; **2d**, 130-15-4; **2f**, 2460-77-7; **3**, 762-72-1; **4a**, 138786-03-5; **4b**, 138786-04-6; **4c**, 138786-05-7; **4d**, 138786-06-8; **4e**, 138786-07-9; **5a**, 2117-24-0; **5b**, 78018-53-8; **5c**, 138786-08-0; **5d**, 30432-51-0; **6**, 138786-09-1; **7**, 81790-10-5; **8**, 138786-10-4; **9**, 7622-93-7; $LiClO_4$, 7791-03-9; furan, 110-00-9; diethyl ether, 60-29-7.

[1] a) P. A. Grieco, J. J. Nunes, M. D. Gaul, *J. Am. Chem. Soc.* **1990**, *112*, 4595; b) Review: H. Waldmann, *Angew. Chem.* **1991**, *103*, 1335; *Angew. Chem. Int. Ed. Engl.* **1991**, *30*, 1306.
[2] The LPDE solution has already been used elsewhere to increase the reaction rate of polar reactions. See also: a) S. Winstein, S. Smith, D. Darwish, *J. Am. Chem. Soc.* **1959**, *81*, 5511; b) R. Herter, B. Föhlisch, *Synthesis* **1982**, 976; c) R. Braun, J. Sauer, *Chem. Ber.* **1986**, *119*, 1269; d) Y. Pocker, J. C. Ciula, *J. Am. Chem. Soc.* **1989**, *111*, 4728.
[3] M. A. Forman, W. P. Dailey, *J. Am. Chem. Soc.* **1991**, *113*, 2761.
[4] P. A. Grieco, J. D. Clark, C. T. Jagoe, *J. Am. Chem. Soc.* **1991**, *113*, 5488.
[5] J. Ipaktschi, A. Heydari, unpublished results.
[6] All compounds gave correct spectroscopic and analytical data.
[7] S. Inoue, K. Saito, K. Kato, S. Nozaki, K. Sato, *J. Chem. Soc. Perkin Trans. 1* **1974**, 2097.
[8] K. Sato, S. Inoue, K. Saito, *J. Chem. Soc. Perkin Trans 1* **1973**, 2289.
[9] S. Inoue, R. Yamaguchi, K. Saito, K. Sato, *Bull. Chem. Soc. Jpn.* **1975**, *47*, 3098.
[10] *Naturally Occuring Quinones* (Ed.: R. H. Thomson) 3rd ed., Academic, New York, **1987**.
[11] S. Araki, N. Katsumura, Y. Butsugan, *J. Organomet. Chem.* **1991**, *415*, 7.
[12] The UV spectrum of benzoquinone with allyltrimethylsilane shows a charge-transfer band at 280 nm.
[13] H.-J. Knölker, P. G. Jones, J.-B. Pannek, *Synlett.* **1990**, 429.

Large Hyperconjugative and Inductive Effects on C-C-X Bond Angles (X = Main-Group Element): The Crystal Structure of Triethylborane and Ab Initio Investigations**

By *Roland Boese,* Dieter Bläser, Norbert Niederprüm, Markus Nüsse, Waldemar A. Brett, Paul von Ragué Schleyer,* Michael Bühl,* and *Nicolaas J. R. van Eikema Hommes*

Remarkable deviations from expected geometries are found in seemingly simple compounds. Several structure determinations of molecules with tricoordinate boron and the structural element CH_3CH_2B revealed abnormally large C-

[*] Priv.-Doz. Dr. R. Boese, Dipl.-Ing. D. Bläser, Dr. N. Niederprüm, M. Nüsse, Dr. W. A. Brett
Institut für Anorganische Chemie der Universität Gesamthochschule Universitätsstrasse 3–5, D-W-4300 Essen 1 (FRG)
Prof. Dr. P. von R. Schleyer, Dr. N. J. R. van Eikema Hommes, Dr. M. Bühl
Institut für Organische Chemie der Universität Erlangen-Nürnberg Henkestrasse 42, D-W-8520 Erlangen (FRG)

[**] This work was supported by the Fonds der Chemischen Industrie, at Erlangen by the Deutsche Forschungsgemeinschaft, and the Convex Computer Corporation. N. J. R. van E. H. was a recipient of an Alexander von Humboldt Foundation Fellowship, and M. B. received a fellowship from the Studienstiftung des Deutschen Volkes.

C-B angles of up to 120.2(5)°.[1] Such large expansions of the tetrahedral angle (109.47°) are not likely to be due to repulsive intramolecular[2] or intermolecular[3] interactions. Although the C-C-B angle is 118.3(1)° in the high-temperature phase of triethylboroxine (**1**),[3] no strongly repulsive interactions are apparent. (The shortest intermolecular nonbonded H···H distances are 2.39 Å).

Is hyperconjugation responsible for the large C-C-B bond angles? To answer this question, we compare the X-ray structure of Et_3B (**2**),[4] which has formally a vacant boron p orbital, with that of the sodium salt of Et_4B^- (**3**),[6] in which no hyperconjugation is possible. We also have carried out ab initio geometry optimizations with the MP2/6-31G* basis set[7] on **2** and **3**, as well as on ethylborane (in various conformations), $CH_3CH_2BH_3^-$, and the whole set of compounds of the type CH_3CH_2X with elements of the second (X = Li, BeH, BH_2, CH_3, NH_2, OH, F) and third periods (Na, MgH, AlH_2, SiH_3, PH_2, SH, Cl). This data allows our findings with the boron compounds to be interpreted in a general framework.

The molecular structure of **2** (Fig. 1 left) is only slightly distorted from the expected C_{3h} symmetry. The B–C distances are 1.573(1) Å (mean value). The shortest nonbonded H···H separations, are 2.50 Å (intramolecular, between the ethyl groups) and 2.44 Å (intermolecular, see packing diagram, Fig. 2) and are not expected to have more than a minor influence on the molecular geometry. The mean C-C-B angle in **2**, 118.9(2)°, is nearly as large as that in triethylboroxine (**1**). The MP2/6-31G* geometry of **2**, computed in C_{3h} symmetry, has the same C-C-B bond angle (118.4°).

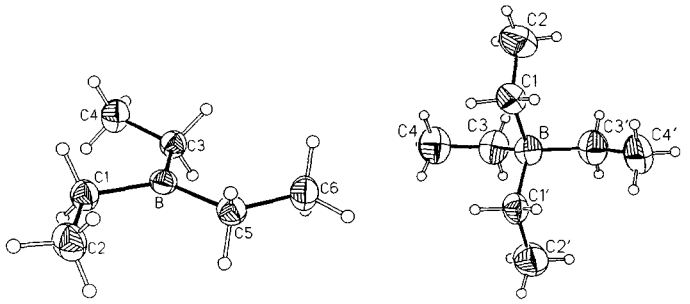

Fig. 1. Left: Structure of **2** in the crystal, the thermal ellipsoids are drawn at the 50% level. Bond lengths [Å] and angles [°], standard deviations 0.001 Å and 0.1°: B-C1 1.575, B-C3 1.573, B-C5 1.572, C1-C2 1.533, C3-C4 1.525, C5-C6 1.530; C1-B-C3 120.2, C1-B-C5 120.0, C3-B-C5 119.7, B-C1-C2 118.7, B-C3-C4 118.7, B-C5-C6 119.3; C2-C1-B-C3 178.4, C2-C1-B-C5 −0.9, C4-C3-B-C1 6.5, C4-C3-B-C5 −174.2, C6-C5-B-C1 −177.1, C6-C5-B-C3 3.7. Right: Structure of **3** in the crystal, the thermal ellipsoids are drawn at the 50% level. The cation and three surrounding dioxane molecules are omitted. Bond lengths [Å] and angles [°]: B-C1 1.643(5), B-C3 1.649(6), C1-C2 1.540(6), C3-C4 1.519(7); C1-B-C1' 107.4(4), C1-B-C3 109.6(2), C1-B-C3' 110.8(3), C3-B-C3' 108.6(4), B-C1-C2 116.4(3), B-C3-C4 116.3(3).

The crystallographic symmetry of **3** is C_2 (Fig. 1 right). The B–C distances (1.646(4) Å, mean value) are greater (by 0.06–0.10 Å) than those in **2** and in tetracoordinated mono- and diethylboron compounds[8] (1.599 Å, mean value). The C-C-B angles in **3**, 116.4(2)°, are in the same range as in related compounds[8] (115.6°, mean value), and only slightly smaller than in **1** and **2**. The shortest intramolecular nonbonded H···H distances between different ethyl groups (2.35 Å) and the shortest intermolecular distances (2.41 Å) should not affect the C-C-B angles to any appreciable extent. Hence, inductive, rather than steric or hyperconjugative effects, must be responsible for the large C-C-B angles in **3**. This is confirmed by both the C-C-B angle of 113.1° which

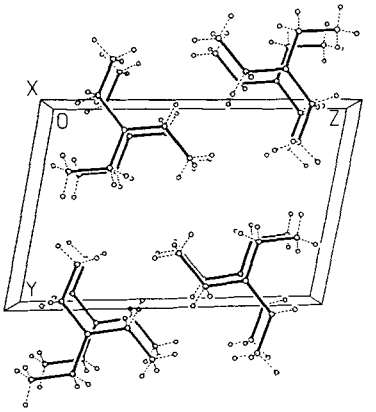

Fig. 2. Packing in **2** in the unit cell, intermolecular H···H separations between the stacks of molecules are 2.44 Å.

we compute for the small parent compound, the anion $CH_3CH_2BH_3^-$, in which steric repulsions are absent, and by the value for **3** in D_{2d} symmetry (116.1°; MP2/6-31G*).

As summarized in Figure 3, the C-C-X angles (ab initio, MP2/6-31G* basis set) in the whole set of compounds of the type CH_3CH_2X (X = Li–F, Na–Cl) range from approximately 105° for X = BH_2 to 118° for X = Li. (A search with the Cambridge Structural Database also reveals that greatly expanded C-C-X angles are common; Table 1.[9]) The general tendency of the C-C-X angles to correlate with the electronegativies (according to Allred–Rochow) of X[12] (element and group electronegativities are very similar) is apparent in Figure 3 (dotted line).

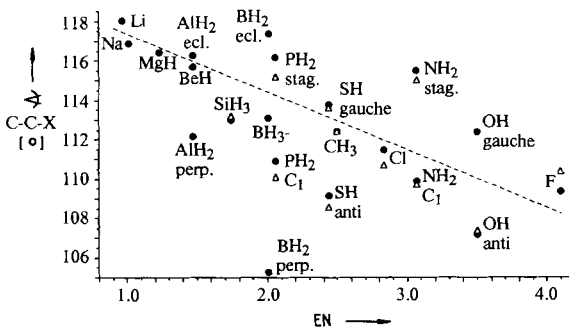

Fig. 3. Electronegativity EN (according to Allred–Rochow) and the C-C-X angles (MP2/6-31G*) of ethyl–main-group element compounds (black dots). Experimental data taken from "*Landolt-Börnstein*", *II*, Vol. 15, Springer, Berlin, **1987**, are included for comparison (triangles). The dotted line indicates the general trend to smaller angles with increasing electronegativity of the substituent (inductive effect). Deviations are due primarily to hyperconjugative effects (see text). Note the large angle differences when two conformations are possible. ecl = eclipsed, stag. = staggered, perp. = perpendicular. For more details see text.

The compounds with the more electronegative substituents have smaller C-C-X angles. This mimics the situation expected for carbocation/anion ion-pairs: more electropositive X substituents lead to the larger angles of the strongly pyramidalized carbanions (for example, in polar organometallic compounds). Thus, the expanded C-C-B angles, $\measuredangle$CCB = 113.1° in $CH_3CH_2BH_3^-$ (MP2/6-31G*) and in EtB_4^-, $\measuredangle$CCB = 116.4° in the X-ray crystal structure and 116.1° in the MP2/6-31G* structure, are primarily the consequence of the sigma (inductive) effect of boron in the absence of a vacant p orbital.

Deviations from such regular behavior (i.e., the points not on the dotted line in Fig. 3) are due primarily to hyperconju-

Table 1. Bond angles α ($\triangleq$ C-C-X, X = main-group element) determined by X-ray crystallography for compounds with the structure element Et-X.

X	n [a]	$\alpha \pm \sigma$[°]	α_{min}[°]	α_{max}[°]
Be	2	115.35 ± 0.95	114.67	116.02
Mg	7	120.73 ± 6.98	111.65	129.58
B	88	115.50 ± 3.38	100.08	128.07
Al	51	116.82 ± 4.78	105.59	133.74
C	3431	113.50 ± 4.53	74.88	159.66
Si	24	116.69 ± 3.88	112.87	132.03
N	3105	118.60 ± 3.41	75.42	145.88
P	1410	115.64 ± 3.89	95.85	137.47
O	1751	110.01 ± 5.44	83.96	164.32
S	245	112.69 ± 3.99	88.83	139.53

[a] n = Number of structures examined [9].

gation effects. Specifically, in the *perpendicular* conformation of CH_3CH_2–BH_2, the empty boron p orbital lies in the C-C-B plane (perp. in Fig. 3). Thus the resulting hyperconjugation with the C–C bond results in a considerable reduction in the C-C-B angle to 105.3°.

In the *eclipsed* conformation, in which the empty boron p orbital is *perpendicular* to the C-C-B plane, the C-C-B angle is influenced indirectly. Hyperconjugation with the vacant p orbital now involves the two equivalent α CH bonds (which have roughly 30° dihedral angles). Electrons are withdrawn from the CH_2 orbital with π symmetry. Hence, the antibonding interactions between the hydrogen atoms are reduced and the orbital which has H···H character has a greater influence. The result is that the H-C-H angle decreases to 103.1° in Et_3B (MP2/6-31G*). The C-C-B angle expands (to 117.4°) as a consequence (the Thorpe–Ingold hypothesis).[13]

When the X group is a π-donor rather than a π-acceptor, negative hyperconjugation with a lone pair results in a wider C-C-X angle. For example, for X = NH_2 in the *staggered* conformation with the N lone pair *anti* to the C-C bond the C-C-X angle is 115.5°. In the *trans* conformations of C_2H_5OH and C_2H_5SH, for example, the smaller C-C-X angles (ca. 107.2°) arise indirectly as summarized in Scheme 1.

Scheme 1. Orientations of the ethyl group relative to the p orbital of the main-group element X. Left, perpendicular conformation **A**; right, eclipsed conformation **B**. When the p orbital in **A** is empty, the C-C-X angle decreases; when occupied, the angle increases. When the p orbital in **B** is empty, the H-C-H angle decreases and the C-C-X angle increases; when occupied, the H-C-H angle increases and the C-C-X angle decreases.

Idealized "sp^3" bond angles of 109.47° require tetrahedral symmetry and thus cannot be expected generally. "The regular tetrahedral angle is the exception rather than the rule in organic chemistry."[14] Figure 3 and Table 1 emphasize the variety of molecular geometries and that many bond angles in simple organic compounds do not fit the widely accepted generalizations.

Received: October 14, 1991 [Z 4968 IE]
German version: *Angew. Chem.* **1992**, *104*, 356

CAS Registry numbers:
2, 97-94-9; **3**, 15523-24-7; **3**·3dioxane, 138785-29-2; EtBeH, 6917-57-3; EtMgH, 63533-53-9; $EtBH_2$, 25070-50-2; $EtAlH_2$, 14914-86-4; $EtCH_3$, 74-98-6; $EtSiH_3$, 2814-79-1; $EtNH_2$, 75-04-7; $EtPH_2$, 593-68-0; EtOH, 64-17-5; EtSH, 75-08-1.

[1] R. Köster, G. Seidel, R. Boese, B. Wrackmeyer, *Chem. Ber.* **1988**, *121*, 597–615.
[2] R. Köster, G. Seidel, R. Boese, *Chem. Ber.* **1990**, *123*, 1013–1028.
[3] R. Boese, M. Polk, D. Bläser, *Angew. Chem.* **1987**, *99*, 239–241; *Angew. Chem. Int. Ed. Engl.* **1987**, *26*, 245–247.
[4] **2** (m.p. = 182.3 K) was crystallized in a capillary by means of a computer-controlled miniature zone-melting procedure [5] at 161 K, the data were collected at 150 K. Nicolet R3/mV diffractometer with a low temperature device of our own construction, $Mo_{K\alpha}$ radiation, program used: SHELXTL-Plus (Version 4.11). Crystal size: 0.3 mm diameter (cylindric). Triclinic, $a = 4.172(1)$, $b = 7.803(1)$, $c = 11.727(2)$ Å, $\alpha = 100.23(1)$, $\beta = 96.35(1)$, $\gamma = 94.60°(1)$, $V = 368.3(1)$ Å^3, $Z = 2$. Space group $P\bar{1}$, $\rho_{calc.} = 0.884$ Mgm^{-3}, $2\theta_{max} = 60°$, 2133 independent intensities, 1815 observed ($F_0 \geq 4\sigma(F)$), 124 parameters, hydrogen atoms refined without constraints and individual isotropic DPs, all other atoms with ADPs. $R = 0.048$, $R_w = 0.058$, $w^{-1} = \sigma^2(F_0) + 6.63 \times 10^{-3} F_0^2$), maximum residual electron density 0.28 eÅ^{-3}.
[5] D. Brodalla, D. Mootz, R. Boese, W. Osswald, *J. Appl. Crystallogr.* **1985**, *18*, 316–319.
[6] Structure determination of **3**, crystallized with three molecules of dioxane: The crystal had to be kept with the mother liquor and transferred below 270 K; cooling below 250 K damages the crystal. Crystal size: 0.33 × 0.27 × 0.18 mm^3. Monoclinic, $a = 18.071(3)$, $b = 10.916(2)$, $c = 15.453(3)$ Å, $\beta = 125.31(1)°$, $V = 2487.4(8)$ Å^3; $Z = 4$, $T = 250$ K, space group $C2/c$, $\rho_{calc.} = 1.283$ Mgm^{-3}, $2\theta_{max.} = 45°$, 2212 independent intensities, 1193 observed ($F_0 \geq 4\sigma(F)$), 141 parameters, hydrogen atoms refined as rigid groups with isotropic DPs for each group, all other atoms were refined with ADPs. $R = 0.056$, $R_w = 0.051$, $w^{-1} = \sigma^2(F_0) + 1.7 \times 10^{-4} F_0^2$, maximum residual electron density 0.26 eÅ^{-3}. Other data are the same as for **1**. Further details of the crystal structure investigations are available on request from the Fachinformationszentrum Karlsruhe, Gesellschaft für wissenschaftlich-technische Information mbH, D-W-7514 Eggenstein-Leopoldshafen 2, on quoting the depository number CSD-320332 for **2**, CSD-320331 for **3**, the authors' names, and the full journal citation.
[7] W. J. Hehre, L. Radom, P. von R. Schleyer, J. A. Pople, *Ab Initio Molecular Orbital Theory*, Wiley, New York, **1986**.
[8] a) R. Köster, G. Seidel, R. Boese, *Chem. Ber.* **1990**, *123*, 2109–2116; b) M. Yalpani, R. Boese, R. Köster, *ibid.* **1990**, *123*, 713–718; c) R. Köster, G. Seidel, G. Müller, R. Boese, B. Wrackmeyer, *ibid.* **1988**, *121*, 1381–1392; d) R. Köster, G. Seidel, R. Boese, B. Wrackmeyer, *ibid.* **1988**, *121*, 597–615; e) M. Yalpani, R. Boese, R. Köster, *ibid.* **1990**, *123*, 707–712.
[9] The data were obtained from the Cambridge Structural Database (CSD), Version from 8.5.1991 with 90296 entries, using the Cambridge Structural Database System (CSDS) Version 4.40. [10] Only crystal structures containing the structure element X–Et (X = second- or third-period element) with R values between 0.001–0.08 were considered. The valencies of the specified elements have not been taken into account. Despite the relatively high standard deviations, the t-test [11] shows that most of the comparisons among the angles involving the various elements are significantly different (except for Be and Si).
[10] F. H. Allen, O. Kennard, R. Taylor, *Acc. Chem. Res.* **1983**, *16*, 146.
[11] R. Kaiser, G. Gottschalk, *Elementare Tests zur Beurteilung von Meßdaten*, B. I.-Wissenschaftsverlag, Mannheim, **1972**, p. 25.
[12] a) T. Clark, G. W. Spitznagel, R. Klose, P. von R. Schleyer, *J. Am. Chem. Soc.* **1984**, *106*, 4412–4419; b) P. von R. Schleyer, *Pure Appl. Chem.* **1987**, *59*, 1647–1660.
[13] See P. von R. Schleyer: *J. Am. Chem. Soc.* **1961**, *83*, 1368–1373.
[14] K. Mislow, *Introduction to Stereochemistry*, Benjamin, New York, **1966**, p. 13.

An Arsanylidensilane ("Arsasilene") and its Derivatization with Tellurium and Benzophenone**

By *Matthias Driess** and *Hans Pritzkow*

Organosilicon compounds with low-coordinated Si atoms and multiple bonds to silicon were of great importance for the recent development of silicon chemistry. In the last ten years the use of, for example, disilenes, silaalkenes, and

[*] Dr. M. Driess, Dr. H. Pritzkow
Anorganisch-chemisches Institut der Universität
Im Neuenheimer Feld 270, D-W-6900 Heidelberg (FRG)

[**] This work was supported by the Fonds der Chemischen Industrie and the Deutsche Forschungsgemeinschaft (SFB 247). We thank Messer-Griesheim GmbH, Duisburg, for chemicals, and Prof. Dr. W. Siebert Heidelberg for his support.

silanimines for the preparation of new classes of organosilicon compounds have proved to be extremely profitable.[1] For investigations into the structure and reactivity of compounds with low-coordinated Si atoms, the synthesis of unsaturated Si compounds of the type $R_2Si{=}E$ with new combinations of element–silicon $(p\text{-}p)_\pi$ bonds and λ^4, σ^3 coordinated Si atoms plays a key role. Therefore, we search for efficient ways to isolate compounds with π bonds between silicon and the heavy homologues of Group 15, i.e. phosphorus, arsenic, antimony, and bismuth. Whereas compounds with a P–Si π bond ("phosphasilenes") **A**[2] are already known, there are so far no examples for the homologous systems **B**–**D**.

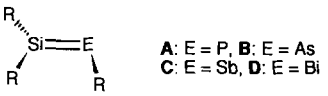

A: E = P, **B**: E = As
C: E = Sb, **D**: E = Bi

Recently we have achieved, starting from Is_2SiF_2 (Is = 2,4,6-iPr$_3$C$_6$H$_2$) and $LiPH_2 \cdot DME$ (DME = dimethoxyethane), in a multiple-step reaction, a simple synthesis of thermally stable and at the same time activated phosphanylidensilanes ("phosphasilenes").[3] It has been shown that this simple synthetic route surprisingly is also suitable for the preparation of **1**, the first arsasilene. Thus, the reaction of Is_2SiF_2 with two equivalents of $LiAsH_2 \cdot DME$ in THF at 20 °C leads quantitatively to the lithiated coupling product **2**, which is stable in THF for several days.

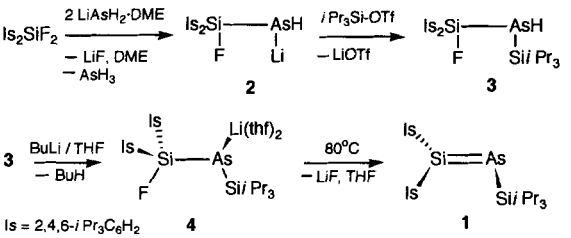

Compound **2**, which is not isolated, can be directly transformed into the disilylarsane **3** (Table 1) with triisopropylsilyl trifluoromethanesulfonate. Lithiation of **3** with one equivalent of nBuLi in a hexane/THF mixture leads to the lithoarsane **4** (Table 1), which is isolated in the form of colorless, extremely air- and moisture-sensitive crystals. The ^{1}H NMR spectrum and an elemental analysis prove that the Li atom in **4**, solvated with two THF molecules, is only threefold coordinated. This result was confirmed by a crystal structure analysis of **4** (Fig. 1).[4]

In contrast to $LiAs(SiMe_3)_2 \cdot DME$,[5] which up to now is the only lithium disilylarsane complex structurally confirmed, and which both in solution and also in the solid state is dimeric, **4** is monomeric in the solid state. The Li atom is distorted trigonal planar, the As atom pyramidal, and the fluoro-substituted Si atom as a result of steric overloading has a highly distorted tetrahedral coordination. In contrast to that, the iPr substituted Si atom is tetrahedrally surrounded. Noteworthy is the short Li–As bond (2.46 Å). The As–Si bond lengths of 2.29 Å (FSi–As) and 2.32 Å (iPrSi–As) are shorter than As–Si single bonds (2.33–2.40 Å) and not significantly different from the value in the dimeric $LiAs(SiMe_3)_2 \cdot DME$ (2.30 Å).[5]

The thermal elimination of LiF and THF from **4** in toluene at ca. 90 °C leads to an intensely red solution of **1**,

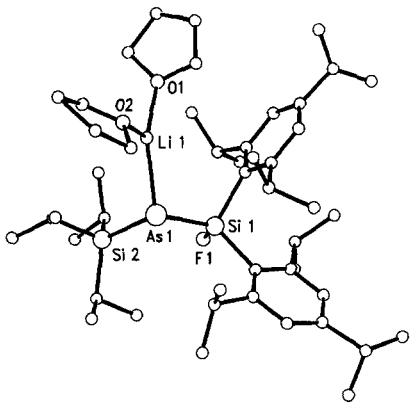

Fig. 1. Molecular structure of **4**. Selected bond lengths [Å] and angles [°]: As1-Si1 2.296(4), As1-Si2 2.320(4), Si1-F1 1.631(8), Li-As1 2.46(3), Li-O1 1.91(3), Li-O2 1.92(4); Si1-As1-Si2 106.4(1), Si1-As1-Li 110.2(7), Si2-As1-Li 109.5(7), As1-Li-O1 143.9(16), As1-Li-O2 114.0(15), O1-Li-O2 101.9(16).

which can be isolated as a spectroscopically pure (^{1}H NMR and mass spectra), deep-red oil (Table 1). In the ^{29}Si NMR spectrum, for the λ^4, σ^3 coordinated Si atom, similar to the analogous phosphasilene,[3] a signal at very low field ($\delta = 179.1$) is observed. The ^{29}Si nuclei of the SiiPr$_3$ group result in a singlet at $\delta = 28.0$. The ^{29}Si chemical shifts of **1**, as with the analogous phosphasilene[3] and other compounds of this type,[2] are noticeably temperature dependent [$\delta(^{29}Si)$ for Si=As at 80 °C: 177.2, for As–SiiPr$_3$: 27.9]; however, they are only slightly influenced by the donor ability of the solvent in contrast to silanimines. Therefore, the

Table 1. NMR spectroscopic and selected mass spectrometric data of **1** and **3**–**6**.

1: ^{1}H NMR (200 MHz, C_6D_6, 300 K): $\delta = 1.35$ (br.d, 54H, SiCHMe_2, o-, p-CHMe_2, $J = 7.0$ Hz), 1.50 (br.m, 3H, SiCHMe$_2$), 2.92 (br.m, 2H, p-CHMe$_2$), 4.00 (br., 2H, o-CHMe$_2$), 4.16 (br., 2H, o-CHMe$_2$), 7.16 (s, 4H, arom. H); ^{29}Si NMR (INEPT): $\delta = 28.0$ (s, SiiPr), 179.0 (s, SiAs); MS (EI, 70 eV): m/z 666 (M^+, 71%), 623 ($M - C_3H_7)^+$, 8), 509 ($(M - Si{i}Pr_3)^+$, 7), 451 ($(M - Si{i}Pr_3 - C_3H_7 - Me)^+$, 8), 433 ($(Is_2Si - 1H)^+$, 100).

3: ^{1}H NMR (200 MHz, C_6D_6, 300 K): $\delta = 1.02$ (br., 18H, SiCHMe_2), 1.11 (d, 12H, p-CHMe_2, $J = 6.9$ Hz), 1.19 (br., 24H, o-CHMe_2), 2.73 (sept, 2H, p-CHMe$_2$, $J = 6.9$ Hz), 3.59 (br.sept 4H, p-CHMe$_2$), 7.04 (s, 4H, arom. H) [a]; ^{19}F NMR (standard $CFCl_3$): $\delta = -125.6$ (s, J(F-Si) = 356 Hz); ^{29}Si NMR (INEPT): $\delta = 13.5$ (d, SiF, J(Si-F) = 355.6 Hz), 14.4 (s, SiiPr); MS (EI, 70 eV): m/z 686 (M^+, 10%), 453 (Is_2SiF^+, 100).

4: ^{1}H NMR (200 MHz, [D_8]toluene, 300 K): $\delta = 1.20$–1.46 (br.m, 65H, SiiPr, CHMe_2 and 8H von THF), 2.77 (sept, 2H, p-CHMe$_2$, $J = 6.9$ Hz), 3.38 (m, 8H, THF), 3.65 (br., 4H, o-CHMe$_2$), 7.09 (s, 4H, arom. H); ^{19}F NMR (standard $CFCl_3$): $\delta = -118.3$ (s, J(F-Si) = 320 Hz); ^{29}Si NMR (INEPT): $\delta = 24.4$ (d, SiF, J(Si-F) = 320.8 Hz), 26.7 (d, SiiPr, J(Si-F) = 3.6 Hz). Correct C,H-analysis.

5: ^{1}H NMR (200 MHz, C_6D_6, 300 K): $\delta = 0.45$–1.64 (br.m, 57H, SiiPr and CHMe_2), 2.75 (sept, 1H, $J = 6.9$ Hz, p-CHMe$_2$), 2.78 (sept, 1H, $J = 6.9$ Hz, p-CHMe$_2$), 3.87 (br., 4H, o-CHMe$_2$), 7.11 (s, 2H, arom. H), 7.19 (s, 2H, arom. H); ^{29}Si NMR (INEPT): $\delta = 18.5$ (s, SiiPr), -44.5 (s, SiTe); ^{125}Te NMR (C_6D_6, standard Me_2Te): $\delta = -1157.5$ (s); MS (EI, 70 eV): m/z 796 (M^+, 21%), 666 ($(M - Te)^+$, 9), 435 (Is_2SiH^+, 100).

6: ^{1}H NMR (200 MHz, C_6D_6, 340 K): $\delta = 1.10$ (d, 18H, SiCHMe_2, $J = 7.2$ Hz), 1.18 (d, 36H, o-, p-CHMe_2, $J = 6.8$ Hz), 1.42 (sept, 3H, SiCH-Me$_2$, $J = 7.2$ Hz), 2.78 (sept, 2H, p-CHMe$_2$, $J = 6.8$ Hz), 4.05 (br., 4H, o-CHMe$_2$), 6.83–7.06 (m, 10H, Ph), 7.62 (s, 2H, arom. H), 7.66 (s, 2H, arom. H); ^{13}C NMR (50 MHz, C_6D_6, 340 K): $\delta = 15.428$ (s, SiCHMe$_2$), 20.224 (s, CHMe_2), 23.731 (s, CHMe_2), 24.901 (br., CHMe$_2$), 34.273 (s, CHMe$_2$), 86.872 (s, AsC), 122.536 (br.), 126.649 (s), 134.713 (s), 150.860 (br.), 151.156 (s), 154.807 (br.); ^{29}Si NMR (INEPT, C_6D_6): $\delta = -3.24$ (s, Si-O), 23.00 (s, SiiPr); MS (EI, 70 eV): m/z 848 (M^+, 2.5%), 666 ($(M - Ph_2CO)^+$, 40), 433 ($(Is_2Si - 1H)^+$, 100); correct C,H-analysis.

[a] AsH signal not found. Below 278 K two anisochronic methyl groups of the SiiPr group are observed.

 © VCH Verlagsgesellschaft mbH, W-6940 Weinheim, 1992 0570-0833/92/0303-0317 $ 3.50+.25/0

^{29}Si NMR spectrum proves that in **1** there is a As–Si π bond with similar polarity relations as is in the P–Si π system.

The high kinetic stability of **1** allowed investigations into the reactivity of this compound. Thus, the oxidation of **1** with elemental tellurium (toluene, 25 °C, 1 d) leads to the yellow, crystalline three-membered ring compound **5**. The structure of the AsSiTe three-membered ring is confirmed by mass spectrometry and ^{29}Si as well as ^{125}Te NMR spectra (Table 1), especially since the ^{29}Si and ^{125}Te chemical shifts are very similar to those of the homologous PSiTe three-membered ring.[6]

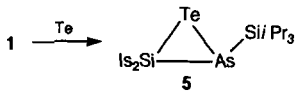

5

Since kinetically stabilized silanimines react with ketones in a metathetical process to give azomethine derivatives ($R_2C{=}NR$) and trimeric cyclosilanones $(R_2SiO)_3$,[7] we investigated whether analogous methylenarsanes "arsaalkenes" are obtained from **1** and ketones $R_2C{=}O$ (R = Ph, *t*Bu). Whereas benzophenone reacts with **1** to give **6** already at 0 °C, with $tBu_2C{=}O$ even at 90 °C for 8 h no reaction is achieved. The composition and structure of **6** are confirmed by mass spectrometry, and NMR spectroscopy, respectively (Table 1). In the mass spectrometer, as a retro reaction of **6** only the fragmentation to $\mathbf{1}^+$ and $Ph_2C{=}O$ is observed.

The crystal structure analysis[8] of **6** shows that as a result of the bulky substituents unusual bonding situations exist (Fig. 2). The SiOCAs four-membered ring is slightly bent

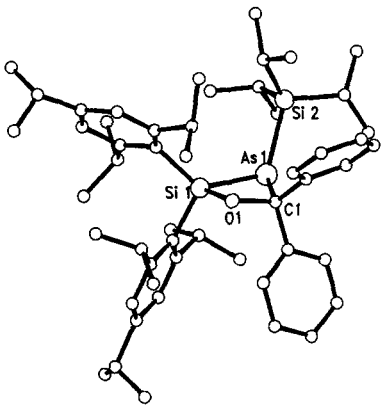

Fig. 2. Molecular structure of **6**. Selected averaged bond lengths [Å] and angles [°]: As1-Si1 2.382(2), As1-Si2 2.393(2), As1-C1 2.057(7), Si1-O1 1.688(4), C1-O1 1.450(8); Si1-As1-C1 68.6(2), As1-Si1-O1 82.5(1), Si1-O1-C1 105.8(3), O1-C1-As1 101.0(4).

(along the As–O axis 11.7° and relative to Si1–C1 16.2°), the Si–As, Si–O, and C–O bond lengths correspond to extended single bonds, and the As atom is tetrahedrally coordinated (sum of angles 299.4°). Of particular note is the long As–C distance (2.060(7) Å), which is 0.1 Å longer than the average single bond (ca. 1.95 Å); this is probably caused by the bulky substituents. The inert behavior of $tBu_2C{=}O$ towards **1** is probably due to steric hindrance.

Under drastic conditions (160 °C, 10 h) **6** actually decomposes into $Is_2Si{=}O$, which immediately *dimerizes* to **7** (in contrast to less bulky silanones, which usually *trimerize*), and the arsaalkenes **8** and **9**.[9] This presents a new way to arsaalkenes[10] via arsasilenes by means of a pseudo Wittig reaction.

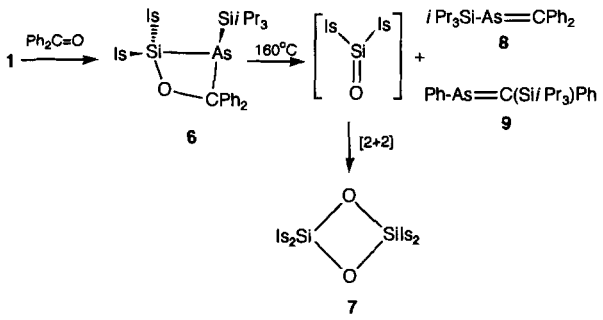

Experimental Procedure

4: A solution of Is_2SiF_2 (5.4 g, 11.44 mmol) in THF (40 mL) was added to $LiAsH_2 \cdot$ DME (3.98 g, 22.88 mmol) and was stirred for 3 h at 0 °C then 16 h at 25 °C. To the orange-yellow solution of **2**, $iPr_3SiOSO_2CF_3$ (3.5 g, 11.44 mmol) was added at −50 °C and then this was stirred for 30 min at 25 °C. Finally, all volatiles were removed at 10^{-2} Torr and the dark brown crude product was taken up in hexane (50 mL) and filtered over a G3 frit. Compound **3** could be crystallized from a concentrated solution. For the further processing to **4** this was not absolutely necessary. Therefore, the filtrate was diluted with THF (10 mL), cooled to −78 °C, and treated with *n*BuLi (11.44 mmol, 2.5 M solution in hexane, Aldrich). The clear orange solution was slowly warmed to 25 °C, the solvent removed in vacuum, and the solid residue recrystallized twice from hexane at −30 °C. Yield: 5.13 g (6.13 mmol, 53.7%), colorless crystals.

1: **4** (912 mg, 1.09 mmol) was dissolved in toluene (5 mL) and heated to 80–90 °C for 14 h. The red solution was completely evaporated and taken up in hexane (5 mL). Me_3SiCl (1 mL) was added and the solution was stirred for 1 d at 25 °C to separate the LiF. The LiCl was filtered off and the filtrate was concentrated in vacuum to give **1** as a deep-red, viscous oil. Yield: 660 mg (0.99 mmol, 91%).

5: **1** (420 mg, 0.63 mmol) was dissolved in toluene (10 mL) and stirred with Te powder (excess) for 1 d at 25 °C. The excess Te was filtered off and the red filtrate was concentrated to ca. 2 mL and left at 10 °C so that after two crystallizations yellow crystals of **5** precipitated. Yield: 199 mg (0.25 mmol, 39.8%), mp = 164 °C.

6: 1 (583 mg, 0.88 mmol) was dissolved in toluene (10 mL) and added to benzophenone (160 mg) dissolved in toluene (5 mL) at ca. 0 °C. The initial deep red color of the solution disappeared immediately. All volatiles were removed at 10^{-2} Torr, and the residue was recrystallized twice from hexane (2 mL) at 25 °. Yield: 621 mg (0.73 mmol, 83.3%), colorless crystals, mp = 135 °C.

Received: October 24, 1991 [Z 4985 IE]
German version: *Angew. Chem.* **1992**, *104*, 350

CAS Registry numbers:
1, 138435-76-4; **2**, 138435-77-5; **3**, 138435-78-6; **4**, 138435-84-4; **5**, 138435-79-7; **6**, 138435-80-0; **7**, 138435-81-1; **8**, 138435-82-2; **9**, 138435-83-3; Is_2SiF_2, 108202-50-2; $LiAsH_2 \cdot$DME, 138435-85-5; $iPr_3SiOSO_2CF_3$, 80522-42-5; Ph_2CO, 119-61-9; Te, 13494-80-9.

[1] Reviews: Disilenes: R. West, *Angew. Chem.* **1987**, *99*, 1231; *Angew. Chem. Int. Ed. Engl.* **1987**, *26*, 1201; Silaalkenes: G. Raabe, J. Michl (*Multiple bonds to silicon*) in *The Chemistry of Organic Silicon Compounds, Part 2* (Eds.: S. Patai, Z. Rappaport), Wiley, New York, **1987**, p. 1044; Silanimines: *ibid.*, p. 1108.

[2] C. N. Smit, F. Bickelhaupt, *Organometallics* **1987**, *6*, 1156; H. M. M. Bastiaans, F. Bickelhaupt, Y. van den Winkel, *Phosphorus Sulfur Silicon Relat. Elem.* **1990**, *49/50*, 333; Y. van den Winkel, H. M. M. Bastiaans, F. Bickelhaupt, *J. Organomet. Chem.* **1991**, *405*, 183; see also [3].

[3] M. Driess, *Angew. Chem.* **1991**, *103*, 979; *Angew. Chem. Int. Ed. Engl.* **1991**, *31*, 102.

[4] Crystal structure analysis of **4**: Monoclinic, $P2_1/n$, $a = 18.933(10)$, $b = 12.053(6)$, $c = 24.306(12)$ Å, $\beta = 111.30(6)°$, $V = 5168$ Å^3, $Z = 4$; 2667 reflections ($I > 2\sigma(I)$, four-circle diffractometer, $Mo_{K\alpha}$ radiation, ω scan), $R = 0.091$, $R_w = 0.097$ (As, Si, F, O anisotropic, C isotropic, H in calculated positions, methyl groups as rigid groups, 332 parameters). A THF molecule and *p*-positioned isopropyl groups are disordered.[11]

[5] G. Becker, C. Witthauer, *Z. Anorg. Allg. Chem.* **1982**, *492*, 28.

[6] Is_2Si-Te-P(Si*i*Pr$_3$): $\delta(^{29}Si) = -66.5$ (d); $\delta(^{125}Te) = -1124.8$ (d). M. Driess, unpublished.

[7] N. Wiberg, *J. Organomet. Chem.* **1984**, *273*, 141; S. Vollbrecht, U. Klingebiel, D. Schmidt-Bäse, *Z. Naturforsch. B* **1991**, *46*, 709.
[8] Crystal structure analysis of **6**: monoclinic, $P2_1/a$, $a = 17.919(18)$, $b = 16.238(16)$, $c = 34.53(3)$ Å, $\beta = 90.83(6)°$, $V = 10047$ Å^3, $Z = 8$; 7501 reflections ($I > 2\sigma(I)$ four-circle diffractometer, $Mo_{K\alpha}$ radiation, ω scan), $R = 0.065$, $R_w = 0.059$ (As, Si, O, C anisotropic, H in calculated positions, isotropic temperature factors, phenyl rings as rigid groups, 921 parameters).[11]
[9] The arsaalkenes **8** and **9** were characterized by ^{1}H NMR as well as ^{13}C NMR spectroscopy and also mass spectrometry. The 1,3,2,4-dioxadisilethane **7** [$\delta(^{29}Si) = -6.38$; MS (EI, 70 eV): m/z 900 (M^+, 84(%), 435 (Is_2SiH^+, 100)] is identical with the product from the oxidation of $Is_2Si{=}SiIs_2$ with O_2: R. West, A. Millevolte, 24th Organosilicon Symposium, April 12-13 1991, El Paso, USA.
[10] T. C. Klebach, H. van Dongen, F. Bickelhaupt, *Angew. Chem.* **1979**, *91*, 423; *Angew. Chem. Int. Ed. Engl.* **1979**, *18*, 395; G. Becker, G. Gutekunst, *Z. Anorg. Allg. Chem.* **1980**, *470*, 144.
[11] Further details of the crystal structure investigation may be obtained from the Fachinformationszentrum Karlsruhe, Gesellschaft für wissenschaftlich-technische Information mbH, D-W-7514 Eggenstein-Leopoldshafen 2 (FRG) on quoting the depository number CSD-55937, the names of the authors, and the journal citation.

Cyclodextrin Derivatives as Chiral Selectors—Investigation of the Interaction with (*R*,*S*)-Methyl-2-chloropropionate by Enantioselective Gas Chromatography, NMR Spectroscopy, and Molecular Dynamics Simulation**

By *Jutta E. H. Köhler, Manfred Hohla, Martina Richters,* and *Wilfried A. König**

Dedicated to Professor Ernst Bayer on the occasion of his 65th birthday

Enantiomeric substrates form energetically and structurally distinguishable host–guest complexes with cyclodextrins and their derivatives. This is shown, for example, in the investigation of chiral substrates in the presence of cyclodextrins by enantioselective chromatography,[1] NMR spectroscopy,[2] and X-ray structure analysis.[3] To understand the host–guest interaction and thereby, the "chiral recognition" it would be very useful to obtain information concerning the spatial relationship between host and guest molecules in molecular complexes.

The model we investigated involves (*R*,*S*)-methyl-2-chloropropionate **1** complexed with heptakis(3-*O*-acetyl-2,6-di-*O*-pentyl)-β-CD (Lipodex D, **2**).[4] On capillary columns coated with **2**, the enantiomers of **1** are resolved with an unusually large separation factor ($\alpha = 2.02$, on a 25 m "fused-silica capillary" at 333 K $\Delta\Delta G^0_{R,S} = 2$ kJ mol^{-1}).

The ^{1}H NMR spectrum of a solution of **1** and **2** in a nonpolar solvent ([D_{12}]cyclohexane, [D_{14}]hexane) shows significantly different signals for (*R*)-**1** and (*S*)-**1**. All signals of the (*S*) enantiomer are shifted to lower field by up to $\Delta\delta = 0.5$ in comparison to the (*R*) enantiomer (Fig. 1). Futhermore,

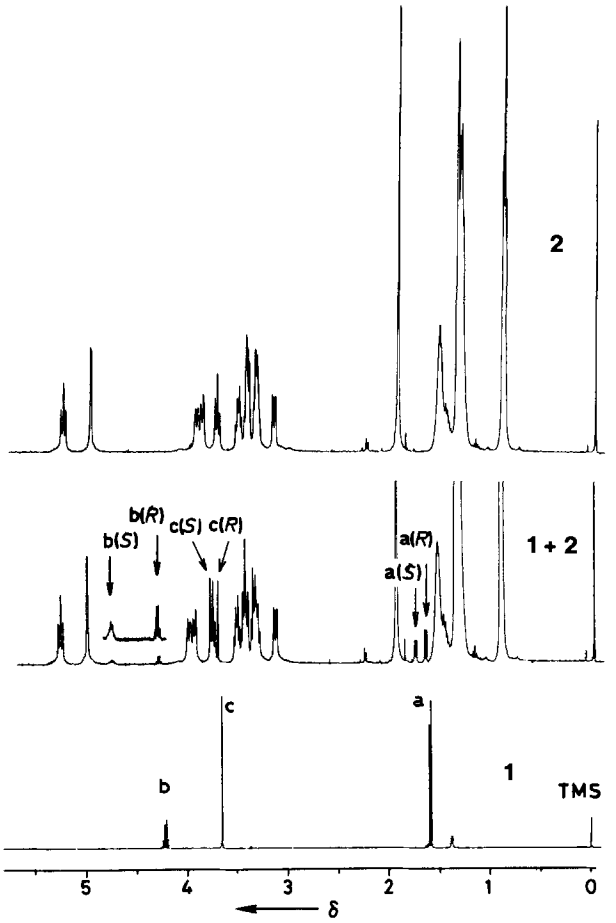

Fig. 1. 400 MHz ^{1}H NMR spectra of (*R*,*S*)-**1** (below) with the signals of the methyl (a), methine (b), and methoxy groups (c), of (*R*,*S*)-**1** and **2** in mol ratio 1:2.25 (middle; the resonance signals a, b, and c show different chemical shifts for the enantiomers) and of **2** (above). All spectra were recorded in [D_{12}]cyclohexane.

the methine proton of (*S*)-**1** does not show a quartet, but a signal of higher order (Fig. 2). This could indicate a nonequivalence of the coupling CH_3 protons as a result of a specific interaction with the chiral host molecule in the inclusion complex.

The differences in the chemical shift values decrease on raising the temperature and also on increasing the host–guest ratio. Similar, though less pronounced effects appeared in the ^{1}H NMR spectra of solutions of **2** and either (*R*,*S*)-methyl-2-bromopropionate, (*R*,*S*)-methyllactate, or (*R*,*S*)-methylmandelate. In every case, the protons of the enantiomer retained more strongly on the GC column also absorb at lower field. Thus, in principle, cyclodextrin derivatives are suitable as chiral shift reagents. A similar example of discrimination for the enantioselective inclusion of enantiomers was reported by A. Collet et al.[5] for bromochlorofluoromethane and a synthetic cryptophane.

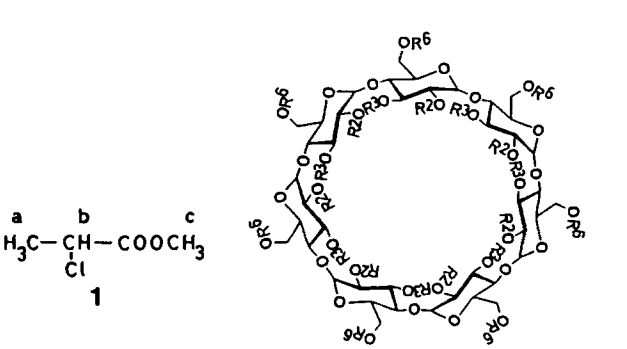

[*] Dr. J. E. H. Köhler, M. Hohla
Consortium für Elekrochemische Industrie
Zielstattstrasse 20, D-W-8000 München 70 (FRG)
Prof. Dr. W. A. König, M. Richters
Institut für Organische Chemie der Universität
Martin-Luther-King-Platz 6, D-W-2000 Hamburg 13 (FRG)

[**] This work was supported by the Deutsche Forschungsgemeinschaft and the Fonds der Chemischen Industrie.

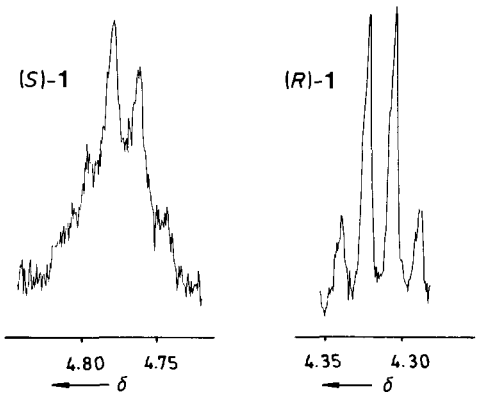

Fig. 2. Resonance signal of the methine proton of (*R*)-**1** (right) and (*S*)-**1** (le Recording conditions as for Figure 1.

To investigate why (*S*)-**1** complexes more effectively wi **2**, a total of four models for molecular dynamics (MD) sir ulations[6] was applied (Fig. 3).

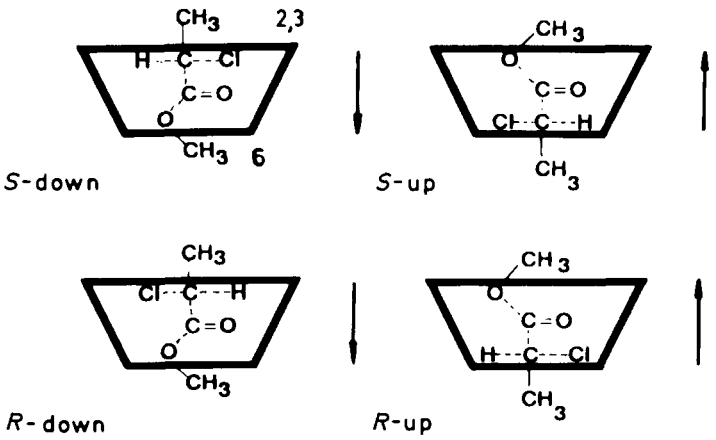

Fig. 3. Molecular dynamic models of complexes from **1** and **2**. The numbers 2, 3, and 6 (in the upper left picture) indicate the position of the substituents at C-2, C-3, and C-6, respectively, of the glucose units of **2**. This position is the same in all four models.

Based on the known X-ray structure data of β-CD,[7] the side chains of **2** were fixed in the 2, 3, and 6 positions of the glucose units, in such a way that they were oriented as evenly as possible vertically upwards (wider opening of the cavity, substituents at C-2 and C-3, see Fig. 3) and downwards (substituents at C-6). The substrates (*S*)-**1** and (*R*)-**1** were placed vertically in both orientations (Fig. 3) in the cavity of **2**.

Following this, the energy was minimized (under vacuum at 0 K) and then an MD simulation using the Discover program (version 2.6) over five picoseconds (ps) was carried out.[8] During the first picosecond the simulation proceeded at a temperature of 3 K, in order to carefully relax the possibly existing large strains of the energy-minimized structures. In the course of the second to fifth picosecond the temperature was 300 K. Both the "*S*-down" and the "*R*-down" complexes proved to be unstable. Already, after the third picosecond, the guest molecule has left the cavity of **2** (Fig. 4a, b). After 5 ps, the host and guest are completely separated. A return is not likely as a result of the high speed of the substrate.

The "*S*-up" complex proved to be the most stable. After the fifth picosecond, the substrate is still found in the cavity of **2** (Fig. 4c). For the "*R*-up" complex, after this time, the guest molecule is outside the cavity but still in the active region of the hydrophobic side-chains (Fig. 4d).

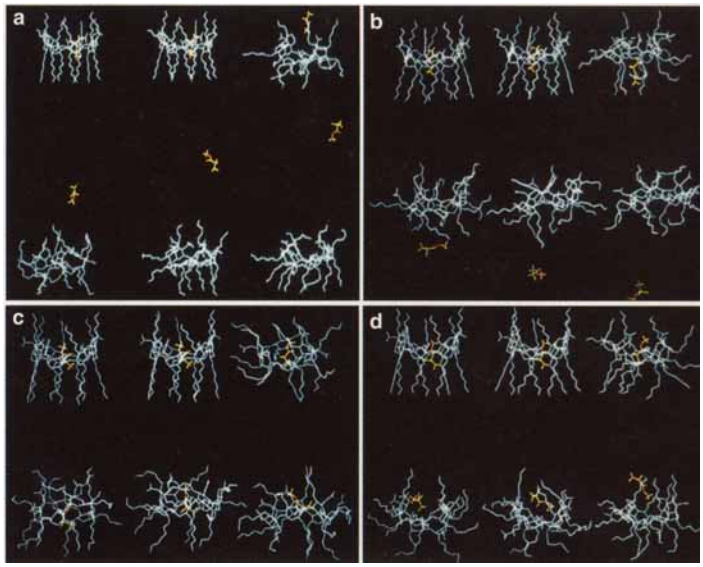

Fig. 4. Molecular dynamic trajectories over 5 ps for the complexes "S-down" (a), "R-down" (b), "S-up" (c), and "R-up" (d) from **1** (yellow and orange) and **2** (blue). The upper left picture shows the starting structure of each, next to which are shown the simulated structures obtained after 1 and 2 ps, and in the second row, those occurring after 3, 4, and 5 ps. Further explanations see text.

These results are in agreement with the GC and NMR results, which show that (*S*)-**1** forms the more stable complex with **2**. Furthermore, NOE measurements on the (*S*)-**1**/**2** and (*R*)-**1**/**2** systems showed that the methoxy group is, in agreement with the "up" orientation of the substrate, in the vicinity of the C-3 proton of the glucose units. A detailed spatial assignment has hitherto not been possible due to the complexity of the NMR spectra.

It should be noted, that a period of 5 ps is not sufficient for an unequivocal result, in the sense of statistical mechanics and with regard to the molecular dynamics. We will continue these studies with the aim to obtain information about the interactions existing for the complexation between host and guest molecules, from the trajectories obtained via simulations over considerably longer periods.

Received: September 17, 1991 [Z 4918 IE]
German version: *Angew. Chem.* **1992**, *104*, 362

CAS Registry numbers:
1, 40705-03-1; (*R*)-**1**/**2**, 138667-23-9; (*S*)-**1**/**2**, 138667-24-0; **2**, 120614-93-9.

[1] T. Koscielski, D. Sybilska, J. Jurczak, *J. Chromatogr.* **1983**, *280*, 131–134; D. W. Armstrong, D. J. Ward, R. D. Armstrong, T. E. Beesley, *Science* **1987**, *232*, 1132–1135; W. A. König, S. Lutz, G. Wenz, *Angew. Chem.* **1988**, *100*, 989–990; *Angew. Chem. Int. Ed. Engl.* **1988**, *27*, 979–980; W. A. König, *Nachr. Chem. Tech. Lab.* **1989**, *37*, 471–476; V. Schurig, H.-P. Nowotny, *Angew. Chem.* **1990**, *102*, 969–986; *Angew. Chem. Int. Ed. Engl.* **1990**, *29*, 939–956.

[2] D. D. MacNicol, D. S. Rycroft, *Tetrahedron Lett.* **1977**, 2173–2176; T. Murakami, K. Harata, S. Morimoto, *Chem. Lett.* **1988**, 533–556.

[3] K. Harata, K. Uekama, M. Otagiri, F. Hirayama, *Bull. Chem. Soc. Jpn.* **1987**, *60*, 497–502; J. A. Hamilton, L. Chen, *J. Am. Chem. Soc.* **1988**, *110*, 5833–5841.

[4] W. A. König, S. Lutz, G. Wenz, E. von der Bey, *HRC8CC J. High Resolut. Chromatogr. Chromatogr. Commun.* **1988**, *11*, 506–509.

[5] J. Canceill, L. Lacombe, A. Collet, *J. Am. Chem. Soc.* **1985**, *107*, 6993–6996.

[6] W. F. van Gunsteren, H. J. C. Berendsen, *Angew. Chem.* **1990**, *102*, 1020–1055; *Angew. Chem. Int. Ed. Engl.* **1990**, *29*, 992–1027.

[7] C. Betzel, W. Saenger, B. E. Hingerty, G. M. Brown, *J. Am. Chem. Soc.* **1984**, *106*, 7545–7557.

[8] J. Maple, U. Dinur, A. T. Hagler, *Proc. Natl. Acad. Sci. USA* **1988**, *85*, 5350-5354; we have used the CVFF force field without cross terms with harmonic potential.

New Intermediate Steps in the Synthesis of Larger Nickel Clusters**

By *Dieter Fenske,** *Harald Krautscheid,* and *Michael Müller*

Phosphane complexes of electron-rich transition metal halides react in organic solvents with silyl derivatives of the elements P, As, Sb, S, Se, and Te with the loss of $SiMe_3Hal$, affording metal-rich clusters.[1] Thus, for example, nickel clusters with 3 to 34 nickel atoms can be isolated from the reaction of $[NiCl_2(PPh_3)_2]$ with $Se(SiMe_3)_2$.[1, 2] These reactions always result in a mixture of cluster complexes, whose structures are influenced by the solvent, the stoichiometric ratio of the starting materials, and the nature of the tertiary phosphanes. To investigate these influences we treated $Se(SiMe_3)_2$ with $[NiCl_2(PR_2R')_2]$ (R = *i*Pr, Phe (Phe = C_2H_4Ph), Et; R' = *i*Pr, Me, Ph) in THF.[3] In addition to the previously discussed cluster complexes we have now been able to isolate and structurally characterize the compounds **1**–**6**.[4, 5]

$[Ni_4Se_3(PPhe_3)_5]$ **1**

$Se(SiMe_3)_2$ → $[NiCl_2(PPhe_3)_2]$ → **3** $[Ni_7Se_5(PiPr_3)_6]$ + $[Ni_8Se_6(PiPr_3)_4]$ **4**

$Se(SiMe_3)_2$ $\xrightarrow{[NiCl_2(PEt_2Me)_2]}$ $[Ni_5Se_4Cl_2(PEt_2Me)_6]$ **2**

$Se(SiMe_3)_2$ → $[NiCl_2(PiPr_3)_2]$ → $[Ni_8Se_6(PEt_2Ph)_6]$ **5** + $[Ni_{21}Se_{14}(PEt_2Ph)_{12}]$ **6**

The cluster complexes **1**–**6** form black crystals whose IR and NMR spectra are not very informative. Following the cluster formation by ^{31}P NMR spectroscopy it can be seen that a) the reactions are only complete after 15–20 days; b) the phosphane selenide $R_2R'PSe$ is always formed as a by-product; c) in the reaction solution, together with other compounds, complexes of the formula $[Ni_3Se_2X_2(PR_2R')_4]$ (X = Cl, $SeSiMe_3$) **7** are always formed.

Complex **7** contains a Ni_3 cluster capped by two μ_3-Se ligands, in which PR_2R' groups and Cl^- or $SeSiMe_3$ ligands are additionally bonded to the Ni centers. It appears that **7** is an important intermediate in the synthesis of metal-rich clusters. The formation of **1** and **2** can be explained as resulting from the reaction of $Se(SiMe_3)_2$ with $[NiCl_2(PPhe_3)_2]$ or $[NiCl_2(PEt_2Me)_2]$ with the reactive Ni–X bonds of **7**.

The structure of **1** (Fig. 1, top) contains a severely distorted Ni_4 tetrahedron (Ni–Ni: 239.3–288.9 pm), in which, as a result of the steric protection from the $PPhe_3$ ligands, only two (of four) faces of the tetrahedron are capped by μ_3-Se (Se1, Se2) ligands. Additionally, Se3 acts as a μ_2-bridge. Due to the phosphanes coordinated to Ni, only Ni3 and Ni4 have similar chemical environments. Ni2 is trigonal-planar, bonded to P2, Se1, and Se2, and Ni1 is tetrahedrally coordinated. Although complex **1** with its 60 VE (valence electrons) fulfills the 18-electron rule for tetrahedral clusters, the Ni_4 cluster is, as mentioned previously, severely distorted.

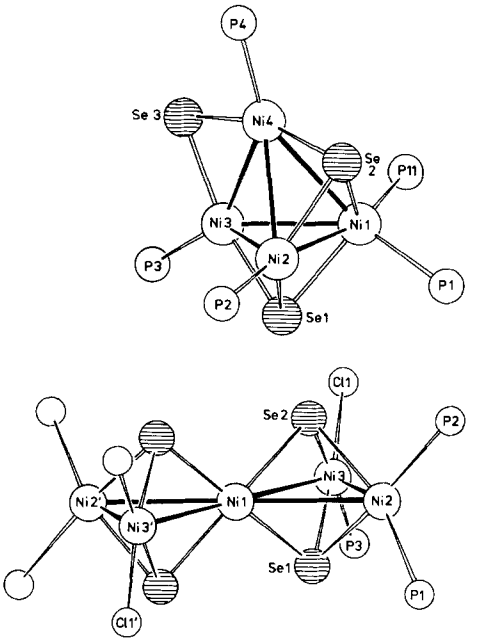

Fig. 1. Molecular structures of **1** (top) and **2** (bottom) (C atoms omitted for clarity). Important distances (± 0.3 pm) and angles (± 0.1°): **1**: Ni1-Ni2 239.3, Ni1-Ni3 283.3, Ni1-Ni4 279.5, Ni2-Ni3 288.9, Ni2-Ni4 288.3, Ni3-Ni4 265.8 (μ_3-Se)-Ni 223.0–238.6, (μ_2-Se)-Ni 221.9–223.4; Ni3-Se3-Ni4 73.3, Ni-(μ_3-Se)-Ni 61.4–79.2, Ni-Ni-Ni 49.4–67.0. **2**: Ni1-Ni2 294.2, Ni1-Ni3 322.8, Ni2-Ni3 298.3, (μ_3-Se)-Ni 229.2–234.5, Ni3-Cl1 223.3; Ni-Se-Ni 78.5–89.2, Ni2-Ni1-Ni3 57.6, Ni1-Ni3-Ni2 56.4, Ni1-Ni2-Ni3 66.0, Ni2-Ni1-Ni2' 180.0, Ni2-Ni1-Ni3' 122.4.

Complex **2** (Fig. 1, bottom) consists of a planar spirocyclic Ni_5 cluster with $\bar{1}$ symmetry which is formed from two vertex-sharing Ni_3 units, both of which are capped by two μ_3-Se ligands. The structural similarity of **2** and **7** is clearly shown by the fact that in **2**, a Ni atom (Ni2) is also bonded to two PEt_2Me ligands, and Ni3 to Cl^- and PEt_2Me ligands. This results in all the Ni atoms exhibiting a slightly distorted square-planar coordination geometry. The structure of **2** is similar to those of $[Pd_5Se_4Cl_2(PPh_3)_6]$, $[NiPd_4S_4Cl_2(PPh_3)_6]$, and a spirocyclic $HgNi_4$ cluster complex recently reported by Kubiak et al.[7] Based on the Ni–Ni distances in **2** (294.2–322.8 pm), it can no longer be assumed that bonding interactions exist between the metal atoms, each of which, after the 80 VE contained in **2** have been formally divided, have 16 VE per Ni center.

Figure 2 shows the structure of **3**, characteristic of which is a mirror plane through the atoms Se1, Se2, Se4, Ni1, Ni2, and Ni5. The structure can be described as consisting of two vertex-sharing tetrahedra. In accordance with the principle for the condensation of clusters this (previously unknown) cluster type contains 102 VE.[15] In the tetrahedron Ni1, Ni3, Ni3', and Ni5 the Ni–Ni distances range from 258.3–280 pm. The shorter bonds connect to Ni5 which is also bonded to the Ni atoms of the second tetrahedron (Ni2, Ni4, and Ni4') which has much shorter Ni–Ni distances (233–234 pm). Similar short Ni–Ni bonds have only previously been found in binuclear complexes such as $[Cp_2Ni_2X_2]$ (X = MeCN, Ph_2C_2, CO).[8] The distances between Ni2, Ni4, and Ni4' of 330 pm are greater than those reported for Ni–Ni bonding.

The polyhedral faces of the bitetrahedra are capped by one μ_3-SeH ligand and four μ_4-Se (Se1, Se2, Se3, Se3') ligands. A topological relationship between the structures of **3**, **7**, and **1** appears to exist. **3** shows an obvious relationship to previously isolated compounds, for example $[Ni_8S_5(PPh_3)_7]$,

[*] Prof. Dr. D. Fenske, Dr. H. Krautscheid, Dipl.-Chem M. Müller, Institut für Anorganische Chemie der Universität Engesserstrasse, Geb.-Nr. 30.45, D-W-7500 Karlsruhe (FRG)

[**] This work was supported by the Deutsche Forschungsgemeinschaft and the Fonds der Chemischen Industrie.

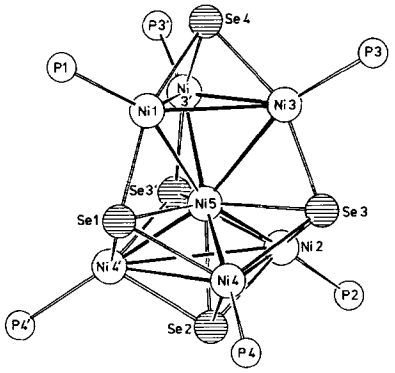

Fig. 2. Molecular structure of **3** (C atoms omitted for clarity). Important distances (± 0.3 pm) and angles (± 0.1°): Ni1-Ni3 274.4, Ni1-Ni5 258.3, Ni2-Ni5 233.0, Ni3-Ni5 259.4, Ni3-Ni3' 280.0, Ni4-Ni5 234.0, Se4-Ni 227.1 und 228.1 (μ_4-Se)-Ni 227.4–251.2, Ni-P 214.3–218.9; Ni1-Se4-Ni3 74.1, Ni2-Se2-Ni5 56.9, Ni2-Se2-Ni4 95.1, Ni2-Se3-Ni4 88.9, Ni3-Se3-Ni4 105.0, Ni2-Ni5-Ni4 96.3, Ni2-Ni5-Ni3 96.5, Ni1-Ni5-Ni2 156.4, Ni1-Ni5-Ni3 64.0, Ni1-Ni3-Ni5 57.8, Ni3-Ni1-Ni5 58.2.

which contains two edge-sharing Ni_5 bipyramids, and $[Ni_9E_9(PPh_3)_6]$ (E = S, Se), consisting of a Ni_9 cluster formed from two face-sharing Ni_6 octahedra.[1, 9] **3** is a probable intermediate on the way to clusters with *trans* face-sharing octahedra of the formula $[Ni_{3n+3}E_{3n+3}(PR_3)_6]$.

The synthesis of **4** (Fig. 3, top) clearly illustrates that other clusters can be formed under the same conditions. Complex **4** consists of a central, almost regular tetrahedron Ni5–Ni8 (indicated by dashed lines in Fig. 3) onto whose tetrahedral faces a further four Ni atoms (Ni1–Ni4) are bonded. The Ni–Ni bonds in the inner tetrahedron (281.1–284.6 pm) are considerably longer than those to the peripheral Ni atoms (247.6–250.1 pm). Alternatively, the eight Ni centers may be considered as being the vertices of a cube, which as a result of strong interactions along the face-diagonals, has been distorted into a dodecahedron consisting of irregular triangles. This distortion is a result of the varying coordination of the Ni atoms.

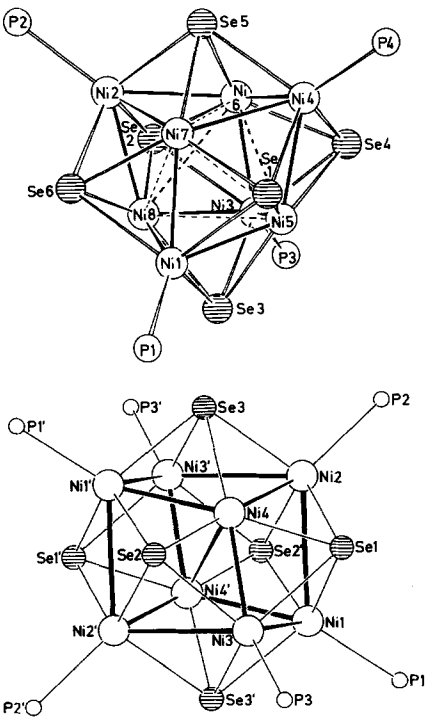

Fig. 3. Molecular structures of **4** (top) and **5** (bottom) (C atoms omitted for clarity). Important distances (± 0.4 pm) and angles (± 0.1°): **4**: Ni-Ni 247.6–250.1 und 281.1–284.6, Ni-Se 227.5–230.1 und 242.2–245.6, Ni-P 218.7–220.0; Ni1-Se1-Ni5 63.7, Ni1-Se1-Ni4 110.9, Ni5-Se1-Ni7 76.6, Ni5-Ni1-Ni7 69.4, Ni1-Ni5-Ni3 107.8, Ni1-Ni5-Ni7 55.1, Ni1-Ni5-Ni6 104.0, Ni6-Ni5-Ni7 60.3. **5**: Ni-Ni4 238.3, Ni4-Ni4' 266.7, Ni1-Ni2 277.9, Ni1-Ni3 274.7, Ni2-Ni3' 273.5, (μ_4-Se)-Ni 225.3–226.3 und 239.9–247.2, Ni-P 221.0–221.6; Ni1-Ni2-Ni3' 92.4, Ni2-Ni1-Ni3 93.5, Ni2'-Ni3-Ni1 93.7, Ni4-Ni2-Ni1 73.3, Ni2-Ni4-Ni3 115.2, Ni2-Ni4-Ni1' 114.2, Ni1'-Ni4-Ni3 113.2, Ni4'-Ni4-Ni3 75.2, Ni2-Ni4-Ni4' 76.8.

Whereas Ni5–Ni8 are each bonded to three Se ligands, Ni1–Ni4 are coordinated to three Se and one $PiPr_3$ ligands. The differing coordination of the Ni atoms probably arises from the large steric demands of the $PiPr_3$ groups.[10] This is shown in the space-filling model for the structure of **4**, in which further coordination of ligands is not possible, since the free coordination sites at Ni5–Ni8 are effectively protected by the *i*Pr groups.

Complex **4** has 112 VE and therefore fits the series of known cubic Ni_8 clusters. A shortening of the Ni–Ni bonds and a distortion of the Ni_8 cube is observed with an increasing deviation from the expected valence electron number (120 VE).[11] The ratio r of the length of the face-diagonal to the length of the edge of the cube can be used as a measure of the distortion. In clusters with 120 VE, for example $[Ni_8S_6(PPh_3)_8]$ or $[Ni_8Se_6(PnBu_3)_8]$, regular Ni_8 cubes (Ni–Ni: 270 pm) are found with $r = 1.41$.[11] In contrast, for $[Ni_8(PPh)_6(PPh_3)_4]$ (Ni–Ni: 251.7–254.1; Ni···Ni: 323–325 pm) containing 112 VE r = 1.28, and in **4** this value is further reduced to 1.14.[12] The differing bonding situations of the Ni centers also have an influence influence on the Ni–Se bond lengths, which for the Ni atoms with the coordination number three (Ni5–Ni8) of 227.5–230.1 pm are about 15 pm shorter than those for the Ni atoms with the coordination number four (Ni1–Ni4) (242.2–245.6 pm).

The controlling influence of the ligands on the cluster structure is clearly illustrated by the molecular structure of **5**. As in **4**, a distorted cube ($\bar{1}$ symmetry) exists, whose cubic faces are capped by μ_4-Se ligands. Six Ni atoms show the coordination number four and are bonded to three Se and one PEt_2Ph ligand (Ni1, Ni2, Ni3, Ni1', Ni2', Ni3'), whereas Ni4 and Ni4'are bonded only to three Se ligands. This coordination deficiency leads to a distortion of the Ni_8 cube along the solid-diagonal (Ni4–Ni4' 266.7 pm). The bonds from Ni4 to Ni1', Ni2, and Ni3 of 238.3 pm are considerably shorter than the other Ni–Ni distances (266.7–277.9 pm). In **5**, as in **4**, the Ni–Se bonds (225.3–226.3 pm) to the Ni centers with the coordination number three are approximately 14–21 pm shorter than those to the Ni centers with the coordination number four. Complex **5** contains 116 VE, four electrons fewer than would be expected for a cubic cluster.

The metal-rich cluster complex **6** can be isolated—depending on the reaction time—from the reaction of $[NiCl_2(PEt_2Ph)_2]$ with $Se(SiMe_3)_2$. Its structure ($\bar{1}$ symmetry) consists of a central Ni_{13} cuboctahedron (Ni5–Ni11 and the inversion-related Ni atoms) of which two Ni_4 faces (Ni5–Ni8, Ni5'–Ni8') are bonded to Ni1–Ni4 forming two cubes (Fig. 4). All Ni–Ni distances lie in the range 257.6–280.0 pm and correspond to the values observed in other selenium-capped Ni clusters.[1] The central, slightly distorted cuboctahedron represents a section of a face-centered cubic packing. Previously reported compounds containing this structure fragment include; $[Pt_6Ni_{38}(CO)_{48}H_2]^{4-}$, $[Pd_{38}(CO)_{28}(PEt_3)_{12}]$ and $[Pd_{23}(CO)_{22}(PEt_3)_{10}]$.[13]

The structure of the Ni_{21} framework can be regarded as an intermediate step to a series of "super clusters", in which a central M_{13} cuboctahedron is surrounded by n shells which contain $(10n^2 + 2)$ metal atoms ($n \geq 2$). This principle proposed by G. Schmid is illustrated by $[M_{55}Cl_6(PPh_3)_{12}]$ (M = Rh, Au).[14] In **6**, Ni1–Ni4 and Ni1'–Ni4' can be con-

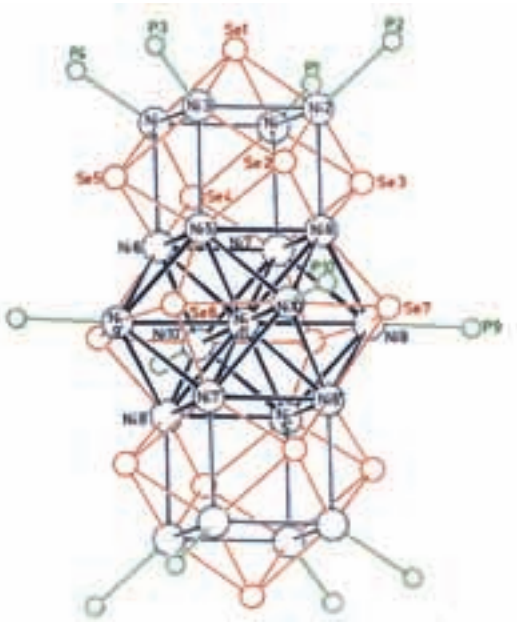

Fig. 4. Molecular structure of **6** (C atoms omitted for clarity). Ni: blue, Se: red, P: green. Important distances (± 0.2 pm) and angles (± 0.1°): In the cuboctahedron: Ni-Ni 260.6–272.4, Ni11-Ni 257.6–280.0; in den Ni_8-Kuben: Ni1-Ni2 263.8, Ni2-Ni3 265.7, Ni3-Ni4 265.1, Ni1-Ni7 262.1, Ni2-Ni8 259.3, Ni3-Ni5 261.4, Ni4-Ni6 262.3, (μ_4-Se)-Ni 231.0–241.9, Ni-P 219.4–225.8; Ni2-Ni1-Ni7 91.1, Ni1-Ni4-Ni3 90.3, Ni6-Ni11-Ni7 61.1, Ni8'-Ni11-Ni5 62.0, Ni7-Ni11-Ni9' 121.4, Ni7-Ni11-Ni9 58.5.

sidered as being part of a second shell, which could contain a maximum of 42 Ni atoms.

The metal framework is stabilized by 14 μ_4-Se capping ligands (Ni–Se 231.0–241.9 pm). Additionally, the Ni periphery (Ni1–Ni4, Ni9, Ni10, and the inversion-related Ni atoms) is bonded to 12 PEt_2Ph groups which provide full protection of the $Ni_{21}Se_{14}$ core. Complex **6** contains 290 VE, which is 16 electrons more than is predicted by the 18-electron rule if all Ni–Ni bonds shown in Figure 4 are considered as two-center two-electron bonds. The principle for condensation of clusters from D.M.P. Mingos affords a valence electron number of 286 which is in good agreement with the valence electron number of **6**.[15]

Received: October 21, 1991 [Z 4983 IE]
German version: Angew. Chem. **1992**, *104*, 309

CAS Registry numbers:
1, 138407-33-7; **2**, 138384-25-5; **3**, 138458-77-2; **4**, 138458-76-1; **5**, 138458-78-3; **6**, 138628-92-9; $[NiCl_2(PEt_2Me)_2]$, 138384-26-6; $[NiCl_2(PPhe_3)_2]$, 128213-14-9; $[NiCl_2(PEt_2Ph)_2]$, 17523-33-0; $[NiCl_2(PiPr_3)_2]$, 17731-65-6; $Se(SiMe_3)_2$, 4099-46-1.

[1] D. Fenske, J. Ohmer, J. Hachgenei, K. Merzweiler, *Angew. Chem.* **1988**, *100*, 1300; *Angew. Chem. Int. Ed. Engl.* **1988**, *27*, 1277.

[2] D. Fenske, J. Hachgenei, J. Ohmer, *Angew. Chem.* **1985**, *97*, 684; *Angew. Chem. Int. Ed. Engl.* **1985**, *24*, 706; *ibid.* **1985**, *97*, 993 and **1985**, *24*, 993; D. Fenske, J. Ohmer, *ibid.* **1987**, *99*, 155 and **1987**, *26*, 148.

[3] **1–6** (Typical procedure): $[NiCl_2(PR_2R')_2]$ (4 mmol) was dissolved in 50 mL of THF. Following addition of $Se(SiMe_3)_2$ (1 mL, 4 mmol) the solution turned dark brown. After two weeks all the volatile components were distilled off at room temperature. Recrystallization of the residue from diethyl ether (**1** and **2**) or heptane (**3**–**6**) afforded crystals suitable for X-ray analysis. Yields 10–40%.

[4] X-ray structure analyses: Stoe Stadi IV, $Mo_{K\alpha}$, empirical absorption correction; data collection and refinement: ω-Scan (profile analysis). **1** 0.5 Et_2O: Crystal data, (230 K): $a = 1416.0(9)$, $b = 1423.9(9)$, $c = 2816.7(14)$ pm, $\alpha = 100.08(4)$, $\beta = 95.09(4)$, $\gamma = 98.56(4)°$, $V = 5491 \cdot 10^6$ pm^3; space group $P\bar{1}$ (No. 2), $Z = 2$, $\mu(Mo_{K\alpha}) = 17.1$ cm^{-1}, $2\theta_{max} = 52°$; 19781 reflections, of which 13018 were unique with $I > 2\sigma(I)$, 739 parameters (Se, Ni, P, C anisotropic), $R_1 = 0.076$, $R_2 = 0.056$. – **2**: Crystal data (200 K): $a = 911.9(5)$, $b = 1201.0(6)$, $c = 2369.9(13)$ pm, $\beta = 107.3(4)°$, $V = 2550 \cdot 10^6$ pm^3; space group $P2_1/n$ (No. 14), $Z = 2$; $\mu(Mo_{K\alpha}) = 48.4$ cm^{-1}, $2\theta_{max} = 54°$; 6367 reflections, of which 3677 were unique with $I > 2\sigma(I)$. 215 parameters (Se, Ni, Cl, P, C anisotropic, the positions of the H atoms were calculated), $R_1 = 0.067$, $R_2 = 0.046$. – **3**: Crystal data (200 K): $a = 1321.5(6)$, $b = 2221.0(11)$, $c = 1326.0(7)$ pm, $\beta = 112.0(3)°$, $V = 3608 \cdot 10^6$ pm^3, space group $P2_1/m$ (No. 11), $Z = 2$; $\mu(Mo_{K\alpha}) = 43.3$ cm^{-1}, $2\theta_{max} = 56°$; 8620 reflections, of which 5417 were unique with $I > 2\sigma(I)$, 313 parameters (Se, Ni, P anisotropic), $R_1 = 0.069$, $R_2 = 0.048$. – **4**: Crystal data (200 K): $a = 1474.8(13)$, $b = 2019.4(12)$, $c = 2070.6(13)$ pm, $\alpha = 98.93(4)$, $\beta = 100.20(4)$, $\gamma = 106.55(3)°$, $V = 5678 \cdot 10^6$ pm^3, space group $P\bar{1}$ (No. 2), $Z = 4$, $\mu(Mo_{K\alpha}) = 63.8$ cm^{-1}, $2\theta_{max} = 50°$; 18936 reflections, of which 11754 were unique with $I > 2\sigma(I)$; 897 parameters (Se, Ni, P, C anisotropic), $R_1 = 0.086$, $R_2 = 0.079$. In the asymmetric unit, two independent molecules of **4** crystallize, however, these can be considered identical within the bounds of standard deviation. **5**: Crystal data (290 K): $a = 1505.6(9)$, $b = 1224.3(6)$, $c = 1985.7(10)$ pm, $\beta = 94.43(4)$, $V = 3649.5 \cdot 10^6$ pm^3; space group $P2_1/n$ (No. 14), $Z = 2$, $\mu(Mo_{K\alpha}) = 100.35$ cm^{-1}, $2\theta_{max} = 52°$; 8461 reflections, of which 5350 were unique with $I > 2\sigma(I)$; 328 parameters (Se, Ni, P, C anisotropic, the positions of the H atoms were calculated), $R_1 = 0.077$, R_2 0.067. – **6**: THF: Crystal data (200 K): $a = 1509.9(19)$, $b = 1647.5(8)$, $c = 1809.9(19)$ pm, $\alpha = 103.44(4)$, $\beta = 96.00(4)$, $\gamma = 115.71(5)°$, $V = 3845 \cdot 10^6$ pm^3; space group $P\bar{1}$ (No. 2), $Z = 1$, $\mu(Mo_{K\alpha}) = 58.02$ cm^{-1}, $2\theta_{max} = 54°$; 15600 reflections, of which 11588 were unique with $I > 2\sigma(I)$, 709 parameters (Se, Ni, P, C anisotropic, the positions of the H atoms were calculated), $R_1 = 0.047$, $R_2 = 0.042$.

[5] Further details of the crystal structure investigation may be obtained from the Fachinformationszentrum Karlsruhe, Gesellschaft für wissenschaftlich-technische Information mbH, D-W-7514 Eggenstein-Leopoldshafen 2 (FRG) on quoting the depository number CSD-55942, the names of the authors, and the journal citation.

[6] D. Fenske, H. Fleischer, H. Krautscheid, J. Magull, *Z. Naturforsch. B.* **1990**, *45*, 127.

[7] D. Fenske, H. Fleischer, H. Krautscheid, C. Oliver, S. Weisgerber, *Z. Naturforsch.* B **1991**, *46*, 1384; Jinkang Gong, Jean Hüang, P. E. Fanwick, C. B. Kubiak, *Angew. Chem.* **1990**, *102*, 407; *Angew. Chem. Int. Ed. Engl.* **1990**, *29*, 396.

[8] R. D. Adams, F. A. Cotton, G. A. Rusholme, *J. Coord. Chem.* **1971**, *1*, 275; O. S. Mills, B. W. Shaw, *J. Organomet. Chem.* **1968**, *11*, 595; A. A. Hock, O. S. Mills, *Advances in the Chemistry of Coordination Compounds*, (Ed.: S. Kirshner), Macmillan, New York, **1961**, p. 640.

[9] D. Fenske, J. Hachgenei, J. Ohmer, *Angew. Chem.* **1985**, *97*, 684; *Angew. Chem. Int. Ed. Engl.* **1985**, *24*, 706; C. A. Ghilardi, S. Midollini, L. Sacconi, *J. Chem. Soc. Chem. Commun.* **1981**, 47.

[10] C. A. Tolmann, *Chem. Rev.* **1977**, *77*, 313.

[11] D. Fenske, J. Magull, *Z. Naturforsch. B* **1990**, *45*, 121; J. K. Burdett, G. J. Miller, *J. Am. Chem. Soc.* **1987**, *109*, 4081; M. Müller, D. Fenske, unpublished results.

[12] D. Fenske, J. Hachgenei, F. Rogel, *Angew. Chem.* **1984**, *96*, 959; *Angew. Chem. Int. Ed. Engl.* **1984**, *23*, 982.

[13] A. Ceriotti, F. Demartin, G. Longoni, M. Manassero, M. Marchionna, G. Piva, M. Sansoni, *Angew. Chem.* **1985**, *97*, 708; *Angew. Chem. Int. Ed. Engl.* **1985**, *24*, 697; E. G. Mednikov, N. K. Eremenko, Y. L. Slovokhotov, Y. T. Struchkov, *J. Organomet. Chem.* **1986**, *301*, C35.

[14] G. Schmid, *Struct. Bonding* **1985**, *62*, 51; G. Schmid, B. Morun, J.-O. Malm, *Angew. Chem.* **1989**, *101*, 772; *Angew. Chem. Int. Ed. Engl.* **1989**, *28*, 778; G. Schmid, *Polyhedron* **1988**, *7*, 2321.

[15] D. M. P. Mingos, *J. Chem. Soc. Chem. Comm.* **1985**, 1352; *Chem. Soc. Rev.* **1986**, *15*, 31; *Acc. Chem. Res.* **1984**, *17*, 311; *J. Chem. Soc. Chem. Comm.* **1983**, 706; D. M. P. Mingos, R. L. Johnston, *J. Organomet. Chem.* **1985**, *280*, 419; *Struct. Bonding* **1987**, *68*, 29; B. K. Teo, G. Longoni, F. R. K. Chung, *Inorg. Chem.* **1984**, *23*, 157.

Synthesis and Structure of $[Ni(PtBu_6)]$ and $[Ni_5(PtBu)_6(CO)_5]$ and Calculations on the Electronic Structure of $[Ni(PtBu)_6]$ and $(PR)_6$, R = tBu, Me**

By *Reinhart Ahlrichs*,* *Dieter Fenske*,* *Hannes Oesen*, and *Uwe Schneider*

Cyclic phosphanes $(PR)_n$ (R = organic group, $n = 3–6$) have already been the subject of numerous studies,[1] and

[*] Prof. Dr. R. Ahlrichs, Dipl.-Chem. U. Schneider
Institut für Physikalische Chemie der Universität
Kaiserstrasse 12, D-W-7500 Karlsruhe (FRG)
Prof. Dr. D. Fenske, Dipl.-Chem. H. Oesen
Institut für Anorganische Chemie der Universität
Engesserstrasse, Geb.-Nr. 30.45, D-W-7500 Karlsruhe (FRG)

[**] This work was supported by the Deutsche Forschungsgemeinschaft and the Fonds der Chemischen Industrie.

they can be used as ligands in transition-metal complexes.[2, 3] For example, upon reaction of $(PR)_n$ with metal carbonyl compounds either derivatives with cyclic phosphane ligands or complexes with PR chains as ligands are obtained. In some cases a ring expansion of the cyclophosphane has also been observed. Thus, the mononuclear complex $[Mo(CO)_4(PEt)_5]$ is obtained upon reaction of $(PEt)_4$ with $[Mo(CO)_6]$.[4] We have now found a simple method for the synthesis of $[Ni(PtBu)_6]$ (**1**).

$NiCl_2$ was allowed to react with $P(SiMe_3)_3$ and $(PtBu)_3$ in THF affording a black solution, from which yellow crystals of **1** could be isolated in about 30% yield. Apparently **1** is formed as a result of a redox reaction of $NiCl_2$ and a ring expansion of the P_3 ring to a P_6 ring. Compound **1** is diamagnetic and decomposes slowly in solution with formation of nickel and $(PtBu)_4$.[5] In the ^{31}P NMR spectrum of **1** a resonance signal is observed at $\delta = -183$ (121.5 MHz, C_6D_6, 25 °C, H_3PO_4 ext. standard), and in the mass spectrum the molecular ion is found with the expected isotopic distribution.

$$NiCl_2 + 2(PtBu)_3 \xrightarrow[-Me_3SiCl]{P(SiMe_3)_3} [Ni(PtBu)_6] \quad \mathbf{1}$$

According to a crystal structure analysis,[6] **1** contains a P_6 ring at the center of which a Ni atom is located (Fig. 1).

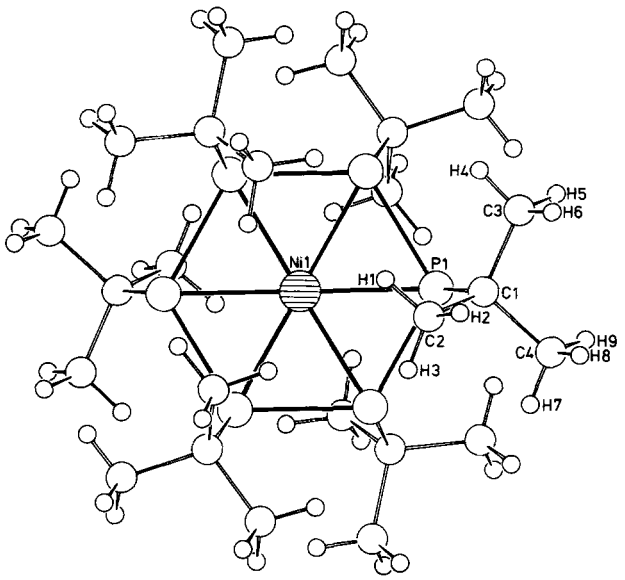

Fig. 1. Crystal structure of **1**. Important bond lengths [pm] and angles [°]: Ni-P 229.0(1), P-C 191.6(1), C-C 151.9–153.1(3), P-P 229.1(7); P-Ni-P 60.0(0), 120.0(0), 180.0(0), Ni-P-C 114.7(1), P-P-C 100.4, 104.5.

The maximum deviation of the atoms from the NiP_6 plane is ±1.1 pm. Three P atoms lie above, while the other three P atoms lie below this plane. The Ni–P distance (229.0(1) pm) is relatively large.[7] For example, in $[(PtBu)_2Ni(PtBu)_4]$ (**2**), a structural isomer of **1**, values of 215–226 pm are found for the Ni–P bond lengths.[8] A further remarkable feature are the unusually long P–P distances (229.1(1) pm) in **1**, which are about 6–12 pm longer than in free $(PPh)_6$ (223.7(5) pm), in **2** (219.6–223.7(4) pm), and in $(PtBu)_3$ (218.5–221.8 pm).[8–10]

The synthesis of **1** is remarkable, since apparently it has not hitherto been possible to isolate free $(PtBu)_6$ or to prepare complexes of this type. As illustrated in Figure 2, the Ni

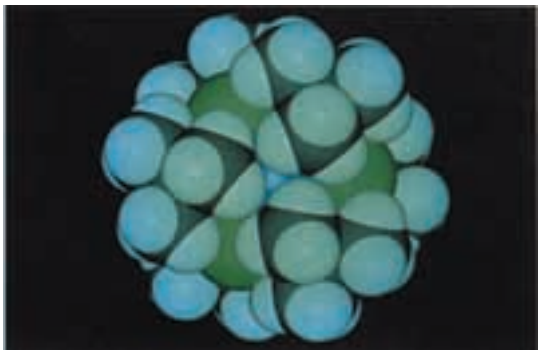

Fig. 2. Space-filling model of **1** (Ni blue, P green, H white).

atom located at the center of the P_6 ring of **1** is, however, so effectively shielded by the *t*Bu groups that this can be regarded as the reason for its stability.

The bonding situation in **1** could be described in terms of the Ni being present in the zero oxidation state. We have therefore attempted to prepare **1** by direct reaction of $(PtBu)_3$ with $[Ni(CO)_4]$ in diethyl ether. Rapid evolution of CO and concomitant formation of a dark solution was observed. After removal of the solvent by distillation, and recrystallization of the residue from pentane, black crystals of **3** were obtained. In the IR spectrum of **3** the ν(CO) vibration can be observed at 1967 cm^{-1}, and in the ^{31}P NMR spectrum four multiplets appear at $\delta = 137$, 253, 727, and 795 (121.5 MHz, C_6D_6, 25 °C, H_3PO_4 ext. standard).

$$(PtBu)_3 \xrightarrow{[Ni(CO)_4]} [Ni_5(PtBu)_3(P_3tBu_3)(CO)_5] \quad \mathbf{3}$$

3 (Fig. 3) can be regarded as an intermediate in the formation of a cluster analogous to $[Ni_8(PPh)_6(CO)_8]$ in which only three Ni atoms are missing for the construction of the

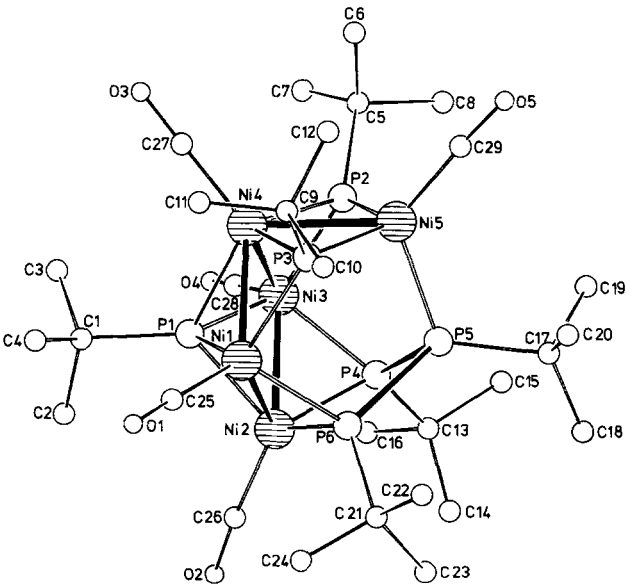

Fig. 3. Crystal structure of **3** (H atoms omitted). Important bond lengths (±0.2 pm) and angles (±0.1°): Ni1-Ni2 259.2, Ni1-Ni4 261.4, Ni2-Ni3 260.1, Ni3-Ni4 259.7, Ni4-Ni5 258.6, Ni-P1 219.5–223.3, Ni-P2 215.1–220.0, Ni-P3 214.8–220.5, Ni-P4 216.9–217.7, Ni5-P5 221.0, Ni-P6 217.0–218.4, P4-P5 225.2, P5-P6 226.2; Ni2-Ni1-Ni4 88.5, Ni1-Ni2-Ni3 91.6, Ni2-Ni3-Ni4 88.7, Ni1-Ni4-Ni3 91.2, Ni1-Ni4-Ni5 87.6, P6-P5-P4 79.7.

Ni_8 cube.[7, 11] This assumption is supported by the geometry of the Ni_5 cluster (Ni–Ni–Ni 87.6–91.6°, Ni–Ni 258.6–261.4 pm). The Ni atoms are each bound in a distorted tetrahedral fashion to a terminal CO ligand and to three P*t*Bu ligands. Different types of phosphane bridges are formed thereby. P1 acts as μ_4-bridging ligand while P2 and P3 act as μ_3-bridging ligands (Ni–P 214.8–223.3). The atoms P4–P6, on the other hand, form a P_3 chain, which is bound as a $\mu_4(\eta^2,\eta^{1'},\eta^{2''}$-ligand to Ni1, Ni2, Ni3, and Ni5 (Ni–P 216.9–220.5 pm). Apparently it is a P_3tBu_3 ligand formed by ring-opening of $(PtBu)_3$. Compound **3** fulfills the 18e-rule (80 VE) if the μ_3- and μ_4-P*t*Bu bridges are considered as 4e donors and the P_3tBu ligand as 8e donor.

To gain insights into the bonding situation and its correlation with the structure and stability of **1**, ab initio calculations[12] were carried out for **1**, $(PtBu)_6$ (**4**), $(PtBu)_4$, and the corresponding methyl compounds. MP2 calculations were also carried out, in so far as the size of the molecules allowed, in an attempt to describe approximately the electron correlation. Starting from the point group D_3, the structure of $(PtBu)_6$ (**4**) converges to a D_{3d} structure (Fig. 4). A lowering of symmetry ($D_{3d} \rightarrow D_3$) by rotation of the *t*Bu groups about the P–C axis by 9° increases the energy only slightly, by 8 kJ mol^{-1}. Within the limits of accuracy of the calculation, however, a D_3 structure cannot be ruled out.

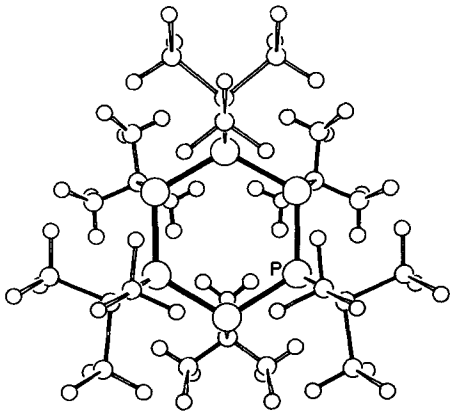

Fig. 4. Calculated molecular structure of $(PtBu)_6$ (**4**).

The P_6 ring has a slightly puckered chair form (deviation of 5.6 pm from the mean plane) with normal P–P distance.[8–10] Apparently the almost planar P_6 ring results from the steric requirement of the *t*Bu group, which is also reflected in the rather long P–C distance. In the case of $(PMe)_6$ (D_{3d}), on the other hand, a deviation from the plane of 32.3 pm and a P–C distance of 187.5 pm (4.1 pm shorter than in **4**) were obtained.

The SCF calculation of $(PtBu)_4$ yielded the structural parameters listed in Table 1. Accordingly, the SCF energy of one and a half molecules of $(PtBu)_4$ is 15 kJ mol^{-1} lower than that of **4**, even though P_4 rings are generally not very stable (as is also reflected in the P–P distance, which is elongated by 1.3 pm compared to that in the P_6 ring). The steric requirement of the *t*Bu group in $(PtBu)_4$ is easier to satisfy than in **4**. It is understandable, therefore, that **1** (in an unknown way) reacts with formation of $(PtBu)_4$. In the calculations for **1**, a closed-shell atomic wave function ($^1A_{1g}$ in D_{3d} and $^1A_1$ in D_3) was used, since **1** is diamagnetic. Subsequent calculations of triplet states always led to higher energy: **4** has no unoccupied low-lying MOs which could accept an electron from Ni. Optimization of the structure led to D_3 symmetry; the energy, however, is only 1.6 kJ mol^{-1} lower than for D_{3d} symmetry.

Table 1. Structure parameters of $(PtBu)_4$, **1**, and **4** calculated by SCF methods [12].

	$(PtBu)_4$	**1**	**4**
Point group	D_{2d}	D_3	D_{3d}
Distances [pm]			
Ni-P	–	231.8	–
P-P	224.0	230.4, 233.3	222.7
P-C	192.3	191.7	191.6
C-C	154.0–154.6	153.5, 154.6	153.5–154.4
Angles [°]			
P-P-P	83.9	120.0	119.7
P-P-C	108.1	102.0, 103.7	102.5
Ni-P-C	–	116.5	–
center-P-C	–	–	119.9
E_{SCF} [au]	−1989.07488	−4490.20551	−2983.60672

A comparison of the calculated structure parameters of **1** (Table 1) with those of the crystal structure analysis shows agreement within 3 pm/3°. This is remarkable, since larger errors were to be expected in the case of the calculation. Noticeable features in comparison with **4** are the longer (by 8 pm) P–P distance and a further planarization of the P_6 ring (deviation of the P atoms of 0.2 pm from the plane). The stability of **1** is obviously not due to cage effects, since **1** is considerably more stable than Ni + **4**.[13]

Population analyses[14] show that Ni is present in the zero oxidation state. The two methods of analysis gave net charges (over all atoms) of less than 0.2e.

The analysis according to Mulliken is particularly informative regarding the bonding situation. It furnishes the following valence populations: **4**: P $3s^{1.67}3p^{3.24}3d^{0.14}$; **1**: P $3s^{1.75}3p^{3.21}3d^{0.15}$, Ni $3d^{9.51}4s^{0.27}4p^{0.05}$. To a first approximation, Ni is present in the electronic configuration $3d^{10}$. The electron transfer in the Ni-4s AO is compensated by back bonding from the Ni-d_{xy}, and Ni-$d_{x^2-y^2}$ AOs (occupation in each case 1.78) to P–P antibonding e* MOs of the ring. This is seen in the strong interaction of these Ni AOs with the MOs of the P_6 ring, which is also reflected in the expansion of the ring. The electronic structure of **1** cannot be described in terms of the 18e rule. Electron correlation effects[13] are decisive for the stability of **1**, as is also the case for other Ni^0 compounds.[15]

Experimental Procedure

1: A suspension of anhydrous $NiCl_2$ (0.8 g, 6.2 mmol) in THF (50 mL) was treated with tri-*tert*-butylcyclotriphosphane (3.26 g, 12.4 mmol) and $P(SiMe_3)_3$ (1.0 g, 4.0 mmol). After a short time the $NiCl_2$ dissolved to give a black solution, from which a yellow oil separated. The solvent was removed by distillation, and the resulting residue was dissolved in pentane (40 mL). After filtration from the insoluble residue, large yellow crystals of **1** crystallized from the filtrate. Yield: 1.08 g (30%).

3: A solution of $(PtBu)_3$ (1 g, 3.8 mmol) in THF (20 mL) was treated at 20 °C with $[Ni(CO)_4]$ (1.29 g, 7.6 mmol). The solution darkened with concomitant evolution of CO. After 2 h the solvent was removed in a vacuum and the residue was recrystallized from pentane. Compound **3** crystalllized in the form of *black crystals*. Yield: 1.45 g (80%).

Received: October 31, 1991 [Z 5001 IE]
German version: *Angew. Chem.* **1992**, *104*, 312

CAS Registry numbers:
1, 138354-03-7; **3**, 138354-04-8; **4**, 138384-29-9; $NiCl_2$, 7718-54-9; $(PtBu)_3$, 61695-12-3; $P(SiMe_3)_3$, 15573-38-3; $[Ni(CO)_4]$, 13463-39-3.

[1] L. Maier, *Helv. Chim. Acta* **1966**, *49*, 1119; M. Baudler, C. Gruner, *Z. Naturforsch. B* **1976**, *31*, 1311; M. Baudler, B. Carlsohn, B. Kloth, D. Koch, *Z. Anorg. Allg. Chem.* **1977**, *432*, 67; W. Hölderich, G. Fritz, *ibid.* **1979**, *457*, 127; M. Baudler, J. Hellmann, *Z. Naturforsch. B* **1981**, *36*, 266.

[2] A. M. Caminade, J. P. Majoral, R. Mathieu, *Chem. Rev.* **1991**, *91*, 575.
[3] H. G. Ang, B. O. West, *Aust. J. Chem.* **1967**, *20*, 1133; M. Baudler, F. Salzer, J. Hahn, *Z. Naturforsch. B* **1982**, *37*, 1529; A. L. Rheingold, M. E. Fountain, *Organometallics* **1984**, *3*, 1471; B. O. West in *Homoatomic Rings, Chains and Macromolecules of Main-Group Elements* (Ed.: A. L. Rheingold), Elsevier, Amsterdam, **1977**, p. 409.
[4] H. G. Ang, J. S. Shannon, B. O. West, *Chem. Commun.* **1965**, 10; M. A. Bush, P. Woodward, *J. Chem. Soc. A* **1968**, 1221.
[5] M. Baudler, J. Hahn, H. Dietsch, G. Fürstenberg, *Z. Naturforsch. B* **1976**, *31*, 1305.
[6] X-ray structure analysis: Stoe Stadi IV, $MO_{K\alpha}$, empirical absorption correction, data collection and refinement: ω-scan, profile analysis. **1**: lattice constants (200 K): $a = b = 1040.9(1)$, $c = 2486.4(4)$ pm, $\alpha = \beta = 90°$, $\gamma = 120°$, $V = 2333.0 \times 10^6$ pm^3; space group $R\bar{3}$ (No. 148), $Z = 3$, $\mu(Mo_{K\alpha}) = 8.8$ cm^{-1}, $2\theta_{max} = 54°$; 1136 reflections, 1047 with $I > 2\sigma(I)$, Ni,P,C anisotropic, H isotropic (84 parameters), $R_1 = 0.026$, $R_2 = 0.033$, $S = 1.28$.—**3**: lattice constants (200 K): $a = 1163.1(9)$, $b = 1181.5(8)$, $c = 1880.0(9)$ pm, $\alpha = 107.75(3)$, $\beta = 90.31(3)$, $\gamma = 118.66(4)°$, $V = 2123.2 \times 10^6$ pm^3; space group $P\bar{1}$ (No. 2), $Z = 2$, $\mu(Mo_{K\alpha}) = 23.3$ cm^{-1}, $2\theta_{max} = 54°$, 9729 reflections refined, 7934 with $I > 2\sigma(I)$, Ni,P,C,O anisotropic, C atoms of the C_4H_9 groups isotropic, H of the CH_3 groups refined as rigid groups (461 parameters). $R_1 = 0.039$, $R_2 = 0.044$, $S = 0.90$.—Further details of the crystal structure investigations are available on request from the Fachinformationszentrum Karlsruhe, Gesellschaft für wissenschaftlich-technische Information mbH, D-W-7514 Eggenstein-Leopoldshafen 2 (FRG), on quoting the depository number CSD-55935, the names of the authors, and the journal citation.
[7] D. Fenske, J. Ohmer, J. Hachgenei, K. Merzweiler, *Angew. Chem.* **1988**, *100*, 1300; *Angew. Chem. Int. Ed. Engl.* **1988**, *27*, 1277.
[8] R. A. Jones, M. H. Seeberger, B. R. Whittlesey, *J. Am. Chem. Soc.* **1985**, *107*, 6424.
[9] J. J. Daly, *J. Chem. Soc.* **1965**, 4789.
[10] J. Hahn, M. Baudler, C. Krüger, Yi-Hung Tsay, *Z. Naturforsch. B* **1982**, *37*, 797.
[11] L. D. Lower, L. F. Dahl, *J. Am. Chem. Soc.* **1976**, *98*, 5046.
[12] The calculations were carried out with a Workstation IBM 6000/320 and the program system TURBOMOLE (R. Ahlrichs, M. Bär, M. Häser, H. Horn, C. Kölmel, *Chem. Phys. Lett.* **1989**, 162, 165). The following basis sets were used: Ni, a Wachters basis of type (14s,11p,6d)/[8s,7p,4d] extended by (2p,1d) (A. J. H. Wachters, *J. Chem. Phys.* **1970**, *52*, 1034); P, (11s,7p,1d)/[6s,4p,1d]. C(P-bound): (8s,4p)/[4s,2p], from: S. Huzinaga, *Approximate Atomic Wavefunctions*, Department of Chemistry Report, University of Alberta, Edmonton, Alberta, Canada, **1971**; remaining C,H: minimum basis (9s,3p)/[2s,1p], and (3s)/[1s], respectively, which were completely energy-optimized for neopentane.
[13] The reaction Ni($3d^{10}$) + **4** → **1** is 168 kJ mol^{-1} exothermic in the SCF approximation. MP2 calculations for the corresponding Me-compounds gave a further stabilization of ca. 613 kJ mol^{-1} by correlation effects, which should also apply in the case of the *t*Bu compound. Since the $^3F(3d^8\,4s^2)$ ground state of Ni is 1.83 eV (176 kJ mol^{-1}) more stable than the $^1S(3d^{10})$ state (A. A. Radzig, B. N. Smirnow: *Reference Data on Atoms, Molecules and Ions*, Springer, Berlin **1985**, p. 157) the stability of **1** can be estimated to a very rough approximation to be 600 kJ mol^{-1}.
[14] R. S. Mulliken, *J. Chem. Phys.* **1955**, *23*, 1833; C. Ehrhardt, R. Ahlrichs, *Theor. Lit. Chim. Acta* **1985**, *68*, 231, and references cited therein.
[15] M. R. A. Blomberg, U. B. Brandemark, P. E. M. Siegbahn, J. Wennerberg, C. W. Bauschlicher, Jr. *J. Am. Chem. Soc.* **1988**, *110*, 6650.

Dynamic Forcing, a Method for Evaluating Activity and Selectivity Profiles of RGD (Arg-Gly-Asp) Peptides

By *Gerhard Müller, Marion Gurrath, Horst Kessler,** and *Rupert Timpl*

A detailed knowledge of the receptor-bound conformation of substrate molecules and of the complementary receptor surface is of primary importance for rational drug design. Provided that the three-dimensional structure of a receptor or of the receptor–substrate complex are unknown, investigations of conformationally restricted model peptides containing biologically relevant recognition sequences offer a straightforward approach to characterize the requirements for binding.[1]

The tripeptide sequence RGD (Arg-Gly-Asp) was identified as a universal cell-recognition sequence within several extracellular matrix proteins. These proteins bind to transmembrane cell surface-receptors, the so-called integrins, and are involved in a variety of physiologically important processes like cell differentiation, platelet aggregation, and tumor metastasis.[2, 3]

We have synthesized several cyclic RGD peptides to study the conformational influence of the RGD sequence on the specificity of different integrin–RGD peptide interactions. In all peptides the same lead sequence was fixed in different conformations by variation of the chirality of selected residues. The peptides show a wide variety of biological activities in inhibition assays of tumor cell **adhesion**.[4] Of primary interest are the cyclic pentapeptides *cyclo*(-Arg-Gly-Asp-D-Phe-Val-) = c(RGD*F*V) (**1**) and *cyclo*(-Arg-Gly-Asp-Phe-D-Val-) = c(RGDF*V*) (**2**). Compared to the prototype linear standard peptide GRGDS and the linear parent sequence of **2**, both peptides inhibit tumor cell adhesion, mediated by the laminin fragment P1, with activities which are two orders of magnitude higher (Fig. 1).

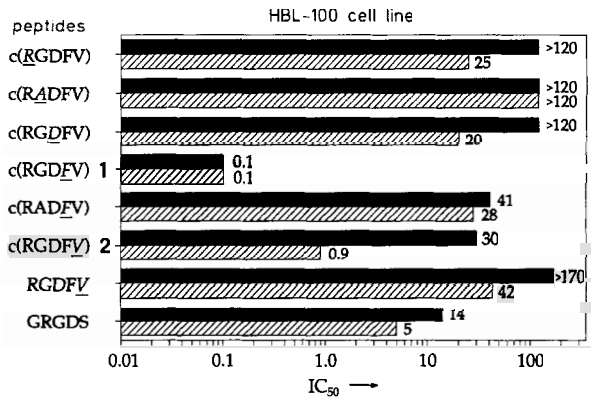

Fig. 1. IC_{50} [10^{-6} M] values of pentapeptides against laminin P1 (hatched) and vitronectin (filled) mediated tumor-cell adhesion. The D amino acid is printed in italics and underlined.

The conformation of the RGD sequence within the cyclic peptides is therefore closely related to the structure in the receptor-bound state. The increased activity of the cyclic peptide **2** compared to the linear precursor peptide RGDFV is due to a smaller loss of conformational entropy of cyclic compounds during binding.

Peptide **1** also inhibits vitronectin-mediated tumor-cell adhesion in a submicromolar range, but **2** is less active there. This demonstrates for the first time that enhanced selectivity can be achieved by conformational restriction of RGD peptides. In the following discussion, this biological observation will be correlated with structural features of the peptides by using molecular dynamics (MD) techniques.

The analysis of the conformations of peptides **1** and **2** results in identical structures for the common βII'γ turn motif. However, the position of the RGD sequences within the underlying structural templates is different in these two compounds. In peptide **1** the RGD sequence forms a tight γ turn with Gly in the central position. The Arg and Asp side chains

[*] Prof. Dr. H. Kessler, Dipl.-Chem. G. Müller, Dipl.-Chem. M. Gurrath
Institut für Organische Chemie der Technischen Universität München
Lichtenbergstrasse 4, D-W-8046 Garching (FRG)
Dr. R. Timpl
Max-Planck-Institut für Biochemie, Martinsried (FRG)

[**] This investigation was supported by the Fonds der Chemischen Industrie (doctoral fellowship for GM), the Studienstiftung des deutschen Volkes (doctoral fellowship for MG), and the Deutsche Forschungsgemeinschaft.

are oriented almost parallel to one another on the same side of the peptide ring. As expected the D residue (Phe) occupies the i + 1 position of the βII′ turn. In contrast the essential Arg and Asp side chains point in opposite directions in peptide **2**, so that the guanidino and carboxy functionalities are separated by a larger distance (Fig. 2).

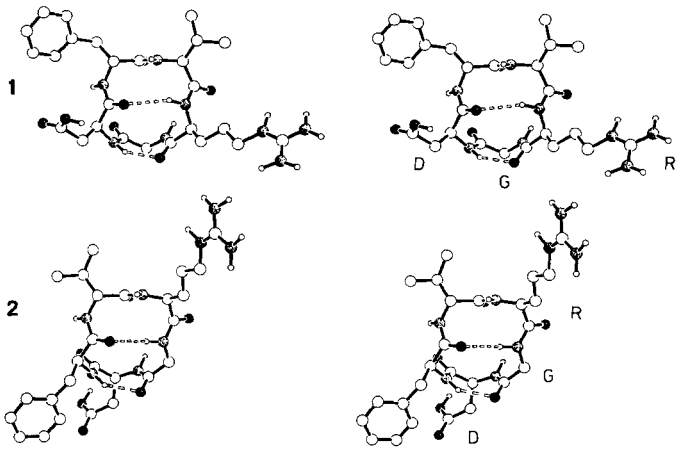

Fig. 2. Stereoplot of the NMR-derived conformations of c(RGDFV) **1** (above) and c(RGDFV) **2** (below). Oxygen atoms are filled, nitrogen atoms are shaded, and carbon atoms are shown as open spheres. Only hydrogen atoms of polar atom groups are shown explicitly. Both conformations are oriented so that the βII′ turn is located in the upper part of the molecule. The hydrogen bonds are indicated as dotted lines.

Based on the results of the inhibition experiments we propose the structure of **2** as the bioactive conformation for the laminin P1 receptor. The significantly different conformation of **1** is thought to be related to the receptor-bound conformation for the vitronectin receptor. This is sufficient to explain the interaction of the c(RGDFV)–laminin P1 receptor and the c(RGDFV)–vitronectin receptor, but not the nonselective binding of the more active peptide **1** to the laminin P1 receptor.

Valuable information was obtained for solving this contradiction from careful examination of the MD simulations. For **1** an unexpected hydrogen-bond pattern results from a 70 ps trajectory of a MD simulation in a dimethyl sulfoxide (DMSO) solvent box.[5] Peptide **1** forms the predicted hydrogen bonds between Arg^1NH and Asp^3CO and between Asp^3NH and Arg^1CO, and surprisingly an additional pair which is similar to that determined for peptide **2** (Table 1).

Table 1. Analysis of hydrogen-bond patterns over the last 70 ps of the 100 ps MD simulations of c(RGDFV) **1** and of c(RGDFV) **2**. r_{DA} = donor-acceptor distance, θ_{DHA} = donor-proton-acceptor angle.

	Donor	Acceptor	r_{DA} [pm]	θ_{DHA} [°]	Population [%]	Turn
1	Arg^1NH	Asp^3CO	341	160	41	βII
	Asp^3NH	Arg^1CO	294	139	85	γ
	Gly^2NH	Phe^4CO	348	135	20	βI *shift*
	Phe^4NH	Gly^2CO	321	134	37	γ_i *shift*
2	Gly^2NH	Phe^4CO	313	161	98	βII′
	Phe^4NH	Gly^2CO	283	142	95	γ

This fact indicates a second accessible conformation for peptide **1**, a finding which could not be extracted from any experimental data.

To verify this assumed receptor-specific transition we employed the method of *dynamic forcing*.[6] Dynamic forcing is a restrained molecular mechanics technique, in which a dihedral restraining is superimposed onto molecular dynamics simulations by extending the force field with an additional harmonic potential function that forces selected torsions into defined target values. For the simulation of **1** the main-chain dihedral angles of peptide **2** served as target values. Peptide **2** was forced to change its conformation to a structure related to that of **1**. By evaluating energetic parameters and by scaling the restraining force constant, dynamic forcing gives an impression of possible transition pathways.

Peptide **1** changes its conformation to the desired target structure of **2** during the initial phase of the 30 ps simulation (Fig. 3, center). The structural analysis of the trajectory

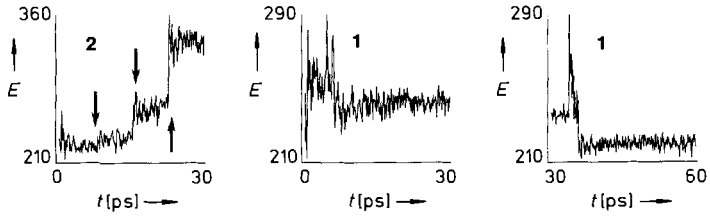

Fig. 3. Analysis of simulations with dynamic forcing for c(RGDFV) **2** (increase of the force constant is marked by arrows) and c(RGDFV) **1** of 0–30 ps as well as for **1** of 30–60 ps. E in kcal mol^{-1}.

shows stable intermediates as "snapshots" of the transition (Fig. 4). The peptide reaches a $\beta II'\gamma_i$ structure via the already populated shifted $\beta I\gamma_i$ conformation. The inverse γ turn (γ_i) then changes into a regular γ turn, so that the βII′γ target conformation, identical to that determined for **2** (Fig. 2, bottom) is adopted. The interconversion of the γ_i into the γ turn is a sterically hindered process as indicated by the energy barrier around 5–7 ps (Fig. 3, center).

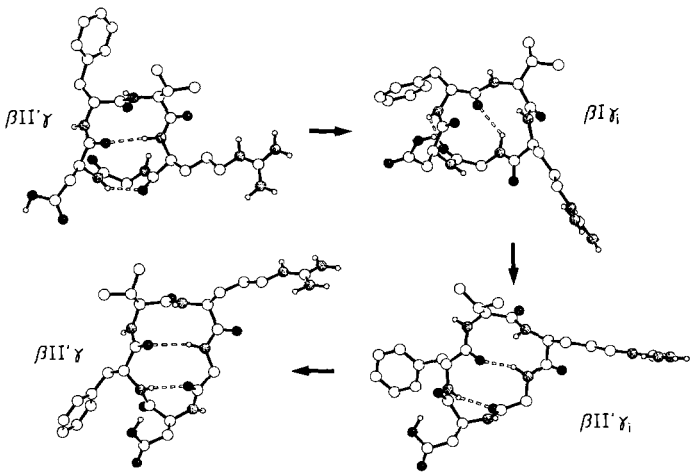

Fig. 4. Monitored intermediates of **1** with stable turn structures during the simulated conformational transition.

Peptide **2** is not able to adopt the target conformation under the same simulation conditions, although the force constant for the restraining term was increased. This is the reason for the stepwise increase in the potential energy profile for **2** in Figure 3 (left). Only energetically unfavorable conformations were observed.

We have extended the simulation of peptide **1** to 60 ps, changing the applied target torsion values after the first 30 ps

in such a way that the peptide is forced back into its initial, NMR-derived conformation. Again the peptide changes to the target structure in the initial phase of the simulation (6 ps) (Fig. 3, right). It is obvious that the NMR-derived conformation is the energetically favored structure, but the conformational transition induced by the laminin P1 receptor is easy to perform.

The positioning of the essential RGD sequence in conformationally restricted molecules that are defined by a rational design principle led to highly active and selective compounds. The combination of biological data and conformational characteristics allows the definition of conformation–activity relationships and furthermore implies a dynamic model of receptor–substrate interactions. Hence, from these computer simulation techniques it was possible to explain the biological profile of RGD peptides.

From the recently published conformational analysis of two native RGD-containing proteins, kistrin[7] and echistatin,[8] members of the disintegrin family, it was not possible to derive a bioactive RGD conformation, because the RGD sequence is located in both proteins in exposed and highly *flexible* loop regions. Our study of conformation–activity relationships with an underlying dynamic aspect demonstrates the importance of taking into account conformational changes of substrate molecules during receptor binding. The receptor exerts a *conformational pressure* on a substrate, enabling different substrate conformations to be induced, depending on the receptor environment.

Experimental Procedure

For structure refinement MD simulations were performed with the GROMOS force field [9] and NMR-derived interproton distances as constraints. The initial structure was built up manually so that no secondary structure elements were preformed. After energy minimization the structure was simulated by MD for 2 ps at 1000 K, 3 ps at 500 K, and further 5 ps at 300 K in vacuum with a distance-restraining force constant of 4000 kJ mol^{-1} nm^{-2}. The obtained conformation served as the initial structure for a 150 ps solvent simulation in a DMSO solvent box [5] with a box length of approximately 3.5 nm containing about 150–180 DMSO molecules. After the first 70 ps MD the distance restraining force constant was reduced from 1000 kJ mol^{-1} nm^{-2} to 500 kJ mol^{-1} nm^{-2} for further 30 ps. The last 50 ps of the 150 ps trajectory were simulated without any restraint to make sure that the obtained conformation after 100 ps restrained MD was a low-energy structure.

For the simulation of the conformational transitions of **1** and **2** the CVFF (*C*onsistent *V*alence *F*orce *F*ield) was employed which is implemented in the DISCOVER (BIOSYM) program package [10]. The force field was extended by a harmonic potential function for the dihedral-angle restraints. These simulations were performed in vacuum over 30 ps. The dihedral-angle restraining force constant was set for the first 7.5 ps at 1 kcal rad^{-2} and was increased in 7.5 ps steps to 2.5 kcal rad^{-2}, 5 kcal rad^{-2}, and 10 kcal rad^{-2}.

Received: October 15, 1991 [Z 4969 IE]
German version: *Angew. Chem.* **1992**, *104*, 341

CAS Registry numbers:
1, 137813-35-5; **2**, 137894-01-0; GRGDS, 96426-21-0.

[1] H. Kessler, *Angew. Chem.* **1982**, *94*, 509–520; *Angew. Chem. Int. Ed. Engl.* **1982**, *21*, 512–523.
[2] M. D. Pierschbacher, E. Ruoslahti, *Nature* **1984**, *309*, 30–33.
[3] S. E. D'Souza, M. H. Ginsberg, E. F. Plow, *Trends Biochem. Sci.* **1991**, *16*, 246–250.
[4] M. Aumailley, M. Gurrath, G. Müller, J. Calvete, R. Timpl, H. Kessler, *FEBS Lett.* **1991**, *291*, 50–54.
[5] D. F. Mierke, H. Kessler, *J. Am. Chem. Soc.*, **1991**, *113*, 9466–9470.
[6] R. S. Struthers, G. Tanaka, S. C. Koerber, T. Solmajer, E. L. Baniak, L. M. Gierasch, W. Vale, J. Rivier, A. T. Hagler, *Proteins: Struct. Funct. Genet.* **1990**, *8*, 295–304.
[7] M. Adler, R. A. Lazarus, M. S. Dennis, G. Wagner, *Science* **1991**, *238*, 491–497.
[8] V. Saudek, R. A. Atkinson, J. T. Pelton, *Biochemistry* **1991**, *30*, 7369–7372.
[9] W. F. van Gunsteren, H. J. C. Berendsen, *Groningen Molecular Simulation (GROMOS) Library Manual Biomos*, Groningen, **1987**.
[10] P. Dauber-Osguthorpe, V. A. Roberts, D. J. Osguthorpe, J. Wolff, M. Genest, A. T. Hagler, *Proteins: Struct. Funct. Genet.* **1988**, *4*, 31–47.

Selective Inhibition of Trypanosomal Triosephosphate Isomerase by a Thiopeptide**

By *Horst Kessler,* Hans Matter, Armin Geyer, Hans-Jürgen Diehl, Matthias Köck, Guido Kurz, Fred. R. Opperdoes, Mia Callens,* and *Rik K. Wierenga*

Dedicated to Professor Gerhard Quinkert on the occasion of his 65th birthday

Although much effort has been invested in the study of sleeping sickness its control has not yet been achieved.[1] The germs causing this tropical disease (*Trypanosoma brucei brucei*) obtain their energy exclusively from glycolysis. Thus, the synthesis of selective inhibitors of glycosomal enzymes of the pathogen is a promising approach.[2] In our investigations of the inhibition of trypanosomal *t*riosephosphate *iso*merase (TIM), EC 5.3.1.1), a key enzyme in this process,[3] we have developed several cyclic hexapeptides which have shown remarkable effectiveness and selectivity.[4] Several determinations of the crystal structure of TIM are known,[5] but the binding site of peptide inhibitors has not been localized until now.

Here we report the improvement of biological activity of a cyclic peptide, which was achieved by conformational changes in the peptide backbone. All side-chain functionalities were unmodified. The selective introduction of a thiocarbonyl group into the cyclic hexapeptide *cyclo*(Gly^1-Pro^2-Phe^3-Val^4-Phe^5-Phe^6) induces a drastic change in the backbone conformation,[6] resulting in a remarkable enhancement in the selective inhibition of trypanosomal TIM. The O/S exchange (*thionylation*) within conformationally restricted peptides can take place with high regioselectivity.[6, 7]

The introduction of a thiocarbonyl group as a modification of a peptide bond is an isosteric replacement of a carbonyl group. The local geometry in the vicinity of this fragment is scarcely influenced.[7] However, by the selective exchange of a CO-NH unit by its sulfur analogue the formation of transannular hydrogen bonds within the peptide can be influenced. The C=S fragment exhibits weaker acceptor properties, and due to its enhanced acidity the neighboring amide proton is a better donor than the oxo analogue. In addition, the larger van der Waals radius of the sulfur and the longer C=S bond limit the $\{\varphi, \psi\}$ conformational space in a characteristic manner: The thiocarbonyl fragment can be positioned at the i + 1 and i + 2 positions of a βI turn but only at the i + 2 position of a βII turn. The unfavorable steric interaction of the sulfur with the side chain of the L-amino acid in the i + 2 position prohibits the adoption of the βII turn.[8]

The thionylation of the peptide described here causes a remarkable increase of its inhibitory effect on trypanosomal TIM. Although the cyclic oxopeptide *cyclo*(Gly^1-Pro^2-Phe^3-Val^4-Phe^5-Phe^6) has only weak biological activity (Table 1), the analogous thiopeptide *cyclo*(Gly^1-Pro^2-Phe^3-Val^4-

[*] Prof. Dr. H. Kessler, Dipl.-Chem. H. Matter, Dipl.-Chem. A. Geyer, Dipl.-Chem. H. J. Diehl, Dipl.-Chem. M. Köck, Dipl.-Chem. G. Kurz
Organisch-chemisches Institut der Technischen Universität München
Lichtenbergstraße 4, D-W-8046 Garching (FRG)
Prof. Dr. F. R. Opperdoes, Dr. M. Callens
International Institute of Cellular and Molecular Pathology
Avenue Hippocrate 75, B-1200 Brüssel (Belgium)
Dr. R. K. Wierenga
European Molecular Biology Laboratory
Meyerhofstraße 1, D-W-6900 Heidelberg (FRG)

[**] This work was supported by the Fonds der Chemischen Industrie, the Deutsche Forschungsgemeinschaft, and a BRIDGE project of the EEC. H. M. and M. K. thank the Fonds der Chemischen Industrie for a grant.

Table 1. Inhibition of TIM by cyclic hexapeptides.

Peptide	IC_{50} [a] [μM] gTIM	R-TIM
cyclo(G-P-F-V-FΨ[CS-NH]F)	6	>100
cyclo(G-P-F-V-F-F)	150	>500
cyclo(P-F-F-K(Z)-W-F) F3-008	3	>125 [b]
cyclo(P-F-T-K(Z)-W-F) 008	7	>125 [b]

[a] Inhibition constants (amount required to inhibit the activity by 50%) for the inhibition of the glycosomal TIM of trypanosomes (gTIM) and the isoenzyme from rabbit muscle (R-TIM). [b] No significant inhibition is found for the isoenzymes from dog muscle, yeast, and *E. coli*.

Phe^{5}Ψ[CS-NH]Phe^6) is one of the most potent inhibitors. For comparison we list the biological activities of the best inhibitors examined so far (Table 1). These inhibitors show high selectivity for the trypanosomal TIM; the isoenzymes from dog or rabbit muscle, yeast, and *E. coli* are not inhibited.

This modification of biological activity by thionylation is induced by the change of the spatial structure. The conformation of both peptides was determined by a combination of NMR spectroscopy and molecular dynamics (MD) simulations. In Figure 1 we show the structures averaged over 80 ps of MD simulations in dimethyl sulfoxide (DMSO).[9] Both peptides exist in solution as two slowly exchanging isomers identified by two separate sets of signals in the NMR spectrum. In both cases the isomers differ in the configuration about the Gly^1-Pro^2 amide bond (*cis*/*trans*). The patterns of the *intra*molecular hydrogen bonding in the two peptides exhibit distinct differences. The oxopeptide contains a βI turn with a hydrogen bond from Gly^1 NH to Val^{4}C=O and a slightly distorted βI turn without the expected hydrogen bonds between Pro^2 and Phe^3 in the i + 1 and i + 2 positions. The *cis*/*trans* isomerization of the Gly^1-Pro^2 amide bond has only a small influence on the overall conformation of the peptide. The spatial structure next to the *cis* peptide bond of the less populated conformer exhibits a turn structure not yet described in cyclic hexapeptides.[10] A βII′ turn is found on the opposite side of this conformation.

The pattern of the hydrogen bonding within the thiopeptide[6] is shifted by one residue in the amino acid sequence relative to the pattern in the oxopeptide. The conformational influence of the thiocarbonyl group forces proline into the i + 2 position of a βII′ turn (*trans* isomer) or a βVIa turn [11] (*cis* isomer; see Scheme 1). Both isomers form hydrogen bonds between Phe^{3}NH and Phe^{6}C=O and between Phe^{6}NH and Phe^{3}C=O, the latter resulting from the altered donor properties of the Phe^{6}NH hydrogen next to the thiocarbonyl fragment. Steric effects have a minor influence on the conformational changes within the βI turn. Both isomers of the thiopeptide have been shown to be very flexible in MD simulations and in experimental relaxation studies.[6]

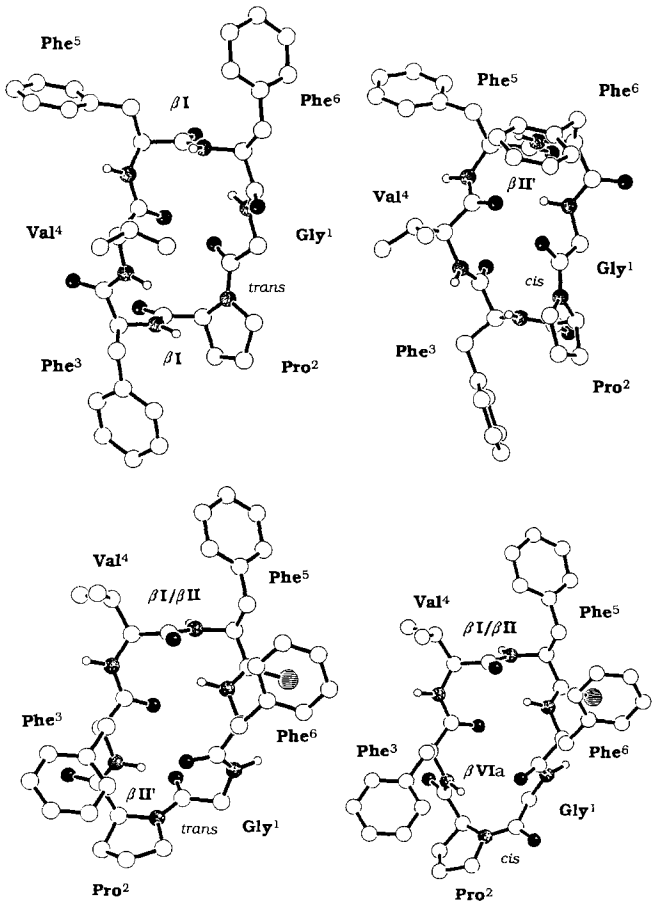

Fig. 1. Conformation of *cyclo*(Gly^1-Pro^2-Phe^3-Val^4-Phe^5-Phe^6) (above) and *cyclo*(Gly^1-Pro^2-Phe^3-Val^4-Phe^{5}Ψ[CS-NH]Phe^6) (below). The *trans* and *cis* isomers about the Gly^1-Pro^2 amide bond are shown on the right and left, respectively. The structures were obtained from 80 ps of MD simulation in DMSO with the GROMOS program [14]. Experimental data from 500 MHz and 600 MHz NOESY and ROESY measurements were used as distance restraints in the calculations. Side-chain conformations (except for Phe^6 in the *cis* isomer of the oxopeptide, upper right) were fixed in the most populated rotamers determined by coupling constants. It was impossible to ascertain the side-chain conformations of Phe^6 in the *cis* isomer of the oxopeptide because of the chemical-shift degeneracy of both diastereotopic C_β hydrogens [15]. The thiopeptide exhibited larger mobility during the MD simulation; here we show only one conformation with the βII turn in the flexible region.

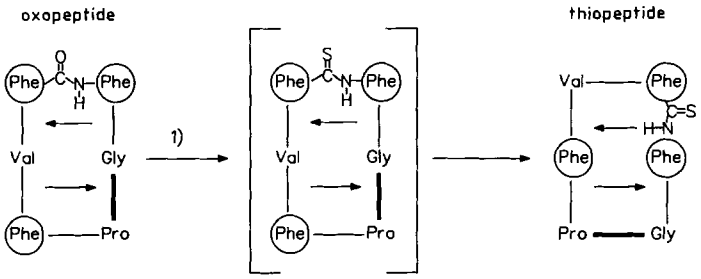

Scheme 1. Change in hydrogen-bonding patterns caused by selective thionylation of a cyclic hexapeptide. The bond in boldface between Gly^1 and Pro^2 in both peptides shows *cis*/*trans* isomerism. Thionylation exclusively at the Phe^5-Phe^6 amide bond was observed under the given conditions. 1) Yokoyama's reagent, 20 equiv, 16 h, room temperature.

Until now conformational control in cyclic hexapeptides has been achieved by the introduction of a D amino acid.[12, 13] A similar role might be conceded to thiocarbamide bonds in the future design of biologically active substances. The structure–activity relationships of the compounds examined so far show that a favorable arrangement of amino acids with aromatic side-chains is important for biological activity. Since the spatial structure of the peptide/TIM complex is not yet known, it is too early to speculate about the interactions leading to the observed biological effects.

Experimental Procedure

100 mg (0.15 mmol) of *cyclo*(Gly-Pro-Phe-Val-Phe-Phe) was suspended in 15 mL of absolute THF and homogenized in an ultrasound bath. 60 mg (15 mmol) of Yokoyama's reagent [6b] was then added, and the mixture was

stirred 16 h at room temperature. Isolation and purification were achieved by flash chromatography (chloroform/methanol 19/1). Yield: 27 mg (26%) *cyclo*-(Gly-Pro-Phe-Val-PheΨ[CS-NH]Phe). For further details see ref. [6].

Received: November 21, 1991 [Z 5031 IE]
German version: *Angew. Chem.* **1992**, *104*, 343

CAS Registry numbers:
TIM, 9023-78-3; *cyclo*(G-P-F-V-FΨ[CS-NH]F), 139409-16-8.

[1] A review is given by B. Clement, *Pharm. Unserer Zeit* **1989**, *18*, 97–111.
[2] a) W. G. J. Hol, R. K. Wierenga, H. Groendijk, R. J. Read, A.-M. W. H. Thunnissen, M. E. M. Noble, K. H. Kalk, F. M. D. Vellieux, F. R. Opperdoes, P. A. M. Michels in *Molecular Recognition* (Ed.): S. M. Roberts), Royal Society of Chemistry, Exeter, **1989**, pp. 84–93; b) W. G. J. Hol, *Angew. Chem.* **1986**, *98*, 765–777; *Angew. Chem. Int. Ed. Engl.* **1986**, *25*, 767–778.
[3] F. R. Opperdoes, P. Borst, *FEBS Lett.* **1977**, *80*, 360–364.
[4] D. A. Kuntz, R. Osowski, M. Schudok, R. K. Wierenga, K. Müller, H. Kessler, *European J. Biochem.* **1992**, submitted.
[5] a) R. K. Wierenga, K. H. Kalk, W. G. J. Hol, *J. Mol. Biol.* **1987**, *198*, 109–121; b) R. K. Wierenga, M. E. M. Noble, J. P. M. Postma, H. Groendijk, K. H. Kalk, W. G. J. Hol, F. R. Opperdoes, *Proteins* **1991**, *10*, 33–49; c) M. E. M. Noble, R. K. Wierenga, A.-M. Lambeir, F. R. Opperdoes, A.-M. W. H. Thunnissen, K. H. Kalk, H. Groendijk, W. G. J. Hol, *ibid.* **1991**, *10*, 50–69; d) E. Lolis, T. Alber, R. C. Davenprot, D. Rose, F. C. Hartman, G. A. Petsko, *Biochemistry* **1990**, *29*, 6609–6618.
[6] a) H. Kessler, A. Geyer, H. Matter, M. Köck, *Int. J. Pept. Protein Res.* **1992**, in press; b) M. Yokoyama, Y. Hasegawa, H. Hatanaka, Y. Kawazoe, T. Imamoto, *Synthesis* **1984**, 827.
[7] D. Seebach, S. Y. Ko, H. Kessler, M. Köck, M. Reggelin, P. Schmieder, M. D. Walkinshaw, J. J. Bölsterli, D. Bevec, *Helv. Chim. Acta* **1991**, in press.
[8] T. F. M. La Cour, *Int. J. Pept. Protein Res.* **1987**, *30*, 564–571.
[9] D. F. Mierke, H. Kessler, *J. Am. Chem. Soc.* **1991**, *113*, 9466–9470.
[10] Because of the *cis* peptide bond between the i + 1 and i + 2 positions, we use the term *pseudo* βI turn since the Φ and Ψ angles correspond to a βI turn.
[11] a) J. S. Richardson, *Adv. Protein Chem.* **1981**, *34*, 167–339; b) S. S. Zimmermann, H. A. Scheraga, *Biopolymers* **1977**, *16*, 811–843.
[12] H. Kessler, *Angew. Chem.* **1982**, *94*, 509–520; *Angew. Chem. Int. Ed. Engl.* **1982**, *21*, 512–523.
[13] M. Aumailley, M. Gurrath, G. Müller, J. Calvete, R. Timpl, H. Kessler, *FEBS Lett.* **1991**, *291*, 50–54.
[14] W. F. van Gunsteren, H. J. C. Berendsen, *Groningen Molecular Simulation (GROMOS) Library Manual, Biomos*, Groningen, **1987**.
[15] The conformation shown has the Phe^6 side-chain with $\chi_1 = 60°$ which is usually unfavored in peptides.

Do Pheromone Receptors that Receive the Same or Similar Signal Molecules Have the Same or Similar Structure?**

By *Hans Jürgen Bestmann,** *Wu Caihong, Claudia Rehefeld, Friedrich Kern,* and *Barbara Leinemann*

Dedicated to Professor Michael Hanack on the occasion of his 60th birthday

When pheromone molecules meet an insect's antenna, opening of ion channels is initiated in the dendritic membrane of nerve cells. The resulting flow of ions through the membrane alters the original rest potential. A receptor potential is set up which is electrotonically distributed over the membrane and later converted into action potentials, which if need be are further conducted via intermediary neurons into the central nervous system and processed there, possibly leading to a particular behavior. The mechanism of formation of the ion channels in the case of pheromones is still largely unknown. Recent investigations[1] suggest that second-messenger cascades are involved as in the case of the olfactory systems of vertebrates.[2] On the basis of structure–activity studies[3] one may assume that a functionally flexible interaction[4] between the signal molecules and a receptor occurs at the beginning of such a cascade, which can be determined by the stereochemistry of the pheromones to a greater or lesser extent.[5]

In the case of butterflies and moths (*Lepidoptera*), chemical communication generally takes place through a mixture of several different molecules which are present in a definite ratio.[3] In many cases the structures of the components of such a pheromone complex differ very slightly, often in the functional end group only. For each component there are receptor cells on the antenna of the respective species which specifically answer to pheromones or compounds derived therefrom, if the latter bear the correct functional end group. Thus, e.g., in the case of *Bombyx mori* one finds an alcohol and an aldehyde receptor for bombykol **1a** and bombykal **1b**,[6] and in the case of *Antheraea* species an acetate and an aldehyde receptor for (6*E*, 11*Z*)-6,11-hexadecadienyl acetate **3a** and the corresponding aldehyde **3b**.[7, 8] Further, often the same molecules are found as components of the pheromone complex in different species, e.g. bombykal **1b** in *Bombyx mori* and in *Manduca sexta*.[9]

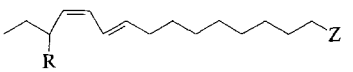

1a, R = H, Z = CH_2OH; **1b**, R = H, Z = CHO
2a, R = Me, Z = CH_2OH; **2b**, R = Me, Z = CHO

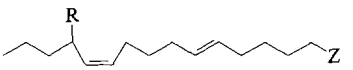

3a, R = H, Z = CH_2O_2CMe; **3b**, R = H, Z = CHO
4a, R = Me, Z = CH_2O_2CMe; **4b**, R = Me, Z = CHO

There now arise the fundamental questions of whether 1) the receptors on the antenna of different species, which should take up the same signal molecules, have the same structure, and whether 2) receptors in the same species, which must receive very similar molecules with only different terminal groups (e.g. **1a** and **1b** or **3a** and **3b**), differ only in the complementary part for the functional end group or also in other parts of the molecule.[10]

To answer these questions we have enlisted the electrophysiological measurement of chiral pheromone derivatives. In earlier studies intended to show whether receptors for achiral signal molecules can differentiate chiral derivatives,[11] we used the electroantennogram technique.[12] In our present experiments single-cell recording has been used,[13] since only this enables accurate statements concerning the above questions. Our investigations led to the following results (cf. Table 1):

Question 1: The "aldehyde receptor" of *Bombyx mori* scarcely differentiates between the enantiomers of 14-methylbombykal **2b**. **2b** is fiftyfold less active than bombykal **1b**. The aldehyde receptor of *Manduca sexta*, on the other hand, differentiates between the two enantiomers of **2b**

[*] Prof. Dr. H. J. Bestmann, Dr. C. Rehefeld, Dipl.-Biol. F. Kern, B. Leinemann
Institut für Organische Chemie der Universität Erlangen-Nürnberg
Henkestrasse 42, D-W-8520 Erlangen (FRG)
Prof. C. Wu
Department of Biology,
Peking University, Beijing 100871 (China)

[**] Pheromones, Part 85. This work was supported by the Deutsche Forschungsgemeinschaft and the Volkswagen-Stiftung. – Part 84: H. J. Bestmann, F. Kern, A. Mineif, H. Platz, O. Vostrowsky, *Z. Naturforsch. C*, in press.

by a factor of 100 with $R > S$. The (*R*)-enantiomer, however, is only ten times less active than the pheromone **1b**.

From these observations it can be concluded that the structures of the two bombykal receptors are different, since a) they differentiate the same chiral derivative to widely different extents, and b) the differences between the activity of the particular pheromone and **2b** differ largely.

Question 2: (*R*)-**2a** interacts with the "alcohol receptor" of *Bombyx mori* three times better than the (*S*)-isomer. It is ten times less active than the pheromone **1a**.

In summarizing all these data it may be concluded that the alcohol and aldehyde receptors in *Bombyx mori* differ not only in the structure of the part necessary for recognition of the functional end group.

Table 1. Results of electrophysiological measurements (single-cell recordings) with optically active pheromone derivatives.

Species	Substance [a]	Comparison	Factor	*n* [b]
Bombyx mori	**2a**	$R > S$	3	20
	1a/(*R*)-**2a**	**1a** > (*R*)-**2a**	10	12
	2b	$R \geq S$	–	20
	1b/(*R*)-**2b**	**1b** > (*R*)-**2b**	50	17
Manduca sexta	**2b**	$S > R$	100	24
	1b/(*R*)-**2b**	**1b** > (*R*)-**2b**	10	11
Antheraea pernyi	**4a**	$S > R$	3	24
	4b	$R > S$	10	22
	3a/(*S*)-**4a**	**3a** > (*S*)-**4a**	100	22
	3b/(*R*)-**4b**	**3b** > (*R*)-**4b**	400	18
Antheraea polyphemus	**4a**	$S > R$	3	20
	4b	$R > S$	50	20
	3a/(*S*)-**4a**	**3a** > (*S*)-**4a**	400	18
	3b/(*R*)-**4b**	**3b** > (*R*)-**4b**	10	12

[a] **2a**: (14 *R*)- and (14 *S*)-enantiomer; **2b**: (14 *R*)- and (14 *S*)-enaniomer; **4a**: (13 *R*)- and (13 *S*)-enantiomer; **4b**: (13 *R*)- and (13 *S*)-enantiomer. [b] *n* = number of measurements.

This is much more evident in the case of *Antheraea pernyi*. The acetate receptor differentiates between the enantiomers of **4a**[14] by a factor of 3, with $S > R$. The (*S*)-enantiomer is less active than the pheromone **3a** by a factor of 100. In the same animal species, the cell specific for the aldehyde differentiates between the enantiomers of **4b** by a factor of 10; but now $R > S$, i.e. the reverse of that in the case of the acetate. (*R*)-**4b** acts three times more weakly than the pheromone **3b**.

In the case of the related species *Antheraea polyphemus* we have the following picture: The enantiomers of the acetate **4a** are differentiated by a factor of 3 with $S > R$, whereby the activity of (*S*)-**4a** decreases by a factor of 400 compared to the pheromone **3a**. In the same species the aldehyde receptor differentiates (*S*)- and (*R*)-**4b** with a factor of 50, and again with $R > S$. (*R*)-**4b** is ten times less active than the pheromone **3b** of the species.

Since, in the two *Antheraea* species, the acetate receptor prefers the (*S*)-enantiomer while the aldehyde receptor prefers the (*R*)-enantiomer, one may conclude that the two receptors must differ in their structure, not only in the region corresponding to the functional end groups of the signal molecule but also at least in the part which intercalates the terminal alkyl group of the pheromone. Also the difference in the decrease of activity between the more active enantiomers of **4a** and **4b** compared to the acetate pheromone **3a** and the aldehyde pheromone **3b** suggests that the receptors have different structures.

In the case of the closely related species *A. pernyi* and *A. polyphemus* the differences between the respective acetate and aldehyde receptors are, however, not so pronounced as in the case of *Bombyx mori* and *Manduca sexta*.

We have suggested that the interaction between pheromone and receptor should be a flexible dynamic process.[3, 4, 11] Upon intercalation the conformations of signal molecule and receptor synchronously change until both are in a definite conformation, bound to each other by noncovalent interactions ("induced fit").[15] It is postulated that the "biologically active" conformation of the signal molecule of the receptor is the most stable.[16] However, as shown here, if for the same molecule in different insect species and for molecules which differ in the functional end group in the same species, receptors with different structure are available, one may assume that the intercalated conformations are also not the same but differ.[17] This means that the biologically active conformation in a few cases only is the thermodynamically most stable and that nature makes use of the many conformations in which signal molecules can occur.

Received: July 22, 1991;
Revised: October 14, 1991 [Z 4812 IE]
German version: *Angew. Chem.* **1992**, *104*, 353

[1] J. Boeckhoff, E. Tareilus, H. Breer, *EMBO J.* **1990**, *9*, 2453; H. J. Breer, J. Boeckhoff, E. Tareilus, *Nature* **1990**, *345*, 65; J. Boeckhoff, K. Raming, H. Breer, *J. Comp. Physiol. B.* **1990**, *160*, 99.

[2] D. Lancelot, U. Pace, G. D. Prestwich, G. J. Blomquist, *Pheromone Biochemistry*, Academic Press, **1987**, p. 592.

[3] Review: H. J. Bestmann, *Verhandlung der Gesellschaft Deutscher Naturforscher und Ärzte, 113. Versammlung Nürnberg 1984*, Wissenschaftliche Verlagsgesellschaft, Stuttgart, **1985**, p. 301.

[4] H. J. Bestmann, P. Rösel, O. Vostrowsky, *Liebigs Ann. Chem.* **1979**, 1189.

[5] Regarding extremely high stereospecificity in the trail pheromones of the ant species *Leptogenys diminuta* cf. S. Steghaus-Kovac, U. Maschwitz, A. B. Attygalle, R. T. S. Frighetto, N. Frighetto, O. Vostrowsky, H. J. Bestmann, *Experientia* **1992**, in press.

[6] K. E. Kaissling, G. Kasang, H. J. Bestmann, W. Stransky, O. Vostrowsky, *Naturwissenschaften* **1978**, *65*, 382.

[7] J. Kochansky, I. Tette, E. F. Taschenberg, R. T. Cardé, K. E. Kaissling, W. L. Roelofs, *J. Insect. Physiol.* **1975**, *21*, 1977; H. J. Bestmann, H. Platz, T. Brosche, J. Erler, A. B. Attygalle, J. Schwarz, O. Vostrowsky, C. Wu, K. E. Kaissling, C. T. Chen, *Z. Naturforsch. C.* **1987**, *42*, 631.

[8] Concerning the receptor specificity in the case of *Antheraea* species see H. J. Bestmann, C. Wu, B. Döhla, K. Li, K. E. Kaissling, *Z. Naturforsch. C.* **1987**, *42*, 435.

[9] The complete pheromone of *Manduca sexta* was first elucidated only recently: J. H. Tumlinson, M. M. Brennan, R. E. Doolittle, E. R. Mitchell, A. Brabham, B. E. Mazomemos, A. H. Baumhover, D. M. Jackson, *Arch. Insect Biochem. Physiol.* **1989**, *10*, 255.

[10] Studies on brown algae show differences in behavioral responses to the same compounds in various species, D. G. Müller, W. Boland, L. Jaenicke, G. Gassmann, *Z. Naturforsch. C.* **1985**, *40*, 457. Brown algae are quite simple organisms in which one could possibly conclude the presence of different receptor structures on the basis of differing behavioral responses. In more highly developed organisms such as lepidoptera this is permitted only in rare cases or not at all. Behavioral responses are the result of signal processing in the *central nervous system*. The questions posed here by us do not however concern the primary interaction between signal molecule and its receptor in the denditric membrane, which finally initiate the opening of the ionic channels.

[11] H. J. Bestmann, H. L. Hirsch, H. Platz, M. Rheinwald, O. Vostrowsky, *Angew. Chem.* **1980**, *92*, 492; *Angew. Chem. Int. Ed. Engl.* **1980**, *19*, 475.

[12] D. Schneider, *Z. Vgl. Physiol.* **1957**, *40*, 9.

[13] K. E. Kaissling, J. Thorson, D. B. Satelle, L. M. Hall, J. D. Hildebrand, *Receptors for Neurotransmitters, Hormones and Pheromones in Insects*, Elsevier/North Holland Biomedical Press, Amsterdam, **1980**, p. 261.

[14] We shall report on the synthesis of the enantiomers of **4** in a separate communication.

[15] H. J. Bestmann, C. Rehefeld, *Naturwissenschaften* **1989**, *76*, 422.

[16] T. Liljefors, B. Thelin, J. N. C. Van der Pers, C. Löfstedt, *J. Chem. Soc. Perkin Trans. 2* **1985**, 1957; T. Liljefors, M. Bengtsson and B. S. Hansson, *J. Chem. Ecol.* **1987**, *13*, 2023; M. Bengtsson, T. Liljefors, B. S. Hansson, C. Löfstedt, S.V. Copaja, *ibid.* **1990**, *16*, 667.

[17] Questions regarding the conformation of signal substances on the receptor are also dealt with by O. L. Chapman, J. A. Klun, K. C. Mattes, R.S. Sheridan, S. Maini, *Science* **1978**, *201*, 926; *J. Am. Chem. Soc.* **1978**, *100*, 4878. It should be noted here that conclusions are drawn about behavioral responses (cf. Ref. [10]). The results obtained deviate from those of electrophysiological measurements (Ref. [11]).

Electrochemical Oxidation of 1-(*p*-Dimethylaminophenyl)-3,3-dimethyltriazene—Cyclic Voltammetric Detection of a Triazene Radical Cation and Dication**

By *Bernhard Gollas* and *Bernd Speiser**

Dedicated to Professor Anton Rieker on the occasion of his 60th birthday

Stable or persistent radical cations have frequently been found as primary products in the oxidation of amines[1] and hydrazines.[2] In the case of triazenes, i.e. compounds with *three* linearly connected nitrogen atoms, apparently no example has hitherto been reported in which the one-electron oxidation product has a lifetime sufficiently long enough for experimental detection. Insights into hypothetical triazene radical cations, however, are of particular interest, since, on the one hand, they are possibly the first intermediates which also occur in the oxidative metabolism of the carcinogenic triazenes in biochemical systems and, on the other, since 1-aryl-3,3-dimethyltriazenes are used against malignant melanoma.[3] Reactions at an electrode can often be regarded as model reactions for biochemical processes.[4] Nevertheless, only few studies have been carried out concerning the anodic oxidation of triazenes.[5, 6] A triazene radical cation has been formulated as unstable intermediate but was not detected experimentally.[5]

For the generation and mechanistic study of the reactivity of triazene radical cations we have oxidized 1-aryl-3,3-dimethyltriazenes **1** at a Pt-anode in anhydrous acetonitrile with nBu$_4$NPF$_6$ as supporting electrolyte.[7] We report here on the one-electron oxidation of the compound **1a** to the radical cation **1a**$^{\bullet+}$, on its further oxidation to the dication **1a**$^{2+}$, and on the decomposition reactions of **1**$^{\bullet+}$ and **1a**$^{2+}$. The reaction mechanism of the triazenes **1b**–**1h** is more complicated and will be discussed elsewhere.

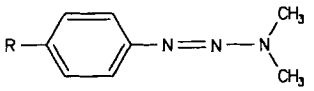

1a R = $(CH_3)_2N$ **1b** R = OC_2H_5
1c R = OCH_3 **1d** R = CH_3
1e R = H **1f** R = Br
1g R = CF_3 **1h** R = NO_2

Figure 1 shows cyclic voltammograms of **1a** at a scan rate of $v = 0.1$ Vs^{-1} in the potential ranges -0.9 to $+1.7$ and -0.4 to $+0.8$ V. The peaks I and II fulfill all criteria required for the pair of peaks of a reversible *one*-electron transfer: the peak current ratio i_p^{II}/i_p^{I} is close to 1 at sufficiently high scan rates ($v \geq 0.2$ Vs^{-1}) and a switching potential $E_\lambda = +0.4$ V; i_p^{I} is proportional to $\sqrt{v}$; the peak potentials E_p^{I} and E_p^{II} are independent of v (formal potential $E^\circ = +0.091 \pm 0.001$ V). The peak potential difference, ΔE_p (0.067 V), is increased only slightly compared to the value for a reversible one-electron transfer. Consistent with this, coulometric measurements gave a value of $n = 1.0$. The potentials do not vary with the concentration of the triazene. From the peak current i_p^{I}, a diffusion coefficient of $D = (2.2 \pm 0.2) \times 10^{-5}$ cm s^{-1} was calculated for **1a** in acetonitrile. For slower scan rates the ratio of the peak currents i_p^{II} and i_p^{I} becomes smaller ($E_\lambda = +0.4$ V; $v = 0.1$ Vs^{-1}: $i_p^{II}/i_p^{I} = 0.96$; $v = 0.01$ Vs^{-1}: $i_p^{II}/i_p^{I} = 0.82$). The initially formed triazene radical cation **1a**$^{\bullet+}$ undergoes further chemical reaction.

[*] Priv.-Doz. Dr. B. Speiser, Dipl.-Chem. B. Gollas
Institut für Organische Chemie der Universität
Auf der Morgenstelle 18, D-W-7400 Tübingen 1 (FRG)

[**] Electrochemistry of Triazenes, Part 1. – This work was supported by the Deutsche Forschungsgemeinschaft.

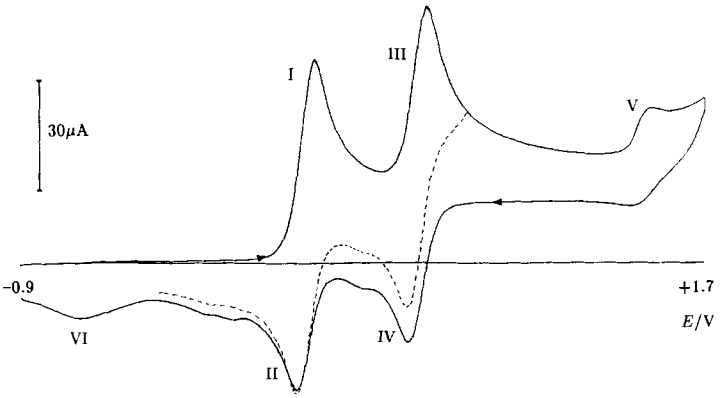

Fig. 1. Cyclic voltammograms of the triazene **1a** in CH_3CN/0.1 M nBu$_4$NPF$_6$ at a Pt electrode ($v = 0.1$ Vs^{-1}, $c = 2.16 \times 10^{-3}$ M) in the potential ranges -0.9 to $+1.7$ V (—), and -0.4 to $+0.4$ V (– – –).

Voltammograms in the region of the first electron transfer from **1a** were analyzed as a function of v using the computer program system EASIEST (*e*lectro*a*nalytical *si*mulation and parameter *est*imation).[8] The rate constant for the reaction of the radical cation determined from the peak potentials and peak current ratios on the basis of the EC model (reversible electron transfer with subsequent irreversible reaction) was found to be $k = 0.01$ s^{-1}. Simulation of the voltammograms with the reaction parameters thus obtained for various values of v confirmed the analysis. Figure 2 shows the agreement between experimental and simulated voltammograms for the fastest and slowest scan rates used.

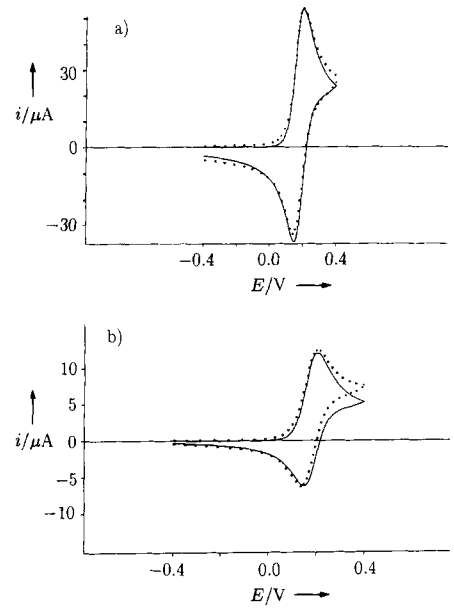

Fig. 2. Experimental (broken) and simulated (solid curve; simulation parameters see text) cyclic voltammograms of the triazene **1a** in the region of the first oxidation; a) $v = 0.2$ Vs^{-1}, b) $v = 0.01$ Vs^{-1}.

The deviations in the upper potential region, especially at $v = 0.01$ Vs^{-1}, are in part explained by the fact that the background current is not taken into account in the simulation. The second electron transfer leading to the dication as well as the electrode reaction leading to follow-up products also contribute quite clearly to the experimental total current in this region.

The electrolysis of **1a** in an ESR spectrometer at room temperature yielded a solution which showed the spectrum of the *N,N,N',N'*-tetramethyl-*p*-phenylenediamine radical cation (Wursters Blue, $\mathbf{2}^{\bullet+}$) (Fig. 3a). Chemical oxidation with $I_2/AgClO_4$ also led to the spectrum of $\mathbf{2}^{\bullet+}$ (*blue* solution). After several successive cycles the cyclic voltammograms of **1a** show small peaks, which, by comparison can be assigned to the two-step oxidation of *N,N,N',N'*-*p*-phenylenediamine **2** to its dication.[9] Products of the preparative electrolysis of **1a** were investigated with the help of CAD mass spectrometry. Here too, the formation of **2** from **1a** was observed. Thus, the reaction of $\mathbf{1a}^{\bullet+}$ is so rapid on the time scale of these experiments that only the product of the decomposition is detected.

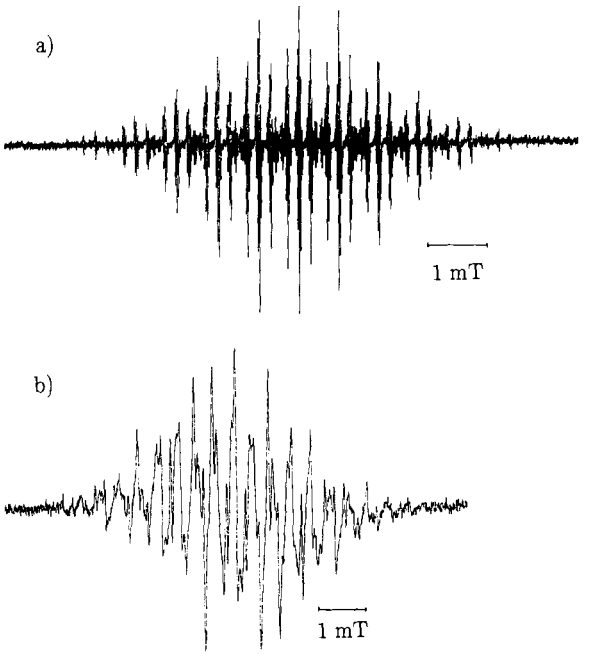

Fig. 3. ESR spectra after the oxidation of **1a** with $I_2/AgClO_4$ in acetonitrile; a) at room temperature, b) at −40 °C.

When the chemical oxidation of **1a** and the ESR investigation were carried out at −40 °C, the now blue-*green* solution gave a spectrum which differed from that of the radical cation $\mathbf{2}^{\bullet+}$ (Fig. 3b). The increased line width possibly arises from exchange phenomena between radical cations and non-oxidized molecules. This second spectrum is also observed upon electrolysis of **1a** at −40 °C and +0.25 V, albeit with poor resolution. In both cases a superposition with the spectrum of $\mathbf{2}^{\bullet+}$ cannot be ruled out. Upon warming the solutions to room temperature after the low-temperature experiments the spectrum of Wursters Blue was obtained, which then—even upon renewed cooling—remained unchanged. Thus, at −40 °C the ESR spectrum of a new species is recorded which converts into $\mathbf{2}^{\bullet+}$; the changes in the spectrum do not represent a temperature effect.

The reaction mechanism for the one-electron oxidation of **1a** is shown in Scheme 1 (left). A similar elimination of N_2 has already been observed in the *thermolysis* of a 1-vinylazopyrazole.[10] Possibly the reaction is initiated by splitting of $\mathbf{1a}^{\bullet+}$ into the corresponding diazenyl radical and the dimethylnitrenium ion. The diazenyl radical would then decompose to N_2 and the dimethylamino-substituted phenyl radical, which in turn would afford $\mathbf{2}^{\bullet+}$ by recombination with the nitrenium ion. On the basis of the measurements presented here, parallel reactions of $\mathbf{1a}^{\bullet+}$ to give non-electroactive and non-paramagnetic products cannot be ruled out.

A value of $n = 0.9$ was measured coulometrically for the second electron transfer (Peaks III/IV); $E^\circ = +0.516 \pm 0.004$ V). Accordingly, this is also a one-electron oxidation, which is consistent with the peak potential difference ($\Delta E_p = 0.069$ V).

The resulting triazene dication $\mathbf{1a}^{2+}$ decomposes more rapidly than $\mathbf{1a}^{\bullet+}$. Whereas the reduction Peak IV strongly decreases with decreasing scan rates, Peak V ($E_p^{ox} = 1.417 \pm 0.008$ V) grows significantly. Thus, the latter can be assigned to a product of the follow-up reaction of the dication. Peak VI ($E_p^{red} = -0.751 \pm 0.009$ V) is only to be observed in the reductive part of the voltammogram when **1a** is previously oxidized to at least the dication stage, but not when only oxidized to the radical cation. Accordingly, a decomposition product of $\mathbf{1a}^{2+}$ is reduced here. Both from a comparison of measurements on *p*-dimethylaminobenzenediazonium tetrafluoroborate **3** as well as from experiments with addition of **3** to the solution of the triazene, we conclude that the Peaks V and VI correspond to the oxidation and reduction of **3**, respectively. In both cases rapid irreversible follow-up reactions occur.

On the other hand, for the decomposition reaction of $\mathbf{1a}^{2+}$, which has already been formulated with a quinone imine structure,[5] splitting into **3** and the dimethylnitrenium ion would be conceivable, whereby the latter reacts to give follow-up products. On the other hand, **3** could be formed from a monocation after deprotonation of $\mathbf{1a}^{2+}$. The cleavage of the N–N bond and the occurrence of the diazonium ion **3** are not, however, to be attributed to the liberation of protons. The latter was postulated by Matřka et al.[5] In the present work, the oxidation of **3** was observed in peak V even

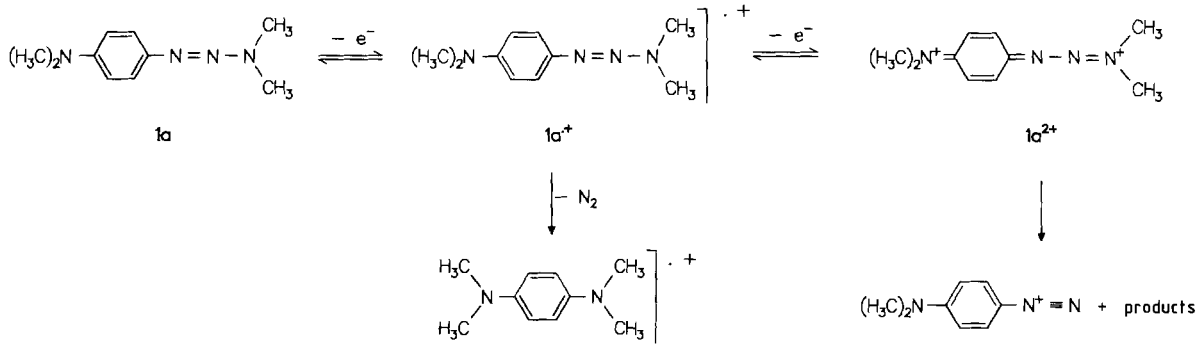

Scheme 1. The electrochemical oxidation of **1a**.

with a tenfold excess of the base 2,6-lutidine. The oxidation to the dication $\mathbf{1a}^{2+}$ is outlined in Scheme 1 (right).

In contrast to the electrochemical oxidation of amines,[11] the primary products of the one- and two-electron oxidation of the triazene **1a** initially decompose with cleavage of an N–N bond and not via solvolysis of an *N*-alkyl group. Compared to the bonding in the radical cations of tetraalkylhydrazines[2] this bond appears in the triazene cations to be labile. Regarding the bonding and the reactivity, the open-shell species $\mathbf{1a}^{\bullet+}$ and the dication $\mathbf{1a}^{2+}$ rather resemble triazenes protonated at N(3).[12]

Received: August 1, 1991;
Revised: September 25, 1991 [Z 4847 IE]
German version: *Angew. Chem.* **1992**, *104*, 336

[1] As new example for tertiary amines see: H. Bock, I. Göbel, Z. Havlas, S. Liedle, H. Oberhammer, *Angew. Chem.* **1991**, *103*, 193–196; *Angew. Chem. Int. Ed. Engl.* **1991**, *30*, 187–190; for secondary amines cf. H. Kainer, K. H. Hausser, *Chem. Ber.* **1953**, *86*, 1563–1570; for primary aryl amines cf. P. Hertl, A. Rieker, B. Speiser, *J. Electroanal. Chem.* **1986**, *200*, 147–158.
[2] S. F. Nelsen, *Acc. Chem. Res.* **1981**, *14*, 131–138.
[3] M. Julliard, G. Vernin, *Ind. Eng. Chem. Prod. Res. Dev.* **1981**, *20*, 287–296.
[4] G. Dryhurst, *Electrochemistry of Biological Molecules*, Academic, New York, **1977**, p. 2; T. Shono, T. Toda, N. Oshino, *J. Am. Chem. Soc.* **1982**, *104*, 2639–2641.
[5] V. Zvěřina, M. Remeš, J. Kroupa, Z. Ságner, M. Matřka, *Coll. Czech. Chem. Commun.* **1972**, *37*, 839–845.
[6] J. Huguet, M. Libert, C. Caullet, *Bull. Soc. Chim. Fr.* **1972**, 4860–4864.
[7] All potentials in this work are referred to an external ferrocene standard; concentrations of **1a**: ca. 10^{-3} M; Bruker Polarograph E310 with Wenking Voltage Scan Generator VSG 72.
[8] B. Speiser, *Anal. Chem.* **1985**, *57*, 1390–1397.
[9] T. Yao, S. Musha, M. Munemori, *Chem. Lett.* **1974**, 939–944.
[10] M. Schulz, L. Mögel, N.-X. Dung, R. Radeglia, *Z. Chem.* **1982**, *22*, 56.
[11] K. K. Barnes, C. K. Mann, *J. Org. Chem.* **1967**, *32*, 1474–1479; P. J. Smith, C. K. Mann, *ibid.* **1969**, *34*, 1821–1826; L. C. Portis, V. V. Bhat, C. K. Mann, *ibid.* **1970**, *35*, 2175–2178.
[12] A. Schmiedekamp, R. H. Smith, Jr., C. J. Michejda, *J. Org. Chem.* **1988**, *53*, 3433–3436.

$[SbCl([15]Crown-5)](SbCl_6)_2$ and $[BiCl([18]Crown-6)(CH_3CN)_2](SbCl_6)_2$: Salts with Antimony(III) and Bismuth(III) Dications

By *Michael Schäfer, Gerlinde Frenzen, Bernhard Neumüller*, and *Kurt Dehnicke**

Dedicated to Professor Wolfgang Beck on the occasion of his 60th birthday

In antimony–crown ether complexes $[SbX_3([15]crown-5)]$ (X = F,Cl (**1**), Br, I) the antimony atom is eightfold coordinated in a sandwich-like fashion by the five O atoms of the crown ether and the three halogen atoms.[1–3] The lone pair on the antimony atom is oriented towards the cavity formed by the crown ether, and according to ^{121}Sb Mössbauer spectroscopic findings contains a high s-part.

By exploiting the steric activity of the lone pair we were able, for the first time, not only to prepare a dication of antimony(III) but also one of bismuth(III), using the same synthetic strategy. In the case of bismuth(III) only the dicationic thiourea complex $[Bi(NO_3)\{SC(NH_2)_2\}_5]^{2+}$ has thus far been reported; it has an octahedral structure, and the lone pair shows no stereochemical activity.[4]

[*] Prof. Dr. K. Dehnicke, Dr. M. Schäfer, Dr. G. Frenzen, Dr. B. Neumüller
Fachbereich Chemie der Universität
Hans-Meerwein-Strasse, D-W-3550 Marburg (FRG)

The dication of antimony(III) is formed as colorless crystals upon reaction of **1** with excess antimony pentachloride in acetonitrile [Eq. (a)].

$$\underset{\mathbf{1}}{[SbCl_3([15]crown\text{-}5)]} + 2\,SbCl_5 \longrightarrow \underset{\mathbf{2}}{[SbCl([15]crown\text{-}5)](SbCl_6)_2} \quad (a)$$

According to the crystal structure analysis[5] the molecular structure contains two symmetry-independent cations which are almost identical; Figure 1 shows the crystal structure of one of them. The antimony atom is surrounded in an almost pentagonal-planar construction by the five O atoms of the crown ether and an axially oriented Cl atom, thus resulting in a structure with almost C_{5v} symmetry. The Sb

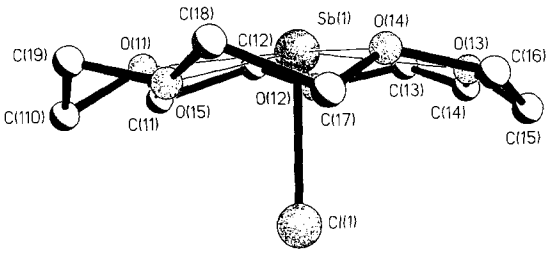

Fig. 1. The crystal structure of one of the two symmetry independent $[SbCl([15]crown\text{-}5)]^{2+}$ ions of **2**. Bond lengths and angles see text.

atom is located only 26 pm (dication **1**) or 17 pm (dication **2**) above the best plane through the five O atoms; it is thus shifted approximately in the direction of the lone pair. The Sb–Cl distances are shortened only slightly, on average from 241.7 pm to 236.5 pm (mean value of both dications), during conversion of the half-sandwich arrangement in **1**[1] into the dication of **2**, whereas the Sb–O distances are shortened drastically from 290 to 232 pm. Thus, they already fall in the range of bond lengths of covalent Sb–O bonds, as are found, for example, for the Sb–O axial distances in SbOF with a fivefold coordinated antimony atom (222 and 230 pm, respectively[6]).

The two resonance signals in the ^{121}Sb Mössbauer spectrum of **2** (Fig. 2) with contributions to the isomeric shift of $-16.8\ mm\,s^{-1}$ and $-3.0\ mm\,s^{-1}$ can be assigned to the an-

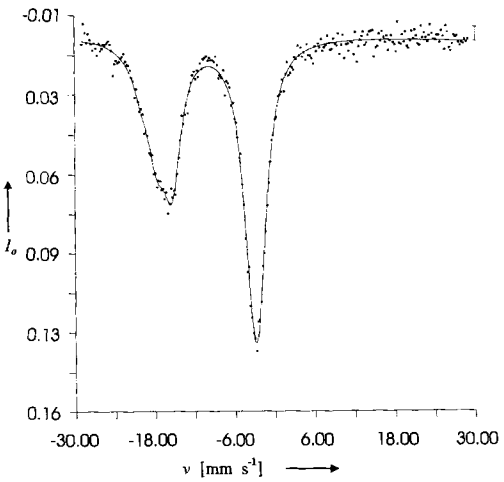

Fig. 2. ^{121}Sb Mössbauer spectrum of **2** at 4.2 K. I_o = resonance absorption, v = isomeric shift.

timony sites of cation and anion, respectively.[7] In the case of the $SbCl_6^-$ ion, whose symmetry deviates only little from O_h, the small electric field gradient leads to a quadrupole splitting ΔE_Q of only 5.1 mm s^{-1}, whereas in the case of the cation of **2** a ΔE_Q value of 16.0 mm s^{-1} is measured. The almost unchanged isomeric shift of **2** in comparison to **1** ($v = 17.0$ mm s^{-1} [2]) is indicative of a comparatively large s-part of the lone pair in both complexes. In contrast, the increase in the quadrupole splitting from 10.2 mm s^{-1} in **1** to 16.0 mm s^{-1} in **2** reflects the relatively large p_x–p_y bonding parts of the five Sb–O bonds of the equatorially arranged crown ether, which correlates well with the short Sb–O distances. Structure and ^{119}Sn Mössbauer investigations on tin–crown ether complexes [SnCl([18]crown-6)]X (X = ClO_4^-, $SnCl_3^-$) led to similar findings.[8, 9]

Reaction of bismuth trichloride with antimony pentachloride in the presence of [15]crown-5 analogously to Equation (a) leads to formation of only the monocation **3** [Eq. (b)].

$$BiCl_3 + [15]\text{crown-5} + SbCl_5 \xrightarrow{CH_3CN} [BiCl_2([15]\text{crown-5})(CH_3CN)]SbCl_6 \quad \textbf{3} \qquad (b)$$

As the crystal structure analysis shows[10] (Fig. 3), the cavity of the crown ether is obviously too small to accommodate the bismuth atom. Actually, the dication **4** is formed,

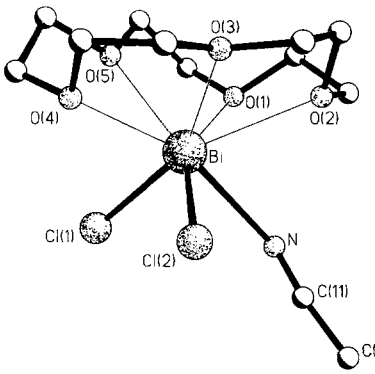

Fig. 3. The crystal structure of the $[BiCl_2([15]\text{crown-5})(CH_3CN)]^+$ ion of **3**. Selected bond lengths [pm] and angles [°]: Bi-Cl(1) 251.5(7), Bi-Cl(2) 248.9, Bi-N 265(3); Cl(1)-Bi-Cl(2) 93.6(3), Cl(1)-Bi-N 82.6(7), Cl(2)-Bi-N 79.7(6).

but only upon using the larger crown ether [18]crown-6 [Eq. (c)]. It should be pointed out that the formation of the dication in **4** is not only dependent on the size of the crown ether but is also determined by the Lewis acidity of the antimony pentachloride, since the corresponding reaction with bismuth trichloride as Lewis acid leads to $[BiCl_2([18]\text{crown-6})]_2^{2+}[Bi_2Cl_8]^{2-}$,[11] i.e. only to the monocation $[BiCl_2([18]\text{crown-6})]^+$. The Bi–Cl and Bi–O bond lengths in this monocation are quite similar to those in **3**.

$$BiCl_3 + [18]\text{crown-6} + 2\,SbCl_5 \xrightarrow{CH_3CN} [BiCl([18]\text{crown-6})(CH_3CN)_2](SbCl_6)_2 \quad \textbf{4} \qquad (c)$$

According to the crystal structure analysis of **4**[12] the cavity of the crown ether is obviously too large to facilitate

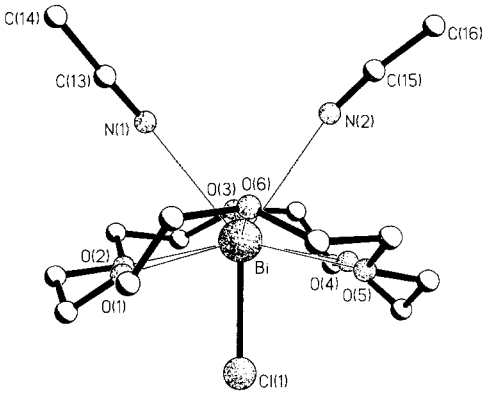

Fig. 4. The crystal structure of the $[BiCl([18]\text{crown-6})(CH_3CN)_2]^{2+}$ ion of **4**. Selected bond lengths [pm] and angles [°]: Bi-Cl(1) 247.9(6), Bi-N(1) 282(2), Bi-N(2) 286(3); Cl(1)-Bi-N(1) 141.0(6), Cl(1)-Bi-N(2) 144.8(5), N(1)-Bi-N(2) 74.1(7).

a coplanar arrangement of the Bi atom with the six O atoms (Fig. 4). Instead, the Bi atom is surrounded by the O atoms of the crown ether in a distorted prismatic fashion and the Cl atoms and the N atoms of the acetonitrile ligands each occupy a prism face. Hence, it is understandable why the acetonitrile ligands cannot coordinate to the side of the molecule away from the crown ether, as in **3**. A conceivable steric activity of the lone pair on the Bi atom cannot be established with certainty, as is usually the case with Bi^{III} compounds.[13] Nevertheless, a possible preferred direction of the lone pair along the Cl–Bi axis cannot be ruled out.

Received: October 5, 1991 [Z 4955 IE]
German version: *Angew. Chem.* **1992**, *104*, 354

CAS Registry numbers:
1, 107198-25-4; **2**, 138694-72-1; **3**, 138694-74-3; **4**, 138694-76-5.

[1] E. Hough, D. G. Nicholson, A. K. Vasudevan, *J. Chem. Soc. Dalton Trans.* **1987**, 427.
[2] M. Schäfer, J. Pebler, B. Borgsen, F. Weller, K. Dehnicke, *Z. Naturforsch. B*, **1990**, *45*, 1243.
[3] M. Schäfer, J. Pebler, K. Dehnicke, *Z. Anorg. Allg. Chem.*, in press.
[4] G. B. Jameson, E. Blaszó, H. R. Oswald, *Acta Crystallogr. Sect. C*, **1984**, *40*, 350.
[5] Crystal data of **2**·1.5 CH_3CN (−65 °C): space group $P2_12_12_1$, a = 1274.9(3), b = 1937.7(4), c = 2765.6(6) pm, Z = 8, Enraf-Nonius CAD4 four-circle diffractiometer, $Mo_{K\alpha}$ radiation, graphite monochromator, ω-scan, θ = 2–23°, 2897 observed independent reflections ($F_o \geq 4\sigma(F_o)$), H atom positions isotropic, R = 0.061, R_w = 0.045 [12].
[6] A. Åström, *Acta Chem. Scand.* **1972**, *26*, 3849.
[7] An isomeric shift of −3.2 mm s^{-1} has been quoted for the $SbCl_6^-$ ion in $[Rb_4Sb^{III}Cl_6]Sb^{V}Cl_6$: D. I. Baltrunas, S. P. Ionov, A. Yu. Aleksandrov, E. F. Makarov, *Chem. Phys. Lett.* **1973**, *20*, 55.
[8] R. H. Herber, G. Carraquillo, *Inorg. Chem.* **1981**, *20*, 3693.
[9] M. G. B. Drew, D. G. Nicholson, *J. Chem. Soc. Dalton Trans.* **1986**, 1543.
[10] Crystal data of **3** (−80 °C): space group $P2_1/n$, Z = 4, Enraf-Nonius CAD4 four-circle diffractometer, $Mo_{K\alpha}$ radiation, graphite monochromator, ω-scan, θ = 2–25°, 2188 observed independent reflections ($F_o \geq 4\sigma(F_o)$), H atom positions with constant temperature factors in calculated positions, disordered Cl atoms on Sb(1) with common temperature factors, $\mu(Mo_{K\alpha})$ = 86.1 cm^{-1}, R = 0.085, R_w = 0.060 [12].
[11] N. W. Alcock, M. Ravindran, G. R. Willey, *J. Chem. Soc. Chem. Commun.* **1989**, 1063.
[12] Crystal data of **4** (−80 °C): space group $P\bar{1}$, Z = 2, Enraf-Nonius CAD4 four-circle diffractometer, $Mo_{K\alpha}$ radiation, graphite monochromator, ω-scan, θ = 1.5–28°, 4388 observed independent reflections ($F_o \geq 4\sigma(F_o)$), H atom positions with constant temperature factors in calculated positions, $\mu(Mo_{K\alpha})$ = 69.9 cm^{-1}, R = 0.089, R_w = 0.079. Further details of the crystal structure investigations are available on request from the Fachinformationszentrum Karlsruhe, Gesellschaft für wissenschaftlich-technische Information mbH, D-W-7514 Eggenstein-Leopoldshafen 2 (FRG), on quoting the depository number CSD-55941, the names of the authors, and the journal citation.
[13] A. F. Wells, *Structural Inorganic Chemistry*, Clarendon Press, Oxford, **1984**.

Quantification of the Reactivity of 3-Aminopropyltriethoxysilane Monolayers with the Quartz-Crystal Microbalance**

By *Dirk G. Kurth* and *Thomas Bein**

Surface reactions have been utilized to construct well-ordered, three-dimensional structures on surfaces and to study surface phenomena in self-assembled films.[1] An important question in surface chemistry is to what extent known reactions from the highly developed fields of synthetic organic and inorganic chemistry can be utilized on surfaces. One aspect is the chemical yield of a reaction conducted according to conventional procedures compared to that of a reaction conducted on a surface. Due to their high mass-sensitivity, piezoelectric devices, that is instruments employing oscillating crystals, have found application in studies of surface phenomena.[2] The method is based on measuring the shift in the resonance frequency of the crystal upon the deposit of mass on the electrode surfaces. For low masses the mass–frequency relationship is linear and obeys the Sauerbrey equation.[3] Although in situ electrochemical reactions on electrode surfaces[4] and the adsorption kinetics of thiols on gold[5] have been studied with piezoelectric devices, the use of quartz-crystal microbalances (QCMs) in quantifying sequential reactions confined to a surface has not been explored.

In this communication, we demonstrate that a reaction confined to a surface can be followed with a QCM. If 3-aminopropyltriethoxysilane (APS) is immobilized on an oxidized aluminium substrate and then allowed to react with chlorodimethylsilane, a surface-immobilized dimethylsilane–ammonium salt forms (Scheme 1). In contrast to the spontaneous organization of some molecular assemblies[6] APS does not form well-ordered, crystalline monolayers.[7] However, we have found that monomolecular layers of APS may be formed by gas-phase adsorption on the substrate.

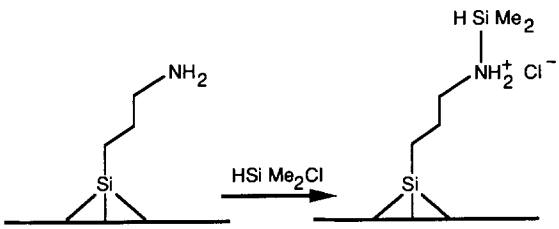

Scheme 1. Schematic representation of the reaction of immobilized APS with chlorodimethylsilane.

In addition to the QCM we have also used reflection absorption IR spectroscopy (RAIR) spectroscopy, ellipsometry, and contact-angle measurements to elucidate the presence and the organization of the reactants and the products on the surface. In our experiments the precleaned substrate (glass slides with a layer of oxidized aluminium)[8] were placed in specially designed glass dishes at room temperature under dried nitrogen and were then exposed to APS vapor for several minutes to several hours. After evacuation of the chamber, the modified slides were exposed to chlorodimethylsilane vapors for 15 minutes. The samples were evacuated and handled under nitrogen until all measurements had been completed.

Figure 1 shows the RAIR spectrum of an APS monolayer on oxidized aluminium.[9] The thickness of the sample was determined by optical ellipsometry to be 6 ± 1 Å.[10] The contact-angle θ_a of this sample was $52 \pm 2°$. The RAIR spectrum shows two peaks at 1610 and 1583 cm^{-1} that are assigned to associated and free amino groups. The amine can undergo hydrogen bonding with the ethoxy, silanol, or surface hydroxy groups, which increases the frequency of the N–H deformation mode.[11] The hydrogen bonding is expected to force the amine group towards the surface, reducing the overall film thickness.

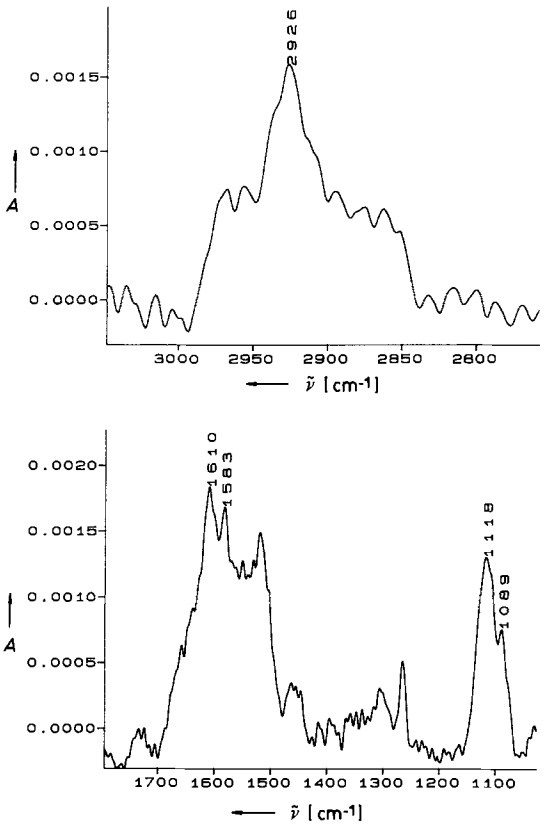

Fig. 1. RAIR spectrum of an APS monolayer on oxidized aluminum. *A*: absorbance (arbitrary units).

Figure 2 shows the QCM response for the adsorption of APS under rigorously dry conditions.[12] Upon exposure to the APS vapor a steady increase in the frequency shift was observed. To remove physisorbed material the reactor was evacuated and rinsed with nitrogen several times. According to the QCM results, the remaining mass is due to chemisorption of a monolayer of APS; the frequency reading of the QCM after evacuation was stable for several days. The frequency change ΔF, measured in several experiments, averages to 48 ± 2 Hz, which is equivalent to 5.2 ± 0.2 APS molecules per nm^2, assuming the attachment of $H_2N(CH_2)_3Si(OEt)$ species on the surface.[13] At this extent of coverage, each APS molecule occupies an average of 1.9 nm^2.[14] The

[*] Prof. Dr. T. Bein, Dipl.-Chem. D. G. Kurth
Purdue University
Department of Chemistry
West Lafayette IN 47907-1393 (USA)

[**] This work was supported by the National Science Foundation (DMR-8706167 and DMR-900695) and by the Department of Energy (New Mexico WERC Program). We thank Herb Tardy of the Sandia National Laboratories for helpful discussions and assistance in the ellipsometric measurements, which were obtained on an instrument at the Center for High Technology Materials at the University of New Mexico. We are also grateful to Alfonso Torres for his help.

data are consistent with the attachment of about one monolayer of APS to the aluminium surface by gas-phase adsorption.

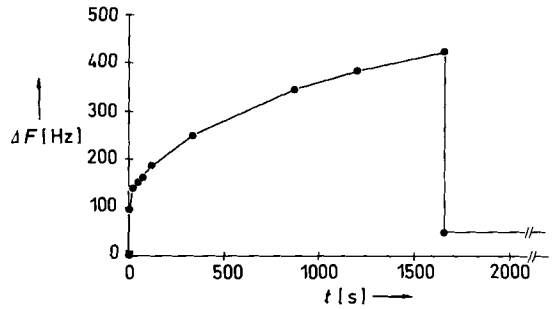

Fig. 2. QCM response for the adsorption of APS under rigorously dry conditions. After evacuation only one monolayer remains on the electrode surface of the QCM.

We conducted subsequent reactions on the APS monolayer with chlorodimethylsilane vapor by placing the slides in a reactor under nitrogen filled with 0.5 mL of the silane, and exposed the slides to the vapors for 15 minutes at room temperature. After this treatment the film thickness had increased by 5 ± 1 Å. The RAIR spectrum is shown in Figure 3. The

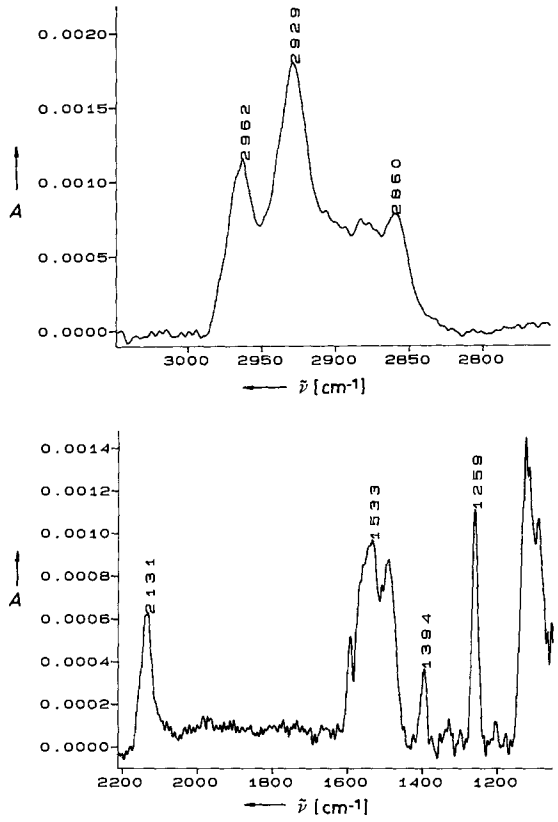

Fig. 3. RAIR spectrum after the reaction of the APS monolayer with chlorodimethylsilane. *A*: absorbance (arbitrary units).

strong bands at 2962, 2860, and 1259 cm^{-1} are assigned to the C–H stretching and deformation modes of the newly attached dimethylsilyl group. The band at 2860 cm^{-1} overlaps with the CH_2 stretching vibration of the propyl group from APS. The band at 2131 cm^{-1} is characteristic for the Si–H stretch. This band is shifted approximately 40 cm^{-1} compared to the comparable band of liquid chlorodimethylsilane (2175 cm^{-1}, transmission spectrum). This shift is attributed to the changed electronic environment after exchange of the chlorine atom.[15] The band at 1394 cm^{-1} is strongly enhanced after the reaction and assigned to the deformation mode of the CH_2 group next to the NH_2^+ group; the band at 1533 cm^{-1} is assigned to the deformation mode of the NH_2^+ group. The contact-angle decreases from $52 \pm 2°$ for the APS film to $41 \pm 3°$ after the reaction. The enhanced wettability of the sample after the reaction is consistent with the formation of an ammonium salt, as indicated by the RAIR data. Apparently, the newly formed overlayer composed of dimethylsilane is disordered and allows penetration of water into the film. This is in agreement with other reports that short-chain *n*-alkylthiols do not form well-ordered monolayers.[16]

The frequency shift in the QCM experiment averaged over several experiments is 33 ± 2 Hz, which is equivalent to 5.3 ± 0.2 additional HMe_2SiCl molecules per nm^2. The data indicate that within the experimental accuracy, all the immobilized amino groups reacted with chlorodimethylsilane from the gas phase. In contrast to reactions with dense self-assembled monolayers, this reaction is quantitative because the APS film is not highly organized.

Received: October 2, 1991 [Z 4948 IE]
German version: *Angew. Chem.* **1992**, *104*, 323

CAS Registry numbers:
Me_2SiHCl, 1066-35-9; $(EtO)_3Si(CH_2)_3NH_2$, 919-30-2.

[1] a) A. Ulman, N. Tillman, *Langmuir* **1989**, *5*, 1418; b) H. Lee, L. J. Kepley, H. Hong, T. E. Mallouk, *J. Am. Chem. Soc.* **1988**, *110*, 618; c) R. Maoz, J. Sagiv, *Langmuir* **1987**, *3*, 1034; d) S. R. Wasserman, Y. Tao, G. M. Whitesides, *ibid.* **1989**, *5*, 1074.

[2] a) C. Lu, A. W. Czanderma in *Applications of Quartz-Crystal Microbalance, Methods and Phenomena, Vol. 7*, Elsevier, New York, **1984**; b) M. D. Ward, D. A. Buttry, *Science* **1990**, *249*, 1000; c) R. Schumacher, *Angew. Chem.* **1990**, *102*, 347; *Angew. Chem. Int. Ed. Engl.* **1990**, *29*, 329; d) R. R. McCaffery, S. Bruckenstein, P. N. Prasad, *Langmuir*, **1986**, *2*, 228.

[3] G. Sauerbrey, *Z. Phys.* **1959**, *155*, 206.

[4] M. R. Deakin, T. Li, O. R. Melroy, *J. Electroanal. Chem.* **1988**, *243*, 343.

[5] R. C. Thomas, L. Sun, R. M. Crooks, A. J. Ricco, *Langmuir* **1991**, *7*, 620.

[6] a) C. Bain, G. M. Whitesides, *Angew. Chem. Adv. Mater.* **1989**, *101*, 522; *Angew. Chem. Int. Ed. Engl. Adv. Mater.* **1989**, *28*, 506; *Adv. Mater.* **1989**, 110; b) R. Nuzzo, E. Korenic, L. Dubois, *J. Phys. Chem.* **1990**, *93*, 767; c) J. Gun, J. Sagiv, *J. Colloid Interface Sci.* **1986**, *112*, 457.

[7] D. Kurth, T. Bein, *J. Phys. Chem.*, submitted.

[8] Ultraclean aluminum (99.999%) was evaporated onto glass slides at a base pressure of 10^{-6} Torr. The aluminum slides were cleaned in a nitrogen or oxygen plasma and exposed to water vapor. An amorphous aluminum oxide–hydroxide layer thus formed had a thickness of 50 Å to 100 Å, as indicated by optical ellipsometry (P. Thiel, T. E. Madey, *Surf. Sci. Rep.* **1987**, *7*, 211 and literature cited therein). Slides prepared this way were completely wetted by water (M. E. Schrader, *Surf.* **1979**, *2*, 541; *Contam. Genesis Detect. Control, Proc. Symp.* **1978**.

[9] RAIR spectra were obtained on a Mattson Polaris FTIR spectrometer with a Harrick attachment and an MCT detector at an angle of incidence of 86°. 1000 scans were collected. The sample spectra were compared to those obtained from precleaned gold reference slides. The spectra were electronically corrected in the baseline with two or three base points at a higher and lower frequencies.

[10] Ellipsometric measurements were made using a Rudolf Research Ellipsometer (43603-200E) with a He–Ne laser at a 70° angle of incidence and a 45°/135° azimuth of the compensator. Film thicknesses were calculated using the complex refractive index of the substrate, determined prior to derivatization, and the bulk refractive index of the film with an algorithm developed at Sandia National Labs (H. L. Tardy, *Ellipse User's Manual and Program Reference*; Report No. 89-0008; Sandia National Laboratories, Albuquerque, NM, USA, **1989**).

[11] K. Nakanishi, P. H. Solomon, *Infrared Absorption Spectroscopy*, 2nd ed., Holden-Day, San Francisco, **1977**.
[12] The QCM measurements were made on polished, AT-cut crystals (AT: orientation of the cut relative to the crystal axes) with aluminum electrodes operated at a frequency of 9 MHz. A surface roughness of 15%, as measured by nitrogen adsorption isotherms, was taken into account.
[13] The bands at 2975, 2888, and 1390 cm^{-1} in the RAIR spectrum reveal the presence of ethoxy groups within the surface-attached APS moiety. The bands at 1089 and 1118 cm^{-1} are characteristic for siloxane oligomers, indicating the loss of ethoxy groups and partial cross-linking on the surface.
[14] C. E. D. Chidsey, D. N. Loiacono, *Langmuir*, **1990**, *6*, 682.
[15] D. Anderson in *Analysis of Silicones* (Ed.: A. Smith), Wiley, New York, **1974**, Chapter 10.
[16] a) M. D. Porter, T. B. Bright, D. L. Allara, C. E. D. Chidsey, *J. Am. Chem. Soc.* **1987**, *109*, 3559; b) C. D. Bain, G. M. Whitesides, *ibid.* **1988**, *110*, 5897.

Synthesis of the Calicheamicin Aryltetrasaccharide Domain Bearing a Reducing Terminus: Coupling of Fully Synthetic Aglycone and Carbohydrate Domains by the Schmidt Reaction**

By *Randall L. Halcomb, Serge H. Boyer,* and *Samuel J. Danishefsky**

The identification of the mechanistically novel, highly potent antitumor agents calicheamicin (**1**)[1a,b] and esperamicin (**2**)[1c,d] as well as neocarzinostatin[2a] and dynemycin[2b] has spurred a variety of initiatives in synthesis,[3] biosimulation,[4] and computation.[5,6] An ultimate goal of the creative interactivity of such efforts is the development of more accessible compounds which manifest higher therapeutic indices than do the natural products.[7]

The aglycone sector of **1** is recognized as the source of the cytoxic diradical effector species.[8] Our laboratory has completed the synthesis of the fully functionalized aglycone, calicheamicinone (**3**).[9] Experiments conducted with the synthetic racemate,[10] showed it to retain the DNA-cleaving properties of the drug **1** though with significantly reduced potency. Suitably activated aglycone retains some of the remarkable capacity for direct hydrogen abstraction from C–H bonds of oligonucleotide constructs[11a,b] however, it lacks any significant sequence selectivity in DNA cleavage of the type manifested by calicheamicin.[12,13]

Recently, enzymatic resolution of intermediates en route to **3** and the descarbamoyl version thereof has been achieved.[14a,b] This advance provides access to enantiomerically pure "late" intermediates in the synthetic sequence. Of course the use of aglycone intermediates of unambiguous absolute configuration obviates the structural ambiguities arising from the employment of a racemate as a coupling component.

The carbohydrate domain is presumed[15,16] to provide the sensitivity to structural nuance responsible for the sequence selectivity manifested by the drug in its cleavage of various oligonucleotide targets. An important synthetic goal was achieved by Nicolaou et al. in their synthesis of the methylglycoside corresponding to the aryltetrasaccharide domain of calicheamicin.[17] Our efforts focussed on the related trisaccharide sector of esperamicin.[18,19] Those studies led to the synthesis of trisaccharide methylglycoside **4a**. Furthermore, it was demonstrated by inference that the fully deprotected system, **4b**, undergoes extremely rapid rearrangement to the azafuranose **5**.[20] Maintenance of the free reducing end was shown to be possible by protecting the nitrogen atom of the hydroxylamino linkage as a Teoc carbamate (see **4c**, Teoc = $Me_3SiCH_2CH_2O_2C$).[18]

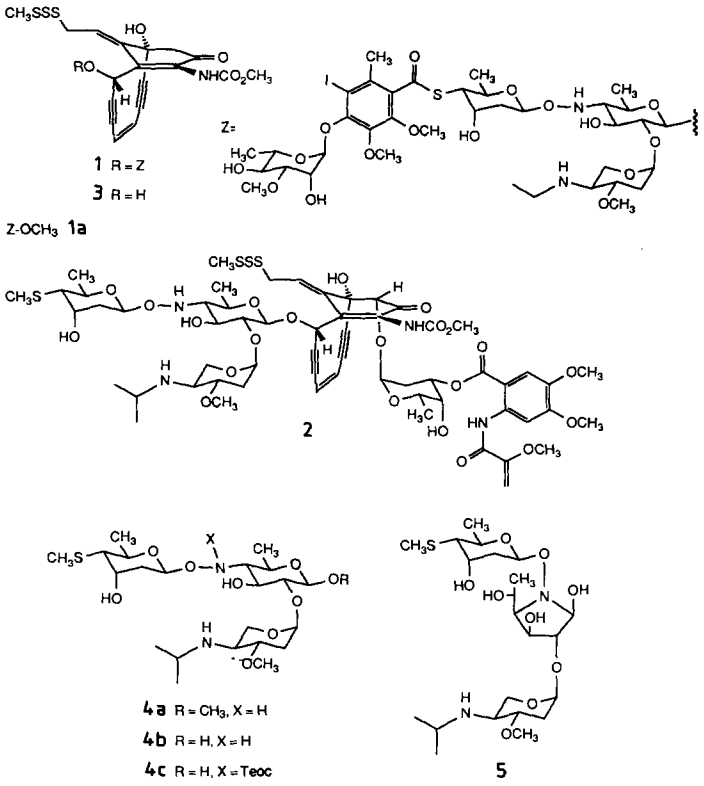

We describe here a) the first synthesis of the aryltetrasaccharide sector of calicheamicin which bears a free reducing terminus and b) the first demonstration that a properly activated aryltetrasaccharide system will indeed function as a glycosyl donor toward enantiomerically pure advanced aglycone intermediates en route to **3**.

Ferrier rearrangement[21] of commercially available diacetyl-L-rhamnal affords **6**,[23] which upon exchange of protecting groups, osmylation, and selective monomethylation,[22] provided a 72% yield of **7** (Scheme 1).[23] The free axial OH group in **7** was acetylated, and the anomeric hydroxyl group was liberated by debenzylation. Compound **8**,[23] thus produced, was converted to the trichloroacetimidate **9**.[24,25] Upon treatment of **9** with $BF_3 \cdot Et_2O$ and phenol **10**,[26] the aryl glycoside **11**[23,27] was obtained in 83% yield. This compound was converted to the axial silyl ether **12**[23] under standard conditions in 91% yield. Selective methoxycarbonylation *para* to the glycosyloxy function[28] gave ester **13**[23] albeit in only 45% yield.

All attempts to convert **13** to **15** by dealkylation, hydrolysis, or other acyl-transfer methods were unsuccessful.[29] However, the desired acid **15**[23] could be obtained by reduction of **13** with diisobutylaluminium hydride followed by

[*] Prof. Dr. S. J. Danishefsky, R. L. Halcomb, S. H. Boyer
Department of Chemistry
Yale University
225 Prospect Street
New Haven, CT 06511 (USA)

[**] This research was supported by PHS (Grant CA 28824). NMR spectra were measured at the Northeast Regional NSF/NMR Facility at Yale University, which was supported by the National Science Foundation NSF Chemistry Division (Grant CHE 7916210). An American Chemical Society Organic Division Fellowship (sponsored by the Monsanto Corporation) and a Pfizer Fellowship to R. L. H. and a Kent Fellowship to S. H. B. are gratefully acknowledged.

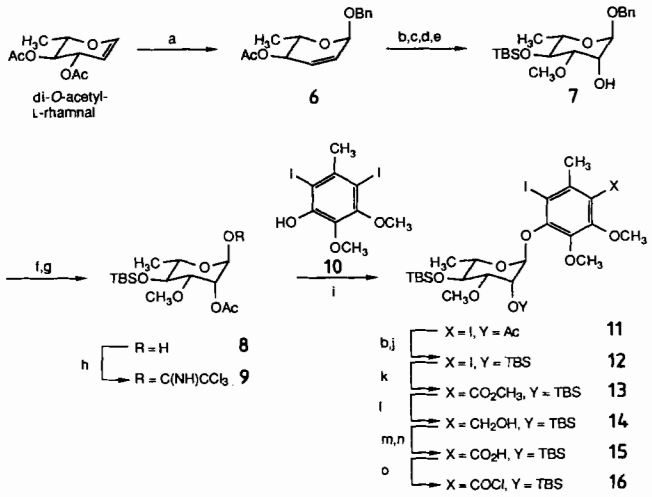

Scheme 1. a) BnOH, CH_2Cl_2, $BF_2 \cdot Et_2O$, room temperature (RT) (91%). b) NaOMe, MeOH. c) $tBuMe_2SiCl$ (TBSCl), imidazole, CH_2Cl_2, RT (96% for b + c). d) OsO_4, *N*-methylmorpholine-*N*-oxide (NMO), acetone, H_2O (96%). e) 1. Bu_2SnO, MeOH, Δ; 2. CH_3I, Bu_4NBr, benzene, Δ (98%). f) Ac_2O, pyridine (99%). g) H_2, $Pd(OH)_2$, MeOH (92%). h) Cl_3CCN, NaH (0.7 equiv), CH_2Cl_2, 0 °C (95%). i) **10**, $BF_3 \cdot Et_2O$, CH_2Cl_2, −48 °C (89%). j) TBSOtf (tf = triflate), pyridine, DMAP, CH_2Cl_2, 0 °C (91% for i + j). k) CO, $Pd(OAc)_2$, MeOH, Et_3N, $Ph_2P(CH_2)_3PPh_2$, dimethyl sulfoxide (DMSO), 65 °C (45%). l) iBu_2AlH, CH_2Cl_2, −78 °C (90%). m) Dess-Martin periodinane (*1,1,1*-triacetoxybenzo[*c*]iodafuranone), CH_2Cl_2, 0 °C → RT (98%). n) $NaClO_2$, H_2O, *t*BuOH, 2-methyl-2-butene, NaH_2PO_4 (98%). o) $(COCl)_2$, RT.

two-step oxidation[30a,b] of the resulting alcohol **14**. Compound **15** was converted to acid chloride **16** for subsequent reactions.

Under mediation by DMAP and Et_3N, **16** acylated the previously reported **17**[18] to afford **18**[23] in 85% yield (Scheme 2). The aryltetrasaccharide domain now could readily be assembled. Alkylation of the nitrogen atom[31] of the Teoc carbamate with the previously reported triflates **19** and **20**[18] provided the aryltetrasaccharides **21**[23] and **22**[23] respectively in yields of approximately 80%.

Hydrazinolysis of the phthalimide group of **21** followed by reductive alkylation[32] of **23**[23] afforded **24** in 98% yield. Cleavage of the *para*-methoxybenzyl (PMB) blocking group was accomplished (75%) using a standard protocol.[33]

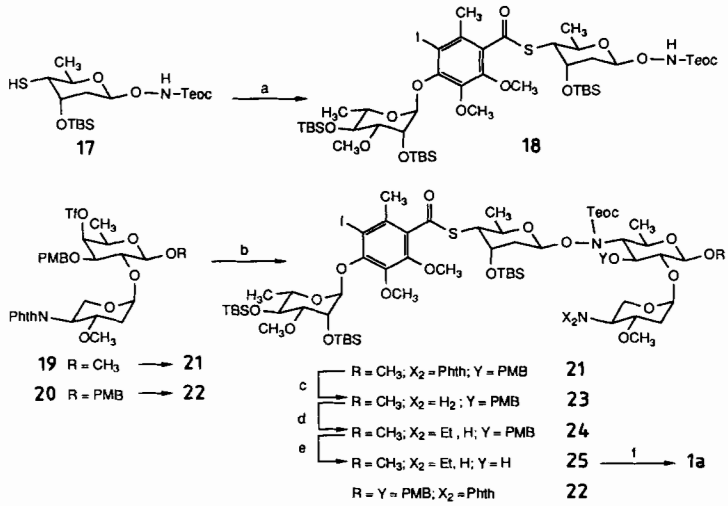

Scheme 2. a) **16**, Et_3N, DMAP, CH_2Cl_2, 0 °C (85% from **15**). b) 1. NaH, **18**, dimethylformamide (DMF), 0 °C → RT; 2. **19** or **20**, DMF, 0 °C (80%). c) H_2NNH_2, EtOH, Δ (91%). d) CH_3CHO, $NaCNBH_3$, $MgSO_4$, MeOH (98%). e) dichlorodicyano-*para*-benzoquinone (DDQ), CH_2Cl_2, H_2O (75%). f) Bu_4NF, THF, 0 °C (60%).

Compound **25**[23] thus obtained was fully desilylated to afford the free methylglycoside **1a** Z-OCH_3.[23] The binding properties of **1a** with various oligonucleotide sequences are currently being evaluated.[34]

The two PMB groups of **22** were simultaneously cleaved[33] to give a 79% yield of **26**.[23] Compound **26** was

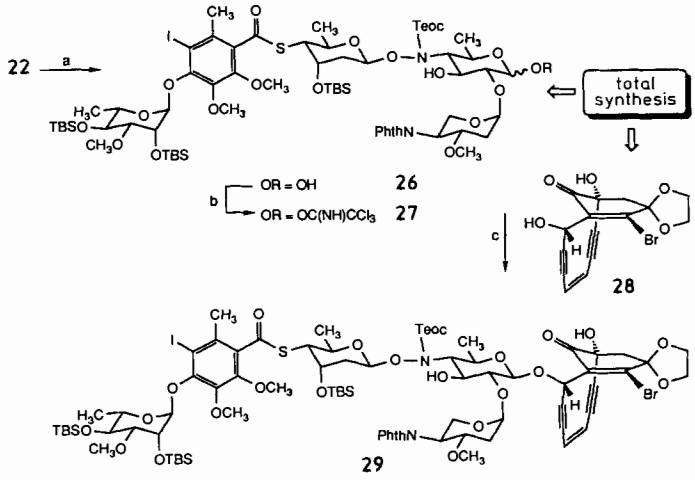

Scheme 3. a) DDQ, CH_2Cl_2, H_2O (79%). b) Cl_3CCN, diazabicycloundecene (DBU), CH_2Cl_2, RT (73%). c) **28**, $BF_3 \cdot Et_2O$, Et_2O/CH_2Cl_2, −78 °C (15%).

Table 1. ^1H NMR data for **1a**, **27**, and **29**. Ar = aryl, A–E: nonaromatic rings, eq = equatorial, ax = axial.

(490 MHz, $CDCl_3$). **1a:** δ = 6.25 (br.s, 1H, ONH), 5.75 (d, 1H, *J* = 1.3 Hz, H-1D), 5.43 (m, 1H, H-1E), 5.06 (dd, 1H, *J* = 10.0, 1.7 Hz, H-1B), 4.49 (m, 1H, H-2D), 4.33 (m, 1H, H-3B), 4.23 (d, 1H, *J* = 7.7 Hz, H-1A), 4.21 (dq, 1H, *J* = 9.7, 6.2 Hz, H-5D), 4.08 (dq, 1H, *J* = 10.7, 6.2 Hz, H-5B), 4.01 (t, 1H, *J* = 9.7 Hz, H-3A), 3.90 (s, 3H, $ArOCH_3$), 3.85 (s, 3H, $ArOCH_3$), 3.80 (dd, 1H, *J* = 8.9, 3.5 Hz, H-4B), 3.78–3.72 (m, 3H, H-3D, H-5E_{eq}, H-5E_{ax}), 3.66 (dd, 1H, *J* = 9.3, 6.2 Hz, H-5A), 3.65 (t, 1H, *J* = 9.6 Hz, H-4D), 3.59 (s, 3H, OCH_3), 3.53 (s, 3H, OCH_3), 3.52–3.48 (m, 2H, H-2A, H-3E), 3.39 (s, 3H, OCH_3), 2.72–2.67 (m, 2H, CH_2N), 2.65–2.60 (m, 1H, H-4E), 2.37 (s, 3H, $ArCH_3$), 2.35 (t, 1H, *J* = 9.8 Hz, H-4A), 2.34–2.29 (m, 1H, H-2E_{eq}), 2.06–2.02 (m, 1H, H-2B_{eq}), 1.82–1.76 (m, 1H, H-2B_{ax}), 1.65–1.55 (m, 1H, H-2E_{ax}), 1.43 (d, 3H, *J* = 6.2 Hz, 3H-6B), 1.35 (d, 3H, *J* = 6.2 Hz, 3H-6A), 1.32 (d, 3H, *J* = 6.2 Hz, 3H-6D), 1.13 (t, 3H, *J* = 7.1 Hz, N-C-CH_3).

27: δ = 8.96 (s, 1H, NH), 7.88–7.82 (m, 2H, ArH), 7.75–7.69 (m, 2H, ArH), 6.48 (d, 1H, *J* = 3.6 Hz, H-1A), 5.48 (d, 1H, *J* = 2.9 Hz, H-1E), 5.38 (d, 1H, *J* = 2.0 Hz, H-1D), 5.40–5.30 (m, 1H, H-1B), 4.54 (dt, 1H, *J* = 11.1, 4.6 Hz, H-4E), 4.47 (t, 1H, *J* = 2.0 Hz, H-2D), 4.50–4.43 (m, 1H), 4.40–4.34 (m, 2H), 4.33–4.21 (m, 3H), 4.20–4.06 (m, 2H), 3.98 (dd, 1H, *J* = 10.6, 3.9 Hz), 3.94–3.80 (m, 3H), 3.88 (s, 3H, $ArOCH_3$), 3.82 (s, 3H, $ArOCH_3$), 3.71 (t, 1H, *J* = 9.0 Hz, H-4D), 3.58 (dd, 1H, *J* = 10.1, 4.7 Hz, H-4B), 3.54 (dd, 1H, *J* = 9.0, 2.4 Hz, H-3D), 3.42 (s, 3H, OCH_3), 3.24 (s, 3H, OCH_3), 2.56–2.51 (m, 1H, H-2E_{eq}), 2.38 (s, 3H, $ArCH_3$), 2.20–2.02 (m, 1H, H-2B_{eq}), 1.83–1.76 (m, 1H, H-2B_{ax}), 1.65–1.55 (m, 1H, H-2E_{ax}), 1.48 (d, 3H, *J* = 6.2 Hz, 3H-6B), 1.28 (d, 3H, *J* = 6.2 Hz, 3H-6A), 1.20 (d, 3H, *J* = 6.1 Hz, 3H-6D), 1.14–1.09 (m, 2H, CH_2Si), 0.93 (s, 18H, 2Si*t*Bu), 0.92 (s, 9H, Si*t*Bu), 0.20–0.10 (m, 18H, 6SiMe), 0.08 (s, 9H, $SiMe_3$).

29: δ = 7.85–7.80 (m, 2H, ArH), 7.72–7.68 (m, 2H, ArH), 6.16 (d, 1H, *J* = 1.2 Hz, C≡C-CH), 5.79 (pseudo-d, 1H, *J* = 9.3 Hz, olefinic H), 5.69–5.63 (m, 2H, H-1E, olefinic H), 5.38 (d, 1H, *J* = 1.6 Hz, H-1D), 5.35–5.26 (br.m, 1H, H-1B), 4.79 (dt, 1H, *J* = 12.7, 5.1 Hz, H-4E), 4.76 (d, 1H, *J* = 8.0 Hz, H-1A), 4.62 (t, 1H, *J* = 11.1 Hz, H-5E_{ax}), 4.46 (t, 1H, *J* = 2.1 Hz, H-2D), 4.36 (br.s, 1H, H-4B), 4.32–4.20 (m, 4H), 4.19–4.00 (m, 6H), 3.94–3.76 (m, 5H), 3.87 (s, 3H, OCH_3), 3.81 (s, 3H, OCH_3), 3.75–3.70 (m, 1H), 3.70 (t, 1H, *J* = 9.0 Hz, H-4E), 3.59 (dd, 1H, *J* = 10.8, 5.1 Hz, H-4B), 3.54 (dd, 1H, *J* = 9.0, 2.4 Hz, H-3D), 3.41 (s, 3H, OCH_3), 3.29 (s, 3H, OCH_3), 2.58 (AB, 2H, *J* = 14.1 Hz, Δν = 156.6 Hz, aglycone-CH_2), 2.54 (m, 1H, H-2E_{eq}), 2.36 (s, 3H, $ArCH_3$), 2.38–2.32 (m, 1H, H-2B_{eq}), 1.86–1.79 (m, 1H, H-2B_{ax}), 1.65–1.55 (m, 1H, H-2E_{ax}), 1.45 (d, 3H, *J* = 6.2 Hz, 3H-6B), 1.23 (d, 3H, *J* = 6.2 Hz, 3H-6A), 1.20 (d, 3H, *J* = 6.0 Hz, 3H-6D), 1.10–1.00 (m, 2H, CH_2Si), 0.94 (s, 18H, 2Si*t*Bu), 0.92 (s, 9H, Si*t*Bu), 0.21–0.10 (m, 18H, 6SiMe), 0.07 (s, 9H, $SiMe_3$).

converted to trichloroacetimidate **27**[35] in the usual manner[25] (Scheme 3). As the aglycone coupling partner we selected an enantiomerically pure version of the previously reported **28**.[14b] In the event, reaction of **27** with **28** under standard Schmidt conditions[25] afforded **29**. Although the yield is modest (15%),[36] this is the first example of the use of the aryltetrasaccharide domain corresponding to calicheamicin as a glycosyl donor.

Now that the feasibility of such a reaction has been demonstrated, many exciting questions present themselves. These are subjects of active pursuit in our laboratory.

Received: October 2, 1991 [Z 4950 IE]
German version: *Angew. Chem.* **1992**, *104*, 314

CAS Registry numbers:
1a, 108212-75-5; **6**, 76404-29-0; **7**, 138785-32-7; **8**, 138785-33-8; **9** α anomer, 138785-31-6; **9** β anomer, 138785-34-9; **10**, 115592-76-2; **11**, 138785-35-0; **12**, 138785-36-1; **13**, 138785-37-2; **14**, 138785-38-3; **15**, 138812-91-6; **16**, 138785-39-4; **17**, 134262-75-2; **18**, 138785-40-7; **19**, 134262-73-0; **20**, 134262-80-9; **21**, 138785-41-8; **22**, 138785-42-9; **23**, 138785-48-5; **24**, 138785-43-0; **25**, 138785-44-1; **26**, 138785-45-2; **27** α anomer, 138785-46-3; **27** β anomer, 138875-06-6; **28**, 134527-43-8; **29** α anomer, 138875-05-5; **29** β anomer, 138785-47-4; di-*O*-acetyl-L-rhamnal, 34819-86-8.

[1] a) M. D. Lee, T. S. Dunne, M. M. Siegel, C. C. Chang, G. O. Morton, D. B. Borders, *J. Am. Chem. Soc.* **1987**, *109*, 3464; b) M. D. Lee, T. S. Dunne, C. C. Chang, G. A. Ellestad, M. M. Siegel, G. O. Morton, W. J. McGahren, D. B. Borders, *ibid.* **1987**, *109*, 3466; c) J. Golik, J. Clardy, G. Dubay, G. Groenewold, H. Kawaguchi, M. Konishi, B. Krishnan, H. Ohkuma, K. I. Saitoh, T. W. Doyle, *ibid.* **1987**, *109*, 3461; d) J. Golik, G. Dubay, G. Groenewold, H. Kawaguchi, M. Konishi, B. Krishnan, H. Ohkuma, K. I. Saitoh, T. W. Doyle, *ibid.* **1987**, *109*, 3462.

[2] a) K. Edo, M. Mizugake, Y. Koide, H. Seto, K. Furihata, N. Otake, N. Ishida, *Tetrahedron Lett.* **1985**, *26*, 331; b) M. Konishi, H. Ohkuma, K. Matsumoto, T. Tsuno, H. Kamei, T. Miyaki, T. Oki, H. Kawaguchi, G. D. van Duyne, J. Clardy, *J. Antibiot.* **1989**, *42*, 1449.

[3] a) S. L. Schreiber, L. L. Kiessling, *Tetrahedron Lett.* **1989**, *30*, 433; b) P. Magnus, F. Bennett, *ibid.* **1989**, *30*, 3637; c) A. S. Kende, C. A. Smith, *ibid.* **1988**, *29*, 4217; d) P. Magnus, R. T. Lewis, J. C. Huffman, *J. Am. Chem. Soc.* **1988**, *110*, 6921; e) P. Magnus, P. A. Carter, *ibid.* **1988**, *110*, 1626.

[4] a) K. C. Nicolaou, Y. Ogawa, G. Zuccarello, H. Kataoka, *J. Am. Chem. Soc.* **1988**, *110*, 7247; b) K. C. Nicolaou, G. Skokotas, S. Furuya, H. Suemune, D. C. Nicolaou, *Angew. Chem.* **1990**, *102*, 1066; *Angew. Chem. Int. Ed. Engl.* **1990**, *29*, 1064.

[5] a) R. C. Hawley, L. L. Kiessling, S. L. Schreiber, *Proc. Natl. Acad. Sci. USA* **1989**, *86*, 1105; b) K. C. Nicolaou, G. Zuccarello, Y. Ogawa, E. J. Schweiger, T. Kumazawa, *J. Am. Chem. Soc.* **1988**, *110*, 4866; c) J. P. Snyder, *ibid.* **1990**, *112*, 5367; d) P. Magnus, S. Fortt, T. Pitterna, J. P. Snyder, *J. Am. Chem. Soc.* **1990**, *112*, 4986.

[6] For a recent review see K. C. Nicolaou, W.-M. Dai, *Angew. Chem.* **1991**, *103*, 1453; *Angew. Chem. Int. Ed. Engl.* **1991**, *30*, 1387.

[7] M. D. Lee, G. A. Ellestad, D. B. Borders, *Acc. Chem. Res.* **1991**, *24*, 235.

[8] a) R. G. Bergman, *Acc. Chem. Res.* **1973**, *6*, 25; b) N. Darby, C. U. Kim, J. A. Salaün, K. W. Shelton, S. Takada, S. Masamune, *J. Chem. Soc. Chem. Commun.* **1971**, 1516.

[9] J. N. Haseltine, M. P. Cabal, N. B. Mantlo, N. Iwasawa, D. S. Yamashita, R. S. Coleman, S. J. Danishefsky, G. K. Schulte, *J. Am. Chem. Soc.* **1991**, *113*, 3850.

[10] a) J. Drak, N. Iwasawa, D. M. Crothers, S. J. Danishefsky, *Proc. Natl. Acad. Sci. USA* **1991**, *88*, 7464; b) Oligonucleotide cleavage experiments with antipodal effectors related to the aglycone are in progress.

[11] a) N. Zein, W. J. McGahren, G. O. Morton, J. Ashcroft, G. A. Ellestad, *J. Am. Chem. Soc.* **1989**, *111*, 6888; b) J. J. De Voss, L. A. Townsend, W. D. Ding, G. O. Morton, G. A. Ellestad, N. Zein, A. B. Tabor, S. L. Schreiber, *ibid.* **1989**, *112*, 9669.

[12] N. Zein, M. Poncin, R. Nilakantan, G. A. Ellestad, *Science* **1989**, *244*, 697.

[13] N. Zein, A. M. Sinha, W. J. McGahren, G. A. Ellestad, *Science* **1988**, *240*, 1198.

[14] a) D. S. Yamashita, V. P. Rocco, S. J. Danishefsky, *Tetrahedron Lett.*, in press; b) V. P. Rocco, S. J. Danishefsky, G. K. Schulte, *ibid.*, in press.

[15] a) S. Walker, K. G. Valentine, D. Kahne, *J. Am. Chem. Soc.* **1990**, *112*, 6428; b) S. Walker, D. Yang, D. Kahne, *ibid.* **1991**, *113*, 4716.

[16] K. C. Nicolaou, E. P. Schreiner, W. Stahl, *Angew. Chem.* **1991**, *103*, 566; *Angew. Chem. Int. Ed. Engl.* **1991**, *30*, 585.

[17] K. C. Nicolaou, R. D. Groneberg, T. Miyazaki, N. A. Stylianides, T. J. Schulze, W. Stahl, *J. Am. Chem. Soc.* **1990**, *112*, 8193.

[18] R. L. Halcomb, M. D. Wittman, S. H. Olson, S. J. Danishefsky, J. Golik, H. Wong, D. Vyas, *J. Am. Chem. Soc.* **1991**, *113*, 5080.

[19] a) J. Golik, H. Wong, D. M. Vyas, T. W. Doyle, *Tetrahedron Lett.* **1989**, *30*, 2497; b) K. van Laak, H. Rainer, H. D. Scharf, *ibid.* **1990**, *31*, 4113.

[20] J. Golik, H. Wong, B. Krishnan, D. M. Vyas, T. W. Doyle, *Tetrahedron Lett.* **1991**, *32*, 1851.

[21] R. J. Ferrier, *Adv. Carbohydr. Chem. Biochem.* **1969**, *24*, 199; A minor amount of the β anomer was also produced (α/β = 6/1).

[22] S. David, S. Hanessian, *Tetrahedron* **1985**, *41*, 643; The ratio of O-3 to O-2-methylation was 4:1.

[23] All new compounds were characterized by NMR and IR spectroscopy, high-resolution mass spectroscopy, and optical rotation. For selected ^{1}H NMR data of compounds **1a**, **27**, and **29** see Table 1.

[24] The trichloroacetimidate **9** existed as an inseparable mixture of anomers (α/β = 10/1).

[25] R. R. Schmidt, *Angew. Chem.* **1986**, *98*, 213; *Angew. Chem. Int. Ed. Engl.* **1986**, *25*, 212.

[26] K. C. Nicolaou, T. Ebata, N. A. Stylianides, R. D. Groneberg, P. J. Carrol, *Angew. Chem.* **1988**, *100*, 1138; *Angew. Chem. Int. Ed. Engl.* **1988**, *27*, 1097.

[27] Also produced was a minor amount of the corresponding β anomer (α/β = 20/1).

[28] Besides **13** the regioisomeric ester (7%), the diester (17%), and recovered starting material (30%) were also isolated.

[29] Products arising from cleavage of the glycoside bond were commonly observed in these attempts.

[30] a) D. B. Dess, J. C. Martin, *J. Org. Chem.* **1983**, *48*, 4155; b) B. O. Lindgren, T. Nilson, *Acta. Chem. Scand.* **1973**, *27*, 888; c) J. C. Bottaro, G. A. Berchtold, *J. Org. Chem.* **1980**, *45*, 1176.

[31] D. Yang, S. H. Kim, D. Kahne, *J. Am. Chem. Soc.* **1991**, *113*, 4715.

[32] R. F. Borch, *Org. Syn.* **1972**, *52*, 124.

[33] Y. Oikawa, T. Yoshioka, O. Yonemitsu, *Tetrahedron Lett.* **1982**, *23*, 885.

[34] J. Aiyar, Yale University, unpublished results.

[35] A mixture of α and β imidates was produced in a 3:1 ratio and was easily separated. Only the α anomer was used in the glycosylation reaction.

[36] An equal amount of the α anomer was also produced. Higher anomeric ratios have been obtained using other optically active aglycone intermediates as coupling partners. These results will be published in due course.

Total Synthesis of Calicheamicin–Dynemicin Hybrid Molecules**

By *K. C. Nicolaou,* Erwin P. Schreiner, Yoshiharu Iwabuchi,* and *Toshio Suzuki*

The discovery of the novel and highly potent anticancer antibiotics of the enediyne class such as calicheamicin γ_1^I

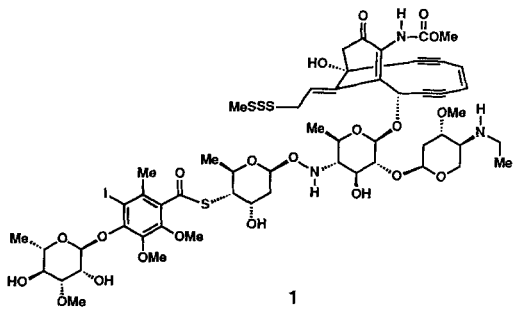

[*] Prof. K. C. Nicolaou, Dr. E. P. Schreiner, Dr. Y. Iwabuchi, Dr. T. Suzuki
Department of Chemistry, The Scripps Research Institute
10666 N. Torrey Pines Road, La Jolla, CA 92037 (USA)
and
Department of Chemistry, University of California, San Diego
La Jolla, CA 92093 (USA)

[**] This work was supported by the National Institutes of Health (USA) and the Scripps Research Institute.

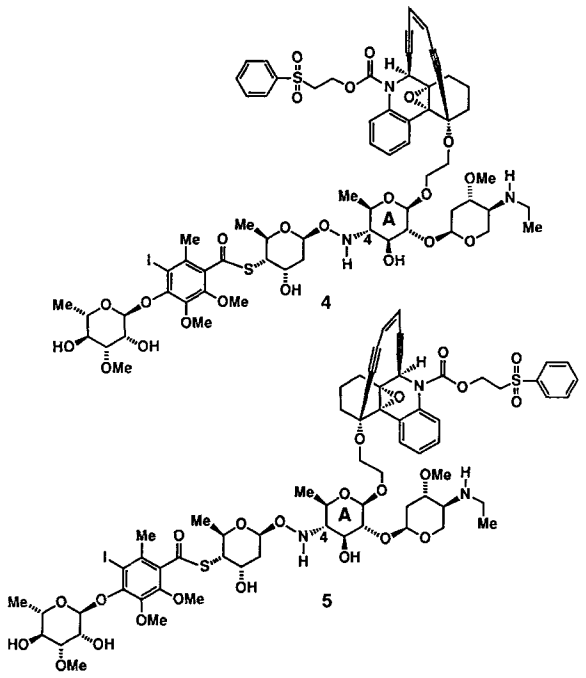

(**1**)[1] and dynemicin A (**2**)[2] generated a great deal of excitement in the chemical, biological, and medical communities.[3] Undoubtedly one of the prime challenges in the field is the design and synthesis of molecules that mimic, combine, or even outperform the biological actions of the natural products.[4] Several reports relating to this subject have already appeared.[3-5] In this communication we report the total synthesis of a series of hybrid molecules that combine the intact oligosaccharide fragment of calicheamicin γ_1^I (**1**) with the "warhead", dynemicin A (**3**), and a triggering device.

Hybrid structures **4** and **5** and their A-4 epimers were constructed according to Scheme 1. Thus the oligosaccharide **6** (Table 1) capped at the anomeric position of ring A with the photoremovable *ortho*-nitrobenzyl ether protecting group was synthesized following modifications of our recently published procedure.[6] Deprotection of **6** by photolysis furnished the free lactol **7** (95% yield), which was then converted into the trichloroacetimidate **8** with catalytic amounts of NaH and excess CCl_3CN in methylene chloride[7] (98% yield).

Coupling of **8** with (±)-**3**[8] under the influence of boron trifluoride–ether led to a mixture of four compounds (70%, ca. 5:5:1:1 ratio) which were separated by high pressure liquid chromatography (silica gel, heptane: diethyl ether, 3:7 → heptane:ethyl acetate, 7:3, gradient). Based on ^{1}H NMR and optical rotation data,[9] the four isomers were tentatively assigned structures **9** (major), A-1 anomer of **9** (minor), **12** (major), and A-1 anomer of **12** (minor).

The two major compounds (β-anomers) **9** and **12** were then taken through the sequence indicated in Scheme 1 to the four final products **4**, **5**, A-4 epimer of **4**, and A-4 epimer of **5** as follows: The triethylsilyl ethers were removed by exposure to HF–pyridine complex to afford compounds **10** (85%) and **13** (85%). The secondary amine was then liberated under carefully controlled conditions (Et_2NH, 0 °C) affording precursors **11** and **14**, respectively, in 68% yield in each case. Finally, reduction of the oxime double bond with sodium cyanoborohydride/boron trifluoride–ether at low temperatures led to a 1:1 mixture of A-4 epimers in 80% total yield for each case. Pure hybrid structures **4**, **5** (Table 1) and their A-4 epimers were obtained by preparative thin-layer chromatography (silica gel, 10% methanol in ethyl acetate). The A-4 stereochemistry was assigned based on ^{1}H NMR data [the A-4 protons for compounds **4** and **5** appear as a pseudotriplet at $\delta = 2.34$ ($J = 10.0, 10.0$ Hz) and 2.27 ($J = 10.0, 10.0$ Hz), respectively, revealing the equatorial orientation of the nitrogen].[6]

Preliminary biological results revealed significant anticancer activity with only two of these agents, namely compounds **4** and **5** which, interestingly, possess the correct stereochemistry for calicheamicin γ_1^I (**1**) at all stereocen-

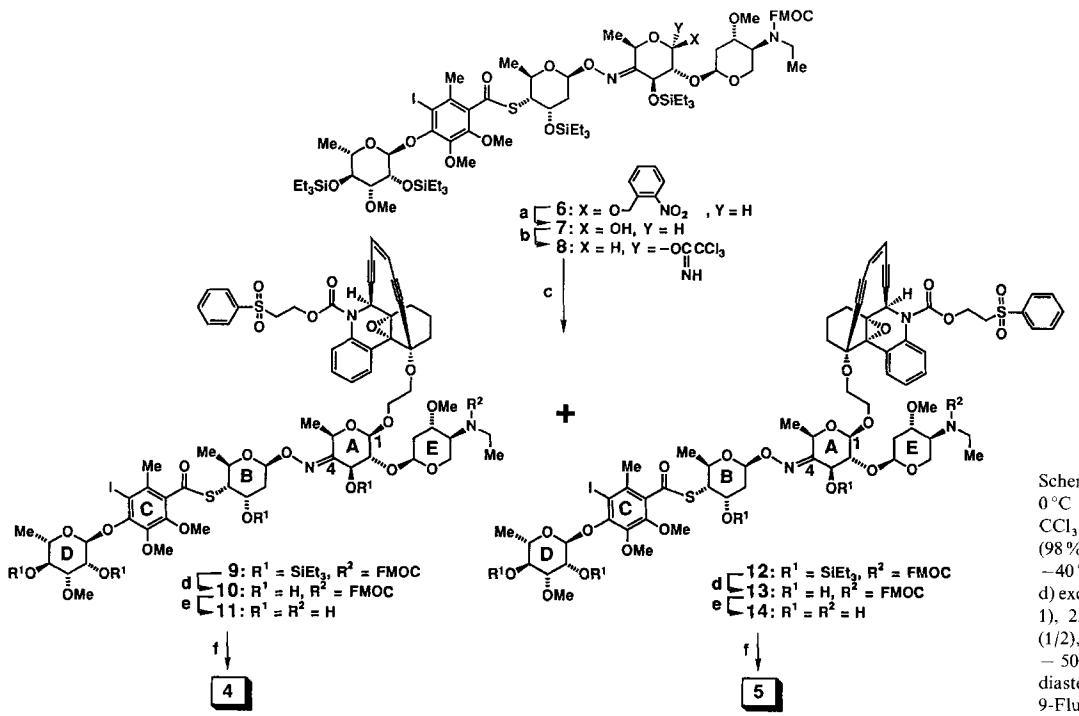

Scheme 1. a) *hv*, THF/H_2O (9/1), 0 °C (95%); b) NaH (cat.), CCl_3CN/CH_2Cl_2 (1/12), 25 °C (98%); c) **3**, CH_2Cl_2, −60 → −40 °C (70%, $\beta:\alpha = 5:1$ ratio); d) excess HF. pyr, CH_2Cl_2/THF (7/1), 25 °C (85%); e) Et_2NH-THF (1/2), 0 °C (68%); f) $NaCNBH_3$, −50 °C (80%, 1:1 mixture of the diastereomers at A-4). FMOC = 9-Fluorenylmethyl carbonate.

Table 1. Selected physical properties and spectroscopic data of **4**, **5** and **6**. eq = equatorial, ax = axial.

4: Colorless oil; $R_f = 0.24$ (silica, 10% methanol in dichloromethane); $[\alpha]_D^{25}$ (CH_2Cl_2, $c = 0.25$) +113.6; IR (film): $\tilde{\nu}_{max} = 2940$, 1720, 1680, 1460, 1410, 1325, 1150, 1070 cm^{-1}; ^1H NMR (500 MHz, $CDCl_3$): $\delta = 8.47-6.92$ (series of multiplets, 9 H, aromat.), 6.34 (br.s, 1 H, ONH), 5.75 (d, $J = 10.0$, 1 H, vinyl), 5.74 (d, $J = 2.1$ Hz, 1 H, D-1), 5.63 (d, $J = 10.0$ Hz, 1 H, vinyl), 5.50 (br.s, 1 H, E-1), 5.34 (br.s, 1 H, propargyl), 5.04 (dd, $J = 10.0$, 2.1 Hz, 1 H, B-1), 4.49 (m, 3 H, D-2, CH_2O), 4.42 (d, $J = 7.9$ Hz, 1 H, A-1), 4.30 (m, 1 H, B-3), 4.19 (dq, $J = 9.5$, 6.0 Hz, 1 H, D-5), 4.16 (m, 1 H, E-5_{ax}), 4.07 (dq, $J = 10.8$, 6.0 Hz, 1 H, B-5), 4.02 (pt (pseudo triplet), $J = 10.0$, 10.0 Hz, 1 H, A-3), 3.97 (m, 2 H, E-3, E-5_{eq}), 3.87–3.79 (series of multiplets, 5 H, A-2, D-3, CH_2O), 3.89 (s, 3 H, CH_3O, aromat.), 3.84 (s, 3 H, CH_3O, aromat.), 3.77 (dd, $J = 10.8$, 2.6 Hz, 1 H, B-4), 3.68–3.56 (series of multiplets, 3 H, A-5, D-4, CH_2O), 3.58 (s, 3 H, CH_3O, D-ring), 3.48 (br.s, 2 H, CH_2O), 3.36 (s, 3 H, CH_3O, E-ring), 2.73 (m, 1 H, E-4), 2.61 (m, 1 H, CH_2N), 2.36 (s, 3 H, CH_3, aromat.), 2.34 (pt, $J = 10.0$, 10.0 Hz, 1 H, A-4), 2.28–1.58 (series of mutliplets, 14 H, B-2_{ax}, B-2_{eq}, CH_2, OH, NH), 1.53 (m, 1 H, E-2_{ax}), 1.42 (d, $J = 6.0$ Hz, 3 H, B-6), 1.30 (d, $J = 6.0$ Hz, 6 H, A-6, D-6), 1.13 (t, $J = 7.0$ Hz, 3 H, CH_3CH_2N); MS: *m/z* (rel. intensity) 1622 ($M^{\oplus}$ + Cs, 17); high resolution MS (FAB^+): calcd for $C_{67}H_{84}IN_3O_{23}S_2Cs$ ($M^{\oplus}$ + Cs): 1622.3036, found 1622.3069

5: Colorless oil; $R_f = 0.24$ (silica, 10% methanol in dichloromethane); $[\alpha]_D^{25}$ (CH_2Cl_2, $c = 0.33$) −119.2; IR (film): $\tilde{\nu}_{max} = 2940$, 1720, 1680, 1460, 1410, 1325, 1150, 1070 cm^{-1}; ^1H NMR (500 MHz, $CDCl_3$): $\delta = 8.45-7.01$ (series of multiplets, 9 H, aromat.), 6.30 (br.s, 1 H, ONH), 5.78 (d, $J = 10.0$, 1 H, vinyl), 5.72 (d, $J = 2.1$ Hz, 1 H, D-1), 5.72 (d, $J = 2.1$ Hz, 1 H, D-1) 5.62 (d, $J = 10.0$ Hz, 1 H, vinyl), 5.42 (br.s, 1 H, E-1), 5.34 (br.s, 1 H, propargyl), 5.02 (dd, $J = 10.0$, 2.1 Hz, 1 H, B-1), 4.48 (m, 2 H, CH_2O), 4.46 (dd, $J = 3.2$, 2.1 Hz, 1 H, D-2), 4.38 (d, $J = 7.4$ Hz, 1 H, A-1), 4.30 (m, 1 H, B-3), 4.18 (dq, $J = 9.5$, 6.0 Hz, 1 H, D-5), 4.06 (dq, $J = 10.8$, 6.0 Hz, 1 H, B-5), 3.99 (pt, $J = 10.0$, 10.0 Hz, 1 H, A-3), 3.98–3.78 (series of multiplets, 7 H, D-3, E-3, E-5_{ax}, E-5_{eq}, CH_2O), 3.87 (s, 3 H, CH_3O, aromat.), 3.82 (s, 3 H, CH_3O, aromat.), 3.73 (dd, $J = 10.2$, 2.2 Hz, 1 H, B-4), 3.61 (m, 2 H, D-4, CH_2O), 3.56 (s, 3 H, CH_3O, D-ring), 3.51 (dd, $J = 10.0$, 7.4 Hz, 1 H, A-2), 3.47 (dq, $J = 10.0$, 6.0 Hz, 1 H, A-5), 3.45 (br.s, 2 H, CH_2O), 3.33 (s, 3 H, CH_3O, E-ring), 2.65 (m, 3 H, E-4, CH_2N), 2.29 (s, 3 H, CH_3, aromat.), 2.27 (pt, $J = 10.0$, 10.0 Hz, 1 H, A-4), 2.24–1.52 (series of multiplets, 14 H, B-2_{ax}, B-2_{eq}, E-2_{eq}, CH_2, OH, NH), 1.47 (m, 1 H, E-2_{ax}), 1.39 (d, $J = 6.0$ Hz, 3 H, B-6), 1.30 (d, $J = 6.0$ Hz, 3 H, D-6), 1.28 (d, $J = 6.0$ Hz, 3 H, A-6), 1.10 (t, $J = 7.0$ Hz, 3 H, CH_3CH_2N); MS: *m/z* (rel. intensity) 1622 ($M^{\oplus}$ + Cs, 30); high resolution MS (FAB^+): calcd for $C_{67}H_{84}IN_3O_{23}S_2Cs$ ($M^{\oplus}$ + Cs): 1622.3036, found 1622.3091

6: Colorless oil; $R_f = 0.58$ (silica, ether/petroleum ether 1/1); $[\alpha]_D^{25}$ (CH_2Cl_2, $c = 0.31$) −17.7; IR (film neat): $\tilde{\nu}_{max} = 2950$, 2875, 1700, 1460, 1240, 1180 cm^{-1}; ^1H NMR (500 MHz, [D_6]DMSO, 340 K): $\delta = 8.04-7.27$ (series of multiplets, 12 H, aromat.), 5.39 (pt, $J = 6.2$, 6.2 Hz, 1 H, B-1), 5.37 (d, $J = 2.1$, 1 H, D-1), 5.12 (d, $J = 14.1$ Hz, 1 H, benzyl), 5.11 (br.s, 1 H, E-1), 4.96 (d, $J = 14.1$ Hz, 1 H, benzyl), 4.80 (q, $J = 6.6$ Hz, 1 H, A-5), 4.60 (d, $J = 6.3$ Hz, 1 H, A-1), 4.42 (pt, $J = 2.1$, 2.1 Hz, 1 H, D-2), 4.40 (m, 1 H, B-3), 4.39–4.31 (m, 2 H, CH_2-FMOC), 4.27 (d, $J = 1.4$ Hz, 1 H, A-3), 4.22 (pt, $J = 6.0$, 6.0 Hz, 1 H, benzyl-FMOC), 4.06 (dq, $J = 9.2$, 6.0 Hz, 1 H, D-5), 3.99 (dq, $J = 10.0$, 6.0 Hz, 1 H, B-5), 3.86 (dd, $J = 6.3$, 1.4 Hz, 1 H, A-2), 3.81 (s, 3 H, CH_3O, aromat.), 3.77 (s, 3 H, CH_3O, aromat.), 3.76–3.63 (series of multiplets, 5 H, B-4, D-4, E-3, E-5_{ax}, E-5_{eq}), 3.54 (dd, $J = 8.9$, 2.1 Hz, 1 H, D-3), 3.39 (s, 3 H, CH_3O, D-ring), 3.24 (m, 1 H, E-4), 3.17 (br.s, 3 H, CH_3O, E-ring), 2.83 (br.s, 2 H, CH_2N), 2.31 (s, 3 H, CH_3 aromat.), 2.23 (m, 1 H, E-2_{eq}), 1.97 (m, 2 H, B-2_{ax}, B-2_{eq}), 1.46 (m, 1 H, E-2_{ax}), 1.43 (d, $J = 6.6$ Hz, 3 H, A-6), 1.28 (d, $J = 6.0$ Hz, 3 H, B-6), 1.17 (d, $J = 6.0$ Hz, 3 H, D-6), 0.92 (m, 36 H, CH_3CH_2Si), 0.85 (br.s, 3 H, CH_3CH_2N), 0.62 (m, 24 H, CH_2Si); MS: *m/z* (rel. intensity) 1906 ($M^{\oplus}$ + Cs, 96); high resolution MS (FAB^+): calcd for $C_{83}H_{128}IN_3O_{21}SSi_4Cs$ ($M^{\oplus}$ + Cs): 906.5937, found 1906.5981

ters.[10] The investigation of the chemistry and biology of these novel hybrid molecules, and the design and synthesis of other molecular assemblies within this class are continuing.

Received: October 14, 1991 [Z 4967 IE]
German version: *Angew. Chem.* **1992**, *104*, 317

[1] M. D. Lee, T. S. Dunne, M. M. Siegel, C. C. Chang, G. O. Morton, D. B. Borders, *J. Am. Chem. Soc.* **1987**, *109*, 3464; M. D. Lee, T. S. Dunne, C. C. Chang, G. A. Ellestad, M. M. Siegel, G. O. Morton, W. J. McGahren, D. B. Borders, *ibid.* **1987**, *109*, 3466.

[2] M. Konishi, H. Ohkuma, K. Matsumoto, T. Tsuno, H. Kamei, T. Miyaki, T. Oki, H. Kawaguchi, G. D. VanDuyne, J. Clardy, *J. Antibiot.* **1989**, *42*, 1449; M. Konishi, H. Ohkuma, T. Tsuno, T. Oki, G. D. VanDuyne, J. Clardy, *J. Am. Chem. Soc.* **1990**, *112*, 3715.

[3] For a review see: K. C. Nicolaou, W.-M. Dai, *Angew. Chem. Int. Ed. Engl.* in press.

[4] For the first examples of designed biological mimics of the enediyne natural products see K. C. Nicolaou, G. Zuccarello, Y. Ogawa, E. J. Schweiger, T. Kumazawa, *J. Am. Chem. Soc.* **1988**, *110*, 4866; K. C. Nicolaou, Y. Ogawa, G. Zuccarello, H. Kataoka, *ibid.* **1988**, *110*, 7247.

[5] For a selected number of synthetic enediyne compounds, see a) P. Magnus, S. M. Fortt, *J. Chem. Soc. Chem. Commun.* **1991**, 554; b) A. G. Myers, P. M. Harrington, E. Y. Kuo, *J. Am. Chem. Soc.* **1991**, *113*, 694; c) P. A. Wender, C. K. Zercher, *ibid.* **1991**, *113*, 2311; d) K. C. Nicolaou, A. L. Smith, S. V. Wendeborn, C.-K. Hwang, *ibid.* **1991**, *113*, 3106; e) T. Doi, T. Takahashi, *J. Org. Chem.* **1991**, *56*, 3465; f) J. N. Haseltine, M. P. Cabal, N. B. Mantlo, N. Iwasawa, D. S. Yamashita, R. S. Coleman, S. J. Danishefsky, G. K. Schulte, *J. Am. Chem. Soc.* **1991**, *113*, 3850; g) M. Hirama, K. Fujiwara, K. Shigematsu, Y. Fukazawa, *ibid.* **1989**, *111*, 4120; h) J. A. Porco, Jr., F. J. Schoenen, T. J. Stout, J. Clardy, S. L. Schreiber, *ibid.* **1990**, *112*, 7410.

[6] K. C. Nicolaou, R. D. Groneberg, T. Miyazaki, N. A. Stylianides, T. J. Schultze, W. Stahl, *J. Am. Chem. Soc.* **1990**, *112*, 8193.

[7] For a review on the trichloroactimindate glycosidation method, see R. R. Schmidt, *Angew. Chem. Int. Ed. Engl.* **1986**, *25*, 212.

[8] For the synthesis of this compound, see K. C. Nicolaou, E. P. Schreiner, W. Stahl, *Angew. Chem. Int. Ed. Engl.* **1991**, *30*, 585; K. C. Nicolaou, C.-K. Hwang, A. L. Smith, S. V. Wendeborn, *J. Am. Chem. Soc.* **1990**, *112*, 7416; K. C. Nicolaou, A. L. Smith, S. V. Wendeborn, C.-K. Hwang, *ibid.* **1991**, *113*, 3106.

[9] ^1H NMR (500 MHz, [D_6]DMSO, 340 °K, δ(A-1 proton); $[\alpha]_D^{23}$, in CH_2Cl_2): 4.47 (d, $J = 6.3$ Hz); +82.1 ($c = 0.36$); **12**: 4.47 (d, $J = 6.3$ Hz); −77.1 ($c = 0.28$). The minor α anomers exhibited the A-1 proton at $\delta = 5.10$ (anomer of **9**) and 5.08 (anomer of **12**) and the following optical rotations ($[\alpha]_D^{23}$) in CH_2Cl_2: +60.5° A-1 anomer of **9** ($c = 0.35$); −79.6° A-1 anomer of **12** ($c = 0.35$). The isomers with the positive rotations (e.g. **9** and its anomer) were tentatively (and cautiously!) assigned the dynemicin A (**2**) absolute stereochemistry, since the latter exhibits a positive rotation. Confirmation of these assignments by other means is in progress.

[10] Molt-4 T-cell leukemia: IC_{50} ca. 1×10^{-10} M for **5** and 1×10^{-9} M for **4**; UCLAP-3 lung carcinoma: IC_{50} ca. 1.6×10^{-7} M for **5** and 7.8×10^{-8} M for **4**. We thank Dr. W. Wrasidlo of The Scripps Research Institute for these studies.

Ligand Effects in Grignard Additions**

By *Manfred T. Reetz*,* *Nicholas Harmat*, and *Rainer Mahrwald*

Dedicated to Professor Günther Maier on the occasion of his 60th birthday

An important method for controlling chemo- and stereoselectivity of "carbanions" consists in titanation with reagents of the type $ClTiL_3$ (L = Cl,OR,NR_2, etc.).[1] Since the sense and extent of selectivity in carbonyl addition reactions depends to a great extent on the nature of the ligands L, such a transmetalation makes possible, inter alia, the exploitation of ligand effects in carbanion chemistry. Although in recent

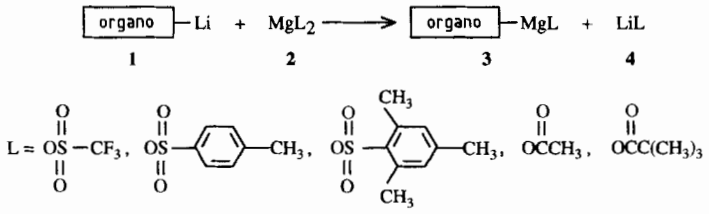

Scheme 1. Magnesiation of carbanions as a means to control chemo- and stereoselectivity (organo = CH_3,nC_4H_9,iC_3H_7, PhC≡C,C_6H_5).

[*] Prof. Dr. M. T. Reetz, Dr. N. Harmat, Dr. R. Mahrwald
Fachbereich Chemie der Universität
Hans-Meerwein-Strasse, D-W-3550 Marburg (FRG)
and
Max-Planck-Institut für Kohlenforschung
Kaiser-Wilhelm-Platz 1, D-W-4330 Mülheim an der Ruhr (FRG)

[**] This work was supported by the Deutsche Forschungsgemeinschaft (SFB 260 and Leibniz-Program) and the Fonds der Chemischen Industrie.

times other metals have been tested along similar lines (e.g., cerium,[2] iron,[3] and ytterbium[4] salts), the potential effects of ligands on selectivity have not been explored to date. This also applies to classical Grignard reagents.[5] We report here the first systematic studies on ligand effects in carbonyl addition reactions of organomagnesium reagents. In order to prepare the new Grignard reagents **3**, organolithium compounds **1** were transmetalated with magnesium salts MgL_2 (**2**). Since we have not yet studied the structure or the Schlenk equilibrium, the diagram for **3** is simply a formal description.[6]

The reagents **3** prepared by this route add to carbonyl compounds as smoothly as the traditional Grignard reagents RMgX (X = Cl, Br, I). At least in the case of the alkyl- and arylmagnesium carboxylates RMgOC(O)R this is not necessarily self-evident, because carboxylate salts have some electrophilic character and could react in the sense of a Gilman ketone synthesis.[7] The first indication of synthetically meaningful ligand effects came about in a simple study regarding chemoselectivity. Upon reacting 1:1 mixtures of an aldehyde (e.g. **5**) and a ketone (e.g. **6**) with one equivalent of the reagents RMgL in competition experiments, the aldehyde reacts essentially exclusively to form adducts **7**. In contrast, classical alkylmagnesium halides lead to about 2:1 mixtures of carbonyl adducts **7** and **8**. Selectivity for aldehydes is also high in the reactions of organotitanium reagents $RTiL_3$; this behavior results from steric effects originating from the bulky ligands L at titanium.[1, 8]

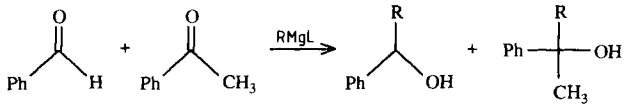

Scheme 2. Product ratio **7**:**8** (depending on RMgL): 55:45 (CH_3MgBr), 95:5 (CH_3MgOTs), 99:1 ($CH_3MgOC(O)C(CH_3)_3$), 60:40 (*n*BuMgBr), 99:1 (*n*BuMgOTs).

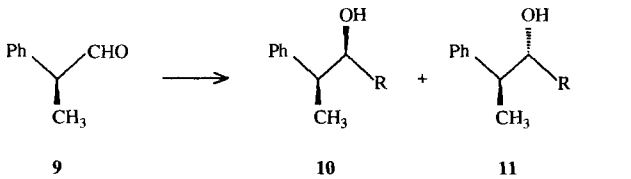

Table 1. Stereoselective Grignard additions to aldehyde **9**.

Reagent	Yield [%]	**10**:**11**
CH_3MgX (X = Cl, Br, I)	>80	≈70:30[9]
CH_3MgOTf [a]	86	90:10
CH_3MgOTs [b]	76	92: 8
$CH_3MgOSO_2C_6H_2(CH_3)_3$	63	94: 6
CH_3MgOAc	83	91: 9
$CH_3MgOC(O)tBu$	87	94: 6
*n*BuMgCl	88	85:15
*n*BuMgOTf	79	91: 9
*n*BuMgOTs	76	93: 7
$nBuMgOSO_2C_6H_2(CH_3)_3$	68	95: 5
*n*BuMgOC(O)*t*Bu	68	95: 5
*i*PrMgI	≈70	80:20[12]
*i*PrMgOC(O)*t*Bu	85	94: 6
PhC≡CMgCl	73	74:26
PhC≡CMgOTs	77	87:13
$PhC{\equiv}CMgOSO_2C_6H_2(CH_3)_3$	56	89:11
PhMgBr	80	72:28
PhMgOTf	74	88:12
PhMgOTs	67	93: 7

[a] Tf = triflate. [b] Ts = tosyl.

In spite of considerable progress, the Cram/anti-Cram problem in addition reactions of α-chiral aldehydes of the type **9** has, in general, still not been solved.[9-12] Table 1 shows that for these aldehydes ligand effects in Grignard additions are also beneficial. The observed Cram selectivity is comparable or higher than in the analogous reactions of organotitanium[10] or other selective organometallic reagents.[11] Furthermore, branched alkyl groups such as isopropyl add readily, which is not possible when using organotitanium reagents due to undesired reduction (e.g., β-hydride elimination.[1]

Another challenge in synthesis is the stereoselective addition of arylmetal reagents to substituted cyclohexanone derivatives, because such "flat" reagents afford 1:1 or 2:1 mixtures of alcohols with axial and equatorial OH groups.[13] In the case of reactions of 4-*tert*-butylcyclohexanone (**12a**), remarkable ligand effects are obtained with the reagents described above (Table 2). Whereas the conventional reagent PhMgBr (and PhLi as well) leads to a 1:1 mixture of **13a** and **14a**, the bulky analog $PhMgOSO_2C_6H_2(CH_3)_3$ gives rise to a diastereoselectivity of 90% in favor of **13a**.[14] In the case of 3-methylcyclohexanone **12b**, axial attack is favored to the extent of 95%!

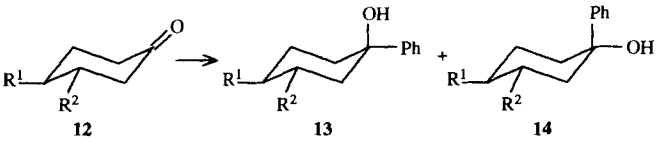

Scheme 3. **12**–**14**: R^1 = *t*Bu, R^2 = H (**a**); R^1 = H, R^2 = CH_3 (**b**).

Table 2. Additions to the cyclohexanone derivatives **12**.

Ketone	Reagent	Yield [%]	**13**:**14**
12a	PhMgBr	94	49:51[13]
12a	PhMgOTf	87	73:27
12a	PhMgOTs	90	85:15
12a	$PhMgOSO_2C_6H_2(CH_3)_3$	82	90:10
12b	PhMgBr	54	59:41[13]
12b	PhMgOTf	85	70:30
12b	PhMgOTs	83	79:21
12b	$PhMgOSO_2C_6H_2(CH_3)_3$	75	95: 5

Finally, nitrogen-based ligands were also tested. For example, reagents **15**[15] and **16**[16] add to 2-phenylpropanal **9** with essentially complete Cram selectivity affording **10** (R = *n*Bu) (*ds* = 97% for **15** and >98% for **16**) in yields of 76% and 69%, respectively. In the usual chemoselectivity test with the aldehyde/ketone pair **5**/**6**, **15** exclusively formed the aldehyde adduct **7** (R = *n*Bu).

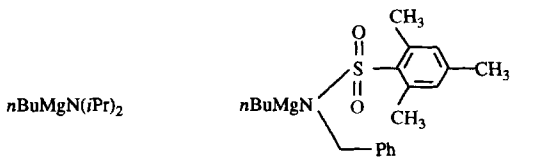

The reactions described herein show that ligand effects in chemo- and stereoselective Grignard reactions can be use-

ful.[17] It remains to be seen whether ligand effects also play a role in aldol additions of magnesium enolates or in Ni- and Pd-catalyzed coupling reactions and Cu-catalyzed conjugate additions of organomagnesium reagents RMgL.

Experimental Procedure

A solution of a magnesium carboxylate $Mg[OC(O)R]_2$ (1.55 mmol) in dry THF (10 mL) was treated with an alkyl- or aryllithium reagent at −78 °C. The temperature was allowed to rise to 0 °C, whereupon the stirred solution was cooled once more to −78 °C. To the homogeneous solution was added a carbonyl compound, and the mixture was stirred at −78 °C for about 0.5 h. After allowing the temperature to reach 0 °C, the mixture was treated with a NH_4Cl solution and worked up analogously to traditional Grignard reactions. Reagents with tosylate ligands are sometimes insoluble. A racemate of aldehyde **9** was used.

Received: November 9, 1991 [Z 5014 IE]
German version: *Angew. Chem.* **1992**, *104*, 333

[1] M. T. Reetz, *Organotitanium Reagents in Organic Synthesis*, Springer, Berlin, **1986**; B. Weidmann, D. Seebach, *Angew. Chem.* **1983**, *95*, 12–26; *Angew. Chem. Int. Ed. Engl.* **1983**, *22*, 31; M. T. Reetz, *Top. Curr. Chem.* **1982**, *106*, 1–54.

[2] T. Imamoto, N. Takiyama, K. Nakamura, T. Hatajima, Y. Kamiya, *J. Am. Chem. Soc.* **1989**, *111*, 4392–4398.

[3] T. Kauffmann, B. Laarmann, D. Menges, K.-U. Voß, D. Wingbermühle, *Tetrahedron Lett.* **1990**, *31*, 507–510.

[4] G. A. Molander, E. R. Burkhardt, P. Weinig, *J. Org. Chem.* **1990**, *55*, 4990–4991.

[5] a) Alkyl- and arylmagnesium iodides show a somewhat lower diastereoselectivity in reactions with α-alkoxy ketones than the analogous bromides or chlorides: E. L. Eliel in *Asymmetric Synthesis, Vol. 2* (Ed.: J. D. Morrison), Academic, New York, **1983**; b) House et al. described the addition of alkylmagnesium alkoxides RMgOR′ to carbonyl compounds, which was accompanied by undesired condensation and reduction; the addition to 4-*tert*-butylcyclohexanone yielded 2:1 mixtures of alcohols with axial and equatorial OH groups, respectively: H. O. House, W. L. Respess, *J. Org. Chem.* **1965**, *30*, 301–303; c) In reactions of 4-*tert*-butylcyclohexanone, reagents of the type $RMgNR'_2$ appear to offer no advantages due to low yields: E. C. Ashby, J. T. Laemmle, *Chem. Rev.* **1975**, *75*, 521–546; E. C. Ashby, G. F. Willard, *J. Org. Chem.* **1978**, *43*, 4094–4098; d) A few chirally modified organomagnesium reagents undergo enantioselective carbonyl additions: T. D. Inch, G. J. Lewis, G. L. Sainsbury, D. J. Sellers, *Tetrahedron Lett.* **1969**, 3657–3660; J. P. Battioni, W. Chodkiewicz, *Bull. Soc. Chim. Fr.* **1972**, 2068–2069; A. I. Meyers, M. E. Ford, *Tetrahedron Lett.* **1974**, 1341–1344; T. Mukaiyama, K. Soai, T. Sato, H. Shimizu, K. Suzuki, *J. Am. Chem. Soc.* **1979**, *101*, 1455–1460; R. Noyori, M. Kitamura, *Angew. Chem.* **1991**, *103*, 34–55; *Angew. Chem. Int. Ed. Engl.* **1991**, *30*, 49; B. Weber, D. Seebach, *Angew. Chem.* **1992**, *104*, 96–97, *Angew. Chem. Int. Ed. Engl.* **1992**, *31*, 84–86.

[6] Since lithium salts **4** are formed in this reaction, complex magnesium- and lithium-containing reagents need to be considered, for example, ate complexes.

[7] In fact, no carbonyl addition reactions were observed with methylmagnesium trifluoroacetate $CH_3MgOC(O)CF_3$ prepared in situ; presumably the more electrophilic C-atom of the carboxylate is attacked by the nucleophile, so that the reagent does not survive or is never formed.

[8] M. T. Reetz, S. Maus, *Tetrahedron* **1987**, *43*, 101–108.

[9] D. J. Cram, F. A. Abd Elhafez, *J. Am. Chem. Soc.* **1952**, *74*, 5828–5835; P. R. Jones, E. J. Goller, W. J. Kauffman, *J. Org. Chem.* **1971**, *36*, 3311–3315.

[10] M. T. Reetz, R. Steinbach, J. Westermann, R. Peter, B. Wenderoth, *Chem. Ber.* **1985**, *118*, 1441–1454.

[11] Y. Yamamoto, K. Maruyama, *J. Am. Chem. Soc.* **1985**, *107*, 6411–6413.

[12] T. Matsumoto, Y. Hosoda, K. Mori, K. Fukui, *Bull. Chem. Soc. Jpn.* **1972**, *45*, 3156–3160.

[13] a) G. D. Meakins, R. K. Percy, E. E. Richards, R. N. Young, *J. Chem. Soc. C* **1968**, 1106–1109; b) R. Luderer, J. E. Woodall, J. J. Pyle, *J. Org. Chem.* **1971**, *36*, 2909–2910.

[14] For electronic reasons the axial attack is actually preferred, but steric factors may override: G. Frenking, K. F. Köhler, M. T. Reetz, *Angew. Chem.* **1991**, *103*, 1167–1170; *Angew. Chem. Int. Ed. Engl.* **1991**, *30*, 1146–1149; see also: Y.-D. Wu, K. N. Houk, *J. Am. Chem. Soc.* **1987**, *109*, 908–910.

[15] Prepared from diisopropylamine and salt-free $(n\text{Bu})_2\text{Mg}$. The degree of diastereoselectivity in the addition of **15** to aldehyde **9** is not influenced by the presence of Li salts.

[16] Prepared by the reaction of the corresponding sulfonamide with $(n\text{Bu})_2\text{Mg}$ (in situ from *n*BuMgCl and *n*BuLi).

[17] Salt effects can also play a role (cf. [6.15]).

Two Stereoisomeric [4.5.5.5]Fenestranes Formed by Intramolecular [2 + 2] Cycloaddition**

By *Reinhart Keese**

Structural modification in the periphery of fenestranes of type **1** leads to the opening of two opposite bond angles ρ and σ at the quaternary central C atom.[1] Whereas the bond angles ρ and σ in all-*cis*-[5.5.5.5]fenestrane (**2a**) are 115°,[2] they are 128.3° and 129.2°, respectively, in a derivative of [4.4.4.5]fenestrane.[3] For all-*cis*-[4.4.4.4]fenestrane **4**, bond angles of 130° have been calculated.[4] The fenestranes of the all-*cis* series hitherto prepared have bond angles between those of **2** and **4**.[1] Stereoisomeric fenestranes that differ from the all-*cis* series by the presence of at least one *trans*-fused bicyclo[x.y.0]octane unit are 'inverted' at the appropri-

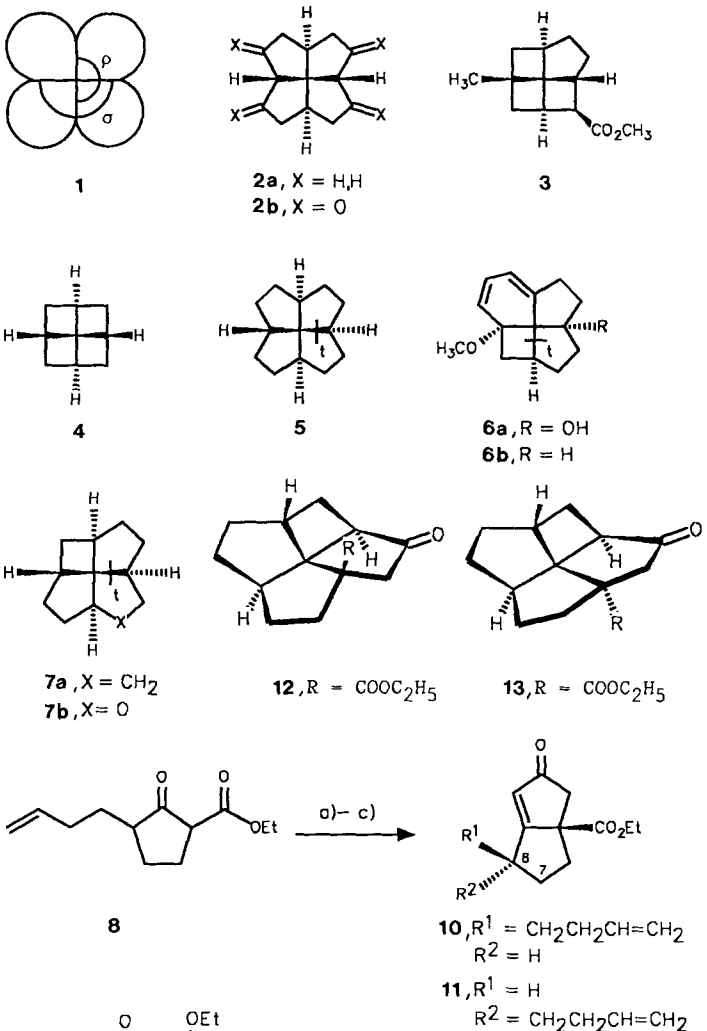

[*] Institute of Organic Chemistry
University of Bern
Freiestrasse 3, 3012 Bern (Switzerland)

[**] This work was supported by the Swiss National Science Foundation. I gratefully acknowledge the skillful experimentation of B. Herzog and thank Priv.-Doz. Dr. P. Bigler and Dr. C. Müller for NMR measurements. Part of these results was presented at the Int. Chem. Congr. of Pacific Basin Chemical Societies, Honolulu, December 1989; cf. *Nachr. Chem. Techn. Lab.* **1990**, *38*, 322.

ate bridgehead. According to our MNDO calculations, these fenestranes have two opposite bond angles at the quaternary C atom that are larger than 109.47°. For example, in *cis-cis-cis-trans*-[5.5.5.5]fenestrane **5** they are 122° and 127.4°.[1a]

Reports on syntheses of stereoisomeric fenestranes are scarce. The mechanistic interpretation of one of the products obtained in the photolysis of 1-[but-3-enyl]-7-methoxyindane implies the formation of the [4.5.5.6]fenestradiene **6**, which contains a *trans*-fused bicyclo[3.2.0]heptane substructure.[5] More recently, P. Grieco et al. reported the synthesis of a derivative of **7a** through Claisen rearrangement in H_2O.[6] Smits and Caple et al. reported the formation of two derivatives of the oxafenestrane **7b**.[7] We describe here the synthesis of the stereoisomeric [4.5.5.5]fenestranes **12** and **13**. The latter compound contains a *trans*-fused bicyclo[3.3.0]-octane unit. The key step of our synthesis is the photochemically induced intramolecular [2 + 2] cycloaddition, which has previously been used only for preparation of all-*cis*-fenestranes.[8]

After double deprotonation with NaH-*n*BuLi, alkylation of ethyl 2-oxocyclopentanoate in the 3-position with 4-bromobutene gave **8**. Annulation of **8** with bromide **9**[9] gave a mixture of **10** and **11**, which could be separated by chromatography.[10] As expected, irradiation of **10** in hexane with a 125 W low-pressure lamp in a quartz vessel gave the fenestrane **12** in 89% yield.

Surprisingly, the endo isomer **11** is also photoreactive and gave in a yield of 86% a single product, which according to detailed NMR studies (2D, NOE and hetero-NOE analysis) is the stereoisomeric *cis-trans-cis-cis*-(4.5.5.5)fenestrane **13** (cf. Table 1).[11] This is the first example of a photochemically induced, intramolecular [2 + 2] cycloaddition at the *endo* side of a bicyclo[3.3.0]oct-1-en-3-one with concomitant formation of a *trans*-fused bicyclo[3.3.0]octane framework. For the parent hydrocarbons of **12** and **13** opposite bond angles (ρ and σ) of 120.8 and 133°, respectively, for ρ and 120° and 126°, respectively, for σ are calculated.[13] At present, the compounds **13**, **3**, **7a**, and the O-containing **7b** are the sole hydrocarbons with $C(C)_4$ subunits that according to MNDO calculations contain two opposite bond angles with an average value of as large as 129°.[13]

Table 1. NMR data of **12** and **13** [a].

assignment [b]	**12** ^{13}C	^1H	**13** [c] ^{13}C	^1H
C(1)H	48.12	2.65 (m)	45.51	2.8 (d, 8.1)
C(2)	218.66	–	221.30	–
$C(3)H_2$	50.27	3.08 (dd, 17.3, 0.8, H_{cis})	45.91	2.5 (d, H_{cis}, 18.0)
		2.38 (dd, 17.3, 1.5, H_{trans})		2.7 (d, H_{trans}, 18.0)
C(4)	55.63	–	59.14	–
$C(5)H_2$	39.81	2.58 (m, H_{cis})	29.10	1.3 (dd, H_{cis})
		≈1.65 (m, H_{trans})		2.2 (m, H_{trans})
$C(6)H_2$	32.01	≈1.66 (m, H_{trans})	32.29	2.25 (m, H_{cis})
		1.85 (m, H_{cis})		1.3 (m, H_{trans})
C(7)H	52.44	2.45 (m)	39.39	2.4 (m)
$C(8)H_2$	32.57	≈1.58 (m, H_{cis})	27.59	2.15 (m, H_{cis})
		≈2.05 (m, H_{trans})		1.8 (m, H_{trans})
$C(9)H_2$	34.68	≈1.75 (m, H_{cis})	32.287	1.5 (m, H_{cis})
		2.07 (m, H_{trans})		1.65 (m, H_{trans})
C(10)H	40.10	2.30 (m)	45.505	2.7 (m)
		≈1.85 (m, H_{trans})		
$C(11)H_2$	25.26	≈2.15 (m, H_{cis})	25.261	1.8 (m)
		≈1.85 (m, H_{trans})		1.8 (m)
C(12)	68.80	–	72.228	–

[a] ^{13}C and ^1H NMR ($CDCl_3$, TMS, chemical shift (δ, J in Hz), Bruker AM400. [b] Sequence according to numbering of the ring system. [c] NOE results: irradiated at $C(X)H_{cis,trans}$: signal enhancement at $C(Y)H_{cis,trans}$ to the ester group; **13**: C(1)H: C(7)H; Hetero-NOE of **13**: $C(3)H_{cis}$: C(1'); C(7)H[$C(6)H_{cis}$]: C(1').

Received: October 19, 1991 [Z 4978 IE]
German version: *Angew. Chem.* **1992**, *104*, 307

CAS Registry numbers:
8, 138608-14-7; **9**, 73542-48-0; **10**, 138608-15-8; **11**, 138608-16-9; **12**, 138608-17-0; **13**, 138665-06-2.

[1] a) W. Luef, R. Keese, *Helv. Chim. Acta* **1987**, *70*, 543; b) *J. Mol. Struct. Theochem.* **1992**, in press.
[2] MNDO results for **2a**; according to X-ray structure analysis of **2b**, bond angles are 115.1° und 117.5°: R. Mitschka, J. Oehldrich, K. Takahashi, J. M. Cook, U. Weiss, J. V. Silverton, *Tetrahedron* **1981**, *37*, 4521. In fenestrindane bond angles of 116.5° bave been found; D. Kuck, H. Bögge, *J. Am. Chem. Soc.* **1986**, *108*, 8107.
[3] Based on the X-ray structure analysis of a derivative of **3**: B. R. Venepalli, W. C. Agosta, *Chem. Rev.* **1987**, *87*, 399.
[4] E.-U. Würthwein, J. Chandrasekhar, E. D. Jemmis, P. von R. Schleyer, *Tetrahedron Lett.* **1981**, *22*, 843.
[5] a) J. Mani, S. Schüttel, Cong Zhang, P. Bigler, C. Müller, R. Keese, *Helv. Chim. Acta* **1989**, *72*, 487; b) Cong Zhang, D. Bourgin, R. Keese, *Tetrahedron* **1991**, *47*, 3059.
[6] a) P. A. Grieco, E. B. Brandes, S. McCann, J. D. Clark, *J. Org. Chem.* **1989**, *54*, 5851; b) P. A. Grieco, J. D. Clark, C. T. Tagoe, *J. Am. Chem. Soc.* **1991**, *113*, 5488.
[7] W. A. Smits, S. M. Buhanjuk, S. O. Simonyan, A. S. Shashkov, Y. T. Struchkov, A. I. Yanovsky, R. Caple, A. S. Gybin, L. G. Anderson, J. A. Whiteford, *Tetrahedron Lett.* **1991**, *32*, 2105.
[8] a) W. G. Dauben, D. M. Walker, *Tetrahedron Lett.* **1982**, *23*, 711; b) M. T. Crimmins, *Chem. Rev.* **1988**, *88*, 1467.
[9] E. Piers, B. Abeysekera, *Can. J. Chem.* **1982**, *60*, 1114.
[10] The compounds **10** and **11**, prepared in analogy to published methods (M. Thommen, P. Gerber, R. Keese, *Chimia* **1991**, *45*, 21), were obtained in 48% (**10**) and 4.8% (**11**) yield.
[11] The spectroscopic data (NMR, IR, MS) and elemental analyses of the new compounds are compatible with the structures given.
[12] For two other intramolecular examples see [7]; an intermolecular cycloaddition at the *endo* side of a bicyclo[3.3.0]oct-1-en-3-one has been observed; D. Bourgin, *Dissertation*, University of Berne, **1991**.
[13] MNDO results: W. Luef, R. Keese, unpublished.

Conformational Preference of the Torand Ligand in Its Complexes with Potassium and Rubidium Picrate**

By *Thomas W. Bell,** *Peter J. Cragg, Michael G. B. Drew, Albert Firestone* and *Daw-Iong A. Kwok**

Torands[1, 2] are unusual host compounds for cationic guests and small hydrogen-bond donors. Among known host families, including crown ethers,[3] cryptands,[4] and spherands,[5] torands are unique in that their macrocyclic perimeters are defined by smaller, completely fused rings. Torand **1**[1] is an unusually planar, highly preorganized system that binds alkali metals rapidly to form 1 : 1 complexes of exceptional stability[1a] when compared with complexes of other nonencapsulating ligands. Despite its binding

[*] Prof. T. W. Bell, Dr. P. J. Cragg, Dr. A. Firestone, Dr. D.-I. A. Kwok
Department of Chemistry, State University of New York
Stony Brook 11794-3400 (USA)
Dr. M. G. B. Drew
Department of Chemistry, The University
Whiteknights, GB-Reading RG6 2AD (UK).

[**] This work was supported by the U.S. National Institutes of Health (NIH) via award GM32937. Funds for the X-ray diffractometers were obtained from the United Kingdom Science and Engineering Research Council and from the NIH (grant 1S10RR0058901). Also acknowledged is a NATO grant for international collaborative research.

strength and preorganization, torand **1** displays weak size-selectivity toward alkali metals. Detailed structural and thermodynamic studies are required to understand these apparent contradictions fully. Described herein are the first X-ray crystal structures of torand complexes; they verify the relative planarity of **1** and reveal its preference for a staggered conformation.

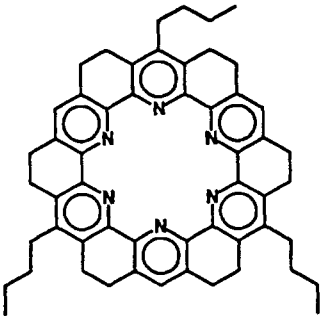

1

Torand **1** forms 1:1 complexes with Li^+, Na^+, K^+, Rb^+, and Cs^+, all of which have been characterized as their picrate salts.[1a,c] Crystal structure analyses of the potassium picrate complex (**1** · K^+)(picrate$^-$) and the rubidium picrate complex (**1** · Rb^+)(picrate$^-$) are reported in this communication. The following article[14] describes the structure of the lithium picrate complex, which crystallizes in 2:2 stoichiometry. Key points of interest regarding these structures are the exact coordination environment of the cation and the conformation of the macrocyclic ligand. Since the perfectly planar conformation of **1** would be destabilized by eclipsed H-C-C-H torsional interactions in the six ethylene fragments, a twist is induced between each pair of pyridine rings. The resulting conformations can be described by eight possible combinations[6] of the six N-C-C-N torsion angles of the central 18-membered ring: (+ + + + + +), (+ + + + + −), (+ + + + − −), (+ + + − + −), (+ + − + + −), (+ + + − − −), (+ + − + − −) and (+ − + − + −). The X-ray structural analyses of both **1** · K^+ and **1** · Rb^+ reveal that **1** adopts the same overall conformation (+ − + − + −), in which the six nitrogen atoms are staggered above and below the best plane of the macrocycle.

Model studies on torands[7] indicated that metal ions having radii in the range of 1.4 to 1.5 Å should match the cavity size when binding in the best plane of **1**. Potassium was expected to fit most exactly because its radius ranges from 1.38 to 1.55 Å for coordination numbers 6 to 9.[8] The X-ray crystal structure of **1** · K^+ depicted in Figure 1[9] shows the K ion lying only 0.21 Å out of the best plane of the six nitrogen atoms, to which it binds approximately equally (K–N distances 2.73–2.85 Å, mean 2.77 Å). The seventh contact is to one of the nitro oxygen atoms of the picrate anion (2.85 Å). The phenoxide oxygen atom is disordered between positions O90A and O90B (Fig. 1) in the ratio of 61:39. In position O90A this oxygen forms the next shortest contact to the potassium ion (3.40 Å); a nitro oxygen atom of a neighboring picrate ion forms the shortest intermolecular K–O contact (3.72 Å). The absolute values of the six N-C-C-N torsional angles in **1** · K^+ range from 14 to 18°. The central 18-membered ring thus deviates from the D_{3d} symmetry observed in many crystalline 18-crown-6 complexes.[3d] This lowering of symmetry is possibly caused by axial coordination to the picrate ion, which is 3.29 Å from the nearest pyridine ring (N13 ··· N91). The angle between the picrate phenyl ring and the pyridine ring is 22.2°.

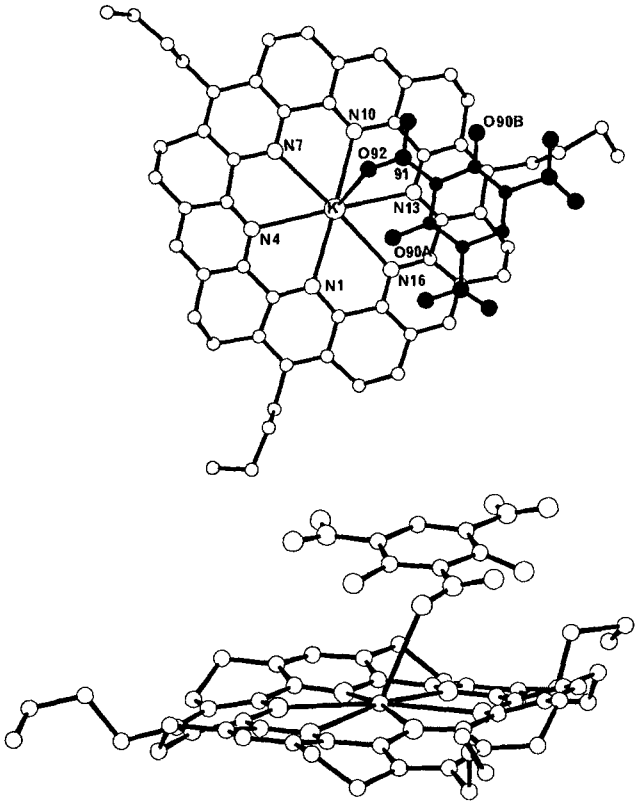

Fig. 1. Structure of **1** · K^+(picrate$^-$) in the solid state (hydrogen atoms omitted, picrate ions shown in black). Top: View perpendicular to the best plane of **1**. Bottom: Side view. Bond lengths [Å] and angles [°] of interest: K-N1 2.728(5), K-N4 2.850(5), K-N7 2.753(7), K-N10 2.738(5), K-N13 2.781(6), K-N16 2.792(6), K-O90A 3.469(9), K-O92 2.836(6), N1-K-N4 59.7(2), N4-K-N7 58.4(2), N7-K-N10 61.0(2), N10-K-N13 61.1(2), N13-K-N16 59.0(2), N16-K-N1 59.9(2), O92-K-N10 71.8(2), O92-K-N13 75.8(2); N1-C-C-N4 16(1), N4-C-C-N7 −14(1), N7-C-C-N10 17(1), N10-C-C-N13 −18(1), N13-C-C-N16 18(1), N16-C-C-N1 −17(1).

The structure of **1** · Rb^+ depicted in Figure 2[9] is similar to that of **1** · K^+ except that the Rb ion is 8-coordinate and is displaced by 1.06 Å from the best plane of the six nitrogen atoms. The six Rb–N distances range from 2.93 to 3.06 Å (mean 2.98 Å); in these complexes, Rb^+ appears to be 0.21 Å larger than K^+, in approximate agreement with Shannon's ionic radii (1.46 Å for 7-coordinate K^+ and 1.61 Å for 8-coordinate Rb^+).[8] The picrate ion in **1** · Rb^+ is bidentate with Rb–O contacts that are 0.21–0.24 Å longer than the K–O contact in **1** · K^+. In keeping with a larger metal-ion radius, torand torsional angles in **1** · Rb^+ (18–22°) are larger than in **1** · K^+. The longer oxygen contacts also allow an increase in the distance between the picrate ion and the nearest pyridine ring (smallest distance: C83 ··· C40, 3.49 Å; angle between picrate phenyl ring and pyridine ring, 4.6°).

The displacement of the metal ion from the torand plane and the larger torsional angles in **1** · Rb^+ produce an alternation of pyridine orientations with respect to the metal ion. Rubidium lies approximately within the planes of three pyridine rings (*para*-C-N-Rb^+ angle 172°) and is significantly displaced from the planes of the other three (*para*-C-N-Rb^+ angle 145°). Interactions between ligands and alkali metal ions are predominantly electrostatic,[10] and this alternation of the alignments of pyridine dipoles should weaken three of the six contacts. Despite the change in metal–macrocycle coordination from hexagonal planar in **1** · K^+ to hexagonal pyramidal in **1** · Rb^+, the torand conformations are remarkably similar. On the average, the N-C-C-N tor-

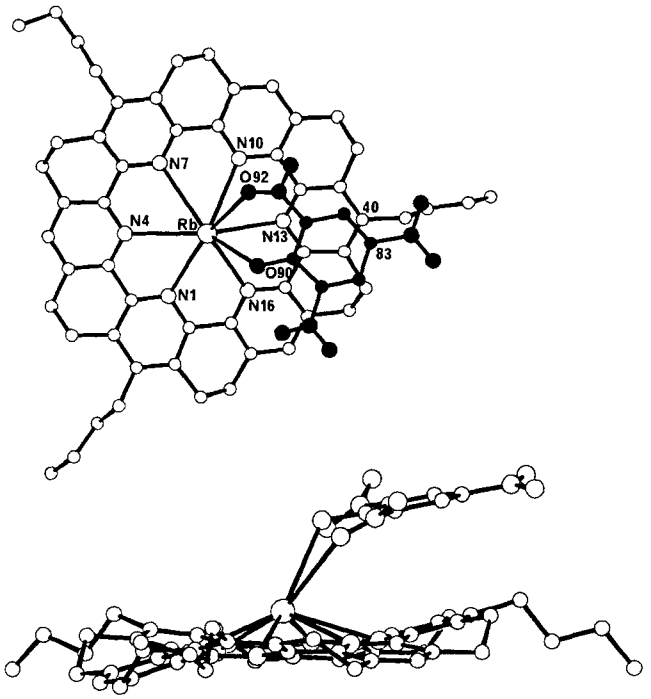

Fig. 2. Structure of **1** · Rb^+(picrate$^-$) in the solid state (hydrogen atoms omitted, picrate ions shown in black). Top: View perpendicular to the best plane of **1**. Bottom: Side view. Bond lengths [Å] and angles [°] of interest: Rb-N1 3.009(8), Rb-N4 3.006(8), Rb-N7 3.061(8), Rb-N10 2.954(8), Rb-N13 2.948(7), Rb-N16 2.926(8), Rb-O90 3.06(1), Rb-O92 3.09(1), N1-Rb-N4 55.0(2), N4-Rb-N7 55.1(2), N7-Rb-N10 55.0(2), N10-Rb-N13 56.1(2), N13-Rb-N16 57.0(2), N16-Rb-N1 56.1(2), O90-Rb-N13 80.0(2), O90-Rb-N16 80.1(2); O92-Rb-N10 62.9(2), O92-Rb-N13 78.6(2), N1-C-C-N4 −22(1), N4-C-C-N7 21(1), N7-C-C-N10 −18(1), N10-C-C-N13 19(1), N13-C-C-N16 −19(1), N16-C-C-N1 22(1).

sional angles decrease by only 4°. This suggests that the (+ − + − + −) conformation is preferred. Preliminary results of molecular mechanics calculations support this conclusion. Although the average O-C-C-O torsional angles in ([18]crown-6) · KNCS[11] and ([18]crown-6)$_2$ · $(RbNCS)_2$[11a,12] also vary by only 4°, more extreme conformational changes are observed in (dibenzo[18]crown-6) · KNCS and (dibenzo[18]crown-6) · RbNCS.[13] The coordination numbers and geometries of potassium and rubidium ions are apparently forced to adjust to the spatial requirements of torand **1**, although the conformations of macrocyclic ligands usually adjust to the bonding demands of metals. Even spherands, which dictate the coordination numbers of alkali metals, adjust their conformation in complexes.[5] On the other hand, axial coordination is not controlled in torands and in other planar macrocyclic ligands; this can lead to considerable variation in structures of complexes, as illustrated in the accompanying article.[14]

Experimental Procedure

1 · K^+(picrate$^-$): A solution of torand **1** [1a] (37 mg, 0.047 mmol) in $CHCl_3$ (3 mL) was washed with 15 mL of an aqueous solution of potassium picrate (40 mg, 0.15 mmol) and of K_2CO_3 (40 mg, 0.29 mmol). The aqueous layer was extracted with CH_2Cl_2 (10 mL), and the combined organic solutions were evaporated to dryness. The residue was recrystallized from n-butyronitrile (8 mL), and the resulting yellow-orange crystals were dried at room temperature (0.1 torr) for 12 hours. Yield: 31 mg (64%).

^{1}H NMR: (10^{-3} M in D_2O-saturated $CDCl_3$, 300 MHz) δ = 8.380 (s, 2H; picrate), 7.503 (s, 3H; pyridine-H), 3.031 (s, 24H; $ArCH_2CH_2Ar$), 2.784 (t, 6H; CH_2Pr), 1.5–1.6 (m, 12H; CH_2CH_2Me), 1.027 (t, J = 7 Hz, 9H; CH_3). IR (KBr): $\tilde{\nu}$[cm^{-1}] = 3080(w), 2940(m), 2920(m), 2840(m), 1630(s), 1600(w), 1540(s), 1485(m), 1445(m), 1425(w), 1370(m), 1350(m), 1320(s), 1290(s), 1270(m), 1250(s), 1210(s), 1180(w), 1150(m), 1095(w), 1060(m), 1030(w), 985(w), 960(m), 930(m), 920(w), 900(m), 775(m), 720(m), 710(m), 700(m). Correct C, H, N analyses. Recrystallization from a CH_2Cl_2 solution layered with CH_3CN gave clear, yellow rectangular crystals. The crystal used for X-ray diffraction studies measured 0.4 × 0.2 × 0.1 mm.

1 · Rb^+(picrate$^-$): A solution of **1** (30.4 mg, 0.039 mmol) in $CHCl_3$ (3 mL) was washed with 25 mL of an aqueous solution of rubidium picrate (32 mg, 0.10 mmol) and 0.2 mL of triethylamine. The $CHCl_3$ solution was evaporated to dryness, and the residue was recrystallized by slow evaporation of the solvent of a solution in ethyl acetate/CH_2Cl_2. The resulting yellow powder was dried for 12 hours at room temperature (0.1 torr). Yield, 33.4 mg (76%).

^{1}H NMR: (D_2O-saturated $CDCl_3$, 300 MHz, δ = 8.387 (s, 2H; picrate), 7.452 (s, 3H; pyridine-H), 2.986 (s, 24H; $ArCH_2CH_2Ar$), 2.751 (t, 6H; CH_2Pr), 1.5–1.6 (m, 12H; CH_2CH_2Me), 1.025 (t, J = 7 Hz, 9H, CH_3). IR (KBr): $\tilde{\nu}$[cm^{-1}] = 3080(w), 2940(m), 2920(m), 2860(m), 2840(m), 1630(s), 1600(w), 1540(s), 1510(m), 1490(m), 1445(m), 1430(m), 1370(m), 1355(m), 1320(s), 1290(s), 1275(s), 1255(s), 1210(s), 1180(w), 1150(m), 1095(w), 1060(m), 1030(w), 995(w), 955(m), 930(w), 915(w), 900(m), 775(m), 720(m), 700(m). Correct C, H, N analyses. The crystal used for X-ray diffraction studies (0.5 × 0.5 × 0.05 mm) was grown from a CH_2Cl_2 solution layered with hexane, and had the composition **1** · Rb^+(picrate$^-$)$(CH_2Cl_2)_{0.5}$.

Received: September 23, 1991 [Z 4927 IE]
German version: *Angew. Chem.* **1992**, *104*, 319

CAS Registry numbers:
1·K^+, 127360-41-2; **1**·Rb^+(picrate$^-$), 127360-43-4; **1**·Rb^+(picrate$^-$)·0.5CH_2Cl_2, 138858-77-2; Li, 7439-93-2; Na, 7440-23-5; Cs, 7440-46-2.

[1] a) T. W. Bell, A. Firestone, R. Ludwig, *J. Chem. Soc. Chem. Commun.* **1989**, 1902–1904; b) T. W. Bell, A. Firestone, *J. Am. Chem. Soc.* **1986**, *108*, 8109–8111; c) A. Firestone, *Dissertation*, State University of New York at Stony Brook, **1988**.

[2] T. W. Bell, J. Liu, *Angew. Chem.* **1990**, *102*, 931–933; *Angew. Chem. Int. Ed. Engl.* **1990**, *29*, 923–925.

[3] a) *Cation Binding by Macrocycles* (Eds.: G. W. Gokel, Y. Inoue), Dekker, New York, **1990**; b) O. A. Raevskii, *Koord. Khim.* **1990**, *16*, 723–748; *Sov. J. Coord. Chem. (Engl. transl.)* **1990**, *16*, 385–405; c) C. J. Pedersen, *Angew. Chem.* **1988**, *100*, 1053–1059; *Angew. Chem. Int. Ed. Engl.* **1988**, *27*, 1021–1027; d) A. V. Bajaj, N. S. Poonia, *Coord. Chem. Rev.* **1988**, *87*, 55–213.

[4] a) J.-M. Lehn, *Angew. Chem.* **1990**, *102*, 1347–1362; *Angew. Chem. Int. Ed. Engl.* **1990**, *29*, 1304–1319; b) J.-M. Lehn, *ibid.* **1988**, *100*, 91–116 and **1988**, *27*, 89–112.

[5] D. J. Cram, *Science (Washington, D. C.)* **1988**, *240*, 760–767.

[6] Some of these combinations represent more than one conformation when enantiomers and the positions of the butyl groups are considered.

[7] a) T. W. Bell, F. Guzzo, M. G. B. Drew, *J. Am. Chem. Soc.* **1991**, *113*, 3115–3122; b) M. G. B. Drew, J. de O. Cabral, M. F. Cabral, F. S. Esho, S. M. Nelson, *J. Chem. Soc. Chem. Commun.* **1979**, 1033–1035.

[8] R. D. Shannon, *Acta Crystallogr. Sect. A* **1976**, *32*, 751–767.

[9] **1** · K^+(picrate$^-$): $C_{60}H_{56}N_9O_7K$, M_r = 1053.5, triclinic, a = 16.872(8), b = 14.993(10), c = 10.107(7) Å, α = 93.1(1), β = 84.9(1), γ = 105.4(1)°, V = 2453.5 Å^3, $\rho_{calcd.}$ = 1.43 g cm^{-3}, space group $P\bar{1}$, Z = 2, $Mo_{K\alpha}$ radiation, λ = 0.71069 Å. The structure was solved by direct methods and refined by the full-matrix least-squares method: K anisotropic. H atoms were generated, riding on the appropriate carbon atoms. The picrate anion's oxygen was disordered over two sites, O90A and O90B, with 61 : 39 occupancy. 2840 reflections (θ_{max} = 25°) were refined to R = 0.074 (R_w = 0.086). **1** · Rb^+(picrate$^-$) · 0.5CH_2Cl_2: $C_{60.5}H_{57}N_9O_7RbCl$, M_r = 1143.1, monoclinic, a = 9.823(2), b = 12.770(2), c = 41.618(8) Å, β = 92.39(2)°, V = 5216(3) Å^3, $\rho_{calcd.}$ = 1.45 g cm^{-3}, space group $P2_1/c$, Z = 4, $Cu_{K\alpha}$ radiation, λ = 1.54178 Å. The structure was solved by direct methods and refined by the full-matrix least-squares method: all non-H atoms anisotropic. H atoms were generated, riding on the appropriate carbon atoms at a distance of 0.95 Å. A molecule of dichloromethane was located at the crystallographic center of inversion with 50% occupancy. 3634 reflections (θ_{max} = 50°) were refined to R = 0.076 (R_w = 0.097). Further details of the crystal structure investigations are available on request from the Director of the Cambridge Crystallographic Data Centre, University Chemical Laboratory, Lensfield Road, Cambridge, CB2 1EW (UK) on quoting the full literature citation. The assistance of R. Subramanian is gratefully acknowledged.

[10] M. Badertscher, M. Welti, P. Portmann, E. Pretsch, *Top. Curr. Chem.* **1986**, *136*, 17–80.

[11] a) M. Dobler, *Ionophores and their Structures*, Wiley, New York, **1981**, p. 133–145; b) P. Seiler, M. Dobler, J. D. Dunitz, *Acta Crystallogr. Sect. B* **1974**, *30*, 2744–2745.

[12] M. Dobler, R. P. Phizackerley, *Acta Crystallogr. Sect. B* **1974**, *30*, 2746–2748.

[13] The angle between benzene rings varies from 46–71°: a) A. Bianchi, J. Giusti, P. Paoletti, S. Mangani, *Inorg. Chim. Acta* **1986**, *117*, 157–164; b) D. Bright, M. R. Truter, *J. Chem. Soc. B* **1970**, 1544–1550.

[14] T. W. Bell, P. J. Cragg, M. G. B. Drew, A. Firestone, D.-I. A. Kwok, *Angew. Chem.* **1992**, *104*, 321; *Angew. Chem. Int. Ed. Engl.* **1992**, *31*, 348.

A Supramolecular Assembly of Two Torands, Two Lithium Ions, and Three Water Molecules **

By *Thomas W. Bell,* Peter J. Cragg, Michael G. B. Drew, Albert Firestone,* and *Daw-Iong A. Kwok**

The preceding article describes structures of crystalline 1:1 complexes between a torand (**1**) and the picrate salts of potassium and rubidium. The sodium and potassium complexes are remarkably stable in chloroform,[1] and the crystal structure of the potassium complex shows axial coordination to picrate. Lithium also forms stable 1:1 complexes with **1**,[2] despite its small size compared with the cavity formed by the central 18-membered ring of **1**. The X-ray structural analysis reported here shows that **1** · Li aggregates in the solid state form a stacked torand dimer threaded by a hydrated chain of two lithium ions.

Torand **1** was treated with an aqueous solution of lithium picrate and lithium hydroxide to give **1** · Li^+(picrate$^-$) · $(H_2O)_{1.5}$, which was crystallized from a mixture of organic solvents. The crystal structure[3] depicted in Figures 1 and 2 shows the aggregation of two molecules of the 1:1 complex with three molecules of water, one of which bridges between the two lithium ions. Figure 1 shows the triclinic unit cell containing two symmetry-related molecules of the 2:2 complex as well as a view of the complex along the axis perpendicular to the torand rings. The picrate ions are not coordinated to lithium, hydrogen-bonded to water, or linked by π stacking to torands. Each molecule of the 2:2 complex is a discrete entity in which the two torands are coaxially stacked, as shown in Figure 1 (bottom). This diagram also shows that the torands are rotated with respect to each other by approximately 30° about the perpendicular axis, producing a pseudo-S_{12} axis. The three water molecules lie nearly on this axis, whereas the two lithium ions are offset, binding unsymmetrically to the torand cavities.

Both lithium ions have approximately tetrahedral coordination geometries, and Li–O bonds to a terminal water molecule and to the bridging water molecule. Each lithium ion is coordinated to a bipyridine fragment through one short Li–N bond (2.04, 2.09 Å), and one longer Li–N bond (2.30, 2.35 Å). For each the next shortest contact is to a third nitrogen atom (both 2.61 Å), suggesting that the torand acts partly as a terpyridyl ligand. The Li–O distances fall in the range 1.86–1.96 Å and are shorter than usually observed for hydrated lithium (1.91–2.34 Å).[4] It is clear, however, that the coordinated oxygen atoms belong to water molecules rather than hydroxide ions because the C–O bond lengths in the picrate ions (1.22, 1.26 Å) are consistent with those observed for a picrate anion (1.22–1.25 Å)[5] rather than picric acid (1.31–1.35 Å).[6]

The two torands in $[\mathbf{1}_2 \cdot Li_2(H_2O)_3]^{2+}$ are clearly in van der Waals contact since the angle between the best planes of the six nitrogen atoms of each is only 3°, and the distances between N_6 centroids is 3.64 Å. On the other hand, the torands are not completely planar and are complementarily folded. The six N-C-C-N torsion angles for each of the central 18-membered rings are given in Figure 2 and show that this folding produces an approximate mirror plane, neglecting the hydrated dilithium chain. The folding plane bisects

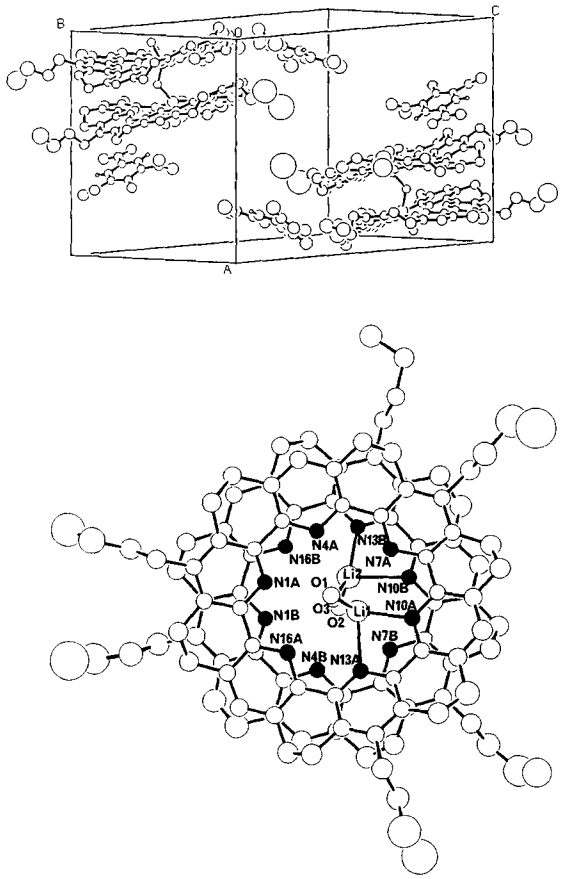

Fig. 1. Structure of $[\mathbf{1}_2 \cdot Li_2(H_2O)_3(picrate)_2]$ in the solid state (hydrogen atoms omitted). Top: Unit cell. Bottom: View along the perpendicular axis. Bond lengths [Å] and angles [°] of interest: Li1-N1A 3.61(2), Li1-N4A 3.38(2), Li1-N7A 2.64(2), Li1-N10A 2.10(2), Li1-N13A 2.30(2), Li1-N16A 3.03(2), Li1-O1 1.90(2), Li1-O3 1.91(2), Li2-N1B 3.46(2), Li2-N4B 3.64(2), Li2-N7B 3.11(2), Li2-N10B 2.26(2), Li2-N13B 2.02(2), Li2-N16B 2.63(2), Li2-O2 1.87(2), Li2-O3 1.96(2); N1A-Li1-N4A 46(1), N4A-Li1-N7A 55(1), N7A-Li1-N10A 71(1), N10A-Li1-N13A 77(1), N13A-Li1-N16A 61(1), N16A-Li1-N1A 48(1), O1-Li1-O3 111(1), O1-Li1-N10A 112(1), O1-Li1-N13A 97(1), O3-Li1-N10A 132(1), O3-Li1-N13A 118(1), N1B-Li2-N4B 46(1), N4B-Li2-N7B 48(1), N7B-Li2-N10B 61(1), N10B-Li2-N13B 79(1), N13B-Li2-N16B 72(1), N16B-Li2-N1 54(1); O2-Li2-O3 111(1), O2-Li2-N10B 96(1), O2-Li2-N13B 113(1), O3-Li2-N10B 113(1), O3-Li2-N13B 113(1).

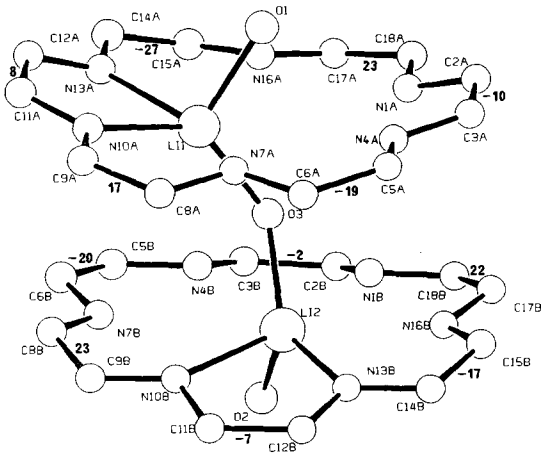

Fig. 2. Structure of $[\mathbf{1}_2 \cdot Li_2(H_2O)_3]^{2+}$ in the solid state. Side view along approximate mirror plane with N-C-C-N torsional angles indicated.

[*] Prof. T. W. Bell, Dr. P. J. Cragg, Dr. A. Firestone, Dr. D.-I. A. Kwok
Department of Chemistry, State University of New York
Stony Brook, New York 11794-3400 (USA)
Dr. M. G. B. Drew
Department of Chemistry, The University
Whiteknights, GB-Reading RG6 2AD (UK)

[**] This work was supported by the U.S. National Institutes of Health (NIH) via award GM32937. Funds for the X-ray diffractometer were obtained from the NIH (grant 1S10RR0058901). Also acknowledged is a NATO grant for international collaborative research. See also preceding communication [13].

torand A through opposite pyridine rings containing N7A and N16A. The six torsional angles fit a $(+--/++-)$ pattern where the position of the mirror plane is indicated by the symbol/. The 30° rotation of torand B with respect to A requires that this folding plane falls between pyridine rings; thus it bisects the CC bonds for N1B-C-C-N4B and N10B-C-C-N13B. These are the smallest torsional angles (−3, −7°), and the remaining torsions nicely fit a $(+-/+-)$ pattern.

The conformations of the torands in $[\mathbf{1}_2 \cdot Li_2(H_2O)_3]^{2+}$ differ significantly from the staggered $(+--+--)$ conformation observed in $\mathbf{1} \cdot K^+$(picrate$^-$) and $\mathbf{1} \cdot Rb^+$(picrate$^-$). This difference is apparently due to the complementary folding observed in the dimer, but why does $\mathbf{1} \cdot Li^+$ crystallize as a 2:2 complex, whereas $\mathbf{1} \cdot K^+$ and $\mathbf{1} \cdot Rb^+$ crystallize as 1:1 complexes with axial coordination by the picrate ion? The answer may be that this supramolecular assembly is stabilized by a hydrogen bonding network. An obvious difference between $\mathbf{1} \cdot Li^+$ and $\mathbf{1} \cdot K^+$ or $\mathbf{1} \cdot Rb^+$ is that the lithium ion does not fill the cavity of **1**, leaving the potential for hydrogen bonding by uncoordinated pyridine-N atoms. Lithium also possesses a larger hydration energy than potassium or rubidium.[7] Coordination to lithium should enhance the ability of water to donate hydrogen bonds, so the structure of $[\mathbf{1}_2 \cdot Li_2(H_2O)_3]^{2+}$ was carefully examined for evidence of OH···N hydrogen bonding.

Both terminal water molecules lie within 3.0 Å of several uncoordinated pyridine-N atoms, but only two of these pyridine rings are oriented with their lone pairs on N directed towards the O atoms. Thus N16A may be hydrogen-bonded to O1 (2.94 Å), and N7B to O2 (2.96 Å). It appears more likely that the bridging water molecule is hydrogen-bonded to inward-directed pyridine-N atoms N1A and N4B. Although these O–N distances are somewhat long (3.07 and 3.08 Å respectively), these nitrogen atoms and the lithium ions are located approximately tetrahedrally around O3 (Li1-O3-N1A 89°, Li1-O3-N4B 109°, Li2-O3-Ni1A 125°, Li2-O3-N4B 90°, N1A-O3-N4B 105°). The combination of weak hydrogen bonds to O3 and van der Waals interactions between the torands can explain the formation of the observed supramolecular assembly as well as the relatively short Li–O bridging distances in the complex.

Among the known crystal structures of lithium complexes,[4, 8–11] the structure of $[\mathbf{1}_2 \cdot Li_2(H_2O)_3]^{2+}$ is unusual in that lithium is unsymmetrically associated with three nitrogen atoms of the macrocycle. In two complexes of planar 15-membered macrocycles containing five sp^2 nitrogen donors,[9] lithium binds symmetrically with Li–N distances ranging from 2.15 to 2.27 Å. While this ligand contains a terpyridyl fragment, the distance between terminal nitrogens in this smaller macrocycle is only 4.13 Å, compared to an average of 4.81 Å in $[\mathbf{1}_2 \cdot Li_2(H_2O)_3]^{2+}$. Average Li–N bond distances are 2.08 Å in complexes with N-containing arene ligands[4] and 2.13 Å in the bipyridine complex of lithium picrate,[8] indicating that lithium is too small to bind symmetrically to a terpyridyl fragment of **1**.

A range of structures has been observed for lithium complexes of crown ethers,[4, 10] and $[\mathbf{1}_2 \cdot Li_2(H_2O)_3]^{2+}$ bears some resemblence to the 1:2 complexes between lithium salts and [12]crown-4. The Li([12]crown-4)$_2^+$ ion is useful for characterizing free anionic species in the solid state.[10a] Again $[\mathbf{1}_2 \cdot Li_2(H_2O)_3]^{2+}$ breaks the rule: lithium normally coordinates to picrate in complexes.[4, 8] Also of relevance are the structures of Li_2([18]crown-6)$(H_2O)_4X_2$ (X = Cl or Br).[10b] One of the two lithium ions in these structures forms three contacts of unequal length to consecutive oxygens of the crown ether. In the 1:2 complex of 18,18′-spirobi([19]crown-6) with $LiI(H_2O)_2$ the metal ion is also coordinated unsymmetrically to three consecutive oxygens of the crown.[10c]

Lithium salts show a pronounced tendency to form hydrated aggregates; key examples are the complexes of [18]crown-6 already mentioned[10b, c] and $[Li_2(H_2O)_6]^{2+}$.[11] In both cases the environments of the lithium ions are approximately tetrahedral, and two lithium and two oxygen atoms form four-membered rings. The linear $Li_2(H_2O)_3$ chain observed in the torand complex is apparently unique, although linear chains of hydrated sodium ions are known.[12] These observations suggest that the design of lithium-selective hosts might profitably accommodate part of the lithium hydration shell. Moreover, the structure of $[\mathbf{1}_2 \cdot Li_2(H_2O)_3]^{2+}$ suggests that longer linear chains of torands might be produced by decreasing the ratio of bridging ligand to metal, paving the way to polymeric materials with potential for ion and electron conductivity.

Experimental Procedure

A solution of torand **1**[1,2] (30 mg, 0.039 mmol) in $CHCl_3$ (3 mL) was washed with 7 mL of an aqueous solution of lithium picrate (30 mg, 0.11 mmol) and of $LiOH \cdot H_2O$ (35 mg, 0.83 mmol). The $CHCl_3$ solution was evaporated to dryness, and the residue was dissolved in ethyl acetate/CH_2Cl_2. Slow evaporation of the solvent yielded yellow needles of $[\mathbf{1}_2 \cdot Li_2(H_2O)_3(picrate)_2]$, which were dried for 12 hours at room temperature (0.1 torr). Yield 32 mg (71%).

^{1}H NMR (10^{-3} M in D_2O-saturated $CDCl_3$, 300 MHz): δ = 8.312 (s, 2H; (picrate), 7.515 (s, 3H; pyridine), 3.044 (s, 24H; $ArCH_2CH_2Ar$), 2.777 (t, 6H; CH_2Pr), 1.5–1.6 (m, 12H; CH_2CH_2Me), 1.020 (t, J = 7 Hz, 9H; CH_3). IR (KBr): $\tilde{\nu}$ [cm^{-1}] = 3400(br), 3080(w), 2940(m), 2840(m), 1630(s), 1600(m), 1540(s), 1510(m), 1485(m), 1450(m), 1430(m), 1375(m), 1350(m), 1320(m), 1290(s), 1270(m), 1250(s), 1210(m), 1150(m), 1095(w), 1060(m), 1030(w), 960(m), 910(m), 900(w), 780(m), 720(m), 700(m). Correct C,H,N analyses. The crystal used for X-ray structural analysis (0.6 × 0.3 × 0.05 mm) was grown from a CH_2Cl_2 solution layered with 10:1 (v/v) ethyl acetate/hexane.

Received: September 23, 1991 [Z 4928 IE]
German version: *Angew. Chem.* **1992**, *104*, 321

CAS Registry number:
$[\mathbf{1}_2 \cdot Li_2(H_2O)_3]^{2+}$, 138877-19-7.

[1] T. W. Bell, A. Firestone, R. Ludwig, *J. Chem. Soc. Chem. Commun.* **1989**, 1902–1904.

[2] a) A. Firestone, *Dissertation*, State University of New York at Stony Brook, **1988**, p. 923–925; b) T. W. Bell, P. J. Cragg, A. Firestone, D.-I. A. Kwok, R. Ludwig, unpublished.

[3] [{**1** · Li(H_2O)}$_2(\mu$-$H_2O)$][picrate)$_2$]: $C_{120}H_{118}N_{18}O_{17}Li_2$, M_r = 2098.2, triclinic, a = 16.818(2), b = 18.692(2), c = 19.392(2) Å, α = 118.145(8), β = 95.72(1), γ = 95.82(1)°, V = 5272(1) Å^3, ρ_{calcd} = 1.322 g cm^{-3}, space group $P\bar{1}$, Z = 2, $Cu_{K\alpha}$ radiation, λ = 1.54178 Å. The structure was solved by direct methods and refined by full matrix least squares; all non-H atoms anisotropic. H atoms were generated, riding on the appropriate carbon atoms at a distance of 0.95 Å. 11630 reflections were measured (θ max = 50°) of which 6816 unique reflections were observed with $F > 3\sigma(F)$, R = 0.071 (R_w = 0.086). Further details of the crystal structure investigation are available on request from the Director of the Cambridge Crystallographic Data Centre, University Chemical Laboratory, Lensfield Road, Cambridge, CB2 1EW (UK) on quoting the full literature citation. The assistance of R. Subramanian is gratefully acknowledged.

[4] U. Olsher, R. M. Izatt, J. S. Bradshaw, N. K. Dalley, *Chem. Rev.* **1991**, *91*, 137–164.

[5] a) S. M. Doughty, J. F. Stoddart, H. M. Colquhoun, A. M. Z. Slawin, D. J. Williams, *Polyhedron* **1985**, *4*, 567–573; b) J. D. Owen, *Acta Crystallogr. Sect. C* **1984**, *40*, 246–248; c) J. A. Hamilton, M. N. Sabesan, L. K. Steinrauf, *J. Am. Chem. Soc.* **1981**, *103*, 5880–5885; d) I. R. Hanson, J. D. Owen, M. R. Truter, *J. Chem. Soc. Perkin Trans. 2* **1981**, 1606–1615; e) V. W. Bhagwat, H. Manohar, N. S. Poonia, *Inorg. Nucl. Chem. Lett.* **1981**, *17*, 207–210; f) *ibid.* **1980**, *16*, 373–375; g) D. L. Hughes, C. L. Mortimer, M. R. Truter, *Inorg. Chim. Acta* **1978**, *28*, 83–89.

[6] a) S.-I. Yamaguchi, M. Goto, H. Takayanagi, H. Ogura, *Bull. Chem. Soc. Jpn.* **1988**, *61*, 1026–1028; b) H. M. Colquhoun, S. M. Doughty, J. F. Stoddart, A. M. Z. Slawin, D. J. Williams, *J. Chem. Soc. Perkin Trans. 2* **1986**, 253–257; c) E. N. Duesler, J. H. Engelmann, D. Y. Curtin, I. C. Paul *Cryst. Struct. Commun.* **1978**, *7*, 449–453; d) F. H. Herbstein, M. Kaftory, *Acta Crystallogr. Sect. B* **1976**, *32*, 387–396.

[7] M. Badertscher, M. Welti, P. Portmann, E. Pretsch, *Top. Curr. Chem.* **1986**, *136*, 17–80.
[8] M. S. Hundal, G. Sood, P. Kapoor, N. S. Poonia, *J. Crystallogr. Spectrosc. Res.* **1991**, *21*, 201–204.
[9] a) E. C. Constable, L. Y. Hung, J. Lewis, P. R. Raithby, *J. Chem. Soc. Chem. Commun.* **1986**, 1719–1720; b) E. C. Constable, M. J. Doyle, J. Healy, P. R. Raithby, *ibid.* **1988**, 1262–1264.
[10] a) P. P. Power, *Acc. Chem. Res.* **1988**, *21*, 147–153; b) T.-L. Chang, M. Zhao, N.-H. Hu, Z.-S. Jin, *Rev. Chim. Miner.* **1987**, *24*, 382–390; c) M. Czugler, E. Weber, *J. Chem. Soc. Chem. Commun.* **1981**, 472–473.
[11] C. L. Raston, C. R. Whitaker, A. H. White, *Aust. J. Chem.* **1988**, *41*, 413–416.
[12] B. Hedman, *Acta Crystallogr. Sect B* **1977**, *33*, 3077–3083.
[13] T. W. Bell, P. J. Cragg, M. G. B. Drew, A. Firestone, D.-I. A. Kwok, *Angew. Chem.* **1992**, *104*, 319, *Angew. Chem. Int. Ed. Engl.* **1992**, *31*, 345.

Idealized Pentagonal-Planar Coordination for Indium in $[(\mu_5\text{-In})\{Mn(CO)_4\}_5]^{2-}$

By *Martin Schollenberger, Bernhard Nuber,* and *Manfred L. Ziegler**

The possible geometries for a pentacoordinated central atom are so similar that they are easily interconvertible.[1] The idealized coordination polyhedrons, the trigonal bipyramid and the square pyramid, occur only very rarely in nature in undistorted form.[2] In almost all cases, however, these two coordination geometries are energetically considerably more favorable than a pentagonal-planar structure. Pentagonal-planar coordination has thus been observed only when interpretation as a virtual pentagonal bipyramid is possible.[3–6] We report here on the anionic complex $[(\mu_5\text{-In})\{Mn(CO)_4\}_5]^{2-}$ (**3**), in which the indium atom is found in the center of a five-membered ring constructed from five $[Mn(CO)_4]$ units. Although this ring is not strictly planar but is distorted towards an envelope conformation, the coordination environment of indium in the center of the ring can best be described as idealized pentagonal planar. This unusual coordination form is forced on the indium exclusively by the steric requirements of its position in the center of a rigid five-membered ring.

Metathesis reactions aimed at constructing carbonylmanganese compounds usually proceed from easily accessible $[Mn(CO)_5]$ derivatives. Because of the high inherent stability of the $[Mn(CO)_5]$ unit, the products as a rule also include the $[Mn(CO)_5]$ fragments. For instance, $InCl_3$ reacts with $Na[Mn(CO)_5]$ by stepwise substitution to form $[\{Mn(CO)_5\}_nInCl_{(3-n)}]$ $(n=1-3)$.[7] We have shown that in metathesis reactions, anionic clusters constructed from three $[Mn(CO)_4]$ moieties afford derivatives in which the $[Mn_3(CO)_{12}]$ unit generally remains intact. Thus $[(\mu\text{-H})Mn_3(\mu\text{-CO})_2(CO)_{10}]^{2-}$ reacts with $InCl_3$ to form $[In\{(\mu\text{-H})Mn_3(CO)_{12}\}_2]^-$ and $[InCl\{(\mu\text{-H})Mn_3(CO)_{12}\}\{Mn(CO)_5\}]^-$.[8]

In contrast, the completely deprotonated form of $K_2[(\mu\text{-H})Mn_3(\mu\text{-CO})_2(CO)_{10}]$, $K_3[Mn_3(\mu\text{-CO})_2(CO)_{10}]$ (**1**),[8,9] affords predominantly the tetranuclear product **2** with excess of $InCl_3$ (Scheme 1).[10–12] In **2** two $[Mn(CO)_4]$ units joined by Mn–Mn bonds are bridged by $[\{Mn(CO)_5\}InCl]^-$ groups. In a broad sense these bridging ligands, which are derivatives of the type R_2In^-, are isoelectronic with bridging methylene ligands R_2C and their homologues R_2Si and R_2Sn.[13–15] The Mn centers are in an idealized octahedral geometry, because the bridging ligands and the equatorial CO groups are approximately coaxially bound. Thus the Mn atoms, the indium centers, and the equatorial CO groups are coplanar. The center of gravity of the molecular ion **2** lies on the crystallographic inversion center, the substituents on the bridging ligands are *trans* to one another, and the Mn–Mn bond in **2** (316.4(2) pm) results in a comparatively small Mn-In-Mn bond angle (72.6(1)°).

Complex **3** is formed as a side product in the synthesis of **2** (Scheme 1).[10,11] It has a very unusual structure (Fig. 1) in which the five $[Mn(CO)_4]$ units are joined to form a five-membered ring of metal atoms; the indium center in the middle of this ring forms bonding interactions with all five manganese atoms.

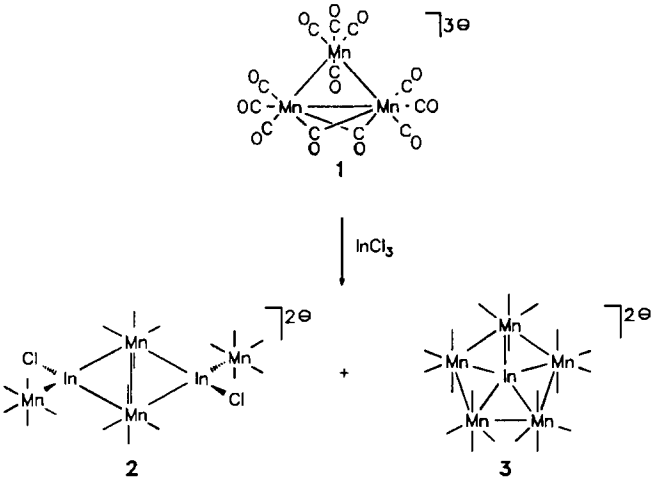

Scheme 1. The reaction of **1** with $InCl_3$. The lines at the manganese atoms of **2** and **3** represent terminal CO ligands.

The conformation of the cyclic $[Mn_5(CO)_{20}]$ building block (isolobal to C_5H_5!) is a flattened envelope (torsion angles [°]: Mn5-Mn1-Mn2-Mn3 −7.0; Mn2-Mn1-Mn5-Mn4 33.1). The Mn3-Mn4-Mn5 plane lies at an angle of 45° to the best plane containing Mn3-Mn2-Mn1-Mn5. The manganese atoms are in an idealized octahedral environment; with respect to the five-membered ring two CO groups are equatorial and two CO ligands are axial at each Mn

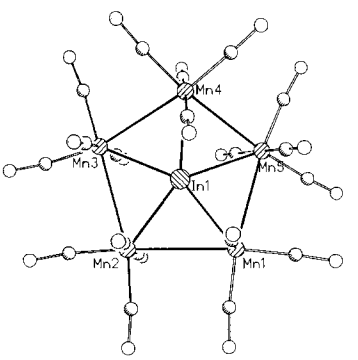

Fig. 1. Structure of **3** in the solid state. Selected distances [pm] and angles [°]: In1-Mn1 265.0(2), In1-Mn2 261.8(3), In1-Mn3 264.6(2), In1-Mn4 265.1(2), In1-Mn5 265.7(2), Mn1-Mn2 320.8(3), Mn1-Mn5 314.2(3), Mn2-Mn3 323.5(3), Mn3-Mn4 317.8(3), Mn4-Mn5 309.5(3); Mn1-In1-Mn2 75.0(1), Mn1-In1-Mn5 72.6(1), Mn2-In1-Mn3 75.8(1), Mn3-In1-Mn4 73.7(1), Mn4-In1-Mn5 71.3(2).

[*] Dipl.-Chem. M. Schollenberger, Dr. B. Nuber, Prof. Dr. M. L. Ziegler[+]
Anorganisch-chemisches Institut der Universität Heidelberg
[+] Deceased April 30, 1991; correspondence about this communication to:
Prof. Dr. G. Huttner
Anorganisch-chemisches Institut der Universität
Im Neuenheimer Feld 270, D-W-6900 Heidelberg (FRG)

atom. The indium lies almost at the center of gravity of the ring spanned by the five manganese atoms (distance 8.5 pm; deviation from the best plane 4.6 pm). Its coordination is approximately pentagonal planar. This unusual coordination form in **3** is exclusively due to the sterically rigid $[Mn_5(CO)_{20}]$ "ligand".

Experimental Procedure

All manipulations were conducted under an inert atmosphere (argon) in the absence of moisture and air. All glass apparatus was evacuated several times on an oil vacuum line and flushed with argon before use. The solvents were dried under argon and freshly distilled.

1: Prepared by published methods [8, 9], this compound contains 30% KOH. For the preparation of **2** and **3**, **1** was freed of KOH by dissolution in acetone and filtration, followed by evaporation of the acetone. KOH-free **1** is pyrophoric.

2 and **3**: THF (8.5 mL) was added to a mixture of **1** (0.58 g, 0.94 mmol) and dry $InCl_3$ (0.87 g, 4.10 mmol). The color changed immediately from green to blue. The solution was stirred for 5 min, methanol (1.5 mL) was added, and the mixture was separated on a chromatography column (MPLC column 46 × 2.6 cm, silica gel 40–63 μ, eluent THF/methanol 10/1). A yellow and a blue fraction that have not yet been able to be characterized were eluted first in low yields. The third violet fraction was treated with $AsPh_4Cl$ monohydrate (100 mg, 0.229 mmol), the solvent removed at 10^{-1} mbar, and the residue taken up in a mixture of *n*-hexane, ethyl acetate, and acetone (5:20:15 mL). The violet mother liquor was filtered off through a G3 Schlenk filter; at +4 °C **2**-$(AsPh_4)_2 \cdot (CH_3)_2CO$ precipitates as red-brown crystals. They are separated from the mother liquor by decantation, washed three times with diethyl ether, and dried in vacuum. Yield: 90 mg (8%, calculated on initial amount of **1**), correct elemental analyses.

The fourth, brown fraction was treated with $AsPh_4Cl$ monohydrate (50 mg, 0.115 mmol), the solvent removed at 10^{-1} mbar, and the residue taken up in ethyl acetate. Excess $AsPh_4Cl$ and KCl remained undissolved. The brown mother liquor was filtered through a G-3 Schlenk filter. At +4 °C, **3**-$(AsPh_4)_2$ precipitated in the form of dark brown crystals, which were separated by decantation from the mother liquor, washed three times with diethyl ether, and dried at 10^{-1} mbar. Yield: 15 mg (2%, calculated on initial amount of **1**), correct elemental analyses. A light brown residue which cannot be eluted remains on the column.

Received: September 30, 1991 [Z4939 IE]
German version: *Angew. Chem.* **1992**, *104*, 329

CAS Registry numbers:
1, 130934-60-0; **2**-$(AsPh_4)_2 \cdot (CH_3)_2CO$, 138407-41-7; **3**-$(AsPh_4)_2$, 138407-43-9; In, 7440-74-6; Mn, 7439-96-5.

[1] F. A. Cotton, G. Wilkinson, *Inorganic Chemistry*, 4th ed., Wiley, New York, **1980**, p. 50.
[2] R. S. Berry, *J. Chem. Phys.* **1960**, *32*, 933–938.
[3] See [1], p. 196.
[4] K. O. Christe, E. C. Curtis, D. A. Dixon, H. P. Mercier, J. C. P. Sanders, G. J. Schrobilgen, *J. Am. Chem. Soc.* **1991**, *113*, 3351–3361.
[5] B. F. Hoskins, C. D. Pannan, *Aust. J. Chem.* **1976**, *29*, 2337–2348.
[6] S. C. Kokkou, C. J. Cheer, *Acta Crystallogr. Sect. C* **1986**, *42*, 1159–1161.
[7] A. T. T. Hsieh, M. J. Mays, *J. Chem. Soc. Dalton Trans.* **1972**, *516*–521.
[8] W. Schatz, H.-P. Neumann, B. Nuber, B. Kanellakopulos, M. L. Ziegler, *Chem. Ber.* **1991**, *124*, 453–463.
[9] B. F. G. Johnson, R. D. Johnston, J. Lewis, B. H. Robinson, *J. Organomet. Chem.* **1967**, *10*, 105–109.
[10] Spectroscopic data of **2** and **3**: **2**-$(AsPh_4)_2 \cdot (CH_3)_2CO$: UV/VIS ($CH_2Cl_2$): λ_{max} [nm] (ε) = 264 (39000), 270 (36800), 320 (23300), 570 (8800); ^1H NMR (300 MHz, [D$_6$]acetone, internal standard [D$_6$]acetone, room temperature): δ = 7.82–7.95 (m, phenyl-H); ^{13}C NMR (75 MHz, [D$_6$]acetone, internal standard [D$_6$]acetone, room temperature): δ = 230.6 (s, carbonyl-C); 135.5, 134.3, 132.0, 122.1 (phenyl-C); IR (KBr): ν [cm^{-1}] = 2064 st, 2030 st, 1979 sst, 1950 sst, 1887 st, 1869 st (C=O). **3**-$(AsPh_4)_2$: UV/VIS (CH_2Cl_2): λ_{max} [nm] (ε) = 264 (43900), 270 (38300), 342 (22400), 490 (12300); ^1H NMR (300 MHz, [D$_6$]acetone, internal standard [D$_6$]acetone, room temperature): δ = 7.82–7.95 (m, phenyl-H); IR (KBr): ν [cm^{-1}] = 1988 sst, 1968 sst, 1947 st, 1938 st, 1926 st, 1912 st, 1902 st, 1887 m, 1880 m, 1864 m (C=O).
[11] Crystal structure of **2** and **3**: **2**-$(AsPh_4)_2 \cdot (CH_3)_2CO$: $C_{69}H_{46}O_{19}As_2In_2Cl_2Mn_4$, M = 1849.29, monoclinic, space group $C2/c$ (no. 15), a = 2462.8(8), b = 1521.0(9), c = 2221.1(8) pm, β = 117.72(2)°, V = 7365(1) × 10^6 pm^3, Z = 4, T = 298 K, θ range 3.0° < 2θ < 52.5°, 7908 measured reflections, 4416 observed reflections ($I > 2\sigma(I)$), 3850 independent reflections ($I > 2.5\sigma(I)$), 396 refined parameters, $R(R_w)$ = 0.064 (0.052). **3**-$(AsPh_4)_2$: $C_{68}H_{40}O_{20}As_2InMn_5$, M = 1716.44, rhombic, space group *Pbca* (no. 61), a = 1930(1), b = 2403(1), c = 2922(1) pm, V = 1355(1) × 10^7 pm^3, Z = 8, T = 298 K, θ range 3.0° < 2θ < 50.0°, 12515 measured reflections, 6410 observed reflections ($I > 2\sigma(I)$), 5652 independent reflections ($I > 2.5\sigma(I)$), 530 refined parameters, $R(R_w)$ = 0.070 (0.056). Measurement on a Siemens (Nicolet-Syntex) R3 four circle diffractometer, $Mo_{K\alpha}$ radiation, graphite monochromator. Further details of the crystal structure investigation may be obtained from the Fachinformationszentrum Karlsruhe, Gesellschaft für wissenschaftlich-technische Information mbH, W-7514 Eggenstein-Leopoldshafen 2 (FRG) on quoting the depository number CSD-55887, the names of the authors, and the journal citation.
[12] Selected distances [pm] and angles [°] for **2**: In1-Mn1 272.5(3), In1-Mn2a 269.2(2), In1-Mn2 265.0(2), In1-Cl1 248.8(4), Mn2-Mn2a 316.4(2); In1-Mn2-Mn2a 54.3(1), In1a-Mn2-Mn2a 53.1(1), Mn2-In1-Mn2a 72.6(1), Mn1-In1-Cl1 100.9(1), Mn1-In1-Mn2 128.8(1), Mn1-In1-Mn2a 130.4(1), Cl1-In1-Mn2a 108.7(1), Cl1-In1-M2 113.9(1).
[13] W. Schulze, H. Hartl, K. Seppelt, *Angew. Chem.* **1986**, *98*, 189–190; *Angew. Chem. Int. Ed. Engl.* **1986**, *25*, 185–186.
[14] G. L. Simon, L. F. Dahl, *J. Am. Chem. Soc.* **1973**, *95*, 783–789.
[15] H. Preut, H.-J. Haupt, *Z. Anorg. Allg. Chem.* **1976**, *422*, 47–53.

Reaction of C_{60} with Dimethyldioxirane—Formation of an Epoxide and a 1,3-Dioxolane Derivative**

By *Yiannis Elemes, Scott K. Silverman, Chimin Sheu, Michelle Kao, Christopher S. Foote,* Marcos M. Alvarez,* and *Robert L. Whetten**

Since their discovery,[1] the fullerenes have attracted much attention.[2–4] Although gram quantities of C_{60} and C_{70} can now be produced,[5, 6] the chemical reactivity of these new compounds is just beginning to be explored, and few products have been completely characterized. Among these are adducts to C_{60} of OsO_4,[7, 8] other metal-complex fragments,[9–11] and diphenylcarbene.[12]

Although C_{60} is easy to reduce and reacts readily with nucleophiles, it is very difficult to oxidize.[13–17] Dioxiranes have been used to make epoxides that are difficult to prepare by other routes.[18–26] We now report that C_{60} reacts with dimethyldioxirane to give an epoxide $C_{60}O$ and a 1,3-dioxolane derivative.

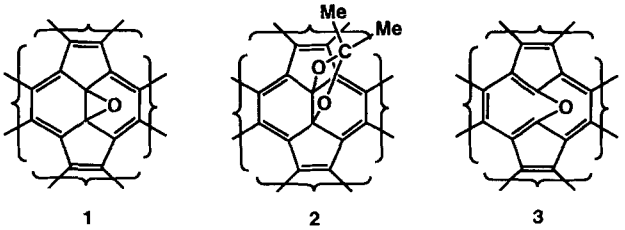

1 **2** **3**

C_{60} reacts with dimethyldioxirane to give two products, **1** and **2**, which in the solid state are stable dark crystals. Solutions of **2** in toluene are yellow, those of **1**, purple (similar to solutions of C_{60}). The UV/VIS spectra of **1** and **2** are shown in Figures 1a and 1b. The FTIR spectrum of **1** is shown in Figure 2a. The ^{13}C NMR spectrum of **1** (Fig. 3a) consists of 17 signals, of which four correspond to two carbon atoms and

[*] Prof. C. S. Foote, Prof. R. L. Whetten, Dr. Y. Elemes, S. K. Silverman, C. Sheu, M. Kao, M. M. Alvarez
Department of Chemistry and Biochemistry
University of California
Los Angeles CA 90024-1569 (USA)

[**] This research was supported by the U.S. National Institutes of Health (GM-20080) and the U.S. National Science Foundation (CHE89-11916). We thank Dr. D. Cox for helpful discussions and a copy of [30].

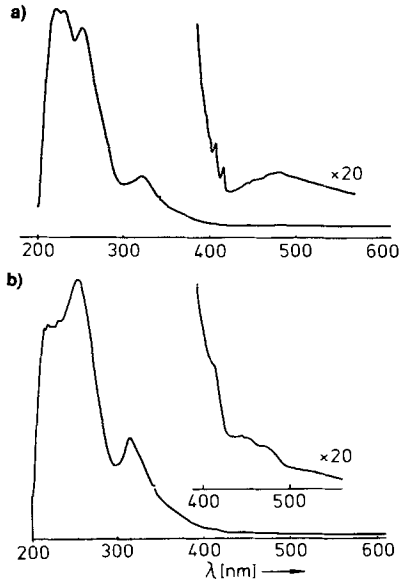

Fig. 1. UV/VIS spectra of a) $C_{60}O$ **1** and b) C_{60}-1,3-dioxolane **2** in *n*-hexane.

thirteen correspond to four carbon atoms. This is the correct number and ratio of peak intensities for a C_{60} adduct of C_{2v} symmetry. The osmium-tetraoxide adduct, of which a detailed NMR study has recently appeared,[27] has the same symmetry.

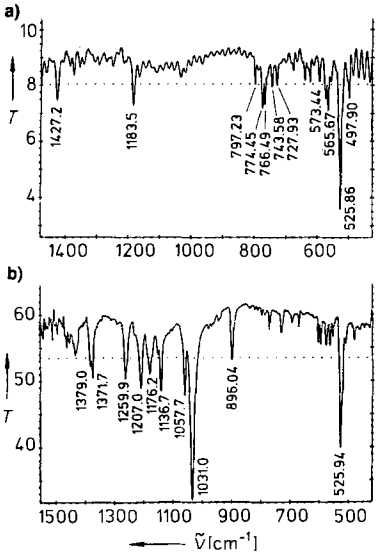

Fig. 2. FTIR spectra (KBr pellets) of a) $C_{60}O$ **1** and b) C_{60}-1,3-dioxolane **2**.

The LD-TOF mass spectrum (laser desorption time-of-flight)[28, 29] of **1** displays a peak for $C_{60}O$ (m/z 736 ± 2, M^+) as well as for C_{60}, which arises from loss of one oxygen atom. The FAB mass spectrum (not shown) shows a weak peak at m/z 736, but the loss of an oxygen atom is much more pronounced here. There is no $C_{60}O$ in the starting material, as shown by the LD-TOF spectrum, and the isolated **1** is not contaminated by C_{60} according to HPLC. Based on the above data, **1** is a monoepoxide of C_{60} with the oxygen bridging the bond connecting two six-membered rings, a bonding situation also found in other C_{60} adducts.[27]

After much of this work had been completed, we received a manuscript from chemists at Exxon and the University of Pennsylvania reporting the preparation of $C_{60}O$ by a photochemical route and by isolation from soot.[30] The properties of their material are in excellent agreement with those reported above. The infrared bands differ slightly in relative intensities, which we attribute to the difference in medium (KBr pellet vs. film). The ^{13}C NMR shifts are quite similar, although the solvents used are different (CS_2 vs. C_6D_6). Both $C_{60}O$ and $C_{70}O$ have also been detected in the gas phase.[31] An oxide of C_{70} is formed in the soot with other fullerenes and has been characterized only by mass and UV/VIS spectrometry.[6] Recent electrochemical studies reported that the dianion of C_{60} reacts with O_2 to form a series of C_{60} oxides which were detected by FAB mass spectrometry but were not otherwise characterized.[32]

Our product is clearly the epoxide **1** rather than the annulene[33] **3**, as shown by the ^{13}C NMR signal at $\delta = 90.92$; an sp^2 C–O should give rise to a signal below $\delta = 140$.[34, 35] Substituted epoxide carbons typically resonate at $\delta = 52$–70.[36] Although the resonance at $\delta = 90.92$ is at low field for epoxide carbons, the downfield shift is probably caused by the anisotropy of the partially broken fullerene, which was also reported in the diphenylcarbene adduct.[12] The similarity of the UV/VIS spectrum of the diphenylcarbene adduct to that of C_{60} was taken as indirect evidence for the open annulene structure, which is clearly implied by the long C–C bond.[37] The UV/VIS spectra of **1** and C_{60} are also quite similar, but the NMR spectrum of **1** provides definitive proof of its epoxide character.

Based on spectral data we identify the second product of the reaction of dimethyldioxirane and C_{60} as 1,3-dioxolane **2**. The FTIR spectrum of compound **2** (Fig. 2b) shows a very strong sp^3 C–O absorption band at 1031 cm^{-1} and a C–H absorption band at 2900 cm^{-1}. The LD-TOF mass spectrum has a molecular ion (m/z 795, M^+, corresponding to C_{60} + dimethyldioxirane) and signals of greater intensity for fragmentation to $C_{60}O$ (loss of acetone) and to C_{60}. The exact molecular mass of M^+ (794) was obtained from the FAB mass spectrum but here, as with **1**, the signal of the C_{60} ion is dominant. The ^{13}C NMR spectrum of **2** (Fig. 3b) also has 17 signals for the C_{60} skeleton, of which 13 correspond to four carbon atoms, and four correspond to two carbon atoms. The resonance at $\delta = 96$ (at lower field than the related signal in **1**) is assigned to the O-bound carbon atoms. The signals at $\delta = 113.04$ (1 C) and 28.92 (2 C) are assigned to the

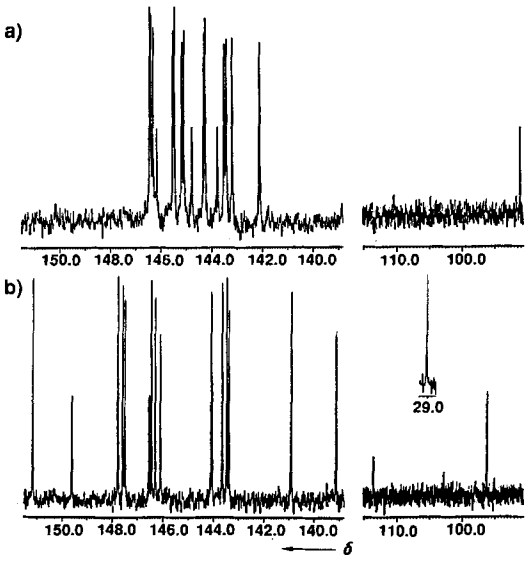

Fig. 3. ^{13}C NMR spectra of a) $C_{60}O$ **1** and b) C_{60}-1,3-dioxolane **2** in CS_2 with [D_6]acetone as internal lock and [Cr(acac)$_3$] as relaxation agent.

ketal and methyl C atoms, respectively. In the ^{1}H NMR spectrum (in CS_2) the methyl hydrogens give rise to a sharp singlet at $\delta = 1.56$.

The 1,3-dioxolane structure can be deduced from the number of signals in the ^{13}C NMR spectrum; the 1,2-isomer would have only a single mirror plane. The same reasons advanced in favor of the epoxide structure for **1** lead us to conclude that adduct **2** also has the closed structure. The fullerene regions of the ^{13}C NMR spectra of the OsO_4 adduct of C_{60} [27] and of **2** are strikingly similar (Fig. 3b), confirming their structural similarity. Hydrolysis of this ketal and oxidation of the resulting diol may offer an attractive and specific route to ring-opened fullerenes.

The determination of the mechanism for the formation of **1** and **2** will require further study. It is particularly surprising that the O–O bond of the dimethyldioxirane opens. To our knowledge, this is the first reported dimethyldioxirane adduct of this type. Small amounts of a 1,3-dioxolane were formed during the epoxidation of *cis*-3-hexene,[38] but this resulted from addition of acetone to the epoxide under the acidic conditions used. When a solution of **1** in acetone/toluene was stirred at 50 °C for 12 h, no change was observed (HPLC). Solutions of **1** in toluene heated at 110 °C for 24 h showed gradual decomposition of **1** to C_{60}. The 1:1 dimethyldioxirane–C_{60} adduct **2** could give epoxide **1** by loss of acetone, or **1** and **2** could be formed in competitive reactions. But no change was observed (HPLC) for solutions of **2** in toluene after they had been heated at 110 °C for 24 h. Thus, the two compounds do not interconvert under more extreme conditions than those required for their formation (and isolation), and the competitive pathway seems likely.

Addition of dimethyldioxirane to C_{60} could proceed by either homolytic or heterolytic cleavage of the O–O bond. Although Wudl et al. report reactions of C_{60} with 1,3-dipoles,[12] the path via diradicals seems more likely in our case.

Experimental Procedure

A solution of C_{60} (200 mg, 0.28 mmol) [39] in toluene (400 mL) was treated with 2.5 mL of a solution of dimethyldioxirane [19] in acetone (0.11 M) at room temperature. After 12 h a brown insoluble material was removed by filtration. The elemental analysis (C 84.97, H 0.94, O 14.09) corresponds to $C_{60}H_{9\ldots10}O_{7\ldots8}$; FTIR (KBr): ν[cm^{-1}] = 527, 1041 (s), 1208, 1174, 2940 (w), 2989 (w). The products were separated by preparative HPLC (C_{18} reverse-phase, acetonitrile/toluene, 55:45 (v:v), detection at 340 nm, 9.5 mL min^{-1}). Baseline peak separation allowed isolation of 12 mg of **2**, 8 mg of **1**, and 66 mg of unreacted C_{60}. Chromatography on alumina also led to separation of **1** and **2**. UV/VIS (*n*-hexane): **1**: λ_{max} [nm] = 228, 249, 319 (s), 405, 416 (w), 478 (br., w); **2**: λ_{max} [nm] = 253, 313 (s), 412, 444, 471 (vw). FTIR (KBr): **1**: $\tilde{\nu}$[cm^{-1}] = 1427, 1184, 774, 766, 566, 526, and others; **2**: three weak bands at 2900 cm^{-1}, others at 1379, 1207, 1176, 1138, 1058, 1031 (s), 896, 526 (s). ^{13}C NMR (125 MHz, CS_2, [D$_6$]acetone as internal lock, [Cr(acac)$_3$] as relaxation agent, 42000 scans, 25 °C): **1**: δ(number of carbon atoms) = 146.32(4), 146.29(4), 146.20(4), 146.04(2), 145.40(4), 145.34(4), 145.05(4), 144.97(4), 144.64(2), 144.18(4), 144.14(4), 143.64(2), 143.38(4), 143.30(4), 143.07(4), 141.99(4), 90.92(2); **2** (same conditions as for **1** except 38000 scans): δ = 151.04(4), 149.47(2), 147.64(4), 147.45(4), 147.36(4), 146.40(2), 146.31(4), 146.17(4), 145.96(4), 143.96(4), 143.93(2), 143.53(4), 143.35(4), 143.26(4), 140.79(4), 139.02(4), 113.04(1), 96.15(2), 28.92(2).

Received: December 23, 1991 [Z 5097 IE]
German version: *Angew. Chem.* **1992**, *104*, 364

[1] H. W. Kroto, J. R. Heath, S. C. O'Brien, R. F. Curl, R. E. Smalley, *Nature* **1985**, *318*, 162.
[2] W. Krätschmer, L. D. Lamb, K. Fostiropoulos, D. R. Huffman, *Nature* **1990**, *347*, 354.
[3] W. Krätschmer, K. Fostiropoulos, D. R. Huffman, *Chem. Phys. Lett.* **1990**, *170*, 167.
[4] H. Ajie, M. M. Alvarez, S. A. Anz, R. D. Beck, F. Dieterich, K. Fostiropoulos, D. R. Huffman, W. Krätschmer, Y. Rubin, K. E. Schriver, D. Sensharma, R. L. Whetten, *J. Phys. Chem.* **1990**, *94*, 8630.
[5] R. Ettl, I. Chao, F. Diederich, R. L. Whetten, *Nature* **1991**, *353*, 149; F. Diederich, R. Ettl, Y. Rubin, R. L. Whetten, R. Beck, M. Alvarez, S. Anz, D. Sensharma, F. Wudl, C. Khemani, A. Koch, *Science* **1991**, *252*, 548.
[6] G. Peters, M. Jansen, *Angew. Chem.* **1992**, *104*, 240; *Angew. Chem. Int. Ed. Engl.* **1992**, *31*, 223.
[7] J. M. Hawkins, T. A. Lewis, S. D. Loren, A. Meyer, J. R. Heath, Y. Shibato, R. J. Saykally, *J. Org. Chem.* **1990**, *55*, 6250.
[8] J. M. Hawkins, A. Meyer, T. A. Lewis, S. Loren, F. J. Hollander, *Science* **1991**, *252*, 312.
[9] P. J. Fagan, J. C. Calabrese, B. Malone, *Science* **1991**, *252*, 1160.
[10] R. S. Koefod, M. F. Hudgens, J. R. Shapley, *J. Am. Chem. Soc.* **1991**, *113*, 8957.
[11] P. J. Fagan, J. C. Calabrese, B. Malone, *J. Am. Chem. Soc.* **1991**, *113*, 9408.
[12] T. Suzuki, Q. Li, K. C. Khemani, F. Wudl, Ö. Almarsson, *Science* **1991**, *254*, 1186.
[13] P.-M. Allemand, A. Koch, F. Wudl, Y. Rubin, F. Diederich, M. M. Alvarez, S. J. Anz, R. L. Whetten, *J. Am. Chem. Soc.* **1991**, 113, 1050.
[14] D. Dubois, K. M. Kadish, S. Flanagan, R. E. Haufler, L. P. F. Chibante, L. J. Wilson, *J. Am. Chem. Soc.* **1991**, *113*, 4364.
[15] P.-M. Allemand, G. Srdanov, A. Koch, K. Khemani, F. Wudl, *J. Am. Chem. Soc.* **1991**, *113*, 2780.
[16] C. Jehoulet, A. J. Bard, *J. Am. Chem. Soc.* **1991**, *113*, 5456.
[17] D. Dubois, K. M. Kadish, S. Flanagan, L. J. Wilson, *J. Am. Chem. Soc.* **1991**, *113*, 7773.
[18] R. W. Murray, R. Jeyaraman, *J. Am. Chem. Soc.* **1984**, *106*, 2462.
[19] R. W. Murray, R. Jeyaraman, *J. Org. Chem.* **1985**, *50*, 2847.
[20] R. W. Murray, S. N. Rajadhyaksha, R. Jeyaraman, *Polycycl. Aromat. Compd.* **1990**, *1*, 213.
[21] L. Troisi, L. Cassidei, L. Lopez, R. Mello, R. Curci, *Tetrahedron Lett.* **1989**, *30*, 257.
[22] S. K. Silverman, C. S. Foote, *J. Am. Chem. Soc.* **1991**, *113*, 7672.
[23] W. Adam, L. Hadjiarapoglou, X. Wang, *Tetrahedron Lett.* **1989**, *30*, 6497.
[24] W. Adam, L. Hadjiarapoglou, B. Nestler, *Tetrahedron Lett.* **1990**, *31*, 331.
[25] W. Adam, L. Hadjiarapoglou, V. Jager, J. Klicic, B. Seidel, X. Wang, *Chem. Ber.* **1991**, *124*, 2361.
[26] W. Adam, L. Hadjiarapoglou, X. Wang, *Tetrahedron Lett.* **1991**, *32*, 1295.
[27] J. M. Hawkins, S. Loren, A. Meyer, R. Nunlist, *J. Am. Chem. Soc.* **1991**, *113*, 7770.
[28] F. Diederich, Y. Rubin, C. B. Knobler, R. Whetten, K. E. Schriver, K. N. Houk, Y. Li, *Science* **1989**, *245*, 1088.
[29] K. E. Schriver, Dissertation, University of California, Los Angeles, **1990**.
[30] K. M. Creegan, J. L. Robbins, W. K. Robbins, J. M. Millar, R. D. Sherwood, P. J. Tindall, D. M. Cox, J. P. McCauley, Jr., D. R. Jones, T. T. Gallagher, A. M. Smith III, *J. Am. Chem. Soc.* **1992**, *114*, 1103.
[31] J. M. Wood, B. Kahr, S. H. Hoke II, L. Dejarme, R. G. Cooks, D. Ben-Amotz, *J. Am. Chem. Soc.* **1991**, *113*, 5907.
[32] W. A. Kalsbeck, H. H. Thorp, *J. Electroanal. Chem.* **1991**, *314*, 363.
[33] E. Vogel, M. Biskup, W. Pretzer, W. A. Böll, *Angew. Chem.* **1964**, *76*, 785; *Angew. Chem. Int. Ed. Engl.* **1964**, *3*, 642.
[34] F. W. Wehrli, T. Wirthlin, *Interpretation of Carbon-13 NMR Spectra*, Heyden, London, **1976**, p. 170ff. and p. 251.
[35] H.-O. Kalinowski, S. Berger, S. Braun, *^{13}C NMR-Spectroscopy*, Thieme, Stuttgart, **1984**, p. 268ff.
[36] H.-O. Kalinowski, S. Berger, S. Braun, *^{13}C NMR-Spectroscopy*, Thieme, Stuttgart, **1984**, p. 320, 327.
[37] X-ray structural analysis: F. Wudl, personal communication.
[38] R. W. Murray, V. Ramachandran, *Photochem. Photobiol.* **1979**, *30*, 187.
[39] H.-D. Beckhaus, C. Rüchardt, M. Kao, F. Diederich, C. S. Foote, *Angew. Chem.* **1992**, *104*, 69; *Angew. Chem. Int. Ed. Engl.* **1992**, *31*, 63.

Ab Initio Investigations of Structure and Stability of $[R_3SiAl]_4$, R = H, Me, *t*Bu**

By *Uwe Schneider, Reinhart Ahlrichs,* Hans Horn,* and *Ansgar Schäfer*

The synthesis of metastable Al^I compounds, for example, AlCl in toluene/ether by Schnöckel et al.,[1] opened new routes in aluminium chemistry.[2] Thus, $Cp^*_4Al_4$,

[*] Prof. Dr. R. Ahlrichs, Dipl.-Chem. U. Schneider, Dr. H. Horn, Dipl.-Chem. A. Schäfer
Institut für Physikalische Chemie und Elektrochemie der Universität Kaiserstrasse 12, D-W-7500 Karlsruhe (FRG)

[**] This work was supported by the Fonds der Chemischen Industrie. We thank Prof. Dr. H. Schnöckel for very helpful discussions and the communication of unpublished results.

$Cp^* = C_5Me_5$, could be synthesized and structurally characterized.[3] The compound shows a central Al_4 tetrahedron, as known from the analogous boron compounds (e.g. B_4Cl_4[4, 5]). Recently, by the reaction of the sodium silane tBu$_3$SiNa with AlCl, the successful synthesis of tBu$_3$SiAl was achieved, which, according to evidence from mass spectrometry, also exists as a tetramer.[6] A structure determination has not been possible up to now because no suitable crystals could be obtained. Herein, we report the results of ab initio calculations on tBu$_3$SiAl and its tetramer, from which statements can be made concerning the structure (Fig. 1) and the relative stability of these compounds.

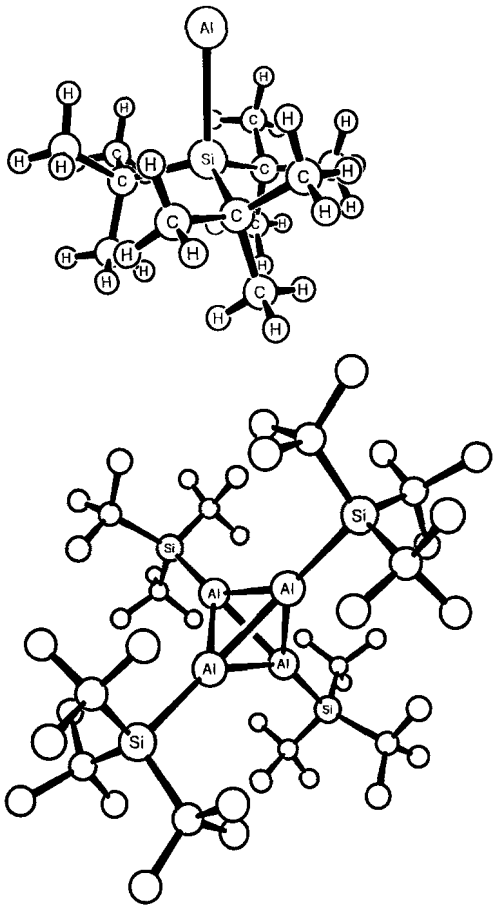

Fig. 1. Calculated structures of tBu$_3$SiAl with C_3 symmetry (top) and [tBu$_3$SiAl]$_4$ with T symmetry (bottom, H atoms are not drawn).

B^I and Al^I compounds have a tendency to form tetramers and higher oligomers, for example, B_9Cl_9.[7] The molecules B_4R_4 (R = Cl, F, H), like the analogous Al_4R_4 species, have already been theoretically intensively investigated.[5, 8, 9] The four lone pairs n(M) of the MR-building blocks are available for bonding in the central M_4 tetrahedron of M_4R_4 (M = B, Al) (Fig. 2). From these in (the local) T_d symmetry, a_1 (bonding) and t_2 (antibonding) MOs are formed by linear combination. The t_2 MOs are stabilized by admixing of contributions of vacant AOs π(M) (e in C_{3v}) of the monomer MR (Fig. 2). This effect is crucial for the stability of M_4R_4 relative to 4 MR.[9] In an alternative view each tetrahedral face can be assigned an electron pair, which occupies a bonding three-center MO.[8, 10]

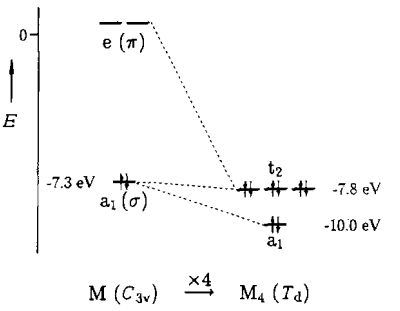

Fig. 2. Qualitative MO diagram of the M_4 tetrahedron in M_4X_4 (T_d). The energies are valid for M = Al, X = $SiMe_3$. For the other molecules the relationships are similar.

The π(M) stabilization competes with a posssible stabilizing π delocalization π(R) → π(M) in the monomers. This explains the decreasing stability of M_4R_4 relative to 4 MR in the series R = H, Cl, F for M = B and R = H, Cl, F, Cp for M = Al, because the π-delocalization in the monomers increases in this order. According to Wade's rules,[11] a stable dianion $M_4R_4^{2-}$ would be expected. Since with the two additional electrons a degenerate level of type t_1, t_2 or e (other MOs are not at disposal in the valence region) would have to be partially occupied, Wade's rules seem to fail for the tetramer.[8]

The ab initio calculations[12] were carried out on IBM RISC 6000 workstations using the TURBOMOLE program[13] within the framework of the SCF approximation partially supplemented by MP2 calculations.[14] With gradient calculations all structural parameters were optimized for each given molecular symmetry.[15] For the molecules H_3SiAl, $[H_3SiAl]_4$, Me_3SiAl and tBu$_3$SiAl force field calculations (analytical second derivatives of the SCF energy with respect to the nuclear coordinates in the corresponding basis) confirmed that the symmetries C_{3v}, T_d, C_{3v}, and C_3, respectively,[16] each lead to a local minimum on the SCF potential energy surface (all calculated vibration frequencies are real).

The important results of the calculations are collected in Table 1. The calculated Al–Al distances in the tetramers vary very little (261.1–263.8 pm). They are similar to the distance in Al_4H_4 (261.7 pm[9]) and are somewhat shorter than a typical Al–Al single bond of 266 pm.[17] The Si–Al distances for $[H_3SiAl]_n$ and $[Me_3SiAl]_n$ decrease from the monomer to the tetramer by approximately 12 pm. The lone pair n(Al) in the monomer is weakly Si–Al antibonding; in

Table 1. Calculated structures and energies of $[R_3SiAl]_n$, $n = 1,4$ [distances in pm, energies in E_{SCF} and E_{MP2} in Hartree, ΔE_{tet} in kJ mol^{-1}, see Eq. (a)].

R	n	Symmetry	Al-Al	Si-Al	Si-R	E_{SCF}	E_{MP2}	ΔE_{tet} (SCF/MP2)
H	1	C_{3v}	–	260.8	149.2	– 532.505179	– 0.125022	–
H	4	T_d	261.6	249.1	148.5	– 2130.172013	– 0.578834	– 397/–604
Me	1	C_{3v}	–	261.3	189.1	– 649.473263	– 0.391149	–
Me	4	T_d	261.1	249.5	188.1	– 2598.055776	– 1.651537	– 427/–655
tBu	1	C_3	–	260.3	197.1	– 1000.443891	–	–
tBu	4	T	263.8	259.4	197.4	– 4001.939364	–	– 430/–

the tetramer this effect is reduced through cage bonding.[9] For [*t*BuSiAl] an almost identical Si–Al distance (ca. 260 pm) was found in the monomer and tetramer, which can be seen as a result of a low steric repulsion between the tBu$_3$Si groups in the tetramer. The Si–Al bond has a relatively small force constant[18] and therefore reacts sensitively to disturbances.

The reaction energy ΔE_{tetr} for the tetramerization of tBu$_3$SiAl is obtained from the SCF approximation as shown in (a). For H_3SiAl and Me_3SiAl, the very similar values

$$\Delta E_{tetr}([t\mathrm{Bu_3SiAl}]_4) = E([t\mathrm{Bu_3SiAl}]_4) - 4E(t\mathrm{Bu_3SiAl}) = -430\ \mathrm{kJ\,mol^{-1}} \quad \text{(a)}$$

-397 and -427 kJ mol^{-1}, respectively, were obtained. The SCF approximation underestimates the tetramerization energy. This is shown by MP2 calculations, which for H_3SiAl showed an addditional contribution of -207 kJ mol^{-1} and for Me_3SiAl of -228 kJ mol^{-1}, which is in agreement with the results for the tetramerization of AlR (R = H, F, Cl,), $\Delta\Delta E \approx -200$ kJ mol^{-1}.[9] If a similar effect is assumed also for tBu$_3$SiAl, then a tetramerization energy of ca. -600 kJ mol^{-1} can be expected.[19] This value corresponds to a bond energy of 150 kJ mol^{-1} per electron pair or tetrahedral face or 100 kJ mol^{-1} per Al–Al pair or tetrahedral edge.

The comparison of [tBu$_3$SiAl]$_4$ with Al_4R_4 (R = H, Cl, F, Cp)[9] shows a consistent picture. Since no π delocalization $\pi(t\mathrm{Bu_3Si}) \rightarrow \pi(\mathrm{Al})$ is expected for tBu$_3$SiAl, the the metal atoms of the tetramer are as strongly bound as in Al_4H_4 (-571 kJ mol^{-1}[9]), in agreement with the calculated distances.

In particular, the bonds in Cp_4Al_4 are significantly weaker than those in [tBu$_3$SiAl]$_4$: in the Cp compound, the Al–Al distance of 276.9 pm (exp.;[3] calc. 279.6 pm[9]) is relatively long, and the tetramerization energy (-160 kJ mol^{-1}, with MP2) is relatively low. These results are in agreement with those found experimentally: [tBu$_3$SiAl]$_4$ can be sublimed at 180 °C, whereas $Cp^*_4Al_4$ in the solid form decomposes at 70 °C.[20]

The compound [tBu$_3$SiAl]$_4$ (see Fig. 1, bottom) is a molecule with a completely nonpolar (hydrophobic) surface. Therefore, it is to be expected that crystals are highly disordered or even show plastic phases. This could be an explanation for the above mentioned difficulties for the structure determination.

According to our calculations, [tBu$_3$SiAl]$_4$ holds a special position among the Al$^{\mathrm{I}}$ compounds: the Al_4 tetrahedron shows optimal stabilization (lacking competition of a π delocalization in the monomer) and is shielded without larger steric hindrance or strains by the substituents.

Received: October 24, 1991 [Z 4986 IE]
German version: *Angew. Chem.* **1992**, *104*, 327

CAS Registry numbers:
H_3SiAl, 138540-84-8; $[H_3SiAl]_4$, 138540-85-9; Me_3SiAl, 138540-86-0; $[Me_3SiAl]_4$, 138540-87-1; tBu$_3$SiAl, 138540-88-2; [tBu$_3$SiAl]$_4$, 138540-89-3.

[1] M. Tacke, H. Schnöckel, *Inorg. Chem.* **1989**, *28*, 2895.
[2] P. Paetzold, *Angew. Chem.* **1991**, *103*, 559; *Angew. Chem. Int. Ed. Engl.* **1991**, *30*, 544.
[3] C. Dohmeier, C. Robl, M. Tacke, H. Schnöckel, *Angew. Chem.* **1991**, *103*, 594; *Angew. Chem. Int. Ed. Engl.* **1991**, *30*, 564.
[4] J. Aihara, *Bull. Chem. Soc. Jpn.* **1983**, *56*, 335.
[5] D. J. Swanton, R. Ahlrichs, *Theor. Chim. Acta* **1989**, *75*, 163.
[6] N. Wiberg in *Frontiers of Organosilicon Chemistry* (Eds.: A. R. Bassindale, P. P. Gaspar), The Royal Society of Chemistry, Cambridge, **1991**, p. 263–270.
[7] P. R. LeBreton, S. Urano, M. Shahbaz, S. L. Emery, J. A. Morrison, *J. Am. Chem. Soc.* **1986**, *108*, 3937; T. Davan, J. A. Morrison, *Inorg. Chem.* **1986**, *25*, 2366.
[8] D. J. Swanton, R. Ahlrichs, M. Häser, *Chem. Phys. Lett.* **1989**, *155*, 329.
[9] R. Ahlrichs, M. Ehrig, H. Horn, *Chem. Phys. Lett.* **1991**, *183*, 227.
[10] A. F. Wells, *Structural Inorganic Chemistry*, Oxford University Press, Oxford, **1984**, p. 1060.
[11] K. Wade, *Chem. Commun.* **1971**, 792; *Adv. Inorg. Chem. Radiochem.* **1976**, *18*, 1.
[12] The following basis sets were used: Al, Si: [11s7p1d/6s4p1d], η(d) = 0.3 and 0.4 repectively; C in R = Me and Si bound in R = tBu: [8s4p/4s2p], primary C in R = tBu: [9s3p/2s1p]; H in R = H: [4s/2s], in R = Me and R = tBu: [3s/1s]. The basis sets for C and H were energy optimized using neopentane as model compound. For the Si bound C, a double-zeta basis set was used to have sufficient flexibility for the description of the Si–C bond.
[13] R. Ahlrichs, M. Bär, M. Häser, H. Horn, C. Kölmel, *Chem. Phys. Lett.* **1989**, *162*, 165.
[14] C. Møller, M. S. Plesset, *Phys. Rev.* **1934**, *46*, 618; MP2 denotes the treatment of electron correlation in the second order of perturbation theory, starting from the Hartree-Fock ground state. In our calculations, we only included the correlation of the valence electrons.
[15] Examples of investigations of AlH and Al_4H_4 with more precise methods (MP2-gradient, coupled cluster (CCSD(T))) showed that correlation effects reduce the Al–Al distance only by 2 pm. The bond energy of the tetramer is underestimated in the MP2 approximation by approximately 50 kJ mol^{-1}. Analogous relationships are also to be expected for the compounds examined here (J. Gauss, personal communication).
[16] tBu$_3$SiAl does not have the highest possible symmetry C_{3v}, because in this case imaginary wave numbers of 99 icm^{-1} and 27 icm^{-1} were obtained for two normal modes. The lowering of symmetry from C_{3v} to C_3, which is caused by steric hindrance of the *tert*-butyl groups, leads to an energy reduction of 20 kJ mol^{-1}. For $[Me_3SiAl]_4$ and [tBu$_3$SiAl]$_4$, for which force field calculations were not possible, T_d and T symmetry respectively were assumed on the basis of these results.
[17] W. Uhl, *Z. Naturforsch. B* **1987**, *42*, 557.
[18] In the framework of the SCF approximation the force constant of the Al–Si bond is 100 N m^{-1} in tBu$_3$SiAl, 94 N m^{-1} in H_3SiAl, 133 N m^{-1} in $[H_3SiAl]_4$.
[19] A MP2 calculation for [tBu$_3$SiAl]$_4$ was unfortunately not possible.
[20] On the basis of its low decomposition temperature (around -60 °C), Cp_4Al_4 could not be investigated in a crystalline form; C. Dohmeier, H. Schnöckel, unpublished.

Chemiluminescence Oscillations Driven by a Flow-through Reactor in the $[Ru(bpy)_3]^{2+}$ Catalyzed Belousov–Zhabotinskii Reaction

By *Harry R. Weigt**

The Belousov–Zhabotinskii (BZ) reaction[1]—in the strict sense the metal-ion-catalyzed oxidation of malonic acid by bromate/sulfuric acid—is already considered a classical model system for the formation of dissipative structures.[2] On exceeding certain critical parameters and for suitable reaction procedures far from the equilibrium, sustained concentration oscillations occur, for example, or even spatially and spatial/temporally organized reaction states.[3] The extremely complicated underlying mechanism has not nearly been elucidated.[4]

An interesting extension of conventional methods is the involvement of electronically excited species on the basis of oscillating chemiluminescence (OCL) arising spontaneously in many BZ systems.[5] The measurement of the OCL has proved to be a convenient, very sensitive technique, which appears to be most highly developed for $[Ru(bpy)_3]^{2+}$ catalyzed BZ systems (bpy = 2,2′-bipyridine).[6] Some of the reasons for this are the remarkable photophysical and photochemical properties of the metal complex,[7] including its CL potential through the excited charge-transfer state.[8] In the

[*] Dr. H. R. Weigt
Fachbereich Physik der Universität
Am Neuen Palais 10, D-O-1571 Potsdam (FRG)

past without exception, however, batch experiments were conducted. As this process is limited fundamentally to transient states and structures, the interpretation in particular of the sometimes very complicated temporal CL behavior appeared problematic. For instance, for a system with the concentrations given in the legend of Figure 1 under batch conditions (i.e., on the way to equilibrium), we found an oscillator lifetime of only 30 min which had a extremely variable oscillation form almost impossible to interpret.

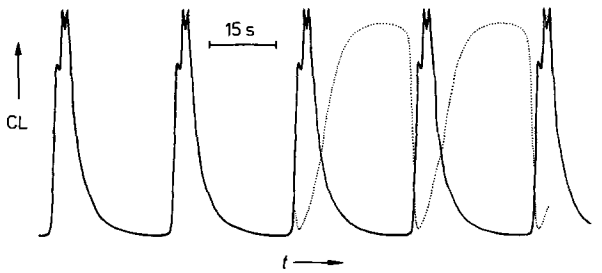

Fig. 1. CSTR-stabilized OCL in $[Ru(bpy)_3]^{2+}$ catalyzed BZ system. Operating parameters: initial concentrations $[mol\,L^{-1}] = 0.053(BrO_3^-)$; 0.35 $(CH_2(COOH)_2)$; 1×10^{-4} $([Ru(bpy)_3]^{2+})$; 1.0 (H_2SO_4); reactor volume = 26 cm^3; $T = 299\,K$; $\dot{V} = 2.2\,mL\,min^{-1}$. CL measurement: $\lambda_{em} = 610$ nm; redox potential (dotted line): potential difference (peak-to-peak) = 40 mV.

Stabilization of the various, only momentarily existing system states over a longer period was achieved with a (stirred) flow-through reactor (CSTR = Continuous-flow Stirred Tank Reactor).[9] This provides a thermodynamically open system through a constant flux of starting materials and simultaneous removal of products. Among the freely variable operating parameters are the flux concentrations, the average residence time of the reactive material (as quotient of the reactor volume and total flow rate) and the reactor temperature. Figure 1 shows the behavior of the system for the chosen set of parameters under flow conditions. Represented are the time-resolved CL intensity[10a] and the simultaneously recorded redox potential.[10b] The OCL is characterized by significantly more features in its oscillogram than in that of the potential. For each oscillation three clearly distinguishable emission peaks are reproduced in a basic pattern. The periodic steep onset of the luminescence corresponds to the beginning of the autocatalytic part of the process (recognized by the drop in the redox potential). The signal shape of the electrode's (integrated) display does, however, not correspond to the characteristic CL peak pattern for this set of parameters.

Even on variation of only the total flow rate $\dot{V}$, a number of OCL modes can be generated. As example Figure 2 shows the behavior for a stepwise decrease of $\dot{V}$. The essential part of a cycle for each $\dot{V}$ is represented. Between the individual stabilized cycles (corresponding to the limit cycle behavior) in this experiment is a period of nonstationary transition behavior lasting of the order of 1 h. The oscillation pictures resulting from the chosen $\dot{V}$ are obtained independent of the operating mode of the reactor and the direction of $\dot{V}$ change. Hysteresis effects, which are conceivable, were not observed. At high flow rates (above $12\,mL\,min^{-1}$) the time-resolved CL structure is characterized by a pronounced side peak (similar to that found for batch experiments a short time after the start[6]), which is deformed to a shoulder as $\dot{V}$ decreases. At $\dot{V} = 3.0\,mL\,min^{-1}$ a second side peak following the first in time is seen, which becomes a needlelike signal. Concomitant with this change is a decrease of the major peak. Below $\dot{V} = 1.0\,mL\,min^{-1}$ the curve shape is markedly

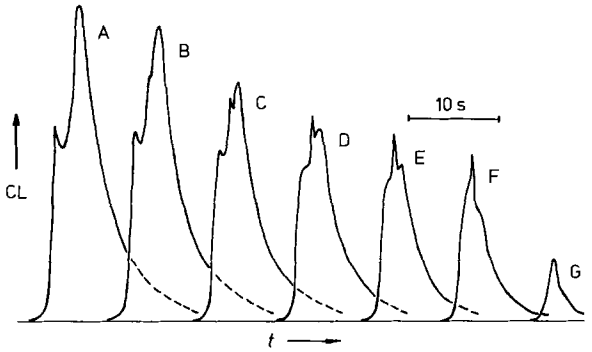

Fig. 2. Dependence of OCL structure on the total volume flow $\dot{V}$. Operating parameters: $\dot{V}\,[mL\,min^{-1}] = 4.0$ (**A**); 3.0 (**B**); 2.5 (**C**); 2.0 (**D**); 1.5 (**E**); 1.0 (**F**); 0.3 (**G**); remaining conditions and CL measurement as in Figure 1.

smoothed; at $0.3\,mL\,min^{-1}$ (corresponding to a relatively large average residence time for the reactants) only a weak kink may be seen in the relatively weak CL signal.

In contrast to the hardly changing curve shape of the potential (for redox as well as Br^--sensitive electrodes), the OCL is apparently a selective indicator representing specific but still coded responses of the system to the variation of the operating parameters. The controlled development of the CL structure will thus be able to contribute supplementary information to that obtained from conventional methods in the discussion on relevant elementary processes.

The CSTR-stabilized OCL also appears interesting in connection with newer investigations on the oxygen effect on BZ oscillators.[12,13] We could confirm the results of Saigusa[13]—extrapolated to flow conditions—to a large extent. When the reaction mixture is enriched with additional oxygen, a transition to an "O_2-induced state"[13] is observed (Fig. 3).[14] This transition is characterized by a noticeably

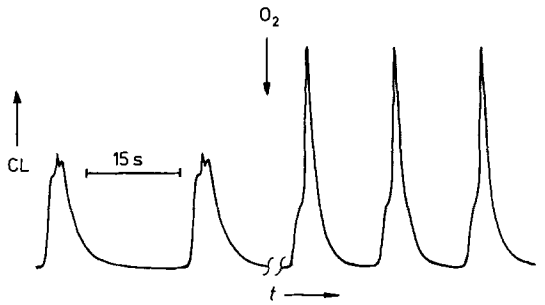

Fig. 3. Oxygen-induced OCL regime in flow experiment [14]. Operating parameters: $\dot{V} = 2.0\,mL\,min^{-1}$; O_2 flow rate = $0.12\,L\,min^{-1}$; remaining conditions and CL measurement as in Figure 1.

different period, CL-amplitude, and oscillation shape. The OCL here undoubtedly points to a phase change. In contrast to Saigusa[13] our system returned to the original undisturbed state after switching off the oxygen flow. This reversibility naturally occurs only in the flow experiment.

Received: October 17, 1991 [Z4974 IE]
German version: *Angew. Chem.* **1992**, *104*, 358

CAS Registry numbers:
$[Ru(bpy)_3]^{2+}$, 15158-62-0; malonic acid, 141-82-2; O_2, 7782-44-7.

[1] a) B. P. Belousov, *Sb. Ref. Radiats. Med.* **1959**, 145; b) A. M. Zhabotinskij, *Selbsterregte Konzentrationsschwingungen* (Russ.), Nauka, Moskau, **1974**.

[2] G. Nicolis, I. Prigogine, *Self-Organisation in Non-Equilibrium systems*, Wiley, New York, **1977**.

[3] a) U. F. Franck, *Angew. Chem.* **1978**, *90*, 1; *Angew. Chem. Int. Ed. Engl.* **1978**, *17*, 1; b) R. J. Field in *Oscillations and Travelling Waves in Chemical systems* (Eds.: R. J. Field, M. Burger), Wiley, New York, **1985**, Chapter 2.
[4] L. Györgi, T. Turanyi, R. J. Field, *J. Phys. Chem.* **1990**, *94*, 7162.
[5] A. D. Karavaev, G. S. Parshin, V. P. Kazakov, *Izvest. Akad. Nauk SSSR, Ser. Khim.* **1980**, 221.
[6] a) F. Bolletta, V. Balzani, *J. Am. Chem. Soc.* **1982**, *104*, 4250; b) H. R. Weigt, H. Ritschel, G. Junghähnel, *Z. Chem.* **1983**, *23*, 152; H. R. Weigt, G. Junghähnel, *ibid.* **1985**, *25*, 382; c) A. D. Karavaev, V. P. Kazakov, G. A. Tolstikov, *Teor. Eksp. Khim.* **1986**, 65.
[7] R. J. Watts, *J. Chem. Educ.* **1983**, *60*, 834.
[8] a) F. E. Lytle, D. M. Hercules, *Photochem. Photobiol.* **1971**, *13*, 123; b) I. Rubinstein, A. J. Bard, *J. Am. Chem. Soc.* **1981**, *103*, 512.
[9] A. Pacault, P. Hanusse, P. De Kepper, C. Vidal, J. Boissonade, *Acc. Chem. Res.* **1976**, *9*, 438.
[10] a) The chemiluminescence was registered with a photomultiplier after including a high-intensity monochromator (Bausch & Lomb) in the circuit. Measurements were performed at an OCL wavelength maximum of 610 nm (spectral width: 10 nm). The OCL spectrum agrees both with the stationary photoluminescence (see [6a,b] and H. R. Weigt, *Dissertation*, Pädagogische Hochschule Potsdam, **1984**) and the oscillating photoluminescence (H. R. Weigt, unpublished); b) the potential was recorded at a platinum redox electrode (MC 20, Meinsberg) relative to a silver chloride electrode (SE 20, Meinsberg).
[11] A. D. Karavaev, V. P. Kazakov, *Teor. Eksp. Khim.* **1990**, 566.
[12] P. Ruoff, R. M. Noyes, *J. Phys. Chem.* **1989**, *93*, 7394.
[13] H. Saigusa, *Chem. Phys. Lett.* **1989**, *157*, 251.
[14] Oxygen (technical quality) was introduced into the lower part of the reactor through a capillary. The gas flow was determined with a flow meter (TG 400, Medingen).

Dimerization of Thiophene to Give a Linear $S(CH)_8S$ Fragment with $[(C_5Me_5)Rh(C_2H_4)_2]$**

By *Robert M. Chin* and *William D. Jones**

Reactions of thiophenes with transition metals as models for studying the hydrodesulfurization of petroleum have aroused increased interest over the past few years.[1] A variety of coordination modes of thiophene have been found,[2] and reactions in which the ring has been cleaved have been reported.[3] The simple insertion of an unsaturated rhodium[4] or iridium[5] metal center into the thiophene C–S bond has also been examined [Eq. (a)], and we report here an example in which C–C bond formation occurs concomitant with the C–S cleavage.

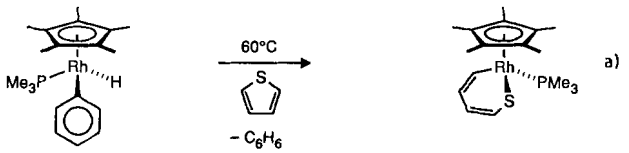

a)

Heating a solution of $[(C_5Me_5)Rh(C_2H_4)_2]$ with a 20-fold excess of thiophene in benzene solution at 90 °C for 15 h was followed by removal of solvent and extraction of the residue with hexane. Upon cooling a red-black precipitate forms. The product is identified as **1** on the basis of NMR and analytical data.[6]

$[(C_5Me_5)Rh]_2[\mu^2\text{-}1,2,3,4,\eta^4\text{-}5,6,7,10\text{-}\eta^4\text{-}S(CH)_8S]$ **1**

The ^1H NMR spectrum shows eight distinct multiplets for the eight methine groups; a COSY spectrum (COSY = *co*rrelated *s*pectroscop*y*) indicates that these groups are attached in a linear array. Two distinct C_5Me_5 resonances are also observed. The ^{13}C NMR spectrum shows two downfield singlet and six upfield doublet resonances, suggesting that six carbons in the chain are attached to metal centers. A $^{13}C/^1H$ HETCOR spectrum (HECTOR = *het*eronuclear *cor*relation) shows that these six carbons are adjacent to each other at an end of the $(CH)_8$ chain. These data led to the formulation of **1** as indicated in Equation (b). Use of α-deu-

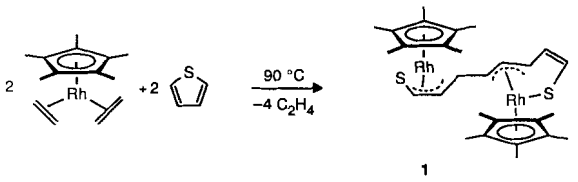

b)

1

teriothiophene in the reaction leads to a product in which the resonances at $\delta = 6.503$, 6.009, 4.165, and 3.245 are diminished in intensity by half, indicating that the $S(CH)_8S$ fragment arises by the coupling of two α thiophene carbons after C–S cleavage.

Confirmation of the structure deduced from NMR results was obtained from a single-crystal X-ray diffraction study.[7] Since the compound proved difficult to crystallize, a preliminary data set was obtained on a small crystal (Fig. 1). A

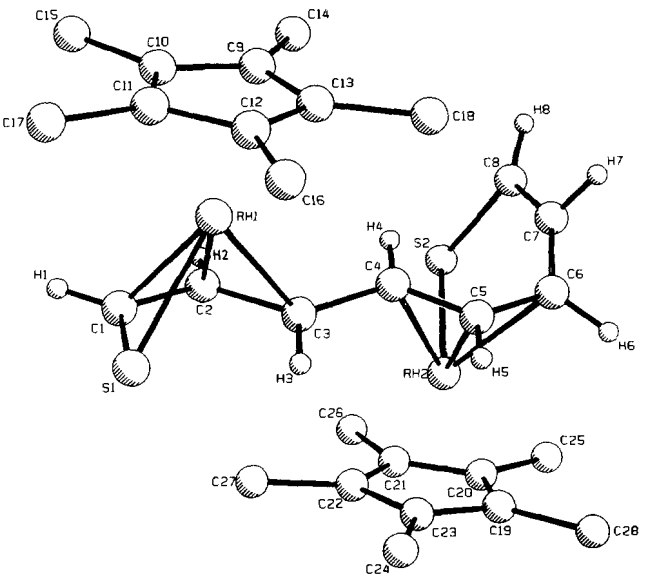

Fig. 1. PLUTO drawing of the structure of **1** in the solid state. Selected distances: Rh(1)-S(1), 2.38(2); Rh(1)-C(1), 2.11(7); Rh(1)-C(2), 2.15(7); Rh(1)-C(3), 2.30(7); Rh(2)-S(2), 2.36(2); Rh(2)-C(4), 2.19(6); Rh(2)-C(5), 2.11(7); Rh(2)-C(6), 2.31(7); S(1)-C(1), 1.65(8); S(2)-C(8), 1.80(7); C(1)-C(2), 1.5(1); C(2)-C(3), 1.54(9); C(3)-C(4), 1.5(1); C(4)-C(5), 1.33(8); C(5)-C(6), 1.4(1); C(6)-C(7), 1.5(1); C(7)-C(8), 1.4(1)

more symmetric molecule with the $S(CH)_8S$ unit bound in a $1,2,3,4\text{-}\eta^4\text{-}7,8,9,10\text{-}\eta^4$ fashion is not observed, despite the fact that $[(C_5Me_5)Rh(\text{polyolefin})]$ complexes are expected to be labile at 100 °C,[8] leading to the conclusion that the structure observed for **1** is thermodynamically preferred.

[*] Prof. W. D. Jones, R. M. Chin
Department of Chemistry University of Rochester, Rochester, NY 14627 (USA)

[**] This work was supported by the National Science Foundation grant CHE-9102318.

Irradiation (310–380 nm, 25 °C) of a 0.034 M solution of $[(C_5Me_5)Rh(C_2H_4)_2]$ in [D_6]benzene containing a ninefold excess of thiophene shows the formation of both a small amount of **1** and another material displaying four low-field resonances in the ^1H NMR spectrum. In addition to a C_5Me_5 resonance at $\delta = 1.504$, multiplets are seen at $\delta =$ 11.843 (ddd, $J = 9.2$, 6.3, 1.6 Hz; 1 H), 9,082 (dd, $J = 8.7$, 6.8 Hz, 1 H), 8.256 (ddd, $J = 9.4$, 7.1, 1.3 Hz, 1 H), and 7.575 (ddd, $J = 9.0$, 7.1, 1.3 Hz, 1 H), suggesting the presence of aldehydic and/or carbenoid hydrogens. This intermediate is tentatively assigned structure **2** [Eq. (c)], and reacts thermal-

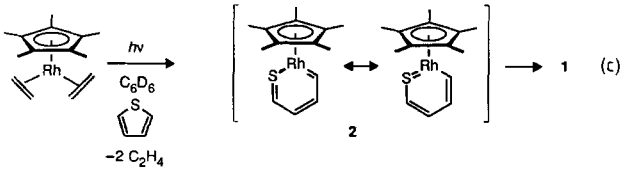

ly to form dimer **1**. A methyl-substituted iridium analogue of **2** which also displays low field resonances for the metallacycle hydrogens, has been isolated as a stable species.[5] Further mechanistic details are under investigation.

Received: October 7, 1991 [Z 4960 IE]
German version: *Angew. Chem.* **1992**, *104*, 340

[1] R. J. Angelici, *Acc. Chem. Res.* **1988**, *21*, 387–394; C. M. Friend, J. T. Roberts, *ibid.* **1988**, *21*, 394–400.
[2] R. J. Angelici, *Coord. Chem. Rev.* **1990**, *105*, 61–76; T. B. Rauchfuss, *Prog. Inorg. Chem.* **1991**, *39*, 259–329.
[3] G. H. Spies, R. J. Angelici, *Organometallics* **1987**, *6*, 1897–1903; J. W. Hachgenei, R. J. Angelici, *J. Organomet. Chem.* **1988**, *355*, 359–378; A. E. Ogilvy, M. Draganjac, T. B. Rauchfuss, S. R. Wilson, *Organometallics* **1988**, *7*, 1171–1177; P. Hübener, E. Weiss, *J. Organomet. Chem.* **1977**, *129*, 105–115.
[4] W. D. Jones, L. Dong, *J. Am. Chem Soc.* **1991**, *113*, 559–564; L. Dong, S. B. Duckett, K. F. Ohman, W. D. Jones, *ibid.* **1992**, *114*, 151–160.
[5] J. Chen, L. M. Daniels, R. J. Angelici, *ibid.* **1990**, *112*, 119–204.
[6] ^1H NMR (400 MHz, C_6D_6, 25 °C): $\delta = 6.503$ (dd, $J = 5.5$, 3.3 Hz, H_8); 6.009 (dt, $J = 3.9$, 1.0 Hz, H_1); 5.492 (dd, $J = 6.4$, 3.9 Hz, H_7); 4.900 (ddd, $J = 8.0$, 3.9, 2.0 Hz, H_2); 4.818 (dd, $J = 6.8$, 4.0 Hz, H_6); 4.165 (ddd, $J = 11.3$, 7.0, 1.0 Hz, H_5); 3.245 (t, $J = 11.0$ Hz, H_4); 2.915 (ddt, $J = 11.0$, 7.9, 1.3 Hz, H_3); 1.681 (s, C_5Me_5); 1.463 (s, C_5Me_5). $^{13}C\{^1H\}$ NMR (100 MHz, C_6D_6, 25 °C): $\delta = 140.14$ (s, H_8); 121.55 (s, H_7); 92.17 (d, $J = 9.5$ Hz, H_1); 87.46 (d, $J = 6.0$ Hz, H_2); 86.14 (d, $J = 6.0$ Hz, H_5); 82.69 (d, $J = 12.1$ Hz, H_6); 76.26 (d, $J = 7.0$ Hz, H_4); 66.70 (d, $J = 10.2$ Hz, H_3); 96.71 (d, $J = 6.7$ Hz, C_5Me_5); 96.82 (d, $J = 5.7$ Hz, C_5Me_5); 10.05 (s, C_5Me_5) 9.08 (s, C_5Me_5). Correct C,H analyses for $Rh_2S_2C_{28}H_{38}$. Isolated yield ca. 50%.
[7] Complex **1** crystallizes in monoclinic space group $P2_1/c$ with $a = 12.810(9)$, $b = 16.118(17)$, $c = 14.025(25)$ Å, $\beta = 109.78(10)°$, and $Z = 4$. Of the 4468 data collected on a $0.1 \times 0.1 \times 0.1$ mm^3 crystal, 791 with $I > 3\sigma(I)$ were used to solve the structure, in which a model was used with the C_5Me_5 ligands refined as rigid groups and only rhodium and sulfur refined anisotropically to give final agreement parameters of $R = 0.105$, $R_w = 0.113$. Further details of the crystal structure investigation are available on request from the Director of the Cambridge Crystallographic Data Centre, University Chemical Laboratory, Lensfield Road, GB-Cambridge CB21EW(UK), on quoting the full journal citation.
[8] A. K. Smith, P. M. Maitlis, *J. Chem. Soc., Dalton Trans.* **1976**, 1773–1777.

BOOK REVIEWS

Book Reviews are written by invitation from the editor. Suggestions for books to be reviewed and for book reviewers are welcome. Publishers should send brochures or (better) books to the following address: Redaktion Angewandte Chemie, Postfach 101161, W-6940 Weinheim, Federal Republic of Germany. The editor reserves the right of selecting which books will be reviewed. Uninvited books not chosen for review will not be returned.

Liquid Crystallinity in Polymers. Principles and Fundamental Properties. Edited by *A. Ciferri*. VCH Publishers, New York/VCH Verlagsgesellschaft, Weinheim, 1991. x, 438 pp., hardcover DM 155.00.—ISBN 0-89573-771-X/3-527-28922-9

The field of liquid crystalline polymers, which has undergone rapid development during the last few years, has already given rise to several multi-author books. The book reviewed here belongs to this category. However, whereas most publications of this kind are collections of articles covering a broad range of topics, an attempt has been made here to make the contributions more closely related to each other. The editors have also imposed a system of priorities with regard to topics, which clearly sets the book in a class apart from previous publications.

The book "Liquid Crystallinity in Polymers" aims to describe the various theoretical approaches towards an understanding of liquid crystalline (LC) polymers, and to compare their predictions with experimental data. LC polymers of both thermotropic and lyotropic types are considered. The book is divided into four parts. Part 1, consisting of two articles, deals with the conformations of LC polymers. First N. Lauprêtre and C. Noel report on the conformational analysis of mesogenic groups in polymers, then G. L. Brelsford and W. R. Krigbaum discuss the theory of persistence lengths in LC polymer chains and the experimental methods used to determine them. Part 2 consists of three articles on theories that attempt to explain liquid crystalline behavior in terms of molecular properties. A. Khoklov reports on theories based on the Onsager equation. A. Abe and M. Ballauff describe the Flory lattice model, then G. Ronca and A. Ten Bosch discuss other theoretical approaches. In Part 3 we at last come to three contributions dealing with the dependence of phase properties on many different variables of the system. Here the editor, A. Ciferri, gives an overview of the phase behavior of rigid and semirigid mesogens, A. Sirigu contributes a discussion of the phase behavior of flexible main-chain polymers, and H. Finkelmann discusses polymers with liquid crystalline side-chains. The fourth and last part of the book is devoted to physics. S. D. Lee and R. B. Meyer discuss the viscosity and elastic properties of liquid crystalline polymers. M. Kleman considers questions and defects and texture, and the final contribution by G. Marrucci is devoted to the rheology of nematic polymers.

All the articles are written by leading experts in their special fields, and together they ensure that the book impressively achieves its purpose of explaining different theoretical approaches and comparing them with experimental results. In addition the numerous literature references at the end of each contribution (typically between 100 and 200 per article) provide a good basis for further reading on each topic. However, concentrating on the specific objective described above has meant that some other equally important aspects of liquid crystalline polymers have had to be left out or only briefly touched on. For example, theoretical models are developed only for the nematic phase, so that smectic phases are assigned only a minor role which understates their importance in liquid crystalline polymers. Other aspects given scant attention include some that are of particular interest to the chemist: relationships between structure and properties, chemical synthesis, and matters relating to technology and applications. Also the strongly theoretical bias means that readers without considerable previous knowledge of solid state physics will find the book difficult to understand, except for Part 3, where the discussions are more understandable for the non-specialist reader and are less narrowly defined in subject matter. For these reasons the book can be recommended primarily for theoretically orientated chemists, technologists and physicists.

In summary, "Liquid Crystallinity in Polymers" achieves its stated purpose very well; however, it is essentially a more specialized work than its rather generally worded title suggests.

Erik Wischerhoff, Rudolf Zentel
Institut für Organische und Makromolekulare Chemie
der Universität Düsseldorf (FRG)

Similarity Models in Organic Chemistry, Biochemistry and Related Fields. (Series: Studies in Organic Chemistry, Vol. 42.) Edited by *R. I. Zalewski, T. M. Krygowski* and *J. Shorter*. Elsevier, Amsterdam, 1991. XV, 694 pp., hardcover, DFl 420.00.—ISBN 0-444-88161-1

Similarity studies of various kinds are currently very much in vogue in the chemical world. Of those scientists involved with such studies, a growing number occupy themselves with so-called similarity modeling. This is the latest name for a field that has steadily evolved from work dating back to the 1960s on the use of Hammett's equation in biological contexts through linear free-energy relationship (LFER) studies to correlation analysis in organic chemistry (CAOC). Today the field has expanded to embrace an overlapping network of methodologies concerned with such things as sophisticated data clustering techniques, a wide variety of quantitative structure–activity relationship (QSAR) procedures, and innovative pattern recognition methods. The motivation behind all the present activity is the possibility of designing chemical species optimally suited for a range of practical applications. The design process typically involves the characterization of the species by appropriate molecular descriptors followed by the clustering of these descriptors by means of similarity modeling. The whole procedure has now been honed to a fine instrument that can, in principle, be used to design molecules of any genre. In practice, however, it is used almost exclusively for the design of molecules that are biologically active such as pharmaceutical drugs.

Because of the potential value of this kind of research, the number of books dealing with similarity modeling has gradually begun to mount. Among notable recent examples, mention might be made of Willett's "Similarity and Clustering in Chemical Information Systems" and the compendium of Johnson and Maggiora (Eds) on "Concepts and Applications of Molecular Similarity". The volume reviewed here may be considered as the third part of a trilogy, each part of which has sought to bring its readers up-to-date on the latest developments in the broad area of molecular structure–property correlations. The first volume, Chapman and Shorter's (Eds.) "Advances in Linear Free Energy Relationships", came out in 1972, and the second volume from the same editors titled "Correlation Analysis in Chemistry: Recent Advances" appeared in 1978. All three volumes are associated with the veteran John Shorter who has been prominent in the field for over a quarter of a century. As was the case for its two predecessors, the third part reflects contemporary thinking in the chemometrics domain. Moreover, all of its eleven contributed chapters are written by important workers in the field. This means the reader has the advantage of several different approaches to and perspectives on state-of-the-art similarity modeling.

The drawbacks of having so many contributors are also clearly in evidence in the considerable amount of overlap in the topics covered. Thus, Chapters 1, 2, 4, 6, 8, and 10 discuss various aspects of the Hammett equation, and solvent effects are treated in Chapters 2, 5, 6, 8, and 9. In general authors have tended to focus on their own specialties to the exclusion of several of the newer trends and developments in similarity modeling. The coverage of the central theme is therefore somewhat patchy and certainly less than comprehensive. Whereas the statistical treatment of data and the role of steric effects are given a heavy emphasis, other equally important topics are dismissed with the briefest mention. Topics that have been short-changed include the burgeoning applications of topological indices, recent developments on molecular shape descriptors, quantitative approaches to the recognition of molecular similarity, and the use of ab initio quantum-chemical methods for the comparison of molecular similarity based on electron densities. The standard of writing of the various chapters is not uniformly high. The contributions from authors whose native language is not English are in most cases badly in need of language editing. In general there seems to be far too much stress in this volume on the more traditional approaches to structure–activity correlations and far too little on some of the more exciting new directions in which the field is now heading.

The breakdown by chapter is as follows: Chapter 1 (Krygowski and Wozniak) starts off with a fairly hefty dose of statistics. The principal discussion is devoted to the statistics of regression analysis and is comprehensive. A number of appropriate examples are provided. The inclusion of such a chapter is a good idea and will be welcomed by many of the practitioners of similarity modeling. It will be especially helpful now that sophisticated software packages such as SPSS offering a variety of statistical options have appeared on the market. In Chapter 2 (Shorter) the application and development of the Hammett equation are reviewed up to the present time. Shorter shows convincingly that the equation still has many important uses, particularly in its multiparametric forms, in spite of the fact that it was first put forward in 1937. Both Chapters 3 (Godfrey) and 4 (Häfelinger) deal with substituent effects, the former with the transmission of these effects in organic systems and the latter with the behavior of hydrogen as a substituent in organic π systems. The authors point out that current models oversimplify the chemistry involved and consequently interpretations based on field, inductive, or resonance effects alone are likely to be inadequate. Chapter 5 (Laurence) illustrates how-

the similarity principle has been applied in both infrared and ultraviolet spectroscopic data correlations with solvent and substituent effects. The principle is revealed as a powerful tool in the organization and analysis of a very large body of data. In Chapter 6 (Langhals) the rather vexing issue of solvent effects is addressed within the context of binary solvent systems. This chapter contains a number of useful tables of relevant parameters. Chapters 7 (Oszczapowicz), 8 (Jaworski and Kalinowski), and 9 (Zalewski) support the notion that similarity modeling is usually the most appropriate means of establishing structure–property relationships in the respective fields of gas chromatography, organic electrochemistry, and food chemistry. The former two make use of linear free-energy relationships whereas the latter applies a principal component analysis and also discusses the mathematical foundations of this type of approach. Chapter 10 (Livingstone) offers a general overview of quantitative structure–activity relationships and is one of the most readable chapters in the book. Not only does it serve as a valuable introduction to neophytes, but it also reports on a number of significant advances made since the late 1970s. This chapter includes a total of 513 references and an appendix listing software suppliers. The final Chapter 11 (Charton) treats the author's own approach to the quantitative description of steric effects. This chapter is also well-written and informative, containing among other things, several tables of atomic radii and two appendixes on the parameters used in regression equations. The index to the volume is adequate, though I would have preferred to have found more multiple entries in it.

As a whole this work is not comprehensive in its coverage; nor it is really suitable for use as an introductory text on the various applications of similarity modeling. Its appeal will be rather to those researchers and others currently engaged in the more conventional approaches to structure–activity relationships in chemistry.

Dennis H. Rouvray
University of Georgia
Athens, Georgia (USA)

Photochemical Technology. By *A. M. Braun, M.-T. Maurette* and *E. Oliveros*, Translated by *D. F. Ollis* and *N. Serpone*. Wiley, Chichester, 1991. XX, 559 pp., hardcover £ 95.00—ISBN 0-471-92652-3

This book on photochemistry (originally published as *Technologie Photochimique,* Presses Polytechniques Romandes, Lausanne, 1986) is the first to be concerned primarily with the technical aspects of such processes, especially in connection with organic photoconversions that have been and are being utilized in economically viable industrial processes. I have not previously encountered a book that gives so much valuable information on experimental procedures and apparatus used in both laboratory scale and pilot plant photochemical reactions. The first chapter is concerned with photochemical principles (e.g., absorption spectroscopy, photophysical decay processes of excited states, energy transfer, etc.). While entirely sufficient for the purpose of this book, this chapter is (appropriately) not as comprehensive as treatments in other well-known photochemistry texts. The chapter on radiometry and actinometry provides more detail on these subjects than I have previously seen in any book, supported by relevant theory, and many figures and tables. The next two chapters, concerned with light sources and filters and photochemical reactors, totaling almost one hundred pages, are remarkable. The information here is of enormous use to anyone planning to carry out photochemical reactions on any scale. Detailed schematic figures of lamps and reactors in ordinary and not so ordinary use are provided, along with extensive tables listing characteristics of various types of lamps, lasers, and filters. The extremely detailed figures, which cannot be found elsewhere, clearly required enormous care and effort to produce.

The rest of the book provides a wealth of information about a number of photochemical conversions that have found diverse industrial applications. Technological details regarding all stages of these processes are given, with abundant references to the patent literature. Again, this kind of information is not available in any other source, and must have taken great effort to compile. Specifically, these chapters cover photonitrosylation, photochlorination, photobromination, sulfochlorination and sulfoxidation, photochemical desulfonation and desulfonylation, photohydrodimerization, photooxidation, and vitamins. While the mechanistic aspects of these reactions are not the main focus, a significant amount of such discussion is included in each case. The economic aspects of these processes are discussed, along with safety considerations. The wealth of useful information is staggering. The authors have clearly shown, for the first time in my experience, the potential as well as the limitations of photochemistry on an industrial scale, and they put the lie to the common criticism that photochemistry is an arcane subject with no significant practical applications. The one important subject that the authors do not treat with the attention it deserves is solar energy conversion, which I hope they will address in a future book or future editions of this book.

In summary, "Photochemical Technology" is a wonderfully useful book which admirably fills an important gap in this field. It is highly recommended to anyone involved in the practice of photochemistry, from students to researchers to engineers. It is an indispensable compendium of easily accessible information, presented in a clear and lucid style that readers at all levels will appreciate. No one involved with photochemistry should fail to include this book in their personal as well as institutional libraries. The authors are to be congratulated for their remarkable achievement.

David I. Schuster
Department of Chemistry
New York University
New York, NY (USA)

Handbook of Thin Layer Chromatography. (Chromatographic Science Series, Vol. 55). Edited by *J. Sherma* and *B. Fried*. Marcel Dekker, New York, 1991. viii, 1047 pp., hardcover $ 165.00 (US and Canada), $ 198.00 (all other countries).—ISBN 0-8247-8335-2

This book is divided into two parts: the first has 13 chapters devoted to theory and general practices of TLC, while the second has 18 chapters dealing with applications based on compound types such as amino acids, peptides, antibiotics, carbohydrates, lipids, natural pigments, inorganics and organometallics, pesticides, pharmaceuticals, steroids, synthetic dyes, and vitamins. There are also chapters on "TLC Coupled with MS", "Thin Layer Radiochromatography", "Applications of Flame Ionization Detectors in TLC", and "Photographic Documentation", in Part 1, and on the application side, on polymers, toxins, and enantiomer separations, as well as phenols, aromatic acids, and indoles

which can be considered as special features and are required to keep pace with the fast developing modern analytical methods vis-à-vis TLC. OPLC, a relatively young thin layer technique still gaining in improvement and popularity, gets proper treatment in the form of a chapter.

Chapter 1 is an introduction to basic techniques, materials, and apparatus involved or required for TLC. Though there are full chapters devoted to theory and mechanism of TLC, sorbents and layers, optimization, development, OPLC, and documentation, each of these, in addition to various other aspects of TLC, has been introduced briefly in Chapter 1, making the chapter a real introduction to present day TLC. Similarly, sample preparation and spotting methods have been sufficiently described.

Though each step in TLC can be optimized, it is far from simple due to the large number of variables involved. General optimization methods and specific strategies for solvent selection have been presented in detail; they can be used to enhance detection limits in post-chromatographic derivatization reactions or to obtain a better separation in the chromatographic development step.

Commonly used sorbents have been characterized in terms of their physical and chemical parameters and chromatographic properties. These include silica gels, aluminas, kieselguhrs, cellusoses, polyamides, and Sephadex®. A brief discussion on RP-plates, amino-, cyano-, and diol-modified precoated silica layers, AE-, CM-, and DEAE- cellulose with modified functional groups to be used for ion exchange TLC, impregnated layers, precoated layer with concentrated zones, and Chiralplates® makes the chapter more useful and suggests wider and versatile applications of TLC. It clearly establishes the advancement in the technique and methodology of TLC since Stahl's fundamental work in developing sorbent materials for TLC which culminated in the first standard handbook (Dünnschichtchromatographie—Ein Laboratoriums-Handbuch, Springer Verlag, Berlin, 1962). Trends and procedures in preparative layer chromatography (PLC) have been discussed and compared for classical PLC with the two forced-flow techniques of over-pressure-layer and rotation-planar chromatography, maintaining the importance of PLC as a successful method for the isolation of synthetic and natural products.

With due regard to the complexity of chromatographic processes, limitations of the existing semiempirical models, and the need to study and understand further the theory of chromatography, the chapter on "Theory and Mechanism of TLC" provides a good review of the basic knowledge about the physical phenomenon, main concepts about efficiency of separation, usefulness of partition and adsorption models used in everyday laboratory practice, and attempts to enhance performance of TLC. The chapter on "Photodocumentation of Thin Layer Chromatograms" views laboratory photography as a sophisticated methodology needed to complement the TLC and analytical process, and serves as a good, useful guide for photographic techniques, equipment and principles for instant photography, especially under UV light.

TLC, like other aspects of research chemistry, is rapidly becoming dominated by instrumentation and automation techniques. This includes areas such as sample application and dosage, chromatogram development, densitometric evaluation by absorbance or fluorescence (200–800 nm), data acquisition, peak location and optimization, spectra recording, multi-wavelength scanning, and integration and calibration, as well as the use of flame ionization detectors (though with applications limited to lipids and related substances), the application of MS with FAB or SIMS as detectors with unique and wider advantages, and the development of the imaging proportional counter (IPC) detector for in situ counting or radioscanning of materials labeled with isotopes without the need to remove labeled material from the TLC plate for scintillation counting. The rapid advances in instrumentation made over the past decade to provide fast, quantitative analysis, as noted above, have been described very well in the Handbook in different chapters. Unfortunately there is no reference to the instrumentation and operational costs, which seem to be high and mostly outweigh advantages due to automation and make TLC far from a simple and inexpensive method. An updated discussion on such aspects would be worthwhile in such a Handbook, indicating a steady period of refinement and growth in the area.

The chapters have been contributed by recognized experts, have a comprehensive, organized plan and present a thorough description and discussion on the topic. The references cited are largely recent ones but also include more significant older literature. A large number of tables and figures have been provided, presenting various suitable TLC methods that have been extensively tried and tested in various laboratories, mentioning detection limits, and minimizing the need to refer to original journals. There are no printing errors. A list of contents of individual chapters would have helped the reader to orientate himself more rapidly to a problem of interest within the multi-authored volume. The glossary and the directory of manufacturers provide useful additional information. The book is a valuable source of information for everybody (specialists and beginners) involved with separation studies in universities, industry, analytical laboratories, clinical analyses, and in the areas of organic synthesis, protein analysis, food and drug analysis, biosynthesis etc. Complete addresses of contributors, suitable for correspondence, would have probably been more meaningful, and a comparatively low price would have encouraged individuals to own a copy.

Jürgen Martens
Fachbereich Chemie
der Universität Oldenburg (FRG)

Carbohydrates as Organic Raw Materials. Edited by *F. W. Lichtenthaler*. VCH Verlagsgesellschaft, Weinheim/VCH Publishers, New York, 1991. x, 367 pp., hardcover DM 148.00.—ISBN 3-527-28280-7/1-56081-131-5

This book is essentially a summary of the sixteen papers presented at the workshop-conference on "Progress and Prospects in the Use of Carbohydrates as Organic Raw Materials", which took place in Darmstadt in April 1990. It is intended mainly for research scientists in industry who need to be aware of the current state of knowledge on the technology of using carbohydrates as renewable raw materials. However, the editor limits the coverage mainly to mono- and disaccharides, and excludes starch and cellulose, which are also very important raw materials. The title of the book leads one to expect a more comprehensive treatment of the subject. In fact, only two of the chapters are concerned specifically with polysaccharides.

Each chapter is clearly set out, consisting of an abstract, which is useful for recapitulating after reading the chapter, followed by the main text, and lastly a bibliography, which is quite extensive in most cases. The subject index too seems to be comprehensive and clear. The frequent changes in the style of the formulas, sometimes within a single chapter, have a rather distracting effect. Synthetic chemists will find that in some cases not enough details of reactant quantities and yields are given.

Chapter 1 has been included in the book as an addition to the conference papers. This reviewer was unable to understand the colored "computer pictures" that are intended to represent hydrophobic and hydrophilic surfaces of sucrose, and they seem superfluous. The six chapters that follow are concerned with the disaccharide sucrose. The first of these describes the esterification and chloride substitution of different OH groups to produce nonionic surfactants and sweeteners. Here we come across the first errors. On page 39 the compound under discussion is D-*galacto*-sucrose, but the formula given is that of D-*gluco*-sucrose; on page 46 the formula shown is not that of the sweetener aspartam, as the caption claims. Chapter 3 describes, with the help of diagrams, the enzymic conversion of sucrose to isomaltulose and higher oligosaccharides using immobilized fructosyltransferases, then goes on to discuss the extraction and uses of 5-hydroxymethylfurfural and levoglucosan. Unfortunately some formula errors have also crept into this chapter (p. 75). In Chapter 4 the synthesis and applications of sucrose-methacrylate gels and sucrose-formaldehyde resins are discussed. One of the uses of these products is for immobilizing and stabilizing transition metal complexes and photoreactive components. It is also suggested that they could be used as drug carriers. In this chapter we also find (on p. 102) a pentavalent carbon atom! Chapter 5 gives a brief account of methods for synthesizing sucrose sulfates. Chapter 6 is a very instructive and competent description of the chemical and enzymic conversion of glucose to various 1-*O*-α-D-glycopyranosides for the production of surfactants and polymerizable vinylsaccharides. Chapter 7 is a clearly written account of the detailed process for the enzymic modification of sucrose.

Next Chapter 8 briefly discusses the microbiological production of polyfructose and its potential use as a carrier material for flavorings and colorants. Chapter 9 gives a detailed account of the history of the disaccharide leucrose, from its discovery and structure determination to its production by a microbiological process and its use as an odor additive in food products. In contrast, the description of methods for obtaining poly-, oligo-, and monosaccharides from sugar-beet pectin is of a very general nature.

In Chapter 11 attention is drawn to the potential uses of the cheaply available saccharides glucose, fructose, lactose, and isomaltulose for industrial-scale syntheses. The chapter contains a number of serious printing errors that need to be corrected. For example, on page 213 the acetylation of D-fructose and ring-opening with PCl_5 suddenly results in the appearance of a benzoylated fructose derivative. Moreover, the continuation from page 213 is found on page 215, and from here one goes to page 214 (confusing); also formula **17** on page 217 needs to be corrected. The chapter continues by describing the synthesis of natural products from carbohydrate precursors, with a few examples. The extensive bibliography to this chapter might also have included a reference to the article by A. Vasella in *Modern Synthetic Methods* **1980**.

The next three chapters are concerned with the use of hydrogen fluoride in carbohydrate chemistry and with a few newer methods for the selective oxidation of D-glucose and of poly- and oligosaccharides, e.g. cyclodextrins. Chapter 15 describes the synthesis of vinyl-substituted sugars and their polymerization to polyvinylsaccharides. The potential applications of these interesting polymers remain to be explored. Lastly, Chapter 16 discusses the possibility of using sucrose as a starting material for the manufacture of dyes, pigments, and carbohydrate-modified organic conductors.

Leaving aside some printing errors and mistakes in diagrams that could have been avoided, this book gives a good and informative account of the potential uses of sucrose, leucrose, and glucose as organic raw materials, more especially by virtue of the extensive bibliography provided. Also, by reading selected chapters, industrial chemists working in this area will find stimulating ideas for the increased exploitation of carbohydrates.

Reinhold Oehrlein
Ciba-Geigy
Basel (Switzerland)

Short-Lived Molecules. By *M. J. Almond.* Ellis Horwood, New York, 1990. 194 pp., hardcover $ 59.95.—ISBN 0-13-798554-1

This book is intended for qualified chemists who do not have a detailed knowledge of the subject described by the title; the readership envisaged ranges from advanced chemistry students to chemists already engaged in research. In particular it is claimed to be of interest to materials scientists in industry, to readers whose work is concerned with catalysis and with photochemistry, and to those with interests in high-temperature processes.

The relatively small size of the book means that the treatment of the subject must be limited to a few examples, and the same also applies to the choice of material and the way in which it is treated. Thus the book claims to be no more than an introduction to the chemistry of short-lived molecules. The author has taken account of this by including a list of references at the end of each chapter, covering published work up to 1988. A noteworthy feature is a systematic compilation of the most important review articles published between 1978 and 1988; this fills in most of the gaps that the book itself has unavoidably had to leave.

After an introduction the author briefly describes most of the experimental techniques now commonly used for generating, detecting, and characterizing short-lived molecules (evaporation, sputtering, flames, shock waves, photolysis, flow systems, matrix isolation techniques, trapping experiments). The literature citations refer the reader on the one hand to fundamental papers on individual techniques, and on the other hand to published work breaking new ground at the forefront of developments in modern experimental methods.

The chapter on the photochemistry of metal carbonyl compounds is the longest in the book (35 pp., 41 references). As an especially important example the photosubstitution of ligands in complexes of the type $M(CO)_6$ (M = Cr, Mo, W) is described in considerable detail, and some problems arising with particular methods of investigation are also discussed. This is followed by an account of the knowledge that has been gained, mainly by matrix spectroscopy, about the short-lived carbonyl complexes that can be generated from various stable precursors ($Fe(CO)_3$, $Mo(CO)_3$, $Mo(CO)_4$, $Mo(CO)_5$ etc.) by splitting off one or more CO ligands. This chapter ends with some considerations regarding multinuclear complexes, and complexes containing CO-related ligands such as NO, ethene, and cyclopentadienyl. The rest of the chapters are concerned with the reactivity of free metal atoms, the chemistry of divalent silicon, aspects of organic photochemistry, high-temperature molecules, ions and radicals, routes to inorganic materials, and the chemistry of the atmosphere and interstellar space.

At first sight this choice of topics seems rather arbitrary, and probably reflects the personal preferences of the author as a guiding principle. However, one can accept this in view

of the aim set out in the introduction, which is to give a selective overview of the field. A similar situation is found with regard to the choice of material within each chapter. In every case one could have made a different choice which would have been at least equally good, and many topics are only touched on very briefly. For example, in the final chapter there is no mention of the buckminsterfullerenes (C_{60} and higher homologues),[*] as important forms of interstellar carbon and constituents of carbon black; however, the manuscript was in preparation at a time before the critical voices doubting this interpretation of the then available spectra had been completely silenced, and one can therefore understand the reasons for the omission.

Altogether the book contains such a wealth of stimulating ideas that the reader whose interest goes deeper is unlikely to be content with the text itself; the references provide easy access to material for more detailed study. Thus the book is a working guide rather than a textbook, and from this standpoint I found it enjoyable reading, and can therefore recommend it for the readership envisaged by the publishers. It would be useful for university and research institute libraries to have copies of the book so that it would also be easily accessible to students.

Ulrich Zenneck
Institut für Anorganische Chemie
der Universität Erlangen-Nürnberg (FRG)

Frontiers in Supramolecular Organic Chemistry and Photochemistry. Edited by *H.-J. Schneider* and *H. Dürr*. VCH Verlagsgesellschaft, Weinheim/VCH Publishers, New York, 1991. xii, 485 pp., hardcover DM 196.00.—ISBN 3-527-28016-2/0-89573-951-8

This book contains twenty articles which, except for the chapters written by the two editors, are based on papers presented at the Workshop on Supramolecular Organic Chemistry and Photochemistry which took place at the end of August 1989 in Saarbrücken, Germany. The main focus of interest here lies not in the individual molecules but in the association of molecules. The activities of the individual research groups in the area of supramolecular chemistry are aimed not only at gaining a deeper understanding of biological systems but also, most importantly, at developing new materials and technologies. In this book (p. 25) Lehn defines the goal as: "... strategies toward properties and functions rather than toward structures ...". The topics covered in this book are concerned with both aspects: they range from the design of ligands and their synthesis, and a description of the formation of complexes containing these ligands, through to the photochemistry of biological systems. The arrangement of the book's contents also essentially follows this pattern.

In the first chapter (pp. 1–28) Jean-Marie Lehn reviews the work of his group, from the start of their investigations of molecular recognition through studies of structures with electronic and ionic conductivity up to work on information and signal processing and molecular self-organization. This is followed by a series of chapters dealing with problems of host–guest interactions, as follows: selectivity and complementarity in molecular recognition, Schneider, pp. 29–56; receptors of the calixarene type, Ungaro, pp. 57–82; metallomacrocycles as host compounds for neutral guests, Reinhoudt, pp. 83–108; the design and synthesis of a biotin receptor, determination of association constants in host–guest complexes, Wilcox, pp. 123–144; azacyclophanes, Murakami, pp. 145–166. The main emphasis is also on synthesis in Stoddart's contribution (pp. 251–264); here, however, in catenanes and rotaxanes one is dealing with noncovalent bonding of a different kind.

Czarnik and Diederich describe some real applications. Czarnik (pp. 109–122) uses changes in the fluorescence properties as a method of analysis in the formation of chelates by anthracene derivatives, while Diederich (supramolecular catalysis, pp. 167–192) has not only used his cyclophanes for binding substrates but has also developed them into catalysts, e.g. for the condensation of benzoin or for the oxidation of aromatic aldehydes.

In the second part of the book the discussion of supramolecular systems is extended beyond host–guest complexes, which are made up of only a few molecules, to micelles, vesicles, membranes and various other systems, many of which have liquid crystalline properties. The topics dealt with are helical clathrates formed by inclusion in amylose (Hui, pp. 203–222), transport through channel-containing membranes (Menger, pp. 193–202), and self-organizing membranes (Fuhrhop, pp. 223–250).

The final part of the book deals with photochemistry in supramolecular structures, i.e. with those photochemical and photophysical properties that distinguish supramolecular structures from the individual molecules of which they are formed. The discussion is mainly concerned with fluorescence and electron transfer phenomena. The ultimate objectives of these studies, for example economically viable processes for the photochemical breakdown of water or the fixing of CO_2 or nitrogen in nonbiological systems, are still far from being attained. These contributions should therefore be regarded as more in the nature of progress reports.

In the area of photochemistry the systems discussed again include complexes made up of a small number of molecules, but also in addition liquid crystals, micelles and biological materials. Thus the topics covered include the photochemistry and photophysics of anthraceno-crown ethers (Bouas-Laurent, pp. 265–286) and of ion pairs and coordination compounds (Balzani, pp. 371–392). Schaffner discusses the photophysics and photochemistry of the biliprotein chromophore with regard to its protein matrix (pp. 421–452). Ringsdorf describes the photoinduced structural changes that occur in some organized supramolecular systems, most of which are liquid crystalline (pp. 311–336), and Willner deals with photoinduced electron transfer in systems of this type (pp. 337–370), whereas Braun discusses oxidation reactions in microheterogeneous media (pp. 393–420). De Schryver describes the use of fluorescence measurements for characterizing micelles. The photochemical part concludes with a chapter on supramolecular photosensitizers (based on ruthenium) for nonbiological photosynthesis (Dürr, pp. 453–476).

Altogether this book is an excellent collection of papers from the Saarbrücken Workshop, and it summarizes the latest developments in a number of different areas that come under the general heading of supramolecular chemistry. The layout of the text is clear and systematic, and there are plenty of figures, some of which are in color. Regrettably, however, the high price will be an obstacle to reaching a large readership.

Ulrich Lüning
Institut für Organische Chemie und Biochemie
der Universität Freiburg (FRG)

[*] See J. F. Stoddart, *Angew. Chem.* **1991**, *103*, 71–72; *Angew. Chem. Int. Ed.* **1991**, *30*, 70–71.

Dienes in the Diels-Alder Reaction. By *F. Fringuelli* and *A. Taticchi*. Wiley, Chichester, 1990. xx, 348 pp., hardcover £ 55.15.—ISBN 0-471-85549-9

Within its 348 pages this book offers no fewer than 165 pages of tables and 63 pages of references. While this may be taken as evidence of the authors' great diligence, it does not make up for the fact that the presentation of the data leaves much to be desired. In their preface the authors indicate that the audience they have in mind includes undergraduate students. Such students should be warned, however, that this book, at the steep price of £ 55, is not a good investment, since only the first of its six chapters can be considered didactic. The first chapter does indeed contain a discussion of the fundamental principles of the Diels–Alder reaction, but since the treatment is somewhat superficial and is compressed into 40 pages, it would have been preferable to omit this chapter altogether and, by way of introducing the subject, to refer the reader to an appropriate and well-received textbook, such as that by W. Carruthers,[*] a recent text that also happens to be less expensive since it is available as a paperback (US $ 36.01 paperback, US $ 73.01 hardcover).

Probably most readers will lose interest in the book after the first chapter. That is where the enumeration begins of 1,3-dienes and their reactions with various dienophiles. The organization is conventional: open chain dienes (Chapter 2), exocyclic dienes (Chapter 3), compounds with one exocyclic and one endocyclic double bond (Chapter 4) and with two endocyclic double bonds, each in a different ring (Chapter 5), and finally, cyclic dienes (Chapter 6). Each of these classes of dienes is introduced by means of representative reactions and individual reactions are then described in extensive tables. In the tables the diene component is listed by structure, whereas each dienophile is described in two ways: firstly, either by full name or by an abbreviation, and secondly by a code classifying reactive centers and substituents. The purpose of this latter listing escapes me.

It is difficult for a reviewer to assess whether the collection of data presented in this volume is really comprehensive. In trying to do so I chose 20 relevant references between 1980 and 1986, which are known to me, but found only 12 of them referred to in the book. Older references cannot be traced here; it was made quite clear in the preface that the literature is covered only between 1978 and 1987. Nevertheless, the extensive tables which list reactants and yields may be useful to academic or industrial research chemists who wish to check their own literature surveys.

This volume is presumably based on an extensive search of Chemical Abstracts. Unfortunately, the references so collected were not placed in any systematic order whatever, alphabetic, numerical or chronological. Thus, Chapter 2 lists 500 references but its first section, 2.1 (1,3-butadienes), starts with reference 456. In Chapter 6 each of the three sections is referenced independently. The first section of this chapter, 6.1 (carbocyclic dienes) (453 references), starts with reference 413. All this is annoying, particularly since many cheap computer programs are available that can execute alphabetical or numerical sorting with ease. With reference to computer software, apparently several different programs of varying quality were employed to draw the formulas in this book: in some cases double bonds are not clearly drawn (e.g., pp. 152, 233, 237), and several drawings are smudged (e.g., the representations of face-selective Diels–Alder reactions, pp. 38 and 63).

What a pity: a great deal of work has gone into this volume, but not enough thought was given to its design and execution.

Axel G. Griesbeck
Institut für Organische Chemie
der Universität Würzburg (FRG)

[*] W. Carruthers, *Cycloaddition Reactions in Organic Synthesis*, Pergamon, Oxford, **1990**. 300 pp., hardcover ISBN 0-08-034713-4, paperback.

Sulfur Analogues of Polycyclic Aromatic Hydrocarbons (Thiaarenes). Environmental Occurrence, Chemical and Biological Properties. (Series: Cambridge Monographs on Cancer Research.) By *J. Jacob*. Cambridge University Press, Cambridge, 1990. XIV, 281 pp., hardcover £ 55.0. – ISBN 0-521-30120-3

This monograph provides chemists, biologists, and medical scientists with information on the sulfur analogues of polycyclic aromatic hydrocarbons, with special regard to their possible environmental effects, in particular their mutagenic and carcinogenic properties. It includes analytical and synthetic aspects, as well as the physical and biological data that are available up to now. As the information on these topics is widely scattered throughout the literature, the authors have performed a valuable service in bringing it together in an encyclopedic compilation, and in presenting, for the first time, comparisons with the corresponding non-sulfur polycyclic arenes that have been studied more thoroughly. Nevertheless, because there are still many gaps in our knowledge of these sulfur compounds, this cannot be more than a first crude attempt. Since many new sulfur-containing polycyclic arenes have recently been synthesized, one must hope that it will soon be possible to fill in the picture in more detail, and to find out whether the sulfur analogues are in fact less carcinogenic than the corresponding arenes.

The monograph is written in a concise and clearly understandable style. It begins with a general part (94 pp.) which gives information on the biological activities of this hitherto relatively little studied class of compounds, deals with questions of nomenclature, and discusses spectroscopic data (UV/VIS, fluorescence, phosphorescence, IR, NMR, mass spectrometry); in some cases these data are presented in the form of tables together with those for the corresponding non-sulfur arenes. This first part also includes general information on the synthesis of the compounds and their isolation, separation and identification, based on oxidations or reductions in combination with a wide variety of chromatographic methods. The picture is completed with information on natural occurrence and on mutagenic formation from the biomass. The biosynthetic building blocks are believed to be hydrogen sulfide from microbial processes, elemental sulfur, and sulfur-containing amino-acids. This explains the instances of occurrence in mineral oil and coal. A carefully compiled bibliography, including also metabolic aspects, is provided.

The second part (132 pp.) gives information on individual thiaarenes. The choice seems rather subjective, but has been determined by the relevance to biological activity. Unfortunately the monocyclic compound thiophene is not included. The compound-specific part begins with bicyclic and ends with nonacyclic compounds. There is a general preponderance of thiaarenes with the sulfur atom in the five-membered ring, i.e. thiophene derivatives. Only a few isolated examples of thiapyrans are included. One quickly gets used to the peculiar notation used for the partial structural formulas.

For example, C_4S–C_6 stands for benzothiophene, C_4S–C_6–C_6 for naphthothiophene, and so on. In any case, this is then followed by the structural formula, the name, and details of synthesis, occurrence, and properties. In each case the data are supported by the names of the authors and the year of publication. The full citation can be found in a special chapter containing nearly 1000 references, arranged alphabetically by authors. There is also an index containing about 900 keywords relating to the thiaarenes listed.

One might criticize by pointing out that, despite the wealth of material, only a modest amount of information on mutagenic and carcinogenic properties is given, and that the manuscript deadline was apparently as early as 1986. Nevertheless, the monograph is an essential first step, and it provides a sound basis for a deeper understanding of the possible environmental effects of sulfur-containing polycyclic arenes and an initial attempt at a comparative study. At the same time it also reveals the disturbing inadequacy of our knowledge of this specialized topic, but on the other hand it points the way to future work, including especially computer-aided molecular modeling studies. Although this is an unconventional book, it can be recommended for everyone interested in the subject.

Roland Mayer
Institut für Organische Chemie
der Technischen Universität Dresden (FRG)

Transition Metals in Total Synthesis. By *P. J. Harrington*. Wiley, Chichester, 1990. xvi, 484 pp., hardcover £ 47.50.—ISBN 0-471-61300-2

The very welcome aim of this book is to demonstrate the value of proven synthetic methods based on organotransition-metal chemistry, by exemplifying their application to key steps in total syntheses. The author states in the preface that it is intended for advanced students as well as experienced chemists.

The well-bound book, whose clean, well-set text contrasts to some extent with the rather unprofessional looking structural formulas, consists of 14 chapters and is provided with a subject index. Each chapter is linked to one or two structurally related target compounds and usually starts with an explanation of their origin and biological activity. This is always followed by a quite detailed description of a certain class of organotransition-metal compounds, covering methods of preparation and typical reactivities. The chapters conclude with a tersely presented ("synform-like") total synthesis of the target molecule(s) in which the previously discussed organometallic compounds are involved in key positions.

In this manner, the book describes a rather limited, but quite relevant selection of synthetically useful methods for C–C-bond formation, in all of which transition-metal complexes are used either as catalysts (e.g. Heck reaction, allylic alkylation, Stille coupling, Vollhardt cyclization), stoichiometric reagents (e.g. Pauson-Khand reaction, Tebbe-Grubbs reactions, Schwartz reaction) or building blocks (e.g. reactions at carbonyl π complexes of Cr, Fe or Co, or the Dötz reaction).

Upon first glance the book makes a favorable impression. It is at once evident that the author made an effort to give the reader a broad overview with the emphasis on the preparative scope of each method. In this he can be excused for occasionally resorting to mere lists, and not even flinching from including ten-page tables. However, in the likewise very detailed explanations of mechanisms it would have been desirable to put a greater emphasis on the basic and common principles of organotransition-metal reactions.

One ground for criticism is the rather frequent mistakes in structural formulas (for example, on page 210 alone, four of the twelve formulas contain a total of six errors); there are the contracted C-rings of two steroids (page 233), the apparently epimerized 17-β-estradiol (page 202), the inadvertently partially hydrogenated arene (page 212), and a product with a shifted methoxy group (page 331). Also the denotation of nonisolable intermediates by square brackets is not applied consistently, which leads to confusion, as too does the fact that in many of the formulas the (relative) stereochemistry is not fully indicated or (sometimes) not given at all.

Apropos stereochemistry: It is unfortunate that in this book little or no distinction is made between absolute and relative configuration. Even the target compounds (with biological activity) are usually introduced as racemates (e.g. (±)-estrone on page 200), and the chosen syntheses then lead likewise to racemic mixtures. Thus, readers who regard the control of absolute configuration as an important objective as well might not be completely convinced of the usefulness of organotransition-metal methods. The term "enantioselectivity" does in fact appear in one of the chapters, but not in the context of a synthesis, and characteristically, of the "chiral" ligands shown there (pp. 74–75) at least two are (according to the formula diagram) meso compounds. That stereochemistry is not exactly the author's favorite topic becomes especially apparent in Chapter 11, where arene tricarbonylchromium complexes are discussed. After convincing the reader that compounds of this type can be chiral, the author states (on page 337): "To illustrate, complexation of racemic 1-indanol can produce as many as four diastereomers. In fact, complexation occurs exclusively on the same face as the hydroxyl group. The pair of diastereoisomeric complexes are separable. Oxidation of the (S)-isomer affords a single complex of indanone". This statement is quite simply wrong at several points. It ought to read: "... as many as four stereoisomers (two diastereomeric pairs of enantiomers). In fact, complexation occurs diastereoselectivity on the same face as the hydroxyl group. The pair of enantiomeric complexes may be separated by classical resolution techniques (via diastereomer formation). Oxidation of the (1S)-isomer...".

There are also other errors that do not exactly inspire confidence, for example, the conversion of a ketone to an epoxide by using the dimsyl anion (p. 140), or the (improbable) occurrence of free cyclobutadiene as an intermediate in the preparation of its $Fe(CO)_3$ complex from 3,4-dichlorocyclobutene (p. 98).

The currentness of the book leaves something to be desired as well. Although there are a handful of literature references for 1987 (mostly to the author's own work) and 1988, the discussions are, on average, considerably less up-to-date than this. Had the author taken the trouble to research the more recent literature, it would have saved him several further embarrassments. For example, it is regrettable that in discussing the Semmelhack syntheses of (±)-acorenone and (±)-acorenone B (Chapter 11) he has failed to mention the work of Uemura et al., which was published in 1986. In stating that "stereospecific synthesis of (intermediates) A and B would improve both syntheses significantly" (p. 343) he reveals his ignorance, as exactly this problem has already been solved by Uemura. In another passage (pp. 318–319) he describes how complexes of benzene derivatives with $Cr(CO)_3$ can be prepared by transcomplexation at 200 °C; here we read: "Thus, the naphthalene complex should be most suitable for preparation of new arene complexes by arene

exchange". It is almost beyond belief that the method introduced several years ago by Kündig and since applied by others, which does in fact use the naphthalene complex as the reagent (at mild 70 °C), is not cited here.

Though the book's flaws are flagrant, its strengths should not be completely ignored. Many of the chapters are quite readable, interesting, and well written from a teaching standpoint. Doubts remain, however, that the author can convince a wider circle of readers of the usefulness of organotransition metal methods, since almost no comparisons with alternative methods of synthesis are made. And when the low cost of a starting material (e.g. 2-methylanisole) is put forward as a "selling point" for a particular synthesis, many readers will be annoyed to discover that the cost of the transition metal reagent required in stoichiometric quantities is many times greater, but not even mentioned. Instead, so many thoroughly sound arguments and good examples could have been put forward as impressive confirmation of the usefulness of transition metals for total syntheses—even for nonracemic target compounds.

To summarize, the author's intentions are entirely laudable, but the value of the book is considerably diminished by the many shortcomings as regards the quality and up-to-dateness of the discussions. Readers who use the book for casual browsing will certainly be able to derive some interesting ideas and insights from it. On the other hand, those looking for a good treatment of the applications of transition metals in organic synthesis, especially beginners in the field, would be better advised to go to other (and also cheaper) monographs, such as that by Collman, Hegedus, Norton, and Finke and/or to a selection of recent review articles on the individual topics. The gap in the market, which this book was intended to fill, remains open.

Hans-Günther Schmalz
Institut für Organische Chemie
der Universität Frankfurt/Main (FRG)

Registered names, trademarks, etc. used in this journal, even when not marked as such, are not to be considered unprotected by law.

© VCH Verlagsgesellschaft mbH, D-W-6940 Weinheim, 1992. – Printed in the Federal Republic of Germany by Konrad Triltsch Druck- und Verlagsanstalt Würzburg.

All rights reserved (including those of translation into foreign languages). No part of this issue may be reproduced in any form — by photoprint, microfilm, or any other means — nor transmitted or translated into a machine language without written permission from the publishers. Only single copies of contributions, or parts thereof, may be made for personal use. This journal was carefully produced in all its parts. Nevertheless, authors, editors, and publisher do not warrant the information contained therein to be free of errors. Readers are advised to keep in mind that statements, data, illustrations, procedural details, or other items may inadvertently be inaccurate.

Valid for users in the USA: The appearance of the code at the bottom of the first page of an article (serial) indicates the copyright owner's consent that copies of the article may be made for personal or internal use, or for the personal or internal use of specific clients. This consent is given on the condition, however, that the copier pay stated per-copy fee through the Copyright Clearance Center, Inc. (CCC), for copying beyond that permitted by Sections 107 or 108 of the U.S. Copyright Law. This consent does not extend to other kinds of copying, such as copying, for general distribution, for advertising or promotional purposes, for creating new collective works, or for resale. For copying from back volumes of this journal see 'Permissions to Photo-Copy: Publisher's Fee List' of the CCC.

Editorial office: Postfach 10 11 61, D-W-6490 Weinheim, Federal Republic of Germany, Telephone (06201) 60 23 15, Telex 465 516 vchwh d, Telefax (06201) 602 328, E-Mail Z16@DHDURZ2 in Earn Bitnet.

Editor: *Peter Gölitz*

Associate editors: *R. H. Schmidt-Radde, K. J. Schneider, A. Stimson.* **Editorial assistant:** *E. Schweikart*

Publishers: VCH Verlagsgesellschaft mbH. (Managing Directors: *Hans Dirk Köhler, Dr. Karlheinz Köpfer*), Pappelallee 3, W-6940 Weinheim, Federal Republic of Germany.

Advertising office (Advertising Manager: *R. J. Roth*): Postfach 10 11 61, D-W-6940 Weinheim, Federal Republic of Germany, Telephone (0 62 01) 60 61 36, Telex 4 67 155, Telefax (0 62 01) 606 156.

ANGEWANDTE CHEMIE
International Edition in English
Volume 31 · Number 4
April 1992
Pages 367–486

Multiple Peptide Synthesis Methods and Their Applications

New Synthetic Methods (87)

By Günther Jung* and Annette G. Beck-Sickinger

Dedicated to Professor Ernst Bayer on the occasion of his 65th birthday

Rapid developments in the biotechnology of new proteins, as well as advances in immunology and the development of pharmaceuticals based on inhibitors and antagonists, have led to immense demands for synthetic peptides. Simultaneous preparation of 100–150 completely different peptides, having chain lengths of up to 20 amino acids can nowadays be achieved using multiple synthesis methods. The yields and qualities of the peptides so obtained are high enough to permit reliable in vivo and in vitro screening for biological activities. Moreover, it is possible to optimize synthetic conditions and to carry out comparative studies on the secondary structures and conformational mapping of proteins. Special multiple synthesis methods facilitate the epitope mapping of larger peptides for diagnostic purposes and for the development of vaccines based on a few hundreds of free or rod-bound peptides that are useful for immunoassays. Multiple methods of peptide synthesis also enable the preparation of so-called peptide libraries which could comprise hundreds of thousands of peptides, and by which new perspectives for the screening of lead structures will be opened up. Peptide synthesis using a combination of photolabile protecting groups and photolithographic procedures enables the assembling of peptide libraries on small plates for use in miniature immunoassays. Furthermore, lipopeptide-antigen conjugates allow both the preparation of peptide-specific and monoclonal antibodies as well as a complete screening of epitopes of B-, T-helper and T-killer cells. Applications in the areas of AIDS diagnosis, the development of vaccines, and screening for the hormone analogues, demonstrate just some of the possibilities that have been opened up by multiple peptide synthesis methods.

1. Peptide Synthesis Through the Ages

Peptide chemistry is currently witnessing a tremendous upswing in technological progress. The numerous possibilities for research using synthetic peptides in the solving of biological problems are becoming increasingly better recognized.[1–8] No other area of organic chemistry seems so dependent on interdisciplinary cooperation as peptide chemistry. The fields of research in modern peptide chemistry include synthesis and analysis, isolation and structure determination, conformational investigations, and molecular modeling. Project-oriented studies are being carried out in conjunction with research groups in pharmacology, physiology, immunology, biology, and biophysics. More and more peptides with unusual amino acids,[9–15] modified peptide bonds,[16–21] linker or spacer molecules,[22, 23] and peptide mimetics[14–26] are being prepared. Highlights of the medicinal chemistry of agonists and antagonists of biologically active peptides and inhibitors have recently been summarized by Hirschmann.[26a] Great progress has also been made in immunology at the molecular level regarding recognition mechanisms, using both synthetic peptides[27a, b] and vaccines.[27c–e] The peptide chemist is continually being con-

[*] Prof. Dr. G. Jung, Dr. A. G. Beck-Sickinger
Institut für Organische Chemie der Universität
Auf der Morgenstelle 18, D-W-7400 Tübingen (FRG)

 © VCH Verlagsgesellschaft mbH, W-6940 Weinheim, 1992 0570-0833/92/0404-0367 $ 3.50+.25/0

fronted with new challenges at ever shorter intervals.[28, 29] There is a greater demand for new strategies, faster syntheses,[28] better coupling reagents and protecting groups, and especially for methods for the simultaneous preparation and analysis of very large numbers of peptides in a short time.

We present here a survey of the latest developments in the area of multiple peptide synthesis (MPS) and address the possibilities of modern analysis for a large number of polypeptides (multiple peptide analysis, MPA). These methods will be illustrated by means of examples showing their characteristic applications.

1.1. Synthetic Partial Sequences of Proteins

In 1963 Anderer[30] prepared virus-neutralizing antibodies using the synthetic *C*-terminal hexapeptide of the protein of tobacco mosaic virus. Since then, the use of synthetic partial sequences of proteins has played a major role in the determination of antigenic determinants. Concomitant with the progress being made in gene technology research and the development of automatic protein sequencers, the number of sequenced proteins is increasing so rapidly that sequences can be ascertained and compared only by using special programs and data banks.[31] Despite the progress made in gene technology, the chemical synthesis of short proteins is presently one of the fastest methods for obtaining experimental information about binding-domains, active centers, and modifications.

Interestingly, Merrifield's decisive concept[32, 33] of an automated peptide synthesis on a solid support, appeared shortly after Anderer's investigations. The Merrifield synthesis[28, 33–36] was a prerequisite for the rapid synthesis of many peptides. Biosynthesis of the sequence analogues of biologically active peptides and proteins has been achieved by the use of side-chain mutagenesis; however, a specific modification by inserting non-proteinogenic amino acids is almost only possible by chemical methods. Owing to the large number of diagnostically and therapeutically interesting proteins, and to the increasing demand for proteins in biochemical research, it is no longer possible to prepare the required protein segments using conventional methods of fragment condensation within a reasonable time.[37–39]

1.2. Biologically Active, Low Molecular Weight Peptides

The number of highly biologically active peptides which can be used as a basis for the development of pharmaceuticals, or can be employed for therapy in the natural form, has increased drastically. Our bodies 'recognize' and react with many more peptides than was previously thought. Bombesin, endothelins, epidermal growth factor (EGF), magainin and neuropeptide Y are just a few examples of a large number of highly active peptides which have been the subject of chemical research in the last few years. Continuous activities are also aimed at modifying other significant peptides such as atrial natriuretic factor, renin, somatostatin, cholecystokinin, pepstatin, calcitonin, bradykinin, enkephalin, angiotensin, vasopressin and oxytocin.[1–8] Knowledge of the structure-activity relationships which disclose the correlation between amino acid sequence, peptide conformation and biological activity is important both for the elucidation of the underlying principles of signal recognition and information transfer, and for pharmacological applications. Furthermore, an understanding of the mechanisms of agonism and antagonism of peptide hormones can be gained only by a systematic modification of peptide and non-peptide analogues.

1.3. Analytical Procedures are Advancing

By improved methods of biological, biochemical and instrumental analysis, it is possible to have access to picomolar (or even less) amounts of novel biologically active materials. Fully automatic gas-phase sequencing according to the method of Edman[40, 41] requires less than 100 pmol of a protein. Furthermore, by using HPLC on-line coupling, the molecular masses of polypeptides over 10000 Da can be determined by ion-spray mass spectrometry;[40, 42] likewise in the lower picomolar range. For amino acid analysis even a few femtomol of peptide suffices in special cases.[40, 43] Consequently, it is more often possible to sequence naturally occurring peptides in the picomolar range, and then to study their biological activities using synthetic compounds and their analogues.[27, 44, 45]

Günther Jung, who was born in Tübingen in 1937, studied chemistry at the Universität Tübingen, where he gained his doctorate in 1967 under the supervision of E. Bayer. After his habilitation (1971) in the natural products area he became Professor of organic chemistry and biochemistry at the Universität Tübingen, after turning down numerous positions at other universities. He spent 1967/68 in the USA as an assistant professor at the Univeristy of Houston, Texas. In 1989 he was awarded the Max Bergmann Medal for his work on lantibiotics. His areas of research include the structural elucidation, mode of action and biosynthesis of larger polypeptide antibiotics and siderophores, structure-activity relationships of the neuropeptide Y, models for transmembrane channels, multiple peptide synthesis methods, B-, T-helper and T-killer cell epitope mapping, and the development of synthetic peptide vaccines.

Annette G. Beck-Sickinger, born 1960 in Aalen (Germany), studied chemistry (Diploma 1986) and biology (Diploma 1990) at the University of Tübingen. After a period of research work with R. A. Houghten at the Scripps Clinic & Research Foundation (La Jolla, California) she returned to Germany and gained her doctorate (1989) under the supervision of Professor G. Jung. From 1990 to 1991 she carried out research as a post-doctorate with Professor Carafoli at the ETH Zürich. She is presently at the University of Tübingen where she is working on her habilitation. Her research interests lie in the areas of peptide-protein interactions, photocrosslinking, and structure-activity relationships of neuropeptides.

2. Multiple Peptide Synthesis—the Logical Step

In order to respond to the rapidly growing demands for a large number of peptides with completely different sequences, several groups have, since 1985, been developing different concepts for a multiple peptide synthesis (Tables 1 and 2). The term multiple peptide synthesis (MPS), also known as simultaneous multiple peptide synthesis (SMPS), denotes the parallel synthesis of many peptides having various lengths and amino acid sequences. In principle, the various methods can be distinguished by the differences in the polymeric support employed, the number of peptides possible, and the amount of products obtained. Typically, if more, than 10 mg of product is obtained, not only the characterization but also a purification step can be carried out. Subsequent modification of the peptide then becomes possible.

The multiple synthesis methods are mostly applied in hormone and inhibitor research. For the identification of relevant side chains, every amino acid of a biologically active peptide can be systematically substituted, the chain lengths can be varied, and *N*- as well as *C*-termini can be modified (Fig. 1).[46] In the original solid-phase synthesis, the various *N*-terminal modifications such as acetylations, biotinylations, succinimidylations or couplings for preparing immunogens could be achieved by portioning the peptide–resin. By contrast, modifications within the peptide chain or at the *C*-terminal segment can only be achieved by multiple methods or by consecutive syntheses. Thus, in the multiple

Table 1. Survey of the multiple peptide synthesis (MPS) methods for preparing more than 50 μM.

Method	Tea bag		R*MPS	PS-grafted PE films	Continuous flow peptide synthesis (CF-SP-MPS)	Synthesizer PSSM-8
Polymer	PS-DVB	PS-DVB	PS-DVB	PS-PE-film	PS-DVB	PS-DVB
Number	<150	<150	25	10	10	8
Amount	50–500 μmol	50–500 μmol	50–500 μmol	500 μmol	20–400 μmol	5–400 μmol
Protecting goup	Boc	Fmoc	Fmoc/Boc	Boc	Fmoc/Boc	Fmoc
Activation	DIC	TBTU/HOBt	any	symmetrical anhydride	HOBt/DIC	HOBt/DIC TBTU, others
Washing cycle	manual with shaking	automatic Labortec 411	manual with shaking	manual	manual with connected reactors	automatic
Computer program	required	required	useful			included
Control	picric acid		ninhydrin		bromophenol blue	
Reference	[49]	[52]	[79]	[90]	[81]	[77]

PS = polystyrene, PE = polyethylene, DVB = divinylbenzene, Boc = *tert*-butoxycarbonyl, Fmoc = fluorenylmethoxycarbonyl, TBTU = *O*-(benzotriazol-1-yl) *N,N,N',N'*-tetramethyluronium tetrafluoroborate, HOBt = 1-hydroxybenzotriazole, DIC = diisopropylcarbodiimide.

Table 2. Multiple peptide synthesis methods for preparing small amounts and diagnostic agents.

Method	Methods with pipetting robots		Multiple column	Pepscan	Spots on paper	Cellulose disks	Cellulose paper	Cotton disks
Polymer	PS-DVB	PS-DVB	Macrosorb-SPR	PE-rods	cellulose	cellulose	cellulose	cellulose
Number	90 or 144	48	96	96/block	96	10	4	10
Amount	5–25 μmol/ tube	25–50 μmol/ tube	7 μmol/ cartridge	300 nmol/ rod	100 nmol/ spot	4–6 μmol/ disc	3 μmol/ cm^2	3 μmol/ cm^2/disk: ∅ 3 cm
Protecting group	Fmoc	Fmoc	Fmoc	Fmoc	Fmoc	Fmoc	Fmoc	Fmoc
Activation	DIC/HOBt or TBTU	PyBOP/ HOBt	Dhbt-ester	Pfp-ester	DIC/HOBt, or TBTU	DIC/HOBt, or TBTU	DIC/HOBt	DIC/HOBt
Washing cycle	automatic TECAN 5032 (Zinsser SMPS 532)	automatic Gilson M 222 (Abimed AMS 422)	manual with multi-pipetting	manual	manual	automatic, continuous flow synthesizer	manual	manual, centri-fugation
Computer program	included	included		required	required	required		
Control			Dhbt		bromo-phenol blue	bromo-phenol blue	bromo-phenol blue	bromo-phenol blue
Reference	[72]	[75]	[78]	[62]	[71]	[83]	[82]	[88]

PyBOP = (benzotriazo-1-yl)-*N*-oxytripyrrolidinophosphonium hexafluorophosphate. Dhbt = 3-hydroxy-4-oxo-3,4-dihydro-1,2,3-benzotriazine, Pfp = pentafluorophenyl.

peptide synthesis it is possible to simultaneously prepare the same peptide bound to different anchors and to cleave it to obtain peptide acid, peptide amide, alkylated amide, hydrazide, or a fully protected fragment.

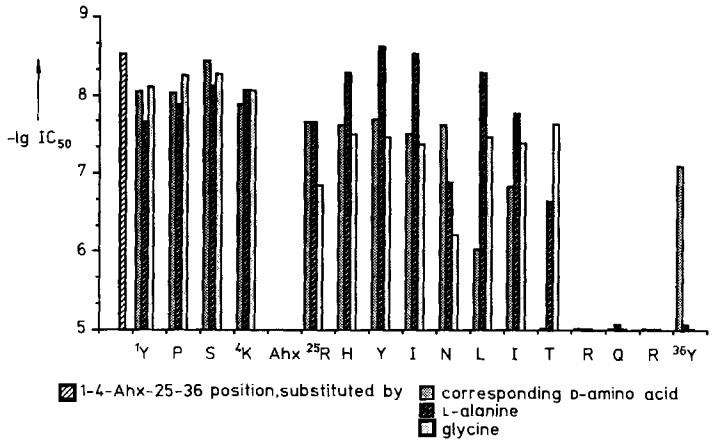

yPSK-Ahx-RHYINLITRQRY	APSK-Ahx-RHYINLITRQRY	GPSK-Ahx-RHYINLITRQRY
YpSK-Ahx-RHYINLITRQRY	YASK-Ahx-RHYINLITRQRY	YGSK-Ahx-RHYINLITRQRY
YPsK-Ahx-RHYINLITRQRY	YPAK-Ahx-RHYINLITRQRY	YPGK-Ahx-RHYINLITRQRY
YPSk-Ahx-RHYINLITRQRY	YPSA-Ahx-RHYINLITRQRY	YPSG-Ahx-RHYINLITRQRY
YPSK-Ahx-rHYINLITRQRY	YPSK-Ahx-AHYINLITRQRY	YPSK-Ahx-GHYINLITRQRY
YPSK-Ahx-RhYINLITRQRY	YPSK-Ahx-RAYINLITRQRY	YPSK-Ahx-RGYINLITRQRY
YPSK-Ahx-RHyINLITRQRY	YPSK-Ahx-RHAINLITRQRY	YPSK-Ahx-RHGINLITRQRY
YPSK-Ahx-RHYiNLITRQRY	YPSK-Ahx-RHYANLITRQRY	YPSK-Ahx-RHYGNLITRQRY
YPSK-Ahx-RHYlnLITRQRY	YPSK-Ahx-RHYIALITRQRY	YPSK-Ahx-RHYIGLITRQRY
YPSK-Ahx-RHYINlITRQRY	YPSK-Ahx-RHYINAITRQRY	YPSK-Ahx-RHYINGITRQRY
YPSK-Ahx-RHYINLiTRQRY	YPSK-Ahx-RHYINLATRQRY	YPSK-Ahx-RHYINLGTRQRY
YPSK-Ahx-RHYINLltRQRY	YPSK-Ahx-RHYINLIARQRY	YPSK-Ahx-RHYINLIGRQRY
YPSK-Ahx-RHYINLITrQRY	YPSK-Ahx-RHYINLITAQRY	YPSK-Ahx-RHYINLITGQRY
YPSK-Ahx-RHYINLITRqRY	YPSK-Ahx-RHYINLITRARY	YPSK-Ahx-RHYINLITRGRY
YPSK-Ahx-RHYINLITRQrY	YPSK-Ahx-RHYINLITRQAY	YPSK-Ahx-RHYINLITRQGY
YPSK-Ahx-RHYINLITRQRy	YPSK-Ahx-RHYINLITRQRA	YPSK-Ahx-RHYINLITRQRG

Fig. 1. Top: Identification of amino acids of the hormone neuropeptide Y (NPY) which interacts with a receptor (rabbit kidney cortex). Using 48 analogues of the heptadecapeptide YPSK-Ahx-RHYINLITRQRY-NH_2 (Ahx = 6-aminohexanoic acid), prepared by the MPS method and by replacing one position each of the sequence by L-alanine, glycine or the corresponding D-amino acid, it was shown that the *C*-terminal tetrapeptide amide RQRY-NH_2 is essential for the interaction, since substitution at these four positions leads to a large decrease in the receptor affinity [57a]. The figure shows the order of the natural amino acid plotted on the x-axis. Receptor-binding data of the analogues are presented as -lg IC_{50} (pIC_{50}) (IC_{50} = concentration in [M] of the half-maximal inhibition of the binding of ^{125}I-NPY is shown by the bars). Bottom: Sequences of the analogues. Left-hand column: small letters symbolize the position substituted by the D-amino acid; center column: substitution by L-alanine A; right-hand column: substitution by glycine G.

Using the systematic scanning of a protein with anti-peptide or anti-protein antibodies, called epitope mapping, usually leads to the detection of sequential B-cell-epitopes. T-helper-cell epitopes (length of 12–17 amino acids) and T-killer-cell epitopes (length of 8–10 amino acids) can be identified with short peptides, which cover the whole sequence of the protein. In addition, conformational mapping, the investigation of the folding of a protein, is possible when overlapping segments (length of 15 to 20 amino acids) are synthesized and systematically investigated by experimental methods for the analysis of the conformation. These scans are more precise when greater numbers of defined peptides from the one protein are used.

In the sequential mapping of a protein for immunological and biochemical investigations, it is often sufficient to have a few milligrams of peptide, if overlapping sequences are used. The length of the sequences and width of the raster are then to be adjusted to the types of investigation and determine the number of peptides to be synthesized (Fig. 2).

If, e.g., the nef-protein of HIV-virus with 208 amino acids (AA) is going to be investigated by using hexapeptide segments and a raster of 1,[47] 203 peptides are required. For the number n of required peptides, the following is generally valid.

$$n = \frac{\text{no. of AAs of protein} - \text{no. of AAs of peptide segment}}{\text{raster number}} + 1 \qquad \text{(a)}$$

Such a fine scanning with overlapping partial sequences is carried out in particular in the determination of immunoglobulin binding-sites (Fig. 2). For investigation of the immunogenicity of protein segments, longer peptides are required but with a less dense raster. Thus, the P6-protein of *Haemophilus influenza Type b*, containing 134 amino acids, could be immunologically mapped using 28 peptides with a raster of 4 and a peptide segment containing 20 amino acids.[48]

3. Different Synthetic Concepts—One Goal

3.1. Peptide Synthesis in a 'Tea Bag'

Houghten's tea-bag method, although published for the first time in 1985,[49] already belongs to the oldest strategies of multiple peptide synthesis. This method is suitable for preparing up to 150 different peptides with a yield of up to 50 mg. Separation of the polymeric support is achieved by sealing it in polypropylene nets before the solid-phase synthesis is begun. For each peptide, such a labeled tea bag of noted solvent stability is filled with ca. 100 mg of polymeric support.[50] Generally polystyrene-divinylbenzene (1%) is used, but it is possible to employ other polymeric supports as long as the size of the smallest particle is larger than the pores of the net (Fig. 3, p. 372).

Deprotection of the α-amino group and washing are simultaneously carried out in a suitable polypropylene, screw-capped bottle, the size of which can be adjusted depending on the number of peptides and the washing volume. The washing volume per tea bag is typically 3–5 mL. For the coupling, tea bags are sorted according to the coupling amino acids and are allowed to react parallel with the activated amino acids in separate reaction vessels. Next, for removal of excess reagents, the tea bags are separately washed twice and then reunited for deprotection. In order to facilitate diffusion of reagents into the resin, washing and coupling steps are carried out with vigorous shaking.

In principle, the tea-bag method is not dependent on protection strategy or activation. Houghten developed this method for the *tert*-butoxycarbonyl (Boc)/benzyl (Bzl) strategy and *N,N'*-diisopropylcarbodiimide (DIC) activation.[49, 51] We employ the superior Fmoc/*t*Bu strategy and *O*-(benzotriazol-1-yl)-*N,N,N,N'*-tetramethyluronium tetrafluoroborate (TBTU) activation,[52] which leads to faster coupling cycles and avoids halogenated solvents.

In comparison to other parallel syntheses, the tea-bag method yields at least 30–50 mg of peptide with a chain

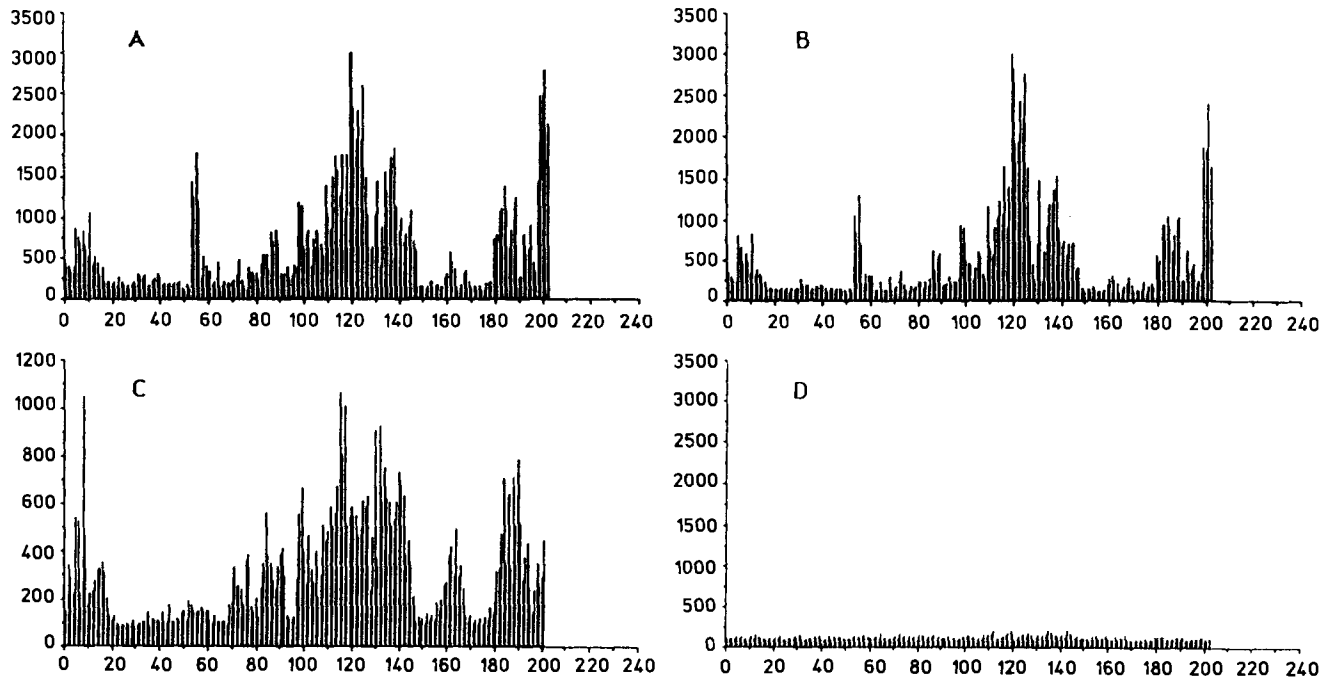

Fig. 2. Epitope screening of the HIV nef-protein by means of Pepscan-ELISA according to Gombert et al. (cf. Section 3.2.1) [47]. The intensity and accumulation of positive peaks in the ELISA indicate continuous (sequential) B-cell-epitopes in distinct sequences, which are recognized by anti-Nef-antibodies. A continuous B-cell-epitope consists of adjacent amino acids within the sequence of a protein. The specificity and affinity of antibodies against discontinuous epitopes, which contain several parts of a protein within different areas of the sequence, might be increased. However, ELISA-assays with peptide-antigens are frequently used with great success. The continuous B-cell epitope of the Nef-protein from three HIV isolates (SF2 (A), BRU (B) and MAL (C)) were determined by binding of antibodies (Fig. 5), which were directed against the Nef-protein, and obtained from HIV positive sera (dilution 1:1200). Serum D is a HIV negative control serum. The ELISA values (optical density × 1000 at 405 nm) were plotted versus the peptide numbers. By testing a representative number of HIV positive sera, several peptides of different length (cf. Fig. 6) showed a very clear limitation of the relevant epitope [47].

length of more than ten amino acids. This amount is sufficient for detailed analyses, spectroscopic investigations (including NMR studies), and a large number of biological tests.

The variability of this method is noteworthy: solvents, activation of amino acids, coupling schemes and further synthetic parameters can be altered from coupling to coupling, as well as during one coupling cycle. Therefore, this procedure is particularly suitable for methodological investigations.[53] Different bases for neutralization,[51] many coupling reagents[53a] and various reagents for the end-capping of non-coupled N^{α}-amino groups[53b] have thus been systematically investigated. From the syntheses of more than a hundred peptides, conclusions can be made concerning the amino acid- and position-dependent coupling efficiency.[54]

Information about the structure-activity relationships of fibrinogen,[55] magainin-2[56] and neuropeptide Y[46, 57] as well as elucidation of antigen-antibody interactions[58] could be obtained by the synthesis of many peptide analogues using the tea-bag method. Furthermore, the tea-bag method has also been used successfully for the conformational mapping of proteins.[59a] The flexibility of this method and the relatively large amounts of peptide obtained have proven advantageous (Fig. 4, p. 373).

Conformational predictions, based on the behavior of peptide sequences in HPLC-chromatography, have recently been published.[60] In this way, e.g., the change in behavior of amphiphilic helices following amino acid substitution has been investigated.[61] For statistically significant evaluations of such investigations, a large number of similar peptides is required. These can only be obtained by multiple synthesis methods. A further advantage of Houghten's MPS method is the low cost, as no investment for instruments is necessary. Since all the steps in this procedure (washing, sorting of the bags, etc.) have to be carried out manually, the method is laborious, which must be considered its major disadvantage. A computer-supported calculation of the synthetic cycles, especially in the sorting steps, becomes indispensible. Moreover, in practice, it becomes impossible to carry out a coupling control for a large number of peptides.[54b, c] However, this method is improved by our own procedure, i.e., the use of a combination of tea-bag synthesis and a semi-automatic synthesizer (Labortec-Bachem, Bubendorf, Switzerland), which allows automation of the washing steps[52] (Fig. 3c).

3.2. Peptide Synthesis without Visible Yields?

3.2.1. Peptide Synthesis on Rods

Peptide synthesis without visible amounts of peptides? – This concept was developed by Geysen et al.[62] Several hundred peptides can be simultaneously prepared using this procedure. The peptides remain permanently bound to the carrier, however, not only during but also following the synthesis. At the end of the synthesis only the protecting groups are removed. Amino-functionalized polyethylene rods (4 mm diameter, 40 mm length) are employed as support. 96 of these so-called 'pins' are fixed into a block con-

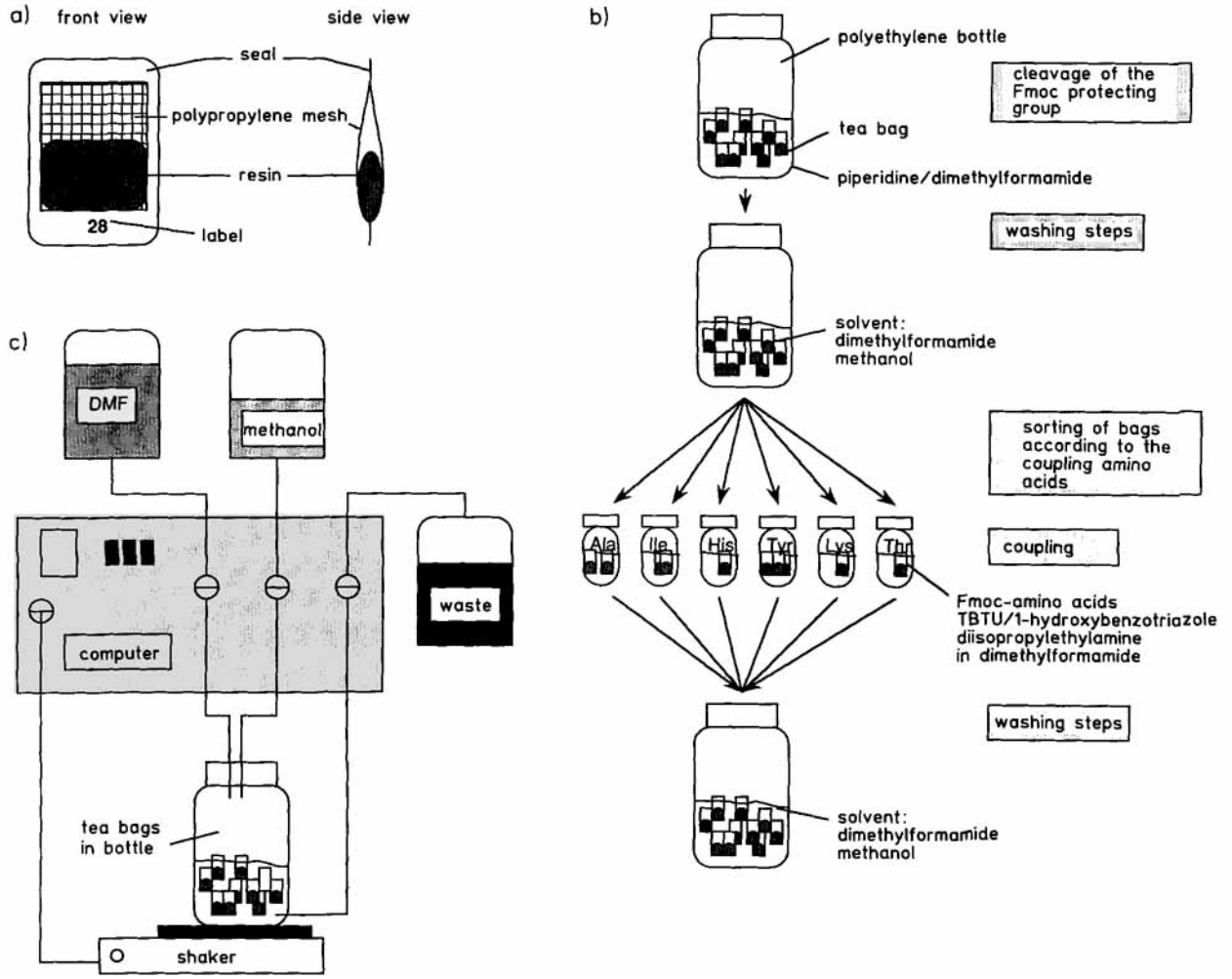

Fig. 3. Schematic representation (a) of a 'tea bag', (b) of the synthetic steps for a multiple peptide synthesis and (c) of the semi-automatic synthesizer [52]. a) Polypropylene net (pore size 64 μm) is labeled and sealed to prepare the bags (3 × 4 cm) [49]. After filling the bags with the polymeric support and sealing the last opening, the bags are tested for leaks and used for the synthesis. One peptide is obtained per bag. b) In a multiple synthesis, cleavage of the N^{α}-protecting group as well as all the washing steps are performed with all the tea bags in a common reaction vessel. For coupling, the bags are sorted for the different amino acids and treated with activated N^{α}-protected amino acids in different vessels. c) Washing of the bags is carried out automatically, whereby addition and removal of solvents by suction are effected by means of computer-controlled valves [52]. TBTU = *O*-(benzotriazol-1-yl)-*N*,*N*,*N*',*N*'-tetramethyluronium tetrafluoroborate, DMF = dimethylformamide, Fmoc = fluorenylmethoxycarbonyl.

taining 8 rows of 12 rods (Fig. 5). The pins are so arranged, that they fit exactly into the wells of the plates used for the *e*nzyme-*l*inked *i*mmuno*s*orbent *a*ssay (ELISA). Washing and deprotecting steps are carried out in large baths. The amount and distribution of the Fmoc-amino acids to be coupled are calculated by a computer program. We were able to make a substantial improvement here by using a computer-controlled stencil, which enabled rapid and accurate pipetting onto the dimethylformamide-stable ELISA plates. After activation, the blocks are placed on the plates and coupling can be carried out. Polyethylene rods cannot swell or shrink, and adsorbed molecules can only be removed with difficulty. Therefore, a thorough washing after each reaction step of the synthetic cycle is of utmost importance. In a new variant, detachable 'heads' and not the rods themselves are functionalized. The blocks themselves can be used several times.

The importance of the pin method lies in the immunoanalytical field.[63-65] Antibodies against large proteins can be tested using overlapping tetra- and nonapeptides in the so-called Pepscan.[65] Mono- or polyclonal sera are distributed in the ELISA-plates and are incubated with the rods. The corresponding specific antibodies in the antisera preferably bind only to the peptide rods having the sequence of a continuing B-cell epitope. Direct application of human sera necessitates some experience in order to suppress non-specific reactions. Since the synthetic peptides cover the entire protein, with only an amino acid shift in each peptide, very accurate analyses of the B-cell epitopes are obtained. In the case of monoclonal antibodies, the continuing binding site can be accurately determined, down to the amino acid (Fig. 6, p. 374).

The VPI-protein from the virus of foot-and-mouth disease,[62] FeLVgp70-protein,[66] the capsular protein of Epstein-Barr virus,[64] and various proteins of HIV-subtypes[47,67] are only a few examples of proteins which have so far been investigated with regard to their antibody binding sites.

If the primary sequence of a protein, against which a monoclonal antibody is directed, is not known, or if it concerns a discontinuous epitope, then this epitope can also be imitated by peptides which do not occur in the protein sequence. Such antibody-binding peptides are called *mimotopes*.[65]

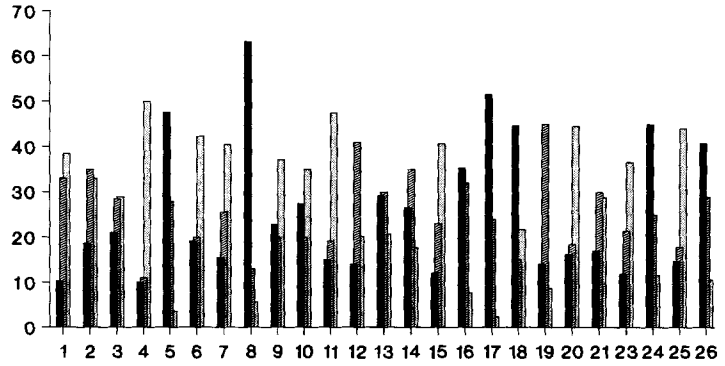

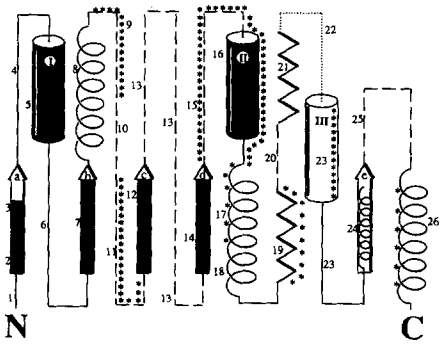

α-helix- and β-sheet conformation of the model

α-helix- and β-sheet conformation: agreement of circular dichroism measurements and model

α-helix- and β-sheet conformation according to circular dichroism measurements in unmodeled regions

random coil according to circular dichroism measurements

epitopes determined by ELISA

Numbers refer to HSV1-TK peptide segments.

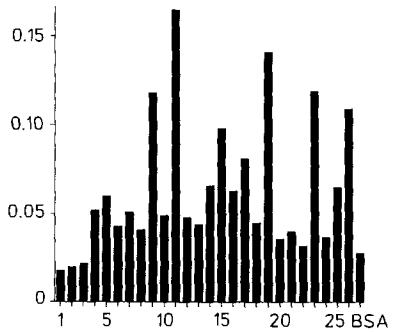

Fig. 4. Conformational analysis (top) and epitope mapping (bottom) of thymidine kinase (376 amino acid residues) from *Herpes simplex* virus [59a]. By using sequential peptides (15 to 17 amino acids) it was possible to refine the three-dimensional models obtained by the molecular dynamic simulation (middle) [59b]. 26 peptides were prepared by the tea bag method (cf. Fig. 3), analytically characterized, and investigated by circular dichroism (CD). Figure 4 (top) shows the calculated percentage of the different conformations for every peptide as derived from the CD spectra. Recognition of the peptides by a thymidine kinase antiserum is shown in Figure 4 (bottom). In the model, the parts on the surface area (B-cell epitope) are better recognized than the peptides from internal segments of the protein. x-Axis: peptide numbers. BSA = bovine serum albumin as negative control; y-axis: ELISA value, relative absorption value.

Such antibody-binding peptides are called *mimotopes*.[65] The mimotope is developed by means of combining D- and L-amino acids and is always controlled by the antibody binding tests (Pepscan-ELISA). However, a high specificity of the monoclonal antibody is required, since one normally begins with screening at the dipeptide level.[65] Carrier-bound mimotopes can be used, e.g., for the isolation of antibodies from antisera by means of affinity chromatography or for blocking an antibody binding site. They are also of interest for the screening of new lead structures.

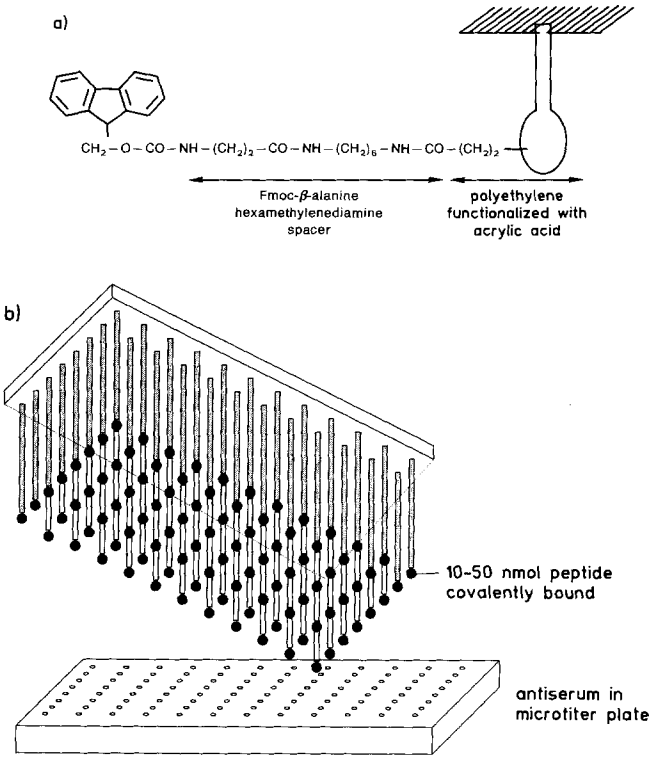

Fig. 5. Schematic representation (a) of a pin and (b) of the block for the pin synthesis. Polyethylene rods (4 × 40 cm) are functionalized with acrylic acid, and N^{β}-Fmoc-β-alanyl-1,6-diaminohexane is introduced as a spacer. Peptide synthesis is carried out on DMF-stable polyethylene microtiter plates. The test is performed by means of pepscan-ELISA, whereby the covalently linked pin-peptides in the usual microtiter plates are investigated for the binding capability of antibodies (cf. Fig. 2). After successful tests, the pins are washed with detergent and are ready to be used for new sera. Use of a single block for up to 50 tests is possible.

In order to obtain free peptides by the pin synthesis method, either an acid-labile anchor has to be inserted between the first amino acid and the polyethylene rods, or special enzymatic or acidolytic cleavage points must be *C*-terminally introduced. For this purpose, R. van der Zee et al.[68a, b] have proposed either Asp-Pro-Gly or Lys-Gly as the *C*-terminal cleavage sequence; the former can be cleaved with formic acid, the latter with trypsin. Neutral cleavage of a Lys-Pro polymer via diketopiperazine formation is another possibility; however, after this cleavage the diketopiperazine adduct is formed and not the free peptide acid.[68c] A better alternative is the use of extremely acid-labile anchors such as 4-(2′,4′-dimethoxyphenylhydroxymethyl)phenoxy and 2-methoxy-4-alkoxybenzyl, which have been fully investigated with regard to their cleavage reactivity.[69] This efficient syn-

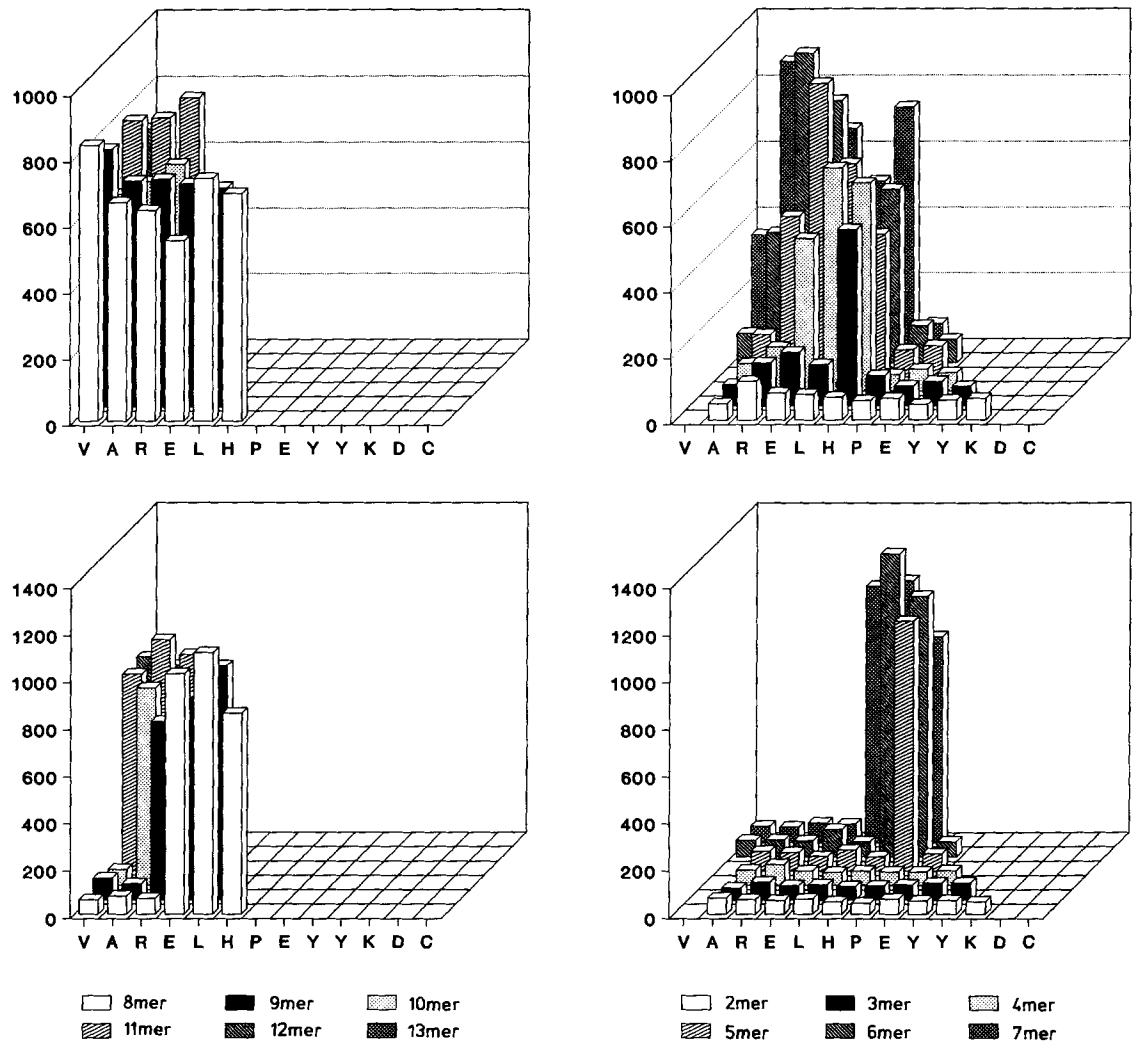

Fig. 6. Epitope fine-mapping, exemplified by two monoclonal antibodies against HIV 1 Nef-protein (Spohn, Universität Tübingen, private communication). The 2- to 13-peptides employed have been prepared by pin synthesis (cf. Fig. 5), and tested by Pepscan-ELISA. Sequences of the tested protein region are plotted on the x-axis (*C*-terminal consensus-sequence of the Nef-protein from various HIV 1-isolates relative to HIV-BRU 193–206). Each bar represents a peptide, whereby an assignment in the direction of the *N*-terminal amino acid takes place. The y-axis shows the absorption in ELISA in mOD at 405 nm, which is a criterion for the binding of antibody. Top: For the production of antibody (Dü6) a mouse was immunized with a lipopeptide immunogen (cf. [27b]) Pam_3Cys-VARELHPEYYKDC without further adjuvant or carrier. The monoclonal antibody obtained recognizes the Nef-protein, the smallest sequence is the tripeptide H-P-E. Bottom: The monoclonal antibody (Dü 106) was obtained by immunization with the Nef-protein. The shortest sequence is the pentapeptide P-E-Y-Y-K.

thetic method, on rods, is suitable for preparing peptides for immunological investigations. It is especially effective for the identification of epitopes which are recognized by monoclonal antibodies and polyclonal sera. Because of the different initial loading and lack of purity controls, however, no quantification should be attempted.[70] Since maximally 300 nmol of peptide can be synthesized per rod, peptide synthesis on rods is not suitable for the structure-activity investigations of hormone analogues.

3.2.2. Spot Synthesis

An inexpensive procedure for the preparation of polymer-bound peptides, used for the screening of sera, has recently been introduced by Frank et al.[71] The first amino acid was coupled to a sheet of cellulose paper (55 × 105 cm). For this purpose, 1 μL aliquots of the coupling reagent (0.3 M solution of Fmoc-amino acid HOBt-ester) were pipetted onto the paper at 49 points with a point separation of 1 cm. The entire sheet was then immersed into appropriate solutions for washing, acetylation, and deprotection. After the last step, an ethanol washing, the paper was dried. Coupling of the next amino acid was then carried out by distribution of the aliquots on the corresponding spots. This could be accomplished manually or by using a pipetting robot. The peptides were not removed from the paper under the cleavage conditions of the side-chain deprotection (20% trifluoroacetic acid, 1% triisobutylsilane); therefore, the sheets can be directly employed for immunological tests. The peptide-bound paper sheet can be subsequently treated and tested in a manner similar to the membranes of the western blot. Frank et al.[54] exemplified this by performing epitope analysis of the immunogen region of cytomegalovirus (hCMV), using 49 peptides, made simultaneously on paper sheets. If free peptides are to be prepared, a cleavage point is introduced

before the first amino acid,[68c] the spots are cut out and the peptides are cleaved separately.

3.3. Fully Automatic Synthesizers are Successful

The tediousness of the tea-bag and pin syntheses has so far prevented employment of these multiple methods in many laboratories. Since during multiple peptide synthesis (Tables 1 and 2), as in solid-phase synthesis,[32-36] deprotection, washing and coupling steps are repeated in every cycle, SMPS should also be automatable. In the meantime, two methods have been realized independently of each other. In both cases a commercially available pipetting robot has been modified and programmed for the requirements of peptide synthesis (Fig. 7).

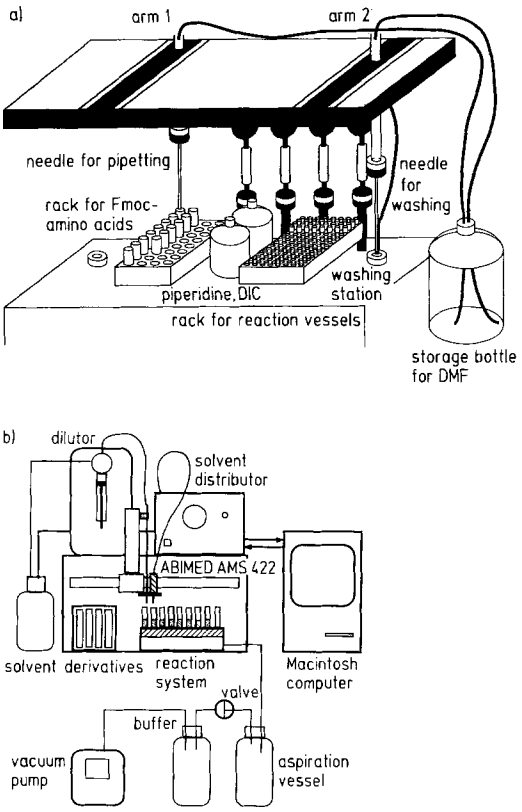

Fig. 7. Schematic representation of the fully automatic multiple peptide synthesizers based on PC-controlled pipetting robots: a) After Schnorrenberg [72]: The robot, with two arms moving in the x, y and z directions, pipettes reagents and derivatives according to the desired sequence. DMF serves as solvent. Suction is effected by two needles ('washing needles') which are equipped with a platinum sieve. b) After Gausepol [75]: Addition of reagents is likewise achieved by means of a pipetting needle. The synthesis takes place in a sintered-glass vessel; suction is achieved by connecting to a vaccum. (Thanks are due to Dr. H. Gausepohl from Abimed, for supplying this Figure).

Schnorrenberg et al.[72] employed a modified Tecan RSP 5052 (Zinsser SMPS 532), a robotic sample processor with two freely moving (in the *x*, *y* and *z* directions) needles attached to two arms. Needle 1 is used for addition of reagents, activated amino acids, and solvents. Needle 2 is equipped with a stainless steel sieve and is used for the removal (by suction) of solvents. Depending on the programming, any kind of glass vessels or Eppendorf tubes can be employed as reaction vessels. Furthermore, as in the tea-bag method, cross-linked polystyrene–divinylbenzene (1%) is used as the polymeric support, and amino acids are predissolved in dimethylformamide/1-hydroxybenzotriazole and activated by addition of *N,N'*-diisopropylcarbodiimide. The synthetic cycle and sequence-dependent amino acid distribution are controlled by a personal computer (Fig. 7a).

Many successful applications, such as investigation of the structure-activity relationships of endothelin[73a] and T-cell epitopes of influenza nucleoproteins,[73b,c] as well as the possible application of various activation methods for amino acids,[74] verify the suitability of this robot for multiple peptide synthesis. By using a device for simultaneous suction in the new synthesizer, version SMPS 532, the solvent consumption is lowered and the time for the synthesis of 48 decapeptides is reduced from three days to just one.

Alternatively, the multiple synthesizer developed by Gausepohl et al.[75] (Abimed AMS 422) is based on the Gilson M222 laboratory robot. The one-arm apparatus, controlled by a personal computer, is equipped with six extra needles for the distribution of reagents. These enable parallel distribution of the reagents and solvents into the $6 \times 8 = 48$ reaction vessels. The bottom of each reaction vessel consists of a sintered-glass filter, so that suction of solvents can be simultaneously carried out by means of a vacuum pump and control valves (Fig. 7b). Therefore, the duration of cycles can be substantially reduced. The use of up to 50 mg of polymeric support per reaction vessel and distribution of the Fmoc-amino acids and activation reagent for the synthesis of peptide-polypropylene pins has been described.[75b] Activation was formerly achieved using benzotriazol-1-yl-oxy-tris(dimethylamino)phosphonium hexafluorophosphate (BOP)/*N*-methylmorpholine; recently the less toxic benzotriazol-1-yl-oxy-tripyrrolidinophosphonium hexafluorophosphate (PyBOP) has been used.

So far, automated multiple peptide synthesis with the help of robotic sample processors is only possible using Fmoc strategy. Open vessels prohibit the use of trifluoroacetic acid which is required in every cycle of the Boc strategy. The parallel, fully automatic synthesis of eight peptides in the range of 5–400 μmol has recently been published by Nokihara et al.[77] The reaction vessels, reservoirs and amino acid derivatives have been supplied on eight tracks. Each track was used for the synthesis of a peptide and contained the complete set of reagents for a synthesis. An arm, on which eight needles are mounted, moves in the *x*-axis for the pipetting of solvents and reagents. The software can be varied with respect to different activation methods and the scale of peptides to be synthesized. This apparatus, however, allows the parallel synthesis of only eight peptides; an expansion is not possible.

Holm and Meldal[78] reduced the time required for the manual parallel synthesis by using a semi-automatic synthesizer. Addition of solutions and solvents into 96 vessels was simultaneously carried out via 96 connections; removal of the solvents was achieved by reduced pressure. Macrosorb-SPR (7 μm) was employed as the polymeric support, Fmoc-amino acid-Dhbt (Dhbt = 3-hydroxy-4-oxo-3,5-dihydro-1,2,3-benzotriazine) esters were used as the activated derivatives, and the colored material thus produced was spectroscopically monitored. This method was used for the

synthesis of 20 tetrapeptides; 100 mg of resin was used in each vessel.[78b]

Wolfe (1978) introduced a semi-automatic synthesizer R^{a}MPS (Dupont) for the parallel synthesis of 25 peptides, each on 50 mg of polystyrene.[79] Addition of the reagents was performed manually by pipetting; suction of the solvents was simultaneously carried out in all vessels by a vacuum pump. This was the first synthesizer with which the idea of multiple peptide synthesis was realized; however, it could not compete with newly developed ones with regard to the capacity, automation, and number of peptides to be synthesized. Nonetheless, it is a moderately priced machine and probably suitable for laboratories which maximally require 25 peptides at a time.

Krchňak et al. introduced a variant for multiple synthesis using the continuous flow procedure at low pressure.[80] Here, up to ten reactors were employed, each of which contained 40–500 mg of polystyrene-divinylbenzene (1%). The solvents used for washing were simutaneously introduced into the corresponding coupling vessels by means of valves and the whole system was operated under nitrogen pressure. Each of the amino acid/1-hydroxybenzotriazole active esters prepared in situ was manually added to the corresponding reactor. The use of Fmoc and Boc strategies for peptide synthesis by this method is described.[81]

3.4. Cellulose as Support in Multiple Syntheses

Functionalized paper is also used as a polymeric support in multiple peptide synthesis. Eichler et al.[82] employed paper strips (Whatman 540) loaded with 1–2 μmol/cm^2 of N^{α}-protected amino acids. Both Boc/Bzl and Fmoc/*t*Bu strategies can be employed in this way. The peptides synthesized can either be detached from the paper, or, after removal of the side-chain protection, they can remain attached to the paper and be employed for the antibody formation test by means of ELISA on paper (dot blot). Coupling cycles, applications and advantages are comparable to those of the tea-bag synthesis (cf. Section 3.1). Further advantages include the simple operation—cutting instead of sealing and filling (as in the tea bags)—as well as lower costs through both the use of cheaper materials and low consumption of washing solvents. However, up to now there is a lack of experience of working with cellulose as a support for peptide synthesis. Moreover, low mechanical stability of the support imposes certain limitations.

Frank et al.[83, 84] described simultaneous multiple peptide synthesis on labeled cellulose paper disks as solid supports (cf. Section 3.2.2.). A peptide is synthesized on each disk using a manually operated multicolumn continuous flow synthesizer. For each coupling the paper disks (diameter 1.55 cm, Whatman 3MM) must be sorted and tightly stacked in columns (1.5 × 10 cm glass tubes). As many as 100 disks can be reacted simultaneously with the same amino acid derivative in one reactor column, but several columns can be used in parallel. Therefore this method is expecially suitable for systematic sequence alteration. A computer program furnishes the correct compilation for a minimal number of cycles. The peptides can either be employed for immunological tests while on the cellulose support, or, after detachment, as free peptides, e.g., for structure-activity relationship studies.[85] Allylic anchor groups[86] have been used for the parallel preparation of protected fragments of parathyroid hormone.[87] A yield of only 8–10 mg of crude peptide somewhat limits the application of the paper disks; owing to the specificity of the column of the apparatus, the size of the disks cannot be varied indefinitely. As already described for other automatic methods, there is a limited flexibility with respect to the synthetic strategy and coupling reagents; savings in time and chemicals are, however, great.

Cotton, the purest form of cellulose, is mechanically much more stable than paper. Lebl et al. have previously used this support for both solid-phase synthesis and in continuous flow peptide synthesis (CPPS).[88] Cotton pieces (3 cm in diameter) have been used for the multiple synthesis of overlapping fragments of CRF (corticotropin releasing factor), whereby decapeptides with yields of 4–6 mg have been obtained.[89] The washing step in this method is interesting; removal of solvents is achieved by centrifugation, similarly to the procedure used in laundry machines. This efficient method of centrifugation for peptide-resins has already been employed by Birr[36] in his automatic centrifugal reactor for peptide synthesis.

3.5. Polystyrene–Polyethylene Film, a New Procedure?

With the use of polystyrene-grafted polyethylene film (PS-PE) as a support, a further variation of multiple peptide synthesis has been accomplished.[90] In this procedure, styrene is polymerized on a polyethylene film using γ-irradiation. Like the tea bags, small pieces of film (1.5 × 3 cm) can be washed and deblocked together, while couplings are carried out simultaneously in separate vessels. Because of the covalent bonding of polystyrene to polyethylene, there are no losses of resin support, and it is also not necessary to prepare polypropylene bags by sealing.

Peptide yields per gram of PS-PE film compare with those of the tea-bag synthesis; therefore, in principle, all the uses described in Section 3.1 are also applicable in this case. Structure-activity investigations of both melittin analogues[91] and parathyroid hormone (PTH)[92] have already been carried out using peptides prepared by this procedure.

4. Multiple Cleavage

With the existing numerous concepts for multiple peptide synthesis, the question of the multiple cleavage of peptides from polymeric supports has to be examined. No problems of this kind are encountered in the case of pin synthesis (Pepscan), since the peptides remain bound to the rods during most applications, and only the side-chain protecting groups are removed. In syntheses using the Fmoc strategy, deprotection is achieved with trifluoroacetic acid. The only commercially available 'multiple cleavage apparatus' has been developed for the tea-bag method and the Boc strategy. 24 peptide–resins can be simultaneously treated with hydro-

gen fluoride.[93] The important problem of multiple cleavage is not discussed in all the other published methods.

A substantial advantage of the Fmoc strategy over the Boc strategy lies in the use of trifluoroacetic acid instead of hydrogen fluoride. Consequently, during cleavage of peptides conventional glass and plastic apparatus can be employed. In our optimized multiple procedure, we pour a slurry of the peptide–resin in deprotecting solvent (trifluoroacetic acid containing scavenger) into Pasteur pipettes which are stopped with glass wool at the outlet; the peptide solution is then separated from the resin by simple filtration under pressure, just by pressing the suction balls of the pipettes. Finally, the peptide is precipitated, as usual, with ether. Owing to the large number of peptides, the centrifuges and lyophilizers employed should have large capacities.

5. Multiple Analysis—a Challenge

Ever since Merrifield developed the synthesis of peptides on polymeric supports, one question which has always arisen, is, 'how pure' are the synthetic products. The 'Merrifield synthesis' could achieve its ultimate goal only with the advent of HPLC and the purification possibilities it offers (cf. also Ref. [28a]). Besides requiring the highest possible separation performance in the chromatographic methods, multiple peptide analysis also calls for the treatment of a large number of samples in a short time.

Reversed-phase HPLC with automatic HPLC-sample distributor and on-line UV spectrometer[49, 94] is an absolute prerequisite. Similarly, fully automatic peptide hydrolysis with on-line amino acid analysis[40, 43, 95] is also required. Commercially available capillary zone electrophoresis (CZE) with an autosampler[96, 97] offers a new possibility for the fast, high-resolution analytical investigation of a large number of synthetic peptides.[98]

One of the best methods for on-line peptide analysis is the combination of LC (or CZE) and mass spectrometry; a combination which is rapidly becoming a routine procedure.[40, 42, 99] High sensitivity, mild ionization and detection of high molecular masses are achieved by electro- and ion-spray ionization. Hence, these methods are suitable for the analysis of peptide solutions (Fig. 8).[98, 100, 101] A microbore-HPLC unit is preferable as the HPLC component because of its low flow rate, since otherwise a solvent at a flow rate of more than 200 μL/min can no longer be removed by existing vacuum systems. A normal HPLC and a T-splitter can also be used; a combination whereby UV and mass spectra of all the peaks are simultaneously recorded. By using an automatic sample distributor without on-line HPLC, up to 60 peptide solutions can be consecutively analyzed by ion-spray mass spectrometry per hour.

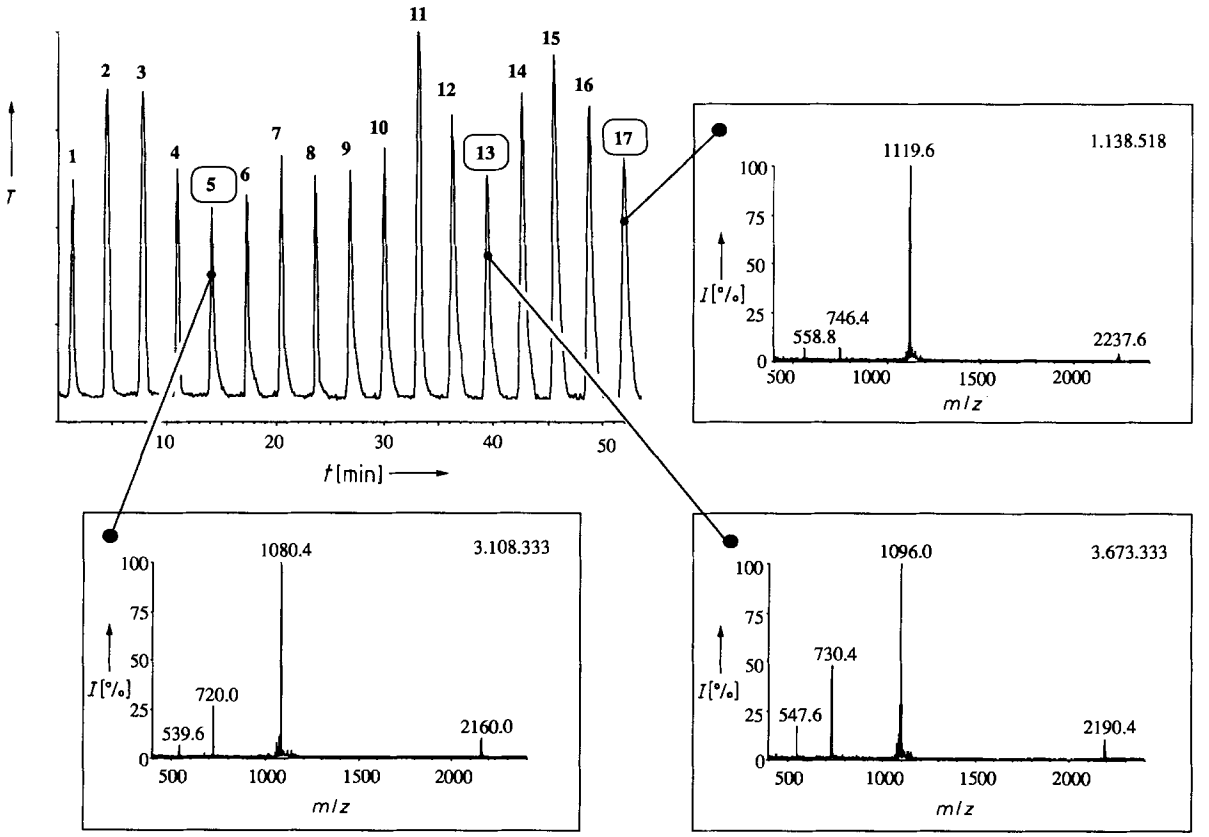

Fig. 8. Analysis of 17 peptide samples by ion-spray mass spectrometry within 55 min [100]. Injection of the dissolved peptides (50 pmol) is performed with an autosampler every 1–3 min. The total ion stream is captured in the spectrometer, and the individual peaks can be analyzed at the end of the run. This ionization method, which is especially suitable for peptides and proteins, produces multiply charged molecular ions. The following masses have been found: Peptide 5: 2159 at $(M + H)^{\oplus}$ 2160, $(M + 2H)^{2\oplus}$ 1080.4, $(M + 3H)^{3\oplus}$ 720.0, $(M + 4H)^{4\oplus}$ 539.6. Peptide 13: 2189.4 at $(M + H)^{\oplus}$ 2190.4, $(M + 2H)^{2\oplus}$ 1096.0, $(M + 3H)^{3\oplus}$ 730.4, $(M + 4H)^{4\oplus}$ 547.6. Peptide 17: 2236.6 at $(M + H)^{\oplus}$ 2237.6, $(M + 2H)^{2\oplus}$ 1119.6, $(M + 3H)^{3\oplus}$ 746.4, $(M + 4H)^{4\oplus}$ 558.8.

6. Peptide Libraries—or: How One Synthesizes Thousands of Peptides

Peptide libraries can consist of thousands of individual peptides which are synthesized as a mixture of peptides or as separate individual peptides. The review in Table 3 summarizes the studies published on this important subject so far. The pharmaceutical industry hopes to elucidate a large number of the novel lead structures by means of these peptide libraries.

parent peptide. Such a procedure can offer great advantages for the development of synthetic vaccines.

Multiple substitutions with conservation of the so-called anchor positions have also been used for the identification of octa- and nonapeptide motifs of the MHC-I molecule-bound peptides which are recognized by cytotoxic T-lymphocytes.[27a, 44]

The method of Houghten et al. for the construction of a peptide library[105] is based on the same principle and employed for the identification of a definite, biologically active

Table 3. Review of the methods for contructing peptide libraries containing more than 1000 peptides.

Methods	Light-controlled synthesis	Expression in phages	Separation methods	Library of free peptides	Mixotopes
Polymer	Aminated glass slides	pIII-protein of fusion-phages	Polymeric beads	PS-DVB	PS-DVB
Procedure	Photolabile N_α protecting group (Nvoc), removal by a process of photolithography, HOBt/DIC coupling	Randomly modified phages [$(NNK)_6$-insertion in pIII-protein] expression of hexapeptides	SPS with Fmoc or Boc strategy, any activation, separation of beads before the coupling, deprotection and washing steps are carried out together	Tea bag SPS, Fmoc or Boc strategy, any activation, coupling of amino acid mixtures at definite positions	SPS, Fmoc or Boc strategy, any activation, coupling of amino acid mixtures at definite positions
Screening	Fluorescence labeled antibodies are detected by fluorescence microscopy	Selection and subcloning of phages, recognition by antibody	Labeled antibodies catalyze a color-reaction and stain the polymeric beads after binding	Combination of biotest and the next synthetic cycle	Not necessary
Identification	Synthesis on localized spots, spatially addressable	DNA sequencing of the genome of phages	Protein sequencing from positively identified peptide-beads	Defined peptide sequences in the last bioassay	Defined synthetic mixtures
Application	Screening of antibodies or soluble receptors	Screening of antibodies or soluble receptors	Screening of antibodies or soluble receptors	Screening of antibodies or soluble receptors	Vaccination, or immunization
Reference	[110]	[108, 109a]	[106, 107]	[105]	[104]

SPS = solid-phase peptide synthesis.

The first publications on parallel, non-separated peptide synthesis appeared in 1990.[102] Inspired by the 'mixed' synthesis of oligonucleotides,[103] mixtures of different amino acids—instead of a single amino acid derivative—have been activated and coupled at definite positions. The resulting analogues have been separated by preparative HPLC, analyzed and characterized; the parallel synthesis of six analogues has been described.[102] It seems that this method is very promising if small amounts ($<0.1-1$ mg) of analogues of a peptide are required. HPLC isolation of the components effects their purification at the same time. Problems are encountered with analogues having very similar structure and containing by-products which cannot be separated simply by RP-HPLC. This phenomenon is mostly unpredictable, especially when several positions are simultaneously substituted, and in the case of larger peptides when their chromatographic behavior is influenced by the formation of secondary structure. Moreover, a structurally dependent, non-uniform coupling of different amino acids leads to dissimilar product distribution.

Gras-Masse et al.[104] have synthesized 7.5×10^5 analogues of the HIV-gp120 sequence. Each peptide consists of 22 amino acids, the substituted positions reflect the variable amino acids of different HIV isolates, and the conserved positions are maintained. These so-called 'mixotopes'[104] are therefore not accidental sequences, but analogues of the sequence. For an oligopeptide having a certain length, the 'anchor amino acids', 'defined positions' and 'mix positions' are distinguished. 'Anchor amino acids' characterize the already known, essential positions of a sequence and are found in all peptides. The number of defined positions determines the number of peptide mixtures which were prepared by Houghten using the tea-bag synthesis.[49-51] For a defined position, 20 so-called 'sublibraries' are needed, each containing one of the 20 amino acids at this position. Consequently two defined positions lead to 400 and three to 8000 peptide mixtures. If amino acids other than the proteinogenic ones are also used, the number of resulting peptides increases rapidly. The remaining positions (mix positions) are coupled as a mixture of all derivatives. Therefore, in the case of 20 amino acids and n mix positions, each sublibrary contains a mixture of 20^n peptides.

Neither an analysis nor a separation is necessary for the identification of a biologically active peptide, only the biological test determines which sublibrary (i.e., which tea bag) contains the active peptide. The thus determined defined position becomes an extra new 'anchor amino acid' in the next synthetic cycle or 'peptide book' of the oligopeptide library. Consequently, a multiple peptide synthesis is necessary for each unknown amino acid position (Table 4).

The sensitivity of the biological test system is a limiting factor for the number of mix positions, which, among other

Table 4. Dependency of the number and content of individual peptides in a peptide mixture (for preparing peptide libraries) on the number of variable positions.

Number of variable positions	Six	Five	Four	Three	Two	One	None [a]
For 20 amino acids:							
Number of peptides in the mixture	64000000	3200000	160000	8000	400	20	
Amount of one peptide in 1 mg product with a mass of 660 amu (hexapeptide)	16 pg 25 fmol	300 pg 0.5 pmol	6 ng 9.4 pmol	125 ng 190 pmol	2.5 μg 4 nmol	50 μg 75 nmol	1 mg 1.5 μmol
Molarity of one peptide, 1 mg mL^{-1}	2.5×10^{-11}	5×10^{-10}	9×10^{-9}	1.9×10^{-7}	4×10^{-6}	8×10^{-5}	1.5×10^{-3}
For 40 amino acids (including D-amino acids):							
Number of peptides in the mixture	4096000000	102400000	2560000	64000	1600	40	
Amount of one peptide in 1 mg product with a mass of 660 amu (hexapeptide)	0.25 pg 0.4 fmol	10 pg 15 fmol	390 pg 590 fmol	16 ng 23 pmol	625 ng 1 nmol	25 μg 40 nmol	
Molarity of one peptide, 1 mg mL^{-1}	4×10^{-13}	1.5×10^{-11}	5.9×10^{-10}	2.3×10^{-8}	10^{-6}	4×10^{-5}	

[a] Normal synthesis.

things, is determined by the binding constants. Having, e.g., 5 mix positions, 1 mg of a peptide mixture contains only 300 pg of each individual peptide. In the case of hexapeptide mixtures in solutions of 1 mg per mL, this corresponds to a concentration of 5×10^{-10} mol L^{-1} (Table 4); therefore, a test is only meaningful in the case of receptor systems with very high affinity.

Well-sorted peptide libraries offer the possibility for discovering active analogues, ligands for receptors or antibodies, and for testing cross-reactivities. Also non-polymer-bound peptide mixtures make it possible to carry out investigations on membrane-bound proteins. If, however, protein segments are to be investigated, it becomes an immensely time-consuming procedure. Problems of the presence of different percentages of various analogues, which are due to the non-uniform couplings, also arise in this case.

In order to avoid these problems, Furka et al.[106] and, later, Lam et al.[107] separated the polymeric supports for the coupling of each of the 20 amino acid derivatives. Uniform couplings can, therefore, be achieved, since the competition between slow and fast couplings no longer exists. Subsequently, the polymer was again mixed, washed and the *N*-terminal protecting group was jointly removed. For the next coupling, the distribution of the polymer in each vessel containing the 20 amino acids is purely statistical. Initially, Furka et al.[106] demonstrated this proportional-mixing method for the synthesis, cleavage, and chromatographic separation of nine tetrapeptides which have been identified by sequencing. This method is suitable for the manual synthesis of a very large number of resin-bound oligopeptides within a relatively short time.

Lam et al.[107] likewise established a library of oligopeptides which remained bound to the polymeric support and were only freed from the side-chain protecting groups. A separation step is not necessary; only the biological activity of the analogues is important. If the polymer is used in the form of beads, only a defined peptide and its failure sequence, determined by the conditions of synthesis, are found on every bead. If, e.g., the peptide of this single bead is recognized by an antibody, the polymer-peptide-antibody complex can be stained by a second antibody carrying a fluorophore or an enzyme, and can hence be distinguished from the polymeric beads containing non-bound peptides. Under a microscope, the positively identified peptide-polymers are separated from the beads having non-bound peptide and the peptide sequence is determined by the Edman degradation. The method is highly efficient and practicable; it can be carried out in every peptide laboratory using standard methods and without the need for elaborate apparatus.

With respect to the scale of synthesis, one should be aware of the following limitations in the use of proportional-mixing methods. The usual loading of 0.5 mmol/g signifies about 200 pmol of peptide per polymeric bead. The number of polymeric beads should be at least ten times higher than the number of peptides, since the loading of each bead fluctuates and, practically, more than one bead is required for the detection and analysis. Assuming that each time only ten beads (200 mesh) are loaded with a defined peptide, and by using only 20 proteinogenic amino acids in several positions, one obtains almost 10 g of peptide–resin for a pentapeptide library, 150 g for the hexapeptide, 3 kg for the heptapeptide, and over 50–100 kg for the octapeptide libraries. If at the same time D-amino acids are also to be used in several positions, then for the large libraries tons of resin will be required. This unreasonable situation can be circumvented by the construction of sublibraries with firm and defined positions, as well as by the use of very small polymeric beads. These possibilities are limited by the sensitivity and capacity of the biological tests and instrumental analysis.

In the molecular biology laboratories of Scott and Smith,[108] and Delvin et al.[109] a completely different kind of epitope library has been developed. Fusion-phages in *E. coli* are transformed through – $(KKN)_{15}$ or $(KKN)_6$ –, where K corresponds to a mixture of all four deoxynucleotides and N to a mixture of guanidine and thymidine. Every triplet KKN can code for all of the 20 amino acids, but only for one stop-codon. The production takes place in p-III protein which is coded by phages and which is expressed at a defined position on the surface of the phages. Identification of the active peptide sequence is again achieved at the DNA level. Phages which bind to the biotin-labeled antibody are isolated over streptavidin (affinity purification), multiplied, and their DNA is isolated and sequenced. Since the pattern of the restriction enzymes of phages and the production site are known, sequencing is less elaborate than expected. This method can represent a simpler procedure for the gene technology laboratories in need of epitope libraries. To what extent interactions with the surface of phages, as well as

changes in the secondary structure of ligands in proteins can impair the desired recognition, however, must be further investigated.

The parallel synthesis of thousands of oligopeptides at defined sites and on the micromolar scale is possible by the method of Fodor et al.[110] In this recently reported novel concept,[111] photolabile nitroveratryloxycarbonyl is used for the amino protection. Irradiation and hence deprotection of a surface area of only 100×100 μm is possible by means of stencils; following this the coupling of the next amino acid is carried out. Suitable choice and the combination of stencils enables the synthesis of 100×100 peptides per cm^2. Since regulation of the mask is carried out analogously to the process of photolithography, it is possible to accurately assign the positions. Detection is achieved in a biological test system, e.g., by fluorescence microscopy using antibodies carrying a fluorescence label. The precision of the method, as well as the efficiency and the application of photolithographic techniques in peptide synthesis, are impressive. However, incompleteness of the photolytic removal of protecting groups in the synthesis of large peptides could pose a problem. Establishment of the method as routine, however, is simply not possible, since it involves large investments in both equipment and personnel. It can however be assumed that this microtechnique will bring advances in the area of biosensor research.

The methods for the construction of peptide libraries introduced in this section open up a new dimension in peptide synthesis. The selection ensues from the biological test systems. For this purpose, the peptides used are often bound to polymers, either *C*-terminally to the polymeric support, or to a protein from phages. This imposes two restrictions: firstly, blocking of the *C*-terminus must not be restrictive, secondly, the biological test system must be active in the soluble or solubilized form. Both prerequisites are often fulfilled for antigen–antibody interactions. All these methods have proven successful, especially in the screening and identification of binding sites of monoclonal antibodies.

Tests on membrane receptors or intact cells, however, require mixtures of free peptides, and these should contain the individual peptides, preferably in detectable amounts. So far, only Houghten's method[105] offers this possibility, but for this method a substantially greater elaboration is required.

7. Natural Peptide Libraries and the Future of Multiple Synthesis Methods

Peptide libraries have not been invented by the human. Nature impressively demonstrates the interaction of individual peptides from natural oligopeptide libraries with highly specifically differentiated proteins from the body's own and foreign sources. By isolation and so-called 'pool-sequencing' it was recently shown to be possible to determine the individual, specific sequence motifs of naturally processed self-peptides for a few defined MHC class I alleles.[27a] Thousands of these self-peptides appear continuously as degradation products of the body's own cellular proteins on the cell surface, bound to a cleft of the major histocompatibility complex (MHC) molecules. Membrane-bound proteins of MHC class I molecules present short peptides to the killer-cell receptors (cytotoxic T-lymphocytes, CTL). The MHC class II proteins present somewhat longer peptides to the T-helper cell receptors, by which the B-cells become prone to stimulation for differentiation and subsequent antibody production. The binding relationships in the cleft of MHC class I molecules are well established.[112] The sequence motifs of the highly complex, natural peptide mixtures show certain anchor amino acids (cf. Fig. 9) in constant positions of the octa- or nonapeptides. The amino acid side chains of the anchors fit into the allele-specific pockets of the MHC cleft, whilst among the other positions a large variability of the amino acids often occurs.[27a]

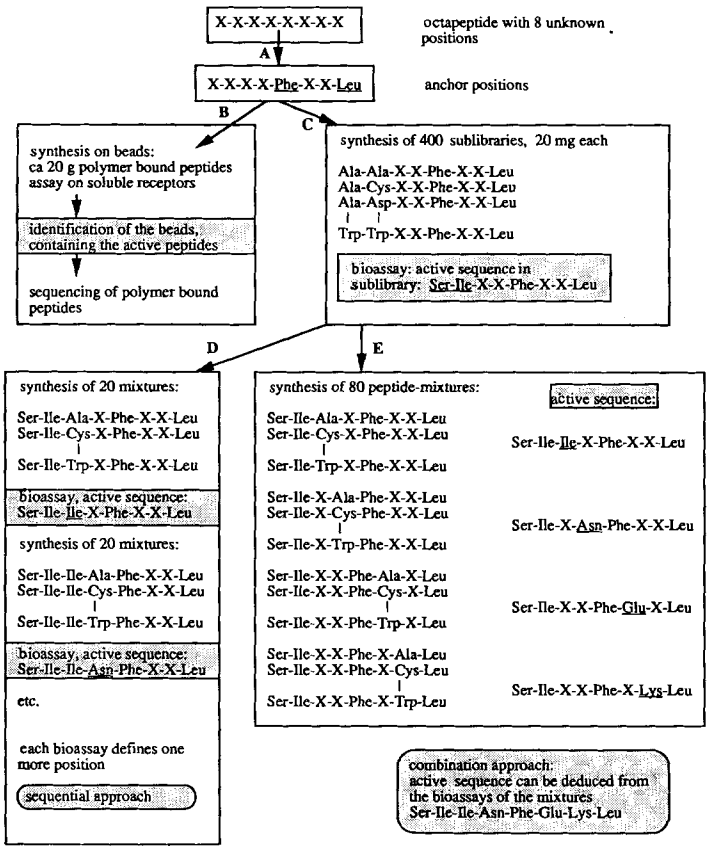

Fig. 9. Possible identification of active sequences exemplified by K^b-restricted CTL-epitope ovalbumin 258–267. Binding to MHC class I receptor of the killer cells serves as the bioassay. Positions 5 (Phe) and 8 (Leu) are known (from the literature) as the anchor positions for binding to the cleft of the MHC class I molecule (**A**) [27a]. Construction of a corresponding peptide library can be performed either by the proportionation method (**B**) or by means of free peptides in sublibraries (**C**). For this purpose 400 sublibraries have to be separated, each with two defined sequences and four variable positions (X). Identification of the variable positions can be achieved either sequentially (**D**) or by combination (**E**). In both cases, 80 further peptide mixtures will be necessary.

A selection could therefore be achieved with the help of two consecutive recognition processes from our body's extensive peptide libraries. First, the binding in the MHC cleft is specific for definite motifs in the peptide sequences, and second, by the cell–cell contact through the ternary interactions of MHC, peptide and T-cell receptor it will be decided whether the origin of presented peptide fragment is from the body itself or a foreign source. The cell which, e.g., carries a

foreign viral peptide is then lysed by the killer cells in the immune system, or it initiates a T-helper cell-mediated antibody reaction against a shell protein of the virus.

The peptide chemist assumes a decisive role in the interdisciplinary research projects discussed in the introductory sections. He has special experience and recognizes the possibilities for new variants of multiple synthesis methods and new analytical procedures. Therefore, he decides in most of the cases which kind of structural variations are to be carried out. The valuable 'tools' which the peptide chemists have so far put at the disposal of pharmacology, immunochemistry, molecular biology, physiology and biophysics have been tailored and have contributed to rapid development in these fields. The successful use of multiple synthesis methods will add new areas to these research fields, whose experimental feasibility seemed utopic until recently.

In this review, the largest fields for the application of products obtained by multiple peptide synthesis could only be briefly referred to; the following must also be mentioned. The development of vaccines can be performed on the molecular level, by investigation of the above-mentioned naturally processed and presented peptides from viral, bacterial and the body's own proteins.[27b,c] The results of bioassays of natural isolates and synthetic peptide mixtures can be compared. By systematic variation and substitution of amino acids the folding tendency of the larger peptides can be studied experimentally, rapidly and more exactly. Furthermore, rapid development of enzyme inhibitors may be achieved, and the screening of new enzymes and enzyme specificities can be carried out by the incorporation of backbone modifications and unusual amino acids.

Multiple synthesis methods will undoubtedly offer surprising new possibilities in many areas including biosensors, and above all, automation for the screening of lead structures in pharmaceutical research.

Thanks are due to the Bundesministerium für Forschung und Technologie, the Deutsche Forschungsgemeinschaft (SFB 323) and the Fonds der Chemischen Industrie for financial support of the project oriented research in multiple peptide synthesis. The multiple methods of peptide synthesis and analysis could not have been achieved in our laboratory without the engagement, substantial ideas and experimental contributions of K.-H. Wiesmüller, F. Gombert, R. Spohn, W. Tröger, H. Dürr, H. Drechsel, E. Hoffmann, J. Metzger, S. Stefanovic and W. Beck. A. G. Beck-Sickinger thanks the Deutsche Forschungsgemeinschaft for a research stipend.

Received: October 21, 1991 [A 858 IE]
German version: Angew. Chem. 104 (1992) 375
Translated by Dr. B. Hemmasi, Tübingen (FRG)

[1] *Peptides 1988, Proc. 20th Eur. Pept. Symp.* (Eds.: G. Jung, E. Bayer), de Gruyter, Berlin, **1989**; and references cited therein.

[2] *Peptides 1990, Proc. 21st Eur. Pept. Symp.* (Eds.: E. Giralt, D. Andreu), Escom, Leiden, **1991**.

[3] *Peptides: Chemistry and Biology, Proc. 10th Am. Pept. Symp.* (Ed.: G. R. Marshall), Escom, Leiden, **1988**.

[4] a) *Peptides, Chemistry, Structure and Biology, Proc. 11th Am. Pept. Symp.* (Eds.: J. E. Rivier, G. R. Marshall), Escom, Leiden, **1990**; b) *Peptides, Chemistry and Biology Proc. 12th Am. Pept. Symp.* (Eds.: J. A. Smith, J. E. Rivier), Escom, Leiden, **1992**.

[5] a) *Innovation and Perspectives in Solid Phase Synthesis: Peptides, Polypeptides and Oligonucleotides, Macro-Organic Reagents and Catalysts – 1990* (Ed.: R. Epton), SPCC, Birmingham, **1990**; b) *Innovation and Perspectives in Solid Phase Synthesis and Related Technologies: Peptides, Polypeptides and Oligonucleotides, 1991* (Ed.: R. Epton), Intercept, Andover, **1992**.

[6] a) *Peptide Chemistry 1987, Proc. 25th Symp. Pept. Chem.* (Eds.: T. Shiba, S. Sakakibara), Protein Research Foundation, Osaka, **1988**; b) *Peptide Chemistry 1988, Proc. 26th Symp. Pept. Chem.* (Ed.: M. Ueki), Protein Research Foundation, Osaka, **1989**.

[7] a) *Forum Peptides, Proc. 1st Int. Forum Pept.* (Eds.: B. Castro, J. Martinez), Centre de Pharmacologie—Endocrinologie, Montpellier, **1984**; b) *Second Forum on Peptides, Vol. 174* (Eds.: A. Aubry, M. Marraud, B. Vitoux), John Libbey Eurotext, London, **1989**.

[8] *The Peptides: Analysis, Synthesis, Biology, Vol. 1–9.* (Ed.: J. Meienhofer et al), Academic, London, **1979–1987**.

[9] a) D. C. Roberts, F. Vellaccio in [8], *Vol. 5*, **1983**, p. 341–449; b) *Peptides* (Eds.: B. Castro, B. Penke, A. Török), de Gruyter, Berlin, **1988**, p. 409–417.

[10] a) C. Toniolo, *Biopolymers* **1989**, *28*, 247–257; b) *Int. J. Pept. Protein Res.* **1990**, *35*, 287–300.

[11] M. Crisma, G. Valle, G. M. Bonora, C. Toniolo, F. Lelj, V. Barone, F. Fraternali, P. M. Hardy, H. L. S. Maia, *Biopolymers* **1991**, *31*, 637–641.

[12] J. Gante, *Synthesis* **1989**, 405–413.

[13] H. Heimgartner, *Angew. Chem.* **1991**, *103*, 271–297; *Angew. Chem. Int. Ed. Engl.* **1991**, *30*, 297–323.

[14] K. Noda, Y. Shimohigashi, N. Izumiya in [8], *Vol. 5*, **1983**, p. 285–339.

[15] a) *Chemistry and Biochemistry of the Amino Acids* (Ed.: G. C. Barrett), Chapman and Hall, London, **1985**; b) *Amino Acids: Chemistry, Biology and Medicine* (Eds.: G. Lubec, G. A. Rosenthal), Escom, Leiden, **1990**.

[16] R. M. Freidinger, *Trends Pharm. Sci. Rev.* **1989**, *10*, 270–274.

[17] a) A. F. Spatola in *Chemistry and Biochemistry of Amino Acids, Peptides and Proteins Vol. 7* (Ed.: B. Weinstein), Dekker, New York, **1983**, p. 267–357; b) D. B. Shorman, A. F. Spatola, W. S. Wire, T. F. Burks, T. M. D. Nguyen, P. W. Schiller, *Biochem. Biophys. Res. Commun.* **1989**, *162*, 1126–1132.

[18] a) D. Tourwé, *Janssen Chim. Acta* **1985**, 3–18; b) J. S. Davies in *Amino Acids and Peptides, Vol 21* (Ed.: J. H. Jones), R. Soc. Chem., London, **1990**, p. 129–173.

[19] A. Aubry, D. Bayenil, J.-P. Mangeot, J. Vidal, S. Sterin, A. Collet, A. Lecoq, M. Marraud, *Biopolymers* **1991**, *31*, 793–801.

[20] a) M. Goodman in [4a], p. 3–29; b) J. M. Bormann, M. Goodman, *Int. J. Pept. Protein Res.* **1984**, *23*, 610–620; c) L. Gazerro, M. Pinori, A. S. Verdini in [5a], p. 403–412.

[21] N. Delaet, M. Elseviers, D. Tourwé, G. Van Binst in [5a], p. 473–480.

[22] G. Jung, A. G. Beck-Sickinger, H. Dürr, W. Gaida, G. Schnorrenberg, *Biopolymers* **1991**, *31*, 613–619.

[23] M. Elseviers, L. Van Der Auwera, H. Pepermans, D. Tourwé, G. Van Binst, *Biochem. Biophys. Res. Commun.* **1988**, *154*, 515–521.

[24] a) B. A. Morgan, J. A. Gainor, *Annu. Rep. Med. Chem.* **1989**, *24*, 243–252; b) S. L. Harbeson, D. H. Rich, *J. Med. Chem.* **1989**, *32*, 1378–1392.

[25] a) G. Hölzemann, *Kontakte (Darmstadt)* **1991**, 3–12; b) G. Hölzemann, *ibid.* **1991**, 55–63.

[26] a) R. Hirschmann, *Angew. Chem.* **1991**, *103*, 1305–1327; *Angew. Chem. Int. Ed. Engl.* **1991**, *30*, 1278–1301; b) W. F. Degrado, *Adv. Protein Chem.* **1988**, *39*, 51–124.

[27] a) K. Falk, O. Rötzschke, S. Stevanović, G. Jung, H.-G. Rammensee, *Nature* **1991**, *351*, 290–296; b) K.-H. Wiesmüller, G. Jung, G. Hess, *Vaccine* **1989**, *7*, 29–33; c) K. Deres, H.-J. Schild, K.-H. Wiesmüller, G. Jung, H.-G. Rammensee, *Nature* **1989**, *342*, 561–564; d) K.-H. Wiesmüller, K. Deres, H. Schild, H. G. Rammensee, G. Jung in [2], p. 857–859; e) H. Schild, K. Deres, K.-H. Wiesmüller, G. Jung, H.-G. Rammensee, *Eur. J. Immunol.* **1991**, *21*, 2649–2654.

[28] a) E. Bayer, *Angew. Chem.* **1991**, *103*, 117–133; *Angew. Chem. Int. Ed. Engl.* **1991**, *30*, 113–129; b) W. Rapp, L. Zhang, R. Häbich, E. Bayer in [1], p. 199–201.

[29] T. Wieland, M. Bodansky, *The world of peptides, A brief history of peptide chemistry*, Springer, Berlin, **1991**.

[30] a) F. Anderer, *Z. Naturforsch. B* **1963**, *18*, 1010–1014; b) *Biochim. Biophys. Acta* **1963**, *71*, 246–248.

[31] a) F. C. Bernstein, T. F. Koetzle, G. J. B. Williams, E. F. Myer, Jr., M. D. Brice, J. R. Rodgers, O. Kennard, T. Shimanouchi, M. Tarsani, *J. Mol. Biol.* **1977**, *112*, 535–542; b) M. G. Dayhoff, R. M. Schwartz, H. R. Chen, W. C. Barker, L. T. Hunt, B. C. Orcott, *Nucleic Acid Sequence Databank* **1981**, *DNA 1*, 51–58; c) *The Swiss Protein Sequence Databank, EMBL, EMBL Data Library and Amos Bairoch* (Geneva University).

[32] R. B. Merrifield, *J. Am. Chem. Soc.* **1963**, *85*, 2149–2154.

[33] a) R. B. Merrifield, *Adv. Enzymol. Relat. Areas Mol. Biol.* **1969**, *32*, 221–296; b) G. Barany, R. B. Merrifield in [8], *Vol. 2.*, **1979**, p. 1–284.

[34] J. M. Stewart, J. D. Young, *Solid Phase Peptide Synthesis*, Pierce Chemical Company, New York, **1984**.

[35] E. Atherton, R. C. Sheppard, *Solid Phase Peptide Synthesis, a Practical Approach*, Oxford University Press, Oxford, **1989**.

[36] C. Birr, *Aspects of the Merrifield Peptide Synthesis*, Springer, Berlin, **1979**.

[37] E. Wünsch et al., *Methoden Org. Chem.*, (Houben-Weyl) 4th Ed. **1974**, Vol. 15a, b.

[38] a) H.-D. Jakubke, H. Jeschkeit, *Aminosäuren, Proteine, Peptide, Eine Einführung* Akademie Verlag, Berlin, **1982**; b) J. Jones, *The Chemical Peptide Synthesis*, University Press, Oxford, **1991**.

[39] M. Bodansky, *Peptide Chemistry, A Practical Textbook*, Springer, Berlin, **1988**.

[40] a) *Techniques in Protein Chemistry* (Ed.: T. E. Hugli), Academic, San Diego, **1989**; b) *Techniques in Protein Chemistry II* (Ed.: J. J. Villafranca), Academic, San Diego, **1991**.

[41] a) *Modern Methods in Protein Research – Review Articles Vol. 2* (Ed.: H. Tschesche), de Gruyter, Berlin, **1985**; b) F. Lottspeich in [41a], p. 347–352; c) *Methods in Protein Sequence Analysis* (Ed.: B. Wittmann-Liebold), Springer, Berlin **1989**; d) *Advanced Methods in Protein Microsequence Analysis* (Eds.: B. Wittmann-Liebold, J. Salnikow, V. A. Erdmann), Springer, Berlin, **1986**.

[42] a) A. P. Bruins, T. R. Covey, J. D. Henion, *Anal. Chem.* **1987**, *59*, 2642–2646; b) A. P. Bruins, L. O. G. Weidolf, J. D. Henion, W. L. Buddle, *ibid.* **1989**, *59*, 2647–2652.

[43] a) K. Ashman, A. Bosserhoff in [41a], p. 155–172; b) F. G. Nolan, N. J. Dovichi, *Anal. Chem.* **1987**, *59*, 2803–2805; c) W. A. König in *Modern Methods in Protein and Nucleic Acid Research—Review Articles* (Ed.: H. Tschesche), de Gruyter, Berlin, **1990**, p. 213–230.

[44] a) O. Rötzschke, K. Falk, K. Deres, H. Schild, M. Norda, J. Metzger, G. Jung, H.-G. Rammensee, *Nature* **1990**, *348*, 252–254; b) O. Rötzschke, K. Falk, S. Stevanović, G. Jung, P. Walden, H.-G. Rammensee, *Eur. J. Immunol.* **1992**, in press; c) K. Falk, O. Rötzschke, K. Deres, J. Metzger, G. Jung, H.-G. Rammensee, *J. Exp. Med.* **1992**, in press; d) O. Rötzschke, K. Falk, H. Schild, M. Norda, H.-G. Rammensee, K. Deres, J. Metzger, S. Stevanović, K.-H. Wiesmüller, G. Jung in [4b], pp. 832–834.

[45] a) H.-P. Weil, A. G. Beck-Sickinger, J. Metzger, S. Stevanović, G. Jung, M. Josten, H.-G. Sahl, *Eur. J. Biochem.* **1990**, *194*, 217–223; b) *Nisin and Novel Lantibiotics* (Ed.: G. Jung, H.-G. Sahl), Escom, Leiden, **1991**.

[46] A. G. Beck-Sickinger, G. Jung, W. Gaida, H. Köppen, G. Schnorrenberg, R. Lang, *Eur. J. Biochem.* **1990**, *194*, 449–456.

[47] F. Gombert, W. Blecha, M. Tähtinen, A. Ranki, S. Pfeiffer, W. Tröger, R. Braun, N. Müller-Lantzsch, G. Jung, H. Rübsamen-Waigmann, K. Krohn, *Virology* **1990**, *176*, 458–466.

[48] H. Rotering, A. G. Beck-Sickinger, K.-H. Wiesmüller, W. Dorner, G. Jung, *J. Infect. Dis.*, submitted.

[49] R. A. Houghten, *Proc. Natl. Acad. Sci. USA* **1985**, *82*, 5131–5135.

[50] R. A. Houghten, *Trends Biotechnol.* **1987**, *5*, 322–324.

[51] R. A. Houghten, J. H. Cuervo, J. M. Ostresh, M. K. Bray, N. D. Frizzell in [3], p. 166–172.

[52] A. G. Beck-Sickinger, H. Dürr, G. Jung, *Pept. Res.* **1991**, *4*, 88–92.

[53] a) J. Ježek, R. A. Houghten in [2], p. 74; b) R. A. Houghten, N. Lynam in [1], p. 214–216.

[54] a) K. Büttner, O. Arad, J. Ostresh, R. A. Houghten in [5a], p. 325–336; b) O. Arad, R. A. Houghten, *Pept. Res.* **1990**, *3*, 42–50.

[55] Z. M. Ruggeri, R. A. Houghten, S. R. Russel, T. S. Zimmermann, *Proc. Natl. Acad. Sci. USA* **1986**, *83*, 5708–5712.

[56] J. H. Cuervo, B. Rodriquez, R. A. Houghten in [4a], p. 124–126.

[57] a) A. G. Beck-Sickinger, W. Gaida, G. Schnorrenberg, R. Lang, G. Jung, *Int. J. Pept. Protein Res.* **1990**, *36*, 522–530; b) A. G. Beck-Sickinger, W. Gaida, G. Schnorrenberg, G. Jung in [2], p. 646–648; c) A. G. Beck-Sickinger, W. Gaida, G. Schnorrenberg, R. E. Lang, J. Metzger, G. Jung in [5a], p. 447–451.

[58] a) C. Pinilla, J. R. Appel, R. A. Houghten in [2], p. 860–861; b) G. L. Jones, H. Edmundson, R. Lord, L. Spencer, R. Mollard, A. Saul in [5a], p. 497–510; c) R. A. Houghten, J. R. Appel, J. M. Sitarik in [3], p. 543–546; d) W. Van't Hof, P. C. Driedijk, M. van der Berg, A. G. Beck-Sickinger, G. Jung, R. C. Aalberse, *Mol. Immunol.* **1991**, 1225–1232.

[59] a) N. Zimmermann, A. G. Beck-Sickinger, G. Folkers, S. Krickl, I. Müller, G. Jung, *Eur. J. Biochem.* **1991**, *200*, 519–528; b) G. Folkers, S. Krickl, S. Trumpp-Kallmeyer, *Arch. Pharm. (Weinheim Ger.)* **1989**, *322*, 409–413; c) A. G. Beck-Sickinger, G. Jung in *Nisin and Novel Lantibiotics* (Eds.: G. Jung, H.-G. Sahl), Escom, Leiden **1991**, p. 218–230.

[60] a) R. A. Houghten, S. T. DeGraw, *J. Chromatogr.* **1987**, *386*, 223-228; b) R. A. Houghten, J. M. Ostresh, *Biochromatography* **1987**, *2*, 80–84; c) K. Büttner, J. Ostresh, R. A. Houghten in [4a], p. 423–425.

[61] a) K. Büttner, R. A. Houghten in [2], p. 478–480; b) S. E. Blondelle, K. Büttner, R. A. Houghten in [2], p. 738–739.

[62] H. M. Geysen, R. H. Meloen, S. J. Barteling, *Proc. Natl. Acad. Sci. USA* **1984**, *81*, 3998–4002.

[63] W. M. M. Schaaper, H. Lankhof, D. J. A. Meijer, W. C. Puijk, R. H. Meloen in *Peptides 1986, Proc. 19th Eur. Pept. Symp.* (Ed.: D. Theodoropoulos), de Gruyter, Berlin, **1987**, p. 577–580.

[64] J. M. Middeldorp, R. H. Meloen, *J. Virol. Methods* **1988**, *24*, 147–159.

[65] a) H. M. Geysen, S. J. Rodda, T. J. Mason, G. Tribbick, P. G. Schoofs, *J. Immunol. Methods* **1987**, *102*, 259–274; b) H. M. Geysen, S. J. Rodda, T. J. Mason, *Mol. Immunol.* **1986**, *23*, 709–715.

[66] K. Singh, P. Sheridan, L. Aldwin, D. E. Nitecki in [4a], p. 898–899.

[67] a) F. O. Gombert, R. Schaude, W. Tröger, G. Jung, H. Rübsamen-Waigmann, W. Blecha, S. Pfeiffer, K. Krohn, M. Tähtinen, V. Ovod, A. Ranki, L. Shi, P. Wernet in [2], p. 872–875; b) U. Rudén, P. A. Broliden, Z. Trojnar, B. Wahren in [2], p. 911–913; c) M. Korkolainen, A. Närvänen, V. Varnies, F. Lillo, S. Kontlo, R. Resculdani, A. Visconti, M.-L. Huhtala in [5a], p. 511–518.

[68] a) R. Van der Zee, W. Van Eden, R. H. Meloen, A. Noordzij, J. D. A. Van Embden, *Eur. J. Immunol.* **1989**, *19*, 43–47; b) V. Van Eden, A. Noordzij, E. H. Hensen, R. Van der Zee, J. D. A. Van Embden, R. H. Meloen in *Vaccine 89 – Modern Approaches to new Vaccine, including prevention of AIDS* (Eds.: R. A. Lerner, H. Ginsberg, R. M. Chanokk, F. Brown), Cold Spring Harbour Laboratories, **1989**, p. 33–37; c) A. M. Bray, N. J. Maeji, H. M. Geysen, *Tetrahedron Lett.* **1990**, *31*, 5811–5814.

[69] a) H. Rink, *Tetrahedron Lett.* **1987**, *28*, 3787–3790; b) K. Barlos, D. Gratos, J. Kallitsis, G. Papaphotin, P. Sotiria, Y. Wenqing, W. Shafer, *ibid.* **1989**, *30*, 3943–3946; c) P. Sieber, *ibid.* **1987**, *28*, 2107–2110; d) M. Mergler, R. Nyfeler, R. Tanner, J. Gosteli, P. Gross, *ibid.* **1988**, *29*, 4009–4012; e) M. Mergler, R. Tanner, J. Gosteli, P. Grogg, *ibid.* **1988**, *29*, 4005–4008.

[70] J. M. Carter, J. A. Lyon in [4a], p. 721–723.

[71] R. Frank, S. Güler, S. Krause, W. Lindenmaier in [2], p. 151–152.

[72] G. Schnorrenberg, H. Gerhardt, *Tetrahedron* **1989**, *45*, 7759–7764.

[73] a) G. Schnorrenberg, R. E. Lang in [4a], p. 1029–1030; b) G. Schnorrenberg, K.-H. Wiesmüller, A. G. Beck-Sickinger, H. Drechsel, G. Jung in [2], p. 202–203; c) K.-H. Wiesmüller, K. Deres, L. Shi, D. Wei, P. Wernet, G. Jung in [5b], in press.

[74] H. Drechsel, K.-H. Wiesmüller, U. Treffer, G. Jung, *Int. J. Pept. Protein Res.*, submitted.

[75] a) H. Gausepohl, M. Kraft, C. Boulin, R. W. Frank in [4a], p. 1003–1004; b) H. Gausepohl, M. Kraft, C. Boulin, R. W. Frank in [5a], p. 487–490.

[76] H. Gausepohl, M. Kraft, C. Boulin, R. W. Frank in [2], p. 206–207.

[77] K. Nokihara, R. Yanamoto, M. Hazana, V. Wakizawa, S. Nakamura in [5b], in press.

[78] a) A. Holm, M. Meldal in [1], p. 208–210; b) M. Meldal, K. Breddam in [5a], p. 533–536.

[79] H. R. Wolfe, *Manual to RAMPS multiple peptide synthesis system*, DuPont/NEN Co., Wilmington, DE, **1987**.

[80] A. Dryland, R. C. Sheppard, *J. Chem. Soc. Perkin Trans. 1* **1986**, 125–137.

[81] a) V. Krchňák, J. Vágner, O. Mach, *Int. J. Pept. Protein Res.* **1989**, *33*, 209–213; b) V. Krchňák, J. Vágner, *Pept. Res.* **1990**, *3*, 182–193; c) in [2], p. 200–201.

[82] J. Eichler, M. Beyermann, M. Bienert, M. Lebl in [1], p. 205–207.

[83] B. Blankenmeyer-Menge, R. Frank, *Tetrahedron Lett.* **1988**, *29*, 5871–5874.

[84] R. Frank, R. Döring, *Tetrahedron* **1988**, *44*, 6031–6040.

[85] a) T. Böldicke, F. Maywald, E. Wingender, J. Collins, R. Frank in [1], p. 220–222; b) T. Böldicke, S. Kindt, F. Maywald, G. Fitzlaff, M. Böcher, R. Frank, J. Collins, *Eur. J. Biochem.* **1988**, *175*, 259–264.

[86] a) H. Kunz, B. Dombo, *Angew. Chem.* **1988**, *100*, 732–734; *Angew. Chem. Int. Ed. Engl.* **1988**, *27*, 711–713; b) C. Birr, G. Becker, T. Nebe, H. Nguyen-Trong, T. Müller, M. Schramm, H. Kunz, B. Dombo, W. Kosch in [4a], p. 1031–1033.

[87] B. Blankenmeyer-Menge, R. Frank in [5a], p. 465–472.

[88] a) M. Lebl, V. Gut, J. Eichler in [4a], p. 1059–1060; b) M. Lebl, J. Eichler, *Pept. Res.* **1989**, *2*, 297–300.

[89] J. Eichler, J. Furkert, M. Bienert, W. Rohde, M. Lebl, in [2], p. 156–157.

[90] a) R. H. Berg, K. Almdal, W. Batsberg Pedersen, A. Holm, J. P. Tam, R. B. Merrifield, *J. Am. Chem. Soc.* **1989**, *111*, 8024–8026; b) R. H. Berg, K. Almdal, W. Batsberg Pedersen, A. Holm, J. P. Tam, R. B. Merrifield in [5a], 453–459.

[91] R. H. Berg, K. Almdal, W. Batsberg Pedersen, A. Holm, J. P. Tam, R. B. Merrifield in [4a], p. 1036–1037.

[92] R. H. Berg, K. Almdal, W. Batsberg Pedersen, A. Holm, J. P. Tam, R. B. Merrifield in [2], p. 149–150.

[93] a) R. A. Houghten, M. K. Bray, S. T. DeGraw, C. J. Kiroy, *Int. J. Pept. Protein Res.* **1986**, *27*, 675–680; b) R. A. Houghten, S. T. DeGraw, M. K. Bray, S.R. Holtmann, N. D. Frizzell, *BioTechniques* **1986**, *4*, 522–528.

[94] a) *High Performance Liquid Chromatography of Proteins and Peptides* (Eds.: M. T. W. Hean, F. E. Regnies, C. T. Wehr), Academic, New York, **1983**; b) *High Performance Liquid Chromatography in Protein and Peptide Chemistry* (Eds.: F. Lottspeich, A. Henschen, K. Hupe), de Gruyter, Berlin, **1981**; c) M.T. W. Hearn *Adv. Chromatogr.* **1982**, *20*, 1–82.

[95] D. Dupont, P. Keim, A. Chui, M. L. Bozzini, K. J. Wilson, *Applied Biosystems User Bulletin* **1988**, *2*, 1–8.

[96] a) F. Foret, P. Boček in *Advances in Electrophoresis Vol. 3* (Eds.: A. Chambach, M. J. Dunn, B. J. Radok), **1989**, VCH, Weinheim, p. 271–347; b) R. A. Wallingford, A. G. Ewing *Adv. Chromatogr.* **1989**, *29*, 1–76.

[97] a) J. W. Jorgenson. K. D. Lukacs, *Science* **1983**, *222*, 266; b) J. W. Jorgenson, K. D. Lukacs, *Anal. Chem.* **1981**, *53*, 1298–1302; c) A. S. Cohen, A. Paulus, B. L. Karger, *Chromatographia* **1987**, *24*, 15–24.

[98] E. Bayer in *Modern Methods in Protein- and Nucleic Acid Research, Review Articles* (Ed.: H. Tschesche), de Gruyter, Berlin, **1990**, p. 133–148.

[99] M. Grolo, T. Takeuchi, D. Ishii, *Adv. Chromatogr.* **1989**, *30*, 167–199.

[100] J. Metzger, G. Jung in [2], p. 341–342.

[101] J. Metzger, G. Jung in *Chemistry of Peptides and Proteins, Vol. 6*, (Eds.: D. Brandenburg, V. Ivanov, W. Voelter), Attempto, Tübingen, **1992**, in press.
[102] F. S. Tjoeng, D. S. Towery, J. W. Bulock, D. E. Whipple, K. F. Fok, M. H. Williams, M. E. Zupec, S. P. Adams, *Int. J. Pept. Protein Res.* **1990**, *35*, 141–146.
[103] a) D. E. Woods, A. F. Markham, A. T. Ricker, G. Goldberger, H. R. Cotten, *Proc. Natl. Acad. Sci. USA* **1982**, *79*, 5661–5665; b) M. D. Edge, A. R. Greene, G. R. Heathcliffe, P. A. Meacak, W. Schuch, D. B. Scanlan, T. C. Atkinson, C. R. Newton, A. F. Markham, *Nature* **1981**, *292*, 756–762.
[104] H. Gras-Masse, J.-C. Ameisen, C. Boutillon, F. Rouaix, M. Bossus, B. Deprez, A. Capron, A. Tartar in [4b], pp. 842–844.
[105] R. A. Houghten, C. Pinilla, S. E. Blondelle, J. R. Appel, C. T. Dooley, J. H. Cuervo, *Nature* **1991**, *354*, 84–86.
[106] a) A. Furka, F. Sebestyén, M. Asgedom, G. Dibó, *Int. J. Pep. Protein Res.* **1991**, *37*, 487–493; b) *Abstr. 14th Int. Congr. Biochem. Vol. 5*, Prag, Tschechoslowakei, **1988**, p. 47; c) *Abstr. 10th Int. Symp. Med. Chem.*, Budapest, Ungarn, **1988**, p. 288.
[107] a) K. S. Lam, S. E. Salmon, E. M. Hersh, V. J. Hruby, W. M. Kazmierski, R. J. Knapp, *Nature* **1991**, *354*, 82–84; b) K. S. Lam, S. E. Salmon, E. M. Hersh, V. J. Hruby, F. Al.-Obeidi, W. N. Kazmierski, R. J. Knapp in Ref. [46], pp. 492–495.
[108] a) J. K. Scott, G. P. Smith, *Science* **1990**, *249*, 386–390; b) G. P. Smith, J. K. Scott in [46], pp. 485–488.
[109] a) J. J. Devlin, L. C. Panganiban, P. E. Devlin, *Science* **1990**, *249*, 404–406; b) S. E. Cwirla, E. A. Peters, R. W. Barrett, W. J. Dower, *Proc. Natl. Acad. Sci. USA* **1990**, *87*, 6378–6382.
[110] S. P. Fodor, J. L. Read, M. C. Pirrung, L. Stryer, A. T. Lu, D. Solas, *Science* **1991**, *251*, 767–773.
[111] G. Kiedrowski, *Angew. Chem.* **1991**, *103*, 839–840; *Angew. Chem. Int. Ed. Engl.* **1991**, *30*, 840–841.
[112] On the basis of the X-ray structure analysis of the MHC-class I protein HLA-A2 (M. A. Saper, P. J. Bjorkman, D. C. Wiley, *J. Mol. Biol.* **1991**, *219*, 277–319) a nonapeptide-HLA-A2 complex was investigated by means of molecular dynamics simulation (N. Zimmermann, O. Rötzschke, K. Falk, D. Rognan, G. Folkers, H.-G. Rammensee, G. Jung, *Angew. Chem.* **1992**, *104* and *Angew. Chem. Int. Ed. Engl.* **1992**, *31*, in press. As a start in structure-activity studies of viral killer-cell epitopes a nonapeptide with retro-inverso Gln-Arg peptide bonding was synthesized for the first time (H. Dürr, M. Goodman, G. Jung, *Angew. Chem.* **1992**, *104* and *Angew. Chem. Int. Ed. Engl.* **1992**, *31*, in press).

Natural Products as Probes of Cellular Function: Studies of Immunophilins

By Michael K. Rosen and Stuart L. Schreiber*

One of the great mysteries of cell biology remains the mechanism of information transfer, or signaling, through the cytoplasm of the cell. Natural products that inhibit this process offer a unique window into fundamental aspects of cytoplasmic signal transduction, the means by which extracellular molecules influence intracellular events. Thus, natural products chemistry, including organic synthesis, conformational analysis, and methods of structure elucidation, is a powerful tool in the study of cell function. This article traces our understanding of a group of natural products from the finding that they inhibit cytoplasmic signaling to their current recognition as mediators of the interaction between widely distributed protein targets. The emphasis of the discussion is primarily structural. The interactions between the natural-product ligands and their protein receptors are analyzed at a molecular level in order to shed light on the molecular mechanisms of the biological functions of these compounds. In the process we hope to illustrate the power of chemical analysis as applied to biological systems. Through chemistry we can understand the molecular basis of biological phenomena.

1. Introduction

Signal transduction refers to the process by which extracellular molecules influence intracellular events. For example, the actions of the hormone insulin are initiated at the cell surface, when extracellular insulin binds to the membrane-bound insulin receptor. This binding triggers a series of membrane-associated events, followed by a cascade of poorly defined intracellular events that result in the transcription of genes that encode metabolic enzymes. Thus, a signal that originates outside the cell is transmitted through the cell membrane, along intermediate carriers in the cytoplasm, and into the nucleus, causing a change in the status of the cell. In recent years, much has been learned about the mechanisms of signal transduction at the membrane and in the nucleus of the cell. In contrast, very little is known about the mechanisms of signal transduction through the cytoplasm of the cell. Despite the importance of such processes, the detailed mechanisms of cytoplasmic signaling remain among the great mysteries of cell biology, a fact that has led the cytoplasm to be referred to as the "black box" of signal transduction.

Natural products chemistry has long played an important role in the elucidation of biological mechanisms. Pioneering synthetic and mechanistic studies of molecules such as steroids, prostaglandins, and porphyrins, to name only a few, have led to fundamental insights regarding the biological functions of these important classes of compounds. Certain natural products are also uniquely suited for the study of the mysterious processes of the cell, including cytoplasmic signaling, due to their interference with these processes. By studying inhibitory natural products bound to their biological receptors, we may gain a detailed understanding of the function of these receptors. Research in this area relies on a combination of the powerful, complementary tools of synthetic chemistry, molecular biology, cell biology, and methods of structure elucidation, including both NMR spectroscopy and X-ray crystallography. This review highlights recent advances in the structural and mechanistic understanding of cytoplasmic signaling that have arisen through application of these techniques to the study of the immunophilins, a family of cytosolic proteins that bind natural products. These advances have culminated in the identification and characterization of pentameric complexes composed of two normally noninteracting protein constituents and a natural product "glue" that binds the proteins together in a biologically significant manner. In the process, it has been discovered that a protein phosphatase is a key cytoplasmic component of a family of signal transduction pathways.

2. Background

FK506[1, 2] and cyclosporin A[3] (CsA) are fungal natural products (Fig. 1) that inhibit Ca^{2+}-dependent[**] signaling pathways in a variety of cell types.[4, 5] In T cells, both agents inhibit the transcription of a number of genes, including that encoding interleukin-2 (IL-2), which are normally activated by stimulation of (by binding of certain extracellular molecules to) the T cell receptor (TCR).[6] In mast cells they inhibit the exocytosis (i.e. movement to the cell surface and fusion with the cell membrane) of secretory vesicles that normally results from stimulation of the IgE receptor.[7] A variety of biochemical and biological data indicate that in both cases inhibition occurs within the cytoplasm and not at the cell surface or in the nucleus.

On a biochemical level FK506 and CsA are also quite similar. Through synthesis of radiolabeled and immobilized derivatives of these agents for use in protein purification, it was discovered that both bind with high affinity to soluble, cytoplasmic receptor proteins[8] (immunophilins;[8, 9] this term is used to denote immunosuppressant binding proteins, as both FK506 and CsA are immunosuppressive drugs[2, 10]). The FK506 receptor has been named FKBP,[11] and the CsA receptor has been named cyclophilin[12] (CyP). Both proteins catalyze the isomerization of *cis* and *trans* amide-bond rotamers of peptide and protein substrates.[11, 12]

[*] Prof. Dr. S. L. Schreiber, M. K. Rosen
Department of Chemistry, Harvard University
Cambridge, MA 02138 (USA)

[**] The terms Ca^{2+}-dependent and -independent in this context refer to signaling pathways that are characterized by the presence or absence, respectively, of an immediate rise in the concentration of intracellular cytoplasmic Ca^{2+} following binding to the cell surface receptor.

The enzymatic activity of FKBP is potently inhibited by binding of FK506 (K_i = 0.4 nM), but not CsA,[11] and the activity of CyP is inhibited by CsA (K_i = 6 nM),[12] but not FK506.

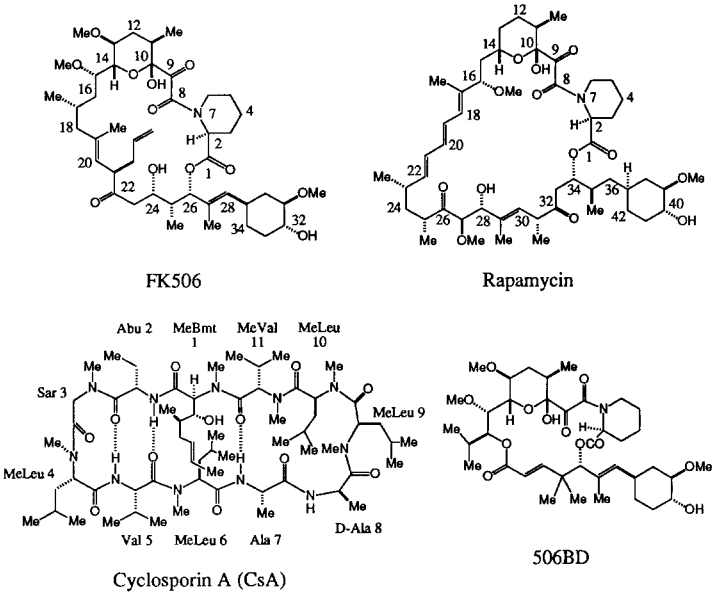

Fig. 1. Chemical formulas of the immunophilin ligands.

Although FK506 is approximately 100 times more effective than CsA in cellular assays, in virtually all other respects the two molecules behave identically in both T cells and mast cells. This similarity in biological function, coupled with the discovery that the molecules inhibit two distinct rotamase enzymes,[*] led to speculation that the biological effects of these agents were due to their rotamase inhibition. It was hypothesized that a necessary step in activation of unknown proteins required for IL-2 transcription in T cells was rotamase-catalyzed isomerization of a peptidyl–prolyl amide bond. Inhibition of this catalysis by FK506 or CsA would then result in inhibition of IL-2 transcription.[13]

Strong evidence against this "rotamase hypothesis" came from biochemical and biological studies of two structurally related molecules: rapamycin,[14, 15] an immunosuppressive fungal natural product and FKBP ligand, and 506BD,[16] a synthetic FKBP ligand (Fig. 1). Given the structural similarities between the three ligands, it is not surprising that, like FK506, rapamycin and 506BD also bind tightly to FKBP and inhibit the rotamase activity of the enzyme (K_i(rapamycin) = 0.2 nM; K_i(506BD) = 5 nM).[15, 16] In fact, NMR and crystallographic studies have demonstrated that FK506 and rapamycin interact with a common domain of FKBP through their common structural elements.[17] Fascinatingly, although FK506 and rapamycin both bind to FKBP and inhibit its rotamase activity, rapamycin does not inhibit the same TCR-mediated signaling pathway that is affected by FK506 and CsA. Rather, it blocks a later Ca^{2+}-independent pathway associated with T cell activation, which is mediated by the IL-2 receptor (IL-2R)[15, 18, 19] (Fig. 2). Even more striking is the fact that 506BD has no inhibitory effect on either of the signaling pathways inhibited by FK506 or rapamycin. Furthermore, it was shown that FK506, rapamycin, and 506BD can all block the actions of the others,

[*] The expression rotamase has the same meaning as PPIase (for peptidyl prolyl *cis–trans* isomerase) an acronym used by others for the description of proteins that catalyze the isomerization of *cis* and *trans* amide-bond rotamers of peptides and proteins.

Stuart L. Schreiber was born in 1956 and was raised in Virginia (USA). He studied as an undergraduate in Charlottsville, Virginia, where he obtained a B.A. in chemistry in 1977 at the University of Virginia. Following Ph.D studies under the direction of R. B. Woodward and Yoshito Kishi at Harvard University, he began his independent career in 1981 in the Department of Chemistry at Yale University. In 1988, he accepted a Professorship at the Department of Chemistry at Harvard. His group is engaged in the study of biological processes through the combined application of synthetic organic chemistry and molecular and structural biology.

Michael Rosen was born in 1965 in Philadelphia, Pennsylvania (USA). He received B.S. degrees in chemistry and chemical engineering from the University of Michigan in 1987. As a Winston Churchill Scholar during 1987–1988 he earned a C.P.G.S. in the Natural Sciences from the University of Cambridge (England) under the direction of Professor Alan R. Battersby. Since that time he has been a graduate student in the research group of Professor Stuart L. Schreiber at Harvard University. His primary interests lie in the structural analysis of proteins and protein–ligand complexes by NMR.

presumably through competitive binding to a common receptor, FKBP. In contrast, the actions of FK506 and rapamycin are unaffected by CsA, which does not bind FKBP; the actions of CsA are also unaffected by FK506, rapamycin, and 506BD, which do not bind CyP.[15, 16, 19, 20] If the biological properties of FK506 and rapamycin were simply due to inhibition of the rotamase activity of FKBP, then they should both interfere with the same pathways. 506BD should also inhibit these same pathways and thus be biologically active. Because this is not the case, it implies that FK506 and rapamycin do *not* act by *eliminating* a function of FKBP; rather they act by *adding* a function to the protein. In a sense, FK506 and rapamycin are prodrugs that are activated by binding to FKBP. CsA is similarly inactive until it binds CyP. This explanation of the immunophilin–ligand complexes as the species responsible for signal inhibition has been termed the "active complex" hypothesis.[8, 9, 15, 16, 21] Genetic studies have also provided strong support for this idea by demonstrating that FKBP is both necessary and sufficient to mediate the actions of rapamycin in yeast,[22, 23] and that CyP mediates the actions of CsA in this organism.[21, 24] Paradoxically, although FK506 and rapamycin are structurally similar and bind to a common protein, FKBP, their FKBP complexes have different biological actions. Furthermore, while CsA is structurally dissimilar to FK506 and binds to CyP, which is unrelated to FKBP, the biological actions of the CyP–CsA complex are indistinguishable from those of the FKBP–FK506 complex. It is interesting to speculate that upon binding to CyP a yet-to-be discovered CyP ligand may provide a complex that has properties indistinguishable from those of the FKBP–rapamycin complex.

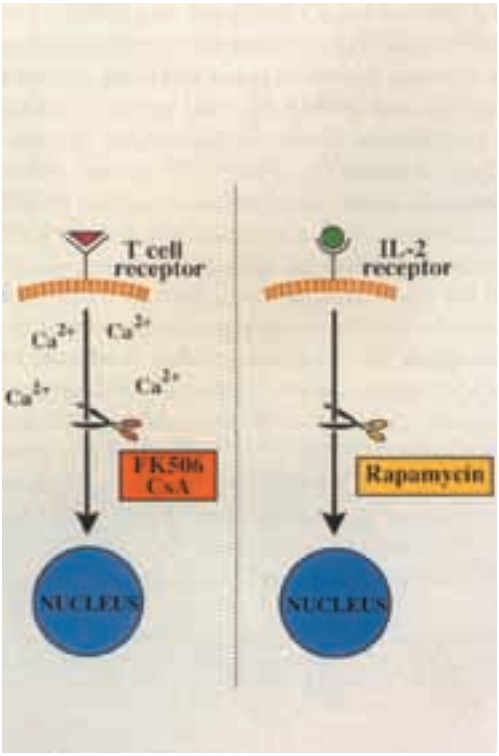

Fig. 2. FK506 and CsA inhibit Ca^{2+}-dependent signaling pathways, while rapamycin inhibits Ca^{2+}-independent pathways. These are illustrated in the T cell by the pathways emanating from the T cell receptor and the IL-2 receptor, respectively, but include signaling pathways in a variety of cell types, including mast cells and neurons.

One obvious, if seemingly unlikely prediction from the above biological data is that the structurally unrelated FKBP–FK506 and CyP–CsA complexes should act, either directly or indirectly (through other proteins), upon a common target molecule that is distinct from the target acted upon by the FKBP–rapamycin complex. The FKBP–FK506 and CyP–CsA target should be a component of Ca^{2+}-dependent signaling pathways such as TCR-mediated transcription in T cells and IgE receptor-mediated exocytosis in mast cells; the FKBP–rapamycin target molecule should be a component of Ca^{2+}-independent signaling pathways such as IL-2R-mediated proliferation in T cells. In both cases, the target should be unaffected by either protein or ligand alone, since only the immunophilin–ligand complexes are active inhibitors (Fig. 3 top).

In fact, we have recently demonstrated that calcineurin (CN), also referred to as protein phosphatase 2B, a calmodulin-dependent serine/threonine protein phosphatase,[25] possesses all the predicted biochemical properties of a target common to both FKBP–FK506 and CyP–CsA.[26] CN is a heterodimeric protein composed of two subunits, calcineurin A (CNA), which contains the calmodulin-binding and phos-

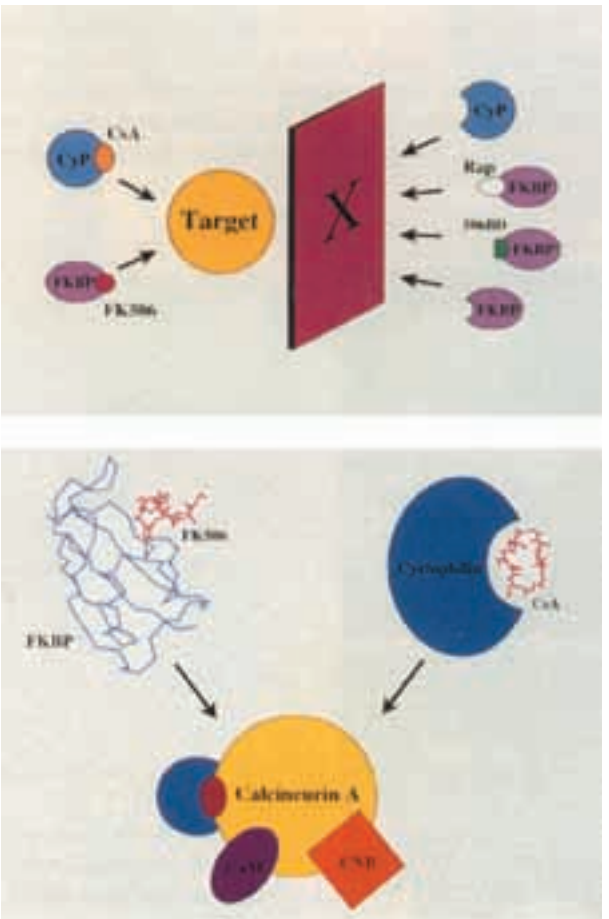

Fig. 3. Top: The CyP–CsA and FKBP–FK506 complexes act on a common target molecule that is not affected by FKBP or CyP alone, or by the FKBP–rapamycin or FKBP–506BD complexes. Bottom: Formation of the pentameric immunophilin-drug-CNA-CNB-calmodulin complex (see text).

phatase active sites, and calcineurin B (CNB), which is a Ca^{2+}-binding protein with, as yet, unknown function. The binding of calmodulin to CNA results in a tenfold increase in the phosphatase activity of the enzyme. In direct binding assays, CN binds to both the FKBP–FK506 and CyP–CsA complexes, but not to FKBP or CyP alone, or to the FKBP–rapamycin complex. In addition, the binding of CN to FKBP–FK506 is inhibited by CyP–CsA (but not by CyP or CsA alone), suggesting that the two complexes compete for the same, or two interacting binding sites. The phosphatase activity of calcineurin, when measured with a phosphopeptide substrate, is potently inhibited by the FKBP–FK506 and CyP–CsA complexes, but is unaffected by FKBP, CyP, FK506, rapamycin, 506BD, or the FKBP–rapamycin complex. Interestingly, it was recently reported that the translocation of a cytosolic component of the transcription factor NF-AT, which regulates IL-2 transcription and is sensitive to FK506, into the cell nucleus due to a rise in intracellular calcium levels is blocked by both FK506 and CsA.[27] The common dependence on intracellular calcium, location in the cytosol, and sensitivity to FK506 and CsA have led us and others to speculate that this component of NF-AT may be a substrate for CN, and that its location in the cell may be dependent on its phosphorylation state.[9, 28, 29] Thus, the inhibition of IL-2 transcription by FK506 and CsA may be the result of their indirect inhibition of the dephosphorylation of a component of NF-AT.

An important question arises from this body of data: How does the binding of FK506 and rapamycin to FKBP and of CsA to CyP change both the ligands and the receptors, enabling the complexes to perform functions the individual components are incapable of performing alone? The remainder of this review will focus on the aspects of ligand–receptor interactions most relevant to this question. In particular, we will discuss the structures of both the natural products and the proteins, and the changes that occur to each upon binding. The pentameric immunophilin-drug-CNA-CNB-calmodulin complexes (Fig. 3 bottom) will then be analyzed in light of the known biochemical data on the interactions between the immunophilin–ligand complexes and calcineurin.

3. Structural Studies of FKBP and its Complexes with FK506 and Rapamycin

3.1. Initial Work

Early structural studies of the FKBP–FK506 and CyP–CsA complexes centered on analysis of the interactions between ligand and receptor. These studies were motivated, in part, by two conflicting proposed mechanisms of rotamase catalysis, and hence of rotamase inhibition by the ligands[30] (Fig. 4). One mechanism involved initial formation of a tetrahedral enzyme–substrate adduct similar to that formed during the hydrolysis of the amide bond by serine or cysteine proteases. Rotation about the C–N bond in the adduct, followed by expulsion of the enzyme nucleophile would result in amide-bond isomerization. This mechanism was supported by studies of Fischer et al.,[12b] who showed that in CyP modification of a cysteine in the active site with *p*-hydroxymercuribenzoic acid eliminated the rotamase activity of the enzyme. Fischer et al.[31] also found an inverse secondary deuterium-isotope effect with substrates containing [α,α-^{2}H]Gly-Pro, indicating a change in hybridization ($sp^2 \rightarrow sp^3$) and thus formation of a covalent bond in the transition state of the reaction. These kinetic data were, however, disputed by Harrison and Stein,[32] who found a normal secondary deuterium-isotope effect using the same substrates. Site-directed mutagenesis studies further demonstrated that none of the cysteine residues in CyP are required for catalysis.[33] These results, coupled with measurement of thermodynamic activation parameters for CyP[32] and FKBP,[34, 35] led to an alternative mechanism of rotamase activity involving binding of a transition-state structure that contains a twisted, or distorted amide bond. In this view, the energy needed to overcome amide bond resonance and isomerize the C–N bond would come from favorable noncovalent interactions between the enzyme and a peptide substrate.

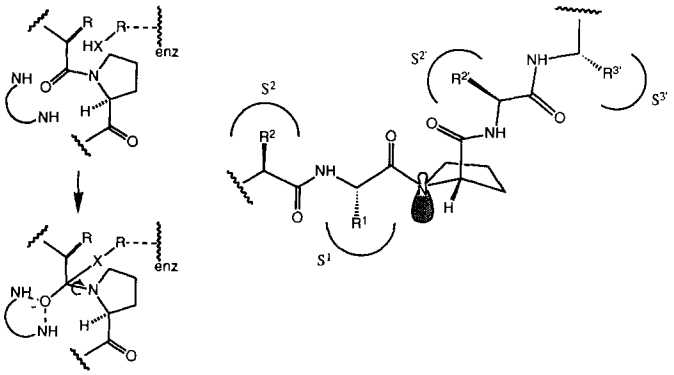

Fig. 4. Two proposed mechanisms of rotamase catalysis. Left: Initial formation of a tetrahedral intermediate. Right: Catalysis by stabilization of a twisted amide bond. enz = enzyme.

The mechanism involving a tetrahedral intermediate led to the consideration that FK506 and rapamycin might bind to FKBP through nucleophilic attack of a side chain of the enzyme on one of the two electrophilic carbonyl carbon atoms of the ligand, C8 or C9. ^{13}C NMR studies of the complex of fully synthetic [8,9-^{13}C]FK506[36] and recombinant human FKBP,[37] however, showed no evidence for formation of a tetrahedral adduct.[30] These studies also demonstrated that FK506 binds to FKBP in a single conformation, although the unbound ligand exists in organic solution as a 2:1 mixture of *cis* and *trans* amide-bond rotamers.

The finding that FK506 and, by inference, rapamycin do not bind covalently to FKBP suggested a possible explanation for the strong interaction between the ligands and their receptor. In the solid state, both FK506 and rapamycin possess a dihedral angle of approximately 90° about the C8–C9 bond. This conformation is also maintained in the complexes of both ligands with FKBP. A dihedral angle of 90° between C8 and C9 and a planar N7–C8 amide group place the keto carbonyl roughly perpendicular to the plane of the pipecolinyl ring (pipecoline = methylpiperidine). Because the pipecolinyl ring most probably mimics the proline ring in natural peptide substrates, the keto carbonyl of FK506 or rapamycin is in the same position as would be a twisted amide carbonyl group of a peptide undergoing rotamase catalysis (Fig. 5). Thus, the perpendicular keto carbonyl groups of FK506 and rapamycin allow the ligands to mimic

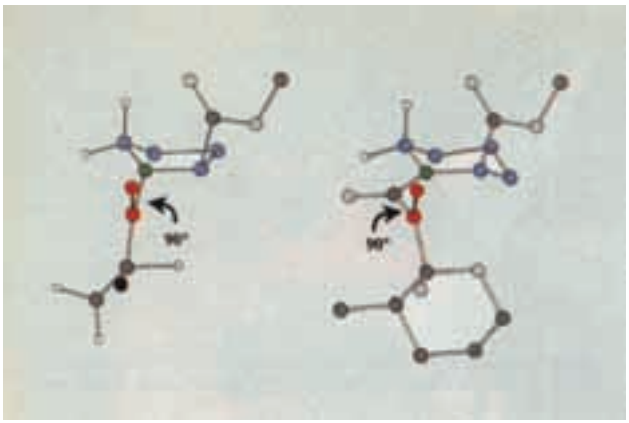

Fig. 5. FK506 and rapamycin may mimic a twisted peptido–prolyl amide bond in a peptide substrate. Left: Model of a twisted amide bond in a peptide substrate. Right: Portion of the crystal structure of free FK506. The analogous carbonyl groups in the two structures are colored red.

a transition-state structure involving a twisted amide bond.[30]

The view of FK506 and rapamycin as twisted amide peptidomimetics was further extended by studies of the substrate specificity of FKBP.[34] In the peptide series succinyl-Ala-Xaa-Pro-Phe-(*p*-nitro)anilide, it was found that peptides with branched hydrophobic amino acids Leu, Ile, and Val as Xaa were greatly favored (up to 1000-fold over peptides with Xaa amino acids with charged side chains as determined by measurement of $K_{cat}K_m^{-1}$ values) with Leu > Ile > Val. Analysis of the structures of FK506 and rapamycin suggested a possible rationale for these observations. Beginning with the pipecolinic acid moiety and proceeding in the "*N*-terminal" direction, both ligands possess a dicarbonyl group, a tertiary hydroxyl group, and a branched aliphatic chain. As illustrated in Figure 6, these can be mapped onto the amide carbonyl group, amide nitrogen atom, and the side chain of a branched aliphatic amino acid residue *N*-terminal to a proline. Thus, the binding of FK506 and rapamycin to FKBP was proposed to result from the ability of the ligands to mimic a Leu-Pro dipeptide with a twisted amide bond.[38]

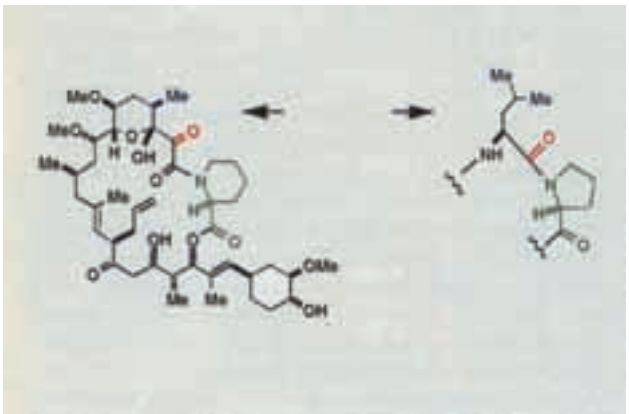

Fig. 6. FK506 (left) and rapamycin may mimic a leucine–proline substrate with a twisted amide bond (right). Analogous atoms are colored alike. Leu is the preferred P1 residue.

3.2. Three-Dimensional Structures

In order to further explain the enzymatic, ligand-binding and biological properties of the immunophilins, we undertook the structure determination of free human FKBP by NMR.[39–41] Our success in this effort was due significantly to the cooperative nature of FKBP, which proved to be soluble and stable, and gave beautiful NMR spectra. Structural studies of the human FKBP–ligand complexes were also undertaken in a fruitful collaboration with Professor Jon Clardy's group at Cornell University. This work resulted in high-resolution crystal structures of both the FKBP–FK506 and FKBP–rapamycin complexes.[42–44] Analyses of the three FKBP structures, showing both the bound and free forms of the protein, have yielded new insights into many aspects of immunophilin function.

3.2.1. Overview of the Structures

All three FKBP structures show the same fold of the protein (Fig. 7 left). The structure is characterized by a five-stranded antiparallel β sheet with a novel +3, +1, −3, +1 loop topology. The strands of the sheet, which run roughly

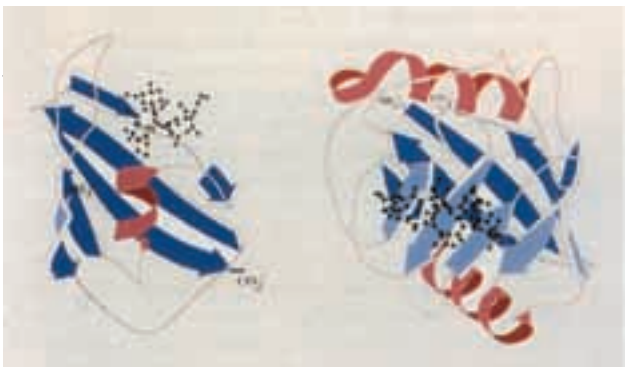

Fig. 7. Richardson diagrams of FKBP (left) and CyP (right). A ball-and-stick model of FK506 is positioned in the ligand-binding site of FKBP[42,44]. A similar model of CsA[69,70] is used to indicate *schematically* the location of the ligand-binding site in CyP[67,68]. We prepared an approximate model of the CyP–CsA complex by docking the structure of bound CsA[69] into the structure of free CyP[68] using reported intermolecular NOEs observed between MeLeu 9 of CsA and Trp 121 of CyP[73]. We thank Professor Ke for providing the CyP coordinates.

perpendicular to the long axis of the molecule, are composed of residues 2–8, 21–30, 35–38 with 46–49 (this strand is interrupted by a loop at residues 39–45), 71–76, and 97–106. A short amphipathic α helix containing residues 57–63 is aligned with the long axis of the protein and lies against the sheet, forming a tightly packed hydrophobic core. The core is composed entirely of aliphatic and aromatic residues, with all but one of the aromatic residues clustered at one end of the molecule. The conserved aromatic and aliphatic side chains of Tyr 26, Phe 36, Phe 46, Val 55, Ile 56, Trp 59, Tyr 82, and Phe 99 line a shallow cleft at the *N*-terminus of the α helix, forming the FK506 and rapamycin binding site. The side chains of these residues are well defined in both the

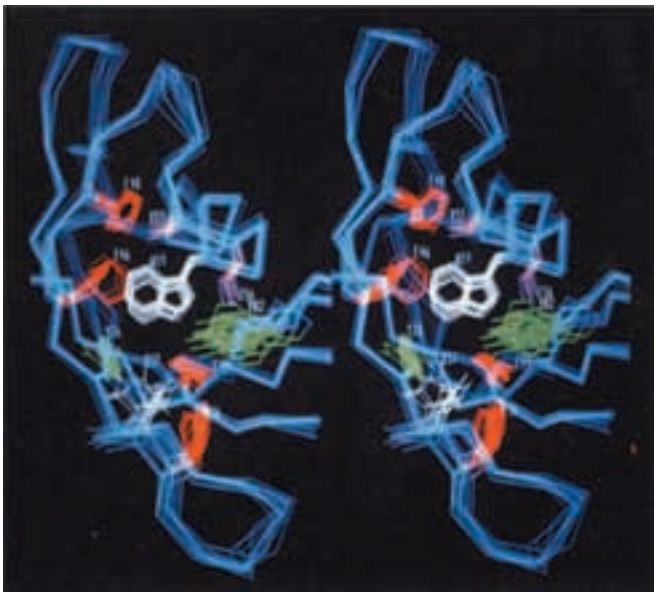

Fig. 8. Stereoview of selected residues in the ligand-binding pocket of FKBP. An overlay of 15 structures of the free protein generated by NOE-restrained molecular dynamics simulation is shown. The orientation is approximately perpendicular to that in Figure 7. (Note the α helix at the upper right and the β strands lining the lower left.) Residues are identified by the one-letter amino acid code. Side chains are colored as follows: Phe = red; Tyr = green; Arg, Asp, Trp = white; Ile, Val = purple. The loops Ser38–Pro45 and Gly83–His94 have been removed for clarity.

ligated and unligated forms of FKBP (Figs. 8 and 9). Both ligands fit tightly into the binding pocket and have a number of similar hydrophobic and hydrogen-bonding interactions with the protein. The FKBP-binding domain of FK506 extends from the C24 hydroxyl group, through the diketo pipecolinyl moiety and the pyranose ring, to the C15 methoxy group. This finding was anticipated on the basis of structural analyses of FK506 and rapamycin and on the biological properties of the two molecules, and led to the design of the FKBP ligand 506BD (see Fig. 1).[16] Most of the trisubstituted cyclohexyl ring (C26–C34) of FK506 and

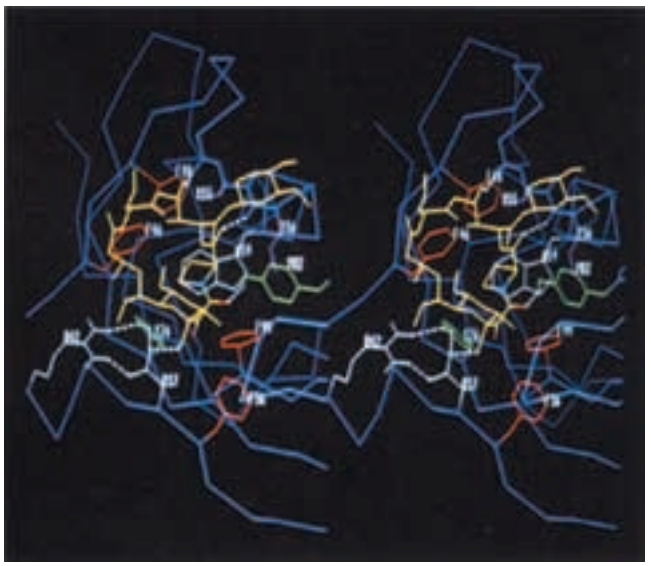

Fig. 9. Stereoview of selected residues in the binding pocket of the FKBP–FK506 complex. Orientation and colors of the side chains are the same as in Figure 8. Bound FK506 is yellow. Hydrogen bonds (see text) are white.

carbon atoms C18–C23 of its macrocycle, including the allyl group, do not contact FKBP and are exposed to solvent. Similarly, the binding domain of rapamycin consists of the region from the C28 hydroxyl group through the pyranose ring; carbon atoms C15–C27 are exposed to solvent. For rapamycin the orientation of the cyclohexyl ring (C34–C42) is different from that in FK506, and makes several contacts to FKBP. The pipecolinyl ring is the most deeply imbedded portion of both ligands (Fig. 9). This moiety is in van der Waals contact with the indole ring of Trp59 at the back of the binding pocket, and with the side chains of Tyr26, Phe46, Val55, Ile56, and Phe99 at the sides of the pocket. In the NMR spectra of the FKBP–FK506 complex the extremely high-field chemical shifts ($\delta = -2$ to 0) of the pipecolinyl methylene hydrogens, and several NOE cross-peaks in the aromatic region also reflect the proximity of this group to aromatic residues of the protein.[17] A number of additional hydrophobic contacts are made between the ligands and the protein. These include interactions between the pyranose ring and residues Tyr26, Asp37, Tyr82, His87, and Ile90, and between the region C24–C26 of FK506, and C28–C32 of rapamycin, and residues Phe46 and Glu54 of FKBP. Thus, the nanomolar binding constants of FK506 and rapamycin may be due, in part, to the complementary hydrophobic surface of FKBP.

The favorable van der Waals interactions between FKBP and both FK506 and rapamycin are complemented by similar arrays of intermolecular hydrogen bonds. Both ligands have identical hydrogen bonds from the C1 ester carbonyl group to Ile56 NH, the C8 amide carbonyl group to the Tyr82 phenolic OH group, and the C10 hemiketal OH group to the Asp37 carboxylate. Despite the differences between the C24–C26 region of FK506 and the C28–C33 region of rapamycin, both also make analogous hydrogen bonds to Glu54 CO, FK506 from the C24 hydroxyl group, and rapamycin from the C28 hydroxyl group. Rapamycin makes one additional hydrogen bond not seen in the FK506 complex, from the C40 hydroxyl group to Glu53 side chain CO group. The pattern of hydrogen bonds involving Ile56 NH, Glu54 CO, and Gln53 CO is reminiscent of the antiparallel β-sheet-like contacts often seen between proteins and peptide ligands. These hydrogen bonds then extend the portions of FK506 and rapamycin that may be described as peptidomimetic to include the region between the C1 ester carbonyl group and the C24 (C28 for rapamycin) hydroxyl group. The structural analogy between the ligands and a tetrapeptide is illustrated in Figure 10. The pipecolinyl ester carbonyl group acts as the proline amide carbonyl group in a Leu-Pro peptide fragment. The region from O1 to C25 (C29 for rapamycin), including the cyclohexyl ring, is roughly equivalent to an aromatic amino acid residue. The C24 hydroxyl group (C28-OH for rapamycin) then represents the amide NH group of the following residue in the chain. Thus, FK506 and rapamycin may bind to FKBP by acting as transition-state analogues of a Leu(or Val)-Pro-Xaa-Yaa peptide substrate. We are currently investigating this hypothesis through synthesis of peptides and peptide analogues designed based on the FKBP–FK506 and FKBP–rapamycin complex structures.[45] Biochemical analyses of these molecules, coupled with structural analysis of their complexes with FKBP (through X-ray crystallography and/or NMR

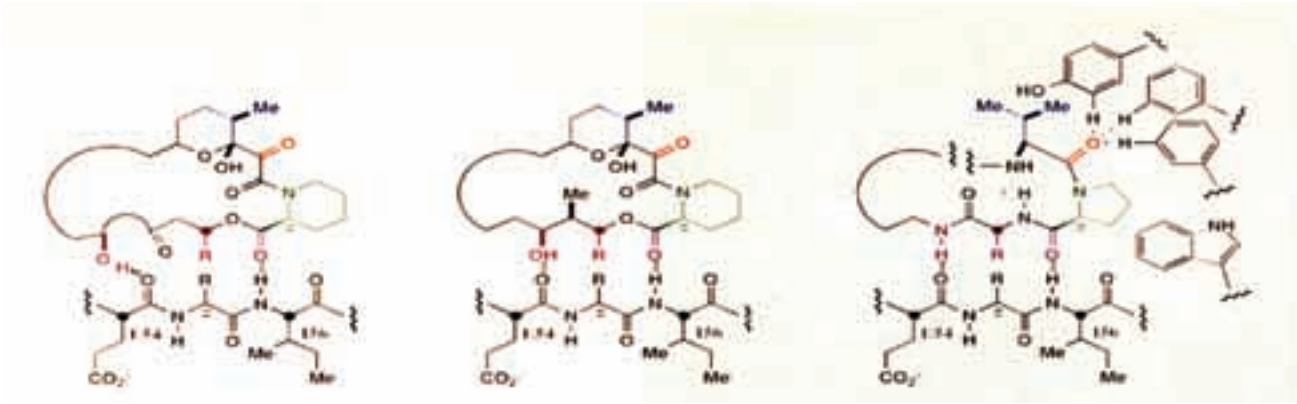

Fig. 10. Schematic illustration of the bonding between FKBP and the ligands rapamycin (left) and FK506 (middle) and a peptide (right). Analogous atoms have the same color.

spectroscopy) will probe the energetic contributions of the various receptor–ligand interactions.

The hypothesis that FK506 and rapamycin are transition-state analogues of an FKBP substrate predicts that in addition to the interactions discussed above there should be significant contacts between the protein and the keto carbonyl groups of the ligands. These same contacts would then stabilize a twisted amide bond in the transition state for rotamase catalysis. Initially we had expected, based on the many known structures of protein–ligand complexes, that the keto carbonyl group (at C9) would be bound by a network of hydrogen bonds or typical electrostatic interactions with charged residues. However, the structures of the two receptor–ligand complexes clearly show that the keto carbonyl group does not make any hydrogen bonds to the protein, nor does it contact any charged residues of the protein. Instead, it is in close proximity to the $C^{\varepsilon}H$ atoms at the edges of three aromatic rings, Tyr26, Phe36, and Phe99 (Fig. 9). Such C–H···O interactions have been observed in small organic molecules[46] and proteins,[47] and it has been proposed that these contribute to the stability of such systems. Theoretical calculations, too, support the notion that C–H···O interactions can stabilize small molecules as well as proteins.[48] However, to our knowledge the FKBP complexes would be the first examples in which this type of interaction contributes significantly to the binding of a ligand to its receptor. It would also represent a novel mechanism of catalysis, wherein transition-state stabilization is achieved through arene–carbonyl interaction.

3.2.2. *Structural Consequences of Binding*

Since neither FKBP nor FK506 or rapamycin are able to bind to or inhibit the phosphatase activity of CN, it is important to analyze the differences between the free and bound forms of both protein and ligands in order to understand the biological actions of the two complexes. How does binding activate FKBP and its ligands, allowing FKBP–FK506 to recognize CN, and FKBP–rapamycin to recognize a different target protein? The existance of both free and bound structures of all components of these complexes now allows this question to be addressed.

3.2.2.1. Comparison of free and bound FKBP

Comparison of the structure of unbound FKBP with those of either of the FKBP–ligand complexes reveals that the majority of residues in the protein binding pocket are not greatly perturbed by ligand binding. In particular, the aromatic and aliphatic residues making direct contact to ligand (Tyr 26, Phe 46, Val 55, Ile 56, Trp 59, and Phe 99) show only small conformational differences between the bound and free structures (compare Figs. 8 and 9). In addition, regions of the protein that are not directly involved in binding (for example, the bulk of the α helix and the β sheet) are also not dramatically different in the bound and free structures. Subtle changes in these regions may prove to be significant, but as will be discussed later in Section 5, this seems unlikely. There are several loops in FKBP, however, that appear to undergo both structural and dynamic changes on ligand binding. Not surprisingly, these loops are located at the rim of the binding pocket. In the structure of free FKBP, the seven residue bulge, Ser 39 to Pro 45, that occurs in the middle of the fifth strand of the β sheet is only poorly characterized by the NMR data (Fig. 11). A lack of medium- and long-range NOEs in this loop, coupled with the relatively weak sequential and intraresidue NOEs further suggest that this region may be disordered, sampling a wide range of conformations. In the crystal structure of the FKBP–FK506 complex this loop is well defined by the electron density. This structure is stabilized by a large number of backbone/backbone and backbone/side-chain hydrogen bonds despite its rather unusual conformation. A similar set of hydrogen bonds is seen in the FKBP–rapamycin complex. However, the high thermal factors observed for residues 40 to 43 in this structure indicate greater mobility or disorder than in the

Fig. 11. α Carbon overlay of ten structures of free FKBP generated by NOE-restrained molecular dynamics simulation. The view is similar to that in Figures 8 and 9. The α helix is colored red (as in Fig. 7). The basic loop Ser39–Pro45 is blue. The loop Gly83–His94 is green.

FK506–FK506 complex. This difference probably reflects different numbers of intermolecular contacts in this region in the two crystal forms.[44] Many of the hydrogen bonds in the region appear to be facilitated by an Asp-Arg-Tyr triad[49] involving the side chains of Asp37, Arg42, and Tyr26 (Fig. 9). This interaction bends the backbone of the loop toward the body of the protein, enabling many hydrogen-bond donors and acceptors to come together. In free FKBP no evidence for these interactions with Arg42 has yet been observed in the NMR data. Further, preliminary NMR analyses of the FKBP–FK506 complex have shown that the chemical shifts of the amide hydrogens of several residues between Ser39 and Pro45 change substantially on binding. Thus, ligand-binding may increase the propensities of residues in this region to form hydrogen bonds, resulting in changes in conformation and/or mobility of the loop. Interestingly, the region from Lys34 to Lys44 is one of the most highly charged (seven of eleven residues are charged) and most basic (net charge +3) sequences of FKBP (see hFKBP12 sequence in Fig. 12). The proximity to the bound ligand, structural changes on ligand binding, and high charge density all suggest that this region may be important in contacting CN in the pentameric complex.

A second region of FKBP that appears to change significantly on ligand binding is the segment from Tyr82 to His94 (green in Fig. 11). This loop is poorly defined in free FKBP. Like the basic loop described above, this segment shows few

```
                                 o          o  o        o      oo•o•o o   o•   ••       oo          o  o
                                 ••o        •  o•     oo••o   •  •••••• •   ••o ••       ••    oo o o••• • •
Mustrans2  16  GVDISPKQDE GVLKVIKREG TGTETPMIGD RVFVHYTGWL LDGTKFD-----SSL DR-K-DKFSFDL  75
    PaORF 117  ARFGVRELTG GVLVSELRRG QGNGIGAATQ -VHVRYRGLL ADGQVFD-----QSE SA---EWFALD-  173
    CtMIP  57  KAGVIELEPN KLHDRVVKEG TGRVLSG-KP TALLHYTGSF IDGKVFD-----SSE KN-K-EPILLPL  115
    LpMIP 117  NKPGVVVLPS GLQYKVINAG NG-VKPGKSD TVTVEYTGRL IDGTVFD-----STE KT-G-KPATFQV  175
   NmFKBP   1           M GSLIIEDLQE SFGKEAVKGK EITVHYTGWL EDGTKFD-----SSL DR-R-QPLTITL   51
   ScFKBP   1     MSEVIEG NVKIDRISPG DGATFPKTGD LVTIHYTGTL ENGQKFD-----SSV DR-G-SPFQCNI   57
   NcFKBP   1     MTIPQLD GLQIEVQQEG QGTRETRRGD NVDVHYKGVL TSGKKFD-----ASY DR-G-EPLNFTV   57
  hFKBP13   1   TGAEGKRK LQIGVKKRVD HCPIKSRKGD VLHMHYTGKL EDGTEFD-----SSL PQ-N-QPFVFSL   58
  bFKBP30  92  SEETLDEGPP KYTKSVLKKG DKTNFPKKGD VVHCWYTGTL QDGTVFDTNIQTSSK KKKNAKPLSFKV  158
  bFKBP12   1           GVQVETISPG DGRTFPKRGQ TCVVHYTGML EDGKKFD-----SSR DR-N-KPFKFVL   50
  hFKBP12   1           GVQVETISPG DGRTFPKRGQ TCVVHYTGML EDGKKFD-----SSR DR-N-KPFKFML   50
                         βββββββ          22  βββββββββββ 11  βββ     β33 11     ββββ2

                 o   ••  oo   o   o  •     o o      o••  o      ooo   o• •o  oo•
                 • oo•••o••o  ••  •  •o o o•  •  oo ••• o• •oo ••••oo•••••• ••••o•o•o
Mustrans2  76  GKGEVIKAWD IAVATMKVGE VCHITCKPEY AYGAAGSPPK IPPNATLVFE VELFEFKGED LTEEED  141
    PaORF 174  S---VIEGWR TALRAMPVGA RWRVVIPSAQ AYGHEGAGDL IPPDAPLVFE IDLLGFR*          227
    CtMIP 116  TK--VIPGFS QGMQGMKEGE VRVLYIHPDL AYGTAGQ--L -PPNSLLIFE VKLIEANDDN VSVTE*  175
    LpMIP 176  S--QVIPGWT EALQLMPAGS TWEIYVPSGL AYGPRSVGGP IGPNETLIFK IHLISVKKSS *       233
   NmFKBP  52  GVGQVIKGWD EGFGGMKEGG KRKLTIPSEM GYGatrrggv IPPHATLIFE VELLKVYE*          109
   ScFKBP  58  GVGQVIKGWD VGIPKLSVGE KARLTIPGPY AYGPRGFPGL IPPNSTLVFD VELLKVN*          114
   NcFKBP  58  GQGQVIKGWD EGLLGMKIGE KRKLTIAPHL AYGNRAVGGI IPANSTLIFE TELVGIKGVQ KGE*  120
  hFKBP13  59  GTGQVIKGWD QGLLGMCEGE KRKLVIPSEL GYGERGAPPK IPGGATLVFE VELLKIERRT EL*   120
  bFKBP30 159  GIGKVIRGWD EALLTMSKGE KARLEIEPEW AYGKKGQPDx ixqpnxLIFE VELVDID*          215
  bFKBP12  51  GKQEVIRGWE EGVAQMSVGQ RAKLTISPDY AYGATGHPGI IPPNATLIFD VELLKLE*          107
  hFKBP12  51  GKQEVIRGWE EGVAQMSVGQ RAKLTISPDY AYGATGHPGI IPPHATLVFD VELLKLE*          107
               2      αααα αααα11  22  βββββββ 311   2'2'3        22  ββββ ββββββ
```

Fig. 12. Manual sequence alignments of known FKBPs. Only the homologous region of each protein is shown. Numbers at the ends of each row are the position of the nearest amino acid in the full protein. Gaps inserted in the sequences are represented by hyphens, *C*-termini are marked with stars, and uncertain assignments are in lowercase. Residues in boldface correspond to residues of hFKBP12 that contact FK506 in the X-ray structure of the complex[42,44]. Degrees of conservation are indicated by solid and open circles above the sequence as follows: •• completely conserved; •o strong preference for one amino acid (at least seven occurrences); • conservative substitutions; o mostly similar amino acids. Below the sequences, the secondary structure of hFKBP12 in the complex with FK506 is shown; α helix is marked with α, antiparallel β strand with β, and β turns with numbers corresponding to type beneath the second and third positions. The following sequences are included: human FKBP12[37], bovine FKBP12[57a], bovine FKBP12[57a], bovine FKBP25[57b], human FKBP13[56], NcFKBP (*Neurospora crassa*)[57c], ScFKBP (*Saccharomyces cerevisiae*)[57d], NmFKBP (*Neisseria meningitidis*)[57e], LpMIP (*Legionella pneumophila* macrophage infectivity potentiator)[57f], CtMIP (*Chlamydia trachomatis*)[57g], PaORF (open reading frame in the *Pseudomonas aeruginosa algR2* gene)[57h], and Mustrans2 (homologue of mouse transition protein 2)[57i].

long-range NOEs, and only weak sequential and intraresidue NOEs. In addition, TOCSY and NOESY NMR spectra provide evidence for two distinct conformations of this loop that interconvert slowly on the NMR time scale.[39] Although the exact nature of this interconversion has not yet been determined, chemical shift perturbations show that it affects several residues between Tyr 82 and His 87.[50] Thus, in the absence of ligand the loop Tyr 82 to His 94 appears to sample at least two, and possibly more, different conformations. In contrast, in both FKBP–ligand complexes this loop shows a single, well-defined conformation that is stabilized by several intraprotein hydrogen bonds and a number of van der Waals contacts to the ligand. In the free protein these contacts would be absent, allowing the loop greater flexibility. These changes suggest that this loop, like that from Ser 39 to Pro 45, may be involved in CN recognition. If this proves to be the case, then the CN binding site could span up to almost 20 Å, and contain regions of both high positive charge density (from the protein) and high hydrophobicity (from the effector domains of the ligands). Mutagenesis studies are currently underway to identify definitively the regions of FKBP that are important in the formation of the ternary complex with CN.

3.2.2.2. Comparison of Free and Bound FKBP Ligands

The differences between bound and free FK506 and rapamycin are also revealing. Free FK506 has been examined with a variety of techniques, including X-ray crystallography,[1] NMR spectroscopy,[51, 52] and theoretical calculations.[53] The structure of the molecule crystallized from organic solvent[1] is shown in Figure 13. In the crystal, FK506 exists in a single conformation with a *cis* amide bond. In contrast, in organic solution it exists as a 2:1 mixture of *cis*:*trans* amide-bond rotamers.[1, 51, 52] The structures of both rotamers were recently determined by NOE–restrained molecular dynamics calculations.[51, 52] Although similar to the crystal structure in some respects, both conformations are significantly different in others. In the FKBP binding domain, the *cis* structure in solution is quite similar to the solid-state structure. However, the two differ in the region surrounding C23, with large deviations in the torsion angles about C20-C21, C21-C22, C23-C24, C24-C25, C25-C26, and C26-C27. Most notably, the cyclohexyl residue extends away from the macrocycle in the solid state, while in solution it is wrapped under the macrocycle due to a C25-C26-C27-C28 dihedral angle of 91°. It is interesting that the *trans* conformer in solution differs from the crystal structure in the FKBP binding domain but is relatively similar in the remainder of the molecule. Other than changes to the torsion angles about C1-C2 and C9-C10, which compensate for the *trans* versus *cis* amide bond, the only other differences between the two structures are in the torsion angles from C16 to C19. An important common feature (see below) of all three unbound conformers is the orientation of the pyranose moiety outside of the macrocyclic ring. In this orientation, the pyranose ring does not make any intramolecular contacts.

Free FK506 has also been studied theoretically.[53] Calculations employing a Monte Carlo search of torsion angles in the macrocycle of the molecule have revealed the presence of

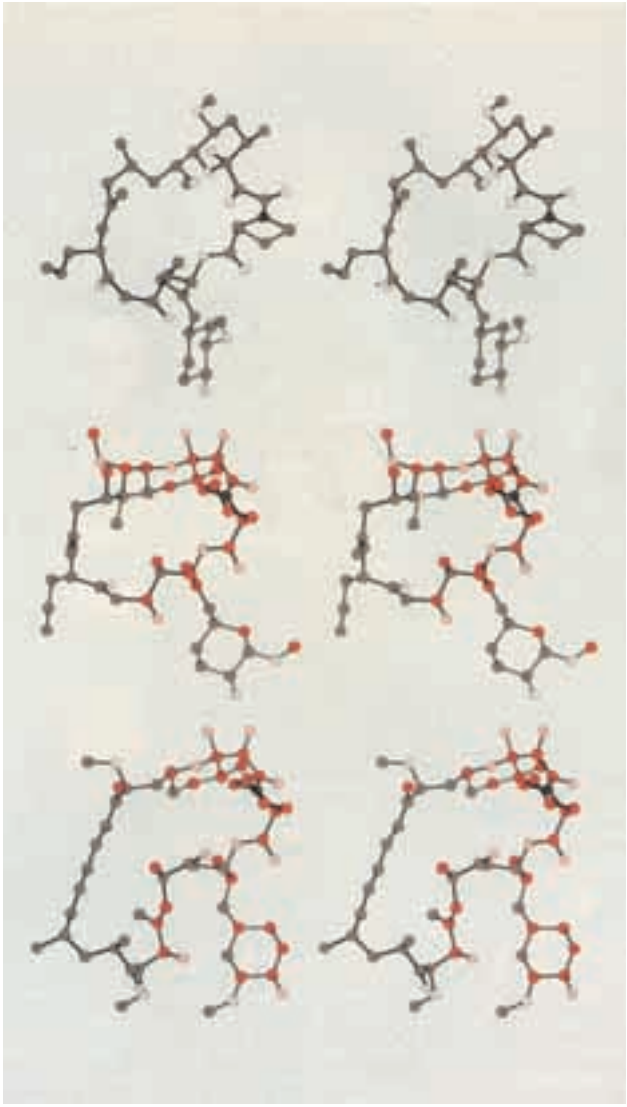

Fig. 13. Stereoviews of the structures of free FK506 (top), bound FK506 (middle), and bound rapamycin (bottom) in the solid state. In middle and bottom pictures, atoms in close contact (< 4 Å) with heavy atoms of FKBP12 are shaded red[42–44].

21 distinct low-energy conformations (within 12 kcal mol^{-1} of the lowest energy structure)[53] including both the *cis* and *trans* amide-bond isomers. Molecular dynamics simulations have also been used to study the structure and dynamics of FK506 in water[53] (the insolubility of the molecule in aqueous media has prevented direct structural analysis in this environment). Over the course of a simulation of 200 ps, beginning with the energy-minimized solid-state structure, FK506 adopted two stable conformations that differed primarily in the torsion angles about C17-C18 and C18-C19. Flexibility was also observed about the C1-C2 and C8-C9 torsions. In general, however, the structure did not deviate significantly from the solid-state conformation during the 200 ps.

The structure of bound FK506[42, 44, 54] (Fig. 13 middle) is dramatically different from the known structures of the free ligand[42, 44] (A necessary caveat at this point is that the structure of FK506 in aqueous solution has not yet been experimentally determined. Thus, the differences between the free and bound forms of the molecule described below do

not necessarily reflect effects of binding, and thus should only cautiously be interpreted as such). This is true of both the solution and solid-state conformations. The most notable change between the crystalline forms is that the amide bond of bound FK506 is *trans*, while in the crystal structure of the free molecule it is *cis*. This change is compensated for by large rotations about the C1–C2, C14–C15, C15–C16, and C16–C17 bonds. Significant changes are also seen in these same torsion angles when either of the free forms in solution is compared to the bound form. The differences in the torsion angles flanking the pyranose ring, C14-C15 and either the amide torsion angle (for the *cis* conformations) or C9-C10 (for the *trans* conformation), result in a rotation of this moiety under the macrocycle in the bound structure. This gives the binding domain a more compact shape and forms a hydrophobic core of the ligand. Overall, these changes result in only a 3 kcal mol^{-1} increase in energy due to unfavorable steric interactions on binding (comparing crystal structures in both the free and bound forms).[42] However, the approximately 150° rotation about the C14–C15, bond does result in steric interaction between the methyl substituents of the C13 and C15 methoxy groups. These groups are roughly *anti* to each other in all forms of the free ligand. But in the bound structure of FK506, the C15 methoxy group is rotated to the outer side of the macrocyclic ring and adopts a gauche + /gauche − orientation with respect to the C13 methoxy group. The energetic consequence of this interaction, which is not present in rapamycin, may be in part responsible for the ligand specificity observed in other FKBPs (see Section 6).

In contrast to FK506, the free and bound conformations of rapamycin are highly similar.[43, 44] The root-mean-square deviation (rmsd) between the bound and free structures is 0.48 Å. Like bound FK506, rapamycin has a *trans* amide bond in the solid state (in organic solution it exists as a 4:1 mixture of *trans*:*cis* amide-bond rotamers). It also has the pyranose ring folded under the macrocycle, and the cyclohexyl moiety extended outward from the body of the molecule. Interestingly, the conformation of the FKBP-binding domain of bound FK506 is virtually identical to that of rapamycin. The rmsd between the two bound ligands from C1 to C13 is 0.12 Å. Thus, the FKBP binding pocket interacts strongly with only one conformation of the two ligands. The fact that rapamycin's FKBP-affinity is twice that of FK506 may, in part, reflect its greater propensity to adopt this conformation.

Although the conformation of FK506 may be significantly altered by binding to FKBP, the same can probably not be said of rapamycin. This is true of both domains of the molecules. While ligation may serve to alter the conformation of FK506, better enabling it to contact CN in the pentameric complex, for rapamycin it appears that this may simply serve to surround the ligand with residues of the protein. Binding may also aid in the transfer of both molecules from the lipid membrane into the aqueous environment of the cytoplasm. It seems likely that since FK506 and rapamycin bind to the same site in FKBP, the selectivity of the two FKBP–ligand complexes arises from the different chemical compositions of the two ligands. These result in two different composite protein–ligand surfaces, enabling the complexes to bind two different targets.

3.3. 506BD

The synthetic FKBP ligand 506BD[16] has proven to be extremely useful in increasing our understanding of the structural basis for the biological actions of FK506 and rapamycin. This molecule contains the common FKBP-binding domain of FK506 and rapamycin, but lacks the effector domain of either ligand.[16] Instead, the geometry of the binding domain is maintained by a simple (both structurally and synthetically) *trans* enoate spacer. The ability of 506BD to bind FKBP and inhibit the biological actions of FK506 and rapamycin, coupled with the inability of the ligand to inhibit signal transmission pathways clearly defined the two-domain (binding and effector) nature of FK506 and rapamycin. In retrospect, however, the success of 506BD as an FKBP ligand was somewhat fortuitous, for the molecule was designed based on the crystal structure of unbound FK506. When 506DB was designed, the conformation of bound FK506 would not be known for almost two years. Because the free and bound structures of FK506 are very different, it is surprising that a linker designed to bridge two points in the free molecule would be able to bridge the same two points in the bound. This is in fact the case. The enoate spacer in 506BD was designed to connect from C16 to C25, a distance of 5.2 Å in unbound FK506.[1] A *trans* enoate was employed in order to accomodate both the *cis* and a possible *trans* amide-bond rotamer. The regions flanking the spacer were also designed to maintain the local conformational preferences seen in the C14–C26 region of FK506. Inspection of bound FK506 revealed that despite the many unanticipated changes detailed above, C16 and C25 are 4.2 Å apart in this conformation. Thus, the same *trans* enoate linker can join these points together without significantly perturbing the bound structure of the binding domain.[16]

3.4. Insights from Protein Sequence

FKBP is only one member of a growing family of FK506- and rapamycin-binding proteins. At least four other proteins that bind the two ligands have been observed and partially characterized in human T cells.[55, 56] In addition, a number of proteins with high homology to FKBP have been identified in various organisms, including other mammals, yeast, and bacteria.[57] Cyclophilins, too, have been identified in a variety of cell types and different organisms.[58] The known FKBPs range in molecular weight from 12 kDa for the archetypal protein (hereafter referred to as FKBP12) to 59 kDa for the phosphorylated FKBP59 found in T cells.[55] Despite their variations in size, all members of the FKBP family that have been sequenced to date (either directly through automated Edman degradation, or indirectly through cloning and sequencing of their complementary DNA (cDNA)) show a common FKBP12-like domain of approximately 12 kDa. An alignment of the sequences of some of these proteins is shown in Figure 12 (see Section 3.2.2.1.) Several features of this alignment are striking. First, although the number of conserved amino acids from approximately residue 25 through the *C*-terminus (residue numbers referenced relative to hFKBP12) is fairly high, the *N*-terminus shows very little homology among the various proteins.

Interestingly, in hFKBP12 residues 1 to 13 and 13 to 29 correspond to the first two of four exons in the genomic DNA encoding the protein.[59] These exons are separated from the remaining two exons, which encode residues 29 to 66 and 67 to 107, by a large intron of 16000 DNA bases. The other introns are much smaller and contain only 109 and 3300 bases. This gene structure suggests that the *N*-terminal regions of the FKBPs may have developed through the recruitment of unrelated exons by the large intron preceeding the common *C*-terminal domain. Thus, analysis of the FKBP12 gene provides an evolutionary explanation for the high variability seen in the *N*-terminal peptide of members of the FKBP family.[59]

Examination of the sequence alignment in light of the structures of unbound FKBP12 and of the two FKBP12–ligand complexes also provides insight into the requirements for stability, ligand binding, and rotamase catalysis of these proteins. A total of 13 residues are exactly conserved in all known FKBPs. Six of these, Gly 33, Gly 69, Gly 83, Gly 28, Leu 97, and Leu 103, are important to the structural integrity of the protein.[57b] The remaining seven, Tyr 26, Phe 36, Asp 37, Val 55, Ile 56, Tyr 82, and Phe 99, line the binding pocket or make important contacts to ligand. Trp 59, which also appears critical for maintaining the structure of the binding pocket is conserved in all but one sequence, where it is replaced by Phe. The high conservation of residues in the FKBP binding pocket suggests that all proteins in the family will bind ligands in a similar manner. In all cases, binding will involve a large number of van der Waals interactions with aromatic and aliphatic residues of the protein, plus several specific hydrogen bonds from the ligand to the protein. The sequence conservation coupled with a view of FK506 and rapamycin as transition-state analogues also suggests that these types of interactions may be necessary for rotamase catalysis. The conserved residues Tyr 26, Phe 36, and Phe 99 may be important for stabilizing the carbonyl group of a twisted amide in the rotamase transition state. The potential of the Tyr 82 phenolic hydroxyl group to form a hydrogen bond and the capacity of the Asp 37 carboxylate group to form a salt bridge may be important as well. Furthermore, it has been suggested that the hydrophobicity of the rotamase active sites of both FKBP and CyP may play a significant role in the enzymatic mechanism of the isomerization reaction.[35, 44, 60] Vapor pressure measurements have shown that peptide bonds are highly solvated in aqueous media.[61] Wolfenden and Radzicka[60] have argued that bound water molecules will inhibit isomerization of the amide bond since the presumably non-resonance-stabilized transition-state structure will be less polar than the starting or product structures. An enzyme that promotes desolvation by providing a hydrophobic binding site will then facilitate isomerization. In support of this hypothesis for catalysis by desolvation[62] are NMR data demonstrating that the isomerization of *N*,*N*-dimethylacetamide is significantly more rapid in methylene chloride than in water.[63] Kofron et al. have discussed a similar mechanism[35] on the basis of theoretical calculations indicating that interactions with water reduce the flexibility of amide bonds.[64] Finally, Van Duyne et al.[44] have noted calculations showing that the dipole along the C–N bond is decreased in a twisted amide relative to the planar species,[65] and that the stability of dipolar species is decreased in low-dielectric environments.[66] Thus, they postulate that the hydrophobic ligand-binding site of FKBP may promote isomerization by destabilizing the strongly dipolar amide bond in a peptide substrate.

4. Structural Studies of Cyclophilin (CyP) and its Complex with Cyclosporin A (CsA)

4.1. Cyclophilin (CyP)

Although the structure of the CyP–CsA complex remains unknown, Kallen et al. and Ke et al. have recently determined the structures of a CyP–tetrapeptide complex and unbound CyP by X-ray crystallography.[67, 68] In addition, Weber et al. and Fesik et al. have also determined the structure of CsA bound to CyP by isotope-edited NMR spectroscopy.[69, 70] The results of these studies provide many clues regarding the structure and biological function of the CyP–CsA complex. As can be seen in Figure 7, the structure of CyP bears no obvious resemblance to that of FKBP12. CyP is composed of an eight-stranded antiparallel β barrel capped at each end by an α helix. The topology of the β strands is $+1, -3, -1, -2, +1, -2, -3$, which results in an unusual loop crossing reminiscent of that seen in FKBP12. The eight-stranded β-barrel structure of CyP is related to the structures of several members of the β-protein family,[71] including bilin-binding protein,[72a] retinol-binding protein,[72b] β-lactoglobulin,[72c] and insecticyanin.[72d] Like CyP, these proteins also bind small hydrophobic ligands. The ligand-binding pocket of β-proteins is in a cleft between the two sheets forming the barrel.[71, 72] In CyP, however, intermolecular NOEs, chemical shift changes on binding, and overall geometry of the protein indicate that the CsA-binding pocket is not located inside the central β barrel.[67, 68] Rather, it is in a cleft at the protein surface formed by one sheet of the barrel and the loop from Lys 118 to His 126. Previous NMR studies indicated that bound CsA contacts the side chains of the single tryptophan residue of CyP, Trp 121, and an unidentified phenylalanine residue.[73] The CyP structure corroborates this data, since Trp 121 sits at one end of the binding pocket, and Phe 60 and Phe 113 are located at its base. The structure also provides an explanation of the inhibition of CyP rotamase activity and CsA binding by modification of cysteine residues with *p*-hydroxymercuribenzoic acid,[12b] as Cys 115 and Cys 62 are both located in the binding pocket. The roles of other residues in the binding cleft, including His 54, Arg 55, Ile 57, Met 61, Asn 102, Gln 111, Leu 122, and His 126 are still unclear. However, the generally high conservation of these residues in the various cyclophilins suggests that they make important contacts to the ligand, and may also be involved in rotamase catalysis. In this regard, it is curious that there are no obvious similarities between the active sites of FKBP12 and CyP.

4.2. Cyclosporin A (CsA)

In the absence of a complete structure of the CyP–CsA complex it is difficult to identify differences between bound and unbound CyP that may be important for interaction

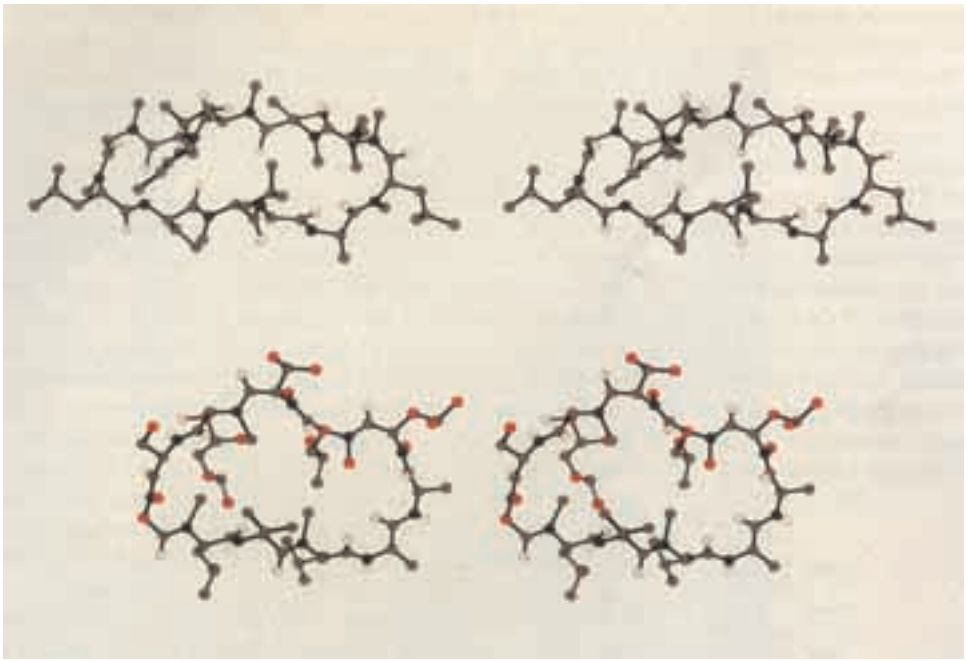

Fig. 14. Stereoviews of free (top) and bound (bottom) CsA. In the structure of bound CsA, atoms with attached hydrogens that show NOE crosspeaks to CyP in a NOESY spectrum (50 ms) of the CyP–CsA complex are shaded red[70].

with CN. However, the existance of both free[74] and bound[69, 70] CsA structures (Fig. 14) does allow such an analysis to be made for the ligand portion of the complex. The conformation of bound CsA is strikingly different from the conformation of the free ligand in the crystalline state and in organic solvents. (The crystal and solution structures of CsA in organic media, for example methylene chloride, are extremely similar, and hence will be referred to jointly as the conformation of the "free" ligand. The insolubility of CsA in aqueous media has prevented detailed structure determination in more biological environments (however, see Quesniaux et al.[75]). Thus, as with the FKBP ligands, comparisons between free and bound CyP ligands should be interpreted cautiously.) Free CsA can be divided into two overlapping domains. The first consists of residues 11–3 and 4–7, which form two strands of an antiparallel β sheet joined by a type β II′ turn at residues 3 and 4. There are hydrogen bonds between Abu 2 NH and Val 5 CO, Val 5 NH and Abu 2 CO, and Ala 7 NH and MeVal 11 CO stabilizing the structure. Notably, all the *N*-methyl groups in this region (11, 2, 4, 6) are directed outside the macrocyclic ring. The second domain consists of residues 7–11, which form an irregular loop stabilized by a hydrogen bond from D-Ala 8 NH to MeLeu 6 CO and a number of van der Waals contacts, including several to the *N*-methyl group of MeVal 11, which is directed into the center of the macrocycle. All amide bonds in the structure are *trans*, except that between MeLeu 9 and MeLeu 10, which is *cis*.

In contrast to free CSA, the bound molecule has no elements of regular secondary structure. In addition, there are no intramolecular hydrogen bonds. Of the seven *N*-methyl groups, only two, those of MeVal 11 and MeLeu 9, are exposed. The remainder are directed into the macrocycle and make a number of intramolecular van der Waals contacts. Correspondingly, all four amide NH groups and ten of eleven amide CO groups are at least partly exposed. On the basis of H/D-exchange rates it was proposed that one amide NH group, that of Abu 2, makes an intermolecular hydrogen bond to CyP. Strikingly, all amide bonds in the bound conformation are *trans*, indicating a high energy barrier to binding.

In addition to determining the structure of bound CsA, Weber et al. and Fesik et al. also identified a number of intermolecular NOEs between ligand and receptor.[69, 70] In particular, many NOEs were observed from aromatic and aliphatic residues of CyP, including the sole tryptophan, Trp 121. These NOEs indicate, as had been previously suggested,[76] that CsA binds in a hydrophobic pocket of the protein. The patterns and locations of protein–ligand NOEs also allowed both groups to determine the regions of CsA that contact CyP in the complex. As indicated in Figure 14 bottom, the amino acid residues 9 through 3 all show a number of intermolecular contacts. Hence, these residues constitute the binding domain of CsA. In contrast, residues 4 through 8 show only intramolecular NOEs, indicating they do not strongly interact with the protein. This suggests that these residues may constitute the region of CsA that is in contact with calcineurin (CN) when simultaneously bound to CyP.

An important tenet of the active complex hypothesis is that the only necessary requirement for signal inhibition by a drug is binding of the immunophilin–drug complex to its relevent biological target (CN in the case of FK506 and CsA). The tight binding of drug to immunophilin is not necessary per se, and as demonstrated with 506BD is also not sufficient to cause inhibition. With this in mind, the identification of distinct binding and possible effector domains of CsA allows explanation of the biochemical and biological data on a wide range of CsA analogues. In most but not all cases there is a direct correlation between CyP binding and inhibitory activity measured in T-cell activation assays.[77, 78] Not surprisingly, most of the analogues that do not bind CyP have been modified in the regions of the drug that contact the protein. For example, the following analogues all

have > 80% decrease in CyP binding and activity in T-cell activation assays relative to CsA: MeAla 9, MeAla 10, MeAla 11, MeLeu 11, α-amino-γ-fluorobutyrate 2.[77] A number of modifications of the MeBmt 1 side chain have similar effects. There are, however, several CsA analogues that do not show a correlation between CyP binding and signal inhibition. These can be divided into two categories: 1) those that do not bind CyP tightly, but are inhibitory and 2) those that do bind CyP, but are not inhibitory. The existence of such compounds has led to speculation that CyP may not be the relevant biological receptor of CsA (that is, not the receptor responsible for the biological actions of the drug).[78] The active complex hypothesis provides an interesting alternative explanation of this data. In the first category there is only one reported molecule, dimethyl-Bmt–CsA (Fig. 15). This compound binds CyP roughly a hundredth as

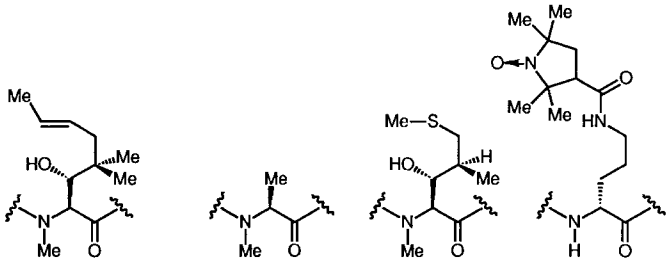

Fig. 15. Modified side chains of CsA analogues whose immunosuppressive activity does not correlate with affinity for CyP. Numbers refer to amino acid positions in CsA.

tightly as CsA, but retains 35% of the inhibitory activity of CsA in T-cell activation assays. It is possible that although dimethyl-Bmt–CsA binds CyP weakly on its own, its binding may be enhanced on binding of the ligand–receptor complex to CN. That is, the additional protein–protein and protein–ligand contacts in the ternary complex may be sufficient to overcome the energetic penalty incurred by the addition of a methyl group to CsA. Investigations of the CyP–dimethyl-Bmt–CsA complex support this possibility and indeed resolve the paradox surrounding this molecule.[79] The second category of CsA analogues consists of compounds with modifications to three residues: MeBmt 1, MeLeu 6, and D-Ala 8. These compounds include, among others, MeAla 6, Me-Thia-Bmt 1, and TPc-D-Orn 8 (Fig. 15). The properties of these molecules are reminiscent of those of 506BD, which binds FKBP but does not interfere with signal transduction in T cells or mast cells. By analogy with 506BD, these molecules contain the elements necessary to interact with CyP, but do not have the proper structure to enable their ligand–receptor complexes to bind to CN. This explanation is consistent with the location of residues 6 and 8 on the effector domain of CsA. In addition, the MeBmt 1 derivatives in the second category all possess modifications of the MeBmt side chain at locations near the side chain of MeLeu 6 on one face of the bound CsA macrocycle. Thus, MeBmt 1 may be important for contacting both CyP and CN in the pentameric complex. In support of these explanations of the various synthetic analogues, results in our laboratory illustrate that for a number of analogues of both FK506 and CsA, inhibition of signal transduction correlates exactly with the ability of complexes of these molecules with their cognate immunophilin receptors to inhibit the phosphatase activity of CN.[79]

The conformation of the CsA effector domain also suggests a possible mode of interaction of the CsA portion of the CyP–CsA complex with CN. The CsA backbone from the carbonyl group of Sar 3 through the amide NH group of Ala 7, with the exception of MeLeu 4, is reminiscent of one strand of a pleated β sheet. This suggests that the interactions between bound CsA and CN may resemble those observed between strands of a β sheet. The carbonyl groups of residues 3 and 5, and the NH group of residue 7 all lie in the plane of the CsA macrocycle, and are directed outward. The amide plane containing Val 5 NH and MeLeu 4 CO is angled relative to the plane of the macrocycle, although Val 5 NH could still be accessible for hydrogen-bonding interactions with CN. Note that the *N*-methyl groups of residues 4 and 6, which might interfere sterically with a regular pattern of hydrogen bonds, are directed into the macrocyclic ring and thus remain unobtrusive. Finally, the side chains of residues 4, 5, and 6 alternate above and below the plane of the CsA macrocycle in a fashion similar to that seen in β sheets. This enables the side chains of MeLeu 4 and MeLeu 6 to participate in stabilizing contacts with the side chains of MeLeu 10 and MeBmt 1 on one face of the macrocycle. These features together result in a regular, accessible surface composed of the side chains of 4, 5, and 6, and the backbone amide groups of residues 3 through 7 that would be able to make a number of hydrophobic and hydrogen-bonding contacts with CN. The structure of this surface suggests that the CsA portion of the CyP–CsA complex may interact with CN in a β-sheet-like structure.

5. Structures of the Pentameric Immunophilin-Drug-CNA-CNB-Calmodulin Complexes

5.1. Contacts between the Immunophilin–Ligand Complexes and CN

It interesting to speculate on which regions of the various immunophilin–ligand complexes are important for contacting their biological targets and which regions impart specificity to the complexes, allowing them to interact with different partners. Is it possible that only the ligand portions of the complexes contact the partner, and that the sole function of the protein is to correctly position the ligand and mold it into the proper conformation for binding? Or can it be that only the protein is important for binding, and that the function of the ligands is to induce or stabilize particular protein conformations that are then able to interact with different biological partners? Or is it possible that a composite surface formed by both ligand *and* receptor is required for binding, and that the ligands and receptors mold each other cooperatively? A variety of evidence suggests that, at least for the FKBP12–ligand complexes, the last possibility is the most likely. The free and bound structures of rapamycin are virtually identical. Thus, rapamycin does not need to interact with FKBP12

in order to take on its biologically active conformation. Yet it is inactive on its own.[22, 23] Comparison of the structure of free FKBP12 with those of its FK506 and rapamycin complexes reveals that regions of the protein that do not contact ligand are not changed significantly by complexation. Thus, the ligands do not exert large allosteric effects on the protein that might facilitate binding to target. This is not surprising, given the relatively small size of FKBP12. More significantly, comparison of the two complexes shows that even in the regions of the structure surrounding the ligands, the two proteins are extremely similar. (The differences observed in the region Gly28–Gly33 are most likely artifacts of crystal packing and therefore are probably not significant.[44]) Given the distinct biological effects of the complexes, it then seems unlikely that only the protein contacts the biological target molecules. This analysis suggests a ternary complex in which both immunophilin and ligand make contacts with the target.

5.2. Structure of the FKBP–FK506 and CyP–CsA Binding Site of Calcineurin

Phosphatase inhibition and binding data[26] on the immunophilin–ligand complexes provide insight into the structures of the pentameric complexes. The ability of CyP–CsA to displace calcineurin and calmodulin from an immobilized FKBP–FK506 reagent demonstrates that the two complexes share either a common binding site or two interacting binding sites on CN.[26] It is not apparent from the available structural data how the two complexes might interact with a common site. The resolution of this issue may require further information on the regions of the two proteins (FKBP12 and CyP) that are involved in CN recognition. The inability of calmodulin or the CNB subunit to bind immunophilin–drug complexes suggests that the binding site(s) probably resides in the CNA subunit.[79] The increased binding of FKBP–FK506 and CyP–CsA to CN in the presence of calmodulin also suggests that the calmodulin- and immunophilin–ligand-binding sites are not independent.[79] The interaction between these sites may be transmitted indirectly, through changes to CN, or more directly, through stabilizing interactions between calmodulin and the immunophilin–ligand complex when both are bound to CNA. A more detailed picture of the immunophilin–ligand binding site may be derived from the substrate-dependence of CN inhibition. The dephosphorylation of a 20-residue phosphopeptide by CN is strongly inhibited by both FKBP–FK506 and CyP–CsA (K_i = ca. 30 nM when measured with bovine CN and human immunophilins[79]). However, dephosphorylation of *p*-nitrophenyl phosphate is actually enhanced by approximately a factor of 3 at similar concentrations of the two immunophilin–drug complexes.[26] These data indicate that the binding site for the complex is not the enzyme active site, but the two sites are probably spatially close to each other. A similar relationship between binding and active sites is seen in the recently solved crystal structure of cyclic AMP-dependent protein kinase bound to a peptide inhibitor.[88] A schematic illustration of this description of the immunophilin–ligand binding site is presented in Figure 16. Thus, our current model of pentameric complex formation

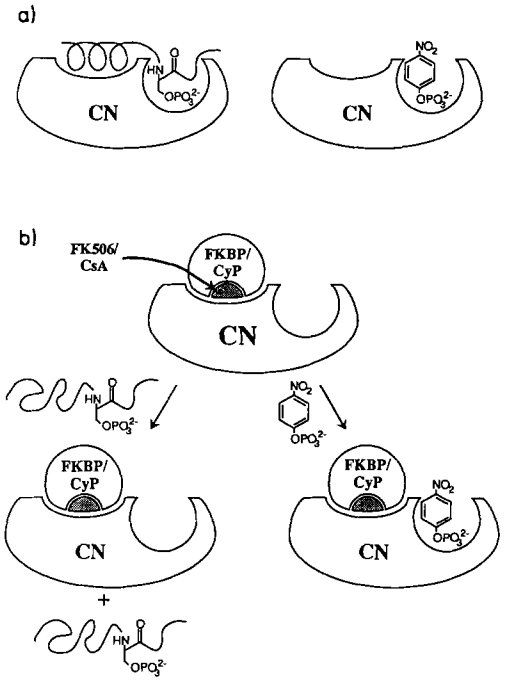

Fig. 16. Model of the binding site of CN in the immunophilin–ligand complex. a) Two different substrates, a phosphopeptide and *p*-nitrophenyl phosphate, are bound to CN. b) Immunophilin–ligand complexes, FKBP12–FK506 and CyP–CsA, affect the enzymatic activity of CN on the two substrates (phosphopeptide and *p*-nitrophenyl phosphate).

involves calmodulin-facilitated binding of FKBP–FK506 or CyP–CsA in a single or in two interacting hydrophobic binding sites that are adjacent to the phosphatase active site present on the A subunit of CN.

6. Additional Roles of the Immunophilins

A variety of data indicate that in addition to mediating the signal inhibition of FK506, rapamycin, and CsA, immunophilins may also have a number of other roles in the cell. For example, FKBP13 is a membrane-associated protein and the predominant FKBP in mast cells.[7, 55, 56] Although FKBP12 and FKBP13 share 43% amino acid sequence identity, and show exact identity for all residues lining the ligand-binding pocket, the two proteins are significantly different in the regions immediately surrounding the binding pocket. In particular, residues in the highly charged basic loop of FKBP12 (Arg40 to Lys44) have been replaced with much different, uncharged residues in FKBP13 (RDRNK → LPQNQ, using the one-letter amino acid code). If this loop is important for binding of the FKBP12–FK506 complex to CN, then these differences imply a different biological role for FKBP13. Indeed, the FKBP13–FK506 complex does not bind CN, although the structural basis for this has not yet been determined.[79] Clues to the biological role of FKBP13 also can be drawn from the protein sequence. Unlike all other known FKBPs, FKBP13 is initially synthesized with a signal peptide at its *N*-terminus that directs the protein into the endoplasmic reticulum (ER).[55, 80] In the ER the peptide is cleaved, leaving the soluble form of the molecule. At its extreme *C*-terminus FKBP13 also contains a possible ER-retention sequence,[81] Arg-Thr-Glu-Leu-CO_2^- (Fig. 12). This causes

the protein to be retained in the ER rather than secreted or directed to other parts of the cell. These two signal peptides indicate that FKBP13 is a resident protein of the ER, and suggest that it may play a role in regulating protein traffic in this organelle. Thus, FKBP13 may be similar in function to the heat-shock proteins[82] and protein disulfide isomerase,[82, 83] which stabilize nascent unfolded or improperly folded polypeptide chains in the ER, preventing their aggregation and precipitation. It is not unreasonable that FKBP13, too, may stabilize unfolded peptides through interactions with its hydrophobic pocket. It may also act as a protein foldase by facilitating the *cis–trans* isomerization of peptidyl–prolyl amide bonds, an event shown to be rate limiting in the in vitro folding of a number of proteins.[84]

Similar roles have also been postulated for two members of the cyclophilin family, CyP-B[58f, 58g] and the protein product of the ninaA gene.[58d, 85] Both these molecules reside in the ER, although CyP-B is a soluble protein whereas ninaA is bound to the membrane through a transmembrane *C*-terminal domain. The ninaA protein, which is located specifically in photoreceptor cells in the eye of *Drosophila melanogaster* is necessary for proper function of the visual pigment rhodopsin. *Drosophila* photoreceptor cells containing a mutant ninaA gene have dramatically reduced levels of rhodopsin, resulting in impaired visual function (the rhodopsin is trapped in the ER[86]). When the mutant gene is replaced with the wild type, rhodopsin function is restored along with normal vision. The actions of ninaA have also been shown to be substrate specific: Of the homologous rhodopsins Rh1, Rh2 (70% amino acid identity to Rh1), and Rh3 (35% amino acid identity to Rh1), only the levels of Rh1 and Rh2 are affected by ninaA mutations. These data suggest that the ninaA cyclophilin is required for the proper trafficking of rhodopsin from the ER to the plasma membrane of the eye.[58d, 85, 86]

Another interesting member of the FKBP family that was discovered using a synthetic rapamycin-based affinity matrix[55] is FKBP25.[57b] This protein consists of two clearly defined domains. The *C*-terminal region consisting of 114 residues is homologous to FKBP12 (42% sequence identity). But the *N*-terminal region consisting of 101 residues does not show significant homology to any known protein. Unlike FKBP12 and FKBP13, which bind FK506 and rapamycin with roughly equal affinity, FKBP25 shows almost 200-fold selectivity for rapamycin over FK506 (K_i(rapamycin) = 0.9 nM; K_i(FK506) = 160 nM). FKBP25 also possesses a possible nuclear localization sequence,[87] consisting of a Lys_4 tetrapeptide and one of two Lys_2 dipeptides. The apparent sequestering of FKBP25 in the nucleus suggests a different role for this protein than for FKBP12 and FKBP13. Rapamycin selectivity, and the presence of an *N*-terminal domain also point to this conclusion. Identification of the role of FKBP25 must wait, however, for a number of analyses. These include confirmation of its presence in the nucleus, determination of the function and structure of its *N*-terminal domain, and assessment of its ability to form inhibitory complexes with FK506 and rapamycin.

The body of data accumulated in the various immunophilins, including those described above, clearly suggest multiple roles for this family of proteins. They are found in virtually all organisms examined to date. They show tissue specificity. They are localized in the cell in compartments ranging from the cytoplasm to the nucleus. They exist in soluble and membrane-bound forms. Finally, nearly all proteins tested to date show rotamase activity, yet the substrate specificity varies from protein to protein. These data, while providing only hints as to the exact nature of the biological roles of this family, do indicate that there are many interesting aspects of immunophilin function that are still unexplored.

7. Summary and Outlook

In summary, a family of natural products was used to identify a new family of protein receptors, named immunophilins. Investigations of these proteins resulted in the understanding that they function as complexes with their cognate immunosuppressive ligands. This led to the use of immunophilin–ligand complexes as probes of cellular signal transduction pathways, allowing the discovery of a common target, calcineurin. Identification of substrates of CN may provide yet a further step in this pathway. In this manner, by beginning with inhibitory natural products, a signal transduction pathway can be investigated molecule by molecule through the black box of the cytoplasm.

It is not unusual for natural products from one organism to bind to proteins in another. Examples of this include many pharmacologically useful compounds including the opiates and antimitotic agents. It is also not unprecedented that ligands are able to enhance the interaction between two proteins. The uniqueness of the immunophilin story resides in the fact that the ligands FK506, CsA, and rapamycin possess both these properties. Not only do they bind to proteins in organisms other than those that produce them, but in binding they enhance the interactions between these proteins and others. Thus, all three of the known natural immunophilin ligands have evolved with two separate but related abilities. It seems difficult to believe that this dual function arose fortuitously, especially if one considers the complex relations between the three ligands described in the introduction of this review.

This quandary leads to a number of basic, and still unanswered questions regarding the function of these fascinating compounds and their biological receptors. To begin with, why do the immunosuppressants FK506, CsA, and rapamycin exist? What purpose does it serve fungi to make compounds with their complicated and interrelated spectrum of properties? Similarly, why do the immunophilins exist? Surely they did not evolve to bind molecules found only in microorganisms. If their purpose is to regulate signal transduction in cells, how are they activated? Are there endogenous molecules whose actions are mimicked by the various immunosuppressants? If so, can we identify these molecules and use their bound structures to design better signal transduction inhibitors? At a more detailed level there are still many questions. What is the physiological role of CN, and what are its natural substrates? Thus, how close are we to defining all of the molecules in the black box of the signal transduction pathway from cell surface receptors to the nucleus? (For a speculative proposal addressing this question see [89].) What is the target of the later acting FKBP–rapamycin complex? Is this molecule related to CN? Finally,

what is the structural basis for the formation of the different ternary immunophilin–ligand–target complexes? Can the structures of these complexes provide us with general knowledge about the mechanisms of molecular recognition? The resolution of these questions will depend, as have the studies that led us to them, on a variety of experimental methods and approaches. It is hoped that by applying the complementary tools of chemistry, biology, and structural analysis, we will be in a position to pose even more exciting questions in the future.

We would like to thank our many friends and colleagues who have been involved in the structural studies of the immunophilins. In particular, our continuing collaborations with Jon Clardy and his group at Cornell University have yielded a wealth of structural insights into the molecular basis of immunophilin function. Our success in determining the solution structure of unbound FKBP12 would also have been impossible without the patience, guidance, and efforts of Stephen Michnick, and the hard work and critical analysis of Tom Wandless and Professor Martin Karplus of the Harvard Chemistry Department. Thanks go out to Mark Albers and Tom Wandless for critiquing the manuscript, Robert Standaert for kindly providing Figure 12, and Dr. Hengming Ke of the University of North Carolina for providing coordinates of CyP (used to prepare Fig. 7) prior to publication. Finally, we owe a great debt to other members of the Schreiber group, including M. A., Jun Liu, Pat Martin, R. S., and T. W. whose commitment and enthusiasm have made the immunophilin project in this laboratory exciting and successful. M. K. R. would like to thank the American Chemical Society Division of Organic Chemistry and Merck, Sharp & Dohme for financial support in the form of a graduate fellowship. Immunophilins research in the S. L. S. laboratory is supported by grants from the National Institutes of General Medical Sciences (GM-38627 and GM-40660).

Received: October 25, 1991 [A 8591E]
German version: *Angew. Chem.* **1992**, *104*, 413.

[1] H. Tanaka, A. Kuroda, H. Marusawa, H. Hatanaka, T. Kino, T. Hoto, M. Hashimoto, T. Taga, *J. Am. Chem. Soc.* **1987**, *109*, 5031–5033.
[2] A. W. Thomson, *Immunol. Today* **1989**, *10*, 6–9.
[3] a) A. Rüegger, M. Kuhn, H. Licht, H. R. Loosli, R. Huguenin, C. Quiquerez, A. von Wartburg, *Helv. Chim. Acta* **1976**, *59*, 1075; b) T. J. Petcher, H. P. Weber, A. Rüegger, *ibid.* **1976**, *59*, 1480; c) R. M. Wenger, *Prog. Chem. Org. Nat. Prod.* **1986**, *50*, 123–168; *Angew. Chem.* **1985**, *97*, 88–96; *Angew. Chem. Int. Ed. Engl.* **1985**, *24*, 77–85.
[4] a) J. E. Kay, C. R. Benzie, M. R. Goodier, C. J. Wick, S. E. A. Doe, *Immunology* **1989**, *67*, 473–477; b) J. E. Kay, S. E. A. Doe, C. R. Benzie, *Cell. Immunol.* **1989**, *124*, 175–181; c) P. Walliser, C. R. Benzie, J. E. Kay, *Immunology* **1989**, *68*, 434–435.
[5] J. E. Kay, A. L. Moore, S. E. A. Doe, C. R. Benzie, R. Schönbrunner, F. X. Schmid, A. P. Halestrap, *Transplantation Proc.* **1990**, *22*, 96–99.
[6] M. J. Tocci, K. A. C. Matkovich, P. Kwok, F. Dumont, S. Lin, S. Degudicibus, J. J. Siekierka, J. Chin. N. I. Hutchinson, *J. Immunol.* **1989**, *143*, 718–726.
[7] T. Hultsch, M. W. Albers, S. L. Schreiber, R. J. Hohman, *Proc. Natl. Acad. Sci. USA* **1991**, *88*, 6229–6233.
[8] S. L. Schreiber, *Science* **1991**, *251*, 283–287.
[9] The focus of this article is primarily structural; for a discussion of the biological aspects of immunophilin research see: S. L. Schreiber, J. Liu, M. W. Albers, R. Karmacharya, E. Koh, P. K. Martin, M. K. Rosen, R. F. Standaert, T. J. Wandless, *Transplantation Proc.* **1991**, *23*, 2851–2857.
[10] a) N. Yoshimura, S. Matsui, T. Hamashima, T. Oka, *Transplantation* **1989**, *47*, 351; b) N. Yoshimura, S. Matsui, T. Hamashima, T. Oka, *ibid.* **1989**, *47*, 356; c) T. Starzl, J. Fung, R. Venkataramman, S. Todo, A. J. Demetris, A. Jain, *Lancet ii* **1989**, 1000–1004.
[11] a) M. W. Harding, A. Galat, D. E. Uehling, S. L. Schreiber, *Nature* **1989**, *341*, 758–760; b) J. J. Siekierka, S. H. Y. Hung, M. Poe, C. S. Lin, N. H. Sigal, *ibid.* **1989**, *341*, 755–757.
[12] a) R. E. Handschumacher, M. W. Harding, J. Rice, R. J. Drugge, D. W. Speicher, *Science* **1984**, *226*, 544–546; b) G. Fischer, H. Bang, C. Mech, *Biomed. Biochim. Acta* **1984**, *43*, 1101–1111; c) G. Fischer, B. Wittmann-Liebold, K. Lang, T. Kiefhaber, F. X. Schmid, *Nature* **1989**, *337*, 476–478; d) N. Takahashi, T. Hayano, M. Suzuki, *ibid.* **1989**, *337*, 473–475.
[13] E. E. Emmel, C. L. Verweij, D. B. Durand, K. M. Higgins, E. Lacy, G. R. Crabtree, *Science* **1989**, *246*, 1617–1620.
[14] A. J. Findlay, L. Radics, *Can. J. Chem.* **1980**, *58*, 579–590.
[15] B. E. Bierer, P. S. Mattila, R. F. Standaert, L. A. Herzenberg, S. J. Burakoff, G. Crabtree, S. L. Schreiber, *Proc. Natl. Acad. Sci USA* **1990**, *87*, 9231–9235.
[16] B. E. Bierer, P. K. Somers, T. J. Wandless, S. J. Burakoff, S. L. Schreiber, *Science* **1990**, *250*, 556–559; b) P. K. Somers, T. J. Wandless, S. L. Schreiber, *J. Am. Chem. Soc.* **1991**, *113*, 8045–8056.
[17] T. J. Wandless, S. W. Michnick, M. K. Rosen, M. Karplus, S. L. Schreiber, *J. Am. Chem. Soc.* **1991**, *113*, 2339–2341.
[18] F. J. Dumont, M. J. Staruch, S. L. Koprak, M. R. Melino, N. H. Sigal, *J. Immunol.* **1990**, *144*, 251–258.
[19] J. E. Kay, L. Kromwel, S. E. A.Doe, M. Denyer, *Immunology* **1991**, *72*, 544–549.
[20] F. J. Dumont, M. R. Melino, M. J. Staruch, S. L. Koprak, P. A. Fischer, N. H. Sigal, *J. Immunol* **1990**, *144*, 1418–1424.
[21] M. Tropschug, I. B. Barthelmess, W. Neupert, *Nature* **1989**, *342*, 953–957.
[22] Y. Koltin, L. Faucette, D. J. Bergsma, M. A. Levy, R. Cafferkey, P. L. Koser, R. K. Johnson, G. P. Livi, *Mol. Cell. Biol.* **1991**, *11*, 1718–1723.
[23] J. Heitman, N. R. Movva, M. N. Hall, *Science* **1991**, *253*, 905–909.
[24] Similar findings with FK506 have been reported: J. Heitman, N. R. Movva, P. C. Hiestand, M. N. Hall, *Proc. Natl. Acad. Sci U.S.A.* **1991**, *88*, 1948–1952.
[25] C. B. Klee, M. H. Krinks, *Biochemistry* **1978**, *17*, 120–126; b) C. B. Klee, T. H. Crouch, M. H. Krinks, *Proc. Natl. Acad. Sci., U.S.A.* **1979**, *76*, 6270–6273.
[26] J. Liu, J. D. Farmer, Jr., J. Friedman, I. Weissman, S. L. Schreiber, *Cell* **1991**, *66*, 807–815.
[27] W. M. Flanagan, B. Corthesy, R. J. Bram, G. R. Crabtree, *Nature* **1991**, *352*, 803–807.
[28] A. L. DeFranco, *Nature* **1991**, *352*, 754–755.
[29] An example of a dephosphorylation-dependent translocation of a cytoplasmic transcription factor into the nucleus has recently been reported: T. Moll, G. Tebb, U. Surana, H. Robitsch, K. Masmyth, *Cell* **1991**, *66*, 743–758.
[30] M. K. Rosen, R. F. Standaert, A. Galat, M. Nakatsuka, S. L. Schreiber, *Science* **1990**, *248*, 863–866.
[31] G. Fischer, E. Berger, H. Bang, *FEBS Lett.* **1989**, *250*, 267–270.
[32] a) R. K. Harrison, R. L. Stein, *Biochemistry* **1990**, *29*, 1684–1689; b) R. K. Harrison, C. G. Caldwell, A. Rosegay, D.Melillo, R. L. Stein, *J. Am. Chem. Soc.* **1990**, *112*, 7063–7064.
[33] J. Liu, M. W. Albers, C. Chen, S. L. Schreiber, C. T. Walsh, *Proc. Natl. Acad. Sci. U.S.A.* **1990**, *87*, 2304–2308.
[34] M. W. Albers, C.T. Walsh, S. L. Schreiber, *J. Org. Chem.* **1990**, *55*, 4984–4986.
[35] J. L. Kofron, P. Kusmic, V. Kishore, E. Colón-Bonilla, D. H. Rich, *Biochemistry* **1991**, *30*, 6127–6134.
[36] M. Nakatsuka, J. A. Ragan, T. Sammakia, D. B. Smith, D. E. Uehling, S. L. Schreiber, *J. Am. Chem. Soc.* **1991**, *112*, 5583–5601.
[37] a) R. F. Standaert, A. Galat, G. L. Verdine, S. L. Schreiber, *Nature* **1990**, *346*, 671–674; b) N. Maki, F. Sekiguchi, J. Nishimaki, K. Miwa, T. Hayano, N. Takahashi, M. Suzuki, *Proc. Natl. Acad. Sci. U.S.A.* **1990**, *87*, 5440–5443.
[38] A caution against interpreting the hemiketal hydroxyl as a mimic of an amide NH is in order: D. K. Donald, M. E. Cooper, M. Furber, E. Wells, R. Hutchinson, F. M. Black, *Tetrahedron Lett.* **1991**, *32*, 1375–1378.
[39] M. K. Rosen, S. W. Michnick, M. Karplus, S. L. Schreiber, *Biochemistry* **1991**, *30*, 4774–4789.
[40] S. W. Michnick, M. K. Rosen, T. J. Wandless, M. Karplus, S. L. Schreiber, *Science* **1991**, *251*, 836–839.
[41] J. A. Moore, D. A. Peattie, M. J. Fitzgibbon, J. A. Thomson, *Nature* **1991**, *351*, 248–250.
[42] G. D. Van Duyne, R. F. Standaert, P. A. Karplus, S. L. Schreiber, J. Clardy, *Science* **1991**, *251*, 839–842.
[43] G. D. Van Duyne, R. F. Standaert, S. L. Schreiber, J. Clardy, *J. Am. Chem. Soc.* **1991**, *113*, 7433–7434.
[44] G. D. Van Duyne, R. F. Standaert, P. A. Karplus, S. L. Schreiber, J. Clardy, unpublished results.
[45] Y. Ikeda, S. L. Schreiber, unpublished results.
[46] R. Taylor, O. Kennard, *J. Am. Chem. Soc.* **1982**, *104*, 5063–5070.
[47] K. A. Thomas, G. M. Smith, T. B. Thomas, R. J. Feldmann, *Proc. Natl. Acad. Sci. U.S.A.* **1982**, *79*, 4843–4847.
[48] K. B. Wiberg, R. F. Waldron, G. Schulte, M. Saunders, *J. Am. Chem. Soc.* **1991**, *113*, 971–978.
[49] A. Horovitz, L. Serrano, B. Avron, M. Bycroft, A. R. Fersht, *J. Mol. Biol.* **1990**, *216*, 1031–1044.

[50] M. K. Rosen, S. W. Michnick, S. L. Schreiber, unpublished results.
[51] P. Karuso, H. Kessler, D. F. Mierke, *J. Am. Chem. Soc.* **1990**, *112*, 9434–9436.
[52] D. F. Mierke, P. Schmieder, P. Karuso, H. Kessler, *Helv. Chim. Acta* **1991**, *74*, 1027–1047.
[53] J. Pranata, W. L. Jorgensen, *J. Am. Chem. Soc.* **1991**, *113*, 9483–9493.
[54] A. M. Petros, R. T. Gampe, Jr., G. Gemmecker, P. Neri, T. F. Holzman, R. Edalji, J. Hochlowski, M. Jackson, J. McAlpine, J. R. Luly, T. Pilot-Matias, S. Pratt, S. W. Fesik, *J. Med. Chem.* **1991**, *34*, 2928–2931.
[55] H. Fretz, M. W. Albers, A. Galat, R. F. Standaert, W. S. Lane, S. J. Burakoff, B. E. Bierer, S. L. Schreiber, *J. Am. Chem. Soc.* **1991**, *113*, 1409–1411.
[56] Y.-J. Jin, M. W. Albers, W. S. Lane, B. E. Bierer, S. L. Schreiber, S. J. Burakoff, *Proc. Natl. Acad. Sci. U.S.A.* **1991**, *88*, 6677–6681.
[57] a) Bovine, 12kDa: W. S. Lane, A. Galat, M. W. Harding, S. L. Schreiber, *J. Protein Chem.* **1991**, *10*, 151; b) Bovine, 25kDa: A. Galat, W. S. Lane, R. F. Standaert, S. L. Schreiber, *Biochemistry*, **1992**, *31*, 2427–2434; c) *Neurospora crassa*; M. Tropschug, E. Wachter, S. Mayer, E. R. Schönbrunner, F. X. Schmid, *Nature* **1990**, *346*, 674; d) *Saccharomyces cerevisiae*, G. Wiederrecht, L. Brizuela, K. Elliston, N. H. Sigal, J. J. Siekierka, *Proc. Natl. Acad. Sci. U.S.A.* **1991**, *88*, 1029; see also [22, 24]; e) *Neisseria meningitidis:* A. C. F. Perry, I. J. Nicolson, J. R. Saunders, *J. Bacteriol.* **1988**, *170*, 1691; R. F. Standaert A. Galat, G. L. Verdine, S. L. Schreiber, *Nature* **1990**, *346*, 671; f) *Legionella pneumophila* – macrophage infectivity potentiator (MIP): N. C. Engleberg, C. Carter, D. R. Weber, N. P. Cianciotto, B. I. Eisenstein, *Infect. Immunity* **1989**, *57*, 1263; g) *Chlamydia trachomatis:* A. G. Lundemose, S. Birkelund, S. J. Fey, P. M. Larsen, G. Christiansen, *Mol. Microbiol.* **1991**, *5*, 109; h) open reading frame in the *Pseudomonas aeruginosa* algR2 gene: J. Kato, L. Chu, K. Kitano, J. D. DeVault, K. Kimbara, A. M. Chakrabarty, T. K. Misra, *Gene* **1989**, *84*, 31; G. Wiederrecht, L. Brizuela, K. Elliston, N. H. Sigal, J. J. Siekierka, *Proc. Natl. Acad. Sci. U.S.A.* **1991**, *88*, 1029; i) Mustrans2 (homologue of mouse transition protein 2; S. Nelki, C. Greenhall, F. Shanahan, K. Dudley, unpublished sequence from the EMBL database (accession number X17068, **1990**).
[58] a) *Neurospora crassa:* M. Tropschug, D. W. Nicholson, F.-U. Hartl, H. Köhler, N. Pfanner, E. Wachter, W. Neupert, *J. Biol. Chem.* **1988**, *263*, 14433–14440; b) *Saccharomyces cerevisiae:* B. Haendler, R. Keller, P. C. Hiestand, H. P. Kocher, G. Wegmann, N. R. Movva, *Gene* **1989**, *83*, 39–46; c) *Escherichia coli*: J. Liu, C. T. Walsh, *Proc. Natl. Acad. Sci. U.S.A.* **1990**, *87*, 4028–4032 (note that the rotamase activity of this protein is not inhibited by CsA); d) *Drosophila melanogaster* ninaA: S. Schneuwly, R. D. Shortridge, D. C. Larrivee, T. Ono, M. Ozaki, W. L. Pak, *Proc. Natl. Acad. Sci. U.S.A.* **1989**, *86*, 5390–5394; B.-H. Shieh, M. A. Stamnes, S. Seavello, G. L. Harris, C. S. Zuker, *Nature* **1989**, *338*, 67–70; e) tomato, maize, *Brassica napus*: C. S. Gasser, D. A. Gunning, K. A. Budelier, S. M. Brown, *Proc. Natl. Acad. Sci. U.S.A.* **1990**, *87*, 9519–9523; f) human CyP-B: E. R. Price, L. D. Zydowsky, M. Jin, C. H. Baker, F. D. McKeon, C. T. Walsh, *Proc. Natl. Acad. Sci. U.S.A.* **1991**, *88*, 1903–1907; g) *Saccharomyces cerevisiae* CyP-B: P. L. Koser, D. Sylvester, G. P. Livi, D. J. Bergsma, *Nucleic Acids Res.* **1990**, *18*, 1643; h) human CyP-C: J. Friedman, I. Weissman, *Cell* **1991**, *66*, 798–806.
[59] A. G. DiLella, R. J. Craig, *Biochemistry* **1991**, *30*, 8512–8517.
[60] R. Wolfenden, A. Radzicka, *Chemtracts Biochem. Mol. Biol.* **1991**, *2*, 52–54.
[61] R. Wolfenden, *J. Am. Chem. Soc.* **1976**, *98*, 1987–1988.
[62] a) S. G. Cohen, V. M. Vaidy, R. M. Schultz, *Proc. Natl. Acad. Aci. U.S.A.* **1970**, *66*, 249–253; b) R. Wolfenden, *Science* **1983**, *222*, 1087–1093.
[63] T. Drakenberg, K. I. Dahlqvist, S. Forsén, *J. Phys. Chem.* **1972**, *76*, 2178–2183.
[64] S. Scheiner, C. W. Kern, *J. Am. Chem. Soc.* **1977**, *99*, 7042–7050.
[65] K. B. Wiberg, K. E. Laidig, *J. Am. Chem. Soc.* **1987**, *109*, 5935–5943.
[66] K. B. Wiberg, R. F. Waldron, G. Schulte, M. Saunders, *J. Am. Chem. Soc.* **1991**, *113*, 971–977.
[67] J. Kallen, C. Spitzfaden, M. G. M. Zurini, G. Wider, H. Widmer, Wüthrich, M. D. Walkinshaw, *Nature* **1991**, *353*, 276–279.
[68] H. Ke, L. D. Zydowsky, J. Liu, C. T. Walsh, *Proc. Natl. Acad. Sci. U.S.A.* **1991**, *88*, 9483–9487.
[69] C. Weber, G. Wider, B. von Freyberg, R. Traber, W. Braun, H. Widmer, K. Wüthrich, *Biochemistry* **1991**, *30*, 6563–6574.
[70] S. W. Fesik, R. T. Gampe, Jr., H. L. Eaton, G. Gemmecker, E. T. Olenicczak, P. Neri, T. F. Holzman, D. A. Egan, R. Edalji, R. Simmer, R. Helfrich, J. Hochlowski, M. Jackon, *Biochemistry* **1991**, *30*, 6574–6583.
[71] L. Sawyer, *Nature* **1987**, *327*, 659.
[72] a) R. Huber, M. Schneider, O. Epp, I. Mayr, A. Messerschmidt, J. Pflugrath, H. Kayser, *J. Mol Biol.* **1987**, *195*, 423–434; b) M. E. Newcomer, T. A. Jones, J. Åqvist, J. Sundelin, U. Eriksson, I. Rask, P. A. Peterson, *EMBO J.* **1984**, *3*, 1451–1454; c) M. Z. Papiz, L. Sawyer, E. E. Eliopoulos, A. C. T. North, J. B. C. Findlay, R. Sivaprasadarao, T. A. Jones, M. E. Newcomer, P. J. Kraulis, *Nature* **1986**, *324*, 383–385; d) H. M. Holden, W. R. Rypniewski, J. H. Law, I. Rayment, *EMBO J.* **1987**, *6*, 1565–1570.
[73] S.W. Fesik, R. T. Gampe, Jr., T. F. Holzman, D. A. Egan, R. Edalji, J. R. Luly, R. Simmer, R. Helfrich, V. Kishore, D. H. Rich, *Science* **1990**, *250*, 1406–1409.
[74] a) H.-R. Loosli, H. Kessler, H. Oschkinat, H.-P. Weber, T. J. Petcher, A. Widmer, *Helv. Chim. Acta* **1985**, *68*, 682–704; b) H. Kessler, M. Köck, T. Wein, M. Gehrke, *ibid.* **1990**, *73*, 1818–1832.
[75] V. F. J. Quesniaux, R. M. Wanger, D. Schmitter, M. H. V. Van Regenmortel, *Int. J. Pept. Prot. Res.* **1988**, *31*, 173–185.
[76] S. L. Heald, M. W. Harding, R. E. Handschumacher, I. M. Armitage, *Biochemistry* **1990**, *29*, 4466–4478.
[77] P. L. Durette, J. Boger, F. Dumont, R. Firestone, R. A. Frankshun, S. L. Koprak, C. S. Lin, M. R. Melino, A. A. Pessolano, J. Pisano, F. A. Schmidt, N. H. Sigal, M. J. Staruch, B. E. Witzel, *Transplantation Proc.* **1988**, *20(2), Suppl 2*, 51–57.
[78] N. H. Sigal, F. Dumont, P. L. Durette, J. J. Siekierka, L. Peterson, D. H. Rich, B. E. Dunlap, M. J. Staruch, M. R. Melino, S. L. Koprak, D. Williams, B. Witzel, J. M. Pisano, *J. Exp. Med.* **1991**, *173*, 619–628.
[79] J. Liu, M. W. Albers, T. J. Wandless, S. Luan, D. G. Alberg, P. J. Belshaw, P. Cohen, C. MacKintosh, C. B. Klee, S. L. Schreiber, *Biochemistry*, in press.
[80] W. T. Wickner, H. F. Lodish, *Science* **1985**, *230*, 400–407.
[81] a) H. R. B. Pelham, *Trends Biochem. Sci.* **1990**, *15*, 483–486; b) H. R. B. Pelham, *Annu. Rev. Cell Biol.* **1989**, *5*, 1–23.
[82] J. E. Rothman, *Cell* **1989**, *59*, 591–601.
[83] R. B. Freedman, *Trends Biol Sci.* **1984**, 438–441.
[84] J. F. Brandts, H. R. Halvorson, M. Brennan, *Biochemistry* **1975**, *14*, 4953–4963; b) F. X. Schmid, R. L. Baldwin, *Proc. Natl. Acad. Sci. U.S.A.* **1978**, *75*, 4764–4768; c) F. X. Schmid, R. Grafl, A. Wrba, J. J. Beintema, *ibid.* **1986**, *83*, 872–876; d) H. P. Bächinger, *J. Biol. Chem.* **1987**, *262*, 17144–17148; e) J. M. Davis, B. A. Boswell, H. P. Bächinger, *ibid.* **1989**, *264*, 8956–8962.
[85] M. A. Stamnes, B.-H. Shieh, L. Chuman, G. L. Harris, C. S. Zuker, *Cell*, **1991**, *65*, 219–227.
[86] N. J. Colley, E. K. Baker, M. A. Stamnes, C. S. Zuker, *Cell* **1991**, *67*, 255–263.
[87] a) P. A. Silver, *Cell* **1991**, *64*, 489–497; b) J. Robbins, S. M. Dilworth, R. A. Laskey, C. Kingwall, *Cell* **1991**, *64*, 615–623.
[88] D. R. Knighton, J. Zheng, L. F. Ten Eyck, V. A. Ashford, N.-H. Xuong, S. S. Taylor, J. M. Sowadski, *Science* **1991**, *253*, 407–414; b) D. R. Knighton, J. Zheng, L. F. Ten Eyck, N.-H.Xuong, S. S. Taylor, J. M. Sowadski, *ibid.* **1991**, *253*, 414–420.
[89] S. L. Schreiber, G. R. Crabtree, *Immunol. Today* **1992**, *13*, 136–142.

On the Influence of Heteroatoms in α- and β-Functionalized Alkyl Transition-Metal Compounds

By Dirk Steinborn*

Dedicated to Professor Rudolf Taube on the occasion of his 60th birthday

The first homoleptic trimethylsilylmethyl transition-metal complexes were synthesized about 20 years ago in the research groups of Wilkinson and Lappert, resulting in a significant advance in the understanding of the thermodynamic and kinetic stability of transition-metal–carbon σ bonds. The relatively high thermal stability of these bonds provides a dramatic contrast to the Köbrich lithium carbenoids XCH_2Li, known for about 30 years and famous for their extraordinarily high reactivity. Both compound classes illustrate that introduction of a heteroatom into an alkyl ligand can have a profound influence on the structure, stability, and reactivity of an alkylmetal compound, opening the possibility of entirely new reactions. Because of their simple and unambiguous structure, α- and β-heteroatom-substituted transition-metal compounds containing the unit [M–CH_2–Y] or [M–CH_2–CH_2–Y] (where Y is an element from the 4th–7th main groups or groups 14–17, not including C[**]) are particularly suitable for studying effects of the nature of a heteroatom center (neutral/cationic, coordinatively saturated/Lewis basic) on structure, stability, and reactivity as a function of the type of complex, the nature of M, and the number of methylene groups separating M and Y. The diversity of stabilizing and destabilizing influences emanating from the heteroatom center generally produces a broad spectrum of reactivity and stability. This is reflected in an impressive way in homogeneous catalysis, where functionalized alkylmetal compounds arise as intermediates, as well as in the electronic influences of functionalized alkyl ligands, which are determined largely by the nature of the heteroelement present.

1. Introduction

Main-group organometallic compounds have been the subject of intensive investigation since the beginning of this century. By contrast, the chemistry of transition-metal–organic complexes experienced its first dramatic development in the 1950s. One important stimulus was certainly the recognition that transition-metal organometallic compounds are capable of catalyzing a vast number of C–C bond-formation processes and functionalizing reactions of unsaturated hydrocarbons, which in turn opens entirely new possibilities in synthetic organic chemistry and has a profound significance in the context of biochemical phenomena as well.[1]

A growing body of knowledge about organometallic chemistry, together with improved preparative techniques and new approaches to the characterization of substances, have made it increasingly possible to study systems containing not only an M–C bond but also other centers of high reactivity. These include complexes with functionally substituted σ-organo ligands. Important prototypes for functionalized organometallic complexes are the ω-heteroatom-substituted alkylmetal compounds **1**, which can contain a neutral, coordinatively saturated heteroatom center ($YR_n = SiR_3$), a neutral, Lewis-basic heteroatom center ($YR_n = NR_2, PR_2, OR, SR, F, Cl, Br, I$), or a cationic heteroatom center ($^+YR_{n+1} = {}^+NR_3, {}^+PR_3, {}^+OR_2, {}^+SR_2$).

$[L_xM\text{-}(CH_2)_m\text{-}YR_n]$ **1a** $\quad [L_xM\text{-}(CH_2)_m\text{-}\overset{+}{Y}R_{n+1}]$ **1b**

R = alkyl, aryl, H; $m \geq 1$; M = metal

The interface between inorganic and organic chemistry is illustrated by **1**. These compounds represent a link between the "purely organic" doubly substituted hydrocarbons **2** and the binuclear organometallic compounds **3**.[2]

$R_nY\text{-}(CH_2)_m\text{-}YR_n$ **2** $\quad [L_xM\text{-}(CH_2)_m\text{-}ML_x]$ **3**

The unambiguous structure of the compounds **1** seems to predestine them for studies of the influence of metals and heteroatoms as a function of the length of the alkylene bridge. The effect of the heteroatom is complex; on one hand the electronic characteristics and the spatial demands of the organo ligand are modified, and reactions that are possible with analogous nonfunctionalized compounds can be suppressed; for example, β-hydride elimination is *not* possible with the α-functionalized alkyls $[L_xMCH_2YR_n]$ (R = alkyl, aryl), even though with the transition-metal alkyls $[L_xMCH_2CHR_2]$ this generally represents a decomposition pathway with low activation energy. On the other hand, heteroelements can also facilitate fundamentally new types of reactivity (Scheme 1).

As a result of manifold reaction pathways and a variety of stabilizing and destabilizing influences, heteroatom-substituted alkylmetal compounds are subject to a wide variation, as illustrated by the organometallic inner complexes (for instance **4**, the first well-characterized compound of type **1**[3]), the carbenoid **5** that decomposes at temperatures as low as −100 °C,[4] and the thermally relatively stable

[*] Doz. Dr. habil. Dirk Steinborn
Institut für Anorganische Chemie der Technischen Hochschule Merseburg
Geusaer Strasse, D-O-4200 Merseburg (FRG)

[**] Other abbreviations: Bz = benzyl; Cp = η^5-C_5H_5; Cp* = η^5-C_5Me_5; cy = cyclohexyl; H_2pc = phthalocyanine; tmeda = *N,N,N',N'*-tetramethylethylenediamine; X = halogen.

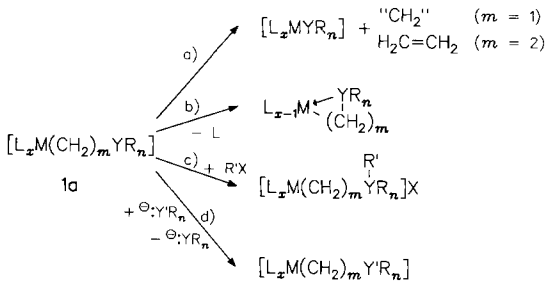

Scheme 1. Some characteristic reactions of **1a**: a) carbenoid reactions ($m = 1$) and fragmentation and β elimination reactions ($m = 2$); b) inner-complex formation; c) ylide ($m = 1$) and "onio" alkyl complex formation ($m \geq 2$); d) substitution of YR_n.

homoleptic[*] alkyl transition-metal compounds **6**.[5] With the synthesis and characterization of **6** the "long search for stable alkyl transition-metal compounds" (Wilkinson, Nobel Prize Lecture 1973[6]) was successfully concluded, leading to fundamental understanding of the stability and reactivity of metal–carbon σ bonds. The significance of the class of compounds **1** is underscored by the potential application of such systems as synthetic building blocks in organic chemistry and as catalysts for homogeneous catalysis, as illustrated by the reagent **7** with its "umpoled" reactivity,[7] as well as by **8**, which is a key intermediate in the Wacker process.[8]

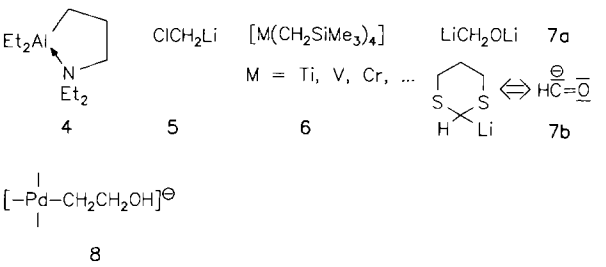

This article provides an overview of the chemistry of the α- and β-functionalized organo-transition-metal compounds **1** ($m = 1, 2$). Several discussions have already appeared of compounds containing γ- and δ-functionalized alkyl ligands together with a Lewis-basic heteroatom (e.g. **4**).[9, 10] The reader is referred to other sources for reviews of the chemistry of α-heteroatom-substituted organo-alkali-metal compounds[11, 12] and metal complexes containing ylide ligands.[13–15]

[*] The term *homoleptic* is applied to σ-organometallic compounds that contain only σ-bonded organo residues. These might also be coordinated further by way of a heteroatom in the sense of intramolecular coordination (organometallic inner or chelate complex).

2. Heteroatom-Substituted Methylmetal Compounds

2.1. Silicon as Heteroatom

2.1.1. Synthesis and Reactivity

Table 1 summarizes broadly applicable synthetic principles relevant to α-functionalized alkylmetal compounds.

Table 1. Principles of synthesis for α-functionalized alkylmetal compounds [a,b].

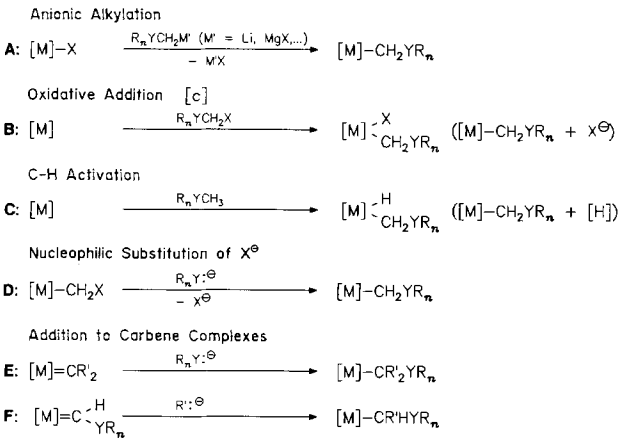

[a] η^2 Coordination can also occur in place of the indicated η^1 coordination provided Y carries a nonbonding pair of electrons. [b] Here and in the following, square brackets around the metal are used to indicate those ligands in a complex that take no direct part in the reaction. The possibility of cleavage or addition of ligands has not been taken into account in the schematic equations, nor has charge balance. [c] Includes reactions that proceed as nucleophilic substitutions with loss of X^-.

Virtually all the metals form trimethylsilylmethyl complexes, and methods **A** and **B** are particularly useful for their synthesis. The isolable homoleptic transition-metal derivatives shown in Table 2 warrant special attention. Their synthesis by anionic alkylation is to some extent attributable to redox reactions (Scheme 2).

Bond strengths for M–CH_2SiMe_3 and M–C_{alkyl} tend to be comparable.[28] The relatively high thermal stability of homoleptic trimethylsilylmethyl complexes has a kinetic origin and is due largely to the absence of β-H atoms (no β-H elimination is possible), the great stability of the Si–C bond,

Dirk Steinborn, born in 1946 in Berlin, studied chemistry from 1965–1969 at the Humboldt-Universität in Berlin and moved in 1970 to the Technische Hochschule Leuna–Merseburg where he completed his doctoral work in 1974 under R. Taube. He then worked for three years in industry. In 1984 he was awarded the degree Dr. sc. nat. for work on nitrogen-substituted alkylmetal compounds and the electronic influence of organo ligands. This was followed in 1986 by a Facultas docendi, after which he was appointed (in 1987) to the faculty of the Technische Hochschule Merseburg. In the same year Steinborn was awarded the Friedrich Wöhler Prize of the Chemischen Gesellschaft. His areas of interest include coordination chemistry, organometallic chemistry and complex catalysis, and bioinorganic chemistry.

Table 2. Homoleptic trimethylsilylmethyl complexes of transition metals.

Compound R = Me_3SiCH_2	Color	$\mu_{eff.}$ [μ_B]	M.p. [°C] ($T_{dec.}$; $t_{1/2}$ [a])	Ref.
Neutral complexes				
9 [TiR_4] [b, c]	pale green-yellow	diamagnetic	0 (137 °C [26]; 110 h)	[16]
10 [ZrR_4] [b, c]	colorless	diamagnetic	10–11 (65 h)	[16]
11 [HfR_4]	colorless	diamagnetic	8–10 (350 h)	[16]
12 [VR_4]	dark green	1.30	43 (95 °C [27])	[17]
13 [$TaMe_3R_2$]	yellow	diamagnetic	(25)	[18]
14 [CrR_4]	purple-red	2.89	40	[17]
15 [Mo_2R_6]	yellow	diamagnetic	99 (100–120 °C [d])	[17, 19]
16 [W_2R_6]	orange-brown	diamagnetic	110	[17, 19]
17 [$MnR_2]_n$	pale orange	2.38 [52]	150 [d]	[20]
Anionic complexes [e]				
18 [LiL_4][LnR_4] [f, g]	colorless ... pink		85...140	[21, 22]
19 [$LiL_4]_2$[UR_6] [h]	light green	2.7 [i]	(30)	[23]
20 [$Li(C_4H_8O_2)]_3$[UR_8]	olive green		(150–154)	[23]
21 Li_2[MnR_4]	reddish brown			[20]
22 [Li(tmeda)]$_2$[MnR_4]	colorless	5.6	168 (dec.)	[24]
23 [Li(tmeda)]$_2$[CoR_4]	blue			[25]

[a] Half-life for the decomposition in benzene at 80 °C for compounds **9** and **10** and at 90 °C for compound **11**. [b] [$M(CH_2SiMe_2Ph)_4$] (M = Ti, Zr), [$Ti(CH_2SiMePh_2)_4$], [$Ti(CH_2SiMe_2Bz)_4$] cf. [16]. [c] Mean bond dissociation enthalpy E_D(Ti–C) = 253 kJ mol^{-1}, E_D(Zr–C) = 310 kJ mol^{-1}. [d] Sublimation temperature in vacuum. [e] Here and in what follows, the square brackets in "ate" complexes are intended only to highlight MC_x coordination. Coordinative interactions are not excluded between the lithium ion and the organic residue (e.g., through multicenter bonding with the σ-bonded C atoms or with the nonbonding electron pairs of Lewis-basic heteroatoms). [f] L = Et_2O, thf, 1/2 tmeda; Ln = Y, Er, Yb, Lu. [g] Regarding the existence of the neutral complex [$Sc\{CH_2SiMe_2(o\text{-}MeOC_6H_4)\}_3$] cf. [49]. [h] L = Et_2O, thf. [i] For L = thf at 273 K.

coordinative saturation of the Si atom, and the increased spatial requirement[29] of the trimethylsilylmethyl ligand (bimolecular decomposition reactions are hindered). In addition to homolytic bond cleavage, thermal decomposition has been shown to involve methylidene and methylidyne complex formation as a consequence of α-H eliminations. It may be that agostic α-CH–M interactions are also relevant, as has been demonstrated for the zirconium complex [$Zr(CH_2SiMe_3)_4\{Me_2P(CH_2)_2PMe_2\}$] (Zr–H = 248 pm, Zr–C = 221.5(9) pm).[30]

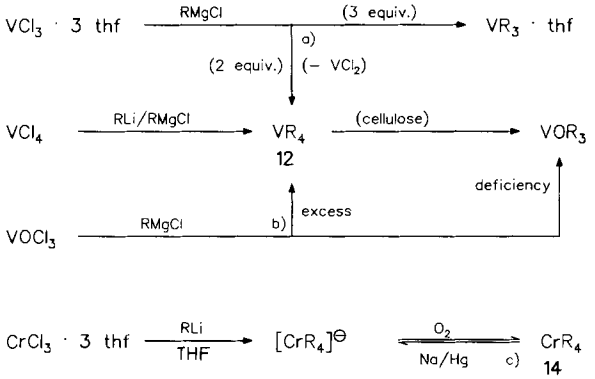

Scheme 2. Synthesis of trimethylsilylmethylvanadium and -chromium compounds [17, 27]. a) Disproportionation; b) reduction; c) $E_{1/2}$ −1.28 V vs. a saturated calomel electrode. R = Me_3SiCH_2.

Homoleptic complexes with terminal and μ_2-trimethylsilylmethylidene and -methylidyne ligands have been prepared, isolated, and characterized (Table 3). μ_3-$CSiMe_3$ ligands appear only in compounds stabilized by complexation,

Table 3. Homoleptic trimethylsilylmethylidene and -methylidyne complexes of transition metals.

Compound R = Me_3SiCH_2	Color	$\mu_{eff.}$ [μ_B]	M.p. [°C] (B.p. [°C]; p [Torr])	Ref.
Methylidene complexes				
24 Li[LuR_2(CHSiMe$_3$)]	greenish white		pyrophoric	[22]
25 [Li(tmeda)]-[LuR_2(CHSiMe$_3$)]	greenish white		113–115 (dec.)	[22]
26 [$LnR(\mu\text{-}CHSiMe_3)]_n$ (Ln = Er, Lu)	pinkish yellow (Ln = Er)		pyrophoric [a]	[22]
27 [MoR_3(CHSiMe$_3$)] [b]	red	1.1	(70; 10^{-3})	[19]
Methylidine complexes				
28 [$Nb_2R_4(\mu\text{-}CSiMe_3)_2$]	red	diamagnetic	152 (dec.)	[17, 31]
29 [$Ta_2R_4(\mu\text{-}CSiMe_3)_2$]	orange	diamagnetic	170 (dec.)	[17, 31]
30 [MoR_3(CSiMe$_3$)]	yellow	diamagnetic	(70; 10^{-3})	[19]
31 [WR_3(CSiMe$_3$)]	yellow	diamagnetic	(70; 10^{-3})	[19]
32 [$W_2R_4(\mu\text{-}CSiMe_3)_2$]	reddish brown	diamagnetic	140–150 [c]	[19, 31, 32]
33 [$Re_2R_4(\mu\text{-}CSiMe_3)_2$]	green		145 (dec.)	[33]

[a] Decomposition temperature for Ln = Er: 380 °C. [b] Isolated as a mixture with **30**. [c] Sublimation temperature at 10^{-3} Torr.

such as [$\{(CO)_3Co\}_3(\mu_3\text{-}CSiMe_3)$].[34] A quasi-aromatic planar dimetallacyclobutadiene structure is present in the binuclear complexes **28**, **29**, **32**, and **33**, in which, depending upon whether the interaction is d^0–d^0, d^1–d^1, or d^2–d^2, the two metal atoms exhibit no bonding, a single bond, or a double bond.[32, 35]

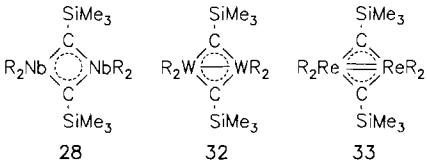

Scheme 3. The methylidyne complexes **28**, **32**, and **33**. The metal–metal distances are 289.7 (**28**), 253.5 (**32**), and 255.7 pm (**33**). R = Me_3SiCH_2.

Compound **32** reacts with alkynes via a π-alkyne complex to give **34** by insertion into the μ_2-$CSiMe_3$ ligand–metal bond. The remarkable fluctuation in μ-allyl ligands probably occurs by way of a μ-cyclopropene complex as intermediate (Scheme 4).[35, 36]

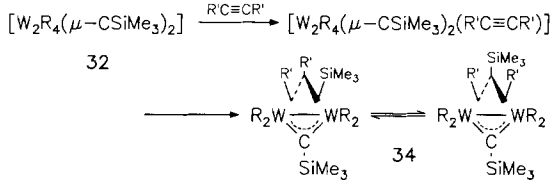

Scheme 4. Reaction of the binuclear complex **32** with alkynes. R = Me_3SiCH_2.

2.1.2. C–H Activation

In the case of trimethylsilylmethyl complexes, intramolecular γ-C–H activation[37] leads to 3-sila-1-metallacyclobutanes[38] (Scheme 5). The M-C-Si-C ring in **39** is nearly planar, with fold angles along the C–C vector of up to 14.3°.[38c] Even the weakly reactive C–H bonds in Me_4Si can be acti-

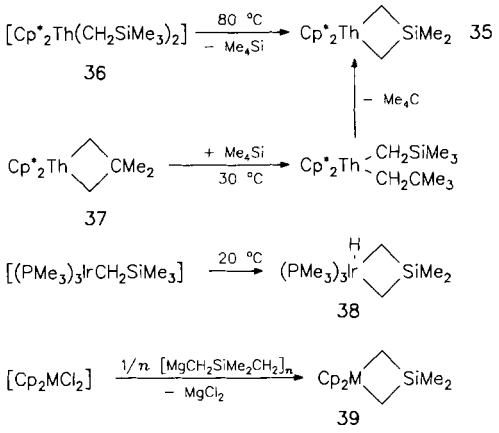

Scheme 5. Synthesis of 3-sila-1-metallacyclobutanes by C–H activation with and without elimination of Me_4Si, as well as by anionic alkylation. M = Ti, Zr, Nb, Mo.

vated intermolecularly! This is shown, for example by the formation of **35** from **37** and Me_4Si.[38d]

The 14 valence-electron (VE) complex fragment **40** ($\widehat{PP} = t\mathrm{Bu_2PCH_2P}t\mathrm{Bu_2}$), whose highly strained four-membered ring (P-Pt-P 74.7(1)° in $[(\widehat{PP})\mathrm{Pt(H)CH_2CMe_3}]$) is responsible for its exceptional reactivity, reacts with Me_4Si by oxidative addition of the C–Si bond to give **42**, a consequence of prior C–H activation.[39] In the case of $\widehat{PP} = \mathrm{cy_2PCH_2CH_2Pcy_2}$ the ring strain is lowered and the reaction ceases at the hydrido complex **41**.[40]

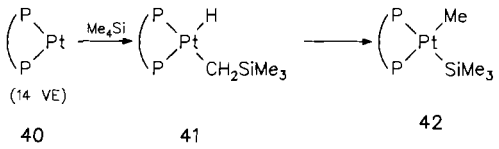

A γ-C–H activation in bis(trimethylsilyl)amide complexes—which can be induced thermally, photochemically, or by bases—leads to azasilametallacyclobutanes[41,42] (Scheme 6).

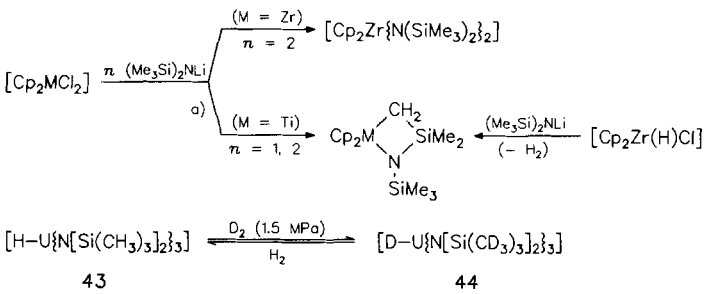

Scheme 6. Synthesis of azasilametallacyclobutanes, which occur as intermediates in the H–D exchange in **43**. a) γ-C–H activation also occurs with 2 equiv $(Me_3Si)_2NLi$ [41]. M = Ti, Zr.

Compounds of this type are key intermediates for the rapid H–D exchange observed in systems like **43**.[43]

2.1.3. η^2-Silaethene Complexes

η^2-Silaethene complexes can be synthesized by Si–H activation or reductive dechlorination from H- or Cl-substituted silylmethyl ligands, respectively (Scheme 7).[44,45] Depending upon the extent of back donation, η^2-silaethene complexes can be characterized either as silametallacyclopropane **48** or π-silene complexes **49**. The experimentally determined Si–

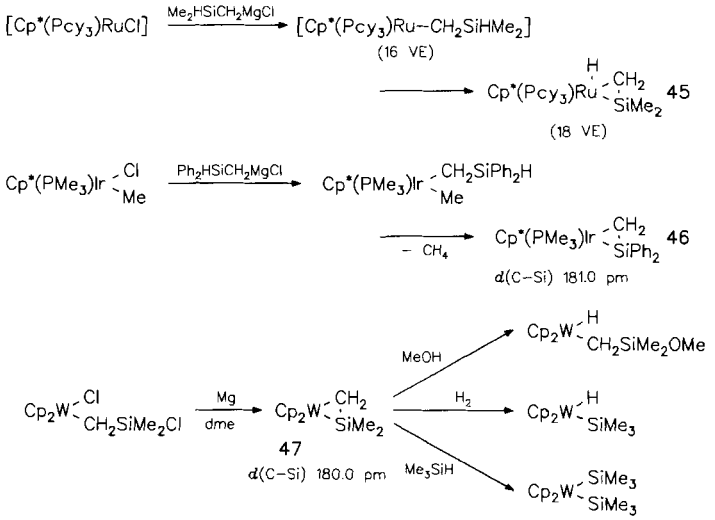

Scheme 7. Synthesis of η^2-silaethene complexes, and characteristic addition reactions involving cleavage of M–Si or M–C bonds.

C bond length of approximately 180 pm indicates partial double-bond character (Si–C ≈ 189 pm; Si=C ≈ 173 pm). The iridium complex **46** is actually quite stable, since no decomposition is observed even at 140 °C in the presence of PMe_3 or upon treatment with hydrogen or UV irradiation.[45] This distinguishes it significantly from comparable

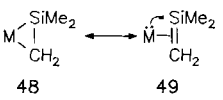

olefin complexes.[46] η^2-Silaethene complexes such as **50** are also accessible by β-H elimination from silylmetal compounds. They are intermediates in the strictly regioselective metal-catalyzed H–D exchange of alkyl silanes (Scheme 8).[47]

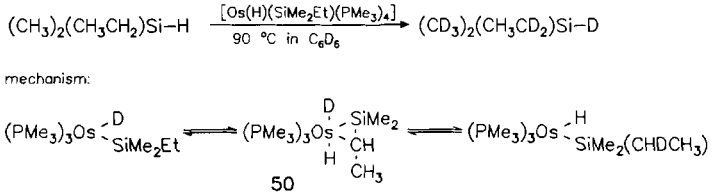

Scheme 8. Metal-catalyzed H–D exchange in alkylsilanes showing the reaction mechanism.

2.1.4. Bis- and Tris(trimethylsilyl)methyl Complexes

The introduction of additional trimethylsilyl residues into trimethylsilylmethyl ligands leads to ligands with considerable spatial demands and a characteristic ability[48] to 1) stabilize metals in their lower coordination states (cf. the overview of homoleptic transition-metal complexes in

Table 4), and 2) produce subvalent main-group-metal alkyls in low oxidation states (cf. the higher homologues of carbenes and alkyl radicals $M[CH(SiMe_3)_2]_n$; M = Ge, Sn, Pb; $n = 2, 3$[54]).

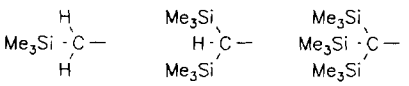

Table 4. Homoleptic bis- and tris(trimethylsilyl)methyl complexes of transition metals.

Compound	Color	$\mu_{eff.}$ [μ_B]	M.p. [°C] (B.p. [°C]; p [Torr])	Ref.
R = $(Me_3Si)_2CH$				
51 [LnR_3] (Ln = La, Sm) [a]				[49]
52 [TiR_3]	blue-green			[50]
53 [VR_3]	blue-green			[50]
54 [CrR_3]	green	3.8	80 [b]	[50]
55 [UR_3]	blue	3.0	60 [b]	[51]
56 [MnR_2]	pale yellow	5.5	8–10 (100–110; 0.5)	[52]
R = $(Me_3Si)_3C$				
57 [MnR_2]	pale yellow	5.1	290 (315 [b])	[53]

[a] An important factor in synthesis according to **A** is the introduction of a Ln alcoholate in place of $LnCl_3$ [49a]. [b] Decomposition temperature.

The structure of bis- and tris(trimethylsilyl)methyl complexes—similar to the case of the homoleptic norbornyl complexes[55]—is characterized in a striking way by the high spatial demands of the ligands and not by the electronic structure of the central atoms. Whereas Mn displays the coordination number 4 in the polymeric compound **17** (see Table 2), the complexes **56** and **57** are linear and monomeric. The coordination number 2 is characteristic for (monomeric) homoleptic tris(trimethylsilyl)methyl compounds: neutral complexes **58**[53, 56] and the anions in **59**[57] are isostructural and isoelectronic. All display strictly linear structures. The structure of **59a** is exceptional in that the compound is a lithate complex.

$[M\{C(SiMe_3)_3\}_2]$ **58**

58: M = Mg (a), Zn (b), Cd (c), Hg (d), Mn (e)

$[Li(thf)_4][M\{C(SiMe_3)_3\}_2]$ **59**

59: M = Li (a), Cu (b), Ag (c)

Compound **54** deviates significantly from planarity (C-Cr-C angle of 117.6°[50]); **51** and **55** are even pyramidal (C-M-C: for M = La, Sm, 110°;[49] for M = U, 107.7°[51]). This is not simply a result of steric factors, but rather is related to an increase in coordination number through agostic γ-methyl–metal interactions, which have also been demonstrated in other bis(trimethylsilyl)methyl complexes.[51, 58] In the case of crystalline $[\{(Me_3Si)_2CH\}_2Mg]_\infty$ there is even an intermolecular agostic interaction $Mg\cdots C'H_3$ (Mg–C' 253.5(4), Mg–H 233.3–251.6 pm, C-Mg-C 140.0(2)°), leading to the unusual coordination number of 3 for magnesium.[59]

The reactivity of bis- and tris(trimethylsilyl)methyl complexes is largely a function of spatial shielding of the central atom: **58b** is stable in boiling hydrochloric acid; it also does not react with bromine.[56a] The Cd and Hg compounds $M[C(SiMe_3)_2(SiMe_2CH{=}CH_2)]_2$ show a similar reactivity; in the case of the Hg compound the vinyl group can be substituted with trifluoroacetic acid at 60 °C without attack on the M–C bond.[60]

The unusually high decomposition temperatures of **58** and $[(Me_2PhSi)_3C–Hg–R]$ (R = CH_2Ph, Ph, Bu) (about 300 °C in the melt!) demonstrate that sterically demanding ligands can also result in stabilization relative to unimolecular radical dissociation, which has been considered in the context of the insufficiently investigated phenomenon of energy transport and energy transfer within a ligand and through a metal.[48, 61]

2.2. Lewis-Basic Heteroatoms

2.2.1. Synthesis of Homoleptic Transition-Metal Complexes

Anionic alkylation (synthesis **A** in Table 1) with $C_5H_{10}NCH_2Li$ has been used to prepare a complete series of homoleptic piperidinomethyl complexes of the 3d elements[62, 63] (Table 5). Treatment of $TiCl_4 \cdot 2thf$ with

Table 5. Homoleptic transition-metal complexes with Lewis-basic heteroatoms.

Compound	Color	$\mu_{eff.}$ [μ_B]	T (dec.) [°C]	Ref.
Aminomethyl complexes ($R = C_5H_{10}NCH_2$)				[62, 63]
60 $Li_4[Ti_2R_6(CNC_5H_{10})_2]$	red	0.39	160–180	
61 $[VR_4]$	brown	1.71	95–105	
62 $[Li(thf)]_2[CrR_4]$	redviolet	4.93	115–125	
63 $Li_2[Cr_2R_6]$	red	0.96/Cr	150–165	
64 $Li_3[CrR_6]$	red	3.93	130–160	
65 $[Li(C_4H_8O_2)]_2[MnR_4]$	pale pink	5.95	140–170	
66a $[Li(thf)]_2[FeR_4]$	yellowish green	5.30	100–120	
66b $[Li(C_4H_8O_2)]_2[FeR_4]$	pale yellow	5.30	100–115	
67a $[Li(thf)]_2[CoR_4]$	blue	4.31	100–115	
67b $[Li(C_4H_8O_2)]_2[CoR_4]$	blue	4.23	100–110	
68 $[Li(Et_2O)]_2[NiR_4]$	yellow	0.33	100–110	
Phosphinomethyl complexes				
69 $[TaMe_3(CH_2PPh_2)_2]$ [a]		diamagnetic		[18]
70 $[La\{\eta^3\text{-}CH(PPh_2)_2\}_3]$	yellow	diamagnetic	>150	[64]
Thiomethyl complex				
71 $[Pd(\mu\text{-}\eta^2\text{-}CH_2SPh)_2]_4$	orange-yellow		164	[65]

[a] Contains traces of tmeda.

$C_5H_{10}NCH_2Li$ leads by α-elimination to the carbyne complex **60**, which probably has a dimeric structure analogous to the μ-trimethylsilylmethylidyne complex **28**. $VCl_3 \cdot 3thf$ can be converted with $C_5H_{10}NCH_2Li$ under redox disproportionation into **61**. $CrBr_2 \cdot 2thf$ reacts with $C_5H_{10}NCH_2Li$ in

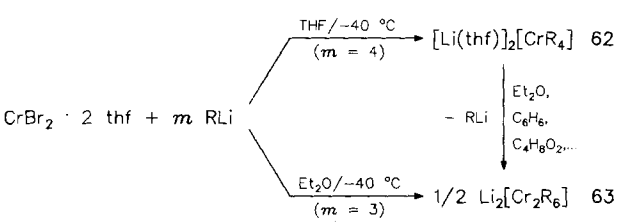

Scheme 9. Synthesis of piperidinomethylchromium(II) complexes. R = $C_5H_{10}NCH_2$.

THF as solvent to give **62**, a high-spin tetraalkylchromate(II) complex, and in ether to give **63** (Scheme 9).

The compounds **60–68** are extremely sensitive to hydrolysis and to air. Reaction with alcohols and $LiAlH_4$ leads, respectively, to protolytic and reductive cleavage of the ligand in the form of *N*-methylpiperidine. A remarkable feature of the homoleptic transition-metal alkyls is their high thermal stability ($T_{dec.} > 100\,^{\circ}C$). These are in every case more stable than the analogous methyl complexes. Apart from the stability of the ligand to β-elimination and its electronic influence, the decisive factor appears here to be a Li–N interaction in the "ate" complexes.

If the halides of the 3d elements from Ti to Ni are treated with thioanisolyllithium at $-78\,^{\circ}C$ and then warmed to room temperature, the result is release of the C_1 to C_3 hydrocarbons with formation of thiophenolate complexes[66] (Scheme 10). The reaction of $CoBr_2 \cdot 2thf$ has been examined in greater detail and shown to produce **74**. The homoleptic thioanisolyl compounds of the 3d elements **72** that are assumed to be intermediates are apparently characterized in general by a low degree of thermal stability due to facile cleavage of the methylene group. Only in the case of palladium has a homoleptic compound **71** (Table 5) been isolated, with μ-η^2-coordination of the thioanisolyl ligand.[65]

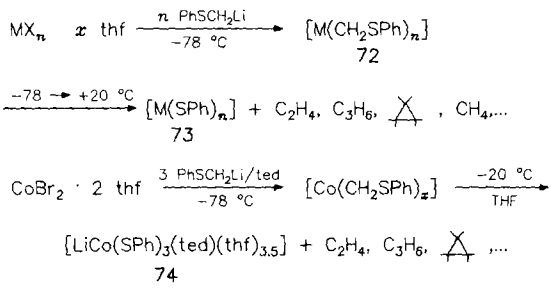

Scheme 10. Reaction of halides of the 3d elements with thioanisolyllithium. In parentheses: fraction of PhSH in sulfur-containing hydrolysis products as percentage. Fe^{II} (88) ≈ Co^{II} (83) > Ni^{II} (58) ≈ Mn^{II} (56) > V^{III} (44) ≈ Ti^{III} (40) > Ti^{IV} (31) ≫ Cr^{III} (9). ted = $N(CH_2CH_2)_3N$.

Reference is made in Table 5 to two stable homoleptic phosphinomethyl transition-metal complexes. The zirconium compounds $[Zr(CH_2YMe)_4]$ (Y = O, S) have been only partially characterized.[67]

2.2.2. Synthesis of Heteroleptic Transition-Metal Complexes

A wide range of heteroleptic transition-metal complexes with functionalized methyl ligands has been prepared; see as a representative example the syntheses of thiomethyl complexes in Scheme 11 and Table 6. The compounds R_nYCH_2M **75** ($R_nY = R_2N$, R_2P, RO, RS; M = Li, MgX) represent readily accessible and reasonably stable starting materials for anionic alkylation (**A**); only $ROCH_2Li$ and $ROCH_2MgX$ decompose as carbenoids at temperatures below $0\,^{\circ}C$.[11, 76] Halomethyl compounds[77] of lithium and magnesium are such thermolabile carbenoids (they decompose between -50 and $-100\,^{\circ}C$[4, 76]) that they are unsuitable for syntheses along route **A**. On the other hand, they can

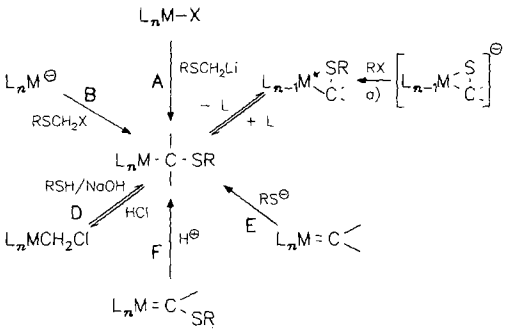

Scheme 11. Synthesis of heteroleptic functionalized methyl transition-metal compounds as illustrated by the example of thiomethyl complexes. a) *S*-Alkylation of thioformaldehyde complexes.

be considerably stabilized by complex formation with transition-metal compounds such as $[Ti(OiPr)_4]$.[78]

An oxidative addition reaction **B** employing the iminium salts $[R_2N{=}CH_2]X$, $ROCH_2Cl$, $RSCH_2Cl$, or CH_2X_2 has been widely used in particular for the synthesis of CO-, Cp-, and PR_3-stabilized complexes. Oxidative addition of methylene halides may be preceded by formation of a CH_2Cl_2 complex.[79]

Table 6. Examples of syntheses according to reaction routes given in Scheme 11.

Synthesis principle	Example	Ref.
A	$[Cp(PPh_3)Ni(\eta^1\text{-}CH_2SPh)]$ **76**	
	$[Cp_2Ti(\eta^1\text{-}CH_2SPh)_2]$ **77**	[68]
B	$Na[pcFe(\eta^1\text{-}CH_2SPh)] \cdot 4thf$ **78**	[68]
B	$[Pd(\eta^1\text{-}CH_2SMe)Cl(PPh_3)_2]$ **79**	
	$\rightleftharpoons [Pd(\eta^2\text{-}CH_2SMe)Cl(PPh_3)]$ **80** + PPh_3	[69]
B/D	$[Cp(CO)_2Fe(\eta^1\text{-}CH_2SMe)]$ **81**	[70]
E [b]	$[Cp(CO)Fe\{\eta^2\text{-}C(SMe)_3\}]$ **82**	[71]
F	$[Cp(CO)_2W\{\eta^2\text{-}CH(SMe)Me\}(CF_3CO_2)]^+$ **83**	[72]
[a]	$[Cp_2(PMe_3)Ti(\eta^2\text{-}CH_2SMe)]^+$ **84**	[73]

[a] *S*-Alkylation of thioformaldehyde complexes affords thiomethyl compounds. See also [74]. [b] For the 1,2 shift of MeS from the carbanionic C atom according to the reverse reaction in **E**, see [71, 75].

η^2-Phosphinomethyl complexes such as **85** are accessible through oxidative addition/nucleophilic substitution of CH_2X_2 starting with phosphidometallates[80] and by reductive cycloelimination from chloromethyl–phosphane complexes.[81] The synthesis of **86** from aminomethyltin compounds apparently proceeds by way of similar intermediates.[82]

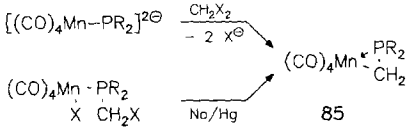

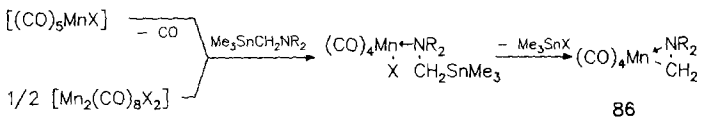

Remarkably mild reaction conditions suffice for C–H activation in the trimethylphosphane–metal(0) complexes of

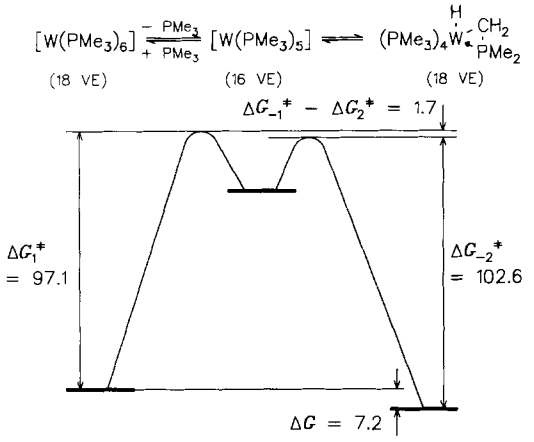

Fig 1. C–H Activation in $[W(PMe_3)_6]$ (data in kJ mol^{-1}). The rate-determining step is the dissociation of PMe_3. In the case of the 16-electron complex $[W(PMe_3)_5]$ oxidative C–H addition is favored over ligand association [83e].

Mo, W, Fe, Ru, and Os, with the formation of hydrido-η^2-phosphinomethyl complexes[83] (cf. Fig. 1). This is a result of high electron density at the metal as a consequence of the powerful σ-donor and weak π-acceptor tendencies of trimethylphosphane. The reversible interconversion of phosphane complexes (**87a**) and η^2-phosphinomethyl complexes **87b** through deprotonation of the phosphane ligands facilitated by amides, organolithium compounds,[84a] or ylides, (cf. Schmidbaur et al.[84b]) or through protolytic cleavage of the M–C bond, illustrates that C–H activation in methylphosphane complexes can also proceed in the sense of an electrophilic substitution (supported by nucleophiles).

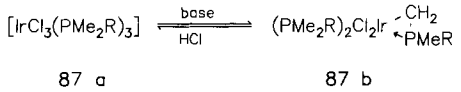

87 a 87 b

C–H bonds in *N*-bound methyl groups are accessible through intramolecular activation in the sense of oxidative addition (**88**) and electrophilic substitution (**89**), which may, given certain structural features and under particular reaction conditions—as in the case of **90**—compete with orthometallation (sp^3 C–H vs. sp^2 C–H activation)[85] (Scheme 12). It would appear that an *N*-methyl C–H activation is also responsible for the unusual isomerization at temperatures as low as 60 °C of a 2,6-bis(*N*,*N*-dimethylaminomethyl)phenyliridium(I) complex into the 2,4 analogue.[86]

Functionalized methylmetal complexes can be prepared from Fischer carbene and carbyne complexes according to **E** and **F** (see Table 1) by nucleophilic addition or migration of a nucleophile from a metal to a carbene carbon atom (Scheme 13).[87] The latter approach is applicable to protonation: with **93**, for example, the first step is protonation of the metal atom, followed by the reverse of an α elimination, in which hydride transfer occurs from the metal to the carbene.[87a, 88] The thermal transformation of the methyl phosphide iridium complex **94** is a result of intramolecular transfer of phosphide to a carbene, preceded by a spontaneous α-H elimination from a methyl ligand. The kinetic and thermodynamic products of the reaction are **95** and **96**, respec-

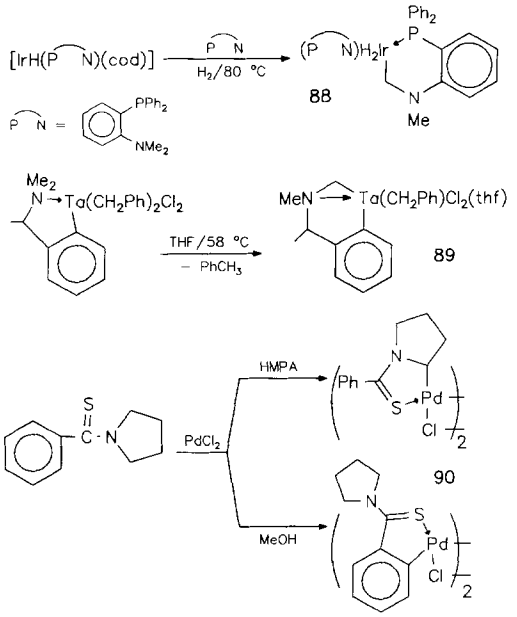

Scheme 12. Intramolecular C–H activation in *N*-methyl groups. HMPA = hexamethylphosphoric triamide.

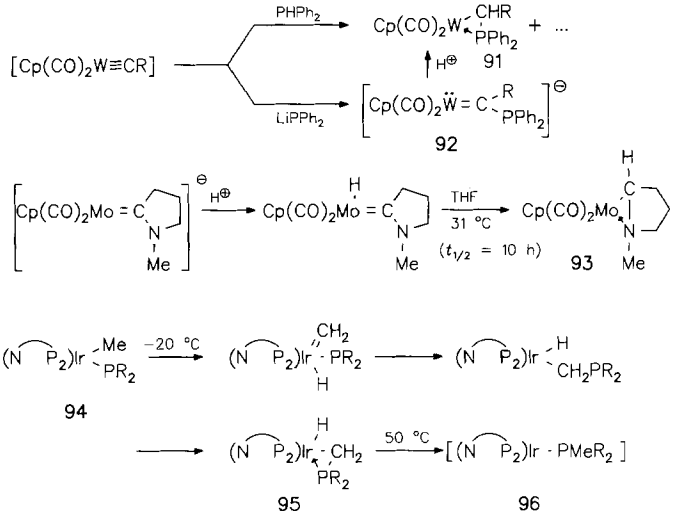

Scheme 13. Functionalized methylmetal compounds from carbyne and carbene complexes. $\widehat{NP}_2 = N(SiMe_2CH_2PPh_2)_2$.

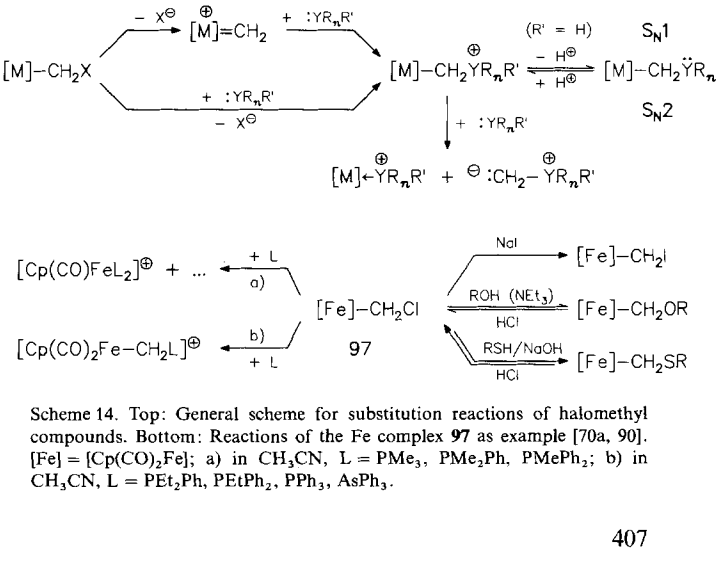

Scheme 14. Top: General scheme for substitution reactions of halomethyl compounds. Bottom: Reactions of the Fe complex **97** as example [70a, 90]. [Fe] = [Cp(CO)$_2$Fe]; a) in CH_3CN, L = PMe_3, PMe_2Ph, $PMePh_2$; b) in CH_3CN, L = PEt_2Ph, $PEtPh_2$, PPh_3, $AsPh_3$.

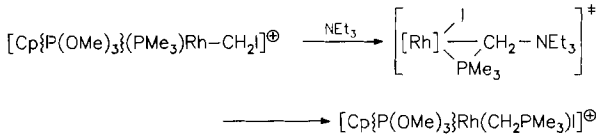

Scheme 15. Isomerization reaction.

tively. Photochemical reaction leads directly to the phosphane complex **96**.[89]

The halogen atom in halomethyl compounds can undergo nucleophilic substitution through a reaction similar to an S_N1 or S_N2 process according to **D** (see Table 1). Neutral nucleophiles lead to ylide complexes, and substitution of the ylide may follow as a competing reaction[70, 90, 91] (Scheme 14). Cleavage of halogen and addition of the nucleophile may occur in the sense of an intramolecular 1,2-shift, as is assumed in the case of the NEt_3-catalyzed isomerization of the Rh complex in Scheme 15.[92] Intramolecular substitutions **D** result in the formation of **98**–**100**[93] from the corresponding halomethyl phospane or phosphide complexes.

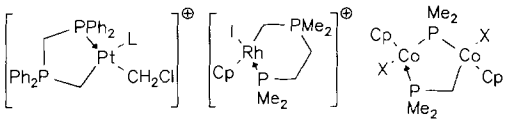

98 99 100

Transfer of a halide to a carbene is also the basis for synthesis of halomethyl complexes from metal halides and diazomethane.[94] Halomethylmetal compounds can also be prepared from formyl complexes,[95] as well as by decarbonylation of haloacetyl complexes.[96]

Photochemical decarboxylation of α-aminocarboxylate complexes **101** results in α-aminomethyl complexes **102** by way of radical intermediates.[97] An important factor in the smooth course of this reaction is the well-known facile elim-

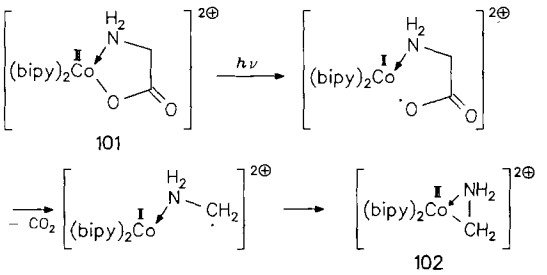

101 102

ination of CO_2 from RCO_2 radicals.

Azomethines can be transformed at nickel(0) centers into aminomethyl complexes, as illustrated by the formation of **103** from $[Ni(cod)_2]$ and *N*-methylsalicylaldimine.[98]

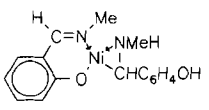

103

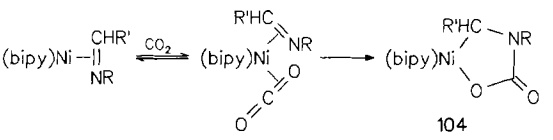

104

Oxidative coupling of the two hetero-π-systems to the five-membered ring heterocycles **104**[99] occurs in the presence of CO_2 under very mild reaction conditions ($T < 0\,^{\circ}C$; atmospheric pressure) with a wide variety of Ni^0 substrates. These and the corresponding reactions with isocyanates[100] demonstrate the ability of transition-metal complexes to accomplish the activation of CO_2.[101]

2.2.3. *Structure and Bonding*

Lewis-basic hetereoelements in functionalized methyl ligands are capable of entering into binding interaction with Lewis-acidic metallic centers, whereby the transition between η^1- and η^2-coordination is rather fluid (Scheme 16). Repulsive M–Y interactions (**105a**) as in $[Cp_2Zr(\eta^1\text{-}CH_2PPh_2)Cl]$ (Zr-C-P 130°)[102a] occur only in exceptional situations. Weak Fe–N interactions (**105c**) have been dis-

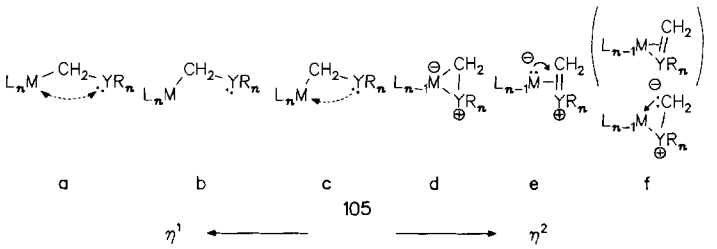

Scheme 16. Interactions between a Lewis-basic heteroatom and a Lewis-acidic metal center.

cussed in the case of $[Cp(CO)_2FeCH_2NMe_2]$.[102b] η^2-Complexes can be described as metallacyclopropanes **105d** ($H_2\overset{\ominus}{\ddot{C}}\text{–}\ddot{Y}R_n$ as ligand) or as heteroolefin complexes **105e** (with $H_2C{=}\overset{\oplus}{Y}R_n$ or $H_2C{=}\overset{\ominus}{\ddot{Y}}R_n$ as ligand), representing differing extents of electron-density transfer from the metal into the π* orbital of the C–Y double bond (cf. the Dewar–Chatt–Duncanson model). An ylide-like structure ("metal ylide", **105f**) involving more or less strong interaction between the ylidic C atom and the metal has been suggested when there is extremely strong M–Y interaction.[80d] In this way it becomes possible to invoke resonance structures corresponding to **105d**–**f** to describe the bonding relationships in η^2-complexes within the context of a valence-bond model.

As a consequence of the weak Lewis basicity of halogen and ether-oxygen atoms, stable η^2-halo complexes are unknown, and η^2-alkoxymethyl complexes are known only for strongly oxophilic central atoms like Zr^{IV}[103] and Mo^{II}.[88a]

η^1-Amino, η^1-phosphino-, and η^1-thiomethyl complexes also have the ability to enter into intermolecular complexation due to the strong Lewis basicity of the heteroatom, leading to $\mu\text{-}\eta^2$ coordination. Both homo- and heterobimetallic compounds have been described, including $[CpNi(\mu\text{-}\eta^2\text{-}$

$CH_2PR_2)_2NiCp]$[81b] and $[Cp_2Zr(\mu\text{-}\eta^2\text{-}CH_2PR_2)_2ML_x]^{n+}$ (ML_x = Rh(cod), $n = 1$; ML_x = $Cr(CO)_4$, $n = 0$).[104]

Bis- and tris(dimethylphosphino)methyl ligands (**106b** and **106c**) show an increasing tendency toward phosphorus coordination. Ligand **106b** is an exceptionally ambident lig-

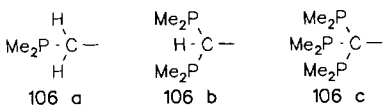

106 a 106 b 106 c

and with a wealth of possibilities for coordination[105] and the ability to stabilize main-group metals in low oxidation states.[106] *P,P*-Coordination dominates with transition metals, whereby the carbanion-like C atom is capable of either inter- or intramolecular coordination of complex fragments, as in **107** and **108**.[107] η^1-*C*-coordination has been demonstrated for $[Hg\{CH(PPh_2)_2\}_2]$.[108] A η^3- (i.e., π-allyl-like) coordination of the ligand is found in a homoleptic

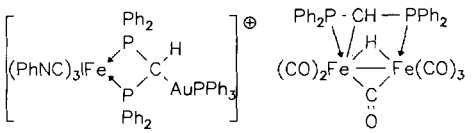

107 108

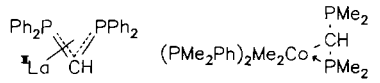

70 109

complex of La^{III} (**70**), a hard central atom with little tendency toward phosphorus coordination (Table 5).[64] Systems of this type, as well as the η^2-*P,C*-coordination found in **109**, apparently represent important intermediates through which ligand fluctuations (e.g., η^2-*P,P*-coordination $\rightleftharpoons$ η^1-*C*-coordination) and rearrangements (e.g., $[L_nM(H)(R_2PCHPR_2)] \rightarrow [L_nM(R_2PCH_2PR_2)]$) may pass.[64, 107c]

2.2.4. Reactivity

A reversible transformation from η^1 to η^2 coordination is generally associated with a thermally or photochemically induced ligand cleavage or addition (Scheme 17). If the α-hydrogen atoms in $[Cp_2Zr(\eta^1\text{-}CH_2PMe_2)Cl]$ are replaced by Me_3Si groups, *C*-nucleophilicity is reduced relative to *P*-nucleophilicity, producing a η^2 compound $[Cp_2Zr\{\eta^2\text{-}C(SiMe_3)_2PMe_2\}Cl]$.[109]

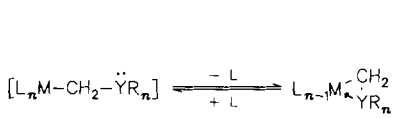

110 111

Scheme 17. Reversible transformation between η^1 and η^2 coordination.

Interactions between metal and heteroelement may influence the reactivity of a complex in a crucial way. It has been demonstrated with halomethyl compounds of Groups 1 and 12 that metal–halogen interaction is a significant factor in carbenoid reactivity (that is, cleavage of the CH_2 group from substituted methyl ligands).[110]

The carbenoid reactivity of thioanisolyl compounds has been closely investigated in the case of the nickel and titanium complexes **76** and **77**, which are transformed into thiophenolato complexes in boiling benzene (Table 7). During the decomposition of **77** small amounts of toluene have been detected as an insertion product of the solvent benzene and the CH_2 group that is cleaved. Norcarane is observed in the presence of cyclohexene. Methylene cleavage apparently proceeds via η^2-thioanisolyl complexes, as shown for **76** in Scheme 18. Because formation of a η^2-thioanisolyl structure

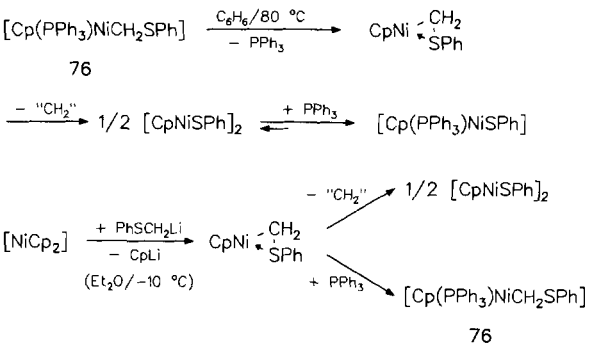

Scheme 18. Proposed mechanism of the thermal decomposition of **76**. The presumed intermediate $[CpNi(\eta^2\text{-}CH_2SPh)]$ can be trapped in high yield with PPh_3 as **76** in the reaction of $[Cp_2Ni]$ with $PhSCH_2Li$ [68].

is effectively prevented by the phthalocyanine ligand, thermal decomposition of **78** occurs in an entirely different way: at 150–170 °C in THF there is homolytic cleavage of the Fe–C bond without formation of a thiophenolato iron complex.[68] It remains an open question what the structural prerequisites for facile methylene cleavage in a η^2-thioanisolyl complex are.

Carbenoid reactivity has not been observed with any of the thioanisolylmercury or -zinc compounds **114**–**117** shown

Table 7. The transformation of thiomethyl complexes into thiolate complexes.

Compound	Reaction Conditions	Products	Ref.
76 $[Cp(PPh_3)NiCH_2SPh]$	Benzene, 80 °C	$[Cp(PPh_3)NiSPh]$, $[CpNiSPh]_2$, PPh_3, C_2H_4, C_3H_6,...	[68]
77 $[Cp_2Ti(CH_2SPh)_2]$	Benzene, 80 °C	$[Cp_2Ti(SPh)_2]$, $[Cp_2TiSPh]_2$, $PhSCH_3$, CH_4, C_3H_6,... [a]	[68]
78 $Na[pcFeCH_2SPh] \cdot 4thf$	THF, 150–175 °C	Na[pcFe], $PhSCH_3$, $PhSCH_2SPh$, PhSSPh,...	[68]
112 $[Cp_2Zr\{CH(SPh)Ph\}_2]$	Toluene, 70 °C	$[Cp_2Zr(SPh)_2]$, PhCH=CHPh	[111]
113 $[Cp_2Zr(Ph)\{CH(SiMe_3)SR\}]$	Toluene, 82 °C	$[Cp_2Zr(SR)\{CH(SiMe_3)Ph\}]$ (R = Me, Ph)	[111]

[a] Trace amounts of $PhCH_3$ and, in the presence of cyclohexene, norcarane.

true for bis(phenylthio)methylmercury compounds.[117]

A β-sulfur-substituted 1,2-diphenylethylzirconium compound has been assumed to be an intermediate in the thermal decomposition of **112** (Table 7).[111] The thermally induced rearrangement of **113** (R = Ph) (Table 7) proceeds in an intramolecular way according to first-order kinetics ($\Delta H^{\neq}$ = 85.0 kJ mol^{-1} at 82 °C).[111] Based on an NMR spectroscopic investigation, the metallathiacyclopropane compound **119** is thought to be in rapid equilibrium with the carbene–mercaptide form **118**, a circumstance reflected in its reactions with

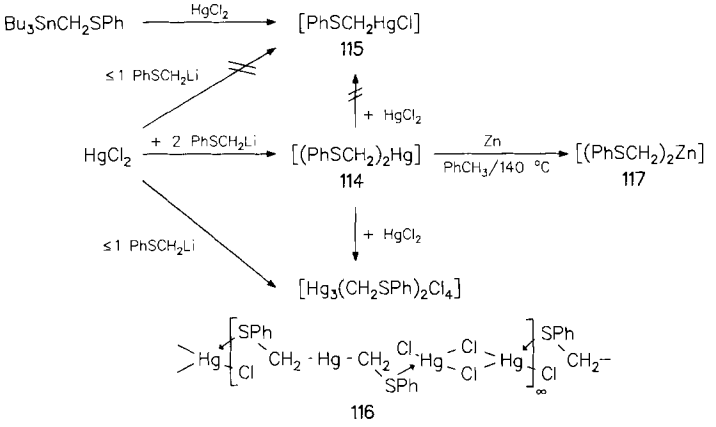

Scheme 19. Thioanisolyl compounds of mercury and zinc [112]. The strong tendency toward formation of **116**—from which $HgCl_2$ is not eliminated even in boiling acetone or THF—is due to mercury's high affinity for sulfur, which is also reflected in the crystal structure of **116** [113].

phosphanes and $[Me_3O]BF_4$, which involve cleavage of the C–S bond in the three-membered ring.[71]

Compounds functionalized with oxygen such as **120** and **121** can also be converted into alkoxide complexes, with the

118 119

elimination of olefins.[115] The zirconium complex **121** is capable of transferring a CH_2 group under relatively mild conditions (40 °C) to the Schwartz reagent. At 80 °C, but only for R = CH_2Ph, it undergoes a Wittig rearrangement.[103, 116]

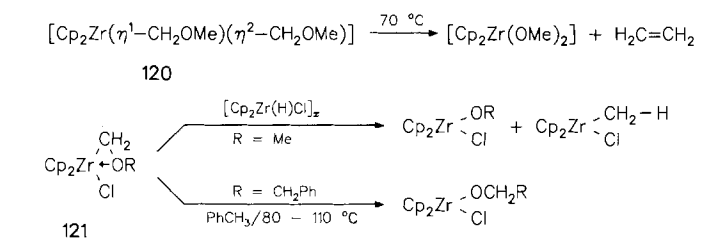

Functionalized methyl ligands support transformations like those shown in Scheme 20. Functionalized organo ligands with dipole stabilization as in complexes **122** have electronic characteristics between those of the ylide ligands **123** (see Section 2.3) and **110**. A wide variety of such systems has been described,[117] and they will not be treated here.

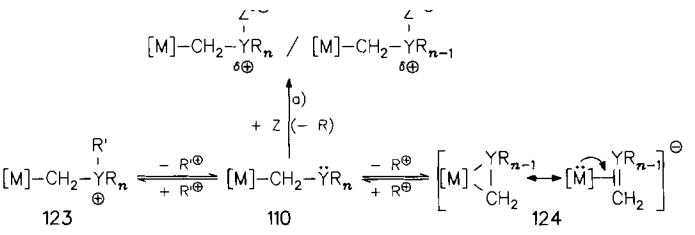

Scheme 20. a) Z represents a substituent that induces the positive end of a dipole at Y; for example, a substituent with a –M effect.

The complexes **124** can be regarded either as metallacyclopropanes or as π complexes [see, for example, the complexes with formaldehyde,[118, 119] thioformaldehyde,[74] imines,[98, 118a, 120] and methylenephosphanes (phosphaalkenes)[121]]. Representative of the reactions of these ligands, the formation of the thioformaldehyde complexes **125** is detailed in Scheme 21.[73, 74] Targeted oxidation of thiomethyl compounds leads to complexes like **126** and **127** with sulfinyl- and sulfonylmethyl ligands. Such ligands are regarded as dipole-stabilized.[122]

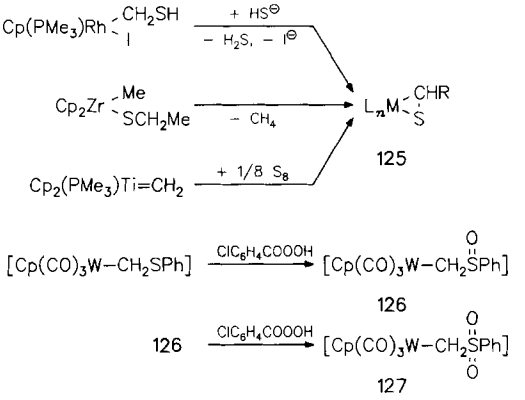

Scheme 21. Synthesis of thioformaldehyde complexes **125**, and oxidation of a thioanisolyl complex.

2.2.5. *Catalytic Aspects*

Aminomethyl complexes like **128** probably occur as intermediates in the synthesis of α-amino acids under the conditions of the "oxo" reaction, starting with aldehydes and acid amides. An aminoacetyl complex can arise from CO insertion into **128**, from which the amino acid is liberated by hydrolysis.[123]

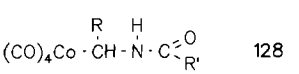

128

Metal-catalyzed hydrogenations of CO proceed to give a broad spectrum of hydrocarbons and oxygen-functionalized compounds depending upon the catalyst and reaction conditions. Such reactions occur by way of α-hydroxyalkyl compounds **129**, where R = H, alkyl (Scheme 22). Further re-

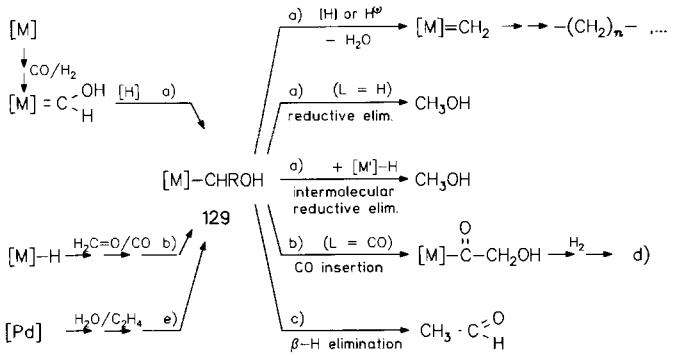

Scheme 22. α-Hydroxyalkyl complexes in catalysis. a) CO hydrogenation. b) Hydroformylation of formaldehyde. c) Wacker process (R = Me; otherwise, R = H). d) Reaction forming C_2 products like ethyleneglycol and glycol aldehyde. Certain ligands L from the coordination sphere of [M] are given above the reaction arrow.

duction or protonation with elimination of water leads to methylene complexes, which are important intermediates in the Fischer–Tropsch synthesis.[124] Reactions of hydrido hydroxymethyl complexes (**129**, L = H) and of **129** with metal hydrides can proceed by intra- or intermolecular reductive elimination to give methanol. CO insertion and subsequent reductive elimination of the acyl group from carbonyl hydroxymethyl complexes (**129**, L = CO) opens the way to C_2 products such as hydroxyacetaldehyde and ethylene glycol.[125]

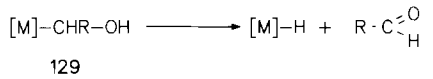

Scheme 23. Decomposition of α-hydroxyalkyl complexes **129** to hydrido complexes and aldehydes.

In general, α-hydroxyalkyl complexes are thermodynamically unstable and decompose to hydrido complexes and aldehydes (Scheme 23; for an exception see [126]). A reaction of this type is utilized in the Wacker process to liberate acetaldehyde.[8] The reverse reaction plays a role in metal-catalyzed formaldehyde hydroformylations and homologations.[125] Model reactions have been used to emulate important elementary steps in the catalytic processes (Scheme 24).[126]

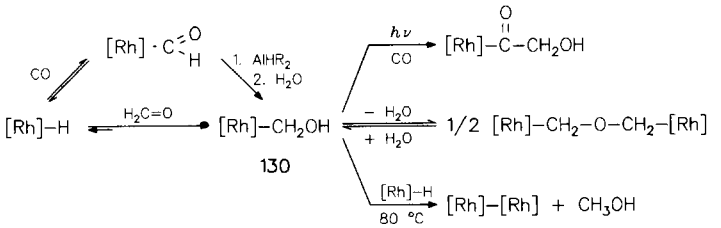

Scheme 24. Reactivity of the hydroxymethyl complexes **130**. [Rh] = octaethylporphyrinrhodium.

Coenzyme-B_{12}-dependent diol dehydratases catalyze the rearrangement of 1,2-diols to aldehydes or ketones. Probably an α,β-dihydroxyalkylcobalt compound[131] is formed first, and this species subsequently—perhaps via radical intermediates—causes isomerization and dehydration of the diol (Scheme 25).[127]

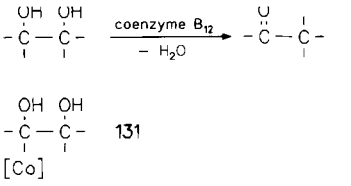

Scheme 25. Dehydration of 1,2-diols to aldehydes or ketones.

α-*S*-functionalized alkylmetal compounds are probably significant as intermediates in catalytic hydrodesulfurization (HDS), used for removing thiophene and other organosulfur compounds from crude petroleum fractions.[73, 128] For example, the hydrogenation of thiophene under HDS conditions may proceed by way of these intermediates, as documented in the formation of **132** through insertion of dihydrothiophene into a Pt–H bond.[128]

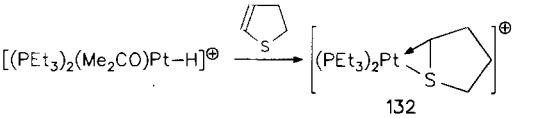

2.3. Ylide Complexes

Ylides must be regarded both as zwitterions and neutral ligands.[13–15] As a result of the neighboring positive charge on the heteroatom—and, in the case of Y = P, S a supplementary $p_\pi d_\pi$ contribution to bonding (Scheme 26)—the

Scheme 26. Resonance structures of ylides.

donor potential at carbon is considerably lower than that of the corresponding alkyl anion. This inhibits intramolecular electron transfer[129] and constitutes an important factor in the stability of ylide complexes. The positive charge on the heteroatom assures (especially with *P*- and *S*-ylides) facile activation of the neighboring C–H bonds, so that various coordination possibilities are present in addition to bonding as a simple σ-donor ligand (Scheme 27).

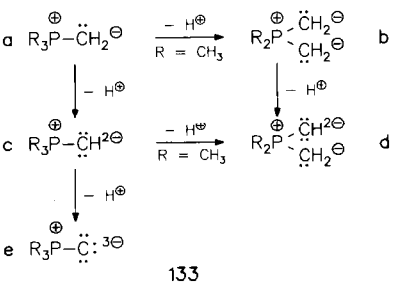

Scheme 27. Coordination possibilities for phosphorus ylides **133**. **a**, **c**, and **e** function as monodentate and b, d as bidentate ligands. **c**/**d** are carbene/alkylidene ligands, and **e** is a carbyne/alkylidyne ligand (R = Me).

Table 8. Homoleptic ylide complexes of transition metals.

Compound [a]	M	Color	$\mu_{eff.}$ [μ_B]	M.p. [°C] (T (dec.) [°C])	Ref.
Phosphorus ylides					
134 $[Ln\{(CH_2)_2PMe_2\}_3]$ [b]				(160...210)	[22, 130]
135 $[Zr_2\{(CH_2)_2PMe_2\}_4(\mu\text{-}CPMe_3)_2]$		yellow	diamagnetic		[131]
136 $[M_2\{\mu\text{-}(CH_2)_2PMe_2\}_4]$	Cr	golden yellow	diamagnetic	165–167 (> 132)	[132, 133]
140	Mo	orange-red	diamagnetic	(256–275)	[132, 133]
137 $[Cr\{(CH_2)_2PMe_2\}_3]$ [c]		red	3.6	59–68	[132]
138 $[Cr\{(CH_2)_2PMe_2\}_2(Ph)(CH_2PMe_3)]$		red		97–105 (dec.)	[132]
139 $[Cr(CH_2PMe_3)_3(C{\equiv}CPh)_3]$		pale yellow	3.82	119–122	[132]
141 $[W(CH_2PPh_3)_3]$		red	diamagnetic	78–79	[134]
142 $[M\{(CH_2)_2PtBu_2\}_2]$	Ni	yellow	diamagnetic	134	[135]
144	Pd	colorless	diamagnetic	154	[135]
147	Pt	colorless	diamagnetic	215 (dec.)	[135]
143 $[M_2\{(CH_2)_2PMe_2\}_2\{\mu\text{-}(CH_2)_2PMe_2\}_2]$	Ni	yellow	diamagnetic	(123)	[135]
145	Pd	colorless	diamagnetic	146	[135]
146 $[Pd\{(CH_2)_2PMe_2\}(CH_2PMe_3)_2]Cl$		colorless	diamagnetic	185–186	[135]
148 $[PtMe_2(CH_2PMe_3)_2]$		colorless	diamagnetic	154	[135]
Sulfur ylides					
149 $[Pd\{(CH_2)_2S(O)Me\}_2]$		colorless	diamagnetic		[136]
150 $[Pd\{(CH_2)_2S(O)Me\}\{CH_2S(O)Me_2\}_2]I$		colorless	diamagnetic		[136]

[a] Selection. In some cases additional compounds have been described with other organic residues on phosphorus. [b] Ln = Y, La, Nd, Gd, Er, Pr, Sm, Ho, Lu. [c] The appropriate phenyl-substituted compound is subject to orthometalation [132].

Apart from the methods **D**–**F** (Table 1), other broadly applicable approaches are available for the synthesis of η^1-ylide complexes (**G**–**I**, Scheme 28). Method **A** with $R_nY(CH_2)_2Li$ and method **K** are particularly valuable for the preparation of η^2 complexes. Many very thermally stable homoleptic phosphorus ylide complexes of transition metals have been prepared (Table 8); for examples of syntheses see Scheme 29.[132, 135]

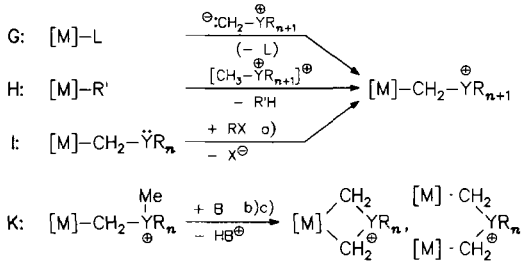

Scheme 28. Synthetic principles for ylide complexes. a) Including R = H. b) B represents a base, which may be coordinated to M. c) Including "transylidation" reactions (B = ylide).

Ylide **133b** plays the role of a bridging ligand (μ-η^2 coordination). The two metal centers may also be subject to M–M bonding. The Group 6 metal complexes **136** and **140** belong to the chromium(II) acetate structural type (symmetry reduced to C_{4h} as a result of a nonplanar five-membered ring).[133] The fourfold bond between the metals leads to very short M–M distances of 189.5(3) pm in **136** and 208.2(2) pm in **140**.

Ligand **133c** is isomeric to **133b** (R = CH_3).[14, 137] The prototropic zirconium complexes **151a** and **b** exist in solution in equilibrium.[138] Complexes with **133c** as ligand can be characterized as (specially substituted) carbene complexes or as metal-substituted phosphorus ylides. Further deprotonation of **133c** leads to **133e**, which forms μ-methylidyne complexes containing M_2C_2 four-membered rings in the cases M = Zr (**135**)[131] and M = Ti.[14, 138]

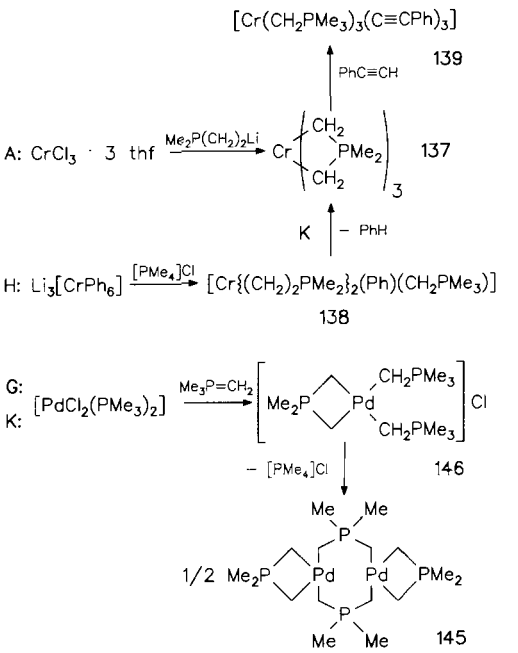

Scheme 29. Examples of the synthesis of homoleptic phosphorus–ylide complexes of transition metals.

Homoleptic palladium complexes **149** and **150** containing sulfur ylides (Table 8) have been described; homoleptic compounds of the main-group elements and metals of Groups 11 and 12 have long been known.[15, 139] The synthesis of **149** and **150** by treatment of $[PdCl_4]^{2-}$ with $(Me_3SO)I$ in aqueous (!) alkaline solution[136] is unusual, and may be relevant to biochemical processes. Of interest from a preparative standpoint is the synthesis of the organometallic com-

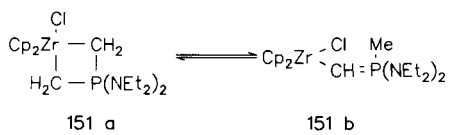

pounds $[Pd\{(CH_2)_2S(O)Me\}(PPh_3)_2]I$ and $[Pd\{(CH_2)_2S(O)Me\}(I)(PPh_3)]$ from the diphosphanepalladium halides and $(Me_3SO)I$ under phase-transfer conditions (CH_2Cl_2/NaOH; $(R_4N)I$ as phase-transfer catalyst).[140]

A great many heteroleptic *P*-, *S*-, and *N*-ylide complexes have been prepared by substitution reactions starting with halomethyl compounds (**D**), by addition of YR_{n+1} (HYR_n) to carbene complexes (**E**), and by alkylation, arylation, or protonation (**I**) (Table 1 and Scheme 28). Protonation is in principle reversible. Ylide addition or substitution reactions of type **G** are restricted to ylides displaying sufficient stability, hence this type of synthesis of *N*-ylide complexes is feasible only with such resonance-stabilized ylides as $R'C(O)-\overset{\ominus}{\underset{\cdot\cdot}{C}}H-\overset{\oplus}{N}R_3$. The *N*-ylide complexes **152** are accessible by isomerization of pyridine–platinacyclobutane complexes (Scheme 30).[141]

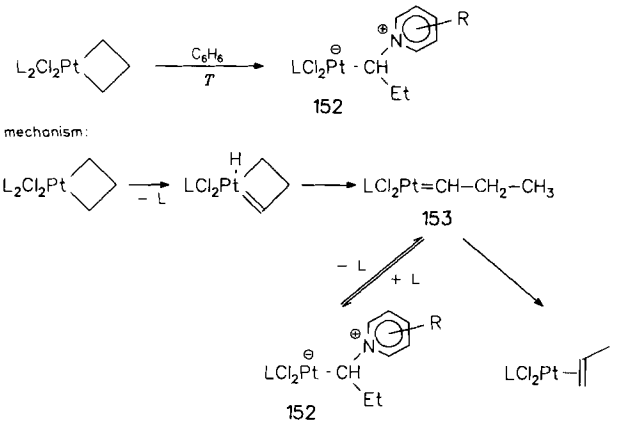

Scheme 30. *N*-Ylide complexes starting with platinacyclobutanes. One possible mechanism is indicated, involving α-H elimination, reductive elimination, and carbene addition. The competitive formation of propene might be explained by a 1,2 hydrogen shift starting with **153** [141b]. L = pyridine, substituted pyridine.

The reactivity of ylide complexes is largely determined by the characteristics of the leaving group YR_{n+1} (HYR_n). Low basicity of the leaving group is thus responsible for the carbenoid reactivity of *O*- and *S*-ylide complexes such as $[Cp(CO)_2FeCH_2ORH]^+$ (in situ) and $[Cp(CO)_2FeCH_2SR_2]^+$ (**154**).[142] Facile synthesis and control over carbenoid reactivity by variation of R are responsible for making **154** attractive as cyclopropanation reagents. This in turn permits one to invoke *O*- and *S*-ylide complexes in place of halomethyl compounds as precursors for substitution reactions corresponding to **D** (Table 1; see, for example, Schemes 11 and 14, as well as the formation of $[\{Cp(CO)_2FeCH_2\}_2NMe_2]^+$ and $[\{Cp^*(CO)_2FeCH_2\}_2SR]^+$ from the amino- and thiomethyliron complexes, respectively).[102b, 143]

3. β-Heteroatom-Substituted Ethylmetal Compounds

3.1. Alkali-Metal and Alkaline-Earth Compounds

β-Substituted alkyllithium and Grignard reagents **155** containing a Lewis-basic heteroatom are unstable (Scheme 31).

Scheme 31. M = Li, MgX; R_nY = R_2N, R_2P, RO, RS, X.

They have been assumed to arise as intermediates in reactions involving ethylene elimination,[144] and in the course of ether cleavages.[145] So far, the synthesis of **156** has only proven possible by reaction of β-bromoethylamines with highly active magnesium at temperatures between −78 °C and −100 °C. It could be shown that decomposition occurred with heterolytic fragmentation as a function of the residue R between −80 °C and −20 °C (Scheme 32).[146]

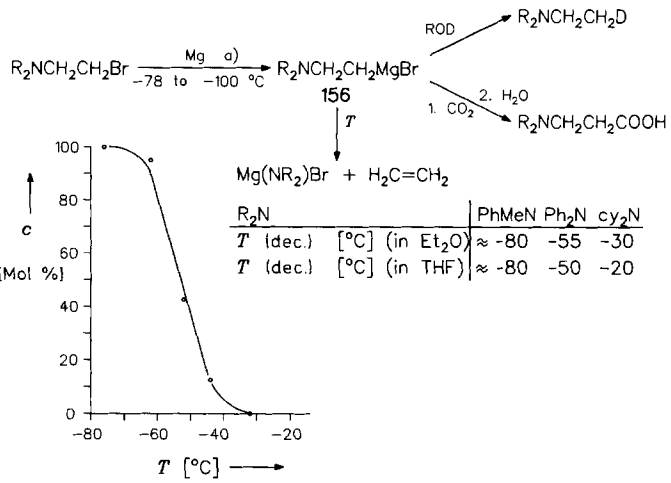

Scheme 32. Synthesis of β-aminoethylmagnesium bromides **156**. The illustration depicts the decomposition curve for $Ph_2NCH_2CH_2MgBr$ in THF as solvent [146]. a) Preparation of highly reactive Mg by reduction of $MgBr_2$ with K according to Rieke.

Stabilization of β-substituted ethyllithium and Grignard reagents can be achieved by suitable modification of the basic structure **155** (Scheme 33).[147] Crucial to increasing the stability are stereoelectronic considerations (**157**; **158**,

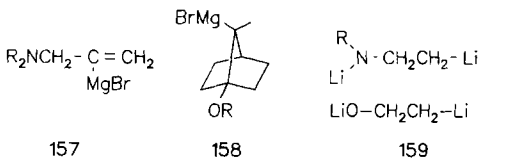

Scheme 33. Decomposition temperatures: **157**, greater than 20 °C; **158**, 130 °C; **159**, −60 °C.

Bredt's rule), increased electronegativity at an sp^2-hybridized C atom (**157**), and, in the case of **159**, a dramatic increase in the basicity of the leaving group LiO^- vs. RO^- or $Li(R)N^-$ vs. R_2N^-.

3.2. Transition-Metal Compounds

Homoleptic transition-metal compounds are unknown, but a wide variety of heteroleptic β-functionalized ethyl tran-

sition-metal compounds has been prepared by oxidative addition of $R_nYCH_2CH_2X$.

The addition of anionic nucleophiles R_nY^- to olefin complexes, which can occur either as a one-step, intermolecular reaction or as an insertion subsequent to coordination of the nucleophile at the metal center, leads to the functionalized ethyl compounds **160** (Scheme 34). Neutral nucleophiles $R_nR'Y$ lead to the compounds **161** with a cationic center in the alkyl ligand ("onio"-ethyl complexes). Complexes **160** and **161** exist in a protonation/deprotonation equilibrium when R' = H.

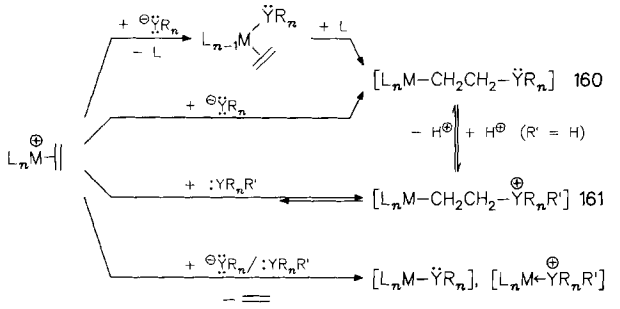

Scheme 34. On the reactivity of nucleophiles toward olefin complexes. Kinetic and thermodynamic data for the conversion of $[Cp(CO)_2Fe(\eta H_2C{=}CH_2]^+$ (**162**) is summarized in Table 9.

Table 9. Kinetic and thermodynamic data for the reaction of $[Cp(CO)_2Fe(\mu^2\text{-}H_2{=}CH_2)]^+$ (**162**) with nucleophiles according to Scheme 34 [148] [a].

162 + Nucleophile			
Addition	MeOH, *t*BuSH, $MeNH_2$, Me_2NH, py, PPh_3 [b], $P(OEt)_3$, MeO^-, CN^- [c]		
Substitution	N_2H_4, N_3^-, I^-, NCO^-, CN^- [c]		
Rate of addition	$cyNH_2 > MeO^- > P(p\text{-}MeOC_6H_4)_3 > PPh_3 >$ py		
$\Delta H^{\neq}$ [kJ mol^{-1}]	52	30	31
$\Delta S^{\neq}$ [JK^{-1} mol^{-1}]	−15	−107	−108

[a] Kinetic studies on the rate of addition confirm that with MeO^- as nucleophile, desolvation makes the major contribution to $\Delta G^{\neq}$ [149]. [b] Addition to the analogous propene complex affords $[Cp(CO)_2FeCH_2CHMePPh_3]^+$, which is readily converted to $[Cp(CO)_2Fe(PPh_3)]^+$ upon cleavage of propene. [c] Dependent on the reaction conditions.

Nucleophilic addition competes with substitution of the olefin. A high degree of electrophilicity like that encountered in cationic olefin complexes favors nucleophilic addition.[150] The electron density at the olefin is also influenced crucially by the donor–acceptor characteristics of the *trans* ligand, which provides an opportunity for directing the addition/substitution competition.[151]

Stereochemical investigations have shown that intermolecular nucleophilic addition is a *trans* process.[152] MO calculations indicate that the LUMO of the olefin increases in energy as a result of symmetric η^2-olefin coordination to a metal-complex fragment. Moreover, activation with respect to ligand-addition reactions occurs only to the extent that the olefin is bound unsymmetrically, tending towards η^1 coordination (see **163**).[153] The insertion of an olefin is a concerted cyclic process. Model calculations on palladium complexes have shown that—consistent with experimental observations—the insertion can be regarded as an orbital-

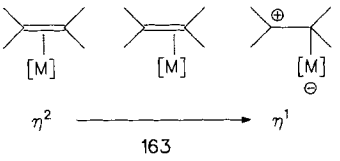

163

controlled reaction, whereas *trans* addition entails both orbital and charge control.[154]

In principle, olefins can also be inserted into $M–YR_n$ bonds, as demonstrated by the regioselective insertion of acrylonitrile as an olefin with an activated double bond to form Pt complex **164**,[155] as well as by the formation of **165**.[156]

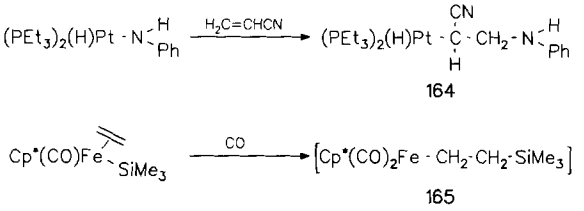

164 165

C–H activations are particularly easy to achieve in *tert*-butyl- and isopropylphosphane complexes in the form of electrophilic substitution or oxidative addition, leading to the formation of metallaphosphacyclobutanes[157] like **166** (M = Pd^{II}, Pt^{II}) and **167** (M = Ru^{II}, Os^{II}, Ir^{III}), containing

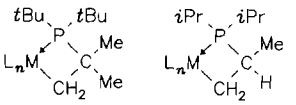

166 167

nonplanar four-membered rings.[158] The reaction is influenced fundamentally by the spatial demands of the phosphane.[159] In the case of $PtBu_2R$ complexes with long-chain R residues there is competition with a δ-C–H activation process (five-membered versus four-membered ring formation).[157b, 160]

The complex fragment $[Cp^*(PMe_3)Ir]$ reacts with *tert*-butyl amines and alcohols not through oxidative addition of the N–H or O–H bond, but rather of a C–H bond to give $[Cp^*(PMe_3)(H)Ir–CH_2CMe_2YR_n]$ (YR_n = NH_2, OH).[161]

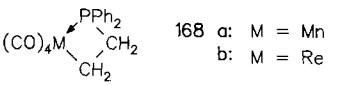

168 a: M = Mn
b: M = Re

Similarly to the formation of α-functionalized derivatives **85** and **86**, the metallaphosphacyclobutane compounds **168** can be prepared by reductive cycloelimination from β-chloroethylphosphane complexes,[81, 162] although the analogous synthesis of $[CpNiCH_2CH_2PR_2]$ proved unsuccessful.[81b] The highly strained four-membered rings in **168a** and **168b** react with SO_2 (and, in the case of **168a**, with CO and CO_2) to cause ring expansion.[163] Not only α-

aminocarboxylates (cf. **101**) but also the β-aminocarboxylates of Co(III) undergo photochemical decarboxylation with the formation of azacobaltacyclobutanes.[97]

3.3. Reactivity

β-Functionalized ethylmetal complexes **160** display in addition to a σ M–C bond with the Lewis-basic heteroelement yet another reactive center. They are accessible through the reactions in Scheme 35.

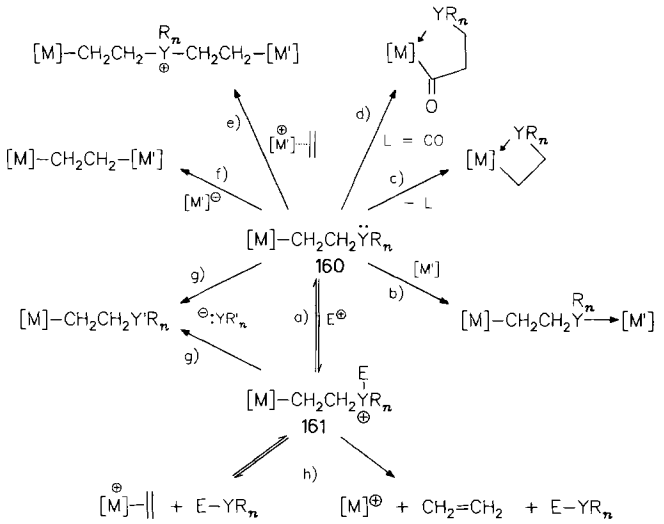

Scheme 35. Reactions of complexes **160**. a) Addition of electrophiles; b)–d) inter- and intramolecular complex formation; c) addition to olefin complexes; f) formation of binuclear complexes by oxidative addition/nucleophilic substitution; g) nucleophilic substitution; h) β-elimination of EYR_n and heterolytic fragmentation.

Reaction route a) represents the addition of electrophiles to $\ddot{Y}R_n$. Particularly important are protonation (reversible!) and alkylation of Y to "onio"-ethyl complexes.

Syntheses b)–d) involve inter- and intramolecular complexation of $-\ddot{Y}R_n$. As a result of ring expansion through insertion (of CO, for example) into the M–C bond the strain in the four-membered ring is reduced. Organometallic inner complex formation decreases the tendency toward β elimination, since the latter requires a coplanar M-C-C-H arrangement.

Route e) is the addition of **160** to metal–olefin complexes. As a result of this reaction the synthesis of **160**/**161** by addition of HYR_n to metal–olefin complexes may become difficult or impossible. Thus, $[L_nPt(C_2H_4)]ClO_4$ reacts with Et_2NH, $EtNH_2$, and NH_3 to give $[(L_nPtCH_2CH_2)_2NEt_2]ClO_4$, $[(L_nPtCH_2CH_2)_3NEt]ClO_4$, and $[(L_nPtCH_2CH_2)_4N]ClO_4$ [L_n = (tmeda)Cl].[164]

In reaction path f) oxidative addition of $X–CH_2CH_2–X$ to metal complexes give ethylene-bridged bimetallic compounds via $[M]–CH_2CH_2–X$ intermediates (example: $[Cp(CO)_2Ru–CH_2CH_2–Ru(CO)_2Cp]$).[2]

Reaction route g) is a nucleophilic substitution of ^-YR_n ($E–YR_n$), especially with $^-Y'R_n$ = Cl, Br, OR, and E–YR = HOR.

β-Elimination of $E–YR_n$ with formation of a metal–olefin complex [route h)] either involves the reverse of the reaction for synthesizing **161** in accord with Scheme 34, or heterolytic fragmentation.

Depending upon the structure of the compound there can be considerable differences in thermal stability, as illustrated by the example of the aminoethyl complexes in Table 10. The

Table 10. On the thermal stability of selected β-aminoethyl complexes.

Compound	Synthesis principle	T (dec.) [°C] $-NPh_2$	$-NPhMe$	$-NC_5H_{10}$	Ref.
169 $Na[pcFeCH_2CH_2NR_2]\cdot x$ thf [a]	**B**	>100	>100	>100	[165a]
170a $[pcFeCH_2CH_2NR_2]\cdot 1/4$ thf	[b]	181	142	114	[165b]
170b $[pcCoCH_2CH_2NR_2]$	**B**	212	180		[165c]
156 $R_2NCH_2CH_2MgBr$	[c]	−50 [d]	−80 [d]	−20 [d, e]	[146]

[a] x = 3–5. [b] Oxidation of **169** with trityl chloride. [c] Cf. Scheme 32. [d] In THF as solvent. [e] R_2N = cy_2N.

exceptionally high stability of the phthalocyanine complexes **169** and **170** can be attributed to strong M–N bonds in the complex, which block all the coordination positions in the vicinity of the M–C bond. Thus, H elimination and bimolecular reactions are effectively ruled out as decomposition processes with low energies of activation. Comparison of the phthalocyanine derivatives **169** and **170** with the Grignard reagents **156** clearly reveals the influential role of the nature of the M–C bond on stability.

Heterolytic fragmentation can be induced in three ways (Scheme 36), namely, 1) by increasing the positive charge on the heteroatom Y through protonation, alkylation, or reaction with other electrophiles;[165, 166] 2) by introduction of a

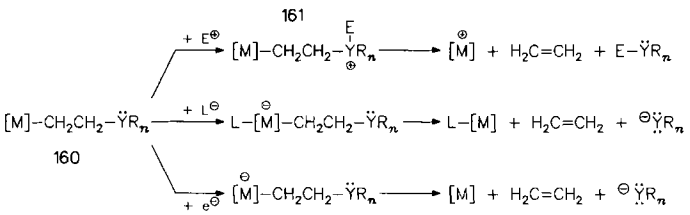

Scheme 36. Fragmentation reactions of the ethyl complexes **160**.

ligand with a strong *trans* effect (e.g., OH^-, CN^-) in a position *trans* to the alkyl ligand;[167] or 3) by reductive M–C bond cleavage.[168] Thus, the tendency toward elimination of, in the case of 1), the nucleofugal group and in the case of 2) and 3), the electrofugal group, as a result of weakening the M–C bonding, is increased.

ROH and R_2NH have been particularly thoroughly investigated as nucleofugal leaving groups, and cobaloximes, cobalamines, and metallophthalocyanines as electrofugal leaving groups. Thus, the exceptionally stable β-aminoethyl(phthalocyanine)iron(II) complexes **168** undergo heterolytic fragmentation upon treatment with electrophiles (Scheme 37). The rate of decomposition is a function both of the position of equilibrium a) and of the nature of the actual fragmentation reaction b). It increases with increasing elec-

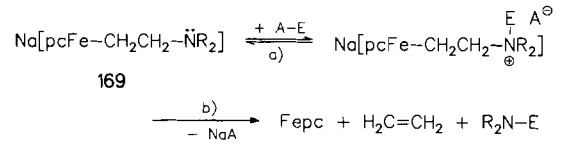

Scheme 37. Heterolytic fragmentation of the phthalocyanine complexes **169**. The reaction rate depends on the electrophile A–E (MeI < MeOH ≈ MeC(O)Cl < $C_7H_7SO_3H$) and on the amino group $-NR_2$ (NPh_2 ≪ NPhMe < NC_5H_{10}).

trophilicity of the attacking agent and with increasingly high nucleophilicity or basicity at the nitrogen of the aminoethyl ligand.[165a] The Fe^{III} and Co^{III} compounds **170** react analogously.[165b, c]

A technique for removal under mild conditions of *C*- and *N*-terminal protecting groups in peptide synthesis is based on the reductive cleavage of M–C bonds in *β-O*-functionalized ethyl(phthalocyanine)cobalt(III).[168a, 169] Reductive cleavage can also be accomplished electrochemically by the use of catalytic amounts of cobalt phthalocyanine.[168b]

3.4. Catalytic Aspects

In the present understanding of the mechanisms of metal-complex-catalyzed functionalization reactions of unsaturated olefins (Scheme 38, top), three principle routes need to be considered: 1) intermolecular addition of HYR_n to an olefin activated by complex formation (cf. Scheme 34), 2) insertion of an olefin into an M–YR_n bond (cf. Scheme 34), and 3) a sequential insertion–elimination (Scheme 34, bottom). The intermediates in mechanisms 1) and 2) are *β*-functionalized alkyl complexes.

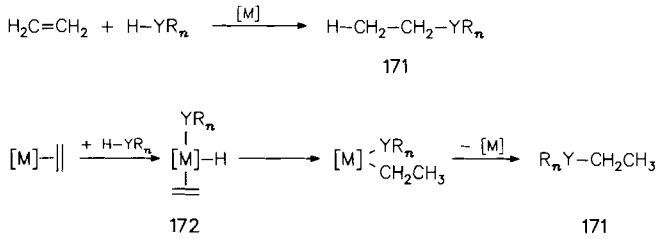

Scheme 38. Functionalization reactions of olefins, illustrated with the example of ethene.

Palladium-catalyzed oxidative functionalization of ethylene with H_2O or HOAc for the synthesis of acetaldehyde and vinyl acetate, respectively, proceeds by way of *β-O*-functionalized alkylpalladium compounds. Results of kinetic and stereochemical investigations of the Wacker process are consistent with an intermolecular addition of H_2O to an ethenepalladium complex with the formation of **8** as an intermediate (Scheme 39). It is not yet certain to what extent the palladium hydride **173** formed by elimination of acetaldehyde then decomposes to Pd^0, to be subsequently reoxidized, or forms the palladium hydroperoxide complex **174** by O_2 insertion.[8] In principle, closure of the C–O bond might also occur through **175**, a suggestion supported by investigations with radioactively labeled oxygen.[8b]

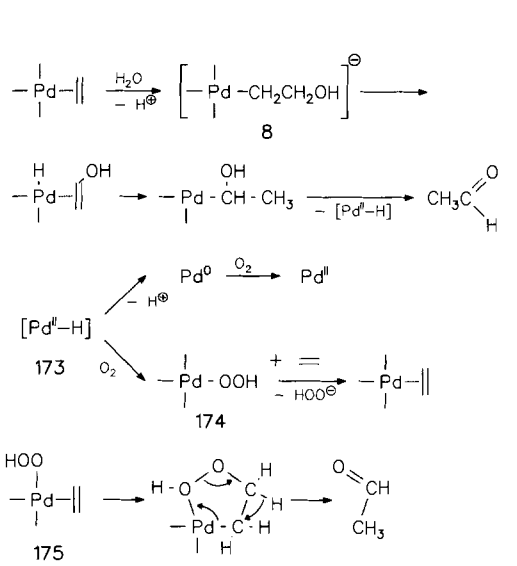

Scheme 39. On the mechanism of the Wacker process.

The mechanism of transition-metal-catalyzed olefin amination (Scheme 38 top: H–YR_n = H–NR_2)[170] and aminomethylation (Scheme 38 top: H–YR_n = H–CH_2NR_2)[171] has not been established (cf. the review in [172]). Intermolecular amine addition with the formation of *β*-amino- or *β*-ammonioethyl complexes is a possibility in the case of rhodium-catalyzed amination, as already demonstrated for the stoichiometric (!) amine additions to olefin complexes of Pt and Pd. In principle Ir complexes are also capable of undergoing N–H addition[173] and olefin insertion into an Ir–amide bond,[155] so an insertion/elimination mechanism cannot be ruled out.

Both insertion/elimination and insertion mechanisms have been discussed for hydrosilylation (Scheme 38 top: H–YR_n = H–SiR_3), corresponding to C–Si bond formation by reductive elimination of Et–SiR_3 from an ethylsilylmetal complex or insertion of ethene into an M–Si bond.[174]

Metathesis reactions might proceed as [2 + 2] cycloadditions by way of metallacyclobutane intermediates such as

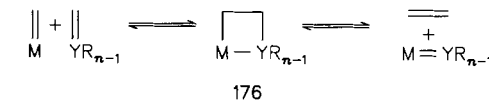

176 (YR_{n-1} = O, NR, CR_2). This has been clearly demonstrated in the case of olefin metathesis (YR_{n-1} = CR_2).[175] Metallaoxetanes (YR_{n-1} = O) have been assumed to be intermediates in metal-assisted or metal-catalyzed oxidations and oxygen-transfer reactions,[176] processes that are extremely important not only in organic synthesis (e.g., oxygenation of olefins according to Sharpless and the Tebbe–Grubbs procedure for deoxygenation of carbonyl compounds) but also in biochemistry (e.g., oxidations catalyzed by cytochrome P-450).

Metallaoxetanes are accessible from metal alcoholates through C–H activation,[177] or from *β*-hydroxyalkyl com-

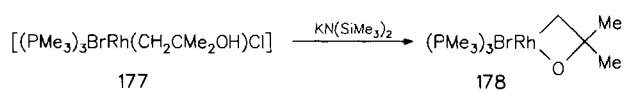

pounds via O–H activation, (**177** → **178**).[178] The four-membered ring in **178** is planar. The relatively short bond lengths for Rh–C (206.9(10) pm in **178** and 213.1(8) in **177**) and C–O (141.6(12) pm in **178** and 145.2(9) in **177**) suggest polarization in the direction metal carbene complex/ketone (see **179**).[178]

179 a 179 b

4. Electronic Characteristics of Functionalized Alkyl Ligands

Important electronic characteristics of ligands are reflected in their electronic influences. This applies specifically to the ability of a ligand L in a complex LML'_x to influence via the central atom other metal–ligand bonds M–L' or the other ligands L' themselves (in their ground state![179]). Such effects have direct consequences for the chemical, physical, and spectroscopic properties of complexes. They also play a significant role in complex-chemical activation or stabilization of ligands, and in ligand-dependent control over reactions catalyzed by metal complexes.[180–182]

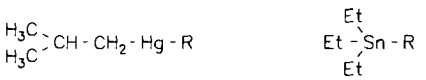

180 181

The electronic influence of L is primarily a feature of L itself, but it also depends upon a number of other very complex and diverse factors. Neglecting all differences related to the types of complexes investigated and to the experimental methods enables a universal parameter P_{trans} for characterizing the *trans* influence to be derived.[183] This points to the potentially very considerable electronic influence of σ-organo ligands that results from the low electronegativity of carbon.

The electronic influence of the σ-organo ligand R on the isobutylmercury and triethyltin compounds **180** and **181** has been characterized by NMR spectroscopy on the basis of $^1J(^{199}Hg,^{13}C_{iBu})$ and $^1J(^{119}Sn,^{13}C_{Et})$ in a consistent and theoretically well-founded way.[184] Here the magnitude of the coupling constant is a measure of the s character of the metal hybrid orbital directed toward the indicator ligand (Me_2CHCH_2 or Et). According to Bent's rule[186] the s character of this orbital decreases with increasing donor character of R. This in turn reduces the coupling constant, so that the latter indeed reflects the electronic influence of R. The accuracy of such predictions in the case of the compound types investigated (for an analysis of other metal alkyls cf. Steinborn et al.[187]) is demonstrated by the validity of Equation (a).[184]

$$1/n \sum_{i=1}^{n} J^i/J^i_s = 1 \qquad (a)$$

$J^i = {}^1J(M,{}^{13}C)$ in **180** and **181**; $J^i_s = {}^1J(M,{}^{13}C)$ in the corresponding symmetrically substituted compounds $[R_2Hg]/[iBu_2Hg]$ and $[R_4Sn]/[Et_4Sn]$; M = ^{199}Hg, $n = 2$; M = ^{119}Sn, $n = 4$. For **180** these conclusions are also supported by pseudopotential ab initio calculations on the compounds [Me–Hg–R].[188]

Figure 2 depicts series of electronic influences for ligands R that have been established according to this theoretically sound procedure.[184] Both series provide as a crude classification of the ligand influence the sequence alkyl > alkenyl ≈

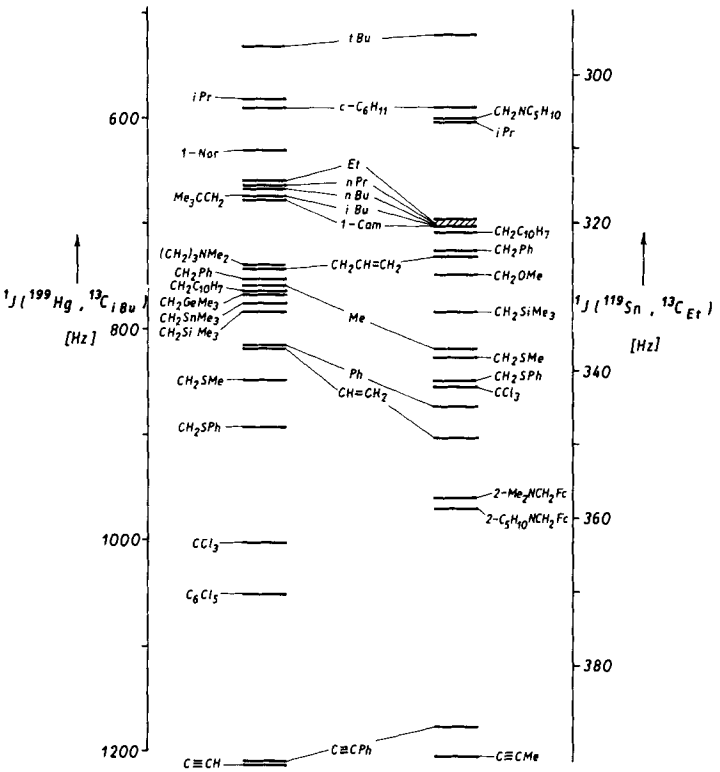

Fig. 2. Electronic influence of R in **180** (scale on the left) and **181** (scale on the right) based on the coupling constants $^1J(^{199}Hg,^{13}C_{iBu})$ and $^1J(^{119}Sn,^{13}C_{Et})$, respectively [184a,c,e, 185]. 1-Nor = 1-norbornyl; 1-Cam = 1-camphenyl; $CH_2C_{10}H_7$ = α-naphthylmethyl; 2-R_2NCH_2Fc = 2-(aminomethyl)ferrocenyl.

aryl > alkynyl, that is, $sp^3 > sp^2 > sp$, though this sequence is subject to some modification as a consequence of secondary effects. Certain calculated and experimental quantities for σ-organo residues are observed to follow similar trends,[1d] including the s character of the valence-hybrid orbitals, the electron affinities of the corresponding radicals, the ionization potentials of the anions, the electronegativities of R, and the acidities of RH, but in none of these cases is there a rigorous correlation over the complete range of investigated organo ligands. This is due to the specificity of metal–ligand bonding and the variation in donor–acceptor characteristics of the metal-complex fragments ML'_x to which R is bonded.

The relationship between the tin compounds **181** and the group electronegativity χ is shown in Figure 3.[182] This is an especially important model quantity, and it can be interpreted as a measure of σ-donor strength. Within the confines of the parent systems (Et, $CH{=}CH_2$, Ph, C≡CH) and the simple alkyl residues (Me, Et, *n*Pr, *i*Pr, *n*Bu, *t*Bu) there is a consistent, but inverse, correlation. Deviations point to peculiarities in bonding characteristics that are also apparent in

a comparison of the electronic ligand influences of R in **180** and **181**.[182]

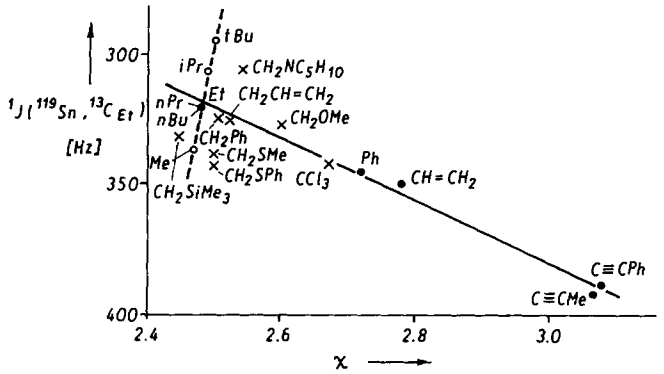

Fig. 3. Dependence of the coupling constant $^1J(^{119}Sn,^{13}C_{Et})$ as a measure of the electronic influence of ligand R in **181** on the electronegativity χ (based on Inamoto) of R [182].

Inconsistencies are particularly striking in the case of the allyl and benzyl ligands, as well as with functionalized methyl ligands whose π or n electrons are capable of entering into conjugative interaction with electrons from the M–C bond (conjugation of the σ–π or σ–n type, or negative hyperconjugation[189]). This is underscored by quantum-chemical calculations, according to which methyl anions are significantly less stabilized by elements of the first complete row (NH_2, OH, F) than by elements of the second row (SiH_3, PH_2, Cl) (see Figure 4).[190] Such results are due largely to

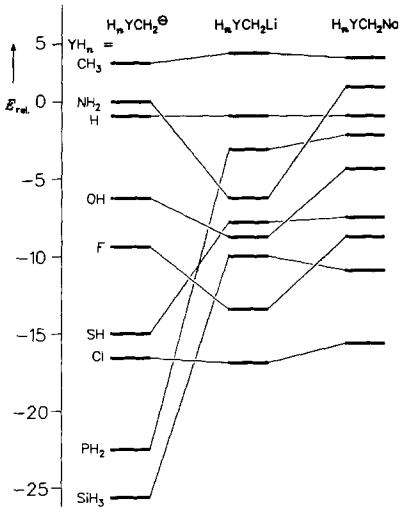

Fig. 4. Comparison of the stabilization energies $E_{rel.}$ of functionalized methyl anions with the corresponding functionalized methyllithium and methylsodium compounds [190].

greater polarization and more strongly developed negative hyperconjugation, and not to a d-orbital contribution. Moving to lithium compounds effectively reduces this additional stabilization. Stabilization of organo alkali-metal-compounds is largely a consequence of the formation of bridged structures (η^2-coordination), which are more prevalent for M = Li than for M = Na. The influence of the heteroatom is also reflected in the thermodynamic stability of lithium compounds, as indicated by investigations into variously substituted alkoxymethyllithium compounds.[191]

The two series of electronic influences shown in Figure 2, which are among the most extensive of their type, facilitate meaningful classification and characterization of a large number of σ-organo ligands in terms of their electronic influences on the basis of a theoretically grounded physical parameter. Such results provide an important foundation for judging structural and bonding effects in organometallic compounds generally.

5. Future Prospects

A geminal or vicinal arrangement of carbanion-like species and heteroatom centers in structural units such as M–CH_2–Y or M–CH_2–CH_2–Y leads to unusual bonding and stability relationships as well as to new types of reactions for complexes.

By contrast, the inductive effect of a heteroatom on the M–C bond is small in the case of the homologous γ- and δ-functionalized alkylmetal compounds. At the same time, 1,ω-eliminations with the formation of cyclopropane/propene or cyclobutane/butene[192] make way for the classical decomposition pathways of alkylmetal compounds.[1] When Y is coordinated to M the result is a five- or six-membered chelate ring, which generally leads to stabilization, permitting, for example, the synthesis of homoleptic γ-aminopropyl transition-metal complexes of Zr, Cr, Mn, and Co[193] as well as advantageous application of γ-aminopropylgallium and -indium compounds in MOVPE processes (MOVPE = *m*etal *o*rganic *v*apor *p*hase *e*pitaxy).[194]

There still remain a great many white (and gray) areas on the "topographic map" of alkylmetal compounds. Complexes with heavier heteroatoms, for example, have been investigated only to a limited extent. These might well prove to be a source of new aspects of reactivity, due in the case of α-stannylmethyl compounds to relatively facile electrophilic cleavage of the Sn–C bond. For example, R_3SnCH_2Li—in contrast to R_3SiCH_2Li—behaves as the equivalent of CH_2^{2-}.[195]

Completion of systematization with increasing reference to more complex systems, more thorough elucidation of the relationships linking structure with reactivity, and a more sophisticated theoretical foundation particularly for the electronic influences of the heteroatom on the M–C bond are certain to bring to light much that is new in this important and interesting area of organometallic chemistry.

Received: June 6, 1991 [A854IE]
German version: *Angew. Chem.* **1992**, *104*, 392
Translated by Dr. W. E. Russey, Huntingdon, PA (USA)

[1] a) *Comprehensive Organometallic Chemistry* (Eds.: G. Wilkinson, F. G. A. Stone, E. W. Abel), Pergamon, Oxford, **1982**; b) P. J. Davidson, M. F. Lappert, R. Pearce, *Chem. Rev.* **1976**, *76*, 219; c) R. R. Schrock, G. W. Parshall, *ibid.* **1976**, *76*, 243; d) R. Taube, H. Drevs, D. Steinborn, *Z. Chem.* **1978**, *18*, 425.
[2] a) W. A. Herrmann, *J. Organomet. Chem.* **1983**, *250*, 319; b) J. R. Moss, L. G. Scott, *Coord. Chem. Rev.* **1984**, *60*, 171; c) C. P. Casey, J. D. Audett, *Chem. Rev.* **1986**, *86*, 339.

[3] G. Bähr, G. E. Müller, *Chem. Ber.* **1955**, *88*, 251.
[4] G. Köbrich, *Angew. Chem.* **1972**, *84*, 557; *Angew. Chem. Int. Ed. Engl.* **1972**, *11*, 473.
[5] C. S. Cundy, B. M. Kingston, M. F. Lappert, *Adv. Organomet. Chem.* **1973**, *11*, 253.
[6] G. Wilkinson, *Angew. Chem.* **1974**, *86*, 664.
[7] E. J. Corey, D. Seebach, *Angew. Chem.* **1965**, *77*, 1134; *Angew. Chem. Int. Ed. Engl.* **1965**, *4*, 1075; D. Seebach, *ibid.* **1979**, *91*, 259 and **1979**, *18*, 239.
[8] a) B. Akermark, B. C. Söderberg, S. S. Hall, *Organometallics* **1987**, *6*, 2608; b) T. Hosokawa, S.-I. Murahashi, *Acc. Chem. Res.* **1990**, *23*, 49.
[9] I. Omae, *Organometallic Intramolecular-coordination Compounds (J. Organomet. Chem. Libr.* **1986**, *18*).
[10] I. Omae, *Coord. Chem. Rev.* **1988**, *83*, 137.
[11] D. J. Peterson, *Organomet. Chem. Rev. Sect. A* **1972**, 295.
[12] A. Krief, *Tetrahedron* **1980**, *36*, 2531.
[13] W. C. Kaska, *Coord. Chem. Rev.* **1983**, *48*, 1.
[14] H. Schmidbaur, *Angew. Chem.* **1983**, *95*, 980; *Angew. Chem. Int. Ed. Engl.* **1983**, *22*, 907.
[15] L. Weber, *Angew. Chem.* **1983**, *95*, 539; *Angew. Chem. Int. Ed. Engl.* **1983**, *22*, 516.
[16] P. J. Davidson, M. F. Lappert, R. Pearce, *Acc. Chem. Res.* **1974**, *7*, 209, and references cited therein.
[17] G. Wilkinson, *Chimia* **1973**, *27*, 165, and references cited therein.
[18] C. Santini-Scampucci, J. G. Riess, *J. Organomet. Chem.* **1980**, *187*, 331.
[19] a) M. H. Chisholm, F. A. Cotton, M. Extine, B. R. Stults, *Inorg. Chem.* **1976**, *15*, 2252; b) R. A. Andersen, M. H. Chisholm, J. F. Gibson, W. W. Reichert, I. P. Rothwell, G. Wilkinson, *ibid.* **1981**, *20*, 3934; c) C. G. Young, E. M. Kober, J. H. Enemark, *Polyhedron* **1987**, *6*, 255.
[20] R. A. Andersen, E. Carmona-Guzman, J. F. Gibson, G. Wilkinson, *J. Chem. Soc. Dalton Trans.* **1976**, 2204.
[21] J. L. Atwood, W. E. Hunter, R. D. Rogers, J. Holton, J. McMeeking, R. Pearce, M. F. Lappert, *J. Chem. Soc. Chem. Commun.* **1978**, 140.
[22] H. Schumann, *Angew. Chem.* **1984**, *96*, 475; *Angew. Chem. Int. Ed. Engl.* **1984**, *23*, 484, and references cited therein.
[23] E. R. Sigurdson, G. Wilkinson, *J. Chem. Soc. Dalton Trans.* **1977**, 812.
[24] R. J. Morris, G. S. Girolami, *Organometallics* **1989**, *8*, 1478.
[25] a) R. Andersen, E. Carmona-Guzman, K. Mertis, E. Sigurdson, G. Wilkinson, *J. Organomet. Chem.* **1975**, *99*, C19; b) R. S. Hay-Motherwell, G. Wilkinson, B. Hussain, M. B. Hursthouse, *Polyhedron* **1990**, *9*, 931.
[26] G. A. Razuvaev, L. I. Vyshinskaya, S. Y. Timoshenko, *Dokl. Akad. Nauk SSSR* **1984**, *276*, 1147.
[27] G. A. Razuvaev, V. N. Latyaeva, L. I. Vyshinskaya, V. V. Drobotenko, *J. Organomet. Chem.* **1981**, *208*, 169; *Dokl. Akad. Nauk SSSR* **1981**, *259*, 127.
[28] J. A. M. Simoes, J. L. Beauchamp, *Chem. Rev.* **1990**, *90*, 629.
[29] L. N. Zakharov, Y. N. Saf'yanov, G. A. Damrachev, *Inorg. Chim. Acta* **1989**, *160*, 77.
[30] J. Z. Cayias, E. A. Babaian, D. C. Hrncir, S. G. Bott, J. L. Atwood, *J. Chem. Soc. Dalton Trans.* **1986**, 2743.
[31] a) W. Mowat, G. Wilkinson, *J. Chem. Soc. Dalton Trans.* **1973**, 1120; b) R. A. Andersen, A. L. Galyer, G. Wilkinson, *Angew. Chem.* **1976**, *88*, 692; *Angew. Chem. Int. Ed. Engl.* **1976**, *15*, 609.
[32] M. H. Chisholm, F. A. Cotton, M. W. Extine, C. A. Murillo, *Inorg. Chem.* **1978**, *17*, 696; M. H. Chisholm, J. A. Heppert, E. M. Kober, D. L. Lichtenberger, *Organometallics* **1987**, *6*, 1065.
[33] M. Bochmann, G. Wilkinson, A. M. R. Galas, M. B. Hursthouse, K. M. A. Malik, *J. Chem. Soc. Dalton Trans.* **1980**, 1797.
[34] D. Seyferth, *Adv. Organomet. Chem.* **1976**, *14*, 97; b) H. T. Schacht, H. Vahrenkamp, *J. Organomet. Chem.* **1990**, *381*, 261.
[35] M. H. Chisholm, J. A. Heppert, J. C. Huffman, *J. Am. Chem. Soc.* **1984**, *106*, 1151.
[36] E. D. Jemmis, B. V. Prasad, *J. Am. Chem. Soc.* **1987**, *109*, 2560.
[37] A. D. Ryabov, *Chem. Rev.* **1990**, *90*, 403.
[38] a) T. H. Tulip, D. L. Thorn, *J. Am. Chem. Soc.* **1981**, *103*, 2448; b) J. W. Bruno, T. J. Marks, V. W. Day, *ibid.* **1982**, *104*, 7357; c) W. R. Tikkanen, J. W. Egan, Jr., J. L. Petersen, *Organometallics* **1984**, *3*, 1646; d) C. M. Fendrick, T. J. Marks, *J. Am. Chem. Soc.* **1984**, *106*, 2214.
[39] P. Hofmann, H. Heiß, P. Neiteler, G. Müller, J. Lachmann, *Angew. Chem.* **1990**, *102*, 935; *Angew. Chem. Int. Ed. Engl.* **1990**, *29*, 880.
[40] M. Hackett, G. M. Whitesides, *J. Am. Chem. Soc.* **1988**, *110*, 1449.
[41] S. J. Simpson, R. A. Andersen, *J. Am. Chem. Soc.* **1981**, *103*, 4063; *Inorg. Chem.* **1981**, *20*, 3627.
[42] D. C. Bradley, H. Chudzynska, J. D. J. Backer-Dirks, M. B. Hursthouse, A. A. Ibrahim, M. Motevalli, A. C. Sullivan, *Polyhedron* **1990**, *9*, 1423.
[43] S. J. Simpson, H. W. Turner, R. A. Andersen, *Inorg. Chem.* **1981**, *20*, 2991.
[44] a) B. K. Campion, R. H. Heyn, T. D. Tilley, *J. Am. Chem. Soc.* **1988**, *110*, 7558; b) T. S. Koloski, P. J. Carroll, D. H. Berry, *ibid.* **1990**, *112*, 6405.
[45] B. K. Campion, R. H. Heyn, T. D. Tilley, *J. Am. Chem. Soc.* **1990**, *112*, 4079.
[46] M. Dziallas, A. Höhn, H. Werner, *J. Organomet. Chem.* **1987**, *330*, 207.
[47] D. H. Berry, L. J. Procopio, *J. Am. Chem. Soc.* **1989**, *111*, 4099.
[48] J. D. Smith, *Pure Appl. Chem.* **1986**, *58*, 623.
[49] a) P. B. Hitchcock, M. F. Lappert, R. G. Smith, R. A. Bartlett, P. P. Power, *J. Chem. Soc. Chem. Commun.* **1988**, 1007; b) M. F. Lappert, R. Pearce, *ibid.* **1973**, 126.
[50] G. K. Barker, M. F. Lappert, J. A. K. Howard, *J. Chem. Soc. Dalton Trans.* **1978**, 734.
[51] W. G. van der Sluys, C. J. Burns, A. P. Sattelberger, *Organometallics* **1989**, *8*, 855.
[52] R. A. Andersen, D. J. Berg, L. Fernholt, K. Fägri, Jr., J. C. Green, A. Haaland, M. F. Lappert, W.-P. Leung, K. Rypdal, *Acta Chem. Scand. Ser. A* **1988**, *42*, 554.
[53] N. H. Buttrus, C. Eaborn, P. B. Hitchcock, J. D. Smith, A. C. Sullivan, *J. Chem. Soc. Chem. Commun.* **1985**, 1380.
[54] a) M. F. Lappert, *Pure Appl. Chem.* **1978**, *50*, 703; b) T. Fjeldberg, A. Haaland, B. E. R. Schilling, M. F. Lappert, A. J. Thorne, *J. Chem. Soc. Dalton Trans.* **1986**, 1551; c) L. M. Engelhardt, B. S. Jolly, M. F. Lappert, C. L. Raston, A. H. White, *J. Chem. Soc. Chem. Commun.* **1988**, 336.
[55] B. K. Bower, H. G. Tennent, *J. Am. Chem. Soc.* **1972**, *94*, 2512; E. K. Byrne, K. H. Theopold, *ibid.* **1987**, *109*, 1282; V. Dimitrov, K.-H. Thiele, D. Schenke, *Z. Anorg. Allg. Chem.* **1985**, *527*, 85.
[56] a) C. Eaborn, N. Retta, J. D. Smith, *J. Organomet. Chem.* **1980**, *190*, 101; b) S. S. Al-Juaid, C. Eaborn, P. B. Hitchcock, C. A. McGeary, J. D. Smith, *J. Chem. Soc. Chem. Commun.* **1989**, 273.
[57] a) C. Eaborn, P. B. Hitchcock, J. D. Smith, A. C. Sullivan, *J. Chem. Soc. Chem. Commun.* **1983**, 827; b) *ibid.* **1984**, 870; c) *J. Organomet. Chem.* **1984**, *263*, C23.
[58] Corresponding compounds with the sterically less demanding trimethylsilylmethyl ligands crystallize as thf adducts.
[59] P. B. Hitchcock, J. A. K. Howard, M. F. Lappert, W.-P. Leung, S. A. Mason, *J. Chem. Soc. Chem. Commun.* **1990**, 847.
[60] G. A. Ayoko, N. H. Buttrus, C. Eaborn, P. B. Hitchcock, J. D. Smith, *J. Organomet. Chem.* **1987**, *320*, 137.
[61] C. Eaborn, K. L. Jones, J. D. Smith, K. Tavakkoli, *J. Chem. Soc. Chem. Commun.* **1989**, 1201.
[62] a) D. Steinborn, *Z. Chem.* **1976**, *16*, 328; b) *ibid.* **1972**, *17*, 347.
[63] D. Steinborn, *Proc. Conf. Coord. Chem. 12th (Smolenice/Bratislava)*, **1989**, 363.
[64] H. H. Karsch, A. Appelt, G. Müller, *Angew. Chem.* **1986**, *98*, 832; *Angew. Chem. Int. Ed. Engl.* **1986**, *25*, 823.
[65] K. Miki, G. Yoshida, Y. Kai, N. Yasuoka, N. Kasai, *J. Organomet. Chem.* **1978**, *149*, 195.
[66] a) R. Taube, D. Steinborn, *J. Organomet. Chem.* **1974**, *65*, C9; b) D. Steinborn, R. Taube, *Z. Anorg. Allg. Chem.* **1985**, *521*, 183.
[67] D. G. H. Ballard, *Adv. Catal.* **1973**, *23*, 263.
[68] a) R. Taube, D. Steinborn, W. Höbold, *J. Organomet. Chem.* **1985**, *284*, 385; b) D. Steinborn, R. Taube, *ibid.* **1985**, *284*, 395.
[69] K. Miki, Y. Kai, N. Yasuoka, N. Kasai, *J. Organomet. Chem.* **1979**, *165*, 79.
[70] a) M. L. H. Green, M. Ishaq, R. N. Whiteley, *J. Chem. Soc. A* **1967**, 1508; b) R. B. King, M. B. Bisnette, *Inorg. Chem.* **1965**, *4*, 482.
[71] G. N. Glavee, R. J. Angelici, *J. Am. Chem. Soc.* **1989**, *111*, 3598.
[72] F. R. Kreißl, F. X. Müller, D. L. Wilkinson, G. Müller, *Chem. Ber.* **1989**, *122*, 289.
[73] J. W. Park, L. M. Henling, W. P. Schaefer, R. H. Grubbs, *Organometallics* **1990**, *9*, 1650.
[74] a) H. Werner, W. Paul, W. Kraup, J. Wolf, G. Müller, J. Riede, *J. Organomet. Chem.* **1988**, *358*, 95; b) S. L. Buchwald, R. B. Nielsen, J. C. Dewan, *J. Am. Chem. Soc.* **1987**, *109*, 1590.
[75] R. A. Doyle, R. J. Angelici, *J. Am. Chem. Soc.* **1990**, *112*, 194.
[76] J. Villieras, *Organometal. Chem. Rev. Sect. A* **1971**, *7*, 81.
[77] Perhalogenated alkyl ligands have not been dealt with here; a review appeared recently over perfluoroalkyl complexes: R. P. Hughes, *Adv. Organomet. Chem.* **1990**, *31*, 183.
[78] T. Kauffmann, R. Fobker, M. Wensing, *Angew. Chem.* **1988**, *100*, 1005; *Angew. Chem. Int. Ed. Engl.* **1988**, *27*, 943.
[79] R. J. Kulawiec, R. H. Crabtree, *Coord. Chem. Rev.* **1990**, *99*, 89.
[80] a) E. Lindner, K. A. Starz, H.-J. Eberle, W. Hiller, *Chem. Ber.* **1983**, *116*, 1209; b) E. Lindner, D. Goth, *J. Organomet. Chem.* **1987**, *319*, 149; c) E. Lindner, M. Stängle, W. Hiller, R. Fawzi, *Chem. Ber.* **1989**, *122*, 823; d) E. Lindner, E. Ossig, M. Darmuth, *J. Organomet. Chem.* **1989**, *379*, 107.
[81] a) E. Lindner, G. Funk, S. Hoehne, *Chem. Ber.* **1981**, *114*, 2465; b) E. Lindner, F. Bouachir, W. Hiller, *Z. Naturforsch. B.* **1982**, *37*, 1146; c) E. Lindner, P. Neese, W. Hiller, R. Fawzi, *Organometallics* **1986**, *5*, 2030.
[82] E. W. Abel, R. J. Rowley, *J. Chem. Soc. Dalton Trans.* **1975**, 1096.
[83] a) H. F. Klein, *Angew. Chem.* **1980**, *92*, 362; *Angew. Chem. Int. Ed. Engl.* **1980**, *19*, 362; b) H. Werner, R. Werner, *J. Organomet. Chem.* **1981**, *209*, C60; c) J. Gotzig, R. Werner, H. Werner, *ibid.* **1985**, *290*, 99; d) R. S. Shinomoto, P. J. Desrosiers, T. G. P. Harper, T. C. Flood, *J. Am. Chem. Soc.* **1990**, *112*, 704; e) D. Rabinovich, G. Parkin, *ibid.* **1990**, *112*, 5381, and references cited therein.
[84] a) S. Al-Jibori, C. Crocker, W. S. McDonald, B. L. Shaw, *J. Chem. Soc. Dalton Trans.* **1981**, 1572; b) H. H. Karsch, H.-F. Klein, H. Schmidbaur, *Angew. Chem.* **1975**, *87*, 630; *Angew. Chem. Int. Ed. Engl.* **1975**, *14*, 637.

[85] a) E. Farnetti, G. Nardin, M. Graziani, *J. Chem. Soc. Chem. Commun.* **1989**, 1264; b) H. C. L. Abbenhuis, D. M. Grove, G. P. M. van Mier, A. L. Spek, G. van Koten, *Recl. Trav. Chim. Pays-Bas* **1990**, *109*, 361; c) Y. Tamaru, M. Kagotani, Z. Yoshida, *Angew. Chem.* **1981**, *93*, 1031; *Angew. Chem. Int. Ed. Engl.* **1981**, *20*, 980.

[86] A. A. H. van der Zeijden, G. van Koten, R. Luijk, R. A. Nordemann, A. L. Spek, *Organometallics* **1988**, *7*, 1549.

[87] a) V. A. Osborn, C. A. Parker, M. J. Winter, *J. Chem. Soc. Chem. Commun.* **1986**, 1185; b) H. Adams, N. A. Bailey, V. A. Osborn, M. J. Winter, *J. Chem. Soc. Dalton Trans.* **1986**, 2127; c) G. A. Carriedo, V. Riera, M. Luz Rodriguez, J. C. Jefferey, *J. Organomet. Chem.* **1986**, *314*, 139.

[88] a) H. Adams, N. A. Bailey, P. Cahill, D. Rogers, M. J. Winter, *J. Chem. Soc. Dalton Trans.* **1986**, 2119; b) A. K. Burrell, G. R. Clark, J. G. Jeffrey, C. E. F. Rickard, W. R. Roper, *J. Organomet. Chem.* **1990**, *388*, 391.

[89] M. D. Fryzuk, K. Joshi, R. K. Chadha, *J. Am. Chem. Soc.* **1989**, *111*, 4498.

[90] G. C. A. Bellinger, H. B. Friedrich, J. R. Moss, *J. Organomet. Chem.* **1989**, *366*, 175, and references cited therein.

[91] G. J. Arsenault, M. Crespo, R. J. Puddephatt, *Organometallics* **1987**, *6*, 2255.

[92] H. Werner, L. Hofmann, R. Feser, W. Paul, *J. Organomet. Chem.* **1985**, *281*, 317.

[93] a) N. W. Alcock, P. G. Pringle, P. Bergamini, S. Sostero, O. Traverso, *J. Chem. Soc. Dalton Trans.* **1990**, 1553; b) H. Werner, L. Hofmann, W. Paul, U. Schubert, *Organometallics* **1988**, *7*, 1106; c) R. Zolk, H. Werner, *J. Organomet. Chem.* **1986**, *303*, 233.

[94] a) W. A. Herrmann, *Angew. Chem.* **1978**, *90*, 855; *Angew. Chem. Int. Ed. Engl.* **1978**, *17*, 800; b) R. McCrindle, G. J. Arsenault, R. Farwaha, A. J. McAlees, D. W. Sneddon, *J. Chem. Soc. Dalton Trans.* **1989**, 761.

[95] D. H. Gibson, S. K. Mandal, K. Owens, W. E. Sattich, J. O. Franco, *Organometallics* **1989**, *8*, 1114.

[96] a) V. Galamb, G. Palyi, R. Boese, G. Schmid, *Organometallics* **1987**, *6*, 861.

[97] A. L. Poznyak, V. I. Pavlovski, *Angew. Chem.* **1988**, *100*, 812; *Angew. Chem. Int. Ed. Engl.* **1988**, *27*, 789.

[98] M. Matsumoto, K. Nakatsu, K. Tani, A. Nakamura, S. Otsuka, *J. Am. Chem. Soc.* **1974**, *96*, 6777.

[99] a) D. Walther, *Z. Chem.* **1989**, *29*, 146; b) D. Walther, E. Dinjus, V. Herzog, *ibid.* **1982**, *22*, 303; c) D. Walther, E. Dinjus, J. Sieler, J. Kaiser, O. Lindqvist, L. Anderson, *J. Organomet. Chem.* **1982**, *240*, 289.

[100] H. Hoberg, *J. Organomet. Chem.* **1988**, *358*, 507.

[101] A. Behr, *Angew. Chem.* **1988**, *100*, 681; *Angew. Chem. Int. Ed. Engl.* **1988**, *27*, 661.

[102] a) P. Hofmann, P. Stauffert, N. E. Schore, *Chem. Ber.* **1982**, *115*, 2153; b) E. K. Barefield, D. J. Sepelak, *J. Am. Chem. Soc.* **1979**, *101*, 6542.

[103] G. Erker, R. Schlund, C. Krüger, *J. Chem. Soc. Chem. Commun.* **1986**, 1403.

[104] a) N. E. Schore, S. J. Young, M. Olmstead, P. Hofmann, *Organometallics* **1983**, *2*, 1769; b) R. Choukroun, A. Iraqi, C. Rifai, D. Gervais, *J. Organomet. Chem.* **1988**, *353*, 45.

[105] R. J. Puddephatt, *Chem. Soc. Rev.* **1983**, *12*, 99.

[106] H. H. Karsch, B. Deubelly, G. Hanika, J. Riede, G. Müller, *J. Organomet. Chem.* **1988**, *344*, 153, and references cited therein.

[107] a) V. Riera, J. Ruiz, *J. Organomet. Chem.* **1986**, *310*, C36; b) G. M. Dawkins, M. Green, J. C. Jeffery, C. Sambale, F. G. A. Stone, *J. Chem. Soc. Dalton Trans.* **1983**, 499; c) H. H. Karsch, *Angew. Chem.* **1982**, *94*, 923; *Angew. Chem. Int. Ed. Engl.* **1982**, *21*, 921.

[108] M. Lusser, P. Peringer, *J. Organomet. Chem.* **1986**, *312*, C61.

[109] H. H. Karsch, B. Deubelly, J. Hofmann, U. Pieper, G. Müller, *J. Am. Chem. Soc.* **1988**, *110*, 3654.

[110] B. J. Wakefield in [1a], *Vol. 7*, p. 1; W. Carruthers in [1a], *Vol. 7*, p. 661.

[111] a) A. S. Ward, E. A. Mintz, M. R. Ayers, *Organometallics* **1986**, *5*, 1585; b) A. S. Ward, E. A. Mintz, M. P. Kramer, *ibid.* **1988**, *7*, 8; c) E. A. Mintz, A. S. Ward, *J. Organomet. Chem.* **1986**, *307*, C52.

[112] a) R. Taube, D. Steinborn, B. Adler, *J. Organomet. Chem.* **1984**, *275*, 1; b) D. Steinborn, U. Sedlak, *Z. Chem.* **1985**, *25*, 376.

[113] J. Sieler, D. Steinborn, O. Lindqvist, L. Andersen, *J. Organomet. Chem.*, in press.

[114] T. Chivers, R. Ram, *Can. J. Chem.* **1977**, *55*, 2554.

[115] G. Erker, R. Schlund, M. Albrecht, C. Sarter, *J. Organomet. Chem.* **1988**, *353*, C27.

[116] S. L. Buchwald, R. B. Nielsen, J. C. Dewan, *Organometallics*, **1989**, *8*, 1593.

[117] P. Beak, D. B. Reitz, *Chem. Rev.* **1978**, *78*, 275.

[118] a) L. D. Durfee, I. P. Rothwell, *Chem. Rev.* **1988**, *88*, 1059; b) J. C. Bryan, J. M. Mayer, *J. Am. Chem. Soc.* **1990**, *112*, 2298; c) S. Gambarotta, C. Floriani, A. Chiesi-Villa, C. Guastini, *Organometallics* **1986**, *5*, 2425.

[119] a) G. Erker, U. Hoffmann, R. Zwettler, P. Betz, C. Krüger, *Angew. Chem.* **1989**, *101*, 644; *Angew. Chem. Int. Ed. Engl.* **1989**, *28*, 630; b) G. Erker, *Acc. Chem. Res.* **1984**, *17*, 103.

[120] M. D. Fryzuk, C. D. Montgomery, *Coord. Chem. Rev.* **1989**, *95*, 1.

[121] H. Werner, W. Paul, J. Wolf, M. Steinmetz, R. Zolk, G. Müller, O. Steigelmann, J. Riede, *Chem. Ber.* **1989**, *122*, 1061.

[122] H.-J. Kneuper, C. Zimmermann, K. Harms, G. Boche, *Chem. Ber.* **1989**, *122*, 1043.

[123] a) J.-J. Parnaud, G. Campari, P. Pino, *J. Mol. Catal.* **1979**, *6*, 341; b) W. Petri, W. Beck, *Chem. Ber.* **1984**, *117*, 3265.

[124] W. A. Herrmann, *Angew. Chem.* **1982**, *94*, 118; *Angew. Chem. Int. Ed. Engl.* **1982**, *21*, 117.

[125] a) J. C. Selover, G. D. Vaughn, C. E. Strouse, J. A. Gladysz, *J. Am. Chem. Soc.* **1986**, *108*, 1455; b) G. D. Vaughn, C. E. Strouse, J. A. Gladysz, *ibid.* **1986**, *108*, 1462; c) G. D. Vaughn, J. A. Gladysz, *ibid.* **1986**, *108*, 1473.

[126] S. L. van Voorhees, B. B. Wayland, *Organometallics* **1985**, *4*, 1887.

[127] G. N. Schrauzer, *Angew. Chem.* **1977**, *89*, 239; *Angew. Chem. Int. Ed. Engl.* **1977**, *16*, 233.

[128] G. N. Glavee, L. M. Daniels, R. J. Angelici, *Organometallics* **1989**, *8*, 1856.

[129] R. Taube, D. Steinborn, H. Drevs, P. N. Chuong, N. Stransky, J. Langlotz, *Z. Chem.* **1988**, *28*, 381.

[130] H. Schumann, F.-W. Reier, *Inorg. Chim. Acta* **1984**, *95*, 43, and references cited therein.

[131] G. W. Rice, G. B. Ansell, M. A. Modrick, S. Zentz, *Organometallics* **1983**, *2*, 154.

[132] a) E. Kurras, U. Rosenthal, H. Mennenga, G. Oehme, *Angew. Chem.* **1973**, *85*, 913; *Angew. Chem. Int. Ed. Engl.* **1973**, *12*, 854; b) E. Kurras, U. Rosenthal, H. Mennenga, G. Oehme, G. Engelhardt, *Z. Chem.* **1974**, *14*, 160; c) E. Kurras, H. Mennenga, G. Oehme, U. Rosenthal, G. Engelhardt, *J. Organomet. Chem.* **1975**, *84*, C13; d) E. Kurras, U. Rosenthal, *ibid.* **1978**, *160*, 35.

[133] F. A. Cotton, B. E. Hanson, W. H. Ilsley, G. W. Rice, *Inorg. Chem.* **1979**, *18*, 2713.

[134] W. C. Kaska, R. F. Reichelderfer, L. Prizant, *J. Organomet. Chem.* **1977**, *129*, 97.

[135] Cf. [14], and references cited therein.

[136] a) I. J. B. Lin, L. Hwan, H. C. Shy, M. C. Chen, Y. Wang, *J. Organomet. Chem.* **1986**, *315*, 135; b) M. C. Cheng, S. M. Peng, J. J. B. Lin, B. H. H. Meng, C. H. Liu, *ibid.* **1987**, *327*, 275.

[137] a) J. C. Baldwin, N. L. Keder, C. E. Strouse, W. C. Kaska, *Z. Naturforsch. B* **1980** *35*, 1289; b) G. Erker, P. Czisch, R. Mynott, Y.-H. Tsay, C. Krüger, *Organometallics* **1985**, *4*, 1310.

[138] H. Schmidbaur, R. Pichl, G. Müller, *Angew. Chem.* **1986**, *98*, 572; *Angew. Chem. Int. Ed. Engl.* **1986**, *25*, 574; *Chem. Ber.* **1987**, *120*, 39.

[139] Y. Yamamoto, *Bull. Chem. Soc. Jpn.* **1987**, *60*, 1189.

[140] R. F. Wu, I. J. B. Lin, G. H. Lee, M. C. Cheng, Y. Wang, *Organometallics* **1990**, *9*, 126.

[141] a) R. J. Puddephatt, *Coord. Chem. Rev.* **1980**, *33*, 149; b) R. J. Al-Essa, S. S. M. Ling, R. J. Puddephatt, *Organometallics* **1987**, *6*, 951.

[142] M. N. Mattson, J. P. Bays, J. Zakutansky, V. Stolarski, P. Helquist, *J. Org. Chem.* **1989**, *54*, 2467.

[143] V. Guerchais, J.-Y. Thepot, C. Lapinte, *J. Chem. Soc. Chem. Commun.* **1989**, 1554.

[144] W. E. Lindsell in [1a], *Vol. 1*, p. 155.

[145] A. Maercker, *Angew. Chem.* **1987**, *99*, 1002; *Angew. Chem. Int. Ed. Engl.* **1987**, *26*, 972.

[146] D. Steinborn, *J. Organomet. Chem.* **1979**, *182*, 313.

[147] a) J. Ficini, G. Sarrade-Loucheur, H. Normant, *Bull. Soc. Chim. Fr.* **1962**, 1219; b) H. H. Grootveld, C. Blomberg, F. Bickelhaupt, *Tetrahedron Lett.* **1971**, 1999; c) J. Barluenga, F. J. Fananas, M. Yus, *J. Org. Chem.* **1979**, *44*, 4798; J. Barluenga, *Pure Appl. Chem.* **1990**, *62*, 595.

[148] a) M. Rosenblum, *J. Organomet. Chem.* **1986**, *300*, 191; b) P. Lennon, M. Madhavarao, A. Rosan, M. Rosenblum, *ibid.* **1976**, *108*, 93, and references cited therein.

[149] T. Ghazy, L. A. P. Kane-Maguire, K. Do, *J. Organomet. Chem.* **1990**, *390*, 91.

[150] a) L. Maresca, G. Natile, *J. Chem. Soc. Chem. Commun.* **1983**, 40; F. P. Fanizzi, F. P. Intini, L. Maresca, G. Natile, F. Gasparrini, *J. Chem. Soc. Dalton Trans.* **1990**, 1019; c) H. Werner, R. Feser, L. Hofmann, *J. Organomet. Chem.* **1985**, *292*, 361.

[151] a) G. Natile, *J. Chem. Soc. Chem. Commun.* **1978**, 654; b) M. Stephenson, R. J. Mawby, *J. Chem. Soc. Dalton Trans.* **1981**, 2112.

[152] a) B. Akermark, J.-E. Bäckvall, K. Zetterberg, *Acta Chem. Scand. Ser. B* **1982**, *36*, 577; b) B. Akermark, K. Zetterberg, *J. Am. Chem. Soc.* **1984**, *106*, 5560.

[153] O. Eisenstein, R. Hoffmann, *J. Am. Chem. Soc.* **1980**, *102*, 6148.

[154] a) S. Sakaki, K. Maruta, K. Ohkubo, *Inorg. Chem.* **1987**, *26*, 2499; b) J.-E. Bäckvall, E. E. Björkman, L. Pettersson, P. Siegbahn, *J. Am. Chem. Soc.* **1984**, *106*, 4369.

[155] R. L. Cowan, W. C. Trogler, *Organometallics*, **1987**, *6*, 2451.

[156] C. L. Randolph, M. S. Wrighton, *J. Am. Chem. Soc.* **1986**, *108*, 3366.

[157] a) R. G. Goel, W. O. Ogini, *Organometallics* **1982**, *1*, 654; b) S. Hietkamp, D. J. Stufkens, K. Vrieze, *J. Organomet. Chem.* **1977**, *139*, 189; c) H. Kletzin, H. Werner, *Angew. Chem.* **1983**, *95*, 916; *Angew. Chem. Int. Ed. Engl.* **1983**, *22*, 873; d) K. Roder, H. Werner, *J. Organomet. Chem.* **1989**, *367*, 321.

[158] J. D. Oliver, D. F. Mullica, W. O. Milligan, *Inorg. Chem.* **1982**, *21*, 3284.

[159] B. L. Shaw, *J. Organomet. Chem.* **1980**, *200*, 307.

1983, *250*, 617; b) B. L. Simms, J. A. Ibers, *ibid.* **1987**, *330*, 279.
[161] D. P. Klein, J. C. Hayes, R. G. Bergman, *J. Am. Chem. Soc.* **1988**, *110*, 3704.
[162] E. Lindner, R. Fawzi, *J. Organomet. Chem.* **1986**, *299*, C47.
[163] a) E. Lindner, G. Funk, *J. Organomet. Chem.* **1981**, *216*, 393; b) A. Behr, U. Kanne, G. Thelen, *ibid.* **1984**, *269*, C1.
[164] G. Annibale, L. Maresca, G. Natile, A. Tiripicchio, M. Tiripicchio-Camellini, *J. Chem. Soc. Dalton Trans.* **1982**, 1587.
[165] a) D. Steinborn, U. Sedlak, R. Taube, *Z. Anorg. Allg. Chem.* **1982**, *492*, 103; b) D. Steinborn, U. Sedlak, R. Taube, C. Wild, A. Henze, P. Franke, *Z. Anorg. Allg. Chem.* **1982**, *492*, 113; c) D. Steinborn, unpublished.
[166] K. L. Brown, S. Ramamurthy, *Organometallics* **1982**, *1*, 413.
[167] a) W. L. Mock, C. Bieniarz, *Organometallics* **1984**, *3*, 1279; b) K. L. Brown, Z. Szeverenyi, *Inorg. Chim. Acta* **1986**, *119*, 149.
[168] a) H. Eckert, I. Ugi, *Liebigs Ann. Chem.* **1979**, 278; b) R. Scheffold, E. Amble, *Angew. Chem.* **1980**, *92*, 643; *Angew. Chem. Int. Ed. Engl.* **1980**, *19*, 629.
[169] H. Eckert, M. Listl, I. Ugi, *Angew. Chem.* **1978**, *90*, 388; *Angew. Chem. Int. Ed. Engl.* **1978**, *17*, 361.
[170] a) D. R. Coulson, *Tetrahedron Lett.* **1971**, 429; b) R. Taube, E. Krukowka, D. Steinborn, DD C 07 C/321 646-7 (**1989**).
[171] a) M. G. Clerici, F. Maspero, A. D'Alfonso, US 4110377, **1978**; b) D. Steinborn, B. Thies, I. Wagner, R. Taube, *Z. Chem.* **1989**, *29*, 333.
[172] a) D. Steinborn, R. Taube, *Z. Chem.* **1986**, *26*, 349; b) J. J. Brunet, D. Neibecker, F. Niedercorn, *J. Mol. Catal.* **1989**, *49*, 235.
[173] A. L. Casalnuovo, J. C. Calabrese, D. Milstein, *J. Am. Chem. Soc.* **1988**, *110*, 6738.
[174] a) *The Chemistry of Organic Silicon Compounds* (Eds.: S. Patai, Z. Rappoport), Wiley, **1989**; b) I. Ojima in [174a], p. 1479; c) T. D. Tilley in [174a], p. 1415.
[175] R. Taube, *Homogene Katalyse*, Akademie-Verlag, Berlin, **1988**.
[176] K. A. Jorgensen, B. Schiott, *Chem. Rev.* **1990**, *90*, 1483.
[177] A. Miyashita, J. Ishida, H. Nohira, *Tetrahedron Lett.* **1986**, *27*, 2127.
[178] A. A. Zlota, F. Frolow, D. Milstein, *J. Am. Chem. Soc.* **1990**, *112*, 6411.
[179] The electronic influence is more narrowly specified as a *trans* (*cis*) influence in the case of a mutual *trans* (*cis*) arrangement of the influencing and affected ligands. This is to be distinguished from the electronic effect (*trans*/*cis* effect), which describes the impact of L on the reaction rate of a ligand-substitution reaction of the type L–[M]–L′ + L″ → L–[M]–L″ + L′. With the electronic effect, the impact of L is thus reflected in both the ground state *and* the transition state [180,181].
335.
[181] D. Steinborn, *Wiss. Zeitschr. Tech. Hochsch. Carl Schorlemmer Leuna-Merseburg* **1986**, *28*, 203.
[182] D. Steinborn, R. Taube, R. Radeglia, *Mitteilungsbl. Chem. Ges. DDR* **1988**, *35*, 278.
[183] M. M. Gofman, V. I. Nefedov, *Inorg. Chim. Acta* **1978**, *28*, 1.
[184] a) D. Steinborn, R. Taube, R. Radeglia, W. Höbold, *J. Organomet. Chem.* **1981**, *210*, 139; b) R. Radeglia, D. Steinborn, R. Taube, *Z. Chem.* **1981**, *21*, 365; c) D. Steinborn, M. Buthge, R. Taube, R. Radeglia, K. Schlothauer, K. Nowak, *J. Organomet. Chem.* **1982**, *234*, 277; d) R. Radeglia, D. Steinborn, R. Taube, *Spectrochim. Acta Part A* **1983**, *39*, 843; e) D. Steinborn, *Z. Chem.* **1985**, *25*, 412.
[185] 1-Nor: V. Dimitrov, K.-H. Thiele, R. Radeglia, *Z. Anorg. Allg. Chem.* **1983**, *503*, 177; CH_2MMe_3 (M = C, Ge, Sn): B. Fabisch, T. N. Mitchell, *J. Organomet. Chem.* **1984**, *269*, 219; $CH_2C_{10}H_7$: J. Scholz, Dissertation, Technische Hochschule Merseburg, **1984**; 1-Cam: D. Schenke, K.-H. Thiele, *J. Prakt. Chem.* **1990**, *332*, 496; R_2NCH_2Fc: C. Krüger, K.-H. Thiele, M. Dargatz, *Z. Anorg. Allg. Chem.* **1989**, *569*, 97; $(CH_2)_3NMe_2$: E. Langguth, K.-H. Thiele, *ibid.* **1985**, *530*, 69.
[186] a) H. A. Bent, *Chem. Rev.* **1961**, *61*, 275; b) W. A. Bingel, W. Lüttke, *Angew. Chem.* **1981**, *93*, 944; *Angew. Chem. Int. Ed. Engl.* **1981**, *20*, 899.
[187] D. Steinborn, R. Taube, R. Radeglia, *J. Organomet. Chem.* **1982**, *229*, 159.
[188] J. Reinhold, N. Steinfeldt, M. Schüler, D. Steinborn, *J. Organomet. Chem.*, in press.
[189] P. v. R. Schleyer, A. J. Kos, *Tetrahedron* **1983**, *39*, 1141.
[190] P. v. R. Schleyer, T. Clark, A. J. Kos, G. W. Spitznagel, C. Rohde, D. Arad, K. N. Houk, N. G. Rondan, *J. Am. Chem. Soc.* **1984**, *106*, 6467.
[191] J. S. Sawyer, T. L. Macdonald, G. J. McGarvey, *J. Am. Chem. Soc.* **1984**, *106*, 3376.
[192] a) K. L. Rollick, W. A. Nugent, J. K. Kochi, *J. Organomet. Chem.* **1982**, *225*, 279; b) W. F. Bailey, R. P. Gagnier, J. J. Patricia, *J. Org. Chem.* **1984**, *49*, 2098.
[193] a) A. Shakoor, K. Jacob, K.-H. Thiele, *Z. Anorg. Allg. Chem.* **1983**, *489*, 115; b) E. Langguth, N. Van Thu, A. Shakoor, K. Jacob, K.-H. Thiele, *ibid.* **1983**, *505*, 127.
[194] H. Schumann, U. Hartmann, W. Wassermann, *Polyhedron* **1990**, *9*, 353.
[195] T. Sato, T. Igarashi, M. Minomura, E. Murayama, *J. Org. Chem.* **1988**, *53*, 1207.

[4 + 4]-Cycloaddition Reactions in the Total Synthesis of Naturally Occurring Eight-Membered Ring Compounds

By *Gerd Kaupp**

Eight-membered rings can be obtained by [4 + 4]-cycloadditions of 1,3-dienes[1] via diradicals or other intermediates. Synthesis of such compounds has been achieved by thermal,[2] photochemical,[3] and by metal-catalyzed[4] processes: these reactions have been the subject of extensive mechanistic studies.[5] The thermal version has generated little interest, except in the case of cycloreversion; the Cope rearrangement of 1,2-divinylcyclobutanes[3] is more commonly used. [4 + 4]-Cycloadditions are also used with 1,3-dipoles or mesoionic heterocycles for the synthesis of six- and seven-membered rings, and also for [6 + 4]-cycloadditions.[2b] Good yields can be obtained with the photolytic reaction when the 1,3-diene is fixed in the *s-cis* configuration. Such is the case for, amongst others, condensed arenes, α-pyrones, and 2-pyridones. Two coupled, linear [4 + 4]-cycloadditions lead to ten-membered rings.[2e] Catalysis by Ni^0 is the obvious method of choice for open-chain 1,3-dienes, favorable coordination (template effect) apparently solving the difficult problem of bringing the terminal groups of the bis-1,3-diene into contact. The choice of typical examples given in Scheme 1 shows that one, two, or four eight-membered rings, which are not connected by zero bridges, can be formed by [4 + 4]-cycloadditions.

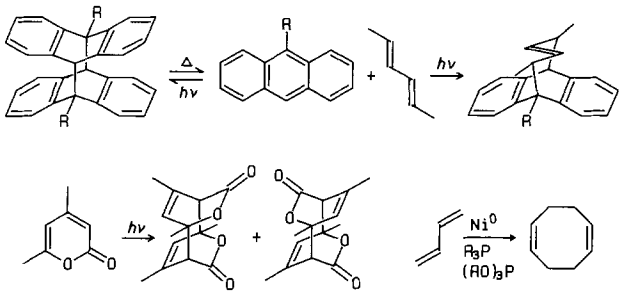

Scheme 1.

Cyclooctanoids (eight-membered ring compounds) can also be found among biologically active natural products such as sesqui-, di-, and sesterterpenes, as well as non-terpenoids. The total synthesis of such compounds has been a challenge for many research groups for years. In spite of intensive efforts, the total synthesis of the chemotherapeutic taxol **13** has not yet been achieved. Less highly functionalized analogues of taxol, which also inhibit the depolymerization of tubulin,[6] are now being prepared. In addition to taxol **13**, some of the best known naturally occurring cyclooctanoids include fusicoccin A (**1**), ophiobolin A (**2**), vinigrol (**3**), epoxybasmenone (**4**), kalmanol (**5**), (+)-asteriscanolide (**8**), crispolide, vulgar olide, cotylenin, variecolin, pleuromutilin, taxusin, and others.

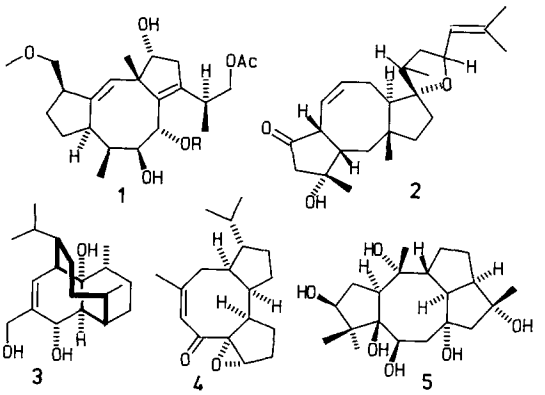

Strategies have been developed for the synthesis of these compounds, in some cases successfully, that do not depend on [4 + 4]-cycloaddition for formation of the eight-membered ring. The concern, unjustly, was that the control of the regio- and stereoselectivity would not be possible and that cross-dimerization with substituted 1,3-dienes would lead to poor yields. Original German work was apparently not so

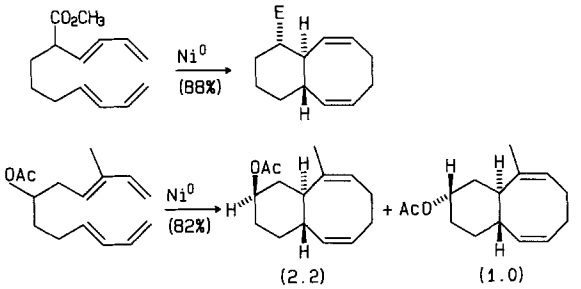

Scheme 2.

accessible in the United States, so that exchange of information concerning cycloaddition strategies in the synthesis of natural products containing eight-membered rings was very slow. It was not until 1986 that Wender et al. at Stanford showed[7] that it was possible to conduct stereoinduced Ni^0-catalyzed [4 + 4]-cycloadditions, even in the presence of oxygen-containing substituents (Scheme 2). Thereafter, the same group achieved the enantioselective synthesis of the cyclooctanoid **8**, a sesquiterpene.[8] With this approach they also plan on exploring further possibilities for the synthesis of cyclooctanoid diterpenes of the taxane series, such as **13**.[9] The key step in the synthesis of **8** was the Ni^0-catalyzed intramolecular [4 + 4]-cycloaddition of **6** (accessible in 11% yield from acrolein in nine steps) to give **7** in 67% yield (leading to a 36% yield of **8** in three further steps): a satisfyingly short and elegant total synthesis.

[*] Prof. Dr. G. Kaupp
Fachbereich 9 – Organische Chemie I – der Universität
Postfach 2503, D-W-2900 Oldenburg (FRG)

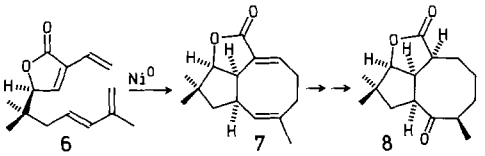

Presumably stimulated by the success of template-controlled syntheses, Sieburth et al. in Stony Brook hoisted the flag for photochemical metal-catalyzed stereoselective [4 + 4]-cycloadditions.[10] This case requires, of course, that two *s-cis*-constrained dienes are connected to each other. The choice thus fell on 2-pyridones. Target molecules are fusicoccin **1** and the cancer chemotherapeutic agent taxol **13** (cf. ref. [6]). The 3,6-bis(2-pyridone) **9**, used as the racemate but undoubtedly separable into the enantiomers, provides favorable prerequisites for the [4 + 4]-photocycloaddition. The nitrogen atoms, the carbonyl groups, and the double bonds are so arranged that further reaction to give **1** by standard methods appears to be possible. Indeed, the epimers **10** were formed by photolysis in good yield (66 and 75%). Moreover, suitable choice of solvent (protic or aprotic) even allowed preferential formation of one of the epimers. What is unfortunately still lacking is a suitable substituent R that can be employed for formation of the other 5-membered ring in **1**, without impeding the photoreaction: an interesting interim result.

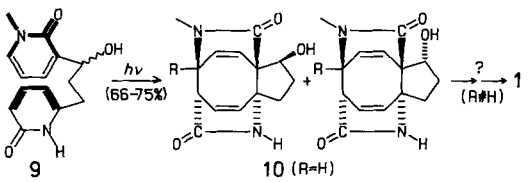

Sieburth et al. also photolyzed the racemic 3,6-bis(2-pyridone) **11**, in which the two rings are connected by a four-membered chain, obtaining both epimers of the secondary alcohol **12** (2:3, 63%). A certain resemblance to taxol **13** is clearly present, but there is still a long way to go. For example, a hydroxyl group is required at the other end of the bridging chain, B should be preferably a methyl group, and a suitable substituent A must be found that allows cyclization to the additional six-membered ring in **13**. Alternatively, it would be better if the methoxymethyl-substituted five-membered ring was already present on the *N*-methylpyridone ring. This interim result must be compared with that from Stanford in 1987, in which the [4 + 4]-cycloaddition was catalyzed with Ni^0.[9] Using conversion of **14** to **15** and **16** to **17** as model reactions allows the eight-membered ring and each of the two six-membered rings to be constructed, although not simultaneously (Scheme 3). A starting compound such as **18**, in which both possibilities are combined, and from which conversion to **13** is feasible with standard reactions after treatment with Ni^0, is not yet known. (A starting material similar to compound **16** was used in work recently published.[11] This starting compound, however, contains a methyl group at C4 and the *tert*-butyldimethylsiloxy group has been shifted from C5 to C7. This could, in connection with the [4 + 4]-cycloaddition (74%), possibly lead to crispolide, but neither this "model" nor **16** is suitable for synthesis of taxol **13**).

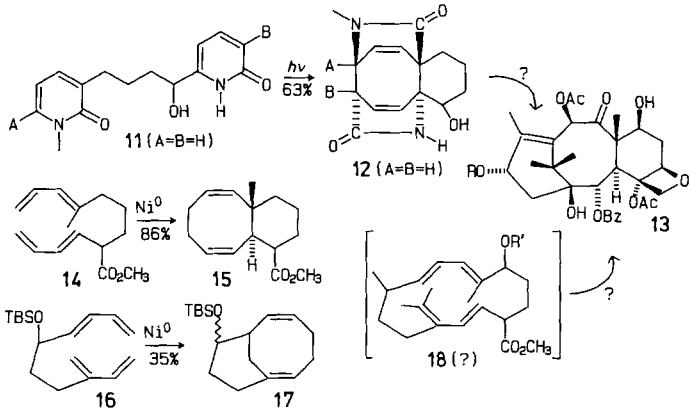

Scheme 3. TBSO = *tert*-butyldimethylsiloxy.

Although Sieburth et al. have not yet reached their goal, their results have nevertheless provided vital new impetus for the total synthesis of naturally occurring cyclooctanoids. The most suitable cycloaddition strategy in each case stands or falls with the accessibility of the bis-diene required. It should always be attempted, by means of stereoselective cycloaddition, to save steps in a total synthesis. The foundation for the application of [4 + 4]-cycloaddition for the most varied experimental conditions already exists. One should also not forget, that *cyclovinylogous* additions[5b] contain still further ideas for saving synthetic steps. For example, eight-membered rings can also be constructed by [2 + 2]-cycloaddition of cyclobutenes or of alkynes to (hetero)cyclohexenes or arenes followed by further ring expansion.[3a, 12] Diels–Alder reactions between components connected by a bridging group with six carbon atoms lead to cyclooctanone-annelated cyclohexenes.[13] Further perspectives for the synthesis of natural products are opened up by the cyclovinylogous [6 + 4]-[2b, 5b] (for ten-membered rings, see **3**, **13**, pleuromutilin), [6 + 6]-[14] and [4 + 4 + 4]-additions[4] (twelve-membered rings, see **5**), are often investigated in parallel with the [4 + 4]-additions. Thus, synthesis strategies aimed at the largest ring present containing no zero bridges should definitely also be considered. The work of Wender[7–9] and Sieburth[10] appears to illustrate a renaissance of cycloaddition reactions of polyenes, with very promising potential.

German version: Angew. Chem. **1992**, 104, 435

[1] H. Bouas-Laurent, J. P. Desvergne, *Stud. Org. Chem. (Amsterdam)* **1990**, *40*, 561–630.

[2] a) J. Wagner, J. Bendig, A. Felber, A. Sommerer, D. Kreysig, *Z. Chem.* **1985**, *25*, 64; b) W. Friedrichsen, W. D. Schröer, T. Debaerdemaeker, *Liebigs Ann. Chem.* **1980**, 1850–1858; W. Friedrichsen, H.-G. Oeser, *ibid.* **1978**, 1161–1186; c) S. A. Ali, M. I. M. Wazeer, *J. Chem. Soc. Perkin Trans. 2* **1986**, 1789–1792; J. Thesing, H. Mayer, *Chem. Ber.* **1956**, *89*, 2159–2167; J. Basan, H. Mayr, *J. Am. Chem. Soc.* **1987**, *109*, 6519–6521; H. Meier, U. Konnert, S. Graw, T. Echter, *Chem. Ber.* **1984**, *117*, 107–126; d) [6 + 2]-cycloadditions with 1,5-dipoles: P. A. Wender, J. L. Mascarenas, *J. Org. Chem.* **1991**, *56*, 6267–6269; e) A. Katritzky, S. I. Bayyuk, N. Dennis, G. Musumarra, E.-U. Würthwein, *J. Chem. Soc. Perkin Trans 1* **1979**, 2535–2541 (classified there as an "allowed" photoreaction).

[3] a) G. Kaupp, *Methoden Org. Chem. (Houben-Weyl) 4th Ed.* **1975**, Vol. 4/5a, p. 278, 360; E. Leppin, *ibid.*, p. 476, 484; V. Zanker, *ibid.*, p. 586, 616; b) Y. Nakamura, T. Kato, Y. Morita, *J. Chem. Soc. Perkin Trans.1* **1982**, 1187–1191.

[4] G. Wilke, *Angew. Chem.* **1963**, *75*, 10–20; *Angew. Chem. Int. Ed. Engl.* **1963**, *2*, 105–115; P. Heimbach, P. W. Jolly, G. Wilke in *Advances in Organometallic Chemistry*, Vol. 8 (eds.: F. G. A. Stone, R. West), Academic Press, New York, **1970**, p. 29ff.; P. W. Jolly, G. Wilke, *The Organic Chemistry of Nickel*, Vol. 2, Academic Press, New York, **1975**.
[5] a) J. Saltiel, R. Dabestani, K. S. Schanze, D. Trojan, D. E. Townsend, V. L. Goedken, *J. Am. Chem. Soc.* **1986**, *108*, 2674–2687, and references cited therein; b) G. Kaupp, E. Teufel, *Chem. Ber.* **1980**, *113*, 3669–3674; G. Kaupp, H.-W. Grüter, E. Teufel, *ibid.*, **1983**, *116*, 630–644; G. Kaupp, D. Schmitt, *ibid.*, **1981**, *114*, 1567–1571; **1980**, *113*, 1458–1471; G. Kaupp, H.-W. Grüter, *ibid.*, **1980**, *113*, 1626–1631; *Angew. Chem.* **1979**, *91*, 943–944; *Angew. Chem. Int. Ed. Engl.* **1979**, *18*, 881–882; G. Kaupp, *Liebigs Ann. Chem.* **1973**, 844–878.
[6] S. Blechert, A. Kleine-Klausing, *Angew. Chem.* **1991**, *103*, 428–429; *Angew. Chem. Int. Ed. Engl.* **1991**, *30*, 412–414; F. Gueritte-Voegelein, D. Guenard, F. Lavelle, M. T. LeGoff, L. Mangatal, P. Potier, *J. Med. Chem.* **1991**, *34*, 992–998.
[7] P. A. Wender, N. C. Ihle, *J. Am. Chem. Soc.* **1986**, *108*, 4678–4679; *Tetrahedron Lett.* **1987**, *28*, 2451–2454.
[8] P. A. Wender, N. C. Ihle, C. R. D. Correia, *J. Am. Chem. Soc.* **1988**, *110*, 5904–5906.
[9] P. A. Wender, M. L. Snapper, *Tetrahedron Lett.* **1987**, *28*, 2221–2224; M. L. Snapper, Stanford University, *Diss. Abstr. Int. B* **1991**, *52*, 248–249.
[10] S. M. Sieburth, J.-l. Chen, *J. Am. Chem. Soc.* **1991**, *113*, 8163–8164.
[11] P. A. Wender, M. J. Tebbe, *Synthesis* **1991**, 1089–1094; the reaction conditions for the conversions **6** → **7** from ref. [8]. and **16** → **17** from ref. [9] are not given here for comparative purposes.
[12] J. G. Atkinson, D. E. Ayer, G. Büchi, E. W. Robb, *J. Am. Chem. Soc.* **1963**, *85*, 2257–2263; D. Bryce-Smith, A. Gilbert, J. Grzonka, *J. Chem. Soc. Chem. Commun.* **1970**, 498–499; W. C. Agosta, W. W. Lowrance, *J. Org. Chem.* **1970**, *35*, 3851–3856; G. Kaupp, M. Stark, *Angew. Chem.* **1977**, *89*, 555–556; *Angew. Chem. Int. Ed. Engl.* **1977**, *16*, 552, and literature cited therein; G. Kaupp, U. Pogodda, A. Atfah, H. Meier, A. Vierengel, *Angew. Chem.* **1992**, *104*, in press; *Angew. Chem. Int. Ed. Engl.* **1992**, *31*, in press; cf. also P. A. Wender, C. J. Manly, *J. Am. Chem. Soc.* **1990**, *112*, 8579–8581 (synthesis of ten-membered rings).
[13] K. Sakan, D. A. Smith, S. A. Babirad, F. R. Fronczek, K. N. Houk, *J. Org. Chem.* **1991**, *56*, 2311–2317; J. S. Yadav, R. Ravishankar, *Tetrahedron Lett.* **1991**, *23*, 2629–2632; R. V. Bonnert, P. R. Jenkins, *J. Chem. Soc. Perkin Trans. 1* **1989**, 413–418.
[14] See, for example L. A. Paquette, J. H. Barrett, D. E. Kuhla, *J. Am. Chem. Soc.* **1969**, *91*, 3616–3624; G. Kaupp, E. Teufel, H. Hopf, *Angew. Chem.* **1979**, *91*, 232–234; *Angew. Chem. Int. Ed. Engl.* **1979**, *18*, 215–217, and references therein for the synthesis of paracyclophanes via *para*-quinodimethanes.

[Ni(P*t*Bu)$_6$]—a Strain on the 18 Electron Rule? **

By *Kurt Dehnicke**

The 18e rule already established in 1927 by Sidgwick has proved to be extremely successful for the understanding of the constitution, structure, and chemical reactions of simple, especially organometallic complexes and has contributed considerably to the development of organoelement chemistry. In the 18e rule the valence electrons of the central atom and the sum of the electrons participating in the bonds of the ligands to the central atom are added together. If the total is 18 electrons, then the compound has achieved the electron configuration of the next noble gas atom and at the same time is diamagnetic. The stability maximum connected with this can be understood from MO theory: All 18 electrons are placed either in bonding or in the most unfavorable case also in nonbonding molecular orbitals. Examples for this are the tetrahedral complexes nickel tetracarbonyl (**1**), the trifluorophosphane derivative (**2**) which is accessible from **1** by ligand exchange, and **3** only recently prepared from the reaction of bis(cyclooctadiene)nickel with phosphabenzene.[1] The total of 18 electrons in these complexes results from the 10d electrons of the nickel atom and a total of eight electrons from the four ligands.

$[Ni(CO)_4]$ **1** $[Ni(PF_3)_4]$ **2** $[Ni(PC_5H_5)_4]$ **3**

However, exceptions to the 18e rule soon became known, such as the V complex **4** with 17e, the Co complex **5** with 19e, and the Ni sandwich complex **6** with 20e constructed analogously to **5**.

$[V(CO)_6]$ **4** $[Co(C_5H_5)_2]$ **5** $[Ni(C_5H_5)_2]$ **6**

[*] Prof. Dr. K. Dehnicke
Fachbereich Chemie der Universität Marburg
Hans Meerwein-Strasse, D-W-3550 Marburg (FRG)

All these complexes (**4**–**6**) are paramagnetic and show a strong tendency to achieve 18 valence electrons: **4** gains an electron to form the $[V(CO)_6]^-$ ion and **5** loses an electron to give the very stable cobaltocenium ion $[Co(C_5H_5)_2]^+$.[2] Complex **5** is also used preparatively as a reducing agent.[3] The decamethyl-substituted derivative of **6** can be oxidized under certain conditions to the dication with 18 valence electrons.[4]

Based on the 18e rule, Wade[5] and Mingos[6] later established the counting rules for cluster molecules. These proved particularly successful for the understanding of the electronic and framework structures of boranes and carboranes and made predictions concerning the *closo* (closed), *nido* (nest), and *arachno* (spider) structures possible.

None of these well-tried rules can be applied to the very recently synthesized nickel complex **7**.[7] According to the

$[Ni(PtBu)_6]$ **7**

crystal structure analysis, the nickel atom of **7** sits in the middle of a near-planar P_6 ring in which the *tert*-butyl groups almost envelop the Ni atom above and below the $[NiP_6]$ plane. Compound **7** is stable at room temperature, diamagnetic, and slowly decomposes in solution to Ni and $(PtBu)_4$. A simple count leads to 22 valence electrons. The results of a standard ab initio calculation[7] carried out very carefully are in excellent agreement with the data from the crystal structure analysis. The P–P distances in the P_6 ring are approximately 8 pm longer than in noncomplexed phosphacycles; also the Ni–P distances are somewhat longer than expected.[8] This fits well to the relatively large spatial requirement of the Ni^0 atom. Furthermore, the Ni atom is in close contact with the six P–P σ bonds of the "P_6 life bouy" and contributes to the extension of the P–P bond through the back bonding from the d_{xy} and $d_{x^2-y^2}$ atomic orbitals into the antibonding e* molecular orbitals of the P_6 ring. How-

ever, the effects of the electron correlation are especially important for the stability of **7**. Apart from the $3d^{10}$ electrons of the Ni atom and the electrons in the six σ P–P molecular orbitals it is the six free electron pairs of the phosphorus atoms (sometimes adding up to a total of 34e!), which participate in the "strong-correlated motion". The influence of the *tert*-butyl groups planarizing the P_6 ring which prepares the ring for the inclusion of the Ni atom is also important. $(PtBu)_6$ in the free state is unknown. According to the ab initio calculation $(PtBu)_6$ should have a near-planar P_6 ring due to the spatial requirement of the *t*Bu groups. The calculations for $(PMe)_6$ showed a strongly puckered P_6 ring with a chair conformation.[7] The spatial requirement of the *tert*-butyl groups can be fulfilled more easily for $(PtBu)_4$ than for $(PtBu)_6$. According to a crystal structure analysis,[9] which is in good agreement with the ab initio calculation,[7] $(PtBu)_4$ contains a nonplanar P_4 ring. This explains why **7** does not decompose to Ni and $(PtBu)_6$ but instead to the tetramer. It has to be noted that the planarizing effect of the *t*Bu groups still has an effect on the structure of $(PtBu)_4$, which among the six known cyclotetraphosphanes shows the smallest P–P torsion angle of 24.5°. [9]

The contribution, which the *t*Bu groups enveloping the Ni atom are able to provide for the stability of **7** towards the decomposition (with the loss of metallic Ni (428 kJ mol^{-1})), can be understood if it is assumed that three H atoms each of the three Me groups of the six *t*Bu moieties above and below the $[NiP_6]$ plane in alternating sequence point at the $[NiP_3]$ segments (Scheme 1). Thus the nickel atom in **7** is coordinated analogously to the cubic close packing of metallic Ni so that it can "feel at home".

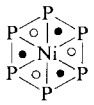

Scheme 1. Schematic representation of the Ni complex **7**. The filled and empty circles show the position of the H atoms of *t*Bu groups above and below the P_6 ring, respectively.

The structure and bonding of **7** are unusual and the method of its synthesis was also unexpected. Apparently due to a labeling mistake the ampule that was thought to contain $PtBu_3$ and was to be used for the peripheral protection in the construction of the nickel clusters[10] actually contained $(PtBu)_3$! Thus, **7** was formed according to Equation (a) in a

$$NiCl_2 + 2(PtBu)_3 \xrightarrow[-ClSiMe_3]{P(SiMe_3)_3} \underset{\mathbf{7}}{[Ni(PtBu)_6]} \qquad (a)$$

redox reaction with the ring opening of the P_3 ring. The product corresponds to a template reaction of Ni^0.

A further product of the ring opening of the P_3 ring of $(PtBu)_3$ could be obtained by the reaction with **1**, which led to the nickel cluster **8**. Besides three :P*t*Bu groups (4e donor) which bridge the nickel atoms, this also contains the open-chain ligand group **9** (8e donor) as a bridging ligand.[6]

$[Ni_5(CO)_5(PtBu)_3(P_3tBu_3)]$ **8**

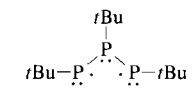

9

A dimerization of **9** in the presence of naked Ni atoms makes the formation of **7** easy to understand. Since it is known that **1** is not a good precursor for Ni atoms, $[Ni(cod)_2]$ would have been a better partner for the synthesis of **7**!

What consequences could that have for the 18e rule? Well, on closer inspection it proves to be very durable. If it is assumed that the four additional electrons in **7** occupy the antibonding doubly degenerate HOMO of the NiP_6 group, then this would partially compensate for the bonding effect of the highest occupied HOMO of the same symmetry. The result is then only a weakening of the Ni–P bonds which is alleviated by the described correlation effect and by the shielding effect of the *t*Bu groups.

The hopes remain that soon the higher homologue of **7**, namely $[Pd(AstBu)_6]$, will be synthesized.

German version: *Angew. Chem.* **1992**, *104*, 437

[1] C. Elschenbroich, M. Nowotny, W. Massa, Universität Marburg, personal communication.
[2] R. D. W. Kemmitt, D. R. Russell in *Comprehensive Organometallic Chemistry, Vol. 5* (Eds.: G. Wilkinson, F. G. A. Stone, E. W. Abel), Pergamon, Oxford, **1982**, p. 245–247.
[3] P. Hofacker, C. Friebel, K. Dehnicke, P. Bäuml, W. Hiller, J. Strähle, *Z. Naturforsch. B* **1989**, *44*, 1161–1166.
[4] U. Kölle, F. Khouzami, H. Lueken, *Chem. Ber.* **1982**, *115*, 1178–1196.
[5] K. Wade, *Adv. Inorg. Chem. Radiochem.* **1976**, *18*, 1–66.
[6] D. M. P. Mingos, *Acc. Chem. Res.* **1984**, *17*, 311–319.
[7] R. Ahlrichs, D. Fenske, H. Oesen, U. Schneider, *Angew. Chem.* **1992**, *104*, 312; *Angew. Chem. Int. Ed. Engl.* **1992**, *31*, 323.
[8] Comparable values for Ni–P distances are 211.5 pm in **3** [1] and 215–226 pm in $[(PtBu)_2Ni(PtBu)_4]$ (R. A. Jones, M. H. Seeberger, B. R. Whittlesey, J. Am. Chem. Soc. 1985, 107 6424–6426), whereas those in **7** are 229.0 pm.
[9] W. Weigand, A. W. Cordes, P. N. Swepston, *Acta Crystallogr. Sect. B* **1981**, *37*, 1631–1634.
[10] D. Fenske, J. Ohmer, J. Hachgenei, K. Merzweiler, *Angew. Chem.* **1988**, *100*, 1300–1320; *Angew. Chem. Int. Ed. Engl.* **1988**, *27*, 1277–1297.

Spectral Hole Burning at Room Temperature and with a Single Molecule: Two New Perspectives**

By *Christoph Bräuchle,**

Although the first experiments concerning spectral hole burning were conducted almost 20 years ago, this field still surprises with new and fascinating results and developments. This may be due to the deep insights into the electronic structure of molecules in solids that can be gained by the high spectral resolution, and the ready application of these fundamental scientific findings in high technology areas such as optical storage. The two phenomena which are discussed in this contribution, namely spectral hole burning at room temperature and spectral hole burning with a single molecule, show this dual significance and were presented at an international conference entitled "Persistent Spectral Hole Burning: Science and Applications" in September 1991 in Monterey, California.

The principle of spectral hole burning is represented schematically in Figure 1.[1] Dye molecules embedded in a solid matrix (crystal or amorphous solids such as polymers and glasses) have different environments, and therefore different local fields. This leads to a distribution of the absorption

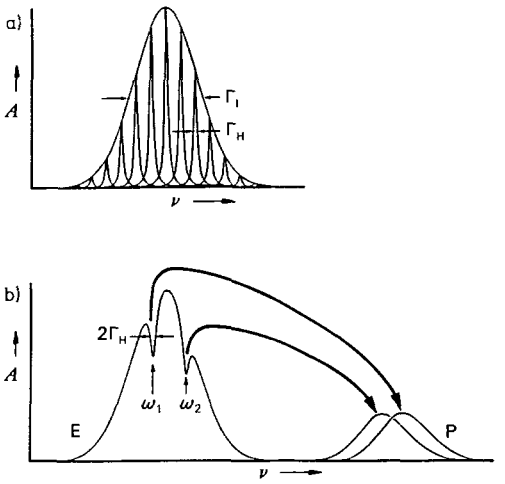

Fig 1. Principle of spectral hole burning. Absorption band a) before the burning, b) after the burning with the frequencies ω_1 and ω_2. A: absorption; ν: frequency; E: starting material; P: product; Γ: line width.

frequencies for the dye molecules, in which the various frequency packets are characterized by their homogeneous line widths Γ_H. The envelope of all frequency packets observable in the experiment is the inhomogeneous broadened absorption band of width Γ_I. At liquid helium temperatures ($T \leq 4.2$ K) the homogeneous line width Γ_H of zero phonon transitions (pure electronic transitions of the molecules without the participation of the phonons of the surrounding solid) becomes very small (10^{-4}–10^{-1} cm^{-1}), whereas the inhomogeneous line width Γ_I remains large (100–1000 cm^{-1}) and many (10^3–10^6) frequency packets are hidden beneath the inhomogeneous absorption band.

The most interesting spectroscopic information about the molecules is contained in the homogeneous absorption bands (their position, width, and form). Thus, for instance, the effective relaxation time T_2 can be obtained directly from Γ_H, which consists of the lifetime of the excited state T_1 and the pure phase relaxation time T_2^* in accordance with $\Gamma_H = 1/(\pi T_2) = 1/(2\pi T_1) + 1/(\pi T_2^*)$. Based on the assumption that spectral diffusion (structural relaxation processes between the burning of the hole and its detection, see discussion below) does not lead to an additional broadening of the hole, the homogeneous absorption band can be obtained from a hole burning experiment. For this, the probe is irradiated with an extremely narrow-band laser ($\Delta\omega \ll \Gamma_H$), so that only one frequency packet absorbs photons. The excited molecules can undergo photochemical reactions (e.g. proton tautomerism in the case of the free base of phthalocyanine dyes), in which their absorption frequency changes. Due to the transition of these molecules from starting materials to products, a spectral hole occurs by the recording of a new absorption spectrum. This is a "negative" of the corresponding absorption band of the frequency packet (Fig. 1b).

However, the burning of a spectral hole does not necessarily require a photochemical reaction, but is also possible photophysically, for example by a change of the state of a so-called *T*wo-*L*evel *S*ystem (TLS). A TLS may correspond to the motion of a segment of a polymer chain or the breaking and forming of a hydrogen bond. Both of these can be characterized by the two energy levels of a double-well potential. There is a large distribution of TLS with different energies and transition probabilities as a result of the many different degrees of freedom especially in an amorphous solid. When embedded molecules interact with such TLS and if these change their state as a result of irradiation, then the absorption frequency of the molecules is shifted, and a spectral hole is detected in the original position. The process can also be considered as a reorientation in the environment of the molecules, without the molecules themselves being changed photochemically.

From this description it becomes clear that spectral hole burning provides information not only about the molecules themselves but also in particular about their environments. Thus, the molecules are probes with which the surrounding solid can be scanned. This becomes especially fascinating when the hole burning is achieved with a single probe molecule. This aspect is the topic of the second part of this contribution. First the application-oriented side of spectral hole burning shall be discussed.

Already in 1978 a high-density optical storage device was proposed on the basis of the permanent spectral hole burning as "Frequency Domain Optical Storage" (FDOS).[1, 2] An overview of the optical and magnetic storage methods and the corresponding storage densities in bit per cm^2 and bit per cm^3, respectively, is given in Figure 2. From this it can be seen that data pit memories already on the market and

[*] Prof. Dr. C. Bräuchle [+]
Institut für Physikalische Chemie der Universität
Sophienstrasse 11, D-W-8000 München 2 (FRG)
[+] Currently guest professor at the University of California, Los Angeles

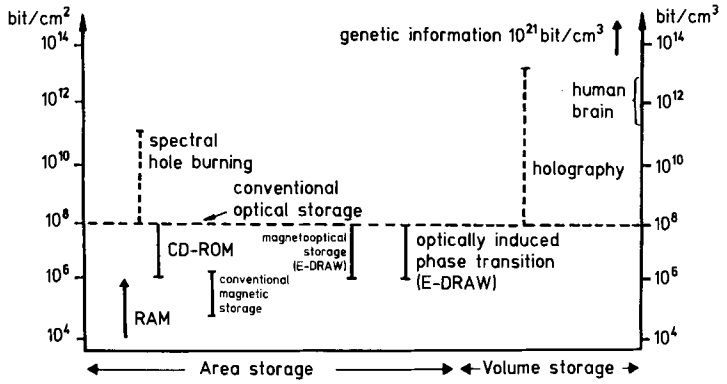

Fig. 2. Overview of the storage methods and their corresponding storage densities. Left axis for area storage, right axis for volume storage.

conventionally referred to as optical, CD-ROM (*C*ompact *D*isk *R*ead *O*nly *M*emory) and the reversible magnetooptical E-DRAW memory (*E*rase *D*irect *R*ead *A*fter *W*rite), have storage densities limited to 10^8 bit per cm^2. This limiting value has physical causes (diffraction limit for the focused laser spot) and can only be improved by a factor of 4 by the use of a frequency-doubled semiconductor laser. So far, for optical data pit storage the laser is only used to give a point-like heating of the material in the focus of the laser; that is, the characteristic properties of laser light, namely its monochromacity and coherence, are not used. However, if the monochromacity of laser light is used, then with the help of the spectral hole burning (FDOS), the storage on the area (two dimensions) can be extended by the storage on the frequency axis as the third dimension, and the storage density can be raised to 10^{11} bit per cm^2 by the writing of typically 1000 spectral holes at each laser-focused spot. If the coherence of laser light is used, information can be stored in the depth of the medium as the third dimension with the help of holography and thus provide a volume storage with a theoretical storage density of 10^{13} bit per cm^3. By the skillful use of holographic methods not only the storage but also the optical processing of information is possible.[3]

In the meantime the storage density of the FDOS memory has been increased further by the utilization of the electric field (Stark effect) as the fourth storage dimension and the combination with holographic detection methods. The resulting storage of 100 holograms in the frequency range of only 1 cm^{-1} has already been demonstrated.[4] It could also be shown here that the application of holographic methods made additional logical connections between the stored information possible and thus opened one way to the optical computer.

Although the methodic possibilities of the FDOS memory have thus been extended considerably, the development of materials suitable for the storage remains a difficult and unresolved problem. This is a result of the various requirements,[1] of which the most important are reversibility, rapid writing, thresholding, and high-temperature hole burning. Reversibility,[1] rapid writing,[1, 5] and thresholding in the form of two-color writing[1, 6, 7] have already been demonstrated on a series of different systems. Thus, in principle, concepts for a corresponding material design have been achieved. However, spectral hole burning is extremely difficult at temperatures greater than 10–20 K. This is mainly a result of the decrease of the zero phonon band relative to the phonon side-band and manifests itself in a very large broadening of the spectral hole with increasing temperature. As a result, at $T > 20$ K either no spectral hole or one which is almost as wide as the total inhomogeneous absorption band is detected.

So far, this situation has been avoided by the use of dye molecules such as porphyrins and phthalocyanines,[8, 9] which only show a weak coupling of the pure electronic transition to the phonons of the solid. Thus, during the electronic transition in the molecule "fewer" phonons in the solid are produced. However, these attempts did not succeed in meeting a further requirement for high-temperature hole burning: the shift of the phonon spectrum of the matrix to higher frequencies. In this way phonon states could be occupied in considerable number only at higher temperature. To increase the rigidity of the polymer matrix and thus raise the phonon frequencies, the polymer matrix was cross-linked.[8] The maximum of the phonon frequency distribution, however, was still at $\omega_0 \leq 25\ cm^{-1}$. Nevertheless, in systems of porphyrins or phthalocyanines in polymers, spectral holes with a hole width of approximately $\Gamma_L \leq 15\ cm^{-1}$ could be burned at liquid nitrogen temperatures and at up to $T \leq 120$ K. Due to the narrow inhomogeneous line width of the systems used, only a multiplexing factor $M = \Gamma_i/\Gamma_L$ of roughly 50 was achieved; that is, 50 holes or bits can be stored in the frequency axis as the third storage dimension in addition to the area.[8] This already shows that compromises must be made with regard to the overall properties of a system. Thus, though hole burning may be conducted at higher temperatures, the resulting storage density is not increased to the extent possible for the hole burning at low temperatures.

Recently, in another approach dye molecules were adsorbed on surfaces.[10] For a system in which quinizarine (1,4-dihydroxyanthraquinone) was adsorbed on γ-Al_2O_3, the coupling of the pure electronic transition to the phonons was significantly lower and ω_0 with 50 cm^{-1} significantly higher than for the same dye in ethanolic glass or polymer matrices. As a result of the greater inhomogeneous line width Γ_i of this system, the multiplexing factor was 70–100 for $T = 80$ K. Since similar effects were also observed for other adsorbate/substrate systems,[10] a new material concept was demonstrated. However, the ultimate aim of hole burning at room temperature has not yet been realized in these studies.

Recently, room-temperature hole burning was achieved with a completely different system, namely substitutionally disordered microcrystals of $SrFCl_{0.5}Br_{0.5}$[11] and $Mg_{0.5}Sr_{0.5}FCl_{0.5}Br_{0.5}$[12] doped with 1 atom% Sm^{2+} ions. The basic strategy for the development of this system[13] is exactly opposite to the one previously described. In the experiments mentioned up to this point the attempt was made to retain the intensity of the zero phonon band also at higher temperatures, and a wide inhomogeneous absorption band could be assumed. In contrast, for the Sm^{2+}-doped systems a wide inhomogeneous absorption band must first be produced, but an intense zero phonon band can be assumed even at room temperature. This is due to the strong shielding of all the inner 4f electron transitions of Sm^{2+} which are used for the spectral hole burning in these systems. For a wide inhomogeneous absorption band of the 4f transitions a

strong disturbance in the environment of the Sm^{2+} ions is necessary. This is produced by the substitutional disorder in $BaFCl_{0.5}Br_{0.5}:Sm^{2+}$ during the statistical exchange of Cl^- or Br^-, relative to $BaFCl:Sm^{2+}$ and $BaFBr:Sm^{2+}$, respectively.[13] The broadening can be further increased by additional statistical variation of the cation, for example in $Mg_{0.5}Sr_{0.5}FCl_{0.5}Br_{0.5}:Sm^{2+}$.[13]

The ratios for the $^5D_0-^7F_0$ transition of the 4f electrons of Sm^{2+} in $SrFCl_{0.5}Br_{0.5}:Sm^{2+}$ at room temperature are illustrated in Figure 3.[11] The calculated multiplexing factor is

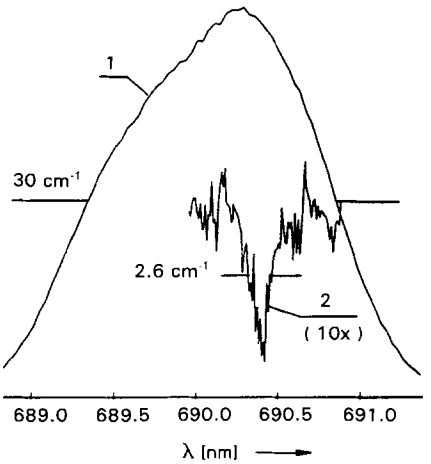

Fig. 3. Inhomogeneous absorption band of the $^5D_0-^7F_0$ transition in microcrystals of $SrFCl_{0.5}Br_{0.5}:Sm^{2+}$ (1) and the spectral hole at room temperature (2).

roughly 10, much smaller than the values obtained at liquid He temperatures. But experiments with the Sm^{2+}-doped systems, even though these are not ideal FDOS meterials, are important nevertheless, since they have shown a new strategy which makes hole burning at room temperature possible and which yields spectral holes of sufficient thermal stability. Interestingly, the Sm^{2+} systems also show reversibility,[11] and two-color writing[6, 11] is possible. The latter means that two different wavelengths for the associated photochemistry are used to write the information, so that on reading at only one wavelength the written information cannot be destroyed (threshold requirement).

A further approach should also be mentioned which uses small particles of variable diameter with dye molecules on their surfaces.[14] Spectral hole burning is possible in such systems, because the resonance absorption varies with the particle size, and the dye molecules are photochemically transformed on particles which fulfill the resonance condition for the wavelength used for the burning. Since temperature dependence does not arise here, spectral hole burning at room temperature is a priori possible. However, it has been shown that the particles must be above a minimum size due to both the resonance requirement and the formation of satellite bands. Thus, the gain of storage density in the frequency dimension is overcompensated by the loss of storage density in the area. So far it remains unclear whether this disadvantage can be overcome.

In all optical storage systems the storage of a bit on a molecule would be the absolute upper limit of a memory on a molecular basis. Almost a year ago a "Highlight" in this journal[15] discussed the first spectroscopic observations by W. E. Moerner et al.[16] and M. Orrit et al.[17] of single pentacene molecules embedded in a *para*-terphenyl crystal. The fascinating results were made possible by high dilution, extremely small sample volume (ca. 200 μm^3), and spectral separation by highly sensitive detection of fluorescence excitation. Despite many unsuccessful attempts to extend the technique to other molecule/matrix systems, pentacene in the *para*-terphenyl crystal seemed to be the only object of study. Thus, in their outlook the authors[15] pointed out that the extension of this experiment to the even more interesting amorphous dye/matrix systems, such as dye molecules in polymers and glasses, remained a significant experimental challenge.

In a post-deadline paper for the Monterey conference, T. Basché and W. E. Moerner[18] were the first to describe the spectroscopic detection of single perylene molecules in an amorphous polyethylene matrix. Figure 4 shows the absorption of single perylene molecules dependent on the laser frequency and the probe location in one dimension. The extension of the method to these new classes of systems, the detailed study of the amorphous state of polymers and other solids possible as a result, and the novel observation of spectral hole burning with a single molecule are of great interest.

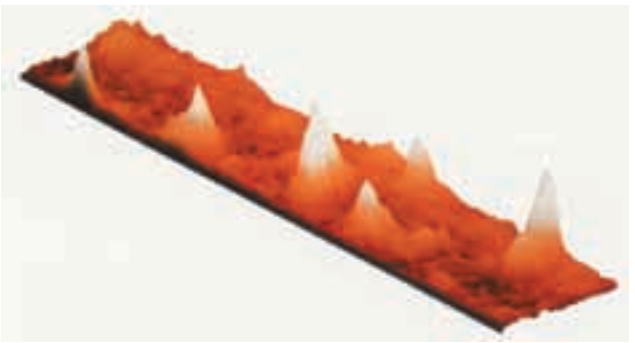

Fig. 4. Fluorescence signals of six single perylene molecules in a polymer film. Each increase corresponds to the fluorescence of one molecule. The frequency of the scanning laser is varied (6.1 GHz), and the laser is moved over the surface of the sample (23 μm) in one dimension. The emission intensities are different because the positions of the molecules relative to the laser focus differ. In some signals the form is changed due to a small amount of spectral diffusion during the scans.

Figure 5 shows such a hole burning experiment.[18] The fluorescence excitation spectrum of a single perylene molecule in a perylene/polyethylene film system (mass ratio $9.5 \times 10^{-7}:1$) was recorded by a laser scan with ± 1 GHz for the center at 448.021 nm. Here a frequency-stable molecule that showed no spectral diffusion was chosen. The latter can be recognized by a sudden stochastic frequency jump of the total absorption band caused by the phonon-induced change of state in a TLS in the environment of the molecule. Since the absorption band of the molecule remained constant in the three laser scans carried out successively a–c in Figure 5 (and five further laser scans before spectrum a was recorded), this molecule can be classified as frequency stable in the sense of the above. After spectrum c was recorded, the laser frequency was altered such that it agreed with the absorption frequency of the molecule. As spectrum d shows, the absorption of the molecule disappeared within 30 s. Surprisingly, after a few minutes the absorption of the molecule returned

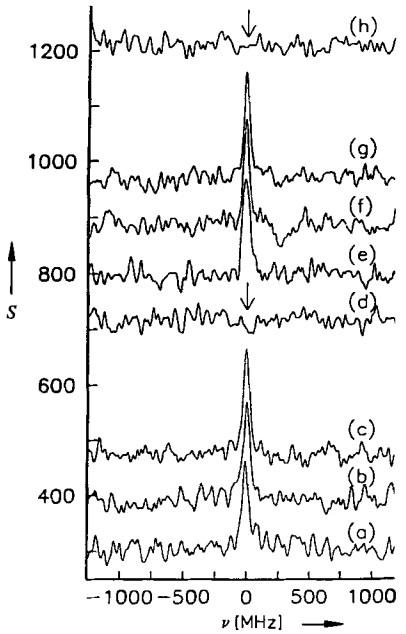

Fig. 5. Spectral hole burning with a single perylene molecule in polyethylene at $T = 1.5\,K$. The meaning of the laser scans a–h is described in the text. ν: laser frequency, S: fluorescence excitation signal in the number of occurences per 100 ms.

to the same location within ± 10 MHz in a frequency-stable form (spectra e to g). After that, a further hole could be burned (spectrum h), and the whole process could be repeated several times. To confirm that a spectral hole had actually been burned, that is that a single molecule had been manipulated by light, Basché and Moerner repeated the reaction at different burning powers of 4.5 to 27 nW. They observed an unequivocal decrease of the average burning time with increasing laser power, whereas the return time was completely stochastic and independent of the power of the laser. Thus it is confirmed that the spectra in Figure 5 reflect spectral hole burning with a single molecule.

The process can be interpreted as follows: A transition in a nearby TLS is activated by the irradiation, and in a quantum jump the absorption frequency of the molecule is shifted to that of the "product state". This lies outside the frequency window of Figure 5, and therefore could not be identified so far. The recurrence of the molecular absorption shows the stochastic return of the TLS into the original state and serves as a clear indication that only a single TLS participates in the process. (Of course, there were also molecules whose absorption frequency did not return to the original value after the burning.)

As a result of their experiments Basché and Moerner were able to prove a hierarchy of the TLS with which the dopant molecule interacts. TLS which are distant from the dopant molecule produce very rapid and small frequency changes. These changes are the main reason for the dephasing and thus for the homogeneous line width Γ_H. Here the interaction of the molecule is averaged over many TLS so that the homogeneous line width should be of the same size for all single molecules. TLS which are closer to the dopant molecule produce much larger and less frequent frequency changes. These TLS are responsible for the sudden frequency jumps, which are observable within the frequency window of the experiment and cause the spectral diffusion. Here each single molecule sees its own local environment, which with these experiments can be observed for the first time. Finally, there are TLS which are the "direct neighbors" of the dopant molecule, which can only be activated by spectral hole burning and cause the largest frequency changes. Some of these TLS return spontaneously to their original state others do not.

Apart from these highly interesting scientific results, Basché and Moerner have also demonstrated the first optical switch or the first optical storage element based on a single molecule in their spectral hole burning with a single molecule. Thus they have reached the absolute limit of optical storage on a molecular basis. In such molecular storage the existence or nonexistence of the molecular absorption at its original frequency position is assigned with a "1" or a "0", respectively. Initial considerations show that storage densities of 10^{14} bit per cm^2 should be possible, taking into account the dilution of the donation molecules. This density would be six orders of magnitude greater than those of commercially available optical storage devices. The application of subdiffraction-limited light with a cross section similar to the absorption cross section of the molecules is of great interest. Thus, the signal-to-noise ratio would also increase greatly, and a more reliable and very rapid detection of the hole burning process or the molecular switch process would be possible.

Apart from the hole burning described here the specific manipulation of a single molecule is only feasible with the help of the tunnel microscope.[19] Both procedures are unique in that they allow us from our macroscopic world to directly address *specific single* molecules or atoms in the microscopic domain, and to manipulate them and receive signals from this domain. Thus, the way to molecular electronics in its true sense, in which information is specifically stored, passed on, and switched by single molecules, has become more feasible.

German version: *Angew. Chem.* **1992**, *104*, 431

[1] *Persistent Spectral Hole Burning: Science and Application* (Ed.: W. E. Moerner), Springer, Berlin, **1988**; J. Friedrich, D. Haarer, *Angew. Chem.* **1984**, *96*, 96; *Angew. Chem. Int. Ed. Engl.* **1984**, *23*, 113.
[2] G. Castro, D. Haarer, R. M. Macfarlane, H. P. Trommsdorff, US 4101976, **1978** ("Frequency selective optical data storage").
[3] C. Bräuchle, N. Hampp, D. Oesterhelt, *Adv. Mater.* **1991**, *3*, 420.
[4] U. P. Wild, A. Rebane, A. Renn, *Adv. Mater.* **1991**, *3*, 453; C. De Caro, A. Renn, U. P. Wild, *Appl. Opt.* **1991**, *30*, 2890.
[5] W. E. Moerner, T. P. Carter, C. Bräuchle, *Appl. Phys. Lett.* **1987**, *49*, 430.
[6] A. Winnacker, R. M. Shelby, R. M. Macfarlane, *Opt. Lett.* **1985**, *10*, 350.
[7] T. P. Carter, C. Bräuchle, V. Y. Lee, W. E. Moerner, *J. Phys. Chem.* **1987**, *91*, 3998.
[8] A. Furusawa, K. Horie, *J. Chem. Phys.* **1991**, *94*, 80; S. Saikan, A. Imaoka, Y. Kanematsu, K. Sokada, K. Kominami, M. Iwamoto, *Phys. Rev. B* **1990**, *41*, 3185.
[9] W. P. Ambrose, W. E. Moerner, *Chem. Phys.* **1990**, *71*, 144.
[10] T. Basché, C. Bräuchle, *J. Phys. Chem.* **1991**, *95*, 7130; B. Sauter, C. Bräuchle, *Chem. Phys. Lett.*, in press.
[11] a) *Technical Digest on Persistent Spectral Hole Burning: Science and Applications, Vol. 16*, (Ed.: Optical Society of America, Washington, DC, USA, **1991**, b) R. Jaaniso, H. Bill in [11 a], p. 146; *Europhys. Lett.* **1991**, *16*, 569.
[12] K. Holliday, C. Wei, M. Croci, U. P. Wild in [11 a], p. 118.
[13] C. Wei, S. Huang, J. Yu, *J. Lumin.* **1989**, *43*, 161.
[14] S. Arnold, C. T. Lin, W. B. Whitten, J. M. Ramsey, *Opt. Lett.* **1991**, *16*, 420.
[15] D. Haarer, L. Kador, *Angew. Chem.* **1991**, *103*, 553; *Angew. Chem. Int. Ed. Engl.* **1991**, *30*, 540.
[16] W. E. Moerner, L. Kador, *Phys. Rev. Lett.* **1989**, *62*, 235; W. P. Ambrose, W. E. Moerner, *Nature* **1991**, *349*, 225.
[17] M. Orrit, J. Bernard, *Phys. Rev. Lett.* **1990**, *65*, 2716.
[18] T. Basché, W. E. Moerner in [11 a], p. PD1; *Nature* **1992**, *355*, 335.
[19] H. Fuchs, T. Schimmel, *Adv. Mater.* **1991**, *3*, 112; D. M. Eigler, E. K. Schweizer, *Nature* **1990**, *344*, 524.

Communications may be submitted in English *or* in German. Further details regarding the submission of communications can be found in the "Notice to Authors" reproduced in the January issue of the journal. Copies thereof may be obtained from the editorial office upon request.

'Bis(oxazolines)' as Ligands for Self-Assembling Chiral Coordination Polymers— Structure of a Copper(I) Catalyst for the Enantioselective Cyclopropanation of Olefins**

By *David A. Evans,* Keith A. Woerpel,* and *Michael J. Scott*

We recently reported that the 1:1 complex of copper(I) trifluoromethanesulfonate (Cu^{I}-triflate, CuOTf) and the chiral 'bis(oxazoline)' **1**[***] forms an effective catalyst for the enantioselective cyclopropanation of olefins with diazoacetic acid esters.[1] This reaction proceeds in 97 to >99% *ee*, and, with the proper choice of ester, disubstituted cyclopropanes can be formed with high *trans* selectivity. Although oxazolines have been previously employed as chiral ligands,[2] bis(oxazolines) have recently shown their utility not only in cyclopropanations,[3, 4] but in other reactions as well.[1, 4, 5] To gain better insights into the coordination chemistry of this versatile C_2-symmetric ligand[6] and to probe the origin of the high enantioselectivity, we attempted to isolate the active catalyst. We report here the X-ray crystal structure of the bis(oxazoline)–CuOTf complex **2**, which forms an unusual chiral, non-racemic, helical coordination polymer. Furthermore, we report on the use of this complex in the highly enantioselective cyclopropanation of olefins and on the determination of the absolute configuration of the products, and we show how our results compare with those reported by other groups.[3, 4]

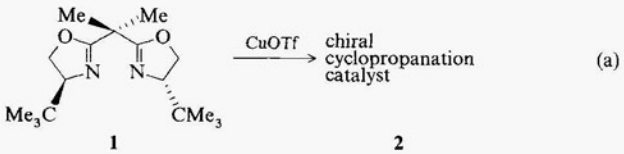

(a)

1 **2**

Bis(oxazoline)[7] **1** and CuOTf·0.5 C_6H_6[8] form a complex in dichloromethane, which was isolated as a white solid [Eq. (a)]. The X-ray crystal structure, shown in Figure 1,[9] shows a single-stranded helical polymer with threefold symmetry where the bis(oxazoline) ligand occupies a bridging position between two nearly linear, two-coordinate copper(I) ions. The structure further reveals that the triflate counterion is dissociated from the metal center. The ligand adopts a conformation wherein the large *tert*-butyl group is directed away from the center of the helix. Accordingly, the bis(oxazoline) **1**, by virtue of its chirality, directs both the assembly of the polymer and the sense of helicity. To date, only one other example of a chiral, non-racemic helical coordination polymer has been reported.[10] Unlike this and other coordination polymers and oligomers which involve multidentate ligands,[11] the structure of complex **2** demonstrates that bidentate ligands are also capable of enforcing macromolecular organization. The complex **2** is also noteworthy since it is one of the few oxazoline–metal complexes characterized by X-ray crystallography.[6b–d] With regard to the metal–ligand bond distances, the Cu–N bond lengths (1.88 Å) are typical for two-coordinate copper(I) and are the same as those of a recently reported two-coordinate CuOTf–bis(imine) complex.[12] Finally, despite the extreme oxygen sensitivity of solutions of copper(I) complex **2**, the solid complex can be stored for months in air without deterioration. Inspection of the crystal structure reveals that the copper(I) atoms are sterically protected from oxidation by the *tert*-butyl groups.

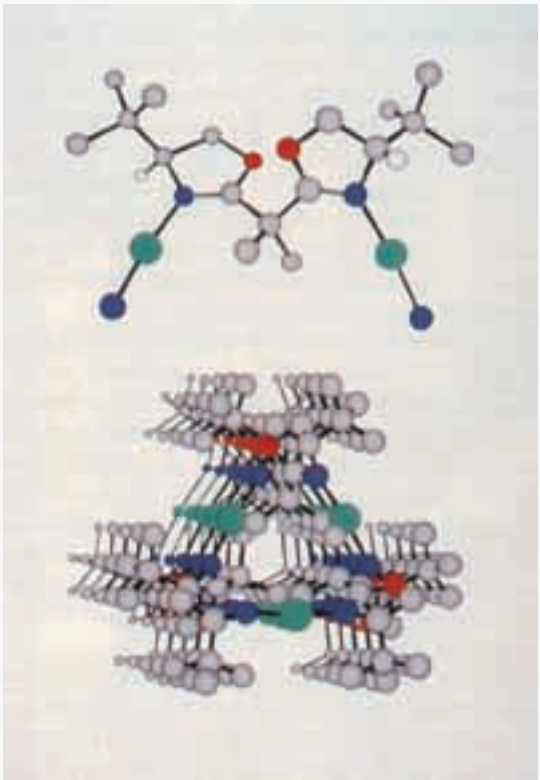

Fig. 1. Top: View of the repeating unit of the cation of **2** in the crystal. Cu–N 1.88(1) Å; N–Cu–N 171.6(4)°. Bottom: The helical cation of **2** as viewed along the three-fold screw axis.

With the knowledge that complex **2** is polymeric in the solid state, we studied its structure in solution using several spectroscopic techniques. Sharp resonances were observed in the ^1H and ^{13}C NMR spectra of **2** at 25 °C ($CDCl_3$), indicating that the complex is not paramagnetic. These spectra also

[*] Prof. D. A. Evans, K. A. Woerpel, and M. J. Scott
Department of Chemistry, Harvard University,
Cambridge, MA 02138 (USA)

[**] Support for this research was provided by the National Science Foundation and the National Institutes of Health. The NIH BRS Shared Instrumentation Grant Program 1 S10 RR01748-01A1 is acknowledged for providing NMR facilities.

[***] According to IUPAC rules of nomenclature, compound 1 is a bis(dihydrooxazolyl)propane.

revealed the presence of only *one* oxazoline moiety, demonstrating equivalence of the two heterocycles caused either by symmetry or fluctionality. Incremental addition of excess ligand **1** (from 0 to >2 equiv) to solutions of **2** led to spectra which again showed a single set of sharp resonances different from those observed for either **1** or **2**. We therefore conclude that rapid ligand redistribution is occurring and that the polymeric structure is disrupted in solution. This was confirmed by variable temperature NMR experiments, since spectra of **2** acquired between −50 and 0 °C lacked symmetry. An IR spectrum of a $CHCl_3$ solution of **2** showed that the C–N double bond absorbance had shifted to longer wavelengths upon coordination. The IR spectrum also showed a strong absorbance at 1280 cm^{-1}, which is indicative of a noncoordinated triflate in $CHCl_3$ solution.[13] Fast-atom bombardment mass spectrometry confirmed that **2** was a complex of **1** and CuOTf, displaying major ions at *m/z* 357, 651, and 506, which correspond to **1**-$^{63}Cu^+$, $(\mathbf{1})_2$-$^{63}Cu^+$, and **1**-$^{63}CuOTf^+$. Attempts to ascertain the molecular weight of the dissolved compound by vapor-pressure methods failed. Regarding the structure in solution, the only conclusions we can make at this time are that the ligand **1** is coordinated to the copper atom and is undergoing rapid ligand redistribution, and that the triflate is fully dissociated from the metal center.

Complex **2** was found to be an effective catalyst for the enantioselective cyclopropanation of olefins by ethyl diazoacetate. A sample of **2** (1 mol%) was employed as the catalyst for the cyclopropanation of styrene by ethyl diazoacetate. The ethyl cyclopropanecarboxylates **3R** and **4R**[14] were isolated in a 73:27 ratio in 75% isolated yield [Eq. (b)]. The enantioselection was found to be 98% *ee* for each isomer, as determined by capillary GLC analysis of the amides obtained by amidation with (*R*)-1-phenylethylamine. These results are similar to those obtained when the catalyst from CuOTf and **1** was prepared in situ.[1]

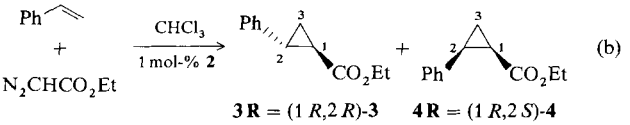

(b)

3R = (1*R*,2*R*)-**3** **4R** = (1*R*,2*S*)-**4**

The absolute configurations of the products **3** and **4** derived from chiral bis(oxazoline) catalysts have been the subject of some confusion.[1, 3a, 4] The sense of asymmetric induction for the major diastereomeric product **3** observed in this study is in agreement with the independent studies of Masamune et al. and Pfaltz et al. employing the pre-catalyst **8** derived from the ligand **7** [Eq. (c)]. However, the absolute configuration of the minor product **4** was not the same in the three reports. In order to resolve this issue, we employed the pre-catalyst **8** in reaction (b) and obtained **3R** (88% *ee*) and **4R** (83% *ee*), which are the same products observed employing catalyst **2**, but **4** was observed to be of the opposite configuration to that reported.[3a] Furthermore, we have also established that the catalyst obtained from **7** and CuOTf also leads to the same products **3R** (98% *ee*) and

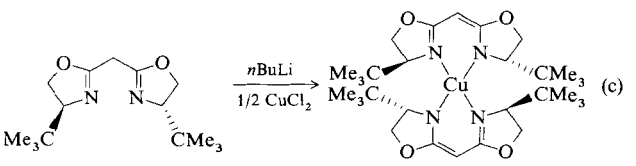

(c)

7 **8**

4R (93% *ee*).[1] To clarify these ambiguities, we investigated the stereochemical relationship between products **3** and **4**.

The esters **3R** (96% *ee*) and **4R** (94% *ee*) were hydrolyzed separately to the corresponding acids **5R** and **6R**. Comparison of the optical rotations of these four compounds with the literature values suggests that the configuration is as shown (Scheme 1).[15] To demonstrate that the *cis*- and *trans*-products have the same configuration at C-1, the *cis* product **4R** was epimerized with potassium bis(trimethylsilyl)amide, which resulted in a mixture of *trans*- and *cis*-esters in a ratio of >100:1 (capillary GLC). The product was found to be the *trans* ester **3S** with a rotation of opposite sign to that of the cyclopropanation product **3R**. Hydrolysis of **3S** afforded

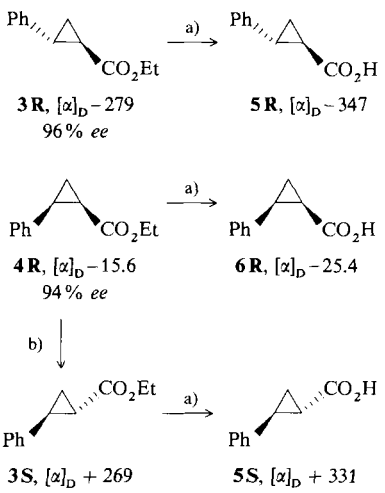

Scheme 1. a) NaOH, $MeOH/H_2O$. b) $KN(SiMe_3)_2$, THF, −78° → 0 °C.

the *trans* acid **5S**, again of opposite optical rotation to the product **5R** obtained from the cyclopropanation product **3R**. We therefore conclude that the reaction products differ in configuration at C-2, the carbon which bears the phenyl group, but both are of the (*R*) configuration at C-1. Finally, we have obtained an X-ray crystal structure of the amide obtained by reaction of **3S** with (*R*)-1-phenylethylamine which confirms that the product is indeed the (*1S,2S*)-isomer. This result, along with the chemical correlation, unambiguously established the stereochemical relationship between the 2-phenylcyclopropanecarboxylate isomers. Thus, we conclude that the Masamune/Pfaltz catalyst derived from **8** and complex **2** effect the same sense of enantioselection.

Received: November 18, 1991 [Z 5027 IE]
German version: *Angew. Chem.* **1992**, *104*, 439

[1] D. A. Evans, K. A. Woerpel, M. M. Hinman, M. M. Faul, *J. Am. Chem. Soc.* **1991**, *113*, 726–728.
[2] a) H. Brunner, U. Obermann, *Chem. Ber.* **1989**, *122*, 499–507; b) H. Brunner, U. Obermann, P. Wimmer, *Organometallics* **1989**, *8*, 821–826; c) G. Balavoine, J. Clinet, I. Lellouche, *Tetrahedron Lett.* **1989**, *30*, 5141–5144.
[3] a) R. E. Lowenthal, A. Abiko, S. Masamune, *Tetrahedron Lett.* **1990**, *31*, 6005–6008; b) R. E. Lowenthal, S. Masamune, *ibid.* **1991**, *32*, 7373–7376.
[4] D. Müller, G. Umbricht, B. Weber, A. Pfaltz, *Helv. Chim. Acta* **1991**, *74*, 232–240.
[5] a) H. Nishiyama, H. Sakaguchi, T. Nakamura, M. Horihata, M. Kondo, K. Itoh, *Organometallics* **1989**, *8*, 846–848; b) H. Nishiyama, M. Kondo, T. Nakamura, K. Itoh, *ibid.* **1991**, *10*, 500–508; c) E.J. Corey, N. Imai, H.-Y. Zhang, *J. Am. Chem. Soc.* **1991**, *113*, 728–729; d) G. Helmchen, A. Krotz, K. T. Ganz, D. Hansen, *Synlett* **1991**, 257–259; e) For a brief review of this family of ligands, see: C. Bolm, *Angew. Chem.* **1991**, *103*, 556; *Angew. Chem. Int. Ed. Engl.* **1991**, *30*, 542–543.
[6] Recently, there have been several papers discussing oxazoline–metal complexes: a) M. Onishi, K. Isagawa, *Inorg. Chim. Acta* **1991**, *179*, 155–156;

b) J. Hall, J.-M. Lehn, A. DeCian, J. Fischer, *Helv. Chim. Acta* **1991**, *74*, 1–6; c) C. Bolm, K. Weickhardt, M. Zehnder, T. Ranff, *Chem. Ber.* **1991**, *124*, 1173–1180; d) C. Bolm, K. Weickhardt, M. Zehnder, D. Glasmacher, *Helv. Chim. Acta* **1991**, *74*, 717–726.

[7] The ligand **1** was prepared by acylation of *tert*-leucinol with 2,2-dimethylpropane-1,3-dioyl dichloride followed by cyclization with triphenylphosphane–carbon tetrachloride–triethylamine, according to the procedure of Vorbrüggen (H. Vorbrüggen, K. Krolikiewicz, *Tetrahedron Lett.* **1981**, *22*, 4471–4474), which proceeds in >60% overall yield.

[8] R. G. Salomon, J. K. Kochi, *J. Am. Chem. Soc.* **1973**, *95*, 3300–3310.

[9] Crystal data: trigonal, P3(1)21, $a = 11.632(2)$ Å, $c = 15.554(7)$ Å, $\alpha = 90.0°$, $\beta = 90.0°$, $\gamma = 120.0°$, $T = 193$ K, $Z = 3$. The heavy atoms were refined anisotropically, and the hydrogen atoms were placed in calculated positions and refined anisotropically. The final residuals for 136 variables refined against 1228 data for which $F_o^2 > 3\sigma F_o^2$ were $R = 6.3\%$, final $R_w = 7.2\%$. Further details of the crystal structure can be obtained from the Director of the Cambridge Crystallographic Data Centre, University Chemical Laboratory, Lensfield Road, Cambridge CB2 1EW (England) on quoting the full journal citation.

[10] J. F. Modder, G. van Koten, K. Vrieze, A. L. Spek, *Angew. Chem.* **1989**, *101*, 1723; *Angew. Chem. Int. Ed. Engl.* **1989**, *28*, 1698–1700.

[11] See, for example: a) J.-M. Lehn, A. Rigault, J. Siegal, J. Harrowfield, B. Chevrier, D. Moras, *Proc. Natl. Acad. Sci. USA* **1987**, *84*, 2565–2569; b) O. J. Gelling, F. van Bolhuis, B. L. Feringa, *J. Chem. Soc., Chem. Commun.* **1991**, 917–919 and references cited therein.

[12] J. F. Modder, J.-M. Ernsting, K. Vrieze, M. deWit, C. H. Stam, G. van Koten, *Inorg. Chem.* **1991**, *30*, 1208–1214.

[13] G. A. Lawrance, *Chem. Rev.* **1986**, *86*, 17–33.

[14] The descriptors '**R**' or '**S**' of compounds **3**–**6** refer to the stereochemistry at C-1, the carbon which bears the carbonyl group.

[15] a) *trans*-2-Phenylcyclopropanecarboxylic acid: Y. Inoue, T. Sugita, H. M. Walborsky, *Tetrahedron* **1964**, *20*, 1695–1699; b) *cis*-2-phenylcyclopropanecarboxylic acid: T. Aratani, Y. Nakanishi, H. Nozaki, *ibid.* **1970**, *26*, 1675–1684.

Synthesis and Structure of the First Trinuclear, Half-Sandwich Carboranegadolinium(III) Cluster **

By *Aderemi R. Oki, Hongming Zhang,* and *Narayan S. Hosmane* *

The cyclopentadienyl ligand and a number of its *C*-substituted derivatives have been widely utilized in organometallic chemistry.[1] Although almost all of the s-, p-, d-, and f-elements have been complexed with these ligands, only a limited number of cyclopentadienyl gadolinium complexes have been structurally characterized.[2] Moreover, no known examples of trinuclear π-organogadolinium complex systems could be found in the literature.[3] However, the first carborane complex of an f-element is the uranium complex $[\{Li^+(thf)_4\}_2\{commo\text{-}3,3'\text{-}UCl_2(3,1,2\text{-}UC_2B_9H_{11})_2\}^{2-}]$, whose bent sandwich structure was determined by X-ray diffraction.[4] Since then, a number of *closo* (half-sandwich), and *commo* (sandwich) lanthanide complexes with *nido*-C_2B_9 and *nido*-C_2B_{10}-carborane ligands have been reported.[5] To date, there have been no reports on any of the carborane gadolinium complexes. Here, we report the synthesis and X-ray structure analysis of the first *closo*-carboranegadolinium(III) cluster complex. To our knowledge, complex **1** also represents the first trinuclear, μ_3-oxygen-bridged, half-sandwich, Gd(III) π-complex of any ligand system known to date.

$[\{\eta^5\text{-}1\text{-}Gd\text{-}2,3\text{-}(SiMe_3)_2\text{-}2,3\text{-}C_2B_4H_4\}_3\{\mu_2\text{-}1\text{-}Li\text{-}2,3\text{-}(SiMe_3)_2\text{-}2,3\text{-}C_2B_4H_4\}_3(\mu_3\text{-}OMe)\{\mu_2\text{-}Li(C_4H_8O)\}_3(\mu_3\text{-}O)]$ **1**

[*] Prof. Dr. N. S. Hosmane, Dr. A. R. Oki, Dr. H. Zhang
Department of Chemistry, Southern Methodist University
Dallas, TX 75275 (USA).

[**] This work was supported by grants from the National Science Foundation (CHE-9100048), the Robert A. Welch Foundation (N-1016), and the donors of the Petroleum Research Fund, administered by the American Chemical Society.

Treatment of the THF-solvated $Li_2[2,3\text{-}(SiMe_3)_2C_2B_4H_4]$ salt **2**[6] with anhydrous $GdCl_3$ in a molar ratio of 2:1 in dry benzene, followed by extraction and crystallization of the product from a solution containing 95% dry *n*-hexane and 5% dry THF resulted in the isolation of light yellow, transparent, and extremely air- and moisture-sensitive crystals of **1** in 58% yield. The paramagnetism of **1** precluded obtaining useful NMR data. However, the solution IR spectrum of **1** exhibits three terminal B–H stretches, presumably due to their interactions with the metals. Fine structures of this kind have been previously observed in the IR spectra of *closo*-$[1,1,1,1\text{-}(thf)_4\text{-}1,2,3\text{-}LnC_2B_9H_{11}]$ ($Ln = Sm^{II}$, Yb^{II}).[5c] The structure of the title compound could be determined unequivocally by X-ray diffraction analysis.[7]

The crystal structure reveals that **1** is a cluster complex consisting of six carborane cages, three THF molecules, three Gd atoms and six Li atoms, and possessing approximately a threefold symmetry-axis that passes through O(100) and O(120) atoms (Fig. 1). The metal atoms construct a tri-

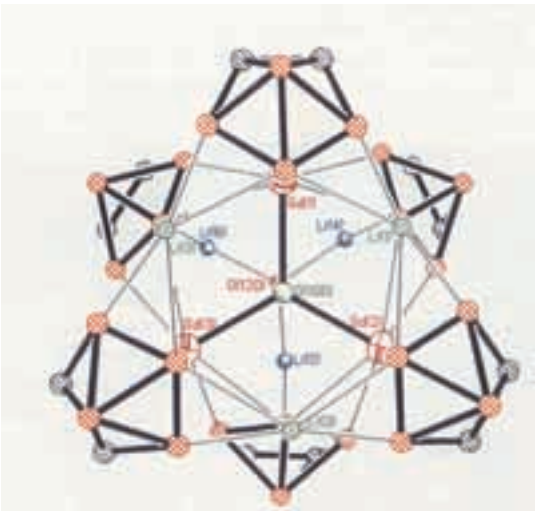

Fig. 1. Perspective view (from above) showing the C_2B_4-carborane cages and the equilateral triangles of Gd and Li atoms in **1**.

capped trigonal prism with gadolinium atoms in the capping positions. While the upper and lower Li-triangular planes [Li(1), Li(2), and Li(3) and Li(4), Li(5) and Li(6), respectively], are parallel (dihedral angle of 1.1°) their dihedral angles to the central Gd_3-triangular plane [Gd(1), Gd(2), and Gd(3)] are 1.0 and 1.4°, respectively. The central μ_3-bridged oxygen atom [O(100)] is located only 0.22 Å above the Gd_3-triangular plane. On the other hand, the methoxy oxygen [O(120)] links the apical Li atoms of three *closo*-lithiacarboranes in a tetrahedral fashion and is located 0.72 Å below the lower Li-plane. The distances of 4.04(3), 4.10(3) and 4.11(3) Å between the cage-bridged and THF-solvated Li metals are considerably longer than the distances in the central Gd_3-triangular plane [3.772(2), 3.778(2) and 3.786(2) Å] and the lower Li_3-plane [2.92(3), 2.96(3) and 2.94(3) Å] consisting of three *closo*-lithiacarborane units. Although Li-triangles eclipse one another, their presence, in staggered conformations, above and below the central plane of three apical Gd atoms is particularly noteworthy (Figs. 1 and 2).

The gadolinium metal atom in each *closo*-gadolinacarborane unit is η^5-bonded to the cage atoms, with Gd–carborane face and Gd–centroid distances ranging from 2.71(2) to 2.80(2) Å and 2.38 to 2.4 Å, respectively. The metal–centroid distances in **1** are slightly shorter than those in the structures of $[(\eta^5\text{-}C_5H_5)_3Gd(thf)]$,[8] $[\{\eta^5\text{-}C_5H_5\}_2Gd(Br)\}_2]$,[9] $[\{\eta^5\text{-}C_5H_5)Gd\}_5(\mu_2\text{-}OMe)_4(\mu_3\text{-}OMe)_4(\mu_5\text{-}O)]$ (**3**),[3] and in the

polymeric complex $[(\eta^5\text{-}C_5H_5)_2Gd(Br)]_\infty$.[9] The *closo*-gadolinacarboranes are also bridged by $[Li^+(thf)]$ moieties with Li–B distances of 2.24(3)–2.40(2) Å. The average Gd–O(100) distance of 2.193(7) Å, observed for **1**, is quite reasonable for a triply-bridged O atom when compared to the Gd–(μ_5-O) distances of 2.42(1) Å in the structure of **3**.[3]

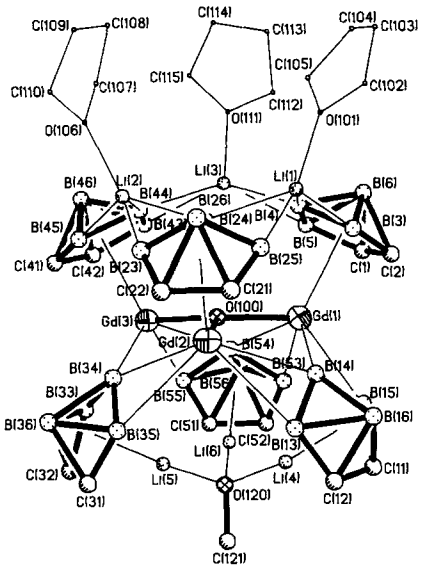

Fig. 2. A side view of **1** showing the atom numbering scheme. The $C_{(cage)}$-$SiMe_3$ groups are omitted for clarity. Selected distances [Å] and angles [°]: Gd(1)-center 1 [C(1) to B(5)]2.379, Gd(2)-center 3 [C(21) to B(25)] 2.386, Gd(3)-center 5 [C(41) to B(45)] 2.399, Gd(1)-O(100) 2.196(7), Gd(2)-O(100) 2.196(7), Gd(3)-O(100) 2.186(7), Li(4)-center 2 [C(11) to B(15)] 1.83, Li(5)-center 4 [C(31) to B(35)] 1.89, Li(6)-center 6 [C(51) to B(55)] 1.82, Li(4)-O(120) 1.87(3), Li(5)-O(120) 1.80(3), Li(6)-O(120) 1.87(2), O(120)-C(121) 1.43(3), Gd(1)-B(Li-carborane) 2.69(2)–2.87(2), Gd(2)-B(Li-carborane) 2.66(1)–2.91(2), Gd(3)-B(Li-carborane) 2.69(2)–2.87(2), Li(1)-B(Gd-carborane) 2.24(3)–2.38(3), Li(2)-B(Gd-carborane) 2.33(3)–2.39(3), Li(3)-B(Gd-carborane) 2.33(3)–2.40(2); center(1)-Gd(1)-O(100) 115.9, center(3)-Gd(2)-O(100) 115.9, center(5)-Gd(3)-O(100) 116.4, Gd(1)-O(100)-Gd(2) 118.4(3), Gd(1)-O(100)-Gd(3) 119.2(3), Gd(2)-O(100)-Gd(3) 119.6(3), center(2)-Li(4)-O(120) 169, center(4)-Li(5)-O(120) 173, center(6)-Li(6)-O(120) 168, Li(4)-O(120)Li(5) 105(1), Li(4)-O(120)-Li(6) 105(1), Li(5)-O(120)-Li(6) 107(1), Li(4)-O(120)-C(121) 114(1), Li(5)-O(120)-C(121) 116(1), Li(6)-O(120)-C(121) 109(1).

As can be seen in Figures 1 and 2, each lithiacarborane complex bridges the two Gd atoms of the central plane with the Gd–B distances ranging from 2.66(1) to 2.91(2) Å. The bonding of the lithium atom to the C_2B_3 face of the carborane units, below the Gd-triangular plane, is pentahapto with the Li-centroid distances ranging from 1.82 to 1.89 Å. However, the average Li–C distance [2.17(3) Å] is significantly shorter than the average Li–B distance of 2.36(3) Å. Slippage of this kind, although more pronounced in the present case, has already been found in the structures of lithium complexes of 1,2-diboratabenzene and 2-boratanaphthalenide.[10] Since each of the six carborane ligands is doubly negatively charged and three Gd^{III} and six Li^I metals are present, for charge compensation an additional $(MeO)^-$ moiety is bound to the apical lithium atoms of the lower triangle of *closo*-lithiacarboranes [average Li–O(120) = 1.85(3) Å] in a tetrahedral fashion (the average Li–O(120)–Li and Li–O(120)–C(121) angles are 106(1) and 113(1)°, respectively) and an O^{2-} unit, that is almost coplanar with the central Gd-plane, is triply-bridged to three Gd atoms in a trigonal-planar geometry with an average Gd–O(100)–Gd angle of 119.1(3)°. The recent report on trinuclear lanthanide complexes of the type $[Ln_3(\mu\text{-}pzMe_2)_6(\eta^2\text{-}pzMe_2)_3\{(\mu_3\text{-}O)Na_2(solv)_2\}]$ (Ln = Yb, solv = THF; Ln = Ho, solv = $pzMe_2$, pz = pyrazolyl) suggests that complexes containing lanthanides other than Gd^{III}, incorporating trinuclear units of the type $[(\mu_3\text{-}O)Ln_3]^{n+}$ with trigonal-planar geometry, can be synthesized.[11] Nonetheless, the exact source of the μ_3-OMe ligand and the μ_3-O ion in **1** is still unknown. Since the methoxide ion could be generated slowly at room temperature from the cleavage of THF by organoalkali metal compounds,[12] a similar reaction could occur between THF and *tert*-BuLi as a side-reaction during the formation of **2**. In any case, we have not only reproduced the yield and the formation of cluster complex **1** but also synthesized the samarium analogue whose molecular geometry is identical with that of **1** as determined by single crystal X-ray diffraction analysis.[13]

The presence of reactive lithiacarborane units suggest that **1** could react with three further equivalents of MX_2 (M = p, d, or f-metal in the oxidation state +II, X = halogen) to give a series of novel, mixed metal, and stacked trinuclear cluster systems in which a new triangle of metal atoms could be bent-sandwiched by two gadolinium cluster complexes. Such an endeavor is currently underway in our laboratories.

Experimental Procedure

1: **2** (6.4 mmol) [6] was allowed to react with anhydrous $GdCl_3$ (0.84 g, 3.18 mmol) in dry benzene (25 mL) at 0 °C for 24 h, during which time the color of the solution turned to yellow. At this point, the heterogeneous product mixture was filtered through a frit in vacuo and the solvent was removed from the filtrate, leaving a pale-yellow solid. This solid was then dissolved in a solvent mixture of hexane (95%) and THF (5%) and filtered in vacuo. After slow removal of the solvents from the second filtrate, a light yellow, highly air and moisture sensitive crystalline solid, identified as **1**, was obtained in 58% yield (1.3 g, 0.61 mmol; moderately soluble in polar and nonpolar organic solvents; m.p. 100–103 °C). Reproducible microanalytical data for the same sample of **1** could not be obtained, as it is extremely sensitive to air and moisture. IR (C_6D_6): $\tilde{\nu}$ [cm^{-1}] = 2500 (sh), 2360 (vs, br), 2250 (s, br) (B–H).

Received: November 27, 1991 [Z 5037 IE]
German version: *Angew. Chem.* **1992**, *104*, 441

CAS Registry numbers:
1, 139524-17-7; **2**, 137627-93-1; $GdCl_3$, 10138-52-0.

[1] a) *Comprehensive Organometallic Chemistry* (Eds.: G. Wilkinson, F. G. A. Stone, E. W. Abel), Pergamon, Oxford, **1982**; b) *Comprehensive Coordination Chemistry* (Eds.: G. Wilkinson, R. D. Gillard, J. A. McCleverty), Pergamon, New York, **1987**; c) *Dictionary of Organometallic Compounds* (Exec. Ed.: J. E. Macintyre), Chapman & Hall, New York, **1984**, and Suppl. Vol. 1–5, **1985–89**; d) F. A. Cotton, G. Wilkinson, *Advanced Inorganic Chemistry*, 5. edition, Wiley, New York, **1988**, and references cited therein.

[2] a) R. D. Rogers, L. M. Rogers, *J. Organomet. Chem.* **1991**, *416*, 201–290; b) W. J. Evans, *Adv. Organomet. Chem.* **1985**, *24*, 131–177; c) W. J. Evans, *Polyhedron* **1987**, *6*, 803–835; d) W. J. Evans, S. L. Gonzales, J. W. Ziller, *J. Am. Chem. Soc.* **1991**, *113*, 7423, and references cited therein.

[3] Although the trinuclear Gd-π-complex system is unknown, recently, the pentanuclear Gd-π-complex **5** was synthesized and its structure determined; see H. Schumann, G. Kociok-Köhn, J. Loebel, *Z. Anorg. Allg. Chem.* **1990**, *581*, 69.

[4] F. R. Fronczek, G. W. Halstead, K. N. Raymond, *J. Am. Chem. Soc.* **1977**, *99*, 1769.

[5] a) M. J. Manning, C. B. Knobler, M. F. Hawthorne, *J. Am. Chem. Soc.* **1988**, *110*, 4458; b) R. Khattar, C. B. Knobler, S. E. Johnson, M. F. Hawthorne, *Inorg. Chem.* **1991**, *30*, 1970; c) M. J. Manning, C. B. Knobler, R. Khattar, M. F. Hawthorne, *ibid.* **1991**, *30*, 2009.

[6] A. R. Oki, H. Zhang, N. S. Hosmane, *Organometallics* **1991**, *10*, 3964.

[7] Crystal data for **1**: $C_{61}H_{203}O_5B_{24}Si_{12}Gd_3Li_6$, M = 2127.1, triclinic, $P\bar{1}$, a = 16.035(7), b = 16.883(6), c = 23.903(9) Å, α = 89.04(3), β = 88.87(3), γ = 67.95(3)°; V = 5996(4) Å^3, Z = 2, ϱ_{calcd} = 1.178 g cm^{-3}, μ = 1.844 mm^{-1}. Of 10077 data collected on Nicolet *R3m/V* diffractometer ($Mo_{K\alpha}$, 2θ = 3.5–38°, 230 K) 9563 reflections were unique and 8103 reflections were observed [$I > 3.0\sigma(I)$]. Data were corrected for Lorentz, polarization, and absorption effects. The structure was solved by heavy-atom methods and refined by block-diagonal least-squares techniques using SHELXTL-Plus (G. M. Sheldrick, *Structure Determination Software Program Package*, Siemens Analytical X-ray Instruments, Inc., Madison, WI, USA, 1990). All non-H atoms, except for the disordered THF [O(101),

C(102) to C(105)] were refined anisotropically. Bonds of the disordered THF were constrained during refinements. No attempts were made to locate the H atoms. The final refinement of **1** converged at $R = 0.053$, $wR = 0.081$, and $GOF = 2.78$ for observed reflections. The maximum and minimum residual electron densities are 0.94 and -0.85 e/Å^3, respectively. Further details of the crystal structure investigation may be obtained from the Fachinformationszentrum Karlsruhe, Gesellschaft für wissenschaftlich-technische Information mbH, D-W-7514 Eggenstein-Leopoldshafen 2 (FRG), on quoting the depository number CSD-56000, the names of the authors, and the journal citation.

[8] R. D. Rogers, R. V. Bynum, J. L. Atwood, *J. Organomet. Chem.* **1980**, *192*, 65.

[9] W. Lamberts, H. Lueken, U. Elsenhans, *Inorg. Chim. Acta* **1986**, *121*, 81.

[10] a) G. E. Herberich, B. Hessner, M. Hostalek, *Angew. Chem.* **1986**, *98*, 637; *Angew. Chem. Int. Ed. Engl.* **1986**, *25*, 642; b) P. Paetzold, N. Finke, P. Wennek, G. Schmid, R. Boese, *Z. Naturforsch. B* **1986**, *41*, 167.

[11] H. Schumann, P. R. Lee, J. Loebel, *Angew. Chem.* **1989**, *101*, 1073; *Angew. Chem. Int. Ed. Engl.* **1989**, *28*, 1033.

[12] R. L. Letsinger, D. F. Pollart, *J. Am. Chem. Soc.* **1956**, *78*, 6079, and references cited therein.

[13] A. R. Oki, H. Zhang, N. S. Hosmane, *J. Am. Chem. Soc.*, submitted for publication.

The polymer dissolves in toluene/dichloroethane under carefully controlled conditions and acid catalysis with formation of oligolides at 100 °C; the triolide is the major component and can be distilled (after the removal of acidic impurities by washing with sodium carbonate solution) to give colorless crystals (mp = 110.0–110.5 °C) in about 50% yield.[8] Crystal structure analysis of the triolide (Fig. 1) shows that the three nearly parallel carbonyl groups point in the same direction and are in effect ready to complex an ion.[9]

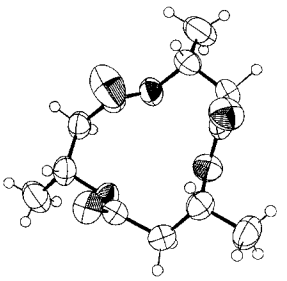

Fig. 1. ORTEP plot [13] of the crystal structure of **1** [14]. The ellipsoids of the thermal vibrations of the atoms correspond to a 50% probability. The radii of the hydrogen atoms are chosen arbitrarily.

The Triolide of (*R*)-3-Hydroxybutyric acid—Direct Preparation from Polyhydroxybutyrate and Formation of a Crown Estercarbonyl Complex with Na Ions

By *Dieter Seebach,* Hans-Martin Müller, H. Michael Bürger,* and *Dietmar A. Plattner*

Besides polypeptides, polynucleotides, and polysaccharides, the polyhydroxyalkanoates (PHA) are a class of biopolymers whose importance in biochemistry and medicine has been recognized only recently.[1, 2] The longest known representative of this class of compounds, poly-(*R*)-3-hydroxybutanoate (PHB),[3] has made its way into the newspapers as a component of the biodegradable plastic BIOPOL.[4] Mixtures of oligolides of 3-hydroxybutanoic acid (HB) were obtained by macrolactonization by the methods of Yamaguchi and Shanzer, and it was possible to isolate pure compounds containing three to ten HB units, albeit in low yield, by chromatographic separation.[5] These oligolides may provide exact structural data relevant to the PHB polyester backbone and should serve as models for testing the hypothesis according to which PHB is involved in the formation of ion channels through cell membranes and even in the passage of DNA into genetically competent bacteria, for example in cloning.[6]

We have now found a remarkably simple way of preparing the triolide **1** ((*R,R,R*)-4,8,12-trimethyl-1,5,9-trioxadodeca-2,6,10-trione) on a 20 g scale directly from the cheap PHB.[7]

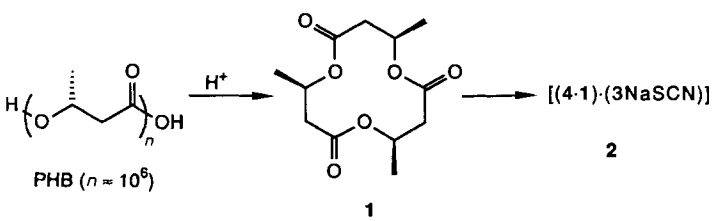

Indeed, crystallizations from acetonitrile solutions containing the triolide and alkali-metal salts yield complexes of a variety of compositions. From a solution of NaSCN and **1** we were able to isolate single crystals of the complex **2** suitable for X-ray structure determination.

The section of the structure shown in Figure 2 reveals the presence of crownlike complexes with one sodium ion coordinated to the three carbonyl oxygen atoms of the triolide (Na–O distances 2.44, 2.50, and 2.53 Å). Comparison of the conformations of the ligand with and without the sodium ion (Fig. 2, bottom) shows that it "adjusts" to the ion by the oxygen atoms moving closer together in the direction of the sodium ion (ion–dipole interaction).

Although numerous structures are known in which keto or amide carbonyl oxygen atoms act as ligands for alkali-metal ions,[10] or in which ether and carbonyl oxygen atoms cooperate in the complexation,[11] or in which only ester carbonyl oxygen atoms are involved in the complexation with other functional groups present in the ring (compare the complexation of alkali-metal ions with depsipeptides, especially with valinomycin[12]), we do not know of any alkali-metal complexes with cyclic ligands containing only ester functionalities such as in **2**. However, in the Ca-polyphosphate-PHB ion-channel proposed by Reusch Ca ions are complexed by ester carbonyl groups.[6]

Experimental Procedure

A mixture of PHB (36 g) and toluene-4-sulfonic-acid monohydrate (15.5 g, 81.5 mmol) in 750 mL of toluene/dichloroethane (4:1) was heated and stirred at reflux for 20 h. The water was removed azeotropically with a Dean-Stark trap (15 h). The clear brown solution was cooled to room temperature, washed with a half-saturated solution of Na_2CO_3 and with saturated NaCl solution, dried over $MgSO_4$, filtered, and evaporated to dryness. The semisolid residue was distilled (100 °C/0.05 Torr). Yield: 15–19 g (42–53%) colorless solid. Mp = 110.0–110.5 °C; $[\alpha]_D^{RT} = -33.9$ ($c = 1.005$, $CHCl_3$); IR (KBr): $\tilde{\nu}$[cm^{-1}] = 2995w, 1745vs, 1725s, 1375s, 1305s, 1295s, 1260m, 1190vs, 1130s, 1110s, 1045s; ^{1}H NMR (400 MHz, $CDCl_3$, 25 °C, TMS): $\delta = 1.30$ (d, $^3J = 6.4$ Hz, 9H; CH_3); $\nu_a = 2.39$, $\nu_b = 2.46$ (ABX, $^3J_{AX} = 2.1$ Hz, $^3J_{BX} = 11.3$ Hz, $^3J_{AB} = 13.5$ Hz, 6H; CH_2); 5.31–5.39 (m, 3H; HC-O); ^{13}C NMR (100 MHz, $CDCl_3$, 25 °C, TMS): $\delta = 20.76$ (CH_3), 42.15 (CH_2), 68.86 (CH), 170.02 (CO); SIMS-

[*] Prof. Dr. D. Seebach, Dipl.-Chem. H.-M. Müller, Dipl.-Chem. H. M. Bürger, Mag. rer. nat. D. A. Plattner
Laboratorium für Organische Chemie der Eidgenössischen Technischen Hochschule
ETH-Zentrum, Universitätstrasse 16, CH-8092 Zürich (Switzerland)

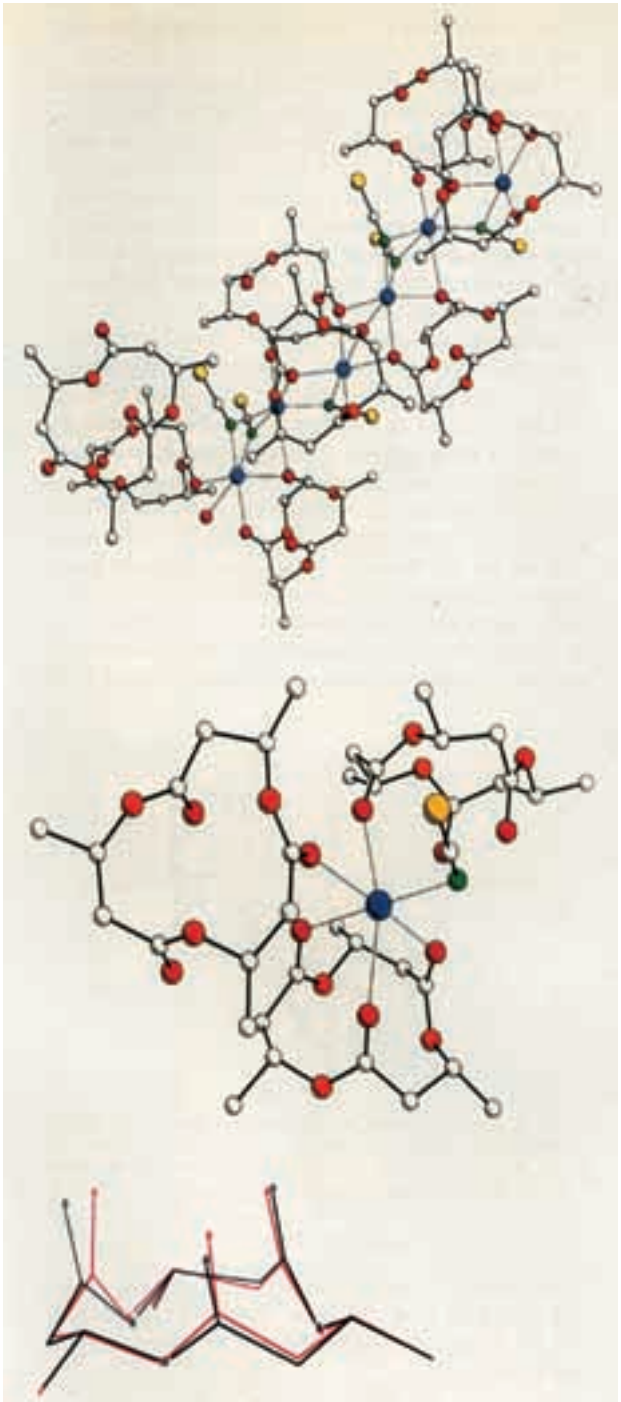

Fig. 2. PLUTO plots of sections of the crystal structure of **2** [15]. All Na ions are hexacoordinated. Top: Chelate-like bonds between two carbonyl oxygen atoms and a Na atom; note the three Na,O,Na,N four-membered rings, in which two Na ions are coordinated to the same carbonyl oxygen atom (Na-O distances in the first ring 2.38 and 2.82 Å, in the other two, 2.44 and 2.63 Å). Note also that one of the four symmetry-independent triolide molecules is uncomplexed. Middle: A section containing a crown estercarbonyl complex with the entire coordination sphere of the corresponding Na ion. Bottom: the overlayed conformations of the free (black) and the crownlike complexed ligand (red). Red spheres = oxygen atoms of CO groups, orange = oxygen atoms of ester groups, white = carbon atoms, yellow = sulfur atoms, green = nitrogen atoms.

MS: *m/z* 281.1 ($[M + Na]^+$, 40), 259.1 ($[M + H]^+$, 100), 155.1 (40); correct elemental analysis; molecular weight (osmom.) = 260.4.

Received: November 27, 1991 [Z 5039 IE]
German version: *Angew. Chem.* **1992**, *104*, 443

CAS Registry numbers:
1, 139629-08-6; *ent*-**1**, 139629-09-7; *rac*-**1**, 139629-10-0; *rac-epi*-**1**, 139683-17-3; **2** (salt), 139683-16-2; **2** (coordination compound), 139683-18-4; PHB homopolymer), 29435-48-1; PHB (repeating unit), 31759-58-7; (*S*)-β-butyrolactone, 65058-82-4; *rac*-β-butyrolactone, 36536-46-6.

[1] Y. Doi, *Microbial Polyesters*, VCH, New York, **1990**; A. J. Anderson, E. A. Dawes, *Microbiol. Rev.* **1990**, *54*, 450–472; A. Steinbüchel, *Nachr. Chem. Tech. Lab.* **1991**, *39*, 1112–1124.
[2] D. Seebach, S. Roggo, J. Zimmermann in *Stereochemistry of Organic and Bioorganic Transformations* (Eds.: W. Bartmann, K. B. Sharpless), VCH, Weinheim, **1987**, pp. 85–126.
[3] M. Lemoigne, *Ann. Inst. Pasteur (Paris)*, **1925**, *39*, 144–173.
[4] P. Holmes, L. Wright, L. Collins (Imperial Chemical Industries) EP 52 459, **1981** (*Chem. Abstr.* **1982**, *97*, 143146r); *Neue Zürcher Zeitung*, December 12, 1986; *The New York Times*, May 3, 1985.
[5] D. Seebach, U. Brändli, P. Schnurrenberger, M. Przybylski, *Helv. Chim. Acta.* **1988**, *71*, 155–167; D. Seebach, U. Brändli, H.-M. Müller, M. Dobler, M. Egli, M. Przybylski, K. Schneider, *ibid.* **1989**, *72*, 1704–1717; H.-M. Müller, M. Dobler, P. Zbinden, D. Seebach, *Chimia* **1991**, *45*, 376.
[6] R. Reusch, H. Sadoff, *Proc. Natl. Acad. Sci. USA* **1988**, *85*, 4176–4180; R. Reusch, *Proc. Soc. Exp. Biol. Med.* **1989**, *191*, 377–381.
[7] ICI Biological Products, PO Box 1, GB Billingham, Cleveland TS23 1LB.
[8] *ent*-**1** (from (*S*)-β-butyrolactone), *rac*-**1** (mp = 67.0–67.5 °C), and *rac-epi*-**1** (mp = 104.0–104.5 °C) (both from *rac*-β-butyrolactone) were also prepared.
[9] According to NMR spectroscopic investigations and the measured dipole moment, the structure in solution does not seem to differ significantly from the structure in the solid state.
[10] D. Seebach, *Angew. Chem.* **1988**, *100*, 1685–1715; *Angew. Chem. Int. Ed. Engl.* **1988**, *27*, 1624–1654; C. Schade, P. von R. Schleyer, *Adv. Organomet. Chem.* **1987**, *27*, 169–247.
[11] S. D. Burke, W. J. Porter, J. Rancourt, R. F. Kaltenbach, *Tetrahedron Lett.* **1990**, *31*, 5285–5288; I. Tajima, M. Okada, H. Sumitomo, *J. Am. Chem. Soc.* **1981**, *103*, 4096–4100.
[12] M. Dobler, *Ionophores and Their Structures*, Wiley & Sons, New York, **1981**.
[13] C. K. Johnson, ORTEP-II, *Report ORNL-5138*, Oak Ridge National Laboratory: Oak Ridge, TN, 1976.
[14] Crystal structure analysis of **1**: $C_{12}H_{18}O_6$. Determination of the cell parameters and collection of the reflection intensities were performed on a Syntex $P2_1$ single-crystal diffractometer ($Mo_{K\alpha}$-radiation, graphite monochromator, $\lambda = 0.7107$ Å); orthorhombic, space group $P2_12_12_1$ (No. 19), $a = 8.929(5)$, $b = 9.842(5)$, $c = 15.331(7)$ Å, $V = 1347.2$ Å^3, $Z = 4$, $\rho_{calc} = 1.27$ g cm^{-3}, $\mu = 0.64$ mm^{-1}, $F(000) = 552$. Complete number of reflections measured: 2806 (2ϑ-scan, $2.5 < 2\vartheta < 50°$); 2375 unique reflections, of which 1768 with $I > 2\sigma(I)$ were used for the determination (Direct Methods, SHELXS-86 [16]) and refinement (SHELX-76 [17]) of the structure. The non-hydrogen atoms were refined anisotropically using a weighting scheme. The positions of the hydrogen atoms were determined from differential *Fourier* syntheses, and they were refined isotropically. The refinement converged finally at $R = 0.052$ ($R_w = 0.059$, number of variables 235).
[15] Crystal structure analysis of **2**: $C_{12}H_{18}O_3 \cdot 0.75$ NaSCN. Determination of the cell parameters and collection of the reflection intensities were performed on a Syntex $P2_1$ single-crystal diffractometer ($Mo_{K\alpha}$-radiation, graphite monochromator, $\lambda = 0.7107$ Å); monoclinic, space group $P2_1$ (No. 4), $a = 9.977(5)$, $b = 26.026(13)$, $c = 12.572(6)$, $\beta = 103.24(2)$, $V = 3177.7$ Å^3, $Z = 8$, $\rho_{calc} = 1.33$ g cm^{-3}, $\mu = 1.52$ mm^{-1}, $F(000) = 1344$. Complete number of reflections measured: 5736 (ω-2ϑ-scan, $2.5 < 2\vartheta < 50°$); learnt-profile method; empirical absorption correction ($0.931 < T < 1.000$); 5498 unique reflections, of which 4896 with $I > 2\sigma(I)$ were used for the determination (Direct Methods, SHELXS-86 [16]) and the refinement (BIG-SHELX-76 [17]) of the structure. The non-hydrogen atoms were refined anisotropically using a weighting scheme; the hydrogen atoms were added to this structure model with constant isotropic temperature factors on calculated positions and refined using the riding model. The refinement converged finally at $R = 0.036$ ($R_w = 0.039$, number of variables 757). Further details concerning the crystal structure analyses may be obtained from the director of the Cambridge Crystallographic Data Centre, University Chemical Laboratory, Lensfield Road, GB-Cambridge CB2 1EW (UK), by indicating the full reference of this paper.
[16] G. M. Sheldrick, *SHELXS-86, Program for the Solution of Crystal Structures*, University of Göttingen, **1986**.
[17] G. M. Sheldrick, *SHELX-76, Program for Crystal Structure Determination*, University of Cambridge, **1976**.
[18] *BIG SHELX-76*, UCLA version, **1985**.

Caro's Acid: Molecular Structure and Association in the Solid State at −130 °C

By *Walter Frank** and *Birgit Bertsch-Frank**

Caro's acid (trioxoperoxosulfuric acid H_2SO_5),[1] one of the best known named compounds in inorganic chemistry, is representative of the class of inorganic peroxoacids. Its high oxidation potential and its instability—which can also result in spontaneous, explosive degradation[2]—complicates the preparation and study of the pure acid. Since the crystallization of the extremely hygroscopic and low-melting compound (m.p. = 47 °C) is also difficult to control, the possibility of obtaining a single crystal for structural analysis was considered doubtful.[3]

Pure H_2SO_5 (**1**) was first prepared by D'Ans and Friedrich, not without danger, by reacting H_2O_2 with HSO_3Cl.[4] If H_2O_2 is treated with SO_3, a reaction which formally yields the desired compound directly, substantial amounts of side products and degradation products are formed.[5] Much simpler is the preparation of defined H_2SO_4/H_2SO_5 mixtures, which when cooled under moisture-free conditions are storable indefinitely, and from which we could crystallize the peroxoacid **1** at low temperature without danger. Methods that have proved useful in the study of thermolabile crystals were employed for the further treatment of the crystalline material.[6]

From the vibration spectra[7, 8] a molecular structure with an intramolecular O-H···O hyrogen bond, in which the hydrogen atom of the peroxo group is close to an oxo oxygen atom, was postulated for crystalline **1**. The actual molecular structure in the solid at −130 ± 3 °C, however, shows that no intramolecular hydrogen bond is present (Fig. 1).[9] The

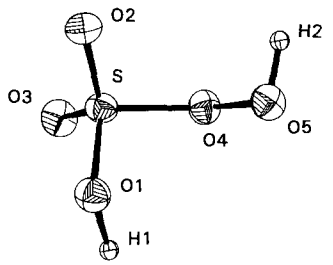

Fig. 1. The molecular structure of Caro's acid in the solid state at −130 °C. The ellipsoids of the thermal movement correspond to a residence probability of 50%; the radius of the hydrogen atoms was chosen arbitrarily. Bond lengths [pm] and angles [°]: O4-O5 146.4(3) (in H_2O_2 145.8(4) [10]), S-O1 152.4(2), S-O2 141.8(2), S-O3 143.2(2) (in H_2SO_4 S-OH 153(2), S-O 142(2) [11]), S-O4 160.2 (in $S_2O_8^{2-}$ anion 164.4(5) [12]), O1-H1 94(4), O5-H2 95(4); O1-S-O2 106.8(1), O1-S-O3 112.9(1), O1-S-O4 104.0(1), O2-S-O3 121.4(2), O2-S-O4 109.3(1), O3-S-O4 101.0(1), S-O4-O5 108.7(2), H1-O1-S 112(2), H2-O5-O4 98(3).

O–O bond length does not differ notably from that of solid hydrogen peroxide,[10] and the S–O distances also lie within the expected range.[13] From them, using simple empirical relationships,[14] we estimated a bond order of about 1 for the bond from S to the peroxo group, about 4/3 for the bond to the OH group, and about 5/3 each for the bonds to the oxo oxygen atoms. Thus, in contrast to H_2SO_4 ($2 \times 7/4$ and $2 \times 5/4$),[11] in H_2SO_5 the character of only three of the S–O bonds is intermediate between that of double and single bonds.

The shape of the molecule (point group symmetry 1) is determined by the conformation of the H1–O1–S–O4–O5–H2 chain and the torsion angles H1-O1-S-O4 (− 68 °), O1-S-O4-O5 (− 59.4 °), and S-O4-O5-H2. The value for the latter of −104° lies between that for the potential minimum for rotation in gaseous H_2O_2 (120 °)[15] and that in solid H_2O_2 enforced by the molecular association (90.2 °). It also gives an impression of the structure modifying forces of the solid state association for **1**.

The molecules in the crystal of **1** are linked in layers parallel to the *a,b* plane by a system of unsymmetric, almost linear O–H···O hydrogen bonds. If the O···O distance (265.6 and 272.1 pm) is used as criterium, the hydrogen bonds are strong.[16] There are only slight differences between these distances and those between the oxygen atoms involved in hydrogen bonding in H_2SO_4 and H_2O_2 [263(2) and 276.1(5) pm, respectively], which explains the relationship between the two halves of the molecule **1** with the parent compounds, the different acidity of the OH and OOH functions, and indirectly the monobasic character of the acid. Further details of the linkage of the associated molecules and layered structure may be seen in Figure 2. Viewed in an

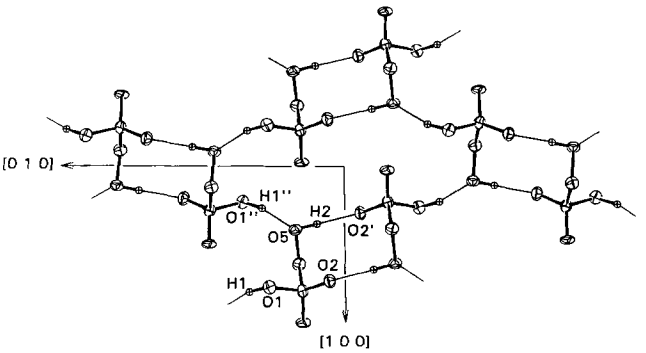

Fig. 2. Hydrogen-bond system and layer structure. Section of a layer of O–H–O linked H_2SO_5 molecules. (Distances [pm]: O1''···O5 265.6(4), H1''···O5 173(5), O5···O2' 272.1(4), H2···O2' 178(5); angles [°]: O5···H1''-O1'' 173(10), O2'···H2-O5 172(10); symmetry coding: ': 1-x, -y, 1-z, '': −0.5 + x, 0.5-y, 1-z).

abstract way[17] a layer may be seen as a (8.4^2) network with the S and O5 atoms as knots or as a (4.4) network of (H_2SO_5) enantiomeric pairs. Only van der Waals forces hold the layers together.

Experimental Procedure

Oleum (65%, 33.1 mL; i.e., 42.9 g (0.535 mol) SO_3) was added to an 87.3% hydrogen peroxide solution (14.3 mL; 17.2 g (0.505 mol) H_2O_2) over a period of 1 h at 0–10 °C. Half an hour thereafter the iodometric and cerimetric analysis of the viscose liquid revealed 62.9% H_2SO_5 and 0.5% unreacted H_2O_2. After many attempts, crystals suitable for a single-crystal X-ray analysis were obtained by slow cooling to −20 °C over 24 h. They were selected and transferred to a glass capillary at low temperature and freed of adhered mother liquor in a stream of argon. All apparatus for the preparation and the structural analysis was of glass and was treated with concentrated H_2SO_4, rinsed with distilled water, and dried in a dust-free environment.

Received: September 25, 1991 [Z 4931 IE]
German version: *Angew. Chem.* **1992**, *104*, 469

CAS Registry numbers:
H_2SO_5, 7722-86-3; H_2O_2, 7722-84-1; oleum, 8014-95-7.

[*] Prof. Dr. W. Frank
Fachbereich Chemie der Universität
Erwin-Schrödinger-Strasse, D-W-6750 Kaiserslautern (FRG)
Dr. B. Bertsch-Frank
Degussa AG, Forschung Anorganische Chemie
Rodenbacher Chaussee 4, D-W-6450 Hanau 1 (FRG)

[1] H. Caro, *Z. Angew. Chem.* **1898**, 845.
[2] J. O. Edwards, *Chem. Eng. News* **1955**, *33*, 3336.

[3] J. Flanagan, W. P. Griffith, A. C. Skapski, *J. Chem. Soc. Chem. Commun.* **1984**, 1574.
[4] J. D'Ans, W. Friedrich, *Z. Anorg. Chem.* **1912**, *73*, 325.
[5] H. Ahrle, *J. Prakt. Chem.* **1909**, *79*, 129.
[6] M. Veith, W. Frank, *Chem. Rev.* **1988**, *88*, 81.
[7] A. Simon, *Z. Anorg. Chem.* **1939**, *242*, 369.
[8] J. L. Arnau, P. A. Giguère, *Can. J. Chem.* **1970**, *98*, 3903.
[9] Crystal structure analysis of **1**: H_2SO_5, $M_r \approx 114.08$, $a = 628.5(3)$, $b = 1420.0(4)$, $c \approx 773.4(3)$ pm, $Z = 8$, $V_c = 0.6902$ nm^3, space group *Pbca*, crystal size $0.69 \times 0.66 \times 0.21$ mm^3, four-circle diffractometer, $Mo_{K\alpha}$ radiation, 912 measured reflections, 713 independent reflections with $I > 0$, numerical absorption correction, 64 refined parameters, $R = 0.047$, $R_w = 0.041$. Further details of the crystal structure investigation may be obtained from the Fachinformationszentrum Karlsruhe, Gesellschaft für wissenschaftlich-technische Information mbH, D-W-7514 Eggenstein-Leopoldshafen 2 (FRG) on quoting the depository number CSD-55888, the names of the authors, and the journal citation.
[10] J. Savariault, M. S. Lehmann, *J. Am. Chem. Soc.* **1980**, *102*, 1298.
[11] C. Pascard-Billy, *Acta Crystallogr.* **1965**, *18*, 827.
[12] B. K. Sivertsen, H. Sorum, *Z. Kristallogr. Mineral.* **1969**, *130*, 449.
[13] Compare with the distances given in the legend of Figure 1. Closer inspection shows that the bond S–O 2 is shorter than S–O 3, although the former participates in an intermolecular hydrogen bond. This finding should be seen, for example, in connection with the variance of the distances between sulfur atoms and terminal oxygen atoms in trimeric sulfur trioxide.
[14] I. D. Brown, D. Altermatt, *Acta Crystallogr. Sect. B* **1985**, *41*, 244.
[15] R. C. Redington, N. B. Olsen, P. C. Cross, *J. Chem. Phys.* **1962**, *36*, 1311.
[16] J. Emsley, D. J. Jones, J. Lucas, *Rev. Inorg. Chem.* **1981**, *3*, 105.
[17] A. F. Wells, *Structural Inorganic Chemistry*, 5. Ed., Clarendon, Oxford, **1984**, p. 81.

Investigations of the Structure and Reactivity of a Stannaketenimine**

By *Hansjörg Grützmacher,* Stefanie Freitag, Regine Herbst-Irmer,** and *George S. Sheldrick*

Dedicated to Professor Hans-Friedrich Grützmacher on the occasion of his 60th birthday

Investigations of the existence or nonexistence of systems with multiple bonds to elements of the higher periods have long entertained experimental and theoretical chemists.[1] In this context compounds with tin–element multiple bonds are interesting; of these only the distannene **1**[2] from Lappert et al. and the stannaethene **2**[3] from Berndt et al. have been characterized by X-ray structural analyses. A number of groups have reported experimental evidence of stannaethenes and stannanimines.[4] Quantum chemical calculations of the tin–carbon and tin–tin "double bond" have also been conducted.[5]

We report here the synthesis and molecular structure of the adduct of diarylstannandiyl **3**[6] and mesitylisocyanide **4**,

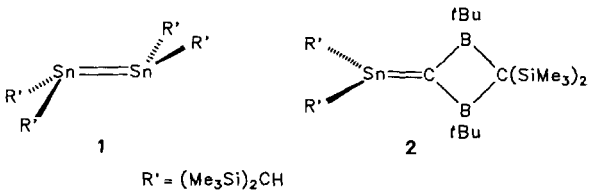

compound **5**, which is formally a stannaketenimine and thus comparable to the silaketenimine $tBu_2Si{=}C{=}NR$ (R = Ph, Mesityl, 2,4,6-$tBu_3C_6H_2$)[7] postulated by Weidenbruch et al. as an intermediate.

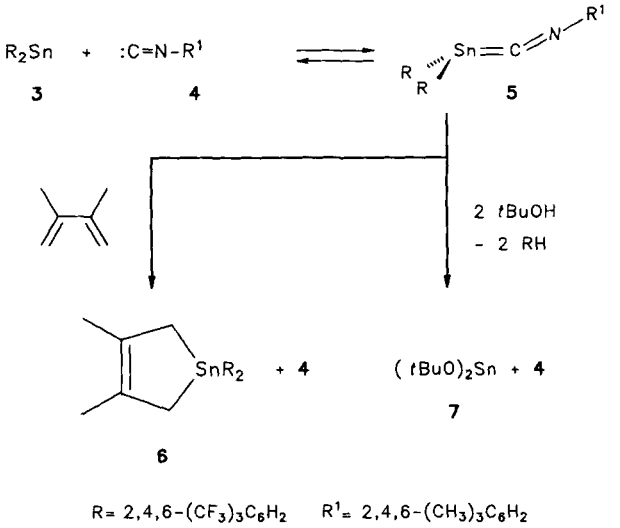

R= 2,4,6-$(CF_3)_3C_6H_2$ R^1= 2,4,6-$(CH_3)_3C_6H_2$

A solution of equimolar amounts of **3** and **4** cooled to −78 °C provided pale yellow crystals of **5**.[8] Crystals suitable for X-ray structural analysis were obtained by sublimation at 40 °C/0.01 Torr. The structure of stannaketenimine **5** shows atoms C11(C20), Sn1, C1, and N1 to have a very bent orientation (Fig. 1). In an idealized ketenimine these atoms

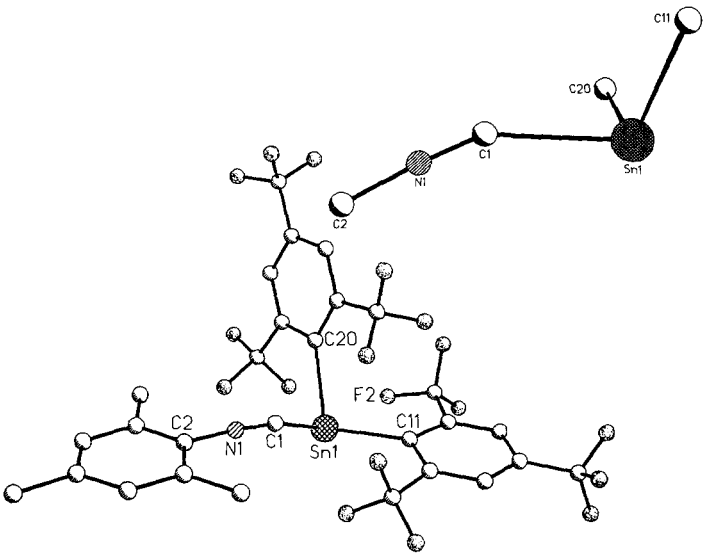

Fig. 1. Structure of **5** in the crystal. Selected bond lengths [Å] and angles [°]: Sn1-C1 2.397(3), Sn1-C11 2.306(2), Sn1-C20 2.314(3), C1-N1 1.158(3), N1-C2 1.405(3), Sn1-F2 2.72; C20-Sn1-C11 102.6(1), C1-Sn1-C11 104.9(1), C1-Sn1-C20 83.4(1), Sn1-C1-N1 153.9(2), C1-N1-C2 175.0(3). The stannaketenimine frame without substituents is shown in the upper right.

would lie in one plane. The comparison of the C11-Sn1-C1 and C20-Sn1-C1 bond angles (104.9(1) and 83.4(1)°, respectively) points out the distortion of the pyramidal coordination geometry of the tin atom; this arises from the relatively short Sn1–F2 contact (2.72 Å).[6] The Sn1–C1 distance of 2.397(3) Å is significantly greater than the distances between Sn1 and the *ipso* carbon atoms C11 and C20 in the aryl rings,

[*] Dr. H. Grützmacher
Anorganisch-chemisches Institut der Universität
Im Neuenheimer Feld 270 D-W-6900 Heidelberg
Dr. R. Herbst-Irmer, S. Freitag, Prof. Dr. G. M. Sheldrick
Anorganisch-chemisches Institut der Universität
Tammannstrasse 4, D-W-3400 Göttingen (FRG)

[**] This work was supported by the Dr.-Otto-Röhm-Gedächtnisstiftung, the Fonds der Chemischen industrie, and the Deutsche Forschungsgemeinschaft (SFB 247).

which correspond to the lengths of single bonds in sterically encumbered tin compounds (2.22–2.30 Å).[10] The C1–N1 bond length (1.158(3) Å) is typical for isocyanides.[11] In the IR spectrum of **5** the C–N stretching vibration (2166 cm^{-1}; KBr) is shifted to higher wave numbers relative to that of **4** (2118 cm^{-1}; KBr), as is also found for isocyanide–transition-metal complexes.

The bent molecular structure of **5** was predicted by the model of Malrieu and Trinquier, which correlates the geometry of a system with (cumulated) double bonds with the singlet–triplet energy difference of the molecular fragments.[13] According to this model the silaketene $H_2Si{=}C{=}O$, which can be described as a silandiyl–carbon monoxide complex, also has a bent structure.[14] The Sn1-C1-N1 angle in **5** deviates 26° from that of the linear Sn1-C1-N1 frame of a pure donor(isocyanide)–acceptor(stannandiyl). This is an indication that the Sn1–C1 interaction in **5** may be described as a "double" π donor–acceptor interaction, similar to that in **1** (Scheme 1). This is weaker than the interaction which is

2 5

Scheme 1. Qualitative MO description of the bonding systems in **2** and **5**.

equivalent to a tin–carbon single bond. Measurement of the temperature-dependence of the ^{119}Sn NMR chemical shifts (Fig. 2) allowed the determination of the dissociation enthalpy $\Delta H^\circ = 29.6 \pm 0.4$ kJ mol^{-1} and the dissociation entropy $\Delta S^\circ = 90 \pm 1$ J $K^{-1} mol^{-1}$ for the dissociation of **5** to **3** and **4**. Not unexpectedly the reaction of adduct **5** with 2,3-dimethylbutadiene and *tert*-butylalcohol affords exclusively reaction products **6** and **7**, which are the products of the reaction of **3** with these reagents.[15]

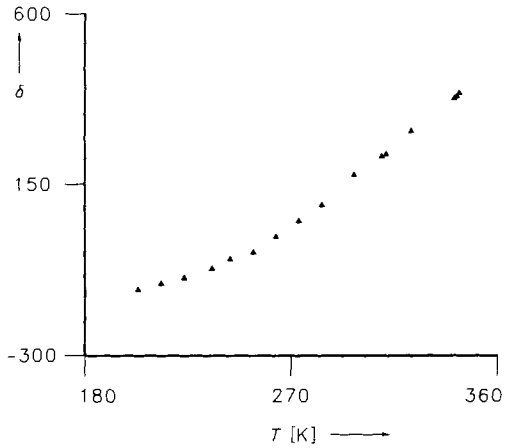

Fig. 2. ^{119}Sn NMR chemical shift of **5** as a function of temperature. The spectra were measured at temperature intervals between −80 to +70 °C in a 10 mm NMR tube with 0.3 g **5** in 0.5 mL C_6D_6 and 2 mL toluene. The ^{119}Sn NMR chemical shift of **3** is known ($\delta \approx 678$)[6], that of **5** was extrapolated to $\delta = -150$. The experimental ^{119}Sn NMR data collected at a number of temperatures was used in the calculation of the dissociation enthalpy and entropy. (Parameter correlation ln*K* vs. 1/T: 0.9935).

Stannaethene **2** with trigonal-planar coordination and the shorter tin–carbon bond (2.025 Å) is formally an adduct of the stannandiyl as Lewis base and the extremely electrophilic carbene $:C(BtBu)_2C(SiMe_3)_2$, which does not exist in this form.[16] In **5**, on the other hand, the stannandiyl is the Lewis acid. In this respect the two bonding systems **2** and **5** are complementary to each other and delineate the range of bonding in the stannaethenes.

Received: September 27, 1991 [Z 4936 IE]
Publication delayed on authors' request.
German version: *Angew. Chem.* **1992**, *104*, 459

CAS Registry numbers:
3, 131079-28-2; **4**, 57116-96-8; **5**, 139015-72-8; **6**, 139015-73-9; **7**, 3275-19-2; 2,3-dimethylbutadiene, 513-81-5.

[1] Relevant reviews: a) *Multiple Bonds and Low Coordination in Phosphorus Chemistry* (Ed.: M. Regitz, O. J. Scherer), Thieme, Stuttgart, **1990**; b) G. Raabe, J. Michl, *Chem. Rev.* **1985**, *85*, 419; c) J. Barrau, J. Escudié, J. Satgé, *ibid.* **1990**, *90*, 283; d) A. H. Cowley, N. C. Norman, *Prog. Inorg. Chem.* **1986**, *34*, 1; e) K. Seppelt, *Angew. Chem.* **1991**, *103*, 399; *Angew. Chem. Int. Ed. Engl.* **1991**, *30*, 361.

[2] D. E. Goldberg, P. B. Hitchcock, M. F. Lappert, K. M. Thomas, A. J. Fieldberg, A. Haaland, B. E. R. Schilling, *J. Chem. Soc. Dalton Trans.* **1986**, 2387, and references cited therein.

[3] H. Meyer, G. Baum, W. Massa, S. Berger, A. Berndt, *Angew. Chem.* **1987**, *99*, 559; *Angew. Chem. Int. Ed. Engl.* **1987**, *26*, 547.

[4] a) D. Seyferth, J. L. Lefferts, *J. Am. Chem. Soc.* **1974**, *96*, 6237; b) V. K. Belsky, N. N. Zemlyansky, I. V. Borisova, N. D. Kolosova, I. P. Beletskaya, *Cryst. Struct. Commun.* **1982**, *11*, 881; c) M. Veith, V. Huch, *J. Organomet. Chem.* **1986**, *306*, 263; d) H. Grützmacher, H. Pritzkow, *Organometallics* **1991**, *10*, 938; e) N. Wiberg, K. S. Vasisht, *Angew. Chem.* **1991**, *103*, 105; *Angew. Chem. Int. Ed. Engl.* **1991**, *30*, 93; f) H. Grützmacher, H. Pritzkow, *ibid.* **1991**, *103*, 976 and **1991**, *30*, 1017.

[5] a) M. J. S. Dewar, G. L. Grady, J. J. P. Stewart, *J. Am. Chem. Soc.* **1984**, *106*, 6771; b) G. Trinquier, J.-P. Malrieu, *ibid.* **1987**, *109*, 5303; c) K. D. Dobbs, W. J. Hehre, *Organometallics* **1986**, *5*, 2057; d) K. K. Baldridge, M. S. Gordon, *J. Am. Chem. Soc.* **1988**, *110*, 4204.

[6] H. Grützmacher, H. Pritzkow, F. T. Edelmann, *Organometallics* **1991**, *10*, 23.

[7] a) M. Weidenbruch, B. Brandt-Roth, S. Pohl, W. Saak, *Angew. Chem.* **1990**, *102*, 93; *Angew. Chem. Int. Ed. Engl.* **1990**, *29*, 90; b) *Polyhedron* **1991**, *10*, 1147.

[8] Experimental procedure: A solution of **3** (2 g, 3 mmol) in dry degassed *n*-hexane (20 mL) was allowed to react with **4** (0.44 g, 3 mmol). The solution was cooled to −78 °C and the resulting yellow crystals were removed by filtration and dried. **5**: Mp = 88 °C; yield: 91%. – ^1H NMR (C_6D_6): $\delta = 1.82$ (s, 3H, CH_3), 1.88 (s, 6H, CH_3), 6.28 (s, 2H, 2,4,6-$(CH_3)_3C_6H_2$), 7.94 (s, 4H, 2,4,6-$(CF_3)_3C_6H_2$). – ^{19}F NMR (C_6D_6): $\delta = -57.7$ (s, 12F, *ortho*-CF_3, satellites: $J(^{119}Sn, ^{19}F) = 244.6$, $J(^{117}Sn, ^{19}F) = 233$ Hz), −63.6 (s, 6F, *para*-CF_3).

[9] Crystal structural analysis of **5** : space group $P\bar{1}$, $a = 8.633(1)$, $b = 8.782(1)$, $c = 20.290(3)$ Å, $\alpha = 89.16(1)$, $\beta = 80.03(1)$, $\gamma = 76.06°$, $V = 1469.0$ Å^3, $Z = 2$, $\mu = 1.01$ mm^{-1} ($Mo_{K\alpha}$), 6822 observed intensities, semiempirical absorption correction, $2\theta_{max} \approx 52°$, 5268 symmetry-independent reflections with $F > 4\sigma(F)$ used for structure solution (Patterson and Fourier methods) and refinement, nonhydrogen atoms anisotrope, H atoms refined with the "riding" model, *para*-CF_3 groups disordered, occupation factor ca. 0.85 : 0.15, with refined distance restraints, $R = 0.0280$, ($R_w = 0.294$, $w^{-1} = \sigma^2(F) + 0.0001\,F^2$). Further details of the crystal structure investigation may be obtained from the Fachinformationszentrum Karlsruhe, Gesellschaft für wissenschaftlich-technische Information mbH, D-W-7514 Eggenstein-Leopoldshafen 2 (FRG) on quoting the depository number CSD-55832, the names of the authors, and the journal citation.

[10] H. Puff, B. Breuer, G. Gehrke-Brinkmann, P. Kind, H. Reuter, W. Schuh, W. Wald, G. Weidenbrück, *J. Organomet. Chem.* **1989**, *363*, 265.

[11] J. A. Green, P. T. Hoffmann in *Isonitrile Chemistry* (Eds.: I. Ugi) (*Org. Chem.* **1971**, *20*, 1).

[12] See I. Ugi, R. Meyer, *Chem. Ber.* **1960**, *93*, 93.

[13] G. Trinquier, J.-P. Malrieu, *J. Am. Chem. Soc.* **1987**, *109*, 5303.

[14] a) C. A. Arrington, J. T. Petty, E. E. Payne, W. C. K. Haskins, *J. Am. Chem. Soc.* **1988**, *110*, 6240; b) M.-A. Pearsall, R. West, *ibid.* **1988**, *110*, 7228; c) T. P. Hamilton, H. F. Schaefer III, *J. Chem. Phys.* **1989**, *90*, 1031.

[15] **6**: M.p. = 81–82 °C; Yield 82%. – ^1H NMR (C_6D_6): $\delta = 1.82$ (s, 6H, CH_3), 2.21 (s, 4H, CH_2, satellites: $^2J(^{119}Sn/^{117}Sn, ^1H) = 47.5$ Hz), 7.82 (s, 4H, aromat. H). – ^{19}F NMR (C_6D_6): $\delta = -59.25$ (s, 12F, *ortho*-CF_3, satellites: $J(^{119}Sn/^{117}Sn, ^{19}F) = 32.2$ Hz), -63.82 (s, 6F, *para*-CF_3). **7**: See M. Veith, *Chem. Rev.* **1990**, *90*, 1, and references cited therein.

[16] R. Wehrmann, H. Klusik, A. Berndt, *Angew. Chem.* **1984**, *96*, 810; *Angew. Chem. Int. Ed. Engl.* **1984**, *23*, 826.

A Straightforward Synthesis of Nitrilimines; X-Ray Crystal Structure of a Nitrilimine Stabilized by Non-Heteroatom Substituents**

By *Régis Réau, Guilaine Veneziani, Françoise Dahan,* and *Guy Bertrand**

Dedicated to Professor Hans-Friedrich Grützmacher on the occasion of his 60th birthday

Recently, the use of heteroatoms has allowed the preparation of stable species that were believed to be only transient intermediates. The most striking example is the synthesis of stable carbenes[1] bearing either a silicon and a phosphorus atom,[2] or two nitrogen atoms.[3] So far, the only known nitrilimines stable at room temperature bear heteroatom substituents (B, Si, P), both at the carbon and nitrogen ends.[4] They were obtained from the reaction of lithiated diazo compounds with electrophiles, a reaction assumed for a long time to give only diazo compounds.[5] Since nitrilimines can rearrange into the more thermodynamically stable diazo compounds,[6] and the concomitant formation of both isomers has never been observed, we believed that nitrilimines were the products of the kinetically controlled reaction, and that they were only isolable because of the stabilizing effect of the heteroatoms.[4c] The primary formation of nitrilimines from the lithiated diazo compounds could imply that the lithium atom is bound to the nitrogen end rather than to the carbon end. Here we report that tin diazo compounds are powerful precursors of nitrilimines as exemplified by the synthesis of the first stable nitrilimine with non-heteroatom substituents. We also demonstrate that the formation of nitrilimines and diazo compounds from lithiated diazo compounds results from competitive attack at either the nitrogen or carbon atom.

The structure of tin diazo compounds is well established in contrast to that of lithium diazo compounds; in the former, the metal is bound to the carbon atom.[7] However, in THF at room temperature, bis(trimethylstannyl)diazomethane (**2**)[8] readily reacts with chloro[bis(diisopropylamino)]-phosphane (**1**) to give quantitatively *C*-[bis(diisopropylamino)phosphino]-*N*-[bis(diisopropylamino)phosphino]-nitrilimine (**3**).[9] In contrast, the reaction of lithiated bis(diisopropylamino)phosphinodiazomethane **4** with chlorophosphane **1** provides the isomeric bis(phosphino)-diazomethane **5**.[10] Nitrilimine did not thermally isomerize

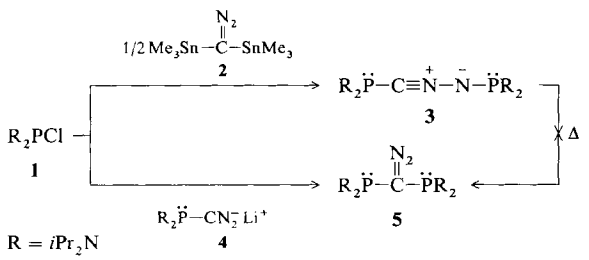

to **5**, clearly demonstrating that **3** is not the product of the kinetically controlled reaction of lithium compound **4** and phosphane **1**; in other words, the electrophilic attack on the carbon and nitrogen ends are two competitive processes.

[*] Dr. G. Bertrand, Dr. R. Réau, G. Veneziani, Dr. F. Dahan
Laboratoire de Chimie de Coordination du CNRS
205, route de Narbonne, F-31077 Toulouse Cédex (France)

[**] This work was supported by the Centre National de la Recherche Scientifique (CNRS).

Since **3** was the first stable nitrilimine bearing two electron-donating substituents, the importance of the electronic effects in stabilization was considered. Indeed, the reaction of tin diazo compound **2** with triphenylmethylchloride in acetonitrile at −30 °C gave rise to nitrilimine **6**, which was isolated as surprisingly air-stable, pale yellow crystals (60 °C decomp., 90% yield). The identification of **6** as a nitrilimine

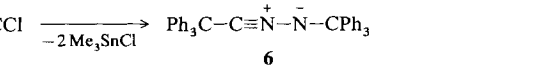

was supported by ^{14}N NMR [$\delta = -182$ (C*N*N)][11] and ^{13}C NMR data [$\delta = 60.71, 76.26$ (Ph_3C), 85.5 (CNN)], and by a strong, broad absorption band in the IR spectrum at 2052 cm^{-1}. The structure of **6** was confirmed by an X-ray structure analysis[12] (Fig. 1). Nitrilimine **6** has a structure

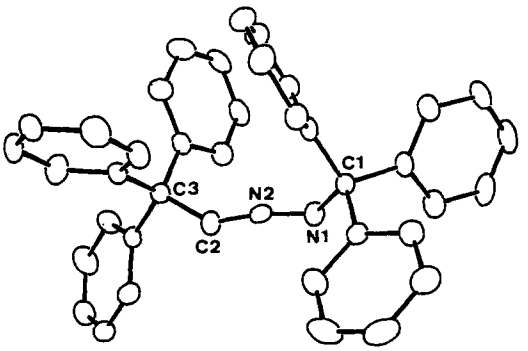

Fig. 1. Molecular structure of **6** in the crystal (ORTEP, ellipsoids at the 35% probability level). Selected bond lengths [Å] and angles [°]: C1-N1 1.530(2), N1-N2 1.262(2), N2-C2 1.173(3), C2-C3 1.503(3), C1-N1-N2 115.2(2), N1-N2-C2 169.4(2), N2 C2-C3 137.3(2), C1-N1-N2-C2 135.7, N1-N2-C2-C3 134.0

similar to the bent allenyl model predicted by theory,[13] and interestingly resembles the previously reported *C*-thiophosphoranyl-*N*-phosphinonitrilimine.[4d] The stability of **6** can only be explained in terms of steric effects, because the triphenylmethyl groups have no apparent electronic interaction with the CNN skeleton. In spite of its bulky substituents, nitrilimine **6** undergoes typical 1,3-dipolar reactions:[14] Compound **6** underwent regio- and stereospecific [2 + 3] cycloaddition with methyl acrylate, methyl propiolate, dimethyl fumarate, and dimethyl maleate, leading to the respective five-membered heterocycles **7**–**10**[9] in high yields.

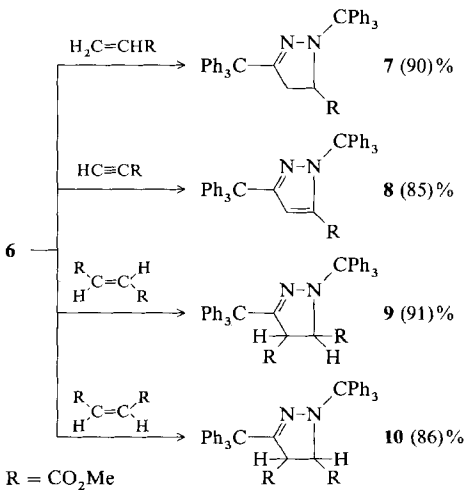

The formation of bis(phosphino)nitrilimine **3** demonstrates the potential of tin diazo compounds as nitrilimines precursors and allows a clarification of the mechanism of the reaction of electrophiles with lithium diazo compounds. The first experimental evidence of an organic nitrilimine and its isolation were separated by 30 years. The crucial step was the stabilization of these 1,3-dipoles by heteroatom substituents.

Experimental Procedure

6: An acetonitrile solution (4 mL) of bis(trimethylstannyl)diazomethane (**2**) (278 mg, 0.757 mmol) was added dropwise to 2 equivalents of triphenylmethylchloride (421 mg, 1.51 mmol) in acetonitrile (6 mL) at $-30\,^{\circ}C$. The solution was stirred for 1 h at $-30\,^{\circ}C$, and **6** precipitated as a pale yellow solid which was washed several times with acetonitrile. Trimethylchlorostannane was removed under vacuum (ca. 15 h) at room temperature. Nitrilimine **6** was recrystallized from THF/Et_2O (358 mg, 90%). Nitrilimine **6** is air stable in the solid state but slowly decomposes in solution above $-20\,^{\circ}C$.

Cycloaddition reactions: A solution of the dipolarophile in THF was added to the stoichiometric amount of nitrilimine **6** in THF at $-30\,^{\circ}C$. The mixture was allowed to warm to room temperature, and the solvent was then removed at 10^{-2} Torr. The solids **7**–**10** were washed several times with pentane and dried in vacuo.

Received: September 30, 1991 [Z 4940 IE]
German version: *Angew. Chem.* **1992**, *104*, 481

CAS Registry numbers:
1, 56183-63-2; **2**, 21803-09-8; **3**, 137320-40-2; **4**, 113533-26-9; **5**, 105309-80-6; **6**, 139130-94-2; **7**, 139130-95-3; **8**, 139136-96-4; **9**, 139130-97-5; **10**, 139130-98-6; methyl acrylate, 96-33-3; methyl propiolate, 922-67-8; dimethyl fumarate, 624-49-7; dimethyl maleate, 624-48-6; triphenylmethylchlorid, 76-83-5.

[1] M. Regitz, *Angew. Chem.* **1991**, *103*, 691–693; *Angew. Chem. Int. Ed. Engl.* **1991**, *30*, 674–676.

[2] a) A. Igau, H. Grützmacher, A. Baceiredo, G. Bertrand, *J. Am. Chem. Soc.* **1988**, *110*, 6463–6466; b) A. Igau, A. Baceiredo, G. Trinquier, G. Bertrand, *Angew. Chem.* **1989**, *101*, 617–618; *Angew. Chem. Int. Ed. Engl.* **1989**, *28*, 621–622; c) G. R. Gillette, A. Baceiredo, G. Bertrand, *ibid.* **1990**, *102*, 1486–1488 and **1990**, *29*, 1429–1431.

[3] A. J. Arduengo, R. L. Harlow, M. Kline, *J. Am. Chem. Soc.* **1991**, *113*, 361–363.

[4] a) M. P. Arthur, A. Baceiredo, G. Bertrand, *J. Am. Chem. Soc.* **1991**, *113*, 5062–5063; b) F. Castan, A. Baceiredo, G. Bertrand, *Angew. Chem.* **1989**, *101*, 1253–1254; *Angew. Chem. Int. Ed. Engl.* **1989**, *28*, 1250–1251; c) F. Castan, A. Baceiredo, D. Bigg, G. Bertrand, *J. Org. Chem.* **1991**, *56*, 1801–1807; d) M. Granier, A. Baceiredo, Y. Dartiguenave, M. Dartiguenave, M. J. Menu, G. Bertrand, *J. Am. Chem. Soc.* **1990**, *112*, 6277–6285.

[5] M. Regitz, G. Mass, *Diazo Compounds, Properties and Synthesis*, Academic Press, London, **1986**.

[6] a) M. Granier, A. Baceiredo, G. Bertrand, *Angew. Chem.* **1988**, *100*, 1397–1398; *Angew. Chem. Int. Ed. Engl.* **1988**, *27*, 1350–1351; b) C. Wentrup, *Helv. Chim. Acta* **1978**, *61*, 1755–1764; c) R. Gleiter, W. Rettig, C. Wentrup, *ibid.* **1974**, *57*, 2111–2124; d) A. Padwa, T. Caruso, S. Nahm, A. Rodrigez, *J. Am. Chem. Soc.* **1982**, *104*, 2865–2871.

[7] a) J. Lorberth, S. H. Shin, H. Donath, S. Wocadlo, W. Massa, *J. Organomet. Chem.* **1991**, *407*, 167–171; b) A. Fadini, E. Glozbach, P. Krommes, J. Lorberth, *ibid.* **1978**, *149*, 297–307.

[8] M. F. Lappert, J. Lorberth, J. S. Poland, *J. Chem. Soc. A* **1970**, 2954–2959.

[9] Selected spectroscopic data: **3**: ^{31}P NMR (THF): $\delta = 96.0$, 45.5 [d, $^4J(^{31}P, ^{31}P) = 9$ Hz]; ^{13}C NMR (C_6D_6): $\delta = 63.3$ [d, $^1J(^{31}P, ^{13}C) = 62.5$ Hz, CNN]; ^{14}N NMR ($CDCl_3$): $\delta = -191.9$ (CNN); IR (THF): $\nu = 2047\ cm^{-1}$(CNN). **7**: ^{13}C NMR ($CDCl_3$): $\delta = 42.2$ (CH_2), 62.8 (CH), 156.5 (CN); ^1H NMR ($CDCl_3$): $\delta = 2.2$ [dd, $J = 16.8$, 11.4 Hz, 1H, CH_2], 2.6 (dd, $J = 16.8$, 9.3 Hz, 1H, CH_2], 3.9 [dd, $J = 11.4$, 9.3 Hz, 1H, CH]. **8**: ^{13}C NMR ($CDCl_3$): $\delta = 115.1$ (CH), 134.6 (CCO_2), 155.1 (CN); ^1H NMR ($CDCl_3$): $\delta = 6.5$ (s, 1H, CH). **9**: ^{13}C NMR ($CDCl_3$): $\delta = 59.8$ (*C*CH), 67.7 (NCH), 150.5 (CN); ^1H NMR ($CDCl_3$): $\delta = 4.1$ [d, $J = 11.4$ Hz, 1H, CCH], 4.3 [d, $J = 11.4$ Hz, 1H, NCH]. **10**: ^{13}C NMR ($CDCl_3$): $\delta = 57.5$ (*C*CH), 67.6 (NCH), 155.6 (CN); ^1H NMR ($CDCl_3$): $\delta = 3.5$ [d, $J = 10.4$ Hz, 1H, CCH], 4.2 [d, $J = 10.4$ Hz, 1H, NCH].

[10] a) A. Baceiredo, A. Igau, G. Bertrand, M. J. Menu, Y. Dartiguenave, M. Dartiguenave, J. J. Bonnet, *J. Am. Chem. Soc.* **1986**, *108*, 7868–7869; b) M. J. Menu, M. Dartiguenave, Y. Dartiguenave, J. J. Bonnet, G. Bertrand, A. Baceiredo, *J. Organomet. Chem.* **1989**, *372*, 201–206.

[11] K. Horchler von Locquenghien, R. Réau, G. Bertrand, *J. Chem. Soc. Chem. Commun.*, **1991**, 1192–1193.

[12] Space group $P2_1/c$, $a = 17.793(2)$, $b = 10.635(1)$, $c = 17.013(2)$ Å, $\beta = 102.41(1)^{\circ}$, $V = 3144.1$ Å^3, $Z = 4$, 6343 measured reflections, 3165 independent observed [$F_o^2 > 3\sigma(F_o^2)$], 404 refined parameters, $R(F_o) = 0.027$ ($R_w = 0.029$). Further details of the crystal structure investigations are available on request from the Fachinformationszentrum Karlsruhe, Gesellschaft für wissenschaftlich-technische Information mbH, D-W-7514 Eggenstein-Leopoldshafen 2, on quoting the depository number CDS-56010, the names of the authors, and the journal citation.

[13] a) P. Caramella, K. N. Houk, *J. Am. Chem. Soc.* **1976**, *98*, 6397–6399; b) P. Caramella, R. W. Gandour, J. A. Hall, C. G. Deville, K. N. Houk, *ibid.* **1977**, *99*, 385–392, and references therein.

[14] a) R. Huisgen, *Angew. Chem.* **1963**, *75*, 604–637 and 742–754; *Angew. Chem. Int. Ed. Engl.* **1963**, *2*, 565–608 and 633–645; b) P. Caramella, P. Grünanger in *1,3 Dipolar Cycloaddition Chemistry* (Ed.: A. Padwa), Wiley, New York, **1984**; c) R. Huisgen, M. Seidel, G. Wallbillich, H. Knupfer, *Tetrahedron* **1962**, *17*, 3–29; d) A. Eckell, R. Huisgen, R. Sustmann, G. Wallbillich, D. Grashey, E. Spindler, *Chem. Ber.* **1967**, *100*, 2192–2213.

Preparation, Ligand Exchange Reactions, and Structure of a Diene(aqua)ruthenium Complex $[(cod)Ru(H_2O)_4](OTs)_2$**

By *Ulrich Kölle,* Gabriele Flunkert, Ralf Görissen, Martin U. Schmidt,* and *Ulli Englert*

Metal ions which together with water are complexed to arenes or olefins, contradict the Jørgensen rule[1] for transition metal complexes (either hard, hard or soft, soft!) and therefore are expected to have special properties. Apart from the well characterized dicationic benzene(aqua)Ru- and Os complexes[2, 3] as well as the recently described tetramethylthiophene-Ru analogue,[4] a series of dicationic cyclopentadienyl(aqua)–metal complexes, some of them less well characterized, of the type $[Cp^{(*)}M(H_2O)_3]^{2+}$ ($Cp^* = \eta^5$-C_5Me_5) is known; $[CpCr(H_2O)_3]^{2+}$,[5] $[Cp^*Co(H_2O)_3]^{2+}$,[6, 7] $[Cp^*Rh(H_2O)_3]^{2+}$,[7, 8] $[Cp^*Ru(H_2O)_3]^{2+}$.[7] These complexes are of differing stabilities. Most recently also a number of olefin(aqua) complexes was prepared.

The dication **1** of the title compound proved to be a surprisingly robust organometallic aqua complex which was prepared in the way shown in Scheme 1 and is the first structurally characterized diene(aqua)–metal complex.

$$RuCl_3 \cdot nH_2O \xrightarrow[EtOH]{C_6H_8} [\{(C_6H_6)RuCl_2\}_2] \xrightarrow[-AgCl]{Ag^+,\,H_2O} [(C_6H_6)Ru(H_2O)_3]^{2+}$$

$$\xrightarrow[H_2O,\,10\,^{\circ}C]{h\nu} [Ru(H_2O)_6]^{2+} \quad (\mathbf{2}) \xrightarrow{cod,\ EtOH} [(cod)Ru(H_2O)_4]^{2+} \quad (\mathbf{1})$$

Scheme 1. Counterions of the dicationic complexes: p-$CH_3C_6H_4SO_3^-$ (OTs) or SO_4^{2-}. cod = 1,5-cyclooctadiene.

The photochemical route convenient for the preparation of $[Ru(H_2O)_6]^{2+}$ (**2**),[7, 10] avoids the somewhat involved reduction of aqueous ruthenic acid by activated lead[11] and makes smaller scale preparations of the hexaaqua-metal ion easier. In contrast to the reaction of **2**-$(OTs)_2$ with 1,3-cyclooctadiene which gave a (η^5-cyclooctadienyl)(η^6-arene) complex,[12] we found that in ethanol with cod only a complexation to the dicationic complex **1** with one cod and four aqua ligands occurred (yields and physical data for this and

[*] Prof. Dr. U. Kölle, Dipl.-Chem. G. Flunkert, Dipl.-Chem. R. Görissen, Dipl.-Chem M. Schmidt, Dr. U. Englert
Institut für Anorganische Chemie der Technischen Hochschule
Professor-Pirlet-Strasse 1, D-W-5100 Aachen (FRG)

[**] This work was supported by the Fonds der Chemischen Industrie. We thank Prof. H. Elias, Institut für Anorganische Chemie der Technischen Hochschule Darmstadt, for the ligand H_2salen and Johnson Matthey, Reading, England for the loan of $RuCl_3$.

the other newly prepared compounds see Table 1). This is, dependent on the anion, soluble in polar organic solvents and particularly soluble in water. In contrast to **2**, the solutions are not air sensitive and also do not decompose or disproportionate when warmed.[13]

Table 1. Yields and selected physical data of the compounds **1**-$(OTs)_2$, **3**, **4**, **5a**–**5c** (as PF_6 salt), and **6**-$(OTs)_2$.

1-$(OTs)_2$: ^{1}H NMR (80 MHz, D_2O, H_2O (δ = 4.65) as standard): δ = 4.4 (br s, 4H; =CH), 2.3 (br s, 8H; CH_2); ^{13}C NMR (D_2O): δ = 28.86 (t, J(C, H) = 132.6 Hz), 89.90 (d, J(C, H) = 161.6 Hz); IR(KBr) $\tilde{\nu}$ [cm^{-1}] = 3271 (br, H_2O), 2960, 2930, 2880 (CH_2, CH_3), 1635 (C=C), 1446 (δ CH_2) 682 (δ HC=CH); correct C,H-analysis

3: Yield 80%; ^{1}H NMR (300 MHz, C_6D_6): δ = 1.75, 2.01 (s, each 3H; CH_3), 5.25 (s, 2H; CH), 1.83, 2.44 (m, each 2H), 2.16 (m, 4H; CH_2), 4.23, 4.57 (m, each 2H; =CH); ^{13}C{^{1}H} NMR (60.2 MHz, C_6D_6): δ = 27.38, 28.12 (CH_3), 98.77 (CH), 186.67, 186.75 (C–O), 28.86, 30.78 (CH_2), 88.99, 92.08 (=CH) [a]

4: ^{1}H NMR (80 MHz, CD_3OD): δ = 3.95 (s, 4H; CH_2), 6.9, 7.2 (m, 8H; arom.), 8.44 (2H=CH), ca. 2 (br m, 8H; CH_2), ca. 5.6 (br m, 4H; =CH)

5a-PF_6: Yield quantitative; ^{1}H NMR (80 MHz, $CDCl_3$): δ = 5.03 (s, 5H; Cp), ca. 4 (br m, 12H, OCH_2; 4H, CH), 3.06 (br s, 2H; H_2O), ca. 2.1 (m, 8H; CH_2), 1.22, 1.27, 1.28 (t, J = 7.1 Hz, each 3H; CH_3); IR (KBr) $\tilde{\nu}$ [cm^{-1}] = 1280 s (P=O), 1112, 1037 s (δ POEt), 839 vs (PF_6^-)

5b-PF_6: from **5a** and NaN_3, yield 70%; ^{1}H NMR (80 MHz, CD_3OD): δ = 4.15 (s, 5H; Cp), ca. 4.1 (br m, 12H, OCH_2; 4H, CH), ca. 2.14 (m, 8H; CH_2), 1.32 (t, J = 7 Hz, 6H; CH_3), 1.27 (t, J = 7 Hz, 3H; CH_3); IR (KBr) $\tilde{\nu}$ [cm^{-1}] = 2060 s (N_3), 1112, 1140 s (δ P(O)OEt)

5c-PF_6 from **5a**-PF_6 and KSCN; ^{1}H NMR almost like **5b**-PF_6; IR (KBr) $\tilde{\nu}$ [cm^{-1}] = 2126, 2077 s (SCN), 1113, 1040 s (δ P(O)OEt)

6-$(OTs)_2$: from **1**-$(OTs)_2$ with 2 bar CO, 20 h, roomtemp., H_2O; ^{1}H NMR (80 MHz, D_2O): δ = 4.40 (br s, 4H; =CH), 2.08 (s, 8H; CH_2), 2.31 (s, 6H; CH_3OTs), 7.68, 7.57, 7.33, 7.23 (m, 8H; arom.); ^{13}C NMR (CD_3OD): δ = 197.5 (br s, CO), 94 (m, =CH), ca. 30 (m, CH_2); IR (KBr) $\tilde{\nu}$[cm^{-1}] = 1984 cm^{-1} (CO)

[a] See also P. Powell, *J. Organomet. Chem.* **1974**, *65*, 89 [6].

In the cyclic voltammogram in dimethylformamide, within the limits +1.9 to ca. −1.2 V (saturated calomel electrode), no electon transfer is observed.

Compound **1** was chemically characterized by ligand exchange reactions, which led to the complexes **3**–**7** (Scheme 2). During these reactions, depending on the ligand, one to four aqua ligands were exchanged. The tripod ligand served as a model for a triaqua ligand moiety.[14] The coordination shown in **5**, to a metal complex fragment with twofold symmetry (see Fig. 3), causes the methyl signals of the OEt groups of the tripod ligand to split into three triplets of equal intensity. The remaining aqua ligand can be easily exchanged for other ligands to form a variety of further complexes **5**.

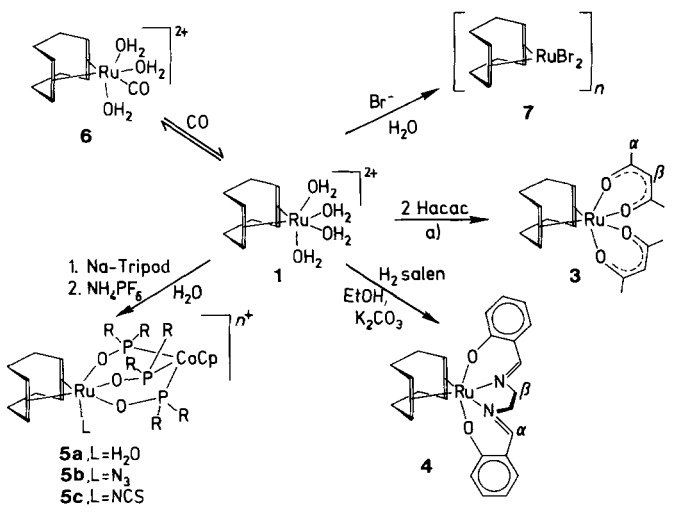

Scheme 2. R = OEt. Hacac = acetylacetone, H_2salen = bis(salicylidene)ethylenediamine. a): EtOH, K_2CO_3, 40 °C, 2 h.

According to the NMR spectra, the salene in **4** coordinates in a similar way to acac in **3** such that a molecule with C_2 symmetry results. Particularly noteworthy is the exchange of an aqua ligand for CO under a mild CO pressure. This reaction corresponds to the recently found carbonylation of **2**-$(OTs)_2$ which afforded the monocarbonyl(aqua) complex.[15] Here, too, the splitting of the cod signals, especially in the ^{13}C NMR spectrum, indicates an unsymmetrical molecular unit and thus, together with the single CO absorption in the IR spectrum, a monocarbonyl complex. With halide ions, for example Br^-, the polymeric dihalide $[(cod)RuBr_2]_x$ immediately precipitates from water. Neither this, nor the analogous chloride could be used, for example with Ag^+ ions in water, to form **1**.

Crystals of **1**-$(OTs)_2$ suitable for a structure determination were obtained by slow evaporation of an aqueous acetone solution. The molecular structure of **1** is shown in Figure 1, and a packing diagram of **1**-$(OTs)_2$ in Figure 2. The complex

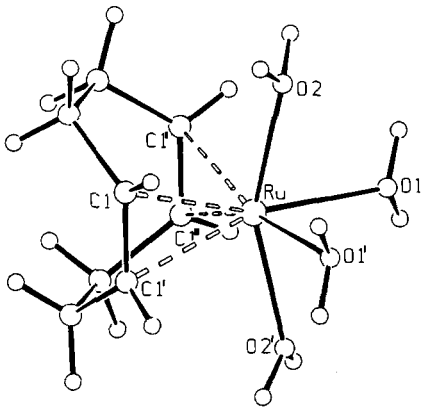

Fig. 1. Crystal structure of **1** (SCHAKAL). Distances [Å]: Ru-O1 2.158(1), Ru-O2 2.095(2), Ru-C1 2.178(1), C1-C1' 1.367(3); Angles [°]: O1-Ru-O1' 86.14(9), O2-Ru-O2' 154.8(1), (middle C1-C1')-Ru-*cis*-O1 93.82, (middle C1-C1')-Ru-*trans*-O1 180, (middle C1-C1')-Ru-O2 99.15, (middle C1-C1')-Ru-(middle C1''-C1''') 86.22.

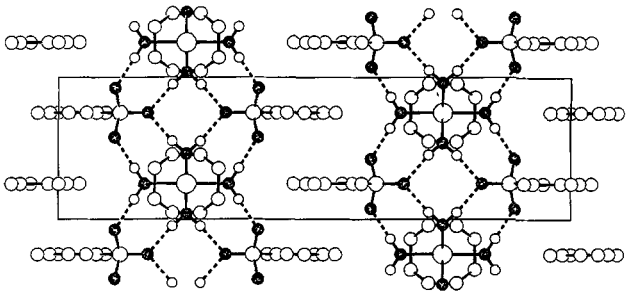

Fig. 2. Packing diagram of **1**-$(OTs)_2$. Oxygen atoms dark. The strands of $[(cod)Ru(H_2O)_4]^{2+}$ ions, each twice H-bonded via tosylate ions, lie along the *c* axis, distance RuO···H···OS 2.746(2), 2.683(2) Å.

contains one (cod)Ru unit, to which are symmetrically coordinated four aqua ligands to yield a highly distorted octahedral arrangement. Two crystallographic mirror planes of the space group *Pmmn* through the Ru, interconvert the two aqua ligand sets as well as the cod halves. Of the aqua lig-

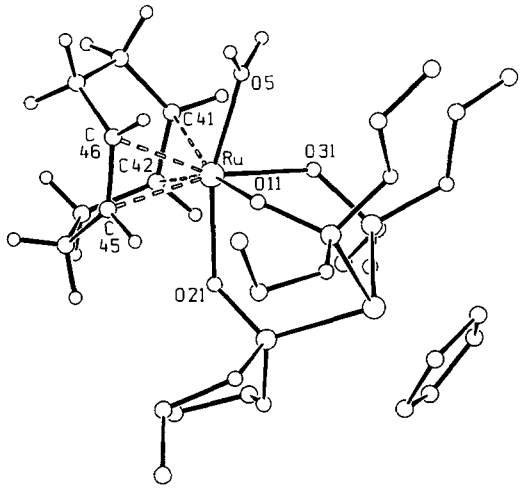

Fig. 3. Crystal structure of **5a**-ClO_4 (SCHAKAL). Distances [Å]: Ru-O11 2.10(2), Ru-O21 2.09(2), Ru-O31 2.10(3), Ru-O5 2.10(2), Ru-C41 2.17(2), Ru-C42 2.17(2), Ru-C45 2.17(3), Ru-C46 2.19(4), C41–C42 1.38(1), C45–C46 1.385(9); Angles [°]: O5-Ru-O11 81.2(6), O5-Ru-O21 162(2), O5-Ru-O31 81.3(7), (middle C41–C42)-Ru-O21 95, (middle C45–C46)-Ru-O5 95.

ands, two are *trans* to an olefin double bond (O1), and two are approximately *trans* to each other (O2) with a O–Ru–O angle for the latter of 155°. Note that the Ru–O1 distances of 2.158(2) Å are significantly longer than those of Ru–O2 (2.095(2) Å. Since all of the water-H atoms are hydrogen-bonded to the sulfonate groups of the anions, as illustrated in Figure 2, whereby the crystalline salt forms a chain structure, this difference has to be attributed to a real *trans* effect of the double bonds. Thus, in **1**, for the first time the influence of the organic ligand on the metal–water bond is structurally evident. The effect could not be derived from the structure of $[(C_6H_6)Ru(H_2O)_3]^{2+}$, the only other compound comparable with $[Ru(H_2O)_6]^{2+}$, because the lack of a threefold crystallographic axis and the different H bonding of the water protons makes the Ru–O distances unequal.

In Figure 3 the cation of the perchlorate **5a**-ClO_4[17] is shown. Of the two possible orientations, the tripod ligand adopts the one that substitutes the O1 and O1′ and O2. Here, the Ru distances to the tripod O atom (2.10(2), and 2.09(2) Å, respectively) are as long as those to the remaining aqua ligand, and correspond to the Ru–O2 distance in **1**-(OTs), i.e. the rigid tripod ligand does not reflect the observed *trans*-effect in the aqua complex. Two oxygen atoms of the disordered ClO_4^- ion connect the cations via H bonds to form dimeric units. The Ru–cod distances as well as the relatively short C=C distances of the coordinated cod double bond, which classify the aqua-Ru complex as a poor back bonding fragment, are the same in the two complexes within the limits of error.

The few measurements carried out so far concerning the kinetics of water exchange in organometallic aqua- and closely related complexes[18] all show a rate of exchange increased by a factor of 10^3–10^5 towards the hexaaqua–metal ions of the same electron configuration. Evidently this kinetic lability is related to the longer metal–water bond. A corresponding relationship was noted for the Ru^{II} acetonitrile complexes $[Ru(CH_3CN)_6]^{2+}$, $[(C_6H_6)Ru(CH_3CN)_3]^{2+}$, and $[(C_5H_5)Ru(CH_3CN)_3]^{+}$, with an increasing exchange rate of the acetonitrile in this order.[19] The kinetic lability together with the thermal stability of the dicationic complex **1**, and the possibility of a reversible CO addition (Scheme 2), hopefully mean that diene(aqua) complexes can also act as effective catalysts.

Experimental Procedure

A solution of $[Ru(H_2O)_6](OTs)_2$ (0.3 g, 0.48 mmol) and cod (1.5 mL) in ethanol (30 mL) was stirred for 4 h at room temperature under an inert atmosphere. This resulted in a color change from red-violet to yellow. The solvent was removed under vacuum, and the residue was taken up in water (5 mL) and extracted three times with hexane (5 mL) to remove the excess cod. A yellow oil remained after the removal of water under vacuum. This was dissolved in acetone/ethanol (4:1), and cooled to −10 °, whereby the salt was obtained in the form of orange-yellow needles. Yield ca. 70–85%.

Received: October 1, 1991
Revised: December 14, 1991 [Z4945IE]
German version: *Angew. Chem.* **1992**, *104*, 445

CAS registry numbers:
1-$(OTs)_2$, 139015-58-0; **2**-$(OTs)_2$, 15694-44-7; **3**, 31742-01-5; **4**, 139015-59-1; **5a**-ClO_4, 139015-67-1; **5a**-PF_6, 139040-89-4; **5b**-PF_6, 139015-63-7; **5c**-PF_6, 139015-65-9; **6**-$(OTs)_2$, 139015-61-5; **7**, 121922-71-2.

[1] C. K. Jørgensen, *Inorg. Chem.* **1964**, *3*, 1201–1202.
[2] Y. Hung, W.-J. Kung, H. Taube, *Inorg. Chem.* **1981**, *20*, 457–463.
[3] a) P. Bernhard, L. Helm, I. Rapaport, A. Ludi, A. E. Merbach, *J. Chem. Soc. Chem. Commun.* **1984**, 302–303; b) M. Stebler-Röthlisberger, W. Hummel, P.-A. Pittet, H.-B. Bürgi, A. Ludi, A. E. Merbach, *Inorg. Chem.* **1988**, *27*, 1358–1363.
[4] E. A. Ganja, T. B. Rauchfuss, C. L. Stern, *Organometallics*, **1991**, *10*, 270–275.
[5] L. O. Spreer, I. Shah, *Inorg. Chem.* **1981**, *20*, 4025–4027.
[6] U. Kölle, B. Fuss, *Chem. Ber.* **1984**, *117*, 753–762.
[7] U. Kölle, W. Kläui, *Z. Naturforsch. B* **1991**, *46*, 75–83.
[8] U. Kölle, *J. Electroanal. Chem. Interfacial Electrochem.* **1990**, *292*, 217–229; A. Nulton, P. Bailey, P. M. Maitlis, *J. Chem. Soc. Dalton Trans.* **1981**, 1997–2002.
[9] Compare D. V. McGrath, R. H. Grubbs, *J. Am. Chem. Soc.* **1991**, *113*, 3611–3613.
[10] W. Weber, P. C. Ford, *Inorg. Chem.* **1986**, *25*, 1088–1092.
[11] P. Bernhard, H.-B. Bürgi, J. Hauser, H. Lehmann, A. Ludi, *Inorg. Chem.* **1982**, *21*, 3936–3941.
[12] M. Stebler-Röthlisberger, A. Salzer, H.-B. Bürgi, A. Ludi, *Organometallics* **1986**, *5*, 298–302.
[13] Following our observations **2** disproportionated in water on mild warming ($E^0(3\,Ru^{2+} \rightarrow 2\,Ru^{3+} + Ru) = -0.014$ V (calculated from the standard potentials from *Handbook of Chemistry and Physics*, 64th Ed., CRC Press, Boca Raton, FL, USA, **1983**, p. D156)
[14] Cf. W. Kläui, *Angew. Chem.* **1990**, *102*, 661–670; *Angew. Chem. Int. Ed. Engl.* **1990**, *29*, 627–637.
[15] G. Laurenczy, L. Helm, A. Ludi, A. E. Merbach, *Helv. Chim. Acta* **1991**, *74*, 1236–1238.
[16] Structure data: space group *Pmmn* (No. 59), $a = 6.931(1)$, $b = 24.911(6)$, $c = 7.516(2)$ Å, $V = 1.9277(8)$ nm^3, $Z = 8/4$, $\rho_{calc} = 1.832$ g cm^{-3}, crystal dimensions $0.4 \times 0.3 \times 0.2$ mm, ENRAF-Nonius CAD4, $Mo_{K\alpha}$, $\lambda = 0.7093$ Å, 293 K, $\omega/2\theta$ scan, $0 < \omega < 30°$, extinction coefficients refined to 0.610×10^{-6}, empirical absorption correction by the ψ scan method, 5485 reflections, of which 4381 $I > 3\sigma(I)$, 1724 independent with $I > 3\sigma(I)$, and $\theta < 30°$ in the structure factor calculation and refinement; nonhydrogen atoms anisotropic, H atoms of the aqua ligands and at C1 isotropic, remaining H atoms not refined, but included in the structure correction. 107 parameters, $R = 0.024$, $R_w = 0.038$ (statistically weighted). Further details from the Fachinformationszentrum Karlsruhe, see [17].
[17] Structure data: space group $P2_1/c$, $a = 12.515(2)$, $b = 12.410(3)$, $c = 23.719(5)$ Å, $\beta = 101.36°$, $V = 3.612(2)$ nm^3, $Z = 4$, $\rho_{calc} = 1.585$ g cm^{-3}, crystal dimensions $0.4 \times 0.3 \times 0.2$ mm, ENRAF-Nonius CAD4, $Mo_{K\alpha}$, $\lambda = 0.7093$ Å, 293 K, ω scan, $3° < \theta < 25°$, 5989 reflections, extinction correction, empirical absorption correction by the ψ scan method; with 3589 unique reflections with $I > 2\sigma(I)$, 434 parameters, $R = 0.046$, $R_w = 0.047$ (statistically weighted). Perchlorate disorder about the Cl–O bond, H bonds ClO_4–H_2O. Further details of the crystal structure investigation may be obtained from the Fachinformationszentrum Karlsruhe, Gesellschaft für wissenschaftlich-technische Information mbH, D-W-7514 Eggenstein-Leopoldshafen 2 (FRG) on quoting the depository number CSD-55845, the names of the authors, and the journal citation.
[18] k_1 for water exchange in $[Ru(H_2O)_6]^{2+} = 1.8 \times 10^{-2}\,s^{-1}$ [11]; in $[(C_6H_6)Ru(H_2O)_3]^{2+} = 11\,s^{-1}$ [3b]; k for water exchange in $[CpCr(H_2O)_3]^{2+} \approx 10\,M^{-1}s^{1}$ [5]; k for the reaction $[Cp^*M(bpy)(H_2O)]^{2+} + SCN^- \rightarrow [Cp^*M(bpy)(SCN)]^{+} = 1.05\,M^{-1}s^{-1}$, M = Co; $111\,M^{-1}s^{1}$, M = Rh; $325\,M^{-1}s^{1}$, M = Ir (J. Schneider, H. Elias, U. Kölle, *J. Serb. Chem. Soc.* **1990**, *55*, 695–700).
[19] W. Luginbühl, P. Zbinden, P. A. Pittet, T. Armbruster, H.-B. Bürgi, A. E. Merbach, A. Ludi, *Inorg. Chem.* **1991**, *30*, 2350–2355.

The Beilstein Test: An Unintentional Dioxin Source in Analytical and Research Laboratories

By *Barbara M. Scholz-Böttcher, Müfit Bahadir,** and *Henning Hopf*

In 1872 F. Beilstein introduced his now classical experiment as an easy proof for halides in organic materials.[1] In this flame test on copper wire, the volatile copper halides are detected by the green color of the flame. Even if there are doubts about its specifity,[2] the Beilstein test is a routine and quick screening test, mainly for chloride, up to the present day.

The combustion of chlorinated organic materials is suspected to generate polychlorinated dibenzo-*p*-dioxins (PCDD) and -furans (PCDF).[3] Main reasons for their formation are the preformed structures in precursor substances as well as a catalyzed de novo synthesis during the combustion. By now it is a well-known fact that even traces of copper(II) chloride have a high catalytic activity on the formation of PCDD and PCDF during thermal treatment. This has been confirmed in model experiments with synthetic matrices as well as fly ash from municipal waste incineration plants.[4-6] The optimal temperature for the formation of PCDD or PCDF is 300 °C.

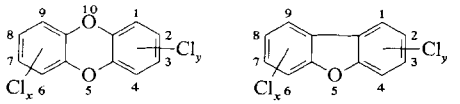

Scheme 1. Structures of polychlorinated dibenzo-*para*-dioxins (PCDD) and dibenzofurans (PCDF). $x = 1-4$, $y = 0-4$.

Aromatic systems arising from a partial, incomplete combustion process are subject to chlorination reactions. Radical mechanisms and chlorination by free halogen, both generated in the presence of $CuCl_2$, have been proposed. Chlorine is released from $CuCl_2$ by thermal activation. In the presence of oxygen, Cu(II) chloride may also act as a catalyst as demonstrated by the Deacon reaction for chlorine generation.[4]

The conditions of the Beilstein test thus provide all prerequisites for PCDD and PCDF formation: appropriate combustion temperatures, chlorinated organic compounds, oxygen, and copper. To prove this assumption, seven chlorinated compounds have been investigated: 2,4-dichloro- (2,4-DCP), 2,4,6-trichloro- (2,4,6-TCP) and pentachlorophenol (PCP) as well as monochlorobenzene (MCB), known to be PCDD and PDCF precursors,[3, 7] and triphenylmethylchloride (Trityl), trichloroethylene (TRI), and polyvinylchloride (PVC), from which PCDD or PDCF generation is only possible from de novo synthesis during the test.[3]

Around 100 mg MCB and TRI were burned in a total of ten tests after dipping the copper wire into the substances and collecting the combustion gases on glass wool and polyurethane foam (PU). About 10 mg of the chlorinated phenols were tested in the same manner. The exact quantities used were calculated by reweighing. In case of PVC 100 mg of polymer was cut into small pieces and burned in five portions; here glass wool was the only adsorbent. The adsorbents were extracted for 8 h with toluene in a soxhlet apparatus. After introducing ^{13}C-labeled 2,3,7,8-substituted PCDD or PCDF isomers that contain between four and eight chloro substituents the sample cleanup was carried out with alkaline alumina according to Hagenmaier et al.[8] The final solution in 100 µL of isooctane octane was analyzed with GC-MS in selected ion monitoring (SIM) mode. Tetrachloro- to octachloro-substituted PCDD or PCDF compounds were quantified by comparison with corresponding ^{13}C-labeled internal standards (isotope dilution technique), whereas monochloro- to trichloro-substituted PCDD or PCDF compounds were calculated from the response factors of tetrachlorinated dioxins and furans (TeCDD and TeCDF).[9]

The main intention of our experiments was to examine whether PCDD and PCDF are formed under the conditions of the Beilstein test, which are typical for combustion in general. It is almost impossible to reproduce exactly the complex reactions under the test conditions. Variations in the temperature gradient depending on the flame position of the copper wire, in the induction periods for each compound and in the amounts used all play a significant role. Since many modifications of the Beilstein test exist, our results may represent just an order of magnitude of PCDD and PCDF generation.

The temperature inside the glass wool reached a maximum at between 300° and 500 °C (Fig. 1) depending on the duration of one single test (10–30 s) and drops immediately after the burner was removed. The temperature of the PU foam never exceed 40 °C; that of the moderate flame lay between 700 °C and 900 °C. Although catalytic effects of PCDD or PCDF formation on the surface of the glass wool or other solid inorganic adsorbents cannot be excluded, this type of sampling for the following GC-MS analysis is the state of the art for the generation and analytical characterization of gaseous combustion products.[10-12]

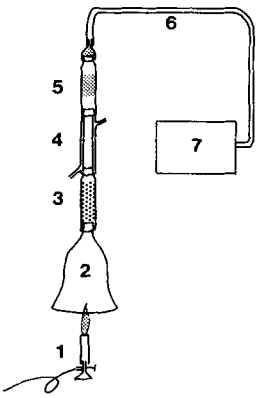

Fig. 1. Apparatus used for the Beilstein test. Bunsen burner (1), funnel (2), tube filled with glass wool (3), water-cooled condensor (4), tube filled with polyurethane foam (5), PVC tubing (6), pump (7).

The Beilstein test led to the formation of PCDD/F for all investigated compounds (Table 1). The toxicity equivalencies (TEQ) relative to 2,3,7,8-TeCDD were calculated using the toxicity factors recommended by the German Federal Health Agency.

Chlorinated phenols are well-known precursors for PCDD and PDCF. In case of PCP and 2,4,6-TCP the direct condensation products, OcCDD and TeCDD, respectively, predominated. 2,3,7,8-TeCDD, however, was not detectable in either case. A chlorine content in PCDD and PCDF higher than expected from the structures of the precursors 2,4,6-TCP and 2,4-DCP was observed, which indicates catalytic effects

[*] Prof. Dr. M. Bahadir, Dr. B. M. Scholz-Böttcher
Institute of Ecological Chemistry and Waste Analysis
of the Technical University
Hagenring 30, D-W-3300 Braunschweig (FRG)
Prof. H. Hopf
Institute of Organic Chemistry of the Technical University of Braunschweig

Table 1. PCDD/DF concentrations in the combustion gas of the Beilstein test (ng per g substance tested). Summation symbols represent the total concentration of furans and dioxins with indicated degree of substitution. Rows labeled 2,3,7,8 refer to the 2,3,7,8-chlorosubstituted derivatives of the compound in the previous row. Cl_4–Cl_8 represent the total concentration of all the tetrachloro- to octachloro-substituted compounds.

Furans/ Dioxins [a]	PCP [ng g^{-1}]	2,4,6-TCP [ng g^{-1}]	2,4-DCP [ng g^{-1}]	MCB [ng g^{-1}]	Trityl [ng g^{-1}]	TRI [ng g^{-1}]	PVC [ng g^{-1}]
ΣMoCDF	–	–	10	–	162	–	–
ΣDiCDF	–	550	143	300	285	31	–
ΣTrCDF	–	1638	8638	90	223	–	–
ΣTeCDF	70	7344	2076	148	254	2	7
2,3,7,8	–	47	–	3	–	–	+
ΣPeCDF	9	1206	686	41	62	3	15
2,3,7,8	–	85	151	16	17	5	14
ΣHxCDF	1026	475	24	49	–	72	44
2,3,7,8	410	371	–	14	–	30	44
ΣHpCDF	6341	1097	381	28	77	474	121
2,3,7,8	4438	975	276	11	39	345	79
OcCDF	141	688	152	20	–	544	93
ΣCl_4–Cl_8	7587	10810	3319	286	392	1095	279
ΣPCDF	7587	12998	4109	676	1062	1126	279
ΣMoCDD	–	–	–	–	–	–	–
ΣDiCDD	–	25	419	–	–	–	–
ΣTrCDD	–	1813	1209	12	–	–	–
ΣTeCDD	114	58813	1848	111	–	–	2
2,3,7,8	–	–	–	–	–	–	–
ΣPeCDD	333	6963	324	168	–	–	–
2,3,7,8	123	16	–	52	–	–	–
ΣHxCDD	2649	6050	371	491	–	–	7
2,3,7,8	1118	144	29	126	–	–	7
ΣHpCDD	61565	3100	1524	391	–	27	43
2,3,7,8	31405	2158	1095	204	–	15	21
OcCDD	270730	14369	26325	145	169	79	56
Cl_4–Cl_8	335091	89295	30419	1306	169	107	108
ΣPCDD	335091	91133	32047	1318	169	107	108
TEQ	852	915	111	31.5	5.2	8.2	7.5

[a] Mo = mono, Di = di, Tr = tri, Te = tetra, Pe = penta, Hx = hexa, Hp = hepta, Oc = octa.

of copper. In the case of 2,4-DCP little direct condensation product, but large amounts of OcCDD were detected. The adsorption efficiency of the filters for less chlorinated PCDD or PCDFs might have been insufficient because of their relatively high vapor pressures.[7] All isomers except MoCDD or MoCDF and DiCDD were generated from MCB. The amounts formed were one order of magnitude less than those of the chlorophenols, because of the necessity of an additional incorporation of oxygen into the molecule. Mainly PCDF isomers were formed by the de novo synthesis in case of Trityl, TRI, and PVC. The direct condensation product of three trichloroethylene molecules is hexachlorobenzene. This might be the reason, why the higher chlorinated PCDD and PCDFs predominated in the Beilstein test.

The generation of PCDD and PCDF during incineration of PVC is still controversial. While on the one hand the influence of PVC on the concentration of PCDD and PCDF in combustion processes is denied,[13] on the other it could be shown that the combustion of PVC in an oxidative atmosphere generates these compounds by interactions of organics with HCl, both of which are generated during the combustion of PVC.[14] In the Beilstein test, PVC serves as a source of organic compounds and chlorine simultaneously, and the copper-catalyzed formation of PCDD and PCDF does occur.

In conclusion, our experiments show that formation of PCDD and PCDF under the conditions of the Beilstein test must be expected. Their generation is due to preformed structures of the starting materials and partly by de novo synthesis. Absolute amounts of 0.4–340 μg PCDD and PCDF and 5–915 ng TEQ per gram of tested compound were obtained. In no case could we detect 2,3,7,8-TCDD itself. This phenomenon is mainly attributed to the substitution pattern of the compounds investigated. The application of 2,4,5-TCP, for example, would very likely have led to a high yield of 2,3,7,8-TeCDD and correspondingly high TEQ, which we tried to avoid in our laboratory.

Based on today's knowledge, the national ADI values (acceptable daily intake) of 2,3,7,8-TeCDD TEQ are set at 1–10 pg per kg body weight, amounting to 70–700 pg for an adult. Depending on the copper target used (e.g., a piece of copper wire or a German Pfennig) between 1 and 5 mg of an unknown compound are usually applied for one Beilstein test. While testing 5 mg 2,4,6-TCP, more than 4500 pg 2,3,7,8-TeCDD TEQ are released. This calculation demonstrates that, depending on the chlorinated compound used, a single Beilstein test can easily exceed the daily tolerance. A long term accumulation, for example, on dust particles, in research and teaching laboratories is likely to occur.

As a conclusion we propose that the Beilstein test for halides should be substituted in a laboratory's daily practice[15] or if a substitution is not practicable, Beilstein tests should be only carried out under a fume hood equipped with a charcoal filter and a UV lamp for decontamination purposes.

Received: October 2, 1991 [Z 4949 IE]
German version: *Angew. Chem.* **1992**, *104*, 477

CAS Registry numbers:
ΣMoCDF, 42934-53-2; ΣDiCDF, 43047-99-0; ΣTrCDF, 43048-00-6; ΣTeCDF, 30402-14-3; 2,3,7,8-TeCDF, 51207-31-9; ΣPeCDF, 30402-15-4; 2,3,7,8-PeCDF, 114464-92-5; ΣHxCDF, 55684-94-1; 2,3,7,8-HxCDF, 114464-90-3; ΣHpCDF, 38998-75-3; 2,3,7,8-HpCDF, 114464-91-4; OcCDF, 39001-02-0; ΣMoCDD, 35656-51-0; ΣDiCDD, 64501-00-4; ΣTrCDD, 69760-96-9; ΣTeCDD, 41903-57-5; 2,3,7,8-TeCDD, 1746-01-6; ΣPeCDD, 36088-22-9; 2,3,7,8-PeCDD, 40321-76-4; ΣHxCDD, 34465-46-8; 2,3,7,8-HxCDD, 132642-81-0; ΣHpCDD, 37871-00-4; 2,3,7,8-HpCDD, 35822-46-9; OcCDD, 3268-87-9; 2,4-dichlorophenol, 120-83-2; 2,4,6-trichlorophenol, 88-06-2; pentachlorophenol, 87-86-5; monochlorobenzene, 108-90-7; triphenylmethyl chloride, 76-83-5; trichloroethylene, 79-01-6; polyvinylchloride, 9002-86-2.

[1] F. Beilstein, *Ber. Dtsch. chem. Ges.* **1872**, *5*, 620–621.
[2] A. Keller, *Nature* **1951**, *167*, 907–908.
[3] O. Hutzinger, H. Fiedler, *VDI Berichte: Dioxin; Eine technische Herausforderung Vol. 634* (Ed.: VDI-Kommission Reinhaltung der Luft), VDI Verlag, Düsseldorf, **1987**, pp. 17–35.
[4] H. Hagenmaier, H. Brunner, R. Haag, M. Kraft, *VDI Berichte DIOXIN*, Düsseldorf, **1987**, pp. 557–584.
[5] L. Stieglitz, H. Vogg, *Formation and Decomposition of Polychlorodibenzodioxins and -furans in Municipal Waste Incineration, Vol. KfK 4379*, Kernforschungszentrum Karlsruhe, **1988**.
[6] K. Jay, L. Stieglitz, *Chemosphere* **1991**, *22*, 987–996.
[7] *Sachstand Dioxine, UBA-Berichte 5/85* (Ed.: Umweltbundesamt), Erich Schmidt Verlag, Berlin, **1985**.
[8] H. Hagenmaier, H. Brunner, R. Haag, H.-J. Kunzendorf, M. Kraft, K. Tichaczek, U. Weberruß, *VDI Berichte DIOXIN*, Düsseldorf, **1987**, pp. 61–89.
[9] Details of the experiments and the analytical procedure applied will be published elsewhere.
[10] E. S. Lahaniatis, D. Bieniek, L. Vollner, F. Korte, *Chemosphere* **1981**, *8*, 935–943.
[11] E. S. Lahaniatis, E. Clausen, D. Bieniek, F. Korte, *Chemosphere* **1985**, *14*, 233–238.
[12] W. Merz, H.-J. Neu, M. Kuck, K. Winkler, S. Gorbach, H. Muffer, *Fresenius Z. Anal. Chem.* **1986**, *325*, 449–460.
[13] K.-G. Malle, *GIT Fachz. Lab.* **1991**, *35*, 757–765.
[14] A. B. J. Oudhuis, P. J. J. Tromp, K. Olie, J. A. Moulijn, *10th international meeting DIOXIN 90, short papers, Combustion, Pulp & Paper, Soil, Remedial action, Destruction, General topics Vol. 3* (Ed.: O. Hutzinger, H. Fiedler), ECO-INFORMA Press, Bayreuth, **1990**, S. 303–306.
[15] The present study was initiated by H. Hopf when during the demonstration of the Beilstein test in an elementary lecture course he noticed that the conditions were "almost ideal" for the formation of dioxins.

Molecular Machines: Molecular Structure of $[(p\text{-Tol}_3P)_{10}Au_{13}Ag_{12}Cl_8](PF_6)$—a Cluster with a Biicosahedral Rotorlike Metal Core and an Unusual Arrangement of Bridging Ligands**

By *Boon K. Teo** and *Hong Zhang*

Further miniaturization poses a major challenge in the development of microelectronics.[1] Progress must rely on the fabrication of components on the nanometer scale ("nanotechnology", molecular machines, molecular computers, etc.[2, 3]). Two approaches for building such devices can be distinguished: the "scaling down" of state-of-the-art microelectronics technology ("top-down" method)[1] and the construction of molecular or supramolecular assemblies with specific functions and properties from smaller building blocks ("bottom-up" method).[4–7] These organized and functional supramolecules and -complexes,[4] constructed either by direct synthesis or by self-assembly, are prototypes of more sophisticated molecular devices.[5] In this regard, the "cluster of clusters" concept proposed by us[8–10] for building large cluster aggregates from smaller clusters is also useful in the design and synthesis of "supraclusters" which may ultimately serve as models for molecular machines of well-defined structures. The driving force for such spontaneous cluster assemblage is the "self-organization self-similarity" principle (fractal) often observed in nature.[8, 11, 12] In this paper, we report a new 25-metal-atom cluster which, along with two recently reported clusters of the series, can be visualized as a molecular rotor with two metal icosahedra sharing a vertex. Hence, this supracluster assemblage may also be termed a "biicosahedral rotor". The ellipsoidal (prolate) metal core measures approximately $1 \times 1 \times 1.5\ nm^3$, suggesting that this series of clusters can be envisaged as a prototype for nanomechanical rotary devices.

Our recent work in the synthesis and structural characterization of a series of phosphine Au–Ag halide clusters gave rise to a new sequence of cluster structures which can be described as vertex-sharing polyicosahedra.[8–10] In these structures, the basic building block is an icosahedron composed of 13 metal atoms (Au_7Ag_6), and the design rule (mode of construction) is vertex-sharing.[8, 9] The first member of this series is the cationic 25-metal-atom cluster **1** (isolated as the PF_6^- salt), which can be considered as two Au-centered Au_7Ag_6 icosahedra sharing one Au atom (nuclearity = $2 \times 13 - 1 = 25$).[10b] The adjacent metal pentagons in **1** are staggered (*s*) with respect to one another, giving rise to three icosahedral (or bicapped pentagonal antiprismatic) cages (*sss* conformation). More recently, the SbF_6^- salt of the cluster cation **2** was shown to have a novel staggered/eclipsed/staggered (*ses*) conformation.[10c] Here, the two middle Ag_5 pentagons are eclipsed (*e*), resulting in a central bicapped pentagonal prismatic cage. The title cluster cation $[(p\text{-Tol}_3P)_{10}Au_{13}Ag_{12}Cl_8]^+$ (**3**), has a new conformation nearly halfway between those observed in **1** and **2**, and an unusual arrangement of the bridging ligands which is distinct from that of **1** or **2**. Larger clusters in this series include the 37-metal-atom dication $[(p\text{-Tol}_3P)_{12}Au_{18}Ag_{19}Br_{11}]^{2+}$[10e] and the 38-metal atom cluster $[(p\text{-Tol}_3P)_{12}Au_{18}Ag_{20}Cl_{14}]$[10f, g] and the 46-metal atom cluster $[(Ph_3P)_{12}Au_{24}Ag_{22}Cl_{10}]$.[10h] In these latter structures, the icosahedral units are linked by (interpenetrating) bicapped pentagonal prisms (as in the *ses* configuration), instead of (interpenetrating) icosahedra (as in the *sss* conformation).[8, 9, 10c] Clusters based on other building blocks and different modes of construction can be found in the literature.[13–19]

$[(p\text{-Tol}_3P)_{10}Au_{13}Ag_{12}Br_8]^+$ **1**

$[(Ph_3P)_{10}Au_{13}Ag_{12}Br_8]^+$ **2**

$[(p\text{-Tol}_3P)_{10}Au_{13}Ag_{12}Cl_8]^+$ **3**

The PF_6^--salt of cluster cation **3** was prepared by the reduction of a mixture of $(p\text{-Tol})_3P$, $HAuCl_4$ and $AgNO_3$, (Au:Ag = 1:1) with $NaBH_4$ in absolute ethanol, followed by the addition of excess NH_4PF_6 in ethanol. The dark red precipitate was filtered and purified by recrystallization from ethanol/hexane. Crystals suitable for X-ray diffraction study were obtained by evaporation of an ethanol/hexane solution of the recrystallized product.[20, 21]

In Figure 1a and b the metal core and the $[P_{10}Au_{13}Ag_{12}Cl_8]$ framework of **3** are depicted. The cluster has ten tri(*p*-tolyl)phosphine and eight chloride ligands. The ten phosphine ligands coordinate to ten peripheral Au atoms

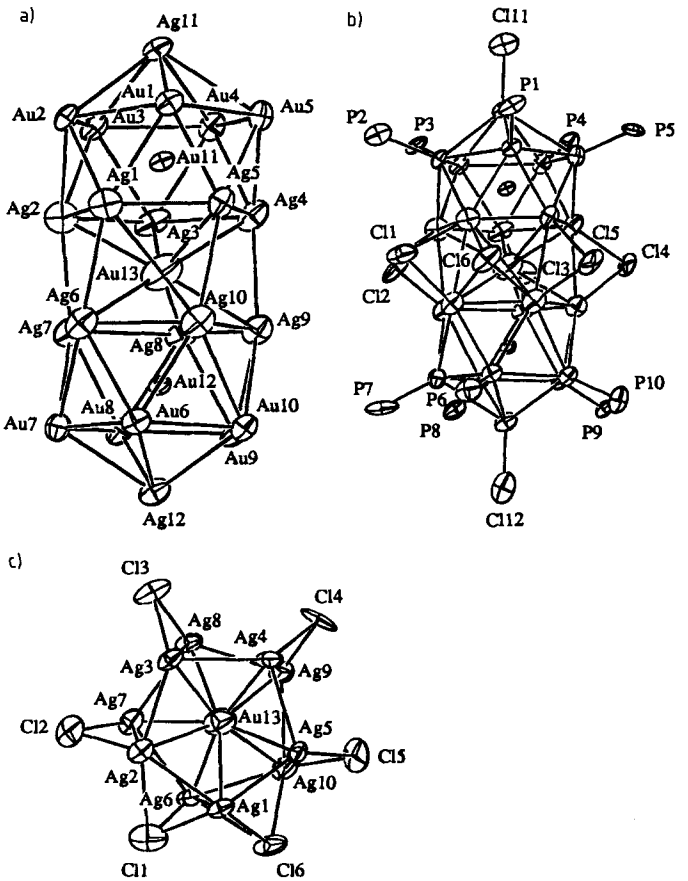

Fig. 1. Crystal structure of **3** (PF_6^- salt). a) Biicosahedral framework of the $Au_{13}Ag_{12}$ core; b) metal–ligand framework ($P_{10}Au_{13}Ag_{12}Cl_8$); c) projection of the two Ag_5 pentagons onto the approximate plane of the six doubly bridging chloride ligands. The cluster has an idealized C_5 axis passing through Ag11, Au11, Au13, Au12, and Ag12. Important distances [Å]: (n = 1–5, m = 6–10): Au11-Au(n) 2.718(av), Au11-Ag(n) 2.804(av), Au11-Ag11 2.86(1), Au11-Au13 2.791(9), Au12-Au(m) 2.719(av), Au12-Ag(m) 2.874(av), Au12-Ag12 2.69(1), Au12-Au13 2.847(9), Au13-Ag(n) 2.91(av), Au13-Ag(m) 2.86(av), Au-P 2.32(av), Ag11-Cl11 2.33(5), Ag12-Cl12, 2.36(5), doubly bridging chloride ligands Cl2-Cl5, Cl-Ag 2.47(av), triply bridging chloride ligands, Cl1-Ag1 2.62(6), Cl1-Ag2 2.93(5), Cl1-Ag6 2.51(5), Cl6-Ag1 2.48(4), Cl6-Ag6 3.07(5), Cl6-Ag10 2.78(5). The six chloride ligands form a distorted hexagon with "nonbonding" (crystallographically independent) distances of Cl6···Cl1 3.66, Cl6···Cl5 3.78, Cl1···Cl2 4.01, Cl2···Cl3 4.93, Cl3···Cl4 5.03, Cl4···Cl5 4.31.

[*] Prof. B. K. Teo, H. Zhang
Department of Chemistry, University of Illinois at Chicago
Chicago, IL 60680 (USA)

[**] This work was supported by a grant from the U.S. National Science Foundation (CHE 9115278). We would also like to thank Prof. P. Pyykkö, Helsinki, for pointing out the importance of relativistic effects.

in a radial fashion. As for the eight chloride ligands, two are terminal (Cl11 and Cl12), while the remaining six are bridging (Cl1-Cl6) (Fig. 1c).

The most interesting feature of the structure of **3** is that the metal framework has neither an *ses* nor an *sss* conformation (cf. Fig. 1c). In fact, it is nearly halfway between these two extremes. As a result, the metal framework has an idealized D_5 symmetry (instead of D_{5d} for *sss* as in **1**, or D_{5h} for *ses* as in **2**). The projection of the four pentagons of metal atoms (two outer Au_5 rings and two inner Ag_5 rings) onto the plane of the bridging ligands gives rise to a ring of 20 metal atoms more or less evenly distributed around the circle (Fig. 2). It is conceivable that in solution, the two metal icosahedra are relatively free to rotate about the shared vertex (Au13),[22] and that the observed solid-state structure is a snapshot of one of many energy minima.

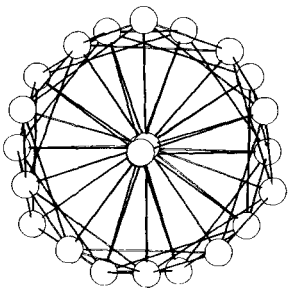

Fig. 2. The projection of the four pentagons of metal atoms in **3** (see Fig. 1a) onto the plane of the bridging ligands.

The arrangement of the six bridging chloride ligands (Cl1–Cl6) which connect the two Ag_5 pentagons (Ag1–Ag5 and Ag6–Ag10) is also rather unusual. Since pentagonal symmetry is incommensurate with the hexagonal net, we expect significant distortions in the arrangement of the bridging ligands. Indeed, as shown in Figure 1c the six bridging ligands can be categorized into two groups: four doubly bridging (Cl2–Cl5) and two triply bridging (Cl1, Cl6) ligands. The coordination of the doubly bridging ligands is more or less symmetrical whereas that of the triply bridging ligands is highly asymmetrical. For example, Cl1 has one long (2.93(5) Å) and two short (2.51(5) and 2.62(6) Å) Cl–Ag distances. The opposite is true for Cl6, which has one short (2.48(4) Å) and two long (2.78(5) and 3.07(5) Å) Cl–Ag distances.

There are several empirical rules for the Au–Ag superclusters that we have structurally characterized: 1. The interstitial or "bulk" atoms in the icosahedral cages are gold atoms; 2. The shared vertices (bicapped pentagonal prismatic cages) are also gold atoms; 3. The phosphine ligands are attached to surface gold atoms; 4. The halide ligands are bonded to silver atoms. These observations can be explained by the fact that gold is substantially more electronegative than silver (2.54 for Au, 1.93 for Ag). This disparity in electronegativity is related to relativistic effects.[23] The more electronegative gold atoms tend to prefer sites of high electron density, including the centers of the icosahedra or the shared vertices (which are centers of the bicapped pentagonal prisms). The more electron-donating phosphine ligands prefer more electronegative Au atoms, whereas the more electron-withdrawing halide ligands prefer the more electropositive Ag atoms.

This metal framework with a conformation halfway between *ses* and *sss* provides strong evidence for the concept of a "cluster of clusters" as applied to this series of vertex-sharing icosahedral Au–Ag superclusters. Further structural evidence comes from the separations between the pentagons: the intraicosahedra Au(1–5)–Ag(1–5) and Au(6–10)–Ag(6–10) interplanar distances of 2.40 Å and 2.52 Å are 0.5 Å shorter than the intericosahedra (inner) Ag(1–5)–Ag(6–10) interplanar distance of 2.91 Å. Moreover, the average intraicosahedral metal–metal distances of 2.772 Å (Au11-centered) and of 2.792 Å (Au12-centered) in **3** are significantly shorter (ca. 0.1 Å) than the average intericosahedral distances of 2.872 Å (Au13-centered). These observations suggest that intraicosahedral bondings are stronger than intericosahedral bonding, thereby reinforcing the cluster of clusters concept in which the individual icosahedron serves as a building block.

Received: October 2, 1991 [Z 4951 IE]
German version: *Angew. Chem.* **1992**, *104*, 447

[1] *Physics and Technology of Submicron Structures* (Eds.: H. Heinrich, G. Bauer, F. Kuchar), Springer, Berlin, **1988**.
[2] a) H. I. Smith, H. G. Craighead, *Phys. Today* **1990**, *43*(2), 24; b) J. N. Randall, M. A. Reed, G. A. Frazier, *J. Vac. Sci. Technol. B* **1989**, *7*, 1398.
[3] a) G. D. Stucky, N. Herron, Y. Wang, M. Eddy, D. Cox, K. Moller, T. Bein, *J. Am. Chem. Soc.* **1989**, *111*, 530; b) G. D. Stucky, J. E. MacDougall, H. Eckert, N. Herron, Y. Wang, K. Moller, T. Bein, *ibid.* **1989**, *111*, 8006.
[4] a) J.-M. Lehn, *Angew. Chem.* **1990**, *102*, 1347; *Angew. Chem. Int. Ed. Engl.* **1990**, *29*, 1304; b) *Pure Appl. Chem.* **1978**, *50*, 871; c) *Angew. Chem.* **1988**, *100*, 91; *Angew. Chem. Int. Ed. Engl.* **1988**, *27*, 89.
[5] a) F. H. Kohnke, J. P. Mathias, J. F. Stoddart *Angew. Chem. Adv. Mater.* **1989**, *101*, 1129; *Angew. Chem. Int. Ed. Engl. Adv. Mater.* **1989**, *28*, 1103; b) P. L. Anelli, N. Spencer, J. F. Stoddart *J. Am. Chem. Soc.* **1991**, *113*, 5131; R. R. Ashton, C. L. Brown, E. J. T. Crystal, K. P. Parry, M. Pietraskiewicz, N. Spencer, J. F. Stoddart, *Angew. Chem.* **1991**, *102*, 1058; *Angew. Chem. Int. Ed. Engl.* **1991**, *30*, 1042.
[6] J. S. Lindsey, *New J. Chem.* **1991**, *15*, 153.
[7] M. P. Byrn, C. J. Curtis, I. Goldberg, Y. Hsiou, S. I. Khan, P. A. Sawin, S. K. Tendick, C. E. Strouse, *J. Am. Chem. Soc.* **1991**, *113*, 6549.
[8] B. K. Teo, H. Zhang, *Proc. Natl. Acad. Sci. USA* **1991**, *88*, 5067, and references cited therein.
[9] Reviews: a) B. K. Teo, H. Zhang, *J. Cluster Sci.* **1990**, *1*, 223; b) *ibid.* **1990**, *1*, 155; c) *Polyhedron*, **1990**, *9*, 1985; d) B. K. Teo, *ibid.* **1988**, *7*, 2317.
[10] a) B. K. Teo, K. Keating, *J. Am. Chem. Soc.* **1984**, *106*, 2224; b) B. K. Teo, H. Zhang, X. Shi, *Inorg. Chem.* **1990**, *29*, 2083; c) B. K. Teo, X. Shi, H. Zhang, *J. Am. Chem. Soc.* **1991**, *113*, 4329; d) B. K. Teo, H. Zhang, *Inorg. Chem.* **1991**, *30*, 3115; e) B. K. Teo, M. Hong, H. Zhang, D. Huang, *Angew. Chem.* **1987**, *99*, 943; *Angew. Chem. Int. Ed. Engl.* **1987**, *26*, 897; f) B. K. Teo, M. Hong, H. Zhang, D. Huang, X. Shi *J. Chem. Soc. Chem. Commun.* **1988**, 204; g) B. K. Teo, H. Zhang, X. Shi *J. Am. Chem. Soc.* **1990**, *112*, 8552; h) B. K. Teo, H. Zhang *Inorg. Chim. Acta* **1988**, *144*, 173; i) *Inorg. Chem.* **1988**, *27*, 414.
[11] B. B. Mandelbrot *The Fractal Geometry of Nature*, Freeman, New York, **1983**.
[12] H. O. Peitgen, P. Richter, *The Beauty of Fractals*, Springer, Heidelberg, **1986**.
[13] A. J. Whoolery, L. F. Dahl, *J. Am. Chem. Soc.* **1991**, *13*, 6683.
[14] J.-F. You, B. S. Snyder, R. H. Holm *J. Am. Chem. Soc.* **1988**, *110*, 6589.
[15] a) R. D. Adams, Z. Dawoodi, D. F. Forest, B. E. Segmuller, *J. Am. Chem. Soc.* **1983**, *105*, 831; b) P. D. Williams, M. D. Curtis, D. N. Duffey, W. M. Butler, *Organometallics* **1983**, *2*, 165; c) B. F. G. Johnson, *Philos. Trans. R. Soc. London, Ser. A* **1982**, *308*, 5.
[16] a) C. M. T. Hayward, J. R. Shapley, M. R. Churchill, C. Bueno, A. L. Rheingold, *J. Am. Chem. Soc.* **1982**, *104*, 7347; b) S. Martinengo, A. Fumagalli, R. Bonfichi, G. Ciani, A. Sironi *J. Chem. Soc., Chem. Commun.* **1982**, 825; c) V. G. Albano, P. L. Bellon *J. Organomet. Chem.* **1969**, *19*, 405; d) R. D. Pergola, F. Demartin, L. Garlaschelli, M. Manassero, S. Martinengo, M. Sansoni, *Inorg. Chem.* **1987**, *26*, 3487; e) A. Fumagalli, S. Martinengo, G. Ciani, A. Sironi, *J. Chem. Soc.; Chem. Commun.* **1983**, 453.
[17] S. R. Drake, K. Henrick, B. F. G. Johnson, J. Lewis, M. McPartlin, J. Morris *J. Chem. Soc., Chem. Commun* **1986**, 928.
[18] a) E. G. Mednikov, N. K. Eremenko, *J. Organomet. Chem.* **1986**, *C35–C37*, 301; b) E. G. Mednikov, N. K. Eremenko, Yu. L. Slovokhotov, Yu. T. Struchkov, *J. Mendeleev Chem. Soc. (Russian)*, cited in [4a]; c) E. G. Mednikov, N. K. Eremenko, Yu. L. Slovokhotov, Yu. T. Struchkov, S. P. Gubin, *J. Organomet. Chem.* **1983**, *258*, 247.
[19] For reviews on metal clusters see, for example, a) K. Kharas, L. Dahl *Adv. Chem. Phys.* **1988**, *70*, 1; b) P. Chini *Gazz. Chim. Ital.* **1979**, *109*, 225; c) *J. Organomet. Chem.* **1980**, *200*, 37; d) P. Chini, G. Longoni, V. G. Albano

Adv. Organomet. Chem. **1976**, *14*, 285; e) *Transition Metal Clusters* (Ed.: B. F. G. Johnson), Wiley-Interscience, Chichester, England, **1980**; f) B. F. G. Johnson, R. E. Benfield *Top. Inorg. Organomet. Stereochem.* (Ed.: G. Geoffroy), **1981**, g) D. Fenske, J. Ohmer, J. Hachgenei, K. Merzweiler *Angew. Chem.* **1988**, *100*, 1300; *Angew. Chem. Int. Ed. Engl.* **1988**, *27*, 1277; h) G. Schmid *Struct. Bonding (Berlin)* **1985**, *62*, 51.

[20] Single crystal X-ray diffraction data were collected with an Enraf-Nonius diffractometer ($Mo_{K\alpha}$ radiation). $[(p\text{-}Tol_3P)_{10}Au_{13}Ag_{12}Cl_8](PF_6)\cdot n$EtOH: monoclinic $P2_1$, $a = 20.410(1)$, $b = 20.767(3)$, $c = 28.182(3)$ Å, $\gamma = 91.71(4)$; $V = 11939.9(4)$ Å^3, $Z = 2$. The tolyl groups and the PF_6^- anion were refined as rigid bodies (see [10g] for details). Anisotropic (heavy atoms)-isotropic (carbon atoms) refinement gave $R_1 = 0.112$ for 6706 independent reflections ($2\theta \leq 46°$) with $I > 3\sigma$.

[21] Further details of the crystal structure are available on request from the Fachinformationszentrum Karlsruhe, Gesellschaft für wissenschaftlich-technische Information mbH in D-W-7514 Eggenstein-Leopoldshafen 2, on quoting the following number CSD-56021, the names of the authors, and the journal citation.

[22] It is interesting to note that the isotropic thermal parameters of all the gold atoms (Au1–Au12) fall within the narrow range of $B = 2$–3 Å^2, with the exception of the shared vertex (Au13) which has a B value of 6.6(2) Å^2. This latter value may signify a greater thermal motion and/or site disorder (split peaks) of the shared vertex. For comparation, the B values of the silver atoms fall within the range of 3–5 Å^2.

[23] a) P. Pyykko, J. Desclaux, *Acc. Chem. Res.* **1979**, *12*, 276; b) K. S. Pitzer *ibid.* **1979**, *12*, 271.

Tris(cyclopentanolato)oxovanadium(v): a Model for the Transition State of Enzymatic Phosphoester Cleavage**

By *Frank Hillerns, Falk Olbrich, Ulrich Behrens,* and *Dieter Rehder**

Dedicated to Professor Reinhard Nast on the occasion of his 80th birthday

(Alkoxo)oxovanadium complexes ("vanadate esters") have come under general scrutiny lately, on one hand because of their potential in generating thin metal-oxide and -carbide layers by gas-phase deposition,[1] and on the other because of the biological importance of vanadium ester compounds. The ester-like bond in vanadate(v) ($H_2VO_4^-$) is discussed, for example, in connection with the vanadate-dependent haloperoxidases from brown marine algae[2] and with the interaction of vanadate with phosphate-metabolizing enzymes and their substrates.[3] Some of these enzymes are inhibited by vanadium—the inhibition of ribonuclease A[4] and T_1,[5] for example, have been well studied. The cleavage (or formation) of the phosphoester bond in RNA proceeds via a pentavalent, trigonal-bipyramidal intermediate.[6] Enzymes take up vanadate esters as substrate in competition to phosphate esters,[3] and their function is thereby blocked. Such vanadate–enzyme complexes, which are stable analogues of the transition state of the phosphorylation reaction, were detected in systematic ^{51}V NMR investigations,[7] but could not be isolated. We have thus conducted model studies with cyclopentanol[8] in order to characterize them better. We show that vanadate esters, unlike phosphate esters, can be pentacoordinate.

In aqueous medium vanadate(v) forms esters with cyclopentanol (ROH) that can be identified by ^{51}V NMR spectroscopy. At physiological pH, the major component of the products is an ester which has the composition $[HVO_3(OR)]^-$ and a formation constant of $K = 0.13(2)$ M^{-1}.[9]

In nonaqueous systems in which the competitive condensation reaction of monovanadate to form oligovanadates does not take place, the formation tendency for vanadate esters is clearly more pronounced than that of the analogous phosphate esters. The ester **1** formed from $VOCl_3$ and *cyclo*-C_5H_9OH[10] shows one signal in the ^{51}V NMR spectrum at concentrations over 100 mM ($\delta = -616$); at lower concentra-

$[VO(cyclo\text{-}C_5H_9O)_3]$ **1**

tions a second signal appears ($\delta = -623$), which increases in intensity as the total concentration decreases (Fig. 1). We

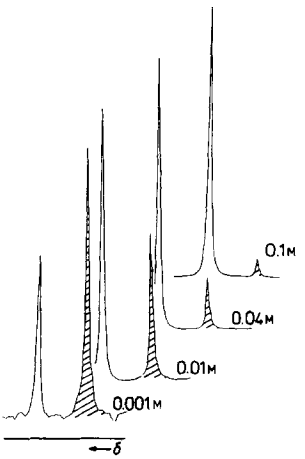

Fig. 1. ^{51}V NMR spectra (94.7 MHz) of $[VO(cyclo\text{-}C_5H_9O)_3]$ (**1**) in $CDCl_3$, showing the position of the equilibrium described in Equation (a) for four concentrations c. The signal at high magnetic field ($\delta(^{51}V) = -623$, hatched) corresponds to the monomer, that at $\delta = -616$ to the dimer. A 2D EXSY (*ex*change *s*pectroscop*y*) experiment shows that the chemical exchange formulated in Equation (a) actually takes place.

have already observed concentration and temperature dependence of $\delta(^{51}V)$ for other vanadyl esters and concluded that at least two species participate in an exchange equilibrium [Eq. (a)].[8b, 11] When R = *cyclo*-C_5H_9 the exchange is so slow even at room temperature that monomer and oligomer can be detected simultaneously.[11] In the concentration

$$n[VO(OR)_3] \rightleftharpoons [\{VO(OR)_3\}_n] \quad \text{(a)}$$

range c of 0.001 to 0.08 M for the vanadyl ester **1**, $n \approx 2$ [Eq. (a)], and the dimerization constant $K = [\text{dimer}]/[\text{monomer}]^2 = 870(50)$ M^{-1}. An X-ray structure analysis of the dimer of **1** showed how the dimerization took place. $[\{VO(cyclo\text{-}C_5H_9O)_3\}_2]$[12] comprises two monomeric units bridged by two alkoxide oxygen atoms (Fig. 2). In each of these units vanadium is in the center of a distorted trigonal bipyramid. The oxo ligand and the bridging alkoxo oxygen atom of the adjacent unit form the apexes. The vanadium atom lies 35 pm above the plane spanned by the three oxygen atoms of the alkoxo ligands (all-*cis* configuration). The distance from the V atom to the bridging O atom (O2) of 183.5(4) pm is distinctly longer than the distances to O3 and O4 [176.2(3) and 176.3(6) pm]. Even longer [229.6(3) pm] is the distance from O2 to the symmetry-related VA of the second monomeric unit of the dimer, which is only a little shorter than these bond lengths in multinuclear oxo–vanadi-

[*] Prof. Dr. D. Rehder, Dipl.-Chem. F. Hillerns, Dipl.-Chem. F. Olbrich, Prof. Dr. U. Behrens
Institut für Anorganische und Angewandte Chemie der Universität
Martin-Luther-King-Platz 6, D-W-2000 Hamburg 13 (FRG)

[**] This work was supported by the Deutsche Forschungsgemeinschaft and the Fonds der Chemischen Industrie.

um compounds with unsymmetric oxygen bridges.[13] The dimer of **1** has C_2 symmetry in the solid state, but C_{2h} symmetry in solution, as deduced from ^1H and ^{13}C NMR spectra of concentrated solutions that only contain the dimer.[14] The mirror plane passes through V, O2, VA, and O2A.

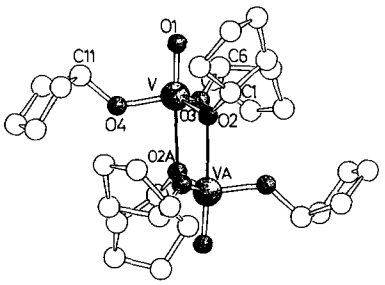

Fig. 2. SCHAKAL representation of $[\{VO(cyclo\text{-}C_5H_9O)_3\}_2]$. Selected bond lengths [pm] and angles [°]: V-O1 159.5(3), V-O2 183.5(4), V-O3 176.2(3), V-O4 176.3(6), V-O2A 229.6(3), O2-C1 142.0(7), O3-C6 143.7(6), O4-C11 144.5(7), V···VA 335.3(2); O1-V-O2 101.0(2), O1-V-O3 101.3(2), O1-V-O4 101.5(2), O1-V-O2A 172.9(2), O2-V-O3 117.5(2), O2-V-O4 118.3(2), O3-V-O4 113.1(2), O2-V-O2A 71.9(2), V-O2-C1 131.5(3), V-O3-C6 130.4(3), V-O4-C11 129.7(4), V-O2-VA 108.0(2).

The following aspects are interesting with reference to the model character of $[\{VO(cyclo\text{-}C_5H_9O)_3\}_2]$ for biological systems with vanadium as coordination center. 1) The short V–O distances [176.3(6) and 176.2(3) pm] are comparable with those found for V–O (apart from the usual single-bond lengths of about 195 pm) in vanadate-dependent peroxidase (172 pm),[2a] suggesting that for the binding of vanadium to this enzyme, serine possibly plays a role. 2) V^V strives for a trigonal bipyramidal coordination sphere in the presence of alkoxo ligands, as discussed for the transition state for the enzymatic phosphoester cleavage; (alkoxo)oxovanadium compounds are therefore analogues of this transition state. 3) This impression is supported by the two different V–OR bond lengths in our model (176.3 and 183.5 pm); a similar asymmetry is also found in the complexes formed from ribonuclease A and uridine and vanadate, in which the V–O distances to the oxygen functions of ribose in the 2′- and 3′-position are given as 170 and 189 pm .[15] 4) The distinct tendency—also in solution—to dimerization is relevant in connection with more recent observations that not only monovanadate but also divanadate (among others) can inhibit phosphorylation enzymes.[16]

Received: October 8, 1991 [Z4956IE]
German version: *Angew. Chem.* **1992**, *104*, 479

CAS-Registry numbers:
$[VO(cyclo\text{-}C_5H_9O)_3]$, 134939-18-7; $[\{VO(cyclo\text{-}C_5H_9O)_3\}_2]$, 139041-31-9.

[1] D. C. Bradley, *Chem. Rev.* **1989**, *89*, 1317.
[2] The participation of side chains of the protein matrix containing OH functions is probable a) in the active site itself for the coordination of vanadium (deduced from EXAFS: J. M. Arber, E. de Boer, C. D. Garner, S. S. Hasnain, R. Wever, *Biochemistry* **1989**, *28*, 7968) and b) on the enzyme surface for the binding of vanadate (deduced from ^{51}V NMR: D. Rehder, H. Holst, W. Priebsch, H. Vilter, *J. Inorg. Biochem.* **1991**, *41*, 171).
[3] M. J. Gresser, A. S. Tracey in *Vanadium in Biological systems* (Ed.: N. D. Chasteen), Kluwer, Amsterdam, **1990**.
[4] B. Borah, C. W. Chen, W. Egan, M. Miller, A. Wlodawer, J. S. Cohen, *Biochemistry* **1985**, *24*, 2058.
[5] D. Rehder, H. Holst, R. Quaas, W. Hinrichs, U. Hahn, W. Saenger, *J. Inorg. Biochem.* **1989**, *37*, 141.
[6] U. Heinemann, W. Saenger, *J. Biomolecul. Struct. Dyn.* **1983**, *1*, 523.
[7] a) A. S. Tracey, J. S. Jaswal, M. J. Gresser, D. Rehder, *Inorg. Chem.* **1990**, *29*, 4283; b) J. Richter, D. Rehder, *Z. Naturforsch. B* **1991**, *46*, 1613. The major component is a 2:2 complex (the complex formation constant at pH 7.9 is 2.2×10^7 M^{-3}); on the basis of the characteristic chemical shift at $\delta(^{51}V) = -523$ (relative to $VOCl_3$), a trigonal bipyramidal configuration at vanadium was deduced.
[8] Structural information for the following (alkoxo)oxovanadium compounds is known: a) $[VO(OMe)_3]_\infty$: C. N. Caughlan, H. M. Smith, K. Watenpaugh, *Inorg. Chem.* **1966**, *12*, 2131; b) $[\{VO(OCH_2CH_2Cl)_3\}_2]$: W. Priebsch, D. Rehder, *Inorg. Chem.* **1990**, *29*, 3013; c) $[VOCl(pin)]_2$ [pin = pinacolate(2-)]: D. C. Crans, R. A. Felty, M. M. Miller, *J. Am. Chem. Soc.* **1991**, *113*, 265.
[9] $\delta(^{51}V) = -560$ (relative to $VOCl_3$) for $HVO_3(OR)^-$ (ROH = cyclopentanol) in D_2O/acetone 3/1 at pD 7.2 and an ionic strength of $I = 1$ M (NaCl). For the determination of the formation constant K from ^{51}V NMR spectra and for the formation constants of other esters derived from vanadate and divanadate, see for example, A. S. Tracey, M. J. Gresser, *Can. J. Chem.* **1988**, *66*, 2570.
[10] F. Hillerns, D. Rehder, *Chem. Ber.* **1991**, *124*, 2249. The freshly prepared compound is a colorless liquid at room temperature; the freezing point is −10 °C. Suitable crystals were obtained by slow cooling to −25 °C. In solution and at room temperature, slow decomposition takes place.
[11] a) K. Paulsen, D. Rehder, D. Thoennes, *Z. Naturforsch. B* **1978**, *33*, 834; b) K. Paulsen, D. Rehder, *Z. Naturforsch. A* **1982**, *37*, 139.
[12] $C_{30}H_{54}O_8V_2$; space group $P3c1$ (no. 165); $a = 1840.5(3)$, $c = 1657.3(3)$ pm, $V = 4862(1) \times 10^6$ pm^3, $\mu = 52.5$ cm^{-1}, $Z = 6$, $\varrho_{ber} = 1.321$ g cm^{-3}; $R = 0.068$, $R_w = 0.050$, 1989 significant reflections, $F_0 > 6\sigma(F_0)$; number of the refined parameters = 182; residual electron density: maximum 0.72, minimum −0.67 e Å^{-1}. The measurement was performed at −100 °C on an Enraf-Nonius CAD4 instrument with $Cu_{K\alpha}$ radiation (graphite monochromator); angular range $2.25 < \theta < 76.5$. Hydrogen atoms were calculated in idealized positions. An absorption correction was applied with the program DIFABS (N. Walker, D. Stuart, *Acta Crystallogr. Sect. A* **1983**, *39*, 158). Further details of the crystal structure investigation may be obtained from the Fachinformationszentrum Karlsruhe, Gesellschaft für wissenschaftlich-technische Information mbH, D-W-7514 Eggenstein-Leopoldshafen 2 (FRG) on quoting the depository number CSD-55997, the names of the authors, and the journal citation.
[13] See for example a) $[V_3O_2(\mu_3\text{-}O)(thf)(O_2CPh)_6]$: F. A. Cotton, G. E. Lewis, G. N. Mott, *Inorg. Chem.* **1982**, *21*, 3127; b) $[V_6O_4(\mu_3\text{-}O)_2(\mu\text{-}O)_4(O_2CPh)_9]$: D. Rehder, W. Priebsch, M. von Oeynhausen, *Angew. Chem.* **1989**, *101*, 1295; *Angew. Chem. Int. Ed. Engl.* **1989**, *28*, 1221.
[14] Only one environment for $cyclo\text{-}C_5H_9$ was observed. ^1H NMR (250 MHz, CD_3Cl): $\delta = 5.53$ (tt, $J = 5.2$ and 3.4 Hz, 1H; α-C), 1.89 (m, 4H; β-C), 1.77 and 1.58 (m, 4H; γ-C). ^{13}C NMR (62.8 MHz, $CDCl_3$): $\delta = 105.3$ (α-C), 36.27 (Cβ), 23.24 (Cγ).
[15] G. Petsko, D. Ringe, cited in [8c], Table 3 as personal communication.
[16] a) D. C. Crans, C. M. Simone, A. K. Saha, R. H. Glew, *Biochem. Biophys. Res. Commun.* **1989**, *165*, 246; b) D. C. Crans, S. M. Schelble, *Biochemistry* **1990**, *29*, 6698.

Oligo(9,10-anthrylenes), Organic Compounds with Stable High-Spin States**

By *Martin Baumgarten, Uwe Müller, Angelika Bohnen,* and *Klaus Müllen**

Stable high-spin states play a central role in the search for organic solids possessing ferromagnetic properties.[1] The "uncoupling" of individual spins has usually been sought in π-conjugated compounds with so-called non-Kekulé structures.[2] The ionic derivatives of oligo(9,10-anthrylenes) **1**[3] ought to be able to form high-spin states, if only because of the almost orthogonal configuration of their individual anthracene components. By theoretical studies, we have been able to show that ferromagnetic coupling is possible in the triplet dianion of 9,9′-bianthryl **2**.[4, 5]

Although the chemical and physical properties of **2** have been thoroughly described,[5, 6] higher oligoanthrylenes **1**, $m > 0$, have not previously been studied. Here we report the

[*] Prof. Dr K. Müllen, Dr M. Baumgarten, Dipl.-Chem. U. Müller, Dipl.-Chem. A. Bohnen
Max-Planck-Institut für Polymerforschung,
Ackermannweg 10, D-W-6500 Mainz (FRG)

[**] This study was supported by the Federal Ministry for Research and Technology.

synthesis of defined, soluble oligomers up to the heptamer (**3a**, **3b**, **4**, **5**). Cyclovoltammetric and ESR characterization of the title compounds provides evidence for their extreme redox activity and, above all, for the possibility of forming high-spin states.

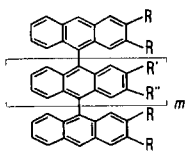

1: R = R' = R'' = H
2: R = R' = R'' = H, $m = 0$
3a: R = R'' = H, R' = $C(CH_3)_2CH_2CH_3$, $m = 1$
3b: R = H, R' = R'' = n-C_6H_{13}, $m = 1$
4: R = n-C_6H_{13}, R' = R'' = H, $m = 2$

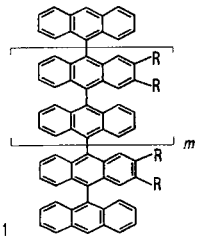

5: R = n-C_6H_{13}, $m = 2$

The starting materials of the trimers **3a**, **b**, are the anthraquinones **6a** or **6b**, alkyl-substituted in the 2- or the 2- and 3-positions, which can easily be prepared by standard procedures.[7, 8] **6a** and **6b** react with 9-lithioanthracene **8a** (2 equiv. diethyl ether, room temperature, 24h) to yield the coupling products **7a** and **7b** respectively. These are then treated with hydrogen iodide and hypophosphorous acid (glacial acetic acid, reflux, 3h), to afford the trianthrylenes **3a** (50%) and **3b** (60%) respectively, after chromatography over silica gel (Table 1). The tetramer **4** is formed by reaction of the 10,10'-bianthronylidene **9** with the lithium compound **8b**[9] (diethyl ether, room temperature, 24h), followed by aromatization with hydrogen iodide/hypophosphorous acid and chromatographic purification (31% yield; Table 1). In contrast to the coupling method described, the palladium-catalyzed reaction of arylboronic acids with arylhalogenides,[10] which is often useful for direct aryl-aryl couplings, yields only dimeric products in this case.

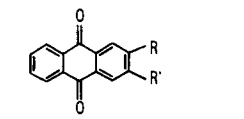

6a: R = $C(CH_3)_2CH_2CH_3$, R' = H
6b: R = R' = n-C_6H_{13}

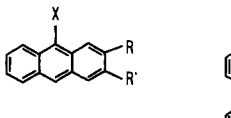

8a: R = R' = H, X = Li
8b: R = R' = n-C_6H_{13}, X = Li
8c: R = R' = n-C_6H_{13}, X = H
8d: R = R' = n-C_6H_{13}, X = Br

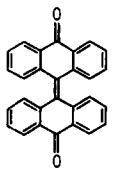

9

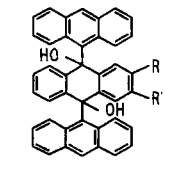

7a: R = $C(CH_3)_2CH_2CH_3$, R' = H
7b: R = R' = n-C_6H_{13}

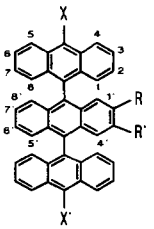

3a: R = $C(CH_3)_2CH_2CH_3$, R' = H, X = X' = H
3b: R = R' = n-C_6H_{13}, X = X' = H
3c: R = R' = n-C_6H_{13}, X = Br, X' = H
3d: R = R' = n-C_6H_{13}, X = X' = Br
3e: R = R' = n-C_6H_{13}, X = Li, X' = H

Bromination of **3b** affords the bromo derivatives **3c** (1 equiv. bromine, carbon tetrachloride, 273 K, 2h) and **3d** (2 equiv. bromine, carbon tetrachloride, 273 K, 3h), and

Table 1. Selected physical and spectroscopic data for **3a**–**3d**, **4**, and **5** [a].

3a: MS (EI 70 eV): m/z 600.3 (M^+); ^{1}H NMR: δ = 8.7 (s, 2H, H-10), 8.22 (m, 4H, H-4,5), 7.5 (m, 4H, H-3,6), 7.35-7.0 (m, 15H, H-1,2,7,8,1',3'-8'), 1.3 (q, 2H, CH_2), 0.85 (s, 6H, CH_3), 0.35 (t, 3H, CH_3).

3b: MS (EI 70 eV): m/z 698.2 (M^+); ^{1}H NMR: δ = 8.74 (s, 2H, H-10), 8.23 (m, 4H, H-4,5), 7.53 (m, 4H, H-3,6), 7.46-7.24 (m, 8H, H-1,2,7,8), 7,11 (m, 4H, H-5'-8'), 6.95 (s, 2H, H-1',4'), 2.35 (t, 4H, CH_2), 1.25-0.8 (m, 16H, CH_2), 0.71 (t, 6H, CH_3).

3c: MS (EI 70 eV): m/z 777.3 (M^+); ^{1}H NMR: δ = 8.76 (m, 3H), 8.24 (m, 2H), 7.67 (m, 2H), 7.57 (m, 2H), 7.5-7.11 (m, 12H), 6.96 (s, 1H), 6.93 (s, 1H), 2.34 (m, 4H, CH_2), 1.57-0.8 (m, 16H, CH_2), 0.73 (m, 6H, CH_3).

3d: MS (EI 70 eV): m/z 856.5 (M^+); ^{1}H NMR: δ = 8.75 (m, 4H, H-4,5), 7.68 (m, 4H, H-3,6), 7.38 (m, 8H, H-1,2,7,8), 7.08 (m, 4H, H-5',6',7',8'), 6.94 (s, 2H, H-1',4'), 2.36 (t, 4H, CH_2), 1.24-0.84 (m, 16H, CH_2), 0.72 (t, 6H, CH_3).

4: MS (FD 4 kV): m/z 1043.8 (M^+); ^{1}H NMR: δ = 8.87 (s, 2H, H-10), 8.21 (m, 2H, H-5), 7.99 (s, 2H, H-4), 7.6-7.15 (m, 22H, H-6-8, 1'-8'), 7.01 (s, 2H, H-1), 2.83 (t, 4H, CH_2), 2.61 (t, 4H, CH_2), 1.8-0.94 (m, 38H, alkyl), 0.67 (t, 6H, CH_3).

5: MS (FD 4 kV): m/z 1739.4 (M^+).

[a] All NMR spectra were measured in $C_2D_2Cl_4$ at 200 MHz and room temperature. Numbering of the anthracene rings follows IUPAC nomenclature rules.

opens a simple route to higher homologues of **1**. Thus, **3c** can be quantitatively converted to the lithio derivative **3e**, and then coupled to **6b** to yield the heptamer **5**, in a reaction sequence analogous to the trimer syntheses. Compound **5** can be isolated by volume exclusion chromatography (18%).

The unusual redox properties of the oligo(9,10-anthrylenes) are demonstrated by cyclovoltammetric studies (Table 2). **3a** can be reversibly converted both into the

Table 2. Redox potentials of the oligoanthrylenes **2** [12], **3a**, **3b**, and **4**, determined by cyclic voltammetry [a].

	$E^1_{1/2}$	$E^2_{1/2}$	$E^3_{1/2}$	$E^4_{1/2}$	$E^5_{1/2}$	$E^6_{1/2}$
Oxidation						
2	1.15 [b]	1.44 [b]				
3a	1.16 [c]	1.33 [c]	1.57 [c]			
3b	1.04	1.33	1.45	2.0		
4	1.0	1.05	1.46	1.59	1.67	1.95
Reduction						
2	−2.17	−2.39	−2.92 [d]	−3.04 [d]		
3a	−2.16	−2.26	−2.68	−2.77 [d]	−2.86 [d]	
3b [f]	−2.15	−2.25				
4	−2.14	−2.29	−2.45	−2.76 [e]	−2.76 [e]	

[a] Oxidation in CH_2Cl_2, reduction in THF; conducting salt: n-Bu_4NPF_6, gold working-electrode, silver wire as quasireference, redox potentials as reversible pairs in V vs a saturated calomel electrode (ferrocene standard 310 mV), scan speed v = 100 mVs^{-1}, T = 273 K. [b] v = 2 Vs^{-1}, lower scan speed led to absorption on the electrode. [c] v = 1 Vs^{-1}, analogous to [b]. [d] electrochemically irreversible, Ecp-output. [e] ΔE < 80 mV. [f] Absorption on the electrode prevented the detection of highly charged species.

mono-, di-, and tricationic forms, and into the mono-, di-, and trianions. For **3b** a tetracation can also be obtained, and for **4** a reversible redox sequence can be detected which proceeds in eleven successive steps from the pentaanion to the hexacation (Fig. 1). All of the first reduction and oxidation potentials are virtually independent of the number of replications, thus excluding the possibility of significant conjugative interactions between the individual subunits. The minor differences between the first reduction potentials of **3a** and **3b** can be explained by the different number of alkyl substituents, which serve to solubilize the molecule and stabilize the cations.

Reduction of oligoanthrylenes with alkali metals permits ESR and ENDOR characterization of the resulting para-

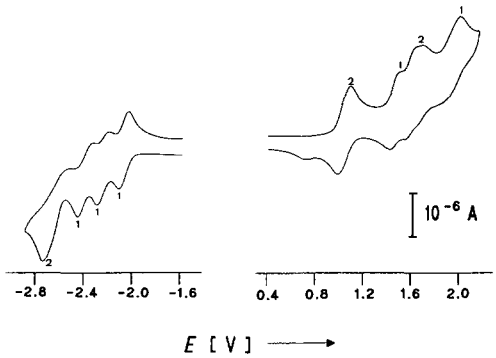

Fig. 1. Cyclic voltammagram of the oxidation and reduction of **4**. Each individual oxidation or reduction step is marked as a one or two electron transition.

magnetic ions in solution. The spin density distribution in the monoradicals is of particular interest here; i.e., the spin localization or delocalization with respect to the individual anthracene units, and the presence of triplet states in the dianions or higher spin multiplicities in the more highly charged forms. The hyperfine coupling constants of the ring protons of the radical monoanion **3b** (K^+/methyltetrahydrofuran (MTHF)) (Table 3) are very similar to those of the anthracene radical anion,[13] and the reduction in symmetry is indicated by the nonequivalence of the 1,4-, and 2,3-protons. This finding is consistent only with a localization of the electron spin on a terminal anthracene residue of $\mathbf{3b}^{\bullet-}/K^+$. The electronic absorption spectra of the monoanions of **2**, **3b** and **4** also demonstrate that in each case one anthracene unit is charged: the respective λ_{max} values are virtually independent of the chain length[14] and reveal the anthracene units to be independent electrophores.

Table 3. Coupling constants a and the respective number of protons in the radical anion of trianthrylene **3b** [a].

H Position	1,4,5,8	2,3,6,7	10
aH	0.286/0.266	0.165/0.136	0.531
Number n	2/2	2/2	1

[a] ENDOR/ESR measurements were carried out at 200 K, solvent: MTHF. Assignment of the hyperfine coupling constants by correlation with Hückel-MO charge densities.

Successive further reduction of $\mathbf{3b}^{\bullet-}$ in frozen solution (T = 150 K) yields an ESR signal which must be assigned to a triplet state of $\mathbf{3b}^{2-}$ (D = 3.85 mT)[5, 15], a quartet state of $\mathbf{3b}^{3-}$ (D = 11.5 mT)[16] and a triplet state of $\mathbf{3b}^{4-}$ (D = 15.2 mT) (Fig. 2A). Analogously, stepwise reduction of **4** affords ESR signals which confirm the initial formation of a triplet state of the dianion $\mathbf{4}^{2-}$ (D = 3.6 mT), and later that of a quartet state of $\mathbf{4}^{3-}$ (D = 11.4 mT); this is transformed into a quintet state of $\mathbf{4}^{4-}$ (D = 8.9 mT)[17] and finally into a triplet state (D = 14.5 mT) of an even more highly charged derivative of **4** (Fig. 2B). Interestingly, for dianions $\mathbf{3b}^{2-}$ and $\mathbf{4}^{2-}$ no $\Delta m_s = 2$ transition could be found, while for the more highly charged derivatives of **3b** and **4** and for $\mathbf{2}^{2-}$ a $\Delta m_s = 2$ transition can be observed at half resonance field. Transitions with $\Delta m_s = 3$ or 4 have not yet been detected, and studies in the L-band are planned.[16, 17]

For diradicals, the characteristic zero field parameters D allow an estimation of the mean distance between the interacting spins by the point-dipole approach[18]. In the case of species $\mathbf{3b}^{2-}$ and $\mathbf{4}^{2-}$ this indicates the charge on each of the

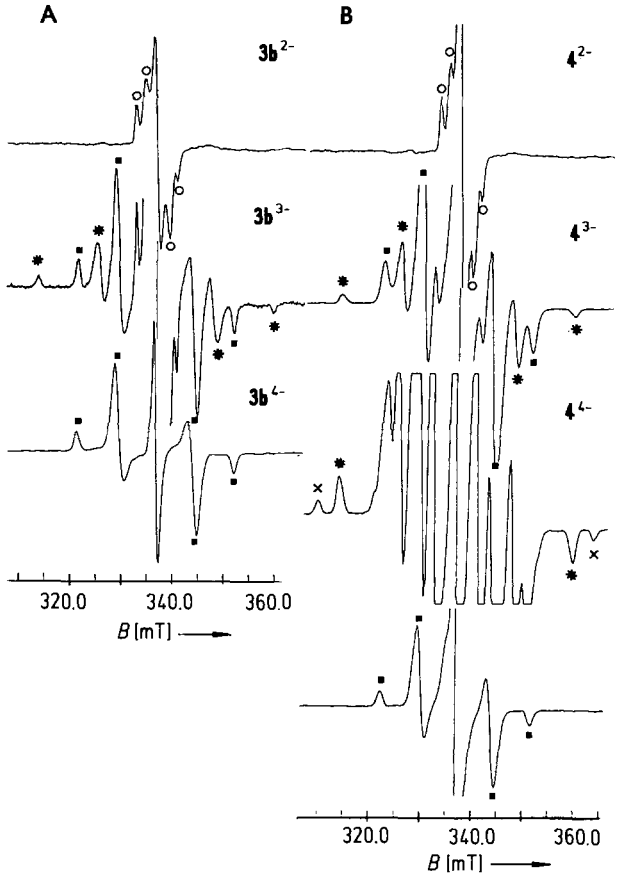

Fig. 2. ESR spectra of the anthrylene radical anions of **3** and **4** (MTHF/K^+/150 K). A: ESR spectra for three reduction steps of **3**, B: ESR spectra for various reduction steps of **4**. In each case, the largest spin state splitting (S = 1, 3/2, 2) is marked. o diradical (small D), * triradical, ■ diradical (large D), × tetraradical. The lowest spectrum of B cannot be assigned to a defined redox state: $\mathbf{4}^{5-}$ or $\mathbf{4}^{6-}$. It shows the interaction between two unpaired electrons on adjacent anthracene units.

terminal electrophores ($\mathbf{3b}^{2-}$: R = 0.89 nm, $\mathbf{4}^{2-}$: R = 0.92 nm).

Since the high-spin systems carry charges, they ought to tend less to coupling reactions than do the well-studied neutral radicals, and should therefore be chemically more stable. Further studies, such as the measurement of the magnetic susceptibilities and the ESR spectra at low temperatures (4–300K) are in progress. The prerequisite for these is the selective generation of definite redox states.

Received: October 19, 1991 [Z4979IE]
German version: *Angew. Chem.* **1992**, *104*, 482

CAS Registry numbers:
2, 1055-23-8; $\mathbf{2}^{\bullet-}$, 34471-67-5; $\mathbf{2}^{2-}$, 42007-24-9; **3a**, 139102-14-0; **3b**, 139102-15-1; $\mathbf{3b}^{\bullet-}$, 139236-40-1; $\mathbf{3b}^{2-}$, 139102-16-2; $\mathbf{3b}^{3-}$, 139236-41-2; $\mathbf{3b}^{4-}$, 139130-61-3; **3c**, 139130-56-6; **3d**, 139130-57-7; **3e**, 139130-58-8; **4**, 139130-59-9; $\mathbf{4}^{\bullet-}$, 139236-43-4; $\mathbf{4}^{2-}$, 139102-17-3; $\mathbf{4}^{3-}$, 139341-68-7; $\mathbf{4}^{4-}$, 139236-42-3; **5**, 139130-60-2; **6a**, 32588-54-8; **6b**, 139102-10-6; **7a**, 139102-12-8; **7b**, 139102-13-9; **8a**, 74391-89-2; **8b**, 139102-11-7; **9**, 434-85-5.

[1] Proceedings of The Symposium on Ferromagnetic and High Spin Molecular Based Materials, Dallas, April 1989: *Mol. Cryst. Liq. Cryst.* **1989**, *176*.
[2] J. S. Miller, A. J. Epstein, W. M. Reiff, *Chem. Rev.* **1988**, *88*, 201–220; T. J. LePage, R. Breslow, *J. Am. Chem. Soc.* **1987**, *109*, 6412–6421; M. Matasashiti, T. Momose, T. Shida, Y. Teki, T. Takui, K. Itoh, *ibid.* **1990**, *112*, 4700–4702; I. Fujita, Y. Teki, T. Takui, T. Kinoshita, K. Itoh, *ibid.* **1990**, *112*, 4074–4075; S. Murata, H. Iwamura, *ibid.* **1991**, *113*, 5547–5556; J. Veciana, C. Rovira, M. I. Crospo, O. Armet, V. M. Domingo, F. Palacio, *ibid.* **1991**, *113*, 2552–2561.

[3] A. Subaric-Leitis, Ch. Monte, A. Roggan, W. Rettig, P. Zimmermann, J. Heinze, *J. Chem. Phys.* **1990**, *93*, 4543–4555.
[4] K. Müllen, M. Baumgarten, N. Tyutyulkov, S. Karabunarliev, *Synth. Met.* **1991**, *40*, 127–136.
[5] H. Hoshino, K. Kimamura, M. Imamura, *Chem. Phys. Lett.* **1973**, *20*, 193–196.
[6] M. Dietrich, J. Mortensen, J. Heinze, *Angew. Chem.* **1985**, *97*, 502–504; *Angew. Chem. Int. Ed. Engl.* **1985**, *24*, 508–510; J. Mortensen, J. Heinze, *J. Electroanal. Chem.* **1985**, *175*, 333–342; O. Hammerich, J. M. Saveant, *J. Chem. Soc. Chem. Commun.* **1979**, 938–940.
[7] O. Bayer, *Methoden Org. Chem. (Houben-Weyl) 4. Aufl. 1952-*, Band 7/3c, **1979**, p. 46.
[8] All new compounds yielded the expected spectroscopic data and elementary analyses (Table 1).
[9] **8b** by reaction of **8d** with butyl lithium; **8d** from **6b** by general methods, see A. Roedig, *Methoden Org. Chem. (Houben-Weyl), 4th ed. 1952–*, Vol. 5/4, **1960**, p. 254, O. Bayer, *Methoden Org. Chem. (Houben-Weyl), 4th ed. 1952–* Vol. 7/3c, **1979**, p. 282.
[10] M. Rehahn, A. D. Schlüter, G. Wegner, W. J. Feast, *Polymer* **1989**, *30*, 1060–1062; U. Fahnenstich, K.-H. Koch, K. Müllen, *Makromol. Chem. Rapid Commun.* **1989**, *10*, 563–569.
[11] This finding is consistent with the electronic absorption spectra of the neutral compounds (CH_2Cl_2, **2**: λ_{max} = 391 nm, **3a**: λ_{max} = 401 nm, **3b**: λ_{max} = 404 nm, **4**: λ^{max} = 406 nm), which reveal only a small bathochromic shift of the longest wavelength band with increasing chain size. This may be caused by the different substitution patterns.
[12] In particular aprotic solvents, **2** can be reversibly charged to both a tetracation and a tetraanion [6].
[13] O. W. Howarth, G. K. Fraenkel, *J. Am. Chem. Soc.* **1966**, *88*, 4514–4515.
[14] $\mathbf{2}^{\bullet-}$: λ_{max} = 669 nm, $\mathbf{3b}^{\bullet-}$: λ_{max} = 671 nm, $\mathbf{4}^{\bullet-}$: λ_{max} = 682 nm (all measurements in THF/K^+).
[15] For the triplet dianion of **2** (K^+/MTHF/150 K) we have measured a *D*-value of 15.8 mT.
[16] J. Brickmann, G. Kothe, *J. Chem. Phys.* **1973**, *59*, 2807–2814; B. Kirste, H. van Willigen, H. Kurreck, K. Möbius, M. Plato, R. Biehl, *J. Am. Chem. Soc.* **1978**, *100*, 7505–7513.
[17] R. D. Dowsing, *J. Magn. Reson.* **1970**, *2*, 332–337; J. A. Novak, R. Jain, D. A. Dougherty, *J. Am. Chem. Soc.* **1989**, *111*, 7618–7619; E. Wasserman, R. W. Murray, W. A. Yager, A. M. Trozzolo, G. Smolinsky, *ibid.* **1967**, *89*, 5076–5078; p. I. Weissmann, T. Kothe, *ibid.* **1975**, *97*, 2537–2538.
[18] A. Carrington, A.-D. McLachlan, *Introduction to Magnetic Resonance*, Harper&Row, New York, **1967**, p. 130.

Bismuth Alkoxide Dimer Complexes Containing Planar $Bi_2(\mu\text{-}OR)_2$ Cores: Syntheses and Structures of $[\{Bi[OCH(CF_3)_2]_3(thf)\}_2]$ and $[\{Bi(OC_6F_5)_3(C_7H_8)\}_2] \cdot 2C_7H_8$**

By *Carolyn M. Jones, Michael D. Burkart,* and *Kenton H. Whitmire**

Recently, metal alkoxide compounds have been receiving attention as precursors to high-temperature superconductors via sol–gel or vapor deposition processes. Current precursors incorporate bulky ligands in order to achieve desirable volatility or solubility. However, more controlled syntheses might be achieved by the use of smaller ligands in order to form complex alkoxide oligomers and clusters with more than one metal constituent. To this end we explored the synthesis of soluble bismuth alkoxides containing nonsterically demanding ligands. Bismuth is an important component in many superconductors with a high transition temperature such as $[Bi_2Sr_2CaCu_2O_8]$ [1a] and $[Sr_2Bi_2Cu_2O_{7+d}]$.[1b] Unfortunately, relatively few bismuth alkoxides have been structurally characterized.[2] We report here the syntheses and structures of two bismuth alkoxide dimer complexes which act as Lewis acceptors.

The reaction of bismuth trichloride with three equivalents of $Na[OCH(CF_3)_2]$ in THF results in the formation of the tris(alkoxide) complex **1** as a THF solvate [Eq. (a)]. The analogous reaction with $NaOC_6F_5$ does not yield a tris(alkoxide) compound;[3] however, refluxing triphenylbismuth with HOC_6F_5 in toluene resulted in the desired product as a toluene solvate [Eq. (b)]. It was previously reported in the literature that trialkylbismuth compounds do not react with alcohols.[4] However, we have found this reaction to be facile for phenols; the reaction of triethylbismuth with HOC_6F_5 or HOC_6H_5 produces a monosubstituted phenoxy-bridged chain polymer.[5]

$$BiCl_3 + 3\,Na[OCH(CF_3)_2] \xrightarrow[-3\,NaCl]{THF} \underset{\mathbf{1}}{[\{Bi[OCH(CF_3)_2]_3(thf)\}_2]} \quad (a)$$

$$BiPh_3 + 3\,HOC_6F_5 \xrightarrow[-3\,C_6H_6]{C_6H_5CH_3} \underset{\mathbf{2}}{[\{Bi(OC_6F_5)_3(C_6H_5CH_3)\}_2]} \quad (b)$$

Compounds **1** and **2** are structurally similar in the solid state; each forms a loose dimer with a planar $[Bi_2(\mu\text{-}OR)_2]$ ring structure (Figs. 1 and 2). The bismuth centers show a distorted octahedral coordination geometry in which two of the sites are occupied by asymmetric bridging alkoxide ligands (for **1**: Bi(1)–O(1), 2.188(7); Bi(1)–O(1A), 2.688(7) Å; for **2**: Bi(2)–O(2), 2.210(8); Bi(2)–O(2A), 2.571(7) Å). A THF molecule (in **1**) or toluene (in **2**) is coordinated in the site *trans* to the shorter bismuth–oxygen bond of the $[Bi_2(\mu\text{-}OR)_2]$ unit. A stereoactive lone pair of electrons occupies one of the octahedral sites *cis* to the bridging alkoxide ligands. Two additional alkoxide ligands complete the octahedron. Compound **2** contains additional lattice toluene.

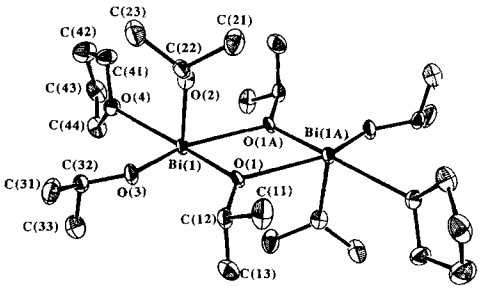

Fig. 1. ORTEP diagram of $[\{Bi[OCH(CF_3)_2]_3(thf)\}_2]$ (1) with thermal ellipsoids drawn at 40% probability level. Fluorine and hydrogen atoms were omitted for clarity. Selected bond distances [Å] and angles [°] not mentioned in text: Bi(1)–O(2), 2.064(8); Bi(1)–O(3), 2.116(7); Bi(1)–O(4), 2.575(7); Bi(1)–O(1)–Bi(1A) 109.1(3); O(1)–Bi(1)–O(1A) 70.9(3); O(1)–Bi(1)–O(2), 90.6(3); O(1)–Bi(1)–O(3), 81.8(3); O(1)–Bi(1)–O(4), 165.8(3); O(2)–Bi(1)–O(1A) 84.1(3); O(2)–Bi(1)–O(3), 90.6(3); O(2)–Bi(1)–O(4), 81.6(3); O(3)–Bi(1)–O(1A) 152.1(2); O(3)–Bi(1)–O(4), 86.4(3); O(4)–Bi(1)–O(1A) 119.7(2).

The NMR spectra of compounds **1** and **2** in C_6D_6 or $[D_8]$toluene suggest that these are not rigid structures in solution as only a single signal is observed for the alkoxy (in **1**) or phenoxy (in **2**) ligands at room temperature. A second signal appears in the ^{19}F NMR spectrum of **1** in $[D_8]$toluene as the temperature is lowered and is the predominant signal at −65 °C. The temperature-dependent NMR spectra may reflect monomer–dimer interconversion; the dimer is the predominant species at low temperature.

[*] Dr. K. H. Whitmire, Dr. C. M. Jones, M. D. Burkart
Rice University, Department of Chemistry
P.O. Box 1892, Houston, TX 77251 (U.S.A.)

[**] We thank the Donors of Petroleum Research Fund (administered by the American Chemical Society) and the Robert A. Welch Foundation for support of this work. Funds for the Rigaku AFC5S diffractometer were provided in part by the National Science Foundation.

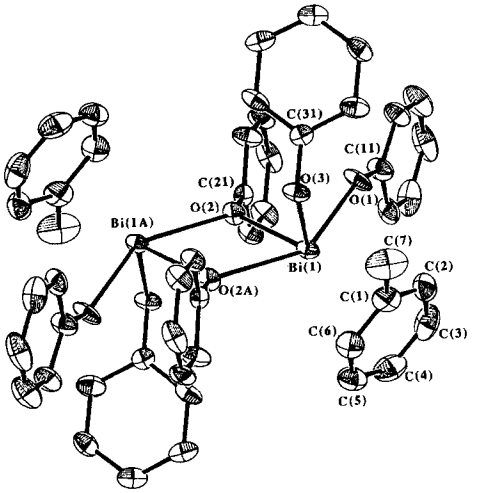

Fig. 2. ORTEP diagram of $[\{Bi(OC_6F_5)_3(C_7H_8)\}_2]\cdot 2C_7H_8$ (**2**) with thermal ellipsoids drawn at 40% probability level. Fluorine atoms on pentafluorophenoxide ligands, hydrogen atoms, and lattice toluene have been omitted for clarity. The carbons of the pentafluorophenoxide rings are numbered sequentially from the *ipso* carbon. Selected bond distances [Å] and angles [°] not mentioned in text: Bi(1)–O(1), 2.147(8); Bi(1)–O(3), 2.088(9); Bi(1)–O(2)–Bi(1A) 112.3(3); O(1)–Bi(1)–O(2), 86.5(3); O(1)–Bi(1)–O(2A), 145.4(3); O(1)-Bi(1)-O(3), 82.7(3); O(2)–Bi(1)–O(2A), 67.7(3); O(2)–Bi(1)–O(3), 92.6(3); O(2A)–Bi(1)–O(3), 76.1(3).

Compound **2** is particularly interesting in that it is a rare example of a bismuth–arene π complex and the first such bismuth alkoxide. The first examples of structurally characterized bismuth–arene complexes were the bismuth trichloride adducts, $[\{1,3,5\text{-}(CH_3)_3C_6H_3\}(BiCl_3)]$ and $[\{(CH_3)_6C_6\}(BiCl_3)]$, described by Schmidbaur.[6a] Two aluminum trichloride adducts of bismuth chloride arene complexes have also been structurally characterized.[6b]. In **2** the distance between the bismuth atom and the toluene ring centroid is slightly shorter than in the bismuth trichloride mesitylene complex (2.96(4) vs. 3.07(2) Å) and is close enough to be considered a real (albeit weak) interaction. The angle between the ring normal and the metal to ring center vector in **2** is 5.7° (vs. 2.1–7.3° for the bismuth trichloride adducts) indicating an η^6-bound toluene molecule.

The bismuth center appears to prefer a "hypervalent" electron configuration in tris(alkoxide) compounds and readily functions as a Lewis acid to alkoxide ligands on other bismuth atoms and to solvent molecules. Steric bulk on the alkoxide ligands can prevent further coordination as in the case of $[Bi\{2,5\text{-}Me_2C_6H_3O\}_3]$.[2a] The bismuth centers in the phenoxy-bridged chain polymers $[BiEt_2(\mu\text{-}OR)]_\infty$ mentioned earlier are four coordinate. The compound $[Bi(OC_2H_4OMe)_3]$ oligomerizes to make each bismuth(III) center five coordinate with a stereoactive lone pair of electrons.[2b] Compound **1** can be thought of as having four electrons in excess of the filled octet while **2** has eight more than needed. A similar situation exists for the bismuth atoms in the bismuth trichloride adducts of Schmidbaur et al. where the lone pairs are *not* stereoactive.[6a] The use of non-sterically demanding alkoxide ligands in **1** and **2** readily allows oligomerization which, together with the Lewis-acceptor properties of the bismuth center, raises the possibility of incorporation of other metal centers to form mixed-metal alkoxide oligomers.

Experimental Procedure

Compound **1**: Bismuth trichloride dissolved in THF was added to a THF solution containing three equivalents of $Na[OCH(CH_3)_2]$ formed in situ by the reaction of the alcohol with excess sodium hydride. A white precipitate resulted immediately Removal of the THF in vacuo was followed by extraction with hot toluene and filtration through Celite. Cooling to room temperature and reduction of volume afforded large colorless crystals of **1**. Compound **1** has been characterized spectroscopically and by single-crystal X-ray diffraction: ^{1}H NMR (C_6D_6): $\delta = 5.58$ (s), 3.39 (m), 1.26 (m); ^{19}F NMR (C_6D_6, 297 K, CF_3COOH): $\delta = 0.34$ (d, $J = 4$ Hz); ([D_8]toluene, 242 K) 0.172 (d, $J = 4$ Hz); IR (nujol) $\tilde{\nu}$ [cm^{-1}] = 1294 (s), 1284 (s), 1258 (s), 1188 (s), 1165 (m), 1138 (s), 1095 (s), 1022 (m), 926 (w), 889 (m), 859 (s), 850 (m), 831 (w), 744 (s), 690 (s), 684 (s). Crystal data for **1**: monoclinic space group $P2_1/n$ (no. 14), $T = -80$ °C, $a = 13.738(7)$, $b = 10.936(7)$, $c = 14.389(8)$ Å, $\beta = 94.53(4)$°, $R = 0.0427$, $R_w = 0.0471$, $S = 1.766$. For 326 parameters, 2786 observed reflections with $I \geq 3\sigma(I)$. Repeated attempts to obtain analytical data were unsuccessful because of fractional loss of THF from analytical samples.

Compound **2**: Triphenylbismuth was refluxed with three equivalents of HOC_6F_5 in toluene for 12 h followed by filtration. A clear yellow solution resulted from which yellow crystals of **2** grew at −20 °C. Compound **2** was characterized spectroscopically and by single-crystal X-ray diffraction: ^{19}F NMR (C_6D_6, CF_3COOH): $\delta = -87.74$ (d), −89.10 (t, $J = 19$ Hz), −94.44 (m); IR (nujol) $\tilde{\nu}$ [cm^{-1}] = 1307 (m), 1162 (m), 1021 (s), 795 (s), 751 (m). Crystal data for **2**: triclinic space group $P\bar{1}$ (no. 2), $T = -80$ °C, $a = 11.086(6)$, $b = 13.378(8)$, $c = 10.771(9)$ Å, $\alpha = 98.58(7)$, $\beta = 95.58(5)$, $\gamma = 95.22(5)$°, $R = 0.0591$, $R_w = 0.0581$, $S = 1.691$ for 411 parameters, 4019 observed reflections with $I \geq 3\sigma(I)$. Several attempts to obtain analytical data were unsuccessful due to fractional loss of toluene from analytical samples. Further details of the crystal structure investigators are available on request from the Director of the Cambridge Crystallographic Data Centre, University Chemical Laboratory, Lensfield Road, GB-Cambridge CB21EW (UK), on quoting the full journal citation.

Received October 19, 1991 [Z 4980 IE]
German version: *Angew. Chem.* **1992**, *104*, 466

CAS Registry numbers:
1, 139242-93-6; **2**, 139242-94-7; **2**·2C_7H_8, 139242-95-8; $HOCH(CF_3)_2$, 920-66-1; HOC_6F_5, 771-61-9; $BiPh_3$, 603-33-8.

[1] a) H. Maeda, Y. Tanaka, M. Fukutomi, T. Asane, *Jpn. J. Appl. Phys.* **1988**, *27*, L209; b) C. Michel, M. Hervieu, M. M. Borel, A. Grandin, F. Deslandes, J. Provost, B. Raveau, *Z. Phys. B-Condensed Matter* **1987**, *68*, 421.
[2] a) W. J. Evans, J. H. Hain, Jr., and J. W. Ziller, *J. Chem. Soc., Chem. Commun.* **1989**, 1628; b) M. A. Matchett, M. Y. Chiang, W. E. Buhro, *Inorg. Chem.* **1990**, *29*, 358.
[3] C. M. Jones, K. H. Whitmire, unpublished.
[4] H. Gilman, J. F. Nelson, *J. Am. Chem. Soc.* **1937**, *59*, 935.
[5] K. H. Whitmire, J. C. Hutchison, A. L. McKnight, unpublished.
[6] a) A. Schier, J. M. Wallis, G. Müller, H. Schmidbaur, *Angew. Chem.* **1986**, *98*, 742; *Angew. Chem. Int. Ed. Engl.* **1986**, *25(8)*, 757; b) W. Frank, J. Weber, E. Fuchs, *ibid.* **1987**, *99*, 68 and **1987**, *26*, 74.

A Nonaromatic Expanded Porphyrin Derived from Anthracene—A Macrocycle which Unexpectedly Binds Anions**

By *Jonathan L. Sessler,* Tarak D. Mody, Debra A. Ford,* and *Vincent Lynch*

Dedicated to Professor James P. Collman on the occasion of his 60th birthday

Porphyrins are among the most versatile ligands, forming complexes with almost every metal cation in the periodic table.[1] However, little record of these species as anion-binding agents[2] has appeared in the literature.[3–5] One reason, perhaps, is that protonated porphyrins, with a core diameter

[*] Professor J. L. Sessler, T. D. Mody, D. A. Ford, Dr. V. Lynch
Department of Chemistry and Biochemistry
University of Texas at Austin
Austin, TX 78712 (USA)

[**] This work was supported by the National Institues of Health (AI 28845). J. L. S. also thanks the NSF for a Presidential Young Investigator Award (1986), the Alfred P. Sloan Foundation for a Research Fellowship (1989–1991), and the Camille and Henry Dreyfus Foundation for a Teacher-Scholar Award (1988–1992). D. A. F. is grateful to the United States Navy for allowing an academic leave and for providing M. S. thesis support.

of approximately 4 Å, are too small to bind anions within the macrocyclic cavity.[2] Quite recently, we have found that certain aromatic "expanded porphyrins" including, sapphyrin[6] and rubyrin[7] are capable of serving both as anion receptors in the solid state[6, 7] and as anion carriers under certain solution-phase conditions.[8] Here, we wish to report the synthesis and crystallographic characterization of a novel, nonaromatic, anthracene-derived Schiff base, the expanded porphyrin **1**. As an X-ray structure analysis shows, the diprotonated form of **1** effectively binds chloride ions.[9, 10] In addition, we present the results of liquid-membrane transport experiments which are consistent with the binding of chloride and fluoride ions in solution.

The synthesis of macrocycle **2**-Cl and its neutral parent **1** is shown in Scheme 1. The critical step is the acid-catalyzed 1:1 condensation of 1,8-diaminoanthracene (**4**)[11] and the diformyl tripyrrane **3**.[12] X-ray quality crystals of the diprotonated macrocycle as its mixed chloride tetrafluoroborate salt, **2**-BF_4, were obtained by slow diffusion of diethyl ether into a solution of dichloromethane/methanol (2:1 v/v) containing **2**-Cl and a small excess of ethereal tetrafluoroboric acid.[10]

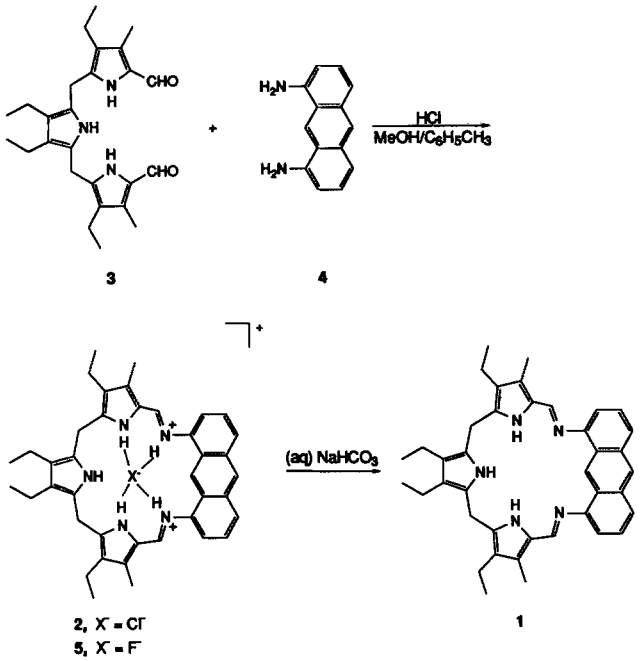

Scheme 1. Synthesis of **1**.

From the X-ray structure analysis,[10] the core of the macrocycle is found to contain a near mirror plane, and the two pyrrole rings A and C of the tripyrrane and the anthracene moiety lie in essentially the same plane (Fig. 1). The

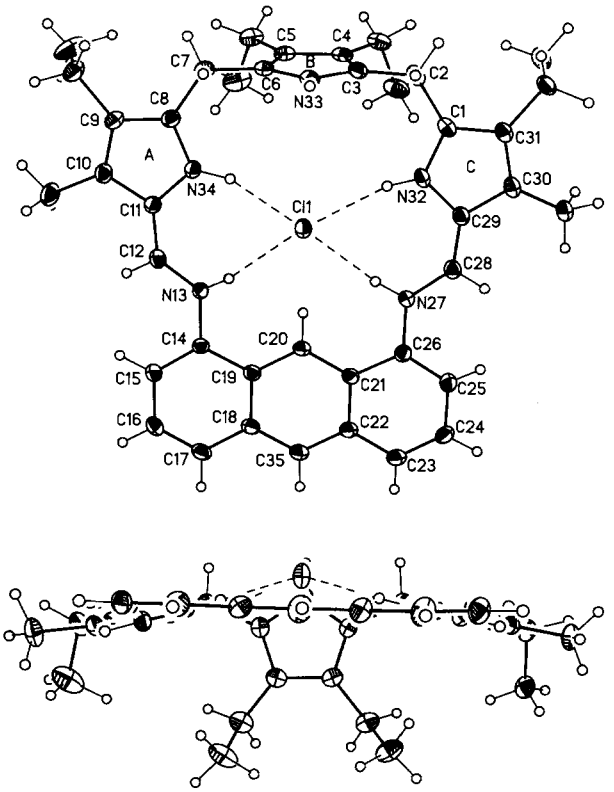

Fig. 1. Structure of **2**-BF_4 in the crystal (thermal ellipsoids at the 30% probability level, H atoms with arbitrary radii). The interactions of the Cl^- ion with the hydrogen atoms of the macrocycle are indicated by dashed lines. Not shown is an H-bonded BF_4^- counterion with an H–F distance of 2.02(3) Å which is nearly directly above N33 of pyrrole ring B. Top: View perpendicular to the plane through the nitrogen atoms. Bottom: Side view showing the nearly perpendicular orientation of the two planar subunits of the macrocycle and the partial encapsulation of the chloride counterion.

Table 1. Data for the characterization of new compounds [a].

1: Mp > 190 °C (decomp.); ^{1}H NMR (300 MHz, $CDCl_3$, TMS): δ = 1.14 (m, 12H; CH_2CH_3), 2.23 (s, 6H; pyrr-CH_3), 2.49 (q, 8H; CH_2CH_3), 3.89 (s, 4H; $(pyrr)_2$-CH_2), 6.91 (d, 2H, H15,25), 7.41 (t, 2H; H16,24), 7.55 (s, 1H; NH), 7.78 (d, 2H; H17,23), 8.32 (s, 2H; CHN), 8.36 (s, 1H; H35), 9.22 (s, 1H, H20); ^{13}C NMR (75.5 MHz, $CDCl_3$): δ = 8.83, 15.66, 16.60, 17.15, 17.63, 22.62, 111.10, 119.35, 121.73, 122.02, 123.60, 124.64, 125.41, 125.92, 126.44, 126.74, 127.83, 131.94, 132.40, 147.44, 151.12. UV/VIS ($CHCl_3$) λ_{max} [nm] (log ε) 332.5 (4.55), 415 (4.33). HRMS (FAB): *m/z* 593.3518 (M^+), calcd for $C_{40}H_{43}N_5$: 593.3519 (±0.0001).

2-Cl: Mp > 190 °C (decomp.), ^{1}H NMR (300 MHz, $CDCl_3$, TMS): δ = 1.04 (t, 6H; CH_2CH_3), 1.14 (t, 6H; CH_2CH_3); 2.23 (s, 6H; pyrr-CH_3), 2.40 (q, 4H; CH_2CH_3), 2.48 (q, 4H; CH_2CH_3), 4.01 (s, 4H, $(pyrr)_2$-CH_2), 7.34 (t, 2H; H16,24), 7.48 (d, 2H; H15,25), 7.77 (d, 2H; H17,23), 8.15 (s, 2H; CHN), 8.40 (s, 1H; H35), 9.16 (s, 1H; NH), 10.14 (s, 1H; H20), 12.90 (s, 2H; $CHNH^+$), 14.43 (s, 2H; NH); ^{13}C NMR (75.5 MHz, $CDCl_3$/CD_3OD): δ = 9.61, 14.06, 15.94, 16.88, 17.61, 23.91, 115.47, 117.33, 118.49, 118.64, 122.00, 122.14, 123.36, 125.65, 127.20, 127.82, 129.85, 131.97, 135.54, 135.69, 138.93, 139.10, 143.88, 154.37. UV/VIS: ($CHCl_3$) λ_{max} [nm] 352, 430. HRMS (FAB): *m/z* 631.3428 (M^+ − Cl), calcd for $C_{40}H_{46}N_5Cl$: 631.3442 (±0.0014)

4: Mp = 154–156 °C; ^{1}H NMR (300 MHz, CD_3OD): δ = 6.72 (d, 2H; H2,7), 7.25 (t, 2H; H3,6), 7.46 (d, 2H; H4,5), 8.30 (s, 1H; H9), 8.55 (s, 1H, H10); ^{13}C NMR (75.5 MHz, CD_3OD): δ = 107.53, 113.45, 118.78, 122.89, 125.84, 126.52, 132.34, 142.17. HRMS (CI): *m/z* 208.1000 (M^+), calcd for $C_{14}H_{12}N_2$: 208.1000

[a] HRMS = high-resolution mass spectroscopy.

central pyrrole ring B is almost perpendicular to this plane; the dihedral angle formed is 79.3°. The chloride anion is bound in pseudo square-planar geometry 0.795 Å above the planar portion of the macrocycle with the four inner hydrogen atoms (H13, H27, H32, H34) pointing towards it. The H–Cl distances range from 2.21(4) to 2.41(4) Å. The N–Cl bond lengths are between 3.11 and 3.25 Å, which is consistent with strong hydrogen bonding.[2d] There is also a hydrogen-bonding interaction between F4 of the BF_4^- and H33 N33 of the central pyrrole unit. In this case the H–F distance is 2.02(3) Å.

The structure of the chloride-containing salt **2**-BF_4 differs from that of the HSCN salt **6** of the nonaromatic texaphyrin-type macrocycle **7**, which we reported previously.[12] For instance, **6** is clearly protonated at only one of the azomethine nitrogens, whereas **2**-BF_4 is clearly quite stable as a diprotonated salt. This may simply reflect effective differences in the basicity of the nitrogen atoms in these two con-

methine(N)–azomethine(N) distances (5.024(1) and 2.60(1) Å for **2**-BF_4 and **6**, respectively). In particular, we suggest that two protons can be accommodated in the cavity macrocycle **1**, whereas in **7** geometric and/or electrostatic repulsions would preclude such a double accommodation.[13] Certain-

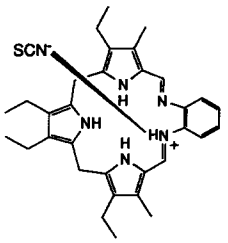

6

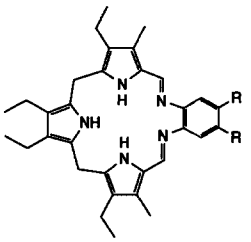

7, R = H
8, R = OCH_3

ly, in **2**-BF_4 the short bonds C11–C12 and C28–C29 (1.373 and 1.386 Å, respectively) are consistent with a model wherein the positive charges on the azomethine centers N13 and N27 are delocalized into the adjacent pyrrole rings A and B (Scheme 2).

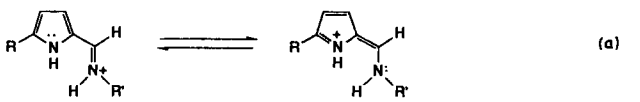

(a)

Scheme 2.

In contrast to other comparable expanded porphyrin–anion adducts like **6**, for **2**-BF_4 the core chloride complex of cation **2** was detected in both the low-resolution and high-resolution FAB (fast atom bombardment) mass spectra. These data lead us to suggest that the chloride anion is bound tightly in **2**-BF_4, at least in the gas phase.

Further insight into the anion-binding properties of macrocycle **1** and its protonated derivatives[14] was obtained from preliminary solution-phase transport experiments using a three-phase model membrane system [AqI]-[CH_2Cl_2]-[AqII] (Aq = aqueous;[15] AqI = 0.5 M HF, adjusted to pH 3.2 with NaOH,[17] and AqII = NaOH (pH 12)). In a first set of experiments compound **1**, via the presumed intermediacy of **5**, was found to accelerate the transport of fluoride ions through the CH_2Cl_2 phase with an initial flux value Φ_{F^-} of 5.03 ± 0.16 μmol h^{-1} under conditions where the nonaromatic texaphyrin-type system **8**[18] proved much less effective as a carrier ($\Phi_{F^-} = 1.60 \pm 0.10$ μmol h^{-1}) and simple passive diffusion in the absence of any added carrier was negligible ($\Phi_{F^-} \leq 0.01$ μmol h^{-1}) (Fig. 2). Under these conditions roughly 13 hours were required in the case of **1** for the transport of 10 mol% of the fluoride ions from AqI through CH_2Cl_2 to AqII. During this time the carrier **1** appeared to be completely stable (no evidence of decomposition or hydrolysis of the macrocycle was found in the UV/VIS spectra and thin-layer chromatograms of the recovered material).[19] However, as expected, a steady decrease in the pH of AqII from 12 to 5 was observed during this monitoring period. This is consistent with fluoride ion transport by the so-called symport mechanism,[20] in which anions and protons are complexed and transported together by the macrocyclic carrier. Mechanistically, therefore, carrier **1** appears to function as a fluoride ion carrier in a manner similar to that of the under identical experimental conditions this new, nonaromatic expanded porphyrin is roughly six times more efficient (per mole) than sapphyrin as a fluoride ion carrier.

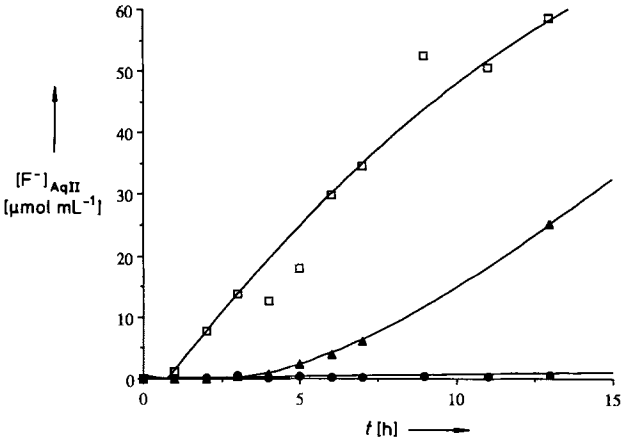

Fig. 2. Course of fluoride transport with macrocycles **1** and **8** with time. Transport experiments were performed with a glass U-tube at 28 °C. Conditions: AqI (1 mL): 0.5 M HF, adjusted to pH 3.2 with NaOH. Membrane; carrier: 1.0 mM, 10 mL CH_2Cl_2. AqII (1 mL): NaOH (pH 12). The release of fluoride ion into the receiving phase, AqII, was monitored at various times by a fluoride combination electrode (Orion). In all cases, the control experiment was performed in the absence of carrier. For anthraphyrin **1** (□) $\Phi_{F^-} = 5.03 \pm 0.16$ μmol h^{-1}. For the nonaromatic texaphyrin **8** (▲) $\Phi_{F^-} = 1.60 \pm 0.10$ μmol h^{-1} and for the control (●), recorded in the absence of carrier, $\Phi_{F^-} \leq 0.01$ μmol h^{-1}.

The transport of fluoride ions was found to be strongly inhibited by chloride ions. For instance, when the transport experiment was repeated with AqI = 0.5 M HF + 0.5 M NaCl (pH 3.2) and AqII = NaOH, (pH 12), Φ_{F^-} was 1.02 ± 0.10 μmol h^{-1}. This strong inhibition could reflect the fact that fluoride ion transport is limited by the formation and/or break-up of a strong, kinetically nonlabile chloride complex. Consistent with this supposition are the following findings: 1) Macrocycle **1** is a relatively ineffective chloride ion carrier and only nominally better than **8** ($\Phi_{Cl^-} = 1.56 \pm 0.16$ μmol h^{-1} and 1.13 ± 0.16 μmol h^{-1} for **1** and **8**, respectively; AqI = 0.1 M HCl + 0.4 M NaCl (pH 1.2); AqII = NaOH (pH 12)). 2) In CH_2Cl_2, chloride ions are bound roughly 14 times more effectively than fluoride ions by the diprotonated macrocycle **1** ($K_{S[Cl^-]} = 2.0 \times 10^5$ M^{-1}, $K_{S[F^-]} = 1.4 \times 10^4$ M^{-1}).[21] These results thus lead us to suggest that this new expanded porphyrin can serve not only as an effective anion carrier but also as an anion-specific receptor.

Experimental Procedure

4: This diamine was obtained by treating 1,8-diaminoanthraquinone [23] (2.00 g, 8.4 mmol, 88% purity) with sodium borohydride (4.0 g, 106 mmol) for 48 h in 100 mL isopropyl alcohol at reflux. The cooled suspension was poured into 250 mL ice water, and the red precipitate was filtered and washed with water several times. The red-brown solid so obtained was then dried under vacuum for 24 h. This solid was then dissolved in chloroform and purified by column chromatography. Initial elution with pure $CHCl_3$ was followed by a gradient elution with CH_3OH in $CHCl_3$ (0–3%). The last fraction, a bright fluorescent yellow solution, was collected and concentrated to dryness to afford a green solid. This solid was recrystallized from dichloromethane and *n*-hexane to yield 0.500 g (33% yield) 1,8-diaminoanthracene (**4**) as bright yellow needles.

2-Cl: This macrocycle was prepared in >90% yield from the acid-catalyzed reaction of **4** and **3**[12] according to the procedure reported earlier for the preparation of the non-aromatic texaphyrin **7**.[12] The red solid isolated was recrystallized from a solution of CH_2Cl_2 and CH_3OH layered with diethyl ether. Single crystals of the diprotonated chloride tetrafluoroborate salt **2**-BF_4 were obtained by slow diffusion of diethyl ether into a dichloromethane/

methanol solution (2:1 v/v) containing **2**-Cl and a small excess of ethereal tetrafluoroboric acid.

1: The neutral form of the macrocycle was obtained in essentially quantitative yield by dissolving **2**-Cl in dichloromethane and stirring vigorously with aqueous sodium bicarbonate for 15 min. The organic layer was then washed with water and brine (2 × each), dried over anhydrous sodium sulfate, and concentrated to dryness. The reddish-brown solid was recrystallized from CH_2Cl_2/CH_3OH to afford **1** as shiny brown needles.

Received: October 21, 1991 [Z 4981 IE]
German version: *Angew. Chem.* **1992**, *104*, 461

CAS Registry numbers:
1, 139312-37-1; **2**-BF_4, 139312-38-2; **3**, 109929-99-9; **4**, 139312-39-3; **5**-BF_4, 139312-40-6; 1,8-diaminoanthraquinone, 129-42-0.

[1] See, for instance *The Porphyrins, Vol. I–VII* (Ed.: D. Dolphin), Academic Press, New York, **1978**; b) *Porphyrins and Metalloporphyrins* (Ed.: K. M. Smith), Elsevier, Amsterdam, **1975**.

[2] a) C. P. Hrung, M. Tsutsui, D. L. Cullen, E. F. Meyer, *J. Am. Chem. Soc.* **1976**, *98*, 7878–7880; b) A. Stone, E. B. Fleischer, *ibid.* **1968**, *90*, 2735–2748; c) N. Hirayama, A. Takenaka, Y. Sasada, E.-I. Watanabe, H. Ogoshi, Z.-I. Yoshida, *J. Chem. Soc. Chem. Commun.* **1974**, 330–331; d) E. Cetinkaya, A. W. Johnson, M. F. Lappert, G. M. MacLaughlin, K. W. Muir, *J. Chem. Soc. Dalton Trans.* **1974**, 1236–1243.

[3] For overviews of anion-binding receptors, see: a) L. F. Lindoy; *The Chemistry of Macrocyclic Ligands*, Cambridge University Press, Cambridge, **1989**, Chapter 5; b) J.-M. Lehn, *Angew. Chem.* **1988**, *100*, 91–116; *Angew. Chem. Int. Ed. Engl.* **1988**, *27*, 89–112; c) F. P. Schmidtchen, *Top. Curr. Chem.* **1986**, *132*, 101–133; e) F. Vögtle, H. Sieger, W. M. Müller, *ibid.* **1981**, *98*, 107–161. See also ref. [4] and [5].

[4] Anion complexation in polyammonium receptors: a) J.-M. Lehn, R. Meric, J.-P. Vigneron, I. Bkouche-Waksman, C. Pascard, *J. Chem. Soc. Chem. Commun.* **1991**, 62–64; b) M. W. Hosseini, A. J. Blacker, J.-M. Lehn, *J. Am. Chem. Soc.* **1990**, *112*, 3896–3904, and references therein. c) M. Mertes, K. B. Mertes, *Acc. Chem. Res.* **1990**, *23*, 413–418, and references therein; d) F. P. Schmidtchen, *Tetrahedron Lett.* **1989**, 4493–4496.

[5] Anion binding in cyclointercaland/cryptand/cyclophane systems: a) R. E. Cramer, V. Fermin, E. Kuqwabara, R. Kirkup, M. Selman, K. Aoki, A. Adeyemo, H. Yamazaki, *J. Am. Chem. Soc.* **1991**, *113*, 7033–7034; b) J. Brodbelt, S. Maleknia, C.-C. Liou, R. Lagow, *ibid.* **1991**, *113*, 5913–5914; c) B. Dietrich, J.-M. Lehn, J. Guilhelm, C. Pascard, *Tetrahedron Lett.* **1989**, *30*, 4125–4128, and references therein.

[6] a) J. L. Sessler, M. J. Cyr, A. K. Burrell, *Synlett* **1991**, 127–133; b) J. L. Sessler, M. J. Cyr, V. Lynch, E. McGhee, J. A. Ibers, *J. Am. Chem. Soc.* **1990**, *112*, 2810–2813.

[7] J. L. Sessler, T. Morishima, V. Lynch, *Angew. Chem.* **1991**, *103*, 1018–1020; *Angew. Chem. Int. Ed. Engl.* **1991**, *30*, 977–980.

[8] a) H. Furuta, M. J. Cyr, J. L. Sessler, *J. Am. Chem. Soc.* **1991**, *113*, 6677–6678; b) J. L. Sessler, D. Ford, M. J. Cyr, H. Furuta, *J. Chem. Soc. Chem. Commun.* **1991**, 1733–1735.

[9] The systematic name for macrocycle **1** is: 4,5,9,31-tetraethyl-10,30-dimethyl-13,27,32,33,34-pentaazaheptacyclo[27.2.1.$1^{3,6}$.$1^{8,11}$.$1^{18,22}$.$0^{14,19}$.$0^{21,26}$]pentatriaconta-3,5,8,10,12,14,16,18,20,22(35),23,25,27,29,31-pentadecaene. We suggest the trivial name, anthraphyrin, for this compound.

[10] X-ray crystal analysis: $(C_{40}H_{45}N_5)^{2+}(Cl^-)(BF_4^-)$; triclinic, $P\bar{1}$ (No. 2), $Z = 2$, $a = 10.695(3)$, $b = 12.048(3)$, $c = 14.774(4)$ Å, $\alpha = 81.35(2)$, $\beta = 74.36(2)$, $\gamma = 88.75(2)°$, $V = 1811.8(9)$ Å^3, $\rho_{calc} = 1.32$ g cm^{-3} (198 K), $F(000) = 756$. Data collected at 198 K on a Nicolet R3 diffractometer, $Mo_{K\alpha}$ radiation, graphite monochromator ($\lambda = 0.7107$ Å), ω-scans to 50° in 2θ; 6418 unique reflections, 4269 with $F_0^2 > 3\sigma(F_0^2)$. The structure was solved by direct methods and refined by full-matrix least-squares (SHELXTL-Plus, Siemens Analytical X-ray Instruments, Inc., Madison, WI, USA) with anisotropic thermal parameters for the non-hydrogen atoms. The positions of the hydrogen atoms were obtained from a ΔF map and refined isotropically. $R = 0.0465$, $wR = 0.0560$, GOF = 1.840 for 640 parameters. The minimum and maximum residual electron density were -0.26 and 0.31 e$^-$ Å^{-3}, respectively. Further details of the crystal structure are available on request from the Director of the Cambrdige Crystallographic Data Centre, University Chemical Laboratory, Lensfield Road, GB-Cambridge CB21EW (UK), on quoting the full journal citation.

[11] Satisfactory spectroscopic and mass spectrometric data were obtained for all new compounds (see Table 1).

[12] J. L. Sessler, M. J. Johnson, V. Lynch, *J. Org. Chem.* **1987**, *52*, 4394–4397.

[13] The structure of **2**-BF_4 also differs from that of tetrapyridyl porphyrin dihydrochloride. This latter system binds one chloride ion above and one below the macrocyclic plane (see ref. [2b]).

[14] The pK_a values of the diprotonated anthraphyrin, pK_{a_1} and pK_{a_2} are 4.0 and 8.5, respectively.

[15] Transport experiments were carried out at 28 °C with the glass U-tube set-up described earlier [8, 16]. The base of the U-tube cell (1.0 cm, i.d.; coated with Sigmacote™ to prevent etching of the glass by HF) was filled with a solution of the carrier (1.0 mM) in CH_2Cl_2 (10 mL). In the arms of the U-tube, the two aqueous phases, AqI and AqII (1.0 mL each), were layered on the CH_2Cl_2 phase. Initial flux values, Φ_{X^-} were calculated from the amount (μmol) of Cl^- and/or F^- transported per hour during the regime of linear dependence at the start and were found to be reproducible within the error ranges quoted in the text. In all cases, the control experiments were performed in the absence of carrier. We are grateful to Dr. Hiroyuki Furuta for his assistance.

[16] H. Furuta, K. Furuta, J. L. Sessler, *J. Am. Chem. Soc.* **1991**, *113*, 4706–4707.

[17] The initital concentration of the free fluoride ions $[F^-]$ was calculated to be approximately 0.25 M under these conditions ($K_{assF} = 6.46 \times 10^{-4}$ M); *The Merck Index*, Med., Merck & Co., Rahway, NJ, **1989**.

[18] J. L. Sessler, T. D. Mody, R. Ramasamy, A. D. Sherry, *New J. Chem.*, in press.

[19] The dimethoxy derivative **8** [18] was used in place of **7** because it proved more stable than this original [12] nonaromatic texaphyrin.

[20] H. Tsukube in *Liquid Membranes: Chemical Applications* (Eds.: T. Araki, H. Tsukube), CRC, Boca Raton, FL, USA, **1990**, p. 27.

[21] Binding strengths were determined from standard Benesi–Hildebrand and/or Scatchard plots of the spectral shifts induced in the optical spectrum (at 421 and 430 nm) as a function of amounts of added F^- and Cl^- (as the tetrabutylammonium salts). Estimated errors are $\leq 25\%$ [22].

[22] K. A. Connors, *Binding Constants: The Measurement of Molecular Complex Stability*, Wiley, New York, **1987**.

[23] We would like to thank Takashi Morishima and Mitsubishi Kasei Co. for kindly providing us with the requisite starting 1,8-diaminoanthraquinone. We are also grateful to Ken Lancaster for synthetic assistance.

Tetrathienylethylenes, a New Class of Electron Donors—Dications Twisted by 90° Stabilized by Formation of Polymethine Units**

By *Takanori Suzuki, Hiroaki Shiohara, Masayuki Monobe, Tomoo Sakimura, Shoji Tanaka, Yoshiro Yamashita,* and *Tsutomu Miyashi**

Recently much attention has been focused on multistage redox systems[1] because of their special properties such as conductivity and organic ferromagnetism. Although thiophene units have been frequently used in thienoquinoid[2] or condensed[3] forms in the design of new molecular skeletons, they have not been used as the end groups of redox systems. In view of the stabilization of a carbenium ion by thiophene units,[4] we have now prepared very simple yet hitherto unknown tetrakis(2-thienyl)ethylenes **1** and found that they are strong two-electron donors whose dications are stabilized by the formation of two polymethine subunits.

Unsubstituted **1a**[5] was prepared in 41% yield by a reductive coupling of bis(2-thienyl)ketone[6] using $TiCl_4/Zn$[7]

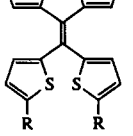

1a: R = H
1b: R = Me
1c: R = SMe

[*] Prof. Dr. T. Miyashi, Dr. T. Suzuki, H. Shiohara, M. Monobe, T. Sakimura
Department of Chemistry, Faculty of Science, Tohoku University
Sendai 980 (Japan)
Dr. S. Tanaka, Prof. Dr. Y. Yamashita
Institute for Molecular Science
Okazaki 444 (Japan)

[**] We thank Dr. Kimio Akiyama and Prof. Dr. Yusaku Ikegami, Institute for Chemical Reaction Science, Tohoku University, for the measurement and evaluation of the ESR spectrum.

in refluxing THF. Reactions of **1a** with excess *n*BuLi in THF at −40 °C followed by treatment with iodomethane or dimethyl disulfide afforded tetrasubstituted derivatives **1b** (R = Me)[5] and **1c** (R = SMe)[5] in 71% and 48% yields, respectively.

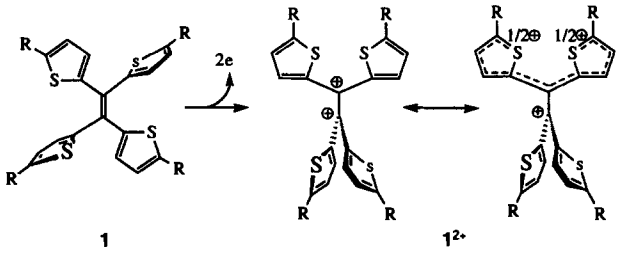

1 1^{2+}

Scheme 1. The conformations of **1** and 1^{2+} according to the X-ray structure analyses of **1c** and $\mathbf{1c}^{2+}$.

The cyclic voltammogram of **1a** shows an irreversible wave similar to that of tetraphenylethylene, but the oxidation potential E^{ox}[8] of the former (+0.91 V) is much lower than that of the latter (+1.36 V). Derivatives **1b** and **1c** substituted at the reactive α position of thiophene undergo reversible one-wave two-electron oxidation (E^{ox} = +0.70 and +0.55 V, respectively). The oxidation potential of **1c** is nearly the same as that of the well-known electron donor dibenzotetrathiafulvalene (E^{ox} = +0.57 V). The blue dication $\mathbf{1c}^{2+}$ generated by electrochemical oxidation in CH_2Cl_2 was isolated as a stable ClO_4^- salt.[5]

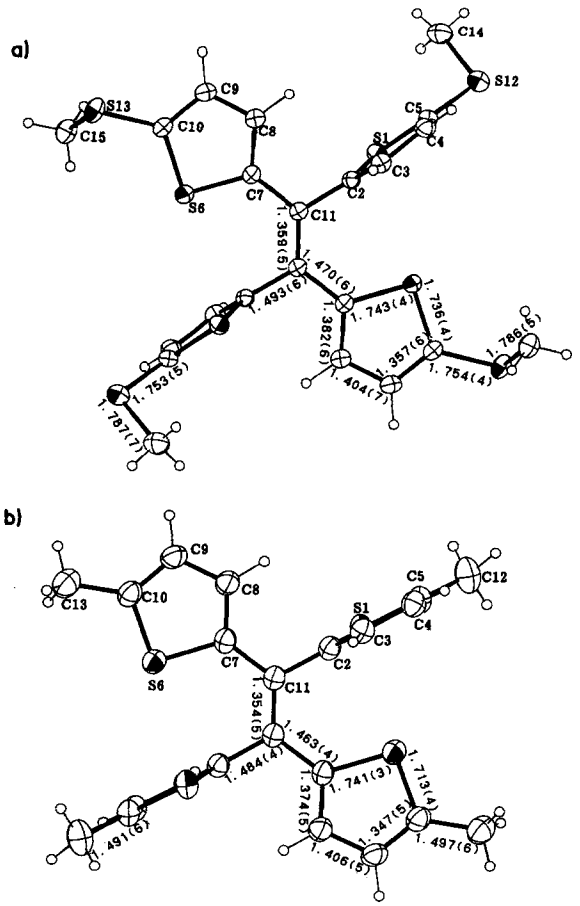

Fig. 1. X-ray crystal structures of the neutral molecules **1c** (a) and **1b** (b). The two halves of each molecule are related by an inversion center. The bond lengths are in Å. Additional bond lengths: S1–C2, S1–C5, C2–C3, C3–C4 and C4–C5 1.728(4), 1.730(5), 1.353(6), 1.418(7), and 1.360(7) for **1c**, and 1.725(3), 1.728(4), 1.360(4), 1.417(5) and 1.351(5) for **1b**, respectively.

The X-ray structural analyses[9] of **1c** and the $\mathbf{1c}^{2+}$ salt revealed that the molecular geometry is drastically changed upon oxidation (Scheme 1). Neutral **1c** possesses a planar *trans*-dithienylethylene structure substituted with two thiophene rings which are orthogonal to the molecular plane (Fig. 1a). In contrast, in $\mathbf{1c}^{2+}$ the two halves of the molecule are twisted around the central C–C bond (Fig. 2). Because $\mathbf{1c}^{2+}$ is penetrated by a crystallographic $\bar{4}$ axis, the rotation angle (90°) is the largest of the reported values for dicationic ethylene derivatives.[10–12] The dithienylcarbenium moiety itself is nearly planar with the largest deviation of 0.44 Å at thiophene S atoms,[13] indicating the delocalization of each positive charge over one half of the molecule. The dihedral angle between two thiophene rings is 35.8°, smaller than that between the two aryl groups in the dication of tetrakis(*p*-methoxyphenyl)ethylene (50.9°).[11]

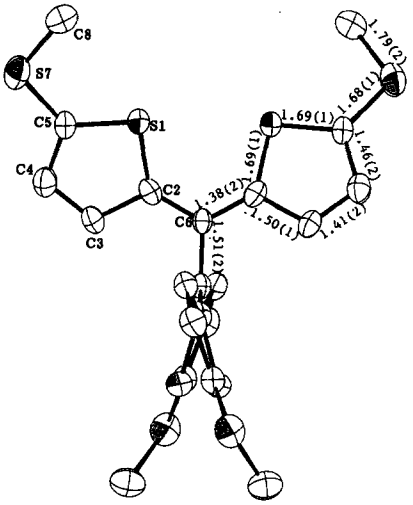

Fig. 2. X-ray crystal structure of the twisted dication in $\mathbf{1c}^{2+} \cdot 2ClO_4^- \cdot CH_2Cl_2$. The central C–C bond lies on a $\bar{4}$ axis, so only one-fourth of $\mathbf{1c}^{2+}$ is crystallographically independent. The bond lengths are given in Å.

Stabilization of cations by delocalization over the polymethine unit[14] was proved recently to be unexpectedly large, even greater than an aromatic [4n + 2]π stabilization.[15] The structural features of $\mathbf{1c}^{2+}$ indicate a conjugated polymethine framework[16] for 1^{2+} ions with 12 electrons distributed over 11 atoms (Scheme 1). Evidence of the formation of the polymethine structure in $\mathbf{1c}^{2+}$ is also provided by the strong UV/VIS absorption[17] at 662 nm (lg ε = 5.16 in CF_3CO_2H) and the alternation of π-electron density as deduced from the ^{13}C NMR chemical shifts (Table 1). In contrast to trithienylcarbenium ions,[4] the largest positive charge is found on C_5 ($\Delta\delta$ = 47.04), not on $C_{ethylene}$ ($\Delta\delta$ = 19.82). The short bond length between S7 and C5 (1.68(1) Å) as well as the small torsion angles C8-S7-C5-S1 (9.3°) and

Table 1. ^{13}C NMR chemical shifts of **1c** and $\mathbf{1c}^{2+}$ [a].

	$C_{ethylene}$	C2	C3	C4	C5	CH3
1c	126.71	144.83	130.60	129.56	140.51	21.64
$\mathbf{1c}^{2+}$	146.53	140.72	149.14	133.61	187.55	20.38
$\Delta\delta$ [b]	19.82	−4.11	18.54	4.05	47.04	−1.26

[a] In $CDCl_3$ (**1c**) and CF_3CO_2D ($\mathbf{1c}^{2+}$). The chemical shifts were assigned on the basis of ^{13}C-^1H coupling and COSY spectra. [b] $\delta(\mathbf{1c}^{2+}) - \delta(\mathbf{1c})$.

C8-S7-C5-C4 (12.8°) indicate that not only the thiophene sulfur atoms but also the thiomethyl sulfur atoms act as end groups of the polymethine units in $\mathbf{1c}^{2+}$ (Scheme 2).

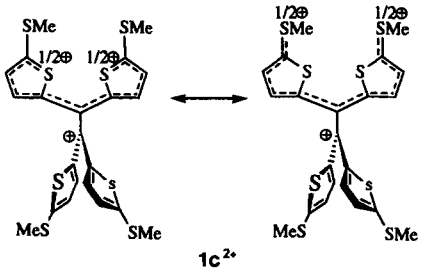

Scheme 2. Participation of the S atoms in the polymethine stabilization in $\mathbf{1c}^{2+}$.

Electrolysis of **1c** in CH_2Cl_2 gave rise to a radical cation which was detected by ESR. Its spectrum indicates that the unpaired electron of $\mathbf{1c}^{+\cdot}$ is delocalized over four equivalent thiophene rings.[18]

The quite similar molecular geometries (Fig. 1b) and redox properties of **1b** and **1c** indicate that $\mathbf{1b}^{2+}$ is also stabilized by the formation of polymethine units. In the electrochemical oxidation of **1b** and in its oxidation with excess $NOBF_4$ in CH_2Cl_2, a deep violet color developed due to $\mathbf{1b}^{2+}$ ($\lambda_{max} = 520$ nm, lg $\varepsilon > 4.65$ at -78 °C). However, attempts to isolate $\mathbf{1b}^{2+}$ as a salt have been unsuccessful; only a brown resin has been obtained.

The dithienylmethylene unit exhibits a strong donating property which may be exploited in new redox systems.[19] Absence of the interactions between *ortho* hydrogen atoms as observed in diarylcarbenium ions[11] makes it possible for dithienylcarbenium units to adopt a nearly planar arrangement, allowing the effective delocalization of positive charge over a polymethine subunit.

Experimental Procedure

1a: To a suspension of low-valent Ti prepared from $TiCl_4$ (5.88 g, 31.0 mmol) and zinc (4.37 g, 66.8 mmol) in 100 mL of dry THF under nitrogen were added dropwise pyridine (2.5 mL, 33.2 mmol) and a dry solution of bis(2-thienyl)ketone (5.76 g, 29.6 mmol) in 15 mL THF. The mixture was heated at reflux for 19 h, then poured into 600 mL of 10% K_2CO_3, and extracted with CH_2Cl_2. The extract was washed with brine and dried over Na_2SO_4. The solvent was evaporated, and the residue was washed with benzene to give pale orange crystals, which were purified by gradient sublimation (185 °C, 4×10^{-2} Torr). 2.16 g of **1a** were obtained in 41% yield.

1b: To a dry THF solution (15 mL) of **1a** (84.0 mg, 0.236 mmol) was added dropwise a solution of *n*BuLi in *n*-hexane (3.2 mL, 1.3 mol dm^{-3}, 4.16 mmol) at -78 °C under nitrogen. The mixture was stirred for 18 h at -40 °C, then iodomethane (3.41 g, 24.0 mmol) was added. The temperature was increased over 1 h to 20 °C, and the mixture was poured into 100 mL of water and extracted with CH_2Cl_2. The extract was washed with brine and dried over Na_2SO_4. Evaporation of the solvent gave an orange solid which was purified by chromatography on SiO_2 (CH_2Cl_2: *n*-hexane, 1:4), giving 69 mg of **1b** in 71% yield.

1c: Following a procedure analogous to that described for **1b**, **1a** (1.07 g, 3.00 mmol) was allowed to react with *n*BuLi in *n*-hexane (32 mL, 1.3 mol dm^{-3}, 41.6 mmol) for 6.5 h at -40 °C; dimethyl disulfide (10.5 g, 111 mmol) was then added. Corresponding workup and chromatographic separation on SiO_2 (CH_2Cl_2: *n*-hexane, 1:9) gave 780 mg of **1c** in 48% yield. The tris(methylthio) derivative **2** was also obtained as yellow crystals (320 mg) in 22% yield.

Received: October 21, 1991 [Z 4982 IE]
German version: *Angew. Chem.* **1991**, *104*, 454

CAS Registry numbers:
1a, 139376-06-0; **1b**, 139376-07-1; **1c**, 139376-08-2; $\mathbf{1c}^{2+} \cdot 2ClO_4^- \cdot CH_2Cl_2$, 139407-25-3; $\mathbf{1c}^{+\cdot}$, 139376-09-3; $\mathbf{1c} \cdot (DDQ)_2$, 139376-10-6; $\mathbf{1c} \cdot (I_2)_4$, 139376-11-7; bis(2-thienyl)ketone, 704-38-1.

[1] K. Deuchert, S. Hünig, *Angew. Chem.* **1978**, *90*, 927; *Angew. Chem. Int. Ed. Engl.* **1978**, *17*, 875.
[2] E. Günther, S. Hünig, K. Peters, H. Rieder, H. G. von Schnering, J.-U.von Schütz, S. Söderholm, H.-P. Werner, H. C. Wolf, *Angew. Chem.* **1990**, *102*, 220; *Angew. Chem. Int. Ed. Engl.* **1990**, *29*, 204; K. Takahashi, T. Suzuki, K. Akiyama, Y. Ikegami, Y. Fukazawa, *J. Am. Chem. Soc.* **1991**, *113*, 4576.
[3] Y. Kono, H. Miyamoto, Y. Aso, T. Otsubo, F. Ogura, T. Tanaka, M. Sawada, *Angew. Chem.* **1989**, *101*, 1254; *Angew. Chem. Int. Ed. Engl.* **1989**, *28*, 1222; A. Ishii, J. Nakayama, J. Kazami, Y. Ida, T. Nakamura, M. Hoshino, *J. Org. Chem.* **1991**, *56*, 78; A. Tsubouchi, N. Matsumura, H. Inoue, *J. Chem. Soc. Chem. Commun.* **1991**, 520.
[4] B. Abarca, G. Asensio, R. Ballesteros, T. Varea *J. Org. Chem.* **1991**, *56*, 3224.
[5] All the compounds gave satisfactory analytical and spectral data. **1a**: pale yellow prisms, m.p. = 196–198 °C; MS (25 eV): *m/z* 356 (M^+, 100), 290 (39); ^{1}H NMR (90 MHz, $CDCl_3$): $\delta = 7.40-7.20$ (m, 4H; H5), 7.00–6.80 (m, 8H; H3,4); IR (KBr): $\tilde{\nu}$ [cm^{-1}] = 3070, 1422, 1348, 1233, 1125, 1049, 850, 778, 700; UV (CH_2Cl_2): λ_{max} [nm] (ε) = 284 (15200), 354 (15000), 370 (15300). – **1b**: pale yellow needles, m.p. = 122.5–123 °C; MS (25 eV): *m/z* 412 (M^+, 100), 364 (18); ^{1}H NMR (200 MHz, $CDCl_3$): $\delta = 6.65$ (d, $J = 3.4$ Hz, 4H; H3), 6.57 (dq, $J = 3.4$, 1.0 Hz, 4H; H4), 2.43 (d, $J = 1.0$ Hz, 12H; CH_3); ^{13}C NMR (50 MHz, $CDCl_3$): $\delta = 142.17$ (C2), 141.81 (C5), 129.67 (C3), 126.74 ($C_{ethylene}$), 124.79 (C4), 15.47 (CH_3); IR (KBr): $\tilde{\nu}$ [cm^{-1}] = 2900, 1456, 1439, 1237, 1223, 810, 791, 774; UV (CH_2Cl_2): λ_{max} [nm] (ε) = 296 (16100, 368 (16200), 382 (17400). – **1c**: yellow needles, m.p. = 98.5–99.5 °C; MS (70 eV): *m/z* 540 (M^+, 100), 525 (29), 494 (25); ^{1}H NMR (200 MHz, $CDCl_3$): $\delta = 6.87$ (d, $J = 3.8$ Hz, 4H; H4), 6.73 (d, $J = 3.8$ Hz, 4H; H3), 2.47 (s, 12H; CH_3); IR (KBr): $\tilde{\nu}$ [cm^{-1}] = 1424, 1314, 964, 804, 772; UV (CH_2Cl_2): λ_{max} [nm] (ε) = 288 (13200), 326 (15500), 404 (18200). – $\mathbf{1c}^{2+} \cdot 2ClO_4^- \cdot CH_2Cl_2$: dark purple prisms, m.p. = 171–175 °C (decomp.); ^{1}H NMR (200 MHz, CF_3CO_2D): $\delta = 7.94$ (d, $J = 4.6$ Hz, 4H; H3), 6.36 (d, $J = 4.6$ Hz, 4H; H4), 2.97 (s, 12H; CH_3); IR (KBr): $\tilde{\nu}$ [cm^{-1}] = 1498, 1422, 1360, 1312, 1184, 1168, 1140, 1106, 1082 (ClO_4^-), 1020; UV/VIS (CF_3CO_2H): λ_{max} [nm] (ε) = 352 (36300), 400 (12900), 446 (24200), 656 (145600), 662 (144000).
[6] R. M. Acheson, K. E. MacPhee, P.G. Philpott, J. A. Barltrop *J. Chem. Soc.* **1956**, 698.
[7] D. Lenoir, *Synthesis* **1977**, 553.
[8] All the potential values in the text are in Volt vs. the standard calomel electrode and were measured by cyclic voltammetry under the same conditions (0.1 mol dm^{-3} Et_4NClO_4 in MeCN, Pt-wire electrode, scan rate 100 mV s^{-1}, E^{ox}(of ferrocene = + 0.38 V). Oxidation number of **1b** was determined from the concentration dependence of peak currents with tetrathiafulvalene as an external standard. In the case of irreversible waves, E^{ox} was calculated as E_{pa} (anodic peak potential) -0.03 V.
[9] **1c**: $C_{22}H_{20}S_8$, M = 540.86, triclinic, space group $P\bar{1}$, $a = 9.581(2)$, $b = 10.887(1)$, $c = 6.031(1)$ Å, $\alpha = 93.39(1)$, $\beta = 93.78(2)$, $\gamma = 81.14(1)$°, $V = 619.5(2)$ Å^3, $Z = 1$, $\rho_{calcd} = 1.450$ g cm^{-3}. A total of 3039 unique data was collected ($Mo_{K\alpha}$, $\lambda = 0.71049$ Å, $\mu = 7.018$ cm^{-1}, $2\theta < 58$°), of which 2867 non-zero reflections were used for structure refinement. $\mathbf{1c}^{2+} \cdot 2ClO_4^- \cdot CH_2Cl_2$: $C_{23}H_{22}S_8O_8Cl_4$, $M = 824.69$, tetragonal, space group $P4/n$, $a = b = 10.819(2)$, $c = 14.202(2)$ Å, $V = 1662.5(5)$ Å^3, $Z = 2$, $\rho_{calcd} = 1.647$ g cm^{-3}. A total of 1916 unique data was collected ($Mo_{K\alpha}$, $\lambda = 0.71049$ Å, $\mu = 8.835$ cm^{-1}, $2\theta < 55$°), of which 936 had $F > 3\sigma(F)$ and were used for structure refinement. **1b**: $C_{22}H_{20}S_4$, M = 412.64, monoclinic, space group $P2_1/c$, $a = 9.578(4)$, $b = 8.496(1)$, $c = 13.178(3)$ Å, $\beta = 101.73(3)$°, $V = 1050.0(6)$ Å^3, $Z = 2$, $\rho_{calcd} = 1.305$ g cm^{-3}. A total of 1811 unique data was collected ($Cu_{K\alpha}$, $\lambda = 1.5418$ Å, $\mu = 41.09$ cm^{-1}, $2\theta < 126$°), of which 1490 had $F > 3\sigma(F)$ and were used for structure refinement. These data sets were collected on an AFC-5R diffractometer at 286 K. Absorption correction was applied for **1b** (Ψ-scan-method). Block-diagonal least-squares refinement gave $R = 0.0460$ for **1c**, 0.1211 for $\mathbf{1c}^{2+} \cdot 2ClO_4^- \cdot CH_2Cl_2$ and 0.0387 for **1b**. Because of the disorder of solvent and a counteranion, the R value of $\mathbf{1c}^{2+} \cdot 2ClO_4^- \cdot CH_2Cl_2$ is very large and the large esds prevent the comparisons of bond lengths. Further details of the crystal structure investigations may be obtained from the Fachinformationszentrum Karlsruhe, Gesellschaft für wissenschaftlich-technische Information mbH, D-W-7514 Eggenstein-Leopoldshafen 2 (FRG), on quoting the depository number CSD-55915, the names of the authors, and the journal citation.
[10] H. Bock, K. Ruppert, K. Merzweiler, D. Fenske, H. Goesmann, *Angew. Chem.* **1989**, *101*, 1715; *Angew. Chem. Int. Ed. Engl.* **1989**, *28*, 1684.
[11] N. C. Baenziger, R. E. Buckles, T. D. Simpson *J. Am. Chem. Soc.* **1967**, *89*, 3405.
[12] Conformations of substituted ethylene dications were studied by ab initio methods, and a planar geometry was predicted for $C_2X_4^{2+}$ (X = F or OH), which suffers no steric repulsion between vicinal substituents. G. Frenking, *J. Am. Chem. Soc.* **1991**, *113*, 2476.
[13] The interatomic distance between two thiophene S atoms (3.19 Å) is shorter than the sum of the van der Waals radii (3.70 Å). However, with respect to the anisotropy of the lone pairs the repulsive or attractive interactions should not very important. D. B. Boyd, *J. Phys. Chem.* **1978**, *82*, 1407.

[14] K. Elbl, C.Krieger, H. A. Staab, *Angew. Chem.* **1986**, *98*, 1024; *Angew. Chem. Int. Ed. Engl.* **1986**, *25*, 1023; H. A. Staab, J. Hofmeister, C. Krieger, *ibid.* **1991**, *103*, 1003 and **1991**, *30*, 1030; H. Bock, K. Ruppert, C. Näther, Z. Havlas, *ibid.* **1991**, *103*, 1194 and **1991**, *30*, 1180.
[15] H. Bock, A. Rauschenbach, K. Ruppert, Z. Havlas, *Angew. Chem.* **1991**, *103*, 706; *Angew. Chem. Int. Ed. Engl.* **1991**, *30*, 714.
[16] S. Dähne, D. Leupold, *Angew. Chem.* **1966**, *78*, 1029; *Angew. Chem. Int. Ed. Engl.* **1966**, *5*, 984; S. Dähne, F. Moldenhauer, *Prog. Phys. Org. Chem.* **1985**, *15*, 77–83.
[17] F. A. Mikhailenko, L. I. Shevchuk, *Synthesis* **1973**, 621.
[18] **1c**$^{+\cdot}$: a^{H}[G] = 2.25 (4H; H3), 0.16 (4H; H4), 0.62 (12H; Me). The observed ESR spectrum could not be simulated by supposing the delocalization of an unpaired electron over two thiophene rings. The full detail of ESR study will be reported elsewhere.
[19] **1c** formed charge-transfer complexes with dichlorodicyanobenzoquinone (DDQ) and iodine. **1c** · $(DDQ)_2 \cdot CH_2Cl_2$: violet prisms, m.p. = 134–137 °C (decomp.); IR (KBr): $\tilde{\nu}$ [cm^{-1}] = 2205, 1570, 1496, 1364, 1306, 1188, 1172, 1022; powder conductivity: σ [$S\,cm^{-1}$] = 5.0×10^{-9}. – **1c** · $(I_2)_4$: violet needles, m.p. = 87–95 °C (decomp.); IR (KBr): $\tilde{\nu}$ [cm^{-1}] = 1492, 1426, 1453, 1308, 1184, 1166, 1138, 1100, 1020; powder conductivity σ [$S\,cm^{-1}$] = 5.3×10^{-8}.

One-Pot Multifunctionalization of Polymethyl Hydrocarbon π Ligands. Maximum Space Occupancy by Double Branching and Formation of Arboroles**

By *Françoise Moulines, Bruno Gloaguen,* and *Didier Astruc**

De Gennes and Hervet successfully predicted[1] that the dendrimer strategy,[2–6] an idea pioneered by Vögtle,[2] leads to space saturation on the outer sphere surface after a few generations. We now show how the maximum number of functional branches in arboroles can be achieved in a one-pot reaction. For this purpose, the acidity enhancement of methyl substituents in polymethyl hydrocarbon ligands by complexation to cationic organo-transition metal fragments[7] is exploited in combination with allylation and benzylation reactions. This polysequential strategy is only limited by steric demand in the products when an excess of reagents is used.

Up to now we had concentrated our attention on the hexafunctionalization of hexamethylbenzene leading to discoid molecules[8] [Eq. (a)].

$$[FeCp(C_6Me_6)]^+ \xrightarrow[R'X]{KOR} [FeCp\{C_6(CH_2R')_6\}]^+ \qquad (a)$$

R = H or *t*Bu; R′ = Me, CH_2Ph, CH_2CHCH_2; X = Br or I.

The deprotonation-allylation sequences of Equation (a) rapidly lead to the replacement of one H in each Me substituent by an allyl group.[8a]. We could now show that continuation of this reaction is possible and leads to the slower introduction of a second allyl group on each benzylic carbon. Thus, using a 20-fold excess of allyl bromide and KOH in dimethoxyethane (DME) at 40 °C, the twelve allyl branches are attached in about 12 days (KOH is replaced several times). Formation of **3**, the first hexaisoalkylbenzene-transition metal complex, via **2** results from 24 reactions starting from the proton reservoir complex **1** (12 deprotonations and 12 alkylations). The overall yield of **3** is only 17.5%, since the growing steric demand induces extensive decomplexation of the $CpFe^+$ fragment.

The structure of **3** is secured by the correct C, H, Fe analyses and by the ^1H and ^{13}C NMR spectra.[9] In particular, the slow, second branching is easily monitored by the new Cp peaks appearing in the ^1H NMR spectra of the reaction samples and by the integration ratio. The Cp peak position is shifted all the more downfield as the number of allyl arms increases from six (δ = 4.65, CD_3CN) to twelve (δ = 5) due to the deshielding effect of the *endo* allyl chains. The allyl group is the only one leading to double branching; alkyl and benzyl halides give only single branching[8c, d] [Eq. (a)] even under drastic conditions.

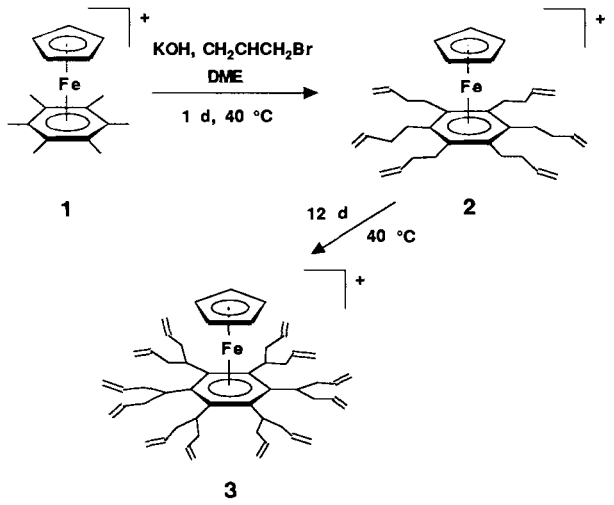

The slow formation and the decomplexation of the dodecafunctional complex **3** show how rapidly spatial crowding is reached. Starting from the durene complex **4** (Scheme 1), we are not confronted with such problems, and double branching proceeds more rapidly at room temperature giving **5** with-

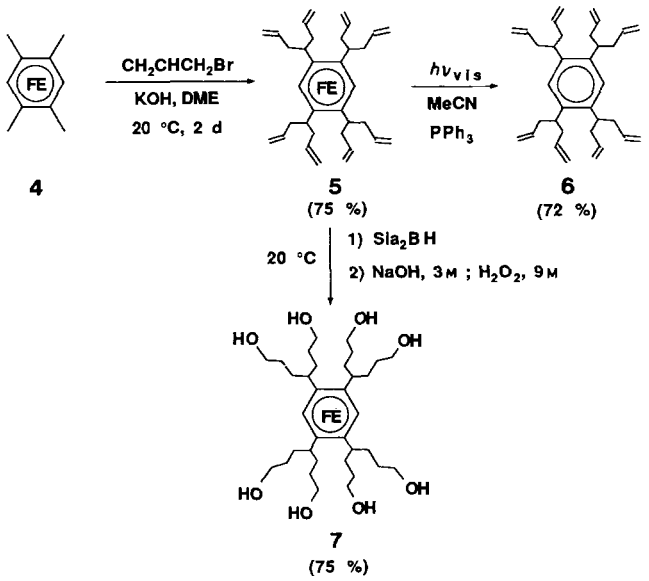

Scheme 1. Syntheses starting from the durene complex **4**. FE = $(\eta_5$-Cp)Fe^+, Sia_2BH = disiamylborane. All cations present as PF_6^- salts.

[*] Prof. D. Astruc, Ing. F. Moulines, Dr. B. Gloaguen
Laboratoire de Chimie Organique et Organométallique
Université Bordeaux I
351, Cours de la Libération, F-33405 Talence Cedex (France)

[**] Financial support from the Centre National de la Recherche Scientifique, the University Bordeaux I and the Region Aquitaine is gratefully acknowledged. We thank Drs Martin Ruppelt, Andrew Van Sickle, David S. Brown, and Bernard Barbe for kind and valuable assistance.

out decomplexation. The octafunctional ligand **6** of **5** can be readily removed by photolysis with visible light.[10] A convenient synthesis of the octol **7** is achieved by hydroboration with subsequent alkaline oxidation[11] (Scheme 1).

The NMR spectra of **3** and **5**–**7** show the directionalities[12a] of the geared, branched substituents. Whereas **3** has a single, blocked directionality, **5** and **7** have independent directionalities (Scheme 2) on the two sides with distinct *endo*- and *exo*-allyl branches on the NMR time scale up to 100 °C.[9] On the other hand, the geared rotation of the branches is faster than the NMR time scale in the free aromatic compound **6** (only one allyl type according to the ^{1}H NMR spectrum up to 500 MHz).

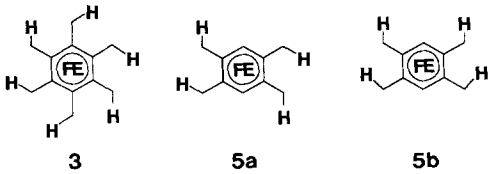

Scheme 2. Orientation of the arms in **3** and **5**. In the case of **5** two orientations are possible (**a** and **b**). The allyl groups are omitted for clarity.

Reaction of **4** with benzyl bromide and KOH in DME at 46 °C afforded pure **8**,[9] and photolysis with visible light, as for **5**, furnished the free ligand **9**. An attempted threefold branching of **10** to give **11** did not give any pure compound even under drastic conditions; the maximum number of benzyl branches achieved being between seven and eight.[12b] This indicates that the steric limit is attained before the third benzylation of the three benzylic carbons (the unusual reaction of **10** with allyl bromide will be described later[12b]).

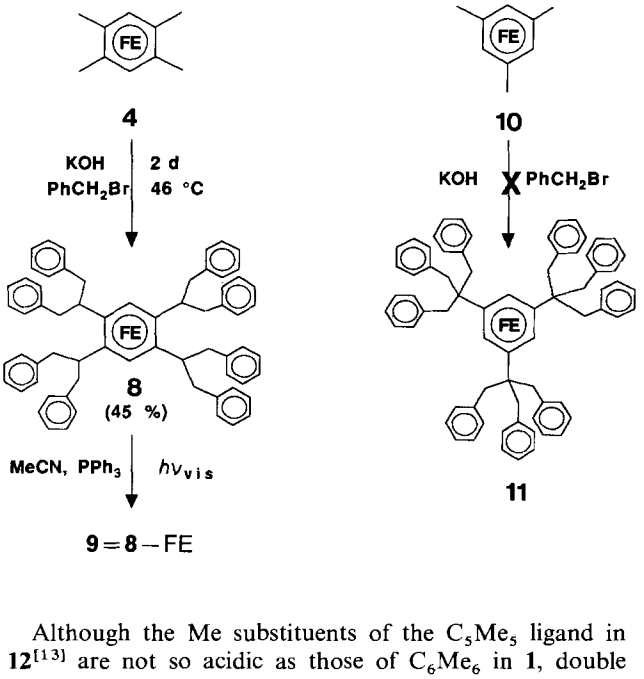

Although the Me substituents of the C_5Me_5 ligand in **12**[13] are not so acidic as those of C_6Me_6 in **1**, double branching is easier because the C–centroid–C angle is larger in C_5Me_5 (72°) than in C_6Me_6 (60°).[14] Thus, decaallylation and decabenzylation of **12** furnish **13** and **14**, respectively.[9] As for **1**, the combination of reduced reactivity and bulk-induced decomplexation limits the yields, and the single directionality (Scheme 3) is blocked on the NMR time scale up to above 100 °C.

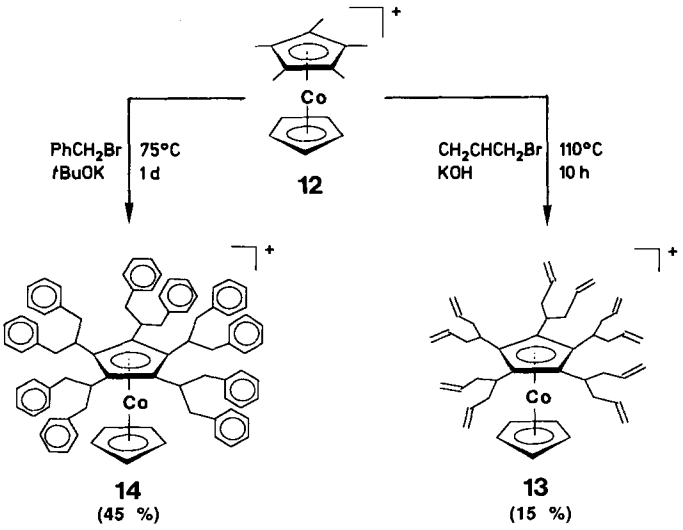

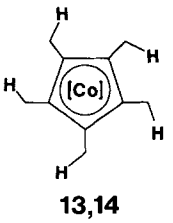

Scheme 3. Orientation of the arms in **13** and **14**; view from above. The allyl and benzyl groups, respectively, are omitted for clarity. [Co] = (η^5-Cp)Co$^+$.

Summarizing, one-pot octa-, deca- and dodecafunctionalization of π ligands can be performed by an activation process which uses cationic transition-metal fragments CpM^+ (M = Fe, Co). This double branching, multiple functionalization approaches the steric limit, as indicated by the low reaction rates, decomplexations, and impossible introduction of three benzyl groups on the three benzylic carbons of **10**. The new molecules have specific topologies and could be used in the future to encapsulate guest substrates (time-selective drug delivery), attach multiple redox centers, and serve as synthons in supramolecular[15, 16] organometallic chemistry.

Received: October 2, 1991 [Z 4984 IE]
German version: *Angew. Chem.* **1992**, *104*, 452

CAS Registry numbers:
1, 53702-66-2; **2**, 116927-70-9; **3**, 139494-26-1; **4**, 83542-60-3; **5**, 139494-28-3; **6**, 139494-23-8; **7**, 139523-80-1; **8**, 139494-30-7; **9**, 139494-24-9; **10**, 32757-45-2; **12**, 126580-33-4; **13**, 139494-32-9; **14**, 139494-34-1; $H_2C{=}CHCH_2Br$, 106-95-6; $PhCH_2Br$, 100-39-0; Sia_2BH, 1069-54-1.

[1] P.-G. de Gennes, H. J. Hervet, *Phys. Lett. (Paris)* **1983**, *44*, 351.
[2] E. Bulheim, W. Wehner, F. Vögtle, *Synthesis* **1978**, 155.
[3] a) G. R. Newkome, Z. Q. Yao, G. R. Baker, V. K. Gupta, *J. Org. Chem.* **1985**, *50*, 2003; b) G. R. Newkome, C. N. Moorefield, G. R. Baker, A. L. Johnson, R. K. Behera, *Angew. Chem.* **1991**, *103*, 1205; *Angew. Chem. Int. Ed. Engl.* **1991**, *30*, 1176, and references cited therein.
[4] D. A. Tomalia, A. M. Taylor, W. A. Goddart III, *Angew. Chem.* **1990**, *102*, 119; *Angew. Chem. Int. Ed. Engl.* **1990**, *29*, 138, and references cited therein.
[5] a) Y. H. Kim, O. W. Webster, *J. Am. Chem. Soc.* **1990**, *112*, 4592; b) H. Uchida, Y. Kabe, K. Yoshino, A. Kawamata, T. Tsumuraya, S. Masamune, *ibid.* **1990**, *112*, 7077.
[6] a) C. J. Hawker, J. M. J. Frechet, *J. Am. Chem. Soc.* **1990**, *112*, 7638; b) I. Amato, *Sci. News (Washington D.C.)* **1990**, *138*, 288; c) Y.-X. Chen, *Youji Huaxue* **1990**, *10*, 289.
[7] D. Astruc, *Acc. Chem. Res.* **1986**, *19*, 377; *Top. Curr. Chem.* **1991**, *160*, 47; Tetrahedron Report No. 157 (*Tetrahedron* **1983**, *39*, 4027); in *The Chem-*

istry of the Metal-Carbon Bond, Vol. 4 (Eds.: F. R. Hartley, S. Patai), Wiley, New York, **1987**, pp. 625–731.

[8] a) F. Moulines, D. Astruc, *Angew. Chem.* **1988**, *100*, 1394; *Angew. Chem. Int. Ed. Engl.* **1988**, *27*, 1347; b) *J. Chem. Soc. Chem. Commun.* **1989**, 614; c) D. Astruc, J.-R. Hamon, G. Althoff, E. Román, P. Batail, P. Michaud, J.-P. Mariot, F. Varret, D. Cozak, *J. Am. Chem. Soc.* **1979**, *101*, 5445; d) J.-R. Hamon, J.-Y. Saillard, A. Le Beuze, M. McGlinchey, D. Astruc, *ibid.* **1982**, *104*, 7549; e) For the preparation of $[FeCp(C_6H_nMe_{6-n})]^+$ salts ($n = 0$ to 6) see I. U. Khand, P. L. Pauson, W. E. Watts, *J. Chem. Soc. C* **1968**, 2257 and Ref. [7] therein.

[9] The new compounds (PF_6^- salts throughout this paper) gave statisfactory elemental and spectroscopic analyses (^1H and ^{13}C NMR). For example, complex **3**: orange vitreous resin: Calcd. for $C_{35}H_{71}FePF_6$: C 70.04, H 7.82, Fe 6.16%; found C 69.81, H 7.74, Fe 6.25% (CNRS Centre, Lyon-Villeurbanne); ^{13}C NMR (62.9 MHz, CD_3CN), two sets of allyl signals for the *endo* and *exo* arms: $\delta = 137$, 138.4 ($CH = CH_2$), 115.7, 118 ($CH = CH_2$), 31.2, 35.7 (CH-CH_2-CH), 38.4 (Ar-CH_2), 104.1 (C_5H_5); ^1H NMR (250 MHz, CD_3CN): $\delta = 5.5$–6 ($CH = CH_2$), 4.8–5.1 ($CH_2 = CH$), 2–2.7 (CH-CH_2-CH), 3.9 ($ArCH$), 5.0 (Cp). IR (KBr): $\tilde{\nu}$[cm^{-1}] = 830 (PF_6^-), 1640 C = C). – Complex **8**: yellow crystals after recrystallization from acetone/ethanol 1/1 at −20 °C; calcd. for $C_{71}H_{67}FeP_4F_6$: C 76.06, H 6.02, Fe 4.98%; found C 76.11, H 6.11, Fe 5.13%; ^{13}C NMR (62.9 MHz, CD_3COCD_3): two sets of benzyl signals for the *endo* and *exo* branches; $\delta = 140.4$, 139.3 (quart. C_6H_5), 127.5, 130 (C_6H_5), 41.2, 42.6 (CH_2), 110.4 (quart. $C_6H_2R_4$), 83.54 ($CH_{Ar,Fe}$); ^1H NMR (250 MHz, CD_3COCD_3): $\delta = 7.45$, 6.31 (C_6H_5, *exo*), 7.14, 6.68 (C_6H_5, *endo*), 3.43, 3.62 (CH_2, *exo*), 2.80, 2.70 (CH_2, *endo*), 6.49 ($CH_{Ar,Fe}$), 5.32 (C_5H_5). – Complex **14**: yellow-brown crystals after recrystallization from acetone/ethanol 1/1. Calcd. for $C_{85}H_{80}CoPF_6$: C 78.2, H 6.18, Co 4.51%; found C 78.31, H 6.07, Co 4.59%; ^{13}C NMR (62.9 MHz, $CDCl_3$): two sets of benzyl signals; $\delta = 41.6$, 44.2 (CH_2), 128–132.5 (CH_{Ar}), 42.3 (CH_2CHCH_2), 108.5 (C_5R_5), 86.3 (C_5H_5). – ^{13}C peaks were assigned using off-resonance and DEPT techniques. The NMR spectra of the other Fe and Co complexes also clearly show *exo* and *endo* arms, contrary to the free arenes **6**.

[10] a) T. P. Gill, K. R. Mann, *Inorg. Chem.* **1983**, *22*, 1986; b) D. Catheline, D. Astruc, *J. Organomet. Chem.* **1984**, *272*, 417.

[11] H. Brown in *Organic Syntheses via Boranes*, Wiley, New York, **1975**, p. 52.

[12] a) K. Mislow, *Chimia* **1986**, *40*, 395; b) J.-L. Fillaut, N. de Beaumont, B. Gloaguen, D. Astruc, unpublished results.

[13] For the preparation of **12**, see: U. Koelle, F. Khouzami, *Angew. Chem.* **1980**, *92*, 658; *Angew. Chem. Int. Ed. Engl.* **1980**, *19*, 640.

[14] B. Gloaguen, D. Astruc, *J. Am. Chem. Soc.* **1990**, *112*, 4607.

[15] J.-M. Lehn, *Angew. Chem.* **1988**, *100*, 92; *Angew. Chem. Int. Ed. Engl.* **1988**, *27*, 89.

[16] F. Vögtle, *Supramolekulare Chemie*, Teubner, Stuttgart, 1989; Supramolecular Chemistry, Wiley, New York, **1991**.

$(H_2Si)_2E_2$ and $(Mes(t\mathrm{Bu})Si)_2E_2$ (E = As, P): Incommensurable Systems of Different Stability with Unusually Long E–E Bonds**

By *Matthias Driess,* Rudolf Janoschek,* and *Hans Pritzkow*

In memoriam Manfred L. Ziegler

We are interested in the influence of silicon as a framework atom on the ring strain and the isomerization ratio (*exo,endo*; *exo,exo*) in phosphabicyclo[1.1.0]butanes.[1] It is already known that the substitution of the two peripheral organophosphandiyl fragments R–P: in tetraphosphabicyclo[1.1.0]butanes **A** by isovalent electronic diorganosilandiyls R_2Si: **B** results in a drastic change of the character of the P–P bridgehead bond. Hence, the P–P bridgehead bond in **A** is ca.0.10 Å *shorter* than in normal diphosphanes with λ^3,σ^3-P atoms (2.20–2.23 Å), whereas derivatives of type **B** show an inverse behavior, i.e. have approximately 0.15 Å *longer* P–P bonds.[2] The relatively short central P–P bond in **A** is attributed to partial π character.[3]

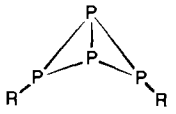

A

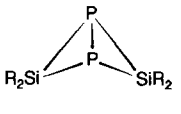

B

The longer bridgehead bond in the P_2Si_2 system **B** can also be explained qualitatively as the silicon in the peripheral position causes a high Baeyer's angle strain. A further characteristic of silicon atoms in the P_2Si_2 system **B** is their ability to avoid very unfavorable steric interactions in the *endo* position by *exo,endo* → *exo,exo* rearrangement (Si inversion).[1, 2] Such an isomerization of 1,3-diphosha-2,4-disilabicyclo[1.1.0]butanes **B** was first observed for the derivatives **1a** and **1b**, in which *tert*-butyl and mesityl groups are substituted at the silicon. In order to understand this new rearrangement at silicon comparative experimental and theoretical investigations are necessary. To learn how the size of the bridgehead atoms influences the length of the central bond and the relative stability of the *exo,endo* and *exo,exo* isomers, we have synthesized the compounds **2**, homologues of **1a** and **1b**, which in the bridgehead positions have arsenic atoms instead of phosphorus.

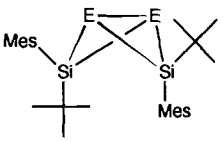

1a, E = P
2a, E = As

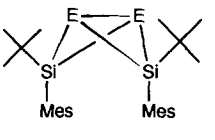

1b, E = P
2b, E = As

Compound **2a** was prepared analogous to **1a** by intramolecular As–As bond formation. The precursors **3** and **4** are also the first known 1,3,2,4-diarsadisiletanes. Compound **3** is formed by the cyclic condensation of Mes-(tBu)$SiCl_2$ (Mes = 2,4,6-trimethylphenyl) and $[LiAsH_2(dme)]$ (dme = dimethoxyethane) in the molar ratio of 1:2. Remarkably, only that isomer of **3** was formed in which the *tert*-butyl groups are in *trans* configuration. The constitution of **3** was confirmed by NMR spectroscopy[4] and an X-ray structure analysis (Fig. 1a).[5]

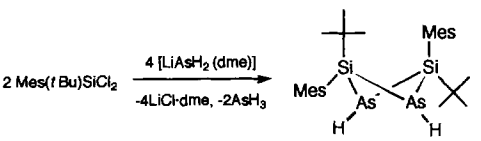

3

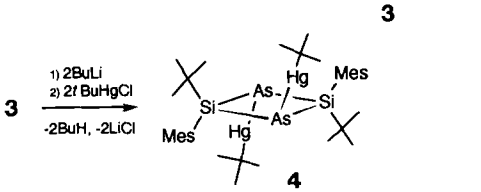

4

[*] Dr. M. Driess, Dr. H. Pritzkow
Anorganisch-chemisches Institut der Universität
Im Neuenheimer Feld 270, D-W-6900 Heidelberg (FRG)
Prof. Dr. R. Janoschek
Institut für Theoretische Chemie der Universität
Mozartgasse 14, A-8010 Graz (Austria)

[**] This work was supported by the Deutsche Forschungsgemeinschaft. We thank Messer-Griesheim GmbH, Duisburg, for chemicals, and Prof. Dr. W. Siebert Heidelberg for his spontaneous, friendly support.

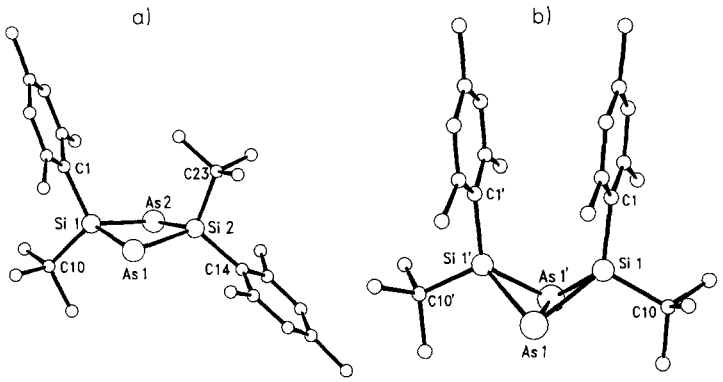

Fig. 1. a) Molecular structure of **3**. Selected bond lengths [Å] and angles [°]: Si-As 2.382-2.401(1), Si-C 1.900-1.914(6): Si-As-Si 83.6(1), As-Si-As 94.2, 94.9(1). b) Molecular structure of **2b**. Selected bond lengths [Å] and angles [°]: As1-As1' 2.602(3), As1-Si1 2.355(3), Si-C 1.904(6), 1.926(4); Si1-As1-Si1' 84.3(1), As1'-As1-Si1 56.5(1), As1-Si1-As1' 67.1(1).

The ^{1}H NMR spectra of **3**[4] are temperature dependent. This can be explained by dynamic effects at the arsenic centers (As inversion, *cis*, *trans* isomerism of the H atoms at the arsenic) analogous to those of the corresponding P_2Si_2 cyclobutanes. The heterocycle in **3** is nonplanar (As1–Si1–As2/As1–Si2–As2 21.5°), and the bond lengths and angles are in the expected range. The nonbonding As–As distance is 3.51 Å.

Double deprotonation of **3** with two equivalents of BuLi and subsequent mercurization with *t*BuHgCl leads to the 1,3-dimercurio derivative **4**,[6] in which according to ^{1}H and ^{29}Si NMR spectra, the *t*BuHg groups are *trans* to one another.

Photolysis of a colorless solution of **4** (0.025 M) in benzene with a 150 Watt light bulb yielded a yellow solution of **2a**, elemental Hg, isobutene, and H_2 after 24 hours. In contrast to **1a**, which under the same reaction conditions rapidly rearranges to **1b** (*exo,exo* isomer),[1] **2a** (*exo,endo* isomer) can be isolated in a pure form.[7] The *exo,endo* configuration of the Si *tert*-butyl groups in **2a** is proved unequivocally by the ^{1}H and ^{29}Si NMR spectra[7] (two types of *t*Bu and Mes groups each; two chemically inequivalent ^{29}Si nuclei).

If a solution of **2a** in hexane is stored for several weeks at 25 °C or irradiated for a longer period (ca. one week), the gradual formation of a small amount of the *exo,exo* isomer **2b** is observed spectroscopically (^{1}H and ^{29}Si NMR)[8] as the only product. At higher temperature or upon irradiation with UV light mainly uncharacterized products result. The compound **2b** was isolated in 8% yield in the form of orange-yellow crystals which were only slightly air sensitive. A crystal structure analysis[9] of **2b** (Fig. 1b) confirms the *exo,exo* configuration.

The fold angle As1–Si1–As1'/As1–Si1'–As1' is 72.8° and therefore differs only slightly from that in **1b** (71.7°).[1] The As–Si bond length (2.355(3) Å) is significantly shorter than that in **3** (average 2.391(1) Å), but nevertheless lies in the characteristic range for As–Si single bonds.[10] The most notable feature of the structure of **2b** is the extremely long As–As bond length of 2.602(3) Å. In contrast, in isostructural molecules with a As–As bridgehead bond,[11] the bond lengths *are shorter* than normal As–As single bonds [d(As–As) ≈ 2.44 Å]. The long As–As bond in **2b** is only comparable with that in realgar As_4S_4 (2.59 Å)[12] and thus very unusual for an As_2 group in a small ring system. To sum up, it can be established that the substitution of phosphorus atoms with arsenic atoms in the bridgehead position considerably increases the stability of the *exo,endo* isomer. In contrast, the change from a P_2 to an As_2 bridge in the bicyclo[1.1.0]butane framework hardly alters the length of the bridgehead bond relative to the single bond. The central As–As bond in the rearranged *exo,exo* product **2b** as well as the P–P bond in the analogous **1b** are ca. 6% longer than a normal single bond.

How can the Si inversion and different stability of *exo,endo* and *exo,exo* isomers be interpreted? For energetic reasons it can be assumed and calculations show that the Si inversion does not occur by homolytic cleavage, but via a transition structure with C_s symmetry (Fig. 2), i.e. for the inversion a SiR_2 unit should rotate 180° about the line that bisects the R–Si–R angle. However, if an ab initio calculation[13] (SCF/6-31G*) under C_s symmetry restriction is carried out for the parent compound $(H_2Si)_2P_2$, this does not result in the required energy minimum for the postulated transition structure (cf. Fig. 2). The energy is higher than the dissociation energy for $(H_2Si)_2P_2 \rightarrow SiH_2 + P_2(SiH_2)$ (SCF: 62.5 kcal mol^{-1}; MP2: 71.0 kcal mol^{-1})

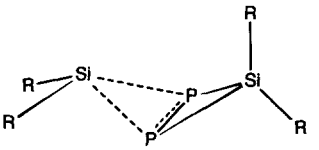

Fig. 2. C_s symmetrical transition structure of the Si inversion in 1,3-diphospha-2,4-disilabicyclo[1.1.0]butane.

Furthermore, the calculations reveal that by a coupling with the ring inversion (D_{2h}) no Si inversion is possible without dissociation. Tetrasilabicyclo[1.1.0]butane shows bond-extension isomerism,[14] which is in agreement with the rapid inversion of the folded bicycle at room temperature, whereas for $(H_2Si)_2P_2$ a relatively high barrier to ring inversion of 52.0 (SCF) and 51.0 kcal mol^{-1} (MP2), respectively, is observed. A second energy minimum for a structure with a longer P–P bridgehead bond could not be found. Possible diradical character of $(H_2Si)_2P_2$, with such long P–P distances as those in the folded equilibrium structure (C_{2v}, 2.360 Å) and the planar transition structure of the ring inversion (D_{2h} 2.667 Å), can be definitely rejected on the basis of the calculation of the multiconfiguration wave functions (MCSCF).[15] A CAS-MCSCF/6-31G* calculation of the wave function[16] with the active orbitals π, π*, and σ* (important for the P–P interaction) afforded as occupation numbers 1.992, 1.899, and 0.109, respectively. These disprove a diradical character (that would have occupation numbers of approximately 1, 1, and 2, respectively) and instead suggest an ionic donor–acceptor representation (Fig. 3).

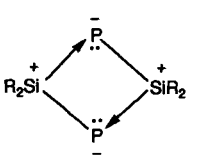

Fig. 3. Valence formula describing the P–P interaction in 1,3-diphospha-2,4-disilabicyclo[1.1.0]butanes.

Similar results were obtained for the folded structure. The atomic charges of −0.483 (on P) and +0.675 (on Si) as well as the high relative energy of the triplet state of 88.4 kcal mol^{-1} (UMP2) are in agreement with this interpretation of the electronic structure. The reliability of the ab

initio calculation of $(H_2Si)_2P_2$ is reflected in the good agreement of the calculated and experimental (substituted system) distances and angles. For the equilibrium structure (C_{2v}) a longer P–P distance of 2.360 Å was calculated, which is only 0.02 Å shorter than the experimental value for **1b**.[1] The negative results of the ab initio calculations regarding the Si inversion suggest that this process in **1a** is only forced to occur by the presence of bulky substituents. Hence, this is no characteristic of the folded P_2Si_2 bicycle. The incomparability of the parent compound and the derivative with bulky substituents is probably also true for diarsadisilabicyclo[1.1.0]butanes. The greater stability of the *exo,endo* isomer **2a** in comparison to **1a** is probably due to unfavorable As–As interactions in the transition state of the Si inversion.

Experimental Procedure

3: To a solution of Mes(*t*Bu)$SiCl_2$ (4 g, 14.54 mmol) in THF (30 mL) at −78 °C, a solution of [$LiAsH_2$(dme)] (5.06 g, 29.08 mmol) in THF (30 mL) was added. This mixture was warmed to −30 °C over a 2 h period, stirred for a further 2 h at this temperature, and then slowly warmed to 28 °C. After 8 h at 28 °C all volatiles were removed at 10^{-2} Torr. The residue was taken up in benzene (30 mL) and filtered. Concentration of the pale yellow, clear filtrate to ca. 5 mL afforded trapezoid-shaped, colorless crystals after 2 d at 28 °C. Yield 2.52 g (4.50 mmol, 62%). Mp = 188–190 °C.

4: To a solution of **3** (1 g, 1.78 mmol) in THF (20 mL), BuLi (227.8 mg, 3.56 mmol, 2.5 M solution in hexane) was added at −78 °C. The initial colorless solution immediately changed to an intense orange-yellow. After 30 min at −40 °C a solution of *t*BuHgCl (1.046 g, 3.56 mmol) in THF was added slowly which resulted in a colorless solution. Following this the solvent was removed, the residue was taken up in hexane (10 mL), filtered, and crystallized at −78 °C. Compound **4** was isolated as colorless, light-sensitive crystals. Yield 1.859 g (1.58 mmol, 89%). Mp = 176 °C (decomp.).

2a: A vigorously stirred benzene solution of **4** (100 mL, 0.025 M) was exposed to light (150 Watt light bulb) for 24 h. The yellow suspension formed was filtered several times over dry silica gel to remove Hg. Any remaining Hg was later removed under vacuum (10^{-3} Torr). Concentration of the intense yellow solution afforded spectroscopically (^{1}H and ^{29}Si) pure **2**. Yield 1.353 g (2.42 mmol, 97%).

2b: A hexane solution of **2a** (60 mL, 0.017 M) was irradiated analogously to that for the preparation of **2a** for 1 week at 25 °C. The solution was concentrated to ca. 1 mL, and within 2 weeks **2b** crystallized out completely (^{1}H NMR control, 45.6 mg, 8%).

Received: October 25, 1991 [Z 4988 IE]
German version: *Angew. Chem.* **1992**, *104*, 449

CAS Registry numbers:
2a, 139136-93-1; **2b**, 139238-72-5; **3**, 139130-91-9; **4**, 139130-92-0; MeS(*t*Bu)$SiCl_2$, 89486-31-7; [$LiAsH_2$(dme)], 138435-85-5; *t*BuHgCl, 38442-51-2.

[1] M. Driess, *Angew. Chem.* **1991**, *103*, 979–981; *Angew. Chem. Int. Ed. Engl.* **1991**, *31*, 1022–1024; M. Driess, H. Pritzkow, M. Reisgys, *Chem. Ber.* **1991**, *124*, 1923.

[2] Tetraphosphabicyclo[1.1.0]butane: E. Niecke, R. Rüger, B. Krebs, *Angew. Chem.* **1982**, *94*, 553; *Angew. Chem. Int. Ed. Engl.* **1982**, *21*, 544; R. Riedel, H.-D. Hansen, E. Fluck, *ibid.* **1985**, *97*, 1050 bzw. **1985**, *24*, 1056; Diphosphadisilabicyclo[1.1.0]butane: M. Driess, A. D. Fanta, D. Powell, R. West, *ibid.* **1989**, *101*, 1087, **1989**, *29*, 1038 respectively: see also [1].

[3] T. Dabisch, W. W. Schoeller, *J. Chem. Soc. Chem. Commun.* **1986**, 896; W. W. Schoeller, C. Lerch, *Inorg. Chem.* **1983**, *22*, 2992.

[4] **3**: ^{1}H NMR (200 MHz, 340 K, C_6D_6): δ = 1.069 (s, 18 H, *t*Bu), 2.074 (s, 6 H, *p*-Me), 2.708 (br., 14 H, *o*-Me and AsH), 6.725 (s, 4 H, aromat. H); ^{29}Si NMR (298 K, INEPT): δ = −14.09(s); MS(EI, 70 eV): *m/z* (%) 560 (M^+, 73.4), 501 ($(M-t\text{Bu}-2\text{H})^+$, 5.9), 267 ($Mes_2SiH^+$, 74.1), 163 (100).

[5] Crystal structure analysis of **3**: Space group $P\bar{1}$, a = 8.739(4), b = 14.280(7), c = 15.336(8) Å, α = 109.79(3), β = 106.17(3), γ = 103.07(3)°, V = 1617 Å^3, Z = 2, 4327 observed reflections ($I > 2\sigma_I$, four-circle diffractometer, $Mo_{K\alpha}$ radiation, ω scan). The refinement (As, Si, C anisotropic, methyl groups as rigid groups) resulted in R = 0.049, R_w = 0.055. **3** crystallized with benzene.[17]

[6] **4**: ^{1}H NMR (200 MHz, 298 K, C_6D_6): δ = 1.191 (s, 18 H, *t*BuSi), 1.327 (s, 18 H, *t*BuHg, $^3J(^1H, ^{199}Hg)$ = 166 Hz), 2.107 (s, 6 H, *p*-Me), 2.729 (s, 12 H, *o*-Me), 6.756 (s, 4 H, aromat. H); ^{29}Si NMR: δ = −2.56(s); correct C,H analysis.

[7] **2a**: ^{1}H NMR spectra temperature dependent as a result of the hindered rotation of the Mes groups; ^{1}H NMR (200 MHz, 298 K, C_6D_6): δ = 0.801 (s, 9 H, *t*Bu), 1.20 (s, 9 H, *t*Bu), 1.331 (s, 3 H, *o*-Me), 1.572 (s, 3 H, *o*-Me), 2.078–2.114 (m, 6 H, *p*-Me), 2.757–2.767 (br., 6 H, *o*-Me), 6.745 (s, 2 H, aromat. H), 6.772 (s, 2 H, aromat. H); ^{29}Si NMR: δ = 1.62 (s, 1 Si), 8.51 (s, 1 Si). – MS (EI, 70 eV): *m/z* (%) 558 (M^+, 25.3), 501 ($(M - t\text{Bu})^+$, 32.4), 267 (Mes_2SiH^+, 20.0), 57 ($C_4H_9^+$, 100).

[8] **2b**: ^{1}H NMR (200 MHz, 298 K, C_6D_6): δ = 1.215 (s, 18 H, *t*Bu), 2.368 (s, 6 H, *p*-Me), 2.770 (s, 12 H, *o*-Me), 6.289 (s, 4 H, aromat. H); ^{29}Si NMR: δ = −25.71 (s). – MS (EI, 70 eV): identical with **2**.

[9] Crystal structure analysis of **2b**: Space group $C2/c$, a = 19.679(20), b = 11.935(10), c = 12.527(10) Å, β = 108.51(3)°, V = 2790 Å^3, Z = 4, 1049 observed reflections ($I > 2\sigma_I$, four-circle diffractometer, $Mo_{K\alpha}$ radiation, ω scan). The molecule has a crystallographic twofold axis. The refinement (As, Si,C anisotropic, methyl and phenyl groups as rigid groups) resulted in R = 0.071, R_w = 0.074.[17]

[10] W. Hönle, H.G. von Schnering, *Z. Naturforsch. B* **1980**, *35*, 789.

[11] [(*t*$Bu_3C_6H_2$)PAs]$_2$: P. Jutzi, U. Meyer, S. Opiela, M. M. Olmstead, P. P. Power, *Organometallics* **1990**, *9*, 1459; [$(Ph_3P)_2PdAs]_2$: D. Fenske, H. Fleischer, C. Persau, *Angew. Chem.* **1989**, *101*, 1740; *Angew. Chem. Int. Ed. Engl.* **1989**, *28*, 1665.

[12] E. J. Porter, G. M. Sheldrick, *J. Chem. Soc. Dalton Trans.* **1972**, 1347.

[13] GAUSSIAN 88: M. J. Frisch, M. Head-Gordon, H. B. Schlegel, K. Raghavachari, J. S. Binkley, C. Gonzalez, D. J. Defrees, D. J. Fox, R. A. Whiteside, R. Seeger, C. F. Melius, J. Baker, R. Martin, L. R. Kahn, J. J. P. Stewart, E. M. Fluder, S. Topiol, J. A. Pople, Gaussian Inc., Pittsburgh, PA, **1988**.

[14] P. von R. Schleyer, A. F. Sax, J. Kalcher, R. Janoschek, *Angew. Chem.* **1987**, *99*, 374–377; *Angew. Chem. Int. Ed. Engl.* **1987**, *26*, 364–366.

[15] R. Janoschek, *Chem. Unserer Zeit* **1991**, *25*, 59–66.

[16] MOLEKEL: H. J. Werner, W. Meyer, *J. Chem. Phys.* **1981**, *74*, 5794; H. J. Werner, E. A. Reinsch, *ibid.* **1882**, *76*, 3144.

[17] Further details of the crystal structure investigation may be obtained from the Fachinformationszentrum Karlsruhe, Gesellschaft für wissenschaftlich-technische Information mbH, D-W-7514 Eggenstein-Leopoldshafen 2 (FRG) on quoting the depository number CSD-55938, the names of the authors, and the journal citation.

New Routes to Alkylidyne-Bridged Ditungsten Compounds Supported by Alkoxide or Siloxide Ligands by the Activation of Ethylene**

By *Stephanie T. Chacon, Malcolm H. Chisholm,* Cindy M. Cook, Mark J. Hampden-Smith,* and *William E. Streib*

Dedicated to Professor E. O. Fischer

Following Fischer's[1] discovery of the carbyne ligand (now more commonly called alkylidyne) numerous other examples emerged with rich and interesting reactivity. The most common synthetic routes to carbyne complexes involve reactions of carbonyl ligands, α-hydrogen atom transfer from alkyl and/or alkylidene ligands, and C–C scission of coordinated alkynes.[2] We describe here two new reactions leading to carbyne-bridged ditungsten compounds, together with the results of labeling studies that reveal potential insight into the reaction pathways involved in these remarkably facile reactions.

The ethyne adduct $[W_2(\mu\text{-}C_2H_2)\{OSi(t\text{Bu})Me_2\}_6(py)]$[3] and ethylene (≥ 1 equiv) react in hexane at −20 °C to give the blue crystalline compound **1**.

$[W_2(H)(\mu\text{-}CCH{=}CHCH_3)\{OSi(t\text{Bu})Me_2\}_6]$ **1**

Compound **1** is also formed if the reaction is carried out at room temperature; however, a competitive reaction leading

[*] Prof. M. H. Chisholm, S. T. Chacon, C. M. Cook, Prof. M. J. Hampden-Smith, Dr. W. E. Streib
Department of Chemistry and Molecular Structure Center
Indiana University, Bloomington, IN 47405 (USA)

[**] This work was supported by the Department of Energy, Office of Basic Sciences, Chemistry Division, and the National Science Foundation. S. T. C. thanks the American Association of University Women Educational Foundation for an American Dissertation Year Fellowship.

to the previously characterized compound $[W_2(\mu\text{-}CCH)\{OSi(t\text{Bu})Me_2\}_5]$[3] is observed. The latter compound does not react with ethylene to give **1** as determined from a separate experiment. The structure of **1** has been determined from an X-ray crystallographic study and is shown in Figure 1.[4] The NMR data obtained for **1** in $[D_8]$toluene at

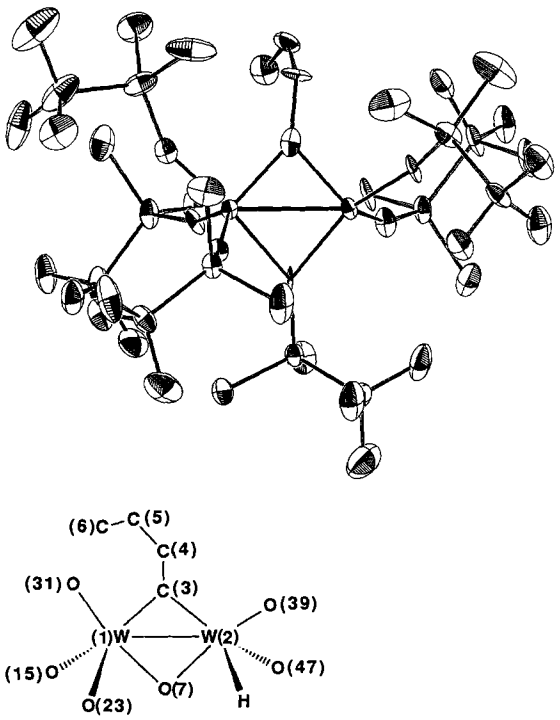

Fig. 1. Top: ORTEP drawing of $[W_2(H)(\mu\text{-}CCH{=}CHCH_3)\{OSi(t\text{Bu})Me_2\}_6]$ (**1**). Hydrogen atoms have been omitted for clarity. Pertinent distances [Å] are W(1)-W(2) 2.658(1), W(1)-O(7) 2.10(1), W(1)-O(15) 1.89(1), W(1)-O(23) 1.86(1), W(1)-O(31) 1.94(1), W(1)-C(3) 1.98(1), W(2)-C(3) 1.92(1), W(2)-O(7) 2.05(1), W(2)-O(39) 1.87(1), W(2)-O(47) 1.92(1). Bottom: The proposed position of the hydride ligand is indicated in the stick drawing.

$-70\,^{\circ}C$ are consistent with the structure found in the solid state (i.e., all siloxy ligands are chemically inequivalent) and, in particular, confirm the presence of the hydride and bridging 2-butenylidyne ligands. At $-70\,^{\circ}C$ the hydride signal shows a coupling to ^{183}W ($I = 1/2$, 14.5% natural abundance) of 145 Hz, while at 22 °C the magnitude of this coupling is only 83 Hz. The relative satellite intensity due to coupling to ^{183}W is notably larger in the room temperature spectrum. This, together with the low-temperature NMR behavior of the $OSi(t\text{Bu})Me_2$ signals, leads us to believe that in the structure of **1**, the hydride ligand occupies a terminal position on W2, which is otherwise only four coordinate. It is evident, however, that a fluxional process involving terminal-bridge interchange of both siloxide and hydride ligands is rapid on the NMR time scale at room temperature.

The compound $[W_2(\mu\text{-}CMe)(OCH_2t\text{Bu})_6(Ot\text{Bu})]$ (**2**), was first discovered as a minor product in the reaction between $[W_2(OCH_2t\text{Bu})_6]$ and ethylene (2 equiv).[5] The origin of the OtBu ligand can reliably be traced to the presence of adventitious tBuOH that was present in the solution as a residual impurity from the preparation of $[W_2(OCH_2t\text{Bu})_6]$ by alcoholysis of $[W_2(Ot\text{Bu})_6]$. The reaction shown in Equation (a)

$$[W_2(OCH_2t\text{Bu})_6(C_2H_4)_2] + t\text{BuOH} \longrightarrow [W_2(\mu\text{-}CMe)(OCH_2t\text{Bu})_6(Ot\text{Bu})] + C_2H_6 \quad (a)$$

2

provides a synthesis of **2** in ca. 50% isolated yields starting from $[W_2(OCH_2t\text{Bu})_6(C_2H_4)_2]$.[6]

The structure of the μ-ethylidyne complex **2**[4] is shown in Figure 2 and the NMR data are consistent with the solid-state structure.

Insight into the reaction pathways leading to the facile formation of compounds **1** and **2** may be gleaned from the following observations involving the use of labeled C_2 compounds: 1) The reaction between $[W_2(\mu\text{-}^{13}C_2H_2)\{OSi(t\text{Bu})Me_2\}_6(py)]$ and C_2H_4 in hexane at $-20\,^{\circ}C$ yields the isotopomer of **1** $[W_2(H)(\mu\text{-}^{13}C^{13}CH{=}CHCH_3)\{OSi(t\text{Bu})Me_2\}_6]$ while the reaction between $[W_2(\mu\text{-}C_2D_2)\{OSi(t\text{Bu})Me_2\}_6(py)]$ and C_2H_4 gives $[W_2(D)(\mu\text{-}CCD{=}CHCH_3)\{OSi(t\text{Bu})Me_2\}_6]$. 2) The reaction between $[W_2(OCH_2t\text{Bu})_6(C_2D_4)_2]$ and tBuOH in hexane yields $[W_2(\mu\text{-}CCD_3)(OCH_2t\text{Bu})_6(Ot\text{Bu})]$ and C_2D_5H as deduced from NMR studies.

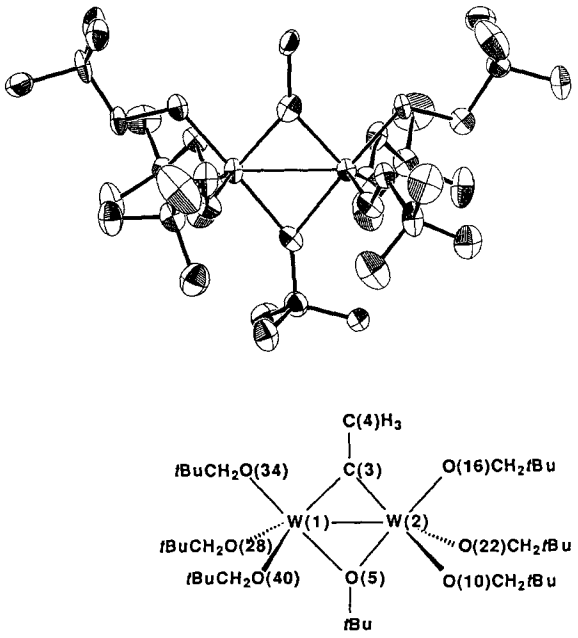

Fig. 2. Top: ORTEP drawing of $[W_2(\mu\text{-}CMe)(OCH_2t\text{Bu})_6(Ot\text{Bu})]$ (**2**). Hydrogen atoms have been omitted for clarity. Pertinent distances are W(1)-W(2) 2.644(1), W(1)-O(5) 2.05(1), W(1)-O(28) 1.90(1), W(1)-O(34) 1.94(1), W(1)-O(40) 1.91(1), W(1)-C(3) 1.94(1), W(2)-O(5) 2.03(1), W(2)-O(10) 1.90(1), W(2)-O(16) 1.94(1), W(2)-O(22) 1.90(1), W(2)-C(3) 1.94(1). Bottom: Stick drawing of **2**.

The stereospecific transfer of H/D atoms and the stereochemistry about the C–C double bond in **1** lead us to suggest that the alkylidyne ligand is formed by initial C–C bond formation to generate a metallacyclopentenyl moiety[7] followed by β-H elimination and reinsertion to generate an alkenyl ligand. By subsequent α-CH activation the hydride and alkenylidyne ligands are formed (see Scheme 1).

The formation of the isotopomer of **2** containing the $[W_2(\mu\text{-}CCD_3)]$ moiety indicates that the ethylidyne H/D atoms arise exclusively from those on ethylene and as such parallels the reaction of ethylene on a Pt^{III} surface that generates the μ_3-ethylidyne ligand.[8]

In conclusion, we have discovered two facile reactions leading to alkylidyne-bridged ditungsten compounds supported by alkoxide or siloxide ligands from ethylene. It seems quite plausible that these are merely the first examples in the reactions of ditungsten alkoxides/siloxides and alkenes.

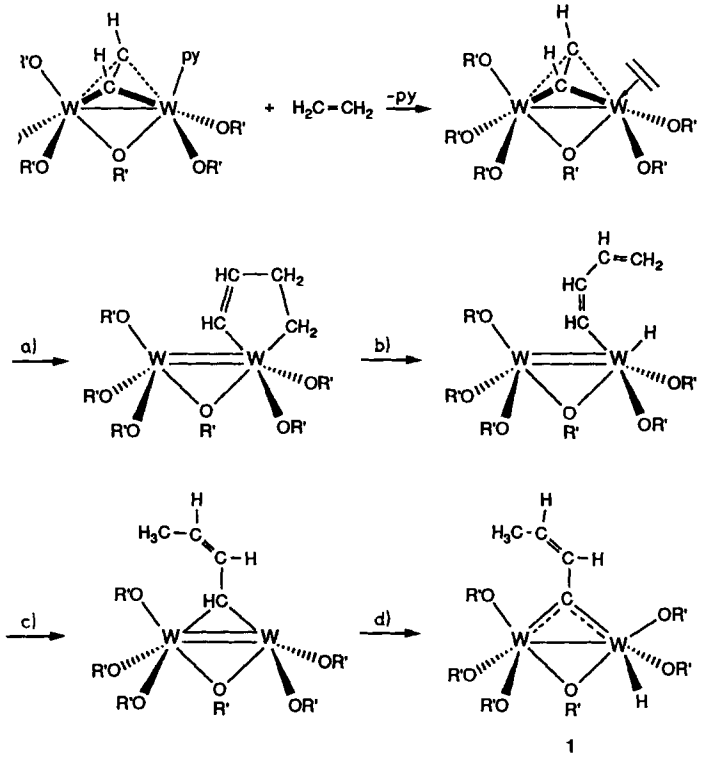

Scheme 1. A possible reaction pathway leading to the formation of **1** from $[W_2(\mu\text{-}C_2H_2)\{OSi(t\text{Bu})Me_2\}_6(py)]$ and ethylene. R′ = Si(*t*Bu)Me_2. a) C–C coupling, b) β-H elimination, c) insertion, d) α-H elimination.

Experimental Procedure

$[W_2(H_a)(C_aC_bH_b{=}C_cH_cC_dH_{3d})\{OSi(t\text{Bu})Me_2\}_6]$ (**1**): A 50 mL Kontes flask charged with black $[W_2(\mu\text{-}C_2H_2)\{OSi(t\text{Bu})Me_2\}_6(py)]$ crystalline solid (330 mg, 0.26 mmol) and a stir bar was placed in a CO_2(s)/ethanol cold bath at −72 °C. Toluene (10 mL) was then added. The heterogeneous mixture was immediately frozen at −196 °C, evacuated, and C_2H_4 (1.31 mmol) introduced through a calibrated vacuum manifold. The flask was immediately placed in a cold bath at −72 °C for 30 min, during which time the mixture became homogeneous, and the brown solution gained a blue tint. The solution was placed at −20 °C for 12 h. Reduction of the volume to ca. 5 mL, and crystallization at −20 °C led to the isolation of deep blue-black crystals of **1**. Combined crystallizations gave **1** in 45% isolated yield.

^{1}H NMR (300 MHz, 22 °C, C_6D_6): δ = 15.76 (s, $J_{W,H}$ = 83 Hz, I = 32%, H_a); 8.22 (dq, $^3J_{Hb,Hc}$ = 11 Hz, $^4J_{Hb,Hd}$ = 1 Hz, H_b); 5.64 (dq, $^3J_{Hc,Hb}$ = 11 Hz, $^3J_{Hc,Hd}$ = 6 Hz, H_c); 1.88 (dd, $^3J_{Hd,Hc}$ = 6 Hz, $^4J_{Hd,Hb}$ = 1 Hz, H_d); 1.10 (s, br, OSi(*t*Bu)Me_2); 0.34 (s, br, OSi(*t*Bu)Me_2).

^{1}H NMR (300 MHz, −70 °C, C_7D_8): δ = 15.56 (s, $J_{W,H}$ = 145 Hz, I = 22%, H_a); 8.22 (dq, H_b); 5.64 (dq, H_c); 1.88 (dd, H_d); (OSi(*t*Bu)Me_2): 1.35, 1.24, 1.14, 1.12, 1.06, 1.02 (s with intensity ratio 1:1:1:1:1:1); (OSi(*t*Bu)Me_2): 0.70, 0.66, 0.48, 0.47, 0.32, 0.30, 0.29, 0.26, 0.21, 0.17, 0.16 (s with intensity ratio 1:1:1:1:1:1:2:1:1:1. The signal of intensity 2 is apparently due to accidental degeneracy).

^{13}C{^{1}H} NMR (75 MHz, 22 °C, C_6D_6): $^{13}C_a{}^{13}C_bH_b{=}{}^{13}C_cH_c{}^{13}C_dH_{3d}$ ligand only; δ = 313.8 (d, $^1J_{Ca,Cb}$ = 45 Hz, $^1J_{C,W}$ = 142 Hz, I = 22%, C_a); 152.0 (dd, $^1J_{Cb,Cc}$ = 70 Hz, $^1J_{Cb,Ca}$ = 45 Hz, C_b); 127.1 (dd, $^1J_{Cc,Cb}$ = 70 Hz, $^1J_{Cc,Cd}$ = 43 Hz, C_c); 16.7 (d, $^1J_{Cd,Cc}$ = 43 Hz, C_d). Chemical shifts and coupling constants are invariant at low temperatures (−70 °C).

^{13}C NMR (gated decoupled) (75 MHz, 22 °C, C_6D_6): δ = 313.8 (dd, $^1J_{Ca,Cb}$ = 45 Hz, $^2J_{Ca,Hb}$ = 10 Hz, C_a); 152.0 (dddd, $^1J_{Cb,Hb}$ = 154 Hz, $^1J_{Cb,Cc}$ = 70 Hz, $^1J_{Cb,Ca}$ = 45 Hz, $^2J_{Cb,Hc}$ = 4 Hz, C_b); 127.1 (dddq, $^1J_{Cc,Hc}$ = 157 Hz, $^1J_{Cc,Cb}$ = 70 Hz, $^1J_{Cc,Cd}$ = 43 Hz, $^2J_{Cc,Hd}$ = 7 Hz, C_c); 16.7 (dq of virtual triplets, $^1J_{Cd,Hd}$ = 126 Hz, $^1J_{Cd,Cc}$ = 43 Hz, $^2J_{Cd,Hb} \approx {}^4J_{Cd,Ha(trans)} \approx$ 11 Hz, C_d giving rise to second-order fine coupling which appears as virtual triplets).

$[W_2(\mu\text{-}CMe)(OCH_2t\text{Bu})_6(Ot\text{Bu})]$ (**2**): $[W_2(OCH_2t\text{Bu})_6(C_2H_4)_2]$ [6] (389 mg, 0.411 mmol) was placed in a 30 mL Schlenk flask equipped with a Teflon-coated stir bar and 10 mL of hexane was added at 0 °C. 100 μL of a 4.4 M *t*BuOH solution in toluene was added by syringe. The solution was allowed to stir for four days and then cooled to −20 °C. Three batches of 30, 48, and 148 mg of crystals were isolated for a total yield of 55% (226 mg, 0.228 mmol).

^{1}H NMR (300 MHz, −40 °C, C_7D_8): δ = 4.54 (s, 3H, CCH_3), $OCH_2C(CH_3)_3$: 4.67 (s, 4H), 3.60 (d, 4H, $^2J_{H,H}$ = 10 Hz), 3.34 (d, 4H, $^2J_{H,H}$ = 10 Hz); 1.97 (s, 9H, $OC(CH_3)_3$; $OCH_2C(CH_3)_3$: 1.35 (s, 18H), 0.86 (s, 36H).

$[W_2(OCH_2t\text{Bu})_6(Ot\text{Bu})(\mu\text{-}{}^{13}C^{13}CH_3)]$: ^{1}H NMR (360 MHz, 22 °C, C_7D_8): δ = 4.47 (dd, 3H, $^1J_{H,C}$ = 130 Hz, $^2J_{H,C}$ = 7 Hz, $^{13}C^{13}CH_3$).

^{13}C{^{1}H} NMR (75 MHz, 22 °C, C_7D_8): δ = 34.4 (d, $^1J_{C,C}$ = 30 Hz, $^{13}C^{13}CH_3$); 297.3 (d, $^1J_{C,C}$ = 30 Hz, $^1J_{C,W}$ = 160 Hz, I = 26%, $^{13}C^{13}CH_3$).

Received: October 28, 1991 [Z 4993 IE]
German version: *Angew. Chem.* **1992**, *104*, 467

CAS Registry numbers:
1, 139524-19-9; **2**, 139563-95-4; $[W_2(\mu\text{-}C_2H_2)\{OSi(t\text{Bu})Me_2\}_6(py)]$, 134384-51-3; $[W_2(OCH_2t\text{Bu})_6(C_2H_4)_2]$, 128659-38-1; $[W_2(\mu\text{-}{}^{13}C_2H_2)\{OSi(t\text{Bu})Me_2\}_6(py)]$, 134384-63-7; $[W_2(\mu\text{-}C_2D_2)\{OSi(t\text{Bu})Me_2\}_6(py)]$, 134384-37-5; $[W_2(OCH_2t\text{Bu})_6(C_2D_4)_2]$, 139524-20-2; $[W_2H(\mu\text{-}{}^{13}C^{13}CH{=}CHCH_3)\{OSi(t\text{Bu})Me_2\}_6]$, 139524-21-3; $[W_2D(\mu\text{-CCD=CHCH}_3)\{OSi(t\text{Bu})Me_2\}_6]$, 139524-22-4; $[W_2(\mu\text{-CCD}_3)(OCH_2t\text{Bu})_6(Ot\text{Bu})]$, 139524-23-5.

[1] E. O. Fischer, G. Kreissl, C. G. Kreiter, J. Müller, G. Huttner, H. Lorenz, *Angew. Chem.* **1973**, *85*, 618; *Angew. Chem. Int. Ed. Engl.* **1973**, *12*, 564.
[2] J. P. Collman, L. S. Hegedus, J. R. Norton, R. G. Finke, *Principles and Applications of Organotransition Metal Chemistry*, University Science Books, Mill Valley, CA, **1987**, pp. 137–146, and references cited therein.
[3] M. H. Chisholm, C. M. Cook, J. C. Huffman, W. E. Streib, *J. Chem. Soc. Dalton Trans.* **1991**, 929.
[4] Crystal data for **1** at −172 °C: a = 14.037(2), b = 18.453(2), c = 11.681(2) Å, α = 91.20(1), β = 106.63(1), γ = 100.35(1)°, Z = 2, ϱ_{calcd} = 1.41 g cm^{-3} and space group $P\bar{1}$. Of the 8821 reflections collected ($Mo_{K\alpha}$, 6° < 2θ < 45°) 7482 were unique and the 6625 having $F_0 > 3\sigma(F)$ were used in the least-squares refinement. In the final cycles of refinement, the non-H atoms were varied with anisotropic thermal parameters. The final residuals are $R(F)$ = 0.0535 and $R_w(F)$ = 0.0527. Crystal data for **2** at −147 °C: a = 12.619(4), b = 18.459(5), c = 10.316(2) Å, α = 91.42(1), β = 102.35(1)°, γ = 70.74(1)°, Z = 2, ϱ_{calcd} = 1.49 g cm^{-3} and space group $P\bar{1}$. Of the 7489 reflections collected ($Mo_{K\alpha}$, 6° < 2θ < 45°) 5810 were unique and the 4999 having $F > 3\sigma(F)$ were used in the least squares refinement. The final residuals are $R(F)$ = 0.0473 and $R_w(F)$ = 0.0466. All non-H atoms were refined anisotropically. Further details of the crystal structure investigations may be obtained from the Fachinformationszentrum Karlsruhe, Gesellschaft für wissenschaftlich-technische Information mbH, D-W-7514 Eggenstein-Leopoldshafen 2 (FRG), on quoting the depository number CSD-56004, the names of the authors, and the journal citation.
[5] M. H. Chisholm, J. C. Huffman, M. J. Hampden-Smith, *J. Am. Chem. Soc.* **1989**, *111*, 5284.
[6] R. H. Cayton, S. T. Chacon, M. H. Chisholm, J. C. Huffman, *Angew. Chem.* **1990**, *102*, 1056; *Angew. Chem. Int. Ed. Engl.* **1990**, *29*, 1026.
[7] The coupling of two alkyne ligands to give a $[W_2(\mu\text{-}C_4R_4)]$ center is well documented in the chemistry of $[W_2(OR)_6]$ compounds. See M. H. Chisholm, D. M. Hoffman, J. C. Huffman, *J. Am. Chem. Soc.* **1984**, *106*, 6806.
[8] L. L. Kesmodel, L. H. Dubois, G. A. Somorjai, *J. Chem. Phys.* **1979**, *70*, 2180.

$[(Ph_3PAu)_6Mn(CO)_3]^+$, a Cluster with Pentagonal-Bipyramidal Structure**

By *Jörg Mielcke*, and *Joachim Strähle**

Dedicated to Professor Ernst Bayer on the occasion of his 65th birthday

The cluster cations $[(Ph_3PAu)_xM(CO)_y]^+$ are obtained from the photolysis of $[Ph_3PAuN_3]$ in the presence of metal carbonyls.[1–6] The composition of the cations is determined by the electronic requirement of the transition metal M, which tries to achieve a stable noble-gas electron configuration (for a qualitative explanation of the bonding see [5]). In the series of cluster cations which we have so far structurally characterized with the metal center Au_xM (x = 4–7), we

[*] Prof. Dr. J. Strähle, Dipl.-Chem. J. Mielcke
Institut für Anorganische Chemie der Universität
Auf der Morgenstelle 18, D-W-7400 Tübingen (FRG)

[**] Cluster synthesis by the photolysis of $[R_3PAuN_3]$, Part 7. This work was supported by the Deutsche Forschungsgemeinschaft and the Fonds der Chemischen Industrie. We thank Degussa AG for tetrachloroauric acid.– Part 6:[6].

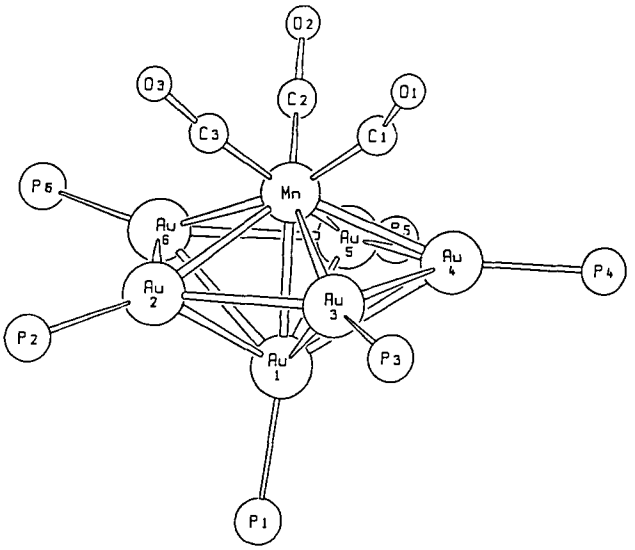

Fig. 1. Crystal structure of **2** (for the phosphane ligands only the P atoms are shown).[12] Important distances [Å] and angles [°]: Au1-Au2 2.812(1), Au1-Au3 2.864(1), Au1-Au4 2.951(1), Au1-Au5 2.802(1), Au1-Au6 2.917(1), Au2-Au3 2.826(1), Au2-Au6 2.948(1), Au3-Au4 2.861(1), Au4-Au5 2.792(1), Au5-Au6 2.920(1), Mn-Au1 2.618(1), Mn-Au2 2.718(1), Mn-Au3 2.671(2), Mn-Au4 2.649(1), Mn-Au5 2.723(2), Mn-Au6 2.622(2), Mn-C1 1.74(1), Mn-C2 1.78(1), Mn-C3 1.775(8), C1-O1 1.22(2), C2-O2 1.22(1), C3-O3 1.181(9), C1-Au4 2.44(1), C2-Au5 2.56(1); Mn-C1-O1 154(1), Mn-C2-O2 165.4(9), Mn-C3-O3 169.0(7).

have now prepared in addition to the Au_6M cluster $[(Ph_3PAu)_6V(CO)_4]^+$ (**1**)[6] also the cluster $[(Ph_3PAu)_6Mn(CO)_3]^+$ (**2**) of analogous formula. Interestingly, despite the same total number of electrons the clusters show different structures. The cluster framework of **1** can be described as a double-capped trigonal bipyramid with the vanadium atom in an equatorial position, whereas **2** forms a pentagonal bipyramid, in which the manganese atom is in an axial position (Fig. 1).

The Au_6Mn cluster **2** is formed in low yield together with $[(Ph_3PAu)_4Mn(CO)_4]^+$, on the photolysis of a solution of $[Ph_3PAuN_3]$ and $[Mn_2(CO)_{10}]$ in THF.[4] Better yields of **2** can be obtained starting from $[Ph_3PAuMn(CO)_5]$.[7] Compound **2** can be isolated after chromatographic separation as the PF_6 salt in the form of orange-red, air-stable, small plate-like crystals. The IR spectrum shows two bands for the $Mn(CO)_3$ group at 1894 and 1838 cm^{-1}. The crystal structure analysis[8] shows that **2** has a pentagonal-bipyramidal structure which is rare for metal clusters. The only other metal cluster known with this structure is $[(Ph_3PAu)_7]^+$.[9] In **2** strong Mn–Au bonds are found, which are between 2.618 and 2.723 Å long (comparable with the corresponding values in the cluster cation $[(Ph_3PAu)_4Mn(CO)_4]^+$ [4]). The Au–Au distances (2.792 to 2.951 Å) lie in the range of values which are found in the homonuclear gold clusters[10] between the peripheral gold atoms. Similar distances are also found in $[(Ph_3PAu)_7]^+$,[9] $[(Ph_3PAu)_4Mn(CO)_4]^+$,[4] and **1**.[6]

The Au_6 frameworks of **1** and **2**, like the metal frameworks Au_xM of other known cluster cations, can be interpreted as icosahedral fragments (Fig. 2).[5] The transition metal M is situated in the center of the incomplete icosahedron.

Compound **2** can be regarded as an analogue of the cyclopentadienyl complex $[CpMn(CO)_3]$, since the pentagonal-pyramidal $[(Ph_3PAu)_6]^+$ part of the framework is similar to the cyclopentadienyl ligand with respect to the structure and the bonding (Fig. 3) .

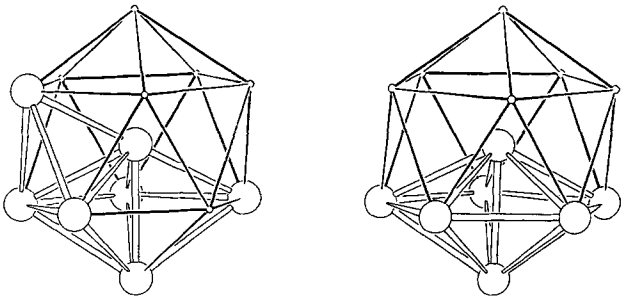

Fig. 2. Representation of the cluster frameworks Au_6M of **1** (left) and **2** (right) as centered icosahedral fragments.

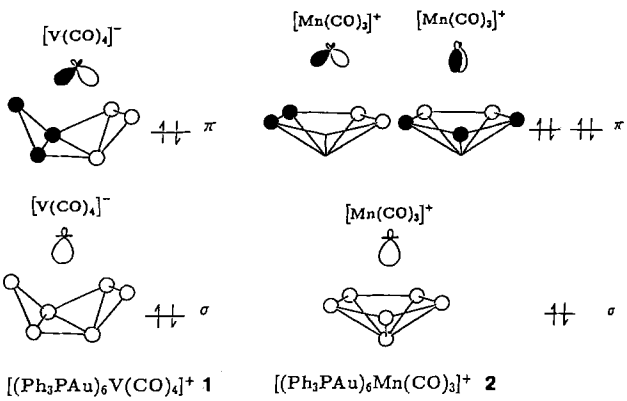

Fig. 3. Schematic representation of the cluster MOs in **1** [6] and **2**. The radial oriented sp-hybrid orbitals of the Ph_3PAu groups are symbolized by circles.

From our experience so far, the clusters $[(Ph_3PAu)_xM(CO)_y]^+$ [1–5] with the same number of valence electrons for the fragment $M(CO)_y$ form the same structure type as shown by the examples $[(Ph_3PAu)_4Co(CO)_3]^+$,[5] $[(Ph_3PAu)_4Mn(CO)_4]^+$,[4] $[(Ph_3PAu)_5Fe(CO)_3]^+$,[3] and $[(Ph_3PAu)_5Mo(CO)_4]^+$.[11] That this is not the case with **1** and **2** can be explained on the basis of the stereochemistry and the bonding. Hence, model studies show that the elliptical form of Au_6V in **1** results in a lower repulsion between the four CO groups and the $(Ph_3PAu)_6$ part of the framework than would be the case with a more spherical structure as exists for the Au_6Mn framework.

To interpret the bonding, the clusters **1** and **2** can be dismantled into the fragments $(Ph_3PAu)_6$, and $V(CO)_4$ or $Mn(CO)_3$, respectively. If the $M(CO)_y$ fragments allocate six electrons for the back bonding to the CO groups, then for **1** this results in a $[(Ph_3PAu)_6]^{2+}$ fragment with four valence electrons for the cluster bonding and a d^6 $[V(CO)_4]^-$ group with two vacant valence orbitals. For **2**, a $(Ph_3PAu)_6$ fragment with six valence electrons and a d^6 $[Mn(CO)_3]^+$ group with three empty orbitals remain. The latter can form a bonding cluster MO with σ symmetry as well as two MOs with π symmetry with the radial oriented sp-hybrid orbitals of the Ph_3PAu groups, whereas for **1** together with a cluster MO with σ symmetry only one MO with π symmetry results (Fig. 3). The structures of **1** and **2** are probably influenced by the π MOs. Since the two π MOs in **2** are arranged perpendicular to one another, a spherical cluster is preferred. In the case of only one π MO, as exists in **1**, the elliptical cluster structure obviously leads to a more effective overlap.

An alternative allocation of the valence electrons of **1** to one $(Ph_3PAu)_6$ fragment with six valence electrons and a d^4 $[V(CO)_4]^+$ group with four vacant valence orbitals could lead to a spherical structure analogous to $[CpV(CO)_4]$. How-

ever, from the explained reasons it is evidently less favored. The spherical structure for $[CpV(CO)_4]$ is determined by the rigid cyclopentadienyl ligand and tolerated due to its lower steric requirement. The more sterically demanding $(Ph_3PAu)_6$ framework is flexible because of the weak gold–gold interactions, and therefore able to adapt to its optimal structure.

Experimental Procedure

A mixture of $[Ph_3PAuMn(CO)_5]$[7] (300 mg, 0.458 mmol), $[Ph_3PAuNCO]$ (229.8 mg, 0.458 mmol), and $[Ph_3PAuN_3]$ (68.95 mg, 0.138 mmol) was irradiated in freshly distilled THF (70 mL) for 30 min using a high-pressure Hg lamp with a nitrogen purge. This produced a deep red-brown solution, which was filtered and evaporated to dryness under vacuum, then dissolved in a little CH_2Cl_2 and chromatographed on a Al_2O_3 column. An initial major fraction contained $[(Ph_3PAu)_4Mn(CO)_4]^+$. The compound **2** was eluted as a second fraction, and after the addition of KPF_6 was isolated as $\mathbf{2}\cdot PF_6$. Orange-red crystals were obtained after recrystallization from CH_2Cl_2/diisopropyl ether in 15% yield. IR: $\tilde{\nu}$ [cm^{-1}] = 1894 (C=O), 1838 (C=O); ^{31}P NMR: (CH_2Cl_2, 32.44 MHz): δ = 40.1; FAB MS: *m/z* 2893.5 ($[(Ph_3PAu)_6Mn(CO)_3]^+ - H$ = $(M-H)^+$), 2630.7 ($(M-PPh_3-2H)^+$), 1628.7 ($(M-2\ AuPPh_3-PPh_3-H)^+$).

Received: October 29, 1991 [Z4995IE]
German version: *Angew. Chem.* **1992**, *104*, 485

CAS Registry numbers:
2-PF_6, 139041-33-1; $[Ph_3PAuMn(CO)_5]$, 14692-78-5; $[Ph_3PAuNCO]$, 24169-91-3; $[Ph_3PAuN_3]$, 20224-83-3; Au, 7440-57-5; Mn, 7439-96-5.

[1] G. Beuter, J. Strähle, *Angew. Chem.* **1988**, *100*, 1099–1100; *Angew. Chem. Int. Ed. Engl.* **1988**, *27*, 1094–1095.
[2] G. Beuter, J. Strähle, *J. Organomet. Chem.* **1989**, *372*, 67–78.
[3] G. Beuter, J. Strähle, *Z. Naturforsch. B* **1989**, *44*, 647–652.
[4] G. Beuter, J. Strähle, *J. Less-Common. Met.* **1989**, *156*, 387–395.
[5] G. Beuter, J. Mielcke, J. Strähle, *Z. Anorg. Allg. Chem.* **1991**, *593*, 35–45.
[6] K. Wurst, J. Strähle, G. Beuter, D. Belli Dell'Amico, F. Calderazzo, *Acta Chem. Scand.* **1991**, *45*, 844–849.
[7] C. E. Coffey, J. Lewis, R. S. Nyholm, *J. Chem. Soc.* **1964**, 1741–1749.
[8] Crystal data for $\mathbf{2}\cdot PF_6$: $P2_1/c$, $a = 23.105(4)$, $b = 13.189(6)$, $c = 37.781(7)$ Å, $\beta = 98.67(2)°$, $Z = 4$, $R = 0.086$ for 6118 unique reflections with $I > 3\sigma(I)$ and 527 refined parameters (Enraf-Nonius CAD4, SDP-Plus, $Mo_{K\alpha}$, ω/θ scans, $3° \le \theta \le 25°$). Empirical absorption correction, anisotropic temperature parameters for the metal and P atoms; some H atoms were considered with calculated positions. Further details of the crystal structure investigation may be obtained from the Fachinformationszentrum Karlsruhe, Gesellschaft für wissenschaftlich-technische Information mbH, D-W-7514 Eggenstein-Leopoldshafen 2 (FRG) on quoting the depository number CSD-55998, the names of the authors, and the journal citation.
[9] J. W. A. van der Velden, P. T. Beurskens, J. J. Bour, W. P. Bosman, J. H. Noordik, M. Kolenbrander, J. A. K. M. Buskes, *Inorg. Chem.* **1984**, *23*, 146–151.
[10] P. G. Jones, *Gold Bull.* **1983**, *16*, 114–124.
[11] G. Beuter, S. Maier, J. Strähle, unpublished.
[12] E. Keller, *SCHAKAL, Fortran program for the reproduction of crystal structures*, Freiburg, **1986**.

The First Structural Characterization of a Metal–Enterobactin Complex: $[V(enterobactin)]^{2-}$ **

By *Timothy B. Karpishin* and *Kenneth N. Raymond**

Our appreciation of the significance of the siderophores[1]—microbial iron sequestering agents—has increased as their role in many diseases caused by pathogenic bacteria or fungi has become clearer. Iron supply, mediated by siderophores, is often the limiting factor in the growth of these organisms.[2] Of the approximately 200 siderophores now characterized, enterobactin (produced by enteric bacteria such as *E. coli* and discovered in 1970[3]) has been prominent and is the most powerful ferric ion chelator known (overall stability constant, $K_f \approx 10^{49}$).[4] The synthesis,[5] biosynthesis[6] and intracellular transport of enterobactin (Fig. 1) and its Fe^{III} complex[7] have all been studied. One

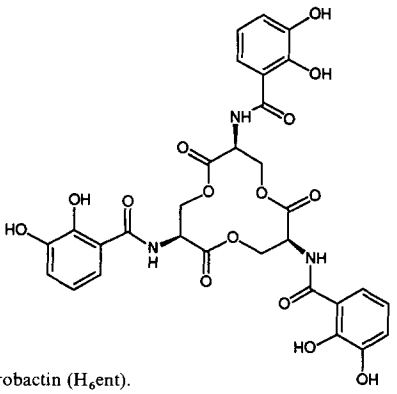

Fig. 1. The formula of enterobactin (H_6ent).

particular goal has been the explanation of the extraordinarily high stability of ferric enterobactin which is typically greater than that of simple model compounds by a factor of 10^6. Studies dealing with this issue have involved spectroscopic[8] and thermodynamic methods,[4] three-dimensional conformational analysis from NMR spectra of the diamagnetic Ga^{III} complex,[9] and molecular mechanics calculations of the free ligand and Fe^{III} complex.[10] The latter two analyses differ markedly in specific aspects of the predicted structure of the ferric enterobactin complex and how that structure affects the biological properties of the siderophore. Although enterobactin will bind many other metal ions in place of Fe^{III},[7b, 11] efforts in several laboratories over a number of years have failed to give crystals for a structure analysis. We report here the first structural characterization of a metal–enterobactin complex: $[V(enterobactin)]^{2-}$.

Reaction of protonated enterobactin, H_6ent,[12] with $VO(acetylacetonate)_2$ and two equivalents of KOH results in the displacement of the vanadyl oxygen[13] and formation of the vanadium(IV) complex, $[V(ent)]^{2-}$.[14] The complex anion is shown in Figure 2.[15] The molecule is a tris chelate complex (three catecholate groups) and has approximate C_3 molecular point symmetry. Since the backbone of enterobactin is based on three L-serine units, the introduction of chirality at the metal center (Δ or Λ) produces a diastereomeric complex ion. The chirality of the Fe^{III}, Cr^{III}, and Rh^{III} enterobactin complexes has been shown from CD spectra to be 100% Δ (a right-handed propeller).[11a, 16] As can be seen from a view down the approximate molecular threefold axis (Fig. 3), $[V(ent)]^{2-}$ also has Δ-configuration.[17]

The Δ configuration of $[Fe(ent)]^{3-}$ has important biological implications. Since the mirror image Λ-ferric enantioenterobactin (which consists of D-serine units) is not as efficient in growth promotion as the native Δ-$[Fe(ent)]^{3-}$,[7e] and since it is known that the tris(catechol) portion of the molecule is essential for recognition by the *E. coli* outer membrane protein,[7b] it has been suggested that it is the Δ chirality at the Fe center that is crucial in the recognition of $[Fe(ent)]^{3-}$. It is thus desirable to understand the interactions that stabilize the Δ isomer in metal–enterobactin complexes. Shanzer et al. have proposed that the preference for

[*] Prof. Dr. K. N. Raymond, T. B. Karpishin
Department of Chemistry, University of California
Berkeley, CA 94720 (USA)

[**] This research was supported by United States National Institutes of Health Grant AI 11744.

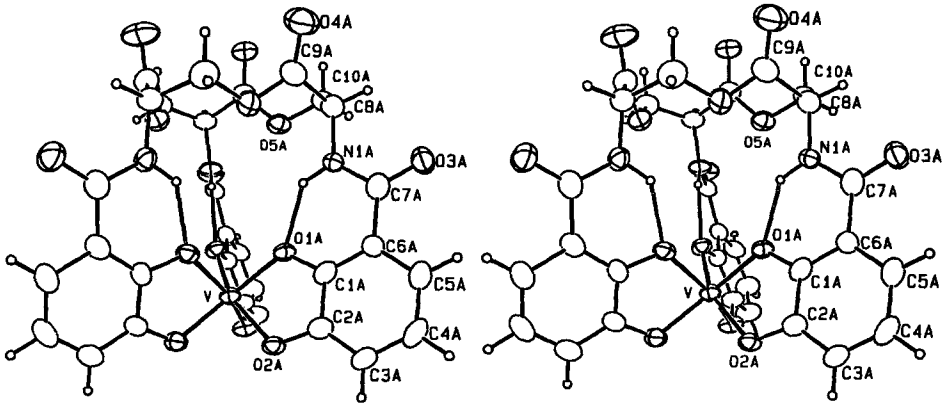

Fig. 2. Stereoview (ORTEP) of the structure of $[V(ent)]^{2-}$. The atoms in the structure are named A, B, and C to denote the threefold symmetry in the molecule. Average bond lengths and angles: V-O1 1.946(7) Å; V-O2 1.939(5) Å; O1-V-O2 79.8(6)°.

the Δ conformation of $[Fe(ent)]^{3-}$ is a result of hydrogen bonding between the amide protons and the ester oxygens of the serine backbone that occurs in the free ligand prior to iron binding.[10] This analysis suggested, however, that these bonds are broken once the ferric complex is formed. We

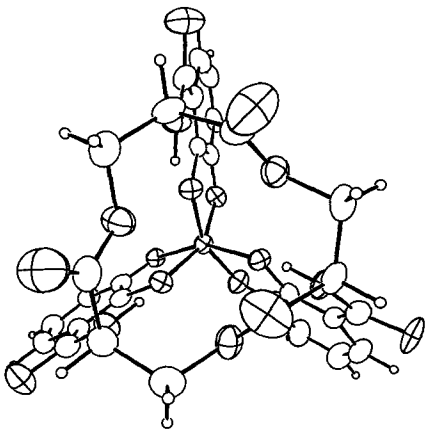

Fig. 3. Structure of $[V(ent)]^{2-}$; view down the approximate molecular threefold axis (ORTEP).

come to the conclusion that the preference for the Δ isomer in metal enterobactin complexes is a result of conformational constraints that exist within the twelve-membered ring, and this can be seen in our structure of $[V(ent)]^{2-}$. If a least-squares plane is defined by the twelve-membered ring atoms of the enterobactin molecule, six atoms (C9A, B, C; C10A, B, C) sit above the plane and six sit below (O5A, B, C; C8A, B, C). At the chiral center C8, the bonds within the twelve-membered ring (to C9 and C10) determine the tilt of the C8–N1 bond. Since each of the catecholamide arms remains planar (vide infra), the tilt of the C8–N1 bonds relative to the plane above sets the handedness of the propeller at the metal center. As a result of non-bonded interactions within the constraints of the twelve-membered ring, C9 sits on average 0.27(4) Å higher above the plane than C10 (Scheme 1). This in turn causes the three bonds from C8 to N1 to tilt as a right-handed propeller (when viewed down the threefold axis) to maintain normal tetrahedral angles at C8.

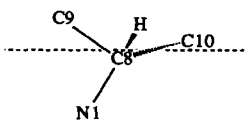

Scheme 1. Orientation of atoms around C8 (see text). The broken line shows the least squares plane.

Although molecular mechanics calculations on $[Fe(ent)]^{3-}$ have assumed ideal octahedral geometry around the iron center with a trigonal twist angle[18] of 60°, that angle in $[V(ent)]^{2-}$ is 28° and in $[Fe(ent)]^{3-}$ is likely to be ≈33°.[19] More accurate modeling of the structure of $[Fe(ent)]^{3-}$ will require incorporation of a coordination geometry intermediate between octahedral and trigonal prismatic.[20]

A very important feature in the structure of $[V(ent)]^{2-}$ is the hydrogen bonding between the amide protons (on N1) and the catechol oxygens (O1) (Fig. 2) forming stable six-membered rings and resulting in the planarity of the catecholamide arms. The average NH···O distance is 1.857(6) Å.[21] This hydrogen bonding between the amide protons and catechol oxygens of metal tris(catecholamide) complexes has been found in every such model compound crystallographically characterized.[22] Although this H-bonding was concluded not to be significant in the structure of $[Ga(ent)]^{3-}$ based on NMR studies,[9] the structures of $[V(ent)]^{2-}$ and the model compounds indicate that such hydrogen bonding plays a key role in the iron (III)–enterobactin complex.

Although the metal ion is somewhat smaller (V^{IV} = 0.58 Å; Fe^{III} = 0.65 Å[23]) the major features seen in this structure must apply also to the native $[Fe(ent)]^{3-}$ complex.[24] From Figure 2 it is clear that the twelve-membered ring is ideally suited as a base from which the three catecholamide binding groups arise. The average V–O1 bond length (1.946(7) Å) is essentially the same as the average V–O2 bond length (1.939(5) Å), indicating that the binding subunits are perfectly positioned by the ring above for coordination to a metal. In contrast, in the V^{III}[22a] and Fe^{III}[16] structures of trencam (a tripodal enterobactin analogue[25] whose Fe^{III} complex has an overall stability constant of $10^{43.6}$), the two M–O bond lengths differ by 0.022 Å and 0.038 Å respectively, indicative of the cap being too small to correctly position the three catecholate groups around the metal center. It is this feature in the design of enterobactin that we believe to be a major contributor to the high stability of the ferric complex relative to model compounds.

In summary, after much speculation regarding the detailed conformation and structure of ferric enterobactin, the major features of this important molecule are revealed by the $[V(ent)]^{2-}$ complex reported here. As the relationship between the structure of the ferric enterobactin complex and its mediation of iron transport into the cell is explored, these

results at last present a definitive answer regarding the key features of the molecular structure.

Received: October 30, 1991 [Z 4999 IE]
German version: *Angew. Chem.* **1992**, *104*, 486

CAS Registry numbers:
K_2[V(ent)], 139131-20-7; $VO(acac)_2$, 3153-26-2; K_2[V(ent)] · 3 DMF, 139238-76-9.

[1] a) B. F. Matzanke, G. Matzanke-Müller, K. N. Raymond in *Iron Carriers and Iron Proteins* (Ed.: T. M. Loehr), VCH Publishers, New York, **1989**, p. 1; b) R. C. Hider, *Struct. Bonding (Berlin)* **1984**, *58*, 25; c) K. N. Raymond, G. Müller, B. F. Matzanke, *Top. Curr. Chem.* **1984**, *123*, 49; d) J. B. Neilands, *Annu. Rev. Biochem.* **1981**, *50*, 715.
[2] a) S. K. Guterman, P. M. Morris, W. J. K. Tannenberg, *Gen. Pharmacol.* **1978**, *9*, 123; b) *Microbial Iron Metabolism* (Ed.: J. B. Neilands), Academic Press, New York, **1974**.
[3] a) J. R. Pollack, J. B. Neilands, *Biochem. Biophys. Res. Commun.* **1970**, *38*, 989; b) I. G. O'Brien, F. Gibson, *Biochim. Biophys. Acta* **1970**, *215*, 393.
[4] L. D. Loomis, K. N. Raymond, *Inorg. Chem.* **1991**, *30*, 906.
[5] a) A. Shanzer, J. Libman, *J. Chem. Soc. Chem. Commun.* **1983**, 846; b) W. H. Rastetter, T. J. Erickson, M. C. Venuti, *J. Org. Chem.* **1981**, *46*, 3579; c) E. J. Corey, S. Battacharyya, *Tetrahedron Lett.* **1977**, *45*, 3919.
[6] F. Rusnak, M. Sakaitani, D. Drueckhammer, J. Reichert, C. T. Walsh, *Biochemistry* **1991**, *30*, 2916, and references cited therein.
[7] a) K. Poole, L. Young, S. Neshat, *J. Bacteriol.* **1990**, *172*, 6991; b) D. J. Ecker, L. D. Loomis, M. E. Cass, K. N. Raymond, *J. Am. Chem. Soc.* **1988**, *110*, 2457; c) D. J. Ecker, B. F. Matzanke, K. N. Raymond, *J. Bacteriol.* **1986**, *167*, 666; d) J. S. Lodge, T. Emery, *ibid.* **1984**, *160*, 801; e) J. B. Neilands, T. J. Erickson, W. H. Rastetter, *J. Biol. Chem.* **1981**, *256*, 3831.
[8] T. B. Karpishin, M. S. Gebhard, E. I. Solomon, K. N. Raymond, *J. Am. Chem. Soc.* **1991**, *113*, 2977.
[9] M. Llinás, D. M. Wilson, J. B. Neilands, *Biochemistry* **1973**, *12*, 3836.
[10] A. Shanzer, J. Libman, S. Lifson, C. E. Felder, *J. Am. Chem. Soc.* **1986**, *108*, 7609.
[11] a) J. V. McArdle, S. R. Sofen, S. R. Cooper, K. N. Raymond, *Inorg. Chem.* **1978**, *17*, 3075; b) S. S. Isied, G. Kuo, K. N. Raymond, *J. Am. Chem. Soc.* **1976**, *98*, 1763.
[12] H_6(ent) · H_2O was isolated from cultures of *E. coli* AN311 as previously described: I. G. Young, F. Gibson, *Methods Enzymol.* **1979**, *56*, 394.
[13] The vanadium(IV) tris(catecholate) complex has previously been prepared using $VO(acac)_2$ as the starting material: S. R. Cooper, Y. B. Koh, K. N. Raymond, *J. Am. Chem. Soc.* **1982**, *104*, 5092.
[14] To 25 mg of H_6(ent) · H_2O (0.036 mmol) in degassed MeOH was added 9.5 mg $VO(acac)_2$ (0.036 mmol). A solution of KOH in degassed MeOH (0.072 mmol) was added via cannula resulting in a deep blue solution which was taken to dryness yielding a blue-black solid, K_2[V(ent)], which is air-stable indefinitely; MS (negative ion-FAB): m/z 715 ([V(ent)]H^-).
[15] Crystals of K_2[V(ent)] · 3 DMF were grown from a DMF solution of the complex by vapor diffusion of Et_2O over a period of six weeks: $K_2VC_{39}H_{42}N_6O_{18}$, $M_r = 1011.95$; monoclinic space group $P2_1$ (No. 4); $a = 13.164(3)$ Å, $b = 10.001(1)$ Å, $c = 16.600(2)$ Å; $\beta = 93.96(1)°$, $V = 2180(1)$ Å^3; $Z = 2$, $\rho_{calcd} = 1.54$ g cm^{-3}. The structure was solved by direct methods using SHELXS. Full matrix least-squares refinement (using the program MOLEN) yielded $R = 0.049$ and $R_w = 0.062$ for 600 parameters and 5551 absorption-corrected reflections with $I \geq 3\sigma(I)$. All non-hydrogen atoms in the complex anion were refined anisotropically. The data $(+h, +k, \pm l$ and Friedel pairs $-h, -k, \pm l)$ were collected on an Enraf-Nonius CAD-4 Diffractometer from $3 \leq 2\theta \leq 45$ using $Mo_{K\alpha}$ radiation. Further details of the crystal structure investigation are available on request from the Fachinformationszentrum Karlsruhe, Gesellschaft für wissenschaftlich-technische Information mbH, D-W-7514 Eggenstein-Leopoldshafen 2 (FRG), on quoting the depository number CSD-56008, the names of the authors, and the journal citation.
[16] T. D. P. Stack, T. B. Karpishin, K. N. Raymond, *J. Am. Chem. Soc.* **1992**, *114*, 1512.
[17] The chirality of the three C8 atoms derived from L-serine (*S*) defines the correct enantiomorph in the crystal structure solution; nonetheless the enantiomorphic *R* structure was also refined as an internal check and yielded $R = 0.054$ and $R_w = 0.067$.
[18] The twist angle (θ) in tris chelate complexes is defined as the projection of the O-M-O angle onto a plane perpendicular to the idealized threefold axis; in O_h, $\theta = 60°$, in D_{3h}, $\theta = 0°$.
[19] The twist angle in Fe^{III} tris(catecholate) complexes is generally 4–6° greater than in V^{IV} complexes with the same ligands (cf. Refs. [22c,d, 24]). This is due to the smaller size of the V^{IV} metal ion [20].
[20] D. L. Kepert, *Inorganic Stereochemistry*, Springer, Heidelberg, **1982**.
[21] The amide hydrogen to oxygen distance was calulated using an idealized N–H bond (1.009 Å): F. H. Allen, O. Kennard, D. G. Watson, L. Brammer, A. G. Orpen, R. Taylor, *J. Chem. Soc. Perkin Trans. II* **1987**, S1.
[22] a) A. R. Bulls, C. G. Pippin, F. E. Hahn, K. N. Raymond, *J. Am. Chem. Soc.* **1990**, *112*, 2627; b) T. J. McMurry, M. W. Hosseini, T. M. Garrett, F. E. Hahn, Z. E. Reyes, K. N. Raymond, *ibid.* **1987**, *109*, 7196; c) T. B. Karpishin, K. N. Raymond, unpublished results; d) T. M. Dewey, K. N. Raymond, unpublished results.
[23] R. D. Shannon, *Acta Crystallogr. Sect. A* **1976**, *32*, 751.
[24] Each of the complexes $[V^{IV}(catecholate)_3]^{2-}$ and $[Fe^{III}(catecholate)_3]^{3-}$ has been previously structurally characterized (cf. [13] and K. N. Raymond, S. S. Isied, L. D. Brown, F. R. Fronczek, J. H. Nibert, *J. Am. Chem. Soc.* **1976**, *98*, 1767) and the most significant differences are in the M–O bond lengths (V: 1.942(8) Å; Fe: 2.015(6) Å).
[25] S. J. Rodgers, C.-W. Lee, C. Y. Ng, K. N. Raymond, *Inorg. Chem.* **1987**, *26*, 1622.

α-Hydroxyaldehyde Derivatives Arising from Oxidation of Plasmalogens**

By *Claudia Meyer*, *Arnulf Lutz*, and *Gerhard Spiteller**

Oxidized lipoproteins of low density (low density lipoproteins, LDL), which can bind to specific macrophage receptors, are known to play a significant role in the onset of atherosclerosis.[1] Polyunsaturated fatty acids of LDL phospholipids are believed to influence the oxidation of LDL,[1, 2] and the resulting aldehydes, like malondialdehyde (MDA) and 4-hydroxy-2-nonenal (4-HNE), react with the free amino groups of LDL proteins.[3] Until now, it was not considered that these aldehydes could also be formed either by hydrolysis or oxidation of plasmalogens such as **1**.[4–6] Plasmalogens make up a high percentage of the lipoprotein phospholipids (20–30% in the ethanolamine fraction).[7] Masked α-hydroxyaldehydes recently detected in tissue lipids are of similar reactivity as 4-HNE.[8–10] In this work we show that masked derivatives of α-hydroxyaldehydes result from oxidation of plasmalogens. These derivatives, once deprotected, could likewise participate in atherogenesis.

Lipids from bovine liver were extracted according to the method of Bligh and Dyer and reduced with lithium aluminum hydride.[9, 11–13] After separation of the fatty alcohols, the lysolipids were isolated by thin-layer chromatography (cyclohexane:ethyl acetate 1:2). The fraction with $R_f = 0.15–0.20$, which was silylated with *N*-methyl-*N*-(trimethylsilyl)trifluoroacetamide and analyzed by GC/MS, contained homologues of structure **2** where R′ = $C_{14}H_{29}$, $C_{16}H_{31}$, and

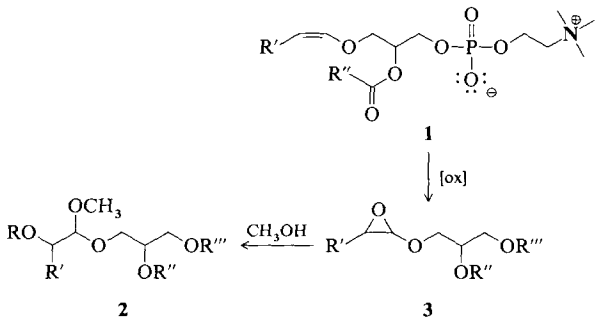

Scheme 1. Hypothesized origin of the mixed acetals **2** from plasmalogens **1**.

[*] Prof. Dr. G. Spiteller, C. Meyer, Dr. A. Lutz
Lehrstuhl Organische Chemie I
Universität Bayreuth
Postfach 101251, D-W-8580 Bayreuth (FRG)

[**] This work was supported by the Deutsche Forschungsgemeinschaft and the Fonds der Chemischen Industrie. We thank M. Glässner for the mass spectral data, D. Laatsch for supplying the glass capillary columns, and Dr. J. Reiner for recording the NMR spectra.

$C_{16}H_{33}$ [R = R″ = R‴ = $Si(CH_3)_3$]. These homologues are masked α-hydroxyaldehydes.

The presence of mixed acetals **2** is understandable if one postulates epoxides **3** as intermediates (Scheme 1). To test this possible pathway to **2**, we studied the plasmalogen model compounds dodec-1-enyl propyl ether (**4**) and 1-*O*-(dec-1-enyl)glycerol-2,3-diacetate (**5**). Vinyl ether **4** was prepared by the procedure of Gigg et al., and the synthesis of **5** was described previously.[9, 13, 14]

Payne epoxidation of **4** or **5** in methanol led to acetals **6a** and **7a–c** which are structurally analogous to **2**.[10, 15]. In ethanol, homologues **6b** and **7d–f** (Schemes 2 and 3) were

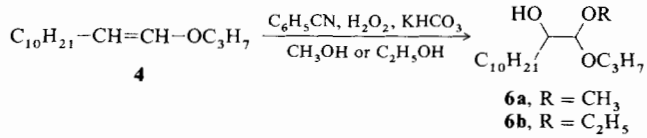

Scheme 2. Payne epoxidation of **4**.

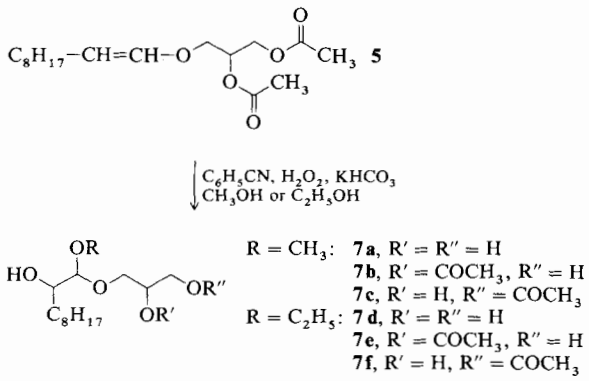

Scheme 3. Payne epoxidation of **5**.

obtained. Compounds containing the α-hydroxyacetal group **8** arise from the attack of alcohols on epoxides **9** or **10** (Scheme 4; analogous to **3** → **2**).[16]

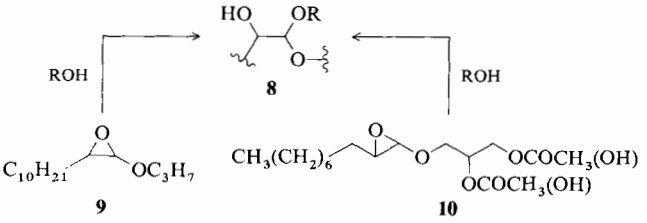

Scheme 4. Attack of alcohol on enol ether epoxides **9** and **10**.

Marmer et al. oxidized plasmalogen model compounds at 86 °C with air.[5] After 5 h, there was a decrease in the concentration of starting material, and the formation of aldehydes was observed. The authors reported that the addition of unsaturated fatty acids to the mixtures accelerated the reaction. In the present work, enol ether **4** was stirred with air in methanol at room temperature for 24 h to yield acetal **6a** plus aldehydes (C10–C12), carboxylic acids (C10–C12), and 1-hydroxy-2-dodecanone. The addition of methyl linoleate to the reaction mixture raised the yield of **6a** by about a factor of 10.

In conclusion, our studies showed that masked α-hydroxyaldehydes could be produced under very mild conditions and without the aid of enzymes. An analogous oxidation of plasmalogens to α-hydroxyaldehydes could also take place in vivo.

Experimental Procedure

2: Example: R′ = C_8H_{17}; TLC (cyclohexane:ethyl acetate 1:2): R_f = 0.14 (R = R″ = R‴ = H); GC (OV 101): RI = 2186/2206 [R = R″ = R‴ = $Si(CH_3)_3$]; MS (70 eV): *m/z* 103 (100%), 73 (76), 219 (76), 147 (32), 129 (28), 279 (12), 259 (8), 205 (2) [R = R″ = R‴ = $Si(CH_3)_3$].

4: Yield: ca. 10%; TLC (cyclohexane:ethyl acetate 10:1): R_f = 0.88; GC (OV 101): RI = 1553/1600 (*cis*/*trans*); MS (70 eV): *m/z* 57 (100%), 99 (44), 43 (40), 82 (26), 68 (14), 226 (M^+, 5); ^{1}H NMR (500 MHz, C_6D_6): *cis*: δ = 0.78 (t, *J* = 7.4 Hz, 3H), 0.90 (t, *J* = 7.0 Hz, 3H), 1.20–1.40 (m, 16H), 1.38–1.46 (m, 2H), 2.35 (dq, *J* = 7.3, 1.4 Hz, 2H), 3.37 (t, *J* = 6.5 Hz, 2H), 4.45 (dt, *J* = 7.3, 6.3 Hz, 1H), 5.85 (dt, *J* = 6.3, 1.4 Hz, 1H); *trans*: δ = 0.82 (t, *J* = 7.4 Hz, 3H), 0.91 (t, *J* = 7.0 Hz, 3H), 1.20–1.40 (m, 16H), 1.46–1.54 (m, 2H), 1.94 (dq, *J* = 7.3, 1.1 Hz, 2H), 3.40 (t, *J* = 6.5 Hz, 2H), 4.83 (dt, *J* = 12.6, 7.3 Hz, 1H), 6.32 (d, *J* = 12.6 Hz, 1H); ^{13}C NMR (500 MHz, C_6D_6): mixture of *cis* and *trans* isomers (ca. 1:3): δ = 10.4, 10.6, 14.3, 22.9, 23.1, 23.4, 24.6, 28.3, 29.5, 29.7, 29.8, 30.0, 30.0, 30.1, 30.4, 31.4, 32.3, 70.5, 73.5, 103.7, 106.8, 145.5, 147.0. In subsequent reactions a mixture of *cis and trans* isomers was employed.

5: Yield: 86%; TLC (cyclohexane:ethyl acetate 4:1): R_f = 0.47; GC (OV 101): RI = 1943/2013 (*cis*/*trans*); MS (70 eV): *m/z* 159 (100%), 43 (87), 57 (44), 99 (23); ^{1}H NMR (500 MHz, $CDCl_3$): *cis*: δ = 0.88 (t, *J* = 6.7 Hz, 3H), 1.21–1.56 (m, 12H), 2.0–2.06 (m, 2H), 2.07 (s, 3H), 2.09 (s, 3H), 3.84 (dd, *J* = 0.7, 5.3 Hz, 2H), 4.17 (dd, *J* = 6.0, 12.0 Hz, 1H), 4.34 (dd, *J* = 3.9, 12.0 Hz, 1H), 4.40 (dt, *J* = 6.1, 7.4 Hz, 1H), 5.19 (dt, *J* = 5.4, 6.1 Hz, 1H), 5.89 (dt, *J* = 1.4, 6.1 Hz, 1H); *trans*: δ = 0.88 (t, *J* = 6.7 Hz, 3H), 1.21–1.38 (m, 12H), 1.86–1.94 (m, 2H), 2.1 (s, 3H), 2.15 (s, 3H), 3.78 (d, *J* = 5.1 Hz, 2H), 4.18 (dd, *J* = 5.8, 12.0 Hz, 1H), 4.43 (dd, *J* = 3.9, 12.0 Hz, 1H), 4.79 (dt, *J* = 7.3, 12.6 Hz, 1H), 5.20–5.28 (m, 1H), 6.21 (dt, *J* = 2.7, 12.6 Hz, 1H).

6a: Yield (Payne epoxidation of **4** in CH_3OH): 22%; TLC (cyclohexane:ethyl acetate 10:1): R_f = 0.23; GC (OV 101): RI = 1835/1848; as trimethylsilyl (TMS) ether: RI = 1911/1924; MS (70 eV): *m/z* 103 (100%), 61 (94), 57 (32), 43 (32), 71 (20), 215 (4), 243 (2), 256 (0.5); as TMS ether: *m/z* 103 (100%), 61 (93), 73 (21), 43 (16), 243 (3), 257 (2), 287 (1), 314 (0.5).

6b: TLC (cyclohexane:ethyl acetate 10:1): R_f = 0.23; GC (OV 101): RI = 1888, as TMS ether: RI = 1940; MS (70 eV): *m/z* 117 (100%), 75 (97), 43 (14), 47 (13), as TMS ether: *m/z* 117 (100%), 75 (80), 73 (12), 257 (8), 301 (6), 243 (4), 315 (3), 345 (1).

7a: TLC (cyclohexane:ethyl acetate 1:2): R_f = 0.14; GC (OV 101): as TMS ether: RI = 2190/2214; MS (70 eV): as TMS ether: *m/z* 219 (100%), 103 (82), 73 (70), 129 (32), 279 (16), 259 (11), 147 (10).

7d: Yield (Payne epoxidation of **5** in C_2H_5OH): 47%; TLC (cyclohexane:ethyl acetate 1:2): R_f = 0.16; GC (OV 101): RI = 2063/2096, as TMS ether: RI = 2216/2236; MS (70 eV): *m/z* 103 (100%), 73 (76), 219 (66), 147 (32), 129 (28), 293 (12), 273 (8), 205 (2).

7e, 7f (mixture): Yield (Payne epoxidation of **5** in C_2H_5OH): 31%; TLC (cyclohexane:ethyl acetate 1:2): R_f = 0.40; GC (OV 101): RI = 2173/2198, as TMS ether: RI = 2261/2277; MS (70 eV): as TMS ether: *m/z* 189 (100%), 73 (63), 129 (55), 147 (8), 273 (7), 175 (6), 215 (5), 263 (9).

10: 1-*O*-(1,2-Epoxydecyl)glycerol-2,3-diacetate: Yield (Payne epoxidation of **5** in acetone): 20% (GC); TLC (cyclohexane:ethyl acetate 3:1): R_f = 0.29; GC (OV 101): RI = 2125/2135; MS (70 eV): *m/z* 43 (100%), 57 (77), 71 (58), 159 (36), 141 (34), 115 (20), 189 (6), 227 (2.5), 257 (0.5), 270 (0.3).

11: TLC (cyclohexane:ethyl acetate 4:1): R_f = 0.41; GC (OV 101): RI (as TMS ether) = 1711; MS (70 eV): *m/z* 43 (100%), 57 (81), 41 (52), 55 (28), 71 (26), 169 (20), 85 (18), 95 (12), 183 (2); as TMS ether: *m/z* 103 (100%), 73 (74), 257 (60), 43 (22), 75 (20), 169 (12), 117 (6), 129 (5), 143 (4); ^{1}H NMR (300 MHz, $CDCl_3$): δ = 0.79–0.89 (m, 3H), 1.13–1.34 (m, 14H), 1.52–1.67 (m, 2H), 2.37 (t, *J* = 7.5 Hz, 2H), 3.12 (s, 1H), 4.20 (s, 2H); ^{13}C NMR (300 MHz, $CDCl_3$): δ = 14.0 (C12), 22.7, 23.7, 29.2, 29.2, 29.4, 29.5, 31.8 (C4–C11), 38.4 (C3), 68.0 (C1), 209.9 (C2).

Received: October 30, 1991 [Z 4996 IE]
German version: *Angew. Chem.* **1992**, *104*, 491

CAS Registry numbers:
2 (TMS ether, R′ = C_8H_{17}), 139199-41-0; **2** (TMS ether, R′ = $C_{14}H_{29}$), 139199-58-9; **2** (TMS ether, R′ = $C_{16}H_{31}$), 139199-60-3; **2** (TMS ether, R′ = $C_{16}H_{33}$), 139199-59-0; **4** (*cis* isomer), 139199-42-1; **4** (*trans* isomer), 139199-43-2; **5** (*cis* isomer), 128262-09-9; **5** (*trans* isomer), 128262-08-8; **6a**, 139199-45-4; **6a** (TMS ether), 139199-46-5; **6b**, 139199-47-6; **6b** (TMS ether), 139199-48-7; **7a**, 139199-49-8; **7b**, 139199-61-4; **7c**, 139199-62-5; **7d**, 136132-48-4; **7d** (TMS ether), 139199-50-1; **7e**, 139199-51-2; **7e** (TMS ether), 139199-53-4; **7f**, 139199-52-3; **7f** (TMS ether), 139199-54-5; **10**, 139199-55-6; **11**, 139199-56-7; **11** (TMS ether), 139199-57-8.

[1] D. Steinberg, S. Parthasarathy, T. F. Carew, J. C. Khoo, J. L. Witztum, *N. Engl. J. Med.* **1989**, *320*, 915–924.

[2] U. P. Steinbrecher, S. Parthasarathy, D. S. Leake, J. L. Witztum, D. Steinberg, *Proc. Natl. Acad. Sci. USA* **1984**, *81*, 3883–3887.
[3] A. M. Fogelman, I. Shechter, J. Seager, M. Hokom, J. S. Child, P. A. Edwards, *Proc. Natl. Acad. Sci. USA* **1980**, *77*, 2214–2218; G. Jürgens, J. Lang, H. Esterbauer, *Biochim. Biophys. Acta* **1986**, *875*, 103–114; U. P. Steinbrecher, J. L. Witztum, S. Parthasarathy, D. Steinberg, *Arteriosclerosis (Dallas)* **1987**, *7*, 135–143.
[4] H. R. Warner, W. E. M. Lands, *J. Biol. Chem.* **1961**, *236*, 2404–2409; L. A. Horrocks, S. Spanner, R. Mozzi, S. Chun Fu, R. A. D. Amato, S. Krakowka, *Adv. Exp. Med. Biol.* **1978**, *100*, 423–438; E. Yavin, S. Gatt, *Eur. J. Biochem.* **1972**, *25*, 431–436 and 437–446.
[5] W. N. Marmer, E. Nungesser, T. A. Foglia, *Lipids* **1986**, *21*, 648–651; T. A. Foglia, E. Nungesser, W. N. Marmer, *ibid.* **1988**, *23*, 430–434.
[6] R. A. Zoeller, O. H. Morand, C. R. H. Raetz, *J. Biol. Chem.* **1988**, *263*, 11590–11596; O. H. Morand, R. H. Zoeller, C. R. H. Raetz, *ibid.* **1988**, *263*, 11597–11606.
[7] J. E. Vance, *Biochim. Biophys. Acta* **1990**, *1045*, 128–134.
[8] A. Lutz, G. Spiteller, *Liebigs Ann. Chem.* **1991**, 563–567.
[9] W. Knörr, Ph.D. Thesis, Universität Bayreuth, **1989**.
[10] A. Lutz, Ph.D. Thesis, Universität Bayreuth, **1991**.
[11] E. C. Bligh, W. J. Dyer, *Can. J. Biochem. Physiol.* **1959**, *37*, 911–917.
[12] H. H. O. Schmid, W. J. Baumann, H. K. Mangold, *Biochim. Biophys. Acta* **1967**, *144*, 344–354.
[13] W. Knörr, G. Spiteller, *J. Chromatogr.* **1990**, *526*, 303–318.
[14] J. Gigg, R. Gigg, *J. Chem. Soc. C* **1968**, 16–21.
[15] G. B. Payne, *Tetrahedron Lett.* **1962**, 763–765.
[16] R. E. Parker, N. S. Isaacs, *Chem. Rev.* **1959**, *59*, 737–799.

Catalysis of the Addition of Allyltrimethylsilane to Aldehydes by Silylating Agents. $Me_3SiB(OTf)_4$, a New, 'Supersilylating' Reagent**

By *Anthony P. Davis* and Marcel Jaspars*

The addition of allylsilanes such as **1** to aldehydes and ketones (Scheme 1)[1] can be induced by catalytic amounts of fluoride ion, stoichiometric amounts of Lewis acids or (as we ourselves showed recently) catalytic amounts of the superacid $H_2OTf^+B(OTf)_4^-$ (Tf = CF_3SO_2).[2] However, it is generally understood that it is not promoted by silylating agents, such as Me_3SiOTf[3,4] and Me_3SiI.[5–7] In the course

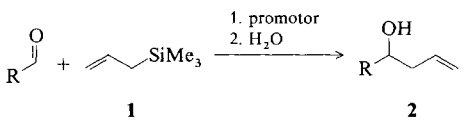

1 **2**

Scheme 1.

of an investigation into the mechanism of the superacid-catalyzed version of the reaction we have re-examined the question of catalysis by 'Me_3SiX', and have made two discoveries which we report herein. The first, perhaps of minor importance, is that Me_3SiOTf and (especially) Me_3SiI are considerably more active than previous reports have suggested. The second, of greater significance, is a new reagent which may fairly be described as a 'supersilylating' agent, is an excellent catalyst for allylations, and promises to have a variety of other applications in organic synthesis.

The results of some experiments involving Me_3SiOTf and Me_3SiI are presented in Entries 1–3 of Table 1. At room temperature and fairly high concentrations, both are capable of catalyzing the addition if given sufficient time. The most reasonable mechanism would appear to be as in Scheme 2; the initial adducts **3** are desilylated during work-up to give homoallyl alcohols **2**. A comparison of entries 2 and 3 in

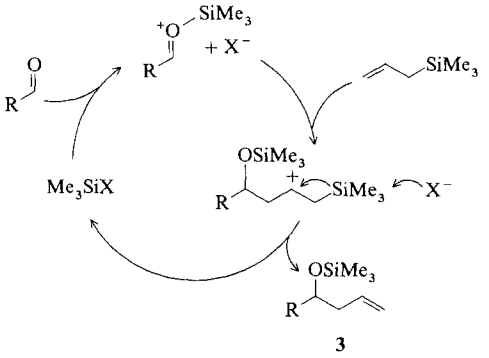

3

Scheme 2.

Table 1 indicates that Me_3SiI is considerably more active than Me_3SiOTf, and also gives a cleaner product. However, neither catalyst could be said to be preparatively useful. Yields are at best moderate, due to the formation of substantial amounts of nonpolar by-products.

Table 1. The addition of allyltrimethylsilane **1** to aldehydes RCHO, catalyzed by silylating agents Me_3SiX. [a]

No.	Aldehyde	Promoter [b]	Reaction time	Yield of **2** [%]
1	PhCHO	Me_3SiOTf (20)	21 h	61 [c, d]
2	$Ph(CH_2)_2CHO$	Me_3SiOTf (20)	23 h	27 [c]
3	$Ph(CH_2)_2CHO$	Me_3SiI (20)	45 min	65 [e]
4	PhCHO	$Me_3Si\,B(OTf)_4$ (1)	5 min	80
5	$Ph(CH_2)_2CHO$	$Me_3Si\,B(OTf)_4$ (0.2)	25 min	93 [f]
6	*n*-C_4H_9CHO	$Me_3Si\,B(OTf)_4$ (1)	20 min	80 [g]
7	*c*-$C_6H_{11}CHO$	$Me_3Si\,B(OTf)_4$ (1)	15 min	84

[a] Unless otherwise stated, the reactions were performed in CH_2Cl_2 at room temperature. [RCHO] = 0.5 M, [**1**] = 0.75 M. The initial adduct **3** was desilylated with MeOH/HCl (aq) and purified by flash chromatography. [b] Numerical values in brackets are amounts of the promoter in mol-%. [c] Desilylative work-up with $NaHCO_3$ (aq). [d] This experiment was mentioned briefly in Ref. [2]. [e] Desilylative work-up with $Na_2S_2O_3$ (aq). [f] Preparative scale experiment (see *Experimental*). [g] Desilylation with ether/HCl (aq) was only partially successful. Yield refers to a ca. 4:1 mixture of **2** and **3**.

In the reactions 4–7 in Table 1 the new 'supersilylating' reagent $Me_3SiB(OTf)_4$ was employed. It can be prepared as a solution in dichloromethane or chloroform simply by adding a solution of Me_3SiOTf to a freshly-prepared sample of $B(OTf)_3$[10] (Scheme 3). An exothermic reaction occurs, leading to a homogeneous, pale yellow solution.[11] The ^{11}B NMR spectrum (CH_2Cl_2, standard $BF_3{\cdot}OEt_2$) of one such solution showed a single resonance at $\delta = -3.17$ ($W_{1/2}$ = 28 Hz). Both the chemical shift and narrow line width are as expected for the 'spherically symmetrical' anion $B(OTf)_4^-$.[12]

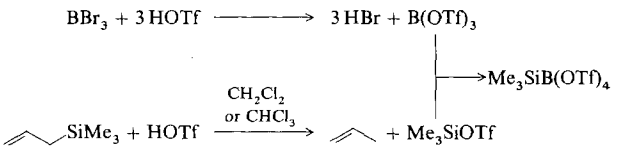

Scheme 3.

[*] Dr. A. P. Davis, M. Jaspars
Department of Chemistry,
Trinity College, IRL-Dublin 2 (Ireland)

[**] This work was supported in part by the Science programme of the European Community. We are grateful to Dr. M. G. Orchard for helpful discussions.

The ^1H NMR spectrum (CD_2Cl_2, standard CH_2Cl_2) contained a single peak at $\delta = 0.58$ and the ^{13}C NMR spectrum (CH_2Cl_2, standard CH_2Cl_2) a single peak for *C*-Si at $\delta = 0.0$ ($^1J_{C,Si} = 54$ Hz) and a quartet for *C*-F at $\delta = 118$ ($^1J_{C,F} = 318$ Hz). The precise structure of the species in these solutions is still uncertain. Two possibilities (representing extremes of a continuum) are (a) an ion pair Me_3Si^+ $B(OTf)_4^-$ [13] and (b) a covalent structure **A** in which the Me_3Si group is exchanging rapidly between the sulfonyl oxygens (to maintain the apparent symmetry in the $B(OTf)_4$ unit). At present we are inclined to prefer the latter because of the unexceptional nature of the ^1H and ^{13}C NMR data.[14]

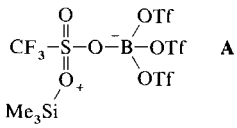

A

Irrespective of its structure, the relevant entries in Table 1 clearly suggest that $Me_3SiB(OTf)_4$ is a very powerful source of electrophilic silyl units. At room temperature it is able to catalyze the addition of allyltrimethylsilane to a variety of simple aldehydes with remarkable efficiency. The reactions are relatively clean, resulting in only trace amounts of the nonpolar by-products referred to above. Particular attention is drawn to the preparative-scale reaction (Entry 5 and *Experimental Procedure*) in which a 93% yield of product was obtained using only 0.2 mol % of catalyst. Despite its reactivity, this reagent is not especially difficult to handle. The dichloromethane solutions may be stored at $-10\,^\circ C$ under argon for several weeks without loss of activity. Considering the many applications which have been found for Me_3SiOTf[15] and Me_3SiI,[16] there is a high probability that $Me_3SiB(OTf)_4$ will prove to be a valuable addition to the synthetic chemists' armory.

Finally, as mentioned above, the original motivation for this work was our curiosity concerning the mechanism of our earlier variant of the addition of allylsilanes to aldehydes, catalyzed by the superacid H_2OTf^+ $B(OTf)_4^-$. Although it is still possible that our first proposal (catalysis by 'H^{++}')[2] is correct, the present work suggests a plausible alternative involving the reaction of the superacid with allyltrimethylsilane to form a supersilylating species within the reaction mixture.

Experimental Procedure

Me_3Si $B(OTf)_4$: Trifluoromethanesulfonic acid (531 μL, 6 mmol) was added to boron tribromide (distilled from Al powder; 190 μL, 2 mmol) at 0 °C. After evolution of HBr had ceased the flask was evacuated for 1 h to give $B(OTf)_3$ as a viscous yellow liquid [10]. In a separate flask, a solution of Me_3SiOTf was prepared by addition of trifluoromethanesulfonic acid (177 μL, 2 mmol) to a solution of allyltrimethylsilane (320 μL, 2 mmol) in CH_2Cl_2 (5 mL)[17], and leaving the resulting mixture to stand for ten minutes. Addition of this solution to the $B(OTf)_3$ at 0 °C resulted in the evolution of heat and formation of a pale yellow solution believed to contain Me_3Si $B(OTf)_4$ (for data, see text).

2: R = $Ph(CH_2)_2$: The above solution of Me_3Si $B(OTf)_4$ in CH_2Cl_2 (0.4 M, 25 μL, 0.01 mmol) was added to a solution of 3-phenylpropanal (665 μL, 5 mmol) and allyltrimethylsilane (112 mL, 7 mmol) in CH_2Cl_2 (10 mL). Analysis by TLC indicated that the aldehyde had been consumed after 25 min. MeOH (1 mL) and hydrochloric acid (36%, 12 drops) were added. Analysis by TLC indicated the desilylation to be complete in 40 min. The mixture was washed with $NaHCO_3$ aq. and extracted with CH_2Cl_2, and the extract was washed with NaCl aq. and dried ($MgSO_4$). Evaporation of the solvent followed by flash chromatography gave 1-phenyl-5-hexen-3-ol (824 mg, 93%) [D. Seebach, R. Imwinkelried, G. Stucky, *Helv. Chim. Acta* **1984**, *70*, 448], ^1H NMR (300 MHz, $CDCl_3$): $\delta = 1.70-2.05$ (m, 3H; O*H* + PhCH_2), 2.10–2.37 (m, 2H; CH_2CHOH), 2.62–2.87 (m, 2H; CH_2CH = CH_2), 3.60–3.72 (m, 1H; *H*COH) 5.05–5.20 (m, 2H; CH = CH_2), 5.70–5.95 (m, 1H; C*H* = CH_2), 7.08–7.29 (m, 5H; Ph). 36 mg of a less polar by-product was also isolated.

Received: October 31, 1991 [Z 5002 IE]
German version: Angew. Chem. **1992**, *104*, 475

CAS Registry numbers:
1, 762-72-1; **2**, R = Ph, 936-58-3; **2**, R = $Ph(CH_2)_2$, 60340-28-5; **2**, R = *n*-C_4H_9, 40575-42-6; **2**, R = *c*-C_6H_{11}, 69036-26-6; **3**, R = *n*-C_4H_9, 139462-61-6; **A**, 139462-62-7; PhCHO, 100-52-7; $Ph(CH_2)_2CHO$, 104-53-0; *n*-C_4H_9CHO, 110-62-3; *c*-$C_6H_{11}CHO$, 2043-61-0.

[1] H. Sakurai, *Pure Appl. Chem.* **1982**, *54*, 1; I. Fleming, J. Dunoguès, R. Smithers, *Organic Reactions* **1989**, *37*, 57.
[2] A. P. Davis, M. Jaspars, *J. Chem. Soc., Chem. Commun.* **1990**, 1176.
[3] T. Tsunoda, M. Suzuki, R. Noyori, *Tetrahedron Lett.* **1980**, *21*, 71.
[4] H. Sakurai, K. Sasaki, A. Hosomi, *Tetrahedron Lett.* **1981**, *22*, 745.
[5] A. Mekhalfia, I. E. Markó, *Tetrahedron Lett.* **1991**, *32*, 4779.
[6] References [3–5] make specific mention of failed attempts to catalyze the addition using the relevant silylating agents. These attempts are contrasted with other reactions which proceed more readily, such as that between allylsilanes and acetals.
[7] Silylating agents have been shown to be active in catalyzing the reactions of more nucleophilic species with aldehydes. For example, both Me_3SiOTf [8] and the combination $Me_3SiCl/SnCl_2$ [9] have been reported to catalyze the addition of silyl enol ethers to conjugated aldehydes, although in the former case only low conversions were achieved.
[8] S. Murata, M. Suzuki, R. Noyori, *Tetrahedron* **1988**, *44*, 4259.
[9] N. Iwasawa, T. Mukaiyama, *Chem. Lett.* **1987**, 463.
[10] For the preparation of $B(OTf)_3$, see: G. A. Olah, O. Farooq, S. M. F. Farnia, J. A. Olah, *J. Am. Chem. Soc.* **1988**, *110*, 2560. Olah et al. have studied the interaction of R_3SiOTf with BCl_3 and BBr_3 by ^{11}B and ^{29}Si NMR spectroscopy but, as far as we are aware, have not reported any preparative applications of these mixtures; G. A. Olah, K. Laali, O. Farooq, *Organometallics* **1984**, *3*, 1337.
[11] $B(OTf)_3$ itself is only slightly soluble in CH_2Cl_2 or $CHCl_3$.
[12] Compare $\delta = -3.55$ ($W_{1/2}$ 53 Hz) for $TfOH_2^+$ $B(OTf)_4^-$ in SO_2ClF at $-35\,^\circ C$; G. A. Olah, K. Laali, O. Farooq, *J. Org. Chem.* **1984**, *49*, 4591.
[13] It has been reported that trimethylsilyl perchlorate is 'weakly ionic' in dichloromethane, according to conductivity measurements; J. B. Lambert, J. A. McConnell, W. Schilf, W. J. Schultz Jr., *J. Chem. Soc. Chem. Commun.* **1988**, 454.
[14] Compare Me_3SiOTf $\delta(H) = 0.50$, $\delta(C) = 0.3$ ($^1J(C,Si) = 60$ Hz); Me_3SiI $\delta(H) = 0.53$, $\delta(C) = 6.5$ ($^1J(C,Si) = 54$ Hz). In particular, the fact that $^1J(C,Si)$ for $Me_3SiB(OTf)_4$ is so similar to the foregoing values suggests that the hybridization at Si is similar to that in Me_3SiOTf and Me_3SiI; K. D. Summerhays, D. A. Deprez, *J. Organometallic Chem.* **1976**, *118*, 19.
[15] H. Emde, D. Domsch, H. Feger, U. Frick, A. Götz, H. H. Hergott, K. Hofmann, W. Kober, K. Krägeloh, T. Oesterle, W. Steppan, W. West, G. Simchen, *Synthesis* **1982**, 1.
[16] G. A. Olah, S. C. Narang, *Tetrahedron* **1982**, *38*, 2225.
[17] T. Morita, Y. Okamoto, H. Sakurai, *Synthesis* **1981**, 745.

The Electronic Structure of $[(\eta^5\text{-}C_5H_5)_2Co_2]$: Comment on the Existence of a Complex with an Unsupported Co–Co Double Bond

By *Harmon B. Abrahamson, Gerald P. Niccolai, D. Michael Heinekey, Charles P. Casey,* and *Bruce E. Bursten**

Schneider et al. have recently reported the synthesis of a dinuclear cobalt complex **1**, formulated as $[Cp_2^*Co_2]$ ($Cp^* = \eta^5\text{-}C_5Me_5$), by the cocondensation of Co atoms and

[*] Prof. B. E. Bursten
Department of Chemistry
The Ohio State University
Columbus, OH 43210 (USA)
Prof. H. B. Abrahamson
Department of Chemistry
University of North Dakota
Grand Forks, ND 58202 (USA)
G. P. Niccolai, Prof. C. P. Casey
Department of Chemistry
University of Wisconsin – Madison
Madison, WI 53706 (USA)
Prof. D. M. Heinekey
Department of Chemistry
University of Washington
Seattle, WA 98195 (USA)

Cp*H in a metal-atom reactor.[1] Crystallographic characterization of compound **1** indicates a very short (2.253 Å) Co–Co distance, which the authors state is consistent with the presence of an unsupported Co–Co double bond. This report of an unsupported Co–Co double bond almost coincides with the reports of two very different organodirhenium complexes, one that contains an unsupported d^2–d^2 double bond[2] and one that has a d^6–d^6 double bond supported only by two semibridging carbonyl ligands.[3]

If it is correctly formulated, **1** is the first compound to contain a "naked" Co–Co double bond. The high symmetry and paramagnetism of **1** also stimulated our interest in the metal–metal bonding in this complex, as we have previously rationalized the paramagnetism of a supported Fe–Fe double bond in a highly symmetrical environment.[4] We therefore report here nonempirical Fenske–Hall molecular orbital investigations of the bonding in the model complex $[Cp_2Co_2]$ (**2**; $Cp = \eta^5$-C_5H_5) and in the related hypothetical hydride complexes $[(CpCo)_2(\mu\text{-}H)_n]$ (**3**: $n = 1$; **4**: $n = 2$; **5**: $n = 3$; **6**: $n = 4$).[5] We believe that the results we present for **2**, when taken with the available physical and chemical data for **1**, mandate a closer examination of whether **1** truly possesses an unsupported Co–Co bond.

As shown in Figure 1 (left), the Cp–Co fragment exhibits the familiar "three-below-two" splitting pattern of the predominantly Co 3d orbitals.[6] With respect to bond formation along the fivefold axis of the Cp–Co fragment, the 3dσ orbital is part of the lower set of orbitals, while the doubly degenerate 3dπ orbitals form the upper set. Figure 1 (center) shows the result of interacting two Cp–Co fragments to form the MO's of **2**. The resultant orbital ordering is essentially the same as that derived by Lichtenberger et al. in their discussion of the bonding in $[(CpM)_2(\mu\text{-}L)_2]$ complexes,[7] and by us in our earlier study of $[(CpRu)_2(\mu\text{-}OMe)_2]$.[8] Even at the short Co–Co bond distance observed in **1**, the splitting induced by the Cp–Co interaction dominates that induced by Co–Co bond formation. As a result, the Co–Co σ* antibonding MO is lower in energy than the doubly degenerate Co–Co π bonding MO's, which are the highest occupied MO's in **2**. If we neglect the small contributions of the Co 4s orbitals to the σ* orbital, there is no net Co–Co σ bond in **2**; the molecule does indeed contain a Co–Co double bond, but both components of this bond have π symmetry.

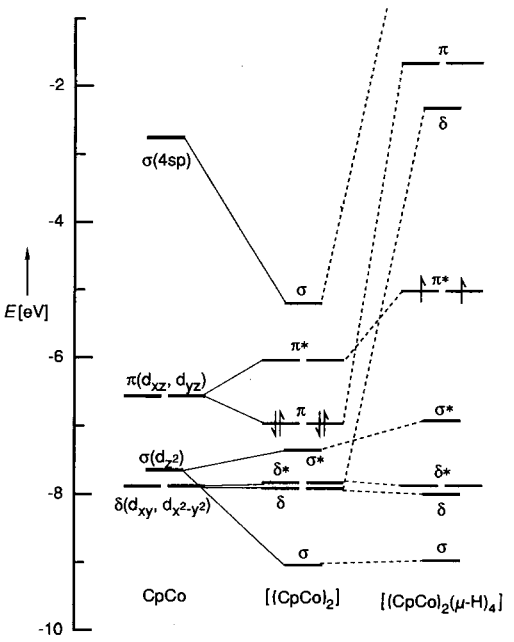

Fig. 1. Co 3d-based molecular orbitals of the Cp–Co fragment, their combination to form the molecular orbitals of $[Cp_2Co_2]$, and the correlation of these orbitals to those of $[Cp_2Co_2(\mu\text{-}H)_4]$.

This description of the bonding in the cyclopentadienyl dimer **2** causes us to question whether the pentomethylcyclopentadienyl dimer **1** has been formulated correctly. First, **1** has an exceptionally short Co–Co bond, yet it seems unlikely that the bond would be so short in the absence of a σ component. Second, ^{1}H NMR spectroscopy reveals a large paramagnetic shift for the Cp* methyl groups of **1** ($\delta = 61.3$ at 30 °C in $[D_8]$toluene).[1] A linear dependence between the paramagnetic shift and $1/T$ suggests that **1** has a high-spin ground state. By contrast, our calculations on **2** are consistent with a singlet ground state, although we observe a rather small (ca. 0.9 eV) splitting between the π HOMO's and the π* LUMO's of **2**. Thus, the lowest lying triplet state could be close enough in energy to the calculated singlet state to allow significant thermal population of the triplet state;[9] however, thermal population of a ππ* triplet state would significantly weaken the Co–Co bond, which is again inconsistent with the observed bond length in **1**. Third, **1** is apparently unreactive toward ethylene and CO,[1] which strikes us, and others,[10] as inconsistent with its electronic structure. The π orbitals of **2** are relatively high in energy for an occupied orbital, whereas the π* orbitals are rather low-lying unoccupied orbitals. Because the Co–Co bond is unsupported, both these sets of frontier orbitals should be spatially accessible to small reactant molecules. Thus, we would expect **1** to be quite reactive toward both electrophiles and nucleophiles. We are particularly surprised that **1** does not react with CO to form the well-known $[(Cp^*Co)_2(\mu\text{-}CO)_2]$ dimer (**7**)[11] or monomeric $[Cp^*Co(CO)_2]$,[12] which can be formed by the reaction of **7** with CO. The Co–Co distance in **7** (2.33–2.34 Å)[11] is consistent with a formal Co–Co double bond; that the bond length in **7** is so similar to that in **1** seems to indicate that CO addition to the unsupported Co–Co double bond would not significantly disrupt the metal–metal bonding. We also note that compound **1** was isolated by chromatography on Al_2O_3 that contained 5% H_2O.[1] That the molecule is unaffected by these manipulations is quite remarkable.

If the compound **1** prepared by Schneider et al. is not $[Cp^*_2Co_2]$, then what could it be? Because the authors have determined the crystal structure of **1**, it seems unlikely that additional second-row or heavier atoms are present. In the crystallographic details the authors point out that there is residual electron density (2.5 e Å^{-3}) located 1.8 Å from each Co atom on the crystallographic twofold axis, which bisects the Co–Co bond. Inasmuch as the magnitude of this electron density is not inconsistent with the presence of a bridging hydride ligand, and the characterization of **1** does not exclude this possibility,[13] we believe that one or more μ-H ligands may be present in the compound. To this end, we have also performed MO calculations on compounds **3**–**6**. Compounds **3** and **5** are formally mixed-valent complexes that are necessarily paramagnetic due to the presence of an odd number of electrons. However, it seems unlikely that the CpCo=CoCp fragment of the monohydride **3** would possess axial symmetry. Compound **4** would be the dihydride analogue of the Co(II) dimers $[(Cp^*Co)_2(\mu\text{-}X)(\mu\text{-}Y)]$ (**8**) prepared by Koelle et al.[14]

Compounds **8** exhibit longer Co–Co bonds than that observed for **1** (for example, Co–Co = 2.49 Å for X = Cl, Y = NMe_2) and are described as paramagnetic complexes with strong antiferromagnetic coupling. Our calculations on

4 indicate a HOMO–LUMO separation of 1.25 eV (slightly larger than that in **2**), so that at the short Co–Co separation a singlet ground state seems more likely than a triplet ground state. In **6**, the four hydride ligands interact strongly with one of the Co–Co δ and both Co–Co π orbitals, leading to significant destabilization of these metal-based orbitals, much as we saw for $[CpReH)_2(\mu\text{-}H)_4]$.[15] As a result of these interactions, the HOMO's of **6** are the half-filled, doubly degenerate Co–Co π* orbitals [Figure 1 (right)], and the molecule is expected to possess a triplet ground state.

Complex **6** has strong precedent in the literature. An analogous Group 8 complex, $[(Cp^*Ru)_2(\mu\text{-}H)_4]$ (**9**), which has two fewer valence electrons than **6** and is diamagnetic, possesses a Ru–Ru bond length of 2.463 Å consistent with its formulation as a hydride-supported metal–metal triple bond.[16] In addition, we have recently demonstrated that $[Cp^*_2Re_2(CO)_4]$ (**10**), which contains a Re–Re double bond supported by two semibridging carbonyls, reacts with H_2 at −80 °C to yield $[Cp^*_2Re_2(CO)_4(\mu\text{-}H)_2]$.[3] Compound **10** is more sterically congested than $[Cp^*_2Co_2]$, suggesting that the latter would also undergo facile addition of hydrogen (an expected by-product of the reaction of Co atoms with Cp*H) to the Co–Co bond.

In summary, we believe that the electronic structure of **2** together with the reactivity exhibited by **1** casts some doubt on whether the latter is truly $[Cp^*_2Co_2]$, and feel that there may be additional hydride ligands present in the observed structure. The presence of one, three, or four bridging hydride ligands could explain the observed magnetic behavior of **1**, and compounds with such supporting ligands would be less reactive than one containing an unsupported Co–Co double bond. We are currently undertaking higher level electronic structure calculations on compounds **2**–**6**, and we hope these comments stimulate further experimental studies of compound **1**.

Received: November 8, 1991 [Z 5010 IE]
German version: *Angew. Chem.* **1992**, *104*, 464

CAS Registry numbers:
2, 139495-49-1; **3**, 139495-50-4; **4**, 139495-51-5; **5**, 139495-52-6; **6**, 139495-53-7.

[1] J. J. Schneider, R. Goddard, S. Werner, C. Krüger, *Angew. Chem.* **1991**, *103*, 1145; *Angew. Chem. Int. Ed. Engl.* **1991**, *30*, 1124.
[2] R. Toreki, R. R. Schrock, M. G. Vale, *J. Am. Chem. Soc.* **1991**, *113*, 3610.
[3] C. P. Casey, H. Sakaba, P. N. Hazin, D. R. Powell, *J. Am. Chem. Soc.* **1991**, *113*, 8165.
[4] J. P. Blaha, B. E. Bursten, J. C. Dewan, R. B. Frankel, C. L. Randolph, B. A. Wilson, M. S. Wrighton, *J. Am. Chem. Soc.* **1985**, *107*, 4561.
[5] Computational details: Molecular orbital calculations employed the Fenske-Hall method [M. B. Hall, R. F. Fenske, *Inorg. Chem.* **1972**, *11*, 768; B. E. Bursten, *Pure & Appl. Chem.* **1991**, *63*, 839) with a Slater-type orbital (STO) basis derived from numerical atomic calculations [B. E. Bursten, J. R. Jensen, R. F. Fenske, *J. Chem. Phys.* **1978**, *68*, 3320. The Co 4s and 4p orbital exponents were both set equal to 2.00. The molecular orbitals were analyzed by Mulliken populations and fragment analysis [D. L. Lichtenberger and R. F. Fenske, *J. Chem. Phys.* **1976**, *64*, 4247]. The metric parameters of **2** were taken from the crystal structure of **1**, and the molecule was idealized to D_{5h} symmetry. The assumed geometries of **3**–**6** were identical to that of **2** except for the addition of symmetrically bridging hydride ligands at a Co–H distance of 1.79 Å.
[6] T. A. Albright, J. K. Burdett, M. H. Whangbo, *Orbital Interactions in Chemistry*, Wiley, New York, **1985**, Chapter 20.
[7] D. L. Lichtenberger, A. S. Copenhaver, J. L. Hubbard, *Polyhedron* **1990**, *9*, 1783.
[8] S. D. Loren, B. K. Campion, R. H. Heyn, T. D. Tilley, B. E. Bursten, K. W. Luth, *J. Am. Chem. Soc.* **1989**, *111*, 4712.
[9] We cannot determine state energies from Fenske–Hall MO calculations. However, the HOMO-LUMO splitting is an upper bound to the energy difference between the singlet ground state and the lowest triplet excited state.
[10] J. Wachter, *Angew. Chem.* **1991**, *103*, 1140; *Angew. Chem. Int. Ed. Engl.* **1991**, *30*, 1120.
[11] a) W. I. Bailey, D. M. Collins, F. A. Cotton, J. C. Baldwin, W. C. Kaska, *J. Organomet. Chem.* **1979**, *165*, 373; b) L. M. Cirjak, R. E. Ginsburg, L. F. Dahl, *Inorg. Chem.* **1982**, *21*, 940.
[12] L. R. Byers, L. F. Dahl, *Inorg. Chem.* **1980**, *19*, 277.
[13] The mass spectrum of **1** could not be obtained due to decomposition, [1] and combustion analysis can not unambiguously rule out bridging hydride ligands, as shown by the theoretical elemental analyses of $[Cp^*_2Co_2]$, $[Cp^*_2CoH_2]$ and $[Cp^*_2Co_2H_4]$:
$[Cp^*_2Co_2]$: Co 30.35, C 61.86, H 7.79%;
$[Cp^*_2Co_2H_2]$: Co 30.19, C 61.54, H 8.26%;
$[Cp^*_2Co_2H_4]$: Co 30.04, C 61.22, H 8.73%;
$[Cp^*_3Co_2]$: Co 22.51, C 68.82, H 8.66%.
The last compound is included because **1** is cocrystallized with $[Cp^*_3Co_2]$, and reference is made to repeated recrystallizations in order to provide analytically pure **1**. Chronically high hydrogen analyses might be interpreted as $[Cp^*_3Co_2]$ in $[Cp^*_2Co_2]$, but the actual values for the analytically pure sample were not stated in [1].
[14] U. Koelle, B. Fuss, M. Belting, E. Raabe, *Organometallics* **1986**, *5*, 980.
[15] B. E. Bursten, R. H. Cayton, *Organometallics* **1988**, *7*, 1349.
[16] a) H. Suzuki, H. Omori, H. L. Lee, Y. Oshida, Y. Moro-oka, *Organometallics* **1988**, *7*, 2243; b) R. E. Marsh, *ibid.* **1989**, 8, 1583.

1,2,4-Cyclohexatriene, an Isobenzene, and Bicyclo[4.4.0]deca-1,3,5,7,8-pentaene, an Isonaphthalene: Generation and Trapping Reactions**

By *Manfred Christl*,* *Martin Braun*, and *Germar Müller*

After Miller and Shi[1] had generated the isomer **1** of dimethylnaphthalene by β elimination of HBr and had trapped it with potassium *tert*-butoxide as well as diphenylisobenzofuran, we asked ourselves whether the isonaphthalene **2** and the isobenzene **3** could also be prepared and subjected to trapping reactions. Two further isobenzenes, namely 1,2,3-cyclohexatriene and cyclohex-1-en-3-yne, were recently generated and intercepted.[2]

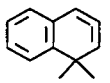

1

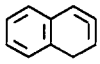

2

3

In connection with our work[3] concerning 1,2-cyclohexadiene and its derivatives,[4] we wanted to liberate **2** and **3** using the Doering–Moore–Skattebøl method. At first, the dibromocyclopropanes **13** and **14** were considered as unsuitable starting materials, since the addition of dibromocarbene, generated from bromoform and a base, to indene and cyclopentadiene only yields 2-bromonaphthalene[5] and bromobenzene, respectively, because of the rapid rearrangement of **13** and **14**.

Therefore, as previously for a precursor of 1-oxacyclohexa-2,3-diene,[6] we used the high energy of the C–F bond and added bromofluorocarbene ($CHBr_2F$, 50% NaOH, $PhCH_2NEt_3Cl$, CH_2Cl_2, ice bath) to indene and cyclopentadiene. We obtained **6**[7, 8] and **10**[7] in 16 and 20% yields,

[*] Prof. Dr. M. Christl, Dr. M. Braun, Dipl.-Chem. G. Müller
Institut für Organische Chemie der Universität
Am Hubland, D-W-8700 Würzburg (FRG)

[**] Cycloallenes, Part 8. This work was supported by the Deutsche Forschungsgemeinschaft and the Fonds der Chemischen Industrie. We thank Prof. Dr. L. Skattebøl, Oslo, for valuable suggestions and Prof. Dr. R. Janoschek, Graz, for the theoretical study of the isobenzene **3** (see following communication [11]).—Part 7: H. Jelinek-Fink, M. Christl, E.-M. Peters, K. Peters, H. G. von Schnering, *Chem. Ber.* **1991**, *124*, 2569-2575.

respectively. Only upon heating, the compounds **6** (130 °C, 3.5 h) and **10** (70 °C, 2 h) decompose to give 2-bromonaphthalene and bromobenzene, respectively.

As hoped, methyllithium causes the Br–Li exchange in **6** and **10**, followed by the loss of LiF. This leads, with ring expansion, to the cyclic allenes **2** and **3**, respectively, as the products of trapping reactions suggest.

Thus, a 14:1 mixture of the [2+2]cycloadducts **4**[7] and **5**[7] of the isonaphthalene **2** was formed by the reaction of **6** in styrene with MeLi in ether at −25 °C in 63% yield. Analogous products were obtained with α-methylstyrene. The use of butadiene as the trapping reagent afforded a 4:2:1 mixture of the [2+2]cycloadduct **7**,[7] and the [4+2]cycloadducts **8**[7] and **9**[7] in 27% yield. In the case of 2,3-dimethylbutadiene, the amount of the [2+2]cycloadduct was significantly larger than that of the [4+2]cycloadducts.

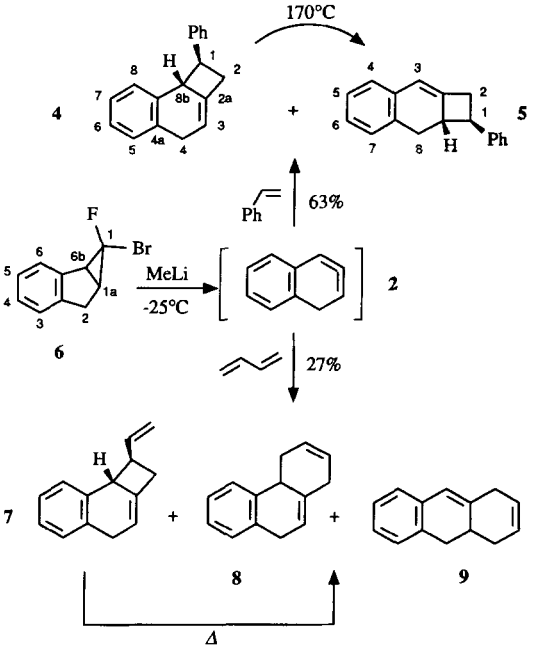

If **10** is allowed to react with MeLi in the presence of styrene, then the [2+2]cycloadduct **11**[7] of **3** and probably its diastereomer are obtained as a 19:1 mixture in 65% yield. The trapping reaction of **3** with α-methylstyrene proceeded analogously.

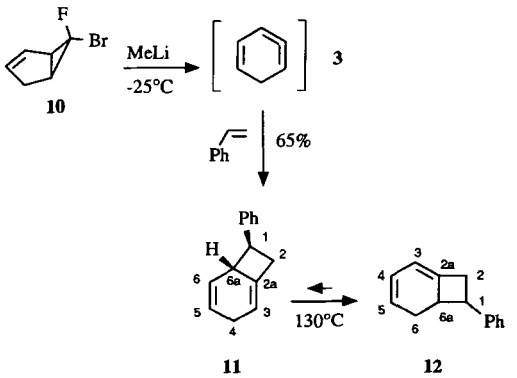

We then investigated whether the dibromocarbene adducts of indene and cyclopentadiene, namely **13** and **14**, respectively, were also stable enough for preparative purposes. Produced from indene and cyclopentadiene, respectively, and tetrabromomethane in ether with MeLi[9] at −60 °C, they are actually stable in solution up to 0 °C as proved by the ^{1}H NMR spectra. We have used these findings to synthesize the cycloadducts of **2** and **3** in one-pot reactions.

Treatment of **13**, prepared at −60 °C, with MeLi in the presence of styrene at −30 °C furnishes the same mixture of **4** and **5** as from the use of **6**. With butadiene instead of styrene, **7**–**9** were again formed. The yields based on indene were, with 40 and 24%, respectively, considerably higher than from the method via **6** (10 to 4%, respectively).

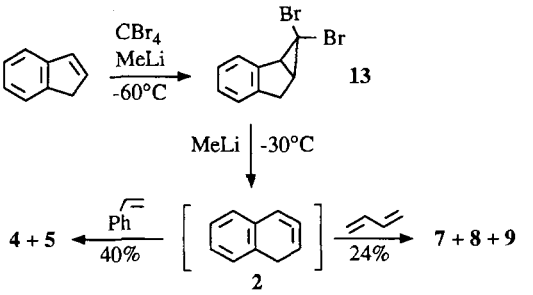

The cycloadducts **11** (49% compared with 13% via **10**), **17**[7] (14%) and **18**[7] (8%), **15**[7] (5%), and **16**[7] (5%), were formed analogously from cyclopentadiene, tetrabromomethane, MeLi, and the trapping reagents styrene and cyclopentadiene (see *Experimental Procedure*) as well as (*E*)-β-methylstyrene and furan, respectively. The 1,4-cyclohexadiene subunits of these compounds and their configurations are proved unequivocally by NMR spectroscopy (cf. Table 1).

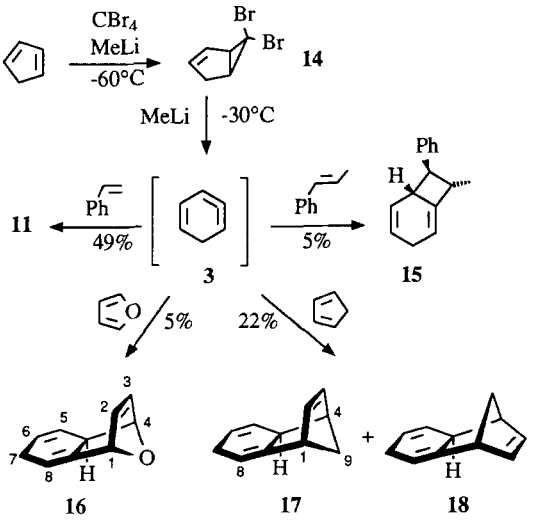

Noteworthy are the reactivities of the different allene π bonds in **2** and **3**. The [4+2]cycloaddition of **2** with butadiene appears to lead, with little selectivity, to a 2:1 mixture of the tetrahydrophenanthrene **8** and the tetrahydroanthracene **9**. Due to the readily occurring thermal rearrangement of the [2+2]cycloadduct **7**, formed at the same time, into **8** and **9** in the ratio 2:1, this result must be confirmed by further investigations. The exclusive participation of the conjugated allene π bond in the [4+2]cycloadditions of **3** results in the

formation of **16**–**18**. We explain this by the more favorable frontier orbital energies in comparison to those of the nonconjugated allene π bond. This is based on the assumption of a one-step mechanism in the sense of the Diels–Alder reaction. In the [2+2]cycloadditions those allene π bonds react which are conjugated with the benzene unit in **2** and the ethylene unit in **3**, respectively. On the basis of previous results,[10] we assume that two-step processes occur with diradical intermediates such as **19** and **20** when styrene is used as the trapping reagent. Apparently, the ring closures of **19** and **20** yield **4** and **11**, respectively, with high selectivity under kinetic control. These are thermodynamically less stable than their conjugated isomers **5** and **12**, respectively.

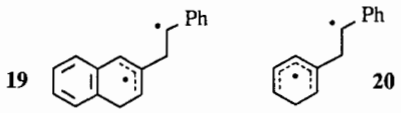

19 **20**

The latter is supported by the thermolyses of **4** and **11**, which lead mainly to **5** (81%)[7] and a 1:3 mixture (64%) of **11** and **12**,[7] respectively. Here, the diradicals **19** and **20** should again be intermediates, because the ring closures **19** → **4** and **20** → **11** are probably reversible above 100 °C. The preferred pathways of **19** and **20** to the nonconjugated products **4** and **11**, respectively, are attributed to the absolute spin density maximum in the benzyl position of the allyl radical moiety of **19**, and in the center of the pentadienyl radical part of **20**, respectively. In the case of **20**, this is the result of a theoretical study, which also describes the nature of the isobenzene **3** (see following communication[11]).

Table 1. Selected physical data of **4**–**18**; ^{1}H NMR (200 or 400 MHz) and ^{13}C NMR (50 or 100 MHz) spectra measured in $CDCl_3$ if not stated otherwise.

4: Mp = 45–47 °C. ^{1}H NMR (C_6D_6): δ = 2.87 (m, 2H; H2), 3.09 (ddd, J(4,4) = 18.8, J(3,4) = 6.3, J(4,8b) = 2.3 Hz, 1H; H4), 3.25 (dm, J(3,4) = 2.9 Hz, 1H; H4), 3.27 (q, mean J(1,2) = J(1,8b) = 8.3 Hz; H1), 3.95 (m; H8b), 5.58 (ddq, mean J(2,3) = J(3,8b) = 1.9 Hz; H3), 6.90–7.90 (m, 9H; H-arene); ^{13}C NMR: δ = 30.6 (t; C4), 38.1 (t; C2), 46.9, 51.7 (each d; C1,8b), 113.7 (d; C3), 125.4, 126.0, 126.1, 126.4, 128.2 (each d; C5,6,7,8, *p*-C), 126.9 (d; *o*-C), 128.6 (d; *m*-C), 136.4, 139.1, 139.4 (each s; C2a,4a,8a), 144.2 (s; *ipso*-C)

5: ^{1}H NMR: δ = 2.77–3.34 (m; 6H), 6.22 (t, line width 2.0 Hz; H3), 6.96–7.38 (m; 9H-arene); ^{13}C NMR: δ = 34.7 (t; C8), 37.7 (t; C2), 45.08, 45.13 (each d; C1,8a), 115.8 (d; C3), 125.7, 125.8, 126.2, 126.7, 128.2 (each d; C4,5,6,7, *p*-C), 126.5 (d; *o*-C), 128.4 (d; *m*-C), 134.3, 135.4 (each s; C3a,7a), 141.8 (s; C2a), 144.1 (s; *ipso*-C)

6: Mp = 71–72 °C. ^{1}H NMR: δ = 2.51 (m, 1H), 3.18 (m, 3H), 7.08–7.22 (m, 3H), 7.32 (m, 1H); ^{13}C NMR: δ = 32.2 (td, J(C,F) = 3.5 Hz; C2), 34.0 (dd, J(C,F) = 12.6 Hz; C1a), 41.3 (dd, J(C,F) = 12.1 Hz; C6b), 82.6 (d, J(C,F) = 315.0 Hz; C1), 124.3, 125.2, 126.7, 127.3 (each d; C3,4,5,6), 137.0 (d, J(C,F) = 2.5 Hz), 143.5 (s; C2a,6a)

7: ^{13}C NMR: δ = 30.4 (t; C4), 36.0 (t; C2), 45.7, 49.8 (each d; C1,8b), 113.0 (d; C3), 113.8 (t), 141.8 (d) (CH = CH_2), 125.3, 126.1 (double intensity), 128.1 (each d; C5,6,7,8), 136.3, 139.0, 139.6 (each s; C2a,4a,8a)

8: ^{13}C NMR: δ = 29.5, 34.9, 36.9 (each t; C1,4,9), 38.0 (d; C4a), 116.4 (d; C10), 125.8, 126.0, 126.6, 126.9, 127.7, 128.3 (each d; C2,3,5,6,7,8), 133.2, 134.8, 137.7 (each s; C4b,8a,10a)

9: ^{13}C NMR: δ = 33.1, 33.5, 33.8 (each t; C1,4,10), 34.3 (d; C4a), 120.7 (d; C9), 125.3, 126.32, 126.34, 126.4, 126.8, 127.5 (each d; C2,3,5,6,7,8); the signals of C4a,8a,10a could not be located precisely because of the low intensity.

10: ^{1}H NMR: δ = 2.31 (ddddd, J = 7.6, 6.5, 2.5, 1.8, 0.7 Hz; H5), 2.60 (br dquin, J = 16.0, 2.4 Hz, 1H; H4), 2.66 (dm, 1H; H4), 2.73 (dtdd, J = 7.6, 2.4, 1.0, 0.4 Hz; H1), 5.64 (dq, J = 5.6, 2.1 Hz), 5.78 (dtd, J = 5.6, 2.2, 0.8 Hz) (H2,3); ^{13}C NMR: δ = 33.3 (td, J(C,F) = 3.0 Hz; C4), 33.5 (dd, J(C,F) = 13.3 Hz), 41.6 (dd, J(C,F) = 12.4 Hz) (C1,5), 82.5 (d, J(C,F) = 316.0 Hz; C6), 124.5 (d; C3), 133.6 (dd, J(C,F) = 1.7 Hz; C2)

11: ^{1}H NMR [a]: δ = 2.66 (m, 2H; H4), 2.91 (ddquin, J(2,2) = 12.5, J(1,2) = 9.0, J(2,3) ≈ mean J(2,4) ≈ J(2,6a) ≈ 1.9 Hz, 1H; H2), 2.98 (ddquin, J(1,2) = 7.2, J(2,3) ≈ mean J(2,4) ≈ J(2,6a) ≈ 1.4 Hz, 1H; H2), 3.19 (≈q, J(1,6a) = 8.3 Hz; H1), 3.35 (≈qtq, mean J(4,6a) = 8.2, J(3,6a) ≈ J(5,6a) ≈ 3.0, J(6,6a) = 1.8 Hz; H6a), 5.44 (m; H3), 5.83 (≈dqd, J(5,6) ≈ 9.4, mean J(4,5) ≈ 3.1, J(3,5) = 0.9 Hz; H5), 5.91 (dq, mean J(4,6) = 1.9 Hz; H6), 7.17–7.33 (m; C_6H_5); ^{13}C NMR: δ = 26.4 (t; C4), 38.4 (t; C2), 46.9 (d; C6a), 50.6 (d; C1), 112.0 (d; C3), 126.2 (d, *p*-C), 126.6 (d; *o*-C), 127.2, 127.3 (each d; C5,6), 128.4 (d; *m*-C), 138.5 (s; C2a), 144.0 (s; *ipso*-C)

12: ^{1}H NMR: δ = 2.18 (ddm, J(6,6) = 17.5, J(6*endo*,6a) = 14.0 Hz; *endo*-H6), 2.40 (dddm, J(6*exo*,6a) = 9.7, J(5,6*exo*) = 6.0 Hz; *exo*-H6), 2.90–3.06 (m, 2H), 3.08–3.30 (m, 2H), 5.55–5.70 (m, 2H), 5.94 (m, 1H), 7.15–7.37 (m; C_6H_5); ^{13}C NMR: δ = 27.8 (t; C6), 38.4 (t; C2), 43.4, 45.9 (each d; C1,6a), 123.0, 125.1, 125.9, 126.1 (each d; C3,4,5, *p*-C), 126.4 (d; *o*-C), 128.5 (d; *m*-C), 138.4 (s; C2a), 144.4 (s; *ipso*-C)

13: ^{1}H NMR ($CDCl_3$/ether): δ = 2.57 (br t, J(1a,2*exo*) ≈ J(1a,6b) ≈ 7.0 Hz; H1a), 2.97 (br d, J(2,2) = 17.7 Hz; *endo*-H2), 3.17 (dd; *exo*-H2), 3.26 (br d; H6b), 7.05–7.17 (m, 3H), 7.28 (br d, J = 7.3 Hz; 1H)

14: ^{1}H NMR ($CDCl_3$/ether): δ = 2.29 (dm; *endo*-4-H), 2.30 (br t; H5), 2.55 (ddt, J(4,4) = 18.6, J(4*exo*,5) = 7.6, J(2,4*exo*) ≈ J(3,4*exo*) ≈ 2.0 Hz; *exo*-H4), 2.73 (≈dt, J(1,5) = 7.2, J(1,4*endo*) = 3.0, J(1,2) = 2.4 Hz; H1), 5.58 (dq, J(2,3) = 5.5, J(2,4*endo*) = 2.2 Hz; H2), 5.77 (dtd, J(3,4*endo*) = 2.2, J(3,5) = 0.8 Hz; H3)

15: ^{13}C NMR: δ = 17.0 (q; CH_3), 26.1 (t; C4), 47.3, 47.6 (each d; C2,6a), 55.6 (d; C1), 109.7 (d; C3), 126.3 (d; *p*-C), 126.7 (d; *o*-C), 127.2, 127.3 (each d; C5,6), 128.4 (d; *m*-C), 143.2, 145.0 (each s; C2a, *ipso*-C)

16: ^{1}H NMR [a]: δ = 2.64–2.73 (m, 2H; H7), 2.90 (m; H4a), 5.18 (m; H1), 5.19 (dm, J(4,4a) ≈ 4.0 Hz; H4), 5.59 (qm; J(4a,8) ≈ mean J(7,8) ≈ 3.5 Hz; H8), 5.80 (br s; H5,6), 6.09 (dd, J(2,3) = 5.7, J(3,4) = 1.6 Hz; H3), 6.43 (br dd, J(1,2) = 1.6 Hz; H2); ^{13}C NMR: δ = 28.0 (t; C7), 40.6 (d; C4a), 80.1, 80.7 (each d; C1,4), 112.9 (d; C8), 126.7, 128.4, 129.9 (each d; C3,5,6), 136.1 (d; C2), 141.7 (s; C8a)

Table 1. (continued)

17: ^{13}C NMR: δ = 28.1 (t; C7), 41.9 (d; C4a), 45.5, 47.4 (each d; C1,4), 50.4 (t; C9), 112.3 (d; C8), 127.4, 130.3, 131.0 (each d; C3,5,6), 136.4 (d; C2), 146.2 (s; C8)

18 [a]: ^{1}H NMR: δ = 1.30 (dtt, J(9,9) = 8.1, J(1,9*syn*) = J(4,9*syn*) = 1.6, J(2,9*syn*) = J(3,9*syn*) = 0.6 Hz; *syn*-H9), 1.67 (dq, J(1,9*anti*) = J(4,9*anti*) = J(4a,9*anti*) ≈ 2.0 Hz; *anti*-H9), 2.11 (dm; H4a), 2.54 (dddt, J(7,7) = 20.0, J(4a,7*endo*) = 11.0, J(5,7*endo*) = 3.0, J(6,7*endo*) = J(7*endo*,8) = 1.7 Hz; *endo*-H7), 2.70 (dddd, J(7*exo*,8) = 6.2, J(6,7*exo*) = 5.2, J(4a,7*exo*) = 4.0 Hz; *exo*-H7), 2.81 (br s; H4), 3.34 (br s; H1), 5.71 (dm; H8), 5.85 (br dd, J(5,6) = 9.0, J(4a,5) = 1.3 Hz; H5), 5.88 (ddddd, J(4a,6) = 3.1, J(6,8) = 0.9 Hz; H6), 6.10 (br dd, J(2,3) = 5.6, J(1,2) = 2.9 Hz; H2), 6.39 (br dd, J(3,4) = 3.1 Hz; H3); ^{13}C NMR: δ = 28.4 (t; C7), 42.6 (d; C4a), 45.2, 48.9 (each d; C1,4), 50.8 (t; C9), 114.7 (d; C8), 129.7, 131.1, 133.0 (each d; C3,5,6), 139.0 (d; C2), 145.2 (s; C8a)

[a] The assignment is based on decoupling and NOE experiments.

Experimental Procedure

11: To a stirred solution of 1,3-cyclopentadiene (2.25 g, 34.0 mmol) and tetrabromomethane (11.3 g, 34.1 mmol) in ether (50 mL), MeLi (34.0 mmol, 34 mL, 1.0 M in ether) was added dropwise at −60 °C under N_2 during 1 h. Then the mixture was warmed to −30 °C, and styrene (20 g, 192 mmol) was added. A further 34.0 mmol of MeLi was then added dropwise over 30 min. The mixture was stirred continually and allowed to warm to 0 °C over a 4 h period. Then water (30 mL) was added and the phases were separated. The aqueous phase was extracted with ether (3 × 30 mL). The combined ether layers were dried with Na_2SO_4, concentrated at 20 °C/20 torr, and the excess styrene was distilled off at 20 °C/0.1 torr. From the residue, colorless **11** (3.04 g, 49%) was distilled at 100 °C (kugelrohr)/0.1 torr, which probably contained ca. 5% of its diastereomer.

17 and **18**: As described above, to a solution of 1,3-cyclopentadiene (8.0 g, 121 mmol) and tetrabromomethane (4.14 g, 12.5 mmol) in ether (10 mL), MeLi (13.1 mmol and 14.6 mmol) was added at −60 and −30 °C, respectively. The final distillation at 60 °C (kugelrohr)/0.1 torr yielded a yellowish liquid (1.56 g). Purification by flash chromatography (SiO_2, pentane) afforded firstly dicyclopentadiene, then **18** (145 mg, 8%), and finally 307 mg of a 5.7:1.0 mixture of **17** (14%) and benzonorbornadiene (2%). Pure **17** was obtained by preparative gas chromatography (column length: 1.5 m, 20% ethylene glycol adipate (EGA) on Volaspher®, 100 °C). A mixture of **17** and **18** was dehydrogenated with 2,3-dichloro-5,6-dicyano-*p*-benzoquinone (DDQ) which yielded benzonorbornadiene (38%).

Received: November 15, 1991 [Z 5024 1E]
German version: *Angew. Chem.* **1992**, *104*, 471

CAS Registry numbers:
2, 139407-87-7; **3**, 124869-33-6; *cis*-**4**, 139407-88-8; *cis*-**5**, 139407-89-9; **6**, 139407-90-2; *cis*-**7**, 139407-91-3; **8**, 139407-92-4; **9**, 139407-93-5; **10**, 139407-94-6; *cis*-**11**, 139244-61-4; *trans*-**11**, 139408-00-7; **12**, 139407-95-7; **13**, 139407-96-8; **14**, 88472-16-6; **15**, 139407-97-9; , **16**, 139407-98-0; **17**, 139407-99-1; **18**, 139492-53-8; $PhCH{=}CH_2$, 100-42-5; $H_2C{=}CHCH{=}CH_2$, 106-99-0; $PhCMe{=}CH_2$, 98-83-9; (*E*)-PhCH=CHMe, 873-66-5; $CHBr_3$, 75-25-2; $CHBr_2F$, 1868-53-7; CBr_4, 558-13-4; indene, 95-13-6; cyclopentadiene, 542-92-7; furan, 110-00-9.

[1] B. Miller, X.Shi, *J. Am. Chem. Soc.* **1987**, *109*, 578–579.
[2] W. C. Shakespeare, R. P. Johnson, *J. Am. Chem. Soc.* **1990**, *112*, 8578–8579.
[3] M. Christl, M. Braun in *Strain and Its Implications in Organic Chemistry* (Eds.: A. de Meijere, S. Blechert), Kluwer, Dordrecht, **1989**, S. 121–131.
[4] R. P. Johnson, *Chem. Rev.* **1989**, *89*, 1111–1124.
[5] W. E. Parham, H. E. Reiff, P. Schwarzentruber, *J. Am. Chem. Soc.* **1956**, *78*, 1437–1440.
[6] M. Christl, M. Braun, *Chem. Ber.* **1989**, *122*, 1939–1946.
[7] The proposed structures of the new compounds are in agreement with the analytical and spectroscopic data (cf. Table 1). The isolation of the compounds was achieved by kugelrohr distillation at 0.1 torr (**5**, **8**–**12**, **16**–**18**), flash chromatography on SiO_2 with pentane (**4**, **7**–**9**, **15**–**18**) or crystallization (**6**, from methanol).
[8] N. V. Volchkov, A. V. Zabolotskikh, M. B. Lipkind, and O. M. Nefedov, (*Izv. Akad. Nauk SSSR, Ser. Khim* **1989**, 1935; *Chem. Abstr.* **1990**, 112, 138661d) describe as a result of the CBrF addition to indene under very similar conditions to those here, not **6**, but 2-fluoronaphthalene which arose from the diastereomer of **6** by rearrangement and subsequent elimination of HBr.
[9] For this method of production of dibromocarbene, see also; W. T. Miller, Jr., C. S. Y. Kim, *J. Am. Chem. Soc.* **1959**, *81*, 5008–5009; L. Skattebøl, *Tetrahedron Lett.* **1961**, 167–172.
[10] S. Harnos, S. Tivakornpannarai, E. E. Waali, *Tetrahedron Lett.* **1986**, *27*, 3701–3704; M. Christl, M. Schreck, *Chem. Ber.* **1987**, *120*, 915–920.
[11] R. Janoschek, *Angew. Chem.* **1992**, *104*, 473; *Angew. Chem. Int. Ed. Engl.* **1992**, *31*, 476.

1,2,4-Cyclohexatriene, an Isobenzene, and its [2+2] Cycloaddition with Styrene: A Theoretical Study**

By *Rudolf Janoschek**

Only a fraction of the 217 constitutional isomers with the general formula C_6H_6 are known. In the preceding communication Christl et al. describe their successful generation of the isobenzene 1,2,4-cyclohexatriene (**1**), which was proven by subsequent trapping reactions.[1] The identification of this interesting compound raises a number of questions. Where does isobenzene fit into the series of C_6H_6 isomers with regard to its heat of formation? What is its equilibrium geometry? Is this a chiral compound, and if so, how high is the barrier to racemization? What evidence is there for a possible diradical character of **1**? Questions arise concerning the chemoselectivity in its [2+2] cycloaddition with styrene. The amount of information in the respective answers can be increased by the comparison of this isobenzene with related known compounds, primarily with 1,2-cyclohexadiene (**2**) which has been investigated experimentally[2] and theoretically.[3]

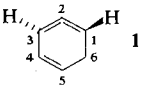

1

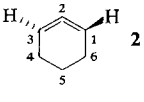

2

[*] Prof. R. Janoschek
Institut für Theoretische Chemie der Universität
Mozartgasse 14, A-8010 Graz (Austria)

[**] I wish to thank Prof. M. Christl, Würzburg for his initiative which sparked this work.

To answer these questions we employed the semiempirical AM1 method.[4] This computational method provides especially reliable results for hydrocarbons; another advantage is the speed with which answers for our list of complicated questions may be obtained. The calculations were conducted with the MOPAC6 program[5] on a STARDENT computer.[6] The bent and twisted allene fragments in **1** and **2** give rise to diradical character which requires a multiconfigurational wave function for its correct description.[7] The calculations were thus carried out with the configuration interaction (CI) formalism, in which all electronic configurations arising from the distribution of two electrons in two orbitals are taken into account. The restricted Hartree–Fock (RHF) open-shell orbitals served in the construction of the configurations. On the energy hypersurfaces numerous stationary points, discussed later in this communication, were characterized either as minima or saddle points (transition structures) by their complete sets of harmonic vibrational frequencies.

The calculated heat of formation of **1**, 93.7 kcal mol^{-1}, is considerably higher than that of benzene (22.0 kcal mol^{-1}). This increase in energy relative to benzene can be understood as arising from three contributions: loss of the stabilization of benzene, ring strain (bent allene), and rehybridization of the C6 center ($sp^2 \rightarrow sp^3$). The heat of formation of **1** correlates well with the values of the known C_6H_6 isomers like fulvene (62.6 kcal mol^{-1}) and Dewar benzene (116.7 kcal mol^{-1}).

A "planar or chiral allene fragment" are the two possible structural alternatives for **1**. Significant calculated structural data are listed in Table 1. The local energy minimum corresponds to a chiral structure with C_1 symmetry. The dihedral angles H-C1-C2-C3 and H-C3-C2-C1 with an average value of $-161°$ are characteristic ($-180°$ corresponds to a planar orientation). The C1-C2-C3 angle of 132.4° is indicative of considerable ring strain. Optical activity for the calculated chiral structure of **1** can be expected only if the energy barrier (activation enthalpy) to racemization is high enough. The corresponding transition structure has C_s symmetry and is only 2 kcal mol^{-1} higher in energy than the C_1 minimum (Fig. 1). The resulting high rate of racemization rules out the observation of optical activity. Isobenzene can thus be designated as dynamically chiral.

Table 1. Structural data for **1** and **2** (bond lengths in Å, angles in degrees), for the energy minima (C_1 and C_2), and for the transition structures (C_s) of the racemizations.

	1		**2**	
	C_1	C_s	C_2	C_s
C1-C2	1.334	1.335	1.329	1.347
C2-C3	1.348	1.377	1.329	1.347
C3-C4	1.456	1.424	1.497	1.488
C4-C5	1.354	1.364	1.538	1.526
C5-C6	1.502	1.486	1.538	1.526
C1-C6	1.493	1.488	1.497	1.488
C1-C2-C3	132.4	131.9	133.7	133.3
H-C1-C2-C3	−159.0	180.0	−154.3	−178.5
H-C3-C2-C1	−163.1	180.0	−154.3	178.5
C5-C4-C3-C2	−23.8	0.0	−29.8	−21.9
C4-C3-C2-C1	12.1	0.0	21.2	0.2

The predictive value of the calculated properties of the new compound **1** can be understood better if the related known 1,2-cyclohexadiene (**2**) is referred to. Significant structural data for both **1** and **2** are provided in Table 1. In the minimum energy structure of **2** (C_2 symmetry) the expanded dihedral angle H-C1-C2-C3 ($-154°$) relative to that

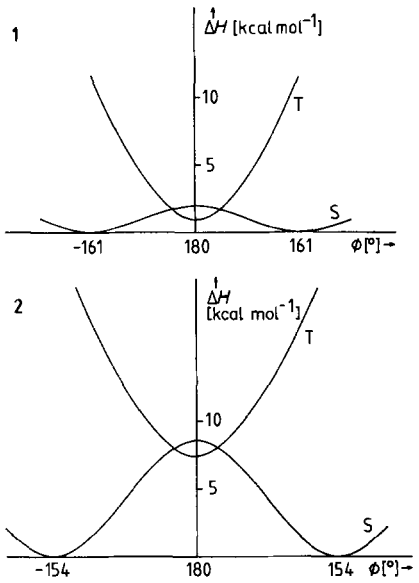

Fig. 1. Enthalpy profile for the racemizations of **1** and **2** over the dihedral angle ϕ = H-C1-C2-C3 = H-C3-C2-C1. These two angles are slightly different in **1** due to its C_1 symmetry (see Table 1); S: singlet, T: triplet.

of **1** is an indication of the higher activation energy for racemization via the C_s transition structure, which with a value of 8.7 kcal mol^{-1} is actually the case. This value is in good agreement with the results of earlier calculations with semiempirical (MNDO-CI, 5.7 kcal mol^{-1}) as well as ab initio methods (MCSCF/3-21G level, 12.1 kcal mol^{-1}; the value given in ref.[3], 13.1 kcal mol^{-1}, was treated with a subsequent zero-point vibration correction). The calculations were supported by experimental evidence: When the generation of **2** and the trapping reaction were carried out at 80 °C, optical activity was lost.[8]

The expected diradical character of bent and almost planar allene fragments is apparent from the relative position of the triplet state. According to Figure 1 the diradical character of the transition structures of **1** and **2** is uncontested, since the triplet state lies about 1 kcal mol^{-1} lower than the singlet state in each case; in both molecules examined the triplet minima and the singlet transition structures have almost identical geometries. The vertical difference in energies between the triplet state and the singlet minima is also low, 11.6 kcal mol^{-1} for **1** and 23.8 kcal mol^{-1} for **2**.

Compound **2** was identified by IR spectroscopy on the basis of the intense asymmetric C=C stretching band of the allene fragment at 1886 cm^{-1}.[9] The calculations described here predict bands of high relative intensity at 1822 cm^{-1} for **1** and 1817 cm^{-1} for **2**.

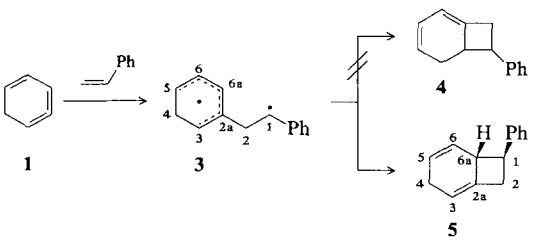

Scheme 1. The [2+2] cycloaddition of isobenzene **1** with styrene via the reactive intermediate **3**. For comparative purposes the numbering scheme for **3** and **5** is the same.

In the context of a discussion of the reactivity of **1** in a [2+2] cycloaddition with styrene the following questions arise: Is there a diradical reactive intermediate **3**? Why is compound **5** formed in this reaction even though adduct **4** with conjugated double bonds is 1.8 kcal mol^{-1} lower in energy? A minimum could be localized for diradical **3**, in which a pentadienyl radical unit is evident in the six-membered ring as vouched for by the structural data in Table 2.

Table 2. Structural data for diradical **3** and adduct **5** (bond lengths in Å, angles in degrees).

	3	**5**
C2a-C6a	1.418	1.523
C2a-C3	1.367	1.328
C3-C4	1.478	1.495
C4-C5	1.478	1.495
C5-C6	1.363	1.342
C6-C6a	1.407	1.480
C2-C2a	1.492	1.500
C1-C2	1.471	1.569
C1-*ipso*-C-phenyl	1.408	1.478
C1-C6a	3.119	1.561
C1-C3	3.491	3.413
C1-C2-C2a-C6a	67.2	10.0
C5-C6-C6a-C2a	−0.1	31.5

A pentadienyl radical unit can be recognized by the nonequivalent bond lengths C2a–C6a and C2a–C3 as well as bonds of almost the same length, C2a–C6a, C6–C6a and C2a–C3, C5–C6. A delocalized description of the single electron in the six-membered ring in the sense of **3** is thus justified. The spin density is maximal on the C6a center, an analogous situation to that in the free pentadienyl radical. Furthermore, the C1-C2-C2a-C6a dihedral angle is markedly less than 90°, which causes the C1–C6a distance to be less than that of C1–C3. Thus the ring closure to **5** is sketched out in the reactive intermediate **3**. Structural data for adduct **5** are provided in Table 2. Both rings in **5** are puckered.

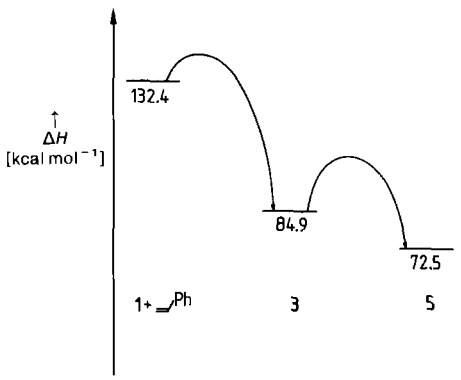

Fig. 2. The enthalpy diagram for the [2+2] cycloaddition reaction of **1** with styrene.

Finally the enthalpy diagram for the [2+2] cycloaddition reaction is sketched in Figure 2.

Received: November 15, 1991 [Z 5025 IE]
German version: *Angew. Chem.* **1992**, *104*, 473

CAS Registry numbers:
1, 124869-33-6; **2**, 14847-23-5; **3**, 139375-80-7; **5**, 139244-61-4; H_2C=CHPh, 100-42-5.

[1] M. Christl, M. Braun, G. Müller, *Angew. Chem.* **1992**, *104*, 471; *Angew. Chem. Int. Ed. Engl.* **1992**, *31*, 473.
[2] Review article on the experimental and theoretical investigations of strained cyclic cumulenes: R. P. Johnson, *Chem. Rev.* **1989**, *89*, 1111–1124.
[3] R. O. Angus, M. W. Schmidt, R. P. Johnson, *J. Am. Chem. Soc.* **1985**, *107*, 532–537.
[4] M. J. S. Dewar, E. G. Zoebisch, E. F. Healy, J. J. P. Stewart, *J. Am. Chem. Soc.* **1985**, *107*, 3902.
[5] J. J. P. Stewart, F. J. Seiler Res. Lab. US Air Force Academy, CO 80840, **1990**.
[6] STARDENT 3040, EDV-Zentrum der Universität Graz.
[7] R. Janoschek, *Chem. Unserer Zeit* **1991**, *25*, 59–66.
[8] M. Balci, W. M. Jones, *J. Am. Chem. Soc.* **1980**, *102*, 7607.
[9] C. Wentrup, G. Gross, A. Maquestiau, R. Flammang, *Angew. Chem.* **1983**, *95*, 551; *Angew. Chem. Int. Ed. Engl.* **1983**, *22*, 542.

Designing Synthetic Cationic Molecular Receptors for Alcohols**

By *Luis Méndez, Raymond Singleton, Alexandra M. Z. Slawin, J. Fraser Stoddart,* David J. Williams,* and *M. Kevin Williams*

In the early days of supramolecular chemistry, the complexation[1] of cationic guests in apolar solvents was achieved largely using neutral hosts. In these instances, strong host–guest associations are a consequence of the electrostatic interactions between the charged guest and the dipoles centered on the heteroatoms within the host. The design of hosts that bind neutral guests successfully has proven to be much more taxing both intellectually and in practice. The principal intermolecular interactions that have been exploited in the complexation[2] of neutral guests by neutral hosts have been hydrogen bonding, π–π stacking interactions, and the hydrophobic effect. In most instances, the host–guest binding has relied upon the simultaneous and cooperative action of several such noncovalent bonding interactions.[3] Guests such as phenols,[4] ureas,[5] barbiturates,[6] and nucleotides[7] have been complexed strongly by sophisticated hosts by means of a combination of hydrogen bonds and/or π–π stacking interactions.

Monohydric alcohols of low molecular weight are particularly difficult to bind selectively with synthetic hosts because a) they possess only a single hydroxyl group, and b) they are soluble in a wide range of solvents. Although there have been a number of reports[8] of selective clathration and inclusion of short-chain alcohols in the solid state, no strong complexation of these relatively featureless substrates has been achieved[9] in solution. Recently, we described[10] the discovery of the complexation of MeOH by monoprotonated, disubstituted 1,7-diaza-12-crown-4 receptor units. Here, we report a) the preparation of some disubstituted 1,7-diaza-4,10-dioxacyclododecanes, b) the quantitative evaluation of their monoprotonated derivatives as hosts for binding short-chain alcohols in solution, and c) the solid-state structures[11] of both the free and complexed hosts.

Compounds **1** and **2** were prepared by reaction of 1,7-diaza-4,10-dioxacyclododecane[12] with benzyl bromide and 2-phenylethyl bromide, respectively, and protonated with one molar equivalent of NH_4PF_6 in MeOH. The formation of **1** · HPF_6 and **2** · HPF_6 is accompanied by the release of NH_3. These salts are highly soluble in CD_2Cl_2, a property which we exploited in ^{1}H NMR spectroscopic studies, in which their complexing ability towards MeOH, EtOH, *n*-PrOH, and *n*-BuOH, and—in some cases—the fully deuterated derivatives was quantitatively evaluated.

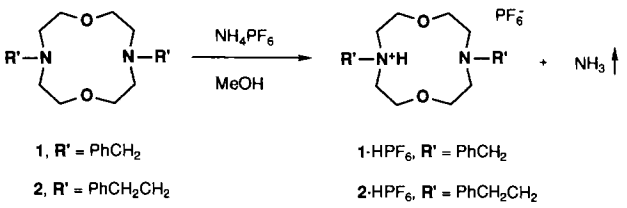

Interestingly, the signals for the OCH_2 protons in **1** · HPF_6 and **2** · HPF_6 are influenced most[13] on complexation with alcohols. The chemical shift dependence of the OCH_2 protons in **1** · HPF_6 and **2** · HPF_6 on the addition of these alcohols formed the basis for the titration method employed to establish 1:1 stoichiometries for the complexes, and used to provide data for a quantitative assessment of complexation strengths (Table 1). The 1:1 stoichiometry of the complex formed between **1** · HPF_6 and [D_4]MeOH was confirmed by the method of continous variations (Fig. 1).[14] The determinations of the association constants K_a were carried out by linearization (according to the Higuchi method[14, 15]) of the binding isotherm obtained from the ^{1}H NMR titrations. The importance of monoprotonation of the receptor is evident from a comparison of the K_a values for **2** and **2** · HPF_6 in Table 1; the K_a value of the protonated receptor is 40 times greater than that of the unprotonated receptor. The strength of complexation of alcohols is also dependent on the nature of the substituents ($PhCH_2$ in **1** and $PhCH_2CH_2$ in **2**). When the phenyl groups are more distant from the hydrogen-bond-

Table 1. The association constants K_a and derived free energies of complexation ΔG^0 for the neutral receptor **2** and the cationic receptors **1** · HPF_6 and **2** · HPF_6 with a range of short-chain alcohols [a] in CD_2Cl_2 at 20 °C.

Receptor	Alcohol	K_a [M^{-1}]	ΔG^0 [kJ mol^{-1}]
2	[D_4]methanol	1.1	−0.25
1 · HPF_6	[D_4]methanol	4.8	−3.81
1 · HPF_6	ethanol	1.6	−1.20
1 · HPF_6	*n*-propanol	2.2	−1.90
2 · HPF_6	[D_4]methanol	47	−9.37
2 · HPF_6	[D_6]ethanol	8.6	−5.23
2 · HPF_6	*n*-propanol	2.9	−2.60
2 · HPF_6	*n*-butanol	3.2	−2.84

[a] Deuterated alcohols were employed in some titration experiments in order to avoid masking the NMR resonances of the receptors.

[*] Prof. J. F. Stoddart
School of Chemistry, University of Birmingham
Edgbaston, Birmingham B15 2TT (UK)
Dr. L. Méndez, Dr. M. K. Williams
Department of Chemistry, The University
Sheffield S3 7HF (UK)
A. M. Z. Slawin, Dr. D. J. Williams
Chemical Crystallography Laboratory
Department of Chemistry, Imperial College
London SW7 2AY (UK)
Dr. R. Singleton
Scimat Limited
Techno Trading Estate, Bramble Road
Swindon SN2 6EZ (UK)

[**] This work was supported by the British Science and Engineering Research Council, Scimat Limited, and the Ministerio de Educación y Ciencia in Spain.

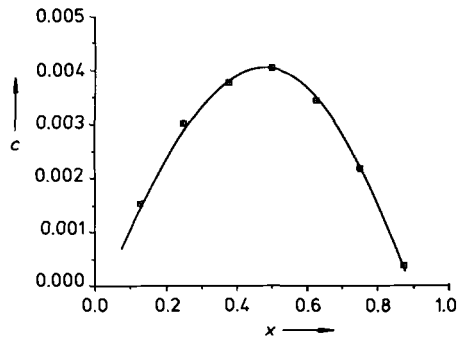

Fig. 1. The concentration c of $\mathbf{1} \cdot HPF_6 \cdot CD_3OD$ relative to CD_3OD versus the mole fraction x of $\mathbf{1} \cdot HPF_6$ in CD_2Cl_2 at 20 °C.

ing centers in the receptors, the complexes formed with MeOH, EtOH, and *n*-PrOH are all stronger.

The disubstituted 1,7-diaza-12-crown-4 derivatives are highly suitable receptors[16] for RNH_3^+ and $R_2NH_2^+$ ions, because they can form two $N \cdots H\text{–}N^+$ hydrogen bonds with the cationic substrates. When these same receptors are monoprotonated, it is possible for them to form simultaneously an $N \cdots H\text{–}O$ hydrogen bond and an $N^+\text{–}H \cdots O$ hydrogen bond with a neutral ROH substrate, because the lone electron-pair on the neutral nitrogen atom acts as a good hydrogen-bond acceptor and the protonated nitrogen atom is a strong hydrogen-bond donor. This two-point binding model (Fig. 2) has been confirmed by an organized sequence of structural investigations which have been carried out in the solid state on neutral and charged—free as well as complexed—disubstituted 1,7-diaza-12-crown-4 derivatives.

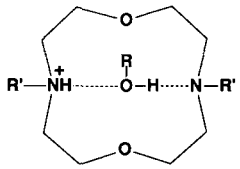

Fig. 2. The two-point binding model showing the hydrogen bonding of an alcohol (ROH) molecule to a monoprotonated disubstituted 1,7-diaza-12-crown-4 derivative.

The single-crystal X-ray structures[17–19] of **1**, $\mathbf{2} \cdot HPF_6$, and $\mathbf{1} \cdot HPF_6 \cdot MeOH$ are illustrated in Figures 3, 4, and 5, respectively. In the solid state, **1** (Fig. 3) possesses crystallographic C_i symmetry, the 12-membered ring adopts a [66] conformation,[20, 21] and the lone electron-pairs of the nitrogen atoms are on opposite faces of the macrocycle. In $\mathbf{2} \cdot HPF_6$ (Fig. 4), the cation assumes an asymmetric and folded geometry; the protonated and unprotonated nitrogen atoms are directed towards each other and form an almost linear hydrogen bond ([$N^+\text{–}H \cdots N$] distance 3.01 Å). The

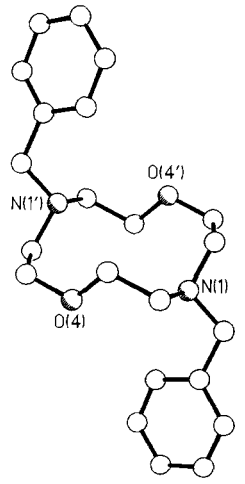

Fig. 3. The structure of **1** in the crystal. The transannular N–N and O–O distances are 4.37 and 4.35 Å, respectively.

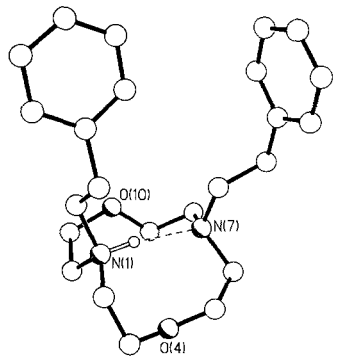

Fig. 4. The structure of $\mathbf{2} \cdot HPF_6$ in the crystal. The transannular N–N and O–O distances are 3.01 and 4.17 Å, respectively. The H-N(7) distance is 2.04 Å and the N(1)-H-N(7) angle is 169°.

solid-state structure of $\mathbf{1} \cdot HPF_6 \cdot MeOH$ (Fig. 5) has crystallographic C_s symmetry with the mirror plane passing through the two oxygen atoms in the monoprotonated disubstituted 1,7-diaza-12-crown-4 derivative. The MeOH molecule also lies in this mirror plane. The 12-membered ring

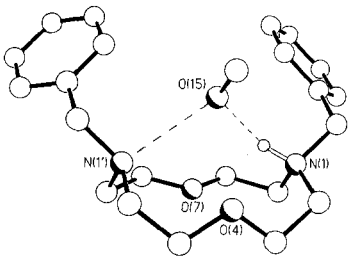

Fig. 5. The structure of $\mathbf{1} \cdot HPF_6 \cdot MeOH$ in the crystal. The transannular N–N and O–O distances are 4.53 and 3.06 Å, respectively. The H-O(15) distance is 1.87 Å and the N(1)-H-O(15) angle is 161°.

adopts a [48] conformation[20] in which both nitrogen atoms are oriented over one face of the macrocycle. The position of the ammonium proton was located from a difference electron-density map, though, of course, because of the crystallographic symmetry constraints, it must alternate between the two nitrogen sites throughout the crystal lattice. The position of the OH proton could not be located. But by inference with the geometry observed[10] in the MeOH complex of the diprotonated analogue $\mathbf{3} \cdot 2HPF_6$ we conclude

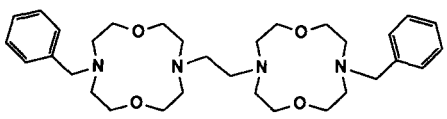

3

that the binding of the MeOH molecule to $\mathbf{1} \cdot HPF_6$ involves combination of $N^+\text{–}H \cdots O$ and $O\text{–}H \cdots N$ hydrogen bonds.[22] The $N^+ \cdots O$ and $O \cdots N$ distances are by symmetry both 2.81 Å.

The two-point binding model for the complexation of alcohols by monoprotonated disubstituted 1,7-diaza-12-crown-4 derivatives has been firmly established. The opportunity now exists to develop this type of complexation between cationic host and neutral guest for the design of receptors that will exhibit selectivity[23] within the homologous series of simple alcohols (CH_3OH, C_2H_5OH, C_3H_7OH) and the

constitutionally isomeric alcohols from C_3H_7OH upwards in molecular weight.

Experimental Procedure

1: 1,7-Diaza-4,10-dioxacyclododecane [12] (200 mg, 1.1 mmol) and Na_2CO_3 (0.61 g, 5.7 mmol) were suspended in dry MeCN (8 mL). Then, benzyl bromide (395 mg, 2.3 mmol) was added dropwise to the suspension under reflux. After 10 h the reaction mixture was cooled and filtered. Evaporation of the solvent from the filtrate under vacuum afforded a residue which was extracted with $CHCl_3$. Chromatography [SiO_2, 35%] NH_3/MeOH/Et_2O/$CHCl_3$ (0.2/10/30/80) afforded **1** [386 mg, 95%, mp = 89–90 °C, *m/z* (EIMS) = 354 (M^+); ^{1}H NMR ($CDCl_3$, 250 MHz): δ = 2.77 (t, 8H, ^3J = 4.5 Hz), 3.61 (t, 8H, ^3J = 4.5 Hz), 3.70 (s, 4H), 7.20–7.45 (m, 10H)]. Single crystals suitable for X-ray crystallography were grown from *n*-hexane.

1 · HPF_6: A solution of **1** (1.0 g, 2.8 mmol) and NH_4PF_6 (0.46 g, 2.8 mmol) in MeOH (20 mL) was stirred under reflux for 8 h. When the reaction mixture cooled, colorless crystals formed, which were filtered and dried under vacuum during 36 h. They were characterized as **1** · HPF_6 [1.1 g, 78%, mp = 170 °C; ^{1}H NMR (CD_2Cl_2, 400 MHz): δ = 3.10 (t, 8H, ^3J = 4.8 Hz), 3.62 (t, 8H, ^3J = 4.8 Hz), 4.10 (s, 4H), 5.40 (br s, 1H), 7.36–7.47 (m, 10H)]. Single crystals of **1** · HPF_6 · MeOH suitable for X-ray crystallography were obtained by gradually cooling a saturated solution of **1** · HPF_6 in MeOH from 60 °C to 20 °C.

2: 1,7-Diaza-4,10-dioxacyclododecane [12] (300 mg, 1.7 mmol) and Na_2CO_3 (1.2 g, 11.3 mmol) were suspended in dry MeCN (40 mL). Then, a solution of 2-phenylethyl bromide (624 mg, 3.5 mmol) in MeCN (5 mL) was added dropwise to the stirred reaction mixture under reflux. After 24 h the reaction mixture was cooled and filtered. Evaporation of the solvent from the filtrate under vacuum afforded an oil which was extracted with boiling hexane. The hexane solution was concentrated under vacuum and cooled in an ice-box. Long colorless needles formed which were identified as **2** [244 mg, 37%, mp = 58–60 °C, *m/z* (EIMS) = 382 (M^+); ^{1}H NMR ($CDCl_3$, 250 MHz): δ = 2.70–2.80 (m, 16H), 3.61 (t, 8H, ^3J = 4.5 Hz), 7.15–7.31 (m, 10H)].

2 · HPF_6: A mixture of **2** (50 mg, 0.13 mmol) and NH_4PF_6 (21.3 mg, 0.13 mmol) in MeOH (2.4 mL) was stirred under reflux during 10 h. The solvent was removed under vacuum, affording an oil which crystallized on addition of Et_2O. After removal of the solvent, the crystals were dried under vacuum and characterized as **2** · HPF_6 [69 mg, 100%, mp = 155–160 °C; ^{1}H NMR (CD_2Cl_2, 400 MHz): δ = 2.89 (t, 4H, ^3J = 4.3 Hz), 3.10–3.18 (m, 12H), 3.74 (t, 8H, ^3J = 4.8 Hz), 5.38 (br s, 1H), 7.17–7.34 (m, 10H)]. Single crystals suitable for X-ray crystallography were grown by slow evaporation of a CH_2Cl_2 solution of **2** · HPF_6.

Received: November 21, 1991 [Z 5032 IE]
German version: *Angew. Chem.* **1992**, *104*, 456

CAS Registry numbers:
1, 139495-32-2; **1**·HPF_6, 139495-34-4; **1**·HPF_6·MeOH, 139495-36-6; **1**·HPF_6·[D_4]methanol, 139495-38-8; **1**·HPF_6·ethanol, 139495-39-9; **1**·HPF_6·*n*-propanol, 139495-40-2; **2**, 139495-33-3; **2**·HPF_6, 139495-35-5; **2**·[D_4]methanol, 139495-37-7; **2**·HPF_6·[D_4]methanol, 139495-41-3; **2**·HPF_6·[D_6]ethanol, 139495-42-4; **2**·HPF_6·*n*-propanol, 139495-43-5; **2**·HPF_6·*n*-butanol, 139495-44-6; 1,7-aza-4,10-dioxacyclododecane, 294-92-8.

[1] Y. Inoue, G. W. Gokel, *Cation Binding by Macrocycles*, Dekker, New York and Basel **1990**.
[2] J. Rebek, Jr., *Angew. Chem.* **1990**, *102*, 261–272; *Angew. Chem. Int. Ed. Engl.* **1990**, *29*, 245–255; K. S. Jeong, T. Tjivikua, A. Muehldorf, G. Deslongchamps, M. Famulok, J. Rebek, Jr., *J. Am. Chem. Soc.* **1991**, *113*, 201–209.
[3] F. Diederich in *Cyclophanes* (Ed.: J. F. Stoddart), The Royal Society of Chemistry, Cambridge, UK, **1991**.
[4] B. J. Whitlock, H. W. Whitlock, Jr., *J. Am. Chem. Soc.* **1990**, *112*, 3910–3915; K. M. Neder, H. W. Whitlock, Jr., *ibid.* **1990**, *112*, 9412–9414.
[5] T. R. Kelly, M. P. Maguire, *J. Am. Chem. Soc.* **1987**, *109*, 6549–6550; T. Bell, J. Liu, *ibid.* **1988**, *110*, 3673–3674; V. Hedge, P. Madhukar, J. D. Madura, R. P. Thummel, *ibid.* **1990**, *112*, 4549–4550; M. Crego, J. J. Raposo, M. J. Sanz, V. Alcázar, M. C. Caballero, J. R. Morán, *Tetrahedron Lett.* **1991**, *32*, 4185–4188.
[6] S.-K. Chang, A. D. Hamilton, *J. Am. Chem. Soc.* **1988**, *110*, 1318–1319.
[7] S. C. Zimmerman, W. Wu, *J. Am. Chem. Soc.* **1989**, *111*, 8054–8055; S. C. Zimmerman, W. Wu, Z. Zeng, *ibid.* **1991**, *113*, 196–201; J. C. Adrian, Jr., C. S. Wilcox, *ibid.* **1989**, *111*, 8055–8057; T. Tjivikua, G. Deslongchamps, J. Rebek, Jr., *ibid.* **1990**, *112*, 8408–8414; T. H. Park, J. Schroeder, J. Rebek, Jr., *Tetrahedron* **1991**, *47*, 2507–2518.
[8] E. Weber, H.-P. Josel, H. Puff, S. Franken, *J. Org. Chem.* **1985**, *50*, 3125–3132; W. Moneta, P. Beret, J.-L. Pierre, *J. Chem. Soc. Chem. Commun.* **1985**, 899–901; D. Worsch, F. Vögtle, *J. Incl. Phenom.* **1986**, *4*, 163–167; K. Kobiro, M. Takahashi, N. Nishikawa, K. Kakiuchi, Y. Tobe, Y. Odaira, *Tetrahedron Lett.* **1987**, *28*, 3825–3826; B. Dung, F. Vögtle, *J. Incl. Phenom.* **1988**, *6*, 429–442; F. Toda, K. Okada, T. C. W. Mak, *Chem. Lett.* **1988**, 1829–1832; J. W. Johnson, A. J. Jacobson, W. M. Butler, S. E. Rosenthal, J. F. Brody, J. T. Lewandoski, *J. Am. Chem. Soc.* **1989**, *111*, 381–383; S. A. Bourne, L. R. Nassimbeni, K. Skobridis, E. Weber, *J. Chem. Soc. Chem. Commun.* **1991**, 282–283; M. Czugler, E. Weber, *J. Incl. Phenom.* **1991**, *10*, 355–366.
[9] However, weak complexes in solution have been observed with cyclophanes: Y. Kikuchi, Y. Kato, Y. Tanaka, H. Toi, Y. Aoyama, *J. Am. Chem. Soc.* **1991**, *113*, 1349–1354; and with cyclodextrins: Y. Matsui, K. Mochida, *Bull. Chem. Soc. Jpn.* **1979**, *52*, 2808–2814; A. B. Ari, J. Szejtli, L. Barcza, *J. Incl. Phenom.* **1983**, *1*, 151–157.
[10] B. L. Allwood, L. Méndez, J. F. Stoddart, D. J. Williams, M. K. Williams, *J. Chem. Soc. Chem. Commun.*, **1992**, 331–333.
[11] Nicolet R3m diffractometer, ω scans, $Cu_{K\alpha}$ radiation (graphite monochromator). The structures were solved by direct methods and refined anisotropically. Further details of the crystal structure investigations are available on request from the Director of the Cambridge Crystallographic Data Centre, University Chemical Laboratory, Lensfield Road, GB-Cambridge CB2 1EW (UK), on quoting the full journal citation.
[12] B. Dietrich, J.-M. Lehn, J.-P. Sauvage, J. Blanzat, *Tetrahedron* **1973**, *29*, 1629–1645.
[13] In the complexation of alcohols by **1** · HPF_6 and **2** · HPF_6, the chemical shift change of the OCH_2 signal was larger than that of the NCH_2 signal in all cases. In the proposed two-point binding model (Fig. 2), the oxygen atom of the alcohol is located sufficiently close to the OCH_2 groups for its lone pairs of electrons to shield the OCH_2 protons. Indeed, an upfield shift ($\Delta\delta$ = 0.06–0.12) of these protons in **1** · HPF_6 and **2** · HPF_6 is observed when they complex alcohols.
[14] K. A. Connors, *Binding Constants. The Measurement of Molecular Complex Stability*, Wiley, New York, **1987**.
[15] M. Nakano, N. I. Nakano, T. Higuchi, *J. Phys. Chem.* **1967**, *71*, 3954–3959.
[16] J. C. Metcalfe, J. F. Stoddart, G. Jones, *J. Am. Chem. Soc.* **1977**, *99*, 8317–8319; J. C. Metcalfe, J. F. Stoddart, G. Jones, W. E. Hull, A. Atkinson, I. S. Kerr, D. J. Williams, *J. Chem. Soc. Chem. Commun.* **1980**, 540–543.
[17] Crystal data for **1**: monoclinic, a = 9.735(1), b = 7.339(1), c = 14.591(2) Å, β = 106.92(2)°, V = 997 Å^3, space group $P2_1/n$, Z = 2 (the molecule is disposed about a center of symmetry), ρ = 1.18 g cm^{-3}, $\mu(Cu_{K\alpha})$ = 6 cm^{-1}, 1148 independent observed reflections with $|F_o| > 3\sigma|F_o|$, $2\theta \leq 116°$, refined to R = 0.038, R_w = 0.040.
[18] Crystal data for **2** · HPF_6: monoclinic, a = 11.218(11), b = 19.882(14), c = 11.480(6) Å, β = 94.98(6)°, V = 2551 Å^3, space group $P2_1/n$, Z = 4, ρ = 1.38 g cm^{-3}, $\mu(Cu_{K\alpha})$ = 16 cm^{-1}, 2670 independent observed reflections with $|F_o| > 3\sigma|F_o|$, $2\theta \leq 116°$, refined to R = 0.094, R_w = 0.102.
[19] Crystal data for **1** · HPF_6 · MeOH: monoclinic, a = 14.263(8), b = 13.088(7), c = 14.916(7) Å, β = 97.23(4)°, V = 2762 Å^3, space group $I2/m$ (body-centered cell chosen because *C*-face-centered cell had $\beta \approx 133°$), Z = 4 (the molecule has crystallographic C_s symmetry), ρ = 1.28 g cm^{-3}, $\mu(Cu_{K\alpha})$ = 15 cm^{-1}, 1629 independent observed reflections with $|F_o| > 3\sigma|F_o|$, $2\theta \leq 116°$, refined to R = 0.098, R_w = 0.112.
[20] J. Dale, *Top. Stereochem.* **1976**, *9*, 199–270.
[21] P. Groth, *Acta Chem. Scand.* **1978**, *32A*, 279–280.
[22] The distance between O(15) and the ether oxygen O(7) is 3.01 Å. A hydrogen bond between these two atoms is not likely, since this distance is almost the same as the transannular O···O distance in **1** · HPF_6 · MeOH and in its diprotonated analogue **3** · $2HPF_6$. The O(15)···O(4) distance is somewhat shorter (2.89 Å) and may be a possible alternative MeO–H···O hydrogen bond.
[23] After this communication was submitted for publication, novel boron-containing crown ethers were reported to bind alcohols, such as MeOH, EtOH, *i*PrOH, and $PhCH_2OH$, with good selectivities in the presence of amines like $PhCH_2NH_2$ or $PhCHMeNH_2$: M. T. Reetz, C. M. Niemeyer, K. Harms, *Angew. Chem.* **1991**, *103*, 1515–1517, 1517–1519; *Angew. Chem. Int. Ed. Engl.* **1991**, *30*, 1472–1474, 1474–1476.

An Opinion on the Heterogeneous Photoreactions of N_2 with H_2O **

By *Jimmie G. Edwards,* Julian A. Davies, David L. Boucher,* and *Abdelkader Mennad*

Artificial photosynthesis of ammonia is an important research goal. In the course of other work,[1] we have reviewed

[*] Prof. J. G. Edwards, Prof. J. A. Davies, Mr. D. L. Boucher, Dr. A. Mennad
Department of Chemistry, University of Toledo
Toledo, OH 43606 (USA)

[**] This work was supported by Dr. H. L. McMaster, CEO, Glasstech, Inc.

reported successful syntheses [2] and have attempted to reproduce, under a variety of conditions, reported ammonia yields by methods using iron-doped metal oxides as catalysts. We find such methods to be ineffective. Our most statistically significant results are presented here, and possible bases for previous reports are suggested. We argue that the likelihood of success with such methods is small and that further research in this direction should be undertaken only after careful consideration.

Schrauzer and Guth [3] first reported the reaction of N_2 with H_2O to make NH_3 by UV irradiation over TiO_2-based catalysts. Others [4–11] have confirmed and extended this photoassisted N_2-fixation (hereafter denoted by pNf) with a wide range of catalyst types. Solar energy was reported to drive pNf; [12] important contribution to the ammonia inventory of the earth by solar driven pNf with desert sands as catalysts was postulated. In one report [13] NH_3 was made at 2–18 mg h^{-1} in a solar reactor. This enticing reaction could be of immense practical importance, and its exploration and elucidation would seem to call for vigorous research activity.

Reported concentrations of ammonia from pNf were at the micromolar level or lower in most cases. The report by Lichtin and Vijayakumar [9] of molar concentrations was a typographical error; concentration units were μM.[14] Ammonia is ubiquitous in nature at micromolar levels.[15] For example, the ammonia concentration in water exposed to air in Antarctica gained 3 μM in 7 h; [16] up to 20 μmol h^{-1} of ammonia is exhaled in human breath.[17] It follows that contamination in artificial photosynthesis experiments must be a major concern. Further concern arises from the fact that ammonia is *oxidized* to NO_2^- by photocatalysis under the very conditions reported to promote *reduction* of N_2 to NH_3.[18–21] Confirmation of the reported pNf should, therefore, include ammonia synthesis and isolation in amounts well above background levels, or failing this, synthesis from isotopically labeled N_2 of equivalently labeled ammonia.

For the proposed stoichiometric reaction [Eq. (a)] [3, 4] a free energy of $\Delta G°(298\ K) = 658$ kJ per mol N_2 is calculated. This energy cannot come from just one photon per nitrogen molecule in the range 300–400 nm used in many reported experiments. Moreover, to avoid an unfavorable equilibrium, the product activity would need to be absurdly low. For example, at equilibrium at 298 K for reactants under standard conditions and an ammonia concentration of 1 μM, the oxygen partial pressure would be 10^{-70} atm. With a more reasonable oxygen activity of 10^{-10} atm, the ammonia concentration at equilibrium would be 6.3×10^{-51} M, which equates to one molecule of ammonia in a volume 240 times that of the earth. Organisms fix nitrogen as ammonia with hydrogen from water through multistep processes which ultimately are light-driven.[22] These naturally occurring reactions developed under evolutionary influences over eons. How remarkable it would be if a surface as common as that of iron-doped titanium dioxide could provide a template suitable for promoting such a complicated process.

$$N_2(g) + 3H_2O(l) \longrightarrow 2NH_3(aq) + 1.5O_2(g) \qquad (a)$$

Since the process involves more than one photon, if reversal of reaction (a) is to be slowed the proposed catalyst must have an almost inconceivably fortuitous set of thermal relaxation sites where photons, or resultant active sites or carriers can activate the system to the next levels. Each site must create through thermal equilibration an energy barrier to reversal as symbolized in Figure 1. Because such barriers must be present to impede the reverse reactions, a minimum of three photons per N_2 molecule would be needed, even in the unlikely case that each of the three steps involved about the same energy. Three 350 nm photons would supply the needed 658 kJ per mol N_2 and three barriers of 130 kJ mol^{-1}. If an electron/hole mechanism [23] is assumed, not three but six photons with energies greater than the band-gap energy of the photocatalyst would be required for the six-electron reduction of N_2 to $2NH_3$.

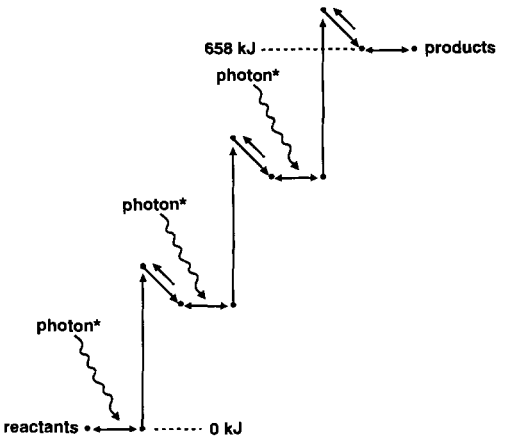

Fig. 1. Schematic, idealized, and generalized representation of a heterogeneous, photocatalytic mechanism requiring three photons with four adsorbed states of progressively higher energy, the higher three with reversal barriers arising from thermal equilibration. This diagram is not intended to represent any known steps in the photosynthesis of NH_3 or any states on the surface of oxide photocatalysts, because none in such a sequence has been established.

To elucidate this process, we did two types of experiments under conditions like those in the reported successful pNf experiments, but with $^{15}N_2$ as the nitrogen source.[24] Type 1: A prospective catalyst powder was saturated with water vapor, sealed in a reaction tube with either liquid water [25] or an atmosphere saturated with water vapor, and N_2(g) enriched to 99% with ^{15}N (hereafter called $^{15}N_2$), and irradiated; twelve irradiation experiments were done. The prospective catalyst powder was either coprecipitated or surface-loaded iron-doped titanium dioxide prepared with due regard to the cautionary notes [26] concerning photocatalyst syntheses. Type 2: A prospective catalyst powder was sealed in a reaction tube with liquid water and $^{15}N_2$ and irradiated. Twenty samples of prospective catalyst were used; all were single or binary oxide xerogels with components chosen from TiO_2, Fe_2O_3, NiO, Al_2O_3, and SiO_2. Twenty-five Type-2 experiments were done.

Both types of experiment used 45-mL quartz reaction tubes closed by quartz stopcocks with Teflon plugs. Stopcocks were covered by aluminium foil, and the tubes were irradiated in a circular rack in the center of which was a double-walled, water-cooled, quartz immersion well containing a 450-W Hanovia medium-pressure mercury lamp. A cylindrical steel reflector surrounded the rack. Reactant water was deionized to $\kappa_w > 19$ MΩcm and its background ammonia content was monitored by a specially developed method.[15] An isotope-ratio mass spectrometer (Europa Scientific Ltd.) was used to analyze for $^{14}N_2$: $^{14}N\,^{15}N$: $^{15}N_2$

ratios.[27] The sensitivity of the analysis was tested on 48 standards made of $^{15}NH_3$ and natural NH_3 such that excess ^{15}N over natural abundance ranged from 0.10 to 50.0 nmol in a sample of 7.14 μmol. The smallest enrichments were detected with a confidence exceeding 99%. One tenth nmol of $^{15}NH_3$ above natural levels was always detected at this confidence level. The samples were also analyzed for oxidized, fixed ^{15}N as NO_2^- and NO_3^- (hereafter denoted by NO_x^-).

In experiments of both types, and with all prospective catalyst powders, amounts of ammonia synthesized (here defined as that detected above natural abundance) varied around zero with a Gaussian distribution. The range in Type 1 was 0 ± 200 to 300 ± 150 pmol (average 15 ± 290 pmol). Amounts of synthesized NO_x^- were 40 ± 130 to 290 ± 750 pmol (average 100 ± 830 pmol). In the control experiments, the amount of synthesized ammonia in nonirradiated water was 100 ± 140 pmol and synthesized NO_x^- was 150 ± 140 pmol. In the control with water and no $^{15}N_2$, the total "fixed nitrogen" was 120 ± 150 pmol.

The amounts of synthesized ammonia from Type 2 were -80 ± 40 to 70 ± 50 pmol (average 1.5 ± 70 pmol), and of synthesized NO_x^- -0.2 to $+2.2$ nmol (average 0.32 ± 0.63 nmol). This outcome was skewed by four results of more than 1 nmol of $^{15}NO_x^-$ (21 experiments yielded 45 ± 180 pmol, 4 experiments 1.8 ± 0.6 nmol). In view of the not unfavorable free energy ($\Delta G°(298\ K) = 7\ kJ\ mol^{-1}$) of reaction (b) there remains some possibility that gaseous N_2

$$N_2(g) + 1.5O_2(g) + 2OH^-(aq) \longrightarrow 2NO_2^-(aq) + H_2O(aq) \qquad (b)$$

can be photooxidized either by O_2 or by an oxidizing prospective catalyst to aqueous NO_x^- in low concentrations. These results provide no evidence for reductive fixation of nitrogen in any of our cases.

In another set of experiments,[21, 28] the degradation of micromolar concentrations of aqueous ammonia under UV radiation in the presence of iron-doped TiO_2 was studied in atmospheres ranging from O_2 through air, N_2 and Ar, to H_2. Values of pH ranged from 1 to 12 and temperatures from 0 °C to 90 °C. In all cases ammonia was degraded in a few hours, and when oxygen was present NO_2^- or NO_3^- was formed. The degradation of ammonia under these conditions has been known for a long time.[18–20]

In this work we failed to fix nitrogen as ammonia under a variety of conditions with prospective catalysts of several types, some like those used in reports of successful pNf. Ammonia is degraded under the very conditions reported to produce it.

Ammonia is known to be pervasive in the background, and contamination from natural sources is an everpresent pitfall in artificial photosynthesis experiments.[16, 17] Known mechanisms for biological photosynthesis of ammonia from water and nitrogen are impressively complex and still not completely understood. Any simpler mechanism involving small molecules and heterogeneous catalysis on metal-oxide substrates would be subject to reversal or side reactions forming thermodynamically more favorable states.[18] There is well-founded interest in the surface chemistry and physics of doped ceramic oxides like TiO_2 under UV radiation,[4] but there is reason to doubt that ammonia can be photosynthesized on such surfaces. Further research on this enticing and fascinating nitrogen-fixation process should be undertaken only after due consideration. In particular, further work in this area should include identification and characterization of the favorable sites on the proposed catalyst which stabilize the necessary intermediate states in the suggested reaction.

Received: November 27, 1991 [Z 5038 IE]
German version: *Angew. Chem.* **1992**, *104*, 489

[1] H. A. McMaster, US 4688522, **1987**, US 4799870, **1989**.
[2] D. L. Boucher, Ph. D. Thesis, University of Toledo, **1992**.
[3] G. N. Schrauzer, T. D. Guth, *J. Am. Chem. Soc.* **1977**, *99*, 7189.
[4] J. Soria, J. C. Conesa, V. Augugliaro, L. Palmisano, M. Schiavello, A. Sclafani, *J. Phys. Chem.* **1991**, *95*, 274.
[5] H. Miyama, N. Fujii, Y. Nagae, *Chem. Phys. Lett.* **1980**, *74*, 523.
[6] Q. Li, K. Domen, S. Naito, T. Onishi, K. Tamaru, *Chem. Lett.* **1983**, 321.
[7] E. Endoh, J. K. Leland, A. J. Bard, *J. Phys. Chem.* **1986**, *90*, 6223.
[8] E. Endoh, A. J. Bard, *Nouv. J. Chim.* **1987**, *11*, 217.
[9] N. N. Lichtin, K. M. Vijayakumar, *J. Indian Chem. Soc.* **1986**, *63*, 29.
[10] M. M. Khader, N. N. Lichtin, G. H. Vurens, M. Salmeron, G. A. Somorjai, *Langmuir* **1987**, *3*, 303.
[11] K. Tennakone, S. Wickramanayake, C.A.N. Fernando, O. A. Ileperuma, S. Punchihewa, *J. Chem. Soc. Chem. Commun.* **1987**, 1078.
[12] G. N. Schrauzer, N. Strampach, L. N. Hui, M. R. Palmer, J. Salehi, *Proc. Natl. Acad. Sci. USA* **1983**, *80*, 3873.
[13] W. A. Mallow, Report: DOE/SF/11939-T1; Order N° DE85 001482. 24. September 1984, U.S. Government Printing Office, Washington, D.C.
[14] N. N. Lichtin, Boston University, private communication, **1989**.
[15] G. T. Richardson, J. A. Davies, J. G. Edwards, *Fresenius J. Anal. Chem.* **1991**, *340*, 392.
[16] C. Saigne, S. Kirchner, M. Legrand, *Anal. Chim. Acta* **1987**, *208*, 11.
[17] T. B. Larson, D. S. Covert, R. Frank, R. J. Charlson, *Science* **1977**, *197*, 161.
[18] G. Gopalarao, *Z. Phys. Chem. Abt. A* **1939**, *184*, 377.
[19] G. Gopalarao, K. S. Murty, *J. Indian Chem. Soc.* **1941**, *12*, 127.
[20] G. Gopolarao, C. I. Varadanam, *J. Indian Chem. Soc.* **1941**, *18*, 361.
[21] M. Kungsawasd, M. S. Thesis, University of Toledo, **1990**.
[22] See papers in *Proc. 7th Int. Congr. on Nitrogen Fixation*, Cologne, FRG, Gustav Fischer Verlag, Stuttgart, **1988**.
[23] J. Augustynski *Struct. Bonding*, **1988**, *69*, 20.
[24] These experiments were similar to the $^{15}N_2$ work of Schrauzer et al. [12]; that report, however, is not clear on which of the results were from $^{15}NH_3$, and no distribution of isotopes in the products was given.
[25] Schrauzer et al. [12] found no photosynthesis of NH_3 in liquid H_2O, but others [2] reported success in this medium.
[26] a) G. N. Schrauzer, T. D. Guth, M. R. Palmer, J. Salehi in *Solar Energy: Chemical Conversion and Storage* (Eds.: R. R. Hautala, R. B. King, C. Kutal), The Humana Press, Clifton, NJ, **1979**. b) G. N. Schrauzer, T. D. Guth, J. Salehi, N. Strampach, L. N. Hui, M. R. Palmer in *Homogeneous and Heterogeneous Photocatalysis* (*NATO ASI Ser. Ser. C* **1986**, *174*, 509).
[27] D. Harris, Crop and Soil Science Dept., Michigan State University, East Lansing, MI 48824.
[28] A. Wang, M. S. Thesis, University of Toledo, **1991**.

Synthesis of Octameric Phosphodiesters of [3,3-Bis(hydroxymethyl)cyclobutyl]adenine and -Thymine as well as their Hybridization Properties**

By *Jean-Michel Henlin, Klaus Jaekel, Peter Moser, Hans Rink, Erich Spieser,* and *Gerhard Baschang**

Two recent publications concerning synthetic nucleosides[1, 2] have prompted us to communicate the results

[*] Dr. G. Baschang, Dr. J. M. Henlin, H. Rink, E. Spieser
Division Pharma, Forschung und Entwicklung, Ciba-Geigy AG
CH-4002 Basel (Switzerland)
K. Jaekel, Dr. P. Moser
Forschungsdienste, Physikalische Methoden, Ciba-Geigy AG

[**] We thank Prof. H. Fritz, Dr. H. Fuhrer, and Dr. E. Keller for the NMR measurements, Dr. D. Müller for mass spectrometric determinations, and F. Ossola for help with the experimental work.

of our own work in this area. Several research groups have shown that the substitution of deoxyribose in nucleosides by oxetanes and cyclobutanes leads to biologically active compounds.[3] We are interested in the oligomeric phosphodiesters of such artificial nucleosides, especially for their ability to form double strands with ribo- and deoxyribonucleic acids i.e. to hybridize. Apart from the complementarity of the nucleic bases very little is known about the special conditions which two pairing strands and especially their phosphodiester backbone must satisfy. Herein, we report about adenyl and thyminyl derivatives of 1,1-cyclobutandimethanol.

Starting from 3-benzyloxy-1,1-cyclobutandimethanol,[4, 5] which was obtained in a slightly modified way, we synthesized the *O*-protected, sulfonated derivative **1** (Scheme 1) in three steps. Direct introduction of thymine with 1,8-diazabicyclo[5.4.0]undec-7-ene (DBU) in dimethyl sulfoxide (DMSO) at 80 °C afforded **2** (52%) together with the N^1,N^3-disubstituted product (34%). With adenine only **3** (90%) was obtained under the same conditions. The adenine group in **3** was protected by benzoyl chloride to give **4** whose subsequent monosubstitution with methoxytritylchloride (MeOTrCl) yielded the *trans*-substituted **5** and the *cis*-substituted **6** after chromatographic separation. In the thymine series we obtained the *trans* derivative **7** and the *cis* derivative **8**. The structures of these isomers were assigned from NOE

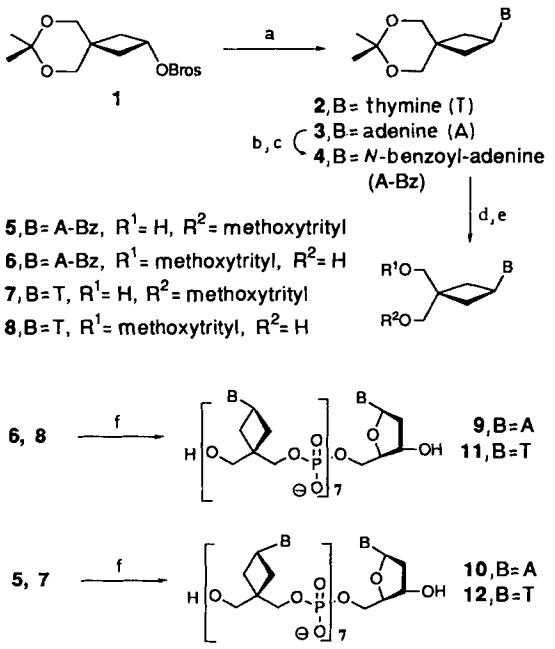

Scheme 1. Synthesis of cyclobutylcarbanucleosides and their octameric phosphodiesters. a) B (3 equiv)/DBU (3 equiv), DMSO, 24h, 80 °C B = A (90%) B = T (52%); b) PhCOCl/pyridine (95%); c) $NH_4OH/THF/H_2O$; d) HCl 2M/dioxane then Na_2CO_3 (70%); e) MeOTrCl/pyridine (**6** (9%) + **5** (27%), and **7** (35%) + **8** (42%), respectively); f) solid-phase synthesis [6,7] (80–87% per coupling step).

experiments. In **5** and **7** irradiation of $H_{1\alpha}$ produced a positive effect on $H_{2\alpha}$, $H_{4\alpha}$, and the methylene protons of the substituted hydroxymethyl group. In contrast in **6** and **8** this effect was observed on the unsubstituted hydroxymethyl group. The four compounds were converted by the phosphotriester method on a solid phase[6, 7] to give octameric phosphodiesters. The thymine-containing oligomers **11** and **12** have thymidine at the end, whereas the adenine-containing oligomers **9** and **10** have deoxyadenosine as the last nucleoside.[8]

The results of the pairing characteristics of the new oligonucleotides both towards ribo- and deoxyribonucleic acids and also towards the complementary homologous oligonucleotides are summarized in Table 1. Apart from the high T_m value[9] of the hybrids of **10** and poly-rU (55 °C), which cannot be explained at the moment, but perhaps indicates a triplex formation, three graded interactions between complementary oligomers can be identified. In contrast, strands with noncomplementary bases showed no cooperative melting properties (see Table 1, footnote [b]). As expected, the T_m values of the hybrids of cyclobutyl oligomers with the complementary DNAs (27 °C, 28 °C) are higher than the T_m values of their hybrids with the less adaptable RNAs (9 °C, 11 °C). The pseudo-α oligomers **10** and **12** lead to lower T_m values than the pseudo-β oligomers **9** and **11**. However, the most interesting result is the unequivocal interaction between the cyclobutyl-A oligomers **9** or **10** and the cyclobutyl-T oligomers **11** or **12** with intermediate T_m values of 18 °C and 20 °C. Hence, following Eschenmoser's example,[10] here is a further synthetic oligonucleotide system, which however, shows interactions with natural RNA and DNA in addition to those with itself.

Table 1. Melting temperatures T_m [°C] and hyperchromicity (in parentheses) of the octameric phosphodiesters [a].

	poly-rA	poly-dA	poly-rU	$(dT)_8$	**11**	**12**
9	[b]	[b]	9 (16%)	28 (25%)	20 (28%)	9 (14%)
10	[b]	[b]	55 (42%)	22 (27%)	18 (28%)	12 (16%)
11	11 (23%)	27 (24%)	[b]			
12		10 (10%)		[b]		
poly-rA				13 (35%)		

[a] All experiments were carried out in phosphate buffer pH = 7.0 and 1M sodium chloride; in physiological NaCl solution the T_m values are approximately 10 °C lower. [b] No determinable T_m value.

Received: November 4, 1991 [Z 5006 1E]
German version: *Angew. Chem.* **1992**, *104*, 492

CAS Registry numbers:
1, 139130-99-7; **2**, 139131-00-3; **2** (N^1,N^3-disubstituted), 139131-09-2; **3**, 139131-61-4; **4**, 139131-02-5; **5**, 139131-03-6; **6**, 139131-04-7; **7**, 139131-05-8; **8**, 139131-06-9; **9**, 139131-07-0; **10**, 139238-73-6; **11**, 139131-08-1; **12**, 139238-74-7; thymine, 65-71-4; adenine, 73-24-5.

[1] T. Maruyama, Y. Sato, T. Horii, H. Shiota, K. Nitta, T. Shirasaka, H. Mitsuya, M. Honjo, *Chem. Pharm. Bull.* **1990**, *38*, 2719–2725.
[2] H. Boumchita, M. Legraverend, C. Huel, E. Bisagni, *J. Heterocycl. Chem.* **1990**, *27*, 1815–1819.
[3] a) S. Hayashi, D. W. Norbeck, W. Rosenbrook, M. Matsukura, J. J. Plattner, S. Broder, H. Mitsuya, *Antimicrob. Agents Chemother.* **1990**, *34*, 287–294; b) D. W. Norbeck, E. Kern, S. Hayashi, W. Rosenbrook, H. Sham, T. Herrin, *J. Med. Chem.* **1990**, *33*, 1281–1285; c) N. Katagiri, H. Sato, C. Kaneko, *Chem. Pharm. Bull.* **1990**, *38*, 288–290; d) Y. Wang, G. W. J. Fleet, R. Storer, P. L. Myers, C. J. Wallis, O. Doherty, *Tetrahedron Asymm.* **1990**, *1*, 527–530; e) Y. Nishiyama, N. Yamamoto, Y. Yamada, T. Daikoku, Y. Ishikawa, K. Takahashi, *J. Antibiot.* **1989**, *42*, 1854–1859; f) Y. Ishikawa, A. Narita, A. Shiozawa, Y. Hayashi, K. Narasaka, *J. Chem.*

Soc. Chem. Commun. **1989**, 1919–1921; g) W. A. Slusarchyk, M. G. Young, G. S. Bisacchi, D. R. Hockstein, R. Zahler, *Tetrahedron Lett.* **1989**, *30*, 6453–6456; h) S. Saito, S. Hasegawa, K. Takahashi, N. Shimada, J. Seki, H. Hoshino, Y. Nishiyama, K. Matsubara, T. S. S. Nagahata, (Nippon Kayaku Kabushiki Kaisha) EPA 0334250, 18. March **1989**; priority: 23. March **1988**, JP 67253/88; *Chem. Abstr.* **1990**, *112*, 179712; i) D. W. Norbeck, J. B. Kramer, *J. Am. Chem. Soc.* **1988**, *110*, 7217–7218; j) W. A. Slusarchyk (E. R. Squibb & Sons), EPA 0352013, 13. July **1989**; priority: 18. July **1988**, US 220849; *Chem. Abstr.* **1990**, *113*, 403444; k) S. Niitsuma, J. Ichikawa, K. Kato, T. Takita, *Tetrahedron Lett.* **1987**, *28*, 3967–3970 and 4713–4714; l) N. Shimada, S. Hasegawa, T. Harada, T. Tomisawa, A. Fujii, T. Takita, *J. Antibiot.* **1986**, *39*, 1623–1925.

[4] M. Avram, C. D. Nenitzescu, M. Maxim, *Chem. Ber.* **1957**, *90*, 1424–1432.

[5] J. Safanda, P. Sobotka, *Collect. Czech. Chem. Commun.* **1982**, *47*, 2440–2447.

[6] J. H. van Boom, G. A. van der Marcel, C. A. A. van Boeckel, G. Wille, C. F. Hoyng in *Chemical and Enzymatic Synthesis of Gene Fragments, A Laboratory Manual* (Eds.: H. G. Gassen, A. Lang), Verlag Chemie, Weinheim, **1982**.

[7] The oligomers were purified on an ion-exchange column "Mono Q HR575", Pharmacia, 5 × 0.7 cm, with a 0.05–1 M NaCl gradient in 10 M triethylamine at 1 *bar*; molecular masses were determined mass spectroscopically by electrospray ionization.

[8] For technical reasons the purchasable resin charged with thymidine and deoxyadenosine, respectively, [3′-(5′-methoxytrityl-*N*-benzoyl-deoxyadenosyl)succinoyl-amidomethyl-polystrene, crosslinked with 1% divinylbenzene] was used. We expected additional information about the disturbing influences of the natural nucleotide from the comparison of T_m values of pseudo-α- (**10**, **12**) and pseudo-β-oligomers (**9**, **11**).

[9] T_m values are obtained in the first approximation as the point of inflection of the function: UV absorption (λ_{max}) = $f(T)$.

[10] A. Eschenmoser, *Nachr. Chem. Tech. Lab.* **1991**, *39*, 795–807.

BOOK REVIEWS

Book Reviews are written by invitation from the editor. Suggestions for books to be reviewed and for book reviewers are welcome. Publishers should send brochures or (better) books to the following address: Redaktion Angewandte Chemie, Postfach 101161, W-6940 Weinheim, Federal Republic of Germany. The editor reserves the right of selecting which books will be reviewed. Uninvited books not chosen for review will not be returned.

Non-Chromatographic Continuous Separation Techniques. By *M. Valcárel* and *M. D. Luque de Castro*. Royal Society of Chemistry, London, 1991. XII, 290 pp., hardcover £ 42.50.—ISBN 0-85186-986-6

The demands being made on the performance of analytical methods are becoming ever more exacting, not only with regard to the quality of the results but also from the standpoints of the speed and economy of the methods used. In recent years there have been great advances in methods of detection, in data processing, and in methods for the delivery of samples to the measuring instruments. The latest challenge presented is to incorporate the sample preparation into the automation of the analytical procedure, so that here too one can achieve higher efficiency and better reproducibility. Non-chromatographic separation techniques offer one approach to this problem, and form the subject of this book.

These techniques are dealt with under three sections. Based on the type of phase transition of the analyte used to achieve separation, the methods are classified as gas-to-liquid systems, liquid-to-liquid systems, and liquid-to-solid systems. Each of these sections is itself divided up in a very logical way, and this systematic treatment is an impressive feature of the book. However, the techniques of field flow fractionation and capillary electrophoresis do not fit into this scheme, and they are treated in a separate, but rather short, section.

Each chapter begins with an introduction to the nature of the problem, followed by a lucid and practically-orientated description of the principles on which the method is based. Next the various modules that make up the system are described, followed in many cases by details of actual instruments and of how the techniques are used. Applications to special types of problems are also described, with the help of clear block diagrams. These include some very original solutions, which reveal the deep knowledge of the subject possessed by the authors, who have themselves made considerable contributions to the development of the techniques.

There is a carefully compiled index, which includes advice on the use of the techniques, and information on the methods used to solve the special problems discussed in the book. There are about 600 literature references (extending up to 1991) giving access to more detailed information.

The book clearly explains the advantages that non-chromatographic separation techniques can offer with regard to precision, sample throughput rate, economy in reagents and reduction of analytical costs. On the other hand the limitations are also clearly explained, especially in the chapter on "leaching". The descriptions of the methods assume that one already has a sample in solution; techniques for handling solid samples are still at an early stage of development.

In their final summing-up the authors explain that their aim has been to familiarize people in the analytical world with these techniques, and so contribute to their becoming established; the book should succeed in this objective. This interesting and very readable monograph is suitable both for the newcomer to the field, seeking a general description of non-chromatographic separation methods, and for the specialist looking for a solution to a particular problem.

Rolf Fischbach
Analytisches Laboratorium
Hoechst AG, Frankfurt/Main (FRG)

Modern NMR Techniques, and Their Applications in Chemistry. (Practical Spectroscopy Series, Vol. 11). Edited by *A. I. Popov* and *K. Hallenga*. Marcel Dekker, New York, 1991. x, 665 pp., hardcover $ 135.00 (USA and Canada), $ 162.00 (all other countries).—ISBN 0-8247-8332-8

The field of NMR spectroscopy is certainly not a branch of science suffering from a lack of literature; at all levels, from simple textbooks all the way through to sophisticated

specialized monographs, this market is fairly well catered for. Still, even for such a well-covered topic as NMR spectroscopy, there are areas in which one would like to see further books published. The book to be discussed here "Modern NMR Techniques and Their Application in Chemistry" is very timely as, for example, the title addresses one of the gaps in the NMR book market. It is certainly a very ambitious title, and since the price of the book is also substantial, high expectations are accordingly raised. Any evaluation will have to be guided by these expectations.

To be quite frank, I am a little disappointed with this book and I feel forced to attest a certain taste of a "misnomer" and at least some lack of "up-to-dateness". My reasons will be explained in greater detail in the following.

What does this book have to offer in its 665 pages? In ten chapters different authors address various aspects of the application of NMR spectroscopy in chemistry. Such a multi-author approach is perfectly acceptable in times of ever-increasing specialization.

Chapter 1, "NMR Properties of Nuclei" (52 pages), is somewhat out of place in a book such as this. This chapter contains the *very* basics of NMR spectroscopy which can be found in numerous variations in many textbooks written for a wide chemistry audience. Moreover, the potential readership of this book can be expected, nowadays, to have this basic knowledge.

Chapter 2, "Fourier Transform NMR: Theoretical and Practical Aspects" (72 pages), is much more useful in this respect. For a chemist, it is easily readable and the topic deserves its own chapter. Again, however, the contents can be found in several other NMR books.

The remaining eight chapters deal with the application of NMR in chemistry. It is very welcome that two chapters (208 pages) are devoted to solid state NMR spectroscopy. However, these two chapters are more likely to cement old prejudices rather than to generate appetite for application. For instance, the chapter "Solid State NMR of Spin-1/2 Nuclei" shows as application examples two figures (on pages 137, 160) from work by Pines et al. and by Herzfeld and Berger which can be considered as truly historical. Over the last ten years these two figures have appeared in a number of review articles and books. Further appetizing examples or an overview of the substantial achievements in this area of research in recent years are missing completely. Similarly the section of CP-MAS NMR spectroscopy is somewhat misleading. Examples given for this methodology are limited to ^{13}C measurements on coals and organic polymers. Fair enough, these *are* very important applications, but by no means do they alone represent what one would call "Modern NMR Techniques and Their Application in Chemistry".

Chapter 4, "Solid-State NMR: Quadrupolar Nuclei", presents a useful discussion of quadrupolar interactions and asymmetry parameters. In this chapter the selection of examples is much broader.

Chapter 5, "Quantitative Analysis by NMR" (46 pages), is again of mainly very basic character. It would have been appropriate for this chapter to address explicitly quantitation problems in solid-state NMR, as it is known that these problems are not quite the same for solutions and solids.

Perhaps it would have been better to combine Chapter 6 "Structural Determination of Organic Compounds" and Chapter 10 "Two-Dimensional NMR Studies of Biomacromolecules" into one chapter. The methodology used for these two topics shows many overlaps and parallels, the essential difference being just the molecular weight of the "objects" under investigation.

Chapter 7, "Structural Determination of Inorganic Compounds", does give a fairly broad overview, including inorganic and organometallic applications, as well as two-dimensional experiments in solution. Solid-state NMR spectroscopy comes off poorly in this chapter; only cement and zeolites are mentioned, and at that, very briefly. This is a real pity, especially since chapters 3 and 4 do not offer much in terms of inorganic applications either. A more detailed discussion, for example on the combined use of solid- *and* solution-state NMR, or on diffraction techniques plus NMR, would have been highly desirable.

Both Chapter 8 "Equilibria Studies in Solutions" and Chapter 9 "Reaction Kinetics and Exchange" are justified by the fact that these aspects of NMR spectroscopy are usually only dealt with very briefly in other textbooks.

To conclude, in my opinion another book on the same subject of modern NMR applications in chemistry approaches the ambitious goals of the refereed book much better. This alternative, edited by P. Granger and R. K. Harris and published in 1990, also uses the multi-author approach; it is quite comparable as regards size and price, and gives a much more up-to-date and broader overview ("Multinuclear Magnetic Resonance in Liquids and Solids—Chemical Applications", NATO ASI Series C, Vol. 322, Kluwer Academic Publishers, 1990, ISBN 0-7923-0986-3).

Angelika Sebald
Bayerisches Forschungsinstitut
für Geochemie und Physik
an der Universität Bayreuth
Bayreuth (FRG)

Preparative Polar Organometallic Chemistry 2. By *L. Brandsma*. Springer, Berlin, 1990. XII, 227 pp., paperback DM 86.00.—ISBN 3-540-52749-4

This second volume, in which preparations and reactions of lithium, sodium and potassium compounds that result from deprotonation at an sp_3-hybridized carbon atom are described, extends the scope beyond that of the first volume (published in 1987) by including also the most important examples of Li, Na and K compounds obtained by deprotonation at an sp_2-hybridized carbon. The care that is taken in the preparation of the "Brandsmas" is now almost legendary – to anyone acquainted with this author's love for experimental detail, especially in the organometallic field, that comes as no surprise. Following the developments during the 1980s that led to lithium, sodium and potassium compounds becoming some of the most important synthetic reagents in organic chemistry, it is extremely useful to now have access also to a wealth of carefully tested laboratory recipes for "sp_3 anions". Thus, this second volume, like the first, belongs in every organic chemistry laboratory!

The volume contains ten chapters as follows: 1. Reactivity of Polar Organometallic Intermediates; 2. Metallation of Aromatic and Olefinic Hydrocarbons; 3. Metallation of Saturated Sulfur Compounds; 4. α-Metallation of Derivatives of Toluene Containing Heterosubstituents; 5. Metallation of Heterosubstituted Allylic and Benzylic Compounds; 6. Metallation of Heterocyclic Compounds; 7. Metallation of Aldimines and Ketimines; 8. Metallation of Nitriles and Isonitriles; 9. Generation of Lithium Halocarbenoids; 10. Metallation of Carbonyl and Thiocarbonyl Compounds. The appendix contains first a very useful "Metallation–Functionalization" index, in the form of a table summariz-

ing the metallations and functionalizations with electrophiles that are described in Chapters 2–10. This is followed by a list of the starting compounds used in the preparations described in Volumes 1 and 2. Next there is an index to the contents of both volumes. Some typical reactions and special techniques are then described, with examples taken from both volumes. Lastly there is a section on the purification and storage of a few relevant reagents and solvents.

To summarize, I can only repeat what I wrote previously by emphatically recommending the second volume, like the first, for everyone concerned with the organometallic chemistry of lithium, sodium and potassium; this is likely to include a great many chemists.

Gernot Boche
Fachbereich Chemie
der Universität Marburg (FRG)

The Chemistry of Polymers. (Royal Society of Chemistry Paperbacks Series). By *J. W. Nicholson*. The Royal Society of Chemistry, London, 1991. XII, 174 pp., paperback £ 14.50.—ISBN 0-85186-413-9

This little book is intended for advanced students, industrial chemists, and newcomers to the field of polymer chemistry, and provides a very brief introduction to the chemistry and physical properties of polymers. It is divided into ten chapters, each consisting of an introduction followed by 10–30 pages on a particular aspect of the subject; these include such varied topics as polymerization reactions, crosslinking, structure, mechanical properties, and decomposition.

Thus the book's title is repeated as a heading for the first chapter, which describes the structures and properties of the main polymers of industrial importance (polyethylene, polystyrene, nylon, etc.) and also several naturally occuring macromolecular substances such as starch and proteins. In the chapter on polymerization reactions special emphasis is put on classifying the reactions according to their kinetics into chain (addition) polymerizations and step (condensation) polymerizations. The basic principles of the reactions are discussed and illustrated by examples; the methods whereby these are scaled up into industrial processes are then described. The following chapter deals with the stereochemistry of polymers, including carbon atoms as chiral centers, and with crystallinity and thermal properties such as the glass transition temperature. Surprisingly, liquid crystalline polymers and their phase transformations are not discussed at this point; this topic is only briefly touched on later, in Chapter 9, which deals with special aspects of polymer chemistry.

In contrast, the various methods for crosslinking oligomers and polymers are described in detail, with particular emphasis on industrial-scale applications. The important chapter on methods for determining the molecular mass distribution of polymers is preceded by a discussion of their solution properties. The longest chapter in the book is that dealing with mechanical properties, including tensile properties and stretching behavior, rubber-like elasticity, and reinforced materials. Here (though not elsewhere) the reader is even referred to other literature for further study. Next the risks of polymers becoming degraded by heat and light are discussed, together with their combustion properties and fire resistance. In this context the use of the antimony-halogen synergistic effect to lower the flammability index of polymers is mentioned.

The idea of the final chapter, which aims to give a heightened awareness of environmental effects, is interesting and potentially valuable. However, it is mainly limited to general statements of an almost political kind about methods of waste disposal; biodegradable polymers are only very briefly mentioned.

In setting out to give an overview of the whole field of polymers, extending as far as their materials science and technology, J. W. Nicholson has had to keep the amount of detail down to a minimum, but unfortunately has not included recommendations for additional or more advanced reading. The book will be of interest and value mainly for newcomers to the field who expect to be involved in technological aspects of polymer chemistry. Detailed physicochemical and organic chemical aspects are not treated. The level of treatment is comparable with the introductory sections to be found in standard textbooks of organic and physical chemistry, but not with standard works on polymer chemistry such as those by Elias and Vollmert.

Martin Baumgarten
Max-Planck-Institut für Polymerforschung,
Mainz (FRG)

Registered names, trademarks, etc. used in this journal, even when not marked as such, are not to be considered unprotected by law.

© VCH Verlagsgesellschaft mbH, D-W-6940 Weinheim, 1992. – Printed in the Federal Republic of Germany by Konrad Triltsch Druck- und Verlagsanstalt Würzburg.

All rights reserved (including those of translation into foreign languages). No part of this issue may be reproduced in any form — by photoprint, microfilm, or any other means — nor transmitted or translated into a machine language without written permission from the publishers. Only single copies of contributions, or parts thereof, may be made for personal use. This journal was carefully produced in all its parts. Nevertheless, authors, editors, and publisher do not warrant the information contained therein to be free of errors. Readers are advised to keep in mind that statements, data, illustrations, procedural details, or other items may inadvertently be inaccurate.

Valid for users in the USA: The appearance of the code at the bottom of the first page of an article (serial) indicates the copyright owner's consent that copies of the article may be made for personal or internal use, or for the personal or internal use of specific clients. This consent is given on the condition, however, that the copier pay stated per-copy fee through the Copyright Clearance Center, Inc. (CCC), for copying beyond that permitted by Sections 107 or 108 of the U.S. Copyright Law. This consent does not extend to other kinds of copying, such as copying, for general distribution, for advertising or promotional purposes, for creating new collective works, or for resale. For copying from back volumes of this journal see 'Permissions to Photo-Copy: Publisher's Fee List' of the CCC.

Editorial office: Postfach 10 11 61, D-W-6490 Weinheim, Federal Republic of Germany, Telephone (06201) 60 23 15, Telex 465 516 vchwh d, Telefax (06201) 602 328, E-Mail Z16@DHDURZ2 in Earn Bitnet.

Editor: *Peter Gölitz*

Associate editors: *R. H. Schmidt-Radde, K. J. Schneider, A. Stimson.* **Editorial assistant:** *E. Schweikart*

Publishers: VCH Verlagsgesellschaft mbH. (Managing Directors: *Hans Dirk Köhler, Dr. Karlheinz Köpfer*), Pappelallee 3, W-6940 Weinheim, Federal Republic of Germany.

Advertising office (Advertising Manager: *R. J. Roth*): Postfach 10 11 61, D-W-6940 Weinheim, Federal Republic of Germany, Telephone (0 62 01) 60 61 36, Telex 4 67 155, Telefax (0 62 01) 606 156.

ANGEWANDTE CHEMIE
International Edition in English
Volume 31 · Number 5
May 1992
Pages 487–664

Transport and Fate of Organic Compounds in the Global Environment

By Karlheinz Ballschmiter*

Dedicated to Professor Heinz Harnisch on the occasion of his 65th birthday

The role of chemistry in our soon-to-be global industrial society requires a global perspective for the discussion of the uptake, transport, and conversion of chemical compounds in the environment. The fate of organic compounds in the volume flow of the atmosphere and hydrosphere can be categorized into transport pathways and adjustments of equilibria in the multiphase system atmosphere–oceans–land surface. The global volume flow in the atmosphere (wind, areas of high and low pressure) and in the hydrosphere (rivers, circulation of water in lakes, ocean currents) alone would account for the transport of organic compounds if they were stable and if all these compounds were molecularly distributed in these phases. However, this particular case is observed only for volatile chlorofluorocarbons and tetrachloromethane. For most organic compounds, complex adsorption/desorption processes on finely dispersed particle phases in the air and water as well as abiotic and biotic transformations determine the transport behavior.

The global fate of a compound includes its accumulation as well as its decomposition in defined environmental compartments. Both phenomenon may have long-term consequences in the affected areas; this is indicated by the accumulation of polychlorobiphenyls and analogous compounds in marine mammals and deep-sea fauna, and is evident in the decomposition of chlorofluorocarbons in the stratosphere. The accepted definition of the level of a risk, the product of the probability of an event and the potential amount of damage, takes on a new dimension when viewed from a global perspective—especially when one further connects the extent of the damage to the possible means of correction. It is the responsibility of scientists to point out the irreparable regional to global consequences directly and indirectly connected to the production of chemicals and to provide suggestions for prevention. Politicians can only react by applying their methods to limit the damage; however, they cannot generate any solutions based on science.

1. Introduction

An account of the pathways and mechanisms whereby organic compounds at low concentrations are transported in the atmosphere, the hydrosphere and the biosphere on a global scale must, within the confines of a review such as this, be limited to describing the basic processes that can occur and indicating their dimensions. The complexity arising from the mixing and separation processes that are possible, whose description involves geography, geophysics, meteorology and oceanography, is further compounded by the wide range of physicochemical and chemical properties of the many compounds that can be regarded as xenobiotics.[*] The list of compounds in the environment that result directly or indirectly from modern industrial civilization is extensive, including such widely varied examples as phosgene,[1] chlorofluoromethanes (F11 and F12),[2] benzene,[3] chlorinated biphenyls,[4] chlorinated dibenzo-*p*-dioxins and dibenzofurans,[5] and acetonitrile.[6]

[*] Prof. Dr. K. Ballschmiter
Analytische Chemie und Umweltchemie der Universität
Albert-Einstein-Allee 11, W-7900 Ulm (FRG)

[*] Greek xenos = foreign, bios = life; harmful chemicals in the environment.

Although attention is mainly focussed on those compounds that are produced and distributed through human activities when one is considering the question of their fate in the global environment, one must not overlook the fact that the observed atmospheric concentrations of some compounds, such as the solvent chloroform,[7] include a biogenic contribution. Likewise formaldehyde, whose occurrence as a pollutant has been much discussed, also has a natural background concentration in the atmosphere as an intermediate product during the 'cold' combustion of methane from sewage or marsh-gas (reaction with 'OH radicals). Both these compounds thus belong to natural evolutionary processes.

For many molecular species there are preferred transport pathways and consequently regions of the environment in which they mainly occur, while for others their occurrence is completely random.[8–15] Accumulation in a specific region can occur as a result of being introduced through use of a product or through being indirectly generated there, or it can arise through transport from another region.

The combined effects of transport and conversion processes can be envisaged as working like a sort of 'environmental chromatography' on a regional or global scale. Thus the global environment can be regarded as a complex chromatographic system in which gas chromatography and liquid chromatography are closely intertwined. The transport behavior of a compound is determined by its molecular properties and by the nature and structure of the transport medium in its various possible sub-phases (e.g. water present as clouds in the atmosphere, or particles and colloids in water).

In order to be able to describe the distribution processes that take place in the real environmental situation, regarding this as a sort of global laboratory, one must have access to the necessary analytical methods which meet the requirements of the task with regard to detection sensitivity, resolution, reliability, and truly representative sampling. The capability to analyze complex mixtures of organic compounds down to extreme trace concentrations forms the essential basis on which to develop a global environmental chemistry encompassing a very wide range of substances.

A knowledge of how xenobiotics (man-made chemicals) become distributed in the environment provides the basis for a discussion of the occurrence and fate of such chemicals, and thus forms part of a study of 'ecotoxicokinetics' that can ultimately be looked at on a global scale.

Toxicokinetics is a branch of toxicology, and describes the processes of resorption, distribution, transformation and elimination that are undergone by a biologically active (toxic) substance within an organism. If we extend the concept of an organism by giving it global dimensions, which are, however, decidedly finite, and we then consider not only direct biological interactions but also, quite generally, all types of interference with the global system of equilibria, such a global 'chemokinetics' is only slightly removed from the conventional approaches of toxicokinetics. The essential difference is that, in such a global 'ecotoxicology', experiments to study the effects are ruled out, or are only possible to a very limited extent; instead one must study events that have already occurred and from these develop strategies for preventing future damage.

A fact that is often overlooked is that the level of a risk is defined as the product of the probability of an event and the amount of damage caused. Where the potential damage is global, only an extremely low occurrence probability can result in a normal (acceptable) risk. Eventually a stage is reached where the occurrence probability must approach zero. Preventing environmental damage is not an entirely new human endeavor—forest plantings to prevent avalanches were essential to safeguard lives in the Alps, as also were dykes on coasts—but the general experience has been that visible local dangers prompt action far more effectively than possible scenarios involving global catastrophe.

Environmental chemicals, apart from a few exceptions, are 'got rid of' on a local or regional basis through emission or by dilution (e.g. via fume extractors, vehicle exhausts, chimneys and by wind, and for liquids through effluent outlets or drainage channels or by rivers); alternatively they are taken up by the environment in a more diffuse and more complex way in the course of or following their use. In principle, therefore, if the basic physicochemical properties (water solubility, vapor pressure, melting point, K_{OC}, K_{OW}, K_{GW}, Henry's constant) and chemical properties (reactivity, decomposition products) of a compound are either known or can be predicted, one can forecast the regional and global mass transport processes that a compound undergoes in the atmosphere[16–20] and hydrosphere,[16, 21–24] and hence the expected long-term consequences of its release into the environment and the subsequent dispersion processes.[25, 26]

The processes whereby organic compounds are transported in the environment can be classified as follows:

Karlheinz Ballschmiter, born 1937 in Petershagen (Pomerania), studied chemistry at the University of Mainz, where, in 1966, he also gained his doctorate and a prize for the best Doctorand in Rheinland-Pfalz. After a two-year spell doing research at the Argonne National Laboratory in Chicago, he habilitated in 1971 in Mainz. In 1973 he moved to the University of Ulm, where at present he is full professor of analytical chemistry and environmental chemistry. In 1982, Ballschmiter received the Merckle Research Prize from the University of Ulm, in 1990 the Philip-Morris Research Prize from the Philip-Morris Foundation, and in 1990 the Fresenius Prize from the German Chemical Society. He is actively engaged in a number of working groups, among them the Advisory Committee on Existing Chemicals of Environmental Relevance (BUA), of the German Chemical Society. His areas of research include the systematic and applications-oriented problems of organic trace analysis and environmental chemistry, as well as investigations of the global occurrence and migration of environmental chemicals and the correlation of chemical structure and final fate of the chemicals.

1. Transport in the technosphere from the site of production to the place of use.
2. Transport in the hydrosphere (surface water, groundwater, lakes, tides, oceans).
3. Transport in the atmosphere (troposphere 0–10 km, stratosphere 10–50 km).
4. Transport in the lithosphere (by groundwater).
5. Transport in the biosphere (migrations of animals etc., food chains, incorporation into eggs and milk, incorporation into the fetus).

There is a continual interchange between mechanisms 2–5, and the transport in the troposphere and that in the upper layers of the hydrosphere, especially in the oceans, can mutually reinforce each other. The phase transitions in each direction involve complex physicochemical processes, and attempts are being made to describe these using simplified models.[8, 9, 14]

In this discussion, transport in the lithosphere (the soil and groundwater) will not be examined in detail. The surface of land, including vegetation, does not have a direct transport function, but rather acts as a local or regional 'source' (e.g., following pesticide spraying), as an intermediate 'store' (e.g., by absorbing a substance deposited from the atmosphere), or as a 'sink' in which a substance is ultimately retained. Groundwater , on the other hand, has a long-term function as a transport medium for environmental chemicals on a local or regional scale.[13, 15]

In trying to assess whether or not a given compound is distributed via a particular transport pathway, the chemist's experience in the laboratory regarding properties such as its water solubility, volatility, volatility in steam, or stability can often be misleading. In particular, descriptions such as 'soluble in water' and 'involatile' need to the reinterpreted when one is concerned with regional and global processes.

A clear and unambiguous classification of the dimensions of transport pathways or of areas of distribution is essential for addressing many problems. The relevant distances or surface areas determine whether one is dealing with a point source (e.g., a town or city), a ribbon-shaped source (e.g., a highway), an extended source (such as an industrial zone), or a diffuse release over a very large area (e.g., Europe, Japan, the USA). On a local scale a chimney stack is a point source, and the same description can also apply to a city, whereas on a continental scale one might even regard the Ruhr region or the industrial belt around Birmingham (UK) as point sources. With regard to the question of a point of measurement, especially for measurements in the lower troposphere, one can only expect to get representative and meaningful results from sources of extended area if the measurements are carried out over a sufficiently long period and are supplemented by further data (time of year, weather conditions, cyclical pattern of work activity, variation through the day). Conclusions can then be drawn regarding, for example, the covariance of emissions of different substances, such as C_1 and C_2 organohalogen compounds in an industrial region, or regarding the intrusion of pollutants into a 'clean air zone'.[27]

A classification into distribution areas of different scales—local, regional or global—is also often applied, although one cannot define rigid distinctions between these. An attempt at such a differentiation is shown in Table 1. Here the term 'national' may take on a special practical significance when considering the spread of a pollutant in the environment. National boundaries are often identical to transitions between zones or patterns of use, and they therefore define sources, without, however, hindering the spread of a compound.

Table 1. Transport on different scales regarding distribution of environmental chemicals.

Description	Distances [km]	Description	Distances [km]
Point	0 to 0.05	National	200 to 1000
Local	0.05 to 10	Continental	1000 to 5000
Regional	10 to 200	Global	5000 to 40000

If one regards the global distribution and transformation behavior of a compound as an experiment, and defines its boundary conditions in terms of appropriate questions, then, assuming that one has suitable analytical methods for measuring the extremely low concentrations present in the unavoidably complex mixtures, it is possible to investigate global environmental chemistry in a retrospective manner.

The study of the chemistry of substances in the environment, 'environmental chemistry', has previously been mainly the domain of physicists and biologists rather than of chemists. However, the concept of the whole planet as a chemical reaction flask is already a reality. The processes that go on within it must now be treated as an integral part of the science that we call chemistry.

2. Global Parameters for Characterizing the Uptake of Chemicals into the Environment

For compounds that are direct products of the chemical industry, including oil processing, some indications of the quantities that one can expect to enter the environment may be obtained from national, regional and global production figures and patterns of use.[28] For some groups of compounds, such as the chlorofluorocarbons (CFCs), the C_1 and C_2 chlorinated solvents, or the BTEX arenes (benzene, toluene, ethylbenzene and xylene), one can easily arrive at such estimates. However, as soon as one moves to the chlorinated ethanes, ethylenes, cyclohexanes, benzenes and biphenyls, compounds that are becoming increasingly important as tracers for studying global distribution pathways, only crude estimates of annual world production, past and present, are available. Also one can only make crude estimates regarding what fraction of the material produced (e.g., the chlorinated benzenes and chlorinated biphenyls) has already entered the environment, or how much can do so in the future. Moreover, nothing is known about the extent to which chemical wastes are disposed of by improper, if not criminal, methods on a regional or global scale; the size of the problem may be considerable, and can only be guessed at.

Emissions of environmental chemicals, which are quite generally correlated with industrial production and thus with the standard of living (e.g., emissions of solvents, detergents, and plasticizers), can be estimated from the annual gross national product of each country, if one assumes that

Table 2. Countries with an annual gross national product (GNP) greater than $ 100000 M or a per head product greater than $ 5000 (1984). [29]

Country	GNP		CO_2 emissions (1986)
	Total $ M	Per head $	Tons per head per year
Federal Republic of Germany	678880	11090	11.7
France	542960	9860	7.0
United Kingdom	480680	8530	11.8
Italy	367040	6440	
Netherlands	135830	9430	
Switzerland	105060	15990	
Sweden	99060	11880	
Canada	330870	13140	
USA	3670490	15490	20.0
Mexico	158310	2060	
Saudi Arabia	116380	10740	
India	197210	260	0.7
China	318310	310	2.4
Japan	1248090	10390	7.6
Brazil	227280	1710	
Australia	184980	11890	15.5

the industrial structure is nearly the same in each case. Table 2 lists the countries that had a gross national product (GNP) of more than $ 100 million or a GNP per head of more than $ 5000 in 1984.[29] The regions where there is substantial industrial production or is likely to be in the future are mainly distributed within a narrow belt in the northern hemisphere, lying roughly within the range 30–55° N. However, China, with approximately 25% of the world's population, would need to increase its GNP per head by a factor of 20–30 to catch up with the present levels in Europe and Japan. Even if one assumes a severe reduction in the rate of world population growth—which is rather unrealistic—the efforts being made by all the political forces to raise the overall GNP per head to that already achieved in the leading industrial countries could alone lead to enormous emissions of pollutants on a global scale.[29] The question of what sort of industrial civilization should be aimed at worldwide, or indeed can have a long-term future, is a very practical one. Can the European-Japanese-US model have a future in the global sense?

GNP is not an appropriate parameter for those chemicals which, although produced in the industrially advanced countries or based on their science and technology, are specifically made for use in other regions of the world, for example in crop growing (rice, maize, cotton, etc.) or in cattle rearing (agents for controlling ectoparasites, tsetse fly, etc.). For these compounds one can arrive at estimates regarding sources on the basis of the structure of the economy and a knowledge of the pattern of use and the regions affected. For example, despite all the prohibitions on the use of 4,4'-DDT (dichlorodiphenyltrichloroethane) in the USA and Western Europe, there has been no significant reduction in the world total production of this insecticide and its use against malaria; the main reasons are its relative cheapness, low toxicity to humans, and the growth of resistance in the insect populations.[30] Up to 1984, 4,4'-DDT and other organochlorine insecticides continued to be produced in the former GDR.

The emissions from diffuse sources (consisting of a multitude of small sources dispersed over a large area) are often underestimated. For example, in Germany alone about 250 tons of material in the form of fine particles is generated each day by abrasion of vehicle tires, making a total of nearly 100000 tons per year. The emission of carbon particles from diesel vehicles now stands at about 60000 tons per year. According to the Federal Office of the Environment in Berlin, the quantity of fuel evaporated during 1988 from the tanks of the approximately 30 million motor vehicles in the then Federal Republic of Germany, when either stationary or traveling, was 362000 tons. A further 46000 tons was evaporated during the refueling of vehicles. Multiplying these figures to correspond to a total of 300 million vehicles gives some idea of the expected global emissions.

In cases where no figures for production and use are available from official statistics, indirect but nevertheless reliable estimates can be calculated from the accumulation of the compounds in non-migratory birds,[31] in non-migratory fish present in rivers, estuaries or in lakes that have no outflow,[32] or which can be found as deposits on foliage, mosses or conifer needles[33] or in lake sediments.[34] Data from the estuaries of large river systems such as the Rhine, Elbe, Rhône, Nile, Volga, Ob, Lena, Amur, Huangho, Congo, Amazon, Rio de la Plata[35] or Mississippi[36] are especially valuable for the information they give about releases into their catchment areas from industrial production, agriculture and aqueous effluents. Menhaden oil, extracted from a plankton-filtering fish that swims in shoals and is of industrial importance, provides an almost ideal means of studying the pollutants burden carried by the warm layer of the Gulf Stream.[32] Similarly, the pollutants burden found in fish from the Caspian Sea gives unequivocal information about the uptake of persistent chemicals carried by the Volga and Ural rivers from the large industrial regions of the former USSR.[37] In cases where the input of a compound or group of compounds from distant sources can be estimated, it is a simple matter to determine the local or regional contribution.[27]

If the rate of uptake of a chemical into the environment cannot be directly estimated, but it is known that this occurs exclusively in the northern hemisphere, or the proportion in the northern hemisphere can be estimated, and if it can also be assumed to be predominantly retained in the atmosphere, then the uptake in the northern hemisphere can be calculated from the concentration in the troposphere of the southern hemisphere, provided that one knows the mean partial lifetimes τ_{phys} (physical translocations) and τ_{chem} (chemical transformations). Such estimates have been made for 1,1,1.2-tetrachloroethane, hexachlorobutadiene and other trace pollutants.[38] Using data for the southern hemisphere ensures that one can assume global mixing to have occurred. These considerations are not valid for compounds whose chemical and physical lifetimes τ_{chem} and τ_{phys} in the atmosphere are short, i.e. on the order of days or weeks, since the time required for movement to the southern hemisphere is typically about one year.

3. The Chemical Stability of Chemicals under Environmental Conditions

How far xenobiotics are transported depends on their physical properties and their chemical stability. For trans-

port to occur requires time. If a compound disappears from the transporting media (air and water) within hours or days through being physically extracted ("translocation") or through a chemical transformation, this sets a limit on the distance over which it is dispersed. Conversely, a global distribution is possible only if there is chemical stability.

The lifetime τ of a compound in a particular compartment of the environment is defined as the reciprocal of the rate of disappearance; thus Equation (1) defines:

$$\text{rate of disappearance} = \tau^{-1} \tag{1}$$

The overall rate is made up of two components [Eq. (2)]:

$$\tau_{total}^{-1} = \tau_{chem}^{-1} + \tau_{phys}^{-1} \tag{2}$$

For the environmental compartment consisting of the atmosphere, τ_{chem}^{-1} (chemical transformation) and τ_{phys}^{-1} (translocation) can each be subdivided into several terms, resulting in Equation (3):

$$\tau_{total}^{-1} = [\tau_{OH}^{-1} + \tau_{O_3}^{-1} + \tau_{NO_2}^{-1} + \tau_{H_2O}^{-1} + \tau_{h\nu}^{-1} + \tau_{therm}^{-1}] + [\tau_D^{-1} + \tau_R^{-1} + \tau_W^{-1}] + \tau_T^{-1} \tag{3}$$

τ_{OH}, τ_{O_3}, τ_{NO_2} and τ_{H_2O} relate to the reactions of the compound in question with 'OH radicals, ozone, NO_2 and H_2O respectively. $\tau_{h\nu}$ and τ_{therm} relate to photolysis and thermal decomposition (as in PAN, (peroxyacetylnitrate) for example), τ_D^{-1} relates to extraction by dry deposition, τ_R^{-1} to extraction in rainfall after particles have acted as condensation nuclei for water droplets in clouds including 'in-cloud' and 'below-cloud' scavenging ("rain-out"), and τ_W^{-1} to absorption in rainfall in the manner of a gas-scrubbing process ("wash-out"). τ_T^{-1}, which relates to extraction through being carried by the wind out of a geographically defined environmental compartment ("transport"). It corresponds to an uptake into a different environmental compartment.

For many compounds the parameters of Equation (3) reduce to a simpler situation, for example as expressed in Equation (4).

$$\tau_{total}^{-1} = \tau_{OH}^{-1} + \tau_D^{-1} + \tau_R^{-1} + \tau_T^{-1} \tag{4}$$

Here the only processes that remain are reactions with 'OH radicals, extraction in the form of particles (deposition plus rain-out), and removal by wind. For a hemisphere one can instead have Equation (5), which includes only the reaction with 'OH radicals and extraction predominantly by wash-out.

$$\tau_{total}^{-1} = \tau_{OH}^{-1} + \tau_W^{-1} \tag{5}$$

3.1. Transformations in the Troposphere

This description refers specifically to the component of the reciprocal lifetime τ_{total}^{-1} that includes chemical reactions. The chemical lifetime τ_{chem} is defined as the time during which the initial concentration c_0 decays to $c_0 e^{-1}$ [Eq. (6)], i.e. to 38.6% of the initial concentration:

$$\tau_{(x)} \equiv c_{0(x)} \rightarrow c_{0(x)} e^{-1} \tag{6}$$

The sum of all transformation reactions in the atmosphere is given by Equation (7):

$$-\frac{dx}{dt} = (k_{OH} c_{OH} + k_{O_3} c_{O_3} + k_{NO_2} c_{NO_2} + k_{H_2O} c_{H_2O}) c_x \tag{7}$$

Normally one can assume $k_{OH} c_{OH} \gg k_{O_3} c_{O_3}$, $k_{NO_2} c_{NO_2}$, $k_{H_2O} c_{H_2O}$ so that the chemical lifetime is essentially determined by the reaction with 'OH radicals. Alkenes are an exception, as their reactions with ozone and with 'OH radicals have comparable rates, i.e. $k_{OH} c_{OH} \simeq k_{O_3} c_{O_3}$.

The product $k_{OH} c_{OH}$ is often written instead in the form K_{OH} as expressed in Equation (8).

$$\tau_{x(OH)} = (k_{OH} c_{OH})^{-1} = K_{OH}^{-1} \tag{8}$$

Hydroxy radicals, which are responsible for the cold combustion of organic substances in the atmosphere, are formed mainly through the action of intense solar radiation on moist air, in which oxygen atoms in the singlet state $O(^1D)$ react with water. Other important mechanisms forming 'OH radicals are the reactions of peroxy radicals ($HO_2^{\cdot}$) with NO or O_3. Table 3 summarizes yet more reactions whereby 'OH radicals are formed.[39] The concentration of 'OH radicals, c_{OH}, fluctuates according to the radiation intensity and the concentrations of the various precursor species. In measurements carried out at Schauinsland in the Black Forest in June 1984, the hydroxy radical concentration increased from 1×10^6 molecules cm^{-3} at 8.00 a.m. to 7×10^6 molecules cm^{-3} at midday.[40] In Washington State (46° N, 117° W) in October 1987 the measured concentrations varied from less than $(0.25 \pm 0.05) \times 10^6$ molecules cm^{-3} in the morning and evening to $(2.9 \pm 0.5) \times 10^6$ molecules cm^{-3} at midday. By contrast, in a city atmosphere the midday concentration rose

Table 3. Formation of 'OH radicals in the atmosphere.

Basic reactions [a]		Source reactions [b]	
Educts	Products	Educts	Products
$O(^1D) + H_2O$	$2\,^{\cdot}OH$	$O_2 + h\nu$ ($\lambda < 242$ nm)	$2O(^1D)$
$O_3 + {}^{\cdot}O_2H$	$^{\cdot}OH + 2O_2$	$O_3 + h\nu$ ($\lambda \leq 315$ nm)	$O(^1D) + O_2$
$NO + {}^{\cdot}O_2H$	$^{\cdot}OH + NO_2$	$O_3 + h\nu$ ($\lambda \geq 330$ nm)	$O(^3P) + O_2$
$O(^1D) + H_2$	$^{\cdot}OH + H$	$N_2O + h\nu$ ($\lambda < 337$ nm)	$O(^1D) + N_2$
$O(^1D) + CH_4$	$^{\cdot}OH + {}^{\cdot}CH_3$	NO_2 ($\lambda \leq 365$ nm)	$O(^1D) + NO$
$O(^3P) + {}^{\cdot}O_2H$	$^{\cdot}OH + O_2$	NO_2 ($\lambda \leq 420$ nm)	$O(^3P) + NO$
$O(^3P) + H_2O_2$	$^{\cdot}OH + {}^{\cdot}O_2H$	$O(^3P) + O_2 + M$	$O_3 + M^*$
$O_3 + H$	$^{\cdot}OH + O_2$	$CH_2O + h\nu$ ($\lambda \leq 330$ nm)	$H^{\cdot} + HCO^{\cdot}$
$HNO_3 + h\nu$	$^{\cdot}OH + NO_2$	$H^{\cdot} + O_2 + M$	$^{\cdot}O_2H + M^*$
$HNO_2 + h\nu$	$^{\cdot}OH + NO$	$HCO^{\cdot} + O_2$	$^{\cdot}O_2H + CO$
$H_2O_2 + h\nu$	$^{\cdot}OH + {}^{\cdot}OH$	$CH_3\text{-}CH_2O + h\nu$	$CH_3^{\cdot} + HCO^{\cdot}$

[a] Formation of 'OH radicals. [b] Formation of precursors of 'OH radicals.

to $(10.1 \pm 3.3) \times 10^5$ molecules cm^{-3}.[40] A new method of measuring 'OH radical concentrations based on the reaction with SO_2 gives time-scale resolutions in the order of minutes, and is expected to greatly improve the detection capabilities for this important atmospheric trace constituent.[41]

According to a photochemical model that takes account of 45 distinct reactions as well as the temperature, pressure and solar radiation intensity, one can expect a globally averaged daytime 'OH concentration of 1.6×10^6 molecules cm^{-3}, compared with a night-time value of 0.013×10^6 molecules cm^{-3}, i.e. about a factor of 100 smaller than the daytime value.[39] In contrast to work by other authors, this model predicts a higher average value for the northern than for the southern hemisphere (0.85×10^6 and 0.78×10^6 molecules cm^{-3} respectively).[39] The average value for the entire troposphere is 0.82×10^6 molecules cm^{-3}. As a global average for the concentration of 'OH radicals in the troposphere a value of $(0.5 \pm 0.1) \times 10^6$ molecules cm^{-3} is generally assumed.[42]

The most important scavenging reactions that remove 'OH radicals from the troposphere are the reactions with CH_4 (Table 4) and with CO. Global variations in the concentrations of these two trace gases in the troposphere are at present the main cause of differences in the average concentration of 'OH radicals.[42]

Table 4. Breakdown of methane by 'OH radicals in the atmosphere, giving formaldehyde, carbon monoxide, and finally CO_2.

Educts	Products	Educts	Products
Breakdown of CH_4:		*Breakdown of HCHO:*	
$CH_4 + {}^{\bullet}OH$	$CH_3^{\bullet} + H_2O$	$HCHO + {}^{\bullet}OH$	$CHO^{\bullet} + H_2O$
$CH_3^{\bullet} + O_2 + M$	$CH_3O_2^{\bullet} + M^*$	$CHO^{\bullet} + O_2$	$CO + {}^{\bullet}O_2H$
$CH_3O_2^{\bullet} + NO$	$CH_3O^{\bullet} + NO_2$	$CHO^{\bullet} + O_2$	$CO_2 + {}^{\bullet}OH$
$CH_3O^{\bullet} + O_2$	$HCHO + {}^{\bullet}O_2H$	$HCHO + h\nu$	$H^{\bullet} + HCO^{\bullet}$
$CH_3O^{\bullet} + NO_2$	CH_3ONO_2	$(\lambda \leq 330$ nm)	
Breakdown of CO:		*Chain scission [a]:*	
$CO + {}^{\bullet}OH$	$CO_2 + H^{\bullet}$	${}^{\bullet}O_2H + {}^{\bullet}O_2H$	$H_2O_2 + O_2$
$H^{\bullet} + O_2 + M$	${}^{\bullet}O_2H + M^*$	$CH_3O_2^{\bullet} + {}^{\bullet}O_2H$	$CH_3OOH + O_2$
${}^{\bullet}O_2H + NO$	${}^{\bullet}OH + NO_2$		

[a] Chain scission results when the concentration of NO is very much smaller than the concentration of $CH_3O_2^{\bullet}$ and $H_2O^{\bullet}$.

The reaction rate constant k_{OH} may be either determined experimentally or calculated approximately from molecular data.[43] The average lifetimes of CFCs in the troposphere, together with their relative ozone depletion potentials (ODP) and greenhouse effect potentials (GHEP), are listed in Table 5. This illustrates the fact that it is necessary to take into account both the occurrence of a compound and its conversion products under environmental conditions. The data show that the compounds that are envisaged as replacements for the older CFCs do not yet unequivocally meet all the environmental requirements.

In Table 6 the values of k_x and $k_x c_x \equiv K_x$ for X = OH, O_3 and NO_2 are compared for several environmental trace compounds.[44] For propene the rates of breakdown by 'OH radicals and by ozone are about the same, and this applies to all alkenes, including the large class of the terpenes. Biogenic terpenes ('pine fragrances') have half-lives varying from minutes to a maximum of 24 hours in the troposphere.[43] In

Table 5. Average lifetimes τ_{OH} in the troposphere, ozone depletion potentials (ODP) and greenhouse effect potentials (GHEP) for various chlorofluorocarbons (CFCs). The abbreviations of the compounds envisaged as successors to the older CFCs are italicized.

CFC		τ_{OH} [years]	ODP	GHEP
F11	CCl_3F	60	1 [a]	1 [a]
F12	CCl_2F_2	120	0.9–1.0	2.8–3.4
F113	CCl_3-$CClF_2$	90	0.8–0.9	1–4
F114	$CClF_2$-$CClF_2$	200	0.6–0.8	3.7–4.1
F115	$CClF_2CF_3$	400	0.4–0.5	7.5–7.6
F22	$CHClF_2$	15.3	0.04–0.06	0.3–0.4
F123	$CHCl_2$-CH_3	1.6	0.01–0.02	0.024
F124	CHClF-CF_3	6.6	0.02	0.09
F141b	CH_3-CCl_2F	7.8	0.07–0.09	0.09–0.1
F124b	CH_3-$CClF_2$	19.1	0.05–0.06	0.03–0.04
F125	CHF_2-CF_3	28.1	0	0.5–0.7
F134a	CH_2F-CF_3	15.5	0	0.3
F143a	CH_3-CF_3	41.0	0	0.7
F152a	CH_3-CHF_2	1.7	0	0.03
F10	CCl_4	50	1.1	0.3
1,1,1-trichloroethane	CH_3-CCl_3	6.3	0.1	0.02

[a] Set at 1 as reference substance.

contrast, polychlorinated terpenes (e.g., polychlorocamphors, toxaphene) are capable of worldwide distribution, a fact demonstrated as long ago as 1979.[45] 500 kilotons of toxaphene were produced between 1947 and 1977.

Table 6. Relative contributions of the reactions with 'OH, O_3 and NO_2 to the lifetime τ_{chem} for some trace organic compounds in the atmosphere [a] [44].

Cpd.	k_{OH} [b]	K_{OH} [c] $[10^{-6}s^{-1}]$	k_{O_3} [b]	K_{O_3} [d] $[10^{-6}s^{-1}]$	k_{NO_2} [b]	K_{NO_2} [e] $[10^{-6}s^{-1}]$
Butane	2.5	1.3	$<10^{-11}$	$<10^{-5}$	3.5×10^{-5}	5×10^{-3}
Toluene	6.2	3.1	$<10^{-8}$	$<10^{-2}$	3.6×10^{-5}	5×10^{-3}
Propene	30	15	10^{-5}	11	7.6×10^{-3}	0.95

[a] $\tau_{chem}^{-1} = \tau_{OH}^{-1} + \tau_{O_3}^{-1} + \tau_{NO_2}^{-1}$; $\tau_{chem} = (K_{OH} + K_{O_3} + K_{NO_2})^{-1}$. [b] $k_{OH}, k_{O_3}, k_{NO_2}$ in $[10^{-12}\,cm^3$ molecules$^{-1}s^{-1}]$. [c] $K_{OH} = 5 \times 10^5\, k_{OH}$. [d] $K_{O_3} = 10^{12}\, k_{O_3}$. [e] $K_{NO_2} = 1.3 \times 10^8\, k_{NO_2}$.

As an example of a typical sequence of reactions in the breakdown of a hydrocarbon by 'OH radicals, Table 4 shows the breakdown of methane. This does not differ fundamentally from the chemistry of the methane flame. For other hydrocarbons too there are many similarities between the chemistry of atmospheric processes and that of flames, since the reacting species are in many cases the same.[46]

The main photooxidants, i.e. reacting species and reaction products involved in the breakdown of organic compounds by 'OH, ozone and NO_x, can be listed on the basis of earlier and more recent studies as follows: 'OH, ${}^{\bullet}O_2H$, $RO_2^{\bullet}$ (R = any organic group, not confined to alkyl), ozone, NO_2, $NO_3^{\bullet}$, N_2O_5, organic nitrates, H_2O_2, methyl hydroperoxide, peroxyacetic acid, peroxyacetyl nitrate, peroxynitric acid, peroxynitrates. Complex reaction cycles can arise, especially under the action of solar radiation; although advances are being made in our knowledge of these, many unanswered questions remain regarding the reaction products (photochemical smog).[42, 43]

In Table 7 an attempt has been made to assign some of the organic compounds that are found in trace concentrations to

Table 7. Classification of organic compounds according to their reactivity with 'OH radicals. The reactivity classes are defined in terms of lifetime τ in days d, k_{OH} in cm^3 molecules$^{-1}s^{-1}$.

Reactivity class	τ [d]	k_{OH}	Compounds
6	5×10^4	$<10^{-16}$–10^{-15}	tetrachloromethane (F10); trichlorofluoromethane (F11); dichlorodifluoromethane (F12); chlorotrifluoromethane (F13); tetrafluoromethane (F14); hexachloroethane
5	5×10^3	10^{-15}–10^{-14}	methane; 1,1,2,2,-tetrachloroethane
4	5×10^2	10^{-14}–10^{-13}	chloromethane; bromomethane; 1,2-dichloroethane; 1,1,1,-trichloroethane; 1,2-epoxyethane; acetonitrile; 1,2-dichloronitrobenzene
3	50	10^{-13}–10^{-12}	dichloromethane; chloroform; 1,2-dibromoethane; tetrachloroethene; isobutyl nitrate; chlorobenzene; 1,2-dichlorobenzene; 1,4-dichlorobenzene; 1,2,4-trichlorobenzene; nitrobenzene
2	5	10^{-12}–10^{-11}	benzene; toluene; ethylbenzene; biphenyl; vinyl chloride; trichloroethene; ethane; methanol; pentyl nitrate; CS_2; *N*-nitrosodimethylamine (DMNA)
1	0.5	10^{-11}–10^{-10}	formaldehyde; acetaldehyde; benzaldehyde; phenanthrene; acenaphthene; cyclohexene; hexachlorocyclopentadiene; styrene; *N*-nitrosodiethylamine (DENA); diethyl ether; chlorotoluidine; morpholine; chloraniline

classes of different reactivities, so that their potential for global distribution can be estimated from the values of τ_{chem} ($\simeq \tau_{OH}$). Table 8 indicates the spread of values predicted for τ_{OH} at two different 'OH radical concentrations for a selection of chlorinated C_1 and C_2 compounds.

Table 8. τ_{OH} for chloromethanes, chloroethanes and chloroethenes in days as a function of the 'OH radical concentration.

Compound	k_{OH} [a]	c^1_{OH} [b] τ_{OH} [d]	c^2_{OH} [c] τ_{OH} [d]
CH_3Cl	0.42×10^{-13}	600	120
CH_2Cl_2	1.4×10^{-13}	170	34
$CHCl_3$	3×10^{-13}	120	24
CCl_4	0.0016×10^{-13}	1.5×10^5	0.3×10^5
CH_3-CCl_3	0.12×10^{-13}	1900	380
CH_2Cl-CH_2Cl	0.65×10^{-13}	400	80
$H_2C{=}CHCl$	68×10^{-13}	3	0.6
$HClC{=}CCl_2$	22×10^{-13}	11	2.2
$Cl_2C{=}CCl_2$	1.7×10^{-13}	140	28

[a] k_{OH} in cm^3 molecule$^{-1}s^{-1}$. [b] $c^1_{OH} = 0.5\times10^6$ [molecule cm^{-3}]. [c] $c^2_{OH} = 2.5\times10^6$ [molecule cm^{-3}]. [d] $\tau \equiv c_o \rightarrow c_o e^{-1} = c_o \times 2.72^{-1}$; τ_{OH} in days.

For the chlorofluorohydrocarbons (CFCs) especially, the long lifetimes in the troposphere, which result in a uniform distribution in the stratosphere and in direct photolysis occurring there, lead to the well-known problems of absorption of thermal radiation and ozone depletion. In the long term it will be necessary to replace the CFCs now in use by alternatives such as F123 ($CHCl_2$–CF_3) and F114b (CH_3–CCl_2F). Both these compounds have a low ozone depletion potential and greenhouse effect potential (Table 5) with long lifetimes in the troposphere, estimated as 1.6 and 7.8 years respectively. For these compounds one expects a uniform global distribution as for 1,1,1-trichloroethane. In refrigeration engineering F12 (CCl_2F_2) is now beginning to be replaced by the fluorocarbon F134a (CH_2F–CF_3). The predicted lifetime of this compound in the troposphere is 15.5 years.

3.2. Transformations in the Hydrosphere and Ecosphere

In the hydrosphere, and also in the ground, xenobiotics undergo conversion not only by reaction with water (hydrolysis) but also, to an important extent, by microbiological breakdown (the "self-cleaning" ability of rivers and seas, and the formation of humus in the soil). The biological transformation of xenobiotics occurs mainly through co-metabolization by non-specific enzymes such as the monooxygenases or hydrolases,[47] and can sometimes come to a stop at one of the subsequent stages (secondary or tertiary persistence, as in the example DDT → DDE (1,1-dichloro-2,2-bis(4-chlorophenyl)ethene)), or can form other xenobiotics of different compound classes (e.g., chlorobenzenes → chlorophenols → chlorocatechols,[48] or chlorobiphenyls → chlorobenzoic acids[49]). Classic examples of biotransformations giving a more toxic product are the hydrodechlorination of trichloro- and tetrachloroethylenes in groundwater to give vinyl chloride,[13] and the conversion of thiophosphoric acid esters into phosphoric acid esters which act as choline-esterase inhibitors. In contrast to this, for chlorinated biphenyls and dibenzo-*p*-dioxins, persistence (*para*-recalcitrance: persistence of Cl_xB compounds with 4,4'- or 2,5-substitution, and of Cl_xDD or Cl_xDF compounds with 2,3,7,8-substitution (chlorinated dibenzo-*p*-dioxines/dibenzofurans)) goes hand-in-hand with biological activity.[4, 50]

The fact that, despite the existence of so many different biological and non-biological mechanisms for the breakdown of pollutants, many compounds are already present on a global scale, clearly shows the severity of the demands now being placed on the ecosphere with regard to the breakdown of xenobiotics. For some time now there has been speculation as to whether microbial transformation does not begin until a threshold concentration is reached.

4. The Concept of Multiphase Equilibrium Distribution

Any system, whether it is the global system consisting of the atmosphere, oceans, biota (living organisms) and the earth's surface or a microsystem such as a garden pond, can be divided into the four basic phases of air, water, lifeforms (e.g., cells) and earth (humus, sediments, rocks). For a molecule these basic phases correspond to different states of aggregation, namely the gaseous state, a solution in water, a solution in fat, or adsorbed on carbon compounds or on silicates. The atmosphere as a compartment of the environment is itself a multiphase system consisting of oxygen and nitrogen, particles with a bimodal size distribution, and water in condensed or solid phases (clouds, mist, rain, hail, snow). Similarly the compartment consisting of the oceans is actually a suspension of particles and colloids together with a multitude of biological subphases ranging from plankton to whales.

In such a multiphase system each molecular species becomes distributed throughout the various phases in different concentrations, determined by the condition that it has the same chemical potential in each phase, depending on its physical and chemical properties (e.g., vapor pressure, water solubility, octanol/water partition coefficient K_{OW}, bioconcentration factor BCF, adsorption coefficient in sediments K_{OC}, Henry's constant $H = P_0 S_{H_2O}^{-1}$, or in the form $K_{GW} = a_{air} a_{H_2O}^{-1}$ for partition between gas and water, and the reduced Henry's constant H/K_{OW} for partition between gas and octanol) (Fig. 1).

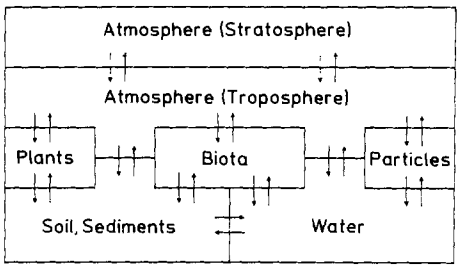

Fig. 1. Multiphase distribution of an environmental chemical in the environmental compartments ground, water, air and biota. The preference for a region is described as geo-, aquo-, aero- or bioaccumulation. For transport in the atmosphere and the hydrosphere, equilibria with the respective particulate phase play a central role.

For the basic phases air, water, ground (including sediments) and living organisms, compounds can be assigned, on the basis of their Henry's constants H, water solubilities, K_{OC} and K_{OW} values, to classes that have a preference for a particular phase and therefore accumulate in that region[51] (see Table 9). By applying multifactorial analysis it is found that for values of H greater than 22 $Pa\,m^3mol^{-1}$ the preferred environmetal compartment is the air for all values of K_{OW}. For $H < 2\ Pa\,m^3mol^{-1}$ either water or ground is the preferred phase, depending on the values of K_{OW}; there is a clear preference for water if $\lg K_{OW} < 4$, and for ground if $\lg K_{OW} > 5$.[52]

Table 9. Correlation between magnitude of physicochemical constants and preferential distribution of a compound between the four environmental compartments (air (H), water (S_{H_2O}), soil (K_{OC}), and biota (K_{OW}) [51].

Preferential concentration	Air H [$Pa\,m^3mol^{-1}$]	Water S_{H_2O} [$mol\,m^{-3}$]	Soil K_{OC}	Biota K_{OW}
low	$<10^{-3}$	10^{-3}	<1	$<10^3$
moderate	10^{-3}–1	10^{-3}–1	1–10^3	10^3–10^5
high	>1	>1	$>10^3$	$>10^5$

According to this concept of multiphase distribution, it is necessary to consider not only the processes of bioaccumulation and geoaccumulation but also aeroaccumulation (enrichment in the atmosphere) and aquoaccumulation (enrichment in the hydrosphere).

A knowledge of the mass fractions in a multiphase distribution, e.g., for a 1:1:1 system (Table 10), or for phase conditions approximating to those of the real world (the unit-world approach proposed by D. Mackay), provides important basic data with regard to the distribution in the environment.[53] Other authors have discussed similar models that are undergoing further refinement or have been applied to limited regions,[25, 26, 54] and models for the transport of xenobiotics to the arctic by air, snow and marine currents.[55]

Table 10. Equilibrium partition ratios of environmental chemicals between the environmental compartments air, water and solid phase according to Mackay level I [56].

Compound	Air [%]	Water [%]	Solid phase [%]	Preferred compartment
CCl_4	99.80	0.19	0.02	air
$CCl_2C{=}CCl_2$	99.45	0.40	0.15	air
hexachlorobutadiene	78.02	2.06	19.93	air, (solid phase)
pentachlorobenzene	48.10	2.10	49.81	air, solid phase
hexachlorobenzene	10.11	0.39	89.50	(air), solid phase
α-HCH [a]	0.28	50.67	49.05	water, solid phase
4,4'-DDT	0.40	0.42	99.18	solid phase
atrazine	0.01	93.15	6.84	water
nitrobenzene	30.49	68.04	1.47	air, water
3,4-dichloraniline	37.07	46.84	16.09	air, water, solid phase
phthalates:				
diethyl-	1.50	95.94	2.55	water
di-*n*butyl-	0.38	9.52	90.1	(water), solid phase
di(2-ethylhexyl)-[b]	1.62	4.74	93.65	solid phase

[a] HCH = hexachlorocyclohexane. [b] DEHP.

Mackay's unit-world model divides the world into 510×10^6 subunits.[53] An average static distribution among these subunits is then calculated, taking into account the phase volumes of atmosphere, biota and sediments (the oceanic system, with regard to its global share of the water phase, is not included), assuming that n moles of substance per year are released into the environment, and using an average value for the breakdown rate, so far as this is known. For example, if we assume that the global rate of release of DDT is 1.6×10^5 tons per year, this method predicts DDT concentrations of 6.2 $ng\,m^{-3}$ in the atmosphere, 5.5 $\mu g\,m^{-3}$ in water, and 0.25 $\mu g\,kg^{-1}$ in organisms. The values actually measured in the environment in air and water are less than these by about a factor of 10^3. The concentrations in fish living near the ocean surface are within about a factor of 10 of the predicted value, whereas for deep-sea fish the concentrations of 4,4'-DDT are greater by a factor of 10^4 (Table 11). These variations, even within the same basic phase, indicate that the unit-world theory gives only a partial description of the actual global distribution. At the same time the results listed in Table 11 illustrate that in practice there are wide differences between the patterns of distribution of individual compounds.[32, 57]

However, in developing theories of the global distribution of compounds one can assume values for their properties and calculate how these will affect the distribution between different environmental compartments. Nevertheless, such model calculations must always ignore the heterogeneity of the actual processes occuring in the atmosphere and oceans. The complexity and heterogeneity of environmental distribution processes can easily be appreciated if one considers an imaginary experiment in which water is regarded as a persistent environmental chemical. All molecules whose properties

are approximately the same as those of water will behave like it, whereas molecules that are unlike water will behave quite differently.

Table 11. Concentrations of organochlorine compounds in the liver of surface and deep-sea fish from the eastern part of the North Atlantic (Saõ Miguel (Azores) and Madeira). [58] All contents in micrograms per kg (ppb) based on fat.

Cpd.	Fresh water (rain) Lake Sete Cidades (Azores)		Salt water Coast (Azores)	Salt water Coast (Madeira)	Salt water Deep-sea (Madeira)
	Carp	Pike	Scorpion fish	Parrot fish	Black scabbard fish
HCH (BHC) [a]					
α-HCH	35	46	7	9	<0.1
β-HCH	<0.1	<0.1	<0.1	<0.1	<0.1
γ-HCH	7	8	1	1	<0.1
δ-HCH	<0.1	<0.1	<0.1	<0.1	<0.1
HCB [b]	13	4	4	2	17
PCB (Cl_xB) [c]					
28 (Cl_3B)	<0.1	2	<0.1	2	45
52 (Cl_4B)	<0.1	7	<0.1	2	105
101 (Cl_5B)	22	14	3	6	305
138 (Cl_6B)	120	38	18	16	930
153 (Cl_6B)	95	22	15	12	570
180 (Cl_7B)	71	16	10	9	410
ΣPCB (60% Cl)	802	234	114	112	5800
DDT group					
4,4'-DDT	<0.1	<0.1	<0.1	<0.1	5060
4,4'-DDE	50	80	3	5	1100
4,4'-DDD	310	128	20	10	3030
4,4'-DDMU	<0.1	22	<0.1	<0.1	d [d]
ΣDDT [e]	360	230	23	15	9190
2,4'-DDT	<0.1	<0.1	<0.1	<0.1	390
2,4'-DDD	<0.1	8	<0.1	<0.1	<0.1
2,4'-DDE	<0.1	4	<0.1	<0.1	<0.1
Chlordane group					
heptachloro	<0.1	<0.1	<0.1	<0.1	<0.1
cis-chlordane	13	14	3	<0.1	250
trans-chlordane	<0.1	4	<0.1	<0.1	80
trans-nonachloro	8	12	3	4	245
oxychlordane	<0.1	3	2	4	20
dieldrin	6	1	13	18	35
mirex	<0.1	d [d]	2	0.1	32
polychloro-terpenes [f]	(+)	++	++	+	+++

[a] HCH = hexachlorocyclohexane, BHC = benzenehexachloride. [b] HCB = hexachlorobenzene. [c] PCB = polychlorobiphenyl. [d] $0.1 < d < 1$. [e] ΣDDT = 4,4'-DDT + 4,4'-DDD + 4,4'-DDE + 4,4'-DDMU; 4,4'-DDD = 1,1-bis(4-chlorophenyl)-2,2-dichloroethane, DDMU = 2,2-di(4-chlorophenyl)-1-chloroethane. [f] Not quantified. Present (+) in the range 50–1000 $\mu g\,kg^{-1}$ (based on fat).

Figures 1 and 2 summarize in schematic form the phase equilibria, the different types of material transport and the physical and chemical removal of substances from the different compartments of the environment. This is a simplified model for the purposes of experimental studies; superimposed upon it in the real world are the climatic zones, the continents, the coasts and the currents flowing in the oceans and in the atmosphere. The approach that we have called the 'Ulm method' starts from observed data on the actual situation (compound distribution patterns and concentrations including their temporal and spatial changes) in representative regions within the global material flow, and sets out to understand these in terms of molecular properties and the basic geophysical processes. The guiding theme of our studies is to address the questions "which compounds?—how much?—where?—why?"[57]

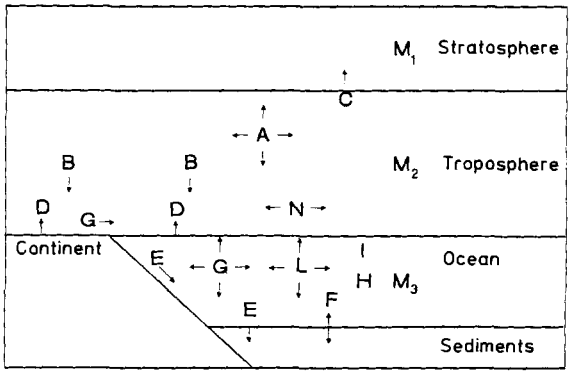

Fig. 2. Parameters of the global distribution of molecules. The following terms collate transport and transformation of an environmental chemical on a global scale: A = transport term (air) $\approx p_o$, K_{OH}^{-1}, $K_{h\nu}^{-1}$, K_{OW}^{-1}, $S_{H_2O}^{-1}$; B = deposition term (air) $\approx S_{H_2O}$, K_{OW}, K_{OC}, p_o^{-1}; C = extraction term stratosphere $\approx p_o$; D = evaporation term (water) $\approx p_o$, p_{H_2O}, K_{OW}^{-1}, $S_{H_2O}^{-1}$; E = sedimentation term $\approx K_{OW}$, K_{OC}, $S_{H_2O}^{-1}$; F = retention term sediment (geoaccumulation) $\approx K_{OC}$, K_{OW}; G = transport term (water) $\approx S_{H_2O}$; H = biotransformation term; I = retention term biophase (bioacccumulation) $\approx K_{OW}$; L = transport term biophase; M = transformation term (abiotic) $\approx K_{h\nu}$, K_{OH}, K_{O_3}, K_{NO_2}, K_{H_2O}, K_{therm}; M_1: stratosphere, M_2: troposphere, M_3: ocean; N = transport term, international commerce.

5. Global Dilution Volumes and Mass Transport

Substances that are released from the belt containing the industrial countries of the northern hemisphere, and become uniformly distributed throughout the world in accordance with their various partition constants Kp_i, have access to the following volumes and surface areas in which dilution and/or retention can take place (see Table 12).[18, 19, 21, 22]

Table 12. Areas, volumes and mass flows in the global context [21]. N = north, S = south; see also Table 13.

1. *Areas* [m^2]		2. *Volumes* [m^3]	
Surface area of the earth	510×10^{12}	Troposphere 0–11 km [a]	5.62×10^{18}
Land area	148×10^{12}	Segments: 0–30°N(S); 30–90°N(S) [b]	1.41×10^{18}
Total ocean surface area	362×10^{12}	Oceans (total)	1.350×10^{18}
Oceans in the northern Hemisphere	155×10^{12}	Pacific Ocean	0.696×10^{18}
		Atlantic Ocean	0.323×10^{18}
Oceans in southern Hemisphere	207×10^{12}	North sea	0.000054×10^{18}
		Baltic sea	0.000023×10^{18}
Pacific Ocean	166×10^{12}		
Atlantic Ocean	84×10^{12}		

3. *Annual evaporation and precipitation into the oceans* [$cm\,year^{-1}$] [63]

	Evaporation	Precipitation	Difference
Atlantic Ocean	104	78	−26
Indian Ocean	138	101	−37
Pacific Ocean	114	121	+7
Arctic Ocean	12	24	+12
All oceans (average)	125	112	−13

Volume evaporated from oceans	$440 \times 10^{12}\ m^3 year^{-1}$
Volume evaporated from land areas	$70 \times 10^{12}\ m^3 year^{-1}$
Total water in the troposphere (global)	$13 \times 10^{12}\ m^3$

[a] Normalized to STP $3.16 \times 10^{18}\ m^3$, weight 40×10^{20} g. [b] Normalized to STP $0.79 \times 10^{18}\ m^3$.

1) The atmosphere: The atmoshere close to the earth consists of the troposphere (0 to 10 km), with a volume of $5.62 \times 10^{18}\ m^3$, and the stratosphere, with a volume about four times greater, these two regions being separated by the tropopause (Fig. 3). The stratosphere extends to about

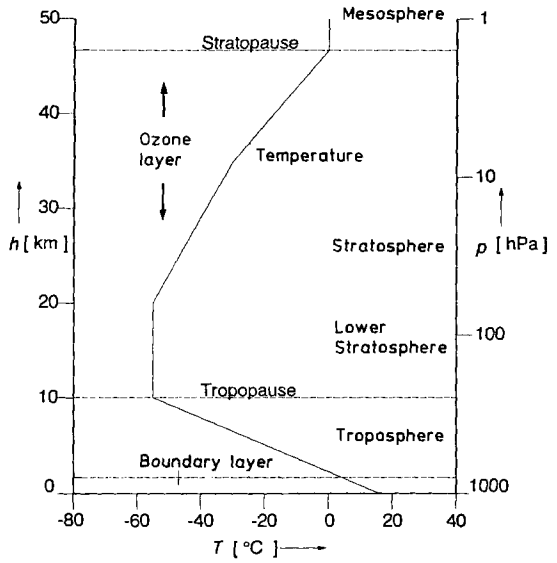

Fig. 3. Schematic representation of the vertical structure of the atmosphere. In the tropics the troposphere, as a region of rapid global mixing processes, reaches an altitude h of 14–16 km, at the Poles of 8–10 km. At middle latitudes (40–50°) it is changeable with diffuse transition to the stratosphere. The boundary layer between the two parts of the lower atmosphere (tropopause) is characterized by a temperature increase, the effect of which, corresponds to inversions in the neighborhood of the earth's surface. The ozone layer in the stratosphere at an altitude of 20–50 km, with a maximum ozone concentration on average at an altitude of 35 km, acts as UV filter. The absorption of radiation leads to an increasing temperature T at higher altitudes in the stratosphere.

50 km. If the volume of air in the troposphere is normalized to STP (standard temperature and pressure) one obtains a value of 3.16×10^{18} m^3. On the basis of the overall circulation consisting of the global wind system, the general circulation, it is useful to divide the troposphere into four roughly equal zones defined by the latitudes 0 to 30° N, 30 to 90° N, and the same in the southern hemisphere, containing circulating air masses that exchange with each other over well-defined time intervals (Fig. 4).

The stratosphere (10–50 km) is a space in which dilution occurs, and for most organic molecules it acts as a sink owing

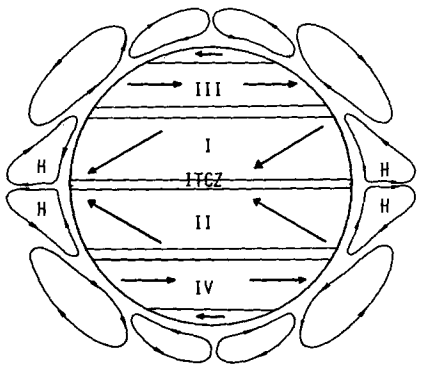

Fig. 4. Schematic representation of global circulation (general circulation) in the troposphere: I north-east tradewind, II south-east tradewind, III northern west-wind belt, IV southern west-wind belt. The climbing air in the intertropic convergence zone (ITCZ) forms, as a low-pressure channel, a distinct boundary layer between the northern and the southern hemisphere. The tradewind regions and the west-wind belt are separated by the so-called horse latitudes over the oceans; this boundary is wave-shaped. Thus, air pockets from the west-wind belt reach into the tradewind region. The indicated vertical movements of air round the circle which symbolizes the earth are here highly exaggerated. On scaling the globe down to a diameter of 1.2 m, the troposphere would form a layer of only ca. 1 mm thick.

to photolysis and reaction with triplet-state oxygen. Even for F12 (CF_2Cl_2) the quantity present on entering the stratosphere becomes reduced to 1% of this value after 40 km.[59] Only CF_4 is completely stable from 0 to a height of 34 km. The main source of CF_4 is aluminum production but it is also commericially available; from an environmental standpoint it is the most stable organic compound made by man.

2) The oceans: The total volume of the oceans is 1.35×10^{18} m^3, of which more than half is accounted for by the Pacific ocean (0.70×10^{18} m^3) The mean depth of the hydrosphere is 3790 m, that of the oceans alone is 4700 m. The volume of the oceans is about a quarter of that of the troposphere. 71% of the earth's surface is covered by sea. The portions of the ocean's surface in relation to the global wind system are: trade wind region 30%, west-wind belt 24%, horse latitudes 20%, intertropical convergence zone (ITCZ) (doldrums) 8%. All other regions sum up to 18%.

3) The ground: The earth's total land surface is 148×10^{12} m^2, of which 10% (14.8×10^{12} m^2) is used for agriculture. If one assumes that the depth to which penetration and exchange occurs is 50 cm, this gives a global dilution volume of 74×10^{12} m^3, of which 7.4×10^{12} m^3 is under cultivation.

For the ocean beds we may assume a penetration depth of 1 cm (since 1–4 mm of sedimentation occurs in 1000 years), giving a dilution volume of only 3.6×10^{12} m^3, which is virtually negligible; consequently one expects to find here the highest concentrations of those environmental chemicals with an affinity for soil that enter the oceans (see HCB, PCB and DDT in Table 11). The deep sea floor is no sink for organic chemicals as the benthic fauna reuses all available organic carbon compounds.

To a first approximation the volumes of the three main compartments available to environmental chemicals are in the ratio 10^6 (troposphere) to 0.25×10^6 (oceans) to 1 (ground). Particular environmental chemicals that show a nearly ideal global distribution as a result of their stability and volatility are the chlorofluorocarbons (CFCs)[60] and tetrachloromethane.[61] The quantities of these that have been released into the environment have become equally distributed between the northern and southern hemispheres ($C_{SH}/C_{NH} \simeq 1$), and the amounts present in the surface waters of the open sea correspond to the partition between the gas phase and the water phase that one expects from the value of K_{GW}.

Whenever the observed concentrations of a substance differ from the equilibrium values expected from the theoretical partition ratios (K_{GW}, K_{OW}, K_{OC}), this means that one phase is enriched and the other is depleted. Since these deviations must be regarded as resulting from globally integrated partition coefficients, they can give valuable information about the actual situation within the corresponding environmental compartments, and thus about real transport phenomena in the global mass flow and the presence of sources and sinks in the atmospheric and oceanic systems. For some halomethanes one finds a non-equilibrium distribution that does not correspond to that expected from the equilibrium partition constants K_{GW}, whereas for tetrachloromethane an equilibrium distribution is observed; this confirms that the upward convection currents off the coast of West Africa due to their increased primary production act as a source of these compounds, including chloroform.[7, 38]

The mass flows that take place during continental and global mixing processes in the atmosphere and hydrosphere are difficult to comprehend, and can only be expressed in terms of many powers of ten. Even for a regional air movement on a front that is 100 km wide and 1000 m high—nothing unusual in weather terms—100×10^9 m^3 of air, with a mass of 126 million tons, is moved for each kilometer of the path.

The mass of the troposphere (0–10 km) in one hemisphere is about 40×10^{14} tons, and the volume in the bottom 3000 m is 1530×10^{15} m^3. To produce in this a global concentration of 1 ng m^{-3} one would need only 1.53×10^3 tons of a substance. For many compounds a concentration of 1 ng m^{-3} can be measured without difficulty using modern analytical methods (optimizing enrichment and detection).

In 1976 alone, the total quantity of the chlorofluorocarbons $CFCl_3$, CF_2Cl_2 and CHF_2Cl (Freons) produced was 822×10^3 tons. These volatile and stable compounds become uniformly distributed throughout both hemispheres before being broken down by photolysis in the stratosphere, with all the consequences, much discussed in recent years, that this entails for the ozone layer there.[64] Because of the structure of our earth, there is nowhere else that CFCs can finally end up other than in the stratosphere. As an alternative sink for CFCs one might consider incorporating them into air used for high-temperature combustion processes (e.g., of coal, oil, petrol, diesel fuel, or incinerated wastes). In the long term such "anthropogenic" sinks could become important locally or regionally for removing stable CFCs that diffuse back from the stratosphere. A sink in the troposphere, whereby a substance is destroyed with the formation of decomposition products, can only be relevant for compounds whose lifetimes τ_{OH} in the troposphere are in the range 0.5 to 2 years as the upper limit (Table 5).

Table 13 summarizes the volumes transported by the most important ocean currents. These data are important when assessing the global flows of environmental chemicals. When one considers the global volumes available for dilution, which are in the ratio 4:1 for the atmosphere and the oceans, and also bears in mind that for many persistent and bioaccumulating environmental chemical (e.g. HCH, HCB, Cl_xB, DDE) the concentrations found are 1 in 100 or higher in volume terms, the importance of the flow of materials in the oceanic system becomes obvious. The time dimensions of the transport processes in the two compartments are different, but are of the same order of magnitude (Table 14).

Table 13. Transport of water by ocean currents [12]. N = north, S = south, W = west, E = east.

Current	Direction of flow	Flow rate [10^6 m^{3}s^{-1}]	Current	Direction of flow	Flow rate [10^6 m^{3}s^{-1}]
Gulf Stream (40° N)	NE	75–115	Peruvian current	N–NW	20
Canaries current	S	15	Pacific equatorial undercurrent	E	30–40
Kuroshio current (North Pacific)	NE	40–50	West wind drift (Antarctic current)	E	150–180
Eastern Australia current	S	30–45			

Table 14. Time-scales of various transport-processes in the atmosphere and the oceans.

Atmosphere	$\bar{v}$ [a]	t [b]	Hydrosphere (Oceans)	$\bar{v}$ [a]	t [b]
Storm	80 km h^{-1}	0.5 d	Surface currents	0.80 m s^{-1}	15 days
Moderate breeze	20 km h^{-1}	4 d	Deep currents	0.01 m s^{-1}	3 years
Depression or anticyclone	300 m h^{-1} (vertical)	–	Upward convection	3 m year^{-1}	–

[a] Average velocity. [b] Time required to travel 1000 km.

If the escape of xenobiotics into the global dilution space is impeded, either temporarily (e.g., by local or regional meteorological inversion conditions in the bottom layer of the troposphere) or permanently (as in inland seas such as the Baltic or Mediterranean), the increase of concentration in these environmental compartments proceeds at a time-lapse.

6. Transport from the Site of Production to the Place of Use

The movement of organic compounds by humans in the course of worldwide economic activities, an aspect of their introduction into the environment that belongs to the technosphere, can only be very crudely quantified; nevertheless, it makes an important contribution to the process of distribution into the environment. This form of transport can be superimposed on the natural distribution processes, as, for example, when the main regions in which 4,4′-DDT is used shift from the northern to the southern hemisphere, or when the use of a pesticide alters in response to long-term or temporary changes in the regional distribution of the target species (as in the case of Dieldrin for locust control), or when its population declines. Such changes shift the release point (or rather the release zone) from which the natural distribution processes start. Moreover, the transportation routes themselves have the potential to become point sources for release into the environment. The tanker accidents that appear so often in the news are just one example. Seasonal variations in the use of a compound or in its release to the environment can have significant effects on a global scale.

In many cases a knowledge of the agricultural land use (e.g., forestry, or a predominance of either crop-growing or cattle-rearing) or of the industrial structure of a region (e.g., coal-mining, oil or gas extraction, metals production, or the various types of chemical industries) can indicate the extent to which particular xenobiotics (solvents, plasticizers, raw materials, wastes, pesticides, etc.) are likely to be continuously transported in and eventually released into the environment.[65]

For the insecticide hexachlorocyclohexane (HCH) it is possible to verify such predictions, since the products used in the northern and southern hemispheres are of different constitution. In the northern hemisphere the product made and used in the largest quantities is the isomer mixture obtained by photochlorination of benzene (known as technical HCH or BHC, benzene hexachloride), of which γ-HCH (lindane) is the main insecticidal component and which contains about 60% α-HCH; pure γ-HCH is used to a lesser extent. On the other hand, in the southern hemisphere (Argentina, Aus-

tralia, New Zealand) only lindane is used in significant amounts. The exchange between the northern and southern hemispheres can be monitored relatively easily by measuring the ratio of the α/γ-HCH isomers in the atmosphere[66] and in the oceanic system (both water and fish).[67] Measurements in the lower troposphere at Réunion in the Indian ocean show that the transfer of α-HCH into the southern hemisphere only takes place very slowly. As similar results are found for hexachlorobenzene,[68] whose main source is definitely in the northern hemisphere, one must assume that for all semivolatile chlorohydrocarbons the interhemisphere exchange in the troposphere occurs only slowly.[66] The barrier responsible for this is the tropical rain belt (20° N to 20° S), where τ_R and τ_W reach their minimum values, so that their reciprocals, which determine the deposition rate, are at a maximum. For γ-HCH, as also for chlorinated biphenyls

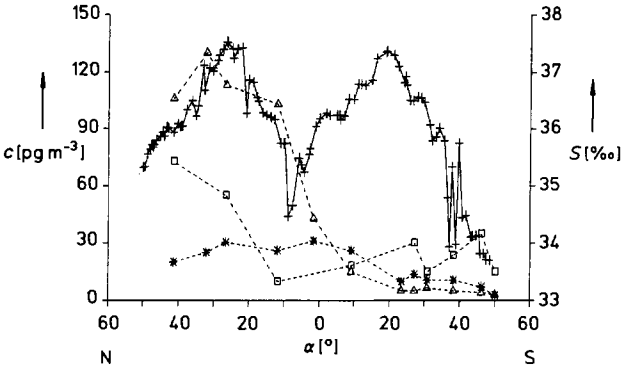

Fig. 5. North/South distribution of the concentration c of α- and γ-hexachlorocyclohexane (α-HCH: Δ, γ-HCH: *) and hexachlorobenzene (HCB: □) in the lower troposphere above the Atlantic Ocean (measurements by FS Polarstern-Ant. IX/1). The intertropic convergence zone (ITCZ) forms a distinct barrier to the entry of α-HCH and HCB in the southern hemisphere. Extraction from the troposphere takes place in the tradewind region over the North Atlantic following increased precipitation, which is indicated by the decrease in salinity (+) of the surface water. N = north, S = south, α = latitude, S = salinity.

(PCBs), there is a nearly uniform distribution in the troposphere above the Atlantic as a result of uptake into both hemispheres (Fig. 5).[68]

7. Molecular and Particle-Mediated Transport in the Atmosphere and Hydrosphere

For environmental chemicals that are equally stable the dimensions of their respective transport pathways are determined by the physics of the transport processes and the relevant removal mechanisms for the transport medium concerned (air or water), and thus by the distribution characteristics expressed by the physical lifetime τ_{phys}. If transport in the environment occurred solely in molecular-dispersed forms involving ideal gases and true solutions, it could be described in terms of the global volume flows in the atmosphere (general circulation and rainfall distribution) and hydrosphere (ocean currents) from a knowledge of the equilibrium partition constants Kp_i. However, for both transport compartments the organic compounds present in air and water undergo a constant exchange between molecular-dispersed forms and adsorption on particles or colloidal association (see Fig. 1). Compounds adsorbed on particles travel much shorter distances than when transported in molecular form in air or as solutions in water, due to both dry and wet deposition processes, both in the atmosphere and through sedimentation in the hydrosphere and bioincorporation as nutrients in the biosphere.

The fraction ϕ of a compound that exists in adsorbed form in water or air depends on the equilibrium partition coefficient Kp and on the volume fraction V_{part} of the particle phase as expressed by Equation (9):

$$\phi = Kp\,V_{part}(1 + Kp\,V_{part})^{-1} \quad (9)$$

Particle concentrations in the atmosphere above continents are typically in the range 10–100 $\mu g m^{-3}$, giving values for V_{part} of 5×10^{-12} to 50×10^{-12}. In clean marine air V_{part} is typically about 0.5×10^{-12} (Table 15). In the surface water of the open sea V_{part} can have values as high as 5×10^{-8}, corresponding to a particulate content of 100 $mg m^{-3}$ (Table 16).

Table 15. Particulate concentrations in the lower troposphere in marine [68, 80] and continental [81] locations.

Marine air [a]	Particulate concentration [$\mu g m^{-3}$]	Continental air	Particulate concentration [$\mu g m^{-3}$]
North Atlantic (middle)	6.71 ± 4.24	Swiss Alps (1550 m)	12.6 [b]
South Atlantic (middle)	9.06 ± 5.25	Rural air (940 m)	25.0 [c]
Pacific (28° N–40° S)	8.44 ± 5.14	Average for 46 cities [d]	79
Indian Ocean	3.52 ± 1.10		
Mediterranean	6.98 ± 2.92		

[a] Concentration of organic carbon (TOC) in marine aerosols (Bermuda) lies between 0.15 and 0.47 $\mu g m^{-3}$. [b] Majority of particles have a diameter less than 1 μm. The values for the measured particulate contents lie in the range 0.51–35.5. [c] Majority of particles have a diameter smaller than 1 μm. Measured values of particulate content lie in the range 5.2–74.4. [d] Measurements carried out in 1975.

In assuming Kp values for adsorption from the atmosphere it is unnecessary to a first approximation to make a correction for the nature of the particles, for example as regards their organic carbon content.[69] For adsorption on sediments, however, a correction is made for the organic carbon content OC, and thus $Kp = f(OC)$. On the other hand the enrichment of, for example, chlorinated biphenyls (Cl_xB) and of aromatic hydrocarbons with two to four rings on suspended particles in the water column follows the simple relationship $c_{part} = K'_p C_{solution}$.

The coefficients K'_p appear not to be correlated with K_{OW}.[70] The build-up of different chlorinated biphenyls on suspended particles was found to take place in the same proportions as their relative concentrations in solution. It was only when the sediments were analyzed that the expected enrichment in the more highly chlorinated PCBs, corresponding to the increase in the K_{OW} values ($K''_p = f(K_{OW})$), was observed.[70]

The extraction of compounds from the multiphase atmospheric system by particles (aerosols) and condensed and solid water phases (fog, spray, rain, hoar-frost, snow) has been very thoroughly studied.[55, 71–75]

The adsorption of gases in multimolecular films is described by the Brunauer–Emmett–Teller (BET) equation [Eq. (10)].

$$\frac{n}{n_\infty} = \frac{bp}{(p^0 - p)[1 + (b-1)p/p^0} \tag{10}$$

This contains the temperature dependence of the adsorption in the form of the vapor pressure p at the temperature T. However, differences in the aerosol surface area per unit volume are only taken into account indirectly via the ratio between the actual surface coverage n [$g\,cm^{-2}$] and the coverage n_∞ needed to give a monomolecular film (b is a numerical parameter).[76] The original BET equation as formulated in 1938 was subsequently put into a more convenient form by C. E. Junge.[69] By making certain simplifying assumptions he arrived at the following expression [Equation (11)] for the adsorbed fraction ϕ of a compound in the atmosphere as a function of the vapor pressure P^0 [Pa] and the available aerosol surface per unit volume θ [cm^2cm^{-3}]:

$$\phi_T = \frac{c\theta}{p^0 + c\theta} (T = \text{constant}) \tag{11}$$

The constant c is a function of the molecular mass, the heat of condensation, and a contribution to the adsorption interaction that is specific to the substance. For physisorption the latter term can be regarded as essentially constant for a wide range of compounds. An average value for c is about 17.2 Pa cm.

From experimental measurements of ϕ for several chlorinated biphenyls (Cl_xB) the specific surface area θ in $cm^2\,cm^{-3}$ can be calculated using the Junge equation [Eq. (11)]. Measurements of $\phi(Cl_xB)$ in the city environment of Ulm and in a forest area in the Schwäbische Alb gave values of $3-6\times10^{-6}$ cm^2cm^{-3} for city air and $1-4\times10^{-6}$ cm^2cm^{-3} for forest air.[77] These results are in agreement with the average values usually calculated for city and rural air from the quantities of aerosols present. For pure air regions the values found for θ are less than 1×10^{-6} cm^2cm^{-3}.[55, 69, 78] For $p^0 = c\theta$ the equation gives an equal partition between the gas and particle phases; the vapor pressure needed to achieve this in 'pure' air is about 1.7×10^{-5} Pa. Pankow and other authors have discussed the molecule-specific parameters of the Junge equation [Eq. (11)], and their findings support Junge's approach.[79]

For solids it has been shown experimentally that p^0 in Equation (11) is best expressed in terms of the vapor pressure p_L^0 existing above the supercooled melt.[72] p_S^0 and p_L^0 are related by Equation (12):

$$\ln(p_L^0 p_S^{0-1}) = S_F(T_m - T)/RT \tag{12}$$

Here T_m is the melting point and T is the temperature of the environment in Kelvin; S_F is the entropy of fusion; an average value of S_F/R is 6.79. For 2,3,7,9-tetrachlorodibenzodioxin (m.p. 305 °C) the vapor pressure p_L^0 above the supercooled melt is 745 times greater than the vapor pressure p_S^0 above the solid substance. Such differences are crucial in determining whether transport in the atmosphere is molecular or particle-mediated, and thus whether the scale of it is regional to continental or only local.[4]

If the ratio of the adsorbed fraction ϕ to the total amount is known, and it is assumed that an aerosol particle remains in the troposphere for an average period of a days, the physical lifetime τ_{D+R} is given by the simple expression in Equation (13), which takes into account the fall-out by both dry

$$\tau_{D+R} = a\phi^{-1} \tag{13}$$

and wet deposition. The average retention time of aerosol particles in the lower troposphere is 7 days, with a range of 2 to 20 days depending on the diameter.[69] For aerosols generated in the sea the average retention time is 1.5 days.[80]

The lower the vapor pressure of a compound and the greater the available aerosol surface, the greater will be the fraction adsorbed. For the insecticide 4,4′-DDT with a vapor pressure of only 4.5×10^{-6} Pa (at 20 °C) the adsorbed fraction for "pure" air is 20%, which means that 80% of the DDT is distributed as molecules in the gas phase. These values become meaningful when one compares the measured background burdens with the saturation concentrations. 4,4′-DDT has a saturation concentration of 1.9 $\mu g\,m^{-3}$ corresponding to the vapor pressure of the solid compound, compared with the experimentally observed concentrations of 1 to 10 $pg\,m^{-3}$ in the atmosphere. Thus the concentrations of 4,4′-DDT in the atmosphere only amount to about $1/10^5$ of the saturation concentration. If instead one takes the saturation concentration as that above the supercooled melt, corresponding to p_L^0, which is greater, the ratio of observed concentration to that at saturation is even smaller. For polychlorobiphenyls (PCBs, Cl_xB) the corresponding values for ϕ are around 0.01, which means that under clean air conditions 99% of the Cl_xB molecules in the multiphase system of the troposphere are in the gas phase. Even for city air that is heavily burdened with aerosols, the proportion of Cl_xB in the gas phase is still about 50%. These calculations apply for temperatures in the range 20–25 °C. However, when one takes into account the fact that the average temperature over the first 4000 m of the troposphere is −11 °C, the partition ratio is considerably shifted in favor of the adsorbed phase. Wet deposition (rain-out), which occurs when the particles act as condensation nuclei for water droplets which subsequently form rain, can then become an important extraction mechanism. As will be shown later, each raindrop is formed from about 10^6 cloud droplets, which means that at least 10^6 condensation nuclei loaded with absorbate are present in a single raindrop. Convection rainfall can also arise, for example from the melting of ice particles that have been formed by cooling to −25 to −50 °C at altitudes of 10–12 km.[82]

For any sufficiently complex mixture of compounds that belong to the same class and have vapor pressures and water solubilities differing over a range of several orders of magnitude, such as the chlorinated biphenyls (209 compounds), the chlorodibenzofurans (135 compounds), or the chlorodibenzodioxins (75 compounds), the Junge equation defines the range of properties that will lead to different partition ratios in the atmosphere. The condition $\phi \simeq 0$ corresponds to the fully molecular-dispersed state (the "all-off" state with negligible adsorption), whereas $\phi \simeq 1$ corresponds to the fully particle-dispersed state ("all-on"), with nearly complete adsorption). In the intermediate region, for related compounds

whose vapor pressures are sufficiently different (e.g., Cl_xB, Cl_xDF, Cl_xDD, $x = 1-2$, $7-8$) there can be a reversal of which of the two states (gas phase or adsorbed phase) predominates. This leads to differences in composition in the retained material (in the atmosphere) and in the fall-out (rain, fog, hoar-frost, snow). This effect has been demonstrated experimentally for polychlorinated biphenyls (Cl_xB) in city areas.[75, 83] In this environmental compartment the particle surface area per unit volume reaches 5×10^{-6} cm^2cm^{-3} or more, and at low temperatures (0–10 °C) this is sufficient to cause differences that result in a depletion of the less volatile chlorohomologues in the atmosphere. In clean marine air at sea level with a temperature of 28 °C (measured at Réunion in the Indian ocean) the distribution of PCBs in the atmosphere is typical of an "all-off" situation. The data listed in Table 15 for particle concentrations in the lower marine atmosphere show that in oceanic regions there are only small global variations. The results found at Réunion thus appear to be of general validity.

On a global scale one would expect that the numerous preferential transport processes, summarized in the global partition equation (Fig. 2), should result in a preponderance of the more volatile PCBs in the lower troposphere. If one assumes that the main source of PCBs is a belt extending from 40° N to 60° N, then as one moves from north to south across the Atlantic Ocean, with only a small change in the concentration in the lower atmosphere, no significant increase in the proportion of the more volatile trichloro- and tetrachlorobiphenyls (e.g., PCB 28 and PCB 52) is found in the more southerly latitudes (Fig. 6).[68] The expected enrichment in the less highly chlorinated compounds is only found when one compares the atmosphere above the Eastern Atlantic with that in central Europe (the Schwäbische Alb region in Germany), in samples in which the sum of the concentrations of all the PCBs is about the same. The concentrations of Cl_xB compounds for $x = 3$ to 7 in the lower atmosphere over the Atlantic show identical trends (Fig. 6).[68] However, their rise and fall is not directly correlated with the temperature of the surface water but with its particulate content, as

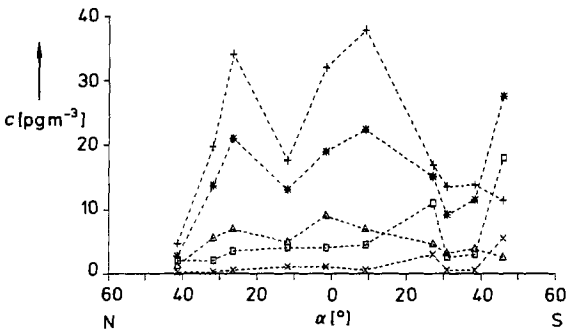

Fig. 6. North/South distribution of the concentration c of chlorinated biphenyls (Cl_xB) 2,4,4'-Cl_3B (PCB 28: Δ), 2,2',5,5'-Cl_4B (PCB 52: +), 2,2',4,5,5'-Cl_5B (PCB 101: *), 2,2',4,4',5,5'-Cl_6B (PCB 153: □) and 2,2',3,4,4',5,5'-Cl_7B (PCB 180: x) in the marine ground layer over the Atlantic ocean measured during a voyage of the FS Polarstern from Bremerhaven to Punta Arenas (Ant IX/1). The profile of the concentrations of PCB 28, 52 and 101 follows the salinity of the surface water. The increase in concentration of PCB 101, 153 and 180 at 48° South results from the extraction of such from the oil-producing areas of South Chile. The often postulated increase in concentration of readily volatile Cl_xB with increasing southern latitude could not be confirmed.

determined by the primary production processes, and with its salinity, as controlled by evaporation and precipitation.

The constancy of the marine PCBs distribution pattern makes it possible to obtain an indication of the amounts of PCBs released from industrial activities (mainly oil production) in the southern parts of Chile and Argentina. These releases are dominated by the more highly chlorinated PCBs with around 60% chlorine content (PCB 153 and PCB 180). Some indications regarding these regional inputs of highly chlorinated PCBs into the South Atlantic from industrial sources had already been obtained from the burdens found in the eggs of the various species of penguins that breed in the Falkland Islands and live at other times in a variety of habitats, including the open sea and the coastal regions of Patagonia.[84]

It is generally believed that in sea water the dissolved molecular fraction is the dominant form, even for compounds such as the PCBs, despite the fact that these are said to be "insoluble" in water by everyday standards. However, in the ocean the same sort of considerations apply as for the atmosphere. The 'particulates' content of sea water, which here includes not only dust and desert sand that enter the water, but also nanoplankton, crustacean shells and mud aggregates, determines how long a compound with limited water solubility remains in the water column. The particulates contents in the surface water of various oceans under open-sea conditions and for water columns in the open sea generally are listed in Table 16. As an approximate rule of

Table 16. Particulate concentrations in oligotrophic fresh-water lakes [70] and in oceans [85].

Surface waters	Particulate concentration [mgm^{-3}]	Water columns [b]	Particulate concentration [mgm^{-3}]
Great Lakes (USA–Canada)	100–500	Surface water (0–500 m)	110
North Atlantic (eastern side)	470	Middle depth (1000–3000 m)	5–20
South Atlantic (middle)	160	Bottom water (> 3000 m)	100
Indian Ocean (middle)	66		
North Atlantic (eastern side) [a]	(100)		
South Atlantic (middle) [a]	(25)		
Indian Ocean (middle) [a]	(10)		

[a] POC = particulate organic carbon content in surface waters. The total organic carbon content in oceanic surface water (TDC) is 0.3–1.0 gm^{-3} in the Sargossa Sea (Atlantic). [b] Average values are quoted.

thumb it can be assumed that 20–25% of the mass of the particulates consists of organic compounds (particulate organic carbon, POC).[85] When one gets to within several hundred meters of the ocean bed the particulates content begins to increase with depth due to resuspension.

The particulate content, including colloids (e.g., humic acids, saffrons), also influences the partition of less volatile and relatively insoluble compounds between surface water and the lowest layer of the troposphere, and this will be discussed later (Section 9).

Lifetimes in the surface waters of the oceans have been calculated for several groups of compounds by Japanese authors.[86] In the case of the hexachlorocyclohexanes they

found for α-HCH (water solubility 5.2×10^{-3} mol m^{-3}) values from 2 to 3.4 years, and for γ-HCH (solubility 2.1×10^{-2} mol m^{-3}) they found 5.1 to 10 years; in contrast, for PCBs with water solubilities ranging from 1.2×10^{-5} to 8×10^{-7} mol m^{-3} the corresponding retention times ranged from an average of 0.1 year (scatter: 0.07 to 0.12) to one of 0.57 year (scatter: 0.38 to 0.76). In each case the values apply for regions with high rates of primary production (150–250 g C m^{-2} a^{-1}) and for those with much lower rates (50–100 g C m^{-2} a^{-1}), which follow a trend reflecting the particulate content in the underlying water column. At a depth of 3200 m in the Sargasso sea in 1979/1980 an average particle-mediated flow of 1.6 μg m^{-2} year^{-1} of PCBs was measured.[87] The lifetimes for the *DDT* group of compounds are similar to those for the PCBs.

Considerably longer lifetimes of 3–5 years have been found for chlorinated biphenyls (Cl_xB) in the open sea surface waters of the Mediterranean.[88] Under deep-sea conditions the shortest lifetimes found were around 30 years.

Several different mechanisms must be distinguished, namely the adsorption on suspended particles, the exchange processes that take place during sedimentation, and the adsorption processes during the transformation of deposited particles (muds) into new sediments. The latter constitutes an entirely new phase whose composition is determined by chemical and biological activity. The early stages of diagenesis involve much chemical activity. Moreover, the solution/adsorbent (liquid/solid) ratio alters from one extreme to the other as the particulate/water system is transformed via the mud state into a new system consisting of a sediment with an interstitial solution.

Adsorption on and within the ground, which is the third important environmental compartment, is a complex process. The Langmuir isotherm equation is based on the assumption that the adsorbing surface is uniform. It was developed to describe the adsorption of gases, which was treated as a dynamic equilibrium.

The Freundlich isotherm was developed to describe adsorption from liquids. It assumes an adsorbing surface with a heterogeneous structure, and the adsorption is then a function of the concentration, as described empirically in Equations (14) and (15).

$$c_S = K c_{solution}^{1/n} \tag{14}$$

$$\lg c_S = n^{-1} \lg c_{solution} + \lg K \tag{15}$$

The Freundlich adsorption isotherm [Equation (15)] has been found to give a better description of the adsorption of organic compounds from dilute solutions and also in the ground,[89–91] since it contains the variable n which can be adjusted to fit the observed data. For very dilute solutions, n should have the value 1, and the simple Nernst distribution should then apply.

If the adsorption is related not to the mass of soil in grams but instead to the carbon content of the soil, the resulting adsorption constant K_{OC} is approximately independent of the nature of the soil as expressed in Equation (16):

$$K_{OC} = \frac{\text{μg of compound (\% org. carbon)}^{-1}}{\text{μg of compound (g of soil)}^{-1}} \tag{16}$$

Further, it has been shown that K_{OC} is only to a first approximation the same for different soils.[90] K_{OC} is directly related to K_{OW}. Both these quantities are often determined by regression analysis from the retention data obtained by C_{18}-RP liquid chromatography when compared with standard substances. However, it is better to calculate K_{OC} from data obtained by C_2-RP liquid chromatography.[91]

8. Transport in the Atmosphere

8.1. The General Circulation—The Global Wind System

The most rapid and effective horizontal and vertical mixing, extending to global dimensions, occurs in the lower 10 km of the atmosphere, i.e. the troposphere (see Fig. 3).[18,19] The transfer through the tropopause into the stratosphere (10–50 km) occurs only slowly, requiring about one year, while the theoretical return flow of organic substances that are photostable (for wavelengths $\lambda_{max} < 200$ nm) requires about four years.[92] Mixing in the stratosphere is much slower than that in the troposphere below.

The 'wind and weather' mass transport processes in the troposphere are associated with low-pressure areas (cyclones) containing upward air flows and high-pressure areas (anticyclones) with downward air flows. These cover a large area, and their time-scale can vary from hours, in regions where convection rainfall occurs, to the more usual periods of days to weeks within each hemisphere. An individual gas molecule or a particle with quasimolecular dynamic behavior ($d \leq 2$ μm) in the atmosphere of the temperate zone of westerly winds will take three to five weeks to travel around the world. With regard to mixing in the northern hemisphere, this means that the entire air mass above central Europe or that over Russia and Siberia travels around the world in an easterly direction about eight to ten times in a year. The contrary air movements that occur on a continental scale are only of regional importance, and can be analyzed in terms of "foreign" air masses that eventually become absorbed into the overall mixing process.

Even a very light breeze of only 4 km h^{-1}, one that can scarcely be felt, will move an air mass from Hamburg to the Alps in eight days. This enables one to easily appreciate the distances traveled by air masses in the average wind speed of 20 km h^{-1} that is generally assumed. Under these conditions it takes only ten days for air to travel from the east coast of the USA to central Europe, while a depression of storm strength would need only two to four days. The jet streams that occur in the tropopause of the tropics and middle latitudes can easily reach wind speeds of 200–500 km h^{-1}.

These global air movements take place in quite different directions in the two hemispheres, and thus affect different regions of distribution. In the middle latitudes (30° to 60° N or S) an easterly movement predominates, i.e. west winds prevail. Between the temperate latitudes and the equator the north-east trade winds and the south-east trade winds in the northern and southern hemispheres respectively converge towards each other, each with a strong east wind component, moving air towards the west (Fig. 7).[20] This convergence,

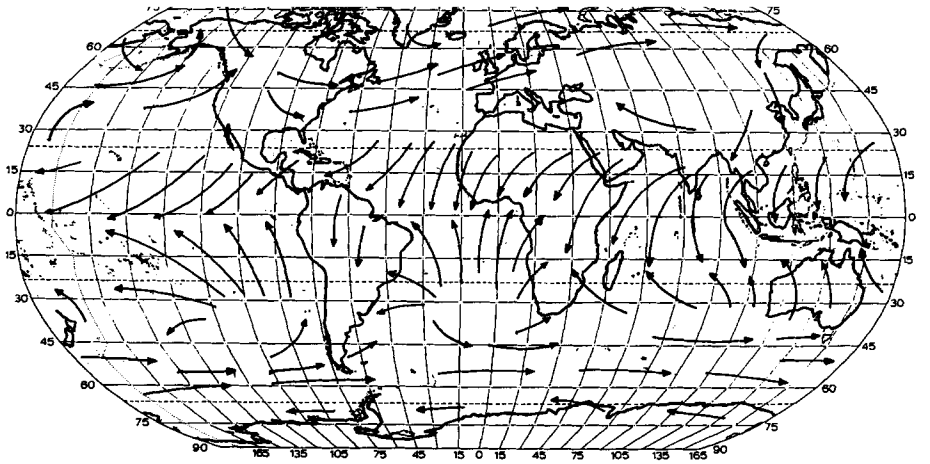

Fig. 7. Scheme of the prevailing winds in the lower troposphere (0–1000/2000 m) during the northern winter. In the northern summer, over the Indian Ocean, the south-east tradewind, as south-west monsoon, reaches out across the equator in a northerly direction as far as the Himalaya Region. The intertropic convergence zone (ITCZ) then shifts to ca. 30° North. Over the Atlantic and Pacific Oceans, the ITCZ shifts only slightly towards the south. The tradewind system remains essentially undisturbed. (See also Figs. 4 and 8.)

with an upward movement where the flows meet (the intertropical convergence zone, ITCZ, forming the so-called Hadley cells north and south of the equator) determines the time-scale for exchange between the hemispheres, which is about one year for gases (see also Fig. 4).[69]

In the continental regions this greatly simplified global "general circulation" is broken up into individual flows unique to their locations. Moreover, during the northern summer the north-east trade wind (north-east monsoon) swings around over the Indian Ocean to become the south-west monsoon, so that the south-east trade winds then extend across the equator towards the north. Thus, in the northern summer, air from the lower troposphere of the southern hemisphere pushes far to the north.[122]

Over the North Atlantic the permanent central Atlantic high (Azores high) results in a clockwise circulation of air which can carry Sahara dust as far as the Antilles (Caribbean) and Bermuda, while in Ireland it is possible to have fine dust carried over from the east coast of North America. The fact that dust from the Sahara is transported on a continental scale (giving reddish-yellow snow in the Alps, for example) vividly illustrates the potential for long-distance transport of substances. Similarly the global spread of radioactive particles from the Chernobyl disaster was a revealing, yet unwanted, experiment.

By carefully studying the weather map on a continental scale one can recognize preferred paths for the flow of air near ground level. Acid rain over Scandinavia (containing H_2SO_3 and H_2SO_4 extracted from the atmosphere) originates not only from central Europe (e.g., the Ruhr and the Saar region—Elsass-Lothringen) but also to a considerable extent from the industrial regions of the United Kingdom. Often the path taken by a typical 'low over the British Isles' is not over the central mountains of Germany towards Scandinavia but a more northerly route.[119]

Vertical air movements, familiar on a local scale as thermals or downward air currents, are manifested on a regional scale as the familiar "highs" (anticyclones) and "lows" (cyclones, depressions). Increased air pressure is caused by downward-moving air masses, and conversely a depression is characterized by rising air. The equatorial calm zones (the doldrums) are caused by regions of rising air masses with virtually no horizontal component of air-flow. The upward air movements in low pressure regions are an important factor in the mixing of the atmosphere, as they transport air that is near the ground, and therefore close to sources, up to higher altitudes.

Diffusion processes are of little importance for mixing in the troposphere, since the diffusion distances are quite insignificant owing to the very short mean free paths; even hydrogen has a mean free path of only 1.6×10^{-5} cm at 0 °C and 1 bar, compared with an average wind speed of 5.5 m s^{-1}. The potential rate of diffusion in the longitudinal direction for hydrogen at STP is only about 0.5 cm s^{-1}.

The planetary system of high- and low-pressure zones which builds up in the atmosphere well above the earth's surface (5–10 km) plays a very important role in global transport in the troposphere (Fig. 8). These circulating systems, whose influence extends far to the north and south, are best described in terms of the pressure relationships existing in the 500 mb region (corresponding to an altitude of about 5 km); they are responsible for the rapid exchange within the

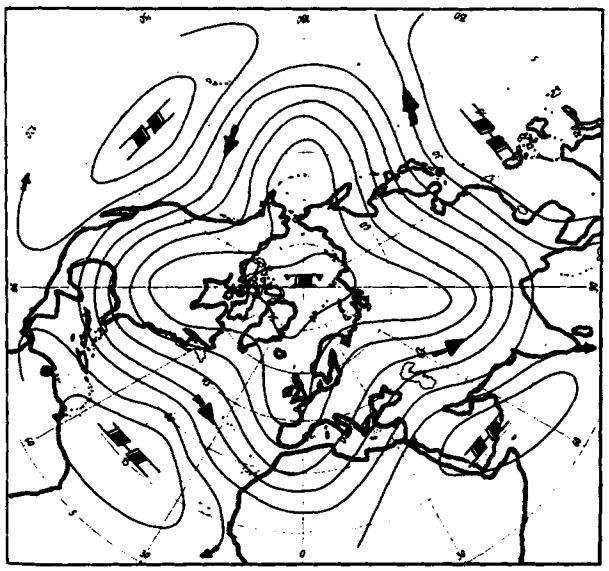

Fig. 8. Schematic representation of the planetary cyclone/anticyclone systems in the free atmosphere (ca. 5 km altitude) of the northern hemisphere. The air current follows the isobars, flowing in an easterly direction (west wind). Higher wave numbers can also occur (four bulges around the central low T). H = high.

equal distribution of trace substances between the two.[17, 18]

If the vertical exchange processes in a local area are slowed down or even halted by inversion layers (warm air lying above cool ground air), it is possible for pollutants such as SO_2, CO, nitrogen oxides, benzene or chlorinated solvents to accumulate in the cooler air near the ground, as their removel is then inhibited. Weather conditions such as these make one acutely aware, in an indirect way, of the 'normal' removal mechanisms in the lower troposphere.

In the stratosphere the temperature layers are such that there is a sort of permanent inversion (see Fig. 3), and the exchange processes are consequently much slower and less turbulent than in the troposphere. Return flows of air from the stratosphere to the troposphere can occasionally occur, usually where there are local disturbances in the tropopause at middle latitudes; these can, for example, act as sources of ozone from the stratosphere.

8.2. Extraction from the Atmosphere

Organic compounds can be removed from the troposphere in a number of ways, as follows:

1) by adsorption on large or very large aerosol particles (2–20 μm) which are then deposited;
2) through rain-out following adsorption on smaller aerosol particles which then act as condensation nuclei for cloud droplets and eventually form raindrops ('hydrometeorites');
3) by adsorption on particles which then collide with cloud droplets or raindrops and are captured;
4) through wash-out of molecules in the gas phase by raindrops, as in a gas scrubbing process;
5) by diffusion through the atmosphere/ocean interface;[16]
6) by moving out into the stratosphere.[92]

Which is the most effective process in a given case depends on the molecular properties (e.g., vapor pressure, polarity, water solubility) and the conditions in the troposphere (temperature, particulate surface area, amount of precipitation, type of rainfall (cyclonal or zenithal), stability of the tropopause, etc.).[58–60]

Relationships have been derived for some of the extraction mechanisms, as detailed below.[53–55, 71, 72]

1) Deposition as dry particles [Eq. (17)],

$$F = v_d c_{part} \tag{17}$$

where F = flow rate [$mol\,m^{-2}\,a^{-1}$] v_d = deposition velocity (for particles with diameters in the range 0.01 to 1 μm values of v_d from 0.02 to 0.5 $cm\,s^{-1}$ can be assumed, corresponding to the potential diffusion velocity of hydrogen in the longitudinal and slower directions), c_{part} = concentration of the compound existing in the adsorbed phase in air = ϕc_{total} [$mol\,m^{-3}$]; ϕ according to Equation (11).

2) Rain-out of particles that have acted as condensation nuclei for water droplets:

$$F = r c_{part} I_R \tag{18}$$

cient, c_{part} = concentration of the compound existing in the adsorbed phase in air = ϕc_{total} [$mol\,m^{-3}$], ϕ according to Equation (11), I_R = annual rainfall [$m\,a^{-1}$].

3) Wash-out of the gas-phase component by absorption [Eq. (19)]:

$$F = \frac{I_R c_{vap}}{H} \tag{19}$$

where F = flow rate [$mol\,m^{-2}\,a^{-1}$] I_R = annual rainfall [$m\,a^{-1}$], $c_{vap} = (1 - \phi)c_{total}$ [$mol\,m^{-3}$], ϕ according to Equation (11), H = Henry's constant = $p^0 S_{H_2O}^{-1} = c_{air}/c_{water}^{-1}\,RT$ [$Pa\,m^3\,mol^{-1}$]. The equilibrium between the gas phase and the raindrops becomes established after only about 10 m of fall.

The extraction by rainfall is also often expressed by the wash-out ratio W, defined by $W = c_{rain}/c_{air}$. W includes not only the extraction from the gas phase W_{vap} but also that from the adsorbed phase W_{part} [Eq. (20)], where W_{part} is the

$$W = W_{part} + W_{vap} \tag{20}$$

product of $c_{rain\,(part)}$ and $c_{air\,(part)}^{-1}$ and W_{vap} is the product of $c_{rain\,(solution)}$ and $c_{air\,(vapor)}^{-1}$, which is equal to RTH^{-1}.

The contributions of W_{part} and W_{vap} to W are determined by the fraction ϕ [Eq. (11)] of the compound that is adsorbed on particles [Eq. (21)]:

$$W = W_{part}\phi + W_{vap}(1 - \phi) \tag{21}$$

W_{part} can vary over a wide range.[72]

4) Extraction of organic compounds by diffusion at the interface atmosphere/ocean.[16] The exchange of molecules through the air/water interface is generally described by the Equation (22) developed by Liss and Slater,[93] which is based on Whitman's two-film model:

$$F = K_l(c_g H^{-1} RT - c_l) = K_g(c_g - HR^{-1}T^{-1}c_l) \tag{22}$$

in which K_l and K_g are the mass-transfer coefficients [$m\,h^{-1}$] in the liquid and gas phases respectively, c_l and c_g are the concentrations in the two phases [$mol\,m^{-3}$], and H is Henry's constant.

5) Extraction of organic compounds by their transport into the stratosphere.[92] In the various removal mechanisms the fraction ϕ [Eq. (11)] of a compound in the atmosphere that is adsorbed on particles evidently plays an important role. The fraction of adsorbed molecules is correlated with the vapor pressure and with the concentration of aerosol particles and/or the particle surface area per cm^3 [Eq. (11)]. Measurements and calculations show that in sea air at 20 °C as much as 90% of C_{24} alkanes[94] and a similar proportion of polychlorobiphenyls[84] remains in the gas phase. Values of ϕ for *n*-alkanes from C_{16} to C_{25} in city air (Barcelona) at an average temperature of 12 °C have been determined.[95] These measurements confirm the theoretically predicted dependence of ϕ on the aerosols specific surface area θ [$cm^2 cm^{-3}$] (Table 17).

The diameters of atmospheric particles show a bimodal distribution, with one maximum at 1.0 μm caused by the aggregation of Aitken particles ($d < 0.2$ μm) and another at

bons; ϕ = adsorbed fraction × (gas-phase fraction)$^{-1}$. (City air, Barcelona, 12 °C). [95]

alkanes	p [Pa] [a]	ϕ	alkanes	c (particles)	ϕ
n-C_{16}	–	<0.01	n-C_{21}	2.8×10^{-3}	0.73
n-C_{17}	9.4×10^{-2}	0.02	n-C_{22}	1.2×10^{-3}	0.89
n-C_{18}	2.9×10^{-2}	0.08	n-C_{23}	6.0×10^{-4}	0.97
n-C_{19}	1.6×10^{-2}	0.23	n-C_{24}	2.7×10^{-4}	0.98
n-C_{20}	6.6×10^{-3}	0.50	n-C_{25}	–	0.99

[a] Pressure p at 12 °C.

10 μm consisting mainly of particles picked up by circular eddies from land and sea surfaces (dust, sandstorm seaspray). The distribution of organic compounds that characterizes their origin often follows the above particle size distribution. The majority of organic compounds are found on particles with diameters less than 2 μm, even though these constitute only 25% of the total particulate mass.[80, 81, 94] For particles collected from the atmosphere near London the burdens of polyaromatic hydrocarbons, PAH (phenanthrene to coronene), showed a clear maximum in the region $d = 0.2$ to 2 μm.[96] Moreover, aerosols with diameters less than 2 μm contain a large proportion of particles generated by combustion processes.[80, 95–97]

With regard to the regional distribution of organic trace substances in the troposphere, this marked preference for adsorption on particles with diameters less than 2 μm can necessitate treating the aerosols as a separate phase in the atmosphere and taking differences of particle size into account. For particles with diameters of 2 μm or less, dry deposition is, to a first approximation, negligible. Such particles behave like molecules, obeying gas dynamics. Their velocities of fall V_d are in the range 0.02 to 0.5 $cm\,s^{-1}$, or 0.7 to 18 $m\,h^{-1}$.[54] In contrast to this, average wind speeds are 20×10^3 $m\,h^{-1}$, and superimposed on these are the downward or upward air velocities in anticyclonic or cyclonic weather conditions respectively, which are of the order of 100 to 300 $m\,h^{-1}$, even if one ignores the thermals in the lowest layer (0–1000 m).

The Junge equation [Eq. (11)] can be extended to apply not only to aerosols but also to extraction by the surfaces of leaves and conifer needles. As well as taking into account the capture of aerosol particles by the fine structures of leaf surfaces, and the interception of rainfall before it reaches the ground (20–30% may fail to reach the ground as run-off from the foliage, branches and trunk), the leaf surfaces themselves can be treated in the same way as the surface of aerosols, with a value of θ [cm^2cm^{-3}] that is related to an average tree height of 10 m. In ecological studies one defines leaf area index (LAI) in m^2m^{-2} as the ratio of the total leaf area, assumed to be one-sided, to the ground area covered by forest or shrubs.[98, 99] For a leaf area index of 5 and an average tree height of 10 m, θ has a value of 10^{-2} cm^2cm^{-3}. For dust-laden city air the highest values of θ are around 4×10^{-6} cm^2cm^{-3}, and thus a typical value of θ for leaf surfaces is 10^3 to 10^4 times greater. In this case an adsorption of 50%, expressed by the value $\phi = 0.5$, would result for a vapor pressure in the range $(1.7 \text{ to } 17) \times 10^{-2}$ Pa. Thus leaf surfaces are of considerable importance for the extraction of substances from the troposphere near ground level.

These theoretical considerations are consistent with measurements of the soil burdens of Cl_xDD and Cl_xDF in different types of terrain in Germany, giving 1.5 ngiTE kg^{-1} for crop-growing land, 7.0 ngiTE kg^{-1} for grazing land, and 40.9 ngiTE kg^{-1} for forest leaf debris.[100] The leaf debris of a forest constitutes a sink which is analogous to ocean sediments.

The rates of fallout per m^2 resulting from deposition of aerosols have been determined for a number of organic compounds.[4] In Iceland in the summer of 1972 the rate of deposition of polychlorinated biphenyls (Cl_xB) by this mechanism was 1.1 $\mu g\,m^{-2}$ per month, whereas in winter the rate fell to 0.05 $\mu g\,m^{-2}$ per month. In the vicinity of Ulm in the Schwäbische Alb region in Germany in the winter of 1986, during a period dominated by high pressure, the rate of deposition of PCBs on the snow surface was 1.3 $\mu g\,m^{-2}$ per month. These rates of deposition are remarkably similar, if one excludes the winter figure for Iceland. This narrow range of deposition rates corresponds to a similarly narrow range of Cl_xB concentrations in the lower troposphere above the continents. In non-industrial regions of both central Europe (Schwäbische Alb (FRG))[66] and North America,[98] where there is very little direct uptake of these compounds, the concentration of Cl_xB in the lower troposphere was in the range 135–170 $pg\,m^{-3}$. In Réunion (Indian ocean) Cl_xB concentrations of about 125 $pg\,m^{-3}$ have been measured.[66]

There is considerable evidence that the Cl_xB concentration in the atmosphere above the oceans is determined by that in the surface water (Fig. 6). The quantity of Cl_xB present in the top 5 m of the ocean, assuming a concentration of 500–1000 $ng\,m^{-3}$,[86, 101, 102] is equal to that in the air column above it extending to a height of 10 km, if one assumes a concentration of 125–200 $pg\,m^{-3}$. The experimentally determined values for $K_{GW} = c_{gas}\,c_{water}^{-1}$ (dimensionless) for various compounds of the Cl_xB series range from 7.9×10^{-3} (for PCB 28, the 2,2′,4′ compound) to 0.4×10^{-3} (for PCB 180, the 2,2′,3,4,4′,5,5′ compound).[103] The concentrations measured in air and water at sea level give values for K_{GW} in the range from 4.1×10^{-3} to 0.1×10^{-3}. Thus the air contains much lower concentrations of Cl_xB than the equilibrium with water predicts. A more detailed comparison of the K_{GW} values found for individual PCBs in both continental and marine environments at ground level is given in Table 18.[77] These data confirm that under environmental conditions the concentrations of the PCBs investigated are lower in the atmosphere, and correspondingly greater in the water, by a factor of 2 to 6, when compared with the lowest

Table 18. Comparison of air/water partition coefficients $K_{GW} = c_{air}\,c_{water}^{-1}$ for PCBs.

Cpd.	Position [a]	$K_{GW} \times 10^3$ Environment [77] [b]	[c]	[d]	[e]	Laboratory [103]
PCB 28	2,4,4′	1.6	0.9	0.8	4.1	7.9 ± 1.2
PCB 52	2,2′5,5′	1.1	1.6	0.7	3.9	8.0 ± 2.0
PCB 101	2,2′,4,5,5′	0.6	0.9	0.3	1.7	3.7 ± 1.3
PCP 138	2,2′3,4′,5,5′	0.2	0.4	0.3	1.3	0.84 ± 0.27
PCB 153	2,2′,4,4′,5,5′	0.2	0.5	0.3	1.0	0.93 ± 0.24
PCB 180	2,2′,3,4,4′,5,5′	0.08	0.13	0.2	0.2	0.40 ± 0.19

[a] Position of the chlorine substituents. [b] Lake on Ulm University campus. [c] North Atlantic (Bermuda). [d] Lagoon, Réunion. [e] Open sea, Réunion.

Table 19. Annual inputs (I) in [$t a^{-1}$] and flow rates (F) in [$\mu g m^{-2} a^{-1}$] for various organochlorine compounds in the oceans [105].

	Atlantic Ocean				Pacific Ocean				Indian Ocean		Total	
	North		South		North		South					
	I	F	I	F	I	F	I	F	I	F	I	F
α/γ-HCH	851	15.5	97	1.9	2460	29.5	471	4.3	698	10.3	4754	12.7
HCB	16.8	0.31	10	0.20	19.9	0.22	18.9	0.17	11.4	0.17	77.1	0.23
DDT + DDE	15.6	0.28	14.0	0.27	66.4	0.74	25.7	0.23	43.3	0.64	165	0.44
ΣPCB	99.7	1.81	13.8	0.27	35.5	0.40	29.1	0.26	52.1	0.77	239	0.64
Σ Chlordane	8.7	0.16	1.0	0.02	8.3	0.09	1.9	0.02	2.4	0.04	22.1	0.06
Dieldrin	16.6	0.03	2.0	0.04	8.9	0.10	9.5	0.09	6.0	0.09	42.9	0.11

measured laboratory values for the gas/water partition constant K_{GW}.[103] A detailed study of the air/water and water/particulate distribution for chlorodibenzo-*p*-dioxins and chlorodibenzofurans in the Baltic similarly showed a higher fraction in the water phase than expected from laboratory results.[104]

The differences between the apparent environmental values of K_{GW} for an oligotrophic lake and for the open ocean are surprisingly small. According to Equation (30) and the results in Table 18 the proportion of Cl_xB present in unassociated solution form varies between 20 and 50%. It is not yet known why the trend of the fraction present in unassociated solution is opposite to that of the water solubilities of the different PCBs. Modeling studies of the uptake of persistent organochlorine compounds into the Arctic ocean gave ratios for hexachlorobenzene (HCB) that are similar to those given here for PCBs; for HCB too the calculations indicate a flow from the water into the atmosphere.[55]

Measurements of Cl_xB concentrations in the surface waters of the North Atlantic during the period 1973–1975 showed a maximum in the region between 5° N and 20° N, where the rainfall is greatest and also the North Equatorial Stream, a continuation of the Canaries Stream, flows.[99] For the corresponding region south of the equator (5° S to 20° S) the concentration of Cl_xB in the surface waters was found to be very much smaller. This region has a rainfall comparable to that in the corresponding northern latitudes, but here the surface water comes from the South Equatorial current and therefore from the South Atlantic. Both sets of results lead to the conclusion that if removal from the atmosphere occurs mainly through rainfall, as Harvey and Steinhauer have assumed, then the PCBs do not cross the intertropical convergence zone (ITCZ), and therefore the interhemisphere exchange in the troposphere must be greatly inhibited in the case of the PCBs. The same has also been found for hexachlorobenzene and α-hexachlorocyclohexane.[66] More recent measurements in the atmosphere at sea level over the Atlantic during two north–to–south and south–to–north crossings by the research ship "Polarstern" have confirmed these results (Fig. 5).[68] However, for PCBs the situation needs to be looked at in greater detail; here one must distinguish between regional and global transport, unless one assumes that the inputs of PCBs into the northern and southern hemispheres are equal (Fig. 6).

A research group has been set up under GESAMP (World Meteorological Organization) to bring together studies on the annual input of trace chemicals from the atmosphere into the global oceanic system.[105] Data are mapped in 10° squares and used to extrapolate. The inputs (in tons $year^{-1}$) and flow rates [$\mu g m^{-2}$ $year^{-1}$] for several chlorohydrocarbons are listed in Table 19. In assembling the data it became clear, not surprisingly, that the available information for the southern hemisphere, and also for organic compounds in general, is rather meager. There have, on the whole, been very few studies up to now of the distribution of trace organic compounds in the atmosphere. In this field, as in others, one detects the influence of the traditional emphasis on inorganic analytical chemistry in the education of chemists, and therefore also of those in related disciplines.

8.3. Transport Pathways in the Global Water Circulation

Rainfall has a key transport role (through rain-out and wash-out) in removing both polar and non-polar involatile organic compounds from the troposphere. Lakes that have no rivers running in or out receive their input of xenobiotics solely from rainfall, and therefore act as catchment basins for this fall-out, which accumulates in water, fish (see Table 11)[58] and sediments.[34]

The total volume of water present on the earth in liquid, vapor and solid forms is 1.384×10^9 km^3, of which 97.4% exists as brine in the oceans. The volume of water evaporated per year from the ocean surface is 440000 km^3, and of this about 400000 km^3 falls directly back into the oceans as rain (Table 12).[22, 63] The quantity of water falling onto land areas as rain is 110000 km^3 per year, of which 40000 km^3, about a third, originates from the oceans, while the rest comes from the continental or "minor" circulation. The total annual global rainfall is 510000 km^3, while the quantity of water present in the troposphere at any time is a mere 14000 km^3. The water in the troposphere undergoes 36 changes a year, i.e. once every 9–10 days, by falling back to the earth's surface as rain. In the tropics the annual rainfall in different latitude zones is 49000 km^3 for 20° N to 10° N, 82000 km^3 for 10° N to the equator, 64000 km^3 for 0 to 10° S, and 50000 km^3 for 10 to 20° S; the total of 245000 km^3 makes up nearly half the world's rainfall. Over the Atlantic and Pacific oceans there is a narrow but continuous belt in which the annual rainfall is as high as 300–400 cm (Fig. 9).[22]

The annual run-off from the continents in the form of rivers is 25000 km^3 in the northern hemisphere and 15000 km^3 in the southern hemisphere. The resulting north to south transport in the oceanic system is balanced by a transport of water vapor from south to north crossing the equator which takes place in the troposphere.

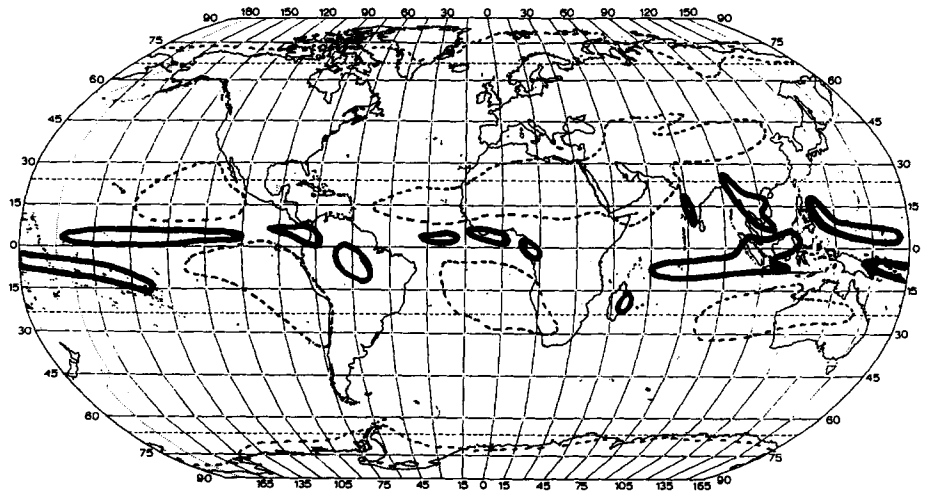

Fig. 9. Global distribution of the areas having the extremes of annual rainfall (areas marked by an unbroken line: annual rainfall > 2000 mm; areas marked by a broken line: annual rainfall < 250 mm). The well-known extremely dry areas on the continents stretch out to the high seas. As areas with high evaporation rates they also supply to the heavy precipitates formed in the ascending air masses in the intertropic convergence zone. These precipitates stemming from high clouds form a curtain of water between the northern and southern hemispheres, with all the consequences of the extraction of organic compounds by rain-out and wash-out.

With regard to the deposition of substances in rainfall, both in solution form and adsorbed on particles, it must be borne in mind that a quantity of rainfall equal to the entire water in the troposphere falls back to the earth's surface 36 times in the course of a year, while large areas are arid and take no significant part in this, and furthermore that about 71% of the earth's surface is occupied by the oceans. Consequently, at least 3/4 of the fall-out from the troposphere due to deposition, rain-out and wash-out reaches the surface of the oceans (Table 12).

Whereas for *ad*sorption processes an important quantity is the available particulate surface area per unit volume, the analogous quantity for *ab*sorption processes is the amount of the condensed water phase per unit total volume. Even in rain-clouds with a high water content, the mass of condensed water per unit volume seldom exceeds 1–4 $g\,m^{-3}$. Table 20 compares values for the ratio of the liquid water phase to the gas phase for haze, fog and clouds. If the water/air partition

Table 20. Phase ratios for water in the condensed phase and air.

	Haze	Fog	Clouds	Drizzle	Rain
Droplet radius [μm]	0.03–0.3	≈10	≈10	100–300	300–2000
Water/Air [cm^3m^{-3}]	10^{-5}–10^{-4}	0.05–0.5	0.1–3	0.1–3	0.1–3
Average phase ratios [a]	$\ll 10^{-7}$	10^{-7}	10^{-6}	10^{-6}	10^{-6}

[a] Average phase ratios water/air in $[m^3m^{-3}]$.

coefficient is known, one can estimate the maximum possible extraction by condensed water ('hydrometeorites'). Water drops of any size are called hydrometeorites. Water droplets in clouds cannot escape from the clouds other than by evaporation. Even for water droplets with a diameter of 200 μm the downward path in 90% saturated air is only 3 cm.[83] About 10^6 cloud droplets need to merge in order to form one average-sized raindrop, and accordingly there are about 10^6 condensation nuclei trapped in each raindrop.

For removal by solvation in the water phase (i.e. in raindrops) the Ostwald solubility α' (α' = solubility in water $[g\,L^{-1}]$/vapor density $[g\,L^{-1}]$) determines the rate at which a compound can be removed by wash-out. α' is the reciprocal of the more usual gas/water partition coefficient K_{GW} [Eq. (24)]:

$$K_{GW} = c_{air}\,c_{water}^{-1} \tag{24}$$

For transport calculations a useful quantity is the retention time or lifetime τ [years], defined, as previously [Eq. (1)], by $\tau = 1/(\text{removal rate})$ leading to:

$$\tau = \text{volume of air column} \times (\alpha' \times \text{rainfall volume})^{-1} \tag{25}$$

or, expressed in terms of K_{GW}:

$$\tau = K_{GW} \times \text{volume of air column} \times (\text{rainfall volume})^{-1} \tag{26}$$

For lindane, assuming a rainfall of 100 cm $year^{-1}$ from an 8000 m column of the atmosphere and a value of 0.2×10^{-4} for K_{GW}, the predicted retention time τ is 58 days. If the rainfall is increased to 300 cm $year^{-1}$, as in the tropics for example, the retention time for lindane is reduced to 19 days. For PCBs containing 60% chlorine (Arodor 1260, Chlorphen A 60), with a K_{GW} value of about 10^{-3},[103] the corresponding retention times for wash-out are about 8 and 2.7 years respectively. Furthermore, the removal of PCBs by wash-out is reduced by the phenomenon of water vapor distillation (similar to steam distillation), which also applies for raindrops.

From a knowledge of the ratio of the condensed water phase to the air volume (Table 20) and of K_{GW} values, one can make theoretical calculations of extraction rates for fog or rain. Measurements show that for semivolatile compounds there are always higher concentrations in rainfall than these calculations predict.[106, 107] Compounds with low solubilities in water are mainly removed with the rain on particles that act as condensation nuclei for fog and rain, at a rate determined by the partition ratio between the gas and absorbed phases. In this context one can regard the raindrops as dust particles that have become weighed down with water. Table 21 lists concentrations of organic compounds in rainwater, measured in a central European city (Hannover).[107]

Table 21. Concentrations of moderately volatile organic compounds in rainwater in Central Europe (Hannover, FRG) [107].

Compound	Concentration [$\mu g L^{-1}$]	Scatter [a] [μL^{-1}]	Compound	Concentration [$\mu g L^{-1}$]	Scatter [a] [$\mu g L^{-1}$]
Alkanes			*Fatty Acids:*		
Σ alkanes (Winter 1989)	15.1	4.4–19.0	Σ fatty acids	27.6	16.2–44.1
(CPI) [b]	(1.5)	(1.2–2.0)	(CPI) [b]	(8.1)	(5.3–15.7)
Σ alkanes (Summer 1989)	40.6	3.9–111.2	n-$C_{15}H_{31}$ COOH	8.7	4.5–16.1
(CPI) [b]	(3.0)	(1.6–5.3)	n-$C_{25}H_{51}$ COOH	1.0	0.5–3.8
Σ alkanes (Fall 1989)	84.4	11.0–151.5			
(CPI) [b]	(1.7)	(1.2–2.1)			
Aldehydes:			*Phenoles:*		
Σ aldehydes	127.4	13.1–359.6	phenol	5.6	1.3–15.4
formaldehyde	110.7	8.1–303.8	3-/4-methylphenol	2.5	0.46–9.9
acetaldehyde	12.0	1.5–20.5	2-nitrophenol	0.18	0.03–0.68
polycyclic hydrocarbons:			4-nitrophenol	5.7	1.2–19.5
Σ PAH (Winter 1989/1990) [c]	0.60	0.12–1.2			
benzo[*a*]pyrene	0.03	0.001–0.19			

[a] Scatter refers to the range over which the measured values scatter. [b] CPI = Carbon preference index, i.e. the ratio of odd-numbered to even-numbered carbon compounds; a CPI greater than 2 indicates that the material is mainly of biological origin. [c] PAH = polycyclic aromatic hydrocarbons.

8.4. Variation of the Lifetimes τ_{OH}, τ_R and τ_W according to Latitude

On a global scale one needs to divide the atmosphere into at least three belts in each hemisphere, corresponding to the major climatic zones: 1) the polar regions (latitudes 90° to 60°; north pole, south pole), 2) the middle latitudes or west wind belts (60° to 30°; north-west and south-west passage), 3) the tropics (30° to 0°; northern and southern tropics). The two tropical belts are separated from each other by the relatively narrow but well-defined intertropic convergence zone (ITCZ) (see also Fig. 4).

The lifetime τ_{OH} of a compound in relation to its reaction with $^{\bullet}OH$ radicals is given by the reciprocal of the product of the rate constant k_{OH} and the concentration of $^{\bullet}OH$ radicals. For calculations relating to long time-scales it is sufficient to assume a global average figure of 0.5×10^6 molecules cm^{-3} for this concentration, but a realistic and more detailed consideration of the distribution behavior of compounds requires one to take into account the large variations of $^{\bullet}OH$ radical concentration with latitude (meridional variation). Whereas the reaction rate constant k_{OH} remains unchanged, the lifetime τ_{OH} decreases by a factor of 10 or more as one moves from the polar regions to the equator.[39, 42]

The concentration of $^{\bullet}OH$ radicals in the troposphere shows an approximate, and very important, correlation with the solar radiation intensity. Striking evidence of this is provided by the diurnal variations, by factors of as much as 100, in the concentrations of $^{\bullet}OH$ radicals.[39]

The lifetimes for rain-out (following adsorption on particles) and wash-out (absorption in raindrops), τ_R^{-1} and τ_W^{-1} respectively, take on a special significance in the regions immediately to the south and north of the ITCZ. The values of τ_{OH}, τ_R and τ_W have their global minima as one crosses the equator. In this connection it should be noted that a movement from the zone between 30° N and 60° N into the zone of larger area between 30° N and the equator is accompanied by streaming in a larger volume equivalent to a dilution which is further accentuated by the mixing-in of air descending from higher altitudes in the region of 30° N due to the trade winds.

If one assumes constant values for the gas/particle and gas/water partition coefficients, the lifetimes τ_R^{-1} and τ_W^{-1} for rain-out and wash-out respectively are influenced to different extents by the amount of rainfall and the average temperature. These latter two parameters also vary according to latitude. Furthermore, τ_R also depends on the average aerosol surface area per unit volume [$cm^2 cm^{-3}$]; for clean marine air this is constant throughout the world to a first approximation. With regard to the variation of temperature with latitude, the important variable is the average sea-level temperature. With increasing altitude the differences in average temperature disappear. The average temperature in each zone follows the annual cycle of solar radiation intensity, with extreme values in the polar regions.

With regard to the transport of organic compounds it is evident that the ITCZ forms an important physical and chemical barrier between the northern and southern hemispheres. Immediately to the north and south of the ITCZ one finds—as already mentioned—the global rainfall maxima, caused by cumulus clouds extending to heights of 10–12 km. The resulting high wash-out rate is accompanied by a marked increase in $^{\bullet}OH$ radical concentration, so that not only the physical but also the chemical lifetimes for compounds with high reactivities towards these radicals are significantly reduced in the tropics. The barrier effect of the ITCZ has been

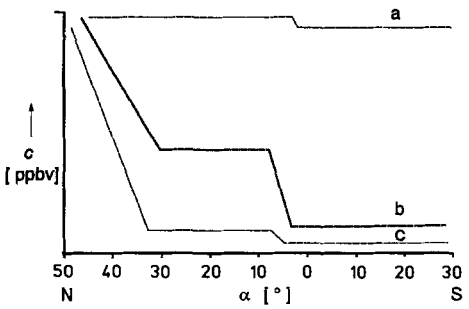

Fig. 10. Plot of the concentration c of tetrachloromethane (a), trichloroethene (c) and tetrachloroethene (b) in the tropospheric boundary layer of the Atlantic Ocean, recorded for a north-south traverse (Bremerhaven-Capetown). The intertropic convergence zone forms an effective barrier for chlorinated ethenes.

clearly demonstrated for a series of organohalogen compounds from C_1 to C_{12}, which have their main sources in the west wind region of the northern hemisphere (Fig. 10).[38] This barrier effect is further accentuated by the partial reversal of the flow direction that occurs in the rising air masses of the Hadley cells, returning a portion of this air back into the hemisphere from whence it has originated (see Fig. 4).

9. Transport from the Surface Waters of the Oceans into the Troposphere

The extent to which the oceans act not only as a "sink" by receiving rainfall but also as a 'source', returning chemicals into the troposphere by normal reverse diffusion, by the water vapor distillation effect, and by forming aerosols (sea spray) from the surface microlayer, is an unanswered question that one can only point to as a subject for future investigation. For nonvolatile compounds such as HBC, PCBs or DDT, our own recent measurements suggest that the concentrations in the upper levels of the ocean (0–50 m) determine those present in the column of the troposphere (0–12 km) above.[68]

Measurements of the concentrations of the hydrocarbons from decane ($C_{10}H_{22}$) to octaeicosane ($C_{28}H_{58}$) in the North Sea about 300 km to the north-west of Scotland gave values of 10 to 100 $\mu g\,m^{-3}$ in the sea and 0.1 to 10 $ng\,m^{-3}$ in the atmosphere above. The theory that the sea is the main source of biogenic alkanes in the marine atmosphere is further supported by the observation that the molecular mass distribution pattern of alkanes in the marine atmosphere, with a maximum at C_{15}, is considerably different from that in air above the continents, with a maximum at about C_{22}–C_{24}.[94, 105]

The basic theory of the exchange between air and water phases was derived in 1974 by Liss and Slater, who based their approach on the two-film theory of exchange at a gas/water interface [Eq. (22)], first described in 1923 by W. G. Whitman.[53, 93] The exchange taking place in the boundary layer between the two phases is determined by the sum of the transition barriers in the partial boundary layers of the gas phase and of the water phase. For substances with a small Henry's constant (p_L/S_L, where $p_L \ll S_L$) the exchange is controlled by the gas phase, whereas for substances with a large Henry's constant ($p_L \gg S_L$) it is controlled by the water phase.

Superimposed on the diffusion processes in the two partial boundary layers are the macroscopic motions occurring in the two phases (wind, disturbances of the water surface, currents). In natural waters (lakes and oceans) one must also take into account the surface microlayer (0–50 μm), which contains higher concentrations of organic substances and constitutes an important additional boundary in relation to molecular dimensions. The two-film theory can also be applied to the exchange between the gas phase and the condensed water phase in the atmosphere (clouds and rain). On the other hand, one needs to remember that the component in the water phase that is not present in free solution form does not take part in the diffusional exchange described by the two-film model.

Alongside the molecular exchange between the gas phase and the water phase we must also consider extraction from the water by sea spray and by the formation of droplets from the films around gas bubbles. The annual global uptake of organic substances into the lower troposphere by the latter mechanisms, thus contributing to the overall marine aerosol formation, is 50×10^6 tons, and this remains in the troposphere for periods determined by the lifetimes of the aerosols produced.[20] The types of compounds transported by these mechanisms, which mainly involve the surface microlayer, are those that tend to become concentrated in this layer, including not only those with surface-active properties but also organochlorine compounds that are relatively nonvolatile and sparingly soluble in water.[102]

The equilibrium distribution that exists in practice between the atmosphere and the warm water layer of the oceans (0–200 m) can be described, in analogy with the definition of Henry's constant, by the expression given in Equation (27).

$$H_{\text{environment}} = c_{\text{air}} RT c_{\text{water}}^{-1} \tag{27}$$

The total concentrations present in the atmosphere and in the water can each be divided into a molecular-dispersed fraction and a bound fraction (ϕ_A for air and ϕ_W for water).

$$H_{\text{environment}} = \frac{[c_{\text{air}}(1-\phi_A) + c_{\text{air}}\phi_A]\,RT}{c_{\text{water}}(1-\phi_W) + c_{\text{water}}\phi_W} \tag{28}$$

The molecular-dispersed fractions $(1-\phi)$ should be related to the true Henry's constant [Eq. (29)], whereby $R = 8.134$ [$Pa\,m^3mol^{-1}K^{-1}$] and $RT = 2.385 \times 10^3$ [$Pa\,m^3mol^{-1}$] at 293 K.

$$H_{\text{ideal}} = c_{\text{air}}(1-\phi_A)c_{\text{water}}^{-1}(1-\phi_W)^{-1}RT \tag{29}$$

If we make the reasonable assumption that the bound fraction in the atmosphere is adsorbed on particles, and that $\phi_A < 0.05$, Equation (29) can be simplified and rearranged to give Equation (30):

$$c_{\text{air}} = c_{\text{water}}(1-\phi_W)\,H_{\text{ideal}}(RT)^{-1} \tag{30}$$

or, after rearranging to give the bound fraction in water to Equation (31).

$$\phi_W = 1 - H_{\text{environment}} H_{\text{ideal}}^{-1} \tag{31}$$

Values of $H_{\text{environment}}$ have been estimated from experimental data for PCBs with different degrees of chlorination (Table 18). It should be possible to calculate H_{ideal} as $p_{(L)}/S_{H_2O(L)}$ using data for the supercooled melt. However, values calculated in this way are found to be 10 to 100 times greater than the values for PCBs determined by direct experiment, and any conclusions regarding ϕ_W based on such calculated values would therefore be invalid.[103] If instead the values from direct laboratory measurements[103] are inserted into Equation (30), it is found that the bound fraction ϕ_W in water for the various PCBs (Cl_xB) ranges from 0.5 to 0.9. However, this means that any calculations regarding thermodynamic equilibria must take into account a considerable correction factor for the difference between the measured concentration c_{analyt} and the effective concentration a. In the classical expression $a = fc_{\text{analyt}}$ the correction factor or activity coefficient includes interaction contributions that can only be crudely estimated at present.

In addition to the adsorption from water onto particulate matter (POM), all compounds with low water solubility are

affected to an equally important extent by various types of interaction (association, hydrophobic interactions) with substances loosely described as dissolved organic matter (DOM);[104a, 109, 110] these include humic acids and saffrons, mainly characterized by their UV absorption around 270 nm. Some compounds such as PCBs are found in laboratory measurements to have increased 'solubility' (better described as 'uptake') in water containing dissolved humic acids. This is of no direct importance in practice, even in the oceans, since the concentrations of these substances in the oceans are very low, but on the other hand the component that is bound in this way does not take part in the direct equilibrium between the atmosphere and the ocean, and is instead included in ϕ_w. In attempting to explain the reduction in the concentrations of PCBs at sea level in the atmosphere over the ocean, where there is increased primary production, these interactions need to be taken into account along with the adsorption on the surfaces of particulates. It is not yet possible to estimate the relative contributions of adsorption and association to ϕ_w.

10. Transport in the Hydrosphere

The importance of water as a transport medium and regional repository for xenobiotics has been strikingly demonstrated during the last few decades, through people's direct experience of the contamination of nearly all streams, rivers and coastal waters. Attempts that are being made at gradually restoring the conditions that existed a few decades ago are the first signs of an international concern over cleaning up the global environment.

10.1. Transport Processes in the Inland Hydrosphere of the Continents

In all parts of the world it is often regarded as an important precondition, when choosing an industrial production site, that one should be able to dispose of part or all of the wastes by having them carried away by surface water. Along with the release of wastes into the lower troposphere by wind, rivers are important disposal routes for all industrial civilizations; even if one does not have the benefit of an island location, they provide a direct outlet to the coast. However, the need to be able to use the surface waters in other ways, especially for drinking water, has given a great impetus to worldwide programs for cleaning up effluents and thus keeping rivers free of pollution.

In the northern hemisphere the volume of water returned annually into the oceans by river is 25000 km^3, while the figure for the southern hemisphere is 15000 km^3. Where a river that has an important function as a waste disposal route empties into an inland sea or a partly landlocked sea in which little exchange occurs, the problems caused by the input of pollutants become apparent more quickly than in the oceanic system. Examples of this are seen in the Caspian Sea, the Black Sea together with the Sea of Marmara, the Mediterranean, the Baltic, and even the North Sea, despite the fact that the water in the latter exchanges with the North Atlantic every three years.

The potential for transport of xenobiotics into and by the groundwater on a local or regional scale is less immediately obvious.[13, 15, 89] Depending on the geological conditions, rainwater seeps downward at a rate of 3 to 5 m per year (excluding limestone karst districts). Groundwater currents have velocities ranging from 10^{-4} to 10^{-6} ms^{-1}, giving transport pathways moving at about 4 km per year. Transport in groundwater resembles the slow sand filtration process used to purify drinking water, and thus the transport of xenobiotics is largely determined by their water solubility. Alongside the transport process there is a slow microbiological transformation caused by microorganisms, most of which generate methane. For trichloroethene and tetrachloroethene, two compounds that are often present as groundwater pollutants, the end-product of these transformations is vinyl chloride, which has a notoriously high biological activity.[13]

In inland seas in temperate zones the surface water and the water at greater depths are at nearly equal temperatures in spring and autumn, and therefore have similar densities. This, combined with the winds that are experienced at these times, usually results in a mixing process extending to considerable depths, known as the spring and autumn deep circulation (dimictic lakes or seas).[111] This circulation can extend to depths of 100 m or more. In summer, in lakes of appreciable depth (more than 20 m), a stable vertical temperature distribution becomes established, with the result that mixing can only occur in the top 6 to 10 m. Consequently, the input of substances through rain or dry deposition produces a concentration gradient. In polar and subpolar regions there is only one mixing process, which occurs in the summer (monomictic lakes or seas); for the rest of the year the "winter temperature distribution" prevails, with the water on the lake bed at $+4\,^{\circ}C$. In the tropics some lakes are monomictic while others are polymictic; here, depending on location and depth, a deep circulation process can take place in the winter as a result of the lower temperature of the surface water. However, more far-reaching circulation processes occur through wind action. An interesting example of this is found in the Caspian Sea, which is really a lake; this has a circulation which undergoes seasonal changes of direction according to the prevailing wind.

Such circulations not only regulate the transport of oxygen down to greater depths, but in a similar way other compounds that do not undergo transport on particulates are carried down to deeper regions.

10.2. Transport Processes in the Oceans

On a continental or global scale the surface currents of the oceans (Fig. 11) have transport functions that are second only to the mixing processes in the troposphere with regard to the quantities moved, the distances involved, and the transport velocities (Table 14). Typical average current velocities range from about 0.4 to 1.5 ms^{-1}, with peak values of about 2.0 ms^{-1}. For an average velocity of 0.8 ms^{-1} the distance traveled in a month is about 2000 km. However, the actual linear displacement can be greatly reduced by meanderings. The average rates of flow at great depths are about 0.01 to 0.02 ms^{-1},[112] so that a typical distance traveled in a year would be about 300 km. According to this, water that

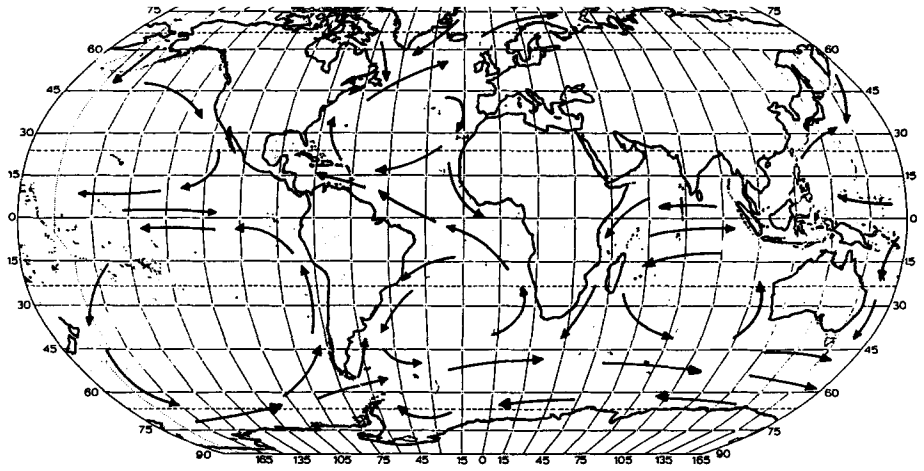

Fig. 11. Currents at the surface of the oceans. The global wind system and the necessities of mass/density balances shape the surface ocean currents. In the Atlantic the Southern equatorial current, which changes over into the Brazil current brings surface water northwards from the southern hemisphere. The surface currents flowing towards the west on the western side of the continent draw cold and nutrient-rich water from deeper layers to the surface. Surface water preferentially sinks at the poles.

sank to great depths in the Antarctic in 1950 should have traveled about 12000 km up to now. During this period deep-sea water should have traveled, in the South Atlantic bottom-water current, the distance of about 9000 km from the Antarctic to the equator.

The surface currents in all the oceans can be approximately represented as several global circulating currents,[24] which together preserve the world balance of mass and energy. In addition there is a further movement in the southern hemisphere, namely the west wind drift that circulates from west to east around the south pole in the Antarctic ocean, and extends to considerable depths. From this Antarctic west wind drift several cold currents branch northwards, on the western sides of South America (the Humboldt current), of South Africa (the Benguela current), and of Australia (the Western Australian current) (Fig. 11). As a result of these movements there is a constant exchange between the surface waters of the oceans. This inter-oceanic exchange at the surface is further reinforced by deep-sea currents that flow in a northerly direction and are also fed by the Antarctic west wind drift, which extends to depths of 4000 to 5000 m (Fig. 12).

A more detailed classification of the surface currents in the oceans reveals branch currents flowing across the equator. The South Equatorial current that flows in a westerly direction in the South Atlantic throws off the Guayana current towards the north, along the coast of the South American continent; this water subsequently flows through the Gulf of Mexico into the Gulf Stream. The upward currents on the western sides of the continents introduce bodies of water that have not previously, or at least not recently, been involved in the transport of xenobiotics.

Where two surface currents meet, their water masses are forced down to greater depths. These 'convergences' form relatively sharp boundaries in the classification of water masses in the world's oceans; in the case of the Antarctic convergence in the South Atlantic there is even a distinct boundary between different types of animals. The descending water masses carry down with them substances that have entered the ocean at the surface.

The descending surface waters at both poles form the oceanic deep currents, which extend well beyond the equator. In the southern hemisphere these ocean-bed currents, which are fed from the west wind drift circulating around the South Pole, flow towards the north (Fig. 12), whereas water from the North Polar Sea flows southwards (Fig. 13), eventually reaching the Indian and Pacific Oceans.[24, 112]

Where surface currents separate (divergences), they draw water upwards from deeper levels. This water is colder and richer in nutrients. There is then an increase in the rate of primary production, which is controlled by the light intensity

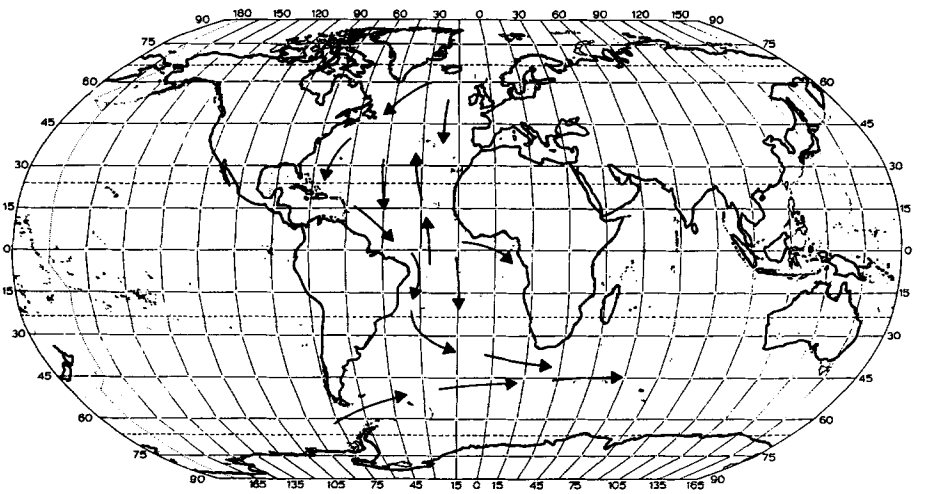

Fig. 12. Flow of Arctic and Antarctic bottom water currents at depths of over 4000 m. The circumpolar Antarctic west-wind drift reaching into the bottom water feeds water masses flowing northward which eventually reach a northerly latitude of 45° North.

and the phosphates content of the water, and corresponding increases occur in the trophic levels that follow.

The system of water layers in the ocean depths must be taken into account in an analysis of the global transport of xenobiotics, even though its effects are on a time-scale measured in decades. For example, it has been found that the distribution pattern of hexachlorocyclohexanes in the water column off Bermuda corresponds to that expected for the water layer in the southern hemisphere from whence it originates.[67, 102]

11. Transport in the Biosphere

The flow of matter in the biophase in the oceanic system, which can be treated to a first approximation as a separate mobile environmental compartment independent of water movements, is often overestimated. The average rate of primary production in the ocean is about 0.01 to 0.03 $kg\,m^{-2}\,year^{-1}$, whereas that on land is typically 50 to 200 times greater. Even in semi-desert regions used for nomadic grazing, a primary production rate of 1 $kg\,m^{-2}$ per year is generally assumed. In its progress down the various levels of the marine food chain, only 10–20% of the biologically generated material is retained at each level.[114]

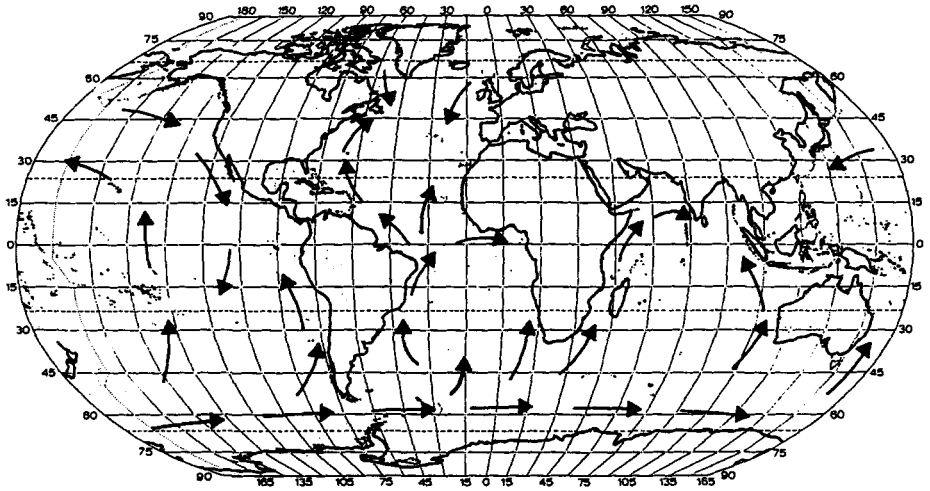

Fig. 13. Scheme of the flow of Arctic deep-water at a depth of ca. 2000 m in the Atlantic ocean. Water of Arctic origin penetrates as far as the southern regions of the Indian Ocean. Flow rates of 10–15 $cm\,s^{-1}$, corresponding to 60–90 $km\,d^{-1}$, are reached.

A model has recently been proposed to describe the delicate balance between the deep ocean currents and the surface currents that are largely determined by wind patterns and alter accordingly.[113] According to this, minor changes in the pattern of air movements caused by small climatic variations in the lower troposphere can have greatly magnified effects on the global oceanic system.

The transport of xenobiotics in the depths of the oceans takes place not only through the downward flows of water that occur mainly in the polar regions, but also by another mechanism, namely the fall-out of organic matter (detritus) in the oceans.[112] Excreted products from animal metabolism, exoskeletons and all kinds of dead organisms, from unicellular blue algae to whales, sink towards the ocean bed. Although many of these constitute food for other organisms, so that many biological cycles constantly interact with each other, the only significance of this for our present purpose is that it delays the transport to greater depths. However, it can also result locally in the accumulation of persistent compounds in trophic levels lower down the food chain.[114] This transport mechanism can be likened to the fall-out of particles from the atmosphere, and the interactions with xenobiotics are rather similar. Compared with transport by water it is quite rapid: the time needed to reach the ocean bed for a typical ocean depth of about 4000 m varies from a few days to several weeks. A rapid input of organic substances can occur when a surface blanket of algae dies and sinks.[114] The actual rate of sedimentation in the oceans, measured by the rate of deposition at the seabed, is about 1–4 mm per thousand years.

The total primary production of phytoplankton in the oceans is about 200×10^9 tons per year, corresponding to $(12-20) \times 10^9$ tons of biologically bound carbon, whereas only about $(10-20) \times 10^9$ tons of zooplankton are produced. These totals are very unevenly distributed in the oceans and there are great variations with time. Only $(0.2-1.5) \times 10^9$ tons per year of the primary production remains by the time we get down to the third and fourth trophic levels (i.e., fish). It is estimated that the maximum annual world fish catch that this can support indefinitely is 0.1×10^9 tons. The present annual fish catch total of 0.07×10^9 tons (Table 22) is already very near to this limit.

From the standpoint of the accumulation of persistent chemicals, the reduction in mass flow by a factor of 10 for each stage to the next trophic level means that there is a corresponding increase in concentration, since little or no

Table 22. Annual world deep-sea fish catches in 10^6 tons fresh weight [29] [a].

Year	Catch [10^6 t]	Year	Catch [10^6 t]
1950–54	24.7	1970–74	67.9
1955–59	32.3	1975–79	72.1
1960–64	46.2	1980–84	75.0
1965–69	59.5	1986	76.0

[a] Breakdown of uses (1982): fresh fish sales 18%, frozen fish 22%, canned fish 13%, dried or salted fish 14%, soaps, fish-meal, pharmaceuticals 33%.

breakdown of these compounds with a release of energy occurs. In certain cases this can result in the accumulation of large burdens of xenobiotics in non-migratory predators (e.g., perch, hawks) that feed on species which migrate large distances (pelagic fish, migratory birds), without the involvement of any other environmental transport mechanisms.

It is evident that transport in the biosphere plays a less important role in the global mass transport of xenobiotics than the flows in the atmosphere and hydrosphere described earlier. Its importance undoubtedly lies in the area of real or potential biological effects of environmental chemicals. The existence of food chains is a fundamental aspect of the biosphere, and the transport of xenobiotics can also have a connection with food chains, depending on the properties of the compounds. In the long term the bioaccumulation or biomagnification of stable (persistent) compounds in food chains must be regarded just as seriously from the environmental standpoint as acute toxic effects.[115] Algae that concentrate stable, strongly lipophilic compounds such as PCBs or the DDT group from the surrounding water pass these on through uptake by zooplankton and by plankton-filtering marine animals or fish. The phenomenon of marine food chains in which whole populations of species undergo a regular daily or nightly migration is another form of transport in and by the biosphere. Since the beginning of evolution deep-sea fauna, through their feeding activities, have been carrying organic compounds from higher to lower levels, and therefore the enormous concentration factors found for stable environmental chemicals in the biophase, e.g. in deep-sea fish (Table 11), are inevitable rather than surprising.[58] Similar effects are also found in marine mammals, which are at the end of the food chain.[115, 116]

The world's fisheries, which have harvested about 75 million tons of fish since 1980, are also a form of transport in the biophase. About 25 million tons of this total consists of 'industrial fish', which is processed rather than consumed directly (Table 22). Populations whose diet includes a high proportion of fish and marine mammals are exposed in a very direct way to the transport of chemicals in the biosphere.

Another transport process which, although it only applies to specific individuals, is nevertheless a basic phenomenon throughout the world and one for which there is no possibility of human intervention, is the partial transfer of persistent lipophilic xenobiotics from the mother to the fetus. This applies not only to humans but to marine mammals such as seals and dolphins.[117] Lipophilic compounds that can be transferred in this way during the gestation period in humans and other mammals include hexachlorobenzene, PCBs with substituents in the 2-, 4- and 5-positions, and the 17 compounds belonging to the 2,3,7,8-substituents of chlorinated dibenzo-*p*-dioxins and dibenzofurans.[50]

Similarly it has been found that persistent chemicals accumulated in the bodies of crustaceans and fish become transfered to their eggs or sperm.

The extent to which these effects can, over long periods, cause irreparable damage at one of the weakest points in the reproduction cycle, thereby threatening the survival of a species, can at present only be a matter for speculation, but the effects certainly cannot be dismissed as being of no significance. In this complex of questions the marine mammals are particularly affected, as nearly all of them are predators at the end of a long food chain. Marine mammals do not have the option of changing their diet or shortening the gestation period, whereas this is not fundamentally ruled out for humans, whether now or in the future.

12. Outlook

During the last 50 years the prediction that many man-made chemicals would reach every corner of the global environment has become a reality. Modern methods of organic trace analysis, used in conjunction with techniques for concentration, separation and detection at the very low concentrations in complex organic mixtures that need to be analyzed, have revealed this situation, but are not the cause of it, as is often naively claimed, even in discussions among chemists.

Bearing in mind the many different mechanisms of global transport that are possible in the atmosphere and in the oceans, it is virtually inevitable that certain compounds, which can be regarded as tracer chemicals in the environment, should be found to be present throughout the world, and should become concentrated in certain parts of the environment as a result of thermodynamic equilibria. This has occurred despite the fact that in many cases their use and distribution in the environment only began as recently as 40 years ago or less, despite limitations on their use in some regions, and despite the fact many of them, unlike pesticides, were not deliberately released into the environment.

It is now becoming apparent that even microbiological breakdown, which, as the converse of biosynthesis, has maintained the carbon cycle since the beginning of evolution, has a limit to its capabilities; otherwise it would not have been possible, within a few decades, for the world's oceans to accumulate easily detectable concentrations of a complex mixture of xenobiotics.

The chemical community has a duty to take note of the presence throughout the world of chemicals that it has produced, either directly or indirectly, and accordingly to reinforce the efforts now being made to develop products that are environmentally friendly in the long term. Biological evolution has avoided the introduction of chemical compounds that are not capable of being broken down again into basic building blocks such as H_2O, CO_2, H_2S, HCl or NH_3. All biosynthetic processes contain within them the mechnisms for biological breakdown of the compounds produced. Should not the chemist learn from nature in this respect? This happened in the past, and must now happen again. The chemist understands, and speaks, the language of molecules. Environmental chemistry is a new chapter in the chemistry of natural products; however, environmental chemistry also requires that we should ask ourselves whether that which is technologically possible and economically successful in a superficial sense can always be justified in a global and long-term context.[118]

Received: March 14, 1991 [A 863 IE]
German version: *Angew. Chem.* **1992**, *104*, 501
Translated by Dr. J. K. Becconsall, Pwllheli (Wales)

[1] H. B. Singh, *Nature* **1976**, *264*, 428–429; B. Dimitriades, B. W. Gay, R. R. Arnts, R. L. Seila, *J. Air Pollut. Control Assoc.* **1983**, *33*, 575–587; S. R. Wilson, P.-J. Crutzen, G. Schuster, D. W. T. Griffith, G. Helag, *Nature* **1988**, *334*, 689–691.

[2] R. G. Prinn in *The Changing Atmosphere* (Eds.: F. S. Rowland, A. S. A. Isaksen), Dahlem Workshop Reports, Wiley, Chichester, **1988**, pp. 33–48.
[3] *Benzol, Stoffbericht No. 24* (Gesellschaft Deutscher Chemiker, Beratergremium für umweltrelevante Altstoffe), VCH, Weinheim, **1988**; *Nichtlimitierte Automobil-Abgaskomponenten,* Projektbericht der Volkswagen AG, Wolfsburg, **1988**.
[4] *PCBs and the Environment, Vol. I; II; III* (Ed.: J. S. Waid), CRC Press, Boca Raton, USA, **1986**; K. Ballschmiter in *Analytiker Taschenbuch, Vol. 7* (Eds.: W. Fresenius, H. Günzler, W. Huber, H. Kelker, I. Lüderwald, G. Tölg, H. Wisser), Springer, Berlin, **1988**, pp. 393–432.
[5] M. Ono, N. Kannan, T. Wakimoto, R. Tatsukawa, *Mar. Pollut. Bull.* **1987**, *18*, 640–643; C. Rappe, L. O. Kjeller, P. Bruckmann, K. H. Hackhe, *Chemosphere* **1988**, *17*, 3–20; B. D. Aitzer, R. A. Hites, *Environ. Sci. Technol.* **1989**, *23*, 1396–1401; R. M. Smith, P. W. O'Keefe, K. M. Aldons, H. Valente, S. P. Connor, R. J. Donnelly, *ibid.* **1990**, *24*, 1502–1506; D. Broman, C. Näf, Y. Zebühr, *ibid.* **1991**, *25*, 1841–1850.
[6] S. Hamm, G. Helas, P. Warneck, *Geophys. Res. Lett.* **1984**, *11*, 1207–1210.
[7] S. A. Penkett in *Atmospheric Chemistry* (Ed.: E. D. Goldberg), Springer, Berlin, **1982**, pp. 329–355; *Interchange of Pollutants between the Atmosphere and the Oceans* (Reports and Studies No. 23, World Meteorological Organization (GESAMP)), Geneva, **1985**; T. J. Class, R. Kohnle, K. Ballschmiter, *Chemosphere* **1986**, *15*, 427–436; *Chloroform, BUA-Stoffbericht 1,* (Gesellschaft Deutscher Chemiker, Beratergremium für umweltrelevante Altstoffe (BUA)), VCH, Weinheim, **1985**; T. J. Class, K. Ballschmiter, *J. Atmos. Chem.* **1988**, *6*, 35–46; *Fresenius Z. Anal. Chem.* **1987**, *327*, 40–41; B. Walter, K. Ballschmiter, *Fresenius J. Anal. Chem.* **1991**, *341*, 564–566; *ibid* **1992**, *342*, in press.
[8] *Fate of Pollutants in the Air and Water Environments, Teil 1, 2* (Ed.: H. J. Suffet), Wiley, New York, **1977**.
[9] W. Brock Nealy, G. E. Blau, *Environmental Exposure from Chemicals, Vol. I, II,* CRC Press, Boca Raton, USA, **1985**.
[10] *Atmosphärische Spurenstoffe und physikalisch-chemisches Verhalten* (Eds.: K. H. Becker, J. Löbel), Springer, Berlin, **1985**.
[11] *The Handbook of Environmental Chemistry The Natural Environment and the Biogeo-chemical Cycles, Vol. 1, Part A–E* (Ed.: O. Hutzinger), Springer, Berlin, **1980–1990**; *Reactions and Processes, Vol. 2, Part A,* Springer, Berlin, **1980**.
[12] *Pollutant Transfer and Transport in the Sea, Vol. I, II* (Ed.: G. Kullenberg), CRC Press, Boca Raton, USA, **1982**.
[13] a) *Halogenorganische Verbindungen (HOV) in Wässern* (HOV-Studie) (Fachgruppe Wasserchemie, Gesellschaft Deutscher Chemiker), **1987**; b) *Vinylchlorid (Chlorethen), BUA-Stoffbericht 35* (Gesellschaft Deutscher Chemiker, Beratergremium für umweltrelevante Altstoffe (BUA)), VCH, Weinheim, **1989**.
[14] *Sources and Fates of Aquatic Pollutants* (Eds.: R. A. Hites, S. J. Eisenreich), Am. Chem. Soc., Washington, **1987**.
[15] *Der Stofftransport im Grundwasser und die Wasserschutzgebietsrichtlinie W 101* (Umweltbundesamt), E. Schmidt, Berlin, **1985**.
[16] A. E. Gill, *Atmosphere-Ocean Dynamics,* Academic, Orlando, **1982**.
[17] H. Reuter, *Die Wissenschaft vom Wetter,* Springer, Berlin, **1978**.
[18] G. H. Liljequist, K. Cehak, *Allgemeine Meteorologie,* 2. Aufl., Vieweg, Braunschweig, **1979**.
[19] E. Heyer, *Witterung und Klima,* Teubner, Leipzig, **1977**.
[20] S. Hastenrath, *Climate and Circulation of the Tropics,* Reidel, Dordrecht, **1985**.
[21] H. G. Gierloft-Emden, *Geographie des Meeres—Ozeane und Küsten, Teil 1,* de Gruyter, Berlin, pp. 603–680.
[22] J. Blüthgen, W. Weischet, *Allgemeine Klimageographie,* de Gruyter, Berlin, **1980**.
[23] L. Hasse, F. Dobson, *Introductory Physics of the Atmosphere and the Oceans,* Riedel, Dordrecht, **1986**.
[24] G. Dietrich, K. Kalle, W. Kraus, G. Siedler, *Allgemeine Meereskunde,* 3rd Edit., Bornträger, Berlin, **1975**.
[25] *Modeling the Fate of Chemicals in the Aquatic Environment* (Eds.: K. L. Dickson, A. W. Maki, J. Cairus, Jr.), Ann Arbor Science, Ann Arbor, **1982**.
[26] *Enviromental Modeling for Priority Setting among Existing Chemicals* (Proceedings, Workshop 11.–13.11.1985; GSF—Projektgruppe Umweltgefährdungspotentiale von Chemikalien), Landsberg, **1985**; Y. Cohen, *Environ. Sci. Technol.* **1986**, *20*, 538–544.
[27] P. Kirschmer, A. Gerlach, *LIS-Ber. 87,* Immissionsmessungen von Chlorkohlenwasserstoffen, Essen **1989**; B. Güthner, T. J. Class, K. Ballschmiter, *Mikrochim. Acta* **1990**, 21–27; H. Frank, W. Frank, H. J. C. Neves, R. Englert, *Fresenius J. Anal. Chem.* **1991**, *340*, 678–683.
[28] A readily accessible and very comprehensive review of world chemicals production is given every year in *Chemical and Engineering News* (American Chemical Society). Production figures for the last ten years are given for specific groups of chemicals and also for some individual compounds, including F11, F12, F22, 1,1,1-trichloroethane and tetrachloroethylene (*Chem. Eng. News,* 24 June 1991, pp. 28–81). For the Federal Republic of Germany the "Stoffberichte" published regularly by the Beratergremium für umweltrelevante Altstoffe (BUA) of the Gesellschaft Deutscher Chemiker include up-to-date figures for production and releases into the environment. These figures can be scaled up with a satisfactory degree of confidence to include production in other countries; however, the figures for environmental releases obtained in this way are likely to be too low, as few countries have more stringent environmental protection regulations than those in Germany. "Stoffberichte" for more than 80 compounds of environmental importance have been published by VCH, Weinheim, and this series of reports is continually being extended.
[29] *United Nations Environment Programme (UNEP): Environmental Data Report,* 2nd Edition, 1989/90 Blackwell, Oxford, **1989**. ISBN 0-631-16987-3. These reports, which are planned to appear at two-yearly intervals, contain a wealth of regional and global data on the situation in the changing environment. Critical discussions of the tabulated data are included.
[30] C. R. Krishnamurti, T. S. S. Dikshith in *Biodegradation of Pesticides* (Eds.: F. Matsumara, C. R. Krishnamurti), Plenum, New York, **1982**, pp. 257–301.
[31] H. Hoerschelmann, K. Polzhofer, K. Figge, K. Ballschmiter, *Environ. Pollut.* **1979**, 247–269.
[32] K. Ballschmiter, M. Zell, *Int. J. Environ. Anal. Chem.* **1980**, *8*, 15–35; M. Zell, K. Ballschmiter, *Fresenius Z. Anal. Chem.* **1980**, *304*, 337–349; K. Ballschmiter, H. Buchert, S. Bihler, M. Zell, *ibid.* **1981**, *306*, 323–339.
[33] E. Bacci, D. Calamari, C. Gaggi, C. Biney, S. Focardi, M. Morosini, *Chemosphere* **1986**, *15*, 747–754; *ibid.* **1988**, *17*, 693–702; S. Paterson, D. Mackay, E. Bacci, D. Calamari, *Environ. Sci. Technol.* **1991**, *25*, 886–871; G. Erikson, S. Jensen, H. Kylin, W. Strachan, *Nature* **1989**, *341*, 42–44.
[34] H. Buchert, S. Bihler, K. Ballschmiter, *Fresenius Z. Anal. Chem.* **1982**, *313*, 1–20; J. M. Czuczwa, R. A. Hites, *Environ. Sci. Technol.* **1986**, *20*, 195–200.
[35] J. C. Colombo, M. F. Khalil, M. Arnac, A. C. Horth, J. A. Catoggio, *Environ. Sci. Technol.* **1990**, *24*, 498–505.
[36] T. J. Leiker, C. E. Rotard, C. R. Barnes, W. E. Pereira, *Chemosphere* **1991**, *23*, 817–830.
[37] K. Ballschmiter, H. Buchert, C. Scholz, M. Zell, *Fresenius Z. Anal. Chem.* **1983**, *316*, 242–246.
[38] T. J. Class, K. Ballschmiter, *Chemosphere* **1986**, *15*, 413–427; *Fresenius Z. Anal. Chem.* **1987**, *327*, 198–204; T. Wiedmann, Diplomarbeit, Ulm, **1989**.
[39] Yu Lu, M. A. K. Khalil, *Chemosphere* **1991**, *23*, 397–444.
[40] V. Patt, *Fresenius J. Anal. Chem.* **1991**, *340*, 633–667; C. C. Felton, I. C. Sheppard, M. J. Campbell, *Environ. Sci. Technol.* **1991**, *24*, 1841–1847.
[41] F. L. Eisele, D. J. Tanner, *J. Geophys. Res.* **1991**, *96*, 9295–9308.
[42] P. J. Crutzen in *Atmospheric Chemistry* (Ed.: E. D. Goldberg), Springer, Berlin, **1982**, pp. 313–328; P. Fabian, *Atmosphäre und Umwelt, Chemische Prozesse, menschliche Eingriffe,* 3rd Edit., Springer, Berlin, **1989**; B. J. Finlayson-Pitts, J. W. Pitts Jr., *Atmospheric Chemistry: Fundamentals and Experimental Techniques,* J. Wiley New York, **1986**, pp. 93–208, 589–644; J. H. Seinfield, *Atmospheric Chemistry and Physics of Air Pollution,* J. Wiley, New York, **1986**, pp. 111–194; R. Prinn, D. Cunnolds, R. Rasmussen, P. Simmonds, F. Alyea, A. Crawford, P. Fraser, R. Rosen, *Science* **1987**, *238*, 945–950; I. S. A. Isaksen in *The Changing Atmosphere* (Eds.: F. S. Rowland, I. S. A. Isaksen), Wiley, New York, **1988**, pp. 141–157; R. I. Cicerone *ibid.*, pp. 49–61; M. A. K. Khalil, R. A. Rasmussen, *Environ. Sci. Technol.* **1990**, *24*, 549–553; *Chemosphere* **1990**, *20*, 227; G. Mégie, *Ozon—Atmosphäre aus dem Gleichgewicht,* Springer, Berlin, **1991**.
[43] H. G. Wagner, R. Zellner, *Angew. Chem.* **1979**, *91*, 707; *Angew. Chem. Int. Ed. Engl.* **1979**, *18*, 663; T. E. Graedel, *Chemical Compounds in the Atmosphere,* Academic, New York, **1978**; T. Mill in *The Handbook of Environmental Chemistry, Reactions and Processes, Vol. 2, Part A* (Ed.: O. Hutzinger), Springer, Berlin, **1980**, pp. 77–105; H. Niki in *Atmospheric Chemistry* (Ed.: E. D. Goldberg), Springer, Berlin, **1982**, pp. 301–312; R. Atkinson, *Chem. Rev.* **1986**, *86*, 69–201; *Environ. Toxicol. Chem.* **1988**, *7*, 435–442; S. Harekeyama, H. Akimoto, N. Washida, *Environ. Sci. Technol.* **1991**, *25*, 1884–1890; D. Grosjean, *ibid.* **1989**, *23*, 1506–1514.
[44] *Umweltbereich Luft* (Fonds der Chemischen Industrie), Verband der Chemischen Industrie, Frankfurt/Main, **1987**.
[45] B. Jansson, R. Vaz, G. Blomquist, S. Jensen, M. Olsson, *Chemosphere* **1979**, *8*, 181; M. Zell, K. Ballschmiter, *Fresenius Z. Anal. Chem.* **1980**, *300*, 387–402.
[46] D. J. Hucknall, *Chemistry of Hydrocarbon Combustion,* Chapman and Hall, London, **1985**, pp. 129–326.
[47] G. Bonse, M. Metzler, *Biotransformationen organischer Fremdsubstanzen,* Thieme, Stuttgart, **1978**; C. M. Menzie in *The Handbook of Environmental Chemistry—Reactions and Processes Vol. 2, Part A* (Ed.: O. Hutzinger), Springer, Berlin, **1980**, pp. 247–302; *Microbial Degradation of Xenobiotics and Recalcitrant Compounds* (Eds.: T. Leisinger, A. M. Look, R. Hutter, J. Nüesch), Academic, London, **1981**. *Microbial Degradation of Organic Compounds* (Ed.: D. T. Gibson), Dekker, New York, **1984**. *Pesticide Transformation Products: Fate and Significance in the Environment* (Eds.: L. Somasundarum, J. R. Coats), Am. Chem. Soc., Washington, **1991**.
[48] K. Ballschmiter, C. Scholz, *Chemosphere* **1980**, *9*, 457–467.

[49] K. Ballschmiter, C. Unglert, H. J. Neu, *Chemosphere* **1977**, *6*, 51–56; K. Furakawa in *Biodegradation and Detoxification of Environmental Pollutants* (Ed.: A. M. Chakrabarty), CRC Press, Boca Raton, USA, **1982**, pp. 33–57; S. Dmochewitz, K. Ballschmiter, *Chemosphere* **1988**, *17*, 111–121.

[50] *Halogenated biphenyls, terphenyls, naphthalines, dibenzodioxins and related products—Topics in environmental health* (Eds.: R. D. Kimbrough, A. A. Jensen), Elsevier, Amsterdam, **1989**.

[51] D. Calamari, University of Milan, private communication, **1991**.

[52] C. C. Travis, J. W. Dennison, A. D. Arms, *Chemosphere* **1987**, *16*, 117–125.

[53] D. Mackay, *Environ. Sci. Technol.* **1979**, *13*, 1218; D. Mackay, S. Paterson, B. Cheung, E. B. Neely, *Chemosphere* **1985**, *14*, 335–374; D. Mackay, S. Paterson, *Environ. Sci. Technol.* **1986**, *20*, 810–816; *ibid.* **1991**, *25*, 427–436.

[54] A. Leo, C. J. Hansch, D. Elkins, *Chem. Rev.* **1971**, *71*, 525; P. J. McCall, D. A. Laskowski, R. L. Swaun, H. I. Dishburger, *Residue Rev.* **1983**, *85*, 231–244; S. J. Eisenreich, G. J. Hollod, R. C. Johnson in *Atmospheric Pollutants in Natural Waters* (Ed.: S. J. Eisenreich), Ann Arbor Science, Ann Arbor, **1981**, pp. 425–444; A. W. Andren, J. W. Strand, *ibid.* **1981**, pp. 459–480.

[55] W. E. Cotham, T. F. Bidleman, *Chemosphere* **1991**, *22*, 165–188.

[56] *Concentrations of industrial organic chemicals measured in the environment: The influence of physico-chemical properties, tonnage and use pattern,* (Technical Report 29, European Chemical Industry Ecology and Toxicology Centre (ECETOC)), Brussels, **1988**.

[57] K. Ballschmiter, *Nachr. Chem. Techn. Lab.* **1979**, *27*, 542–546; *ibid.* **1985**, *33*, 206–208; *Wiss. Fortschr.* **1987**, *637*, 111–113; K. Ballschmiter in [13a], pp. 394–403; K. Ballschmiter, M. Zell, *Int. J. Environ. Anal. Chem.* **1980**, 15–35; M. Zell, K. Ballschmiter, *Fresenius Z. Anal. Chem.* **1980**, *300*, 387–402; *ibid.* **1980**, *304*, 337–349; K. Ballschmiter, H. Buchert, S. Bihler, M. Zell, *ibid.* **1981**, *306*, 323–339; K. Ballschmiter, C. Scholz, H. Buchert, M. Zell, K. Figge, K. Polzhofer, H. Hoerschelmann, *ibid.* **1981**, *309*, 1–7; H. Buchert, S. Bihler, P. Schott, H. P. Röper, H.-J. Pachur, K. Ballschmiter, *Chemosphere* **1981**, *10*, 945–956; H. Buchert, S. Bihler, K. Ballschmiter, *ibid.* **1982**, *313*, 1–20; K. Ballschmiter, H. Buchert, C. Scholz, M. Zell, *Fresenius Z. Anal. Chem.* **1983**, *316*, 242–246; P. Kirschmer, K. Ballschmiter, *Int. J. Environ. Anal. Chem.* **1983**, *14*, 275–284. P. Kirschmer, U. Reuter, K. Ballschmiter, *Chemosphere* **1983**, *12*, 225–230; T. Class, K. Ballschmiter, *Fresenius Z. Anal. Chem.* **1986**, *325*, 1–7; *ibid.* **1987**, *327*, 198–204; R. Wittlinger, K. Ballschmiter, *Chemosphere* **1987**, *16*, 2497–2513; W. Krämer, K. Ballschmiter, *Fresenius Z. Anal. Chem.* **1988**, *330*, 524–526; H. Buchert, T. Class, K. Ballschmiter, *ibid.* **1989**, *333*, 211–217; R. Wittlinger, K. Ballschmiter, *ibid.* **1990**, *336*, 193–200.

[58] W. Krämer, H. Buchert, U. Reuter, M. Biscoito, D. G. Maul, G. Le Grand, K. Ballschmiter, *Chemosphere* **1984**, *13*, 1255-1267.

[59] P. Fabian, D. Gönner, *Fresenius Z. Anal. Chem.* **1984**, *319*, 890–897.

[60] R. H. Gammon, J. Cline, D. Wisegarver, *J. Geophys. Res.* **1982**, *87*, 9441–9454.

[61] R. I. Hunter-Smith, P. W. Balls, P. S. Liss, *Tellus Ser. B* **1983**, *35*, 170–176; T. J. Class, K. Ballschmiter, *Chemosphere* **1986**, *15*, 413–427; *Tetrachlormethan, BUA-Stoffbericht 45,* (Gesellschaft Deutscher Chemiker, Beratergremium für umweltrelevante Altstoffe (BUA)), VCH, Weinheim, **1990**.

[62] T. J. Class, K. Ballschmiter, *J. Atmos. Chem.* **1988**, *6*, 35–46.

[63] H. D. Holland, *The Chemistry of the Atmophere and Oceans,* Wiley, New York, **1978**, pp. 56–80.

[64] *Vorsorge zum Schutz der Erdatmosphäre,* 3rd Edit. (Der Deutsche Bundestag, Enquete Kommission), Economica, Bonn, **1990**; F. S. Rowland, *Environ. Sci. Technol.* **1991**, *25*, 622–628; S. A. Penkett, *ibid.* **1991**, *25*, 631–635; G. Mégie, *Ozon—Atmosphäre aus dem Gleichgewicht,* Springer, Berlin, **1991**.

[65] *Lehrbuch der Ökologischen Chemie,* (Ed.: F. Korte), Thieme, Stuttgart, **1987**, pp. 25–34, 104–140.

[66] R. Wittlinger, K. Ballschmiter, *Fresenius J. Anal. Chem.* **1990**, *336*, 193–200; K. Ballschmiter, R. Wittlinger, *Environ. Sci. Technol.* **1991**, *25*, 1103–1111.

[67] R. Fischer, W. Krämer, K. Ballschmiter, *Chemosphere* **1991**, *23*, 889–900.

[68] J. Schreitmüller, K. Ballschmiter, unpublished results, DFG-Projekt Ba 371/11-2.

[69] C. E. Junge in *Fate of Pollutants in the Air and Water Environments, Part I* (Ed.: I. H. Suffet), Wiley, New York, **1977**, pp. 7–26; G. Czeplak, C. E. Junge, *Adv. Geophys.* **1974**, 18, 57–72.

[70] J. E. Baker, S. J. Eisenreich, B. J. Eadie, *Environ. Sci. Technol.* **1991**, *25*, 500–509.

[71] C. E. Junge, *J. Geophys. Res.* **1972**, *77*, 5183–5200; R. A. Duce, E. K. Durrsma, *Mar. Chem.* **1977**, *5*, 319–339; A. H. Woodcock, *J. Meteorol.* **1953**, *10*, 362–371.

[72] T. F. Bidleman, *Environ. Sci. Technol.* **1988**, *22*, 361–367.

[73] C. Lenenberger, J. Czuczwa, E. Heyerdahl, W. Giger, *Atmos. Environ.* **1988**, *22*, 695–705.

[74] W. Voldner, H. Schroeder, *Atmos. Environ.* **1989**, *23*, 1949–1961.

[75] J. C. Duinker, F. Bouchertall, *Environ. Sci. Technol.* **1989**, *23*, 57–62.

[76] S. Brunauer, P. H. Emmett, E. Teller, *J. Am. Chem. Soc.* **1938**, *60*, 309–319.

[77] R. Fischer, Dissertation, Universität Ulm, **1990**; J. Schreitmüller, Diplomarbeit, Universität Ulm, **1990**.

[78] K. T. Whitby, *Atmos. Environ.* **1978**, *12*, 135–159.

[79] J. F. Pankow, *Atmos. Environ.* **1987**, *21*, 2275–2283.

[80] C. E. Junge, *J. Geophys. Res.* **1972**, *77*, 5183–5200; J. M. Prospereo, *ibid.* **1979**, *84*, 725–731; E. J. Hoffman, R. A. Duce, *ibid.* **1974**, *79*, 4474–4477; E. Lipiatou, J. O. Grimalt, M. Colom-Altes, R. Simo, J. Albaiges, *J. Polycycl. Aromat. Comp.* **1992**, in press.

[81] I. J. Shak, *J. Air Pollut. Control Assoc.* **1986**, *36*, 254–257; B. C. Gälli, P. R. Bürkli, W. P. Nyffeler, P. W. Schindler, *Int. J. Environ. Anal. Chem.* **1989**, *35*, 111–118.

[82] F. Möller, *Einführung in die Meteorologie – Physik der Atmosphäre,* BI—Hochschultaschenbücher, Bibliographisches Institut, Mannheim, **1973**, pp. 211–217; H. Reuter, *Die Wissenschaft vom Wetter,* Springer, Berlin, **1978**, p. 53–67, p. 109; H. R. Pruppacher in *Chemistry of Multiphase Atmospheric Systems* (Ed.: W. Jaeschke), Springer, Berlin, **1986**, pp. 133–190.

[83] R. Wittlinger, K. Ballschmiter, *Chemosphere* **1987**, *16*, 2497–2513.

[84] K. Ballschmiter, C. Scholz, H. Buchert, M. Zell, K. Figge, K. Polzhofer, H. Hoerschelmann, *Fresenius Z. Anal. Chem.* **1981**, *309*, 1–7.

[85] M. Ewing, E. Thomdike, *Science* **1965**, *147*, 1291–1294; M. B. Jacobs, M. Ewing, *ibid.* **1969**, *163*, 380–386; D. C. Gordon, *Deep Sea Res.* **1971**, *18*, 1127–1134.

[86] S. Tanabe, R. Tatsukawa, *J. Oceanogr. Soc. Jpn.* **1983**, *39*, 55–62; R. Tatsukawa, S. Tanabe in *PCB's in the Environment, Vol. I* (Ed.: J. S. Waid), CRC Press, Boca Baton, USA, **1986**, pp. 143–161.

[87] A. H. Knap, *Nature* **1986**, *319*, 572–574.

[88] K. A. Burns, J. P. Villeneuve, *Mar. Chem.* **1987**, *20*, 337–359.

[89] R. P. Schwarzenbach, J. Westall, *Environ. Sci. Technol.* **1981**, *15*, 1360–1367; R. P. Schwarzenbach, W. Giger, E. Höhn, J. K. Schneider, *ibid.* **1983**, *17*, 472–479; D. M. Di Toro L. M. Horzempa, *ibid.* **1982**, *16*, 595–602.

[90] K. Kawamoto, K. Urano, *Chemosphere* **1989**, *19*, 1223–1231; H. Kishi, N. Kogure, Y. Hashimoto, ibid. **1990**, *21*, 867–876.

[91] G. Szabo, S. L. Prosser, R. A. Buckman, *Chemosphere* **1990**, *21*, 495–505.

[92] T. Shimazaki, *Minor constituents in the middle atmosphere,* Terra Science/Reidel, Tokio/Dordrecht, **1985**.

[93] W. G. Whitman, *Chem. Metall. Eng.* **1923**, *29*, 146; P. S. Liss, P. G. Slater, *Nature* **1974**, *247*, 181–184; D. Mackay, P. J. Leinonen, *Environ. Sci. Technol.* **1975**, *9*, 1178–1180.

[94] G. Ketseridis, J. Hahn, R. Jaenicke, C. E. Junge, *Atmos. Environ.* **1976**, *10*, 603–610; G. Ketseridis, R. Eichmann, *Pure Appl. Geophys.* **1978**, *116*, 274–282; E. J. Ledat, I. L. Laseter, *Science* **1974**, *186*, 261–263; R. Eichmann, P. Neuling, G. Ketseridis, J. Han. R. Haenicke, C. E. Junge, *Atmos. Environ.* **1979**, *13*, 587–599; *ibid.* **1980**, *14*, 695–703.

[95] J. Albaigés, J. M. Bayona, P. Fernandez, J. Grimault, A. Rosell, R. Simó, *Mikrochim. Acta* **1991**, 13–27.

[96] S. O. Baek, M. E. Goldstone, P. U. W. Kirk, J. N. Lester, P. Perry, *Chemosphere* **1991**, *22*, 503–520.

[97] E. D. Goldberg, *Black Carbon in the Environment—Properties and Distribution,* Wiley, New York, **1985**.

[98] J. B. Manchester-Neesweg, A. W. Andren, *Environ. Sci Technol.* **1989**, *23*, 1138–1148.

[99] H. Walter, S. W. Breckle, *Ökologie der Erde, Vols. 2, 3,* Fischer, Stuttgart, **1984**.

[100] W. Rotard, W. Christmann, W. Knoth, *Dioxin 91, 11h Int. Symp. on Chlorinated Dioxins and Rel. Comp.,* September 23–27 **1991**, Poster, Research Triangel Park, NC, USA.

[101] G. R. Harvey, W. G. Steinhauer, *J. Mar. Res.* **1976**, *34*, 561–575; *Atmos. Environ.* **1974**, *8*, 777–782

[102] W. Krämer, K. Ballschmiter, *Fresenius Z. Anal. Chem.* **1988**, *330*, 524–526.

[103] S. Brunner, E. Hornung, H. Sauth, E. Wolff, O. G. Piringer, I. Altschuh, R. Brüggemann, *Environ. Sci. Technol.* **1990**, *24*, 1751–1754.

[104] D. Broman, C. Näf, C. Rolff, Y. Zebühr, *Environ. Sci. Technol.* **1991**, *25*, 1850–1864.

[105] *The atmospheric input of trace species to the world oceans* (Report and Studies No. 38, GESAMP, World Meteorological Organization (WMO)), Geneva, **1989**.

[106] D. E. Wells, S. J. Johnstone, *Water Air Soil Pollut.* **1978**, *9*, 271–280; E. Atlas, C. S. Giam, *ibid.* **1988**, *38*, 19–36; C. Neuenberger, J. Czuczwa, E. Heyerdahl, W. Giger, *Atmos. Environ.* **1988**, *22*, 695–705; W. Rsad, Y. Cohen, H. Sakugawa, I. R. Kaplan, *Environ. Sci. Technol.* **1991**, *25*, 2012–2023.

[107] K. Levsen, S. Behnert, H. D. Winkeler, *Fresenius J. Anal. chem.* **1991**, *340*, 665–671; K. Levsen, S. Behnert, B. Priess, M. Svoboda, H. D. Winkeler, I. Zietlow, *Chemosphere* **1990**, *21*, 1027–1061; G. Brooks Avery, J. D. Willey, C. A. Wilson, *Environ. Sci. Technol.* **1991**, *25*, 1875–1880.

[108] J. Hahn in *Atmosphärischer Spurenstoffe* (Ed.: R. Jaenicke), Deutsche Forschungsgemeinschaft, VCH, Weinheim, **1987**, pp. 121–144; B. R. T.

Simoneit, J. N. Cardoso, N. Robinson, *Chemosphere* **1990**, *21*, 1285–1301.

[109] Y. P. Chin, W. J. Weber, *Environ. Sci. Technol.* **1989**, *23*, 978–984; R. Lara, W. Ernst, *Chemosphere* **1989**, *19*, 1655–1664; A. Sabljic, R. Lara, W. Ernst, *ibid.* **1989**, *19*, 1665–1676; J. F. Pankow, S. W. McKenzie, *Environ. Sci. Technol* **1991**, *25*, 2046–2053.

[110] J. F. McCarthy, L. E. Robertson, L. W. Burns, *Chemosphere* **1989**, *19*, 1911–1920.

[111] J. Schwoerbel, *Einführung in die Limnologie*, Fischer, Stuttgart, **1977**.

[112] H. Stommel, A. B. Arons, *Deep Sea Res.* **1960**, *6*, 217; I. L. Reid, R. J. Lynn, *ibid.* **1971**, *18*, 1063–1088.

[113] T. F. Stocker, D. G. Wright, *Nature* **1991**, *351*, 729–730.

[114] R. V. Tait, *Meeresökologie*, Thieme, Stuttgart, **1971**; K. J. Kötting, E. F. Kilian, R. Schnetter, *Einführung in die Meeresbiologie, Vols. 1, 2*, Vieweg, Braunschweig, **1982**; P. Müller, *Biogeographie*, Ulmer, Stuttgart, **1980**; V. Smetacek, *Spektrum Wiss.* **1991**, No. 12, 58–63.

[115] S. Tanabe, T. Mori, R. Tatsukawa, *Chemosphere* **1983**, *12*, 1269–1275; *Bioakkumulation in Nahrungsketten* (Deutsche Forschungsgemeinschaft), VCH, Weinheim, **1987**; *Polychlorierte Biphenyle: Bestandsaufnahme über Analytik, Vorkommen, Kinetik und Toxikologie* (Deutsche Forschungsgemeinschaft), VCH, Weinheim, **1988**; D. W. Connell, *Bioaccumulation of Xenobiotic Compounds*, CRC Press, Boca Raton, USA, **1990**.

[116] D. W. Kuehl, B. C. Butterworth, J. Cibal, P. Marguis, *Chemosphere* **1991**, *22*, 849–858; Kuehl D. W., R. Haebler, C. Potter, *Chemosphere* **1991**, *22*, 1071–1084.

[117] R. F. Addison, S. R. Kerr, J. Dall, *J. Fish. Res. Board Can.* **1973**, *30*, 595–60; R. F. Addison, P. F. Brodie, *ibid.* **1977**, *34*, 937–942; S. Tanabe, R. Tatsukawa, K. Maruyama, N. Miyazaki, *Agri. Biol. Chem.* **1982**, *46*, 1249–1254; A. Schecter, O. Päpke, M. Ball, *Chemosphere* **1990**, *21*, 1017–1022; S. Mößner, T. R. Spraker, P. R. Becker, K. Ballschmiter, *ibid.* **1992**, in press.

[118] W. Jost, *Globale Umweltprobleme*, Steinkopf, Darmstadt, **1974**; *Chemiepolitik, Gespräch über eine Kontroverse* (Ed.: M. Held), VCH, Weinheim, **1988**; *Menschheit und Erde (Spektrum Wiss.*, Sonderheft 9, **1990**).

Reaction Dynamics of Aligned Molecules

By Franz Josef Comes

Dedicated to Professor Heinz Harnisch on the occasion of his 65th birthday

Photofragmentation—also termed 'half collision'—is a method to comprehend the complicated process of a chemical reaction (the 'full collision') better. The use of polarized light enabled the study of the spectroscopy of aligned molecules, yielding information about the photochemically produced intermediate state—the transition state. Even though stable reaction products were studied, the forces responsible for the motions of the fragments can be visualized. In this way a model can be constructed that represents the part of the potential hypersurface responsible for the observed motions. The application of this spectroscopic method to hydrogen peroxide H_2O_2 has become a classic example. The complex decomposition of hydrazoic acid, HN_3, represented a challenge, and its successful solution proves the general applicability of this method.

1. Introduction

The goal of reaction dynamics is to derive the mechanism of a chemical reaction from the microscopic properties of its atomic constituents. The summation of microscopic processes yields the macroscopically observed overall reaction. Until now, the situation was usually reversed: the observed reaction was used to deduce possible microscopic steps. The macroscopic reaction rate, however, is a parameter averaged over all microscopic reactant and product states of the involved particles and, hence, does not yield a direct insight into the microscopic events. While macroscopic rate laws yield very useful facts about the quantitative course of the reaction, they provide only limited information on important intra- and intermolecular motions that describe the course of the reaction on the microscopic level.

In order to deduce which forces disrupt some bonds and create others during the course of a reaction, it is necessary to extract information about the potential energy surface from experimental results. The desired forces are then simply the derivatives of this potential energy. This goal could in principle be reached with the help of quantum mechanics. It is well known, however, that real systems are suitable for exact quantum mechanical treatments only in rare cases.

To describe the course of a chemical reaction that is initiated by the collision of two reactants and ends (for simplicity's sake) in two products, the involved particles must be characterized not only by their energies, but also by their various momentums. When E_N^i and $\vec{p}_N$ represent the internal energy and the linear momentum, respectively, of particle N, this reaction is described by Scheme 1.

The goal of reaction dynamics, namely to understand the interactions between the particles involved in the reaction,

$A(E_A^i, \vec{p}_A) + BC(E_{BC}^i, \vec{p}_{BC})$	reactants
$\rightarrow (ABC)^*(E_{ABC}^i, \vec{p}_{ABC})$	transition state
$\rightarrow AB(E_{AB}^i, \vec{p}_{AB}) + C(E_C^i, \vec{p}_C)$	products

Scheme 1. Two reactants with specific internal energies and linear momenta react to form two products.

[*] Prof. Dr. F. J. Comes
Institut für Physikalische und Theoretische Chemie der Universität
Niederurseler Hang, W-6000 Frankfurt am Main 50

can be achieved by suitable preparation of the reactants. The use of molecular-beam and laser techniques has provided important advances for experimental studies of reaction dynamics. In the simplest case of a molecular-beam experiment, A particles in a beam are directed onto BC particles, which could also be within a beam. The scattering of the products AB and C as a result of the reaction is then observed. In these single collision experiments the particles are usually provided with a well-defined collision energy (translational energy). This makes it possible to study the scattering as a function of collision energy and impact direction ($\vec{p}$ is fixed).

Laser irradiation excites particles into specific states, thereby fixing their internal energy, E^i. In particular, it can be used to transform the molecule ABC directly, without a preceding collision, into an activated state $(ABC)^*$, which dissociates to form products AB + C. In this way a unimolecular reaction can be initiated through the conversion of internal energy. The decomposition of the activated molecule can also occur before any redistribution of internal energy in the complex $(ABC)^*$. In this process, also termed 'half collision', the fragmentation of $(ABC)^*$ into AB + C is of interest. It can be measured by observing the distribution of the internal energy with respect to angle, velocity, and state. The quantum state distribution of E^i can be measured with suitable methods such as chemiluminescence in the infrared or visible light range, laser-induced fluorescence (LIF), or resonance-enhanced multiphoton ionization (REMPI). The velocity distribution of the products can be measured with Doppler spectroscopy.

These state-selective chemical processes yield a detailed description of the chemical reaction and provide information about the events during the transformation of reactants to products. The investigation can either focus on the transient particle $(ABC)^*$ itself, for example, with real-time measurements in the pico- or even femtosecond range, or on the stable final products.[1] In the latter case, variables integrated over the entire course of the reaction are observed.

The method of Doppler and polarization spectroscopy belongs to the class of experiments that yield information from stable reaction products.[2] Nevertheless, from the vector properties of the fragments a detailed picture of the course of the reaction can be obtained.[3] These results there-

fore complement those from reactive scattering. The velocity or the angular momentum of the fragments yields information on the form of the potential surface near the transition state from which the translational or rotational energy arises. It is a fascinating idea to use these vector properties to determine the forces that cause them.

Doppler and polarization spectroscopy utilizes the ability to obtain spatially aligned molecules through the use of plane-polarized light.[3] The spatial asymmetry that occurs during the fragmentation of aligned molecules makes it possible, in conjunction with a narrow band laser, to perform a type of subdoppler spectroscopy that differs from its usual form with statistically distributed molecules. Both the width *and* the shape of the Doppler-broadened line become sources of information. From the vectorial properties of the fragments, for example, their velocity or angular momentum, conclusions can be drawn about the dynamics of the process. To do this, these quantities that are defined in the molecular frame are related to variables that caused the primary alignment in the external (laboratory) reference frame. The resulting vector correlations contain the information on dynamics in the form of details about the forces that led to the observed distribution of the vector quantities. Specifically, information can be deduced about the symmetry and lifetime of the transition state, as well as the shape of the potential surface, expressed in molecular coordinates relevant to the fragmentation.

Theory can contribute considerably to the understanding of the observed phenomena. Quantum mechanical calculations yield the shape of the multidimensional potential energy surface responsible for the nuclear motions during the reaction. Theory can also forecast the nuclear dynamics under selected initial conditions for the motions. Thus a direct comparison between experimental observations and theoretical predictions becomes possible. In addition, the detailed data furnished by modern spectroscopic techniques provide the opportunity to test theoretical approaches.

The following sections explain the spectroscopic method for obtaining the information described above. The method is illustrated by discussing the fragmentation reaction of hydrogen peroxide (H_2O_2), which has proven to be the classic example for the procedure. This molecule has a number of favorable properties for the application of the method and hence is the best studied molecule in this context. The knowledge gained from this investigation is then used to study another molecule, hydrazoic acid (HN_3). The fragmentation in this case is a complex process. Ab initio calculations of the potential surfaces show that these results are in full agreement with quantum mechanical predictions.

2. Doppler and Polarization Spectroscopy: the H_2O_2 Molecule as an Example

2.1. Background

The ability of molecules to absorb electromagnetic radiation is described by the absorption cross section σ. From energy considerations, the radiation required for fragmentation is, in general, UV light. The electric dipole approximation uses the transition moment $\vec{\mu}$ to describe the absorption-induced transition from initial to final states. $\vec{\mu}$ is a vector quantity and refers to molecular coordinates.

Light is characterized as an electromagnetic wave by the electric field vector $\vec{E}$. If this vector oscillates only in one plane, the light is called linearly or plane polarized. To maximize absorption at a given wavelength, $\vec{E}$ (defined by the polarization of the light in the laboratory frame) and $\vec{\mu}$ (defined in the molecular frame) must be parallel, since σ is defined according to (1) by the scalar product of $\vec{E}$ and $\vec{\mu}$. In the other extreme, when $\vec{E}$ and $\vec{\mu}$ are perpendicular the absorption cross section vanishes.

$$\sigma(\lambda) \approx (\vec{E}\vec{\mu})^2 \qquad (1)$$

The absorption of light correlates the two coordinate systems so that after absorption the excited molecules are a subgroup of aligned particles situated in an environment of statistically oriented, that is, disordered, particles. If the light was polarized in the z direction, the transition dipole moments point preferentially in the z direction. The distribution has a $\cos^2(\theta)$ dependence (1), with $\theta = \sphericalangle(\vec{E} = \vec{z}, \vec{\mu})$. The spatial intensity distribution has the same shape as the p_z orbital known from quantum mechanics.

The use of plane-polarized light makes it therefore possible to observe decomposition processes in which the excited and subsequently decomposing molecules have a certain alignment relative to the polarization direction of the excita-

Franz Josef Comes, born in 1928, obtained his Diplom in Physics in Mainz, and his doctorate at the Max-Planck-Institut für Chemie (Otto-Hahn-Institut) in Mainz working with Paneth on the study of meteorites by mass spectrometry. After this excursion into geophysics and cosmochemistry, he worked on the problems of molecular spectroscopy and reaction kinetics at the University of Bonn with Groth where he obtained his habilitation in 1964 and became Professor in 1969. In 1970 he was awarded the Fritz-Haber Prize of the Deutsche Bunsengesellschaft for fundamental work on photodissociation, photoionization, and molecular and photoelectron spectroscopy. After a guest professorship at the University of Southern California, Los Angeles, followed by a period as guest in the synchrotron group of Desy in Hamburg, he accepted the chair of Physical Chemistry at Frankfurt University in 1972. His interests include the application of lasers in chemistry, in particular in studies on reaction dynamics. Other fields of research are atmospheric chemistry and applications of the photovoltaic effect, in particular for the development of solar cells from amorphous silicon and germanium.

tion radiation and, hence, relative to a given spatial direction. This alignment of excited molecules does not stem from an application of an orienting force, but rather from the fact that only those molecules with $\vec{\mu}$ accidentally aligned parallel to the polarization direction are excited with maximum probability and induced to dissociate. The fragments to be observed stem exclusively from aligned reactant molecules. As the alignment of the molecules is correlated with their symmetry, the fragments' flight paths will, in general, display a spatial asymmetry caused by repulsive forces during the dissociation.

During photolysis, the fragments gain energy from the decomposition process. This energy is distributed among the degrees of freedom. The distribution is specific for each decomposition process. It is the goal of dynamics studies to analyze just this distribution. The different forms of energy of the products, for example, the kinetic energy E_{kin}, or the rotational energy E_{rot} (both scalar quantities), are related to vector quantities such as the velocity $\vec{v}$ or the angular momentum $\vec{J}$ of the fragments. To determine these variables, the analysis must leave the system undisturbed, that is, it must proceed without collisions, during the entire time interval from the beginning of molecular fragmentation to the identification of products. Only those spectroscopic observables are required that are associated with the *nascent* products of the fragmentation.

One method which fulfills these criteria for observing nascent species is based on fast spectroscopy with a time resolution in the nanosecond regime. This temporal resolution is sufficient, as the experiments are performed under reduced pressures, usually a few millitorr. Under these conditions the interval between two collisions falls in the microsecond time scale.

One possible experimental arrangement is to use a photolysis flash a few nanoseconds in duration to excite the reactant molecules. After a delay of at least the duration of one flash, a second flash, the probe flash, is employed to detect the products. This kind of experiment is called a pump-and-probe experiment and will be discussed in detail in Section 3.

An important initial piece of data for the application of Doppler and polarization spectroscopy is the energy content of the products, expressed by scalar quantities. For the photolysis of H_2O_2 with UV radiation [Eq. (2)] the two OH

$$H_2O_2 + h\nu \longrightarrow OH + OH \qquad (2)$$

product molecules exhibit an energy distribution that is very favorable for Doppler spectroscopy, since the energy is primarily translational in nature. According to Equation (3) the

$$E_{exc} = E_{h\nu} + E^i(H_2O_2) - E_{diss} \qquad (3)$$

absorbed light energy $E_{h\nu}$ together with the thermal energy $E^i(H_2O_2)$ from the experimental temperature T is shared between the two products after subtraction of the dissociation energy, E_{diss}. When the photolysis wavelength λ is 266 nm, about 90% of E_{exc} is kinetic energy and 10% is rotational energy. There is no measurable vibrational energy.[4] At this photolysis energy, the two OH product molecules acquire a velocity of about 3700 ms^{-1}, which is significantly faster than that of thermal particles. Therefore the OH fragments are, for all practical purposes, monoenergetic with respect to their velocity, which leads to extraordinarily sharp Doppler profiles.

2.2. Spatial Anisotropy; the $\langle\vec{\mu}\vec{v}\rangle$ Correlation

The simplest example of a fragmentation is the decomposition of a molecule AB into the fragments A and B, for which the transition dipole moment $\vec{\mu}$ is assumed to be perpendicular to the A–B axis, along which the dissociation will proceed. All molecules with their dissociation axes in a plane orthogonal to the direction of $\vec{\mu}$ have then the same probability for excitation.

Figure 1 shows two possible cases. Due to cylindrical symmetry, all directions in this plane are equivalent. If the fragments are to be observed by optical means (e.g. laser-induced fluorescence), the Doppler effect caused by the fragment velocity is the same for all directions in the plane. If, however, the observer is looking at the fragments down the direction of $\vec{\mu}$, perpendicular to the plane, no Doppler effect (i.e., no line broadening) will be registered. In this special case the velocity of the escaping fragments has no component in the direction of the observation. From the spatial asymmetry in the Doppler effect of the dissociation products, the linear momentum $\vec{p}$ of the fragments can be determined.

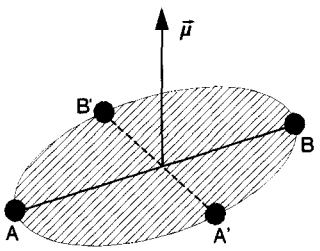

Fig. 1. After excitation of A–B by plane-polarized light, the transition dipole moments of the majority of excited molecules are aligned. All other orientations of the molecular axis (e.g. A'–B') in the plane perpendicular to $\vec{\mu}$ are equivalent and lead to the same alignment.

In reality, not only molecules with their transition moments $\vec{\mu}$ aligned with the electric field vector $\vec{E}$ are excited, but also those with a transition dipole moment at an angle to $\vec{E}$, that is, those that do have a finite component in the direction of $\vec{E}$. For an oblique position of $\vec{\mu}$ with respect to $\vec{E}$, the excitation probability simply follows a $\cos^2$ function [Eq. (1)]. Hence, molecules aligned parallel to $\vec{E}$ represent the largest contribution to the total excitation and, therefore, to the total fragmentation as well.

The H_2O_2 molecule in its electronic ground state exhibits only C_2 symmetry, which contains only the presentations A and B. The electronic singlet states can only be ^1A or ^1B. As the ground state is ^1A, the transitions $^1A \leftarrow {}^1A$ and $^1B \leftarrow {}^1A$ must be considered. For the first case, the corresponding transition dipole moment $\vec{\mu}$ must lie along the C_2 axis for symmetry reasons. It is therefore perpendicular to the O–O bond axis, as shown in Figure 2. Doppler spectroscopy (see later in this section) reveals that the first excited state of H_2O_2 is an ^1A state.[5, 6] At higher excitation energies, both ^1A and ^1B excited states are observed.[7] For the excitation

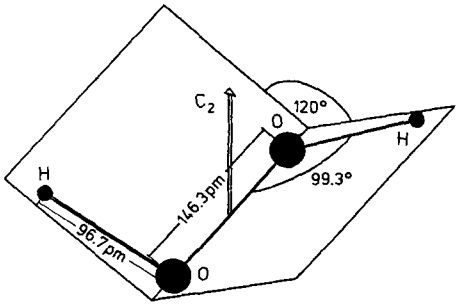

Fig. 2. Equilibrium configuration of H_2O_2, indicating the position of the C_2 axis. $\vec{\mu}$ is parallel to C_2 for the $^1A \leftarrow {}^1A$ transition.

to a ^1B state, $\vec{\mu}$ must lie, again for symmetry reasons, in a plane perpendicular to the C_2 axis, which therefore must contain the O–O bond axis. In addition, quantum mechanical calculations have shown that for excitation to the lowest lying ^1B state, the corresponding $\vec{\mu}$ is directed nearly exactly along the O–O axis.[8]

On irradiation with light of wavelength 266 nm, excitation of H_2O_2 leads solely to the ^1A state.[4, 5] When the polarization is in the z direction, the oxygen atoms of excited species will lie predominantly in the xy plane, due to the position of $\vec{\mu}$ perpendicular to the O–O bond [Eq. (1)]. If the excited molecule dissociates without a time delay, the two fragments will be expelled with the same high velocity $\vec{v}$ along the dissociation direction (the O–O axis). All directions in the xy plane are equivalent due to the cylindrical symmetry of the system.

If, as in Figure 3a and b, the fragments are observed by the probe laser along the x direction, OH fragments that

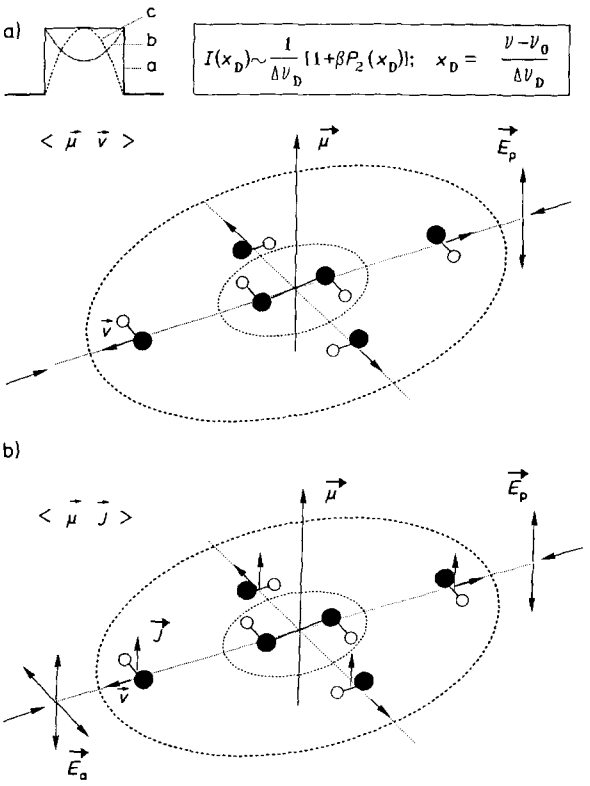

Fig. 3. Pictorial views of the vector correlations: a) $\langle \vec{\mu}\vec{v} \rangle$ correlation, b) $\langle \vec{\mu}\vec{J} \rangle$ correlation.

move directly towards or away from the detector in the x direction cause a maximum Doppler shift. Particles moving perpendicular to this direction (i.e., along the y or z axes) show no Doppler effect at all, because only the velocity component along the observation direction is Doppler active. There are no fragments with $\vec{v}$ along the z direction, a consequence of the spatial anisotropy in the distribution of the fragment velocities $\vec{v}$, which, in turn, results directly from the primary alignment of the reactant molecules.

For randomly (isotropically) aligned reactant molecules, the Doppler effect causes a rectangular pulse (Fig. 3a, curve a), if an infinite resolution (i.e., infinitesimal laser band width) and a monochromatic fragment velocity are assumed.

In the present example (the excitation to the ^1A state of H_2O_2 by z polarized light) no fragments with velocity vectors along the z direction will be formed. Such particles would not cause an observable Doppler effect along the x direction. As compared to the isotropic case, this leads to a lack of particles that show no Doppler effect. Therefore, the rectangular profile will experience a decrease in intensity at the center of the line, which is seen as a dip at the center (curve b in Figure 3a).

If the observation direction were along the z axis, profile c would result. Most of the fragments move in the xy plane and exhibit no Doppler effect along the z direction. From an experiment under the above conditions that results in profiles b and c one can conclude that, in the case of H_2O_2, the excited state has ^1A symmetry. The asymmetry of the velocity distribution determined from the Doppler effect yields information about the molecular symmetry of the excited state. The form of the velocity profiles is given by the equation shown in Figure 3a, where β represents the asymmetry parameter which contains the actual physical information. P_2 is the second Legendre polynomial for $\cos\theta$. In the isotropic case, $\theta = 0$. For the present example of H_2O_2, $\beta = -1$. For the excitation only to the lowest lying ^1B state ($\vec{\mu}$ aligned along the O–O axis) profiles b and c would be observed for the opposite detector orientations.

This example illustrates the correlation of $\vec{\mu}$ of the reactant molecule with the velocity vector $\vec{v}$ of its fragments (the $\langle \vec{\mu}\vec{v} \rangle$ correlation).

The discussion so far has shown Doppler profiles for given sets of conditions. The photolysis of H_2O_2 at 266 nm will now be used to illustrate actual experimental results (Fig. 4). An analysis of the profiles yields an asymmetry parameter of $\beta = -0.71$, rather different from -1,[5] which causes prediction and experimental results to differ. There are two conceivable reasons for this deviation. On one hand, the excitation at 266 nm may not exclusively yield the ^1A excited state, but a mixture of ^1A and ^1B states, thereby lowering the observed asymmetry. This would agree with the tendency of β to be as close to zero as possible, but can be excluded because measurements with different wavelengths, for example, 308 and 248 nm, yield the same results. On the other hand, the assumption of immediate dissociation of the excited molecule may not be justified.

In reality, a molecule requires a certain amount of time for fragmentation. During this interval, the molecule will, for instance, continue to rotate due to its thermal energy, leading to a rotation of the molecular coordinate system with respect to the laboratory frame. This rotation, in turn, causes

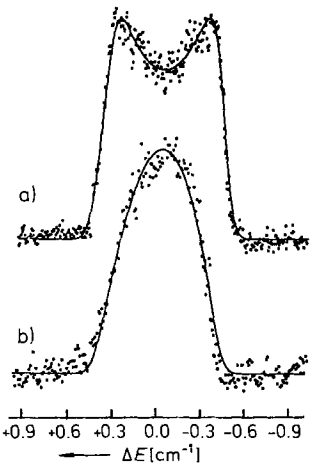

Fig. 4. Spectra of the $Q_1(4)$ transition (see also Section 2.3) of OH [5] for an arrangement of lasers where a) excitation and probe lasers are coaxial and polarized in parallel directions, b) pump and probe lasers are perpendicular to each other and polarization directions are as in a). A value of -0.71 is obtained for the asymmetry parameter β.

a lowering of the profile asymmetry, due to the change in the original alignment of the molecules. The observed value of β therefore decreases.

As has been shown by Bush and Wilson,[9] the average lifetime τ of the excited molecule can be calculated from the experimental value of β and the angular velocity of the reactant molecule. This velocity can be deduced from the rotational constants and the temperature of the molecules. From the experimentally determined β for H_2O_2 an average lifetime of $\tau = 60$ fs is obtained. As this is in the order of the period of one molecular vibration, we conclude that the H_2O_2 molecule decomposes along the fastest possible pathway after excitation. The potential surface of the excited state along the dissociation coordinate must therefore be purely repulsive. The application of Doppler spectroscopy yields, for the first time, information about the potential surface for the excited state that leads to fragmentation. One of the major goals of Doppler and polarization spectroscopy is to determine the shape of this potential surface; its gradients, in the proper coordinates, then describe the forces that cause the motion of the molecular fragments.

2.3. Rotational Asymmetry; $\langle \vec{\mu}\vec{J} \rangle$ Correlation

The fragmentation of H_2O_2 forms two diatomic OH molecules. In this section we are interested in the rotation of these fragments. The angular momentum $\vec{J}$ of diatomic molecules is perpendicular to the internuclear axis. For detection, the OH fragments are excited to the $^1\Sigma_g^+$ state. The J selection rules allow R, P, and Q transitions. For R and P transitions ($\Delta J = \pm 1$), the corresponding transition moment $\vec{\mu}_F$ of the OH fragment is perpendicular to $\vec{J}$. For Q transitions ($\Delta J = 0$), $\vec{\mu}_F$ is parallel to $\vec{J}$. If the output of the probe laser ($\vec{E}_p$) is also plane polarized, the alignment of the fragments relative to a given reference frame can be measured. For Q transitions, $\vec{\mu}_F$ parallel to $\vec{E}_p$ implies maximum excitation probability and means that $\vec{J}$ is parallel to $\vec{E}_p$ as well ($\vec{J} \parallel \vec{E}_p$). For R and P transitions, $\vec{\mu}_F$ is parallel to $\vec{E}_p$ when $\vec{J}$ is perpendicular to $\vec{E}_p$ ($\vec{J} \perp \vec{E}_p$).

At any given observation and polarization direction for the probe laser, the intensity ratios of bands stemming from R (or P) and Q transitions reflect the alignment of the angular momentum vector in space. One obtains a further vector correlation between the alignment of the reactant molecule, due to its transition dipole moment $\vec{\mu}$, and the fragment's angular momentum $\vec{J}$. This is generally referred to as alignment.

Figure 3b shows an expanded picture of the H_2O_2 fragmentation; the rotation of the fragments is now included. The present example is simplified as all $\vec{J}$ vectors are perpendicular to the xy plane. This, however, is irrelevant for the illustration of the $\langle \vec{\mu}\vec{J} \rangle$ correlation.

Both the $\langle \vec{\mu}\vec{J} \rangle$ and the $\langle \vec{\mu}\vec{v} \rangle$ vector correlations contain one piece of data each from the laboratory frame (the spatial alignment of $\vec{\mu}$ is determined by $\vec{E}$ of the excitation radiation) and the molecular coordinate system ($\vec{v}$ and $\vec{J}$ are determined by the molecular geometry).

2.4. The $\langle \vec{v}\vec{J} \rangle$ Correlation

The finite lifetime of the fragmenting molecules perturbs their original alignment in space. Therefore the $\langle \vec{\mu}\vec{v} \rangle$ and $\langle \vec{\mu}\vec{J} \rangle$ vector correlations are progressively lost with increasing lifetimes. However, the information on the dynamics of the molecular fragmentation is still present. If the fragment rotation is caused by a particular intramolecular motion, for instance, a bending oscillation, the velocity $\vec{v}$ and the angular momentum $\vec{J}$ of the fragments will always be preferentially perpendicular to each other (see later in this section). It is therefore necessary to eliminate the effects of the excited species' rotation before the fragmentation on the resulting observation, in order to recognize the correlation of $\vec{v}$ and $\vec{J}$ clearly. If $\vec{v}$ and $\vec{J}$ are correlated to $\vec{\mu}$, they must also be correlated to each other. However, this correlation, contrary to those discussed so far, is no longer connected to the laboratory frame, because both $\vec{v}$ and $\vec{J}$ are only associated with fragment motions. It is therefore necessary to find a transformation that identifies the correlation of $\vec{v}$ and $\vec{J}$. A formalism for this transformation has been developed by R. N. Dixon.[10] The $\langle \vec{v}\vec{J} \rangle$ correlation provides information that is independent of the lifetime of the excited reactant molecule, but contains the sought after results even if the molecule fragments, for example by predissociation, after a lifetime that is comparatively long for a dissociation process. For the case of fragmenting glyoxal (ethanedial), P. Houston et al. showed by analysis of CO fragments that the $\langle \vec{v}\vec{J} \rangle$ correlation is retained even after an excited-state lifetime of 1 μs (several thousand molecular vibrational periods), if the molecule was initially aligned.[11]

The $\langle \vec{v}\vec{J} \rangle$ correlation thus enables the elimination of effects of rotations of the parent molecule, even though these rotations cause a loss of the original molecule alignment. Even for molecules which decompose after a long lifetime, the full decay dynamics can be obtained by analyzing the $\langle \vec{v}\vec{J} \rangle$ correlation.

What kind of information does the $\langle \vec{v}\vec{J} \rangle$ correlation yield? Consider the decomposition of a planar molecule. If the fragmentation occurs from a motion within the molecular plane (Fig. 5a), the velocity vectors will also lie in this plane.

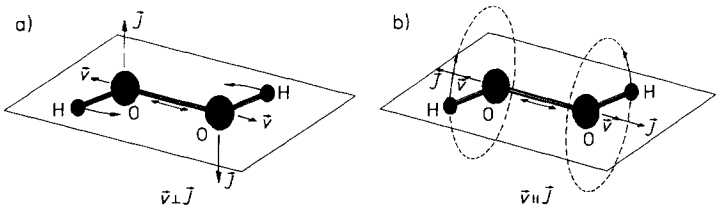

Fig. 5. Dependence of the orientation of $\vec{v}$ and $\vec{J}$ for H_2O_2 on the active mode of fragmentation. a) $\vec{v} \perp \vec{J}$; the active mode is a bending motion. b) $\vec{v} \parallel \vec{J}$; the active mode is a torsional motion.

A bending vibration in the plane causes a fragment rotation with an angular momentum vector perpendicular to the plane, leading to a perpendicular correlation between $\vec{v}$ and $\vec{J}$. More generally, any fragmentation stemming from a planar motion of the molecule yields a perpendicular correlation of $\vec{v}$ and $\vec{J}$. The value of the bipolar moment β_{vJ} described below is $-1/2$. If, however, the fragment rotation is caused by a torsional motion (Fig. 5b), $\vec{J}$ is parallel to $\vec{v}$ ($\beta_{vJ} = +1$).

Dixon has shown that the asymmetry parameter β can be expressed as the sum of bipolar moments $\beta_{\mu v}$, $\beta_{\mu J}$, β_{vJ}, and $\beta_{\mu vJ}$, which describe the correlation of the indicated fragment properties [Eq. (4)].[10]

$$\beta = \left[\frac{b_2\beta_{\mu v} + b_3\beta_{vJ} + b_4\beta_{\mu vJ}}{b_0 + b_1\beta_{\mu J}}\right] \quad (4)$$

Dixon also determined the numerical values of b_0 to b_4 for the various experimental geometries. This is done by observing R, P, and Q bands in different geometries.

The photolysis of H_2O_2 shows that the bipolar moments β_{vJ} are positive for the above described rotational states of the OH fragments. For an excitation wavelength of 193 nm, which was used for extensive experimental studies[12] as well as for dynamics calculations,[13] the value of β_{vJ} is close to $+1$, indicating that $\vec{v}$ and $\vec{J}$ of the fragments are nearly parallel. The intramolecular motion that causes the fragmentation is thus a torsional motion of the molecule.

This interesting result can have two origins. Torsional vibration, the lowest energy vibration of H_2O_2, is excited even at room temperature in the electronic ground state. It is possible that the fragment motions are caused by this torsional excitation. The more interesting case, however, is present when the observed OH torsion is a result of the shape of the excited state's potential surface. When the reactant molecules are strongly cooled, they lose internal energy. If the measured correlation still remains unchanged, the excited state must have caused the observed effect.

Experimentally, this is done by cooling the molecules in a molecular beam by adiabatic expansion to close to absolute zero. No significant change in the correlation was detected indicating that the source of the fragment torsion is to be found in the shape of the potential surface of the excited state.[7, 14]

2.5. The $\langle \vec{J}_A \vec{J}_B \rangle$ Correlation; Simultaneous Excitation of Several States

Doppler and polarization spectroscopy is potentially able to resolve further details of the molecular decay. For this to be feasible, the spectral resolution of the detector needs to be increased. For the experiments described so far, it was sufficient to resolve the absorption bands enough to determine the asymmetry parameter β. However, when viewed in detail, these bands are found to be composites of a number of bands. Further spectral resolution yields therefore added information about the fragmentation process.

The decomposition of a species containing four atoms into two diatomic products (e.g. $H_2O_2 \rightarrow OH(A) + OH(B)$) can lead to different values for the $\langle \vec{v}\vec{J} \rangle$ correlation. If $\beta_{vJ} = 1$, a torsional motion of the parent molecule is the driving force for fragmentation. The identical daughter fragments, OH(A) and OH(B), will have identical rotational energies, but opposite directions of rotation. This pair formation leads to another vector correlation, the $\langle \vec{J}_A \vec{J}_B \rangle$ correlation. OH(A) and OH(B) are formed in pairs, where $\vec{J}_A = -\vec{J}_B$. The ratio of the absolute values of $\vec{J}_A$ and $\vec{J}_B$ will be 1:1. Any deviation of the $\langle \vec{J}_A \vec{J}_B \rangle$ correlation from this ratio can be interpreted as a sign of additional motions within a plane of the parent molecule.

Thus a problem arises: how can one observe the two OH fragments which are created simultaneously from a single parent molecule? Experiments show that each molecule in the photolysis of H_2O_2 yields two OH fragments, but the rotational states of the fragments are differently populated. For a specific excitation energy, the parent molecule is apparently capable of reacting along different decay paths. According to Figure 6, the distribution of rotational states has a maximum at a particular rotational quantum number.

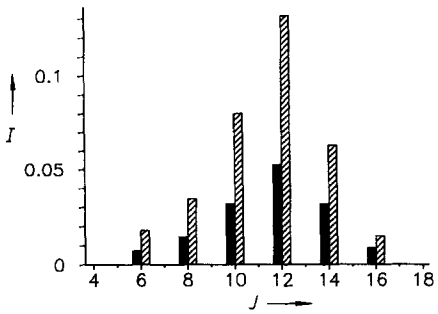

Fig. 6. Distribution of rotational states for the OH products after simultaneous excitation (193 nm) of cooled H_2O_2 into the $\tilde{A}\,^1A$ (▨) and $\tilde{B}\,^1B$ (■) states. For clarity, only data for even quantum numbers (J) are shown. I = population of the rotational level in arbitrary units.

However, it is in principle possible that OH fragments in lower rotational states are preferentially paired with those in higher states, which would depend only on the specific dynamics of the decomposition.

The different aspects of this method will be demonstrated on a simple example, for which three possible decomposition channels are assumed (Scheme 2).

$$H_2O_2 + h\nu \longrightarrow H_2O_2^*$$

$$H_2O_2^* \longrightarrow OH^{(A)}(J_i) + \begin{Bmatrix} OH^{(B)}(J_{i-1}) + \Delta E_{kin}(i, i-1) \\ OH^{(B)}(J_i) + \Delta E_{kin}(i, i) \\ OH^{(B)}(J_{i+1}) + \Delta E_{kin}(i, i+1) \end{Bmatrix}$$

Scheme 2. Decomposition channels for H_2O_2 as reason for the distribution of rotational states over the OH fragments.

Since in the decomposition of H_2O_2 the fragments have no vibrational energy, only rotational energy specified by its quantum number J, and kinetic energy, signified by ΔE_{kin}, are present. Each of the three paths exhibits a different combination of rotating fragments, differing in their kinetic energy according to the principle of conservation of energy. If we observe OH fragments in the J_i state, the processes of Scheme 2 contribute to the Doppler width of the measured rotation band. The corresponding kinetic energies are $\Delta E_{kin}(i,i-1)$, $\Delta E_{kin}(i,i)$, and $\Delta E_{kin}(i,i+1)$. The expected Doppler band is therefore in fact composed of three bands of different width, in accordance with the different amounts of kinetic energy that are released during the fragmentation (Fig. 7). The heights of the individual bands are proportional

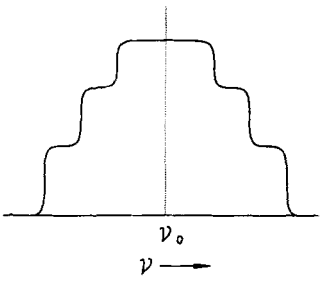

Fig. 7. Coincident pair formation. Schematic representation of a Doppler band for a case with three decay channels (see Scheme 2).

to the relative contribution of the corresponding decay channel. Hence, the desired information can be obtained from the wings of the band profiles. The spectral resolution of the analysis laser must be considerably increased to be able to reveal this information. High-resolution spectroscopy, that is, the analysis of the wings of a Doppler-broadened rotation band, makes it possible to examine simultaneously formed product pairs and to determine the so-called pair formation probabilities. This is exactly the $\langle \vec{J}\vec{J} \rangle$ correlation. This correlation expresses the probability of finding the counterpart of a fragment in the J_i state in the states J_{i+1}, J_i, and J_{i-1}.

2.6. Vector Correlations for the Simultaneous Excitation of Several Dissociation Continua

Both the ^1A and the ^1B states of H_2O_2 are excited simultaneously with light of wavelength 193 nm, because it contains sufficient energy, in contrast to a wavelength of 266 nm (Section 2.2). As described above, the transition dipole moment $\vec{\mu}$ of the lowest lying ^1A state lies along the C_2 axis, which is perpendicular to the O–O bond. Ab initio calculations for the ^1B state showed that the corresponding $\vec{\mu}$ lies nearly along the O–O axis. Therefore, if the excitation to the ^1A state causes a band shape similar to curve b in Figure 3a, the excitation to the ^1B state must lead to the complementary band shape, curve c, in Figure 3a (and vice versa). This is simply because those parent molecules excited to the ^1A state are preferentially aligned along an axis perpendicular to the O–O bond. For molecules excited to the ^1B state, the preferred alignment is in the perpendicular direction, along the O–O axis. When both states are excited simultaneously, the two band shapes overlap. For infinite detector resolution, the profile is square for approximately equal excitation probabilities for both states. The measured asymmetry parameter β_{obs} is composed of the weighted contributions of the two simultaneously initiated fragmentation processes [Eq. (5)].

$$\beta_{obs} = a\beta_A + (1-a)\beta_B \quad (5)$$

The variable a is wavelength dependent and indicates the fraction of the total excitation that is attributable to the ^1A state. The contribution of the ^1B state is $(1-a)$.

The analysis of vector correlations from a continuous absorption spectrum (a dissociation continuum) makes it possible to solve complicated problems such as the simultaneous participation of several excited states quantitatively.

From the vector correlations the contribution of each of the simultaneously excited states to the rotational excitation of the formed fragments can be calculated. In fact, the states ^1A and ^1B contribute about 65% and 35%, respectively, to the total absorption. The distribution of rotational states is nearly identical (Fig. 6).[6] The latter finding is in exact agreement with the decay dynamics computations performed by Staemmler et al. with ab initio techniques based on potential surfaces of the molecule in both excited states.[13, 15] These potential surfaces clearly show two things: the excited states are purely repulsive in nature (also found by using the $\langle \vec{\mu}\vec{v} \rangle$ correlation) and they are strongly repulsive with respect to the torsion coordinate (predicted by the $\langle \vec{v}\vec{J} \rangle$ correlation). The H_2O_2 molecule in its ^1A excited state exhibits a strong tendency to convert to the *trans*-planar conformation, whereas in the ^1B state the opposite motion towards the *cis*-planar conformation prevails. In both cases a torsional motion is excited. As the gradients of both potential surfaces are nearly equal in absolute value, the distributions of rotational states are also expected to be equal, as was shown experimentally (Fig. 6).

These specific details of the fragmentation reaction can be illustrated more clearly by choosing the isotopically substituted molecule D_2O_2 as example. In addition, the study of D_2O_2 can also serve to test these methods if the results are compared with predictions based on the experiments described above. Replacing the H atoms with heavier deuterium atoms moves the fragment's center of gravity closer to the deuterium position. Forces that repulse the two fragments therefore have more leverage, and a higher fraction of the total energy is expected to be in the form of rotational energy. This enhanced motion, which will manifest itself as planar motion, will shift the values for the $\langle \vec{v}\vec{J} \rangle$ correlation towards the negative as planar motions lead to negative correlations. The $\langle \vec{\mu}\vec{v} \rangle$ correlation will be even more negative than before.

The results of this experiment indicate an increase in the rotational energy of the OD fragments by 30% compared to OH. Both correlations were found to behave exactly as predicted: both $\langle \vec{v}\vec{J} \rangle$ and $\langle \vec{\mu}\vec{v} \rangle$ become slightly more negative.[16] This good agreement of experimental findings with theoretical predictions is an excellent proof for the power of this spectroscopic method.

3. Experimental Considerations

In Section 2, conditions for the successful application of Doppler and polarization spectroscopy were outlined. One

of these conditions was the absence of collisions involving the spectroscopically studied molecules. As also mentioned, a possible solution is to perform pump-and-probe experiments at reduced pressures while employing a temporal resolution in the nanosecond regime. This means that both pump and probe lasers must operate in the pulsed mode. To observe the spatial anisotropy of the fragment velocities, the Doppler profiles must be obtained in both coaxial and perpendicular beam directions. For the observation of the $\langle \vec{\mu}\vec{J} \rangle$ correlation is it necessary to polarize the two laser beams in mutually perpendicular directions. For the photolysis laser, it is sufficient to have available a number of fixed frequencies, so that the excitation of either a single absorption continuum or the simultaneous excitation of several continua is possible. The analysis laser must possess a narrow bandwidth and must be tunable in the UV range, so that different molecules can be studied. The last condition necessitates frequency doubling of the radiation.

In our experiments the probe laser is used according to the principles of laser-induced fluorescence. The molecule to be observed is excited by resonance absorption, and the resulting total fluorescence is measured without any prior spectral resolution. The spectrum obtained is called a fluorescence-excitation spectrum. This method is state-selective, which is absolutely necessary, and very sensitive, but usually requires a time delay of several pulse lengths between photolysis and probe pulses to reduce the effect of stray radiation caused by the stronger photolysis laser.

Figure 8 shows schematically a possible experimental setup that complies with the requirements described above.[17] The photolysis and probe beams pass through the sample chamber perpendicular to each other; the parallel arrangement of the probe laser is indicated by dashed lines. The observation direction along which the fluorescence is measured is perpendicular to both laser beams.

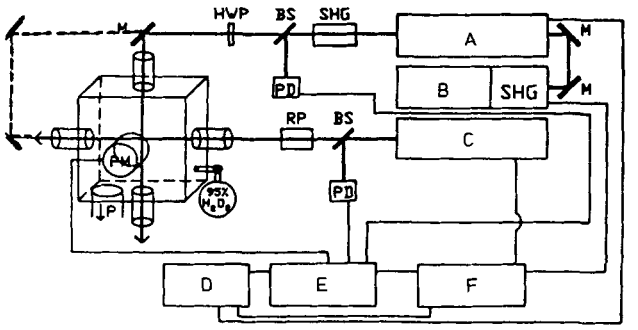

Fig. 8. Diagram of the apparatus for Doppler and polarization spectroscopy. M: mirror, BS: beam splitter, SHG: second harmonic generator (frequency doubler), PD: photodiode, RP: polarizer, PM: photomultiplier, P: pump, A: dye laser, B: Nd-YAG laser, C: ArF laser, D: computer, E: boxcar integrator, F: trigger.

The molecules to be studied are prepared either under quasi-static conditions or in a molecular beam. Quasi-static in this context means that the gas is under reduced pressure, but is kept flowing slowly, so that no secondary products can accumulate during the analysis. The molecular-beam experiment is performed in the form of an ultrasonic expansion to cause adiabatic cooling in order to permit the observation of particles at temperatures close to 0 K. These conditions yield molecules in their lowest energy states, thereby making it possible to neglect their internal energy in the analysis.

The $\langle \vec{J}\vec{J} \rangle$ correlation experiment requires a further increase in the spectral resolution. A diagram of the apparatus is not shown to conserve space, but it should be mentioned that a laser with high spectral resolution is necessary; for our H_2O_2 experiment, a continuous laser was employed. The output of this laser must be converted into intense light pulses, which is achieved by using a dye laser amplifier.[18] As follows from Equation (6), the pulse width Δt of this dye

$$\Delta\nu\Delta t \approx 1 \qquad (6)$$

laser must be chosen small enough to make the necessary frequency resolution possible (in the case of OH detection, $\Delta\nu \leq 100$ MHz). In order to convert this frequency resolution into the desired spectral resolution, the reactant molecules for the H_2O_2 experiment must be cooled by adiabatic expansion in the molecular beam.

4. Results of High-Resolution Doppler Spectroscopy: The Impact Parameter

Because of conservation of energy, the excess energy available to the fragments, E_{exc}, can be deduced from the photolysis energy, if the energy necessary for dissociation is taken into account [see Eq. (3)]. On application of the law of conservation of momentum, the internal energy of the fragments can be calculated. The conservation of angular momentum makes it possible to determine the impact parameter that affects the repulsion of the formed fragment pair. To apply this last principle the angular momentums involved must be analyzed in detail. The $\langle \vec{J}_A \vec{J}_B \rangle$ correlation is an important source of information, since its value indicates the distribution of angular momentum among simultaneously formed fragments. For H_2O_2 decomposition, the $\langle \vec{J}_A \vec{J}_B \rangle$ correlation indicates to what extent the fragments' rotational energy stems from a torsional motion of the parent H_2O_2 molecule. Particularly important, the fraction of the fragment's rotation due to other motions of the parent molecule can be deduced. This fraction should be directly related to the deviation of the $\langle \vec{J}_A \vec{J}_B \rangle$ correlation from a 1:1 ratio. The deviation, in turn, is dependent on the contribution of the orbital angular momentum to the total angular momentum of the fragments, from which the desired impact parameter can be calculated. If its value is vanishingly small, the repulsion of the two fragments can be treated like a central collision of the centers of gravity of the two fragments. Hence, the impact parameter yields information about the deviation of the collision from a central one.

The photolysis of H_2O_2 yields two chemically identical OH radicals as products. As discussed earlier, there are no fundamental reasons that prevent those two particles from being formed in different rotational quantum states. If the initial states of the two simultaneously formed species are completely uncorrelated, the probability of pair formation is the *product* of the formation probabilities of each separate species [Eq. (7)]. If the initial states are completely correlated, as would be the case had they been formed exclusively

from a torsional motion of the parent molecule, Equation (8) will hold. The determination of the probability matrix $P(J_A J_B)$ will yield information about possible correlations.

$$P(J_A J_B) = P(J_A)P(J_B) \tag{7}$$

$$P(J_A J_B) = \delta(J_A J_B)P(J_A)$$
$$\text{where } \delta(J_A J_B) = \begin{cases} 1 \text{ for } J_A = J_B \\ 0 \text{ for } J_A \neq J_B \end{cases} \tag{8}$$

Figure 9 shows the matrix elements as a function of J_A and J_B.[18] In general, the matrix elements on the diagonal are the largest. Therefore, the maximum probability process is the formation of fragments with equal rotational energy. However, the observed distribution of P shows a width at half height of about three rotational states.

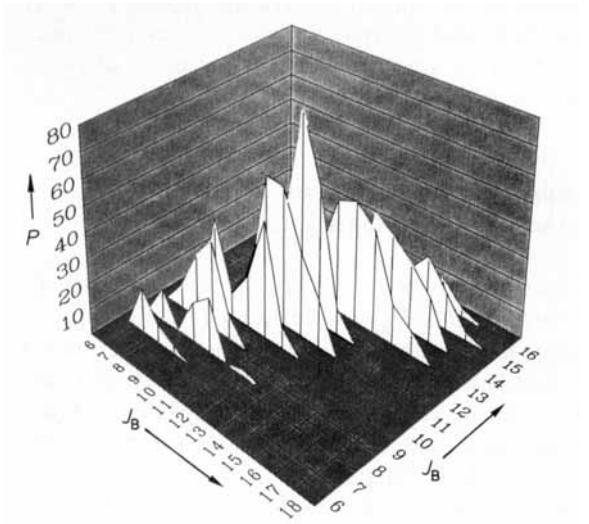

Fig. 9. Pair formation probability $P(J_A J_B)$ for the photofragmentation of H_2O_2 at 193 nm.

The primary result that can be gleaned from Figure 9 is that the 1:1 correlation of J_A and J_B could also be caused by a bending motion of the parent molecule. However, this would lead to a negative $\langle \vec{v}\vec{J} \rangle$ correlation. A strongly positive $\langle \vec{v}\vec{J} \rangle$ correlation is found instead, which must be due to a torsional motion. Therefore it is expected that $\vec{J}_A = -\vec{J}_B$. Deviations from this relationship are caused by additional bending motions of the rotamers. Studies at an excitation wavelength of 193 nm showed that the torsional contribution to the total rotation is 70%.[19]

As discussed earlier, the rotational motion of the fragments is governed by the law of conservation of angular momentum, which applies to the entire system. If the molecular beam contains cooled reactant molecules, their angular momentum will be close to zero. Therefore, if the angular momentum of the absorbed photon is ignored, the total angular momentum is composed of the angular momentums of the product molecules, $\vec{J}_A$ and $\vec{J}_B$, and any orbital angular momentum $\vec{L}_{AB}$. The law of conservation of angular momentum takes the form shown in Equation (9), and the limits of possible values for $\vec{L}_{AB}$ are given by Equation (10). The orbital angular momentum L_{AB} can be expressed as Equation (11) where μ represents the reduced mass of the system, v_{AB} represents the relative velocity, which can be determined accurately, and b is the impact parameter. The impact parameter acts as the lever that causes L_{AB}.

$$\vec{J}_A + \vec{J}_B + \vec{L}_{AB} = 0 \tag{9}$$

$$J_A + J_B \geq L_{AB} \geq |J_A - J_B| \tag{10}$$

$$L_{AB} = \mu b \, v_{AB} \tag{11}$$

According to the vector correlations, J_A and J_B are essentially oriented in an antiparallel manner. Therefore, the value of L is given by the difference ΔJ of J_A and J_B, yielding Equation (12) for b, where $\Delta\nu_D$ represents the Doppler line width and ν_0 the resonance frequency.

$$b = \frac{\Delta J \, \nu_0}{\Delta\nu_D \, c \, m_{OH}} \tag{12}$$

When the value of ΔJ found from Figure 9 is inserted, the impact parameter b is found to be (1.0 ± 0.3) pm.[18] This calculated impact parameter is smaller than the distance between the center of gravity of the OH group and the oxygen atom, which implies that the repulsive force does not act directly along the O–O bond, but rather along a line joining the two centers of gravity of the OH fragment pair. Therefore the simple picture of an oxygen–oxygen repulsion does not describe the dissociation of H_2O_2 in sufficient detail.

5. The Fragmentation of HN_3—a Complex Case

The study of the H_2O_2 decomposition by Doppler and polarization spectroscopy yielded a nearly complete characterization of this fragmentation. It indicated which forces are active during the dissociation and led to the observed energy distribution in the products. The fragmentation was shown to be a direct process, which occurs on a purely repulsive potential surface with a duration of only 60 fs. Now, as for all experimental methods, a question arises regarding general applicability, especially to more complex problems. The study of hydrazoic acid, HN_3, was chosen as example. The following discussion shows that its fragmentation could be studied in as much detail as that of H_2O_2.

HN_3 is a molecule containing four atoms, which absorbs UV radiation to decompose into two diatomic fragments. The first absorption continuum, which has its maximum absorption at 265 nm, yields the fragmentation reaction (13).[20, 21]

$$HN_3(^1A') + h\nu \longrightarrow HN_3(^1A'') \longrightarrow NH(a^1\Delta) + N_2(^1\Sigma_g^+) \tag{13}$$

The products of this reaction are NH, in a metastable excited electronic state, and N_2, in its electronic ground state. At first glance this molecule provides more favorable conditions for the study of the fragmentation reaction than H_2O_2: two different products are formed, which can be observed separately by spectroscopy. However, the potential surface proved to be significantly more complicated. In the following discussion, only the decay channel leading to the $v'' = 0$ vibrational state of $NH(^1\Delta)$ will be considered. The excited vibrational states that are also formed during the fragmentation will not be taken into account.[22]

At a photolysis wavelength of 193 nm, a second decay path yields hydrogen atoms, $H(^2S)$. These were identified by LIF employing the Ly_α radiation[17] of a frequency-tripled dye laser.[23] The other fragment is most probably the triatomic N_3, as expressed in Equation (14). N_3 was indeed observed. However, because this species could also be a product of (15), the mechanism of (14) has not yet been

$$HN_3 + h\nu \longrightarrow H(^2S) + N_3(\tilde{X}^2\Pi) \quad (14)$$

$$NH(^1\Delta) + HN_3 \longrightarrow NH_2 + N_3 \quad (15)$$

proved even though the experimental data indicate that N_3 is a primary product of the photolysis.[24] Since the decay channel described by (14) has not yet been examined with Doppler and polarization spectroscopy, this aspect of the fragmentation of HN_3 will not be discussed further.

The first important step of the analysis concerns the distribution of energy. From an argument analogous to that which led to Equation (3), an expression for the excess energy can be deduced [Eq. (16), where μ is the reduced mass of

$$E_{exc} = \langle E_{rot}(NH)\rangle + \langle E^i(N_2)\rangle + \tfrac{1}{2} m_{NH}^2 \langle v_{NH}\rangle^2/\mu \quad (16)$$

the system and $\langle v_{NH}\rangle$ the average velocity of the NH fragment]. This equation contains only the average rotational energy of the NH species, $\langle E_{rot}(NH)\rangle$, because in the present treatment there is *no* excitation of NH vibration.

All energy measurements, as well as the vector correlations discussed below, are performed exclusively on the NH fragment, which is identified by LIF through the measurement of the NH fluorescence stemming from the $c^1\Pi \rightarrow a^1\Delta$ transition produced by radiation from the probe laser. N_2 is more difficult to observe spectroscopically. Equation (17) is derived from Equation (16) to calculate the average internal energy of the N_2 fragment.

$$\langle E^i(N_2)\rangle = E_{exc} - \langle E_{rot}(NH)\rangle - \tfrac{1}{2} m_{NH}^2 \langle v_{NH}\rangle^2/\mu \quad (17)$$

From the beginning the distribution of this energy among the rotational and vibrational degrees of freedom is not determined. Of the excess energy, 51% is found as kinetic energy of the fragments; hence the contribution of the internal energy to the total is 49%. This internal energy is distributed in an extremely dissimilar way between the two fragments—the N_2 molecule receives 94% of it. Only 6% is present as rotational energy of the NH fragment. By using the laws of conservation of energy and momentum, the velocities of the two products are calculated to be 3320 ms^{-1} for NH and 1770 ms^{-1} for N_2.[22] The high NH velocity is the most significant result. High-resolution experiments, as used for the study of simultaneous pair formation, show that the N_2 velocity distribution is very narrow, indicating that, similar to the H_2O_2 case, sharp Doppler profiles can be expected.

Changing the photolysis wavelength from 280 nm to 266 nm, 283 nm, and 308 nm indicates the complex nature of the fragmentation, because the kinetic energy, and therefore the velocity of the particles, remains essentially unchanged. Moreover, the change in photon energy does *not* lead to a change in the NH rotation, which implies that the excess energy is exclusively utilized for excitation of N_2. This implication has very important consequences for the shape of the potential surface (Table 1).[25]

Table 1. Excess energies and energies of fragments [cm^{-1}] from the decomposition of HN_3 at different wavelengths.

	248 nm		266 nm		283 nm		308 nm	
	NH	N_2	NH	N_2	NH	N_2	NH	N_2
E_{exc}	21950		19210		~16970		14100	
E_{kin}	6800	3640	7040	3770	6430	3440	6950	3720
E_{rot}	700	10810	700	7700	~700	6400	690	2740

A further strong indication of the complexity of the HN_3 decomposition reaction comes from observations of the Λ states of the NH fragments. The study of the various Λ states of $NH(^1\Delta)$ and $ND(^1\Delta)$ at an excitation wavelength of 308 nm indicates equal population of the $^1\Delta(A')$ and $^1\Delta(A'')$ states but different vector correlations with evidence of a remarkable isotope effect. This suggests a distinctly nonplanar dissociation geometry of the fragmentation product in the $^1\Delta(A')$ state.[26]

In its ground state, HN_3 is planar.[27] The three nitrogen atoms form a nearly linear chain, while the H atom is at an angle of 71.2° to this chain. The absorption at 266 nm causes the transition $\tilde{A}^1A'' \leftarrow \tilde{X}^1A'$, which has its corresponding transition dipole moment $\vec{\mu}$ perpendicular to the plane of the molecule. The population of rotational states in NH has its maximum at $J = 5$ and shows a slight inversion in the lower quantum states.[22]

The experimental setup for the study of the HN_3 photolysis reaction is exactly the same as described in Section 3. The different photolysis wavelengths were generated by using the fourth harmonic of a Nd-YAG laser (266 nm), or the radiation of either a KrF (248 nm) or XeCl (308 nm) laser. The arrangement of the analysis laser remained unchanged.

Measurements of the asymmetry parameter of the R, P, and Q transitions in the occupied rotational states of the NH fragment were performed for the different experimental geometries mentioned earlier. They yield the bipolar moments $\beta_{\mu v}$, $\beta_{\mu J}$, and β_{vJ} [Eq. (4)] for each rotational state, which describe the vector correlations between the transition dipole moment $\vec{\mu}$ of the parent molecule and the velocity v or the angular momentum $\vec{J}$ of the NH fragment and between $\vec{v}$ and $\vec{J}$ of the NH fragment itself. The values of $\beta_{\mu v}$ deserve special attention. As shown in Figure 10a, the lowest energy NH rotation results in a value for $\beta_{\mu v}$ of -0.4, which is close to the absolute minimum for this quantity (-0.5), indicating an almost perpendicular alignment of $\vec{\mu}$ and $\vec{v}$. However, $\beta_{\mu v}$ increases with increasing rotational energy, finally becoming positive for $J > 9$.[22] This behavior for $\beta_{\mu v}$, which is observed for $\beta_{\mu J}$ as well, is also found at an excitation wavelength of 308 nm. Only minor differences are seen.[25]

Although $\beta_{\mu J}$ is very small and only slightly dependent on the NH rotation, it is always positive, indicating that $\vec{\mu}$ of the parent molecule and $\vec{J}$ of the NH products are oriented predominantly parallel to each other. The resulting β_{vJ} is positive and increases for the higher quantum states (Fig. 10b). This last result shows that a torsional motion of HN_3 is responsible for the fragment's rotation and that its influence increases with increasing rotational excitation of the NH species. The negative value for the $\langle \vec{\mu}\vec{v}\rangle$ correlation ($\beta_{\mu v}$ close to -0.5) is expected for a planar dissociation geome-

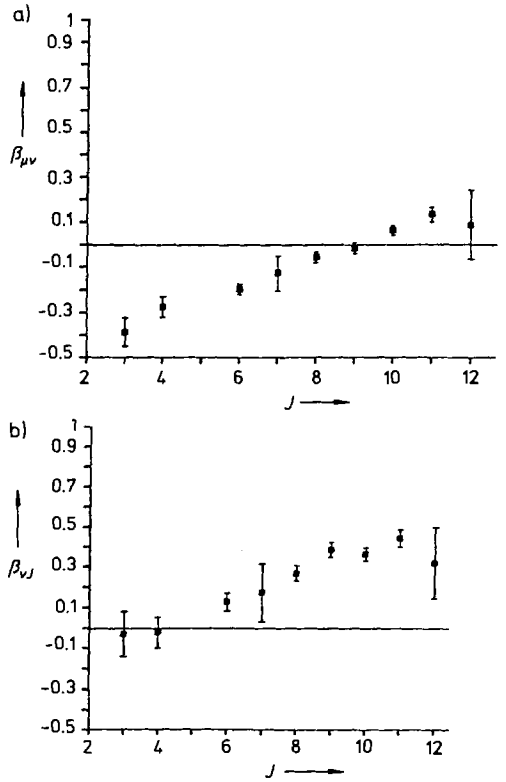

Fig. 10. Vector correlations expressed as the asymmetry parameter β for the NH fragment from the photofragmentation of HN_3 at 266 nm as a function of rotational quantum number of NH [22]. a) $\beta_{\mu\nu}$; b) $\beta_{\nu J}$.

try. When $\vec{\mu}$ and $\vec{v}$ become more parallel ($\beta_{\mu\nu}$ becomes more positive), the plane in which the NH fragment velocity is developed is tilted towards the direction of $\vec{\mu}$ leading simultaneously to a higher rotational excitation. Of all HN_3 vibrational modes, only the ν_6 (a″) mode satisfies this criterion. This is a bending vibration directed out of the original plane of the molecule. The excited state potential surface should therefore exhibit a large (negative) gradient with increasing angle between the three N atoms. The unequal distribution of the angular momenta is a direct result of such a geometry: the location of the centers of gravity of the fragments ensures that the N_2 species receives significantly more angular momentum than the NH fragment. For N_2, the center of gravity lies between the two N atoms, whereas for NH the center of gravity is nearly coincident with the nitrogen atom because the H atom is light. During the evolution of the fragment rotation from the bending motion of the parent molecule, the N_2 fragment is readily induced to rotate, while NH behaves nearly like a single atom and is provided primarily with orbital angular momentum.

Two experimental results support the above conclusion regarding the N_2 fragment. At a photolysis wavelength of 283 nm, REMPI spectroscopy showed that the produced N_2 is only rotationally excited, with an average rotational quantum number of 56. The distribution of the rotation is Gaussian, with a small half-height width of $\Delta J \approx 13$.[28] (An important consequence is the narrow velocity distribution, which is also determined by ΔJ.) The second confirmation stems from studies of simultaneous pair formation, which also show purely rotationally excited N_2 molecules for various photolysis energies. The rotational energy distribution in these cases is also narrow. For $\lambda = 248$ nm, the average rotational quantum number is 70.[29] The spectral resolution in the observation of pair formation by analysis of NH fragments is not sufficient to resolve the rotational states of N_2 by an LIF technique, because the difference in rotation constants of NH and N_2 is too large. Nevertheless, it can be said that the energy of N_2 is rather incompatible with vibrational excitation. If a Gaussian distribution is assumed, the maximum population of the rotational states of N_2 for an excitation at 248 nm occurs at $J = 70$, with a half-height width of $\Delta J = 18$.

Further information about the shape of the potential surface can be obtained from pair formation correlations. This correlation limits the possible motions of the system. According to Figure 11, maximum N_2 rotation occurs when NH rotation is at a minimum.[29] Furthermore, for high N_2

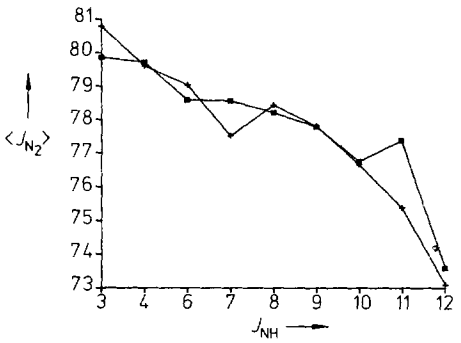

Fig. 11. Pair formation correlation for N_2 and NH for the photofragmentation of HN_3 at 248 nm [29]. $\langle J_{N_2} \rangle$ is the average rotational quantum number of the N_2 fragment. ■: photolysis under quasi-static conditions, +: molecular-beam experiment.

rotation $\langle \vec{\mu}\vec{J} \rangle$ is positive. This $\langle \vec{\mu}\vec{J} \rangle$ correlation is reduced to nearly zero with decreasing rotational excitation of N_2. A positive $\langle \vec{\mu}\vec{J} \rangle$ correlation for N_2 indicates that the rotation vectors of the fragments are more likely to be parallel to the transition dipole moment. For HN_3 this means that they are perpendicular to the original plane of the molecule, which leads to the conclusion that the high N_2 rotation is primarily caused by a motion of the parent molecule that lies *in* the molecular plane. This is the ν_5 bending motion. The potential surface gradient for this motion is therefore initially steeper. With decreasing N_2 and increasing NH rotation, the bending motion is increasingly out of this plane. From the $\langle \vec{\mu}\vec{v} \rangle$ correlation for NH it is known that, for higher NH rotations the bending motion perpendicular to the original plane (ν_6) becomes more important for the decomposition dynamics.

The vector correlations predict that the potential surface has large gradients for angle variations that occur in the original plane or perpendicular to it. These projections are fully confirmed by new ab initio calculations of this potential surface.[30] The theoretical predictions state that, in the vicinity of the N_2–NH equilibrium distance, the forces are directed much more strongly into the ν_5 rather than the ν_6 motion. Only with increasing N_2–NH distance, does the potential for the out-of-plane motion become steeper. This effect of changing from the ν_5 to the ν_6 mode during the process of decomposition influences the NH fragment rotation in such a way that a torsional motion is developed, which can be readily recognized by the positive $\langle \vec{v}\vec{J} \rangle$ correla-

tion. This correlation is very small for small NH rotations. These findings are in full agreement with the observation that small NH rotations are correlated with large N_2 rotations, which are caused by the ν_5 vibration in the original plane of the molecule.

As was discussed for the photodecomposition of H_2O_2, the product–pair correlations can be used in conjunction with the law of conservation of angular momentum to obtain information about the impact parameter. As the rotation of NH is small while that of N_2 is exceptionally large, the orbital angular momentum is determined primarily by the N_2 rotation. The orbital angular momentum can be determined by using Equations (10)–(12) developed for the H_2O_2 case [Eq. (18)].

$$L_{N_2-NH} = \mu_{N_2-NH} b v_{N_2-NH} \tag{18}$$

For the excitation at 266 nm, the most probable rotational quantum number is 70. Therefore, by using the experimentally observed fragment velocities, the impact parameter b is calculated to be approximately 0.9 Å.[22] This is somewhat larger than the equilibrium distance between the centers of gravity of the N_2 fragment and HN_3. The impact parameter decreases for lower excitation energies (283, 308 nm), which could indicate a smaller amplitude for the bending motion in these cases.

The preceding discussion demonstrates that Doppler and polarization spectroscopy is a powerful tool which yields an exact description of the forces that are acting during the decomposition of the transition state, not only for H_2O_2 but also for the more complex example, HN_3. It is possible to gain insight into the molecular motions of femtosecond duration occurring in chemical reactions. While conclusions are drawn from quantities that are integrated over the course of the reaction, the resulting information yields a complete description of the entire reaction path.

Conclusions

The studies of molecules with Doppler and polarization spectroscopy are performed with a spectral resolution that allows the exact determination of the band profile of an absorption line, which contains all necessary information. For this to be feasible, complete resolution of the rotational fine structure is essential. Further information from the spectrum is gleaned from the spin of the electron and the Λ splitting. Even nuclear spin effects can be observed. These subtle aspects of the spectral information have, with one exception, not been discussed here, in order not to exceed the limits of an introductory description of the potential of Doppler and polarization spectroscopy.

There is already a fairly large number of molecules that have been examined in several laboratories.[3] The analysis of pair formation, however, has so far only been applied to the two examples described in this review. This method renders possible a characterization of the fragmentation reaction that goes beyond the description given by the vector correlations between $\vec{\mu}$, $\vec{v}$, and $\vec{J}$. The examples were meant to show the potential of the method and the conclusions that can be drawn from it. The description of the photodecomposition process illustrates how a molecular system moves on the molecular level from an unstable excited state to a stable final state, providing insight into the nature of the reaction path of a chemical reaction and into how the molecules distribute the energy absorbed during a chemical process. As the motions of these products is a true image of the forces that cause them, it is possible to deduce the forces from properties of the products. Doppler and polarization spectroscopy, as well as time-resolved spectroscopy at extremely short lifetimes, are complementary methods for the investigation of important intramolecular events, which are of great importance to the understanding of reaction dynamics.

Experimental results cited herein were taken from several doctoral and master's (Diplom) theses. I am grateful to all collaborators for their enthusiastic efforts. I want to thank Dr. K.-H. Gericke, Prof. E. A. Reinsch and Prof. R. N. Dixon, whose collaboration and critical contributions were essential for the success of the investigations discussed in this review. The work was supported by the Deutsche Forschungsgemeinschaft.

Received: October 15, 1990
Revised version: December 12, 1991 [A 862 IE]
German version: *Angew. Chem.* **1992**, *104*, 529
Translated by Dr. W. C. A. Wilisch, Pasadena, California (USA)

[1] a) J. L. Knee, A. H. Zewail, *Spectroscopy* **1988**, *3*, 4; b) F. J. Comes, K.-H. Gericke, A. U. Grunewald, S. Klee, *Ber. Bunsenges. Phys. Chem.* **1988**, *92*, 273.
[2] R. N. Zare, D. R. Herschbach, *Proc. IEEE* **1963**, *51*, 173; R. N. Zare, *Dissertation Harvard University Cambridge*, **1964**.
[3] J. P. Simons, *J. Phys. Chem.* **1984**, *88*, 1287; *Molecular Photodissociation Dynamics* (Eds.: M. N. R. Ashfold, J. E. Baggott) Royal Society of Chemistry, London, **1987**; G. E. Hall, P. L. Houston, *Annu. Rev. Phys. Chem.* **1989**, *40*, 375.
[4] K.-H. Gericke, S. Klee, F. J. Comes, R. N. Dixon, *J. Chem. Phys.* **1986**, *85*, 4463.
[5] S. Klee, K.-H. Gericke, F. J. Comes, *J. Chem. Phys.* **1986**, *85*, 40.
[6] M. P. Docker, A. Hodgson, J. P. Simons, *Chem. Phys. Lett.* **1986**, *128*, 264.
[7] A. U. Grunewald, K.-H. Gericke, F. J. Comes, *J. Chem. Phys.* **1987**, *87*, 5709.
[8] E. A. Reinsch, *Chem. Phys. Lett.* **1987**, *141*, 369.
[9] Q. E. Bush, N. R. Wilson, *J. Chem. Phys.* **1972**, *56*, 3638, 3655.
[10] R. N. Dixon, *J. Chem. Phys.* **1986**, *85*, 1866.
[11] I. Burak, J. W. Hepburn, N. Sivakumar, G. E. Hall, Q. Shawala, P. L. Houston, *J. Chem. Phys.* **1987**, *86*, 1258.
[12] A. U. Grunewald, .-H. Gericke, F. J. Comes, *Chem. Phys. Lett.* **1986**, *132*, 121.
[13] R. Schinke, *J. Phys. Chem.* **1988**, *92*, 4015; R. Schinke, R. Staemmler, *Chem. Phys. Lett.* **1988**, *145*, 486.
[14] A. U. Grunewald, K.-H. Gericke, F. J. Comes, *Chem. Phys. Lett.* **1987**, *133*, 501.
[15] a) U. Meier, Dissertation, Ruhr-Universität Bochum, **1988**; b) U. Meier, V. Staemmler Bochum, personal communication.
[16] S. Klee, K.-H. Gericke, F. J. Comes, *Ber. Bunsenges. Phys. Chem.* **1988**, *92*, 429.
[17] Ly_α is the resonance radiation of the hydrogen atom. It is the first line of the Lymann series at 126.1 nm.
[18] K.-H. Gericke, H. G. Gläser, C. Maul, F. J. Comes, *J. Chem. Phys.* **1990**, *92*, 411.
[19] A. U. Grunewald, K.-H. Gericke, F. J. Comes, *J. Chem. Phys.* **1988**, *89*, 345.
[20] F. Rohrer, F. Stuhl, *J. Chem. Phys.* **1988**, *88*, 4788.
[21] J. R. McDonald, R. G. Miller, A. P. Baronavski, *Chem. Phys. Lett.* **1977**, *51*, 57.
[22] K.-H. Gericke, R. Theinl, F. J. Comes, *Chem. Phys. Lett.* **1989**, *164*, 605.
[23] K.-H. Gericke, M. Lock, F. J. Comes, *Chem. Phys. Lett.*, in press.
[24] T. Haas, K.-H. Gericke, *Ber. Bunsenges. Phys. Chem.* **1991**, *95*, 1289.
[25] K.-H. Gericke, T. Haas, M. Lock, R. Theinl, F. J. Comes, *J. Phys. Chem.* **1991**, *95*, 6104.
[26] K.-H. Gericke, M. Lock, R. Fasold, F. J. Comes, *J. Chem. Phys.*, in press.
[27] B. Winnewisser, *J. Mol. Spectrosc.* **1980**, *82*, 220.
[28] J. Chu, P. Marcus, P. J. Dagdigian, *J. Chem. Phys.* **1990**, *93*, 257.
[29] T. Haas, Diplomarbeit, Universität Frankfurt am Main, **1990**.
[30] U. Meier, V. Staemmler, *J. Phys. Chem.* **1991**, *95*, 6111.

Molecules with Large Cavities in Supramolecular Chemistry

By Christian Seel and Fritz Vögtle*

Dedicated to Professor Heinz Harnisch on the occasion of his 65th birthday

Supramolecular chemistry is a new area of research that has rapidly developed from pure synthetic chemistry, and its novelty has led to interdisciplinary cooperation between organic and inorganic chemistry, biochemistry, physical and theoretical chemistry, and physics. Whereas *molecular chemistry* essentially deals with the covalent bonding of atoms, supramolecular chemistry is predominantly involved in the study of the weaker intermolecular interactions resulting in the association and self-organization of several components to form larger aggregates (supramolecules). The first crown ether discovered by the subsequent Nobel prizewinner Pedersen was more the fortuitous reaction product of an impurity, but nowadays, some twenty-five years later, chemists are able to tailor host molecules to special requirements. Host compounds having a cyclophane skeleton make an important contribution, since their aromatic structural units ensure the necessary rigidity of the molecular structures and thereby improve the preorganization of the coordination sites for the cooperative binding of the guests. During the course of the rapid development of supramolecular chemistry such a large number of synthetic hosts has been developed and their interaction with guests studied in such depth that we must restrict ourselves here to a discussion of a particular group of host compounds, namely cavity-supporting macrobicyclic and macrooligocyclic phanes, which bear a similar relation to open-chain and monocyclic hosts as the metal-complexing cryptands to the podands and crown ethers. The molecular architecture of these three-dimensionally bridged macrooligocycles is a challenge for synthetic chemistry. (Not only the size and shape of the intramolecular cavity, but also the provision of the latter with suitable coordination centers have to be included in the synthesis strategy.) The capacity for the envelopment of guests from all sides and the expedient *endo* functionalization often also produce a particularly strong binding of host and guest, outstanding selectivities with regards to molecular recognition, and special properties of the supramolecular complexes.

1. Introduction

The first triply bridged cyclophanes were the molecule **1**,[1] obtained by Cram in 1958 from a paracyclophane by intramolecular coupling (path E in Scheme 1), and the symmetrical [n.n.n]phanes **2**,[2] prepared by Dale and Hubert in 1965 by double cyclotrimerization of terminal diynes (path H in Scheme 1). A general route to such molecules was achieved with the synthesis of [3.3.3]phanes such as **3** (Tos = p-SO_2-C_6H_4Me) from two readily accessible trifunctionalized halves (paths A and D in Scheme 1) (Vögtle, 1970).[3] The

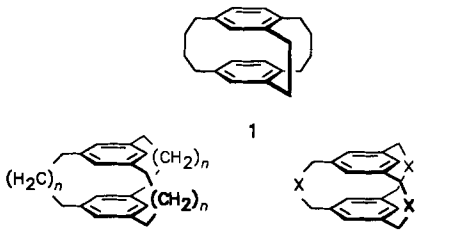

2: n = 5–7 **3**: X = S, SO_2, N-Tos

subsequent optimization of the cyclization reactions, the application of the dilution principle,[4] and chromatographic and analytic methods, and the discovery of the "cesium effect"[5] made it possible to transform polyfunctionalized starting compounds often in surprisingly high yields into macrocyclic three-dimensional compounds of comparably large molecular masses (well over 2000 Daltons) rather than into polycondensed products.

The development of synthetic host compounds, triggered by the crown ether chemistry founded by Pedersen, proceeded in parallel to this.[6] This research led to the realization that specifically directed complexing, molecular recognition, and ion transport through membranes can be achieved with synthetic ligands as well as with natural receptors. The "three-dimensional crowns" conceived by Lehn, namely the cryptands, illustrate the considerable influence that the three-dimensional envelopment of the guest by the host has on the complex stability and complexing selectivity.[7] With the inclusion of durene by a diphenylmethanophane, Koga (1980)[8] was one of the most successful pioneers in combining host–guest chemistry and cyclophane chemistry;[9] reports of other work in this field followed in quick succession.[10]

In the same year we attempted to imitate the inclusion properties of cyclodextrins with large-cavity benzocryptands.[11] The first efficient macrobicyclic hosts with a cyclophane framework were conceived at the beginning of the 1980s by Collet (1981, see Section 4.3.),[12] Diederich (1984, see Section 4.3.),[13] and us (1984, see Section 3.1.).[14]

In this review article we will discuss the qualitative and quantitative expansion of the studies of cyclophane-type macrooligocyclic hosts[15] in the more general field of supramolecular chemistry.[9d, 16] We will focus on their endoreceptor properties, that is, on the inclusion of guest components

[*] Prof. Dr. F. Vögtle, Dr. C. Seel
Institut für Organische Chemie und Biochemie der Universität
Gerhard-Domagk-Strasse 1, D-W-5300 Bonn 1 (FRG)

in the cavity interior. In this discussion it will become evident that cavity-enclosing hosts with optimum preorganization[17] of their bonding centers often produce effects unobtainable with open-chain molecules.

2. Synthetic Strategies

A whole range of various strategies for synthesizing large, multiply bridged molecular skeletons is described in the literature. Common to all strategies is the stepwise assembly of easily accessible structural subunits according to a "molecular building-block principle"[15] (molecular LEGO[18]). Depending on the strategy, the starting compounds of the decisive cyclization step have completely different structures and functional groups. In the "simplest" case five components, namely two spacers and three bridge units are joined together by sixfold bond formation (path A in Scheme 1). Multistep reaction paths in which only two molecules are necessary in the final cyclization step (paths C and D) or in which ring closure occurs intramolecularly (paths E, F, G) are synthetically more time-consuming and complex, though in general more promising.

Cyclization to form triply bridged macrocycles proceeds most often through the formation of carbon–heteroatom bonds, especially through *N*-alkylations[19] and *N*-acylations. In general the yields are higher the fewer the bonds formed simultaneously. For example, from the one-pot reaction (path A in Scheme 1) of two equivalents of triamine **4** with three equivalents of diacid chloride **5**, we obtained the bicyclic compound **7** in only 1.5% yield (Scheme 2).[14] If on the other hand triacid chloride **6** is treated with **4** in a 1:1 cyclization (path D in Scheme 1), **7** is obtained in at least 13% yield. In the same way, a whole family of new macrobi-

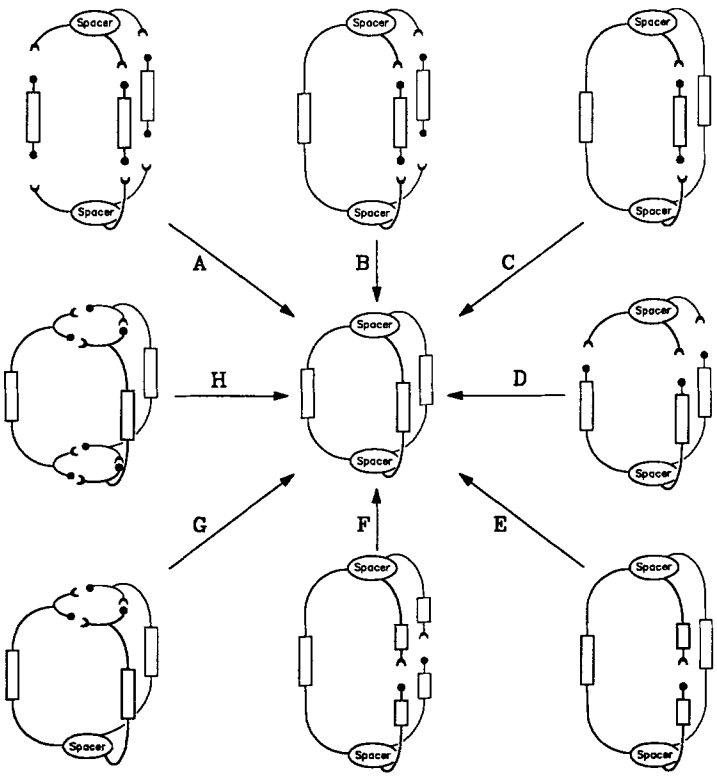

Scheme 1. Synthetic strategies for triply bridged cyclophane hosts. A: five components, six bonds; B: three components, four bonds; C: two components, two bonds; D: two components, three bonds; E: one bond; F: two bonds; G: three bonds; H: three components, six bonds.

Fritz Vögtle, born in 1939 in Ehingen/Donau, studied chemistry in Freiburg as well as chemistry and medicine in Heidelberg. There he received his Ph.D. for research with H. A. Staab on the valence isomerization of double Schiff bases. After his habilitation on steric interactions inside cyclic compounds, he was H2/H3 professor in Würzburg from 1969 to 1975. He then accepted a position as director of the Institut für Organische Chemie und Biochemie in Bonn. He is interested in the field of supramolecular chemistry and molecular recognition and after working on topics concerning crown ethers, podands, and siderophores, he has concentrated on compounds with large intramolecular cavities, ligands for supramolecular photochemistry, concave dyes, molecular tweezers, and ball- and tube-shaped molecules. His further areas of research are deformed, strained, and chiral/helical molecules, cyclophanes, and compounds with appealing architecture.

Christian Seel was born in 1963 in Bonn and studied chemistry there from 1983 to 1988. In his Diplomarbeit with F. Vögtle he synthesized macrobicyclic ligands for metal ions. In 1991 he received his Ph.D. in the same research group for his work on macrooligocyclic host compounds with large cavities for the complexation of organic guests.

cyclic hosts with three donor units (catechol, bipyridine, diaza crowns) or three hydrophobic structure elements (diphenylmethane, *o*-terphenyl) is now accessible.[15]

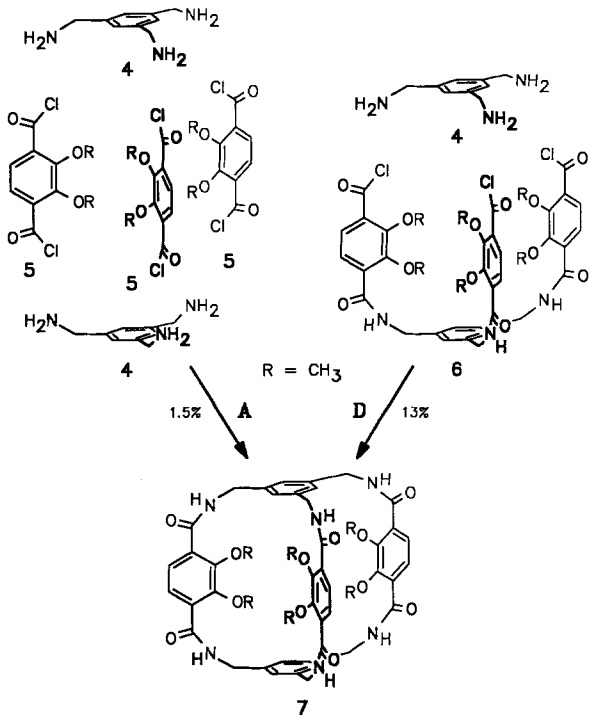

Scheme 2. Two pathways for forming the macrobicyclic tris(catechol) **7**.

The efficiency of the cyclization by multiple lactam formation is also demonstrated by the synthesis of the tetraazo double-decker porphyrin **8**, obtained in 18% yield and involving a fourfold linkage.[20]

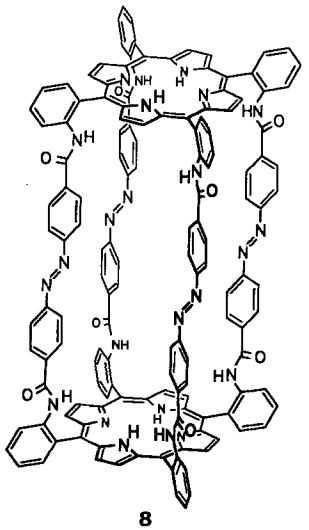

The simultaneous multiple condensation of aldehydes with amines to form Schiff bases leads to surprisingly good results in the formation of large, molecular cavities: With this method[21] Lehn et al. prepared the hexaimine cryptand **9** in 60% yield,[22] and Lindsey and Mauzerall obtained (after subsequent hydrogenation) the quadruply bridged porphyrin **10** in yields as high as 80–95%.[23]

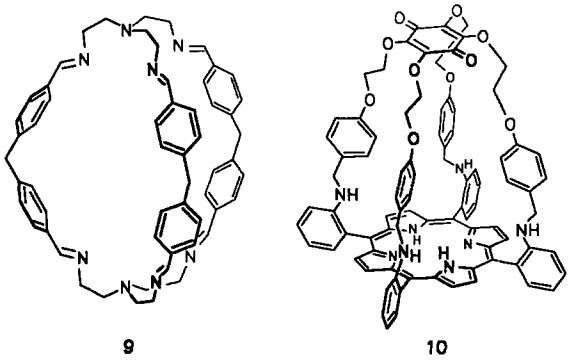

We successfully synthesized the tris(paraquat) cage **13** by sixfold quaternization of three 4,4'-bipyridine molecules (**11**) with two triphenylbenzene spacers **12** (Scheme 3).[24]

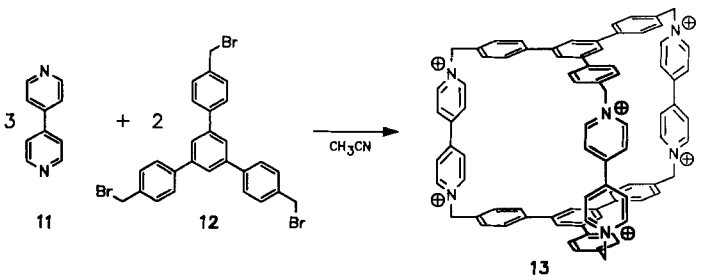

Scheme 3. Synthesis of the macrobicyclic tris(paraquat) **13**.

The ring closures by ether and sulfide linkages universally employed in crown ether and cyclophane chemistry have only rarely been used in the preparation of large molecular cavities. Examples include Cram's "carcerands", in which two bowl-shaped cavitands are linked by four sulfide or acetal bridges (see Section 4.5).

Last but not least, we must mention some cyclization methods in which not carbon–heteroatom bonds, but instead carbon–carbon bonds are formed.[25] An example is the alkyne coupling according to Eglinton; its application in the cyclodimerization of tris(propargyl ether) **14** to form the tris(diyne) **15** in 20–30% yields was described by Breslow

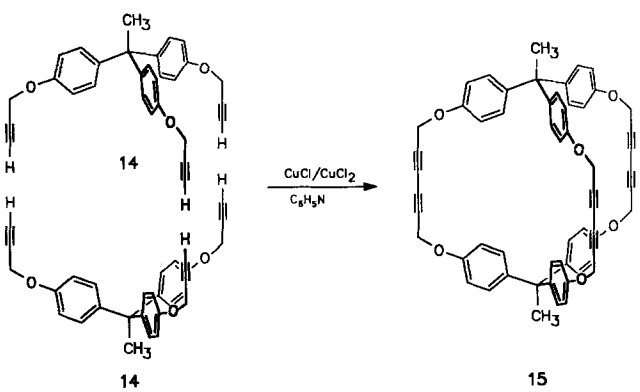

Scheme 4. Formation of the cage molecule **15** by triple alkyne coupling.

(Scheme 4, see also Section 4.3).[26] Bicyclic cage molecules are also accessible by intramolecular coupling of dialkynes and tetraalkynes (paths E and F in Scheme 1) (Whitlock, see Section 4.3, Lehn.[27]).

In the "cryptophane" host family developed by Collet et al. (see also Section 4.3),[28] the cyclotriveratrylene spacers (or their derivatives) are formed by intramolecular condensation of three veratrole units in the decisive step of the synthesis (path G in Scheme 1), thus simultaneously with the macrobicyclic skeleton (Scheme 5).

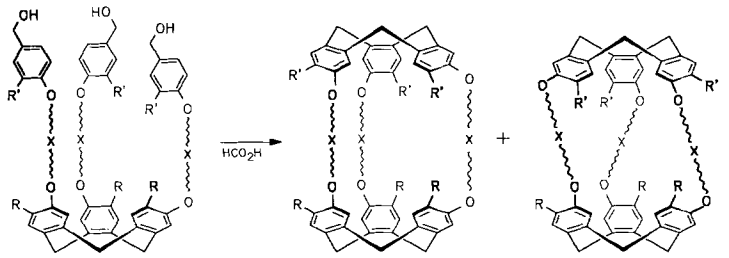

Scheme 5. Cryptophane synthesis by intramolecular condensation of a cyclotriveratrylene unit.

The first known purely carbo(bi)cyclic[29, 30] large cavity is found in the dodecacarboxylic acid **17**, which was obtained by sixfold malonic ester alkylation of three molecules of tetraester **16** with two trihalide units **12** (Scheme 6).[31]

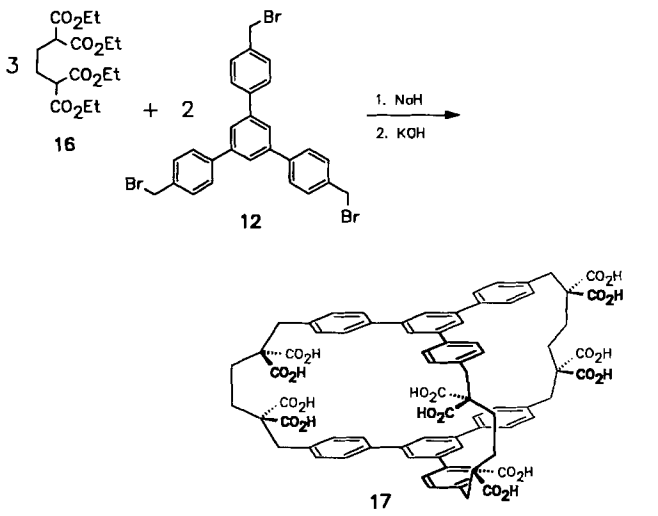

Scheme 6. Formation of the first molecule with an all-carbon framework containing a large cavity.

3. Metal Complex Formation—Large Cavities for Small Ions

3.1. Macrobicyclic Siderands

Siderophores (Greek: iron carriers) are defined as generally hexadentate chelate ligands of low molecular weight that are produced by microorganisms as growth factors for extracellular iron uptake by the complexation of Fe^{III}.[32] Iron plays an indispensable role in many oxidation and reduction processes in the cell. Iron(III) is not directly biologically available on account of its very low solubility at physiological pH values. By complexing with siderophores it is converted into a soluble, transportable form; the "sideroplexes" (iron complexes of the siderophores) can then be absorbed by membrane receptors on the cell surface.[33] The geometrical conditions and the chirality of the coordination center and of the anchor skeleton as well as the arrangement and nature of the peripheral functional groups are decisive in this connection. In recent years a large number of "siderands" (artificial siderophores) have been synthesized and investigated with regards to their complex-forming properties and biological activity. The intention was to elucidate the iron-transport phenomena, the structural requirements placed on the complexes and cell receptors, and the decomplexation mechanisms.[32]

Many siderophores contain three catechol units, the six oxygen atoms of which in the deprotonated form can coordinate metal ions in an octahedral fashion. The prototype of the catechol siderophores is enterobactin (**18**).[34] In its Fe^{III} complex **19** the donor centers are wound in the form of a Δ-*cis* helix around the metal ion.[35] The formation constant K_{ass} for complex **19** is approximately 10^{52} M^{-1} and is the largest yet measured for a natural substance.[36] Numerous

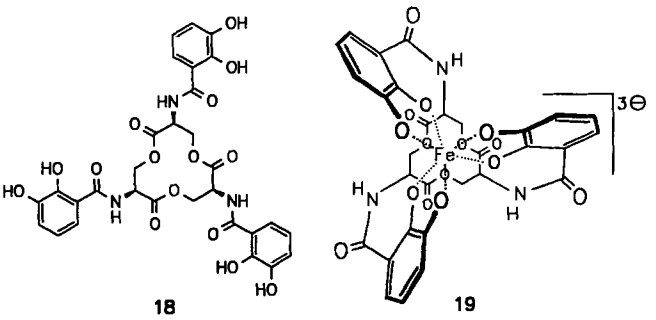

synthetic analogues of enterobactin have been developed in the last decade, in particular by Raymond et al.[32b] In these analogues the catechol units are fixed to freely movable sidearms of various linear, branched, or cyclic anchor skeletons. For example, in "MECAM" (**20**) the hydrolysis-sensitive cyclotriester of **18** is replaced by a benzene ring.[37] The formation constant of the Fe^{III} complex is 10^{46} M^{-1}.[38]

We prepared the macrobicyclic siderand **21** in 1984 with the aim of obtaining a chelate ligand with an optimally preorganized donor geometry.[14] In this case the catechol units are integrated in a large cage framework to restrict their conformational mobility. The skeleton is flexible enough, however, to permit an octahedral arrangement of the donor oxygen atoms in the complex. The spatial preorientation and three-dimensional "clamping" of the binding centers contributes decisively to the extremely strong bonding of the metal ion to **21** ("macrobicyclic effect").[39] This new type of ligand has the highest hitherto measured formation constant of an iron(III) complex: $K_{ass} \approx 10^{59}$ M^{-1}.[40] This complex is stable even at pH 3; **21** is found to be clearly superior to open-chain compounds in competition experiments.[41]

In 1987 Raymond et al. synthesized the related macrobicyclic ligand **22** ("bicapped TRENCAM").[42] The X-ray

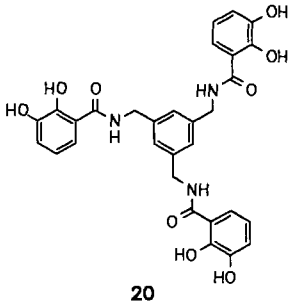

20

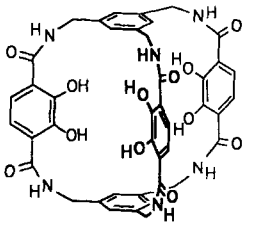

21

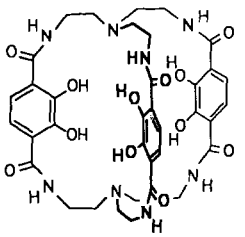

22

structure analysis of its iron(III) complex revealed that the metal ion has a trigonal-prismatic coordination sphere previously unknown for such complexes, which is stabilized by six intramolecular hydrogen bonds between the amide protons and the adjacent catechol oxygen atoms (Fig. 1).[43]

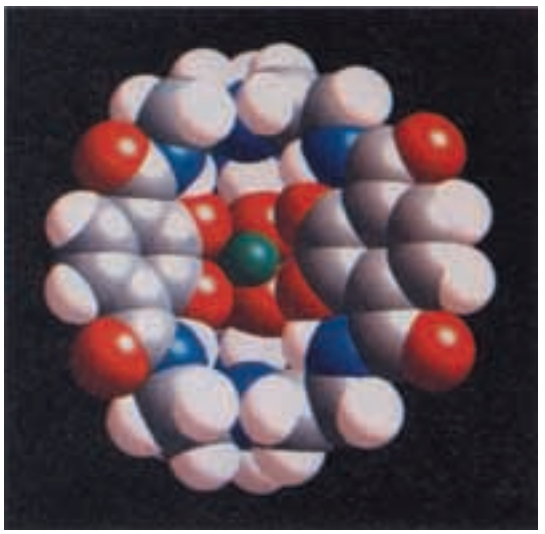

Fig. 1. Crystal structure of the Fe^{III} complex of siderand **22** with trigonal-prismatic coordination sphere of the cation. (All color diagrams were prepared on HP 825 SRX with MOLEK 9000, P. Bischof, ISKA, D-W-6140 Bensheim.)

The volume of the cavity enclosed by the bicyclic molecular framework of **21** can be successively enlarged according to our building-block principle by incorporating larger spacers (1,3,5-triphenylbenzene and 1,1,1-triphenylethane units) instead of the central benzene rings.[44] Thus, the ligand **23** provides sufficient room for a convergent and cooperative arrangement of the six methoxy groups during the inclusion of a metal cation in the interior of the cavity.[45] This ligand forms alkali-metal complexes whose stabilities are comparable to those of complexes of crown ethers with alkali metals. Ligand **23** (R = benzyl) is size-selective; cesium ($\lg K_{ass}$ = 5.3 ± 0.5) is bound roughly six times more strongly than potassium.

Pierre et al. have just recently performed the template synthesis of the Fe^{III} complex of the macrobicyclic siderand **24**, whose donor centers are formed by *o,o'*-dihydroxybiphenyl instead of pyrocatechol units.[46, 47]

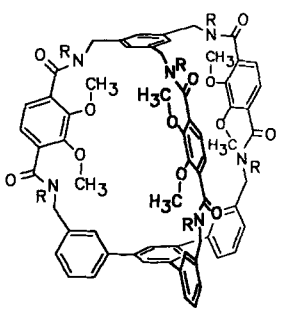

23

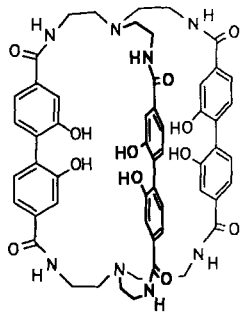

24

3.2. Cagelike Ligands with Three Bipyridine Units

For some years intensive efforts have been made to develop efficient molecular systems for photoinduced charge-separation, the first step in the photochemical utilization of solar energy.[48] Attention is focused in particular on supramolecular electron-transfer photosensitizers,[49] that is, molecules that are able to absorb light and consequently oxidize or reduce other molecules in reversible processes. Ruthenium(II)–bipyridine complexes are of particular interest because of their stability and special combination of lifetime, reactivity, redox potentials, and the chemoluminescence of their lowest excited state.[50]

The relatively rapid radiationless deactivation of the lowest excited state is problematical in complexes such as $[Ru(bpy)_3]^{2+}$ (**25**). This ^{3}MLCT state (MLCT = Metal-to-Ligand Charge-Transfer) is rapidly adopted after excitation to the first excited singlet state on account of the strong spin-orbit coupling of ruthenium (A and B in Scheme 7a) and is decisive for the luminescence properties and energy-transfer and electron-transfer processes of the system. A further disadvantage of this complex is its photodissociation (D in Scheme 7a), which proceeds by a (thermally excited) radiationless transition (C in Scheme 7a) to a distorted ^{3}MC

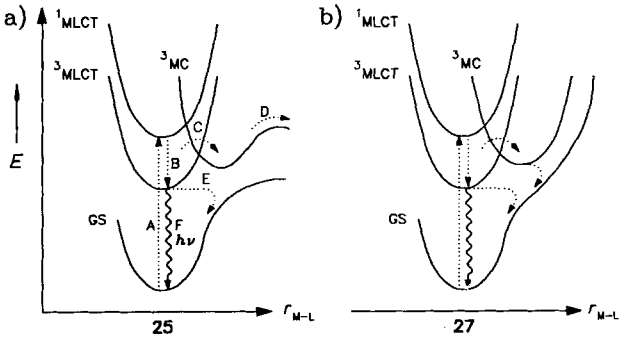

Scheme 7. Energy potentials of the ruthenium complexes **25** and **27** (LC: ligand-centered, MLCT: metal-to-ligand charge-transfer, MC: metal-centered, GS: ground state, r_{M-L}: metal–ligand distance). For A–F see text.

state (MC = Metal-Centered) with subsequent cleavage of one of the six ruthenium–nitrogen bonds.[48–50]

One possible way of improving the photostability is to increase the energy difference between the ^{3}MLCT and ^{3}MC states. Whereas the energy level of the latter cannot be increased, it is possible to reduce the ^{3}MLCT energy by suitable derivatization of the bipyridine units. This leads, however, to an enhanced (thermally independent) radiationless transition to the ground state (E in Scheme 7a) and thus to a drastic reduction of the lifetime of the ^{3}MLCT state and a lower photochemical quantum yield.

Alternatively, photodissociation can be prevented by clamping the bipyridine units in a bicyclic framework as in **26** (Scheme 7b). The photochemical properties of such complexes are hardly different than those of **25** as long as the first coordination sphere of the metal is not disturbed by steric effects. The rigidity of such a ligand furthermore reduces the rate of the thermally activated radiationless decomposition processes.[51]

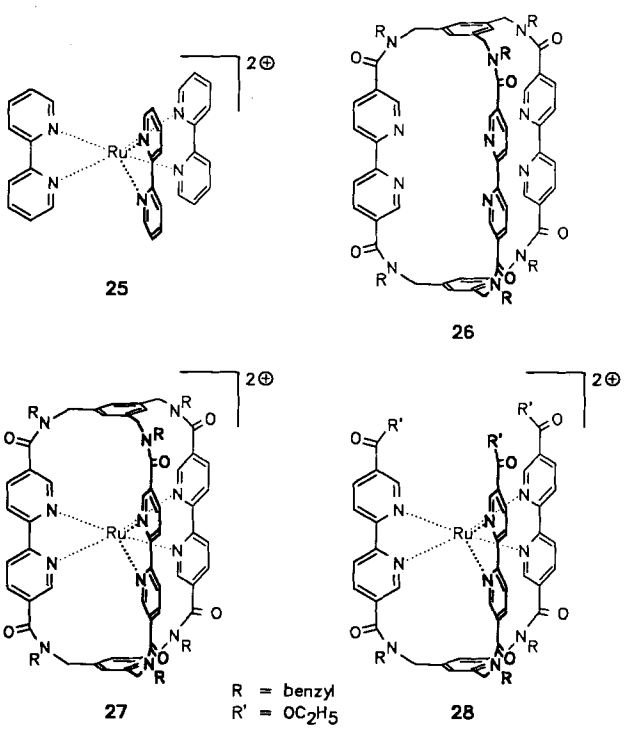

Examination of Corey–Pauling–Koltun (CPK) models show that the tris(bipyridine) cage ligand **26**[52] is able to provide the strictly octahedral coordination sphere required by ruthenium(II). (In the schemes and figures the complexes are not depicted as octahedral for reasons of clarity.) In this case the host molecule together with its three chelate units is coiled in the form of a "triple helix" around the guest ion (Fig. 2). The electron-withdrawing amide groups in the cage complex should lower the energy level of the ^{3}MLCT state and thus reduce its lifetime. Since, however, the carbonyl groups are approximately vertical to the plane of the arene units as is evident in the model, their $-$M effect is weakened. This is demonstrated by the fact that in the absorption spectrum of the cage complex **27**[53] the d $\rightarrow \pi^*$ band (^{3}MLCT band) has a distinctly smaller red-shift compared to

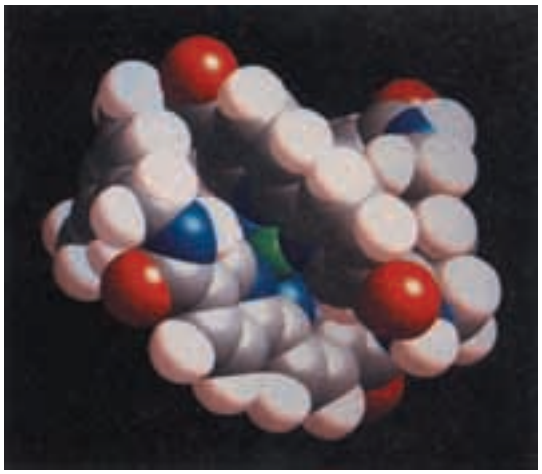

Fig. 2. Space-filling model of the cage complex **27** [according to MM2 calculations (MOLEK 9000 on HP 825 SRX) based on the crystal structure of **25**].

$[Ru(bpy)_3]^{2+}$ (**25**), than that in the case of the less rigid semicage complex **28**.[54, 55]

Similar effects are found in the luminescence band in the emission spectrum (90 K), which is attributed to the transition of the ^{3}MLCT state to the ground state (F in Scheme 7a). At 90 K the lifetime of the excited state is controlled by the energy difference relative to the ground state, and is 4.8 μs for both **25** and **27**. In contrast to this, however, the lifetime of the emission state of the cage complex at room temperature is twice as long as that of the bipyridine complex **25** (1.7:0.8 μs). At room temperature the lifetime is governed by the thermally activated transition from the ^{3}MLCT state to the geometrically distorted ^{3}MC state. The latter is sterically unfavorable for the cage complex, and accordingly the quantum yield of the photodissociation is at least four orders of magnitude less than in the reference complex **25**.

In **27** the shielding of the relevant orbitals of the metal ion from all sides causes the quenching of the ^{3}MLCT state by oxygen to be five times smaller than in $[Ru(bpy)_3]^{2+}$ (**25**). Table 1 provides a summary of the photophysical data of the complexes discussed.[51]

Table 1. Some photochemical data of the Ru^{II} complexes **25**, **27**, and **28**.

Complex	Absorption		Emission		Emission		Photodissociation
	298 K		298 K		90 K		298 K
	λ_{max} [nm]	ε	λ_{max} [nm]	τ [μs] [a]	λ_{max} [nm]	τ [μs] [a]	Φ_p [b]
25	452	13000	615	0.8	582	4.8	1.7×10^{-2}
27	455	10400	612	1.7	597	4.8	$<10^{-6}$
28	477	9500	640	0.45	620	1.9	$<10^{-5}$

[a] Lifetime of the ^{3}MLCT state. [b] Quantum yield of the photodissociation.

It is found that the photochemical properties of tris(bipyridine) complexes are substantially improved if the donor centers are integrated in tailor-made macrobicyclic molecular frameworks.[56] At similar absorption and emission behaviors, there is a greater photostability of the complexes as well as a substantially longer lifetime of the excited state responsible for the luminescence.

The cavity within the framework of ligand **26** is predestined for the octahedral coordination of transition-metal ions. This is also demonstrated by the fact that its Fe^{II} complex is stable even to powerful oxidizing agents such as hydrogen peroxide.[52] Hosts with insufficient conformational flexibility, such as the smaller cryptand **29**[57] synthesized from 6,6'-disubstituted bipyridine units, prove less favorable with regards to an octahedral coordination sphere.[58]

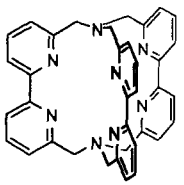

29

Lanthanide ions such as europium(III) and terbium(III) do not place such high demands on the orbital geometry of the ligand field as ruthenium(II). Lanthanide ions are of photochemical interest since their cryptates exhibit a distinct emission at room temperature, whereas their simple aqua complexes are not luminescent. This is attributed to the fact that the three-dimensional envelopment of the ions by the ligand impedes the radiationless deactivation by solvent molecules. The stable, photoactive cryptates of ligand **29** are effective molecular "A-ET-E luminophores" (A-ET-E = Absorption Energy-Transfer Emission), which reemit the UV light absorbed by the ligand (excitation at 320 nm), after intramolecular energy-transfer from $\pi \rightarrow \pi^*$ states to excited metal-states, as visible light (emission at 570–700 nm, Fig. 3). The

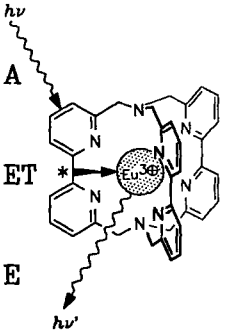

Fig. 3. A-ET-E light conversion processes of the europium(III) cryptate of **29**.

disadvantage of these cryptates is the low quantum-yield of these energy conversions, since in addition to emission, intensive ligand-internal, radiationless deactivation is always observed (Lehn, Balzani et al.).[59]

With the two "tren" caps (tren = tris(2-aminoethyl)amine), the macrobicyclic ligand **30** has two further metal-coordination centers in addition to the bipyridine units. The tritopic cryptand **30** forms trinuclear complexes such as **31**, which to our knowledge is the first trisilver cage complex. Figure 4 shows the structure resulting from the X-ray analysis of the tetrafluoroborate of **31**.[60]

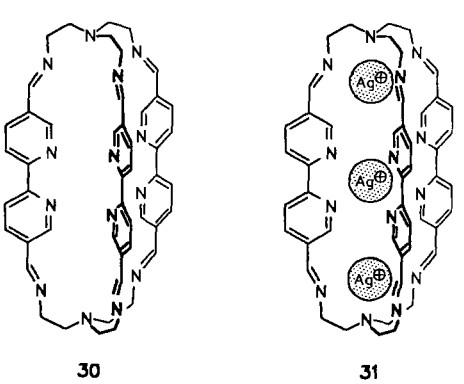

30 **31**

Fig. 4. Crystal structure of the trisilver cage complex **31**.

4. Complexation of Organic Molecules with Cagelike Host Compounds

4.1. Binding Forces in Complexes with Organic Guests

In the complexation of organic guest molecules the intermolecular interactions that lead to binding are essentially weaker than those in the complexation of metal ions. The requirements in terms of the steric and functional complementarity and spatial preorganization of the host compounds are correspondingly high. In addition, suitable binding niches or cavities have to be considerably larger than in ligands for metal complexes, often calling for a greater synthetic effort.

In the molecular recognition of organic molecules with polar or protic functional groups, the formation of hydrogen bonds between the host and the guest is most often the driving force of the complex formation. For example, Rebek et al. have reported a whole family of niche-shaped hosts with different functional groups forming hydrogen bonds[61] and a self-replicating system based thereon.[62] A catalyst for nucleophilic condensations is also based on a network of hydrogen bonds (Kelly),[63] as are the supramolecular complexes of tris(melamine) compounds with cyanuric acid (Whitesides).[64] The molecular tweezers of Wilcox,[65] the urea ligand of Thummel[66] as well as Bell's torands[67] and Hamilton's diamidopyridine cycles[68] are further examples of hosts which bind guests by means of multiple hydrogen bonds.[69]

The binding forces that occur in the complexing of nonpolar organic molecules by nonpolar binding sites of corresponding host compounds are weaker; such binding forces include van der Waals interactions (London dispersion forces), arene stacking, cation–π interactions, dipole-induced-

dipole interactions and electron-donor–acceptor interactions. Last but not least the influence of solvent, which comes under the heading of the "hydrophobic effect", exerts a great influence in complexation.[70]

Recognizing that hydrophobic interactions decisively influence substrate binding in biological systems, Diederich et al.[71] investigated the solvent dependence of the binding strength in the complexation of aromatic guest molecules in studies involving water-soluble cyclophane hosts with hydrophobic cavities.[72] They showed that aromatic guests such as perylene or pyrene can be complexed even in a nonpolar solvent such as carbon disulfide and also in aromatic solvents (benzene). The complex formation constants are particularly large in water, as well as in trifluoroethanol and ethylene glycol. The constants decrease in the transition from polar protic solvents to dipolar aprotic solvents and are weakest in nonpolar solvents such as carbon disulfide. In this connection the free energy of binding shows a good correlation with the Dimroth–Reichardt parameter $E_T(30)$.[73, 74] This empirical parameter of solvent polarity is related to macroscopic properties such as the dielectric constant, dipole moment, cohesion, and polarizability. Since the shape of the host–guest complexes does not essentially alter when the solvent is changed,[75] the differences in the binding strength cannot be attributed to variable van der Waals interactions between the partners; they are instead related to solvation. If it is energetically favorable for a solvent to solvate the nonpolar surfaces of the host and guest, then association of the binding partners is promoted little or not at all. In the case of weak solvation, however, complex formation is supported correspondingly. The most important properties of the solvent that determine these influences are the cohesion interactions and the polarizability.[76] If the solvent molecules have strong cohesive interactions (like protic solvents, in particular water), the solvation of nonpolar molecular surfaces and cavities is unfavorable with respect to enthalpy. The solvent molecules on the surface can participate in fewer hydrogen bonds than those in the bulk and consequently are higher in energy. In the case of the association of two nonpolar surfaces, for example, in the inclusion of aromatic guests in molecular cavities, the surface solvent molecules are released into the bulk and their energy content is lowered, thereby promoting complex formation (enthalpic hydrophobic effect). At the same time a strongly positive entropy term comes into play: the ordered solvent cage enveloping the host and guest molecules is destroyed at the binding sites, and the molecules released are transformed into a less-ordered state (entropic hydrophobic effect).

The polarizability determines, in addition to the interatomic distances, the attractive potential of the London dispersion interactions. In weakly polarizable solvents such as alcohols and water (oxygen atoms and hydroxyl groups are substantially less polarizable than for example aliphatic and aromatic hydrocarbon groups), the dispersion forces between the solvent molecules and the nonpolar host and guest surfaces are weaker than those between the binding sites of the complex components. The situation is different in the case of easily polarizable solvents. Here the dispersive interactions between solvent, host, and guest are of comparable magnitude, and accordingly the driving force for complex formation exerted by the solvent is only weak or even completely absent.

Because of their favorable interactions with the binding sites of the host and guest, lipophilic solvent molecules such as chloroform or benzene may in fact be regarded as only weak competitors for the host receptor site. But due to their large excess, they effectively compete with the guest molecules. Water, in contrast, is the most favorable medium for the complexation of nonpolar compounds; however, it cannot promote complexation more strongly than can be expected because of its physical properties, namely the strong cohesive forces and low polarizability.[72]

The investigation of the complexation of imidazole with a macrobicyclic host shows furthermore that the size and shape of the solvent molecules may also influence the stability of host–guest complexes (Still and Chapman). Bulky solvent molecules, which cannot penetrate the cavity and solvate the binding sites as readily as smaller solvent molecules, give rise to higher binding constants.[77]

Cyclophane hosts can complex aromatic guest compounds even in nonpolar organic solvents,[72] which shows the importance of arene–arene interactions in the formation of corresponding supramolecules. These attractive forces between π systems are found, for example, in the packing of aromatic molecules in the crystal[78] and in phenomena such as vertical base-stacking, which stabilizes the double-helix structure of DNA, as well as the intercalation of drugs and other agents in the DNA strand.[79] An analysis of the crystal structures of a series of proteins shows the influence that the nonbonding interactions of aromatic side-chains have on the tertiary structure.[80, 81] Interacting arene pairs are defined as those in which the centers of the stacked rings are less than 700 pm apart.[80a] Arrangements in which a positively polarized hydrogen atom at the edge of one aromatic ring is directed toward the π-electron cloud of another ring are frequently observed (Fig. 5a).[82] A special case of these edge-to-face arrangements is the so-called T-stacking, in which the interplanar angle is approximately 90°, and the center of gravity of one ring is situated on the symmetry axis of the other ring.[83] The global minimum of the potential energy is also located

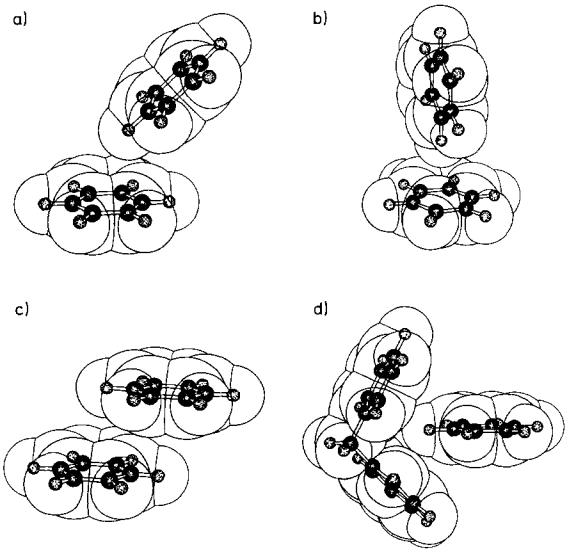

Fig. 5. Several arrangements of interacting benzene rings (π-stacking). a) Edge-to-face stacking. b) T-stacking. c) Offset face-to-face stacking. d) Edge-in-angle stacking (Software: SCHAKAL, E. Keller, Freiburg.)

here: for two benzene rings whose centers are 500 pm apart a potential energy of $E \approx -10.0\ \mathrm{kJ \times mol^{-1}}$ was calculated (Fig. 5b).[80b] A local minimum lies in an offset face-to-face stacking, in which one or two hydrogen atoms of both systems lie over the electron cloud of the partner molecule (Fig. 5c).[81] On the other hand frontal face-to-face stacking is unfavorable on account of the strong repulsion of the π-electron clouds. For inclusion in the niche of a diphenylmethane unit (a subunit often used in cyclophane hosts; see Section 4.3) the aromatic guest approaches the surfaces of the two phenylene rings with its edge. This double edge-to-face arrangement can be termed accordingly edge-in-angle stacking (Fig. 5d).

Hunter and Sanders developed a simple model to clarify the strict geometrical requirements for the interactions between aromatic systems.[84] In this model the σ frame and the π electrons are considered separately, and the charge distribution of the molecule is described by a set of point charges. The positive σ skeleton is sandwiched between two negative π-electron clouds. It is concluded that the arene–arene interaction does not involve, for example, an electronic attraction between the two π systems, but that the attractive π–σ interactions between the electron clouds and the positively polarized hydrogen atoms overcompensate for the unfavorable π–π repulsion.

Van der Waals interactions may have a considerable influence on the strength of arene pairing. Since this is proportional to the area of the π overlap, however, this influence cannot be dominating. This would necessarily involve a maximum overlap and thus favor a cofacial arrangement. Whereas electrostatic forces determine the geometry of the arrangement, van der Waals interactions and solvophobic interactions contribute only to the magnitude of the stacking energy.

Electron-donor–acceptor interactions are also important for the selective binding in host–guest complexes and in biological systems. For example, Diederich and Ferguson found that electron-rich host molecules (donors) and electron-poor guest compounds (acceptors) form particularly stable complexes; however, charge transfer was not observed in this connection.[85] Stoddart's template syntheses of catenanes constructed from electron-rich aromatic crown ethers and cyclic bis(paraquat) units,[86] as well as Hünig's preparation of macroheterocyclic, viologen-analogue onium host compounds by means of a phenanthrene template[87] are also based on effects of this type (and T-stacking effects). Electron-donor–acceptor interactions are also the driving force in the complex formation of "cyclo-bisintercalands" (Lehn)[88] and—in addition to hydrogen bonds—in tweezer molecules (Zimmerman,[89] Harmata[90]). Hamilton et al. demonstrated the influence that the distribution of the partial charges within the π-electron systems has on the orientation (face-to-face or edge-to-face) of a guest (additionally bound by hydrogen bonds) relative to the arene surfaces of the host.[91] Dougherty et al.[92] explained the strength of the complexation of quaternary ammonium salts by a cyclophane receptor by the occurrence of ion–dipole interactions,[93] whereby the positive charge of the guest is "solvated" by the electron-rich surface of the aromatic rings. This effect is also observed in the complexation of aromatic guests by azoniacyclophanes (Schneider[94]).[69]

4.2. Molecular Recognition of Organic Molecules by Hydrogen Bonds and Ionic Interactions (Ion Bridges)

Following the donor–spacer concept[15] for the synthesis of macrobicyclic ligands, we prepared a series of hosts with increasingly larger intramolecular cavities by replacing the benzene anchor groups in ligands such as **21** and **26** by larger spacers, for example 3,3′,3″- or 4,4′,4″-trisubstituted triphenylbenzene units).[44,95] Varying the bridge building-blocks allows one to adapt the complexing properties of the macrobicyclic hosts to the binding character of many different types of guests. Using this principle we were able to prepare basic and acidic endoreceptors for the inclusion of respective hydrogen-bond donor and acceptor guests, and nonpolar endoreceptors for complexing hydrophobic molecules (Scheme 8).[15]

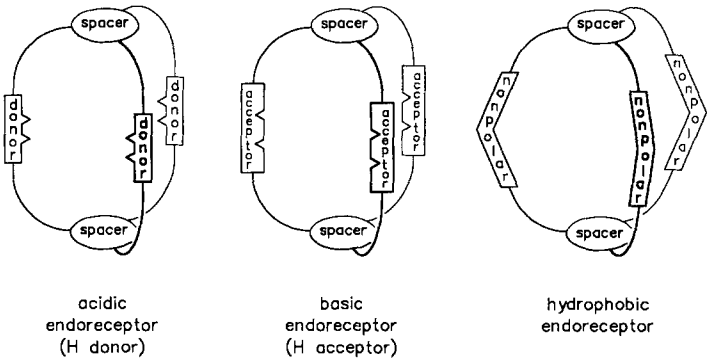

Scheme 8. Types of endoreceptors.

The internal walls of the tris(bipyridine) compounds **32**–**34** with the six basic heteroarenes are virtually lined with hydrogen-bond acceptors.[95] These hosts are thus tailor-made for

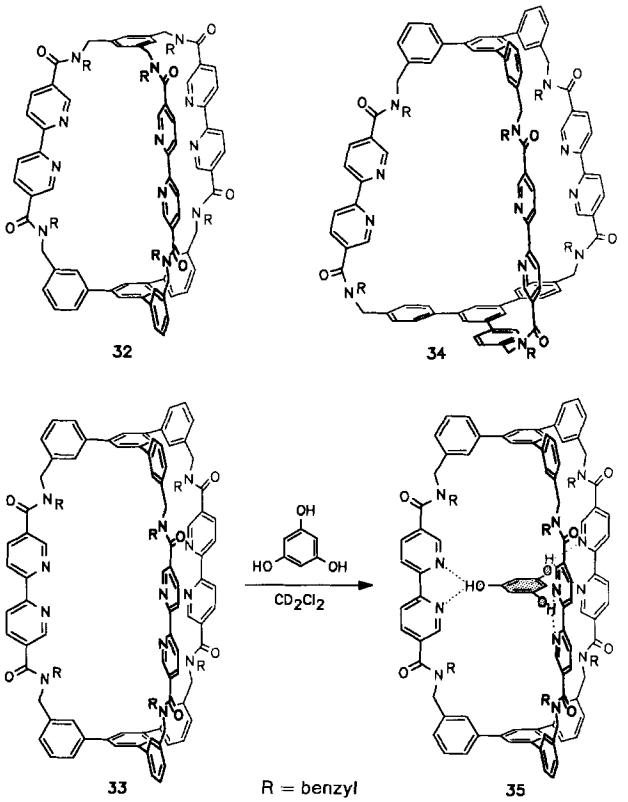

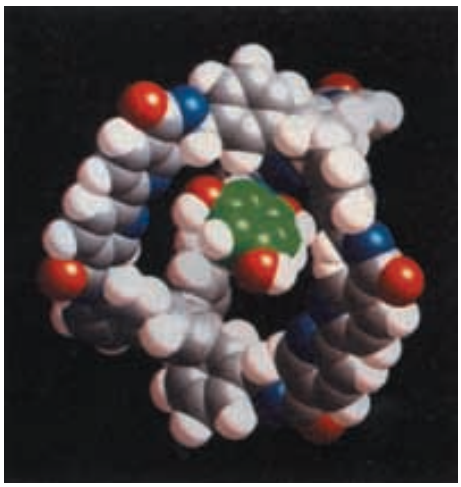

Fig. 6. Space-filling model of the phloroglucinol inclusion complex **35**. The *N*-benzyl groups are not shown; the carbon atoms of the guest are colored green.

encapsulating sterically and functionally complementary trihydroxybenzenes. Such guests, which are otherwise sparingly soluble in the organic phase (CH_2Cl_2), are solubilized by the hosts and bound by means of multiple hydrogen bonds in the cavity. The complexation can thus be detected not only by ^1H NMR spectroscopy (the spectra exhibit signals for both host and guest), but can also be followed macroscopically by the dissolution of the suspended guests. An association constant K_{ass} of $1.1 \times 10^4\ M^{-1}$ was determined (in CH_2Cl_2) for the phloroglucinol (1,3,5-trihydroxybenzene) complex **35** (Fig. 6); however, pyrogallol (1,2,3-trihydroxybenzene) and other compounds not complementary to the structure of the receptors are discriminated (Table 2).

Table 2. Selective coupling of organic guests by tris(bipyridine) hosts in CD_2Cl_2 [a].

Guest	**32**	**33**	**34**
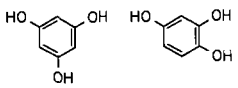	+	+	−
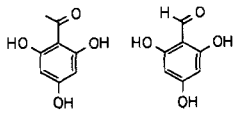	+	+	+
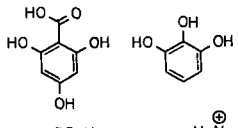	−	−	−
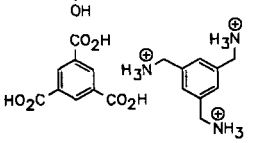	−	−	−

[a] (+ = complexation, − = no noticeable complexation.)

The hosts **32**–**34** also react sensitively to the introduction of methyl or ammonium groups into the guest molecules: 2,4,6-trihydroxytoluene or 2,4,6-trihydroxyaniline hydrochloride are not complexed. The more strongly acidic nitrophloroglucinol simply forms, like picric acid, 1:3 complexes.

In contrast to the tris(bipyridine) hosts, the macrobicyclic ligand **36** has pronounced proton-donor character (acidic endoreceptor, see Scheme 8) because of the six hydroxyl groups of the catechol units. As a consequence, it complexes organic molecules with basic functional groups as long as the pK_S and pK_B values are mutually compatible.[96] In experiments with strongly basic triamines, saltlike aggregates are formed as the result of an acid–base reaction. On the other hand, purine and pyrimidine bases and similar, less basic compounds can be solubilized by **36** in dichloromethane, *in* which they are otherwise only sparingly soluble. Host **36** is

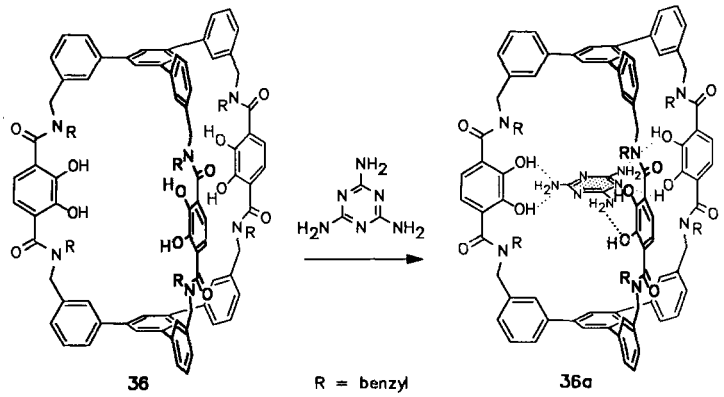

clearly superior to open-chain catechol compounds on account of the better preorganization of its binding centers due to the clamping in the cage framework. Furthermore, in transport experiments based on solid–liquid–liquid extractions the rate of transport of the aforementioned guests through an organic phase and into an aqueous acidic solution is substantially increased by host **36**. Figure 7 shows the space-filling model of the adenine complex of **36**.

If three crown ether building-blocks are held in place by two spacers, then macropentacyclic structures are obtained whose cavities contain three coordination centers for metal ions or

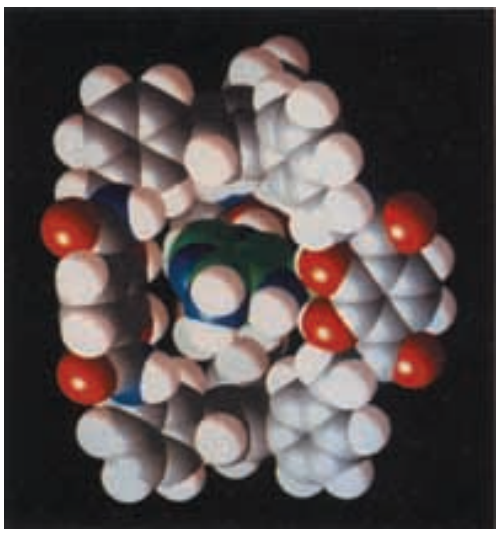

Fig. 7. Space-filling model of the adenine inclusion complex of the host **36**. The *N*-benzyl groups are not shown; the carbon atoms of the guest are colored green.

proton donors.[11] The water-soluble triscrowns **37**–**39** form 3:1 complexes with salts such as KSCN;[97] however, cooperative binding of cations was not observed. In addition, hosts **38** and **39** bind various naphthalenediols, whereas phenol as well as di- and trihydroxybenzenes and triammonium salts are not appreciably complexed.

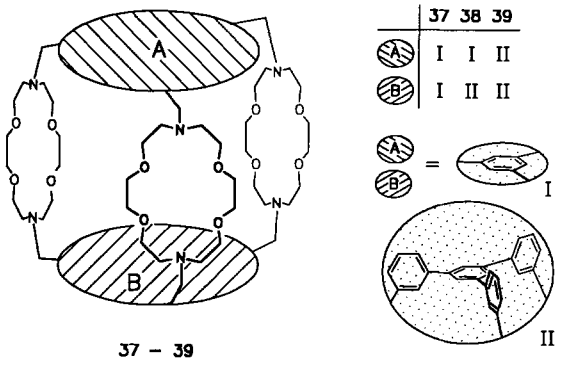

37 – 39

In the host compounds **40**, **42**, and **44** a cyclophanelike subunit is bridged with a crown ether building-block.[98] The crown ether part serves as a site for hydrogen bonds or ion bridges, whereas the cyclophane part offers lipophilic groups a nonpolar environment. The hosts are consequently ditopic receptors for organic guests, which in addition to hydrophobic subunits also contain polar protic or cationic structure elements. Thus, the basket-shaped[99] molecule **40** in $CDCl_3$ solubilizes for example ammonium *p*-nitrophenolate by the formation of the complex **41**.[100] Through the binding of the ammonium ion to the crown ether unit the phenolate is drawn into the host cavity and fixed by the ion bridge. The ionic centers are thus shielded from the lipophilic solvent by the host framework, while at the same time the arene ring of the guest is positioned between the naphthalene units.

In a similar manner the cylindrical hosts **42** and **44** (Saigo[101] and Hamilton[102]) are able to incorporate various alkylammonium ions. The complexation of ω-phenylalkylammonium ions **43** by **42** proceeds with cooperative interaction if the guests are optimally adapted to the host in terms of their chain length. If the ammonium group docks on the crown, the terminal phenyl ring comes into contact with the nonpolar cyclophane unit when **43** has $(CH_2)_5$ or $(CH_2)_6$ chains. The resulting gain in stability is reflected in the association constants; with K_{ass} values of roughly $1.7 \times 10^3\ M^{-1}$, they are three to six times higher than those measured for guests with shorter or longer chains (determined by NMR spectroscopy in $CDCl_3/CD_3OD$ 4:1).[101]

Lehn et al. have reported on the molecular recognition of dicarboxylates[103] by the macrobicyclic receptor **45**.[104] In its protonated form this receptor forms inclusion complexes with the dianions of aliphatic α,ω-dicarboxylic acids. Adipate ($K_{ass} = 2.6 \times 10^3\ M^{-1}$) is the most complementary in terms of size and is more strongly bound than larger and smaller homologues. The terephthalate complex **46** ($K_{ass} = 2.5 \times 10^4\ M^{-1}$),

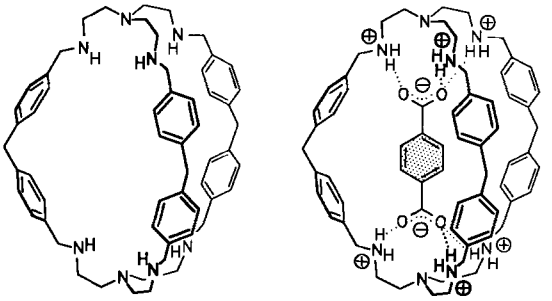

45 **46**

in which hydrophobic interactions as well as electrostatic interactions play a role, is one order of magnitude more stable. The X-ray structure analysis of **46** shows the envelopment of the guest by the host, and its fixation by the formation of three hydrogen bonds between each carboxyl group and the ammonium groups (Fig. 8).

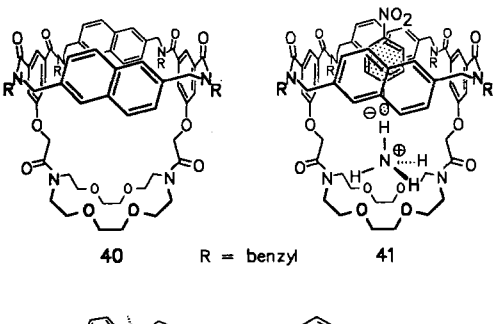

40 R = benzyl **41**

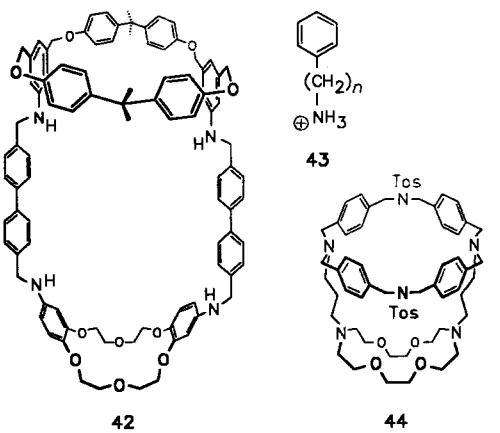

42 **44**

Fig. 8. Crystal structure of the terephthalate inclusion complex **46**. The hydrogen atoms are not shown; the carbon atoms of the guest are colored green.

Whitlock et al. have reported on a series of macrobicyclic host compounds **47**–**48** ("phenol sticky hosts"), which contain, in addition to rigid, hydrophobic naphthalene walls, a pyridine unit as "docking site".[105, 106] These polycycles bind phenols in nonpolar solvents with a high degree of efficiency and electronic and stereochemical specificity.

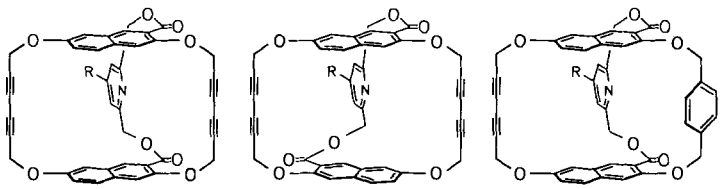

47a (*meso*) R = $N(CH_3)_2$ **47b** (±) **48a** : R = $N(CH_3)_2$ **48b** : R = H

The isomeric hosts **47a** (*meso*) and **47b** (±) are formed in the same cyclization reaction in a 2:1 ratio.[105] In the ligands **48a** and **48b** one of the two hexadiyne units of **47a** is replaced by a *p*-xylylene group. The distance between the naphthalene spacers is thereby reduced, with the result that the cavity is better adapted to the size of the guests.[106] Furthermore, as also demonstrated by the crystal structure, favorable edge-to-face interactions (T-stacking) occur between the guest and *p*-xylylene ring (Fig. 9). Accordingly, *p*-nitrophenol is four times more strongly bound by **48a** than by **47a** ($K_{ass} = 0.6 \times 10^4\ M^{-1}$ and $2.3 \times 10^4\ M^{-1}$). The (±) isomer **47b** binds even more weakly than the *meso* host **47a**, presumably due to its lesser conformational flexibility and the consequently larger steric barrier in complex formation. Here it is found that greater rigidity does not necessarily confer better ligand properties.

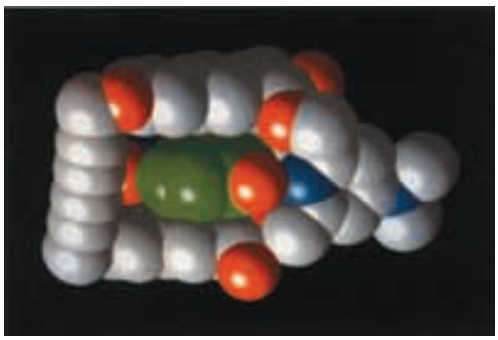

Fig. 9. Crystal structure of **48a** with intercalated *p*-nitrophenol. The hydrogen atoms are not shown; the carbon atoms of the guest are colored green.

An important factor for molecular recognition by formation of hydrogen bonds is the optimum adjustment of the basicity of one component and the acidity of the other. For example **48b**, which is less basic due to the absence of the dimethylamino group, is a weaker host than **48a**. Complexation also does not occur if the guests are more acidic than *p*-nitrophenol, for instance 3,5-dinitrophenol or benzoic acids. In contrast to binding by hydrogen bonds, simple proton-transfer thus does not necessarily result in the formation of supramolecular structures (cf. the complexation properties of the hosts **32**–**36**).

The macrobicyclic hosts **49** and **50** of Still et al.[77] employ multiple hydrogen bonds to bind organic guests with donor and acceptor functionalities arranged in a manner complementary to the cyclourea units and amide groups of the molecular cavities.[107, 108] Various heteroarenes are thus incorporated. For example, the binding energy for the complex of 4-pyridone and **49** is approximately $-21\ kJ\,mol^{-1}$. Compounds such as pyridine or *N*-substituted imidazoles are discriminated, since they do not possess proton-donor properties.[107]

Host **50** complexes amides of primary amines. The binding results from interactions between the amide hydrogen atoms of the guest and the cyclourea unit of the host, as well as between the carbonyl group of the guest and the amide protons of the host. The molecular framework of **50** contains two asymmetric bridgehead carbon atoms with (*S*) configuration. In the case of amides with a center of chirality adjacent to the nitrogen atom, the (*S*) enantiomers are more tightly bound than the (*R*) enantiomers, since they are better adapted to the host geometry. Although the enantioselection is not high, it is nevertheless significant. For the two isomers of *N*-(1-phenylethyl)acetamide, for example, $\Delta\Delta G_{ass}$ is $1.7\ kJ\,mol^{-1}$ ($CDCl_3$) [$\Delta G = -12.7\ kJ\,mol^{-1}$ (*S*) enantiomer and $-11.0\ kJ\,mol^{-1}$ (*R*) enantiomer].[108]

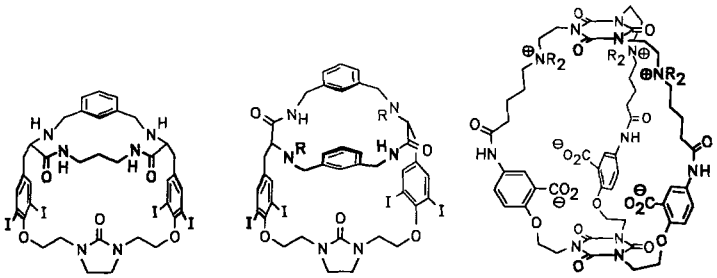

49 **50** : R = benzyl **51**

The water-soluble bicyclic compound **51** (R = CH_3) is a ditopic host for zwitterionic amino acids (Askew).[109] The framework of the host contains three quaternary ammonium groups as well as three carboxylate groups, which in the case of inclusion of appropriate guests may be oriented towards the cavity.[110] The host binds γ-aminobutyric acid (GABA) with an association constant of $3.2 \times 10^3\ M^{-1}$ (D_2O). Glycine, which is too small, and 6-aminocaproic acid, which is too large, are only weakly bound.

Macrobicycles with chelate building-blocks integrated into the molecular skeleton are able to fix guests in the cavity by means of ionic interactions in addition to hydrogen bonds. The cage molecule **52**, with its convergently arranged phenanthroline bridges,[111] has three coordination sites for metal ions. The intramolecular cavity is essentially too large for 1:1 complexes of type **27** to be formed. Indeed, it offers so much space that three cations including three "guest ligands" can be accommodated (Fig. 10). In the hepternary complexes **52a** and **52b** three 2,9-disubstituted phenanthroline molecules are incorporated as copper(I) complexes. The 1:3:3 stoichiometry (*m/z* 2765 and 2307) and the *endo* conformation are unambiguously confirmed by spectroscopy. This stoichiometry is not observed for the complexes of

Fig. 10. Space-filling model of the hepternary supramolecular complex **52b**. The carbon atoms of the guest ligands are colored green.

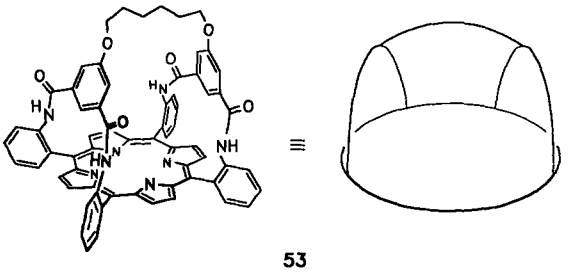

53

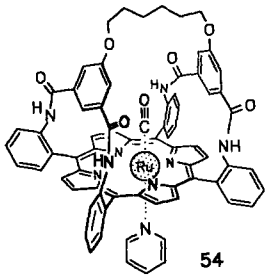

54

phenanthroline derivatives with space-filling substituents in the 4 and 7 positions.[112]

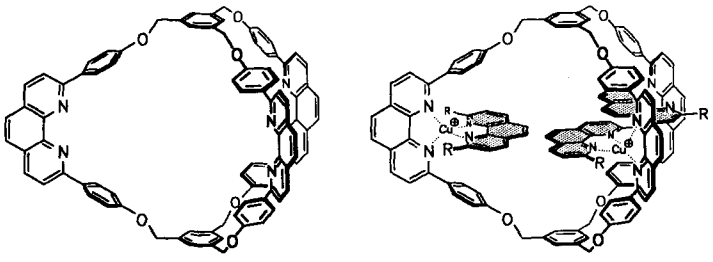

52

52a : R = *p*-tolyl
52b : R = CH_3

A series of multiply bridged porphyrins with intramolecular cavities is described in the literature.[113] The "capped porphyrins" (Baldwin,[114] Basolo,[115] Ibers,[116] Lindsey,[23]; for example **11**), the "pocket porphyrins" (Collman)[117] and the quadruply linked "double-decker porphyrins" ("stratibisporphyrins"; Kagan, Bruice,[118] Vögtle[20]; for example **8**) may be mentioned in this context. The porphyrinophanes developed by Collman et al. and termed "picnic basket porphyrins" (PBPs) because of their shape, will be illustrated with the example of **53**.[119] The rigid skeleton encloses a cavity that shields one face of the porphyrin unit, which (similarly to the crown ethers in the hosts **40**, **42**, and **44**) serves as binding sites for metal cations and additionally coordinated "guest ligands". PBPs are model compounds for the active center of cytochrome P-450 monooxygenases.[120]

Ru^{II} complexes of PBP **53** can be formed with $[Ru_3(CO)_{12}]$; the free, axial positions of the metal ions are then occupied by a CO ligand and a solvent molecule (pyridine (Py) or THF). The complexes exist in two regioisomeric forms: in one the CO ligand is located in the interior of the cavity, in the other outside the cavity. Equilibrium experiments have shown that the CO_{out}–Py_{in} complex is thermodynamically more stable than the CO_{in}–Py_{out} isomer **54** ($\Delta E \geq 8.2$ kJ mol^{-1}).[119a]

If sterically unprotected Ru^{II} porphyrins are exposed to molecular oxygen, the metal is irreversibly oxidized. This proceeds presumably via a μ-peroxo dimer, in which two porphyrin units are connected by an O_2 bridge.[119] In order to obtain more stable complexes, one must prevent this dimerization. In the PBPs one face of the porphyrin is shielded by the molecular skeleton. The other side can be blocked by tightly coordinating ligands. Such a ligand is 1,5-dicyclohexylimidazole (DCI), which is sterically too demanding to be able to occupy the cavity, with the result that complex **55** is formed regiospecifically. The weakly binding THF molecule can now easily be replaced by O_2 (complex **56**). The N_2 complex **58** may be obtained from **55** via the Ru^{III}-Cl-PBP complex **57** (Scheme 9).[119b]

Whereas the dioxygen complex **56** is only metastable in an O_2 atmosphere (half-life 90 min), the nitrogen complex **58** is

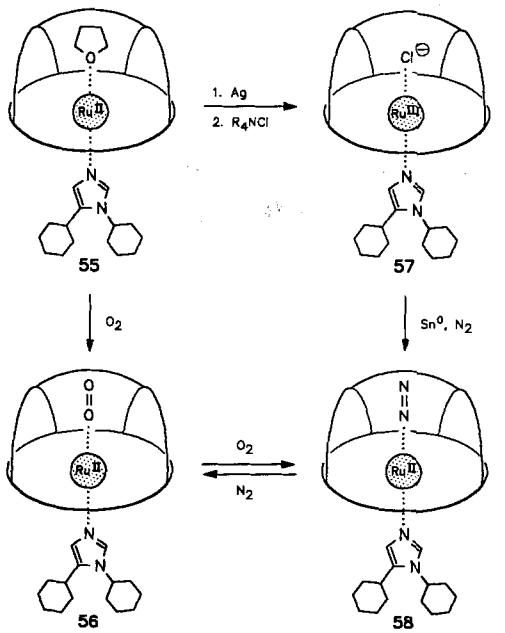

55 **57** **56** **58**

Scheme 9. Formation of the oxygen and nitrogen complexes of PBP by exchange of the *in* ligands.

stable for weeks under inert gas. The IR spectroscopic data of **56** indicate that molecular oxygen is reduced to the superoxide ion O_2^-, and **56** may be regarded as a Ru^{III}–O_2^- complex. Complex **56** is not paramagnetic, and consequently there are no unpaired electrons, which is why it is assumed that there is an additional bond between the metal and the directly coordinating oxygen atom.[119b]

4.3. Complexation of Neutral Molecules by van der Waals Interactions

In 1955 Stetter and Roos were the first to become interested in large cyclophanes as potential inclusion hosts for small organic compounds.[121] The crystalline 1:1 complexes of their bis(benzidine) cycles with solvent molecules (benzene, dioxane) were subsequently shown, however, to be clathrates and not inclusion complexes.[122] At the beginning of the 1980s Koga led the way in the development of water-soluble host compounds for organic guests. In his tetraazacyclophanes two diphenylmethane units form hydrophobic niches and make the incorporation of nonpolar molecules in the aqueous phase and in the crystal possible.[8]

In 1984 Diederich and Dick synthesized the first macrobicyclic hosts **59a** and **59b** for complexing neutral molecules.[13] (The numerous monocyclic analogues cannot be

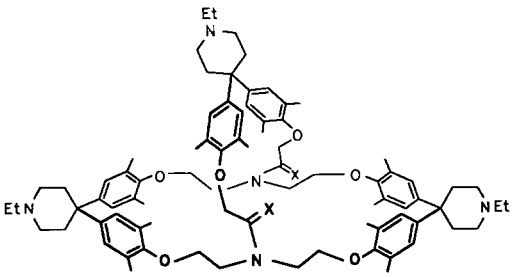

59a : X = O
59b : X = 2H

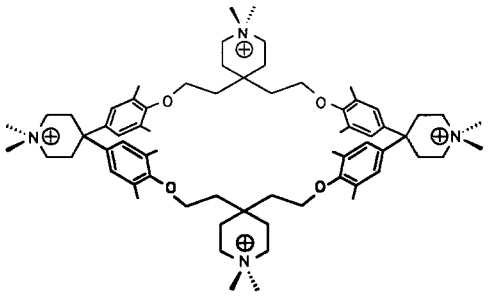

60

discussed individually within the scope of this article, but are described in detail elsewhere.[9d, 71]) The protonated piperidinium rings on the three diphenylmethane building-blocks confer water-solubility on the macrobicycles and their complexes. Due to the spiro linkage, the ionic centers are located on the periphery and thus do not interfere with the markedly nonpolar character of the cavity.

Host **59a** complexes flat aromatic guests in aqueous phase. The association constants are of a comparable order of magnitude to those of the monocyclic comparison compound **60**.[123] For the pyrene complex they were determined by liquid–liquid extraction to be $3.1 \times 10^6\ M^{-1}$ for **59a**[75] and $1.8 \times 10^6\ M^{-1}$ for **60**.[123] The envelopment of the guests by monocycle **60** is obviously very effective. In **59a** the hydrophobic character of the cavity is decreased by the solvation of the two polar amide groups. This unfavorable effect is obviously even more pronounced in the case of **59b**, which contains two protonated, highly solvated amine nitrogen atoms as bridgeheads, and its binding capacity for nonpolar guests in aqueous phase is clearly reduced. The situation is reversed in organic solvents (see Section 4.1): the solvation of the more polar amide groups is stronger than that of the (in this case non-protonated) amine functions. The extra energy expended in the desolvation in the complexing step reduces the binding strength. The association constants for the pyrene complexes in methanol were found to be $3.4 \times 10^4\ M^{-1}$ for **59b** and only $65\ M^{-1}$ for **59a** (UV titration).[75]

Another host with three diphenylmethane units is the macrobicyclic hexaamine **61**, which can be obtained from a relatively short synthesis (analogous to path A in Scheme 1).[124, 125] The six tertiary amino groups in the molecular framework of **61** not only impart solubility in aqueous HCl, but the resulting protonation prevents the collapse of the large discus-shaped cavity by means of the mutual repulsion of the positive charges. This host molecule exhibits a remarkable capacity for complexing various condensed arenes with complementary size and shape, such as triphenylene, perylene, or pyrene. The binding constant for the latter in methanol was found to be $10^{2.5}\ M^{-1}$. The com-

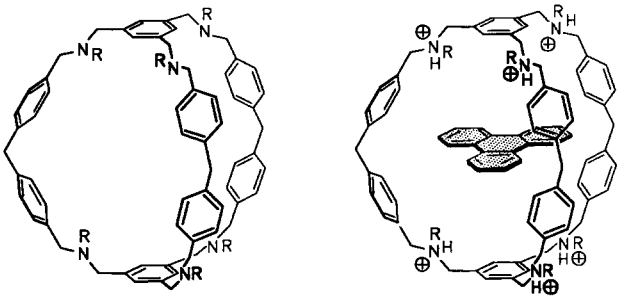

61 R = CH_3 **62**

plexation has drastic effects on the ^1H NMR signals. Not only are the proton signals of the guest shifted to higher field ($\Delta\delta \approx 1.5$), but also the otherwise broad signals of the host compound become sharper and resolve into multiplets; high-field and low-field shifts are also observed (see Fig. 11 for the triphenylene complex **62**). The conformational flexibility of the host framework is restricted by the inclusion of a guest, and the cavity shape is adapted to the guest ("induced fit").

Compounds that are too small, such as benzene and naphthalene, or too large, like coronene, are not appreciably complexed by the receptor model compound. Nor is anthracene bound appreciably, though phenanthrene is, a discrimination that has not hitherto been observed. Also, methyl-substituted and partially hydrogenated derivatives of arenes are not recognized as guests, even if the analogous parent com-

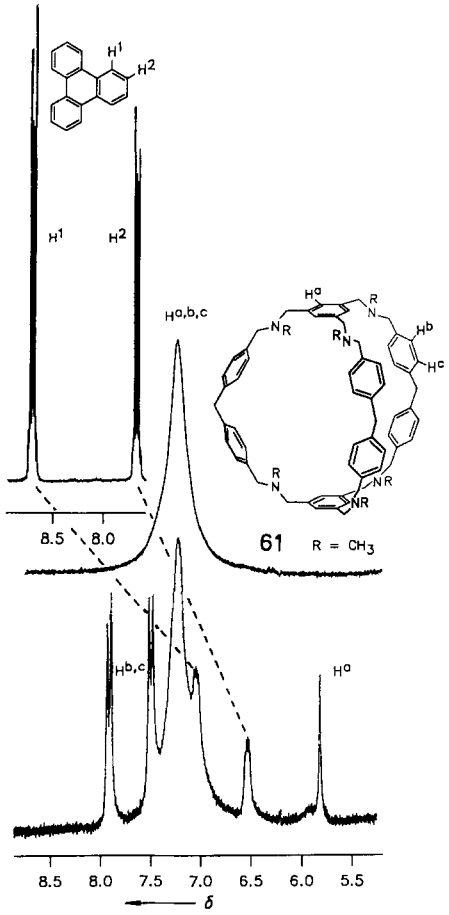

Fig. 11. Effect of complexation on ^{1}H NMR signals of the guest and host as illustrated by triphenylene and **61**. Top: guest triphenylene (CD_2Cl_2/D_3COD); center: host **61** (DCl/D_2O); bottom: host–guest complex **62** (DCl/D_2O).

pounds are included. Aliphatic CH_2 and CH_3 groups obviously prevent a favorable inclusion in the niches of the diphenylmethane units, as is possible with the arene parent compounds. The attractive interactions with an edge-in-angle arrangement of two aromatic systems are exhibited in this case (see Section 4.1). Table 3 provides a summary of complexed and discriminated compounds. Fig. 12 shows the space-filling model of the triphenylene complex **62**. On account of selective complexation, pyrene for example could be separated from decahydropyrene, and triphenylene from dodecahydrotriphenylene in phase-transfer (liquid–liquid and solid–liquid) experiments.[124, 126] Phenanthrene can be successfully separated from a mixture with naphthalene in *n*-hexane by the U-tube method.[124]

Table 3. Selective complexation of condensed arenes by host **61** in aqueous solution.

Complexed	Not appreciably complexed
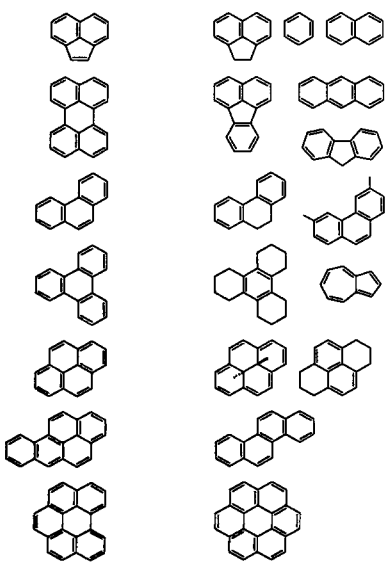	

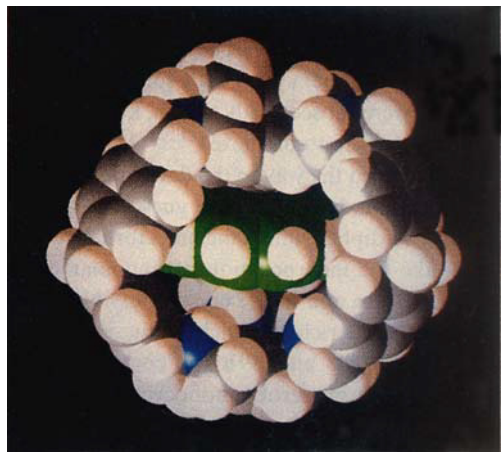

Fig. 12. Space-filling model of the triphenylene inclusion complex **62**. The carbon atoms of the guest are colored green.

The two macrobicyclic hosts **63a** and **63b** illustrate an interesting case of configurational isomerism: the acid-soluble hexaamines are "*in/out* isomers", which cannot be interconverted by conformational changes. They are obtained in a ratio of about 1:1 in the cyclization.[127] The differing size of the molecular cavities resulting from the stereochemical differences has a drastic influence on the complexation behavior. Whereas naphthalene and 2,6- and 2,7-dihydroxynaphthalene are bound by both hosts in aqueous acidic solution, only the larger *out/out* isomer **63a** is able to incorporate adamantane and 1-adamantanethiol. To our knowledge this is the first time that the complexation of an alicyclic hydrocarbon has been successfully achieved (complex **64**).

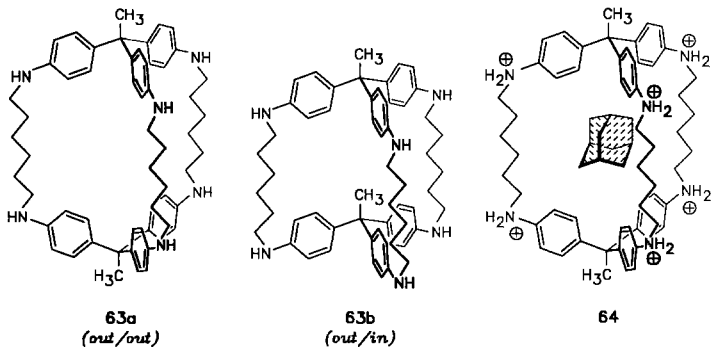

Collet et al. developed a family of host molecules whose skeletons are constructed from two cyclotribenzyl units (e.g.

cyclotriveratrylene, CTV), which are linked to one another by three alkyldiether bridges. These cryptophanes exhibit an interesting behavior in their complexation of halomethanes.[128]

The inclusion of halomethanes is evident in the strong upfield shifts of the signals of the guests in the ^{1}H NMR spectra ($\Delta\delta > 4$). The crystal structure analyses of the CH_2Cl_2 complexes of the isomeric cryptophanes C (**65**) and D (**66**) demonstrate that the guests are incorporated in the cavity between the two bowl-shaped spacers.[128] Interestingly, only the CH_2Cl_2 complex of the (+) enantiomer crystallized from a racemic solution of (±)-cryptophane D (**66**) in CH_2Cl_2/acetone (enantiomer separation by crystallization, Fig. 13).[129]

The chirality of the host molecule **65** effects the enantioselective inclusion of the likewise asymmetric bromochlorofluoromethane.[130] Investigations with enriched CHBrClF and pure enantiomers of cryptophane C (**65**) showed that the complexes in which the host and guest have the same rotational direction (*p* complex) are more stable than in the other case (*n* complex, $\Delta\Delta G \approx 1.1$ kJ mol^{-1} in $CDCl_3$).

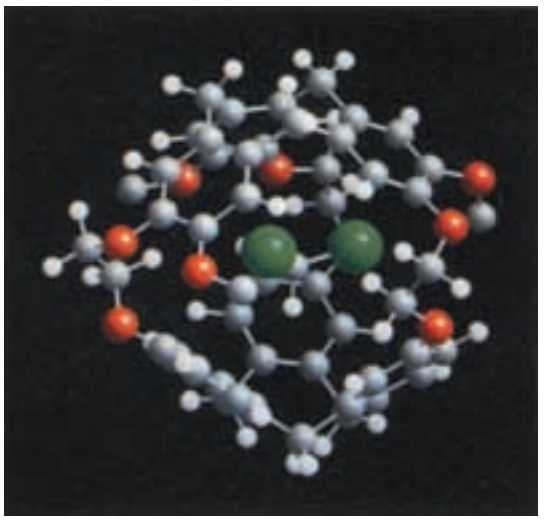

Fig. 13. Ball-and-stick model of the crystal structure of (+)-cryptophane D (**66**) with one CH_2Cl_2 molecule in the cavity (side view). The chlorine atoms of the guest are colored green.

The complex stabilities depend greatly on the size of the guest molecules (and of the solvent molecules[77]). In accord with Diederich's observations[71a, 131], it is found that the "best" guests are somewhat smaller than might be assumed from the CPK models. Cryptophane E (**67**) binds in (CD_2Cl_2)$_2$ a whole series of halomethanes, ranging in size from methyl iodide to carbon tetrachloride.[28, 132] The largest formation constant was found for the complex with the medium-sized chloroform ($K_{ass} = 470$ M^{-1}), whereas the smaller dichloromethane ($K_{ass} = 120$ M^{-1}) and the bulkier bromoform ($K_{ass} = 40$ M^{-1}) are bound substantially more weakly. Cryptophane A (**68**) on the other hand,[12] which has a smaller cavity and smaller portals, binds CH_2Cl_2 more strongly than $CHCl_3$ ($K_{ass} = 475$ M^{-1} and 230 M^{-1}, respectively).[133] A water-soluble derivative of **68**, the hexacarboxylic acid **69**, behaves in the opposite way. The stability constant K_{ass} of the complex with $CHCl_3$ is 7700 M^{-1}, but "only" 5000 M^{-1} with CH_2Cl_2. Probably because of the larger lipophilic surface and the resultant larger number of solvate molecules to be "stripped" in the complexing, the driving force of the hydrophobic effect is stronger for the binding of chloroform than of dichloromethane.[133]

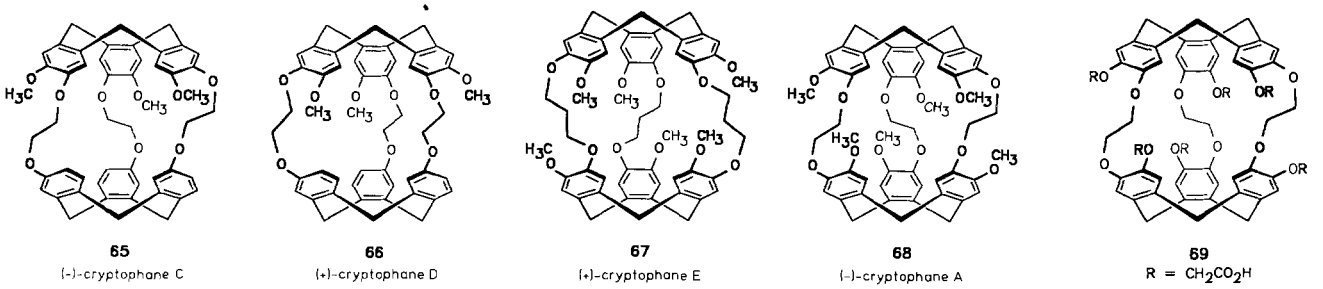

65 (-)-cryptophane C

66 (+)-cryptophane D

67 (+)-cryptophane E

68 (-)-cryptophane A

69 R = CH_2CO_2H

Other macrobicyclic hosts with a predominantly nonpolar molecular framework include the tris(diyne) compounds **15**[26] and **70**.[134] The aromatic spacers as well as the diacetylene bridges impart a marked rigidity and prevent the frame from collapsing. The ether oxygen atoms acting as "hinges" enable the molecule to twist, however, and thus adapt to the size of the incorporated guests.[135]

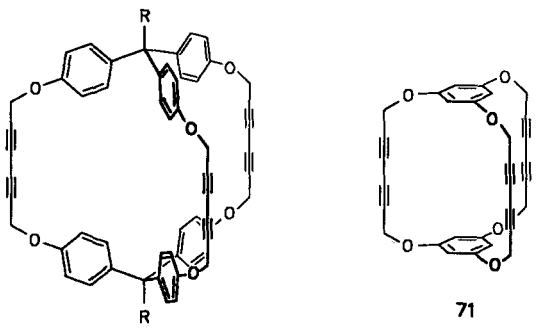

15: R = CH_3
70: R = H

71

Crystals of **15** obtained from benzene strikingly illustrate this adaptation (Breslow et al.). The triphenylethane units are twisted helically so that a solvent molecule is rigidly clamped in the cavity interior between two oppositely situated phenylene rings of the host (Fig. 14). This is a typical example of

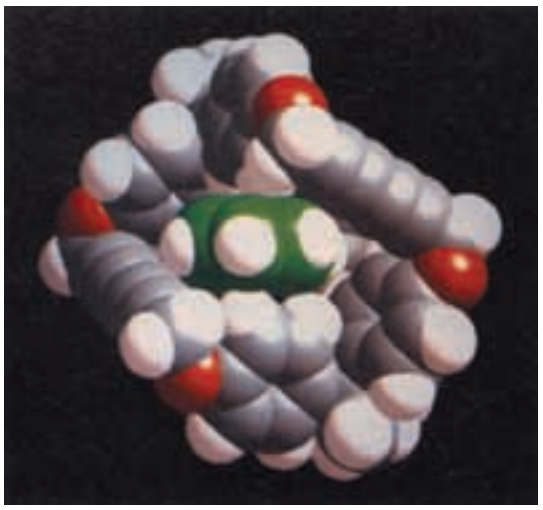

Fig. 14. Crystal structure of the macrobicyclic host **15** with intercalated benzene. The unit cell contains four further benzene molecules, two of which are also incorporated in the host framework. The carbon atoms of the guest are colored green.

a multiple edge-to-face interaction (T-stacking, see Section 4.1, Fig. 5).[26]

The inclusion complex of host **70** with acetonitrile is comparable.[134] The guest can take two alternative positions in the host cavity, one of which is illustrated in Figure 15. Through π-stacking and electron-donor–acceptor interactions, the two aromatic units of one of the three bridges of the macrobicyclic host are attracted to the interposed guest, and thus have a smaller interspacing than the remaining units. The IR spectrum of the complex exhibits a considerable shift of the nitrile band to smaller wavenumbers (2219 cm^{-1} compared to 2254 cm^{-1} in free acetonitrile), which could indicate a lengthening of the C–N bond on account of the intermolecular interactions.[134]

Fig. 15. Crystal structure of the acetonitrile inclusion complex of the host **70**. Only one of the two occurring orientations of the guest in the cavity is shown. The carbon atoms of the guest are colored green.

The smaller tris(diyne) **71** with two benzene spacers instead of triphenylmethane units also incorporates acetonitrile in the crystal. Here, too, the nitrile band is shifted 35 cm^{-1} in the IR spectrum. However, in contrast to **70**, in this case the methyl group of the guest is situated between the arene units of the host, and not the nitrile group. This arrangement can be interpreted as a consequence of a σ–π interaction between the acidic protons of the CH_3 group and the electron-rich (π-basic) tris(alkoxy)benzenes (Fig. 16).[136]

Fig. 16. Crystal structure of the acetonitrile inclusion complex of the host **71**. The carbon atoms of the guest are colored green.

4.4. Catalytically Active Host Compounds

Starting from bis(diphenylmethano)cyclophanes, Diederich developed the supramolecular catalysts **72**–**74**. In the hosts **72** and **73** a thiazolium ring and a phenol ring, respectively, are arranged as catalytically acting groups above the molecular cavity, in other words above the binding site for aromatic guests. The thiazolium group is the active center in thiamine

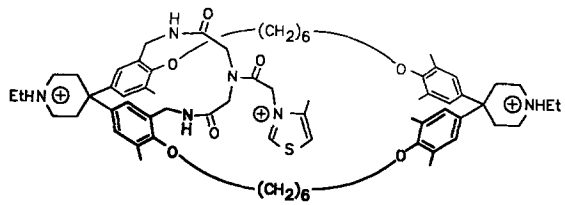

72

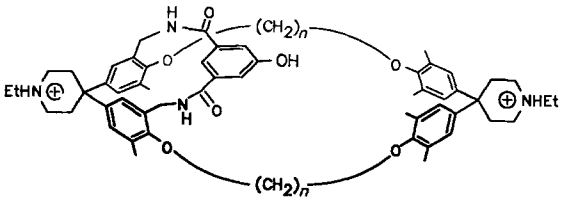

73a: $n = 4$
73b: $n = 6$

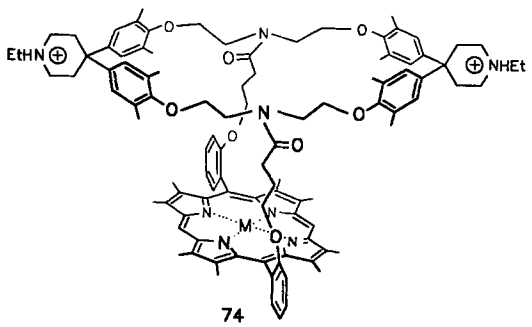

74

pyrophosphate (TPP), which serves as an important cofactor in many enzymes catalyzing C–C bond formation and cleavage.[137] The cavity of the enzyme model **72** provides sufficient space to accommodate two benzaldehyde molecules and fix them at a favorable distance relative to the thiazolium ring, with the result that benzoin is formed in high yield.[138]

The phenolic OH group of **73a** and **73b** is an effective nucleophile at physiological pH values,[137] and the two hosts thus act as synthetic esterases ("α-chymotrypsin mimics").[139] With 4-nitro-1-naphthyl acetate as substrate, significant differences are observed in the acceleration of the transacylation step: a factor of 178 in the case of **73a** compared to a factor of 14 in the case of **73b**. The cavity of **73a** is sufficiently large to permit an approach of the phenol and ester groups in the complex favorable for the reaction (productive complexing). The situation is different with the smaller host **73b**, which is also able to complex the aromatic residue readily, but only unproductively. The phenol residue of a second host molecule thus acts as catalytic center in this case.

The porphyrin-bridged cyclophane **74**[140] is a synthetic model compound for the natural cytochrome P-450 enzymes,[120] which as monooxygenases are involved in the catabolism of lipophilic substrates. They contain as an essential structural feature an iron(II) hemoporphyrin in the vicinity of a hydrophobic substrate binding site. In **74** the cyclophane part, which is linked by two bridges to the porphyrin ring, forms such a binding site. In trifluoroethanol the Fe^{III} complex of **74** incorporates acenaphthylene ($K_{ass} = 1.05 \times 10^3\ M^{-1}$) and oxidizes this guest selectively to acenaphthen-1-one, in the presence of iodosobenzene as oxygen carrier. Phenanthrene on the other hand, which is likewise strongly but unproductively bound ($K_{ass} = 1.33 \times 10^3\ M^{-1}$), inhibits catalysis competitively without being attacked itself.

4.5. Multiply Bridged Cage Host Compounds

The macropentacyclic host molecule **75** has a rigid, cubic framework whose six sides are formed by tetraaza[3.3.3.3]-paracyclophane units (Murakami).[141] Because of its water-solubility in the protonated state, **75** is able to incorporate both neutral and anionic organic guests in its cavity by utilizing hydrophobic interactions.[142] The cavity in the octa-

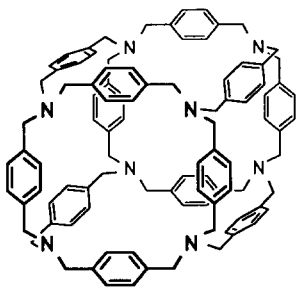

75

cation of **75** is no longer sufficiently lipophilic due to the strong solvation, and consequently no complex formation is observed.[143] In contrast the tetracation of **75** binds, for example, *N*-phenyl-1-naphthylamine with an association constant K_{ass} of $8.8 \times 10^4\ M^{-1}$ (pH 4). With the structurally related 8-anilinonaphthalene-1-sulfonate (ANS) electrostatic forces of attraction are also involved as driving forces: The binding of the guest ($K_{ass} = 1.6 \times 10^5\ M^{-1}$ at pH 4) is about twice as strong.[142]

Cram et al. designed a new family of molecular "container compounds": the carcerands **76a**[144] and **76b**,[145] which are constructed of two quadruply bridged "cavitand" subunits,[146] and have a virtually closed molecular surface. Once guests have been trapped in the cavity they can be released again only by destruction of the molecular framework. Inclusion complexes of all neutral molecules and ions present in the cyclization reaction have been detected: solvent molecules (THF, *N,N*-dimethylformamide, *N,N*-dimethylacetamide, and dimethyl sulfoxide), cesium ions of the auxiliary base, and even argon and freon from the inert-gas atmosphere. The complexes can be separated chromatographically, and there is consequently an exchange of information between the guest in the interior and the host environment. According to Cram these "carceplexes" provide a new phase of matter for the incorporated guests. The interior of the carceplexes is a definable mixture of free space and space-filling guests ("guest plus vacuum in varying proportions").[144]

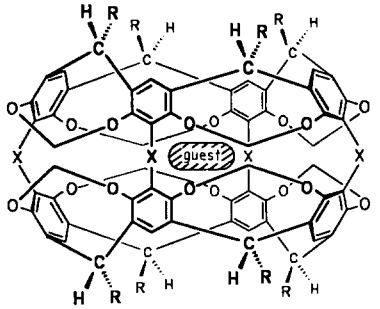

76a : R = CH_3, X = CH_2SCH_2
76b : R = CH_2CH_2Ph, X = OCH_2O
76c : R = CH_2CH_2Ph, X = Y
76d : R = CH_2CH_2Ph, X = Z

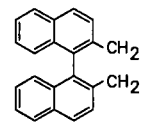

If the cavitand halves are held in position with larger bridges (as in **76c**[147] and **76d**[148]) or with only three instead of four units,[149] the windows in the equator plane of the cage molecules are consequently widened and the shielding of the cavity is thus less complete. Consequently the "hemicarceplexes" can be decomplexed by heating in solvents consisting of bulky molecules. The free "hemicarcerands" can then form new inclusion complexes on treatment with other solvents or solutions of suitable guests. The steric barriers in these processes are relatively high and the complexes are correspondingly stable ("constrictive binding").

5. Future Outlook

Molecules with an aesthetic architecture reminiscent of macroscopic structures have always held a particular fasci-

nation for the synthetic chemist.[150] In this review article we have discussed the not insubstantial contribution made by large host molecules with intramolecular cavities and suitable endoreceptor properties in supramolecular chemistry and, in this context, particularly in the elucidation of the principle of molecular recognition. Despite much success in this field, by no means all the objectives have been achieved. For example the synthetic receptors for sugars,[151] steroids,[152] lipids, peptides, and nucleotides,[61a, 65, 68, 153] and the separation of enantiomers are certainly open to improvement.[154] One may also anticipate the insights provided by the investigations of dendrimers[155] (cascade molecules,[156] arborols[157]), which have recently been in the forefront of attention.

In the future, interest will extend over and above molecular recognition to desired functions. Biological systems with their outstanding properties often serve as examples in this connection. The first steps on the path to efficient and readily accessible bioorganic and bioinorganic catalysts that imitate highly specific enzymatic catalytic processes have already been taken, though many challenges still remain. Transport phenomena of all types are also worthwhile subjects for study, for example the transport of ions or molecules with mobile carriers[126] or transport by means of molecular channels or tubes through cell membranes.[158] From the medical aspect sequestering agents would be important in removing toxic and radioactive metals and other poisons from the body, or also as drug carriers for transporting drugs to targeted disease sites. Such complex-forming agents may also be imagined in fluorescence- or radiolabeling of antibodies[159] for early recognition of metastases (tumor imaging). Efforts will also continue in the transmission of information, such as occurs in nerve pathways, and in developing molecular wires, antennae, light converters, rectifiers, transistors, and systems for the photochemical splitting of water.[16]

With its multidisciplinary character, supramolecular chemistry offers a broad spectrum for scientists of all fields, and in the future will not only provide important incentives for basic research but also for innovative applications.

We wish to thank all co-workers who by their efforts and knowledge have contributed to the success of our research in the field of large molecular cavities. We also wish to thank W. Schmidt, Dr. A. Schröder, and in particular P.-M. Windscheif for preparing some of the diagrams for this review article. We are grateful to Professor A. von Zelewsky (Freiburg, Switzerland), Prof. V. Balzani (Bologna, Italy), and their co-workers for the fruitful cooperation in the field of supramolecular photochemistry. We also thank colleagues who have provided crystal structure data. Our work was supported by the Deutsche Forschungsgemeinschaft and the Bundesministerium für Forschung und Technologie.

Received: July 22, 1991 [A 864]
German version: *Angew. Chem.* **1992**, *104*, 542

[1] D. J. Cram, R. A. Reeves, *J. Am. Chem. Soc.* **1958**, *80*, 3094–3103.
[2] J. Hubert, J. Dale, *J. Chem. Soc.* **1965**, 3160–3170.
[3] a) F. Vögtle, *Liebigs Ann. Chem.* **1970**, *735*, 193–195; b) V. Boekelheide, R. A. Hollins, *J. Am. Chem. Soc.* **1970**, *92*, 3512–3513; c) F. Vögtle, P. Neumann, *J. Chem. Soc. Chem. Commun.* **1970**, 1464–1465.
[4] P. Knops, N. Sendhoff, F. Vögtle, *Top. Curr. Chem.* **1991**, *161*, 3–36.
[5] A. Ostrowicki, E. Koepp, F. Vögtle, *Top. Curr. Chem.* **1991**, *161*, 37–68. Some authors dispute the existence of a specific cesium effect, see for example C. Galli, L. Mandolini, *J. Org. Chem.* **1991**, *56*, 3045–3047.
[6] C. J. Pedersen, *Angew. Chem.* **1988**, *100*, 1053–1059; *Angew. Chem. Int. Ed. Engl.* **1988**, *27*, 1021–1027.
[7] J.-M. Lehn, *Struct. Bonding (Berlin)* **1973**, *16*, 1–69.
[8] a) K. Odashima, A. Itai, Y. Iitaka, K. Koga, *J. Am. Chem. Soc.* **1980**, *102*, 2504–2505; b) *J. Org. Chem.* **1985**, *50*, 4478–4484.
[9] a) P. M. Keehn, S. M. Rosenfeld, *Cyclophanes I, II* in *Organic Chemistry, a Series of Monographs, Vol. 4* (Ed.: H. H. Wasserman), Academic Press, New York, **1983**; Vol. 45; b) *Cyclophanes* (Ed. F. Vögtle); Part I: *Top. Curr. Chem.* **1983**, *113*; Part II: *ibid.* **1983**, *115*; c) F. Vögtle, *Cyclophan-Chemie*, Teubner, Stuttgart, **1990**; d) F. Diederich, *Cyclophanes, Monographs in Supramolecular Chemistry*, (Ed.: J. F. Stoddart), Royal Society of Chemistry, Cambridge, **1991**.
[10] a) I. Tanaka, I. Tajima, Y. Hayakawa, M. Okada, M. Bitoh. T. Ashida, H. Sumitomo, *J. Am. Chem. Soc.* **1980**, *102*, 7873–7876; b) S. J. Abbot, A. G. M. Barrett, C. R. A. Godfrey, S. B. Kalindjian, G. W. Simpson, D. J. Williams, *J. Chem. Soc. Chem. Commun.* **1982**, 796–797; c) F. Vögtle, H. Puff, E. Friedrichs, W. M. Müller, *ibid.* **1982**, 1398–1400; d) C. D. Gutsche, *Acc. Chem. Res.* **1983**, *16*, 161–170, and references cited therein.
[11] N. Wester, F. Vögtle, *Chem. Ber.* **1980**, *113*, 1487–1493. see C. Pascard, C. Riche. M. Cesario, F. Kotzyba-Hibert, J.-M. Lehn, *J. Chem. Soc. Chem. Commun.* **1982**, 557–560.
[12] J. Gabard, A. Collet, *J. Chem. Soc. Chem. Commun.* **1981**, 1137–1139.
[13] F. Diederich, K. Dick, *Angew. Chem.* **1984**, *96*, 789–790; *Angew. Chem. Int. Ed. Engl.* **1984**, *23*, 810–811.
[14] W. Kiggen, F. Vögtle, *Angew. Chem.* **1984**, *96*, 712–713; *Angew. Chem. Int. Ed. Engl.* **1984**, *23*, 714–715.
[15] F. Ebmeyer, F. Vögtle in *Bioorganic Chemistry Frontiers 1*, Springer, Berlin, **1990**, p. 143–159; F. Vögtle, *Kem. Kemi* **1989**, *16*, 796–798; F. Ebmeyer, F. Vögtle in *Inclusion-Compounds Vol. 4* (Eds. J. Atwood, E. Davies, D. MacNicol), Oxford Science Publications, Oxford, **1991**, p. 263–282.
[16] a) F. Vögtle, *Supramolekulare Chemie*, Teubner, Stuttgart, **1989**; *Supramolecular Chemistry, an Introduction*, Wiley, Chichester **1991**; b) *Frontiers in Supramolecular Organic Chemistry and Photochemistry* (Eds.: H.-J. Schneider, H. Dürr), VCH, Weinheim, **1990**; c) V. Balzani, F. Scandola, *Supramolecular Photochemistry*, Horwood, Chichester, **1991**; d) J. Fuhrhop, *Bioorganische Chemie*, Thieme, Stuttgart, **1982**; e) H. Dugas, *Bioorganic Chemistry*, Springer, Berlin, **1989**; f) M. L. Bender, M. Komiyama, *Cyclodextrin Chemistry*, Springer, Berlin, **1978**; g) C. D. Gutsche, *Calixarenes* in *Monographs in Supramolecular Chemistry*, (Ed.: J. F. Stoddart), Royal Society of Chemistry, Cambridge, **1989**; h) *Host Guest Complex Chemistry* (Eds.: F. Vögtle, E. Weber); Part I: *Top. Curr. Chem.* **1981**, *98*; Part II: *ibid.* **1982**, *101*; Part III: *ibid.* **1983**, *121*; i) *Bioorganic and Biomimetic Chemistry* (Eds.: F. Vögtle, E. Weber); Part I: *ibid.* **1985**, *128*; Part II: *ibid.* **1986**, *132*; Part III: *ibid.* **1986**, *136*; j) J.-M. Lehn, *Angew. Chem.* **1988**, *100*, 91–116; *Angew. Chem. Int. Ed. Engl.* **1988**, *27*, 89–114; k) J.-M. Lehn, *ibid.* **1990**, *102*, 1347–1362 bzw. **1990**, *29*, 1304–1319.
[17] D. J. Cram, *Angew. Chem.* **1986**, *98*, 1041–1060; *Angew. Chem. Int. Ed. Engl.* **1986**, *25*, 1039–1058.
[18] F. H. Kohnke, J. P. Mathias, J. F. Stoddart, *Angew. Chem. Adv. Mater.* **1989**, *101*, 1129–1136; *Angew. Chem. Int. Ed. Engl. Adv. Mater.* **1989**, *28*, 1126–1133; *Adv. Mater.* **1989**, 275–282.
[19] F. Ebmeyer, F. Vögtle, *Chem. Ber.* **1989**, *122*, 1725–1727.
[20] K. H. Neumann, F. Vögtle, *J. Chem. Soc. Chem. Commun.* **1988**, 520–522.
[21] According to our experience this method is restricted to specially preorganized oligoamines and only certain dialdehydes: M. Bauer, F. Kochendörfer, M. Kreysel, W. M. Müller, F. Vögtle, unpublished. Cf. ref. [60, 147].
[22] J. Jazwinsky, J.-M. Lehn, D. Lilienbaum, R. Ziessel, J. Guilhem, C. Pascard, *J. Chem. Soc. Chem. Commun.* **1987**, 1691–1694. Analogous macrobicycles with heteroarene units: a) D. McDowell, J. Nelson, *Tetrahedron Lett.* **1988**, *29*, 385–386; b) V. McKee, *Polyhedron* **1989**, *8*, 1143–1145.
[23] J. S. Lindsey, D. C. Mauzerall, *J. Am. Chem. Soc.* **1982**, *104*, 4498–4450.
[24] In this reaction, which is difficult to reproduce, the analogous open-chain tris(bipyridinium) compound could also be isolated and fully characterized. Because of its six positive charges the macrobicycle **13** could not be detected by mass spectrometry; however, its ^{1}H and ^{13}C NMR spectra are in accord with the cage-like structure. F. Kochendörfer, Dissertation, Universität Bonn, **1989**. Cf. Lit. [86, 87].
[25] A one-pot Wittig reaction in which a macrobicyclophane framework is constructed with sixfold bond formation is described: H.-K. Högberg, O. Wennerström, *Acta Chem. Scand. Ser. B.* **1982**, *36*, 661–667.
[26] D. O'Krongly, S. R. Denmeade, M. Y. Chiang, R. Breslow, *J. Am. Chem. Soc.* **1985**, *107*, 5544–5545.
[27] S. Claude, J.-M. Lehn, J.-P. Vigneron, *Tetrahedron Lett.* **1989**, *30*, 941–944.
[28] Review: A. Collet, *Tetrahedron* **1987**, *43*, 5725–5759. A shorter synthetic pathway (path H) is described in J. Canceill, A. Collet, *J. Chem. Soc. Chem. Commun.* **1988**, 582–584.
[29] P. R. Ashton, N. S. Isaacs, F. H. Kohnke, G. Stagno d'Alcontres, J. F.

Stoddart, *Angew. Chem.* **1989**, *101*, 1269–1271; *Angew. Chem. Int. Ed. Engl.* **1989**, *28*, 1261–1263.
[30] P. R. Ashton, N. S. Isaacs, F. H. Kohnke, J. P. Mathias, J. F. Stoddart, *Angew. Chem.* **1989**, *101*, 1266–1269; *Angew. Chem. Int. Ed. Engl.* **1989**, *28*, 1258–1261.
[31] T. Merz, H. Wirtz, F. Vögtle, *Angew. Chem.* **1986**, *98*, 549–550; *Angew. Chem. Int. Ed. Engl.* **1986**, *25*, 567–568.
[32] a) *Microbial Iron Transport: A. Comprehensive Treatise*, Academic Press, New York, **1974**, b) K. N. Raymond, G. Müller, B. F. Matzanke, *Top. Curr. Chem.* **1984**, *123*, 49–102; c) *Siderophores from Microorganisms and Plants* (Eds.: M. J. Clarke, J. B. Goodenough, J. A. Ibers, C. K. Jørgensen, D. M. P. Mingos, J. B. Neilands, G. A. Palmer, D. Reinen, P. J. Sadler, R. Weiss, R. J. P. Williams *(Struct. Bonding (Berlin)* **1984**, *58*); d) R. J. Bergeron, *Chem. Rev.* **1984**, *84*, 587–602; e) *Iron. Siderophores and Plant Diseases* (Ed.: T. R. Swinburne), *(Nato ASI Ser. Ser. A* **1986**, *117*); f) *Iron Transport in Microbes, Plants and Animals* (Eds.: G. Winkelmann, D. van der Helm, J. B. Neilands), VCH, Weinheim, **1987**; g) M. J. Miller, *Chem. Rev.* **1989**, *89*, 1563–1579; h) *Iron Carriers and Iron Proteins* (Ed.: T. M. Loehr), *Physical Bioinorganic Chemistry, Vol. 5*, VCH, Weinheim, **1989**.
[33] a) R.C. Hider, D. Bickar, I. E. G. Morrison, J. Silver, *J. Am Chem. Soc.* **1984**, *106*, 6983–6987; b) M. E. Cass, T. M. Garrett, K. N. Raymond, *ibid.* **1989**, *111*, 1677–1682.
[34] a) J. R. Pollack, J. B. Neilands, *Biochem. Biophys. Res. Commun.* **1970**, *38*, 989–992; b) I. G. O'Brien, F. Gibson, *Biochim. Biophys. Acta* **1970**, *215*, 393–402.
[35] a) S. S. Isied, G. Kuo, K. N. Raymond, *J. Am. Chem. Soc.* **1976**, *98*, 1763–1767; b) J. V. McArdle, S. R. Sofen, S. R. Cooper, K. N. Raymond, *Inorg. Chem.* **1978**, *17*, 3075–3078; c) J. B. Neilands, T. J. Erickson, W. H. Rastetter, *J. Biol. Chem.* **1981**, *256*, 3831–3832.
[36] W. R. Harris, C. J. Carrano, S. R. Cooper, S. R. Sofen, A. Avdeef, J. V. McArdle, K. N. Raymond, *J. Am. Chem. Soc.* **1979**, *101*, 6097–6104.
[37] a) W. R. Harris, F. L. Weitl, K. N. Raymond, *J. Chem. Soc. Chem. Commun.* **1979**, 177–178; b) M. C. Venuti, W. H. Rastetter, J. B. Neilands, *J. Med. Chem.* **1979**, *22*, 123–124.
[38] W. R. Harris, K. N. Raymond, *J. Am. Chem. Soc.* **1979**, *101*, 6534–6541.
[39] $Pb^{2\oplus}$ and $Bi^{3\oplus}$ complexes see M. Magerstädt, O. A. Gansow, L. K. Pannell, F. Vögtle, W. Kiggen, *Nucl. Med. Biol.* **1990**, *17*, 409–412.
[40] We thank Prof. R. C. Hider, A. D. Hall, and P. D. Taylor, University of Essex and King's College, London, for determining the constants. K. N. Raymond et al. discuss these values in [43d].
[41] W. Kiggen, F. Vögtle, S. Franken, H. Puff, *Tetrahedron* **1986**, *42*, 1859–1872.
[42] T. J. McMurry, S. J. Rodgers, K. N. Raymond, *J. Am. Chem. Soc.* **1987**, *109*, 3451–3453.
[43] a) T. J. McMurry, M. W. Hosseini, T. M. Garrett, F. E. Hahn, Z. E. Reyes, K. N. Raymond, *J. Am. Chem. Soc.* **1987**, *109*, 7196–7198; b) K. N. Raymond, T. J. McMurry, T. M. Garret, *Pure Appl. Chem.* **1988**, *60*, 545–548; c) T. J. McMurry, K. N. Raymond, US-A 4939254, **1990**; d) T. M. Garret, T. J. McMurry, M. W. Hosseini, Z. E. Reyes, F. E. Hahn, K. N. Raymond, *J. Am. Chem. Soc.* **1991**, *109*, 2965–2977.
[44] P. Stutte, W. Kiggen, F. Vögtle, *Tetrahedron* **1987**, *43*, 2065–2074.
[45] J. Peter-Katalinić, F. Ebmeyer, C. Seel, F. Vögtle, *Chem. Ber.* **1989**, *122*, 2391–2393.
[46] A siderophore cryptand with three endocyclic hydroxamate groups: Y. Sun, A. E. Martell, *J. Am. Chem. Soc.* **1989**, *111*, 8023–8024.
[47] J. L. Pierre, P. Baret, G. Gellon, *Angew. Chem.* **1991**, *103*, 75–76; *Angew. Chem. Int. Ed. Engl.* **1991**, *30*, 85–86.
[48] a) *Photochemical Conversion and Storage of Solar Energy* (Ed.: J. S. Conolly), Academic, New York, **1981**; b) *Photochemical Conversion and Storage of Solar Energy* (Ed.: J. Rabani) Weizmann, Israel, **1981**; c) *Energy Resources through Photochemistry and Catalysis* (Ed.: M. Graetzel), Academic, New York, **1983**; d) *Photochemical Energy Conversion* (Eds.: J. R. Norris, Jr., D. Meisel), Elsevier, New York, **1989**; e) *Photoconversion Processes for Energy and Chemicals* (Eds.: D. O. Hall, G. Grassi), Elsevier, New York, **1989**.
[49] a) V. Balzani, A. Juris, F. Scandola in *Homogeneous and Heterogeneous Photocatalysis* (Eds.: E. Pelizzetti, N. Serpone), Reidel, Dordrecht, **1986**; b) *Supramolecular Photochemistry* (Ed.: V. Balzani), Reidel, Dordrecht, **1987**; c) H. Hennig, D. Rehorek, *Photochemische and Photokatalytische Reaktionen von Koordinationsverbindungen*, Akademie Verlag, Berlin, **1987**; d) V. Balzani, *Pure Appl. Chem.* **1990**, *62*, 1099–1102.
[50] a) K. Kalyanasundaram, *Coord. Chem. Rev.* **1982**, *46*, 159–244; b) E. A. Seddon, K. R. Seddon, *The Chemistry of Ruthenium*, Elsevier, New York, **1984**; c) V. Balzani, N. Sabbatini, F. Scandola, *Chem. Rev.* **1986**, *86*, 319–337; d) F. Barigelletti, A. Juris, V. Balzani, P. Belser, A. von Zelewsky in *Photochemistry and Photophysics of Coordination Compounds* (Eds.: H. Yersin, A. Vogler), Springer, Heidelberg **1987**, p. 79; e) R. A. Krause, *Struct. Bonding (Berlin)* **1987**, *67*, 1–79; f) A. Juris, V. Balzani, F. Barigelletti, S. Campagna, P. Belser, A. von Zelewsky, *Coord. Chem. Rev.* **1988**, *84*, 85–277; g) V. Balzani, F. Barigelletti, L. De Cola, *Top. Curr. Chem.* **1990**, *158*, 31–71; h) P. Belser, *Chimia* **1990**, *44*, 226–236.
[51] F. Barigelletti, L. De Cola, V. Balzani, P. Belser, A. von Zelewsky, F. Vögtle, F. Ebmeyer, S. Grammenudi, *J. Am. Chem. Soc.* **1989**, *111*, 4662–4668.
[52] a) S. Grammenudi, F. Vögtle, *Angew. Chem.* **1986**, *98*, 1119–1121; *Angew. Chem. Int. Ed. Engl.* **1986**, *25*, 1119–1121; b) S. Grammenudi, M. Franke, F. Vögtle, E. Steckhan, *J. Inclusion Phenom. Mol. Recognit. Chem.* **1987**, *5*, 695–707.
[53] P. Belser, L. De Cola, A. von Zelewsky, *J. Chem. Soc. Chem. Commun.* **1988**, 1057–1058.
[54] L. De Cola, F. Barigelletti, V. Balzani, P. Belser, A. von Zelewsky, F. Vögtle, F. Ebmeyer, S. Grammenudi, *J. Am. Chem. Soc.* **1988**, *110*, 7210–7212.
[55] Oligonuclear complexes of open-chain tris(bipyridine) ligands are described: L. De Cola, P. Belser, F. Ebmeyer, F. Barigelletti, F. Vögtle, A. von Zelewsky, V. Balzani, *Inorg. Chem.* **1990**, *29*, 495–499; see also Lit. [50h].
[56] See also the complexes of sepulchrates and similar bicyclic heteroaliphatic compounds, for example: P. Bernhard, A. M. Sargeson, F. C. Anson, *Inorg. Chem.* **1988**, *27*, 2754–2760, and references cited therein. See also H. Takemura, T. Shinmyozu, T. Inazu, *Tetrahedron Lett.* **1988**, *29*, 1789–1792.
[57] a) J.-C. Rodríguez-Ubis, B. Alpha, D. Plancherel, J.-M. Lehn, *Helv. Chim. Acta.* **1984**, *67*, 2264–2269; b) A. Caron, J. Guilhelm, C. Riche, C. Pascard, B. Alpha, J.-M. Lehn, J.-C. Rodríguez-Ubis, *ibid.* **1985**, *68*, 1577–1582; c) B. Alpha, E. Anklam, R. Deschenaux, J.-M. Lehn, M. Pietraszkiewicz, *ibid.* **1988**, *71*, 1042–1052; d) J.-M. Lehn, J.-B. Regnouf de Vains, *Tetrahedron Lett.* **1989**, *30*, 2209–2212.
[58] H. Dürr, K. Zengerle, H.-P. Trierweiler; *Z. Naturforsch.* B. **1988**, *43*, 361–367.
[59] a) B. Alpha, J.-M. Lehn, G. Mathis, *Angew. Chem.* **1987**, *99*, 259–261; *Angew. Chem. Int. Ed. Engl.* **1987**, *26*, 266-268; b) B. Alpha, V. Balzani, J.-M. Lehn, S. Perathoner, N. Sabbatini, *ibid.* **1987**, *99*, 1310–1311 and **1987**, *26*, 1266–1267; see also c) J.-M. Lehn, M. Pietraszkiewicz, J. Karpiuk, *Helv. Chim. Acta.* **1990**, *73*, 106–111.
[60] J. de Mendoza, E. Meza, J.-C. Rodríguez-Ubis, P. Vázquez, F. Vögtle, P.-M. Windscheif, K. Rissanen, J.-M. Lehn, D. Lilienbaum, R. Ziessel, *Angew. Chem.* **1991**, *104*, 1365–1367; *Angew. Chem. Int. Ed. Engl.* **1991**, *30*, 1331–1333. A similar cage ligand with three 4,4'-disubstituted bipyridine units: O. Kocian, R. J. Mortimer, P. D. Beer, *Tetrahedron Lett.* **1990**, *31*, 5069–5072.
[61] a) Review: J. Rebek, Jr., *Angew. Chem.* **1990**, *102*, 261–272; *Angew. Chem. Int. Ed. Engl.* **1990**, *29*, 245–256, and references cited therein; b) J. S. Nowick, P. Ballester, F. Ebmeyer, J. Rebek, Jr., *J. Am. Chem. Soc.* **1990**, *112*, 8902–8906. π-Stacking interactions are also of great importance in complexes of these systems (see below in this section).
[62] T. Tjivihua, P. Ballester, J. Rebek, Jr., *J. Am. Chem. Soc.* **1990**, *112*, 1249–1250.
[63] T. R. Kelly, G. J. Bridger, C. Zhao, *J. Am. Chem. Soc.* **1990**, *112*, 8024–8034, and references cited therein.
[64] C. T. Seto. G. M. Whitesides, *J. Am. Chem. Soc.* **1991**, *113*, 712–713, and references cited therein.
[65] J. C. Adrian, Jr., C. S. Wilcox, *J. Am. Chem. Soc.* **1991**, *113*, 678–680, and references cited therein.
[66] V. Hegde, P. Madhukar, J. D. Madura, R. P. Thummel, *J. Am. Chem. Soc.* **1990**, *112*, 4549–4550, and references cited therein.
[67] T. W. Bell, J. Liu, *Angew. Chem.* **1990**, *102*, 931-933; *Angew. Chem. Int. Ed. Engl.* **1990**, *29*, 923–925, and references cited therein.
[68] F. Garcia-Tellado, S. Goswami, S.-K. Chang, S. J. Geib, A. D. Hamilton, *J. Am. Chem. Soc.* **1990**, *112*, 7393–7394; Review: A. D. Hamilton, *J. Chem. Educ.* **1990**, *67*, 821–828, and references cited therein.
[69] This list of examples does not claim to be complete.
[70] a) W. P. Jenks, *Catalysis in Chemistry and Enzymologie*, McGraw-Hill, New York, **1969**, Chapter 8; b) C. Tanford, *The Hydrophobic Effect: Formation of Micelles and Biological Membranes*, 2nd ed., Wiley, New York, **1980**, c) A. Ben-Naim, *Hydrophobic Interaction*, 2nd ed., Plenum, New York, **1983**; d) A. Fersht, *Enzyme Structure and Mechanism*, 2nd ed., Freeman, New York, **1985**, Chapter 11.
[71] Reviews: a) F. Diederich, *Angew. Chem.* **1988**, *100*, 372–396; *Angew. Chem. Int. Ed. Engl.* **1988**, *27*, 362–386; b) F. Diederich, *J. Chem. Educ.* **1990**, *67*, 813–820. Recent work could not be considered here: S. B. Ferguson, E. M. Sandford, E. M. Seward, F. Diederich, *J. Am. Chem. Soc.* **1991**, *113*, 5410–5419; D. B. Smithrud, T. B. Wyman, F. Diederich, *ibid.* **1991**, *113*, 5420–5426.
[72] D. B. Smithrud, F. Diederich, *J. Am. Chem. Soc.* **1990**, *112*, 339–343.
[73] C. Reichardt, *Solvents and Solvent Effects in Organic Chemistry*, 2nd ed., VCH, Weinheim, **1988**, Chapter 7.
[74] See also H.-J. Schneider, R. Kramer, S. Simova, U. Schneider, *J. Am. Chem. Soc.* **1988**, *110*, 6442–6448.
[75] F. Diederich, K. Dick, D. Griebel, *J. Am. Chem. Soc.* **1986**, *108*, 2273–2286.
[76] S. B. Ferguson, E. M. Seward, F. Diederich, E. M. Sanford, A. Chou, P. Inocencio-Szweda, C. B. Knobler, *J. Org. Chem.* **1988**, *53*, 5593–5595.
[77] K. T. Chapman, W. C. Still, *J. Am. Chem. Soc.* **1989**, *111*, 3075–3077. See

also in Section 4.3 the solubility dependence of halomethane complexation by cryptophanes, see [28].
[78] a) R. W. G. Wyckoff, *Crystal Structures of Benzene Derivatives, Vol. 6*, Interscience, New York, **1969**; b) G. R. Desiraju, A. Gavezzotti, *J. Chem. Soc. Chem. Commun.* **1989**, 621–623.
[79] W. Saenger, *Principles of Nucleic Acid Structure*, Springer, New York, **1984**.
[80] a) S. K. Burley, G. A. Petsko, *Science* **1985**, *229*, 23–28; b) S. K. Burley, G. A. Petsko, *J. Am. Chem. Soc.* **1986**, *108*, 7995–8001.
[81] R. O. Gould, A. M. Gray, P. Taylor, M. D. Walkinshaw, *J. Am. Chem. Soc.* **1985**, *107*, 5921-5927.
[82] In crystals of arenes this type of packing is termed "herringbone stacking". See [78 b].
[83] See also G. Karlström, P. Linse, A. Wallqvist, B. Jönsson, *J. Am. Chem. Soc.* **1983**, *105*, 3777-3782.
[84] C. A. Hunter, J. K. M. Sanders, *J. Am. Chem. Soc.* **1990**, *112*, 5525–5534. See also C. A. Hunter, *J. Chem. Soc. Chem. Commun.* **1991**, 749–751.
[85] S. B. Ferguson, F. Diederich, *Angew. Chem.* **1986**, *98*, 1127–1129; *Angew. Chem Int. Ed. Engl.* **1986**, *25*, 1127–1129.
[86] a) P. R. Ashton, T. T. Goodnow, A. E. Kaifer, M. V. Reddington, A. M. Z. Slawin, N. Spencer, J. F. Stoddart, C. Vicent, D. J. Williams, *Angew. Chem.* **1989**, *101*, 1404–1408; *Angew. Chem. Int. Ed. Engl.* **1989**, *28*, 1396–1400; b) P. R. Ashton, C. L. Brown, E. J. T. Chrystal, T. T. Goodnow, A. E. Kaifer, K. P. Parry, D. Philp, A. M. Z. Slawin, N. Spencer, J. F. Stoddart, D. J. Williams, *J. Chem. Soc. Chem. Commun.* **1991**, 634–639; c) D. Philp, J. F. Stoddart, *Synlett* **1991**, 445–458. With regard to electron-donor–acceptor and arene–arene interactions see also J.-Y. Ortholand, A. M. Z. Slawin, N. Spencer, J. F. Stoddart, D. J. Williams, *Angew. Chem.* **1989**, *101*, 1402–1404; *Angew. Chem. Int. Ed. Engl.* **1989**, *28*, 1394–1396, and references cited therein.
[87] M. Bühner, W. Geuder, W.-K. Gries, S. Hünig, M. Koch, T. Poll. *Angew. Chem.* **1988**, *100*, 1611–1614; *Angew. Chem. Int. Ed. Engl.* **1988**, *27*, 1553–1556. Non-bonded pairing of viologen radical cations by π–π interactions ("pimerization"): W. Geuder, S. Hünig, A. Suchy, *Tetrahedron* **1986**, *42*, 1665–1677.
[88] J. Jazwinski, A. J. Blacker, J.-M. Lehn, M. Cesario, J. Guilhem, C. Pascard, *Tetrahedron Lett.* **1987**, *28*, 6057–6060.
[89] S. C. Zimmerman, W. Wu, *J. Am. Chem. Soc.* **1989**, *111*, 8054–8055, and references cited therein. See also J. F. Blake, W. L. Jorgensen, *ibid.* **1990**, *112*, 7269–7278.
[90] M. Harmata, C. L. Barnes, *J. Am. Chem. Soc.* **1990**, *112*, 5655–5658.
[91] A. V. Muehldorf, D. Van Engen, J. C. Warner, A. D. Hamilton, *J. Am. Chem. Soc.* **1988**, *110*, 6561–6562.
[92] D. A. Stauffer, R. E. Barrans, Jr., D. A. Dougherty, *Angew. Chem.* **1990**, *102*, 953–956; *Angew. Chem. Int. Ed. Engl.* **1990**, *29*, 915–918, and references cited therein.
[93] See also C. A. Deakyne, M. Meot-Ner (Mautner), *J. Am. Chem. Soc.* **1985**, *107*, 474–479.
[94] a) H.-J. Schneider, T. Blatter, S. Simova, I. Theis, *J. Chem. Soc. Chem. Commun.* **1989**, 580–581; b) H.-J. Schneider, D. Ruf, *Angew. Chem.* **1990**, *102*, 1192–1194; *Angew. Chem. Int. Ed. Engl.* **1990**, *29*, 1159–1161; c) H.-J. Schneider, T. Blatter, P. Zimmermann, *ibid.* **1990**, *102*, 1194–1195 and **1990**, *29*, 1161–1162; d) H.-J. Schneider, *ibid.* **1991**, *103*, 1419–1439 and **1991**, *30*, 1417–1437.
[95] F. Ebmeyer, F. Vögtle, *Angew. Chem.* **1989**, *101*, 95–96; *Angew. Chem. Int. Ed. Engl.* **1989**, *28*, 79–80.
[96] C. Seel, F. Vögtle, *Angew. Chem.* **1991**, *103*, 433–436; *Angew. Chem. Int. Ed. Engl.* **1991**, *30*, 442–445.
[97] a) F. Vögtle, A. Wallon, W. M. Müller, U. Werner, M. Nieger, *J. Chem. Soc. Chem. Commun.* **1990**, 158–161; b) A. Wallon, U. Werner, W. M. Müller, M. Nieger, F. Vögtle, *Chem. Ber.* **1990**, *123*, 859–867.
[98] In this connection see speleands and similar compounds: a) J. Canceill, A. Collet, J. Gabard, F. Kotzyba-Hibert, J.-M. Lehn, *Helv. Chim. Acta* **1982**, *65*, 1894–1897; M. Dhaenens, L. Lacombe, J.-M. Lehn, J.-P. Vigneron, *J. Chem. Soc. Chem. Commun.* **1984**, 1097–1099; b) J. W. H. Smeets, L. van Dalen, V. E. M. Kaats-Richter, R. J. M. Nolte, *J. Org. Chem.* **1990**, *55*, 454–461, and references cited therein.
[99] L. Wambach, F. Vögtle, *Tetrahedron Lett.* **1985**, *26*, 1483–1486; B. Dung, F. Vögtle, *J. Inclusion Phenom. Mol. Recognit Chem.* **1988**, *6*, 429–442.
[100] C. Seel, Dissertation, Universität Bonn, **1991**.
[101] K. Saigo, N. Kihara, Y. Hashimoto, R.-J. Lin, H. Fujimura, Y. Suzuki, M. Hasegawa, *J. Am. Chem. Soc.* **1990**, *112*, 1144–1150.
[102] A. D. Hamilton, P. Kazanjian, *Tetrahedron Lett.* **1985**, *26*, 5735–5738.
[103] Complexation of inorganic anions by oligocyclic phanes: a) Ref. [11]; b) D. Heyer, J.-M. Lehn, *Tetrahedron Lett.* **1986**, *27*, 5869–5872; c) T. Fujita, J.-M. Lehn, *ibid.* **1988**, *29*, 1709–1712. See also F. P. Schmidtchen, *Nachr. Chem. Tech. Lab.* **1988**, *36*, 8–17.
[104] J.-M. Lehn, R. Méric, J.-P. Vigneron, I. Bkouche-Waksman, C. Pascard, *J. Chem. Soc. Chem. Commun.* **1991**, 62–64; see also Ref. [22].
[105] a) R. E. Sheridan, H. W. Whitlock, Jr., *J. Am. Chem. Soc.* **1986**, *108*, 7120–7121; b) *ibid.* **1988**, *110*, 4071–4073. c) K. M. Neder, H. W. Whitlock, Jr., *ibid.* **1990**, *112*, 9412–9414; See also S. P. Miller, H. W. Whitlock, Jr., *ibid.* **1984**, *106*, 1492–1494; M. E. Haeg, B. J. Whitlock, H. W. Whitlock, Jr., *ibid.* **1989**, *111*, 692–696.
[106] B. J. Whitlock, H. W. Whitlock, Jr., *J. Am. Chem. Soc.* **1990**, *112*, 3910–3915; J. E. Cochran, T. J. Parrot, B. J. Whitlock, H. W. Whitlock *ibid.* **1992**, *114*, 2269–2270.
[107] J. D. Kilburn, A. R. MacKenzie, W. C. Still, *J. Am. Chem. Soc.* **1988**, *110*, 1307–1308.
[108] P. E. J. Sanderson. J. D. Kilburn, W. C. Still, *J. Am. Chem. Soc.* **1989**, *111*, 8314–8315.
[109] B. C. Askew, *Tetrahedron Lett.* **1990**, *31*, 4245–4248.
[110] "Concave Benzoic Acids": U. Lüning, C. Wangnick, K. Peters, H. G. von Schnering, *Chem. Ber.* **1991**, *124*, 397–402; there see also "concave bases", and references cited therein.
[111] F. Bitsch, C. O. Dietrich-Buchecker, A.-K. Khémiss, J.-P. Sauvage, A. Van Dorsselaer, *J. Am. Chem. Soc.* **1991**, *113*, 4023–4025; and references cited therein.
[112] F. Vögtle, I. Lüer, V. Balzani, N. Armaroli, *Angew. Chem.* **1991**, *103*, 1367–1369; *Angew. Chem. Int. Ed. Engl.* **1991**, *30*, 1333–1336.
[113] Reviews: a) J. E. Baldwin, P. Perlmutter, *Top. Curr. Chem.* **1984**, *121*, 181–220; b) B. Morgan, D. Dolphin, *Struct. Bonding (Berlin)* **1987**, *64*, 115–268.
[114] J. E. Baldwin, J. H. Cameron, M. J. Crossley, I. J. Dagley, S. R. Hall, T. Klose, *J. Chem. Soc. Dalton Trans.* **1984**, 1739–1746, and references cited therein.
[115] T. Hashimoto, R. L. Dyer, M. J. Crossley, J. E. Baldwin, F. Basolo, *J. Am. Chem. Soc.* **1982**, *104*, 2101–2109, and references cited therein.
[116] M. R. Johnson, W. K. Seok, J. A. Ibers, *J. Am. Chem. Soc.* **1991**, *113*, 3998–4003.
[117] K. Kim, J. Fettinger, J. L. Sessler, M. Cyr, J. Hugdahl, J. P. Collman, J. A. Ibers, *J. Am. Chem. Soc.* **1989**, *111*, 403–405, and references cited therein.
[118] a) N. E. Kagan, D. Mauzerall, R. B. Merrifield, *J. Am. Chem. Soc.* **1977**, *99*, 5484–5486; b) B. C. Bookser, T. C. Bruice, *ibid.* **1991**, *113*, 4208–4218; and references cited therein.
[119] a) J. P. Collman, J. I. Brauman, J. P. Fitzgerald, P. D. Hampton, Y. Naruta, J. W. Sparapany, J. A. Ibers, *J. Am. Chem. Soc.* **1988**, *110*, 3477–3486; b) J. P. Collman, J. I. Brauman, J. P. Fitzgerald, J. W. Sparapany, J. A. Ibers, *ibid.* **1988**, *110*, 3486–3495; c) J. P. Collman, X. Zhang, R. T. Hembre, J. I. Brauman, *ibid.* **1990**, *112*, 5356–5357.
[120] *Cytochrom P-450: Structure, Mechanism and Biochemistry* (Ed.: P. R. Ortiz de Montellano), Plenum, New York, **1986**.
[121] H. Stetter, E.-E. Roos, *Chem. Ber.* **1955**, *88*, 1390–1395.
[122] R. Hilgenfeld, W. Saenger, *Angew. Chem.* **1982**, *94*, 788–789; *Angew. Chem. Int. Ed. Engl.* **1982**, *21*, 781–782.
[123] F. Diederich, K. Dick, *J. Am. Chem. Soc.* **1984**, *106*, 8024–8036.
[124] F. Vögtle, W. M. Müller, U. Werner, H.-W. Losensky, *Angew. Chem.* **1987**, *99*, 930–932; *Angew. Chem. Int. Ed. Engl.* **1987**, *26*, 901–903.
[125] Similar macrobicycles see: a) U. Werner, W. M. Müller, H.-W. Losensky, T. Merz, F. Vögtle, *J. Inclusion Phenom. Mol. Recognit. Chem.* **1986**, *4*, 379–385; b) A. Wallon, J. Peter-Katalinić, U. Werner, W. M. Müller, F. Vögtle, *Chem. Ber.* **1990**, *123*, 375–379.
[126] a) M. Kirch, J.-M. Lehn, *Angew. Chem.* **1975**, *87*, 542–543; *Angew. Chem. Int. Ed. Engl.* **1975**, *14*, 555–556; b) J.-M. Lehn, *Pure Appl. Chem.* **1979**, *51*, 979–997; c) J. D. Lamb, R. M. Izatt, J. J. Christensen, *Progr. Macrocyclic Chem.* **1981**, *2*, 41–181; d) ref. [123]; e) W. H. Mandeville, G. M. Whitesides, *J. Org. Chem.* **1986**, *51*, 3257–3261; f) A. Harada, S. Takahashi, *J. Chem. Soc. Chem. Commun.* **1987**, 527–528; g) ref. [87]; h) V. Prelog, M. Dumić, *Helv. Chim. Acta* **1986**, *69*, 5–11; i) ref. [16j], p. 104–107; j) D. G. Rethwisch, A. Subramanian, G. Yi, J. S. Dordick, *J. Am. Chem. Soc.* **1990**, *112*, 1649–1650; k) W. F. Nijenhuis, A. R. van Doorn, A. M. Reichwein, F. de Jong, D. N. Reinhoudt, *ibid.* **1991**, *113*, 3607–3608; l) H. Furuta, K. Furuta, J. L. Sessler, *ibid.* **1991**, *113*, 4706–4707; m) ref. [96].
[127] a) J. Franke, F. Vögtle, *Angew. Chem.* **1985**, *97*, 224–225; *Angew. Chem. Int. Ed. Engl.* **1985**, *24*, 219–220; b) H. Schrage, M. Franke, F. Vögtle, E. Steckhan, *ibid.* **1986**, *98*, 335–337 and **1986**, *25*, 336–338; c) H. Schrage, F. Vögtle, E. Steckhan, *J. Inclusion Phenom. Mol. Recognit. Chem.* **1987**, *6*, 157–165.
[128] J. Canceill, M. Cesario, A. Collet, J. Guilhem, C. Pascard, *J. Chem. Soc. Chem. Commun.* **1985**, 361–363.
[129] J. Canceill, M. Cesario, A. Collet, J. Guilhem, C. Riche, C. Pascard, *J. Chem. Soc. Chem. Commun.* **1986**, 339–341.
[130] J. Canceill, L. Lacombe, A. Collet, *J. Am. Chem. Soc.* **1985**, *107*, 6993–6996.
[131] F. Diederich, K. Dick, D. Griebel, *Chem. Ber.* **1985**, *118*, 3588–3619.
[132] J. Canceill, L. Lacombe, A. Collet, *J. Am. Chem. Soc.* **1986**, *108*, 4230–4232; J. Canceill, M. Cesario, A. Collet, J. Guilhem, L. Lacombe, B. Lozach, C. Pascard, *Angew. Chem.* **1989**, *101*, 1249–1252; *Angew. Chem. Int. Ed. Engl.* **1989**, *28*, 1246–1249.
[133] J. Canceill, L. Lacombe, A. Collet, *J. Chem. Soc. Chem. Commun.* **1987**, 219–221.
[134] F. Vögtle, R. Berscheid, W. Schnick, *J. Chem. Soc. Chem. Commun.* **1991**, 414-416.
[135] Macrobicyclic tris(diynes) with phosphorane spacers see: a) B. P. Friederichsen, H. W. Whitlock, Jr., *J. Am. Chem. Soc.* **1989**, *111*, 9132–9134; b) B. P. Friederichsen, D. R. Powell, H. W. Whitlock, Jr., *ibid.* **1990**, *112*, 8931–8941.

[136] F. Vögtle, M. Nieger, R. Berscheid, *J. Chem. Soc. Chem. Commun.* **1991**, 1364–1366.
[137] a) J. H. Fendler, E. J. Fendler, *Catalysis in Micellar and Macromolecular Systems*, Academic, New York, **1975**; b) C. Walsh, *Enzymatic Reaction Mechanisms*, Freeman, San Francisco, **1979**; c) L. Stryer, *Biochemistry*, Freeman, San Francisco, **1979**; d) *Enzyme Mechanisms* (Eds.: M. I. Page, A. Williams) Royal Society of Chemistry, London, **1987**; e) *Mechanistic Principles of Enzyme Activity* (Eds.: J. F. Liebman, A. Greenberg), VCH Publishers, New York, **1989**; f) ref. [70a, d].
[138] H.-D. Lutter, F. Diederich, *Angew. Chem.* **1986**, *98*, 1125–1127; *Angew. Chem. Int. Ed. Engl.* **1986**, *25*, 1125–1127, and references cited therein.
[139] a) G. Schürmann, F. Diederich, *Tetrahedron Lett.* **1986**, *27*, 4249–4252; b) F. Diederich, G. Schürmann, I. Chao, *J. Org. Chem.* **1988**, *53*, 2744–2757, and references cited therein.
[140] D. R. Benson, R. Valentekovich, F. Diederich, *Angew. Chem.* **1990**, *102*, 213–216; *Angew. Chem. Int. Ed. Engl.* **1990**, *29*, 191–194.
[141] a) Y. Murakami, J. Kikuchi, T. Hirayama, *Chem. Lett.* **1987**, 161–164; b) Y. Murakami, J. Kikuchi, *Pure Appl. Chem.* **1988**, *60*, 549–554. Cf. Y. Murakami, J. Kikuchi, H. Tenma, *J. Chem. Soc. Chem. Commun.* **1985**, 753–755. A chiral variant has recently been described: Y. Murakami, T. Ohno, O. Hayashida, Y. Hisaeda, *J. Chem. Soc. Chem. Commun.* **1991**, 950–952.
[142] Y. Murakami, J. Kikuchi, T. Ohno, T. Hirayama, *Chem. Lett.* **1989**, 881–884.
[143] Y. Murakami, J. Kikuchi, T. Ohno, T. Hirayama, H. Nishimura, *Chem. Lett.* **1989**, 1199–1202. Recent publications that could not be considered here: Y. Murakami, T. Ohno, O. Hayashida, Y. Hisaeda, *ibid.* **1991**, 1595–1598; Y. Murakami, J.-I. Kikuchi, T. Ohno, T. Hirayama, Y. Hisaeda, H. Nuhimura, *ibid.* **1991**, 1657–1660.
[144] a) D. J. Cram, S. Karbach, Y. H. Kim, L. Baczynskyj, K. Marti, R. S. Sampson, G. W. Kalleymeyn, *J. Am. Chem. Soc.* **1988**, *110*, 2554; b) J. A. Bryant, M. T. Blanda, M. Vincenti, D. J. Cram, *ibid.* **1991**, *113*, 2167–2172.
[145] a) J. C. Sherman, D. J. Cram, *J. Am. Chem. Soc.* **1989**, *111*, 4527–4528; b) J. C. Sherman, C. B. Knobler, D. J. Cram, *ibid.* **1991**, *113*, 2194–2204.
[146] D. J. Cram, S. Karbach, H.-E. Kim, C. B. Knobler, E. M. Maverick, J. L. Ericson, R. C. Helgeson, *J. Am. Chem. Soc.* **1988**, *110*, 2229–2237, and references cited therein. See also ref. [16g]. A carcerand based on calixarenes has been described recently: T. Arimura, S. Matsumoto, O. Teshima, T. Nagasaki, S. Shinkai, *Tetrahedron Lett.* **1991**, *32*, 5111–5114.
[147] M. L. C. Quan, D. J. Cram, *J. Am. Chem. Soc.* **1991**, *113*, 2754–2755; M. L. C. Quan, C. B. Knobler, D. J. Cram, *J. Chem. Soc. Chem. Commun.* **1991**, 660–662.
[148] J. K. Judice, D. J. Cram, *J. Am. Chem. Soc.* **1991**, *113*, 2790–2791.
[149] M. E. Tanner, C. B. Knobler, D. J. Cram, *J. Am. Chem. Soc.* **1990**, *112*, 1659–1660. The stabilization of cyclobutadiene in a hemicarcerand was recently reported: D. J. Cram, M. E. Tanner, R. Thomas, *Angew. Chem.* **1991**, *103*, 1048–1051; *Angew. Chem. Int. Ed. Engl.* **1991**, *30*, 1024–1028.
[150] F. Vögtle, *Reizvolle Moleküle der Organischen Chemie*, Teubner, Stuttgart, **1989**; *Fascinating Molecules in Organic Chemistry*, Wiley, Chichester, **1992**.
[151] a) K. Kurihara, K. Ohta, Y. Tanaka, Y. Aoyama, T. Kunitake, *J. Am. Chem. Soc.* **1991**, *113*, 444–450; b) C.-Y. Huang, L. A. Cabell, E. V. Anslyn, *Tetrahedron Lett.* **1990**, *31*, 7411–7414.
[152] a) K. Odashima, H. Kawakami, A. Miwa, I. Sasaki, K. Koga, *Chem. Pharm. Bull.* **1989**, *37*, 257–267; b) S. Kumar, H.-J. Schneider, *J. Chem. Soc. Perkin Trans. 2* **1989**, 245–250; c) D. R. Carcanague, F. Diederich, *Angew. Chem.* **1990**, *102*, 836–838; *Angew. Chem. Int. Ed. Engl.* **1990**, *29*, 769–771.
[153] M. W. Hosseini, A. J. Blacker, J.-M. Lehn, *J. Am. Chem. Soc.* **1990**, *112*, 3896–3904.
[154] a) I. Takahashi, K. Odashima, K. Koga, *Tetrahedron Lett.* **1984**, *25*, 973–976; b) ref. [130]; c) J. Rebek, Jr., B. Askew, P. Ballester, M. Doa, *J. Am. Chem. Soc.* **1987**, *109*, 4119–4120; d) D. A. Lightner, J. K.Gawronsky, W. M. D. Wijekoon, *ibid.* **1987**, *109*, 6354–6362; e) M. A. Petti, T. J. Sheppod, R. E. Barrans, Jr., D. A. Dougherty, *ibid.* **1988**, *110*, 6825–6840; f) C. B. Knobler, F. C. A. Gaeta, D. J. Cram, *J. Chem. Soc. Chem. Commun.* **1988**, 330–333; g) F. Diederich, M. R. Hester, M. A. Uyeki, *Angew. Chem.* **1988**, *100*, 1775–1777; *Angew. Chem. Int. Ed. Engl.* **1988**, *27*, 1705–1707; h) P. P. Castro, T. Georgiadis, F. Diederich, *J. Org. Chem.* **1989**, *54*, 5835–5838; i) W. H. Pirkle, T. C. Pochapsky, *Chem. Rev.* **1989**, *89*, 347–362; k) A. Echavarren, A. Galán, J.-M. Lehn, J. de Mendoza, *J. Am. Chem. Soc.* **1989**, *111*, 4994–4995; l) ref. [108]; m) ref. [9d], Chapter 6; n) ref. [141].
[155] Review: D. A. Tomalia, A. M. Naylor, W. A. Goddard III, *Angew. Chem.* **1990**, *102*, 119–138; *Angew. Chem. Int. Ed. Engl.* **1990**, *29*, 138–157.
[156] E. Buhleier, W. Wehner, F. Vögtle, *Synthesis* **1978**, 155–158.
[157] G. R. Newkome, Z.-Q. Yao, G. R. Baker, V. K. Gupta, P. S. Russo, M. J. Saunders, *J. Am. Chem. Soc.* **1986**, *108*, 849–850; G. R. Newkome, G. R. Baker, S. Arai, M. J. Saunders, P. S. Russo, K. J. Theriot, C. N. Moorefield, L. E. Rogers, J. E. Miller, T. R. Lieux, M. E. Murray, B. Phillips, L. Pascal, *ibid.* **1990**, *112*, 8458–8465, and references cited therein.
[158] J.-M. Lehn, J. Malthête, A.-M. Levelut, *J. Chem. Soc. Chem. Commun.* **1985**, 1794–1796; L. Jullien, J.-M. Lehn, *Tetrahedron Lett.* **1988**, *29*, 3803–3806; V. E. Carmichael, P. J. Dutton, T. M. Fyles, T. D. James, J. A. Swan, M. Zojaji, *J. Am. Chem. Soc.* **1989**, *111*, 767–769; F. Vögtle, A. Schröder, D. Karbach, *Angew. Chem.* **1991**, *103*, 582–584; *Angew. Chem. Int. Ed. Engl.* **1991**, *30*, 575–577.
[159] *Radiolabeled Monoclonal Antibodies* (Ed.: S. C. Srivasta) Plenum, New York, **1988**; T. A. Kaden, *Nachr. Chem. Tech. Lab.* **1990**, *38*, 728–732.

Distorted Molecules: Perturbation Design, Preparation and Structures

By Hans Bock,* Klaus Ruppert, Christian Näther, Zdenek Havlas, Hans-Friedrich Herrmann, Claudia Arad, Ilka Göbel, Andreas John, Jochen Meuret, Sabine Nick, Andreas Rauschenbach, Wolfgang Seitz, Torsten Vaupel, and Bahman Solouki

Dedicated to Professor Heinz Harnisch occasion of his 65th birthday

The structure of a molecule can change considerably as its energy and thus its electron distribution within the time-domain of dynamic relaxation varies. Based on comparison of approriate measured data of related compounds and supported by quantum chemical calculations, therefore, charge-perturbed and/or sterically overcrowded molecules can be designed. Their preparation, handling, and structural characterization, frequently under extreme and especially largely aprotic conditions, provides some surprises. New structural principles become evident and old-fashioned ones are confirmed. Thus the contact-ion aggregates that form on ultrasonically supported reduction of unsaturated hydrocarbons with sodium metal partly contain dibenzene sodium sandwiches. Vicinal dimethylamino substituents or isoelectronic isopropyl groups cause steric overcrowding and facilitate oxidation to molecular cations by energetically favorable delocalization of the generated positive charge. Molecules and molecular ions in which an even number of π electrons are distributed over a σ skeleton containing an odd number of centers preferentially form cyanine subunits. This is demonstrated by the novel ethene dication and dianion salts with central C–C single bonds and molecular halves twisted relative to each other. Altogether in two years well over 50 structures have been determined. Much has been learned from them, especially about electron transfer and contact ion-pair formation in aprotic solvents. Nevertheless, we had to realize that answers to many questions, above all "what crystallizes, how, and why", are still out of reach.

"Actually, everything is more complicated".
(Foreword from a Ph.D. thesis, Frankfurt University)

1. Starting Point: Structural Estimates from Measured Data and Approximate Energy Hypersurface Calculations

Even the predominantly preparative chemist profits considerably if he looks at his spectra from the additional point of view that these represent 'molecular state fingerprints'.[1] One example each from the gas phase and from solution will serve to illustrate both the approach and the gain of information.

1.1. The Structure of $H_3CS–C{\equiv}C–SCH_3$ in the Gas Phase

The gas-phase thermolysis of bis(methylthio)cyclobutene-1,2-dione at 720 K according to real-time gas analysis by photoelectron (PE) spectroscopy proceeds largely selectively by elimination of two energetically favorable leaving molecules of CO ($\Delta H^0_{f,273} = -110\,kJ\,mol^{-1}$) to form bis(methylthio)acetylene.[2] Two preferred conformations are conceivable for the latter in its ground state: the methylthio substituents are either coplanar or perpendicular to each other (Scheme 1). The possibilities can be evaluated from a

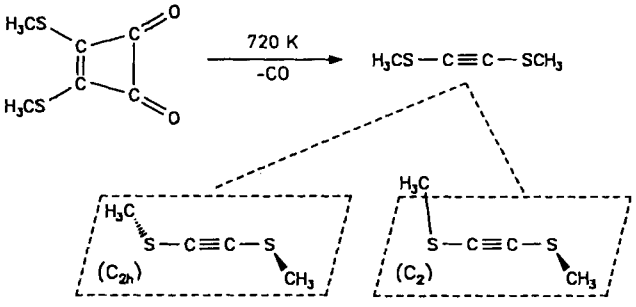

Scheme 1. Simulated synthesis of bis(methylthio)acetylene in the gas phase and its two preferred conformations.

calculation of an approximate one-dimensional MNDO energy hypersurface, in which only one of the total of $(3n - 6) = 30$ degrees freedom for the molecule containing $n = 12$ centers, namely the dihedral angle ω(C-SCCS-C) (Scheme 2), is considered.

[*] Prof. Dr. H. Bock, Dipl.-Chem. K. Ruppert, Dipl.-Chem. C. Näther, Dipl.-Chem. I. Göbel, Dipl.-Chem. A. John, Dipl.-Chem. J. Meuret, Dipl.-Chem. S. Nick, Dipl.-Chem. A. Rauschenbach, Dipl.-Chem. W. Seitz, Dipl.-Chem. T. Vaupel, Dr. B. Solouki
Institut für Anorganische Chemie der Universität
Niederurseler Hang, D-W-6000 Frankfurt am Main 50 (FRG)
Dr. Z. Havlas
Institute of Organic Chemistry and Biochemistry
Czechoslowakian Academy of Sciences
Flemingovo Nam 2, CS 16610 Prague (Czechoslowakia)
H.-F. Herrmann
Hoechst AG
Postfach 80 03 20, D-W-6230 Frankfurt am Main 80 (FRG)

[**] Structure of Charge-Perturbed and Sterically Overcrowded Molecules, Part 20, and Molecular Properties and Models, Essay 24. Part 19: H. Bock, W. Seitz, Z. Havlas, J. W. Bats, unpublished; Essay 23: [34].

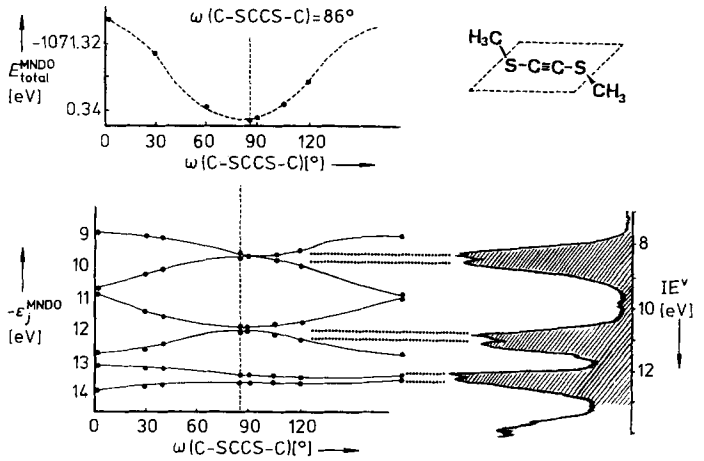

Scheme 2. Top: One-dimensional energy hypersurface for bis(methylthio)acetylene as a function of its dihedral angle ω(C-SCCS-C). Bottom: Koopmans's correlation of the eigenvalue pattern with the six lowest vertical ionization energies. IE^V, determined by PE spectroscopy. The intensity of the bands in the PE spectrum is given in counts per second (cps).

The MNDO potential minimum is found at a dihedral angle of 86°, and the MNDO eigenvalues calculated for the C_2 conformation reproduce via Koopmans's correlation, $-\varepsilon_j^{MNDO} = IE_n^V$, three double bands observed in the PE spectrum (Scheme 2). An independent structure determination of $H_3CS-C\equiv C-SCH_3$ by electron diffraction in the gas phase[3] confirms the preferred conformation deduced from the energy hypersurface minimum and by comparison of the measured vertical ionization energies with the calculated eigenvalue pattern. The dihedral angle is consistently determined to be 86°.[3]

1.2. The Structures of Radical Cations $R_2NNR_2^{\bullet\oplus}$ in Solution

The oxidation of silyl-substituted hydrazine derivatives by the oxygen-free and selective one-electron-transfer oxidation reagent $AlCl_3/CH_2Cl_2$[4] yields their radial cations[1a, 4, 6] in their doublet ground states [Eq. (a)].

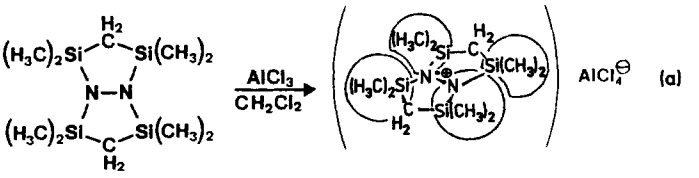

(a)

The high-resolution ESR spectrum including the ^{29}Si coupling (natural abundance 4.5%) of the planarized 1,5-diaza-2,4,6,8-tetrasilabicyclo[3.3.0]octane derivative can be simulated satisfactorily.[5] Problems, however, result on comparison with analogous silyl hydrazine radical cations such as $((H_3C)_3Si)_2N^{\bullet\oplus}$-$N(Si(CH_3)_3)_2$;[5] they can be resolved by reference to approximate quantum chemical calculations for the model compound $H_2N-NH_2^{\bullet\oplus}$, which reveal a

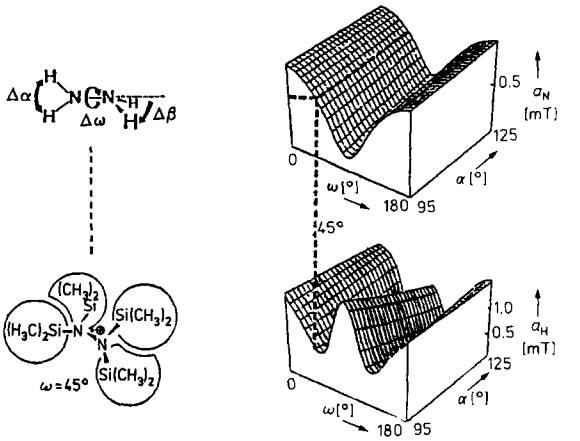

Scheme 3. INDO hypersurfaces for the dependence of the coupling constants a_N and a_H of $H_2N-NH_2^{\bullet\oplus}$ on angles ω and α, and estimated structure (---) for the sterically overcrowded tetrakis(trimethylsilyl)hydrazine radical cation in solution [5, 6].

Hans Bock obtained his Ph.D. in 1958 from the Ludwigs Maximilians University in Munich, submitting a thesis on reactions of the rocket-fuel hydrazine, and his habilitation in 1964 based on investigations concerning relations between color and constitution of azo compounds. In the following three years as a visiting fellow at the Federal Institute of Technology in Zurich, the three-volume book "The HMO Model and its Application" was compiled under the guidance of his mentor and friend Edgar Heilbronner and later translated into English, Japanese, and Chinese. In 1968 he received the Chemistry Award of the Academy of Science in Göttingen and the offer of an inorganic professorship at the Johann Wolfgang Goethe University of Frankfurt. Preparative nonmetal chemistry, in combination with physical measurements and quantum-chemical calculations has remained the trademark of his research group: Short-lived molecules, some of them found in interstellar space, are generated under nearly unimolecular conditions and identified by their PE-spectroscopic ionization fingerprints; radical ions and their ion pairs in aprotic solution are characterized by their ESR/ENDOR signal patterns and their respective molecular states; the accompanying structural changes are discussed based on calculated energy hypersurfaces. Professor Bock, a dedicated university teacher, has won numerous honors, among them the Frederic Stanley Kipping Award of the American Chemical Society and the Wilhelm Klemm Award of the German Chemical Society. The University of Hamburg bestowed an honorary Ph. D. degree on him in 1988. Since 1977 he has been an External Scientific Member of the Max Planck Society, and since 1981 an Adjunct Professor of The University of Michigan, Ann Arbor.

different angular dependence of the dominant couplings a_N and a_H[5, 6] (Scheme 3).

For the structure of tetrakis(trimethylsilyl)hydrazine radical cation in solution a twisting angle between the two molecular halves of 45° is deduced (Scheme 3), caused by the mutual repulsion of the four bulky $(H_3C)Si$ groups.[1a, 5] The corresponding INDO energy hypersurface for the unsubstituted hydrazine radical cation (Scheme 4) predicts a completely planar geometry about the N centers (symmetry D_{2h}) as well as an N–N distance shortened relative to that in H_2NNH_2 by 17 pm (!) to 128 pm due to the formation of a two-center/three-electron multiple bond.[5, 6]

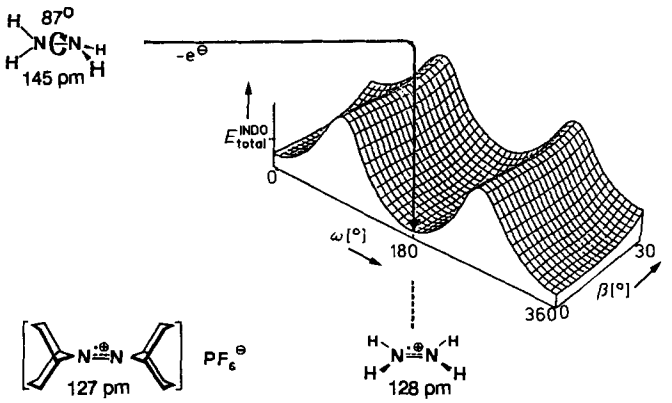

Scheme 4. INDO energy hypersurface for $H_2N^{\cdot\oplus}NH_2$ and N–N bond length in the hexafluorophosphate salt of a tetraalkylhydrazine radical cation (cf. text).

Both predictions were confirmed shortly afterwards by the structure determination for the salt of a tetraalkylhydrazine radical cation, kinetically stabilized by steric wrapping. Accordingly, the radical cation is planar and exhibits an N–N distance of 127 pm.[7]

1.3. The Quintessence: The Structures of Molecules in Particular Molecular States

The examples selected from several investigations by PE spectroscopy in the gas phase[8] as well as ESR/ENDOR spectroscopy in solution[9] (Schemes 1 to 4) confirm that suitable correlations of experimental and quantum chemical molecular-state data together with approximate energy hypersurface calculations do indeed allow satisfactory estimates of the structures of short-lived, and therefore not isolable compounds.

Molecular states are—as documented for example by photochemical synthesis steps or by redox reactions—the real chemical 'building blocks'. They can be ordered with respect to both energy[1a, d] (Fig. 1) and time scales[10] (Fig. 2).

For closer elaboration of the abundant molecular-state data along of energy and time scales (Fig. 1 and 2),[1c, 8] PE and electron spin resonance (ESR/ENDOR)[9, 11] techniques are chosen as representative, because they proved to be useful in the planning of the structure investigations reported here. 'Vertical' ionization energy patterns, which are measured with a time resolution less than 10^{-15} s, can be correlated by applying Koopmans's theorem, $IE_n^v = -\varepsilon_j^{SCF}$ to the eigenvalues calculated for the neutral molecule[1, 8] (cf. Scheme 2). In contrast, ESR/ENDOR signal patterns are recorded with a considerably smaller time resolution of greater than 10^{-8} seconds, that is, long after the activation of molecular dynamics at about 10^{-13} seconds, and the spin populations ρ_μ detected for the individual radical ion centers μ can be rationalized, for example according to the McConnell relation, $\rho_\mu \propto c_{j\mu}^2$, by comparison with the squared orbital coefficients $c_{j\mu}^2$ calculated for them.[11] The measurement techniques complement each other, especially for radical cations, because of their different time resolution and together with approximate hypersurface calculations (Scheme 3 and 4) allow reliable estimates of structural changes of molecules M on adiabatic one-electron oxidations $M \rightarrow M^{\cdot\oplus} + e^{\ominus}$.

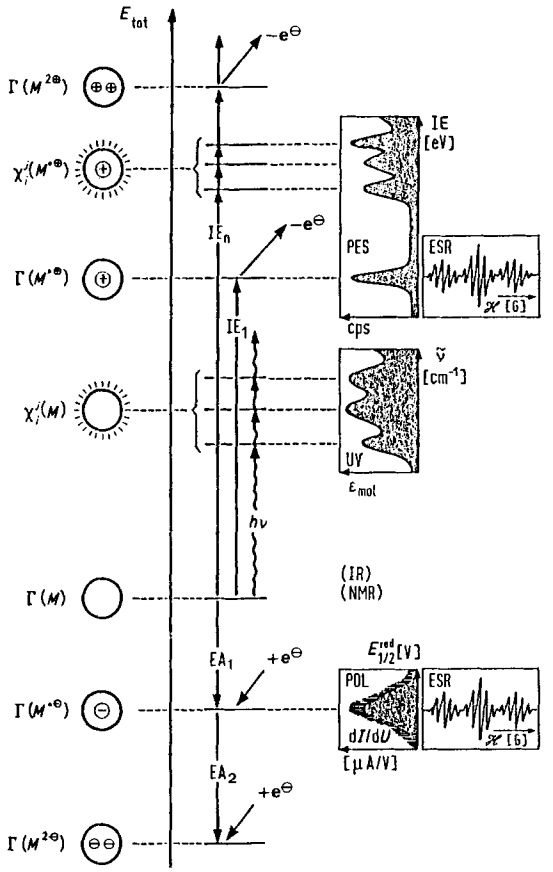

Fig. 1. A: Schematic energy scale for electronic ground (Γ) and excited (χ_i^j) states of a neutral molecule M and its radical cations $M^{\cdot\oplus}$ or dications $M^{2\oplus}$ generated by ionization or oxidation and its radical anions $M^{\cdot\ominus}$ and dianions $M^{2\ominus}$ resulting from electron insertion. B: Representative methods used in the reported investigations are UV, PE, ESR, and ENDOR spectroscopy as well as polarography (POL) or cyclic voltammetry (CV).

Many sets of molecular-state data (Fig. 1) can be advantageously discussed on the basis of a qualitative molecular-state model supported by quantum chemical calculations, which only considers the connection between the centers, their spacial arrangement, their effective nuclear potentials, and the resulting electron distribution[1] (Scheme 5). These rather drastic simplifications, however, accentuate that each

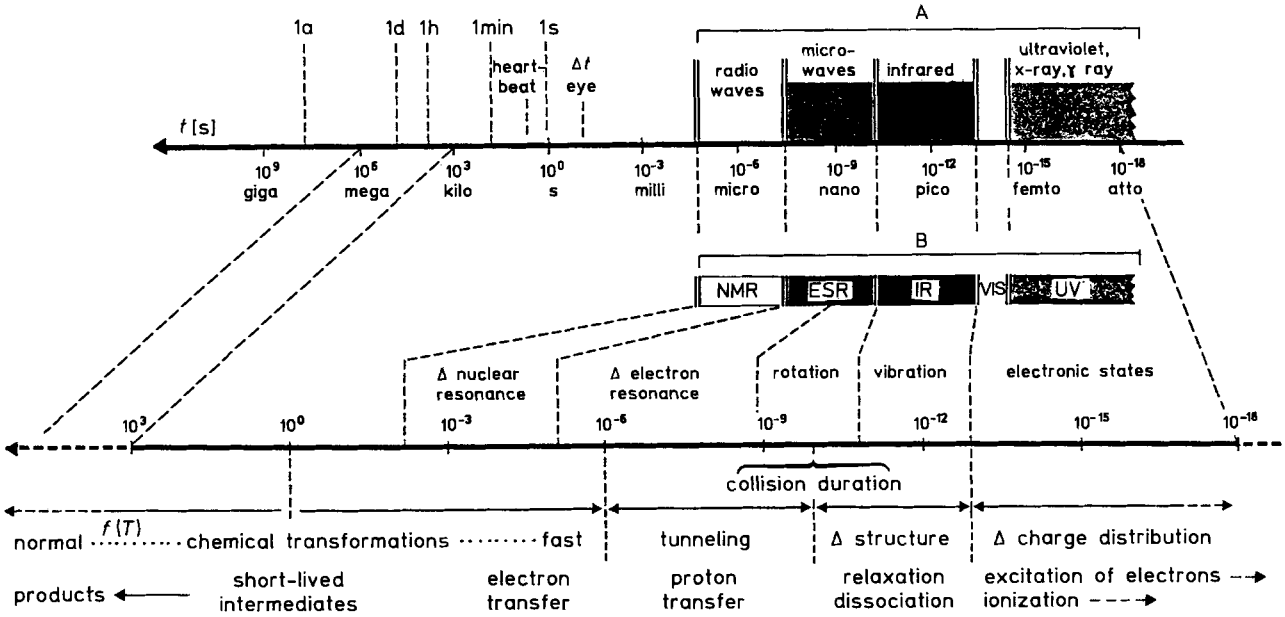

Fig. 2. Schematic time scale for molecular states and their changes (in seconds, the time unit intermediate between the duration of a human heart-beat and the transmission of stimuli by the eye) [10].

molecular state defined accordingly must possess an individual structure, and that changes in its energy and its charge distribution (Fig. 1) will always provoke structural changes through the inherent molecular dynamics (Fig. 2).

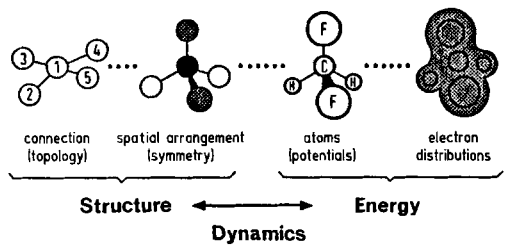

Scheme 5. Qualitative molecular-state model.

The following syntheses of charge-perturbed molecules, their growth as single crystals, and their structural characterization all started from considerations of the molecular states based on appropriate experimental data and supplementary quantum chemical calculations.

2. Organic Compounds of Alkali Metals Containing Inter- and Intramolecular Dibenzenesodium Sandwiches—Examples for the Usefulness of Quantum Chemical Structure Calculations

Perphenyl-substituted unsaturated hydrocarbons such as tetraphenylethene,[12, 13] tetraphenylallene,[14, 15] or tetraphenylbutadiene[16, 17] can be reduced at alkali-metal mirrors in aprotic conditions under argon; 1,1-diphenylethene forms a C–C bond to yield the tetraphenylbutane-1,4-diyl dianion.[18] In all the reduction products obtained as well as in many known[19] alkali metal–organic contact ion aggregates, the negative charge of the molecular anions and dianions is compensated by the alkali–metal cations, which are usually solvated and in some of the sodium compounds reported here are complexed in dibenzene sandwiches. In addition, the discussion of these novel molecular-anion salts demonstrates the usefulness of prior and subsequent chemical calculations.[14–18]

2.1. Tetraphenylethene

Ethene, the simplest monounsaturated hydrocarbon exhibits interesting molecular-state properties. On energy increase of 418 kJ mol^{-1} by $\pi \rightarrow \pi^*$ excitation, it switches from its ground state $\tilde{X}(^1A_g)$ of D_{2h} symmetry into its $\tilde{A}(^1B_{1u})$ state, for which after vibronic relaxation two perpendicular H_2C molecular halves are postulated.[20]

Stimulated by this spectroscopic result, we have estimated by approximate energy hypersurface calculations for varying dihedral angles ω which structural changes are to be expected for redox reactions of ethene.[12, 21] For the ground state of the neutral molecule, the well-established D_{2h} gas-phase structure is reproduced (Scheme 6, ○). For a fictive electron insertion that does not account for the stabilizing effects of countercations the calculated enthalpies of formation ΔH_f^{MNDO} predict an energy increase, and because of its shallower potential trough (Scheme 6: △) the structure of ethene radical anions might deviate slightly from planarity. The insertion of a second electron, enforced with rather crude quantum chemistry under an unrealistic energy increase, however, should twist the negatively charged molecular halves considerably relative to each other (Scheme 6, □).

Despite of considerable concern that the semiempirical results for the ethene dianion calculated without explicit account of the electron correlation are likely to be classified as 'se non e vero, e ben trovato',[23] we have chosen phenyl substituents for an improved charge delocalization and

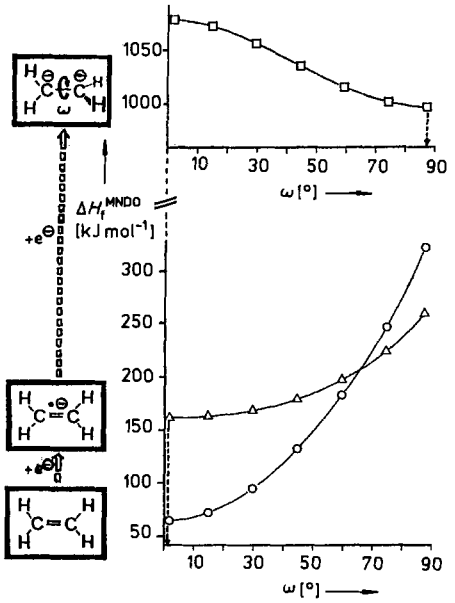

Scheme 6. MNDO enthalpies of formation for ethene, its radical anion, and its dianion as a function of the dihedral angle $\omega(H_2C\text{-}CH_2)$.

treated tetraphenylethene[23] in aprotic diethylether ($c_{H\oplus} < 1$ ppm) under argon with a sodium metal mirror generated at 10^{-4} mbar (Fig. 3a). The stringlike structure determined for the isolated green and extremely air-sensitive crystals exhibiting a metallic luster in a cold (210 K) N_2 flow (Fig. 3b) may be described in stages (Fig. 3c to e) as follows: Twofold reduction of the unsaturated hydrocarbon to its dianion[24] elongates the C–C double bonds by 13 pm (!) to a C–C single bond. The molecular halves, in which the negative charge is energetically favorably delocalized as in a cyanine ($C_6 \cdots C^{\ominus} \cdots C_6$, cf. Section 6), are twisted by 56° (Fig. 3c). In the contact ion pair formed (Fig. 3d), the $Na^{\delta\oplus}$ counterion solvated by two ether molecules is coordinated to a chain of six carbon centers, which stretches from phenyl ring I over the central C–C bond to phenyl ring III. The contact ion-pair units are connected to form an infinite string by the dibenzenesodium sandwich links (Fig. 3b).

For the formation of the twofold reduction product of tetraphenylethene with the unexpected polymeric structure of the contact ion triples, the following speculations, which are partly supported by experiment, can be forwarded[12] (cf. Section 4): Tetraphenylethene shows a planar $C_2C{=}CC_2$ skeleton, around which the four phenyl groups are twisted by angles between 45° and 53°,[23] thereby largely covering the central π cloud of ethylene by their *ortho* hydrogens (Fig. 3a). On single-electron transfer the radical anion is formed. Since its structure remains similar to that of the sterically overcrowded neutral molecule, it presumably only forms solvent-separated radical ion pairs $M^{\bullet}_{solv}{}^{\ominus} \cdots Na^{\oplus}_{solv}$, and therefore preferentially disproportionates, especially in ether solution, according to $2\,M^{\bullet\ominus} \rightarrow M + M^{\ominus\ominus}$ yielding the dianion. Considerable structural changes that lay bare the central C–C bond (Fig. 3c) accompany the second electron transfer to generate the dianion, which can be stabilized by formation of contact ion pairs $[M^{2\ominus}Na^{\oplus}(OR_2)_2]^{\ominus}$ (Fig. 3d). Under the reaction conditions, a polymer chain linked by dibenzene sodium sandwiches (Fig. 3e) crystallizes (Fig. 3b).

2.2. Tetraphenylallene

Who would have possibly suspected that the twofold reduction of organic molecules—often formulated as the inadmissably simplified equation $M + 2e^{\ominus} \rightarrow M^{2\ominus}$—takes such a complicated pathway in the case of tetraphenylethene? The knowledge gained spurred us on to numerous investigations, for instance, into the analogous reduction of tetraphenylal-

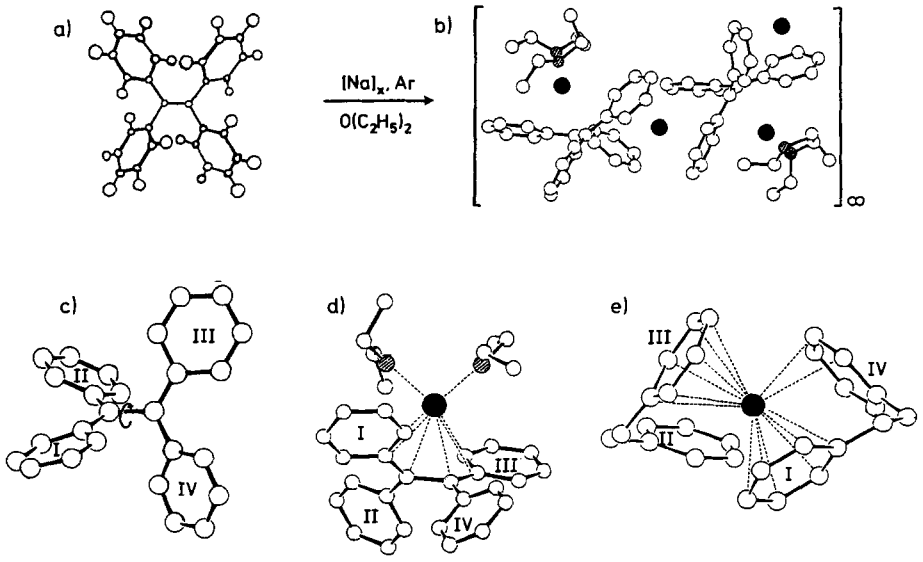

Fig. 3. Results of single crystal structure analyses of a) tetraphenylethene and b) its dianion salt, which is generated by a twofold reduction with sodium metal in diethyl ether and consists of a chain of contact ion pairs d) between $Na^{\delta\oplus}$ counterions solvated by two ether molecules and the dianion c). The chain is connected by dibenzenesodium sandwich links e) [12]. The following structural details are emphasized (●: Na, ◍: O; cf. also Scheme 13): In the tetraphenylethene dianion c) the negatively charged molecular halves are joined by a C–C single bond 149 pm long and twisted relative to each other by 56°. In the contact ion pair d), the sodium countercation solvated by two ether molecules is embedded in a cradle of six carbon centers, which extends from ring I across the central CC bond to ring II. The contact distances amount to 270–283 pm for $Na^{\delta\oplus} \cdots C$ and to an average of 232 pm for $Na^{\delta\oplus} \cdots O$. The contact ion-pair units d) are linked by 14-fold coordinated $Na^{\delta\oplus}$ centers e) at nine $Na^{\delta\oplus} \cdots C$ distances between 276 and 298 pm and five between 302 and 309 pm forming an infinite polymer chain.

lene with sodium.[14] From the reaction mixture, crystals of a salt containing the anion can be grown, in which the $Na^{\delta\oplus}$ counterion surprisingly is embedded in an intramolecular dibenzene sandwich [Eq. (b)].

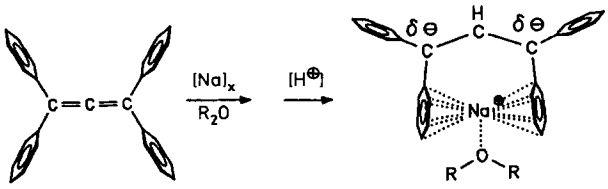

(b)

The course of the reaction had been suggested by comprehensive energy hypersurface calculations, each fully geometry-optimized, for the parent compound allene, chosen as model to save CPU-time[14] (Scheme 7). Clearly the gas phase structure of allene[27] is satisfactorily reproduced in the MNDO total energy minimum. Single-electron insertion to form the radical anion should reduce the dihedral angle $\omega(H_2C\cdots CH_2)$ to about half. For further reduction to the dianion, a considerable energy difference ($\Delta\Delta H_f^{MNDO}$ $(D_2 \rightarrow C_{2v}) \approx 660$ kJ mol^{-1}) is predicted, which must cause drastic structural deformations: Thus the molecular skeleton should be both planarized and bent ($\sphericalangle$ CCC $\approx 160°$). The resulting largely localized and accordingly extremely basic carbon σ lone pair ($q_u^{MNDO} = -0.78$) might be protonated, for example by the solvent, to form an allyl anion in which the negative charge would then be energetically far more favorably distributed over the two outer carbon centers ($\Delta\Delta H_f^{MNDO} \approx 780$ kJ mol^{-1}).

Well forecast? The structure of the extremely air-sensitive black crystals with a metallic luster, determined in a cold N_2 flow (200 K), confirms the quantum chemical planning of the experiment (Scheme 7) in detail: A tetraphenylallyl anion has been formed, exhibiting inter-carbon distances of 139 pm and a C-C-C bending angle of 130°. Unexpected and unique (according to a literature search[25, 26, 28]) therefore, is only the cage of the two phenyl rings opposite to each other containing the $Na^{\delta\oplus}$ counterion and closed by a coordinated diethyl ether molecule in W conformation as a solvent-plug.

To rationalize the surprising formation of the intramolecular dibenzenesodium sandwich, again extensive MNDO energy hypersurface calculations have been performed chosing for the sake of reduced CPU-time diphenylallylsodium diethyl ether as an appropriate model compound.[29] The

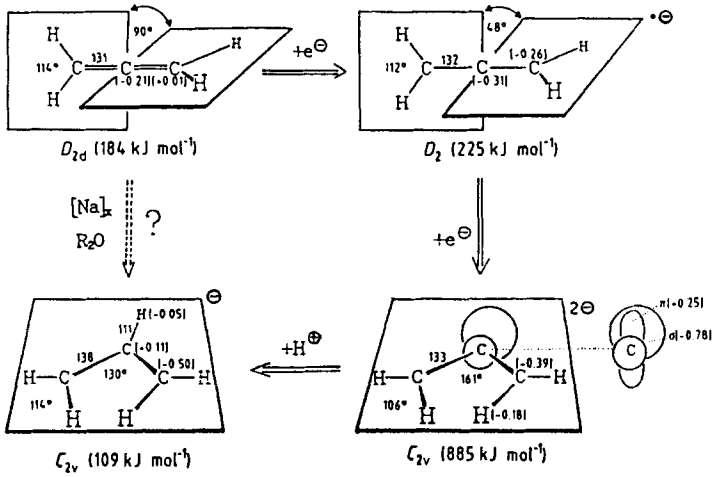

Scheme 7. Geometry-optimized MNDO energy hypersurface calculations for the course of the reduction allene → allyl anion (cf. text; bond lengths in pm, heats of formation in parentheses and charge orders in square brackets).

structure corresponding to the minimum of the MNDO total energy (Fig. 4b) reproduces all essential experimental observations (Fig. 4a) in a satisfactory approximation and suggests, in addition, the following plausible explanation for the formation of the intramolecular dibenzenesodium sandwich: In the energetically favorable C_2 structure of the diphenylallyl anion, the phenyl rings facing each other are twisted each by 41° out of the C-C-C allyl plane. A total negative charge of $\sum q_C = -0.47$ is calculated for their five outer ring-carbon centers, which exceeds the charge of a single terminal allyl-carbon center of $q_C = -0.36$ (Fig. 4c). If, therefore, the $Na^{\delta\oplus}$ counterion is fixed to one of the outer allyl-C centers, it moves along a barrier-free trough of the MNDO hypersurface between the two acute-angled phenyl rings into the center of the largest possible contact ion-pair interaction (Fig. 4b). The total charge at the $Na^{\delta\oplus}$ center is calculated to be +0.34 and in the isolated sodium salt containing the allyl anion, therefore, largely covalent complexation should prevail. The ether solvent-plug of the hydrocarbon cage reduces the MNDO enthalpy of formation considerably.

2.3. 1,1-Diphenylethene

A third example of the reductions of phenyl-substituted unsaturated hydrocarbons with alkali metals illustrates additional facets: If 1,1-diphenylethene is treated with either

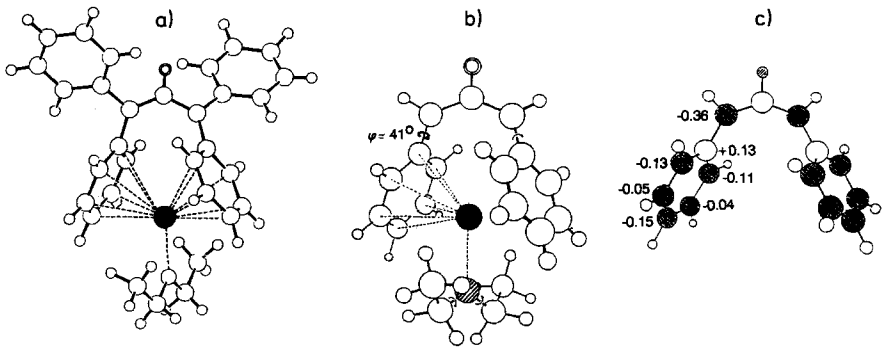

Fig. 4. a) Single crystal structure of tetraphenylallylsodium diethyl ether (●: Na, ◎: O, ○: H); b) MNDO geometry-optimized structure of the diphenyl derivative; c) charge distribution of the diphenyl derivative (cf. text). Selected bond lengths [pm] [14] and angles [°]: GH_{allyl} 99, $C\text{-}C_{phenyl}$ 146, φ(C-phenyl(Na)) 56, Na···C 272–310, Na···O 225. Calculated: φ(C-phenyl(Na)) 41, Na···C 260–273, Na···O 251.

sodium or lithium in aprotic diethyl ether solution under argon, the salts of the 1,1,4,4-tetraphenylbutane-1,4-diyl dianion [Eq. (c)] result through C-C bond formation[30] as

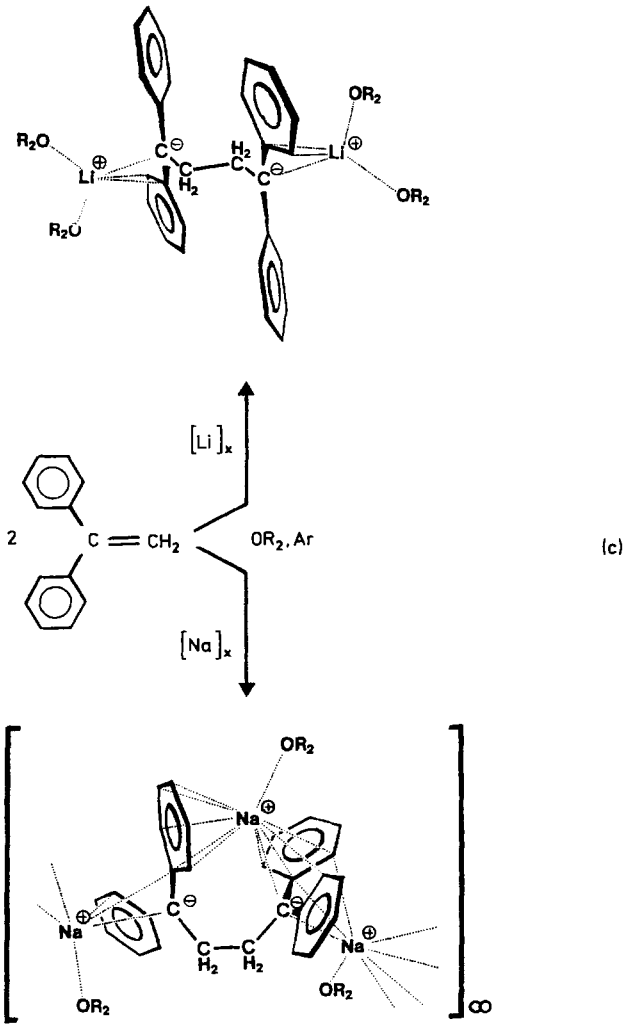

(c)

hydrolysis-sensitive intermediates of a 1,1,4,4-tetraphenylbutane synthesis. This has been proven for both contact ion triples by their single crystal structures[18] (Fig. 5).

On two-electron reduction of 1,1-diphenylethylene with lithium or sodium, distinct types of contact ion triples thus result, the structures of which (Fig. 5) obviously depend on the differing cation solvation energies (see Scheme 9a) and

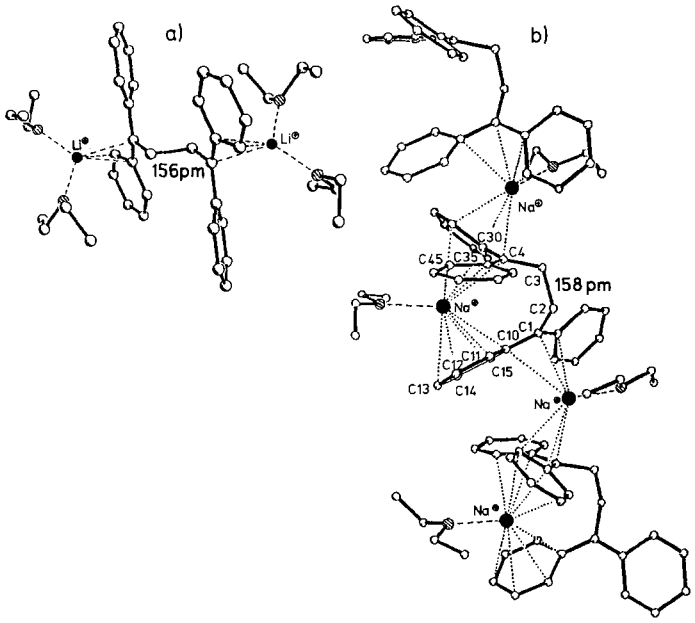

Fig. 5. Single crystal structures of a) 1,1,4,4-tetraphenylbutane-1,4-diyldilithium tetrakis(diethyl ether) and b) 1,1,4,4-tetraphenylbutane-1,4-diyldisodium bis(diethyl ether). The contact distances [pm] are: $Li^{\oplus}\cdots O$ 193, $Li^{\oplus}\cdots C$ 232 to 258, $Na^{\oplus}\cdots O$ 235 and $Na^{\oplus}\cdots C$ 273 to 305 (for further structural data see ref. [18] as well as Scheme 13).

may also be influenced by their different radii (see Scheme 9b). The monomeric dilithium compound solvated by four diethyl ether molecules exhibits an antiperiplanar ethane conformation ($^{\ominus}C$–H_2C–CH_2–$C^{\ominus}$). In contrast, the polymer string of the disodium aggregate solvated by only two diethyl ether molecules consists of contact ion pair anions $[M^{2\ominus}Na^{\oplus}OR_2]^{\ominus}$, which again contain intramolecular dibenzenesodium sandwich subunits. These are bridged by synclinal $^{\ominus}C$–CH_2–CH_2–$C^{\ominus}$ chains (Fig. 4a) and are connected by each η^3-coordinated, ether-solvated $Na^{\delta\oplus}(OR_2)$ cations. The negative charges on the two carbanion centers that are separated by an ethane bridge, are only partly delocalized into the phenyl rings. The resulting repulsive interaction stretches the central C–C single bond to 156 pm (Fig. 5a) and even to 158 pm (Fig. 5b).

Extensive quantum chemical calculations have been performed on the disodium salt of tetraphenylbutane-1,4-diyl dianion containing another intramolecular dibenzenesodium sandwich (cf. Section 2.2) aimed especially at detecting the effect of optimum charge distribution in the formation of

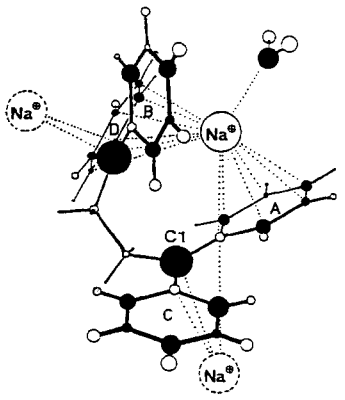

	$M^{2\ominus}$	$[M^{2\ominus}Na^{\oplus}(OH_2)]^{\ominus}$	$(Na^{\oplus}\cdots[\ ]\cdots Na^{\oplus})$
$\Delta\Delta H_f^{MNDO}$ [kJ mol^{-1}]	0	−1130	−1970
$\sum q^{MNDO}$ (M)	−2	−1.53	−1.15
$\sum q^{MNDO}$ (Ring A)	−0.30	−0.27	−0.12
$\sum q^{MNDO}$ (Ring B)	−0.30	−0.21	−0.06
$\sum q^{MNDO}$ (Ring C)	−0.36	−0.19	−0.13
$\sum q^{MNDO}$ (Ring D)	−0.36	−0.23	−0.09
q(C1)	−0.27	−0.34	−0.41

Scheme 8. MNDO model calculations for a hydrated link of the chain from a polymeric string of tetraphenylbutane-1,4-disodium (cf. Fig. 5b and text).

contact ion aggregates. The differences both in the heats of formation $\Delta\Delta H_f^{MNDO}$ and in the charge distribution q_μ^{MNDO} between the dianion $[M^{2\ominus}Na^{\oplus}(OH_2)]^{\ominus}$ and the corresponding chain subunit $Na^{\oplus}\cdots[M^{2\ominus}Na^{\oplus}(OH_2)]^{\ominus}\cdots Na^{\oplus}$ (Scheme 8) have been estimated by using the experimentally determined structure (Fig. 5b) as starting point.

As expected, the MNDO model calculations (Scheme 8) demonstrate that in contact ion pairs the enthalpy of formation is drastically lowered. The charges $\sum q_\mu^{MNDO}$ of the various dianion phenyl rings drop considerably, especially for the chain structure subunit $(Na^{\oplus}\cdots[M^{\ominus\ominus}Na^{\oplus}(OH_2)]^{\ominus}\cdots Na^{\oplus})$ in which, however, the additional outer ligands have been neglected. On the other hand, the charges q_{C1} at the butane diyl centers remain approximately constant. In summary, the preferred formation of an intramolecular $Na^{\delta\oplus}(OR_2)$ sandwich is supported quantum chemically also in the case of the tetraphenylbutane-1,4-diyl dianion.[18]

2.4. Why Dibenzenesodium Sandwiches in Particular?

Altogether three novel "hydrocarbon oysters with solvated sodium pearls" have been presented so far: the polymeric string of the tetraphenylethylene dianion salt[12] (Fig. 3b) with an intermolecular dibenzenesodium subunit, and with intramolecular ones, the monomeric tetraphenylallyl anion complex[14] (Fig. 4a) and the polymeric tetraphenylbutane-1,4-diyl dianion aggregate[18] (Fig. 5b). They all form under the rather brutal conditions of sodium metal reduction in ether solution, add new facets to the fascinating world of alkali-metal–organic compounds,[19] and in addition, illustrate the usefulness of quantum chemical calculations for the prediction and rationalization of hitherto unknown structures.

Nevertheless, many questions on the topic "what crystallizes, how, and why" (Section 8.2) remain unanswered. Let us begin with the formation of the inter- and intramolecular dibenzenesodium subunits possibly already in solution (Section 4). Analogous structural arrangements are also known in $Li^{\oplus}$ complexes[19, 25] and in salts of other phenyl-substituted hydrocarbon anions, but as half-sandwiches or with η^3-coordination.[19, 26]. There is hardly any doubt that competing solvation effects play an important and presumably essential role, because the enthalpies of hydration doubles from $[Cs^{\oplus}(H_2O)_{10}]$ (248 kJ mol^{-1}) to $[Li(H_2O)_{25}]$ (500 kJ mol^{-1})[31] (Scheme 9a). In addition, but with the necessary caution, the potential influence of the countercations' radii will be emphasized: Starting point is the correlation of first vertical ionization potentials of the alkali atoms as a measure of their effective nuclear charges (as defined according to Slater[32]) versus their atomic (r_{Met}), covalent (r_{Met-}), and ionic radii ($r_{Met\oplus}$) as well as their radii defined for 80% ionic character ($r_{Met^{\delta\oplus}}$)[19] (Scheme 9b).

The radius of the ring of maximum π electron density of benzene can be estimated at 120 pm by inserting the bond length $d_{CC} = 139$ pm into the formula for the inner circle radius of a regular hexagon, $r_{inner} = d\sqrt{3}/2$. If the radii ratios (Scheme 9b) do play some role, it would therefore be the $Na^{\delta\oplus}$ counterion which preferentially offers itself for six-membered ring sandwich formation.[18] Other single-crystal structures determined since then agree with this hypothesis.

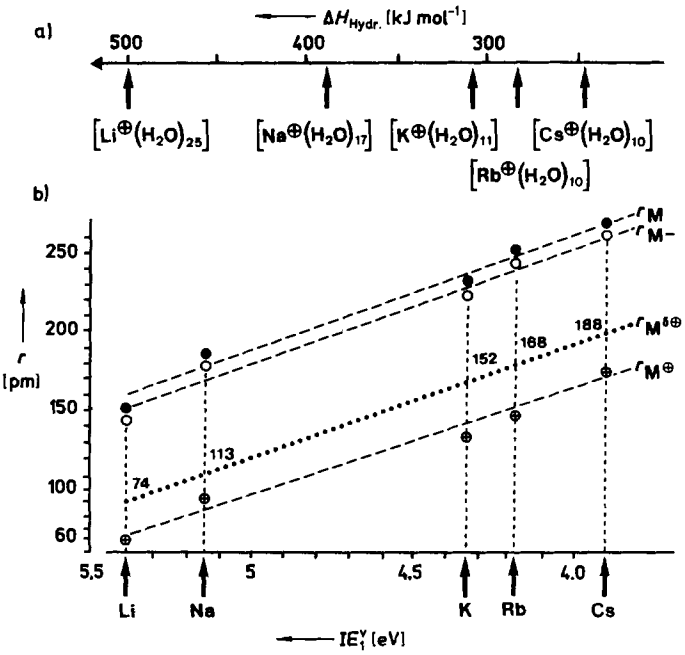

Scheme 9. a) Enthalpies of hydration for alkali-metal cations [31]; b) correlation of the atomic, covalent, and ionic radii (numbers given are for 80% ionic character [19]) with the first vertical ionization energies of alkali-metal atoms.

For instance, the sterically more rigid (biphenyl-2,2'-diyl) diphenylethenesodium diethyl ether[13] [Eq. (d)] contains within its complicated layer-lattice η^6-complexed six-membered fluorene rings exhibiting $Na^{\delta\oplus}$ contact distances between 281 and 298 pm. The other hemisphere of the tenfold coordinated $Na^{\delta\oplus}$ centers shows only a η^3-allylic bonding to the six-membered ring of the next-neighbor diphenylethene molecular half through contact distances of 269, 275, and 295 pm.[13]

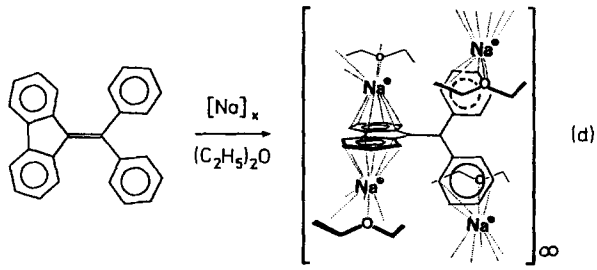

Counter examples, however, exist and should not be concealed. The most interesting one resulted from the numerous attempts to grow single crystals of the reduction products of tetraphenylbutadiene with sodium in the chelating solvent, dimethoxyethane(DME) (cf. Section 3.2): The structure obtained from our so far largest X-ray data set of 9000 registered reflexes proved that the unit cell of the almost black, dark-red crystals exhibiting a metallic luster contained one contact ion triple $[M^{2\ominus}(Na^{\oplus}dme_2)_2]$[33] and one dianion $[M^{2\ominus}]$ with two separated, octahedrally solvated counterions $[Na^{\oplus}(dme)_3]$[33] [Eq. (e)].

From this unexpected structure one may gather that the favorable charge delocalization along a butene-1,4-diyl chain leads to a preference for the η^3-allyl coordination over the η^6-sandwich complexation to the phenyl rings (Eq. (c)

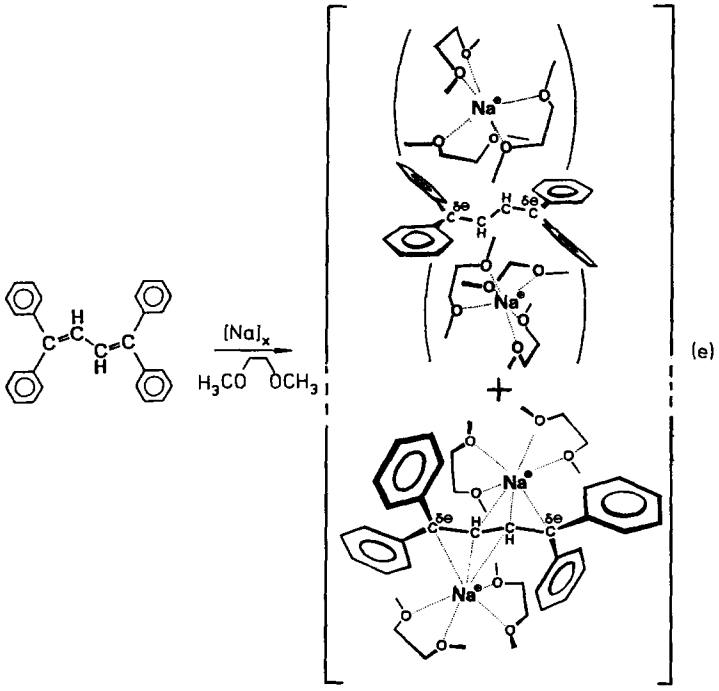

and Fig. 5), and that the stronger solvation by the chelating solvent dimethoxyethane relative to diethyl ether is energetically comparable to the η^3-allyl coordination to the butene-1,4-diyl dianion.

As pointed in the foreword 'actually, everything is more complicated'. Thus on reduction of perylene with sodium in dimethoxyethane a contact ion triple results, in which the dianion again forms η^6-half-sandwich subunits with only doubly solvated $Na^{\delta\oplus}$ counterions[33] [Eq. (f)].

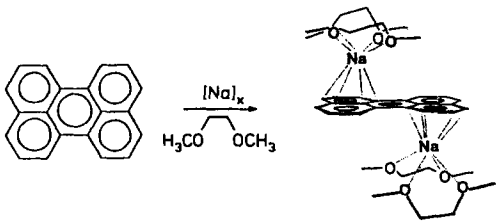

Within the context elaborated (Scheme 9 and Eq. (e)), the structure found may be rationalized at first glance by assuming that in competition between a η^6-sandwich coordination of the $Na^{\delta\oplus}$ counterions and threefold solvation by DME, here the former wins. Possibly, however, the stacking of the contact ion triples in the crystal provides a decisive contribution (Section 8.2).

This section's question, 'why dibenzenesodium sandwiches in particular?', cannot be answered straightforwardly due to their multifaceted aspects. Additional experiments planned to reduce unsaturated hydrocarbons containing six-membered rings by varying both the alkali metal as well as the solvent will help to elucidate the origin of the obviously favorable benzenesodium sandwich formation and, above all, contribute to the interesting competition between countercation solvation and their π coordination to molecular anions of unsaturated hydrocarbons.

3. Structural Changes on Reduction of Unsaturated Hydrocarbons

According to molecular state considerations (Section 1.3), every redox reaction inevitably is accompanied by structural changes due to the changes in energy coupled to the uptake or removal of electrons. Atoms and ions change their radii, diatomic molecules their bond lengths, and larger molecules with more degrees of freedom often preferentially their bond angles.[1d, 34] Because a discussion of all the individual data for the present structures of the organic compounds of alkali metals and especially of their comparison with the many literature values[19] would exceed the scope of this review, three variations characteristic for the reduction of unsaturated hydrocarbons to their molecular anions have been selected for illustration.

3.1. C–C Bond Formation

1,1-Diphenylethene is reduced by lithium or sodium metal to dianion salts of tetraphenylbutane-1,4-diyl[18] (Eq. (c) and Fig. 5). Presumably, the C–C bond formation on dimerization is initiated by a heterogeneous surface reaction, but proceeds in the anionic polymerization of hydrocarbons such as the copolymerizations of styrene on technical scale within the liquid phase.[18] Because of their more general relevance, MNDO/CI energy hypersurface calculations[35] have been performed for the model system ethylene to obtain some insight into the pathway of the C–C bond formation for the intermediates of the reduction isolated as single crystals (Scheme 10).

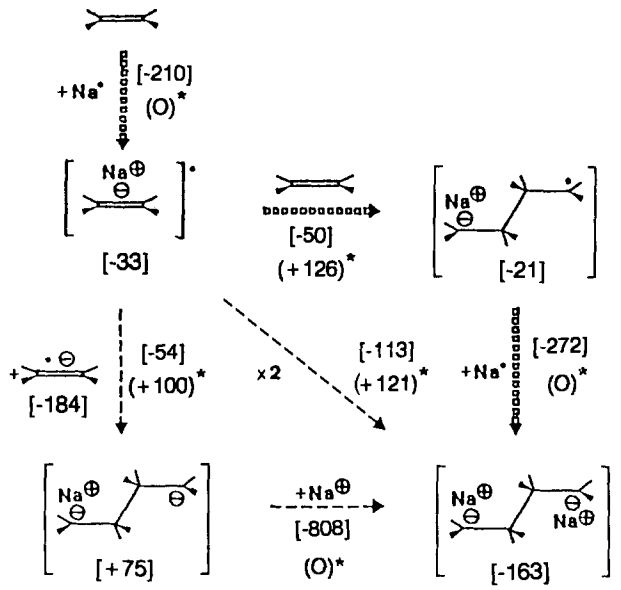

Scheme 10. MNDO/CI calculations for C–C bond formation on reduction of ethene with sodium (enthalpy differences $\Delta\Delta_f^{MNDO}$ in square brackets and activation enthalpies in parentheses, each in kJ mol^{-1}).

The following tentative reduction pathway (Scheme 10: ⇒) is proposed:[18] At the sodium mirror the energetically preferred contact ion-pair radical $[H_2C{=}CH_2^{\bullet\ominus}Na^{\oplus}]$ forms and adds surplus ethylene to the $Na^{\oplus}$ butane-1-yl radical,

which is further reduced to the diamagnetic triple ion $[Na^{\oplus}H_2C^{\ominus}-CH_2-CH_2-CH_2^{\ominus}Na^{\oplus}]$. Phenyl substituents lower all enthalpy values.[35]

3.2. CC Double Bond Shift

On reduction of 1,1,4,4-tetraphenylbutadiene by sodium in dimethoxyethane as well as by potassium in diethyl ether, which again (cf. Fig. 5) yield contact ion aggregates of different structure[16] (Fig. 6), the alternation in the bond lengths of the C_4 chain is reversed.

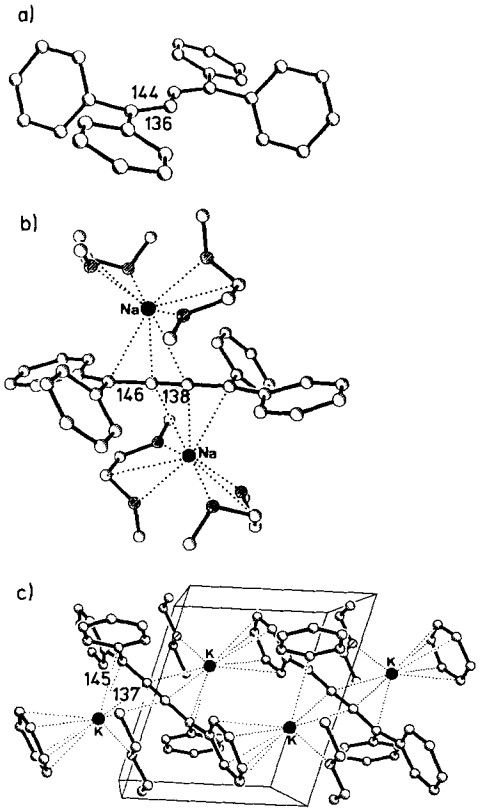

Fig. 6. Single crystal structures of a) 1,1,4,4-tetraphenylbutadiene and of its b) monomeric Na/DME and c) polymeric $K/O(C_2H_5)_2$ reduction products.

The reaction with sodium in the chelating dimethoxyethane solvent yields a monomeric contact ion triple, in which on each side of the central C_4 chain a doubly solvated $Na^{\oplus}$ counterion is coordinated in a η^3 fashion [Fig. 6b and Eq. (e)]. In contrast, the reduction with potassium in diethyl ether as a weaker solvating ligand produces crystals with a complex layer structure of infinite polymer chains (Fig. 6c), in which the tetraphenylbut-2-ene-1,4-diyl dianions are connected by altogether ninefold coordinated, but each only singly ether-solvated $K^{\oplus}$ counterions alternately in η^3- and η^4-modes. Despite these structural differences, caused by the decreasing solvation of the countercations and their increasing radii (Scheme 9), the two-electron reduction of tetraphenylbutadiene to its dianion[19] is accompanied in both of them by equally large eye-catching C=C bond shifts along the C_4 chain. The two outer, C–C double bonds (136 pm) are elongated by about 10 pm towards a C–C single bond, whereas the inner C···C partial π bond is shortened by 6 pm to 138 pm. The negative charges are predominantly located at the chain ends C_1 and C_4, and again (cf. Scheme 8) are only partly delocalized into the phenyl rings as can be gathered from their connecting CC bond lengths of 144 and 148 pm and their twist angles of 23° and 51°. Remarkable among the several structural changes that occur on two-electron reduction of 1,1,4,4-tetraphenylbutadiene,[16] are also the opened angles at the inner butene centers (129°), presumably due to the Coulomb repulsion between the outer carbanion centers, as well as the interior angles at the *ipso* carbon centers of the phenyl substituents ("*ipso*-angles") decreased to 114°. The changes at the *ipso* angles will be discussed subsequently in a general context.

3.3. Variation of *ipso* Angles in Six-Membered Rings of Benzene Derivatives

This rather frequent structural distortion in planar six-membered rings shall be illustrated here by three spectacular observations[36–38] (Scheme 11). In the 2-dimethylamino-

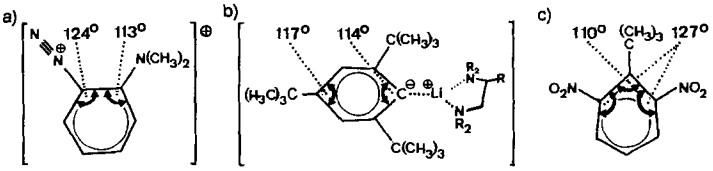

Scheme 11. Selected examples of *ipso* angles of benzene derivatives perturbed by substituents (R = CH_3).

benzenediazonium cation (Scheme 11a), the planar six-membered ring (interior angle sum of 720°) exhibits *ipso* angles widened to 124° at the (diazonium)acceptor-substituted center but closed to 113° at the (dimethylamino)donor-substituted center.[36] The (pentamethylethylenediamine)$Li^{\oplus}$ salt of the supermesityl carbanion (Scheme 11b) also contains a planar six-membered ring, which, however, is stretched along the $C^{\ominus}\cdots Li^{\oplus}$ axis, that is, the *ipso* angles at the $C^{\ominus}$ center and at the *para* carbon are reduced to 114° and 117°, respectively.[37] The structural data for 2-*tert*-butyl-1,3-dinitro-benzene (Scheme 11c) prove that even uncharged benzene derivatives can show considerable ring distortions and that steric effects (Section 7) may also play some role. The *ipso* angles at the (nitro)acceptor-substituted centers are enlarged to 127° (!), and that at the sterically overcrowded (*tert*-butyl)donor center is squeezed to 110° (!).

A generalization of changes in the *ipso* angles observed for six-membered rings, which are extensively documented and discussed in the literature,[37, 39] is achieved by a presumably nonlinear correlation with substituent perturbation parameters ξ[37] (Scheme 12). Accordingly, the corresponding angles for benzene (Scheme 12, X = H) are changed in different ways on substitution: donor substituents exert a strong angle-diminishing and acceptor groups a smaller angle-widening effect.

In the structures of the sodium salts of the phenyl-substituted hydrocarbon anions and dianions presented in Fig-

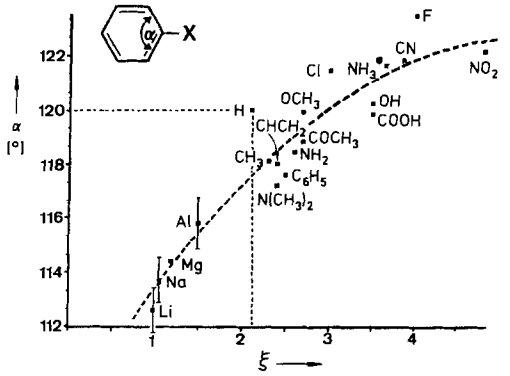

Scheme 12. Correlation of the *ipso* angles (α) of benzene derivatives with substituent electronegativities ξ [37].

ures 3 to 5, considerable distortions of the six-membered rings are observed (Scheme 13).

In the tetraphenylethene dianion, both the rings I and III (Scheme 13a and b) participate in the $Na^{\oplus}$ contact ion-pair from the front and in the dibenzenesodium sandwich subunit from the back. However, ring IV that does not exhibit any $Na^{\delta\oplus}$ contacts is more strongly perturbed (Scheme 13c). The *ipso* angle is reduced to 113° and its sub-

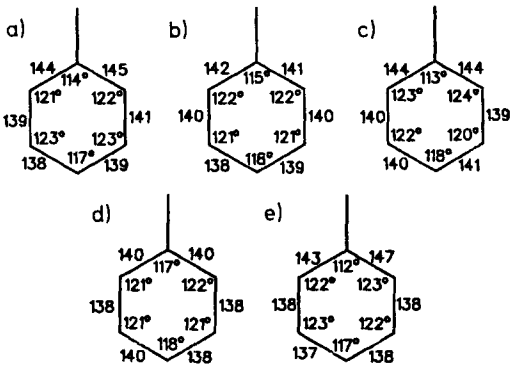

Scheme 13. Representative six-membered ring distortions in phenyl-substituted hydrocarbon anions (Fig. 4) and dianions (Fig. 3 and 5). a) Ring I, b) ring III, c) ring IV of Figure 3e; d) the sandwich-forming ring of Figure 4a; e) the sandwich-forming ring C10–C15 of Figure 5b.

tending bonds are each increased to 144 pm by the negative charge at the carbon anionic center 146 pm away (Fig. 3 and Scheme 12). In contrast, in the six-membered rings forming the intramolecular dibenzenesodium sandwich in the tetraphenylallyl anion (Scheme 13d and Fig. 4a), the C–C bond lengths are balanced to a large extent due to the pronounced η^6 coordination, and the *ipso* angle is reduced only to 117° because of the rather small negative partial charge at the adjacent allylic carbon center. The strongest distortion in all the sodium salt structures investigated is found in the sandwich-forming phenyl ring of the butane-1,4-diyl dianion (Scheme 13e). It is caused by the considerable negative partial charge at the adjacent $C^{\ominus}$ center of the saturated C_4 chain (C_1 in Scheme 8): the *ipso* angle shrinks to 112° and the subtending bonds are as elongated as in ring IV of the tetraphenylethene dianion (Scheme 13c).

Summarizing, the *ipso* angle reductions in the phenyl-substituted contact ion aggregates, the skeletal twisting and bond lengthening observed (Section 2), and the C–C bond formation and C=C bond shift discussed in more detail in Sections 3.1 and 3.2 all illustrate the striking structural changes that can accompany the reduction of unsaturated hydrocarbons M to their anions $M^{\ominus}$ and dianions $M^{2\ominus}$.

4. Structures of Radical Anion Salts—The Tip of the Iceberg of Equilibria Networks in Solution?

4.1. Proof of Single-Electron Reduction Products in Solution and the Crystallization of Fluorenone–Sodium–Bis(dimethoxyethane)

The structures of alkali-metal salts of phenyl-substituted hydrocarbon anions presented so far exclusively concern diamagnetic end products of two-electron reductions by alkali metals at room temperature (Sections 2 and 3.2). In essence, they prove the surprising formation of inter- (Fig. 3) and intramolecular (Figs. 4 and 5) dibenzenesodium sandwich subunits, the C–C connection to dianions (Fig. 5) and their protonation (Fig. 4), as well as their crystallization partly to monomeric contact ion multiples (Figs. 4, 5a, and 6b) and partly to cation-bridged polymer chains (Figs. 3b, 5b, and 6c). Proposals for their formation have been forwarded repeatedly, based on additional experimental as well as quantum chemical information (see e.g. Fig. 4 or Schemes 7 and 10). However, despite an ocean of known organic compounds of alkali metals[19] exhibiting fascinating structures, both the effects of the countercations and their solvation on the crystallizing product (Section 2.4) and many other details of the redox processes involved (Scheme 14) remain sunk at unknown depths. To sound

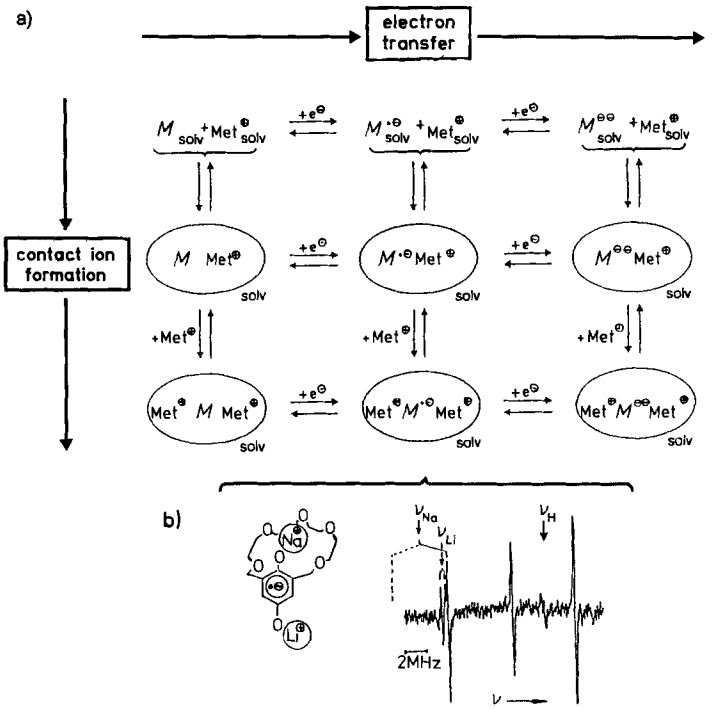

Scheme 14. a) A two-dimensional cut through the multidimensional network of equilibria in reduction reactions; M = molecule, Met = metal. b) ENDOR characterization of a radical cation consisting of a contact ion triple in aprotic THF solution ($c_{H^{\oplus}} < 1$ ppm) at 200 K [43a].

them out would be of interest also for the many chemical and biochemical reactions that are controlled by ion-pair interactions.[40] From a structural point of view especially, the question arises whether a single negative charge may already cause the drastic distortions observed in the single-electron oxidation of tetraalkylhydrazines (Section 1.2).

The study of these aspects remains a dream: reduction reactions in solution proceed by a multidimensional network of electron transfer, solvation, complex formation, and aggregation equilibria[41] (Scheme 14a), which often are decisively influenced by the reaction conditions as, for instance, negligible proton activities, the solvent chosen (solv), the concentrations of the reactants, or the temperature. Depending on the reaction conditions and the counterions $Met^{\oplus}$, a molecule M may pass through the network of equilibria by different routes.[42,43] Thus for the crystallization of tetraphenylethenedisodium bis(diethyl ether), a pathway via $\{M^{2\ominus} + Met^{\oplus}\}$ has been proposed, whereas the formation of the "shape-selective" radical cation triple formed by a macrocyclic polyether radical anion[43a] (Scheme 14b) should proceed via $\{M + Na^{\oplus}\}$ and $\{[M^{\bullet\ominus}Na^{\oplus}]^{\bullet} + Li^{\oplus}\}$. In general, although contact ion pairs of radical anions can be structurally characterized in solution at low temperatures by their ESR/ENDOR signal patterns,[11,43,44] they often decompose by disproportionation according to the equation $2M^{\bullet\ominus} \rightarrow M + M^{\ominus\ominus}$ on attempted isolation.

Fluorenone has been chosen as a suitable model compound for the planned preparation of a radical contact ion pair $[M^{\bullet\ominus}M^{\oplus}]$. The relatively large difference of $\Delta\varepsilon_{\frac{1}{2}}^{red} = -1.29 - (-1.95) = 0.66$ V[45a] for its two lowest and each reversible halfwave reduction potentials suggest that the fluorenone radical anion has a rather low tendency to disproportionate, and its radical contact ion-pairs have already been investigated at low temperature in tetrahydrofurane glasses.[45b] The ultrasonically activated stoichometric reaction of fluorenone in dimethoxyethane with sodium metal under Ar in aprotic conditions ($c_{H^{\oplus}} < 1$ ppm) at 260 K yields a dark red solution, from which on slow cooling to 230 K red needles with a greenish metallic luster crystallize.[46] The structure determination of the extremely air-, moisture- and temperature-sensitive crystals in a stream of nitrogen at 180 K proves that a contact ion pair-dimer has been formed (Scheme 15).

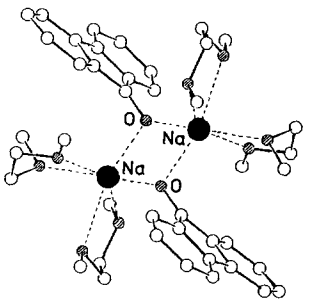

Scheme 15. Structure of the dimeric contact ion pair, fluorenonesodium bis(dimethoxyethane) [46].

The presumably first[46,47] single crystal structural analysis of a radical contact ion-pair dimer provides a wealth of information. The obviously preferred sixfold coordination of the doubly DME-solvated $Na^{\oplus}$ counterions enforces the formation of a $Na_2^{\oplus}O_2^{\delta\ominus}$ parallelogram with $d_{NaO} = 228$ and 240 pm. The structure depicts the aggregation of contact ion pairs[41] within the multidimensional equilibrium network (Scheme 14a) and agrees with the results of the solid state ENDOR measurement.[45b]. It should be kept in mind for speculations about the pathway of the reduction of organic carbonyl compounds by sodium metal to 1,2-diols HOR_2C-CR_2OH.[48] Each $Na^{\oplus}$ counterion is positioned 115 pm above the molecular plane of the fluorenone radical anion with which it interacts most strongly and 28 pm from the π_{CO} plane. This allows a direct spin transfer from the radical anion, which according to the frequently applied empirical Hirota rules[11,43,44] corresponds to the positive sign of the ^{23}Na ENDOR coupling[44] measured and thus provides structural evidence to substantiate them. In contrast, the interesting question from the structural point of view concerning the distortions due to one negative charge has a disappointing answer: On single-electron reduction of fluorenone, only small changes are observed because the charge is extensively delocalized over the 113 center molecular skeleton; for example, the C=O bond is only marginally lengthened from 122[49] to 128 pm.[46]

4.2. Solvent-Separated Radical Ion Pairs of Tetraphenylbutadiene and -Butatriene

The successful low-temperature reduction of fluorenone with sodium and the single-crystal growth of the contact ion-pair dimer $[fluorenone^{\bullet\ominus}Na^{\oplus}]_2$ in the joint solvent cage of four dimethoxyethane molecules stimulated an extensive literature search for further structure determinations of salts containing radical anions of unsaturated hydrocarbons. However, only solvent-separated[19] radical ion pairs were discovered such as $[biphenyl^{\bullet\ominus}][K^{\oplus}(tetraglyme)]$,[50a] $[terphenyl^{\bullet\ominus}][Na^{\oplus}(dme)_3]$,[50b] or $[TCNE^{\bullet\ominus}][Cp_2Fe^{\oplus}](H_3CCN)$ (TCNE = tetracyanoethene).[50c] Interesting facets are that TCNE also exhibits a rather large difference of 1 V between its first and second half-wave reduction potentials,[51] and that despite the presence of hydrocarbon radical anions, alkali-metal countercations can be completely solvated by polyethers (see [Eq. (e)], Section 2.4). Such structures prove in addition that here, other than in many known donor/acceptor molecular complexes,[52] the complete electron transfer to the hydrocarbon component under formation of the corresponding radical anion has taken place.

Extending the reduction of phenyl-substituted unsaturated hydrocarbons by alkali metals (Section 2 and 3), we have treated 1,1,4,4-tetraphenylbutadiene with lithium shavings[53] and tetraphenylbutatriene with a sodium mirror,[53] each 1:2 in the chelating solvent dimethoxyethane at room temperature. Unexpectedly, crystals of dark red $[tetraphenylbutadiene^{\bullet\ominus}][Li^{\oplus}(dme)_3]$ (Fig. 7a) and violet $[tetraphenylbutatriene^{\bullet\ominus}][Na^{\oplus}(dme)_3]$ (Fig. 7b) have been isolated.

The structural analyses prove that in both cases a threefold solvation of the cation by DME is preferred to π complexation by the hydrocarbon skeleton. The resulting "naked" radical anions enable a direct structural comparison (Scheme 16) with the neutral molecules M[16] (Fig. 6)[54]

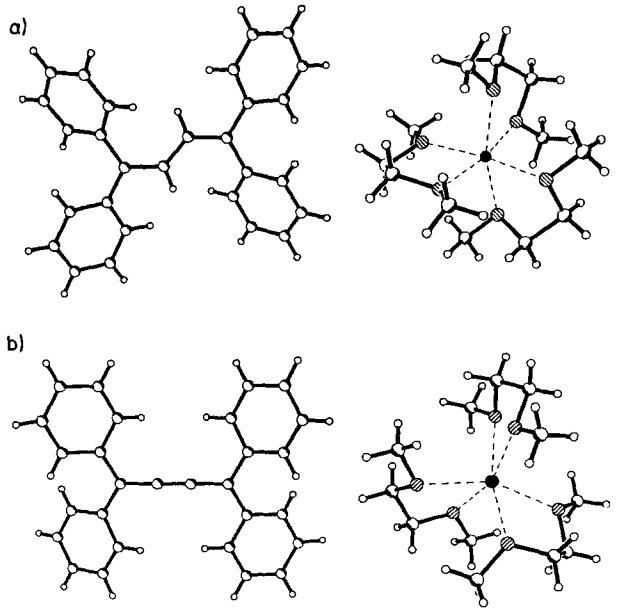

Fig. 7. Single crystal structures of the solvent-separated salts of radical anions a) 1,1,4,4-tetraphenylbutadienelithium tris(dimethoxyethane); b) tetraphenylbutatrienesodium tris(dimethoxyethane) (● = $Li^{\oplus}$, $Na^{\oplus}$; ◍ = O; for structural details see Scheme 16).

as well as with the likewise "naked" dianion $M^{2\ominus}$ of 1,1,4,4-tetraphenylbutadiene [Eq. (e)].

With increasing charge $M \rightarrow M^{\bullet\ominus} \rightarrow M^{\ominus\ominus}$, the length of the outer C–C bonds within the C_4 chain increases, while the central C–C bonds decrease in length (Scheme 16). These

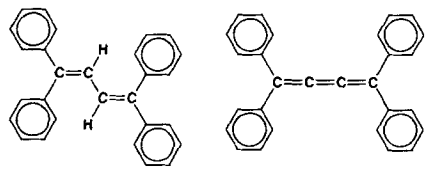

M	136	144	135	126
$M^{\bullet\ominus}$	142	139	139	124
$M^{\ominus\ominus}$	146	137		

Scheme 16. Comparison of CC bond lengths along the C_4 chains of tetraphenylbutadiene and -butatriene, and their dependence on the total charge.

structural changes are more pronounced for tetraphenylbutadiene, because of the Coulomb repulsion between the negative charges, which are predominantly localized at the ends of the chain. The synthesis of the unknown tetraphenylbutriene dianion, for which quantum chemical calculations predict a significant kink[54] in the C_4 chain, is presently being attempted by the deprotonation of 1,1,4,4-tetraphenylbut-2-yne.[53]

4.3. Staple and Spatial Lattice Structures of the Alkali-metal Salts of 2,3-Diphenylquinoxaline and Tetracyanoethene Radical Anions

Radical anion salts of the fluorenonesodium type (Scheme 15) exhibiting isolated contact ion pairs are still a rarity. Recently, the novel intramolecular sodiocryptatium **A**[55] has been added, in which one of the three α,α′-bipyridyl bridges of the cryptand has been recognizably reduced to its radical anion. The C–C bond between the two six-membered rings is shortened from 149 to 142 pm and, in addition, the two $Na^{\oplus} \cdots N^{\delta\ominus}$ contact distances of 259 pm are shorter than the others of 283 pm.

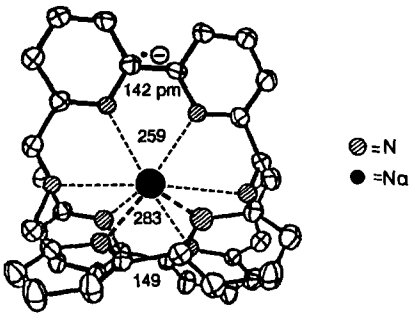

A

The radical anion salts of organic compounds, which are topical because of their magnetic properties,[56a] frequently crystallize in either separated stacks favored by flat molecular skeletons or, in case of more pronounced "salt character", spatial lattice structures. From the multitude of known compounds,[19a] the following ones are selected as being representative: [hexaazaoctadecahydrocoronene$^{\bullet\oplus}$][TCNE$^{\bullet\ominus}$],[56c] [tetracyano-*p*-quinodimethane$^{\bullet\ominus}$$Rb^{\oplus}$]$_{\infty}$,[56b] [chloranil$^{\bullet\ominus}$$K^{\oplus}$],[56c] and the also solvent-free [TCNE$^{\bullet\ominus}$$Cs^{\oplus}$]$_{\infty}$.[56d] We have also isolated single crystals of the cation-solvated radical anion salts [2,3-diphenylquinoxaline$^{\bullet\ominus}$$K^{\oplus}$(dme)]$_{\infty}$ (Fig. 8a),[57] [TCNE$^{\bullet\ominus}$$Na^{\oplus}$(dme)]$_{\infty}$ (Fig. 8b),[58] and [TCNE$^{\bullet\ominus}$$K^{\oplus}$(dme)] (Fig. 8c)[59] after reduction in the chelating solvent, dimethoxyethane.

To faciliate rationalization of their three-dimensional lattices, these structures (Fig. 8) are characterized as follows: [2,3-Diphenylquinoxaline$^{\bullet\ominus}$$K^{\oplus}$(dme)]$_{\infty}$ (Fig. 8a) crystallizes in layers of the radical anions, which stack in the perpendicular direction. The anions are alternately turned around the stacking axis,[57] presumably to achieve optimum packing (cf. Section 8.2). Between these stacks, the singly DME-solvated $K^{\oplus}$ counterions are found. Their eightfold coordination[57] illustrated in detail shows a clearly recognizable η^3 complexation to the quinoxaline nitrogen lone pair and two adjacent carbon centers of the phenyl rings, which are each twisted by 55° out of the molecular plane. The $C \cdots K^{\oplus}$ contact distances of 312 and 333 pm are considerably larger than the ones to the electron-rich O and N centers of 277 and 281 pm.[57] [TCNE$^{\bullet\ominus}$$Na^{\oplus}$(dme)]$_{\infty}$ and [TCNE$^{\bullet\ominus}$$K^{\oplus}$(dme)] (Figs. 8b and c) exhibit structural differences due to the size of the countercations: $Na^{\oplus}$ forms altogether six contacts to four TCNE$^{\bullet\ominus}$ and one DME molecule;[58] $K^{\oplus}$ formally seven to four TCNE$^{\bullet\ominus}$ and two DME molecules.[59] In the crystal lattice of the sodium salt,[58] the TCNE$^{\bullet\ominus}$ radical anions are arranged in parallel strings shifted relative to each other, and because they are connected by the singly DME-solvated $Na^{\oplus}$ counterions between them, they form "infinite tubes" (Fig. 8b). In the potassium salt, the TCNE$^{\bullet\ominus}$ subunits are packed in stacks; they form undulating parallel

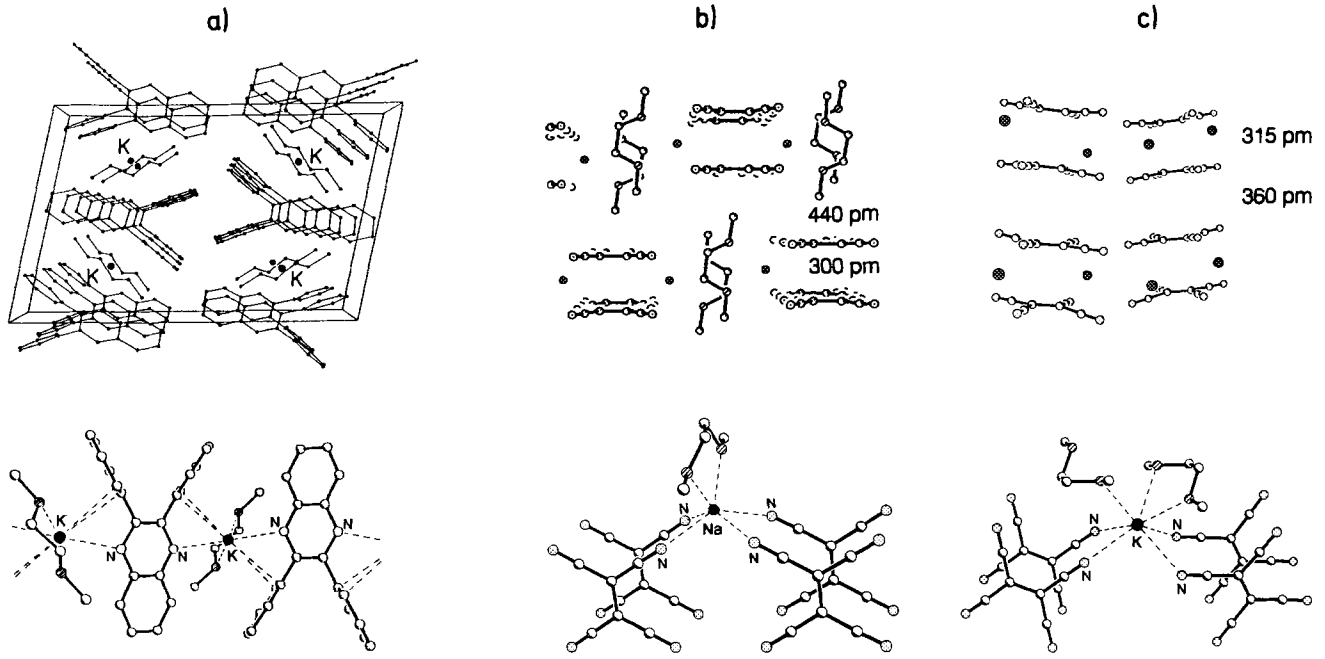

Fig. 8. Single crystal structures of radical anion salts containing solvated countercations. a) [2,3-diphenylquinoxaline$^{\cdot\ominus}$K$^{\oplus}$(dme)]$_\infty$: unit cell perpendicular to the radical-anion stacks (top) and details of the polymer string (bottom); b) [TCNE$^{\cdot\ominus}$Na$^{\oplus}$(dme)]$_\infty$: view along the 100 direction (top) and coordination sphere around the Na$^{\oplus}$ cations (bottom); c) [TCNE$^{\cdot\ominus}$K$^{\oplus}$(dme)]$_\infty$: layers viewed along the 010 direction (without dme) (top) and coordination sphere around the K$^{\oplus}$ cations (bottom). ● = counterions, ◍ = O, ◎ = N; see text and Scheme 18.

layers alternately 360 and 315 pm apart; the K$^{\oplus}$ counterions are interspersed in the smaller gap[59] (Fig. 8c).

The effect of a single negative charge on the molecular skeleton of the TCNE radical anion is of special interest, because its "naked" dianion in the complex salt [Cp$_2^*$Co$^{\oplus}$]$_2$[TCNE$^{2\ominus}$] comprises two molecular halves connected by a C–C single bond 149 pm long and twisted by 87° (!) relative to each other[24b, 56a] (Table 1). These fundamental structural changes can be rationalized analogously to those in the tetraphenylethene dianion (Fig. 3b), by the formation of two energetically favorable cyanine subunits (see Section 6.1) during the second reduction step $M^{\cdot\ominus} \rightarrow M^{\ominus\ominus}$, and can be reproduced quantum chemically (cf. Scheme 6). Similar although considerably smaller effects are expected and observed for the insertion of only a single electron $M \rightarrow M^{\cdot\ominus}$ (Table 1): The central C–C bond is elongated by 3 pm to 7 pm depending on the cation, and the molecular halves are twisted by 19°.

Table 1. Bond distances d_{CC} and $d_{CC(N)}$ [pm] and dihedral angles $\omega(C_2C\text{-}CC_2)$ [°] for tetracyanoethene TCNE, its radical anion [TCNE$^{\cdot\ominus}$] with different countercations, and its dianion salt [M$^{2\ominus}$] (average values in parentheses).

	TCNE	TCNE$^{\cdot\ominus}$				TCNE$^{2\ominus}$
		[Cp$_2^*$Fe$^{\oplus}$]	Na$^{\oplus}$ (dme)	K$^{\oplus}$ (dme)	Cs$^{\oplus}$	[Cp$_2^*$Co$^{\oplus}$]$_2$
	[59]	[50c]	[58]	[59]	[56d]	[50c]
d_{CC}	136	139	142	142	(143)	149
ω	0	0	8	12	18	87
$d_{CC(N)}$	143	142	142	142	(142)	139

The introductory question whether one negative charge can cause similarly drastic structural changes as a single positive charge in the special case of electron-rich molecules (Section 1.2), can therefore by affirmed according to the known structures of molecular anion salts only for the formation of intramolecular contact ion pairs (Section 2.2). The structural differences between the radical anions presented here (Scheme 15, Figs. 7 and 8) and to the neutral compounds are usually significantly smaller than those between them and the molecular dianions. This fact supports the proposals forwarded for their formation via solvent-separated radical ion pairs (Section 2.1).

In general, the radical anions $M^{\cdot\ominus}$ that often decompose in solution are stabilized on insertion into a crystal lattice, as expected. In addition to the informative structure comparison with the corresponding neutral molecules M and their dianions $M^{2\ominus}$, however, the single-crystal structures of radical anion salts provide varied and interesting insights into the multidimensional network of electron transfer, solvation, contact ion complexation or aggregation equilibria (Scheme 14a), which determines for the particular molecule, counterion, solvent, and reaction conditions the isolated end products. Also in this respect their investigation deserves intensified effort.

5. Molecular Polycations and Their Design—Examples of the Usefulness of Suitable Data

5.1. Vertical Ionization in the Gas Phase and Adiabatic Oxidation in Solution

These electron removal processes take place at different points in the "chemical" time scale (Fig. 2). Vertical ionization occurs in less than 10^{-15} seconds, that is, faster than the vibrational processes which start at about 10^{-13} seconds.

The radical cation states (Fig. 1) observed in photoelectron spectra therefore exhibit the "frozen" structure of the neutral molecule. In contrast, the oxidation in solution at more than 10^{-8} seconds is slower and thus allows energetically favorable structural changes in the resulting radical cation through its $(3n-6)$ degrees of freedom. This time dependence of all molecular redox reactions in solution[34] will be illustrated by the example of the "electron-rich" bis-(dimethylamino)disulfide[9d] (Scheme 17).

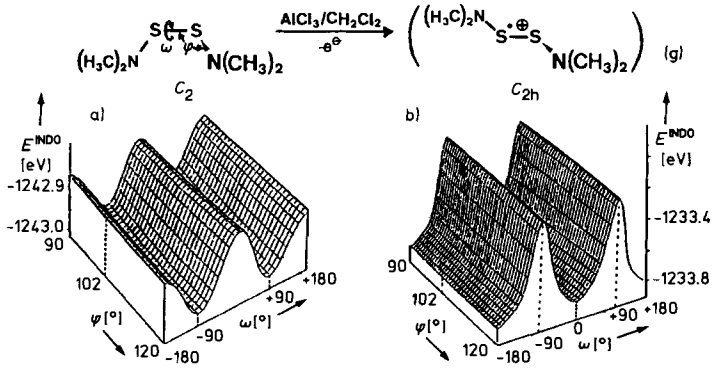

Scheme 17. INDO energy surfaces for the model compound H_2NSSNH_2 used to rationalize the oxidation of the experimentally studied bis(dimethylamino)disulfide [Eq. (g)]: Dependence of the INDO energy for a) vertical ionization and b) adiabatic oxidation on the dihedral angle ω(NS-SN) and on the obtuse angle φ(S-S-N) of H_2NSSNH_2.

The vertical ionization of $(H_3C_2N\text{–}SS\text{–}N(CH_3)_2$ at 8.02 eV produces its radical cation ground state of unchanged C_2 symmetry (Scheme 17a), in which the positive charge generated is largely delocalized over the N and S lone pairs. The first adiabatic ionization energy is observed at 7.2 eV, that is, about 0.8 eV = 77 kJ mol^{-1} lower.[9d] Adiabatic one-electron oxidation with $AlCl_3$ in CH_2Cl_2[4] generates a planarized radical cation of C_{2h} symmetry (Scheme 17b) as proven by the ESR spectrum registered with a time resolution of greater than 10^{-8} s. Accompanying INDO closed- and open-shell energy hypersurface calculations for the model compound $H_2N\text{–}SS\text{–}NH_2$ (Scheme 17) support—as for $H_3CS\text{–}C{\equiv}C\text{–}SCH_3$ (Scheme 2) or $R_2N\text{–}NR_2^{\bullet\oplus}$ (Schemes 3 and 4)—the structures inferred from the experimental data and predict a dihedral angle ω(NS-SN) of 90° for the neutral compound (Scheme 17a) and 0° for its planarized radical cation (Scheme 17b).

There are many rules of thumb for the "art of oxidation", which facilitate planning and performing of redox reactions and reduce problems in the ensuing effort to isolate multiply oxidized molecules and, especially, to grow single crystals; for instance:

1) For the gas phase ionization of medium-sized molecules with IE_1^V between 6 and 11 eV, considerably higher energies are needed than obtained on electron insertion, for which electron affinity values EA_1 often remain below 1 eV.

2) The oxidation potential of about +1.6 eV[4] determined for the system $AlCl_3/CH_2Cl_2$, which due to its lack of oxygen proves especially advantageous for air- and water-sensitive nonmetal compounds,[1a, 4, 60] corresponds to a first vertical ionization energy $IE_1^V < 8$ eV[4] and can be increased on exchange of the Lewis acid $AlCl_3$ by $SbCl_5$. For the single-electron transfer involved, both structurally characterized radical-cation salts $[M^{\bullet\oplus}][AlCl_4^{\ominus}]$[61] and $ClH_2C\text{–}CH_2Cl$[61] detected by gaschromatography in the reaction mixture suggest that the carbocation presumably generated by $Cl^{\ominus}$ abstraction $AlCl_3 \rightarrow AlCl_4^{\ominus}$ from CH_2Cl_2 could be reduced according to $CH_2Cl^{\oplus} + e^{\ominus} \rightarrow CH_2Cl^{\bullet}$ to a chloromethyl radical, which reacts further, for example, by dimerization.

3) Aprotic conditions ($c_{H\oplus} < 1$ ppm), which can be achieved by additional treatment of the solution with Al_2O_3 heated to glowing in vacuo,[62] are also essential for oxidations $M \rightarrow M^{\bullet\oplus} \rightarrow M^{\oplus\oplus}$, because in the second redox half-system reduction necessarily occurs to a more electron-rich and therefore often easily protonated species.

4) In order to chose as selective as possible an oxidizing reagent to avoid side and successive reactions, the measurement of an electrochemical series for the evaluation of optimum redox conditions is strongly recommended. From the series for dimethylformamide(DMF)[63] (Scheme 18) it follows, for instance, that 3,6-di(*tert*-butyl)catecholate salts are

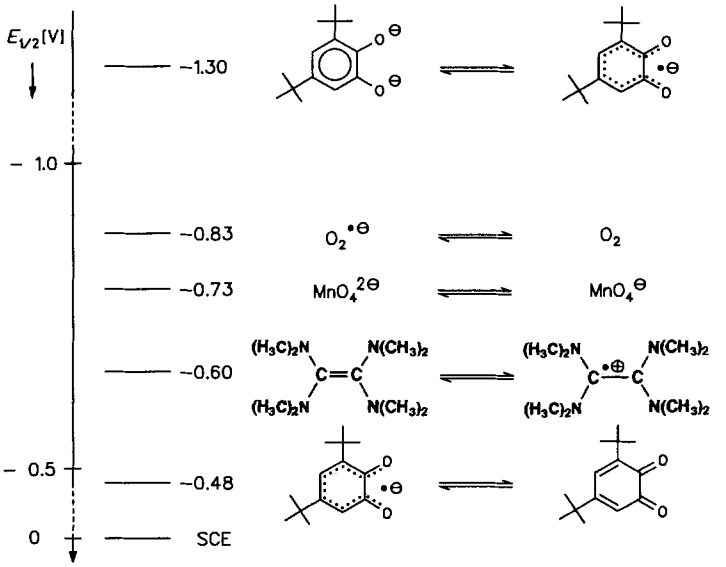

Scheme 18. Part of an electrochemical series in DMF [63].

oxidized by a purple $KMnO_4$ solution only to the semiquinone radical anion and not to the *ortho*-quinone [Eq. (h)], or that $KMnO_4$ is reduced by hyperoxide radical anion salts selectively, and because O_2 escapes, quantitatively to the dark green manganate(VI) dianion[63] [Eq. (i)].

5) The two redox reactions [Eq. (h) and (i)], chosen as examples, also illustrate the advantageous use of crown

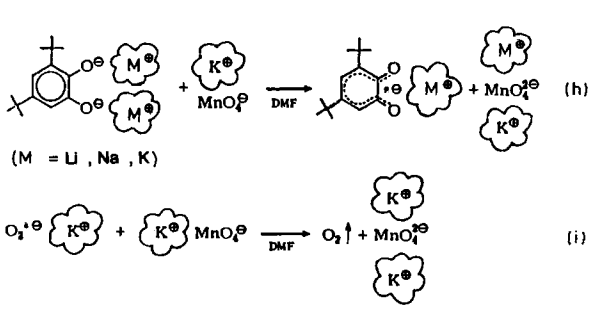

ethers[64a] or cryptands[64b] with cation-selective diameter as "solubility broker" for insoluble salts.

6) The often favorable reversibility of redox processes can be proven by cyclic voltammetry, although the different oxidation conditions at the electrode surface have to be taken into account. As spectacular example, hexaazaoctadecahydrocoronene is presented. Four consecutive reversible one-electron oxidation steps have been observed[56a] (Scheme 19) and in perfect accord, salts $M^{n\oplus}(X^{\ominus})_n$ with oxidation numbers $n = 1$ to 4 were isolated and structurally characterized.

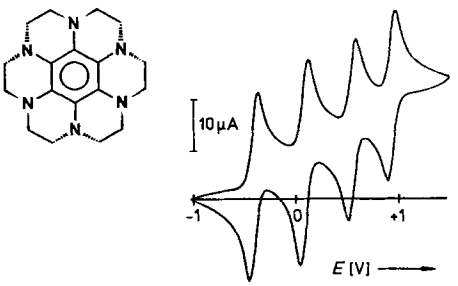

Scheme 19. Cyclic voltammogram of hexaazaoctadecahydrocoronene [50c].

For multiple oxidations, several additional "rules of thumb" exist. Thus larger molecules are more easily oxidized if the positive charge is effectively delocalized, for example, into suitable donor substituents. The resulting molecular cations can be kinetically stabilized by steric shielding by bulky groups. On the other hand, however, with increasing molecular size often only small structural changes are observed. For a given molecule, quantum chemical calculations are invaluable.[21]

Essential requirements for successful multiple oxidations of organic molecules and the isolation of their polycation salts are therefore: the right intuition—advantageously based on a knowledge of perturbation effects in chemically related known compounds and its verification by suitable experimental data from PE spectroscopy, cyclic voltammetry, or ESR/ENDOR spectroscopy, as well as quantum chemical calculations—a portion of luck in selecting the oxidizing reagent as well as the solvent, and, last but not least, skilled hands, which optimize—as before in the preparation of dibenzenesodium sandwich (Section 2) and other radical contact ion complexes (Section 4)—the redox and crystal growth conditions.

5.2. Salts of Dications of Tetrakis(dimethylamino)ethene, Tetramethoxythianthrene and Tetrakis(dimethylamino)-*para*-benzoquinone

All precursors for the salts of dications discussed in this section are tetrasubstituted by donor groups, because even the double ionization to energetically favorable dications $M^{2\oplus}$ require energies between 12 eV and 15 eV.

5.2.1. *Tetrakis(dimethylamino)ethene*

The rather unusual molecule[65] exhibits a first vertical ionization energy of only 6.13 eV (Fig. 9a), that is, only 1 eV higher than that of the sodium atom at 5.14 eV (Scheme 9). Reaction with oxygen-free water, therefore, oxidizes the electron-rich compound M containing four electron pairs on the N centers—presumably under evolution of hydrogen—to its radical cation $M^{\cdot\oplus}$ characterized by ENDOR spectroscopy[67] (Fig. 9b). Halogens such as Cl_2 or Br_2 accomplish a two-electron oxidation to the dication $M^{2\oplus}$[21,65] [Eq. (j)].

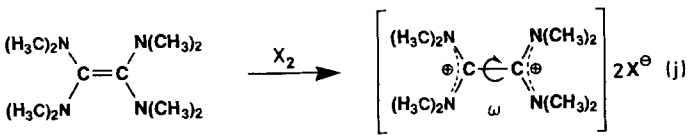

The dichloride, dibromide, or bis(hexafluorophosphate) salts can be isolated, single crystals grown, and their structures determined[21,68] (Fig. 9c), for which quantum chemical calculations[21] predict C–C single bonds and molecular halves twisted relative to each other (Scheme 6 and Section 6).

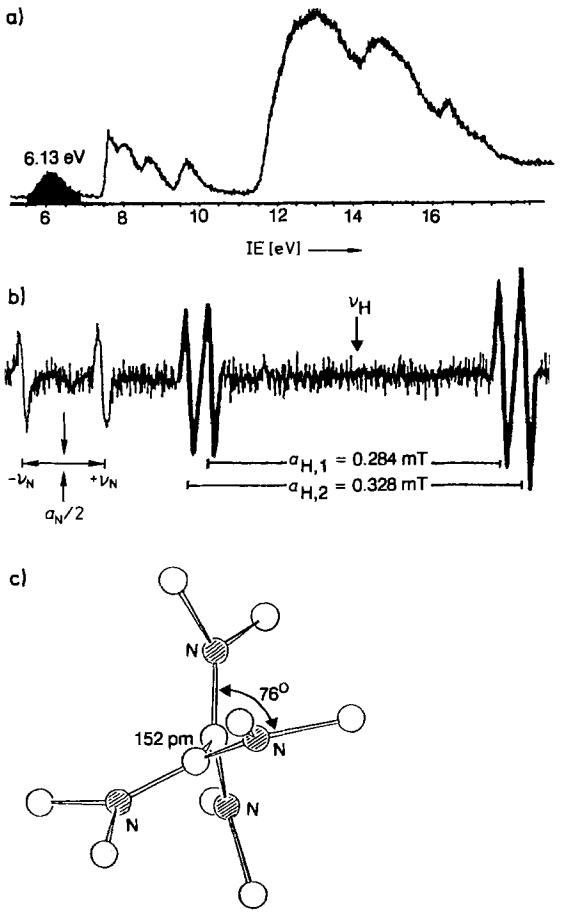

Fig. 9. Tetrakis(dimethylamino)ethene: a) Helium (I) photoelectron spectrum (intensity in cps) in the gas phase; b) ENDOR spectrum of the radical cation in water showing the ^{14}N coupling and two different ^{1}H couplings; c) single crystal structure of the dications [21] of $[((H_3C)_2N)_2{}^{\oplus}\text{–}{}^{\oplus}C(N(CH_3)_2)_2](Cl^{\ominus})_2$.

A more drastic structural change of a molecule on two-electron oxidation than observed for tetrakis(dimethylamino)ethene can hardly be imagined! On comparison with

the neutral compound (Section 7.2), both molecular halves are now twisted by 76°, the C–C double bond is stretched by 14 pm (!) to a C–C single bond, and the $(H_3C)_2N$ pyramids become completely planar. A rationalization is offered by the energetically favorable charge delocalization in two cyanine subunits $>N\cdots C^{\oplus}\cdots N<$ each containing three centers and four π electrons (Section 6.1).

5.2.2. *2,3,6,7-Tetramethoxythianthrene*

Contrary to the corresponding hydrocarbon anthracene with 14π-electrons, 2,3,6,7-tetramethoxythianthrene is not planar but folded as a butterfly (Fig. 10a). The same structure has been determined for the parent compound $C_{12}H_8S_2$[69b] and rationalized by the increase in its number of π electrons by two relative to planar anthracene on sulfur

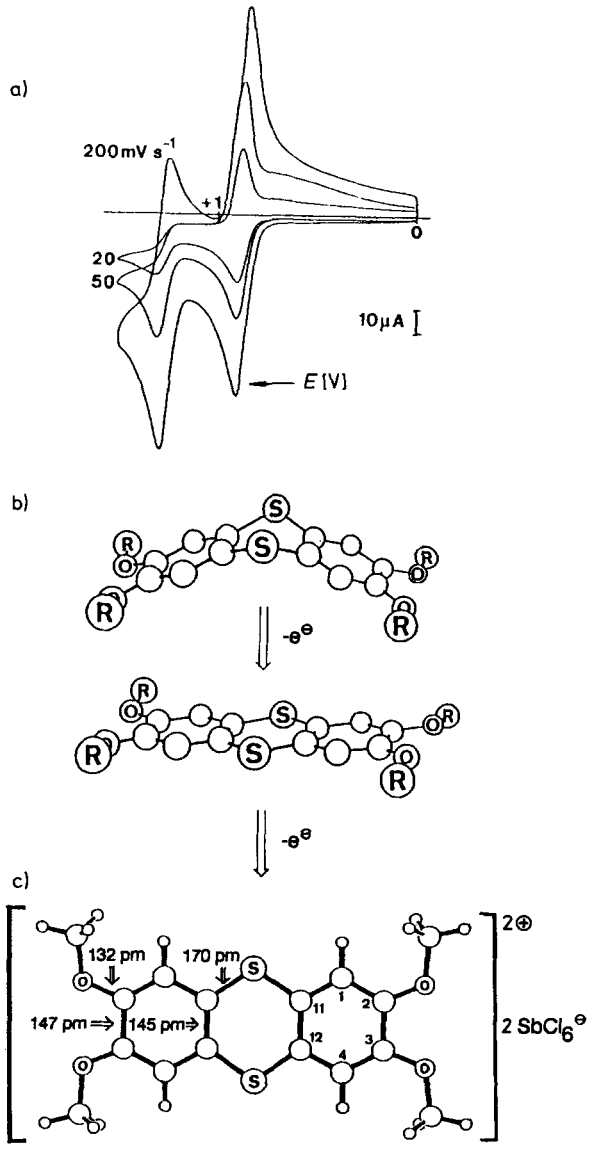

Fig. 10. 2,3,6,7-Tetramethoxythianthrene: a) Cyclic voltammograms in Al_2O_3-dried CH_2Cl_2/0.1 M $Bu_4N^{\oplus}ClO_4^{\ominus}$ under argon (recording velocities between 20 and 200 mVs^{-1}); b) structure diagrams for the one-electron oxidation to the radical cation [69a,c] and for the bis(hexachloroantimonate) dication salt [70] (cf. Table 2).

inclusion. One-electron oxidation by $NO^{\oplus}SbCl_6^{\ominus}$ or I_2 generates a blue radical cation, the σ skeleton of which is already planarized[69c] (Fig. 10b), although the "ideal" 14π electron configuration is still exceeded by 1. Cyclic voltammetric measurements under aprotic conditions and with increased recording velocity[70] show, in addition to the first half-wave potential at +0.88 V, a second reversible oxidation step at 1.27 V (Fig. 10b). Reaction with $SbCl_5$ in CH_2Cl_2 (cf. Section 5.1) under argon and aprotic conditions ($c_{H^{\oplus}}$ <1 ppm) yields a green solution, from which black rhombic crystals with a metallic luster grow after several days, which shine dark red when viewed under a cool-light lamp. The structure determination at low temperature[70] produces an unexpected result (Fig. 10b).

In contrast to any expectation of "aromaticity" for the tetramethoxythianthrene dication, which now contains 14π electrons for the three annelated six-membered rings, a π system enlarged by the methoxy oxygens to a total of 18 centers is found, the σ skeleton of which exhibits shortened O–C bonds and elongated C–S bonds 132 and 170 pm long, respectively, as well as lateral and inner C–C bonds of the outer rings stretched to 147 pm and 145 pm (Fig. 10c). A comparison with the essential bond distances d_{CX} of the neutral molecule M and the radical cation $M^{\bullet\oplus}$[69c] (Table 2) suggests that the structure of the dication $M^{2\oplus}$ can be best described by two fourfold connected, positively charged chains H_3CO–CCC–$S^{\oplus}$–CCC–OCH_3. This assumption is

Table 2. Bond lengths of 2,3,6,7-tetramethoxythianthrene and its molecular cations.

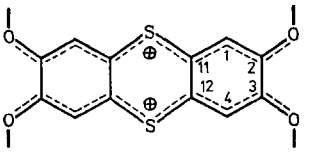

d_{CX} [pm]	M	$M^{\bullet\oplus}$	$M^{2\oplus}$
C2-C3	141.0	143.0	147.2
C11-C12	138.3	139.5	145.3
C1-C2	138.0	136.2	138.7
C1-C11	139.7	140.0	140.1
C11-S	177.6	172.3	169.5
C2-O	136.9	134.9	131.5

supported by geometry-optimized MNDO calculations,[70] which satisfactorily reproduce both the structure and the color of the dication. The enthalpies of formation ΔH_f^{MNDO} [$kJ\,mol^{-1}$] are calculated to be −311 for tetramethoxythianthrene M, +406 for its radical cation $M^{\bullet\oplus}$ and +1501 for its dication $M^{2\oplus}$, form which adiabatic ionization energies $IE_1^a(M \rightarrow M^{\bullet\oplus}) \approx 7.4$ eV and $IE_1^a(M^{\bullet\oplus} \rightarrow M^{\oplus\oplus}) \approx 11.4$ eV are estimated. Their sum, approximately 18.8 eV = 1810 $kJ\,mol^{-1}$, illustrates the energies required for the twofold ionization of molecules in the gas phase (Section 5.1). The energy needed for twofold oxidation in solution, however, can be considerably reduced by solvation. Thus for the dication of tetrakis(dimethylamino)-*p*-benzoquinone presented next, the MNDO enthalpies of formation are calculated to be lower by about 500 $kJ\,mol^{-1}$ for geometry-optimized solvation by eight water molecules.

5.2.3. *Tetrakis(dimethylamino)-p-benzoquinone*

p-Benzoquinone, the textbook example for two consecutive and each reversible single-electron transfer reductions of organic π systems, can be "umgepolt" by four dimethylamino substituents[60d] (Scheme 20). Tetrakis(dimethylamino)-*p*-benzoquinone, therefore, can be both reduced to its semiquinone radical anion as well as oxidized to its semiquinone radical cation[61d] (Fig. 11a).

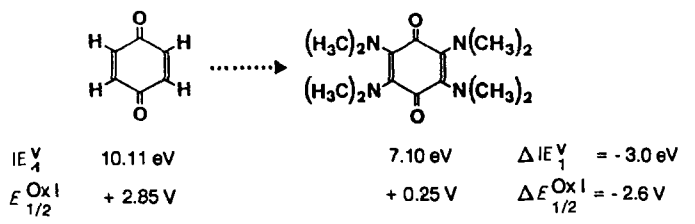

Scheme 20. First vertical ionization energies and half-wave oxidation potentials of *p*-benzoquinone and its tetrakis(dimethylamino) derivative.

This rather unusual redox behavior of the electron-rich compound containing four N lone pairs is due to delocalization of the positive charge into the dimethylamino substituents. The oxidation by $SbCl_5/CH_2Cl_2$ allows the preparation of a black dication salt $M^{2\oplus}[SbCl_6^{\ominus}]_2$[71] (Fig. 11b), the single crystal structure of which has been determined as has that of the likewise black, sterically overcrowded neutral compound *M* (Section 7.1, Scheme 31). Accordingly, and contrary to the expectation from the irreversible second oxidation potential (Fig. 11a), the molecular skeleton of tetrakis(dimethylamino)-*p*-benzoquinone survives on removal of two electrons (Fig. 11b). Two 6π electron/5-center cyanine chains[71] are formed, which are twisted relative to each other by 35°, thereby reducing the steric strain in the neutral compound (Scheme 31).

In detail, the C–C double bonds are stretched by 9 pm (!) towards C–C single bonds, the different C–C bond lengths adjacent to the O=C groups become equal, the C–N bonds shorten by up to 10 pm (!) and all dimethylamino groups planarize. The charge distribution q_μ^{AM1} (Fig. 11c) calculated for the quantum chemically reproducible structure[71] is in accord with a delocalization of the positive charges along the two N-C-C(O)-C-N$^\oplus$ cyanine chains (Section 6.1) predominantly into the peripheral methyl groups.

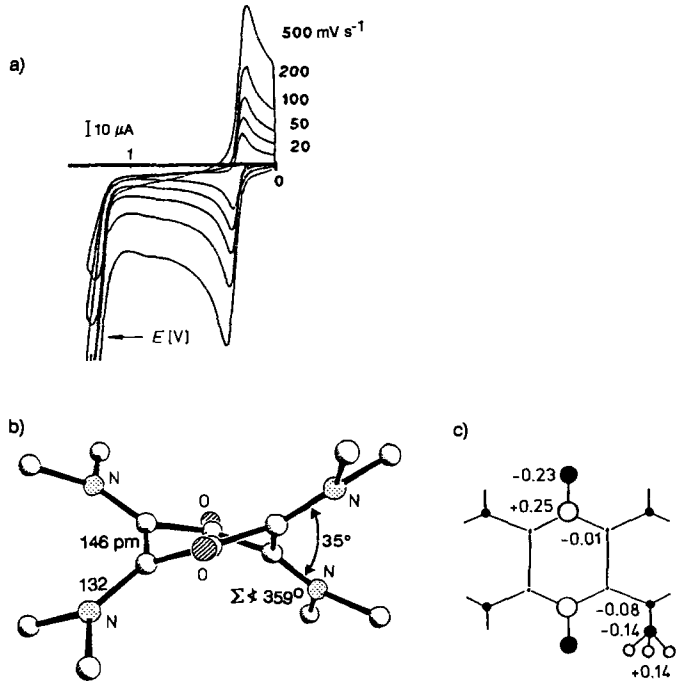

Fig. 11. Tetrakis(dimethylamino)-*p*-benzoquinone: a) Cyclic voltammograms in DMF/0.1 M $Bu_4N^{\oplus}ClO_4^{\ominus}$ (v = 20 to 500 mVs^{-1}, ΔE_1 = 70 mV, ΔE_2 irreversible); b) single crystal structure of the dication bis(hexachloroantimonate); c) AM1 charge distribution.

5.3. Perspectives: Molecular Polycations by Oxidative Coupling or by Acid/Base Reactions

Polycation salts of molecules can be obtained not only by decrease in the number of electrons in a molecule, enforced by oxidation, $M - n(e^{\ominus}) \rightarrow M^{n\oplus}$ (Sections 5.1 and 5.2), but also by several other routes. Representative examples[72–75] will illustrate their preparation by oxidative coupling $2M - 2(e^{\ominus}) \rightarrow [M^{\oplus} - {}^{\oplus}M]$ as well as by multiple acid/base reactions such as amination $MX_n + n(B) \rightarrow [MB_n^{\oplus}](X^{\ominus})_n$, protonation $M + 2(H^{\oplus}) \rightarrow [H^{\oplus}M^{\oplus}H]$ or cation chelatation $M + 2(Met^{\oplus}) \rightarrow [Met^{\oplus}M^{\oplus}Met]$, and highlight the structural changes observed.

5.3.1. *4,4'-Di(tert-butyl)-1,2'-dipyridinium Diperchlorate*

Oxidation of suitably substituted *N*-aminopyridinium salts yields—possibly via a tetrazene intermediate[76]—dipyridinium salts (Scheme 21). Single crystals could be grown only after anion exchange $Br^{\ominus} \rightarrow ClO_4^{\ominus}$. Their structure determined in a nitrogen flow at 100 K, in which all hydrogen centers have been located,[72a] causes some headache concerning the dihedral angle (ω = 84°) between the two each planar pyridinium rings connected by an N–N single bond of 143 pm: the isoelectronic correspondence >C=C< → >N$^{\oplus}$–$^{\oplus}$N< would suggest planarity as has

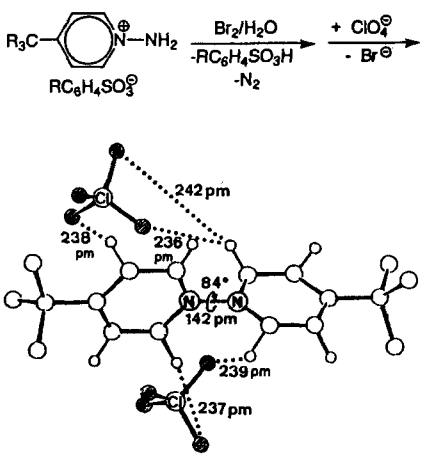

Scheme 21. Preparation and structure of 4,4'-di-*tert*-butyl-1,1'-dipyridinium diperchlorate.

been proven, for instance, for biphenyl planarized in the solid state[77] or for sterically shielded tetraalkylhydrazine dications.[78]

Comprehensive MNDO energy hypersurface calculations[72a] predict that a substantial enthalpy of 75 kJ mol^{-1} is required to enforce coplanarity of the two pyridinium rings in the dication, which may be classified as being anomeric.[79] However, the distances between some ring hydrogens and the perchlorate counter anions are only between 236 pm and 242 pm (Scheme 21) and, therefore, within the range of hydrogen bonds.[80, 81] The short intermolecular distances support the unexpected twisting of the two molecular halves of the 1,1-dipyridinium dication to almost perpendicular to each other, which according to the MNDO calculations should lead to a favorable charge distribution.

5.3.2. *Tetrakis(dimethylaminopyridinio)-p-benzoquinone Tetrakis(triflate)*

Among the derivatives of *p*-benzoquinone, the unusual molecular properties of the fourfold dimethylaminopyridinio-substituted dark red tetracation marks it as being special: the two reversible half-wave reduction potentials are lowered by +1.24 V and by +1.30 V to +0.73 V and to +0.16 V(!). Its rather elegant one-pot preparation from chloranil in almost quantitative yield proceeds by a fast transamination via the first-formed 4-dimethylamino-*N*-trimethylsilylpyridinium triflate with elimination of R_3SiCl[82] (Scheme 22).

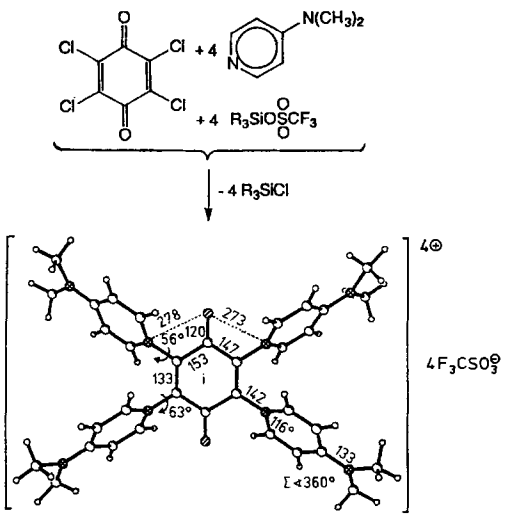

Scheme 22. Preparation and structure of tetrakis(dimethylaminopyridinio)-*p*-benzoquinone tetrakis(triflate); i: center of inversion, R = CH_3 (cf. text for details).

The structure determination[72b] shows layers of the bulky tetracations, each interspersed with two disordered independent triflate anions and two whose contact distances to the centers of the longer C–C(O) bonds are 280 pm. The C–C bonds flanking the quinone groups attract attention because of differing lengths of 147 pm and 153 pm (Section 6.2), as do the completely planarized dimethylamino groups. They are connected by a rather short CN distance of only 132 pm to the pyridine ring, which exhibits an *ipso* angle at the nitrogen center of only 116° (Scheme 12). The intramolecular O···N distance is shorter than the sum of the interference radii (290 pm, Section 7.1). MNDO calculations predict for each pyridinio- and amino-nitrogen center a charge of −0.2 and thus support an extensive delocalization of the four positive charges over the whole cyanine-like distorted molecular skeleton (Scheme 22).

5.3.3. *N,N,N′,N′-Tetraisopropyl-p-phenylenediammonium Bis(tetrachloroaluminate)*

This salt of a "nonredox" dication crystallized on attempts to oxidize the *N*-tetraisopropyl-substituted *p*-phenylenediamine (which exhibits the surprisingly low first ionization energy of only 6.6 eV[73]) with $AlCl_3/CH_2Cl_2$ (Section 5.1). Instead of the possibly rather hydrolysis-sensitive product[73] containing one electron less than the well-investigated "Wurster's Blue" salts,[83] however, the compound containing a doubly protonated dication was isolated. Although its structure (Scheme 23) does not exhibit any unexpected pecularities, it is—like numerous analogous literature examples—well suited to disclose differences between oxidized and protonated molecular cations.

The structural comparison (Scheme 23) documents that the (R)N–C_{phenyl} bonds are elongated on protonation of the neutral molecule, but shortened on its oxidation. In the diammonium salt, the different isopropyl groups are twisted by 56 and 77° out of the plane of the ring; on electron removal $M \rightarrow M^{\bullet\oplus}$, the dihedral angle ω(CC-NC) closes from 23 to 0° and the dimethylamino groups are completely planarized. The *ipso* angles in the arene ring (Scheme 12) reflect the dissimilar charge delocalization: for $R_2HN^{\oplus}$ acceptor groups they amount to 122°, while for the R_2N donor groups twisted by 117° and 116° they are below the normal value of 120° as expected.

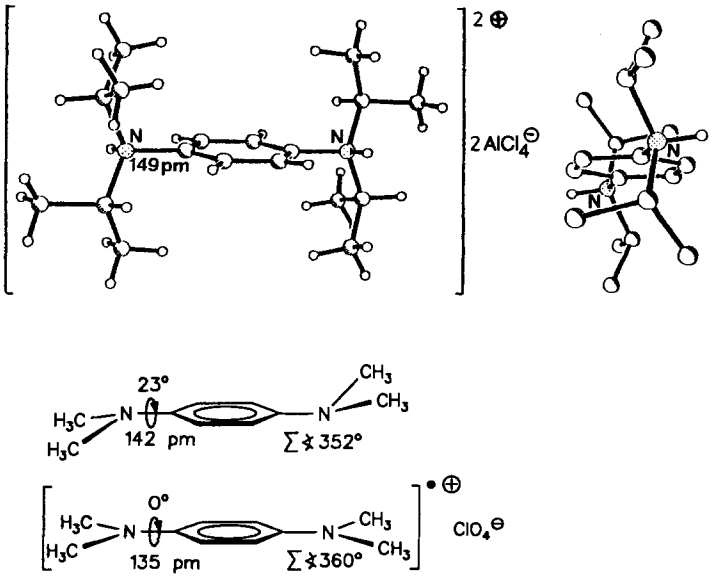

Scheme 23. Two views of the structure of *N,N,N′,N′*-tetraisopropyl-*p*-phenylenediammonium bis(tetrachloroaluminate) [74] and selected structural data for *N,N,N′,N′*-tetramethyl-*p*-phenylenediamine [84] as well as its "Wurster's Blue" perchlorate [83c].

5.3.4. Tetra(2'-pyridyl)pyrazine Dichloride and Bis(tetraphenylborate)—Examples for "Chemical Mimesis" Involving Inter- and Intramolecular Hydrogen Bridges

Increasing interest in conformational changes, particularly of biochemical importance, prompted the selection of tetra(2'-pyridyl)pyrazine as a model compound:[62] it contains six N electron pairs in five almost rigid rings that, however, are flexible around the connecting C–C bonds. We succeeded in growing single crystals of its HCl adduct and its diprotonated $^{\ominus}B(C_6H_5)_4$ salt and determined their structures[74] (Scheme 24), which due to the "naked" $Cl^{\ominus}$ and the phenyl-embedded $R_4B^{\ominus}$ counterions exhibit different hydrogen bonds.

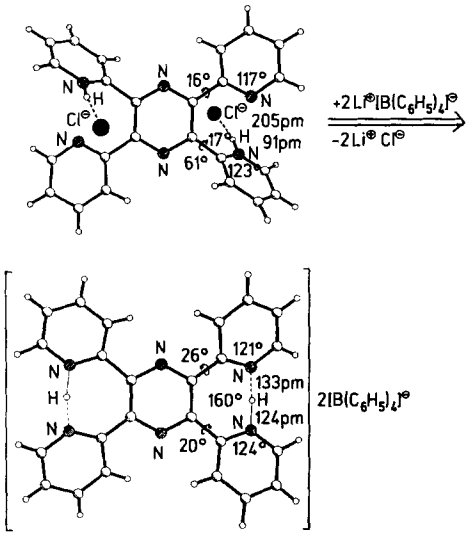

Scheme 24. Comparison of the structures of the dichloride and bis(tetraphenylborate) salts of diprotonated tetra(2'-pyridyl)pyrazine [74].

In the neutral molecule tetrakis(2'-pyridyl)pyrazine, neighboring pyridine rings are twisted out of the pyrazine ring plane by 50° in the same direction; the C-N-C ring angles are 117°.[74] On twofold HCl addition, diagonally opposite pyridine rings are protonated and their twist angles increase to 61° due to H bonds of 205 pm[81] to the electron-rich chloride ions. Simultaneously, the *ipso* angles at the pyridinio nitrogens (Scheme 12) increase to 123° as expected. Resalting by addition of lithium tetraphenylborate and recrystallization of the salt now containing phenyl-embedded and therefore no longer protonable counteranions, generates intramolecular hydrogen bonds between each pair of adjacent pyridine rings, the *ipso* angles of which increase to more than 120°[74] (Scheme 24). The H bonds are almost symmetrical, exhibiting N ··· H distances of 124 pm and 133 pm and a 160° angle at the H center. At present we are also attempting the crystallization of an analogous salt in which both protons are substituted by metal ions $Met^{\oplus}$:[75] to form the two anticipated energetically favorable $Met^{\oplus}$-tris(*N*-chelates), all pyridine substituents would have to rotate around their bonds to the pyrazine rings. We have succeeded in growing crystals of many other compounds with unusual hydrogen bonding.[75]

In concluding this outlook, it should be emphasized that molecular polycations, accessible by many different routes, are indeed attractive subjects of research; a plethora of available experimental data, from vertical ionization energies to adiabatic half-wave oxidation potentials in solution (Section 5.1), offers inspiring hints, and the structural changes observed, from the twisted ethene dication through the stretched dication of thianthrene to the twisted dication of *p*-benzoquinone (Section 5.2), are tremendous. From the wealth of known nonmetallic multiple cations, the planar rings $S_4^{2\oplus}$, $N_2S_2^{2\oplus}$ and $S_4N_4^{2\oplus}$, the dumbbell-shaped $S_7^{\oplus}$-S_5-$S_7^{\oplus}$ or the prismane $Te_6^{4\oplus}$ are quoted as representative. Together with the preceding discussion of "nonredox" polycations accessible by protonation, alkylation, amination, or metal cation chelation, for example, they round off the various perspectives required to predict and to prepare molecules perturbed by positive charges and to draw conclusions from their structures.

6. Structural Changes Accompanying Redox Reactions: More Favorable Charge Delocalization on Cyanine Distortion

6.1. Ethene and Six-Membered Ring Dianions and Dications as Prototypes

The remarkable structural changes on reduction of unsaturated hydrocarbons (including C–C bond formation, double-bond shift, or the substituent-dependent decrease or increase of *ipso* angles in six-membered rings) have already been emphasized (Section 3). On twofold reduction of ethene derivatives the double bond is stretched to a single bond and the two negatively charged molecular halves twist relative to each other (Sections 2.1 and 4.3). The twofold oxidation of donor-substituted ethenes distort the molecular skeleton in a similar way (Section 5.2).

In close analogy, the C=C bonds within the six-membered ring of the tetrakis(dimethylamino)-*p*-benzoquinone dication are also elongated and the two positively charged subunits R_2N–CC(O)C–$NR_2^{\oplus}$ are likewise distorted to a twist conformation. The literature provides additional examples such as the dications of 1,2,4,5-tetrakis- and hexakis(dimethylamino)benzene[86] (Scheme 25).

The structural changes in ethene and six-membered ring dianions and dications (Scheme 25) can be rationalized by a simple model based on the "coupling principles in organic dyes",[87a] developed more than 25 years ago. Although discussed then in terms of energetically favorable π-charge delocalization, of special importance are the changes in the σ framework.[88] In general, cyanine chains are characterized by the distribution of an even number n of π electrons over an odd number N of π centers.[87] The prototypes selected (Scheme 25) are classified as follows: ethene dianions with two cyanine-like subunits (Scheme 25a: $n = 4$, $N \approx 3$ or 25b: $n = 6$, $N = 5$), ethene dication also with two cyanine-like subunits (Scheme 25c: $n = 4$, $N = 3$), and six-membered ring dications with two cyanine-like subunits (Scheme 25d to f: $n = 6$, $N = 5$, partly branched). The C–C distances between the cyanine-like subunits lie in the range 146 (d) to

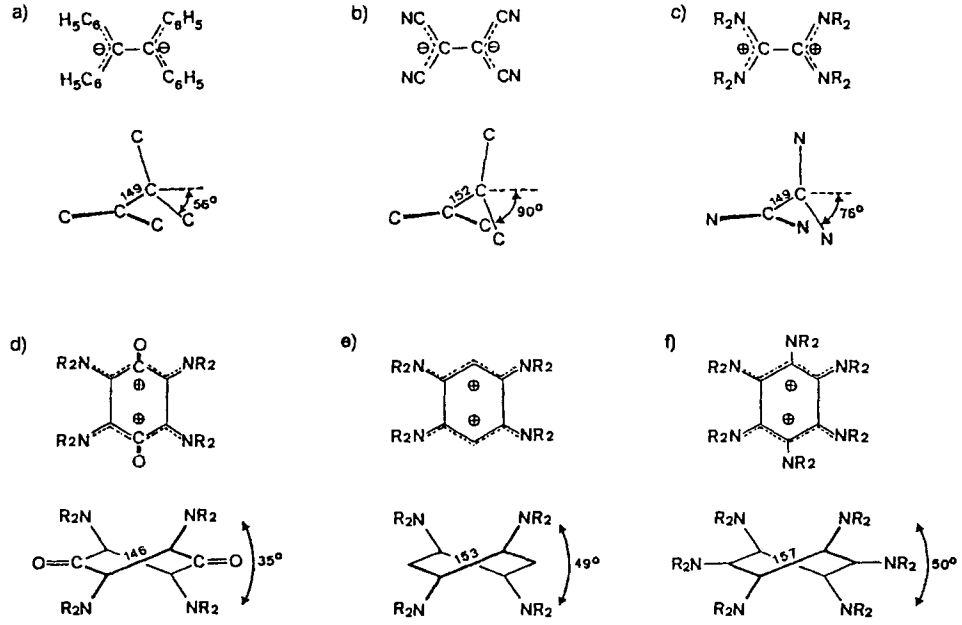

Scheme 25. Prototypes of dianions and dications of ethene and six-membered ring compounds with cyanine-like distortions. a) Cf. Fig. 3 [12]; b) see Table 1 [50c]; c) see Fig. 9c [21]; d) see Fig. 11b [71]; e) [86a]; f) [86b].

157 pm (f) and the corresponding dihedral angles ω in the range 35 (d) to 90° (b).

6.2. The Cyanine Principle

Many other molecules also exhibit cyanine-like distorted structures. Thus in contrast to 2,5-bis(trimethylsilyl)-*p*-benzoquinone[89a] (Scheme 26a), in the 2,5-dialkylamino derivatives with a similarly planar six-membered ring (Scheme 26b), an equilibration of the bond lengths along the NCCCO chains can be recognized.[89b] Drastic structural changes are observed in the planar dianion salt[90a] of 2,5-dihydroxy-*p*-benzoquinone,[90b] which is prepared by an acid/base reaction without any changes in the number of π electrons (Scheme 26c and d).

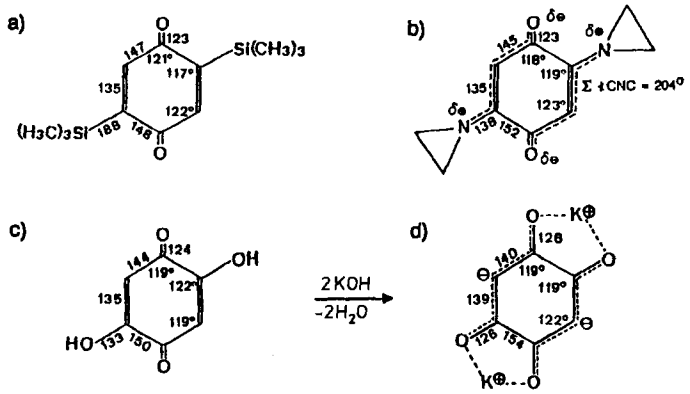

Scheme 26. Comparison of the structures of selected *p*-benzoquinone derivatives (cf. text).

The cyanine principle[87] so far has been explored predominantly based on parametrized π-LCAO/MO calculations[87a, b, 91] and the long-wavelength excitation energies of cyanine chains simulated by applying the approach of an "electron in a box" (FEM).[92] Because of the considerable changes in the molecular σ skeleton, we have repeated semiempirical[87c] calculations for the essential building blocks of the compounds presented as prototypes (Schemes 25 and 26) using the AM1 procedure[93] and fully optimizing the geometry of each example.[94] For the neutral compounds, strongly alternating bond lengths along their central NCCCN or OCCCN chains are calculated (Scheme 27; **I** and **III**), whereas in the cyanine cation $NCCCN^{\oplus}$ the bonds are already largely equalized (Scheme 27, **II**). In addition, and especially for the merocyanine derivative (**III**) and the tetramethyl-1,5-diazapentadiene cation (**II**), a pronounced charge alternation is predicted.

Combination of two cyanine subunits such as $R_2N\text{-}CCC\text{-}NR_2^{\oplus}$ (**II**) to approximate the dication of tetrakis(dimethylamino)benzene (Scheme 25e), or two merocyanines (**III**) to simulate 2,5-bis(dimethylamino)-*p*-benzoquinone

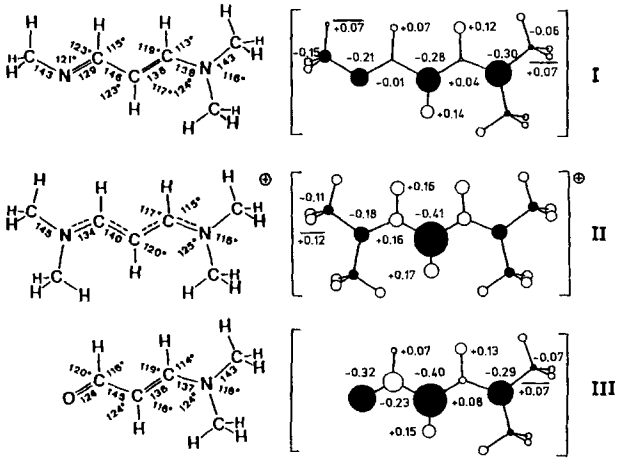

Scheme 27. Geometry-optimized AM1 structural data (left) and charge distributions (right) for cyanine building blocks with different end groups (cf. text).

(Scheme 26b) according to a "molecules in molecule" approximation yields after each complete geometry-optimization the AM1 structural parameters and charge distributions shown in Scheme 28.

Both calculated structures resemble the experimentally determined ones (Schemes 25e and 26b) even in detail (bond lengths ± 2 pm, bond angles $\pm 2°$). Thus for 1,2,4,5-tetrakis(dimethylamino)benzene dication, the elongated ring C–C bonds of 153 pm are calculated to be 152 pm, and even the twist angle between the cyanine subunits of 49° is satisfactorily reproduced (Scheme 28, 54°). Again alternating

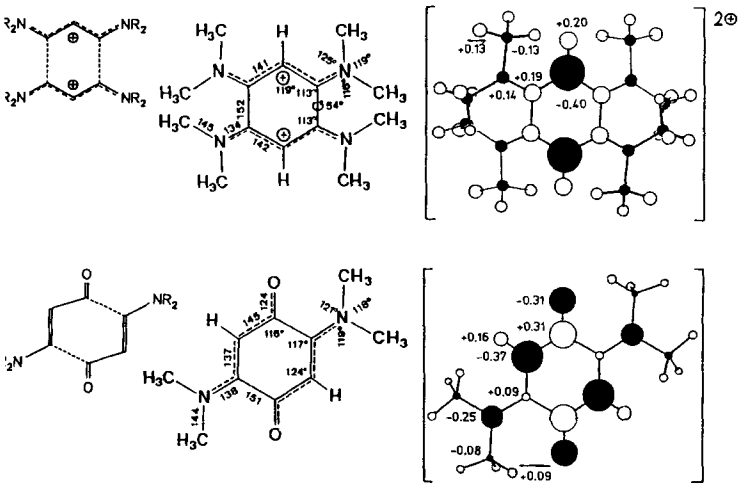

Scheme 28. Geometry-optimized AM1 structural data (left) and charge distributions (right) for 1,2,4,5-tetrakis(dimethylamino)benzene dication and for 2,5-bis(dimethylamino)-*p*-benzoquinone.

charge distributions result along the R_2N–CCC–NR_2 chains, and according to the considerable average contribution of +0.26 calculated for each H_3C group, the positive charges are preferentially located on the periphery of the molecule. Within the six-membered ring positive partial charges are predicted for all C centers of the long C–C ring bonds and accordingly, the electron density between them should be lowered. The cyanine distortion, that is, the bond equalization along the 6-electron/5-center subunits, also becomes apparent in 2,5-bis(dimethylamino)-*p*-benzoquinone, especially on comparison with its merocyanine building blocks (Scheme 27, **III**) and as expected, the calculations predict long C–C bonds between the two cyanine chains (Scheme 28, 151 pm). The appropriate C centers are again positively charged and, therefore, offer a plausible explanation for the—on first sight rather strange—different lengths of the C–C bonds that flank the O=C groups in 2,5-bis-(dimethylamino)-*p*-benzoquinones. Note also that the amino substituents should be close to planar (sum of angles at the nitrogen centers are about 359°), the molecular skeletons are slightly twisted and for each of the four H_3C groups a total charge of +0.19 is calculated (Scheme 28).

Consequently, it is the energetically favorable, alternating ($\sigma + \pi$) charge distribution along the cyanine chains that causes the bonds between the partially positively charged ring-C centers to stretch and thereby facilitates the twisting between the molecular halves. Even when starting from hexagonal six-membered ring skeletons, the quantum chemical ($\sigma + \pi$) geometry optimization does not lead to a local energy minimum with enhanced cyclic delocalization, which often is misleadingly termed "aromatic". On the contrary, a preferred distribution of an even number of π electrons over a distorted σ skeleton with an odd number N of centers results.[88] Hence, the cyanine principle is a general[87] and powerful structural perturbation concept.[21, 70, 71, 86, 91]

6.3. Cyanine Perturbations: Multifarious Possibilities and CSD Search

Already 25 years ago, before the ethene and six-membered ring distortions were widely known (Scheme 25 and 26), the "test compounds" for cyanine perturbations[87a] depicted in Scheme 29 were proposed.

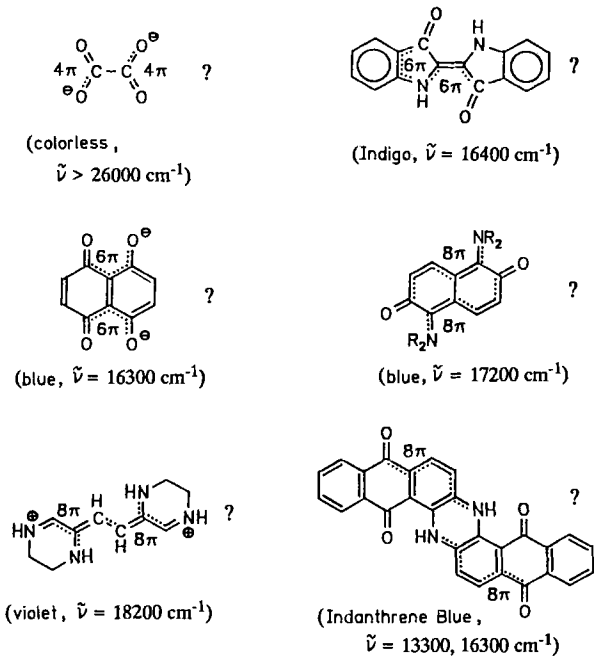

Scheme 29. Potential test compounds proposed to substantiate cyanine distortions.

A search in the Cambridge Structure Data (CSD) file reveals that for many of the proposed test compounds either no entries are detected or unexpected structures are found. For instance, the potassium salt of the oxalate dianion[95] is planar—possibly due to advantageous stack packing—but nevertheless shows an unexpectedly long bond length of 157 pm. Indigo is also planar[96a] (as is thioindigo[96b] in which no intramolecular hydrogen bonds form), and the bonds lengths of between 135 pm and 158 pm for its five-membered rings as well as its C–C double bond of 132 pm do not suggest any merocyanine-like equalization. The same applies to the known structure of "Indanthrene Blue".[97] In contrast, cyanine-like skeletal distortions are[87b] reported, for instance, for tetramethyloxamide,[98] (5-dimethylamino-2,4-pentadienylidene)dimethylammonium perchlorate,[99] the tetracyanoethylene dianion[56] (see also Scheme 25), or the sodium salt of 3-hydroxyprop-2-enal[100] (Scheme 30).

Convincing skeletal changes are also observed for 5,8-dihydroxy-1,4-naphthoquinone[101a] on complexation of

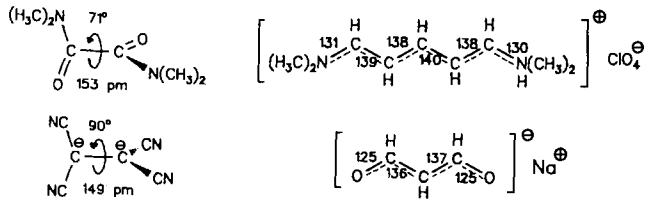

Scheme 30. Compounds displaying cyanine-like skeletal distortions.

$Cu^{2\oplus}$ ions[101b] [$r_{Cu^{2\oplus}} = 72$ pm, see Scheme 30 and Eq. (k)]. The C–OH and C=O bonds, differing by 10 pm in the free quinone, and, the flanking C–C bonds become equal and the central ring C–C bond is elongated. Analogous effects have

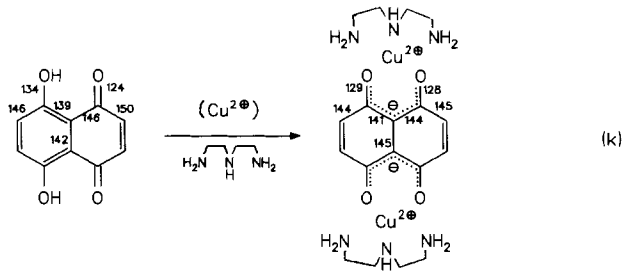

(k)

been determined for 1,8-dimethylaminonaphthalene, the prototype "proton sponge",[81] on salt formation [Eq. (l)], for example with $HOTeF_5$[102a, b] or with the *C*-hydroxy-*ortho*-carborane 1,2-HO-C(Ph)$C_2B_{10}H_{10}$.[102c, d] The proto-

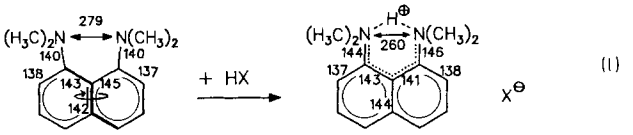

(l)

nation simultaneously removes the steric strain caused by the two dimethylamino substituents in the naphthalene *peri* positions, which widens the N···N distance to 279 pm under considerable distortion of the molecular framework. Because the N···$H^{\oplus}$···N hydrogen bond formed is only slightly tilted out of the molecular plane, the effect of the positive charge on the σ skeleton becomes apparent.[88] An analogous effect occurs on cation complexation [Eq. (k)].

Summa summarum, the cyanine structure perturbation principle constitutes, if applied with caution and sense of proportion, a heuristic rule useful in devising experiments. For an improved evaluation, however, a quantum chemical geometry-optimization of the target molecule or molecular ion is recommended[93] (Schemes 6, 26 and 28). If the "cyanine intuition" is confirmed, especially as regards the resulting charge distribution (Section 5.2 and 6.2), then the probability of scoring a large number of hits for surprising structures is high [cf. Schemes 25 or Eq. (k)]. Since various combinations of donor and acceptor substituents for the manifold classes of compounds are conceivable and positively charged molecular ions can be prepared not only by redox reactions (Section 5.1) but also by protonation, alkylation, amination, or cation chelation (Section 5.3), a wide area for future research opens. The results to be expected might also provide answers to the "what came first, the hen or the egg" question:[88] can an energetically favorable π delocalization provoke structural distortions or is an already distorted σ skeleton a prerequisite?

7. Steric Overcrowding by Substituents $-Si(CH_3)_3$, $-N(CH_3)_2$ or $-CH(CH_3)_2$

7.1. Selected Literature Examples and Interference Radii

Sterically overcrowded and, therefore, structurally distorted molecules and molecular ions already have been repeatedly discussed or quoted, for example, tetrakis(trimethylsilyl)hydrazine radical cation (Section 1.2), tetraphenylethene (Section 2.1), and 1,3-dinitro-2-*tert*-butylbenzene (Scheme 11c). The "umgepolten" molecule 1,2,4,5-tetrakis(dimethylamino)-*p*-benzoquinone, which exhibits unusual properties (Scheme 20), displays a sterically enforced chair conformation in the solid state[71] (Scheme 31).

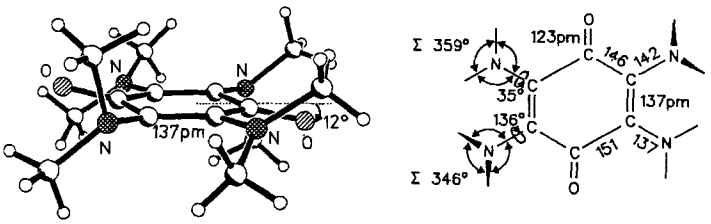

Scheme 31. Single crystal structure of tetrakis(dimethylamino)-*p*-benzoquinone.

The voluminous $(H_3C)_2N$ substituents[81] in which the interference radius of each methyl group is about 200 pm press the O=C bonds lying between them out of the central C_4 skeletal plane of the quinone in opposite directions by interplanar angles OCC_2-CC_2 of 12°. The dimethylamino groups are twisted and flattened and connected to the centers of the six-membered ring by varying CN bond distances. The resulting different n_N/π- and σ-CN-interactions deform the quinone skeleton. Thus the lengths of the C–C bonds adjacent to the O=C groups differ by 5 pm, providing another example for merocyanine-like distortions of dialkylamino-substituted quinones (Section 6.2).

From the thousands of documented molecules whose frameworks are distorted through steric overcrowding by bulky substituents groups, hexakis(*tert*-butyl)disilane[103a] is selected here because of its spectacularly stretched Si–Si bond, and octachlorotetraradialene[104] because of its drastically changed angles (Scheme 32). The disilane derivative contains cogwheel-like, intermeshed *tert*-butyl groups, and its space-filling model shows an ellipsoid with an almost closed surface of hydrogens (omitted in Scheme 32). It exhibits Si–C bonds stretched to 199 pm and an especially interesting Si–Si central bond of 270 pm, longer than that of $(H_3C)_3Si$-$Si(CH_3)_3$ by an exceptional 36 pm.[103] The Pauling bond order, $n = 10^{[d(1) - d(n)]/60}$ ($d(1)$ = length of a normal single bond, $d(n)$ = length of the bond in question), of the

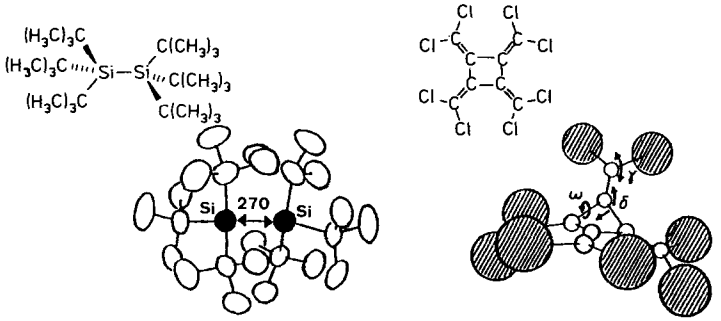

Scheme 32. Single crystal structures of hexakis(*tert*-butyl)disilane and of octachlorotetraradialene.

latter amounts to only 0.26, and therefore interactions within the "van der Waals skin" have to contribute considerably to the cohesion of this and other strange organosilicon molecules.[105] In contrast, octachlorotetraradialene (Scheme 32) releases its steric strain almost exclusively by the angle changes. In a completely planar molecule, the four Cl···Cl contact distances between adjacent Cl_2C groups would be only 270 pm,[104] which is considerably smaller than the sum of two van der Waals radii for chlorine (Scheme 34, 360 pm). The four-membered ring folds to give a dihedral angle ω(CC-CC) of 27°, and the Cl_2C groups are tilted alternately up and down as a result of additional bending at the two double-bond centers by $\delta = 194°$ and $\gamma = 188°$, accomplishing an apparently still tolerable Cl···Cl contact distance of 332 pm.[104]

However, whoever bases his predictions for hexakis(dimethylamino)benzene on the drastic changes of bond lengths and angles possible (Scheme 32) or on the undulating six-membered rings of sterically overcrowded benzene derivatives such as $C_6(CF_3)_6$,[106a] $C_6(Si(CH_3)_3)_6$,[106b] and $C_6(NO_2)_3(N(CH_3)_2)_3$[106c] and expects that its six bulky $(H_3C)_2N$ substituents should cause a more severe structural distortion than in tetrakis(dimethylamino)-*p*-benzoquinone (Scheme 31) will be bitterly disappointed. Its C_6N_6 skeleton[86b] (Scheme 33) exhibits approximately C_{6h} symmetry (!) and all of its bond lengths and angles are found to be within normal tolerance limits.

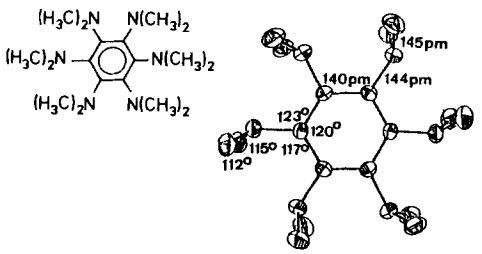

Scheme 33. Single crystal structure of hexakis(dimethylamino)benzene.

A qualitative estimate of the space filled by substituents is also of importance for the "kinetic stabilization" of those thermodynamically stable molecules that can be generated in the gas phase under unimolecular conditions but rapidly polymerize on condensation.[107, 108] Embedding them in "alkyl cotton" consisting of inert substituents renders possible the isolation of derivatives or short-lived parent compounds such as $H_2C = NH$[107a] or $H_2Si = CH_2$[107b]. For an estimate, the "interference", "interaction", or "van der Waals" radii[109] are often taken into consideration (Scheme 34); they are derived from ionic radii or molecular structures,[109a] de Broglie wavelengths, collision cross-sections, or critical data,[109b] as well as from force-field calculations.[103c] They are angle- and direction-dependent[109a, d] and are occasionally unrealistically overestimated.[103e] For a definition, it has been proposed that the van der Waals volume of a molecule cannot be penetrated by that of another at thermal energies corresponding to room temperature.[109b] Some frequently used literature values[109a, f] are contrasted with the C–C distances in the basic hydrocarbons ethene, benzene, and naphthalene in Scheme 34 to provide a scale.

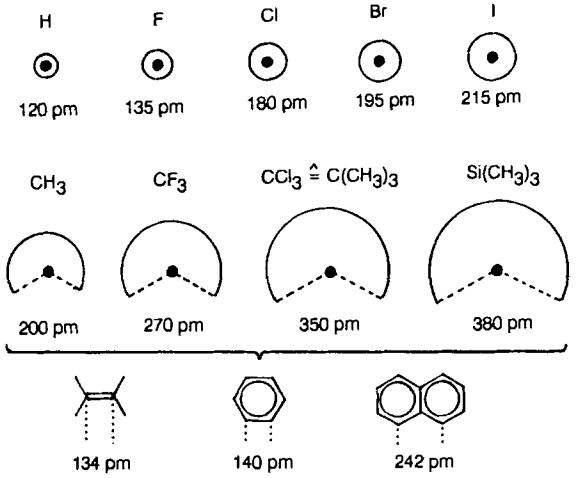

Scheme 34. Comparison of interference radii of frequent substituents with the C–C distances in basis hydrocarbons.

Despite the obvious usefulness of interference radii for qualitative estimates, restrictions are advisable. To begin with single-center substituents, which allow more straightforward remarks, the structures of planar tetrachloro- and tetraiodoethene determined by gas-phase electron diffraction[110] display distances between vicinal and especially between the geminal halogen centers that are far smaller than the sum of the interference radii (Schemes 34 and 35).

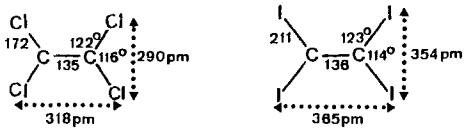

Scheme 35. Structures of tetrachloro- and tetraiodoethene in the gas phase.

As concerns Hal_2C groups, therefore, the assumption of a spherical electron-density distribution around the individual halogen centers[109a, d] is unjustified as expected. On the other hand, the intermolecular contacts, for example, in octachlorotetraradialene (Scheme 32) can still be discussed within the concept of interference radii. The Cl···Cl distances of 332 pm, resulting after the angles changes specified, are compressed by about 8% relative to the sum of van der Waals radii of 360 pm (Scheme 34). Two additional structural ob-

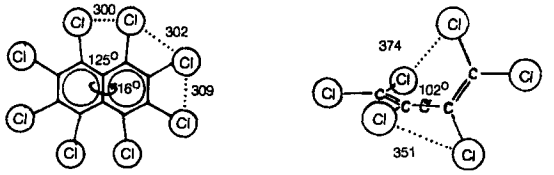

Scheme 36. Single crystal structure of octachloronaphthalene and gas-phase structure of hexachlorobutadiene.

servations for perchlorinated unsaturated hydrocarbons round off the impression (Scheme 36): One of the shortest intramolecular Cl···Cl distances of 300 pm has been determined between the *peri* positions of chiral octachloronaphthalene (symmetry D_2)[111] and in *gauche* hexachlorobutadiene (symmetry C_2), the molecular halves containing the two double bonds are twisted by 102° relative to each other[112] to avoid Cl···Cl contact distances of only about 270 pm that would result for a planar *trans* configuration.

For substituent *groups*, the interference radii (Scheme 34) represent only the maximum value for unhindered rotation and, therefore, can be considerably undercut with space-saving and, in particular, staggered conformations (see, for instance, Scheme 33). Thus, in the intermeshed structure of hexakis(*tert*-butyl)disilane (Scheme 32), the shortest intramolecular C···C distance between the molecular halves amounts to 334 pm and, therefore, is 17% shorter than the sum of the van der Waals radii of two methyl groups (400 pm, Scheme 34).

The preceding remarks on advantages, rules of thumb, and recommendations for caution concerning the use of interference radii are necessarily incomplete. Within the scope given, the dynamic aspects[109c, d] (Fig. 2) or the usefulness of structure predictions by force-field[103c] and energy-hypersurface calculations[1, 6] (Sections 1.1 and 5.1), which are nowadays possible also for larger molecules on fast work stations, can only be indicated. For the following own contributions to studies on sterically overcrowded molecules, a combination of partly intuitive interference radii considerations, measurement of characteristic molecular properties, and as careful as possible a quantum chemical exploration of the pathways through the space spanned by the $(3n-6)$ degrees of freedom of n-atom ensembles and containing numerous local minima proved to be advantageous.

7.2. Prototype Molecules from Frankfurt: $((H_3C)_3Si)_3Si$–$Si(Si(CH_3)_3)_3$, $((H_3C)_2N)_2C{=}C(N(CH_3)_2)_2$ and $N(CH(CH_3)_2)_3$

All three selected molecules have been investigated, because their space-filling substituent groups allow an energetically favorable delocalization of the positive charge in their radical cation ground states, accessible by vertical ionization or adiabatic oxidation (Section 5.1).

7.2.1. *Hexakis(trimethylsilyl)disilane*

In accordance with the parametrized $\sigma_{SiSi}/\sigma_{SiSi}$ interaction model,[1a, 8h, 113] the title compound exhibits the lowest first vertical ionization energy of all disilane derivatives investigated so far[104] (Scheme 37).

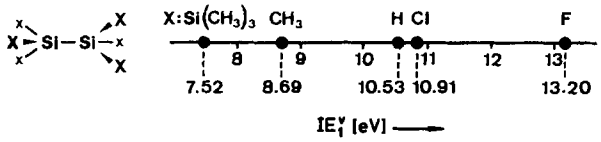

Scheme 37. First vertical ionization energies of disilane derivatives.

Hexakis(trimethylsilyl)disilane crystallizes in the space group $R\bar{3}c$ with 12 molecules of D_3 symmetry per unit cell.[114] The steric overcrowding by 18 peripheral methyl groups (Scheme 38) is especially evident in the stretched central Si–Si bond of 240 pm and the other six of 239 pm, in the dihedral angles ω(SiSi-SiSi) of 43 and 77°, as well as in intramolecular C···C distances as short as 351 pm, which demonstrate the interlocking of the methyl groups since the interference radii us for CH_3 is about 200 pm (Scheme 34). The intermeshing of the molecular halves obviously reduces the substituent compression considerably, because the more sterically strained hexakis(*tert*-butyl)derivative (Scheme 32) exhibits comparable dihedral angles ω(CSi-SiC) of 45 and 75°.[115]

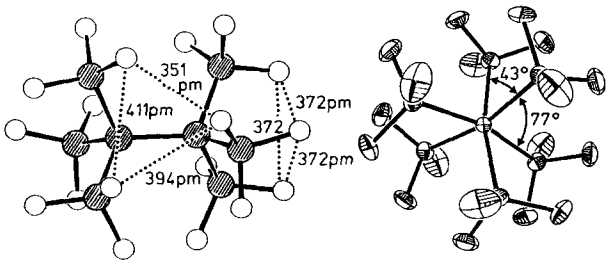

Scheme 38. Single crystal structure of hexakis(trimethylsilyl)disilane. Left: side view; right: view along the Si-Si axis.

A ^{1}H NMR spectrum recorded at 190 K does not show any signal splitting for the 42 equivalent methyl hydrogen centers; the rotational barriers must therefore be smaller than 20 kJ mol^{-1}. Regrettably, no persistent radical cation can be generated despite the low first vertical ionization energy (Scheme 37) and in agreement with the irreversible first oxidation potential in aprotic solution (Section 5.1).

7.2.2. *Tetrakis(dimethylamino)ethene*

The extremely electron-rich molecule M[65] containing four nitrogen electron pairs exhibits a first vertical ionization of only 6.13 eV[66] and therefore is immediately oxidized like sodium metal on dissolving in water, presumably according to $2M + 2H_2O \rightarrow 2(M^{\oplus}OH^{\ominus}) + H_2$ (Section 5.2). The ENDOR spectrum[67] of its radical cation (Fig. 9), which could not be isolated so far, inexplicably shows two different ^{1}H couplings. This observation, together with the structurally proven cyanine-like deformation of its dication (Sections 5.2 and 6.1), prompted the determination of the structure of neutral compound[116] (Fig. 12). Since it melts at

0 °C, a single crystal had to be grown on the goniometer needle in a cold N_2 flow.[116] In the gas-phase electron diffraction experiment, the evaporation temperature of the hardly volatile compound had to be kept below 100 °C[116] because of potential thermal decomposition.[65]

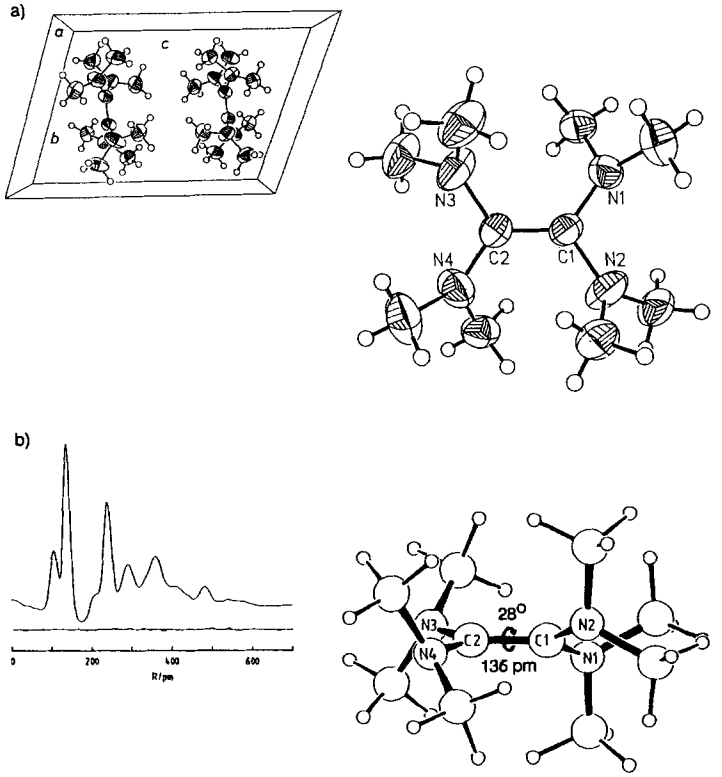

Fig. 12. Structures of tetrakis(dimethylamino)ethene. a) Single crystal determination: unit cell containg 2 molecules (intermolecular H···H distances > 243 pm) and averaged (disordered) molecular structure. Important distances and angles: C-C 135, C-N 140, N-C(H) 141–145 pm; $\omega(N_2C\text{-}CN_2)$ 28°. b) Gas-phase determination: radial distribution function and molecular structure. Important distances and angles: C-C 136, C-N 140, N-C(H) 141 to 145 pm, $\omega(N_2C\text{-}CN_2)$ 28°, N-C-N 118°, ω(CC-NC) 55°; angle sum around N 351°.

The solid-state and the gas–phase structure of tetrakis (dimethylamino)ethene agree well;[116] small deviations can be traced especially to the disordering of the dimethylamino groups in the crystal. The steric overcrowding by the four bulky $(H_3C)_2N$ substituents[71, 81, 86b] becomes visible in their considerable flattening (Fig. 12b: angle sum around N 351°) and, in particular, in the twisting of the two molecular halves relative to each other (Fig. 12: $\omega(N_2C\text{-}CN_2) = 28°$). This is further substantiated on comparison with the dihedral angles of other ethene derivatives:[117] The present world record is held by bis(biphenyl-2,2′-diyl)ethenes with up to 40° twist and, in addition, a C-C bond stretched to 139 pm. Tetrakis(*tert*-butyl)ethene is still unknown and molecules that closely resemble it, tetrakis(trimethylsilyl)- and tetrakis(1-methyl-cyclopropyl)ethene, are twisted by 29.5°[118] and 20°.[117] Tetrakis(isopropyl)ethene, isoelectronic to the title compound, surprisingly contains a planar $C_2C{=}CC_2$ skeleton,[117] which also suggests a considerable spatial demand for the nitrogen lone pairs.

The single crystal data of tetrakis(dimethylamino)ethene as well as the gas-phase data, which exclude packing effects (Fig. 12), enable rationalization of essential molecular properties. The low first vertical ionization energy[66] cannot be explained by considerably reduced n_N/π-interactions relieved by the 40° turn of the N lone pairs out of an averaged π plane ($\cos^2 40° = 0.6$),[1b] but can be traced directly to the considerable flattening of the dimethylamino groups, because triisopropylamine, which also displays an almost planar NC_3 skeleton[119] (see Fig. 13), shows an extremely low value for IE_1^V of only 7.18 eV. The associated lowering of the N inversion barrier simultaneously provides a molecular dynamics argument (Fig. 2) for the single ^1H NMR signal measured at room temperature.[65] In conclusion it should not be concealed that the structure of the neutral molecule does not resolve the mystery of the two different ^1H ENDOR couplings for its radical cation $M^{\bullet\oplus}$ (Fig. 9); increased efforts, therefore, are being dedicated to the growth of a single crystal of a radical cation salt $[M^{\bullet\oplus}]X^{\ominus}$.

7.2.3. *Triisopropylamine*

The triisopropylamine molecule[119] constitutes an excellent example for conclusions about structure drawn from suitable data (Section 1). Initial target of the investigations was the preparation of a trialkylamine with a low first vertical ionization energy, that is, a radical cation ground state in which the positive charge is stabilized by the surrounding alkyl groups and which could potentially also be oxidized adiabatically to attempt the isolation of its radical cation salts $[M^{\bullet\oplus}]X^{\ominus}$ (Section 5.1). Indeed triisopropylamine, accessible according to the literature by a three-step synthesis including $CN \rightarrow CH_3$ Grignard exchange, exhibits a rather low first ionization energy of only 7.18 eV (Fig. 13a), which is 1.3 eV (!) below that of trimethylamine and comparable to that of a phosphorus ylide.[120] To our bewilderment, however, a reversible one-electron oxidation potential recorded by cyclic voltammetry was noticed (Fig. 13b), because this can only be expected when all H–C bonds are perpendicular to the N lone pair and thus prevents the usual H elimination from an intermediate immonium cation $R_2N^{\oplus}{=}CR_2$.[119] Certainty about a flattened radical cation structure was provided by the ESR spectrum showing exclusively a N triplet (Fig. 13c), which meant that potential couplings of the 21 (!) hydrogens were smaller than the signal width. Quantum chemical geometry-optimization supported a planar NC_3 skeleton in the radical cation and suggested the same for the neutral molecule.

According to a careful literature search, triisopropylamine is the first trialkylamine for which a sterically enforced planarization of the NC_3 pyramid and the associated formation of a p-type nitrogen lone pair could be structurally proven.[121] This structure (Fig. 13d) is in accord with all the experimental data obtained so far and also with the results of quantum chemical calculations (Fig. 13a–c),[119] which predict a small dipole moment and a charge distribution polarized according to the effective nuclear charges from the negative nitrogen to the positive isopropyl groups. The rather low inversion enthalpies estimated for varying C-N-C angles by MNDO FORCE and AM1 calculations suggest for triisopropylamine a shallow double-minimum potential.

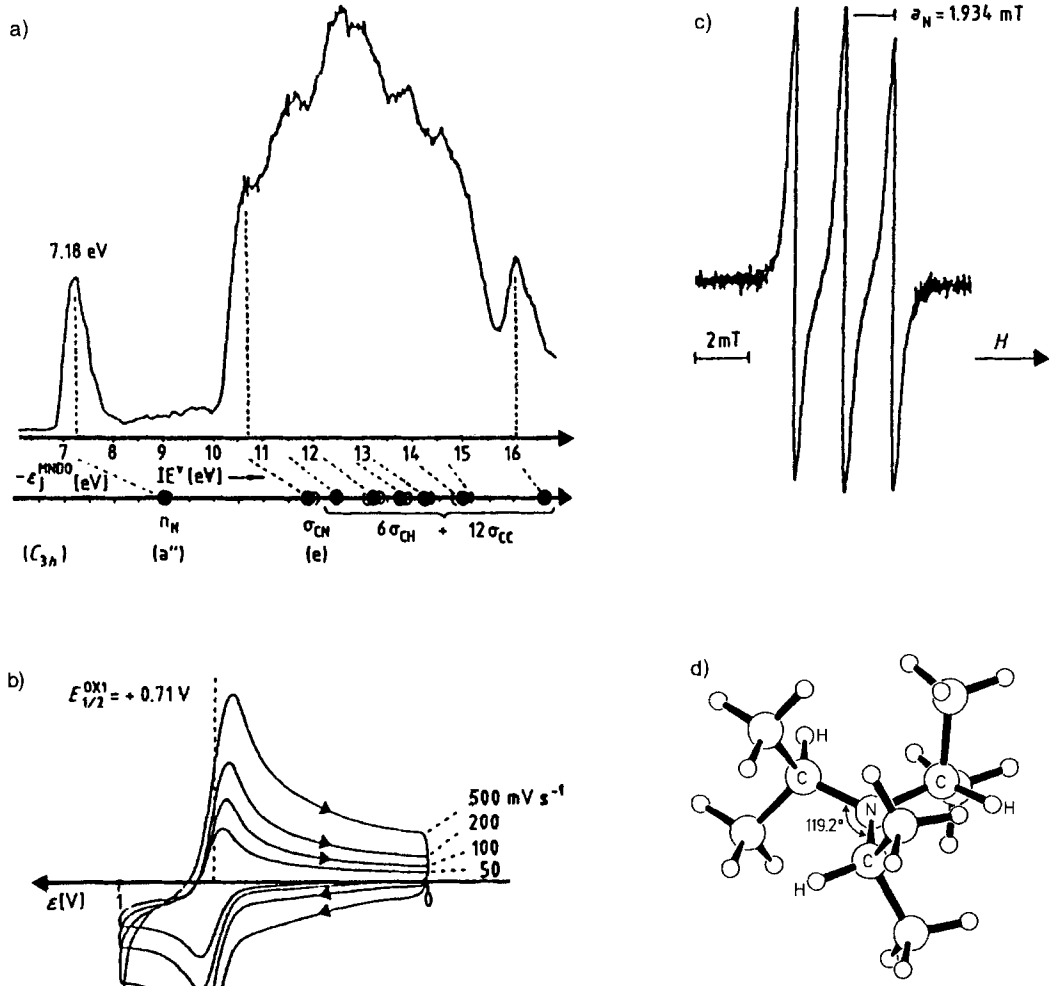

Fig. 13. Selected measurements for triisopropylamine: a) He(I)-PE spectrum up to 16 eV with Koopmans's assignment based on MNDO eigenvalues; b) cyclic voltammograms in THF/0.1 M $Bu_4N^{\oplus}ClO_4^{\ominus}$ at 243 K (recording velocities $v = 50$ to 500 mVs^{-1}); c) ESR spectrum of the radical cation generated by SbF_5/CH_2Cl_2 at 200 K; d) structure in the gas phase determined by electron diffraction.

Single crystals of the salt $((H_3C)_2HC)_3NH^{\oplus}Cl^{\ominus}$ have been grown in the interim; and their structure was determined at 90 K[122] (Scheme 39). Although we had hoped for

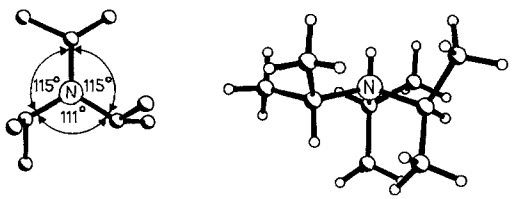

Scheme 39. Single crystal structure of triisopropylammonium hydrochloride at 90 K.

a protonation of the p-like nitrogen lone pair of the almost planar triisopropylamine molecule, the structural changes observed demonstrate an interesting possibility for the arrangement of three bulky isopropyl groups around a four-coordinate center: one takes up a horizontal position. The angle sum about N of 341° confirms the deviation from an ideal tetrahedron (angle sum = 327°), and angles of 115° on both sides of the horizontal isopropyl group illustrate that steric strain still exists. From interference radii considerations (Scheme 34), it is remarkable that the C-N-C angle between two other $(H_3C)_2HC$ substituents can be compressed to 111°.

In conclusion, the relationship between structural effects due to charge perturbation and steric overcrowding must be emphasized, although they have been dealt with separately for didactic reasons. Tetraphenylethene was chosen as a suitable example for a reduction reaction (Section 2.1). The cyanine-like distortion in its dianion (Fig. 3 and Section 6.1), that is the elongation of the C=C bond by 13 pm and the

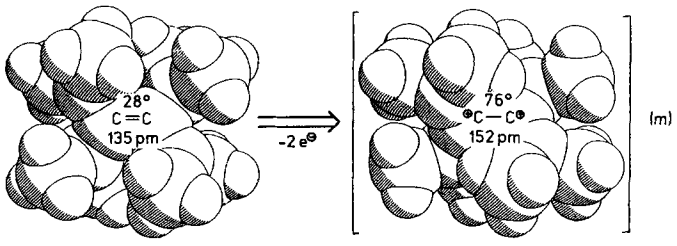

twisting of the molecular halves by 56°, renders possible the formation of a contact ion pair at the previously shielded central C–C bond. The same applies to the double oxidation of tetrakis(dimethylamino)ethene [Eq. (m)], in which both charge perturbation and relief of steric compression operate in the same direction.

Once more, this evidence shows that molecular states—despite interesting individual facets (Scheme 5)—have to be considered as an entity (Figs. 1 and 2) and that "actually, everything is more complicated".

8. Summary and Perspectives

This review reports essential results of two years' structural investigation starting from and stimulated by suitable molecular-state data as well as their quantum chemical calculation. It contains more than 30 structures determined for the products of the reduction of unsaturated phenyl-substituted hydrocarbons with alkali metals (Sections 2 and 3), for radical contact ion pairs (Section 4), for molecular polycation salts (Sections 5 and 6), as well as for sterically distorted compounds (Section 7). A selection of literature observations supplement and extend the review. Our current intensified investigations will allow us to acquire experience in the design, preparation, and growth of single crystals of charge-perturbed and sterically overcrowded molecules as well as in their quantum chemical interpretation.

8.1. Useful Rules of Thumb for the Design and Preparation of Distorted Molecules

Experimental data, structural parameters, and quantum chemical results can be summarized in molecular state considerations, which in addition allow the comparison of perturbations of chemically related molecules and molecular ions.[11] This point of view provides the following interdependent, frequently useful, and partly obvious rules of thumb both for the design of distorted molecules and for their preparation:

1) Suitable molecular-state data such as (adiabatic) half-wave redox potentials or (vertical) ionization energies, which can be either measured, calculated, or estimated from correlations between related compounds, usually provide valuable hints for highly selective electron-transfer reactions (cf. for example, Section 5a).

2) UV/VIS spectra, often satisfactorily reproduced by CI calculations (cf. Section 5.2), and especially the isobestic points observed, can be helpful in optimizing difficult crystal growth conditions and, above all, in the selection of the solvent.

3) ESR/ENDOR spectra and their temperature dependence prove valuable in the attempts to crystallize paramagnetic molecular-ion salts; the spin populations obtained simultaneously can usually be correlated with calculated charge distributions.

4) Known structural parameters often offer only unsatisfactory predictions for strong charge perturbation in molecular ions. Similarly the interference radii estimated from them are a poor indicator for severe overcrowding in molecules and often only cover some aspects of the many degrees of freedom (cf. Sections 6.5 and 7.1). On the other hand, correlations with substitution perturbations frequently allow the discovery of stimulating consequences (Sections 2.3 and 3.3).

5) In general, energy hypersurface and partly also force-field calculations under full geometry-optimization allow the reproduction of structures of molecules (Sections 2.6 and 7), of molecular anions and their contact ion aggregates (Sections 2, 3, 4, and 6), as well as of molecular cations (Sections 5 and 6) in a satisfactory way and even their correct prediction. Metal countercations always have to be taken into account (Sections 2 and 3), and counteranions in case of hydrogen bond formation (Section 5.3).

6) Discussions of appropriate data based on quantum chemical results, the reliability of which can be tested in suitable correlations, will always provide a wealth of additional aspects (cf. for example Sections 1.1, 2.1, 5.2, or 6.2).

7) Comparisons between experimental and/or calculated molecular-state data (Section 1.3) based on first and second order perturbation arguments provide reliable conclusions,[92b] but leave room for fantasy on the evaluation of "chemically related compounds". They can increase the hit probability in the design of distorted molecules considerably.

Most important is the success of the preparative effort. A satisfactory solution of the multiparameter problem of striking optimum conditions for the growth of frequently temperature-, air-, proton-, and light-sensitive single crystals definitely needs a grain of luck, as does their suitability for the structure determination.

8.2. What We Still Do Not Know

Despite all the fascination for this research area, which was new to us, and the achieved quantum chemical comprehension of some molecular structures, we cannot disguise our disatisfaction with regard to the question "what crystallizes, how, and why?" This problem is inherent in crystallization, which as prototype of molecular self-organization[123] is presently again[124] receiving much world-wide attention.[103c, 125] Thus, further improved force-field calculations enable the rationalization of interactions in the crystal—as exemplified by diphenyl, which is twisted by 40° in the gas phase but planar in the crystal.[103c] Structures of hydrocarbons within certain space groups can be reproduced by a molecular cluster approach: specified arrangements are generated by symmetry operators and their energies calculated approximately; tetramethyldibenzocyclooctene ($P\bar{1}$) is quoted as a successful example.[125] Dipole moments do not exert any significant influence on the crystallization in certain space groups.[125b] Better suited are presumably stronger interactions such as caused by multiple hydrogen bonds or by the Coulomb attraction between separated stacks of disklike donor and acceptor components in organic conductors.

The specific example of molecular anion salts also shows that more is unknown than is known. Thus the effects of countercations and of their solvation on the resulting crystal structure have been investigated only sporadically (cf. Sections 2.4 or 3.2) and remain largely uncomprehended.

Serendipity led to the discovery that, for instance, the tetracyanoethene radical anion under comparable conditions in dimethoxyethane solution crystallizes with solvent in salts $[TCNE^{\cdot\ominus}Met^{\oplus}(dme)_1]_\infty$ containing six-coordinate $Na^{\oplus}$ or seven-coordinate $K^{\oplus}$ ions, but without solvent with $Cs^{\oplus}$ as $[TCNE^{\cdot\ominus}Cs^{\oplus}]_\infty$ (Section 4.3). The tetraphenylbutadiene dianion is found within the very same crystal either in η^3-coordination with two $[Na^{\oplus}(dme)_2]$ counterions, or "naked" with completely solvent-separated $[Na^{\oplus}(dme)_3]$ ions (Section 2.4). Even more confused is the situation in ether solutions: the reductions of organic hydrocarbons with alkali metals take place through a network of equilibria (Sections 3.1 and 4.1) until the molecular anions or dianions, generated partly by protonation, C–C bond formation, or double-bond shift (Sections 2.2, 3.1, and 3.2), finally crystallize, sometimes in intra- or intermolecular dibenzenesodium sandwich structures (Section 2.4). Despite all tentative interpretations, here again many questions remain unanswered, from "how is the electron transferred from the metal mirror?" through "do the solutions contain metal atoms or metal clusters?" back to the initial "what role is played by solvent cages especially during the crystallization?"[126] Without further specification, a comparably large number of questions on oxidation reactions—although partly of different type—need answers.

Altogether, more questions are raised than answered in this report or, put positively, there is a lot of stimulation for numerous future experiments.

Our report covers two years of fascination by structures of charge-perturbed and sterically overcrowded molecules. Within this period, former "gas-men" and "solution-ladies" turned into "stone age people", to take a primordial morning look using a cold-light lamp at the crystals growing from deep-coloured solutions in Schlenk traps under argon. We like to express our gratefulness to all, who have helped us in our learning process. Above all, thanks go to my friend and former colleague Dieter Fenske (now Technical University Karlsruhe), who together with his co-workers K. Merzweiler and H. Goesmann, supported our first steps in the use of a four-circle diffractometer. My present colleague, Robert Schlögl, and Dr. W. Bensch from his group, have generously provided the measurement time as well as their experience in solution of structures. Support also came from Professor E. Egert and his co-workers Dr. J. W. Bats and Dr. M. Dyrbusch. Joint research projects link us with Dr. W. Bensch (University of Frankfurt), with Dr. H. Borrmann, Dr. W. Hönle, Professor H. G. von Schnering, and Professor A. Simon (Max-Planck Institute for Solid State Research, Stuttgart-Büsnau), with Dr. E. Herdtweck and Professor W. A. Herrmann (Technical University, Munich), as well as with Professor H. Oberhammer and his co-worker S. Liedle (University Tübingen). Generous financial grants have been provided by the Deutsche Forschungsgemeinschaft and Land Hessen, the research project has also been supported by the Fonds der Chemischen Industrie, the Alexander von Humboldt (Z. H.) and the Adolf-Messer-Foundations.

Received: October 9, 1991 [A 865 IE]
German version: *Angew. Chem.* **1992**, *104*, 564

[1] See, for example, a) H. Bock, *Angew. Chem.* **1989**, *101*, 1659–1682; *Angew. Chem. Int. Ed. Engl.* **1989**, *28*, 1627–1650; b) H. Bock, R. Dammel, *ibid.* **1987**, *99*, 518–540; **1987**, *26*, 504–528; c) H. Bock, B. Solouki, *ibid.* **1981**, *93*, 425–442; **1981**, *20*, 427–444; d) the essay dedicated to Erich Hückel on occasion of his 80th birthday on "Molecular states and Molecular Orbitals" (H. Bock, *ibid.* **1977**, *89*, 631–655; **1987**, *16*, 613–637).

[2] H. Bock, W. Ried, U. Stein, *Chem. Ber.* **1981**, *114*, 673.

[3] B. Beagley, V. Ulbrecht, S. Katsumata, D. R. Lloyd, J. A. Connor, G. A. Hudson, *J. Chem. Soc. Faraday Trans. II* **1977**, *73*, 1278.

[4] H. Bock, U. Lechner-Knoblauch, *J. Organomet. Chem.* **1985**, *294*, 295.

[5] H. Bock, W. Kaim, H. Nöth, A. Semkow, *J. Am. Chem. Soc.* **1980**, *102*, 4421; *Angew. Chem.* **1978**, *90*, 308; *Angew. Chem. Int. Ed. Engl.* **1978**, *17*, 286; see also [9e].

[6] H. Bock, R. Dammel, B. Roth, "Molecular State Fingerprints and Semiempirical Hypersurface Calculations" in ACS Symposium Series 232 American Chemical Society, Washington D.C. 1983, p. 139–165.

[7] a) S. F. Nelsen, W. C. Hollinsed, C. R. Kessel, J. C. Calabrese, *J. Am. Chem. Soc.* **1978**, *100*, 7876; b) S. F. Nelsen, S. C. Blackstock, K. J. Haller, *Tetrahedron* **1986**, *42*, 6106.

[8] For further structure estimates from gas-phase investigations by PE spectroscopy, see e.g. a) H. Bock, B. Solouki, G. Bert, P. Rosmus, *J. Am. Chem. Soc.* **1977**, *99*, 1663; *Chem. Phys.* **1977**, *22*, 453; b) H. Bock, U. Stein, A. Semkow, *Chem. Ber.* **1980**, *113*, 3208; c) H. Bock, H. Müller, *Inorg. Chem.* **1984**, *23*, 4365; d) H. Bock, R. Dammel, *Angew. Chem.* **1985**, *97*, 128; *Angew. Chem. Int. Ed. Engl.* **1985**, *24*, 111; e) H. Bock, B. Solouki, H. W. Roesky, *Inorg. Chem.* **1985**, *24*, 4425; f) H. Bock, H. P. Wolf, G. Tschmutowa, *J. Chem. Soc. Chem. Commun.* **1986**, 1068; H. Bock, H. P. Wolf, *ibid.* **1990**, 690; g) H. Bock, R. Dammel, *J. Am. Chem. Soc.* **1988**, *110*, 5261; [1b]; h) H. Bock, B. Solouki in *The Chemistry of Organosilicon Compounds*, (Ed.: S. Patai), Wiley-Interscience, London, **1989**, p. 556–653; [1a]; i) H. Bock, L. Cederbaum, W. von Niessen, P. Paetzold, P. Rosmus, B. Solouki, *Angew. Chem.* **1989**, *101*, 77; *Angew. Chem. Int. Ed. Engl.* **1989**, *28*, 88.

[9] For further structure information from investigation by ESR/ENDOR spectroscopy on radical ions, see e.g. a) H. Bock, W. Kaim, M. Kira, H. Osawa, H. Sakurai, *J. Organomet. Chem.* **1978**, *164*, 295; b) H. Bock, W. Kaim, P. L. Timms, P. Hawker, *Chem. Ber.* **1980**, *113*, 3196; c) H. Bock, B. Roth, G. Maier, *ibid.* **1984**, *117*, 172; *Angew. Chem.* **1980**, *92*, 213; *Angew. Chem. Int. Ed. Engl.* **1980**, *19*, 209; d) H. Bock, W. Schulz, U. Stein, *Chem. Ber.* **1981**, *114*, 2623; e) H. Bock, W. Kaim, *Acc. Chem. Res.* **1982**, *15*, 9; f) H. Bock, B. Hierholzer, H. Kurreck, W. Lubitz, *Angew. Chem.* **1983**, *95*, 817; *Angew. Chem. Int. Ed. Engl.* **1983**, *22*, 787; *Angew. Chem. Suppl.* **1983**, 1088–1105; g) H. Bock, B. Hierholzer, *ibid.* **1988**, *100*, 1127 and **1988**, *27*, 1069; h) H. Bock, B. Hierholzer, P. Rittmeyer, *Z. Naturforsch. B* **1988**, *44*, 187.

[10] The time scale in Figure 2 has been drawn according to the data given in N. Wiberg, *Lehrbuch der Anorganischen Chemie*. 91st–100th ed., de Gruyter, Berlin, **1985**, p. 346.

[11] See, for example, H. Kurreck, B. Kirste, W. Lubitz, *Electron Spin Double Resonance Spectroscopy of Radicals in Solution*, VCH, Weinheim, **1988**.

[12] H. Bock, K. Ruppert, D. Fenkse, *Angew. Chem.* **1989**, *101*, 1717; *Angew. Chem. Int. Ed. Engl.* **1989**, *28*, 1685.

[13] H. Bock, K. Ruppert, E. Herdtweck, W. A. Herrmann, *Helv. Chim. Acta*, in press.

[14] H. Bock, K. Ruppert, Z. Havlas, D. Fenske, *Angew. Chem.* **1990**, *102*, 1095; *Angew. Chem. Int. Ed. Engl.* **1990**, *29*, 1042.

[15] Z. Havlas, S. Nick, H. Bock, *Int. J. Quantum Chem.*, im Druck.

[16] H. Bock, C. Näther, K. Ruppert, *J. Chem. Soc. Chem. Commun.*, in press.

[17] H. Bock, C. Näther, Z. Havlas, unpublished.

[18] H. Bock, K. Ruppert, Z. Havlas, W. Bensch, W. Hönle, H. G. von Schnering, *Angew. Chem.* **1991**, *103*, 1197; *Angew. Chem. Int. Ed. Engl.* **1991**, *30*, 1183.

[19] See e.g. a) C. Schade, P. von R. Schleyer, *Adv. Organomet. Chem.* **1987**, *27*, 169; b) W. N. Setzer, P. von R. Schleyer, *ibid.* **1985**, *24*, 353.

[20] For an overview on the present state of the still not fully elucidated ethene ($\pi \rightarrow \pi^*$) excitation cf. M. B. Robin, *Higher Excited States of Polyatomic Molecules, Vol. 2*, Academic Press, New York, **1975**, S. 2f.

[21] H. Bock, K. Ruppert, K. Merzweiler, D. Fenske, H. Goesmann, *Angew. Chem.* **1989**, *100*, 1715; *Angew. Chem. Int. Ed. Engl.* **1989**, *18*, 1684.

[22] "If it is not true, then it is well invented", G. Bruno, *Gli eroici furori*, Paris, **1585**.

[23] A. Hoekstra, A. Vos, *Acta Crystallogr Sect. B* **1975**, *31*, 1722.

[24] Other known dianions of ethene derivatives $X_2C{=}CX_2$ have, for example, been prepared as follows: a) X_2C = fluorenylidene (M. Walczack, G. D. Stucky, *J. Organomet. Chem.* **1975**, *97*, 313), by deprotonation of bifluorene with LiR; b) X = CN (D. A. Dixon, J. S. Miller, *J. Am. Chem. Soc.* **1987**, *109*, 3656), by reduction of tetracyanoethene with $[(CP^*_2)Co]$; c) X = $Si(CH_3)_3$ (A. Sekiguchi, T. Nakanishi, C. Kabuto, H. Sakurai, *J. Am. Chem. Soc.* **1989**, *111*, 3748), by reduction with lithium metal in THF. None of these ethene dianion salts forms a stringlike structure, presumably because in a) the dianion is sterically shielded, in b) the $Co^{\oplus}$ counterion is embedded in a sandwich and in c) the THF-solvated $Li^{\oplus}$ ions are localized on both sides of the C–C double bond because of their small radius.

[25] For the unusual sandwichlike coordination of sodium, an extensive literature search produced the following parallels: a) Lithium-7b*H*-inde-

no[1,2,3-*jk*]fluorenide (D. Bladauski, H. Dietrich, H. J. Hecht, D. Rewicki, *Angew. Chem.* **1977**, *89*, 490; *Angew. Chem. Int. Ed. Engl.* **1977**, *16*, 474) contains one dodecahapto-coordinated $Li^{\oplus}$ ion between the coaxial phenyl rings which are separated by a distance of 386 pm; b) In lithium 1,1,3,3-biphenyl-2,2'-diylpropenide diethyl ether (D. Bladauski, D. Rewicki, *Chem. Ber.* **1977**, *110*, 3920), the Li-di(η^6-phenyl)-sandwich structure is opened by 56° due to the additional R_2O solvation; c) $(H_5C_6)_3CNA \cdot TMEDA$ also shows a stringlike structure (H. Köster, E. Weiss, *J. Organomet. Chem.* **1979**, *168*, 273), but $Na^{\oplus}$ ion prefers a relatively short bond of 264 pm to the central carbanion carbon center rather than a polyhapto coordination to the phenyl groups; d) In 1,3-diphenylallyllithium diethyl ether (G. Boche, H. Ethrod, M. Marsch, W. Massa, G. Baum, W. Mahdi, *Angew. Chem.* **1986**, *98*, 84; *Angew. Chem. Int. Ed. Engl.* **1986**, *25*, 104), instead of an intramolecular dibenzenelithium sandwich, a polymer chain is formed. See also [19].

[26] Numerous alkali-metal cation half-sandwich compounds are known (cf. [19]). In addition, the contact-ion triples a) terphenyl disodium-hexakis(tetrahydrofuran) should be mentioned (J. H. Noordick, H. M. Doesburg, P. A. J. Prick, *Acta Crystallogr. B* **1981**, *37*, 1659) and b) bis-(dimethoxyethanelithium) salt of the 1,2,4,5-tetrakis(trimethylsilyl)-benzene dianion (A. Sekiguchi, K. Ebata, C. Kabuto, H. Sakurai, *J. Am. Chem. Soc.* **1991**, *113*, 7081), which each contain a sodium or lithium ion on both sides of a benzene ring, and c) the intramolecular phosphonium-bisbenzylide complexes of $Na^{\oplus}$ and $K^{\oplus}$ (H. Schmidbaur, U. Deschler, B. Milewski-Mahrla, B. Zimmer-Gasser, *Chem. Ber.* **1981**, *114*, 608).

[27] Y. Ohsima, S. Yamamoto, N. Nakata, K. Kuchiku, *J. Phys. Chem.* **1987**, *91*, 4696. For tetraphenylallene we have obtained the following structure parameters from a single-crystal structure determination: C=C 132 pm, ∢ C=C=C 173.5°, $\omega(C_2C\text{-}CC_2)$ 87° (H. Bock, R. Ruppert, unpublished).

[28] Selected examples of structure determinations for allyle ions of alkali metals: a) $C_3H_3Li \cdot PMDTA$ (E. Weiss, U. Schürmann, H. Dietrich, W. Mahdi, *J. Organomet. Chem.* **1987**, *332*, 299); b) $C_3H_3Li \cdot TMEDA$ (H. Köster, E. Weiss, *Chem. Ber.* **1982**, *115*, 3422); c) 1,3-diphenylallyllithium diethyl ether [25e].

[29] For this purpose the following parameters have been optimized [14]: $U_{ss} = -4.611$ eV; $U_{pp} = -2.3643$ eV; $\xi_s = 0.73384$ a.u.; $\xi_p = 0.82957$ a.u.; $\beta_s = 1.14529$ eV; $\beta_p = -1.14101$ eV; $\alpha = 1.26193$ Å^{-1}; $g_{ss} = 7.20$ a.u.; $g_{sp} = 5.18$ a.u.; $g_{pp} = 5.43$ a.u.; $g'_{pp} = 4.233$ a.u., $h_{sp} = 0.6428$ a.u.

[30] The reductive C-C bond formation e.g. of silylated ethenes by reaction with alkali metals has been reported for $Ph_3SiHC=CH_2$ (J. J. Eisch, R. J. Beuhler, *J. Org. Chem.* **1963**, *28*, 2876) and for $(Me_3Si)_2C=CH_2$ (M. Kira, T. Hino, Y. Kubota, N. Matsuyama, H. Sakurai, *Tetrahedron Lett.* **1988**, *29*, 6939). Crystal structures cannot be found in the Cambridge Structural Data File: the reaction course is supported by deuterolysis, by reoxidation, as well as by ring closure with R_2SiCl_2 to silacyclopentane derivatives.

[31] N. Wiberg, *Lehrbuch der Anorganischen Chemie*, 91st–100th ed., de Gruyter, Berlin, **1985**, p. 954.

[32] J. C. Slater, *Phys. Rev.* **1930**, *36*, 57; cf K. F. Purcell, J. C. Kotz, *Inorganic Chemistry*, Saunders, Philadelphia, **1977**, p. 44f.

[33] H. Bock, C. Näther, K. Ruppert, Z. Havlas, *J. Am. Chem. Soc.*, in press.

[34] Cf. the examples given in H. Bock, *GIT-Fachz. Lab.* **1991**, *35*, 557.

[35] The MNDO/Cl calculations have been performed by using the program SCAMP. All configurations from the six inner, partly occupied molecular orbitals were considered in each case. As reaction coordinate the distance C···C between the linked C centers has been chosen, and the structures have been pointwise completely geometry-optimized. For Na, the optimized parameters [29] have been applied.

[36] J. D. Dunitz, J. D. Wallis, *Helv. Chim. Acta* **1984**, *67*, 1374.

[37] T. Maezke, D. Seebach, *Helv. Chim. Acta* **1989**, *72*, 624, and references cited therein.

[38] R. Norrestam, L. Schepper, *Acta Chem. Scand. A* **1981**, *35*, 91.

[39] See, for example, A. Domenicano, P. Murray-Rust, A. Vaciago, *Acta Crystallogr. Sect. B* **1983**, *39*, 457 and their preceding publications cited.

[40] See, for example, a) J. M. Lehn, *Angew. Chem.* **1990**, *102*, 1347; *Angew. Chem. Int. Ed. Engl.* **1990**, *29*, 1304; *ibid.* **1988**, *100*, 91 and **1988**, *27*, 89; b) *Cation Binding by Macrocycles* (Eds.: Y. Inone, G. W. Gokel), Dekker, New York, **1990**; for an overview of the older literature c) *Ions and Ion Pairs in Organic Reactions, Vol. 1, Vol. 2* (Ed.: M. Swarc), Wiley-Interscience, New York, **1972** and **1977**. See also [1a, 10b, f] and references cited therein.

[41] See, for example, S. W. Mao, K. Nakamura, N. Hirota, *J. Am. Chem. Soc.* **1974**, *96*, 5341 and references cited therein.

[42] See, for example, H. Bock, *Polyhedron* **1988**, *7*, 2429 and references cited therein.

[43] a) H. Bock, H.-F. Herrmann, *J. Am. Chem. Soc.* **1989**, *111*, 7622. For other own ESR/ENDOR investigations on paramagnetic contact-ion pairs and contact-ion triples in solution, see e.g. b) H. Bock, B. Hierholzer, F. Vögtle, G. Hollmann, *Angew. Chem.* **1984**, *96*, 74; *Angew. Chem. Int. Ed. Engl.* **1984**, *23*, 57; c) H. Bock, B. Solouki, P. Rosmus, R. Dammel, P. Hänel, B. Hierholzer, U. Lechner-Knoblauch, H. P. Wolf in *Organosilicon and Bioorganosilicon Chemistry*, (Ed.: H. Sakurai), Ellis Horwood, Chichester, **1985**, p. 45–73; [1a]; d) H. Bock, B. Hierholzer, P. Schmalz, *Angew. Chem.* **1987**, *99*, 811; *Angew. Chem. Int. Ed. Engl.* **1987**, *26*, 791; e) H. Bock, P. Hänel, H.-F. Herrmann, H. tom Dieck, *Z. Naturforsch. B* **1988**, *43*, 1240; f) H. Bock, B. Hierholzer, D. Jaculi, *ibid.* **1988**, *43*, 1247; g) H. Bock, P. Hänel, H.-F. Herrmann, *ibid.* **1990**, *45*, 1197; h) H. Bock, P. Dickmann, H.-F. Herrmann, *ibid.* **1991**, *46*, 326.

[44] See, for example, W. Lubitz, M. Plato, K. Möbius, R. Biehl, *J. Phys. Chem.* **1979**, *83*, 3402 and references cited therein.

[45] a) H. O. Honse, L. E. Huber, M. J. Umen, *J. Am. Chem. Soc.* **1972**, *94*, 8471; b) M. Guerra, P. Palmieri, G. F. Pedulli, *Chem. Phys.* **1978**, *33*, 45; cf. also H. von Willingen, C. F. Mulks, *J. Chem. Phys.* **1981**, *75*, 2135.

[46] H. Bock, H.-F. Herrmann, D. Fenske, H. Goesmann, *Angew. Chem.* **1988**, *100*, 1125; *Angew. Chem. Int. Ed. Engl.* **1988**, *27*, 1067.

[47] In [19a] terphenyldisodium hexa(tetrahydrofuran) is also quoted [26a] in which, however, the two threefold THF-solvated sodium ions are located with contact distances between 278 pm and 286 pm above and below the central phenyl ring.

[48] See, for example, J. March, *Advanced Organic Chemistry*, Wiley, New York, **1985**, p. 110ff. From fluorenone the diol is formed in 95% yield. (W. E. Bahmann, *J. Am. Chem. Soc.* **1933**, *55*, 1179).

[49] H. R. Luss, D. G. Smith, *Acta Crystallogr. Sect. B* **1972**, *28*, 884.

[50] Selected examples: a) E. de Boer, A. A. K. Klaassen, J. J. Mooij, J. H. Noordick, *Pure Appl. Chem.* **1979**, *51*, 73; b) J. H. Noordick, H. M. Doesburg, P. A. J. Prock, *Acta Crystallogr. Sect.B* **1981**, *37*, 1659; c) J. S. Miller, J. C. Calabrese, H. Rommelmann, S. R. Chittipedi, J. H. Zhang, W. M. Reiff, A. J. Epstein, *J. Am.Chem. Soc.* **1987**, *109*, 769; cf [24b].

[51] P. H. Rieger, I. Bernal, W. H. Reinmuth, G. S. Fraenkel, *J. Am. Chem. Soc.* **1963**, *85*, 683.

[52] See, for example T. M. Bockmann, J. K. Kochi, *J. Am. Chem. Soc.* **1988**, *110*, 1294, and references cited therein.

[53] H. Bock, C. Näther, C. Arad, unpublished.

[54] See C. Liang, L. C. Allen, *J. Am. Chem. Soc.* **1991**, *113*, 1873, and references cited therein, especially H. Irngartinger, W. Götzmann, *Angew. Chem.* **1986**, *98*, 359; *Angew. Chem. Int. Ed. Engl.* **1986**, *25*, 340.

[55] L. Echogoyen, A. DeCian, J. Fischer, J.-M. Lehn, *Angew. Chem.* **1991**, *103*, 884; *Angew. Chem. Int. Ed. Engl.* **1991**, *30*, 838.

[56] Selected examples: a) J. S. Miller, D. A. Dixon, J. C. Calabrese, C. Vazquez, P. J. Krusic, M. D. Ward, E. Wassermann, R. L. Harlow, *J. Am. Chem. Soc.* **1990**, *112*, 381; b) R. J. van der Wal, B. van Bodegom, *Acta Crystallogr. Sect. B* **1979**, *35*, 2003, and references cited therein.; c) M. Kouno, H. Kobayashi, F. Marumo, Y. Saito, *Bull. Chem. Soc. Jpn.* **1973**, *46*, 1987; G. Zanotti, A. Del Pra, *Acta Crystallogr. Sect. B* **1980**, *36*, 313; d) H. Bock, K. Ruppert, *Inorg. Chem.*, in press.

[57] H. Bock, A. John, C. Näther, unpublished.

[58] H. Bock, C. Näther, K. Ruppert, *Z. Anorg. Allg. Chem.*, in press

[59] H. Bock, K. Ruppert, D. Fenske, H. Goesmann, *Z. Anorg. Allg. Chem.* **1991**, *595*, 275, and references cited therein.

[60] Examples of radical cations, generated by $AlCl_3/CH_2Cl_2$ single-electron oxidation and characterized by ESR/ENDOR spectroscopy (review: H. Bock, *Rev. L'Actualite Chim.* **1986**, *3*, 36ff.) a boron/nitrogen heterocycles (H. Nöth, W. Winterfeld, W. Kaim, H. Bock, *Chem. Ber.* **1979**, *112*, 2494); b) tetra(*tert*-butyl)tetrahedrane [9c]; c) silicon-substituted π systems [1a, 9e,f] and trialkylamines [1a, 9a]; d) tetrakis(dimethylamino)-*p*-benzoquinone (H. Bock, P. Hänel, W. Kaim, U. Lechner-Knoblauch, *Tetrahedron Lett.* **1985**, *26*, 5115; e) sulfur compounds: see [9d,h] as well as α-lipoic acid (H. Bock, U. Stein, A. Semkow, *Chem. Ber.* **1980**, *113*, 3208.

[61] O. Graalmann, M. Hesse, U. Klingebiel, W. Clegg, M. Haase, G. M. Sheldrick, *Angew. Chem.* **1983**, *95*, 630; *Angew. Chem. Int. Ed. Engl.* **1983**, *22*, 621.

[62] See, for example, H. Bock, D. Jaculi, *Z. Naturforsch. B* **1991**, *46*, 1091, and references cited therein.

[63] H. Bock, D. Jaculi, *Angew. Chem.* **1984**, *96*, 298; *Angew. Chem. Int. Ed. Engl.* **1984**, *23*, 305.

[64] a) See, for example, J. Pedersen, *Angew. Chem.* **1988**, *110*, 1053; *Angew. Chem. Int. Ed. Engl.* **1988**, *27*, 1021; b) J. M. Lehn, *Acc. Chem. Res.* **1978**, *11*, 49; [13b].

[65] N. Wiberg, *Angew. Chem.* **1968**, *80*, 809; *Angew. Chem. Int. Ed. Engl.* **1968**, *7*, 766.

[66] B. Solouki, H. Bock, unpublished. Cf. also B. Cetinkaja, G. H. King, S.S. Krishnamurthy, M. F. Lappert, J. B. Pedley, *Chem. Commun.* **1971**, 1370.

[67] H. Bock, B. Hierholzer, *Angew. Chem.* **1988**, *100*, 1127; *Angew. Chem. Int. Ed. Engl.* **1988**, *27*, 1069.

[68] Cf. also K. Elbl-Weiser, C. Krieger, H. A. Staab, *Angew. Chem.* **1990**, *102*, 183; *Angew. Chem. Int. Ed. Engl.* **1990**, *29*, 211.

[69] a) G. Klar, W. Hinrichs, J. Riedel, *J. Chem. Res.* **1982**, 334; b) I. Rowe, B. Post, *Acta Crystallogr.* **1958**, *11*, 372; c) G. Klar, W. Hinrichs, P. Berges, *Z. Naturforsch. B* **1987**, *42*, 169: The interplanar angles in $M^{+\oplus}SbCl_6^{\ominus}$ and $M^{+\oplus}I^{\ominus}$ are 180° and 172°, respectively.

[70] H. Bock, A. Rauschenbach, K. Ruppert, Z. Havlas, *Angew. Chem.* **1991**, *103*, 706; *Angew. Chem. Int. Ed. Engl.* **1991**, *30*, 714.

[71] H. Bock, K. Ruppert, C. Näther, Z. Havlas, *Angew. Chem.* **1991**, *103*, 1194; *Angew. Chem. Int. Ed. Engl.* **1991**, *30*, 1180.
[72] a) H. Bock, S. Nick, W. Bensch, *Z. Naturforsch.*, in press; b) H. Bock, S. Nick, J. W. Bats, *Tetrahedron Lett.*, in press.
[73] H. Bock, I. Göbel, K. Ruppert, unpublished.
[74] H. Bock, T. Vaupel, C. Näther, K. Ruppert, Z. Havlas, *Angew. Chem.* **1992**, *104*, 348 *Angew. Chem. Int. Ed. Engl.* **1992**, *31*, 299.
[75] Further unpublished investigations concerning novel hydrogen bonds: H. Bock, W. Seitz, Z. Havlas, J. W. Bats as well as H. Bock, S. Nick, C. Näther.
[76] D. G. Doughty, E. E. Glover, *J. Chem. Soc. Perkin Trans. 1* **1977**, 1593; cf. also M. P. Sammes, H. K. Wah, A. R. Katritzky, *ibid.* **1977**, 327, and references cited therein.
[77] The crystal structure of biphenyl (G. P. Charbonneau, Y. Delugeard, *Acta Crystallogr. Sect. B* **1976**, *32*, 1420) showing a dihedral angle $\omega = 0°$ and a C–C distance of 149 pm can be reproduced by force-field calculations (J.-H. Lii, N. L. Allinger, *J. Am. Chem. Soc.* **1989**, *111*, 8576). In the gas phase, however, phenyl rings are twisted relative to each other by $\omega = 44°$ and a C–C distance of 151 pm is observed (A. Almenningen, O. Bastiansen, L. Fernholt, B. N. Cyvin, S. J. Cyvin, S. Sandal, *J. Mol. Struct.* **1985**, *128*, 59).
[78] On oxidation $M \rightarrow M^{\oplus} \rightarrow M^{\oplus\oplus}$ the N–N bond distance of 149 pm in 2,7-diazatetracyclo[6.2.2.2.^{3,6}.0.^{2,7}]tetradecane decreases first to 133 pm and then to 127 pm, and the N centers are increasingly planarized (angle sums 336°, 355°, and 360°). The dication possesses a dihedral angle $\omega(C_2N^{\oplus}\text{-}^{\oplus}NC_2)$ of 0° [7b]. In contrast, the threefold bridged dication $N^{\oplus}(CH_2CH_2CH_2CH_2)_3N^{\oplus}$ shows a N–N single bond of 153 pm (R. W. Alder, A. G. Orpen, J. M. White, *J. Chem. Soc. Commun.* **1985**, 949).
[79] See, for example, P. von R. Schleyer, E. D. Jemmis, G. W. Spitznagel, *J. Am. Chem. Soc.* **1985**, *107*, 6393; K. B. Wiberg, M. A. Murko, *ibid.* **1989**, *111*, 4821.
[80] See, for example, Q.-C. Yang, M. F. Richardson, J. D. Dunitz, *Acta Crystallogr. Sect. B* **1989**, *45*, 312; K. Wozniak, T. M. Krygowski, B. Karinki, W. Jones, E. Grech, *J. Mol. Struct.* **1990**, *240*, 111; P. Prince, F. R. Fronczek, R. D. Gandor, *Acta Crystallogr. Sect. C* **1990**, *46*, 1720; G. R. Desiraju, *Acc. Chem. Res.* **1991**, *10*, 290, and references cited therein.
[81] Cf. especially H. A. Staab, T. Saupe, *Angew. Chem.* **1988**, *100*, 895; *Angew. Chem. Int. Ed. Engl.* **1988**, *27*, 865; T. Barth, C. Krieger, F. A. Neugebauer, H. A. Staab, *ibid.* **1991**, *103*, 1006 and **1991**, *30*, 1030.
[82] R. Weiss, N. J. Salomon, G. E. Mies, R. Roth, *Angew. Chem.* **1986**, *98*, 925; *Angew. Chem. Int. Ed. Engl.* **1986**, *25*, 917.
[83] Wurster's Blue radical cations: a) first publication: C. Wurster, R. Sendtner, *Ber. Dtsch. Chem. Ges.* **1879**, *12*, 1803; b) ESR investigations for example, F. B. Kaufmann, *J. Am. Chem. Soc.* **1976**, *98*, 5339, and references cited therein.; c) structure determination e.g. J. L. de Boer, A. Vos, *Acta Crystallogr. Sect. B* **1972**, *28*, 835, 839; d) Wurster's Blue radical anion: F. Gerson, U. Krynitz, H. Bock, *Angew. Chem.* **1969**, *81*, 786; *Angew. Chem. Int. Ed. Engl.* **1969**, *8*, 767.
[84] I. Ikemoto, G. Katagiri, S. Nishimura, K. Yakushi, H. Kuroda, *Acta Crystallogr. Sect. B* **1979**, *35*, 2264.
[85] See, for example, A. F. Wells, *Structural Inorganic Chemistry*, 5th ed., Clarendon Press, Oxford, **1984**, p. 703, 829.
[86] a) K. Elbl, C. Krieger, H. A. Staab, *Angew. Chem.* **1986**, *98*, 1024; *Angew. Chem. Int. Ed. Engl.* **1986**, *25*, 1023; b) J. M. Chance, B. Kahr, A. B. Buda, J. P. Toscano, K. Mislow, *J. Org. Chem.* **1988**, *53*, 3226.
[87] a) S. Dähne, D. Leupold, *Angew. Chem.* **1966**, *78*, 1029; *Angew. Chem. Int. Ed. Engl.* **1966**, *5*, 984, and references cited therein as well as parts of the review S. Dähne, K. Hoffmann, *Prog. Phys. Org. Chem.* **1990**, *18*, 1–64; b) S. Hünig, lecture at the 2nd International Colour Symposium, Elmau, **1964** (Abstract: Verlag Chemie, Weinheim, **1966**); c) J. Fabian, A. Mehlhorn, *Theor. Chim. Acta* **1975**, *36*, 351.
[88] S. Shaik, P. C. Hiberty, J.-M. Lefour, G. Ohanessian, *J. Am. Chem. Soc.* **1987**, *109*, 363.
[89] a) H. Bock,S. Nick, K. Ruppert, unpublished; cf. S. Nick, Diplomarbeit, Universität Frankfurt, **1989**; b) T. Ito, T. Sakurai, *Acta Crystallogr. Sect. B* **1973**, *29*, 1594; cf. also R. Kulpe, *ibid.* **1969**, *26*, 1411; *J. Prakt. Chem.* **1970**, *312*, 909; S. Kulpe, B. Schulz, H. Schrauber, *ibid.* **1974**, *316*, 199.
[90] a) S. Kulpe, *J. Prakt. Chem.* **1974**, *316*, 353; b) D. Semmingsen, *Acta Chem. Scand. B* **1977**, *31*, 11.
[91] J. Fabian, A. Mehlhorn, *J. Mol. Struct. (THEOCHEM)* **1984**, *109*, 17, and references cited therein. Cf. also K. D. Nolte, S. Dähne, *J. Prakt. Chem.* **1976**, *318*, 993; H. Ichikawa, J. Aihara, S. Dähne, *Bull. Soc. Jpn.* **1989**, *62*, 2798, and references cited therein.
[92] See, for example, a) H. Kuhn, *Helv. Chim. Acta* **1949**, *32*, 2247; *J. Chem. Phys.* **1949**, *17*, 1198 "Neuere Verfahren zur Behandlung von π-Elektronen-Symstemen" in *Optische Anregung Organischer Systeme*, Verlag Chemie, Weinheim, **1966**; b) E. Heilbronner, H. Bock, *The HMO-Model and its Application Vol. 1*, Wiley and Sons, Chichester 1979, p. 1–130.
[93] M. J. S. Dewar, E. G. Zoebisch, E. F. Healey, J. J. P. Stewart, *J. Am. Chem. Soc.* **1985**, *107*, 3902.
[94] Z. Havlas, S. Nick, H. Bock, unpublished.
[95] G. Jovanovski, J. O. Thomas, I. Olovsson, *Acta Crystallogr Sect. B* **1987**, *43*, 85; A. Sequeira, S. Srikanta, R. Chidambaram, *ibid.* **1970**, *26*, 77 as well as quotients of preceding structure determinations.
[96] a) P. Süsse, M. Steins, V. Kupcik, *Z. Kristallogr.* **1988**, *184*, 269; b) W. Haase-Wessel, M. Ohmasa, P. Süsse, *Naturwissenschaften* **1977**, *64*, 435.
[97] M. Baily, *Acta Crystallogr.* **1955**, *8*, 182.
[98] G. Adiwidjaja, J. Voß, *Chem. Ber.* **1977**, *110*, 1159.
[99] M. Hondo, C. Katayama, J. Tanaka, *Acta Crystallogr. Sect. B* **1986**, *42*, 90; Cf. also S. Kulpe, B. Schulz, *Z. Chem.* **1978**, *18*, 146; J. Dale, O. Eriksen, P. Groth, *Acta Chem. Scand. B* **1987**, *41*, 653 and references cited in each.
[100] P. Groth, *Acta Chem. Scand. A* **1987**, *41*, 117.
[101] a) P. D. Cradwick, D. Hall, M. K. Wood, *Acta Crystallogr. Sect. B* **1977**, *33*, 2380; b) C. G. Pierpont, L. C. Francesconi, D. N. Hendrickson, *Inorg. Chem.* **1978**, *17*, 3470.
[102] a) H. Einspahr, J.-B. Robert, R. E. Marsh, J. D. Roberts, *Acta Crystallogr. Sect. B* **1973**, *29*, 1611; b) P. K. Miller, K. D. Abney, A. K. Rappe, O. P. Anderson, S. H. Strauß, *Inorg. Chem.* **1988**, *27*, 2255; c) D. A. Brown, W. Clegg, H. M. Colquhoun, J. A. Daniels, I. R. Stephenson, K. Wade, *J. Chem. Soc. Chem. Commun.* **1987**, 889; d) M. R. Truter, B. L. Vickery, *J. Chem. Soc. Dalton Trans.* **1972**, 395; D. Pyzalka, R. Pyzalki, T. Borowiak, *J. Crystallogr. Spectrosc. Res.* **1983**, *13*, 211.
[103] a) N. Wiberg, H. Schuster, A. Simon, K. Peters, *Angew. Chem.* **1986**, *98*, 100; *Angew. Chem. Int. Ed. Engl.* **1986**, *25*, 79. b) Many structures of other sterically overcrowded organosilicon molecules are reviewed by W. S. Sheldrick in *The Chemistry of Organic Silicon Compounds* (Eds.: S. Patai, Z. Rappoport), Wiley, Chichester, **1989**, p. 227–303 or at E. Lukevics, O. Pudowa, R. Sturkovich, *Molcular Structure of Organosilicon Compounds*, Wiley, New York. **1989**.
[104] F. P. van Remoortere, F. P. Boer, *J. Am. Chem. Soc.* **1970**, *92*, 3355.
[105] Cf. M. Weidenbruch, B. Blintjer, K. Peters, H. G. von Schnering, *Angew. Chem.* **1986**, *98*, 1090; *Angew. Chem. Int. Ed. Engl.* **1986**, *25*, 1129 and references cited therein.
[106] a) M. H. Couldwell, B. R. Penford, *J. Cryst. Mol. Struct.* **1979**, *6*, 59; b) A. Sekiguchi, K. Ebata, C. Kabuto, H. Sakurai, *J. Am. Chem. Soc.* **1991**, *113*, 1464; c) J. M. Chance, B. Kahr, A. B. Buda, J. S. Siegel, *ibid.* **1989**, *111*, 5940, as well as the references quoted for each different benzene distortion.
[107] See, for example, a) $H_2C{=}NH$ (H. Bock, R. Dammel, *Angew. Chem.* **1987**, *99*, 503; *Angew. Chem. Int. Ed. Engl.* **1987**, *26*, 489); $R_2Si{=}NSiR_3$ with $R = C(CH_3)_3$ (N. Wiberg, K. Schurz, G. Reber, G. Müller, *J. Chem. Soc. Chem. Commun.* **1986**, 591); b) $H_2Si{=}CH_2$ (P. Rosmus, H. Bock, B. Solouki, G. Maier, G. Mihm, *Angew. Chem.* **1981**, *93*, 616; *Angew. Chem. Int. Ed. Engl.* **1981**, *20*, 598), $R_2Si{=}CR_2$ with $R = Si(CH_3)_3$, Adamantyl (A. G. Brook, J. W. Harris, J. Lemmon, M. El Sheikh, *J. Am. Chem. Soc.* **1979**, *101*, 83).
[108] Other frequently applied bulky substituent groups are mesityl, e.g. for $R_2Si{=}SiR_2$ (G. Raabe, J. Michl, *Chem. Rev.* **1985**, *85*, 419), and "supermesityl" $((H_3C)_3C)_3H_2C_6$, z.B. for RP = PR (M. Yoshifuji, I. Shima, N. Inamoto, K. Hirotsu, T. Higuchi, *J. Am. Chem. Soc.* **1981**, *103*, 4587); cf. also [37].
[109] a) L. Pauling, *The Nature of the Chemical Bond.* Verlag Chemie, Weinheim, **1962**, p. 242–247; b) A. Bondi, *J. Phys. Chem.* **1964**, *68*, 441; c) N. L. Allinger, Y. H. Yuh, J.-H. Lii, *J. Am. Chem. Soc.* **1989**, *111*, 8551, 8556, 8576; d) H.-B. Bürgi, J. D. Dunitz, *Acc. Chem. Res.* **1983**, *16*, 153; e) E. A. Braude, E. S. Waight, *Progress in Stereochemistry, Vol 1*, Butterworths, London, **1954**; f) cf. D. Seebach, *Angew. Chem.* **1990**, *102*, 1363; *Angew. Chem. Int. Ed. Engl.* **1990**, *29*, 1320 (Schemes 7 and 9).
[110] T. G. Strand, *Acta. Chem. Scand.* **1967**, *21*, 2111.
[111] F. H. Herbstein, *Acta Crystallogr. Sect. B* **1979**, *35*, 1661.
[112] G. Gundersen, *J. Am. Chem. Soc.* **1975**, *97*, 6342.
[113] The original publications (H. Bock, W. Enßlin, *Angew. Chem.* **1971**, *83*, 435; *Angew. Chem. Int. Ed. Engl.* **1971**, *10*, 404; H. Bock, W. Enßlin, F. Feher, R. Freund, *J. Am. Chem. Soc.* **1976**, *98*, 668), which first report on the charge delocalization in the radical cations of Si_n chains and rings are not quoted in the review by R. West in *The Chemistry of Organic Silicon Compounds* (Eds.: S. Patai, Z. Rappoport), Wiley, Chichester, **1989**, p. 1208–1240 (132 references).
[114] H. Bock, J. Meuret, K. Ruppert, *J. Organomet. Chem.*, in press.
[115] A. Simon, Max-Planck-Institut for Festkörperforschung, Stuttgart, personal communication, **1991**.
[116] H. Bock, H. Borrmann, Z. Havlas, K. Ruppert, H. Oberhammer, A. Simon, *Angew. Chem.* **1991**, *103*, 1733; *Angew. Chem. Int. Ed. Engl.* **1991**, *30*, 1678.
[117] W. Luef, R. Keese, "Strained Olefins: Structure and Reactivity of Nonplanar Carbon–Carbon Double Bonds *Topics in Stereochemistry*, Vol. 20 (Eds. E. Eliel, S. H. Wilen), Wiley & Sons, New York, **1991**.
[118] A. Sekiguchi, T. Nakanishi, C. Kabuto, H. Sakurai, *J. Am. Chem. Soc.* **1989**, *111*, 3748, and references cited therein.
[119] H. Bock, I. Göbel, Z. Havlas, S. Liedle, H. Oberhammer, *Angew. Chem.* **1991**, *103*, 193; *Angew. Chem. Int. Ed. Engl.* **1991**, *29*, 187, and references cited therein.
[120] K. A. Ostoja-Starzewski, H. Bock, *J. Am. Chem. Soc.* **1976**, *98*, 8486.
[121] The first vertical ionization $IE_1^v = 7.13$ eV for 1-azabicyclo[3.3.3]-

undecane, called manxine, also suggests a largely flattened molecular skeleton (S. F. Nelsen, *J. Org. Chem.* **1984**, *49*, 1891). In contrast, the bicyclic macrocycle (G. R. Newkome, N. Majestic, F. Fronczek, J. L. Atwood, *J. Am. Chem. Soc.* **1979**, *101*, 1047), for which a structural determination yields an angle sum of 360° for the N center, is neither a trialkylamine nor can the NC_3 planarization be traced to sterical overcrowding.

[122] H. Bock, I. Göbel, W. Bensch, unpublished.

[123] J. Dunitz, lecture at the X. IUPAC Conference on Physical Organic Chemistry, Haifa, **1990**. Cf. also J. Dunitz, *X-Ray Analysis and the Structure of Organic Molecules*, Cornell Univ. Press, **1979**, p. 321 ff.

[124] See, for example, A. I. Kitaigorodsky, *Molecular Crystals and Molecules*, Academic Press, New York, **1973**, and references cited therein.

[125] See, for example, a) A. Gavezotti, *J. Am. Chem. Soc.* **1991**, *113*, 4622, and references cited therein.; b) J. K. Whitesell, R. E. Davis, L. S. Saunders, R. J. Wilson, J. P. Feagius, *J. Am. Chem. Soc.* **1991**, *113*, 3627; c) H. S. Rzepa, M. L. Webb, A. M. Z. Slavin, D. J. Williams, *J. Chem. Soc. Chem. Commun.* **1991**, 765; d) G. R. Desiraju, *Crystal Engineering, The Design of Organic Solids* (*Mater. Sci. Monogr.* **1989**, *54*).

[126] Cf. A. S. Ellabondy, C. J. Bender, J. Kim, D.-H. Shin, M. E. Kuchenmeister, G. T. Babcock, J. L. Dye, *J. Am. Chem. Soc.* **1991**, *113*, 2347, and references cited therein.

ANGEWANDTE CHEMIE

A Journal of the Gesellschaft Deutscher Chemiker

Reviews planned or recently published

The Enchanting Alkaloids of Yuzuriha
C.H. Heathcock

Transition Structures of Hydrocarbon Pericyclic Reactions
K.N. Houk, Y. Li, J. D. Evanseck

Natural Products as Probes of Cellular Function
S.L. Schreiber, M.K. Rosen

Synthetic Approaches towards Molecular and Polymeric Carbon
F. Diederich, Y. Rubin

Cubanes: Starting Materials for the 1990s and the New Century
P.E. Eaton

Optically Anomalous Crystals
B. Kahr, J.M. McBride

Chemistry and Biology of the Enediyne Anticancer Antibiotics
K.C. Nicolaou, W.M. Dai

Scanning Tunnel Microscopy and Atomic Force Microscopy in Organic Chemistry
J. Frommer

Synchotron X-Ray and Neutron Diffraction Studies in Solid-State Chemistry
A.K. Cheetham, A.P. Wilkinson

What subscribers and authors have to say about Angewandte Chemie:

Jean-Marie Lehn, Université Louis Pasteur, Strasbourg:

"I consider Angewandte Chemie as one of the top not only chemical but scientific journals... It presents the highly effective combination of well chosen, exciting and thorough review articles, reflecting timely topics that cover a very broad range in science, with short but informative communications reporting specific advances of particular interest for chemistry. It is also carefully produced and nicely presented, which adds to the reading pleasure."

VCH

Special Rate for ACS members: US$ 165.00
US$ 190.00 (air mail)*

To subscribe please call 1-800-422-8824

Annual subscription rate 1992 for institutions: US$ 581.00 (air mail)*

The Folding of Squalene; An Old Problem has New Results

By *Rolf Bohlmann**

The importance of steroids in reproduction[1] and sexual differentiation has been known since the sixties. Other classic applications of steroids in medical therapy include the corticoids as anti-inflammatory agents and steroidglycosides from Digitalis for the treatment of heart deficiencies. Synthetic organic chemistry received a strong push from the solution of the regio- and stereochemical questions raised by this class of compounds. The realization of the enantioselective total synthesis of several steroids on an industrial scale was a major milestone in steroid research,[1, 2] which may have falsely led many researchers to believe that this topic is now closed.

The previously mentioned effects of steroids are observed in nature and optimized in part by the results of biological and chemical research. This is not true for antihormones, which counteract the effects of hormones. Because this process is not observed in nature, no directed searches for antihormones were undertaken. Thus the discovery of the first highly active antiandrogens was purely serendipitous.[3]

Hormonal effects can be switched off by means other than through antihormones. The results of basic research on steroid biogenesis imply other methods.[4] The biogenesis of different hormones from cholesterol requires many reactions, which are catalyzed by a number of enzymes. When the exact sequence and the enzymes involved are known, one can prevent the biogenesis of a hormone by hindering a specific enzyme necessary for its synthesis.

A success in this sense[5] is the development of selective aromatase inhibitors,[6] which interfere with the formation of estrogen and thus reduce its effect. Examples of aromatase inhibitors in the development of the treatment of hormone-dependent tumors are the steroids formestane **1** and atamestane **2**,[7] as well as the non-steroid fadrozole **3**.

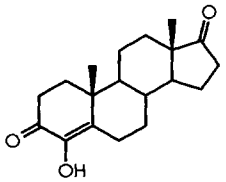

1

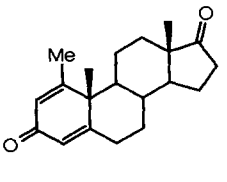

2

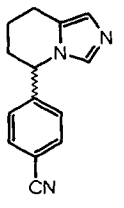

3

These examples show how important basic research is for the recognition of new applications. Despite the possible total syntheses of steroids and diverse partial syntheses, many questions remain unanswered. In this context the importance of several more recent reports regarding the biogenesis of steroids is apparent.

The most remarkable step in the biosynthesis of cholesterol is certainly the folding of squalene and the fourfold cyclization of 2,3-oxidosqualene (**4**) to lanosterol (**5**). This remarkable reaction is mediated by sterolcyclase in only one step (Scheme 1). The purification of this especially interesting enzyme was not achieved for a long time, because it is a membrane-bound system with low stability and solubility; however, Corey et al. recently succeeded in purifying the enzyme.[8] The key to success was the clever choice of an affinity matrix, which mimicked the hydrogen bonds and the hydrophobic frame of squalene.

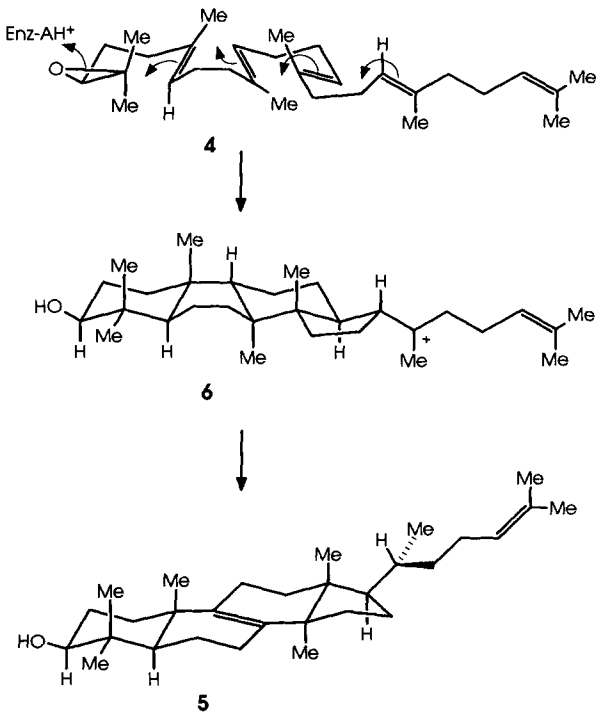

Scheme 1. Fourfold cyclization of oxidosqualene **4** to lanesterol (**5**).

The precleaned microsomes containing sterolcyclase were concentrated by chromatography on DEAE-sepharose and DEAE-cellulose, and the active fraction was subsequently purified on the affinity column. The isolated enzyme can be stored at 0 °C at least 14 days without loss of activity. Thus, the cloning of the sterolcyclase gene and eventually the solution of the structure of the enzyme should be possible.

As long as the three-dimensional structure of an enzyme is not known, its mode of action can be studied only by treating natural or synthetic model compounds with the enzyme preparations. Changes in constitution can be studied especially well with isotopically labeled compounds. Several research groups verified the constitutional correctness of the folding of squalene by experiments with variously labeled starting material. Therefore, it is quite surprising that in this well-known reaction the stereochemistry of the 17 and 18 positions is apparently understood correctly only now.

[*] Dr. R. Bohlmann
Institut für Arzneimittelchemie der Schering AG
Müllerstrasse 170-178, D-W-1000 Berlin 65 (FRG)

Cationic protosterol **6** derived from squalene has a side chain in the 17β position according to the latest investigations,[9] not an 17α side chain as all previous investigations assumed. This mistake made the stereochemistry of the neighboring C20 difficult to decipher. The erroneous configuration of this center would have required an unusually long 120° twist, instead of a shorter 60°, in the enzyme. In order to explain this inconsistency various hypthotheses were proposed employing "nonclassical" carbocations and so-called X groups on the enzyme.

Further support of the 17β stereochemistry in intermediate **7** of the sterol biogenesis is provided by the result of the incubation of the 20-oxa analogue **8** of 2,3-oxidosqualene.

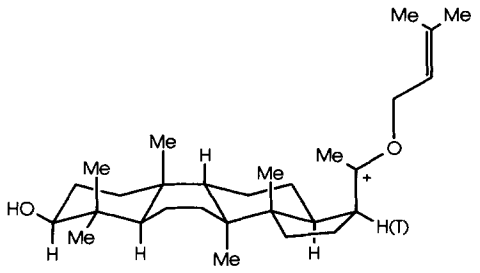

7

Surprisingly, the thermodynamically instable 17β-acetyl derivative **9** forms stereoselectively. Compound **9** can be converted via the 3-*tert*-butyldimethylsilyl ether to the more stable 17α isomer by heating with 1% sodium hydroxide solution at 50 °C for 2h. The 18-tritio derivative of compound **7** was also prepared and cyclized. As expected, the tritium was detected in the 17α position of the labeled **9**. The tritium was removed completely by the basic isomerization mentioned above.

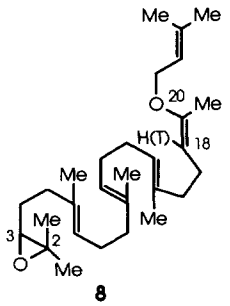

8

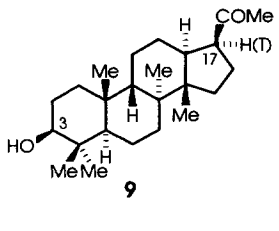

9

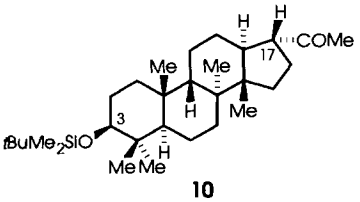

10

These results motivated new studies of the stereochemistry of the biotransformation of 20,21-dehydro-2,3-oxidosqualene (**11**).[11] These investigations showed that only the (18*E*) isomer **11** is converted by the purified enzyme into protostanediol **12**. The structure of this compound was determined from ^{1}H NMR spectra of a derivative.

Again the formation of the five-membered ring generates the 17β side chain. The regioselectivity of the hydroxylation displays a preference for C20. With reference to the (18*E*) double bond in 20,21-dehydro-2,3-oxidosqualene **11**, the new C–C and C–O bonds formed are *trans* diaxial.

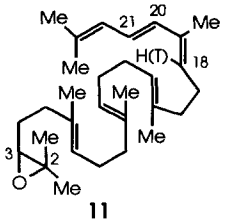

11

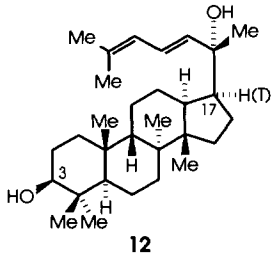

12

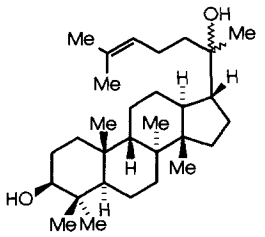

13

Insight into the complex mechanistic and stereochemical relationships of these reactions was made possible by elegant research in preparative organic chemistry. A new enantioselective total synthesis of protostendiol **13**[11] was developed for purposes of comparison. The enantioselective step is an aldol cyclization[12] of the triketone **14** in the presence of (*S*)-phenylalanine and (+)-camphor sulfonic acid. After a

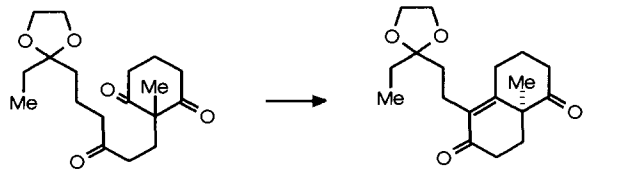

14 **15**

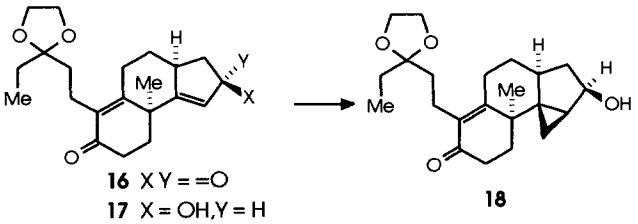

16 X Y = =O
17 X = OH, Y = H **18**

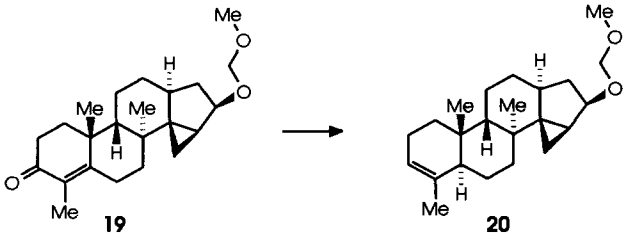

19 **20**

reaction time of 24 days at 23 °C endione was isolated in 77% yield and with 98% *ee*. Subsequent regio- and stereoselective annelation in three steps provided the tricyclic diendione **16**. One reaction in this sequence required one equivalant of mercuric chloride as a catalyst.

The molecule was elaborated further by a regio- and stereoselective reduction of enone **16** to the 16β alcohol **17**, in which the five-membered ring was set up for the introduction of the 14,15β methylene group in **18**. This group served as precursor for the 14β methyl group and also directed the introduction of the 17α side chain. In the last part of the synthesis starting from enone **19**, an allyl–diazene rearrangement[13] was used to establish the not easily accessible A/B-*trans* ring junction in **20**.

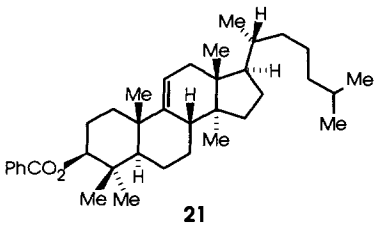

21

After a total of over 20 steps with an overall yield of less than 3% the synthesis was concluded by the conversion of **13** into dihydroparkeolbenzoate **21** and comparison with authentic material. This "success" is relative when one recalls that the natural biosynthesis of protostendiol **13** requires a single step. The simple replacement of hydrogen for a methyl group in oxidosqualene **4**, however, diverts the enzymatic pathway leading to the formation of a different product.[14]

The recent results cited here show how complex questions can be approached today by the complementary efforts in biochemistry, microbiology, molecular biology, and synthetic chemistry.

German version: *Angew. Chem.* **1992**, *104*, 596

CAS Registry number:
Squalene 111-02-4.

[1] R. Wiechert, *Angew. Chem.* **1977**, *89*, 513–520; *Angew. Chem. Int. Ed. Engl.* **1977**, *16*, 506–513.
[2] R. Wiechert, *Angew. Chem.* **1970**, *82*, 331–342; *Angew. Chem. Int. Ed. Engl.* **1970**, *9*, 321–332.
[3] U. Eder, G. Sauer, R. Wichert, *Angew. Chem.* **1971**, *83*, 492–493; *Angew. Chem. Int. Ed. Engl.* **1971**, *10*, 496–497.
[4] a) A. Eschenmoser, L. Ruzicka, O. Jeger, D. Arigoni, *Helv. Chim. Acta* **1955**, *38*, 1890–1904; b) D. M. Harrison, *Nat. Prod. Rep.* **1988**, *5*, 387–415.
[5] *Sterol Biosynthesis Inhibitors, Pharmaceutical and Agrochemical Aspects* (Eds.: D. Berg, M. Plempel), Ellis Horwood, Chichester, VCH, Weinheim, **1988**, p. 534.
[6] P. E. Loenning, D. C. Johannessen, *Drugs Today* **1991**, *27*(2), 117–132.
[7] a) U. Kerb, G. Sauer, R. Wiechert, D. Henderson, Y. Nishino, S. Beier, EP-B 0129500; Y. Nishio, M. R. Schneider, H. Michna, M. F. El Etreby, *J. Steroid Biochem.* **1989**, *34*, 435–437.
[8] E. J. Corey, S. P. T. Matsuda, *J. Am. Chem. Soc.* **1991**, *113*, 8172–8174.
[9] E. J. Corey, S. C. Virgil, *J. Am. Chem. Soc.* **1991**, *113*, 4025–4026.
[10] E. J. Corey, S. C. Virgil, S. Sarshar, *J. Am. Chem. Soc.* **1991**, *113*, 8171–8172.
[11] E. J. Corey, S. C. Virgil, *J. Am. Chem. Soc.* **1990**, *112*, 6429–6431.
[12] H. Hagiwara, H. Uda, *J. Org. Chem.* **1988**, *53*, 2308–2311.
[13] E. J. Corey, G. Wess, Y. B. Xiang, A. K. Singh, *J. Am. Chem. Soc.* **1987**, *109*, 4717–4718.
[14] E. J. Corey, S. C. Virgil, D. R. Liu, S. Sarshar, *J. Am. Chem. Soc.* **1992**, *114*, 1524–1525

Perlithiated and Hyperlithiated Methane

By *Adalbert Maercker**

In 1983 when Schleyer, Pople, et al.[1] prophesied the considerable stability of hexalithiomethane (CLi_6) on the basis of ab initio calculations, certainly no one expected that experimental proof of this hyperlithiated methane with a hexacoordinated carbon atom would follow only a few years later. But H. Kudo[2] at the Japan Atomic Energy Research Institute achieved just this! Because the calculations are only relevant for discrete molecules in the gas phase, it was logical to search for these molecules with mass spectrometry first. It was a long journey with many setbacks,[3] and even January 1990 the goal was still far off. The method of choice was Knudsen-effusion mass spectrometry, which was previously used to detect Li_4O and Li_5O.[4] Unfortunately, the changes in the original[3] apparatus leading to those successful experiments were not reported.

Crystalline dilithioacetylene (C_2Li_2) was heated to 1000 K in a molybdenum Knudsen cell with a radio-frequency generator. The resulting mixture of gases was introduced directly under high vacuum ($< 10^{-5}$ Pa) into a quadrupole mass spectrometer through a 0.3 mm wide orifice [Eq.(a)]. Besides

$$C_2Li_2(s) \xrightarrow{1000\,K} Li(g) + Li_2(g) + CLi_3(g) + CLi_4(g) + CLi_6(g) \qquad (a)$$

CLi_3 and CLi_4, which had already been identified (although curiously in the reverse order of intensity),[3] traces of CLi_6 were detected for the first time. Three signals in the intensity ratio of 0.1 : 0.5 : 1.0 were observed at m/z 52 ($[^{12}C^6Li_2{}^7Li_4]^+$ and $[^{13}C^6Li_3{}^7Li_3]^+$), m/z 53 ($[^{12}C^6Li^7Li_5]^+$ and $[^{13}C^6Li_2{}^7Li_4]^+$), and m/z 54 ($[^{12}C^7Li_6]^+$ and $[^{13}C^6Li^7Li_5]^+$).

These signals in the expected intensity ratio were not detected in the background spectrum or when the ionization energy was less than 9 eV (the optimal setting was 13.0 eV). The mass spectrum from the original report is shown in Figure 1.

The existence of CLi_6 is thus certain; however, the theoreticians still do not agree on the bonding relationships.[1, 5, 6] Schleyer et al.[1] as well as Reed and Weinhold[5]

[*] Prof. A. Maercker
Institut für Organische Chemie der Universität
Adolf-Reichwein-Strasse, D-W-5900 Siegen (FRG)

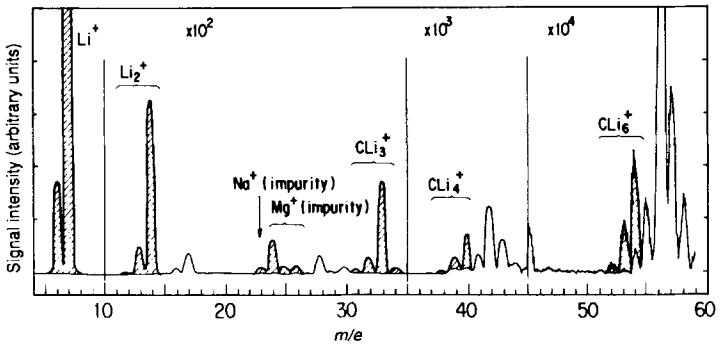

Fig. 1. Mass spectrum of the gas mixture formed from C_2Li_2(s) in a Knudsen cell at 1052 K. Shaded regions: molecular peaks; the thin line is the background spectrum.

doubt that the carbon atom is hypervalent, strictly speaking, and assign two of the total of ten valence electrons to Li–Li bonds which build a metal cage around the central atom. Ritchie[6] disregards these Li–Li bonds on the basis of Bader's electron density analysis, a method which provided rather curious results for other lithium compounds as well. Preparative organic chemists can most likely contribute little to the understanding of these findings. It should be mentioned that pentalithiomethane (CLi_5), also predicted by calculations to be very stable,[1] has not yet been found by Kudo.[2, 3] This neutral molecule should not be confused with the cation CLi_5^+, which Lagow[7] detected by mass spectrometry in 1982 from the flash vaporization of tetralithiomethane (CLi_4).

In contrast to the hyperlithiated methane CLi_6, perlithiated methane CLi_4 is accessible by synthesis; however, its preparation is by no means trivial. CLi_4 was first prepared, again in a Knudsen cell, from the cocondensation under vacuum of lithium vapor and tetrachloromethane on a cold-finger cooled with liquid nitrogen [Eq.(b)].[8] This technique although optimized still provides a maximum of 40% tetralithiomethane together with 58% $C_2Li_2$and traces of other compounds. Unfortunately, it has not yet been possible to separate the resulting mixtures of polylithiated hydrocarbons, and even the separation from the lithium matrix is difficult.[8]

$$CCl_4 + 8\,Li(g) \xrightarrow[-4\,LiCl]{750\,^\circ C} CLi_4 \xleftarrow[-4\,LiCl]{8\,t\text{BuLi/cyclopentane}} C(HgCl)_4 \qquad (b)$$

For the synthesis of larger amounts of tetralithiomethane there is currently no practical alternative to mercury–lithium exchange.[9] Tetralithiomethane is a gray, extremely pyrophoric solid. Because it is insoluble in hydrocarbons, it can be washed free of the excess *tert*-butyllithium and di-*tert*-butylmercury easily. The salt-free product can be obtained if one starts with tetrakis(ethylmercurio)methane; however, lithium chloride does not generally interfere with subsequent reactions.

Perlithiated hydrocarbons such as tetralithiomethane have been termed "lithiocarbons" in analogy to "hydrocarbons". Much more easily accessible than the perlithioalkanes are certain perlithioalkynes, since butyllithium can remove quantitatively not only the hydrogen atoms on sp-hybridized carbon atoms, but also those of the methyl group of propyne, for example [Eq.(c)].[10]

$$HC{\equiv}C{-}CH_3 \xrightarrow[hexane]{n\text{BuLi}} \underset{(75\%)}{C_3Li_4} \qquad (c)$$

C_5Li_4 can be synthesized analogously from 1,3-pentadiyne. Finally, the family of perlithiated hydrocarbons includes trivial compounds like dilithioacetylene (C_2Li_2) and dilithiodiacetylene (C_4Li_2) composed completely of sp-hybridized carbon atoms. Calculations have already been conducted for hexalithiobenzene (C_6Li_6),[11] and experimental evidence is eagerly awaited.

German version: *Angew. Chem.* **1992**, *104*, 598

CAS Registry numbers:
C_2Li_2, 1070-75-3; CLi_3, 70378-93-7; CLi_4, 38827-79-1; CLi_6, 91992-21-1.

[1] P. von R. Schleyer, E.-U. Würthwein, E. Kaufmann, T. Clark, J. A. Pople, *J. Am. Chem. Soc.* **1983**, *105*, 5930–5932.
[2] H. Kudo, *Nature*, **1992**, *355*, 432–434.
[3] H. Kudo, *Chem. Lett.* **1989**, 1611–1614; H. Kudo, personal communication from January 16, 1990.
[4] C. H. Wu, *Chem. Phys. Lett.* **1989**, *139*, 357–359.
[5] A. E. Reed, F. Weinhold, *J. Am. Chem. Soc.* **1985**, *107*, 1919–1921.
[6] J. P. Ritchie, S. M. Bachrach, *J. Am. Chem. Soc.* **1987**, *109*, 5909–5916.
[7] E. D. Jemmis, J. Chandrasekhar, E.-U. Würthwein, P. von R. Schleyer, J. W. Chinn, Jr., F. J. Landro, R. J. Lagow, B. Luke, J. A. Pople, *J. Am. Chem. Soc.* **1982**, *104*, 4275–4276; J. W. Chinn, Jr., R. J. Lagow, *ibid.* **1984**, *106*, 3694–3695.
[8] C. Chung, R. J. Lagow, *J. Chem. Soc. Chem. Commun.* **1972**, 1078–1079; F. J. Landro, J. A. Gurak, J. W. Chinn, Jr., R. J. Lagow, *J. Organomet. Chem.* **1983**, *249*, 1–9.
[9] A. Maercker, M. Theis, *Angew. Chem.* **1984**, *96*, 990–991; *Angew. Chem. Int. Ed. Engl.* **1984**, *23*, 995–996; A. Maercker, M. Theis, *Organomet. Synth.* **1986**, *3*, 398–400; Review: A. Maercker, M. Theis, *Top. Curr. Chem.* **1987**, *138*, 1–61.
[10] Review: R. West, *Adv. Chem. Ser.* **1974**, *130*, 211-221.
[11] Y. Xie, H. F. Schaefer III, *Chem. Phys. Lett.* **1991**, *179*, 563–567.

Model Compounds for Metal Oxides on SiO_2 Surfaces

By *Frank T. Edelmann**

Numerous important processes in the petrochemical industry are catalyzed by metal oxides immobilized on SiO_2 supports.[1] Highly selective catalysts of this type play a significant role in the oxidation of hydrocarbons[2] and the oxidative coupling of methane,[3] as well as in the metathesis[4] and polymerization[5] of olefins and alkynes. Despite highly refined methods of analysis, mechanistic studies and structural investigations of immobilized compounds are still extremely difficult. The exact nature of the SiO_2 surfaces themselves is often a subject of controversy.[6] Thus, much current research is concerned with the synthesis and characterization of compounds which may model the specific surface morphologies of SiO_2 supports and their interactions with metal oxides on the molecular level.

One compound that is much better suited for modeling the SiO_2 surface than Me_3SiOH or Ph_3SiOH, trisilanol **1**, was prepared by Feher et al.[7] Compound **1** is formed in the kinetically controlled hydrolysis of cyclohexyltrichlorosilane [Eq.(a)]. Under the specified reaction conditions, complete

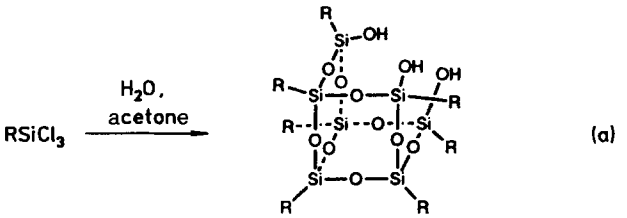

hydrolysis of $c\text{-}C_6H_{11}Si(OH)_3$ requires about three years! However, preparatively useful quantities of **1** can be "harvested" after only a few weeks.[7] The comparison of the molecular structure of **1** (**A**) with the (111) octahedral face of the cristobalite modification of SiO_2 (**B**) reveals an astonishing geometrical relationship. Common to both structural units is a concave silicon–oxygen cavity, whose outer rim is formed by six silicon and six oxygen atoms. The arrangement of potential O-donor centers is also quite similar.

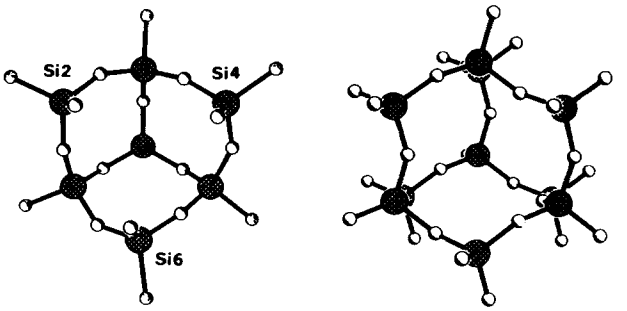

[*] Dr. F. T. Edelmann
Institut für Anorganische Chemie der Universität
Tammannstrasse 4, D-W-3400 Göttingen (FRG)

*P*olyhedral *oligom*etalla*ses*qui*s*iloxanes (POMSS) are accessible by the reaction of **1** with suitable metal compounds. For example a typical POMSS, **2**, is formed in the reaction of **1** with $[(n\text{PrO})_3\text{VO}]$, $[(Me_3SiCH_2)_3VO]$, or $VOCl_3$.[9] A monomer/dimer equilibrium between **2** and **3** exists in solution [Eq.(b)]. Compound **2** can realistically be considered a

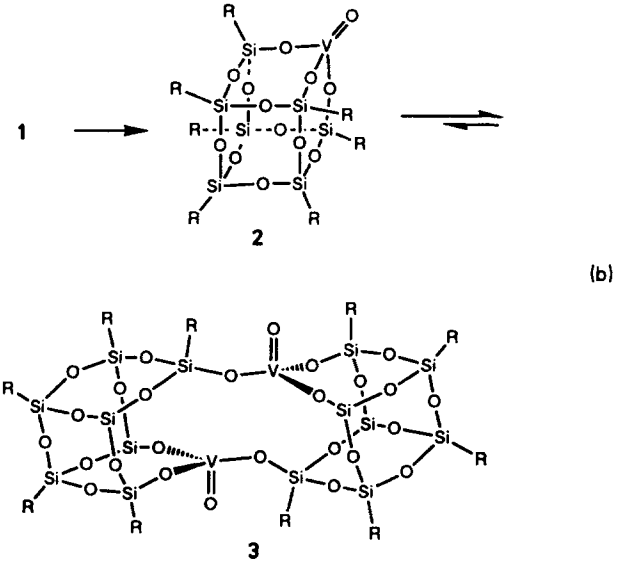

model for a vanadium-containing heterogeneous catalysts, since it is capable of polymerizing ethylene and 1,3-butadiene. In contrast, the comparable vanadiumsiloxide $[(Ph_3SiO)_3VO]$ is inactive under identical reaction conditions!

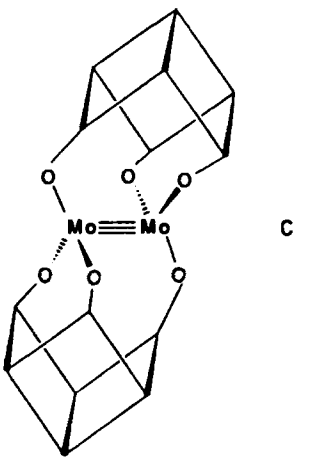

Only a few of the wealth of results are highlighted here. Parts of zeolite structures[10] as well as the silylation of silica[11] can also be modeled by **1**. The reaction of $[Mo_2(O\text{t}Bu)_6]$ with two equivalents of **1** in the absence of Lewis base results in the cleavage of all the O*t*Bu ligands and formation of the dinuclear complex **4**; the central Mo–Si

framework of **4** is shown in **C**. Here an intact Mo≡Mo unit is fixed to both SiO ligands.[12]

$[Mo_2\{(c\text{-}C_6H_{11})_7Si_7O_{12}\}_2]$ **4**

Feher's trisilanol **1** is formally a heptameric condensation product of $c\text{-}C_6H_{11}Si(OH)_3$. The direct synthesis of a model compound for metal oxides on SiO_2 surfaces from a stable silantriol was first described by Roesky et al.[13] Controlled hydrolysis of tBuSiCl$_3$ in the presence of aniline furnishes tBuSi(OH)$_3$, which does not undergo condensation, in 94% yield. Undulating layers are found in the crystal in which the silantriol units are interconnected by hydrogen bonds. tBuSi(OH)$_3$ reacts with Re_2O_7 in a molar ratio of 1:1 with condensation and substitution giving rise to the tetranuclear rhenium siloxide shown in Figure 1.

$$4\ t\text{BuSi(OH)}_3 + 4\ Re_2O_7 \longrightarrow [\{t\text{BuSiO(ReO}_4)\}_4] + 2\ Re_2O_7 \cdot H_2O + 4\ H_2O \quad (c)$$

Compound **5** is the first well-defined, structurally characterized transition-metal complex synthesized from a silantriol. Its synthesis demonstrates a new approach to preparing soluble, metal-containing silicates.

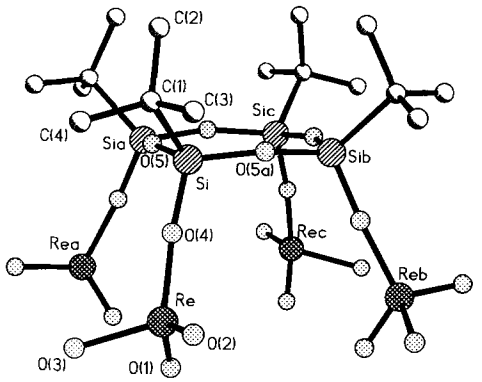

Fig. 1. Structure of **5** in the crystal.

Even the smallest of these model compounds can be considered a true highlight. Until recently metal complexes with SiO ligands were completely unknown.[14] Complexes of type $[M(SiO)L_n]$ could not be detected in matrix studies, much less be isolated.[15] A significant step in the direction towards Si analogues of metal carbonyls was achieved by Schnöckel et al. with their IR spectroscopic proof of [PdSiO] (**6**).[16] This complex is formed when SiO and palladium atoms are deposited simultaneously on a helium-cooled copper surface. According to the spectroscopic data, **6** has a linear, Si-bridged structure. The absorption band of the SiO stretching vibration is at 1246.3 cm^{-1}. The experimental and theoretical results show that the bonding relationships in **6** are comparable to those in [PdCO], that is, that in SiO ligands the σ-donor bond is also reinforced by π-acceptor contributions.

German version: *Angew. Chem.* **1992**, *104*, 600

[1] Y. I. Yermakov, B. N. Kuznetsov, V. A. Zakharov, *Catalysis by Supported Complexes*, Elsevier, New York, **1981**; b) *New Horizons in Catalysis* (Eds.: T. Setyama, K. Tanabe), Elsevier, New York, **1980**; c) F. R. Hartley, *Supported Metal Complexes*, Reidel, Boston, **1985**; d) *Tailored Metal Catalysis* (Ed.: Y. Iwasawa), Reidel, Boston, **1986**.

[2] G. I. Golodets, *Heterogeneous Catalytic Reactions Involving Molecular Oxygen*, Elsevier, New York, **1983**.

[3] a) J. A. Sofranko, J. J. Leonhard, C. A. Jones, *J. Catal.* **1987**, *103*, 302; b) C. A. Jones, J. J. Leonhard, J. A. Sofranko, *ibid.* **1987**, *103*, 311; c) K. J. Zhen, M. M. Khan, C. H. Mak, K. B. Lewis, G. A. Somorjai, *ibid.* **1985**, *94*, 501; d) M. M. Khan, G. A. Somorjai, *ibid.* **1985**, *91*, 263.

[4] a) V. Dragutan, A. T. Balkaban, M. Dimonie, *Olefin Metathesis and Ring Opening Polymerizations of Cycloolefins*, Academic Press, New York, **1986**; b) K. J. Ivin, *Olefin Metathesis*, Academic Press, New York, **1986**.

[5] a) H. Sinn, W. Kaminsky, *Adv. Organomet. Chem.* **1980**, *18*, 99; b) M. P. McDaniel, *Adv. Catal.* **1985**, *33*, 47.

[6] *Kirk-Othmer Encyclopedia of Chemical Technology*, (Eds.: M. Grayson, D. Eckroth), 2nd ed., Wiley, New York, **1978**, p. 397–400, and literature cited therein.

[7] F. J. Feher, D. A. Newman, J. F. Walzer, *J. Am. Chem. Soc.* **1989**, *111*, 1741.

[8] K. Kihara, *Z. Kristallogr.* **1978**, *148*, 237.

[9] F. J. Feher, J. F. Walzer, R. L. Blanski, *J. Am. Chem. Soc.* **1991**, *113*, 3618.

[10] J. J. Feher, K. J. Weller, *Organometallics* **1990**, *9*, 2638.

[11] F. Feher, D. A. Newman, *J. Am. Chem. Soc.* **1990**, *112*, 1931.

[12] T. A. Budzichowski, S. T. Chacon, M. H. Chisholm, F. J. Feher, W. Streib, *J. Am. Chem. Soc.* **1991**, *113*, 688.

[13] N. Winkhofer, H. W. Roesky, M. Noltemeyer, W. T. Robinson, *Angew. Chem.* **1992**, *104*, 670; *Angew. Chem. Int. Ed. Engl.* **1992**, *31*, 599.

[14] H. Werner, *Angew. Chem.* **1990**, *102*, 1109; *Angew. Chem. Int. Ed. Engl.* **1990**, *29*, 1077.

[15] a) J. S. Anderson, J. S. Ogden, *J. Chem. Phys.* **1969**, *51*, 4189; b) M. Auwärter, *Angew. Chem.* **1975**, *87*, 227; *Angew. Chem. Int. Ed. Engl.* **1975**, *14*, 207.

[16] T. Mehner, R. Köppe, H. Schnöckel, *Angew. Chem.* **1992**, *104*, 653, *Angew. Chem. Int. Ed. Engl.* **1992**, *31*, 638.

The Epidemic Spread of Fullerene Research**

By *Tibor Braun**

A recent review in this journal[1] has motivated me to share the results of our studies which examine fullerene research from a different angle.

In general the spread of new achievements in science follows a rule according to which the number of researchers attracted by the new achievement is graphically represented by an S-shaped curve.[2] At the start, diffusion of the basic idea is rather slow. After a while, a steep increase follows, and finally the "saturation" point is reached when the rate of diffusion slows down. The growth process has been described by Goffman[3,4] who modeled the transmission of ideas as an epidemic process. In general, the "epidemic" process in a medical sense is based on the conversion of a susceptible state to an infective one whereby the transition is caused by exposure to some infectious material. The process is relevant not only to infectious disease but can be generalized for many situations. All that is needed is the appropriate interpretation of the components of the process, that is, susceptible, infective, and removed populations, infectious material, intermediary host, latency period, disease, etc. People are susceptible to certain ideas and resistant to others. Once individuals are "infected" with an idea the chances are good that they may infect others after some period of time. Such a process can result in an intellectual "epidemic" (Table 1).[3] We considered the recent discovery[5,6] and outbreak of research on fullerenes a topical example of an intellectual epidemic.

Table 1. The epidemic model according to Goffman et al. [3].

Components of the epidemic process	Epidemic disease	Intellectual epidemic
Agent	Infectious material (bacteria, virus)	Idea
Infective population	Ill people	Authors of papers
Susceptible population	People who may be infected given effective contact with the infectious material	Readers of papers who may be infected given effective contact with the idea
Removal	Immunity or death	Loss of interest or death

A database on the fullerene papers published between 1980 and 1991 has been compiled using the CD-ROM version of the Science Citation Index. The compiled database is restrictive, since it includes only papers published in refereed journals. A statistical evaluation of the database was then conducted. As evident from Figure 1, the increase in the number of publication on fullerenes has been really spectacular. In Tables 2–5 the distribution of fullerene papers according to countries, institutions, authors, and journals is given.

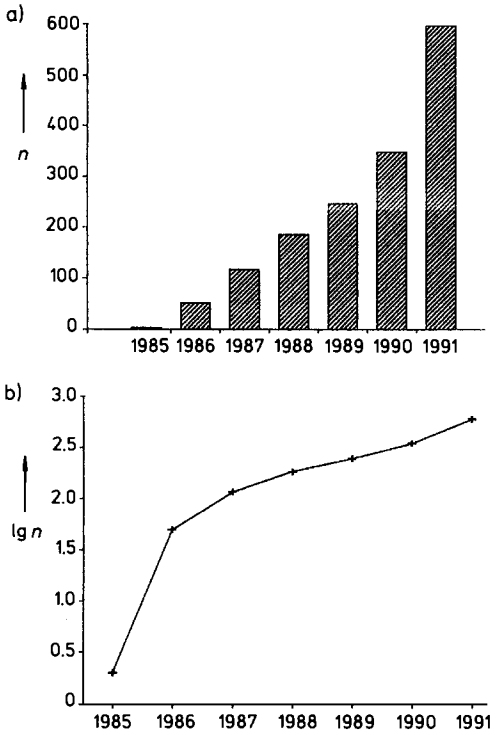

Fig. 1. Increase in the number of publications on fullerene research since 1985. a) Linear scale, b) logarithmic scale.

As expected, the USA is way ahead of the pack in the fullerene publication race with the UK, Germany, Japan, France, and Sweden in the next positions. As is often the case in basic research, most of the fullerene research has been done at universities, but as Table 3 indicates industrial re-

Table 2. Competition in fullerene research according to country.

Country [a]	No. of papers	Country [a]	No. of papers
USA	484	Netherlands	6
England	68	Czechoslovakia	6
Federal Republic of Germany	46	Israel	6
Japan	36	Norway	5
France	17	Australia	4
Sweden	15	Belgium	4
USSR	9	Austria	4
Switzerland	9	Hungary	<4
Italy	8	Poland	<4
Yugoslavia	8	Romania	<4
Wales	8	Peoples' Republic of China	<4
German Democratic Republic	7	Denmark	<4
Canada	6	Scotland	<4

[a] The key terms used by SCI for countries do not reflect the political changes of the last few years.

[*] Prof. T. Braun
Department of Inorganic and Analytical Chemistry
L. Eötvös University, P.O. Box 123
H-1443 Budapest (Hungary)

[**] The author would like to emphasize that the data in this letter is based on and extracted from a database which is not a comprehensive bibliography of the fullerene literature. The database does include most of the research articles on this topic published in refereed journals. Editorial note: Confirmation of the data presented in the tables with two research groups active in the fullerene area revealed that the collated numbers are conservative. In any case, the trend indicated is certainly correct.

Table 3. Institutions leading in fullerene research.

Institution	No. of papers	Institution	No. of papers
AT & T Bell Laboratories	37	Sandia National Laboratories	8
Rice University	37	University of Arizona	8
University of California, Los Angeles	25	Hokkaido University	7
		University of Exeter	7
University of Sussex	20	Czechoslovak Academy of Sciences	6
Exxon Research & Engineering Corp.	14	Dupont Co.	6
IBM Corp., Almaden	12	University of California, Los Alamos Natl. Lab.	6
University of California, Berkeley	10	University of Sheffield	5
Chalmers University of Technology	9	University of Trondheim	5
University of California, Santa Barbara	9		

search laboratories are quite well represented. The "high flyers" among the authors are, of course, the discoverers of the fullerenes; however, the competition is not far behind (Table 4).

Table 4. Leading authors in fullerene research.

Author	No. of papers	Author	No. of papers
Kroto, H. W.	39	McElvany, S. W.	12
Smalley, R. E.	39	Chibante, C. P. F.	12
Haddon, R. C.	20	Rosen, A.	11
Diederich, F.	19	Osawa, E.	10
Curl, R. F.	19	Krätschmer, W.	10
Slanina, Z.	18	Rudzinski, J. M.	9
Heath, J. R.	18	Harter, W. G.	7
Whetten, R. L.	15	Wang, Y.	6
Fowler, P. W.	14	Wastberg, B.	6
Rubin, I.	13	Weeks, D. E.	6
Bethune, D. S.	13	Brendsdal, E.	6
Huffman, D. R.	13	Creasy, W. R.	6
Meijer, G.	12		

The first two papers on the most important advances in fullerene research were published in *Nature*. At the moment, however, the most important channels of publication are four chemistry journals (Table 5). The interdisciplinarity of the topic is nicely illustrated by the listings for the journals *Zeitschrift für Physik, Astronomy and Astrophysics, Computers and Mathematics,* and *Journal of Materials Research.*

In the epidemic model of scientific communication in the field of fullerene research, we have considered all researchers having the background necessary for becoming involved in this topic as susceptibles. In our database individuals are categorized as infectives the year their first paper is published. The total population of fullerene authors represents the infective population.

The Goffman model treats the epidemic process with a system of differential equations which describe the rates of change of the number of susceptible, infective, and removed individuals. Both stochastic and deterministic versions of the model have been discussed. Here we present a simplified

Table 5. The most important channels of publication for articles on fullerene research.

Journal	No of papers
Chemical Physics Letters	76
Journal of Chemical Physics	50
Journal of the American Chemical Society	37
Nature	37
Science	27
Journal of Physical Chemistry	26
Zeitschrift für Physik D	16
Astrophysical Journal	14
Journal of the Chemical Society	14
Chemical and Engineering News	9
Physical Review Letters	8
THEOCHEM	8
International Journal of Quantum Research	8
Thermochimica Acta	7
Astronomy and Astrophysics	6
International Journal of Mass Spectrometry	6
Journal of Chemical Education	6
Theoretica Chimica Acta	5
Angewandte Chemie International Edition in English	4
Chemical Reviews	4
Computers and Mathematics	4
Journal of Materials Research	4
Accounts of Chemical Research	3

graphical version of the model by showing the change in the number of fullerenes authors (infectives) versus time. Figure 2 shows the corresponding curve (dI/dt vs. t). An epidemic growth is evident beginning in 1990.

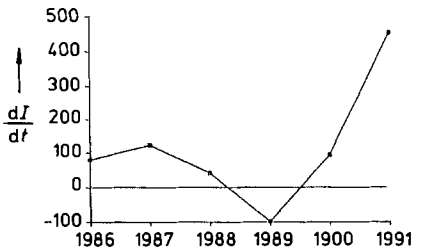

Fig. 2. Yearly increase in the the number of authors I in fullerene research.

A more complicated question to answer is who may be considered the true instigator of this epidemic. Although there was a synergetic aspect to the research beginning with the original discovery in 1985[5] and the many studies which followed, the real outbreak of the epidemic can be related to the publication of the paper on solid C_{60} by Krätschmer, Huffman, et al.[6]

Received: March 21, 1992
German version: *Angew. Chem.* **1992**, *104*, 602

[1] H. W. Kroto, *Angew. Chem.* **1992**, *104*, 113; *Angew. Chem. Int. Ed. Engl.* **1992**, *31*, 111.
[2] T. Braun, E. Bujdosó, A. Schubert, *The Literature of Analytical Chemistry: A Scientometric Evaluation*, CRC Press, Boca Raton, FL, USA, **1987**.
[3] W. Goffman, V. A. Nevil, *Nature* **1964**, *204*, 225.
[4] W. Goffman, *Nature* **1966**, *210*, 786.
[5] H. W. Kroto, J. R. Heath, S. C. O'Brien, R. F. Curl, R. E. Smalley, *Nature* **1985**, *318*, 162.
[6] W. Krätschmer, L. D. Lamb, K. Fostiropoulos, D. R. Huffman, *Nature* **1990**, *347*, 354.

Communications may be submitted in English *or* in German. Further details regarding the submission of communications can be found in the "Notice to Authors" reproduced in the January issue of the journal. Copies thereof may be obtained from the editorial office upon request.

Tetraferrioazaallenium—Product of a Novel Reaction of Coordinated CN^-**

By *Wolf Peter Fehlhammer* Andreas Schröder, Joachim Fuchs,* and *Ernst-Ulrich Würthwein*

Dedicated to Professor Wolfgang Beck on the occasion of his 60th birthday

The mobility of the cyano ligand in the dinuclear complex anion $[Fe_2(CN)Cp_2(CO)_3]^-$ opens up new possiblities for its chemistry.[1] For the first time reactions can also occur at the bridging position in which the *N*-nucleophilicity of the primary terminal CN^- is drastically increased. Herein we report the aprotic cleavage of the CN triple bond with dicarboxylic acid chlorides under very mild conditions and the fixation of the resulting μ-carbidoiron fragment to a second cyanodiiron complex anion.

The alkylation and protonation of the terminal CN ligand of $[Fe_2(CN)Cp_2(CO)_3]^-$ led directly to *bridging* aminocarbyne ligands (CNR_2 and CNH_2, respectively); a monoalkylation to give the isocyanide was achieved only with bulky alkyl groups, a monoprotonation to give CNH was unsuccessful.[2a] On the other hand, even with excess acylation agent only μ-(*mono*acyl)isocyanide complexes of the type **1** were obtained,[2b] and the reaction with succinyl dichloride, in which the formation of the *di*acylaminocarbyne cation **2** should be entropically favored, yielded mainly the tetranuclear complex **3**, that is, the acylation of two cyano complex anions was favored. Oxalyl chloride, for which an intramolecular diacylation is not possible, reacted analogously to give **4**.

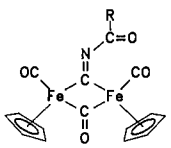

1

[Fe]=Fe(Cp)CO

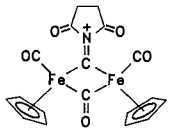

2

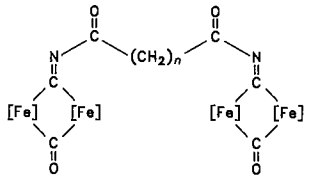

3 $n=2$
4 $n=0$

During the synthesis of **3** (*Experimental Procedure*) a small quantity of red crystals precipitated from the reaction solution, to which we initially attributed no significance. However, the saltlike product showed an IR spectrum with unusually few bands, reminiscent of the parent carbonyl compound $[\{FeCp(CO)_2\}_2]$, and a strikingly low nitrogen content; according to the ^1H NMR spectrum, apart from cyclopentadienyl no further organic ligands are present. Later this product proved to be identical with **5a**, the major product from the reaction of $Na[Fe_2(CN)Cp_2(CO)_3]$ with phthaloyl dichloride, which follows a completely unexpected course.

From the stable red substance **5a**, which crystallizes readily in 59% yield, the salts **5b** (anion = BF_4), **5c** (PF_6), **5d** (ClO_4), **5e** (BPh_4) can be prepared by anion exchange. The analyses of the salts gave nitrogen contents which were in agreement with only ca. 1/2 N atom per $Fe_2Cp_2(CO)_3$ unit. Together with the molecular mass of the cation determined by positive ion FAB mass spectrometry, this suggested the formulation of a CNC-bridged tetranuclear complex. We have now analyzed the often observed white growths from the red crystals and identified them as sodium phthalimide, which is plausible both chemically and from the balanced equation [see Eq. (1)].

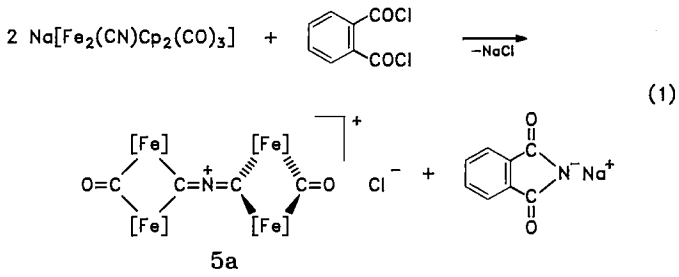

5a

(1)

In order to assign the IR bands ^{13}C-labeled $[Fe_2(^{13}CN)Cp_2(CO)_3]^-$ was treated with phthaloyl chloride, and by the subsequent Cl/BPh_4 exchange converted into $[^{13}C]$ **5e**,

$[Cp_2(OC)_3Fe_2(^{13}CN^{13}C)Fe_2Cp_2(CO)_3]BPh_4$ $[^{13}C]$ **5e**

whose IR band at 1741 cm^{-1} shows the largest bathochromic shift ($-22\ cm^{-1}$) and thus indicates a high ν_{as}(CNC) contribution. Two singlets each for the Cp ligands in the ^1H and ^{13}C NMR spectra and two ^{13}C resonance signals of the terminal CO ligands seem at first glance to be more indicative of a bent azaallyl unit with *exo* and *endo* Fe centers than of a linear azaallenium structure with equivalent iron atoms. However, from the X-ray structure analysis of **5e**[3] the latter is seen to be the case. Figure 1 (top) shows the crystal structure of the cation of **5e**; in Figure 1 (bottom) a space-filling model of **5e** is shown. The cation is constructed from two *cis* configurated $Fe_2Cp_2(\mu\text{-}CO)(CO)_2$ units bonded through an almost linear ($\sphericalangle$ C7–N–C8 = 172.3(9)°) CNC bridge. Further clear evidence for a formulation as a tetraferrioazaallenium ion comes from the identical C7–N (1.24(1) Å) and C8–N (1.24(1) Å) distances, which are typical for CN double bonds, as well as from the angle of 87.1(1)° between the Fe1Fe2C7N and Fe3Fe4C8N planes. The

[*] Prof. Dr. W. P. Fehlhammer, Prof. Dr. J. Fuchs, Dr. A. Schröder
Institut für Anorganische und Analytische Chemie der Freien Universität
Fabeckstrasse 34–36, D-W-1000 Berlin 33 (FRG)
Prof. Dr. E.-U. Würthwein
Institut für Organische Chemie der Universität
Orléans-Ring 23, D-W-4400 Münster (FRG)

[**] This work was supported by the Fonds der Chemischen Industrie and the Bundesminister für Bildung und Wissenschaft within the framework of research area "Synthese und Strukturauflärung niedermolekularer Verbindungen". We thank Prof. H. Kaesz for valuable suggestions.

angle is halved by the C_2 axis through the N atom—the only (although not crystallographic) symmetry element of the axially chiral cation, which thus possesses *two* sets of equivalent Cp and terminal CO ligands. This structure is obviously retained in solution and is also in agreement with the previously discussed results from NMR spectroscopy.

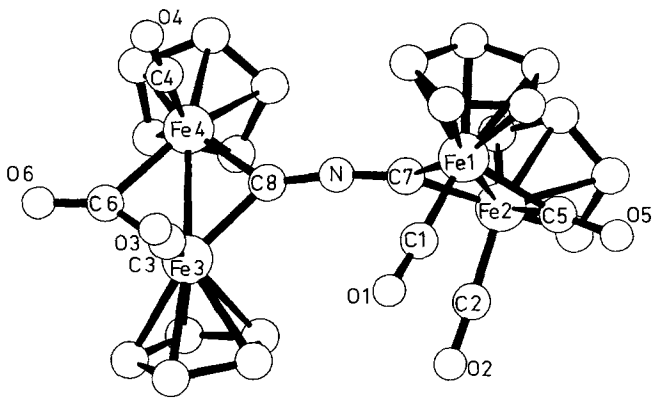

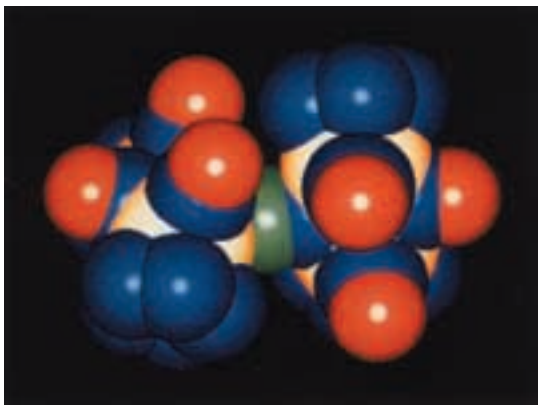

Fig. 1. Top: crystal structure of **5e** (SCHAKAL). Selected distances [Å] and angles [°]: Fe1-Fe2 2.529(4), Fe3-Fe4 2.529(4), Fe1-C7 1.900(8), Fe2-C7 1.851(9), Fe3-C8 1.916(9), Fe4-C8 1.912(10), C7-N 1.24(1), C8-N 1.24(1); C7-N-C8 172.3(9). Torsion angles [°]: Fe1Fe2C5/Fe1Fe2C7 161.9, Fe3Fe4C6/Fe3Fe4C8 166.9, Fe1Fe2C7N/Fe3Fe4C8N 87.1.
Bottom: space-filling model of **5e**. Color code: Fe (yellow), C (blue), O (red), and N (green).

Linear azaallenium ions are found both in purely organic salts such as **6**,[4a] and also in mono- and dinuclear organometallic complexes such as $[Cr(CO)_5C{=}N{=}CtBu_2]X$ ($\sphericalangle$ CNC = 171.7(4)°[5]), and **7** ($\sphericalangle$ CNC = 172.9(4)°),[6] respectively. Also calculations on the corresponding tetralithi-

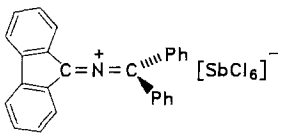

6

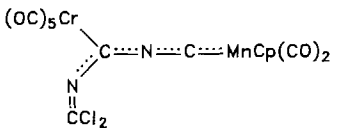

7

ated model compounds demonstrated that the cumulene form $Li_2C{=}N{=}Li_2^+$ with D_{2d} symmetry was lowest in energy. It shows almost the same C=N bond lengths (1.236 Å) as **5e**.[7] The same is true for the C=N bond lengths calculated by ab initio 6-31G* geometry optimization[8] in the parent compound 2-azaallenium $H_2C{=}N{=}CH_2^+$ (D_{2d}, 1.237 Å[9]), which are significantly shorter than those in the arene-substituted derivative **6** (1.27–1.28(1) Å[4a]). The continual preference for the cumulene over the tautomeric bent 2-azaallylium form as well as the agreement of the measured and calculated C=N bond lengths in the given examples show that substituents of metal complex fragments have no special structure-determining influence on the C=N=C framework. In contrast to this, lone pair donor substituents (-OR, $-NR_2$) result in marked C=N bond lengthening and bending at the N atom.[4b]

For the mechanism of formation of **5**, the only notable comment that can be made at this time is that the CN bond even in *mono*acylisocyanide bridges is greatly extended[10] ($[Fe_2Cp_2(\mu\text{-}CNCOC_6F_5)(CO)_3]$: C–N = 1.261(6) Å,[2b] $[Fe_2Cp_2\{\mu\text{-}CNC(O)SEt\}(CO)_3]$: C–N = 1.24(1) Å[11]), and consequently the most likely event upon *di*acylation is a CN bond cleavage. However, since there is no evidence at all for the existence of *N-di*acylated cyano bridges, we favor a reaction pathway via the bis(μ-acylisocyanide diiron) complex **8**.[12]

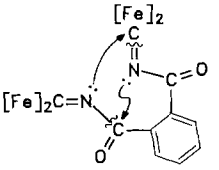

8

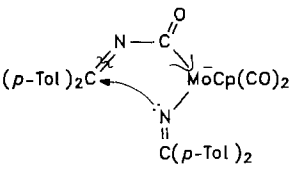

9

A similar mechanism was formulated for the distantly related azaallenium formation from a ketimide and $[Mo(Cl)Cp(CO)_3]$, in which the latter plays the role of phthaloyl dichloride. CN bond cleavage and new linkage probably take place in this mechanism in a 2:1 (ketimide/Lewis acid) adduct **9** with the variation that the heterocumulene remains π bonded in the complex assembly and the formally triply negatively charged N atom is again found in the cyanate byproduct.[13] Finally a 2:1 (*N*-acylaldimine/Et^+) intermediate analogous to **8** was proposed for the alkylation of *N*-benzylidene carboxamides, which leads to higher and lower oxidized 2-azaallenium salts by a formal disproportionation.[14]

Furthermore, interesting parallels can be drawn between [Eq. (1)] and the transformations of CO in clusters as well as on surfaces. These reactions, studied particularly in connection with the Fischer–Tropsch synthesis, are also characterized by a primary (e.g. acyl-supported (!)[15, 16]) C≡O bond cleavage, which however generally leads to *isolable* μ-carbido complexes.[17] However, reaction sequences of the form schematically summarized in Equation (2) occur whose formal similarity with the reaction sequence discussed here [Eq. (3)] is very surprising.[18]

$$[M_x]CO \rightarrow [M_x]\,C \xrightarrow{CO} [M_x]CCO \qquad (2)$$

$$[Fe_2]CN\{\rightarrow [Fe_2]C\} \xrightarrow{NC[Fe_2]} [Fe_2]CNC[Fe_2] \qquad (3)$$

Experimental Procedure

3 (**5a**): To $Na[Fe_2(CN)Cp_2(CO)_3]$ (1.00 g, 1.80 mmol)[1] in THF (40 mL) at −60 °C was added succinyl dichloride (140 mg, 0.90 mmol). The green solution changed immediately to red. Within 3 h a small amount of a bright red precipitate was formed, which was collected on a cooled frit (−30 °C) and dried under vacuum. This substance was identical with **5a** (see below). The filtrate was concentrated to dryness, and the residue was first precipitated from THF/ether, then recrystallized from a concentrated THF solution at −78°. This resulted in

a dark red powder (260 mg, 37%; m.p. 176–180 °C), which from analysis contained 2 mol THF. IR(KBr): $\tilde{\nu}$ [cm^{-1}] = 1989 vs, 1966 s, (ν($CO_{term.}$)), 1802 vs, br (ν($CO_{bridging}$)), 1727 s (ν(C=O)), 1685 s, br (ν(CN)); MS (80 eV, inlet temperature 150 °C): *m/z* 788 (5%) [M^+], 760(4), 732(2), 704(3) [$M^+ - n$CO, n = 1–3], 436(8), 408(4), 380(11) [$Fe_2Cp_2(CO)_nCNR^+$, n = 3–1], 268(12) [$Fe_2Cp_2CN^+$], 242(33) [$Fe_2Cp_2^+$], 186(100) [$FeCp_2^+$].

5a: A vigorously stirred solution of Na[$Fe_2(CN)Cp_2(CO)_3$] (1.00 g, 1.80 mmol) in THF (40 mL) was treated with phthaloyl dichloride (185 mg, 0.90 mmol) in THF (10 mL) at −60 °C. Within a few minutes the solution changed from green to dark red and was then allowed to warm to room temperature. The mixture was stirred for 4 h, the solvent then removed under vacuum, and the residue taken up in acetone and filtered. By the addition of a little ether an off-white product settled out initially. It was identified as sodium phthalimide by comparison with an authentic sample. Further addition of ether led to the precipitation of dark red **5a** (770 mg, 59% yield; m.p. 210 °(decomp.)), which was recrystallized from acetone/*n*-hexane. IR(THF): $\tilde{\nu}$ [cm^{-1}] = 2001 vs, 1964 s (ν($CO_{term.}$)), 1826 s (ν($CO_{bridging}$)), 1777 vs, br (ν(C=N=C)); ^{1}H NMR (270 MHz, CD_3OD, 25 °C): δ = 5.52, 5.25 (both s; Cp); positive-ion FAB-MS (DMSO/glycine/xenon/5 × 10^{-5} Torr): *m/z* 690 (19%) [M^+], 662(6), 634(29), 606(9), 578(11), 550(17), 522(8) [$M^+ - n$CO, n = 1–6], 513(7), 485(10), 457(14), 429(20), 401(8) [$Fe_3Cp_3(CNC)(CO)_n^+$, n = 4–0], 324(43) [$Fe_2Cp_2(CN)(CO)_2^+$], 268(21) [$Fe_2Cp_2CN^+$], 186(100) [$FeCp_2^+$], 147(22) [$FeCpCN^+$].

The complexes **5b**–**5e** were prepared from **5a** by anion exchange with the corresponding alkali metal salts in methanol. **5e**: brick-red rhombic crystals, m.p. 240 °C (decomp.). $\tilde{\nu}$ [cm^{-1}] = 2011 vs, 1983 s (ν($CO_{term.}$)), 1834 s (ν($CO_{bridging}$)), 1774 vs, br (ν(C=N=C)), 1600 m, 1549 m (ν(Ph)); ^{1}H NMR ([D$_6$]DMSO): δ = 7.32–6.78 (m, 20 H. Ph), 5.61, 5.29 (both s, 20 H; Cp); ^{13}C NMR ([D$_6$]DMSO): δ = 261.3 (C=N=C), 259.6 ($CO_{bridging}$), 210.8, 209.9 ($CO_{term.}$), 135.5, 125.2, 121.4 (Ph), 90.3, 89.7 (Cp).

All new compounds gave correct elemental analyses (C,H,Fe,N).

Received: December 5, 1991 [Z 5058 IE]
German version: *Angew. Chem.* **1992**, *104*, 604

[1] W. P. Fehlhammer, A. Schröder, F. Schoder, J. Fuchs, A. Völkl, B. Boyadjiev, S. Schrölkamp, *J. Organomet. Chem.* **1991**, *411*, 181–191.

[2] a) W. P. Fehlhammer, F. Schoder, G. Beck, K. H. Trylus, unpublished results; b) W. P. Fehlhammer, A. Schröder, W. Sperber, J. Fuchs, *Chem. Ber.* **1992**, in press.

[3] Crystallographic data of **5e**: dark red rhombic crystals from acetone/*n*-hexane (− 25 °C). Space group $Pca2_1$, a = 23.351(2), b = 10.822(1), c = 17.526(2) Å, V = 4428.9 Å^3, Z = 4; STOE four-circle diffractometer, $Mo_{K\alpha}$ radiation, 4 ≤ 2θ ≤ 50°, ω scan; 4252 measured reflections, of which 3105 were observed ($I > 2\sigma(I)$), 622 refined parameters. Structure solution with direct methods. Several hydrogen atoms were localized in difference Fourier syntheses, however without refinement. R = 0.059 (R_w = 0.039). Programs used: X-ray 76, Multan-77, DIFABS, Schakal-88. Further details of the crystal structure investigation may be obtained from the Fachinformationszentrum Karlsruhe, Gesellschaft für wissenschaftlich-technische Information mbH, D-W-7514 Eggenstein-Leopoldshafen 2 (FRG) on quoting the depository number CSD-56039, the names of the authors, and the journal citation.

[4] a) M. Al-Talib, I. Jibril, E.-U. Würthwein, J. C. Jochims, G. Huttner, *Chem. Ber.* **1984**, *117*, 3365–3373; b) R. Kupfer, E.-U. Würthwein, M. Nagel, R. Allmann, *ibid.* **1985**, *118*, 643–652.

[5] F. Seitz, H. Fischer, J. Riede, *J. Organomet. Chem.* **1985**, *287*, 87–101.

[6] G. Beck, W. P. Fehlhammer, *Angew. Chem.* **1988**, *100*, 1391–1394; *Angew. Chem. Int. Ed. Engl.* **1988**, *27*, 1344–1347.

[7] However, the Li–C bonds in $Li_2C{=}N{=}CLi_2^+$ (D_{2d};E_{tot} (MP2/6-31G*//6-31G*, see literature [8]) = −160.21516 Hartree can be interpreted as being to a large extent ionic, which is also indicated by the planar-linear D_{2h} structure only 1.8 kcal mol^{-1} richer in energy. It represents the transition state of the cumulene rotation (cf. however D_{2h} $H_2C{=}N{=}CH_2^+$: E_{rel} = 76.4 (!) kcal mol^{-1}) from the 3-21G frequency analysis. The Fe–C bonds in **5** are in contrast far more covalent, i.e. the complexes **5** structurally are more like $H_2C{=}N{=}CH_2^+$. A further transition state with tetralithio-2-azaallylium structure (C_{2v};E_{rel} = 25.0 kcal mol^{-1}) and two bridging lithium atoms between the carbon atoms is significantly richer in energy.

[8] J. S. Binkley, R. A. Whiteside, K. Raghavachari, R. Seeger, D. J. DeFrees, H. B. Schlegel, M. J. Frisch, J. A. Pople, L. R. Kahn, *GAUSSIAN 82*, Carnegie Mellon University, **1984**.

[9] E.-U. Würthwein, *J. Org. Chem.* **1984**, *49*, 2971–2978.

[10] In contrast terminally coordinated isocyanide ligands show CN bond lengths of about 1.14 Å. For the terminal *acyl*isocyanide ligand in [$Cr(CO)_5${4-CNC(O)$C_6H_4NO_2$}] a value of 1.167(10) Å was determined: A. Schröder, W. P. Fehlhammer, unpublished results.

[11] L. Busetto, L. Carlucci, V. Zanotti, V. G. Albano, D. Braga, *J. Chem. Soc. Dalton Trans.* **1990**, 243–250.

[12] When the electrophilic attack that preferably takes place at the oxygen atom in *N*-methylene carboxamides (see [4b]) and at the iminoacyl nitrogen atom in μ-iminoacylisocyanide diiron complexes (A. Schröder, W. Sperber, J Fuchs, W. P. Fehlhammer, *Chem. Ber.*, submitted) is considered, an *intra*molecular *O*-acylation should, however, also be discussed.

[13] H. R. Keable, M. Kilner, *J. Chem. Soc. Dalton Trans.* **1972**, 153–158.

[14] R. Kupfer, E.-U. Würthwein, *Chem. Ber.* **1986**, *119*, 857–871.

[15] A. Ceriotti, P. Chini, G. Longoni, G. Piro, *Gazz. Chim. Ital.* **1982**, *112*, 353.

[16] J. W. Kolis, E. M. Holt, M. A. Drezdzon, K. H. Whitmire, D. F. Shriver, *J. Am. Chem. Soc.* **1982**, *104*, 6134–6135.

[17] In contrast, the CN bond of the isoelectronic CN^- and related CN compounds (HCN, NCCN, RCN) surprisingly is *not* cleaved on metal surfaces: M. E. Kordesch, W. Feng, W. Stenzel, M. Weaver, H. Conrad, J. *Electron Spectrosc. Relat. Phenom.* **1987**, *44*, 149-162; J. S. Somers, M. E. Kordesch, R. Hemmen, T. Lindner, H. Conrad, A. M. Bradshaw, *Surf. Sci.* **1988**, 198, 400-412. Methyl isocyanide appears to isomerize preferentially: C. M. Friend, J. Stein, E. L. Muetterties, *J. Am. Chem. Soc.* **1981**, 103, 767-772. In clusters, nitriles and isocyanides, however, can be hydrogenated stepwise to amine or ammonia, see for example M. A. Andrews, H. D. Kaesz, *ibid.* **1979**, *101*, 7238-7244 and 7255-7259; W. Berndhardt, H. Vahrenkamp, *Angew. Chem.* **1984**, *96*, 362-363; *Angew. Chem. Int. Ed. Engl.* **1984**, *23*, 381; D. E. Coons, J. C. V. Laurie, R. C. Haltiwanger, M. Rakowski DuBois, *J. Am. Chem. Soc.* **1987**, *109*, 283-285; R. D. Adams, *Acc. Chem. Res.* **1983**, *16*, 67-72.

[18] Review: D. Shriver, M. J. Sailor, *Acc. Chem. Res.* **1988**, *21*, 374–379.

Photodimerization of Cinnamic Acid in the Solid State: New Insights on Application of Atomic Force Microscopy**

By *Gerd Kaupp**

Still in its infancy, atomic force microscopy (the abbreviation AFM is also used for the atomic force microscope)[1] is an extremely sensitive surface imaging technique suitable for studying organic solid-state reactions. The microscope scans surfaces with atomic tips to give images of van der Waals forces or contours of constant van der Waals forces with magnification up to atomic resolution. An important field of research is the photochemistry of organic crystals.[2] The application of AFM promises new insights into this field where, especially for topochemically allowed photoreactions, information is urgently required, because these conversions mostly do *not* proceed topotactically. Furthermore, multiproduct topochemistry[3] and many exceptions to topochemistry are known.[4, 5] Finally, the formation of new crystalline or amorphous phases are traditionally *not* treated by topochemistry even if a "reaction cavity principle" is additionally invoked; instead solid solutions are suspected, without proof, up to high conversions (e.g., 50%).[4]

Since AFM studies on gas/solid reactions have revealed six fundamental mechanisms for phase transformation (formation of flat coverings, volcanoes, craters, floes, valleys/ridges, and propagating zones),[2b, 6] the formation of new crystalline phases[7] during the classic reactions of topochemistry was an obvious choice for investigation. These are the photolyses of α-*trans*-cinnamic acid (α-**1**) to form α-truxillic acid (**2**) and of β-*trans*-cinnamic acid (β-**1**) to form β-truxinic acid (**3**).[7]

We now report our AFM observations, which confirm the existence of surface reactions involving substantial material

[*] Prof. G. Kaupp
FB 9 – Organische Chemie I der Universität
Postfach 2503, D-W-2900 Oldenburg (FRG)

[**] This work was supported by the Fonds der Chemischen Industrie, Schering AG, L.O.T. GmbH, and Digital Instruments. We thank Prof. W. Rammensee and J. Schreuer for the determination of the Miller indices of the crystal faces.

transport during the phase transformation, although at exactly this point minimal atomic and molecular movement has been postulated.[2a, 7]

If the smooth, shiny (010) faces of single crystals of α-**1** are irradiated ($\lambda > 300$ nm), not only α-truxillic acid (**2**) forms,[7] but also an as yet unknown minor product (2–3% at 0–70 °C);[8] however, no benzaldehyde or (*Z*)-cinnamic acid is observed. Modification β-**1** affords β-truxinic acid (**3**) as overwhelming major product. Under the best possible control of the phase purity of β-**1**, **3** and **2** are obtained in 96:4 ratio by exposure to sunlight while maintaining the temperature at 20 °C (β-**1** → α-**1** conversion takes place above 45 °C).[7] Our surface photolyses at 0–20 °C confirmed that besides **3** and a little of **2**, no other dimer is formed from β-**1**. Traces of (*Z*)-cinnamic acid are formed only when the reaction is far advanced (0.75% at 50% conversion), and again no benzaldehyde can be detected. The photolyses are thus highly selective, and contamination by side products is almost entirely suppressed.

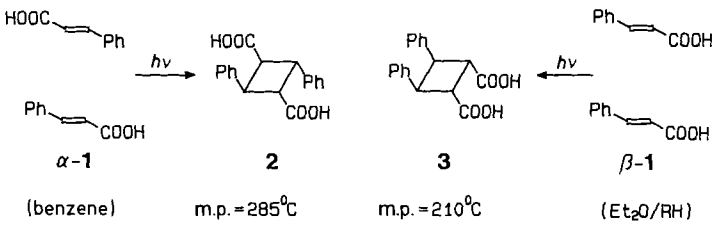

When the largest surfaces of the crystals are mounted as near horizontal as possible in the AFM (<10° deviation), the progress of the reaction involving phase transformation can be followed for very low conversion by direct scanning of the van der Waals surface.[8] The (010) surface of the single crystals of α-**1** is very smooth (Fig. 1a). Low steps and hills (< 40 nm) can be recognized. The hills grow on exposure to air in three days, up to three times their original height, and are probably composed of hydrated **1** (see below). On irradiation (1 min) of the fresh surface, in contrast to previous suppositions,[7, 9] an oriented surface reaction occurs (Fig. 1b,c), which forms a thin covering on the surface. This is divided into zones by parallel furrows, which intersect the *c* axis at an angle of about 45°. The trenches which probably compensate for a density increase after the photoreaction (density of the crystals according to X-ray analysis: α-**1** 1.242;[7] **2** 1.35 g cm^{-3}[9]) are 1600–3200 nm apart. Thus, a horizontal material transport takes place during the formation of the new crystalline[7] phase. According to the depth of the trenches (Fig. 1b, c), the new phase is approximately 100 nm thick, corresponding to about 300 molecular layers, which is the initial penetration depth of the 313 nm light that predominantly causes the excitation under the given reaction conditions.[8]

Perpendicular to the major furrows and emanating from them, ice-floelike upheavals begin to form (vertical transport components) (Fig. 1b,c), which on further photolysis (10 min, separate experiment) develop into layered plates about 100 nm thick (Fig. 1d). However, this makes the crystal cloudy, permeated with cracks parallel to the original trenches, and it can only be scanned with the AFM at a few places at this stage.[2b] The clearly directed transport processes cannot be explained by the topochemical reaction cavity principle and would not be expected on that basis.

Figures 1b–d are not artifacts caused by hydration of the product. Figure 1e shows that hydration occurs to a small extent after exposing the sample of Figures 1b,c to air for 3 h.[10] In this process, volcanolike[2b, 6] hills up to 100 nm high (gas/solid reaction[11]) are formed. Also at this point, the solid material—according to the powder records in reference [7] it is crystalline—can be scraped off with a needle under the stereomicroscope parallel to the main crystal face.

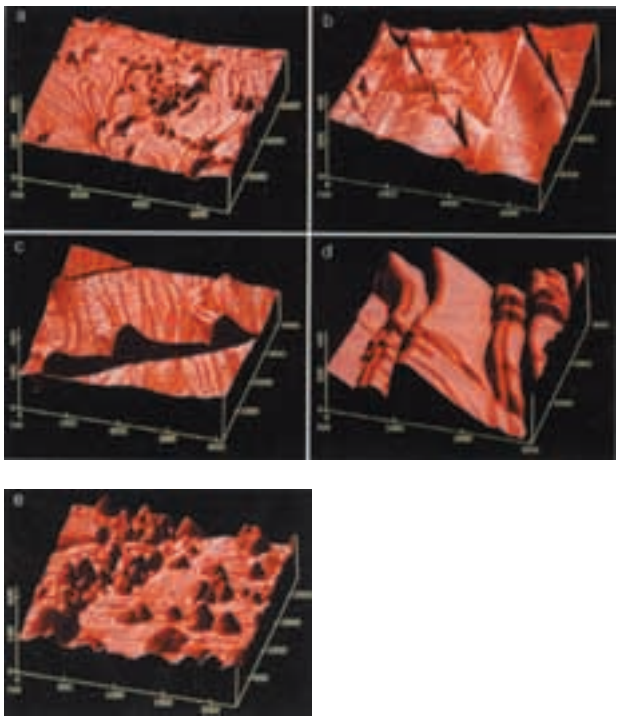

Fig. 1. AFM images of the main crystal face (010) of α-**1**: a) fresh, b) 0° after 1 min irradiation, c) 180° after 1 min irradiation, d) 90° after 10 min irradiation, e) surface 1b,c after 3 h exposure to air at 18 °C.

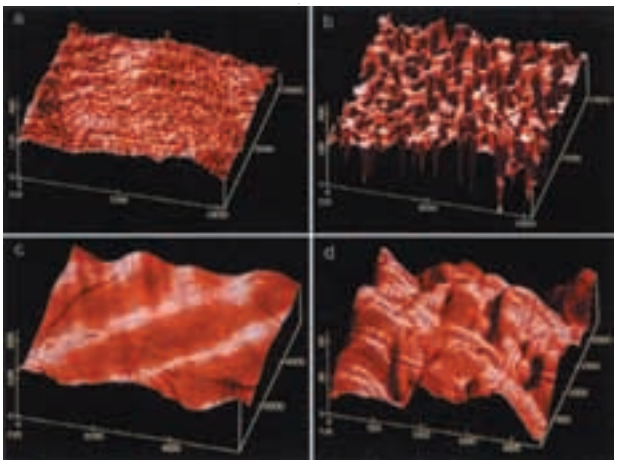

Fig. 2. AFM images of the main crystal face (100) of β-**1**: a) fresh, b) after 1 min irradiation, c) after 7 min irradiation, d) surface 2c after 10 h exposure to air at 18 °C.

In the case of β-**1**, both the main surface (100) and the almost half as wide side edge (010) can be studied with AFM. Figures 2a and 3a show that there are considerable differences. The main face is smoother (Fig. 2a), while the narrow edges reveal a floelike structure (Fig. 3a). Both in air and under high vacuum the irradiation (1 min) of the main face leads to crater formation (Fig. 2b), that of the side edge to

volcano formation (Fig. 3b). This is accompanied by substantial material transport. The typical crater depths are 200 nm for a diameter of 500 nm, and the volcanoes are about 400 nm high. Interestingly, complementary phase transformations thus take place on crystal surfaces perpendicular to each other. On further irradiation (7 min) complete leveling of both surfaces occurs. At this point, therefore, material is very effectively transported vertically in the direction of the original crystal faces (Fig. 2c, 3c). These unexpectedly complicated surface transformations could not be predicted from the topochemical reaction cavity principle.[4] They are good starting points for the elucidation of the molecular mechanism of material transport on photolysis,[12] as are the characteristic differences in the crystal faces before irradiation (Fig. 2a, 3a).

Surprisingly, even after photolysis the characteristics of the irradiated main and side faces are different. This suggests that different phases of β-truxinic acid (**3**) are formed. After 10 h hydration[10] in air, extended hills and valleys (Fig. 2d) or round craters (Fig. 3d) are observed as typical gas/solid reactions.[6, 11] No detailed interpretation of this remarkable difference is yet possible.

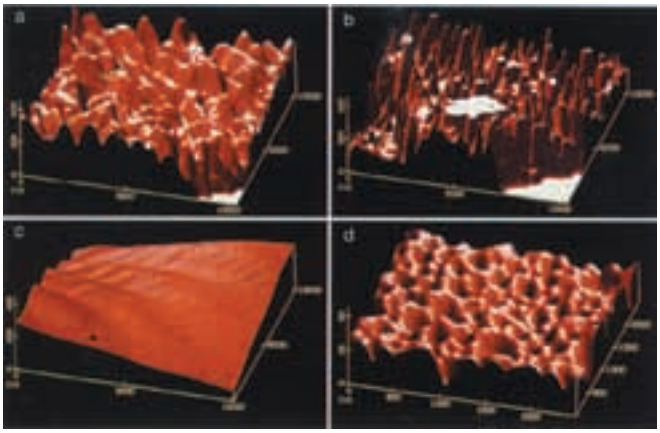

Fig. 3. AFM images of the side face (010) of β-**1**: a) fresh, b) after 1 min irradiation, c) after 7 min irradiation, d) surface 3c after 10 h exposure to air at 18 °C.

The AFM results show that photoreactions on solids take place on the surface when irradiation is selective. Compression by the crystal environment is not apparent even for low conversion. It appears that the chemical formation of new phases for photoreactions and gas/solid reactions are related processes.[6] Since the light does not penetrate very deeply into the crystal and has considerable intensity gradients, the progress of the photodimerization reaction as surface reaction that proceeds increasingly toward the interior of the crystal when the photoproducts do not absorb is probable in any case, whether topochemically "allowed" or "forbidden".[13] The AFM images are immediately discernible and open up completely new, unexpected details that cannot be obtained with other techniques (including electron microscopy). Clearly atomic force microscopy is a technique with which processes hardly understood till now can be studied, in particular new phase formation in crystal reactions under the common (and even preparative) practices of selective irradiation, because here the important details for the mechanism are not averaged out as, for instance, in X-ray structural analyses but are directly visible and interpretable.

From the crystal packing determined by X-ray methods, the orientation that has a geometric advantage for the reaction can be deduced, in particular for long, extended molecules. X-ray structural analysis is the method of choice for the study of the very rare single crystal to single crystal photodimerizations[14] and provides densities as well as molecular orientations that are extremely significant for the interpretation of phase transformation mechanisms. Nevertheless, with the unsuspected and remarkable transport phenomena made visible by AFM, the many exceptions[3–5] to the topochemical postulate become easier to understand. From here a new beginning is possible.

Received: September 30, 1991
Revised: March 12, 1992 [Z4941IE]
German version: *Angew. Chem.* **1992**, *104*, 606

CAS Registry number:
1, 140-10-3.

[1] G. Binnig, C. Quate, C. Gerber, *Phys. Rev. Lett.* **1986**, *56*, 930. AFM instruments have been available commercially in Germany since October 1990.

[2] a) G. M. J. Schmidt et al. in *Solid State Photochemistry* (Ed.: D. Ginsburg), Verlag Chemie, Weinheim, **1976**; b) first AFM applications: G. Kaupp, lectures at the 10th Int. Conf. Chem. Org. Solid State (Vancouver, July 7–12, 1991) and the 15th Int. Conf. Photochem. (Paris, July 27–August 2, 1991).

[3] G. Kaupp, E. Zimmermann, *Angew. Chem.* **1981**, *93*, 1107–1108; *Angew. Chem. Int. Ed. Engl.* **1981**, *20*, 1018–1019; for the related X-ray structural analysis: E. Kaftory, G. Kaupp, **1983**, unpublished; our analysis shows the necessary twofold symmetry that is not present in results published later, but essentially agrees with these in all other details (in contrast to the product distribution and the interpretation of their results): C. R. Theocharis, W. Jones, J. M. Thomas, M. Motevalli, M. B. Hursthouse, *J. Chem. Soc. Perkin Trans. 2* **1984**, 71–76; H. Frey, G. Behmann, G. Kaupp, *Chem. Ber.* **1987**, *120*, 387–393; G. Kaupp, H. Frey, G. Behmann, *ibid.* **1988**, *121*, 2135–2145; S. Mohr, *Tetrahedron Lett.* **1979**, 3139–3140; *ibid.* **1980**, 593–594.

[4] This inability is particularly noticeable for the photodimerization of anthracene and 9-anthracenecarbonitrile: see the discussion in M. D. Cohen, *Angew. Chem.* **1975**, *87*, 439–447; *Angew. Chem. Int. Ed. Engl.* **1975**, *14*, 386–394; M. D. Cohen, *Mol. Cryst. Liq. Cryst.* **1979**, *50*, 1–10. In the "reaction cavity principle" formulated there it is postulated that the product molecules must fit into the cavity as well as possible for solid solutions to form in the starting crystal, and that the product crystallizes out when the solubility limit is exceeded. For cinnamic acid, it is suspected that up to 50% conversion might occur prior to recrystallization.

[5] Dynamic calculations: S. V. Ramamurthy, K. Venkatesan, *Chem. Rev.* **1987**, *87*, 433–481; surface effects: E. A. Chandross, J. Ferguson, *J. Chem. Phys.* **1966**, *45*, 3564–3567; D. P. Craig, P. Sarti-Fantoni, *Chem. Commun.* **1966**, 742–743; crystal defects: M. D. Cohen, Z. Ludmer, J. M. Thomas, J. O. Williams, *ibid.* **1969**, 1172–1173; exitons and phonons: S. R. Kearsley in *Studies in Organic Chemistry 32, Organic Solid State Chemistry* (Ed.: G. R. Desiraju), Elsevier, Amsterdam, **1987**, Chap. 3; electron microscopy: G. M. Parkinson, M. J. Goringe, S. Ramdas, J. O. Williams, J. M. Thomas, *J. Chem. Soc. Chem. Comm.* **1978**, 134–135.

[6] G. Kaupp, *Mol. Cryst. Liq. Cryst.*, **1992**, *211*, 1–15.

[7] M. D. Cohen, G. M. J. Schmidt, F. I. Sonntag, *J. Chem. Soc.* **1964**, 2000–2013; G. M. J. Schmidt, *ibid.* **1964**, 2014–2021.

[8] NanoScope II, Digital Instruments, Santa Barbara, CA, USA; head D; XY: 333 ÅV^{-1}; Z: 100 ÅV^{-1}; 400 × 400 points; max. 15000 nm XY and 4000 nm Z; standard square-pyramidal Si_3N_4 tips with 45° vertex angle; cantilever with spring constant 0.12 Nm^{-1}; force ca. 10^{-8} N attractive; plane-fit and low-pass filter. Irradiation after removal of the scanner *n* min from 5 cm distance, with water-cooled Hg high-pressure lamp Hanau 150 W through Solidex at 18 °C in normal atmosphere; the same site of the crystal is found routinely within 500 nm or better. The measurements made several times on fresh crystals were reproducible. In addition the crystals were irradiated externally under vacuum (5×10^{-4} Torr) at 0 °C, mounted on the AFM without delay and measured. The same features were observed. For the product analysis by HPLC, the irradiated surface was scraped off (RP-18, H_2O/CH_3CN, phosphate buffer pH 2.0); **1**: UV (CH_3OH): λ_{max} = 273 nm (lgε = 4.34); **α-1**: monoclinic platelets ($P2_1/n$, a = 7.76, b = 17.98, c = 5.65 Å, β = 97.4°) from hot benzene by slow cooling [7], solid state absorption: λ_{max} (E_{rel}) = 240 (1.00), 296 (sh, 0.945), 304 (0.995), 318 (0.955), 365 (sh, 0.09), 390 (sh, 0.04) nm, at 334 nm; E_{rel} = 0.55; according to ^{1}H NMR analysis (see G. Montaudo, S. Caccamese, U. Librando, *Org. Magn. Reson.* **1974**, *6*, 534–536), the minor product of the photolysis does not conform to the ε-truxillic acid found by R. Stoermer

and E. Laage (*Chem. Ber.* **1921**, *54*, 77–85) as minor product; β-**1**: weakly arched, saber-shaped crystal aggregates with monoclinic single crystals strung together in the form of a ladder ($P2_1/a$, $a = 31.3$, $b = 4.04$, $c = 6.05$ Å, $\beta = 90.3°$), about half as thick as they are wide, with convex arched narrow faces, from diethyl ether by layering with petroleum ether at 4 °C [7], solid state absorption: λ_{max} (E_{rel}) = 241 (0.98), 282 (sh, 0.97), 308 (1.00), 315 (1.00), 364 (sh, 0.39), 390 (sh, 0.26), 440 (sh, 0.11) nm.

[9] E. D. Eanes, G. Donnay, *Z. Kristallogr., Kristallgeometr., Kristallphys., Kristallchem.* **1959**, *111*, 368–371; here conclusions that the product **2** does not show any preferred orientation were made from X-ray diffraction recordings and have been explicitly confirmed in [7].

[10] Neither of **2** nor of **3** are hydrates known; we thank Prof. M. Lahav for confirmation that truxillic and truxinic acids are hygroscopic.

[11] G. Kaupp, *Mol. Cryst. Liq. Cryst.* **1988**, *161*, 119–143.

[12] G. Kaupp, W. Rammensee, unpublished.

[13] G. Wegner proposed irradiation into the outermost absorption edge of the crystals. It remains to be seen whether in this way and in contradiction to [7] single crystal to single crystal transformations occur while maintaining the space group (e.g. maintaining $P2_1/n$ instead of forming Cc in the case of **2** [9]).

[14] H. Nakanishi, W. Jones, J. M. Thomas, M. B. Hursthouse, M. Motevalli, *J. Chem. Soc. Chem. Comm.* **1980**, 611; H. Nakanishi, W. Jones, J. M. Thomas, *Chem. Phys. Lett.* **1980**, *71*, 44–48; D. A. Dougherty, C. S. Choi, G. Kaupp, A. B. Buda, J. M. Rudzinski, E. Osawa, *J. Chem. Soc. Perkin Trans. 2* **1986**, 1063–1070.

Photodimerization of Anthracenes in the Solid State: New Results from Atomic Force Microscopy**

By *Gerd Kaupp**

The technique of atomic force microscopy (AFM) enables the phase transformations in topochemical photoreactions to be studied in detail for the first time.[1] The elucidation of the dimerization reaction of anthracenes seems to be most important, because here the most serious violations of the topochemical rules are observed. Already the [4 + 4] photodimerization of anthracene is topochemically forbidden.[2] Anthracene derivatives that crystallize in the α type, for example 9-Cl-, 9-Br-, 9-CH_3-, 9-CO_2CH_3-, and 9-$CONH_2$-anthracene,[3] give the topochemically allowed head/tail dimers. On the other hand, only two of the anthracene derivatives crystallizing in the β type, 1,5-dichloro- and 1-(2,4-dichlorophenyloxycarbonyl)anthracene form the anticipated head/head dimers. The β type crystals of 9-Cl-, 9-CHO-, and 9-CN-anthracene yield exclusively the "wrong" head/tail photodimers, and many other β type crystals such as 9-Br-, 9-CO_2CH_3-, 9-CO_2H-, and 1,10-dichloroanthracene are photostable despite favorable intermolecular distances.[3] The attempts at explanation up to now [4, 5] have not implicated the formation of the new phases and mention the possibility of surface reactions only sporadically. We report here on phase transformations on the crystal surface of typical anthracene derivatives that are observed by atomic force microscopy upon selective irradiation into the long-wavelength absorption band. Such irradiation techniques have been used in all previous investigations.[5] We found no fundamental differences between topochemically allowed and forbidden reactions, but in all cases observed formation of new phases that build features that look like floes.

[*] Prof. G. Kaupp
FB 9 – Organische Chemie I der Universität
Postfach 2503, D-W-2900 Oldenburg (FRG)

[**] This work was supported by the Fonds der Chemischen Industrie, Schering AG, L.O.T. GmbH, and Digital Instruments. We thank Prof. W. Rammensee and J. Schreuer for the determination of the Miller indices of the crystal surfaces.

Anthracene (**1a**) crystallizes from ethanol in monoclinic prismatic scales. The main crystal face (001) reveals small corrugations and 2–4 nm high steps under the AFM (Fig. 1a). After two minutes irradiation in air or under high vacuum, the dimer **2a** forms, in spite of being topochemically forbidden.[2] Figure 1 shows clearly that the phase change

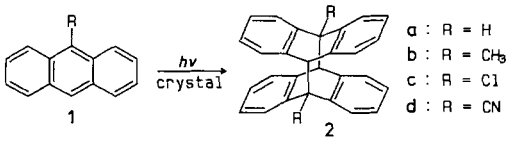

of the crystalline product involves substantial vertical transport of material (perpendicular to the a/b plane). Hilly ridges up to 16 nm high form along the steps, while at the foot of each step a furrow appears. Since the reaction **1a** → **2a** is not accompanied by a decrease in the density (the density of monoclinic anthracene calculated from X-ray structural analysis is 1.24,[6] that of orthorhombic dianthracene, 1.28[7]), horizontally layered material is piled up on the original steps. On longer light exposure (5 and 12 min) the hills grow to a maximum height of about 50 nm, merging together increasingly to form floes (Fig. 1c, d). The surface material becomes

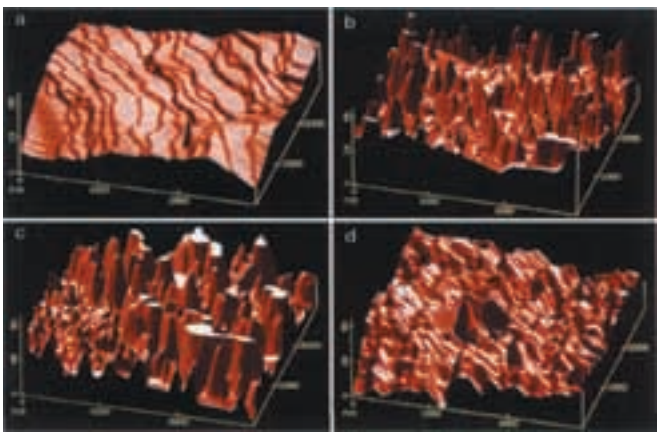

Fig. 1. AFM images of the main crystal face (001) of **1a**: a) fresh; b) after irradiation for 2 min; c) after irradiation for 5 min; d) after irradiation for 12 min.

easily detachable under the stereomicroscope. The penetration of the photochemically active light (predominantly λ = 365 nm) can be estimated to about 200 nm if an ε value of about 7000, that is, comparable with solution spectra, is assumed for the solid-state absorption.[8] The molecular regrouping takes place within this range, and only then does the light penetrate into deeper layers.[9] Figure 1 contains much more direct information than electron microscopy images with 9000-fold magnification, in which the origin of slightly changing contrasts is unclear.[10]

To exclude thermal effects during photolysis and to demonstrate the reliability of the AFM measurements the nonreactive anthracene-9-carboxylic acid **1**, R = CO_2H (crystallized from CH_3OH, platelets, main crystal face (100); Fig. 2a, b), and 9,10-dibromoanthracene (from benzene, triclinic, main crystal face (010); Fig. 2c, d) were irradiated. Identical images were obtained before and after exposure to

light in air for 20 and 30 minutes, respectively, even at high sensitivity, and the same sites of the crystals could be found again.

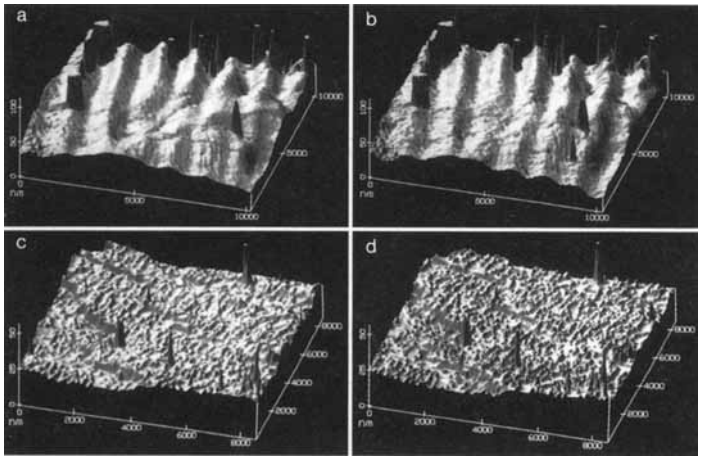

Fig. 2. AFM images of the main crystal faces of 9-anthracenecarboxylic acid (100) a) before and b) after irradiation for 20 min and of 9,10-dibromoanthracene (010) c) before and d) after irradiation for 10 min.

The derivatives 9-methylanthracene (**1b**, monoclinic prisms from toluene) and 9-chloroanthracene (**1c**) crystallize in the α type, pairing head to tail, and yield—as predicted from topochemical considerations—the head/tail photodimers **2b**[11] and **2c**, respectively. Here too, substantial transport processes are shown to take place in the vertical direction from the beginning of the exposure. Although the (100) face of **1b** is quite rough, Figures 3a and b depict very clearly already after 1 min irradiation hill- and floelike growths of considerable height (up to 150 nm). Longer exposure times (5 min, Fig. 3c) do not increase the height but the breadth of the ridges. The greater magnification at the same stage (Fig. 3d) shows the presence of well-formed floes clearly separated, which form an easily detachable white crust.

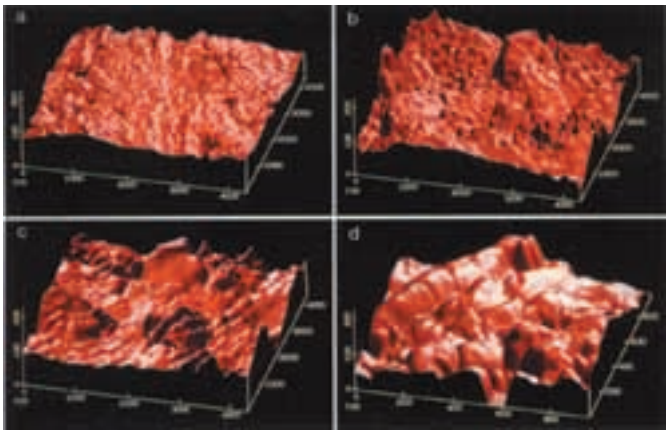

Fig. 3. AFM images of the main crystal face (100) of **1b**: a) fresh; b) after irradiation for 1 min; c), d) after irradiation for 5 min.

Cracks can now be seen under the stereomicroscope. The assumption of minimal atomic and molecular movement during the formation of solid solutions in the crystal's interior[2] can clearly *not* be supported by these observations.

In 9-chloroanthracene (**1c**, platelets from dichloroethane) the floe formation is particularly pronounced when the morphologically dominant face (interplanar spacing $d =$ 7.015(4) Å; a clearcut assignment to one of the two reported modifications of **1c**[3] was not possible) is irradiated for 1 min (Fig. 4). The floes are slightly tilted and at different heights up to 80 nm take on a preferred direction. After 5 min irradiation this direction is approximately maintained, but the floes have become much more substantial and have partly merged. Thus, a horizontal transport immediately follows the vertical, and in this second phase of the reaction the photodimerization in and on the floes is probably completed.

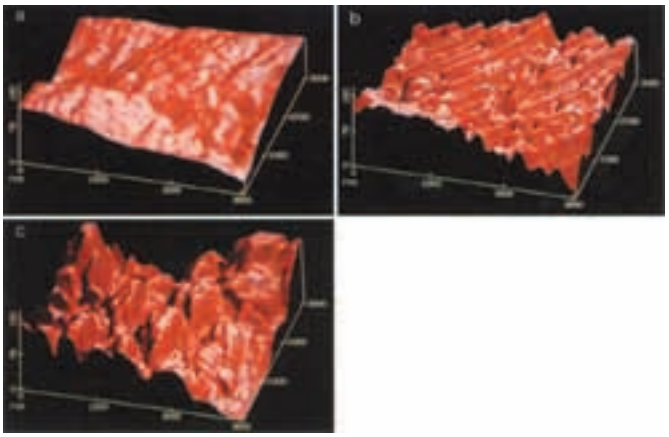

Fig. 4. AFM images of the main crystal face (100) of **1c**: a) fresh; b) after irradiation for 1 min; c) after irradiation for 5 min.

Till now the behavior of 9-anthracenecarbonitrile (**1d**), which crystallizes in the β type, seemed the most difficult to understand, since despite favorable topochemical prerequisites, instead of the head/head dimer the "wrong" head/tail dimer **2d** is formed.[3, 11] In Figure 5 it is apparent that already after 1 min irradiation, ridges of quite different heights (30 or 200 nm) develop with a preferred direction approximately along the original corrugations. These grow and finally form more and more pronounced floelike structures (Fig. 5),

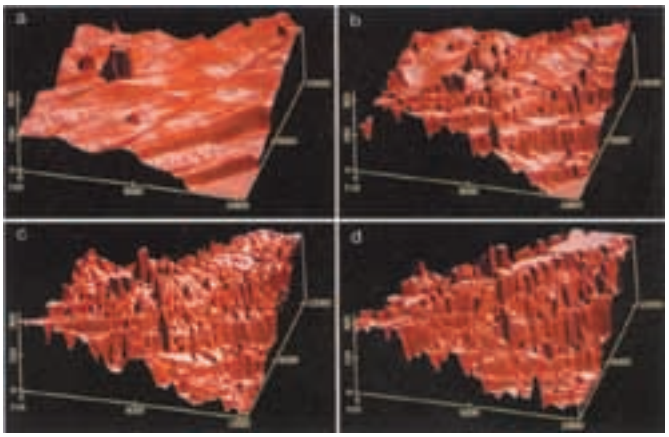

Fig. 5. AFM images of the (010) face of **1d**: a) fresh; b) after irradiation for 1 min; c) after irradiation for 6 min; d) after irradiation for 20 min.

analogous to the behavior **1a**, **b**, and **c**. The densities determined by X-ray crystallography are 1.30 for orthorhombic **1d**[12] and 1.309 for triclinic **2d**.[13] Thus here, irrespective of the crystal system, there is no special mechanism, as might have been presumed, because in this reaction every second anthracenecarbonitrile molecule must formally rotate through 180°.

The AFM results reemphasize[1] that photoreactions of solids take place at the surface, when the long-wavelength band is selectively irradiated. Again, compressions by the crystalline environment do not play a decisive role even at low conversion. This makes quite plain that new phase formations must not be overlooked in the elucidation of solid-state photolyses. Also one must consider that despite a complete reorientation of the molecules (Fig. 1, 3, 4, 5) the packing of the original molecules in the crystal definitely provides an advantage in regioselectivity, which is indeed taken advantage of when no opposing factors override and when additional electrostatic effects (in the corresponding head/tail diradical, in contrast to **3d**) favor the ring closure.

Although the density is not decreased in these photodimerizations, local pressure nevertheless apparently builds up in the stacklike crystals of **1**,[3] which finally leads to reorientation and transport vertical to the largest faces of the original crystals. The resulting dimers **2** are thicker and shorter than the flat disks of **1**, which leads not to volcano[1] formation but to floe formation when the original surfaces are broken preferably at weak points. Figures 1, 3, 4, and 5 show this feature for the first time in rich detail for real (not averaged) surfaces.

On the basis of these AFM images showing comprehensive transport phenomena, it is not surprising that the anthracene reaction centers situated far apart[2] can come together for reaction.[14]

The explanation for the complete absence of the head/head dimer of 9-anthracenecarbonitrile in favor of **2d**[3] must be founded in the known diradical mechanism[15] and its polar effects:[16] the diradical **3d**, while favored electronically and also by the crystal packing, has the disadvantage of electrostatic repulsion on bond formation between the two radical centers. It would therefore rather cleave to form two molecules of **1d**. A permanent chemical change only occurs when two molecules of **1d** meet in opposite orientations of the crystal packing. Apparently the versatile transport phenomena provide ample opportunity. Alternatively, the same result could be achieved if a labile head/head dimer (see [11]) forms as intermediate from **3d** in low yields and initiates the phase transformation (as occurs with the isolable dimers **2**) to finally decompose thermally via **3d** (see also [5]).

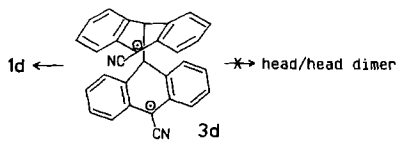

These results of AFM investigations lay the foundations of new, more comprehensive theories on the reactivity of organic crystals. The static picture of crystal reactivity as deduced from X-ray crystallography must be complemented by the dynamics of phase transformation. Such dynamics could be deduced from X-ray crystallography only in the case of single crystal to single crystal or at least topotactic conversions. Further knowledge of nontopotactic reactions will be gleaned from irradiation with polarized light of different intensities and through the as yet technically unattainable AFM study of very narrow crystal edges.

Experimental Procedure

For details of the AFM measurements, see [1]. The crystals were grown from saturated solutions by slow evaporation of the solvent at room temperature, separated by suction, and washed. Selection was aided by a stereomicroscope. The crystal was mounted directly on the AFM with its main face horizontal and irradiated at a distance of 5 cm with a Hanau 150 W Hg high-pressure lamp through Solidex at 18 °C or under high vacuum at a distance of 15 cm at 0 °C for eight to ten times longer. All measurements were repeated several times with fresh crystals. After the measurements at the original site, other sites of the same surface were examined to ensure that the photoreaction took place everywhere and was not perhaps limited to special regions. Analysis of the products was undertaken by HPLC on material scraped from the irradiated crystal. For preparative control experiments, ^{1}H NMR spectroscopy was employed. Only a negligible amount of anthraquinone formation occurred on exposure to air (< 5% of the conversion in all cases).

To determine the Miller indices of the crystal face, several single crystals were introduced into an X-ray diffractometer (Philips PW 1800) in the same orientation as for the AFM measurements. The *d* values were determined and the surface parameters calculated from the known lattice parameters.

Received: October 26, 1991
Revised version: March 12, 1992 [Z 4990 IE]
German version: *Angew. Chem.* **1992**, *104*, 609

CAS Registry numbers:
1a, 120-12-7; **1b**, 779-02-2; **1c**, 716-53-0; **1d**, 1210-12-04.

[1] G. Kaupp, *Angew. Chem.* **1992**, *104*, 606; *Angew. Chem. Int. Ed. Engl.*, **1992**, *31*, 592.
[2] M. D. Cohen, *Angew. Chem.* **1975**, *87*, 439–447; *Angew. Chem. Int. Ed. Engl.* **1975**, *14*, 386–394; *Mol. Cryst. Liq. Cryst.* **1979**, *50*, 1–10.
[3] G. M. J. Schmidt, *Pure Appl. Chem.* **1971**, *27*, 647–678; stacked structures: M. D. Cohen, Z. Ludmer, Y. Yakhot, *Phys. Status Solidi. B* **1975**, *67*, 51–61; J. P. Cox, G. A. Sim, *Acta Crystallogr. Sect. B* **1979**, *35*, 404–410.
[4] V. Ramamurthy, K. Venkatesan, *Chem. Rev.* **1987**, *87*, 433–481; E. A. Chandross, J. Ferguson, *J. Chem. Phys.* **1966**, *45*, 3564–3567; D. P. Craig, P. Sarti-Fantoni, *Chem. Commun.* **1966**, 742–743; M. D. Cohen, Z. Ludmer, J. M. Thomas, J. O. Williams, *ibid.* **1969**, 1172–1173; G. M. Parkinson, M. J. Goringe, S. Ramdas, J. O. Williams, J. M. Thomas, *J. Chem. Soc. Chem. Commun.* **1978**, 134–135.
[5] G. Wegner proposed that single crystal to single crystal transformations be attempted by irradiation into the outermost absorption edge. It remains to be seen whether in this way the space group of the starting crystal is also fixed in the dimer (which always crystallizes in a different space group), or whether the "correct" head/head dimer of **1d** forms.
[6] A. M. Mathieson, J. M. Robertson, V. C. Sinclair, *Acta Crystallogr.* **1950**, *3*, 245–247.
[7] M. Ehrenberg, *Acta Crystallogr.* **1966**, *20*, 177–182; C. S. Choi, P. L. Marinkas, *Acta Crystallogr. Sect. B* **1980**, *36*, 2491–2493.
[8] Anthracene solid-state spectrum (diffuse reflection): $\lambda_{max}(E_{rel})$ = 351(sh, 0.86), 365(0.95), 385(1.00), 407(0.93) nm; light polarized parallel to the crystal's *b* axis penetrates less deeply through the main face into the crystal, because the extinction coefficient (21300) is three times larger than for light polarized perpendicular to the *b* axis (7040): A. Bree, L. E. Lyons, *J. Am. Chem. Soc.* **1956**, 2662–2670.
[9] The highly resolved floes (initially perpendicular to the surface but later tilted) out of **2a** appear from their spacing and length to have nothing in common with the approximately 50000 nm long and 2000 nm thick needles parallel to the *a* axis or the lances of similar length and about 20000 nm wide obtained by Sarti-Fantoni et al. after several hours irradiation at low intensity: D. Donati, G. G. T. Guarini, P. Sarti-Fantoni, *Mol. Cryst. Liq. Cryst.* **1973**, *21*, 289–297.
[10] A. P. Rood, D. Emerson, H. J. Milledge, *Proc. R. Soc. London A* **1971**, *324*, 37–43; the "network parallel to the *a,b* planes of the anthracene crystal" ("image intensifier" because of rapid destruction by the electron beam) that was described on the grounds of the contrast obtained in electron microscopy appears equally unclear: J. M. Thomas, E. L. Evans, J. O. Williams, *ibid.* **1972**, *331*, 417–427.
[11] In contrast, on irradiation of **1b** in solution, apart from **2b** the thermolabile head/head dimer forms (G. Kaupp, E. Teufel, *Chem. Ber.* **1980**, *113*, 3669–3674). Its presence was overlooked previously. Reliable estimates of the stability of a 9,10-head/head dimer of **1d** are not available.

[12] H. Rabaud, J. Clastre, *Acta Crystallogr.* **1959**, *12*, 911-915.
[13] C. R. Theocharis, W. Jones, *J. Chem. Soc. Faraday Trans. 1* **1985**, *81*, 857-874.
[14] It must be checked whether the details about the epitaxy in at least six orientations of the crystals of dimer **2a** should be reinterpreted, because this report assumes crystallization solely in the interior of the anthracene crystal: M. M. Julian, *J. Chem. Soc. Dalton Trans.* **1972**, 558-560; D. P. Craig, J. Rajikan, *J. Chem. Soc. Faraday Trans.* **1978**, *74*, 292-303.
[15] G. Kaupp, *Justus Liebigs Ann. Chem.* **1973**, 844-878; *ibid.* **1977**, 254-275; for UV/VIS diradical spectra there is already a review available [M. J. Johnston in *Handbook of Photochemistry, Vol. 2* (Ed.: J. C. Scaiano), CRC Press, Boca Raton, FL, USA **1989**, Chap. 2], but it does not even mention the first 1,4-diradical spectra [G. Kaupp, E. Teufel, H. Hopf, *Angew. Chem.* **1979**, *91*, 232-234; *Angew. Chem. Int. Ed. Engl.* **1979**, *18*, 215-217], although their resolution is much better than the later spectra of the Scaiano/Johnston group and others.
[16] G. Kaupp, H.-W. Grüter, *Angew. Chem.* **1979**, *91*, 943-944; *Angew. Chem. Int. Ed. Engl.* **1979**, *18*, 881-882; *Chem. Ber.* **1980**, *113*, 1458-1471.

Cyclometallaborazines: Borazines with Metal Atoms as Ring Building Blocks: $PhB(MeN)_3(TiCl_2)_2$**

By *Hans-Joachim Koch, Herbert W. Roesky,* Rakesh Bohra, Mathias Noltemeyer,* and *Hans-Georg Schmidt*

Dedicated to Professor Anton Meller on the occasion of his 60th birthday

Borazine was first reported by A. Stock and E. Pohland in 1926.[1] The number of borazines substituted at the ring framework is legion. However, to our knowledge no derivatives are so far known, which contain transition-metal atoms as building blocks in the borazine framework. Only quadrinomial boron-containing metallacycles have already been reported.[2-4]

Methyl-bis[(methyl(trimethylsilyl)aminophenyl)boryl]-amine (**1**), prepared by Nöth et al.,[5] served as the starting material for the synthesis of the target compound and should react with titanium halides via ring closure to give **2**. However, the reaction of **1** with titanium tetrachloride in the molar ratio 1:1 in $CHCl_3$ did not afford **2**, but led instead to a red-brown powder **3** and the substituted borazine **4**[6] in almost quantitative yields (49% each) [Eq. (a)].

We obtained deep red crystals of **3** from THF (also soluble in MeCN) which were suitable for X-ray crystallography. The results of the structure analysis are shown in Figure 1.[7]

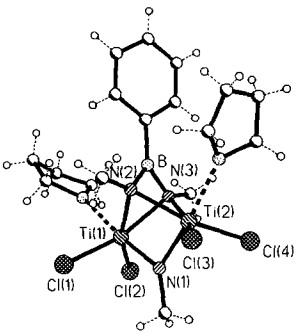

Fig. 1. Crystal structure of **3** with two coordinated THF molecules. Selected distances [pm] and angles [°]: Ti(1)-Ti(2) 273.6(1), Ti(1)-N(1) 188.9(3), Ti(1)-N(2) 212.8(3), B-N(2) 145.3(6), B-N(3) 144.7(5), Ti(2)-N(1) 186.3(3), Ti(2)-N(2) 213.5(3); Ti(1)-N(1)-Ti(2) 93.6(1), Ti(1)-N(2)-Ti(2) 79.9(1), Ti(1)-N(3)-Ti(2) 79.7(1).

These confirm that **1** reacts with titanium tetrachloride via the insertion of two titanium dichloride units to give **3**. An increase in the yield of **3** cannot be achieved by the reaction of **1** and titanium tetrachloride in the ratio 1:2. Also, a by-product, which could explain the reaction pathway could not be isolated. Only a change in solvent from $CHCl_3$ to hexane led to the unstable intermediate **5**.

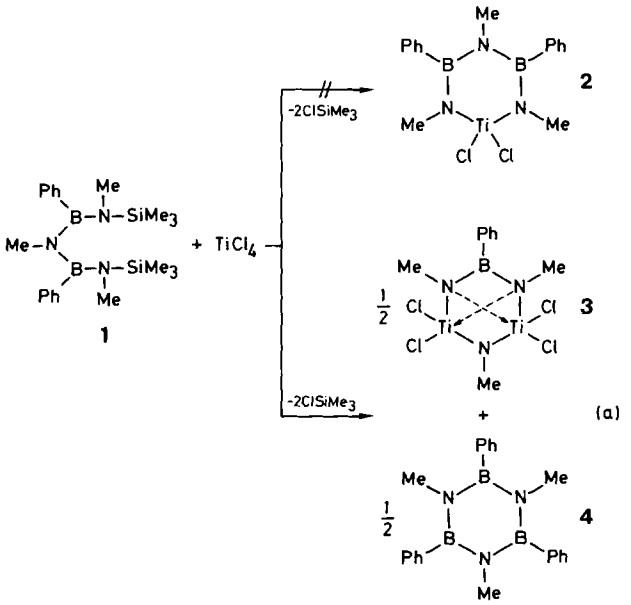

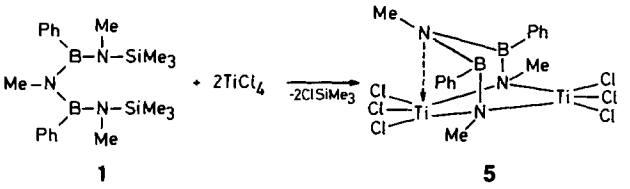

Together with **5**, compound **4**, traces of **3**, and a red-brown TiN-containing polymer were also formed. Compound **5** is yellow, crystalline, and is obtained in a yield of 17.5%. The crystal structure analysis showed two molecules of **5** in the asymmetric unit.[8]

On the basis of the structures of **3** and **5** (Fig. 2) as well as the experimental results the following reaction sequence seems plausible: in the first step, **1** reacts with two equivalents of titanium tetrachloride to give **5**. Compound **5** then decomposes very rapidly via an S_{Ni} reaction to give **3** and one equivalent of $PhBCl_2$. The $PhBCl_2$ then reacts with a further equivalent of **5** to give **4**, whereby two equivalents of titanium tetrachloride are liberated which themselves then react again with **1**.

The structure of **3** can be described as a geometric body whose surface consists of four, bent, irregular squares, or as a tetrahedron whose apexes are N(2), N(3), Ti(1), and Ti(2), which on the N(2)–N(3) edge is bridged by a boron atom and on the Ti(1)–Ti(2) edge is bridged by a nitrogen atom. The

[*] Prof. Dr. H. W. Roesky, H.-J. Koch, Prof. R. Bohra, Dr. M. Noltemeyer, H.-G. Schmidt
Institut für Anorganische Chemie der Universität
Tammannstrasse 4, D-W-3400 Göttingen (FRG)

[**] This work was supported by the Volkswagen-Stiftung, the Deutsche Forschungsgemeinschaft, and the Fonds der Chemischen Industrie.

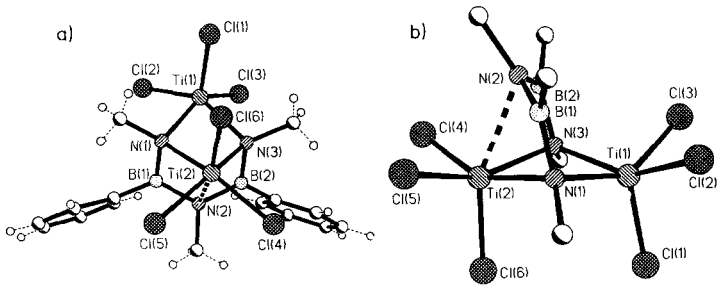

Fig. 2. Crystal structure of **5**. a) top view, b) side view. Selected distances [pm] and angles [°]: Ti(1)-Ti(2) 326.4(1), Ti(1)-N(1) 209.6(4), Ti(1)-N(3) 210.8(3), B(1)-N(1) 145.0(6), B(2)-N(2) 147.2(7), B(2)-N(3) 146.3(6), Ti(2)-N(1) 210.7(3), Ti(2)-N(3) 212.2(4); Ti(1)-N(1)-Ti(2) 101.9(2), N(1)-Ti(1)-N(3) 75.6(1).

reason for this nonplanar configuration are the strong intramolecular Ti–N interactions [Ti(1)–N(3) 213.0(3) and Ti(2)–N(2) 213.5(3) pm], which, if the THF ligands are considered, lead to a distorted octahedral environment of the titanium atoms. The lengths of the Ti–N bonds to the threefold coordinated nitrogen atom [Ti(1)–N(1) 188.9(3) and Ti(2)–N(1) 186.3(3) pm] are similar to that in $[(\eta^5\text{-}C_5H_5)TiCl_2N(SiMe_3)_2]$ [187.9(3) pm].[9] Shorter Ti–N bonds are found in the compounds $[Ph_2P(S)N{=}TiCl_2\cdot 3\,C_5H_5N]$ [172.0(2) pm][10] and $[(\eta^5\text{-}C_5Me_5)Ti(Cl){=}NtBu\cdot C_5H_5N]$ [169.8(4) pm].[11] The Ti–N bonds to the fourfold coordinated nitrogen atoms are significantly longer [Ti(1)–N(2) 212.8(3) and Ti(2)–N(3) 214.1(3) pm].

Compound **5** can best be described as a bicyclo[3.1.1]heptane derivative. The titanium atoms are coordinated differently, whereas Ti(1) is surrounded in a distorted tetragonal pyramidal manner, Ti(2) is surrounded in a distorted octahedral manner [intramolecular Ti(2)–N(2) interactions (244.4 pm)]. The other Ti–N bond lengths (average 210.2 pm) correspond to those in $[Ph_2P\{\mu\text{-}N(SiMe_3)\}_2TiCl_2\{NPPh_2N(SiMe_3)_2\}]$[12] (average 210.3 pm). Similar Ti–Cl distances to those in **5** (average 222.1 pm) are present in $[(\eta^5\text{-}C_5H_5)TiCl_2N(SiMe_3)_2]$[13] (average 227.1 pm).

The boron–nitrogen framework of **1** is influenced very little by the titanium atoms in **5**, as a comparison of the structures of **5** and **1**[14] shows; the B–N distances are only an average of 2.9 pm longer in **5**. In contrast, the Ti–Ti distances for **3** and **5** are significantly different [273.6(1) and 326.4(2) pm, respectively]. This may be explained by the variation of the bridge lengths in **3** (N–B–N) and in **5** (N–B–N–B–N). Compound **5** can only be stored for a long period of time as a crystalline solid under inert conditions. In solution, **5**, in contrast to **3**, is very unstable and decomposes within 2–3 minutes to give **3** and **4**.

Experimental Procedure

3: To a solution of **1** (2.05 g, 5.0 mmol) in $CHCl_3$ (40 mL), $TiCl_4$(0.95 g, 5.0 mmol) in $CHCl_3$ (20 mL) was added dropwise at room temperature. The suspension was refluxed for 4h, then allowed to cool to room temperature and a red-brown precipitate was filtered off. Finally the powder was extracted several times in $CHCl_3$ and thus compounds **3** (0.99 g, 2.4 mmol, 49%) and **4** (0.84 g, 2.4 mmol, 49%) were obtained. **3**: m.p. = 135 °C (decomp); IR(nujol/KBr): $\tilde{\nu}$[cm^{-1}] = 2955vs, 2925vs, 1461s, 1377s, 721m. Correct C, H, N, Cl analyses. ^{11}B NMR (80.21 MHz, CD_3CN, $OEt_2\cdot BF_3$ ext.): δ = 24.1 (s). – ^{1}H NMR (250.13 MHz, CD_3CN, TMS ext.): δ = 7.5 (m, Ph, 5H), 4.5 (s, Me, 3H), 3.6 (s, Me, 6H). – EI-MS: *m/z* 413 (M^+, 14%).

5: To a suspension of **1** (2.05 g, 5.0 mmol) in hexane (40 mL), $TiCl_4$ (1.90 g, 10.0 mmol) in hexane (20 mL) was added dropwise at room temperature. The reaction mixture was refluxed for 3h and subsequently filtered whilst still hot. Yellow crystals of **5** together with a red -brown solid, precipitated out from the filtrate at −25 °C. The crystals were sorted out. Yield 0.50 g (0.88 mmol, 17%). m.p. = 105 °C (decomp). IR(nujol/KBr): $\tilde{\nu}$[cm^{-1}] = 1660m, 1498m, 1456vs, 1378vs, 1262s, 1181s, 1111s, 988s, 702s, 518vs. Correct C, H, N, Cl analyses. ^{11}B-NMR (80.21 MHz, C_6D_6, $OEt_2\cdot BF_3$): δ = 2.2(s). – ^{1}H-NMR (250.13 MHz, C_6D_6, TMS ext.): δ = 7.3 (m, Ph, 10H), 3.8 (s, Me, 6H), 2.7 (s, Me, 3H).

Received: August 21, 1991 [Z 4881 IE]
Publication delayed at authors' request
German version: *Angew. Chem.* **1992**, *104*, 612

[1] A. Stock, E. Pohland, *Chem. Ber.* **1926**, *59*, 2215–2223.
[2] D. Fest, C. D. Habben, A. Meller, G. M. Sheldrick, D. Stalke, F. Pauer, *Chem. Ber.* **1990**, *123*, 703–706.
[3] H. Braunschweig, P. Paetzold, R. Boese, *Chem. Ber.* **1990**, *123*, 485–487.
[4] P. Paetzold, K. Delpy, R. P. Hughes, W. A. Herrmann, *Chem. Ber.* **1985**, *118*, 1724–1725.
[5] H. Nöth, M. J. Sprague, *J. Organomet. Chem.* **1970**, *22*, 11–22.
[6] H. Nöth, W. Tinhof, *Chem. Ber.* **1974**, *107*, 3806–3817.
[7] a) Crystal structure analysis of **3**·2THF Space group $P2_1/c$, a = 1588.9(3), b = 903.1(1), c = 1814.7(4) pm, β = 102.30(1)°, V = 2.5442(13) nm^3, Z = 4, ρ_{calcd} = 1.45 Mg m^{-3}, $\mu(Mo_{K\alpha})$ = 1.06 mm^{-1}, 7440 measured reflections to $2\theta_{max}$ = 45°, 2776 observed reflections with $|F| > 3\sigma(|F_0|)$ were used for the structure refinement. R = 0.039 (wR = 0.046, weighting scheme $w^{-1} = \sigma^2(F) + 0.0004F^2$). b) Further details of the crystal structure investigation may be obtained from the Fachinformationszentrum Karlsruhe, Gesellschaft für wissenschaftlich-technische Information mbH, D-W-7514 Eggenstein-Leopoldshafen 2 (FRG) on quoting the depository number CSD-55828, the names of the authors, and the journal citation.
[8] Crystal structure analysis of **5**: Space group $P2_1$, a = 879.4(1), b = 2288.0(4), c = 1183.9(1) pm, β = 91.52(1)°, V = 2.3811(5) nm^3, Z = 4, ρ_{calcd} = 1.59 Mg m^{-3}, $\mu(Mo_{K\alpha})$ = 1.35 mm^{-1}, 5412 measured reflections to $2\theta_{max}$ = 45°, semiempirical absorption correction, 4930 observed reflections with $|F| > 3\sigma|F_0|$ were used for the structure refinement. R = 0.029 (wR = 0.030, weighting scheme $w^{-1} = \sigma^2(F) + 0.0004F^2$).[7b]
[9] Y. Bai, H. W. Roesky, M. Noltemeyer, *Z. Anorg. Allg. Chem.* **1991**, *595*, 21–26.
[10] H. W. Roesky, H. Voelker, M. Witt, M. Noltemeyer, *Angew. Chem.* **1990**, *102*, 712–713; *Angew. Chem. Int. Ed. Engl.* **1990**, *29*, 669.
[11] Y. Bai, M. Noltemeyer, H. W. Roesky, *Z. Naturforsch. B*, **1991**, *46*, 1357–1363.
[12] M. Witt, H. W. Roesky, D. Stalke, F. Pauer, T. Henkel, G. M. Sheldrick, *J. Chem. Soc. Dalton Trans.* **1989**, 2173–2177.
[13] Y. Bai, H. W. Roesky, M. Noltemeyer, *Z. Anorg. Allg. Chem.*, in press.
[14] Crystal structure analysis of **1**: Space group $P2_1/c$, a = 1173.2(1), b = 1360.8(1), c = 3209.0(2) pm, β = 91.33(2)°, V = 5.122(3) nm^3, Z = 8, ρ_{calcd} = 1.06 Mg m^{-3}, $\mu(Mo_{K\alpha})$ = 0.14 mm^{-1}, 7967 measured reflections to $2\theta_{max}$ = 45°, empirical absorption correction, 4148 observed reflections with $|F| > 3\sigma(|F_0|)$ were used for the structure refinement. R = 0.077 (wR = 0.074, weighting scheme $w^{-1} = \sigma^2(F) + 0.0006F^2$). [7b]

$[t\text{BuSiO(ReO}_4)]_4$, a Model Compound for Metal Oxides on Silicate Surfaces—Synthesis from the Stable Triol $t\text{BuSi(OH)}_3$ and Re_2O_7**

By *Norbert Winkhofer, Herbert W. Roesky,* Mathias Noltemeyer,* and *Ward T. Robinson*

Dedicated to Professor Heinz Harnisch on the occasion of his 65th birthday

Transition metal oxides on silicon dioxide supports find wide application as catalysts in the petrochemical industry.[1, 2] But to a large extent, the processes taking place on the catalyst surface are not understood. Their study is hindered by the complicated structure of these silicate surfaces, making the synthesis of model substances essential. Feher et al.[3, 4] succeeded in preparing the heptameric condensation

[*] Prof. Dr. H. W. Roesky, N. Winkhofer, Dr. M. Noltemeyer, Prof. Dr. W. T. Robinson
Institut für Anorganische Chemie der Universität
Tammannstrasse 4, D-W-3400 Göttingen (FRG)

[**] This work was supported by the Deutsche Forschungsgemeinschaft and the Fonds der Chemischen Industrie.

product of cyclohexylsilanetriol, providing a series of transition-metal derivatives of cubic siloxanes and their derivatives; starting from formal condensation products of phenylsilanetriol, Shklover et al. and Struchkov et al.[5, 6] characterized a cobalt- and a nickelsiloxane cluster.

For some time we have been interested in the suitability of di(*tert*-butyl)silanolate as an anchor for metal oxide fragments. Starting from di(*tert*-butyl)silanediol, we can indeed attach metal complex fragments in high and moderately high oxidation states.[7]

As far as we know, syntheses from free silanetriols have not yet been described, a deficiency which needs to be remedied because this route is expected to be similar to the practical preparation of siloxane catalysts, and the surfaces of the resulting products should thus have similar morphologies to the catalyst surfaces. However, suitable silanetriols were not available. Silanetriols are postulated as intermediates in the industrial preparation of silicon;[8] but on account of their extreme tendency to undergo condensation reactions, most silanetriols cannot be isolated in substance. The few exceptions have large organic residues.[9–12] Their synthesis is in part laborious and sometimes the condensation reactions can be suppressed only for a short while. Preparation by hydrolysis reactions requires very special reaction conditions, as detailed below.

In 1955 already Wiberg et al. described the hydrolysis of tBuSiCl$_3$.[13] They obtained the tetrameric compound (tBuSiO$_{1.5}$)$_4$. Recently the same reaction was conducted under different conditions by P. D. Lickiss et al. affording the dimeric [tBu(OH)$_2$Si]$_2$O.[14] We report here the preparation of the primary hydrolysis product tBuSi(OH)$_3$ (**1**). This compound is exceptionally stable to condensation and precipitates in high yield from a simple reaction with commercially available starting materials.

For its preparation we basically followed the method of Takiguchi.[9] tBuSiCl$_3$ was dissolved in dry diethyl ether and added dropwise to an emulsion of stoichiometric quantities of water and aniline cooled in ice. Removal of the hydrochloride and concentration of the filtrate caused **1** to precipitate as colorless crystals in 94% yield. The exact reaction conditions are crucial. The hydrolysis product **1** is soluble in water, dimethyl sulfoxide (DMSO), and tetrahydrofuran, but almost insoluble in hexane or chloroform. In the ^{1}H NMR spectrum ([D$_6$]DMSO) we observed two signals [$\delta = 0.85$ (tBu), 5.50(OH)] and in the ^{29}Si NMR spectrum (D$_2$O) a singlet ($\delta = -38.8$). The X-ray crystal structure analysis[15] revealed that molecules of **1** are linked by hydrogen bonds to form corrugated layers (Fig. 1). Interactions between the layers are prevented by the hydrophobic *tert*-butyl groups. Cyclohexylsilanetriol also occurs in a similar structure,[12] but (Me$_3$Si)$_3$CSi(OH)$_3$[11] and (Me$_3$Si)$_3$SiSi(OH)$_3$[11] form cagelike structures.[12] As yet these are the only silanetriols whose structures are characterized. The Si–O bond lengths [161.3(4), 163.4(3), 163.1(4) pm] and the Si-O-Si angles [105.8(2), 110.5(2), 106.6(2)°] are comparable with those of known compounds.[11, 12] The hydrogen atoms were all located experimentally, and the interatomic O–O distances (O1···O3 270.5, O1···O2 270.4 pm) are consistent with strong hydrogen bonding.

The reaction of **1** with Re_2O_7 in a 2:1 molar ratio affords [tBuSiO(ReO$_4$)]$_n$ (n = 3, 4) after cleavage of water and exchange of H for ReO$_3$ [Eq. (a)]. The initial precipitate is a

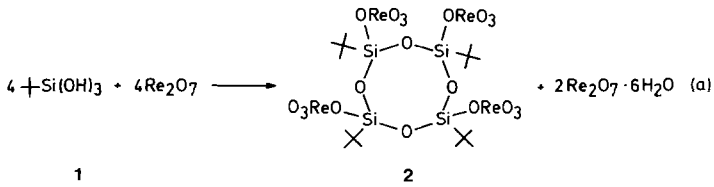

fine gray, very air-sensitive powder. Recrystallization from boiling acetonitrile gave transparent crystals of **2** ($n = 4$) suitable for X-ray structure analysis. All ReO$_3$- and tBu-containing units are *cis* to one another (Fig. 2).[16]

Taking the ^{1}H NMR and ^{29}Si data into account we assume that **2** rearranges rapidly in solution, forming the thermodynamically more stable modification on crystallization. To our knowledge it is the first defined, structurally proven transition-metal compound synthesized from a silanetriol. It thus opens a new way to soluble metal-containing silicates. We are now investigating indications from mass spectrome-

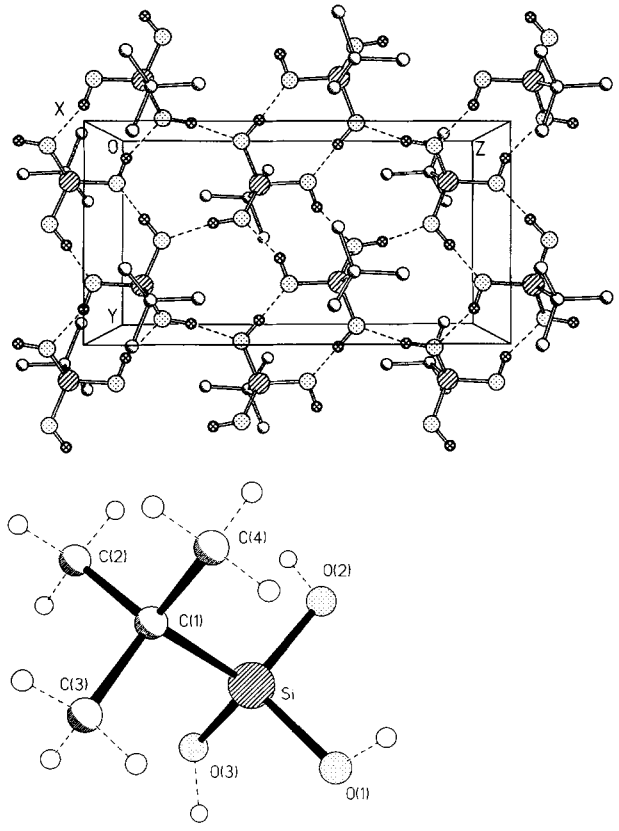

Fig. 1. Top: Packing of **1** in the crystal. The Si, O, and C atoms are represented as in the lower part of the figure. H atoms are shown as crosshatched spheres. Bottom: Structure of **1** in the solid state; bond lengths and angles given in text.

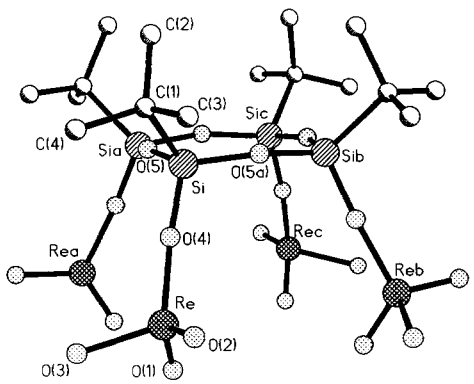

Fig. 2. Structure of **2** in the solid state [16].

try that the analogous six-membered ring is formed as an intermediate or side product.

Experimental Procedure

1: tBuSiCl$_3$ (25 g, 0.13 mol) were dissolved in dry diethyl ether (about 100 mL). This solution was added dropwise over a period of one hour to a vigorously stirred emulsion of water (7.1 mL, 0.39 mol) and aniline (35.7 mL, 36.5 g 0.39 mol) in dry diethyl ether (about 1.5 L) cooled in ice. After the addition the mixture was stirred for a further 12 h while warming to room temperature. Thereafter the precipitated hydrochloride was filtered off, and the clear filtrate concentrated by distillation (34 °C, 760 Torr). Soon small needlelike crystals formed. The crystals were filtered off when the volume reached approximately 200 mL. From the crystalline product (12.4 g, 0.09 mol), crystals suitable for X-ray analysis could be selected. The mother liquor was concentrated under reduced pressure till a few mL remained. A further 4.3 g of amorphous material was obtained. The total was thus 16.7 g (0.12 mol, 94%). Decomposition at 206 °C; correct C, H analyses. MS (EI): m/z 136 $[M]^+$. IR (Nujol/KBr): $\tilde{\nu}$ [cm^{-1}] = 3100w, 1038w, 1010w, 914s, 886s, 844w, 808w, 721w. ^{1}H NMR (80 MHz, [D$_6$]DMSO, TMS ext.): δ = 0.85 (s, 9H; tBu), 5.50 (br s, 3H; OH); ^{29}Si NMR (49 MHz, D$_2$O, TMS ext.): δ = −36.8.

2: Re_2O_7 (2.42 g, 5.0 mmol) and **1** (1.36 g, 10.0 mmol) were placed in a flask, suspended in toluene (40 mL), and heated for 4 h at reflux. This procedure afforded a whitish gray suspension and a few drops of a black oily substance (0.77 g), which were separated by filtration. Removal of the solvent from the filtrate under vacuum left a yellowish oil, which when mixed with 5 mL of pentane spontaneously yielded a white solid. This was filtered off and dried for three days at 10^{-2} Torr at room temperature (yield: 1.73 g, 1.2 mmol, 49%). Extraction with boiling acetonitrile and subsequent crystallization at room temperature furnished square single crystals. Decomposition at 138 °C; correct C, H analyses; MS (EI): m/z 1347 (35%) $[M-t\text{Bu}]^+$, 57 (100%) $[t\text{Bu}]^+$; IR (Nujol/KBr): $\tilde{\nu}$ [cm^{-1}] = 1261s, 1095s, 1018s, 955w, 800s, 722w; ^{1}H NMR (400 MHz, CD_3CN, TMS ext.): δ = 0.95–1.05 (m, 10H; tBu), 1.05–1.15 (m, 9H; tBu); ^{29}Si NMR (79 MHz, CD_3CN, TMS ext.): δ = −52.89 – −59.22 (m).

Received: August 26, 1991 [Z4891 IE]
Publication delayed at authors' request
German version: *Angew. Chem.* **1991**, *104*, 670

CAS Registry numbers:
1, 138385-77-0; **2**, 138407-44-0; tBuSiCl$_3$, 18171-74-9.

[1] Y. I. Yermakov, B. N. Kuznetsov, V. A. Zakharov, *Catalysis by Supported Complexes*, Elsevier, New York, **1981**; T. Setyama, K. Tanabe, *New Horizons in Catalysis*, Elsevier, New York, **1980**.
[2] W. A. Herrmann, J. G. Kuchler, J. K. Felixberger, E. Herdtweck, W. Wagner, *Angew. Chem.* **1988**, *100*, 420–422; *Angew. Chem. Int. Ed. Engl.* **1988**, *27*, 394–395.
[3] F. J. Feher, *J. Am. Chem. Soc.* **1986**, *108*, 3850–3852.
[4] F. J. Feher, D. A. Newman, J. F. Walzer, *J. Am. Chem. Soc.* **1989**, *111*, 1741–1748; F. J. Feher, J. F. Walzer, *Inorg. Chem.* **1991**, *30*, 1689–1694.
[5] Yu. E. Ovchinnikov, V. E. Shklover, Yu. T. Struchkov, M. M. Levitsky, A. A. Zhdanov, *J. Organomet. Chem.* **1988**, *347*, 253–267.
[6] M. M. Levitsky, O. I. Schegolikhina, A. A. Zhdanov, V. A. Igonin, Yu. E. Ovchinnikov, V. E. Shklover, Yu. T. Struchkov, *J. Organomet. Chem.* **1991**, *401*, 199–210.
[7] H. W. Roesky, A. Mazzah, D. Hesse, M. Noltemeyer, *Chem. Ber.* **1991**, *124*, 519–521.
[8] *Ullmanns Enzykl. Tech. Chem.* 4th ed. **1982**, *21*, 511–543.
[9] T. Takiguchi, *J. Am. Chem. Soc.* **1959**, *81*, 2359–2361.
[10] Z. Michalska, Z. Lasocki, *Bull. Acad. Pol. Sci. Ser. Sci. Chim.* **1971**, *19*, 757–763.
[11] S. S. Al-Juaid, N. H. Buttrus, R. I. Damja, Y. Derouiche, C. Eaborn, P. B. Hitchcock, P. D. Lickiss, *J. Organomet. Chem.* **1989**, *371*, 287–295.
[12] H. Ishida, J. L. Koenig, K. C. Gardner, *J. Chem. Phys.* **1982**, *77*, 5748–5751.
[13] E. Wiberg, W. Simmler, *Z. Anorg. Allg. Chem.* **1955**, *282*, 330–344.
[14] P. D. Lickiss, S. A. Lister, A. D. Redhouse, C. J. Wisener, *J. Chem. Soc. Chem. Commun.* **1991**, 173–174.
[15] **1**: $C_4H_{12}O_3Si$, space group $P2_1/c$, monoclinic, a = 9.192(2), b = 6.715(1), c = 12.758(2) Å, β = 91.10(2)°, (Stoe AED2, Rev. 6.2), $Mo_{K\alpha}$ (λ = 0.71073 Å), V = 787.4(2) Å^3, Z = 4, ϱ_{calcd} = 1.15 Mgm^{-3}. R = 5.74, R_w = 0.0632. for 726 observed reflections with $F > 3.0\,\sigma(F)$. Hydrogen atoms could be detected from the difference Fourier synthesis. They were positioned geometrically and refined with a riding model. Further details of the crystal structure investigation may be obtained from the Fachinformationszentrum Karlsruhe, Gesellschaft für wissenschaftlich-technische Information mbH, D-W-7514 Eggenstein-Leopoldshafen 2 (FRG) on quoting the depository number CSD-55829, the names of the authors, and the journal citation.
[16] **2**: $C_4H_9O_5ReSi$, space group $P4/n$, tetragonal, a = 13.260(2), b = 10.500(2) Å, (Stoe-Huber R3m/V), $Mo_{K\alpha}$ (λ = 0.71073 Å), V = 1846.2(5) Å^3, Z = 8, ϱ_{calcd} = 2.528 Mgm^{-3}. The poor quality of the crystals did not permit a good refinement, no further details will be given here.

Cyclophosphazene Metal Oxides, a New Class of Compounds, and Model Compounds for the Polymerization of Phosphazenes**

By *Reinhard Hasselbring, Herbert W. Roesky,** and *Mathias Noltemeyer*

Dedicated to Professor Wolfgang Beck on the occasion of his 60th birthday

Cyclometallaphosphazenes[1] are of significance since they are precursors for interesting polymers[2] and the low-valent metal atoms can participate in cycloadditions.[3] For kinetic reasons the polymers should be free from halogen atoms. This could be achieved if phosphazene oxide and metal oxide building blocks were combined.

The reaction of the acyclic, completely silylated phosphazene **1**[4] with Re_2O_7, by elimination of siloxane, led to the first cyclophosphazene metal oxide **2**. Since **2** only dissolves upon heating in polar solvents such as dimethylsulfoxide (DMSO), pyridine, acetonitrile, or water with decomposition, only the absence of silyl protons can be determined by NMR spectroscopy. However, elemental analysis, mass spectrometry, and IR spectroscopy confirm the composition of **2**. The compound is air- and water-stable at room temperature.

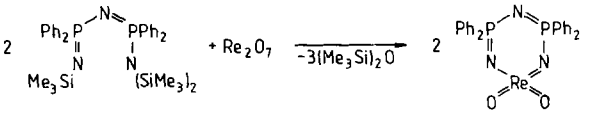

1 **2**

If **2** is allowed to react with an excess of ArNCO (Ar = 2,6-diisopropylphenyl) a mixture of products is obtained, which contains the cyclophosphazene metal imides **3** and **4**. At first, **3** crystallized as deep red needles from toluene/n-hexane at −25 °C, then after ca. three weeks **4** appeared in the form of orange prisms. The crystals of **4** were

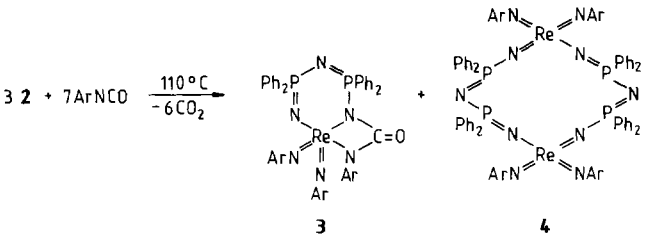

3 **4**

suitable for a single crystal X-ray structure analysis, whereas suitable single crystals of **3** could only be obtained from acetonitrile at room temperature. The molecular structure of **3** is shown in Figure 1.

The [2+2] cycloaddition of the isocyanate at the ReN double bond of **2** (or **5**) leads to a distorted square-pyramidal arrangement of the ligands at the rhenium center in **3**. An otherwise possible planarity of the six-membered ring is

[*] Prof. Dr. H. W. Roesky, R. Hasselbring, Dr. M. Noltemeyer, Institut für Anorganische Chemie der Universität Tammannstrasse 4, D-W-3400 Göttingen (FRG)

[**] This work was supported by the Deutsche Forschungsgemeinschaft and the Fonds der Chemischen Industrie.

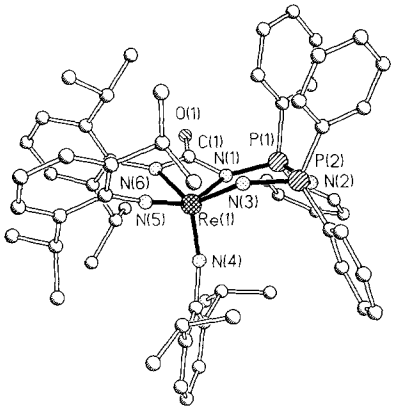

Fig. 1. Molecular structure of **3** [5]. Selected distances [pm] and angles [°]: Re(1)-N(1) 219.9(3), Re(1)-N(3) 186.2(3), Re(1)-N(4) 174.2(3), Re(1)-N(5) 176.2(3), Re(1)-N(6) 204.8(3), P(1)-N(1) 163.8(3), P(1)-N(2) 159.5(4), P(2)-N(2) 160.1(4), P(2)-N(3) 161.7(3), N(1)-C(1) 137.6(5), N(6)-C(1) 138.0(5), O(1)-C(1) 121.3(5); N(1)-Re(1)-N(3) 86.1(1), N(1)-Re(1)-N(4) 94.9(1), N(3)-Re(1)-N(4) 110.6(1), N(1)-Re(1)-N(5) 150.2(1), N(3)-Re(1)-N(5) 100.8(1), N(4)-Re(1)-N(5) 109.3(1), N(1)-Re(1)-N(6) 61.0(1), N(3)-Re(1)-N(6) 127.4(1), N(4)-Re(1)-N(6) 112.0(2), N(5)-Re(1)-N(6) 93.0(1), N(1)-P(1)-N(2) 109.7(2), N(2)-P(2)-N(3) 117.9(2), Re(1)-N(1)-P(1) 131.8(2), P(1)-N(2)-P(2) 120.8(2), Re(1)-N(3)-P(2) 132.7(2).

therefore removed (average deviation from the plane: 20 pm). The bond length between Re(1) and N(1) (219.9 pm) lies in the range of a coordinated bond;[6] all other bonds within the ring system are shorter than single and longer than double bonds. N(1) and N(6) can also be considered as donor atoms of an unsymmetrical Re^{VII} ureato complex.[7]

In the dimetallatetraimidophosphazene **4** (Fig. 2),[8] which is only isolated in very small quantities, the Re centers show an almost tetrahedral coordination, and the twelve-membered ring is puckered.[9] We assume that **4** is formed by a [2+2] dimerization of **5** (via **6**).

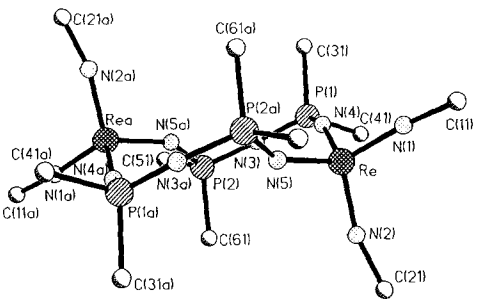

Fig. 2. Molecular structure of **4** (for the aryl groups only the C atoms directly bonded are shown). Selected distances [pm] and angles [°]: Re-N(1) 174.5(4), Re-N(2) 174.3(5), Re-N(4) 183.2(6), Re-N(5) 184.0(6), P(1)-N(3) 157.7(4), P(1)-N(4) 159.0(7), P(2)-N(3) 158.4(6), N(5)-P(2a) 159.8(7), N(1)-Re-N(2) 110.9(2), N(1)-Re-N(4) 107.8(3); N(2)-Re-N(4) 112.3(3), N(1)-Re-N(5) 110.0(3), N(2)-Re-N(5) 106.7(3), N(4)-Re-N(5) 109.1(3), N(3)-P(1)-N(4) 120.5(3), P(1)-N(3)-P(2) 139.1(5), Re-N(4)-P(1) 159.6(4), Re-N(5)-P(2a) 147.9(3), N(3)-P(2)-N(5a) 117.0(3).

Regarding the structure and mechanism the comparison with the well-studied λ^5-azaphospholes is interesting. In that case, an equilibrium is formed between the monomer and dimer (which so far we have not been able to establish for cyclometallaphosphazenes), and [2+2] cycloadditions of ketones and aldehydes are possible. However, ring systems such as **4** are unknown.[10]

It is improbable that **2** is already present as a twelve-membered ring since the mass spectrum gives no indications

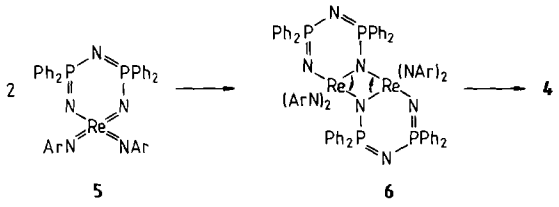

of it. On the other hand, compound **4** is mass spectrometrically clearly different from **3**. However, it appears plausible that **2** is dimeric (analogous to **6**) in the solid state, since the only known cyclotriazaphosphorin metal oxide $[N{=}PPh_2{-}N{=}C(4\text{-}CF_3C_6H_4){-}N{=}ReO_2]_2$, which has been established by a single crystal structure investigation, is also dimeric.[11]

In the presence of Lewis acids, the polymerization of $P_3N_3Cl_6$ leads to the corresponding polymer. Therefore, the formation of a phosphonium ion is assumed, which, as the rhenium atom in **5**, initiates the cycloaddition.[12] It is apparent that if the [2+2] selfaddition is continued to yet larger molecules, it could represent a novel polymerization mechanism by cyclophosphazenes.

Experimental Procedure

2: **1** (4.0 g, 6.3 mmol) in THF (30 mL) was added dropwise to a solution of Re_2O_7 (1.5 g, 3.1 mmol) in THF (30 mL). After 5–6 h, only a fine powdery white product precipitated out of the dark solution. The mixture was stirred for a further 2 d at room temperature, then the solid was filtered off and washed with THF. Yield 2.5 g (63%); m.p. 234 °C; ^{1}H NMR (80.13 MHz, [D$_6$]DMSO, TMS ext.): δ = 7.0 – 8.0 (m); IR (KBr): ν [cm^{-1}] = 1438 m, 1270 s, 1214 s, 1135 s, 1129 vs, 1110 s, 935 s (Re = O), 920 s (Re = O), 721 m, 705 m, 692 m, 575 m, 532 s, 500 m; MS (70 eV): *m/z* 631 (M^+, 100%, ^{187}Re).

3 and **4**: **2** (0.4 g, 0.63 mmol) and ArNCO (1 mL, excess) were refluxed in toluene (5 mL) with evolution of CO_2 for 16 h. After the removal of all volatiles under vacuum at 80 °C, the remaining solid was recrystallized from toluene/*n*-hexane at −25 °C. Yield of **3** 0.35 g, (48%); m.p. 240 °C; ^{1}H NMR (250.133 MHz, $CDCl_3$, TMS ext.): δ = 0.6 (d, 12 H), 0.8 (d, 6 H), 0.9 (d, 12 H), 1.1 (d, 6 H), 3.5 (m, 6 H), 6.8–8.0 (m, 29 H); ^{31}P NMR (101.246 MHz, $CDCl_3$, 85% H_3PO_4 ext.): δ = 17.2 (d), 18.2 (d); IR (nujol): ν [cm^{-1}] = 1671 vs, 1256 s, 1198 s, 1120 s, 1056 s; MS (70 eV): *m/z* 1152 (M^+, 5%, ^{187}Re), 949 (M^+ − ArNCO, 100%). Yield of **4**: ca. 5 mg; m.p. 270 °C; MS (70 eV) : *m/z* 1898 (M^+, 100%, ^{187}Re).

Received: December 4, 1991 [Z 5052 IE]
German version: *Angew. Chem.* **1992**, *104*, 613

CAS Registry numbers:
1, 141088-20-2; **2**, 141088-21-3; **3**, 141088-22-4; **3**·CH_3CN, 141088-25-7; **4**, 141088-23-5; **4**·2 toluene, 141088-24-6; Re_2O_7, 1314-68-7; 2,6-diisopropylphenylisocyanate, 28178-42-9.

[1] H. W. Roesky, K. V. Katti, U. Seseke, M. Witt, E. Egert, R. Herbst, G. M. Sheldrick, *Angew. Chem.* **1986**, *98*, 447–448; *Angew. Chem. Int. Ed. Engl.* **1986**, *25*, 477–478; H. W. Roesky, K. V. Katti, U. Seseke, H.-G. Schmidt, E. Egert, R. Herbst, G. M. Sheldrick, *J. Chem. Soc. Dalton Trans.* **1987**, 847–849; K. V. Katti, H. W. Roesky, M. Rietzel, *Inorg. Chem.* **1987**, *26*, 4032–4035; K. V. Katti, U. Seseke, M. Witt, H. W. Roesky, *Phosphorus Sulfur* **1987**, *30*, 421–423.

[2] H. W. Roesky, M. Lücke, *Angew. Chem.* **1989**, *101*, 480–481; *Angew. Chem. Int. Ed. Engl.* **1989**, *28*, 493.

[3] G. Hogarth, P. C. Konidaris, *J. Organomet. Chem.* **1990**, *399*, 149–152; R. S. Pilato, C. E. Housmekerides, P. Jernakoff, D. Rubin, G. L. Geoffroy, A. L. Rheingold, *Organometallics* **1990**, *9*, 2333-2341; W.-H. Leung, G. Wilkinson, B. Hussain-Bates, M. B. Hursthouse, *J. Chem. Soc. Dalton Trans.* **1991**, 2791-2794.

[4] R. Hasselbring, H. W. Roesky, M. Rietzel, M. Noltemeyer, *Phosphorus, Sulfur, Silicon Relat. Elem.*, in press.

[5] a) $C_{61}H_{71}N_6OP_2Re\cdot CH_3CN$, M_r = 1193.4, monoclinic, $P2_1/c$, a = 2083.6(4), b = 1257.5(3), c = 2301.5(5) pm, β = 98.67(3)°, V = 5.962(3) nm^3, Z = 4, ρ_{calcd} = 1.330 Mg m^{-3}, $\mu(Mo_{K\alpha})$ = 2.162 mm^{-1}, 15935 measured reflections to $2\theta_{max}$ = 45°, semiempirical absorption correction, 7018 observed reflections with $F > 3\sigma(F)$ were used for the solution and refinement of the structure. R = 0.033 (wR = 0.037, weighting scheme $w^{-1} = \sigma^2(F) + 0.0004F^2$). b) Further details of the crystal structure investigation may be obtained from the Fachinformationszentrum

Karlsruhe, Gesellschaft für wissenschaftlich-technische Information mbH, D-W-7514 Eggenstein-Leopoldshafen 2 (FRG) on quoting the depository number CSD-56045, the names of the authors, and the journal citation.
[6] W. A. Herrmann, D. W. Marz, E. Herdtweck, *J. Organomet. Chem.* **1990**, *394*, 285–303.
[7] W. A. Herrmann, G. Wechselbaumer, R. A. Paciello, R. A. Fischer, E. Herdtweck, J. Okuda, D. W. Marz, *Organometallics* **1990**, *9*, 489–496. The structures of the addition products with isocyanates mentioned in this contribution have not been proven.
[8] $C_{96}H_{108}N_{10}P_4Re_2 \cdot 2$toluene, $M_r = 2082.5$, triclinic, $P\bar{1}$, $a = 1281.1(3)$, $b = 1505.8(3)$, $c = 1524.5(3)$ pm, $\alpha = 70.67(3)$, $\beta = 65.36(3)$, $\gamma = 87.74(3)°$, $V = 2.506(1)$ nm^3, $Z = 1$, $\rho_{calcd} = 1.38$ Mg m^{-3}, $\mu(Mo_{K\alpha}) = 2.56$ mm^{-1}, 8314 measured reflections to $2\theta_{max} = 45°$, semiempirical absorption correction, 5783 observed reflections with $F > 3\sigma(F)$ were used for the solution and refinement of the structure. $R = 0.040$ ($wR = 0.046$, weighting scheme $w^{-1} = \sigma^2(F) + 0.0008F^2$). See also [5b].
[9] **4** is nonplanar. However, an almost complete equalizing of the bond lengths takes place so that the formulation of single- and double bonds occurs at random to account for the formal oxidation states.
[10] W. S. Sheldrick, D. Schomburg, A. Schmidpeter, T. von Criegern, *Chem. Ber.* **1980**, *113*, 55–69; A. Schmidpeter, H. Tautz, F. Schreiber, *Z. Anorg. Allg. Chem.* **1981**, *475*, 211–231; R. O. Day, R. R. Holmes, H. Tautz, J. H. Weinmaier, A. Schmidpeter, *Inorg. Chem.* **1981**, *20*, 1222–1229.
[11] R. Hasselbring, H. W. Roesky, M. Noltemeyer, unpublished results. The endocyclic ReN bond of the Re_2N_2 unit is 203 pm long. The ReN distance which is not influenced is 183 pm. These values show that the bond lengthening up until bond breakage gradually depends on factors such as the addition partners or the substituents at the Re.
[12] H. R. Allcock, *Phosphorus-Nitrogen Compounds*, Academic Press, New York, **1972**, chapter 15; R. O. Day, A. Schmidpeter, R. R. Holmes, *Inorg. Chem.* **1983**, *22*, 3696–3699.

O–H Bond Activation in the Gas Phase: The Reactions of Water and Methanol with $[FeCH_3]^+$ **

By *Ofer Blum, Detlef Stöckigt, Detlef Schröder,* and *Helmut Schwarz**

Dedicated to Professor Heinz Harnish on the occasion of his 65th birthday

Although water and methanol are among the cheapest available resources, very little has been done to utilize their economically attractive, robust O–H bond by transition-metal-mediated catalysis.[1] The O–H bonds in water and methanol has been cleaved by transition metals in solution,[1] in solid noble gas matrices,[2, 3] on surfaces,[4] or on iron clusters,[5] resulting in potentially useful metal hydroxides or metal alkoxides. In the gas phase, iron and manganese carbonyl anions[6] and $[HCr(CO)_3]^-$ activate water readily.[7] C–H cleavage predominates in the reaction of methanol with $[Mn(OC)_3]^-$[8] and $[V(OC)_5]^-$.[9, 10] Oxophilic early transition-metal cations (V^+)[11] and neutral metal atoms (Sc, Y, and La)[12] form metal oxides upon reactions with water and methanol. Mo^+ dehydrogenates methanol, but because no labeling experiments were performed, the mechanism 1,1- or 1,2-elimination could not be deduced.[13] 1-Propanol and higher *n*-alcohols react with late transition-metal cations by C–H rather than O–H functionalization.[14] Fe^{II} alkoxides of the general structure $[FeO(CH_2)_nCH_2OH]^+$ ($n = 1-7$) were, however, recently observed to expel molecular hydrogen unimolecularly, and labeling experiments demonstrate that in the course of H_2 evolution the CH_2OH group of the Fe^{II} alkoxide is oxidized to an aldehyde group.[15a] The Fe^+ mediated CH_4 loss from *o*-methoxyphenol was explained in terms of an *ortho* effect resulting in the cleavage of the phenolic O–H bond.[15b] Water or methanol[16] activation by cationic, late transition-metal fragments is as yet unknown. Here we report the O–H bond activation of water and methanol by cationic $[FeCH_3]^+$ and suggest a mechanism that is in keeping with the experimental findings, especially the unusually large kinetic deuterium isotope effects for these reactions.

$$[FeCH_3]^+ + H_2O \xrightarrow{0.94} FeOH^+ + CH_4 \quad (a)$$
$$[FeCH_3]^+ + H_2O \xrightarrow{0.06} [(H_3C)Fe(OH_2)]^+ \quad (b)$$

$[FeCH_3]^+$ generated under FTICR conditions (FTICR = Fourier Transform Ion Cyclotron Resonance)[17] reacts slowly with water to afford mainly $[FeOH]^+$ and CH_4 [Eq. (a)]. At longer reaction times, the secondary adduct products $[FeOH(OH_2)_n]^+$ ($n = 1, 2$) are observed [Eq. (b)]. Control experiments for various trapping and cooling periods and different relative pressures of water and argon brought no substantial change in the branching ratio or the reaction rates, indicating that the activation of water is not caused by excited $[FeCH_3]^+$. A rate constant of $6(\pm 1) \times 10^{-12}$ cm^3 molecule^{-1}s^{-1} is obtained for the slightly exothermic reaction (a)[24] (-6 kcal mol^{-1}[25]). However, since its efficiency ($k_{prod.}/k_{coll.}$) is only 0.3% of the calculated collision limit ($k_{ADO}(H_2O) = 1.9 \times 10^{-9}$ cm^3 molecule^{-1}s^{-1}[26]) a significant activation energy is involved. A substantial kinetic isotope effect $k_H/k_D \geq 20$ is calculated from the rates of reactions (a) and (c).[27]

$$[FeCH_3]^+ + D_2O \xrightarrow{0.04} FeOD^+ + CH_3D \quad (c)$$
$$[FeCH_3]^+ + D_2O \xrightarrow{0.96} [(H_3C)Fe(OD_2)]^+ \quad (d)$$

Only the O–H bond is activated in methanol [Eq. (e)], as evidenced by the products in [Eq. (f)]. Loss of CH_2O [Eq. (g)], observed at longer reaction times, is indicative of the generation of $[FeOCH_3]^+$.[28] A rate constant of $4(\pm 0.8) \times 10^{-10}$ cm^3 molecule^{-1} s^{-1} and an efficiency of 25% ($k_{ADO}(CH_3OH) = 1.7 \times 10^{-9}$ cm^3 molecule^{-1} s^{-1})[26] were observed for reaction (e). Reaction (f) showed a deuterium isotope effect ($k_H/k_D = 15 \pm 3$).

$$[FeCH_3]^+ + CH_3OH \longrightarrow [FeOCH_3]^+ + CH_4 \quad (e)$$
$$[FeCH_3]^+ + CH_3OD \longrightarrow [FeOCH_3]^+ + CH_3D \quad (f)$$
$$[FeOCH_3]^+ + CH_3OX \longrightarrow [HFe(XOCH_3)]^+ + CH_2O \quad (g)$$
$$(X = H, D)$$

The reactions of both water and methanol with $[FeCH_3]^+$ are thought to follow the mechanism depicted in Scheme 1. The initial ligation of the dipolar water or methanol mole-

[*] Prof. Dr. H. Schwarz, Dipl.-Chem. D. Stöckigt, Dipl.-Chem. D. Schröder
Institut für Organische Chemie der Technischen Universität
Straße des 17. Juni 135, D-W-1000 Berlin 12 (FRG)
O. Blum
Department of Organic Chemistry
The Weizmann Institute of Science, Rehovot 76100 (Israel)

[**] Financial support of our work by the Volkswagen-Stiftung, Deutsche Forschungsgemeinschaft, and Fonds der Chemischen Industrie is gratefully appreciated. We are indebted to Professor D. K. Bohme for helpful discussions.

cules to the $[FeCH_3]^+$ cation is favored by the attractive forces between them. Observation of the adduct $[H_3CFe(OX_2)]^+$ (X = H, D) supports this claim. The low reaction efficiency and the observation of a large kinetic isotope effect reveal the existence of a kinetic barrier for the breaking of the O–X bond (X = H, D). The unusual magnitude of the deuterium kinetic isotope effect renders a multicentered transition structure[29] unlikely for the O–H activation, for which a lower k_H/k_D value is anticipated. The O–H cleavage is therefore assumed to take place while the oxygen is ligated to the metal center (Scheme 1: $[H_3CFe(ROH)]^+ \rightarrow [CH_3Fe(H)OR]^+$). A direct hydrogen transfer from the oxy-

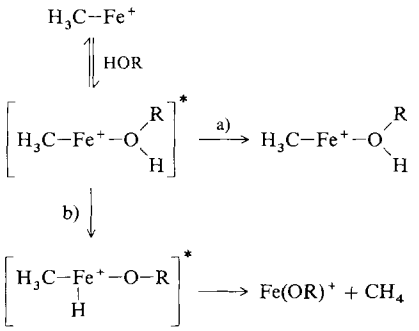

Scheme 1. The proposed mechanism of the O–H bond activation by $[FeCH_3]^+$ (R = H, CH_3). a) Relaxation by collision with argon atoms (R = H); b) slow reaction.

gen atom to the carbon of the methyl group cannot be ruled out, but is unlikely.[30] Such a mechanism is expected to be influenced by the distance between the hydrogen-donating and -accepting atoms, which is not expected to change significantly if R is a hydrogen atom or a methyl group.

An activation of the O–H bond two orders of magnitude faster in methanol than in water can be explained by the 15 kcal mol^{-1} weaker O–H bond strength[25] in methanol. This mechanism, which corresponds to an O–H oxidative addition mechanism, is supported by the striking difference (three orders of magnitude) between the reaction rates of $[FeCH_3]^+$ and $[Fe(^{18}OH)]^+$ with water, the latter occurring at 50% of the collision-rate. There must be a fundamental mechanistic difference between the two processes. The exchange reaction $[Fe(^{18}OH)]^+ + H_2{}^{16}O \rightleftarrows [Fe(^{16}OH)]^+ + H_2{}^{18}O$ is more likely to proceed by hydrogen transfer mechanism to a lone electron pair on the oxygen atom (Eigen mechanism) rather than by oxidative insertion.

Received: December 3, 1991 [Z 5047 IE]
German version: *Angew. Chem.* **1992**, *104*, 637

CAS Registry numbers:
$[FeCH_3]^+$, 90143-29-6; H_2O, 7732-18-5; D_2O, 7789-20-0; CH_3OH, 67-56-1; CH_3OD, 4206-31-9.

[1] Review: H. E. Bryndza, W. Tam, *Chem. Rev.* **1988**, *88*, 1163; also see: D. S. Glueck, L. J. N. Winslow, R. G. Bergman, *Organometallics* **1991**, *10*, 1462, and references cited therein.
[2] a) J. W. Kauffman, R. H. Hauge, J. L. Margrave, *J. Phys. Chem.* **1985**, *89*, 3541, 3547; b) S. C. Chang, R. H. Hauge, Z. H. Kafafi, J. L. Margrave, W. E. Billups, *J. Am. Chem. Soc.* **1988**, *110*, 7975.
[3] M. Park, R. H. Hauge, Z. H. Kafafi, J. L. Margrave, *J. Chem. Soc. Chem. Commun.* **1985**, 1570.
[4] J. B. Benziger, R. H. Madix, *J. Catal.* **1980**, *65*, 36, and references cited therein.
[5] B. H. Weiller, P. S. Bechthold, E. K. Parks, L. G. Pobo, S. J. Riley, *J. Chem. Phys.* **1989**, *91*, 4714.
[6] R. N. McDonald, A. K. Chowdhury, M. T. Jones, *J. Am. Chem. Soc.* **1986**, *108*, 3105.
[7] K. R. Lane, R. R. Squires, *J. Am. Chem. Soc.* **1985**, *107*, 6403.
[8] R. N. McDonald, M. T. Jones, *Organometallics* **1987**, *6*, 1991.
[9] S. W. Buckner, S. L. VanOrden, *Organometallics* **1990**, *9*, 1093.
[10] O–H activation of methanol for similar systems was assumed previously: J. Allison, S. W. McElvany, *Organometallics* **1986**, *5*, 416.
[11] R. R. Squires, P. J. Marinelle, *J. Am. Chem. Soc.* **1989**, *111*, 4101.
[12] K. Liu, J. M. Parson, *J. Chem. Phys.* **1978**, *68*, 1794.
[13] H. Huang, R. W. Holman, M. L. Gross, *Organometallics* **1986**, *5*, 1857.
[14] a) S. Karraß, T. Prüsse, K. Eller, H. Schwarz, *J. Am. Chem. Soc.* **1989**, *111*, 9018; b) T. Prüsse, H. Schwarz, *Organometallics* **1989**, *8*, 2856; c) T. Prüsse, J. Allison, H. Schwarz, *Int. J. Mass Spectrom. Ion Processes* **1991**, *107*, 553.
[15] a) T. Prüsse, H. Schwarz, *Helv. Chim. Acta* **1991**, *74*, 1739; b) A. J. Bjarnason, J. W. Taylor, J. A. Kinsinger, R. B. Cody, D. A. Weil, *Anal. Chem.* **1989**, *61*, 1889.
[16] The C–O cleavage in methanol by Fe^+ or $[Fe(CD_3OH)]^+$ is endothermic (ca. 11 kcal mol^{-1}) and is probably caused by excited iron cations: J. Allison, D. P. Ridge, *J. Am. Chem. Soc.* **1979**, *101*, 4998.
[17] The apparatus (a Spectrospin-CMS-47X Fourier Transform ion cyclotron resonance instrument equipped with an external ion source [18]) and its operation have been previously described [19]. Briefly, Fe^+ is formed through laser desorption/ionization [20] by focusing the beam of a Nd:YAG laser (Spectron Systems, fundamental frequency 1064 nm) onto a stainless steel target. The ions are extracted from the source and transferred into the analyzer cell by a system of electrostatic potentials. The external ion source, transfer system, and ICR cell are differentially pumped by three turbomolecular pumps. After deceleration, the ions are trapped in the field of the superconducting magnet (Oxford Instruments, maximum field strength of 7.05 T). The $^{56}Fe^+$ isotope is isolated by using FERETS [21], and allowed to react with pulsed-in CH_3I to generate $[FeCH_3]^+$ [22]. H_2O or CH_3OH was present at a stationary pressure of $1-2\times10^{-8}$ mbar. Argon was present as a buffer gas with a constant pressure of $0.2-1.5\times10^{-7}$ mbar for collisional quenching of any excited states formed in laser desorption/ionization and for removal of translational energy remaining from the transfer to the ICR cell. Prior to the reaction of $[FeCH_3]^+$ with D_2O the FTICR instrument was flushed with D_2O (5×10^{-7} mbar; 6 h). Nevertheless, H_2O molecules remained adsorbed to the cell wall. An 8% hydrogen content was deduced from the ratio between the adducts $[H_3CFe(OHD)]^+$ and $[H_3CFe(OD_2)]^+$. In the case of CH_3OD the residual CH_3OH content was derived from i) internal ion source ionization of CH_3OD (15 eV), and ii) the isotope distribution of the adduct $[HFe(XOCH_3)]^+$ after long reaction times. The parameters for the absolute pressure determinations are taken from [23]. All functions of the instrument were controlled by a Bruker Aspect 3000 minicomputer.
[18] a) P. Kofel, M. Allemann, H. Kellerhals, K. P. Wanczek, *Int. J. Mass Spectrom. Ion Processes* **1985**, *65*, 97; b) P. Kofel, M. Allemann, H. Kellerhals, K. P. Wanczek, *Adv. Mass Spectrom.* **1985**, *10*, 885.
[19] a) K. Eller, H. Schwarz, *Int. J. Mass Spectrom. Ion Processes* **1989**, *93*, 243; b) K. Eller, W. Zummack, H. Schwarz, *J. Am. Chem. Soc.* **1990**, *112*, 621; c) K. Eller, Dissertation, Technische Universität Berlin, D 83, **1991**.
[20] B. S. Freiser, *Talanta* **1985**, *32*, 697.
[21] R. A. Forbes, F. M. Laukien, J. Wronka, *Int. J. Mass Spectrom. Ion Processes* **1988**, *83*, 23.
[22] D. B. Jacobson, B. S. Freiser, *J. Am. Chem. Soc.* **1985**, *107*, 5876.
[23] J. E. Bartmess, R. M. Georgiadis, *Vacuum* **1983**, *33*, 149.
[24] The formation of the adduct $[H_3CFe(OH_2)_2]^+$ is probably due to collisional stabilization and depends on the argon pressure. Its observed formation rate at an argon pressure of 1×10^{-7} mbar is ca. 1×10^{-21} cm^6 molecule^{-2} s^{-1}. However, radiative association cannot be excluded.
[25] Thermochemical data: S. G. Lias, J. E. Bartmess, J. F. Liebman, J. L. Holmes, R. D. Levin, W. G. Mallard, *J. Phys. Chem. Ref. Data* **1988**, *17*, Suppl. 1.
[26] The ADO (averaged dipole orientation) ion-molecule collision rate constant is calculated according to T. Su, M. T. Bowers, *Int. J. Mass Spectrom. Ion Phys.* **1973**, *23*, 347.
[27] Because reaction of $[FeCH_3]^+$ with D_2O was slow, the pressures of D_2O and Ar were increased to 1.5 and 3.0×10^{-7} mbar, respectively. This experiment is affected by a residual hydrogen content in D_2O [17], and almost all $[Fe(OH)]^+$ stems from this source. For this reason the value given for the kinetic isotope effect represents a lower limit. Accordingly, the correction of the branching ratios given in reactions (c) and (d) for the different pressure was neglected.
[28] a) D. Schröder, H. Schwarz, unpublished; b) T. J. Carlin, L. Sallons, C. J. Cassady, D. B. Jacobson, B. S. Freiser, *J. Am. Chem. Soc.* **1983**, *105*, 6320.
[29] For example as is proposed for C–H activation of alkanes by atomic transition-metal ions: P. A. M. von Koppen, J. Brodbelt-Lustig, M. T. Bowers, D. V. Dearden, J. L. Beauchamp, E. R. Fisher, P. B. Armentrout, *J. Am. Chem. Soc.* **1990**, *112*, 5663.
[30] A quantum mechanical proton tunneling mechanism can be invoked, but the energy dependence of the reaction is yet to be investigated: R. P. Bell, *The Tunnel Effect in Chemistry*: Chapman and Hall, New York, **1980**, Chapters 3 and 4.

Sequential Insertion of ^3He and ^4He in $C_{60}^{\bullet+}$**

By *Thomas Weiske* and *Helmut Schwarz**

Dedicated to Professor Edward W. Schlag on the occasion of his 60th birthday

For the preparation of endohedral fullerene complexes, in which an atom or molecule M is trapped inside the cavity,[1] and for which the symbol $M@C_x$ was proposed,[2] so far two methods have been adopted: 1) During the laser vaporization of doped graphite, any atoms M accidently attached to the inside of the growing carbon sheet are included. Typical examples are $M@C_{60}$ (M = La, Ni, Na, K, Rb, Cs), $La@C_x$ (x = 70, 74, 82) and the doubly doped $Y_2@C_{82}$.[2, 3] 2) In a bimolecular high-energy collision, atoms M penetrate the shell of the fullerenes. As a result of the mechanism of the collision process, only small inert atoms have a chance of being fired into the cage, from which there is no easy escape due to high barriers. In mass spectrometric experiments, so far, He, Ne, and Ar have been inserted into $C_{60}^{\bullet+}$ and $C_{70}^{\bullet+}$.[4] Recently the production of a neutral $He@C_{60}$ cluster was also achieved by the gas-phase reduction of the corresponding radical cation.[5] A shrinkage of the cage ("shrink-wrap" mechanism[6]) with the retention of the inserted atom, which occurs upon intense excitation with the loss of C_2 or multiple units of C_2, is common to all endohedral complexes. On further excitation, if the cage becomes too small to surround the "imprisoned" atom, the fullerene is blown apart (Scheme 1).

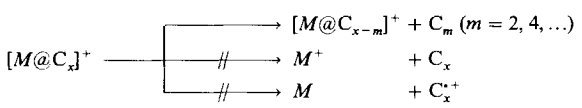

Scheme 1.

Herein we report the sequential insertion of one ^3He *and* one ^4He atom in $C_{60}^{\bullet+}$.[7] The experiment was carried out using a BEBE tandem mass spectrometer (B magnetic and E electric sectors).[8] Technical details of the experiment can be taken from the work describing the neutralization of $[He@C_{60}]^{\bullet+}$,[5] since the considerations there are also valid for the double penetration of the $C_{60}^{\bullet+}$ cage discussed here.

A mixture of C_{60} and C_{70} (> 90% C_{60}) is vaporized in the ion source by heating to 550 °C and ionized with electrons (70 eV). For the production of $[He@C_{60}]^{\bullet+}$, the field strength of the magnet B1 is chosen such that the $C_{60}^{\bullet+}$ ions (m/z 720) are transmitted; the electrical sector E1 has a field strength which allows ions with a kinetic energy of E_K = 5000 eV to pass. Since, for the inelastic collision of $C_{60}^{\bullet+}$ with ^3He in the collision chamber located between B1 and E1 (transmission, T = 40%) the kinetic energy of $C_{60}^{\bullet+}$ is reduced by the center-of-mass-energy, E_{cm}, of the collision complex (E_{cm} = 21 eV for $C_{60}^{\bullet+}$ ions being accelerated to 5000 eV), the accelerating potential is increased by this same value. Under these conditions only $[^3He@C_{60}]^{\bullet+}$ (m/z 723) and inelastically scattered $^{12}C_{60}^{\bullet+}$ ions pass the sector E1. The insertion of a further helium atom occurs by inelastic collisions with stationary ^4He gas in the collision chamber (40% T) located between E1 and B2. Obviously, in this case the inelastically scattered $C_{60}^{\bullet+}$ ions also react with ^4He. The product ions of the bimolecular reactions are recorded by a "linked scan" of B2/E2 = constant[9] (Fig. 1).

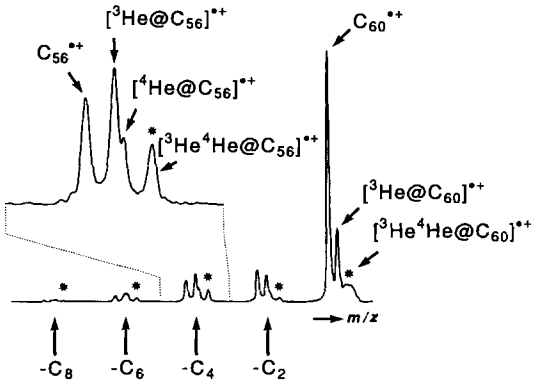

Fig. 1. Sequential insertion of ^3He and ^4He in $C_{60}^{\bullet+}$ by bimolecular high energy collisions:

$C_{60}^{\bullet+} \xrightarrow{^3He} [^3H@C_{60}]^{\bullet+} \xrightarrow{^4He} [^3He^4He@C_{60}]^{\bullet+}$

The signals marked with a star correspond to the formation of insertion products containing one ^3He *and* one ^4He atom.

The "triplet" structure of the $C_x^{\bullet+}$ ions (x = 60–52) with the mass differences Δm = 3, 7 (Fig. 1) proves the consecutive insertion of the two helium atoms ^3He and ^4He.[10] Furthermore, the insert in Figure 1 proves that with improved resolution also the product of the reaction of inelastically scattered $C_{60}^{\bullet+}$ with ^4He becomes visible.

The experiment described here provides a method for the construction of endohedral fullerene adducts of the general structure $AB@C_x$. Crucial to the method is the ability of finding the appropriate "energy windows" necessary for obtaining optimal effective cross sections of the high energy collisions of $C_{60}^{\bullet+}$ ions with the stationary target atoms.

Received: January 25, 1992 [Z 5149 IE]
German version: *Angew. Chem.* **1992**, *104*, 639

CAS Registry numbers:
$C_{60}^{\bullet+}$, 108739-25-9; $[C_{60}{}^3He]^{\bullet+}$, 140225-41-8; $[C_{60}{}^3He^4He]^{\bullet+}$, 140360-31-2.

[*] Prof. Dr. H. Schwarz, Dr. T. Weiske
Institut für Organische Chemie der Technischen Universität
Strasse des 17. Juni 135, D-W-1000 Berlin 12 (FRG)

[**] This work was supported by the Deutsche Forschungsgemeinschaft and the Fonds der Chemischen Industrie. We thank Dr. Wolfgang Krätschmer, Heidelberg, for the gift of C_{60}.

[1] Theoretical studies: a) A. Rosen, B. Wästberg, *J. Am. Chem. Soc.* **1988**, *110*, 8701; b) J. Cioslowski, *ibid.* **1991**, *113*, 4139; c) J. Cioslowski, E. D. Fleischmann, *J. Chem. Phys.* **1991**, *94*, 3730; d) A. H. H. Chang, W. C. Ermler, R. M. Pitzer, *ibid.* **1991**, *94*, 5004; e) D. Bakewies, W. Thiel, *J. Am. Chem. Soc.* **1991**, *113*, 3704; f) B. Wästberg, A. Rosen, *Phys. Scr.* **1991**, *44*, 276; g) J. Cioslowski, *Spectroscopic and Computational Studies of Inclusion Compounds*, Kluwer, Dordrecht, in press; h) P. P. Schmidt, B. I. Dunlap, C. I. White, *J. Phys. Chem.* **1991**, *95*, 10537.

[2] Y. Chai, T. Guo, C. Jin, R. E. Haufler, L. P. C. Chibante, J. Fure, L. Wang, J. M. Alford, R. E. Smalley, *J. Phys. Chem.* **1991**, *95*, 7564.

[3] a) J. R. Heath, S. C. O'Brien, Q. Zhang, Y. Lin, R. F. Curl, H. W. Kroto, F. K. Tittel, R. E. Smalley, *J. Am. Chem. Soc.* **1985**, *107*, 7779; b) F. D. Weiss, J. C. Elkind, S. C. O'Brien, R. F. Curl, R. E. Smalley, *ibid.* **1988**, *110*, 4464; c) J. H. Weaver, Y. Chai, G. H. Kroll, C. Jin, T. P. Ohuo, R. E. Haufler, T. Guo, J. M. Alford, J. Conceicao, L. P. C. Chibante, A. Jain, G. Palmer, R. E. Smalley, *Chem. Phys. Lett.*, submitted.

[4] a) T. Weiske, D. K. Böhme, J. Hrušák, W. Krätschmer, *Angew. Chem.* **1991**, *103*, 898; *Angew. Chem. Int. Ed. Engl.* **1991**, *30*, 884; b) T. Weiske, J. Hrušák, D. K. Böhme, H. Schwarz, *Chem. Phys. Lett.* **1991**, *186*, 459; c) T. Weiske, D. K. Böhme, H. Schwarz, *J. Phys. Chem.* **1991**, *95*, 8451; d) M. M. Ross, J. H. Callahan, *ibid.* **1991**, *95*, 5720; e) K. A. Caldwell, D. E. Giblin, C. S. Hsu, D. Cox, M. L. Gross, *J. Am. Chem. Soc.* **1991**, *113*, 8519;

f) K. A. Caldwell, D. E. Giblin, M. L. Gross, *ibid.*, in press; g) E. E. B. Campbell, R. Ehrlich, A. Hielscher, J. M. A. Frazar, I. V. Hertel, *Z. Phys. D.*, in press; h) T. Weiske, J. Hrušák, D. K. Böhme, H. Schwarz, *Helv. Chim. Acta* **1992**, *75*, 79; i) R. C. Mowrey, M. M. Ross, J. H. Callahan, *J. Phys. Chem.*, in press; j) Z. Wan, J. F. Christian, S. C. Anderson, *J. Phys. Chem.*, in press; k) J. Hrušák, D. K. Böhme, T. Weiske, H. Schwarz, *Chem. Phys. Lett.*, in press.

[5] T. Weiske, T. Wong, W. Krätschmer, J. K. Terlouw, H. Schwarz, *Angew. Chem.* **1992**, *102*, 180; *Angew. Chem. Int. Ed. Engl.* **1992**, *31*, 183.

[6] a) R. F. Curl, R. E. Smalley, Spektr. Wissensch. **1991**, No. 12, p. 88; *Sci. Am.* **1991**, *265*, No. 4, p. 32; b) R. E. Smalley in *Large Carbon Clusters* [*ACS Symp. Ser. 481* (Eds.: G. S. Hammond, V. J. Kuck)], *Am. Chem. Soc.*, Washington, DC, **1992**, p. 141.

[7] The negligible insertion of two ^{4}He atoms in C_{70}^{+} under multiple-collision conditions in one collision cell was described by Gross et al. [see 4e].

[8] a) R. Srinivas, D. Sülzle, T. Weiske, H. Schwarz, *Int. J. Mass Spectrom. Ion Processes* **1991**, *107*, 369; b) R. Srinivas, D. Sülzle, W. Koch, C. H. DePuy, H. Schwarz, *J. Am. Chem. Soc.* **1991**, *113*, 5970.

[9] a) C. G. Macdonald, M. J. Lacey, *Org. Mass Spectrom.* **1984**, *19*, 55; b) J. R. Chapman, *Practical Organic Mass Spectrometry*, Wiley, Chichester, **1985**, Chapter 6.

[10] We have also carried out the reverse sequence, i.e. initial insertion of ^{4}He and then ^{3}He ($C_x^{\cdot+}$ triplets with Δm = 4, 7). As a result of the energetics of the inelastic collisions [see 4f,i,j] we were not surprised to observe that the relative transmittances for the production of $[^3He^4He@C_x]^{\cdot+}$ are different from those for $[^4He^3@C_x]^{\cdot+}$ (x = 60–52). Analogous considerations are also valid for the production of $[^4He_2@C_x]^{\cdot+}$ ($C_x^{\cdot+}$ triplet with Δm = 4, 8).

Formation of a 2,5-Diborabicyclo[2.1.1]hexane Derivative and Its Conversion to a Tetracarbahexaborane**

By *Markus Enders, Hans Pritzkow,* and *Walter Siebert**

Dedicated to Professor Wolfgang Beck on the occasion of his 60th birthday

Preparative and theoretical investigations into the stability of the C_4B_2 compounds **A**,[1] **B**,[2] and **C**[3] have shown that the conversion of the organoborane into the carborane structure is controlled by the substituents R bound to boron. With one amino and one methyl substituent the carborane is still stable; two amino substituents (R = N iPr$_2$) lead to the bicycle **D**. The temperature-dependent ^{1}H NMR spectra indicate that **C** and **D** are in equilibrium.[3]

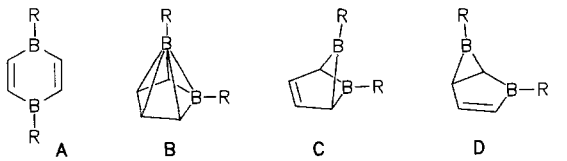

Herein we report a new reaction path to the tetracarbahexaborane **B** from the unsaturated organoborane **1**, a framework isomer of **D** (Scheme 1). In **1**, as in **D**, two sp^2 hybridized B and C atoms as well as two sp^3 hybridized C atoms are present in the C_4B_2 framework; a *nido*-carborane formation is not hindered by the substituent at boron but by the two π systems. After rearrangement of **1** into a 1,3-diboretane bridged by the two isopropylidene groups in the 2,4-position and by H migration, the carborane **2** with an isopropyl and an isopropenyl substituent is formed, whose constitution was determined by the measurement of nuclear Overhauser effects (NOE) in the proton NMR.

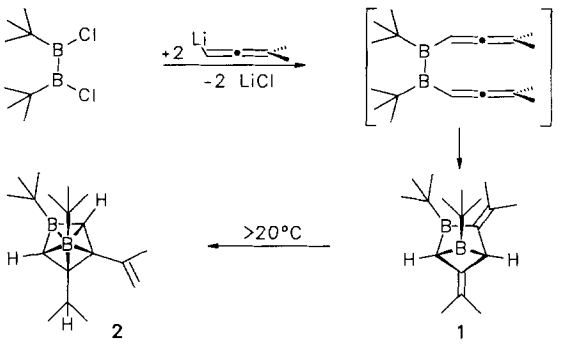

Scheme 1. ^{11}B NMR data for **1**: δ = 33, 66; for **2**: δ = −42, 24.

Whereas amino-substituted diallenylborane and diallenyldiborane(4) derivatives are stable,[4] the bicycle **1** is unexpectedly formed from the reaction of 1,2-di-*tert*-butyl-1,2-dichlorodiborane(4)[5] with 3,3-dimethylallenyllithium in 48% yield. The crystal structure analysis of **1** (Fig. 1)[6] shows a 1-boretane bridged in the 2,4-position. The strong

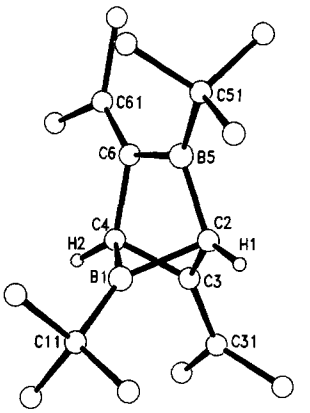

Fig. 1. Molecular structure of **1**. Selected distances [Å] and angles [°]: B1-C3 1.744(9), B1-C2 1.658(8), B1-C4 1.595(9), C2-C3 1.491(7), C3-C4 1.501(7), C3-C31 1.370(6), C2-B5 1.521(7), C4-C6 1.483(7), B5-C6 1.584(8), C6-C61 1.344(6); C2-B1-C4 86.1(5), C2-C3-C4 95.9(5) B1-C2-C3 67.0(4), B1-C4-C3 68.5(4).

folding of the four-membered ring (angle between the planes C4-B1-C2 and C2-C3-C4 is 105°) leads to a short distance between B1 and C3 of 1.74 Å. This indicates a 1,3-transannular interaction between the free p orbital at B1 and the exocyclic double bond at C3, which also explains the remarkable high-field shift in the ^{11}B NMR spectrum (δ = 33). A comparable interaction is found in the Diels–Alder dimer of 2,3,4,5-tetramethyl-1-phenylborole.[7] Also in agreement with this is the fact that the exocyclic substituents (C11 at B1, C31 at C3) do not lie in a plane with the other substituents at B1 and C3 (as is expected by sp^2 hybridized atoms), but are bent toward the center of the ring (8 and 16°, respectively), which favors a transannular interaction.

In the ^{1}H NMR spectrum of **1** the hydrogen atoms of the boretane give rise to two doublets (δ = 3.62, 3.90,

[*] Prof. Dr. W. Siebert, Dipl.-Chem. M. Enders, Dr. H. Pritzkow
Anorganisch-Chemisches Institut der Universität
Im Neuenheimer Feld 270, D-W-6900 Heidelberg (FRG)

[**] This work was supported by the Deutsche Forschungsgemeinschaft (SFB 247), the Fonds der Chemischen Industrie, and the BASF AG.

^4J(H,H) = 5.6 Hz), and for two of the four inequivalent methyl groups of the isopropylidene substituents a quartet (^4J(H,H) = 0.6 Hz) is observed. In the ^{13}C NMR spectrum at room temperature six primary and three quarternary C atoms are observed, and the B–CH atoms show two broad signals at δ = 73.1 and 56.6. Additionally, the quaternary C3 atom at δ = 141 and a broad signal for the C atoms of the *tert*-butyl groups bound to boron are observed on cooling to 250 K.

By framework rearrangement and migration of a hydrogen atom from one isopropylidene group to the other and simultaneously raising the coordination numbers of the boron atoms from three to four and six, respectively, the racemate of **2** is formed. The ^{11}B NMR spectrum shows two signals at δ = 24.1 and −41.9 for the basal and apical boron atom, respectively. The existence of an isopropenyl unit (δ = 5.20 (m,1H), 5.05 (m,1H), 1.85 (m,3H)) and a diastereotopic isopropyl group (δ = 3.01 (sept,1H), 1.02 (d,3H), 0.99 (d,3H)) in the ^{1}H NMR spectrum proves that the H migration has occurred. The two H atoms on the carborane framework produce two doublets at δ = 4.38 and 4.33.

If the methyl protons of the isopropyl group are irradiated, one H atom (δ = 4.38) of the basal CH groups and one H atom of the isopropenyl group (δ = 5.20) show an NOE (8% and 3%). When the CH_3 group of the isopropenyl substituent is irradiated, it is exactly the other way around (NOE at δ = 4.33 (9%) and 5.05 (6%)). This shows that the C_3H_5 and C_3H_7 groups are adjacent and have one H substituent each as a neighbor.

The reaction introduced here is novel since the organoborane **1** can be isolated before the formation of the *nido*-tetracarbahexaborane **2** occurs. Compared with the endocyclic ones in the 1,4-diboracyclohexadiene, the exocyclic double bonds of **1** hinder a rapid rearrangement to the carborane. Only after framework rearrangement and migration of a H atom, one electron of each localized π bond can be made available for cluster formation; thus **1** is kinetically stabilized. The surprising formation of **1** and the rearrangement to **2** are subject to further investigations.

Experimental Procedure

1: To a solution of 1-bromo-3,3-dimethylallene (4.41 g, 30 mmol) in diethyl ether (20 mL), *n*-butyllithium (2.5 M solution, 12 mL) was added at −78 °C. After 30 min 1,2-di-*tert*-butyl-1,2-dichlorodiborane(4) (3.10 g, 15 mmol) in pentane (30 mL) was added dropwise. This was warmed to room temperature, filtered, and after the removal of the solvent distilled as a green-yellow liquid. Yield 1.93 g (47.6%), b.p. 70 °C/10^{-3} Torr, m.p. 65 °C(pentane). ^{1}H NMR (C_6D_6): δ = 0.98 (s, 9H), 1.28 (s, 9H), 1.55 (q, 3H, ^4J(H,H) = 0.6 Hz), 1.66 (q, 3H, ^4J(H,H) = 0.6 Hz), 1.85 (s, 3H), 1.98 (s, 3H), 3.62 (d, 1H, ^4J(H,H) = 5.6 Hz), 3.90 (d, 1H, ^4J(H,H) = 5.6 Hz). – ^{11}B NMR (C_6D_6): δ = 33, 66 (1:1). – ^{13}C NMR ([D_8]toluene, 250 K): δ = 18.5 (B-C_q), 22.6 (CH_3C), 22.7 (CH_3C), 23.9 (CH_3C), 26.5 (CH_3C), 29.2 ((CH_3)$_3$C), 29.3 ((CH_3)$_3$C), 56.5 (B-CH), 73.4 (B-CH), 115.7 (C_q), 126.3(C_q), 141 (B-C_q), 148.2 (C_q). – EI-MS: *m/z* 270 ($M^{\oplus}$, 3.0), 57 ($C_4H_9^+$, 85.6), 56 ($C_4H_8^+$, 100), 41 ($C_3H_5^+$, 88.2).

2: A solution of **1** (30 mg, 0.11 mmol) in [D_8]toluene was heated in an NMR tube to 100 °C. After 90 minutes only the signals of the carborane **2** are present in the ^{1}H NMR spectrum. The reaction half-time is approximately 15 minutes. ^{1}H NMR(C_6D_6): δ = 0.85 (s, 9H), 0.99 (d, 3H, ^3J(H,H) = 6.7 Hz), 1.02 (d, 3H, ^3J(H,H) = 6.7 Hz), 1.36 (s, 9H), 1.85 (m, 3H), 3.01 (sept, 1H, ^3J(H,H) = 6.7 Hz), 4.33 (d, 1H, ^4J(H,H) = 3.5 Hz), 4.38 (d, 1H, ^4J(H,H) = 3.5 Hz), 5.05 (m,1H), 5.20 (m,1H). – ^{11}B NMR(C_6D_6): δ = 24.1, -41.9 (1:1). – ^{13}C NMR ([D_8]toluene, 230 K): δ = 12 (B-C_q), 17.5 (B-C_q), 21.5 (CH_3), 24.2 (CH_3), 24.4 (CH_3), 26.4 ($CH(CH_3)_2$), 31.7 ((CH_3)$_3$C), 32.1 ((CH_3)$_3$C), 79.5 (B-CH), 80.5 (B-CH), 110.1 (C_q), 117.3 (=CH_2), 119.7 (C_q), 136.8 (CCH_3). – EI-MS: *m/z* 270 ($M^{\oplus}$, 100), 255 ($M^{\oplus}$ − CH_3, 22.1), 227 ($M^{\oplus}$ − C_3H_7, 26.9), 213 ($M^{\oplus}$ − C_4H_9, 66.2).

Received: October 18, 1991 [Z 4975 IE]
German version: *Angew. Chem.* **1992**, *104*, 628

CAS Registry numbers:
1, 139565-05-2; **2**, 139565-06-3; $(CH_3)_3CB(Cl)B(Cl)C(CH_3)_3$, 72428-47-8; $(CH_3)_2C{=}C{=}CHBr$, 6214-32-0.

[1] P. L. Timms, *J. Am. Chem. Soc.* **1968**, *90*, 4585–4589; G. E. Herberich, B. Heßner, *J. Organomet. Chem.* **1978**, *161*, C36–C40; *Chem. Ber.* **1982**, *115*, 3115–3127.
[2] P. Binger, *Tetrahedron Lett.* **1966**, 2675–2680; S. M. van der Kerk, P. H. M Budzelaar, A.L.M. van Eekeren, G. J. M. van der Kerk, *Polyhedron* **1984**, *3*, 271–280; R. N. Camp, D. S. Marynick, G. D. Graham, W. N. Lipscomb, *J. Am.Chem. Soc.* **1978**, *100*, 6781–6783.
[3] G. E. Herberich, H. Ohst, H. Mayer, *Angew. Chem.* **1984**, *96*, 975–976; *Angew. Chem. Int. Ed. Engl.* **1984**, *23*, 969.
[4] M. Enders, H. Pritzkow, W. Siebert, *Chem. Ber.*, in press.
[5] W. Biffar, H. Nöth, H. Pommerening, *Angew. Chem.* **1980**, *92*, 63–64; *Angew. Chem. Int. Ed. Engl.* **1980**, *19*, 56; H. Klusik, A. Berndt, *J. Organomet. Chem.* **1982**, *234*, C17–C19.
[6] 1: Space group $P\bar{1}$, a = 9.123(6), b = 9.664(9), c = 12.261(10) Å, α = 95.04(7), β = 91.82(6), χ = 115.88(6)°, V = 966 Å^3, Z = 2; 1347 observed reflections ($I > 1.5\sigma_I$, R = 0.089, Rw = 0.089. Further details of the crystal structure investigation may be obtained from the Fachinformationszentrum Karlsruhe, Gesellschaft für wissenschaftlich-technische Information mbH, D-W-7514 Eggenstein-Leopoldshafen 2 (FRG) on quoting the depository number CSD-56006, the names of the authors, and the journal citation.
[7] P. J. Fagan, E. G. Burns, J. C. Calabrese, *J. Am. Chem. Soc.* **1988**, *110*, 2979–2981.

Equilibria between Nonclassical and Classical Boron Compounds, Competition between Aromaticity in Two and Three Dimensions**

By *Holger Michel, Dirk Steiner, Sigrid Wočadlo, Jürgen Allwohn, Nicolaos Stamatis, Werner Massa,* and *Armin Berndt**

Dedicated to Professor Anton Meller on the occasion of his 60th birthday

Nonclassical boron compounds **2** are considerably lower in energy [1] than their classical isomers **1** and **3**.[2, 3] This can be explained by the three-dimensional aromaticity of **2**.[1, 4] Conversion of the benzo derivatives **4** into **5**, during which the two-dimensional aromaticity of the fused benzene ring would be lost, could not be observed for compounds of type **4**.[5, 6] Therefore, is the three-dimensional aromaticity in

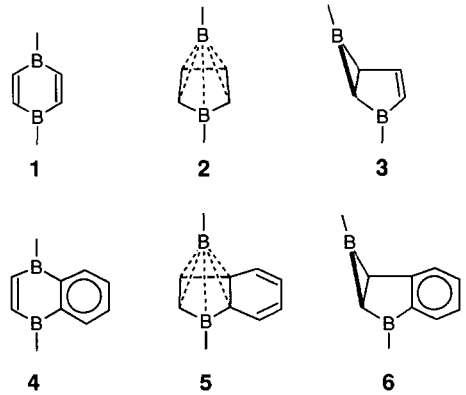

[*] Prof. Dr. A. Berndt, H. Michel, D.Steiner, S. Wačadlo, Dr. J. Allwohn, N. Stamatis, Prof. Dr. W. Massa
Fachbereich Chemie der Universität
Hans-Meerwein-Strasse, D-W-3550 Marburg (FRG)

[**] This work was supported by the Deutsche Forschungsgemeinschaft and the Fonds der Chemischen Industrie. We thank Prof. B. Bogdanović, Max-Planck-Institut für Kohlenforschung, Mülheim, for information concerning the production of highly reactive magnesium (cf. [11]).

tetracarbahexaboranes(6) unable to compete with the two-dimensional aromaticity in benzene rings? Herein we report on rapidly established equilibria between the nonclassical and classical boron compounds **5a, b** and **6a, b**, respectively, which are the result of a competition between these two kinds of aromaticity.

Compounds **5a** and **5b** are formed by the reaction of **7a**[8] and **7b**[9], respectively, with Bogdanović magnesium.[11, 12]

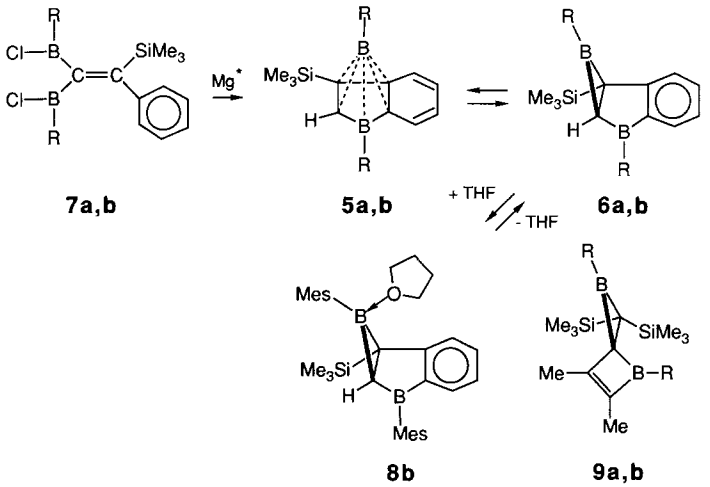

Scheme 1. **a**, R = *t*Bu; **b**, R = 2,4,6-trimethylphenyl (Mes); Mg* = highly reactive Mg (prepared as described by Bogdanović).

The structure of **5a** was deduced from the chemical shifts in the ^{11}B NMR spectrum, which with $\delta = -50.7$ and $+24.1$ correspond approximately to the typical values of tetracarbahexaboranes(6)[3] at $\delta \approx -45$ and $+18$ for apical and basal boron atoms, respectively. The structure of **5b** was confirmed by a crystal structure analysis (Fig. 1).[13]

The distances in **5b** agree satisfactorily with those calculated for the parent compound $C_4B_2H_6$ (**2**),[1] and with those determined from microwave spectroscopy;[15] only the distances between the apical boron and carbon atoms of the fused ring are significantly longer (ca. 15 pm). Corresponding longer distances were also observed for the π complexes of other benzoboroheterocycles.[5] B1 lies 127(3) pm above the almost-planar, BC_4 five-membered ring (deviations from a best plane max. 5(3) pm), towards which the plane of the six-membered ring (max. deviation 3(3) pm) is slightly inclined with an interplanar angle of 4.7(4)°. The C4–C5 and C3–C8 bonds of 145.6(9) and 148.8(9) pm, respectively, are considerably longer than in benzene. The moderate quality of the crystal structure data could be responsible for the fact that the 1,3-diene character of the C5–C6–C7–C8 arrangement of atoms is not more clearly recognizable. As predicted for three-dimensional arenes, which have a five-membered ring with a capping boron,[4] the C2–Si bond is inclined towards the cap from the plane of the five-membered ring (ca. 5.6(3)°).

The signals in the ^{11}B NMR spectrum of a solution of **5b** ($\delta = +9$ and $+47$ at room temperature), lie well outside the range of the typical chemical shifts of tetracarahexaboranes(6). The NMR signal positions of the boron atoms and those of the carbon atoms C1 to C4 for **5b** are strongly dependent on the temperature (Table 1).

Table 1. Chemical shifts of the framework atoms of **5a** ⇌ **5b**, **5b** ⇌ **6b**, and **8b** at different temperatures.

	δ(**5a** ⇌ **6a**)			δ(**5b** ⇌ **6b**)			δ(**8b**)	
T[°C]	−90 [a]	25 [b]	125 [b]	−80 [c]	30 [d]	130 [b]	−80 [a]	30 [a]
B1 [d]	−52.2 [e]	−50.7	−49.3	−24 [f]	9	32	–	15
B2	22.1 [e]	24.1	25.6	34 [f]	47	57	–	65
C1	84.8	85.9	85.7	88.5	67.6	62.0	53.3	54.0
C2	83.0	84.3	84.3	77.6	57.9	52.5	47.2	48.3
C3	124.9	126.3	126.6	130.5	148.1	156.3	170.0	168.4
C4	108.8	111.4	112.2	117.7	134.4	142.4	148.8	148.2
C_5	123.4	124.4	124.4	124.5	124.0	125.3	122.5	122.8
to	125.4	126.2	126.0	125.2	124.5	125.5	125.6	125.6
C_8 [g]	130.3	131.3	131.1	131.0	131.3	133.0	130.3	130.3
	132.3	134.1	134.1	131.6	132.8	134.8	133.2	133.3

[a] In [D_8]THF. [b] In *o*-[D_{10}]xylene. [c] In CD_2Cl_2. [d] Numbering of the atoms as in crystal structures (see Figs. 1 and 2). [e] In pentane at −60 °C. [f] At −40 °C. [g] Without assignment.

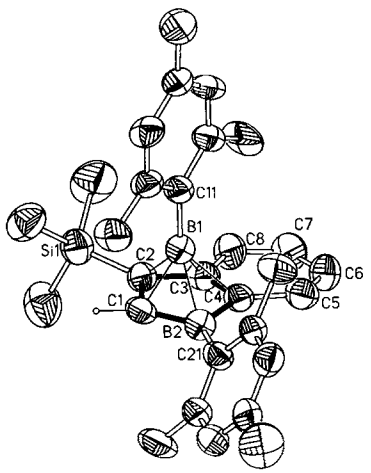

Fig. 1. XP diagram [14] of a molecule of **5b**. The ellipsoids of thermal vibration are drawn at the 50% probability level. Important distances [pm] and angles [°]: B1-C1 167.3(9), B1-C2 171.9(9), B1-C3 184.3(10), B1-C4 186.5(10), B1-B2 187.0(11), B2-C1 149.3(10), C1-C2 150.2(8), C2-C3 144.0(9), C3-C4 141.7(9), C4-B2 156.9(10), C4-C5 145.6(9), C5-C6 140.0(10), C6-C7 139.6(11), C7-C8 136.2(10), C8-C3 148.8(9); B2-C1-B1 72.1(5), B2-C1-C2 114.4(5), C1-C2-C3 102.5(5), C2-C3-C4 113.4(6), C3-C4-B2 109.2(6), C4-B2-C1 99.8(5), C3-C2-Si 133.8(5), C1-C2-Si 123.6(4).

The formation of adducts with Lewis bases is also unusual for tetracarbahexaboranes(6). From **5b** and THF the adduct **8b** is formed, whose crystal structure is shown in Figure 2.[13] The five-membered ring unit is planar with the fused benzene ring (max. deviation from the best plane 5(1) pm), the B1–C1–C2 three-membered ring is bent towards this plane by 114.4(2)°. The C4–C5 and C3–C8 bonds of 141.1(4) and 139.6(4) pm, respectively, are of comparable length to those in benzene. The unusual shortening of the C5–C6 and C6–C7 distances (137.3(5) and 135.8(6) pm, respectively) is probably at least in part due to the anisotropic vibration of the participating atoms mainly within the ring plane (displacements ratio $U3/U1 = 2.4$ to 2.8). The C–B distances in the B1–C1–C2 three-membered ring[16] are significantly shorter than the C–B1 distances in **5b**, the C1–C2 and C2–C3 distances are significantly longer—as is to be expected for a change from multiple-center to two-center bonds.[17]

The ^{13}C NMR spectrum of **8b** in $CDCl_3$ at room temperature is similar to that of **5b** and an equivalent of THF, on cooling it resembles more and more that of **5b** in THF. Apparently **5b** forms a loose adduct with THF. Compound **5a** does not add a THF molecule even in THF at −80 °C.

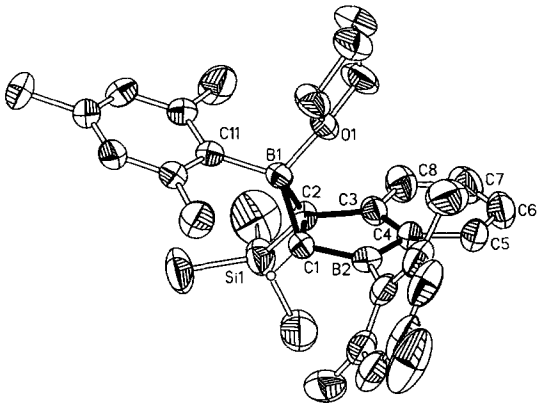

Fig. 2. XP diagram [14] of a molecule of **8b**. The ellipsoids of thermal vibration are drawn at the 50% probability level. Important distances [pm] and angles [°]: B1-C1 162.6(4), B1-C2 158.7(4), B1-O1 158.6(4), B2-C1 152.8(5), C1-C2 157.6(4), C2-C3 151.4(4), C3-C4 140.0(4), C4-B2 156.8(5), C4-C5 141.1(4), C5-C6 137.3(5), C6-C7 135.8(6), C7-C8 140.5(5), C8-C3 139.6(4); B2-C1-B1 121.4(3), B2-C1-C2 109.2(2), C1-C2-C3 102.8(2), C2-C3-C4 114.1(3), C3-C4-B2 109.0(3), C1-B2-C4 104.7(3), C1-B1-C2 58.7(2), C3-C2-Si 116.9(2), C1-C2-Si 113.7(2), C11-B1-O1 109.2.

Nondissociating adducts of type **8** were obtained from **5a,b** and 4-*tert*-butylpyridine. The facile adduct formation is in contrast to the low reactivity of tetracarbahexaboranes(6); thus hexaethyltetracarbahexaborane(6) does not react with trimethylamine oxide even on refluxing in toluene.[19]

All these results can be explained if rapid equilibria between the nonclassical compounds **5a,b** and the classical **6a,b** are assumed. The unusual position of the signals in the NMR spectra result from the weighted-average values $\delta = p\delta_B + (1-p)\delta_A$ of the chemical shifts (δ_A and δ_B) of the components (populations p and $1-p$) participating in the equilibrium ($K = p/1-p$). Their temperature dependence indicates the change of the equilibria with temperature corresponding to $\Delta G = \Delta H - T\Delta S = -RT\ln K$.

Since the ^{11}B NMR signals for **5a** $\rightleftharpoons$ **6a** lie in the range expected for tetracarbahexaboranes(6), it follows that the equilibrium lies mainly on the side of **5a** even at +125 °C. The ^{11}B NMR signals for **5b** $\rightleftharpoons$ **6b**, which are totally different from the expected values for these carboranes, show that already at room temperature comparable quantites of **5b** and **6b** are present. If the following are assumed for the estimation of δ_A and δ_B a) the chemical shifts of **5a** at low temperature are also valid for **5b**, b) the NMR data of the framework atoms of the five-membered rings **6a,b** can be estimated from that of the five-membered ring of **8b**, and c) the $\delta(^{11}B)$ values of the three-membered rings **6a,b** can be estimated from the $\delta(^{11}B)$ of the three-membered rings of **9a** (83[20]) and **9b** (72[21]), then these together with the stated equations and the data[22] in Table 1 result in the thermodynamic approximate values given in Table 2.

Table 2. Thermodynamic parameters of the equilibria **5a** $\rightleftharpoons$ **6a** and **5b** $\rightleftharpoons$ **6b**.

	ΔH [kJ mol^{-1}]	ΔS [J mol^{-1} K^{-1}]	ΔG [kJ mol^{-1}]
5a $\rightleftharpoons$ **6a**:	5.4 ± 0.8	−12.6 ± 8.4	8.8 ± 2.9
5b $\rightleftharpoons$ **6b**:	8.8 ± 0.8	31.9 ± 5.4	−0.8 ± 1.7

The enthalpy differences between **5a,b** and **6a,b** are considerably smaller than the energy difference of 157.0 kJ mol^{-1} calculated for the parent compounds $C_4B_2H_6$ of **2** and **3**.[1] This can be explained by the cancellation of the two-dimensional aromaticity in the benzene ring of **5**. Thus, the equilibria between the nonclassical compounds **5a,b** and classical **6a,b** result from the competition between the two- and three-dimensional aromaticity.

Received: December 2, 1991 [Z 5048 IE]
German version: *Angew. Chem.* **1992**, *104*, 629

CAS Registry numbers:
5a, 139704-27-1; **5b**, 139704-28-2; **6a**, 139704-25-9; **6b**, 139704-26-0; **7a**, 93109-79-6; **7b**, 139704-24-8; **8b**, 139704-29-3; phenyl(trimethylsilyl)acetylene, 2170-06-1; 1,2-dichloro-1,2-dimesityldiborane(4), 114978-52-8.

[1] P. H. M. Budzelaar, S. M. van der Kerk, K. Krogh-Jespersen, P. von R. Schleyer, *J. Am. Chem. Soc.* **1986**, *108*, 3960–3967, and references cited therein.
[2] This is not valid for the systems **1** and **3**, in which the electron-deficient centers are compensated by strong π donors, i.e. the boron atoms have substituents such as F, OMe, NR_2, and ferrocenyl.
[3] G. E. Herberich, H. Ohst, H. Mayer, *Angew. Chem.* **1984**, *96*, 975–976; *Angew. Chem. Int. Ed. Engl.* **1984**, *23*, 969–970, and references cited therein.
[4] E. D. Jemmis, P. von R. Schleyer, *J. Am. Chem. Soc.* **1982**, *104*, 4781–4788.
[5] A. Feßenbecker, H. Schulz, H. Pritzkow, W. Siebert, *Chem. Ber.* **1990**, *123*, 2273–2278.
[6] Also napthalene dications isoelectronic with **4** are not converted into nonclassical dications isoelectronic with **5** [7].
[7] K. Lammertsma, G. A. Olah, C. M. Berke, A. Streitwieser, Jr., *J. Am. Chem. Soc.* **1979**, *101*, 6658–6659, and references cited therein.
[8] H. Klusik, C. Pues, A. Berndt, *Z. Naturforsch. B* **1984**, *39*, 1042–1045.
[9] Compound **7b** (analogous to **7a**) is accessible from phenyl(trimethylsilyl)acetylene and 1,2-dichloro-1,2-dimesityldiborane(4) [10].
[10] R. Hunold, J. Allwohn, G. Baum, W. Massa, A. Berndt, *Angew. Chem.* **1988**, *100*, 961–963; *Angew. Chem. Int. Ed. Engl.* **1988**, *27*, 961–963.
[11] The highly reactive magnesium was produced using the method of B. Bogdanović (personal communication) by the thermolysis of magnesium anthracenide, MgA [12]. For this, MgA (12 g, 28.6 mmol) was refluxed in toluene (150 mL) until the orange color had disappeared. For the separation of the anthracene formed, the solvent pipetted off as soon as the magnesium has settled, should be as hot as possible. The Mg was washed twice (100 mL each time) with first toluene, then toluene/ether (1:1), then ether, it was finally taken up as a suspension in ether (100 mL). To this suspension, a solution of **7b** (12.0 g, 23.8 mmol) was added and the resulting mixture was stirred at room temperature for ca. 15 h. Then the ether was removed under vacuum, the residue taken up in pentane and filtered over a G4 frit to remove the $MgCl_2$ and finally washed with further pentane (2 × 30 mL). The pentane solution was concentrated to ca. 50 mL and crystallized at −18 °C.
5b: Yellow crystals, yield 7.6 g (74%), m.p. 82 °C; from **7a**, the analogue **5a** (m.p. 62–63 °C) was obtained, which can only be separated from a further reaction product, with large losses, by crystallization.
[12] B. Bogdanović, S. T. Liao, K. Schlichte, U. Westeppe in *Organometallic Synthesis, Vol. IV*, (Eds.: R. B. King, J. J. Eisch), Elsevier, Amsterdam, **1988**, p. 410.
[13] Crystal structure analyses using four-circle diffractometer (CAD4, Enraf-Nonius) with $Cu_{K\alpha}$ radiation: **5b**: $C_{29}H_{36}B_2Si$, space group $P\bar{1}$, $a = 810.1(3)$, $b = 974.0(4)$, $c = 1717.4(6)$ pm, $\alpha = 96.67(2)$, $\beta = 103.26(2)$, $\gamma = 94.80°$, $Z = 2$, 1909 unique reflections $F_0 > 5\sigma(F)$ measured at −15 °; No absorption correction ($\mu = 8.6$ cm^{-1}). The hydrogen atoms at partially found, partially calculated positions were kept "riding" in groups with common isotropic temperature factors. For all other atoms except boron anisotropic temperature factors were used. Refinement by the block-diagonal matrix method with threefold blocking.[14] 298 parameters, $R = 0.071$, $wR = 0.056$ (weights $w = 1/\sigma^2(F_0)$). The moderate residuals and the high standard deviations can be attributed to a decomposition of the crystal during the measurement. **8b**: $C_{33}H_{44}B_2OSi$, space group $P2_1/c$, $a = 922.8(1)$, $b = 1862.6(1)$, $c = 1805.7(3)$ pm, $\beta = 91.10°$, $Z = 4$, 3504 unique reflections $F_0 > 3\sigma(F)$ measured at −15 °; empirical absorption correction (ψ scans, $\mu = 8.3$ cm^{-1}, crystal size 0.4 × 0.4 × 0.5 mm^3), extinction correction. The structure was solved by direct methods.[14] All H atoms could be localized and refined, however, in the last cycles they were considered in the calculations "riding" on their bond partners in groups with common isotropic temperature factors. For all other atoms anisotropic temperature factors were used. The refinement of the 349 parameters with full matrix and with weights $w = 1/\sigma^2(F_0)$ resulted in $R = 0.061$, $wR = 0.059$. Further details of the crystal structure investiga-

tion may be obtained from the Fachinformationszentrum Karlsruhe, Gesellschaft für wissenschaftlich-technische Information mbH, D-W-7514 Eggenstein-Leopoldshafen 2 (FRG) on quoting the depository number CSD-56043, the names of the authors, and the journal citation.
[14] G. M. Sheldrick, SHELXTL-Plus. Release 4.0 for Siemens R3 Crystallographic Research Systems. Siemens Analytical X-Ray Instruments, Madison , WI USA, **1989**.
[15] J. P. Pasinski, R. A. Beaudet, *J. Chem. Phys.* **1974**, *61*, 683–691; *J. Chem. Soc. Chem. Commun.* **1973**, 928–929.
[16] Similar distance were observed in boratiranes: M. A. Kropp, M. Baillargeon, K. M. Park, K. Bhamidapaty, G. B. Schuster, *J. Am. Chem. Soc.* **1991**, *113*, 2155–2163, and references cited therein.
[17] The relatively short B2–C1 distance (152.8(5)) together with the long C1–B1 distance (162.6(4)) (in comparison to C2–B1 (158.7(4))) indicates C–B hyperconjugation of the C–B bond of the strained three-membered ring with the empty p-orbital at B2, cf. [18].
[18] A. Höfner, B. Ziegler, W. Massa, A. Berndt, *Angew. Chem.* **1989**, *101*, 188–190; *Angew. Chem. Int. Ed. Engl.* **1989**, *28*, 186–187.
[19] P. Binger, *Tetrahedron Lett.* **1966**, 2675–2680.
[20] R. Wehrmann, H. Klusik, A. Berndt, *Angew. Chem.* **1984**, *96*, 369–370; *Angew. Chem. Int. Ed. Engl.* **1984**, *23*, 369–370.
[21] **9b** is analogous to **9a** accessible from 2-butyne and the borandiylborirane (there **6**) described in the literature (see [10]).
[22] Only for C1 can the $\delta(^{13}C)$ of **5a** not be considered as the limiting value for $\delta(^{13}C)$ of **5b**.

Solid-State NMR Spectroscopic and X-Ray Diffraction Studies of the Low-Temperature Structural Transformation of Hydrated Porous Aluminophosphate VPI-5**

By *João Rocha, Waclaw Kolodziejski, Ian Gameson,* and *Jacek Klinowski**

The aluminophosphate molecular sieve VPI-5 contains 18-membered rings of aluminum and phosphorus atoms, linked via oxygen atoms (Scheme 1).[1, 2] The large channel diameter of ca. 1.2 nm gives the material potential for the separation of large molecules and for catalytic cracking of heavy fractions of petroleum. Several attempts have been made to determine the structure of VPI-5 in detail.[3–6] The most recent refinement of the X-ray diffraction data in the space group $P6_3$ by McCusker et al.[6] is fully consistent with ^{27}Al and ^{31}P NMR spectra.[7–9] A double-rotation NMR study of hydrated VPI-5 has resolved two resonances from tetracoordinated Al and one due to hexacoordinated Al in a 1:1:1 intensity ratio.[10] The signals from tetracoordinated Al are not resolved in the ordinary ^{27}Al MAS (magic-angle spinning) NMR spectrum, and it is of interest to establish whether their quadrupole interaction parameters are sufficiently different for the material to be profitably studied by quadrupole nutation NMR spectroscopy.[11] We have carried out variable-temperature X-ray powder diffraction analyses in tandem with ^{1}H, ^{27}Al, ^{31}P, and ^{27}Al quadrupole nutation MAS NMR studies in the range 180–294 K, using fast spinning rates. These are the first variable-temperature quadrupole nutation studies using MAS. We report that in the range 190–220 K, hydrated VPI-5 undergoes a reversible structural transformation.

The only discernible changes in the X-ray diffraction patterns on cooling the sample from 273 K to 173 K occur in the region shown in Figure 1. All patterns are consistent with earlier work.[6] The (211)-(002), (311)-(102) and (320)-(112) pairs of reflections, unresolved at 273 K, separate on cooling, while the (202) and (410) reflections begin to merge. The explanation is quite straightforward. Measurement of the positions of the (200) and (220) reflections shows that on cooling, the *a* lattice parameter remains essentially unchanged at 1.897 nm. This is not the case with the *c* parameter which

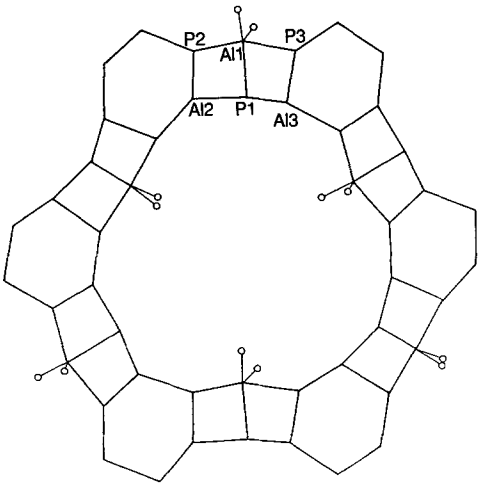

Scheme 1. One layer of the framework structure of hydrated VPI-5 ($P6_3$ symmetry) taken from the stereoscopic view along the [001] direction according to McCusker et al. [6] Aluminum and phosphorus atoms, linked via oxygen atoms (not shown for clarity) are located at the apices of the polygons. P2 and P3, and Al2 and Al3 sites are inequivalent. P sites and Al2 and Al3, are all tetracoordinated. The Al1 site is hexacoordinated as a result of bonding to four bridging oxygens and two "framework" water molecules. Other intracrystalline water is not shown.

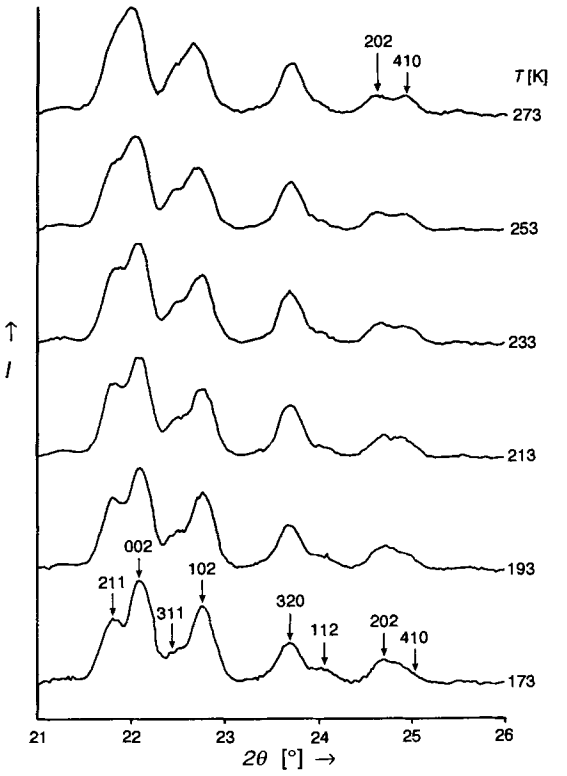

Fig. 1. Variable-temperature X-ray powder diffraction patterns of hydrated VPI-5 between 273 K and 173 K (*I* stands for intensity).

[*] Dr. J. Klinowski, Dr. J. Rocha, Dr. W. Kolodziejski, Dr. I. Gameson
Department of Chemistry, University of Cambridge
Lensfield Road, Cambridge CB2 1EW (UK)

[**] We are grateful to Unilever Research, Port Sunlight, and the University of Aveiro for support, and to Heyong He for providing the sample.

steadily decreases from 0.810 nm at 273 K to 0.805 nm at 173 K. Thus, the position of all the (*hk0*) reflections remains unchanged, while the higher the value of *l* in the (*hkl*) reflections, the more rapid the shift in peak position to higher 2θ (corresponding to smaller interplanar distance). Thus, the (002) reflection moves away from the (211) reflection, as does (112) from (320). Similarly, the separation between the (311) and (102) reflections increases on cooling. In summary, X-ray crystallographic studies showed that the changes in peak positions are continuous, and do not indicate that any phase transition occurs. All the changes are accounted for only by the contraction of the crystallites along the *c* direction.

The ^{27}Al MAS NMR spectra of VPI-5 (Fig. 2a) show two signals in a 2:1 intensity ratio centered at $\delta = 40$ (tetracoordinated Al) and $\delta = -18$ (hexacoordinated Al), respectively. The latter displays a characteristic second-order quadrupole powder pattern which changes significantly with temperature, and can be simulated to yield the quadrupole constant, C_Q, the asymmetry parameter, η, and the isotropic chemical shift, δ_{iso} (Fig. 2b and Fig. 3).

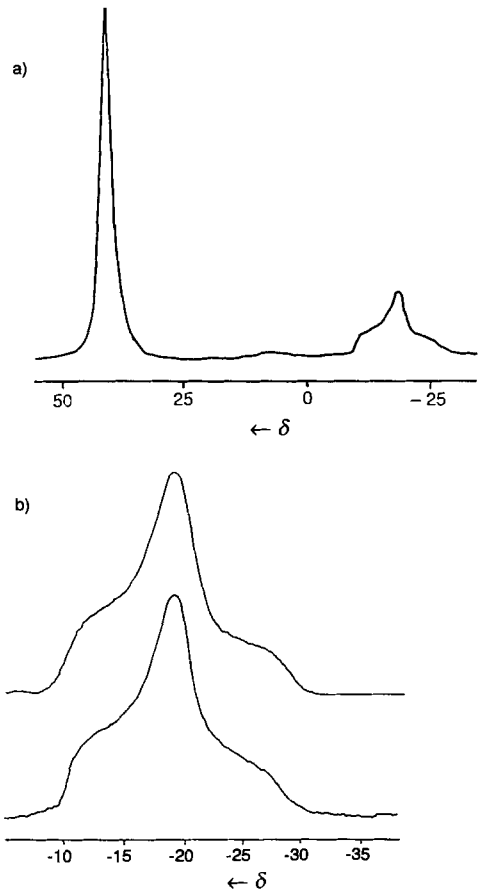

Fig. 2. (a) Room temperature (294 K) ^{27}Al MAS NMR spectrum of hydrated VPI-5 recorded with a spin frequency of 12 kHz. (b) Experimental (lower trace) and simulated (upper trace) second-order quadrupole patterns given by the hexacoordinated Al signal ($C_Q = 3.50$, $\eta = 0.91$, $\delta = -9.9$).

On cooling, the full-width-at-half-maximum Δ of the 40 ppm signal also changes considerably and at 235 K and 180 K ^{1}H decoupling produces a substantial line narrowing. Figure 3 indicates that some structural transformation occurs at 190–220 K. The room temperature quadrupole nutation

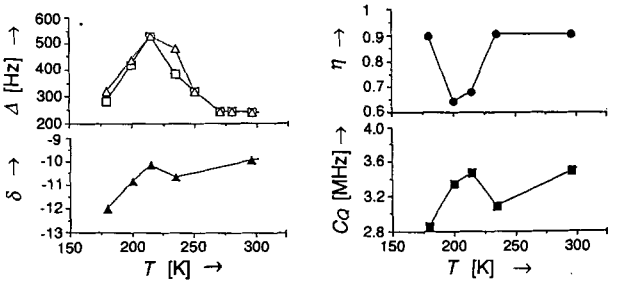

Fig. 3. Variation of full-width-at-half-maximum Δ of the ^{27}Al MAS NMR signal from tetracoordinated Al and isotropic chemical shift δ_{iso} and quadrupole parameters η and C_Q obtained by simulation of the hexacoordinated Al signal (see Fig. 2b), as a function of temperature. In the Δ plot the solid and dashed lines link points obtained from spectra recorded with and without ^{1}H decoupling, respectively. Note that all curves go through a maximum at 190–220 K.

spectrum (Fig. 4, top) has one signal at $\omega_{rf}/2\pi$ and two signals between $\omega_{rf}/2\pi$ and ca. $3\omega_{rf}/2\pi$. This shows that the two signals from tetracoordinated Al, which overlap in the ordinary MAS NMR spectrum, have slightly different quadrupole interaction parameters. The relatively weak spectral feature at $\delta = 38$ and $3\omega_{rf}/2\pi$ is due to a small amount of impurities. At 215 K, the two resonances from tetracoordinated Al are still present, but are less well resolved since the two-dimensional spectrum broadens along F_2 (Fig. 4, middle). However, at 191 K the nutation spectrum is significantly different. In particular, only one signal from tetracoordinated Al is observed (Fig. 4, bottom). On the other hand, at all temperatures studied, the ^{31}P MAS NMR spectra (not shown) display three resonances in a 1:1:1 intensity ratio.[9] It is difficult to imagine how the structure could possibly have *two* crystallographically nonequivalent aluminum sites, but *three* phosphorus sites. We conclude that two of the three aluminum sites are not resolved in the quadrupole nutation 191 K spectrum, because their quadrupole interaction parameters and isotropic chemical shifts are similar.

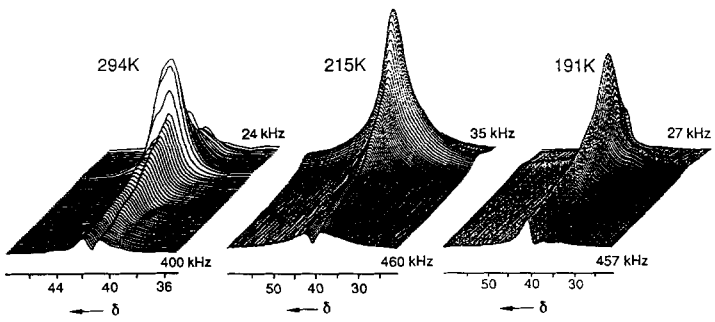

Fig. 4. ^{27}Al quadrupole nutation MAS NMR spectra of hydrated VPI-5 at several temperatures in the region of the signals of tetracoordinated Al.

The room temperature ^{1}H MAS NMR spectrum of hydrated VPI-5 (not shown) displays a broad signal at $\delta = 5$, due to water molecules in the large 18-membered channels. Below room temperature this signal broadens and a rather abrupt change occurs between 200 K and 180 K when a tenfold increase in Δ is observed. This suggests that the motion of the water molecules is effectively frozen. The transformation is fully reversible.

A comparison of the X-ray diffraction and NMR results nicely illustrates the fundamental difference between the two techniques: the spatial range of their sensitivity. NMR spectroscopy is essentially a submolecular technique, and in the case of VPI-5 the ^{31}P and ^{27}Al nuclei are sensitive only to their immediate environment involving at most tens, rather than thousands, of surrounding atoms. Unlike X-ray diffraction, NMR is not sensitive to long-range order. It is clear that the temperature-induced structural changes in VPI-5, as in silicalite,[15-17] involve only very minor modifications in atomic positions, which NMR is far better suited to monitor. Local changes in atomic environments, which can be separately monitored by NMR, may correspond to the same long-range symmetry.

Experimental Procedure

VPI-5 was prepared according to Davis et al. [12] using di-*n*-propylamine (DPA) as a template, hydrated for 12 h (25 wt % water) over a saturated solution of NH_4Cl. Elemental analysis indicates that the DPA content in the samples corresponds to about one molecule per three unit cells.

Powder X-ray diffraction patterns were collected with a Philips PW-1380 horizontal goniometer using $Cu_{K\alpha}$ radiation with a curved graphite monochromator in the diffracted beam. The low-temperature attachment [13,14] contained 30 mg of the sample in symmetrical transmission geometry, packed between two beryllium windows 1 mm apart. The temperature of the sample holder was controlled by a closed-cycle helium refrigerator. Data were collected between $3° \leq 2\theta \leq 60°$ in 0.025° steps with counting for 5 s per point. The temperature was lowered from 273 to 173 K in 5 K steps, at a rate of 1 K min^{-1} and allowing 15 mins for thermal equilibration before each measurement.

^{27}Al MAS NMR spectra were recorded on a Bruker MSL-400 spectrometer at 104.26 MHz (9.4 T) with very short, 0.6 μs (less than 10°), radiofrequency pulses and 0.4–0.5 s recycle delays. The 4 mm double-bearing zirconia rotors were spun in nitrogen gas at 8–12 kHz in the 180–294 K range. Quadrupole nutation spectra were recorded with a radiofrequency field of 115 ± 5 kHz and with MAS at 8–12 kHz. 40 to 64 data points were collected in the t_1 dimension in increments of 0.5 and 1 μs, the damping of the t_1 FID being ca. 30 μs. A sine-bell digitizer filter and zero filling were used in the t_1 dimension and the FIDs were doubly Fourier transformed in the magnitude mode. The chemical shifts are relative to external $[Al(H_2O)_6]^{3+}$. ^1H MAS NMR spectra were recorded at 400.13 MHz with a spinning rate of 7 kHz. In all NMR experiments the temperature was varied in steps of 5–20 K and 15 minutes were allowed for equilibration.

Received: November 15, 1991 [Z 5023 IE]
German version: *Angew. Chem.* **1992**, *104*, 616

[1] M. E. Davis, C. Saldarriaga, C. Montes, J. M. Garces, C. Crowder, *Nature* **1988**, *331*, 698–699.
[2] M. E. Davis, C. Saldarriaga, C. Montes, J. M. Garces, C. Crowder, *Zeolites* **1988**, *8*, 362–366.
[3] C. E. Crowder, J. Garces, M. E. Davis, *Adv. X-Ray Anal.* **1988**, *32*, 507–514.
[4] J. W. Richardson, Jr., J. V. Smith, J. J. Pluth, *J. Phys. Chem.* **1989**, *93*, 8212–8219.
[5] R. R. Rudolf, C. E. Crowder, *Zeolites* **1990**, *10*, 163–168.
[6] L. B. McCusker, C. Baerlocher, E. Jahn, M. Bülow, *Zeolites* **1991**, *11*, 308–313.
[7] M. E. Davis, C. Montes, P. E. Hathaway, J. P. Arhancet, D. L. Hasha, J. M. Garces, *J. Am. Chem. Soc.* **1989**, *111*, 3919–3927.
[8] P. E. Grobet, J. A. Martens, I. Balakrishnan, M. Mertens, P. A. Jacobs, *Appl. Catal.* **1989**, *56*, L21–L25.
[9] J. Rocha, W. Kolodziejski, H. He, J. Klinowski, *J. Am. Chem. Soc.*, in press.
[10] Y. Wu, B. F. Chmelka, A. Pines, M. E. Davis, P. J. Grobet, P. A. Jacobs, *Nature* **1990**, *346*, 550–552.
[11] A. Samoson, E. Lippmaa, *J. Magn. Reson.* **1988**, *79*, 255–268.
[12] M. E. Davis, C. Montes, P. E. Hathaway, J. M. Garces in *Zeolites: Facts, Figures, Future* (Eds.: P. A. Jacobs, R. A. van Santen), Elsevier, Amsterdam, **1989**, p. 199.
[13] I. Gameson, *Ph.D. Thesis*, University of Cambridge, **1987**.
[14] I. Gameson, T. Rayment, *Chem. Phys. Lett.* **1986**, *123*, 145–149.
[15] J. Klinowski, T. A. Carpenter, L. F. Gladen, *Zeolites* **1987**, *7*, 73–78.
[16] C. A. Fyfe, J. H. O'Brien, H. Strobl, *Nature* **1987**, *326*, 281–283.
[17] H. Strobl, C. A. Fyfe, G. T. Kokotailo, C. T. Pasztor, *J. Am. Chem. Soc.* **1987**, *109*, 4733–4734.

Bis(*P*,*P*-di-*tert*-butylphosphinic-*N*-isopropylamidato-*N*,*O*)nickel(II), a Paramagnetic Planar Complex

By *Thomas Frömmel, Wilfried Peters, Hartmut Wunderlich,* and *Wilhelm Kuchen**

Nickel complexes of the general type **1** are mainly monomeric in noncoordinating solvents and the Ni centers are tetracoordinated. Depending on R and R′ they are either dia- or paramagnetic ($\mu_{eff} \approx 3.1-3.3$ B.M. at room temperature).[1] The electronic spectrum of the diamagnetic compounds of this series shows no absorption bands at wave numbers < 10000 cm^{-1}, whereas in the spectra of the paramagnetic complexes, an absorption band at ca. 6500 cm^{-1} as well as a broad band of relatively high intensity with a maximum at ca. 16500 cm^{-1} are observed. The spectra of the paramagnetic complexes could be explained with ligand field theory under the simplifying assumption of T_d symmetry (instead of C_2 symmetry). On the basis of these magnetic and spectroscopic criteria we assigned a planar or tetrahedral coordination geometry to the different complexes **1**. That these criteria were valid for **1** could be proven by X-ray crystallographic investigations, which showed a planar *trans*-NiN_2S_2 chromophore for **1a** and a distorted-tetrahedral structure for **1c**.[1c]

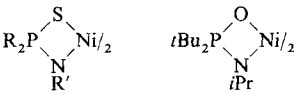

1 **2**

a, R = *t*Bu, R′ = Et; **b**, R = Me, R′ = *cyclo*-C_6H_{11}; **c**, R = *t*Bu, R′ = *cyclo*-C_6H_{11}

However, several compounds **1** show anomalous magnetic moments ($\mu_{eff} < 2.8$ B.M., spin-only value for two unpaired electrons), which vary strongly with temperature for the dissolved complexes. Thus, for example, **1a** is diamagnetic in the solid state and shows no absorption bands < 10000 cm^{-1} in the remission spectrum. In solution, however, this complex is paramagnetic ($\mu_{eff} = 1.52$ (353 K) to 0.98 B.M. (273 K)) and shows a weak absorption at ca. 6500 cm^{-1}. On the other hand, **1b** shows anomalous magnetic behavior both in the solid state ($\mu_{eff} = 1.18$ B.M. (280 K), Curie–Weiss behavior between 290 and 90 K), and also in solution ($\mu_{eff} = 2.56$ (343 K) to 0.65 B.M. (233 K)). In both cases the characteristic absorptions for tetrahedral complexes of the type **1** are observed, here amongst others one at 6600 cm^{-1}. We explained these results by the formation of a conglomerate of the two isomers in solid **1b** and in the solutions of **1a** and **1b** by an isomeric equilibrium (a), which is shifted to the right with increasing temperature.[1d]

$$\underset{\text{(diamagnetic)}}{\text{planar}} \rightleftarrows \underset{\text{(paramagnetic)}}{\text{tetrahedral}} \qquad \text{(a)}$$

We synthesized the phosphinic amidato complex **2** according to Equation (b). Complex **2** forms olive-green crystals

$$2[t\text{Bu}_2\text{P(O)N}i\text{Pr}]\text{Li} \xrightarrow[-2\,\text{LiCl},\ -2\,\text{PPh}_3]{[\text{NiCl}_2(\text{PPh}_3)_2]} \mathbf{2} \qquad \text{(b)}$$

[*] Prof. Dr. W. Kuchen, Dipl.-Chem. T. Frömmel, Dr. W. Peters, Dr. H. Wunderlich
Institut für Anorganische Chemie und Strukturchemie der Universität Universitätsstrasse 1, D-W-4000 Düsseldorf (FRG)

which are highly soluble in aprotic organic solvents and which decompose gradually on the addition of moist air. The complex is monomeric in benzene.

Complex **2** shows the following characteristics: Magnetic properties: $\mu_{eff} = 3.40$ B.M. (297 K), Curie–Weiss behavior from 293 to 90 K (solid state!); $\mu_{eff} = 3.49$ B.M. (293 K), Curie–Weiss behavior from 293 to 190 K (solution in CD_2Cl_2!). Electronic spectra ($\tilde{\nu}$[cm^{-1}]; ε[L $mol^{-1}cm^{-1}$] in parentheses): 6800 (77), 12220 (36), 16780 (152), 18330 (162) (in toluene); 7300 (in transmission, single-crystal recording);[2] 7300, 17300 (in remission, powder spectrum, $BaSO_4$ as standard). The ^{31}P NMR spectrum of **2** shows a resonance at $\delta = -835$ (CD_2Cl_2, 293 K), which in contrast to that of the analogous thio complex [1c, 9] ($\delta = +127$, 293 K, toluene) is strongly shifted to high field.[1d] Thus, in contrast to **1b**, **2** shows Curie–Weiss behavior as well as a magnetic moment both in the solid state *and* in solution as is usually observed for tetrahedral Ni^{II} complexes. Furthermore, a distinct absorption band is found in the electronic spectra of both phases at a wave number $< 10000\ cm^{-1}$, which is shifted by $500\ cm^{-1}$ to higher values in the spectra of the solid. However, also the appearance of the solid and solution spectra of **2** are different in other ways (in contrast to the corresponding spectra of **1c** which are almost identical).[1d]

On the basis of the criteria mentioned, **2** should be tetrahedral both in the solid state and in solution. Therefore, we were even more surprised when the crystal structure analysis[3] showed that the Ni^{II} center is tetracoordinated but that this complex contains the exactly planar *trans*-NiN_2O_2 chromophore (Fig. 1).[4] Thus, to our knowledge **2** is the first paramagnetic planar Ni^{II} complex whose coordination geometry has been confirmed by X-ray crystallography.

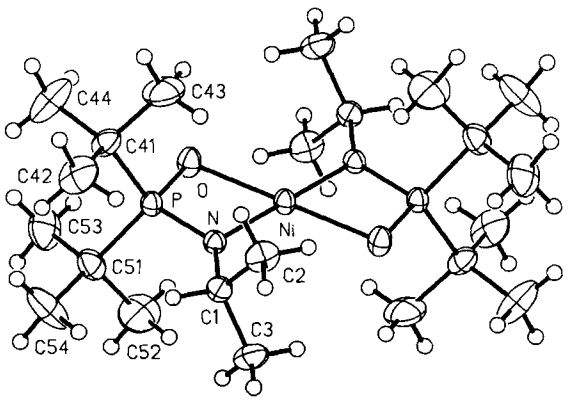

Fig. 1. Molecular structure of **2** (ellipsoids drawn with 25% probability). The complex has $\bar{1}$-C_i symmetry. A higher coordination number for the Ni atoms than four can be excluded since the following shortest distances to atoms of neighboring molecules are calculated: Ni–H 509, Ni–C 586 pm. Selected distances [pm] and angles [°] with standard deviations in parentheses: Ni-N 190.3(2), Ni-O 210.3(2), P-O 151.7(2), P-N 160.4(2), P-C41 184.9(3), P-C51 185.5(3), N-C1 148.0(3); N-Ni-O 74.2(1), Ni-N-P 94.5(1), N-P-O 101.7(1), P-O-Ni 89.6(1), Ni-N-C1 131.4(2), P-N-C1 134.0(2) [5].

According to simple ligand field theory both a low-spin and a high-spin form can be considered for planar Ni^{II} complexes. However, experience so far has shown that the spin-pairing energy is always smaller than term splitting for planar complexes due to the field strength of the ligand and a possible lowering of the symmetry of the ligand field. In contrast to **1**, this is no longer the case for **2** probably as a result of the exchange of S for O. Accordingly, in the electronic spectrum of **2** absorption bands are found at energies which are comparable to those of the tetrahedral complexes **1**. Therefore, in the case of **2**, an assignment of the coordination geometry only on the basis of magnetic and spectroscopic criteria is not possible .

Whether the planar structure of **2** is also retained in solution is as yet unknown. The magnetic behavior of the complex in both phases is almost identical, however, as mentioned, the electronic spectra of **2** in the solid state and in solution are different.

Experimental Procedure

Magnetic measurements were carried out according to Faraday (solid) and Evans (solution).[6] ^{31}P NMR spectroscopy: Bruker AM 200 (81.026 MHz, CD_2Cl_2, 293 K, 85% H_3PO_4).

2: tBu$_2$P(O)NHiPr (92 mmol) (colorless needles from toluene, m.p. 194 °C, $\delta(^{31}P) = 57$ (toluene), prepared from tBu$_2$PNHiPr [7] and 30% H_2O_2 in toluene as according to the literature [8]) in THF (20 mL) was treated with n-butyllithium (92 mmol, 1.6 M solution in hexane) and stirred at room temperature for 2 h. This reaction mixture was slowly added to $[NiCl_2(PPh_3)_2]$ (46 mmol). After the resulting clear solution was stirred for a further 2 h, the solvent was removed under vacuum at room temperature. The residue was taken up in a little toluene and the suspension was centrifuged and the clear solution obtained was kept in the refrigerator for some time. As a result, **2** was obtained as olive-green, hydrolysis-sensitive crystals, which do not change notably up to ca. 270 °C. Yield ca. 45%.

$C_{22}H_{50}N_2NiO_2P_2$ ($M_r = 495.3$), correct elemental analysis, molecular masses (cryoscopic in benzene): 503 (0.207 molal), 507 (0.092 molal); ^1H NMR (200 MHz, CD_2Cl_2, 293 K, TMS): $\delta_{PCCH} = 0.5$, $\delta_{PNCH} = 199$, $\delta_{NCCH} = 14.7$. Because of the strong broadening of the signals no fine structure was observed.

Received: November 21, 1991 [Z 5033 IE]
German version: *Angew. Chem.* **1992**, *104*, 632

[1] a) W. Peters, M. Fuchs, H. Sicius, W. Kuchen, *Angew. Chem.* **1985**, *97*, 217–218; *Angew. Chem. Int. Ed. Engl.* **1985**, *24*, 231–233; b) M. Fuchs, W. Kuchen, W. Peters, *Chem. Ber.* **1986**, *119*, 1569–1580; c) A. Deeg, W. Kuchen, D. Langsch, D. Mootz, W. Peters, H. Wunderlich, *Z. Anorg. Allg. Chem.* **1991**, *606*, 119–132; d) D. Langsch, *Dissertation*, Universität Düsseldorf, **1989**.

[2] We thank Dipl.-Chem H. J. Mink, Institut für Theoretische Chemie der Universität Düsseldorf (Direktor Prof. Dr. H.-H.Schmidtke) for the single-crystal transmission spectra which were recorded with a Bruker IFS-113v spectrometer.

[3] $C_{22}H_{50}N_2NiO_2P_2$ ($M_r = 495.3$): Space group $P2_1/n$ (fully reduced cell, original choice 2), $a = 901.1(1)$, $b = 1507.0(2)$, $c = 1062.2(1)$ pm, $\beta = 97.42(1)°$, $V = 1.4303(3)$ nm^3, $Z = 2$, $\rho_{calcd.} = 1.15$ mg mm^{-3}, $\mu = 0.81$ mm^{-1}. Crystal size $0.4 \times 0.45 \times 0.45$ mm^3, Syntex/Siemens four-circle diffractometer $P2_1/P3$, 4568 reflections ($4 < 2\theta < 60°$, $Mo_{K\alpha}$, $\lambda = 71.073$ pm, graphite monochromator, ω:2θ scan, of 4185 symmetrically independent reflections 2675 observed ($F > 3\sigma_F$). Solution and refinement: SHELXTL-PLUS, $w^{-1} = \sigma^2F + 0.0009F^2$, 133 parameters, $R = 0.049$, $Rw = 0.060$. Further details of the crystal structure investigation may be obtained from the Fachinformationszentrum Karlsruhe, Gesellschaft für wissenschaftlich-technische Information mbH, D-W-7514 Eggenstein-Leopoldshafen 2 (FRG) on quoting the depository number CSD-55891, the names of the authors, and the journal citation.

[4] **2** forms crystals with edge lengths of between 0.4 and 2 mm, of which the smaller were selected for the crystal structure determination and the larger for the magnetic and spectroscopic measurements. To ensure there were no inhomogenetities of the material the crystallographic data and the single crystal transmission spectrum were redetermined for cleaved pieces of a large crystal. Here, the pairing of the *trans*-planar chromophore with the absorption band at 7300 cm^{-1} was confirmed.

[5] The Ni–N–P–O four-membered ring is planar within ±0.5 pm , the bond angles at N (94.5(1)°), P (101.7(1)°) and Ni (74.2(1)°) are significantly smaller than in **1c** (100.5(1), 102.1(1), and 80.7(1)°, respectively), here only the angle at O (89.6(1)°) is significantly greater than the corresponding angle at S in **1c** (76.6(1)°). The Ni–N distance (190.3(2) pm) in **2** is unexpectedly short in comparison to that in **1c** (194.7(1) pm).

[6] D. F. Evans, *J. Chem. Soc.* **1959**, 2003–2005.

[7] W. Kuchen, D. Langsch, W. Peters, *Phosphorus, Sulfur Silicon* **1990**, *54*, 55–61.

[8] W. McFarlane, B. Wrackmeyer, *J. Chem. Soc. Dalton* **1976**, 2351–2355.

[9] In the meantime, an X-ray structure determination has shown that the complex bis(*P*,*P*-di-*tert*-butylthiophosphinic-*N*-isopropylamidato-*N*,*S*)-nickel(II), the thio analogue of **2**, has a distorted tetrahedral structure.

"Artificial Metabolisms" for the Asymmetric One-Pot Synthesis of Branched-Chain Saccharides**

By *Wolf-Dieter Fessner** and *Christiane Walter*

Dedicated to Professor George A. Olah on the occasion of his 65th birthday

The employment of biocatalysts—either as whole cells or as isolated enzymes—in asymmetric synthesis is enjoying increasing attention because of the usually high levels of optical induction, the high selectivities, and the mild reaction conditions.[1] The advantages of their usage are particularly well documented for the conversion of polyfunctionalized compounds such as carbohydrates.[2]

In the context of our program directed at the employment of C–C bond forming aldolases in asymmetric de novo syntheses[3] we have been searching for new means to make the essential substrate dihydroxyacetone phosphate (DHAP) efficiently available.[4] Here we detail the development of multienzyme systems that allow one to exploit regenerating raw materials as an economical source of DHAP for aldol additions using the fructose 1,6-bisphosphate aldolase (FruA). The investigations of these enzyme cascade reactions had been initiated, firstly because of the potential preparative benefit, and secondly to gain insight by qualitative and (semi)-quantitative studies in vitro into the complex kinetic effects operative in such a multiply regulated multienzyme system.[5]

Since the overwhelming number of common enzymes display sufficient activity around pH 7.0, they can be readily combined to ensembles that catalyze specific serial or parallel conversions of shared substrates. By this means, structurally profound conversions become realizable as simple one-pot procedures. Starting with the central function of the FruA in glycolysis to cleave and—in combination with triose phosphate isomerase—symmetrize fructose 1,6-bisphosphate ($Fru1,6P_2$) into C_3 fragments (a reaction that preparatively delivers DHAP in situ[6]), we have assembled additional steps in such a manner (Scheme 1) that glucose, fructose, or sucrose become alternatively accessible as possible precursors. All enzymes involved (cf. caption to Scheme 1) are commercially available, inexpensive, and well characterized.[7, 8] Because this reaction scheme comprises an unusual accumulation of coupled reactions as a new combination of natural, catabolic processes with a nonphysiological, anabolic synthetic component by application of pure isolated enzymes in vitro its designation as *artificial metabolism* seems justified.

We have tested experimentally three different variants for the production of $Fru1,6P_2$: 1) fructose is gradually phosphorylated twice; 2) glucose is first phosphorylated, then isomerized into the ketose form before the second phosphorylation (no adequate enzyme preparation was available to us for the more cost-efficient direct isomerization of glucose into fructose, path②[9]); 3) sucrose is hydrolyzed by invertase to provide both monosaccharides that independently, but convergently, react via the first two pathways, and thereby advantageously exploit the acceptance of the hexokinase

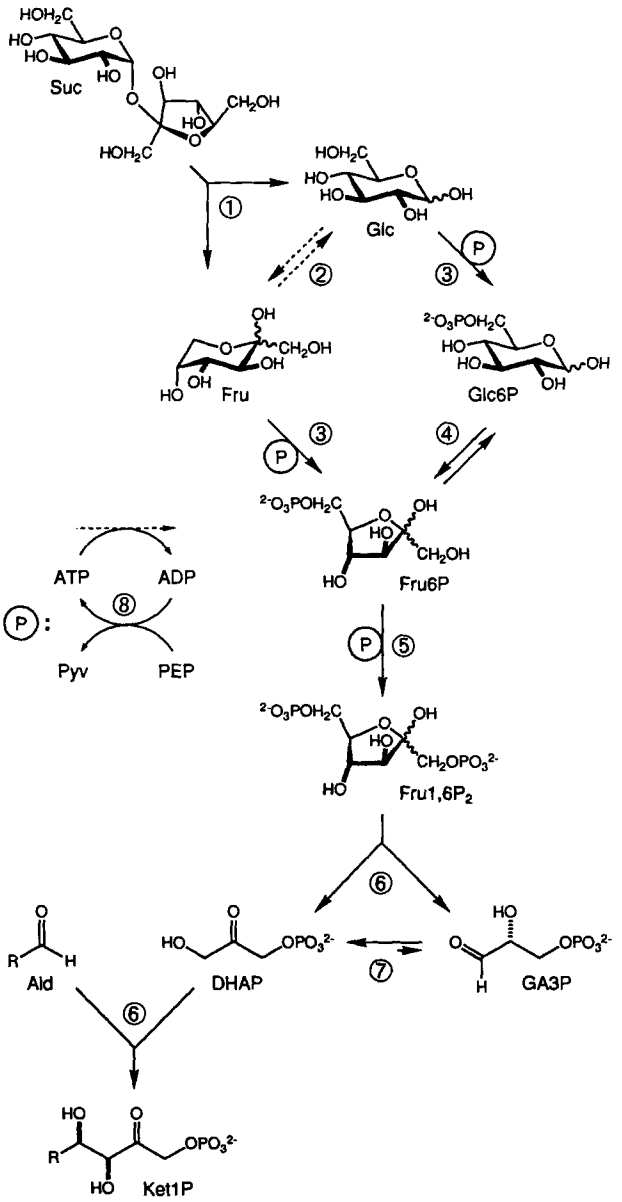

Scheme 1. Multienzymatic one-pot synthesis of ketose 1-phosphates. Cofactor regenerating cycles at phosphorylation steps were detached for clarity (encircled "P"). Abbreviations: Suc = D-sucrose; Glc = D-glucose; Fru = D-fructose; Glc6P, Fru6P = D-glucose(fructose) 6-phosphate; $Fru1,6P_2$ = D-fructose 1,6-bisphosphate; GA3P = D-glyceraldehyde 3-phosphate; DHAP = dihydroxyacetone phosphate; Ald = aldehyde; Ket1P = ketose 1-phosphate; ADP, ATP = adenosine di(tri)phosphate; Pyv = pyruvate; PEP = phosphoenol pyruvate. Enzymes involved are: ① = invertase (EC 3.2.1.26); ② = xylose isomerase (EC 5.3.1.5); ③ = hexokinase (EC 2.7.1.1); ④ = glucose 6-phosphate isomerase (EC 5.3.1.9); ⑤ = fructose 6-phosphate kinase (EC 2.7.1.11); ⑥ = fructose 1,6-bisphosphate aldolase (EC 4.1.2.13); ⑦ = triose phosphate isomerase (EC 5.3.1.1); ⑧ = pyruvate kinase (EC 2.7.1.40).

for both of the free sugars. As a consequence, from glucose and fructose or from sucrose, a total of two or four DHAP equivalents are acquired, respectively. Two other variations, such as the use of sucrose ($Suc + P_i \rightarrow Fru + Glc1P$) or α-glucane phosphorylase ($Glc_n + P_i \rightarrow Glc_{n-1} + Glc1P$)—attractive because of the reduction in required equivalents of phosphate donor—had to be discarded as impractical because of high enzyme costs or rheological complications.

A kinetic analysis of the longest sequence, which starts from sucrose and involves six enzyme-catalyzed reaction steps (Fig. 1), revealed the following effects: 1) fructose and

[*] Dr. W.-D. Fessner, C. Walter
Institut für Organische Chemie und Biochemie der Universität
Albertstrasse 21, D-W-7800 Freiburg (FRG)

[**] Enzymes in Organic Synthesis, Part 3. This research was supported by the Deutsche Forschungsgemeinschaft (Grant Fe 244/2–1), the Wissenschaftliche Gesellschaft Freiburg, and the Fonds der Chemischen Industrie. The generous gift of recombinant bacterial strains by Prof. Dr. D. G. Fraenkel, Harvard Medical School, Boston, is gratefully acknowledged. We thank Dipl.-Chem. O. Eyrisch and Dipl.-Chem. G. Sinerius for samples of purified PFK-2 from *E. coli* and 7, respectively.—Part 2: [3b].

glucose are phosphorylated by hexokinase at almost identical rates; 2) the increase of Fru6P is retarded because of its equilibration to the thermodynamically more stable Glc6P; 3) v_{max} of the fructose 6-phosphate kinase (phosphofructokinase, PFK) remains the limiting factor even at a twofold higher dosage of the enzyme; 4) only on reaching a relatively high concentration of Fru6P (≥ 10 mM[10]) does a period of approximately linear production of Fru1,6P_2 (ca. 20–35 h) commence. The two latter facts are in accord with inhibition

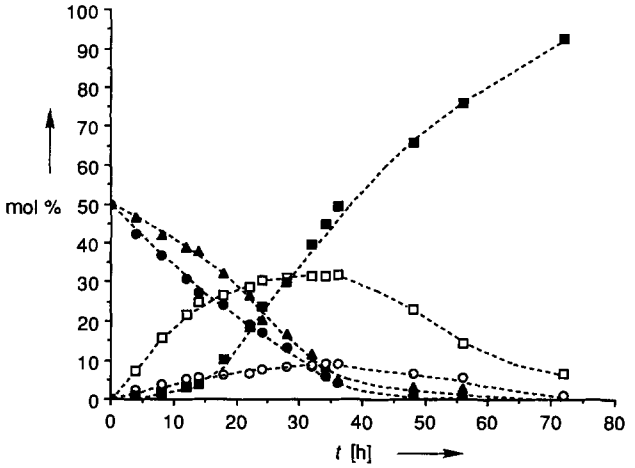

Fig. 1. Progress of the multienzymatic synthesis of fructose 1,6-bisphosphate from sucrose according to Scheme 1 (100 mM Suc, 500 mM PEP, 10 mM $MgCl_2$, 1 U of HK, 3 U of PK, 2 U of PFK, 0.25 U of PGI; 0.5 mL; pH 6.8; 25 °C), determined by assays according to [7b]. For analytical reasons, all consecutive reactions were started *after* the hydrolysis of sucrose by invertase (100 U) was completed. ● = D-Glucose; ▲ = D-fructose; □ = D-glucose 6-phosphate; ○ = D-fructose 6-phosphate; ■ = D-fructose 1,6-bisphosphate.

studies that had identified the PFK as the central regulatory element of glycolysis suffering from inhibition by numerous effectors (e.g. by ATP, PEP, pyruvate). Consequences of the multiple inhibition become distinctly apparent at higher concentrations of all reactants. These complications can indeed be effectively reduced (Fig. 2) by using the allosterically less regulated isoenzyme from *E. coli*, the PFK-2.[11] While the activity of the mammalian enzyme, for example, is almost completely suppressed ($< 5\%$) in the presence of ≥ 150 mM of PEP, the microbial enzyme maintains at least 30% of its activity even at considerably higher PEP concentrations (> 300 mM), which indicates the prevalence of non-competitive inhibition.

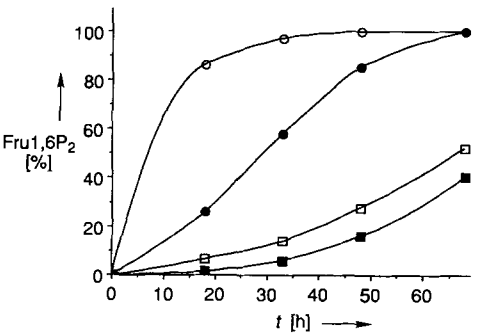

Fig. 2. Comparison of multienzymatic syntheses of fructose 1,6-bisphosphate from sucrose as the result of the type of fructose 6-phosphate kinase (PFK) and variation of the PEP concentration. a) PFK from rabbit muscle (● 25 mM, ■ 100 mM PEP); b) PFK-2 from *E. coli* (○ 25 mM, □ 100 mM PEP). Assays according to [7b].

Subsequently, it proved rather unproblematic to combine to this the cleavage and synthesis steps employing the FruA from rabbit muscle, and thereby to arrive at a total of seven cooperatively acting enzymes. While formation of Fru1,6P_2 by consumption of the enol ester PEP is irreversible, the FruA-catalyzed syntheses are reversible. For reasons of charge entropy, however, the overall equilibrium is shifted towards the singly phosphorylated products, a tendency which may be further promoted by a slight excess of aldehyde. Due to the inherently smaller conversion rates of the aldolase for non-natural substrate analogues the aldol addition becomes the limiting step relative to all preceding reactions. This fact requires for its compensation a higher dosage of the FruA at a level inversely proportional to the substrate quality. We have tested the capacity of the method in preparation reactions (0.1–5 mmol Suc ≙ 0.4–20 mmol DHAP) with a series of aldehydes, which had been selected specifically also for reasons of increasing steric hindrance, in order to allow the further mapping of the substrate acceptance of the FruA from rabbit muscle (Scheme 2).[6]

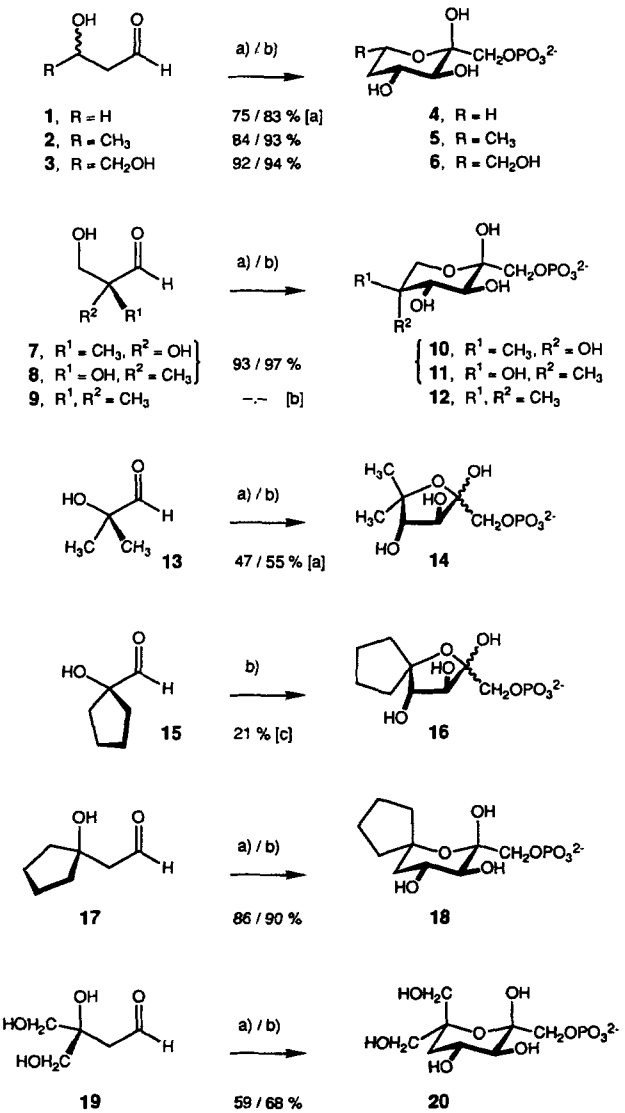

Scheme 2. Enzymatic aldol additions. a) Multienzymatic one-pot synthesis according to Scheme 1 starting from sucrose, glucose, or fructose. b) Synthesis starting from pure fructose 1,6-bisphosphate using FruA-TPI catalysis. [a] Aldehyde was added after quantitative conversion of PEP. [b] No formation of aldol adduct detectable. [c] Reaction was prematurely terminated (conversion corrected yield $\geq 50\%$).

Table 1. NMR data of the aldol adducts [a].

6: ^{1}H NMR: δ = 4.06 (m, 6-H), 3.96 (ddd, 4-H), 3.87 (dd, 1_a-H), 3.79 (dd, 1_b-H), 3.66 (dd, 7_a-H), 3.58 (dd,7_b-H), 3.49 (d, 3-H), 1.97 (ddd, 5_{eq}-H), 1.47 (quart, 5_{ax}-H), $J_{1a,1b}$ = 11.1, $J_{1a,P}$ = 7.7, $J_{1b,P}$ = 5.7, $J_{3,4}$ = 9.6, $J_{4,5ax}$ = 11.5, $J_{4,5eq}$ = 5.1, $J_{5ax,5eq}$ = 12.6, $J_{5ax,6}$ = 12.2, $J_{5eq,6}$ = 2.1, $J_{6,7a}$ = 3.3, $J_{6,7b}$ = 6.1, $J_{7a,7b}$ = 12.1; ^{13}C NMR: δ = 98.3 (C-2), 73.2 (C-3), 69.7 (C-6), 68.2 (C-4), 67.1 (C-1), 64.3 (C-7), 34.7 (C-5), $J_{C-1,P}$ = 4.9, $J_{C-2,P}$ = 7.2.

10: (74%): ^{1}H NMR: δ = 3.93 (dd, 1_a-H), 3.88 (d, 6_{ax}-H), 3.83 (dd, 1_b-H), 3.77 (d, 4-H), 3.65 (d, 3-H), 3.51 (d, 6_{eq}-H), 1.20 (s, CH_3), $J_{3,4}$ = 10.0, $J_{6ax,6eq}$ = 12.5; ^{13}C NMR: δ = 98.3 (C-2), 75.8 (C-5), 73.4 (C-4), 68.8 (C-3), 67.7 (C-1), 66.8 (C-6), 20.8 (CH_3).

11: (26%): ^{1}H NMR: δ = 3.90 (m, 1-H), 3.85 (d, 4-H), 3.80 (d, 6_{ax}-H), 3.57 (d, 3-H), 3.39 (d, 6_{eq}-H), 1.27 (s, CH_3), $J_{3,4}$ = 10.0, $J_{6ax,6eq}$ = 11.7.

14: ^{1}H NMR: δ (β anomer; 86%) = 4.14 (d, 3-H), 4.01 (d, 4-H), 3.74 (d, 1-H), 1.36 (s, CH_3), 1.18 (s, CH_3), $J_{1,P}$ = 6.8, $J_{3,4}$ = 9.0; δ (α anomer; 14%) = 4.11 (d, 3-H), 4.01 (d, 4-H), 3.83 (d, 1-H), 1.32 (s, CH_3), 1.27 (s, CH_3), $J_{3,4}$ = 7.5, ^{13}C NMR: δ = 99.2 (C-2), 80.6 (C-5), 80.4, 75.8 (C-3, -4), 67.0 (C-1), 28.4, 23.3 (2 CH_3), $J_{C-1,P}$ = 4.3, $J_{C-2,P}$ = 7.8.

18: ^{1}H NMR: δ = 4.07 (ddd, 4-H), 3.82 (dd, 1_a-H), 3.68 (dd, 1_b-H), 3.55 (d, 3-H), 2.10 (dd, 5_{eq}-H), 1.70 (t, 5_{ax}-H), 1.86–1.47 (m, cyclopentane H), $J_{1a,1b}$ = 10.8, $J_{1a,P}$ = 6.8, $J_{1b,P}$ = 5,3, $J_{3,4}$ = 9.8, $J_{4,5ax}$ = 11.7, $J_{4,5eq}$ = 4.5, $J_{5ax,5eq}$ = 12.7; ^{13}C NMR: δ = 99.6 (C-2), 73.2 (C-3), 72.8 (C-6), 67.3 (C-1), 66.5 (C-4), 42.5, 41.1 (C-1′, -4′), 37.7 (C-5), 24.1, 21.6 (C-2′, -3′), $J_{C-1,P}$ = 3.2, $J_{C-2,P}$ = 8.1.

20: ^{1}H NMR: δ = 4.12 (ddd, 4-H), 3.93–3.49 (m, 7-, 8-H), 3.43 (d, 3-H), 2.05 (5_{eq}-H), 1.73 (t, 5_{ax}-H), $J_{3,4}$ = 11.8, $J_{4,5ax}$ = 11.3, $J_{4,5eq}$ = 6.8, $J_{5ax,5eq}$ = 13.5; ^{13}C NMR: δ = 99.1 (C-2), 78.9 (C-6), 72.7 (C-3), 68.4 (C-1), 65.2 (C-4), 65.1, 63.4 (C-7, -8), 34.1 (C-5), $J_{C-1,P}$ = 4.1, $J_{C-2,P}$ = 7.3.

[a] NMR spectra were measured in D_2O at pH 7.0 after ion exchange into the Na^+ form. ^{1}H NMR data (400.1 MHz) are given relative to sodium 3-(trimethylsilyl)-[$^2H_4$]-propionate (TSPNa) (δ = 0.00) as the standard, ^{13}C NMR data (100.6 MHz) relative to CH_3CN (δ = 1.30); coupling constants in Hz.

These studies revealed that geminal dialkyl substitution at C-2 is indeed still tolerated. However, with derivatives of glycol aldehyde (third substituent OH; **7/8** > **13** > **15**) the borderline is reached: similar to the situation for pivaldehyde, higher homologues (e.g., **9**) are no longer accepted. Inhibition of the enzymes by high concentrations of aldehydes proved problematic for individual cases only (e.g. the gradual release of acrolein from **1**[12] required its protracted addition). Relative to alternative syntheses starting from pure Fru1,6P$_2$ (cf. Scheme 2, method b) comparable yields are achieved with the multienzyme reactions. Limitations are encountered with very poor substrate analogues ($v_{rel} \leq 1\%$[6]) such as **15**, since isolation of the products from other phosphorylated components becomes quite difficult. Altogether this method makes available (Table 1) a selection of alkylated (**10**/**11**, **14**), spiro-annulated (**16**, **18**), and branched chain saccharides (**20**) or deoxy sugars (**4**,[12] **5**,[6] **6**) that can be produced only with difficulty by using classical synthetic methodology. A systematic investigation of these unusual sugar derivatives will be possible upon application of aldolases with a different stereochemical preference.[3]

In summary, we have demonstrated that multienzyme systems constructed around aldol additions are practical and efficient techniques to achieve complex transformations of saccharides and related compounds, and that these techniques, in which aldolases play a key role as valuable catalysts for the broadly applicable, highly diastereoselective C–C bond formation, can advantageously be applied to the exploitation of regenerable resources.

Experimental

An aqueous solution of sucrose (1.71 g, 5 mmol) containing PEP-K (5.10 g, 25 mmol) $MgCl_2$ (100 mg, 0.5 mmol), and a catalytic quantity of ATP (60 mg, 100 μmol) was adjusted to pH 6.8. After addition of an aqueous solution of **3** (50 mmol; total volume 200 mL) the mixture was incubated with invertase (yeast; 1000 U), pyruvate kinase (rabbit muscle; 300 U), hexokinase (yeast; 100 U), glucose 6-phosphate isomerase (yeast; 25 U [7a]), fructose 6-phosphate kinase (rabbit muscle; 200 U), fructose 1,6-bisphosphate aldolase (rabbit muscle; 500 U), and triose phosphate isomerase (yeast; 500 U) at room temperature. Conversion was monitored by thin-layer chromatography (saturated ammonia/EtOH 1:1) and by enzymatic assays for PEP/pyruvate and Fru1,6P$_2$ [7a]. The sugar phosphate **6** produced was isolated by application of ion exchange techniques [3a].

Received: December 18, 1991 [Z 5078 IE]
German version: *Angew. Chem.* **1992**, *104*, 643

CAS Registry numbers:
1, 2134-29-4; **2**, 107-89-1; **3**, 34764-22-2; **4**, 140361-14-4; **5**, 117626-09-2; **6**, 140361-15-5; 7, 140460-10-2; **8**, 140460-11-3; **9**, 597-31-9; **10**, 140361-16-6; **11**, 140361-17-7; **13**, 20818-81-9; **14**, 140361-18-8; **15**, 63457-91-0; **16**, 140361-19-9; **17**, 140361-20-2; **18**, 140361-21-3; **19**, 140361-22-4; **20**, 140361-23-5; PEP-K, 124080-08-6; DHAP, 57-04-5.

[1] a) G. M. Whitesides, C.-H. Wong, *Angew. Chem.* **1985**, *97*, 617–638; *Angew. Chem. Int. Ed. Engl.* **1985**, *24*, 617–638; b) J. B. Jones, *Tetrahedron* **1986**, *42*, 3351–3403; c) D. H. G. Crout, M. Christen in *Modern Synthetic Methods* (Ed: R. Scheffold), Springer, Berlin, **1989**, pp. 1–114; d) S. Servi, *Synthesis* **1990**, 1–25; e) R. Csuk, B. I. Glänzer, *Chem. Rev.* **1991**, *91*, 49–97.

[2] a) E. J. Toone, E. S. Simon, M. D. Bednarski, G. M. Whitesides, *Tetrahedron* **1989**, *45*, 5365–5422; b) D. G. Drueckhammer, W. J. Hennen, R. L. Pederson, C. F. Barbas, C. M. Gautheron, T. Krach, C.-H. Wong, *Synthesis* **1991**, 499–525.

[3] a) W.-D. Fessner, G. Sinerius, A. Schneider, M. Dreyer, G. E. Schulz, J. Badia, J. Aguilar, *Angew. Chem.* **1991**, *103*, 596–599; *Angew. Chem. Int. Ed. Engl.* **1991**, *30*, 555–558. b) W.-D. Fessner, O. Eyrisch, *ibid.* **1992**, *104*, 76–78 and **1992**, *31*, 56–58.

[4] Chemical synthesis: R. L. Pederson, J. Esker, C.-H. Wong, *Tetrahedron* **1991**, *47*, 2643–2648. Enzymatic synthesis: D. C. Crans, G. M. Whitesides, *J. Am. Chem. Soc.* **1985**, *107*, 7019–7027.

[5] a) M. de Luca, L. J. Kricka, *Arch. Biochem. Biophys.* **1983**, *226*, 285–291; b) G. F. Betts, D. K. Srivastava, *J. Theor. Biol.* **1991**, *151*, 155–167.

[6] M. D. Bednarski, E. S. Simon, N. Bishofberger, W.-D. Fessner, M.-J. Kim, W. Lees, T. Saito, H. Waldmann, G. M. Whitesides, *J. Am. Chem. Soc.* **1989**, *111*, 627–635.

[7] a) Commerical enzymes were from Sigma. Activities were measured photometrically according to standard procedures; cf. A. U. Bergmeyer, *Methods of Enzymatic Analysis*, 3rd ed, VCH, Weinheim **1984**. The preparations of hexokinase and pyruvate kinase contained appreciable amounts of glucose 6-phosphate isomerase. b) Concentrations of sugars and their derivatives were determined enzymatically analogous to Scheme 1 via their DHAP equivalents by adding the retrograde enzymes/cofactors successively to the photometric standard assay (glycerophosphate dehydrogenase/NADH).

[8] Phosphoenol pyruvate can be readily prepared on a molar scale: B. L.Hirschbein, F. P. Mazenod, G. M. Whitesides, *J. Org. Chem.* **1982**, *47*, 3765–3766.

[9] Xylose(glucose) isomerase, technically important for the production of HFC (Gluc/Fru syrup), is only supplied in immobilized form.

[10] K_m of the rabbit muscle PFK for Fru6P is ≈ 43 μM; T. A. W. Koerner, R. J. Voll, A.-L. E. Ashour, E. S. Younathan, *J. Biol. Chem.* **1976**, *251*, 2983–2986.

[11] The enzyme was isolated according to known procedures from an overexpressing recombinant strain: a) J. Babul, *J. Biol. Chem.* **1978**, *253*, 4350–4355; b) F. Daldal, J. Babul, V. Guixé, D. F. Fraenkel, *Eur. J. Biochem.* **1982**, *126*, 373–379; c) F. Daldal, *J. Mol. Biol.* **1983**, *168*, 285–305.

[12] J. R. Durrwachter, D. G. Drueckhammer, K. Nozaki, H. M. Sweers, C.-H. Wong, *J. Am. Chem. Soc.* **1986**, *108*, 7812–7818.

The First Reaction of S_5N_6; Structure of a Complex Containing an $S_2N_3^-$ Ligand**

By *Paul F. Kelly, Alexandra M. Z. Slawin, David J. Williams,* and *J. Derek Woollins**

Despite its long history[1] the chemistry of sulfur–nitrogen compounds continues to provide a rich store of unexpected, and at times inexplicable, reactions. This is particularly the

[*] Dr. J. D. Woollins, Dr. P. F. Kelly, A. M. Z. Slawin, Dr. D. J. Williams
Department of Chemistry
Imperial College of Science, Technology and Medicine
South Kensington, London SW7 2AY (UK)

[**] This work was supported by the British Science and Research Council and the Wolfson Foundation.

case for reactions involving metal species. For example, S_4N_4 reacts with the palladium compound **1** to give **2**, **3**,[2] and **4**.[3]

$(PPh_4)_2[Pd_2Cl_6]$ **1** $(PPh_4)_2[Pd_2Cl_6(S_2N_2)]$ **2**

$(PPh_4)_2[Pd_2Cl_4(S_3N_2)]$ **3** $(PPh_4)[PdCl_2(S_2N_2H)]$ **4**

The formation of such diverse products challenges our ability to construct rational mechanisms for sulfur–nitrogen reactions. Typically, the starting material for such a reaction is one of a handful of sulfur–nitrogen reagents such as S_4N_4, $S_4N_5^-$, $S_3N_3^-$, or $S_3N_3Cl_3$. One species which has not, however, found use in the preparation of sulfur–nitrogen metallacycles is S_5N_6;[4, 5] indeed to the best of our knowledge no reactions of any nature have been reported for S_5N_6. This is undoubtedly due in part to the problems in handling it, since the compound is both extremely explosive and very air-sensitive. Here, we report the first successful reaction of S_5N_6.

Stirring a mixture of **1** and S_5N_6 in CH_2Cl_2 for 12 h yielded three products which were crystallized from the resulting solution by slow diffusion of Et_2O. IR spectroscopy reveals two of the products to be **2** and **3**. The third product, **5**, was characterized by X-ray crystallography.[6] The anion in **5** is

$(PPh_4)[PdCl_2(S_2N_3)]$ **5**

essentially planar, with a maximum deviation of 0.10 Å for Cl(1) (Fig. 1). The PdS_2N_3 ring is planar to within 0.035 Å

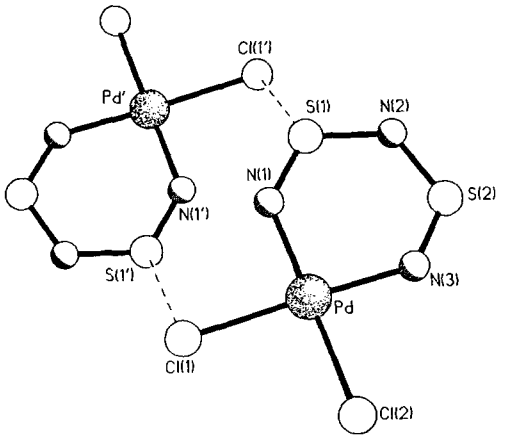

Fig. 1. Structure of a pair of the symmetry-related anions in **5**. Selected bond lengths [Å] and angles [°]: Pd-Cl(1) 2.336(2), Pd-Cl(2) 2.321(2), Pd-N(1) 1.950(6), Pd-N(3) 1.953(6), N(1)-S(1) 1.484(6), N(3)-S(2) 1.489(6), S(1)-N(2) 1.601(7), S(2)-N(2) 1.607(7); Cl(1)-Pd-Cl(2) 92.1(1), N(1)-Pd-N(3) 93.7(2), Pd-N(1)-S(1) 132.2(4), Pd-N(3)-S(2) 132.1(4), N(1)-S(1)-N(2) 120.2(4), N(3)-S(2)-N(2) 120.0(3), S(1)-N(2)-S(3) 121.6(4). Non-bonding contacts: Cl(1)···S(1') 3.56, N(1)···N(1') 3.30, S(1)···N(1') 3.41.

(N(3)) and slightly twisted (ca. 5°) with respect to the $PdCl_2$ plane. The anion has non-crystallographic C_{2v} symmetry; the equivalent ring bond lengths and angles are equal to within statistical significance. Whereas in previously reported MS_2N_3 rings[7–11] (containing the trianionic $S_2N_3^{3-}$ ligand) there is very little variation in the S–N bond lengths within the ring, here there is a marked difference in the lengths of the bonds between the S atoms and bridgehead N atom (average 1.604 Å) and between the S atom and the coordinated N atom (average 1.486 Å). Furthermore, we believe these latter distances to be amongst the shortest S–N bonds yet observed in S–N rings. The only noticeable slight asymmetry in the anion is in the Pd–Cl bond lengths (2.336(2) versus 2.321(2) Å for Cl(1) and Cl(2) repectively). This difference we attribute to a weak intermolecular interaction between Cl(1) and S(1'), 3.56 Å across a crystallographic center of symmetry (Fig. 1).[12] The Pd–N distances are normal. There are no short cation–anion contacts. MS_2N_3 metallacycles have been previously reported, but in all cases the S_2N_3 ligand has been assigned a -3 charge, whereas here it is monoanionic. One example of a protonated $S_2N_3^{3-}$ ligand has been described, the complex anion in **6**.[13] However, from the X-ray analysis there is no evidence

$(AsPh_4)[W(O)Cl_3S_2N_3H)]$ **6**

of protonation of any of the nitrogen atoms of **5**; this is further reinforced by IR studies. Careful measurement of the spectrum of **5** including difference spectra with **1** and **2** does not reveal the presence of any ν(NH) vibrations. ν(NH) vibrations in metal-sulfur-nitrogen systems are usually readily apparent. In the anion of **6**, a medium intensity band at 3275 cm^{-1} is observed.

The reaction of S_5N_6 with **1** demonstrates the usefulness of this S–N compound in the formation of new structural types. The formation of **5** suggests that the $S_2N_3^-$ ligand also has a potentially important role in the chemistry of S–N metallacycles.

Experimental Procedure

5: A mixture of solid S_5N_6 [5] (0.13 g, 0.53 mmol) (**Caution**: explosive!) and **1** (0.286 g, 0.26 mmol) was treated with CH_2Cl_2 (50 mL) and the resulting solution stirred 12 h, during which time it slowly darkened and then lightened in color. The volume was reduced under vacuum to a few mL and the solution filtered then layered with Et_2O. Slow diffusion for 24 h yielded a mass of crystalline product which was washed with Et_2O and dried under vacuum. Three different types of crystals were present in the resulting mixture: brown plates together with orange needles and very dark black-red plates. The crystals were separated manually. The brown plates and orange needles were identified by IR spectroscopy as **2** (115 mg, 37%) and **3** (45 mg, 15%), respectively. Correct C,H,N-analysis. IR (without PPh_4 bands) $\tilde{\nu}$ [cm^{-1}] = 1126(m), 858(vs), 409(m), 308(m).

Received: December 11, 1991 [Z 5066 IE]
German version: *Angew. Chem.* **1992**, *104*, 620

[1] P. F. Kelly, J. D. Woollins, *Polyhedron* **1986**, *5*, 607–632; T. Chivers, F. Edelmann, *ibid.* **1986**, *5*, 1661–1699.
[2] P. F. Kelly, A. M. Z. Slawin, D. J. Williams, J. D. Woollins, *Polyhedron* **1991**, *10*, 2337-2340.
[3] V. C. Ginn, P. F. Kelly, A. M. Z. Slawin, D. J. Williams, J. D. Woollins, *J. Chem. Soc. Dalton Trans.*, **1992**, 963–968.
[4] T. Chivers, J. Proctor, *J. Chem. Soc. Chem. Commun.* **1978**, 642–643.
[5] H. W. Roesky, M. N. S. Rao, T. Nakajima, W. S. Sheldrick, *Chem. Ber.*, **1979**, *112*, 3351–3357.
[6] **5**: $C_{24}H_{20}Cl_2N_3PPdS_2$, $M_r = 622.8$, monoclinic, $a = 13.095(2)$, $b = 14.048(3)$, $c = 13.912(3)$ Å, $\beta = 99.89(2)°$, $V = 2521$ Å^3, space group $P2_1/n$, $Z = 4$, $\varrho_{calc.} = 1.641$ g cm^{-3}, $\mu(Mo_{K\alpha}) = 11.96$ cm^{-1}. Data were measured on a Siemens P4 diffractometer, $Mo_{K\alpha}$ radiation, graphite monochromator, ω scan. The structure was solved by direct methods, and all the non-hydrogen atoms were refined anisotropically. $R = 0.052$ for 2958 independent observed reflections [$3 \leq 2\theta \leq 50°$, $|F_o| > 3\sigma$ ($|F_o|$)]. Further details of the crystal structure investigation are available on request from the Director of the Cambridge Crystallographic Data Centre,

University Chemical Laboratory, Lensfield Road, Cambridge CB2 1EW (UK) on quoting the full journal citation.
[7] H. Wadle, E. Conradi, U. Müller, K. Dehnicke, *Z. Naturforsch. B* **1986**, *41*, 796–798.
[8] H. W. Roesky, J. Schimkowiak, M. Noltemeyer, G. M. Sheldrick, Z. *Naturforsch. B* **1986**, *41*, 175–178.
[9] H. W. Roesky, J. Anhaus, H. G. Schmidt, G. M. Sheldrick, M. Noltemeyer, *J. Chem. Soc. Dalton Trans.* **1983**, 1270–1279.
[10] T. A. Kabanos, A. M. Z. Slawin, D. J. Williams, J. D. Woollins, *J. Chem. Soc. Chem. Commun.* **1990**, 193–194.
[11] N. Burford, T. Chivers, R. T. Oakley, A. W. Cordes, P. N. Swepston, *J. Chem. Soc. Chem. Commun.* **1980**, 1204–1205.
[12] It is noteworthy that the out-of-plane twist of the $PdCl_2$ plane with respect to the PdS_2N_3 plane is such as to reduce the intermolecular Cl···S distance.
[13] E. Conradi, H. Wadle, U. Müller, K. Dehnicke, *Z. Naturforsch. B* **1986**, *41*, 48–52.

Enantioselective Synthesis of 3-Substituted 2-Ketoesters**

By *Dieter Enders,* Hubert Dyker,* and *Gerhard Raabe*

Dedicated to Professor Günther Maier on the occasion of his 60th birthday

As phosphoenolpyruvate (PEP) **A**, pyruvic acid plays a central role in the biosynthesis of sialic acids and ulosonic acids,[1] whereby phosphoenolpyruvate undergoes C–C linkage to aldehydes by means of aldol reactions catalyzed by aldolases. Important natural products such as *N*-acetylneuraminic acid, 3-deoxy-D-*manno*-octulosonic acid (KDO), and 3-deoxy-D-*arabino*-2-heptulosonic acid 7-phosphate (DAHP), the precursor of shikimic acid, are formed in this way. Chemical equivalents of phosphoenolpyruvate—metalated derivatives of pyruvic acid, for example chiral hydrazones **B** (R = H), or more generally derivatives of 2-ketocarboxylic acids[2]—can be considered d^2 synthons **C**.[3] In recent years several such systems have been examined,[4] but to our knowledge no efficient general reagent for the transfer of the synthon **C** to electrophiles in diastereo- and enantioselective reactions is available.

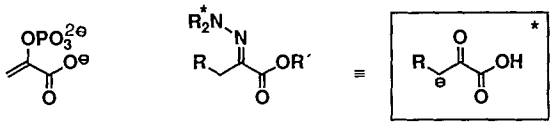

A (PEP) **B** **C**

We now report on the synthesis of a chiral, homologous PEP equivalent **B** (R = CH_3) by the application of our SAMP-/RAMP- hydrazone method[5, 6] and the use of **B** in the synthesis of highly enantio-enriched 3-substituted 2-ketoesters. Our initial attempts at metalating hydrazones of methyl and *tert*-butyl pyruvate and trapping them with electrophiles were unsuccessful and led primarily to self-acylated products. Only after we sterically blocked the ester reactivity as the 2,6-di-*tert*-butyl-4-methoxyphenyl ester[7] was the direct manipulation of the corresponding azaenolates possible. The two-step synthesis of 2-ketoester **1** succeeded in a simple fashion and in excellent yields by the esterification of ethyl oxalyl chloride with the lithium salt of 2,6-di-*tert*-butyl-4-methoxyphenol followed by the chemoselective nucleophilic addition of methyl or ethyl Grignard reagents to the unsymmetrical ethyl aryl oxalate (Scheme 1).

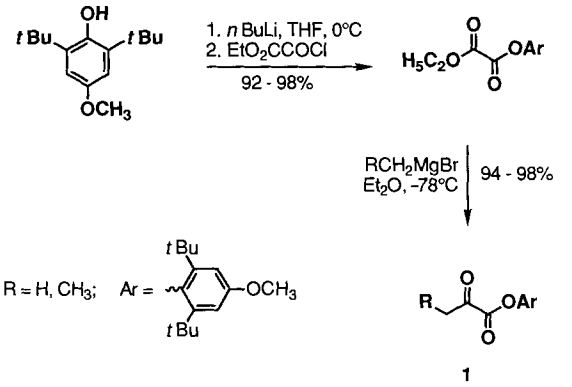

Scheme 1. Synthesis of 2-ketoester **1**.

The reaction of 2-ketoester **1** with (*S*)-1-amino-2-methoxymethylpyrrolidine (SAMP)[6, 8] provided the (*E*)-configured hydrazone (*S*)-**2** as a pale yellow solid in almost quantitative yield. The subsequent metalation with 2.2 equivalents of Lochmann–Schlosser base in tetrahydrofuran at −90 to −78 °C yielded highly reactive azaenolates, which were alkylated by a number of alkyl halides at −100 °C in good yields (51–72%) and with high diastereomeric excesses (*de* = 85 to >95%) to furnish hydrazones (*S,S*)-**3**. If less base was used, the alkylation did not go to completion. By the oxidative cleavage with ozone the alkylated hydrazones were converted in good yields and without racemization to the final products (*S*)-**4**, which were purified by flash chromatography (Scheme 2). This last step is not suitable for compounds like (*S,S*)-**3d** which are easily oxidized by ozone. In such cases the SAMP hydrazone can be converted to ketoesters (*S*)-**4** with boron trifluoride–ether in acetone/water with the addition of paraformaldehyde. This method was previously employed in a similar way for the cleavage of dimethylhydrazones.[9] In comparison to the oxidative cleavage this method gave somewhat better yields; however, reac-

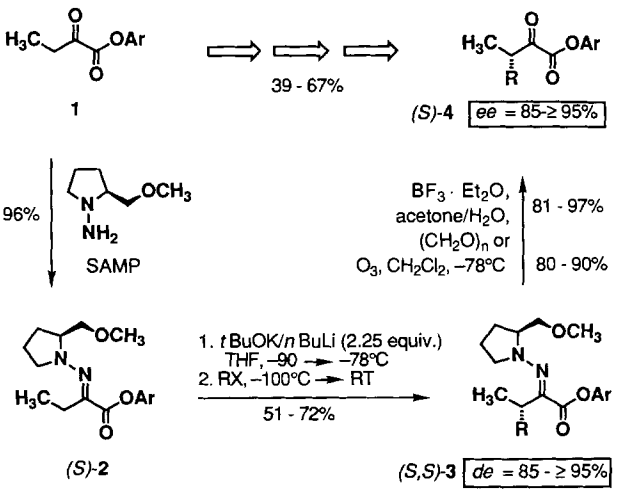

Scheme 2. Enantioselective synthesis of the 3-substituted 2-ketoester **4**.

[*] Prof. Dr. D. Enders, Dipl.-Chem. H. Dyker, Dr. G. Raabe
Institut für Organische Chemie der Technischen Hochschule
Professor-Pirlet-Strasse 1, D-W-5100 Aachen (FRG)

[**] This research was supported by the Fonds der Chemischen Industrie and the companies Degussa, BASF, Bayer, and Hoechst (donation of chemicals). H.D. thanks the Fonds der Chemischen Industrie for a Kekulé fellowship.

tion times of one to two days were required (monitored by thin-layer chromatography).

The enantiomeric excess of the 3-substituted ketoester (*S*)-**4a** was determined by a ^{1}H NMR shift experiment with Eu(hfc)$_3$, and proved that the cleavage with ozone and boron trifluoride–ether proceeded without racemization. In the other cases the enantiomeric excesses are based on the diastereomeric excesses of hydrazones **3** as determined by ^{13}C NMR spectroscopy. The enantiomers (*R*)-**4** are accessible simply by changing the chiral auxilliary (RAMP instead of SAMP), as was demonstrated for (*R*)-**4e** and (*R*)-**4h**.

Table 1. The highly enantio-enriched 3-substituted 2-ketoesters **4** prepared by the enantioselective alkylation of 2-ketoesters **1** via the SAMP hydrazones (*S*)-**2**.

3/4	RX	Yield **3** [%]	Yield **4** [a] [%]	$[\alpha]_D^{RT}$ ($c = 1$, $CHCl_3$)	*ee* [b] [%]
a	EtI	61–65	87 (97) [c]	13.2	93 (*S*)
b	*n*BuI	51–60	90 (96)	9.5	≧95 (*S*)
c	*i*PrI	58–61	90 (–)	32.0	93 (*S*)
d	$(CH_3)_2C{=}CHCH_2Br$	57–70	– (84–90)	–0.6	≧95 (*S*)
e	$PhCH_2Br$	54–62 [d]	80–88 (85)	19.4	≧95 (*S*)
e [e]	$PhCH_2Br$	65 [d]	– (81)	–19.2	≧95 (*R*)
f	$PhCH_2OCH_2Cl$	72	82 (–)	–0.3	92 (*S*)
g	$PhCH_2O(CH_2)_2I$	63	85 (–)	–3.4	88 (*S*)
h	$PhCH_2O(CH_2)_3I$	55–67	81 (92)	–2.6	85 (*S*)
h [e]	$PhCH_2O(CH_2)_3I$	59	80 (–)	2.8	85 (*R*)

[a] Yield of the pure ketoester **4** after cleavage of hydrazone **3** with ozone or $BF_3 \cdot Et_2O$ (in parentheses). [b] Determined by ^{1}H NMR shift experiments with Eu(hfc)$_3$ and/or by ^{13}C NMR spectroscopy of the hydrazone intermediate, whose absolute configuration is given in parentheses. [c] m.p. 56–57 °C. [d] m.p. 78–79 °C. [e] RAMP was used as the chiral auxiliary.

The absolute configuration of hydrazones **3**, and thus also of ketoesters **4**, was determined by X-ray structure analysis of (*S*,*S*)-**3e** (Fig. 1).[10] The (*S*) configuration found at the newly formed stereogenic center is in agreement with that predicted by the postulated mechanism for electrophilic substitutions via SAMP/RAMP hydrazones.[14]

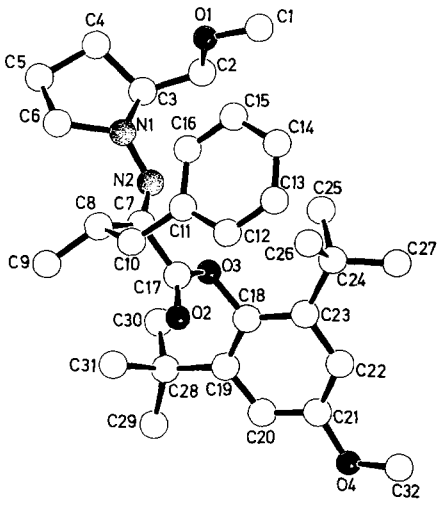

Fig. 1. Structure of (*S*,*S*)-**3e** in the crystal (Schakal plot[15]).

This method permits for the first time the highly enantioselective transfer of a homologous pyruvate unit to electrophiles.[16] Preliminary enzyme-mimetic applications of this new procedure to asymmetric aldol reactions are promising and should allow a simple and stereoselective approach to important natural products and drugs.[17]

Experimental Procedure

A solution of 6.6 mmol Lochmann–Schlosser base was prepared by the addition of a solution of *n*BuLi in *n*-hexane (4.4 mL, 1.5 M) to a solution of potassium *tert*-butoxide (0.74 g) in THF (20 mL) at –78 °C under argon. This solution was cooled to –90 °C, and hydrazone (*S*)-**2** (1.3 g, 3 mmol) dissolved in THF (4 mL) was added. The reaction mixture was stirred for 2 h and allowed to warm to –78 °C. The reaction mixture was then cooled to –100 °C, and a solution of 6.6 mmol of the alkyl halide in 3 mL of THF was added dropwise. The reaction temperature was held at –100 °C for 2 h before the solution was allowed to warm to 0–10 °C over 12 h. The solution was neutralized by the addition of glacial acetic acid (0.4 g, 6.6 mmol) in water (2 mL) and then extracted with ether (200 mL). After the phases were separated, the ethereal phase was washed with a buffer solution (10 mL, pH 7) and saturated NaCl solution (10 mL) and dried over $MgSO_4$. The solvent was removed in vacuum, and the crude hydrazone was purifed by flash chromatography (silica gel, petroleum ether/ethyl acetate 9:1).

For the cleavage, 1 mmol of the hydrazone was dissolved in CH_2Cl_2 (50 mL) and cooled to –78 °C under argon. Ozone was passed through the solution at that temperature until the reaction was complete (reaction progress monitored by TLC). After the excess ozone was dispelled with argon, the reaction mixture was allowed to warm to room temperature. The solvent was removed in vacuum, and the product was purified by flash chromatography (silica gel, petroleum ether/ethyl acetate/isopropanol 95:5:1). Alternatively, the hydrazone was dissolved in 10 mL acetone and 1 mL water, and $BF_3 \cdot Et_2O$ (0.38 mL, 3 mmol) was added dropwise. Paraformaldehyde (0.15 g, 5 mmol) was then added, and the reaction mixture was stirred 15 h at room temperature. To ensure complete reaction another portion of $BF_3 \cdot Et_2O$ (0.38 mL, 3 mmol) was added, and the reaction mixture was stirred another 12–24 h (reaction progress again monitored by TLC). Solvent was removed in vacuum, and the residue was taken up in ether, washed with saturated NH_4Cl solution (5 mL) and saturated NaCl solution (5 mL), and dried over $MgSO_4$. After evaporation of the solvent the crude product was purifed by flash chromatography as described above.

Received: December 3, 1991 [Z 5051 IE]
German version: *Angew. Chem.* **1992**, *104*, 649

[1] F. M. Unger, *Adv. Carbohydr. Chem. Biochem.* **1980**, *38*, 323; R. Schauer, *ibid.* **1982**, *40*, 132.
[2] a) J. M. Brown in *Compr. Org. Chem.* (Eds.: D. H. R. Barton, W. D. Ollis), Pergamon Press, Oxford, **1979**, Vol.2, p. 779; b) A. J. L. Cooper, J. Z. Ginos, A. Meister, *Chem. Rev.* **1983**, *83*, 321.
[3] D. Seebach, *Angew. Chem.* **1979**, *91*, 259; *Angew. Chem. Int. Ed. Engl.* **1979**, *18*, 239.
[4] a) C. G. Wermuth, *Bull. Soc. Chim. Fr.* **1966**, 1435; b) R. R. Schmidt, R. Betz, *Angew. Chem.* **1984**, *96*, 420; *Angew. Chem. Int. Ed. Engl.* **1984**, *23*, 430; c) R. Metternich, W. Lüdi, *Tetrahedron Lett.* **1988**, *29*, 3923; d) A. Esswein, R. Betz, R. R. Schmidt, *Helv. Chim. Acta* 1989, 213; e) E. R. Koft, P. Dorff, R. Kullnig, *J. Org. Chem.* **1989**, *54*, 2936; f) A. Dondoni, G. Fantin, M. Fogagnolo, *Tetrahedron Lett.* **1989**, *30*, 6063; g) A. Dondoni, G. Fantin, M. Fogagnolo, P. Merino, *Tetrahedron Lett.* **1990**, *31*, 4513; h) A. Dondoni, P. Merino, *J. Org. Chem.* **1991**, *56*, 5294; i) I. Tapia, V. Alcazar J. R. Moran, C. Caballero, M. Grande, *Chem. Lett.* **1990**, 697; j) D. R. Williams, J. W. Benbow, *ibid.* **1990**, *31*, 5881; k) A. G. M. Barrett, D. Dhanak, S. A. Lebold, M. A. Russel, *J. Org. Chem.* **1991**, *56*, 1894.
[5] D. Enders in *Asymmetric Synthesis* (Ed.: J. D. Morrison), Academic Press, Orlando, **1984**, Vol. 3, p. 275.
[6] D. Enders, P. Fey, H. Kipphardt, *Org. Synth.* **1987**, *65*, 173, 183.
[7] a) C. H. Heathcock, M. C. Pirrung, S. H. Montgomery, J. Lampe, *Tetrahedron* **1981**, *37*, 4087; b) R. Häner, D. Seebach, *Chimia* **1985**, *39*, 356; c) M. P. Cooke, Jr., *J. Org. Chem.* **1986**, *51*, 1638; T. Vettiger, D. Seebach, *Liebigs Ann. Chem.* **1990**, 189.
[8] a) D. Enders, P. Fey, H. Kipphardt, *Org. Prep. Proc. Int.* **1985**, *17*, 1; b) D. Enders, H. Eichenauer, *Chem. Ber.* **1979**, *112*, 2933.
[9] R. E. Gawley, E. J. Termine, *Synth. Commun.* **1982**, *12*, 15.
[10] Suitable single crystals were obtained by crystallization from *n*-hexane. Orthorhombic, space group $P2_12_12_1$ (19), $a = 9.600(2)$, $b = 13.109(1)$, $c = 24.331(6)$ Å. $V = 3062.0$ Å^3, $M_{calc} = 522.73$, and $Z = 4$ provide a calculated density $\rho = 1.134$ g cm^{-3}. Total number of electrons per elemental cell $F(000) = 1136$, $Cu_{K\alpha}$ radiation ($\lambda = 1.54179$ Å, graphite monochromator), $\mu = 5.93$ cm^{-1} (no absorption correction). Enraf-Nonius four-circle diffractometer, $\Omega/2\theta$ scans, 20 °C. Of 3581 independent reflections ($+h+k+l$) 2625 were observed ($I > 2\sigma(I)$, $R_m = 0.01$), $\sin\theta/\lambda_{max} = 0.628$ for solution and refinement. The structure was solved with direct methods (GENSIN[11] and GENTAN[12] of the XTAL3.0 program package[13]). Positions of the hydrogen atoms were calculated. 344 parameters were refined, $R = 0.090$ ($R_w = 0.097$), residual electron density

0.3 eÅ^{-3}. Further details of the crystal structure investigation may be obtained from the Fachinformationszentrum Karlsruhe, Gesellschaft für wissenschaftlich-technische Information mbH, D-W-7514 Eggenstein-Leopoldshafen 2 (FRG) on quoting the depository number CSD-56193, the names of the authors, and the journal citation.
[11] „GENSIN", V. Subramanian, S. R. Hall, *XTAL 3.0 Reference Manual* (Eds.: S. R. Hall, J. M. Stewart), Universities of Western Australia and Maryland **1990**.
[12] „GENTAN", S. R. Hall *XTAL 3.0 Reference Manual* (Eds.: S. R. Hall, J. M. Stewart), Universities of Western Australia and Maryland **1990**.
[13] *XTAL 3.0 Reference Manual* (Eds.: S. R. Hall, J. M. Stewart), Universities of Western Australia and Maryland **1990**.
[14] a) D. Enders, *Chem. Scr.* **1985**, *25*, 139; b) D. Enders, G. Bachstädter, K. A. M. Kremer, M. Marsch, K. Harms, G. Boche, *Angew. Chem.* **1988**, *100*, 1580; *Angew. Chem. Int. Ed. Engl.* **1988**, *27*, 1522.
[15] E. Keller, *Chem. Unserer Z.* **1986**, *20*, 178.
[16] All new compounds provided correct elemental analyses and spectra (NMR, IR, MS).
[17] D. Enders, H. Dyker, unpublished results.

Biochemical Degradation of Cyanamide and Dicyandiamide**

By *Lydia M. Estermaier,* A. Heidemarie Sieber, Friedrich Lottspeich, Dagmar H. M. Matern,* and *Guido R. Hartmann*

Dedicated to Professor Heinz Harnisch on the occasion of his 65th birthday

Nitrate is the predominant form of nitrogen in the soil available to most plants grown under normal field conditions and is taken up as such as a source of nitrogen. It is produced from ammonium ions by oxidation catalyzed by soil microorganisms (nitrification).[1] Due to the cation exchange properties of soil, NH_4^+ is more easily accumulated than NO_3^- which is rapidly lost by leaching.[2] Most artificial fertilizers contain nitrogen in the form of nitrate or ammonium ions. However, the first synthetic compound used as nitrogen fertilizer was cyanamide, which is synthesized from calcium carbide and atmospheric nitrogen in an exothermic reaction. Despite its relatively high cost, cyanamide is still used in agriculture and horticulture as a nitrogen fertilizer, particularly in the form of its calcium salt, because of its other useful properties. In addition to its ability to provide nitrogen it acts also as a herbicide (defoliating weeds),[3] pesticide, fungicide, and bactericide.[4] In this last function it is also utilized for the deodorization of liquid manure. Cyanamide is also active in halting the dormancy of grape vines[5] and other fruits. This discovery opened a new field of application as plant growth regulator.

Dicyandiamide, the product of dimerization of cyanamide, is applied in agriculture as an inhibitor of nitrification. It prevents the oxidation of NH_4^+ by *Nitrosomonas europea*[6] and thereby stabilizes the supply of nitrogen available in the soil.

The mechanism of the biological degradation of these compounds poses an interesting ecological problem. When applied to fields, cyanamide usually disappears within a couple of days, depending on the soil and its moisture content. It was clear from the beginning that some catalytic mechanism must be involved in the degradation. For a long time it was thought that inorganic catalysts present in the soil are involved in this process, until the experiments of Ernst[7] clearly showed the preponderance of biological mechanisms, although the biochemistry of this particular degradation was not elucidated.

An inducible enzyme, cyanamide hydratase (EC 4.2.1.69), highly specific for the hydration of cyanamide (but not dicyandiamide) to urea, was first detected in the soil fungus *Myrothecium verrucaria*[8] and purified to homogeneity.[9] However, it is unlikely that this enzyme is generally responsible for the biological degradation of cyanamide in the soil, since it is expressed by the fungus only in the complete absence of any other nitrogen source, and expression immediately stops if another nitrogen source becomes available.

Hofmann et al.[10] described another enzymatic activity in extracts of commercial soybean flour which catalyzes the disappearance of cyanamide. We have purified this cyanamide-degrading enzyme from soybean flour (type I, not roasted, Sigma, Munich) in six steps to apparent homogeneity. Its molecular mass is about 600000, and it consists of six identical subunits. The first 23 amino acids at the *N*-terminus of the subunit were sequenced using the methodology described by Eckerskorn et al.[11] The sequence was the same as that at the *N*-terminus of urease from jack bean.[12] These findings suggested that the isolated enzyme may be identical to urease from soybean.

We therefore tested the commercially available, highly purified urease from jack bean (*Canavalia ensiformis*) (type VII, Sigma, Munich) for its ability to degrade cyanamide. Such a comparison disclosed that jack bean urease indeed exhibited the same specific enzymatic activity (310 ± 20 nmol min^{-1} mg^{-1}), and the same K_m value (0.15 ± 0.05 M) with cyanamide as substrate as the enzyme from soybean. Similarly the optimum of pH (7.0) and temperature (70 °C) was the same. In the reaction two moles of ammonia were formed for each mole of cyanamide consumed. Obviously urease catalyzed a cyanamide hydrolase reaction [Eq.(a)].

$$H_2N\text{-}CN + 2H_2O \longrightarrow 2NH_3 + CO_2 \qquad (a)$$

Additional evidence that urease is responsible for the cyanamide hydrolase activity was provided by the effect of specific inhibitors of urease;[13, 14] all of them inhibited the cyanamide hydrolase activity (Table 1).

To determine the substrate specificity we have tested not only cyanamide but also cyanamide derivatives such as *N*-formylcyanamide, acetylcyanamide, and benzoylcyanamide for hydrolysis by urease. But even with a 100-fold greater enzyme concentration than that used in the experiments with unsubstituted cyanamide and with prolonged incubation times up to 24 h, no hydrolysis was detectable.

Since cyanamide is hydrolyzed by urease we investigated also cyanic acid as a substrate. In contrast to cyanamide, cyanic acid is rather unstable at pH 7.0 and decomposes rapidly without addition of a catalyst. Nevertheless, the degradation of this compound is also distinctly enhanced by

[*] Dr. L. M. Estermaier, A. H. Sieber, Dipl.-Chem. D. H. M. Matern, Prof. Dr. G. R. Hartmann (deceased)
Institut für Biochemie der Universität
Karlstrasse 23
D-W-8000 Munich 2 (FRG)
Dr. F. Lottspeich
Laboratorium für Molekulare Biologie – Genzentrum
D-W-8033 Martinsried (FRG)

[**] These investigations have been supported by SKW Trostberg AG and the Fonds der Chemischen Industrie. We are very grateful to Prof. M. H. Zenk and Dr. T. Kutchan, Munich, for generous help with plant cell cultures and for discussions and to Dr. R. J. Youngman, Trostberg, for information. We wish to thank Prof. K. Kobashi, Toyama, for *N*-isopentenoylphosphoric trisamide and Prof. A. Böck and G. Müller, Munich, for the supply of bacterial strains.

Table 1. Effect of inhibitors of jack bean urease on cyanamide hydrolase activity. The conditions of incubation were similar to those of the cyanamide hydratase assay [9], but with 10 mM Tris/HCl buffer 7.4 at 50 °C (Tris: tris(hydroxymethyl)aminomethane). Cyanamide or urea were determined as described [9,23]. *N*-isopentenoylphosphoric trisamide [14] was obtained from Professor K. Kobashi, Toyama. *N*-phenylphosphoric trisamide was synthesized according to Kobayashi [24].

Inhibitor	Concentration [μM]	Cyanamide hydrolase activity [a] [%]	Urease activity [b] [%]
sodium fluoride	20000	48	34
acetohydroxamic acid	20	45	48
hydroquinone	40	45	48
N-isopentanoylphosphoric trisamide	5	60	4
N-phenylphosphoric trisamide	50	34	34

[a] 530 urease units $\times mL^{-1}$ were applied for the cyanamide hydrolase reaction; [b] 3 urease units $\times mL^{-1}$ were applied for the urease reaction.

urease. One mole of ammonia is formed per mole of depleted CNO^-, which suggests reaction (b).

$$HO\text{-}CN + 2HOH \longrightarrow H_2CO_3 + NH_3 \qquad (b)$$

Obviously urease exhibits cyanase (EC 3.5.5.3) activity.[15] As in the case of cyanamide (Table 1), low concentrations (5–30 μM) of phenylbisamidophosphate and phenylphosphoric trisamide inhibited the enzymatic hydrolysis of cyanate although only by 30 to 55%.

A relatively large number of compounds structurally related to urea or cyanamide are hydrolyzed by urease from jack bean, although the rate of hydrolysis is 100 to 1000 times less lower than with urease (Table 2). Obviously, at a low level of

Table 2. Compounds related to urea or cyanamide as substrate of jack bean urease. In our experiments the incubation conditions at 38 °C of Dixon et al. [16] were applied. Cyanamide and dicyandiamide were determined according to [9, 25].

Substrate	k_{cat} [s^{-1}]	K_m [M]	Ref.
urea ($H_2N\text{-}CO\text{-}NH_2$)	3500	0.003	[a]
semicarbazide ($H_2N\text{-}CO\text{-}NH\text{-}NH_2$)	30	0.06	[16]
hydroxyurea ($H_2N\text{-}CO\text{-}NH\text{-}OH$)	12	0.002	[16]
methylurea ($H_2N\text{-}CO\text{-}NH\text{-}CH_3$)	0.075	0.22	[16]
dicyandiamide ($H_2N\text{-}C(NH)\text{-}NH\text{-}CN$)	1.0	0.25	[a]
cyanamide ($H_2N\text{-}CN$)	8.6	0.2	[a]
acetamide ($H_2N\text{-}CO\text{-}CH_3$)	0.55	0.75	[16]

[a] This work.

activity the substrate specificity of urease is rather broad but not unlimited, since derivatives such as guanylurea and cyanourea were not degraded at all, even when we used a urease concentration 100 times higher. Related in structure to cyanourea is dicyandiamide. Thus we have tested also dicyandiamide as a possible substrate of urease.

Unexpectedly, this compound hydrolyzed. The K_m value was almost the same and the k_{cat} value was only nine times less than that for cyanamide (Table 2). Furthermore, the reaction showed a similar dependence on pH and temperature as the enzymatic hydrolysis of cyanamide suggesting that both hydrolytic reactions are catalyzed by the same enzyme.

Analysis of the reaction products revealed that the enzymatic hydrolysis of dicyandiamide led to approximately equal amounts of cyanourea and ammonia. This suggests the following hydrolytic reaction [Eq.(c)].

$$H_2N\text{-}C(NH)\text{-}NH\text{-}CN + HOH \longrightarrow H_2N\text{-}CO\text{-}NH\text{-}CN + NH_3 \qquad (c)$$

This hydrolysis is rather substrate-specific, since guanidine, for example, is not hydrolyzed by urease. Recently, a *Rhodococcus* species was discovered[17] which also degrades dicyandiamide to cyanourea. However, the stoichiometry of this reaction was not determined. The catalysis of the conversion of dicyandiamide to cyanourea belongs to a type of enzymatic reaction that is different from the other reactions catalyzed by urease (urea aminohydrolase) such as the hydrolysis of cyanate or cyanamide. With dicyandiamide as substrate, the hydrolysis of an imino group is catalyzed. Arginine deiminase (EC 3.5.3.6) is another enzyme that catalyzes such a reaction. In contrast to dicyandiamide, hydroxyurea is hydrolyzed by urease to NH_3, CO_2, and H_2NOH.[18]

These findings demonstrate the broad range of reactions that can be catalyzed by the enzyme urease. With respect to the mechanism of catalysis, the question arises of whether all these reactions are catalyzed at the same active center or if urease belongs to the class of "double-headed" enzymes with separate active centers for the various catalytic activities. In this context it may be of interest to note that neither hydroxyurea, hydroquinone, acetohydroxamic acid, nor *N*-isopentenoyl phosphoric trisamide inhibit the hydrolysis of dicyandiamide at a concentration (50 μM) which inhibits the cyanamide hydrolase or urea amido hydrolase activity of urease.

Urease is a widely distributed enzyme found also in plants,[19] and a particularly rich source is the seeds of *Leguminosae*. Therefore it was not surprising that extracts of all such seeds (soybean, mung bean, bush bean, lentil, pea) and of leaves from lentil, pea, and lupine exhibited cyanamide hydrolase activity.

Most of cyanamide and dicyandiamide used in agriculture is applied to the soil. Therefore it is likely that microorganisms in the soil are mainly responsible for the biological conversion and degradation of these compounds. Urease is widely distributed among microorganisms.[19] The question arises whether urease from bacteria in the soil also degrades cyanamide. The answer is not obvious, because bacterial ureases differ from each other and from the plant enzymes in parameters such as size, number of subunits, and nickel content.[20] (Nickel is an essential cofactor for urease activity.) *Bacillus pasteurii* is a gram-positive eubacterium with a particularly high urease activity which occurs in the soil. Its urease consists of four identical subunits (M_r 65000) with a total mass of about 230000,[21] whereas the urease from jack bean consists of six identical subunits (M_r 96600) with a holoenzyme molecular mass of 590000.[13] We compared the substrate-degrading activity of a commercially available preparation of urease from *Bacillus pasteurii* (type X, partially purified powder, 100–200 units per mg, Sigma, Munich) with that of the enzyme from jack bean using urea, cyanamide, and dicyandiamide (Table 3). The plant enzyme was more active than the bacterial urease. This may have been due to the higher purity or due to the fact that both enzymes were not tested under saturating substrate concentrations for technical reasons. Dicyandiamide was metabolized to equal amounts of cyanourea and ammonia by the bacterial urease in an identical manner to the plant enzyme.

Table 3. Hydrolysis of cyanamide and dicyandiamide by urease from jack bean or from *Bacillus pasteurii*. The assay was carried out with 20 mM substrate in 10 mM Tris/HCl pH 8.0 at 50 °C. The disappearance of urea, cyanamide, and dicyandiamide was measured by colorimetric assays as in [23, 9, 25].

Substrate	nmol substrate metabolized at pH 8.0 and 50 °C per min and mg protein by urease from	
	jack beam	*B. pasteurii*
urea	366000 [a]	55000 [d]
cyanamide	176 [b]	9 [e]
dicyandiamide	8 [c]	0.2 [f]

[a] 1.2, [b] 104, [c] 520, [d] 1.2, [e] 436, [f] 8720 units of urease used in the assay.

Inhibitors of urease activity reduced the cyanamide hydrolase activity of the bacterial enzyme (Table 4). This supports the conclusion that the bacterial urease is also responsible for the catalysis of cyanamide degradation. In agreement with the observations made with plant urease, the degradation of dicyandiamide by the bacterial enzyme is not susceptible to inhibition by 15 mM NaF, 100 μM hydroquinone, 50 μM isopentenoylphosphoric trisamide, or 50 μM *N*-phenylphosphoric trisamide.

Table 4. Inhibition of cyanamide hydrolase activity of urease from *Bacillus pasteurii* by urease inhibitors. The enzyme was preincubated with the inhibitor in 10 mM Tris/HCl pH 7.4 for 15 min at 50 °C before addition of substrate.

Inhibitor	Inhibitor concentration [μM]	Cyanamide hydrolysis [a] [%]	Inhibitor concentration [μM]	Urea hydrolysis [b] [%]
sodium fluoride	20000	37	40000	42
acetohydroxamic acid	20	27	20	44
hydroquinone	100	40	40	31
N-phenylphosphoric trisamide	50	46	50	63
N-isopentenoyl-phosphoric trisamide	20	76	0.5	19

[a] 1092 urease units per mL (2 h incubation). [b] 4.4 urease units per mL (15 min incubation).

Cyanamide hydrolase activity was also detected at pH 7.4 and 50 °C in urease containing crude extracts of other soil bacteria such as *Proteus vulgaris, Proteus mirabilis, Klebsiella oxytoca*, and *Mycobacterium phlei* in the range of 0.5–4 nmol cyanamide degradation per min and mg protein.

The fertilizers urea and cyanamide must both be degraded in the soil before they can fulfill their physiological role as suppliers of nitrogen for plants. Urea is degraded efficiently by urease, which is ubiquitous in microorganisms in the soil. Thus in the application of urea as a fertilizer, the abundance of urease may lead to a transitory massive formation of toxic ammonia (ammonium ions) with adverse effects on seed germination, seedling growth, and early plant growth. To eliminate these effects the addition of small amounts of urease inhibitors has been suggested.[22]

For the fertilizer cyanamide the situation is different. Enzymes that degrade cyanamide specifically seem to be much less abundant in the soil. So far only one, cyanamide hydratase, has been discovered[8] and characterized.[9] Its high substrate-specificity for cyanamide poses the interesting question of how this enzyme provides the microorganism with a selective advantage for survival and reproduction, since cyanamide is not found in nature.

An alternative cyanamide-hydrolyzing enzyme is the ubiquitous urease, as we demonstrated above. It catalyzes this reaction much more slowly than the hydrolysis of urea, with the consequence that a massive and instantaneous production of ammonia in the soil is prevented. Thereby the rate of the subsequent nitrification and leakage of nitrate formed from the soil is also diminished.

Because cyanamide and dicyandiamide are not found in nature, the question of how such chemicals are metabolized when they are purposely or inadvertantly released into the environment is raised. One might expect that a biological degradation would not occur, because there has been insufficient time for natural selection and development of suitable degrading microorganisms. However, many such chemicals, including cyanamide, disappear relatively rapidly in nature. In this context one should not overlook the fact that in contrast to the usual conditions in the laboratory the exposure time for degradative processes in natural ecosystems is much longer. It follows that enzymatic processes with much lower reaction rates, like that of the hydrolysis of cyanamide or dicyandiamide by urease from plants and bacteria, may contribute to the removal of toxic synthetic chemicals in the natural environment. For the investigation of enzymes that could be relevant for the metabolism of such chemicals it is therefore important that measurements of substrate specificity should not be limited too narrowly to compounds closely related in structure to the natural substrate and those metabolized with high rates. As was shown here, the substrate specificity of enzymes at low catalytic activity is apparently much broader than previously assumed. It suggests the necessity for further work in this area to develop enzyme assays with much higher sensitivity.

Received: November 4, 1991 [Z 5123 IE]
German version: *Angew. Chem.* **1992**, *104*, 655

[1] L. Beevers, R. H. Hageman in *The Biochemistry of Plants, Vol. 5*, (Ed.: B. J. Miflin), Academic Press, New York, USA **1980**, pp.115–168.
[2] K. Rathsack, *Landwirtsch. Forsch.* **1978**, *31*, 347–358.
[3] a) B. Rademacher, A. Flock, *Z. Acker- Pflanzenbau* **1951**, *94*, 1–54; b) H. Uhl, *ibid.* **1952**, *95*, 121–158; c) R. Heitefuss, H. Bodendörfer, R.-R. Paeschke, *Z. Pflanzenkr. Pflanzenschutz* **1977**, *84*, 641–662.
[4] a) A. Amberger, *Z. Pflanzenernähr. Bodenkd.* **1968**, *119*, 1–10; b) H. Dannenhauer, A. Resz, F. Grossmann, *Z. Pflanzenkr. Pflanzenschutz* **1983**, *90*, 468–478.
[5] Y. Shulman, G. Nir, S. Lavee, *Sci. Hortic.* **1983**, *19*, 97–104.
[6] B. Zacherl, A. Amberger, *Fert. Res.* **1990**, *22*, 37–44.
[7] D. Ernst, *Z. Pflanzenernähr. Düng. Bodenkd.* **1967**, *116*, 34–44.
[8] H. Stransky, A. Amberger, *Z. Pflanzenphysiol.* **1973**, *70*, 74–87.
[9] U. H. Maier-Greiner, B. M. Obermaier-Skrobranek, L. M. Estermaier, W. Kammerloher, C. Freund, C. Wülfing, U. I. Burkert, D. H. Matern, M. Eulitz, M. Breuer, Ö. I. Küfrevioglu, G. R. Hartmann, *Proc. Natl. Acad. Sci. USA* **1991**, *88*, 4260–4264.
[10] E. Hofmann, E. Latzko, A. Süss, *Z. Pflanzenernähr. Düng. Bodenkd.* **1954**, *66*, 193–202.
[11] C. Eckerskorn, W. Mewes, H. Goretzki, F. Lottspeich, *Eur. J. Biochem.* **1988**, *176*, 509–519.
[12] K. Takishima, T. Suga, G. Mamiya, *Eur. J. Biochem.* **1988**, *175*, 151–165.
[13] R. L. Blakeley, B. Zerner, *J. Mol. Catal.* **1984**, *23*, 263–292.
[14] K. Kobashi, S. Takebe, A. Numata, *J. Biochem. (Tokyo)* **1985**, *98*, 1681–1688.
[15] P. Anderson, *Biochemistry* **1980**, *19*, 2882–2888.
[16] N. E. Dixon, P.W. Riddles, C. Gazzola, R. L. Blakeley, B. Zerner, *Can. J. Biochem.* **1980**, *58*, 1335–1344.
[17] S. Hallinger, P. R. Wallnöfer, H. Goldbach, A. Amberger, *Naturwissenschaften* **1990**, *77*, 332–334.
[18] W. N. Fishbein, T. S. Winter, J. D. Davidson, *J. Biol. Chem.* **1965**, *240*, 2402–2406.
[19] F. J. Reithel in *The Enzymes, Vol. 4* (Ed.: P. D. Boyer), Academic Press, New York, USA **1971**, pp.1–21.
[20] M. J. Todd, R. P. Hausinger, *J. Biol. Chem.* **1987**, *262*, 5963–5967.
[21] S. Christians, H. Kaltwasser, *Arch. Microbiol.* **1986**, *145*, 51–55.
[22] a) J. M. Bremner, M. J. Krogmeier, *Proc. Natl. Acad. Sci. USA* **1988**, *85*, 4601–4604; b) J. M. Bremner, M. J. Krogmeier, *ibid.* **1989**, *86*, 8185–8188.
[23] J. C. Polacco, *Plant Physiol.* **1976**, *58*, 350–357.
[24] E. Kobayashi, *Bull. Chem. Soc. Jpn.* **1973**, *46*, 183–186.
[25] K. Vilsmeier, *Z. Pflanzenernähr. Bodenkd.* **1982**, *145*, 503–505.

Oxygen Activation on Nickel(II)tetrahydrosalen Complexes with the Formation of Nickel(II)dihydrosalen Complexes**

By *Arnd Böttcher, Horst Elias,* Lutz Müller,* and *Helmut Paulus*

The activation of oxygen in the coordination sphere of transition-metal center is equally important for chemistry and biology and has been known for a long time for Fe-, Co- and Cu-containing active sites of natural systems and the analogous model complexes.[1] In recent years, Ni^{II} complexes with macrocyclic N_5 ligands have been reported,[2] which are also capable of both O_2 addition and activation. Herein, we report for the first time, Ni^{II} complexes with the open-chain N_2O_2 ligand system of tetrahydrosalen **3** (*N,N'*-bis(2-hydroxybenzyl)-1,2-diaminoethane), which are also O_2 active when they constain a specific substitution pattern on the benzene ring of the ligand. Furthermore, the first X-ray structure analysis of such a complex was achieved and it could be shown that in solution O_2 addition takes place at low temperature. At room temperature only one of the C–N bonds of the coordinated tetrahydrosalen ligand is oxidatively dehydrogenated to give dihydrosalen.

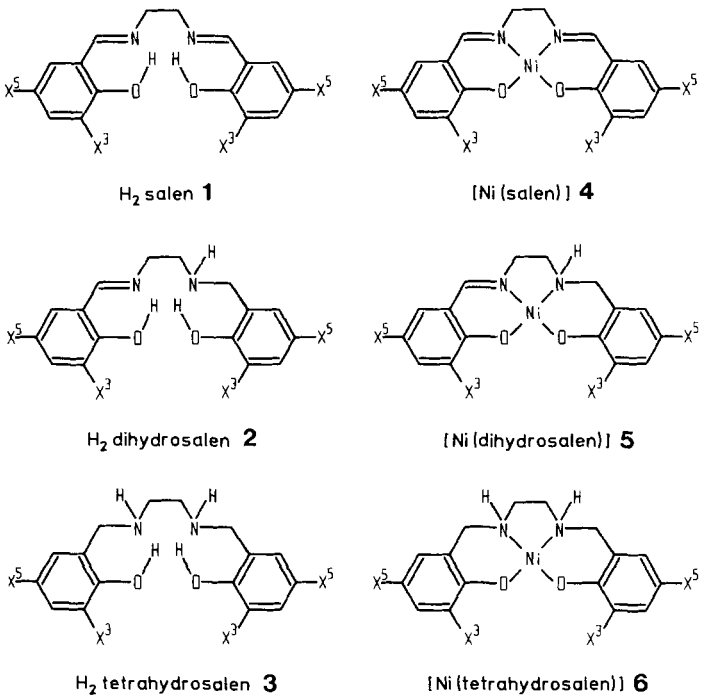

Scheme 1. Compounds **1**–**6**: **a**, $X^3 = X^5 = H$; **b**, $X^3 = t$Bu, $X^5 = H$; **c**, $X^3 = t$Bu, $X^5 = Me$; **d**, $X^3 = t$Bu, $X^5 = Cl$.

In comparison to the extensive literature[3] on Ni^{II} salen complexes and also their application as catalysts,[4] only little is known about the corresponding tetrahydrosalen complexes. [Ni(tetrahydrosalen)] **6a**[5] is pale blue, and the Ni atom is probably coordinated in an octahedral fashion[6] as a result of intermolecular Ni–O interactions ($\mu_{exp} = 2.94$ μ_B). However, an X-ray crystallographically determined structure of **6a** is not known. The introduction of bulky substituents (X^3 = *tert*-butyl) prevents intermolecular association for **6b**–**d**. The ligands **3b**–**d** obtained by hydrogenation of **1b**–**d** form cherry-red 1:1 neutral complexes with Ni^{2+} ions, which absorb at $\lambda_{max} = 512-514$ nm in solution ($\varepsilon_{max} = 970-1100\ M^{-1}cm^{-1}$), and are practically diamagnetic ($\mu_{exp} = 0.35$ μ_B for **6c** at 23 °C).

The X-ray structure analysis of **6b**·acetone[7] confirms that the Ni atom is coordinated in a square-planar fashion (Fig. 1). The NiO_2N_2 plane shows a slight tetrahedral distortion (angle between the two chelate six-membered rings is 13.5°), and the two benzene rings are bent slightly upwards and downward, respectively. The Ni–O distances (186.6 and 185.0 pm) and Ni–N distances (193.0 and 189.0 pm) differ only slightly. This is also true for the C–N distances N1–C7 (147.6 pm) and N2–C10 (139.2 pm), however, the shorter C–N distance is still much longer than the C=N bonds in **4a** (129.3 and 130.1 pm[8]). The Ni–Ni distance between the isolated complex units is 538 pm, and the acetone molecule is not coordinated.

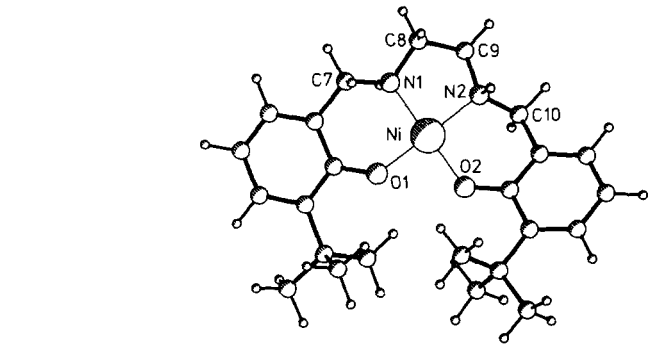

Fig. 1. Crystal structure of **6b**·acetone. Selected bond lengths [pm] and angles [°]: Ni-O1 186.6(3), Ni-O2 185.0(3), Ni-N1 193.0(4), Ni-N2 189.0(4), N1-C7 147.6(5), N1-C8 148.1(5), N2-C9 146.6(6), N2-C10 139.2(6); O1-Ni-O2 86.7(1), O1-Ni-N1 93.4(1), N1-Ni-N2 86.4(2), O2-Ni-N2 93.9(2).

The cherry-red solutions of **6b**–**d** in acetone slowly become yellow-orange in air. Figure 2 shows for **6c** that there is an isosbestic point. The observed changes do not occur when the solutions are saturated with N_2. The correspond-

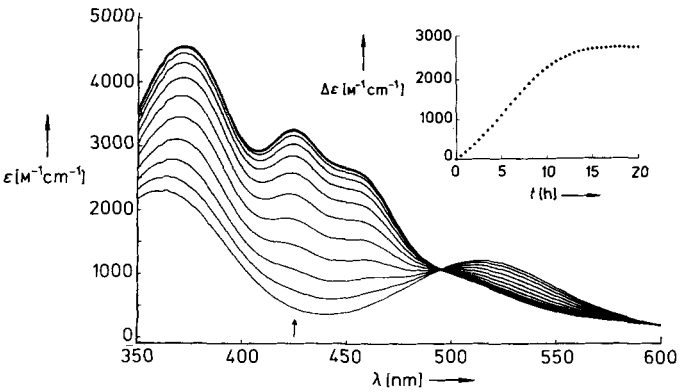

Fig. 2. Spectral changes for the reaction of **6c** with dioxygen in acetone ([**6c**] = 1.24×10^{-4} M, $d = 1$ cm, $T = 20$ °C, $\Delta t = 90$ min) and change of the absorbance at 425 nm with time.

[*] Prof. Dr. H. Elias, Dipl.-Ing. A. Böttcher, Dipl.-Ing. L. Müller
Anorganische Chemie III, Eduard-Zintl-Institut, Technische Hochschule, Hochschulstrasse 10, D-W-6100 Darmstadt (FRG)
Dr. H. Paulus
Strukturforschung, Fachbereich Materialwissenschaft, Technische Hochschule Darmstadt

[**] This work was supported by the Verband der Chemischen Industrie. Arnd Böttcher thanks the Studienstiftung des Deutschen Volkes and the Verband der Chemischen Industrie.

ing complexes [CuL] and [FeLCl] (H_2L = **3b–d**), like the free ligands **3b–d**, are not O_2 active.

Unexpectedly, upon reaction with air under the given conditions, **6b–d** are not dehydrogenated to **4b–d**, but only as far as **5b–d**. This can, for example, be confirmed for **6c** by the characterization of the product **5c** (IR: $\tilde{\nu}$(N–H) = 3180 cm^{-1} together with $\tilde{\nu}$(C=N) = 1620 cm^{-1}; MS (FD): *m/z* 466 for $\mathbf{5c}^{\oplus}$ (100%); ^1H NMR: $(CH_2)_2$ bridge protons at different field; C, H, N analysis), and also of the free ligand **2c** by IR and ^1H NMR spectroscopy as well as mass spectrometry (liberation of **2c** by cyanide treatment of **5c**). Furthermore, the VIS spectrum of **5c** (Fig. 3) shows characteristic absorption features of both **4c** and **6c**; however, it differs significantly from the spectrum of a 1:1 mixture of **4c** and **6c**. The λ_{max} and ε_{max} values are almost the same as those of the complex **5a** synthesized by a different method.[9]

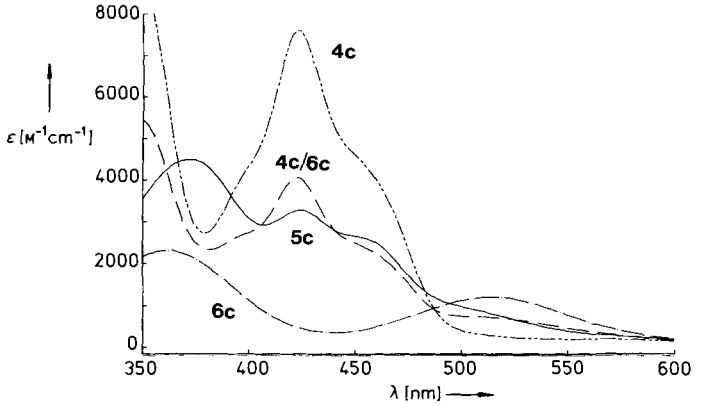

Fig. 3. VIS spectra of **4c**, **5c** (end spectrum from Fig. 2), **6c** and a 1:1 mixture of **4c** and **6c** in acetone ($c = 1.24 \times 10^{-4}$ M, d = 1 cm, T = 20 °C).

The effect of the substituents X[5] on the rate of the reaction of the Ni complexes with O_2 decreases in the order $CH_3 > Cl > H$. If the protons of the ethylene bridge in **6c** are replaced by methyl groups, the reaction becomes considerably slower. For the influence of the solvent on the rate v, the following is approximately [10, 11] valid: v(acetone):v(MeOH):v(toluene, CH_2Cl_2):v(DMF) = 100:15:3:1. The reaction rate in pyridine is virtually zero. Complexes **4b–d** and **5b–d** do not add pyridine (py); in contrast, the complexes **6b–d**, are considerably more Lewis-acidic (see [Eq. (a)]). For example, $K_1 = 0.37$ and $K_2 = 15.8\ M^{-1}$ are

$$\mathbf{6c} + 2\,py \underset{}{\overset{K_1}{\rightleftharpoons}} \mathbf{6c}\cdot py + py \overset{K_2}{\rightleftharpoons} \mathbf{6c}\cdot(py)_2 \qquad (a)$$

obtained for the **6c**/py/acetone system. The adduct **6c**·$(py)_2$ can also be isolated as a solid.

Further results are: 1) If a N_2 saturated solution of **6c** in acetone is allowed to react with acetone saturated with O_2 at −70 °C in a "stopped-flow" spectrophotometer,[12] a sudden ($t_{1/2}$ < 2.5 ms) change of the VIS spectrum is observed, which indicates an O_2 addition. 2) The reaction **6c** → **5c** is first order with regard to the concentration of O_2 and **6c**.[13] 3) During the reaction of **6c** → **5c**, PPh_3 is converted completely into $O{=}PPh_3$ ($[PPh_3]_0 = [\mathbf{6c}]_0$).

Thus, solutions of **6b–d** are O_2 active in that by oxidative dehydrogenation of a C–N bond the dihydrosalen complexes **5b–d** are formed. The rate of the reaction is dependent upon the substituents and the solvent; the Lewis acidity of the Ni center is of great significance for this process.

The described reaction pathway of nickel(II) tetrahydrosalen complexes is of interest for the preparative chemistry (asymmetrical synthesis), for the bioinorganic chemistry of nickel and for catalysis. Further investigations into the stoichiometry and the mechanism of the reaction,[14, 15] and also the role of the solvent[16] are in progress.

Experimental Procedure

1c: 2-Hydroxy-3-tert-butyl-5-methylbenzaldehyde (0.12 mol) in ethanol (200 mL) was slowly reacted with ethylenediamine (0.06 mol). After warming, yellow **1c** crystallized (95%); m.p. 147 °C. ^1H NMR (60 MHz, $CDCl_3$): δ = 1.3 (s, 18H; *t*Bu), 2.1 (s, 6H; CH_3), 3.75 (s, 4H; CH_2), 6.65 (m, 4H; aryl-H), 7.9 (s, 2H; CH); IR (KBr): $\tilde{\nu}$ [cm^{-1}] = 1620 (C=N).

3c: To **1c** (0.03 mol) in glacial acetic acid (50 mL), solid $Na[BH_3(CN)]$ (0.09 mmol) was added with stirring over 2 h at 20 °C. Then the colorless solution was set to pH 7 with NaOH. Extraction with CH_2Cl_2 and crystallization from ethanol/petrolether afforded needlelike crystals of **3c** (55%); m.p. 137 °C. ^1H NMR (300 MHz, $CDCl_3$): δ = 1.4 (s, 18H; *t*Bu), 2.3 (s, 6H; CH_3), 2.9 (s, 4H; CH_2), 4.0 (s, 4H; CH_2), 6.9 (m, 4H; aryl-H); IR(KBr): $\tilde{\nu}$ [cm^{-1}] = 3290 (N-H); MS (70 eV): *m/z* 412 ($M^{\oplus}$, 63%).

6c: **3c** (2 mmol) in methanol (50 mL) was allowed to react with $[Ni(AcO)_2]\cdot 4H_2O$ and NaOH (4 mmol) (each in a little methanol) with stirring and under an N_2 atmosphere. After the reaction solution was warmed and concentrated, red crystals of **6c** precipitated (70%); m.p. 285 °C (decomp.). ^1H NMR (300 MHz, [D_6]acetone): δ = 1.35 (s, 18H, *t*Bu), 2.1 (s, 6H; CH_3), 2.5 (m, 4H; CH_2), 2.95 (dd, ^2J(H,H) = 12 Hz, ^3J(H,H) < 2 Hz, 2H; CH_2), 3.4 (br.s, 2H; NH), 4.15 (ps t, ^2J(H,H) = ^3J(H,H) = 12 Hz, 2H; CH_2), 6.4–6.7 (m, 4H; aryl-H); IR(KBr): $\tilde{\nu}$ [cm^{-1}] = 3180 (N-H), 3140 (N-H); UV/VIS (acetone): λ_{max}[nm](ε) = 362 (2240), 514 (1100); MS(FD): *m/z* 468 ($M^{\oplus}$, 100%). All C, H, N analyses correct. The complexes **6b** and **6d** can be prepared analogously starting from the corresponding aldehydes.

Oxygen oxidation of **6c**: O_2 was passed through a solution of **6c** (0.1 mmol) in acetone (50 mL) for 48 h at 20 °C. By concentration, red-brown, microcrystalline **5c** was obtained (84%); m.p. 345 °C (decomp.). ^1H NMR (300 MHz, [D_6]acetone): δ = 1.35 (s, 18H; *t*Bu), 2.15 (s, 6H; CH_3), 2.5 (m, 1H; CH_2), 2.7 (m, 1H; CH_2), 3.0 (dd, ^2J(H,H) = 12 Hz, ^3J(H,H) = 2.5 Hz, 1H; CH_2), 3.4 (m, 1H; CH_2), 3.7 (br.s, 1H; NH), 4.3 (ps t, ^2J (H,H) = ^3J(H,H) = 12 Hz, 1H; CH_2), 5.35 (t, ^3J(H,H) = 4.5 Hz, 1H; CH_2), 6.4–6.7 (m, 2H; aryl-H), 6.8–7.0 (m, 2H; aryl-H), 7.6 (s, 1H; CH); IR(KBr): $\tilde{\nu}$ [cm^{-1}] = 3180(N-H), 1620 (C=N); VIS (acetone): λ_{max}[nm](ε) = 424 (3240); MS(FD): *m/z* 466 ($\mathbf{5c}^{\oplus}$, 100 %); correct C,H,N-analysis.

Oxidation of PPh_3: O_2 was passed through a solution of **6c** (0.05 mmol) and PPh_3 (0.05 mmol) in acetone (50 mL) for 48 h at 20 °C, after which the acetone was removed. MS(FD): m/z 466 ($\mathbf{5c}^{\oplus}$, 27%), 278 ($PPh_3O^{\oplus}$, 100); no signal at 262 (PPh_3). MS(FD) of the starting mixture: m/z 468 ($\mathbf{6c}^{\oplus}$,100%), 262 ($PPh_3^{\oplus}$, 12).

Received: November 14, 1991 [Z 5022 IE]
German version: *Angew. Chem.* **1992**, *104*, 635

CAS Registry numbers:
1b, 72138-54-6; **1c**, 139526-27-5; **1d**, 139526-28-6; **2b**, 139564-05-9; **2c**, 139526-29-7; **2d**, 139526-30-0; **3b**, 91129-01-0; **3c**, 63551-07-5; **3d**, 139564-04-8; **5b**, 139526-34-4; **5c**, 139526-35-5; **5d**, 139526-36-6; **6b**, 139526-32-2; **6b**·C_3H_6O, 139526-38-8; **6c**, 139526-31-1; **6c**·$(py)_2$, 139526-37-7; **6d**, 139526-33-3; PPh_3, 603-35-0; $O{=}PPh_3$, 791-28-6.

[1] A. E. Martell, D. T. Sawyer, *Oxygen Complexes and Oxygen Activation by Transition Metals*, Plenum, New York, **1988**.
[2] a) E. Kimura, A. Sakonaka, R. Machida, *J. Am. Chem. Soc.* **1982**, *104*, 4255; b) E. Kimura, R. Machida, *J. Chem. Soc. Chem. Commun.* **1984**, 499; c) E. Kimura, R. Machida, M. Kodama, *J. Am. Chem. Soc.* **1984**, *106*, 5497; d) Y. Kushi, R. Machida, E. Kimura, *J. Chem. Soc. Chem. Commun.* **1985**, 216; e) R. Machida, E. Kimura, Y. Kushi, *Inorg. Chem.* **1986**, *25*, 3461; f) D. Chen, J. Motekaitis, A. E. Martell, *ibid.* **1991**, *30*, 1396.
[3] M. D. Hobday, T. D. Smith, *Coord. Chem. Rev.* **1972–1973**, *9*, 311.
[4] H. Yoon, T. R. Wagler, K. J. O'Connor, C. J. Burrows, *J. Am. Chem. Soc.* **1990**, *112*, 4568.
[5] The complexes **5** and **6** are chiral. We have omitted the correct description of the compounds *rac*-**5a–5d** and *rac*-**6a–6d** in the interest of the length of the text.
[6] M. J. O'Connor, B. O. West, *Aust. J. Chem.* **1967**, *20*, 2077.
[7] Crystals of **6b**·acetone suitable for a X-ray structure analysis were obtained from acetone at room temperature. Crystal structure data: $C_{24}H_{34}N_2O_2Ni \cdot C_3H_6O$, long prisms, $0.25 \times 0.55 \times 1$ mm^3, M = 499.31 g mol^{-1}, monoclinic, space group $P2_1/c$, a = 13.552(4), b = 7.958(3), c = 24.807(7) Å, β = 93.43(2)°, V = 2670.36 Å^3, Z = 4, ρ_{calcd} = 1.24 g cm^{-3}, μ = 7.50 cm^{-1}, $Mo_{K\alpha}$ radiation (λ = 0.71069 Å), Stoe-Stadi-4 diffractometer, 4707 independent reflections, 330 reflections not ob-

served ($I > 2\sigma(I)$), $R = 0.0618$, $R_w = 0.0566$ (SHELX-76, SHELXS-86). The structure was solved by direct methods, the H atoms were geometrically set under the assumption of a constant C–H distance of 108 pm. Further details of the crystal structure investigation may be obtained from the Fachinformationszentrum Karlsruhe, Gesellschaft für wissenschaftlich-technische Information mbH, D-W-7514 Eggenstein-Leopoldshafen 2 (FRG) on quoting the depository number CSD-55996, the names of the authors, and the journal citation.

[8] A. G. Manfredotti, C. Guastini, *Acta Crystallogr. Sect. C* **1983**, *39*, 863.

[9] A. Berkessel, *Bioorg. Chem.* **1991**, *19*, 101.

[10] The solvents applied do not vary greatly in their O_2 solubility.[11]

[11] *Gmelins Handbuch der Anorganischen Chemie, Sauerstoff*, 8th ed, 3rd delivery, Verlag Chemie, Weinheim, **1958**, p. 482.

[12] K. J. Wannowius, F. Sattler, H. Elias, *GIT Fachz. Lab.* **1985**, *29*, 1138.

[13] The variation of the O_2 concentration was achieved as follows; the acetone saturated with O_2 was so diluted with N_2 saturated acetone, that 80, 60, 40, and 20% O_2 saturation occurred. The reaction was carried out at 20 °C using the "initial rate method".

[14] It is conceivable that the O_2 adduct $\mathbf{6c}\cdot O_2$ has partially the character of a Ni^{III} superoxide.[15]

[15] A. Berkessel, J. W. Bats, C. Schwarz, *Angew. Chem.* **1990**, *102*, 81; *Angew. Chem. Int. Ed. Engl.* **1990**, *29*, 106.

[16] A referee has rightly pointed out that the high rate of the reaction in acetone could be a result of the intermediate formation of a dioxirane.

Ring Expansion of a 1,2-Diphosphaspiropentane: Formation of a Diphosphamethylenecyclobutane and a 1,4-Diphosphanorbornadiene

By *Catherine Garot, Guita Etemad-Moghadam, Jean-Paul Declercq, Antoine Dubourg,* and *Max Koenig**

Studies of highly strained small-ring compounds have led to an improved understanding of chemical bonding, intramolecular interactions, and reaction mechanisms.[1, 2] Substantial progress has been made on the synthesis and reactivity of oxa-[3] and aza-[4] spiropentanes, the heterocyclic analogues of the well-known and highly strained spiropentane system.[5] All these spiropentanes rearrange to methylenecyclobutane.[6] We now report the first rearrangement of a diphosphaspiropentane not only to the expected diphosphamethylenecyclobutane but also to the unexpected 1,4-diphosphanorbornadiene.

When the diphosphaspiropentane **1**[7] ($\delta^{31}P = -116$) was heated at 100 °C for 5 h in degassed toluene solution, a ring expansion reaction was observed leading to **2** (70%) and **3** (30%) (Scheme 1). The reaction was promoted by addition of azobisisobutyronitrile (AIBN).

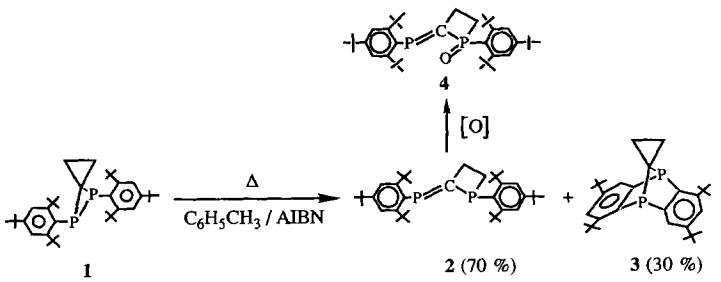

Scheme 1. Thermolysis of **1**.

[*] Dr. M. Koenig, C. Garot, Dr. G. Etemad-Moghadam
University Paul Sabatier, URA CNRS 454
F-31062 Toulouse Cedex (France)
Prof. Dr. J. P. Declercq
University of Louvain-la-Neuve (Belgium)
Dr. A. Dubourg
University of Montpellier (France)

Whereas **3** is stable towards air and moisture, **2** is partially oxidized upon contact with air and gives the phosphane oxide **4**. The preferential oxidation of $\lambda^3\sigma^3$ phosphorus atom is probably the consequence of steric effects and the well-known higher stability of phosphane oxide ($\lambda^5\sigma^4$) over phosphaalkene oxides ($\lambda^5\sigma^3$).[8] The compounds **2**, **3**, and **4** are fully

Table 1. Selected physical data for compounds **2**–**4** [a].

2: ^{31}P NMR: $\delta = 232$ (d, P=), 45 (d, P), $^2J_{PP} = 57$ Hz. ^1H NMR: $\delta = 1.18$ (s, 9H, *p*-tBu), 1.30 (s, 9H, *p*-tBu), 1.35, 1.37 (s, 18H, *o*-tBu), 1.59 (s, 18H, *o*-tBu), 2.32 (m, 4H, CH_2), 7.30 (m, 2H, CH_{Ar}), 7.50 (m, 2H, CH_{Ar}). ^{13}C NMR: $\delta = 27.2$ (d, $^1J_{CP3} = 15$ Hz, CH_2), 30.2 (s, CH_2), 31.6, 31.8 (s, *p*-(*Me*)$_3$C), 32.2 (s, *o*-(*Me*)$_3$C), 32.9 (d, $^4J_{CP} = 7$ Hz, *o*-(*Me*)$_3$C), 33.9 (m, *o*-(*Me*)$_3$C), 34.5 (s, *p*-(Me)$_3$*C*), 35.08 (d, $^3J_{CP} = 6.3$ Hz, *o*-(Me)$_3$*C*), 39.3 (s, *o*-(Me)$_3$*C*), 39.4 (s, *o*-(Me)$_3$*C*), 119.7, 121.7 (s, CH_{Ar}), 122.4 (d, CH_{Ar}), 137.9 (dd, $^1J_{CP3} = 63.0$ Hz, $^3J_{CP2} = 10.7$ Hz, C_{ipso}), 139.25 (m, C_{ipso}), 148.0 (s, $C_{p\text{-}Ar}$), 149.3 (s, $C_{p\text{-}Ar}$), 150.4 (m, $C_{o\text{-}Ar}$), 153.3 (d, $J_{CP} = 4.4$ Hz, $C_{o\text{-}Ar}$), 195.5 (dd, $^1J_{CP2} = 71.0$ Hz, $^1J_{CP3} = 24.6$ Hz, P-C = P). MS (DCI/NH_3): $m/z = 593$ (M^+, 100%).

3: ^{31}P NMR: $\delta = 29$. ^1H NMR: $\delta = 0.85$ (m, 4H, CH_2), 1.18 (s, 18H, tBu), 1.70 (s, 18H, *o*-tBu), 7.40 (q, 2H, Ar), 8.12 (m, 2H, Ar). ^{13}C NMR: $\delta = 9.18$ (t, $^2J_{CP} = 10.4$ Hz, CH_2), 29.34 (s, C-*spiro*), 31.4 (s, (*Me*)$_3$C), 32.13 (t, $^4J_{CP} = 5.5$ Hz, *o*-(*Me*)$_3$C), 34.65 (s, (Me)$_3$*C*), 37.20 (s, *o*-(Me)$_3$*C*), 121.75 (s, CH_{Ar}), 126.57 (pseudo-t, $^3J_{CP} = 17.6$ Hz, CH_{Ar}), 149.27 (pseudo-t, $J_{CP} = 17.0$ Hz, C-*ipso*), 150.12 (pseudo-t, C_{Ar}), 153.66 (pseudo-t, $^2J_{CP} = 8.6$ Hz, C-*ipso*), 155.50 (pseudo-t, $^2J_{CP} = 6$ Hz, C_{Ar}). MS (DCI/NH_3): $m/z = 479$ (M^+, 100%).

4: ^{31}P NMR: $\delta = 270$ (d, P^{II}), 40 (d, P^{III}), $^2J_{PP} = 76$ Hz. ^1H NMR: $\delta = 1.18$ (s, 9H, *p*-tBu), 1.26 (s, 9H, *p*-tBu), 1.34 (s, 18H, *o*-tBu), 1.66 (s, 18H, *o*-tBu), 2.39 (m, 4H, CH_2), 7.32 (m, 2H, CH_{Ar}), 7.40 (m, 2H, CH_{Ar}). ^{13}C NMR: $\delta = 27.2$ (d, $^1J_{CP3} = 14.6$ Hz, CH_2), 30.2 (s, CH_2), 31.1 (s, *p*-(*Me*)$_3$C), 31.4 (s, *p*-(*Me*)$_3$C), 32.4 (d, $^4J_{CP3} = 5.7$Hz, *o*-(*Me*)$_3$C), 33.3 (d, $^4J_{CP} = 8.8$ Hz, *o*-(*Me*)$_3$C), 33.9 (s, *o*-(*Me*)$_3$C), 34.8 (s, *p*-(Me)$_3$*C*), 38.0 (d, $^3J_{CP} = 11.0$ Hz, *o*-(Me)$_3$*C*), 40.9 (s, *o*-(Me)$_3$*C*), 40.94 (s, *o*-(Me)$_3$*C*), 121.6 (s, CH_{Ar}), 122.2 (s, CH_{Ar}), 123.1 (d, $^3J_{CP3} = 12.0$ Hz, CH_{Ar}), 150.1 (s, $C_{p\text{-}Ar}$), 152.3 (s, $C_{p\text{-}Ar}$), 153.4 (d, $^2J_{CP3} = 8.0$ Hz, $C_{o\text{-}Ar}$), 154.3 (s, $C_{o\text{-}Ar}$), 157.7 (s, $C_{o\text{-}Ar}$), 158.0 (s, $C_{o\text{-}Ar}$), 192.6 (dd, $^1J_{CP2} = 67.5$ Hz, $^1J_{CP3} = 61.0$ Hz, P-C = P). MS (DCI/NH_3): $m/z = 609$ (M^+, 100%).

[a] ^1H NMR (250 MHz, C_6D_6, 25 °C, TMS), ^{13}C NMR (62.90 MHz, C_6D_6, 25 °C, TMS), ^{31}P NMR (32.44 MHz, C_6D_6, 25 °C, 85% H_3PO_4 (ext.)). Mass spectrometer: Ribermag R1010 for DCI (NH_3)

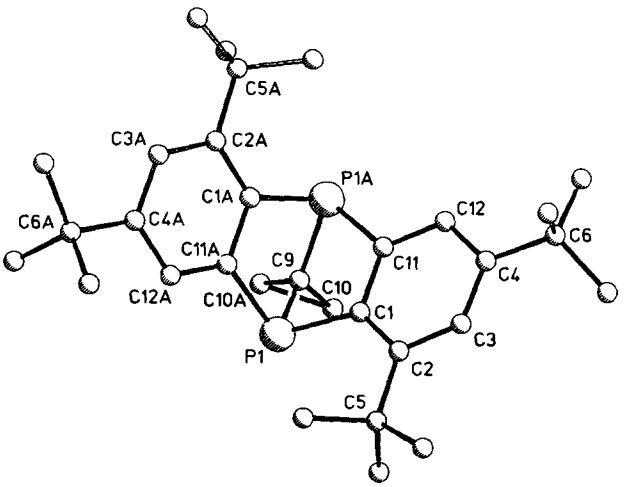

Fig. 1. Molecular structure of **3**. Hydrogen atoms have been omitted for clarity. Selected bond lengths [Å] and angles [°]: P_1-P_{1A} 3.170, P_1-C_9 1.813(4), P_{1A}-C_9 1.823(4), P_1-C_1 1.860(3), P_1-C_{11A} 1.840(4), P_{1A}-C_{1A} 1.865(4), P_{1A}-C_{11} 1.841(3), C_{1A}-C_{11A} 1.413(4), C_1-C_{11} 1.408(4), P_1-C_9-P_{1A} 104.7(2), C_9-P_1-C_1 91.1(2), C_1-P_1-C_{11A} = C_{1A}-P_{1A}-C_{11} 96.1(2), C_{11A}-P_1-C_9 90.4(2), C_{11}-P_{1A}-C_9 89.8(1), C_{1A}-P_{1A}-C_9 91.5(2), C_{10}-C_9-P_1 122.6(3), C_{10A}-C_9-P_1 122.0(4), C_{10}-C_9-P_{1A} 121.1(4), C_{10}-C_9-C_{10A} 59.8(4). Plane 1: P_1-P_{1A}-C_{11}-C_1; Plane 2: P_1-P_{1A}-C_{1A}-C_{11A}; Plane 3: C_9-C_{10A}-C_{10}; Plane 4: C_2-C_1-C_{11}-C_{12}; Plane 5: C_{2A}-C_{1A}-C_{11A}-C_{12A}; Plane 6: C_9-P_1-P_{1A}. Angles between normals to planes: Plane 1–Plane 2 71.71, Plane 1–Plane 3 90.86, Plane 4–Plane 5 69.94, Plane 3–Plane 6 90.97, Plane 4–Plane 6 56.71, Plane 5–Plane 6 126.45, Plane 1–Plane 4 3.00, Plane 2–Plane 5 1.64.

characterized by ^{31}P, ^{13}C and ^{1}H NMR spectroscopy, IR spectroscopy, and mass spectrometry, as well as by elemental analysis. The structure of the novel heteropolycycle **3**[9] has been confirmed by an X-ray diffraction analysis[10] (Fig. 1).

Compound **2** arises as a result of the expected P–P and C–C bond ruptures (via **5** and **6**, see Scheme 2), whereas 1,4-diphosphanorbornadiene **3** forms quite surprisingly from the common biradical intermediate **5** on cleavage of an *ortho-tert*-butyl group from each of the aryl residues. The anionic[11] and photochemical[12] ring-opening of functionalized diphosphiranes occur via diphosphaallyl anions or diphosphiranyl radical intermediates, respectively. On the other hand, we did not detect any intermediate in their thermal ring-opening which allows us to specify the most likely mechanism (radicalar, biradicalar, or concerted).[13, 14]

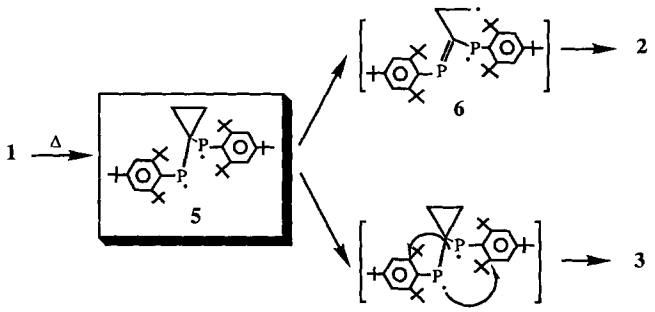

Scheme 2. Proposed mechanism for the formation of **2** from **3** and **1**.

The reaction of **1** to afford **3** via **5** must be promoted by the free rotation of aryl groups ($\Delta G^{\neq} = 10$ kcal mol^{-1} at 20 °C for **1**) and the higher strain of the PCP angle in **1**. A similar aromatic substitution involving phosphorus radicals[15] and silylated[16] radicals has been already described for the thermolysis of germaphosphenes and disilacyclopropanes. An analogous rearrangement involving aryl groups has been observed by Niecke et al., who explained the reaction by abstraction of isobutene.[17]

Whereas the ^{31}P NMR spectrum of **3** displays a singlet ($\delta = 29$), the X-ray structure reveals that the bond lengths and angles around each P atom are slightly different (Fig. 1). The angular sum around each phosphorus atom (277°) is higher than the corresponding value (269°) obtained by Mathey in 1-phosphanorbornadiene.[18]

Experimental Procedure

A colorless solution of **1** (0.115 g, 0.194 mmol) in 2.0 mL of degassed toluene was heated in the presence of AIBN (0.320 g, 1.94 mmol, 10 equiv) at 100 °C for 5 h. The solution became yellow. After removal of the solvent, the residue was taken up in hexane. Filtration followed by thin-layer chromatography of the mixture (Merck precoated preparative TLC plates: silica gel 60 F_{254}) with hexane/toluene (90/10) as eluent, and recrystallization from toluene at room temperature afforded 50 mg (44%) of yellow needles of **2**, 23 mg (30%) of pale yellow crystals of **3** (m.p. 232 °C), and 31 mg (26%) of **4**.

Received: November 9, 1991 [Z 5012 IE]
German version: Angew. Chem. **1992**, *104*, 619

CAS Registry numbers:
1, 140389-76-0; **2**, 140389-77-1; **3**, 140389-78-2; **4**, 140389-79-3.

[1] A. de Meijere, *Angew. Chem.* **1979**, *91*, 867; *Angew. Chem. Int. Ed. Engl.* **1979**, *18*, 809–886.
[2] K. B. Wiberg, *Angew. Chem.* **1986**, *98*, 312; *Angew. Chem. Int. Ed. Engl.* **1986**, *25*, 312–322.
[3] a) J. K. Crandall, D. R. Paulson, *J. Org. Chem.* **1968**, *33*, 3291–3294. b) J. R. Salaün, J. M. Conia, *J. Chem. Soc., Chem. Commun.* **1971**, 1579–1580.
[4] a) J. K. Crandall, W. W. Conover, *ibid.* **1973**, 33–34. b) D. H. Aue, R. B. Lorens, G. S. Helwig, *Tetrahedron Lett.* **1973**, 4795–4798. c) J. K. Crandall, W. W. Conover, *J. Org. Chem.* **1974**, *39*, 63–66.
[5] R. Boese, D. Bläser, K. Gomann, U. H. Brinker, *J. Am. Chem. Soc.* **1989**, *111*, 1501–1503.
[6] T. Miyashi, Y. Takahashi, H. Ohaku, K. Yokogawa, S. I. Morishima, T. Mukai, *Tetrahedron Lett.* **1990**, *31*, 2411–2414.
[7] a) B. M. Trost, *Acc. Chem. Res.* **1974**, *7*, 85–92; b) L. Weber, E. Lücke, R. Boese, *Organometallics* **1988**, *7*, 978; c) M. Gouygou, C. Tachon, R. El-Ouatib, O. Ramarijaona, G. Etemad-Moghadam, M. Koenig, *Tetrahedron Lett.* **1989**, *30*, 177–178.
[8] R. Appel in *Multiple bonds and Low Coordination in Phosphorus Chemistry* (Eds. M. Regitz, O. J. Scherer) G. Thieme Verlag, Stuttgart **1990**, 259.
[9] a) Y. Kobayashi, I. Kumadaki, H. Hamana, S. Fujino, *Tetrahedron Lett.* **1977**, 3057–3058; b) Y. Kobayashi, S. Fujino, I. Kumadaki, *J. Am. Chem. Soc.* **1981**, *103*, 2465–2466.
[10] $C_{31}H_{44}P_2$, $M_r = 478.6$ g mol^{-1}; crystal size 0.6 × 0.5 × 0.3 mm, Huber diffractometer, $Mo_{K\alpha}$ radiation, measurement at room temperature; unit cell dimensions: $a = 10.544(2)$, $b = 12.516(2)$, $c = 13.207(3)$ Å, $\alpha = 75.98(2)$, $\beta = 65.48(3)$, $\gamma = 75.66(2)°$, $V = 1516.9(7)$ Å^3; $Z = 2$, $\varrho_{calcd} = 1.05$ g cm^{-3}. F (000) = 520; triclinic, space group $P\bar{1}$; no absorption correction; $\mu = 0.17$ mm^{-1} ($\lambda = 0.71069$ Å); $2\theta_{max} = 55°$. 6978 independent reflections and 4169 observed with $I > 2.5\,\sigma(I)$. Structure solved by direct methods (SHELXS-86). Anisotropic least-squares refinement (F values) using SHELX-76 program for C and P atoms. H atoms included in theoretical positions. R = 0.068; $R_w = 0.076$ with $w = 1/(\sigma^2(F) + 0.001839\,F^2)$; S = 1.55; Further details of the crystal structure investigation are available on request from the Fachinformations-Zentrum Karlsruhe, Gesellschaft für wissenschaftlich-technische Information mbH, W-7514 Eggenstein-Leopoldshafen 2 (FRG), on quoting the depository number CSD-56009, the names of the authors, and the journal citation.
[11] M. Gouygou, C. Tachon, M. Koenig, G. Etemad-Moghadam, *New J. Chem.* **1989**, *13*, 315–317.
[12] M. Gouygou, C. Tachon, M. Koenig, A. Dubourg, J. P. Declercq, J. Jaud, G. Etemad-Moghadam, *J. Org. Chem.* **1990**, *55*, 5750–5755.
[13] M. Gouygou, J. Bellan, J. Escudié, C. Couret, A. Dubourg, J. P. Declercq, M. Koenig, M., *J. Chem. Soc., Chem. Commun.* **1989**, 593–595.
[14] G. Pfister-Guillouzo, M. Koenig, unpublished.
[15] M. Andrianarison, C. Couret, J. P. Declercq, A. Dubourg, J. Escudié, J. Satgé, *J. Chem. Soc., Chem. Commun.* **1987**, 921–923.
[16] M. Ishikawa, S. Matsuzawa, H. Sugisawa, F. Yano, S. Kamitori, T. Higuchi, *J. Am. Chem. Soc.* **1985**, *107*, 7706–7710.
[17] E. Niecke, B. Kramer, M. Nieger, *Organometallics*, **1991**, *10*, 10–11.
[18] F. Mathey, F. Mercier, C. Charrier, *J. Am. Chem. Soc.* **1981**, *103*, 4595–4597.

One-Dimensional $M^{III}Cu^{II}$ Compounds with an Unprecedented, Tubelike Structural Motif (M = Rare-Earth Metal)

By *Olivier Guillou, Robert L. Oushoorn, Olivier Kahn*, Kamal Boubekeur*, and *Patrick Batail**

The reaction of the dianionic copper(II) complex $[Cu(pba)]^{2-}$ (pba = 1,3-propylenbis (oxamato) ≙ *N,N'*-trimethylendioxamidic acid tetranion) with a divalent metal ion M^{II} in a solvent S affords a bimetallic compound with a chainlike structure and the formula $M[Cu(pba)] \cdot nS$.[1–5] Compounds of this kind exhibit the characteristic behavior of one-dimensional ferrimagnets, that is, the plot of the product of the molar magnetic susceptibility χ_m and the temperature T versus temperature has a minumum. When the

[*] Prof. Olivier Kahn, O. Guillou, R. L. Oushoorn[+],
Laboratoire de Chimie Inorganique, URA CNRS No. 420
Université de Paris-Sud
F-91405 Orsay (France)

[+] Permanent address: Department of Chemistry
Leiden University
NL-Leiden (The Nederlands)

Dr. P. Batail, Dr. K. Boubekeur
Laboratoire de Physique du Solide, URA CNRS No. 002
Université de Paris-Sud
F-91405 Orsay (France)

temperature is lowered further $\chi_m T$ increases, which is typical for ferromagnets. Moreover, some of these compounds display a spontaneous magnetization and behave as molecular magnets below a critical temperature T_c.[5] To the best of our knowledge, the highest T_c value reported so far for this kind of material is 30 K.[4]

If the divalent ion M^{II} is replaced by a trivalent ion M^{III}, compounds of higher dimensionality with the formula $M_2[Cu(pba)]_3 \cdot nS$ may be expected. These may favor the onset of a magnetic ordering, in particular if M^{III} carries a high local spin. For this reason we are interested in the synthesis of compounds of the type $M_2[\{Cu(pba)\}_3] \cdot nS$ in which M is a rare-earth-metal ion. Our first attempt yielded compounds of type **1**(M) in which some of the pba ligands

$[M_2(ox)][\{Cu(pba)\}_3Cu(H_2O)_5] \cdot 20\,H_2O$ **1**(M)

had been hydrolyzed to oxalato (ox) ligands bridging the M^{III} ions.[6] With a more exotic method of preparation, we also succeeded in synthesizing the compounds of type **2**(M).

$M_2[\{Cu(pba)\}_3] \cdot 23\,H_2O$ **2**(M)

All compounds with M = La, Ce, Pr, Nd, Sm, Eu, and Gd are isomorphous; however, smaller, trivalent rare-earth-metal ions (from Tb to Yb and Y) lead to a completely different structure. We report here on the remarkable and quite unexpected structure of **2**(Sm) and on the magnetic properties of some of the **2**(M) compounds in which the metal M comprises the series from La to Gd.

We previously demonstrated that the construction of **1** (Gd) was based on the two-dimensional association across oxalato groups of the single $Gd_2[\{Cu(pba)\}_3]$ units leading to the puckered ladderlike structure **I** represented in Figure 1. We then anticipated that **I** could be shifted (e.g. a 90° twist to **I'**) and eventually associated within different structural motifs depending on the method of synthesis and/or the nature of the rare-earth metal. The molecular architecture of **2**(M) is based solely on the condensation of two such "ladders" to **II** (Fig. 1) furnishing a remarkable infinite tubelike structural motif unprecedented in this chemistry.[7] In the pairing of the ladders the ladder "rungs" are redistributed; this demonstrates the conformational flexibility of the $[Cu(pba)]^{2-}$ unit. These units undergo a collective criss-cross shift creating an infinite structural motif with an essentially square cross section and quasi-fourfold symmetry. Thus, we have found the delicate inner framework of elegant simplicity (Fig. 2, view down the *c* axis of the pseudo-tetragonal unit cell; this corresponds to a 90° twist of projection **II** in Fig. 1 out of the plane of the paper). It is readily seen in Figure 2 that the inner $[Cu(pba)]^{2-}$ units, the ladder rungs, intertwine by alternately switching from one edge of a ladder frame to the nearest one orthogonal, thus fusing **I** and **I'** (Fig. 1). Of particular interest is the helixlike pattern of the intertwined ladder rungs, also apparent in Figures 1 and 2. For lack of space we restrict the discussion to several of the **2**(M) complexes and their magnetic properties:[8]

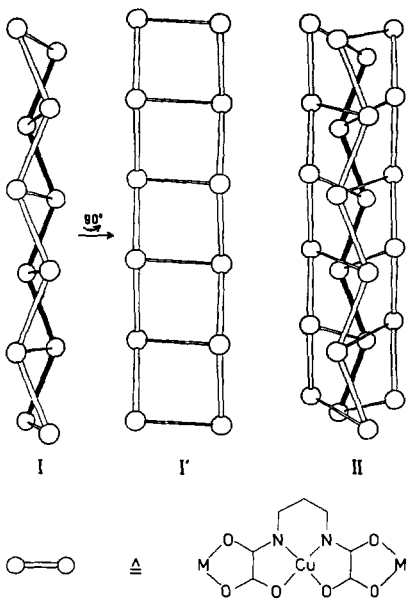

Fig. 1. **I** and **I'** are two representations of the ladderlike structural motif found in **1**(M) from two different views. The condensation of two such orthogonal ladders and the redistribution of the ladder rungs (see text) leads to the tubelike structural motif **II**, which is found in **2**(M).

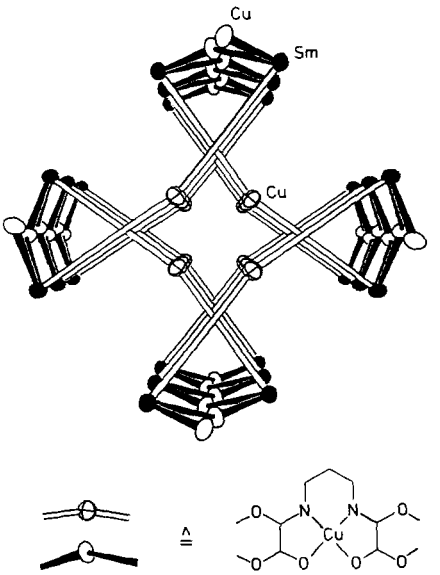

Fig. 2. Schematic representation of the structure of **2**(M) as exemplified by **2**(Sm); view along the *c* axis of the unit cell. The Cu atoms are also shown. The rare-earth-metal atom is surrounded by nine O atoms, of which six are from Cu(bpa) units and three are from water molecules. The Cu atom has square-pyramidal coordination; two O atoms and two N atoms of the pba ligand make up the base, and an O atom of a water molecule forms the apex of the coordination polyhedron. The Sm–Cu separations range from 5.675 to 5.742 Å, and the length of the Sm–Sm rung of the ladder is 11.357 Å.

1) For the **2**(La) compound, which possesses a diamagnetic rare-earth-metal ion, $\chi_M T$ (χ_M is the molar magnetic susceptibility per M_2Cu_3 unit) decreases slightly when the temperature is lowered below 20 K. This indicates that an antiferromagnetic interaction between the Cu^{II} spin carriers take place which is obviously propagated through the La^{III} ion.

2) For **2**(Ce), **2**(Pr), and **2**(Sm), $\chi_M T$ also decreases as T decreases, which may be due to both crystal-field effects around the rare-earth-metal ion and weak antiferromagnetic interactions.

3) **2**(Nd) exhibits a nonmagnetic ground state with $\chi_M T$ approaching zero as T approaches absolute zero. This result is quite unexpected since the local ground state of Nd^{III} is

$^4I_{9/2}$. A perfect compensation of the local magnetic moments within the one-dimensional tubelike network should not happen.

4) The magnetic behavior of **2**(Gd) is totally different from that of the other compounds. Both the temperature dependence of the magnetic susceptibility χ_M at a field strength of 0.1 T and the field dependence of the magnetization M at 2 K have been measured. The results of the former investigation are presented in Figure 3. To temperatures of roughly 30 K,

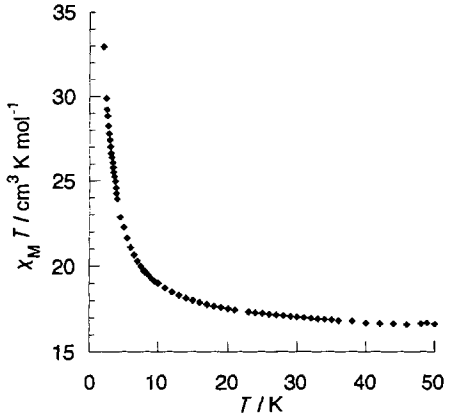

Fig. 3. Plot of $\chi_m T$ versus T for **2**(Gd). Magnetic field strength 0.1 T.

$\chi_M T$ is constant and equal to 16.8 cm^3 K mol^{-1}, as is expected for two Gd^{III} and three Cu^{II} ions that do not interact. When the temperature is lowered, $\chi_M T$ increases more and more rapidly and reaches 33 cm^3 K mol^{-1} at 1.8 K. These data could be fitted with the Curie–Weiss law $\chi_M = C(T-\theta)$ and a Weiss constant $\theta = 1.2$ K, and clearly indicate that the local spins of Gd ($S = 7/2$) tend to align parallel. However, these values do not indicate whether the local spins of Cu ($S = 1/2$) align along the same direction (ferromagnetic behavior) or along the opposite direction (ferrimagnetic behavior). The answer to this question is provided by magnetization measurements. In the low-field regime (from 0 to ca. 0.3 T), M is directly proportional to H, and the slope of the plot is in perfect agreement with the value obtained from the magnetic susceptibility measurements previously discussed. There is no indication of spin decoupling, that is, a change of sign of d^2M/dH^2. When the field is increased further, the magnetization approaches the saturation value $M_S = 17\ N\beta$ (or 95000 cm^3 G mol^{-1}) corresponding to the value anticipated for all local spins aligned along the direction of the external field. The susceptibility and magnetization data are complementary, and unambiguously show that even in the absence of an external magnetic field the local spins tend to align parallel. The Gd^{III} and Cu^{II} ions interact ferromagnetically through the oxamato bridge despite the Gd^{III}–Cu^{II} separation of 5.7 Å. Gd^{III}–Cu^{II} ferromagnetic interactions in discrete molecular species have already been reported.[9, 10]

The versatility of the crystal structures and physical properties of those rare-earth-metal–copper compounds open quite interesting perspectives for novel materials.

Experimental Procedure

2(M): An aqueous solution of $Na_2[Cu(pba)] \cdot 6H_2O$[2,11] (0.05 M) was added dropwise to an aqueous solution of the rare-earth-metal chloride (0.1 M) with vigorous stirring. The solution was stirred for a while, then the light blue precipitate was removed by filtration. The dark blue solution was kept in a temperature-controlled bath at 70 °C. Large cubelike, dark-blue crystals formed within ca. 48 h. The isomorphism of the compounds containing La, Ce, Pr, Ne, Sm, Eu, and Gd was assumed from Debye–Scherrer photographs.

Received: December 19, 1991 [Z 5080 IE]
German version: *Angew. Chem.* **1992**, *104*, 658

[1] O. Kahn, *Struct. Bonding (Berlin)* **1987**, *68*, 89.
[2] Y. Pei, M. Verdaguer, O. Kahn, J. Sletten, J. P. Renard, *Inorg. Chem.* **1987**, *26*, 138.
[3] O. Kahn, Y. Pei, M. Verdaguer, J. P. Renard, J. Sletten, *J. Am. Chem. Soc.* **1988**, *110*, 782.
[4] K. Nakatani, P. Bergerat, E. Codjovi, C. Mathonière, O. Kahn, *Inorg. Chem.* **1991**, *30*, 3978.
[5] O. Kahn in *Magnetic Molecular Materials* (Eds.: D. Gatteschi, O. Kahn, J. S. Miller, F. Palacio) *NATO ASI Ser. Ser. E* **1991**, *198*, 35.
[6] O. Guillou, P. Bergerat, O. Kahn, E. Bakalbassis, K. Boubeker, P. Batail, M. Guillot, *Inorg. Chem.* **1992**, *31*, 110.
[7] **2**(Sm): $M_r = 1548.0$, space group *Pcc2*, $a = 16.076(5)$, $b = 16.079(3)$, $c = 21.256(10)$ Å, $V = 5494(3)$ Å^3, $Z = 4$, $\rho_{calc.} = 1.85$ g cm^{-3}, CAD4-F diffractometer, 12049 reflections, $2° \le 2\theta \le 50°$ ($MO_{K\alpha}$ radiation, $\lambda = 0.71073$ Å), 4834 symmetry-independent reflections, 1549 with $I \ge 2\sigma(I)$ for the refinements. $R = 0.078$, $R_w = 0.089$, $w^{-1} = \sigma^2(F) + 0.07\ F_o^2$. Enraf-Nonius SDP program. Further details of the crystal structure investigations may be obtained from the Fachinformationszentrum Karlsruhe, Gesellschaft für wissenschaftlich-technische Information mbH, D-W-7514 Eggenstein-Leopoldshafen 2 (FRG), on quoting the depository number CSD-56038, the names of the authors, and the journal citation.
[8] The magnetic data were obtained with two apparatus, namely a Faraday-type magnetometer (range of operation to 4.2 K) and a SQUID magnetometer (range of operation to 1.8 K). The SQUID magnetometer used in the low-field regime (a few G) as well as the high-field regime (up to 8 T).
[9] C. Benelli, A. Caneschi, D. Gatteschi, O. Guillou and L. Pardi, *Inorg. Chem.* **1990**, *29*, 1751, and references cited therein.
[10] N. Matsumoto, M. Sakamoto, H. Tamaki, H. Okawa, S. Kida, *Chem. Letters* **1989**, 853.
[11] K. Nonoyama, H. Ojima, M. Nonoyama, *Inorg. Chim. Acta* **1976**, *20*, 127.

A Cyclometalated Aryloxy(chloro)neopentylidene-tungsten Complex: A Highly Active and Stereoselective Catalyst for the Metathesis of *cis*- and *trans*-2-Pentene, Norbornene, 1-Methylnorbornene, and Ethyl Oleate**

By *Jean-Luc Couturier, Christophe Paillet, Michel Leconte, Jean-Marie Basset,** and *Karin Weiss*

The design of versatile, highly active, and well-characterized catalysts remains one of the main objectives of the research in olefin metathesis.[1] In the past few years, it has been shown that some neopentylidene–tungsten(VI) complexes with alkoxide,[2, 3] imido,[3] or aryloxide ligands[4] are efficient homogeneous metathesis catalysts. Aryloxides prove to be particularly useful ligands since their steric and electronic properties can be varied substantially by changing the nature, the number, and the position of the substituents on the phenoxide ligand. With these ligands, it has been possible to control both the activity and the stereoselectivity

[*] Dr. J.-M. Basset, J.-L. Couturier, Dr. C. Paillet, Dr. M. Leconte
Institut de Recherches sur la Catalyse
Laboratoire Propre du CNRS, conventionné à l'Université Claude Bernard-Lyon 1 and
Ecole Supérieure de Chimie Industrielle de Lyon
2, Avenue Albert Einstein, 69626 Villeurbanne Cédex (France)
Dr. K. Weiss
Laboratorium für Anorganische Chemie der Universität Bayreuth
Postfach 10 12 51, D-W-8580 Bayreuth (FRG)

[**] This work was supported by the Société Nationale Elf-Aquitaine and by the Commission of the European Communities. We thank Prof. R. R. Schrock (Massachusetts Institute of Technology) for giving us a preprint of [6b].

of the metathesis reaction.[4, 5] We report here the synthesis and the catalytic properties of a new 2,6-diphenylphenoxy (neopentylidene)tungsten derivative, which has the cyclometalated structure **1a**/**1b** (Scheme 1).

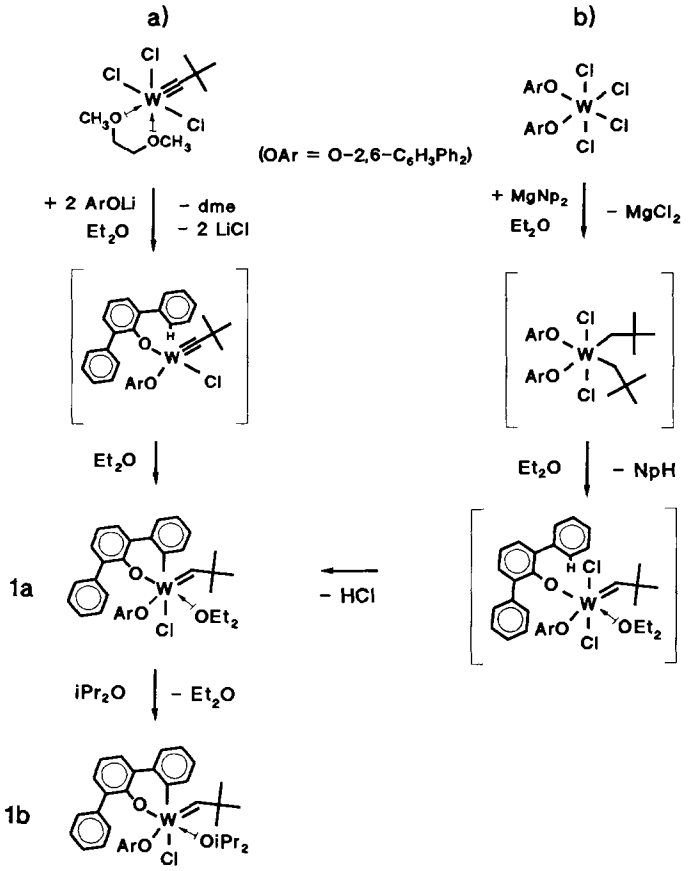

Scheme 1. Two routes for the synthesis of the cyclometalated complexes **1a** and **1b**. Because X-ray structure data are not available, the structures are still hypothetical and are derived from that proposed by R. R. Schrock et al. for the starting complex $[WCl_3(CCMe_3)(dme)]$ [6] and from the known complex $[WCl_4(O\text{-}2,6\text{-}C_6H_3Ph_2)_2]$ [7].

The tungsten complexes **1a**/**1b** can be obtained by two independent routes. Reaction of $[WCl_3(CCMe_3)(dme)]$[6] (dme = dimethoxyethane) with two equivalents of LiOAr (OAr = O-2,6-$C_6H_3Ph_2$) in diethyl ether leads to the orange-brown solid **1a**, which likely arises from path a). The reaction of $[WCl_4(O\text{-}2,6\text{-}C_6H_3Ph_2)_2]$[7] in diethyl ether with one equivalent of $MgNp_2 \cdot$ dioxane (Np = neopentyl) leads, after purification by exchange of diethyl ether with diisopropyl ether, to the orange-brown solid **1b**.[8] The probable sequence of reactions leading to **1b** is path b). **1a** and **1b** were characterized by elemental analyses and ^1H and ^{13}C NMR spectroscopy.[9]

The key step of the two syntheses is the different intramolecular activation of the C–H bond of the arene substituent on the d^0 metal which leads to a stable cyclometalated structure.[10–12] In path a) C–H activation leads to the addition of a hydrogen atom to the carbyne ligand forming a carbene and simultaneous cyclometalation. In path b) the C–H activation leads to the elimination of HCl. The role of the weakly coordinated ether is probably crucial in path a) in which a pentacoordinated W^{VI} center with a possible agostic C–H bond is the precursor of the carbene complex formed via a four-center transition state; this type of sequence is often discussed for the electrophilic activation of C–H bonds.[13]

Complexes **1a** and **1b** are excellent catalysts for olefin metathesis. For example, with **1a** the metathesis equilibrium of 500 equivalents of *cis*-2-pentene or *trans*-2-pentene is reached in 1 min at 25 °C (the equilibrium mixture consists of 2-butene, 2-pentene, and 3-hexene in the approximate ratio of 1:2:1).[1a] **1a** is also highly stereoselective: Extrapolation to 0% conversion shows that the *trans*/*cis* ratios of 2-butene (C_4) and 3-hexene (C_6) in the metathesis of *cis*-2-pentene are 0.01 and 0.00, respectively[14] (at equilibrium, *trans*/*cis* $C_4 \approx 3$ and *trans*/*cis* $C_6 \approx 6$). In the metathesis of *trans*-2-pentene, the *cis*/*trans* ratios of both C_4 and C_6 are equal to 0.004 at 0% conversion. These high stereoselectivities with retention of configuration of the starting olefin are maintained even at high conversions (Figs. 1 and 2). When the

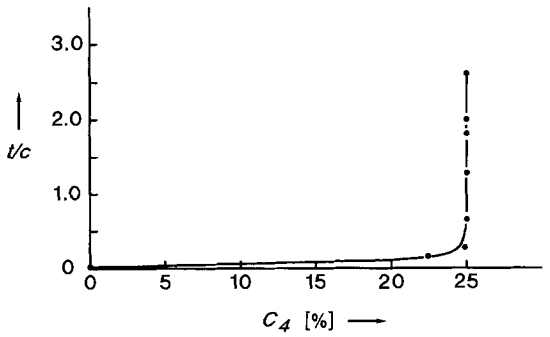

Fig. 1. Metathesis of *cis*-2-pentene catalyzed by **1a**: Plot of the ratio of *trans*- to *cis*-2-butene (*t*/*c*) versus the yield of 2-butene (C_4). *cis*-2-Pentene/**1a** molar ratio = 500/1, $T = 25\,°C$, solvent C_6H_5Cl.

equilibrium of productive metathesis is nearly reached (roughly 25% yield in 2-butene), there is a dramatic change of the configuration of the products due to secondary metathetical isomerization reactions that progressively lead to the ultimate equilibrium *trans*/*cis* ratios.

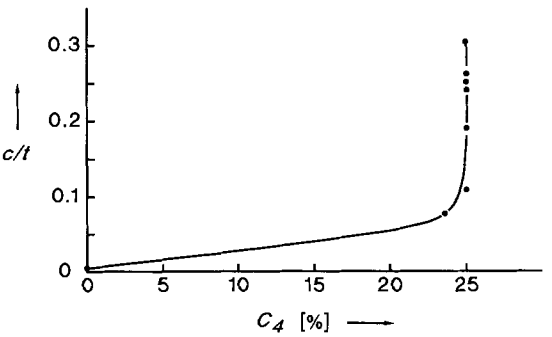

Fig. 2. Metathesis of *trans*-2-pentene catalyzed by **1a**: Plot of the ratio of *cis*- to *trans*-2-butene (*c*/*t*) versus the yield of 2-butene (C_4). *trans*-2-Pentene/**1a** molar ratio = 500/1, $T = 25\,°C$, solvent C_6H_5Cl.

To our knowledge such high stereoselectivities observed almost up to thermodynamic metathesis equilibrium have never been reported in metathesis of 2-pentene with any highly active tungsten-based catalyst. The extremely high retention of configuration of the starting olefin is easily explained on the basis of the favored configuration of the tungstacyclobutane intermediate with two equatorial (e) alkyl groups in the 1 and 3 positions (Scheme 2).[15] One can

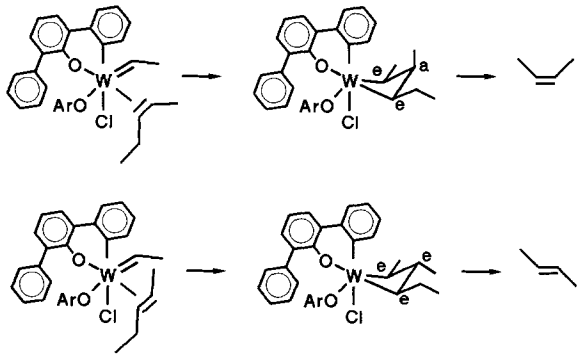

Scheme 2. The two favored tungstacyclobutane intermediates with 1,3-diequatorial alkyl substituents that lead to *cis*-2-butene (in the metathesis of *cis*-2-pentene) and to *trans*-2-butene (in the metathesis of *trans*-2-pentene).

assume that these favored conformations are particularly stabilized by the bulky ligands on tungsten and/or by the rigidity generated by the cyclometalation.

With **1a**, 500 equivalents of norbornene are polymerized at 25 °C in less than one minute.[16] ^{1}H and ^{13}C NMR spectra ($CDCl_3$, 25 °C) indicate that 70% of the C=C bonds have *cis* configuration. This value is in agreement with earlier results found in norbornene metathesis with other stereoselective aryloxy(chloro)carbene-tungsten catalysts.[17]

Polymerization of 1-methylnorbornene with **1a** or **1b** provides a completely head-tail, predominantly syndiotactic poly-1-methylnorbornene with 100% *cis* C=C bonds.[18] Such extremely high stereoselectivity can also be explained on the basis of the favored configuration of the tungstacyclobutane intermediate with the two bulkiest alkyl substituents in 1,3-diequatorial positions (Scheme 3).[20]

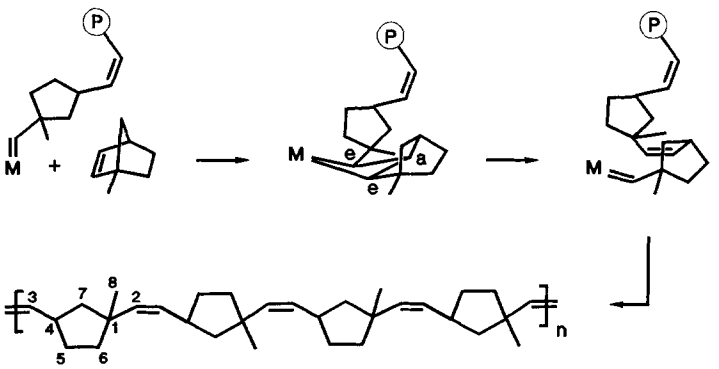

Scheme 3. In the ring-opening metathesis polymerization of 1-methylnorbornene with **1a** or **1b** the favored reaction path leads to the formation of a head-tail, *cis* polymer.

Very promising preliminary results were obtained in the metathesis of ethyl oleate (ethyl-9-octadecenoate), an olefin bearing a functional group (Scheme 4). **1a** can convert selectively roughly 50% of 500 equivalents of ethyl oleate[21] into 9-octadecene and diethyl 9-octadecenedioate in 60 min at 25 °C (Fig. 3; the equilibrium mixture consists of ethyl oleate, 9-octadecene, and the diester in the approximate ratio of 2:1:1). To our knowledge, this is the highest activity reported so far for homogeneous catalysts in the metathesis of this type of substrate.[3, 22]

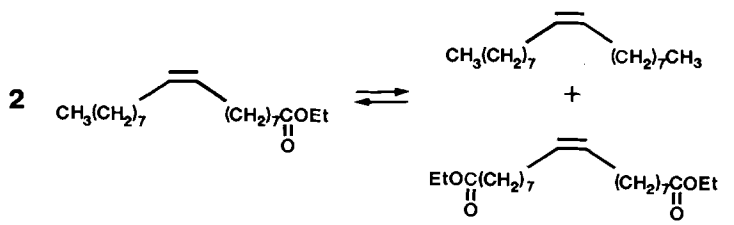

Scheme 4. The equilibrium metathesis reaction of ethyl oleate leads to 9-octadecene and diethyl 9-octadecenedioate.

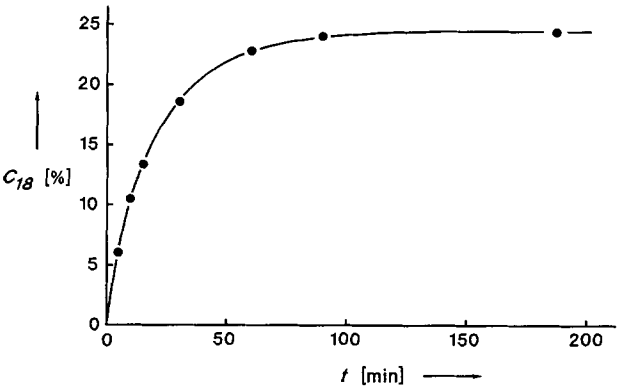

Fig. 3. Metathesis of ethyl oleate catalyzed by **1a**: Plot of the yield of 9-octadecene (C_{18}) versus the reaction time. Ethyl oleate/**1a** molar ratio = 500/1, T = 25 °C, solvent C_6H_5Cl.

Received: August 7, 1991
Revised: December 19, 1991 [Z 4856 IE]
German version: *Angew. Chem.* **1992**, *104*, 622

[1] a) K. J. Ivin, *Olefin Metathesis*, Academic Press, London, **1983**; b) K. J. Ivin in *Olefin Metathesis and Polymerization Catalysts* (Eds.: Y. Imamoglu, B. Zumreoglu-Karan, and A. J. Amass), Kluwer Academic Publishers, Dordrecht, **1990**, p. 1.

[2] a) J. Kress, M. Wesolek, J. A. Osborn, *J. Chem. Soc. Chem. Commun.* **1982**, 514–516; b) J. Kress, A. Aguero, J. A. Osborn, *J. Mol. Catal.* **1986**, *36*, 1–12.

[3] C. J. Schaverien, J. C. Dewan, R. R. Schrock, *J. Am. Chem. Soc.* **1986**, *108*, 2771–2773.

[4] F. Quignard, M. Leconte, J.-M. Basset, *J. Chem. Soc. Chem. Commun.* **1985**, 1816–1817.

[5] a) J.-M. Basset, M. Leconte, J. Ollivier, F. Quignard, Fr. Pat. 8309876, **1983**, SNEA, US-Pat. 4550216, **1985**, SNEA; b) Fr. Pat. 8501930, **1985**, SNEA, US-Pat. 4654462, **1987**, SNEA; c) Fr. Pat. 8611978, **1986**, SNEA, US-Pat. 4861848, **1989**, SNEA; d) F. Quignard, M. Leconte, J.-M. Basset, *J. Mol. Catal.* **1985**, *28*, 27–32; e) *ibid.* **1986**, *36*, 13–29.

[6] a) R. R. Schrock, D. N. Clark, J. Sancho, J. H. Wengrovius, S. M. Rocklage, S. F. Pedersen, *Organometallics* **1982**, *1*, 1645; b) R. R. Schrock, J. Sancho, S. F. Pedersen, *Inorg. Synth.* **1989**, *26*, 44–51.

[7] F. Quignard, M. Leconte, J.-M. Basset, L.-Y. Hsu, J. J. Alexander, S. G. Shore, *Inorg. Chem.* **1987**, *26*, 4272–4277.

[8] In our first study [4] we found that reaction of one equivalent of $MgNp_2$ with $[WCl_4(O\text{-}2,6\text{-}C_6H_3Ph_2)_2]$ in Et_2O led to a compound **A1** whose ^{1}H NMR spectrum ($CDCl_3$) showed a signal at $\delta = 8.7$ for a hydrogen atom bound to a carbene; **A1** proved essentially inactive in the metathesis of *cis*-2-pentene. We have now some indications that suggest that **A1** is a dimeric neopentylidene species (not yet totally identified) resulting from the dimerization of **1a** or **1b**. This dimerization seems to be rather fast in solution (especially in $CHCl_3$ and CH_2Cl_2) but can also be observed in the solid state where the reaction is slower.

[9] Characteristic ^{1}H (100 MHz) and ^{13}C (25 MHz) NMR data for **1a** (C_6D_6, 25 °C): δ(W = CHCMe$_3$) = 10.11 ($J_{W,H}$ = 14 Hz), δ(W = CHCMe_3) = 0.57; δ(W = CH) = 296.66 ($J_{C,H}$ = 130.5, $J_{C,W}$ = 166 Hz), δ(W-C_{ipso}) = 183.15 ($J_{C,W}$ = 115 Hz), δ(W = CHCMe$_3$) = 45.24, δ(W = CHCMe_3) = 31.82. The corresponding data for **1b** are practically identical.

[10] M. R. Churchill, J. W. Ziller, J. H. Freudenberger, R. R. Schrock, *Organometallics* **1984**, *3*, 1554–1562.

[11] R. R. Schrock, R. T. DePue, J. Feldman, K. B. Yap, D. C. Yang, W. M. Davis, L. Park, M. DiMare, M. Schofield, J. Anhaus, E. Walborsky, E. Evitt, C. Krüger, P. Betz, *Organometallics* **1990**, *9*, 2262–2275.

[12] a) J. L. Kerschner, P. E. Fanwick, I. P. Rothwell, *J. Am. Chem. Soc.* **1987**, *109*, 5840–5842; b) J. L. Kerschner, I. P. Rothwell, J. C. Huffman, W. E. Streib, *Organometallics* **1988**, *7*, 1871–1873; c) J. L. Kerschner, P. E. Fanwick, I. P. Rothwell, J. C. Huffman, *ibid.* **1989**, *8*, 1431–1438.

[13] M. E. Thompson, S. M. Baxter, A. R. Bulls, B. J. Burger, M. C. Nolan, B. D. Santarsiero, W. P. Schaefer, J. E. Bercaw, *J. Am. Chem. Soc.* **1987**, *109*, 203–219.

[14] For the metathesis of *cis*-2-pentene, the stereoselectivity at 0% conversion is accurately determined by plotting the *trans*/*cis* ratio of 2-butene vs. the *trans*/*cis* ratio of 2-pentene and by extrapolating at *trans*/*cis*-2-pentene = 0 (in the case of *trans*-2-pentene, *cis*/*trans* C_4 is plotted vs. *cis*/*trans* C_5).[15]

[15] M. Leconte, J.-M. Basset, *J. Am. Chem. Soc.* **1979**, *101*, 7296–7302.

[16] The catalyst is deactivated by addition of benzaldehyde; polynorbornene is recovered after addition of THF to the reaction mixture, precipitation with methanol, filtration, and drying.

[17] Dj. Boutarfa, F. Quignard, M. Leconte, J.-M. Basset, J. G. Hamilton, K. J. Ivin, J. J. Rooney in *Transition Metal Catalyzed Polymerizations: Ziegler-Natta and Metathesis Polymerizations* (Ed.: R. P. Quirk), Cambridge University Press, Cambridge, **1988**, p. 695.

[18] The 100% head-tail, 100% *cis* structure of the poly-1-methylnorbornene obtained with **1a** or **1b** was deduced from ^1H and ^{13}C NMR spectra of the polymer;[19] $^{13}C\{^1H\}$ NMR (62.8 MHz, $CDCl_3$): δ = 29.29 (C-8), 33.02 (C-5), 38.14 (C-4), 41.82 (C-6), 44.13 (C-1), 50.02 (C-7), 135.08 (C-3), 139.47 (C-2) (see Scheme 3 for the numbering of the carbon atoms). The predominantly syndiotactic structure was deduced from the ^{13}C NMR spectrum of the hydrogenated polymer [19].

[19] J. G. Hamilton, K. J. Ivin, J. J. Rooney, *Br. Polym. J.* **1984**, *16*, 21–33.

[20] J.-M. Basset, Dj. Boutarfa, E. Custodero, M. Leconte, C. Paillet in *Olefin Metathesis and Polymerization Catalysts* (Eds.: Y. Imamoglu, B. Zumreoglu-Karan, A. J. Amass), Kluwer Academic Publishers, Dordrecht, **1990**, p. 45.

[21] Ethyl oleate (Sigma, 99%) was used immediately after the ampules were opened and the contents purified by passage through a column of activated alumina.

[22] J. C. Mol, *J. Mol. Catal.* **1991**, *65*, 145–162.

Diastereoselective Complexation of Temporarily Chirally Modified Ligands: Enantioselective Preparation and Configurational Assignment of Synthetically Valuable η^6-Tricarbonylchromium-1-tetralone Derivatives**

By *Hans-Günther Schmalz,* Birgitta Millies, Jan W. Bats,* and *Gerd Dürner*

Dedicated to Professor Gerhard Quinkert on the occasion of his 65th birthday

Chiral transition-metal complexes of achiral π-ligands offer as synthetic building blocks new strategies for the total synthesis of biologically active compounds. If under the influence of the chiral metal-complex substructure, new, permanent chirality centers are generated (diastereoselectively), the competitiveness of such syntheses depends to a large extent on the accessibility of the starting materials in optically active form. In the course of a project in which we want to take advantage of the specific reactivity of η^6-arenetricarbonylchromium complexes[1] for the total synthesis of the antiinflammatory pseudopterosines[2] such as **1**, we required complex **2** (Scheme 1).

The reported techniques[3] for the preparation of nonracemic η^6-tricarbonylchromium complexes of achiral arene ligands are all based on the resolution of racemic mixtures (involving high losses) and did not satisfy our criteria. Here

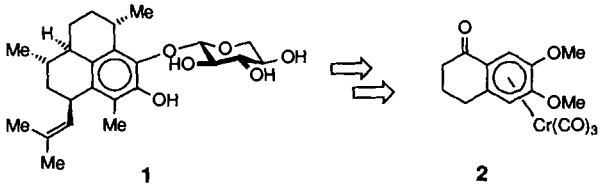

Scheme 1.

we describe an efficient enantioselective method for the preparation of **2** and other η^6-tricarbonylchromium-1-tetralone derivatives in defined and selectable absolute configuration.

The heart of our process (Scheme 2) is the diastereoselective complexation[4] of the tetralol derivatives **4**, which are obtained by enantioselective catalytic reduction of the tetralones **3** according to the method of Corey, Bakshi, and Shibata (CBS reduction).[5] A study initially carried out with

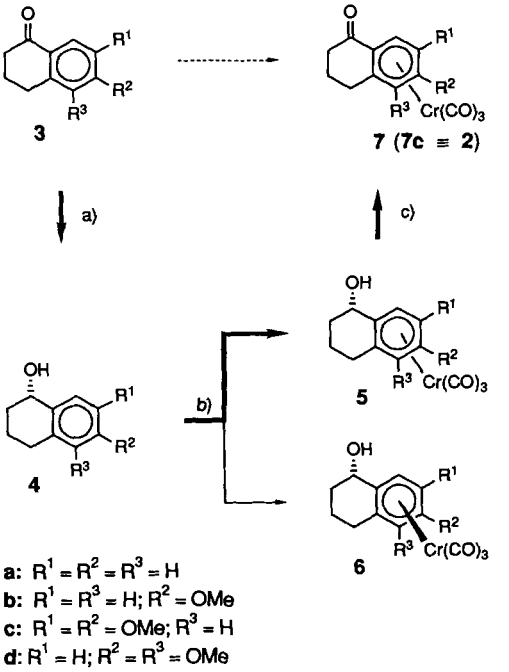

Scheme 2. Preparation of nonracemic η^6-tricarbonylchromium-1-tetralone derivatives by a) enantioselective reduction, b) diastereoselective complexation, and c) reoxidation (for reaction conditions and yields see text and Table 2).

Table 1. Diastereoselective complexation of the alcohols *rac*-**4**.

Alcohol	Complexation Method [a]	Reaction Time [h]	Ratio [b] *rac*-**5**:*rac*-**6**	Yield [c] [%]
rac-**4a**	**A**	5	>99:1	91
rac-**4b**	**A**	5	>99:1	94
rac-**4c**	**A**	5	>99:1	92
rac-**4d**	**A**	5	>99:1	94
rac-**4a**	**B**	30	90:10	65
rac-**4b**	**B**	39	70:30	62
rac-**4c**	**B**	41	52:48	28
rac-**4a**	**C**	50	98:2	70
rac-**4b**	**C**	45	99:1	70
rac-**4c**	**C**	30	96:4	86
rac-**4d**	**C**	27	93:7	74

[a] **A**: $[Cr(CO)_3$(naphthalene)] (1.2 equiv), THF (1.5 equiv), Et_2O, 70 °C (pressure); **B**: $[Cr(CO)_6]$ (1.1 equiv), nBu_2O/THF (10:1), reflux; **C**: $[Cr(CO)_6]$ (1.1 equiv), cat. THF, nBu_2O/heptane (1:1), reflux. [b] Determined by HPLC analysis of the crude product mixture. [c] Yield of isolated diastereomerically pure *rac*-**5**.

[*] Dr. H.-G. Schmalz, Dipl.-Chem. B. Millies, Dr. J. W. Bats, Dr. G. Dürner
Institut für Organische Chemie der Universität
Niederurseler Hang, D-W-6000 Frankfurt/Main 50 (FRG)

[**] This work was supported by the Fonds der Chemischen Industrie and the Bundesministerium für Forschung und Technologie (project 0318801B, "gezielte Synthese biologisch aktiver Moleküle"). We thank Prof. Dr. G. Quinkert, Frankfurt, for support.

racemic compounds (Table 1)[6] revealed that the complexation that employ Kündig's reagent, tricarbonyl(naphthalene)chromium (method **A**),[7] always afforded (as anticipated)[4] the *syn*-tetralol complexes *rac*-**5** with excellent yields and diastereoselectivities. The substantially better accessible reagent $[Cr(CO)_6]$ gave completely unsatisfactory results under standard conditions (method **B**),[4b, 8] in particular in the synthetically relevant case of *rac*-**4c**.[9] However, by changing the solvent mixture (from nBu_2O/THF = 10:1 to nBu_2O/heptane = 1:1; method **C**) good yields and selectivities were obtained with $[Cr(CO)_6]$ as well.

The transformations carried out in the optically active series are summarized in Table 2.[6] Borane reduction of ketones **3** in the presence of catalyst **9**,[5] which is readily accessible from D-proline via the intermediate **8**, always lead to high chemical (97–99%) and optical yields (Table 2) of the alcohols **4**, from which the pure *syn*-complexes **5** were prepared by complexation and chromatographic separation of the diastereomers. Finally, oxidation with Ac_2O/dimethyl sulfoxide (DMSO)[10] afforded the optically active ketone complexes **7** (and **2**).

Table 2. Preparation of the nonracemic complexes **7** (and **2**) from the ketones **3** according to Scheme 2.

Ketone	Complexation Method [a]	Product	Yield [b] [%]	$[\alpha]_D^{20}$ (in $CHCl_3$)	*ee* [c] [%]
3a	**A**	**7a**	77	−802	92
3b	**A**	**7b**	71	−712	86
3c	**A**	**2**	70	−805	85
3c	**C**	**2**	66	−818	85
3d	**A**	**7d**	85	−400	94

[a] **A**: $[Cr(CO)_3$(naphthalene)] (1.2 equiv), THF (1.5 equiv), Et_2O, 70 °C (sealed ampule); **C**: $[Cr(CO)_6]$ (1.1 equiv), cat. THF, nBu_2O/heptane (1:1), reflux. [b] Total yield calculated on amount of ketone **3** used. [c] The enantiomeric purity of the reduction products **4**, determined by ^1H NMR spectroscopy of the acetates in the presence of d-Eu(hfc)$_3$ (**4a**, **4c**, and **4d**) or d-Pr(hfc)$_3$ (**4b**), or by gas chromatography on a chiral phase (**4a** and **4b**), agreed well (±2%) with the enantiomeric purities of the ketone complexes determined by ^1H NMR spectroscopy in the presence of d-Eu(hfc)$_3$ (**2**) or d-Pr(hfc)$_3$ (**7b** and **7d**) and/or by comparison of the chiroptical data with reference values (**7a** and **2**).

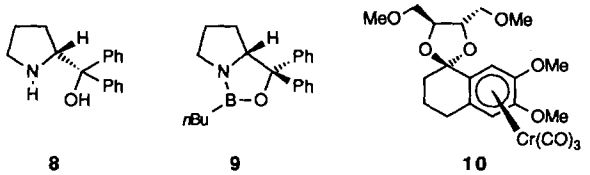

8 **9** **10**

An X-ray crystal structure analysis[11] of the chiral ketal **10**[12] (Fig. 1) revealed its relative and absolute configuration. Hydrolysis of the ketal function of **10** furnished enantiomerically pure *ent*-**2** (m.p. (decomp.) 176 °C; $[\alpha]_D^{20}$ + 974, c = 0.097 in $CHCl_3$).

The absolute configuration of **2** and thus also those of the precursors **4c** and **5c** were thereby established. Circular dichroism (CD) spectra of the tetralone complexes (Fig. 2) indicated the configurational uniformity of compounds **2**, **7a**, **7b**, and **7d**, which confirmed the earlier assignment for **7a** derived by indirect means.[4a] Furthermore, the absolute configuration of the CBS reduction products obtained by using **9** as catalyst corresponds to expectation.[5] Thus, neither the enantioselection of the CBS reduction nor the characteristics of the CD spectra of the ketone complexes are (significantly) affected by the synthetically valuable methoxy substituents.

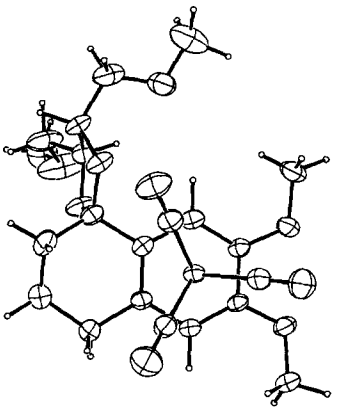

Fig. 1. Structure of **10** in the solid state [11].

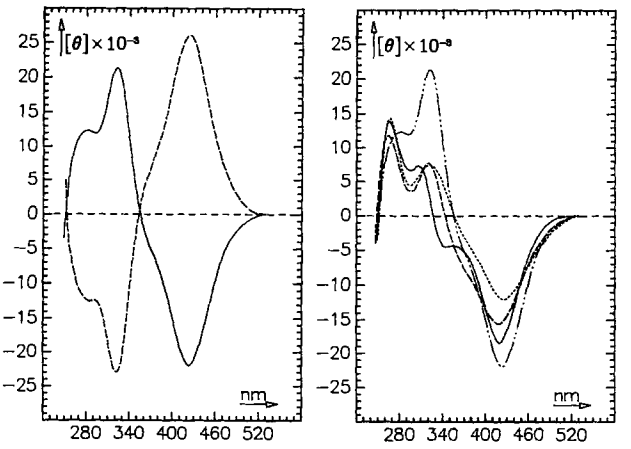

Fig. 2. CD spectra (in MeOH) of ketone complexes; left: **2** (85% *ee*; ——), and *ent*-**2** (>99% *ee*; – – –); right: **2** (85% *ee*; –·–·–), **7a** (92% *ee*; ——); **7b** (85% *ee*; – – –), and **7d** (94% *ee*; ····).

The complexes **7** and their enantiomers, which are also accessible through application of the catalyst *ent*-**9** prepared from L-proline, are expected to serve as valuable building blocks in synthesis. One might anticipate that further enantiomeric enrichment can be achieved through the crystallization of suitable intermediates.

Experimental Procedure

All reactions were performed in the absence of light under argon in degassed, dry solvents.

4c: A solution of $BH_3 \cdot Me_2S$ in THF (0.48 M, 13.2 mL) was added dropwise over 8 h at about 20 °C to 25 mL of a THF solution containing both 2.15 mmol of **9** (prepared from 546 mg of **8** and 241 mg of $nBuB(OH)_2$ by heating for 16 h in 25 mL of toluene in the presence of 4 Å molecular sieves and subsequent removal of the toluene in vacuum) and 2.21 g (10.7 mmol) of **3c**. After the addition of 5 mL of 95% MeOH, all volatile components were removed in vacuum and the residue was flash-chromatographed with hexane/EtOAc (1:1). Yield: 2.18 g (98%, m.p. 72–74 °C).

5c: **4c** (1.0 g, 4.8 mmol), $[Cr(CO)_6]$ (1.28 g, 1.2 equiv), nBu_2O and *n*-heptane (30 mL each), and THF (1 mL) was heated at 150 °C (weak reflux) in an oil bath for 30 h. Removal of the solvent in vacuum and flash chromatography of the residue with CH_2Cl_2/EtOAc (15:1) yielded 1.42 g (86%) of **5c** (m.p. 143–145 °C, decomp.) and about 0.1 g of a mixture of **6c** and unchanged **4c**.

2: A mixture of **5c** (1.31 g, 3.8 mmol) in DMSO (30 mL) and Ac_2O (20 mL) was stirred for 3.5 h at room temperature. The mixture was partitioned between 200 mL of cold 20% NaOH and 300 mL of Et_2O under ice cooling, and the aqueous phase was extracted several times with Et_2O. The combined organic solutions were washed with brine and dried over Na_2SO_4. Flash chromatography with hexane/CH_2Cl_2/EtOAc (10:10:1 to 5:5:1) afforded **2** (1.01 g, 78%) as an orange solid. M.p. 176–178 °C, decomp.; $[\alpha]_D^{20}$ −818, c = 0.111 in $CHCl_3$; IR(KBr): $\tilde{\nu}$ [cm^{-1}] = 1959(s), 1896(s), 1869(s), 1682(s), 1437(m), 1287(s); ^1H NMR (270 MHz, $CDCl_3$): δ = 6.00 (s, 1H), 5.11 (s, 1H), 3.85 (s, 3H), 3.80 (s, 3H), 2.91 (m, 1H), 2.69 (m, 2H), 2.36 (m, 1H), 2.11 (m, 2H); ^{13}C NMR (62.9 MHz, $CDCl_3$, additional DEPT): δ = 21.9(CH_2), 28.0(CH_2), 37.3(CH_2), 56.7(CH_3), 57.3(CH_3), 74.3(CH), 75.5(CH), 87.8, 109.9, 130.5, 135.5, 196.0, 231.3.

Received: December 4, 1991 [Z 5055 IE]
German version: *Angew. Chem.* **1992**, *104*, 640

[1] a) J. P. Collman, L. S. Hegedus, J. R. Norton, R. G. Finke, *Principles and Applications of Organotransition Metal Chemistry*, University Science Books, Mill Valley, CA, USA, **1987**, Chap. 20; b) V. N. Kalinin, *Russ. Chem. Rev.* **1987**, *56*, 682–700; c) M. Uemura, H. Nishimura, T. Minami, Y. Hayashi, *J. Am. Chem. Soc.* **1991**, *113*, 5402–5410.

[2] a) S. A. Look, W. Fenical, R. S. Jacobs, J. Clardy, *Proc. Natl. Acad. Sci. USA* **1986**, *83*, 6238–6240; b) S. A. Look, W. Fenical, G. K. Matsumoto, J. Clardy, *J. Org. Chem.* **1986**, *51*, 5140–5145; c) V. Roussis, Z. Wu, W. Fenical, S. A. Strobel, G. D. Van Duyne, J. Clardy, *ibid.* **1990**, *55*, 4916–4922.

[3] a) A. Solladié-Cavallo in *Advances in Metal-Organic Chemistry, Vol. 1* (Ed.: L. S. Liebeskind), JAI Press, Greenwich, CT, USA, **1989**, p. 99–133 and references cited therein.; b) K. Schlögel in *Organometallics in Organic Synthesis 2* (Eds.: H. Werner, G. Erker), Springer, Berlin, **1989**, p. 63; c) S. G. Davies, C. L. Goodfellow, *Synlett* **1989**, 59–61; *J. Chem. Soc. Perkin Trans. I.* **1989**, 192–193; d) S. Top, G. Jaouen, C. Baldoli, P. Del Buttero, S. Maiorana, *J. Organomet. Chem.* **1991**, *413*, 125–135, and references cited therein.

[4] a) G. Jaouen, A. Meyer, *J. Am. Chem. Soc.* **1975**, *97*, 4667–4672; b) S. G. Davies, C. L. Goodfellow, *J. Organomet. Chem.* **1988**, *340*, 195–201; c) B. Ohlson, C. Ullenius, S. Jagner, C. Grivet, E. Wenger, E. P. Kündig, *ibid.* **1989**, *365*, 243–267, and references cited therein.; J. Brocard, L. Pelinski, J. Lebibi, M. Mahmoudi, L. Maciejewski, *Tetrahedron*, **1989**, *45*, 709–720, and references cited therein.

[5] a) E. J. Corey, R. K. Bakshi, S. Shibata, *J. Am. Chem. Soc.* **1987**, *109*, 5551–5553; b) E. J. Corey, R. K. Bakshi, S. Shibata, C. P. Chen., V. K. Singh, *ibid.* **1987**, *109*, 7925–7926; c) T. K. Jones, J. J. Mohan, L. C. Xavier, T. J. Blacklock, D. J. Mathre, P. Sohar, E. T. Turner Jones, R. A. Reamer, F. E. Roberts, E. J. J. Grabowski, *J. Org. Chem.* **1991**, *56*, 763–769, and references cited therein.

[6] All compounds were characterized by the usual spectroscopic methods and gave correct elemental analyses.

[7] E. P. Kündig, C. Perret, S. Spichiger, G. Bernardinelli, *J. Organomet. Chem.* **1985**, *286*, 183–200.

[8] C. A. L. Mahaffy, P. L. Pauson, *Inorg. Synth.* **1979**, *19*, 154.

[9] A time-resolved study of the reactions by means of HPLC showed that (in contrast to the complexation of 1-indanol [c]) the *syn*/*anti* ratio (**5**:**6**) decreases continuously during the conversions. This loss of selectivity, which is attributable to a change of the $Cr(CO)_3$ group to the opposite π face, is more pronounced (faster), the more methoxy substituents are present on the arene ring. In our laboratory the complete diastereoselection described by Davies et al. in [4b] for the complexation of *rac*-**4a** under similar conditions (19 h reaction time, 36% yield) could not be observed.

[10] S. G. Levine, B. Gopalakrishnan, *Tetrahedron Lett.* **1982**, *23*, 1239–1240.

[11] X-ray crystal structure analysis of **10**: Enraf-Nonius CAD4 diffractometer, $Cu_{K\alpha}$ radiation, $2\theta = 120°$; empirical absorption correction based on ψ scans; structure determination with direct methods (SHELXS 86); the positions of the C and O atoms were determined by difference syntheses, and the hydrogen atoms in calculated positions were not refined. $C_{21}H_{26}CrO_9 \cdot 0.5\,EtOAc$, trigonal, space group $P3_221$, $a = b = 11.5377(7)$, $c = 32.438(2)$ Å, $V = 3739.6(8)$ Å^3, $Z = 6$, $\rho_{calcd} = 1.379$ g cm^{-1}; 2159 independent reflections, of which 2104 with $I > 0$ were used, $R = 0.057$, $R_w = 0.055$. The residual density was less than 0.54 e Å^{-3}. The absolute configuration was deduced from anomalous scattering of the Cr atom ($R = 0.095$, $R_w = 0.092$ for the enantiomorphic structure in the space group $P3_121$). Further details of the crystal structure investigation may be obtained from the Fachinformationszentrum Karlsruhe, Gesellschaft für wissenschaftlich-technische Information mbH, D-W-7514 Eggenstein-Leopoldshafen 2 (FRG) on quoting the depository number CSD-55874, the names of the authors, and the journal citation.

[12] Preparation of **10** (m.p. 101 °C; $[\alpha]_D^{20}$ +160, $c = 0.51$ in $CHCl_3$): H.-G. Schmalz, B. Millies, unpublished.

N-Lithiomethyl-*N*,*N*′*N*″,*N*″-tetramethyldiethylenetriamine: The First Alkyllithium Compound which is Monomeric in Hydrocarbons

By *Gerhard W. Klumpp*,* *Hendrikus Luitjes*, *Marius Schakel*, *Franciscus J. J. de Kanter*, *Robert F. Schmitz* and *Nicolaas J. R. van Eikema Hommes*

In hydrocarbon solution alkyllithium compounds usually exist as tetramers or hexamers.[1, 2] Addition of suitable Lewis bases B (ethers, tertiary amines) converts the hexamers into Lewis-base complexes with a tetrameric alkyllithium unit $[R_4Li_4] \cdot n\,B$ ($n = 1–4$)[1]. Further dissociation into dimer complexes $[R_2Li_2] \cdot 4\,B$ is observed only at very low temperatures in THF, and even trace amounts of hydrocarbons suffice to prevent it.[3] By contrast, the presence of polydentate Lewis bases such as *N*,*N*,*N*′,*N*′-tetramethylethylenediamine (TMEDA), which corresponds to two bases B,[3] or *N*,*N*,*N*′,*N*″,*N*″-pentamethyldiethylenetriamine (PMDTA), which corresponds to three bases B,[4] is advantageous. If the organic groups contained in the aggregates are bulky (R = *tert*-butyl, neopentyl), the aforementioned favorable conditions even allow the formation of complexed monomers $[RLi] \cdot 3\,B$, and dimers $[R_2Li_2] \cdot 4\,B$ are formed in ether.[4].

Due to the chelate effect, intramolecular Lewis-base groups lead to particularly stable complexes. Hence, we have synthesized secondary alkyllithium compounds containing two Lewis-base units. In hydrocarbon solution at room temperature, they exist exclusively as dimers.[5] We have now observed that *N*-lithiomethyl-*N*,*N*′,*N*″,*N*″-tetramethyldiethylenetriamine (**1**), recently prepared by us[6] and containing three Lewis-base groups, is monomeric in hydrocarbon solutions at about 5 °C. As far as we know, this is unprecedented for an alkyllithium compound. Cryoscopy of solutions of crystals of **1**[7] in benzene yielded a value of 1.06 for the degree of aggregation. At 195 K, ^6Li NMR spectra of

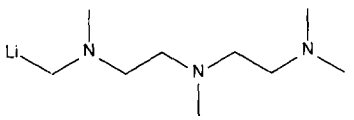

1

solutions of crystalline **1** (^6Li-labeled) in pentane exhibit signals at $\delta = 1.75$ (species A) and 1.35 (species B)[**] in an intensity ratio of 1.27:1 which coalesce, regardless of the concentration of **1**, at 227.7 K (36.80 MHz) and 232.2 K (58.88 MHz), respectively.[8] 1:1:1-Triplets at δ = 51.0 and 52.9 [$^1J(^{13}C,^6Li) = 13.9$ Hz] could be recognized in the 100.61 MHz ^{13}C NMR spectrum at 225 K, proving that A and B are monomers whose α carbon atoms bind to a single lithium atom.[9] At low temperatures, other signals in the C,H-decoupled ^{13}C NMR spectra[10] and in the ^1H NMR spectra[11] of pentane solutions of **1**, also indicate the presence of two species in the above ratio. At higher temperatures the signal patterns attributable to (stereo)isomers and diastereotopicity coalesced, and finally the spectra corre-

[*] Prof. Dr. G. W. Klumpp, Drs.-Ing. H. Luitjes, Dr. M. Schakel, Dr. F. J. J. de Kanter, R. F. Schmitz
Scheikundig Laboratorium, Vrije Universiteit
De Boelelaan 1083, NL-1081 HV Amsterdam (The Netherlands)
Dr. N. J. R. van Eikema Hommes
Institut für Organische Chemie der Universität Erlangen-Nürnberg

[**] In the following text the experimentally observed species A and B are distinguished from the calculated structures **1a** and **1b**.

sponding to the averaged structure **1** were obtained. At 275 K ^{13}C-^{6}Li coupling had vanished. A/B interconversion as well as exchange processes, known for ordinary[2a] and for intramolecularly coordinated[5] alkyllithium compounds, are possible causes of the temperature-dependence. The existence of **1** as a monomer is presumably due to steric hindrance of aggregation and to intramolecular Li–N coordination.

MNDO calculations[12] yielded structures **1a**(A) and **1b**(B) as the most stable states of **1**. Remarkably, in **1a, b** N2 and N3 coordinate to lithium as expected ($d_{N2[N3]-Li}$ = 2.22 [2.22] Å), while N1 interacts only weakly, at most (d_{N1-Li} = 2.67 Å). Despite the tricoordinate nature of lithium implied by this result, the enthalpies of formation obtained for **1a, b** are lower than those calculated for potential dimers of **1** containing coordinatively saturated tetracoordinated lithium.[12] Unfavorable steric effects in the dimers seem to be

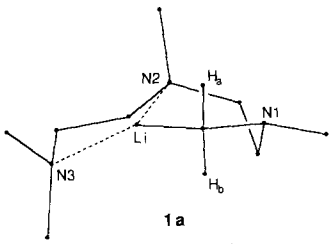

1a

E_{rel} = 0 kJ mol^{-1}

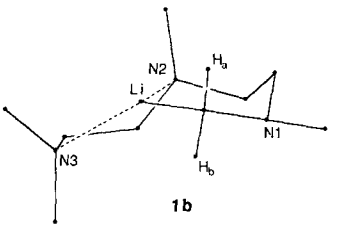

1b

E_{rel} = 4 kJ mol^{-1}

responsible for their higher enthalpies of formation. The enthalpy of activation calculated for the transformation **1a**(A) → **1b**(B), essentially corresponding to an inversion of N1, amounts to 40 kJ mol^{-1}.[12] This is in satisfactory agreement with the experimental value, $\Delta H^{\ddagger}_{A\rightarrow B} = \Delta H^{\ddagger}_{B\rightarrow A} = 43 \pm 3$ kJ mol^{-1} ($\Delta S^{\ddagger}_{A\rightarrow B} = -28 \pm 13$ J mol^{-1}K^{-1}, $\Delta S^{\ddagger}_{B\rightarrow A} = -26 \pm 13$ J mol^{-1}K^{-1}), derived from the coalescence temperatures T_c of the ^{6}Li resonance signals and of two pairs of ^{13}C signals of A/B (100.61 MHz; NCH_2, $\delta = 56.60 + 56.32$, $T_c = 235.5$ K; $(NCH_2)'$, $\delta = 63.24 + 61.36$, $T_c = 255.2$ K).[14]

Two coalescence phenomena were observed for the signals of the CH_2Li protons: Due to fast A/B interconversion the original four resonance signals of the diastereotopic protons H_a and H_b in A(**1a**) and B(**1b**), respectively, fuse at about 258 K to form two very broad signals[15] (H_a and H_b, respectively, in the averaged structure), which for their part coalesce into a broad singlet[16] at approximately 275 K [$\Delta G^{\ddagger}$ (275 K) ca. 53 kJ mol^{-1}]. This indicates fast exchange and, as a consequence, equivalence of the two diastereotopic protons of the averaged structure. Equivalence of H_a and H_b in A(**1a**) and B(**1b**) is not induced by **1a**/**1b** interconversion, and, according to theoretical studies, inversion of C^-, another possible cause, should only occur in aggregates with comparable ease.[17] Do **1a, b**(A, B), monomeric derivatives of α-aminomethyllithium containing two additional Lewis-base centers, invert easier and in a different way than monomeric methyllithium? The loss of ^{13}C-^{6}Li coupling at higher temperatures suggests Li–C bond breaking in the monomer (allowing for inversion of C^-) or intermolecular Li–C exchange involving dimers of higher energy. Inversion of N2 (MNDO enthalpy of activation 51 kJ mol^{-1})[12] could also lead to H_a/H_b exchange. Clarification of the actual mode requires additional studies.

Stable intramolecular organolithium complexes like **1a, b** and other members of this class of compounds prepared by us[5] are models for labile intermolecular Lewis-base complexes [RLi] · 3 B, [R_2Li_2] · 4 B, and [R_4Li_4] · 4 B, and to some degree their properties (structure, dynamics, reactivity) should be exemplary for those of these solvent- and temperature-dependent components of organolithium reagents, which are of such importance in synthesis.[5, 19]

Received: September 23, 1991 [Z 4924 IE]
German version: *Angew. Chem.* **1992**, *104*, 624

CAS Registry number: **1**, 129537-50-4.

[1] H. L. Lewis, T. L. Brown, *J. Am. Chem. Soc.* **1970**, *92*, 4664–4670.
[2] a) Recently, octamers and nonamers were also proven to be present in cyclopentane solutions of primary alkyllithium compounds (G. Fraenkel, M. Henrichs, J. M. Hewitt, B. M. Su, M. J. Geckle, *J. Am. Chem. Soc.* **1980**, *102*, 3345–3350; R. D. Thomas, R. M. Jensen, T. C. Young, *Organometallics* **1987**, *6*, 565–571); b) Menthyllithium is dimeric in benzene (W. H. Glaze, C. H. Freeman, *J. Am. Chem. Soc.* **1969**, *91*, 7198–7199.
[3] D. Seebach, R. Hässig, J. Gabriel, *Helv. Chim. Acta.* **1983**, *66*, 308–337; W. Bauer, D. Seebach, *ibid.* **1984**, *67*, 1972–1988.
[4] W. Bauer, W. R. Winchester, P. von Ragué Schleyer, *Organometallics* **1987**, *6*, 2371–2379; G. Fraenkel, A. Chow, W. R. Winchester, *J. Am. Chem. Soc.* **1987**, *112*, 6190–6198.
[5] W. Moene, M. Vos, F. J. J. de Kanter, G. W. Klumpp, A. L. Spek, *J. Am. Chem. Soc.* **1989**, *111*, 3463–3465; F. J. J. de Kanter, G. W. Klumpp, K. Kolthof, W. Moene, M. Vos, A. L. Spek, unpublished results; M. Vos, F. J. J. de Kanter, M. Schakel, N. J. R. van Eikema Hommes, G. W. Klumpp, *J. Am. Chem. Soc.* **1987**, *109*, 2187–2188.
[6] M. Schakel, M. P. Aarnts, G. W. Klumpp, *Recl. Trav. Chim. Pays-Bas* **1990**, *109*, 305–306.
[7] Crystals of **1** are stable indefinitely at −80 °C. In pentane **1** (ca. 0.2 M) decomposes at room temperature with a half-life of about 18 h (2 **1** → $Me_2NLi + C_2H_2 + Li(NMe)C_2H_4NMe_2$ + PMDTA). During the preparation of the cryoscopy experiment, solutions of **1** in benzene (0.083 M) had to be kept at room temperature for about 20 min. Solutions for NMR studies, which were subjected to the same conditions, contained no detectable decomposition products. We are still trying to obtain an X-ray structure analysis of **1**.
[8] Two solutions, differing in concentration by a factor of 10, were examined. Chemical shifts are based on 1 M LiBr in THF as external standard [δ (50% LiBr in H_2O): −1.04, δ (2-lithiobutane in C_6D_6): 0.77] and are not corrected for volume magnetic susceptibility.
[9] H. Günther, D. Moskau, P. Bast, D. Schmalz, *Angew. Chem.* **1987**, *99*, 1242–1250.
[10] ^{13}C NMR (62.89 MHz, pentane, 195 K [265 K], TMS): δ = 43.58 ($N(3)Me_2$, A or B), 43.80 ($N(3)Me_2$, B or A), 48.73 ($N(3)Me_2$, B), 49.57 ($N(3)Me_2$, A) [45.96], 44.79 (N(1)Me, A), 45.42 (N(1)Me, B) [45.10], 52.48 (N(2)Me, B), 54.41 (N(2)Me, A) [53.18], 51.34 (NCH_2, B), 52.26 (NCH_2, A), 56.32 (NCH_2, B), 56.60 (NCH_2, A), 57.62 (NCH_2, A + B), 61.36 (NCH_2, B) 63.24 (NCH_2, A) [52.78, 56.83, 57.88, 62.18]; (100.61 MHz, 225 K) δ = 51.0 (between 225 and 235 K also visible in 62.89 MHz spectrum) + 52.9 (CH_2Li, $^{1}J(^{13}C, ^{6}Li)$ = 13.9 Hz) [51.74].
[11] ^{1}H NMR (250 MHz, [D_{12}]pentane, 195 K [300 K], TMS): δ = 2.40 + 2.10 [2.28] (s + s, ca. 3H + ca. 3H; $N(3)Me_2$, A + B), 2.33 (s, ca. 1.5H; N(2)Me, A), 2.35 (s, ca. 1.5H; N(2)Me, B) [2.37], 2.31 [2.35] (s, 3H; N(1)Me, A + B), ca. 2 (overlapping signals; NCH_2), 1.63 + 1.19 (d + d, ^{2}J(H, H) = 10.4 Hz, 1H; CH_2Li, B + A, coalescence at ca. 258 K), 0.67 + 0.30 (d + d, ^{2}J(H, H) = 10.4 Hz, 1H; CH_2Li, A + B, coalescence at ca. 258 K) [1.03].
[12] In order to correct for known deficiencies of MNDO calculations (overestimation of C–Li bond strength and nonbonding repulsions) 60 kJ mol^{-1} was added to the calculated energy of $(\mathbf{1})_2$,[13] and 21 kJ mol^{-1} was added to all calculated activation enthalpies (N. J. R. van Eikema Hommes, P. von Ragué Schleyer, unpublished results).
[13] E. Kaufmann, K. Raghavachari, A. E. Reed, P. von Ragué Schleyer, *Organometallics* **1988**, *7*, 1597–1607.
[14] Method: H. Shanan-Atidi, K. H. Bar-Eli, *J. Phys. Chem.* **1970**, *74*, 961–963. Although upon increase of temperature all other A/B signal pairs recognizable at low temperature also coalesced, partial overlap with other temperature-dependent signals restricted exact determination of coalescence temperatures to the four cases given. Rate constants evaluated from the estimated coalescence temperatures [241 K (100.61 MHz) and 255 K (62.89 MHz)] of the N(1)$^{13}CH_3$ and N(2)$^{13}CH_3$ A/B signal pairs correspond to those of the A/B exchange as calculated for the respective temperatures from the activation parameters. The linewidths of the pairs of ^{13}C signals $[N(3)Me]_A$ + $[N(3)Me]_B$ and $[N(3)Me']_A$ + $[N(3)Me']_B$ are considerably larger than those of the other signals, and coalescence took place between the measurements at 215 and 225 K (62.89 MHz) without prior

loss of identity of the A and B component in the (better resolved) low-field pair. This suggests that the sequence, Li-N(3) decoordination, inversion of N(3), and Li-N(3) recoordination, causes fast Me/Me' exchange, while A/B exchange is still slow on the ^{13}C NMR time scale.

[15] $\Delta\nu_{1/2}$ ca. 70 Hz. The low-field resonances were obscured by the signals of the residual protons of the solvent [D_{12}]pentane.

[16] $\Delta G^{\neq} = 19.13\, T_c\{9.97 + \log(T_c/\Delta\nu^{-1})\}$, $\Delta\nu$ ca. 230 Hz.

[17] The value of $\Delta G^{\neq}$ (281 K) for stereomutation of C^- in aggregated alkyllithium compounds is ca. 60 kJ mol^{-1} [18]. Calculations for methyllithium indicated the barrier for inversion of C^- in the monomer to be ca. 55 kJ mol^{-1} higher than in the aggregates[13]. On this basis the value of $\Delta G^{\neq}$ (275 K) for inversion of C^- in **1a, b** is expected to be ca. 110 kJ mol^{-1}.

[18] G. Fraenkel, W. E. Beckenbaugh, P. P. Yang, *J. Am. Chem. Soc.* **1976**, *98*, 6878–6885.

[19] B. O. T. Kammermeier, G. W. Klumpp, K. Kolthof, M. Vos, *Tetrahedron Letters* **1991**, *32*, 3111–3114.

Addition of Benzyl Radicals to Alkenes: The Role of Radical Deformation in the Transition State**

By *Károly Héberger, Manfred Walbiner*, and *Hanns Fischer**

Rate constants for the addition of alkyl radicals to alkenes are influenced strongly by polar and steric effects from substituents of radicals and alkenes. Since the reactions are exothermic ($\Delta H = -50$ to -150 kJ mol^{-1}), the overall reaction enthalpies and radical stabilizations play a minor role, and the transition states are early. This also allows the rationalization of polar effects in terms of orbital interactions of the unperturbed reactants.[1] Calculated transition-state structures vary little with changes in either radical or substrate. As indicated by Figure 1, the forming bond is rather long (215–240 pm), yet the angle of attack is tightly prescribed (107–110°). The alkene center attacked is markedly though not strongly deformed; the other center is hardly affected. Most calculations yield pyramidalized radical centers.[2]

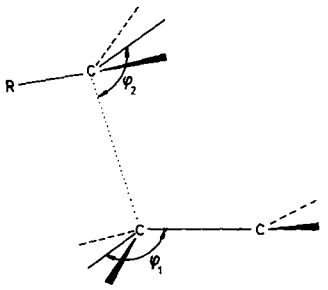

Fig. 1. Transition-state structure for the addition of an alkyl radical to an alkene. Calculated angles for $CH_3 + C_2H_4$: $\varphi_1 = 160°$, $\varphi_2 = 100°$, versus $\varphi_1 = 180°$, $\varphi_2 = 90°$ in the initial state and $\varphi_1 = 125°$, $\varphi_2 = 110°$ in the product state [2d].

In continuation of our previous work on the kinetics of radical additions,[3] we have now determined rate constants for the reaction of benzyl radicals and some *para*-substituted derivatives with a series of monosubstituted and 1,1-disubstituted alkenes. Benzyl is resonance-stabilized by about 50 kJ mol^{-1},[4] and little is known about addition rates of such radicals. The addition of benzyl is estimated to be exothermic, but less so than that of other alkyl radicals.[5] A comparison with rate constants for the addition of other radicals, for instance *tert*-butyl,[3a, b] should reveal the influence of the reaction enthalpy. Furthermore, the SOMO (SOMO = *S*ingly *O*ccupied *M*olecular *O*rbital) energy of benzyl (IP = 7.2 eV) is close to that of *tert*-butyl (IP = 6.7 eV).[6] The latter has clearly nucleophilic behavior,[3a, b] hence benzyl should also be a nucleophilic radical. On *para*-substitution of benzyl, its SOMO energy varies from about -7.9 to -6.3 eV,[6] whereas the stabilization energy is nearly unaffected.[4b] Previously, for *tert*-butyl, a strong dependence of the rate constants on the LUMO energies of the alkenes ($-2.48 \le EA \le -0.21$ eV) had been observed.[3a, b] It might be expected that a similar variation of the benzyl SOMO energy by substitution would cause a similarly strong polar effect.[1]

Figure 2 shows rate constants for the addition of benzyl and, for comparison, *tert*-butyl[7] as a function of the alkene LUMO energy. The linear correlation[3] with the alkene electron affinities for benzyl is significant (lg k_{296} [M^{-1}s^{-1}] = 3.36 + 1.14 EA, 24 measurements, correlation coefficient $r = 0.87$) but weaker than that for *tert*-butyl (lg k_{296} [M^{-1}s^{-1}] = 5.95 + 1.61 EA, 21 measurements, $r = 0.89$). As expected, benzyl is less nucleophilic. The large scatter of the data is not due to experimental error.

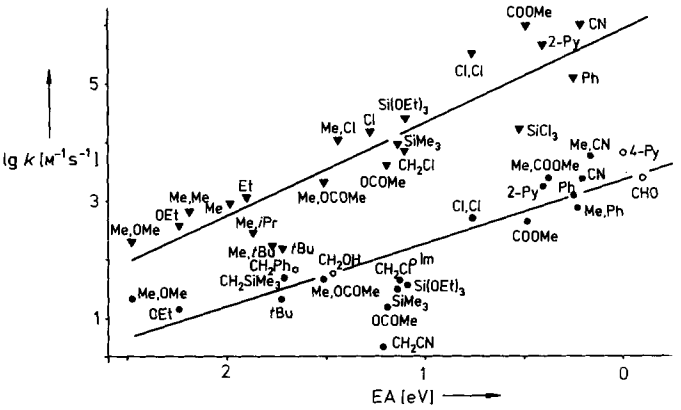

Fig. 2. Rate constants for the addition of benzyl (●○) and *tert*-butyl (▼) to alkenes $H_2C = CY^1Y^2$ (○: EA estimated) in toluene at (23 ± 1) °C. The labels next to the symbols for the benzyl and *tert*-butyl radicals indicate the substituents Y^1 and Y^2 of the alkene. If only one substituent is specified, then $Y^1 = H$ (see also Table 1). Im = imidazolyl, 2-Py = 2-pyridyl, 4-Py = 4-pyridyl.

In general, benzyl radicals react much more slowly than *tert*-butyl with all alkenes, and it is tempting to attribute this to the smaller exothermicity of the addition. However, this is contradicted by the findings that the increased exothermicity in the formation of benzyl-type radicals from styrenes does not increase the rates correspondingly. Moreover, the measured difference in activation energies for the additions of benzyl and *tert*-butyl is on the average 20 kJ mol^{-1}; this is too large to be accommodated by the enthalpy difference of only 38 kJ mol^{-1}. Table 1 presents rate constants for addition of the different *para*-substituted benzyl radicals to selected alkenes. To a first approximation all the radicals show the same weakly nucleophilic behavior. There are differences in detail, but there is no obvious correlation with the radical SOMO energies[6] nor with σ-scales for benzyl substituents.[8] Thus, polar orbital interactions appear to be asym-

[*] Prof. Dr. H. Fischer, Dr. K. Héberger[+], Dipl.-Chem. M. Walbiner
Physikalisch-Chemisches Institut der Universität
Winterthurerstrasse 190, CH-8057 Zürich (Switzerland)

[+] Permanent address: Institute for Chemistry
Hungarian Academy of Sciences, Budapest
Postfach 17, H-1524 (Hungary)

[**] This work was supported by the Schweizerischen Nationalfonds zur Förderung der wissenschaftlichen Forschung.

Table 1. Rate constants for the addition of *para*-X-substituted benzyl radicals to alkenes $H_2C = CY^1Y^2$ in $M^{-1}s^{-1}$ at (23 ± 1) °C.

Y_1, Y_2	X = OMe [a]	Me [a]	H [c]	F [a]	CN [b]
H, OEt	12	32	14	18	260
H, *t*Bu	15	49	18	25	57
H, CH_2CN	28	10	3	8	<10
H, OCO Me	36	25	14	27	20
Cl, Cl	1050	490	550	810	890
H, COOMe	2450	3000	450	1200	680
H, Ph	2300	2300	1300	2400	3400
H, CN	1800	2100	2200	3250	1400

[a] Solvent 2-propanol. [b] Solvent *p*-cyanotoluene. [c] Solvent toluene.

metric: Variations in the energy of the alkene LUMO influence the addition of the radical more than corresponding changes in the radical SOMO energy.

The results are compatible with the calculated properties of the transition states (Fig. 1). Detailed analyses of activation energies for methyl additions to alkenes[2a, d] have revealed large repulsive contributions of the deformation energies required for pyramidalization. For the addition of the methyl radical the main contribution comes from the alkene deformation, though the radical is more pyramidalized. This is understandable since the methyl radical has a flat and broad potential energy surface for out-of-plane deformation;[2a, d] the same probably holds for the *tert*-butyl radical which rapidly inverts in a double minimum potential.[9] The molecular frame of benzyl radicals is considerably stiffer, as supported by the very small temperature-dependence of the hyperfine couplings of the α protons.[10] If, like methyl radicals, benzyl radicals also have to be pyramidalized at the attacking carbon to reach the region of dominating attractive interactions, then a larger radical deformation energy is required. This increases the activation energy and decreases the reactivity. Also, both mesomeric and inductive effects decrease upon deformation of the radical, which may explain the low *para*-substituent effects (Table 1). A comparison of the reactivities of various alkyl radicals further supports this view: Most alkyl radicals are nucleophilic like *tert*-butyl and even methyl, despite its much lower SOMO energy of −9.8 eV.[1, 3] Only strong acceptor substituents change the radical character to ambi- or electrophilic.[1, 2, 3, 11]

We suggest that benzyl and other stabilized radicals react comparatively slowly with alkenes because they resist pyramidalization more strongly than other species and not because of the lower exothermicity of the addition. Our results give no hint to the details of the transition-state structure, and calculations would be very helpful in this respect.

Experimental Procedure

The rate constants were measured by kinetic ESR spectroscopy [3] employing photochemical generation of benzyl by α-cleavage of symmetric ketones [12] or by reaction of *tert*-butoxy radicals from the photolysis of di-*tert*-butyl peroxide with *p*-cyanotoluene. The addition obeyed pseudo-first-order kinetics as shown by variation of alkene concentrations. For fast reacting alkenes, product radicals could be detected whose structures confirmed addition to the unsubstituted alkene center. Rate data are averages from 5–10 individual experiments and have standard deviations of at most 30%. Very small rate constants were difficult to measure and may be somewhat high, since side-reactions may have interfered to some extent.

Received: October 14, 1991 [Z 4966 IE]
Revised: January 2, 1992
German version: *Angew. Chem.* **1992**, *104*, 651

[1] a) B. Giese, *Angew. Chem.* **1983**, *95*, 771–782; *Angew. Chem. Int. Ed. Engl.* **1983**, *22*, 753–763; b) J. M. Tedder, *ibid.* **1982**, *94*, 433–442 and **1982**, *21*, 401–410.

[2] a) R. Arnaud, R. Subra, V. Barone, F. Lelj, S. Olivella, A. Solé, N. Russo, *J. Chem. Soc. Perkin Trans.* **1986**, *2*, 1517–1524; b) K. N. Houk, M. N. Paddon-Row, D. C. Spellmeyer, N. G. Rondan, S. Nagase, *J. Org. Chem.* **1986**, *51*, 2874–2879; c) T. Fueno, M. Kamachi, *Macromolecules* **1988**, *21*, 908–912; d) C. Gonzales, C. Sosa, H. B. Schlegel, *J. Phys. Chem.* **1989**, *93*, 2435–2440; e) M. Zipse, J. He, K. N. Houk, B. Giese, *J. Am. Chem. Soc.* **1991**, *113*, 4324–4325.

[3] a) K. Münger, H. Fischer, *Int. J. Chem. Kinet.* **1985**, *17*, 809–829; b) H. Fischer in *Substituent Effects in Radical Chemistry* (Eds.: Z. Janousek, R. Merényi), Reidel, Dordrecht, **1986**, pp. 123–142; c) I. Beranek, H. Fischer in *Free Radicals in Synthesis and Biology* (Ed.: F. Minisci), Kluwer, Amsterdam, **1989**, pp. 303–316.

[4] a) M. S. Conradi, H. Zeldes, R. Livingston, *J. Phys. Chem.* **1979**, *83*, 2160–2161; b) A. M. de P. Nicholas, D. R. Arnold, *Can. J. Chem.* **1986**, *64*, 270–276.

[5] a) For example for benzyl + ethene: $\Delta H = -62\ kJ\,mol^{-1}$, for *tert*-butyl + ethene: $\Delta H = -100\ kJ\,mol^{-1}$. H_f° values from a) H. Hippler, J. Troe, *J. Phys. Chem.* **1990**, *94*, 3803–3806; b) D. Gutman, *Acc. Chem. Res.* **1990**, *23*, 375–380; c) S. W. Benson, *Thermochemical Kinetics*, Wiley, New York, **1976**.

[6] Vertical ionization energies from a) F. A. Houle, J. L. Beauchamp, *J. Am. Chem. Soc* **1979**, *101*, 4067–4073; *ibid.* **1978**, *100*, 3290–3294; b) K. Hayashibara, G. H. Kruppa, J. L. Beauchamp, *ibid.* **1986**, *108*, 5441–5443; c) A. G. Harrison, P. Kebarle, F. P. Lossing, *ibid.* **1961**, *83*, 777–780. After correction of early data according to Ref. [6b, c] the IPs of *para*-X-substituted benzyl radicals are for X = OCH_3, 6.32 eV; for X = CH_3, 6.96 eV; for X = F, 7.28 eV; for X = CN, 7.86 eV.

[7] We thank H. Rubin, this Institute, for the data for *tert*-butyl not provided in Ref. [3a, b].

[8] a) J. M. Dust, D. R. Arnold, *J. Am. Chem. Soc.* **1983**, *105*, 1221–1227, 6531; b) T. H. Fisher, A. W. Meierhofer, *J. Org. Chem.* **1978**, *43*, 224–228; c) S. Dinctürk, R. A. Jackson, M. Townson, H. Agirbas, N. C. Billingham, G. March, *J. Chem. Soc. Perkin Trans.* **1981**, *2*, 1121–1126; d) X. Creary, M. E. Mehrsheik-Mohammadi, S. McDonald, *J. Org. Chem.* **1987**, *52*, 3254–3263.

[9] J. Pacansky, M. Yoshimine, *J. Phys. Chem.* **1986**, *90*, 1980–1983.

[10] For $\cdot CH_3$ $da/dT \cong 1.8 \times 10^{-4}\ mT\,K^{-1}$, whereas the hyperfine coupling of the α protons of benzyl is practically constant over 600 K: *Magnetic Properties of Free Radicals* in *Landolt-Börnstein Vol. II/9b, II/17c* (Ed.: H. Fischer) Springer, Berlin, **1978**, **1987**.

[11] K. Riemenschneider, H. M. Bartels, R. Dornow, E. Drechsel-Grau, W. Eichel, H. Luthe, Y. M. Matter, W. Michaelis, P. Boldt, *J. Org. Chem.* **1987**, *52*, 205–212.

[12] S. Chiavarelli, G. Settimj, H. M. Alves, *Gazz. Chim. Ital.* **1956**, *87*, 109–1128.

Proof of the Catalytic Activity of a Naked Metal Cluster in the Gas Phase**

By *Patrick Schnabel, Konrad G. Weil,* and *Manfred P. Irion**

Naked metal clusters in the gas phase are usually characterized by a high degree of coordinative unsaturation. They are not only suitable as model substances for heterogeneous catalysis but should themselves be highly selective and effective catalysts. Thus, the search for such new catalysts is often given as a reason for the investigation of their chemical behavior. However, in spite of numerous efforts[1, 2] to our knowledge no synthesis catalyzed by a gas phase metal cluster has so far been reported.[3]

Recently we observed that from a distribution of iron cluster ions Fe_n^+ ($n = 2–13$), which were stored in the ICR cell of a Fourier transform ion cyclotron resonance (FT-ICR) mass spectrometer[4] and were exposed to the reactive gas NH_3 at ca. 10^{-7} mbar, only Fe_4^+ reacted through

[*] Dr. M. P. Irion, Dipl.-Ing. P. Schnabel, Prof. Dr. K. G. Weil
Institut für Physikalische Chemie der Technischen Hochschule
Petersenstrasse 20, D-W-6100 Darmstadt (FRG)

[**] This work was supported by the Deutsche Forschungsgemeinschaft, the Fonds der Chemischen Industrie, and the Röhm-Stiftung. It is part of P. Schnabel's dissertation (Darmstadt, D17).

dehydrogenation of ammonia to give the intermediates $[Fe_4(NH)]^+$ and $[Fe_4(NH)_2]^+$.[8] Ammonia synthesis is presumed to proceed via intermediates formed from (NH) and the iron atoms on the solid catalyst surface,[9] which are similar to the ions we observed. Nevertheless this reaction could not be considered as an example of gas phase catalysis by a naked metal cluster.

Now for the first time clear indications of such catalytic activity have been obtained. If Fe_4^+ ions are isolated by a radio frequency (RF) ejection pulse[11] from Fe_n^+ ions stored in an ICR cell and are exposed to the hydrocarbons ethene or cyclopropane (at ca. 10^{-7} mbar), dehydrogenation reactions occur which for ethene lead to a complex consisting of Fe_4^+ and up to four acetylene ligands. Collision-induced dissociation (CID) with xenon as collision gas leads to the formation of carbides for adducts with less than three acetylene ligands. However, for those adducts whose ligands have attained C_6H_6 stoichiometry, CID leads to the simultaneous loss of all C and H atoms already at a center-of-mass collision energy[12] of ca. 3.2 eV.[10a] This observation together with the kinetic behavior of the adducts[10b] suggest that neutral benzene is liberated in the CID process. (This statement cannot be proven directly from the experiment; however, for reasons of stability we would rather exclude other C_6H_6 isomers.) The naked Fe_4^+ ion is left and in principle can initiate a new cycle.

In 1981 Kappes and Staley were the first to prove such catalytic cycles in the gas phase in an analogous procedure with the simple metal ion Fe^+. Here, N_2O oxidized the hydrocarbons C_2H_6, C_2H_4, C_2H_2, C_3H_4, C_3H_6, C_3H_8, and even CO.[13] Recently the oxidation of ethane was studied in greater detail by Schwarz et al. using FT-ICR as well.[14] Analogous to our results the reaction of $[Fe(CO)_n]^+$ with C_2H_2 gave the adduct ions $[Fe(C_2H_2)_m]^+$ ($m = 1-4$). Neutralization reionization mass spectrometry (NRMS) of $[Fe(C_2H_2)_3]^+$ indicated a partial cyclotrimerization of the ligands to give C_6H_6. Here, too, the addition of the third C_2H_2 ligand occurred more easily than the addition of the previous ones; in all probability CID also effected the release of neutral benzene.[15] Our results lead us to the conclusion that the metal cluster ion Fe_4^+ catalyzes the formation of benzene from ethene (Scheme 1). Clear proof of this conjecture had been missing till now.

Through an optimization of the experimental conditions for the ion transfer to the ICR cell[4] we achieved such an increase in the intensities of the ions stored and detected

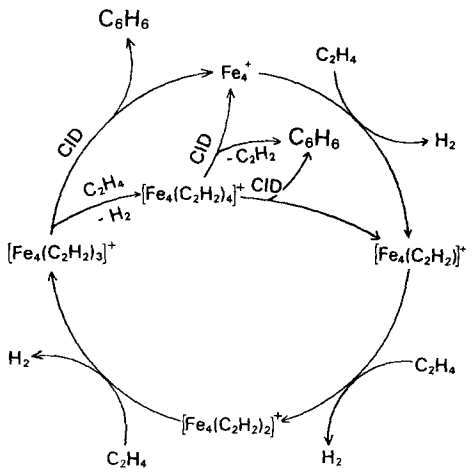

Scheme 1. Catalytic cycle of the metal cluster ion Fe_4^+ for the synthesis of benzene from ethene.

there that several successive reaction steps could be carried out with them. To prove beyond doubt that the same Fe_4^+ ions induce the synthesis of benzene twice, it was neccessary to carry out the MS^5 experiment shown in Scheme 2.[16]

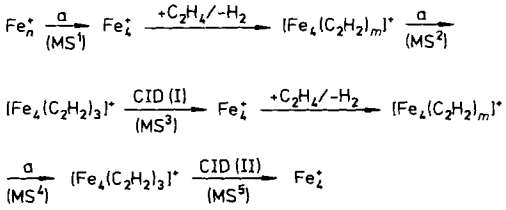

Scheme 2. Complex MS^5 experiment to prove the recovery of the catalyst Fe_4^+ for the reaction with ethene. a = isolation; $m = 1-3$.

Figure 1 shows the FT mass spectrum of the sputtered and stored/cooled Fe_n^+ cluster ions in the size range $n = 3-8$, and Figure 2a shows the signal of the Fe_4^+ ions isolated from them. By the reaction of the Fe_4^+ ions with ethene the spec-

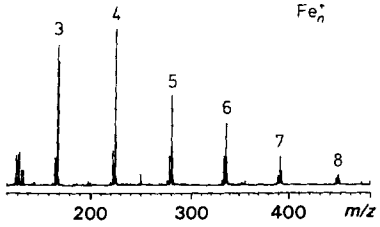

Fig. 1. FT mass spectrum of the Fe_n^+ cluster ions stored/cooled in the ICR cell in the size range $n = 3-8$.

trum of the adduct ions $[Fe_4(C_2H_2)_m]^+$ ($m = 1-3$; Fig. 2b) is obtained. In the next step (Fig. 2c), the ion $[Fe_4(C_2H_2)_3]^+$ is selected and then excited by a RF pulse at its resonance frequency to a translational energy of ca. 36.3 eV. The prima-

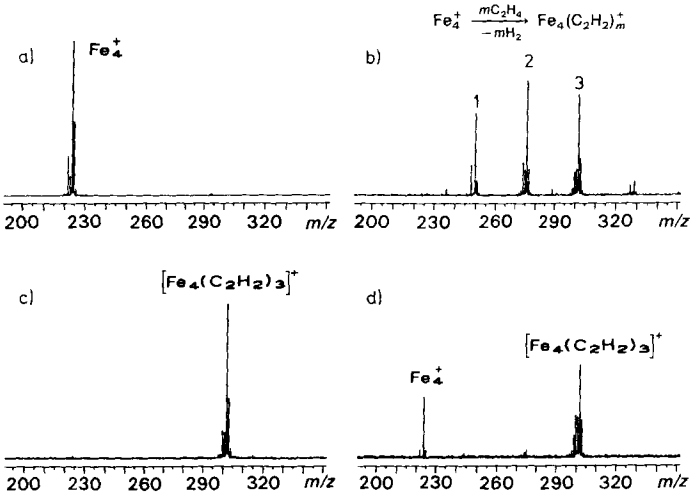

Fig. 2. a) Signal of the isolated Fe_4^+ cluster ions (1st generation). b) FT mass spectrum of the adduct ions $[Fe_4(C_2H_2)_m]^+$ ($m = 1-3$) from the reaction $Fe_4^+ + mC_2H_4 \rightarrow [Fe_4(C_2H_2)_m]^+ + mH_2$ (1st generation; the signal intensities were increased by factor of 2.0). c) Signal of the isolated adduct cluster ions $[Fe_4(C_2H_2)_3]^+$. (1st generation; the signal intensities were increased by factor of 1.5). d) FT mass spectrum of the mother and fragment ions following CID of $[Fe_4(C_2H_2)_3]^+$, 1st generation with xenon as collision gas ($p \approx 10^{-7}$ mbar; $E_{cm} \approx 11$ eV).

ry ion source constantly releases xenon as a background gas into the vacuum up to a pressure of ca. 10^{-7} mbar, which leads to a great number of collisions of the ions excited to a larger cyclotron orbit and thus to their dissociation ($E_{cm} \approx 11$ eV [12]). Finally, the signals of the residual mother ion and the new fragment ion Fe_4^+ are shown in Figure 2d. The whole reaction cycle is repeated once again in an analogous way in Figure 3. (Although the observed intensity inevitably decreases with every step, in this experiment even at the end it is still three to four times more intense than the background noise.)

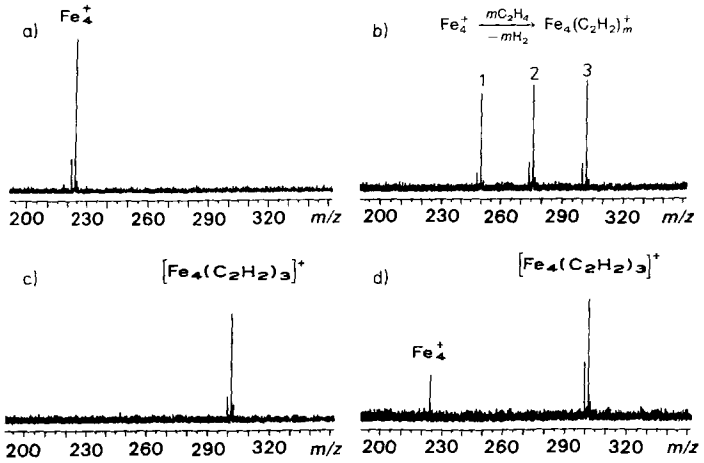

Fig. 3. a) Signal of the isolated Fe_4^+ cluster ions (2nd generation; the signal intensities were increased by a factor of 2.5). b) FT mass spectrum of the adduct ions $[Fe_4(C_2H_2)_m]^+$ ($m = 1-3$) following the reaction of Fe_4^+ with C_2H_4 as in Figure 2b (2nd generation; the signal intensities were increased by a factor of 2.0). c) Signal of the isolated adduct cluster ions $[Fe_4(C_2H_2)_3]^+$ (2nd generation). d) FT mass spectrum of the mother- and fragment ions following CID of $[Fe_4(C_2H_2)_3]^+$, 2nd generation with xenon as collision gas ($p \approx 10^{-7}$ mbar; $E_{cm} \approx 11$ eV).

Thus, the originally produced Fe_4^+ ions have run through the same reaction cycle twice. This demonstrates that a naked metal cluster in the gas phase can indeed act as a catalytic center and repeatedly build up a larger molecule from smaller units.

Received: December 11, 1991 [Z 5067 IE]
German version: *Angew. Chem.* **1992**, *104*, 633

CAS Registry numbers:
Fe_4^+, 73145-65-0; Fe^0, 7439-89-6; ethene, 74-85-1; ethyne, 74-86-2; benzene, 71-43-2.

[1] *J. Chem. Soc. Faraday Trans.* **1990**, *86*, 2343–2551 (Proceedings 25th Faraday-Symposium: "Large Gas Phase Clusters"), in which notably: A. Kaldor, D. M. Cox, pp. 2459–2463.
[2] *Z. Phys. D.* **1991**, *19, 20* (Proceedings ISSPIC-5).
[3] A. Kaldor, D. M. Cox, M. R. Zakin, *Adv. Chem. Phys.* **1988**, *70*, 220.
[4] The FT-ICR mass spectrometer used was home-built with a cubic ICR cell of side length 80 mm, placed in the homogeneous field of an Oxford Instruments 7.05 T superconducting magnet and a Spectrospin data system. Via an Aspect 3000 computer it provided the cell with pulses, registered and Fourier transformed the transient signal.[5] The metal cluster ions are produced by the bombardment of the corresponding metal foil in an external chamber with 20 keV Xe^+ ions from a duoplasmatron ion source [6]. They are injected into the differentially pumped ICR cell by a system of ion optics. A grid in front of the cell decelerates the external ions electrostatically and controls their entrance into the cell. By using a home-made piezoelectric valve at a distance of 8 cm, neon is pulsed in up to ca. 10^{-4} mbar, which by means of collisions helps in trapping the incoming ions and cools them to approximately room temperature.[7] To initiate chemical reactions with the thus thermalized ions, gases can be admitted via continually adjustable leak valves or via a second pulsed valve. Whereas in earlier experiments mainly the first possibility was used [8,10] the ethene in this case was added through the second pulsed valve.
[5] For more details see a) M. P. Irion, A. Selinger, *Z. Phys. Chem.* **1989**, *161*, 233; b) M. P. Irion, A. Selinger, R. Wendel, *Int. J. Mass Spectrom. Ion Processes* **1990**, *96*, 27; c) A. Selinger, P. Schnabel, W. Wiese, M. P. Irion, *Ber. Bunsenges. Phys. Chem.* **1990**, *94*, 1278.
[6] See for example a) F. M. Devienne, J.-C. Roustan, *Org. Mass Spectrom.* **1982**, *17*, 173; b) I. Katakuse, T. Ichihara, Y. Fujita, T. Matsuo, T. Sakurai, H. Matsuda, *Int. J. Mass. Spectrom. Ion Processes* **1985**, *67*, 229.
[7] P. Schnabel, M. P. Irion, K. G. Weil, *Ber. Bunsenges. Phys. Chem.* **1991**, *95*, 197.
[8] a) M. P. Irion, A. Selinger, P. Schnabel, *Z. Phys. D* **1991**, *19*, 393; b) M. P. Irion, P. Schnabel, A. Selinger, *Ber. Bunsenges. Phys. Chem.* **1990**, *94*, 1291; c) M. P. Irion, P. Schnabel, *J. Phys. Chem.* **1991**, *95*, 10596.
[9] G. Ertl in *Catalysis Science and Technology, Band 4* (Eds.: J. R. Anderson, M. Boudart), Springer, Berlin, **1983**, p. 257–282.
[10] a) P. Schnabel, M. P. Irion, K. G. Weil, *J. Phys. Chem.* **1991**, *95*, 9688; b) *Chem. Phys. Lett.* **1992**, *190*, 255.
[11] An ion type of a certain mass/charge ratio is isolated in the ICR cell from ions of other masses, by intentionally exciting the ions of unwanted types by a radio frequency (RF) "ejection pulse" thus eliminating them from the cell. A particular variant of this technique is "FERETS" (R. A. Forbes, F. A. Laukien, J. Wronka, *Int. J. Mass Spectrom. Ion Processes* **1988**, *83*, 23).
[12] The center-of-mass energy, E_{cm}, defines the maximum energy, which is transmitted by the collision of a molecule M with an ion I. It is obtained from the masses m_i from the following formula: $E_{cm} = E_{Lab} \cdot m_M/(m_I + m_M)$.
[13] M. M. Kappes, R. H. Staley, *J. Am. Chem. Soc.* **1981**, *103*, 1286.
[14] D. Schröder, H. Schwarz, *Angew. Chem.* **1990**, *102*, 1466; *Angew. Chem. Int. Ed. Engl.* **1990**, *29*, 1431.
[15] D. Schröder, D. Sülzle, J. Hrusak, D. K. Böhme, H. Schwarz, *Int. J. Mass Spectrom. Ion Processes* **1991**, *110*, 145.
[16] A complex experiment with several mass spectrometric steps (MS^n) requires in a conventional instrument n sectors separated in space. However, in an instrument with ion storage (FT-ICR, quadrupole ion trap) the whole experiment is conducted in the time domain and nothing more than a software extension to include all the pulses is needed. The number n of possible steps is dependent upon the number of mother ions stored originally and the overall efficiency of the MS^n process (fraction of the number of end product ions and the number of original ions) [17]. In FT-ICR the finite ICR cell plate distance limits the cyclotron radius of the ions and thus the maximum number of steps. Supposedly, the practical limit lies at $n = 5$ or $n = 6$ at most [18]. However, already in 1984 MS^5 was demonstrated on organic ions (FT-ICR at 1.4 T magnetic field strength) [19]. With the application of high magnetic fields the experimentalist will run out of ideas rather than of steps to be actually achieved for the MS^n experiment; for example a magnetic field strength of 7 T should allow even MS^{20} [20].
[17] S. A. McLuckey, G. L. Glish, G. J. van Berkel, *Int. J. Mass Spectrom. Ion Processes* **1991**, *106*, 213.
[18] D. Schröder, H. Schwarz, *Angew. Chem.* **1990**, *102*, 925; *Angew. Chem. Int. Ed. Engl.* **1990**, *29*, 910.
[19] J. C. Kleingeld, Dissertation, Amsterdam, **1984**.
[20] B. S. Freiser in *Techniques for the Study of Ion-Molecule Reactions* (Eds.: J. M. Farrar, W. H. Saunders, Jr.), Wiley, New York, **1988**, p. 76–78.

Evidence for [PdSiO] from IR Spectroscopy**

By *Thomas Mehner, Ralf Köppe,* and *Hansgeorg Schnöckel**

Dedicated to Professor Wolfgang Beck on the occasion of his 60th birthday

For a long time simple, coordinatively unsaturated transition-metal carbonyls have been known to exist under matrix conditions. Lately theoretical methods have also been used to study these small molecules such as [PdCO].[1–3] Attempts to generate transition-metal complexes with SiO as ligand in solid argon led to the preparation of [AgSiO].[4] Several theoretical[5,6] and experimental investigations[7] are concerned with the clarification of the bonding relationships in this species. Apparently it is an ion pair Ag^+SiO^-,[9]

[*] Prof. Dr. H. Schnöckel, Dr. T. Mehner, Dipl.-Chem. R. Köppe
Institut für Anorganische Chemie der Universität
Meiserstrasse 1, D-W-8000 Munich 2 (FRG)

[**] This work was supported by the Deutsche Forschungsgemeinschaft and the Fonds der Chemischen Industrie.

as is shown by the formation of SiO^- with Na^+ or K^+.[10] Here we report the first transition-metal complex containing SiO as ligand in solid argon. With respect to bonding it is similar to carbonyl complexes.

When SiO and palladium atoms were condensed together with argon on a helium-cooled copper surface, we observed in the IR spectrum (Fig. 1) besides the absorption of molecular SiO at 1226.0 cm^{-1} a new band at 1246.3 cm^{-1}, which we assigned to the complex [PdSiO] (**1**).[8] Moreover, the complex [PdCO] (**2**) is generated ($\tilde{\nu} = 2050.0\ cm^{-1}$), since CO (2138 cm^{-1}) is always present in these experiments as impurity.

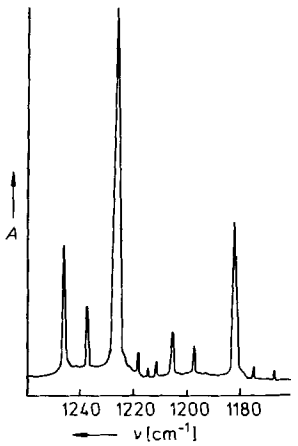

Fig. 1. Section of the IR matrix spectrum after the condensation of Pd atoms with $Si^{16}O/Si^{18}O$.

Annealing the matrix doubles the intensity of the band due to **1** and leads to an additional absorption band at 1237.1 cm^{-1}. Simultaneously [$Pd(CO)_2$] (2044 cm^{-1}) is formed from **2** and CO. Since under these conditions no palladium carbonyl complex with more than one Pd atom is generated, the absorption at 1237 cm^{-1} may be attributed to the complex [(OC)Pd(SiO)] formed from CO and **1**. The formation of [$Pd(SiO)_2$] can be ruled out because the dimerization of SiO is energetically more favorable than the coordination of a second SiO to **1**.[11, 12]

At high CO concentrations (Ar/CO mixtures of 20:1), [(OC)Pd(SiO)] (1237 cm^{-1}) is observed alongside the complexes [$Pd(CO)_n$] ($n = 2-4$) even without annealing. Since no CO absorption is detected,[13] the assignment for the absorption at 1237 cm^{-1} is based initially on theoretical consideration of the bonding in possible products that can form under these conditions but also on the specific experimental conditions under which this absorption is observed.[15]

Qualitative confirmation of the assignment of the SiO band of **1**[16] is provided by the position of the SiO band of the isotopomer [$PdSi^{18}O$] at 1205.8 cm^{-1}. Absorption by the isotopomers with ^{29}Si and ^{30}Si are not observed. They apparently lie beneath the band at 1237.3 cm^{-1} ([(CO)Pd(SiO)]) and 1226.0 cm^{-1} (uncoordinated SiO). The band at 1237.1 cm^{-1} is shifted to 1197.1 cm^{-1} by ^{18}O substitution, which similarly indicates a Si=O vibrational band.

Conclusive confirmation for the assignment of the band at 1246.3 cm^{-1} to [PdSiO] (**1**) is found in normal-coordinate analysis on assumption of a simple valence force field (f(PdSi/SiO) = 0). The measured $^{16}O/^{18}O$ shift of the SiO stretching frequency is satisfactorily reproduced only for a linear silicon-bridged Pd-Si-O molecule[17] on assumption of a Pd–Si frequency of 375 cm^{-1}. The SiO force constant in **1** is calculated to be 8.92 mdyn $Å^{-1}$ (SiO in argon: 9.02) and that of Pd–Si, 2.69 mdyn $Å^{-1}$.

The linear, silicon-bridged structure for **1** (deduced from the spectroscopic data) and the force constants (based on experiment) were confirmed convincingly by ab initio calculations. The relativistic model potential of Sakai et al.,[18] as implemented in the program package CADPAC 4.0[19] that we applied here, was used as basis set for palladium. The quality of this basis[20] was tested by calculations of the excitation energy $4d^{10}(^1S) \rightarrow 4d^9 5s^1(^3D)$ at MP-2 level (exp.: 91.7, calcd: 80.0 kJ mol^{-1}) and by optimization of the geometry of PdH ($^2\Sigma^+$) (exp.: r(PdH) = 153.5, calcd: r(PdH) = 151 pm). The basis sets for Si, C, and O were of TZ2P quality.[21] We performed all calculations at MP2 level taking into account basis-set superposition error.

The results for the structure and for the atomic charges from Mulliken population analyses are summarized in Table 1. The geometry and the force constants correspond to those deduced from the spectra. The Pd–Si bond in **1** is surprisingly strong, since the enthalpy of reaction for Pd + SiO → [PdSiO] is −182 kJ mol^{-1} (basis-set superposition error is taken into account). It is thus of the same order as that for the formation of [PdCO] (−162 kJ mol^{-1}). Furthermore, the frequencies resulting from the calculations (Table 2) confirm the experimental blue shift of the SiO band observed when SiO is coordinated in [PdSiO] ($\Delta\nu_{exp.} = -20.3$, $\Delta\nu_{calcd} = -25.5\ cm^{-1}$).[22]

Table 1. Calculated (MP2) geometries, force constants, and atomic charges (Mulliken) for the linear molecules [PdCO] (**2**) and [PdSiO] (**1**), and the isolated molecules CO and SiO.

	r(Pd-X) [Å]	r(X-O) [Å]	f(PdX) [mdyn $Å^{-1}$] [a]	f(XO) [mdyn $Å^{-1}$] [a]	q(Pd)	q(X)	q(O)
[PdCO]	1.86	1.158	2.85	15.42	0.09	0.19	−0.28
[PdSiO]	2.15	1.528	2.45	8.86	0.0	0.75	−0.75
CO [b]	–	1.134	–	18.38	–	0.09	−0.09
SiO [c]	–	1.529	–	8.69	–	0.51	−0.51

[a] f(PdC/CO) = 0.66 mdyn $Å^{-1}$, f(PdSi/SiO) = 0.007 mdyn $Å^{-1}$. [b] $E_{tot}^{MP2} = -113.143575$ Hartree. [c] $E_{tot}^{MP2} = -364.293021$ Hartree.

Table 2. Measured and calculated (MP2) frequencies for CO, SiO, [PdCO], and [PdSiO] (frequencies in cm^{-1}, intensities in parentheses in km mol^{-1}).

	ν(Pd-X) exp.	ν(Pd-X) calcd	ν(XO) exp.	ν(XO) calcd	δ(PdXO) exp.	δ(PdXO) calcd
SiO			1226.0	1203.4 (9.9)		
[PdSiO]	–	359.0 (6.4)	1246.3	1228.9 (65.6)	–	164.3 (8.9)
CO			2138.0	2133.0 (30.2)		
[PdCO]	–	462.0 (27.2)	2050.0	1969.2 (632.2)	–	343.7 (30.4)

The similar bonding situation in **1** and **2** suggested by these results is underscored by population analyses. The charges on palladium show similar distributions for these Pd complexes (**2**: Pd $4p^{5.97}5s^{0.45}4d^{9.39}p^{0.10}{}_{Pol}$; **1**: $4^{5.97}5s^{0.39}4d^{9.52}p^{0.12}{}_{Pol}$). The theoretical and experimental results presented here show that the bonding relationships in [PdSiO] can be compared with those in [PdCO]; that is, the σ donor bond is strengthened by π acceptor components. The proportion of σ and π bonding, however, differs in **2** and **1**, resulting in a red shift in the frequency of the uncoordinated ligand on coordination in **2**, but a blue shift in **1**.

Received: October 31, 1991 [Z 5000 IE]
German version: *Angew. Chem.* **1992**, *104*, 653

CAS Registry numbers:
SiO, 10097-28-6; Pd, 7440-05-3; [PdSiO], 139495-54-8; [PdCO], 41772-86-5; [(OC)Pd(SiO)], 139523-85-6; CO, 630-08-0.

[1] G. W. Smith, E. A. Carter, *J. Phys. Chem.* **1991**, *95*, 2327, and references cited therein.

[2] C. M. Rohlfing, P. J. Hay, *J. Chem. Phys.* **1985**, *83*, 4641.

[3] P. Schwerdtfeger, J. S. McFeaters, J. J. Moore, D. M. McPherson, R. P. Cooney, G. A. Bowmaker, M. Dolg, D. Andrae, *Langmuir*, **1991**, *7*, 116.

[4] T. Mehner, H. Schnöckel, M. J. Almond, A. J. Downs, *J. Chem. Soc. Chem. Commun.* **1988**, 117.

[5] G. E. Quelch, R. S. Grev, H. F. Schaefer III, *J. Chem. Soc. Chem. Commun.* **1989**, 1498.

[6] J. S. Tse, *J. Chem. Soc. Chem. Commun.* **1990**, 1179.

[7] B. Chenier, H. A. Joly, J. A. Howard, B. Mile, P. L. Timms, *J. Chem. Soc. Chem. Commun.* **1990**, 581.

[8] SiO was synthesized by passing O_2 over hot silicon (1200 °C); Pd atoms were generated by vaporization of the metal at 1450 °C. The cryostat and vaporization conditions have been described previously: R. Ahlrichs, R. Becherer, M. Binnewies, H. Borrmann, M. Lakenbrink, S. Schunck, H. Schnöckel, *J. Am. Chem. Soc.* **1986**, *108*, 7905. The IR spectra were recorded on an IFS-113 v and an IFS-66 v FT-IR spectrometer in absorption with the help of a reflection unit.

[9] R. Köppe, H. Schnöckel, C. Jouany, F. X. Gadea, J. C. Barthelat, *Heteroat. Chem.*, in press.

[10] R. Köppe, H. Schnöckel, *Heteroat. Chem.*, in press.

[11] H. Schnöckel, T. Mehner, H. S. Plitt, S. Schunck, *J. Am. Chem. Soc.* **1989**, *111*, 4578.

[12] From an ab initio calculation for linear [(OC)Pd(SiO)] (E_{tot}^{MP2} = −573.873915 Hartree; r(CO) = 1.135, r(PdC) = 2.02, r(PdSi) = 2.25, r(SiO) = 1.525 Å) erhält man folgende Reaktionsenergien.
[PdCO] + SiO → [(OC)Pd(SiO)] $\Delta E = -107.4$ kJ mol^{-1}
[PdSiO] + CO → [(OC)Pd(SiO)] $\Delta E = -87.4$ kJ mol^{-1}
Pd + CO + SiO → [(OC)Pd(SiO)] $\Delta E = -296.4$ kJ mol^{-1}

[13] The corresponding bands in the carbonyl region are possibly hidden by the CO bands of the various carbonylpalladium complexes.

[14] E. P. Kündig, M. Moskovits, G. A. Ozin, *Can. J. Chem.* **1972**, *50*, 3587.

[15] The lowering of the frequency on changing from [PdSiO] to [Pd(SiO)(CO)] is reasonable, because the Pd–Si bond is weakened as a result of a smaller backbonding component. The Si–O bond and its stretching frequency should thus be more similar to the their counterparts in uncoordinated SiO (1226 cm^{-1}). This is also supported by ab initio calculations [12]: both the Pd–C distance in **2** and the Pd–Si distance in **1** are shorter than in [Pd(SiO)(CO)]. The bonding relationships in **2** and [Pd(CO)$_2$] yield additional evidence for the correctness of these arguments: The CO force constant f(CO) is a bonding parameter free from coupling influences. Its value in **2** of 16.97 mdyn Å^{-1} is smaller than that in [Pd(CO)$_2$] (17.16 mdyn Å^{-1} [14]). Thus the CO bond of free CO (f(CO) = 18.36 mdyn Å^{-1} in an argon matrix) more closely resembles that of [Pd(CO)$_2$] than that of **2**. Consequently both the CO bond in **2** and the SiO bond in **1** become more like the bond in uncoordinated CO or SiO on addition of a CO ligand at Pd.

[16] $\tilde{\nu}$(Si^{16}O) = 1226.0; $\tilde{\nu}$(Si^{18}O) = 1182.2 cm^{-1} in an argon matrix.

[17] In an oxygen-bridged complex, the silicon isotope shifts (Pd–O–^{29}Si and Pd–O–^{30}Si) would be much smaller and would therefore be able to be observed as they would not overlap with strong absorptions of other compounds such as [(SiO)Pd(CO)] or SiO. Calculation of the frequencies for [Pd^{29}SiO] and [Pd^{30}SiO] confirm that these bands are hidden by overlap.

[18] Y. Sakai, E. Miyoshi, M. Klobukowski, S. Huzinaga, *J. Comput. Chem.* **1987**, *8*, 226.

[19] R. D. Amos, J. E. Rice, CADPAC: The Cambridge Analytic Derivatives Package, issue 4.0, Cambridge, **1987**.

[20] The 5s and 4d as well as the 4p electrons are treated explicitly in triple-zeta contraction to include any possible contribution of these electrons to the bond formation. As suggested by Sakai and Huzinaga et al. [18], we added two p-like polarization functions (Pd (MP) (5p8s5d2p)/[3p3s3d2p].

[21] S. Huzinaga, *Approximate Atomic Functions. Technical Report 1971*; University of Alberta, Canada, **1971**.

[22] The structural data and bond energies we calculated for [PdCO] agree well with earlier MP2 calculations [2] (where r(Pd–C) = 1.882, r(C–O) = 1.185 Å, ∢(PdCO) = 180°, Pd–C bond energy = −156 kJ mol^{-1}). In a new detailed theoretical work [3], many computational methods and better basis sets than in our calculations were used to investigate the bonding relationships in **2**. Among the computational methods incorporating electron correlation (MP2, MP3, CISD, CISC), the MP2 calculation yielded the largest bond energy (−109 kJ mol^{-1}); that is, also in our MP2 calculations the strength of the Pd–Si bond is a little overestimated: the Pd–Si distance is too small and the bond energy (Pd + SiO → [PdSiO]) too large. This is in accord with the difference in the frequency shift calculated by us (ν_{CO}(CO)-ν_{CO}(PdCO)) of 164 or 122 cm^{-1} [3] and the experimental value of 88 cm^{-1}.

The Structure of C_{60}: Orientational Disorder in the Low-Temperature Modification of C_{60} **

By *Hans-Beat Bürgi, Eric Blanc, Dieter Schwarzenbach,* Shengzhong Liu, Ying-jie Lu, Manfred M. Kappes,* and *James A. Ibers*

The availability of gram quantities of fullerenes[1] and the discovery of superconductivity in C_{60} doped with an alkali metal[2] have led to a broad spectrum of investigations dealing with diverse chemical and physical properties of solid C_{60}. Models of the structure of C_{60} are the starting point for much of this work. In particular for investigations of the solid-state properties, reliable information on the crystal and molecular structure of C_{60} is indispensable.

On the assumption of icosahedral symmetry, the molecules of C_{60} are approximately spherical. They crystallize in a cubic close-packed arrangement.[3] Above 249 K, the molecules are orientationally disordered in the crystal (the probable space group is $Fm\bar{3}m$). X-ray data of C_{60} measured at 110 K on a merohedrally twinned crystal were interpreted in terms of an ordered model in the space group $Pa\bar{3}$ with molecular site symmetry $\bar{3}$.[3] However, the lengths of bonds which are chemically equivalent and related by the icosahedral symmetry $m\bar{3}\bar{5}$ of the molecule differ considerably in this model; the distances also show deviations of up to 0.1 Å from those determined in an electron-diffraction study on gaseous C_{60}.[4] It was noted[3] that the agreement between the observed and calculated structure amplitudes is not nearly as good as would be expected from the internal agreement among symmetry-equivalent reflections, and it was suggested that there may be deficiencies in the model concerning thermal motion or twinning. Analysis[5] of the atomic displacement tensors $\boldsymbol{U}$ from ref.[3] and subsequent inspection of the residual displacements with the graphics program PEANUT[6] showed them to be incompatible with the expected motion of rigid molecules and also suggested the presence of disorder in the structure. In an independent study of C_{60} based on neutron-diffraction measurements on a powder at 5 K[7] and a Rietveld refinement with bond angles restrained to idealized values, the same packing as in ref.[3] was found with bond lengths in good agreement with those obtained from electron-diffraction studies of gaseous C_{60} and with no indication of disorder. The agreement of observed and calculated diffraction profiles was satisfactory. Displacement parameters were not reported in ref.[7]

We have now carried out additional analyses of the single-crystal X-ray diffraction data of ref.[3] collected at 110 K ($Cu_{K\alpha}$) and also of data collected in a similar manner from a second twinned crystal at 153 K ($Cu_{K\alpha}$) and from a third twinned crystal at 200 K and 100 K ($Mo_{K\alpha}$). These analyses show that at these temperatures the molecules are statistically distributed in two orientations: one with a large population (major orientation) as has been found in the earlier

[*] Prof. D. Schwarzenbach, E. Blanc
Institute of Crystallography, University of Lausanne
BSP, CH-1015 Lausanne (Switzerland)
Prof. H.-B. Bürgi
Laboratory of Crystallography, University of Bern
S. Liu, Y.-J. Lu, Prof. M. M. Kappes, Prof. J. A. Ibers.
Department of Chemistry, Northwestern University

[**] This research was supported by the Swiss National Science Foundation, grants 31-194.91 (H.-B.B.) and 20-28 930.90 (D.S.), the U.S. National Science Foundation, grant CHE-892 2754 (J.A.I.), the Northwestern University Materials Research Center, NSF grant DMR-8821571 (M.M.K.), and the Science and Technology Center for Superconductivity, NSF grant DMR-8809854 (J.A.I.). Note added in proof (April 28, 1992): After this paper was submitted, the results of a high-resolution neutron-diffraction experiment on C_{60} powder were published [13].

analyses,[3, 7] and one with small population (minor orientation) related to the major one by an approximate 180° rotation of the molecule about its crystallographic threefold axis. From the population parameter, free-energy differences between the two orientations are estimated. An approximate value of the energy barrier to reorientation is obtained from the molecular libration amplitudes.

Initial coordinates of the ten crystallographically independent atoms defining the molecule in the major orientation were taken from ref.[3] Those of the molecule in the minor orientation were generated from the coordinates of ref.[3] by a rotation of 180° about the $\bar{3}$([111]) axis. The resulting model was then easily refined by the least-squares method with the use of various distance and displacement parameter restraints. For fixing the shape of a molecule 45 distances between nearest and next-nearest neighbors (up to 2.5 Å) were restrained. The orientation of a shape-restrained molecule is defined by a single positional parameter describing the rotation about the $\bar{3}$ axis. Effective rigid-body motion of a molecule was achieved with 82 rigid-link restraints on the displacement parameters.[8] This motion is described by four parameters, namely two mean-square libration amplitudes and two mean-square translation amplitudes parallel and perpendicular to the $\bar{3}$ axis. All restraints had weights of 10^8. The numbers of reflections used in the refinements with intensities larger than three standard deviations were 1296, 783, 740, and 855 at 100 K, 110 K, 153 K, and 200 K, respectively. The corresponding lattice constants are 14.050(6), 14.052(5), 14.061(5), and 14.067(6) Å. The following models were refined:

A: Minimal model: The shape of the molecule was restrained to icosahedral symmetry, and the thermal displacements to rigid-body motion. The ratio of the two nonequivalent bond lengths $d_{6,6}/d_{5,6}$ was fixed at the value 1.401/1.458 obtained by electron diffraction of C_{60} molecules in the gas phase.[4] If the restraints were given very large weights, this model would be characterized effectively by 14 independent variable parameters: the scale factor, the twinning parameter as described by ref.[3], the population factor of the major orientation, the diameter of the molecule, and one positional and four displacement parameters for each of the two orientations.

B: Intermediate model: Thermal displacements were restrained to rigid-body motion, but positional parameters of all ten atoms in both orientations were refined without restraints (except at 200 K where two distances were fixed). This model is described by 71 effective variable parameters.

C: Maximal model: The molecule with the major orientation was refined without any restraints; displacements of the minor molecule were restrained to rigid-body motion. This model is described by 127 effective variable parameters.

The resulting R values, population parameters, bond lengths, and rigid-body mean-square displacements are reported in Table 1; results of the type C refinements at 153 K and the type B refinements at 200 K are found in ref.[9] Results obtained with the data measured at 100 K are similar to those at 110 K but with larger standard deviations. Therefore, only the population parameter $P(100\text{ K}) = 0.780(5)$ is, reported here (type A refinement, $R(F^2) = 0.096$, $S = 1.105$). The twinning parameter was in all cases equal to 0.5, that is, within the estimated standard deviation, indicating equal volume fractions of the twin domains. A completely unrestrained refinement of the data at 110 K with 183 variables converged to a goodness of fit only insignificantly lower than that obtained with the maximal model; some displacement tensors of the minor orientation were negative. We believe that the data do not contain sufficient information to enable all these parameters to be determined reliably.

The refinement of the diffraction data of the twinned crystals leads to two main conclusions: 1) A model with idealized but disordered molecules of C_{60} explains the experimental data much better than a model with ordered C_{60} molecules ($R(F^2) = 0.08$ vs. 0.14 in ref.[3]). 2) Not much additional information on the geometry and the thermal motion of C_{60} may be gained from models with fewer restraints; improvement of the reliability factors is marginal even though the number of variable parameters increases dramatically (Table 1).

Table 1. Results of the refinements of types A–C. P is the population parameter of the major orientation M; that of the minor orientation m is given by $1-P$. $d_{6,6}$ is the average length of a C=C bond in Å shared by two C_6 rings; $d_{5,6}$ is the average length of a C–C bond shared by C_6 and C_5 rings; values for the minor orientation agree well with those for the major orientation. L_1 and L_2 are the mean-square libration amplitudes in $(°)^2$ parallel and perpendicular to the $\bar{3}$ axis. Estimated standard deviations referring to the last figure are given in parentheses; for the averaged distances, they are derived from the deviance of the sample. S is the goodness of fit with an expectation value of 1 for a perfect model.

	110 K			153 K		200 K
	A	B	C	A	B	A
P	0.764(3)	0.769(4)	0.786(5)	0.696(3)	0.698(4)	0.660(6)
$d_{6,6}M$	1.3909	1.387(3)	1.399(7)	1.3894	1.385(3)	1.3894
$d_{5,6}M$	1.4475	1.450(3)	1.445(5)	1.4459	1.450(2)	1.4459
L_1M	4.9(1)	4.9(1)	5.8(4)	6.8(1)	6.8(1)	8.3(4)
L_2M	4.5(1)	4.5(1)	4.0(4)	6.1(1)	5.9(1)	7.9(4)
L_1m	6.7(3)	6.1(4)	3.6(5)	8.6(3)	8.5(3)	13.1(7)
L_2m	5.1(3)	5.2(4)	3.5(5)	6.6(3)	7.0(3)	8.0(7)
S	1.152	1.110	1.074	1.111	1.090	1.140
$R(F^2)$	0.081	0.077	0.069	0.083	0.079	0.092
$R(F)$	0.037	0.034	0.031	0.039	0.037	0.071

The general packing pattern of C_{60} is as described in ref.[3, 7]. Each molecule has twelve neighbors in a cuboctahedral environment, i.e. six in the equatorial plane in Figure 1 perpendicular to the crystallographic $\bar{3}$ axis, and three above and three below this plane. However, in the disordered struc-

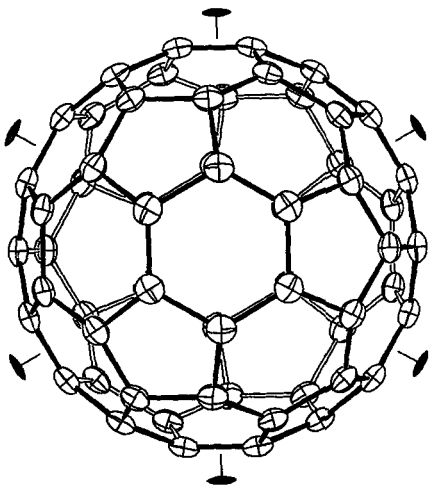

Fig. 1. View down the $\bar{3}$ axis of the molecule, type B refinement at 110 K, major orientation, ellipsoids with 50% probability of occupation. The upper half of the molecule is identified with "filled", the lower half with "empty" bonds. The empty bonds can also be interpreted to represent the upper half of a C_{60} molecule in the minor orientation. On the assumption of icosahedral molecular symmetry, there are non-crystallographic twofold axes perpendicular to the $\bar{3}$ axis and passing through the centers of short C=C bonds (C6–C9 of Fig. 2).

ture there are now in principle four different types of intermolecular contacts (Fig. 2a–d) instead of just one as in the ordered structure (Fig. 2a). Because of its icosahedral symmetry, a C_{60} molecule always presents six C=C bonds to its six neighbors in the equatorial plane, irrespective of its orientation. If the neighbor is in the major orientation, the C=C

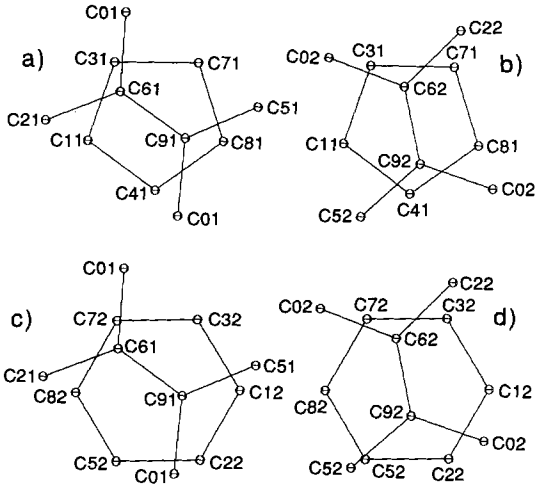

Fig. 2. Intermolecular contacts of C_{60} in the solid state. The molecular orientations are: a) C=C(major)–C_5(major), b) C=C(minor)–C_5(major), c) C=C(major)–C_6(minor), d) C=C(minor)–C_6(minor). The second number of the atom identifier is 1 for the major and 2 for the minor orientation.

bond is presented to a C_5 ring, if it is in the minor orientation to a C_6 ring. In the same way, each of the six neighbors out of the equatorial plane presents one C=C bond to the central molecule irrespective of their orientations. These C=C bonds are seen by C_5 or C_6 rings of the central molecule depending on whether it is in the major or minor orientation. The number and lengths of the shortest intermolecular distances are very similar for all four contacts (Table 2, Fig. 2), especially for contacts a and b. In summary, the surroundings of a molecule and presumably its packing energy are not very dependent on the orientation of its neighbors. All molecules have nearly the same effective potential energy with two not very different minima.

Table 2. Shortest intermolecular contacts. Type B refinement at 110 K (see Fig. 2).

C61-C31	3.140(9)	C62-C31	3.178(12)
C61-C11	3.280(5)	C62-C71	3.245(10)
C91-C81	3.275(3)	C92-C41	3.282(8)
C91-C41	3.387(3)	C92-C81	3.385(8)
C61-C72	3.128(29)	C62-C72	3.159(30)
C61-C82	3.360(13)	C62-C32	3.278(25)
C91-C32	3.464(25)	C92-C52	3.575(11)
C91-C12	3.507(8)	C92-C22	3.592(10)

On the assumption that the disordered structure is in thermodynamic equilibrium, the free-energy difference of the two molecular orientations can be derived from the population factors, $\Delta G = RT \ln (P^{-1}-1)$. Refinement with the minimal model (type A) gives 1.05(3), 1.07(2), 1.05(2), and 1.10(5) kJ mol^{-1} at 100 K, 110 K, 153 K, and 200 K, respectively. The corresponding enthalpy and entropy differences, $\Delta H = 1.06(5)$ kJ mol^{-1} and $\Delta S = 0.0(4)$ J mol^{-1}K^{-1}, reproduce the four experimental populations within one estimated standard deviation. Extrapolation to 5 K yields a population of the minor orientation of about 10^{-12}, in agreement with the interpretation of the neutron-diffraction data[7] in terms of an ordered structure.[10] Energies calculated from refinements of type C differ by only about 10%. The small energy difference between alternative molecular orientations gives quantitative meaning to the small differences in packing distances described above. Analogous determinations of thermodynamic quantities have been described for conformational interconversions and intramolecular proton transfer.[11]

There are two probable mechanisms for the rotation of the molecule from the major to the minor orientation. One of them is a rotation by $\pm 60°$ (or, less likely, by 180°) about the crystallographic $\bar{3}$ axis; the observed angles derived from the type A refinement at 110 K are $182° \pm 120°$. The other mechanism is a rotation by 41.8° (assuming ideal $m\bar{3}\bar{5}$ symmetry) about one of the three molecular twofold axes perpendicular to the $\bar{3}$ axis shown in Figure 1. This rotation replaces the C_6 ring perpendicular to the $\bar{3}$ axis by one of its three neighboring C_6 rings. The energy barrier to rotation can be estimated from the average mean-square libration amplitudes assuming a sinusoidal approximation to the reorientation potential.[12] For the 60° rotation of C_{60} about the $\bar{3}$ axis, the barrier obtained from L_1 of Table 1, assuming the sixfold term to be dominant, is about 34 kJ mol^{-1} (results from L_1 of major site, type A refinements are 34.3, 33.9, and 36.4 kJ mol^{-1} for 110, 153, and 200 K, respectively). The activation barrier for the 41.8° rotation is likely to be of about the same height, since the mean-square libration amplitude L_2 perpendicular to the $\bar{3}$ axis differs by only about 10% from L_1.

Finally, the C=C and C–C distances between mean carbon positions in the crystal are about 0.01 Å shorter than the mean distances of 1.401(10) and 1.458(6) Å obtained by electron diffraction measurements of gaseous C_{60}.[4] The differences of 0.002 Å between the results of type A refinements can be accounted for by a librational bond-length correction. Results of the type B and type C refinements without shape restraints are consistent with those of the type A refinement. It has been suggested[7] that the distances in C_5 rings involved in short intermolecular contacts are longer than those in C_5 rings not involved in such contacts. Our type B refinements show that for the major orientation the difference is only 0.001 and 0.003 Å at 110 K and 153 K, respectively. This difference is negligible.

Received: February 7, 1992 [Z 5177 IE]
German version: *Angew. Chem.* **1992**, *104*, 667

CAS Registry number:
C_{60}, 99685-96-8.

[1] W. Krätschmer, L. D. Lamb, K. Fostiropoulos, D. R. Huffmann, *Nature* **1990**, *347*, 354–358.
[2] A. F. Hebbard, M. J. Rosseinsky, R. C. Haddon, D. W. Murphy, S. H. Glarum, T. T. M. Palstra, A. P. Ramirez, A. R. Kortan, *Nature* **1991**, *350*, 600–601.
[3] S. Liu, Y.-J. Lu, M. M. Kappes, J. A. Ibers, *Science* **1991**, *254*, 408–410 and references therein.
[4] K. Hedberg, L. Hedberg, D. S. Bethune, C. A. Brown, H. C. Dorn, R. D. Johnson, M. de Vries, *Science* **1991**, *254*, 410–412.
[5] V. Schomaker, K. N. Trueblood, *Acta Crystallogr. Sect. B* **1968**, *24*, 63–76.
[6] a) W. Hummel, J. Hauser, H.-B. Bürgi, *J. Mol. Graphics* **1990**, *8*, 214–220; b) W. Hummel, A. Raselli, H.-B. Bürgi, *Acta Crystallogr. Sect. B* **1990**, *46*, 683–692.
[7] W. I. F. David, R. M. Ibberson, J. C. Matthewman, K. Prassides, T. J. S. Dennis, J. P. Hare, H. W. Kroto, R. Taylor, D. R. M. Walton, *Nature* **1991**, *353*, 147–149.
[8] a) J.-J. Didisheim, D. Schwarzenbach, *Acta Crystallogr. Sect. A* **1987**, *43*, 226–232; b) F. L. Hirshfeld, *ibid.* **1976**, *32*, 239–244.

[9] Further details of the crystal structure determination may be obtained from the Fachinformationszentrum Karlsruhe Gesellschaft für wissenschaftliche Information mbH, D-W-7514 Eggenstein-Leopoldshafen 2 (FRG) by quoting the identification number CSD-56171, the authors, and the literature reference.
[10] It is highly unlikely that the populations obtained at four different temperatures with three different crystals agree with the equation for ΔG by accident. The systematic temperature-dependence of P is strong evidence for thermodynamic equilibrium. The time necessary to start measurement after the desired temperature of the crystal has been established is tens of minutes and is certainly sufficient for equilibration.
[11] a) G. A. Sim, *J. Chem. Soc. Chem. Commun.* **1987**, 1118–1120; b) C. J. Simmons, B. J. Hathaway, K. Amornjarusiri, B. D. Santarsiero, A. Clearfield, *J. Am. Chem. Soc.* **1987**, *109*, 1947–1958; c) G. A. Sim, *Acta Crystallogr. Sect. B* **1990**, *46*, 676–687; d) R. Destro, *Chem. Phys. Lett.* **1991**, *181*, 232–233.
[12] E. M. Maverick, J. D. Dunitz, *Mol. Phys.* **1987**, *62*, 451–459.
[13] W. I. F. David, R. M. Ibberson, T. J. S. Dennis, J. P. Hare, K. Prassides, *Europhys. Lett.* **1992**, *18*, 219–225. For the temperature range 90–260 K the same model as ours was suggested. From the population parameters of David et al. we calculate $\Delta H = 1.35(1)$ kJ mol^{-1} and $\Delta S = 1.6(4)$ J mol^{-1} K^{-1}; these values agree essentially with our results. David et al. do not provide intra- and intermolecular distances or libration amplitudes.

Selenonium Hexafluoroantimonate, $H_3Se^+SbF_6^-$**

By *Rolf Minkwitz,* Andreas Kornath,* and *Wolfgang Sawodny*

Dedicated to Professor Alois Haas on the occasion of his 60th birthday

Despite the central significance of the oxonium ion in classic acid–base theory, established and stable H_3O^+ salts were first prepared by K. O. Christe [1] in 1975 by the protonation of water in the super-acidic systems HF/SbF_5 and HF/AsF_5. The considerably less basic hydrogen sulfide is protonated in the same systems, however, the sulfonium salts formed are noticeably more thermolabile than the oxonium salts. $H_3S^+SbF_6^-$ [2] is stable for a short time at room temperature whereas $H_3S^+AsF_6^-$ [3] decomposes at 263 K. The homologous hydrogen selenide is a medium-strong acid [4] even in water, and its basicity is so low that the formation of selenonium ions only occurs under extreme conditions.

The selenonium salt **1** is formed almost quantitatively in HF/SbF_5 at 195 K [Eq. (a)]. However, from the less acidic HF/AsF_5 no salt can be isolated. A telluronium salt cannot be isolated even from HF/SbF_5. H_2Te decomposes spontaneously into the elements at 190 K.

$$H_2Se + HF + SbF_5 \longrightarrow \underset{\mathbf{1}}{H_3Se^+SbF_6^-} \qquad (a)$$

Compound **1** is a colorless solid which is stable (exclusion of air) for ca. one week at 195 K. However, at 213 K, **1** decomposes within minutes with the reformation of its starting materials, and then H_2Se undergoes further decomposition into the elements. Subsequently, the ions H_2Se^+, HSe^+, Se^+, and HF^+ are recorded in the mass spectrum (EI, 70 keV) of **1**.

[*] Prof. Dr. R. Minkwitz, Dipl.-Chem. A Kornath
Fachbereich Chemie der Universität
Postfach 50 05 00, D-W-4600 Dortmund 50 (FRG)
Prof. Dr. W. Sawodny
Fachbereich Chemie der Universität
Postfach 4066, D-W-7900 Ulm (FRG)

[**] This work was supported by the Minister für Wissenschaft und Forschung of Nordrhein-Westfalen and the Bundesminister für Forschung und Technologie.

From an ab initio calculation [5] C_{3v} symmetry can be assumed for the discrete H_3Se^+ ion (d(SeH) = 146.5 pm, $\sphericalangle$(HSeH) = 95.65°), for which four IR- and Raman-active vibrations ($\Gamma_{vib} = 2A_1 + 2E$) are expected. Their experimentally determined positions and intensities (Fig. 1) can be compared with the vibrational frequencies of the isoelectronic AsH_3 [6] given in Table 1. Therefore, an unequivocal assignment is possible.

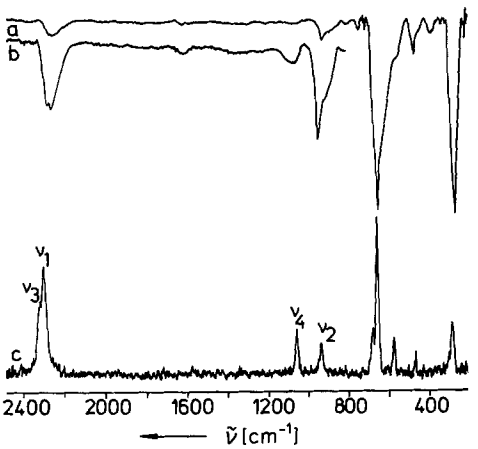

Fig. 1. a) IR spectrum of solid $H_3Se^+SbF_6^-$ (without trituration) between CsBr plates in a low-temperature cell at 163 K. b) Region of the cationic vibrations intensified. c) Raman spectrum of solid $H_3Se^+SbF_6^-$ at 78 K with the cationic vibrations marked.

Table 1. Vibrational frequencies [cm^{-1}] of $X_3Se^+SbF_6^-$ and AsX_3 (X = H, D).

$H_3Se^+SbF_6^-$		$D_3Se^+SbF_6^-$		AsH_3	AsD_3	Assignment
Raman	IR	Raman	IR	IR	IR	[a]
2320 (43)	2312 m	1677 (31)	1647 s	2185	1534	$\nu_3(a_1)\nu_{as}EX_3$
2302 (100)	2280 m	1662 (71)	[b]	2122	[b]	$\nu_1(a_1)\nu_sEX_3$
1057 (34)	1064 vw	756 (12)	753 w	1005	714	$\nu_4(e)\delta_{as}EX_3$
936 (23)	931 m	702 (9)	714 sh	906	660	$\nu_2(e)\delta_sEX_3$
680 (32)		676 (29)				
657 (78)	657 s	658 (100)	655 s			νSbF_6^-
578 (21)		576 (28)				
472 (11)	477 m	470 (19)	479 m			
	395 m					
289 (32)		294 (46)				δSbF_6^-
	275 s		277 s			

[a] E = As, Se. [b] ν_1 and ν_3 are not resolved.

A calculated force field [7] gives a valence force constant f_r of 3.107 N cm^{-1} and a deformation force constant f_α of 0.334 N cm^{-1}. Thus, the valence force constant is slightly below the value obtained from the anharmonic approximation of H_2Se (f_r = 3.12 N cm^{-1}); [8] for the transition to the cationic H_3Se^+, an increase in the valence force constant is expected. The observed decrease is probably a result of hydrogen bonds in the solid and is in agreement with a lowering of the symmetry in the anion, for which more vibrations than expected were measured (Table 1). The same effect is observed for H_3O^+ salts. [1]

Experimental Procedure

H_2Se and D_2Se were prepared and purified from Al_2Se_3 and H_2O, and D_2O, respectively, according to the literature [9]. SbF_5 was fractionally distilled and HF and DF were dried with fluorine.
In a 30 mL KEL-F reactor dried with fluorine (!), SbF_5 (1 mmol) was dissolved in HF or DF (2 g). The solution was frozen at 77 K and layered with HF or DF

(0.5 g). H_2Se or D_2Se (1 mmol), respectively, were condensed into the reaction mixture and it was slowly warmed to 195 K. The selenonium salt 1 precipitated as a colorless solid on thawing. Excess HF or DF was removed under a dynamic vacuum at 195 K.

Received: December 4, 1991 [Z 5053 IE]
German version: *Angew. Chem.* **1992**, *104*, 648

[1] K. O. Christe, C. J. Schack, R. D. Wilson, *Inorg. Chem.* **1975**, *14*, 2224; K. O. Christie, P. Charpin, E. Sovlie, R. Bougon, J. Fawcett, D. R. Russell, *ibid.* **1984**, *23*, 3756.
[2] K. O. Christe, *Inorg. Chem.* **1975**, *14*, 2230.
[3] R. Minkwitz, V. Gerhard, *Z. Naturforsch. B* **1989**, *44*, 364.
[4] A. Dean, *Lange's Handbook of Chemistry* (Ed.: N. A. Lange), McGraw-Hill, New York, USA, **1985**, Chapter 5, p. 15.
[5] D. A. Dixon, D. S. Marynick, *J. Am. Chem. Soc.* **1977**, *99*, 6101.
[6] E. Lee, C. K. Wu, *Trans. Faraday Soc.* **1939**, *35*, 1366.
[7] General Valence Force-Field (GVFF) force constants [Ncm^{-1}] A_1: $F_{11} = 3.089$, $F_{12} = -0.221$, $F_{22} = 0.295$ E: $F_{33} = 3.116$, $F_{34} = 0.263$, $F_{44} = 0.354$: $f_r = 3.107$, $f_a = 0.334$. Vibration frequencies calculated from the force field and measured ( ) frequencies [cm^{-1}]: H_3Se^+: 2331 (2320, 2312 (2302), 1060 (1057), 951 (936); D_3Se^+: 1662 (1677), 1648 (1662), 751 (756), 679 (702).
[8] D. M. Cameron, W. C. Sears, H. H. Nielsen, *J. Phys. Chem.* **1939**, *7*, 994.
[9] G. R. Waitkins, R. Shutt, *Inorg. Synth.* **1946**, *2*, 183.

Preparative-Scale Separation of C_{60} and C_{70} on Polystyrene Gel**

By *Andreas Gügel, Michael Becker, Dirk Hammel, Lutz Mindach, Joachim Räder, Thomas Simon, Manfred Wagner,* and *Klaus Müllen**

An efficient method for the separation of fullerenes is currently of great importance, because of the world-wide research activities centered around this class of compounds[1]. A mixture of C_{60}/C_{70} was hitherto separated on a milligram scale only, which is due to the very low solubility of the material in common chromatographic solvents[2]. A simple, reproducible, inexpensive, and automatic separation procedure is presently not available. Size exclusion chromatography, which has a number of advantages over the conventional liquid chromatographic methods, displays all of the prerequisites required to solve these problems.[3]

The carbon-cluster mixture employed consisted of about 80% C_{60}, 18% C_{70}, and 2% higher molecular weight fullerenes. The separation was carried out on two different columns (PL-Gel 20 × 600 mm, 10 μm, 500 Å, and Shodex 20 × 600 mm, 5 μm, 50 Å). The elugrams with chloroform and toluene were nearly identical on both columns (Fig. 1): C_{60} elutes before C_{70}, and both have a retention time greater than the total permeation limit.

Thus, adsorption or "matrix" effects involving a form of partition or adsorption phenomena are superimposed on size exclusion, resulting in excessive retention and peak-tailing. Another compound exhibiting this unusual behavior is elemental sulfur, which is also retained beyond the total permeation limit. Because the C_{60}/C_{70} mixture is more soluble in toluene, which improves efficiency, this solvent was used as eluent in all further preparative separations (the solubility is about 6 mg mL^{-1} in toluene).

[*] Prof. Dr. K. Müllen, Dipl.-Chem. A. Gügel, Dipl.-Chem. M. Becker, Dipl.-Chem. D. Hammel, L. Mindach, Dr. J. Räder, Dipl.-Chem. T. Simon, Dipl.-Chem. M. Wagner
Max-Planck-Institut für Polymerforschung
Ackermannweg 10, D-W-6500 Mainz (FRG)

[**] Note added in proof (April 27, 1992): A communication appeared in the March 13th issue of *J. Org. Chem.* in which similar results were reported: M. S. Meier, J. P. Selegue, *J. Org. Chem.* **1992**, *57*, 1924–1926.

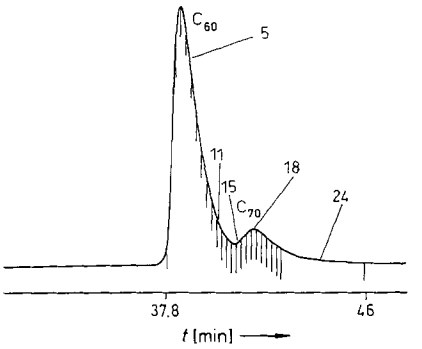

Fig. 1. Separation of C_{60} and C_{70} with cut coints for fractions 5, 11, 15, and 18; column: 20 × 600 mm; stationary phase: PL-gel, 10 μm, 500 Å; mobile phase: 7 mL min^{-1} toluene; detector: UV at 329 nm.

The best fraction cut points for separation were found by investigating certain subfractions (Fig. 1) with field desorption (FD) mass spectrometry[4]. The mass spectra shown (Fig. 2) provide further evidence for the high purity of the products separated. The ^{13}C NMR spectrum of combined fractions 1–11 does not contain a peak arising from C_{70}[4].

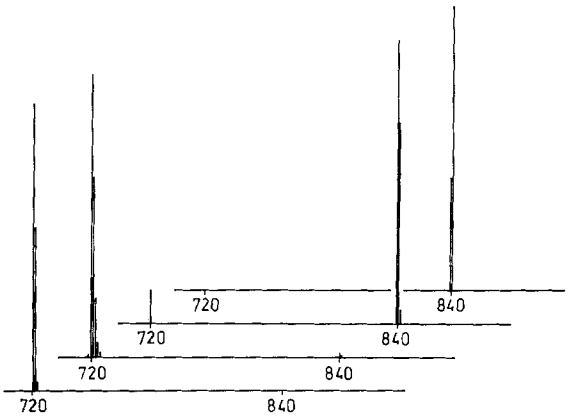

Fig. 2. FD mass spectra of subfractions 5, 11, 15, and 18 (from bottom to top).

With a flowrate of 7 mL toluene per min and repetitive, periodic injections of 6 mL portions of a C_{60}/C_{70} solution, the separation of about 5 g of a C_{60}/C_{70} mixture within 24 h becomes possible. In addition, the eluent can be recovered completely[5].

Moreover, unlike other chromatographic methods like chromatography at higher temperatures,[2a] an extension of the described procedure to larger scale separations is possible simply by increasing the inner diameter of the column.

Experimental Procedure

Apparatus[5]: Elution pump: Master pump M 305 with a 25 SC pump head; injection pump: M 303 with a 25 SC pump head, detector: UV detector M 115 with 0.3 μL flow-through type cell (light path: 0.1 mm); fraction collector 201 C; column: 20 × 600 mm filled with PL-gel (10 μm 500 Å).

Procedure: At 10 min intervals 6 mL of the fullerene solution is injected into the elution stream through a T-connection joining elution and injection pump, and the column. Thus more than one substance zone is present on the column simultaneously and material can be collected continuously. The recovery rate is greater than 90%.

Received: February 14, 1992 [Z 5189 IE]
German version: *Angew. Chem.* **1992**, *104*, 666

[1] See for example: H. W. Kroto, A. W. Allaf, S. P. Balm, *Chem. Rev.* **1991**, *91*, 1213–1235; C. Keller, *GIT Fachz. Lab.* **1991**, *35*, 1098–1108; F. Diederich, R. L. Whetten, *Angew. Chem.* **1991**, *103*, 695–697; *Angew. Chem. Int. Ed. Engl.* **1991**, *30*, 678–680; H. D. Beckhaus, C. Rüchardt, M. Kao. F. Diederich, C. S. Foote, *Angew. Chem.* **1992**, *104*, 69–70; *Angew. Chem. Int. Ed. Engl.* **1992**, *31*, 63–64; W. Krätschmer, L. D. Lamb, K. Fostiropoulos, D. F. Huffmann, *Nature* (London) **1990**, *347*, 354.

[2] See for example: a) W. H. Pirkle, C. J. Welch, *J. Org. Chem.* **1991**, *56*(25), 6973–6974; b) R. Taylor, J. P. Hare, A. K. Abdul-Sada, H. W. Kroto. *J. Chem. Soc. Chem. Commun.* **1990**, *20*, 1423–1425.

[3] B. J. Hunt, S. R. Holding, *Size Exclusion Chromatography*, Chapman and Hall, New York, **1989**; W. W. Yau, J. J. Kirkland, D. D. Bily, *Modern Size-Exclusion Liquid Chromatography*, John Wiley & Sons, New York, **1979**.

[4] The FD mass spectra were recorded on a ZAB 2 – SE – FPD (VG-Instruments). Subfraction 24 contains the higher fullerenes C_{76}, C_{78}, C_{82}, C_{84}. The ^{13}C NMR spectrum [(125 MHz; $C_2D_2Cl_4$, 40 °C): $\delta = 143.13$ (10000 scans)] was recorded on a Bruker AMX-500 spectrometer.

[5] Pumps, detector, and fraction collector from Gilson (Abimed Analysen-Technik GmbH, Langenfeld); columns from the firm Polymer Standards Service, Mainz. It was shown that the peak separation and therefore the amount of material separable per time unit can be distinctly improved by operating two columns in sequence: A. Gügel, K. Müller, unpublished.

Palladium(0)-Catalyzed Three-Component Coupling Reaction of Allyl Benzoates, Carbon Monoxide, and Zincioesters**

By *Yoshinao Tamaru,* Kengo Yasui, Hidenobu Takanabe, Shuji Tanaka,* and *Keigo Fugami*

"Masked acyl-anion equivalents"[1] have been extensively studied in a last few decades, and many useful methods for the synthesis of ketones have been developed. In planning ketone synthesis, however, the most obvious and straightforward strategy is the connection of two substituents to the carbon atom in carbon monoxide, that is, carbon dioxide is converted directly into a carbonyl group. In principle, two routes are conceivable (Scheme 1). Very recently both the ionic route A[2] and the radical variant B[3] have been realized.

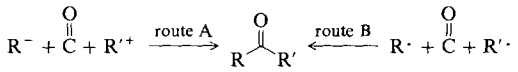

Scheme 1.

Here we report a novel one-pot method of preparing unsymmetrically substituted ketones of types **5** and **6** with a three-component coupling reaction of carbon monoxide, an allyl benzoate, and an organozinc compound as outlined in Scheme 2. The latter two components correspond to R^+ and R^- in route A in Scheme 1. This reaction can be performed very easily: An allyl benzoate **1** is mixed with an organozinc compound (ethyl γ-iodozinciobutyrate (**2**), ethyl β-iodozinciopropionate (**3**), or diethylzinc (**4**)) and a catalytic amount of $[Pd(PPh_3)_4]$. The resulting mixture is stirred under 1 atm of carbon monoxide (a balloon) at an appropriate temperature. The results are summarized in Table 1.

[*] Prof. Dr. Y. Tamaru,* K. Yasui, H. Takanabe, Dr. S. Tanaka, Dr. K. Fugami
Department of Applied Chemistry, Faculty of Engineering
Nagasaki University
Bunkyo, Nagasaki 852 (Japan)

[**] This work was supported by grants from Ministry of Education, Science and Culture (Japan) and Yamada Science Foundation.

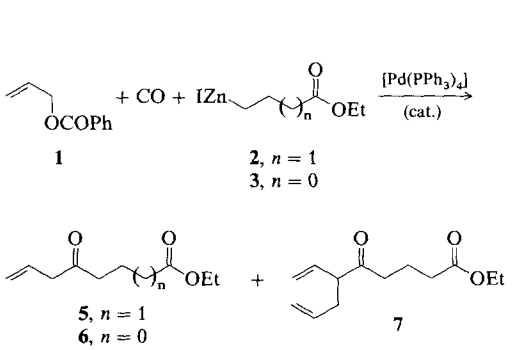

Scheme 2. The allyl groups in **1**, **5**, **6**, and **7** represent a number of derivatives, see Tables 1 and 2.

The course of the reaction is highly dependent on the solvent system. The use of an aprotic dipolar solvent, such as hexamethylphosphoric triamide (HMPA) or *N,N*-dimethylacetamide (DMA), in a small excess to **2** or **3** is essential for the selective formation of **5** or **6**, respectively. The reactions are rather complicated otherwise. For instance, if the reaction of run 7 in Table 1 is conducted in the absence of HMPA (at room temperature for 40 h and then at 35 °C for 40 h; 100% conversion), a complex mixture of products including **6a** (27%), γ-(2-butenyl)-γ-(β-ethoxycarbonylethyl)-γ-butyrolactone (28%, based on benzoate), and many other unidentified products results.[4] The lactone apparently arises from one equivalent of **1a**, one equivalent of carbon monoxide, and two equivalents of **3**. In sharp contrast to **2** and **3**, diethylzinc (**4**) gave the best results for reactions conducted in the absence of HMPA and at lower temperatures (run 9 in Table 1).[5]

Table 1. Pd^0-catalyzed three-component coupling reaction of allyl benzoates **1** with carbon monoxide and the organozinc compounds **2**,**3**, and **4** [a].

No.	**1** (X = OCOPh)	Zn cmpd. [b] (1.5 equiv)	Reaction conditions [c]	Product (% yield) [% conversion] [d]
1	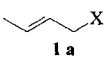 **1a**	**2**	tol./HMPA, RT, 17 h	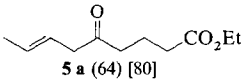 **5a** (64) [80]
2	**1a**	**2**	THF/HMPA, 40 °C, 30 h	**5a** (58) [87]
3	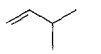 **1b**	**2**	tol./HMPA, RT, 24 h	**5a** (37) [85]
4	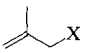 **1c**	**2**	tol./HMPA, RT, 24 h	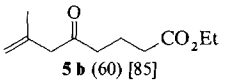 **5b** (60) [85]
5	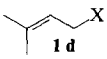 **1d**	**2**	THF/DMA, 40 °C, 24 h	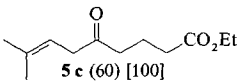 **5c** (60) [100]
6	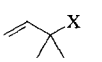 **1e**	**2**	tol./HMPA, RT, 24 h	**5c** (85) [100]
7	**1a**	**3**	THF/HMPA, RT, 60 h	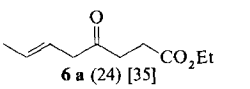 **6a** (24) [35]
8	**1e**	**3**	THF/HMPA, RT, 90 h	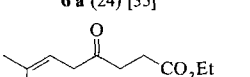 **6c** (24) [44]
9	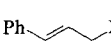 **1f**	**4**	tol., 0 °C, 24 h	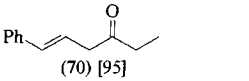 (70) [95]

[a] All reaction mere conducted with 0.05 equiv. of $[Pd(PPh_3)_4]$ under 1 atm of CO. [b] See experimental procedure. [c] tol = toluene, RT = room temperature. [d] Yields refer to the isolated, homogeneous product based on the corresponding starting allyl benzoate **1**.

Table 2. The respective Pd^0-catalyzed coupling reactions of allyl benzoate **1g** and *cinnamyl* benzoate **1f** with carbon monoxide and γ-zincioesters **2** [a] providing the ketones **5d** and **5e**, and the diallyl compounds **7a** and **7b**.

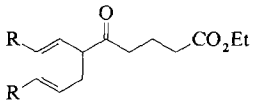

7a, R = H
7b, R = Ph

No.	**1** [b]	**2** [c] (equiv)	Solvent	Me_3SiCl (equiv)	*t*[h]	Product (% Yield) [d]	
1	**1g**	1.5	tol./HMPA	0	30	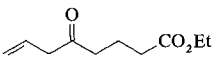 **5d** (40)	**7a** (28)
2	**1g**	3.0	THF/HMPA	0	30	**5d** (43)	**7a** (26)
3	**1g**	3.0	THF/HMPA	4.0 [e]	30	**5d** (78)	**7a** (0)
4	**1f**	3.0	THF/HMPA	0	22	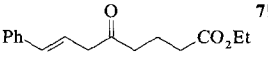 **5e** (70)	**7b** (5)
5	**1f**	3.0	THF/HMPA	4.0	40	**5e** (64)	**7b** (0)
6	**1f**	3.0	THF/DMA	4.0	20	**5e** (74)	**7b** (0)

[a] All reactions were conducted with 0.05 equiv. of $[Pd(PPh_3)_4]$ under 1 atm of CO (100% conversion). [b] X = OCOPh. [c] See experimental procedure. [d] Yields refer to the isolated, homogeneous product based on the corresponding starting allyl benzoate **1**. [e] Reaction in tol./HMPA yielded a complex mixture of products.

Under the conditions optimized for the other allyl benzoates (Table 1), the reaction of **2** with allyl benzoate **1g** provided a considerable amount of the doubly allylated product **7a** in addition to **5d** (run 1 in Table 2). The ratio of **5d** to **7a** did not change when the solvent system and the molar ratios of reactants were changed (run 2 in Table 2). In the reaction of **2** with cinnamyl benzoate (**1f**) **7b** was formed, though in lower yield (run 4 in Table 2). Addition of Me_3SiCl promoted the selective formation of **5**, seemingly at the expense of **7** (runs 3, 5, and 6 in Table 2). We have no mechanistic explanation as of yet.[6]

This Pd^0-catalyzed, selective three-component coupling reaction of allyl benzoates, carbon monoxide, and **2** or **3** is especially remarkable, since other types of products are formed in similar reactions: 1) 1,5-hexadienes and diethyl suberate for the Pd^0-catalyzed reaction of allyl benzoates and **2**[7] and 2) diethyl 4-oxopimelates for the Pd^0-catalyzed reaction of 1-ethoxy-1-siloxycyclopropanes (a presumable precursor of ethyl β-palladiopropionates) and carbon monoxide.[8] It should be also noted that allyl benzoates with isomeric allyl groups provided the same ketone with the lowest possible number of substituents at the position α to the carbonyl group (runs 1 and 3, and 5 and 6 in Table 1). This suggests a mechanism involving a π-allylpalladium species as a common intermediate for carbonylation reaction.[9]

Experimental Procedure

5d (run 3 in Table 2): To a solution of $[Pd(PPh_3)_4]$ (0.10 mmol) in 10 mL of dry THF under 1 atm of CO (a balloon) were successively added 2 mmol of **1g**, 8 mmol of Me_3SiCl (stored over Na), and the supernatant (15 mL) of a solution of **2** [0.4 M, prepared from ethyl γ-iodobutyrate (0.4 M), HMPA (0.6 M), and Zn-Cu couple (1.2 equivalents relative to ethyl γ-iodobutyrate) in THF] [10]. The mixture was stirred at room temperature for 30 h, then diluted with ethyl acetete, and washed with aqueous NH_4Cl solution. The organic phase was dried ($MgSO_4$) and concentrated. The residue was chromatographed with hexane-benzene (30 × 1.5 cm, silica gel 60), affording 0.287 g (78%) of **5d**: Bp (0.5 mm Hg) = 105 °C; IR (neat): $\tilde{\nu}$ [cm^{-1}] = 1728, 1643, 1033, 920. ^1H NMR (400 MHz, $CDCl_3$, TMS): δ = 1.25 (t, J = 7.1 Hz, 3H), 1.89 (quint, J = 7.3 Hz, 2H), 2.32 (t, J = 7.3 Hz, 2H), 2.53 (t, J = 7.3 Hz, 2H), 3.17 (d, J = 7.0 Hz, 2H), 4.12 (q, J = 7.1 Hz, 2H), 5.14–5.18 (m, 2H), 5.91 (ddt, J = 17.2, 10.3, 7.0 Hz, 1H); ^{13}C NMR (100 MHz, $CDCl_3$, TMS): δ = 14.1, 18.7, 33.2, 41.0, 47.7, 60.2, 118.7, 130.4, 173.0, 207.6; MS *m/z* Calcd for $C_{10}H_{16}O_3$: 184.1100. Found: 184.1116.

7a (run 1 in Table 2): **7a** (28%) could be easily separated from **5d** (40%) by chromatography over silica gel. Bp (0.5 mm Hg) = 115 °C; IR (neat): $\tilde{\nu}$[cm^{-1}] = 3080, 1732, 1715, 1032, 920. ^1H NMR (400 MHz, $CDCl_3$, TMS): δ = 1.25 (t, J = 7.1 Hz, 3H), 1.87 (quint J = 7.3 Hz, 2H), 2.25 (m, 1H, coalescing to dd, J = 13.8, 7.0 by irradiation at δ = 5.70), 2.30 (t, J = 7.3 Hz, 2H), 2.48 (d.t, J = 17.6, 7.3 Hz, 1H), 2.49 (m, 1H), 2.60 (dt, J = 17.6, 7.3 Hz, 1H), 3.18 (dt, J = 8.8, 7.0 Hz, 1H), 4.12 (q, J = 7.1 Hz, 2H), 4.98–5.07 (m, 2H), 5.15–5.20 (m, 2H), 5.64–5.75 (m, 2H). ^{13}C NMR (100 MHz, $CDCl_3$, TMS): δ = 14.2, 18.7, 33.3, 35.1, 40.4, 57.2, 60.3, 116.7, 118.2, 135.3 135.8, 173.1, 209.5. MS *m/z* Calcd for $C_{13}H_{20}O_3$: 224.1413. Found: 224.1413.

Received: August 18, 1991
Revised: February 5, 1992 [Z 4875 IE]
German version: *Angew. Chem.* **1992**, *104*, 662

CAS Registry numbers:
1, 583-04-0; **1a**, 50555-04-9; **1b**, 65001-62-9; **1c**, 829-53-8; **1d**, 5205-11-8; **1e**, 31398-79-5; **2**, 104089-17-0; **3**, 104089-16-9; **4**, 557-20-0; **5a**, 140462-80-2; **5b**, 140462-84-6; **5c**, 140462-85-7; **5d**, 140462-88-0; **5e**, 140462-89-1; **6a**, 140462-81-3; **6c**, 140462-86-8; **7a**, 140462-82-4; **7b**, 140462-83-5; *trans*-6-phenyl-5-hexen-3-one, 140462-87-9.

[1] a) B. M. Trost, E. Vedejs, *Organic Synthesis*, Part II, ACS Audio Courses, **1979**, pp. 1–30; b) W. Carruthers, *Some Modern Methods of Organic Synthesis*, Cambridge University Press, **1986**, pp. 43–47.
[2] a) S. Gambarotta, H. Alper, *J. Org. Chem* **1981**, *46*, 2142–2144; b) D. Seyferth, R. C. Hui, *J. Am. Chem. Soc.* **1985**, *107*, 4551–4553; c) B. H. Lipshutz, T. R. Elworthy, *Tetrahedron Lett.* **1990**, *31*, 477–480; d) I. Ryu, Y. Hayama, A. Hirai, N. Sonoda, A. Orita, K. Ohe, S. Murai, *J. Am. Chem. Soc.* **1990**, *112*, 7061–7063; e) N. Satyanarayana, H. Alper, *J. Chem. Soc. Chem. Commun.* **1991**, 8–9.
[3] I. Ryu, H. Yamazaki, K. Kusano, A. Ogawa, N. Sonoda, *J. Am. Chem. Soc.* **1991**, *113*, 8558–8560.
[4] A detailed study is under progress. Results will be reported in due course.
[5] For example, under conditions similar to those of run 9 in Table 1 in the presence of HMPA *trans*-6-phenyl-5-hexen-3-one was isolated only in 9% isolated yield (45% conversion).
[6] At first, we assumed that **7** was formed by a further allylation of **5** via its zinc dienolate. Thus we added Me_3SiCl to quench the allylation by forming the dienyl silyl ether of **5**. However, this assumption proved to be wrong. When treated with an excess of D_2O, neither the reaction mixture of run 3 in Table 2 nor the mixture of **5** and **2** (3 equiv, at room temperature, 30 min), gave **5** deuteriated at the methylene group flanked by the ketocarbonyl and olefin groups.
[7] H. Ochiai, Y. Tamaru, K. Tsubaki, Z. Yoshida, *J. Org. Chem.* **1987**, *52*, 4418–4420.
[8] S. Aoki, E. Nakamura, I. Kuwajima, *Tetrahedron Lett.* **1988**, *29*, 1541–1544.
[9] a) J. Tsuji, K. Sato, H. Okumoto, *J. Org. Chem.* **1984**, *49*, 1341–1344; b) S. Murahashi, Y. Imada, Y. Taniguchi, S. Higashiura, *Tetrahedron Lett.* **1988**, *29*, 4945–4948.
[10] Y. Tamaru, H. Ochiai, T. Nakamura, Z. Yoshida, *Org. Synth.* **1988**, *67*, 98–104.

[2,3] Wittig Rearrangements of Nonconjugated Secondary α-Lithioethers: Proof of Stereospecificity and Inversion of the Configuration of the Carbanion C Atom**

By *Rolf Hoffmann* and *Reinhard Brückner**

[2,3] Wittig rearrangements[1] are one-step symmetry-allowed isomerizations of α-metallated allyl ethers **2** to homoallylalkoxides **3**. *Primary* lithioethers of type **2** (R = H), which can be generated by the treatment of *primary* α-stannyl allyl ethers **1** (R = H) with *n*BuLi, rearrange in THF at −78 °C.[2] Analogous tin/lithium exchange reactions with *secondary* α-stannyl methoxymethyl and benzyloxymethyl ethers are stereoselective and lead to lithioethers with retention of configuration.[3] These intermediates are pyramidal and configuratively stable at −78 °C long enough to react with Me_2SO_4, acetone, Me_3SiCl, Bu_3SnI,[3] and other electrophiles[5] with retention of this configuration. Thus we anticipated that a *secondary* α-lithioether **2** (R = chiral alkyl group) would undergo a [2,3] rearrangement faster than it would stereoisomerize. We set out to prepare such lithioethers **2** with defined relative configuration at the carbanion C atom, allow them to rearrange to **3**, and then determine whether this [2,3] Wittig rearrangement proceeds with retention (→ **3a**) or inversion (→ **3b**) of configuration. We report here the results of our investigation.

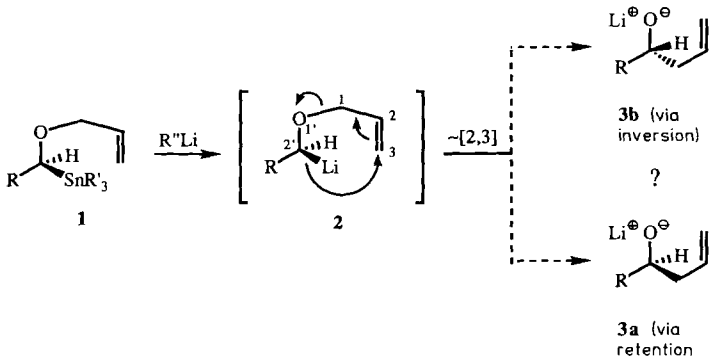

1 **2**

Nonconjugated secondary α-(trialkylstannyl)acetals[3] and (trialkylsilyl)ethers[6] are readily available from α-(trialkylstannyl)alcohols. In contrast, nonconjugated secondary α-(trialkylstannyl)ethers have not yet been prepared from this same type of precursor in a single operation.[7] This difficulty may explain why α-stannyl allyl ethers of type **1** (R = alkyl), which we require as a precursor of **2**, have not yet been described.

We have succeeded in synthesizing stannyl allyl ether **6** which belongs to this product type (Scheme 1). The synthesis makes use of the facile replacement of the Cl atom in α-chloroallyl ether **5** by $LiSnBu_3$. This approach was reported for *acyclic* α-(trialkylstannyl)ethers in a single case,[7c] whereas applications to the more stable *cyclic* analogues have been reported a number of times.[5b, 7c, 8] The stannylether **6** was obtained from **5** in >72% yield as a 1:1 mixture of diastereomers. Flash chromatography on silica gel provided *syn*-**6** (isomeric purity 92:8 based on the ^1H NMR integration of the C*H*-O-CH_2-CH=CH_2 resonances) and *anti*-**6** (isomeric purity 90:10).[10]

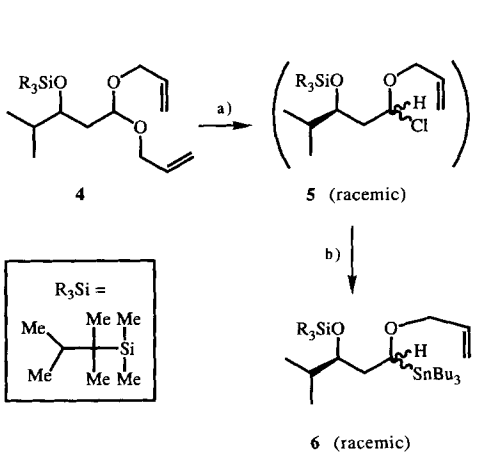

4 **5** (racemic) **6** (racemic)

Scheme 1. a) AcCl, CH_2Cl_2, 40 °C, 3 h; removal of the solvent by evaporation at 0 °C → room temperature. b) $LiSnBu_3$, THF, −78 °C, 1 h (72% from **4**).

Table 1. Spectroscopic data for compounds *syn*-**7**, *anti*-**7**, *syn*-**9**, and *anti*-**9**. ^1H NMR (600 MHz, $CDCl_3$, TMS); ^{13}C NMR (50 MHz, $CDCl_3$, TMS); coupling constants in Hz.

(1*S**,3*S**)-4-Methyl-1-(2-propenyloxy)-1-(tributylstannyl)-3-pentanol *syn*-**7**: ^1H NMR: δ = 0.85–0.97 (m, 5-H_3, 4-CH_3, 3 × 4″-H_3, 3 × 2″-H_2), 1.32 (tq, $J_{3'',2''} = J_{3'',4''} = 7.3$, 3 × 3″-$H_2$), 1.42–1.57 (m, 3 × 1″-$H_2$), 1.65 (dqq, $J_{4,3} = J_{4,5} = J_{4,4\text{-Me}} = 6.8$, 4-H), AB signal ($\delta_A = 1.73$, $\delta_B = 1.97$, $J_{AB} = 14.7$, additional splitting due to $J_{A,1} = J_{A,3} = 2.2$, $J_{B,1} = 11.9$, $J_{B,3} = 9.8$, 2-H_2), 3.52 (ddd$_c$, $J_{3,2\text{-}H^B} = 9.5$, $J_{3,4} = 5.3$, 3-H), 3.70 (s, OH), AB signal ($\delta_A = 3.85$, $\delta_B = 3.95$, $J_{AB} = 12.2$, additional splitting due to $J_{A,2'} = 5.9$, $J_{A,allyl} \approx 1$, $J_{B,2'} = 5.0$, $J_{B,allyl} \approx 1$, 1′-H_2), 4.11 (dd, $J_{1,2\text{-}H^A} = 11.9$, $J_{1,2\text{-}H^B} = 2.9$, 1-H), 5.16 (dd, $J_{3'\text{-}H_{cis},2'} = 10.5$, $J_{gem} = 1.3$, 3′-H_{cis}), 5.25 (dt, $J_{3'\text{-}H_{trans},2'} = 17.2$, $J_{gem} = J_{allyl} = 1.6$, 3′-$H_{trans}$), 5.89 (ddt, $J_{2',3'\text{-}H_{trans}} = 17.2$, $J_{2',3'\text{-}H_{cis}} = 10.7$, $J_{2',1'} = 5.3$, 2′-H). ^{13}C NMR: δ = 9.44 (3 × C-1″), 13.63 (3 × C-4″), 17.57, 18.54 (C-5, 4′-CH_3), 27.45, 29.18 (3 × C-2″, 3 × C-3″), 33.74 (C-4), 38.55 (C-2), 72.18 (C-1′), 78.52, 80.13 (C-1, C-3), 116.94 (C-3′), 134.43 (C-2′).

(1*R**,3*S**)-4-Methyl-1-(2-propenyloxy)-1-(tributylstannyl)-3-pentanol *anti*-**7**: ^1H NMR: δ = 0.88–0.95 (m, 3 × 2″-H_2, 3 × 4″-H_3), 0.96 (d, $J_{5,4} = 6.8$, 5-H_3, 4-CH_3), 1.32 (tq, $J_{3'',2''} = J_{3'',4''} = 7.3$, 3 × 3″-$H_2$), 1.44–1.58 (m, 3 × 1″-$H_2$), AB signal ($\delta_A = 1.80$, $\delta_B = 2.04$, $J_{AB} = 14.8$, additional splitting due to $J_{A,1} = 6.2$, $J_{A,3} = 1.6$, $J_{B,3} = 9.7$, $J_{B,1} = 3.9$, 2-H_2), 3.38 (d, $J_{OH,3} \approx 1$, OH), 3.47–3.55 (m, 3-H), AB signal ($\delta_A = 3.86$, $\delta_B = 3.96$, $J_{AB} = 12.5$, additional splitting due to $J_{A,2'} = 5.5$, $J_{B,2'} = 5.6$, 1′-H_2), 4.19 (dd, $J_{1,2\text{-}H^A} = 6.1$, $J_{1,2\text{-}H^B} = 3.8$, 1-H), 5.16 (dd, $J_{3'\text{-}H_{cis},2'} = 10.5$, $J_{gem} = 1.3$, 3′-H_{cis}), 5.25 (dd, $J_{3'\text{-}H_{trans},2'} = 17.2$, $J_{gem} = 1.6$, 3′-H_{trans}), 5.88 (ddt, $J_{2',3'\text{-}H_{trans}} = 17.2$, $J_{2',3'\text{-}H_{cis}} = 10.4$, $J_{2',1'} = 5.5$, 2′-H). ^{13}C NMR: δ = 9.54 (3 × C-1″), 13.64 (3 × C-4″), 18.09, 18.68 (C-5, 4-CH_3), 27.44, 29.19 (3 × C-2″, 3 × C-3″), 33.86 (C-4), 37.06 (C-2), 72.01 (C-1′), 76.49, 77.75 (C-1, C-3), 116.82 (C-3′), 134.65 (C-2′).

(4*S**,6*S**)-6-[Dimethyl-(1,1,2-trimethylpropyl)siloxy]-7-methyl-1-octen-4-ol *syn*-**9**: ^1H NMR: δ = 0.13, 0.15 (2s, 2 × $SiCH_3$), 0.83 (d, $J_{8,7} = 7.0$, 8-H_3, 7-CH_3), 0.85, 0.87 (2s, 2 × 1′-CH_3), 0.88–0.92 (m, 2′-CH_3, 3′-H_3), 1.48–1.56 (m, 5-H_2), 1.65 (qq, $J_{2'\text{-H},2'\text{-Me}} = J_{2',3'} = 6.9$, 2′-H), 1.78–1.90 (m, 7-H), 2.19–2.29 (m, 3-H_2), 2.96 (s, OH), 3.75–3.82 (m, 4-H, 6-H), 5.11 (d, $J_{1\text{-}H_{cis},2} = 9.9$, 1-$H_{cis}$), 5.12 (d, $J_{1\text{-}H_{trans},2} = 17.2$, 1-$H_{trans}$), 5.85 (ddt, $J_{2,1\text{-}H_{trans}} = 17.2$, $J_{2,1\text{-}H_{cis}} = 10.1$, $J_{2,3} = 7.1$, 2-H). ^{13}C NMR: δ = −2.63, −2.11 (2 × $SiCH_3$), 16.42, 18.00, 18.48, 18.64, 20.21, 20.42 (2 × 1′-CH_3, C-3′, 2′-CH_3, C-8, 7-CH_3), 24.94 (C-1′), 33.23, 34.05 (C-7, C-2′), 37.28, 42.13 (C-3, C-5), 69.95, 76.69 (C-4, C-6), 117.46 (C-1), 134.92 (C-2).

(4*R**,6*S**)-6-[Dimethyl-(1,1,2-trimethylpropyl)siloxy]-7-methyl-1-octen-4-ol *anti*-**9**: ^1H NMR: δ = 0.11, 0.14 (2s, 2 × $SiCH_3$), 0.84–0.90 (m, 2 × 1′-CH_3, 2′-CH_3, 3′-H_3, 8-H_3, 7-CH_3), AB signal ($\delta_A = 1.47$, $\delta_B = 1.61$, $J_{AB} = 14.5$, additional splitting due to $J_{A,4} = 10.1$, $J_{A,6} = 3.1$, $J_{B,6} = 6.9$, $J_{B,4} = 2.3$, 5-H_2), 1.65 (qq, $J_{2',2'\text{-Me}} = J_{2',3'} = 6.9$, 2′-H), 1.86 (dqq, $J_{7,6} = J_{7,7\text{-Me}} = J_{7,8} = 6.6$, 7-H), 2.22 (dd, $J_{3,2} = J_{3,4} = 6.6$, 3-H_2), 2.65 (s, OH), 3.70 (ddd, $J_{6,5\text{-}H^B} = J_{6,7} = 6.4$, $J_{6,5\text{-}H^A} = 3.2$, 6-H), 3.89–3.95 (m, 4-H), 5.11 (d(b), $J_{1\text{-}H_{cis},2} \approx 10$, 1-$H_{cis}$), 5.11 (d(b), $J_{1\text{-}H_{trans},2} \approx 18$, 1-$H_{trans}$), 5.83 (ddt, $J_{2,1\text{-}H_{trans}} = 17.2$, $J_{2,1\text{-}H_{cis}} = 10.2$, $J_{2,3} = 7.1$, 2-H). ^{13}C NMR: δ = −2.37 (2 × $SiCH_3$), 17.58, 18.53, 18.67, 19.05, 20.34, 20.52 (2 × 1′-CH_3, C-3′, 2′-CH_3, C-8, 7-CH_3), 24.97 (C-1′), 33.04, 34.10 (C-7, C-2′), 38.48, 42.66 (C-3, C-5), 67.67, 75.28 (C-4, C-6), 117.58 (C-1), 134.95 (C-2).

[*] Prof. R. Brückner, Dipl.-Chem. R. Hoffmann
Institut für Organische Chemie der Universität
Am Hubland, D-W-8700 Würzburg (FRG)

[**] This research was supported by the Deutsche Forschungsgemeinschaft (Sonderforschungsbereich 347 "Selektive Reaktionen metallaktivierter Moleküle") and the Fonds der Chemischen Industrie. We thank Prof. C. Griesinger and Dipl.-Chem. M. Sattler (Universität Frankfurt) for the 600 MHz ^1H NMR spectra.

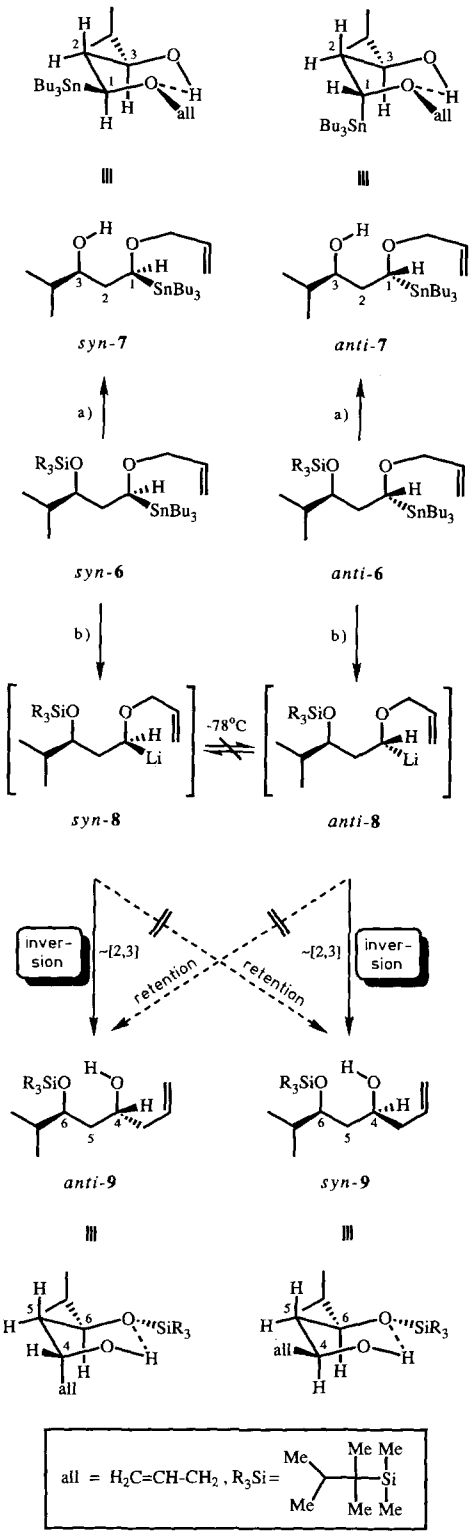

Scheme 2. a) $Bu_4N^+F^-$ (>10 equiv), THF, 60 °C, 6 h (71% *syn*-**7** and 67% *anti*-**7**, respectively). b) *n*BuLi (1.05 equiv), THF, −78 °C, 15 min (67% *anti*-**9** and 89% *syn*-**9**, respectively).

The stannylethers *syn*- and *anti*-**6** were treated with *n*BuLi at −78 °C in THF in separate experiments. Presumably they are converted by tin/lithium exchange to the corresponding lithioethers *syn*- and *anti*-**8** with retention of configuration. The reaction temperature of −78 °C and the total reaction times of 15 min precluded a subsequent epimerization *syn*-**8**⇄*anti*-**8** according to the premises described in the introduction of this report. These conditions were sufficient for complete reaction, and after the Wittig rearrangement the silylated alcohols **9** were collected in yields of 67 to 80%.

Both rearrangements were highly stereoselective: *syn*-**6** provided *anti*-**9** (isomeric purity 95:5 according to the ^1H NMR integration of the 4-H/6-H resonances), and *anti*-**6** furnished *syn*-**9** (isomeric purity 93:7).[13] Because the starting stannylethers *syn*- and *anti*-**6** themselves contained 8 and 10% diastereomers respectively, diastereomeric purity did not apparently suffer in this reaction. The stereochemical complementarity of the two Wittig rearrangements means that they proceed with stereospecificity.

Because lithio allyl ethers could also arise from the [1,2] variation of the Wittig rearrangement,[2, 11b, 14, 15] we had to establish with certainty which mechanism led to the rearrangement product **9**. To this aim we prepared lithioether **12** from **11** according to a procedure described recently,[16] in which the C–S bond of a O,S acetal is cleaved reductively. The isomerization of **12** furnished exclusively **13a** and **13b**,[18] products of a [2,3] rearrangement; product **10** which would be expected from a [1,2] rearrangement was not observed.

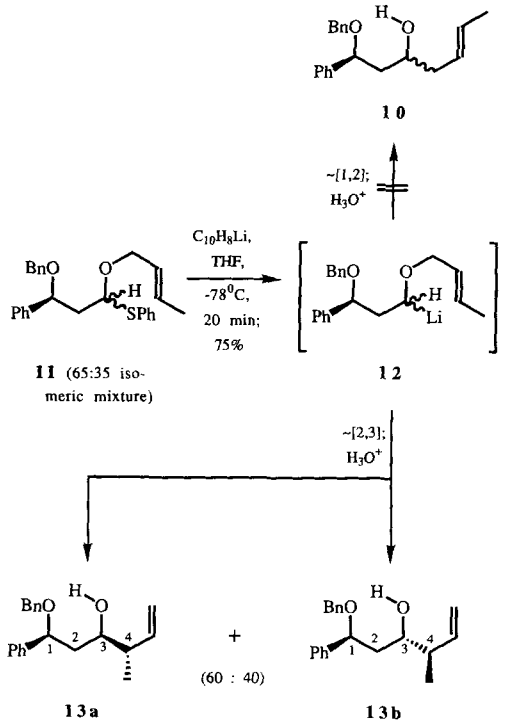

According to this result it is most probable that *syn*-**8** → *anti*-**9** and *anti*-**8** → *syn*-**9** are also [2,3] Wittig rearrangements. Thus we could show that the [2,3] Wittig rearrangement of nonconjugated secondary α-lithio allyl ethers proceeds with inversion of the configuration of the carbanion carbon. The same conclusion was also reached by T. Nakai et al.[19] Our findings are in agreement with the transition state calculated by Wu, Houk, and Marshall[4b] for the [2,3] Wittig rearrangement of Li-CH_2-O-CH_2-CH=CH_2 and correspond to the stereochemical relationships seen in the [1,2] Wittig rearrangement of a nonconjugated tertiary lithio allyl ether.[15, 20]

Received: January 17, 1992 [Z 5129 IE]
German version: *Angew. Chem.* **1992**, *104*, 646

CAS Registry numbers:
4, 140410-48-6; **5** (isomer 1), 140410-49-7; **5** (isomer 2), 140410-50-0; **syn-6**, 140410-51-1; **anti-6**, 140437-97-4; **syn-7**, 140410-52-2; **anti-7**, 140410-53-3;

syn-9, 140410-54-4; **anti-9**, 140410-55-5; **11** (isomer 1), 140410-56-6; **11** (isomer 2), 140410-57-7; **13a**, 140410-58-8; **13b**, 140679-69-2; $C_{10}H_8Li$, 7308-67-0.

[1] Reviews: a) T. Nakai, K. Mikami, *Chem. Rev.* **1986**, *86*, 885–902; b) K. Mikami, T. Nakai, *Synthesis* **1991**, 594–604; c) J. A. Marshall in *Comprehensive Organic Synthesis* (Eds.: B. M. Trost, I. Fleming), *Vol. 3, Carbon-Carbon σ-Bond Formation* (Ed.: G. Pattenden), Pergamon Press, Oxford, **1991**, pp. 975–1014; d) R. Brückner in *Comprehensive Organic Synthesis* (Eds.: B. M. Trost, I. Fleming), *Vol. 6, Heteroatom Manipulation* (Ed.: E. Winterfeldt), Pergamon Press, Oxford, **1991**, pp. 873–908; e) R. Brückner, *Kontakte (Darmstadt)* **1991**, (2) 3–14, *ibid.* **1991**, (3) 3–15.

[2] W. C. Still, A. Mitra, *J. Am. Chem. Soc.* **1978**, *100*, 1927–1928.

[3] W. C. Still, C. Sreekumar, *J. Am. Chem. Soc.* **1980**, *102*, 1201–1202.

[4] a) P. von R. Schleyer, T. Clark, A. J. Kos, G. W. Spitznagel, C. Rohde, D. Arad, K. N. Houk, N. G. Rondan, *J. Am. Chem. Soc.* **1984**, *106*, 6467–6475; b) Y.-D. Wu, K. N. Houk, J. A. Marshall, *J. Org. Chem.* **1990**, *55*, 1421–1423; c) M. Marsch, K. Harms, O. Zschage, D. Hoppe, G. Boche, *Angew. Chem.* **1991**, *103*, 338–339, *Angew. Chem. Int. Ed. Engl.* **1991**, *30*, 321–323.

[5] Repesentative examples of stereoselective reactions of α-chiral nonconjugated α-lithioethers: with D_2O or RCHO: a) T. Cohen, M.-T. Lin, *J. Am. Chem. Soc.* **1984**, *106*, 1130–1131; with an enone: b) D. K. Hutchinson, P. L. Fuchs, *ibid.* **1987**, *109*, 4930–4939; with an α-chloroboronester: c) D. S. Matteson, P. B. Tripathy, A. Sarkar, K. M. Sadhu, *ibid.* **1989**, *111*, 4399–4402; with an epoxide: d) S. D. Rychnovsky, *J. Org. Chem.* **1989**, *54*, 4982–4984; with an amide: e) J. M. Chong, E. K. Mar, *Tetrahedron* **1989**, *45*, 7709–7716; with CO_2: f) P. C.-M. Chan, J. M. Chong, *Tetrahedron Lett.* **1990**, *31*, 1985–1988.

[6] R. J. Linderman, A. Ghannan, *J. Am. Chem. Soc.* **1990**, *112*, 2392–2399.

[7] Syntheses of stannylethers **1**, R = Alkyl: a) J.-P. Quintard, B. Elissondo, M. Pereyre, *J. Org. Chem.* **1983**, *48*, 1559–1560; see also J.-P. Quintard, B. Elissondo, T. Hattich, M. Pereyre, *J. Organomet. Chem.* **1985**, *285*, 149–162; b) A. Duchêne, J.-P. Quintard, *J. Chem. Soc. Chem. Commun.* **1987**, 29–30; c) J. S. Sawyer, A. Kucerovy, T. L. Macdonald, G. J. McGarvey, *J. Am. Chem. Soc.* **1988**, *110*, 842–853; d) J.-i. Yamada, H. Abe, Y. Yamamoto, *ibid.* **1990**, *112*, 6118–6120; e) R. J. Linderman, D. M. Graves, W. R. Kwochka, A. F. Ghannan, T. V. Anklekar, *ibid.* **1990**, *112*, 7438–7439.

[8] a) P. Lesimple, J.-M. Beau, P. Sinaÿ, *J. Chem. Soc. Chem. Commun.* **1985**, 894–895; b) P. Lesimple, J.-M. Beau, P. Sinaÿ, *Carbohyd. Res.* **1987**, *171*, 289–300.

[9] W. C. Still, M. Kahn, A. Mitra, *J. Org. Chem.* **1978**, *43*, 2923–2925.

[10] We determined the configuration of **6** by NMR spectroscopy (Table 1) after desilylation of the separated diastereomers to the β-hydroxyethers *syn*- and *anti*-7 (Scheme 2). These should be in the conformations shown in Scheme 2, based on those found for other β-hydroxyethers[11] and γ-hydroxyalcohols[12]. The *syn* isomer of 7 should have the fixed preferred conformation shown, since the substituents of C-1 and C-3 could thus be oriented equatorial; *anti*-7 may be a mixture of two chair conformations in equilibrium (in Scheme 2 only one of these is shown for clarity) with each having one axial and one equatorial substituent. *One* relevant consequence of this relationship for the structural assignments is that the sum $\delta(^{13}C\text{-}1) + \delta(^{13}C\text{-}3)$ of the ^{13}C NMR chemical shifts in *syn*-7, 158.65, is 4.41 greater than that in *anti*-7 [$\delta(^{13}C\text{-}1) + \delta(^{13}C\text{-}3) = 154.24$] [11a]. The coupling constants of the protons in the 2-position with their neighbors in the 3- and 1-positions provide further stereochemical evidence: Especially large ax/ax couplings for one 2-H are observed only for *syn*-7 ($J_{2,1} = 11.9$ Hz, $J_{2,3} = 9.8$ Hz), and especially small eq/ax couplings are observed for the other 2-H ($J_{2,1} = J_{2,3} = 2.2$ Hz). In the diastereomer assigned the *anti* configuration one observes different pairs of J_{vic} values (2-H_A: $J_{2,1} = 6.1$ Hz, $J_{2,3} = 1.6$ Hz; 2-H_B: $J_{2,3} = 9.7$ Hz, $J_{2,1} = 3.9$ Hz).

[11] a) R. W. Hoffmann, U. Weidmann, *Chem. Ber.* **1985**, *118*, 3980–3992; b) H. Priepke, R. Brückner, *ibid.* **1990**, *123*, 153–168.

[12] L. P. Kuhn, R. A. Wires, *J. Am. Chem. Soc.* **1964**, *86*, 2161–2165; S. Kiyooka, H. Kuroda, Y. Shimasaki, *Tetrahedron Lett.* **1986**, *27*, 3009–3012; J.-M. Lancelin, F. Paquet, J.-M. Beau, *ibid.* **1988**, *29*, 2827–2830.

[13] The assignment of *syn*- and *anti*-**9** was possible by NMR spectroscopy (Table 1) in the same manner as that used in the differentiation of *syn*- and *anti*-7. The interpretation of the data is again based on a hydrogen-bonded chairlike structure with a six-membered ring (Scheme 2). The ^{13}C NMR criterion mentioned above (see [10]) could be applied to the oxygen-bearing ^{13}C centers again. According to this, the *syn* diastereomer has a sum, $\delta(^{13}C\text{-}4) + \delta(^{13}C\text{-}6) = 146.64$, 3.69 greater than that of *anti*-**9** [$\delta(^{13}C\text{-}4) + \delta(^{13}C\text{-}6) = 142.95$]. The ^1H NMR spectrum of this last diastereomer supports the *anti* configuration, because the vicinal couplings of the diastereotopic protons in the 5-position (5-H_A: $J_{5,4} = 10.1$ Hz, $J_{5,6} = 3.1$ Hz; 5-H_B: $J_{5,6} = 6.9$ Hz, $J_{5,4} = 2.3$ Hz) are modulated similarly to the J_{vic} values of the analogous protons in the 2-position of *anti*-7 (9.7, 3.9 Hz; 6.1, 3.6 Hz). The $J_{5,4}$ and $J_{5,6}$ coupling constants for *syn*-**9** could not be obtained, because the signal of 5-H_2 is of higher order even in the 600 MHz spectrum, and the resonance frequencies of 4-H and 6-H are the same at this field strength. Desilylation of *syn*-**9** provided a diol, in which the axial 5-H with large diaxial couplings ($J_{5,4} = J_{5,6} = 10.2$ Hz) and the equatorial 5-H with small eq/ax couplings ($J_{5,6} \approx J_{5,4} \approx 1$–2 Hz) are clearly distinguished.

[14] T. Sugimura, L. A. Paquette, *J. Am. Chem. Soc.* **1987**, *109*, 3017–3024.

[15] R. Hoffmann, R. Brückner, unpublished results.

[16] a) C. A. Broka, T. Shen, *J. Am. Chem. Soc.* **1989**, *111*, 2981–2984; b) B. Kruse, R. Brückner, *Chem. Ber.* **1989**, *122*, 2023–2025.

[17] Method: T. Cohen, M. Bhupathy, *Acc. Chem. Res.* **1989**, *22*, 152–161.

[18] Compounds **13a** and **13b** were isolated as a mixture and were inseparable by flash chromatography[9]. The relative configurations of C-3 and C-1 were deduced from the analysis of the vicinal H,H coupling constants of the protons in the 2-position as was done for **7** [10] and **9** [13]. The configurations of C-4 and C-3 were assigned based on an analogous assignment by Broka et al. [16a].

[19] T. Nakai, unpublished results. We thank Prof. Nakai (Tokyo Institute of Technology) for this information.

[20] Comment during the correction of the manuscript (March 5, 1992): Since this communication was submitted E. J. Verner and T. Cohen (*J. Am. Chem. Soc.* **1992**, *114*, 375–377) have proved the stereoselectivity and inversion of the configuration at the carbanion carbon atom in the ring-expanding [2,3] Wittig rearrangement of *trans*-α-lithio-α'-alkenyltetrahydropyrans to 3-cyclohepten-1-ols. Because the [1,2] Wittig rearrangement competed, a common mechanism leading to both the [2,3] and [1,2] products is not completely ruled out, that is the first may arise from a multistep process.

A Novel Polyoxotungstate Containing a *triangulo* Ni^{II}_3 Cluster with Ferromagnetic Exchange Interactions and an $S = 3$ Ground State**

By *Carlos J. Gómez-García, Eugenio Coronado,** and *Lahcène Ouahab*

Heteropolyoxometalate complexes are proving especially valuable for the study of the magnetic interactions in metallic clusters[1] as well as between delocalized electrons of reduced species ("heteropolyblues") and paramagnetic metal atoms.[2] Many of these molecular metal-oxide clusters have structures that permit the inclusion of magnetic clusters. A good example of this ability is provided by the series of isomorphous complexes $[M_4(H_2O)_2(PW_9O_{34})_2]^{-10}$ ($M = Co^{2+}$, Cu^{2+}, Zn^{2+}, Mn^{2+}). The structural analysis of the Co and Cu compounds[3,4] shows the presence of a rhombus-like tetrameric M_4O_{16} cluster between two $(PW_9O_{34})^{9-}$ units. The magnetic properties of these compounds have shown[5] that the pairwise interactions between the Cu^{2+} ions are antiferromagnetic, but between the Co^{2+} ions ferromagnetic. Despite the different sign of the exchange, in both complexes the ground state is magnetic. The Cu^{2+} cluster has an $S = 1$ ground state resulting from different competing antiferromagnetic exchange windows ("spin frustration") in the rhombus; the Co^{2+} cluster has a doublet ground state (with $M_s = \pm 2$) arising from the splitting of the (effective) $S = 2$ spin state as a consequence of the exchange anisotropy.

We attempted to prepare the Ni^{2+} complex of this series and obtained a novel polyoxotungstate containing a ferromagnetically coupled trinuclear Ni^{2+} cluster. This compound was characterized by elemental analysis, IR spec-

[*] Prof. Dr. E. Coronado, Dr. C. J. Gómez-García
Departamento de Química Inorgánica
Universidad de Valencia
Dr. Moliner 50, E-46100 Burjasot (Spain)
Dr. L. Ouahab
Laboratoire de Chimie du Solide et Inorganique Moléculaire
Université de Rennes I-CNRS-URA 254
Av. Général Leclerc, F-35042 Rennes Cedex (France)

[**] This work is supported by the Comisión Interministerial de Ciencia y Tecnología (MAT89-177), the Program of Spanish-French Integrated Actions (69 B), and by the Institució Valenciana d'Estudis i Investigació. C. J. G.-G. thanks the Ministerio de Educación y Ciencia for a grant.

troscopy, magnetic measurements, and X-ray structural analysis[6] and can be formulated as below:

$K_6Na[Ni_3(H_2O)_3PW_{10}O_{39}H_2O]\cdot 12H_2O$ **1**

The anion of this salt has an unexpected structure (Fig. 1): An equilateral triangular Ni_3^{II} unit, formed by three edge-sharing NiO_6 octahedra, is coordinated by the ligand $(PW_9O_{34})^{9-}$ (α-B isomer), which has three vacant coordination sites, and a WO_6 octahedron. The tungsten atom of

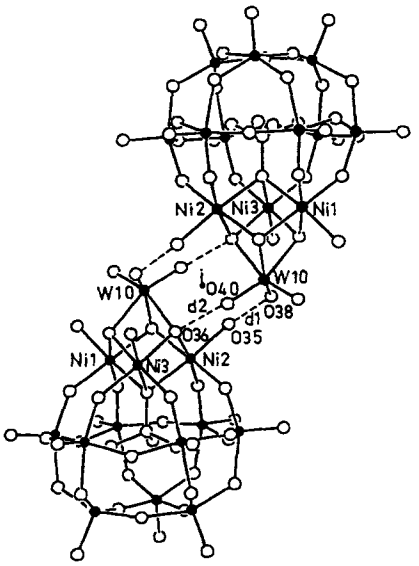

Fig. 1. Structure of the cluster anion $[Ni_3(H_2O)_3PW_{10}O_{39}H_2O]^{7-}$ showing the arrangement of the clusters in centrosymmetrical pairs and the hydrogen bridges (d_1 = 2.68(2) Å, d_2 = 2.73(2) Å). The black circles are the W atoms.

WO_6 forms a distorted $[Ni_3WO_4]$ cubane-type core with the triangular Ni_3^{II} unit. Moreover, these anion clusters are associated pairwise by hydrogen bonds, as sketched in Figure 1, in such a way that the triangular Ni_3^{II} units are parallel and well-isolated magnetically. Figure 1 shows that there are two different hydrogen-bond interactions: One involves O36 (a μ-oxo group) of one cluster and O40 of the neighboring cluster; the other one involves O35 from a water molecule coordinated to Ni2 and O38 of the neighboring cluster. On this basis, one can assign O38 to an oxo anion and O40 to a water molecule. Thus, the coordination around W10 contains a water molecule, in agreement with the Lipscomb's principle.[7]

The results of magnetic measurements on this complex are displayed in Figures 2 and 3. At 1 kG the magnetic moment gradually increases as the temperature is decreased, from 6 $\mu_B mol^{-1}$ at 150 K to a plateau of 8.1 $\mu_B mol^{-1}$ below 5 K (Fig. 2). Such behavior clearly demonstrates that the intracluster Ni–Ni spin coupling is ferromagnetic with negligible intercluster interactions. The magnetic properties of this cluster are largely due to interactions between $^3A_2$ nickel(II) ions as propagated by bridging oxygen atoms. Because this cluster forms a Ni_3 equilateral triangle, these results have been interpreted with an isotropic exchange Hamiltonian operator that assumes that the three pairwise interactions are equal, that is, $\mathcal{H} = -2J(S_1S_2 + S_1S_3 + S_2S_3)$. The susceptibility expression of such a system can be derived from Kambe's treatment.[8] From this expression a close agree-

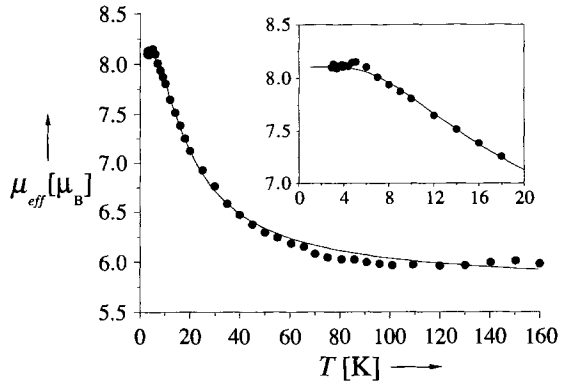

Fig. 2. Plot of μ_{eff} versus T for **1** in a magnetic field of 1.0 kG. The solid line represents the best fit from the Heisenberg exchange model: J = 2.9 cm^{-1}, and g = 2.35.

ment with the experiment in the overall temperature range has been obtained from the following set of parameters: J = 2.9 cm^{-1} and g = 2.35 (solid line in Fig. 2). These parameters lead to an energy diagram in which the ground state has S = 3, and is roughly 17.5 cm^{-1} lower in energy than the lowest lying excited states S = 2. This is the largest spin ground state reported in a heteropolyoxometalate. The existence of very weak intercluster interactions between the S = 3 ground states is detected in the magnetization measurements performed at T = 2 K in magnetic fields between 1 kG and 50 kG (Fig. 3). A typical Brillouin curve is observed which tends to a saturation value of approximately 6 μ_B above 25 kG. As we can see in Figure 3, these data show deviations from the theoretical curve for S = 3 due to intercluster interactions.

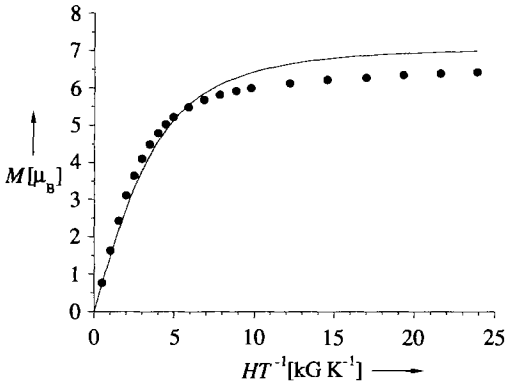

Fig. 3. Magnetization data of the title compound at 2 K. The solid line represents the behavior of a cluster with an S = 3 ground state with a Landé factor g = 2.3.

The unusual ferromagnetic spin coupling of this cluster is related to the Ni-O-Ni angles, which are of two types, those that are close to 90° (92.0(5)°, 92.2(5)°, and 92.1(4)°) involving a common oxygen atom from the PO_4 group, and those that are about 100° (100.5(70°, 100.4(7)°, and 100.7(6)°) corresponding to the three bridging oxygen atoms shared with W10. These angles are in the range in which the Ni–Ni ferromagnetic exchange pathways are dominant (90 ±14°). In this context it should be noted that other nickel ferromagnets are known.[9–11] But in contrast to the title compound, all these complexes show a cubane-type framework and significant intercluster interactions. It is interesting that despite the

structural differences, the *triangulo* cluster has similar exchange couplings to those reported in the cubane clusters ($3-11\ cm^{-1}$).

This kind of heteropolyanionic magnetic cluster could serve in the construction of building blocks for the development of new magnetic molecular materials. In this respect, there is a considerable effort directed to the preparation of molecular magnets based on high-spin molecules.[12] The major difficulty is to interconnect these units in order to build up an extended lattice. Heteropolyoxometalates offer the advantage that they maintain their identity in aqueous and non-aqueous solutions. Thus, these can be associated with suitably chosen cations, for example organic radicals of the type $TTF^{\bullet+}$ and its derivatives, to give extended lattices. This characteristic has been very recently exploited to obtain inorganic/organic charge-transfer salts from diamagnetic heteropolyanions and π-donor organic radicals.[13-15] To our knowledge no studies have been reported with magnetic polyoxoanions.

Experimental Procedure

Compound **1** was prepared following a procedure similar to that reported by Finke [16] for the cobalt derivative of the series $[M_4(H_2O)_2(PW_9O_{34})_2]^{10-}$: $Ni(NO_3)_2 \cdot 6H_2O$ (0.4070 g, 1.4 mmol) was dissolved in distilled water (15 mL). To this light green solution solid $Na_8HPW_9O_{34} \cdot 19H_2O$ (2 g; prepared as described by Finke and dried for 1 h at 140 °C) was added slowly with stirring and gentle warming. KCl (5 g) was then added slowly, and a yellow-green precipitate immediately appeared which was then filtered off. The filtrate was diluted to ca. 50 mL and warmed gently. Slow evaporation of the solvent at room temperature gives after some days a mixture of green needles of **1** and a yellow crystalline powder which were collected and separated carefully. **1** provided a correct elemental analysis. Metal analyses and IR spectra of the yellow powder suggest that this salt contains the anion identified by Knoth et al. [17] as $[Ni_3(H_2O)_2(PW_9O_{34})_2]^{12-}$.

Received: August 6, 1991
Revised: February 5, 1992 [Z 4855 IE]
German version: *Angew. Chem.* **1992**, *104*, 660

[1] a) V. E. Simmons, *Dissertation*, Boston University, **1963**; *Diss. Abstr.* **1963**, *24*, 1391; b) L. C. W. Baker, V. E. S. Baker, S. H. Wasfi, G. A. Candela, A. H. Kahn, *J. Am. Chem. Soc.* **1972**, *94*, 5499; c) *J. Chem. Phys.* **1972**, *56*, 4917; d) G. F. Kokoszka, F. Padula, A. S. Goldstein, E. L. Venturini, L. Azevedo, A. R. Siedle, *Inorg. Chem.* **1988**, *27*, 59.
[2] N. Casañ-Pastor, *Dissertation*, Georgetown University, **1988**.
[3] a) H. T. Evans, C. M. Tourné, T. J. R. Weakley, *J. Chem. Soc. Dalton Trans.* **1986**, 2699; b) T. J. R. Weakley, H. T. Evans, J. S. Showell, G. F. Tourné, C. M. Tourné, *J. Chem. Soc. Chem. Commun.* **1973**, 139.
[4] T. J. R. Weakley, R. G. Finke, *Inorg. Chem.* **1990**, *29*, 1235.
[5] a) C. J. Gómez-García, N. Casañ-Pastor, E. Coronado, L. C. W. Baker, G. Pourroy, *J. Appl. Phys.* **1990**, *67*, 5995; b) N. Casañ-Pastor, J. Bas, E. Coronado, G. Pourroy, L. C. W. Baker, *J. Am. Chem. Soc.*, in press; c) C. J. Gómez-García, E. Coronado, J. J. Borras-Almenar, *Inorg. Chem.*, in press.
[6] **1**: Parallelipipedal crystals, Enraf-Nonius CAD4 diffractometer, $M_r = 3215.43$, triclinic, space group $P\bar{1}$, $a = 10.896(6)$, $b = 12.869(5)$, $c = 20.373(6)$ Å, $\alpha = 94.67(6)$, $\beta = 101.12(8)$, $\gamma = 110.72(8)°$, $V = 2586.6$ Å^3, $Z = 2$, $\rho_{calc.} = 4.218\ g cm^{-3}$, $Mo_{K\alpha}$ radiation ($\lambda = 0.71073$ Å, $\mu = 243.36\ cm^{-1}$), structure solved by direct methods and successive Fourier difference synthesis, refinement of 671 variables with anisotropic thermal parameters gave $R(F) = 0.048$ and $R_w(F) = 0.063$ by using 6030 absorption corrected reflections with $|F| \geq 3\sigma(F)$. Further details of the crystal structure determination may be obtained from the Fachinformationszentrum Karlsruhe, Gesellschaft für wissenschaftlich-technische Information mbH, D-W-7514 Eggenstein-Leopoldshafen 2 (FRG), on quoting the depository number CSD-56123, the names of the authors, and the journal citation.
[7] W. N. Lipscomb, *Inorg. Chem.* **1965**, *4*, 132.
[8] E. Sinn, *Coord. Chem. Rev.* **1970**, *5*, 313.
[9] W. L. Gladfelter, M. W. Lynch, W. P. Schaefer, D. N. Hendrickson, H. B. Gray, *Inorg. Chem.* **1981**, *20*, 2390.
[10] A. P. Ginsberg, *Inorg. Chim. Acta Rev.* **1971**, *5*, 45.
[11] J. A. Bertrand, A. P. Ginsberg, R. I. Kaplan, C. E. Kirkwood, R. L. Martin, R. C. Sherwood, *Inorg. Chem.* **1971**, *10*, 240.
[12] J. K. McCusker, E. A. Schmitt, D. N. Hendrickson in *Magnetic Molecular Materials* (Eds.: D. Gatteschi, O. Kahn, J. S. Miller, F. Palacio), *NATO ASI Ser., Ser. E* **1991**, *198*, 297.
[13] a) L. Ouahab, M. Bencharif, D. Grandjean, *C. R. Acad. Sci., Sér. 2* **1988**, *307*, 749; b) A. Mhanni, L. Ouahab, O. Pena, D. Grandjean, C. Garrigou-Lagrange, P. Delhaes, *Synth. Met.* **1991**, *41-43*, 1703; c) S. Triki, L. Ouahab, D. Grandjean, J. M. Fabre, *Acta Crystallogr. Sect. C* **1991**, *47*, 645; d) S. Triki, L. Ouahab, J. Pandiou, D. Grandjean, *J. Chem. Soc. Chem. Commun.* **1989**, 1068.
[14] C. Bellitto, D. Attanasio, M. Bonamico, V. Fares, P. Imperatori, S. Patrizio, *Mater. Res. Soc. Symp. Proc.* **1990**, *173*, 143.
[15] A. Davidson, K. Boubekeur, A. Pénicaud, P. Auban, C. Lenoir, P. Batail, G. Hervé, *J. Chem. Soc. Chem. Commun.* **1989**, 1373.
[16] R. G. Finke, M. W. Dorege, P. J. Domaille, *Inorg. Chem.* **1987**, *26*, 3886.
[17] W. H. Knoth, P. J. Domaille, R. L. Harlow, *Inorg. Chem.* **1986**, *25*, 1577.

Metallacumulenes: Activation of Diynes and Access to a Novel Bis(Alkenylallenylidene)-ruthenium Complex with the Structural Unit $R_2C{=}C{=}C{=}Ru{=}C{=}C{=}CR_2$**

By *Nadine Pirio, Daniel Touchard, Pierre H. Dixneuf,* Mohammed Fettouhi,* and *Lahcène Ouahab*

Dedicated to Professor Wolfgang Beck on the occasion of his 60th birthday

Delocalized π-electron systems may endow metal-containing polymers and their organometallic precursors with the properties of electronic conductors, non-linear optical materials, or liquid crystals.[1] It has been shown recently that simple unsymmetrical *trans*-bis(acetylide)platinum complexes display non-linear optical properties[2] and that diynyl–metal polymers behave like liquid crystals.[3] Thus much attention is currently being directed to the preparation of new rod-shaped organometallic compounds containing two unsaturated chains such as the ynyl–metal moities $(RC{\equiv}C)_2M$, $(RC{\equiv}C{-}X{-}C{\equiv}C)_2M$, or $[MC{\equiv}C{-}X{-}C{\equiv}C]_n$[2-5] or acetylide-vinylidene-metal complexes.[6, 7] Our interest in the activation of diynes and the search for new metallacumulenes[8] has led us to discover an interesting synthetic method to new rod-shaped unsaturated ruthenium complexes including a *trans*-bis(diynyl)ruthenium complex and a metallacumulene containing a $>C{=}C{=}C{=}Ru{=}C{=}C{=}C<$ arrangement.

The reaction of the *cis* complex **1**[9] with the diynyltin compound **2** in dichloromethane at room temperature afforded the *trans*-chloro(diynyl)ruthenium compound **3** in 30% yield (Scheme 1). We attempted to generate the metallacumulene intermediate **I** (dppm = bis(diphenyldiphosphino)methane) by displacement of the Me_3SiO^- group.

$[(dppm)_2(Cl)Ru{=}C{=}C{=}C{=}C{=}CPh_2)]PF_6$ **I**

Treatment of **3** in methanol with $HBF_4 \cdot Et_2O$ provided the red (alkenylallenylidene)ruthenium complex **4** in 39% yield.

[*] Prof. P. H. Dixneuf, N. Pirio, Dr. D. Touchard
Laboratoire de Chimie de Coordination Organique
URA CNRS 415, Campus de Beaulieu
Université de Rennes
F-35042 Rennes (France)
M. Fettouhi, Dr. L. Ouahab
Laboratoire de Cristallochimie, URA CNRS 254
Université de Rennes

[**] This work was supported by the CNRS and MENJS. N. P. thanks the MRT for a grant.

This product most likely resulted from the addition of methoxide to the electrophilic C3 carbon atom of the cation of intermediate **I**.

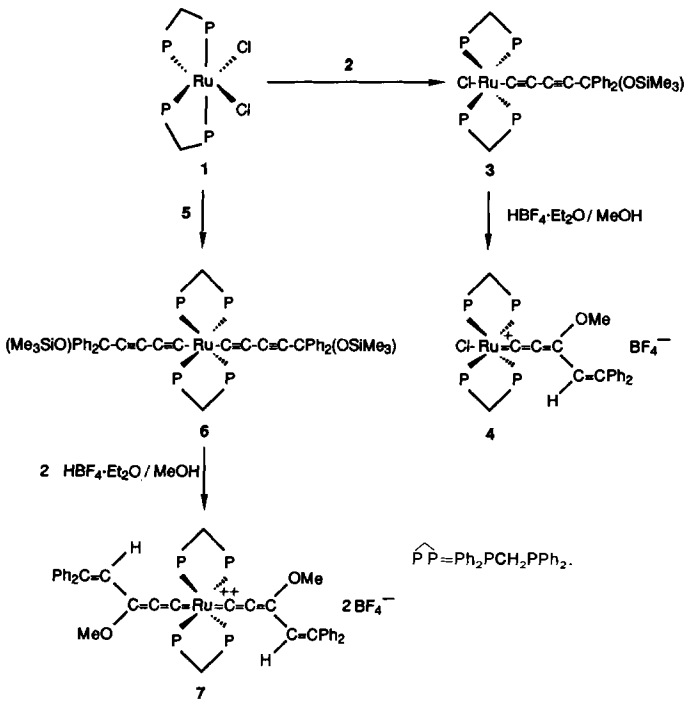

Scheme 1. **2**: $Bu_3Sn-C\equiv C-C\equiv C-CPh_2(OSiMe_3)$; **5**: $HC\equiv C-C\equiv C-CPh_2(OSiMe_3)$.

The transformation of **3** into **4** suggested that the introduction of two *trans* diynyl groups at the ruthenium center would make a bis(alkenylallenylidene)ruthenium complex accessible. Reaction of complex **1** with an excess of **2** did not lead to the substitution of both chloro ligands. The desired bis(diynyl)ruthenium complex **6** was produced much more simply by the direct reaction of **1** with an excess of diyne **5** (6 equiv) in the presence of $HNiPr_2$ in 24% yield [IR (KBr): $\tilde{\nu}$ [cm^{-1}] = 2020 (m, C≡C), 2175 (s, (C≡C)].

The reaction of complex **6** under the same conditions as those required for the conversion of **3** to **4** gave a 76% yield of the novel violet bis(alkenylallenylidene)ruthenium complex **7** [IR (KBr): $\tilde{\nu}$[cm^{-1}] = 1958 (s, C=C=C)]. The symmetric structure of the dication of **7** was evident from the NMR spectra, because of the magnetic equivalence of the PCH_2P protons and the ^{13}C nuclei of the allenylidene group [δ = 233.68 (quint, Ru=*C*, ^2J(P,C)=14.3 Hz), 138.93 (quint, Ru=C=*C*, ^3J(P,C) = 1.6 Hz), 164.96 (s, Ru=C=C=*C*)]. Structural characterization of the dication of **7** revealed that both allenylidene groups and the ruthenium atom are almost in the same plane (Fig. 1).[10] The molecule is centrosymmetric, and the C3′-C2′-C1′-Ru-C1-C2-C3 arrangement is almost linear. Compared to the Ru–C1 and the C1–C2 bond lengths in the cation of the mono(allenylidene)ruthenium complex **8**, (1.884(5) and 1.255(8) Å respectively),[11] the

$[(PMe_3)_2(\eta^5\text{-}C_5H_5)Ru=C=C=CPh_2]PF_6$ **8**

Ru–C1 bond of **7** is long (1.994(7)Å) and the C1-C2 bond short (1.22(1)Å). Apparently the C1–C2 bond has partial triple-bond character, possibly due to conjugation with the methoxy group at C3, which is indicated by a short C3–O

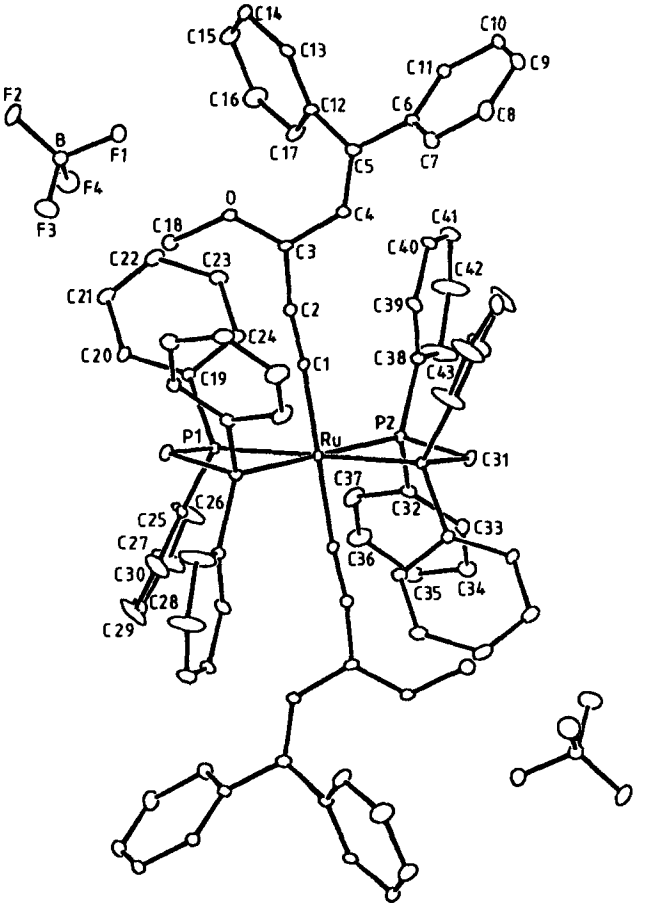

Fig. 1. Crystal structure of **7**. Selected bond lengths [Å] and angles [°]: Ru-C1 1.997(7), O-C3 1.292(9), O-C18 1.46(1), C1-C2 1.22(1), C2-C3 1.39(1), C3-C4 1.45(1), C4-C5 1.36(1); C′1-Ru-C1 180.0, C3-O-C18 121.3(8), Ru-C1-C2 175.0(7), C1-C2-C3 171.4(9), O-C3-C2 122.1(9), O-C3-C4 117.8(7), C2-C3-C4 120.1(7), C3-C4-C5 123.2(8).

bond (1.292(9) Å). The structural parameters thus indicate a substantial contribution of the mesomeric forms **B** and **C** as shown in Scheme 2. In the transformation of compound **6**

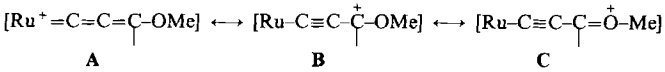

Scheme 2.

into **7** we assume that two consecutive eliminations of Me_3SiO^- and additions of methanol lead to the highly conjugated, rod-shaped metallacumulene intermediates **II** and **III**, and finally to **7** (Scheme 3).

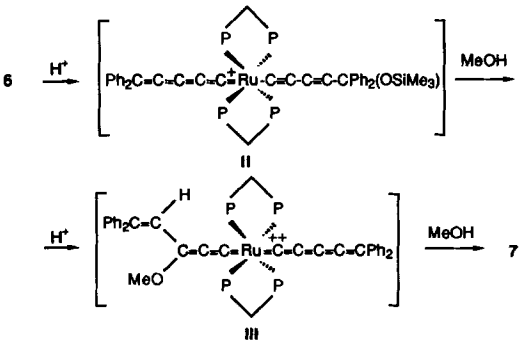

Scheme 3.

Experimental Procedure

All operations were carried out under nitrogen in anhydrous solvent.
3: $^{31}P\{^1H\}$ NMR (CD_2Cl_2, 121.50 MHz): $\delta = -6.47$ (s, PPh_2); $^{13}C\{^1H\}$ NMR (CD_2Cl_2, 75.47 MHz): $\delta = 125.97$ (quint, Ru-*C*≡C, $^2J(P,C) = 15.2$ Hz), 93.48 (s, Ru-C≡*C*), 80.24, 76.51, 63.79 (s, Ru-C≡C-*C*≡*C*-*C*Ph_2); IR (KBr): $\tilde{\nu}$[cm^{-1}] = 2024 (m, C≡C), 2176 (s, C≡C). Correct elemental analysis (C, H, Cl).

4: $^{31}P\{^1H\}$ NMR (CD_2Cl_2, 121.50 MHz): $\delta = -11.72$ (s, PPh_2); $^{13}C\{^1H\}$ NMR (CD_2Cl_2, 75.47 MHz): $\delta = 252.76$ (quint, Ru=*C*, $^2J(P,C) = 13.5$ Hz), 155.71 (s, =*C*Ph_2), 154,15 (s, Ru=C=C=*C*), 150.18 (quint, Ru=C=*C*, $^3J(P,C) = 2.2$ Hz); ^{13}C NMR (CD_2Cl_2, 75.47 MHz): $\delta = 124.43$ (d, *C*H=, $^1J(C,H) = 163.8$ Hz); IR (KBr): ν[cm^{-1}] = 1955 (s, C=C=C). Correct elemental analysis (C, H).

6: A solution of **5** (0.62 g, 2 mmol) and $NHiPr_2$ (3 mmol) in 60 mL of dichloromethane was added to **1** (0.47 g, 0.5 mmol) and $NaPF_6$ (0.34 g, 2 mmol). The solution was stirred at room temperature for 4 h, and its color changed from orange to brown. The crude product was filtered through 30 g of alumina with ether. Recrystallization from THF/pentane (1:3) gave 0.18 g (24%) of **6** as yellow crystals. $^{31}P\{^1H\}$ NMR (CD_2Cl_2, 121.50 MHz): $\delta = -4.21$ (s, PPh_2); $^{13}C\{^1H\}$ NMR (CD_2Cl_2, 75.47 MHz): $\delta = 131.18$ (quint, Ru-*C*≡C, $^2J(P,C) = 15.2$ Hz), 96.42 (s, Ru-C≡*C*), 80.27, 76.60, 64.96 (s, Ru-C≡C-*C*≡*C*-*C*Ph_2). Correct elemental analysis (C, H, P).

7: To a solution of **6** (90 mg, 0.06 mmol) in 20 mL of methanol was added $HBF_4 \cdot Et_2O$ (0.6 mmol). The yellow solution immediately turned blue and then violet. The reaction mixture was stirred for 2 h, the solvent was removed, and the product was washed with ether. Recrystallization from dichloromethane hexane (1:2) afforded 70 mg (76%) of violet crystals of **7**. $^{31}P\{^1H\}$ NMR (CD_2Cl_2, 121.50 MHz): $\delta = -9.14$ (s, PPh_2); $^{13}C\{^1H\}$ NMR (CD_2Cl_2, 75.47 MHz): $\delta = 233.68$ (quint, Ru=*C*, $^2J(P,C) = 14.3$ Hz), 165.58 (s, =*C*Ph_2), 164.96 (s, Ru=C=C=*C*), 138.93 (quint, Ru=C=*C*, $^3J(P,C) = 1.6$ Hz); ^{13}C NMR (CD_2Cl_2, 75.47 MHz): $\delta = 122.01$ (d, *C*H=, $^1J_{CH} = 150.4$ Hz); IR (KBr): $\tilde{\nu}$ [cm^{-1}] = 1958 (s, C=C=C). Correct elemental analysis (C, H, P).

Received: November 19, 1991 [Z 5028 IE]
German version: *Angew. Chem.* **1992**, *104*, 664

CAS Registry numbers:
1, 79982-54-0, **2**, 140389-67-9; **3**, 140389-68-0; **4**, 140389-70-4; **5**, 124686-50-6; **6**, 140389-71-5; **7**, 140389-73-7; **I**, 140389-75-9.

[1] a) J. R. Ferraro, J. M. Williams, *Introduction to Synthetic Electrical Conductors*, Academic, Orlando, FL, USA, **1987**, Chapter 3; b) P. N. Prasad in *Non-linear Optical and Electron Active Polymers* (Ed.: D. R. Ulrich), Plenum, New York, **1988**; c) D. S. Chemla in *Non-linear Optical Properties of Organic Molecules and Crystals Vol. 1* (Ed.: J. Zyss), Academic, Orlando, FL, USA, **1987**.

[2] H. B. Fyfe, M. Mlekuz, D. Zargarian, N. J. Taylor, T. B. Marder, *J. Chem. Soc. Chem. Commun.* **1991**, 188–190, and references therein.

[3] S. Takahashi, Y. Takai, H. Morimoto, K. Sonogashira, *J. Chem. Soc. Chem. Commun.* **1984**, 3–5, and references therein.

[4] a) S. J. Davies, B. F. G. Johnson, M. S. Khan, J. Lewis, *J. Chem. Soc. Chem. Commun.* **1991**, 187–188; b) S. J. Davies, B. F. G. Johnson, J. Lewis, M. S. Khan, *J. Organomet. Chem.* **1991**, *401*, C43–C45; c) B. F. G. Johnson, A. K. Kakkar, M. S. Khan, J. Lewis, *ibid.* **1991**, *409*, C12–C14; d) S. J. Davies, B. F. G. Johnson, J. Lewis, P. R. Raithby, *ibid.* **1991**, *414*, C51–C53. Short review of metalla-enes and metallaynes: M. H. Chisholm, *Angew. Chem.* **1991**, *103*, 690; *Angew. Chem. Int. Ed. Engl.* **1991**, *30*, 673.

[5] N. Hagihara, K. Sonogashira, S. Takahashi, *Adv. Polym. Sci.* **1981**, *41*, 149–179.

[6] A. K. McMullen, J. P. Selegue, J. G. Wang, *Organometallics* **1991**, *10*, 3421–3423.

[7] M. Schäfer, J. Wolf, H. Werner, *J. Chem. Soc. Chem. Commun.* **1991**, 1341–1343.

[8] A. Romero, A. Vegas, P. H. Dixneuf, *Angew. Chem.* **1990**, *102*, 210–211; *Angew. Chem. Int. Ed. Engl.* **1990**, *29*, 215–216.

[9] B. Chaudret, G. Commenges, R. Poilblanc, *J. Chem. Soc. Dalton Trans.* **1984**, 1635–1639.

[10] Crystal data for **7**: violet rhombic crystals, Enraf-Nonius CAD4 diffractometer, monoclinic, space group $P2_1/c$ (No. 14), $a = 16.076(4)$, $b = 11.514(5)$, $c = 20.778(6)$ Å, $\beta = 103.53(2)°$, $V = 3739.1$ Å^3, $Z = 2$, $\rho_{calcd} = 1.364$ g cm^{-3}, $\mu = 3.535$ cm^{-1} ($Mo_{K\alpha}$ radiation). The structure was solved by direct methods and successive Fourier difference synthesis. The H atoms were found by Fourier synthesis and were also placed at idealized positions. Non-hydrogen atoms were refined with anisotropic thermal parameters to $R(F) = 0.058$ and $R\omega(F) = 0.073$ by using 2719 absorption-corrected reflections with $I \geq 3\sigma(I)$. Further details of the crystal structure determination are available on request from the Fachinformationszentrum Karlsruhe, Gesellschaft für wissenschaftlich-technische Information mbH, D-W-7514 Eggenstein-Leopoldshafen 2, FRG, on quoting the depository number CDS-56005, the names of the authors, and the journal citation.

[11] J. Selegue, *Organometallics* **1982**, *1*, 217–218.

Ag_5GeO_4, a New Semiconducting Oxide**

By *Martin Jansen** and *Christoph Linke*

The reader of this article may assume a serious printing error in the formulation of the title compound as Ag_5GeO_4; it is correct, however, and the unusual composition of this new oxide has been confirmed beyond doubt by X-ray analysis[1] and energy-dispersive electron beam microanalysis.[2]

We have previously indicated that the characteristic separation of the silver partial structure (by the formation of short silver–silver contacts) and the anionic parts in silver-rich oxides can only be understood if attractive interactions are assumed between the Ag^+ ions despite the closed d^{10} configuration.[3] This assumption is supported by a wealth of structural examples and, particularly, by the connections between this structural feature and characteristic properties of the substances.[4] Also the otherwise inexplicable features in the crystal structures of zinc and cadmium metal are classified here. Since the aggregates of silver(I) cations can be interpreted topographically as sections from the structure of silver metal and as a result an unoccupied 5s orbital should be present as a low-lying acceptor level, we assumed that in this bonding situation silver should tend towards subvalence. Actually, single subvalent silver compounds such as Ag_2F[5] or Ag_3O[6] are known. We believe that the synthesis of Ag_5GeO_4 is an indication that our assumption could be generally valid. The high tendency of formation of Ag_5GeO_4 is shown in that despite the oxidizing conditions during the preparation (high-pressure oxygen) decomposition into Ag (or $1/2\,Ag_2O$) and Ag_4GeO_4 does not occur.

Ag_5GeO_4 is formed by a solid-state reaction (*Experimental Procedure*) from mixtures of Ag_2O, Ag, and GeO_2, or Ag and GeO_2 under the oxidizing conditions of the high-pressure oxygen synthesis. The reaction product is air-stable and consists of yellow-tinged shiny metallic crystals. The decomposition via loss of oxygen begins at 520 °C.

The crystal structure (Fig. 1) contains almost regular tetrahedral orthogermanate ions with dimensions which are in agreement with numerous corresponding examples.[7] Therefore the silver skeleton must be completely responsible for the "anomaly" in the valency. In systems in which we assume bonding d^{10}–d^{10} interactions,[4] the Ag–Ag dis-

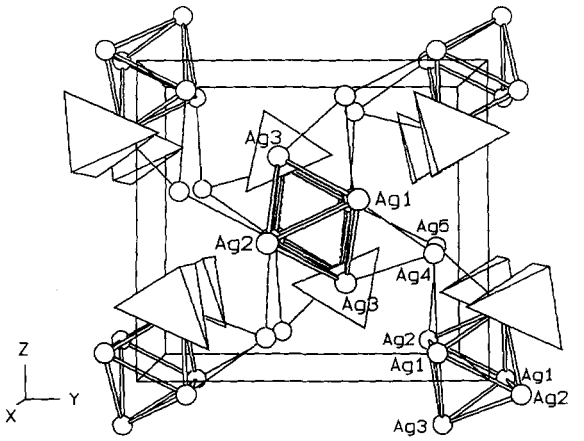

Fig. 1. Diagram of the crystal structure of Ag_5GeO_4 in perspective along [100].

[*] Prof. Dr. M. Jansen, C. Linke
Institut für Anorganische Chemie
Gerhard-Domagk-Strasse 1, D-W-5300 Bonn 1 (FRG)

[**] This work was supported by the Deutsche Forschungsgemeinschaft (Leibnitz-Programm) and the Fonds der Chemischen Industrie.

tances characteristically lie between 289 pm (atom distance in silver metal) and 340 pm (van der Waals contact distance).[8] By the crystal chemical analysis of the solid-state structure of Ag_5GeO_4, however, distances are encountered which in contrast to the ones given are significantly shortened. The silver atoms of the crystallographically independent positions Ag1 to Ag3 form an octahedral cluster with a center of inversion (site symmetry) with significantly shorter distances (274 to 284 pm).

The other Ag–Ag contacts lie in the normal range for silver-rich oxides above 300 pm (with the exception of 291 pm for Ag2–Ag4). The shortening of the silver-silver distances within the Ag_6 cluster indicates that it includes the excess electrons resulting from a simple count ($10 \times Ag^+$, $2 \times GeO_4^{4-}$). This can be expressed by the formula $[Ag_6]^{4+}[Ag_4(GeO_4)_2]^{4-}$. Precisely two electrons occupy the lowest bonding molecular orbital (A_{1g}) in the Ag_6^{4+} unit, which is thus the most electron-poor octahedral cluster so far.

It is now known that M_6 clusters often are centered by nonmetal atoms. Since furthermore, a $[Ag_6O^{4+}]$ unit with monovalent silver would carry the same overall charge as the previously described cluster, we checked the area of the Ag_6 octahedron for residual electron density and the distances of silver to the center of the octahedron: from both criteria we were able to exclude the presence of nonmetal atoms such as C, N, and O.

Because the formation of a "two-electron six-center bond" alone is probably not sufficient to provide the driving force for the formation of the cluster, once again the not yet completely understood d^{10}–d^{10} interactions come into play as additional bonding components. In agreement with this interpretation, particularly with the assumption of an extensive localization of the excess valence electrons in the Ag_6^{4+} clusters, the substance is diamagnetic (measured range: 4–298 K) and shows an electrical resistance of 5 MΩcm at room temperature. The inclusion of silver in the cluster leads to the characteristically one-sided coordinations of the silver atoms by oxygen. It is either a trigonal threefold coordination with bond angles of around 90° at silver (Ag1 and Ag2), which thus occupies the apex of a trigonal pyramid, or a highly bent twofold coordination (Ag3) with bond angles also of around 90°. The germanate tetrahedra project, each with one edge, into the spaces between two Ag_6 octahedra (Fig. 2). The conditions of formation and the stability of the

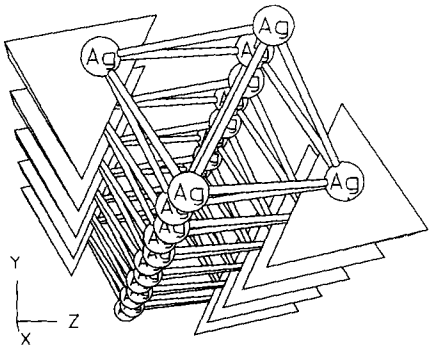

Fig. 2. Relative arrangement of the Ag_6^{4+} clusters and the orthogermanate ions in Ag_5GeO_4.

new compound lead us to expect that other suboxides can also be prepared. Paradoxically, the synthesis of this suboxide can be achieved under increased oxygen pressure. Possible explanations for this are a high thermodynamic stability of the new compound or the fixation of the silver activity by the silver metal always present in the reaction set up, and at the same time a kinetic inhibition of the establishment of an equilibrium between the oxygen activity in the gas phase and in the solid state.

Experimental Procedure

Intimate mixtures of the starting materials Ag_2O and GeO_2 in the molar ratio 5:1 or Ag_2O, Ag, and GeO_2 in the molar ratio 2.5:5:2 were allowed to react in a silver crucible in a high-pressure oxygen autoclave at ($p(O_2) \approx 500$ bar and 320 °C with the addition of a little water as an accelerator (reaction time 10–14 d). GeO_2 (Strem 99.999%); Ag powder was precipitated with hydrazine hydrate as reducing agent at room temperature from a weak ammonia/$AgNO_3$ solution; Ag_2O was obtained by precipitation with potassium hydroxide from a nitric acid/$AgNO_3$ solution. The Ag_2O thus obtained was thoroughly washed and dried in a desiccator over KOH.

Received: December 14, 1991 [Z 5071 IE]
German version: *Angew. Chem.* **1992**, *104*, 618

CAS Registry numbers:
Ag_5GeO_4, 141043-50-7; Ag_2O, 20667-12-3; GeO_2, 1310-53-8; Ag, 7440-22-4.

[1] Monoclinic, space group $P2_1/n$, $a = 636.94(8)$, $b = 991.03(15)$, $c = 923.21(10)$ pm, $\beta = 91.391(12)°$, $V = 5.828(9) \times 10^8$ pm^3, $Z = 4$, Enraf-Nonius CAD 4 four-circle diffractometer, $Mo_{K\alpha}$ radiation, graphite monochromator, $\omega/2\theta$ scan with $2\theta \leq 80°$, empirical absorption correction, 2496 independent reflections with $F_o > 4\sigma(F_o)$, anisotropic temperature factors, $R = 0.061$, $Rw = 0.054$, $w = 1/\sigma^2(F)$, SHELX-76 (G. M. Sheldrick, University of Cambridge, **1976**). Further details of the crystal structure investigation may be obtained from the Fachinformationszentrum Karlsruhe, Gesellschaft für wissenschaftlich-technische Information mbH, D-W-7514 Eggenstein-Leopoldshafen 2 (FRG) on quoting the depository number CSD-56192, the names of the authors, and the journal citation.

[2] EDAX PV 9800; electron microscope Zeiss DSM 940, acceleration voltage 25 kV, found ratio Ag:Ge = 5.07:1.

[3] M. Jansen, Habilitationsschrift, Universität Gießen, **1978**; M. Jansen, *J. Less-Common Met.* **1980**, *76*, 285-292.

[4] M. Jansen, *Angew. Chem.* **1987**, *99*, 1136–1146. *Angew. Chem. Int. Ed. Engl.* **1987**, *26*, 1098–1110.

[5] G. Argay, F. Naray-Szabo, *Acta Chim. Sci. Hung.* **1966**, *49*, 329–337

[6] W. Beesk, P. G. Jones, H. Rumpel, E. Schwarzmann, G. M. Sheldrick, *J. Chem. Soc. Chem. Commun.* **1981**, 664–665.

[7] E'Halvax, H. Voellenke, *Monatsh. Chem.* **1985**, *116*, 1367–1376; A. Wittmann, H. Voellenke, *Z. Kristallogr. Kristallgeom. Kristallphys. Kristallchem.* **1969**, *128*, 66–71; G. S. Smith, P. B. Isaacs, *Acta Crystallogr.* **1964**, *17*, 842–846.

[8] A. Bondi, *J. Phys. Chem.* **1964**, *68*, 441–451.

Self-Replication by Condensation of 3-Aminobenzamidines and 2-Formylphenoxyacetic Acids**

By *Andreas Terfort* and *Günter von Kiedrowski**

The development of artificial self-replicating systems[1] has been envisioned as an intriguing and challenging task for bioorganic and supramolecular chemistry.[2] The goal is to elaborate the structural, functional, and dynamic principles that played a role in the evolution of the earliest life forms on earth and that might form a framework for the future development of synthetic systems capable of evolution.[3] As originally demonstrated in 1986, the smallest conceivable model of a self-replicating system is the autocatalytic synthesis of a self-complementary template molecule.[4] Attempts to realize this principle[4–9] utilized self-complementary oligodeoxynucleotides,[4] oligonucleotide analogues,[5–7] and hybrid molecules incorporating a nucleotide constituent.[8] In

[*] Dr. G. von Kiedrowski, Dipl.-Chem. A. Terfort
Institut für Organische Chemie der Universität
Göttingen, Tammannstraße 2, D-W-3400 Göttingen (FRG)

[**] Financial support by Deutsche Forschungsgemeinschaft and Fonds der Chemischen Industrie is acknowledged. We thank Reinhart Machinek for helpful suggestions and support on the ^{1}H NMR measurements.

all these systems the autocatalytic synthesis follows a rate law that is half order with respect to the template concentration (square-root law).[1a-c, 4-8] The growth of autocatalyst concentration is therefore parabolic in the ideal case.[1a-c, 6]

We have attempted to realize self-replication using the simplest possible organic constituents and without any nucleobase for molecular recognition. Our concept is to employ the amidinium–carboxylate salt bridge[10] as a substitute for base pairing. A titration of benzamidinium tetrafluoroborate with cesium acetate monitored by ^{1}H NMR spectroscopy in [D$_6$]dimethyl sulfoxide ([D$_6$]DMSO) confirmed that the amidinium–carboxylate salt bridge is sufficiently stable in the solvent chosen ($K = 350 \pm 50$ M^{-1} at $T = 35$ °C). Condensation of 3-aminobenzamidines **1** with 2-formylphenoxyacetic acids **2** yielded anils of the type **3**,[11] which can exist in conformations in which the recognition sites are aligned roughly parallel to each other according to force-field calculations (MMX). These molecules should act as autocatalysts since they should be able to bind constituents **1** and **2** forming ternary complexes **4** in which the condensation should proceed more easily due to a preorganization effect.

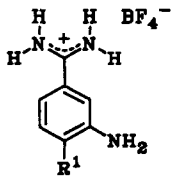

1

a: R^1 = *t*Bu
b: R^1 = Me

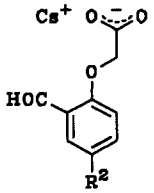

2

a: R^2 = NO_2
b: R^2 = H

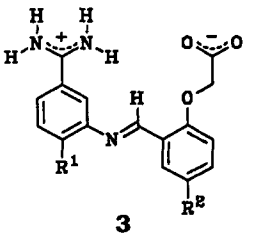

3

a: R^1 = *t*Bu , R^2 = NO_2
b: R^1 = Me, R^2 = NO_2
c: R^1 = *t*Bu , R^2 = H

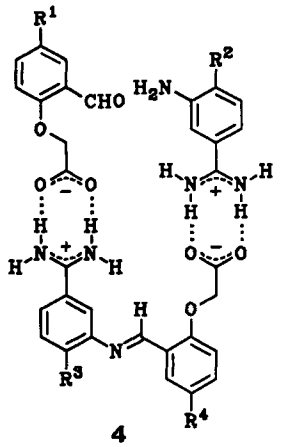

4

a: R^1 = R^4 = NO_2
R^2 = R^3 = *t*Bu
b: R^1 = NO_2, R^2 = Me
R^3 = *t*Bu , R^4 = H

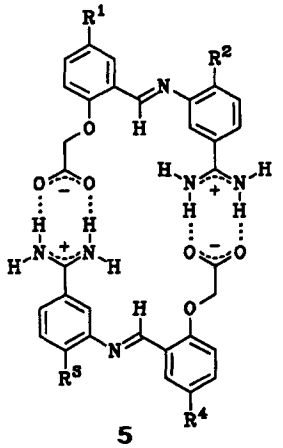

5

a: R^1 = R^4 = NO_2
R^2 = R^3 = *t*Bu
b: R^1 = NO_2, R^2 = Me
R^3 = *t*Bu , R^4 = H
c: R^1 = R^4 = H
R^2 = R^3 = *t*Bu

In fact, experimental evidence for an autocatalytic reaction channel was observed for the synthesis of **3a** from **1a** and **2a** when the reaction was monitored by ^{1}H NMR spectroscopy: the higher the initial concentration of **3a** in the reaction mixtures, the faster its formation.[12] The experimental time traces could be satisfactorily approximated by a

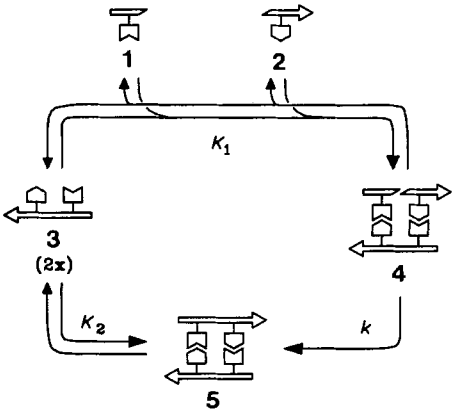

square-root model.[13, 14] Under the given reaction conditions ([D$_6$]DMSO, $T = 50$ °C), the autocatalytic synthesis of **3a** is faster than the nonautocatalytic synthesis by a factor of $\varepsilon = 16.4 \pm 4.4$ M$^{-1/2}$. Thus, the autocatalytic efficiency ε[15] may be compared to that of our system of 1986 ($\varepsilon = 24$ M$^{-1/2}$) as well as to that of the Rebek system ($\varepsilon = 22$ M$^{-1/2}$).[6] The reaction of **1b** and **2a** in the presence of the anil **3c**, which is a structural analogue of the reaction product **3b**, yielded an unexpected result, however. The formation of **3b** in [D$_6$]DMSO at $T = 27$ °C was monitored by ^{1}H NMR spectroscopy up to 25% conversion.

Anil **3c** accelerated the synthesis of **3b** by a factor of 370 M^{-1}. Figure 1 provides evidence that the rate increase roughly corresponds to the initial concentration of **3c**. This finding is remarkable because the catalysis by the structurally analogous self-complementary template **3c** is thus no longer described by a square-root law, but for the first time by a first-order relationship. First-order catalysis is expect-

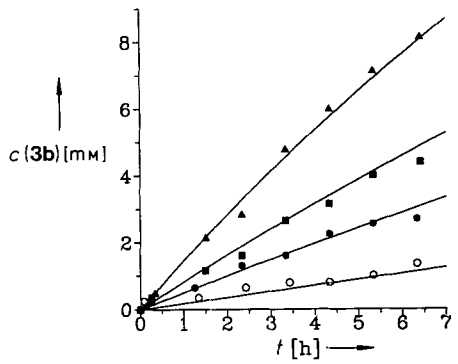

Fig. 1. Reaction rate for the synthesis of anil **3b** in the presence (from bottom to top) of 0, 0.1, 0.2, 0.4 equiv of template **3c** as monitored by ^{1}H NMR spectroscopy. Reaction conditions: 50 mM **1b**, 50 mM **2a**, $T = 27$ °C, solvent [D$_6$]DMSO. ^{1}H NMR frequency: 80 MHz. The set of theoretical curves was calculated using SimFit [14] and the following reaction model: 1) **1b** + **2a** ⇌ **3b** + H_2O. 2) **1b** + **2a** + **3c** → **3b** + **3c** + H_2O. Results: $k_1 = (1.99 \pm 0.15) \times 10^{-5}$ M^{-1}s^{-1}, k_{-1} (no exact solution possible) = $(0.1 \pm 7.3) \times 10^{-5}$ M^{-1}s^{-1}, $k_2 = (7.31 \pm 0.26) \times 10^{-3}$ M^{-2}s^{-1}.

ed, if the concentration of the ternary complex **4b** (formed from **1b**, **2a**, and **3c**) is higher than that of the catalyst duplex **5c**.[16] In this case, the salt bridges in the ternary complex are expected to be more stable than those in the catalyst duplex. Current studies aim to provide experimental support for this hypothesis.

The existence of first-order catalysis by a self-complementary template molecule suggests that self-replication with ex-

ponential autocatalysis should be feasible if the proper model system is used. The strategy might be to search for linking reactions which modulate the molecular recognition process. The linkage must generate a template molecule that forms less stable salt bridges with itself than with its precursors. Current studies aim to couple the modulation of molecular recognition with the generation of chiral template molecules to find an approach towards asymmetric autocatalysis.

Received: October 18, 1991 [Z 4976 IE]
German version: *Angew. Chem.* **1992**, *104*, 626

[1] Reviews: a) G. von Kiedrowski in *40 Jahre Fonds der Chemischen Industrie* (Ed.: Verband der Chemischen Industrie), VCI publications, Frankfurt, **1990**; b) G. von Kiedrowski, *Origins Life*, in press; c) L. E. Orgel, *Cold Spring Harbor Symp. Quant. Biol.* **1987**, *7*, 9–16; d) G. F. Joyce, *ibid.* **1987**, *7*, 41–51.

[2] a) G. M. Whitesides, *Angew. Chem.* **1990**, *102*, 1247–1257; *Angew. Chem. Int. Ed. Engl.* **1990**, *29*, 1209–1218; b) J. S. Lindsey, *New J. Chem.* **1991**, *15*, 153–180.

[3] Cf. essays in *Artificial Life. The Proceedings of an Interdisciplinary Workshop on the Synthesis and Simulation of Living Systems Held September, 1987 in Los Alamos, New Mexico* (Ed.: C. G. Langton), Addison-Wesley, Redwood City, USA, **1989**.

[4] G. von Kiedrowski, *Angew. Chem.* **1986**, *98*, 932–934; *Angew. Chem. Int. Ed. Engl.* **1986**, *25*, 932–935.

[5] G. von Kiedrowski, B. Wlotzka, J. Helbing, *Angew. Chem.* **1989**, *101*, 1259–1261; *Angew. Chem. Int. Ed. Engl.* **1989**, *28*, 1235–1237.

[6] G. von Kiedrowski, B. Wlotzka, J. Helbing, M. Matzen, S. Jordan, *Angew. Chem.* **1991**, *103*, 456–459, 1066; *Angew. Chem. Int. Ed. Engl.* **1991**, *30*, 423–426, 892.

[7] W. S. Zielinski, L. E. Orgel, *Nature* (London) **1987**, *327*, 346–347.

[8] T. Tjivikua, P. Ballester, J. Rebek, Jr., *J. Am. Chem. Soc.* **1990**, *112*, 1249–1250; J. S. Nowick, Q. Feng, T. Tjivikua, P. Ballester, J. Rebek, Jr., *ibid.* **1991**, *113*, 8831–8839.

[9] Meanwhile, template-free approaches towards self-replicating systems were also reported: P. A. Bachmann, P. Walde, P. L. Luisi, J. Lang, *J. Am. Chem. Soc.* **1990**, *112*, 8200–8201; cf. M. Zeleny, G. J. Klir, K. D. Hufford in ref. [3], pp. 125–139.

[10] For other supramolecular applications of salt-bridges with guanidinium and amidinium salts see: a) G. Müller, J. Riede, F. P. Schmidtchen, *Angew. Chem.* **1988**, *100*, 1574–1577; *Angew. Chem. Int. Ed. Engl.* **1988**, *27*, 1516–1518; b) A. Echaverren, A. Galan, J.-M. Lehn, J. de Mendoza, *J. Am. Chem. Soc.* **1989**, *111*, 4994–4995; c) M. Göbel, D. Reckenbeil in *Chemiedozententagung* **1991** (Ed.: D. Döpp), University of Duisburg, Duisburg, **1991**.

[11] Compounds **1** were equipped with alkyl groups to increase the solubility of the corresponding anils sufficiently. Synthesis of compounds **1** will be described elsewhere. 2-Formylphenoxyacetic acids were used instead of the corresponding 2-formylbenzoic acids, since in the latter case it was not possible to prevent an intramolecular attack of the carboxylic group on the anil bond (ring closure).

[12] Compounds **1a** and **2a** (each 50 mM in [D_6]DMSO) were allowed to react in the presence of 0, 0.11, 0.26, and 0.37 mol % of **3a** in NMR tubes sealed by melting. The formation of phenoxyacetic acid **3a** was monitored at a frequency of 500 MHz by observing the following resonances: $\delta = 1.32/1.42$ (*t*Bu **1a**/**3a**), 7.22/7.56 (3′-H **1a**/**3a**), 10.39/8.86 (C*H* = O/C*H* = N). The formation of **3a** is reversible; the equilibrium constant was determined as $K = 5.73 \pm 1$ at $T = 50\,^{\circ}C$. The concentration of the primary adduct is below the limit of detection for the given NMR technique.

[13] The following reaction model based upon the square-root law was chosen for the evaluation of the experimental time courses of NMR integrals with the computer program SimFit [14]: 1) **1a** + **2a** ⇌ **3a** + H_2O. 2) **1a** + **2a** + 0.5 **3a** → 1.5 **3a** + H_2O. The apparent rate constants—as determined by SimFit—are ($T = 50\,^{\circ}C$): $k_1 = (1.50 \pm 0.24) \times 10^{-4}\ M^{-1}s^{-1}$, $k_{-1} = k_1/5.73\ M^{-1}s^{-1}$, $k_2 = (2.46 \pm 0.25) \times 10^{-3}\ M^{-3/2}s^{-1}$.

[14] G. von Kiedrowski, **1991**, unpublished. Program SimFit (Nonlinear *Fit*ting by Dynamic *Sim*ulation) processes the kinetic data of experimental concentration–time traces for any given reaction model. As many as 16 different experiments with varying initial concentrations can by evaluated in a single run. Reaction equations are introduced as input at run-time (i.e. no compiling and linking prior to program start), the program then generates the corresponding set of differential equations and the concentration derivatives (Jacobi matrix). The user may choose either the Runge–Kutta algorithm or a modified Gear algorithm as the method of integration. Nonlinear curve-fitting (by least squares) may be achieved either with the simplex algorithm or with the Newton–Raphson algorithm. The output includes the calculated concentration profiles, the rate constants, and the corresponding variances and covariances. The program supports the input of symbolic assignments of the concentrations of mechanistic species to observable concentrations (expressions with sums and differences). Thus, it is also applicable in those kinetic studies where only the total concentrations can be monitored (e.g. in the case of intermediate complexes which form and dissociate rapidly). In our laboratory, SimFit has proven a valuable tool for a large number of mechanistic studies.

[15] The autocatalytic efficiency ε has been defined as the factor by which the rate of the autocatalytic synthesis exceeds that of the nonautocatalytic synthesis, for a template concentration of 1 M [6].

[16] Normally a square-root law is expected, since a template duplex of type **5** should be more stable than a ternary complex of type **4** for entropic reasons.

BOOK REVIEWS

Book Reviews are written by invitation from the editor. Suggestions for books to be reviewed and for book reviewers are welcome. Publishers should send brochures or (better) books to the following address: Redaktion Angewandte Chemie, Postfach 101161, W-6940 Weinheim, Federal Republic of Germany. The editor reserves the right of selecting which books will be reviewed. Uninvited books not chosen for review will not be returned.

Organic Electrochemistry. An Introduction and a Guide. 3rd Edition (revised and enlarged). Edited by *H. Lund* and *M. M. Baizer*. Marcel Dekker, New York, 1991. XXII, 1550 pp., hardcover $ 234.00.—ISBN 0-8247-8154-6

For nearly twenty years now, "Baizer and Lund" has had the status of a proven and highly regarded standard work, which is oriented specifically towards organic chemists, and provides a broad survey of the many wide-ranging applications of organic electrochemistry. This revised and enlarged third edition takes account of the rapid developments occurring in the field, resulting in a book that contains nearly 400 more pages than the second edition. The revision has

been carried out in a responsible and critical way, so that not only have several chapters on recent developments been added, but also some on topics that are now less important have been taken out, transfering those parts that are still relevant into other chapters. The editors have succeeded in enlisting 30 internationally recognized and experienced scientists, all actively engaged in the research and teaching of their specialist areas, to write the 36 chapters.

Compared with the two earlier editions the structure of the book has changed only slightly. It begins with four chapters, totaling 250 pages, in which the basic principles and methods of electrochemistry are described. At several points here a deliberate decision has been made to avoid too detailed a mathematical description. Chapter 5 will certainly be very useful for newcomers to the field, as it offers much practical advice on how to carry out electrochemical experiments. The part of the book that follows is arranged in traditional organic chemistry style, classified according to types of electrodes and electrophoric groups, and consisting of over 350 pages. Reactions at the cathode are dealt with first, for hydrocarbons, halides, nitro compounds and related substances, carbonyl compounds, azomethines, and carboxylic acids and derivatives. This is followed by reactions at the anode, for hydrocarbons, carboxylic acids, nitrogen compounds, oxygen compounds, and sulfur compounds. Four further chapters then deal with the electrochemistry of heterocycles, electrochemical reactions as key steps in the synthesis of natural products and pharmaceuticals, the importance of electrochemistry in the exploitation of biomasses, and electrochemical reactions of organometallic compounds and coordination compounds. This part of the book is followed by detailed discussions of the various types of electrode reactions (reductive coupling, oxidative coupling, detachment and removal of protecting groups, anodic substitution, anodic fluorination). Here, of course, a small degree of overlapping with other chapters is unavoidable. A separate chapter is also devoted to the stereochemical aspects of organic electrode reactions. This is followed by three chapters on indirect electrochemical synthesis. Under the heading "Present and Future Applications" some topical applications-orientated areas are discussed, including industrial electrochemistry, electrochemical polymerization processes, modified electrodes, conducting polymers, and photoelectrochemistry. This section concludes with an assessment of future needs and opportunities.

From the organic chemist's viewpoint this book makes easy reading and is clear and comprehensible. The editors have succeeded in an exemplary way in welding together the individual contributions to make a consistent whole. However, the book does not always live up to its claim of being an introduction to electrochemistry, as the reader is too often referred to other textbooks, especially in the presentation of the fundamental principles. Also many of the methods are only described very briefly. Nevertheless, this only diminishes the book's usefulness very slightly; it impresses through the expert and skillful choice of material, and the wealth of helpful advice that is offered. Access to original publications for more advanced study is facilitated by the inclusion of about 7000 references, backed up by an index of authors, making the book also a valuable source of information for the scientist active in this field. Regrettably, though, the subject index is very scanty for a work of this size, and it is difficult to understand why.

Despite the reservations expressed above, the book can be recommended without hesitation, as the new "Lund and Baizer" is certain to be appreciated as a valuable guide and a mine of information that one cannot afford to be without. Manuel Baizer, who was the prime mover behind this book, sadly died 2½ years before the completion of the third edition; along with Henning Lund he deserves our sincere gratitude. Unfortunately the high price will be an obstacle to the book reaching a wide readership, and regrettably it will, therefore, not be to hand in every laboratory. It is certainly a must for every library.

Michael Schmittel
Institut für Organische Chemie
der Universität Freiburg (FRG)

Biochemical Messengers. Hormones, Neurotransmitters and Growth Factors. By *D. G. Hardie*. Chapman & Hall, London, 1991. X, 311 pp., paperback £ 13.95.—ISBN 0-412-30350-7

The human body consists of over 50 billion cells. Volvox, the simplest multicellular organism, already consists of 50000 cells. An organism only exists when these interact cooperatively. Cooperation implies communication: messages must be sent from cell to cell, and in these the transmitting cell must give specific information which the receiving cell can process and convert into appropriate reactions. In higher animal organisms there are two large communication systems, one consisting of neurones and the other of hormones. Both systems are based on essentially the same principles, which is not surprising since there is no doubt that they have developed in ways that are connected. Both use molecular messengers and depend for their functioning on complicated molecular signal processing systems. Because of their fundamental importance, both are among the most intensively studied fields of current research. This monograph provides an overview of the present state of knowledge in these areas.

Hardie's book encompasses the whole of this very broad subject. It begins with the "first messengers", the messenger molecules of the hormonal and nervous systems, which usually only travel as far as the plasma membrane of the receiver cell. There the information they carry is converted, through receptors and their signal transduction mechanisms, into "second messengers" and their associated intracellular effects. Hardie describes their structures, their biosynthesis, and the cell biology involved in their storage and distribution. After an excursion into the neurobiology of nerve impulse transmission, he then continues, via the biochemical messengers, to the most exciting part of the story, the receptors. Their experimental identification and characterization, their structures, and the way in which they function, form the subject matter of the middle section of the book. The concluding chapters deal with the regulation of cell division, and with gene regulation by steroid hormone receptors that bond directly to the DNA of the cell nucleus.

Is it appropriate to write monographs dealing with areas of research that are still in a state of flux? The publication of books is inevitably a slower and more cumbersome process than that of review articles, and consequently a book may already be partly out of date by the time it appears. In any case, specialists and researchers obtain their information mainly from the primary literature or from relevant review articles. However, monographs such as that reviewed here are not intended for the specialist. Hardie is here writing for advanced students of biochemistry, biology, and pharmacology. From the research scientist's standpoint his book is best regarded as a first point of entry. As a textbook for advanced students it can be recommended unreservedly. It is clearly

written, readable, up-to-date (covering the literature up to 1989), and contains few errors. Above all it identifies features of regulatory mechanisms that are common to widely different fields of molecular biology. This is a useful text for readers with a broad area of interest, written by a competent author with a good overview of the subject; it offers an ideal basis for a course or seminar on regulatory mechanisms.

Ferdinand Hucho
Institut für Biochemie
Freie Universität Berlin (FRG)

Iron Oxides in the Laboratory. Preparation and Characterization. By *U. Schwertmann* and *R. M. Cornell*. VCH Verlagsgesellschaft, Weinheim/VCH Publishers, New York, 1991. XIV, 137 pp., hardcover DM 118.00.—ISBN 3-527-26991-6/0-89573-858-9

Even on first thumbing through this little book, which has a substantial binding and is pleasing to handle, one is impressed by the clear arrangement of its contents. Anyone who has at some time struggled with the study of iron aquoxides will, after reading it for a short time, join this reviewer in exclaiming "If only this had been available then!". Schwertmann and Cornell save the beginner from having to do a lot of tedious literature searching, and they give much valuable advice regarding the "perversity" of the chemistry that can help to prevent failures.

The first few chapters explain the structural relationships between the oxides and hydroxides of iron, and describe the preparative techniques, methods of investigation, and special synthetic methods. These are followed by nine chapters on the various compounds; five of these deal with iron hydroxides, three with iron oxides, and one with basic iron salts, including also doped variants of these in some cases.

Very detailed methods are given for unambiguously preparing each of nine important iron compounds, analyzing them, and storing them for use as reference materials; these are goethite, lepidocrocite, feroxyhyte, ferrihydrite, akaganeite, hematite, magnetite, maghemite, and iron(III)-oxyhydroxy sulfate. In future this will be the standard work always referred to in connection with iron oxides and hydroxides.

According to an old saying, even the most excellent of carpets must have its small defects, so as not to incur the wrath of Allah. Here they include the missing literature citations on pages 29 to 33, and the absence of a cross-reference to the oxalate extraction test for characterizing goethite (page 46). In describing hydrolysis reactions (e.g., on page 57) it would have been desirable to give the formula of the hydrated starting species, and to mention the oligomeric intermediate products. In describing the preparation of goethite a consistent procedure should have been given: on page 64 the caustic solution is added to the solution of the metal salt, whereas a little later (p. 72) the metal salt solution is added to the caustic solution. This fails to take account of the fact that the isoelectric point of the primary precipitate suspension is approached from the acidic side in one case and from the basic side in the other. The nature of the impurities that become incorporated into the primary precipitate, and can affect the properties of the end-product, is quite different in the two cases.

To this reviewer the title of the monograph is a small source of annoyance, which cannot be blamed on the authors. A more suitable title would contain the generic term "iron aquoxides" introduced by Glemser (*Angew. Chem.* **1961**, *73*, 785), although this has, unfortunately, not been generally adopted. Perhaps this different way of looking at things might stimulate an increased interest in the catalytic, magnetic, electronic, electrochemical, and photovoltaic properties of iron aquoxides (including the "iron oxides" extracted from aqueous systems), which are very sensitive to the presence of hydroxide groups, even in sub-trace concentrations.

The list of groups to whom the book is likely to be of interest might well be extended to include the authors of future monographs!

Dieter H. Buß
Institut für Anorganische Chemie
der Universität Göttingen (FRG)

Protective Groups in Organic Synthesis. 2nd Edition. Edited by *T. W. Greene* and *P. G. M. Wuts*. Wiley, Chichester, 1991. XVI, 473 pp., hardcover £ 47.50.—ISBN 0-471-62301-6

Ten years after the publication of the first edition of this very successful book, Theodora W. Green and Peter G. M. Wuts have now prepared a second edition taking into account the latest state of knowledge on the use of protective groups. The division of subject matter is the same as in the first edition. The book starts by describing the functions that protective groups are intended to achieve. The protective groups used for different compound types or groups are then dealt with in turn: those for hydroxy groups, including 1,2- and 1,3-diols, in Chapter 2, for phenols and catechols in Chapter 3, for carbonyl compounds in Chapter 4, for carboxy groups in Chapter 5, for thiol groups in Chapter 6, and for amino groups in Chapter 7. Lastly, Chapter 8 compares the labilities and stabilities of commonly used protective groups under different conditions (basic, acidic, oxidative, etc.), summarizing these in "reactivity charts"; the charts are identical to those in the first edition.

The material in the new edition is impressively up-to-date. The literature has been comprehensively covered up to 1988, with partial coverage up to 1990 for work published in American journals and in Tetrahedron Letters. For each protective group described, methods for its introduction and subsequent detachment are indicated, though often only by giving the reagents together with a literature reference. Generalized reaction equations are given in a few instances, but more usually only the equation for a special case. In this way the authors have achieved a high density of information. The form of presentation adopted inevitably means that the special properties of protective groups, even of some very important ones, are treated too briefly, or sometimes even not at all. This applies, for example, to the stereospecific neighbor group effects of acetates in the synthesis of glycosides. Also there is no mention of the Koenigs-Knorr and related syntheses. However, this was no doubt deliberate on the part of the authors, since it is unmistakably evident that their main area of interest and experience is in the synthesis of the many natural products containing hydroxy and carbonyl groups, which is also reflected in the relative emphasis given to the various protective groups discussed. Consequently, it is essential that the reader interested in using a particular protective group in experimental work should consult the original literature that is cited. A further reason for this is that the authors have deliberately prefered to cite more recent examples of applications, and on grounds of economy they have made the proviso that the citations do not neces-

sarily include the original publication in which the use of a particular protective group was first proposed.

Despite these reservations, the book can be recommended as an excellent and very useful source of information for all chemists concerned with the synthesis of polyfunctional compounds. Its coverage has been extended from that of the first edition to include *N*-protecting groups for five-membered heterocycles and amides, but the latest developments in the use of protective groups that can be removed enzymically were, of course, too recent to be included (H. Waldmann, *Kontakte (Merck)* **1991** (3), 33). The second edition of "Protective Groups in Organic Synthesis" should be available at all times in every organic preparative laboratory.

Horst Kunz
Institut für Organische Chemie
der Universität Mainz (FRG)

Elementary Introduction to Spatial and Temporal Fractals. (Series: Lecture Notes in Chemistry, Vol. 55.) By *L. T. Fan, D. Neogi* and *M. Yashima*. Springer, Berlin, 1991. IX, 168 pp., paperback DM 44.00.—ISBN 3-540-54212-4

The importance of fractals for describing complex structures and complicated phenomena is now generally recognized, and in the last few years quite a number of books explaining the basic concepts of fractals in an easily understandable way have appeared. The book reviewed here is such a one; it gives an introduction to spatial and temporal fractals, and is intended particularly for students and research scientists working in the area of chemistry. The main emphasis is on definitions, methods and applications; detailed mathematical derivations are kept to a minimum. It is roughly 150 pages in length, and is clearly divided into four parts followed by a detailed appendix.

In the first part the concepts and definitions of fractals are explained. Topological and Hausdorff–Besicovitch fractals and Euclidean dimensions are compared. Line, surface, and volume fractals are also explained.

The second part contains examples that the reader can easily understand using the knowledge gained from the first part. The reader progresses via Cantor sets and Koch curves to coastal perimeters. Particular attention is devoted to methods for determining the fractal dimensions of irregular surfaces. The concept of multifractals is also touched on briefly, and it is shown that complex objects cannot always be fully characterized by a single exponent; instead this may require a distribution of exponents. The justification for this procedure in terms of information theory is not gone into here. Almost every book on fractals has to include a discussion of growth models; here the authors confine their attention to the best known of these, namely the Eden model and the diffusion-generated aggregation model. Transport and dynamic processes in fractal structures are not treated, and accordingly only those characteristic exponents that are of importance for structural analysis are discussed.

The third part of the book deals with temporal fractals. These are also taken to include time series arising from measurements as a function of time, for example, data on the prices of commodities as these vary with time. Such price variations often do not show a normal (Gaussian) distribution. Fluctuations of this sort can be analyzed in terms of stable distributions and fractional Brownian motions. Here a distinction is also made between the properties of self-affinity and self-similarity. The Hurst method for determining the characteristic exponents of discrete time series is described. Only in the final section of this part do the authors deal with "real" time fractals. These include stochastic processes in which the intervals between successive events have a distribution characterized by a divergent average interval. However, the fundamental importance of temporal fractals for the interpretation of dispersive transport processes and slow relaxation phenomena is scarcely mentioned.

The last part is devoted to chaos phenomena. The authors clearly explain the role of the strange attractor in characterizing chaos in deterministic nonlinear systems, and that of the Liapunov exponents in predicting trajectories. The relationship between fractals and chaos is made clear by a consideration of the fractal dimensions of the strange attractor.

The appendix should prove useful for readers interested in practical applications. Here the fractal properties for three particular cases are examined, by determining the fractal dimensions for the perimeter of coal particles, for the surface of rice hulls, and for the pressure fluctuations in multiphase flow systems. Each case study begins with a theoretical introduction, which is followed by a description of the experimental arrangement, and finally a discussion of the results with the help of figures and tables.

This book serves very well the needs of the reader who has no previous knowledge of the subject, and wishes to acquire the necessary background for an understanding of fractals, especially for applications to chemistry, in a way that does not make exacting demands. The price of DM 44.00 is appropriate for a book at this level.

Gerd Zumofen
Laboratorium für Physikalische Chemie
der Eidgenössischen Technischen Hochschule,
Zürich (Switzerland)

Molecular Mechanism for Sensory Signals. By *E. M. Kosower*. Princeton University Press, Princeton NJ (USA), 1991. XVI, 438 pp., hardcover $ 79.50.—ISBN 0-691-08553-6

The elucidation of the molecular mechanisms of sensory perception, signal transduction, and the processing and storage of the information thus obtained is one of the most fascinating research areas of modern biology and biochemistry. Many different approaches are being followed, involving a very wide variety of disciplines ranging from molecular biology to neurobiology, and from molecular structure determination to the study of neuronal networks. E. M. Kosower has performed a valuable service in bringing together in a single publication a survey of the current knowledge on this complex subject.

At the beginning of the book the author defines a hierarchical classification of the world of living organisms, which is made up of levels of organization of varying complexity. A consideration of how these individual levels fit together provides explanations for many apparently unconnected results. This approach from the viewpoint of systems and functions is becoming increasingly important in modern biology. It is a concept to which E. M. Kosower frequently refers back in this book, thereby making many of the relationships easier to understand.

It is only very recently that detailed knowledge has been gained about the mechanism of vision, the olfactory system, the sense of taste, and the transduction of signals. From this a number of common principles and levels of function have been recognized; the receptors, which belong to the lowest level, appear to have similar structures (containing seven

transmembrane helices) in different organisms. This is found not only for bacterial receptors, such as the archaebacterial photoreceptors, but also for eukaryontic receptors such as rhodopsin. At the next level the signal is amplified and converted into a cellular response. A system in which this has been studied especially thoroughly is the G-protein cascade in the mechanism of vision. The transmission, processing and storage of signals is made possible by the communication between neurons. As illustrative examples the author has chosen the nicotinic acetylcholine receptor and the sodium ion channels. The book ends with a discussion of the problems of learning and memory.

A wealth of information is presented in this book, not least through the comprehensive bibliography, which contains 1394 references and provides detailed coverage of results reported up to about 1989. For this reason it could be thoroughly recommended as an introduction to this field, were it not for the author's somewhat individual presentation and interpretation of the results. He gives prominence to his own molecular models of rhodopsin, of the acetylcholine nicotine receptor, and of the sodium ion channel. These ideas regarding their molecular structures are intellectually appealing and are enjoyable to read, and they also allow one to specify some predictions that any theory should satisfy. Nevertheless, one should always bear in mind that these models have not yet been experimentally verified, and that (at least in the case of rhodopsin) some of the details appear to be contradicted by the most recent results.

The data given are often unnecessarily detailed, which is annoying as they are only of interest as examples. Thus, it is not particularly useful to give the structures of so many odor substances and to list the amino acid sequences in such detail as here. Also it is questionable whether secondary structural features such as the α-helix or β-folding need to be described yet again in a book about the molecular mechanisms of sensory perception. Moreover, the quality of the diagrams in these descriptions is very disappointing compared with, for example, those found in textbooks of biochemistry.

To summarize, there are difficulties in the way of recommending this book for a wide readership. However, for those who are interested in an unorthodox treatment of the subject, and who already have at least some relevant knowledge, the book is well worth reading.

Martin Engelhard
Max-Planck-Institut für Ernährungsphysiologie,
Dortmund (FRG)

Electron Deficient Boron and Carbon Clusters. Edited by *G. A. Olah, K. Wade* and *R. E. Williams*. Wiley, Chichester, 1991. xii, 379 pp., hardcover. £ 47.50.—ISBN 0-471-52795-5

For some decades now, we chemists have had access to the theoretical tools needed for the correct quantitative description of bonding in molecules, and nowadays, thanks to developements in computers and programs, they are available for everyone to use. Nevertheless, it still remains true that for the majority of molecules one can, to a good approximation, describe the bonding by assuming the limiting case of localized two-center two-electron bonds. An adequately good approximation often provides qualitative insights that might be obscured by using other, quantitatively more accurate, theoretical methods. In this respect the majority of *classical* molecules can be contrasted to those types of molecules that are still regarded as "exotic" and cannot be described even to a crude approximation in terms of two-center localized bonding; these are the *nonclassical* molecules, to which the Lewis description cannot be applied because they are electron-deficient. Although elements belonging to any part of the Periodic Table can be involved in the formation of nonclassical molecules, it is boron compounds that continue to provide the most striking examples.

The monograph reviewed here, which is dedicated to W. N. Lipscomb on the occasion of his 70th birthday, consists of fourteen articles, eleven of which are on boron cluster compounds. A contribution by T. C. Flood describes some remarkable studies of the oxidative addition of C–H bonds to soluble osmium and iridium complexes, but does not cover electron-deficient boron and carbon compounds. There is only one contribution dealing with carbon clusters, namely that by G. A. Olah on the hypercoordinated nonclassical carbonium ions of which $CH_5^{\oplus}$ is the prototype; this article, a sequel to a recently published monograph on the subject,[*] clearly brings out the relationships between carbon and boron clusters and is well worth reading. These relationships are also emphasized in the editors'short introduction to the book. In their other contributions the editors go beyond their own research in order to explore more general relationships. Olah's article has already been mentioned. R. E. Williams returns to the simple "styx" rules developed by Lipscomb. These state that the bonding skeleton of the boron hydrides and their heteroatom derivatives can be described qualitatively in terms of two-electron bonding between two or three centers, namely between two or three boron atoms or between one hydrogen atom and one (*endo* B–H) or two (B–H–B bridging) boron atoms, provided that where several canonical distributions of these four bond types are possible, resonance is assumed. Williams defines formal charges and derives the structure and the dynamic behavior of the *nido* cluster compounds from the distribution of these charges over the molecule. Boron hydride specialists will benefit from the wealth of knowledge presented here by this doyen of cluster systematics. In a shorter and more general contribution, K. Wade also starts from charge distributions in localized bonding structures according to the styx model to continue with an MO approach to such charge distributions involving more than three centers.

A completely different theoretical approach is described by M. Bühl and P. von R. Schleyer, who report laborious ab initio calculations of the geometries of some boron hydrides and hydroborates. The essential conclusion is that the calculated geometries are better than those determined experimentally, taking as a criterion the ^{11}B NMR signals calculated by the IGLO method; it is well known that these match the observed NMR signals strictly, depending on the correctness of the assumed molecular geometry. A contribution by D. M. P. Mingos and D. J. Wales is concerned with the mechanism of the "diamond-square-diamond" process, in which a polyhedral lattice opens up along one edge of its triangular network to form a square, then closes up again in a direction perpendicular to the original one. (A striking example of this is the Berry pseudorotation.)

The remaining seven articles deal with synthetic, structural, or mechanistic aspects. L G. Sneddon and S. D. Kang describe some new *hypho* clusters and point out that there are regions in these open cluster structures which contain classical bonds. The rest of the contributions are concerned with recent developments, some of the most impressive ones coming from the Fehlner and Greenwood/Kennedy groups in the

[*] G. A. Olah, G. K. S. Prakash, R. E. Williams, L. D. Field, K. Wade, *Hypercarbon Chemistry*, Wiley, New York, **1987**.

field of metalloboranes and from the Greenwood/Greatrex group in the field of borane thermolysis. However, there are also some contributions in which larger portions have already been reported in one or even several previous publications, and even figures have been reproduced unchanged. It is apparent from these articles that the monograph was stimulated by a symposium on electron-deficient clusters held at the Loker Hydrocarbon Research Institute in January 1989.

To summarize, the book contains articles of general importance alongside others of a more specialized nature, representing more or less novel developments. It is a must for the boron chemist and can be recommended for purchase by large libraries.

Peter Paetzold
Institut für Anorganische Chemie
der Technischen Hochschule Aachen (FRG)

Chemical Bonding Theory. By *B. Webster*. Blackwell Scientific Publications, Oxford, 1990. x, 276 pp., paperback £ 14.95.—ISBN 0-632-01621-3

This book is an introduction to the theory of the chemical bond, and has deliberately been kept concise. It is intended for undergraduate students and for lecturers teaching at that level. Although the latter will find the breadth and depth of the monograph insufficient, the division of the subject matter and the choice of topics can be recommended as an attractive basis for preparing lectures. It consists of four chapters (1. Electron Pairs and the Formation of Molecules, 2. The Orbital Model of Atomic Structure, 3. Diatomic Molecules, 4. Polyatomic Molecules) which cover both the basic older methods and some quite recent approaches to the description of the chemical bond.

In Chapter 1, after discussing electron pairing according to the Lewis description, an account is given of the VSEPR approach of Nyholm and Gillespie. However, at the end of the chapter, after an example of the so-called hypervalence phenomenon (SF_6), the author fails to point out the important fact that the chemical bonding involved can also be explained by the MO theory without this concept.

In Chapter 2 a description of the principle of building up atomic structures is followed by a short section on spectroscopy, ending with an account of spin-orbit interactions as manifested in the Russell-Saunders coupling. Aspects treated include the ionization energy, electron affinities, the effective nuclear charge, atomic radii and polarizabilities. As is often the case, solid state chemical aspects are treated in a very fragmented way, and in the wrong chapter. However, it is pleasing that here, in contrast to some much more comprehensive treatments such as that by Huheey, at least a general derivation of the Madelung factor is given (not just for AB-type compounds, as is often misleadingly given). With the help of the exercise problems the concept is then developed into a genuinely useful aid even for students. After introducing relationships between atomic radii and explaining their significance, proximity diagrams as developed by W. B. Pearson and fields in the region of the structure are then applied to the discussion of relationships between structure and bonding, including even some that are highly topical.

Diatomic molecules are used as model systems to develop molecular orbitals, followed by considerations of the polarity of the chemical bond and again of radii. Here the arguments could have been treated in more detail and some aspects expanded on, such as the ideas of Drago et al. and Fajans regarding acid–base behavior. On the other hand adequate space is devoted in this monograph to the dynamics of diatomic molecules, including topics such as the analysis of rotational–vibrational spectra and the relevant selection rules. The section ends with a description of Berlin zones, and some modern ideas regarding electron density.

More complex MO bonding schemes and their symmetry properties are then treated, together with ligand field theory, taking some polyatomic molecules as examples. In this context possible distortions are also discussed, including the Jahn–Teller effect and Walsh diagrams. The last section deals with electron number rules for polyhedral molecules, taking borane derivatives as examples.

The book is completed by tables of data, answers to the exercise problems, a bibliography and an index of contents, all of which are again concise but well-chosen. The explanations of the aims that are included with each chapter and the exercise problems are especially welcome and useful. The monograph is very suitable for revision purposes, and is published in the form of a reasonably-priced paperback.

The author has undoubtedly based the book on his own teaching experience, and has tried throughout to combine older basic knowledge with highly topical recent findings—and he has done this in only 270 pages. Consequently in some parts the leaps in the arguments presented are too great, and the student will need to refer to books that treat these matters in more depth. However, brevity is the soul of wit—this book can be well recommended.

Reinhard Nesper
Laboratorium für Anorganische Chemie
der Eidgenössischen Technischen Hochschule
Zürich (Switzerland)

Introduction to Zeolite Science and Practice. (Series: Studies in Surface Science and Catalysis, Vol. 58.) Edited by *H. van Bekkum, E. M. Flanigen* and *J. C. Hansen*. Elsevier, Amsterdam, 1991. XVI, 754 pp., hardcover HFl 395.00.—ISBN 0-444-88969-8

This book is based on lectures given at a summer school held in 1989. Zeolites have for many years played a very important role in industry. In particular, the use of zeolites in catalytic cracking has led to enormous savings by increasing the production of gasoline and raising its octane value. Zeolites will become even more important in the future. Because of their stability and capability of regeneration they offer the possibility of developing a new generation of catalysts and processes, which will also take account of environmental acceptability as a high priority. This becomes clearly evident in the book, for example in Chapter 16, in which W. F. Hölderich and H. van Bekkum discuss the use of zeolites in organic synthetic chemistry, and introduce applications as catalysts for isomerizations, rearrangements, alkylations, acylations, etc. Whereas the latter chapter is concerned with the development potential of zeolites as catalysts, in Chapter 15 I. E. Maxwell and H. H. J. Stork give a survey of modern applications in the secondary processing of oil and natural gas that are already carried out on an industrial scale, such as catalytic cracking, the conversion of synthesis gas into gasoline constituents, of methanol into gasoline constituents (MTG) and olefins (MTO), and of light paraffins into arenes (the Cyclar process). In some cases the usefulness of zeolite catalysts is limited by the tendency to coke formation, a problem discussed by H. G. Karge in Chapter 14. He considers, among other aspects, the role of acidic centers and

the localization of coke deposition (within the porous structure of the zeolite, or on the outer surfaces of the crystallites). Chapter 13 (H. W. Kouwenhoven and B. de Kroes) is concerned with the preparation of zeolite catalysts. The main emphasis is on the manufacture of catalysts for the fluidized catalytic cracking (FCC) process, which is the most important method for producing gasoline constituents from higher-boiling products. Many of the reactions used for the conversion of hydrocarbons are acid-catalyzed, and in Chapter 12 P. A. Jacobs and J. A. Martens give an introduction to acid-catalyzed reactions on zeolites. Especially useful here is the section dealing with shape-selective catalysis on acidic zeolites, which is one of the most important areas of application of zeolite catalysts. In (shape-selective) catalytic reactions and selective adsorption/separation processes, the rate of diffusion is a key variable, and this is discussed in Chapter 11 by M. F. M. Post. Chapter 10 by R. P. Townsend is concerned with ion exchange in zeolites; the use of zeolite NaA as an alternative to phosphate in detergents is based on its ion exchange properties. In Chapter 9 R. A. van Santen, D. P. de Bruyn, C. J. J. den Ouden, and B. Smit give an introduction to the theory and modeling of zeolites; they discuss theories of the lattice stability of zeolites and of adsorption and acidity, computer modeling of zeolites, and the simulation of adsorption and diffusion. Chapters 7 and 8 are concerned with methods for characterizing zeolites. In Chapter 7 J. H. C. von Hoff and J. W. Roelefsen discuss methods for determining structure and defects, pore size, chemical composition, acidity, morphology, and particle size. In Chapter 8 G. Engelhardt describes the application of solid state NMR spectroscopy to studies of zeolites. He discusses the capabilities of ^{29}Si and ^{27}Al NMR spectroscopy using the magic-angle-spinning (MAS) technique, and the important question of determining the relative proportions of framework and non-framework aluminum and of "NMR-invisible" aluminum ions. MAS-NMR spectroscopy with ^{17}O, ^{11}B, ^{1}H, ^{13}C, or ^{31}P as the observed species also has potential applications to non-zeolitic molecular sieves.

Chapters 4 to 6 are concerned with the synthesis of molecular sieves. In Chapter 4 J. O. Jansen and S. T. Wilson in turn review the synthesis of zeolites and of molecular sieves, respectively, with $AlPO_4$ as the starting material. The details concerning the synthesis of relatively large single cyrstals of some of the zeolites will undoubtedly arouse much interest. In Chapter 5 on "Modified Zeolites" R. Szostak describes secondary and post-synthesis treatments, such as the various methods for extracting aluminum from the zeolite framework. In Chapter 6 R. A. Schoonheydt discusses the transition from the two-dimensional clay minerals to the pillared clays with three-dimensional structures, which exhibit molecular sieve properties. In these the diameter of the channels is greater than in zeolites, and consequently the critical molecular diameter up to which molecules can undergo conversion in the cavity system is greater.

At the beginning of the book the editors list the special characteristics of zeolites: a uniform pore system, an interior surface that is accessible to reacting molecules, exchangeability of the ions, and the possibility of tailoring the size of the pore entrances and the acidity to suit particular applications. In Chapter 1 these characteristics are discussed in lucid detail by L. Moscou, thereby smoothing the way for newcomers to the subject. In Chapter 2 E. M. Flanigen presents a historical outline of the synthesis and use of zeolites. The structures of zeolites are discussed in Chapter 3 by H. van Koningsveld. Appendix I lists the structural characteristics of some of the most important molecular sieves, and Appendix II contains information on pore sizes and on structural isotypes. Both these appendixes are especially useful for the beginner. The detailed subject index enables one to quickly locate information on desired topics.

Each chapter begins with the fundamentals, then goes on to describe the latest results, citing publications up to 1989. The clear arrangement of the contents makes for easy readability. However, it would have been better to use the Geneva nomenclature throughout for the subject headings. This is a very useful book for beginners as well as specialists, and it can be recommended for everyone with an interest in this field.

Michael Nimz
Institut für Anorganische und Analytische Chemie
der Technischen Universität Berlin (FRG)

Carbonylation. By *H. M. Colquhoun, D. J. Thompson* and *M. V. Twigg*. Plenum Press, New York/London, 1991. XI, 296 pp., hardcover $ 65.00.—ISBN 0-306-43747-3.

This book is devoted to transition metal based carbonylation chemistry leading to the synthesis of carbonyl compounds. Following discussion of concepts and practical aspects, it is organized according to the type of organic compound being synthesized (e.g., aldehydes, amides). The last chapter deals with recipes for catalyst preparation and recovery.

The brief introduction provides a good perspective of carbonylation chemistry, past and present. Why this book is timely is well-reasoned in this chapter.

The second chapter is entitled "Reaction Mechanisms in Carbonylation Chemistry". What an excellent contribution, especially for organic chemists! This chapter deals with the nature of metal–CO bonding, elementary steps in catalytic processes (e.g., oxidative addition), and new mechanistic patterns in carbonylation reactions. The explanation of catalysis is first-class, and the critical analysis which the authors provide here and throughout the text is refreshing. There are a few weak points; for example, while electrophilic attack on carbon monoxide is adequately explained, a more in-depth treatment of nucleophilic attack at carbonyl carbon would have been useful. Nevertheless, this logically organized examination of mechanism and synthesis in carbon monoxide chemistry is the best in the literature.

The third chapter is concerned with the handling of carbon monoxide in the laboratory, and the techniques used in the experiments. This is essential for anyone contemplating research in carbonylation reactions.

The following seven chapters include critical accounts of the synthesis of aldehydes, ketones, carboxylic acids, esters, amides (including anhydrides, aryl halides, urethanes, ureas, and isocyanates), lactones, and lactams. The organizational aspects are excellent, and the authors also highlight areas where further research is desirable. The treatment of the subject in each case is very good, and occasionally includes natural product syntheses. Nevertheless, more details could have been provided in some cases. For instance, the mechanism of the Stille reaction is interesting and merited coverage on pedagogic grounds. Also, no reference is made in the book to the interesting work of Sue Thomas and co-workers on the conversion of α,β-unsaturated ketone complexes to ketenes with carbon monoxide. An inconsistency is the notation of the oxidation state of the metal, which is designated in equations, schemes, etc. in some chapters, but not in others.

 © VCH Verlagsgesellschaft mbH, W-6940 Weinheim, 1992 0570-0833/92/0505-0662 $ 3.50+.25/0

A chapter is devoted to a thoughtful analysis of decarbonylation reactions, the reverse of carbonylation processes. This transformation is useful in certain situations, and clearly more work is required in this area.

The final chapter provides experimental procedures for the synthesis of many of the catalysts described in the book. This is a useful contribution, as is the description of methodology for the recovery of metals.

In conclusion, this impressive book is well-written, enjoyable to read, and will be of genuine value to chemists.

Cathleen Crudden, Howard Alper
University of Ottawa
Ottawa (Canada)

Chemometrics. Applications of Mathematics and Statistics to Laboratory Systems. By *R. G. Brereton*. Ellis Horwood, Chichester, 1990. 307 pp., hardcover $ 76.50.—ISBN 0-13-131 350-9

The purpose of this monograph, which is published as an independent volume in the "Ellis Horwood Series in Chemical Computation, Statistics and Information", is to familiarize the experimental chemist with the capabilities and advantages of chemometric methods.

The book proceeds mainly by using simple examples to briefly explain the principle of each of the chemometric methods described, then illustrating how they can be applied to real chemical and analytical problems. This approach has the advantage that the emphasis is on understanding the mathematical and statistical methods used. In describing computer-based methods the author frequently gives details of the wide choice of software that is commercially available, and is in most cases adequate for the purpose. A brief account of the development of chemometrics is followed by an introductory survey of up-to-date literature on chemometrics. The following six chapters describe, in a clearly organized division of subject matter, the most important chemometric methods and their applications.

The chapter on experimental design describes the use of sequential methods such as simplex optimization, factorial plans, multilinear regression methods and variance analysis for the quantitative modeling and optimization of chemical experiments. Next the author describes both well-established methods (control card techniques, the cusum method, autocorrelation analysis) and newer methods (the autoregressive moving average method, the variogram, the Kriging method and the Nyquist frequency) that are used as aids in investigating time series in chemistry and for dealing with the complicated problem of representative sampling. Chapter 4 describes the many different methods for selecting and optimizing the conditions for analyses, such as principal component analysis, information theory, classification procedures, simplex methods, and Fourier and Hadamard transformations. The next two chapters are concerned with the application of univariate and multivariate methods in signal processing. Here there is some overlapping with topics in the previous chapter (e.g. Fourier transformation and principal component analysis), which is an unavoidable consequence of the wide range of uses of chemometric methods. Techniques described under the heading of univariate signal processing include moving average calculations, deconvolution of signals and Kalman filtering. The discussion of factor analysis as a tool for multivariate signal processing omits to give details of the estimation of communalities; however, there is a brief description of the modern method of target transformation factor analysis. In the section on multivariate calibration some important regression methods using latent variables, such as principal component regression and PLS regression, are mentioned but only described very briefly.

The final chapter, which deals with pattern recognition, includes comprehensive descriptions of unsupervised learning methods, especially algorithms for cluster analysis, and the supervised learning methods using either "hard" (linear discrimination analysis, linear learning machine, K nearest neighbors) and "soft" (SIMCA) techniques, as well as "fuzzy" methods.

The user will need to supplement the reading of the short appendix on important mathematical operations by also studying appropriate monographs on mathematical statistics. The appendix does not deal with the use of "robust" statistical methods.

The typography is relatively free of errors, apart from a few exceptions (e.g. Equation 3.5 and Table 5.20), and is very clear. This monograph, with its clear layout of subject matter and the easily understood and well chosen examples of applications in chemistry and analysis, offers a good basic grounding for the experimental chemist who wishes to become involved in chemometrics; also readers who already use mathematical and statistical methods in their area of work will find here new ideas for applying chemometric methods.

Jürgen Einax
Institut für Anorganische und Analytische Chemie
der Universität Jena (FRG)

Bonding and Structure: Structural Principles in Inorganic and Organic Chemistry. (Series: Inorganic Chemistry. Series editor: *J. Burgess*.) By *N. W. Alcock*. Ellis Horwood, Chichester, 1990. 321 pp., hardcover $ 50.95.—ISBN 0-13-465253-3

The introductory remarks in a book on chemical bonding and structure can provide a very good indication of its underlying philosophy; here, in a chapter entitled "The Evidence", the author clearly states his position: all that we require to know are the positions of the atoms in space and the resulting total energy. In the first forty pages the reader is given a good brief survey of the experimental methods whereby structural information can be obtained (X-ray diffraction, NMR, IR, electron diffraction, neutron diffraction, etc.) and of the sorts of structural phenomena that can appear. Already one becomes aware of two things: 1) crystal structures dominate the discussion from the start, and 2) quantum chemistry, which has now developed into a very reliable method for determining molecular structures and one that can no longer be overlooked, is here ignored. Moreover, the author fails to keep to the promise made in the title, as the book is mainly concerned with inorganic solids.

In a 100-page chapter entitled "Ideal Bonds" the properties of metallic, ionic and covalent bonds are described. The description of the underlying quantum mechanical principles is extremely brief and lacks clarity. The LCAO concept is dismissed in a few lines. In discussing the stationary state wavefunctions of hydrogen the real and complex representations are mixed up. The 1s wave function is given in Equation (1),

$$\psi(r) = 2a_0 - 6.5\exp(-r/a_0) \quad (1)$$

and this is even emphasized by putting it in a frame. One of the d functions, although correctly drawn, is thereafter wrongly described as d_z^2. How could this possibly lead to a conical nodal surface? The molecular cationic form of hydrogen is first written as H_2^+, but then appears for several pages as H_+^2. Also printing errors of all kinds are scattered through the text. We find, again within a frame, the statement: "The probability of finding an electron at a given point is given by ψ^2". Thus no distinction is made between probability and probability density, and as a consequence the significance of the volume element dv is completely ignored. The tetrahedral structure of methane is explained in terms of hybridization, with the remark that "One electron can easily be promoted from the 2s to the 2p level"—no mention is made of the energy needed for this process. Is an energy of 97 kcal mol^{-1} small?—and if so, relative to what standard? Next the molecular orbitals of methane are wrongly shown, and it is stated that the LUMO is threefold degenerate. Space does not allow all the other inconsistencies in this chapter to be listed. After describing several types of double bond and the VSEPR model, Hund's rule is stated in such a confused way that one recognizes it only from the heading above the frame; thus we read: "Electrons occupy separate orbitals rather than being paired up" and "The electrons are aligned parallel rather than antiparallel". What remains here of the precise formulation given by Hund in 1927, which leads directly to unambiguous statements in spectroscopy? Finally it is even claimed that the bent structure of the NO_2 radical is a consequence of the Jahn–Teller effect.

It comes as a relief to find that the second part of the book is entitled "Real Bonds and Real Compounds". Here again metals and alloys occupy a central position, but hydrogen bonds and donor–acceptor bonds are also described. In the second of these the "printer's devil" has ensured total confusion by showing, in contradiction of the text, a double occupancy for the acceptor orbital on the boron atom in the key figure to illustrate the B–N bond. Transition metal complexes are described in detail, but the reader will fail to gain an understanding here of the Jahn–Teller effect, since no distinction is made between the concepts of configurations and states. The reader can skip over a whole section on main-group elements, as it reintroduces antiquated devices that have long since been thrown out (the use of d-functions for main-group elements). The same also applies to the section on aromaticity, which is based on Hückel orbitals and completely ignores the developments of the past ten years.

For which readers can this book be recommended? Certainly not for the chemistry students for whom the author intended it. Instead the last 50 pages, which are the book's saving grace, will provide the advanced specialist in solid state chemistry with some information on complex crystal structures, ceramic materials, ionic conductors, ferroelectric materials, nonlinear optics, magnetic interactions, superconductors and semiconductors.

Rudolf Janoschek
Institut für Theoretische Chemie
der Universität Graz (Austria)

Registered names, trademarks, etc. used in this journal, even when not marked as such, are not to be considered unprotected by law.

© VCH Verlagsgesellschaft mbH, D-W-6940 Weinheim, 1992. – Printed in the Federal Republic of Germany by Konrad Triltsch Druck- und Verlagsanstalt Würzburg.

All rights reserved (including those of translation into foreign languages). No part of this issue may be reproduced in any form — by photoprint, microfilm, or any other means — nor transmitted or translated into a machine language without written permission from the publishers. Only single copies of contributions, or parts thereof, may be made for personal use. This journal was carefully produced in all its parts. Nevertheless, authors, editors, and publisher do not warrant the information contained therein to be free of errors. Readers are advised to keep in mind that statements, data, illustrations, procedural details, or other items may inadvertently be inaccurate.

Valid for users in the USA: The appearance of the code at the bottom of the first page of an article (serial) indicates the copyright owner's consent that copies of the article may be made for personal or internal use, or for the personal or internal use of specific clients. This consent is given on the condition, however, that the copier pay stated per-copy fee through the Copyright Clearance Center, Inc. (CCC), for copying beyond that permitted by Sections 107 or 108 of the U.S. Copyright Law. This consent does not extend to other kinds of copying, such as copying, for general distribution, for advertising or promotional purposes, for creating new collective works, or for resale. For copying from back volumes of this journal see 'Permissions to Photo-Copy: Publisher's Fee List' of the CCC.

Editorial office: Postfach 10 11 61, D-W-6490 Weinheim, Federal Republic of Germany, Telephone (06201) 60 23 15, Telex 465 516 vchwh d, Telefax (06201) 602 328, E-Mail Z16@DHDURZ2 in Earn Bitnet.

Editor: *Peter Gölitz*

Associate editors: *R. H. Schmidt-Radde, K. J. Schneider, A. Stimson.* **Editorial assistant:** *E. Schweikart*

Publishers: VCH Verlagsgesellschaft mbH. (Managing Directors: *Hans Dirk Köhler, Dr. Karlheinz Köpfer*), Pappelallee 3, W-6940 Weinheim, Federal Republic of Germany.

Advertising office (Advertising Manager: *R. J. Roth*): Postfach 10 11 61, D-W-6940 Weinheim, Federal Republic of Germany, Telephone (0 62 01) 60 61 36, Telex 4 67 155, Telefax (0 62 01) 606 156.

ANGEWANDTE CHEMIE
International Edition in English
Volume 31 · Number 6
June 1992
Pages 665–804

The Enchanting Alkaloids of Yuzuriha**

By Clayton H. Heathcock*

The oriental plant Yuzuriha (*Daphniphyllum macropodum*) elaborates a fascinating family of polycyclic, squalene-derived alkaloids that provide a test for state-of-the-art methods of organic synthesis. The intriguing structures of these natural products have inspired us to design and explore two rather different approaches for their laboratory synthesis. This article recounts and contrasts these two different syntheses. The first approach was based on a method of synthetic design that emphasizes efficient construction of the polycyclic skeleton of the molecule (Corey's "network analysis"). A strategic bond was identified and the synthesis planned around the late formation of this bond. The synthesis that was designed by this approach proceeded smoothly until the point where it was necessary to remove functional groups that had been incorporated solely for the purpose of forming the strategic bond. Although the problems were eventually overcome, the resulting synthesis was too long and did not control the configuration of one of the stereocenters. The second approach was based on a possible biosynthesis of one of the alkaloids and provided surprisingly easy access to the simpler members of the family. The success of this synthesis led to a concrete proposal about the biosynthesis of the alkaloids and to the discovery of the astonishing transformation depicted in Scheme 27. In this marvelous reaction, an acyclic squalene derivative is converted by successive treatment with ordinary commodity chemicals into a pentacyclic alkaloid. The transformation involves the formation of four carbon–carbon bonds, two carbon–nitrogen bonds, and one carbon–hydrogen bond!

1. Isolation and Structural Elucidation of the Alkaloids

In the Orient there grows a tree that the Japanese call "Yuzuriha," which, loosely translated, means to transfer leaves from hand to hand. The unusual name arose from the uncommon growth habit of Yuzuriha (*Daphniphyllum macropodum* Miquel), which develops an entire new set of leaves each spring before shedding the previous year's leaves later in the summer. Since antiquity, extracts of the bark and leaves of Yuzuriha have been used as a folk remedy for asthma. The first attempt to identify the active principles of the plant was made by the Japanese organic chemist Yagi, who reported in 1909 the isolation of an amorphous material, m.p. 75–84 °C, which he named daphnimacrine.[2] However, with the methods available at the time, no further progress could be made. It now appears that Yagi's daphnimacrine was a mixture of several alkaloids.

It was not until the 1960s that modern methods of structural analysis were equal to the task of deciphering the intricate structures of the alkaloids of Yuzuriha. As in many other cases, it was the group of Yoshimasa Hirata in Nagoya that finally succeeded in isolating two pure substances, daphniphylline (**1**)[3] and yuzurimine (**2**),[4] in 0.01% and 0.015%

[*] Prof. C. H. Heathcock
Department of Chemistry
University of California
Berkeley, CA 94720 (USA)

[**] This review article grew out of a series of lectures presented in Germany in July 1990, as the Merck-Schuchardt Lectureship. The full details of our work on the total synthesis of *Daphniphyllum* alkaloids are reported in a series of articles recently published in the *Journal of Organic Chemistry*: see ref. [1].

yields (based on dry weight of the plant material), respectively.[5] In the following decade, other *Daphniphyllum* alkaloids were identified, including daphmacrine (**3**),[6] macrodaphnine (**4**),[7] methyl homosecodaphniphyllate (**5**),[8] daphnilactone A (**6**),[9] daphnilactone B (**7**),[10] and yuzurine (**8**).[11]

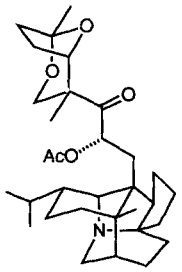

1

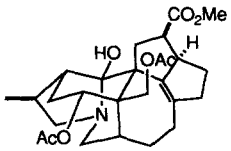

2

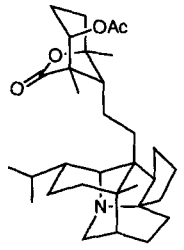

3

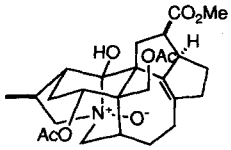

4

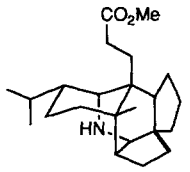

5

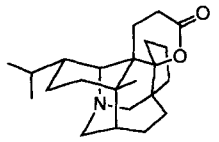

6

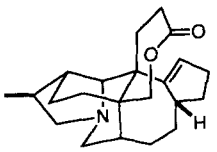

7

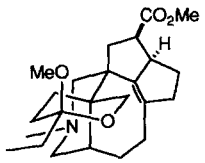

8

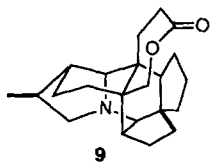

9

A total of 33 alkaloids from Yuzuriha have now been isolated and characterized. In addition, there was a report in 1990 of the isolation of a structurally related alkaloid, bukittinggine (**9**), obtained from the leaves and branches of *Sapium baccatum* collected near the town of Bukittinggi in West Sumatra, Indonesia.[12]

The 34 *Daphniphyllum* alkaloids, including bukittinggine, fall into seven skeletal classes: 1) daphnane (with 7 members), 2) secondaphnane (with 4), 3) daphnilactone A (with 1), 4) daphnilactone B (with 2), 5) yuzurimine (with 10), 6) daphnigracine (with 9), and 7) bukittinggine (with 1). Since the structures of compounds **1**–**9** have all been determined by single-crystal X-ray analysis, the structures, including absolute configuration, of all of the *Daphniphyllum* alkaloids are firmly established.

2. The First Synthetic Approach: Network Analysis

The seductive polycyclic structures of the *Daphniphyllum* alkaloids issue a siren call to the chemist interested in the de novo construction of complex organic molecules.When I first decided to answer this call about twelve years ago, the initial synthetic target that I selected was the C_{22} relative of daphniphylline, methyl homodaphniphyllate (**10**). There were two principal reasons for this choice. First, with only two functional groups and two independent stereocenters (indicated by arrows on its structure),[13] alkaloid **10** appears to be one of the simplest members of the group, its unusual pentacyclic structure notwithstanding. Second, the daphniphylline skeleton was thought to be archetypal of the family because daphniphylline is both wide-spread and abundant.

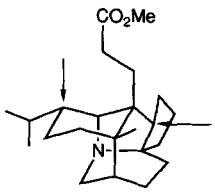

10

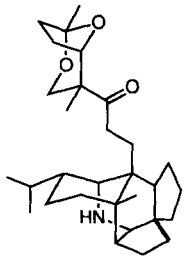

11

Clayton H. Heathcock was born in 1936 in San Antonio, Texas. After completing his secondary education in San Antonio and his undergraduate education at Abilene Christian College, he joined the Champion Paper and Fibre Company in Pasadena, Texas as Supervisor of the Chemical Tests Group in 1958. In 1960 he left this position and matriculated at the University of Colorado, where he did graduate work on steroidal nitrogen compounds with Alfred Hassner; he obtained his Ph.D. in 1963. He spent 1963–1964 in Gilbert Stork's laboratory at Columbia and joined the University of California at Berkeley as Assistant Professor in 1964. He has remained at Berkeley throughout his entire career and served as Chairman of the Department of Chemistry from 1986 through 1989. Professor Heathcock has also chaired the Organic Chemistry Divison of the American Chemical Society, the National Institutes of Health Medicinal Chemistry Study Section, and the Gordon Conference on Stereochemistry. He has served as Editor of Organic Syntheses and is currently Editor-in-Chief of the Journal of Organic Chemistry. His honors include the Ernest Guenther Award (1986), the American Chemical Society Award for Creative Work in Organic Synthesis (1990), the A. C. Cope Scholar Award (1990), and the Prelog Medal (1991). In 1978 he was a recipient of an Alexander von Humboldt United States Senior Scientist Award and was hosted in Germany by Professors Hans Bestmann and Paul Schleyer at Erlangen. In addition to his interest in natural product synthesis, Professor Heathcock has worked extensively in the area of stereocontrolled synthesis of acyclic compounds, and is particularly known for his work on the aldol and Michael addition reactions.

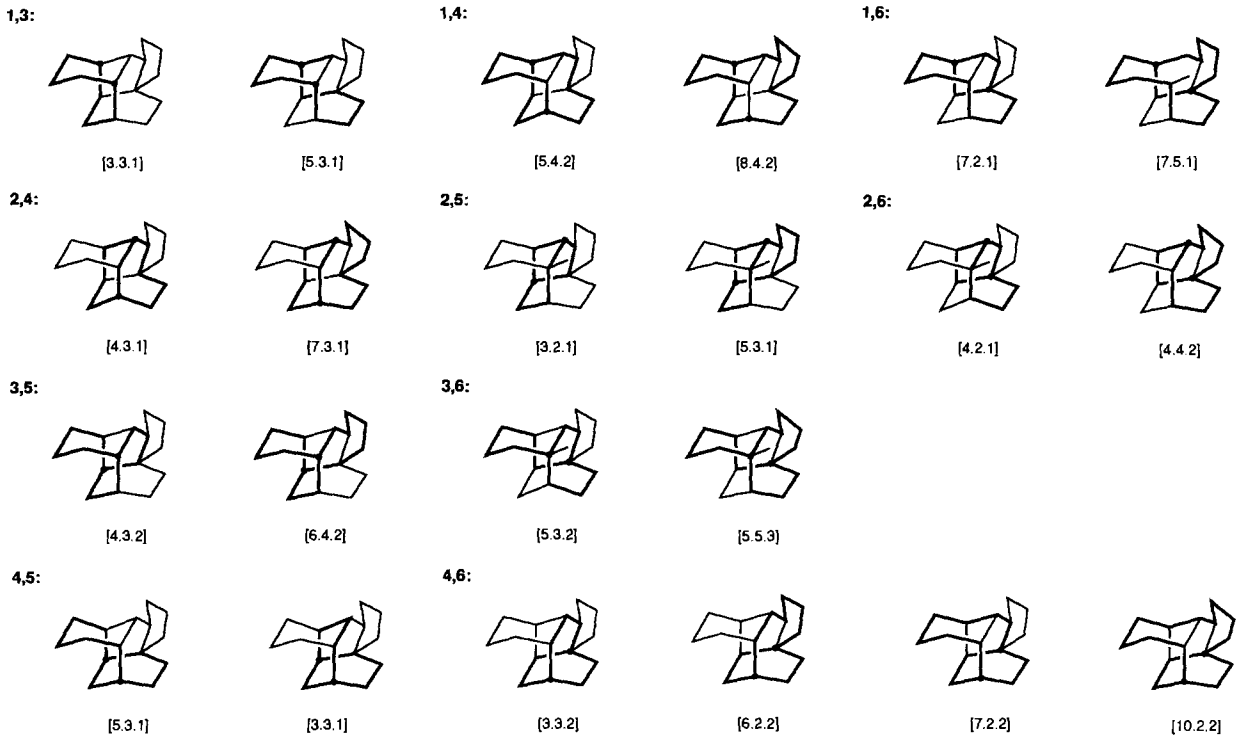

Scheme 1. For the numbering of the atoms see structure **II** (below).

For example, one large-scale extraction of *D. macrododum* leaves yielded 100 g of daphniphylline and only 1.1 g of secodaphniphylline (**11**).[14] It will become clear in the sequel that this reasoning was fallacious and that our identification of **10** as an inaugural goal was unfortunate.

With the target identified, it was neccessary to develop a synthetic plan. Inspection of the structure of alkaloid **10** suggested that the primary obstacle to be overcome is assembly of the intricate pentacyclic skeleton. This is often the case in the synthesis of polycyclic compounds, and Corey has articulated a formal method of analyzing such problems. Corey's formalism, first used in connection with his synthesis of the sesquiterpene longifolene,[15] is called network analysis.[16] A polycyclic molecule will have embedded within its skeleton several bicyclic systems, some fused and some bridged. The basic premise of network analysis is that it is easier to synthesize fused-ring systems than bridged ones.

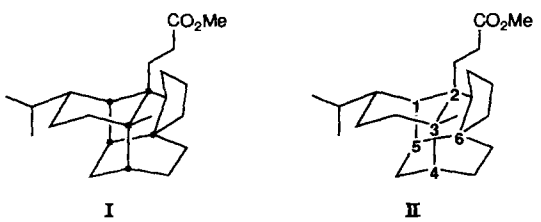

I **II**

The goal of the analysis is to identify the bond or bonds that are common to the most bridged bicyclic systems (the "maximally bridging" bonds), and to "retrosynthetically" remove these bonds, thereby achieving maximum structural simplification of the synthetic target. To locate the bridged-ring systems within the skeletal network of a polycyclic compound, one must first identify the atoms that can be bridgehead atoms in at least one bridged bicyclic system. The bridgehead atoms for methyl homodaphniphyllate are shown by the bold dots in structure **I**. The next step is to consider the bridgehead atoms in pairs and to identify all of the possible bridged bicyclic systems that exist. For the methyl homodaphniphyllate skeleton, the 22 bridged bicyclic systems shown in Scheme 1 are identified. Close examination of the 22 bridged bicyclic subsystems identified in Scheme 1 reveals that one skeletal bond is common to them all. Accordingly, this skeletal bond is identified as the strategic bond.[14] If this bond is retrosynthetically removed, the problem is simplified to the construction of the tetracyclic skeleton shown in Scheme 2. Although the skeleton of hypothetical target **A** is simpler than that of **10**, our stereochemical problem has become more complex, since **A** has five stereocenters. Nevertheless, the goal of network analysis is to

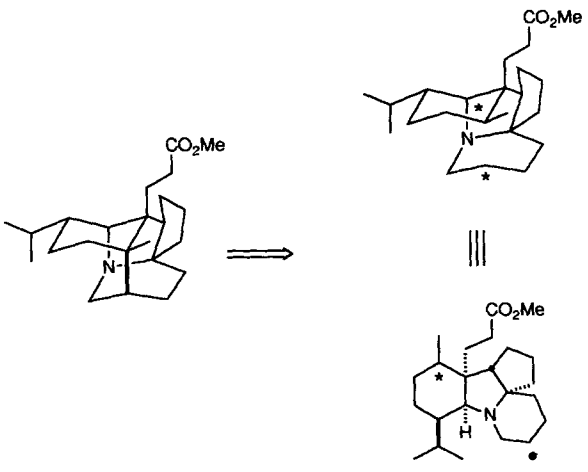

Scheme 2. **A**

identify possible synthetic precursors that have fewer bridged bicyclic systems, and skeleton **A** is clearly indicated as an appropriate target by this approach.

3. Functionality is Necessary to Create the Strategic Bond: "Consonant" and "Dissonant" Relationships

Network analysis only provides a target, not a method of synthesis. There remains the problem of devising a plan to synthesize the target and, equally important, a method of forming the strategic bond. For this purpose, we considered enol/enolate chemistry, namely, intramolecular aldol and intramolecular Michael reactions. For either of these reactions, we need functional groups either at or adjacent to the termini of the strategic bond. Four possible intramolecular aldol reactions are depicted in Scheme 3. A negative aspect

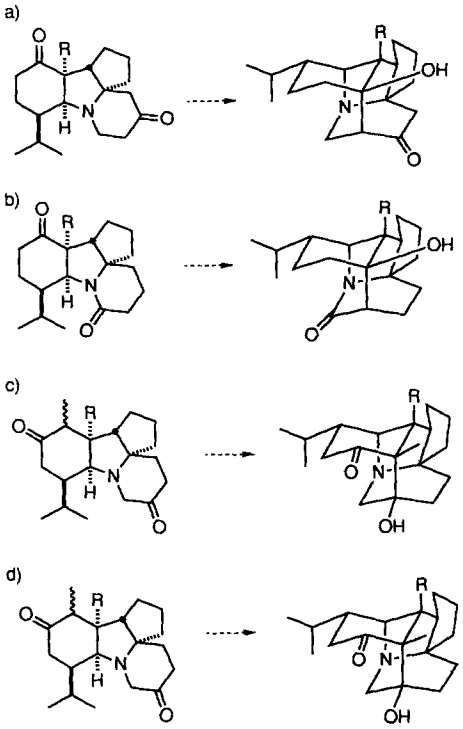

Scheme 3.

of possibilities a) and b) is the necessity of converting a bridgehead hydroxy group into a methyl group after the strategic bond has been formed. Although possibilities c) and d) are superior in this regard, they still would require a clumsy refunctionalization, replacement of a bridgehead hydroxy group by hydrogen, in addition to removal of the unwanted carbonyl group. Scheme 4 sketches three possible intramolecular Michael reactions that would provide the daphnane skeleton. These routes appear to be superior to the intramolecular aldol routes, because it would only be necessary to remove two carbonyl groups after the strategic bond is formed. Furthermore, there is ample precedent for the formation of six-membered rings by both base- and acid-catalyzed intramolecular Michael reactions.

However, the three possible Michael reaction substrates shown in Scheme 4 are not equally amenable to synthesis. In particular, the tetracyclic amino diketone **D** would be much more difficult to synthesize using standard methods than **B** or **C**. Compound **D** differs from **B** and **C** in its intrinsic functionality pattern. That is, in both **B** and **C** the amino

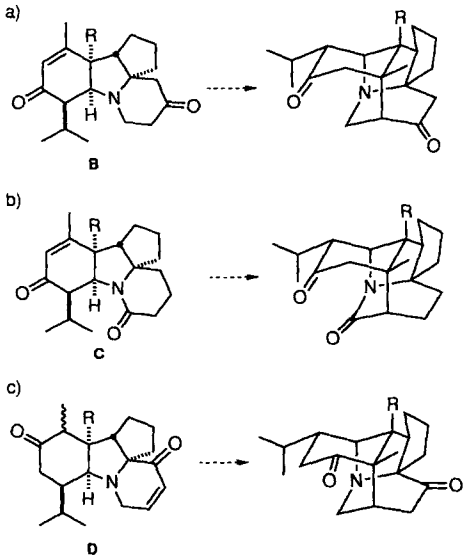

Scheme 4.

function is either β to a carbonyl group or attached directly to one. In **D**, however, the amino group is α and γ to the two carbonyl groups. The experienced synthetic chemist knows several methods to construct the array N–C–C–C=O (Mannich reaction, conjugate addition of an amino group to an α, β-unsaturated carbonyl function, acylation of an enamine, etc.) or N–C=O (amide formation), but few to construct the structural element N–C–C=O. The difference was recognized long ago by Lapworth, who formulated "the rule of alternating polarities,"[17] and formalized more recently by Evans in terms of "consonant" and "dissonant" bifunctional relationships.[18,19] The basic idea is that the presence of a heteroatom in a molecular skeleton can be viewed as imparting an intrinsic pattern of alternating electrophilicity and nucleophilicity to the atoms making up the skeleton. The situation is illustrated for a carbonyl group and an amino group in Scheme 5. Thus, the oxygen atom of a carbonyl group renders the carbonyl carbon atom itself and the β carbon atoms electrophilic, whereas the α and γ carbon atoms are intrinsically nucleophilic. The inherent difficulty in synthesizing α- and γ-amino ketones, relative to β-amino ketones and amides, is clearly seen from the diagrams at the bottom of Scheme 5. In the former case the two functional groups impart conflicting intrinsic polarities to the skeleton. Therefore, in the synthesis of α and γ-amino ketones it would be necessary to modify inherent polarity when constructing the skeleton. Of course, the reader will be aware that a considerable amount of research over the last two decades has been directed at reversing the innate electrophilicity or nucleophilicity of a given carbon atom through various contrivances. This strategy has been called "charge reversal" or "umpolung."[20] However, the use of

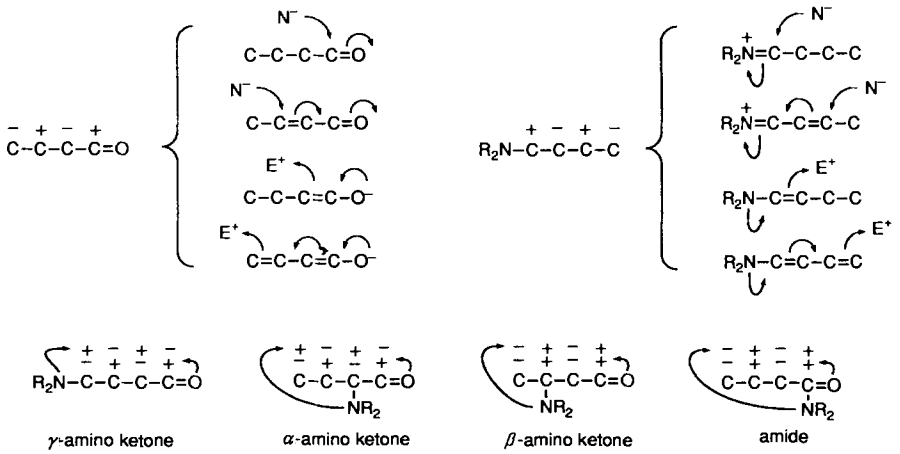

Scheme 5.

umpolung in a synthesis usually requires extra steps, expensive reagents, or esoteric reaction conditions. Since the goal of modern research should be to simplify synthetic routes, umpolung (and the use of protecting groups) must always be regarded as a compromise that is made when a given problem cannot be solved in a more direct manner. In the end, the best solution to a synthetic problem is a well-designed synthesis that takes maximum advantage of the natural functionality of the molecule to be synthesized.[21]

4. The First Synthesis of a *Daphniphyllum* Alkaloid: A Bittersweet Victory

The foregoing analysis directed our attention to the tetracyclic amino diketones **B** and **C** as potential synthetic intermediates for construction of the daphnane skeleton. Of these two possibilities, **B** appeared more attractive because of the great difference in acidity and ease of enolization of a ketone relative to a lactam carbonyl group. Accordingly, this compound became the focus of our attention. The synthesis of a tetracyclic amino diketone with the skeleton of **B** is summarized in Scheme 6. Keto acid **12**[22] and amino ketal **13**[23] were coupled using the mixed anhydride method to obtain a keto amide, which was cyclized by treatment with anhydrous acid. The cyclization reaction involves the reaction of a transient enol ether as the nucleophilic component in an intramolecular Mannich reaction with an acylalkylidenammonium (acylimmonium) ion, a reaction that was first observed by Wenkert et al.[24] The two-step conversion of **12** and **13** to the crystalline tricyclic ketal lactam **14** proceeded in excellent overall yield and was carried readily out on a multigram scale.

Treatment of the lithium enolate of lactam **14** with the benzyl ether of 3-bromopropanol[25] provided **15**, which was treated with the Lawesson reagent[26] to obtain the thiolactam. Surprisingly, thiation of the lactam carbonyl was accompanied by partial replacement of one of the dioxolane oxygen atoms, and it was necessary to remove and reinstall the protecting group before proceeding with the synthesis. In

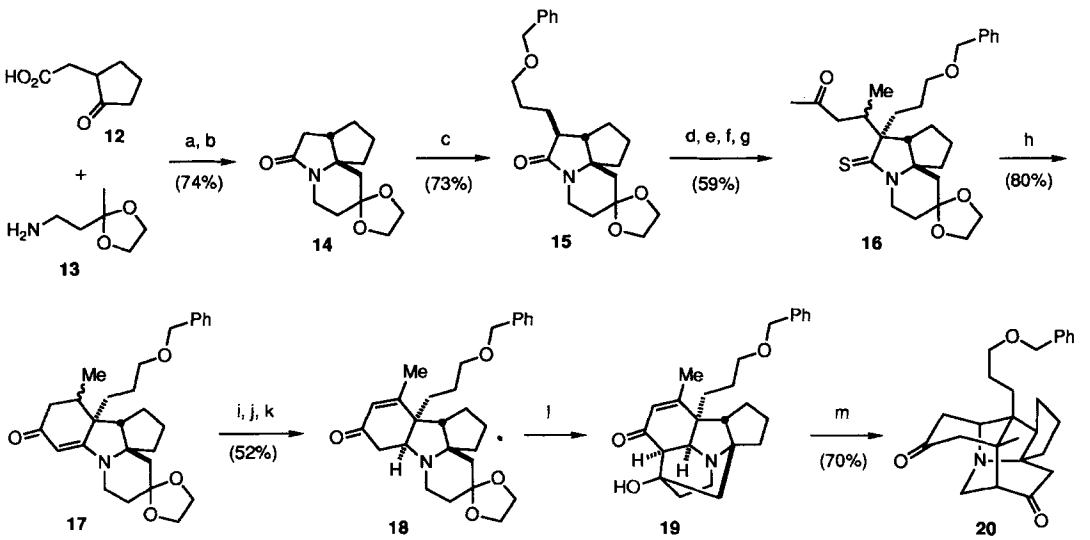

Scheme 6. a: i) **12**, Et_3N,$ClCO_2Et$; ii) **13**. b: *p*-toluenesulfonic acid, toluene, reflux. c: lithium diisopropylamide (LDA), $PhCH_2OCH_2CH_2CH_2Br$. d: Lawesson reagent. e: H_3O^+. f: $(CH_2OH)_2$, H^+. g: LDA, $CH_3COCH{=}CHCH_3$. h: i) $Et_3O^+BF_4^-$; ii) Et_3N. i: i) $Me_3O^+BF_4^-$; ii) $NaBH_4$; iii) H_3O^+. j: i) lithium-2,2,6,6-tetramethylpiperide (LTMP), THF, −78 °C; ii) PhSeCl. k: *m*-chloroperbenzoic acid. l: H_3O^+, acetone. m: MeONa, MeOH.

light of our philosophy with regard to protecting groups articulated at the end of the previous section, this unproductive maneuver constitutes a distinct flaw in the synthesis. However, as will soon be revealed, the entire approach turned out to be flawed for another reason, so there was little incentive to work out more appropriate thiation conditions. Treatment of the lithium enolate of the thiolactam with pent-3-en-2-one afforded **16** as a 6:1 mixture of diastereomers at the methyl-bearing stereocenter in about 80% yield.[27]

The fourth ring was closed by treatment of **16** successively with $Et_3O^+BF_4^-$ and triethylamine to give vinylogous amide **17**. Having reached our first goal of an intermediate with the skeleton of **B** (see Scheme 4), it was necessary to relocate the double bond and set the stage for formation of the strategic bond. This was accomplished by a three-step sequence wherein the double bond of **17** was reduced by successive treatment with $Me_3O^+BF_4^-$, $NaBH_4$, and aqueous acid to obtain a saturated amino ketone. The double bond was then reintroduced by deprotonation with LTMP in THF at $-78\,^\circ C$ and treatment of the resulting enolate with phenylselenyl chloride. Compound **18** was obtained in about 50% overall yield.

With **18** in hand, we could finally test the proposed intramolecular Michael addition and formation of the strategic bond of daphnane. To this end, compound **18** was subjected to aqueous acidic conditions in order to hydrolyze the ketal and thus obtain the enedione corresponding to structure **B** in Scheme 4. The infrared spectrum of the product revealed the presence of a saturated carbonyl group, not the desired α,β-unsaturated carbonyl function. Furthermore, the product clearly contained a hydroxy group. Unexpectedly (but predictably), the initial enedione had undergone an intramolecular aldol reaction under the acidic conditions. Fortunately, this unexpected cyclization was of no real concern, because the aldol cannot dehydrate for geometric reasons, and it is known that aldols are easily reversible under the basic conditions required for the intramolecular Michael reaction. Thus, treatment of aldol **19** with methanolic sodium methoxide smoothly furnished the amino diketone **20**, the first synthetic material having the pentacyclic daphnane skeleton.

With the path to methyl homodaphniphyllate thus illuminated, three tasks remained before us. The first was installation of the final three carbon atoms, in the form of the isopropyl group. Second, there was the seemingly trivial task of removing the two carbonyl oxygens atoms which, having served their synthetic purpose, were now superfluous. Finally, it was necessary to correctly refunctionalize the three-carbon side chain. At this point, a brief detour was forced upon us. In an attempt to introduce the isopropyl group, compound **18** was formylated, and the resulting keto aldehyde was treated with oxalyl chloride to obtain the β-chloro enone **21**. When this material was treated with lithium dimethylcuprate in ether at room temperature, rearranged enone **22** was the only identifiable product (Scheme 7). At first glance, the transformation of **21** into **22** appears astonishing. Although the product is an enone, as expected, the isopropyl and methyl groups seem to have been miraculously relocated. However, the explanation is ordinary and, in fact, the reaction could have been anticipated. Enolate **23**, formed after reaction with the second equivalent of cuprate, simply undergoes β elimination to give a cyclohexadienone, **24**, which undergoes 1,4-addition at the methyl-bearing double bond. Ironically, the same intrinsic polarization that had made this skeleton easy to assemble also provided the seed of its destruction!

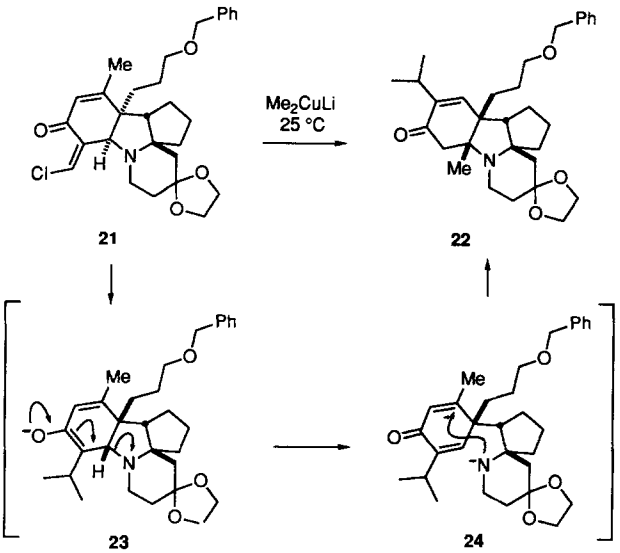

Scheme 7.

The retro-Michael problem was solved in a relatively straightforward fashion. As shown in Scheme 8, the lithium enolate of **18** reacted with acetaldehyde to provide aldol **25**, which was treated with sulfuric acid in aqueous acetone. Careful examination of the reaction intermediates disclosed that the aldol dehydrated rapidly and that the ethylene ketal hydrolyzed more slowly to **26**. This substance, now deprived of the possibility of β elimination or intramolecular aldol reaction by the presence of the ethylidene group, smoothly cyclized to the pentacyclic enedione **27**, which was obtained in about 70% yield.

Efforts were next directed toward introduction of the final carbon atom of methyl homodaphniphyllate. We had planned to accomplish this task by conjugate addition of lithium dimethylcuprate to **27** an had anticipated no problems with the maneuver, since the isopropyl group in the natural product occupies an equatorial position. However, our estimation proved to be overly optimistic. Although **27** reacted smoothly with lithium dimethylcuprate, the product was a mixture of diones, epimeric at the isopropyl-bearing stereocenter, in a ratio of 4:1. This development presented us with three problems: First, the isomers equilibrated with great ease, even on attempted separation by column chromatography on silica gel. Second, although molecular modeling suggested that the desired isomer **29** would predominate in the equilibrium, the calculated strain energies of the two isomers were so close that we had no confidence that this isomer was, in fact, the major product. Finally, and most importantly, many attempts to remove the two carbonyl groups utterly failed. Although space does not permit a complete catalog of the methods that were evaluated for deoxygenation of **28** and **29**, it is sufficient to say that a great many reactions were tested, ranging from simple Wolff–Kishner

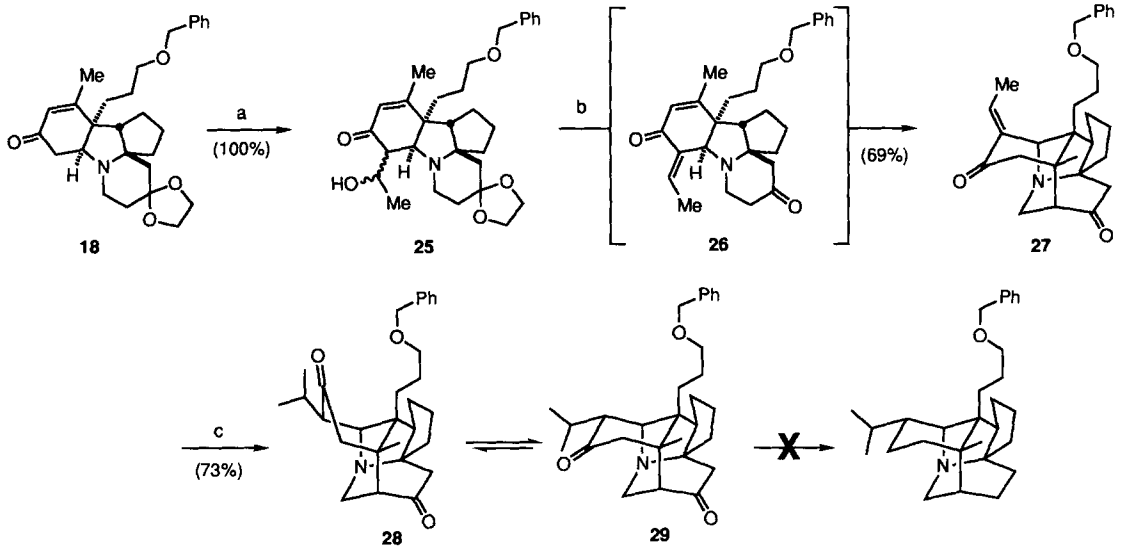

Scheme 8. a: LDA, CH_3CHO; b: H_2SO_4, acetone; c: Me_2CuLi, Et_2O.

reduction to various strategies designed to proceed through free radical intermediates. The origin of the problem seemed to be the sterically hindered environment of the carbonyl next to the isopropyl-bearing center.

We eventually found a way around the impasse. As summarized in Scheme 9, the initial lithium enolate resulting from reaction of lithium dimethyl cuprate with **27** was phosphorylated to obtain **30**, which itself was deprotonated and phosphorylated to arrive at the bis(enol phosphate) **31**. Ireland reduction[28] of **31** provided the unsaturated amino alcohol **32**. The three-step process accomplished introduction of the final methyl group and removal of the two carbonyl groups, albeit in a rather heavy-handed way; the overall yield was only 38%.

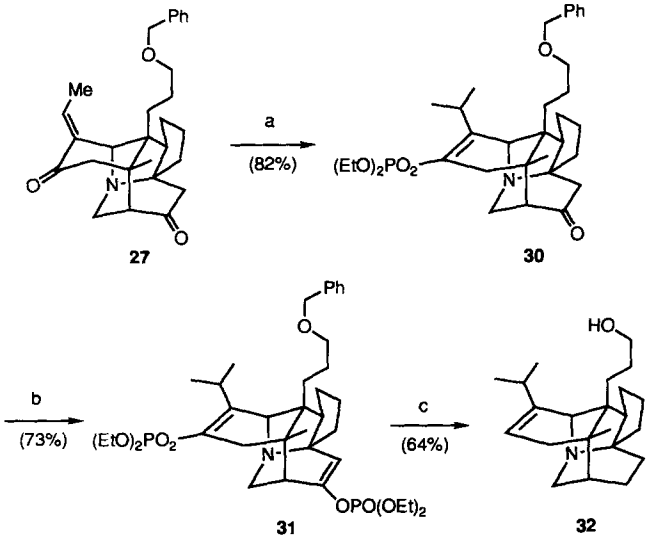

Scheme 9. a: i) Me_2CuLi, ii) $(EtO)_2POCl$. b: i) LDA, THF, hexamethylphosphoric triamide (HMPA); ii) $(EtO)_2POCl$. c: Li, $EtNH_2$.

Having finally dispatched the unwanted carbonyl groups, we had only to adjust the functionality of the three-carbon side chain and reduce the double bond to complete the first synthesis of a *Daphiphyllum* alkaloid. We had not anticipated problems with saturation of the double bond, because molecular models of **32** showed that the same methylene group (indicated with an arrow in Scheme 10) that had impeded removal of the carbonyl oxygen atom now stood squarely in the path of any reagent seeking access to the "bottom face" of the cyclohexene double bond. For this reason, we were rather confident that hydrogenation would occur from the "top face", delivering the daphnane skeleton with the proper configuration at the isopropyl-bearing carbon. However, events proved otherwise. Initial hydrogenations over rhodium did give only one product, but the one having the wrong configuration at the new stereocenter! Subsequent investigations showed that the stereochemical outcome of the reduction was responsive to changes in catalyst and solvent, and we embarked on an extensive program of process development. However, even under the best conditions we could find (Scheme 10), we were able to achieve no better than a 1:1 mixture of the diastereomeric amino

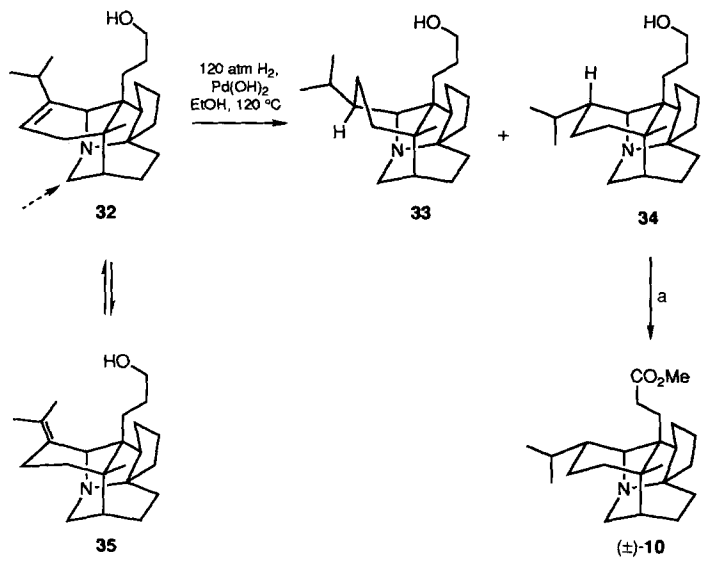

Scheme 10. a: i) Separation; ii) Jones oxidation; iii) 6 M HCl, MeOH.

alcohols **33** and **34** with the respective unnatural and natural configuration at the new stereocenter. Once again, nature had thwarted our simplistic plans. Because hydrogenation of the hindered double bond is slow, it is likely that isomerization occurs to give some isomer, perhaps **35**, in which the bottom face of the double bond is not as hindered as it appears to be in **32**. Nevertheless, amino alcohol diastereomers **33** and **34** were separable by chromatography, and the latter isomer was transformed by succesive oxidation and esterification into racemic methyl homodaphniphyllate, (±)-**10**.

By obtaining a few milligrams of (±)-**10**, we had achieved the first total synthesis of one of the alkaloids of Yuzuriha. However, the problem of finding a truly efficient route to these fascinating natural products had still not been solved. The synthesis just described was not especially long, given the state of synthetic art and the complexity of the target. Only 19 steps were required, starting with keto acid **12** and amino ketal **13**. Although the method of network analysis did identify a facile assembly for the pentacyclic skeleton, the concluding stages of the synthesis, which were occasioned by the need to remove the activating carbonyl groups, were awkward and failed to control one of only two independent stereocenters in the molecule. Thus, the very heuristic that had so simplified the synthetic design had also endowed the synthesis with its Achilles heel.

5. A Fresh Look at the Problem: Dissection of the Target Along Probable Biosynthetic Lines

Even while we were struggling with removal of the two carbonyl oxygen atoms and stereocontrolled reduction of the double bond in **32**, we turned our minds back to the original design. Where had we gone wrong? In examining our assumptions, we reconsidered the reasons for selecting methyl homodaphniphyllate as our first target. Because it is widespread and abundant relative to the other *Daphniphyllum* alkaloids, we had made the mistake of bestowing it with singular importance and elected it as our original synthetic goal. However, an examination of the daphnane and seco-

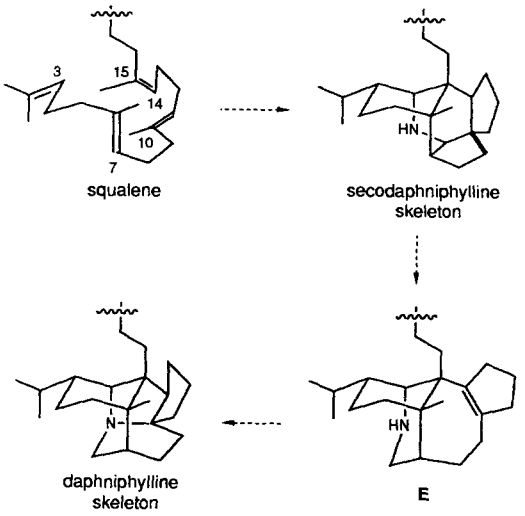

Scheme 11.

daphnane carbon skeletons reveals an important difference. As shown in Scheme 11, the unbroken squalene molecule can be identified in the pentacyclic structural unit of secodaphniphylline but not in that of daphniphylline. That is, in order for squalene to be converted into secodaphniphylline, four C–C bonds must be created: C10 to C14; C6 to C15; C3 to the C15 methyl group; and C7 to the C10 methyl group. The nitrogen atom is inserted between the C10 and C15 methyl groups. In daphniphylline, on the other hand, the nitrogen atom has been inserted between C10 and its methyl group, which has also become bonded to C7. Although circumstantial, the evidence is strong that secodaphniphylline prededes daphniphylline biosynthetically. A reasonable biosynthetic link between secodaphniphylline and daphniphylline is an unsaturated amine with the partial structure **E**.[29]

The perception of this biosynthetic progression was significant, since it suggested the probability of some reasonable chemical path for the conversion of secodaphniphylline to daphniphylline by way of a ring-opened intermediate such as **E**. If we could discover the path, we could use it as a better route to **10**. A natural consequence of this line of thought was a redirection of our attention to the skeleton of seco-

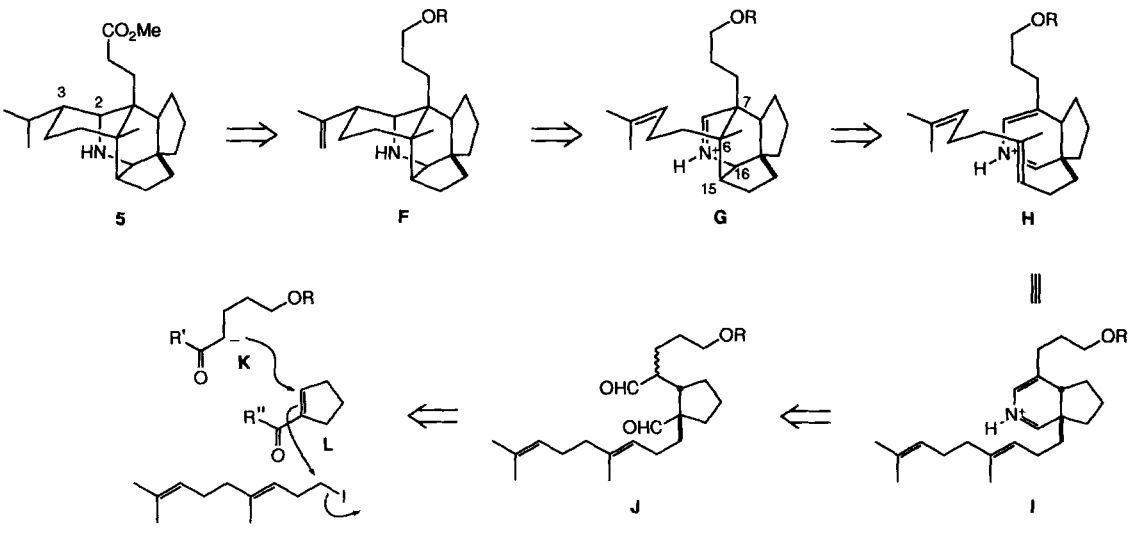

Scheme 12.

daphniphylline, as exemplified by its C_{22} congener, methyl homosecodaphniphyllate (**5**). Although a retrosynthetic analysis centered about the primacy of the pentacyclic network was again possible, we feared that the inevitable end of such a plan would be another struggle to remove necessary but unwanted functional groups. Thus, we abandoned the strategic bond approach in favor of synthetic plans by which the skeleton might be assembled without the wasteful use of auxiliary functional groups. How does nature forge the skeleton of secodaphniphylline from its triterpene raw material? The plan that emerged from these contemplations is summarized in Scheme 12. A key element was the dissection of the skeleton along probable biosynthetic lines. That is, in the retrosynthesis, bond disconnections were made so as to preserve the squalene chain for as long as possible until we recognized an obvious solution based on available materials and methods. This reasoning forced us to consider formation of the C2–C3 bond as the final carbon–carbon bond-forming operation in the formation of secodaphniphylline. Homoallylic amine **F** contains a reasonable retron for the desired transform,[30] which can be viewed as an ene or aza-Prins reaction. Once **G** had been identified as a possible synthetic intermediate, it was natural to take the next step and consider the possible formation of bonds between C6 and C7 and then between C15 and C16. It then became clear that a compound with the part structure of **I** might easily arise from reaction of a monocyclic dialdehyde **J** with ammonia. Up to this point, the plan being developed might even parallel the biosynthesis of the alkaloid. However, with the perception of dialdehyde **J** as an attractive intermediate, a decidedly nonbiosynthetic possibility occurred to us. Compound **J** might be obtained in one grand, triply convergent step by the assembly of an enolate **K**, some α,β-unsaturated carbonyl compound **L**, and homogeranyl iodide (**36**)!

6. Biomimetic Synthesis of Methyl Homosecodaphniphyllate: The Ruggeri Tetracyclization Reaction

The exciting plan was soon put into practice. Successive treatment of the lithium enolate of amide **37** with the α,β-unsaturated ester **38** and homogeranyl iodide (**36**)[31] provided a mixture of three diastereomeric adducts in a total yield of 99%. Compound **39**, the major isomer, was isolated in 87% yield. Two minor isomers were isolated as a 2:1 mixture in a combined yield of 12%. It is not insignificant that the entire carbon skeleton of alkaloid **5** is assembled in this one convergent step. The next task that stood before us was transformation of the ester and amide groups of **39** into aldehyde groups. A good deal of experimentation led to the three-stage protocol summarized in Scheme 13. Treatment of **39** with excess DIBAL gave hydroxy amide **40**, which was hydrolyzed by treatment with KOH in aqueous ethanol. Acidification of the saponification mixture furnished lactone **41** as a 1:1 mixture of diastereomers; epimerization of the benzyloxypropyl center had occurred under the harsh alkaline conditions. However, the configuration at this position is of no consequence because it is destined to have sp^2 hybridization at a later stage in the synthesis. Reduction of **41** with lithium aluminum hydride gave an equimolar mixture of epimeric diols **42** in nearly quantitative yield.

The way was now prepared for the most crucial stage of the plan. Oxidation of diols **42** by the Swern method[32] gave a dialdehyde that turned out to be rather vulnerable to a retro-Michael fragmentation. Consequently, a procedure was developed whereby the material was formed and used in situ. Thus, after the Swern oxidation was complete, gaseous ammonia was passed over the surface of the stirring methylene chloride solution. Concentration of the reaction

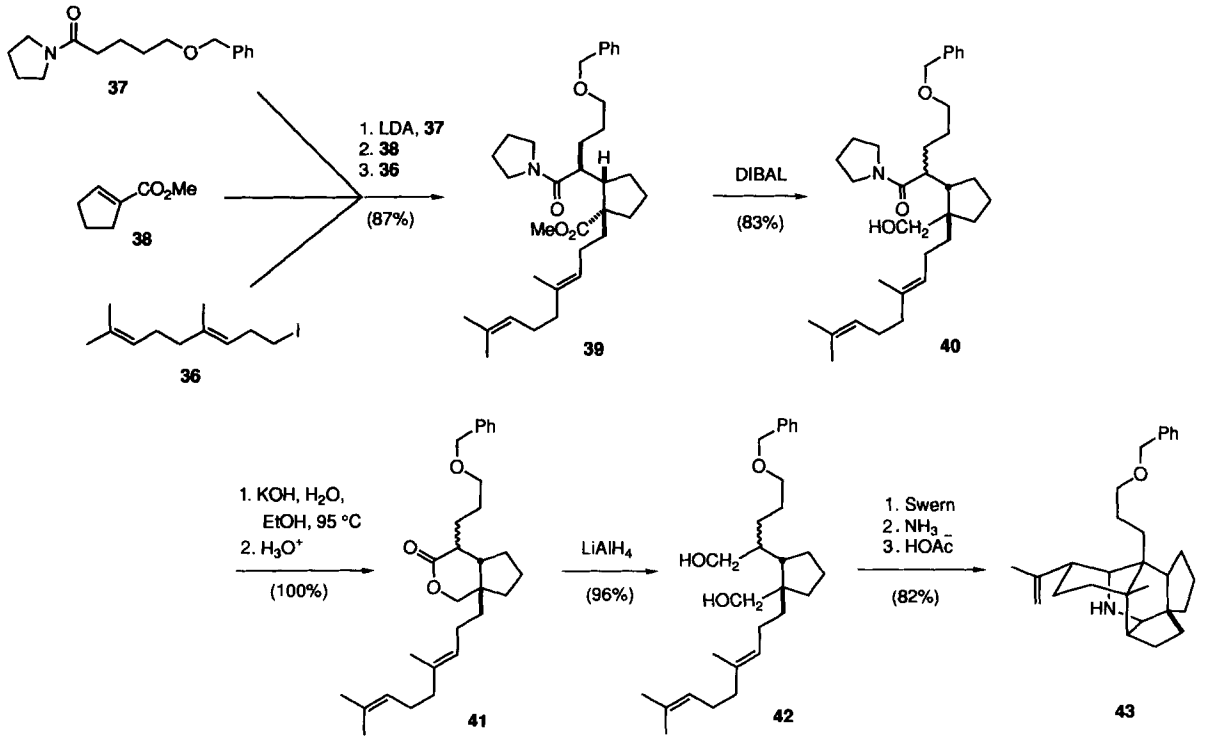

Scheme 13. DIBAL = diisobutylaluminum hydride.

solution gave a residue that was taken up in acetic acid containing NH_4OAc. This mixture was heated at 70 °C and worked up in the normal manner to obtain pentacyclic amine **43** in 82% yield. The structure of **43** was eventually proven by its conversion to (±)-methyl homosecodaphniphyllate.

Several intermediates in the conversion of diols **42** into pentacyclic amine **43** have been isolated (Scheme 14). As has already been discussed, the initial Swern oxidation provided the dialdehydes **44**. When the reaction was terminated after

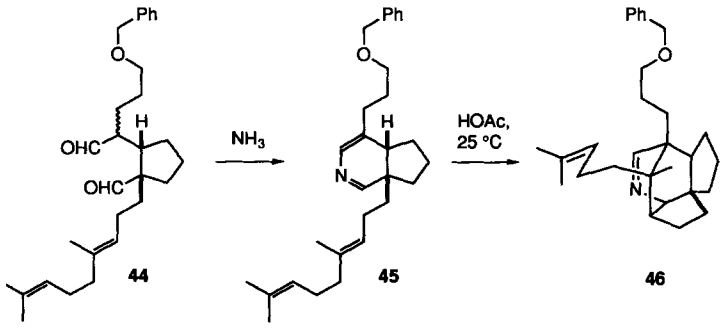

Scheme 14.

addition of ammonia and before treatment with acetic acid, azadiene **45** was isolated. This material was rapidly transformed into the tetracyclic imine **46** upon being dissolved in acetic acid. Analysis by thin-layer chromatography indicated that the Diels–Alder reaction was complete in less than five minutes. The Diels–Alder step is strongly catalyzed by acid, since the thermal conversion of **45** to **46** has a half-life of about 2 h in refluxing toluene.

7. Serendipity: The "Vollhardt Ammonia" Incident

At this point, a remarkable bit of serendipity will be described. One day, after repeating the tetracyclization process with the goal of obtaining a quantity of pentacyclic amine **43**, one of my co-workers brought me the seemingly impossible news that he had followed the standard protocol that had been developed over a period of about two years and, inexplicably, had obtained the saturated pentacyclic amine **47** instead of the normal product. After having been slandered with various aspersions ranging from amnesia to mixing up his NMR tubes, the co-worker repeated the remarkable transformation and finally succeeded in convincing me that the product of the reaction was, indeed, **47**. Where had the double bond gone? A careful inventory of the materials used revealed one important clue. During the preceding week, our lecture bottle of ammonia had been exhausted and my co-workers had borrowed a new bottle from my colleague, Professor Vollhardt. Mass spectral examination of the "Vollhardt ammonia" revealed it to be methylamine, its label notwithstanding. Initially, this realization brought us no great comfort. The problem was now even more mysterious. Not only were we faced with the quandary of a disappearing double bond, but now we also had to deal with a disappearing methyl group! The explanation was eventually provided by another of my colleagues, Professor Pedersen, who suggested the mechanism shown in Scheme 15. Reaction of di-

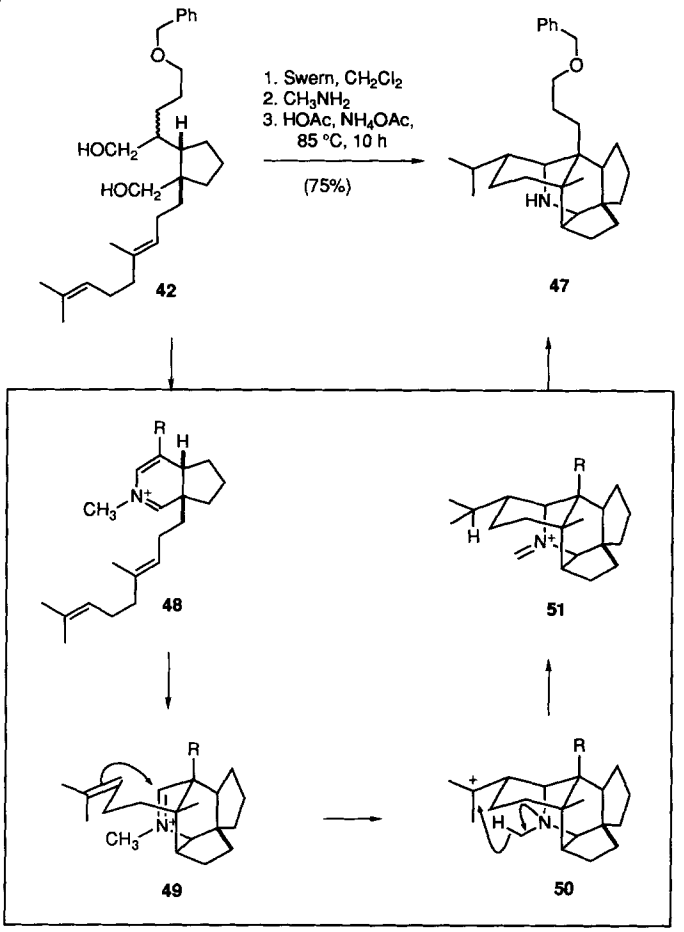

Scheme 15.

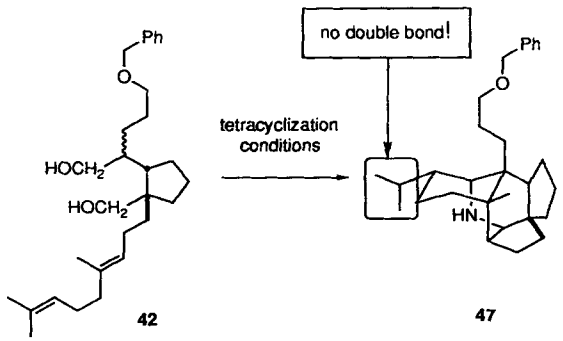

aldehyde **44** with the primary amine is postulated to lead to **48**, which reacts with acetic acid at room temperature to give the tetracyclic immonium salt **49**. In fact, an impure intermediate with NMR spectral features consistent with structure **49** has been isolated from the reaction mixture. Further cyclization of **49** is postulated to provide the amino cation **50**, a substance ideally constructed to undergo intramolecular hydride transfer to give **51**,[33] which is hydrolyzed on workup to afford **47**.

After achieving an efficient synthesis of amine **43**, we only had to modify the functionality of the three-carbon side

chain to complete the synthesis of methyl homosecodaphniphyllate. The alkene was readily hydrogenated with Pd/C as catalyst (Scheme 16). Analysis of the reaction mixture by ^{1}H NMR showed that amine **47** was rapidly produced, along with a small amount of amino alcohol **52**. Addition of a

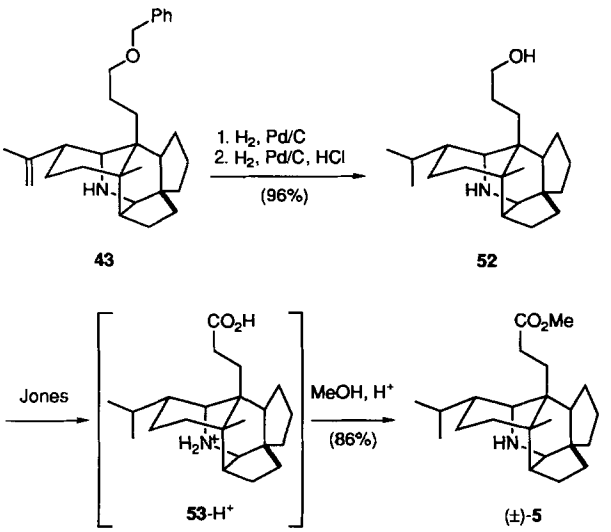

Scheme 16.

small amount of hydrochloric acid increased the rate of hydrogenolysis considerably and permitted complete conversion into **52**, which was isolated as the hydrochloride salt in 96% yield. This material was directly converted to amino acid **53** by oxidation with excess Jones reagent.[34] Finally, compound **53** was converted into racemic methyl homosecodaphniphyllate, (±)-**5**, by Fischer esterification. Comparision of the ^{1}H NMR spectra and R_f values showed the synthetic material to be identical to an authentic sample of the natural alkaloid.[35]

The total synthesis of (±)-methyl homosecodaphniphyllate requires only nine steps and proceeds in 48% overall yield from the simple starting materials **36**, **37**, and **38**. Amide **37** and ester **38** are each made in two steps from commercially available materials. The synthesis of iodide **36** is more complicated, requiring four steps form geraniol. The longest linear sequence requires thirteen steps from geraniol and proceeds in 18% overall yield. The key steps in the synthesis are the tandem Michael addition–alkylation reactions, which assemble all of the carbon atoms necessary for the skeleton, and the tetracyclization reaction, which provides the complete pentacyclic skeleton in one operation. The only disappointing sequence is the conversion of amide **39** to diol **42**; three steps are expended for what would appear to be straightforward functional group manipulations. However, this was the only workable method that we could find for this conversion, and the overall yield for the three steps is quite respectable. All of the steps in the sequence have been carried out on gram scale, and we have used the route to synthesize more than 3.5 g of (±)-methyl homosecodaphniphyllate, several times as much of the alkaloid as has ever been isolated from natural sources. Finally, the synthesis is wholly stereospecific, in contrast to our initial synthesis of methyl homodaphniphyllate.

8. Stealing Another Page from Mother Nature: Conversion of the Secodaphnane Skeleton to the Daphnane Skeleton

In spite of this success, the original problem that we had set before ourselves was only partially solved; we still had to discover a method to rearrange the secodaphnane skeleton to the daphnane skeleton. It has already been pointed out that the desired rearrangement might be realized in two stages by fragmentation of a secodaphnane to an unsaturated amine with structure **E**, which could undergo transannular addition to the double bond. Two possible fragmentation modes of the secodaphnane skeleton are summarized in Scheme 17. Both of these hypothetical transformations are

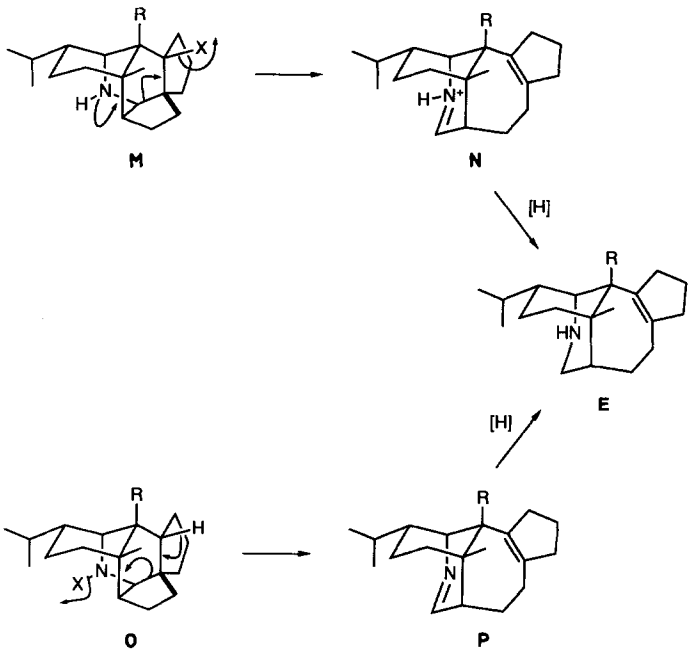

Scheme 17.

Eschenmoser–Grob fragmentation reactions.[36] The first is more conventional and would convert an angulary functionalized secodaphnane **M** into an immonium ion **N**. The second possibility is less well known and involves movement of electrons in the opposite direction, converting an *N*-functionalized secodaphnane **O** into the imine **P**. In either case, we would have to reduce the carbon–nitrogen double bond of the initial fragmentation intermediate to obtain **E**.

Both of the possibilities in Scheme 17 have been investigated. However, because of the constraints of space, I will only discuss the results of the more traditional fragmentation. Since X must be a heteroatom, and since the three-carbon side chain terminated in a heteroatom, it occurred to us that it would be economical to arrange for the same heteroatom to serve both functions. The substrate for the fragmentation would, therefore, be hexacyclic amino ether **54** (Scheme 18). The necessary cyclization substrate would then be the azadiene **55**. If we followed the same route that was already discussed for the synthesis of methyl homosecodaphniphyllate, we would need tricyclic lactone **56**, which might be available by an intramolecular Reformatsky reaction of **57**, followed by cyclization of the resulting bromo alcohol.

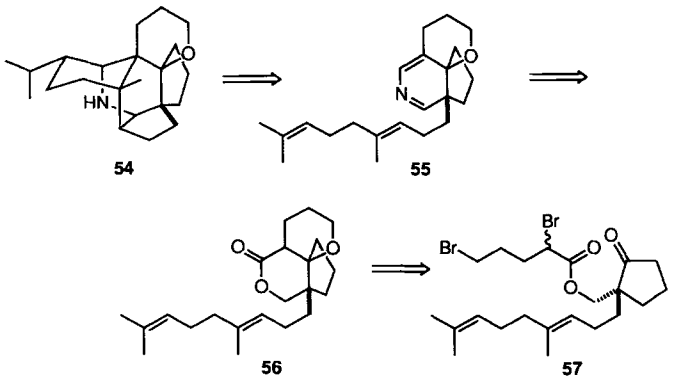

Scheme 18.

To prepare a suitable substrate for the proposed Reformatsky double annulation process, we started with enol ether **58**, which was conveniently prepared from the corresponding β-keto ester. Alkylation of the lithium enolate of **58** with homogeranyl iodide (**36**) provided **59**, which was reduced with lithium aluminum hydride to alcohol **60** (Scheme 19). Esterification with 2,3-dibromopentanoyl bromide[37] provided keto ester **57** after acidic hydrolysis of the enol ether. This material was treated with activated zinc, prepared by treatment of $ZnCl_2$ with sodium naphthalenide in THF,[38] to obtain the tricyclic lactone ether **56**. Although the Reformatsky reaction was rapid, the ensuing cyclization of the zinc alkoxide **61** was slow in pure THF. For this reason, HMPA was added immediately after addition of **57** to the activated zinc suspension. The relative configuration of **56** was assigned on the basis of a single-crystal X-ray structure analysis of a related compound having a methyl group in place of the homogeranyl group.

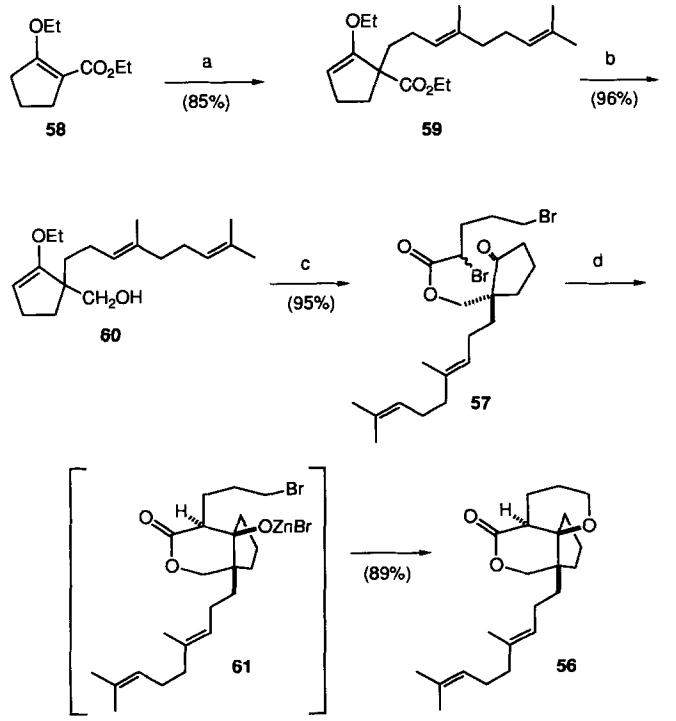

Scheme 19. a: i) LDA; ii) **36**. b: $LiAlH_4$. c: i) $BrCH_2CH_2CH_2CH_2BrCOBr$; ii) H_3O^+. d: Zn, THF, HMPA.

As shown in Scheme 20, reduction of lactone **56** provided diol **62** in high yield. Application of the tetracyclization protocol to this diol was successful, although the yield of the hexacyclic amino ether **63** was lower than that of the cyclization of diol **42**. However, given the fact that **62** has an ether linkage to a tertiary carbon atom that is allylic in some of the tetracyalization intermediates, we were more than pleased with the optimized yield of 47%. Hydrogenation of the double bond over Adams catalyst proceeded in quantitative yield to provide the saturated hexacyclic amino ether **54**. To

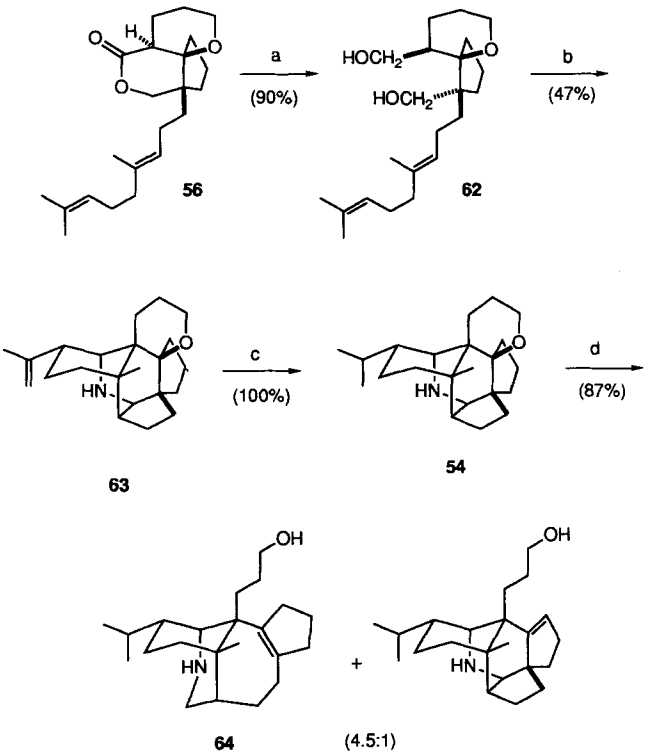

Scheme 20. a: $LiAlH_4$. b: i) Swern oxidation; ii) NH_3; iii) HOAc, 55 °C. c: H_2, PtO_2. d: DIBAL, toluene, reflux 36 h.

bring about the fragmentation suggested in Scheme 17 we needed a Lewis acid to activate the alkoxy leaving group and a reducing agent to reduce the immonium ion expected to result. We thought that a dialkylaluminium hydride might fulfill both functions and perhaps also activate the nucleofugal group by deprotonation of the secondary amine. To this end, **54** was treated with excess DIBAL in refluxing toluene for 72 hours to obtain the desired unsaturated amino alcohol **64** (71% yield), accompanied by some of the simple elimination product **65** (16% yield).

With unsaturated amino alcohol **64** in hand, we were poised for the second stage of the proposed secodaphnane → daphnane isomerization. To this end, **64** was subjected to Jones oxidation and the resulting amino acid treated with sulfuric acid in refluxing methanol of afford unsaturated amino ester **65** (Scheme 21). We were not surprised when **65** was recovered unchanged from other acidic media (e.g., refluxing formic acid, *p*-toluenesulfonic acid in refluxing benzene). Under these acidic conditions the amine is presumably firmly protonated and therefore not nucleophilic even if the double bond also happens to become protonated.

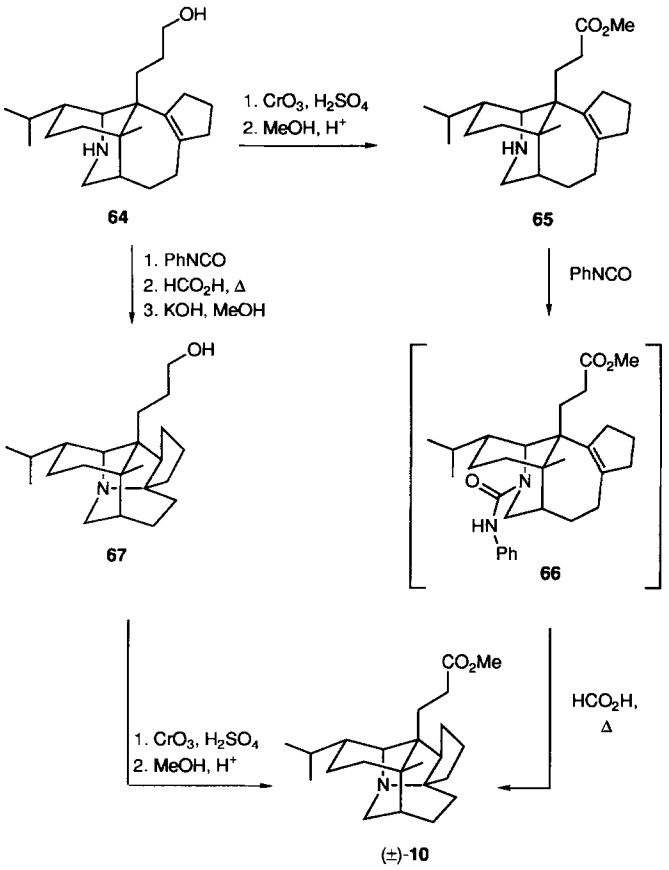

Scheme 21.

However, the *N*-phenylurea derivative **66**, formed by the reaction of **65** with phenyl isocyanate, cyclized smoothly in refluxing formic acid to provide (±)-methyl homodaphniphyllate (**10**) in 63% overall yield. In an alternative sequence of steps, unsaturated amino alcohol **64** was treated sequentially with phenyl isocyanate, refluxing formic acid, and methanolic potassium hydroxide to furnish (±)-homodaphniphyllol (**67**). Jones oxidation of this material and Fischer esterification of the resulting amino acid provided (±)-**10** in an overall yield of about 70%. These successful

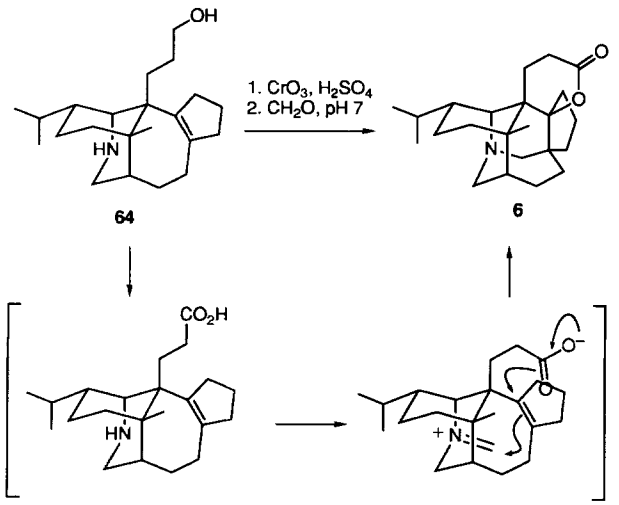

Scheme 22.

cyclizations therefore permitted us finally to solve the problem of a stereocontrolled synthesis of methyl homodaphniphyllate. The synthesis of (±)-**10** by this route required a total of 13 steps from homogeranyl iodide and proceeded in 11% overall yield.

Compound **64** was also converted into racemic daphnilactone A, (±)-**6**, as shown in Scheme 22. Oxidation of **64** delivered the corresponding amino acid, which was treated directly with aqueous formaldehyde at pH 7 to obtain (±)-**6**, whose ^{1}H NMR spectrum and R_f value are identical to those of an authentic sample provided by Professor Yamamura. The complete synthesis of daphnilactone A required 11 steps from homogeranyl iodide and proceeded in 8% overall yield.

9. Transformation of a Squalene Derivative into a Pentacyclic Alkaloid in a Simple One-Pot Transformation

The goal of this project was purely synthetic—we were challenged as molecular architects and engineers by the fascinating structural complexity of the alkaloids of Yuzuriha. Although we applied in our second retrosynthetic analysis a biosynthetic philosophy in performing disconnections that preserved the squalene chain to the extent possible, the resulting synthesis was not truly biomimetic in the sense that it paralleled a known biosynthetic pathway. However, the analysis led us to discover the exceptionally facile tetracyclization process. Could it be that the process actually is biomimetic? A credible biosynthesis is put forth in Scheme 23. The rough outlines of this proposal are as follows: Step 1 is an oxidative transformation of squalene (**68**) into a dialdehyde, **69**.[39] In step 2 it is proposed that some primary amine, perhaps pyridoxamine [40] or an amino acid, condenses with one of the carbonyl groups of **69**, giving imine **70**. Step 3 is the prototopic rearrangement of a 1-azadiene to a 2-azadiene, a process that is well-precedented for the imines formed from α,β-unsaturated carbonyl compounds and benzylamine.[41] Although potassium *tert*-butoxide was used for the prototopic rearrangement of benzylimines, one can imagine that an imine derived from pyridoxamine or an amino acid would rearrange under much milder conditions. Because the 2-azadiene that would result from the foregoing rearrangement is an enimine, its double bond is not especially nucleophilic. However, if some nucleophilic species adds to the imine double bond, as in step 4, the product **72** is a nucleophilic enamine. The subsequent cyclization to give **73** has an exact precedent in vitro in the work of Schreiber, Meyers, and Wiberg.[42] In steps 6–9 the resulting bicyclic dihydropyran derivative **74** is transformed into a dihydropyridine derivative **77** similar to the intermediate in the in vitro conversion of **42** into **43**. Other possible scenarios can be envisioned for the metamorphosis of **74** into **77**. According to our supposition of the biosynthesis **77** would then be converted into **78** by a catalyzed Diels–Alder reaction and the final ring would result from an ene-like cyclization, giving **79**, the putative primordial *Daphniphyllum* alkaloid. Because of the likelihood that **79** is the first pentacyclic substance to occur in the biosynthesis of the al-

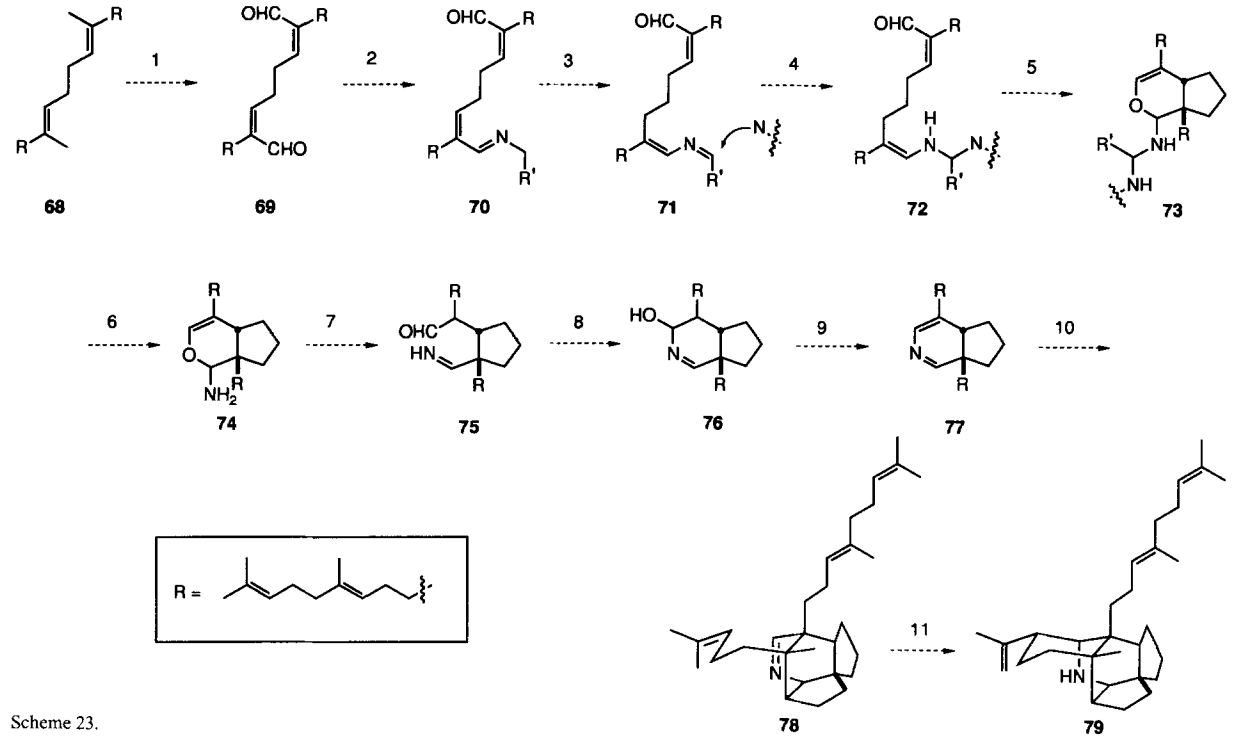

Scheme 23.

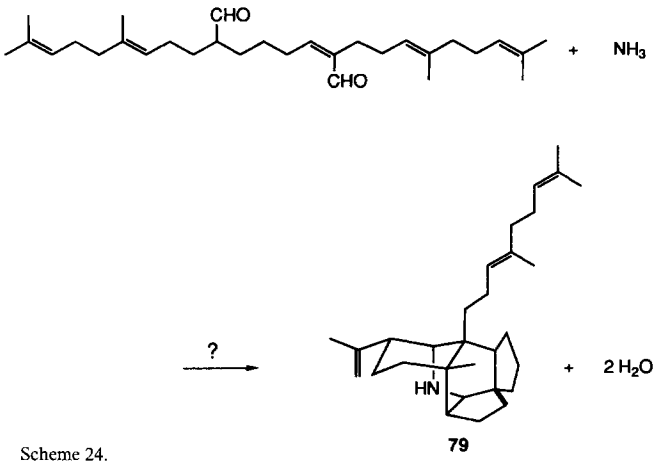

Scheme 24.

kaloids of Yuzuriha, we have named it protodaphniphylline.[43]

How much of this proposed biosynthesis might we be able to imitate in the laboratory? We thought it possible that we could intercept the proposed scheme at the stage of intermediate **72** or the corresponding dialdehyde (Scheme 24). We therefore set about the relatively simple task of preparing a suitable squalene derivative to put this proposition to the test. The route adopted is summarized in Scheme 25. Alkylation of the lithium enolate of *tert*-butyl acetate with homogeranyl iodide (**36**) afforded ester **80**, which was alkylated with the dimethyl acetal of 4-bromobutanal [44] to provide **81**. Hydrolysis of the acetal gave aldehyde **82**, which was condensed with the lithium enolate of **80** to obtain β-hydroxy esters **83** as a mixture of diastereomers. Elimination

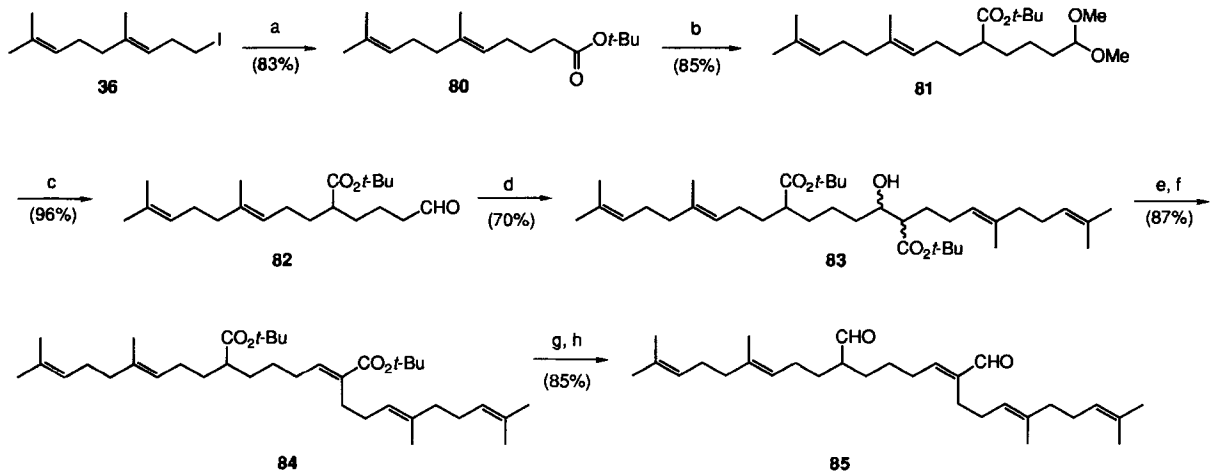

Scheme 25. a: Li enolate of *tert*-butyl acetate. b: i) LDA; ii) $BrCH_2CH_2CH_2CH(OMe)_2$. c: H_3O^+. d: Li enolate of **80**. e: CH_3SO_2Cl, Et_3N. f: 1,8-diazabicyclo[5.4.0]undec-7-ene (DBU), toluene, Δ. g: DIBAL. h: Swern oxidation.

was accomplished by treatment of the methanesulfonate of **83** with DBU in toluene at 80 °C. Diester **84** was obtained in excellent yield, accompanied by approximately 10% of the *Z* isomer. After chromatographic separation to the stereoisomeric diesters, **84** was converted into the *E* dialdehyde **85** as shown in Scheme 25. The pure *Z* isomer **86** was prepared by a slightly different route wherein the C10–C11 double bond was formed by Peterson olefination.

The pentacyclization process was first investigated under the conditions that had served for the teracyclization of **42** to **43** (Scheme 26). Thus, a solution of either **85** or **86** in CH_2Cl_2 was treated with ammonia and triethylamine hydrochloride at room temperature for 16 hours, after which time TLC showed that starting material had been consumed. At this point the solvent was evaporated under vacuum and the resulting residue taken up in acetic acid and heated at 80 °C for 2 hours. Workup gave protodaphniphylline (**79**) in 15 ± 2% yield. Although the yield in this biomimetic synthesis is not high, it must be acknowledged that a profound structural change has occurred—five rings and six σ bonds have been created through the action of the most common of chemical reagents, ammonia and acetic acid.

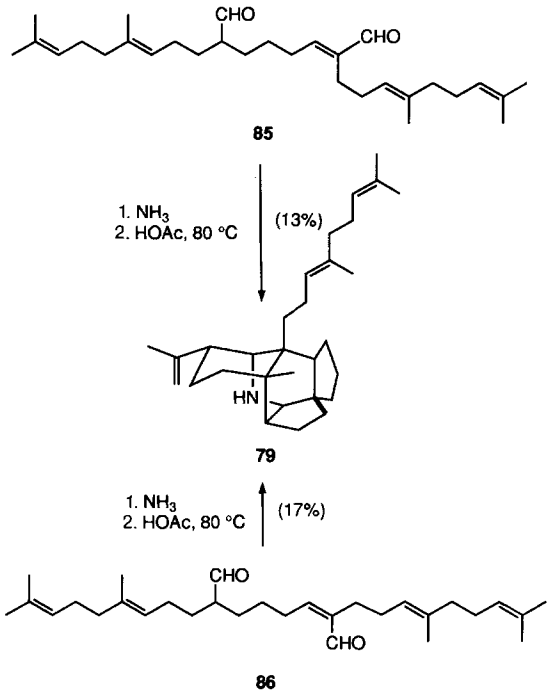

Scheme 26.

A considerable amount of process development eventually resulted in a somewhat more complicated two-pot protocol wherein **85** or **86** was treated sequentially with KOH under phase-transfer conditions, ammonia in DMSO, and acetic acid, to obtain **79** in obout 50% overall yield. However, it was our unexpected experience with the "Vollhardt ammonia" (methylamine) that eventually provided the best solution to the pentacyclization problem. Because the low yield in the pentacyclization of **85** and **86** with ammonia was presumably due to poor selectivity in the formation of the first carbon–carbon bond, we reasoned that the more nucleophilic *N*-methylenamine derived from methylamine might improve upon the 15% yield observed with ammonia. Indeed, when dialdehyde **85** was treated with methylamine and the crude reaction product heated in acetic acid at 80 °C for 11 hours, dihydro-protodaphniphylline **87** was obtained in 65% yield (Scheme 27).

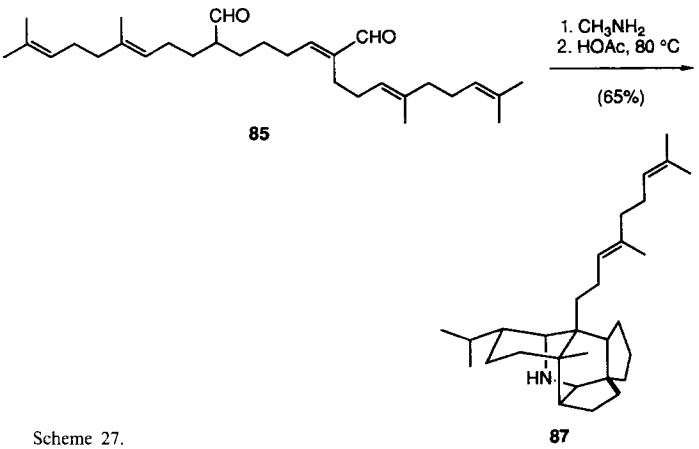

Scheme 27.

10. Epilogue and Editorial

If progress in important fields such as medicine, biochemistry, and materials science is to continue, it is essential that we be able to synthesize literally any structure that the imagination can conceive. The goal of research in organic synthesis is to reach a level of sophistication where this ability can be taken for granted. Yet, there is abroad an insidious notion that organic chemists have already become so adept at synthesis that further academic exercises such as that described here are no longer necessary, that there is no longer any need for research in multistep synthesis. I believe that, in part, this difficulty stems from a confusion of the adjectives effective ("adequate to accomplish a purpose" [45]) and efficient ("performing or functioning in the best possible and least wasteful manner" [45]). In fact, although chemists *have* over the last half-century become rather adept at constructing small amounts of very complicated molecules, we generally cannot prepare most desired organic compounds in an efficient, practical, and truly cost-effective manner. We *can* synthesize almost any given molecule and demonstrate that we have done it. However, this is due more to the development of high-powered separation and analytical tools (HPLC, capillary GC, TLC, FT-NMR spectroscopy) than to some discontinuous change in our ability to solve synthesis problems. That is, because we can carry out separations and establish structure with minute amounts of material, it is possible to do synthesis on very small scale. Thus, we can carry out multistep synthesis in a much shorter period of time than was possible ten or twenty years ago, since more time can be devoted to the development of new chemistry and less to the time-consuming "bringing up of material". This maturity should be considered a normal step in the development of a productive science, not a sign that all of the problems have been solved and that the field no longer merits investigation. Problems of synthesis still abound, as is known by anyone who practices the art. Our textbooks are

filled with hundreds of synthetic methods, all of which have limitations that will never be discovered unless the methods are tested in the challenging arena of the synthesis of multifunctional compounds. Although our approaches to problems have matured, we need even more mature strategies of synthesis. There is no reason that organic chemists should not be able to surpass nature's virtuosity in the synthesis of complex organic structures. In fact, we are still very far from this goal in most cases.

The cascade of reactions depicted in Scheme 27 represents a significant advance in our ability to orchestrate molecular reorganization. In this magnificent process an acyclic dialdehyde is transformed by ordinary commodity chemicals into a pentacyclic product by the formation of four carbon–carbon bonds, two carbon–nitrogen bonds, and one carbon–hydrogen bond. Furthermore, the process occurs with very high stereoselectivity and in excellent yield. However, it should not be misunderstood that even this highly efficient synthesis is perfect, because compromises have still been made. For example, the synthesis outlined in Scheme 25 still required the use of a protecting group (the dimethyl acetal) and involved the use of ester functions as surrogates for aldehyde groups. The inability to deal more directly with these issues demonstrates that there are still frailties in the science of synthesis, infirmities that will, no doubt, one day be cured through further research in multistep synthesis.

I am indebted to the talented and enthusiastic group of coworkers who performed the difficult experiments upon which this review article is based. The original methyl homodaphniphyllate synthesis was carried out by graduate student Mark Sanner and postdoctoral associates Sander Mills and Steven Davidsen. The tetracyclization reaction was discovered and perfected by graduate student Roger Ruggeri, who also applied it to the total synthesis of daphnilactone A and methyl homodaphniphyllate. Graduate student Marvin Hansen applied the Ruggeri cyclization to the synthesis of methyl homosecodaphniphyllate. The felicitous discovery of the methylamine cyclization was made by graduate student John Kath, who has also completed a total synthesis of the C_{30} alkaloid, (−)-codaphniphylline. The pentacyclization process and synthesis of protodaphniphylline were accomplished by postdoctoral associate Serge Piettre, who also carried out important mechanistic experiments that are described in detail in ref. [1c]. *The marvelous transformation of dihydrosqualene dialdehyde* ***85*** *into dihydroprotodaphniphylline was carried out by postdoctoral associate John Ragan. Not discussed here for lack of space are total syntheses of the C_{30} alkaloid (−)-secodaphniphylline (**11**, ref.* [1d]*) and (±)-bukittinggine (7, ref.* [1e]*), which were carried out by postdoctoral colleague Jeff Stafford. Also not covered here is unpublished research by graduate student Daisy Joe, who has explored the alternative mode of fragmention suggested in Scheme 17 and uncovered some fascinating rearrangements of the secodaphnane skeleton. I am also pleased to acknowledge the financial support of the National Science Foundation for a research grant.*

Received: August 30, 1991 [A 860 IE]
German version: *Angew. Chem.* **1992**, *104*, 675.

[1] a) C. H. Heathcock, S. K. Davidsen, S. Mills, M. A. Sanner, *J. Org. Chem.* **1992**, *57*, 2531; b) C. H. Heathcock, M. M. Hansen, R. B. Ruggeri, J. C. Kath, *ibid.* **1992**, *57*, 2544; c) C. H. Heathcock, S. Piettre, R. B. Ruggeri, J. A. Ragan, J. C. Kath, *ibid.* **1992**, *57*, 2554; d) C.H. Heathcock, J. A. Stafford, *ibid.* **1992**, *57*, 2566; e) C. H. Heathcock, J. A. Stafford, D. N. Clark, *ibid.* **1992**, *57*, 2575; f) C. H. Heathcock, R. B. Ruggeri, K. F. McClure, *ibid.* **1992**, *57*, 2585.

[2] S. Yagi, *Kyoto Igaku Zasshi* **1909**, *6*, 208.

[3] a) N. Sakabe, Y. Hirata, *Tetrahedron Lett.* **1966**, 965; b) H. Irikawa, N. Sakabe, S. Yamamura, Y. Hirata, *Tetrahedron* **1968**, *24*, 5691.

[4] N. Sakurai, N. Sakabe, Y. Hirata, *Tetrahedron Lett.* **1966**, 6309.

[5] Among the many other complex natural products whose structures were elucidated by Professor Hirata and his co-workers include the following: a) aplysin: S. Yamamura, Y. Hirata, *Tetrahedron* **1963**, *19*, 1485; b) tetrodotoxin: T. Goto, Y. Kishi, S. Takahashi, Y. Hirata, *ibid.* **1965**, *21*, 2059; c) dihydroteleocidin B: H. Harada, Y. Sakabe, Y. Hirata, Y. Tomiie, I. Nitta, *Bul. Chem. Soc. Jpn.* **1966**, *39*, 1773; d) K. Yamada, S. Takada, S. Nakamura, Y. Hirata, *Tetrahedron* **1968**, *24*, 199, 1255; e) palytoxin: D. Uemura, K. Ueda, Y. Hirata, H. Naoki, H. Iwashita, *Tetrahedron Lett.* **1982**, *22*, 2781; f) halichondrins: D. Uemura, K. Takahashi, T. Yamamoto, C. Katayama, J. Tanaka, Y. Okumura, Y. Hirata, *J. Am. Chem. Soc.* **1985**, *107*, 4796; Y. Hirata, D. Uemura, *Pure Appl. Chem.* **1986**, *58*, 701.

[6] a) T. Nakano, Y. Saeki, C. S. Gibbons, J. Trotter, *Chem. Commun.* **1968**, 600; b) C. S. Gibbons, J. Trotter, *J. Chem. Soc. B* **1969**, 840.

[7] T. Nakano, B. Nilsson, *Tetrahedron Lett.* **1969**, 2883.

[8] a) K. Sasaki, Y. Hirata, *J. Chem. Soc. B* **1971**, 1565; b) M. Toda, Y. Hirata, S. Yamamura, *Tetrahedron* **1972**, *28*, 1477.

[9] K. Sasaki, Y. Hirata, *J. Chem. Soc. Perkin Trans. 2* **1972**, 1411; *Tetrahedron Lett.* **1972**, 1275.

[10] K. Sasaki, Y. Hirata, *Tetrahedron Lett.* **1972**, 1891.

[11] S. Yamamura, K. Sasaki, M. Toda, Y. Hirata, *Tetrahedron Lett.* **1974**, 2023.

[12] D. Arbain, L. T. Byrne, J. R. Cannon, V. A. Patrick, A. H. White, *Aust. J. Chem.* **1990**, *43*, 185.

[13] Of course, alkaloid **10** actually has more than two stereocenters, but stereoisomerism is not possible at several of them for geometric reasons. For example, inversion of configuration at either of the carbons joined by the bold bond in Scheme 2 would lead to diastereomers far too strained for existence. Thus, for practical reasons, the relative configurations of these bridgehead atoms are interdependent.

[14] M. Toda, Y. Hirata, S. Yamamura, *Tetrahedron* **1972**, *28*, 1477.

[15] E. J. Corey, M. Ohno, P. A. Vatakencherry, R. B. Mitra, *J. Am. Chem. Soc.* **1961**, *83*, 1251; *ibid.* **1964**, *86*, 478.

[16] E. J. Corey, W. J. Howe, H. W. Orf, D. A. Pensak, G. Petersson, *J. Am. Chem. Soc.* **1975**, *97*, 6116; see also E. J. Corey, *Angew. Chem.* **1991**, *103*, 469; *Angew. Chem. Int. Ed. Engl.* **1991**, *30*, 455.

[17] A. Lapworth, *Mem. Proc. Manchester Lit. Philos. Soc.* **1920**, *64*, (3), 1; see also R. Robinson, *J. Chem. Soc.* **1947**, 989 and M. D. Salzman, *Chem. Brit.* **1986**, 543.

[18] D. A. Evans, G. C. Andrews, *Accounts Chem. Res.* **1974**, *7*, 147.

[19] For recent discussions of the Lapworth and Evans formalisms, see: a) J. Klein, *Tetrahedron* 1988, *44*, 503; b) Y. Cohen, J. Klein, M. Rabinowitz, *J. Am. Chem. Soc.* **1988**, *110*, 4734; c) F. Serratosa, *Organic Chemistry in Action: The Design of Organic Synthesis*, Elsevier, Amsterdam, **1990**.

[20] D. Seebach, *Angew. Chem.* **1979**, *91*, 259; *Angew. Chem. Int. Ed. Engl.* **1979**, *18*, 239.

[21] In the American southwest, where I was born and raised, this principle was recognized long ago in the folk saying that "it is always easier to ride a horse in the direction he wants to go."

[22] a) R. P. Linstead, E. M. Meade, *J. Chem. Soc.* **1934**, 935; b) A. Kötz, *Liebigs Ann. Chem.* **1933**, *55*, 1168.

[23] A. M. Islam, R. A. Raphael, *J. Chem. Soc.* **1955**, 3151.

[24] E. Wenkert, R. V. Stevens, K. G. Dave, *J. Am. Chem. Soc.* **1968**, *90*, 6177.

[25] C. H. Heathcock, E. F. Kleinman, E. S. Binkley, *J. Am. Chem. Soc.* **1982**, *104*, 1054.

[26] a) S.-O. Lawesson, R. Shabana, S. Scheibye, K. Clausen, S. O. Olesen, *Nouv. J. Chem.* **1980**, *4*, 47. b) S.-O. Lawesson, I. Thompson, K. Clausen, S. Scheibye, *Organic Syntheses Collective Volume 7*, Wiley, New York **1990**, p. 372.

[27] This reaction and related Michael additions of the corresponding oxolactam launched a productive investigation of the stereochemistry of the Michael addition of preformed lithium enolates: a) C. H. Heathcock, M. A. Henderson, D. A. Oare, M. A. Saner, *J. Org. Chem.* **1985**, *50*, 3019; **1990**, *55*, 132; b) C. H. Heathcock, D. A. Oare, *ibid.* **1985**, *50*, 3022; *ibid.* **1990**, *55*, 157; d) D. A. Oare, C. H. Heathcock, *Tetrahedron Lett.* **1986**, *27*, 6169; e) D. A. Oare, C. H. Heathcock, *Top. Stereochem.* and **1989**, *19*, 227.

[28] R. E. Ireland, G. Pfister, *Tetrahedron Lett.* **1969**, 2145.

[29] The traditional nomenclature that has been used by the Nagoya group has been employed in this review and other publications from Berkeley. The reader will note however, that the use of the prefix "seco" in the name of alkaloid **11** is not fully consistent with the structure of the material, which has the same number of rings and skeletal bonds as daphniphylline. Equally mysterious is the origin of "homo" in the common names of **5** and **10**. The Chemical Abstracts Service uses the name daphnane for the C_{22} skeleton of homodaphniphyllic acid and 1,12-secodaphnane for the C_{22} skeleton corresponding to the unknown, but hypothetical biosynthetic link with the structure **E**. In the Chemical Abstracts nomenclature system, the C_{22} skeleton corresponding to methyl homosecodaphniphyllate is 12,16-cyclo-1,12-secodaphnane.

[30] Corey defines a "transform" as the "reverse of a synthetic reaction" and a "retron" of a given transform as "the enabling structural unit for that transform." For example, the basic retron of a Diels–Alder transform is a six-membered ring with one double bond: E. J. Corey, X.-M. Cheng, *The Logic of Chemical Synthesis*, Wiley, New York, **1989**, p. 6. See also E. J. Corey, *Angew. Chem.* **1991**, *103*, 469; *Angew. Chem. Int. Ed. Engl.* **1991**, *30*, 455.
[31] J. P. McCormick, D. C. Barton, *J. Org. Chem.* **1980**, *45*, 2566.
[32] D. Swern, A. J. Mancusco, *Synthesis* **1981**, 165.
[33] Intramolecular hydride shifts of this type are precedented: T. Cohen, A. Onopchenko, *J. Org. Chem.* **1983**, *48*, 4531.
[34] C. Djerassi, R. R. Engle, A. Bowers, *J. Org. Chem.* **1956**, *21*, 1547.
[35] We thank Professor S. Yamamura (Keio University) for providing us with the comparison sample.
[36] a) A. Eschenmoser, A. Frey, *Helv. Chim. Acta* **1952**, *35*, 1660; b) C. A. Grob, W. Baumann, *ibid.* **1955**, *38*, 594; c) C. A. Grob, *Experientia* **1957**, *13*, 126; d) C. A. Grob, F. Ostermayer, *Helv. Chim. Acta* **1962**, *45*, 1119; e) A. Eschenmoser, D. Felix, G. Ohloff, *ibid.* **1967**, *50*, 708, 2108; f) C. A. Grob, P. W. Schiess, *Angew. Chem.* **1967**, *79*, 1; *Angew. Chem. Int. Ed. Engl.* **1967**, *6*, 1; g) C. A. Grob, H.R. Kiefer, H. J. Lutz, H. J. Wilkens, *Helv. Chim. Acta* **1967**, *50*, 416; h) C. A. Grob, *Angew. Chem.* **1969**, *81*, 543; *Angew. Chem. Int. Ed. Engl.* **1969**, *8*, 535.
[37] N. Isenberg, I. Barkocy, S. R. Parker, *Angew. Chem.* **1963**, *75*, 1205; *Angew. Chem. Int. Ed. Engl.* **1964**, *3*, 63.
[38] R. T. Arnold, S.T. Kulenovic, *Synth. Commun.* **1977**, *7*, 223.
[39] Terpenoids have been described in which two methyl groups are in the aldehyde oxidation state. Petrodial is one example: S. Isoe, Y. Ge, K. Yamamoto, S. Katsumura, *Tetrahedron Lett.* **1988**, *29*, 4591.
[40] Pyridoxamine is a well-known nitrogen donor in alkaloid biosynthesis: a) D. R. Dalton, *The Alkaloids, A Biogenetic Approach*, Dekker, New York, **1976**; b) M. Akhtar, V. C. Emery, J. A. Robinson in *The Chemistry of Enzyme Action* (Ed.: M. I. Page), Elsevier, Amsterdam, **1984**, p. 303.
[41] S. K. Malhotra, D. F. Moakley, F. Johnson, *J. Am. Chem. Soc.* **1967**, *89*, 2794.
[42] S.L. Schreiber, H. V. Meyers, K.B. Wiberg, *J. Am. Chem. Soc.* **1986**, *108*, 8274.
[43] S. Piettre, C. H. Heathcock, *Science (Washington, D. C.)* **1990**, *248*, 1532.
[44] a) E. Vedejs, M. J. Arnost, J. P. Hagen, *J. Org. Chem.* **1979**, *44*, 3234; b) J. S. Petersen, S. Töteberg-Kaulen, H. Rapoport, *ibid.* **1984**, *49*, 2948; c) M. E. Kuehne, J. C. Bohnert, *ibid.* **1981**, *46*, 3443.
[45] *The Random House Dictionary of the English Language*, Random House, New York, **1979**.

ANGEWANDTE CHEMIE
A Journal of the Gesellschaft Deutscher Chemiker

Reviews planned or recently published

The Enchanting Alkaloids of Yuzuriha
C.H. Heathcock

Transition Structures of Hydrocarbon Pericyclic Reactions
K.N. Houk, Y. Li, J. D. Evanseck

Natural Products as Probes of Cellular Function
S.L. Schreiber, M.K. Rosen

Synthetic Approaches towards Molecular and Polymeric Carbon
F. Diederich, Y. Rubin

Cubanes: Starting Materials for the 1990s and the New Century
P.E. Eaton

Optically Anomalous Crystals
B. Kahr, J.M. McBride

Chemistry and Biology of the Enediyne Anticancer Antibiotics
K.C. Nicolaou, W.M. Dai

Scanning Tunnel Microscopy and Atomic Force Microscopy in Organic Chemistry
J. Frommer

Synchotron X-Ray and Neutron Diffraction Studies in Solid-State Chemistry
A.K. Cheetham, A.P. Wilkinson

What subscribers and authors have to say about Angewandte Chemie:

Jean-Marie Lehn, Université Louis Pasteur, Strasbourg:

"I consider Angewandte Chemie as one of the top not only chemical but scientific journals... It presents the highly effective combination of well chosen, exciting and thorough review articles, reflecting timely topics that cover a very broad range in science, with short but informative communications reporting specific advances of particular interest for chemistry. It is also carefully produced and nicely presented, which adds to the reading pleasure."

VCH

Special Rate for ACS members: US$ 165.00
US$ 190.00 (air mail)*

To subscribe please call 1-800-422-8824

Annual subscription rate 1992 for institutions: US$ 581.00 (air mail)*

Transition Structures of Hydrocarbon Pericyclic Reactions

By Kendall N. Houk,* Yi Li, and Jeffrey D. Evanseck

Twenty-five years after the discovery of a vast class of organic reactions named "pericyclic reactions" by Woodward and Hoffmann, ab initio quantum mechanics provides a detailed analysis of the geometries, energies, and electronic characteristics of the transition structures of these reactions. Common features are found in all these reactions, and generalizations permit prediction of other transition-structure geometries and energies. At the same time, great diversity is observed—from strongly bonded, rigid, closed-shell entities to weakly interacting, flexible diradical structures.

1. Introduction

1.1. Pericyclic Reactions—Definitions, Examples, and Remaining Questions

In 1965 a series of communications that shook the chemical world appeared.[1] The discoveries reported by R. B. Woodward and Roald Hoffmann culminated in their review, "The Conservation of Orbital Symmetry" which was published in this journal four years later.[2] This work captured the imaginations of chemists by revealing simple theoretical principles that profoundly influence chemical reactions. Since then the properties of molecular orbitals and their interactions have been widely used to predict stereochemistries and mechanisms of organic reactions.

Pericyclic reactions were defined by Woodward and Hoffmann as "reactions in which all first-order changes in bonding relationships take place in concert on a closed curve".[2] An enormous amount has been learned about pericyclic reactions in the last few decades, but there remains intriguing mystery and stimulating controversy about the transition structures of these processes. In this article, we summarize research that defines the nature of pericyclic transition structures as obtained from ab initio quantum mechanical calculations.

Some typical thermally allowed pericyclic reactions and both Woodward–Hoffmann and common names are shown in Figure 1. These reactions all involve six-electron bonding changes. On the right side, rough representations of transition structures for the concerted reactions are sketched. Since this first systematic definition of pericyclic reactions, there has been considerable interest in the nature of the transition structures of such reactions and the theoretical underpinnings of the Woodward–Hoffmann rules.[3] The Woodward–Hoffmann treatment showed that "thermally allowed" reactions could occur by concerted mechanisms, because strong bonding could be maintained throughout the reaction. Other theoretical treatments of these reactions have assumed aromatic transition states,[4] but occasionally very unsymmetrical ("highly asynchronous") transition structures have been advocated.[5]

Pericyclic reactions are widely applicable in synthesis.[6] A few examples are shown in Figure 2. Several masterpieces in synthesis by Woodward, such as that of the steroid hormone,

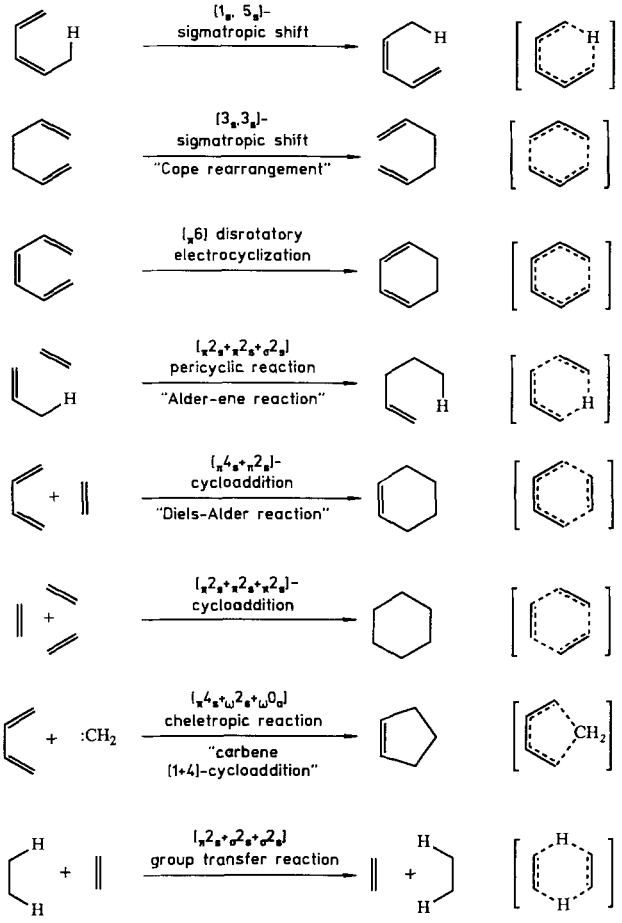

Fig. 1. Examples of common types of pericyclic reactions involving six electrons.

cortisone (Fig. 2a), were based upon the Diels–Alder reaction.[7a] Ireland's group's lasalocid A synthesis (Fig. 2b) used a [3,3] sigmatropic shift, the Ireland version of the Claisen rearrangement,[7b] while electrocyclic openings of benzocyclobutenes and electrocyclization of a hexatriene (Fig. 2c) were important steps in syntheses of xylopinine by Kametani et al.[7c]

There are also pericyclic reactions involved in important biological processes. Ergosterol undergoes a series of photochemical and thermal pericyclic reactions to form Vitamin D_2 (Fig. 3a).[8] The chorismate → prephenate rearrangement, which occurs in the biosynthesis of aromatic amino acids in plants, is a Claisen rearrangement catalyzed (perhaps by altering the mechanism) by the enzyme, choris-

[*] Prof. Dr. K. N. Houk, Dr. Y. Li, Dr. J. D. Evanseck
Department of Chemistry and Biochemistry
University of California, Los Angeles
Los Angeles, CA 90024-1569 (USA)

mate mutase (Fig. 3b).[9] The electrocyclic formation of a biradical that reacts with DNA is the origin of activity of the esperamicin and calicheamicin series of antibiotics (Fig. 3c).[10] This biradical mechanism has prompted wide interest in these types of reactions and in the use of thermal rearrangements to generate reactive intermediates for biological action.[11]

The mechanisms of pericyclic reactions have attracted great interest and have frequently generated heated controversy. Thermally allowed pericyclic reactions may also follow stepwise mechanisms with biradical intermediates, rather than concerted mechanisms. Diels–Alder and other cycloadditions, as well as sigmatropic shifts involving two π systems are the pericyclic reactions most often claimed to occur with the intermediacy of biradicals. The first two reactions in Figure 4 involve the addition of one π system to another, and relatively stable biradicals can be written for potential intermediates in such processes. Also shown are the measured activation enthalpies along with the best available estimates of energies to form biradical intermediates. The difference between these energies has been called the "energy of concert" by Doering et al.[12] Diels–Alder and other cycloadditions have small to moderate energies of concert, while reactions such as sigmatropic hydrogen shifts and electrocyclizations usually have large energies of concert. The concerted mechanism through an aromatic transition state is the norm for thermally allowed reactions, although substituents may induce alterations of transition structures and even of reaction mechanisms.

Only calculations can provide information about the geometrical arrangement of constituent atoms for short-lived species like transition structures.[13] It has recently become possible to calculate the details of transition-state geometries and energetics rather than rely upon the approximate descriptions inferred from experimental data. In this article we describe how transition-structure calculations are performed, what type of information can be obtained, and how reliable these data are, depending upon the computational level. We provide a detailed picture of the shapes and bonding present in transition structures of pericyclic reactions. Our major emphasis is on the reactions of the simplest hydrocarbons, but data on substituted cases are also provided for several reactions to show how the energies and geometries are changed by substituents.

We try to give more quantitative meaning to concepts such as "early" and "late" transition states, "synchronicity", and

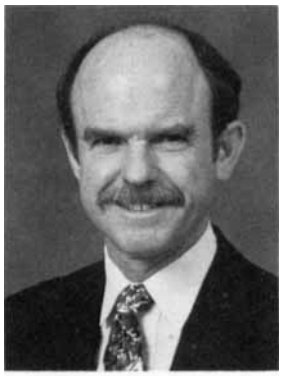

K. N. Houk is Professor and Chairman of the Department of Chemistry and Biochemistry at the University of California, Los Angeles (UCLA). He was born in Nashville, Tennessee, in 1943, and grew up in Bozeman, Montana, and Chicago. He studied at Harvard University, where he received the Ph.D. with Professor R. B. Woodward in 1968. He then joined the faculty of Louisiana State University, moved to the University of Pittsburgh in 1980, and to UCLA in 1986. He was a 1981 recipient of the Alexander von Humboldt Foundation Senior U.S. Scientist Award and had the opportunity to be a guest professor at Erlangen, Cologne, Darmstadt, and Munich. He is the recipient of the Arthur C. Cope Scholar Award of the American Chemical Society (1989) and the James Flack Norris Award in Physical Organic Chemistry (1991). He was Director of the National Science Foundation Chemistry Division from 1988–1990.

Yi Li is a Research Associate at UCLA. He was an undergraduate at Wuhan University, China, attended the University of Pittsburgh under the Chemistry Graduate Program organized by William von Eggers Doering, and received his Ph.D. in 1988 at UCLA with K. N. Houk.

Jeffrey D. Evanseck was born in 1961 and began studies at Purdue University (1980) with William L. Jorgensen. He received his doctorate under K. N. Houk at the University of California, Los Angeles, in 1990 on the theoretical studies of reactive intermediates. He is presently a postdoctoral fellow with Martin Karplus at Harvard University applying theoretical methods to understand enzymatic catalysis.

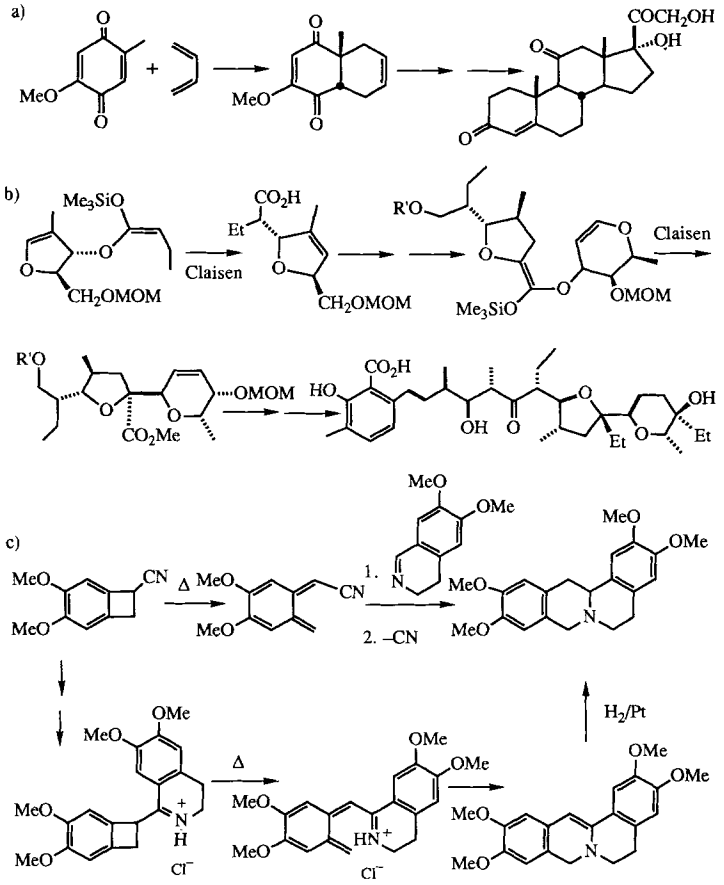

Fig. 2. Examples of natural product syntheses using pericyclic reactions. a) Cortisone [7a]. b) Lasalocid A [7b]; MOM = methoxymethyl, R' = benzyl. c) Xylopinine [7c].

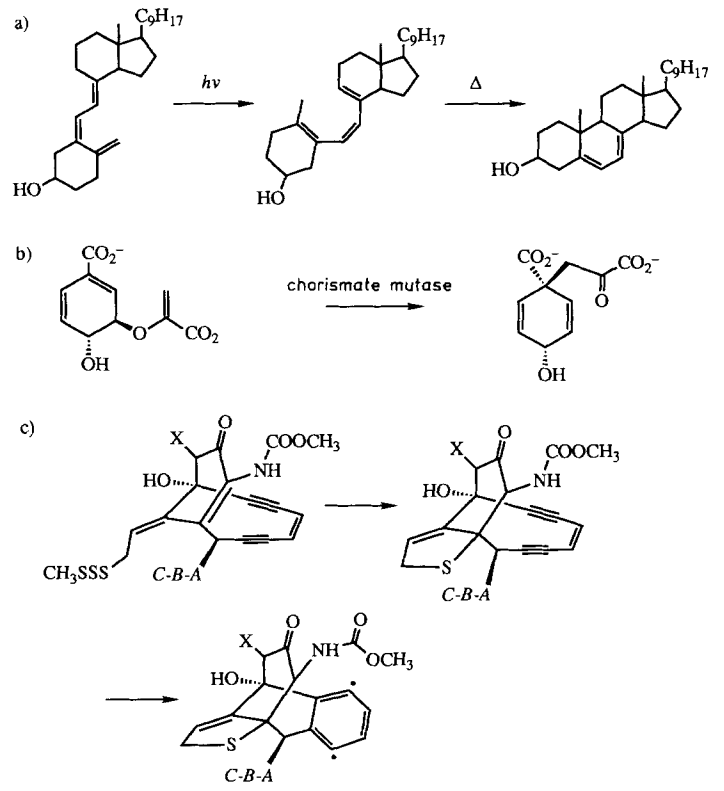

Fig. 3. Examples of pericyclic reactions found in biological processes. a) Precalciferol → vitamin D_2; b) chorismate → prephenate; c) formation of reactive diradicals from esperamicin/calicheamicin, *C-B-A* = sugar residue.

"aromatic transition states". Our goal is to paint memorable semiquantifiable images of transition structures and to develop generalizations for quantitative predictions about geometries, energies, and other properties of transition structures for pericyclic reactions.

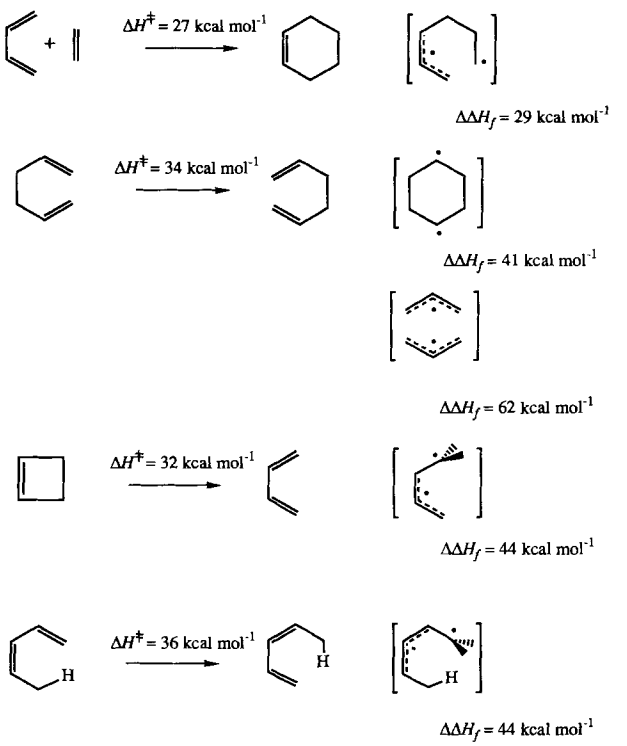

Fig. 4. Experimental activation energies $\Delta H^{\ddagger}$ compared to estimated energies of biradical intermediates $\Delta\Delta H_f$, relative to the reactants, of some pericyclic reactions.

1.2. Transition Structures and Transition States

A "transition structure" corresponds to a saddle point which separates two energy minima on a theoretical potential energy surface.[14–16] It is closely related, but not identical, to a "transition state", which is the quasi-thermodynamic state defined in Eyring's transition state theory.[17] A transition state is situated at a free energy maximum along the reaction path that connects two energy minima. The free energy, ΔG, differs from the enthalpy, ΔH, by $-T\Delta S$. ΔH is equal to the difference of potential energy E, plus RT, zero-point energy, and the thermal corrections (see Fig. 5a and Section 1.5).

In transition-state theory, the rate of an elementary reaction is determined by the difference between the free energies of the transition state and the reactants, as well as the rate of passage through the region of the transition state.[17, 18] When a reaction has a relatively large barrier and a slowly varying entropy in the region of the potential energy maximum, the transition state corresponds closely to the potential energy maximum of the reaction (Fig. 5b). The transition-state geometry will then be essentially the same as the transition-structure geometry. When the reaction has a low barrier or a rapidly varying entropy in the region of the potential energy maximum, the transition state may be at a

geometry quite different from that of the calculated transition structure (Fig. 5c).

Quantum mechanical calculations incorporating the Born–Oppenheimer approximation can be used to determine the potential energies of molecules with any arrangement of the nuclei. When a large number of these calculations are performed, a potential energy hypersurface for a vibrationless system is obtained. The regions of greatest interest on this multidimensional surface are those corresponding to stationary points. A stationary point has all zero first derivatives of the energy with respect to the 3N − 6 independent spatial degrees of freedom. Energy minima are those stationary points at which all force constants (second derivatives of the energy with respect to the 3N − 6 coordinates of the atoms) are positive. The saddle points for transition structures have one, and only one, negative second derivative; the remaining 3N − 7 second derivatives are positive. The negative second derivative corresponds to a force constant for the motion along the reaction coordinate. This is also referred to as an "imaginary vibrational frequency", since the vibrational frequency is proportional to the square root of the force constant.[16]

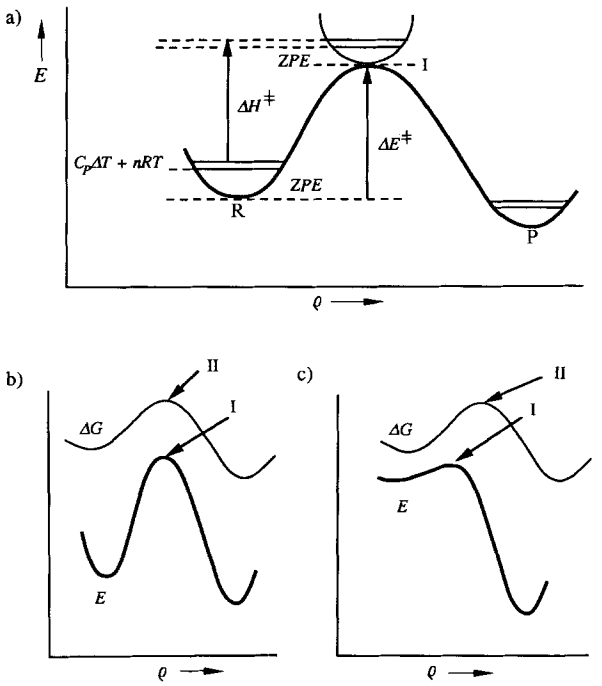

Fig. 5. a) Relationship of ΔH and E along a reaction path ρ. ZPE = zero-point energy, R = reactants, P = products, I = transition structure. The transition structure (I) and transition state (II) coincide in b), but not in (c).

1.3. The Location of Transition Structures with Ab Initio Techniques

It is possible to find both minima and saddle points efficiently, because modern programs such as GAUSSIAN 90 and GAMESS calculate analytically the first and second derivatives of the energy with respect to all geometrical variables.[19, 20] In practice, some explorations of the potential energy surface in the regions of the stationary points are required, and then various programmed procedures can be used to find a point which has all first derivatives as close as desired to zero. In general, it is more difficult to locate transition structures than it is to locate energy minima.[21] In some cases, symmetry restrictions are used to facilitate location of a transition structure, in which case vibrational frequencies are calculated for all 3N − 6 degrees of freedom to verify that the stationary point represent a transition structure. While it is possible to verify that an energy minimum has been found, no procedure exists to ensure that it is the global minimum. Similarly, the authenticity of a transition structure can be proven by a frequency calculation, but only a complete search of the potential energy surface can prove this to be the lowest energy transition structure. In the absence of such complete searches, we generally rely upon limited searches of the potential surface guided by our chemical intuition.

1.4. Ab Initio Computational Methods and Theoretical Levels

Most of the calculations from our group described here use ab initio molecular orbital calculations[16] and the programs developed by Pople and his group over the last two decades.[19] Ab initio calculations are quantum mechanical calculations in which the Schrödinger equation is approximated by using the Hartree–Fock (HF) equations[22] without introduction of arbitrary parameters. The molecular orbitals of a molecule are formed from a linear combination of one-electron functions that describe the atomic orbitals of each atom. This set of functions is the basis set. "Small" basis sets restrict the mathematical description of the atomic orbitals, while "large" basis sets provide a more flexible description, which is also more costly to use in computations. The Hartree–Fock limit, the best approximation that can be achieved with the HF equations, can be approached with the use of large basis sets. We have used the basis sets developed by Pople and co-workers, ranging from the "minimal" STO-3G basis set to the rather large 6-311G** basis set. These are implemented in the GAUSSIAN 82–90 programs[19] and have been described in detail by Hehre et al.[16]

In the HF description of molecules, electron–electron repulsion is calculated as the repulsion between a single electron and the average distribution of all the other electrons obtained iteratively starting form an approximated electron distribution (the *self-consistent field* method, SCF). Such calculations are in error because they neglect the instantaneous correlation of electron motion which reduces the electron repulsion. One of the less expensive methods for estimating the effect of electron correlation is the many-body perturbation expansion method of Møller and Plesset.[23] The perturbation series terminated at n'th order is termed MPn theory. Configuration interaction is another method for calculating "dynamical correlation energy", in which alternative distributions of electrons over the MO's (configurations) are mixed with the lowest energy configuration to form a better wave function.

Multiconfiguration self-consistent field (MCSCF) calculations are used for systems that are poorly represented by a

single configuration of occupied orbitals.[24] Such methods correct for "nondynamical correlation energy". One of the common MCSCF methods is the complete active space (CASSCF) method which mixes together all configurations involving the "active" orbitals. These are defined as those orbitals which undergo significant bonding changes during the reaction.[25a] For example, in a breaking σ bond, there are two electrons in two orbitals, the σ and σ^* orbitals, which constitute the "active space". Pulay et al. described a computational method to choose the active space.[25b] The MCSCF calculations described in this review were performed with GAMESS, a general purpose quantum chemistry program by Dupuis et al.[20]

The choice of a theoretical method is dependent upon the accuracy demanded, the nature of problem to be solved, and the size of molecule. For the calculations of geometries of stable molecules, correlation energy is generally of little consequence. As we shall show, the same is also true for many types of concerted pericyclic transition structures, even though distorted bond lengths and angles are involved, which might be expected to cause the development of biradical character in the wave function. On the other hand, nondynamical correlation does have a dramatic effect upon the geometries of transition structures of forbidden reactions. Correlation energy corrections are always required for the calculation of reasonable activation energies, since correlation energy is larger for transition structures than it is for stable molecules.

1.5. Quantities Obtained from Calculations

The stationary points obtained by the procedures described in the previous section are located on the potential energy surface for vibrationless systems, as shown in Figure 5a. However, a real molecule has vibrational energy, even at 0 K, so that some corrections must be made in order to obtain energies that are directly comparable to experimental quantities. The largest of these is the zero-point energy $1/2\sum h\nu_i$, which is the vibrational energy that a molecule has even at 0 K. This is calculated from vibrational frequencies ν_i, which can be calculated routinely for optimized stationary points, at least in the harmonic approximation. At higher temperatures a molecule will have additional vibrational energy $C_P\Delta T$, which can also be calculated from vibrational frequencies. Addition of $P\Delta V (= \Delta nRT)$ to the internal energy gives the enthalpy of a molecule at a given temperature. Finally, the entropy of a molecule and a transition state at a given temperature can be calculated from the masses, moments of inertia, and vibrational frequencies.[26] Since moments of inertia and vibrational frequencies can be calculated, the former with great accuracy and the latter about 10% too large,[27] the enthalpies, entropies, and free energies of gas-phase stable molecules and transition states can be calculated readily. From the geometry of a transition structure and its vibrational force constants, kinetic isotope effects can be calculated by applying the equation of Bigeleisen and Goeppert-Mayer.[28] The results can then be compared with the experimentally observed values.[29] This method is one of the few means for studying the details of potential surfaces experimentally.[30]

Other properties of transition structures can be obtained from ab initio calculations as well. First of all, calculations provide geometrical details of the transition structure and its electronic structure. The geometry and electron distribution are of great importance for understanding the interactions of the transition structure with its environment, as in the case of reactions in solution or reactions that are catalyzed by enzymes or other catalysts. Calculations also reveal the shapes and energies of the frontier orbitals, which can be used qualitatively to assess the interactions of these orbitals with those of the substituents to predict substituent effects on rates. In addition, bond orders of various partial bonds in the transition structure can also be calculated by various methods,[31] or by Pauling's or other empirical bond length–bond order methods.[32] This type of analysis facilitates the understanding of the nature of partial bonds in the transition structures.[33] Finally, it is conceptually useful to distinguish between a thermodynamic contribution to an activation barrier and an intrinsic barrier. The contributions of intrinsic reaction barriers, defined according to Marcus theory for a reaction $A-B+C\rightarrow A+B-C$ as the mean of the barriers for the reactions $A-B+A\rightarrow A+B-A$ and $C-B+C\rightarrow C+B-C$,[34] can be evaluated systematically to understand the origin of substituent effects.[35]

2. Does Theory Give Reliable Chemical Information about Transition Structures and Energetics? Three Case Studies

There is no general method to determine experimental geometries of transition states.[13] Since exact calculations also are not possible for typical organic reactions, we can only perform calculations at increasingly higher levels of theory until there are no further significant changes in geometries or energies. In Sections 2.1–2.3 we demonstrate how different theoretical levels perform on predictions of geometries and energies for three types of pericyclic reactions. This establishes the validity of the results to be presented later in this paper.

2.1. The [1,5] Sigmatropic Hydrogen Shift in (*Z*)-1,3-Pentadiene

The transition structure corresponding to the $[1_s,5_s]$ hydrogen shift in (*Z*)-1,3-pentadiene is particularly easy to reproduce by a variety of calculations. This is because there are really no alternative mechanisms of similar energy: C–H dissociation followed by recombination would require at least 58 kcal mol^{-1}; a 90° rotation of one terminus, followed by hydrogen transfer would require about 44 kcal mol^{-1};[36] the experimental activation energy is only 36 kcal mol^{-1}.[37] With these additional considerations, the Woodward–Hoffmann rules provide a completely reliable guide to stereochemistries in concerted reactions that have no alternative reaction pathways (sigmatropic hydrogen shifts, electrocyclizations) and a somewhat less firm guide to mechanisms and stereochemistries in cycloadditions, cheletropic reactions, and non-hydrogen sigmatropic shifts, for which several mechanistic paths have rather similar energies.

Transition structures for the degenerate [1,5] hydrogen shift in 1,3-pentadiene calculated at various ab initio levels[38,39] and with several methods of Dewar et al.[40] are shown in Figure 6.[41] At the pictorial level, the geometries

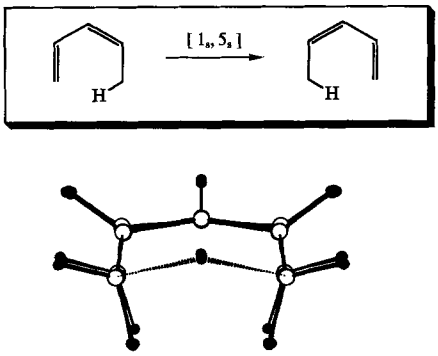

Fig. 6. Superimposed transition structures of the [1,5] sigmatropic hydrogen shift in pentadiene obtained with AM-1, STO-3G, 3-21G, 6-31G, 6-31G*, 6-31G**, MP2/3-21G, and MP2/6-31G* methods.

obtained from all of these calculations are the same! However, on a detailed level, the STO-3G minimal basis set gives results which are quite different from those obtained with better basis sets. The RHF/3-21G geometry is close to that obtained with the 6-31G** basis. The main difference between the RHF and MP2 optimized structures is elongation of bond lengths, but even this is generally limited to only a few hundredths of an Ångstrøm. The MP2 structures are more sensitive to the size of the basis set than the RHF structures. Even so, the overall result is that angles differ by only a few degrees and bond lengths differ by 0.04 Å at most in the various types of calculations. The RHF/3-21G structure is remarkably close to that obtained at the MP2/6-31G* level. For such hydrocarbon reactions with no comparable mechanistic alternatives, the 3-21G transition-structure geometries give bond lengths within several hundredths of an Ångstrøm of the MP2/6-31G* values.[39]

Although the transition structure can be obtained readily, and a reasonable activation energy can be obtained with some additional computational effort (see Section 2.4), the isotope effect calculated for this process is too low, and a tunneling correction must be made to obtain a calculated value near the experimental value.[29c]

2.2. The Cyclobutene → Butadiene Electrocyclization

As shown in Figure 7, the transition-structure geometries for the cyclobutene ring opening are very similar regardless of the level of theory employed.[42-44] The largest deviation in the bond lengths is seen in the elongated cleaving C–C bond which differs by 0.14 Å in the various calculations. The two-configuration (TCSCF) geometry is "latest" (most bond breaking) at 2.238 Å, while the RHF/STO-3G geometry is "earliest" at 2.102 Å. The RHF/3-21G geometries are similar to the MP2/6-31G* optimized geometry. The MP2/3-21G geometry deviates most from the MP2/6-31G* geometry; good MP2 calculations require a reasonably large basis set. In all calculations, the nonplanarity of the carbon skeleton is pronounced, and the C=C–C=C torsional angle ranges from 12° to 16°.

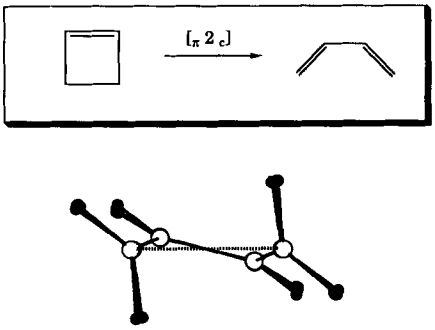

Fig. 7. Superimposed transition structures the electrocyclic ring opening of cyclobutene obtained with AM-1, STO-3G, 3-21G, 4-31G, 6-31G, 6-31G*, 6-31G**, MP2/3-21G, and MP2/6-31G* methods.

The geometries of ground state molecules calculated at either RHF/3-21G or the correlated MP2/6-31G* levels are in excellent agreement with the experimental geometries. For example, the experimental and MP2/6-31G* (value in parentheses) C–C bond lengths of cyclobutene are: C1–C2 1.342 Å (1.345 Å), C2–C3 1.517 Å (1.512 Å), and C3–C4 1.566 Å (1.564 Å). The maximum deviation for cyclobutene is less than 0.005 Å for bond lengths and less than 1.5° for bond angles.

2.3. The Diels–Alder Cycloaddition Reaction

The Diels–Alder reaction between 1,3-butadiene and ethene is exothermic by 40 kcal mol^{-1} and has a reaction barrier of 27 kcal mol^{-1}.[45] There is a reasonable alternative to the concerted mechanism, since thermochemical estimates suggest that the activation barrier for a diradical intermediate is only a few kcal mol^{-1} higher than the experimental activation barrier.[12] Nevertheless, in spite of a long dispute over the reaction mechanism of the Diels–Alder reaction between 1,3-butadiene and ethene, the transition structures located at various levels of theory[46-49] for a concerted mechanism are remarkably similar. Figure 8 shows the geometries of these transition structures obtained by semi-

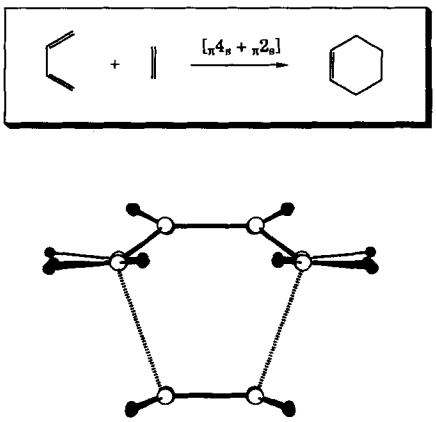

Fig. 8. Superimposed transition structures of the Diels–Alder reaction between butadiene and ethene obtained with AM-1, 3-21G, 6-31G*, MP2/6-31G*, MCSCF/3G, and MCSCF/4-31G methods.

empirical methods,[46] ab initio HF and MP2 calculations,[47,48] and MCSCF techniques.[49] The optimized bond lengths usually agree within a few hundredths of an Ångstrøm in these calculations. The bond lengths of the forming C–C bonds show the largest variation, ranging from 2.20 Å to 2.28 Å. Inclusion of electron correlation tends to lengthen the forming C–C bond. Dewar's early semiempirical methods predicted very asynchronous transition structures, but AM1 and PM3 both predict concerted transition structures similar to the ab initio predictions.[46a]

These three cases provide a sense of the expected accuracy of the calculated transition structures. For the RHF/3-21G or MP2/6-31G* geometries generally described here, the bond lengths are expected to vary at most by a few hundredths of an Ångstrøm from actual ones, while angles will vary by a few degrees at most. The RHF/3-21G geometries are quite good for hydrocarbon transition structures, but MP2/6-31G* optimizations are recommended. For molecules with heteroatoms, calculations with the 6-31G* basis set are necessary to achieve the reliability achieved by the 3-21G basis set for hydrocarbons. Once again, MP2/6-31G* is recommended when feasible. Pople et al. recently described an ab initio method to obtain geometries and bond dissociation energies within a few kcal mol^{-1} of experimental results for much more demanding cases than studied here.[50] This method requires MP2/6-31G* geometry optimizations; these calculations agree well with experimental values, and no significant improvement is achieved at higher levels. However, to obtain accurate energies, much higher levels of theory are required.

2.4. Calculations of Reaction Energetics

In order to compare the experimental activation energies to those calculated for vibrationless systems, the values for the vibrationless cases were calculated from the experimental activation energies by correcting for the thermal vibrational energies and zero-point energies, calculated at the RHF/3-21G level. The experimental activation energies are 36.1 ± 2.2 kcal mol^{-1} for the [1,5] hydrogen shift,[37] 32.9 ± 0.5 kcal mol^{-1} for the conrotatory electrocyclic ring opening of cyclobutene,[51] and 26.5 ± 2 kcal mol^{-1} for the Diels–Alder reaction between butadiene and ethene.[45] The corresponding calculated activation energies (vibrationless) are 39.7 kcal mol^{-1} for the [1,5] shift,[39a] 34.5 kcal mol^{-1} for the conrotatory electrocyclic ring opening of cyclobutene,[44] and 27 kcal mol^{-1} for the Diels–Alder reaction.[47a] The heat of reaction has been adjusted similarly from -11.4 kcal mol^{-1} to -10.9 kcal mol^{-1} for cyclobutene ring opening.[44] The heat of reaction for the Diels–Alder reaction between butadiene and ethene is -34 kcal mol^{-1} when zero-point energies are removed. Table 1 compares experimental and calculated activation energies and heats of reaction for each of these three cases discussed.

A systematic investigation of the effects of the basis set reveals that the minimal STO-3G basis performs exceptionally poorly, but the 3-21G results are in reasonable agreement with higher level RHF calculations. For the [1,5] hydrogen shift, the calculated $\Delta E^{\neq}$ with the 6-31G* basis set approaches the Hartree–Fock limit of 58–59 kcal mol^{-1}, which is about 20 kcal mol^{-1} above the experimental value. For the cyclobutene ring opening, the $\Delta E^{\neq}$ at the RHF level converges to about 46–47 kcal mol^{-1}, which is approximately 12 kcal mol^{-1} larger than the experimental value. The smaller error on correlation of the energies for cyclobutene ring opening is related to the fact that only four electrons are involved in bonding changes, rather than six electrons in the [1,5] hydrogen shift. For the Diels–Alder reaction, the calculated reaction barrier at the RHF level is about 20 kcal mol^{-1} higher than the experimental value. Here, six electrons are involved.

These "correlation energies of activation", that is, the gap between the Hartree–Fock and the experimental activation energies, are different for different reactions. Correlation energy increases as the size of the system—measured by the number of electrons—increases. The correlation energy of the transition structures increases, because partially formed and partially broken bonds have larger correlation errors than fully formed bonds. As demonstrated in the previous examples, the correlation energy is higher when six electrons are involved in bonding changes than when four electrons are involved. The "correlation energy of activation" is 3–4 kcal mol^{-1} per electron in the examples studied here. This quantity provides a rough estimate of activation energies when only RHF quantities are available. A substituent perturbs the energies of the reactants and transition structure, but does not alter the number of electrons involved in bonding processes. Consequently, relative activation energies for the parent and substituted analogs are often reasonable even without inclusion of correlation energy.

At the MP2 level, the calculated reaction barrier with the 6-31G* basis set is in good agreement with experimental

Table 1. Calculated reaction barriers and energies [kcal mol^{-1}] for the [1,5] hydrogen shift of (*Z*)-1,3-pentadiene (I), the electrocyclic ring opening of cyclobutene (II), and the Diels–Alder reaction of butadiene with ethene (III). The subscript rxn means reaction.

	I	II		III	
Computational level	$\Delta E^{\neq}$	$\Delta E^{\neq}$	ΔE_{rxn}	$\Delta E^{\neq}$	ΔE_{rxn}
RHF/STO-3G	64.3	79.7	−12.5	36.0	−104.7
RHF/3-21G	54.8	41.6	−18.0	35.9	−43.1
RHF/4-31G		41.9	−20.1	−42.6	−34.4
RHF/6-31G	56.5	41.9	−20.3		
RHF/6-31G*	58.7	46.9	−10.6	45.0	
RHF/6-31G*//3-21G	58.7	46.2	−13.5	45.1	
RHF/6-31G**	58.1	46.5	−18.4		
MP2/3-21G	39.3	32.7	−22.0		
MP2/6-31G*	36.5	36.8	−7.8	17.6	
MP2/6-31G*//RHF/3-21G	37.6	36.6	−8.1	17.0	
MP2/6-31G**//MP2/6-31G*	36.5	36.8			
MP3//MP2/6-31G*	44.7	40.2		26.9 [a]	
MP4(DQ)//MP2/6-31G*	46.3	40.5			
MP4(SDQ)//MP2/6-31G*	46.1	39.8		29.0 [a]	
MP4(SDTQ)//MP2/6-31G*	41.1	36.6		21.9 [a]	
MCSCF		39.4 [b]	−5.0 [b]	32.7 [c]	
MCSCF		35.8 [d]	−6.2 [d]	33.3 [e]	
MINDO/3-CI [f]		48.9	−1.1	28.2	
MNDO [f]		49.9	−2.0	45.4	−53.9
AM1 [f]		35.3	−15.9	23.8	−56.5
experimental $\Delta E^{\neq}$	38.8 ± 2.2	34.5 ± 0.5		25.1 ± 2	
Arrhenius E_a	36.1 ± 2.2	32.9 ± 0.5		26.5 ± 2	
experimental ΔH_{rxn}	0.0		−10.9		−38.4

[a] With RHF/6-31G* geometries [47b]. [b] TCSCF (DZ) [42b]. [c] CAS2/3G [49]. [d] CISD (DZ) [42b]. [e] CAS1/4-31G [49]. [f] These methods calculate ΔH and not ΔE.

value for the [1,5] hydrogen shift. As more terms in the Møller–Plesset perturbation series are included, the calculated $\Delta E^{\ddagger}$ oscillates, but appears to converge slowly. The activation energy for the [1,5] hydrogen shift estimated with high order MP perturbation theory and the 6-311G** basis set would be approximately 39 kcal mol^{-1}, which is within experimental uncertainty of the observed value of 38.8 $\pm$ 2.2 kcal mol^{-1}.[39]

For the calculations on the cyclobutene ring opening, a quite high level of correlation energy is required in order to reproduce both the experimental activation energy and heat of reaction. The level that is capable of reproducing the heat of reaction may not necessarily be able to reproduce the activation energy. Both $\Delta E^{\ddagger}$ and the ΔE_{rxn} obtained at the MP4(SDTQ)/6-31G*//MP2/6-31G* level are within 2.5 kcal mol^{-1} of the corresponding experimental values.[44]

For the Diels–Alder reaction, the MP2 correlation energy correction overestimates the effect of electron correlation and lowers the $\Delta E^{\ddagger}$ too much. The activation energy at the MP2/6-31G* level is 7 kcal mol^{-1} less than the experimental value; higher level correlation energy corrections are required for the calculation of activation energy. Nevertheless, RHF/3-21G gives a reasonable geometry for the transition structure, as a comparison with the MP2/6-31G* and CASSCF calculations shows.

These results suggest that the geometries of pericyclic transition structures of hydrocarbons can be calculated at the RHF/3-21G level but the MP2/6-31G* level is better when possible, while activation energies must be calculated at least at the MP2/6-31G* level and even this level is often inadequate. Because the correction of correlation energy appears to be characteristic of bond types in the reactant and transition structures, it is possible to make empirical energy corrections based upon the HF limit of activation energy.

3. Classification of Pericyclic Reactions

Woodward and Hoffmann described five categories of pericyclic reactions: cycloaddition reactions, electrocyclic reactions, sigmatropic shifts, cheletropic reactions, and group transfer reactions.[2] There are some, like ene reactions, which do not fit conveniently into this classification scheme—we have named these reactions "miscellaneozations".[52] Another class of reactions was named dyotropic shifts by Reetz.[53]

It is convenient here to classify these reactions further according to the types of bond transformations involved (see also Fig. 1). Molecular reorganizations with no change in the number of π or σ bonds (heats of reaction near zero) include some sigmatropic shifts and group transfers. Transformations of one π bond to one σ bond (1π-to-1σ transformations) include electrocyclic and ene reactions; unstrained reactions of this type are exothermic by about 23 kcal mol^{-1}. The 2π-to-2σ transformations include cycloadditions and cheletropic reactions, and the 3π-to-3σ transformations include three-component cycloadditions such as [2 + 2 + 2] reactions. These two types of reactions are exothermic ($\Delta H \approx -46$ and -69 kcal mol^{-1}, respectively). Based upon the Hammond postulate[54] or Bell–Evans–Polanyi principle,[55] a gradual shift from a central to an earlier transition state is expected along this enthalpy series. This is the order of presentation that we have chosen here, subdivided by the number of electrons involved in the reaction.

4. Transition Structures of Pericyclic Reactions

The best available theoretical transition structures of all types of thermally allowed pericyclic reactions of hydrocarbons will be described in this article, followed by a description of how substituent effects alter transition-structure energies and geometries. In each case, the computational level and the person who performed the calculations are listed if the results have not yet been published. Finally, the features common to all the processes will be summarized.

4.1. Sigmatropic Shifts

A sigmatropic shift involves the migration of a σ bond along one or two π systems. These reactions have been analyzed by Woodward and Hoffmann, who described the electronic structures of transition states in terms of two weakly interacting radicals.[2] Transition structures which have been calculated for sigmatropic reactions do show some resemblance to the geometries of radical fragments. However, the energies of interaction between these fragments are substantial, and diradical intermediates are not generally formed.

4.1.1. [1,2] Sigmatropic Shifts

The dependence of the activation energies of [1,2] shifts upon the number of electrons involved dramatically demonstrates the power of orbital symmetry considerations. The symmetry-allowed two-electron [1,2] shifts in carbocations are facile. In fact, the bridged ("nonclassical") ethyl and vinyl cations that might be thought of as transition structures between classical cations are actually minima on potential energy surfaces obtained by high-level calculations.[56] These ions, like pericyclic transition structures,[4] can be considered to be "aromatic" because of cyclic delocalization of two electrons. Singlet methylcarbene and vinylidene also undergo rapid [1,2] hydrogen shifts to form the much more stable ethene and acetylene, respectively. Transition structures were found to be only slightly higher in energy than the singlet carbenes with inclusion of electron correlation energy corrections.[57] For the [1,2] hydrogen shift of three-electron hydrocarbon radicals[58] and four-electron hydrocarbon anions,[59] transition structures are comparable in energy to the fragments formed in stepwise dissociation–recombination pathways. The barriers for the [1,2] shifts of radicals or of anions are high, because the transition structures are nonaromatic and antiaromatic, respectively.

4.1.2. [1,3] Sigmatropic Shifts

The [1,3] sigmatropic hydrogen shift in propene has been studied extensively.[38, 60–62] The allowed [1_s,3_a] transition structure (Fig. 9) is very contorted and similar in energy to

an allyl radical plus a hydrogen atom which would be formed in a dissociation–recombination mechanism. At the CASSCF/6-31G* level, the partial C···H bond is 1.61 Å long and the C–C bond length is approximately halfway between that of a double and a single bond; the structure thus indeed resembles an allyl radical. The terminal carbons are pyramidalized to maintain partial bonding to the migrating hydrogen.

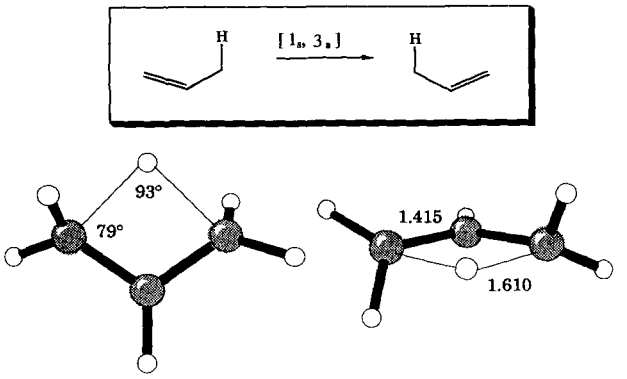

Fig. 9. Two views of the CASSCF/6-31G* transition structure of the $[1_s,3_s]$ sigmatropic hydrogen shift in propene (J. W. Storer).

The symmetry-forbidden suprafacial $[1_s,3_s]$ hydrogen shift is an unfavorable pathway. Both unrestricted Hartree–Fock (UHF) and MCSCF calculations predict a transition structure that resembles a trimethylene diradical.[62] The calculated energy of this species is about 60 kcal mol^{-1} less stable than propene. There is no experimental evidence for a thermal, concerted [1,3] hydrogen shift in simple hydrocarbon systems.

4.1.2.1. [1,3] Sigmatropic Hydrogen Shift of a Radical Cation

The $[1_s,3_s]$ sigmatropic shift in the radical cation of propene has been studied at the MP2 level with UHF/6-31G* geometries.[63] The transition structure has C_s symmetry and resembles the trimethylene radical cation, which corresponds to an energy minimum.[63] The calculated activation energy is 30 kcal mol^{-1}, which is significantly lower than the barrier for this reaction of propene (approximately 60 kcal mol^{-1}). This demonstrates a general principle: forbidden reactions can be made relatively facile by removal of an electron. This is because a forbidden transition state, like the one described above, will always have a very much lower ionization potential than the reactant. This difference in ionization potential is the amount by which the activation energy is lowered by electron detachment. The low ionization potential of the transition state is caused by the avoided HOMO–LUMO crossing that occurs in forbidden reactions.

4.1.2.2. [1,3] Sigmatropic Methyl Shifts

The only geometrically reasonable, thermally allowed methyl shift of 1-butene is the $[1_a,3_s]$ shift (Fig. 10).[64] Steric interactions between the methyl hydrogens and the allyl moiety are indicated by the unusually long forming and breaking C···C bonds (2.5 Å). This distance is about 0.3 Å longer than partial C–C single bonds described earlier for strain-free pericyclic transition structures. Indeed, there is likely to be very little bonding at 2.5 Å, particularly since the p orbital of the migrating center does not point directly at C1 or C3 of the allyl moiety. The calculated activation energy at the MP2/6-31G*//3-21G level is 96 kcal mol^{-1}, which is larger than the required 72 kcal mol^{-1} for the cleavage of the C–C bond.[65] Berson and Salem suggested that a concerted symmetry-forbidden $[1_s,3_s]$ sigmatropic shift would be more favorable than a stepwise process, because subjacent orbital interactions would stabilize the forbidden transition state.[66] However, as in the corresponding hydrogen shift, the transition structure of the $[1_s,3_s]$ methyl shift resembles a 2-methyltrimethylene diradical. Both the allowed and forbidden processes are calculated to have activation energies comparable to, or higher than, the energy required for C–C bond cleavage and recombination. No unequivocal experimental examples of [1,3] sigmatropic alkyl shifts are known in acyclic systems. However, in cyclic or bicyclic systems, where the migrating group is connected to the alkene, examples are plentiful, and some of these are described below.

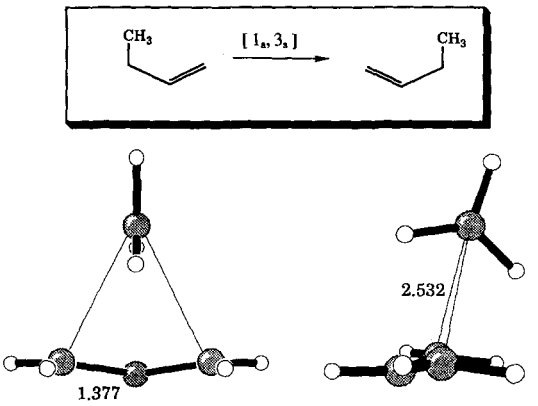

Fig. 10. The RHF/3-21G transition structures of the $[1_a,3_s]$ sigmatropic methyl shift in 1-butene (J. W. Storer).

4.1.2.3. [1,3] Sigmatropic Shifts Involving the Methylene Group

Many [1,3] methylene shifts have been observed experimentally,[67] such as the methylenecyclopropane rearrangement, the vinylcyclopropane to cyclopentene rearrangement, the degenerate analogue—the "walk" rearrangement of bicyclo[2.1.0]pentene—and rearrangements of many bicyclic alkenes such as bicyclo[3.2.0]hept-2-ene to norbornene. These reactions are geometrically constrained to be suprafacial on the allyl system, while the migrating carbon may undergo reaction with either retention or inversion.

Figure 11 shows the transition structure for the allowed $[1_a,3_s]$ vinylcyclopropane → cyclopentene rearrangement.[64] The cyclopropane ring is nearly open, with the breaking C–C bond equal to 2.21 Å, while the formation of the new C–C bond is lagging behind with a bond length of 2.56 Å. The π

system resembles that of an allylic radical (C–C bond lengths of 1.38 Å and 1.39 Å). Inversion of the migrating methylene carbon takes place in the transition structure. The calculated reaction barrier at the RHF level is 84 kcal mol^{-1}. Although MCSCF calculations yield a lower value for the reaction barrier, the transition structure becomes even more diradical in nature, and the stepwise mechanism is likely to be comparable in energy to the concerted path.[68]

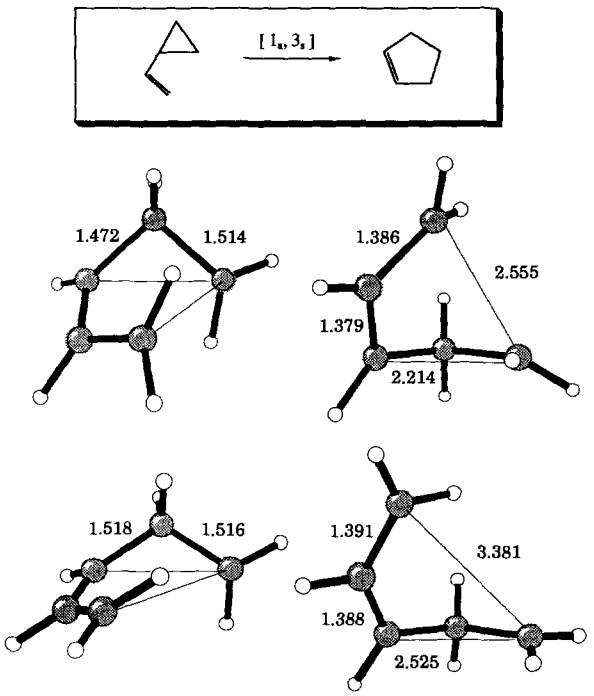

Fig. 11. The RHF/6-31G* (top) and of the CASSCF/3-21G transition structures (bottom) of $[1_a,3_s]$ sigmatropic vinylcyclopropane–cyclopentene shift (J. W. Storer).

The transition structure for the "walk" rearrangement of bicyclo[2.1.0]pentene is shown in Figure 12.[69] The partial C···C single bonds are 2.24 Å long, and the partial double bonds are similar to those of the allyl radical. The cyclobutene ring is planar, a fact which indicates little pyramidalization of the allyl termini or bonding with the migrating group. The calculated activation energy of the concerted

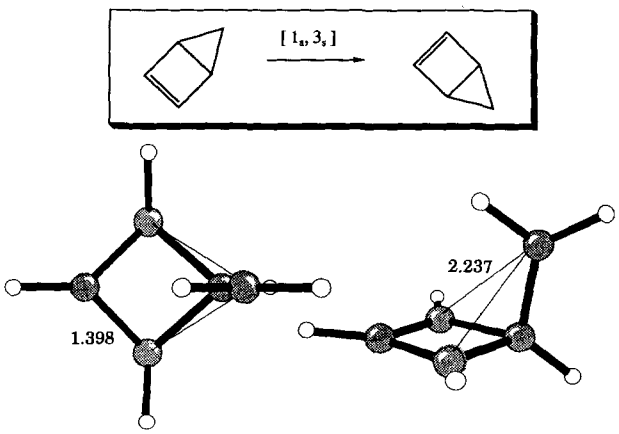

Fig. 12. The RHF/3-21G transition structure of $[1_a,3_s]$ sigmatropic methylene shift in bicyclo[2.1.0]pentene [69a].

[1,3] shift at MP2/6-31G* level is in good accord with the estimated experimental value of 35 kcal mol^{-1}. The forbidden $[1_s,3_s]$ pathway was predicted to be at least 8 kcal mol^{-1} less favorable.[69a]

Better calculations are needed to provide definitive evidence for mechanism, but it appears that [1,3] shift transition structures have much diradical character, and stereochemistries may be controlled by orbital symmetry only when the migrating carbon is forced by the carbon skeleton to interact strongly with the allyl system.

4.1.3. [1,4] Sigmatropic Shifts

The *cis*-1-methylallyl cation may undergo a thermally allowed $[1_s,4_a]$ or a forbidden $[1_s,4_s]$ sigmatropic hydrogen shift. However, attempts to locate transition structures at the RHF/6-31G* level gave instead a bridged C_{2v} minimum (Fig. 13a).[70] This is a hydrogen-bridged nonclassical cation intermediate.

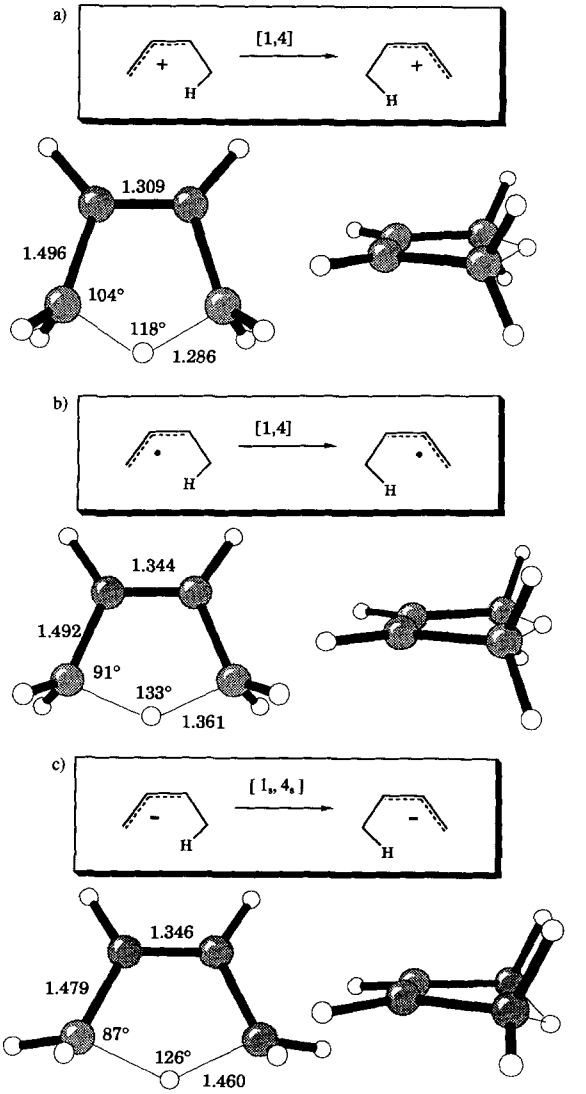

Fig. 13. a) The RHF/6-31G* structure of the hydrogen-bridged butenyl cation (S. M. Ernst). b) The UMP2/6-31G* transition structure of the [1,4] sigmatropic hydrogen shift in the butenyl radical (Y. Li). c) The RHF/6-31G* transition structure of [1,4] hydrogen shift in the butenyl anion (Y. Li).

Transition structures can been located for the [1,4] hydrogen shift in the methylallyl radical and methylallyl anion.[71] The [1,4] hydrogen shift of the methylallyl radical has a transition structure with C_{2v} symmetry (Fig. 13b). The partial C···H bond length is 1.36 Å; the C-C-C bond angle is bent (113°). The central C–C bond is essentially a double bond (1.34 Å), while the terminal C–C bonds are single bonds, 1.49 Å long. This very interesting result shows that the transition structure for this hydrogen shift appears formally like a bridged three-center–three-orbital system, C···H···C. The analogous hydrogen transfer between two methyl radicals has a C···H bond length of 1.3 Å. The double bond in the transition structure only weakly overlap with the C···H···C system, since the H···C-C-C torsional angle is 0°.

Figure 13c shows the transition structure for the allowed $[1_s,4_s]$ hydrogen shift in the 1-methylallyl anion. The migrating hydrogen is only slightly out of the plane defined by the carbons; the H···C-C-C torsional angle is 15°. The terminal methylene groups are rotated in order to maintain bonding with the migrating hydrogen. As with the radical, the terminal C–C bond lengths (1.48 Å) are longer than the central C–C bond (1.35 Å), and the partial H···C bond length is 1.46 Å. The calculated reaction barrier is 30 kcal mol^{-1} at the MP2/6-31G* single-point level, indicating a less favorable process than the [1,4] hydrogen shift in the methylallyl cation.

For the "walk" rearrangement of methylene in the bicyclic cation, a transition structure has been located at the RHF/3-21G level (Fig. 14a).[70] The calculated activation energy for the allowed $[1_a,4_s]$ methylene shift is 18 kcal mol^{-1}, while the experimental value is 15 kcal mol^{-1}.[72] The forbidden process (Fig. 14b) has a very distorted geometry and a predicted activation energy of 33 kcal mol^{-1}.

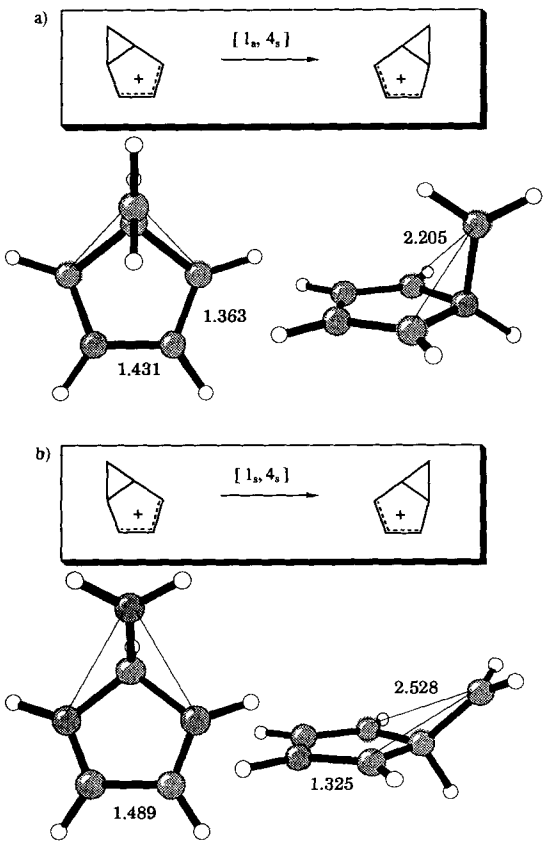

Fig. 14. The RHF/3-21G transition structures of the [1,4] sigmatropic methylene shift in bicyclo[3.1.0]hexenyl cation (S. M. Ernst): a) the $[1_a,4_s]$ pathway; b) the $[1_s,4_s]$ pathway.

4.1.4. *[1,5] Sigmatropic Shifts*

The transition structure for the [1,5] sigmatropic hydrogen shift has been studied extensively, as described earlier.[38–40] For the hydrogen shift in (*Z*)-1,3-pentadiene, the migrating hydrogen projects out of the C1-C2-C4-C5 plane in the transition structure (H···C-C-C torsional angle of 30°, Fig. 15). The partial C···H bond length is 1.41 Å, and the C-H-C angle is 133°. The C–C bonds are 1.40 and 1.42 Å in length; the terminal C–C bonds are the longer bonds. Two hydrogen atoms attached to the terminal carbon atoms are quite near each other. This will cause severe steric interactions when the hydrogens are replaced by larger groups.

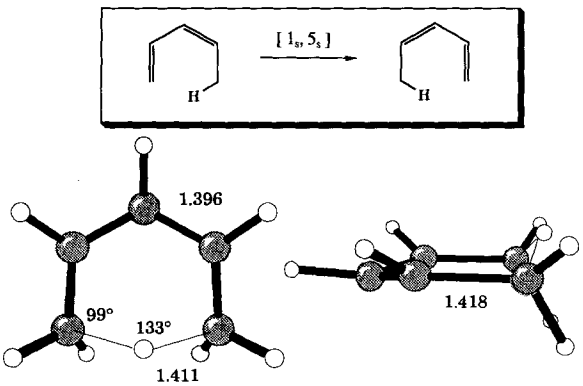

Fig. 15. The MP2/6-31G* transition structure of the $[1_s,5_s]$ sigmatropic hydrogen shift in pentadiene [39a].

Figure 16 shows the transition structure for the [1,5] hydrogen shift in cyclopentadiene. The cyclopentadiene ring and all nonmigrating hydrogen atoms are virtually coplanar. The migrating hydrogen atom is 79° out of the plane. The C–C bond lengths, except that bridged by the migrating hydrogen, correspond to those in aromatic systems, and the

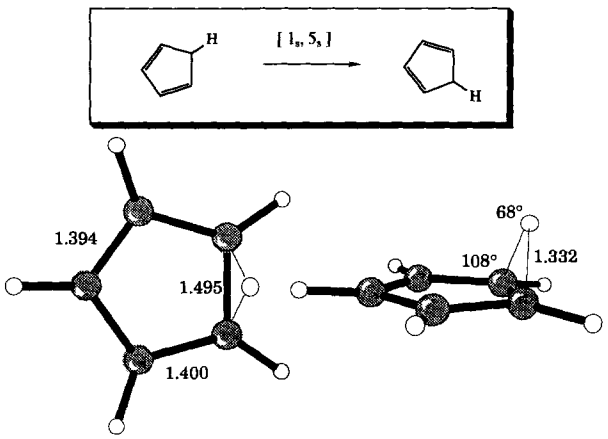

Fig. 16. The RHF/3-21G transition structure of the $[1_s,5_s]$ sigmatropic hydrogen shift in cyclopentadiene [39c].

partial C···H bond lengths are very short. This reaction has a low activation energy of 21 kcal mol^{-1}.[39] It is substantially different from the pentadiene case, because of the close proximity of the migration origin and terminus, which permits good overlap of the hydrogen orbitals with orbitals on both migration origin and terminus.

The transition structure for the thermally allowed [1_s,5_s] sigmatropic methyl shift in *cis*-1,3-hexadiene is shown in Figure 17.[73] The carbon atoms partially bonded to the migrating methyl group are pyramidalized and oriented to maintain interactions with the migrating group. Nevertheless, the degree of bonding is small for the C–C bond length of 2.17 Å, and the predicted activation energy is 73 kcal mol^{-1} at the MP2/6-31G* level. In contrast, the reaction barrier of the corresponding [1,5] hydrogen shift in pentadiene is only 38 kcal mol^{-1}, indicating strong bonding in the transition structure. For the [1,5] methyl shift of 1,3-hexadiene, a stepwise mechanism is comparable in energy to the concerted mechanism. The methyl group cannot take part in multicenter bonding as well as a hydrogen atom can, as described in Section 4.1.5.

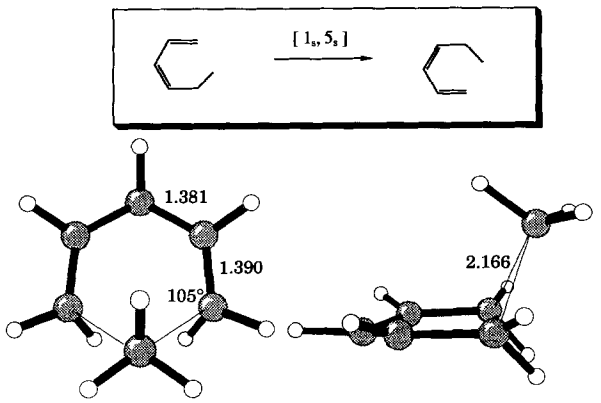

Fig. 17. The RHF/3-21G transition structure of the [1_s,5_s] sigmatropic methyl shift in *cis*-1,3-hexadiene (F. Jensen).

There are many examples of [1,5] methyl shifts in cyclopentadiene systems, and the experimental activation enthalpies are in the range of 40–44 kcal mol^{-1} for simple methyl-substituted cyclopentadienes.[74] Figure 18 shows the transition structure for the allowed [1_s,5_s] methyl shift of 5-methylcyclopentadiene.[73] The partial C···C single bond length is 1.99 Å, while the C···C double partial bonds resemble aromatic double bonds. Little pyramidalization occurs at the carbon centers of the cyclopentadiene ring, even at those two that are formally partially bonded to the migrating methyl group. The calculated reaction barrier at the RHF/3-21G level is 53 kcal mol^{-1}, which should correspond to an actual barrier of about 33 kcal mol^{-1}. The [1,5] shift of a methyl group along a cyclopentadiene is relatively facile, due to the good overlap of a methyl orbital with the orbital on adjacent carbon atoms of a cyclopentadiene ring. This is reflected in the 1.99 Å C···C bond length for the migrating methyl, as compared to 2.17 Å in the hexadiene case. Hydrogen migration is still much more facile.

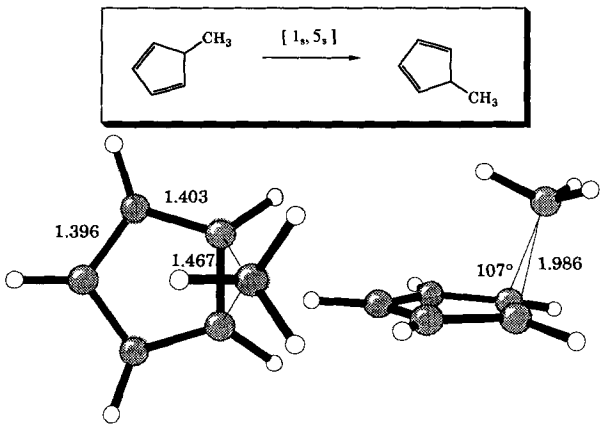

Fig. 18. The RHF/3-21G transition structure of the [1_s,5_s] sigmatropic methyl shift in methylcyclopentadiene (F. Jensen).

The [1,5] sigmatropic methylene shift in bicyclo[4.1.0]-heptadiene (norcaradiene) has been studied at the HF/3-21G level.[73] There are only two possible transition structures for the [1,5] methylene shift: the allowed [1_s,5_s] and the forbidden [1_a,5_s] rearrangements. Figure 19 shows the transition structure located for the allowed process. The activation energy of the [1,5] sigmatropic methylene shift in norcaradiene itself is not known experimentally. The calculated activation energy at the MP2/6-31G* single point level is 53 kcal mol^{-1} for the allowed [1_s,5_s] methylene shift, and 87 kcal mol^{-1} for the forbidden [1_a,5_s] reaction. These results seem to contradict the observed stereochemistry; the reaction is believed to proceed almost exclusively with inversion of the migrating alkyl group in substituted cases.[75] It is likely that the reaction takes place via a diradical mechanism. The calculated activation energy and the geometry of the transition structure (Fig. 19) indicate little or no bonding between the methylene group and the termini of the pentadienyl group. If the rate of recombination of the biradical is much faster than rotation around the C–C bond, the reaction could proceed stereospecifically with inversion of the migrating carbon.

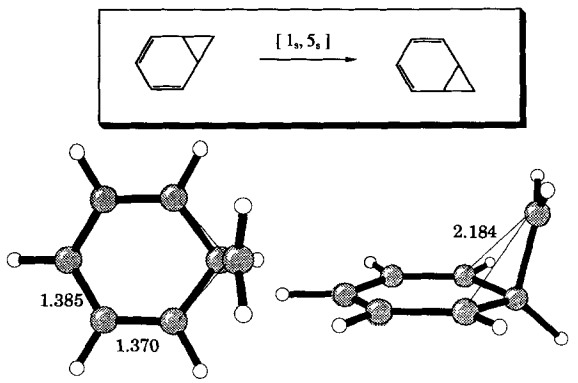

Fig. 19. The RHF/3-21G transition structure of the [1_s,5_s] sigmatropic methylene shift in norcaradiene (S. M. Ernst).

4.1.5. [1,7] Sigmatropic Shifts

Hess, Schaad, and others have reported a transition structure for the allowed [1_s,7_a] hydrogen shift.[38] The RHF/3-21G optimized transition structure of C_2 symmetry is given

in Figure 20.[73] The calculated activation energy is 44 kcal mol^{-1} at the RHF/3-21G level, which is 11 kcal mol^{-1} lower than that for the [1,5] hydrogen shift at the same level of theory. With inclusion of electron correlation, the reaction barrier is estimated to be about 25 kcal mol^{-1}, which is in the range of the experimental estimation.[76] The lower barrier is due to better overlap of the orbitals of the partial C···H bonds and the π system than can occur in the [1,5] shift.[73]

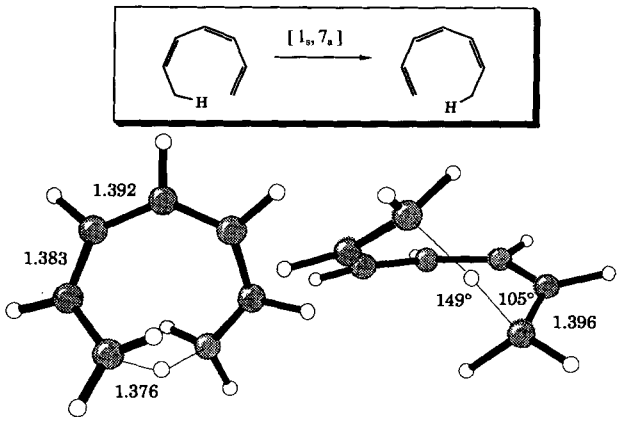

Fig. 20. The RHF/3-21G transition structure of the [1s,7a] sigmatropic hydrogen shift in heptatriene [38].

All of the sigmatropic hydrogen shifts can be considered to involve a C···H···C array, optimally arranged for hydrogen transfer, interacting to a greater or lesser extent with the unsaturated system joining the two carbons involved in the hydrogen transfer. This is further demonstrated by comparisons of the transition structures of sigmatropic hydrogen shifts with those involving intermolecular hydrogen atom transfers (Fig. 21).[77] For the sigmatropic hydrogen shifts, the C···H lengths are 1.33–1.41 Å, about the same as in the transition structure for hydrogen atom transfer between methane and a methyl group. The same comparison holds for methyl shifts. At the UHF/6-31G* level, hydrogen atom transfer from methane to methyl has an activation energy which is 37 kcal mol^{-1} less than that for methyl group transfer.

There are several differences between hydrogen atom and methyl group shifts. The allowed and geometrically feasible hydrogen shifts all have substantial energies of concert. That is, stepwise mechanisms have considerably higher activation energies than observed reactions. On the other hand, there is little or no energy of concert for the alkyl group shifts, which all have transition structures involving very little bonding between radical fragments. The reaction barriers of alkyl shifts are considerably higher than those of the corresponding hydrogen shifts. This arises because hydrogen can readily form reasonably strong bonds simultaneously to two groups. This is difficult for an alkyl group, regardless of whether frontside or backside attack occurs. This is a consequence of the poor overlap achievable between the directional orbital of an alkyl group and two other orbitals simultaneously.

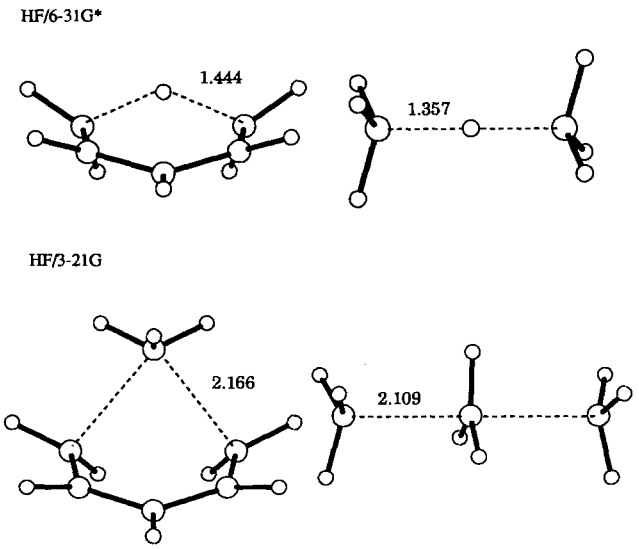

Fig. 21. Comparison of the 6-31G* transition structures of sigmatropic hydrogen shifts with intermolecular hydrogen transfer (top) and the 3-21G transition structures of sigmatropic methyl shifts with intermolecular methyl transfer (bottom).

4.1.6. [3,3] Sigmatropic Shifts

The [3,3] sigmatropic shift, as well as all other higher order sigmatropic shifts, have the possibility of two stepwise mechanisms: fragmentation to two allyl (or other conjugated radical) fragments and recombination, or formation of a diradical by addition of the termini of the two π bonds to each other, followed by cleavage. The concerted pathway may involve transition structures which resemble either one of these extremes. There may even be multiple competing concerted pathways for these processes.[78]

The degenerate Cope rearrangement of 1,5-hexadiene is a case where the precise mechanism is still a matter of uncertainty. A variety of computational techniques have been applied.[79–82] Ab initio CASSCF calculations predict a closed-shell, delocalized, "aromatic" transition state for the Cope rearrangement (Fig. 22).[79] The partial σ bonds are

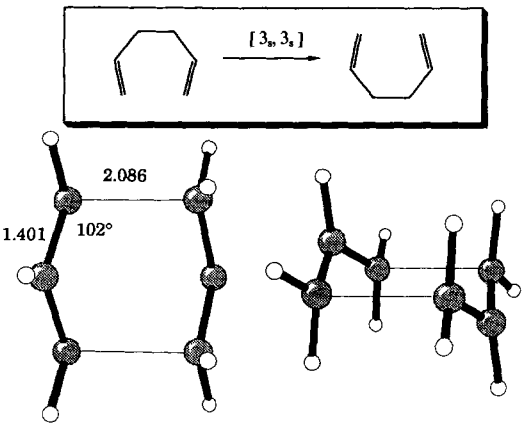

Fig. 22. The CASSCF/3-21G transition structure of [3s,3s] sigmatropic shift (Cope rearrangement) of 1,5-hexadiene [79].

2.09 Å long, which is in the normal range. Transition structures of both chair and boat conformations have been located. The chair is preferred, which is in good agreement with

the experimental observations based upon the stereochemistry of the reaction.[83] The calculated activation entropy for the chair transition structure is in good agreement with the experimental value, but the calculated value is too small for the boat conformation. The experimental isotope effects for Cope rearrangement can be reproduced by the aromatic transition structures from concerted mechanisms,[70] and the 1,4-diyl is estimated to have a significantly higher energy than the observed transition state.[84] Nevertheless, a very high level of calculation will be required to match all available experimental data.[84c]

A variety of other Cope rearrangements of various unsaturated hydrocarbons have also been studied at the RHF/3-21G level.[70] Figure 23 shows the transition structure for the [3,3] sigmatropic rearrangement of 1,5-hexadiyne to form 1,2,4,5-hexatetraene. In the transition structure, the forming

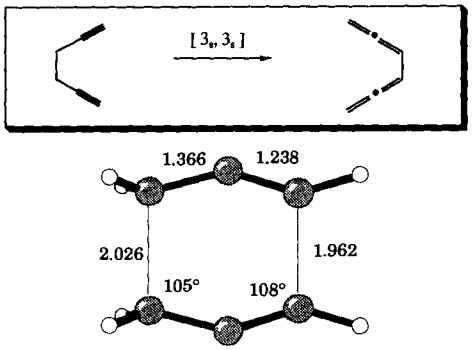

Fig. 23. The RHF/3-21G transition structure of [3s,3s] sigmatropic shift of 1,5-hexadiyne (S. M. Ernst and K. Black).

C···C bond length is 1.96 Å and the breaking C···C bond length is 2.03 Å. The $HC{\equiv}C{-}CH_2{-}$ fragments are bent substantially from linear to a bond angle of 147°. The calculated reaction barrier at the MP2/6-31G* level is 37 kcal mol^{-1}, which is close to the experimental value of 34 kcal mol^{-1}.[85]

Transition structures for the degenerate rearrangement of hexa-1,2-dien-5-yne and the rearrangement of hex-1-en-5-yne to 1,2,5-hexatriene are shown in Figures 24 and 25, respectively.[70, 86] RHF calculations favor the concerted mechanisms for each of these processes, but like the Cope

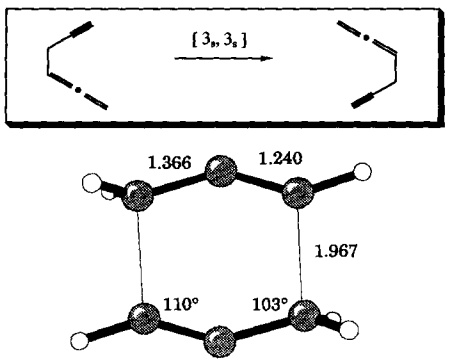

Fig. 24. The RHF/3-21G transition structure of [3s,3s] sigmatropic shift of hexa-1,2-dien-5-yne (S. M. Ernst and K. Black).

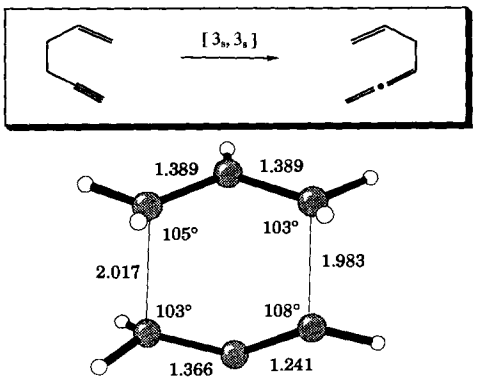

Fig. 25. The RHF/3-21G transition structure of [3s,3s] sigmatropic shift of hex-1-en-5-yne (S. M. Ernst and K. Black).

rearrangement itself, diradical mechanisms are expected to be not too different in energy from concerted mechanisms.[87]

4.2. Group Transfers

Feller, Schmidt, and Ruedenberg reported ab initio studies of the concerted dihydrogen transfer between ethene and ethane.[88] The concerted transition structure has D_{2h} symmetry (Fig. 26).[89] The C···H bonds of the transferring

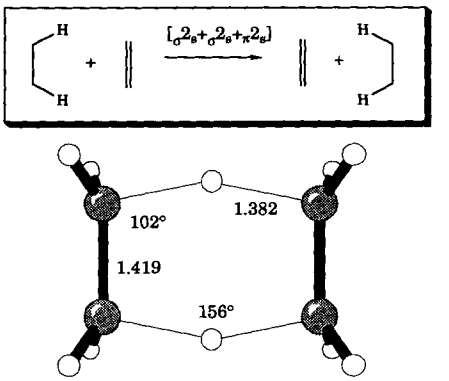

Fig. 26. The CASSCF/3-21G transition structure of hydrogen transfer between ethene and ethane [89].

hydrogens are stretched to 1.38 Å, while the C–C bonds have the usual aromatic-like bond lengths. The partial σ C···H bonds can be described as three-center (C···H···C) three-electron bonds as in sigmatropic hydrogen shifts. The calculated reaction barrier is 71 kcal mol^{-1} at the MCSCF level and 51 kcal mol^{-1} at the MP2/6-31G*//3-21G level.[71] Several molecules have been observed to undergo the concerted dihydrogen transfer reaction.[90]

Figure 27 shows the transition structures for the hydrogen transfer from *cis*-2-butene to 1,3-butadiene.[71] In both *endo* and *exo* transition structures, the partial H···C bond lengths are 1.38 Å, and the butadiene fragments have the usual partial C···C double bond lengths of 1.38–1.40 Å. The *endo* transition structure is predicted to be more stable than the *exo* by 2 kcal mol^{-1}, and the reaction barrier is predicted to be 45 kcal mol^{-1} via the *endo* transition structure at the

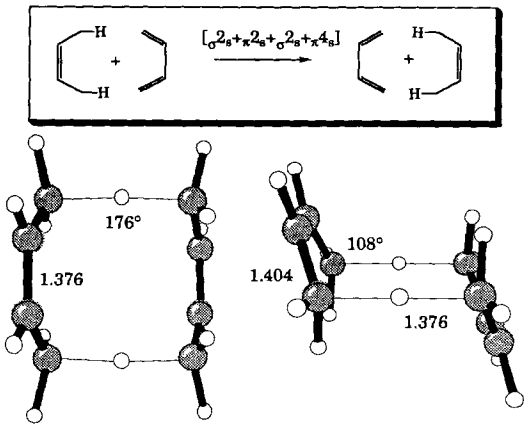

Fig. 27. The RHF/3-21G transition structure of hydrogen transfer between 2-butene and butadiene (Y. Li).

MP2/6-31G*//3-21G level. An example of this reaction is known for a polycyclic case.[91]

4.3. Electrocyclic Reactions

Electrocyclic reactions involve the cyclization of conjugated π systems or the reverse ring-opening process. The reactions may be conrotatory or disrotatory, and generally follow the Woodward–Hoffmann predictions, unless some geometrical constraints such as incorporation into a small ring prevent the allowed process.[92]

4.3.1. Allyl → Cyclopropyl Rearrangements

According to the Woodward–Hoffmann rules, the symmetry-allowed cyclopropyl cation opening to form the allyl cation is disrotatory, while that of the anion is conrotatory. The disrotatory conversion of the cyclopropyl cation to allyl cation is exothermic with a vanishingly small barrier according to MP2 calculations.[93] As shown in Figure 28, the breaking C···C bond length is only 1.56 Å in the transition structure, nearly the same as in the cyclopropyl cation. Indeed, experimental data indicate that the ring opening occurs

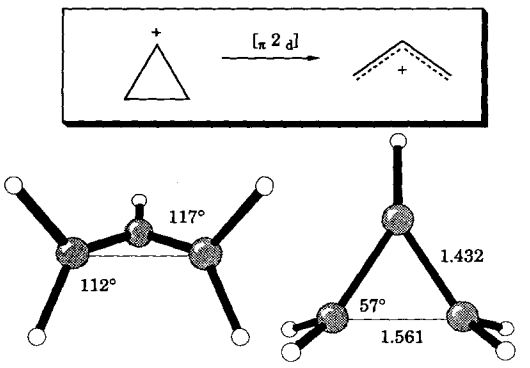

Fig. 28. The MP2/6-31G* transition structure of disrotatory electrocyclic ring opening of the cyclopropyl cation [93]. In this and subsequent drawings of electrocyclic reactions, the angles between the inward and outward rotating hydrogens and the breaking or forming single bond are given.

in concert with ionization in the reactions of cyclopropyl halides and tosylates.[94]

The cyclopropyl radical opens to form the allyl radical with a significant barrier of approximately 20 kcal mol^{-1}.[95] Similarly, the exothermic (-43 kcal mol^{-1}) conrotatory ring opening of the cyclopropyl anion has a reaction barrier of 20 kcal mol^{-1} at the MP2/6-31 + G* level.[96] The breaking C···C bond is stretched to 1.94 Å, and the C–C double bond lengths are 1.45 Å in the transition structure (Fig. 29).

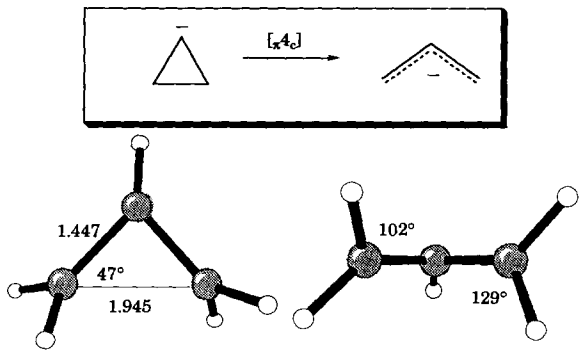

Fig. 29. The MP2/6-31 + G* transition structure of conrotatory electrocyclic ring opening of the cyclopropyl anion (E. A. Kallel).

All carbons are pyramidalized in the transition structure, and the hydrogen atom on the central carbon atom is bent significantly out of the C-C-C plane.

4.3.2. The Butadiene → Cyclobutene Rearrangement

The transition structure for the cyclobutene conrotatory electrocyclic ring opening has been studied extensively.[42–44] Early interest in this reaction focused on the difference in energy between the thermally allowed conrotatory and the thermally forbidden disrotatory processes.[42b,c] There appears to be no concerted C_s transition structure for the forbidden disrotatory process, and experimental and theoretical estimates place the allylmethylene diradical resulting from the rotation of only one of the newly formed methylene and groups of butadiene about 9–11 kcal mol^{-1} above the conrotatory transition structure.[42b]

The concerted conrotatory transition structure obtained at the MP2/6-31G* level is shown in Figure 30. The breaking single bond has stretched from 1.56 Å in cyclobutene to 2.13 Å in the transition structure. The single bond flanking the breaking bond has contracted from 1.51 Å to 1.41 Å; this change of 0.09 Å is about 50% the total change from reactant to product. The conversion of the double bond of cyclobutene to a single bond lags considerably behind the other bond length changes; it has stretched only 0.03 Å in the transition structure, which is only 30% of the total bond extension during the reaction.

These changes are consistent with a description of the reaction in which the major bonding changes occurring to form the transition structure is stretching and twisting of the σ bond, accompanied by the beginnings of interaction of the orbitals at the rotating termini with the π orbitals of the

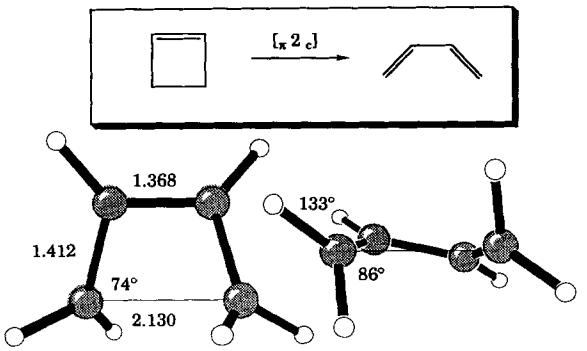

Fig. 30. The MP2/6-31G* transition structure of conrotatory electrocyclic ring opening of cyclobutene [44a].

double bond. Such interaction only becomes substantial when the σ bond is quite long, raising the σ orbital energy, and when rotation has occurred sufficiently to allow σ–π* and σ*–π overlaps. The overlaps are also facilitated by the nonplanarity of the carbon skeleton.[44d] After the transition structure is reached, the energy rapidly decreases toward the s-*cis*-butadiene skew geometry. This analysis helps us understand the substituent effects described in Section 5.1.

The electrocyclic ring opening of benzocyclobutene is analogous, and may be regarded formally as either a 4π- or an 8π-electron process. Figure 31 shows the transition structure for this ring-opening reaction.[97] The cyclobutene motions are very similar to those of the transition structure of the parent cyclobutene ring opening, even though the cyclobutene opening is *exothermic* by 10 kcal mol^{-1}, while the benzocyclobutene opening is *endothermic* by 15 kcal mol^{-1}. The breaking C···C single bond is slightly longer than that in the cyclobutene transition structure, consistent with the fact that the transition structure occurs later in this endothermic reaction.

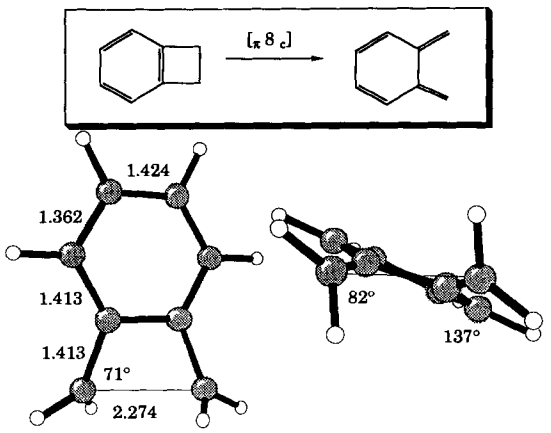

Fig. 31. The RHF/3-21G transition structure of conrotatory electrocyclic ring opening of benzocyclobutene (D. C. Spellmeyer).

4.3.3. The Pentadienyl → Cyclopentenyl Rearrangement

Figure 32a shows the transition structure for the conrotatory electrocyclic conversion of the pentadienyl cation to the cyclopentenyl cation.[96] In the transition structure, the partial C···C single bond is 2.27 Å long, and all partial double bonds have identical bond lengths of 1.39 Å. The activation energy is nearly zero for this highly exothermic process (− 27 kcal mol^{-1}), but the qualitative features are very similar to those for the cyclobutene electrocyclic reaction.

The transition structure for the 6π-electron disrotatory ring opening of cyclopentenyl anion to the more stable pentadienyl anion is shown in Figure 32b.[98] The partial single bond in the transition structure is 2.18 Å in length, while the lengths of the partial double bonds range from 1.39 to 1.44 Å. The calculated reaction barrier is 20 kcal mol^{-1} at the MP2/6-31 + G* single point level.

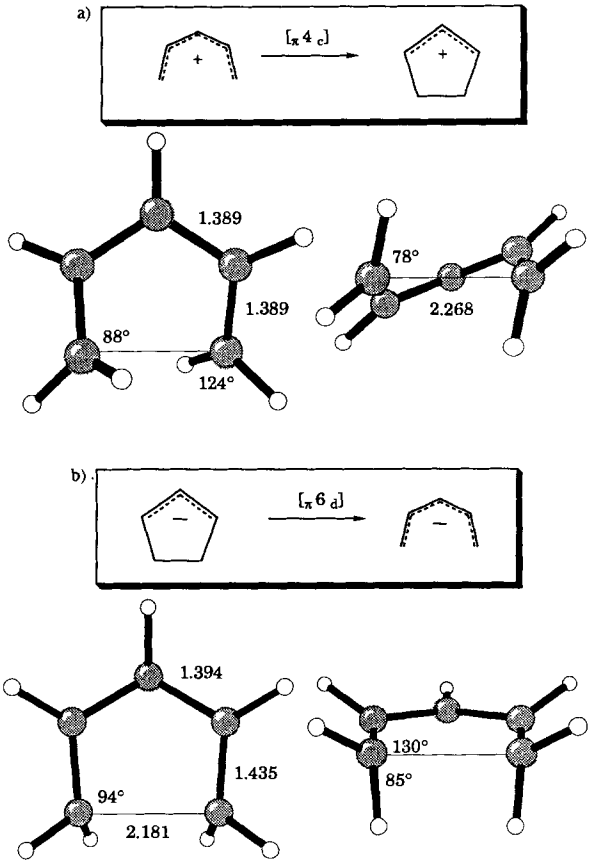

Fig. 32. a) The MP2/6-31G* transition structure of electrocyclization of the pentadienyl cation (E. A. Kallel). b) The RHF/6-31 + G* transition structure of cyclopentenyl anion electrocyclic ring opening (J. D. Evanseck).

4.3.4. The Hexatriene → Cyclohexadiene Electrocyclization

The transition structure for the disrotatory ring closure of *cis*-1,3,5-hexatriene to form 1,3-cyclohexadiene is shown in Figure 33.[97,99] The partial single-bond length is 2.24 Å, and the double-bond lengths are in the range of 1.39 to 1.40 Å. Two hydrogen atoms are in close proximity at the bonding termini, which destabilizes the transition structure to some extent. The boat shape of this transition structure permits the interaction of the π system at carbon atoms 2–4 of the triene with the forming σ bond between carbon atoms

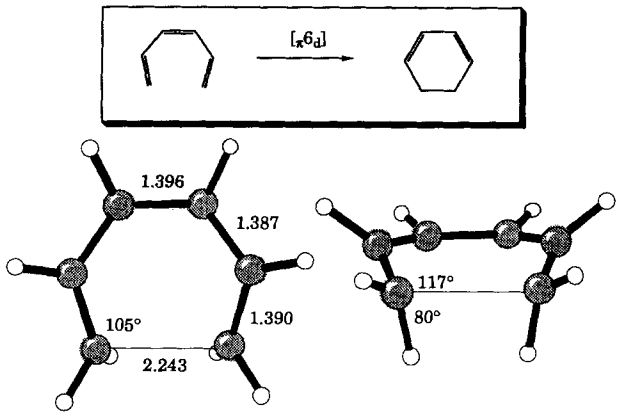

Fig. 33. The RHF/6-31G* transition structure of disrotatory electrocyclization of hexatriene [99].

1 and 6 to be maintained throughout the reaction. The MP2/6-31G* activation energy of 26 kcal mol^{-1} for the ring closure is in good agreement with experimental value of 29 kcal mol^{-1}.[100]

4.3.5. The Hexenediyne → Benzenediyl Electrocyclization

The 6π-electron electrocyclization of hex-3-ene-1,5-diyne gives benzene-1,4-diyl, which opens to form hexenediyne with a rearranged carbon skeleton (Fig. 34).[11e] Bergman et al. studied simple versions of this reaction extensively,[101] but there has been much recent excitement about this process since the discovery that the natural substances, esperamicin and calicheamicin, undergo this type of reaction.[10] In cells, the resulting diradicals abstract hydrogens from DNA to cause double-strand DNA cleavage and cell death.[10]

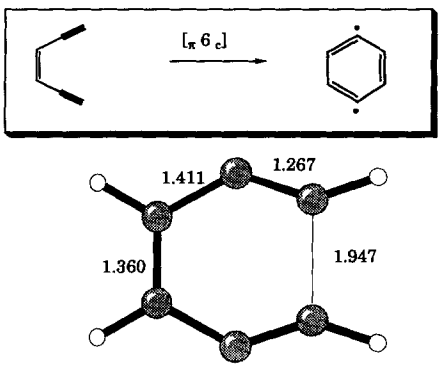

Fig. 34. The CASSCF/MIDI1 transition structure of electrocyclization of hex-3-en-1,5-diyne [11e].

The reaction has also been studied at the semiempirical and MCSCF levels.[11c,d] Generation of the benzene ring compensates for the loss of a bond involved in generation of the diradical, so that the parent system has a relatively ordinary activation barrier for hydrocarbon pericyclic processes. However, ground state strain can lower the barrier so that the cyclization occurs readily at room temperature. Although the reaction might be considered as the addition of two alkynes, it does exhibit geometrical features similar to other pericyclic reaction transition structures.

4.3.6. The Octatetraene → Cyclooctatriene Electrocyclization

The transition structure of this conrotatory eight-electron electrocyclic process is shown in Figure 35.[98] Although the process is clearly conrotatory, the two termini of the partially formed σ bond are aligned nearly perfectly, not twisted as in the conrotatory cyclobutene → butadiene interconversion. The coiled arrangement of the eight carbon atoms permits excellent π overlap throughout the ring in the transition structure. There is also excellent overlap of the π system with the forming C···C bond. The calculated activation energy at the MP2/6-31G* level is 8 kcal mol^{-1}, while Huisgen has found an enthalpy of activation for a substituted tetraene of 22 kcal mol^{-1}.[102]

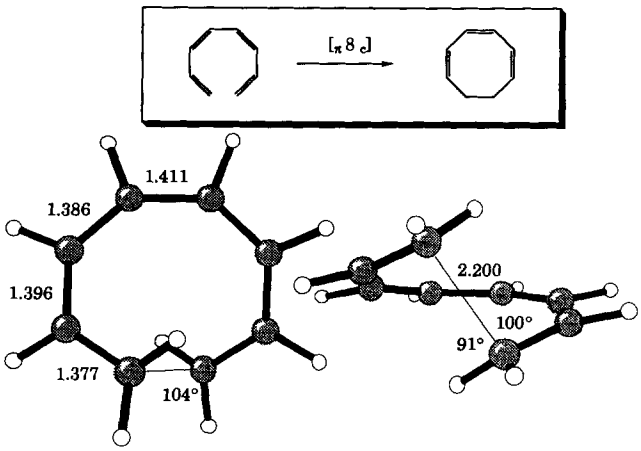

Fig. 35. The RHF/6-31G* transition structure of conrotatory electrocyclic ring opening of cyclooctatriene (J. D. Evanseck).

4.4. The Ene Reaction

The ene reaction is related both to cycloadditions and to sigmatropic hydrogen shifts. One π bond is converted to a σ bond, and a hydrogen atom is transferred at the same time. It has been called a homodienyl [1,5] shift in intramolecular examples.[103] The reaction occurs even with simple unactivated hydrocarbons, although it is best known for the reaction of alkylethylene with electron-deficient molecules such as alkenes, ketones, or azo compounds substituted by electron-withdrawing groups, or singlet oxygen.

The transition structure for the ene reaction of propene with ethene to form 1-pentene is shown in Figure 36.[104] It has an envelope conformation, like that of cyclopentane, but with two long C–C bonds, and the transferring hydrogen atom is placed in one of these long bonds. The forming C···C single bond length is about 2.0 Å, while the two partial C···H bond lengths are 1.22 and 1.52 Å. The calculated reaction barrier at the MP2/6-31G* level is 32 kcal mol^{-1}.

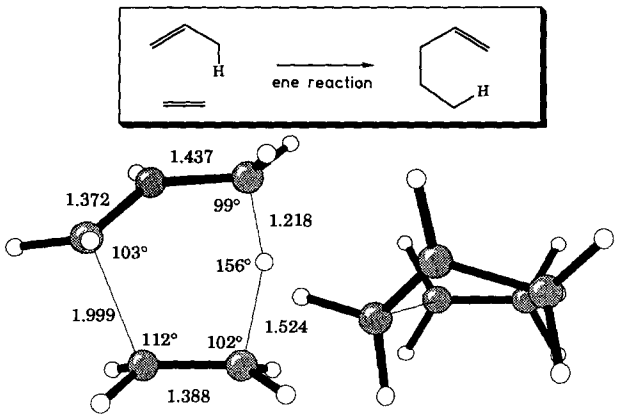

Fig. 36. The RHF/3-21G transition structure of the ene reaction between propene and ethene [104].

The hypothetical diradical, pentane-1,4-diyl, is expected to be close in energy to the concerted transition structure. Nevertheless, the observed stereospecificity of substituted cases implies that the reactions are concerted.[105]

4.5. Hydrogen Additions and Extrusions

The concerted addition of H_2 to ethene is a forbidden four-electron process which will occur in a stepwise fashion. When six electrons are involved, the reaction is thermally allowed. The transition structure for the concerted [1,4] addition of a hydrogen molecule to butadiene is shown in Figure 37.[106] It has forming H···C and breaking H···H bond lengths of 1.60 Å and 0.92 Å, respectively. The H···C-C angle of attack is 96°. The activation energy of the [1,4] addition is predicted to be 36 kcal mol^{-1} at the MP2/6-31G*//HF/3-21G level. The addition of hydrogen to butadiene is exothermic by 36 kcal mol^{-1} at the same level of theory.

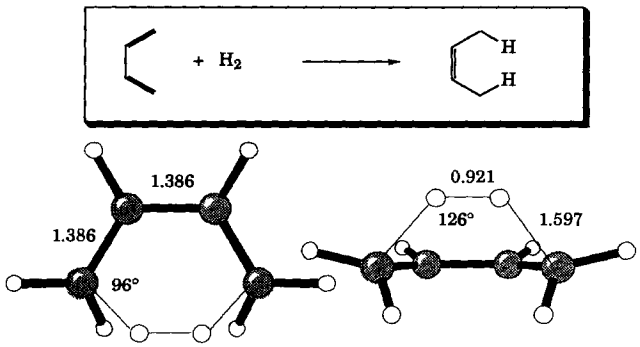

Fig. 37. The RHF/3-21G transition structure of butadiene hydrogenation (A. Dorigo).

Lee and co-workers recently reported experimental studies of the rotational, vibrational, and translational energy distribution of the H_2 formed from elimination from 1,4-cyclohexadiene.[107] They infer from these studies that the transition structure should have a tight H–H distance and that "the H atoms are more likely to move in a plane parallel to the two double bonds rather than perpendicular to it".[107] Thus, the hydrogens are predicted to experience a helicopter-like spinning with respect to the plane of the forming benzene ring. Calculations on this system predict a C_{2v} transition structure (Fig. 38),[71] so that the spinning must be induced by dynamic effects taking place beyond the transition state. The experimental activation energy for the elimination of hydrogen from cyclohexadiene is 44 kcal mol^{-1}, and the reaction is exothermic by 6 kcal mol^{-1}.[108] The calculated quantities at the MP2/6-31G* are 50 and 3 kcal mol^{-1}, respectively.

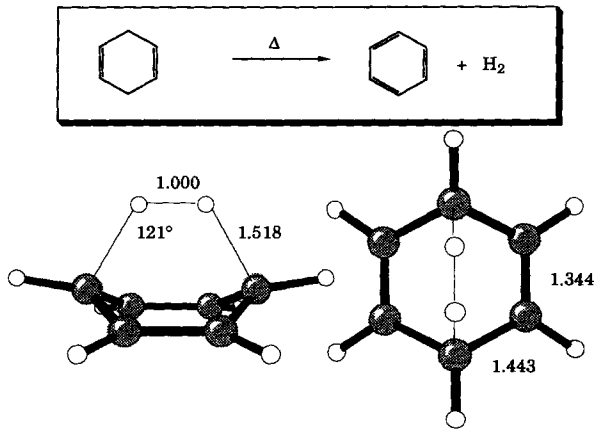

Fig. 38. The RHF/6-31G* transition structure of benzene hydrogenation (Y. Li).

4.6. Cheletropic Reactions

Cheletropic reactions are pericyclic reactions in which two bonds are made or broken to a single atom. This class of reactions includes such common processes as the addition of carbenes to olefins, the loss of CO from cyclopentenones, the loss of N_2 from cyclic *N*-nitrides, and the loss of SO_2 from sulfolene (Fig. 39).

These reactions may be either suprafacial or antarafacial on the olefinic component, and either linear or nonlinear on the chelefuge, the fragment containing the single atom at which the two forming or breaking bonds terminate. This

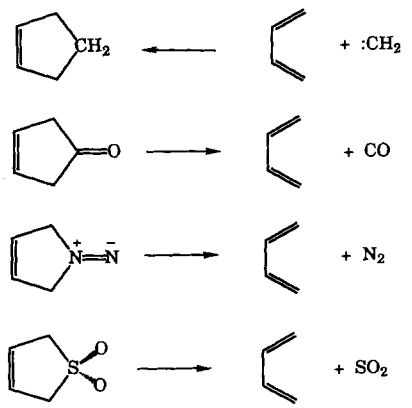

Fig. 39. Examples of cheletropic reactions.

leads to a total of four possible reaction pathways. Direct experimental distinction between all of the mechanistic possibilities cannot be made easily. For three-membered rings (e.g., addition of singlet carbenes to olefins,[109] or loss of SO_2 from thiirane 1,1-dioxides[110]), cheletropic reactions are observed to be suprafacial on the olefin, suggesting that the nonlinear pathway is followed. For five-membered rings, suprafacial reactions are also observed.[111] For seven-membered rings, antarafacial reactions are observed.[112] This suggests that the linear pathways are followed for the larger rings, but calculations have special importance in establishing stereochemistries of such reactions, because of the difficulties of determining them experimentally.

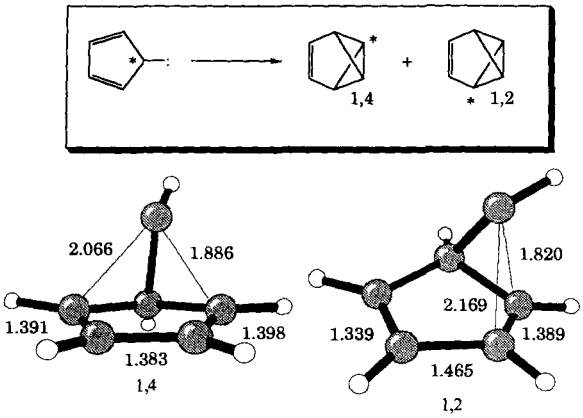

Fig. 40. The HF/3-21G transition structures of 1,4- (left) and 1,2-addition (right) of the carbene in methylene cyclopentadiene [117].

4.6.1. Carbene Additions

Singlet carbene additions to alkenes involve the approach of the vacant π orbital of the singlet carbene to the occupied π orbital of the alkene and subsequent rotation of the methylene fragment to complete cyclopropane formation.[113] This is the classic nonlinear cheletropic mechanism, proposed by Hoffmann twenty-five years ago.[114]

Zurawski and Kutzelnigg studied the ab initio potential energy surface for the addition of singlet methylene to ethene.[115] This study indicates the absence of a barrier, with the energy decreasing monotonically along the entire reaction path. The minimum energy pathway does follow the nonlinear trajectory proposed by Hoffmann. For a variety of substituted carbenes, this nonlinear pathway is followed, but the transition structure varies from a relatively late transition structure for stabilized carbenes (e.g. CF_2) to an early one for unstabilized carbenes (e.g. CCl_2).[116]

4.6.2. Carbene Additions to Dienes

Singlet carbenes may undergo either 1,2- or 1,4-cycloadditions with conjugate dienes. The 1,2-addition is much more favorable than the 1,4-addition. The latter only becomes more favorable in the case of a few intramolecular reactions when the 1,2-addition is made sterically difficult. An example is the singlet cyclopenta-2,4-dienyl carbene to form benzvalene. Transition structures have been located for both 1,2- and 1,4-cycloadditions as shown in Figure 40.[117] The reaction barrier of the 1,4-cycloaddition is 5 kcal mol^{-1} lower than that of the 1,2-addition. In this intramolecular reaction, the ring skeleton constraints prevent the transition structure for the 1,2-addition from achieving the ideal geometry, so that the 1,4-addition becomes more favorable.

4.7. Cycloaddition Reactions

Cycloadditions are reactions involving the addition of two or more unsaturated molecules to each other to form a new ring. Two nomenclature systems are in common use. According to Huisgen's system,[118] a cycloaddition is classified by the number of atoms between the termini involved in ring formation. Thus, Diels–Alder and 1,3-dipolar cycloadditions are (4 + 2) and (3 + 2) cycloadditions, respectively. Parentheses are used to enclose the atom numbers. In the Woodward–Hoffmann system,[2] the number of π electrons involved in bonding changes in the two reactants are used. Thus, Diels–Alder and 1,3-dipolar cycloadditions are both [4 + 2] cycloadditions. Square brackets enclose the numbers of electrons. The latter system will be used here.

4.7.1. [2 + 2] Cycloadditions

According to the Woodward–Hoffmann rules, the $[2_s + 2_s]$ cycloaddition is not a thermally allowed process, while the allowed $[2_a + 2_s]$ process requires a geometrically difficult transition state and should be unfavorable except in unusual circumstances. There have been many theoretical studies of the [2 + 2] reactions involving ethene,[119] acetylene,[120] allene,[121] and ketene.[122] MCSCF calculations on the dimerization of ethene show that there is no symmetrical transition structure for the $[2_s + 2_s]$ process, and the reaction involves two steps with a tetramethylene biradical intermediate.[119] Doubleday et al. has proposed that this intermediate is a free energy minimum because of unfavorable entropy upon cleavage or cyclization.[119c] Figure 41 a shows the *anti* transition structure which leads to the *anti*-butanediyl. The barrier to ring closure includes a contribution from rotation about the central C–C bond. The forming C···C bond length of 1.8–1.9 Å is shorter than those in

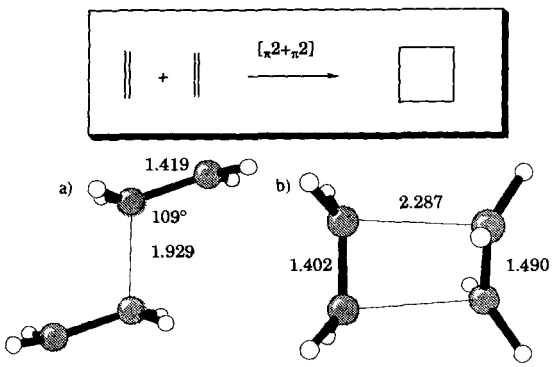

Fig. 41. The MCSCF/3G transition structures of the cyclodimerization of ethene [119b]. a) The nonconcerted $[{}_{\pi}2_s + {}_{\pi}2_s]$ reaction; b) the concerted $[{}_{\pi}2_s + {}_{\pi}2_a]$ reaction.

the concerted reactions discussed in the following sections, while the second bond is not formed at all. All carbon atoms involved in bond formation as well as those at the forming radical are pyramidalized. A transition structure has also been reported for the allowed $[_\pi 2_s + {}_\pi 2_a]$ pathway, but it is very high in energy due to steric repulsions between hydrogens (Fig. 41 b).

By contrast, ketene reacts with ethene via a transition structure that is rather similar to the carbene transition structure.[122b] As shown in Figure 42, the forming bond from ethene to the electrophilic ketene carbonyl carbon is very short while the second bond to the methylene carbon atom is very long. There is zwitterionic character; a charge

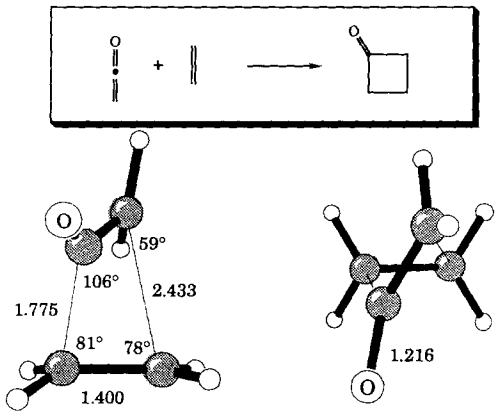

Fig. 42. The MP2/6-31G* transition structure of $[_\pi 2_s + {}_\pi 2_a]$ cycloaddition between ethene and ketene [122].

transfer of 0.2 electrons from ethene to ketene is revealed in this gas-phase calculation.

4.7.2. [4 + 2] Diels–Alder Reactions

The parent Diels–Alder reaction of 1,3-butadiene with ethene to form cyclohexene is the prototype thermally allowed cycloaddition. It has been studied extensively both by semiempirical[46] and ab initio techniques.[47–49] A lively debate over mechanism went on for more than 10 years, because ab initio RHF and MCSCF calculations predict a symmetric transition structure for a route with no intermediates, while semiempirical or ab initio UHF calculations predict a two-step mechanism involving a diradical intermediate. While the concerted, synchronous nature of the prototype reaction is now agreed upon, there is still discussion about the mechanisms of substituted cases.[123]

Figure 43 shows the butadiene–ethene transition structure according to MP2/6-31G* calculations. Several interesting features of the transition structure are summarized here. The angles of attack are approximately tetrahedral, so that the diene and ethene do not approach each other in parallel planes, but instead, the planes are canted with respect to each other. The out-of-plane bending of the hydrogens at C2 and C3 of the diene is quite remarkable, since these hydrogens are nearly coplanar with the attached and germinal carbons in both reactant and product. This pyramidalization of the orbitals on C2 and C3 occurs in order to maximize overlaps

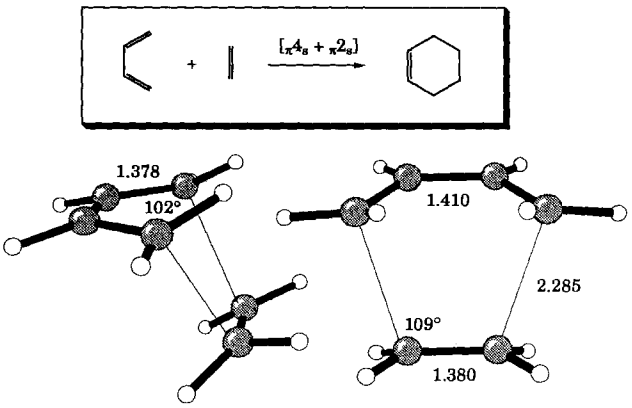

Fig. 43. The MP2/6-31G* transition structure of $[_\pi 4_s + {}_\pi 2_s]$ cycloaddition between butadiene and ethene (R. J. Loncharich).

of the p orbitals at these carbon atoms with the orbitals of forming C···C bonds.[124]

Transition structures have also been located for several other hydrocarbon Diels–Alder reactions. Figure 44 shows the transition structure for the reaction between butadiene and acetylene.[125] The transition structures for the reaction

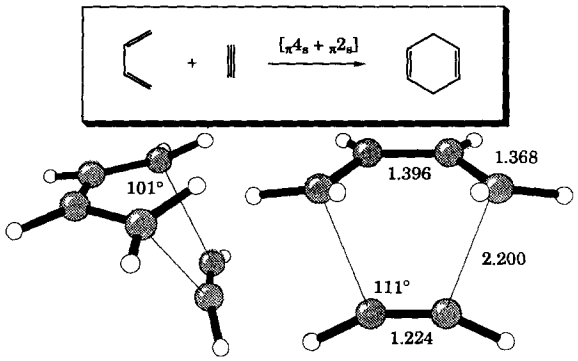

Fig. 44. The RHF/3-21G transition structure of $[_\pi 4_s + {}_\pi 2_s]$ cycloaddition between butadiene and acetylene (M. McCarrick).

between cyclopentadiene and ethene,[126] and cyclobutadiene and ethene[71] are shown in Figure 45 and 46, respectively. Although the reactivity increases from 1,3-butadiene

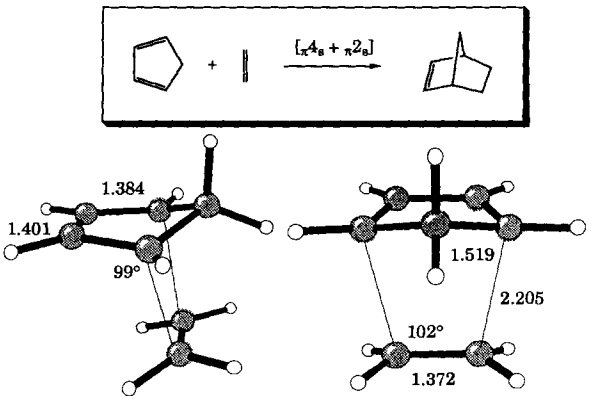

Fig. 45. The RHF/3-21G transition structure of $[_\pi 4_s + {}_\pi 2_s]$ cycloaddition between cyclopentadiene and ethene [126].

over cyclopentadiene to cyclobutadiene, the forming C···C single bond lengths are remarkably constant (2.2 Å) in all of these transition structures. The relative activation energies are related to the reaction exothermicity and to how well the distances between the termini of butadiene and the termini of ethene correspond.

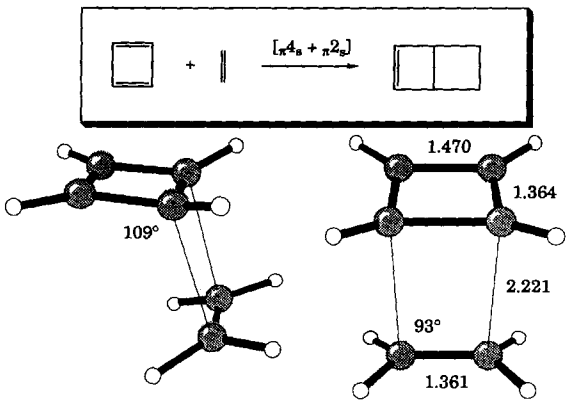

Fig. 46. The RHF/3-21G transition structure of $[\pi 4_s + \pi 2_s]$ cycloaddition between cyclobutadiene and ethene (Y. Li).

The Diels–Alder reaction between benzene and alkenes or alkynes has been suggested to have a strong preference for the concerted pathway and an energy of concert of 23 kcal mol^{-1}.[12] Figure 47 shows the transition structure for the Diels–Alder reaction between benzene and ethene.[71]

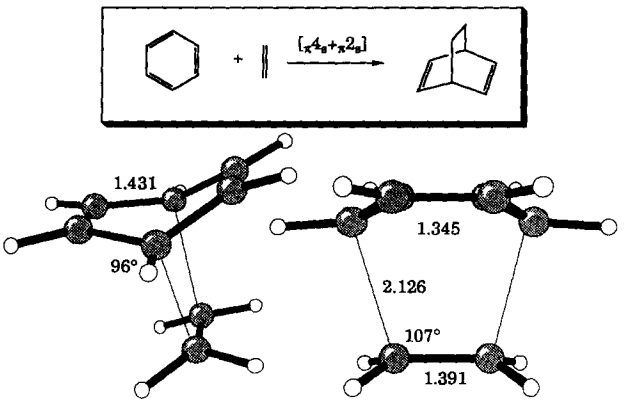

Fig. 47. The RHF/3-21G transition structure of $[\pi 4_s + \pi 2_s]$ cycloaddition between benzene and ethene (Y. Li).

The forming single C···C bond length is 2.13 Å in the transition structure. The benzene moiety is distorted out-of-plane, and the C–C bond lengths of the benzene ring are alternately 1.34 and 1.43 Å. In spite of the distortions, the barrier of this reaction is about the same as that of the prototype Diels–Alder reaction. Thus, the cyclic delocalization of the aromatic ring is maintained in the transition structure. The biradical intermediates which would be formed along nonconcerted path will be very unfavorable due to the significant loss of benzene aromaticity.

Similarly, a concerted transition structure has been located for the Diels–Alder reaction between benzene and acetylene

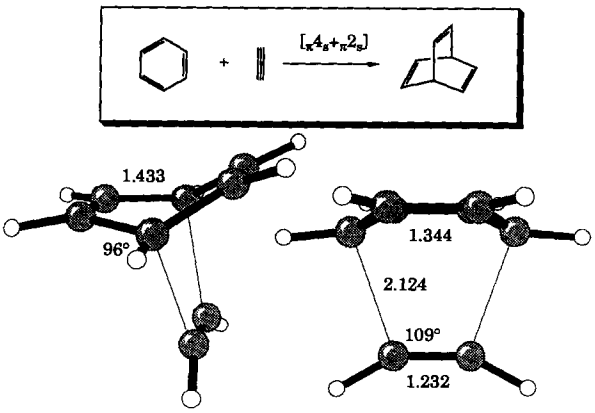

Fig. 48. The RHF/3-21G transition structure of $[\pi 4_s + \pi 2_s]$ cycloaddition between benzene and acetylene (Y. Li).

(Fig. 48).[71] The benzene moiety is almost identical to that in the transition structure of ethene plus benzene, and the forming C···C single bond lengths are 2.12 Å. The calculated reaction barrier at the MP2/6-31G* single point level is 35 kcal mol^{-1}, which is close to the experimental activation energy of 40 kcal mol^{-1}.[127]

4.7.3. [6 + 4] Cycloadditions

Figure 49 shows potential C_s transition structures for the [6 + 4] cycloaddition reaction between *cis*-hexatriene and butadiene.[71] Vibrational frequency calculations indicate two imaginary frequencies for the *endo* stationary point, while the *exo* is an authentic transition structure. The *exo* transition structure is predicted to be 5 kcal mol^{-1} more stable than the *endo* conformation, in full accord with the Woodward–Hoffmann prediction.[2] The forming single-bond lengths are 2.18 Å, and the partial double-bond lengths are in the range of 1.38 Å to 1.40 Å. The patterns of bond alternation resemble those in hexatriene and butadiene, indicating the early nature of these transition structures.

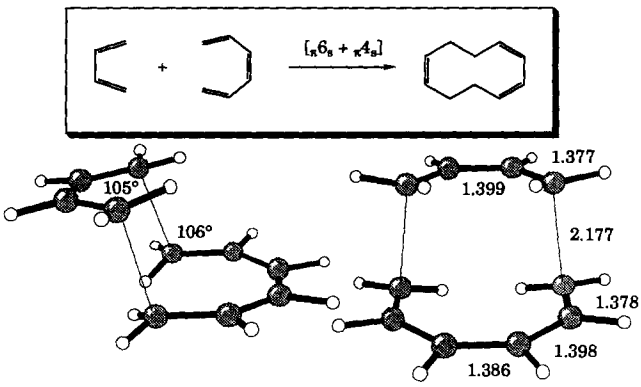

Fig. 49. The RHF/3-21G transition structure of $[\pi 6_s + \pi 4_s]$ cycloaddition between *cis*-hexatriene and butadiene (Y. Li).

For the [6 + 4] cycloaddition between cycloheptatriene and butadiene, both *endo* and *exo* transition structures have also been located (Fig. 50).[71] The *exo* transition structure is

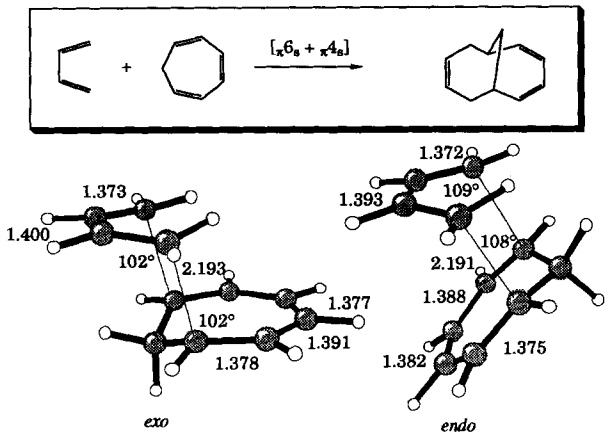

Fig. 50. The RHF/3-21G *exo* and *endo* transition structures of $[_{\pi}6_s + {}_{\pi}4_s]$ cycloaddition between cycloheptatriene and butadiene (Y. Li).

9 kcal mol^{-1} more stable than the *endo*, which may be attributed to the destabilization of the *endo* transition structure by both steric effects and secondary orbital interactions. A similar *exo* preference was found for the [6 + 4] cycloaddition of cyclopentadiene and tropone (Fig. 51).[71] The *exo* transition structure is 10 kcal mol^{-1} more stable than the *endo* stationary point which is, once again, not an authentic transition structure. This reaction has been observed experimentally to give exclusively the *exo* adduct,[128] as predicted by Woodward and Hoffmann.[2] All these transition structures have very similar forming C···C distances of about 2.2 Å.

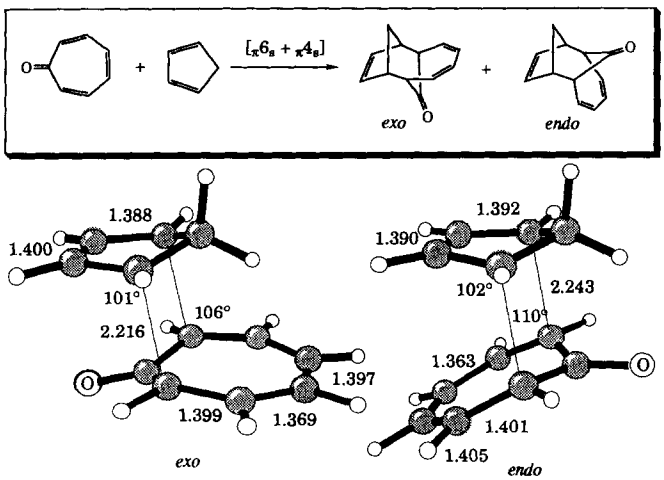

Fig. 51. The RHF/3-21G *exo* and *endo* transition structures of $[_{\pi}6_s + {}_{\pi}4_s]$ cycloaddition between tropone and cyclopentadiene (Y. Li).

4.7.4. [2 + 2 + 2] Cycloadditions

Although cyclotrimerizations are highly exothermic, such reactions are difficult because of unfavorable entropic factors and extremely high reaction barriers. Theoretical studies on the concerted cyclotrimerization of acetylene to benzene have been reported;[129] a very large reaction barrier is predicted. Transition structures have been located for the [2 + 2 + 2] cyclotrimerization of three molecules of acetylene (Fig. 52),[129b] and three molecules of ethene (Fig. 53). For

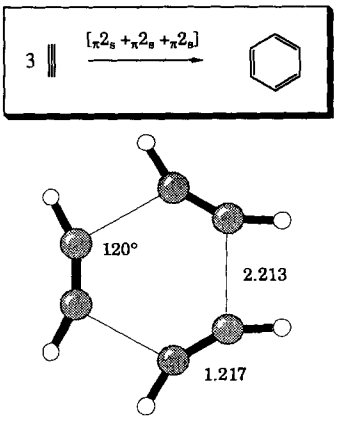

Fig. 52. The RHF/6-31G* transition structure of $[_{\pi}2_s + {}_{\pi}2_s + {}_{\pi}2_s]$ cyclotrimerization of acetylene [129b].

the highly exothermic [2 + 2 + 2] cycloadditions, transition structures are early, and the forming C···C bond lengths are 2.2–2.3 Å. These reactions have high intrinsic reaction barriers because of the necessity of disrupting the closed-shell nature of three molecules in the transition state.

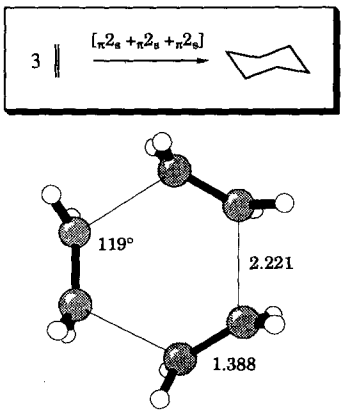

Fig. 53. The MP2/6-31G* transition structure of $[_{\pi}2_s + {}_{\pi}2_s + {}_{\pi}2_s]$ cyclotrimerization of ethene (Y. Li).

5. How Do Substituents Alter Transition Structures?

We have surveyed the hydrocarbon pericyclic reactions and have found a number of features which are common to them all. Substituents may have profound effects on the energies and geometries of the transition structures. In this section, two examples are described. The first case is an example of a reaction for which substituents induce very small changes in geometry, but have large effects of rates and stereoselectivities. This is typical for cases in which diradical alternative mechanisms are much less accessible than the concerted mechanisms, such as electrocyclic reactions and sigmatropic hydrogen shifts. The second example demonstrates a case where substituents alter both the geometry and energy of the transition structure. This will be the case when diradical and concerted mechanisms are close in energy, as in cycloadditions and sigmatropic carbon shifts.

5.1. Cyclobutene Ring Opening

Table 2 summarizes the activation energies of ring openings of a number of substituted cyclobutenes.[44] Also listed are the bond lengths of the breaking C···C bond in each of the transition structures. It is evident that the activation energies of ring openings of substituted cyclobutenes are influenced dramatically by the substituents, but the geometries of the transition structures change very little. Of particular note, a change in activation energy of nearly 20 kcal mol^{-1} is reflected in rather minor changes in geometry. The breaking C···C bond length, the most sensitive measure of geometry alteration, changes by only ± 0.02 Å for substituents at the 3-position rotating outward. Upon inward rotation, larger changes occur.

Table 2. The relative activation energies [kcal mol^{-1}] and lengths of the breaking C···C bond [Å] of transition structures for the substituted cyclobutene ring opening reactions (RHF/3-21G).

Substituent	$\Delta\Delta E^{\ddagger}$ [a]	$\Delta\Delta E^{\ddagger}$ [b]	C3-C4 [a]	C3-C4 [b]
3-NH_2	−11.5	6.0	2.128	2.227
3-OH	−8.8	8.4	2.125	2.181
3-F	−4.2	12.7	2.118	2.154
3-CH_3	−1.7	4.7	2.143	2.175
H	0.0	0.0	2.138	2.138
3-CN	−3.3	1.0	2.140	2.175
3-CHO	−3.6	−8.2	2.143	2.152
3-NO	−4.5	−7.1	2.119	2.129
1-OH	1.9		2.135	
1-F	0.9		2.159	
1-CH_3	1.9		2.145	
1-CHO	−1.1		2.157	

[a] For outward rotation of the substituents on C3 and C4. [b] For inward rotation of these substituents.

Amino and hydroxyl substituents both raise the activation energy substantially upon inward rotation. Repulsive interactions arise between the substituent and the remote terminus of the breaking bond, which cause the length of the breaking bond to increase by almost 0.1 Å and 0.05 Å, for NH_2 and OH, respectively. As shown in Figure 54, the transition structures for the outward and inward electrocyclic opening of 3-aminocyclobutene are nevertheless very similar to each other and to that for the ring opening of cyclobutene. The outward rotating amino group lowers the activation energy by 12 kcal mol^{-1}, while the inward rotating amino group raises the activation energy by 6 kcal mol^{-1}. In spite of the enormous 10^{13} difference in rate constants expected at room temperature for this 18 kcal mol^{-1} difference in activation energy, the geometries are changed very little.

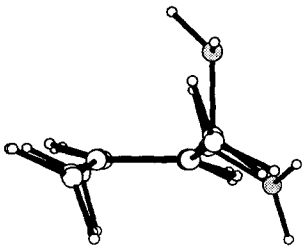

Fig. 54. Transition structures of 3-aminocyclobutene ring openings. The transition structures for the outward and inward rotation of the amino group are superimposed on the transition structure for cyclobutene opening. The nitrogen atom is shaded.

The origin of the stereoselective substituent effects for the ring opening of cyclobutene has been discussed at length.[44] Figure 55 summarizes the theory we have developed. In the

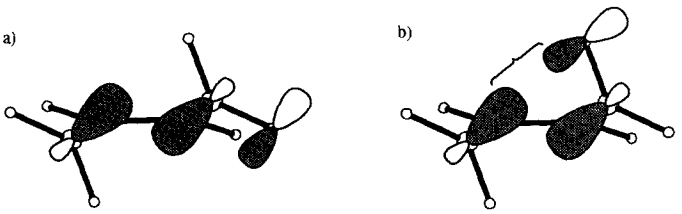

Fig. 55. Orbital interactions in the transition structures for outward (a) and inward (b) rotation of a substituent in cyclobutene ring opening reactions.

transition structure the σ bond is stretched and twisted and interacts weakly with the cyclobutene π bond. A lone pair or π orbital from an outwardly rotating substituent overlaps with the σ and σ* orbitals of the partially broken C···C bond. This overlap results in stabilization. Upon inward rotation, the substituent orbital overlaps not only with the σ and σ* orbitals at the terminus to which the substituent is attached, but also overlaps strongly with the other terminus. If the substituent orbital is doubly occupied, this results in strong destabilization, because a cyclic four-electron antiaromatic interaction occurs.

We have shown that the preference for outward rotation increases as the substituent becomes a more powerful donor. If the substituent is a powerful acceptor, then inward rotation is favored, because a cyclic two-electron interaction occurs. These stereoselective effects of the substituent dictate the direction of the conrotatory opening. Because this is related to the direction of twist, or torque, upon the breaking bond, we have called this type of stereoselectivity, "torquoselectivity".[130]

A substituent on the cyclobutene double bond has a much smaller effect on the activation energy of the reaction (see Table 2), since the π bond for which the substituent is attached interacts only slightly with the breaking σ bond in the transition structure.

5.2. Diels–Alder Reaction

Although the prototype Diels–Alder reaction has been studied extensively, there have been relatively few theoretical investigations of Diels–Alder reactions involving substituents. The transition structures of a series of Diels–Alder reactions have now been investigated.[126, 131, 132] Figure 56 compares the transition structures for the reactions between butadiene and ethene, acrylonitrile, 1,1-dicyanoethene, acrolein, and an adduct of acrolein and a model Lewis acid, BH_3. These were all obtained at the RHF/3-21G level, but many have been studied at higher levels as well.

The activation energies decrease by more than 14 kcal mol^{-1} from the prototype reaction to the acid-catalyzed example. There is a corresponding change from a synchronous reaction towards a diradical or zwitterionic species, where the formation of one bond is far advanced and of the other is in the initial stages. However, these calculations indicate

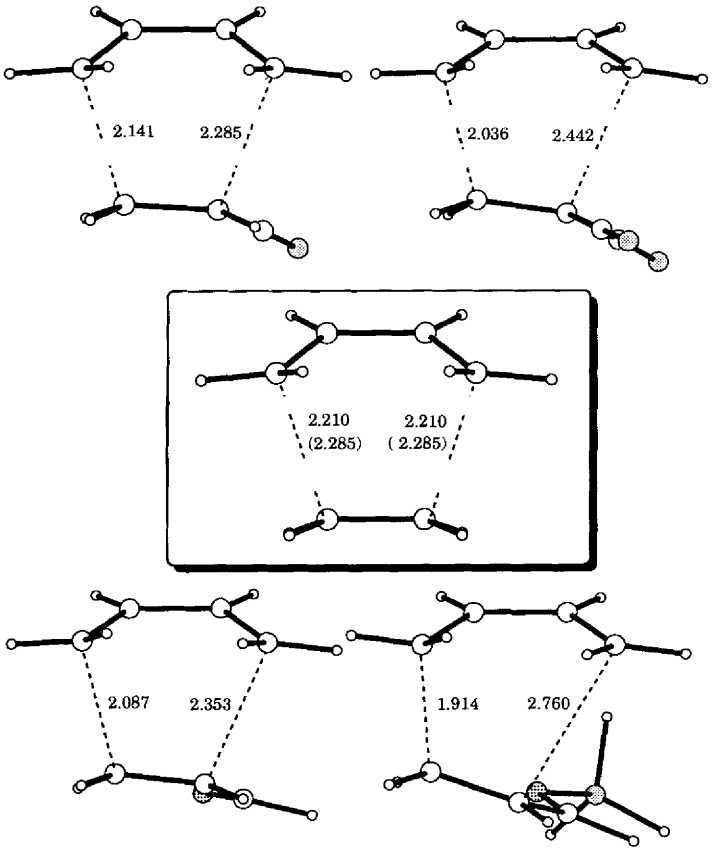

Fig. 56. Transition structures of Diels–Alder reactions between butadiene and acrylonitrile, 1,1-dicyanoethylene, acrolein, and acrolein catalyzed by BH_3. In the center the transition structure for the prototype reaction between butadiene and ethene is shown.

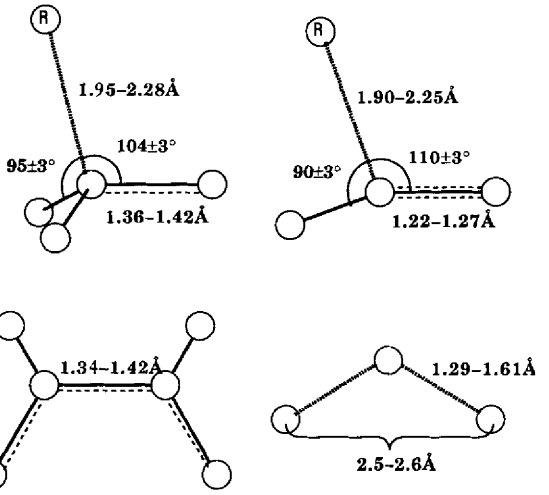

Fig. 57. Summary of geometrical features of transition structures in pericyclic reactions.

that each of these species are transition structures, not intermediates, in the gas phase. When the butadiene → acrolein reaction was studied with MP2/6-31G* geometry optimizations,[132] the asynchronicity of bond formation increased. The difference between the two forming bond lengths was 0.45 Å in this case. However, the species remains a transition structure, if a highly asynchronous one.[132]

In the noncatalyzed reactions the average forming C···C bond length remains nearly constant: the bond to the carbon atom bearing the substituent stretches, while the bond forming to the unsubstituted carbon atom contracts. Only in the Lewis acid catalyzed case, where appreciable charge separation occurs and essentially only one bond is forming in the transition state, is there deviation from this average bond length. The catalyzed reaction might become a stepwise process involving a zwitterion intermediate in solution because of considerable charge separation in the transition structure.

6. Generalizations About Transition Structures in Pericyclic Reactions

The transition structures for pericyclic reactions of hydrocarbons described in this article show remarkable constancy of structure. Figure 57 summarizes the structural fragments found in these reactions. Partially formed or broken C···C single-bond lengths range from 1.95–2.28 Å. This is a value about 50% longer than a normal single bond. This range of 0.3 Å is slightly wider than the range of lengths of single bonds observed experimentally in stable molecules.[133] This is shown graphically in the Figure 58. In transition structures, the partial double bonds range from 1.34–1.42 Å, which is almost double the range observed in aromatic bonds. In the few examples which we have studied theoretically, bonds intermediate between double and triple range in length from 1.22–1.27 Å. The range of partial C···H bond lengths is 1.29–1.61 Å. This is a fairly large range, but more

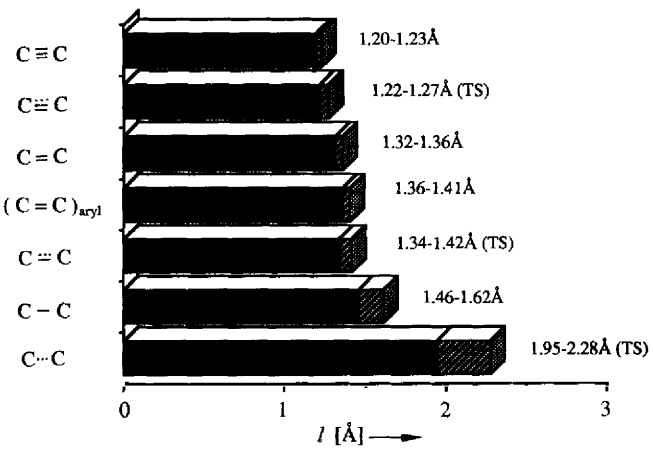

Fig. 58. Carbon–carbon bond-length ranges for normal molecules observed in X-ray structural analyses or calculated for transition structures (TS). Three dots indicate a partial σ bond.

predictable is the distance between the carbon atoms involved in the hydrogen transfer. These distances range from 2.5 to 2.6 Å in a variety of structures we have studied.

The bond angles also follow relatively simple generalizations. The attack on unsaturated linkages for the most part occurs in direction which is expected to lead to bonds in the products of addition—for example, around 109° on an alkene (to give a tetrahedral angle in the product) and in the vicinity of 120° on an alkyne. Since partial bonds are in-

volved, the degree of pyramidalization of sp^2 carbons or bending of sp carbons is intermediate between reactant and product geometries. In general, maximum bonding is maintained in all of these transition structures.

It is also notable that cyclic geometries, substituents, and the "earliness" or "lateness" of these transition structures do not have a large influence on transition-structure geometries. Consequently, we expect the transition structure of a wide variety of substituted molecules to conform to these generalizations.

6.2. Transition State Energies

Because pericyclic reactions include quite a range of reaction types, it might be supposed that the activation energies would vary very widely. While that is indeed the case, particularly for substituted molecules, there is nevertheless a large number of hydrocarbon pericyclic reactions which have experimental activation energies around 32–36 kcal mol^{-1}. A number of these, and a few heterocyclic reactions for comparison, are shown in Figure 59. There are, of course, other reactions that deviate from this generalization. The [2 + 2 + 2] cycloaddition of three ethenes, for which we predict an activation energy of 43 kcal mol^{-1}, and the methylene addition to ethene predicted to have no enthalpic barrier, are examples of large deviations. Substituents also have a large influence on reaction rates either by directly stabilizing or destabilizing the transition structure or by introducing strain into either the reactants or transition state. Nevertheless, many hydrocarbon pericyclic reactions do have activation energies around 32–36 kcal mol^{-1}. This is probably related to the fact that all of these reactions involve the breaking of π or σ bonds and simultaneous formation of partial bonds. The transition states of these reactions are found just at that point on the potential energy surface where the destabilization of the reactants arising from distortion away from the reactant geometries is overcome by stabilization arising from formation of new bonds.

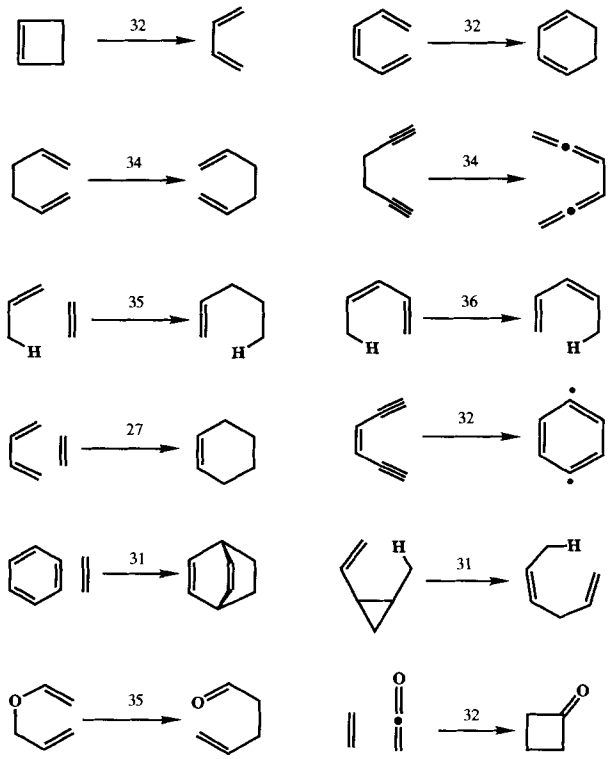

Fig. 59. Examples of pericyclic reactions with activation energies ranging from 31 to 36 kcal mol^{-1} as well as the Diels–Alder reaction prototype (between butadiene and ethene).

We dedicate this review to Professor Roald Hoffmann and to the memory of Robert Burns Woodward, whose brilliant insights created this field. We made the discoveries summarized here during the last decade in our laboratories at Pittsburgh and U.C.L.A. supported by a group of brilliant co-workers. In alphabetical order, they are David M. Birney, Kersey Black, Frank K. Brown, Pierluigi Caramella, Andrea E. Dorigo, Susan M. Ernst, Frank Jensen, E. Adam Kallel, Richard J. Loncharich, Jiri Mareda, Margaret McCarrick, Michael N. Paddon-Row, Nelson G. Rondan, David C. Spellmeyer, Joey W. Storer, Bert Thomas IV, Xuebao Wang, and Yun-dong Wu. Special mention should be made to Dr. Nelson Rondan (Dow Chemical) and Professor Michael Paddon-Row (University of New South Wales) who did the first calculations which inspired this review. We are very indebted to them for their essential contributions. Our thanks are due to the National Science Foundation and the National Institutes of Health for financial support of our research on pericyclic reactions. The calculations reported were made possible by the UCLA Office of Academic Computing and a joint study with the IBM Corporation, which supplied time on the IBM 3090/600J, and the National Science Foundation Supercomputer Centers at San Diego, Pittsburgh, Illinois, and Cornell. We also acknowledge the indispensable contributions of Professor John A. Pople and his group through their development of the GAUSSIAN programs.

Received: July 5, 1991 [A 861 IE]
German version: *Angew. Chem.* **1992**, *104*, 711

[1] R. B. Woodward, R. Hoffmann, *J. Am. Chem. Soc.* **1965**, *87*, 2046, 4389; R. Hoffmann, R. B. Wodward, *ibid.* **1965**, *87*, 395, 2511.
[2] R. B. Woodward, R. Hoffmann, *Angew. Chem.* **1969**, *81*, 797; *Angew. Chem. Int. Ed. Engl.* **1969**, *8*, 781; *The Conservation of Orbital Symmetry*, Verlag Chemie, Weinheim, **1970**.
[3] a) K. Fukui, *Tetrahedron Lett.* **1965**, 2009, 2427; *Acc. Chem. Res.* **1971**, *4*, 57; b) *Orbital Symmetry Papers* (Eds.: H. E. Simmons, J. F. Bunnett), American Chemical Society, Washington, DC, USA, **1976**.
[4] a) H. E. Zimmerman, *Acc. Chem. Res.* **1971**, *4*, 272; b) M. J. S. Dewar, *Angew. Chem.* **1971**, *83*, 859; *Angew. Chem. Int. Ed. Engl.* **1971**, *10*, 761.
[5] M. J. S. Dewar, *J. Am. Chem. Soc.* **1984**, *106*, 209.
[6] G. Desimoni, G. Tacconi, A. Barco, G. P. Pollini, *Natural Products Synthesis Through Pericyclic Reactions*, American Chemical Society, Washington, DC, USA, **1983**.
[7] a) R. B. Woodward, F. Sondheimer, D. Taub, K. Heusler, W. M. McLamore, *J. Am. Chem. Soc.* **1952**, *74*, 4223; b) R. E. Ireland, S. Thaisrivangs, C. S. Wilcox, *ibid.* **1980**, *102*, 1155; c) T. Kametani, M. Kajiwara, T. Takahashi, K. Fukumoto, *J. Chem. Soc. Perkin Trans.* **1975**, *1*, 737; T. Kametani, K. Ogasawara, T. Takahashi, *Tetrahedron* **1973**, *29*, 73.
[8] M. P. Rappold, E. Havinga, *Recl. Trav. Chim. Pays-Bas* **1960**, *79*, 369; E. Havinga, J. L. M. *Tetrahedron* **1961**, *16*, 146; for a recent study, see: J. D. Enas, G. Y. Shen, W. H. Okamura, *J. Am. Chem. Soc.* **1991**, *113*, 3873, and references cited therein.
[9] S. G. Sogo, T. S. Widlanski, J. H. Hoare, C. E. Grimshaw, G. A. Berchtold, J. R. Knowles, *J. Am. Chem. Soc.* **1984**, *106*, 2701; b) Y. Asano, J. J. Lee, T. L. Shieh, F. Spreafico, C. Kowal, H. G. Floss, *ibid.* **1985**, *107*, 4314.
[10] a) J. Golik, J. Clardy, G. Dubay, G. Groenewold, H. Kawaguchi, M. Konishi, B. Krishnan, H. Ohkuma, K. Saitoh, T. W. Doyle, *J. Am. Chem. Soc.* **1987**, *109*, 3461; J. Golik, G. Dubay, G. Groenewold, H. Kawaguchi, M. Konishi, B. Krishnan, H. Ohkuma, K. Saitoh, T.W.

Doyle, *ibid.* **1987**, *109*, 3462; b) M. D. Lee, T. S. Dunne, M. M. Siegel, C. C. Chang, G. O. Morton, D. B. Borders, *ibid.* **1987**, *109*, 3464; c) M. D. Lee, T. S. Dunne, C. C. Chang, G. A. Ellestad, M. M. Siegel, G. O. Morton, W. J. McGahren, D. B. Borders, *ibid.* **1987**, *109*, 3466; d) N. Zein, M. Poncin, R. Nilakantan, G. A. Ellestad, *Science* **1989**, *244*, 697; e) see also K. C. Nicolaou, W.-M. Dai, *Angew. Chem.* **1991**, *103*, 1453; *Angew. Chem. Int. Ed. Engl.* **1991**, *30*, 1387.

[11] a) K. C. Nicolaou, Y. Ogawa, G. Zuccarello, H. Kataoka, *J. Am. Chem. Soc.* **1988**, *110*, 7247; b) K. C. Nicolaou, G. Zuccarello, Y. Ogawa, E. J. Schweiger, T. Kumazawa, *ibid.* **1988**, *110*, 4866; c) J. P. Snyder, *ibid.* **1989**, *111*, 7630; **1990**, *112*, 5367; d) P. Magnus, S. Fortt, T. Pitterna, J. P. Snyder, *ibid.* **1990**, *112*, 4986; e) N. Koga, K. Morokuma, *ibid.* **1991**, *113*, 1907.

[12] W. von E. Doering, W. R. Roth, R. Breuckmann, L. Figge, H.-W. Lennartz, W.-D. Fessner, H. Prinzbach, *Chem. Ber.* **1988**, *121*, 1, and references cited therein.

[13] Femtosecond transition-state spectroscopy studies of chemical reactions may change this; see: a) M. O. Trulson, G. D. Dollinger, R. A. Mathies, *J. Am. Chem. Soc.* **1987**, *109*, 587; b) A. H. Zewail, *Science* **1988**, *242*, 1645; c) I. W. M. Smith, *Nature* **1987**, *328*, 760.

[14] K. Müller, *Angew. Chem.* **1980**, *92*, 1; *Angew. Chem. Int. Ed. Engl.* **1980**, *19*, 1.

[15] This definition has been put into common use by John A. Pople.

[16] a) W. J. Hehre, L. Radom, P. von R. Schleyer, J. A. Pople, *Ab Initio Molecular Orbital Theory*, Wiley, New York, **1986**; b) For a recent review on the concepts and terminology of ab initio quantum chemistry see J. Simons, *J. Phys. Chem.* **1991**, *95*, 1017.

[17] S. Glasstone, K. J. Laidler, H. M. Eyring, *The Theory of Rate Processes*, McGraw-Hill, New York, **1941**.

[18] a) J. I. Steinfeld, J. S. Francisco, W. L. Hase, *Chemical Kinetics and Dynamics*, Prentice Hall, New Jersey, **1989**; b) R. D. Levine, R. B. Bernstein, *Molecular Reaction Dynamics*, Oxford University Press, New York, **1987**; c) D. G. Truhlar, M. S. Gordon, *Science*, **1990**, *249*, 491.

[19] a) J. S. Binkley, R. A. Whiteside, K. Raghavachari, R. Seeger, D. J. DeFrees, H. B. Schlegel, M. J. Frisch, J. A. Pople, L. R. Kahn, *GAUSSIAN 82*, Carnegie-Mellon University, Pittsburgh, PA, USA, **1982**; b) M. J. Frisch, J. S. Binkley, H. B. Schlegel, K. Raghavachari, C. F. Melius, R. L. Martin, J. J. P. Stewart, F. W. Bobrowicz, C. M. Rohlfing, L. R. Kahn, D. J. DeFrees, R. Seeger, R. A. Whiteside, D. J. Fox, E. M. Fleuder, J. A. Pople, *GAUSSIAN 86*, Carnegie-Mellon Publishing Unit, Pittsburgh, **1984**; c) M. J. Frisch, M. Head-Gordon, H. B. Schlegel, K. Raghavachari, J. S. Binkley, C. Gonzalez, D. J. DeFrees, D. J. Fox, R. A. Whiteside, R. Seeger, C. F. Melius, J. Baker, R. L. Martin, L. R. Kahn, J. J. P. Stewart, E. M. Fluder, S. Topiol, J. A. Pople, *GAUSSIAN 88*, Gaussian Inc., Pittsburgh, PA, **1988**; d) The Carnegie-Mellon Quantum Chemistry Archive, Carnegie-Mellon University, Pittsburgh, PA 15213 (USA); e) M. J. Frisch, M. Head-Gordon, G. W. Trucks, J. B. Foresman, H. B. Schlegel, K. Raghavachari, M. A. Robb, J. S. Binkley, C. Gonzalez, D. J. DeFrees, D. J. Fox, R. A. Whiteside, R. Seeger, C. F. Melius, J. Baker, R. L. Martin, L. R. Kahn, J. J. P. Stewart, S. Topiol, J. A. Pople, *GAUSSIAN 90*, Gaussian Inc., Pittsburgh, PA, **1990**.

[20] M. Dupuis, D. Spangler, J. J. Wendoloski, *GAMESS*, National Resource for Computations in Chemistry, Software Catalog, University of California, Berkeley, CA, USA, **1980**, Program QG01; see also M. W. Schmidt, K. K. Baldridge, J. A. Boatz, J. H. Jensen, S. Koseki, M. S. Gordon, K. A. Nguyen, T. L. Windus, S. T. Elbert, *OCPE Bulletin*, **1990**, *10*, 52.

[21] a) F. Bernardi, M. A. Robb in *Ab Initio Methods in Quantum Chemistry I* (Ed.: K. P. Lawley), Wiley, New York, **1987**, p. 156–248; b) H. B. Schlegel in *New Theoretical Concepts for Understanding Organic Reactions* (Eds.: J. Bertran, I. G. Csizmadia), Kluwer Academic Publishers, Boston, **1989**, p. 33.

[22] a) C. C. J. Roothaan, *Rev. Mod. Phys.* **1951**, *23*, 69; b) G. G. Hall, *Proc. R. Soc. London A* **1951**, *205*, 541; c) UHF: J. A. Pople, R. K. Nesbet, *J. Chem. Phys.* **1954**, *22*, 571.

[23] C. Møller, M. S. Plesset, *Phys. R.* **1934**, *46*, 618.

[24] a) F. Bernardi, A. Bottoni, J. J.W. McDouall, M. A. Robb, H. B. Schlegel, *Faraday Symp. Chem. Soc.* **1984**, *19*, 137; b) A. C. Wahl, G. Das in *Methods of Electronic Structure Theory: Modern Theoretical Chemistry, Vol. 3, Part 2* (Ed.: H. F. Schaefer III, Plenum, New York, **1979**, p. 51; c) R. Shepard, *Adv. Chem. Phys.* **1987**, *69*, 63.

[25] a) B. O. Roos, *Int. J. Quantum Chem. Symp.* **1980**, *14*, 175; *Adv. Chem. Phys.* **1987**, *69*, 399; b) P. Pulay, T. P. Hamilton, *J. Chem. Phys.* **1988**, *88*, 4926.

[26] S. W. Benson, *Thermochemical Kinetics*, Wiley-Interscience, New York, **1976**.

[27] a) J. A. Pople, H. B. Schlegel, R. Krishnan, D. J. DeFrees, J. S. Binkley, M. J. Frisch, R. A. Whiteside, R. A. Hout, W. J. Hehre, *Int. J. Quantum Chem. Symp.* **1981**, *15*, 269; b) A. B. Hess, Jr., L. J. Schaad, P. L. Polavara, *J. Am. Chem. Soc.* **1984**, *106*, 4348.

[28] a) J. Bigeleisen, M. Goeppert-Mayer, *J. Chem. Phys.* **1947**, *15*, 261; b) J. Bigeleisen, M. Wolfsberg, *Adv. Chem. Phys.* **1958**, *1*, 15; c) C. J. Collins, N. S. Bowman, *Isotope Effects in Chemical Reactions*, Van Nostrand Reinhold, New York, **1970**.

[29] a) J. E. Baldwin, V. P. Reddy, B. A. Hess, Jr., L. J. Schaad, *J. Am. Chem. Soc.* **1988**, *110*, 8554; b) J. E. Baldwin, V. P. Reddy, L. J. Schaad, B. A. Hess, Jr., *ibid.* **1988**, *110*, 8555; c) L. Chantranupong, T. A. Wildman, *ibid.* **1990**, *112*, 4151.

[30] *Isotopes in Organic Chemistry* (Eds.: E. Buncel, E. E. Lee), Elsevier, Amsterdam, **1987**.

[31] a) J. P. Foster, F. Weinhold, *J. Am. Chem. Soc.* **1980**, *102*, 7211; A. E. Reed, L. A. Curtiss, F. Weinhold, *Chem. Rev.* **1988**, *88*, 899; b) I. Mayer, *Chem. Phys. Lett.* **1983**, *97*, 270; *Int. J. Quantum Chem.* **1986**, *29*, 477.

[32] L. Pauling, *J. Am. Chem. Soc.* **1947**, *69*, 524.

[33] a) S. J. Formosinho, *Tetrahedron* **1986**, *42*, 4557; b) L. Valko, P. Simon, *Chem. Phys.* **1985**, *99*, 447.

[34] R. A. Marcus, *J. Phys. Chem.* **1968**, *72*, 891.

[35] J. R. Murdoch, *J. Am. Chem. Soc.* **1983**, *105*, 2159; 2660, 2667.

[36] H. E. O'Neal, S. W. Benson in *Free Radicals, Vol. 2* (Ed.: J. K. Kochi), Wiley, New York, **1973**, p. 275–359.

[37] a) W. R. Roth, J. König, *Ann. Chem.* **1966**, *699*, 24; b) W. R. Roth, *Chimia* **1966**, *229*, 20.

[38] a) G. J. M. Dormans, H. M. Buck, *J. Mol. Struct. (THEOCHEM)* **1986**, *136*, 121; b) *J. Am. Chem. Soc.* **1986**, *108*, 3253; c) B. A. Hess, Jr., L. J. Schaad, J. Pancir, *ibid.* **1985**, *107*, 149; d) B. A. Hess, Jr., L. J. Schaad, *ibid.* **1983**, *105*, 7185.

[39] a) F. Jensen, K. N. Houk, *J. Am. Chem. Soc.* **1987**, *109*, 3139; b) S. D. Kahn, W. J. Hehre, N. G. Rondan, K. N. Houk, *ibid.* **1985**, *107*, 8291; c) N. G. Rondan, K. N. Houk, *Tetrahedon Lett.* **1984**, *25*, 2519; d) M. J. S. Dewar, E. F. Healy, J. M. Ruiz, *J. Am. Chem. Soc.* **1988**, *110*, 2666.

[40] M. J. S. Dewar, K. M. Merz, J. J. P. Stewart, *J. Chem. Soc. Chem. Commun.* **1985**, 166.

[41] Location of a typical MP2/6-31G* transition structure of six heavy atoms requires 3 CPU hours of Cray Y-MP using the GAUSSIAN 90. The full details of these transition structures, in the form of GAUSSIAN archive entrees, are available from the authors upon request.

[42] a) M. J. S. Dewar, E. G. Zoebisch, E. F. Healy, J. J. P. Stewart, *J. Am. Chem. Soc.* **1985**, *107*, 3902; M. J. S. Dewar, S. Kirchner, *ibid.* **1971**, *93*, 4290, 4291; 4292; b) J. Breulet, H. F. Schaefer III, *ibid.* **1984**, *106*, 1221; c) F. Bernardi, S. De, M. Olivucci, M. A. Robb, *ibid.* **1990**, *112*, 1737, and references cited therein.

[43] a) K. Hsu, R. J. Buenker, S. D. Peyerimhoff, *J. Am. Chem. Soc.* **1971**, *93*, 2117; *ibid.* **1972**, *94*, 5639; R. J. Buenker, S. D. Peyerimhoff, K. Hsu, *ibid.* **1971**, *93*, 5005; b) W. Thiel, *ibid.* **1981**, *103*, 1420; c) J. W. McIver, Jr., A. Komornicki, *ibid.* **1972**, *94*, 2625; d) G. Frenking, N. Heinrich, *Theor. Chim. Acta* **1984**, 65; e) A. Jensen, H. Kunz, *ibid.* **1984**, *65*, 33; f) T. A. Halgren, W. N. Lipscomb, *Chem. Phys. Lett.* **1977**, *49*, 225.

[44] a) D. C. Spellmeyer, K. N. Houk, *J. Am. Chem. Soc.* **1988**, *110*, 3412; b) N. G. Rondan, K. N. Houk, *ibid.* **1985**, *107*, 2099; *ibid.* **1984**, *106*, 7989; c) W. Kirmse, N. G. Rondan, K. N. Houk, *ibid.* **1984**, *106*, 1871; d) E. A. Kallel, Y. Wang, K. N. Houk, *J. Org. Chem.* **1989**, *54*, 6006; e) E. A. Kallel, K. N. Houk, P. Hörstermann, W. R. Roth, unpublished.

[45] a) M. Kraus, M. Vavruska, V. Bazant, *Coll. Czech. Chem. Commun.* **1957**, *22*, 484; b) L. Kuchler, *Trans. Faraday Soc.* **1939**, *35*, 874; c) C. K. Lewis, J. Bergmann, R. Manjoney, R. Paddock, b. L. Kalra, *J. Phys. Chem.* **1984**, *88*, 4112; d) D. Rowley, H. Steiner, *Discuss. Faraday Soc.* **1951**, *10*, 198; e) S. R. Smith, A. S. Gordon, *J. Phys. Chem.* **1961**, *65*, 1124; f) D. C. Tardy, R. Ireton, A. S. Gordon, *J. Am. Chem. Soc.* **1979**, *101*, 1508; g) W. J. Tsang, *Chem. Phys.* **1965**, *42*, 1805; W. Tsang, *Int. J. Chem. Kinet.* **1970**, *2*, 311; h) M. Uchiyama, T. Tomioka, A. Amano, *J. Phys. Chem.* **1964**, *68*, 1878.

[46] a) M. J. S. Dewar, S. Olivella, J. J. P. Stewart, *J. Am. Chem. Soc.* **1986**, *108*, 5771; M. J. S. Dewar, S. Olivella, H. S. Rzepa, *ibid.* **1978**, *100*, 5650, and references cited therein.; b) J. W. McIver, Jr., *Acc. Chem. Res.* **1974**, *7*, 72; c) M. V. Basilevsky, A. G. Shamov, V. A. Tikhomirov, *J. Am. Chem. Soc.* **1977**, *99*, 1369; M. V. Basilevsky, V. A. Tikhomirov, I. E. Chenlov, *Theor. Chim. Acta* **1971**, *23*, 75; d) O. Kikuchi, *Tetrehedron*, **1971**, *27*, 2791; e) J. Pancir, *J. Am. Chem. Soc.* **1982**, *104*, 7424.

[47] a) K. N. Houk, Y.-T. Lin, F. K. Brown, *J. Am. Chem. Soc.* **1986**, *108*, 554; F. K. Brown, K. N. Houk, *Tetrahedron Lett.* **1984**, *25*, 4609; b) R. D. Bach, J. J. W. McDouall, H. B. Schlegel, *J. Org. Chem.* **1989**, *54*, 2931.

[48] a) R. E. Townshend, G. Ramunni, G. Segal, W. J. Hehre, L. Salem, *J. Am. Chem. Soc.* **1976**, *98*, 2190 b) L. A. Burke, *Theor. Chim. Acta* **1985**, *68*, 101; L. A. Burke, G. Leroy, *ibid.* **1977**, *44*, 219; L. A. Burke, G. Leroy, M. Sana, *ibid.* **1975**, *40*, 313; c) M. Ortega, A. Oliva, J. M. Lluch, J. Bertran, *Chem. Phys. Lett.* **1983**, *102*, 317.

[49] F. Bernardi, A. Bottoni, M. J. Field, M. F. Guest, I. H. Hillier, M. A. Robb, A. Venturini, *J. Am. Chem. Soc.* **1988**, *110*, 3050; F. Bernardi, A. Bottoni, M. A. Robb, M. J. Field, *J. Chem. Soc. Chem. Commun.* **1985**, 1051.

[50] J. A. Pople, M. Head-Gordon, D. J. Fox, K. Raghavachari, L. A. Curtiss, *J. Chem. Phys.* **1989**, *90*, 5622.

[51] a) W. Cooper, W. D. Walters, *J. Am. Chem. Soc.* **1958**, *80*, 4220; b) R. W. Carr, Jr., W. D. Walters, *J. Phys. Chem.* **1965**, *69*, 1073.

[52] K. N. Houk in *Pericyclic Reactions, Vol. 2* (Eds.: A. P. Marchand, R. E. Lehr), Academic Press, New York **1977**.

[53] M. T. Reetz, *Tetrahedron* **1973**, *29*, 2189.

[54] G. S. Hammond, *J. Am. Chem. Soc.* **1955**, *77*, 334.

[55] a) R. P. Bell, *Proc. R. Soc. London A* **1936**, *154*, 414; b) M. G. Evans, M. Polanyi, *Trans. Faraday Soc.* **1938**, *34*, 11.

[56] a) W. A. Lathan, W. J. Hehre, J. A. Pople, *J. Am. Chem. Soc.* **1971**, *93*, 808; b) P. C. Hariharan, W. A. Lathan, J. A. Pople, *Chem. Phys. Lett.* **1972**, *14*, 385; c) B. Zurawski, R. Ahlrichs, W. Kutzelnigg, *ibid.* **1973**, *21*, 309; d) J. Weber, A. D. McLean, *J. Am. Chem. Soc.* **1976**, *98*, 875; e) J. Weber, M. Yoshimine, A. D. McLean, *J. Chem. Phys.* **1976**, *64*, 4159; f) H. Lischka, H.-J. Köhler, *J. Am. Chem. Soc.* **1978**, *100*, 5297; g) K. Raghavachari, R. A. Whiteside, J. A. Pople, P. von R. Schleyer, *ibid.* **1981**, *103*, 5649; h) E. D. Jemmis, K. S. Sarma, P. N. V. Pavankumar, *THEOCHEM* **1985**, *22*, 305.

[57] a) J. A. Pople, *Pure Appl. Chem.* **1983**, *55*, 343; b) J. A. Pople, R. Krishnan, M. J. Frisch, J. S. Binkley, P. von R. Schleyer, *J. Am. Chem. Soc.* **1983**, *105*, 6389; c) R. Krishnan, M. J. Frisch, J. A. Pople, *Chem. Phys. Lett.* **1982**, *85*, 145; d) C. E. Dykstra, H. F. Schaefer III, *J. Am. Chem. Soc.* **1978**, *100*, 1378; e) J. D. Evanseck, K. N. Houk, *J. Phys. Chem.* **1990**, *94*, 5518.

[58] a) L. B. Harding, *J. Am. Chem. Soc.* **1981**, *103*, 7469; b) Y. Osamura, T. Takeughi, K. Nishimoto, *Bull. Chem. Soc. Jpn.* **1988**, *61*, 3387; c) T. P. Hamilton, H. F. Schaefer III, *J. Phys. Chem.* **1989**, *93*, 7560.

[59] W.-K. Li, R. H. Nobes, L. Radom, *THEOCHEM* **1986**, *29*, 121.

[60] W. R. Rodwell, W. J. Bouma, L. Random, *Int. J. Quantum Chem.* **1980**, *18*, 107.

[61] a) R. A. Poirier, D. Majlessi, T. J. Zielinski, *J. Comput. Chem.* **1986**, *7*, 464; b) S. Schröder, W. Thiel, *J. Am. Chem. Soc.* **1986**, *108*, 7985.

[62] F. Bernardi, M. A. Robb, H. B. Schlegel, G. Tonachini, *J. Am. Chem. Soc.* **1984**, *106*, 1198.

[63] a) T. Clark, *J. Am. Chem. Soc.* **1987**, *109*, 6838; *ibid.* **1989**, *111*, 761; b) P. Du, D. A. Hrovat, W. T. Borden, *ibid.* **1988**, *110*, 3405; c) M. T. Nguyen, L. Landuyt, L. G. Vanquickenborne, *Chem. Phys. Lett.* **1991**, *182*, 225.

[64] J. W. Storer, K. N. Houk, unpublished results.

[65] D. F. McMillen, D. M. Golden, *Annu. Rev. Phys. Chem.* **1982**, *33*, 483.

[66] a) J. A. Berson, L. Salem, *J. Am. Chem. Soc.* **1972**, *94*, 8917; b) J. A. Berson, *Acc. Chem. Res.* **1982**, *5*, 406.

[67] For a review of "walk" rearrangement see: a) F.-G. T. Klärner, *Top. Stereochem.* **1984**, *15*, 1; b) R. F. Childs, *Tetrahedron*, **1982**, *38*, 567.

[68] a) J. J. Quirante, F. Enriquez, J. M. Hernando, *J. Mol. Struct. (THEOCHEM)* **1990**, *204*, 193; b) J. J. Gajewski, M. P. Squicciarini, *J. Am. Chem. Soc.* **1989**, *111*, 6717; c) M. R. Willcott III, V. H. Cargle, *ibid.* **1967**, *89*, 723; *ibid.* **1969**, *91*, 4310.

[69] a) F. Jensen, *J. Am. Chem. Soc.* **1989**, *111*, 4643; b) P. N. Skancke, K. Yamashita, K. Morokuma, *ibid.* **1987**, *109*, 4157.

[70] S. M. Ernst, K. Black, K. N. Houk, unpublished results.

[71] Y. Li, K. N. Houk, unpublished results.

[72] T. S. Sorensen, A. Rauk in *Pericyclic Reactions, Vol. 2* (Eds.: A. P. Marchand, R. E. Lehr), Academic Press, New York, **1977**.

[73] F. K. Jensen, K. N. Houk, unpublished results.

[74] For a review of thermal [1, j]-sigmatropic rearrangement: C. W. Spangler, *Chem. Rev.* **1976**, *76*, 187, and references cited therein.

[75] W. T. Borden, J. G. Lee, S. D. Young, *J. Am. Chem. Soc.* **1980**, *102*, 4841.

[76] J. L. M. A. Schlatmann, J. Pot, E. Havinga, *Recl. Trav. Chim. Pays-Bas* **1964**, *83*, 1173.

[77] a) E. Wünsch, J. M. Lluch, A. Oliva, J. Bertran, *J. Chem. Soc. Perkin Trans. 2* **1987**, 211; b) T. A. Wildman, *Chem. Phys. Lett.* **1986**, *126*, 325; c) G. Leroy, M. Sana, A. Tinant, *Can. J. Chem.* **1985**, *63*, 1447; d) M. T. Rayez-Meaume, J. J. Dannenberg, J. L. Whitten, *J. Am. Chem. Soc.* **1978**, *100*, 747.

[78] M. J. S. Dewar, E. F. Healy, *Chem. Phys. Lett.* **1982**, *141*, 521.

[79] K. Morokuma, W. T. Borden, D. A. Hrovat, *J. Am. Chem. Soc.* **1988**, *110*, 4474.

[80] M. Bearpark, F. Bernardi, M. Olivucci, M. A. Robb, *J. Am. Chem. Soc.* **1990**, *112*, 1732.

[81] a) M. J. S. Dewar, C. Jie, *J. Am. Chem. Soc.* **1987**, *109*, 5983; b) E. A. Halevi, R. Rom, *Isr. J. Chem.* **1989**, *29*, 311.

[82] Y. Osamura, S. Kato, K. Morokuma, D. Feller, E. R. Davidson, W. T. Borden, *J. Am. Chem. Soc.* **1984**, *106*, 3362.

[83] W. von E. Doering, V. G. Toscano, G. H. Beasley, *Tetrahedron* **1971**, *27*, 5299.

[84] a) W. T. Borden, R. J. Loncharich, K. N. Houk, *Annu. Rev. Phys. Chem.* **1988**, *39*, 213; b) see W. R. Roth, H.-W. Lennartz, W. von E. Doering, L. Birladeanu, C. A. Guyton, T. Kitagawa, *J. Am. Chem. Soc.* **1990**, *112*, 1722; c) Note added in proof: The best available calculations predict concerted and diradical mechanisms of similar energy: M. Dupis, C. Murray, E. R. Davidson, *J. Am. Chem. Soc.* **1991**, *113*, 9756.

[85] a) W. D. Huntsman, H. J. Wristers, *J. Am. Chem. Soc.* **1967**, *89*, 342; b) K. A. Owens, J. A. Berson, ibid. **1990**, *112*, 5973.

[86] K. Black, K. N. Houk, unpublished results.

[87] K. A. Owens, J. A. Berson, *J. Am. Chem. Soc.* **1990**, *112*, 5973.

[88] D. F. Feller, M. W. Schmidt, K. Ruedenberg, *J. Am. Chem. Soc.* **1982**, *104*, 960.

[89] D. K. Agrafiotis, H. S. Rzepa, *J. Chem. Soc. Chem. Commun.* **1987**, 902.

[90] Intramolecular hydrogen transfers are well known, for examples; see: L. A. Paquette, M. A. Kesselmayer, R. D. Rogers, *J. Am. Chem. Soc.* **1990**, *112*, 284, and references cited therein.

[91] H. Geich, W. Grimme, K. Proske, *J. Am. Chem. Soc.* **1992**, *114*, 1492.

[92] J. E. Baldwin in *Pericyclic Reactions., Vol. 2* (Eds.: A. P. Marchand, R.E. Lehr), Academic Press, New York, **1977**, p. 173.

[93] P. von R. Schleyer, M. Bremer, *J. Org. Chem.* **1988**, *53*, 2362.

[94] P. von R. Schleyer, T. M. Su, M. Saunders, J. C. Rosenfeld, *J. Am. Chem. Soc.* **1969**, *91*, 5174.

[95] S. Olivella, A. Sole, J. M. Bofill, *J. Am. Chem. Soc.* **1990**, *122*, 2160, and references cited therein.

[96] E. A. Kallel, K. N. Houk, unpublished results.

[97] C. W. Jefford, G. Bernardinelli, Y. Wang, D. C. Spellmeyer, A. Buda, K. N. Houk, *J. Am. Chem. Soc.* **1992**, *114*, 1157.

[98] J. D. Evanseck, K. N. Houk, unpublished results.

[99] J. E. Baldwin, V. P. Reddy, L. J. Schaad, B. A. Hess, Jr., *J. Am. Chem. Soc.* **1988**, *110*, 8554, 8555.

[100] a) K. E. Lewis, H. Steiner, *J. Chem. Soc.* **1964**, 3080; b) V. A. Pichko, B. Y. Simkin, V. I. Minkin, *Dokl. Phys. Chem. (Engl. Transl.)* **1987**, *292*, 910.

[101] R. R. Jones, R. G. Bergman, *J. Am. Chem. Soc.* **1972**, *94*, 660.

[102] R. Huisgen, A. Dahmen, H. Huber, *J. Am. Chem. Soc.* **1967**, *89*, 7130.

[103] R. Loncharich, K. N. Houk, *J. Am. Chem. Soc.* **1988**, *110*, 2089.

[104] R. Loncharich, K. N. Houk, *J. Am. Chem. Soc.* **1987**, *109*, 6947.

[105] For reviews see a) B. B. Snider, *Acc. Chem. Res.* **1980**, *13*, 426; b) E. C. Keung, H. Alper, *J. Chem. Educ.* **1972**, *49*, 97; c) H. M. R. Hoffmann, *Angew. Chem.* **1969**, *81*, 597; *Angew. Chem. Int. Ed. Engl.* **1969**, *8*, 556.

[106] A. E. Dorigo, K. N. Houk, unpublished results.

[107] E. F. Cromwell, D.-J. Liu, M. J. J. Vrakking, A. H. Kung, Y. T. Lee, *J. Chem. Phys.* **1990**, *92*, 3230.

[108] S. W. Benson, R. Shaw, *Trans. Faraday Soc.* **1967**, *63*, 985.

[109] a) N. G. Rondan, K. N. Houk, R. A. Moss, *J. Am. Chem. Soc.* **1980**, *102*, 1770; b) Y. Apeloig, M. Karni, P. J. Stang, D. P. Fox, *ibid.* **1983**, *105*, 4781; c) G. L. Closs, *Top. Stereochem.* **1968**, *3*, 193.

[110] a) N. P. Neureiter, *J. Am. Chem. Soc.* **1966**, *88*, 558; b) F. G. Bordwell, J. M. Williams, Jr., E. B. Hoyt, Jr., B. B. Jarvis, *ibid.* **1968**, *90*, 429.

[111] a) D. M. Lemal, S. D. McGregor, *J. Am. Chem. Soc.* **1966**, *88*, 1335; b) W. L. Mock, *ibid.* **1975**, *97*, 3666.

[112] a) B. I. Sonobe, T. R. Fletcher, R. N. Rosenfeld, *J. Am. Chem. Soc.* **1984**, *106*, 4352, 5800; b) D. I. Schuster, L. Wong, J. M. Van der Veen, *ibid.* **1985**, *107*, 7045; c) T. R. Darling, J. Pouliquen, N. J. Turro, *ibid.* **1974**, *96*, 1247.

[113] a) P. S. Skell, Y. Garner, *J. Am. Chem. Soc.* **1956**, *78*, 5430; b) W. von E. Doering, W. A. Henderson, Jr., *ibid.* **1958**, *80*, 5274; c) P. S. Skell, M. S. Cholod, *ibid.* **1969**, *91*, 7131.

[114] R. Hoffmann, *J. Am. Chem. Soc.* **1968**, *90*, 1475.

[115] B. Zurawski, W. Kutzelnigg, *J. Am. Chem. Soc.* **1978**, *100*, 2654.

[116] See [109a].

[117] J. D. Evanseck, J. Mareda, K. N. Houk, *J. Am. Chem. Soc.* **1990** *112*, 73.

[118] R. Huisgen, *Angew. Chem. Angew. Chem.* **1963**, *75*, 604, 742; *Angew. Chem. Int. Ed. Engl.* **1963**, *2*, 565, 633.

[119] a) F. Bernardi, M. Olivucci, J. J. W. McDouall, M. A. Robb, *J. Am. Chem. Soc.* **1987**, *109*, 544; b) F. Bernardi, A. Bottoni, M. A. Robb, H. B. Schlegel, G. Tonachini, *ibid.* **1985**, *107*, 2260; c) J. Doubleday, Jr., M. Page, J. W. McIver, Jr., *J. Mol. Struct. (THEOCHEM)* **1988**, *163*, 331.

[120] B. A. Hess, L. J. Schaad, D. N. Reinhoudt, *Int. J. Quantum Chem.* **1986**, *29*, 345.

[121] D. J. Pasto, *J. Am. Chem. Soc.* **1979**, *101*, 39.

[122] a) F. Bernardi, A. Bottoni, M. Olivucci, M. A. Robb, H. B. Schlegel, G. Tonachini, *J. Am. Chem. Soc.* **1988**, *110*, 5993; b) F. Bernari, A. Bottoni, M. A. Robb, A. Venturini, *ibid.* **1990**, *112*, 2106; b) X. Wang, K. N. Houk, *ibid.* **1990**, *112*, 1754.

[123] M. J. S. Dewar, A. B. Pierini, *J. Am. Chem. Soc.* **1984**, *106*, 203.

[124] F. K. Brown, K. N. Houk, *J. Am. Chem. Soc.* **1985**, *107*, 1971.

[125] M. McCarrick, K. N. Houk, unpublished results.

[126] K. N. Houk, R. J. Loncharich, J. F. Blake, W. L. Jorgensen, *J. Am. Chem. Soc*, **1989**, *111*, 9172.

[127] a) G. Huybrechts, W. Leemans, B. Male, *Int. J. Chem. Kinet.* **1982**, *14*, 997; b) H.-D. Martin, T. Urbanek, R. Braun, R. Walsh, *ibid.* **1984**, *16*, 117.

[128] a) R. C. Cookson, B. V. Drake, J. Hudec, A. Morrison, *Chem. Commun.* **1966**, 15; b) S. Ito, *Bull. Chem. Soc. Jpn.* **1966**, *39*, 1351; c) K. N. Houk, R. B. Woodward, *J. Am. Chem. Soc.* **1970**, *92*, 4143, 4145; d) L. A. Paquette, S. J. Hathaway, P. F. T. Schirch, *J. Org. Chem.* **1985**, *50*, 4199, and references cited therein. e) H. H. Rigby, T. L. Moore, S. Rege, *ibid.* **1986**, *51*, 2398; f) A. L. Hohnson, H. E. Simons, *J. Am. Chem. Soc.* **1966**, *88*, 2591; g) S. Ito, Y. Fujise, M. C. Woods, *Tetrahedron Lett.* **1967**, 1059.

[129] a) A) K. N. Houk, R. W. Gandour, R. W. Strozier, N. G. Rondan, L. A. Paquette, *J. Am. Chem. Soc.* **1979**, *101*, 6797; b) R. D. Bach, G. J. Wolber, H. B. Schlegel, *ibid.* **1985**, *107*, 2837.

[130] K. N. Houk in *Strain and Its Implications in Organic Chemistry* (Eds.: A. de Meijere, S. Blechert), Kluwer, Dordrecht, **1989**.

[131] a) D. M. Birney, K. N. Houk, *J. Am. Chem. Soc.* **1990**, *112*, 4127; b) R. J. Loncharich, F. K. Brown, K. N. Houk, *J. Org. Chem.* **1989**, *54*, 1129.

[132] J. W. Storer, L. Raimondi, K. N. Houk, unpublished.

[133] a) O. Ermer, P. Bell, J. Schäfer, G. Szeimies, *Angew. Chem.* **1989**, *101*, 503; *Angew. Chem. Int. Ed. Engl.* **1989**, *28*, 473; b) P. E. Eaton, R. Gilardi, M. Maggini, *J. Am. Chem. Soc.* **1988**, *110*, 7232; c) G. M. Anstead, R. Srinivasan, C. S. Peterson, S. R. Wilson, J. A. Katzenellenbogen, *ibid.* **1991**, *113*, 1378; d) K.-D. Plitzko, B. Rapko, B. Gollas, G. Wehrle, T. Weakley, D. T. Pierce, W. E. Geiger, Jr., R. C. Haddon, V. Boekelheide, *ibid.* **1990**, *112*, 6545.

Synthetic Bilayer Membranes: Molecular Design, Self-Organization, and Application

By Toyoki Kunitake*

Lipid bilayers are a most central building block of the biological molecular organization. Their two-dimensional self-assembly is essential to the generation of biological shapes and sizes on the molecular level. The observation that a totally synthetic amphiphile in water is spontaneously assembled to a bilayer structure suggested that bilayer formation is a general physicochemical phenomenon that is not restricted to particular structures of biolipid molecules. Bilayer formation is now observed for a large variety of synthetic amphiphiles which contain one, two, three, or four alkyl tails. The flexible alkyl tail may be replaced by perfluoroalkyl chains. The supramolecular structures obtained therefrom can be related to the component's molecular structure in many cases. The structural variety and the ease of molecular design make the synthetic bilayer an attractive vehicle for organizing covalently bound functional units and guest molecules. In addition, stable monolayers on water, planar lipid membranes (BLM), and free-standing cast films are obtainable because of the self-assembling property of bilayer-forming compounds. These molecular organizations display common supramolecular features. The use of the cast film as a molecular template provides exciting potential for the production of novel two-dimensional materials.

1. Introduction

Biomembranes provide one of the most important structural units in the organization of the biological cell. In 1964 Bangham and Horne[1] demonstrated that the bilayer structure forms spontaneously from aqueous lipid dispersions, thus establishing that among the constituents of biomembranes, the lipid bilayer plays a most central role in maintaining biological molecular organization. Their discovery led to extensive research on biomembrane mimics and liposomes.

Attempts to prepare a bilayer assembly from amphiphilic compounds different from the natural lipid were conducted concurrently. For example, Gebicki and Hicks observed formation of globular aggregates ("Ufasome") when they dispersed thin films made of oleic acid and linoleic acid in water.[2] Hargreaves and Deamer[3] obtained vesicles by codispersion of fatty acids and higher alcohols. Vesicular aggregates have also been described for 1:1 mixtures of saturated fatty acids (C_{12} to C_{18}) and lysolecithin. However, these aggregates were not sufficiently stable and provided no definite evidence for the isolated bilayer structure.[**]

Many investigators have discussed reasons why some of the polar lipid molecules can form two-dimensionally aligned assemblies. For example, Brockerhoff interpreted the structural features of membrane lipids in terms of a tripartite structure: hydrophobic aliphatic double chain, hydrophilic head group, and the (hydrogen belt) region linking these two moieties.[4] Tanford proposed that bilayer formation can be accounted for by purely geometrical consideration of the volume of the hydrophobic core and the surface area occupied by the head group in membrane lipids.[5] Israelachvili, Mitchell, and Ninham[6] emphasized the role of molecular geometry in determining the structures of lipidic or amphiphilic assemblies and asserted that the packing constraint of a component molecule decided the surface curvature, that is, the morphology of resulting molecular aggregates.

These theories certainly explain the formation of bilayer membranes from biological lipids; however, they do not provide guiding rules that enable us to design novel bilayer-forming compounds.

When we set out to develop new bilayer-forming compounds in 1976, we assumed that the unique structure of the polar head group of biolipid molecules was determined by the biosynthetic and physiological requirements rather than by the physical chemistry of membrane formation. Our first candidates were, therefore, simple double-chain ammonium salts. Didodecyldimethylammonium bromide (**1**, $n = 12$)

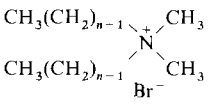

1

gives a clear aqueous dispersion by sonication. When this dispersion was negatively stained by uranyl acetate and observed by electron microscopy, the formation of single- and multiwalled vesicles with a layer thickness of 30–50 Å was recognized (Fig. 1). Their aggregation characteristics such as critical aggregate concentration and molecular weight were consistent with a bilayer vesicle. This result was the first example of a totally synthetic bilayer membrane.[7]

The exceptional behavior of double-chain ammonium salts as aqueous dispersions has been noted many years ago. Ralston, Eggenberger, and DuBrow studied the aggregation behavior of these salts by conductometry and found an unusual dependence of the equivalent conductivities at low concentrations.[8] Kunieda and Shinoda prepared the phase

[*] Prof. Dr. T. Kunitake
Department of Chemical Science and Technology, Faculty of Engineering
Kyushu University, Fukuoka 812 (Japan)

[**] Spontaneous vesicle formation in aqueous mixtures of cationic and anionic single-chain surfactants was described recently: E. W. Kaler, A. K. Murthy, B. E. Rodringuez, J. A. N. Zasadzinski, *Science* **1989**, *245*, 1371.

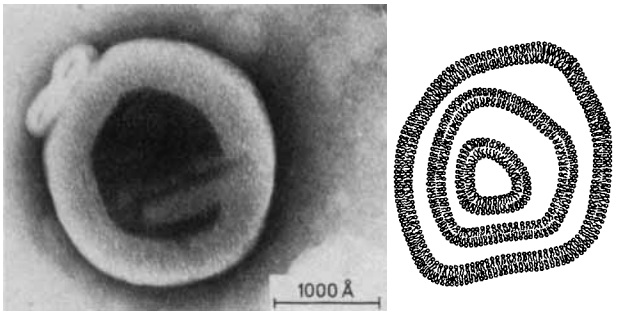

Fig. 1. Electron micrograph (left, negatively stained with UO_2^{2+}) and schematic illustration (right) of the multiwalled vesicle of **1** ($n = 12$).

diagram of these ammonium salts and indicated the transitions between molecular dispersion, liquid crystalline dispersion, and liquid crystal.[9] These dispersions were, however, never referred to as bilayer membranes.

It is important to make a distinction between liquid crystalline dispersions and bilayer membranes. As pointed out by Gray and Winsor,[10] it is the intermicellar forces—that is, the lattice forces—rather than forces from jointing or close packing which determine the viscosities and stabilities of the mesophases. In contrast, a bilayer membrane should be able to exist as an isolated entity without relying on the lattice forces for maintaining its structural integrity. The presence of lamellar multibilayer structures does not warrant the formation of bilayer membranes. We need to show the existence of isolated bilayer structures. The formation of bilayer membranes requires a self-assembling property greater than that of liquid crystalline dispersions.

In the following, we review the molecular design of bilayer-forming molecules, their aggregate morphologies, and some applications. Instead of attempting to prepare an exhaustive catalogue of those compounds, we present the design principle of component amphiphiles and the molecular organization they produce. The molecular design will be discussed in terms of the module concept given in Figure 2. This concept can cover most, if not all, of the types of bilayer-forming compounds. The functional aspects will be discussed only briefly in the last section.

Excellent reviews on various aspects of synthetic bilayer membranes have been published: Fendler prepared an extensive list of amphiphiles that are capable of bilayer formation (up to 1982);[11] routes to functional vesicle membranes have been discussed by Fuhrhop and Mathieu;[12] an extensive review on polymeric bilayer membranes was published by Ringsdorf, Schlarb, and Venzmer[13] in this journal. The last topic is, therefore, not discussed here.

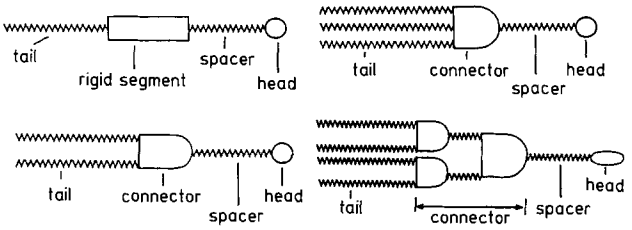

Fig. 2. Structual elements (modules) of bilayer-forming amphiphiles.

2. Bilayer Membranes of Double-Chain Amphiphiles

2.1. Molecular Design and Aggregation Behavior

Many double-chain amphiphiles have been synthesized as analogues of natural lecithin molecules, and their bilayer formation examined. The required molecular modules are tail, connector, spacer, and head groups.

Subsequent to our initial finding,[7] we conducted a systematic survey on the aggregation behavior of dialkylammonium salts with different tail lengths (Table 1).[14] All the

Table 1. Aggregation behavior of dialkyldimethylammonium bromides $R^1R^2Me_2N^+Br^-$ (**1**) [a].

R^1	R^2	Solution [b]	Electron Micrograph	M [c]	T_c [d] [°C]
$C_{22}H_{45}$	$C_{22}H_{45}$	colloidal	lamella		70
$C_{18}H_{37}$	$C_{18}H_{37}$	colloidal	lamella	10^7	45
$C_{16}H_{33}$	$C_{16}H_{33}$	colloidal	lamella & vesicle	–	
$C_{14}H_{29}$	$C_{14}H_{29}$	colloidal	vesicle & lamella	5×10^6	16
$C_{12}H_{25}$	$C_{12}H_{25}$	clear	vesicle	$7 \times 10^5 - 1 \times 10^6$	n.d. [e]
$C_{18}H_{37}$	$C_{16}H_{33}$	colloidal	lamella	2×10^8	31
$C_{18}H_{37}$	$C_{14}H_{29}$	colloidal	vesicle & lamella		
$C_{18}H_{37}$	$C_{12}H_{25}$	clear	vesicle	8×10^6	n.d. [e]
$C_{18}H_{37}$	$C_{10}H_{21}$	clear	vesicle	3×10^6	
$C_{18}H_{37}$	C_8H_{17}	clear	unstructured		
$C_{16}H_{33}$	CH_3	clear	unstructured		

[a] The data are mostly taken from [14] and appended by later experiments. [b] Appearance of the 10 mM solution after sonication. [c] Molecular weight by light scattering. [d] Phase transition temperature. [e] Not determined.

Toyoki Kunitake was born in 1936 in Kurume-shi, Fukuoka-ken, Japan. After completing his M.Sc. in the Faculty of Engineering at Kyushu University in 1960, he studied chemistry under C. C. Price at the University of Pennsylvania, graduating with a Ph.D. degree in 1962. He then spent a year as post-doctorate with C. G. Nieman at the Department of Chemistry, California Institute of Technology, before returning to Kyushu as Associate Professor in 1963. He was promoted to Professor in the Faculty of Engineering in 1974. Besides the field of synthetic bilayer membranes his research interests cover ultrathin films and Langmuir–Blodgett films, surface monolayers, and supramolecular aggregates.

double-chain compounds give colloidal solutions by sonication, and the molecular (aggregate) weights determined by light scattering lie between 10^6 and 10^7. Electron microscopy indicates the presence of vesicles (Fig. 1) and lamellae (Fig. 3), when both alkyl chains are at least ten carbon atoms long. Their layer thicknesses are 30–40 Å, in agreement with

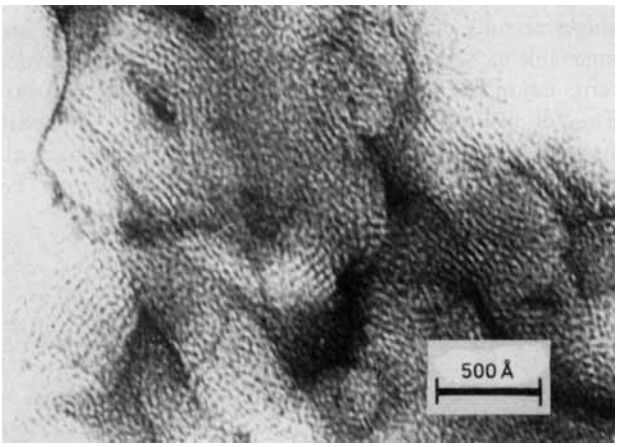

Fig. 3. Electron micrograph (negatively stained with UO_2^{2+}) of lamellar bilayers of **1** ($n = 14$).

the bilayer assemblage. Detection of the gel → liquid crystal phase transition by differential scanning calorimetry (see Section 2.3) strongly suggests the presence of aligned alkyl chains in the aggregate. These ammonium bilayers were extensively characterized.[15–18] The aggregate morphology is naturally affected by the method of dispersion.[17] Carmona-Ribeiro and Chaimovitch reported that large unilamellar vesicles (diameter, 0.5 μm) were obtainable by the solvent vaporization method.[19]

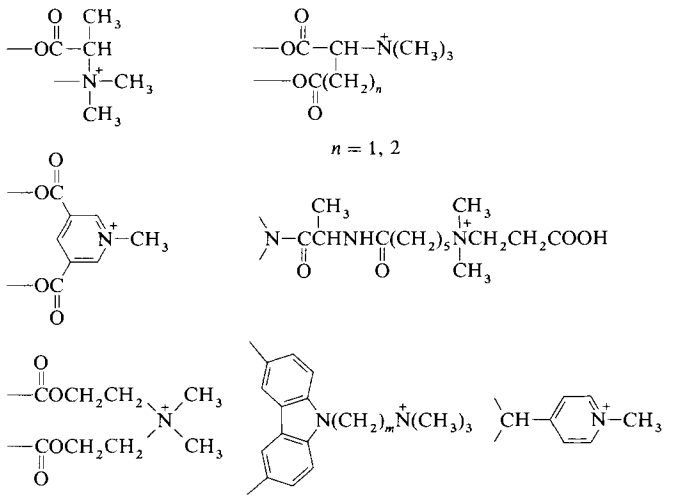

Fig. 4. Connectors of double-chain ammonium amphiphiles [21–25].

The dimethylammonium head can be modified by other substituents or replaced by the sulfonium group.[20] The connector portion that links the hydrophobic alkyl chains and the hydrophilic head group can be varied (Fig. 4). The major function of this unit is to help promote alignment of the alkyl chains. In the dialkyldimethylammonium salts of Table 1, the ammonium head group is directly bonded to alkyl tails without spacer units. A spacer unit that intervenes between the head group and the connector unit exerts significant influence on the molecular orientation in the bilayer. As discussed in Section 6, the length of the methylene chain functioning as spacer is critical in formation of helical superstructures.

Double-chain amphiphiles with anionic head groups form bilayer membranes. Examples with sulfonate (**2**), phosphate (**3**), and carboxylate (**4**) head groups are given in Table 2.[26]

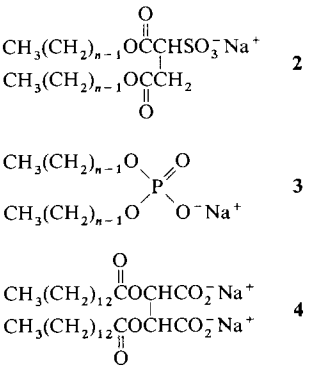

Stable bilayer membranes are formed again when the alkyl chain contains more than ten carbon atoms. The presence of vesicles and lamellae is confirmed by electron microscopy, and their molecular weights are 10^6–10^7. Mortara et al.[27] similarly noted vesicle formation from dihexadecyl phosphate at an early stage in this research.

Table 2. Aggregation behavior of anionic, dialkyl amphiphiles [26] [a].

Compound	Solution	Electron Micrograph	M	T_c [°C]
2 ($n = 16$)	colloidal	lamella	–	45
2 ($n = 12$)	colloidal	large vesicle	2.2×10^7	28
2 ($n = 10$)	clear	large vesicle	1.9×10^6	
3 ($n = 16$)	colloidal	lamella	1.2×10^7	67
3 ($n = 12$)	colloidal	vesicle	2×10^7	33
3 ($n = 10$)	clear	vesicle	4.4×10^6	
4 ($m = 13$)	slightly turbid	vesicle		

[a] See footnotes to Table 1.

The oxyethylene oligomer is conveniently used for preparing nonionic, bilayer-forming compounds.[28] The aggregation behavior of these compounds is summarized in Table 3 for **5** and **6**. In the case of **5** ($n = 8$), bilayer formation is not detected and the molecular weight of the aggregates (ca. 10^5) is smaller than those for typical bilayer aggregates ($> 10^6$).

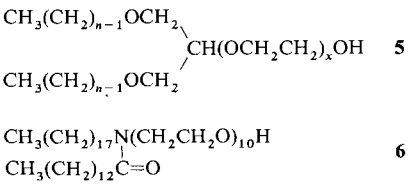

Table 3. Aggregation behavior of nonionic amphiphiles [28] [a].

Compound (n, x)	cmc [b] [μ M]	Electron Micrograph	M	T_c [°C]
5 (8, 6)		unstructured	5×10^5	
5 (8, 10)	50	unstructured	4×10^5	
5 (8, 12)	60	unstructured	6×10^5	
5 (12, 10)	2	irregular vesicles	turbid	
5 (12, 15)	2	vesicles and lamellae	1.2×10^7	n.d.
5 (12, 28)	1	lamellae	1.2×10^7	
5 (14, 15)		vesicles		22 [c], 30
5 (16, 15)			turbid	40–44
5 (16, 12)	1	paired bilayers	2.7×10^7	41
5 (16, 30)	1	lamellae	4.6×10^7	n.d.
5 (18, 15)		disks		51, 55 [c]
6		fragments of lamellae	1.5×10^7	

[a] See also footnotes to Table 1. [b] Critical aggregate concentration. [c] Major DSC peak.

The longer chain analogues **5** (n = 12) and **5** (n = 16) produce bilayer aggregates which exhibit different morphologies. For instance, **5** (12, 15) gives single-compartment vesicles, whereas **5** (16, 15) produces paired bilayers (Fig. 5).

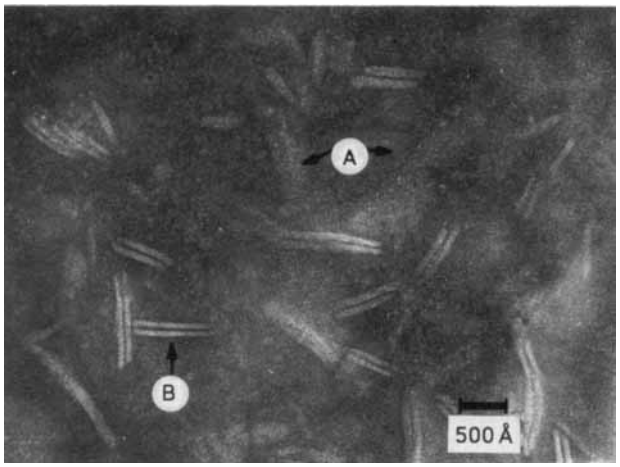

Fig. 5. Electron micrograph of an aqueous dispersion of **5** (16, 15). A top view (arrow A), and a side view (arrow B) of paired bilayers.

Zwitterionic groups such as **7**, **8**, **9**, and **10** were also used as the head group of double-chain amphiphiles.[23, 28]

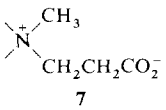

7

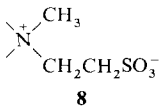

8

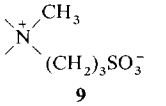

9

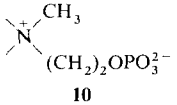

10

2.2. Molecular Alignment in Bilayer Assemblage

The detailed molecular arrangement in some of the synthetic bilayers mentioned above has been elucidated by X-ray crystallography. Kajiyama et al.[29] estimated the bilayer thickness of a series of simple double-chain ammonium amphiphiles **1** from widths between dark striations in electron micrographs of negatively stained samples. They also determined the layer thickness of powder samples. Comparisons of these data with the molecular lengths suggested that the component molecules were tilted with respect to the bilayer surface by 32 to 47° depending on the alkyl chain length.

Okuyama et al. succeeded for the first time in preparing single crystals of a synthetic bilayer compound that are amenable to X-ray structural analysis.[30] The structure determination has been conducted for **1** (n = 14, 16, and 18). They all give intrinsically identical structures,[31, 32] apart from the chain length. As an example, the packing structure of the monohydrate of **1** (n = 18) is given in Figure 6. The

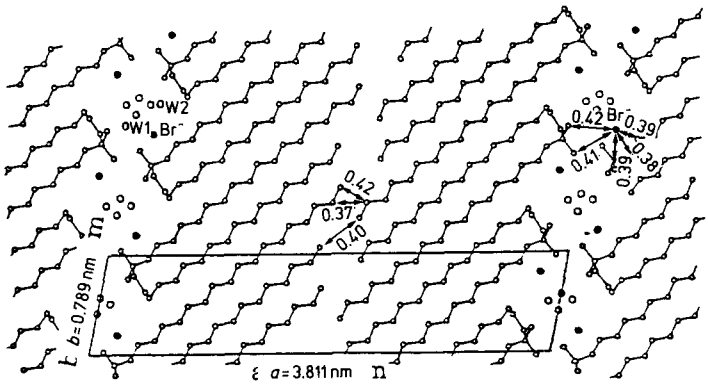

Fig. 6. The packing structure of a single crystal of the monohydrate of **1** (n = 18).

most important aspects in this structure are as follows: a) Br^- and N^+ centers form a hydrophilic plane parallel to the bilayer surface; b) the component molecules are tilted by 45° relative to the bilayer surface; c) one of the octadecyl chains assumes the *trans* zigzag conformation, whereas the other chain shows a folded conformation (*ggtgg*) near the hydrophilic group and the *trans* zigzag conformation towards the alkyl chain end. The chain tilting is caused by the balance between the molecular cross-sections of the hydrophobic portion (40 Å^2 for two methylene chains) and the hydrophilic portion (57 Å^2 for the *bc* plane of the unit lattice). This packing structure is very similar to that found for phosphatidylcholine.[11] The tilt structure was always found for double-chain amphiphiles with the glutamate connector.[33, 114] It is noteworthy that the ammonium amphiphile with two identical chains assumes the unsymmetrical chain packing. This seems to be a common requirement of chain packing among double-chain amphiphiles in order to attain the two-dimensionality.

2.3. Phase Transition and Phase Separation

Phase transition and phase separation are the two, most fundamental properties related to bilayer assemblage. Phase transition is schematically illustrated in Figure 7.

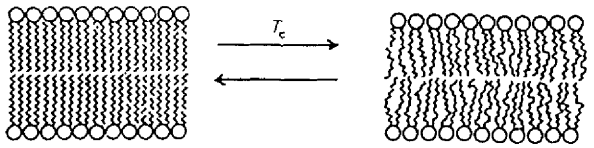

Fig. 7. A schematic illustration of the phase transition, crystalline $\rightleftharpoons$ liquid crystalline at the phase transition temperature T_c.

One of the simplest bilayer-forming amphiphiles, **1** ($n = 18$) shows a remarkably complex phase behavior.[9, 34] We are interested here only in dilute dispersions. The gel→liquid crystal phase transition is commonly observed for dilute aqueous dispersions of double-chain amphiphiles. Figure 8 depicts DSC (differential scanning calorimetry) thermograms for aqueous dispersions of **1** ($n = 12$, 14, 16, 18, and 22). The phase transition temperature, T_c, increases with increasing lengths of the alkyl tail. Many of the bilayer dispersions prepared by sonication give broader DSC peaks. The molecular organization in these well-dispersed samples may not be uniform. In contrast, DSC samples frozen to $-50\,^{\circ}C$ give sharper single peaks, probably because more regular, multilamellar dispersions are formed.

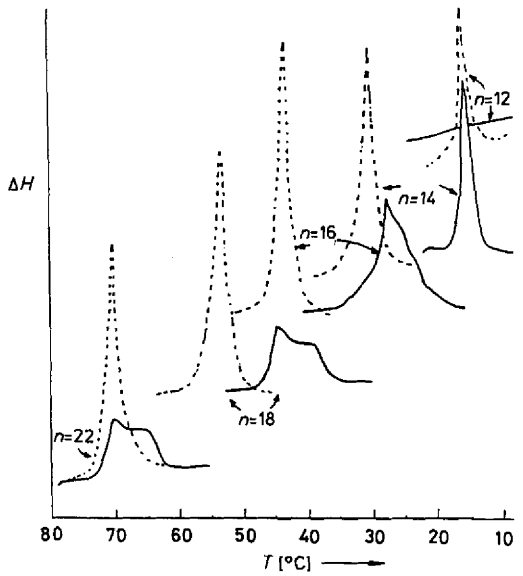

Fig. 8. DSC curves of bilayers of 1–2 wt% of **1** in water. — Samples prepared by the sonication method; - - - samples prepared by the dispersion method or the freezing method.

These data are consistent with the phase transition ranges estimated by other methods: reaction rates in the bilayer matrix, NMR line broadening of the crystalline bilayer, fluorescence spectral changes of probe molecules, turbidity changes, and the extent of positron annihilation.[35] The difference in T_c between the sonicated and frozen samples depends on the molecular structure of the component amphiphile, as shown in Scheme 1. In the case of the simple dimethyldioctadecylammonium amphiphile, **1** ($n = 18$), the sonicated sample has a T_c 9 °C lower than the frozen sample. In other dioctadecylammonium amphiphiles, which possess more complex head and/or connector groups, the differences are much smaller. Uniform bilayer organizations appear to be maintained when hydrogen bonding and/or dipolar interaction are expected between component molecules.

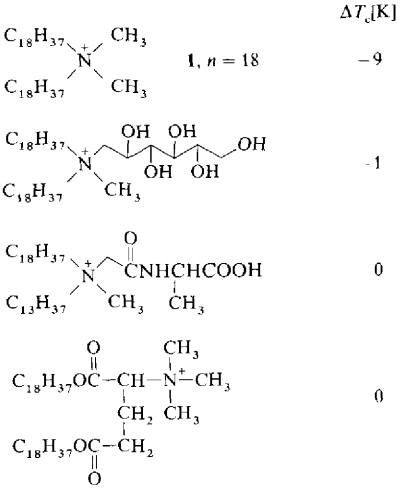

Scheme 1. Difference in T_c of aqueous dispersions of double-chain amphiphiles generated by sonication or freezing.

We compiled DSC date (T_c, enthalpy and entropy change) for the whole family of bilayer-forming, double-chain amphiphiles.[36, 37] The design of a novel bilayer with desired phase transition behavior is now possible. The correlations between this behavior and molecular structure are summarized as follows:

1) The entropy change of the phase transition falls within the range of $60-220\ J\,K^{-1}mol^{-1}$ for stable bilayers of all double-chain amphiphiles including natural lipids. This indicates that all phase transition processes are closely related (chain melting).

2) The variation of the DSC data can be discussed in terms of the structural element of component amphiphiles: a) T_c, ΔH, and ΔS values increase with increasing lengths of tails and spacers, except when diethanolamine is connector; b) enhanced interactions among connectors raise T_c values. However, the corresponding changes in ΔS are not straightforward; c) head-group interactions (electrostatic and/or hydrogen bonding) raise T_c. When the interaction is not very strong, the DSC data (T_c, ΔH and ΔS) for bilayers of different surface charges (cationic, anionic, and neutral) does not vary. Bulky substituents at the head group cause T_c lowering; d) the presence of flexible units (ether and ester) either in the tail or in the spacer leads to T_c lowering. A *cis* double bond (as in the oleoyl group) has the same effect.

Phase separation of synthetic bilayer membranes has been detected by the presence of the component peak in DSC, by λ_{max} shifts in absorption spectroscopy, and by excimer emission in fluorescence spectroscopy. An example of the absorption spectral method is shown in Figure 9.[38] Azobenzene-

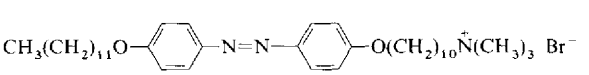

11

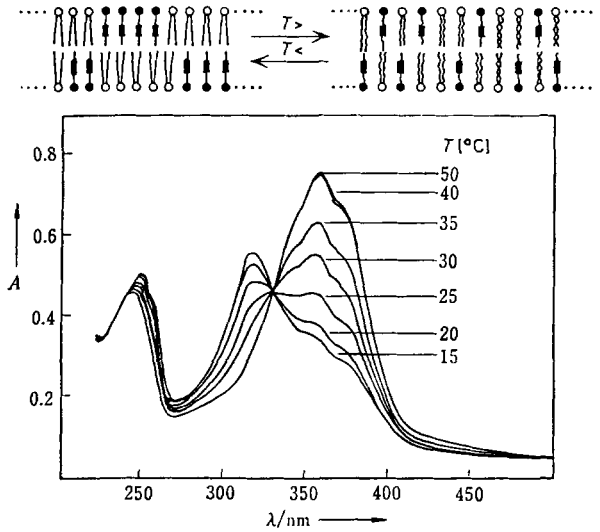

Fig. 9. Spectral changes in the absorption spectrum as a result of phase separation in a 1:10 mixed bilayer of **11** and **1** ($n = 18$).

containing bilayers give large spectral shifts caused by relative orientation and stacking of the azobenzene units (see Section 3.2). A 1:10 mixed dispersion of azobenzene-containing amphiphile **11** and dialkyldimethylammonium amphiphile **1** ($n = 18$) shows λ_{max} at 355 nm in the high-temperature region, indicating the presence of the isolated azobenzene species. By lowering the temperature, a new peak due to formation of the clustered azobenzene component appears at 315 nm. The spectral change corresponds to the phase transition of the matrix bilayer. This property has been exploited in novel applications of bilayers such as detection of chemical signals[39] and control of chemical reactions.[40]

The limited miscibility of hydrocarbons and fluorocarbons is used for controlled formation of separate domains, as will be discussed in Section 5.

2.4. Bilayer Morphology

Bilayer membranes dispersed in water give in many cases vesicular and lamellar morphologies. Unusual morphologies like the paired leaflet of Figure 5 are also noted. Nonbilayer aggregates have been described for phospholipids.[41] Similarly, Murakami et al. reported that there were interconversions between bilayer and nonbilayer morphologies.[42, 43] In contrast to the charged lipids **12** and **13**, which form typical vesicles and lamellae, their nonionic counterpart **14** is dispersed as nonlamellar network aggregates in the neutral pH range (Fig. 10), but is transformed into multilamellar vesicles in the deprotonated form. Addition of cationic **12** also transforms the nonlamellar aggregate into vesicles. An equimolar mixture of the cationic and anionic amphiphiles leads to nonlamellar networks with repeating distances of 70 and 130 Å in the liquid crystalline temperature region. Small-angle X-ray diffraction suggested the formation of a face-centered cubic lattice.[44]

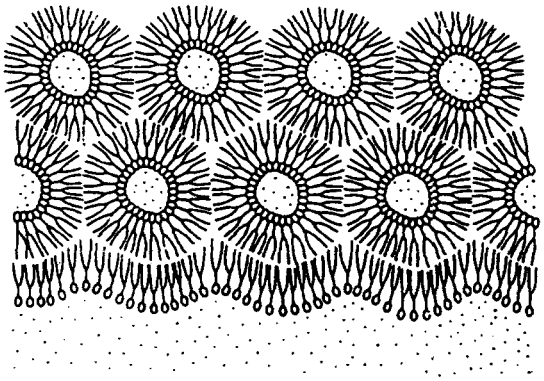

Fig. 10. Nonlamellar network aggregates of the neutral form of **14** [43].

Dynamic morphological changes are intrinsic to many physiological functions of the biological cell. The corresponding study on synthetic bilayer membranes is limited. Rupert et al. examined the ability of vesicles of **1** ($n = 12$) to undergo fusion.[45, 46] They found that dianions such as dipicolinate promoted fusion of vesicles with a diameter of at least 3000 Å, whereas smaller vesicles did not readily fuse despite their aggregation. The fusion was facile when the vesicles were in an overall fluid state. This research group also showed that the lamellar to hexagonal II phase transition proceeded by Ca^{2+}-induced fusion of didodecyl phosphate vesicles.[47] Salt-induced aggregation of dimethyldioctadecylammonium chloride and sodium dihexadecyl phosphate vesicles has been discussed by Carmina-Ribeiro and Chaimovitch.[48]

Optical microscopy is convenient for real-time observation of the morphology change. Evans et al. used video-enhanced contrast-differential interference contrast microscopy to observe dynamic changes of aggregate morphologies of simple double-chain ammonium amphiphiles (**1**, $n = 12$).[49] H. Hotani showed a few years ago that dark-field optical microscopy was particularly advantageous for studying the finer details of biological structures.[50] These investigations confirmed that several transformation pathways existed for various morphologies of liposomes: biconcave, elliptical, regular polygonal, etc.

We applied this technique to examine the morphology of **1** ($n = 12$).[51] The dynamic changes observed are remarkably similar to those of the phospholipids mentioned above. For example, a tubule attached to a vesicle is elongated with time while the vesicle shrinks (Fig. 11 a). A vesicle with protuberance, is converted into a spherical vesicle via an irregular intermediate (Fig. 11 b), and a tadpole and a tripod interconvert (Fig. 11 c). Electron microscopy of freeze-fracture replicas of this dispersion shows that elongated tubules branch

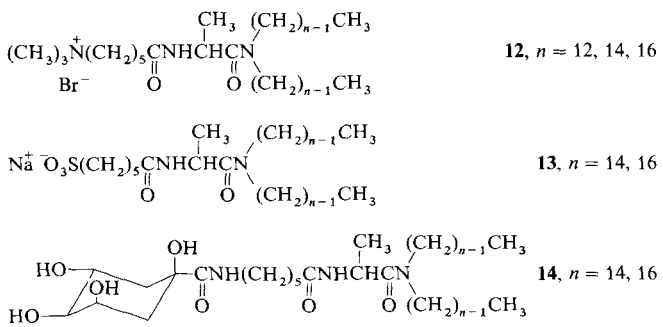

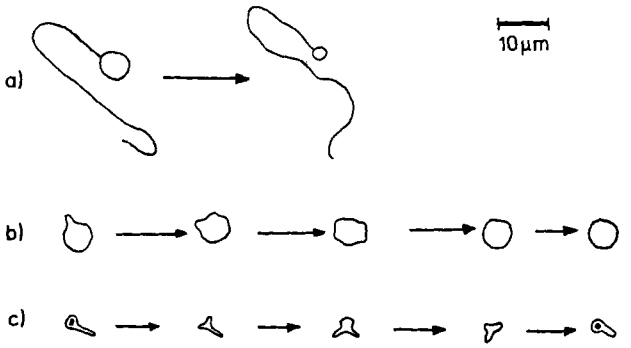

Fig. 11. Schematic illustration of morphological transformation of an aqueous dispersion of **1** ($n = 12$).

into smaller tubules and fibers, which, in turn, are transformed into trains of very small vesicles (diameter, 300–400 Å). The dark-field optical microscopy was further em-

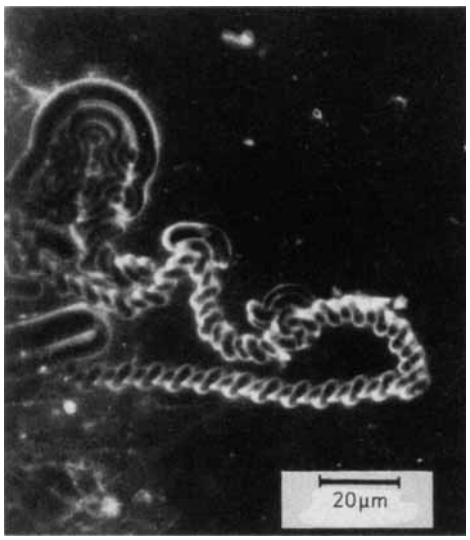

Fig. 12. Dark-field optical micrograph of an aqueous dispersion of **15** ($n = 2$).

ployed for observation of Myelin figures and double-helical fibers of bilayers of double-chain ammonium amphiphile **15** (Fig. 12)[52] The latter morphology was observed for egg-yolk lecithin.

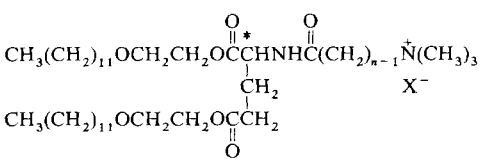

15, $n = 2$ (X = Cl), 11 (X = Br)

3. Bilayer Membranes of Single-Chain Amphiphiles

3.1. Molecular Design

Attachment of two alkyl chains, instead of one, to a single head group should enhance molcular orientation in aggregates because their conformational mobility is restricted. The larger liquid crystalline region in the phase diagram of double-chain amphiphiles compared with that of single-chain counterparts is consistent with this view. If this were the case, stable bilayer membranes would be produced even from single-chain amphiphiles whose conformations are restricted by incorporation of rigid segments or by intermolecular interactions.

Figure 13 illustrates a design principle of a bilayer-forming, single-chain amphiphile. A conventional liquid crys-

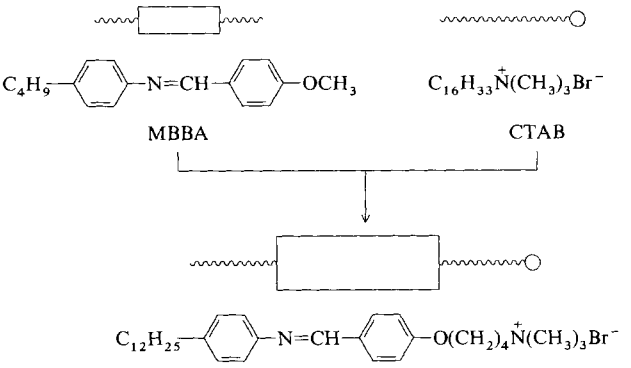

Fig. 13. Design of a single-chain bilayer component by combining the structural features of a compound capable of a liquid crystal transition (MBBA) and a tenside (CTAB).

talline material, MBBA, contains a rigid Schiff base unit connected to a flexible alkyl chain. A micelle-forming surfactant, CTAB, contains a trimethylammonium head group and a hexadecyl chain. The combination of the structural features of these two compounds results in a novel amphiphile that should form aqueous aggregates with a molecular orientation better than that of the conventional micelle. It contains a hydrophilic head, a spacer, a rigid segment, and a flexible tail as structural modules.

Within this structural framework (as in **16** and **17**), the lengths of the methylene chain of the spacer and of the hydrocarbon tails were varied, and their aggregation behavior examined (Table 4).[53] Molecular aggregation detected by

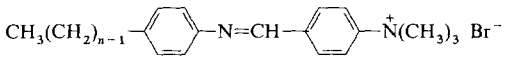

16, $n = 0, 4, 7, 12$

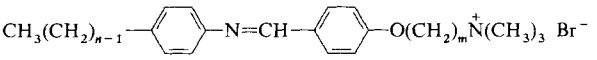

17, $n = 0, 4, 7, 12$, $m = 4, 10$

surface tension measurements occurs at concentrations of 10^{-4}–10^{-5} M except for **16** ($n = 0$) and **17**(0, 10), which did not show any appreciable lowering of surface tension. The critical aggregate concentration is lowered by lengthening of the hydrocarbon tail (C_n portion), but is affected little by the length of the intervening methylene group (C_m portion). The critical aggregate concentrations for **16** ($n = 4$) and **17** (4, 10) lie in the common range of $(2-3) \times 10^{-4}$ M. The critical

aggregate concentration for **16** ($n = 12$) contrasts sharply with that of **17** (0, 10) or **17** (4, 10). In terms of the hydrophile–lipophile balance, these compounds should show similar results. Since this is not so, the location of the rigid segment must determine, to a large extent, the tendency of these amphiphiles to align at the air–water interface.

Table 4. Aggregate behavior of single-chain amphiphiles.

Amphiphile	n	m	cmc [a] [mM]	M [b]	Electron Micrograph
	0		>10	$<10^4$	unstructured
16	4		0.22	1×10^5	unstructured
	7		0.06	8×10^6	lamella
	12		0.01	4×10^6	vesicle and lamella
	4,	4	0.16	8×10^6	unstructured
	7,	4	0.01	2×10^7	lamella
	12,	4	0.01	4×10^6	vesicle
17	0,	10	>10	4×10^6	unstructured
	4,	10	0.33	6×10^6	unstructured
	7,	10	0.02	2×10^7	vesicle
	12,	10	0.01	1×10^7	lamella

[a] Critical aggregate concentration. [b] Molecular weight determined by light scattering.

The average molecular weight of most of the aggregates is 10^6–10^7. Therefore, the average aggregation numbers are in the range of 10^3–10^5. The electron microscopic observation establishes the structural requirement for the formation of a stable bilayer. The development of the bilayer structure is improved with increasing chain lengths of the flexible tail (C_n portion), the minimal chain length being probably between $n = 7$ and $n = 4$. It is worthy of emphasis that **16** ($n = 4$) and **17** (4, 10) fail to form well-organized assemblies in spite of their formation of very large aggregates. A certain tail length is required for an amphiphile to align in aqueous aggregates as well as at the air-water interface.

A systematic variation of lengths of flexible tail and spacer was also conducted for azobenzene-containing, single-chain amphiphiles **18**.[54] Among the total of 21 compounds, the

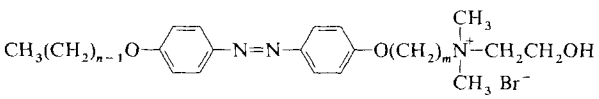

18

formation of stable bilayer membranes as judged by three criteria was concluded for the following combinations of tail length n and spacer length m: $n = 12/m = 2$–$12/n = 10$, $m = 5$–$10/n = 8$, $m = 10$. These results indicate that the tail length is more critical than the spacer length in bilayer formation.

The subsequent studies on molecular design of the single-chain amphiphile established that the kind of head group could be varied as much as those of the double-chain counterpart (cationic, anionic, nonionic, and zwitterionic)[55, 56] and that the rigid segment is extensively variable[57, 58] (Scheme 2). An extensive list of this class of single-chain compounds was compiled.[59] Cho et al. recently reported that an ammonium derivative of cholesterol formed bilayer

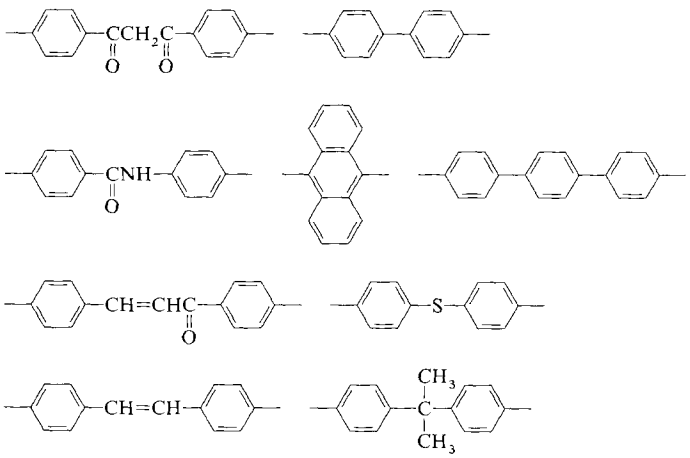

Scheme 2. Examples of rigid segments for single-chain bilayer-forming amphiphiles. For more examples see Scheme 3.

vesicles.[60] It has to be noted that „the rigid segment" implies the structural unit which promotes molecular alignment by intermolecular stacking and other intermolecular interactions. The aromatic „rigid segment" of Scheme 2 promotes intermolecular stacking. The molecular alignment can be improved in single-chain ammonium amphiphiles by strong hydrogen-bonding capability.[61]

3.2. Molecular Orientation within the Bilayer

A systematic structural variation of single-chain amphiphiles indicated that a certain length of the flexible tail was required for bilayer formation. The role of the spacer methylene chain, in contrast, was not clear. The crucial influence of the spacer length on bilayer assembly was first clarified in relation to absorption spectra of the azobenzene bilayer of **18**. Figure 14 shows representative spectral variations which depend on the molecular structure. All the bi-

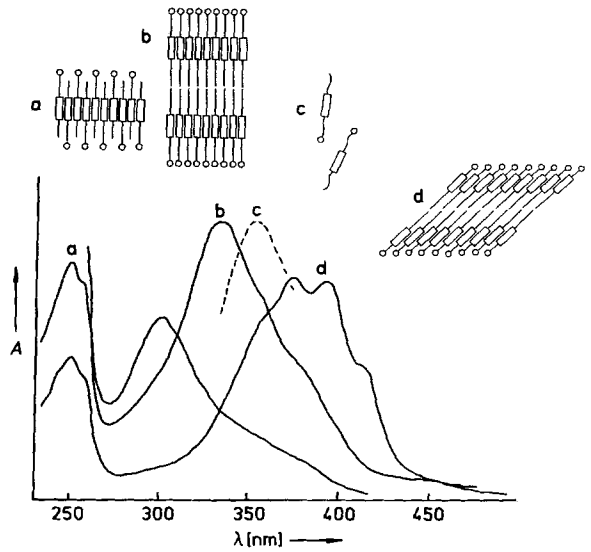

Fig. 14. Absorption spectra and the packing modes of bilayers of **18** (n, m). a) $n = 8$, $m = 10$; H-aggregate; b) $n = 12$, $m = 10$; c) absorption of monomeric azobenzene derivatives; d) $n = 12$, $m = 5$, J-aggregate.

layer components contain the identical azobenzene chromophore, yet their spectral patterns are quite different. λ_{max} covers a wide range from 300 nm for **18** (8, 10) to 390 nm for **18** (12, 5). The observed λ_{max} variation needs to be explained in terms of the chromophore interaction (orientation and aggregation) in the aggregate. According to the molecular exciton model of Kasha,[62] the blue shift for the bilayer of **18** (8, 10) relative to the absorption of the isolated chromophore (λ_{max} 355 nm) results from a parallel orientation of the neighboring transition dipoles (the H-aggregate, Fig. 14a), and a red shift for the bilayer of **18** (12, 5) is attributable to the tilted chromophore orientation (the *J*-like aggregate, Fig. 14d). The other bilayers of **18** (10, 4), **18** (12, 10), and **18** (12, 6) apparently have intermediate orientations (Fig. 14b).

The interdigitated bilayer structure was first proposed for the bilayer of **18** (8, 10) on inspection of the X-ray diffraction of its cast multibilayer film.[63] More recently, Okuyama and co-workers determined its structure from a single crystal (Fig.15).[64] The parallel azobenzene packing is appropriate

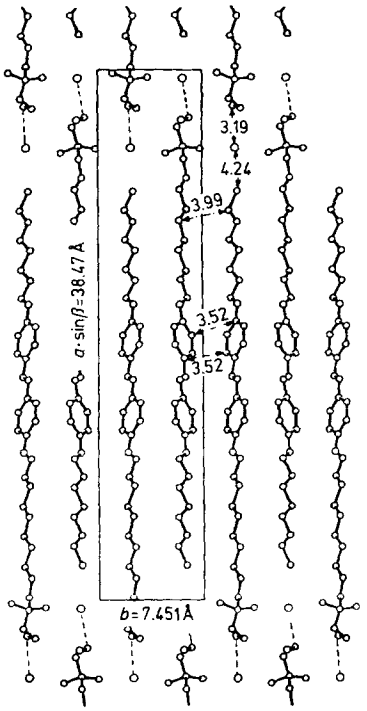

Fig. 15. The packing structure of a single crystal of **18** (8, 10).

for its particular molecular structure, since the cross section of the ammonium head group is about twice the cross section of the hydrophobic portion and the lengths of spacer and tail are very similar.

The crystal structure of the bilayer of **18** (12, 5) is shown in Figure 16.[65] A typical bilayer structure is formed. The tilt angle of the molecular axis from the layer normal amounts to 62°. This inclination is required in the bilayer assemblage in order to match the cross sections of the head group and the hydrophobic chain. The J-aggregate formation inferred from the spectroscopic data is consistent with the crystal structure. The spacer length of $m = 5$ appears essential for the tilted packing, because analogous tilted arrangements are observed for the bilayers with the common $m = 5$ spacer and different tail lengths of $n = 6$, 8, and 10.[66, 67]

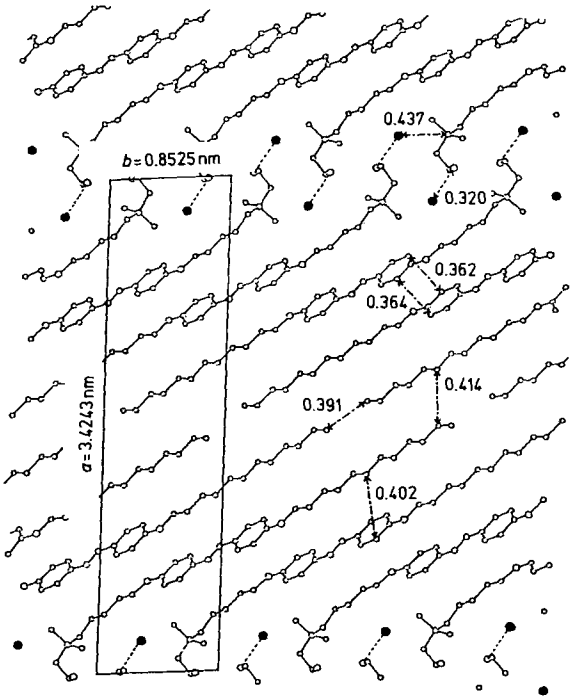

Fig. 16. The packing structure of a single crystal of **18** (12, 5).

X-ray photoelectron spectroscopy (XPS) is also useful for estimation of the molecular packing in single crystals. Nakayama et al.[68] examined the N_{1S} spectrum of a single crystal of **18** (12, 5). The calculated intensity ratio of the azobenzene nitrogen center to the ammonium nitrogen center agreed with the experimental pattern if the molecular axis was assumed to incline ca. 60° to the bilayer normal at the outermost surface of the crystal. This inclination is in close agreement with that determined by X-ray diffraction.

The variation of the molecular alignment with methylene chain lengths is not restricted to bilayers of azobenzene derivatives. Partially interdigitated structures were proposed for **16** ($n = 10$, 12, 14).[69] We very recently prepared a series of single-chain amphiphiles **19** which contain the σ-hydroxydiphenylazomethine unit as rigid segment.[70] The spectral shifts in the absorption spectrum and the layer thickness

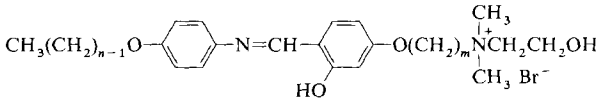

19:(n, m) = (8, 10), (12, 5), (12, 10)

determined by X-ray diffraction of cast films indicated that the effect of alkyl chain lengths on the molecular packing is virtually identical with those of the azobenzene-containing bilayer.

3.3. Morphology of Bilayers

Single-chain amphiphiles form bilayer vesicles and lamellae, similar to those of double-chain amphiphiles. The rigid segment in these amphiphiles promotes regular molecular orientation. The effect of the chemical structure of the rigid segment on aggregate morphologies has been studied systematically for a series of single-chain ammonium amphiphiles.[57] Electron microscopy indicates the formation of aqueous aggregates with various morphologies: the representative cases are globule, vesicle, lamella, rod, tube, and disk (Fig. 17). These morphologies can be explained as arising from different characteristics of the rigid segment, as summarized in Scheme 3. When the rigid segment is biphenyl or azobenzene, globular aggregates (probably collections of small bilayer fragments) are formed. The diphenylazomethine group is structurally similar to the azobenzene group, but their behavior as rigid segment is quite different. The amphiphile with a diphenylazomethine rigid segment produces much better developed bilayer membranes as a result of the dipolar interaction between the diphenylazomethine groups. In the case of the symmetrical rigid segments (biphenyl and azobenzene), the extensive organization appears less favored.

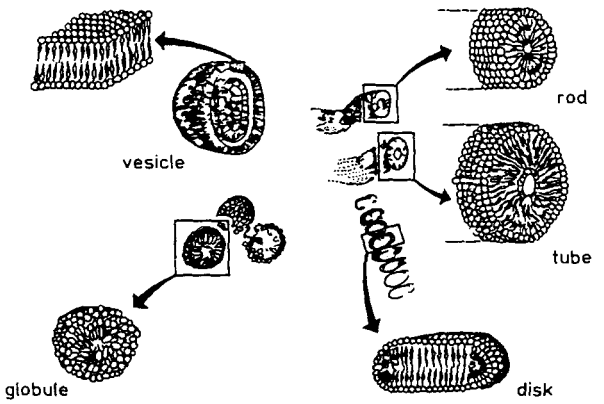

Fig. 17. Aggregate morphologies of single-chain amphiphiles.

A structural feature common to the third group of single-chain ammonium amphiphiles is that they contain bent rigid segments. The bending is either due to single-atom connection of two benzene rings, to rotation of the single bond, or to *meta* substitution. The contrasting behavior of the straight and bent ammonium amphiphiles is interesting. The straight molecules tend to assemble in a neat, two-dimensional arrangement (membrane), but the bent molecules give rise to curvatures which result in a radial molecular arrangement (rodlike and tubular structures). Double *meta* substitution at the rigid segment produces less organized aggregates.

The disk structure contains two kinds of molecular arrangement. One is the two-dimensional arrangement (flat portion) as in the typical bilayer membrane, and the other is a highly curved arrangement (side of the disk) as in the rodlike structure. The fourth group of amphiphiles can assume both the extended and bent conformations, which may be used advantageously to produce the two kinds of molecular packing involved in a disk.

These morphological correlations suggest that the surface curvature of an aggregate is controlled by appropriate mixing of different classes of amphiphiles. Amphiphile **17** (12, 4) gives well-developed, multilamellar vesicles (Fig. 18a). Replacement of this rigid segment with the diphenyl ether unit results in a tubular morphology (Fig. 18b). A 1:1 mixture of

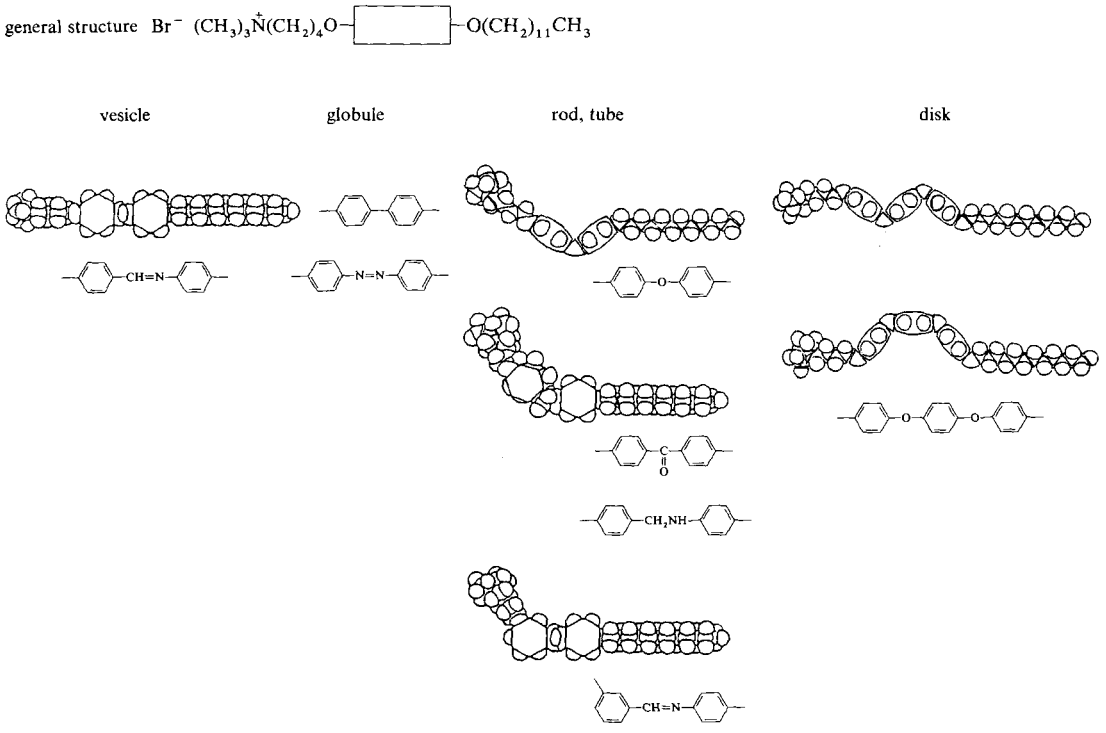

Scheme 3. Schematic representation of the morphology of aggregates and the rigid segments which gives rise to them.

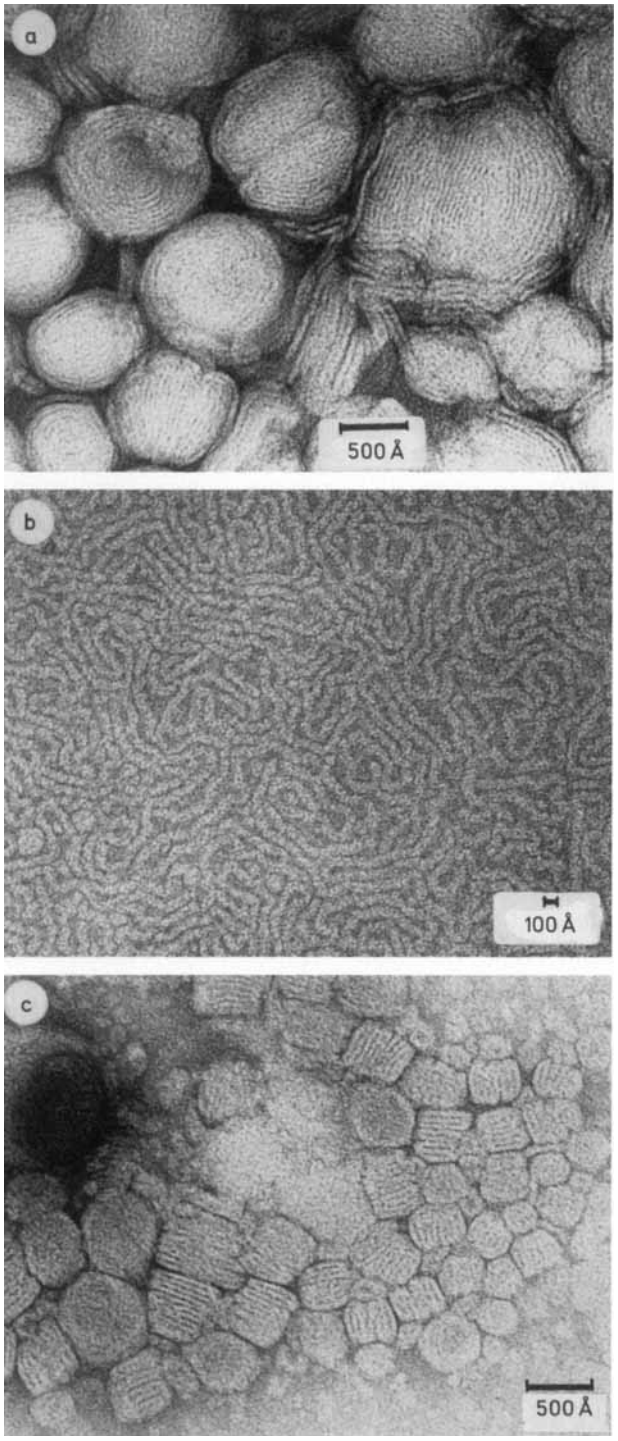

Fig. 18. Electron micrographs of aqueous bilayer dispersions of single-chain ammonium amphiphiles (negatively stained by UO_2^{2+}). a) **17** (12, 4); b) **20**; c) a 9:1 mixture of **17** (12, 4) and **20**.

these amphiphiles gives tubular aggregates very similar to Figure 18b. When the molar ratio is 7:3, an obscure mixture of tubes and lamellae is found. A 9:1 mixture produces stacked disks (or stacked patches of bilayers) with a layer thickness of 40–50 Å (Fig. 18c). It is conceivable that the flat portion of the disk is mainly composed of **17** (12, 4), and that **20** is concentrated along the side of the disk where large curvature is required.

A related morphology control is found for a mixture of **17** (12, 4), and **21**. Cosonication of multiwalled vesicles of **17** (12, 4) and globular **21** gives single-walled vesicles.

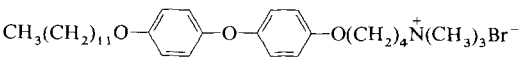

20

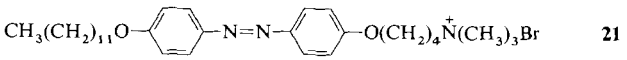

21

4. Molecular Membranes of Multichain and Two-Headed Amphiphiles

4.1. Triple-Chain Amphiphiles

As discussed in Section 1, the hydrophile–lipophile balance is not the most crucial factor that determines bilayer formation. Certain degrees of imbalance will be accommodated by the stabilization gained by molecular alignment. Compounds **22**–**24** are examples of triple-chain ammonium amphiphiles that were tested for bilayer formation.[71]

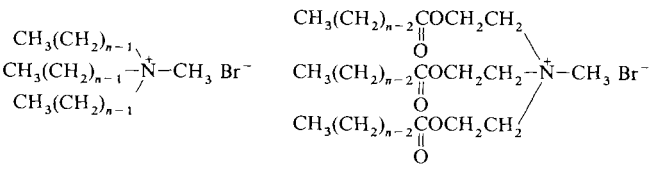

22, $n = 12, 16$ **23**, $n = 12, 16$

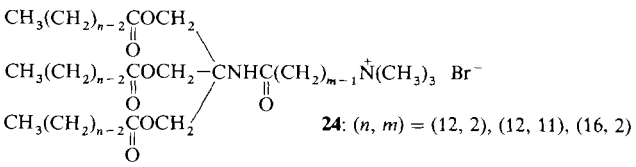

24: $(n, m) = (12, 2), (12, 11), (16, 2)$

Simple triple-chain compounds **22** do not seem to give well-developed bilayer structures. Amphiphiles **23** and **24** form stable bilayer membranes in water, as inferred from their huge molecular weights, the presence of a phase transition, and electron microscopic observation. The CPK molecular

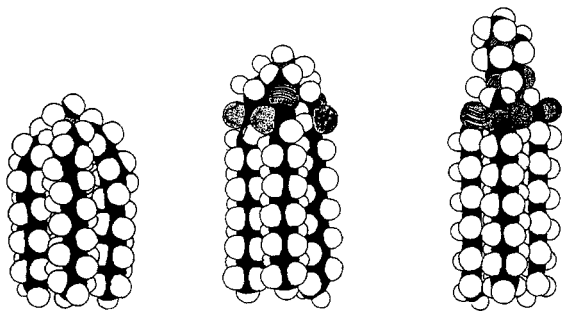

22, n=12 **23**, n=12 **24** (12, 2)

Fig. 19. CPK model of triple-chain amphiphiles with different connectors. The parallel alignment of the alkyl chains in **22** is inferior to that in **23** and **24**.

models of these amphiphiles with different connector structures (Fig. 19) endorse these experimental observations. In the case of **22** ($n = 12$), the long alkyl chains cannot be aligned at locations close to the ammonium group because of its tetrahedral configuration. In contrast, the alkyl chains of **23** ($n = 12$) can be well aligned. The compact chain packing is produced by the presence of the ester unit, and the ammonium head can protrude without conformational constraint. The same situation is found for **24** (12, 2), again due to the presence of the ester linkage.

4.2. Quadruple-Chain Amphiphiles

Very recently, we discovered that even quadruple-chain ammonium amphiphiles such as **25** are suitable for two-dimensional molecular alignment.[72] These compounds give

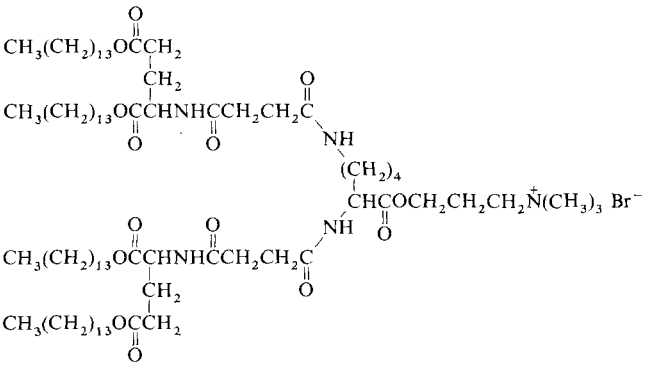

25

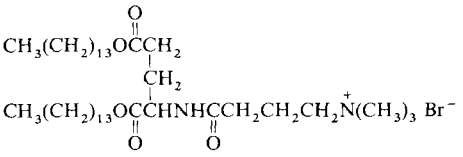

26

transparent aqueous dispersions at 20 mM, and display typical bilayer characteristics. Electron microscopy indicates the formation of vesicles and tapelike aggregates. A DSC experiment showed the presence of the phase transition peak. The transition behavior of **25** is not very different from that of the corresponding double-chain amphiphile **26**. The chain alignment is strongly dependent on the kind of the connector. The chiral unit in **25** and **26** should produce different chiral binding sites at the membrane surface.

The native counterpart of these amphiphiles is four-chained cardiolipin. It is interesting to note, however, that cardiolipin cannot form a stable bilayer assembly by itself.

4.3. Two-Headed Ammonium Amphiphiles

Some archeobacteria contain another class of membrane lipids. One of those lipid components is a macrocyclic amphiphile that spans the bilayer thickness.[73] Covalent bonding of alkyl chain ends of synthetic bilayer components would produce two-headed amphiphiles which may form monolayer membranes in water.

Structural extention of single-chain, bilayer-forming amphiphiles to two-headed amphiphiles results in molecular structures such as **27**–**29**.[74] Two ammonium groups at the ends of a molecule are connected by a single chain that is composed of methylene chains and aromatic unit. They are all dispersed in water as stable aggregates with molecular weights of 10^6–10^7. Electron microscopy shows that lamellae and rodlike structures are formed. As shown in Figure 20, **27** (10 mM) gives highly developed lamellae with layer thickness of 30–40 Å. This figure corresponds to the extended molecular length; therefore, the bisammonium molecule is aligned normal to the layer plane. Molecular elongation and increase in the flexible hydrocarbon chain as in **28** (molecular length, 67 Å) leads to the appearance of tubular structures (diameter 70–100 Å), with dark striations (deposits of uranyl acetate) in the middle. The flexible methylene chain in the center of the molecule would allow the bent molecular packing required for the tubular morphology (Fig. 20b).

The rigid lamella of Figure 20a can be transformed into single-walled vesicles as in Figure 20c by cosonication with cholesterol in the ratio 3:1. The vesicles are 1000–3000 Å in diameter and 60–70 Å in layer thickness. We propose that cholesterol molecules are preferentially located in the outer half of the membrane, thus creating surface curvature suitable for vesicle formation (see Fig. 21a). Remarkable transformations of morphology of lecithin vesicles by addition of lysolecithin and cholesterol were reported in a landmark paper of Bangham and Horne in 1964.[1]

Another way of creating curvature is the use of unsymmetrical bisammonium compounds. Attachment of a decyl chain to one of the ammonium heads of **27** changes the aggregate morphology from lamella to multiwalled ves-

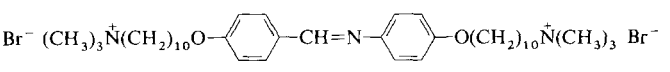

27

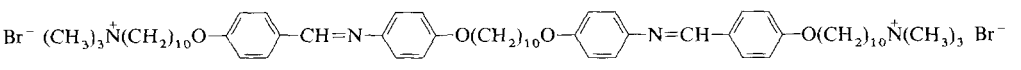

28

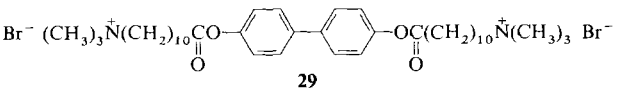

29

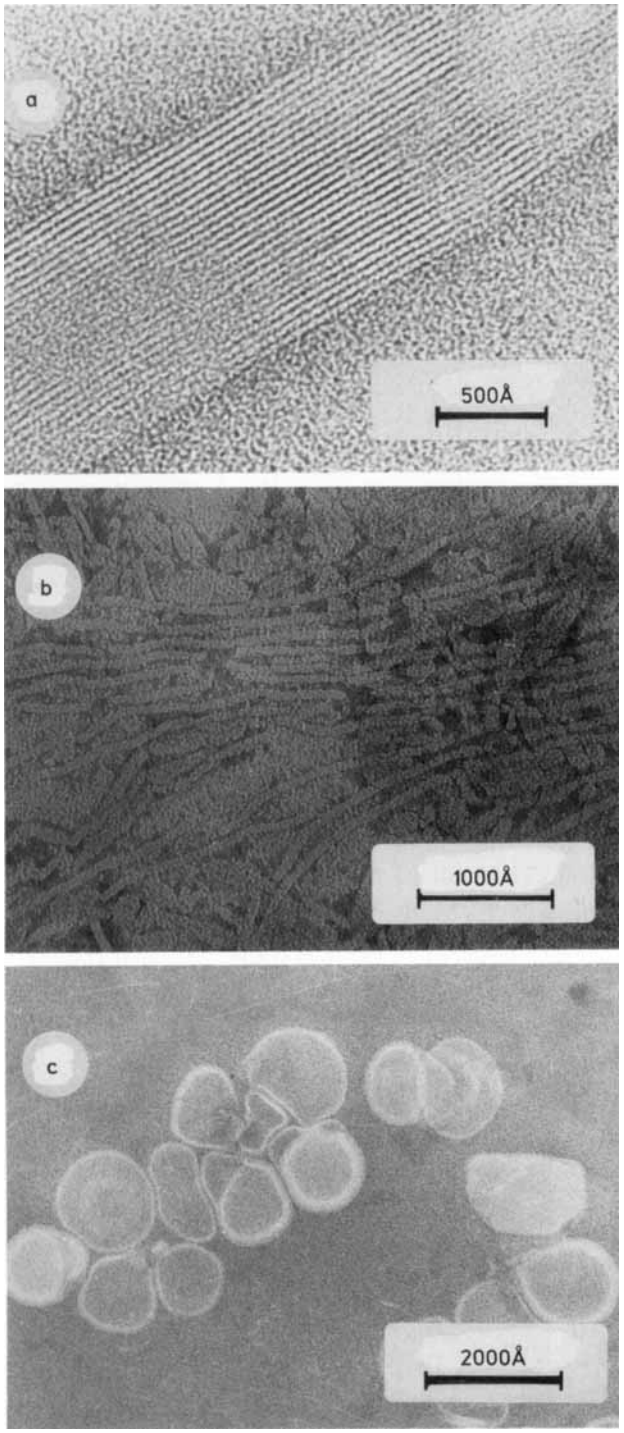

Fig. 20. Electron micrographs of aqueous dispersions of two-headed ammonium amphiphiles (stained by UO_2^{2+}). a) **27**; b) **28**; c) **27** + 1/3 cholesterol.

icles.[75] The decyl-substituted ammonium head in **30** seems to be more populous in the outer surface (Fig. 21 b).

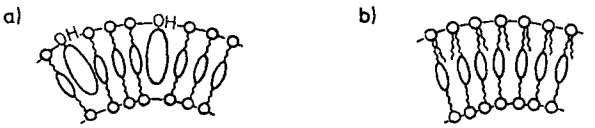

Fig. 21. Creation of surface curvatures in monolayer membranes. a) **27** + 1/3 cholesterol; b) **30**.

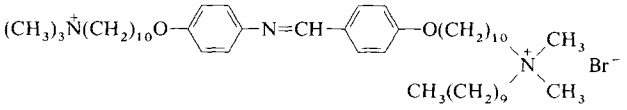

30

Formation of monolayer vesicles was reported by Fuhrhop and co-workers from single-chain amphiphiles with two viologen head groups (**31**).[76] They subsequently

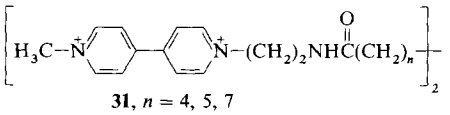

31, $n = 4, 5, 7$

conducted extensive research on this type of compounds, the bolaamphiphiles. For example, they prepared a series of macrocyclic compounds with two polar head groups and studied their vesicle formation.[77]

Amphiphiles related to **27**–**31** can be designed by combining only one end of the alkyl chain in double-chain amphiphiles.[78] Bisammonium compound **32** and related ionene oligomers **33** can form monolayer membranes.

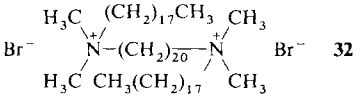

32

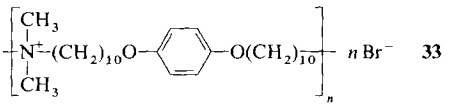

33

5. Bilayer Membranes of Fluorocarbon Amphiphiles

A new class of bilayer membranes are derived by replacement of hydrocarbon chains with fluorocarbon chains. They are single-, double-, and triple-chain compounds; for example, **34**–**38**.[79–82]

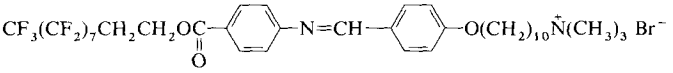

34

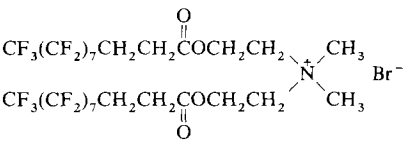

35

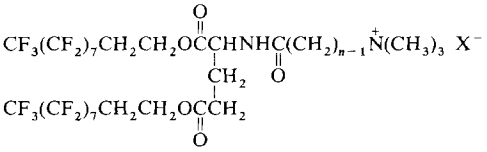

36, $n = 2-11$, X = Cl, Br

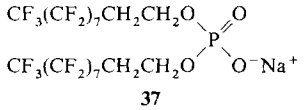

37

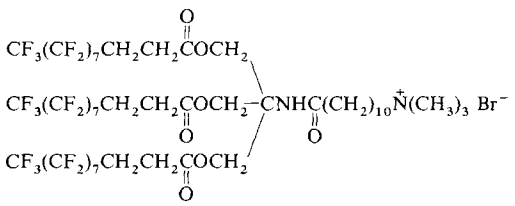

38

Sonication of these amphiphiles in water produces clear to translucent dispersions. Electron microscopic observation after the negative staining reveals the existence of the bilayer structure (vesicles and/or lamellae). For instance, **35** gives well-dispersed, single-walled vesicles. A related hydrocarbon (dodecanoate) amphiphile produces multi-walled vesicles. Double-chain **39**, which possesses both fluorocarbon and hydrocarbon tails gives even better developed single-

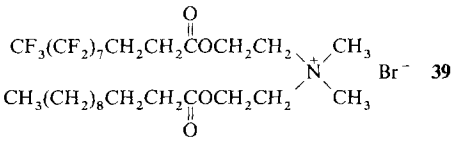

39

walled vesicles. Those amphiphiles which differ only in the tail portion (fluorocarbon vs. hydrocarbon) show aggregation morphologies that are fairly similar. Single-chain amphiphile **34** and triple-chain amphiphiles like **38** also produce bilayer aggregates.

Fluorocarbon bilayers exhibit small endothermic peaks in DSC thermograms. The phase transition temperature (T_c) of the fluorocarbon bilayers is detected at temperatures 20–30 °C higher and have smaller enthalpy changes than those of hydrocarbon bilayers. The smaller enthalpy changes to be an inherent property of bilayers made from fluorocarbon amphiphiles.

Figure 22 illustrates, as an example, the variation of fluorescence depolarization P of diphenylhexatriene embedded in bilayer membranes of the triple-chain amphiphiles.[82] At low temperatures, the P values are large irrespective of the number of fluorocarbon chains, but they decrease sharply near T_c, leading to large P differences. These data indicate that 1) the membranes are equally rigid at low temperatures, 2) the fluidity increases (decrease in P) at the temperature regions which correspond to the respective DSC peaks, and 3) the membrane fluidity of the liquid crystalline bilayer (at $T > T_c$) decreases with increasing number of fluorocarbon chains.

Fluorocarbons are not readily miscible with the corresponding hydrocarbon compounds. This is exemplified by the formation of heterogeneous micelles from fluorocarbon and hydrocarbon surfactants.[83] In the same vein, fluorocarbon and hydrocarbon bilayers show limited miscibilities. This situation can be improved by adding unsymmetrical components such as **39**. The improved miscibility is also

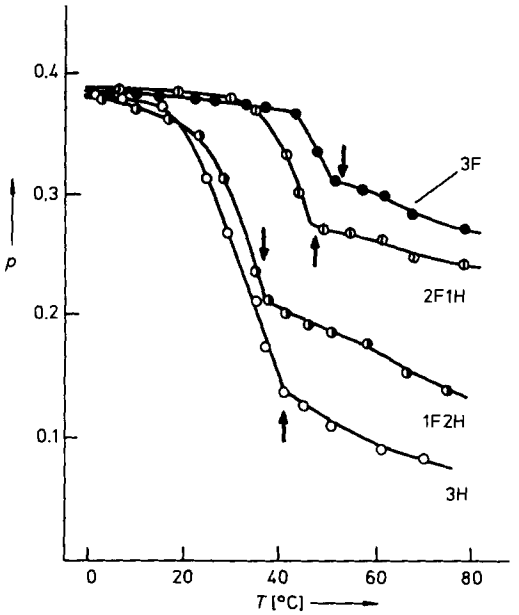

Fig. 22. Fluidity of fluorocarbon bilayers, measured by fluorescence depolarization P of diphenylhexatriene embedded in them. The arrows indicate the T_c values determined by DSC. 3F = **38**, 3H = **24** (12, 11); in 2F1H one and in 1F2H two fluorohydrocarbon chains of **38** are replaced by hydrocarbon chains of **24** (12, 11).

demonstrated in the case of triple-chain bilayer components. As shown schematically in Figure 23, the hydrocarbon component (3H) and the fluorocarbon component (3F) are hardly miscible. Upon addition of a partially fluorocarbon-

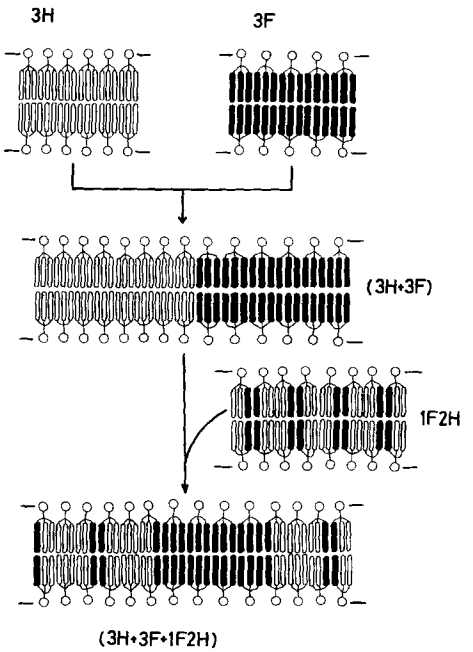

Fig. 23. Miscibility of bilayer membranes of triple-chain amphiphiles containing fluorohydrocarbon and hydrocarbon chains, before and after addition of a mixed amphiphile.

tailed amphiphile 1F2H, the original two components become more miscible.

General aggregation behavior of the fluorocarbon amphiphiles is closely related to that of the corresponding hy-

drocarbon compounds. However, the bilayer properties are very different for the two systems: First, fluorocarbon bilayers are much less permeable than hydrocarbon bilayers toward ions and small molecules. Second, these two membrane components tend to form separate domains, and the phase separation has been effectively used for controlled permeation and catalysis.[81]

6. Chiral Bilayer Membranes

As discussed in Section 2, the amino acid unit acts as a useful module in the design of bilayer-forming compounds. Some of the resulting chiral bilayers of single-chain and double-chain amphiphiles display much enhanced circular dichroism (CD).[84, 85] These data suggested that the chiral components were arranged asymmetrically in fixed spatial dispositions as a result of the formation of higher order structures.

A fairly simple, double-chain amphiphile, L-**40** forms single- and double-walled vesicles with diameters of 300–1000 Å, when dispersed in water by sonication (Fig. 24a).[86]

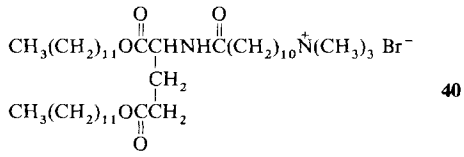

40

These vesicles are slowly transformed into the helical morphology which is made of twisted tapes, as shown in Fig. 24b). Further ageing gives tubes with helical streaks. These helices and tubes are better observed by dark-field optical microscopy (Fig. 24c)[87] and by high-resolution scanning electron microscopy (Fig. 24d).[88] An advantage

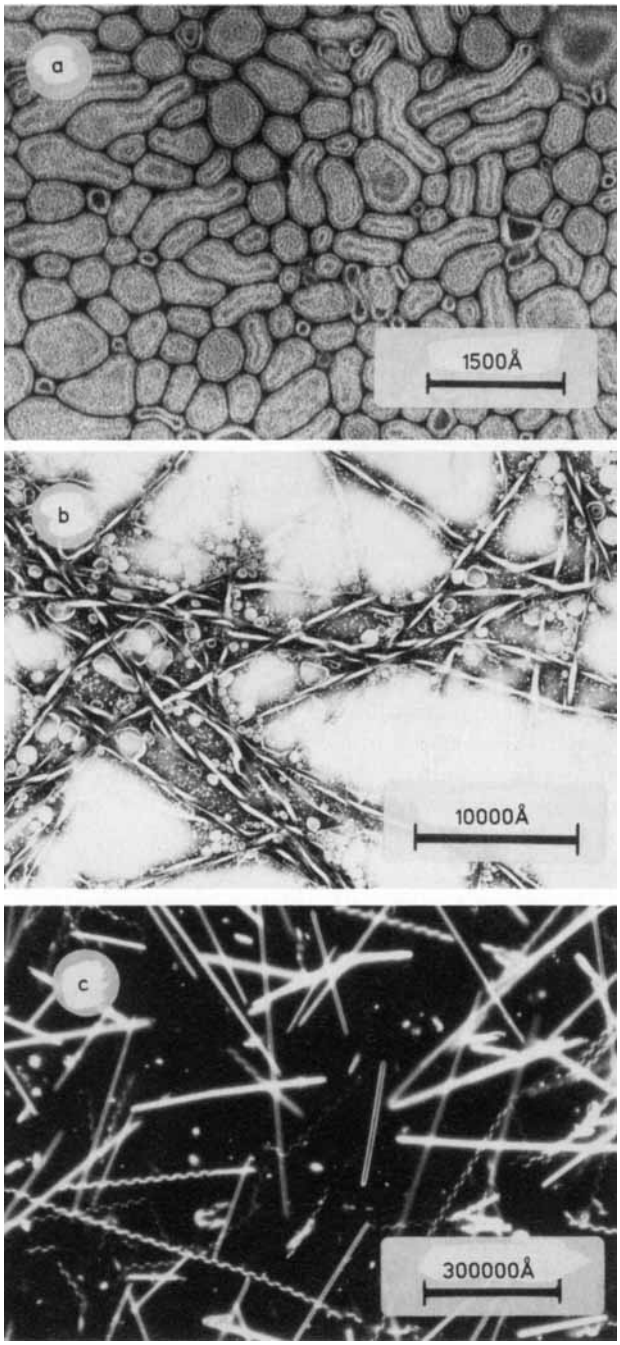

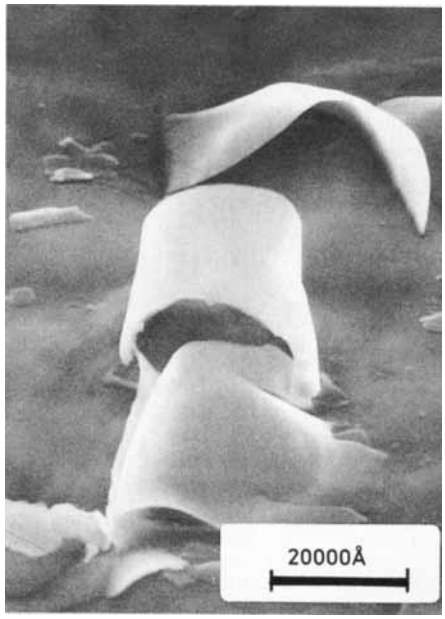

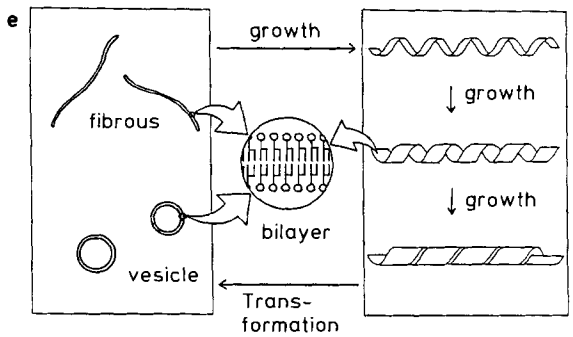

Fig. 24. Formation of helical superstructures from bilayer membranes of chiral ammonium amphiphiles. a) Electron micrograph of aqueous vesicles of L-**40**; no ageing, stained with UO_2^{2+}. b) Electron micrograph of the helical superstructure of L-**40**; stained by UO_2^{2+}. c) Dark-field optical micrograph of the helical superstructure of L-**40**. d) Electron micrograph (high resolution scanning electron microscopy) of the helical superstructure of L-**40**. e) A schematic illustration of helix formation.

of the latter two microscopic methods is that direct images are obtainable. The growth and degradation processes of the helices in water is observable by optical microscopy at a resolution of 1 μm, and the three-dimensional structure of the molecular aggregate can be determined by the scanning electron microscope at a theoretical resolution of less than 10 Å.

The helical superstructure is maintained only in the crystalline state. When the aqueous dispersion of L-**40** (T_c of the bilayer, 33 °C) is warmed to 35 °C, the helices and tubes are all converted into large flexible vesicles. The melting process can be observed directly by optical microscopy.

Enantiomeric amphiphile D-**40** similarly showed a slow growth of helices. These are left-handed, in contrast to the right-handed helices of the L enantiomer. In the case of its racemic bilayer, initially formed vesicles are converted into rodlike aggregates without formation of helices.

Helix formation is sensitive to the molecular structure. It is not observed for a closely related amphiphile with a shorter spacer length: CH_2 instead of $(CH_2)_{10}$. The shorter spacer may interfere with the regular molecular arrangement, since this amphiphile instead forms smooth single-walled vesicles.

The helical superstructure has been obtained for other bilayer-forming amphiphiles. Single-chain ammonium amphiphile **41** gives helical superstructures accompanied by CD enhancement.[89] Cho and Park reported helical superstructures formed by cationic cholesterol-containing polymers.[60] Yamada et al.,[90] concurrently with our initial finding, observed that dialkyl amphiphiles with the oligoglutamate head group **42** produced helical superstructures (twisted ribbons with a layer thickness of 30–40 Å). Single- and double-chain phosphate amphiphiles can form helical superstructures as well.[91] Tubular aggregates, which are products of helical growth, are found in a dispersion of a diacetylenic phosphocholine lipid.[92] Related helical fibers of lipid bilayers were obtained from *N*-octylaldonamides.[93, 94]

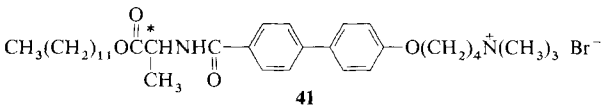

41

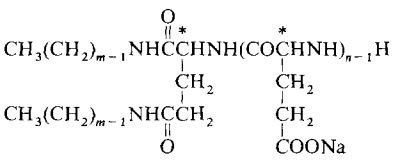

42, $m = 12, 16$

7. Applications and Further Developments

In the preceding sections we described molecular design and basic physicochemical properties of synthetic bilayer membranes. Since a multitude of physiological functions involve biomembranes, functional applications of synthetic bilayers should be numerous. They are briefly described in the following.

7.1. Models and Substitutes of the Biomembrane

The basic structural and physicochemical features of synthetic bilayer membranes are common to those of bilayer membranes of natural lipids. Therefore, lipid components of biological membranes may be replaced with their synthetic counterpart. For example, Ringsdorf and co-workers[95] reconstituted ATPase in a polymerized bilayer membrane of a diacetylenic amphiphile. O'Brien et al.[96] used partially polymerized vesicles of a dienoyl phosphatidylcholine to incorporate rhodopsin without denaturation. We have shown recently that myoglobin, the water-soluble heme protein, can be embedded in the interbilayer region of cast films of synthetic amphiphiles without denaturation.[97] The spatial orientation of myoglobin is fixed apparently by electrostatic attraction between the positively charged residue of the protein surface and the negative phosphate unit of the bilayer membrane. Interestingly, the membrane-bound myoglobin displayed redox reactivity.[98] This functional conversion opens an exciting future for composite molecular systems that are composed of natural and artificial molecules.

Murakami and co-workers recently carried out an extensive investigation on the use of functionalized synthetic bilayers as enzyme-like reaction sites for vitamin B_6-dependent transamination and β-replacement reactions,[99] and vitamin B_{12}-dependent carbon-skeleton rearrangements.[100]

7.2. Substrate Trapping and Reaction Control

Synthetic bilayer vesicles can retain ions and molecules in the inner aqueous phase, just like liposomes of biolipids. In addition, a large number of polymerized synthetic vesicles have been investigated to obtain stabilized drug carriers.[11] The trapping capability leads to separation of chemical species inside and outside the vesicles. This has been studied by many research groups in order to mimic the conversion of solar energy in the photosynthetic reaction center.[101] Other organic reactions were also affected by reactant separation by bilayers and by flip-flop exchanges of reaction bilayer components.[102]

The molecular organization and the physical state (phase separation and phase transition) of bilayers can be used as effective means to control reactions. For instance, phase separation (domain formation) of two reacting species produce a unique feature of reactivity.[40] It is possible to construct a surface receptor which performs discrimination, transduction, and amplification of chemical signals by inducing phase separation.[39]

7.3. Designed Organization of Functional Units

The two-dimensional feature of bilayer membranes is particularly advantageous for designed alignment of photonic, electronic, and magnetic functional units. A correlation be-

tween the chemical structure and the component alignment as discussed in Section 3.2 is useful in this respect. A bilayer of an azobenzene derivative, which possesses a tilted (J-like) molecular packing (see Fig. 14), shows highly efficient electron transfer and energy transfer within the bilayer and to a membrane-bound cyanine dye. These efficient transfers are not observed for analogous bilayers with parallel chromophore stacking.[103]

Some oppositely charged dye molecules are bound to the bilayer surface in a specific manner. For example, anionic cyanine dyes are bound to ammonium bilayer membranes in water either as the monomeric species, as H-aggregates, or as J-like aggregates.[104]

When the polar head of bilayers is a chelating group that binds transition metal ions, electron spins are aligned at the membrane surface. A single-chain amphiphile with the cyclam head group forms a bilayer Cu^{II} chelate, which displays a strong antiparamagnetic interaction.[105] Modifications of the metal complex organization should give rise to interesting magnetic and optical properties.

7.4. Surface Monolayers, Langmuir–Blodgett (LB) Films, and Planar Lipid Membranes (BLM)

Most of the bilayer-forming amphiphiles can form stable monolayers at the air-water interface. That the molecular orientations in monolayers and in the corresponding LB films are closely related to those in aqueous bilayers was demonstrated by absorption spectroscopy.[106] The self-assembling property of these amphiphiles is particularly suitable for enhancing the monolayer stability and the subsequent deposition as LB films. Stable BLMs are also formed from many double-chain ammonium amphiphiles.[107] The extent of alkyl chain alignment critically affects the life time. Common structural features exist for the aggregation behavior of aqueous bilayers, surface monolayers, and BLMs (planar bilayers). Therefore, the molecular design discussed in this article is useful for developing new LB films and BLMs.

7.5. Cast Films and Their Use as Molecular Templates

The outstanding self-assembling property of bilayer membranes is fully demonstrated by the formation of free-standing cast films. Transparent films with regular, multilayer structures are readily obtained when aqueous dispersions of synthetic bilayer membranes are spread on solid supports,[63, 108] as is the case with some phospholipids.[109] It is remarkable that flexible, self-supporting films are obtainable from non-covalent molecular aggregates. Unique molecular sensors and permeation control have been realized by application of these cast films.[110]

The macroscopic anisotropy of the cast film has been used to incorporate planar metal complexes into designed spatial arrangements.[111] More recently, Ishikawa and Kunitake[112] demonstrated that anionic porphyrins are incorporated into cast films of ammonium bilayer membranes in specific spatial orientations, depending on the optimized electrostatic attraction of the negative charge on the porphyrin ring and the positively charged bilayer surface. This methodology should lead to designed molecular systems.

Because of the stability of synthetic bilayers as independent entities, the regular bilayer organization is maintained even when guest molecules are introduced in the interbilayer space of a cast film. Cross-linking of a polymerizable guest and the subsequent removal of the bilayer matrix by solvent extraction produces multilayers of two-dimensional molecular networks.[113, 114] This approach is also applicable to synthesis of molecularly controlled siloxane networks[115, 116] and to the hydrolysis of $FeCl_2$ in a cast film to obtain oriented iron oxide particles.[117] It is clear that cast multibilayer films serve as superb templates for preparation of two-dimensional organic and inorganic materials. Sol–gel condensation of inorganic starting materials in the multibilayer matrix results in novel ceramics with molecular precision.

7.6. Bilayer Assembly in Organic Media

The major driving force of self-assembly of biomembranes and synthetic molecular membranes is the hydrophobic interaction. It is lost in organic solvents with which alkyl tails of the membrane component are miscible. We recently took advantage of the immiscibility of fluoroalkyl chains with conventional organic solvents, in order to prepare bilayer assemblies in organic media.[118, 119] The principle of their molecular design is common to that of aqueous bilayer membranes, although the hydrophilic head group has to be replaced with flexible hydrocarbon groups such as in **43**. Compartmentalization of the molecular space and novel organization of functional molecules are just two examples of the versatile possibilities we can envisage for this system.

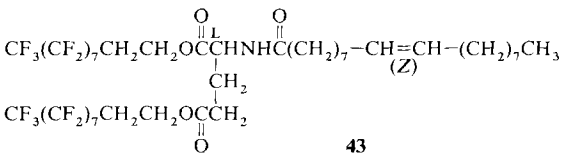

43

Our research described in this review was made possible only through dedication of our co-workers. The author wishes to express his gratitude to these people. He also appreciates the help of Ms. R. Ando, Ms. C. Tsuda, and Mr. T. Nishimi in the preparation of the manuscript.

Received: August 6, 1991 [A 867 IE]
German version: *Angew. Chem.* **1992**, *104*, 692

[1] A. D. Bangham, R. W. Horne, *J. Mol. Biol.* **1964**, *8*, 660.
[2] J. M. Gebicki, M. Hicks, *Nature*, **1973**, *3243*, 232.
[3] W. R. Hargreaves, D. W. Deamer, *Biochemistry*, **1978**, *17*, 3759.
[4] H. Brockerhoff in *Bio Organic Chemistry, Vol. 3* (Ed.: E. E. von Tamelen), Academic Press, New York, **1977**, p. 1.
[5] C. Tanford, *The Hydrophobic Effect. Formation of Micelles, Polymers and Biological Membranes*, Wiley Interscience, New York, **1973**, Chap. 9.
[6] J. N. Israelachvili, D. J. Mitchell, B. W. Ninham, *J. Chem. Soc. Faraday Trans. 2* **1976**, 1525.
[7] T. Kunitake, Y. Okahata, *J. Am. Chem. Soc.* **1977**, *99*, 3860.
[8] A. W. Ralston, D. N. Eggenberger, P. L. DuBrow, *J. Am. Chem. Soc.* **1948**, *70*, 977.
[9] H. Kunieda, K. Shinoda, *J. Phys. Chem.* **1978**, *82*, 1710.

[10] G. W. Gray, P. A. Winsor in *Lyotropic Liquid Crystals* (Ed.: S. Friberg), American Chemical Society, Washington, **1976**, Chap. 1, p. 10.
[11] J. H. Fendler, *Membrane Mimetic Chemistry*, Wiley-Interscience, New York, **1982**, Chap. 6.
[12] J.-H. Fuhrhop, J. Mathieu, *Angew. Chem.* **1984**, *96*, 124; *Angew. Chem. Int. Ed. Engl.* **1984**, *23*, 100.
[13] H. Ringsdorf, B. Schlarb, J. Venzmer, *Angew. Chem.* **1988**, *100*, 117; *Angew. Chem. Int. Ed. Engl.* **1988**, *27*, 113.
[14] T. Kunitake, Y. Okahata, K. Tamaki, F. Kumamaru, M. Takayanagi, *Chem. Lett.* **1977**, 387.
[15] K. Deguchi, J. Mino, *J. Colloid Interface Sci.* **1978**, *65*, 155.
[16] U. Herrmann, J. H. Fendler, *Chem. Phys. Lett.* **1979**, *64*, 270.
[17] Y. Y. Lim, J. H. Fendler, *J. Am. Chem. Soc.* **1979**, *101*, 4023.
[18] K. Kano, A. Romero, B. Djermoune, H. H. Ache, J. H. Fendler, *J. Am. Chem. Soc.* **1979**, *101*, 4030.
[19] A. M. Carmona-Ribeiro, H. Chaimovitch, *Biochem. Biophys. Acta.* **1983**, *733*, 172.
[20] T. Kunitake, Y. Okahata, *Chem. Lett.* **1977**, 1337.
[21] T. Kunitake, N. Nakashima, S. Hayashida, K. Yonemori, *Chem. Lett.* **1979**, 1413.
[22] E. J. R. Sudhölter, J. B. F. N. Engberts, D. Hoekstra, *J. Am. Chem. Soc.* **1980**, *102*, 2467.
[23] Y. Murakami, A. Nakano, K. Fukuya, *J. Am. Chem. Soc.* **1980**, *102*, 4235.
[24] J.-H. Fuhrhop, H. Bartsch, D. Fritsch, *Angew. Chem.* **1981**, *93*, 797; *Angew. Chem. Int. Ed. Engl.* **1981**, *20*, 804.
[25] T. Kunitake, M. Shimomura, Y. Hashiguchi, T. Kawanaka, *J. Chem. Soc. Chem. Commun.* **1985**, 833.
[26] T. Kunitake, Y. Okahata, *Bull. Chem. Soc. Jpn.* **1978**, *51*, 1877.
[27] R. A. Mortara, R. H. Quina, H. Chaimovitch, *Biochem. Biophys. Res. Commun.* **1978**, *81*, 1080.
[28] Y. Okahata, S. Tanamachi, M. Nagai, T. Kunitake, *J. Colloid Interface Sci.* **1981**, *82*, 401.
[29] T. Kajiyama, A. Kumano, M. Takayanagi, Y. Okahata, T. Kunitake, *Contemp. Top. Polym. Sci.* **1984**, *4*, 829.
[30] K. Okuyama, Y. Soboi, K. Hirabayashi, A. Harada, A. Kumano, T. Kajiyama, M. Takayanagi, T. Kunitake, *Chem. Lett.* **1984**, 2117.
[31] K. Okuyama, Y. Soboi, N. Iijima, K. Hirabayashi, T. Kunitake, T. Kajiyama, *Bull. Chem. Soc. Jpn.* **1988**, *61*, 1485.
[32] K. Okuyama, N. Iijima, K. Hirabayashi, T. Kunitake, M. Kusunoki, *Bull. Chem. Soc. Jpn.* **1988**, *61*, 2337.
[33] H. Okada, Kyushu University, unpublished.
[34] M. Kodama, T. Kunitake, S. Seki, *J. Phys. Chem.* **1990**, *94*, 1550.
[35] Y. Okahata, R. Ando, T. Kunitake, *Ber. Bunsenges. Phys. Chem.* **1981**, *85*, 789.
[36] T. Kunitake, R. Ando, Y. Ishikawa, *Mem. Fac. Eng. Kyushu Univ.* **1986**, *46*, 221.
[37] J.-M. Kim, T. Kunitake, *Mem. Fac. Eng. Kyushu Univ.* **1989**, *49*, 93.
[38] M. Shimomura, T. Kunitake, *Chem. Lett.* **1981**, 1001.
[39] M. Shimomura, T. Kunitake, *J. Am. Chem. Soc.* **1982**, *104*, 1757.
[40] T. Kunitake, H. Ihara, Y. Okahata, *J. Am. Chem. Soc.* **1983**, *105*, 6070.
[41] For example V. Luzzati in *Biological Membranes* (Ed.: D. Chapman), Academic Press, New York, **1968**, p. 71.
[42] Y. Murakami, A. Nakano, J. Kikuchi, T. Takaki, K. Uchimura, *Chem. Lett.* **1983**, 1891.
[43] Y. Murakami, J. Kikuchi, T. Takaki, K. Uchimura, A. Nakamo, *J. Am. Chem. Soc.* **1985**, *107*, 2161.
[44] Y. Murakami, J. Kikuchi, T. Takaki, K. Uchimura, *Bull. Chem. Soc. Jpn.* **1986**, *59*, 515.
[45] L. A. M. Rupert, D. Hoekstra, J. B. F. N. Engberts, *J. Am. Chem. Soc.* **1985**, *107*, 2628.
[46] L. A. M. Rupert, J. B. F. N. Engberts, D. Hoekstra, *J. Am. Chem. Soc.* **1986**, *108*, 3920.
[47] L. A. M. Rupert, J. F. L. van Breemen, E. F. J. van Bruggen, J. B. F. N. Engberts, D. Hoekstra, *J. Membr. Biol.* **1987**, *95*, 255.
[48] A. M. Carmina-Ribeiro, H. Chaimovitch, *Biophys. J.* **1986**, *50*, 621.
[49] For example D. F. Evans, B. W. Ninham, *J. Phys. Chem.* **1986**, *90*, 226.
[50] H. Hotani, *J. Mol. Biol.* **1984**, *178*, 113.
[51] N. Nakashima, S. Asakuma, T. Kunitake, H. Hotani, *Chem. Lett.* **1984**, 227.
[52] N. Kimizuka, T. Takasaki, T. Kunitake, *Chem. Lett.* **1988**, 1911.
[53] T. Kunitake, Y. Okahata, *J. Am. Chem. Soc.* **1980**, *102*, 549.
[54] M. Shimomura, R. Ando, T. Kunitake, *Ber. Bunsenges. Phys. Chem.* **1983**, *87*, 1134.
[55] Y. Okahata, T. Kunitake, *Ber. Bunsenges. Phys. Chem.* **1980**, *84*, 550.
[56] Y. Okahata, H. Ihara, M. Shimomura, S. Tawaki, T. Kunitake, *Chem. Lett.* **1980**, 1169.
[57] T. Kunitake, Y. Okahata, M. Shimomura, S. Yasunami, K. Takarabe, *J. Am. Chem. Soc.* **1981**, *103*, 5401.
[58] M. Shimomura, H. Hashimoto, T. Kunitake, *Chem. Lett.* **1982**, 1285.
[59] T. Kunitake, R. Ando, Y. Ishikawa, *Mem. Fac. Eng. Kyushu Univ.* **1986**, *46*, 245.
[60] I. Cho, J. G. Park, *Chem. Lett.* **1987**, 977.
[61] T. Kunitake, N. Yamada, N. Fukunaga, *Chem. Lett.* **1984**, 1089.
[62] M. Kasha in *Spectroscopy of the Excited State* (Ed.: B. D. Bartolo), Plenum Press, New York, **1976**, p. 337.
[63] T. Kunitake, M. Shimomura, T. Kajiyama, A. Harada, K. Okuyama, M. Takayanagi, *Thin Solid Films* **1984**, *121*, L89.
[64] G. Xu, K. Okuyama, M. Shimomura, *Polym. Prepr. Japan* **1989**, *38*, 2407.
[65] K. Okuyama, H. Watanabe, M. Shimomura, K. Hirabayshi, T. Kunitake, T. Kajiyama, N. Yasuoka, *Bull. Chem. Soc. Jpn.* **1986**, *59*, 3351.
[66] H. Watanabe, K. Okuyama, H. Ozawa, K. Hirabayashi, M. Shimomura, T. Kunitake, N. Yasuoka, *Nippon Kagaku Kaishi* **1988**, 55.
[67] K. Okuyama, C. Mizuguchi, G. Xu, M. Shimomura, *Bull. Chem. Soc. Jpn.* **1989**, *62*, 3211.
[68] Y. Nakayama, T. Takahagi, F. Soeda, A. Ishitani, M. Shimomura, K. Okuyama, T. Kunitake, *Appl. Surf. Sci.* **1988**, *33/34*, 1307.
[69] A. Harada, K. Okuyama, A. Kumano, T. Kajiyama, M. Takayanagi, T. Kunitake, *Polym. J.* **1986**, *18*, 281.
[70] Y. Ishikawa, T. Nishimi, T. Kunitake, *Chem. Lett.* **1990**, 165.
[71] T. Kunitake, N. Kimizuka, N. Higashi, N. Nakashima, *J. Am. Chem. Soc.* **1984**, *106*, 1978.
[72] N. Kimizuka, H. Ohira, M. Tanaka, T. Kunitake, *Chem. Lett.* **1990**, 29.
[73] For example S. C. Kushwaha, M. Kates, G. D. Sprott, I. C. P. Smith, *Biochem. Biophys. Acta* **1981**, *664*, 156.
[74] Y. Okahata, T. Kunitake, *J. Am. Chem. Soc.* **1979**, *101*, 5231.
[75] S. Yasunami, Masters Thesis, *Kyushu University*, **1980**.
[76] E. Baumgartner, J.-H. Fuhrhop, *Angew. Chem.* **1980**, *92*, 564; *Angew. Chem. Int. Ed. Engl.* **1980**, *19*, 550.
[77] J.-H. Fuhrhop, H.-H. David, J. Mathieu, V. Liman, H.-J. Winter, E. Boekema, *J. Am. Chem. Soc.* **1986**, *108*, 1785.
[78] T. Kunitake, A. Tsuge, K. Takarabe, *Polym. J. (Tokyo)* **1985**, *17*, 633.
[79] T. Kunitake, Y. Okahata, S. Yasunami, *J. Am. Chem. Soc.* **1982**, *104*, 5547.
[80] T. Kunitake, S. Tawaki, N. Nakashima, *Bull. Chem. Soc. Jpn.* **1983**, *56*, 3235.
[81] T. Kunitake, N. Higashi, *Makromol. Chem. Suppl.* **1985**, *14*, 81.
[82] T. Kunitake, N. Higashi, *J. Am. Chem. Soc.* **1985**, *107*, 692.
[83] For example P. Mukerjee, A. Y. S. Yang, *J. Phys. Chem.* **1976**, *80*, 1388.
[84] T. Kunitake, N. Nakashima, M. Shimomura, Y. Okahata, K. Kano, T. Ogawa, *J. Am. Chem. Soc.* **1980**, *102*, 6642.
[85] T. Kunitake, N. Nakashima, K. Morimitsu, *Chem. Lett.* **1980**, 1347.
[86] N. Nakashima, S. Asakuma, J.-M. Kim, T. Kunitake, *Chem. Lett.* **1984**, 1709.
[87] N. Nakashima, S. Asakuma, T. Kunitake, *J. Am. Chem. Soc.* **1985**, *107*, 509.
[88] Y. Ishikawa, T. Nishimi, T. Kunitake, *Chem. Lett.* **1990**, 25.
[89] T. Kunitake, N. Yamada, *J. Chem. Soc. Chem. Commun.* **1986**, 655.
[90] K. Yamada, H. Ihara, T. Ide, T. Fukumoto, *Chem. Lett.* **1984**, 1713.
[91] J.-M. Kim, Y. Ishikawa, T. Kunitake, *J. Chem. Soc. Perkin Trans. 2*, **1991**, 885.
[92] P. Yager, P. E. Schoen, *Mol. Cryst. Liq. Cryst.* **1964**, *106*, 371, and subsequent publications by these authors.
[93] B. Pfannemuller, W. Walte, *Chem. Phys. Lipids* **1985**, *37*, 227.
[94] J.-H. Fuhrhop, U. Liman, V. Koesling, *J. Am. Chem. Soc.* **1988**, *110*, 6840.
[95] N. Wagner, K. Dose, H. Koch, H. Ringsdorf, *FEBS Lett.* **1981**, *132*, 313.
[96] P. N. Tyminski, L. H. Latimer, D. F. O'Brien, *Biochemistry* **1988**, *27*, 2696.
[97] I. Hamachi, S. Noda, T. Kunitake, *J. Am. Chem. Soc.* **1990**, *112*, 6744.
[98] I. Hamachi, S. Noda, T. Kunitake, *J. Am. Chem. Soc.*, **1991**, 113, 9625.
[99] Y. Murakami, J. Kikuchi, K. Akiyoshi, N. Shiratori, *Isr. J. Chem.* **1987/1988**, *28*, 23.
[100] Y. Murakami, Y. Hisaeda, T. Ohno, Y. Matsuda, *Chem. Lett.* **1986**, 731.
[101] T. Kunitake, *New J. Chem.* **1987**, *11*, 141.
[102] For example R. A. Moss, T. Fujita, S. Ganguli, *Langmuir* **1990**, *6*, 1197.
[103] M. Shimomura, T. Kunitake, *J. Am. Chem. Soc.* **1987**, *109*, 5175.
[104] N. Nakashima, R. Ando, H. Fukushima, T. Kunitake, *J. Chem. Soc. Chem. Commun.* **1982**, 707.
[105] T. Kunitake, Y. Ishikawa, M. Shimomura, *J. Am. Chem. Soc.* **1986**, *108*, 327.
[106] For example N. Kimizuka, T. Kunitake, *Colloids Surf.* **1989**, *38*, 79.
[107] S. Kato, T. Kunitake, *Chem. Lett.* **1991**, 261.
[108] N. Nakashima, R. Ando, T. Kunitake, *Chem. Lett.* **1983**, 1577.
[109] For example W. L. Hubell, H. M. McConnell, *Proc. Natl. Acad. Sci. USA* **1989**, *64*, 20.
[110] Y. Okahata, H. Ebato, *Anal. Chem.* **1989**, *61*, 2185.
[111] T. Kunitake, Y. Ishikawa, M. Shimomura, H. Okawa, *J. Am. Chem. Soc.* **1986**, *108*, 2059.
[112] Y. Ishikawa, T. Kunitake, *J. Am. Chem. Soc.* **1991**, *113*, 621.
[113] S. Asakuma, T. Kunitake, *Chem. Lett.* **1989**, 2059.
[114] S. Asakuma, H. Okada, T. Kunitake, *J. Am. Chem. Soc.* **1991**, *113*, 1749.
[115] K. Sakata, T. Kunitake, *Chem. Lett.* **1989**, 2159.
[116] K. Sakata, T. Kunitake, *J. Chem. Soc. Chem. Commun.* **1990**, 504.
[117] H. Okada, K. Sakata, T. Kunitake, *Chem. Mater.* **1990**, *2*, 89.
[118] Y. Ishikawa, H. Kuwahara, T. Kunitake, *J. Am. Chem. Soc.* **1989**, *111*, 8530.
[119] Y. Ishikawa, H. Kuwahara, T. Kunitake, *Chem. Lett.* **1989**, 1737.

Are Denser Packings of Spheres than Closest Packings Possible? How Many Closest Packings of Spheres Exist?

By *Ulrich Müller**

In 1611 Johannes Kepler wrote a humorous 24-page epistle which was a New Year's present to his benefactor in Prague, the Imperial Councilor Wackher von Wackenfels.[1] Here he proposed an explanation of the hexagonal shape of snowflakes: Water vapor, once it feels the penetrating coldness, freezes into little spheres with some definite size which he calls vapor spheres (*sphaere vapidae*). The vapor spheres in contact with one another adopt the arrangement that we nowadays call cubic closest packing of spheres and which we know to be the structural principle of many metals and of the solid noble gases. For this packing Kepler asserted, "It is the tightest possible; in no other arrangement can more spheres be accommodated in the same vessel."[2] The term closest packing of spheres shows that chemists, physicists, and crystallographers have long intuitively accepted Kepler's assertion; however, it was not proven mathematically until 1991 by W. Y. Hsiang.[3]

For periodically ordered packings of spheres, i.e. lattice packings, Gauss furnished the proof of the highest packing density, although he did not mention packings of spheres at all.[4] However, he introduced the concept of a lattice, and by relating it to the Seeber's theorems[5] on number theory he stated: the volume V of the (primitive) unit cell of a lattice will always satisfy the condition $V\sqrt{2} \geq abc$ if the face and body diagonals of the cell are not shorter than the lattice parameters a, b, and c. The upper limit of the space filling of a lattice packing of equal spheres follows from this condition as was shown by Minkowski.[6] The primitive unit cell of the cubic closest packing of spheres fulfilling Gauss's condition is a rhombohedral cell with the cell edges $a = b = c = 2r$ and the volume $V = \frac{1}{2}a^3\sqrt{2}$ ($r =$ radius of a sphere). This volume is exactly equal to the limiting value of the Gauss condition: $V\sqrt{2} = (\frac{1}{2}a^3\sqrt{2})\sqrt{2} \geq a^3$ (it also is identical for any other closest packing of spheres). A crystal lattice having a smaller unit cell volume, i.e. with greater packing density, is therefore not possible for a packing of equal spheres. This statement, however, is valid only when there is a crystal lattice.

Just as chemists presently have caught the buckyball fever, crystallographers are fiercely discussing the topic of quasi crystals. Quasi crystals have symmetry (e.g. fivefold rotation axes or icosahedral symmetry), and there is a near order around the atoms, but they have no three-dimensional periodical order. Could a quasi-crystalline packing of spheres exist having a higher degree of space filling than a cubic closest packing of spheres? Since the twelve spheres surrounding a central sphere of the same size in an icosahedral arrangement are not in contact with each other, a larger space filling seems possible at first (the coordination number in a closest packing of spheres is 12). Mathematicians have repeatedly furnished proofs with upper limits for the space filling, with values that have been decreasing over the years in the third or fourth decimal place, e.g. 0.77964 (1958), 0.77844 (1986), and finally 0.77836 (1988). There have also been repeated attempts to design nonperiodical packings of spheres, for instance with fivefold symmetry[7] or consisting of shells with icosahedral symmetry,[8] but not even the space filling of a closest packing of spheres was ever achieved.

The central idea of Hsiang's proof concerns the domains of influence of the spheres (also called the Wirkungsbereich, Voronoi domain, Dirichlet domain, or Wigner–Seitz cell). The domain of influence of a sphere is the polyheron made up of the set of planes perpendicular to the lines that connect the sphere under consideration to the surrounding spheres and passing through the midpoints of these lines. (For spheres in contact with each other these are the tangent planes between the spheres.) Kepler described the domain of influence of a sphere in the cubic closest packing by considering the seeds in a pomegranate. Initially the seeds are round, but later as the rind hardens and the seeds continue to grow, they become tightly packed and squeezed together, filling the remaining space and finally taking the shape of rhombic dodecahedra (Fig. 1). In an arbitrary packing of spheres the domains of influence fill the space completely, so that the space filling results from the ratio of the sphere volume to the mean volume of all domains of influence. The domain of influence of the cubic closest packing of spheres, the rhombic dodecahedron, has a volume of $4\sqrt{2}$ when the sphere radius is $r = 1$. With the sphere volume $\frac{4}{3}\pi$ we thus calculate the well-known degree of space filling of the cubic closest packing of spheres to be $\frac{4}{3}\pi/(4\sqrt{2}) = \frac{1}{6}\pi\sqrt{2} = 0.7404805$.

The smallest possible local domain of influence of a single sphere results when it is coordinated icosahedrally;[9] this domain of influence is a pentagonal dodecahedron (Fig. 1). It has a volume of $10\sqrt{2(65 - 29\sqrt{5})}$, which yields a local space filling of 0.7546974. This value had been suspected to be the upper limit for sphere packings but was never proven.[9] Since space cannot be completely filled by pentagonal dodecahedra, other spheres must have different domains of influence. What is the minimum mean volume of all domains of influence?

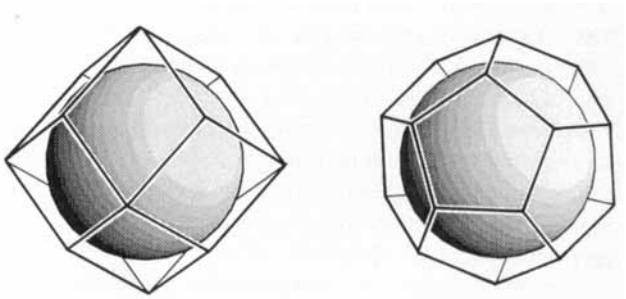

Fig. 1. Rhombic dodecahedron (left) and pentagonal dodecahedron (right) enclosing spheres of equal size.

[*] Prof. Dr. U. Müller
FB Chemie der Universität
Hans-Meerwein-Strasse, D-W-3550 Marburg (FRG)

Table 1. Number of possible stacking variants of closest packings of spheres depending on the space group type [15]. N = number of layers per packet.

N	$P6_3/mmc$	$P6_3mc$	$P\bar{6}m2$	$P\bar{3}m1$	$P3m1$	$R\bar{3}m$	$R3m$	total
2	1 [a]	–	–	–	–	–	–	1
3	–	–	–	–	–	1 [b]	–	1
4	1	–	–	–	–	–	–	1
5	–	–	–	1	–	–	–	1
6	1	–	1	–	–	–	–	2
7	–	–	–	3	–	–	–	3
8	2	–	2	2	–	–	–	6
9	–	–	–	3	3	1	–	7
10	3	–	6	5	2	–	–	16
11	–	–	–	11	10	–	–	21
12	3	1	12	11	15	1	–	43
24	30	70	990	984	57208	6	2	59290
36	252	3514	65268	65240	159005154	28	42	159139498
48	2040	173740	4192200	4192080	488667525580	120	620	488676086380

[a] Hexagonal closest packing. [b] Cubic closest packing, space group $Fm\bar{3}m$.

In addressing this question Hsiang considered a second shell of spheres, consisting of 42 to 44 spheres around the 12 spheres of the first shell; including the central sphere this amounts to a total of 55 to 57 spheres. His impressive goal was to analyze all possible configurations and to derive the domains of influence of the spheres of the first shell. Most configurations could be eliminated because the volumes are too large; for other configurations it had to be shown that they are close to certain key configurations. The distinction of these cases makes up the greater part of the proof which extends over more than 150 pages. First a new method for estimating the volume of local domains of influence was used to prove that the global space filling cannot exceed the local space filling in a pentagonal dodecahedron. Then after introducing the concept of semiglobal space-filling, he derived the maximum global space-filling; it is 0.7404805.

Hsiang first circulated his proof among mathematicians who now have the opportunity to check its correctness. In other circles his work became known by two communications.[10, 11]

Another problem that had never been solved was the question of the possible number of different closest packings of spheres that all have the same space filling as cubic closest packing. For stacks of hexagonal layers of spheres, any stacking sequence of layers with the positions A, B, and C is possible as long as no two layers of the same position are adjacent; therefore, the number of stacking variants is infinite. But how many arrangements are possible for periodical stackings in which a packet of a given number of layers is repeated? First of all, we have to make a clarifying statement: if we take the cubic closest packing of spheres and consider a stacking direction inclined towards the layer plane $A \rightarrow B \rightarrow C \rightarrow A$..., then we have a translationary equivalent layer after one layer (one layer per packet). However, if we only consider a stacking direction perpendicular to the layers, the packet is repeated only after three layers, $(ABC) \rightarrow (ABC)$... An inclined stacking of a packet having N layers will always result in a rhombohedral structure which can be described in a hexagonal setting with packets consisting of $3N$ layers. In the following we will only consider the perpendicular stacking direction.

For a small number of layers per packet the possible stacking sequences can be written down and counted.[12–14] The method for calculating the number of possibilities for an arbitrary number of layers per packet was first demonstrated in 1981 by McLarnan.[15] This approach is based on Pólya's theorem,[16] (which can also be used to calculate the number of isomers of organic compounds). If, in addition, some group theory and White's extension of Pólya's theorem are included,[17, 18] the number of stacking variants with a given symmetry (space group) can also be calculated. Table 1 lists some of the numbers calculated by McLarnan. The table illustrates why it is a significant progress to be able to calculate the numbers with dependence on symmetry: The largest numbers result for low symmetries, whereas in the higher symmetry space group types $P6_3/mmc$ and $R\bar{3}m$ the numbers are relatively small. Chemically reasonable crystal structures are usually only those with higher symmetry. The method described by McLarnan[18] can also be adapted for the calculation of the number of crystal structure types possible with particular space groups for any kind of compound, provided that some definite packing principle can be stated.[19]

I thank Prof. Dr. E. Krafft for helping me locate Kepler's papers.

German version: *Angew. Chem.* **1992**, *104*, 744

[1] J. Kepler, *Strena seu de nive sexangula*, G. Tampach, Frankfurt, **1611**. Reprinted in: *Johannes Kepler – gesammelte Werke* (Eds.: W. van Dyck, M. Caspar, F. Hammer), Vol. IV, C. H. Beck, München, **1941**, p. 261–280. English translation: *On the Six-Cornered Snowflake*, Oxford University Press, **1966**.

[2] "Coaptatio fiet arctissima: ut nullo praetera ordine plures globuli in idem vas compingi queant."

[3] W. Y. Hsiang, Reports PAM-530 and PAM-535. Center for Pure and Applied Mathematics, University of California, Berkeley, **1991**. *Bull. Brazilian Math. Soc.*, in press.

[4] C. F. Gauss, *Werke II*. Königliche Gesellschaft der Wissenschaften, Göttingen, **1876**, pp. 188–196.

[5] L. A. Seeber, *Untersuchungen über die Eigenschaften der positiven ternären quadratischen Formen*, Freiburg, **1831**.

[6] H. Minkowski, *Nachr. Ges. Wiss. Göttingen Math. Phys. Kl.* **1904**, 311.

[7] B. G. Bagley, *Nature* **1965**, *208*, 674; *ibid.* **1970**, *225*, 1040.

[8] A. L. Mackay, *Acta Crystallogr.* **1962**, *15*, 916.

[9] L. Fejes Tóth, *Lagerungen in der Ebene auf der Kugel and im Raum*, Springer, Berlin, **1953**, p. 171.

[10] I. Stewart, *New Scientist* **1991**, *130*, No. 1777, 29.

[11] N. Max, *Nature* **1992**, *355*, 115.

[12] G. Hägg, *Ark Kemi Mineral. Geol. B* **1943**, *16*, 1.

[13] G. S. Zhdanov, *Dokl. Akad. Nauk SSSR* **1945**, *48*, 40.

[14] P. A. Beck, *Z. Kristallogr.* **1967**, *124*, 101.

[15] T. J. McLarnan, *Z. Kristallogr.* **1981**, *155*, 269.

[16] G. Pólya, *Acta Math.* **1937**, *68*, 145.

[17] D. E. White, *Discrete Math.* **1975**, *13*, 277.

[18] T. J. McLarnan, *Z. Kristallogr.* **1981**, *155*, 277.

[19] U. Müller, *Acta Crystallogr. Sect. B* **1992**, *48*, in press.

Oxazaborolidines and Dioxaborolidines in Enantioselective Catalysis**

By *Braj B. Lohray**, and *Vidya Bhushan*

The success of enantioselective catalysts depends on the nature of the metal and the structure and electronic properties of the chiral ligands. A number of highly efficient and useful catalysts are now available for various reactions.[1] Boranes serve as chiral reagents for a number of asymmetric reactions. One of the earliest examples of borane catalysts for the reduction of ketones (or ketoxime ethers) to secondary alcohols (or amines) was reported by Itsuno et al.,[2] in which (*S*)-valinol was used as chiral ligand. Simultaneously, Corey et al.[3a] investigated the enantioselective reduction of ketones with THF · BH_3 and (*S*)-diphenylprolinol borane adduct as catalyst. Later they also employed other oxazaboroles, for example, **1**, R = Me, *n*Bu, as catalysts and used other boranes as reducing agents.[3b,c] (The catalysts **1**, which are easily accessible in both the *R* and the *S* form, are termed CBS reagents.) These afforded excellent yields and enantioselectivities (80–99% *ee*) under very mild reaction conditions (0–25 °C). The reaction (Scheme 1) requires both

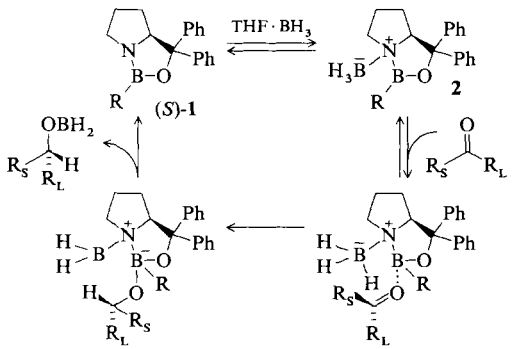

Scheme 1. Possible mechanism of the borane-catalyzed enantioselective reduction of ketones with THF · BH_3.

reagents: neither the catalyst (*S*)-**1** nor THF · BH_3 alone are able to reduce the ketone in considerable yield. Thus, the active reducing species, the "chemzyme" has been postulated to be an intermediate complex **2**, which is formed from (*S*)-**1** and BH_3. Mathre et al. from industry[4a] have modified the preparation of (*S*)-**1** and used it for the synthesis of MK-0471, a carboanhydrase inhibitor.[4b] Martens et al.[4c] reported the use of oxazaborolidines derived from (*S*)-indole-2-carboxylic acid for asymmetric reduction of aromatic ketones, though in lower selectivity.

Two particularly recent examples of borane-catalyzed reductions will now be described: Corey and Link[5] have reported a general method for the synthesis of α-amino acids using (*S*)-**1** (R = *n*Bu) as the chiral catalyst for the enantioselective reduction of alkyl (trichloromethyl) ketones by catecholborane. The (2*R*)-1,1,1-trichloroalkan-2-ol thus obtained was treated with NaOH (4 equiv) and NaN_3 (2 equiv) at 23 °C affording (*S*)-α-azido acids, which were subsequently reduced to α-amino acids. Bringmann and Hartung[6] have synthesized substituted chiral biaryls by the reduction of substituted 2-pyranones with THF · BH_3 in the presence of oxazaborolidines.

Brown et al.[7] achieved the enantioselective addition of diethylzinc to several aldehydes in high yield and optical purity (up to 96% *ee*) by using (4*S*,5*R*)-3,4-dimethyl-5-phenyl-1,3,2-oxazaborolidine. Because B–O and B–N bonds are shorter than metal-oxygen and -nitrogen bonds, there is a better chance that the boron catalysts will be more effective.

Yamamoto et al.[8] suggested that acyloxyboranes might behave as mixed anhydrides because of the electronegative trivalent boron atom and could serve as effective catalysts for various reactions. The chiral acyloxyborane (CAB) **3** prepared by the reaction of monoacylated tartaric acid with one equivalent of THF · BH_3 in dichloromethane at 0 °C is an excellent catalyst for the asymmetric allylation of aldehydes by allylsilanes (Scheme 2).[8] The reaction proceeds at

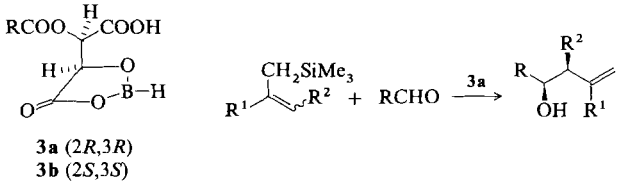

3a (2*R*,3*R*)
3b (2*S*,3*S*)

Scheme 2. Asymmetric allylation with allylsilanes in the presence of 20 mol % **3a**. R = 2,6-dimethoxyphenyl.

−78 °C to furnish predominantly *erythro* homoallylic alcohols (*erythro*:*threo* = 80:20 to 97:3) regardless of the configuration of the allylsilanes. CAB is an equally effective catalyst for the Diels–Alder reactions[9] of a variety of dienes with several dienophiles (α,β-unsaturated acids and aldehydes) under very mild reaction conditions (−78 °C) (Scheme 3). Good to excellent diastereo- (99:1 to 88:12) and

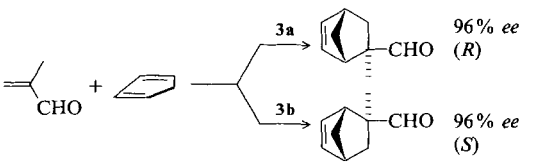

Scheme 3. Diels–Alder reactions enantioselectively catalyzed with 10 mol % **3**.

enantioselectivities (80–97% *ee*) have been observed in most of the cases. The reactive species is assumed to be 1,3,2-dioxaborolidine **3** and the dienophile.

Yamamoto et al.[10] have extended these studies to Diels–Alder reactions catalyzed by *N*-arylsulfonyl 1,3,2-oxazaborolidine **4**. The stereoselectivity with these catalysts is relatively inferior to that observed with **3**. Similar observations have been reported by Helmchen et al.[11] for the Diels–Alder reaction of cyclopentadiene and methacrolein (*exo*:*endo* = 99:1, 64% *ee* for the *exo* isomer) or crotonaldehyde (*exo*:*endo* = 3:97; 72% *ee* for the *endo* isomer). Use of bulkier aryl substituents such as 2,4,6-triisopropyl- and 2,4,6-tri-*t*-butylphenyl in **4** had little influence on the diastereoselectivity of the cycloaddition.

[*] Dr. B. B. Lohray, Dr. V. Bhushan
Division of Organic Chemistry
National Chemical Laboratory
Pune 411008 (India)

[**] N.C.L. communication no. 5394.

Corey and Loh[12] have reported that the Diels–Alder reaction of cyclopentadiene and 2-bromoacrolein, which is catalyzed by oxazaborolidines **4** derived from *N*-tosyl-(*S*)-tryptophan, in dichloromethane at −78 °C gives (*R*)-bromoaldehyde **5** (*exo*:*endo* = 97:3, 96% *ee*) in 1 h. The observed stereoselectivity in this case is opposite to that normally observed for oxazaborolidines **4** generated from *N*-tosyl derivatives of (*S*)-valine or (*S*)-hexahydrophenylalanine. These results suggest a transition state **6** for the synthesis of **5**,[12] in which the dienophile assumes an orientation parallel to the indole ring because of the π–π donor–acceptor interactions. The CAB **3** not only catalyzes allyl transformations (Scheme 2) but also asymmetric aldol reactions between silylenol ethers and aldehydes (Scheme 4).

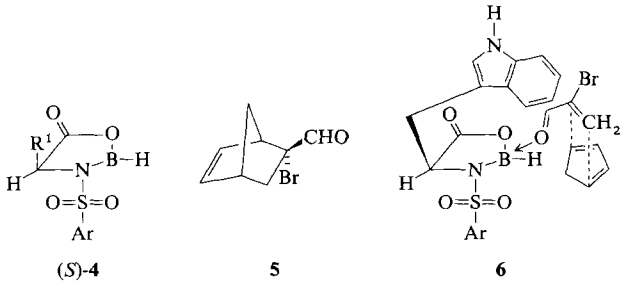

(*S*)-**4** **5** **6**

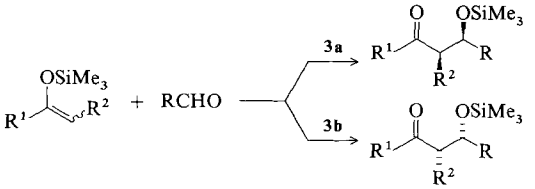

Scheme 4. Aldol reactions enantioselectively catalyzed with 20 mol % **3**.

Yamamoto et al.[13] used 20 mol % of CAB **3** in propionitrile at −78 °C as a highly efficient catalyst for the condensation of several *E* and *Z* silylenol ethers and ketene acetals with a variety of aldehydes (yields 49–97%, 80–97% *ee*). Interestingly, regardless of the configuration of the enol ethers, the *erythro* isomer always predominated (*erythro*:*threo* = 80/20 to >95/<5).

Aromatic and α,β-unsaturated aldehydes always provided higher diastereo- (*erythro*:*threo* ≥ 94:6) and enantioselectivities (92–97% *ee*) than saturated aldehydes. Polar solvents improved the selectivity by decreasing the association of the catalyst with the formation of oligomers as observed by Helmchen.[11]

Kiyooka et al.[14] and Masamune et al.[15] used oxazaborolidine **7** under stoichiometric and substoichiometric (ie, as chiral catalysts) conditions, respectively, as the catalyst for aldol reactions. Masamune suggested that the initial aldol adduct **8** must undergo ring closure (as indicated by arrow in Scheme 5 to release the final product **9** and to regenerate the catalyst. In many cases, slow addition of the aldehyde to the reaction mixture proved beneficial (permits enough time for **8** to undergo ring closure) for improving the enantioselectivity of the reaction. Thus, α,α-disubstituted *N*-arylsulfonylglycines were used for the preparation of the oxazaborolidine **7**, which resulted in catalytic asymmetric aldol processes providing β-hydroxy esters of >97% *ee* from α-unbranched aldehydes (RCH_2CHO) and 84–96% *ee* with α-branched aldehydes (R_2CHCHO). The reaction proceeds smoothly in propionitrile at −78 °C if the aldehydes are added slowly over 3.5 h affording high yields (68–89%) of the adduct.

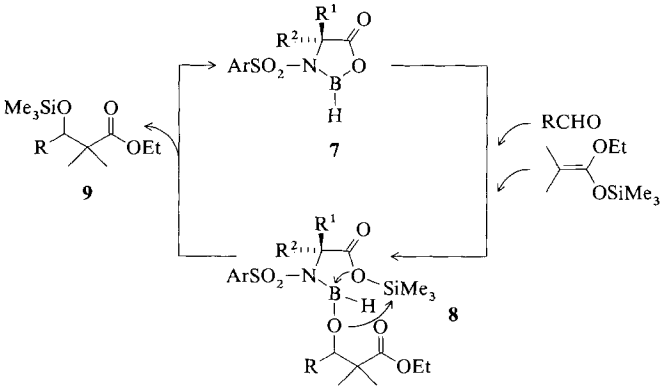

Scheme 5. Oxazaborolidine in aldol reactions.

In summary, oxaza- or dioxaborolidines have been found to be effective catalysts for several reaction types and probably in the future other applications will be discovered for such catalysts.

German version: *Angew. Chem.* **1992**, *104*, 740

[1] *Asymmetric Synthesis, Vol. 5* (Ed.: J. D. Morrison), Academic Press, Orlando, FL, USA, **1985**; R. Noyori, M. Kitamura in *Modern Synthetic Methods, Vol. 5* (Ed.: R. Scheffold), Springer, Berlin, **1989**, p. 115.

[2] S. Itsuno, Y. Sakurai, K. Ito, A. Hirao, S. Nakahama, *Bull. Chem. Soc. Jpn.* **1987**, *60*, 395.

[3] a) E. J. Corey, R. K. Bakshi, S. Shibata, *J. Am. Chem. Soc.* **1987**, *109*, 5551; b) E. J. Corey, *Pure Appl. Chem.* **1990**, *62*, 1209; c) E. J. Corey, R. K. Bakshi, *Tetrahedron Lett.* **1990**, *31*, 611.

[4] a) D. J. Mathre, T. K. Jones, L. C. Xavier, T. J. Blacklock, R. A. Reamer, J. J. Mohan, E. T. T. Jones, K. Hoogsteen, M. W. Baum, E. J. J. Grabowski, *J. Org. Chem.* **1991**, *56*, 751; b) *ibid.* **1991**, *56*, 763; c) J. Martens, C. Dauelsberg, W. Behnen, S. Waldbaum, *Tetrahedron Asymmetry* **1992**, *3* 347.

[5] E. J. Corey, J. O. Link, *J. Am. Chem. Soc.* **1992**, *114*, 1906.

[6] G. Bringmann, T. Hartung, *Angew. Chem.* **1992**, *104*, 782; *Angew. Chem. Int. Ed. Engl.* **1992**, *31*, 761.

[7] N. N. Joshi, M. Srebnik, H. C. Brown, *Tetrahedron Lett.* **1989**, *30*, 5551.

[8] K. Furuta, M. Mouri, H. Yamamoto, *Synlett* **1991**, 561.

[9] a) K. Furuta, Y. Miwa, K. Iwanaga, H. Yamamoto, *J. Am. Chem. Soc.* **1988**, *110*, 6254; b) K. Furuta, S. Shimizu, Y. Miwa, H. Yamamoto, *J. Org. Chem.* **1989**, *54*, 1481.

[10] M. Takasu, H. Yamamoto, *Synlett* **1990**, 194.

[11] a) D. Sartor, J. Saffrich, G. Helmchen, *Synlett* **1990**, 197; b) D. Sartor, J. Saffrich, G. Helmchen, C. J. Richards, H. Lambert, *Tetrahedron: Asymmetry* **1991**, *2*, 639.

[12] E. J. Corey, T.-P. Loh, *J. Am. Chem. Soc.* **1991**, *113*, 8966.

[13] a) K. Furuta, T. Maruyama, H. Yamamoto, *J. Am. Chem. Soc.* **1991**, *113*, 1041; b) *Synlett* **1991**, 439.

[14] S. Kiyooka, Y. Kaneko, M. Komura, H. Matsuo, M. Nakano, *J. Org. Chem.* **1991**, *56*, 2276.

[15] E. R. Parmee, O. Tempkin, S. Masamune, *J. Am. Chem. Soc.* **1991**, *113*, 9365.

Penetrated Ion Pairs: a New Form of Ion Pair

By *Gernot Boche**

Since the pioneering work of Grunwald[1], Winstein et al.,[2] and Fuoss et al.[3] the terms *contact*, *tight*, or *intimate ion pair* and *solvent-separated* or *loose ion pair* have become well known in the chemical world.[4] More recently, Marcus coined another phrase, the *solvent-shared ion pair*.[5] The simplest representations of these ion pairs are shown in Scheme 1.

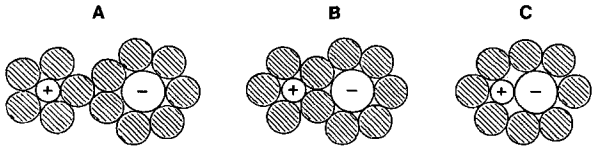

Scheme 1. Schematic representation of a solvent-separated ion pair **A**, a solvent-shared ion pair **B**, and a contact ion pair **C**.

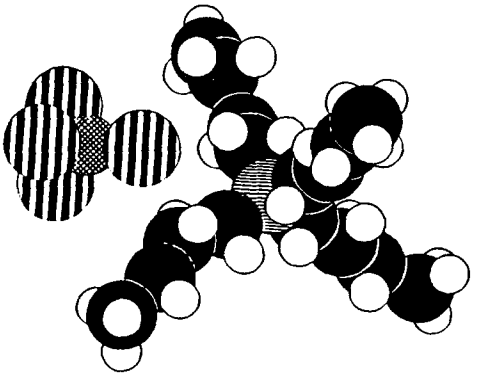

Scheme 2. Penetration of a BF_4^- ion into the empty spaces between the alkyl chains of a tetrabutyl ammonium ion. C atoms are represented by black, H atoms by white, N atoms by fine-hatched, F atoms by coarse-hatched, and B atoms by cross-hatched spheres.

In solvent-separated ion pairs the solvation shells of the cation and the anion touch each other, in solvent-bridged ion pairs the ions share solvent molecules, and in contact ion pairs cation and anion are directly bound to each other and are surrounded by a common solvation shell. There are very few cases in which all three forms have been structurally confirmed; one example is fluorenyllithium, by crystal structure investigations. The cation in fluorenyllithium·2quinuclidine is bound to two C atoms of the fluorenyl anion, an example of a contact ion pair.[6] The ethylenediamine molecules in [fluorenyllithium·2ethylenediamine]$_\infty$ form a three-dimensional network with the Li^+ ions fourfold coordinated to the NH_2 groups. The N-H bridged fluorenyl anions are embedded in this network; thus, cation and anion share the ethylenediamine "solvent" molecules. Models for solvent-separated ion pairs are 1,ω-bis(9-lithio-fluoren-9-yl)ethane and -hexane, each of which crystallizes with eight tetrahydrofuran molecules; each Li^+ ion is tetrahedrally surrounded by four "solvent" molecules. The THF molecules have no bonding contact with the anion.

Recently, greater emphasis has been placed on structural details of the interaction of cation and anion for more complex ion pairs in solution. $^6Li,^1H$ HOESY measurements on fluorenyllithium in different solvents have provided the most accurate information so far concerning this compound,[9] which has been intensively studied. The structure of the ion pair from *N*-allyl-*N*-ethyl-*N*-methylanilinium-*p*-toluenesulfonate, in which the *p*-toluenesulfonate anion can be bound to four different sides of the chiral ammonium ion, was investigated by dipole moment measurements in various solvents.[10]

The interpenetration of the ions is the most recent discovery, which was originally deduced from conductivity measurements on tetraalkylammonium salts with alkyl chains of varying length, and with different anions.[11] The empty spaces between the alkyl chains can be occupied to a certain degree by smaller ions as shown in Scheme 2. Thus, ion pairs are formed whose van der Waals volume is smaller than the sum of the volumes of the single ions.

More precise information on the position of an "anion in the cation" was provided by $^1H,^1H$ and $^{11}B,^1H$ NOE investigations on tetra-*n*-butyl ammonium borohydride:[12] the BH_4 anion and the quaternary nitrogen atom of the cation must be in close contact, since each of three of the BH_4^- hydrogen atoms is in van der Waals contact with two α-CH_2 protons and one β-CH_2 proton of the alkyl chain.

Investigations concerning the interactions of the two ions in ion pairs such as 1-benzyl-15-methoxycinchonanium hydroborate (**1**) are of practical signifiance for the stereoselective synthesis.[13] Cations such as that of **1** are applied in

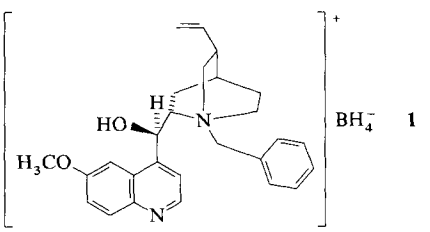

1

phase transfer catalyzed reactions, in which the cation transports the anion into the organic phase. In this phase the chirality of the cation can lead to induction of the BH_4^- reaction. Hence, it is important to know which structure(s) the ion pair forms so that the cause of the chiral induction can be traced and more effective chiral catalysts can be applied. The complete assignment of the protons in the ^1H NMR spectrum of the chiral ion pair **1** and the investigation of the interionic contacts was achieved with a combination of COSY and ROESY NMR spectroscopy. The investigation showed that BH_4^- can penetrate the cationic center at two of the four faces of the trigonal pyramidal coordination polyhedron of the quaternary nitrogen. If this result is compared with the model representations of ion pairs shown in Scheme 1, it is clear which details of the structure of ion pairs are nowadays

[*] Prof. Dr. G. Boche
Fachbereich Chemie der Universität Marburg
Hans-Meerwein-Strasse, D-W-3550 Marburg (FRG)

accessible by NMR spectroscopy. It seems appropriate at this point to mention the term molecular recognition.

A recent publication about a photochemical investigation[14] also provides inside information into important aspects of a structure with penetrated ion pairs. Whereas trimethinecyanine borates in which the borate possesses different substituents than the 4-(1-triptycyl)phenyl groups in **2**, form *trans* → *cis* isomerizations of a double bond on irradiation, this does not happen for **2**.

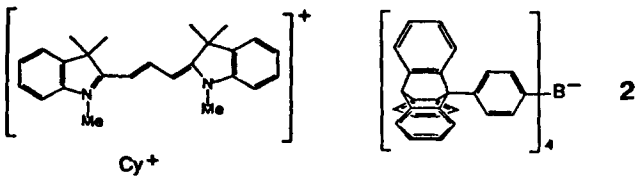

2

Model calculations showed that there is sufficient space in **2** for the penetration of the trimethinecyanine cation (Cy^+) between the 4-(1-triptycyl)phenyl substituents of the borate. However, as soon as the anion has been penetrated by the Cy^+ ion, the cation cannot start the rotation that would lead to the *trans* → *cis* isomerization without cooperative movements in the borate. Figure 1 shows the difference in the ion pair character depending on the borate substituents: the trimethinecyanine cation (red) can penetrate the borate with 4-(1-triptycyl)phenyl groups (Fig. 1, top), whereas a contact ion pair occurs for the $(C_6F_5)_4B$ anion (Fig. 1, bottom).

In summary, the realization that there are *penetrated ion pairs* is a result of recent structure investigations of ion pairs. The importance of this new form of ion pair is already shown by the few examples known.

German version: *Angew. Chem.* **1992**, *104*, 742

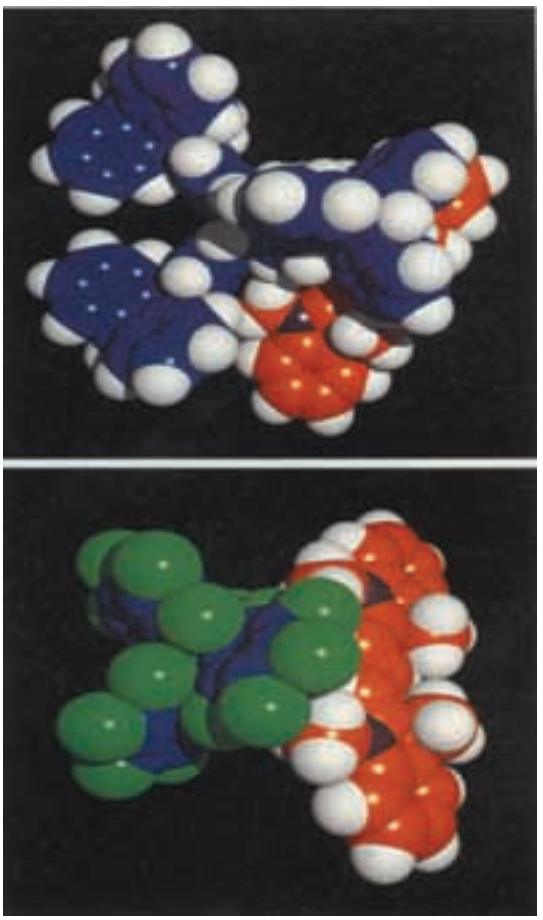

Fig. 1. Top: **2** occurs as a penetrated ion pair. Bottom: If $(C_6F_5)_4B^-$ is used as anion then a contact ion pair is formed.

[1] E. Grunwald, *Anal. Chem.* **1954**, *26*, 1696–1701.

[2] S. Winstein, E. Clippinger, A. H. Fainberg, G. C. Robinson, *J. Am. Chem. Soc.* **1954**, *76*, 2597–2598.

[3] a) R. M. Fuoss, H. Sadek, *J. Am. Chem. Soc.* **1954**, *76*, 5897–5901; b) *ibid.* **1954**, *76*, 5905–5909.

[4] Some review articles and books with further literature citations: a) J. Smid, *Angew. Chem.* **1972**, *84*, 127–144; *Angew. Chem. Int. Ed. Engl.* **1972**, *11*, 112–127; b) I. P. Beletskaya, *Russ. Chem. Rev. Engl. Transl.* **1975**, *44*, 1067–1090; c) T. E. Hogen-Esch, *Adv. Phys. Org. Chem.* **1977**, *15*, 153–266; d) M. Szwarc, *Ions and Ion Pairs in Organic Reactions, Vol. 1, Vol. 2*, Wiley-Interscience, New York, **1972** and **1974**; e) C. Reichardt, *Solvents and Solvent Effects in Organic Chemistry*, VCH, Weinheim, **1990**.

[5] Y. Marcus, *Ion Solvation*, Wiley, Chichester, **1985**.

[6] J. J. Brooks, W. Rhine, G. D. Stucky, *J. Am. Chem. Soc.* **1972**, *94*, 7339–7346.

[7] S. Buchholz, K. Harms, M. Marsch, W. Massa, G. Boche, *Angew. Chem.* **1989**, *101*, 57–59; *Angew. Chem. Int. Ed. Engl.* **1989**, *28*, 72–73.

[8] B. Becher, V. Enkelmann, K. Müllen, *Angew. Chem.* **1989**, *101*, 501–503; *Angew. Chem. Int. Ed. Engl.* **1989**, *28*, 458–460.

[9] D. Hoffmann, W. Bauer, P. von R. Schleyer, *J. Chem. Soc. Chem. Commun.* **1990**, 208–211.

[10] M. K. Begum, E. Grunwald, *J. Am. Chem. Soc.* **1990**, *112*, 5104–5110.

[11] A. P. Abbott, D. J. Schiffrin, *J. Chem. Soc. Faraday Trans.* **1990**, *86*, 1453–1459.

[12] T. C. Pochapsky, P. M. Stone, *J. Am. Chem. Soc.* **1990**, *112*, 6714–6715.

[13] T. C. Pochapsky, P. M. Stone, *J. Am. Chem. Soc.* **1991**, *113*, 1460–1462.

[14] X. Xang, A. Zaitsev, B. Sauerwein, S. Murphy, G. B. Schuster, *J. Am. Chem. Soc.* **1992**, *114*, 793–794.

Communications may be submitted in English *or* in German. Further details regarding the submission of communications can be found in the "Notice to Authors" reproduced in the January issue of the journal. Copies thereof may be obtained from the editorial office upon request.

Self-Assembly of a Cu_4 Complex with Coplanar Copper(I) Ions: Synthesis, Structure, and Electrochemical Properties**

By *Marie-Thérèse Youinou,* Noureddine Rahmouni, Jean Fischer*, and *John A. Osborn*

Ligands containing multiple binding sites are of interest for the construction of structural and reactivity models of certain metallobiomolecules as well as polyelectronic systems.[1] The ligand 3,6-bis(2'-pyridyl)pyridazine (dppn)[2] complexes a variety of metal ions,[3] and given our interest in dicopper-containing proteins, the binuclear copper(II) complexes of dppn attracted our attention.[4] Therefore, we studied the interaction of copper(I) ions with this ligand and report here the structure and some properties of the resultant complexes.

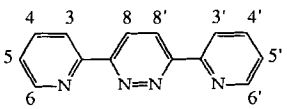

Scheme 1. Structure of the dppn ligand. The numbering is based on the interpretation of its NMR spectra.

When 2 equivalents of dppn were added to 1 equivalent of $[Cu(CF_3SO_3)]_2 \cdot C_6H_6$[5] in benzene, a brown precipitate was isolated (85% yield) and recrystallized as brown crystals from acetone and ether. Microanalytical results combined with the FAB^+ mass spectrum (FAB = Fast Atom Bombardment) indicate that the isolated product is the tetrameric complex **1**.

$[Cu_4(dppn)_4](CF_3SO_3)_4$ **1**

The ^1H and ^{13}C NMR spectra of **1** reveal the molecule to be highly symmetric, with a pattern of resonances similar to that of the free ligand. Additionally, the IR spectrum of **1** indicates that dppn binds in a tetradentate fashion.[4a] X-ray quality crystals of $\mathbf{1} \cdot 2CH_3OH$ were obtained from a 1:1:1 mixture of methanol/acetone/ethanol.

The structure determination[6] shows that the complex consists of discrete $[Cu_4(dppn)_4]^{4+}$ ions and uncoordinated triflate ions with two methanol molecules of crystallization. The structure of the complex cation (Fig. 1), which has crystallographically imposed C_2 symmetry about the Cu1–Cu2 diagonal, is best described as a planar arrangement of four copper atoms lying at the vertices of a slightly distorted rhombus, with sides of length 3.566(1) and 3.582(1) Å and interior angles of 78.72(4) and 101.28(3)°. The four copper atoms are spanned by four dppn ligands, two lying above the Cu_4 mean plane and two below. The distorted tetrahedral environment about each copper(I) ion is provided by two different dppn ligands, each of which supply a pyridine and a pyridazine nitrogen donor atom. Each of the individual

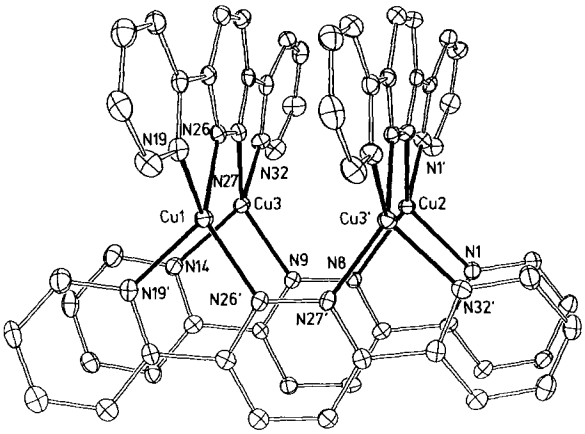

Fig. 1. Top: ORTEP drawing of the crystal structure of $\mathbf{1} \cdot 2CH_3OH$, showing the 50% probability thermal ellipsoids. The hydrogen atoms are omitted for clarity. Selected bond distances [Å] and angles [°] are as follows: Cu1-Cu3 3.566(1), Cu2-Cu3 3.582(1), Cu1-N19 and Cu1-N19' 2.022(5), Cu1-N26 and Cu1-N26' 1.979(5), Cu2-N1 and Cu2-N1' 2.041(5), Cu2-N8 and Cu2-N8' 1.990(5), Cu3-N9 1.991(5), Cu3-N14 1.999(6), Cu3-N27 1.974(5), Cu3-N32 2.005(6); Cu3-Cu1-Cu3' 78.72(4), Cu1-Cu3-Cu2 101.28(3), N19-Cu1-N19' 107.2(3), N19-Cu1-N26 and N19'-Cu1-N26' 80.2(2), N19-Cu1-N26' and N19'-Cu1-N26 134.2(2), N26-Cu1-N26' 127.4(3), N1-Cu2-N1'105.5(3), N1-Cu2-N8 and N1'-Cu2-N8' 79.9(2), N1-Cu2-N8' and N1'-Cu2-N8 132.0(2), N8-Cu2-N8' 131.8(3), N9-Cu3-N27 132.5(2), N9-Cu3-N32 117.5(2), N14-Cu3-N27 119.3(2), N14-Cu3-N32 131.1(2), N9-Cu3-N14 81.8(2), N27-Cu3-N32 81.7(2). Bottom: Representation of $\mathbf{1} \cdot 2CH_3OH$ using the Chem-Ray program.

[*] Dr. M.-T. Youinou, Dr. N. Rahmouni, Prof. J. Fischer, Prof. J. A. Osborn
Laboratoire de Chimie des Métaux de Transition et de Catalyse
Université Louis Pasteur
4, rue Blaise Pascal, F-67000 Strasbourg (France)

[**] This work was supported by the Centre National de la Recherche Scientifique. The authors thank Prof. J. W. Lauher (Stony Brook University, USA) for providing us with his program Chem-Ray and N. Brand for technical assistance.

rings involved in the chelation is planar, but within each dppn ligand the pyridine and pyridazine rings are slightly twisted about the exocyclic C–C bond with dihedral angles of 9(1)°, which are larger than those previously observed in other dinuclear complexes.[4a] Thus the dppn ligand is sufficiently flexible to adjust to the stereochemical requirements of the Cu_4 unit. A striking feature is the almost parallel orientation of the pairs of dppn ligands which are separated by a distance of 3.47 Å, leading to significant π-stacking interactions most likely responsible for the distorsion from the ideal Cu_4 square to the observed rhombus. Distorted tetrahedral Cu_4 units such as the Cu_4X_4 cubane structures are well known,[7] but **1** appears to be a rare example of a planar arrangement of four copper atoms each possessing a tetrahedral geometry.[8] Interestingly, the symmetry evident in the NMR spectra (^1H, ^{13}C) would indicate that, in solution, the Cu_4 framework is either square or oscillating between rhombic structures.

The electrochemical properties of **1** were studied by cyclic voltammetry in DMF.[9] A first series of four successive waves of equal height was observed with $E_{1/2}$ at −0.88, −1.01, −1.16, and −1.32 V (vs. SCE). Peak separations (Δi_p) of between 60 to 70 mV, independent of scan rates (50–250 mVs^{-1}), indicate that **1** undergoes four reversible one-electron processes. In contrast, the reduction of the free ligand begins at −2.07 V and is irreversible. The observed sequence can be interpreted tentatively as a stepwise reduction of each dppn ligand in the tetrameric complex. A second set of reversible waves, presumably due to a second reduction of the ligands, was detected at significantly more negative potentials, −1.74, −1.99, and −2.21 V. The eighth expected reduction step could not be observed, most likely due to its proximity to the reduction potential of the solvent. The remarkable stability of complex **1** during these multielectronic processes would appear to result from reduction taking place mainly on the ligand, as already observed in some ruthenium complexes with bipyridine ligands[10] or copper(I) complexes with catenands;[11] the metal and its stereochemistry would then be largely unchanged.[12] One also may suggest that the reduced states may further be stabilized by interligand π interactions. The metal thus serves not only to lower the reduction potential of the dppn ligand, but also to hold the dppn ligands in parallel proximity.

The formation of **1** appears to result from a spontaneous self-assembly process. When, however, $[Cu(CF_3SO_3)]_2 \cdot C_6H_6$ in acetone was added to an approximatively threefold excess of dppn (per copper atom), a dark green precipitate formed that analyzed as **2**. As expected **2** shows no significant EPR signal and is probably polymeric.[13] Complex **2** is not soluble in most common solvents but can be dissolved in a donor solvent such as CD_3CN. Upon dissolution of **2** the ^1H NMR spectrum reveals immediate formation of **1** and the concomitant liberation of four equivalents of dppn [Eq. (a)]. In solution, the formation of **1** thus appears to be under thermodynamic control. Self-assemblage does not inevitably follow a direct path to **1**; detours such as the formation of **2** can occur if they are rapid and reversible.

$$4\ \underset{\mathbf{2}}{[Cu(dppn)_2(CF_3SO_3)]} \rightleftharpoons \underset{\mathbf{1}}{[Cu_4(dppn)_4](CF_3SO_3)_4} + 4\ dppn \qquad (a)$$

$[Cu(dppn)_2(CF_3SO_3)]$ **2**

In summary, this system involves a ligand which provides two chelating sites and possesses a quasi-rigid, planar structure. Such preorganization, coupled with the stereochemical and coordination demands of the metal ion, predictably leads to the formation of the tetranuclear structure **1**, as long as solvation and anion interactions are minimized. The π-stacking interactions of the dppn ligands may also play an important role in causing closure to the tetranuclear form rather than yielding a polymeric chain structure. The potential of such an electron reservoir to serve as a relay in multielectronic reduction processes is being pursued.

Experimental Procedure

dppn: The ligand 3,6-bis(2'-pyridyl)pyridazine was prepared [2] and characterized. ^1H NMR (200.1 MHz, $(CD_3)_2CO$, 25 °C): δ = 8.75 and 8.73 (m and s, 6H, 8 + 8'; 3 + 3' and 6 + 6'), 8.04, (dt, 2H, 4 + 4'), 7.54 (ddd, 2H, 5 + 5'). ^{13}C NMR (50.3 MHz, $(CD_3)_2CO$, 25 °C): δ = 158.83 (2 + 2'); 154.15 (7 + 7'); 150.28 (6 + 6'); 137.81 (4 + 4'); 125.48 and 125.24 (3 + 3', 8 + 8'); 121.68 (5 + 5').

The syntheses of complexes **1** and **2** were carried out under inert atmosphere with dried and degassed solvents.

1: To a stirred solution of $[Cu(CF_3SO_3)]_2 \cdot C_6H_6$ [5] (0.125 g, 0.25 mmol) in warm benzene (10 mL) was added dropwise under nitrogen a solution of dppn (0.117 g, 0.5 mmol) in warm benzene (10 mL). The reaction mixture was allowed to stir for 15 min. The brown precipitate which formed immediately was filtered, washed with benzene, and recrystallized by diffusion of Et_2O into an acetone solution of the complex (yield 85%). – Correct C,H,N-analysis. MS (FAB^+, NBA): *m/z* 1488.4 ($[M - 2CF_3SO_3]^+$, 8%), 1402.8 ($[M - CF_3SO_3 - dppn]^+$, 68%), 1253.9 ($[M - 2CF_3SO_3 - dppn]^+$, 33%), 956.9 ($[M - 2CF_3SO_3 - 2dppn - Cu]^+$, 15%), 508.9 ($[M - 3CF_3SO_3 - 3dppn - 2Cu]^+$, 75%), 297.0 ($[M - 4CF_3SO_3 - 3dppn - 3Cu]^+$, 100%); ^1H NMR (200.1 MHz, $(CD_3)_2CO$, 25 °C): δ = 9.15 (s, 2H, 8 + 8'), 8.57 (br. d, 2H, 3 + 3', J_{3-4} = 7 Hz), 8.37 (m, 2H, 6 + 6', J_{5-6} = 4.2 Hz), 8.10 (dt, 2H, 4 + 4', $J_{4-5} = J_{4-3}$ = 7 Hz, J_{4-6} = 1.4 Hz), 7.48 (ddd, 2H, 5 + 5', J_{3-5} = 1.1 Hz); ^{13}C NMR (50.3 MHz, $(CD_3)_2CO$, 25 °C): δ = 155.20 (2 + 2'), 150.22 (6 + 6', 148.46 (7 + 7'), 139.90 (4 + 4'), 129.23 and 128.72 (3 + 3', 8 + 8'), 124.68 (5 + 5'). UV/VIS (PC): λ_{max} [nm] (ε) = 441 (31 500); 294 (134 000); IR (Nujol): $\tilde{\nu}$ [cm^{-1}] = 1600 (s), (pyridazine); 1265 (br. s), $(S\text{-}O)_{asym}$; 1030 (s), $(S\text{-}O)_{asym}$; 1015 (w, sh.) 1005 (w), (pyridine).

The analogous BF_4^- or ClO_4^- salts can be prepared by adding dppn to $[Cu(CH_3CN)_4]X$ ($X = BF_4^-, ClO_4^-$) in CH_3CN (ratio 1:1) followed by addition of C_6H_6. In the preparation of the PF_6^- derivative, CH_2Cl_2 was preferred as solvent, since the complex then precipitated directly.

2: To a stirred solution of dppn (0.070 g, 0.3 mmol) in acetone (10 mL) was added dropwise under nitrogen a solution of $[Cu(CF_3SO_3)]_2 \cdot C_6H_6$ (0.030 g, 0.060 mmol) in acetone (5 mL) (after elimination of the copper(0) traces due to some decomposition of $[Cu(CF_3SO_3)]_2 \cdot C_6H_6$ in acetone). Stirring for 15 minutes resulted in the complete precipitation of the dark green solid (yield 50% with respect to copper).—Correct C,H,N-analysis. MS (FAB^+, NBA): *m/z* 531.0 ($[M-CF_3SO_3]^+$, 30%); 297.0 ($[M-CF_3SO_3-dppn]^+$, 100%); minor peaks (< 5%) typical of **1** indicate some transformation of **2** into **1** by dissolution in the matrix and prevent the detection of higher peaks if a polymeric nature of **2** was to be confirmed. IR (Nujol): $\tilde{\nu}$ [cm^{-1}] = 1600(s), 1575(w), 1567(w), (pyridazine); 1287(s) and 1255(s), $(S\text{-}O)_{asym}$; 1035(s), $(S\text{-}O)_s$; 1050(w), 1007(w), 995(w), (pyridine). EPR (solid state, RT): 0.1% Cu(II) impurities.

Received: December 14, 1991 [Z 5070]
German version: *Angew. Chem.* **1992**, *104*, 771

CAS Registry numbers:
1, 140875-24-7; **1** · $2CH_3OH$, 140875-25-8; **2**, 140901-22-0; $[Cu_x(dppn)_4]^{3+}$, 140875-26-9; $[Cu_x(dppn)_4]^{2+}$, 140875-27-0; $[Cu_x(dppn)_4]^+$, 140875-28-1; $[Cu_x(dppn)_4]$, 140875-29-2.

[1] a) J. A. Ibers, R. H. Holm, *Science* **1980**, *209*, 223-235; b) S. J. Lippard *Angew. Chem.* **1988**, *100*, 353–371; *Angew. Chem. Int. Ed. Engl.* **1988**, *27*, 344–361; c) Z. Tyeklar, K. D. Karlin, *Acc. Chem. Res.* **1989**, *27*, 241–248.
[2] W. A. Butte, F. H. Case, *J. Org. Chem.* **1961**, *26*, 4690–4692.
[3] a) J. E. Andrew, P. W. Ball, A. B. Blake, *Chem. Commun.* **1969**, 143–144; b) P. W. Ball, A. B. Blake, *J. Chem. Soc. A* **1969**, 1415–1422; c) J. E. Andrew, A. B. Blake, L. R. Fraser, *J. Chem. Soc. Dalton Trans.* **1975**, 800–805; d) A. Tiripicchio, A. M. Manotti Lanfredi, M. Ghedini, F. Neve, *J. Chem. Soc. Chem. Commun.* **1983**, 97–98; e) M. Ghedini, F. Neve, F. Morazzoni, C. Oliva, *Polyhedron* **1985**, *4*, 497–503; f) M. Ghedini, M. Longeri, F. Neve, *Inorg. Chim. Acta* **1987**, *132*, 223–228; g) G. Denti, L. Sabatino, G. De. Rosa, A. Bartolotta, G. Di Marco, V. Ricevuto, S. Campagna, *Inorg. Chem.* **1989**, *88*, 3309–3313.

[4] a) M. Ghedini, G. De Munno, G. Denti, A. M. Manotti Lanfredi, A. Tiripicchio, *Inorg. Chim. Acta* **1982**, *57*, 87–93; b) G. De Munno, G. Denti, P. Dapporto, *ibid.* **1983**, *74*, 199–203; c) A. M. Manotti Lanfredi, A. Tiripicchio, M. Ghedini, G. De Munno, *Acta Crystallogr. Sect. B.* **1982**, *38*, 1165–1168; d) P. Dapporto, G. De Munno, G. Brono, M. Romeo, *ibid. Sect. C* **1983**, *39*, 718–720.

[5] R. G. Solomon, J. K. Kochi, *J. Chem. Soc. Chem. Commun.* **1972**, 559–560.

[6] X-ray structure analysis of $1 \cdot 2CH_3OH$ ($C_{62}H_{48}N_{16}O_{14}S_4F_{12}Cu_4$), $M = 1851.55$; brown crystals ($0.175 \times 0.160 \times 0.055$ mm^3); monoclinic, space group $P2/n$ with $a = 13.438(4)$, $b = 13.121(4)$, $c = 20.322(6)$ Å, $\beta = 93.44(2)°$, $V = 3576$ Å^3, $Z = 2$, $\varrho_{calcd} = 1.719$ g cm^{-3}, $F(000) = 1864$, $\mu = 3.33$ cm^{-1}. A suitable crystal of $\mathbf{1} \cdot 2CH_3OH$ (obtained by slow recrystallization from a mixture of methanol/acetone/ethanol (1:1:1) at room temperature) was selected on a cooled plate and mounted from the mother liquor. 5142 reflections were collected on a Philips PW 1100/16 diffractometer at -100 °C with Ni-filtered $Cu_{K\alpha}$ radiation $\lambda = 1.5418$ Å ($\theta/2\theta$ scan, $8° < 2\theta < 144°$). The systematic absences $h0l$ ($h + l = 2n + 1$) together with the E statistics and the NZ test suggested the space group $P2/n$ (a nonstandard setting of $P2/c$, No. 13). Successful structure solution and refinement confirmed this choice. The structure was solved by a combination of Patterson, difference Fourier, and full matrix least-squares methods). $R = 0.0538$ and $R_w = 0.0793$ for 2841 reflections having $I > 3\sigma(I)$ and 506 variables. Further details of the crystal structure investigation are available on request from the Director of the Cambridge Crystallographic Data Centre, University Chemical Laboratory, Lensfield Rd, GB-Cambridge CB2 1EW (UK), on quoting the full journal citation.

[7] B. J. Hathaway in *Comprehensive Coordination Chemistry, Vol. 5* (Ed.: G. Wilkinson) Pergamon Press, Oxford, **1987**, pp. 533–774.

[8] a) R. G. Vranka, E. L. Amma, *J. Am. Chem. Soc.* **1966**, *88*, 4270–4271; b) A. M. Manotti Lanfredi, A. Tiripicchio, A. Camus, N. Marsich, *J. Chem. Soc. Chem. Commun.* **1983**, 1126–1128.

[9] Cyclic voltammogram of **1** in dry DMF (0.03 mM) containing 0.1 M tetrabutylammonium perchlorate was measured at room temperature under argon using a classical three-electrode setup with a platinum coil working electrode, a glassy carbon counter electrode, and a AgBr/Ag^0 reference electrode; potentials were referenced to ferrocene (+0.39 V) as internal standard but were quoted relative to the saturated calomel electrode (SCE).

[10] Y. Ohsawa, M. H. DeArmond, K. W. Hanck, D. E. Morris, *J. Am. Chem. Soc.* **1983**, *105*, 6522–6524.

[11] C. Dietrich-Buchecker, J. P. Sauvage, J. M. Kern, *J. Am. Chem. Soc.* **1989**, *111*, 7791–7805.

[12] In contrast, the electrochemical oxidation of **1** was ill-defined and irreversible, undoubtedly because of the instability of Cu^{II} in a tetrahedral environment.

[13] The IR spectrum of **2** shows, besides a monochelating behavior for the dppn ligands, that the triflate anion is coordinated in a bridged fashion.

Alkoxyalkyl-Substituted β-Diketonate Complexes of Barium and Copper: Evidence for Inter- and Intramolecular Stabilization**

By *William S. Rees, Jr.,* Celia R. Caballero,* and *Werner Hesse*

In memorium Manfred L. Ziegler

There is much current interest in the development of new methods for the preparation of electronic materials.[1] Such explorations include sol–gel processing for powder or bulk samples[2] and chemical vapor deposition (CVD) for thin film coatings.[3] Several barium-containing materials systems are of interest because of their demonstrated properties.[4] In an exploration aimed at increasing the vapor pressure of barium-containing compounds while retaining vapor-phase thermal stability—two key features of a useful CVD source compound[3]—we recently examined the intermolecular stabilization of barium-bis-β-diketonates,[5] intramolecular stabilization of barium-bis-η^5-cyclopentadienide compounds,[6] and intramolecular stabilization of barium-bis(oligoalkoxyalkoxides).[7] Whereas each of these new types of compounds offers significant advantages over existing CVD sources,[8] each also suffers some limitation which prohibited broad application in the preparation of thin films.

The limitation of the class of compounds $[Ba\{C_5H_4(CH_2)_nER_m\}_2]$ ($n = 2, 3$; ER_m = OMe, OEt, NMe_2) is their pyrophoric nature;[6] $[\{Ba(tmhd)_2 \cdot 2NH_3\}_2]$ (tmhd = 2,2,6,6-tetramethylheptane-3,5-dionate) is not stable over extended times at the temperatures required for CVD;[5] and the class of compounds $[Ba\{O(CH_2CH_2O)_nR\}_2]$ ($n = 2, 3$; R = Me, Et) is unstable in the vapor phase.[7] We now report the preparation of a new class of ligands, namely the alkoxyalkyl-substituted β-diketones, and their application in the preparation of novel families of both main-group and transition element complexes.

Following our investigation of the decrease in the degree of association of $[\{Ba(tmhd)_2\}_{3,4}]$ by intermolecular addition of Lewis bases[5] and the isolation of monomeric clamshell type oligoalkoxyalkoxides,[7] we now report the successful extension of these discoveries to include intramolecular stabilization of compounds based on the well-known β-diketonate ligand framework by incorporation of an ethereal "scorpion tail". The synthesis of the ligand 2,2-dimethyl-8-methoxyoctane-3,5-dione (**1**) utilizes the Claisen condensation [Eq. (a)]. This synthesis currently is unoptimized; nevertheless, the yield of **1** (66%) is sufficient to permit useful exploration of its properties as a ligand after deprotonation at the acidic methylene position between the two carbonyl groups.

$$Me_3CCOMe + MeO_2C(CH_2)_3OMe \xrightarrow[2.\ HCl(aq)]{1.\ NaH,\ \Delta;\ DME,\ 18\,h} MeOH + \underset{\mathbf{1}}{Me_3CCOCH_2CO(CH_2)_3OMe} \quad \text{(a)}$$

DME = dimethoxyethane

Following Equation (b) CuL_2 (HL = **1**) was prepared from deprotonated **1** and a Cu^{+2} salt.[9] The structure of the

$$2\,HL + Cu(NO_3)_2 \xrightarrow[NH_4OH]{EtOH/H_2O} \underset{\mathbf{2}}{[CuL_2]} + 2\,NH_4NO_3 + H_2O \quad \text{(b)}$$

product $[CuL_2]$ (**2**) was determined by X-ray diffraction (Fig. 1).[9] The ligands are packed on top of each other in the unit cell (Fig. 1b), and an intermolecular, weakly coordinating fifth oxygen atom is 2.987 Å from the copper center. The in-plane Cu–O distances are all 1.90 ± 0.02 Å, and the observed geometry is almost perfectly square-planar (deviation < 0.02 Å). The wavelength of the most intense absorption in the UV spectrum (λ_{max} = 298 nm) does not indicate any significant amount of a five-coordinate complex (square-based pyramid) in solution, since for $[Cu(acac)_2]$, which is known to have a four-coordinate square-planar central atom, λ_{max} is 295 nm (both spectra obtained in THF). Thus, we explain

[*] Prof. Dr. W. S. Rees, Jr., Dr. C. R. Caballero, Dr. W. Hesse
Department of Chemistry and Materials Research and Technology Center
The Florida State University
Dittmer Laboratory of Chemistry Unit One, MS: B-164
Tallahassee, FL 32306-3006 (USA)

[**] This project was supported by the United States Defense Advanced Research Projects Agency contract number MDA 972-88-J-1006 and the Deutsche Forschungsgemeinschaft (postdoctoral fellowship for W. H.). We also thank D. A. Moreno for collecting the UV/VIS data for compound **2**, and CAChe for permitting a trial calculation on the hypothesized geometry of compound **3**.

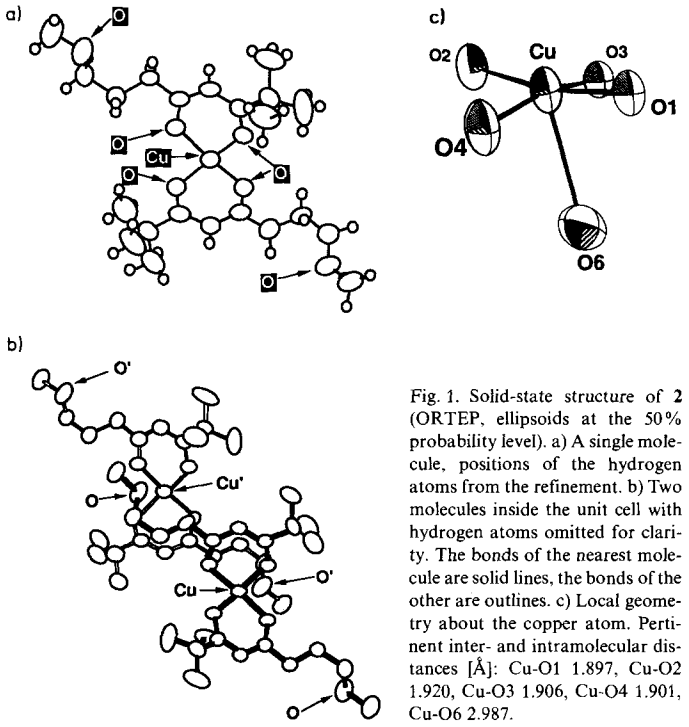

Fig. 1. Solid-state structure of **2** (ORTEP, ellipsoids at the 50% probability level). a) A single molecule, positions of the hydrogen atoms from the refinement. b) Two molecules inside the unit cell with hydrogen atoms omitted for clarity. The bonds of the nearest molecule are solid lines, the bonds of the other are outlines. c) Local geometry about the copper atom. Pertinent inter- and intramolecular distances [Å]: Cu-O1 1.897, Cu-O2 1.920, Cu-O3 1.906, Cu-O4 1.901, Cu-O6 2.987.

this very weak interaction between each copper atom and a fifth oxygen atom in the solid state as more the consequence of molecular packing and not strong domination by tight-binding intermolecular interactions.

Following Equation (c) $[BaL_2]$ (**3**) was prepared by a redox reaction of elemental barium and HL (**1**) accompanied by evolution of $H_{2(g)}$. This new barium compound was purified by distilling off the excess HL, and its composition was confirmed by elemental analysis. It is a monomer in benzene. To our knowledge, this is the first barium compound with β-diketonato ligands which is a liquid at room temperature.[10] Based on the data currently available, it would appear that the metal center is six-coordinate. Examination of space-filling molecular models lends some credence to this suggestion (Fig. 2). Recent publications have appeared describing intermolecular Lewis-base stabilization of monomeric barium-bis-β-diketonates either by crown ethers,[11] or by linear oligoethers.[12] However, to our knowledge compound **3** is the first example of a base-free monomeric barium(II) β-diketonato complex. Current work is aimed at expanding this newly discovered class of ligands.

$$HL_{excess} + Ba \longrightarrow \underset{\mathbf{3}}{[BaL_2]} + H_2 \qquad (c)$$

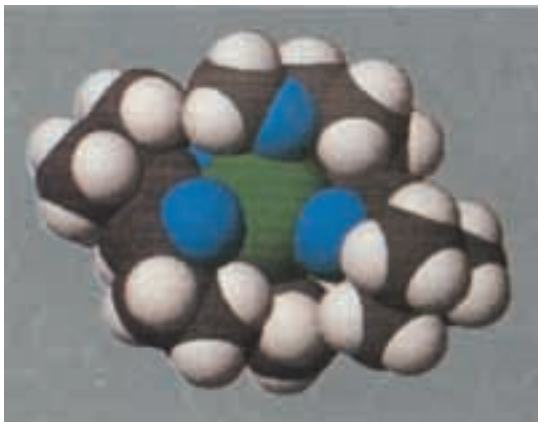

Fig. 2. Space-filling model of the hypothesized structure of compound **3** obtained from the molecular mechanics program of CAChe. Hydrogen atoms are white, carbon black, barium green, and oxygen blue.

Experimental Procedure

1 (HL): Under dry, pure N_2, 44.0 g (0.50 mol) of pinacolone were added dropwise at room temperature to a rapidly stirred suspension of 49.4 g (0.37 mol) of $MeO(CH_2)_3COOMe$ and 15.5 g (0.67 mol) of NaH in 190 mL of freshly distilled DME. After the addition was complete, the mixture was heated at reflux with vigorous stirring for 18 h. After the reaction mixture was cooled to room temperature, 70 mL of concentrated aqueous HCl were added to the orange-brown suspension. A small amount of a white, water-soluble residue remained. The aqueous fraction was extracted with Et_2O (5 × 200 mL), and the combined organic fractions were dried over anhydrous $MgSO_4$, filtered, and concentrated on a rotary evaporator. Distillation of the residue gave pure **1** (b.p. 45 °C at 0.01 mm Hg) in 65.5% yield (49.0 g).

Spectroscopic data of **1**: ^1H NMR (300 MHz, $CDCl_3$): $\delta = 1.10$ [s; $C(CH_3)_3$], 1.85 (m; $CH_2CH_2CH_2$), 2.35 (t; CH_2CO), 3.30 (s; CH_3-O), 3.35 (t; O-CH_2), 5.50 (s; $COCH_2CO$); $^{13}C\{^1H\}$ NMR (75 MHz, $CDCl_3$): $\delta = 25.13$ ($C(CH_3)_3$), 26.83 ($CH_2CH_2CH_2$), 35.02 ($COC(CH_3)_3$), 58.17 (O-CH_2CH_2), 71.35 (CH_3-O), 94.98 ($COCH_2CO$), 195.50 ($COC(CH_3)_3$), 200.10 (CH_2COCH_2). IR (KBr, neat $\tilde{\nu}$[cm^{-1}]): 2960 s, 2920 m, 2860 w, 1720 w, 1700 w, 1600 s, 1480 w, 1460 w, 1360 w, 1270 w, 1120 m, 1020 w.

2: In an open beaker were combined 1.21 g (6.45 mmol) of $Cu(NO_3)_2$, 20 mL of distilled H_2O, 1.53 g (7.64 mmol) of **1**, 20 mL of 95% EtOH, and sufficient $NH_4OH_{(aq)}$ to create a homogeneous, dark blue solution (ca. 6 mL). The solution was extracted with Et_2O (3 × 50 mL). The organic fractions were combined, dried over anhydrous $MgSO_4$, filtered, concentrated to 20 mL, layered with 60 mL of hexane, cooled to −20 °C, and allowed to stand for 48 h. Crystals were collected by filtration and air-dried (m.p. 55–56 °C). Crystals of **2** suitable for X-ray diffraction were obtained by cooling a hexane solution of the compound (− 20 °C, 20 h).

3: Under dry, pure N_2, 3.41 g (17.0 mmol) **1** were added all at once at room temperature to a flask containing a magnetic stirring bar and 0.87 g (6.30 mmol) of freshly cut cubes of elemental Ba. The reaction mixture was stirred until no visible metal fragments remained (5–6 h). Excess **1** was removed by distillation (10^{-2} mm Hg, 45 °C) leaving a clear viscous liquid identified as **3** in almost quantitative yield.

Analytical data of **3**: Satisfactory C,H-analysis; molecular weight (cryoscopic in benzene): calcd. 535, found 600 g mol^{-1}; TGA (N_2, 1 atm): 85% to 270 °C, 46% to 460 °C, 39% to 600 °C; ^1H NMR ($CDCl_3$): $\delta = 1.00$ (s), 1.10 (s), 1.85 (br, m), 2.10 (br, m), 2.40 (s), 3.20 (s), 3.40 (br, m), 5.30 (s).

Received: January 2, 1992 [Z 5106 IE]
German version: *Angew. Chem.* **1992**, *104*, 786

[1] See for example: *Better Ceramics Through Chemistry IV* (Eds.: B. J. J. Zelinski, C. J. Brinker, D. E. Clark, D. R. Ulrich), *Mater. Res. Soc. Symp. Proc.* **1990**.
[2] C. J. Brinker, G. W. Scherer, *Sol-Gel Science*, Academic Press, New York, **1990**.
[3] G. B. Stringfellow, *Organometallic Vapor Phase Epitaxy: Theory and Practice*, Academic Press, New York, **1989**.
[4] a) $YBa_2Cu_3O_{7-\delta}$: C. W. Chu, P. H. Hor, R. L. Meng, L. Gao, Z. J. Huang, Y. Q. Wang, J. Bechtold, D. Campbell, M. K. Wu, J. Ashburn, C. Y. Huang, *Phys. Rev. Lett.* **1987**, *58*, 405–407; b) $(TlO)_mBa_2Ca_{n-1}Cu_nO_x$ ($m = 1, 2$; $n = 1, 2, 3$): Z. Z. Sheng, A. M. Hermann, *Nature* **1988**, *27*, 138–139. c) $BaTiO_3$: T. L. Rose, E. M. Kelliner, A. N. Scoville, S. E. Stone, *J. Appl. Phys.* **1984**, *55(10)*, 3706.
[5] W. S. Rees, Jr., M. W. Carris, W. Hesse, *Inorg. Chem.* **1991**, *30*, 4479.
[6] W. S. Rees, Jr., K. A. Dippel in *Chemical Processing of Advanced Materials* (Ed.: L. Hench), Wiley, New York, in press.
[7] W. S. Rees, Jr., D. A. Moreno, *J. Chem. Soc. Chem. Commun.* **1991**, 1759.
[8] For an excellent review on the early work in this area see: L. M. Tonge, D. S. Richeson, T. J. Marks, J. Zhao, J. Zhang, B. W. Wessels, H. O. Marcy, C. R. Kannewurf in *Electron Transfer in Biology and the Solid State: Inorganic Compounds With Unusual Properties, Part III* (Eds.: M. K. Johnson, R. B. King, D. M. Kurtz, Jr., C. Kutal, M. L. Norton, R. A. Scott), *Adv. Chem. Ser.* **1990**, *226*, 351–368.
[9] A crystal of **2** (0.8 × 0.6 × 0.3 mm) was affixed to a glass fiber with two-component epoxy cement. Data collection was carried out at room temperature in the $\omega/2\theta$ scan mode in the range $2° < 2\theta < 55°$, employing an

automated Enraf-Nonius CAD 4 diffractometer with $Mo_{K\alpha}$ (0.71073 Å) radiation. The space group was $P\bar{1}$ (No. 2), with $a = 9.444(2)$ Å, $b = 10.773(2)$ Å, $c = 13.220(2)$ Å, $\alpha = 68.72(1)°$, $\beta = 81.49(1)°$, $\gamma = 84.32(1)°$, $V = 1238$ Å^3, $Z = 2$, and $\rho_{calc} = 1.240$ g cm^{-3}. Two standard reflections (0$\bar{2}$5, 312), measured every hour, gave <2% intensity deviation over the duration of data collection. Of 6010 measured reflections, 4356 were observed and 3616 with $I > 2\sigma(I)$ were used for structure solution and refinement employing the SDP computer programs by Enraf-Nonius. The final cycle of least-squares refinement of 262 parameters gave residuals of $R = 0.058$ and $R_w = 0.064$ and greatest unassigned electron density of $0.880\ e^- \cdot Å^{-3}$. Further details of the crystal structure investigation are available on request from the Fachinformationszentrum Karlsruhe, Gesellschaft für wissenschaftlich-technische Information mbH, D-W-7514 Eggenstein-Leopoldshafen 2, on quoting the depository number CSD-56191, the names of the authors, and the journal citation.

[10] For a thorough compilation of data of metal β-diketonate complexes see: R. C. Mehrotra, R. Bohra, D. P. Gaur, *Metal β-Diketonates and Allied Derivatives*, Academic Press, New York, **1978**.

[11] J. A. T. Norman, G. P. Pez, *J. Chem. Soc. Chem. Commun.* **1991**, 971.

[12] a) P. Van der Sluis, A. L. Spek, K. Timmer, H. A. Meinema, *Acta Crystallogr. Sect. C 46*, **1990**, 1741; b) R. Gardiner, D. W. Brown, P. S. Kirlin, A. L. Rheingold, *Chem. Mater.* **1991**, *3*, 1053.

The First Complex with a $\sigma^2\pi^4$ Triple Bond between Vanadium Atoms in a Ligand Framework of Fourfold Symmetry—$[V_2\{(p\text{-}CH_3C_6H_4)NC(H)N(p\text{-}C_6H_4CH_3)\}_4]$**

By *F. Albert Cotton*,* *Lee M. Daniels*, and *Carlos A. Murillo**

In memoriam Rosa Víquez de Murillo

The chemistry of compounds containing metal-to-metal multiple bonds has been widely developed in the last two decades. Many of the compounds structurally characterized possess frameworks of structure type **1** (*n* refers to the bond order between the metal atoms). However, progress in the related chemistry of metals in the 3d transition series, with the exception of chromium, has been slow.[1] Only one other complex with a first-row metal with this structure is known, $[Co_2\{(p\text{-}CH_3C_6H_4)NNN(p\text{-}C_6H_4CH_3)\}_4]$.[2] A triple bond between vanadium atoms has been claimed for two compounds **2**,[3] in which the coordination number of the metal atom is greater than in a structure of type **1**. The latter structure is probably best described as an edge-sharing bioctahedron. We now report the structural characterization of the first dinuclear vanadium(II) compound of this type, tetrakis(*N*,*N*′-di-*p*-tolylformamidato)divanadium(II).

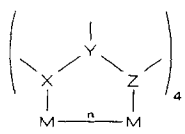

1

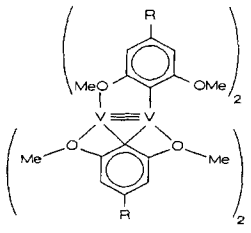

2 R = H, OMe

Theoretical calculations have clearly indicated the possible existence of molecules of type **1**, with vanadium-to-vanadium triple bonds between 2.0 and 2.1 Å in length.[4] This presented a challenge for the synthetic chemist. Unfortunately, the chemistry of vanadium(II) had not been widely investigated until recent years.[5] We thus decided to undertake a comprehensive study of the chemistry of V^{II} with the goal of eventually characterizing a compound of the type **1**.[6]

In addition to the high instability towards air of most of the V^{II} compounds, one of the major difficulties in their preparation is the lack of good starting materials.[7] Early work indicated that *N*-donors such as amines bind to vanadium(II) quite strongly.[7, 8] However, reactions of vanadium complexes containing monocoordinated amines, such as pyridine, or chelating amines, such as tetramethylendiamine (TMEDA), led mainly to mononuclear vanadium(II) compounds. In no single instance did such starting materials provide any of the type **1** compounds, even when suitable ligands were used.[8d]

It became clear that an amine-free starting material was needed. A potentially bridging ligand with only *N*-donor groups was very appealing, but we did not want to generate a complex with a forced configuration that could raise a question as to the presence of a metal-to-metal bond. We decided that the *N*,*N*′-di-*p*-tolylformamidato (dfm) ligand was a good candidate. It has two potential *N*-donor centers and is able to adopt various configurations depending on the requirements of the metal atoms.

Compounds in which dfm (or a closely related ligand) bridges a metal-to-metal bond have been structurally characterized for M = Cr,[9] Mo,[10] W,[9] Re,[11] Ru,[12] Os,[13] Co,[2] Rh,[14] and Ir.[15] Compounds with a similar framework but without metal-to-metal bonds are also known for M = Ni and Pd.[16] The dfm ligand is also capable of forming a bridge between Cu^I or Ag^I ions, although in this case the stoichiometry is different, namely $[M_2(dfm)_2]$.[17] The metal-to-metal distances vary from 1.930(2) Å in $[Cr_2(dfm)_4]$ to 2.705(6) Å in $[Ag_2(dfm_2)]$. The torsion angle (N-M-M-N) also changes from a very few degrees to about 27° in the cation $[Ni_2(dfm)_4]^+$.[16]

Dfm can also act as a chelating ligand, the most relevant example of which is found in the mononuclear vanadium(II) compound $[V(dfm)_2(py)_2]$ formed by the reaction of $[VCl_2(py)_4]$ (py = pyridine) with Li(dfm) in toluene.[7d]

The title compound, $[V_2(dfm)_4] \cdot$ toluene has been fully characterized by various physical and chemical techniques including X-ray crystallography.[18] It is of the same type as other dinuclear formamidato complexes having four bridging ligands. Its structure, depicted in Figure 1, is homologous to that of the dimolybdenum[10] and ditungsten[9] complexes.

The vanadium(II)-to-vanadium(II) separation of 1.978(2) Å is the second shortest bond length found for the $[M_2(dfm)_4]$ species. Only the Cr_2 unit of $[Cr_2(dfm)_4]$ has a shorter M–M distance (1.930(2) Å). This bond is roughly 0.3 Å shorter than the vanadium-to-vanadium distance found in the complexes of type **2** and 0.47 Å shorter that the V–V bond in $[\{PhNC(Me)O\}_4V_2(tmeda)]$.[8d] The vanadium-to-nitrogen separations of 2.092(4) Å and 2.120(4) Å are also much shorter than the typical distance of 2.2 Å found in a host of mononuclear vanadium(II) compounds in which there is pyridine or tmeda.[7, 8] This is probably an indication of the higher basicity of the dfm ligand. The M–N bond is only slightly longer than that found in $[Cr_2(dfm)_4]$ (average 2.047 Å). The vanadium-to-vanadium distance and the small

[*] Prof. Dr. F. A. Cotton, Dr. L. M. Daniels, Prof. Dr. C. A. Murillo [+]
Laboratory for Molecular Structure and Bonding
Texas A & M University
College Station, TX 77843 (USA)

[+] Permanent address: Department of Chemistry
University of Costa Rica
Ciudad Universitaria (Costa Rica)

[**] We are grateful to the Vicerrectoría de Investigación, U.C.R. (Grant No. 115-87-516) for support of work at the University of Costa Rica and to the National Science Foundation for support of work at Texas A & M University. We also thank Dr. Hong Chen for assistance with some of the spectroscopic data.

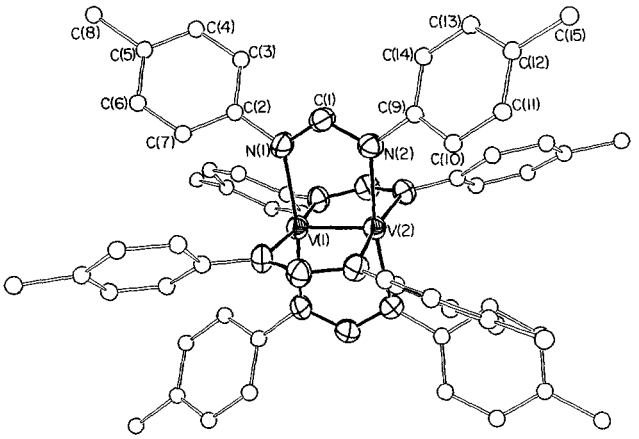

Fig. 1. ORTEP perspective drawing of the molecular structure of $[V_2(dfm)_4]\cdot$ toluene with ellipsoids at the 30% probability level. The carbon atoms of the tolyl groups are drawn as arbitrarily sized spheres.

"formal shortness ratio"[11] (FSR) supports the presence of a fairly strong bond. The FSR of 0.808 is very similar to those of the homologous series with metal–metal quadruple bonds: 0.814 (Cr), 0.840 (Mo), and 0.838 (W). However, a striking difference is found in the magnetic anisotropy, $\Delta\chi$ of the M–M bond. The change in the chemical shift of the methine proton is very large. Relative to the nickel analogue $\Delta\delta$ for the title complex is 4.08. The calculated $\Delta\chi$ value of 7300×10^{-36} m^3 molecule^{-1} is the highest known for any of the dinuclear $[M_2(dfm)_4]$ compounds.[19]

The electronic absorption spectrum (toluene solution) shows two bands (24700, 21300 cm^{-1}) and a shoulder (18200 cm^{-1}) which following some preliminary SCF-Xα-SW calculations[20] can probably be assigned to the N $\rightarrow\delta$, $\pi\rightarrow\delta^*$, and $\pi\rightarrow\delta$ transitions, respectively. These are on the edge of a rapidly rising absorption into the UV which probably arises from one or more L $\rightarrow$ M charge-transfer transitions.

Experimental Procedure

All syntheses were carried out under an inert atmosphere (argon) and with dry and deoxygenated solvents. $[V_2(dfm)_4]\cdot$ toluene was prepared by the reduction of $VCl_3(thf)_3$ [21] (0.80 g, 2.14 mmol) with one equivalent of $NaHBEt_3$ in 20 mL of THF at -70 °C and further addition of a cold suspension of Li(dfm) (4.28 mmol) in 20 mL of THF. After the temperature of the bath reached 20 °C, the red solution was stirred for 30 min. The solvent was then removed under vacuum. The dried solid was extracted with 35 mL of toluene and the solution was kept at -70 °C overnight. The long fiberlike, copper-colored crystals formed were filtered and quickly washed with small amounts of hexane (0.55 g, 52% yield). Upon recrystallization from toluene and layering with hexane, red block-shaped crystals of $[V_2(dfm)_4]\cdot$ toluene formed. Both crystalline forms gave the same NMR spectrum; that of the copper-colored crystals showed only a negligible amount of toluene. The compound is diamagnetic (by NMR). ^{1}H NMR (200 MHz, C_6D_6, 25 °C): $\delta = 1.99$ (s, $-CH_3$), 6.00 and 6.63 (d, $-C_6H_4-$), 10.24 (s, -NCHN-). UV/VIS(toluene): λ_{max} [nm] = 550 (b. sh), 470, 405.

Received: January 14, 1992 [Z5120IE]
German version: *Angew. Chem.* **1992**, *104*, 795

CAS Registry numbers:
$[V_2(dfm)_4]$, 140633-84-7; $[V_2(dfm_4)]\cdot$ toluene, 140633-85-8; $[VCl_3(thf)_3]$, 19559-06-9; Li(dfm), 75344-35-3.

[1] F. A. Cotton, R. A. Walton, *Multiple Bonds Between Metal Atoms*, 1st ed., Wiley, New York, **1982**, 2nd ed., in press.
[2] F. A. Cotton, R. Poli, *Inorg. Chem.* **1987**, *26*, 3652–3653.
[3] a) F. A. Cotton, M. Millar, *J. Am. Chem. Soc.* **1977**, *99*, 7886–7891; b) F. A. Cotton, G. E. Lewis, G. N. Mott, *Inorg. Chem.* **1983**, *22*, 560–561.
[4] F. A. Cotton, M. P. Diebold, I. Shim, *Inorg. Chem.* **1985**, *24*, 1510–1516.
[5] F. A. Cotton, G. Wilkinson, *Advanced Inorganic Chemistry*, 5th ed., Wiley, New York, **1988**, pp. 675–676.
[6] For further discussion see for example F. A. Cotton, L. R. Falvello, R. Llusar, E. Libby, C. A. Murillo, W. Schwotzer, *Inorg. Chem.* **1986**, *25*, 3423–3428, and references cited therein.
[7] a) Ref. [6]; b) F. A. Cotton, C. A. Murillo, *Ing. Cienc. Quim.* **1985**, *9*, 1–2. c) F. A. Cotton, E. Libby, C. A. Murillo, G. Valle, *Inorg. Synth.* **1990**, *27*, 306–310. d) F. A. Cotton, R. Poli, *Inorg. Chim. Acta* **1988**, *141*, 91–98. e) F. A. Cotton, L. M. Daniels, M. L. Montero, C. A. Murillo, unpublished results.
[8] See for example a) P. Dapporto, F. Mani, C. Mealli, *Inorg. Chem.* **1978**, *17*, 1323–1329; b) J. J. H. Edema, A. Meetsma, S. Gambarotta, *J. Am. Chem. Soc.* **1989**, *111*, 6878–6880; c) J. J. H. Edema, W. Stauthamer, F. van Bolhuis, S. Gambarotta, W. J. J. Smeets, A. L. Spek, *Inorg. Chem.* **1990**, *29*, 1302–1306; d) J. J. H. Edema, A. Meetsma, F. van Bolhuis, S. Gambarotta, *ibid.* **1991**, *30*, 2056–2061; e) J. J. H. Edema, S. Gambarotta, A. Meetsma, A. L. Spek, N. Veldman, *ibid.* **1991**, *30*, 2062–2066; f) J. J. H. Edema, S. Gambarotta, S. Hao, C. Bensimon, *ibid.* **1991**, *30*, 2584–2586.
[9] F. A. Cotton, T. Ren, *J. Am. Chem. Soc.*, **1992**, *114*, 2237–2242.
[10] F. A. Cotton, X. Feng, M. Matusz, *Inorg. Chem.* **1989**, *28*, 594–601.
[11] F. A. Cotton, T. Ren, *J. Am. Chem. Soc.*, **1992**, *114*, 2495–2501.
[12] F. A. Cotton, T. Ren, *Inorg. Chem.* **1991**, *30*, 3675–3679.
[13] F. A. Cotton, T. Ren, J. L. Eglin, *Inorg. Chem.* **1991**, *30*, 2559–2563.
[14] J. L. Bear, C.-L. Yao, R. S. Lifsey, J. D. Korp, K. M. Kadish, *Inorg. Chem.* **1991**, *30*, 336–340.
[15] F. A. Cotton, R. Poli, *Polyhedron* **1987**, *6*, 1625–1628.
[16] F. A. Cotton, M. Matusz, R. Poli, X. Feng, *J. Am. Chem. Soc.* **1988**, *110*, 1144–1154.
[17] F. A. Cotton, X. Feng, M. Matusz, R. Poli, *J. Am. Chem. Soc.* **1988**, *110*, 7077–7083.
[18] Crystal data for $V_2N_8C_{60}H_{60}\cdot C_7H_8$, $T = 298$ K: $M_r = 1087.2$, space group $P4/n$, $a = 13.214(6)$, $c = 17.427(5)$ Å, $V = 3043(3)$ Å^3, $Z = 2$, $\varrho_{calcd} = 1.19$ g cm^{-3}, $\mu(Cu_{K\alpha}) = 29.4$ cm^{-1}, Rigaku AFC5R, $4° \le 2\theta \le 120°$. 4971 reflections were collected; 2282 unique, 1179 having $I > 3\sigma(I)$. The data were corrected for absorption (ψ-scans) and an overall decay of 14.4%. Initial positions were taken from the homologous structure of $[W_2(dfm)]\cdot$ toluene [9]. The coordinates and isotropic temperature factor for the methine H atom were included in the refinement. Positions for other hydrogen atoms in the complex were calculated. Disordered solvent molecules reside on the fourfold axis between the metal complexes. The toluene molecules were modeled as two rigid groups with the methyl groups pointing in opposite directions along the fourfold axis. The final cycles of refinement led to $R = 0.049$ and $R_w = 0.068$. Further details of the crystal structure investigation may be obtained from the Cambridge Crystallographie Data Centre, University Chemical Laboratory, Lensfield Road, GB-Cambridge CB2 1EW (UK) on quoting the names of the authors and the journal citation.
[19] The magnetic anisotropy was calculated using the McConnell equation $\Delta\delta = \Delta\chi\,[(1 - 3\cos^2\theta)/12\pi r^3]$, where $\Delta\delta = 4.08$, $\theta = 90°$, $r = 3.62$ Å. See ref. [9] for further discussion.
[20] The SCF-Xα-SW calculations were carried out for the model system $[V_2(HNCHNH)_4]$ and will be reported elsewhere. Also see the work on $[Mo_2(HPO_4)_4]^{2-}$ in M. D. Hopkins, V. M. Miskowski, H. B. Gray, *J. Am. Chem. Soc.* **1986**, *108*, 959–963.
[21] L. Manzer, *Inorg. Synth.* **1982**, *21*, 135–140.

How High is the Barrier for the Valence Isomerization of Cyclobutadiene?**

By *Günther Maier,* Reinhard Wolf,* and *Hans-Otto Kalinowski*

"Our current knowledge about cyclobutadiene[1] allows this chapter to be terminated. It is now secured textbook material," wrote one of us (G.M.) three years ago.[1d] This statement did not remain unchallenged,[2] although even at the time two existing gaps were indicated. The first concerns the UV spectrum of cyclobutadiene that still is not clearly established. The spectrum must show an absorption maximum

[*] Prof. Dr. G. Maier, Dipl.-Chem. R. Wolf, Dr. H.-O Kalinowski
Institut für Organische Chemie der Universität
Heinrich-Buff-Ring 58, D-W-6300 Giessen (FRG)

[**] Small rings, Part 73. This research was supported by the Fonds der Chemischen Industrie. – Part 72: G. Maier, D. Volz, J. Neudert, *Synthesis*, in press.

above 254 nm, because irradiation of cyclobutadiene with longer wavelengths causes its rapid cleavage into two molecules of acetylene.[1d] The extinction of this band is so small that experimental determination has failed so far. The second question still open concerns the activation energy of the valence isomerization of cyclobutadiene. We report here on the first reliable experimental determination of this barrier.

The "Masamune Route"[3a, b] for the synthesis of sterically hindered cyclobutadienes can be applied to cyclopropenyldiazomethane derivatives **1a–d**. Irradiation of cyclobutadienes **2a** and **2b**, available from **1a** and **1b**, respectively, led to tetra-*tert*-butyl- (**3a**)[4a] and tri-*tert*-butyl(trimethylsilyl)-tetrahedrane (**3b**).[4b] The analogous deazotization of the

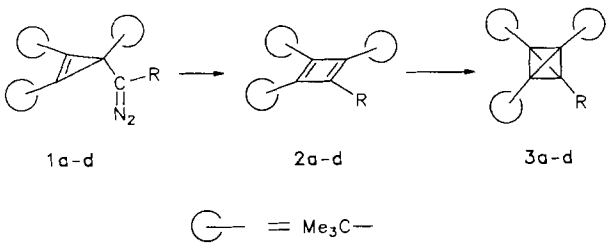

1-3	a	b	c	d
R	CMe_3	$SiMe_3$	$SiMe_2Ph$	$SiMe_2(OCHMe_2)$

diazo compound **1c** (yellow crystals, m.p. 33 °C) and **1d** (orange oil) in the presence of CuCl provided cyclobutadiene–CuCl complexes which were treated with 1,2-bis(diphenylphosphino)ethane to furnish the free cyclobutadienes **2c** (dark red crystals, m.p. 55 °C, 40%) and **2d** (dark red crystals, m.p. 45 °C, 50%). Photoisomerization of **2c** and **2d** yielded the corresponding tetrahedranes **3c** (colorless plates, m.p. 58 °C) and **3d** (colorless, waxy crystals, m.p. 77 °C) (**2c** → **3c**: $\lambda > 300$ nm, 10%; **2d** → **3d**: $\lambda = 254$ nm, 40%). The structures of the two new stable tetrahedranes **3c** and **3d**[5] and their precursors were assigned on the basis of the spectroscopic data given in Table 1. Tetrahedrane **3c** was also characterized by X-ray structure analysis.[6]

The ^{13}C NMR spectra of the silyl-substituted cyclobutadienes **2b–d** are temperature dependent. This is especially interesting since the constitution of these cyclobutadienes offers the possibility of observing the valence isomerization of the two rectangular forms with dynamic NMR spectroscopy. If in cyclobutadiene **2d**, for example, the rectangular structures **A** or **B** are frozen, then the two diagonal atoms C-1 and C-3 and their substituents are magnetically nonequivalent; in a square structure they would be equivalent. However, a single signal would also be found if a fast equilibrium **A** ⇄ **B** existed, feigning a square structure. Until now it has never been possible to observe separate NMR signals for C-1 and C-3, not even for tri-*tert*-butylcyclobutadiene (**2**, R = H).[7a] Application of Saunders' isotopic per-

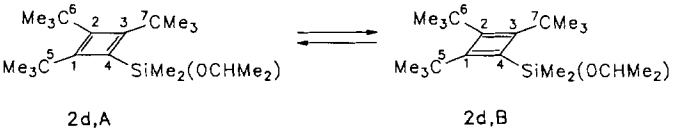

turbation method to the same cyclobutadiene derivative with a perdeutero *tert*-butyl group in the 1 position proved that this system has a double minimum.[7b]

If a solution of **2d** in propane/[D_{10}]diethyl ether (ca. 80:20) is cooled to −60 °C, a single ^{13}C NMR signal at $\delta = 167.7$ is found for C-1/C-3 and at $\delta = 35.3$ for C-5/C-7. As the temperature is lowered these signals become broader and each gradually resolves into two separate signals, which at −158 °C again have the usual half width. The downfield signal ($\delta = 167.7$) is split into two signals at $\delta = 178.4$ and 157.3; the second signal ($\delta = 35.3$) now appears as two signals at $\delta = 36.0$ and 34.6. The coalescence temperature T_c for C-1/C-3 is −123 °C (150 ± 5 K), for C-5/C-7, the T_c is −145 °C (128 ± 3 K; this determination for C-5/C-7 is somewhat more precise than that for C-1/C-3). Thus there are two independent probes for the determination of the free energy of activation for the valence isomerization of **2d**. The values provided are 5.8 ± 0.2 (C-5/C-7, $\Delta\nu = 134$ Hz) and 6.0 ± 0.2 (C-1/C-3, $\Delta\nu = 2120$ Hz) kcal mol^{-1}. The line-shape analysis in the region of the intermediate exchange of the C atoms 5 and 7 furnished the following activation parameters: $\Delta H^{\neq} = 5.3 \pm 0.3$ kcal mol^{-1}, $\Delta S^{\neq} = -4.8 \pm 0.1$ cal K^{-1} mol^{-1}, $\Delta G^{\neq} = 5.9 \pm 0.3$ kcal mol^{-1}, $E_a = 6.6 \pm 0.3$ kcal mol^{-1}.

What does the experimentally determined barrier $\Delta G^{\neq} = 5.8$ kcal mol^{-1} (24.4 kJ mol^{-1}) imply? This value is less than that calculated for the parent compound ($\Delta E^{\neq} = 8.1$–13.4 kcal mol^{-1}),[1d, 8] but agrees remarkably well with the latest results of CI calculations (CI = *C*onfiguration *I*nteraction). Multiconfigurational reference wave functions form the basis of this calculational method, and the zero-point vibration is also taken into account in the determination of $\Delta H^{\neq}$. The CAS(4,4)-CEPA calculational method provides, according to Janoschek,[8b, c] an activation enthalpy of $\Delta H^{\neq} = 6.2$ kcal mol^{-1}. If one considers that the bond alternance in the cyclobutadiene ring system depends very little on the substitution pattern,[1d, 9] then the good agreement between the value determined for **2d** and the calculated activation barrier for the parent compound is not surprising.

Low-temperature ^{13}C NMR measurements with a highest field NMR spectrometer[10] confirmed the barrier of 5.8 kcal mol^{-1} for **2d**. In addition, an analogous coalescence phenomenon was observed for C-1 and C-3 of **2c** under these measurement conditions. At temperatures above −150 °C

Table 1. NMR spectroscopic data (^1H NMR: 400 MHz, ^{13}C NMR: 100.6 MHz, δ values relative to TMS) for compounds **1c,d**, **2c,d** and **3c,d**. All compounds provided correct elemental analyses.

1c: ^1H NMR: $\delta = 7.6$–7.3 (m, 5H; Ph), 1.1 (s, 18H; 2*t*Bu), 1.0 (s, 9H; *t*Bu), 0.5 (s, 6H; $SiMe_2$); ^{13}C NMR: $\delta = 138.7$, 134.1, 129.1, 127.7 (Ph), 128.1 (C = C), 42.4 (CN_2), 40.1 (quart. C), 36.8 (CMe_3), 31.1 ($2CMe_3$), 30.9 ($2CMe_3$), 30.4 (CMe_3), −0.9 ($SiMe_2$)[a]

1d: ^1H NMR: $\delta = 4.0$ (sept, 1H, $J = 6.0$ Hz; $CHMe_2$), 1.2 (s, 18H; 2*t*Bu), 1.1 (d, 6H, $J = 6.0$ Hz; $CHMe_2$), 0.9 (s, 9H; *t*Bu), 0.3 (s, 6H; $SiMe_2$); ^{13}C NMR: $\delta = 128.0$ (C=C), 65.5 ($CHMe_2$), 42.3 (CN_2), 39.9 (quart. C), 36.2 (CMe_3), 31.6 ($2CMe_3$), 31.4 ($2CMe_3$), 30.4 (CMe_3), 25.7 ($CHMe_2$), 0.0 ($SiMe_2$)[a]

2c: ^1H NMR: $\delta = 7.8$–7.2 (m, 5H; Ph), 1.3 (s, 9H; *t*Bu), 1.2 (s, 18H; 2*t*Bu), 0.5 (s, 6H; $SiMe_2$); ^{13}C NMR: $\delta = 168.4$ (C-1/C-3), 149.1 (C-2), 142.3 (Ph), 140.4 (C-4), 134.4, 128.9, 128.1 (Ph), 34.0 ($2CMe_3$), 32.5 (CMe_3), 31.0 (CMe_3), 30.1 ($2CMe_3$), 2.6 ($SiMe_2$)[b]

2d: ^1H NMR: $\delta = 3.9$ (sept, 1H, $J = 6.0$ Hz; $CHMe_2$), 1.4 (s, 18H; 2*t*Bu), 1.3 (s, 9H; *t*Bu), 1.2 (d, 6H, $J = 6.0$ Hz; $CHMe_2$), 0.4 (s, 6H; $SiMe_2$); ^{13}C NMR: $\delta = 168.1$(C-1/C-3), 148.4 (C-2), 141.9 (C-4), 64.9 ($CHMe_2$), 35.5 ($2CMe_3$), 33.3 (CMe_3), 32.6 (CMe_3), 31.1 ($2CMe_3$), 27.0 ($CHMe_2$), 3.0 ($SiMe_2$)[b]

3c: ^1H NMR: $\delta = 7.8$–7.2 (m, 5H; Ph), 1.2 (s, 27H; 3*t*Bu), 0.6 (s, 6H; $SiMe_2$) ^{13}C NMR: $\delta = 140.6$, 134.1, 129.0, 127.8 (Ph), 31.3 ($3CMe_3$), 27.1 ($3CMe_3$), 13.9 (3C-*t*Bu), 0.3 ($SiMe_2$), −22.1 (C-$SiMe_2$)[b]

3d: ^1H NMR: $\delta = 4.1$ (sept, 1H, $J = 6.0$ Hz; $CHMe_2$), 1.2 (s, 27H; 3*t*Bu), 1.15 (d, 6H, $J = 6.0$ Hz; $CHMe_2$), 0.4 (s, 6H; $SiMe_2$); ^{13}C NMR: $\delta = 64.7$ ($CHMe_2$), 31.2 ($3CMe_3$), 27.1 ($3CMe_3$), 26.2 ($CHMe_2$), 14.0 (3C-*t*Bu), 2.1 ($SiMe_2$), −22.4 (C-$SiMe_2$)[b]

[a] In $CDCl_3$. [b] In C_6D_6.

only a single broad signal is observed; at $-168\,^{\circ}C$ the resolution into two separate signals is recognizable. The coalescence temperature $T_c = -158\,^{\circ}C$ ($115 \pm 5\,K$) and the shift difference $\Delta\delta = 17.1$ furnish a free energy of activation of $4.5 \pm 0.2\ kcal\,mol^{-1}$ for **2c**. In the case of **2b**, coalescence cannot be observed even with the highest field NMR spectrometer. It is estimated that the coalescence temperature of **2b** is probably another 35 K lower, that is, at about 80 K. If the shift difference is similar to that of **2c**, this would correspond to a barrier of $\Delta G^{\ddagger} \approx 3.5\ kcal\,mol^{-1}$. The activation barriers determined for **2d** and **2c** have an important consequence. Carpenter's kinetic study[11] of the automerization of 1,2-dideuteriocyclobutadiene ($\Delta H^{\ddagger}$ between 1.6 and 10 $kcal\,mol^{-1}$, $\Delta S^{\ddagger}$ between -17 and $-32\ cal\,K^{-1}mol^{-1}$) kindled a discussion[12] on the extent of the effect of heavy-atom tunneling in this process. According to most calculations[12] the tunneling rate is so high that the "thermal" barrier is practically inconsequential.

This prognosis certainly does not hold for the valence isomerization of cyclobutadienes **2**, whose ring C atoms must be moved along with their large substituents. In this context, one should recall that heavy-atom tunneling has not been proved experimentally by means of dynamic NMR spectroscopy, not even for the migration of unsubstituted C atoms.[13]

The upshot is that the valence isomerization of cyclobutadiene **2d** proceeds with an energy barrier of $\Delta G^{\ddagger} = 5.8\ kcal\,mol^{-1}$. For **2c** the free energy of activation is even lower ($4.5\ kcal\,mol^{-1}$), and for **2b** a further decrease of about 1 $kcal\,mol^{-1}$ is estimated. These reactions are faster than earlier calculations had predicted. Nevertheless, we rule out the participation of heavy-atom tunneling.[14]

Received: January 20, 1992 [Z 5132 IE]
German version: *Angew. Chem.* **1992**, *104*, 764

CAS Registry numbers:
1c, 140633-74-5; **1d**, 140633-75-6; **2c**, 140633-76-7; **2d**, 140633-77-8; **3c**, 140633-78-9; **3d**, 140633-79-0; **3**, R = $SiHMe_2$, 140633-80-3; **3**, R = $CHMe_2$, 140633-81-4.

[1] Summaries of the cyclobutadiene problem: a) M. R. Cava, M. J. Mitchell, *Cyclobutadiene and Related Compounds*, Academic Press, New York, **1967**; b) G. Maier, *Angew. Chem.* **1974**, *86*, 491–505; *Angew. Chem. Int. Ed. Engl.* **1974**, *13*, 425–438; c) T. Bally, S. Masamune, *Tetrahedron* **1980**, *36*, 343–370; d) G. Maier, *Angew. Chem.* **1988**, *100*, 317–341; *Angew. Chem. Int. Ed. Engl.* **1988**, *27*, 309–332.

[2] a) B. R. Arnold, J. Michl, *Spectroscopy of Cyclobutadiene* in *Kinetics and Spectroscopy of Carbenes and Biradicals* (Ed.: M. S. Platz), Plenum, New York, **1990**, pp. 1–35; b) H. Hopf, *Angew. Chem.* **1991**, *103*, 1137–1139; *Angew. Chem. Int. Ed. Engl.* **1991**, *30*, 1117.

[3] a) S. Masamune, N. Nakamura, M. Suda, H. Ona, *J. Am. Chem. Soc.* **1973**, *95*, 8481–8483; b) P. Eisenbarth, M. Regitz, *Chem. Ber.* **1982**, *115*, 3796–3810.

[4] a) G. Maier, F. Fleischer, *Tetrahedron Lett.* **1991**, *32*, 57–60; b) G. Maier, D. Born, *Angew. Chem.* **1989**, *101*, 1085–1087; *Angew. Chem. Int. Ed. Engl.* **1989**, *28*, 1050–1052.

[5] Besides the four stable tetrahedrane derivatives **3a–3d** (isotopomers of **3a** have been prepared in which either the quaternary center of one of the *tert*-butyl groups is ^{13}C-labeled or the hydrogens are replaced by deuterium atoms [1d], we have synthesized two other less stable tetrahedranes: In the reaction of **3d** with lithium aluminum hydride the isopropoxy substituent is replaced with a H atom. The tri-*tert*-butyl(dimethylsilyl)tetrahedrane thus formed [**3**, R = $SiHMe_2$: ^1H NMR(C_6D_6): $\delta = 4.8$ (sept, 1H, $J = 3.6$ Hz; $SiHMe_2$), 1.1 (s, 27H; 3 *t*Bu), 0.3 (d, 6H, $J = 3.6$ Hz; $SiHMe_2$); ^{13}C NMR(C_6D_6): $\delta = 31.2$ (3 CMe_3), 27.0 (3 CMe_3), 14.3 (3 *C*-*t*Bu), -0.8 ($SiMe_2$), -24.7 (*C*-$SiMe_2$)] is indefinitely stable only below $-25\,^{\circ}C$, in accord with the "corset principle"[1d]. The same holds for tri-*tert*-butyl(isopropyl)tetrahedrane [**3**, R = $CHMe_2$: ^1H NMR(C_7D_{14}): $\delta = 2.7$ (sept, 1H, $J = 6.8$ Hz; $CHMe_2$), 1.2 (s, 27H; 3 *t*Bu), 1.15 (d, 6H, $J = 6.8$ Hz; $CHMe_2$); ^{13}C NMR(C_7D_{14}): $\delta = 31.9$ (3 CMe_3), 27.6 (3 CMe_3), 24.8 ($CHMe_2$), 21.9 ($CHMe_2$), 10.1 (3 *C*-*t*Bu), 4.8 (*C*-$CHMe_2$)], which is accessible by the reaction sequence **1** → **2** → **3** but decomposes within a few minutes at room temperature in the presence of air (F. Fleischer, planned dissertation, Universität Giessen).

[6] R. Boese, unpublished results. We thank Priv. Doz. Dr. R. Boese, Universität-Gesamthochschule Essen, for the structure determination.

[7] a) G. Maier, U. Schäfer, W. Sauer, H. Hartan, R. Matusch, J. F. M. Oth, *Tetrahedron Lett.* **1978**, *21*, 1837–1840; b) G. Maier, H.-O. Kalinowski, K. Euler, *Angew. Chem.* **1982**, *94*, 706–707; *Angew. Chem. Int. Ed. Engl.* **1982**, *21*, 693–694.

[8] a) H. Ågren, N. Correia, A. Flores-Riveros, H. J. A. Jensen, *Int. J. Quantum Chem. Quantum Chem. Symp.* **1986**, *19*, 237–246; b) R. Janoschek, J. Kalcher, *ibid.* **1990**, *38*, 653–664; c) R. Janoschek, *Chem. Unserer Zeit* **1991** *25*, 59–66.

[9] The determination of the bond alternance in compounds like **2a** and **2b** by X-ray diffraction is difficult because of disorder. The X-ray data obtained for **2a** are consistent with the calculated differences in the bond lengths of the parent compound (0.22 Å) if the data are "averaged" by superimposing one rectangular ring on another one which is rotated by 90°: J. D. Dunitz, C. Krüger, H. Irngartinger, E. F. Maverick, Y. Wang, M. Nixdorf, *Angew. Chem.* **1988**, *100*, 415–417; *Angew. Chem. Int. Ed. Engl.* **1988**, *27*, 387–389.

[10] 150.9 MHz ^{13}C NMR spectrometer. We thank Bruker, Karlsruhe (FRG), for conducting these measurements.

[11] a) D. W. Whitman, B. K. Carpenter, *J. Am. Chem. Soc.* **1980**, *102*, 4272–4274; b) *ibid.* **1982**, *104*, 6473–6474.

[12] a) B. K. Carpenter, *J. Am. Chem. Soc.* **1983**, *105*, 1700–1701; b) M.-J. Huang, M. Wolfsberg, *ibid.* **1984** *106*, 4039–4040; c) M. J. S. Dewar, K. M. Merz, Jr., J. J. P. Stewart, *ibid.* **1984**, *106*, 4040–4041; d) P. Čársky, R. J. Bartlett, G. Fitzgerald, J. Noga, V. Špirko, *J. Chem. Phys.* **1988**, *89*, 3008–3015; e) R. Lefebvre, Moiseyev, *J. Am. Chem. Soc.* **1990**, *112*, 5052–5054.

[13] M. Saunders, C. S. Johnson, Jr., *J. Am. Chem. Soc.* **1987**, *109*, 4401-4402. According to these authors there is no need to discuss a heavy-atom tunneling effect (M. J. S. Dewar, K. M. Merz, Jr. *ibid.* **1986**, *108*, 5634-5635) for the norbornyl cation (C. S. Yannoni, V. Macho, P. C. Myhre, *ibid.* **1982**, *104*, 907-909, 7380–7381).

[14] For the unsubstituted cyclobutadiene a value of $\Delta G^{\ddagger} = 5.8\ kcal\,mol^{-1}$ would already require a rate constant that is consistent with the fast automerization at $-50\,^{\circ}C$ as measured by Carpenter, but not with the results of Michl (A. M. Orendt, B. R. Arnold, J. G. Radziszewski, J. C. Facelli, K.-D. Malsch, H. Strub, D. M. Grant, J. Michl, *J. Am. Chem. Soc.* **1988**, *110*, 2648-2650) based on the estimated exchange rates [$k(25\,K) \geq 10^3\ sec^{-1}$] from the solid-state ^{13}C NMR spectrum of doubly ^{13}C-labeled cyclobutadiene. The influence of the substituents on the exchange rate is difficult to estimate. The reduction of the barrier in the series **2d** to **2c** to **2b** supports the notion that the rate of valence isomerization increases with increasing steric hindrance. This could be explained by the fact that the substitution raises the energy of the rectangular ground-state more than that of the transition state: a) W. T. Borden, E. R. Davidson, *J. Am. Chem. Soc.* **1980**, *102*, 7958-7960; b) *Acc. Chem. Res.* **1981**, *14*, 69–76; c) K. Mislow, W. D. Hounshell, unpublished. See footnote [24] in ref. [14b].

Origin of the Stabilization of Vinyldiazonium Ions by β-Substitution; First Crystal Structure of an Aliphatic Diazonium Ion: β,β-Diethoxyethenediazonium Hexachloroantimonate**

By *Rainer Glaser,* Grace Shiahuy Chen,* and *Charles L. Barnes*

Dedicated to Professor Andrew Streitwieser on the occasion of his 65th birthday

In contrast to aromatic diazonium ions, most aliphatic diazonium ions are highly reactive intermediates that spontaneously lose N_2,[1,2] making the characterization of these important intermediates quite difficult. Aliphatic diazonium

[*] Prof. Dr. R. Glaser, G. S. Chen, Dr. C. L. Barnes
Department of Chemistry, University of Missouri
Columbia, MO 65211 (USA)

[**] This research was supported by the Petroleum Research Fund of the American Chemical Society and the Research Council of the University of Missouri (92-RC-023-BR). The X-ray diffractometer and the Bruker 500 MHz NMR spectrometer were partially funded by the National Science Foundation (CHE 90-11804 and CHE 89-08304, respectively). This research is part of the projected Ph.D. dissertation of G. S. Chen.

ions have been observed in superacid media[3] and in the gas phase.[4] Alkanediazonium ions have been stabilized by transition metals, but in these complexes the diazonium ions are bent and differ greatly from the free ions.[5] Bott discovered that various β,β-disubstituted ethenediazonium ions[6] are rather stable while the parent system is not.[2] This was attributed to the resonance stabilization of the β substituents. Bertrand et al. recently reported on the alkylation of a diazomethylenephosphorane which gives rise to stable C_β P-analogues of ethenediazonium ions, best described as phosphonio-substituted diazoalkanes.[7]

In this article, we report the first crystal structure analysis of an aliphatic diazonium ion, β,β-diethoxyethylenediazonium ion (**1**) in **1**-$SbCl_6$. With this crystal structure, we provide for the first time experimental information with which theoretical structural studies can be judged. The ab initio structures of **1** and its dimethoxy analogue **2**, 1,1-dimethoxyethene (**3**), and 1,1-dimethoxyethenium ion (**4**) also have been determined for the examination of the importance of individual mesomeric resonance forms.

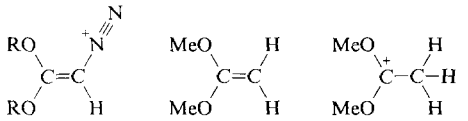

1, R = Et
2, R = Me

3 **4**

1-$SbCl_6$ was prepared by direct alkylation of diazoacetic ester with triethyloxonium hexachloroantimonate in 1,2-dichloroethane as described by Bott.[6] The white needles of **1**-$SbCl_6$ obtained after recrystallization from 1,2-dichloroethane were characterized by elemental analysis and by infrared and ^1H and ^{13}C NMR spectroscopy. IR spectra of **1**-$SbCl_6$ were recorded in CH_2Cl_2 and in the solid state (KBr). In the solution spectrum, the characteristic N–N stretching vibration appears at 2193 cm^{-1} while two bands[6] arise for this N–N stretching mode in the solid-state spectrum at 2192 and 2161 cm^{-1}. The ^1H (italics) and ^{13}C NMR chemical shifts are summarized in Scheme 1. The ^1H

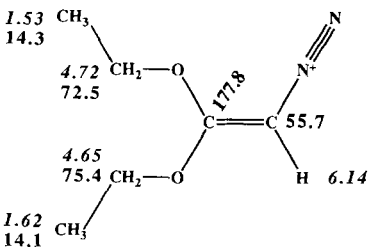

Scheme 1. ^{13}C and ^1H (italics) NMR chemical shifts of **1**.

signals were assigned based on the observed NOE between the vinylic H and the *trans*-CH_2 hydrogen atoms and the two-dimensional ^1H–^1H and ^1H–^{13}C COSY spectra. The signal for the vinylic H at $\delta = 6.14$ is most diagnostic. Unexpectedly, the ^{13}C NMR signal of the α C atom shows a lower intensity than that of the quaternary β C atom, but a DEPT experiment[8] clarified the assignment of these signals.

Single crystals suitable for X-ray crystallography were obtained from a solution of **1**-$SbCl_6$ in 1,2-dichloroethane which was covered with a layer of dry hexane and left standing in a dry box under N_2. Colorless single crystals formed at the interface after three days.[9]

The asymmetric unit of the orthorhombic unit cell of **1**-$SbCl_6$ contains two symmetry-independent cations **A** and **B** (Fig. 1) as suggested by the solid-state IR spectrum. **A** and **B** are surrounded by $SbCl_6^-$ ions, and all chlorine atoms are more than 3.35 Å away from the cations. The β N atoms are

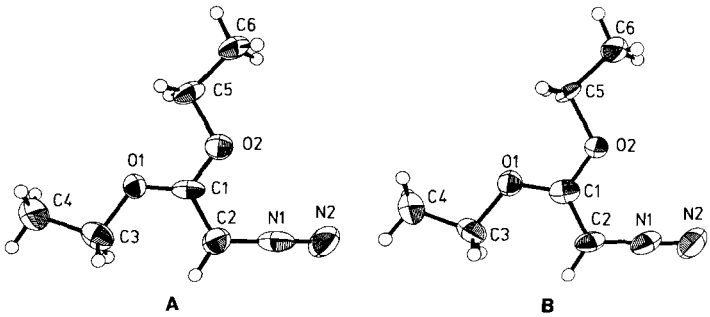

Fig. 1. Crystal structures of the two symmetry-independent β,β-diethoxyethenediazonium ions **A** and **B**. For bond lengths and angles see text.

coordinated by four chlorine atoms, and some of these chlorine atoms occupy bridging positions between the β N and α C atoms. The β C atoms in **A** and **B** are relatively close to two chlorine atoms (>3.4 Å). The ions **A** and **B** have the same conformation, and deviate from local C_s symmetry only slightly. C–O s-*trans* and s-*cis* conformations are preferred for the C_β–O bonds that are *cis* and *trans* with regard to the N_2 group, respectively, and all conformations are s-*trans* about both the Et–O and C–C bonds. Significant structural differences are evident for **A** and **B** (Table 1). The C–N bond in **A** is about 0.05 Å longer than in **B** while both of the C_β–O bonds, and the *cis* C1–O2 bond in particular, are shorter. Angular differences are small except for the *trans* ethyl group. **A** and **B** both exhibit C1–C2 bond lengths of 1.37–1.38 Å and N–N bond lengths of 1.10 Å. The bond angles involving the C1–C2 bond indicate attractive interactions between the N_2 group and the proximate ethoxy group. The C1-C2-N1 and C2-C1-O2 angles are less than 120°, whereas the corresponding angles C1-C2-H and C2-C1-O1 are larger. Importantly, the Et-O-C_β angles indicate approximately sp^2-hybridized O atoms, and the C_β–O distances are comparatively short.

The C_s structure of the diethoxyethenediazonium ion with the conformation of **1** was optimized with the 3-21G and 6-31G* basis sets (Fig.2). Conformational analysis of **2** suggests than this conformation is the most stable one.[11] The ab initio structures agree well with the average experimental values. Bond lengths generally are over- and underestimated at the lower and higher levels of calculation, respectively, but these differences are of about the same magnitude as the experimental uncertainties. The most significant deviations between the calculated and the solid-state structure occur for the Et-O-C_β angles (larger by 3.6–5.8°) and for the N–N bond length (underestimated by 0.01–0.02 Å).[12] Note that both the C_β–O and the Et–O bonds are consistently longer for the *cis* ethoxy group. The C1-C2-H angle is predicted to be significantly larger than the sp^2 hybridization angle.

The structural parameters of the CNN units in diazo compounds and diazonium ions are similar,[13] and thus provide little information regarding contributions of the mesomeric resonance forms of **I**–**IV** (Scheme 2). The C–C and the O–C bond lengths probably are the parameters best suited for this

Table 1. Selected important structural parameters of the crystal and ab initio structures of β,β diethoxyethenediazonium ion [a].

Parameter [b]	crystal			ab initio [c,d]			
	A	B	A–B	3-21G	Δ	6-31G*	Δ
C1-C2	1.378(15)	1.374(14)	0.004	1.3819	0.006	1.3913	0.015
C2-H	–	–	–	1.0617	–	1.0651	–
C2-N1	1.371(16)	1.325(15)	0.046	1.3493	0.001	1.3526	0.005
N1-N2	1.102(15)	1.104(15)	−0.002	1.0912	−0.012	1.0841	−0.019
O2-C1	1.268(12)	1.324(13)	−0.056	1.2957	0.000	1.2780	−0.018
O1-C1	1.257(13)	1.296(13)	−0.039	1.2951	0.019	1.2753	−0.001
C5-O2	1.477(12)	1.493(11)	−0.016	1.5057	0.021	1.4683	−0.017
C3-O1	1.468(13)	1.469(13)	−0.001	1.4954	0.027	1.4590	−0.010
C6-C5	1.500(16)	1.479(14)	0.021	1.5165	0.027	1.5094	0.020
C4-C3	1.561(17)	1.488(16)	0.073	1.5173	−0.007	1.5102	−0.014
C1-C2-H	–	–	–	126.16	–	128.02	–
C1-C2-N1	118.8(10)	116.6(9)	2.2	117.64	−0.1	116.41	−1.3
N2-N1-X	89.6(14)	89.3(12)	0.3	89.93	0.5	90.87	1.4
C2-C1-O2	118.0(10)	119.0(10)	−1.0	118.69	0.2	118.39	−0.1
C2-C1-O1	122.1(9)	125.6(10)	−3.5	123.96	0.1	123.74	−0.1
C5-O2-C1	117.4(8)	117.9(7)	−0.5	123.31	5.7	122.02	4.4
C3-O1-C1	121.9(8)	117.8(8)	4.1	125.69	5.8	123.41	3.6
C6-C5-O2	107.4(8)	106.4(7)	1.0	105.22	−1.7	106.64	−0.3
C4-C3-O1	107.3(9)	105.9(9)	1.4	105.69	−0.9	107.05	0.5

[a] Length in Å and angles in degrees. Standard deviations given in parentheses refer to the last digit(s). [b] For atom numbering see Figure 1. X is a dummy atom connected to N1, *cis* with C1; X-N1 is perpendicular to C2-N1. C1 = C_β, C2 = C_α; N_α is attached to C_α. [c] C_s structure. [d] Δ values are the deviations of the ab initio structures from the *average* values of the crystal structure.

analysis. The short C_β–O bonds and the large Et-O-C_β angles indicate that the Lewis structures of types **III** and **IV** contribute significantly. This importance of **III** and **IV** can be

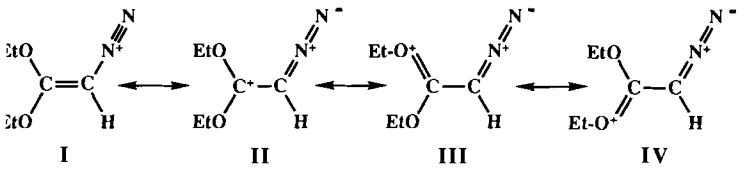

Scheme 2. Resonance forms I–IV of 1.

demonstrated convincingly by comparison[14] of **2** with **3** and **4** (Fig. 2). Note the structural similarities of **1** and **2**. The C_β–O bond lengths in the carbenium ion **4** are only moderately shorter than in **2** (0.015–0.026 Å) while the O–CH_3 bonds are slightly longer (0.008–0.012 Å). In contrast, the C_β–O bonds in **3** are significantly longer (>0.074 Å), and the H_3C–O bonds are shorter (>0.035 Å) than in both **2** and **4**. Thus, the characteristic shortening of the C_β–O bonds and the concomitant lengthening of the H_3C–O bonds in the carbenium ion **4** are also clearly evident in **2**. This finding stresses the importance of resonance forms **III** and **IV**. The longer C–C bonds in **1** and **2** compared to **3** provides evidence for the importance of all of the resonance forms **II**–**IV**. Oxosubstituted carbenium ("oxenium") ions[15] as well as dioxo derivatives[16] ("dioxenium" ions) are known, and a few crystal structures of the former have been reported. Childs et al.[15a] determined the crystal structure of two hydroxycarbenium ions; their short C–OH bond lengths (1.288–1.302 Å) indicate significant contributions of the oxenium ion resonance form.[17]

These results point out the crucial importance of the O-stabilized carbenium-type resonance forms **II**–**IV** in understanding the stability of the β-substituted alkenediazononium ion. Our conclusions are in agreement with topological electron density analysis of other β-substituted ethenediazonium ions[2d] as well as of the unsubstituted system[2a] which suggest electronic structures with overall *neutral* dinitrogen

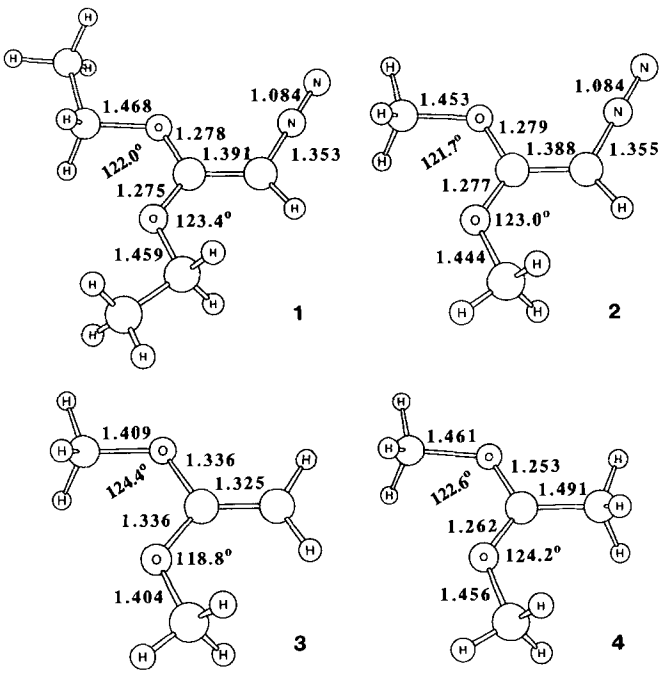

Fig. 2. RHF/6-31G*-optimized C_s structures of **1**–**4**.

fragments. Moreover, the ^{13}C NMR chemical shifts of **1** are indicative of electron depletion at C_β which is also in agreement with the additions of nucleophiles to the β carbon atom in the chemistry of β,β-disubstituted ethenediazonium ions.[18]

Experimental Procedure

Caution: Oxonium salts are toxic and carcinogenic. All experimental work was carried out in a glove box under dry N_2. Solvents were dried over P_4O_{10}; hexane was dried over molecular sieves.

1: To a stirred solution of diazoacetic ester (2.08 g, 18 mmol) in 15 mL of 1,2-dichloroethane was added triethyloxonium hexachloroantimonate (2.6 g, 6 mmol). The resulting mixture was allowed to react 24 h at room temperature. Upon addition of 40 mL of CCl_4 **1** precipitated. The crude product was purified by recrystallization. A saturated solution of **1** in dichloroethane at room tem-

perature was treated with CCl_4 until the crystallization of **1** was observed. Recrystallization at 5 °C furnished 2.08 g of the pure salt **1** as white needles; m.p. 110–112 °C; yield 24%.

^{1}H NMR (500 MHz, CD_2Cl_2, 25 °C, TMS): $\delta = 1.53$ (t, $J = 7$ Hz, 3H), 1.62 (t, $J = 7$ Hz, 3H), 4.65 (q, $J = 7$ Hz, 2H), 4.72 (q, $J = 7$ Hz, 2H), 6.14 (s, 1H); ^{13}C NMR (CD_2Cl_2): $\delta = 14.14$ (CH_3), 14.28 (CH_3), 55.75 (CH), 72.47 (CH_2), 75.41 (CH_2), 177.8 (C1). – Correct elemental analyses (C,H,N,Cl).

Received: December 4, 1991 [Z 5054 IE]
German version: *Angew. Chem.* **1992**, *104*, 749

CAS Registry numbers:
1, 3883-93-0; **2**, 140834-35-1; **3**, 116-11-0; **4**, 41798-19-0; ethyl diazoacetate, 623-73-4; triethyloxonium hexachloroantimonate, 3264-67-3.

[1] Reviews: a) K. Bott, *Angew. Chem.* **1979**, *91*, 279; *Angew. Chem Int. Ed. Engl.* **1979**, *18*, 259; b) K. Bott, *Alkenediazonium Compounds in The Chemistry of the Functional Groups. Suppl. C.* (Eds.: S. Patai, Z. Rappoport), Wiley, New York, **1983**, p. 671; c) K. Laali, G. A. Olah, *Rev. Chem. Intermed.* **1985**, *6*, 237.

[2] a) R. Glaser, *J. Phys. Chem.* **1989**, *93*, 7993; b) R. Glaser *J. Comput. Chem.* **1990**, *11*, 663; c) R. Glaser, G. S.-C. Choy, M. K. Hall, *J. Am. Chem. Soc.* **1991**, *113*, 1109; d) R. Glaser, C. J. Horan, E. Nelson, M. K. Hall, *J. Org. Chem.* **1992**, *57*, 215; e) R. Glaser, C. J. Horan, G. S.-C. Choy, *ibid.* **1992**, *57*, 995.

[3] a) J. R. Mohrig, K. Keegstra, *J. Am. Chem. Soc.* **1967**, *89*, 5492; b) J. R. Mohrig, K. Keegstra, A. Maverick, R. Roberts, S. J. Wells, *J. Chem. Soc. Chem. Commun.* **1974**, 780; c) M. Avaro, J. Levisalles, J. M. Sommer, *Chem. Commun.* **1968**, 410; d) J. F. McGarrity, D. P. Cox, *J. Am. Chem. Soc.* **1983**, *105*, 3961.

[4] a) M. S. Foster, J. L. Beauchamp, *J. Am. Chem. Soc.* **1972**, *94*, 2425; b) M. S. Foster, A. D. Williamson, J. L. Beauchamp, *Int. J. Mass. Spectrom. Ion Phys.* **1974**, *15*, 429; c) T. B. McMahon, T. Heinis, G. Nicol, J. K. Hovey, P. Kebarle, *J. Am. Chem. Soc.* **1988**, *110*, 7591.

[5] a) M. F. Lappert, J. S. Poland, *Chem. Commun.* **1969**, 1061; b) B. W. Day, T. A. George, S. D. Iske, *J. Am. Chem. Soc.* **1975**, *97*, 4127; c) W. A. Herrmann, *Angew. Chem.* **1975**, *87*, 358; *Angew. Chem. Int. Ed. Engl.* **1975**, *14*, 355; d) G. L. Hillhouse, B. L. Haymore, *Inorg. Chem.* **1979**, *18*, 2423; e) W. A. Herrmann, M. L. Ziegler, K. Weidenhammer, *Angew. Chem.* **1976**, *88*, 379; *Angew. Chem. Int. Ed. Engl.* **1976**, *15*, 368.

[6] K. Bott, *Tetrahedron* **1966**, 1251.

[7] J. M. Sotiropoulos, A. Baceiredo, K. Horchler von Locquenghien, F. Dahan, G. Bertrand, *Angew. Chem.* **1991**, *103*, 1174; *Angew. Chem. Int. Ed. Engl.* **1991**, *30*, 1154.

[8] a) D. M. Doddrell, D. T. Pegg, M. R. Bendall, *J. Magn. Reson.* **1982**, *48*, 323; b) Delay time was 1 s. c) The lower intensity of the methine signal most likely is the result of broadening due to quadrupolar coupling to ^{14}N.

[9] X-ray data of **1**: were collected at −100 °C on an Enraf-Nonius CAD4 diffractometer with $Mo_{K\alpha}$ radiation. The needle-shaped crystal was mounted on a glass fiber approximately along the long axis of the needle. The data was corrected for Lorentz and polarization effects. An empirical absorption correction was applied using ψ scans, giving relative transmittance factors between 0.90 and 0.99. The structure was solved by Patterson techniques and refined in the space group $Pca2_1$ with $Z = 8$. Though the antimonate ions are related by a pseudo center of symmetry, the organic cations do not agree with this symmetry element. The acentric space group reported is therefore correct. The polarity of the crystal could not be determined, probably as a result of the pseudocentrosymmetrically related antimonates. Refinement included anisotropic thermal parameters for the non-hydrogen atoms. The hydrogen atoms were included in the model at calculated positions; the orientation of the methyl hydrogen atoms were established in a difference Fourier map. Full-matrix least-square refinements gave final $R = 0.032$, $R_w = 0.044$ and $S = 1.20$ for 2203 reflections with $I > 2.5\,\sigma(I)$. The final Fourier map includes four peaks of about 0.8 $e^-Å^{-3}$ near the antimony atoms, but no other features above 0.5 $e^-Å^{-3}$. All calculations were performed with the NRCVAX suite of programs.[10] Further details of the crystal structure investigation are available on request from the Director of the Cambridge Crystallographic Data Centre, University Chemical Laboratory, Lensfield Road, GB-Cambridge CB2 1EW (UK), on quoting the full journal citation.

[10] E. J. Gabe, Y. Le Page, J.-P. Charland, F. L. Lee, *J. Appl. Chem.* **1989**, *22*, 384.

[11] It is certainly reasonable to assume that the methyl and the methylene groups in the ethoxy fragments are staggered and in the *s-trans* conformation with respect to the C3–C4 and C5–C6 bonds. The dimethyl compound therefore serves well in the investigation of the conformational preferences about the four C–O bonds. R. Glaser, G. S. Chen, unpublished results.

[12] The former is likely to be a crystal-packing effect requiring relatively little energy (bending modes), and the latter reflects the importance of electron correlation in predictions of the N–N bond length as discussed in ref. [2c].

[13] R. Glaser, G. S. Chen, unpublished ab initio studies.

[14] a) **2**–**4** were optimized at the RHF/3-21G- and RHF/6-31G* levels. Analytic computation of the Hessian matrices at the lower level showed all of these structures to be minima. b) Investigation of the protonation of vinyl ethers: K. Ösapay, I. Delhalle, K. M. Nsunda, E. Rolli, R. Houriet, L. Hevesi, *J. Am. Chem. Soc.* **1989**, *111*, 5028.

[15] a) R. F. Childs, R. Faggiani, C. J. L. Lock, M. Mahendran, S. D. Zweep, *J. Am. Chem. Soc.* **1986**, *108*, 1692; b) S. K. Chadda, R. F. Childs, R. Faggiani, C. J. L. Look, *ibid.* **1986**, *108*, 1694.

[16] F. Perron-Sierra, M. A. Promo, V. A. Martin, K. F. Albizati, *J. Org. Chem.* **1991**, *56*, 6188.

[17] Conclusions based on a comparison of **1**–**4** with this ion are difficult to impossible because of the difference in C substituents (phenyl and cyclopropyl as opposed to CHN_2) as well as the number and type (HO or RO) of O substituents.

[18] a) K. Bott, *Chem. Ber.* **1987**, *120*, 1867; b) *Tetrahedron Lett.* **1985**, *26*, 3199.

Cyclohexadienyl-Type Cationic Intermediates in the Friedel–Crafts Alkylation of Benzene Derivatives with the 9-Fluorenyl Cation—Observation by Laser Flash Photolysis**

By *Frances Cozens, Jianhui Li, Robert A. McClelland,** and *Steen Steenken**

There have been a number of recent reports of the use of laser flash photolysis to directly study carbocations under conditions where they are actually found as intermediates in organic reactions.[1] This approach allows the measurement of absolute rate constants for the further reactions of the cation. Previously, reactivities of short-lived cations had been examined only in terms of *relative* rate constants, obtained, for example, from competition experiments in which an intermediate not observed directly partitions between two nucleophiles. One fundamental reaction that has seen considerable investigation in the latter regard is electrophilic aromatic substitution. In this paper we demonstrate that flash photolysis can be employed to *directly* study the key steps in such a reaction. In particular, *both* cationic intermediates of a Friedel–Crafts alkylation can be observed, the initial electrophile *and* the cyclohexadienyl cation, the "σ complex" formed by addition to the arene.

The experiments employed the 9-fluorenyl cation (Fl^+), generated photochemically from 9-fluorenol (Fl-OH) in 1,1,1,3,3,3-hexafluoroisopropyl alcohol (HFIP)[2] (Scheme 1). This system has several features that make it useful for studying reactions with arenes: 1) The photoheterolysis of 9-fluorenol is very clean in this solvent with no competing reactions such as photohomolysis. 2) The solvent itself is relatively unreactive to cations, so that the added arenes can compete for the cation. 3) 9-Fluorenol has sufficient absorbance to be excited at 300–310 nm, a range in which simple aromatic compounds have essentially *no* absorbance.

Indeed, the rates (k_{obsd}) for the exponential decrease of Fl^+ (due to reaction with solvent[2]) increase in the presence of alkenes and arenes, with the expected linear dependence on the concentration of the additive. The second-order rate con-

[*] Prof. Dr. R. A. McClelland, F. Cozens, J. Li
Department of Chemistry, University of Toronto
Toronto, Ontario M5S 1A1 (Canada)
Prof. Dr. S. Steenken
Max-Planck-Institut für Strahlenchemie
Stiftstrasse 34–36, D-W-4330 Mülheim (FRG)

[**] This work was supported by the Natural Sciences and Engineering Research Council of Canada and the Petroleum Research Fund, administered by the American Chemical Society.

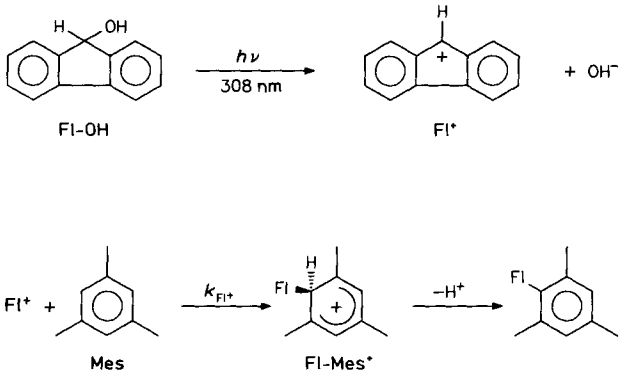

Scheme 1.

stants k_{Fl^+}, determined from the slope of the plot of k_{obsd} versus the concentration of the additive are given in Table 1. For benzene and the monosubstituted benzenes **1**–**5** the rate constants are strongly dependent on the substituents; a plot of log k_{Fl^+} versus σ_p^+ is linear with a slope ϱ of -5.0 ($r = 0.999$). The rate constants, however, approach a plateau at anisole. This "saturation effect" can also be seen in the data for the methylated benzenes, in which additional methyl substituents have little effect after *m*-xylene (compare **5**–**9**). Styrene and its derivatives **10a–e** and 1-methylcyclohexene (**11**) react with the same rate constant, 3×10^9 M^{-1}s^{-1}. This value is probably close to the diffusion limit, at least as based on the observation that there is *no* dependence on substituent in this series.

Table 1. Rate constants for the reaction of π nucleophiles with the 9-fluorenyl cation Fl^+ (k_{Fl^+}) [a] and for the reaction of *n*-nucleophiles with $FlMes^+$ (k_{FlMes^+}) [b].

Reaction with Fl^+		Reaction with Fl-Mes$^+$	
Nucleophile	k_{Fl^+} [M^{-1}s^{-1}]	Nucleophile	k_{FlMes^+} [M^{-1}s^{-1}]
benzene (**1**)	3.3×10^5	$(CF_3)_2CHOH$	5×10^4 s^{-1} [c]
fluorobenzene (**2**)	7.9×10^5	MeOH	3.3×10^6
biphenyl (**3**)	2.8×10^6	EtOH	3.0×10^6
toluene (**4**)	1.1×10^7	iPrOH	1.9×10^6
anisole (**5**)	1.7×10^9	tBuOH	1.3×10^6
m-xylene (**6**)	1.1×10^9	Br^-	2.8×10^9
mesitylene (**7**)	1.9×10^9		
1,2,3,5-$(Me)_4C_6H_2$ (**8**)	1.7×10^9		
pentamethylbenzene (**9**)	1.5×10^9		
$ArCH{=}CH_2$ **10a–e** [d]	$(3.0 \pm 0.2) \times 10^9$		
1-methylcyclohexene (**11**)	2.9×10^9		
$(CF_3)_2CHOH$	$(2-5) \times 10^4$ s^{-1} [c]		

[a] Experiments were carried out at 20 ± 1 °C with solutions of 0.1–0.2 mM 9-fluorenol in HFIP, and excitation at 308 nm. The decay of the cation was monitored at 515 nm, and five to seven concentrations of nucleophile were employed. k_{Fl^+} was obtained as the slope of k_{decay} versus [nucleophile]. [b] Determined by monitoring the rate of decay of Fl-Mes$^+$ at 370 nm as a function of [nucleophile] in a solution of 1 mM 9-fluorenol and 2 mM mesitylene in HFIP. [c] Pseudeo-first-order rate constant for the decay in solvent alone. Number varies depending on water content [2]. [d] Ar = 4-$MeOC_6H_4$ (**a**), 4-MeC_6H_4 (**b**), C_6H_5 (**c**), 4-BrC_6H_4 (**d**), 3-BrC_6H_4 (**e**).

For the photolysis in the presence of selected arenes, experiments were conducted with excitation at 300 nm in a Rayonet reactor, followed by GC analysis of the products. The expected products of electrophilic substitution were observed (Table 2). Authentic samples of these adducts were prepared by the reaction of the appropriate aryl Grignard compounds and fluorenone followed by reduction.[3–5] The product of the capture of Fl^+ by HFIP, 9-(1′,1′,1′,3′,3′,3′-hexafluoroisopropoxy)fluorene,[2] was also present, and together with the substituted arenes quantitatively accounted for all the photolyzed 9-fluorenol. The solvolysis of 9-bromofluorene in HFIP in the presence of toluene, a thermal reaction proceeding via Fl^+, gave a product distribution identical to that of the photochemical reaction (of 9-fluorenol), establishing that the latter also proceeds by way of the free, ground state, 9-fluorenyl cation.

Table 2. Products from the photolysis of 9-fluorenol in the presence of arenes.

Arene	Product(s)
benzene	9-phenylfluorene
toluene	(9-fluorenyl)toluenes, *o*:*m*:*p* = 5:5:90
anisole	(9-fluorenyl)anisoles *o*:*p* = 55:45, *m* < 0.1
m-xylene	(9-fluorenyl)-1,3-dimethylbenzenes 2:4:5 = 0.1:98:2
mesitylene	1-(9-fluorenyl)-2,4,6-trimethylbenzene

As determined from product analysis following photolysis in the presence of both benzene and toluene, the statistically corrected ratio of the rate constants for *para* substitution of toluene compared to reaction with benzene is 200. This quantity can also be calculated from the directly measured rate constants as $[6 \times 0.90 \times k_{Fl^+}\text{(toluene)}]/[k_{Fl^+}\text{(benzene)}] = 180$; the factors 6 and 0.9 represent the statistical correction for benzene and the fraction of *para* product with toluene, respectively. A similar competition between toluene and mesitylene also results in product ratios predictable from the ratio in absolute rate constants (observed mesitylene: *p*-toluene product ratio (statistically corrected) = 70, calculated $[\frac{1}{3} \times k_{Fl^+}\text{(mesitylene)}]/[0.9 \times k_{Fl^+}\text{(toluene)}] = 63$). There has been some discussion as to the consistency of kinetic data based on competition experiments,[6] but in the present case there is clearly excellent agreement with the time-resolved data.

As illustrated for mesitylene in Figure 1, the cyclohexadienyl cation of "σ complex" that results from the reaction of Fl^+ with the arene can be directly observed. In the *absence* of mesitylene, the 9-fluorenyl cation Fl^+ produced by the 308 nm photolysis of 1 mM 9-fluorenol in HFIP decays to zero with $k = (2-5) \times 10^4$ s^{-1}.[2] In the *presence* of mesitylene, however, the disappearance of Fl^+ is much

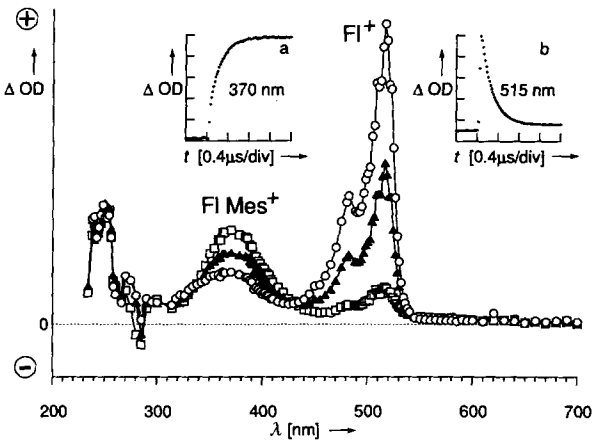

Fig. 1. Absorption spectra of transient species observed upon 308 nm excitation of a solution of 1 mM 9-fluorenol in HFIP (air-saturated) in the presence of 2 mM mesitylene. Spectra were recorded 100 ns (circles), 250 ns (triangles), and 800 ns (squares) after the laser flash. Inset b shows the decrease of the concentration of Fl^+ due to reaction with mesitylene (Mes), inset a the concomitant buildup of the resulting cation Fl-Mes$^+$ (timescale 0.4 μs per division; OD = optical density).

faster, and a new absorbance centered at 365 nm grows in at the same rate as the absorbance of the cation at 515 nm decays (see insets a) and b) in Fig. 1). The 1:1 transformation is also documented by the isosbestic points at 335 and 430 nm.

After reaching a maximum the absorbance at 365 nm eventually decreases again and decays to zero with a rate constant of $5 \times 10^4\ s^{-1}$. This new transient is identified as the 1-(9′-fluorenyl)-2,4,6-trimethylbenzenium ion, Fl-Mes$^+$ (Scheme 1).[7] In support of the assignment of the transient species absorbing at 365 nm to a cyclohexadienyl cation is the fact that the 2,4,6-trimethylbenzenium ion, which is obtained by photoprotonation of mesitylene in HFIP,[8] decays in HFIP with a rate constant of $1 \times 10^5\ s^{-1}$ and has λ_{max} at 355 nm, in agreement with the spectrum of the cation in strong acids.[9–11] The 2,4,6-trimethylbenzenium ion has an additional absorption band at 250–260 nm.[8–11] A band in this spectral region is also apparent in Figure 1, although there is overlap with absorbance[2] due to Fl$^+$.

As a further characterization of the species absorbing at 355 and 260 nm, its reactivity with O_2 (none) and with *n*-nucleophiles was determined. The results (Table 1) show the species to be highly electrophilic, as expected for cyclohexadienyl cations.[8, 12] It is interesting that the rate constants are of a factor 2–6 smaller than those[12] of the corresponding cyclohexadienyl cations produced by addition of *para*-substituted phenyl cations to mesitylene.

Transient σ complexes (cyclohexadienyl cations) were also observed in the reaction of Fl$^+$ with *m*-xylene, anisole, and the tetra- and pentamethylbenzenes, but not with toluene or the less reactive arenes. The latter observation is explained by assuming that the rate of disappearance of the cyclohexadienyl cation is larger than its rate of formation.

There have been suggestions that, depending on the reactivity of the electrophile, transition states in arene substitutions resemble either the σ complex or a π complex.[13] Very fast reactions have been assumed to occur via the latter and to lead to low intramolecular selectivity, such as, with toluene, *ortho*:*para* ratios near 2:1. However, we have found that this concept is not necessarily correct: The reactions of Fl$^+$ with aromatic compounds are very fast, and yet there is significant intra- as well as intermolecular selectivity. The former is reflected by the low yield of *ortho* product from toluene, the latter in the large ratio of rate constants for the reactions of Fl$^+$ with toluene and benzene.

In summary, although the rate constants for the reaction of the 9-fluorenyl cation with arenes measured by laser flash photolysis are large, the system exhibits selectivity patterns indicative of a transition state that has characteristics of the intermediate cyclohexadienyl cation. Such a species has been observed with the more reactive arenes, so that in the same experiment both cationic intermediates of a Friedel–Crafts reaction could be studied directly.

Received: January 21, 1992 [Z 5138 IE]
German version: *Angew. Chem.* **1992**, *104*, 753

CAS Registry numbers:
1, 71-43-2; **2**, 462-06-6; **3**, 92-52-4; **4**, 108-88-3; **5**, 100-66-3; **6**, 108-38-3; **7**, 108-67-8; **8**, 527-53-7; **9**, 700-12-9; **10a**, 637-69-4; **10b**, 622-97-9; **10c**, 100-42-5; **10d**, 2039-82-9; **10e**, 2039-86-3; **11**, 591-49-1; Fl$^+$, 62683-97-0; Fl-Mes$^+$, 141046-51-7; MeOH, 67-56-1; EtOH, 64-17-5; *i*-PrOH, 67-63-0; *t*-BuOH, 75-65-0; Br$^-$, 24959-67-9; 9-fluorenol, 1689-64-1.

[1] R. A. McClelland, V. M. Kanagasabapathy, S. Steenken, *J. Am. Chem. Soc.* **1991**, *113*, 1009.
[2] R. A. McClelland, N. Mathivanan, S. Steenken, *J. Am. Chem. Soc.* **1990**, *112*, 4857.
[3] T. H. Siddall, W. E. Stewart, *Tetrahedron Lett.* **1968**, 5011.
[4] T. H. Siddall, W. E. Stewart, *J. Org. Chem.* **1969**, *34*, 233.
[5] M. Oki, *Angew. Chem.* **1976**, *88*, 67; *Angew. Chem. Int. Ed. Engl.* **1976**, *15*, 87.
[6] See for example G. A. Olah, J. A. Olah, T. Ohyama, *J. Am. Chem. Soc.* **1984**, *106*, 5284; J. H. Ridd, *Acc. Chem. Res.* **1971**, *4*, 248; L. M. Stock, H. C. Brown, *Adv. Phys. Org. Chem.* **1963**, *1*, 35.
[7] Results of experiments at very low mesitylene concentration (<0.5 mM) suggest that the alkylation step may be reversible. Detailed studies with this and other systems are currently in progress.
[8] S. Steenken, R. A. McClelland, *J. Am. Chem. Soc.* **1990**, *112*, 9648.
[9] G. Dallinga, E. L. Mackor, A. A. Verrijn Stuart, *Mol. Phys.* **1958**, *1*, 123.
[10] G. P. Smith, A. S. Dworkin, R. M. Pagni, S. P. Zingg, *J. Am. Chem. Soc.* **1989**, *111*, 525.
[11] H. J. Bakoss, R. J. Ranson, R. M. G. Roberts, A. R. Sadri, *Tetrahedron*, **1982**, *38*, 623.
[12] S. Steenken, P. Maruthamuthu, R. A. McClelland, *J. Am. Chem. Soc.*, in press.
[13] G. A. Olah, *Acc. Chem. Res.* **1971**, *4*, 420.

Selective Binding of Sugar to β-Cyclodextrin: A Prototype for Sugar–Sugar Interactions in Water**

By *Yasuhiro Aoyama,** *Yoshiro Nagai, Jun-ichi Otsuki, Kenji Kobayashi*, and *Hiroo Toi*

Oligosaccharides play important roles in biological information transfer, especially in the intercellular recognition.[1] Selective complexation of sugars in apolar organic media is a rapidly growing area of research in the field of molecular recognition.[2] The object of the present work is to shed light on the oligosugar–sugar interactions *in water*; we report here on the first example: β-cyclodextrin (β-CD)[3] selectively binds aldopentoses.

8-Anilinonaphthalene-1-sulfonate (ANS, in this study as Mg^{2+} salt) is known to form a 1:1 complex with β-CD in water [Eq. (a)], thereby undergoing a significant enhancement of its fluorescence intensity *I* (from 25 arbitrary units for free ANS to 400 for the complex). A binding constant

$$\beta\text{-CD-ANS} \underset{K_{ANS}}{\overset{ANS}{\rightleftharpoons}} \beta\text{-CD} \underset{K}{\overset{guest}{\rightleftharpoons}} \beta\text{-CD-guest} \qquad (a)$$

K_{ANS} of $95\ M^{-1}$ was obtained by fluorimetric titration (pH 6.8 at 25 °C; literature values: 77, 64, 110, and 65[4]). The fluorescence intensity of ANS (1.0×10^{-4} M) at a fixed β-CD concentration (1.2×10^{-2} M) was reduced in the presence of aldopentoses and their derivatives [D-ribose (D-**1**), D- and L-arabinose (D- and L-**2**), D-xylose (D-**3**), D-lyxose (D-**4**), D-2-deoxyribose (D-**5**), and methyl β-D-ribopyranoside (D-**6**)], as well as of aliphatic alcohols [*tert*-butanol (**7**), cyclohexanol (**8**), and *cis*- and *trans*-1,2-cyclohexanediol (**9c** and **9t**)]. In marked contrast, aldohexoses and their derivatives

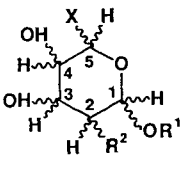

15

1-4 : X=R¹=H, R²=OH
5 : X=R¹=R²=H
6 : X=H, R¹=CH₃, R²=OH
10-12 : X=CH₂OH, R¹=H, R²=OH
13 : X=CH₃, R¹=H, R²=OH
14 : X=R¹=CH₃, R²=OH

[*] Prof. Dr. Y. Aoyama, Y. Nagai, J. Otsuki, Dr. K. Kobayashi, Dr. H. Toi
Department of Chemistry, Nagaoka University of Technology
Kamitomioka, Nagaoka, Niigata 940-21 (Japan)

[**] This work was supported by a Grant-in-Aid for Scientific Research on Priority Areas (No. 03214106) from the Japanese Government.

[D-glucose (D-**10**), D-galactose (D-**11**), D-mannose (D-**12**), D- and L-fucose (D- and L-**13**; fucose = 6-deoxygalactose), and methyl α-D-fucopyranoside (D-**14**)] showed almost no effect. Typical correlations between the difference in intensity ΔI ($I - I_0$) and the concentration of the guest are shown in Figure 1 for selected guests (D-**1**, L-**2**, D-**5**, D-**6**, **9t**, and D- and L-**13**.

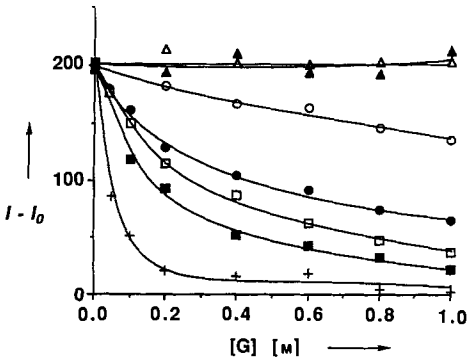

Fig. 1. Correlations between ΔI ($I - I_0$) and the concentration of the guest [G] (excitation at 348 nm and emission at 520 nm) for D-**1** (●), L-**2** (○), D-**5** (□), D-**6** (■), **9t** (+), D-**13** (▲), and L-**13** (△) under conditions of $[ANS]_0 = 1.0 \times 10^{-4}$ M and $[\beta\text{-CD}]_0 = 1.2 \times 10^{-2}$ M at pH 6.8 and 25 °C. I_0 = fluorescence intensity for ANS without guest.

The reduction in fluorescence intensity can be interpreted in terms of competitive inhibition of the ANS binding as a result of β-CD–guest complexation [Eq. (a), guest is **1**–**14**]. More direct evidence for the selective guest binding came from the ^{13}C NMR results. Sugars **1**–**6** and alcohols **7**–**9** (1.0×10^{-1} M) caused characteristic site-specific changes in the ^{13}C chemical shifts δ_C of β-CD (1.0×10^{-2} M). Sugars **10**–**14**, on the other hand, gave practically no effect. Some typical examples are shown in Table 1.

Table 1. Shifts ($\Delta\delta_C$) in ^{13}C NMR signals for β-CD (1.0×10^{-2} M) in the presence of guests (1.0×10^{-1} M) in D_2O.

guest	Δδc [a]						K[M^{-1}] [b]
	C1	C2	C3	C4	C5	C6	
D-**5**	+0.10	+0.05	+0.08	+0.07	+0.02	−0.01	9.4
D-**6**	+0.15	+0.06	+0.10	+0.07	+0.03	−0.07	14
7	+0.21	+0.17	+0.13	+0.17	+0.06	−0.04	56
D-**10**	ca. 0	ca. 0	ca. 0	ca. 0	ca. 0	ca. 0	ca. 0
D-**11**	ca. 0	ca. 0	ca. 0	ca. 0	ca. 0	ca. 0	ca. 0
L-**13**	ca. 0	ca. 0	ca. 0	ca. 0	ca. 0	ca. 0	ca. 0

[a] The chemical shifts (relative to external TMS) of β-CD in the absence of any guest are δ_C = 102.9 (C1), 82.2 (C2), 74.1 (C3), 73.1 (C4), 72.9 (C5), 61.4 (C6): P. Colson, H. J. Jennings, I. C. P. Smith, *J. Am. Chem. Soc.* **1974**, *96*, 8081–8087. A positive sign for $\Delta\delta_C$ indicates a downfield shift. [b] Binding constants for the β-CD–guest complexation determined by fluorimetric analysis (cf. Table 2).

Analysis of the competitive inhibition data[5, 6] gave the binding constants [K, Eq. (a)] shown in Table 2. The trend in the constants for guests **5**, **6**, **7**, **10**, **11**, and **13** parallels the complexation-induced shifts in δ_C ($\Delta\delta_C$, Table 1). They decrease in the general order **8** > **9c** ≈ **9t** ≈ **7** > **1**–**6**. The decreasing order in the aldopentose series (**6** > **5** > **1** > **4** > **3** > **2**) is essentially the decreasing order of hydrophobicities.[7] These results suggest that hydrophobic interactions make an important contribution to the present oligosugar–sugar complexation, but it can not be the sole governing factor. First, the correlation between K and P (lipophilicity)[8] established for the β-CD-alcohol complexation[5] suggests that even the lipophilicity of **6** is not enough to allow its binding to β-CD. Second, fucose (**13**) is more hydrophobic than aldopentoses **1**–**4**, and its methyl glycoside **14** is the most hydrophobic among sugars investigated here; nevertheless, they are not bound by β-CD. There is, however, a rather surprising selectivity between aldopentoses **1**–**6** and aldohexoses **10**–**14**. This selectivity can hardly be due to favorable furanose binding, since the furanose contents for xylose (**3**) and lyxose (**4**) in water are approximately 0[9] and *pyranoside* **6** is in fact best bound. Thus, the absence (aldopentoses) or the presence (aldohexoses) of a substituent X on C5 of a pyranose ring must be the crucial factor.

Table 2. Binding constants K for the β-CD–guest complexation [a].

guest	K [M^{-1}]	guest	K [M^{-1}]	guest	K [M^{-1}]
D-**1**	5.3	D-**6**	14	D-**11**	ca. 0
D-**2**	0.7	**7**	56[b]	D-**12**	ca. 0
L-**2**	0.7	**8**	460[c]	D-**13**	ca. 0
D-**3**	1.0	**9c**	71	L-**13**	ca. 0
D-**4**	4.3	**9t**	61	D-**14**	ca. 0
D-**5**	9.4	D-**10**	ca. 0		

[a] The binding constants are average values obtained from fluorescence measurements for at least three different guest concentrations at pH 6.8 and 25 °C. Estimated errors are ≤20%. [b] Literature value [5]: 47. [c] Literature value [4]: $(2.0 \times 10^{-3})^{-1} = 500$.

The inhibitory effect of both hydrophilic 5-CH_2OH (for **10**–**12**) and hydrophobic 5-CH_3 groups (for **13**–**14**) suggests that the inhibition is steric in origin. This may rule out an *axial* binding mode, in which the substituent X exerts a minimal steric effect but some hydrophilic ring-OH groups of a bound sugar are exposed to the hydrophobic wall of β-CD. If, on the other hand, the polar cluster composed of 1-, 2-, 3-, and 4-OH groups of a bound pyranose stays in a relatively polar region in the vicinity of the rim of β-CD, the remaining ring oxygen atom and C5 bearing substituent X can for steric reasons be accommodated in the cavity when X is H, but not when X is CH_2OH or CH_3.

In summary, hydrophobic contributions to the present β-CD–sugar complexation are evident. However, polar interactions of the OH groups of bound sugar with bulk water and/or the OH groups of β-CD are also extremely important in determining the structure of the complex and hence the selectivity of the sugar binding.

Received: December 16, 1991 [Z 5075 IE]
German version: *Angew. Chem.* **1992**, *104*, 785

CAS Registry numbers:
D-**1**, 50-69-1; D-**1**·β-CD, 141172-89-6; D-**2**, 10323-20-3; D-**2**·β-CD, 141172-90-9; L-**2**, 5328-37-0; L-**2**·β-CD, 141173-63-7; D-**3**, 58-86-6; D-**3**·β-CD, 141172-91-0; D-**4**, 1114-34-7; D-**4**·β-CD, 141172-92-1; D-**5**, 533-67-5; D-**5**·β-CD, 141197-86-0; D-**6**, 17289-61-1; D-**6**·β-CD, 141172-93-2; **7**, 75-65-0; **7**·β-CD, 141172-94-3; **8**, 108-93-0; **8**·β-CD, 70843-37-7; **9c**, 1792-81-0; **9c**·β-CD, 141172-95-4; **9b**, 1460-57-7; **9b**·β-CD, 141173-01-5; D-**10**, 50-99-7; D-**10**·β-CD, 141172-96-5; D-**11**, 59-23-4; D-**11**·β-CD, 141172-97-6; D-**12**, 3458-28-4; D-**12**·β-CD, 141172-98-7; D-**13**, 3615-37-0; D-**13**·β-CD, 141172-99-8; L-**13**, 2438-80-4; L-**13**·β-CD, 141173-04-8; D-**14**, 1128-40-1; D-**14**·β-CD, 141173-00-4; ANS Mg^{2+} salt, 18108-68-4; ANS Mg^{2+} salt·β-CD, 141173-02-6; β-cyclodextrin, 7585-39-9.

[1] I. Eggene, B. Fenderson, T. Toyokuni, B. Dean, M. Stroud, S. Hakomori, *J. Biol. Chem.* **1989**, *264*, 9476–9484; N. Kojima, S. Hakomori, *ibid.* **1989**, *264*, 20159–20162.

[2] Y. Aoyama, Y. Tanaka, S. Sugahara, *J. Am. Chem. Soc.* **1989**, *111*, 5397–5404; R. P. Bonar-Law, A. P. Davis, B. A. Murray, *Angew. Chem.* **1990**, *102*, 1497–1498; *Angew. Chem. Int. Ed. Engl.* **1990**, *29*, 1407–1408.
[3] M. L. Bender, M. Komiyama, *Cyclodextrin Chemistry*, Springer, Berlin, **1977**; W. Saenger, *Angew. Chem.* **1980**, *92*, 343–361; *Angew. Chem. Int. Ed. Engl.* **1980**, *19*, 344–362; R. Breslow, *Acc. Chem. Res.* **1980**, *13*, 170–177; I. Tabushi, *ibid.* **1982**, *15*, 66–72.
[4] I. Tabushi, N. Shimizu, T. Sugimoto, M. Shiozuka, K. Yamamura, *J. Am. Chem. Soc.* **1977**, *99*, 7100–7102; J. Franke, F. Merz, H. W. Lorensky, W. M. Muller, W. Werner, F. Vögtle, *J. Inclusion Phenom.* **1985**, *3*, 471–478; G. C. Catena, F. V. Bright, *Anal. Chem.* **1989**, *61*, 905–909; H.-J. Schneider, T. Blatter, S. Simova, *J. Am. Chem. Soc.* **1991**, *113*, 1996–2000.
[5] Y. Matsui, K. Mochida, *Bull. Chem. Soc. Jpn.* **1979**, *52*, 2808–2814.
[6] K. A. Connors, *Binding Constants*, Wiley-Interscience, New York, **1987**, pp. 175–183.
[7] M. Janado, Y. Yano, *J. Solution Chem.* **1985**, *14*, 891–902; K. Miyajima, K. Machida, M. Nakagaki, *Bull. Chem. Soc. Jpn.* **1985**, *58*, 2595–2599.
[8] *P* is the partition coefficient of an alcohol in the diethyl ether/water sytem; for **6**, $P \approx 0$.
[9] S. J. Angyal, V. A. Pickles, *Aust. J. Chem.* **1972**, *25*, 1695–1710.

Assistance by Electrophiles in Photoinduced Alkylidyne–Carbonyl Coupling**

By *Andreas Mayr,** *Cecilia M. Bastos, Richard T. Chang, John X. Haberman, Katrina S. Robinson,* and *Deirdre A. Belle-Oudry*

Dedicated to Professor Wolfgang Beck on the occasion of his 60th birthday

The coupling of alkylidyne and carbonyl ligands may be induced in different ways.[1] In most reactions, including the first example discovered by Kreissl et al.,[2] alkylidyne–carbonyl coupling is induced by the addition of a strongly nucleophilic ligand to the metal center. There is some indication that the coupling of alkylidyne and carbonyl ligands may also be induced by electrophiles. Schrock et al.[3] reported that the reaction of $[W(CH)Cl(PMe_3)_4]$ with CO in the presence of aluminum reagents such as $(AlCl_3)_2$ gives $[W(\eta^2\text{-}HCCOAlCl_3)Cl(CO)(PMe_3)_3]$. Lippard et al.[4] demonstrated the formation of disiloxyalkyne ligands upon reaction of the siloxymethylidyne complex $[Ta\{COSi(iPr)_3\}(CO)(dmpe)_2]$ [dmpe = bis(dimethylphosphinoethane)] with silylating agents. Related alkyne ligands of the type RCCOE (E = electrophile) are easily accessible by the addition of electrophiles to η^2-ketenyl ligands obtained by nucleophile-induced alkylidyne–carbonyl coupling.[5] Geoffroy et al.[6] were able to demonstrate that ketenyl complexes may also be generated by irradiation of alkylidyne carbonylmetal complexes in the presence of nucleophiles. It was proposed that the role of the nucleophile was that of trapping a photochemically generated ketenyl metal complex. The possibility that some alkylidyne–carbonyl coupling reactions may be induced by electrophiles, and the well-established reactivity of η^2-ketenyl ligands towards electrophiles, suggested that electrophiles may also be effective in assisting the photoinduced process. Here we report that in photoinduced alkylidyne-carbonyl coupling reactions electrophiles are effective reagents for trapping the coupling products.

[*] Prof. A. Mayr,* Dr. C. M. Bastos, R. T. Chang, J. X. Haberman, K. S. Robinson, D. A. Belle-Oudry
Department of Chemistry
State University of New York at Stony Brook
Stony Brook, NY 11794-3400 (USA)

[**] We thank John D. Franolic, Raju Subramanian, and Prof. Stephen A. Koch for the X-ray crystallographic studies. This work was supported by the Petroleum Research Fund administered by the American Chemical Society, and by the National Science Foundation.

Irradiation of the alkylidyne carbonyltungsten complexes *cis*-**1a**, **b** with visible light in the presence of electrophiles ECl affords the alkyne complexes *trans*-**2a**–**e**.[7, 8] The reactions are accompanied by the photochemical *cis–trans* isomerization of complexes **1**.[9] Thus, the same results are obtained when the *trans* isomers of complexes **1** are used as the starting materials. In the absence of light, either no reaction or a different outcome is observed under otherwise similar conditions. The reaction of *trans*-**1a** with HCl was previously reported to give the alkylidene complex *trans*-$[W(CHPh)Cl_2(CO)(PMe_3)_2]$[9].

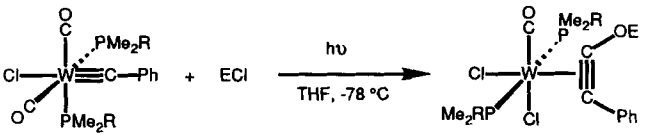

1a: R = Me
1b: R = Ph

2a: R = Me, E = H
2b: R = Me, E = $C(O)CMe_3$
2c: R = Me, E = $C(O)C_6H_4$-4-OMe
2d: R = Ph, E = $C(O)CMe_3$
2e: R = Me, E = $Si(CMe_3)_2Ph$

Complexes **2a**–**e** belong to a well-established group of metal complexes with four-electron-donor alkyne ligands[10] and were characterized by spectroscopic methods.[11] In the ^1H NMR spectra the virtual triplets for the phosphine methyl groups indicate the mutual *trans* arrangement of the phosphine ligands.[12] In the ^{13}C NMR spectra the alkyne ligands give rise to two resonances between $\delta = 190$ and 230, chemical shifts characteristic of four-electron-donor alkyne ligands.[10] The carbonyl ligand of complexes **2b**–**e** gives rise to a single absorption in the IR spectrum. In dichloromethane solution complex **2a** exhibits two IR absorptions at 1925 and 1940 cm^{-1} indicating the presence of two isomers; however, in the solid-state spectrum (KBr) only one CO absorption is found.

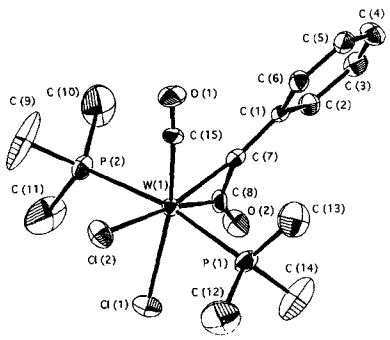

Fig. 1. Crystal structure of **2a**. Selected bond lengths [Å] and angles [°]: W1-C7 2.05(1), W1-C8 1.97(1), W1-C15 2.01(1), W1-P1 2.511(3), W1-P2 2.512(3), W1-Cl1 2.528(3), W1-Cl2 2.454(3), C7-C8 1.32(1); C1-C7-C8 135(1), C7-C8-O2 136(1).

The solid-state structures of the ynol complex **2a** (Fig. 1) and of the alkynyl ester complex **2c** (Fig. 2) were determined by X-ray crystallography.[13] The structural parameters (Table 1) are not unusual, but the orientation of the ynol ligand in complex **2a** is opposite to that expected. In complexes of the type $[WX_2(alkyne)(CO)L_2]$ the alkyne ligands

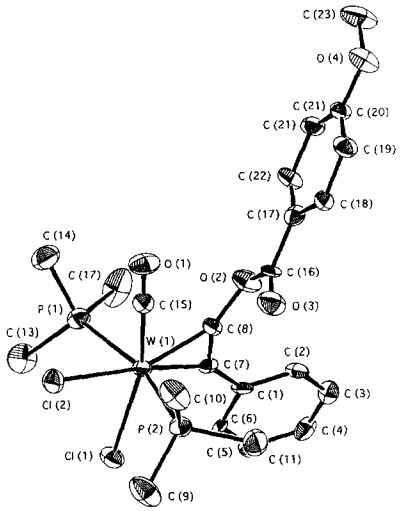

Fig. 2. Crystal structure of **2c**. Selected bond lengths [Å] and angles [°]: W1-C7 2.03(1), W1-C8 1.99(1), W1-C15 1.96(1), W1-P1 2.507(4), W1-P2 2.522(4), W1-Cl1 2.518(3), W1-Cl2 2.479(3), C7-C8 1.28(1); C1-C7-C8 137(1), C7-C8-O2 135(1).

prefer the orientation parallel to the W–CO axis for electronic reasons.[10] Alkyne ligands of the type RCCOR′ are expected to prefer the orientation with the oxygen-substituted carbon atom proximal to the carbonyl ligand (**A**).[14] This situation is found in the solid-state structure of the alkynylester complex **2c**. In the ynol complex **2a** the oxygen-substituted end of the alkyne ligand is oriented distal to the carbonyl ligand (**B**). This electronically less stable orientation is presumably stabilized by a hydrogen bond between the OH group of the ynol ligand and the chloro ligand Cl 1. Even though the OH hydrogen atom was not found in the X-ray structure analysis, the O2-Cl1 distance of 3.022(9) Å is suitable for a hydrogen bond.[15] The presence of two ν(CO) frequencies in the IR spectrum of **2a** in solution indicates that the hydrogen bond between the OH group and the chloro ligand stabilizes the electronically less favorable orientation **B** to such an extent that both conformers **A** and **B** are present in comparable amounts in solution.

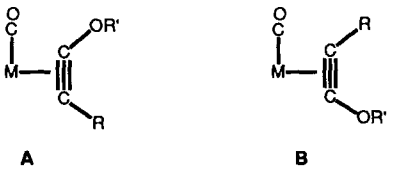

In two other structurally characterized ynol tungsten complexes **3**[16] and **4**[17] the OH group is stabilized by hydrogen bonding to cocrystallized donor solvent molecules, whereby the ynol ligand in **4** also adopts the electronically less favorable orientation. The synthesis of **3** by irradiation of **5** in

$[W(acac)Cl(PhCCOH)(CO)_2] \cdot OEt_2$ **3**
$[W(\eta^5\text{-}C_5H_5)(Me\text{-}4\text{-}C_6H_4CCOH)(CO)(PMe_3)][BF_4] \cdot OCMe_2$ **4**
$[W(CPh)Cl(CO)_4]$ **5**

the presence of acetylacetone was reported by Fischer and Friedrich.[16] It is now recognized as the first example of photoinduced alkylidyne–carbonyl coupling.[6] Based on the results reported here it appears that this reaction may also represent the first example of an electrophile-assisted photoinduced alkylidyne–carbonyl coupling.[11] Formation of **3** could involve initial substitution of the chloro ligand and one carbonyl ligand in **5** by acetylacetone, accompanied by elimination of hydrogen chloride. The liberated HCl could then trap a photochemically generated ketenyl complex to give the final product.

The reaction of photochemically generated ketenyl ligands with electrophiles is an efficient method for the assembly of metal-coordinated ynols and alkyne derivatives, such as alkynyl esters and alkynyl silylethers, from three components: alkylidyne ligand, carbonyl ligand, and electrophile. This method may prove useful in the synthesis of such compounds. The reactions of organic alkynyl esters has been investigated only in recent years,[18] and very little is known about their coordination chemistry. Several complexes of alkynyl esters were previously prepared by acylation of stable ketenyl metal complexes.[19]

Experimental Procedure:

In a typical procedure, one equivalent of the electrophile was added to a solution of **1a, b** in THF at −78 °C. (For the synthesis of **2a**, slightly moist $AlCl_3$ was used as the source of HCl.) The mixture was irradiated from a distance of 10–20 cm with a regular 300 W projector lamp for approximately 2–3 h. During this time the color of the solution changed from light yellow to blue. Compounds **2a–e** were purified by chromatography on silica gel at −30 °C (10% THF/CH_2Cl_2 for **2a**, CH_2Cl_2 for **2b**, and 2% THF/CH_2Cl_2 for **2c–e**) and recrystallization from CH_2Cl_2/hexane (isolated yields: 80% for **2a**, 68% for **2b**, 77% for **2c**, and 51% for **2d**). Complex **2e** is obtained in 20% yield in only about 80% purity.

Received: December 20, 1991 [Z 5086 IE]
German version: *Angew. Chem.* **1992**, *104*, 802

CAS Registry numbers:
1a, 107133-58-4; **1b**, 140903-07-7; **2a**, 140926-02-9; **2b**, 140903-08-8; **2c**, 140903-09-9; **2d**, 140903-10-2; **2e**, 140903-11-3; $ClC(O)CMe_3$, 3282-30-2; $ClC(O)C_6H_4$-4-OMe, 100-07-2; $ClSi(CMe_3)_2Ph$, 140903-06-6.

[1] A. Mayr, C. M. Bastos, *Prog. Inorg. Chem.*, in press.
[2] F. R. Kreissl, A. Frank, U. Schubert, T. L. Lindner, G. Huttner, *Angew. Chem.* **1976**, *88*, 649; *Angew. Chem. Int. Ed. Engl.* **1976**, *15*, 632.
[3] S. J. Holmes, R. R. Schrock, M. R. Churchill, H. J. Wasserman, *Organometallics* **1984**, *3*, 476.
[4] R. N. Vrtis, S. Liu, C. P. Rao, S. G. Bott, S. J. Lippard, *Organometallics* **1991**, *10*, 275.
[5] a) F. R. Kreissl, W. Sieber, M. Wolfgruber, *Angew. Chem.* **1983**, *95*, 503; *Angew. Chem. Int. Ed. Engl.* **1983**, *22*, 493; *Angew. Chem. Suppl.* **1983**, 631; b) *Z. Naturforsch. B* **1983**, *38*, 1419.
[6] J. B. Sheridan, D. B. Pourreau, G. L. Geoffroy, A. L. Rheingold, *Organometallics*, **1988**, *7*, 289.
[7] G. A. McDermott, A. M. Dorries, A. Mayr, *Organometallics* **1987**, *6*, 925.
[8] **1b**: IR (CH_2Cl_2): $\tilde{\nu}$ [cm^{-1}] = 2002 (s), 1930 (s) (CO).
[9] A. Mayr, M. A. Kjelsberg, K. S. Lee, M. F. Asaro, T. Hsieh, *Organometallics* **1987**, *6*, 2610.
[10] J. L. Templeton, *Adv. Organomet. Chem.* **1989**, *29*, 1.
[11] Characteristic spectroscopic data of the complexes **2a–e**. **2a**: ^{1}H NMR (300 MHz, $CDCl_3$, 25 °C, TMS): δ = 1.36 (virt. t, J = 4.2 Hz, 18H; PMe_3), 7.3–7.8 (m, 5H; Ph), 10.30 (br, 1H; OH); ^{13}C NMR ($CDCl_3$, 25 °C): δ = 194.3 (PhCCO), 229.3 (PhCCO), 238.5 (CO); IR (KBr): $\tilde{\nu}$ [cm^{-1}] = 3250 (m, OH), 1941 (s, CO); (CH_2Cl_2, 25 °C): $\tilde{\nu}$ [cm^{-1}] = 1940, 1925 (CO). **2b**: ^{1}H NMR (300 MHz, $CDCl_3$, 25 °C, TMS): δ = 1.41 (virt. t, J = 4.4 Hz, 18H; PMe_3), 1.45 (s, 9H; CMe_3), 7.40–8.14 (m, 5H; Ph); ^{13}C NMR ($CDCl_3$, 25 °C): δ = 173.0 (C=O), 212.1 (PhCCO), 224.2 (PhCCO), 233.8 (t, J(P,C) = 6.2 Hz, CO); IR (KBr): $\tilde{\nu}$ [cm^{-1}] = 1945 (s, CO), 1744 (m, C=O).
2c: ^{1}H NMR (300 MHz, $CDCl_3$, 25 °C, TMS): δ = 1.43 (virt. t, J = 4.3 Hz, 18H; PMe_3), 3.91 (s, 3H; MeO), 7.0–8.3 (m, 9H; Ph, C_6H_4); ^{13}C NMR ($CDCl_3$, 25 °C): δ = 165.6 (C=O), 213.2 (PhCCO), 225.8 (t, J(P,C) = 5 Hz; PhCCO), 233.4 (t, J(P,C) = 6 Hz; CO); IR (KBr): $\tilde{\nu}$ [cm^{-1}] = 1954 (s, CO), 1742 (m, C=O).
2d: ^{1}H NMR (300 MHz, $CDCl_3$, 25 °C, TMS): δ = 1.18 (s, 9H; CMe_3), 1.63 (virt. t, J = 4.4 Hz, 6H; PMe_2Ph), 1.85 (t, ^2J(P,H) = 4.4 Hz, 6H; PMe_2Ph), 7.1–7.6 (m, 15H; Ph, C_6H_4); ^{13}C NMR ($CDCl_3$, 25 °C): δ = 171.9 (C=O), 213.3 (t, J(P,C) = 4.5 Hz; PhCCO), 223.3 (t, J(C,P) = 4.5 Hz; PhCCO), 233.2 (t, J(P,C) = 6.0 Hz; CO); IR (CH_2Cl_2): $\tilde{\nu}$ [cm^{-1}] = 1945 (s, CO), 1744 (m, C=O).

2e: ^{1}H NMR (300 MHz, $CDCl_3$, 25 °C, TMS): $\delta = 1.22$ (s, 9H; CMe_3), 1.40 (virt. t, $J = 4.3$ Hz, 18H; PMe_3), 6.9–7.8 (m, 15H; Ph, $SiPh_2$); ^{13}C NMR ($CDCl_3$, 25 °C): $\delta = 211.9$ (PhCCO), 225.3 (PhCCO), 233.3 (CO); IR (CH_2Cl_2): $\tilde{\nu}$ [cm^{-1}] = 1943 (s, CO), 1649 (w, CCO).

[12] J. M. Jenkins, B. L. Shaw, *J. Chem. Soc. (A)* **1966**, 1407.

[13] Crystallographic data for **2a** and **2c**. **2a**: $C_{15}H_{24}Cl_2O_2P_2W$, $M = 553.06$, $P2_1/n$ (No. 14), $a = 8.668(2)$, $b = 25.76(1)$, $c = 9.541(4)$ Å, $\beta = 102.79(4)°$, $V = 2078(3)$ Å^3, $Z = 4$, $\rho_{calcd} = 1.768$ g cm^{-3}, $\gamma(Mo_{K\alpha}) = 60.93$ cm^{-1}, 1533 unique observed reflections, $3° < 2\theta < 47.9°$, $R = 0.029$, $R_w = 0.037$. **2c**: $C_{23}H_{30}Cl_2O_4P_2W$, $M = 687.19$, $Pca2_1$ (No. 29), $a = 15.584(1)$, $b = 12.599(1)$, $c = 13.962(1)$ Å, $\beta = 90.0°$, $V = 2741.3(1)$ Å^3, $Z = 4$, $\rho_{calcd} = 1.665$ g cm^{-3}, $\mu(Mo_{K\alpha}) = 46.40$ cm^{-1}, 2206 unique observed reflections, $3° < 2\theta < 60°$, $R = 0.035$, $R_w = 0.034$. All intensity measurements were made at room temperature, using $Mo_{K\alpha}$ radiation (graphite monochromator, $\lambda = 0.71069$ Å), and a variable-rate, ω-2θ scan technique. Empirical absorption corrections were applied. The structures were solved by conventional heavy-atom methods and refined by the full-matrix least-squares method. All calculations were performed using the TEXRAY programs. For **2c**, both enantiomers were examined. Further details of the crystal structure investigations can be obtained from the Fachinformationszentrum Karlsruhe, Gesellschaft für wissenschaftlich-technische Information mbH, D-W-7514 Eggenstein-Leopoldshafen 2 (FRG), by quoting the depository number CSD-56078, the names of the authors, and the journal citation.

[14] a) D. C. Brower, K. R. Birdwhistell, J. L. Templeton, *Organometallics* **1986**, *5*, 94; b) W. J. Sieber, M. Wolfgruber, N. H. Tran-Huy, H. R. Schmidt, H. Heiss, P. Hofmann, F. R. Kreissl, *J. Organomet. Chem.* **1988**, *340*, 341.

[15] D. Mootz, J. Hocken, *Angew. Chem.* **1989**, *101*, 1713; *Angew. Chem. Int. Ed. Engl.* **1989**, *28*, 1697.

[16] E. O. Fischer, P. Friedrich, *Angew. Chem.* **1979**, *91*, 345; *Angew. Chem. Int. Ed. Engl.* **1979**, *18*, 327.

[17] J. A. K. Howard, J. C. Jeffery, J. C. V. Laurie, I. Moore, F. G. A. Stone, A. Stringer, *Inorg. Chim. Acta* **1985**, *100*, 23.

[18] P. J. Stang, M. Boehshar, H. Wingert, T. Kitamura, *J. Am. Chem. Soc.* **1988**, *110*, 3272.

[19] K. A. Belsky, M. F. Asaro, S. Y. Chen, A. Mayr, *Organometallics*, in press.

Ion-Selective Hydrazone–Azine Tautomerism of a 14-Membered Macrocylic Ligand**

By *Thomas W. Bell** and *Andrew T. Papoulis*

Bridged pyridine ligands,[1] including torands,[2] are versatile complexing agents for metal ions. In the course of current efforts to incorporate pyrrole rings into torands using the Piloty rearrangement of azines,[3] we have discovered a novel 14-membered azamacrocycle **1**. The binding of lithium and the smaller alkaline-earth metal ions by this ligand is accompanied by pronounced changes in its UV/VIS absorption characteristics. Ion-selective optical sensors based on metal complexation are of current interest for analytical applications.[4]

Macrocyclic ligand **1** was synthesized in two steps from 9-*n*-butyl-2,3,7,8-tetrahydro-1*H*,6*H*-acridine-4,5-dione **2**[5] (Scheme 1). Slow addition of **2** to a large excess of hot methanolic hydrazine gave (*E*,*Z*)-dihydrazone **3** as a yellow precipitate. Condensation of diketone **2** with dihydrazone **3** in hot methanol gave macrocycle **1** as a yellow-orange solid in 38–47% yield with most methods of addition of the reactants. However, when higher dilution was achieved by simultaneous, slow addition of **2** and **3** to hot methanol, **1** was produced in 82% yield. The ^{1}H NMR spectrum of **1** in $CDCl_3$ is consistent with the apparently unique bis(vinylhydrazone) structure shown in **1a** rather than the expected bis(azine) tautomer **1b**. The resonance of the vinyl protons is observed at $\delta = 6.0$, and the downfield shift of the internal NH protons ($\delta = 14.3$) is consistent with their intramolecular hydrogen bonding to the transannular pyridine nitrogen atoms. Addition of trifluoroacetic acid to the $CDCl_3$ solution apparently gives **1** · 2H$^+$ since the vinyl proton resonances are no longer observed and the acidic protons give a broad resonance centered at $\delta = 19$. As suggested by the presence of enamine moieties in structure **1a**, DDQ selectively aromatizes two rings of **1** to give bis(arylhydrazone) macrocycle **4**, which still possesses two internal hydrogens ($\delta = 17.6$).

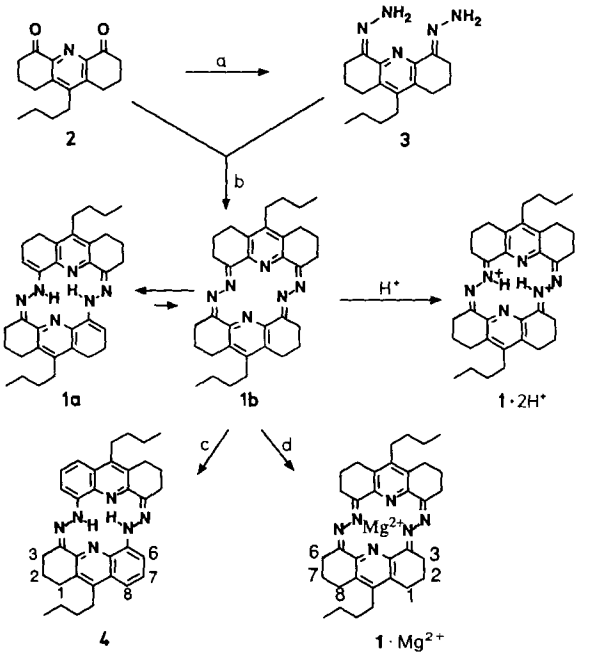

Scheme 1. a: Hydrazine, MeOH (55%); b: MeOH (82%); c: Dichlorodicyanobenzoquinone (DDQ), toluene (63%); d: $Mg(NO_3)_2 \cdot 6H_2O$, CH_3CN (33%).

Macrocycles **1** and **4** both contain 14-membered rings with four of the six nitrogen atoms in the correct positions to coordinate metal ions. To do this **4** must either lose the internal protons or tautomerize to the bis(azo) form, whereas **1** should readily form metal complexes by tautomerization to the bis(azine) form **1b**. Thus **1** reacts with $Mg(NO_3)_2$ in CH_3CN to form **1** · $Mg(NO_3)_2$, which was isolated as a yellow solid. FAB-MS, ^{1}H NMR, ^{13}C NMR, and FT-IR data are in keeping with the C_2 symmetric structure. Apparently **1** · $Mg(NO_3)_2$ does not possess a horizontal mirror plane, since two-proton multiplets are observed in the ^{1}H NMR spectrum at $\delta = 2.8$ and 3.3 displaying geminal coupling ($J = 17$ Hz). This feature suggests that **1** exists in a puckered conformation in the complex, possibly due to axial coordination of Mg^{2+} by NO_3^- on only one face. Ring methylene

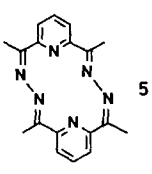
5

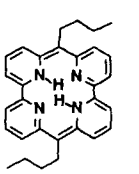
6

[*] Prof. T. W. Bell, A. T. Papoulis
Department of Chemistry, State University of New York
Stony Brook, NY 11794-3400 (USA)

[**] This work was supported by the National Institutes of Health (PHS grant GM 32937). The 600 MHz spectrometer was purchased with funds from the National Institutes of Health (RR05547A), the National Science Foundation (CHE 8911350), the Center for Biotechnology, and the State University of New York, Stony Brook.

protons of **1** thus serve as stereochemical probes which are absent in reported complexes of bis(azine) macrocycle **5**.[6, 7]

Tautomerism of **1a** to **1b** during complexation produces dramatic changes in the UV-VIS absorption spectrum of the ligand. Figure 1 shows that the largest change is the disappearance of the absorption band at $\lambda_{max} = 380$ nm upon complexation of Mg^{2+}. The spectra shown in Figure 1 were

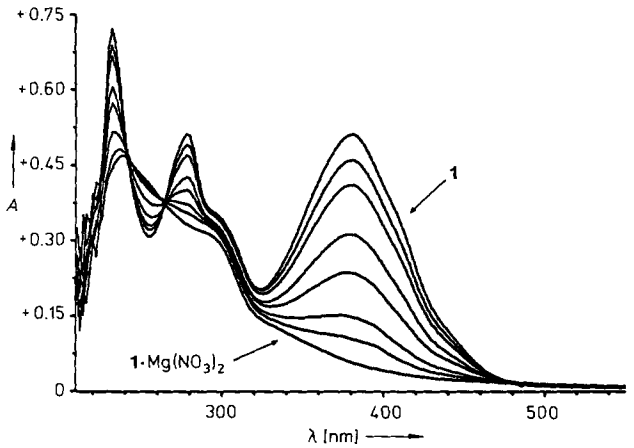

Fig. 1. Overlayed plots of the UV/VIS spectra of **1** and **1** · $Mg(NO_3)_2$ in CH_2Cl_2 (1.9×10^{-5} M). Wavelengths in nm; A = absorbance.

obtained from dissolved samples of **1** and **1** · $Mg(NO_3)_2$ in CH_2Cl_2. The same spectroscopic changes were observed when solid $Mg(NO_3)_2 \cdot 6\,H_2O$ was added to a solution of **1** in CH_2Cl_2. To test the selectivity of **1** in extractions, solutions of **1** in CH_2Cl_2 were exposed to alkali-metal and alkaline-earth nitrates and chlorides. We followed the complexation by measuring changes in the ratio of absorbances at $\lambda = 380$ and 265 nm (the isosbestic point). The results of this study (Fig. 2) show that the optical response is selective for small cations of high charge density such as Li^+, Mg^{2+}, and Ca^{2+}. It is not clear why the nitrate and chloride salts of individual cations respond differently, but this effect may be related to solubility differences in CH_2Cl_2. Anion effects on the stability of crown ether complexes and on the extractability of salts from aqueous into organic solution have been observed.[8]

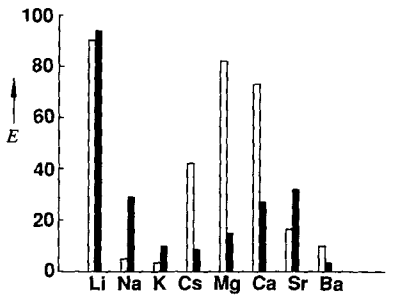

Fig. 2. Spectroscopic changes observed for solutions of **1** in CH_2Cl_2 (2.1×10^{-5} M) exposed for one day to metal salts. Extraction efficiency $E = [R(\mathbf{1}) - R(obs)]/[R(\mathbf{1}) - R(\mathbf{1} \cdot Mg(NO_3)_2)]$, where $R = A_{380}/A_{265}$. ■: Cl^- anion, □: NO_3^- anion.

Ion-selective optical response has also been reported for the bis(bipyridyl) macrocycle **6**, which solubilizes lithium chloride in CH_2Cl_2 with decolorization.[9]. In nonpolar solvents this ligand exists in the intramolecularly hydrogen-bonded form shown in **6**, as indicated by the presence of NH resonances in the ^1H NMR spectrum at $\delta = 15.0$. Although **1**, **4**, **5**, and **6** all contain 14-membered, fully unsaturated rings, the presence of cross-conjugated pyridine rings reduces the diamagnetic ring current expected in (4n + 2) annulenes, an effect observed in *meta*-fused benzannulenes.[10]. Thus, the NH resonances of **1**, **4**, and **6** all appear at relatively low field. It is noteworthy that the macrocyclization leading to **1** proceeds in higher yields than that providing **5**. The latter was prepared in 7% yield by cyclization of the bis(diacetylpyridine) azine and could not be isolated from reaction of 2,6-diacetylpyridine with 2,6-diacetylpyridine(dihydrazone).[7] As was recently pointed out by Thilgen and Vögtle,[11] metal-free macrocyclic bis(azines) are rarely reported, apparently because azines are produced under equilibrium control. The yield of the macrocyclization furnishing **1** appears to be influenced partly by precipitation of the product and partly by kinetic product distribution. Relative to 2,6-diacetylpyridine, **2** is apparently preorganized for macrocyclization by the acridine framework. A predetermined conformation can produce unusual and useful effects.

Experimental Procedure

3: A solution of 1.0 g (3.7 mmol) of diketone **2** [5] in 50 mL of methanol was added dropwise over 3.5 h to a rapidly stirred, boiling solution of 3.5 mL (3.6 g, 110 mmol) of anhydrous hydrazine in 50 mL of methanol. The resulting yellow solution was heated at reflux under N_2 for 30 min, then cooled to room temperature. Methanol was removed under vacuum, and 100 mL of water was added to the residue. The resulting mixture was extracted with $CHCl_3$ (3 × 50 mL), and the combined extracts were dried over Na_2SO_4 and concentrated. Ethyl acetate was added, producing a yellow precipitate, which was allowed to stand at 5 °C for several hours and was then collected by vacuum filtration. Drying in vacuo gave 0.61 g (55%) of **3** as a light yellow solid. M.p. 175–192 °C (decomp.). ^1H NMR (300 MHz, $CDCl_3$): $\delta = 0.96$ (t, $^3J(H,H) = 6.6$ Hz, 3H; CH_3), 1.42 (m, 4H; $CH_2CH_2CH_3$), 1.96 (m, 4H; H2, H7), 2.53–2.64 (m, 6H; H1, H8, $ArCH_2nPr$), 2.77 (m, 4H; H3, H6), 5.5 (s, 2H; (*E*)C = NNH_2), 8.7 (br s, 2H; (*Z*)C = NNH_2); ^{13}C NMR (75 MHz, $CDCl_3$): $\delta = 149.0$, 147.5, 145.9, 145.3, 135.8, 131.5, 130.4, 33.7, 30.7, 28.2, 26.5, 24.9, 23.6, 23.0, 22.9, 20.9, 13.7. FT-IR (KBr): $\tilde{\nu}$ [cm^{-1}] = 3355 s (NH_2), 3273 m (NH_2), 3192 m (NH_2), 2935 s (CH), 2912 s (CH), 2842 s (CH), 1634 m (C = N). MS (70 eV): *m/z* 299 (M^+, 13), 211 (100%). – Correct C,H,N-analysis.

1: Separate solutions of 50 mg (0.18 mmol) of **2** and 55 mg (0.18 mmol) of **3** in 30 mL of methanol were added dropwise over 5 h to 20 mL of rapidly stirred, boiling methanol. The resulting mixture was heated at reflux under N_2 for 14 h, then cooled to room temperature. The precipitate was collected by filtration, washed several times with methanol, and dried in air to give 80 mg (82%) of **1** as a yellow solid. M.p. 190 °C (decomp.). ^1H NMR (300 MHz, $CDCl_3$): $\delta = 0.98$ (t, $^3J(H,H) = 6.6$ Hz, 6H; CH_3), 1.47 (m, 8H; $CH_2CH_2CH_3$), 2.01 (m, 4H; H2), 2.50 (m, 4H, H7), 2.67 (t, $^3J(H,H) = 7.2$ Hz, 4H; $ArCH_2nPr$), 2.78 (t, $^3J(H,H) = 6.3$ Hz, 4H; H1), 2.82–2.91 (m, 8H; H3, H8), 5.99 (t, $^3J(H,H) = 4.8$ Hz, 2H; H6), 14.28 (s, 2H; NH). ^{13}C NMR (75 MHz, $CDCl_3$): $\delta = 147.2$, 147.0, 144.8, 137.1, 135.6, 132.6, 129.6, 99.0, 34.3, 31.1, 28.6, 26.9, 24.3, 23.2, 22.9, 21.7, 13.7. FT-IR (KBr): $\tilde{\nu}$ [cm^{-1}] = 3178 s (NH), 2943 s (CH), 2849 s (CH), 1637 s (C = N). UV/VIS (CH_2Cl_2): λ_{max}[nm](ε) = 380 (27000), 296 (19000), 278 (27000). FAB-MS (Xe^+, 6–8 kV): *m/z* 535 ($M + 1$, 100%). Correct C,H,N-analysis for $C_{34}H_{42}N_6 \cdot (H_2O)_{0.5}$.

4: To a solution of 200 mg (0.37 mmol) of **1** in 300 mL of toluene was added 170 mg (0.75 mmol) of DDQ. The reaction mixture was stirred at room temperature under N_2 for one day and then filtered. The filtered solid was rinsed thoroughly with toluene, and the filtrates were combined and concentrated under vacuum. Recrystallization from toluene gave 125 mg (63%) of **4** as a brownish-red solid. M.p. 244–254 °C (decomp.). ^1H NMR (300 MHz, $CDCl_3$): $\delta = 1.00$ (t, $^3J(H,H) = 6.6$ Hz, 6H; CH_3), 1.55 (m, 8H; $CH_2CH_2CH_3$), 2.03 (m, 4H; H2), 2.79 (t, $^3J(H,H) = 6$ Hz, 4H; $ArCH_2nPr$), 2.94 (m, 8H; H1, H3), 7.17 (d, $^3J(H,H) = 8.4$ Hz, 2H; H6), 7.30 (m, 2H; H7), 7.47 (d, $^3J(H,H) = 7.8$ Hz, 2H; H8), 17.61 (s, 2H; NH). FT-IR: (KBr): $\tilde{\nu}$ [cm^{-1}] = 3429 br (NH), 3060 s (ArH), 2952 s (CH), 2854 s (CH), 1603 s (C = N). FAB-MS (Xe^+, 6–8 KV): *m/z* 530 (M^+, 100%). UV/VIS (CH_2Cl_2): λ_{max}[nm] (ε) = 266 (33000), 302 (16000), 358 (20000), 374 (22000), 404 (25000), 438 (13000), 464 (18000). Correct C,H,N-analysis for $C_{34}H_{38}N_6(H_2O)$.

1 · $Mg(NO_3)_2$: To a mixture of 96 mg (0.37 mmol) of $Mg(NO_3)_2 \cdot 6\,H_2O$ and 50 mL of acetonitrile was added 200 mg (0.37 mmol) of **1**. The mixture was heated at reflux under N_2 for 15 min. until all of **1** dissolved. The resulting dark yellow solution was cooled to room temperature and concentrated with a rotary evaporator. Drying in vacuo gave 277 mg of a dark amber glass. Recrystallization from ethanol gave 85 mg (33%) of a yellow solid. M.p. 170 °C (decomp.).

^{1}H NMR (600 MHz, $CDCl_3$): [12] δ = 0.96 (t, ^3J(H,H) = 6.9 Hz, 6H; CH_3), 1.40 (m, 4H; $CH_2CH_2CH_3$), 1.45 (m, 4H; $CH_2CH_2CH_3$), 1.94 (m, 2H; H7), 2.05 (m, 4H; H2), 2.26 (m, 4H; H3, H7), 2.63 (m, 4H; $ArCH_2nPr$), 2.79 (ddd, ^2J(H,H) = 17.2 Hz, ^3J(H,H) = 9.8 Hz, ^3J(H,H) = 4.9 Hz, 2H; H1), 2.94 (m, 10H; H1, H6, H8), 3.34 (ddd, ^2J(H,H) = 17.5 Hz, ^3J(H,H) = 4.8 Hz, ^3J(H,H) = 4.8 Hz, 2H, H3); ^{13}C NMR (75 MHz, $CDCl_3$): δ = 159.1, 157.6, 153.0, 144.6, 144.3, 139.1, 136.3, 33.6, 29.8, 28.5, 26.3, 25.2, 25.0, 23.1, 22.4, 20.3, 13.6. FT-IR (KBr): $\tilde{\nu}$ [cm^{-1}] = 3370 br (H_2O), 2942 s (CH), 2860 s (CH), 1619 m (C = N). FAB-MS (Xe$^+$, 6–8 kV): *m/z* 620 ($M-NO_3$, 100), 557 ($M-HN_2O_6$, 21.2%). UV/VIS (CH_2Cl_2): λ_{max}[nm] (ε) = 238 (25000), 296 (16000). Correct C,H,N-analysis for $C_{34}H_{42}N_8O_6Mg(H_2O)_{0.5}$.

Received: December 9, 1991 [Z 5061 IE]
German version: *Angew. Chem.* **1992**, *104*, 792

CAS Registry numbers:
1b, 140926-56-3; **2**, 140926-54-1; **3**, 140926-55-2.

[1] T. W. Bell, S. K. Sahni in *Inclusion Compounds, Vol. 4, Key Organic Host Systems* (Eds.: J. L. Atwood, J. E. D. Davies, D. D. MacNicol), Oxford University Press, Oxford, **1991**, p. 325.
[2] T. W. Bell, A. Firestone, R. Ludwig, *J. Chem. Soc. Chem. Commun.* **1989**, 1902; T. W. Bell, P. J. Cragg, M. G. B. Drew, A. Firestone, D.-I. A. Kwok, *Angew. Chem.* **1992**, *104*, 319; *Angew. Chem. Int. Ed. Engl.* **1992**, *31*, 345; *ibid.* **1992**, *104*, 321 and **1992**, *31*, 348.
[3] M. F. Marshalkin, L. N. Yakhontov, *Zh. Org. Khim.* **1978**, *14*, 1729; *J. Org. Chem. USSR (Engl. Transl.)* **1978**, *14*, 1610.
[4] A. Kumar, E. Chapoteau, B. P. Czech, C. R. Gebauer, M. Z. Chimenti, O. Raimondo, *Clin. Chem. (Winston-Salem, NC)* **1988**, *34*, 1709; M. Takagi in *Cation Binding by Macrocycles*, (Eds.: Y. Inoue, G. W. Gokel), Dekker, New York, **1990**, 465; F. Vögtle, M. Bauer, C. Thilgen, P. Knops, *Chimia* **1991**, *45*, 319.
[5] T. W. Bell, A. Firestone, *J. Am. Chem. Soc.* **1986**, *108*, 8109; T. W. Bell, Y.-M. Cho, A. Firestone, K. Healy, J. Liu, R. Ludwig, S. D. Rothenberger, *Org. Synth.* **1990**, *69*, 226.
[6] V. L. Goedken, Y. Park, S.-M. Peng, J. M. Norris, *J. Am. Chem. Soc.* **1974**, *96*, 7693.
[7] W. Radecka-Paryzek, *Inorg. Chim. Acta* **1979**, *34*, 5.
[8] F. De Jong, D. N. Reinhoudt, *Stability and Reactivity of Crown Ether Complexes*, Academic Press, New York, **1981**, 30.
[9] S. Ogawa, R. Narushima, Y. Arai, *J. Am. Chem. Soc.* **1984**, *106*, 5760.
[10] A. T. Balaban, M. Banciu, V. Ciorba, *Annulenes, Benzo-Hetero-Homo-Derivatives and Their Valence Isomers*, CRC Press, Boca Raton, Fl, USA, **1987**, 142–143.
[11] C. Thilgen, F. Vögtle, *Chem. Ber.* **1991**, *124*, 671.
[12] The spin systems were identified according to results of a COSY experiment.

Synthesis, Structure, and Thermolysis of an Unusual Azaphosphasiliridine**

By *Matthias Driess** and *Hans Pritzkow*

Dedicated to Professor Friedrich Bickelhaupt on the occasion of his 60th birthday

The reactivity of disilenes, phosphaalkenes, and diphosphenes towards organoazides and diorganodiazomethanes leads to new five- and three-membered heterocycles, in which the bonding is of particular interest.[1] It was observed that disilenes can react with organoazides and diazomethanes by a [2 + 3] or [2 + 1] cycloaddition depending on electronic and steric factors. In contrast, phosphaalkenes only react by [3 + 2] cycloaddition, and diphosphenes react with diazoalkanes to give stable diphosphiranes. Of particular interest is the [2 + 1] cycloaddition of disilenes, which for the reaction with alkylazides and aryldiazomethane derivatives leads to **A** and **B**, respectively; however, for the reaction with alkenes there are no examples.

[*] Dr. M. Driess, Dr. H. Pritzkow
Anorganisch-chemisches Institut der Universität
Im Neuenheimer Feld 270, D-W-6900 Heidelberg (FRG)

[**] This work was supported by the Deutsche Forschungsgemeinschaft (SFB 247). We also thank Prof. Dr. W. Siebert (Heidelberg) for his support.

Whereas beginning from **A**, compounds of the type **C** are readily accessible by N_2 elimination, starting from **B** (R' = aryl) the analogous formation of **D** is not observed.[1] However, a disilirane **D** (R' = H) is accessible from the reaction of CH_2N_2 with tetrakis(2,6-dimethylphenyl)disilene,[2] although an intermediate could not be observed. Recently we described a simple, high-yield access to stable phosphanylidensilanes (phosphasilenes),[3] so that it is now possible to investigate the reaction pathways of such compounds with diazoalkanes and other cycloaddition partners. Herein we report the synthesis and structure of the first azaphosphasiliridine **1** and its stepwise conversion to the thermolysis products **2**–**4**.

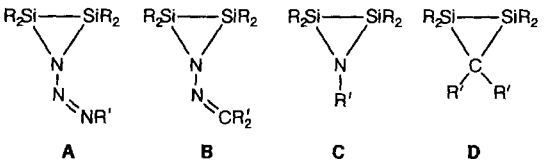

The reaction of the phosphasilene $Is_2Si{=}P{-}Si(iPr)_3$ (Is = 2,4,6-$iPr_3C_6H_2$) with diphenyldiazomethane led to the [2 + 1] cycloadduct **1**[4] in 87% yield, which was isolated in the form of yellow crystals (Scheme 1). The composition of

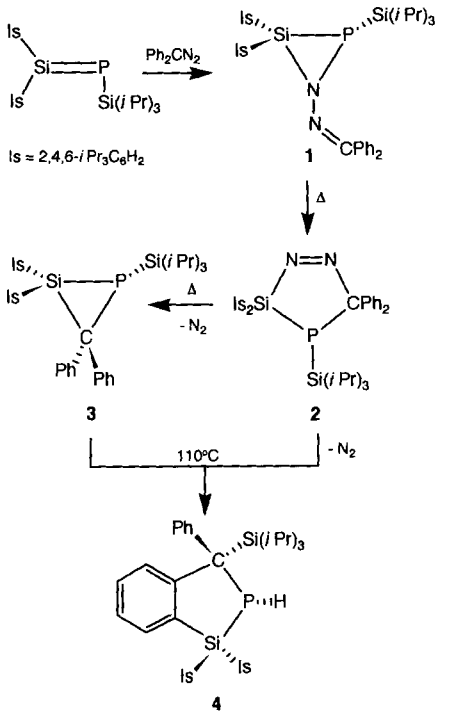

Scheme 1. Synthesis of the heterocycles **1**–**4**.

1 was deduced from the mass spectrum[4] and a correct elemental analysis. The ^{31}P NMR spectrum shows a singlet at δ = – 25.6. In the ^{29}Si spectrum a ^{14}N/^{15}N relaxation-broadened doublet is observed for the Si atom in the three-membered ring at extremely high field (δ = – 86.0) and with an unusually small $^1J_{Si,P}$ coupling constant (J = 3.9 Hz). In contrast, the corresponding coupling constant for the ^{29}Si nucleus of the $Si(iPr)_3$ group (99.5 Hz) is very large. In cyclic, three-membered phosphasilanes the ^{29}Si chemical shifts of the ring atoms lie between δ = – 31.3 and δ = –75.3 and show values of 72.5 to 121.7 Hz for the $^1J_{P,Si}$ coupling constants.[5]

The ^{29}Si chemical shifts for compounds of the type **A**–**C** are typically found at around $\delta = -53$.[1] Since the constitution of **1** could not be unequivocally proved from the NMR data, an X-ray structure determination was carried out (Fig. 1).[6]

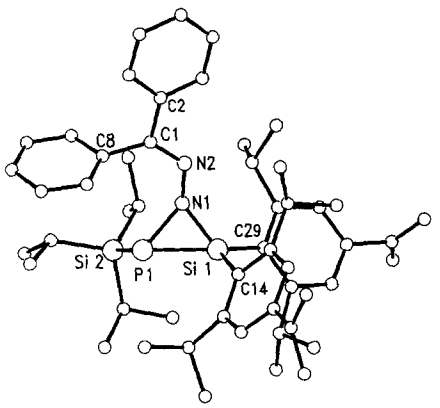

Fig. 1. Crystal structure of **1**. Selected distances [Å] and angles [°]: P1-Si1 2.237(2), P1-Si2 2.298(2), P1-N1 1.817(3), Si1-N1 1.729(3), N1-N2 1.375(4), N2-C1 1.287(5); Si1-P1-Si2 112.9(1), Si1-P1-N1 49.2(1), Si2-P1-N1 109.2(1), P1-Si1-N1 52.7(1), P1-N1-Si1 78.2(1), P1-N1-N2 136.3(3), Si1-N1-N2 133.2(2), N2-C1-C2 114.6(4), N2-C1-C8 129.3(4).

The endocyclic P1–Si1 distance (2.237(2) Å) is significantly shorter than the exocyclic P1–Si2 (2.298(2) Å) distance; however, it is typical for Si–P distances in three-membered cyclophosphasilanes.[5] Notable differences were also found for the N1–P1 and N1–Si1 distances. In comparison to azadiphosphiridines,[7] in which N–P distances of 1.698 and 1.710 Å were observed, the N1–P1 distance (1.817(3) Å) in **1** is extremely long. In contrast to azadiphosphiridines (sum of angles 359.9°), the N1 atom is not coordinated in a planar fashion (347°). Obviously, an ideal, planar conformation at the N1 atom in **1** is prevented as a result of the bulky substituents. Thus, no N–P bond strengthening is possible as was previously discussed for azadiphosphiridines and 1,3,2,4-diazadiphosphetidines.[7] The endocyclic angles at the phosphorus (49.2°) and nitrogen atom (78.2°) in **1** correspond approximately to the values in the azadiphosphiridine derivatives. The sum of the exocyclic, basal bond angles at the Si1 atom (359°) is similar to that in three-membered rings with two Si atoms and one heteroatom,[8] in which the coordination geometry at the silicon and phosphorus atom could be interpreted with the Dewar–Chatt–Duncanson model when described as a π complex. The two planes Si2–P1–Si1/Si1–C29–C14 are twisted into one another by 24°, which would be consistent with a description of **1** as a π complex from phosphasilene and the nitrene form of diphenyldiazomethane.

Thermolysis experiments have shown that **1**, despite its bulky substituents, can undergo rearrangement reactions which can be controlled. After a yellow solution of **1** in toluene was heated for 12h at 95°C, a deep orange solution was obtained whose ^{31}P NMR spectrum showed that **1** had completely rearranged into a mixture consisting of **2** ($\delta = -101.9$), **3** ($\delta = -197.4$), and a small quantity of **4** ($\delta = -100.7$) in the ratio of approximately 3:1:0.5. Although so far the isolation of **2** and **3** has not been successful, an unequivocal characterization is possible on the basis of the ^{31}P and ^{29}Si NMR data. In the ^{29}Si NMR spectrum (INEPT pulse sequence) a relaxation-broadened doublet (as for **1**) at $\delta = -6.1$ ($^1J_{P,Si} = 3.6$ Hz) is detected for the Si atom present in the ring of **2**, whereas the analogous ^{29}Si nucleus in **3** shows a sharp doublet at $\delta = -54.4$ ($^1J_{P,Si} = 49.7$ Hz). The ^{29}Si NMR data assigned to compound **3** are identical with that of comparable cyclophosphasilanes and other three-membered rings containing Si atoms.[5, 8] The NMR spectroscopic assignment for **2** and **3** is also proved by the fact that after the 3:1 mixture was heated for two days at 80°C, the concentration of **3** significantly increases at the expense of that of **2** (ca. 1:1, ^{31}P NMR control), without the appearance of new signals or an increase in the small amount of **4**.

If the thermolysis is now carried out at 110°C for 48h, the ^{31}P NMR spectrum shows that compound **4**[10] is the only product. Compound **4** could be isolated in the form of analytically pure, colorless crystals by crystallization from hexane. The constitution of **4** was also completely established by an X-ray crystal structure analysis (Fig. 2).[11]

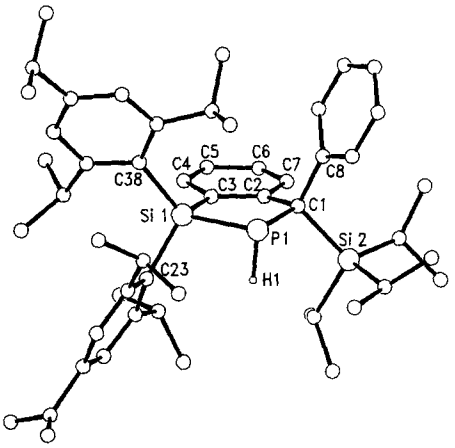

Fig. 2. Crystal structure of **4**. Selected distances [Å] and angles [°]: P1-C1 1.912(2), Si1-P1 2.267(1), Si2-C1 1.973(2), Si1-C3 1.879(2), C1-C2 1.544(3), C2-C3 1.409(3); Si1-P1-C1 95.8(1), P1-Si1-C3 93.6(1), P1-C1-C2 110.5(1), C1-C2-C3 122.0(2), C2-C3-Si1 117.1(1).

The $SiPC_3$ five-membered ring is almost planar. The long P1–C1 distance of 1.912(2) Å is surely a result of the steric hindrance of the substituents at the chiral C1 atom. In the crystal, as in solution (25°C), only one of the two possible diastereomers is found, that in which the H atom at the phosphorus atom occupies a position *trans* to the phenyl group at the C1 atom. Although only tentative statements can be made so far concerning the mechanism of the rearrangement of **3** into **4**, the formation of **4** is worth consideration regarding two aspects. On the one hand, the ring strain of **3** affects the cleavage of a C_{sp2}–H bond at the phenyl ring under simultaneous loss of the Si1–C1 bond and a 1,2-silyl shift of the $Si(iPr)_3$ group from the phosphorus to the saturated C1 atom, whereby the H atom, which was originally attached to the C3 atom, becomes attached to the phosphorus atom. On the other hand, it should be noted that these processes probably occurring in a radical fashion, obviously proceed so effectively that only **4** is obtained (^{31}P NMR control).

Experimental Procedure

1: Ph_2CN_2 (311 mg, 1.60 mmol) in hexane (2 mL) was added to a solution of $Is_2Si{=}P{-}Si(iPr)_3$ (1 g, 1.60 mmol) in toluene (30 mL) at 0°C. The reaction solution immediately changed color from red-orange to bright yellow. After removal of the solvent at 10^{-2} Torr, the residue was taken up in hexane (ca. 2 mL) and left to stand for 12h at room temperature. Compound **1** was isolated in the form of air-stable, bright yellow crystals. More of **1** could be obtained by

concentration of the mother liquor. Yield: 1.13 g (1.38 mmol, 87%); m.p. 150–153 C (decomp.).

4: **1** (435 mg, 0.53 mmol) was dissolved in toluene (1 mL) and heated at 110 °C for ca. 2.5 d (^{31}P NMR control). Following the thermolysis only the presence of **4** could be proven. The volatiles were removed at 25 °C and 10^{-2} Torr, and the residue was crystallized from hexane (ca. 1 mL). Yield: 372 mg (0.47 mmol, 89%) colorless crystals; m.p. 205–206 °C.

Received: January 17, 1992 [Z 5131IE]
German version: *Angew. Chem.* **1992**, *104*, 775

CAS Registry numbers:
1, 140410-24-8; **2**, 140437-96-3; **3**, 140410-25-9; **4**, 140410-26-0; $Is_2Si{=}PSi(iPr)_3$, 134456-72-7; Ph_2CN_2, 883-40-9.

[1] a) Disilene toward R_2CN_2 and RN_3: G. R. Gillette, R. West, *J. Organomet. Chem.* **1990**, *394*, 45; H. Piana, U. Schubert, *ibid.* **1988**, *348*, C19; b) Phosphaalkene toward R_2CN_2 and RN_3: T. A. Van der Knaap, T. C. Klebach, F. Visser, R. Lourens, F. Bickelhaupt, *Tetrahedron* **1984**, *40*, 991; T. Allspach, M. Regitz, G. Becker, W. Becker, *Synthesis* **1986**, 31; c) Diphosphene toward R_2CN_2: J. Bellan, G. Etemad-Moghadam, M. Payard, M. Koenig, *Tetrahedron Lett.* **1986**, *27*, 1145; G. Etemad-Moghadam, J. Bellan, C. Tachon, M. Koenig, *Tetrahedron* **1987**, *43*, 1793; M. Yoshifuji, S. Sasaki, T. Niitsu, N. Inamoto, *Tetrahedron Lett.* **1989**, *30*, 187.

[2] S. Masamune, S. Murakami, H. Tobita, *J. Am. Chem. Soc.* **1983**, *105*, 7777.

[3] M. Driess, *Angew. Chem.* **1991**, *103*, 979; *Angew. Chem. Int. Ed. Engl.* **1991**, *30*, 1022.

[4] **1**: ^{1}H NMR (200 MHz, C_6D_6, 295 K): $\delta = 0.615$ (d, 3H, SiCH*Me*$_2$, J (H,H) = 6.5 Hz), 0.769–1.466 (m, 45H, SiC*H*Me$_2$ and *o*-, *p*-CH*Me*$_2$), 1.553 (d, 3H, CH*Me*$_2$, J (H,H) = 6.8 Hz), 1.804 (d, 3H, CH*Me*$_2$, J (H,H) = 6.8 Hz), 2.699 (sept, 2H, *p*-C*H*Me$_2$, J (H,H) = 6.5 Hz), 3.515 (sept, 1H, *o*-C*H*Me$_2$, J (H,H) = 6.6 Hz), 3.914 (br., 1H, *o*-C*H*Me$_2$), 4.620 (br., 1H, *o*-C*H*Me$_2$), 4.942 (sept. 1H, *o*-C*H*Me$_2$, J (H,H) = 6.5 Hz), 6.964–7.623 (m, 14H, *arom.* H); MS (El, 70 eV): m/z 817 (M^+, 0.1%), 788 ($(M - N_2)^+$, 5), 632 ($(M - N_2 - Si(iPr)_3)^+$, 10), 623 ($(M - N_2 - CPh_2 + 1H)^+$, 32), 433 ($(Is_2Si - 1H)^+$, 100).

[5] M. Baudler, H. Jongebloed, *Z. Anorg. Allg. Chem.* **1979**, *458*, 9; K. F. Tebbe, *Z. Anorg. Allg. Chem.* **1980**, *468*, 202; M. Weidenbruch, M. Herrndorf, A. Schaefer, K. Peters, H. G. von Schnering, *J. Organomet. Chem.* **1985**, *295*, 7; M. Baudler, T. Pontzen, *Z. Anorg. Allg. Chem.* **1982**, *491*, 27.

[6] **1**: Space group $P2_1/n$, $a = 12.977(7)$, $b = 18.066(9)$, $c = 21.671(11)$ Å, $\beta = 96.27(4)°$, $V = 5050$ Å^3, $Z = 4$. 9231 measured reflections, 4898 observed. Non-hydrogen atoms were anisotropically refined, H atoms given in calculated positions or as part of a rigid group (CH_3) with groupwise temperature factors. $R = 0.061$, $R_w = 0.063$ (587 variables) [12].

[7] E. Niecke, A. Nickloweit-Lüke, R. Rüger, *Angew. Chem.* **1981**, *93*, 406; *Angew. Chem. Int. Ed. Engl.* **1981**, *20*, 385; E. Niecke, A. Nickloweit-Lüke, R. Rüger, B. Krebs, H. Grewe, *Z. Naturforsch. B* **1981**, *36*, 1566; 1,3,2,4-Diazadiphosphetidine: D. A. Harvey, R. Keat, A. N. Keith, K. W. Muir, D. R. Rycraft, *Inorg. Chim. Acta* **1979**, *34*, 201; M. L. Thomson, R. C. Haltivanger, A. D. Norman, *J. Chem. Soc. Chem. Commun.* **1979**, 647.

[8] Si-Si-O: H. B. Yokelson, A. J. Millevolte, G. R. Gillette, R. West, *J. Am. Chem. Soc.* **1987**, *109*, 6865; Si-Si-S: R. West, D. J. Young, K. J. Haller, *ibid.* **1985**, *107*, 4942; Si-Si-Se and Si-Si-Te: R. Peng-Koon Tan, G. R. Gillette, D. R. Powell, R. West, *Organometallics* **1991**, *10*, 546; Si-C-C: D. Seyferth, D. C. Annarelli, *J. Am. Chem. Soc.* **1975**, *97*, 2273; see also [1] and [2].

[9] R. S. Grev, H. F. Schaefer III, *J. Am. Chem. Soc.* **1987**, *109*, 6577; D. Cremer, E. Kraka, *ibid.* **1985**, *107*, 3800; D. Cremer, J. Gauss, E. Cremer, *THEOCHEM* **1988**, *46*, 531.

[10] **4**: ^{1}H NMR (200 MHz, C_6D_6, 295 K): $\delta = 0.344$ (br., 6H, SiCH*Me*$_2$), 0.945 (d, 3H, CH*Me*$_2$, J (H,H) = 6.6 Hz), 1.079–1.450 (m, 45H, CH*Me*$_2$ and SiC*H*Me$_2$), 2.698 (sept, 1H, *p*-C*H*Me$_2$, J (H,H) = 6.6 Hz), 2.709 (sept, 1H, *p*-C*H*Me$_2$, J (H,H) = 6.6 Hz), 3.543 (d, 1H, PH, J (P,H) = 183.7 Hz), 3.571 (br., 2H, *o*-C*H*Me$_2$), 3.814 (br., 2H, *o*-C*H*Me$_2$), 6.869–7.276 (m, 9H, *arom.*H), 7.753 (br., 2H, *arom.*H), 7.967 (m, 1H, *arom.*H), 8.373 (m, 1H, *arom.*H); ^{31}P NMR (81 MHz): $\delta = -100.68$ (d, J(P,H) = 183.9 Hz; ^{29}Si NMR (INEPT): $\delta = -0.74$ (d, Is_2Si-P, J(Si,P) = 23.5 Hz), 6.95 (s, Si(*i*Pr)); MS (El, 70 eV): m/z 788 (M^+, 24%), 745 ($(M - iPr)^+$, 12), 630 ($(M - Si(iPr)_3 - 1H)^+$, 100).

[11] **4**: Space group $P2_1/n$, $a = 11.917(6)$, $b = 17.487(9)$, $c = 23.784(12)$ Å, $\beta = 97.95(4)°$, $V = 4909$ Å^3, $Z = 4$. 8970 measured reflections (four-circle diffractometer, $Mo_{K\alpha}$ radiation, ω scan), 5753 observed ($I > 2\sigma I$). Non-hydrogen atoms anisotropic, H atoms in observed positions isotropically refined, except protons of the methyl groups (rigid groups). $R = 0.052$, $R_w = 0.059$ (638 variables)[12].

[12] Further details of the crystal structure investigations may be obtained from the Fachinformationszentrum Karlsruhe, Gesellschaft für wissenschaftlich-technische Information mbH, D-W-7514 Eggenstein-Leopoldshafen 2 (FRG) on quoting the depository number CSD-56208, the names of the authors, and the journal citation.

Estradiols Modified by Metal Carbonyl Clusters as Suicide Substrates for the Study of Receptor Proteins: Application to the Estradiol Receptor**

By *Anne Vessières, Siden Top, Colette Vaillant, Domenico Osella, Jean-Paul Mornon*, and *Gérard Jaouen**

The intimate association of a hormone with its receptor is known to be implicit in the triggering of hormone action; however, mechanistic detail is largely unknown.[1] One approach to identifying the specific amino acids in the receptor implicated in the binding of the hormone is affinity labeling, that is, the use of molecules that will recognize the site of association and bind irreversibly.[1] It is well known that complexation by an organometallic moiety may dramatically alter the properties and reactivity of an organic substrate, and make possible reactions that are difficult or impossible by conventional procedures.[2] Extrapolation of this concept to the biological domain suggests that organometallic complexation of a bioligand may also alter its properties allowing access to information on the nature of recognition.

In studies of the estradiol–receptor complex, it has been postulated that the association site is acidic in nature and may contain an SH group.[3] It also has been demonstrated that the hydroxyl groups at C-3 and C-17 of estradiol are necessary for effective recognition.[1] In addition, substitution studies show that the 17α position can tolerate fairly large substituents without severely diminishing recognition.[4] We thus set about synthesizing the organometallic hormone derivatives **1**–**5** with the aim of binding estradiol

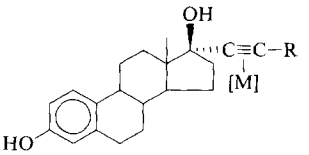

1, R = Me, [M] = $[Co_2(CO)_6]$
2, R = Me, [M] = $[Mo_2Cp_2(CO)_4]$
3, R = H , [M] = $[Os_3(CO)_{10}]$
4, R = H , [M] = $[Ru_3(CO)_{10}]$
5, no R, [M] = $[Ru_3(CO)_9H]$

covalently to its receptor. We hoped to make use of the fact that the transformation of alcohols to their corresponding carbenium ions is facile when the C atom with the hydroxyl group is stabilized by an organometallic moiety. These species may in turn demonstrate strong alkylating properties.[5]

The preparation of **1** and **2** has been described previously.[6] The trimetallic Os and Ru complexes **3** and **4** were synthesized by reaction of ethynylestradiol with the activated clusters $[M_3(CO)_{10}](MeCN)_2$ (M = Os, Ru) and display characteristic chemical shifts in the ^{1}H NMR spectra for the

[*] Prof. Dr. G. Jaouen, Dr. A. Vessières, Dr. S. Top, Dr. C. Vaillant
Ecole Nationale Supérieure de Chimie de Paris
URA CNRS 403, 11 rue P. et M. Curie
F-75231 Paris Cedex 05 (France)
Prof. Dr. D. Osella
Dipartimento di Chimica Inorganica, Turin (Italy)
Dr. J.-P. Mornon
Université Pierre et Marie Curie, Paris (France)

[**] This work was supported by the Centre National de la Recherche Scientifique, Pirmed, Inserm, MRT, and Medgenix. We thank J. Harrod for helpful discussions and Johnson Matthey for a generous loan of precious metals.

coordinated acetylenic proton at $\delta = 8.98$ and 8.33, respectively. Direct heating of $[Ru_3(CO)_{12}]$ with ethynylestradiol in benzene yields the hydrido complex **5**, in which migration of the acetylenic proton to the cluster framework is evidenced by the upfield shift of the ^1H NMR signal at $\delta = -20.45$.

The Relative Binding Affinities (RBA) of these compounds for the estradiol receptor have been determined and are reported in Table 1. The molybdenum complex **2** displays a strong affinity for the estradiol receptor (RBA 33%), while the dinuclear cobalt complex **1** has a good though weaker affinity (RBA 18%). The trinuclear ruthenium complex **4** maintains an acceptable affinity (RBA 8%); however, the other trimetallic complexes studied display a markedly weaker interaction (RBA $\approx$ 2%). A comparison of the RBA values of these complexes reveals a steady decrease in affinity, which may be roughly correlated to the increasing steric hindrance in the 17α position.

Table 1. RBA of the estradiol receptor and the inactivation of the receptor in the presence of the organometallic hormone derivatives **1**–**5**.

Compound	RBA [%] [a]	Inactivation [%] [b]
1	18	80
2	33	22
3	2.5	65
4	8	68
5	2.6	62

[a] The affinity to the estradiol receptor was determined in a competition radioreceptor binding assay with lamb uterine cell extracts (prepared as described in [14]) and [^{3}H]estradiol as a tracer [7]. [b] The inactivation of the estradiol receptor by **1**–**5** was determined by the incubation of the lamb uterine cell extracts (0.3 nmol) with 10 nmol of the hormone derivative. The fraction of the hormone derivative not bound was removed by treatment with charcoal/dextran. The remaining amount of reversibly bound hormone derivative was measured by protamine sulfate precipitation assay after exchange with 10 nm [^{3}H]estradiol (16–20 h, 20 °C).

Following this initial study we set out to investigate the possible existence of a covalent bond between the hormone derivatives and the receptor by receptor inactivation studies. The results shown in Table 1 indicate that these complexes may be separated into three categories: The first contains the cobalt complex **1** which causes a strong inactivation of the estradiol receptor (80%), the second consists of the trinuclear osmium and ruthenium complexes **3**, **4**, and **5**, capable of moderate inactivation (65%), and the third consists of the molybdenum complex **2** which produces only weak inactivation of the receptor (22%). These preliminary experiments with uterine preparations suggest that the 17β OH function of the hormone labeled with an organometallic fragment may be selectively activated at the association site of the estradiol receptor. This may occur by reaction with an acidic species to generate a carbenium ion-like reactive intermediate. Ideally a nucleophile should be located very close to this suggested acidic group to react instantly with the transient electrophile.

The carbenium ion analogues of these hormone complexes may be generated in the presence of acids. Measurement of their pK_{R^+} values was performed with H_2SO_4 according to the method of Deno et al., in a 1:1 mixture of MeCN and H_2O using the appropriate coefficients.[8] Due to the limited stability of the trinuclear hormone complexes in solution, and the additional complication of an equilibrium between the alcohol, carbenium ion, and elimination products,[9] measurements were made on the model compounds **6**–**9** (Table 2).

Table 2. pK_{R^+} Values for the model compounds **6**–**9** [a].

Compound	**6**	**8**	**9**	**7**
pK_{R^+}	−5.5 [b]	−3.4	−1.4	+3 [b]

[a] The pK_{R^+} values for the alcohols in aqueous H_2SO_4/MeCN solution was determined spectroscopically according to the method of Deno et al. [15]. The model compound corresponding to **5** could not be synthesized. [b] Value from ref. [9c].

Complexes **6**, **8**, and **9** all display a negative values of pK_{R^+}, indicative of highly reactive carbocations. The dimolybdenum species is again the anomaly with a positive pK_{R^+} and is expected to be weakly reactive towards nucleophiles. This behavior corresponds to the relative deactivating effect of the labeled hormones (Table 1).

$HC{\equiv}C{-}CH_2OH$
|
[M]

6, [M] = $[Co_2(CO)_6]$, **7**, [M] = $[Mo_2Cp_2(CO)_4]$
8, [M] = $[Os_3(CO)_{10}]$, **9**, [M] = $[Ru_3(CO)_{10}]$

The postulated acidic character at the association site of the receptor necessary for the generation of the carbenium ion, may be due to Brønsted or Lewis acids, or in this case the doubly charged, positive metal ions.[10] Preliminary results showed that the model compound 2-ferrocenylethanol couples with methylcysteinate not only in the presence of CF_3COOH, but also Zn^{2+} and Mg^{2+}.[11] The reaction occurs exclusively at the sulfur atom leaving the nitrogen atom untouched. Interestingly, recent work has suggested the presence of metal dications in the estradiol-binding domain.[12] Furthermore, deactivation studies with MMTS (methyl methane thiosulfate), a highly specific reagent for the SH group,[13] shows a 90% efficiency in deactivating the estradiol receptor.[14] This result suggests that the organometallic hormone derivatives are cysteine-specific reagents.

To ascertain the formation of a covalent bond between the organometallic hormone derivatives and the estradiol receptor, compound **1** was prepared in two radioactive forms: [^{3}H]**1** is tritiated at the 2 and 4 positions with a specific activity of 1.26 TBq mmol^{-1} (34.2Ci/mmole), and [^{14}C]**1** is labeled with ^{14}CO on the cluster unit (specific activity 500 GBq mmol^{-1}, 135 mCi mmol^{-1}). Under conditions suitable for the displacement of the tritiated estradiol from its specific receptor (e.g. treatment with Dextran-coated charcoal at 37 °C for 30 min), [^{3}H]**1** and [^{14}C]**1** remained bound indicating the establishment of an irreversible association between the estradiol receptor and the organometallic hormone. Moreover, the results obtained with [^{14}C]**1** indicated that no decomplexation occurs during the irreversible binding of the organometallic hormone derivatives to the receptor. Further investigations are needed to pinpoint the location of this particular cysteine residue in the receptor and clarify the effect of even bulkier cluster units in affinity labeling.

Recently the complete complementary DNA of the estradiol receptor was cloned and sequenced for the human,[15] chicken, mouse, rat, xenopus (a type of African aquatic frog), and rainbow trout, and their homologues were discussed.[1] In the human estradiol receptor (hER)[15] the hormone-binding domain contains only four cysteine residues (Cys) at positions 381, 417, 447, and 530. The sequence after Cys 447 is conserved in all the receptors (consensus domain

451–471),[16] and the sequence before Cys 530 is highly preserved in all the estradiol receptors sequenced so far.[1] This specific region has recently been identified by point mutations as the key steroid-binding domain of the estrogen receptor.[17]

Furthermore, according to Hydrophobic Cluster Analysis (HCA),[18] the lysine-cysteine-lysine sequence (529–531) appears to be situated at the threshold of the suggested hormone-binding site.[19] This relatively peripheral location of the strong sulfur nucleophile of Cys 530 explains the deactivating effect of the bulky alkynylestradiol clusters **1**–**5**. Finally two independent studies based on the radiosequencing of peptide fragments and truncation experiments have also implicated the region of Cys 530 in the binding of estradiol.[20]

Experimental Procedure

4: To a solution of $[Ru_3(CO)_{12}]$ (100 mg, 0.16 mmol) in 10 mL CH_2Cl_2 and 3 mL CH_3CN at 0 °C was added a solution of Me_3NO (26 mg, 0.35 mmol) in 7 mL CH_2Cl_2 dropwise over 15 min. The solution was allowed to stir for 1 h, then filtered through silica gel, and concentrated to dryness. The orange $[Ru_3(CO)_{10}](MeCN)_2$ was redissolved in 20 mL THF, and ethynylestradiol (46 mg, 0.16 mmol) was added as a solid. The resulting deep orange solution allowed to stir for 1 h. Removal of the solvent and purification by thin-layer chromatography on silica gel eluting with CH_2Cl_2/CH_3CN/pentane (3:1:6) provided a bright orange product, $[Ru_3(CO)_{10}$(ethynylestradiol)], in 47% yield.

^1H NMR (250 MHZ, CD_3COCD_3, 20 °C): $\delta = 7.24$ (d, H1), 6.71 (dd, H2), 6.68 (d, H4), 8.03 (s, O-H3), 4.30 (s, O-H17), 1.15 (s, Me-13), 8.33 (s, ≡CH); ^{13}C NMR (62.87 MHz, $CDCl_3$, 20 °C): $\delta = 153.4$ (C3), 138.1 (C5), 132.2 (C10), 126.5 (C1), 115.2 (C4), 112.7 (C2), 85.5 (C17), 48.6 (C13), 15.1 (C18), 192.8 (C19), 136.7 (C20), 197.7 (CO); IR (pentane): $\tilde{\nu}$ [cm^{-1}] = 2096vw, 2059s, 2052w, 2029m, 2011m, 1884w (CO).

3 was prepared in a similar manner from $[Os_3(CO)_{10}]$ in 63% yield.

^1H NMR (250 MHz, $CDCl_3$, 20 °C): $\delta = 7.18$ (d, H1), 6.65 (dd, H2), 6.56 (d, H4), 6.67 (s, O-H3), 4.47 (s, O-H17), 0.92 (s, Me-13), 8.98 (s, ≡CH); ^{13}C NMR (62.87 MHz, $CDCl_3$, 20 °C): $\delta = 153.5$ (C3), 138.1 (C5), 132.4 (C10), 126.5 (C1), 115.3 (C4), 112.8 (C2), 92.5 (C17), 47.8 (C13), 15.1 (C18), 169.3 (C19), 115.4 (C20), 174.5 (m, CO); IR (CH_2Cl_2): $\tilde{\nu}$ [cm^{-1}] = 2098w, 2059m, 2050m, 2022s, 2014s, 1845vw (CO).

Spectroscopic data of **5**: ^1H NMR (250 MHz, CD_3COCD_3, 20 °C): $\delta = 7.22$ (d, H1), 6.73 (dd, H2), 6.62 (d, H4), 8.10 (s, O-H3), 4.80 (s, O-H17), 1.01 (s, Me-13), −20.45 (s, Ru-H); ^{13}C NMR (62.87 MHz, $CDCl_3$, 20 °C): $\delta = 153.9$ (C3), 138.1 (C5), 132.4 (C10), 126.5 (C1), 115.2 (C4), 112.7 (C2), 90.7 (C17), 48.6 (C13), 15.0 (C18), 103.8 (C19), 162.9 (C20), 197.1 and 188.5 (s, s, CO, 1:2). IR (CH_2Cl_2): $\tilde{\nu}$ [cm^{-1}] = 2096w, 2070s, 2050s, 2017s, 1986w (CO).

Received: December 16, 1991 [Z 5073 IE]
German version: *Angew. Chem.* **1992**, *104*, 790

CAS Registry numbers:
1, 101859-59-0; [^{3}H]-**1**, 141555-08-0; [^{14}CO]-**1**, 141611-90-7; **2**, 101859-58-9; **3**, 141583-41-7; **4**, 141555-06-8; **5**, 141555-07-9; **6**, 12264-12-9; **7**, 84079-77-6; **8**, 141583-42-8; **9**, 141583-43-9; $[Os_3(CO)_{10}](MeCN)_2$, 61817-93-4; $[Ru_3(CO)_{10}](MeCN)_2$, 103257-53-0; $Ru_3(CO)_{12}$, 15243-33-1; ethynyl estradiol, 57-63-6.

[1] T. Ojasoo, J. P. Raynaud, J. P. Mornon, in *Comprehensive Medicinal Chemistry, Vol. 3: Membranes and Receptors* (Ed.: J. C. Emmet), Pergamon, Oxford, **1990**, pp. 1175–1225, and references therein.
[2] a) G. Jaouen in *Transition Metal Organometallics in Organic Synthesis Vol. II* (Ed.: H. Alper), Academic Press, New York, **1978**, Chap. 2; b) A. D. Ryabov, *Angew. Chem.* **1991**, *103*, 945–955; *Angew. Chem. Int. Ed. Engl.* **1991**, *30*, 931–941.
[3] a) J. A. Katzenellenbogen, K. E. Carlson, D. F. Heiman, D. W. Robertson, L. L. Wei, B. S. Katzenellenbogen, *J. Biol. Chem.* **1983**, *258*, 3487–3495; b) E. V. Jensen, D. J. Hurst, E. R. DeSombre, P. W. Jungblut, *Science (Washington, DC)*, **1967**, *158*, 385–387.
[4] A. Vessières, G. Jaouen, M. Gruselle, J. L. Rossignol, M. Savignac, S. Top, S. Greenfield, *J. Steroid Biochem.* **1988**, *30*, 301–305.
[5] K. M. Nicholas, *Acc. Chem. Res.* **1987**, *20*, 207–214.
[6] M. Savignac, G. Jaouen, C. A. Rodger, R. E. Perrier, B. G. Sayer, M. J. McGlinchey, *J. Org. Chem.* **1986**, *51*, 2328–2332.
[7] A. Vessières, S. Top, A. A. Ismail, I. S. Butler, M. Louer, G. Jaouen, *Biochemistry* **1988**, *27*, 6659–6666.
[8] a) N. C. Deno, J. J. Jaruzelski, A. Schriesheim, *J. Am. Chem. Soc.* **1955**, *77*, 3044–3051; b) C. A. Bunton, M. Carrasco, W. E. Watts, *J. Chem. Soc. Perkin Trans. 2* **1979**, 1267–1273.
[9] a) S. Aime, A. J. Deeming, *J. Chem. Soc. Dalton Trans.* **1981**, 828–832; b) S. Ermer, R. Karpelus, S. Miura, E. Rosenberg, A. Tiripicchio, A. M. M. Lanfredi, *J. Organomet. Chem.* **1980**, *187*, 81–90; c) M. Gruselle, C. Cordier, M. Salmain, H. El Amouri, C. Guérin, J. Vaisserman, G. Jaouen, *Organometallics* **1990**, *9*, 2993–2997.
[10] a) E. Kimura, T. Koike, *Comments Inorg. Chem.* **1991**, *11*, 285–301; b) B. L. Allee, D. S. Auld in *Perspectives in Biochemistry* (Ed.: H. Neurath), American Chemical Society, Washington, D.C., **1991** Chap. 6, pp. 69–81.
[11] B. Misterkiewicz, R. Dabard, A. Darchen, H. Patin, *C. R. Acad. Sci. Ser. 2* **1989**, *309*, 875–880; b) S. Top, G. Jaouen, unpublished results.
[12] N. Medici, S. Minucci, V. Nigro, C. Abbondanza, I. Armetta, A. M. Molinari, G. A. Puca, *Biochemistry* **1989**, *28*, 212–219.
[13] J. E. Bodwell, N. J. Holbrook, A. Munck, *Biochemistry* ***1984***, *23*, 1392–1398.
[14] A. Vessières, C. Vaillant, M. Salmain, G. Jaouen, *J. Steroid Biochem.* **1989**, *34*, 301–305.
[15] S. Green, P. Walter, V. Kumar, A. Krust, J. M. Bornert, P. Argos, P. Chambon, *Nature* **1986**, *320*, 134–139.
[16] J. P. Mornon, V. Bissery, C. Gaboriaud, A. Thomas, T. Ojasoo, J. P. Raynaud, *J. Steroid Biochem.* **1989**, *34*, 355-361.
[17] S. E. Fawell, J. A. Lee, R. White, M. G. Parker, *Cell* **1990**, *60*, 953–962.
[18] L. Lemesle-Varloot, B. Henrissat, C. Gaboriaud, V. Bissery, A. Morgat, J. P. Mornon, *Biochimie* **1990**, *72*, 555–574.
[19] L. Lemesle-Varloot, T. Ojasoo, J. P. Mornon, J. P. Raynaud, *J. Steroid Biochem. Mol. Biol.*, **1992**, *41*, 369–388.
[20] a) K. W. Harlow, D. N. Smith, J. A. Katzenellenbogen, G. L. Greene, B. S. Katzenellenbogen, *J. Biol. Chem.* **1989**, *264*, 17476–17485; b) S. E. Fawell, J. A. Lees, M. G. Parker, *Molec. Endocrinol.* **1989**, *3*, 1002–1005.

"Kinetically Enhanced Metalation"—How Substituents Direct *ortho* Lithiation**

By *Nicolaas J. R. van Eikema Hommes* and *Paul von Ragué Schleyer**

Many organic molecules with functional groups are lithiated by RLi selectively in the vicinity of these functional groups. Roberts and Curtin[1] were the first to suggest the now commonly accepted rationalization of this phenomenon: Complexation of the lithium atom to the substituent, for example in benzene derivatives, facilitates the removal of an *ortho* hydrogen atom by the anion R^-. "Directed *ortho* metalation"[2] and "complex-induced proximity effects"[3] have become designations to describe a large class of highly important synthetic reactions.[2–5] However, there is only circumstantial evidence that complex formation between the lithiating reagent and the substrate is really essential. We now propose a new explanation which emphasizes that the directing and activating effects of electronegative substituents are transition-state phenomena.[5, 6]

If strong complexation were responsible for the high regioselectivity, the reactions should proceed more slowly since the complexation energy would have to be overcome in going to the transition state. However, if the energy of the transition state is lowered more than that of the initial complex, the reactions will be accelerated, as is observed experimentally.

Although a complex of *n*-butyllithium and anisole in [D_8]toluene has actually been identified[7] (e.g. by means of HOESY NMR spectroscopy, a method which also reveals agostic interactions,[8, 9] i.e. small distances between lithium and the *ortho* hydrogen atoms), no reaction occurs in this

[*] Prof. Dr. P. von Ragué Schleyer, Dr. N. J. R. van Eikema Hommes
Institut für Organische Chemie der Universität Erlangen-Nürnberg
Henkestrasse 42, D-W-8520 Erlangen (FRG)

[**] This work was supported by the Deutsche Forschungsgemeinschaft, the Fonds der Chemischen Industrie, and the Convex Computer Corporation. N. J. R. v. E. H. thanks the Alexander von Humboldt Foundation for a research fellowship.—Presentations during the course of this work have been made at the VIIth Int. Congress on Quantum Chemistry, Menton, France, **1991** (abstract L33), the 201st American Chemical Society National Meeting, Atlanta, GA, USA, **1991** (abstract ORGN 129), and the XIVth Int. Conference on Organometallic Chemistry, Detroit, MI, USA, **1990** (abstracts, p. 18).

Table 1. Absolute and relative energies and Natural charges [a].

Species [b]	E_{abs}	E_{rel}	C1	CX	X	Li	H	H^-
LiH	7.99615					0.72		−0.72
H_2	1.14410						0.00	
X = *H*								
C_6H_6	231.47041		−0.23	−0.23			0.23	
C_6H_6-LiH **1**	239.49395	−15.8	−0.25	−0.25	0.26	0.68	0.26	−0.70
T.S. C_6H_7Li **2**	239.43502	+18.7	−0.57	−0.24	0.21	0.93	0.12	−0.38
C_6H_5Li **3**	238.31504	+2.0	−0.65	−0.28	0.20	0.91		
X = *O*								
C_6H_5OH	306.50932		−0.33	0.38	−0.76		0.23	
C_6H_5OH-LiH **4**	314.53547	−17.6	−0.29	0.35	−0.83	0.70	0.25	−0.71
T.S.*o*-C_6H_7LiO **5**	314.49557	+5.0	−0.51	0.29	−0.86	0.93	0.13	−0.39
o-HOC_6H_4Li **6**	313.37715	−12.8	−0.62	0.25	−0.88	0.91		
X = *F*								
C_6H_5F	330.49849		−0.31	0.47	−0.40		0.25	
C_6H_5F-LiH **7**	338.51592	−12.4	−0.30	0.44	−0.46	0.72	0.26	−0.73
T.S.*o*-C_6H_6LiF **8**	338.48265	+6.5	−0.50	0.36	−0.49	0.93	0.14	−0.40
o-FC_6H_4Li **9**	337.36753	−13.2	−0.63	0.33	−0.50	0.92		
FC_6H_5-LiH **10**	338.51686	−12.8	−0.29	0.47	−0.38	0.68	0.26	−0.70
T.S.*p*-C_6H_6LiF **11**	338.46445	+17.9	−0.59	0.47	−0.40	0.93	0.13	−0.38
p-FC_6H_4Li **12**	337.34597	+0.3	−0.68	0.45	−0.41	0.91		

[a] Absolute energies (MP2/6-31 + G*//6-31G*) are given in Hartree, energies (E_{rel}) relative to those of the separated reactants are corrected for zero-point vibrational energy differences and are given in kcal mol^{-1}. [b] T.S. = transition state.

hydrocarbon solvent even at room temperature. When *N*,*N*,*N*′,*N*′-tetramethylethylenediamine (TMEDA) is added, lithiation takes place even though the anisole–butyllithium complex is no longer present! Furthermore, no complex between fluorobenzene and *n*-butyllithium can be detected in toluene, even though F is known to be a better *ortho*-directing group than OMe.[10]

In the present ab initio study[11] of the mechanism of the lithiation of aromatic compounds, we consider the reactions of lithium hydride (as a model for organolithium reagents[12]) with benzene, phenol (as a model for anisole), and fluorobenzene. Calculated structures are shown in Figures 1–3. Total and relative energies [MP2/6-31 + G*//6-31G* with zero-point energy corrections (ZPE)] and selected Natural charges[13] are given in Table 1.

The π complex **1** of lithium hydride and benzene is computed to be 15.8 kcal mol^{-1} more stable than the separated species. The complexation of LiH with phenol and with fluorobenzene is quite exothermic; for **4** the complexation energy (17.6 kcal mol^{-1}) is somewhat more than for **10**

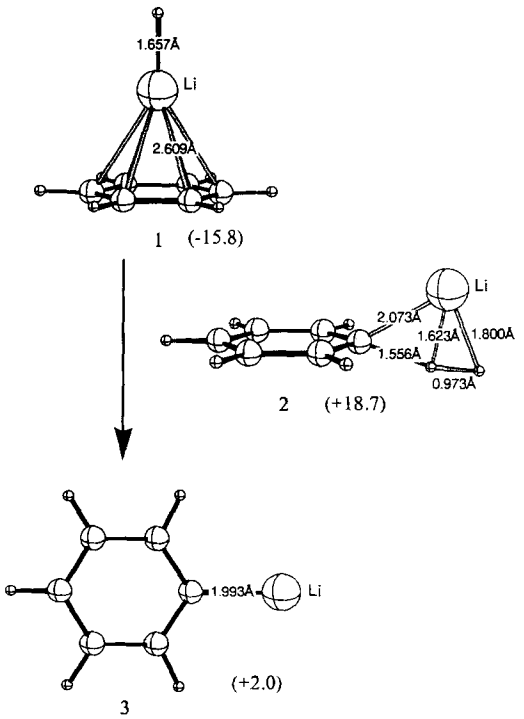

Fig. 1. Calculated structures for the lithiation of benzene with lithium hydride.

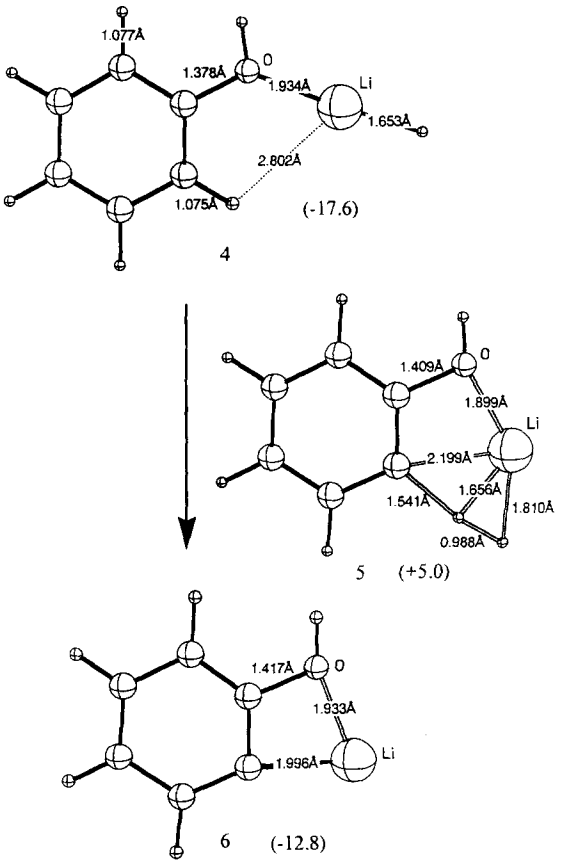

Fig. 2. Calculated structures for the lithiation of phenol with lithium hydride.

(12.8 kcal mol^{-1}). These values are in line with the results of the aforementioned NMR experiments in which anisole but not fluorobenzene forms a detectable complex with the lithium reagent in [D_8]toluene.[7]

Interestingly, in the most stable complex of C_6H_5F and LiH, **10**, the lithium atom is coordinated to the aromatic ring (with the shortest distance to C(4)) rather than to the fluorine. The complexation to fluorine in **7** is computed to be 0.4 kcal mol^{-1} less favorable. Hence, one might expect fluorobenzene to be less reactive than benzene and to be metalated in the *para* position, provided that complex formation is the determining factor for reactivity and regioselectivity. Experimentally, the opposite is observed: Fluorobenzene is metalated in the *ortho* position rapidly at $-50\,^{\circ}C$ in THF, while benzene is unreactive under the same conditions.[10, 14]

(30.6 kcal mol^{-1} relative to the precursor complex). The overall reaction energies show a similar trend: The calculated reaction energies for the *ortho* lithiation of phenol and fluorobenzene are -12.8 and -13.2 kcal mol^{-1}, respectively, while values of $+2.0$ and $+0.3$ kcal mol^{-1} are computed for lithiation of benzene and *para* lithiation of fluorobenzene. As expected from the calculated complex structures the *para*-metalation of fluorobenzene is similar to that of benzene in this respect as well.[15]

The transition structures (**2**, **5**, **8**, and **11**) are also strongly influenced by the substituents. In **2** (Fig. 1) and **11** (Fig. 3) the C-Li-H-H groupings lie in the plane of symmetry perpendicular to the aromatic ring. In contrast, the transition structures **5** (Fig. 2) and **8** (Fig. 3) are planar, with the lithium atoms coordinated intramolecularly by oxygen and by fluorine, respectively. However, the geometries of the C-Li-H-H moieties are very similar in all the transition structures (e.g. H–H = 0.985 ± 0.015 Å, see Figs. 1–3).

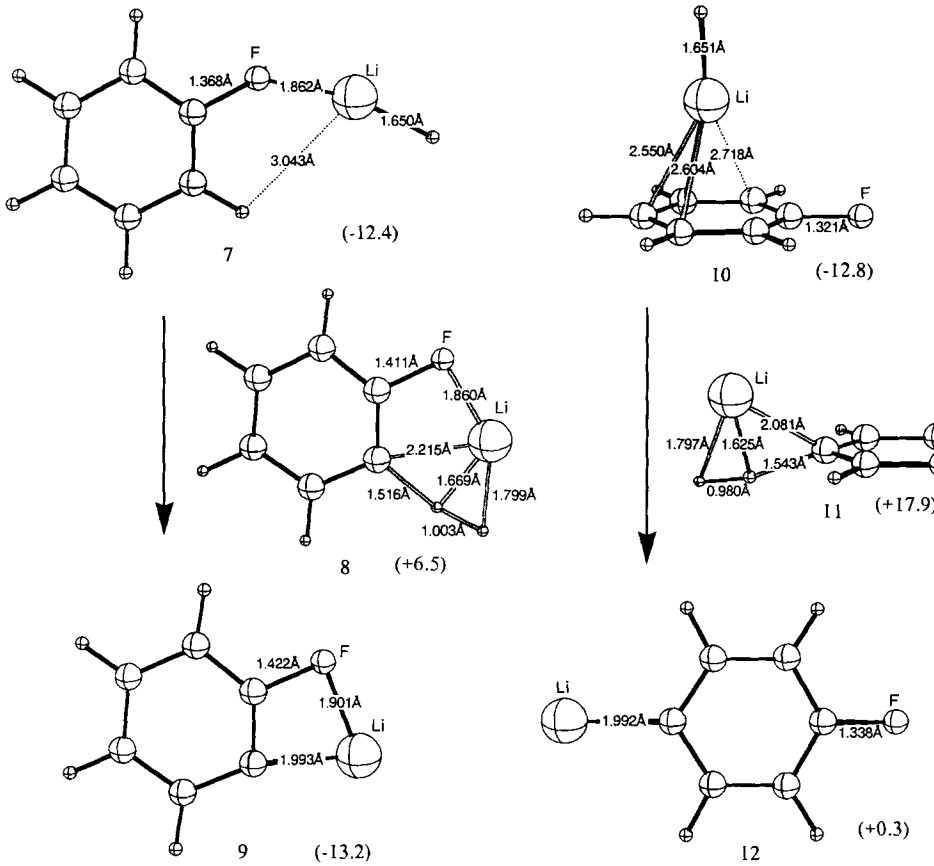

Fig. 3. Calculated structures for the lithiation of fluorobenzene with lithium hydride. Left: Complexation by the fluorine substituent. Right: Complexation by the aromatic ring.

In the complex between phenol and lithium hydride, **4**, *no* signs of agostic activation[8, 9] of the *ortho* hydrogen atom by lithium are evident. The C2–H bond (1.075 Å) is actually shorter than the C6–H bond (1.077 Å). Furthermore, the Li–H2 separation of 2.8 Å is far too large to allow any significant interaction.

In contrast, the effect of electronegative substituents on lowering the activation energies is dramatic. The calculated activation barrier for the lithiation of benzene is 18.7 kcal mol^{-1} relative to the separated reactants and thus 34.5 kcal mol^{-1} relative to the precursor complex. For phenol, these values are 5.0 and 22.6 kcal mol^{-1}, respectively, while those for the *ortho* lithiation of fluorobenzene are 6.5 and 18.9 kcal mol^{-1}. For the *para* lithiation of fluorobenzene, a reaction which is not observed experimentally, we compute a much higher activation barrier of 17.9 kcal mol^{-1}

The Natural charges on Lithium, the *ipso* carbon C1, the migrating hydrogen atom, and the hydride ion (Table 1) are also very similar in all the transition structures. The charge on the migrating hydrogen atom is very low, that is, metalation should be considered in this sense to be a transfer of a hydrogen atom, rather than a proton.[16]

Electronegative *ortho* substituents stabilize the transition states for aromatic lithiation in two ways. First, an electrostatically favorable arrangement of charges is provided (Scheme 1): lithium (positive), *ipso* carbon (negative), *ortho* carbon (positive), and the substituent (negative). Second, the strong coordination of Li–O and Li–F (apparent from their separations which are shorter in the transition structures

than in both the precursor complexes and products, see Figs. 2 and 3) compensates for the effective decrease in the coordination of lithium resulting from the partial bonding in the transition structure. The combination of these effects

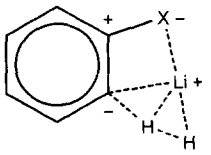

Scheme 1. Charge distribution in the transition state of the *ortho* lithiation of aromatic compounds.

leads to a substantial decrease of the activation energy, and is the cause of the strong preference for *ortho* metalations and other regioselective metalations.[3] This conclusion can be expected to be general. We propose "kinetically enhanced metalation" as a more appropriate designation for the accelerating effects of *ortho* substituents.

Received: December 3, 1991 [Z 5050 IE]
German version: *Angew. Chem.* **1992**, *104*, 768

CAS Registry numbers:
3, 591-51-5; **6**, 72332-11-7; **9**, 348-53-8; **12**, 1493-23-8; LiH, 7580-67-8; C_6H_6, 71-43-2; C_6H_5OH, 108-95-2; C_6H_5F, 462-06-6; anisole, 100-66-3.

[1] J. D. Roberts, D. Y. Curtin, *J. Am. Chem. Soc.* **1946**, *68*, 1658.
[2] V. Snieckus, *Chem. Rev.* **1990**, *90*, 879.
[3] P. Beak, A. I. Meyers, *Acc. Chem. Res.* **1986**, *19*, 356.
[4] For extensive bibliographies see W. N. Setzer, P. von R. Schleyer, *Adv. Organomet. Chem.* **1985**, *24*, 353; C. Schade, P. von R. Schleyer, *ibid.* **1987**, *27*, 169.
[5] G. W. Klumpp, *Recl. Trav. Chim. Pays-Bas* **1986**, *105*, 1
[6] B. O. T. Kammermeier, G. W. Klumpp, K. Kolthof, M. Vos, *Tetrahedron Lett.* **1991**, *32*, 3111.
[7] W. Bauer, P. von R. Schleyer, *J. Am. Chem. Soc.* **1989**, *111*, 7191.
[8] M. Brookhart, M. L. Green, *J. Organomet. Chem.* **1983**, *250*, 395.
[9] G. Erker, W. Frömberg, K. Angermund, R. Schlund, C. Krüger, *J. Chem. Soc. Chem. Commun.* **1986**, 372; N. Koga, S. Obara, K. Morokuma, *J. Am. Chem. Soc.* **1984**, *106*, 4625; W. Bauer, M. Feigel, G. Müller, P. von R. Schleyer, *ibid.* **1988**, *110*, 6033.
[10] See for example H. W. Gschwend, H. R. Rodriguez, *Org. React.* **1979**, *26*, 1.
[11] a) GAUSSIAN 90, Revision I: M. J. Frisch, M. Head-Gordon, G. W. Trucks, J. B. Foresman, H. B. Schlegel, K. Raghavachari, M. Robb, J. S. Binkley, C. Gonzalez, D. J. DeFrees, D. J. Fox, R. A. Whiteside, R. Seeger, C. F. Melius, J. Baker, R. L. Martin, L. R. Kahn, J. J. P. Stewart, S. Topiol, J. A. Pople, Gaussian Inc. Pittsburgh, PA, USA, **1990**; b) CADPAC : R. D. Amos, J. E. Rice, *The Cambridge Analytical Derivatives Packages, Version 4.0*, Cambridge, **1989**, c) 6-31G* Basis set: P. C. Hariharan, J. A. Pople, *Theor. Chim. Acta* **1973**, *28*, 213; M. M. Francl, W. J. Pietro, W. J. Hehre, J. S. Binkley, M. S. Gordon, D. J. DeFrees, J. A. Pople, *J. Chem. Phys.* **1982**, *77*, 3654; d) 6-31+G* Basis set: G. W. Spitznagel, T. Clark, J. Chandrasekhar, P. von R. Schleyer, *J. Comput. Chem.* **1982**, *3*, 363; e) Møller-Plesset theory: J. A. Pople, J. S. Binkley, R. Seeger, *Int. J. Quantum Chem. Symp.* **1976**, *10*, 1, and references therein.
[12] Similar activation energies were calculated (MP2/6-31 + G*//6-31G*) for the metalation of methane by methyllithium (32.9 kcal/mol: E. Kaufmann, P. von R. Schleyer, *J. Comput. Chem.* **1989**, *10*, 437) and by lithium hydride (30.3 kcal/mol: E. Kaufmann, S. Sieber, P. von R. Schleyer, *J. Am. Chem. Soc.* **1989**, *111*, 121). In these studies, the use of larger basis sets led to a modest lowering of the activation barriers.
[13] A. E. Reed, L. A. Curtiss, F. Weinhold, *Chem. Rev.* **1988**, *88*, 899, and references therein.
[14] H. Gilman, T. S. Soddy, *J. Org. Chem.* **1957**, *22*, 1715.
[15] The experimental heat of alcoholysis of *ortho*-lithioanisole is 8.8 kcal mol^{-1} lower than that of phenyllithium [5]. The effects of solvents and of aggregation (see the abstracts cited in [**]) will be discussed in detail in subsequent publications.
[16] See N. J. R. van Eikema Hommes, P. von R. Schleyer, Y. -D. Wu, *J. Am. Chem. Soc.* **1992**, *114*, 1146.

A New, High-Yield Synthesis of Tetraphosphacubanes**

By *Thomas Wettling, Bernhard Geissler, Ronald Schneider, Stefan Barth, Paul Binger,* and *Manfred Regitz**

Dedicated to Professor H.-G. Kuball on the occasion of his 60th birthday

Recently we reported that *tert*-butylphosphaacetylene **2a**[1] can be cyclooligomerized, although only in 8% yield, to the tetraphosphacubane **7a** by heating without solvent to 130 °C.[2] Among known cyclooligomers of **2a**,[3,4] as well as cubanes with P/Si[5] and P/Al[6] combinations of atoms, **7a** is special: strong participation of the "lone pair" on phosphorus in the σ bond between the phosphorus and the framework carbon atoms[7] leads to the NMR resonance signals occurring at extreme positions for the two nuclei (^{31}P NMR: $\delta = +257.4$, ^{13}C NMR: $\delta = -29.1$).[2] To establish whether this effect also influences the reactivity at phosphorus and also whether the phosphorus atoms can now be functionalized, a selective, high-yield access to the pentacycle **7a** was necessary. The pentacycle is the result of two separate cyclodimerization steps; the first is known in principle [8] and the second is basis of this article.

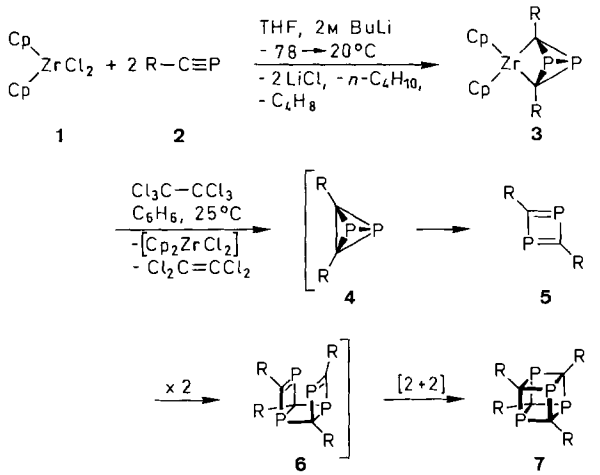

1 2 3 4 5 6 7

2-7a: R = *t*Bu
b: R = CMe_2Et
c: R = 1-adamantyl

The dimeric complex **3a** is the starting material,[8] accessible from bis(cyclopentadienyl)zirconium dichloride (**1**) and 2 mol of the phosphaalkyne **2a** in the presence of magnesium in 53% yield. However, it was obtained reproducibly in 70% yield if the magnesium was replaced by 2 equivalents of *n*-butyllithium and the reaction was carried out at −78 °C.[9]

From previous investigations it is known that reactions of **3a** with halogens and metal or nonmetal halides lead to the

[*] Prof. Dr. M. Regitz, Dr. T. Wettling, Dipl.-Chem. B. Geissler, Dr. R. Schneider, Dipl.-Chem. S. Barth
Fachbereich Chemie der Universität
Erwin-Schrödinger-Strasse, D-W-6750 Kaiserslautern (FRG)
Prof. Dr. P. Binger
Max-Planck-Institut für Kohlenforschung
Kaiser-Wilhelm-Platz 1, D-W-4330 Mülheim an der Ruhr (FRG)

[**] Phosphorus compounds, Part 55. This work was supported by the Volkswagen-Stiftung and the Fonds der Chemischen Industrie. Part 54: U. Bergsträsser, J. Hoffmann, M. Regitz, *Tetrahedron Lett.* **1992**, *33*, 1049–1052.

exchange or elimination of the [Cp_2Zr] fragment as well as the incorporation of halogen into the reaction products.[10] We report herein the removal of the metal residue with a mild halogenation reagent which is followed by the second dimerization step.

The reagent of choice is hexachloroethane,[11] whose reaction with **3a** in benzene at room temperature leads smoothly to the pentacycle **7a** (70%); to our knowledge there are no comparable reactions known. The cyclotetramerization **2a** → **7a** can therefore be achieved in an overall yield of 50%. If the same reaction sequence is applied to the *tert*-pentylphosphaacetylene **2b**, then **3b** [red crystals, 70%, m.p. ≥ 300 °C (decomp.), ^{31}P NMR: $\delta = -247.3$, ^{13}C NMR: $\delta = 133.1$ (t, $^1J_{P,C} = 70.5$ Hz, framework C)] and **7b** [pale-yellow crystals, 75%, m.p. 264 °C, ^{31}P NMR: $\delta = +248.3$, ^{13}C NMR: $\delta = -25.8$ (framework C)][12] are accessible in an analogous way. 1-adamantylphosphaacetylene **2c**, can be converted smoothly into the zirconium complex **3c** [orange-red crystals, 65%, m.p. ≥ 300 °C (decomp.), ^{31}P NMR: $\delta = -257.4$, ^{13}C NMR: $\delta = 131.0$ (t, $^1J_{P,C} = 62.6$ Hz, framework C)]; however, the subsequent yield of **7c** [30%, ^{31}P NMR: $\delta = +245.3$, ^{13}C NMR: $\delta = -21.6$ (framework C)] is reduced by the formation of an isomer whose structure has so far not been confirmed.[13]

A reasonable explanation for the reaction **3** → **7** involves the intermediates **4**–**6**, which could not be proved directly; **5** and **6** are probably also intermediates in the thermal cyclotrimerization of **2a** to **7a**.[2] The thermal isomerization of tetra-*tert*-butyltetrahedrane to the corresponding cyclobutadiene is known in carbon chemistry.[14]

That the zirconium complex **3a** can be converted into the 2,4-di-*tert*-butyl-1,3-diphosphet (**5a**) with hexachloroethane by the elimination of the [Cp_2Zr] fragment is considered plausible from the following experiment: If **3a** is complexed with nonacarbonyldiiron, then **8** is formed [red-brown crystals, 63%, ^{31}P NMR: $\delta = -134.4$, -272.5 (for each d, $^1J_{P,P} = 106.8$ Hz), ^{13}C NMR $\delta = 125.5$ (dd, $^1J_{P,C} = 70.9$ and 64.8 Hz, framework C)]. If this iron complex is treated with

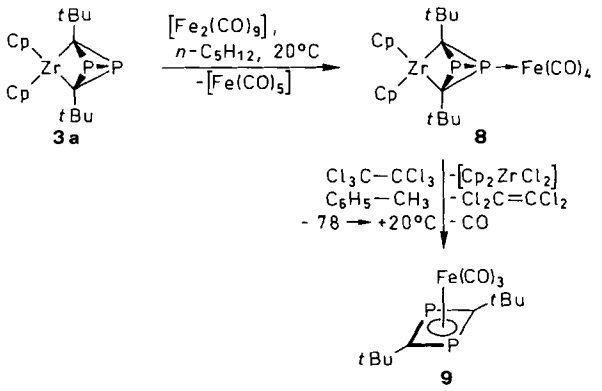

the halogenation reagent, then the complex stabilized diphosphet **9** is formed.[15] However, we do not see the possibility of proving the free diphosphet **5a** under similar conditions.

Experimental Procedure

3a: To a stirred solution of the zirconium compound **1** (2.9 g, 10.2 mmol) in THF (40 mL) at −78 °C (exclusion of air and moisture), 1.6 M *n*-butyllithium in *n*-hexane (12.5 mL, 20.4 mmol) was added dropwise. After 1 h the phosphaalkyne **2a** [1] (2.0 g, 20.0 mmol) was added to this solution at the same temperature. The mixture was allowed to warm up and the solvent was removed at 30 °C/10^{-3} mbar. The residue was dissolved in ether (20 mL) and filtered over a D3 frit. The filtrate was concentrated and cooled to −78 °C which afforded **3a**. Yield: 3.0 g (70%) orange-red crystals; m.p. ≥ 300 °C (decomp.). IR, ^{13}C and ^{31}P NMR spectra are identical with those of an authentic sample. [8]

7a: A solution of the zirconium complex **3a** (1.4 g, 3.3 mmol) in benzene (10 mL) was treated with hexachloroethane (0.79 g, 3.3 mmol) and stirred for 5 d at 25 °C. The solution was pipetted from the precipitated [Cp_2ZrCl_2], concentrated at 25 °C/10^{-2} mbar and the residue was subjected to kugelrohr distillation [155 °C (oven temperature)/10^{-2} mbar]. Yield: 0.47 g (70%) pale yellow crystals; m.p. 241 °C (from *n*-pentane). IR, ^{13}C and ^{31}P NMR spectra are identical to those of an authentic sample. [2]

Received: November 29, 1991 [Z 5042 IE]
German version: *Angew. Chem.* **1992**, *104*, 761

CAS Registry numbers:
1, 1291-32-3; **2a**, 78129-68-7; **2b**, 117972-60-8; **2c**, 101055-70-3; **3a**, 109613-89-0; **3b**, 140438-16-0; **3c**, 140438-17-1; **7a**, 121097-72-1; **7b**, 140438-14-8; **7c**, 140438-15-9; **8**, 140438-18-2; **9**, 126859-53-8; [$Fe_2(CO)_9$], 15321-51-4; Cl_3CCCl_3, 67-72-1.

[1] Most recent review concerning phosphaalkynes M. Regitz and P. Binger in *Multiple Bonds and Low Coordination in Phosphorus Chemistry* (Eds.: M. Regitz, O. J. Scherer), Thieme, Stuttgart, **1990**, pp. 58–111.
[2] T. Wettling, J. Schneider, O. Wagner, C. G. Kreiter, M. Regitz, *Angew. Chem.* **1989**, *101*, 1035–1037; *Angew. Chem. Int. Ed. Engl.* **1989**, *28*, 1013–1014.
[3] (η^4-1-Methylnaphthalene)(η^6-toluene)iron-catalyzed cyclooligomerization: D. Hu, H. Schäufele, H. Pritzkow, U. Zenneck, *Angew. Chem.* **1989**, *101*, 929–931; *Angew. Chem. Int. Ed. Engl.* **1989**, *28*, 900–902.
[4] High-temperature cyclohexamerization via the loss of *t*Bu-C≡C-*t*Bu: T. Wettling, U. Bergsträsser, M. Regitz, *J. Chem. Soc. Chem. Commun.* **1992**, in press.
[5] M. Baudler, G. Scholz, K.-F. Tebbe, M. Feher, *Angew. Chem.* **1989**, *101*, 352–354; *Angew. Chem. Int. Ed. Engl.* **1989**, *28*, 339–341.
[6] A. H. Cowley, R. A. Jones, P. R. Harris, D. A. Atwood, L. Contreras, C. J. Burek, *Angew. Chem.* **1991**, *103*, 1164–1166; *Angew. Chem. Int. Ed. Engl.* **1991**, *30*, 1143–1145.
[7] R. Gleiter, K.-H. Pfeifer, M. Baudler, G. Scholz, T. Wettling, M. Regitz, *Chem. Ber.* **1990**, *123*, 757–760.
[8] P. Binger, B. Biedenbach, C. Krüger, M. Regitz, *Angew. Chem.* **1987**, *99*, 798–799; *Angew. Chem. Int. Ed. Engl.* **1987**, *26*, 764–765.
[9] R. Schneider, Dissertation, Universität Kaiserslautern, **1991**.
[10] P. Binger, T. Wettling, R. Schneider, F. Zurmühlen, U. Bergsträsser, J. Hoffmann, G. Maas, M. Regitz, *Angew. Chem.* **1991**, *103*, 208–211; *Angew. Chem. Int. Ed. Engl.* **1991**, *30*, 207–210.
[11] For the application in organophosphorus chemistry see R. Appel, K. Geissler, H. Schöler, *Chem. Ber.* **1977**, *110*, 376–378; R. Appel, V. Barth, F. Knoch, *Chem. Ber.* **1983**, *116*, 938–950.
[12] The thermal cyclotetramerization at 180 °C afforded only 2% of **7b**.
[13] Approximately 10% (from ^{31}P NMR spectroscopy); ^{31}P NMR: $\delta = -236.7$, -159.2, $+77.8$, $+80.9$. From the thermal reaction of **2a**, a product is formed with the same P/C framework; cf. footnote [14] in ref. [2].
[14] Review: G. Maier, *Angew. Chem.* **1988**, *100*, 317–341; *Angew. Chem. Int. Ed. Engl.* **1988**, *27*, 309–332.
[15] It is identical (from the comparison with the IR, ^{31}P and ^{13}C NMR spectra) to the product obtained from **2a** and [$Fe_2(CO)_9$]: P. Binger, B. Biedenbach, R. Schneider, M. Regitz, *Synthesis* **1989**, 960-961.

Photolithographic Immobilization of Biopolymers on Solid Supports**

By *Lawrence F. Rozsnyai, David R. Benson, Stephen P. A. Fodor,** and *Peter G. Schultz**

The ability to immobilize biomolecules on solid supports in a spatially defined fashion would find considerable application in techniques ranging from atomic force mi-

[*] Dr. S. P. Fodor
Affymax Research Institute
4001 Miranda Ave., Palo Alto, CA 94304 (USA)
Prof. P. G. Schultz, L. F. Rozsnyai, D. R. Benson
Department of Chemistry
University of California
Berkeley, CA 94720 (USA)

[**] This research was supported by the Director, Office of Energy Research, Office of Basic Energy Sciences, Division of Material Sciences, and also by the Division of Energy Biosciences of the U.S. Department of Energy (DE-AC03-76SF00098). The authors acknowledge the helpful assistance of Suzanne Gruber and Steven Sundberg.

croscopy[1] to the generation of receptor arrays for biosensors and parallel ligand-binding assays.[2] Photolithography has been extensively used to spatially direct the formation of electrical circuits and, more recently, the synthesis of peptides and oligonucleotides.[3] We now report the use of photolithographic techniques to spatially direct the covalent attachment of biomolecules to a functionalized glass surface. Antibodies have been crosslinked to a benzophenone-derivatized glass surface in a 500×500 μm checkerboard pattern and subsequently detected by means of epifluorescence microscopy.

Benzophenone was chosen as the crosslinking agent by virtue of its chemical stability, relatively low-energy absorption ($\lambda_{max} \approx 350$ nm), and high efficiency in photochemical crosslinking.[4, 5] Moreover, because the n,π* triplet state of benzophenone reacts with a wide variety of C–H bonds, it should be generally useful for immobilizing many different biomolecules with a wide range of functional groups (including both proteins and nucleic acids).[5] Silica substrates were first derivatized with *t*-butyloxycarbonyl (Boc)-protected 3-aminopropyltriethoxysilane, then deprotected by treatment with 50% trifluoroacetic acid/CH_2Cl_2, and washed with ethyldiisopropylamine/CH_2Cl_2 followed by dimethylformamide (DMF), CH_2Cl_2, and EtOH.[3] The *N*-hydroxysuccinimide (NHS) ester[6] of 3-benzoylbenzoic acid (100 mM in DMF) was then coupled to the aminopropylated glass substrate (Fig. 1). The derivatized substrate was washed with DMF, CH_2Cl_2, and EtOH, and the free NH_2 groups were capped by treatment with acetic anhydride/dimethylaminopyridine. The coupling efficiency of benzoylbenzoic acid was estimated to be approximately 80%.[7]

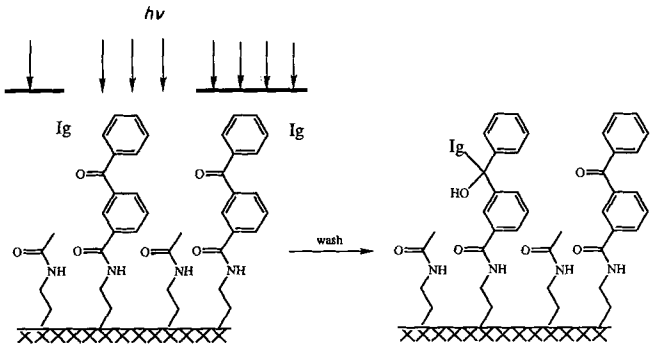

Fig. 1. Light-directed spatially defined immobilization of protein on a solid support.

In order to determine whether spatially addressable crosslinking could be achieved, we attempted to generate a 500×500 μm checkerboard array of photoimmobilized immunoglobulin (Ig) molecules. A 5 μM solution of rabbit IgG (Ig**1**) (in 150 mM NaCl, 10 mM Na_2HPO_4, pH 7.4 (PBS buffer), and 0.05% tween 20) was applied to the benzophenone-derivatized surface and irradiated through a 500×500 μm checkerboard mask (Fig. 1).[3] After a 30 minute irradiation with the 300–400 nm output of a high-pressure mercury arc lamp (12 mW cm^{-2}), the surface was washed with PBS, 1% bovine serum albumin (BSA), and 0.05% tween buffer. Photoimmobilized Ig**1** was labeled by incubating the substrate with fluorescently tagged goat anti-rabbit IgG (Ig**2**). The fluorescent regions of the silica substrate were detected by scanning the substrate in an epifluorescence microscope ($\lambda_{ex} = 488$ nm; $\lambda_{em} > 520$ nm).[8]

The presence of a fluorescent checkerboard pattern (Fig. 2) demonstrates that antibody Ig**1** is bound covalently to the support in specific regions by spatially localized photocrosslinking. Unexposed areas of the checkerboard image appear dark, whereas irradiated regions appear light, due to to the presence of the fluorescent Ig**2** · Ig**1** complex. A photocrosslinking experiment carried out under the same conditions, but with acetylated silica substrate lacking benzophenone, did not yield a checkerboard pattern, and the fluorescence intensities were similar to underivatized substrate. These experiments demonstrate that light-directed immobilization of protein occurs by a photochemical reaction with benzophenone.

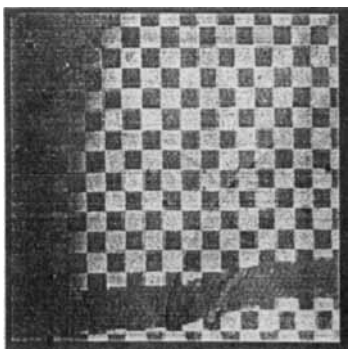

Fig. 2. Spatially localized crosslinked and fluorescence labeling. Light areas correspond to areas of increased fluorescence intensity.

A quantitative comparison between the fluorescence intensity of the checkerboard glass substrate and standardized fluorescent beads (Flow Cytometry Standards) yields an approximate density of one crosslinked antibody per 5000 nm^2. For comparison, the average end-to-end distance of the two ends of the Fab arms of the antibody is approximately 200 Å.[9] The contrast of the fluorescent checkerboard image in this case is 5:1 (after subtracting the background fluorescence of derivatized substrate not exposed to Ig**1** or Ig**2**), representing the ratio of covalently bound antibody (Ig**1**) to noncovalently bound antibody (Ig**1** and/or Ig**2**). However, in other cases lower fluorescence contrast ratios were obtained, presumably due to nonspecific antibody binding.[10] The degree of nonspecific binding is likely to vary as a function of the biomolecule and detection method used in each experiment.

We have demonstrated that proteins can be immobilized on surfaces in spatially defined arrays by the use of photoaffinity labels and photolithography. This method should be generally applicable to a wide range of biopolymers with a variety of functional groups. An important next step is the development of site-selective photoactive or photocaged crosslinking reagents.[11] In addition, it should be possible to construct spatially defined arrays of biomolecules for general use in developing novel biosensors or ligand-binding assays.

Received: December 19, 1991 [Z 5083 IE]
German version: *Angew. Chem.* **1992**, *104*, 801

[1] P. K. Hansma, V. B. Elings, O. Marti, C. E. Bracker, *Science* **1988**, *242*, 209.
[2] C. R. Lowe, *Biosensors* **1985**, *1*, 3.
[3] S. P. A. Fodor, J. L. Read, M. Pirrung, L. Stryer, A. T. Lu, D. Solas, *Science* **1991**, *251*, 768. See also G. von Kiedrowski, *Angew. Chem.* **1991**, *103*, 839; *Angew. Chem. Int. Ed. Engl.* **1991**, *30*, 822.

[4] a) J. T. Kauer, S. Erickson-Vitanen, H. R. Wolfe, W. F. De Grado, *J. Biol. Chem.* **1986**, *261*, 10695, b) W. T. Miller, E. T. Kaiser, *Proc. Natl. Acad. Sci. USA* **1988**, *85*, 5429, c) T. Tao, C. J. Scheiner, M. Lamkin, *Biochemistry* **1986**, *25*, 7633.
[5] a) R. Breslow, *Acc. Chem. Res.* **1980**, *13*, 170, b) C. Helene, *Photochem. Photobiol.* **1972**, *16*, 519.
[6] G. W. Anderson, J. E. Zimmerman, F. M. Gallahan, *J. Am. Chem. Soc.* **1964**, *86*, 1839.
[7] A section of a silica substrate bearing nitroveratryloxycarbonyl (NVOC)-protected amino groups was photodeprotected [3] and then derivatized with the NHS ester of 3-benzoylbenzoic acid. A second section of the substrate was then deprotected and derivatized with the NHS ester of biotin. Any unreacted sites in the first section (due to incomplete coupling of benzophenone) will also react with the biotin NHS ester. The entire surface was then treated with fluorescein-streptavidin (Molecular Probes Inc., Eugene, OR (USA)). The coupling efficiency of benzophenone was then determined by comparison of the fluorescence intensities of the two sections.
[8] Zeiss Axioskop 20, 488 nm excitation from an argon ion laser, Spectra-Physics model 2025. Fluorescence emission above 520 nm was detected with a cooled photomultiplier (Hamamatsu-943-02).
[9] I. Pilz, E. Schwarz, W. Palm, *Eur. J. Biochem.* **1977**, *75*, 195.
[10] The use of acetylated or nonacetylated support did not significantly affect the degree of nonspecific antibody binding.
[11] A caged biotin analogue has recently been shown useful for noncovalent photolithographic immobilization of biopolymers: S. Sundberg, R. Barrett, C. Holmes, *Biophys. J.* **1992**, *61*, 1171.

First Atropo-Enantioselective Ring Opening of Achiral Biaryls Containing Lactone Bridges with Chiral Hydride-Transfer Reagents Derived from Borane**

By *Gerhard Bringmann** and *Thomas Hartung*

Dedicated to Professor Gerhard Quinkert on the occasion of his 65th birthday

Rotationally restricted biaryl compounds from natural and synthetic sources have attracted ever more attention because of their biological activity but also as chiral auxiliaries. For the regio- and stereocontrolled construction of even extremely sterically congested biaryl systems, the lactone-bridged biaryls have proved to be very useful intermediates.[1, 2] They are easily accessible through Pd-catalyzed intramolecular aryl coupling of the molecular halves, which are joined by an ester linkage.[3, 4] Most of these bridged biaryls (if containing *ortho* substituents of "normal" size) are not differentiated into stable atropisomers, since at room temperature they undergo a rapid "helimerization".[5, 6]

This suggests the possibility of cleaving the lactone bridge atropisomer-selectively to form the configuratively stable ring-opened products. By utilizing achiral *H*- or *O*-nucleophiles for chiral substrates (i.e., under internal asymmetric induction) or chiral *O*- and *N*-nucleophiles for achiral substrates (i.e., under external asymmetric induction),[7] we performed this reaction atropodiastereoselectively and demonstrated its application in natural product synthesis. Recently we extended this principle to the atropo-enantioselective ring opening of achiral lactones with chiral *H*-nucleophiles using chirally modified aluminum hydrides.[8] The major problems were the lack of chemical reactivity of the reagents, which had in most cases been developed for chemoselective reduction, for example, of ketones, their tendency to function simultaneously as *N*-nucleophiles, and the mediocre selectivities (in the most favorable case, 88:12 and not attainable for all substrates), as well as the laborious workup. We now report atropo-enantioselective biaryl syntheses by stereoselective reduction of achiral biaryl lactones with modified boranes.

For this purpose, we selected the oxazaborolidines developed by Itsuno et al.[9] and Corey et al.[10] of the type $\mathbf{3}\cdot BH_3$ and $\mathbf{4}\cdot BH_3$, which had already been extremely successfully applied for the enantioselective reduction of ketones, where they gave excellent optical and chemical yields, and required very short reaction times;[9, 10] even a catalytic reaction procedure ("CBS" procedure,[10] "molecular robot"[11]) was possible. The *B*-alkylated compounds **3b** and **3c** were first prepared,[12] analogously to the synthesis of **4b** and **4c**.[10, 13, 14]

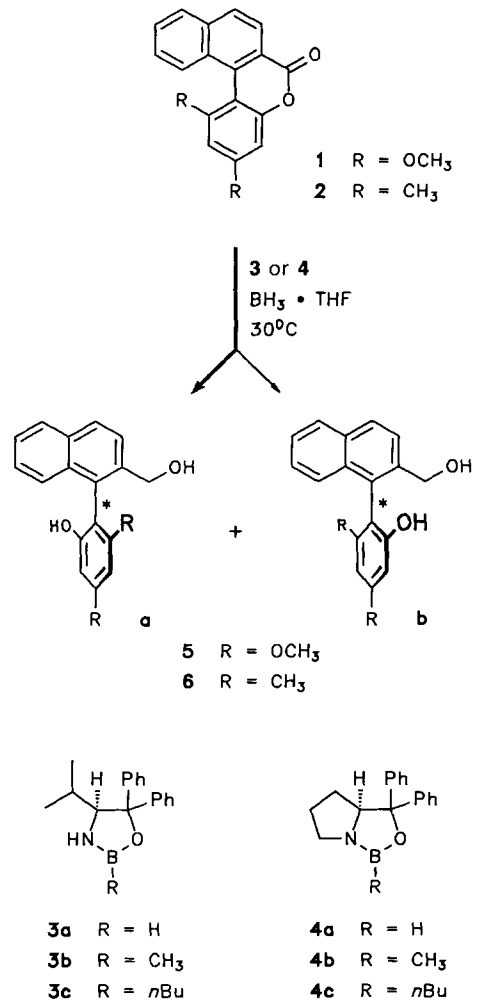

As substrates we used the configuratively labile, axially prostereogenic bridged biaryls **1** and **2**, which can easily be synthesized by esterification and intramolecular aryl coupling[4] from 1-bromo-2-naphthoic acid and 3,5-dimethoxy- or -dimethylphenol. The results of the ring-opening experiments are summarized in Table 1.

The efficiency of the process can be seen in the good results already obtained for the monocyclic derivatives **3a–c**, but in particular for the excellent atropisomeric ratios attained with the bicyclic reagents **4a–4c**, which are at least 90:10 for prac-

[*] Prof. Dr. G. Bringmann, Dipl.-Chem. T. Hartung
Institut für Organische Chemie der Universität
Am Hubland, D-W-8700 Würzburg (FRG)

[**] Novel Concepts in Directed Biaryl Synthesis, Part 12. This work was supported by the Deutsche Forschungsgemeinschaft (SFB 347: Selective Reactions of Metal-Activated Molecules) and by the Fonds der Chemischen Industrie. Part 11: Reference [2].

tically quantitative yields in all cases. By far the highest asymmetric induction is obtained with the *B*-methyl and *B*-*n*-butyl derivatives **4b** and **4c**, independent of the lactone used.

Table 1. Ratios for the atropisomers on reduction of **1** and **2** with the chirally modified boranes **3**·BH_3 and **4**·BH_3 in THF at 30 °C [a].

Lactone	Oxazaborolidine	Alcohol	Ratio [b] **5a**:**5b** or **6a**:**6b**
1	**3a**	**5**	93:7
1	**3b**	**5**	89:11
1	**3c**	**5**	85:15
1	**4a**	**5**	91:9
1	**4b**	**5**	97:3
1	**4c**	**5**	95:5
2	**3a**	**6**	84:16
2	**3b**	**6**	88:12
2	**3c**	**6**	84:16
2	**4a**	**6**	90:10
2	**4b**	**6**	98.5:1.5
2	**4c**	**6**	97:3

[a] All transformations were conducted on an analytic scale (0.03 mmol lactone) in the lactone/oxazaborolidine/BH_3·THF ratio of 1/3/4. [b] The ratio of atropisomers was determined by analytic HPLC on a chiral stationary phase. **5a**/**b**:[8] Chiralcel OF (Daicel), petroleum ether (b.p. 56–64 °C)/*i*PrOH/HCO_2H = 85/15/0.05; the alcohol eluted first is **5b**. **6a**/**b**:[12] Chiralcel OD (Daicel), petroleum ether (b.p. 56–64 °C)/*i*PrOH = 90/10; the alcohol eluted first is **6a**.

The practicality of this stereoselective synthesis is increased by the discovery that when the reaction is performed on a preparative scale, the atropisomeric ratios achieved (e.g., 98.5:1.5 for the reduction of **2** with **4b**) can be improved still further by a simple crystallization step that effortlessly yields enantiomerically pure material (**6a**:**6b** > 99.9:0.1).

Experimental Procedure

3b: A solution of (*S*)-(−)-2-amino-3-methyl-1,1-diphenylbutan-1-ol (510 mg, 2.0 mmol) [9] in dry toluene (10 mL) was treated with trimethylboroxine (190 μL, 171 mg, 1.36 mmol) and stirred for 0.5 h at 20 °C. Thereafter the solution was concentrated to 2 mL, and twice treated with 5 mL of toluene and destilled. After removal of the solvent, colorless crystals of **3b**[12] were obtained in quantitative yield. M.p. 99.5–101 °C, $[\alpha]^{20}_D$ −221.8 (*c* = 1.66, THF).

3c: A solution of (*S*)-(−)-2-amino-3-methyl-1,1-diphenylbutan-1-ol (510 mg, 2.0 mmol) and *n*-butylboronic acid (205 mg, 2.01 mmol) in toluene (30 mL) was heated for 24 h under reflux; water was removed with a Dean–Stark trap. Workup analogous to that of **3b** gave a quantitative yield of **3c**[12] as colorless oil; $[\alpha]^{20}_D$ −185.7 (*c* = 1.89, THF).

6a (*preparative* atropo-enantioselective ring opening of **2** with **4b**): A solution of BH_3·THF (0.80 mmol in 4 mL, 0.2 M) was treated with a 0.2 M solution of oxazaborolidine **4b** (3 mL, 0.60 mmol) in THF at 0 °C under argon. After the addition the mixture was warmed to 30 °C, and a solution of the lactone **2** in THF (0.20 mmol, 55 mg in 6 mL) was added dropwise over 10 min. The reaction solution was stirred for a further 30 min at 30 °C, upon which it was hydrolyzed by addition of water (5 ml) and HCl (2 M, 2 mL). After extraction into ether, the organic phase was dried over $MgSO_4$, and the solvent destilled off in vacuum. Chromatography of the residue on a short silica gel column (CH_2Cl_2) afforded the alcohol **6a** [12] (**6a**:**6b** = 98.5:1.5); yield 52.5 mg (94%), m.p. 141–142 °C, $[\alpha]_D^{20}$ −31.6 (*c* = 0.51, CH_3OH). A subsequent crystallization from dichloromethane/petroleum ether furnished enantiomerically pure material (**6a**:**6b** > 99.9:0.1).

Received: December 27, 1991 [Z 5089 IE]
German version: *Angew. Chem.* **1992**, *104*, 782

CAS Registry numbers:
1, 138435-70-8; **2**, 138435-72-0; **3a**, 117349-13-0; **3b**, 140834-48-6; **3c**, 140834-49-7; **4a**, 110205-59-9; **4b**, 112022-81-8; **4c**, 129145-37-5; **5a**, 140834-50-0; **5b**, 140834-51-1; **6a**, 140834-52-2; **6b**, 140834-53-3; (*S*)-(−)-2-Amino-3-methyl-1,1-diphenylbutan-1-ol, 78603-95-9; Trimethylboroxine, 823-96-1; *n*-Butylboronic acid, 4426-47-5.

[1] G. Bringmann, R. Walter, R. Weirich, *Angew. Chem.* **1990**, *102*, 1006–1019; *Angew. Chem. Int. Ed. Engl.* **1990**, *29*, 977–991.
[2] G. Bringmann, R. Walter, R. Weirich, *Methods Org. Chem. (Houben Weyl), 4th. Ed. 1952* –, Vol. E 22, C2, in press.
[3] D. E. Ames, A. Opalko, *Tetrahedron* **1984**, *40*, 1919–1925.
[4] G. Bringmann, T. Hartung, L. Göbel, O. Schupp, C. L. J. Ewers, B. Schöner, R. Zagst, K. Peters, H. G. von Schnering, C. Burschka, *Liebigs Ann. Chem.* **1992**, 225–232.
[5] G. Bringmann, H. Reuscher, *Angew. Chem.* **1989**, *101*, 1725–1726; *Angew. Chem. Int. Ed. Engl.* **1989**, *28*, 1672–1673.
[6] G. Bringmann, J. R. Jansen, *Synthesis* **1991**, 825–827.
[7] G. Bringmann, R. Walter, C. Ewers, *Synlett* **1991**, 581–583.
[8] G. Bringmann, T. Hartung, *Synthesis*, **1992**, 433–435.
[9] S. Itsuno, K. Ito, *J. Org. Chem.* **1984**, *49*, 555–557; S. Itsuno, M. Nakano, K. Miyazaki, H. Masudo, K. Ito, A. Hirao, S. Nakahama, *J. Chem. Soc. Perkin Trans. 1* **1985**, 2039–2044.
[10] E. J. Corey, R. K. Bakshi, S. Shibata, *J. Am. Chem. Soc.* **1987**, *109*, 5551–5553; E. J. Corey, R. K. Bakshi, S. Shibata, C.-P. Chen, V. K. Singh, *ibid.* **1987**, *109*, 7925–7926; E. J. Corey, S. Shibata, R. K. Bakshi, *J. Org. Chem.* **1988**, *53*, 2861–2863.
[11] E. J. Corey, *Angew. Chem.* **1991**, *103*, 469–479; *Angew. Chem. Int. Ed. Engl.* **1991**, *30*, 455–465.
[12] All new compounds were completely characterized by ^1H NMR, IR, and mass spectra, as well as elemental analysis.
[13] E.J. Corey, R. K. Bakshi, *Tetrahedron Lett.* **1990**, *31*, 611–614.
[14] D. J. Mathre, T. K. Jones, L. C. Xavier, T. J. Blacklock, R. A. Reamer, J. J. Mohan, E. T. Turner Jones, K. Joogsteen, M. W. Baum, E. J. J. Grabowski, *J. Org. Chem.* **1991**, *56*, 751–762.

Matrix-Assisted Laser Desorption Mass Spectrometry of Lignins**

By *Jürgen O. Metzger,* Christine Bicke, Oskar Faix, Wilfried Tuszynski, Raimond Angermann, Michael Karas,* and *Kerstin Strupat*

As component of the lignocelluloses, the skeletal substance of terrestrial plants, lignin is the most common biopolymer besides the polysaccharides cellulose and hemicelluloses. As side product of the cellulose recovery over 50 million tons of technical lignins is produced yearly worldwide, and its use as renewable raw material with a view to protecting the environment is a challenge for chemists. Knowledge about lignins is still fragmentary.[1–3] It is certain that its monomeric precursor in conifers is predominantly coniferyl alcohol (**1a**); in deciduous trees sinapyl alcohol (**1b**) is an additional precursor, as is *p*-cumaryl alcohol (**1c**) in grasses and herblike dicotyledons.[1] According to Freudenberg,[4] these alcohols polymerize to give lignin, by a radical mechanism. However, the biosynthesis path from the monomers to the macromolecule has not yet been unambiguously elucidated.[2] At any rate lignin is fundamentally different from other biopolymers like proteins, nucleic acids, and polysaccharides, in

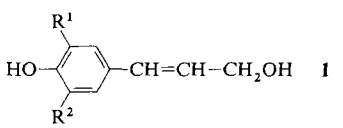

1

a: $R^1 = OCH_3$, $R^2 = H$; **b**: $R^1 = R^2 = OCH_3$; **c**: $R^1 = R^2 = H$.

[*] Prof. Dr. J. O. Metzger
Fachbereich Chemie der Universität
Carl-von-Ossietzky-Strasse 9–11, D-W-Oldenburg (FRG)
Dipl.-Chem. C. Bicke, Priv. Doz. Dr. O. Faix
Bundesforschungsanstalt für Forst- und Holzwirtschaft, Hamburg (FRG)
Dr. W. Tuszynski, Dipl.-Phys. R. Angermann
Fachbereich Physik der Universität Oldenburg
Dr. M. Karas, K. Strupat
Institut für Medizinische Physik der Universität Münster

which the type of linkage and order of the units is stipulated; in lignin at least ten types of binding are found to different extents linking the phenylpropane units into a completely irregular three-dimensional polymer.[5]

To determine the constitutional makeup of lignin by chemical degradation methods is extremely labor-intensive and time-consuming and nevertheless gives no clear answers. In the ^{13}C NMR spectrum, about forty different carbon atoms can be assigned.[5] The molecular weight determination is problematic, because lignins tend strongly toward molecular aggregation in solution.[2] Mass spectrometry has hitherto been used as analytical method for the study and characterization of lignins only in the form of pyrolysis mass spectrometry, in which only monomeric, and to a small extent dimeric, pyrolysis products are detected.[6]

The study of polymers in general, and biopolymers in particular, by mass spectrometry has, however, made enormous advances in recent years with the development of new "soft" ionization techniques such as secondary ion (SI),[7] fast atom bombardment (FAB),[8] and ^{252}Cf plasma desorption (PD) mass spectrometry,[9] as well as various spray processes like ion spray,[10] and in particular, matrix-assisted laser desorption (MALD).[11] The accessible mass range has been steadily extended. Thus MALD mass spectrometry has provided proof of proteins of at least 250000 Da.[12] The protonated quasi-molecular ion was detected, but fragmentation was not observed with this method. MALD-MS was also used successfully for oligosaccharides like maltodextrins and dextrans. The mass spectrum showed peaks for the individual oligomers at well-defined spacings corresponding to the monomeric units, and enabled the determination of the molecular weight distribution up to about 10000 Da.[13] A series of linear polymers like polystyrene and polyethyleneglycol of average molecular weight $\bar{M}_n < 10000$ Da were studied mainly with SIMS.[14]

The lack of a rapid, sensitive, and powerful method for characterizing small amounts of lignins prompted us to investigate the potential of the soft ionization techniques for lignins. Although FAB-MS and PDMS brought no success, MALD-MS provided the breakthrough in the application of mass spectrometry to lignins.

Milled-wood lignin from birch (*Betula alba*), which was well-characterized by classical methods of lignin chemistry,[15] was mixed in the mass ratio 1:15 without further purification with 2,5-dihydroxybenzoic acid as matrix in acetone/water (9:1). A little of the solution (1 μL corresponding to 50 ng of lignin) was placed onto a silver support, dried, and mounted in a time of flight mass spectrometer, as described in reference [12]. A nitrogen laser with a wavelength of 337 nm and an impulse duration of less than 5 ns was used for desorption. The resolution is relatively low ($m/\Delta m = 50$), and the signals thus relatively broad. The peak centroids can, however, be determined with quite good precision (standard deviation $\pm 0.1\,\%$).[12]

The obtained mass spectrum (Fig. 1) shows a wide molecular weight distribution of several hundred to larger than 16000 Da. The center of gravity of the distribution lies around 2600 ± 100 Da, which agrees quite well with the number average of the molecular weight $\bar{M}_n$ of birch lignin determined by gel chromatography.[15] The broad distribution curve (Fig. 1) has a pronounced fine structure up to about 2000 Da (Fig. 2), which may be assigned to oligomeric lignin molecules. These oligomers are not all the same, but themselves show a broad molecular weight distribution. Clear groups of oligomers—from trimers of ca. 600 Da to nonamers of ca. 1800 Da—can be distinguished. The center of gravity of the peaks of oligomeric groups yields the number average of

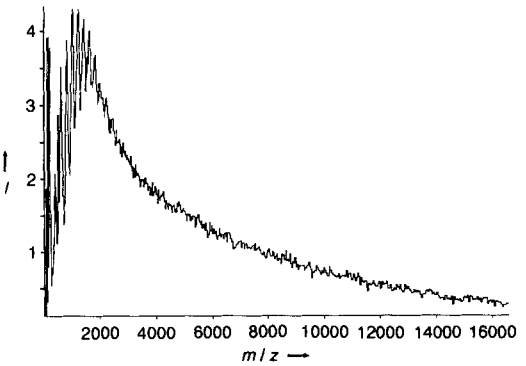

Fig. 1. MALD mass spectrum of birch lignin. Sum of twenty single spectra. I = relative intensity in arbitrary units, molecular weight M_r in Da (m/z).

their molecular weight $\bar{M}_n$. This number average divided by the degree of oligomerization gives an average formula weight of between 214 and 204 Da for one phenylpropane unit of these oligomers, which agrees well with the chemically determined average formula weight of birch lignin (209 Da). The conclusion is that the ionized lignin molecules are probably protonated, since a cationization with Na^+, as observed for sugars,[13] would lead to distinctly higher average molecular weights.

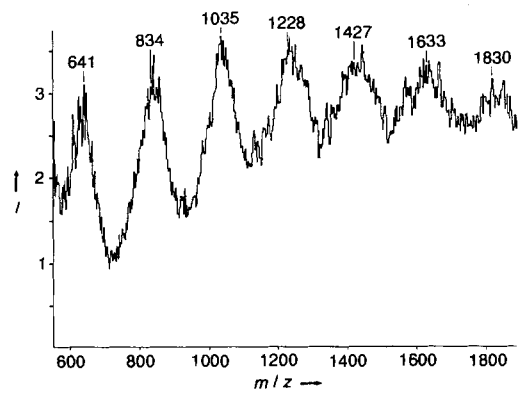

Fig. 2. Fine structure of the MALD mass spectrum in the range 600–1800 Da for birch lignin (section of Fig. 1). The numbers over the peak maxima give the center of gravity of the distribution of the oligolignol signals. I in arbitrary units, M_r in Da.

Figure 2 shows that superimposed on the fine structure of the oligomers (Fig. 1) is a hyperfine structure, which is depicted, expanded, for tetramers in Figure 3. Many tetramers with different molecular weights can be recognized. Two sequences with $\Delta m = 30$ Da (826, 856, 886; and 776, 805, 834, 866) confirm the existence of guaiacyl and syringyl propane building blocks in birch lignin, which differ only by the mass of a methoxy group ($\Delta m = 30$), and indicate that tetramers with four guaiacyl units, three guaiacyl and one syringyl unit, etc. to four syringyl units are present. The center of gravity of the molecular weight distribution of the tetramers lies between m/z 826 (two syringyl and two guaiacyl units) and m/z 856 (three syringyl and one guaiacyl units), which shows that the statistical distribution of the monomers in lignin (syringyl:guaiacyl ≈ 1.4) is already present in the low oligomers. The distribution of the different linkages in lignin identified by chemical degradation[5] also seems to correspond in the low oligomers and in the polymer, as a molecu-

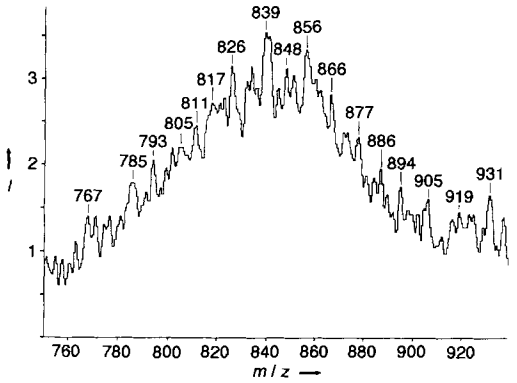

Fig. 3. Hyperfine structure of the MALD mass spectrum in the range for tetramers of birch lignin (section of Fig. 2).

lar mass analysis of the many different tetramers shows. The hyperfine structure of the MALD mass spectrum contains the coded information that enables an increasingly detailed analysis of the complex construction of lignin.

Apart from birch lignin the lignin from a conifer (Chinese redwood, *Metasequoia glyptostroboides*)[17] was studied. The MALD mass spectrum revealed a broad distribution of several hundred to larger than 12000 Da and again directly yielded the number average molecular weight $\bar{M}_n = 2300 \pm 100$. The fine structure of the peaks up to 2000 Da is assigned to oligomers from trimers to decamers (Fig. 4). In contrast to

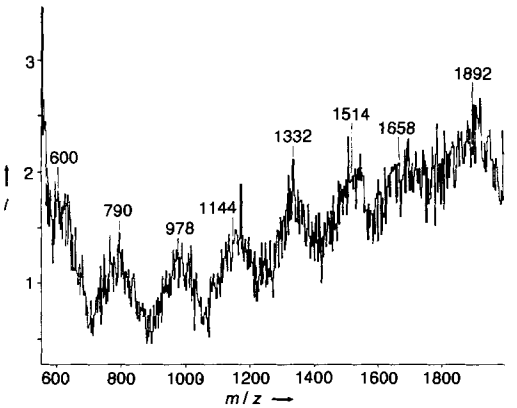

Fig. 4. Fine structure of the MALD spectrum of a conifer lignin (Chinese redwood) from 600 to 2000 Da. Section of the complete spectrum. The numbers above the peak maxima give the center of gravity of the molecular weight distribution for each oligomer range.

birch lignin (Fig. 2), the chemically determined average formula weight of a phenylpropane unit is 190 Da, because conifer lignin consists almost exclusively of guaiacyl propane units. This value is also confirmed by the MALD mass spectrum. As for birch lignin, the hyperfine structure reveals several different oligolignols of the same degree of oligomerization in which the monomers are linked by various binding types.

The results presented here show that MALD mass spectrometry is a fast, sensitive, and extremely powerful micromethod for the characterization of lignins, which yields the molecular weight distribution directly. Up to nonamers (birch lignin) or decamers (conifer lignin) were detected and their average molecular weights determined. In addition, the technique revealed that many different oligomers with the same degree of oligomerization are present in lignin, which reflect the variety and statistical distribution of binding types. It can be expected that the development of MALD mass spectrometry will extend the accessible mass range to lignins of substantially higher molecular weight. An improvement in the spectrometric resolution will enable the fine structure of even the high polymers and the hyperfine structure of the middle range polymers to be analyzed. It remains to be seen whether a subsequent collision-induced fragmentation and application of MS/MS techniques will allow sequencing. Furthermore our results show that mass spectrometry can be used on cross-linked and irregular polymers, which is of significance for many technically important polymers.

Received: November 4, 1991 [Z 5003 IE]
German version: *Angew. Chem.* **1992**, *104*, 777

CAS Registry number:
Milled-woodlignin, 8068-00-6.

[1] *Lignins – Occurrence, Formation, Structure and Reactions* (Eds.: K. V. Sarkanen, C. H. Ludwig), Wiley-Interscience, New York, **1971**.
[2] D. A. I. Goring in *Lignin – Properties and Materials* (Eds.: W. G. Glasser, S. Sarkanen), *ACS Symp. Ser.* **1989**, *397*.
[3] D. Fengel, G. Wegener, *Wood – Chemistry, Ultrastructure, Reactions*, Gruyter, Berlin, New York, **1989**.
[4] K. Freudenberg, A. C. Neish, *Constitution and Biosynthesis of Lignin*, Springer, Berlin, New York, **1968**.
[5] H. Nimz, *Angew. Chem.* **1974**, *86*, 336; *Angew. Chem. Int. Ed. Engl.* **1974**, *13*, 313; G. Krüger, *Chemie Unserer Zeit* **1976**, *10*, 21.
[6] J. O. Metzger, *Fresenius Z. Anal. Chem.* **1979**, *295*, 45, and references cited therein.
[7] A. Benninghoven, *Chem. Phys. Lett.* **1970**, *6*, 616.
[8] M. Barber, R. S. Bordoli, R. D. Sedgwick, A. N. Tyler, *J. Chem. Soc. Chem. Commun.* **1981**, 325.
[9] R. D. Mac Farlane, D. F. Torgersen, *Science* **1976**, *191*, 920.
[10] J. W. Metzger, W. Beck, G. Jung, *Angew. Chem.* **1992**, *104*, 235; *Angew. Chem. Int. Ed. Engl.* **1992**, *31*, 226, and references cited therein.
[11] M. Karas, F. Hillenkamp, *Anal. Chem.* **1988**, *60*, 2299.
[12] M. Karas, U. Bahr, A. Ingendok, F. Hillenkamp, *Angew. Chem.* **1989**, *101*, 805; *Angew. Chem. Int. Ed. Engl.* **1989**, *28*, 760.
[13] B. Stahl, M. Steup, M. Karas, F. Hillenkamp, *Anal. Chem.* **1991**, *63*, 1463.
[14] I. V. Bletsos, D. M. Hercules, D. van Leyen, B. Hagenhoff, E. Niehuis, A. Benninghoven, *Anal. Chem.* **1991**, *63*, 1953.
[15] Elementary analysis: 60.05% C; 5.79% H; 34.16% O; 21.50% MeO; MeO per phenylpropane unit 1.41; average formula mass of one phenylpropane unit 208.8; $\bar{M}_w \approx 9700$; $\bar{M}_n \approx 2600$ [16].
[16] O. Faix, *Das Papier*, **1976** (10A), V1.
[17] Elementary analysis: 62.91% C, 5.88 H, 32.21% O, 15.98 MeO; MeO per phenylpropane unit 0.96; average formula mass of one phenylpropane unit 190.0; $\bar{M}_w \approx 7800$; $\bar{M}_n \approx 2300$ [16].

Transition Metal in a Cube—A Discrete Eight-Coordinate $[Mn^{2+} \subset [2.2.2]$cryptand$]$ as a Body-Centered Cube with an N_2O_6 Donor Set**

By *Karl S. Hagen**

Discrete eight-coordinate complexes of the actinides, lanthanides, and early transition metals are fairly common. However, only two high-symmetry, idealized, polyhedrons are generally observed; the dodecahedron (DD, D_{2d} point group) and the square antiprism (SAP, D_{4d}).[1-3] Various calculations based on interligand repulsion[3,4] or Hückel methods[5] obtain higher energy surfaces for other geometries, such as the hexagonal bipyramid (HB, D_{6h}), bicapped trigonal antiprism (BTAP, D_{3d}), end-bicapped trig-

[*] Prof. K. S Hagen,
Department of Chemistry, Emory University
1515 Pierce Drive, Atlanta, GA 30322 (USA)

[**] This research was supported in part by the University Research Committee of Emory University.

onal prism (ETP, D_{3h}), bicapped trigonal prism (BTP, C_{2v}) square prism (SP, D_{4h}), and the cube (C, O_h) (Scheme 1). The rare eight-coordinate complexes of the middle to late transition elements are generally coordinated by bidentate ligands with a small bite such as NO_3^- (51.8–53.7°).[6] However, sandwich complexes with tetradentate crown ethers are known for Mn^{II}[7] and Fe^{II},[8] as well as Ag^{I},[9] and we have recently utilized tetraaza macrocyclic ligands to prepare analogous SAP sandwich complexes of the small divalent first row transition metals, Fe^{II} and Mn^{II}.[10]

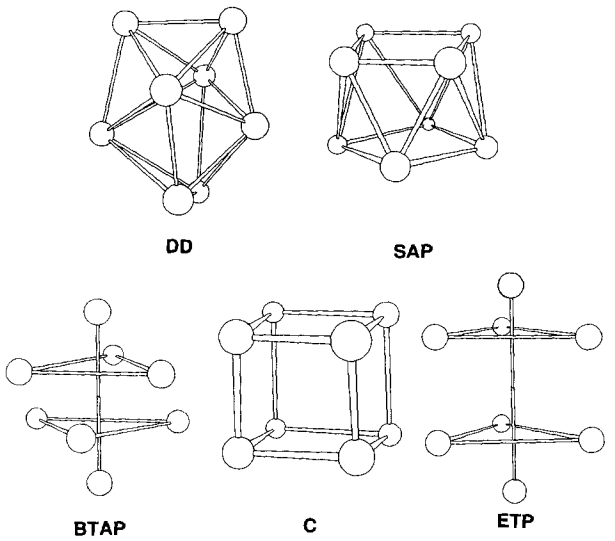

Scheme 1.

Since macrobicyclic ligands have been used to impart unusual kinetic, thermodynamic, or stereochemical properties to six-coordinate metal complexes,[11] one might expect uncommon eight-coordinate structures with ligands such as Lehn's macrobicyclic, diazapolyoxa cryptand ligands.[12] Such is the case for the [2.2.2]cryptates[13] of the large cations Cs^+[14] and K^+,[15] which exhibit a small trigonal distortion from the rare ETP geometry. The Na^+ [2.2.2]cryptates[15] have a trigonal twist closer to BTAP geometry. One might expect a further twist to BTAP or C geometries with smaller spherical cations such as high-spin d^5 Mn^{2+}. No transition-metal [2.2.2]cryptates have yet been isolated, although studies indicate weak binding in protic solution,[17] but this should not preclude their isolation from aprotic media.

Indeed, we have isolated the $CF_3SO_3^-$ salt of [$Mn^{2+} \subset$ [2.2.2]cryptand] (**1**), the first discrete eight-coordinate complex of a transition metal having idealized cubic symmetry, and the first transition-metal complex with this ligand. Although numerous structural studies of cryptates of alkali metals, alkaline earth metals, and of some lanthanides are available,[18] only two structures of transition-metal cryptates have been reported. These are the seven-coordinate Co^{II}[19] and six-coordinate Ni^{II}[20] cryptates with the smaller [2.2.1]cryptand.[13]

The complex **1** (Fig. 1) consists of the Mn^{II} ion encapsulated within the cryptand and located at a crystallographic D_3 site, well separated from the $CF_3SO_3^-$ anions. The triad passes through the Mn atom and the two nitrogen atoms and the three diads pass through the Mn center and bisect each C3–C3′ bond. Eightfold coordination for Mn in **1** (with crystallographically imposed BTAP symmetry) is established by the six O atoms (equivalent by symmetry) and the two symmetry-related N atoms. As emphasized in Figure 2, these atoms are disposed at the eight vertices of the cube about the Mn atom, which gives the Mn^{II} cryptate idealized cubic geometry (O_h point group). Deviations of the MnN_2O_6 atoms from the best fit to a perfect body-centered cube with edge length 2.777 Å (Fig. 2) are only 0.007 Å for N and 0.073 Å for O.

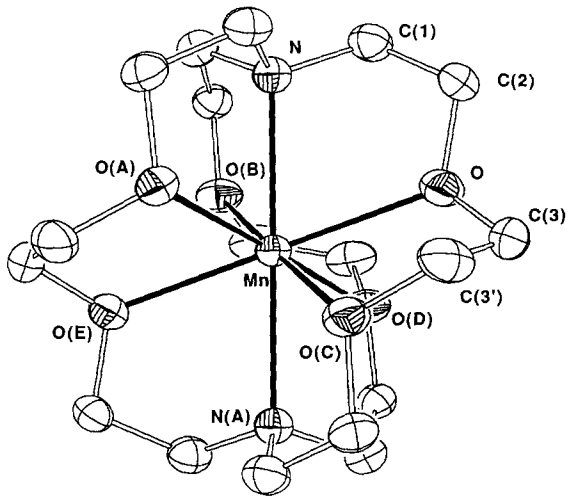

Fig. 1. ORTEP structure of **1** showing the 50% probability thermal ellipsoids and atomic labeling scheme. Selected interatomic distances [Å] and angles [°] are as follows: Mn-N 2.406(4), Mn-O 2.393(2), N···N(A) 4.81, O···O(E) 4.79; N-Mn-O 69.4(1), N-Mn-O(C) 110.6(1), O-Mn-O(A) 108.3(1), O-Mn-O(C) 69.4(1), O-Mn-O(D) 74.0(1), O-Mn-O(E) 177.3(1), N(1)-Mn-N(1′) 111.4(2), N(1)-Mn-N(3) 144.2(2).

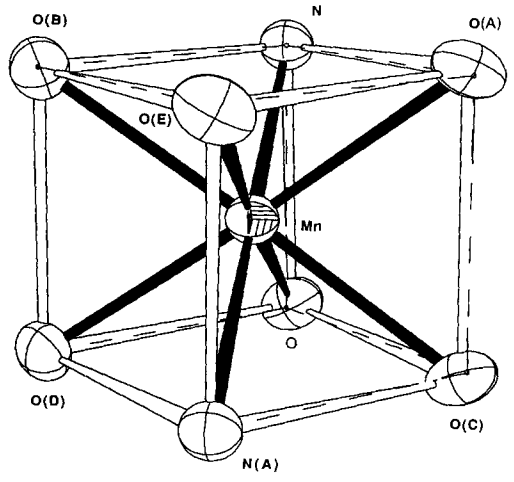

Fig. 2. Structure of **1** showing the body-centered cubic arrangement of oxygen and nitrogen donor atoms about Mn^{2+} as a best fit to a perfect cube having edge length 2.777 Å (dashed lines). Angles [°] and lengths [Å] for the cube: all O-N-O(A) 90.5, N-O-O(C) 92.6, N-O-O-(D) 89.3, O(C)-O-O(D) 87.6; N···O 2.733, O···O(C) 2.724, O···O(D) 2.881 Å.

The edge lengths of the cube are N···O 2.733 Å, O···O 2.724 Å for donor atoms which make up five-membered rings (with the Mn and two CH_2 units), and O···O 2.881 Å between O donor atoms of separate sectors of the cryptand. The L-Mn-L bite angles within five-membered rings are 69.4(1)°, but 74.0(1)° when the two O atoms are not part of the same ring. The mean deviation from the ideal of any one of the four atoms which define a face of the cube is 0.017 Å, and the distance of the Mn ion to each of the six faces is 1.383 Å. The Mn–O bond lengths (2.393(2) Å) are identical by symmetry and within experimental error the same as the

Mn–N bond lengths (2.406(4) Å). As expected with a higher coordination number, Mn to ligand bonds are considerable longer than those of six-coordinate Mn^{II} complexes, but are similar to those found in the square-antiprismatic complex, $[Mn(cyclen)_2]^{2+}$ (2.384–2.435 Å)[10] (cyclen = 1,4,7,10-tetraazacyclododecane). The only other examples of discrete cubic complexes are $[La(bpyO_2)_4]^{3+}$[21] ($bpyO_2$ = 2,2′-bipyridine-*N*,*N*′-dioxide) and $(Et_4N)_4[U(NCS)_8]$.[22]

The great flexibility of the [2.2.2]cryptand is manifested in the cube's N ··· N diagonal distance of 4.462 Å, which is the smallest yet observed for [2.2.2]cryptates[18] and is considerably less than the 6.1 Å for [$Cs^+ \subset$ [2.2.2]cryptand],[14] and 6.872 Å in the empty cryptand.[23] The metal has induced a twisting of the ligand about the triad resulting in an oblique (*ob*) arrangement of the C3–C3′ groups compared to the parallel (*lel*) configuration of the cryptand and cryptates of larger cations. This creates a chiral dication which is isolated as a racemic mixture in a centrosymmetric space group. The large change in ligand conformation compared to the uncomplexed cryptand and lack of crystal field stabilization energy for a high-spin d^5 Mn^{II} ion[24] suggests that there is little kinetic stability to this complex. Yet the complex is stable in anhydrous acetonitrile where its solution EPR spectrum is distinct from that of $Mn(CF_3SO_3)_2$.[24b] A pure powder of **1** exhibits a broad signal at $g = 2.03$, although powder and orientated single-crystal samples of **1** in a diamagnetic matrix (1% in [Cd ⊂ [2.2.2]cryptand] $(CF_3SO_3)_2$)[25] exhibit well-resolved multiline axial spectra with a small zero-field splitting, $D = 220$ gauss (Fig. 3).

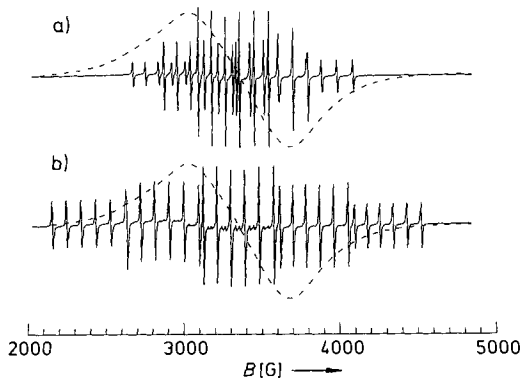

Fig. 3. EPR spectra (X-band) of **1** in a [Cd ⊂ [2.2.2]cryptand]$(CF_3SO_3)_2$ matrix (1%) at 21 °C. The spectrum of a single crystal with the field a) perpendicular to the unique axis and b) parallel to it. The dashed lines represent the signal of an undiluted, powdered sample of **1**.

Experimental Procedure

The triflate salt of **1** is isolated as colorless, analytically pure,[26] crystallographic quality,[27] hexagonal plates in 80% yield, by diffusing diethyl ether into an anhydrous acetonitrile solution of an equimolar mixture of $Mn(CF_3SO_3)_2 \cdot 2CH_3CN$ and the ligand under a dry, dinitrogen atmosphere.

Received: October 1, 1991
Revised version: March 12, 1992 [Z 4944 IE]
German version: *Angew. Chem.* **1992**, *104*, 804

CAS Registry numbers:
1 $(CF_3SO_3)_2$, 141319-70-2; [Cd ⊂ [2.2.2]cryptand]$(CF_3SO_3)_2$, 141394-64-1.

[1] S. J. Lippard, *Prog. Inorg. Chem.* **1967**, *8*, 109–193.
[2] M. G. B. Drew, *Coord. Chem. Rev.* **1977**, *24*, 179–275.
[3] D. L. Keppert, *Prog. Inorg. Chem.* **1978**, *24*, 179–249.
[4] I. G. Shterev, G. S. Nikolov, N. Trendafilova, R. Kirov, *Polyhedron* **1991**, *10*, 393–402.
[5] J. K. Burdett, R. Hoffmann, R. C. Fay, *Inorg. Chem.* **1978**, *17*, 2553–2568.
[6] C. Bellitto, L. Gastaldi, A. A. G. Tomlinson, *J. Chem. Soc. Dalton Trans.* **1976**, 989; J. G. Bergman, F. A. Cotton, *Inorg. Chem.* **1966**, *5*, 1208.
[7] B. B. Hughes, R. C. Haltiwanger, C. G. Pierpont, M. Hampton, G. L. Blackmer, *Inorg. Chem.* **1980**, *19*, 1801–1803.
[8] K. Meier, G. Rihs, *Angew. Chem.* **1985**, *97*, 879–880; *Angew. Chem. Int. Ed. Engl.* **1985**, *24*, 858–859.
[9] P. G. Jones, T. Gries, H. Grützmacher, H. W. Roesky, J. Schimkowiak, G. M. Sheldrick, *Angew. Chem.* **1984**, *96*, 357–358; *Angew. Chem. Int. Ed. Engl.* **1984**, *23*, 376.
[10] M. Sakuta, K. S. Hagen, unpublished.
[11] a) J. E. Parks, B. E. Wagner, R. H. Holm, *J. Am. Chem. Soc.* **1970**, *92*, 3500–3502; b) E. Larsen, G. N. La Mar, B. E. Wagner, J. E. Parks, R. H. Holm, *Inorg. Chem.* **1972**, *11*, 2652–2668; c) A. M. Sargeson, *Chem. Br.* **1979**, *15*, 23–27; d) A. M. Sargeson, *Pure Appl. Chem.* **1984**, *56*, 1603–1619; e) P. Comba, A. M. Sargeson, L. M. Engelhardt, J. M. Harrowfield, A. H. White, E. Horn, M. R. Snow, *Inorg. Chem.* **1985**, *24*, 2325–2327; f) T. J. McMurray, M. W. Hosseini, T. M. Garrett, F. E. Hahn, Z. E. Reyes, K. N. Raymond, *J. Am. Chem. Soc.* **1987**, *109*, 7196–7198.
[12] J.-M. Lehn, *Acc. Chem. Res.* **1978**, *11*, 49–57; J.-M. Lehn, *Science* **1985**, *227*, 849–856.
[13] Abbreviations used: [2.2.2]cryptand: 4,7,13,16,21,24-hexaoxa-1,10-diazabicyclo[8.8.8]hexaxosane; [2.2.1]cryptand: 4,7,13,16,21-pentaaoxa-1,10-diazabicyclo[8.8.5]tricosane; cyclen: 1,4,7,10-tetraazacyclododecane. An inclusion complex is represented by the symbol ⊂.
[14] a) D. Moras, B. Metz, R. Weiss, *Acta Crystallogr. Sect. B* **1973**, *29*, 388–396; b) R. H. Huang, D. L. Ward, M. E. Kuchenmeister, J. L. Dye, *J. Am. Chem. Soc.* **1987**, *109*, 5561.
[15] D. Moras, B. Metz, R. Weiss, *Acta Crystallogr. Sect. B* **1973**, *29*, 383–388.
[16] D. Moras, R. Weiss, *Acta Crystallogr. Sect. B* **1973**, *29*, 396–403.
[17] a) F. Arnaud-Neu, B. Spiess, M.-J. Schwing-Weill, *Helv. Chim. Acta* **1977**, *60*, 2633–2643; b) G. Anderegg, *ibid.* **1981**, *64*, 1790–1795.
[18] R. Hilgenfeld, W. Saenger in *Host Guest Complex Chemistry/Macrocycles* (Eds.: F. Vögtle, E. Weber): Springer, Berlin, **1985**, p. 43–124.
[19] F. Mathieu, R. Weiss, *J. Chem. Soc. Chem. Commun.* **1973**, 816.
[20] S. B. Larso, J. N. Ramsden, S. H. Simonsen, J. J. Lagowski, *Acta Crystallogr. Sect. C* **1983**, *39*, 1646–1648.
[21] A. R. Al-Karaghouli, R. O. Day, J. S. Wood, *Inorg. Chem.* **1978**, *17*, 3702–3706.
[22] R. Countryman, W. S. McDonald, *J. Inorg. Nucl. Chem.* **1971**, *33*, 2212.
[23] B. Metz, D. Moras, R. Weiss, *J. Chem. Soc. Perkin II* **1976**, 423–429.
[24] a) The magnetic moment at room temperature is 5.7 μ_B in the solid state and in CD_3CN solution. b) EPR in CH_3CN (21 °C), **1**-$(CF_3SO_3)_2$: $g = 2.03$, $A_{iso} = 91$ G, $Mn(CF_3SO_3)_2$: $g = 2.02$, $A_{iso} = 93$ G.
[25] K. S. Hagen, unpublished. X-ray analysis: [Cd ⊂ [2.2.2]cryptand]-$(CF_3SO_3)_2$ crystallizes in the trigonal space group $P321$, $a = 8.968(3)$ Å, $c = 10.677(7)$ Å, $V = 743.7(6)$ Å^3, $Z = 1$. The host complex shows a more marked trigonal distortion from cubic symmetry than does **1** (Cd-N 2.389 Å, Cd-O 2.498(3) Å).
[26] Correct C,H,N,S analyses for **1**-$(CF_3SO_3)_2$. The salt does not melt below 330 °C.
[27] X-ray analysis: **1**-$(CF_3SO_3)_2$ crystallizes in the trigonal space group $P\bar{3}c1$, $a = 8.905(3)$ Å, $c = 21.140(8)$ Å, $V = 1449.6(9)$ Å^3, $\varrho_{calcd} = 1.671$ g cm^{-3}, $Z = 2$. 702 reflections, $T = 225$ K, $Mo_{K\alpha}$ radiation ($\lambda = 0.71073$ Å), $2\theta = 60°$, single-crystal X-ray diffractometer; structure solution by Patterson interpretation and expansion (SHELXS-86) and difference Fourier methods. $R = 0.0398$, $R_w = 0.056$. Further details of the crystal structure investigation are available on request from the Director of the Cambridge Crystallographic Data Centre, University Chemical Laboratory, Lensfield Road, GB-Cambridge CB21EW (UK), on quoting the full journal citation.

Titration of C_{60}: A Method for the Synthesis of Organofullerenes**

By *Andreas Hirsch,** *Antonio Soi,* and *Heinrich R. Karfunkel*

The synthesis of well-defined organofullerenes is still very challenging. There are only few reports on the preparation of isomerically pure single compounds.[1–4] The possible organic reactions of C_{60} are: 1) the addition of nucleophiles,[5, 6] 2) the addition of dienes and 1,3-dipoles,[3, 6] and

[*] Dr. A. Hirsch, A. Soi
Institut für Organische Chemie der Universität
Auf der Morgenstelle 18, D-W-7400 Tübingen (FRG)
Dr. H. R. Karfunkel
Ciba Geigy AG, Basel (Switzerland)

[**] This work was supported by the Deutsche Forschungsgemeinschaft.

3) the addition of radicals.[7] Because C_{60} is a polyfunctional molecule, a myriad of products is formed after treatment with an excess of a reagent, for example a nucleophile.[6] It is impossible to isolate isomerically pure single compounds from such reaction mixtures.

To control nucleophilic additions to only one double bond in C_{60} and to maximize the yield of the monoadducts, we titrated dilute solutions of C_{60} in toluene with *tert*-butyllithium and ethylmagnesium bromide. The concentrations of C_{60}, the monoaddition product, and higher addition products upon addition of the nucleophile was determined quantitatively by high-pressure liquid chromatography (HPLC). For this purpose the initially formed fullerides were protonated with methanolic HCl to give $C_{60}HtBu$ **1** and $C_{60}HEt$ **2** (Scheme 1). In this way the formation of products and the

$$C_{60} + t\text{BuLi} \longrightarrow C_{60}t\text{BuLi} \xrightarrow{H^+} \underset{\mathbf{1}}{C_{60}HtBu}$$

$$C_{60} + \text{EtMgBr} \longrightarrow C_{60}\text{EtMgBr} \xrightarrow{H^+} \underset{\mathbf{2}}{C_{60}HEt}$$

Scheme 1. Synthesis of the organofullerenes **1** and **2**.

consumption of C_{60} could be followed very closely from the calculated peak areas (Fig. 1). The UV/VIS spectrum of each peak was simultaneously recorded by means of diode array scans (200–500 nm) allowing the unambiguous assignment of the HPLC peaks to the compounds based on their optical spectra. Because other anionic nucleophiles like amides, hydrides, alkoxides, and thiolates react similarly with C_{60},[6] this synthetic method should allow access to a large variety of monofunctionalized fullerenes as isomerically pure single compounds.

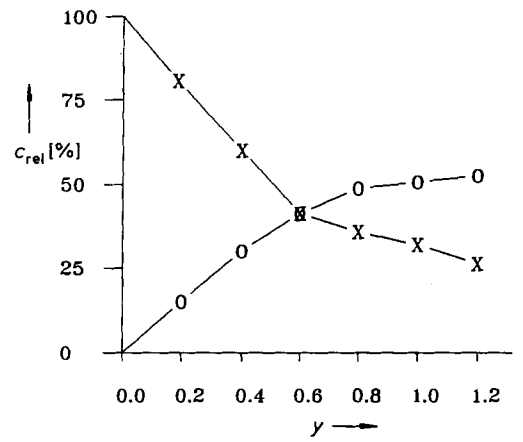

Fig. 1. Results of the titration of the reaction of C_{60} with *tert*-butyllithium. X = amount of C_{60} in % relative to the starting concentration c_A ($c_A = 1.66 \times 10^{-5}$ mol L^{-1}), o = concentration of **1** relative to that of C_{60}; y = equivalents of *t*BuLi. For details see *Experimental Procedure*.

The maximum yield of **1** was about 50%. If the concentration of remaining C_{60} becomes too low, side reactions like $C_{60}t\text{BuLi} + t\text{BuLi} \rightarrow C_{60}t\text{Bu}_2\text{Li}_2$, though heterogeneous, become increasingly important (Fig. 2). In a control experiment an overtitration was carried out: After the addition of about 1.2 equivalents of *t*BuLi the concentration of **1** decreased again, and the concentration of higher addition products increased markedly. The titration with the less reactive ethylmagnesium bromide provided **2** in a maximum yield of about 80%. In this case the formation of higher addition products takes place to a much smaller extent. The chromatograms in Figure 2 show the appearance of five smaller peaks at higher retention times attributed to higher addition products (bis- to hexaadducts). Whereas the UV/

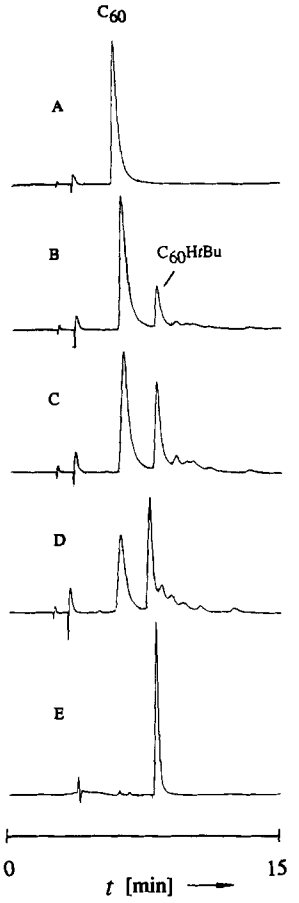

Fig. 2. HPLC control of the reaction of C_{60} with *t*BuLi (also see *Experimental Procedure*). C_{60} before the addition of *t*BuLi (A) as well as after the addition of 0.4 equiv (B), 0.8 equiv (C), and 1.2 equiv *t*BuLi (D). The chromatogram of purified **1** is shown in E. Experimental conditions: Beckman silica gel column (25 × 0.4 cm); particle size 5 μm; eluent *n*-hexane; pressure 4700 kPa; flow rate 0.8 mL min^{-1}; detection at 340 nm.

VIS features of **1** and **2** are very similar to those of C_{60}, the spectra of the higher homologues (diode array scans) are more and more structureless, resulting in a broad tailing from 200 nm into the visible region. Almost the same behavior was observed in the fulleroid series $C_{61}Ph_2$–$C_{66}Ph_{12}$.[3]

Compounds **1** and **2** were purified by preparative reverse-phase HPLC.[8] Here, the higher addition products eluted first and were collected together. The mass spectrum of the mixture of *tert*-butyl adducts shows the peaks of the bis-, tris-, and tetraadducts (*m/z* 836, 894, and 952, respectively).[9] Compounds **1** and **2** were characterized by mass spectrometry, and UV/VIS and ^1H NMR spectroscopy (Table 1). The ^1H NMR spectra exhibit only one signal for the fullerene protons at low field and only one type of ethyl or *tert*-butyl group. Thus only one isomer of either **1** or **2** were formed, namely the product formed by the addition to a six-ring/six-ring double bond (a 6–6 bond). The presence of low-field signals gives evidence of the strong electron-withdrawing influence of the fullerene core. ^1H NMR spectra of mixtures of the higher addition products show two characteristic trends: 1) As the number of substituents increases, the electron-withdrawing influence of the fullerene core decreases (smaller downfield shifts) and 2) higher addition products consist of different regioisomers which produce many signals, finally leading to very broad NMR signals.[6, 10]

Table 1. Selected physical data for the monoadducts **1** and **2**.

1: $M = 778.78$; MS(FAB): m/z 779 (M^+, 15%), 720 ($M^+ - C_4H_9 - H$, 100%); UV/VIS(*n*-hexane): λ_{max}[nm] = 213, 248 (sh), 257, 308 (sh), 326, 408 (sh), 435, 464, 484, 640; IR(KBr): $\tilde{\nu}$[cm^{-1}] = 2959 (s), 2922 (s), 2866 (w), 1462 (s), 1427 (m), 1396 (w), 1369 (s), 1188 (m), 1094 (m), 902 (m), 763 (w), 730 (s), 582 (w), 572 (w), 567 (w), 553 (w), 542 (w), 526 (s) und 513 (w); ^{1}H NMR(400 MHz, CS_2/$CDCl_3$, 25 °C): δ = 6.67 (s, 1H; CH), 2.09 (s, 9H; CH_3). Analysis calculated for $C_{64}H_{10}$: C 98.71, H 1.29%; found C 98.82, H 0.97%.

2: $M = 750.73$; MS(FAB): m/z 750 (M^+, 20%), 748 ($M^+ - 2H$, 25%), 721 ($M^+ - C_2H_5$, 100%); UV/VIS(*n*-hexane): λ_{max}[nm] = 214, 248 (sh), 258, 308 (sh), 326, 408 (sh), 436, 465, 484, 640; IR(KBr): $\tilde{\nu}$[cm^{-1}]: 2959 (m), 2922 (s), 2866 (m), 1452 (s), 1427 (m), 1380 (m), 1261 (m), 1184 (m), 1101 (w), 580 (w), 572 (w), 563 (w), 553 (w), 542 (w), 526 (s), 523 (w); ^{1}H NMR(250 MHz, CS_2/$CDCl_3$, 25 °C): δ = 6.45 (s, 1H; CH), 3.52 (q, ^3J(H,H) = 7.4 Hz, 2H; CH_2), 2.09 (t, ^3J(H,H) = 7.4 Hz, 3H; CH_3).

The experimental findings for **1** and **2** are confirmed by the results of AM1 calculations (MOPAC 6.0)[11]. Calculations were performed on $C_{60}H_2$, $C_{60}HCH_3$, and $C_{60}HtBu$ as 5–6 as well as 6–6 adducts. The 6–6 adducts were shown to be considerably more stable (Table 2); their heats of formation are about 20 kcal mol^{-1} lower than those of the 5–6 adducts. The carbons atoms with the substituents are sp^3-hybridized. The calculated bond length between these carbon atoms is about 1.57 Å and the bond order 0.93. The fullerene protons are deshielded (Mulliken charge in **1** is +0.16), which is in agreement with the downfield shift of the ^{1}H NMR signal (δ = 6.67). Calculations on the intermediate $C_{60}tBu^-$ show that the negative charge is not delocalized (Fig. 3).[12] The highest electron density is found on the C atom next to the sp^3 carbon atom across the 6–6 bond.

Table 2. Calculated energies (AM1 heats of formation) [kcal mol^{-1}] of $C_{60}HtBu$, $C_{60}HCH_3$, and $C_{60}H_2$ as 5–6 and 6–6 adducts.

	$C_{60}HtBu$	$C_{60}HCH_3$	$C_{60}H_2$
5–6	940.2	947.7	950.0
6–6	922.1	929.2	931.2

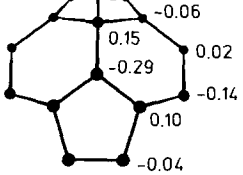

Fig. 3. Electron densities (Mulliken charges) of the affected pyracylene unit of the intermediate $C_{60}tBu^-$ obtained from AM1 calculations.

The titration method described allows the quantitative control of nucleophilic additions to C_{60} necessary for the synthesis and separation of specific addition products in reasonable yields. The attack of one 6–6 bond leads to the formation of single isomers. This method allows access to the organofullerenes C_s-$C_{60}RR'$ and D_{2d}-$C_{60}R_2$ in which R and R′ can be C, H, N, P, O, or S substituents.

Experimental Procedure

For a typical experiment, 30 mg of C_{60} was dissolved in 50 mL of toluene. From this solution 200 µL was used to prepare a dilution series in *n*-hexane (1.66, 0.83, 0.42, and 0.17 [10^{-5} mol L^{-1}] in 10 mL) for HPLC calibration. This allows the subsequent determination of all concentrations of C_{60} and the monoadduct within this range. The nucleophile *tert*-butyllithium (1.7 M in pentane) or ethylmagnesium bromide (0.4 M in THF) was added in portions of 0.2 equivalents relative to C_{60}. To minimize the formation of higher addition products care was taken (rapid stirring and slow addition) to avoid high local concentrations of the nucleophiles in the reaction mixture. A dark precipitate of the lithium or magnesium fullerides formed immediately, which was suspended homogeneously with stirring. After each addition of the nucleophile, 200 µL of the suspension was removed, quenched with 200 µL of 0.01 M HCl, and diluted with *n*-hexane to 10 mL for quantitative HPLC analysis. For the comparison of the concentrations of C_{60} to those of **1** or **2**, the extinction coefficients at the HPLC detection wavelength (340 nm) were determined. After the titration was over, the reaction mixture was quenched with 4 mL of 0.01 M HCl in methanol causing all of the precipitate to dissolve immediately. After evaporation of the solvent **1** and **2** were isolated by preparative HPLC.

Received: March 27, 1992 [Z 5265 IE]
German version: *Angew. Chem.* **1992**, *104*, 808

[1] J. M. Hawkins, T. A. Lewis, S. D. Loren, A. Meyer, J. R. Heath, Y. Shibato, R. J. Saykally, *J. Org. Chem.* **1990**, *55*, 6250.
[2] Y. Elemes, S. K. Silverman, C. Sheu, M. Kao, C. S. Foote, M. M. Alvarez, R. L. Whetten, *Angew. Chem.* **1992**, *104*, 364; *Angew. Chem. Int. Ed. Engl.* **1992**, *31*, 351.
[3] T. Suzuki, Q. Li, K. Khemani, F. Wudl, Ö. Almarson, *Science* **1991**, *254*, 1186.
[4] P. J. Fagan, J. C. Calabrese, B. Malone, *Science* **1991**, *252*, 1160.
[5] A. Hirsch, Q. Li, F. Wudl, *Angew. Chem.* **1991**, *103*, 1339; *Angew. Chem. Int. Ed. Engl.* **1991**, *30*, 1309.
[6] F. Wudl, A. Hirsch, K. Khemani, T. Suzuki, P.-M. Allemand, A. Koch, H. Eckert, G. Srdanov, H. Webb in *Fullerenes* (Eds.: G. S. Hammond, V. J. Kuck) (*ACS Symp. Ser.* **1992**, *481*, 161).
[7] P. J. Krusic, E. Wasserman, P. N. Keizer, J. R. Morton, K. F. Preston, *Science* **1991**, *254*, 1183.
[8] Beckman reversed-phase column C18, ultrasphere ODS with the dimensions 25 × 1 cm, particle size 5 µm; eluent chloroform–acetonitrile 60:40, pressure 7600 kPa, flow rate 3.2 mL min^{-1}; detection at 340 nm and with several diode array scans.
[9] The reason that masses of $C_{60}H_3tBu_3$ and $C_{60}H_6tBu_6$ are not seen either in the FAB or the FD mass spectra is because of their low concentration as well as the tendency of the *tert*-butyl groups to fragment. The peak m/z 720 is the strongest signal, although there is no C_{60} detectable by HPLC.
[10] G. A. Olah, I. Busci, C. Lambert, R. Aniszfeld, N. J. Trivedi, D. K. Sensharma, G. K. S. Prakash, *J. Am. Chem. Soc.* **1991**, *113*, 9287.
[11] J. J. P. Stewart, Programm QCPE-445, MOPAC 6.0 **1990**; M. J. S. Dewar, E. G. Zoebisch, E. F. Healy, J. J. P. Stewart, *J. Am. Chem. Soc.* **1985**, *107*, 3902.
[12] The AM1 calculations of the anions $C_{60}CH_3^-$ and $C_{60}H^-$ gave almost the same results.

A New Reaction Type in the Conversion of Enamines with 1,4-Diphenyl-2-butene-1,4-dione to Give Cage Compounds**

By *Gerd Kaupp,* Uwe Pogodda, Adnan Atfah,* Herbert Meier,** and *Anita Vierengel*

Complex addition, elimination, and substitution reactions in organic chemistry can be classified systematically if not more than four bonds are formed and broken, and when up to two rearrangements are involved.[1] For more complicated cases, at most only individual steps can be interpreted; such

[*] Prof. Dr. G. Kaupp, Dipl.-Chem. U. Pogodda
FB 9 – Organische Chemie I der Universität
Postfach 25 03, D-W-2900 Oldenburg (FRG)
Dr. A. Atfah
Department of Chemistry, Yarmouk University
Irbid (Jordan)
Prof. Dr. H. Meier, A. Vierengel
Institut für Organische Chemie der Universität
Postfach 39 80, D-W-6500 Mainz (FRG)

[**] This work was supported by the Deutsche Akademische Austauschdienst (Stipend for A. A.) and the Fonds der Chemischen Industrie.

considerations must, of course, be mechanistically plausible. We report here on fertile preparative reactions of 1,4-diphenyl-2-butene-1,4-dione ("dibenzoylethylene") with enamines in which six bonds are formed or broken and which also involve a rearrangement. The cage compounds **3** are formed selectively from **1** and **2**.

The reaction of **1a–1d** with **2** gives useful yields in spite of its complexity. The reaction can be interpreted most simply as the result of an ene addition followed by a [2+2+2] cycloaddition of two carbonyl groups to the enamine double bond (tandem reaction). In the conversion **1a** → **3a** it was possible to identify the intermediate **Za**: workup by column chromatography gave the hydrolysis product of the intermediate enamine, 2-(1,2-dibenzoylethyl)cyclopentan-1-one. Elucidation of the structure of the products **3a–d** and their differentiation from the possible alternatives **4** was achieved with the usual spectral data. Definitive proof was provided by ^{1}H,^{1}H(COSY)-, and ^{1}H,^{13}C-correlated 2D NMR spectra together with NOE difference spectra. The vicinal couplings 11-H/10-H,H′/9-H,H′/8-H/7-H/6-H,H′ were demonstrated unequivocally in the COSY 45 recording. This coupling route is, however, in agreement with both structures **3a** and **4a**. Differentiation was made possible by NOE difference spectra: the spatial proximity of the three CH_2 groups is only given in **3a**. Accordingly, positive nuclear Overhauser effects could be measured for the interactions 9-H′/6-H and 10-H′/6-H together with an INDOR effect for the coupled protons 9-H′ and 10-H′.

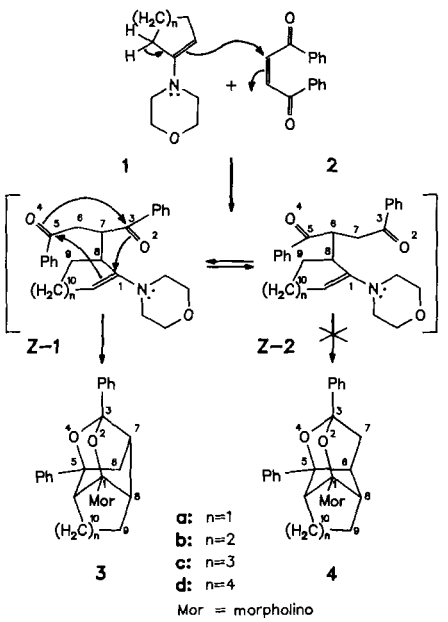

The heteropolycycle in **3a–d** was hitherto unknown. Moreover, the type of reaction is unusual, and its thermal realization has been observed here for the first time. Previously, only two distantly related photochemical examples of the second of the formulated reaction steps were known, i.e. the [2+2+2] cycloaddition of a 1,4-diketone to an alkene.[2]

The usefulness of this type of reaction is increased considerably by the observed regiospecificity. This specificity can be understood on the basis of semiempirical PM3 calculations:[3] the enthalpy of formation of **3a** (−185.07 kJ mol^{-1}) is 3.5 kJ mol^{-1} more negative than that of **4a** (−181.59 kJ mol^{-1}). Moreover, compound **3a** is both thermodynamically and kinetically favored. As added confirmation, therefore, the reactive conformers **Z-1** and **Z-2** were sought as energy minima, with the least possible distance between the reactive centers, and completely optimized. According to these calculations **Z-1** is 25.6 kJ mol^{-1} more stable than **Z-2**. This result is a satisfactory argument for the regioselectivity (formation of **3** but not of **4**), as the distances relevant for reaction of these completely geometrically optimized conformers are comparable (Table 1): for energetic reasons **Z-2** is not involved.

The most obvious mechanistic explanation for the reaction of **Z-1** can be assumed as follows: The C5–C11 bond is formed first, leading to a relatively stable zwitterion (enamine + ketone), followed by formation of the bonds C3–O4 and C1–O2. The difference in charge density (Table 1) between the centers C5 and C11 is considerable (larger in **Z-1a** than **Z-2a**). The difference in charge density between C3 and O4 in the zwitterion is larger than in the educt; the same is also true for the centers C1 and O2, as the C3–O4 bond is formed.

Table 1. Relevant distances (from PM3 calculations) d and total charge density differences ΔQ for **Z-1a**, **Z-2a**, **3a**, and **4a**.

Compound	d [Å] (ΔQ) C5–C11 [a]	C3–O4	C1–O2	Σd [Å]
Z-1a	3.731 (0.567)	3.060 (0.607)	3.476 (0.177)	10.267
3a	1.438	1.433	1.577	
Z-2a	3.409 (0.545)	2.970 (0.625)	4.001 (0.187)	10.380
4a	1.438	1.435	1.564	

[a] Numbering as in structure **3a** and analogously in **4a**.

The selectivity of the reaction of **2** with **1a–d** is surprising, because other unsaturated 1,4-diketones, such as 1,4-diphenyl-2-butyne-1,4-dione ("dibenzoylacetylene") (**5**), react with **1** in a known fashion by [2+2] cycloaddition to give the bicyclic cyclobutenes **6**, which—with the exception of **6a**—undergo immediate isomerization to the monocyclic 1,3-dienes **7**[4].

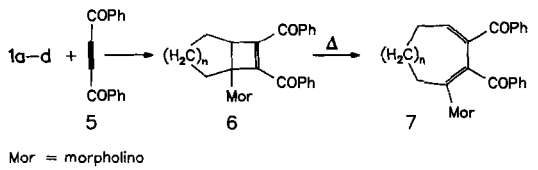

Of critical importance for this new type of reaction is the high preference of compound **2** to undergo ene addition, which presumably proceeds by way of an iminium/enolate zwitterion and which is completed by a protonation/deprotonation step. This allows the fertile synthesis, in a single step, of new oxygenated heteropolycycles with stable acetal- and N,O-acetal groups.[5] Easily available derivatives of **2** or **1** should permit access to a variety of new spherical oxygenated heterocycles; at the same time the regioselectivity is of particular interest because the products could be biologically active on account of the acetal function.[6]

Experimental Procedures

To a solution of **2** (470 mg, 2.0 mmol) in 10 mL of hot methanol was added 2.4 mmol of enamine **1a–d** and the resulting mixture allowed to stand at room temperature for 2–3 d. The product crystallized out and was recrystallized from methanol. **3a**: Yield 30%, m.p. 133–135 °C; **3b**: 22%, m.p. 196–198 °C; **3c**: 84%, m.p. 202–204 °C; **3d**: 80%, m.p. 153–155 °C. The mother liquor still contains some **3**, but no **4** could be detected by ^{1}H NMR spectroscopy. 2-(1,2-

Dibenzoylethyl)cyclopentan-1-one was isolated from the first mother liquor of **3a** by column chromatography on SiO_2 using CH_2Cl_2 as eluent [16% in the crude product from **3a**; ^1H NMR: ^3J(2-H, 1-H') = 4.0 Hz, ^3J(1-H',2-H') = 8.6 and 4.8 Hz; ^{13}C NMR (100 MHz, $CDCl_3$): δ = 218.7, 201.1, 197.7, 136.5, 135.9, 133.2, 133.1, 128.8 (2C), 128.5 (4C), 128.1 (2C), 49.7 (d), 41.0 (d), 38.3, 36.9, 26.1, 20.6; MS (70 eV): *m/z* 320 ($M^{\oplus}$, 1.5%), 215(2), 105(100). **3a**: ^1H NMR (400 MHz, $CDCl_3$): δ = 2.75 [7-H, dd, ^3J(7-H, 6-H') = 5.6 Hz, ^3J(7-H, 8-H) = 8.3 Hz], 2.60 (8-H, m), 2.59 (6-H, d, ^2J = 11.6 Hz), 2.34 [11-H, d, ^3J(11-H, 10-H) = 5.3 Hz], 2.00 [6-H, dd, ^2J = 11.6 Hz, ^3J(6-H', 7-H) = 5.6 Hz], 1.88 (10-H, m), 1.85 (9-H, m), 1.67 (9-H, m), 1.44 (10-H, m); ^{13}C NMR (100 MHz, $CDCl_3$): δ = 110.1 (C-3), 105.5 (C-1), 88.7 (C-5), 52.8 (C-7), 44.2 (C-11), 43.7 (C-8), 36.4 (C-6), 25.0 (C-10), 22.6 (C-9); MS (70 eV): *m/z* 389 (10%), 302 (7), 284 (27), 159 (24), 151 (39), 105 (100), 77 (48). The homologs (**3b–d**) gave similar ^1H and ^{13}C NMR spectra which are completely in accordance with their structure.

Addition of 5 mmol of enamine **1a–d** to a boiling solution of **5** (936 mg, 4.0 mmol) in 15 mL of toluene gave **6** or **7**, which crystallized out after standing for 1–3 d at room temperature. The product was recrystallized from toluene/petroleum ether.

6a: Yield 79%, m.p. 125–127 °C, ^{13}C NMR (75 MHz, $CDCl_3$): δ = 192.2, 190.6, 150.1, 145.3, 137.0, 136.3, 133.2, 133.1, 128.6 (2C), 128.5 (2C), 128.4 (2C), 128.3 (2C), 80.5, 67.1, 49.9, 49.6, 29.8, 25.3, 24.2; **7b**: 80%, m.p. 179–181 °C, ^{13}C NMR (75 MHz, $CDCl_3$): δ = 198.1, 194.8, 164.7, 143.4, 141.5 (2C), 138.6, 131.4, 131.0, 129.6 (2C), 129.0 (2C), 127.9 (2C), 127.7 (2C), 110.4 (C-2), 66.4, 51.5, 29.5, 28.4, 22.9, 22.6; **7c**: 95%, m.p. 151–153 °C, δ(C-2) = 108.4; **7d**: 97%, m.p. 202–204 °C, δ(C-2) = 110.5.

Received: November 6, 1991 [Z 5009 IE]
German version: *Angew. Chem.* **1992**, *104*, 783

CAS Registry numbers:
1a, 936-52-7; **1b**, 670-80-4; **1c**, 7182-08-3; **1d**, 17344-01-3; **2**, 4070-75-1; **3a**, 140410-16-8; **3b**, 140410-17-9; **3c**, 140410-18-0; **3d**, 140410-19-1; **5**, 1087-09-8; **6a**, 140410-20-4; **7b**, 140410-21-5; **7c**, 140410-22-6; **7d**, 140410-23-7.

[1] G. Kaupp, *Top. Curr. Chem.* **1988**, *146*, 57–98.
[2] Photolysis of 1,2-dibenzoylbenzene with norbornene and photolysis of 2-acetonyl-1-acetyl-1,2-dihydronaphthalene-8-carboxylic acid methyl ester: Y. Shigemitsu, S. Yamamoto, T. Miyamoto, Y. Odaira, *Tetrahedron Lett.* **1975**, 2819–2820; L. Y. Chow, X. Y. Liu, S. Hu, *J. Chem. Soc. Chem. Commun.* **1988**, 1047–1048. These reactions are, however, entirely different from those of **2** with **1a–d**.
[3] QCPE-MOPAC version 5.01, scalar version from D. Gerson for IBM 3090, adjusted for vector computer Convex. We thank B. Hubert, Computer Center, University Oldenburg, for help with the adjustment.
[4] The hydrolysis of **7** (EtOH, HCl/H_2O) gives the corresponding 2,3-dibenzoyl-3-cycloalkenones.
[5] Treatment of **3** for several days with trifluoroacetic acid gave the expected benzoyl phenyl bicycloalkanolones and morpholine.
[6] Cf. the thoroughly investigated ring system of the monoterpene glucoside peoniflorin (CAS registry number: 23180-57-6), which can be differentiated from that of **3** in that the atoms 6 and 8 are bridged (with CH_2), but not 8 and 11 (or 12, 13, 14, respectively) (numbering according to structure **3**) [see, for example, K. Yamasaki, M. Kaneda, O. Tanaka, *Tetrahedron Lett.* **1976**, 3965–3968], and the ring system in pillaromycin (1,11-condensed ring instead of 8,11-bridging; numbering according to structure **3**) [M. Asai, *Chem. Pharm. Bull.* **1970**, *18*, 1699–1705; 1706–1712; 1713–1719; 1720–1723], and that in the corresponding diterpenes from *Euphorbia latex* [R. J. Schmidt, F. J. Evans, *Phytochemistry* **1978**, *17*, 1436–1437].

$[(CO)_3(PPh_3)_2OsAg(O_2CCF_3)]$: A Model for an Intermediate on the Reaction Coordinate in Electron Transfer**

By *Lin Song* and *William C. Trogler**

Electron-transfer reactions have been investigated extensively in recent years; however, there is little information available on X-ray structures of precursor complexes because they are short lived and unstable. The Marcus theory of electron transfer between a donor D and acceptor A postulates association between the reactants to form a metastable D–A complex, as a precursor to electron transfer.[1] This mechanism has possible relevance to electron-transfer reactions in living organisms.[2, 3]

Silver(I) salts have been widely used as one-electron oxidants to generate organic and organometallic radicals; they form the basis for the photographic industry. In previous work the formation of an intermediate was observed spectroscopically on oxidation of *trans*-$[Fe(CO)_3(PPh_3)_2]$ with $AgPF_6$, but isolation and further characterization of the short-lived species was not possible.[4] The decay of the intermediate involved in this redox reaction yielded the $[Fe(CO)_3(PPh_3)_2]^+$ radical and metallic silver. Spectroscopic data also suggest that the one-electron oxidation of $[Ru_2(\mu\text{-}CO)(CO)_4\{\mu\text{-}(MeO)_2PN(Et)P(OMe)_2\}_2]$ by silver(I) salts occurs by an inner-sphere intermediate, but attempts to obtain single crystals of the intermediate proved unsuccessful.[5] Here we report the molecular structure of a metal–metal bonded intermediate in one such reaction, which serves as a structural model for a precursor complex in electron-transfer reactions between organometallic species and silver(I) salts.

The heavy metal complex **1** adopts the same trigonal-bipyramidal structure as the analogous Fe complex,[6, 7] and it is more prone to one-electron oxidation.[8] Although the

trans-$[Os(CO)_3(PPh_3)_2]$ **1**

oxidation of **1** with $Ag(O_2CCF_3)$ is thermodynamically favorable in CH_2Cl_2, it becomes less exoergic in THF (Table 1). By performing the reaction in THF, followed by extraction with benzene, we have been able to crystallize the Os–Ag complex **2**, an apparent precursor to the Os(0) → Ag(I) electron-transfer reaction. This 1:1 complex provides

$[(CO)_3(Ph_3P)_2OsAg(O_2CCF_3)]$ **2**

astructural evidence for a metal–metal bonded intermediate in the Ag^+ oxidation of an organometallic compound. This complex also differs from the majority of 1:2 adducts known to form between Ag^+ and transition-metal complexes.[9]

Table 1. Redox properties of $Ag(O_2CCF_3)$ and $[Os(CO)_3(PPh_3)_2]$ obtained from cyclic voltammetry measurements [a].

Solvent	$(E_P)_{red}(Ag^+)$ [V]	$(E_P)_{ox}(Os^0)$ [V]	ΔE_P [V] [b]
THF	0.17	0.13	+0.04
CH_2Cl_2	0.41	0.04 [c]	+0.37
CH_3CN	−0.20 [d]	0.08	−0.28

[a] Experimental conditions: $[AgO_2CCF_3] = 2 \times 10^{-3}$ M, $[Os(CO)_3(PPh_3)_2] = 1 \times 10^{-3}$ M, (in CH_3CN limited by solubility to less than 0.5×10^{-3} M, supporting electrolyte $[Bu_4NPF_6] = 0.1$ M, $T = 23 \pm 2$ °C, scan rate = 200 mVs^{-1}, platinum working electrode, platinum auxiliary electrode, $Ag/AgNO_3$ (0.1 M in CH_3CN) reference electrode, no IR compensation. [b] $\Delta E_P = (E_P)_{red}(Ag^+) - (E_P)_{ox}(Os^0)$. [c] $(E_P)_{ox}$ of **2** is 0.55 V under the same experimental conditions. [d] Ag^+ is stabilized in CH_3CN because $[Ag(CH_3CN)_4]^+$ forms.

An X-ray structural analysis of **2** reveals that it has a distorted trigonal-bipyramidal geometry about Os, and Ag^+ approaches Os in the equatorial plane (Fig. 1). The Ag–Os bond forms 69.0° and 73.5° angles with the neighboring CO

[*] Prof. W. C. Trogler, L. Song
Department of Chemistry, 0506
University of California, San Diego
9500 Gilman Drive, La Jolla, CA 92093-0506 (USA)

[**] This work was supported by a National Science Foundation Grant (CHE-88-15958).

groups, which can be regarded as semibridging.[10] This type of slight structural rearrangement about the metal center was also reported for the 1:2 adduct $[Ag\{Rh(CO)(PPh_3)(\eta\text{-}C_5H_5)\}_2](PF_6)$, which can be viewed as a silver-stabilized radical cation.[11] The linear geometry of the two semibridging CO groups in **2** suggests a net repulsive Ag–CO interaction.[12] The Lewis-base nature of 18-electron osmium complexes containing CO and phosphane ligands has been previously demonstrated by the formation of metal–metal bonded adducts,[13] although the structure about Os in those complexes is nearly octahedral. The coordination environment about Ag^+ in **2** is nearly linear, as often occurs for silver(I). The Ag–Os separation of 2.712(1) Å is consistent with a Os $\rightarrow Ag^+$ dative metal–metal bonding interaction.

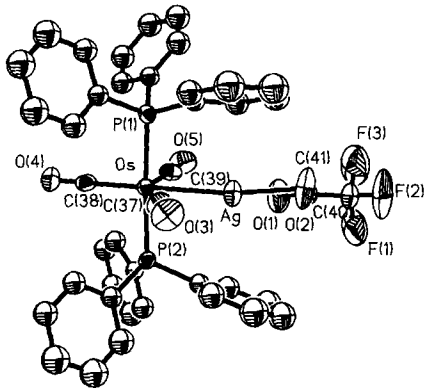

Fig. 1. Structure of **2** (ORTEP, thermal ellipsoids at 50% probability). Selected bond lengths [Å] and angles [°]: Os-Ag 2.712(1), Os-P(1) 2.386(2), Os-P(2) 2.396(2), Os-C(37) 1.936(11), Os-C(38) 1.904(12), Os-C(39) 1.912(10), Ag-O(2) 2.287(12), C(37)-O(3) 1.142(14), C(38)-O(4) 1.145(15), C(39)-O(5) 1.165(12), C(41)-O(1) 1.223(19), C(41)-O(2) 1.233(15), P(1)-Os-P(2) 174.5(1), P(1)-Os-Ag 91.8(1), P(2)-Os-Ag 85.4(1), Ag-Os-C(37) 73.5(4), Ag-Os-C(39) 69.0(3), C(37)-Os-C(38) 113.7(5), C(38)-Os-C(39) 103.8(4), Os-Ag-O(2) 170.8(2).

IR spectra of **2** measured in solution show that its carbonyl stretching frequency shifts more than 30 cm^{-1} to higher energy than that of **1**.[14] The oxidation potential of **2** in CH_2Cl_2 is also 0.51 V more positive than that of **1** according to cyclic voltammetry measurements (Table 1). When **2** is dissolved in THF a weak triplet signal appears in the EPR spectrum ($g = 2.006$, $A_P = 16.3$ G (THF); $g = 2.005$, $A_P = 15.0$ G (toluene)) with hyperfine coupling to the two phosphane ligands. The intensity of the triplet signal decreases and eventually disappears, as metallic silver and other species are observed. We attribute the EPR signal to the short-lived $[Os(CO)_3(PPh_3)_2]^+$ radical, which forms slowly from **2** in solution. For comparison, the solution EPR spectrum of $[(Fe(CO)_3(PPh_3)_2]^+$ in CH_2Cl_2 exhibits a triplet signal at $g = 2.053$ and $A_P = 18.7$ G.[15]

Complex **2** remains stable in CH_3CN for several hours, but it yields metallic silver and other oxidation products in CH_2Cl_2 and THF. The electron-transfer process occurs faster in CH_2Cl_2 than in THF. These stabilities parallel the estimated driving potential (ΔE_P) shown in Table 1. The final products of the Os(0)–Ag(I) electron transfer in THF are $[Os(CO)_2(PPh_3)_2(\eta^2\text{-}O_2CCF_3)](O_2CCF_3)$ and **1**, from disproportionation of the 17-electron $[Os(CO)_3(PPh_3)_2](O_2CCF_3)$ radical.[16] In CH_2Cl_2 the known complex *trans*-$[OsCl_2(CO)_2(PPh_3)_2]$ forms.[17]

Both Xα calculations and qualitative crystal-field considerations predict that the HOMO in trigonal-bipyramidal **2** should be a degenerate d_{xy}, $d_{x^2-y^2}$ derived orbital in the equatorial plane (z axis taken as axial).[15] The X-ray structure of **2** suggests that the Lewis acid $Ag(O_2CCF_3)$ binds to this frontier orbital from which the electron is ultimately removed. The ability of Ag^+ to oxidize organometallics by an inner-sphere metal–metal bonded intermediate may explain its high effectiveness in such oxidations. The strength of the metal–metal bond and the further geometric reorganization necessary in the Os and Ag coordination spheres apparently provides sufficient activation energy for electron transfer, which permits isolation of **2**. Nucleation effects may also be important. We have observed an induction period (followed by zero-order kinetics) in the further electron-transfer reaction of **2** in CH_2Cl_2 that appears to correlate with the formation of metallic silver. The measured redox potential for Ag^+ refers to its reduction to the bulk metal. In **2** electron transfer would produce initially a solvated silver atom, which might be a higher energy intermediate.

Experimental Procedure

All experiments were performed under a nitrogen atmosphere and with dried solvents. Complex **1** was prepared by the method of Collman and Roper [6].

Complex **2**: 10 mL of THF was added into a mixture of **1** (40 mg, 0.050 mmol) and $Ag(O_2CCF_3)$ (11 mg, 0.050 mmol) with stirring in the dark. THF was removed under vacuum after 10 min, and the pale brown residue was extracted with 15 mL of benzene and filtered. The benzene solution was concentrated to about 5 mL and 30 mL of pentane was added to yield 14 mg of **2** (27%). Crystals of **2** · 0.5 C_6H_6 suitable for an X-ray diffraction study were obtained by storing the benzene/pentane mixture at 5 °C for several days.

Received: November 15, 1991 [Z 5020 IE]
German version: *Angew. Chem.*, **1992**, *104*, 806

[1] R. A. Marcus, *Annu. Rev. Phys. Chem.* **1964**, 155.
[2] H. B. Gray, B. G. Malmström, *Biochemistry* **1989**, *28*, 7499.
[3] R. A. Marcus, N. Sutin, *Biochim. Biophys. Acta* **1985**, *811*, 265.
[4] P. K. Baker, N. G. Connelly, B. M. R. Jones, J. P. Maher, K. R. Somers, *J. Chem. Soc. Dalton Trans.* **1980**, 579.
[5] D. W. Engel, R. J. Haines, E. C. Horsfield, J. Sundermeyer, *J. Chem. Soc. Chem. Commun.* **1989**, 1457.
[6] J. P. Collman, W. R. Roper, *J. Am. Chem. Soc.* **1967**, *88*, 3504.
[7] J. K. Stalick, J. A. Ibers, *Inorg. Chem.* **1969**, *8*, 419.
[8] $E_{1/2} = 0.065$ V for $[Fe(CO)_3(PPh_3)_2]$ in CH_2Cl_2 vs. Ag/0.1 M $AgNO_3$ as reference electrode in acetonitrile: M. J. Therien, W. C. Trogler, *J. Am. Chem. Soc.* **1986**, *108*, 4037; $E_{1/2} = -0.005$ V for $[Os(CO)_3(PPh_3)_2]$ under the same experimental conditions.
[9] a) A. Sykes, K. R. Mann, *J. Am. Chem. Soc.* **1988**, *110*, 8252; b) R. Usón, *J. Organomet. Chem.* **1989**, *372*, 171; c) D. M. P. Mingos, M. J. Watson, *Transition Met. Chem.* **1991**, *16*, 285; d) D. J. Liston, Y. J. Lee, W. R. Scheidt, C. A. Reed, *J. Am. Chem. Soc.* **1989**, *111*, 6643; e) P. Braunstein, T. M. G. Carneiro, D. Matt, A. Tiripicchio, M. T. Carmellini, *Angew. Chem.* **1986**, *98*, 721; *Angew. Chem. Int. Ed. Engl.* **1986**, *25*, 748; f) R. Usón, J. Forniés, M. Tomás, I. Ara, J. M. Casas, A. Martin, *J. Chem. Soc. Dalton Trans.* **1991**, 2253.
[10] X-ray crystal structure analysis of **2** · 0.5 C_6H_6: monoclinic, $P2_1/n$, $a = 11.042(2)$, $b = 13.431(3)$, $c = 27.709(5)$ Å, $\beta = 101.05(1)°$, $V = 4033.2(14)$ Å^3, $Z = 4$, $\varrho_{calcd} = 1.744$ g cm^{-3}, $\mu = 3.767$ mm^{-1}, $Mo_{K\alpha}$ radiation, graphite monochromator, 7134 independent reflections, for 4332 of which $F_0 \geq 6.0\sigma(F_0)$, $3° \leq 2\theta \leq 55°$, empirical absorption correction from psi scan data. Structure solution by direct methods, $R = 0.044$, $R_w = 0.066$. Further details of the crystal structure analysis can be obtained from the Fachinformationszentrum Karlsruhe, Gesellschaft für wissenschaftlich-technische Information mbH, D-W-7514 Eggenstein-Leopoldshafen 2 (FRG) on quoting the depository number CSD-55999, the names of the authors, and the journal citation.
[11] a) N. G. Connelly, A. R. Lucy, *J. Chem. Soc. Chem. Commun.* **1981**, 43; b) N. G. Connelly, A. R. Lucy, J. D. Payne, A. M. R. Galas, W. E. Geiger, *J. Chem. Soc. Dalton Trans.* **1983**, 1879.
[12] C. Q. Simpson, M. B. Hall, *J. Am. Chem. Soc.* **1992**, 114, 1641.
[13] a) F. W. B. Einstein, T. Jones, R. K. Pomeroy, P. Rushman, *J. Am. Chem. Soc.* **1984**, *106*, 2707; b) H. B. Davis, F. W. B. Einstein, P. G. Glavina, T. Jones, R. K. Pomeroy, P. Rushman, *Organometallics* **1989**, *8*, 1030;

c) R. J. Batchelor, H. B. Davis, F. W. B. Einstein, R. K. Pomeroy, *J. Am. Chem. Soc.* **1990**, *112*, 2036.
[14] IR of **1**: ν(CO) 1890 cm^{-1} (CH_2Cl_2); 1892 cm^{-1} (THF); IR of **2**: ν(CO): 1925(s), 1946(s), 2006(w) cm^{-1}, $\nu(O_2CCF_3^-)$: 1674 cm^{-1} (CH_2Cl_2); ν(CO): 1927(s), 1946(s), 2010(w) cm^{-1}, $\nu(O_2CCF_3^-)$: 1676 cm^{-1} (THF).
[15] M. J. Therien, W. C. Trogler, *J. Am. Chem. Soc.* **1986**, *108*, 3697.
[16] The intensities of the absorbances of ν(CO) at 1975 and 2045 cm^{-1} and $\nu(O_2CCF_3^-)$ at 1694 and 1644 cm^{-1} increase in a constant ratio. Compared with $\nu(O_2CCF_3^-)$ of 1676 cm^{-1} in **2** and 1692 cm^{-1} in $[Bu_4N](O_2CCF_3)$, the hypsochromic shift of one $O_2CCF_3^-$ group (1694 cm^{-1}) corresponds to an ionic $O_2CCF_3^-$ unit and the bathochromic shift of a second $O_2CCF_3^-$ group (1644 cm^{-1}) is typical for the formation of a bidentate complex. Therefore the absorbances are assigned to $[Os(CO)_2(PPh_3)_2(\eta^2\text{-}O_2CCF_3)](O_2CCF_3)$ The other absorbance at 1892 cm^{-1} is identical to that of **1**.
[17] IR spectrum of the final product from thermal reation of **2** in CH_2Cl_2: ν(CO): 1977(s) and 2046(s) cm^{-1}, $\nu(O_2CCF_3^-)$: 1691 cm^{-1}. For comparison the known $[OsCl_2(CO)_2(PPh_3)_2]$, prepared by the method of Collman and Roper [6], caused these absorptions to increase when added to the same solution. The uncoordinated $O_2CCF_3^-$ group in $[Bu_4N](O_2CCF_3)$ has an absorbance at 1691 cm^{-1} in CH_2Cl_2.

Reagents with Hypervalent Iodine: Formation of Convenient Chiral Synthetic Intermediates by Fragmentation of Carbohydrate Anomeric Alkoxy Radicals**

By *Pedro de Armas*, *Cosme G. Francisco*, and *Ernesto Suárez**

Carbohydrates owe their present importance in part to their use as chiral template precursors for a variety of complex non-carbohydrate substances.[1] In this context many efforts have been made in recent years to develop a new and efficient methodology to create or destroy asymmetric centers by chemical manipulation. The proposed reactions must be compatible with the temporary protective groups that might be employed in this type of synthesis. Special attention has been devoted to the preparation of four-carbon chiral building blocks of the threose and erythrose series,[2] which have been used in the synthesis of several polyhydroxylated natural products.[3]

During the past few years, we have examined several compounds with hypervalent iodine that can generate alkoxy radicals, in order to promote β-fragmentation reactions.[4] A new synthesis of medium-sized lactones and spirolactones was developed by use of these reagents on appropriate oxabicyclic hemiacetals.[5] We now report a new method for the synthesis of four-carbon chiral building blocks of the D- and L-erythrose types by β-fragmentation of the C1–C2 carbon bond of suitably protected D- and L-arabinose, D-ribose, and 2-deoxy-D-ribose (Scheme 1). The reaction has also been extended to the synthesis of five-carbon chiral building blocks of the arabinose type by β-fragmentation of D-mannose and D-glucose derivatives.

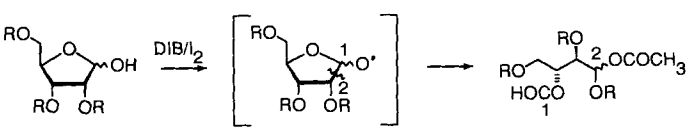

Scheme 1. DIB =(diacetoxyiodo)benzene.

Cleavage of the C1–C2 carbon bond in carbohydrate chemistry can be performed by several methods such as those of Ruff, Wohl, Weerman etc., but they suffer from several drawbacks, for instance, the number of steps required, low yields, and inconveniently strong reaction conditions.[6] Although sodium periodate and lead tetraacetate are routinely used to test for the presence of vicinal diols,[7] they have hardly been used in synthesis to cleave the C1–C2 carbon bond.[8]

The carbohydrate derivative was treated with (diacetoxyiodo)benzene (DIB) and iodine in cyclohexane under the con-

Table 1. β-Fragmentation of carbohydrate anomeric alkoxy radicals [a]

Entry	Substrate [b]	Conditions DIB [mmol]	I_2 [mmol]	time [h]	Product	Yield [%]
1	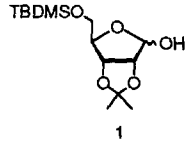 **1**	1.2	1	3	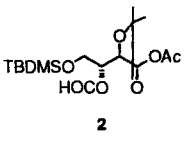 **2**	84
2		1.2	0.1	24		36
3		1.2	0	24		no reaction
4	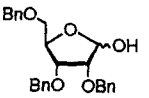 **3**	1.2	1	4	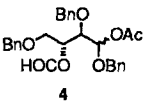 **4**	85
5	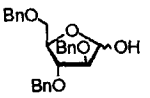 **5**	1.2	1	8	**4**	91
6	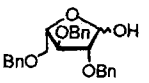 **6**	1.2	1	8	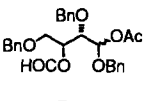 **7**	89
7	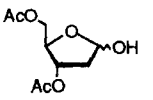 **8**	2.2	1	96	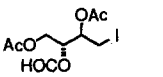 **9**	44
8		1.7	1	0.3 [c]		44
9	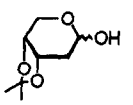 **10**	1.2	1	6	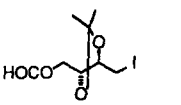 **11**	58
10	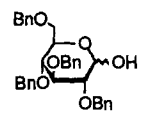 **12**	1.2	1	32	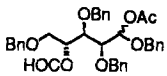 **13**	81
11	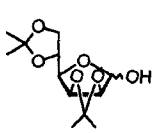 **14**	1.2	1	8	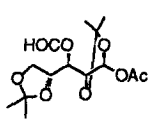 **15**	85

[a] 0.3 mmol scale at 20 °C in cyclohexane (30 mL $mmol^{-1}$). [b] TBDMS = *tert*-butyldimethylsilyl, Bn = benzyl. [c] Under reflux.

[*] Prof. E. Suárez, Dr. P. de Armas, Dr. C. G. Francisco
Instituto de Productos Naturales y Agrobiolgía del C.S.I.C.
Carretera de la Esperanza 2, 38206 La Laguna, Tenerife (Spain)

[**] This work was supported by the Investigation Programme no. PB87-0406 of the Dirección General de Investigación Cientifica y Técnica.

ditions specified in Table 1. The reaction conditions were determined with the readily available 5-*O*-(*tert*-butyldimethylsilyl)-2,3-*O*-isopropylidene-D-ribofuranose (**1**),[9] which gave a major stereoisomer at C1 (ca. 95:5) of the erythrose derivative **2** (entry 1). The proposed stereochemistry at C1 is based on the observed *trans* coupling constant between H1 and H2 ($J_{H1,H2} = 1.96$ Hz). The presence of iodine was necessary for the reaction to take place (entry 3), and lower yields were observed when catalytic amounts were used (entry 2). The reaction mechanism seems to involve the initial formation of the anomeric alkoxy radical followed by β-fragmentation and subsequent trapping of the carbon radical formed at C1 by an acetoxy radical from the reagent. At this point the anomeric carbon is a part of a formate group that forms an ester with the alcohol at C3 (Scheme 1).

A differently protected erythrose building block **4** was obtained from 2,3,5-tri-*O*-benzyl-D-ribofuranose (**3**)[10] (entry 4). Substrate **3**, which lacks the steric bias of the previous example, was found to give a mixture (ca. 1:1) of stereoisomers at C1.

The reaction course does not seem to be dependent on the configuration of the alcohol at C2, since D- and L-2,3,5-tri-*O*-benzylarabinofuranose (**5** and **6**, respectively) were fragmented analogously to substrate **3** to give D- and L-erythrose building blocks **4** and **7**, respectively, in similar yields (compare entry 4 with entries 5 or 6).

β-Fragmentation of 2-deoxy-D-ribofuranose (**8**) and -pyranose derivatives (**10**)[11] gave rise to two potentially interesting synthetic intermediates, the 1-iodo-2,3,4-trihydroxybutane derivatives **9** and **11**, respectively; although yields were lower (entries 7–9), the generation of the formyl group allows subsequent selective modifications of these building blocks to be carried out.

The reaction was also extended to hexoses (entries 10 and 11); thus the 2,3,4,6-tetra-*O*-benzyl-D-glucopyranose (**12**) and 2,3:5,6-di-*O*-isopropylidene-D-mannofuranose (**14**) were transformed into the D-arabinose derivatives **13** and **15**. In the glucopyranose a mixture (ca. 1:1) of C1 stereoisomers of **13** is observed, where the formyl group forms an ester with the hydroxyl group at C4, whereas in the mannofuranose a single stereoisomer is obtained, the formate group being at C3 (the observed *trans* coupling constant between H_1 and H_2 was $J_{H1,H2} = 2.1$ Hz). The spectroscopic data of compounds **2**, **9**, **11**, and **15** are summarized in Table 2.

The fragmentation reaction is independent of ring size; thus, similar yields were obtained for furanose and pyranose derivatives (compare entries 7–8 with 9, and 10 with 11).

We consider that some features of the reported procedure are remarkable: for example, the mild reaction conditions, compatible with the protective groups most widely used in carbohydrate chemistry; the regioselectivity observed during the fragmentation; and also the fact that the reaction outcome does not depend on C2 configuration, the protective groups, or ring size. The generation of the formate group and of the masked aldehyde that permits a flexible use of the resulting building blocks is very valuable. This reaction can also be considered a convenient method to descend the aldose series of carbohydrates and compares well with those reported.[6]

Table 2. Spectroscopic data for **2**, **9**, **11**, and **15**. IR ($CHCl_3$); ^1H and ^{13}C NMR at 200 and 50.3 MHz, respectively, in $CDCl_3$ with internal TMS standard (assignments by DEPT, ^1H-^1H COSY, and ^1H-^{13}C HETCOR).

2: $[\alpha]_D = -33$ (c = 0.18, $CHCl_3$); ^1H NMR: $\delta = 0.05$ (s, 6H, Si $(CH_3)_2$), 0.88 (s, 9H, $SiC(CH_3)_3$), 1.45 (s, 3H, isopropylidene-CH_3), 1.48 (s, 3H, isopropylidene-CH_3), 2.09 (s, 3H, CO-CH_3), 3.78 (dd, $J = 4.67$, 11.32 Hz, 1H, C4-H_a), 3.85 (dd, $J = 4.07$, 11.35 Hz, 1H, C4-H_b), 4.42 (dd, $J = 2.31$, 5.30 Hz, 1H, C2-H), 5.09 (pseudo-q, 1H, C3-H), 6.31 (d, $J = 1.96$ Hz, 1H, C1-H), 8.10 (s, 1H, OCOH). ^{13}C NMR: $\delta = -5.57$ and -5.49 ($Si(CH_3)_2$), 18.23 ($SiC(CH_3)_3$), 21.18 (CO-CH_3), 25.82 ($SiC(CH_3)_3$), 26.59 (isopropylidene-CH_3), 27.22 (isopropylidene-CH_3), 61.35 (C4), 72.75 (C3), 80.51 (C2), 95.90 (C1), 112.77 (isopropylidene-C), 159.99 (OCOH), 169.95 (*C*O-CH_3). IR: $\tilde{\nu}$ [cm^{-1}] = 1729. FABMS (NaI): *m/z* 385 ($[M+Na]^{\oplus}$, 15%).

9: $[\alpha]_D = -25$ (c = 0.24, $CHCl_3$); ^1H NMR: $\delta = 2.07$ (s, 3H, CO-CH_3), 2.13 (s, 3H, CO-CH_3), 3.31 (dd, $J = 6.29$, 11.17 Hz, 1H, C1-H_a), 3.44 (dd, $J = 4.25$, 11.19 Hz, 1H, C1-H_b), 4.22 (dd, $J = 5.84$, 12.4 Hz, 1H, C4-H_a), 4.37 (dd, $J = 3.24$, 12.45 Hz, 1H, C4-H_b), 5.01 (m, 1H, C2-H), 5.35 (m, 1H, C3-H), 8.08 (s, 1H, OCOH). ^{13}C NMR: $\delta = 2.25$ (C1), 20.54 (CO-CH_3), 20.69 (CO-*C*H3), 61.34 (C4), 69.98 (C2), 71.18 (C3), 159.26 (OCOH); 169.41 (*C*O-CH_3), 170.24 (*C*O-CH_3). IR: ν[cm^{-1}] = 1737. FABMS (glycerol, NaCl, NaI): *m/z* 345 ($[M+H]^{\oplus}$, 24%).

11: $[\alpha]_D = -22$ (c = 0.16, $CHCl_3$); ^1H NMR: $\delta = 1.39$ (s, 3H, isopropylidene-CH_3), 1.50 (s, 3H, isopropylidene-CH_3), 3.18 (dd, $J = 6.37$, 10.6 Hz, 1H, Cl-H_a), 3.25 (dd, $J = 7.15$, 10.22 Hz, 1H, Cl-H_b), 4.16-4.55 (m, 4H, C2-H, C3-H, C4-H_2), 8.11 (s, 1H, OCOH). ^{13}C NMR: $\delta = 0.67$ (Cl), 25.43 (isopropylidene-CH_3), 27.97 (isopropylidene-CH_3), 61.71 (C4), 74.77 (C3), 77.55 (C2), 109.95 (isopropylidene-C), 160.38 (OCOH). IR: ν [cm^{-1}] = 1725. FABMS (NaI): *m/z* 323 ($[M+Na]^{\oplus}$, 40%).

15: $\alpha_D = -47$ (c = 0.18, $CHCl_3$); ^1H NMR: $\delta = 1.25$ (s, 3H, isopropylidene-CH_3), 1.35 (s, 3H, isopropylidene-CH_3), 1.50 (s, 6H, 2 × isopropylidene-CH_3), 2.09 (CO-CH_3), 3.86 (dd, $J = 5.79$, 8.76 Hz, 1H, C5-H_a), 4.06 (dd, $J = 6.15$, 8.73 Hz, 1H, C5-H_b), 4.27 (pseudo-q, C4-H), 4.48 (dd, $J = 2.82$, 2.55 Hz, 1H, C2-H), 5.29 (dd, $J = 3.22$, 6.92 Hz, 1H, C3-H), 6.11 (d, $J = 2.1$ Hz, 1H, Cl-H), 8.15 (s, 1H, OCOH). ^{13}C NMR: $\delta = 21.08$ (CO-*C*H_3), 25.21 (isopropylidene-CH_3), 26.43 (isopropylidene-CH_3), 26.70 (isopropylidene-CH_3), 27.03 (isopropylidene-CH_3), 66.15 (C5), 71.05 (C3), 74.04 (C4), 81.29 (C2), 96.67 (C1), 109.72 (isopropylidene-C), 113.58 (isopropylidene-C), 159.81 (OCOH), 170.06 (*C*O-CH_3). IR: ν [cm^{-1}] = 1732. FABMS (glycerol, NaCl): *m/z* 317 ($[M-H]^{\ominus}$, 8%)

Experimental Procedure

A solution of 5-*O*-(*tert*-butyldimethylsilyl)-2,3-*O*-isopropylidene-D-ribofuranose (**1**) [9] (100 mg, 0.33 mmol) in dry cyclohexane (10 mL) containing (diacetoxyiodo)benzene (127 mg, 0.39 mmol) and iodine (84 mg, 0.33 mmol) was stirred at room temperature (20 °C) for 3 h. The reaction mixture was then poured into water and extracted with ether. The organic layer was washed with aqueous sodium thiosulfate and water. Chromatography of the residue (Chromatotron, Merck silica gel 60 PF 254, *n*-hexane/ethyl acetate 9:1 v/v) gave **2** (99 mg, 84%).

Received: December 2, 1991 [Z 5049 IE]
German version: *Angew. Chem.* **1992**, *104*, 746

CAS Registry numbers:
1, 68703-51-5; **2**, 141062-52-4; **3** (α anomer), 89615-45-2; **3** (β anomer), 89361-52-4; **4**, 141062-53-5; **5**, 37776-25-3; **6**, 77870-89-4; **8**, 141062-54-6; **9**, 141062-55-7; **10**, 65236-75-1; **11**, 141062-56-8; **12**, 38768-81-9; **13**, 141062-57-9; **14**, 40036-82-6; **15**, 141062-58-0; (diacetoxyiodo)benzene, 3240-34-4; iodine, 7553-56-2.

[1] S. Hanessian, *Total Synthesis of Natural Products. The Chiron Approach*, Pergamon Press, Oxford **1983**. S. Hanessian, G. Rauncourt, *Pure Appl. Chem.* **1977**, *49*, 1201. B. Fraser-Reid, T. F. Tom, K. M. Sun in *Organic Synthesis, Today and Tomorrow* (Eds.; B. M. Trost, C. R. Hutchinson), Pergamon Press, Oxford, **1981**. T. D. Inch, *Tetrahedron* **1984**, *40*, 3161–3213. K. L. Bhat, S.-Y. Chen, M. M. Joullié, *Heterocycles* **1985**, *23*, 691–729. *Trends in Synthetic Carbohydrate Chemistry* (Eds.: D. Horton, L. D. Hawkins, G. J. McGarvey), American Chemical Society, Washington, **1989**.

[2] T. Hudlicky, H. Luna, J. D. Price, F. Rulin, *Tetrahedron Lett.* **1989**, *30*, 4053–4054. B. R. Baker, K. Hewson, *J. Org. Chem.* **1957**, *22*, 966. A. S. Perlin, *Methods Carbohydr. Chem. Vol. 1*, **1962**, p. 67. M. Kiso, A. Hasegawa, *Carbohydrate Res.* **1976**, *52*, 95. C. E. Ballow, *J. Am. Chem. Soc.* **1957**, *79*, 165. T. Mukaiyama, K. Suzuki, T. Yamada, F. Tabusa, *Tetrahedron* **1990**, *46*, 265–276. T. Mukaiyama, K. Suzuki, T. Yamada, *Chem. Lett.* **1982**, 929–932.

[3] D. R. Williams, F. D. Klingler, *J. Org. Chem.* **1988**, *53*, 2134–2136. G. Stork, S. Raucher, *J. Am. Chem. Soc.* **1976**, *96*, 1583–1584. P. T. Ho, *Can. J. Chem.* **1980**, *88*, 858–860.

[4] R. Freire, R. Hernández, M. S. Rodríquez, E. Suárez, A. Perales, *Tetrahedron Lett.* **1987**, *28*, 981–984. C. G. Francisco, R. Freire, M. S. Rodríguez, E. Suárez, *ibid.* **1987**, *28*, 3397–3400. R. Hernández, J. J. Marrero, E. Suárez, *ibid.* **1988**, *29*, 5979–5982. R. Hernández, J. J. Marrero, D. Melián, E. Suárez, *ibid.* **1988**, *29*, 6661–6664. R. Hernández, J. J. Marrero, E. Suárez, *ibid.* **1989**, *30*, 5501–5504.

[5] R. Freire, J. J. Marrero, M. S. Rodríguez, E. Suárez, *Tetrahedron Lett.* **1986**, *27*, 383–387. M. T. Arencibia, R. Freire, A. Perales, M. S. Rodríguez, E. Suárez, *J. Chem. Soc., Perkin Trans. 1*, **1991**, 3349–3360.

[6] L. Hough, A. C. Richardson in *The Carbohydrates Vol. 1A*, (Eds.: W. Pigman, D. Horton), 2nd ed., Academic Press, San Diego, **1972**, p. 127–138.
[7] A. S. Perlin in *The Carbohydrates Vol. 1B*, (Eds.: W. Pigman, D. Horton), 2nd ed., Academic Press, New York, **1980**, pp. 1167–1215.
[8] Y. Nakahara, K. Beppu, T. Ogawa, *Tetrahedron Lett.* **1981**, *22*, 3197–3200. M. Kinoshita, A. Hagiwara, S. Aburaki, *Bull. Chem. Soc. Japan* **1975**, *48*, 570. M. Kinoshita, S. Mariyama, *ibid.* **1975**, *48*, 2081. S. Aburaki, N. Konishi, M. Kinoshita, *ibid.* **1975**, *48*, 1254. H. R. Schuler, K. Slessor, *Can. J. Chem.* **1977**, *55*, 3280. J. P. H. Verheyden, A. C. Richardson, R. S. Bhatt, B. D. Grant, W. L. Fitch, J. G. Moffatt, *Pure Appl. Chem.* **1978**, *51*, 1363.
[9] B. Kaskar, G. L. Heise, R. S. Michalak, B. R. Vishnuvajjala, *Synthesis* **1990**, 1031–1032.
[10] L. Chan, G. Just, *Tetrahedron* **1990**, *46*, 151–162.
[11] E.J. Corey, A. Marfat, G. Goto, F. Brion, *J. Am. Chem. Soc.* **1980**, *102*, 7984–7985.

Table 1. Formation of heteroaromatic carboxylic acids from methylated heterocycles with cells of *Pseudomonas putida* ATCC 33015 grown on *p*-xylene

Starting material	Product	Yield [%]
2,5-dimethylpyrrole	5-methylpyrrole-2-carboxylic acid	40
3,5-dimethylpyrazole	5-methylpyrazole-3-carboxylic acid	80
2,5-dimethylfuran	5-methylfuran-2-carboxylic acid	40
3-methylthiophene	thiophene-3-carboxylic acid	70
4-methylthiazole	thiazole-4-carboxylic acid	80
3-methylpyridine	pyridine-3-carboxylic acid	50
2-chloro-6-methylpyridine	6-chloropyridine-2-carboxylic acid	90
2-chloro-3-ethyl-6-methylpyridine	6-chloro-5-ethylpyridine-2-carboxylic acid	10
2,4-dimethylpyridine	2-methylpyridine-4-carboxylic acid (90%) 4-methylpyridine-2-carboxylic acid (10%)	40
2,5-dimethylpyrazine	5-methylpyrazine-2-carboxylic acid	90
2,3,6-trimethylpyrazine	5,6-dimethylpyrazine-2-carboxylic acid	90
3-chloro-2,5-dimethylpyrazine	6-chloro-5-methylpyrazine-2-carboxylic acid	90

Enzymatic Oxidation of Methyl Groups on Aromatic Heterocycles: A Versatile Method for the Preparation of Heteroaromatic Carboxylic Acids**

By *Andreas Kiener**

Chemical oxidation reactions used for the industrial scale preparation of heteroaromatic monocarboxylic acids from heteroaromatic compounds bearing one or more methyl groups are often nonspecific and lead to the formation of undesired by-products. To overcome this problem we have been interested in developing a biological oxidation method for this type of reaction. Although enzymatic oxidations of alkyl side chains on heteroarenes by bacteria and fungi have been described,[1] none of these biotransformations have been used for the preparation of aromatic heterocyclic carboxylic acids or their hydroxymethyl derivatives. This communication describes a versatile enzymatic method capable of selectively oxidizing a single methyl group on heteroarenes on a pilot plant scale.

The wild-type strain *Pseudomonas putida* ATCC 33015 was used as the biocatalyst in our investigations. This microorganism can grow on toluene, *m*-xylene, or *p*-xylene as sole carbon and energy source.[2] Both the biochemistry[3, 4] and genetics[5, 6] of the xylene degradative pathway have been extensively studied. *p*-Xylene, for example, is oxidized by xylene monooxygenase to 4-methylbenzylalcohol, which is then further oxidized by benzylalcohol and benzylaldehyde dehydrogenase to 4-methylbenzoic acid. The aromatic carboxylic acid is converted by toluate dioxygenase and dihydroxycyclohexadienecarboxylate dehydrogenase into 4-methylcatechol prior to the cleavage of the aromatic ring by catechol dioxygenase. The cleavage product is then transformed into Krebs-cycle intermediates. Investigations on the substrate specificity of key enzymes in the xylene degradative pathway have focused mainly on substituted aromatic carbocycles.[7] Only a few publications concerning heterocycle oxidation have appeared. One example is the bacterial formation of indigo initiated by hydroxylation of indole by xylene monooxygenase.[8]

We have now demonstrated that *P. putida* grown on *p*-xylene as sole carbon and energy source was capable of oxidizing many methylated heteroaromatic five- and six-membered rings to the corresponding monocarboxylic acids (Table 1). The carboxylic acids accumulated in the fermentation broth and were isolated for analysis. In most cases the generated heteroaromatic carboxylic acids were not further degraded, which indicates that aromatic heterocycles are poor substrates for toluate dioxygenase (none of the heterocycles supported the growth of *P. putida*). As shown in Table 1, biotransformations of 2,3,6-trimethylpyrazine and 3-chloro-2,5-dimethylpyrazine were also regiospecific; this was expected since substituents *ortho* to a methyl group prevent hydroxylation by xylene monooxygenase.[6] The oxidation product of 2,4-dimethylpyridine, however, contained a mixture of 2-methylpyridine-4- and 4-methylpyridine-2-carboxylic acid. The formation of 6-chloro-5-ethylpyridine-2-carboxylic acid from 2-chloro-3-ethyl-6-methylpyridine showed that the enzymatic oxidation was specific for the methyl group. In no experiment did we detect the formation of dicarboxylic acids or the direct hydroxylation of the heteroaromatic ring.

The performance of this biocatalyst system was studied in more detail on 2,5-dimethylpyrazine (DMP). The oxidation product, 5-methylpyrazine-2-carboxylic acid (MPCA), is an intermediate for the production of 5-methylpyrazine-2-carboxylic acid 4-oxide, a drug with antilipolytic activity.[9] The chemical oxidation of DMP to MPCA along any routes still remains inefficient.[10] Resting cell suspensions furnished with more than 30 mM (3.2 $g L^{-1}$) DMP showed a strong accumulation of 2-hydroxymethyl-5-methylpyrazine, which was only partially oxidized to MPCA. However, high product concentrations and high yields were achieved by performing the biotransformation with growing cells. For this reason a mixture of 75% (v/v) *p*-xylene and 25% (v/v) DMP was supplied as growth substrate in large-scale fermentations. Figure 1 shows the accumulation of up to 20 g MPCA L^{-1} during 54 h bacterial growth on a 20 L scale. 2-Hydroxymethyl-5-methylpyrazine was detected in the medium during early stages of fermentation. The biotransformation was terminated when bacterial growth entered the stationary phase (MPCA concentrations $>15 g L^{-1}$ inhibited the growth of *P. putida*). At the end of the fermentation, MPCA was the only oxidation product of DMP detected in the fermentation broth by HPLC analysis.

Biotransformations up to a volume of 1000 L following a slightly modified fermentation procedure were performed to assess the potential of this biological oxidation method for industrial application: The maximal product concentration was 24 g MPCA L^{-1} (at a yield >95%); the concentration of DMP at the end of the biotransformation was below

[*] Dr. A. Kiener
Lonza AG
Biotechnology Research Department
CH-3930 Visp (Switzerland)

[**] I thank R. Glöckler and K. Heinzmann for technical assistance, and Dr. M. Bokel and Dr. M. Hauck for analysis of oxidation products. Fermentations on pilot-plant scale were performed by Dr. M. Rohner.

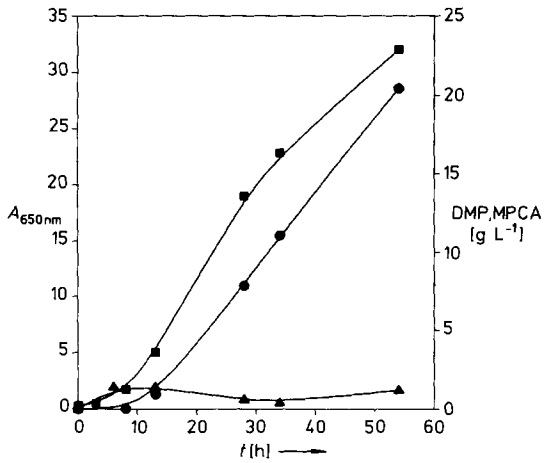

Fig. 1. Microbial oxidation of 2,5-dimethylpyrazine (DMP) to 5-methylpyrazine-2-carboxylic acid (MPCA). Absorption of the cell suspension at 650 nm (■); concentration of DMP (▲) and MPCA (●). After 52 h of fermentation the growth substrate was changed to 100% *p*-xylene.

0.1 g L^{-1}. No bacterial metabolites from *p*-xylene which could hamper product purification were detected in the broth.

In summary, our experiments showed that *P. putida* is a useful biocatalyst for the selective oxidation of a methyl group on aromatic heterocycles to the corresponding monocarboxylic acid. The yield and conditions of the oxidation reactions described here have been optimized only for 2,5-dimethylpyrazine. Nevertheless, in order to develop a general method for the biological oxidation of a methyl group on aromatic heterocycles, we will now focus on the isolation of various mutants defective in the xylene-degradative pathway so that further degradation of certain heteroaromatic carboxylic acids can be prevented or benzylalcohol dehydrogenase inactivated to permit the production of hydroxymethylated compounds.

Experimental Procedure

Starter cultures of *P. putida* were grown in 300 mL Erlenmeyer flasks containing 100 mL of a mineral salt medium (H. G. Kulla, F. Klausener, U. Meyer, B. Lüdeke, T. Leisinger, *Arch. Microbiol.* **1983**, *135*, 1–7) at pH 7. A 10 mL polypropylene tube containing 1 mL *p*-xylene as carbon source was inserted into the Erlenmeyer flask. The xylene vapor formed during incubation at 30 °C on a rotatory shaker was sufficient for cell growth. For large-scale fermentations (20–1000 L) xylene was added directly to the growth medium. The xylene concentration in the fermenter was regulated by measuring the absorbance of fermenter exhaust air at 214 nm with an ISCO UA-5 absorbance detector (ISCO, P.O. Box 5347, Lincoln, NE 68505, USA). The electronic signal of the detector was coupled with a dosage pump for xylene in such a way that the concentration of the growth substrate was about 0.1 mM. Best transformation rates were obtained under substrate-limited growth.

For small-scale biotransformations, methylated heterocycles (10 mM were added to 20 mL suspensions of cells grown on *p*-xylene ($A_{650nm} = 10$) in mineral salt medium in 300 mL sealed flasks to prevent the loss of volatile compounds and incubated for 16 h at 30 °C on a rotatory shaker. Xylene was omitted during biotransformation. The concentrations of oxidation products in cell-free solution were analyzed by thin-layer chromatography. For incomplete conversions the balance of the yield was, in most cases, unoxidized starting material.

Received: December 4, 1991 [Z 5057 IE]
German version: *Angew. Chem.* **1992**, *104*, 748

CAS Registry numbers:
2,5-dimethylpyrrole, 625-84-3; 3,5-dimethylpyrazole, 67-51-6; 2,5-dimethylfuran, 625-86-5; 3-methylthiophene, 616-44-4; 4-methylthiazol, 693-95-8; 3-methylpyridine, 108-99-6; 2-chloro-6-methylpyridine, 18368-63-3; 2-chloro-3-ethyl-6-methylpyridine, 138538-40-6; 2,4-dimethylpyridine, 108-47-4; 2,5-dimethylpyrazine, 123-32-0; 2,3,6-trimethylpyrazine, 14667-55-1; 3-chloro-2,5-dimethylpyrazine, 95-89-6; 5-methylpyrrole-2-carboxylic acid, 3757-53-7; 5-methylpyrazole-3-carboxylic acid, 402-61-9; 5-methylfuran-2-carboxylic acid, 1917-15-3; thiophene-3-carboxylic acid, 88-13-1; thiazole-4-carboxylic acid, 3973-08-8; pyridine-3-carboxylic acid, 59-67-6; 6-chloropyridine-2-carboxylic acid, 4684-94-0; 6-chloro-5-ethylpyridine-2-carboxylic acid, 138538-41-7; 2-methylpyridine-4-carboxylic acid, 4021-11-8; 4-methylpyridine-2-carboxylic acid, 4021-08-3; 5-methylpyrazine-2-carboxylic acid, 5521-55-1; 5,6-dimethylpyrazine-2-carboxylic acid, 13515-06-5; 6-chloro-5-methylpyrazine-2-carboxylic acid, 138538-39-3.

[1] K. Kieslich, *Microbial Transformations*, Thieme, Stuttgart, **1976**, p. 292–523.
[2] D. T. Gibson, *Microbial Degradation of Organic Compounds*, Marcel Dekker, New York, **1984**.
[3] S. Harayama, M. Rekik, M. Wubbolts, K. Rose, R. A. Leppik, K. N. Timmis, *J. Bacteriol.* **1989**, *171*, 5048–5055.
[4] J. P. Shaw, S. Harayama, *Eur. J. Biochem.* **1990**, *191*, 705–714.
[5] S. J. Assinder, P. A. Williams, *Adv. Microb. Physiol.* **1990**, *31*, 1–69
[6] M.-A. Abril, C. Michan, K. N. Timmis, J. L. Ramos, *J. Bacteriol.* **1989**, *171*, 6782–6790.
[7] M. G. Wubbolts, K. N. Timmis, *Appl. Environ. Microbiol.* **1990**, *56*, 569–571.
[8] N. Mermod, S. Harayama, K. N. Timmis, *Biotechnology*, **1986**, *4*, 321–324.
[9] P. P. Lovisolo, G. Briatico-Vangosa, G. Orsini, R. Ronchi, R. Angelucci, *Pharmacol. Res. Commun.* **1981**, *13*, 151–161.
[10] G. P. Borsotti, M. Foa, N. Gatti, *Synthesis*, **1990**, 207–208.

One-Pot Syntheses of Novel Arene Tricarbonyl Chromium Macrocycles and Macrobicycle: Structure of a Pentanuclear Trichromium(0)-Dicopper(I) Cryptate**

By *Marie-Thérèse Youinou,** *Jean Suffert,** and *Raymond Ziessel**

Polyaza receptor molecules with large cavities have recently received a great deal of attention as hosts for metal ions which form binuclear or polynuclear complexes,[1,2] in view of their potential as supramolecular catalysts.[3] Schiff-base condensation of the tris(2-aminoethyl)amine (tren) with suitable dicarbonyl compounds provides N_8 cryptands in good yield.[4] Although macrocycles synthesized from difunctional metal complexes were reported previously,[5,6] such macrobicycles have not yet been prepared. The use of such subunits may provide new photoactive, electroactive, and chiral cryptates. We have recently reported new molecular tweezer ligands based on chiral arene tricarbonyl chromium subunits. Their complexation properties with rhodium(I)[7] and copper(I)[8] as well as their photochemical[9] and electrochemical[10] behavior were studied.

Pursuing this work, we now report a very efficient route, through condensation of various amines with a terephthalaldehyde tricarbonyl chromium complex, to macrocyclic ligands **1** and **2**, macrobicyclic ligands **3**, and a novel trichromium(0)-dicopper(I) cryptate **4**.

The reaction of equimolecular amounts of 1,3-bis(aminomethyl)benzene and chromium(0) complex **6** (synthesized from its precursor **5**[11]) in chloroform gave pure macrocycle

[*] Dr. M.-T. Youinou
Laboratoire de Chimie des Métaux de Transition et de Catalyse
UA au CNRS n° 424, Institut Le Bel
Université Louis Pasteur
4, rue Blaise Pascal, F-67000 Strasbourg (France)
Dr. J. Suffert
Laboratoire de Pharmacologie Moléculaire
UPR au CNRS n° 421, Centre de Neurochimie
5, rue Blaise Pascal, F-67084 Strasbourg Cedex (France).
Dr. R. Ziessel
Ecole Européenne des Hautes Etudes des Industries Chimiques de Strasbourg
IPCMS/GMI, URM au CNRS n° 46
1, rue Blaise Pascal, F-67008 Strasbourg Cedex (France)

[**] This work was supported by the Centre National de la Recherche Scientifique. RZ thanks Prof. J. M. Lehn for research facilities.

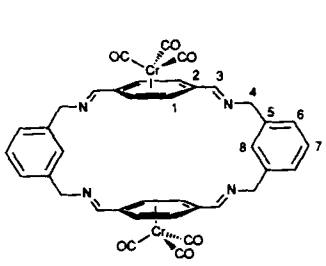

1

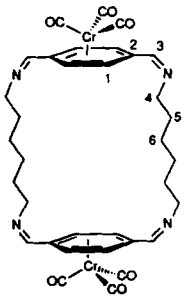

2

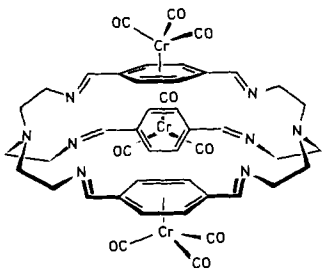

3

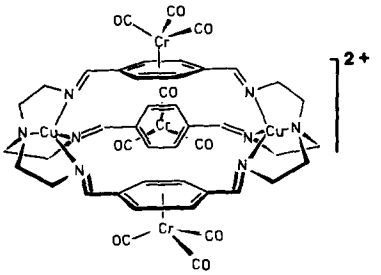

4

1 in 75% yield after recrystallization. If the reaction is carried out in anhydrous tetrahydrofuran, macrocycle **1** is also formed (55% yield); then the ^{1}H NMR spectrum shows an additional singlet at $\delta = 10.92$ ppm, corresponding to four protons. The rapid H–D exchange detected for these protons in D_2O suggests that two water molecules are present, which interact weakly with the macrocycle through hydrogen bonding with alkylidenamine units. The significant deshielding of the water protons probably indicates the formation of an inclusion complex containing two water molecules in the intramolecular cavity of the receptor;[12] the water protons are then expected to be in the deshielding cone of the arene–chromium subunit. To our knowledge, the strength of this effect is very unusual although a similar behavior was observed in the diprotonated form of a spheroidal macrotricycle ligand but the chemical shift for the water protons was much lower ($\delta = 7.32$[12c]). It is also worth noting that condensation of 1,3-bis(aminomethyl)benzene with terephthalaldehyde in anhydrous tetrahydrofuran gave the expected macrocycle, which polymerized after a few hours even at low temperature (−30 °C). It therefore demonstrates that the coordination of the tricarbonyl chromium subunits leads to a stabilization of the alkylidenamine bonds, probably as a result of both electronic[13a] and steric effects. Surprisingly, the use of flexible diamines such as 1,6-diaminohexane also gave macrocycle **2** in an excellent yield (75%).

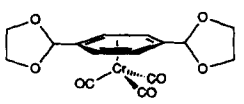

5

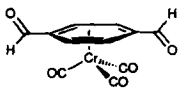

6

Macrobicycle **3** was prepared by addition of dialdehyde **6** (3 equiv) to a solution of tren (2 equiv) in acetonitrile at room temperature. Precipitation of the corresponding macrobicycle hexaimine from the reaction mixture yielded a yellow solid (95% yield, $\lambda_{max} = 430.4$ nm, $\varepsilon = 6600$). Interestingly, this one-pot cyclization which leads to the creation of six bonds does not require high dilution conditions since the expected product precipitates readily from the reaction mixture.

Treatment of cryptand **3** with $[Cu(CH_3CN)_4]ClO_4$[14] in a 1:2 ratio gave the orange-red complex **4** (yield 85%, $\lambda_{max} = 448.4$ nm, $\varepsilon = 12000$), which was fully characterized. In particular, its ^{1}H NMR spectrum was markedly different from that of the macrobicycle **3**: the signals of the alkylidenamine, the complexed aromatic, and the methylene protons α to the alkylidenamine bonds were shifted downfield,

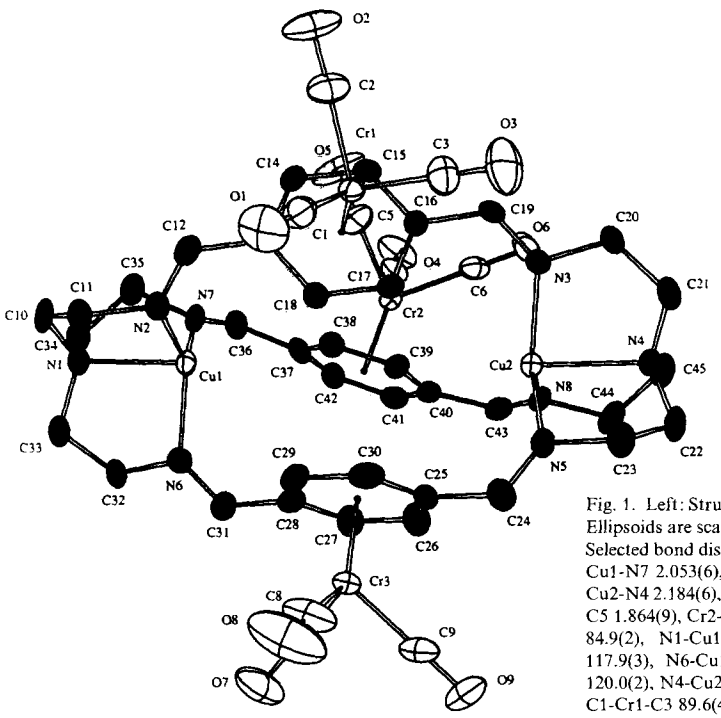

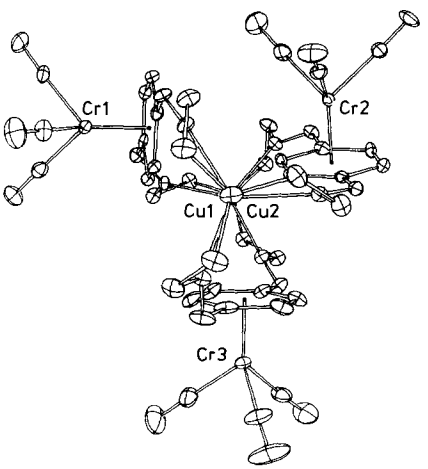

Fig. 1. Left: Structure (ORTEP plot) of **4** · 0.5 CH_2Cl_2 showing the numbering scheme used. Ellipsoids are scaled to enclose 50% of the electronic density. Hydrogen atoms are omitted. Selected bond distances [Å] and angles [°] are as follows: Cu1-N2 1.949(6), Cu1-N6 1.983(6), Cu1-N7 2.053(6), Cu1-N1 2.207(6), Cu2-N5 1.985(6), Cu2-N3 1.995(6), Cu2-N8 2.020(6), Cu2-N4 2.184(6), Cr1-C1 1.846(9), Cr1-C2 1.849(9), Cr1-C3 1.847(9), Cr2-C4 1.860(9), Cr2-C5 1.864(9), Cr2-C6 1.862(9), Cr3-C7 1.83(1), Cr3-C8 1.82(1), Cr3-C9 1.82(1); N1-Cu1-N2 84.9(2), N1-Cu1-N6 85.6(2), N1-Cu1-N7 82.4(2), N2-Cu1-N6 128.9(3), N2-Cu1-N7 117.9(3), N6-Cu1-N7 110.4(3), N3-Cu2-N4 85.6(2), N3-Cu2-N5 126.3(3), N3-Cu2-N8 120.0(2), N4-Cu2-N5 85.7(2), N4-Cu2-N8 84.9(2), N5-Cu2-N 111.7(3), C1-Cr1-C2 86.7(4), C1-Cr1-C3 89.6(4), C2-Cr1-C3 89.0(4). Right: Viewed along the bridgehead N-N axis.

whereas the methylene protons α to the bridgehead nitrogens were not affected. The most significant shift ($\Delta\delta = 0.42$) observed for the alkylidenamine protons was due to coordination of the copper(I) cations. In addition, the IR stretching band ν(C=N) was shifted 30 cm^{-1} by the copper complexation, as previously observed for other related compounds[8] and for copper(I) Schiff's base complexes.[15] Additionally, the crystal structure of cryptate **4** was determined[16] (Fig. 1). The hexaimine cavity has an elongated ellipsoidal shape (with a separation of 11.041(9) Å between the bridgehead nitrogens N1 and N4). The two copper atoms are 6.655(1) Å apart and inside the molecular cavity, whereas the three chromium atoms span a triangle outside the cavity (Cr1 ··· Cr2 6.349(2), Cr1 ··· Cr3 7.415(2), Cr2 ··· Cr3 7.217(2) Å). Each copper(I) ion is similarly coordinated in a distorded tetrahedral fashion to three alkylidenamine nitrogens (Cu1-N2 1.949(6), Cu1-N6 1.983(6), Cu1-N7 2.053(6), Cu2-N5 1.985(6), Cu2-N3 1.995(6), Cu2-N8 2.020(6) Å) and to one bridgehead nitrogen at a longer distance (Cu1-N1 2.207(6) and Cu2-N4 2.184(6) Å). As expected, the geometry about the three chromium atoms is very similar to that of the closely related complex $[C_6H_6Cr(CO)_3]$,[17] which has comparable distances and angles. Furthermore, the mean plane of the phenyl ring containing C13 through C18 is roughly perpendicular to those containing C25 through C30 (89.4(3)°) and C37 through C42 (82.3(3)°). More interestingly, the angle of 165.5(2)° between the mean planes of the phenyl rings involved in coordination with Cr3 and Cr2 (C25 through C30 and C37 through C42 respectively) illustrates the distorsion of the core complex, leading to the absence of a threefold axis of symmetry. When comparing the structure of the same hexaimine macrobicyclic ligand coordinated to two Ag^+ ions (approximate D_3 symmetry[4c]) one may suggest the specific role of the tricarbonylchromium entity in the overall conformation of the core.

Cryptand **3** is the first cage constructed from a difunctional metal complex and cryptate **4** represents a novel pentanuclear entity, containing two encapsulated Cu(I) ions and three photo- and/or electroactive complex fragments in the periphery of the molecular cavity. The synthesis of optically pure receptors from chiral arene tricarbonyl chromium building blocks for use in enantioselective recognition of chiral molecules now seems feasible.

Experimental Procedure

All syntheses were carried out under inert atmosphere with dried and degassed solvents.

1: To a solution of freshly distilled 1,3-bis(aminomethyl)benzene (0.25 g, 1.85 mmol) in anhydrous $CHCl_3$ (40 mL) under argon at room temperature was added a solution of **6** (0.5 g, 1.85 mmol) in $CHCl_3$ (40 mL) within 30 min. After 96 h the solvent was removed under vacuum, the residue dissolved in hot THF, and the mixture cooled and kept at −30 °C overnight. The orange-yellow solid was filtered, washed with Et_2O, and dried under vacuum: Yield 75%.

UV/VIS (CH_2Cl_2): λ_{max} [nm] (ε) = 428.6 (2500), 326.4 (11000), 229.2 (36000). ^1H NMR (for numbering see the structural formula of **1**): (200.1 MHz, [D$_8$]THF, 25 °C): δ = 4.90 (s, 8H; H4), 6.21 (s, 8H; H1), 7.17 (d, 4H, ^3J(H,H) = 6.8 Hz; H6), 7.30 (t 2H, ^3J(H,H) = 6.8 Hz, H7), 7.59 (s, 2H; H8), 8.11 (s, 4H; H3); ^{13}C NMR (100.6 MHz, [D$_8$]THF, 25 °C): δ = 65.25 (C4), 94.64 (C1), 104.47 (C2), 127.18 (C6), 127.57 and 129.76 (C7 or C8), 142.41 (C5), 160.79 (C3), 234.06 (CO). MS (FAB$^+$, *m*-nitrobenzyl alcohol matrix): *m/z* 741.3 (M^+ + H), 656.3 (M^+ − 3CO), 572.3 (M^+ − 6CO), 519.2 (M^+ − 6CO − Cr − H). IR (CH_2Cl_2): $\tilde{\nu}$ [cm^{-1}] = 2960 (CH_2), 1980, 1915 (C=O), 1610 (C=N). Correct C,H,N analyses.

2: A solution of **6** (250 mg, 0.926 mmole) in THF (15 mL) was added slowly to a stirred solution of 1.6-diaminohexane (108 mg, 0.926 mmol) in anhydrous THF (20 mL). After 24 h, the solvent was removed under vacuum, and the residue recrystallized in THF/Et_2O. The deep orange solid was filtered, washed with Et_2O and dried under vacuum: Yield 95%.

UV/VIS (CH_2Cl_2) λ_{max} [nm] (ε) = 423.8 (4100), 327.4 (14900), 232.0 (47200). ^1H NMR (for numbering see structural formula of **2**) (200.1 MHz, $CDCl_3$, 25 °C): δ = 1.39 (m, 8H; H6), 1.67 (m, 8H, H5), 3.58 (t, 8H, ^3J(H,H) = 6.6 Hz, H4), 5.85 (s, 8H; H1), 7.84 (s, 4H; H3); ^{13}C NMR (50.3 MHz, $CDCl_3$, 25 °C): δ = 27.72 (C6), 31.46 (C5), 61.83 (C4), 92.24 (C1), 102.13 (C2), 157.32 (C3), 232.08 (CO). MS (FAB$^+$, *m*-nitrobenzyl alcohol matrix): *m/z* 701.0 (M^+ + H), 565.1 (M^+ − 3CO). IR ($CHCl_3$): $\tilde{\nu}$ [cm^{-1}] = 2930 (CH_2), 1980, 1915 (C=O), 1610 (C=N). Correct C,H,N analyses.

3: To a stirred solution of tris(2-aminoaethyl)amine (0.105 g, 0.715 mmol) in anhydrous CH_3CN (30 mL) under argon was added at room temperature, a solution of **6** (0.290 g, 1.07 mmol) in CH_3CN (15 mL) within 2 hours. During the addition the color of the solution turned orange, and a yellow precipitate formed rapidly. After 15 h the solid was filtered, washed with Et_2O, and recrystallized in CH_2Cl_2/hexane at −20 °C: Yield: 95%.

UV/VIS (CH_2Cl_2) λ_{max} [nm] (ε) = 430.4 (6600), 331.4 (26000), 229.6 (75000). ^1H NMR (200.1 MHz, $CDCl_3$, 25 °C): δ = 2.68 (m, 12H; CH_2), 3.72 (m, 12H; CH_2), 5.55 (s, 12H; complexed arene H), 7.77 (s, 6H, N=CH). ^{13}C NMR (50.3 MHz, [D$_6$]DMSO, 25 °C): δ = 51.67, 57.11, 93.51, 103.50, 157.38, 233.15. MS (FAB$^+$, *m*-nitrobenzyl alcohol matrix): *m/z* 995.1 (M^+ + H), 911.2 (M^+ − 3CO + H), 859.2 (M^+ − Cr − 3CO + H), 827.2 (M^+ − 6CO + H). IR (CH_2Cl_2): $\tilde{\nu}$ [cm^{-1}] = 2965 (CH_2), 1968, 1905 (C=O), 1655 (C=N). Correct C,H,N analyses.

4: To a stirred solution of **3** (50 mg, 0.05 mmol) in anhydrous CH_2Cl_2 (5 mL) under argon was added at room temperature a colorless solution of $[Cu(CH_3CN)_4]ClO_4$ (33 mg, 0.1 mmol) in anhydrous CH_3CN (5 mL). The color of the solution turned deep red instantaneously, showing rapid Cu(I) complexation. After 48 h the solution was filtered over celite. Slow diffusion of pentane produced complex **4** as crystals suitable for X-ray analysis. Yield 86%.

UV/VIS (CH_3CN) λ_{max} [nm] (ε) = 448.4 (12000), 332.2 (34000), 217.2 (11800). ^1H NMR (200.1 MHz, CD_3CN, 25 °C): δ = 3.08 (m, 12H, CH_2), 3.79 (m, 12H; CH_2), 5.98 (s, 12H; complexed arene H), 8.19 (s, 6H; N=CH): ^{13}C NMR (50.3 MHz, CD_3CN, 25 °C): δ = 51.68, 60.77, 91.37, 101.66, 161.81, 238.83. MS (FAB$^+$, *m*-nitrobenzyl alcohol matrix): *m/z* 1220.6 (M^+ − ClO_4), 1084.7 (M^+ − ClO_4 − $Cr(CO)_3$), 948.8 (M^+ − ClO_4 − 2Cr(CO)$_3$), 812.9 (M^+ − ClO_4 − 3Cr(CO)$_3$), 713.0 (M^+ − 2ClO_4 − 3Cr(CO)$_3$), 649.1 (M^+ − 2ClO_4 − 3Cr(CO)$_3$ − Cu). IR (CH_3CN): $\tilde{\nu}$ [cm^{-1}] = 1970, 1920 (C=O), 1625 (C=N). Correct C,H,N analyses for $[C_{45}H_{42}Cr_3N_8O_9Cu_2](ClO_4)_2$.

Received: December 14, 1991 [Z 5072 IE]
German version: *Angew. Chem.* **1992**, *104*, 796

CAS Registry numbers:
1, 141249-72-1; **2**, 141249-73-2; **3**, 141249-74-3; **4**, 141249-76-5; **4** · 0.5 CH_2Cl_2, 141249-77-6; **6**, 57560-53-9; 1,3-bis(aminomethyl)benzene, 1477-55-0; 1,6-diaminohexane, 124-09-41; tris(2-aminoethyl)amine, 4097-89-6.

[1] a) J. P. Lecomte, J. M. Lehn, D. Parker, J. Guilhem, C. Pascard, *J. Chem. Soc. Chem. Commun.* **1983**, 296–298; b) J. Comarmond, B. Dietrich, J. M. Lehn, R. Louis, *ibid.* **1985**, 74–76; c) A. Bencini, A. Bianchi, E. Goria-España, M. Micheloni, P. Paoletti, *Inorg. Chem.* **1988**, *27*, 176–180; d) A. Bencini, A. Bianchi, E. Goria-España, S. Mangani, M. Micheloni, P. Orieli, P. Paoletti, *ibid.* **1988**, *27*, 1104–1107.

[2] J. de Mendoza, E. Mesa, J. C. Rodriguez-Ubis, P. Vasquez, F. Vögtle, P. M. Windscheif, K. Rissanen, J. M. Lehn, D. Lilienbaum, R. Ziessel, *Angew. Chem.* **1991**, *103*, 1365–67; *Angew. Chem. Int. Ed. Engl.* **1991**, *30*, 1331–1333.

[3] J. M. Lehn, *Angew. Chem.* **1988**, *100*, 91–114; *Angew. Chem. Int. Ed. Engl.* **1988**, *27*, 89–112.

[4] a) J. Jazwinski, J. M. Lehn, D. Lilienbaum, R. Ziessel, J. Guilhem, C. Pascard, *J. Chem. Soc. Chem. Commun.* **1987**, 1691–1694; b) D. McDowell, J. Nelson, *Tetrahedron Lett.* **1988**, *29*, 385–386; c) M. G. B. Drew, D. McDowell, J. Nelson, *Polyhedron* **1988**, *7*, 2229–2232; d) O. Kocian, R. J. Mortimer, P. D. Beer, *Tetrahedron* Lett. **1990**, *31*, 5069–5072; e) J. Hunter, J. Nelson, C. Harding, M. McCann, V. McKee, *J. Chem. Soc. Chem. Commun.* **1990**, 1148–1151; f) M. P. Ngwenya, A. E. Martell, J. Reibenspies, *ibid.* **1990**, 1207–1208.

[5] C. Baldoli, P. Del Buttero, S. Maiorana, A. Pagagni, *J. Chem. Soc. Chem. Commun.* **1985**, 1181–1182.

[6] P. D. Beer, *Chem. Soc. Rev.*, **1989**, *18*, 409–450; b) S. Jagadishwar Rao, C. I. Milberg, R. C. Petter, *Tetrahedron Lett.*, **1991**, *32*, 3775–3778, and references cited therein.

[7] J. Suffert, R. Ziessel, *J. Organomet. Chem.* **1989**, *359*, C45–49.

[8] R. Ziessel, J. Suffert, *J. Chem. Soc. Chem. Commun.* **1990**, 1105–1107.

[9] R. M. Everly, R. Ziessel, J. Suffert, D. R. McMillin, *Inorg. Chem.* **1991**, *30*, 559–561.

[10] C. Diaz, J. P. Gisselbrecht, M. Gross, J. Suffert, R. Ziessel, *J. Organomet. Chem.* **1991**, *401*, C 54-60.

[11] E. W. Neuse, *J. Organomet. Chem.* **1975**, *99*, 287–295, and references cited therein.

[12] a) G. W. Gokel, B. J. Garcia, *Tetrahedron Lett.* **1977**, *4*, 317–320; b) I. Golberg, *Acta Cryst.* **1978**, *B34*, 3387–3390; c) E. Graf, Dissertation; Université Louis Pasteur, Straßburg, **1979**, p. 62; d) S. Buoen, J. Dale, P. Groth, J. Krane, *J. Chem. Soc. Chem. Commun.* **1982**, 1172–1174.

[13] A. Ceccon, G. Catelani, *J. Organomet. Chem.* **1974**, *72*, 179–188.
[14] B. J. Hathaway, D. G. Holah, J. D. Poslethwaite, *J. Chem. Soc.* **1961**, 3215–3218.
[15] A. Toth, C. Floriani, M. Pasquali, A. Chiesi-Villa, A. Gaetoni-Manfredotti, C. Guastini, *Inorg. Chem.* **1985**, *24*, 648–653.
[16] Crystal structure analysis of $4 \cdot 0.5CH_2Cl_2$: $C_{45}H_{42}N_8O_{17}Cl_2Cr_3Cu_2 \cdot 0.5CH_2Cl_2$, triclinic, space group $P\bar{1}$; $a = 13.107(3)$, $b = 18.674(5)$, $c = 11.795(3)$ Å, $\alpha = 104.61(2)$, $\beta = 101.51(2)$, $\gamma = 81.80(2)^\circ$, $M = 1363.31$, $V = 2724.4$ Å^3, $Z = 2$, $\varrho_{calcd.} = 1.662$ g cm^{-3}, $F(000) = 1372$, $Mo_{K\alpha}$ radiation, $\lambda = 0.71073$ Å, $\mu(Mo_{K\alpha}) = 15.58$ cm^{-1}. CAD-4-diffractometer, 20 °C; 7815 reflections, of which 4637 with $I > 3\sigma(I)$. Non-hydrogen atoms with the exception of the disordered oxygen atoms of one ClO_4^--group refined anisotropically. 709 variables, $R = 0.060$, $R_w = 0.084$. Further details of the crystal structure investigation are available on request from the Director of the Cambridge Crystallographic Data Centre, University Chemical Laboratory, Lensfield Road, GB-Cambridge CB2 1EW (UK), on quoting the full journal citation.
[17] B. Rees, P. Coppens, *Acta Crystallogr. Sect. B* **1973**, *29*, 2516–2535.

2,2′,5,5′-Tetra-*tert*-butyl-1,1′-diazaplumbocene—a Stable Azacyclopentadienyl Compound of Lead**

By *Norbert Kuhn,* Gerald Henkel,* and *Stefan Stubenrauch*

Dedicated to Professor Wolfgang Beck on the occasion of his 60th birthday

Azacyclopentadienides[1] and other π ligands[2, 3] formally derived from the cyclopentadienide ion by the exchange of CH fragments for heteroatoms are applied successfully in the complex chemistry of the transition metals; however, attempts at the coordination on main group element centers analogous to the rapidly developing chemistry of the cyclopentadienyl complexes[4] have so far not been very successful. Heterometallocenes of divalent group 14 elements, which have been the focus of attention since the discovery of the decamethylsilicocene,[5] are unknown apart from a small number of tin complexes with boron-containing ligands.[6] With the recently demonstrated stabilization of the diazametallocene structure by steric shielding of the nitrogen atoms in complexes of the type **1**, M=Fe,[7a] Co,[7b] now also the coordination of two azacyclopentadienyl ligands to divalent main group element centers is possible as is shown for example for lead. By the lithiation of 2,5-di-*tert*-butylpyrrole

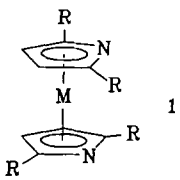

1

2 and subsequent reaction with $PbCl_2$, the stable diazaplumbocene **3** is accessible in good yields (Scheme 1). Compound **3** is the first heteroplumbocene and at the same time also the first azacyclopentadienyl compound of a main group element with classical π coordination.[8]

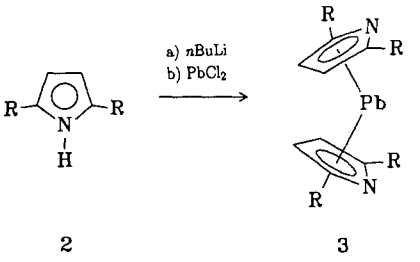

2 3

Scheme 1. R = *tert*-butyl.

Unlike the well-known plumbocene itself,[9, 10] **3** is monomeric in the solid state (Fig. 1.). The crystal structure analysis[11] shows the tilting of the ring planes (Pyr_z–Pb–Pyr'_z 142.7°) also observed for the decamethylplumbocene.[12] This occurs as a result of the stereochemically active lone pair at the metal center,[13] which only allows a parallel arrangement of the ring ligands for strong and uniform steric loading such as in $[(C_5Me_5)_2Si]$[5] and $[(C_5Ph_5)_2Sn]$.[14] The shift of the central atom ("slip") in the direction of the nitrogen atoms N1 and N2 lying opposite to the carbon atoms C2 and C3 and C14 and C15 is identifiable from the Pb–C bond lengths. This is contrary to the geometry of the diazametallocenes **1** and can be seen as the result of the tilted structure; a similar "slip" occurs in the decamethylplumbocene.[12]

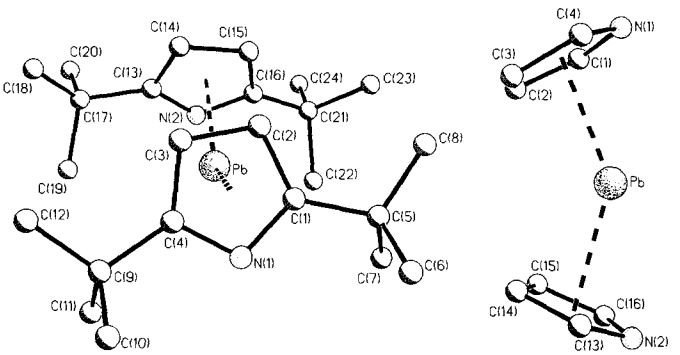

Fig. 1. Plan view and side view of the crystal structure of **3** (without hydrogen atoms, in the side view also without *tert*-butyl groups). Selected bond distances [Å] and valence angles [°] with standard deviations: Pb-N(1) 2.878(12), Pb-C(1) 2.752(14), Pb-C(2) 2.628(11), Pb-C(3) 2.672(11), Pb-C(4) 2.814(12), Pb-N(2) 2.854(12), Pb-C(13) 2.719(19), Pb-C(14) 2.604(18), Pb-C(15) 2.625(14), Pb-C(16) 2.832(13), N(1)-C(1) 1.389(14), N(1)-C(4) 1.373(20), C(1)-C(2) 1.420(25), C(2)-C(3) 1.415(19), C(3)-C(4) 1.426(20), N(2)-C(13) 1.341(21), N(2)-C(16) 1.350(16), C(13)-C(14) 1.398(16), C(14)-C(15) 1.425(22), C(15)-C(16) 1.433(17); N(1)-C(1)-C(2) 111.9(13), N(1)-C(4)-C(3) 111.9(10), C(1)-N(1)-C(4) 104.7(12), C(1)-C(2)-C(3) 105.6(12), C(2)-C(3)-C(4) 105.9(14), N(2)-C(13)-C(14) 111.3(13), N(2)-C(16)-C(15) 109.0(13), C(13)-N(2)-C(16) 108.5(11), C(13)-C(14)-C(15) 105.3(13), C(14)-C(15)-C(16) 105.7(11).

The steric relief in **3** also caused by the tilting of the ring ligands enables a reduction of the torsion angle N1–Pyr_z–Pyr'_z–N2 to 17.2° in contrast to ca. 85° in **1**.[7] An eclipsed conformation with heteroatoms in the *syn* position can be forced in derivatives of the coplanar diazaferrocene by fixing the nitrogen atoms to the bridging metal centers.[15] In contrast to **3**, the significantly extended distance between the central atom and the ring planes (Pyr_z–Pb 2.477, Pyr'_z 2.459 Å) in decamethylplumbocene can be interpreted as a result of repulsive steric interactions between the tilted C_5Me_5 ligands. For the carbocyclic plumbocene this cannot even be balanced by a staggered arrangement of the ligands.

[*] Prof. Dr. N. Kuhn, Prof. Dr. G. Henkel, Dipl.-Chem. S. Stubenrauch
Fachbereich 6 der Universität-Gesamthochschule
Lotharstrasse 1, D-W-4100 Duisburg 1 (FRG)

[**] Heterocycles as ligands, part 14. This work was supported by the Deutsche Forschungsgemeinschaft and the Fonds der Chemischen Industrie. Part 13: [7b].

Compound **3** can be compared with its carbocyclic analogue **4**[16] only in solution, since **4** was not structurally characterized. The ^{207}Pb–^{1}H and ^{207}Pb–^{13}C coupling constants of **3** ($^{2}J_{Pb,H} = 33.6$, $^{1}J_{Pb,C2} = 5.8$, $^{1}J_{Pb,C3} = 31.8$ Hz) are smaller than those of **4**, which might indicate a larger percentage of ionic bonding in **3**. The significant deshielding of the carbon atoms contained in the ring in **3** (δ C2,C5 = 161.71, C3,C4 = 105.19) in comparison with the pyrrole **2** (δ C2,C5 = 139.51, C3,C4 = 102.70) is contrary to the coordination shift in the azacyclopentadienyl compounds of the transition metals.[1, 7, 17] The exchange of two

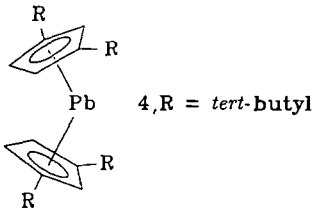

4, R = *tert*-butyl

CH fragments contained in the ring of **4** for nitrogen atoms leads to a significant deshielding of the Pb atom [δ(^{207}Pb) = −4142 in **3** in contrast to −4756 in **4**]. The mass spectrum (EI) shows, probably as a result of the low thermal capacity of **3** (decomposition above 104 °C), the molecular peak only in low intensity.

The synthesis of the diazoplumbocene **3** shows that the azacyclopentadienyl ligand is also suitable for the formation of low molecular weight main group element π complexes. This opens up new possibilities in the coordination chemistry of pyrrole and its derivatives.

Experimental Procedure

To a suspension of $PbCl_2$ (1.39 g, 5.2 mmol) and 2,5-$C_4R_2H_2NLi$ (R = *tert*-butyl) (1.94 g, 10.5 mmol) in toluene (50 mL), THF (2 mL) was added, and the mixture was stirred for 2 h. After the removal of the volatiles the residue was extracted with *n*-pentane (40 mL). After recrystallization yellow crystals of **3** were obtained. Yield 2.50 g, (85%). M.p. 104 °C (decomp).

^{1}H NMR (60 MHz, C_6F_6, TMS int.): δ = 5.51 (4H; C(3,4)-H; ^{2}J (^{207}Pb, ^{1}H) = 33.6 Hz), 1.39 (s, 36H; Me); ^{13}C NMR (75.43 MHz, C_6H_6, TMS int.): δ = 161.71 (C2,C5; ^{1}J(^{207}Pb, ^{13}C) = 5.8 Hz), 105.19 (C3,C4; ^{1}J(^{207}Pb, ^{13}C) = 31.4 Hz), 33.31 (qC), 32.69 (Me); ^{207}Pb NMR (62.7 MHz, C_6H_6, $PbMe_4$ ext.): δ = −4142. – MS (70 eV, EI): *m/z* 564 (M^+, 1%), 386 (M^+ − pyr, 20), 164 (pyr − H^+ − Me, 100), and further fragments.

Received: December 19, 1991 [Z 5081 IE]
German version: *Angew. Chem.* **1992**, *104*, 766

CAS Registry numbers:
2, 3760-56-3; **3**, 140633-73-4; $PbCl_2$, 7758-95-4.

[1] Compare N. Kuhn, *Bull. Soc. Chim. Belg.* **1990**, *99*, 707; J. Zakrezewski, *Heterocycles* **1990**, *31*, 383; D. L. Kershner, F. Basolo, *Coord. Chem. Rev.* **1987**, *79*, 279.

[2] Reviews: F. Mathey, *J. Organomet. Chem.* **1990**, *400*, 149; O. J. Scherer, *Angew. Chem.* **1990**, *102*, 1137; *Angew. Chem. Int. Ed. Engl.* **1990**, *29*, 1104; W. Siebert, *Pure Appl. Chem.* **1988**, *60*, 1345; J. F. Nixon, *Chem. Rev.* **1988**, *88*, 1327; G. Schmid, *Comments Inorg. Chem.* **1985**, *4*, 17.

[3] G. E. Herberich, U. Englert, M. Hostalek, R. Laven, *Chem. Ber.* **1991**, *124*, 17; P. Jutzi, A. Karl, P. Hofmann, *Angew. Chem.* **1980**, *92*, 496; *Angew. Chem. Int. Ed. Engl.* **1980**, *19*, 484, and references cited therein.

[4] Review: P. Jutzi, *J. Organomet. Chem.* **1990**, *400*, 1; P. Jutzi, *Pure Appl. Chem.* **1990**, *62*, 1035; *ibid.* **1989**, *61*, 1731; *Adv. Organomet. Chem.* **1986**, *26*, 217.

[5] P. Jutzi, D. Kanne, C. Krüger, *Angew. Chem.* **1986**, *98*, 163; *Angew. Chem. Int. Ed. Engl.* **1986**, *25*, 164.

[6] H. Wadepohl, H. Pritzkow, W. Siebert, *Organometallics* **1983**, *2*, 1899; G. Schmid, D. Zaika, R. Boese, *Angew. Chem.* **1985**, *97*, 581; *Angew. Chem. Int. Ed. Engl.* **1985**, *24*, 602.

[7] a) N. Kuhn, K. Jendral, R. Boese, D. Bläser, *Chem. Ber.* **1991**, *124*, 89; b) N. Kuhn, M. Köckerling, S. Stubenrauch, D. Bläser, R. Boese, *J. Chem. Soc. Chem. Commun.* **1991**, 1368.

[8] A bridging coordination of the azacyclopentadienyl ligand is observed in several alkali metal complexes with the additional use of the lone pair on the nitrogen atom: N. Kuhn, G. Henkel, J. Kreutzberg, *Angew. Chem.* **1990**, *102*, 1179; *Angew. Chem. Int. Ed. Engl.* **1990**, *29*, 1143; K. Gregory, M. Bremer, P. von R. Schleyer, P. A. A. Klusener, L. Brandsma, *ibid.* **1989**, *101*, 1261 bzw. **1989**, *28*, 1224.

[10] The plumbocene monomeric in the gas phase is converted to a coordination polymer by the transition in the solid state; C. Panattoni, G. Bombierie, U. Croatto, *Acta Crystallogr.* **1966**, *21*, 823; A. Almenningen, A. Haaland, T. Motzfeld, *J. Organomet. Chem.* **1967**, *7*, 97.

[11] **3**: (133 K): trigonal, $P3_2$ $a = 12.748(6)$, $c = 12.748(6)$ Å, $V = 3764.28$ Å^3, $Z = 6$, $\rho_{calcd} = 1.492$ g cm^{-3}, $Mo_{K\alpha}$ radiation, $2\theta_{max} = 48^{\circ}$, 4510 independent reflections, 4126 observed reflections ($F_0 > 3.92\sigma(F_0)$), $R = 0.0343$, $Rw = 0.0342$, $w = [\sigma^2(Fo) + (0.01F_0)^2]^{-1}$. There are two symmetry independent molecules in the crystal with only a few differences in the molecular geometry; for the discussion the data of the Pb1 containing molecule were used. Further details of the crystal structure investigation may be obtained from the Fachinformationszentrum Karlsruhe, Gesellschaft für wissenschaftlich-technische Information mbH, D-W-7514 Eggenstein-Leopoldshafen 2 (FRG) on quoting the depository number CSD-56037, the names of the authors, and the journal citation.

[12] J. L. Atwood, W. E. Hunter, A. H. Cowley, R. A. Jones, C. A. Stewart, *J. Chem. Soc. Chem. Commun.* **1981**, 925.

[13] The bonding geometry of metallocenes of the divalent Group 14 elements has been discussed for example for stannocene and its derivatives; compare P. D. Lickiss in *Chemistry of Tin* (Ed.: P. G. Harrison), Blackie & Son, Glasgow, **1989**, Chapter 7.

[14] M. J. Heek, C. Janiak, J. J. Zuckerman, *J. Am. Chem. Soc.* **1984**, *106*, 4259.

[15] N. Kuhn, E.-M. Horn, R. Boese, D. Bläser, *Chem. Ber.* **1989**, *122*, 2275.

[16] P. Jutzi, R. Dickbreder, *J. Organomet. Chem.* **1989**, *373*, 301.

[17] N. Kuhn, A. Kuhn, E.-M. Lampe, *Chem. Ber.* **1991**, *124*, 997, and references cited therein.

Benzo-1,2,3-triselenolium Trifluoromethanesulfonate—a C_2Se_3 Radical Cationic Salt with Unusual Solid-State Structure**

By *Gotthelf Wolmershäuser** and *Gert Heckmann*

Ring compounds containing S atoms with a 7π electron framework are often unusually stable.[1, 2] In contrast, there are hardly any of the homologous Se compounds known. However, we recently proved the existence of such an unstable compound with the radical **1**. Compound **1** was formed by the reduction of the corresponding cationic 6π electron species.[3] If the N atom in **1** is replaced by Se^+, then the benzo-1,2,3-triselenolium radical cation **2** is obtained, which contains a new 7π-electron heterocycle.

1

2

To our knowledge **2** is the first selenium-centered radical cation with a cyclic C_2Se_3 unit. There are two possible synthetic routes for the preparation of **2**. A reaction step which occurs in both cases is the addition of Se to a Se–halogen bond (Scheme 1). Compound **2**-Cl is formed at room temperature by the reaction of *o*-$C_6H_4Se_2Cl_2$[3] (**3**) with two equivalents of gray selenium in 72% yield. Alternatively, $(C_6H_4Se_2)_x$[4]

[*] Dr. G. Wolmershäuser, Dipl.-Chem. G. Heckmann
Fachbereich Chemie der Universität
Erwin-Schrödinger-Strasse, D-W-6750 Kaiserslautern (FRG)

[**] This work was supported by the Deutsche Forschungsgemeinschaft. We thank Prof. Dr. D. Dormann and Dr. H. Winter, Physikalisches Institut der Universität Karlsruhe, for the magnetic measurements.

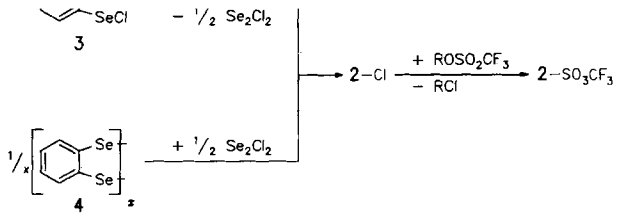

Scheme 1. R = $SiMe_3$

(**4**) can be allowed to react with Se_2Cl_2 under the same reaction conditions. Compound **2**-Cl is a dark blue solid, which is almost insoluble in organic solvents. Readily soluble salts are obtained if the Cl^- is exchanged for complex anions such as $SO_3CF_3^-$. Thus, from the reaction of **2**-Cl with trimethylsilyl trifluoromethanesulfonate and subsequent extraction with acetonitrile a deep violet solution of **2**-SO_3CF_3 is formed, from which gold-colored, metallic shiny crystals precipitate on removal of the solvent.

The X-ray crystal structure[5] shows that **2**-SO_3CF_3 is dimeric in the solid state[6, 7] (Fig. 1). The five-membered heterocycle is almost planar (maximum deviation of the atoms from the plane is 0.09 Å) and coplanar to the C_6 ring. The dimers are formed by two rings which are superimposed and are arranged almost parallel to one another. This conformation allows almost identical interactions for all Se atoms and thus, despite the Coulombic repulsion, an effective spin pairing between the two cations. The average Se–Se distance between the monomeric units in the rings is 3.2 Å, significantly longer than a Se–Se single bond (2.35 Å); however, it is also considerably shorter than the van der Waals distance (4 Å). Somewhat weaker Se···Se interactions between the monomeric units (3.57 Å and 3.76 Å in the direction of the *a* axis, and 3.72 Å along the *c* axis) additionally cause a cross linkage of the planes (Fig. 2). Cation–anion interactions (Se···O = 2.7–3.0 Å), in which two oxygen atoms of two trifluoromethanesulfonate anions bridge the four Se–Se bonds of a dimer, contribute to the reduction of the coulombic repulsion of the cations.

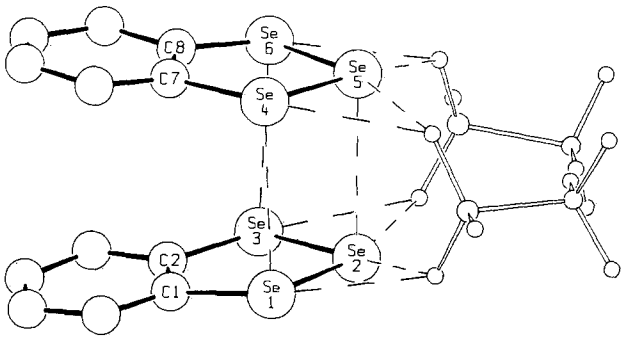

Fig. 1. Crystal structure of **2**-SO_3CF_3. Selected bond distances [Å] and angles [°]: Se1-Se2 2.298(5), Se2-Se3 2.293(5), Se1-C1 1.91(4), Se3-C2 1.88(3), C1-C2 1.41(4), Se4-Se5 2.280(5), Se5-Se6 2.276(5), Se4-C7 1.89(3), Se6-C8 1.85(3), C7-C8 1.38(3), Se1-Se4 3.278(4), Se2-Se5 3.153(4), Se3-Se6 3.246(4); C1-Se1-Se2 99(1), Se3-Se2-Se1 97.2(2), C2-Se3-Se2 98(1), C7-Se4-Se5 98.9(8), Se6-Se5-Se4 97.6(2), C8-Se6-Se5 96.9(9).

The ESR spectrum of **2**-SO_3CF_3 in acetonitrile shows a singlet of low intensity (g = 2.0758 G) with a half-intensity width of about 26.5 G. However, the use of trifluoroacetic acid as the solvent increases the signal intensity considerably, which is an indication of a solvent-dependent dissociation equilibrium. The ion pairs observed in the solid state are probably more strongly dissociated in polar protic solvents so that the coulombic repulsion between the radical cations can become effective. Quite obviously the dimeric structure of **2** is also favored in solution.

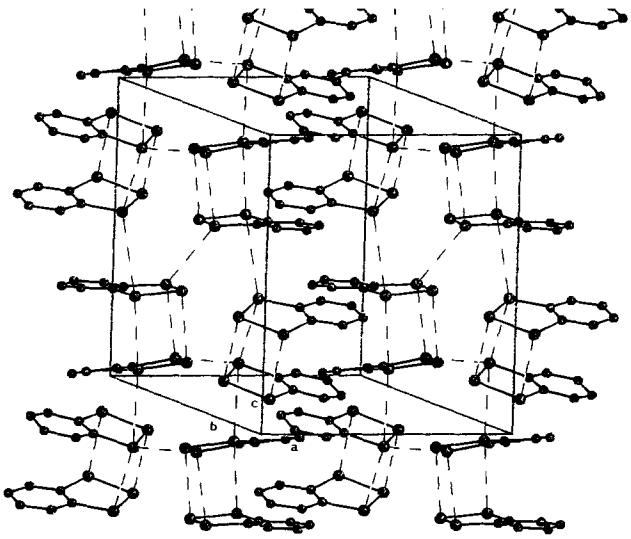

Fig. 2. Arrangement of **2**-SO_3CF_3 in the solid state.

Experimental Procedure

2-SO_3CF_3: A solution of Se_2Cl_2 (0.70 g, 3 mmol) in dichloromethane (5 mL) was added dropwise to a yellow suspension of "[3,4][7,8]dibenzotetraselenocin"(0.72 g, 1.5 mmol)[4] in dichloromethane (30 mL) at room temperature. After 3h the gray-black reaction mixture was allowed to react with trimethylsilyl trifluromethansulfonate (0.5 mL, 3 mmol). The gold, shiny microcrystalline solid was separated after 1h, washed several times with dichloromethane, and dried under vacuum; Yield 0.91 g (64%), m.p. 208 °C.

Received: December 19, 1991 [Z 5079 IE]
German version: *Angew. Chem.* **1992**, *104*, 752

CAS Registry numbers:
2-Cl, 140468-63-9; **2**-SO_3CF_3, 140468-65-1; **3**, 140468-66-2; **4**, 107658-48-0.

[1] R. J. Gillespie, J. P. Kent, J. F. Sawyer, *Inorg. Chem.* **1981**, *20*, 3784.
[2] T. S. Cameron, R. C. Haddon, S. M. Mattar, S. Parsons, J. Passmore, A. P. Ramirez, *J. Chem. Soc. Chem. Commun.* **1991**, 358.
[3] G. Wolmerhäuser, W. Kaim, G. Heckmann, A. Lichtblau, *Z. Naturforsch. B*, **1992**, *47*, 143.
[4] D. J. Sandman, J. C. Stark, L. A. Acampora, L. A. Samuelson, G. W. Allen, S. Jansen, M. T. Jones, B. M. Foxmann, *Mol. Cryst. Liq. Cryst.* **1984**, *107*, 1.
[5] a) **2**-SO_3CF_3: Gold, shiny crystals were obtained from acetonitrile; monoclinic, $P2_1/c$, a = 12.163(7), b = 15.831(4), c = 13.218(6) Å, β = 92.51(2)°, V = 2542(2) Å^3, Z = 4. 3615 independent reflections ($Mo_{K\alpha}$; 1.5° ≤ θ ≤ 26°), of which 1752 were observed with ($I > 2\sigma(I)$; 161 parameters, R = 0.099, R_w = 0.078. b) SHELXS-86 and SHELX-76 were used for the solution and refinement and SCHAKAL-88 was used for drawing the structure. Further details of the crystal structure investigation may be obtained from the Fachinformationszentrum Karlsruhe, Gesellschaft für wissenschaftlich-technische Information mbH, D-W-7514 Eggenstein-Leopoldshafen 2 (FRG) on quoting the depository number CSD-56079, the names of the authors, and the journal citation.
[6] Also the results of magnetic measurements are consistent with this. The surprisingly small Curie constant of $C = 1.24 \times 10^{-3}$ emu mol^{-1} K^{-1} indicates an antiferromagnetic spin pairing.
[7] However, stacks of monomers with a layer distance of 4.1 Å occur in crystals of 4,5-bis(trifluoromethyl)-1,2,3-trithiolium hexafluoroarsenate [2].

Hydrogen Shift in a Parent Compound *Z,Z*-1,3,5-Heptatriene and Its Monodeuterium Analogue

By *Mikhail E. Gurskii, Ilya D. Gridnev, Yuri V. Il'ichev, Anatoly V. Ignatenko,* and *Yuri N. Bubnov**

The [1,7] sigmatropic shift of hydrogen was observed for the first time by Havinga and Schlatmann in the interconversion of vitamin D and precalciferol.[1] The facile antarafacial [1,7] hydrogen shift predicted by Woodward and Hoffmann[2] stimulated a wider study of the phenomenon. Since then the kinetics of [1,7] hydrogen shifts in analogues of the provitamin D_3 system and related compounds[3] have been reported often. There are also some investigations of [1,7] hydrogen shifts in aromatic[4] and open-chain hydrocarbons.[5]

Nevertheless the shift for the parent compound *Z,Z*-1,3,5-heptatriene (**1**) has not been reported. The kinetics of its [1,7] hydrogen shift is important for comparison with quantum mechanics calculations, which have been performed only for **1**.[6] We have now found an easy route to **1** and its deutero-analogue **2**.

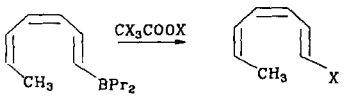

1: X=H
2: X=D

Scheme 1. Synthesis of **1** and **2** from **4**.

During our study on the [1,3] sigmatropic shifts of boron in the allylic type organoboranes we synthesized 2,4,6-heptatrienylborane (**3**), which possesses unusual dynamic properties: besides the [1,3] boron shifts which easily interconvert isomers **3a**–**d**, a [1,7] hydrogen shift occurs in the *Z,Z* isomer **3d** (Scheme 2).

The vinylic borane **4**, the product of the [1,7] H shift, is thermodynamically more stable than the initial heptatrienyl-

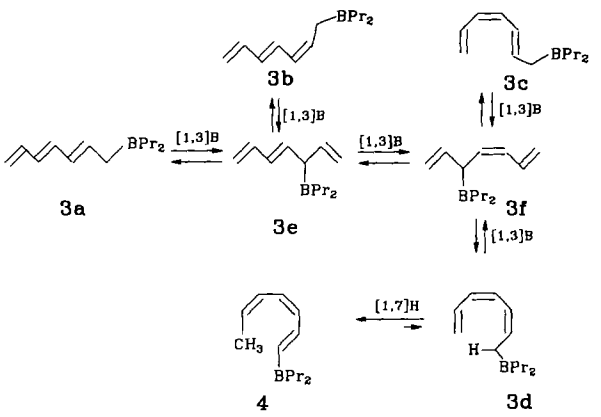

Scheme 2. Dynamic properties of **3**.

[*] Professor Dr. Yu. N. Bubnov, Dr. M. E. Gurskii, Dr. I. D. Gridnev, Dr. A. V. Ignatenko
N. D. Zelinsky Institute of Organic Chemistry
Leninsky prosp., 47, Moscow, 117913 (Russia)
Dr. Yu. V. Il'ichev
Department of Chemistry, Moscow State University.

treatment of **4** with acetic acid or [D_4] acetic acid gives **1** or **2** (Scheme 1).

The [1,7] hydrogen shift in **1** is too slow to measure accurately from the NMR spectra (Fig. 1) by line shape analysis. Moreover **1** dimerizes and polymerizes readily, except when dissolved in a nonpolar solvent. Nevertheless we have man-

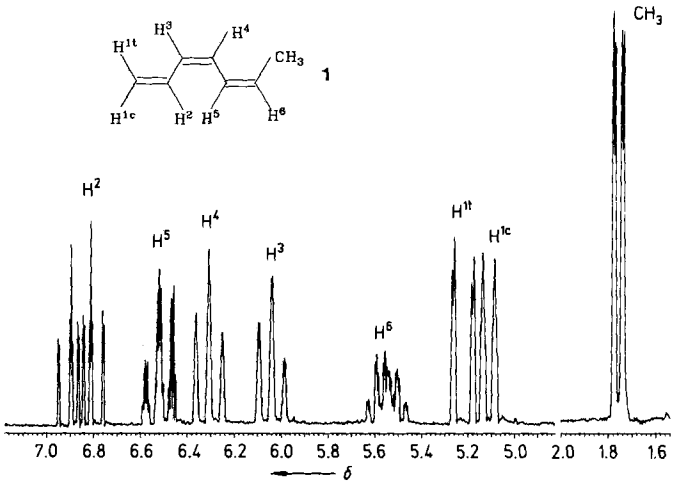

Fig. 1. ^{1}H NMR spectrum of **1** (200 MHz, C_6D_6, 25 °C, TMS).

aged to observe the degenerate [1,7] hydrogen shift in **1** directly by two-dimensional chemical exchange NMR spectroscopy; the results are presented in Figure 2.

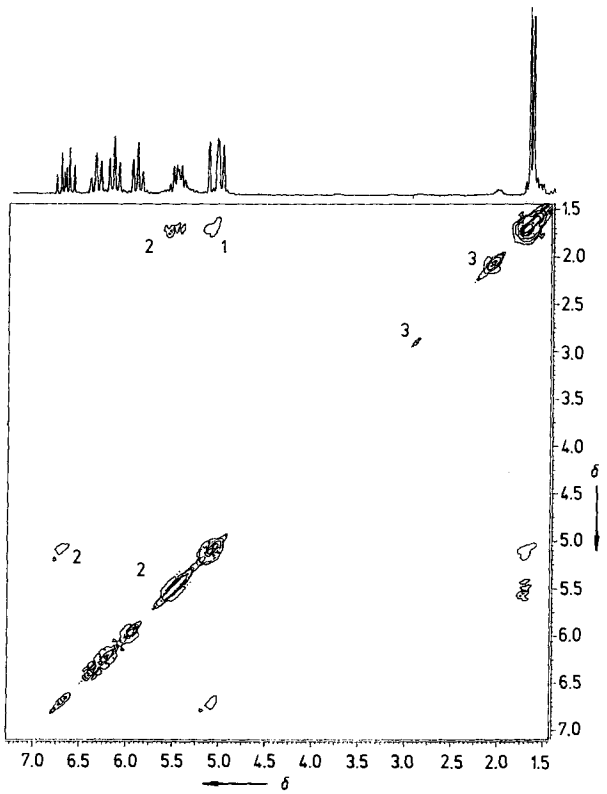

Fig. 2. Direct observation of the degenerate [1,7] hydrogen shift in **1**. Contour plot of ^{1}H NOESY spectrum for **1** (200 MHz, neat liquid, 140 °C, mixing time 0.5 s). 1: Cross-peak caused by the exchange between positions 1 and 7; 2: NOE cross-peaks for the protons adjacent to the exchanging hydrogen; 3: the signals of the dimer of **1** formed during the acquisition of the spectra.

We used the [1,7] hydrogen shift in the labeled compound **2** for the kinetic measurements. As shown in Scheme 3, the [1,7] shift in **2** leads to the exchange of deuterium between positions 1 and 7. The [1,7] deuterium shift in **2c** is degenerate and does not affect the distribution of deuterium between positions 1 and 7. Therefore, deuterium substitution only should affect the rate of [1,7] hydrogen shift slightly, and the reaction can be described as in Scheme 4, where k_H is the rate constant of the [1,7] hydrogen shift for a single hydrogen atom. Therefore the equilibrium ratio of **2c** and the sum of **2a** and **2b** should be 3:2. This agrees well with the experimental findings (see Fig. 3).

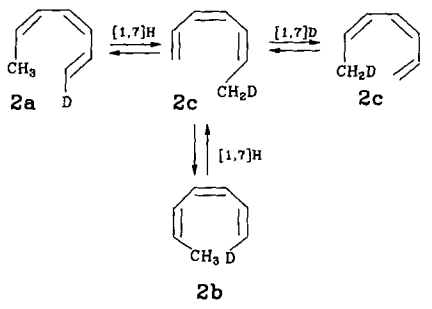

Scheme 3. Dynamic properties of **2**.

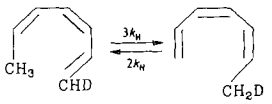

Scheme 4. Kinetic description of the nondegenerate [1,7] hydrogen shift in **2**.

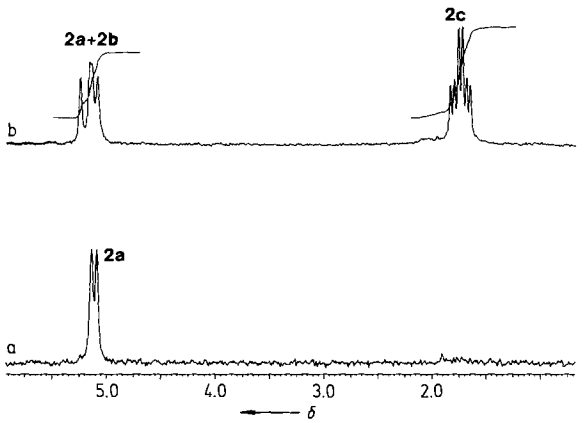

Fig. 3. ^{2}H NMR spectra of the compounds **2a–c** (31 MHz, decane, 25 °C). a) Initial spectrum of **2a**. b) The spectrum of the same sample after 2 h heating at 130 °C. The signals of **2a**, **2b**, and **2c** are clearly visible; the ratio of the intensities for the signals **2c** and **2a** + **2b** is 7:5.

The [1,7]-shift kinetics of **2**, linearized according to Scheme 4, are given in Figure 4a. The concentrations of **2c** and sum of the concentrations of **2a** and **2b** were obtained from the ^{2}H NMR spectra by the integration of the signals at δ = 5.1–5.2 and at 1.7.

The Arrhenius plot presented in the Figure 4b shows a good linear correlation and gives expression (a) for the rate constant k_H of the [1,7] hydrogen shift in the parent compound **1**.

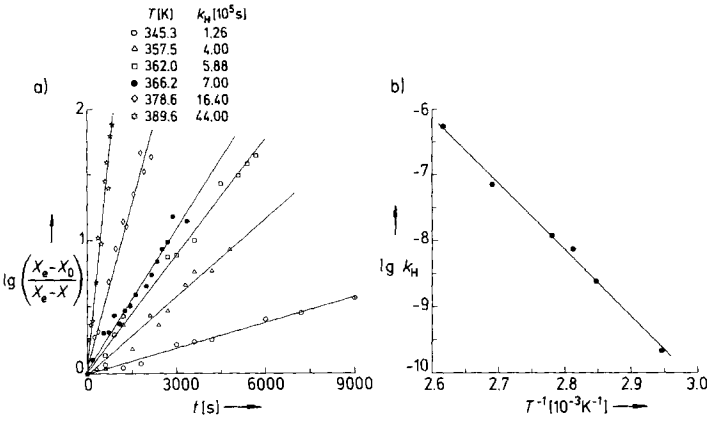

Fig. 4. a) Plots of **2c** concentrations X vs time, linearized according to the Scheme 4. X_0 are the initial concentrations, X_e the equilibrium concentrations of **2c** at each temperature. b) Plot of lg k_H vs T^{-1}.

$$k_H = 1.6 \times 10^8 \, e^{-\frac{87 \pm 3 \text{ kJ mol}^{-1}}{RT}} \, s^{-1} \quad (a)$$

A comparison of the activation parameters in (a) with those reported earlier for the [1,5] hydrogen shift in *Z*-1,3-pentadiene[7] (E_A = 152 kJ mol^{-1}, $A = 2.8 \times 10^{11}$ s^{-1}) shows that our experimental results support the theoretical prediction that [1,7] hydrogen shifts have a lower activation energy but a more negative entropy of activation than [1,5] hydrogen shifts.[6, 8]

Experimental Procedure

The spectral data (see Table 1) were obtained on the Brucker AC-200P, Bruker AM-300 (NMR), UR-20 (IR), and Varian MAT-311A (HRMS) spectrometers.

3a–d was obtained from heptatrienyllithium in hexane/THF [9] and chlorodipropylborane with the yield 70%; b.p. 75 °C (2 Torr), n_D^{20} 1.5115. IR: $\tilde{\nu}$ [cm^{-1}] = 1584, 1629, 3010, 3023, 3091; ^{11}B NMR (64 MHz, neat, 25 °C, $BF_3 \cdot Et_2O$): δ = 85.1. Satisfactory C,H,B analyses.

4: **3** was heated neat in a sealed tube for 1 h at 100 °C (water bath). The equilibrium mixture of **4** (92%) and **3** (8%) was obtained: n_D^{20} 1.5029. IR: $\tilde{\nu}$ [cm^{-1}] = 1556, 1598, 1729, 3017, 3045. ^{11}B NMR (64 MHz, neat, 25 °C, $BF_3 \cdot Et_2O$): δ = 76.6 (**4**), 85.1 (**3**).

1 was obtained from acetic acid and **4** (yield 65%); n_D^{20} 1.5199. IR: $\tilde{\nu}$ [cm^{-1}] = 1570, 1620, 3034, 3050, 3090. ^{13}C NMR (50 MHz, neat, 25 °C, TMS): δ = 131.55 (C2), 128.65 (C3), 126.77 (C6), 123.90 (C4), 123.80 (C5), 116.93 (C1), 12.99 (C7). High-resolution MS (M^+) *m/z* 94.0763, calcd for C_7H_{10} 94.0782.

Table 1. Chemical shifts δ and coupling constants J [Hz] for the compounds **1** [a], **3**, and **4** (without BPr_2 ligands).

Compound	δH1 ($J_{1,2}$)	δH2 ($J_{2,3}$)	δH3 ($J_{3,4}$)	δH4 ($J_{4,5}$)	δH5 ($J_{5,6}$)	δH6 ($J_{6,7c}$)	δH7c (^2J)	δH7t ($J_{6,7t}$)
1 [b]	1.70 (7.2)	5.55 (10.6)	6.52 (10.6)	6.31 (10.6)	6.03 (10.6)	6.85 (10.6)	5.11 (2.2)	5.21 (16.9)
3a	2.19 (8.4)	5.85 (14.9)	6.08 (9.8)	6.28 (14.7)	6.17 (9.8)	6.43 (9.8)	5.08 (1.9)	5.21 (17.0)
3b	2.29 (8.5)	5.70 (10.3)	[c] (11.5)	6.61 (15.3)	[c] (10.1)	6.92 (10.1)	[c]	(16.8)
4	1.81 (7.2)	5.63 (10.3)	6.81 (10.8)	6.55 (11.8)	6.31 (10.6)	7.87 ($J_{6,7}$ = 16.6)	6.68	

[a] The spectral characteristics for the compounds **2** are the same as for the compound **1**, except for: **2a**: 6.85 (ddt, ^3J(H,D) = 1.7 Hz), the signal of H7c is absent; **2b**: 6.85 (ddt, ^3J(H,D) = 2.6 Hz), the signal of H7*t* is absent; **2c**: 1.68 (dt, ^2J(H,D) = 2.2 Hz). [b] The numbering of the atoms for compound **1** in this table is reversed to make it the same as for the compounds **3** and **4**. [c] The signals overlap with the signals of the major isomer.

2 was obtained from **4** and [D_4] acetic acid (yield 68%); n_D^{20} 1.5211. IR: $\tilde{\nu}$ [cm^{-1}] = 1710, 1712, 2200. High-resolution MS (M^+) m/z 95.0853, calcd for C_7H_9D 95.0845.

Kinetic measurements were performed in the probe of the AC-200P NMR spectrometer for the 10% solutions of **2** in *n*-nonane; temperature control was carried out by a VT-1000 variable temperature unit (Bruker).

Received: December 20, 1991 [Z 5084 IE]
German version: *Angew. Chem.* **1992**, *104*, 762

CAS Registry numbers:
1, 30915-44-7; **2a**, 141090-25-7; **2b**, 141090-26-8; **2c**, 141090-27-9; **3a**, 141090-28-0; **3b**, 141090-29-1; **3c**, 141090-30-4; **3d**, 141090-31-5; **4**, 141090-32-6.

[1] a) E. Havinga, J. L. M. A. Schlatmann, *Tetrahedron* **1961**, *16*, 146–152; b) J. L. M. A. Schlatmann, J. Pot, E. Havinga, *Recl. Trav. Chim. Pays-Bas* **1964**, *83*, 1173–1184.

[2] R. B. Woodward, R. Hoffman, *Angew. Chem.* **1969**, *81*, 797–869; *Angew. Chem. Int. Ed. Engl.* **1969**, *8*, 781–850.

[3] a) J. A. Palenzuela, H. Y. Elnagar, W. H. Okamura, *J. Am. Chem. Soc.* **1989**, *111*, 1770–1776; b) J. D. Enas, G. Y. Shen, W. H. Okamura, *ibid.* **1991**, *113*, 3873–3881; c) K. M. Wu, W. H. Okamura, *J. Org. Chem.* **1990**, *55*, 4025–4036.

[4] a) H. Heimgartner, H.-J. Hansen, H. Schmid, *Helv. Chim. Acta* **1970**, *53*, 173–176; b) *ibid.* **1972**, *55*, 1828–1845.

[5] a) P. Courtot, R. Rumin, *Tetrahedron Lett.* **1970**, 1849–1852; b) *Bull. Soc. Chim. Fr.* **1972**, 4238–4250; c) J. E. Baldwin, V. P. Reddy, *J. Am. Chem. Soc.* **1987**, *109*, 8051–8056; d) *ibid.* **1988**, *110*, 8223–8228; e) *J. Org. Chem.* **1988**, *53*, 1129–1132.

[6] B. A. Hess, L. J. Schaad, J. Pancir, *J. Am. Chem. Soc.* **1985**, *107*, 149–154.

[7] W. R. Roth, J. König, *Justus Liebigs Ann. Chem.* **1966**, *699*, 24–32.

[8] C. W. Spangler, *Chem. Rev.* **1976**, *76*, 187–217.

[9] R. B. Bates, W. H. Deines, D. A. McCombs, D. E. Potter, *J. Am. Chem. Soc.* **1969**, *91*, 4608.

Synthesis of a Lipophilic Cyclodextrin–[2]-Rotaxane**

By *Gerhard Wenz,* Eva von der Bey,* and *Lothar Schmidt*

For a long time cyclodextrins **1** have been known to include smaller guest molecules in aqueous solution.[1] Several attempts have been made to exploit their well-defined topology in the construction of "interlocking" molecules like catenanes,[2] rotaxanes,[3] and polyrotaxanes.[4] In aqueous solution, however, the preparative possibilites are limited because of side reactions. In order to provide cyclodextrins for use as host molecules in inert organic solvents, we synthesized a series of lipophilic cyclodextrin derivatives.[5] As a result we discovered that per(3-*O*-acyl-2,6-di-*O*-alkyl)cyclodextrins

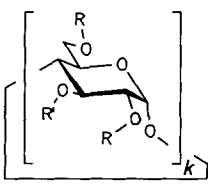

1 k=6,7,8, R=R'=H

1a k = 7, R = *n*-butyl, R' = acetyl

1b k = 7, R = *n*-pentyl, R' = acetyl

[*] Dr. G. Wenz, Dr. E. von der Bey
Max-Planck-Institut für Polymerforschung
Ackermannweg 10, D-W-6500 Mainz (FRG)
Dr. L. Schmidt[+]
Fachbereich Physikalische Chemie der Philipps-Universität Marburg

[+] ^{252}Cf-PD mass spectrum

[**] This research was supported by the Bundesministerium für Forschung und Technologie (BEO/22/0319055A), Henkel KGaA, and Wacker-Chemie GmBH. We thank C. Lepilleur and J. Thiel for optimizing the synthesis and Prof. H. Jungclas, Universität Marburg, and Prof. G. Wegner for discussions.

complex cationic guest molecules and neutral ones as well.[6] Here we describe how the complexation of a guest molecule can be employed in the construction of a [2]-rotaxane.

We chose heptakis(3-*O*-acetyl-2,6-di-*O*-butyl)-β-cyclodextrin (**1a**) as the host and a substituted pyridinium ion as the guest. Compounds **5a** and **5b**, 4,4'-bipyridyl derivatives blocked on one side, were synthesized for the construction of the rotaxane according to Scheme 1. Alcohols **2a** and **2b** were prepared from triphenylmethane and esterified with *p*-toluyl chloride. The methyl groups of esters **3** were brominated, and the bromomethyl compounds **4** were treated with excess 4,4'-bipyridyl providing pyridinium bromides **5**.

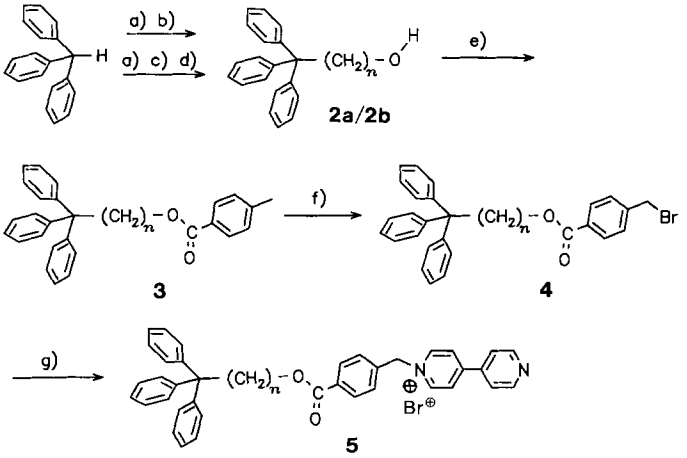

Scheme 1. Synthesis of the rotaxane building blocks **5** from triphenylmethane. **a**, n = 1; **b**, n = 6. Reagents: a) *n*BuLi, b) paraformaldehyde, c) 6-(*tert*-butyldimethylsilyloxy)hexylbromide, d) Bu_4NF, e) *n*BuLi, *p*-toluyl chloride, f) NBS, AIBN, g) 4,4'-bipyridyl.

^{1}H NMR experiments show that the region around the pyridinium group of **5** is indeed complexed by **1a**. For example, the signals of the benzylic protons of **5a** and **5b** shift markedly downfield upon addition of **1a**, whereas the signals of the trityl group remain unchanged. The dependence of the chemical shift of the benzylic protons on the concentration of the host **1a** (Fig. 1) allows the calculation of a stability constant K_s of 150 M^{-1} for the complex **1a** · **5a**, and 450 M^{-1} for **1a** · **5b**.[5a]

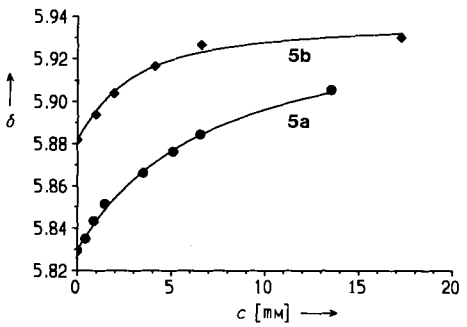

Fig. 1. Chemical shift δ of the benzylic protons of 0.58 M **5a** and 1.25 mM **5b** in CD_3CN at 20 °C as a function of the concentration c of the host **1a**.

The attempt to synthesize a rotaxane by quaternizing the pyridine unit in **1a** · **5a** with the bromide **4a** led only to the dumbbell-shaped **6a** (Scheme 2). Thus the alkylation only

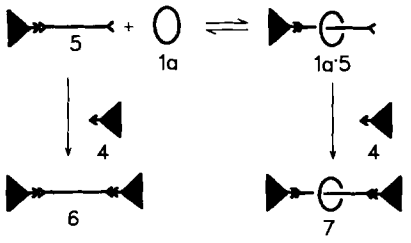

Scheme 2. Construction of rotaxane 7 from the complex **1a** · **5b**.

occurs outside the complex. In contrast, rotaxane **7** was detected in the reaction of **1a** · **5b** with **4b**. The ^{252}Cf-PD mass spectrum[7] of the reaction mixture (Fig. 2a) shows a pronounced signal at *m/z* 3293, the molecular mass of **7**.

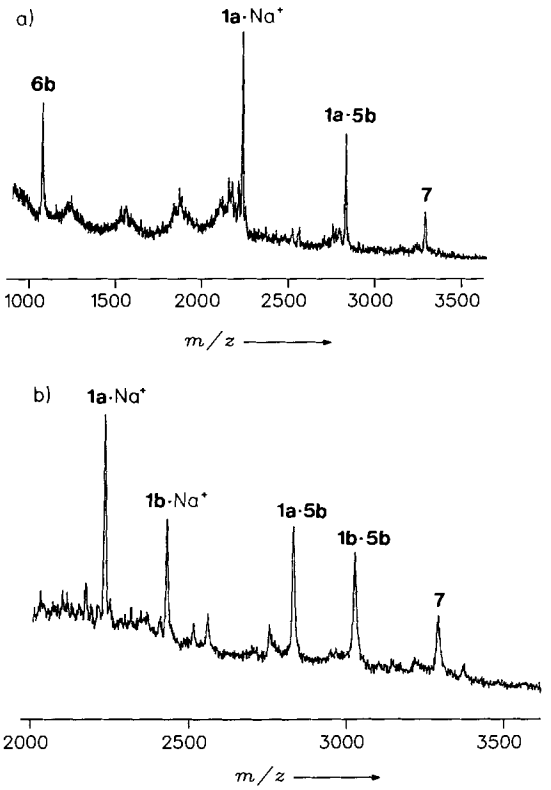

Fig. 2. Mass spectra [7] of the reaction mixture of rotaxane 7 a) before and b) after equilibration with host **1b**.

Because ^{252}Cf-plasma desorption mass spectrometry is very "soft", signals of host–guest complexes were also evident in the mass spectrum. For example, the signal at *m/z* 2833 arose from **1a** · **5b**, and that at *m/z* 2236 from **1a** · Na^+. Thus the signal at *m/z* 3293 could also be due to a loose association of **1a** and **6b** rather than rotaxane **7**. In a control experiment the reaction mixture of **1a**, **5b**, and **4b** was equilibrated with a second host, heptakis(3-*O*-acetyl-2,6-di-*O*-pentyl)-*β*-cyclodextrin (**1b**), whose molecular weight is *m/z* 196 higher than that of **1a**. All associations of **1a** should be recognizable in the mass spectrum because of the exchange of the host. The signal of the rotaxane, on the other hand, should remain unchanged. This is indeed the case (Fig. 2b): In the mass spectra of the aforementioned mixture after the equilibration with **1b** two new signals at *m/z* 2432 and *m/z* 3028 are observed and assigned to **1b** · Na^+ and **1b** · **5b**, respectively. Since no signal at *m/z* 3489 is found, the presence of rotaxane **7** is assured.

Compound **7** was isolated from the reaction mixture in 20% yield.[18] According to the ^{1}H NMR spectrum the C_7 symmetry of the host is retained and the mirror symmetry of the dumbbell is broken by the permanent complexation of the asymmetric host compound (Fig. 3). It is especially noticeable that the signals of the benzylic protons are split into an AB system γ and a singlet γ'. This strong splitting is probably related to the preferred complexation of one half of the dumbbell. The AB system results from the diastereotopic interaction of the benzylic protons with the host.

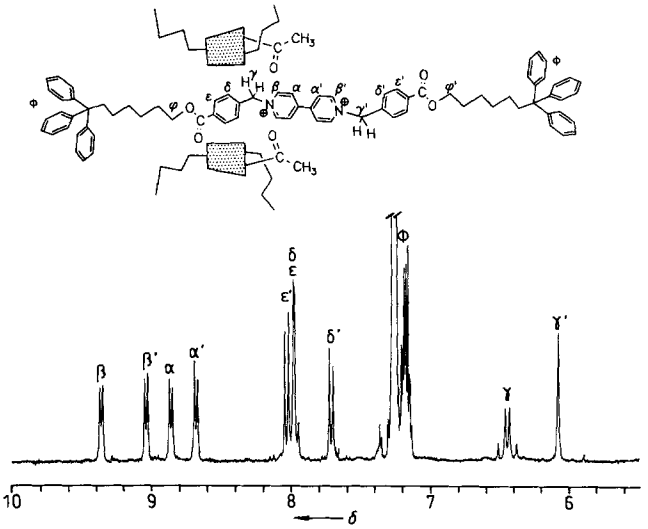

Fig. 3. Structural formula and part of the ^{1}H NMR spectrum of 7. The signals were assigned based on homonuclear decoupling experiments; the low-field signals were assigned to the complexed side.

These first results show that the outcome of a rotaxane synthesis critically depends on the length *n* of the spacer. This is most likely caused by steric interactions between the host and the blocking group. Which of the two triphenylmethyl blocking groups causes the most steric hindrance in the transition state is open for further investigations.

Experimental Procedure

Silica gel Si-60 (40–65 μm) was used for the chromatography. All compounds provided correct elemental analyses. The IR spectra support the assigned structures; ^{1}H NMR: 300 MHz, 20 °C, TMS; ^{13}C NMR: 75.46 MHz, 20 °C, TMS.

1a: Heptakis(2,6-di-*O*-butyl)-*β*-cyclodextrin[5d] (1.92 g, 1 mmol) was allowed to react with acetic anhydride (0.61 g, 6 mmol) and 4-dimethylaminopyridine (0.043 g, 0.35 mmol) in 10 mL CH_2Cl_2 at 40 °C for 3d. The reagents were replenished every day. After workup and chromatography with CH_2Cl_2/*tert*-butyl methyl ether (1/1) **1a** (1.5 g, 68%) was obtained as a colorless oil. ^{1}H NMR($CDCl_3$): δ=0.89 (t, J = 7.3 Hz, 3H), 0.92 (t, J = 7.3 Hz, 3H) 1.26–1.43 (m, 4H), 1.43–1.62 (m, 40H), 2.05 (s, 3H), 3.29 (dd, J = 3.2, 10.1 Hz, 1H), 3.35–3.58 (m, 5H), 3.81 (t, J = 9.1 Hz, 1H), 3.94 (m, 2H), 5.03 (d, J = 3.3 Hz, 1H), 5.18 (t, J = 9.3 Hz, 1H); ^{13}C NMR($CDCl_3$): δ = 13.9, 13.95, 19.0, 19.4, 21.0, 31.8, 69.3, 70.8, 71.2, 73.0, 77.2, 78.4, 98.6, 169.5.

1b: Synthesis (from heptakis(2,6-di-*O*-pentyl)-*β*-cyclodextrin [5d]; yield 76%) and characterization analogous to that of **1a**.

2a: Triphenylmethyllithium was converted to **2a**[9].

2b: A solution of triphenylmethyllithium (8.3 g, 34 mmol) in 100 mL THF under Ar was cooled to −78 °C, and *n*BuLi (1.6 M, 32 mL, 51 mmol) was added dropwise. The reaction mixture was stirred at 20 °C for 24h, then 6-(*tert*-butyldimethylsilyloxy)hexylbromide[10] (10 g, 36 mmol) was added. After being stirred at 20 °C for another 24h, the reaction mixture was treated with Bu_4NF (1.1 M in THF, 50 mL, 55 mmol) and heated at reflux for 2d. Workup with water/chloroform, chromatography with CH_2Cl_2, and recrystallization from petroleum ether/cyclohexane (3/1) provided 6.08 g **2b** (53%). M.p. 74.5 °C; ^{1}H NMR($CDCl_3$): δ = 1.08 (m, 2H), 1.32 (m, 5H), 1.47 (J = 7.0 Hz,

2H), 2.56 (m, 2H), 3.56 (t, J = 6.6 Hz, 2H), 7.16 (m, 3H), 7.26 (m, 12H); ^{13}C NMR($CDCl_3$): δ = 25.6, 25.7, 30.1, 32.7, 40.5, 56.6, 62.9, 125.7, 127.7, 129.2, 147.6.

3a: To a solution of **2a** (1 g, 3.6 mmol) in THF under Ar cooled to −78 °C was added *n*BuLi (1.6 M, 2.25 mL, 3.6 mmol). After 15 min *p*-toluyl chloride (0.5 mL, 3.8 mmol) was added, and the reaction mixture was stirred at 20 °C for 1 d. After workup and recrystallization from cyclohexane/CH_2Cl_2 (9/1) 0.97 g **3a** (65%) were obtained. M.p. 154 °C, ^{1}H NMR($CDCl_3$): δ = 2.35 (s, 3H), 5.31 (s, 2H), 7.12 (d, J = 8.1 Hz, 2H), 7.20–7.32 (m, 15H), 7.58 (d, J = 8.1 Hz, 2H); ^{13}C NMR($CDCl_3$): δ = 21.5, 56.8, 70.9, 126.5, 127.3, 128.0, 129.0, 129.2, 129.5, 143.5, 145.0 166.3.

3b: In analogy to the above procedure, **2a** (1.5 g, 4 mmol) was allowed to react with *p*-toluyl chloride (0.68 mL, 4.4 mmol). Purification by chromatography (eluent CH_2Cl_2/petroleum ether (3/2)) furnished 1.25 g **3b** (62%) as a yellow oil. ^{1}H NMR($CDCl_3$): δ = 1.15 (m, 2H), 1.41 (m, 4H), 1.71 (m, 2H), 2.43 (s, 3H), 2.61 (m, 2H), 4.28 (t, J = 8.6 Hz, 2H), 7.17–7.31 (m, 17H), 7.95 (d, J = 8.0 Hz, 2H); ^{13}C NMR($CDCl_3$): δ = 21.6, 25.6, 25.9, 28.7, 30.0, 40.4, 56.4, 64.7, 125.7, 125.6, 127.7, 129.0, 129.2, 129.5, 142.6, 147.4, 166.3.

4a: A mixture of **3a** (1.04 g, 2.65 mmol), *N*-bromosuccinimide (NBS) (0.52 g, 2.9 mmol), and 2,2′-azodiisobutyronitrile (AIBN; 20 mg) was dissolved in 5 mL CCl_4 and 10 mL $CHCl_3$ and heated at reflux for 3 d. Each day the same amounts of NBS and AIBN were added again. Finally the reaction mixture was filtered at 20 °C. The filtrate was concentrated and dissolved in $CHCl_3$. Precipitation of the product with petroleum ether provided 0.75 g **4a** (60%). ^{1}H NMR($CDCl_3$): δ = 4.42 (s, 2H), 5.31 (s, 2H), 7.17–7.29 (m, 15H), 7.33 (d, J = 8.5 Hz, 2H), 7.63 (d, J = 8.5 Hz, 2H); ^{13}C NMR($CDCl_3$): δ = 32.1, 56.9, 71.2, 126.6, 126.5, 127.3, 128.0, 129.0, 129.3, 129.5, 143.5, 145.0, 166.3.

4b: Analogous to the above reaction, the bromination of **4a** furnished compound **4b** as a yellow oil, yield 80%. ^{1}H NMR($CDCl_3$): δ = 1.15 (m, 2H), 1.45 (m, 4H), 1.65 (m, 2H), 2.55 (m, 2H), 4.25 (t, J = 8.6 Hz, 2H), 4.50 (s, 2H), 7.08 7.28 (m, 15H), 7.62 (d, J = 8.0 Hz, 2H), 8.03 (d, J = 8.0 Hz, 2H); ^{13}C NMR($CDCl_3$): δ = 25.6, 25.8, 28.7, 30.0, 40.4, 32.1, 56.6, 65.1, 125.7, 126.6, 127.7, 128.9, 129.2, 130.0, 142.5, 147.5, 166.0.

5a: Solutions of **4a** (235 mg, 0.5 mmol) in 3 mL CH_3CN and 4,4′-bipyridyl (78 mg, 0.5 mol) in 1 mL $CHCl_3$ were mixed and stirred at 20 °C for 24 h. Then *tert*-butyl methyl ether was added, and **5a** was removed by filtration. Yield 98 mg (31%). ^{1}H NMR(CD_3CN): δ = 5.34 (s, 2H), 5.86 (s, 2H), 7.20–7.33 (m, 15H), 7.46 (d, J = 8.2 Hz, 2H), 7.72 (d, J = 8.2 Hz, 2H), 8.35 (m, 4H), 8.98 (m, 4H); ^{13}C NMR([D_6]DMSO): δ = 56.4, 62.5, 70.2, 121.9, 125.9, 126.5, 128.0, 128.8, 129.4, 130,0, 139.2, 140.7, 144.6, 145.5, 150.9, 152.9, 164.6.

5b: A procedure analogous to that for **5a**, starting with **4b** (220 mg, 0.41 mmol) and 4,4′-bipyridyl (130 mg, 0.82 mol), provided 140 mg **5b** (49%). ^{1}H NMR (CD_3CN): δ = 1.05 (m, 2H), 1.40 (m, 4H), 1.63 (m, 2H), 2.56 (m, 2H), 4.23 (t, J = 8.5 Hz, 2H) 5.91 (s, 2H), 7.15–7.25 (m, 15 H), 7.59 (d, J = 8.0 Hz, 2H), 7.92 (d, J = 8.0 Hz, 2H), 8.05 (d, J = 8.5 Hz, 2H), 8.32 (d, J = 7.0 Hz, 2H), 8.86 (d, J = 8.5 Hz, 2H), 8.99 (d, J = 7.0 Hz, 2H); ^{13}C NMR([D_6]DMSO): δ = 30.3, 30.4, 33.2, 34.3, 44.6, 61.4, 67.5, 70.0, 127.3, 130.9, 131.2, 133.0, 134.0, 134.3, 135.0, 135.8, 144.3, 146.3, 150.8, 152.4, 155.8, 158.0, 170.4.

6a: 4,4′-Bipyridyl (64 mg, 0.4 mmol) in 4 mL CH_3CN and **4a** (571 mg, 1 mmol) in 2 mL $CHCl_3$ were mixed and stirred at 20 °C for 24 h. The resulting yellow precipitate was filtered, washed with $CHCl_3$, and redissolved in hot CH_3CN/$CHCl_3$ (3/1). The slow addition of petroleum ether caused the precipitation of 168 mg **6a** (38%). Yellow solid, m.p. 171 °C. ^{1}H NMR(CD_3CN): δ = 5.35 (s, 4H), 5.86 (s, 4H), 7.21–7.31 (m, 30H), 7.45 (d, J = 8.2 Hz, 4H), 7.72 (d, J = 8.2 Hz, 4H), 8.39 (d, J = 7.1 Hz, 4H), 8.99 (d, J = 7.1 Hz, 4H); ^{13}C NMR([D_6]DMSO): δ = 56.4, 62.7, 70.3, 126.5, 127.2, 128.0, 128.8, 12.0, 129.4, 130.2, 139.0, 144.4, 145.9, 149.3, 164.5.

7: To a solution of **5b** (100 mg, 0.14 mmol) and **1a** (620 mg, 0.28 mmol) in 3 mL CH_3CN was added a solution of **4b** (152 mg, 0.28 mmol) in 0.5 mL $CHCl_3$. The reaction mixture was stirred at 20 °C for 3 d before being separated in four portions by middle-pressure chromatography (column size 30 × 1.5 cm, packed with Si-60 (18–32 μm) from ICN Biomedicals, deactivated with CH_2Cl_2/CH_3OH (7/1)). Elution first with *tert*-butyl methyl ether gave **1a** and **4b**, then with CH_2Cl_2/CH_3OH (7/1) provided **7**: Yield 92 mg (20%), yellow oil. ^{1}H NMR (CD_3CN): δ = 0.81 (t, J = 7.3 Hz, 21H), 0.88 (t, J = 7.3 Hz, 21H), 1.03 (m, 4H), 1.21 (m, 14H), 1.28–1.42 (m, 32H), 1.43–1.54 (m, 14H), 1.61 (m, 4H), 1.88 (s, 21H), 2.57 (m, 4H), 3.12 (dd, J = 3.2, 10.3 Hz, 7H), 3.26–3.56 (m, 42H), 3.69 (t, J = 9.5 Hz, 14H), 4.21 (t, J = 6.4 Hz, 2H), 4.28 (t, J = 10.3 Hz, 7H), 4.93 (d, J = 2.6 Hz, 7H), 4.96 (t, J = 10.1 Hz, 7H), 6.09 (s, 2H), 6.42 (d, J = 14.6 Hz, 1H), 6.46 (d, J = 14.6 Hz, 1H), 7.13–7.30 (m, 30H), 7.72 (d, J = 8.4 Hz, 2H), 7.98 (m, 4H), 8.03 (d, J = 8.4 Hz, 2H), 8.68 (d, J = 6.8 Hz 2H), 8.85 (d, J = 6.8 Hz, 2H), 9.03 (d, J = 6.8 Hz, 2H), 9.38 (d, J = 6.8 Hz, 2H).

Received: December 27, 1991 [Z 5094IE]
German version: *Angew. Chem.* **1992**, *104*, 758

CAS Registry numbers:
1a, 138451-90-8; **1a** Na salt, 141172-87-4; **1a** · **5b** complex, 141172-86-3; **1b**, 120614-93-9; **1b** Na salt, 141172-88-5; **1b** · **5b** complex, 141197-79-7; **2a**, 896-32-2; **2b**, 141172-76-1; **3a**, 141172-77-2; **3b**, 141172-78-3; **4a**, 141172-79-4; **4b**, 141172-80-7; **5a**, 141172-81-8; **5b**, 141172-82-9; **6a**, 141172-83-0; **6b**, 141172-84-1; 7, 141172-85-2; 6-(*tert*-butyldimethylsilyloxy)hexyl bromide, 129368-70-3; triphenylmethane, 519-73-3; *p*-toluyl chloride, 874-60-2; 4,4′-bipyridyl, 553-26-4; heptakis-(2,6-di-O-pentyl)-β-cyclodextrin, 121801-65-8 heptakis-(2,6-di-O-butyl)-β-cyclodextrin, 136781-90-3.

[1] Reviews: J. Szejtli, *Cyclodextrin Technology* in *Topics in Inclusion Science* (Ed.: J. E. D. Davies), Kluwer, Dordrecht, **1988**.
[2] First attempts: A. Lüttringhaus, F. Cramer, H. Prinzbach, F. M. Henglein, *Justus Liebigs Ann. Chem.* **1958**, *613*, 185, synthesis of other catenanes: E. Wasserman, *J. Am. Chem. Soc.* **1960**, *82*, 4433; G. Schill, A. Lüttringhaus, *Angew. Chem.* **1964**, *76*, 567; *Angew. Chem. Int. Ed. Engl.* **1964**, *3*, 546; C. O. Dietrich-Buchecker, J.-P. Sauvage, *Chem. Rev.* **1987**, *87*, 795; P. R. Ashton, T. T. Goodnow, A. E. Kaifer, M. V. Reddington, A. M. Z. Slawin, N. Spencer, J. F. Stoddart, C. Vicent, D. J. Williams, *Angew. Chem.* **1989**, *101*, 1404; *Angew. Chem. Int. Ed. Engl.* **1989**, *28*, 1396.
[3] H. Ogino, *J. Am. Chem. Soc.* **1981**, *103*, 1303; synthesis of other rotaxanes: I. T. Harrison, S. Harrison, *ibid.* **1967**, *89*, 5723; D. Phip, J. F. Stoddart, *Synlett* **1991**, 445.
[4] Main-chain polyrotaxanes: N. Ogata, K. Sanui, J. Wada, *J. Polym. Sci. Polym. Lett.* **1976**, *14*, 459; G. Wenz, B. Keller, *Angew. Chem.* **1992**, *104*, 201; *Angew. Chem. Int. Ed. Engl.* **1992**, *31*, 197; side-chain polyrotaxanes: M. Born, H. Ritter, *Makromol. Chem. Rapid Commun.* **1991**, *12*, 471.
[5] a) G. Wenz, E. von der Bey in *Proc. 4th Int. Cyclodextrins* (Eds.: O. Huber, J. Szejtli), Kluwer, Dordrecht, **1988**, p. 133; b) E. von der Bey, M. Gottlieb, G. Wenz in *Min. 5th Int. Symp. Cyclodextrins* (Ed.: D. Duchene), Editions de Santé, Paris, **1990**, p. 82; c) G. Wenz, P. Mischnick, R. Krebber, M. Richters, W. A. König, *J. High Resolut. Chromatogr.* **1990**, *13*, 724; d) G. Wenz, *Carbohydr. Res.* **1991**, *214*, 257.
[6] A. Hochgesand, G. Wenz in *Min. 5th Int. Symp. Cyclodextrins* (Ed.: D. Duchene), Editions de Santé, Paris, **1990**, p. 322.
[7] ^{252}Cf plasma desorption mass spectra (^{252}Cf-PDMS) were measured from films from CH_3CN; see H. Jungclas, L. Schmidt, H.-W. Fritsch, P. Köhl, *Biotec* **1990**, *2* (2), 30.
[8] An additional product, **6b**, was identified by ^{252}Cf-PDMS, *m/z* 1079.
[9] L. W. Jones, M. W. Seymour, *J. Am. Chem. Soc.* **1928**, *50*, 1150.
[10] Synthesis analogous to E. J. Corey, A. Venkateswarlu, *J. Am. Chem. Soc.* **1972**, *94*, 6190.

Retro-Inverso Amide Bonds between Trifunctional Amino Acids**

By *Hansjörg Dürr, Murray Goodman*, and *Günther Jung**

Dedicated to Professor Ralph Hirschmann on the occasion of his 70th birthday

During the last decade numerous modifications of the peptide backbone[1] were introduced mainly to increase proteolytic stability of peptide-derived drugs. Among these variations the retro-inverso amide bond[2] is outstanding in preserving the essence of the primary structure. The synthesis requires a substituted malonic acid and a 1,1-diaminoalkyl moiety. Most of the retro-inverso peptides reported so far contain no functionalized side chains at the inverted residues.[1] However, for their intended use in drug development the trifunctional amino acids are even more important. We report here the synthesis of the first partially modified retro-inverso analogue of a T-cell epitope of the influenza nucleoprotein designed to fit into the groove of the major histocompatibility complex (MHC) class I molecule.[3] For the first time, the amide bond between the more complex amino acids glutamine and arginine was inverted by combination of solution and solid-phase synthesis.

[*] Prof. Dr. G. Jung, H. Dürr
Institut für Organische Chemie der Universität
Auf der Morgenstelle 18, D-W-7400 Tübingen (FRG)
Prof. Dr. M. Goodman
Department of Chemistry, University of California at San Diego (USA)

[**] This work was been supported by the Fonds der Chemischen Industrie. H. Dürr is recipient of a doctorate stipend from the Studienstiftung des Deutschen Volkes.

We used [*I,I*-bis(trifluoroacetoxy)iodo]benzene (TIB), also named iodobenzene bistrifluoroacetate (IBTFA), for the synthesis of optically pure *N*-acyl-1,1-diaminoalkanes directly from their peptide amide precursors.[2a] The mild reaction conditions and the one-step procedure made this approach the most favorable for generating the 1,1-diaminoalkyl moiety of retro-inverso peptides, with the exception of sulfur-containing amino acid side chains sensitive to oxidation, and the indole and phenol rings. Applying TIB to glutamine and asparagine causes rearrangement of their amide groups to 2,4-diaminobutyric acid and 2,3-diaminopropionic acid, respectively. Hofmann rearrangement with TIB can also be carried out with peptide amides covalently linked to a polymer support.[4] The malonic acid derivatives are usually synthesized by alkylation of malonic acid diesters with an alkyl halide containing the corresponding side chain.

The synthesis of the glutamyl–arginine pre-retro-inverso dipeptide is summarized in Scheme 1. Alkylation of ethyl *tert*-butylmalonate (**1**) with (*N*-benzyloxycarbonyl)-3-chloropropylamine yields the malonyl ornithine derivative **2**. After hydrogenolysis of the benzyloxycarbonyl protecting group, the guanidino group is introduced with amino-iminomethanesulfonic acid.[5] The crude derivative **3** is allowed to react with 4-methoxy-2,3,6-trimethylbenzenesulfonylchloride (Mtr-Cl) in order to obtain the malonate–arginine derivative **4** with a protected side chain.[6] Simultaneously, the basic medium necessary to deprotonate the guanidino group saponifies the ethyl ester and m(*R,S*)Arg(Mtr)-O*t*Bu **4**[7] is obtained in 30% overall yield after column chromatography on silica gel with chloroform/methanol/acetic acid (85:15:2) as eluent.

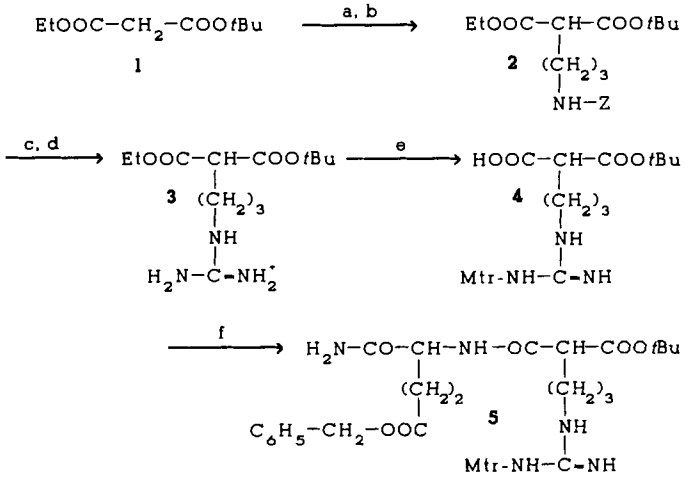

Scheme 1. Synthesis of the glutamyl–arginine pre-retro-inverso dipeptide. a) NaH/DMF, −15 °C to 22 °C, 1 h; b) (*N*-benzyloxycarbonyl)-3-chloropropylamine/DMF, 50 °C, 16 h; c) Pd(C)/H_2, methanol/acetic acid (95:5), 12 h; d) amino-imino-methanesulfonic acid/dioxane/10% Na_2CO_3 aq., 72 h; e) 4 N NaOH/acetone/Mtr-Cl, 2 h; f) H-(D)Glu(Bzl)-NH_2/HOBt/DCC/dichloromethane, 18 h.

The racemic derivative **4** is activated with dicyclohexylcarbodiimide (DCC) and 1-hydroxybenzotriazole (HOBt) in dichloromethane for coupling to D-glutamic acid α-amide-γ-benzyl ester (H-(D)Glu(Bzl)-NH_2) to yield the pre-retro-inverso dipeptide **5**. The resulting diastereomers **5a** and **5b** can be purified and separated on a silica gel column (eluent: chloroform/methanol 9:1). The identity and purity (>98%) of **5a** and **5b** is confirmed by TLC, HPLC, and ^{1}H NMR and ion spray mass spectrometry (IS-MS).[8] The *C*-terminally free pre-retro-inverso dipeptide **6** can be obtained by cleavage of the *t*Bu ester in trifluoroacetic acid (TFA)/dichloromethane/anisole (50:48:2; 1 h).

H_2N-(D)Glu(Bzl)-m(*R,S*)Arg(Mtr)-OH **6**

The retro-inverso killer-cell epitope (CTL epitope) of the influenza nucleoprotein[3] can be built up by Merrifield synthesis by using **6** as a template (Scheme 2). The *C*-terminal

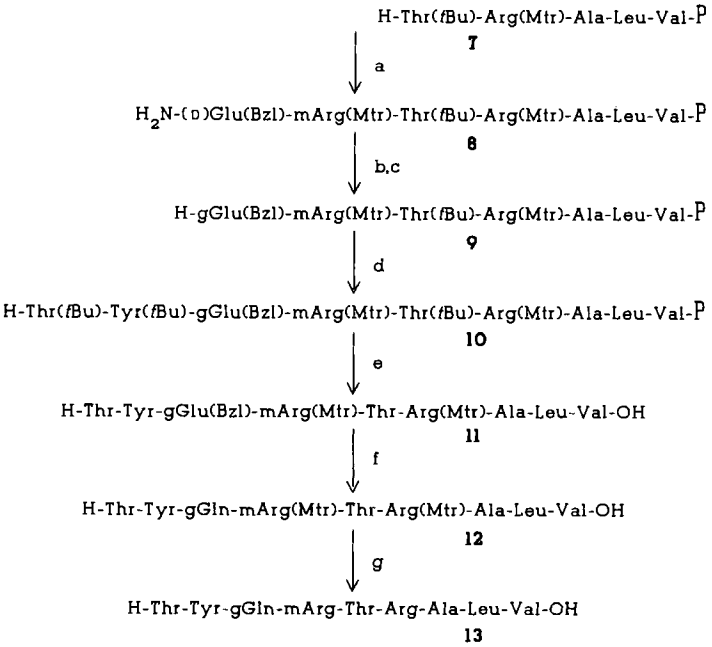

Scheme 2. Synthesis of the partially modified retro-inverso CTL epitope of influenza nucleoprotein (P = *p*-benzyloxybenzylalcohol–polystyrene–1% divinylbenzene). a) **6**/DCC/HOBt/dichloromethane, 36 h; b) [*I,I*-bis(trifluoroacetoxy)iodo]benzene (TIB)/DMF–H_2O (9:1), 3 h; c) *N*-ethylmorpholine/DMF, 5 min; d) Fmoc-amino acid/DCC/HOBt/DMF, 2 h; e) TFA/thioanisole/thiocresol/water (82:8:8:2), 2 h; f) NH_3/methanol, −15 °C to 22 °C, 100 h; g) TFA/thioanisole/thiocresol/water (82:8:8:2), 40 °C, 1 h. All amino acids are of L configuration except for m(*R,S*)Arg. For the structural formula of H_2N-(D)Glu(Bzl)-mArg(Mtr) see Scheme 1 [7].

resin-bound pentapeptide **7** is synthesized automatically by applying Fmoc-strategy on *p*-benzyloxybenzylalcohol–polystyrene–1% divinylbenzene.[9] After the coupling with template **6**, the Hofmann rearrangement with TIB is applied on compound **8** to generate the 1,1-diaminoglutamate derivative **9**. The resin is washed, neutralized, and the compound immediately elongated to the complete nonapeptide **10**. The retro-inverso nonapeptide is cleaved from the resin and partially deprotected to yield **11**. Ammonolysis of the 1,1-diamino-*O*-benzylglutamate residue produces the 1,1-diaminoglutamine derivative **12**. The final product **13** is obtained by trifluoroacetic acid treatment, followed by preparative reverse-phase HPLC. All compounds with exception of **9** are characterized by HPLC, IS-MS and amino acid analysis.[10] No racemization could be detected for **12** by chiral-phase gas chromatography. Interestingly, the retro-inverso CTL epitope **13** is about 10^5 less potent than the natural antigen, which is active in picomolar level in the in vitro killer assay.[3a] At present we are performing competion as-

says to find out whether the epitope backbone modification leads to blocking of the MHC groove or inhibits the T-cell receptor binding.

Received: December 27, 1991 [Z 5098 IE]
German version: *Angew. Chem.* **1992**, *104*, 773

[1] a) A. F. Spatola in *Chemistry and Biochemistry of Amino Acids, Peptides and Proteins* (Ed.: B. Weinstein), Dekker, New York, **1983**, pp. 267–357; b) B. A. Morgan, J. A. Gainor, *Annu. Rep. Med. Chem.* **1989**, *24*, 243–252; c) M. Goodman, R. Rone, N. Manesis, M. Hassan, N. Mammi, *Biopolymers* **1987**, *26*, S25–S32.

[2] a) P. Pallai, M. Goodman, *J. Chem. Soc. Chem. Commun.* **1982**, 280–281; b) N. Chaturvedi, M. Goodman, C. Bowers, *Int. J. Pept. Protein Res.* **1981**, *17*, 72–88.

[3] a) K. Deres, H.-J. Schild, K.-H. Wiesmüller, G. Jung, H.-G. Rammensee, *Nature* **1989**, *342*, 561–564; b) K. Falk, O. Rötzschke, S. Stevanovic, G. Jung, H.-G. Rammensee, *ibid.* **1991**, *351*, 290–296; c) O. Rötzschke, K. Falk, K. Deres, H.-J. Schild, M. Noda, J. Metzger, G. Jung, H.-G. Rammensee, *ibid.* **1990**, *348*, 252–254.

[4] A. Pessi, M. Pinori, A. S. Verdini, G. C. Viscomi, *J. Chem. Soc. Chem. Commun.* **1983**, 195–197.

[5] K. Kim, Y.-T. Lin, H. S. Mosher, *Tetrahedron Lett.* **1988**, *29*, 3183–3186.

[6] M. Fujino, M. Wakimasu, C. Kitada, *Chem. Pharm. Bull.* **1981**, *29*, 2825–2831.

[7] The prefix m represents the malonic acid residue, whereas the g represents the geminal diamino alkyl residue preceeding the derived amino acid in the three-letter notation.

[8] TLC on silica gel (chloroform/methanol/acetic acid, 85:15:2), $R_f = 0.55$ (**5a**), 0.45 (**5b**); ^{1}H NMR: (360 MHz, $CDCl_3$) **5a**: $\delta = 7.68$ (d, 1H, NH), 7.34 (s, 5H, arene), 6.75 (s, 1H, NH), 6.53 (s, 1H, arene), 5.88 (s, 1H, NH), 5.10 (s, 2H, benzyl), 4.43 (m, 1H, α-CH(Glu)), 3.83 (s, 3H, OCH_3), 3.27 (t, 1H, α-CH(mArg)), 3.20 (m, 2H, CH_2), 2.68 (s, 3H, CH_3), 2.60 (s, 3H, CH_3), 2.51 (t, 2H, CH_2), 2.12 (s, 3H, CH_3), 2.10 (m, 2H, CH_2), 1.86 (m, 2H, CH_2), 1.55 (m, 2H, CH_2), 1.44 (s, 9H, *t*Bu); **5b**: $\delta = 7.97$ (d, 1H, NH), 7.37 (s, 5H, arene), 7.00 (s, 1H, NH), 6.60 (s, 1H, NH), 6.59 (s, 1H, arene), 5.15 (s, 2H, benzyl), 4.46 (m, 1H, α-CH(Glu)), 3.90 (s, 3H, OCH_3), 3.39 (t, 1H, α-CH(mArg)), 3.17 (m, 2H, CH_2), 2.75 (s, 3H, CH_3), 2.67 (s, 3H, CH_3), 2.58 (t, 2H, CH_2), 2.18 (s, 3H, CH_3), 2.12 (m, 2H, CH_2), 1.88 (m, 2H, CH_2), 1.59 (m, 2H, CH_2), 1.46 (s, 9H, *t*Bu); IS-MS: (689.1) mol. mass 688.8.

[9] R. Dölling, K.-H. Wiesmüller, J. Metzger, M. Kleemann, H. Dürr, G. Jung in *Peptides 1990* (Eds.: E. Giralt, D. Andreu), Escom, Leiden, **1991**, p. 72–73.

[10] Analytical data for **13**: Amino acid analysis: Ala 1.1(1), Arg 0.9(1), Gln 0(0), Leu 0.9(1), Thr 1.8(2), Tyr 0.8(1), Val 1.0(1); IS-MS: (1108.0) mol. mass 1107.6.

Synthesis and Structure of the Cluster $[NaAu_{12}Se_8]^{3-}$: An Inorganic Cryptand Complex**

By *Song-Ping Huang* and *Mercouri G. Kanatzidis**

The increased interest in the synthesis and structural characterization of soluble metal selenide complexes is due largely to the structural abundance and diversity of these compounds.[1–3] Frequently, for a given metal ion M, more than one compositionally and structurally different selenide complex may be formed and isolated from the M/Se_x^{2-} system.[4–7] For example, during our systematic investigation of the reactions between Au^+ and several Se_x^{2-} ($x = 2–5$) ligands, we have isolated and structurally characterized three different species. First, Au^+ can reduce the pentaselenide ligand Se_5^{2-} to yield a Au^{3+} compound $[Au_2Se_2(Se_4)_2]^{2-}$.[5a] Second, when shorter polyselenide ligands such as Se_4^{2-}, Se_3^{2-}, and Se_2^{2-} are used, the seven- and eight-membered rings of dimeric Au^+ polyselenides, $[Au_2(Se_2)(Se_3)]^{2-}$ and $[Au_2(Se_2)(Se_4)]^{2-}$ are formed.[5b] The formation of either seven- or eight-membered rings can be controlled by the selection of a particular ligand size and a suitable organic counterion. This deviates from the general belief that the metal ions, rather than the size of polychalcogenide ligands used, determine the structures of metal complexes isolable from solution.[1–3, 8, 9] In order to avoid the Au^+/Au^{3+} redox chemistry and explore the reactivity of Au^+ towards other selenides, we used the shortest possible ligand, Se^{2-}. In the Au^+/Se^{2-} system, both the redox chemistry and the ligand size effect cease to operate, while a new factor, the interaction of Au^+ with an alkali-metal ion (i.e. Na^+) surprisingly emerges as a structure-directing force. Here we report a novel cluster, $[NaAu_{12}Se_8]^{3-}$ (**1**), which contains a Na^+ ion encapsulated in a cryptate-like fashion.

The structure of $(Et_4N)_3$-**1** was established by single-crystal X-ray diffraction analysis.[10] The crystal lattice comprises Et_4N^+ cations and $[NaAu_{12}Se_8]^{3-}$ anions. The $[NaAu_{12}Se_8]^{3-}$ anion forms an almost perfect cube with twelve linearly coordinated Au atoms positioned at the midpoints of the edges and eight Se atoms, each with trigonal geometry, occupying the corners of the cube, as shown in Figure 1. The captured Na^+ ion is situated on a crystallographic inversion center, which is also the center of the cube; the distances to the Au atoms lie between 3.327(3) Å and 3.467(3) Å. The Au–Se distances are normal and comparable to those found in $[Au_2(Se_2)(Se_3)]^{2-}$ and $[Au_2(Se_2)(Se_4)]^{2-}$.[5b] The affinity of the $[Au_{12}Se_8]^{4-}$ cage for Na^+ is reminiscent of the behavior of the organic-based cryptands.

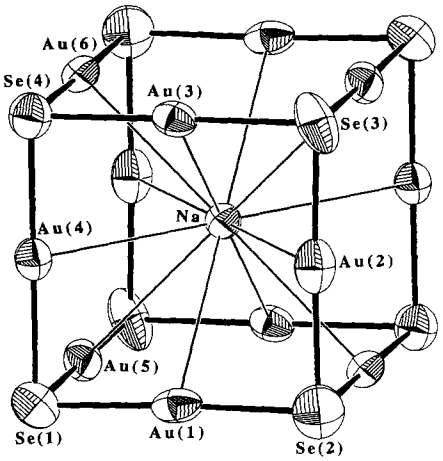

Fig. 1. The structure of $[NaAu_{12}Se_8]^{3-}$ (ORTEP) showing the atom-labeling scheme. Selected bond distances [Å] and bond angles [°]: Au(1)-Se(1) 2.400(7), Au(1)-Se(2) 2.414(8), Au(2)-Se(2) 2.402(8), Au(2)-Se(3) 2.400(8), Au(3)-Se(3) 2.417(7), Au(3)-Se(4) 2.408(6), Au(4)-Se(1) 2.428(7), Au(4)-Se(4) 2.401(6), Au(5)-Se(1) 2.399(7), Au(5)-Se(3) 2.404(7), Au(6)-Se(2) 2.401(7), Au(6)-Se(4) 2.402(6), Na-Au(1) 3.451(2), Na-Au(2) 3.391(3), Na-Au(3) 3.272(3), Na-Au(4) 3.369(3), Na-Au(5) 3.467(3), Na-Au(6) 3.306(2); Se(1)-Au(1)-Se(2) 177.8(2), Se(2)-Au(2)-Se(3) 177.8(2), Se(3)-Au(3)-Se(4) 178.0(2), Se(1)-Au(4)-Se(4) 179.6(2), Se(1)-Au(5)-Se(3) 178.2(3), Se(2)-Au(6)-Se(4) 179.1(2), Au(1)-Se(1)-Au(4) 85.8(2), Au(1)-Se(1)-Au(5) 90.5(2), Au(4)-Se(1)-Au(5) 85.9(2), Au(1)-Se(2)-Au(2) 91.1(3), Au(1)-Se(2)-Au(6) 88.2(2), Au(2)-Se(2)-Au(6) 86.7(2), Au(2)-Se(3)-Au(3) 86.0(2), Au(2)-Se(3)-Au(5) 92.1(2), Au(3)-Se(3)-Au(5) 88.0(2), Au(3)-Se(4)-Au(4) 92.4(2), Au(3)-Se(4)-Au(6) 89.5(2), Au(4)-Se(4)-Au(6) 93.2(2).

[*] Prof. Dr. M. G. Kanatzidis, S.-P. Huang
Department of Chemistry, Michigan State University
East Lansing, MI 48824 (USA)

[**] This work was supported by the Petroleum Chemical Research Fund, administered by the American Chemical Society, and the National Science Foundation (Presidential Young Investigator Award, CHE-8958451). The single-crystal X-ray diffractometers used in this work were purchased by a grant from the National Science Foundation (CHE-8908088). We also thank the Center for Electron Optics at Michigan State University for the use of the electron microscope facilities.

$[NaAu_{12}Se_8]^{3-}$ is a rare example of an inorganic cryptate. Although one might be amazed by the structural simplicity of $[NaAu_{12}Se_8]^{3-}$, the assembly and stabilization of this unique complex reveal a chemical logic. First of all, the strong preference of Au^+ for linear coordination and the trigonal pyramidal geometry of Se^{2-} account for the construction of a cube with edges and corners occupied by atoms. In addition, the cavity size of the cube, which is predetermined by both the Au^+ and the Se^{2-} radii, happens to be a perfect fit for an alkali metal ion, in this case Na^+. A feature worthy of note in a cube is that the distances from the center to its corners are longer than the distances from the center to the midpoints of its edges. Consequently, the Na^+ ion must interact with the twelve Au atoms rather than the eight Se atoms. It has been found that the Au^+ has an affinity for the positively charged alkali-metal ions, and these interactions have precedents in other Au^+ chalcogenide complexes, for example $[KAu_9Te_7]^{4-}$,[12] $[K_2Au_4Te_4(en)_4]^{2-}$ (en = ethylenediamine),[12] and $[K_2Au_4Te_4(dmf)_2]^{2-}$ (dmf = *N*,*N*-dimethylformamide).[13] Thus, the formation of $[NaAu_{12}Se_8]^{3-}$ may not be coincidental, but results instead from the combination of cube-cavity size and the tendency of Au^+ to interact with alkali-metal ions. It should be noted that the S^{2-} ligand can also form cubelike molecules with Au^+ or Cu^+ ions.[14, 15] The $[Cu_{12}S_8]^{4-}$ cube is highly distorted on the edges because the Cu^+ ions deviate from the ideal linear coordination geometry because of attractive $Cu\cdots Cu$ d^{10}–d^{10} interactions.[16] However, no alkali-metal ion is encapsulated in either of the compounds.

A comparison of the volume of the $[Au_{12}S_8]^{4-}$ and $[Au_{12}Se_8]^{4-}$ clusters shows that the sulfide cluster is 12% smaller than its selenide analogue (98 Å^3 vs 111 Å^3). This explains why the corresponding $[NaAu_{12}S_8]^{3-}$ cannot be made. It suggests, however, that $[LiAu_{12}S_8]^{3-}$ may be accessible. On the other hand, the volume of the $[Au_{12}Te_8]^{4-}$ (i.e. 136 Å) is 23% larger than that of the $[Au_{12}Se_8]^{4-}$, which suggests that K^+, Rb^+, or even Cs^+ might be good candidates for inclusion. Attempts to synthesize the $[KAu_{12}Te_8]^{3-}$ have resulted in isolation of only the $[K_2Au_4Te_4(dmf)_2]^{2-}$,[13] which contains a one-dimensional array of $[Au_4Te_4]^{2-}$ sheets held together by ionic interactions between K^+ and Au^+. Work with Rb^+ and Cs^+ is in progress.

The encapsulation of the Na^+ ion in $[Au_{12}Se_8]^{4-}$ may not be due only to the right cavity size but also to a tendency of the cube to reduce its high negative charge. When the synthesis was carried out with K_2Se no corresponding $[KAu_{12}Se_8]^{3-}$ species was found, presumably because of the inability of K^+ to fit into the $[Au_{12}Se_8]^{4-}$ cage. The empty $[Au_{12}Se_8]^{4-}$ cage could not be isolated thus far. It should be mentioned that complete encapsulation of sodium ions by metal chalcogenide complexes was also found in $[Na_2\{Fe_6S_9(SMe)_2\}_2]^{6-}$,[17] where the Na^+ ions cause the aggregation of two Fe_6S_9 clusters, and in the recently reported $[Na_2Fe_{18}S_{30}]^{8-}$,[18] where two Na^+ ions are entirely complexed by the toroidal $Fe_{18}S_{30}$ cluster.

The solid-state far-IR spectrum of $[Et_4N]_3$-**1** shows a single absorption at 236 cm^{-1}. This can be unambiguously assigned to the Au–Se stretching vibration. The same assignment was made in the far-IR spectra of $[Au_2(Se_2)(Se_3)]^{2-}$ and $[Au_2(Se_2)(Se_4)]^{2-}$.[5b] A solution of $[Et_4N]_3$-**1** in DMF is brownish yellow and shows a featureless UV/VIS spectrum. This solution gave a single ^{23}Na NMR signal at $\delta = -12.0$ (relative to $NaBPh_4$ in DMF at $\delta = 0$). The upfield shift of the resonance signal indicates not only that the sodium ion remains encapsulated when the cluster dissolves but also that the Na^+ ion is electronically somewhat "naked" compared to the highly solvated Na^+ ion of the $NaBPh_4$ solution. This is a consequence of the special environment of the Na^+ ion in the cube. The ^{77}Se NMR spectrum of $[Et_4N]_3$-**1** in DMF also shows a single resonance signal at $\delta = 758$ (relative to Ph_2Se_2 in DMF at $\delta = 460$). The NMR data suggest that in solution, **1** retains its structural integrity and are consistent with O_h symmetry.

In summary, the polynuclear gold(I) selenide cluster was made by the reaction of AuCN with Na_2Se in the presence of Et_4NCl. The cluster can act as an inorganic cryptand to capture an alkali-metal ion. The stabilization of the cage structure and the apparent importance of interactions between alkali metals and gold raises interesting implications for the exploitation of such interactions in the synthesis of new cagelike compounds.

Experimental Procedure

All manipulations were carried out in a glove box under a nitrogen atmosphere. Na_2Se was prepared by dissolving the stoichiometric amount of the elements in liquid ammonia. Solvents were all dried and distilled under N_2. AuCN was used as obtained.

Addition of 25 mL of diethyl ether to 20 mL of a reaction mixture of AuCN (45 mg, 0.2 mmol), Na_2Se (25 mg, 0.2 mmol), and Et_4NCl (33 mg, 0.2 mmol) in methanol afforded a pale yellow powder. Collection and recrystallization of this product with a slow diffusion technique in DMF/ether solution (ca. 1:1, total volume 20 mL) over a period of two weeks gave amber-colored, cubelike single crystals of $(Et_4N)_3[NaAu_{12}Se_8]$. The overall yield of the synthesis was estimated at approximately 33% based on the AuCN. Semiquantitative elemental analyses of the compound were carried out by energy dispersive X-ray microanalysis (EDS) with a scanning electron microscope. It revealed that the product contains gold and selenium in a 3:1 ratio. The experimentally measured X-ray diffraction pattern of $(Et_4N)_3$-**1** matches that calculated from the X-ray single crystal data, indicating that it is a homogeneous product.

Received: January 8, 1992 [Z 5111 IE]
German version: *Angew. Chem.* **1992**, *104*, 799

CAS Registry number:
$(Et_4N)_3$-**1**, 141319-68-8.

[1] M. G. Kanatzidis, *Comments Inorg. Chem.* **1990**, *10*, 161–195.
[2] M. A. Ansari, J. A. Ibers, *Coord. Chem. Rev.* **1990**, *100*, 223–266.
[3] J. W. Kolis, *Coord. Chem. Rev.* **1990**, *105*, 195–219.
[4] a) R. W. M. Wardle, C.-N. Chau, J. A. Ibers, *J. Am. Chem. Soc.* **1987**, *109*, 1859–1866; b) J.-H. Liao, M. G. Kanatzidis, *ibid.* **1990**, *112*, 7400–7402.
[5] a) M. G. Kanatzidis, S.-P. Huang, *Inorg. Chem.* **1989**, *28*, 4667–4669; b) S.-P. Huang, M. G. Kanatzidis, *ibid.* **1991**, *30*, 3572–3575.
[6] a) S.-P. Huang, M. G. Kanatzidis, *Inorg. Chem.* **1991**, *30*, 1455–1466; b) M. G. Kanatzidis, S. Dhingra, *ibid.* **1989**, *28*, 2024–2026.
[7] D. Fenske, S. Magull, K. Dehnicke, *Z. Naturforsch. B* **1991**, *46*, 1011–1014.
[8] M. Draganjac, T. B. Rauchfuss, *Angew. Chem.* **1985**, *97*, 745–760; *Angew. Chem. Int. Ed. Engl.* **1985**, *24*, 742–757.
[9] A. Müller, *Polyhedron* **1986**, *5*, 323–340.
[10] Crystal data for $(Et_4N)_3[NaAu_{12}Se_8]$: triclinic $P\bar{1}$, $Z = 2$, $a = 11.956(4)$, $b = 12.733(4)$, $c = 10.784(3)$ Å, $\alpha = 103.94(3)$, $\beta = 108.96(3)$, $\gamma = 113.63(2)°$, $V = 1285(2)$ Å^3 at 23 °C. $2\theta_{max}$ ($Mo_{K\alpha}$) = 45.0°. Number of reflections measured 3557. Number of reflections having $F_o^2 > 3\sigma(F_o^2)$: 1872. $\rho_{calcd} = 4.40$ g cm^{-3}. An empirical absorption correction based on Ψ scans and a DIFABS correction [11] after isotropic refinement of all atoms were applied, $\mu = 396$ cm^{-1}. The minimum and maximum transmission was 0.75 and 1.39, respectively. The structure has an asymmetric unit of $(Et_4N)_{1.5}[Na_{0.5}Au_6Se_4]$. In addition to the Na^+ ion, one of the tetrahedral Et_4N^+ cations was found to occupy a crystallographic inversion center, causing positional disorder of the ethyl groups on this cation site. The refinement of the atoms in this cation was carried out with a disorder model where all the C sites except for a terminal one (i.e. C16) are half-occupied. C16 could not be found, but its position was calculated and included in the structure factor calculation. The structure was solved by direct methods with the program MITHRIL and refined with TEXSAN single crystal analysis software. Final $R = 0.072$ and $R_w = 0.084$. Further details of the crystal structure investigations may be obtained from the Fachinformationszentrum Karlsruhe, Gesellschaft für wissenschaftlich-technische Information mbH, D-W-7514 Eggenstein-Leopoldshafen 2

(FRG), on quoting the depository number CSD-56044, the names of the authors, and the journal citation.
[11] N. Walker, D. Stuart, *Acta Crystallogr. Sect. A* **1983**, *39*, 158–166.
[12] R. C. Haushalter, *Angew. Chem.* **1985**, *97*, 412–413; *Angew. Chem. Int. Ed. Engl.* **1985**, *24*, 432–433.
[13] M. G. Kanatzidis, S.-P. Huang, *Phosphorous Sulfur Silicon Relat. Elem.*, in press.
[14] G. Marbach, J. Strähle, *Angew. Chem.* **1984**, *96*, 695–696; *Angew. Chem. Int. Ed. Engl.* **1984**, *23*, 715–716.
[15] P. Betz, B. Krebs, G. Henkel, *Angew. Chem.* **1984**, *96*, 293–294; *Angew. Chem. Int. Ed. Engl.* **1984**, *23*, 311–312.
[16] a) P. K. Mehrotra, R. Hoffmann, *Inorg. Chem.* **1978**, *17*, 2187–2189; b) K. M. Merz, R. Hoffmann, *ibid.* **1988**, *27*, 2120–2127.
[17] J.-F. You, B. S. Snyder, G. C. Papaefthymiou, R. H. Holm, *J. Am. Chem. Soc.* **1990**, *112*, 6589–6591.
[18] J. F. You, B. S. Snyder, R. H. Holm, *J. Am. Chem. Soc.* **1988**, *110*, 6589–6591.

Chemical Attachment of Organometallics to Proteins in Reverse Micelles**

By *Alexander D. Ryabov,* Alexey M. Trushkin, Lidia I. Baksheeva, Raisa K. Gorbatova, Irina V. Kubrakova, Vadim V. Mozhaev, Boris B. Gnedenko and Andrey V. Levashov*

Enzymes capable of a direct electron exchange with an electrode are at present arousing great interest. In increasing numbers, native enzymes have been shown to be electrochemically active under appropriate conditions.[1] These mediatorless electron relays have, however, an effective alternative in the pseudo-mediatorless systems, where a mediator of the electron transport is bound to a redox enzyme.[2, 3] Different mediators are known,[4, 5] but ferrocene derivatives[6] and osmium complexes[7] accommodate best the functioning of FAD-dependent oxidases. The rich biochemistry of ferrocenes[8] also makes elaboration of simple procedures for their attachment to proteins essential. An obstacle here is the low aqueous solubility of ferrocenes, and, as a result, the known procedures[9] are often heterogeneous in nature. Moreover, the modification is usually carried out in the presence of large to moderate concentrations of urea, which causes protein denaturation (unfolding). Such procedures might be rather invasive, since a protein will not necessarily refold into the native conformation.

A possible alternative that eliminates the solubility problem on one hand, and does not involve unfolding on the other, is a reverse micelle "microreactor" successfully used recently for the modification of α-chymotrypsin and other biomolecules with fatty acid chlorides.[10] Now we report on the modification of GO[*] by FcCOOH in the presence of DCC/*N*-hydroxysuccinimide in reverse micelles of AOT in *n*-octane.

The size of the reverse micelle microreactor can be adjusted to any protein by varying the degree of hydration, that is, the water to surfactant molar ratio, $w_0 = [H_2O]/[AOT]$.[11] In our case, the size of the inner cavity corresponded to a two-subunit GO molecule of the molecular mass 160 kDa achieved when the ratio $[H_2O]/[AOT]$ is 23. The correspondence between the size of the inner cavity of reverse micelle microreactor and the enzyme precludes the unfolding, and hence, only surface amino groups of GO are exposed to modification. Such an approach to modification of surface groups seems to be less laborious and more general than that based on oxidation oligosaccharides at the periphery of enzymes.[9d] As a modifier, we used FcCOOH activated by DCC/*N*-hydroxysuccinimide in acetonitrile solvent.[12] Acetonitrile, the molar amount of which is a factor of 75 lower than that of water, probably does not affect the size of reverse micelles but appears to be an important component, since no modification is observed when the activation is carried out in either benzene, or *n*-octane. Activated FcCOOH is readily attached to NH_2 groups of GO solubilized in the aqueous phase of reverse micelles.

The modified GO does not differ much from native GO. Only five ferrocene residues are attached per molecule of GO (electrothermal atomic absorption spectrometry), far fewer than with the procedures involving urea, where usually more than 10 species are introduced.[9] Electrophoregrams of the native and modified enzymes (SDS, polyacrylamide gel) are practically identical. In both cases only the bands from monomeric units of 80 kDa are developed, which rules out aggregation. Measured with the Clark electrode, the kinetics of dioxygen consumption by modified GO resembles that by the native enzyme, but the modified GO is 22% as active as the native one. The modification thus does not change the enzyme crucially. Rather, it introduces a novel feature displayed in Figure 1, where cyclic voltammograms of the ferrocene-bound enzyme are shown both in the absence and in the presence of D-glucose.

Even in the absence of the substrate (trace a, Fig. 1 left), a peak from pendant ferrocene is observed at 0.27 V. The role of ferrocene units as mediators for the electron transfer becomes clear on consecutive addition of D-glucose (traces b–e). The plot of current versus D-glucose concentration is practically linear in the range 0.01–0.15 M. The response also increases with the temperature reaching maximum at 40 °C and then decreases because the enzyme is inactivated. It was interesting to compare the *operational* thermostability of the native and modified GO preparations at 55 °C by measuring the catalytic current. For native GO, we measured the decrease in the peak current in the presence of added FcCOOH and D-glucose. Naturally, only D-glucose was added to modified GO. Both current/time plots yielded the observed first-order rate constants of thermoinactivation (k_{obs}) of $(5.0 \pm 0.2) \times 10^{-4}$ and $(6.0 \pm 0.8) \times 10^{-4}\ s^{-1}$ for native and modified GO, respectively (0.5 M D-glucose, pH 5). Hence, this modification of GO by hydrophobic ferrocene residues does not significantly decrease its operational stability.

The observation of a true ferrocene electrochemical signal (Fig. 1 left, trace a) suggests that the organometallic moiety is pendant, and hence covalently bound to GO through a spacer rather than adsorbed on its surface. The traces ob-

[*] Prof. A. D. Ryabov,[+] A. M. Trushkin, L. I. Baksheeva, Dr. R. K. Gorbatova
Division of Chemistry, G. V. Plekhanov Russian Economic Academy
Stremyanny per. 28, 113054, Moscow (Russia)
Dr. I. V. Kubrakova
Institute of Geochemistry and Analytical Chemistry, Russian Academy of Sciences, Moscow (Russia)
Dr. V. V. Mozhaev, B. B. Gnedenko, Dr. A. V. Levashov
Department of Chemistry, Moscow State University (Russia)
[+] Alexander von Humboldt fellow (1991-1992) at
Institut für Anorganische Chemie
Universität Witten/Herdecke
Stockumerstrasse 10, D-W-5810 Witten-Annen (FRG)

[**] This work was partly supported by Grant No 7-192 of the All-Union State Scientific and Technological Program "Advanced Methods of Bioengineering" (CIS). We thank Mr. S. Vakula for technical assistance.

[*] Abbreviations: GO = glucose oxidase, BSA = bovine serum albumin, AOT = aerosol OT [bis(2-ethylhexyl)sodium sulfosuccinate], FcH = ferrocene, FcCOOH = hydroxycarbonylferrocene, DCC = dicyclohexylcarbodiimide, SDS = sodium dodecyl sulfate.

served in the presence of D-glucose are very similar to those obtained by Heller et al. for GO with ferrocene residues covalently attached through a short spacer,[9d] but not to those reported by Cass et al. for the mixtures of native GO and added FcCOOH,[6] for which the current sharply increases with increasing potential, reaching limiting values. No ferrocene signals were detected when the modification of GO was carried out in the absence of DCC and/or *N*-hydroxysuccinimide, and addition of D-glucose did not increase the current, since a small amount of mediator can produce a signal in the presence of the substrate. Noncovalent attachment might be expected for proteins like BSA. In fact, even ferrocene without functional groups (FcH) can be adsorbed on the surface of BSA in the reverse micelle microreactor. Naturally, no activating couple is needed in this case. The preparation isolated is again electrochemically active, but the current is seen at much more positive potentials (Fig. 1 right, trace b) suggesting[13] that FcH is buried inside the BSA globule and, therefore, strongly deshielded by the amino acid residues. Despite this, BSA modified thus, as in the case of covalently modified protein,[14] is able to act as a mediator and couples with native GO (Fig. 1 right, trace c).

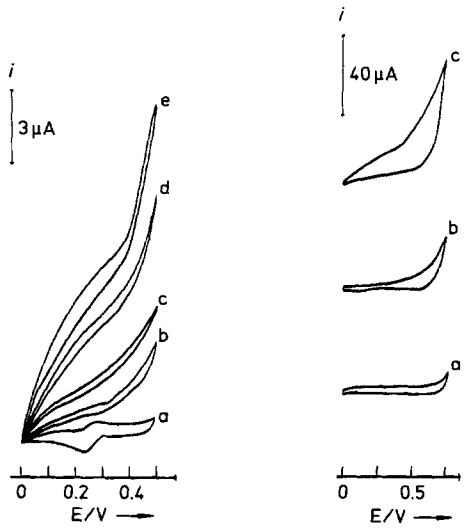

Fig. 1. Left: Cyclic voltammograms of GO modified with FcCOOH at different concentrations of D-glucose: a) 0, b) 0.031, c) 0.046, d) 0.077 and e) 0.154 M. GO 2 mg mL^{-1}. Scan rate 2.5 mV s^{-1}. Right: Cyclic voltammograms of BSA with adsorbed FcH: a) native BSA (2 mg mL^{-1}), b) BSA with adsorbed ferrocene (2 mg mL^{-1}), c) as in b) but in the presence of GO (4 mg mL^{-1}) and D-glucose (0.2 M). Scan rate 5 mV s^{-1}.

In conclusion, the procedures reported enable both covalent binding or adsorption of organometallics on protein surfaces in the reverse micelle microreactors. This may find applications not only in creation of electron relays and new catalysts, but also in the utilization of organometallics as heavy metal probes in electron spectroscopy and other fields of organometallic biochemistry.[8]

Experimental Procedure

GO (β-D-glucose: oxygen 1-oxydoreductase, EC 1.1.3.4) from *Aspergillus niger* and BSA were purchased from Boehringer and Serva, respectively. Dicyclohexylcarbodiimide and *N*-hydroxysuccinimide were obtained from Merck and Sigma, respectively, AOT from Serva, and ferrocene from Reakhim. FcCOOH was prepared as described elsewhere [15]. Cyclic voltammograms were obtained on a potentiostat P-5827M equipped with an XY-recorder. A standard three-electrode cell was used with Ag/AgCl as reference, Pt wire as ancillary, and pyrographite plate (ca. 1.00 cm^2) as working electrode. The latter was always polished with a fine Al_2O_3 powder before the electrochemical measurements. The 2 mL cell was thermostated with water from a 2290 MULTITEMP Thermostatic circulator (LKB). The measurements were made at pH 6.0 (0.1 M phosphate buffer) under aerobic conditions. Potentials are given relative to Ag/AgCl throughout.

GO/Fc-COOH conjugate: GO (30 mg) dissolved in 6 mL borate buffer (0.05 M, pH 9.0) was solubilized in 50 mL of *n*-octane containing AOT (6.67 g, 0.015 mol). Activation of the ferrocene carboxylic groups: FcCOOH (6.3 mg, 0.027 mmol), DCC (6.3 mg, 0.030 mmol), and *N*-hydroxysuccinimide (3.7 mg, 0.027 mmol) were dissolved in 0.25 mL acetonitrile. (Larger amounts of acetonitrile should be avoided because of possible phase separation.) The acetonitrile solution was kept at ca. 5 °C for 30 min, then for 1 h at room temperature, and subsequently added to the enzyme solubilized in reverse micelles of AOT in *n*-octane. The resulting pseudohomogeneous solution was allowed to stand at 20 °C for 24 h and then at 5 °C for 1 h. Cold acetone (100 mL) was added to the mixture to induce the precipitation of GO modified with ferrocene residues. The preparation was centrifuged, thoroughly washed with cold acetone to remove possible admixtures of FcCOOH, and dried in vacuo.

BSA/ferrocene adsorbate: BSA (8.4 mg) was dissolved in the 1.2 mL borate buffer and solubilized in 6 mL of *n*-octane with 1.66 g AOT (0.0038 mol). FcH (1.4 mg, 0.0075 mmol) dissolved in 0.6 mL *n*-octane was added to the micellar solution, and the resulting mixture was kept and worked up as above (18 mL acetone was used).

Received: December 27, 1991 [Z 5102 IE]
German version: *Angew. Chem.* **1992**, *104*, 788

[1] a) S. D. Varfolomeev, *Methods Enzymol.* **1988**, *137*, 430–440; b) R. M. Paddock, E. F. Bowden, *J. Electroanal. Chem.* **1989**, *260*, 487–494; c) L. H. Guo, H. A. O. Hill, G. A. Lowrance, *J. Electroanal. Chem.* **1989**, *266*, 379–396; d) A. Szues, G. D. Hitchens, J. O. M. Bockris, *Bioelectrochem. Bioenergetics* **1989**, *21*, 133–148; e) S.-i. Yabuki, H. Shinohara, M. Aizawa, *J. Chem. Soc. Chem. Commun.* **1989**, 945–946; f) P. De Taxis Du Poet, S. Miyamoto, T. Murakami, J. Kimura, I. Karube, *Anal. Chim. Acta* **1990**, *235*, 255–263; g) M. Shaolin, X. Huaiguo, Q. Bidong, *J. Electroanal. Chem.* **1991**, *245*, 133–138; h) J. Kulys, R. D. Schmid, *Bioelectrochem. Bioenerg.* **1990**, *24*, 305–311.

[2] P. N. Bartlett, V. Q. Bradford, *J. Chem. Soc. Chem. Commun.* **1990**, 1135–1136.

[3] A. Heller, *Acc. Chem. Res.* **1990**, *23*, 128–134.

[4] M. L. Fultz, A. R. Durst, *Anal. Chim. Acta* **1982**, *140*, 1–18.

[5] G. K. Budnikov, O. Yu. Kargina, I. F. Abdullin, *Zh. Anal. Khim.* **1989**, *44*, 1733–1752.

[6] A. E. G. Cass, G. Davis, G. D. Francis, H. A. O. Hill, W. J. Aston, I. J. Higgins, E. V. Plotkin, L. D. L. Scott, A. P. F. Turner, *Anal. Chem.* **1984**, *56*, 667–671; M. J. Green, H. A. O. Hill, J. Chem. Soc. Faraday Trans. 1, **1986**, *82*, 1237–1243.

[7] Y. Degani, A. Heller, *J. Am. Chem. Soc.* **1989**, *111*, 2357–2358; B. A. Gregg, A. Heller, *Anal. Chem.* **1990**, *62*, 258–263; *J. Phys. Chem.* **1991**, *95*, 5976–5980.

[8] Review: A. D. Ryabov, *Angew. Chem.* **1991**, *103*, 945–955; *Angew. Chem. Int. Ed. Engl.* **1991**, *30*, 931–941.

[9] a) Y. Degani, A. Heller, *J. Phys. Chem.* **1987**, *91*, 1285–1289; b) *J. Am. Chem. Soc.* **1988**, *110*, 2615–2620; c) P. N. Bartlett, R. G. Whitaker, M. J. Green, J. Frew, *J. Chem. Soc. Chem. Commun.* **1987**, 1603–1604; d) W. Shuhmann, T. J. Ohara, H.-L. Schmidt, A. Heller, *J. Am. Chem. Soc.* **1991**, *113*, 1394–1397.

[10] a) A. V. Levashov, A. V., Kabanov, Yu. L. Khmelnitsky, I. V. Berezin, K. Martinek, *Dokl. AN SSSR* **1984**, *278*, 246–248; b) A. V. Kabanov, A. L. Klibanov, V. P. Torchilin, K. Martinek, A. V. Levashov, *Bioorg. Khim.* **1987**, *13*, 1321–1324; c) A. V. Kabanov, A. V. Ovcharenko, N. S. Melik-Nubarov, A. I. Bannikov, V. Yu. Alakhov, V. I. Kiselev, P. G. Sveshnikov, O. I. Kiselev, A. V. Levashov, E. S. Severin, *FEBS Lett.* **1989**, *250*, 238–240.

[11] N. L. Klaychko, A. V. Pshezhetsky, A.V. Kabanov, S. V. Vakula, K. Martinek, A. V. Levashov, *Biol. Membr.* **1990**, *7*, 467–472.

[12] For details on the chemistry of the activation procedure see reviews: a) Y. S. Klausner, M. Bodansky, *Synthesis* **1972**, 453–463; b) E. W. Colwin in *Comprehensive Organic Chemistry. The Synthesis and Reactions of Organic Compounds* (Eds.: D. Barton, W. D. Ollis), Pergamon Press, Oxford, **1983**, *Vol. 2*, pp. 634–635.

[13] A. D. Ryabov, E. M. Tyapochkin, S. D. Varfolomeev, A. A. Karyakin, *Bioelectrochem. Bioenerg.* **1990**, *24*, 257–262.

[14] F. Mizutani, M. Asai, *Denki Kagaku oyobi Kogyo Butsuri Kagaku* **1988**, *56*, 1100–1101.

[15] K. L. Rinehart, Jr., K. L. Motz, S. Moon, *J. Am. Chem. Soc.* **1957**, *79*, 2749–2754.

Anti-Bredt Enol Ethers by Transannular Cyclization of Cycloalkynols

By *Heiner Detert, Christina Anthony-Mayer,* and *Herbert Meier**

Since the original definition of the Bredt rule,[1] bridgehead olefins have been a challenge for chemists interested in synthesis. Whereas the preparation and the unusual properties of isocyclic anti-Bredt compounds have been the subject of a large number of investigations, heterocyclic systems of this structure variant are almost unknown.[2]

For the isolation of such compounds in pure form, the ring bearing the *trans* double bond must contain at least eight atoms. For the bicyclic enol ethers **1** this condition is satisfied when $m + n \geq 6$. The geometric strain[3] vanishes when $m + n \geq 8$ and $m,n \geq 3$; in oxabicycloalkenes with larger rings, angle deformations should make only a minor contribution to the total steric strain. Of compounds of type **1**, so far only 9-oxabicyclo[3.3.1]non-1-ene ($m = n = 3$), first synthesized by Wiseman, is known.[4, 5]

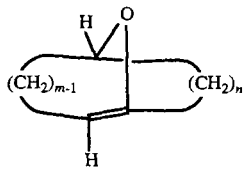

1 (m,n = 1,2,3...)

We report here on a new entry to **1** by thermal isomerization of cycloalkynols. In this process the OH group undergoes transannular addition to the triple bond. By starting from cyclooctan-4-ol-1-one semicarbazone, which exists predominantly as an internal semiaminal **2** (readily soluble in dioxane), the 1,2,3-selenadiazoles **3** (m.p. 134 °C) and **4** (oily liquid) can be synthesized.[6] After separation by column chromatography on silica gel, thermolysis at 160–180 °C/15 Torr gives 3-cyclooctyn-1-ol (**5**) and 4-cyclooctyn-1-ol (**6**), respectively.[7]

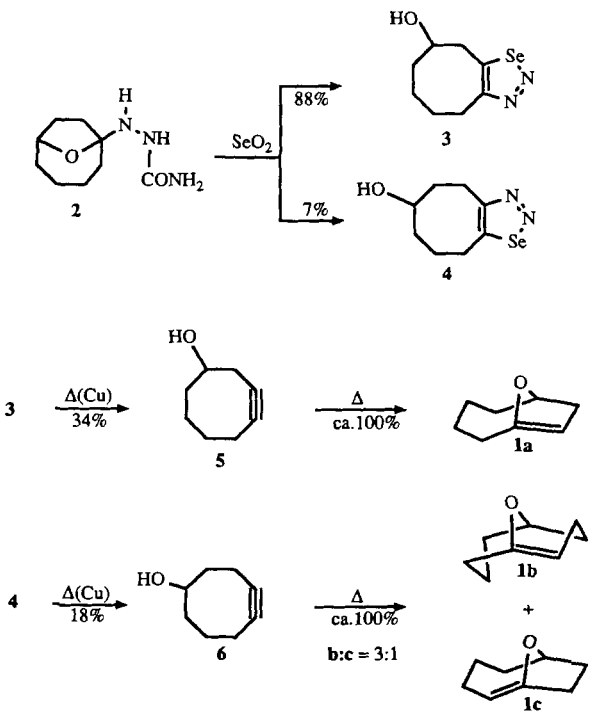

Above 180 °C the cycloalkynols rearrange completely into the anti-Bredt enol ethers. Whereas **5** is converted regiospecifically into 9-oxabicyclo[4.2.1]non-6-ene (**1a**), **6** gives a 3:1 mixture of 9-oxabicyclo[3.3.1]non-1-ene (**1b**) and 9-oxabicyclo[4.2.1]non-1-ene (**1c**). Although strained cycloalkynes possess a low-lying LUMO,[8] nucleophilic attack of the OH group on the triple bond is unexpected; alcohols normally hydrogenate strained, deformed triple bonds smoothly to double bonds.[9, 10] In this manner (*Z*)-cyclooctene is formed from cyclooctyne.[10]

The anti-Bredt enol ethers are suprisingly stable towards further rearrangements or dimerization. They add water regioselectively under acid catalysis, leading to the corresponding semiacetals and their associated tautomeric cycloalkanolones. Compounds **1a–c** react as electron-rich dienophiles with electron-poor dienes such as tetraphenylcyclopentadienone in inverse Diels–Alder reactions to give the corresponding cycloadducts even at room temperature (with almost quantitative yields).

The question can be raised whether the cycloalkynol–oxabicycloalkene rearrangement is limited to highly strained cycloalkynes, and whether the driving force is the partial relief of strain. For this investigation we have prepared 5-cyclodecyn-1-ol (**7**), again using the selenadiazole method. Compound **7** also rearranges thermally, forming a 2:1 mixture of 11-oxabicyclo[4.4.1]undec-1-ene (**1d**)[11] and 11-oxabicyclo[5.3.1]undec-1-ene (**1e**). This rearrangement is therefore not restricted to strained systems!

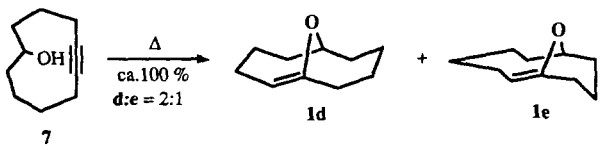

7

Compound **7** undergoes a quite different transannular reaction in the presence of acid. Hanack et al. have observed an isomerization with formation of a carbon–carbon bond generating bicyclo[4.4.0]decan-2-one and bicyclo[5.3.0]decan-2-one under these conditions.[12]

Table 1. Selected ^{1}H and ^{13}C NMR shifts of oxabicycloalkenes **1** ($CDCl_3$, TMS int.).

Compound	–CH–O	O–C=	=CH–
1a	4.58	–	4.90
	84.3	158.9	107.4
1b	4.65	–	5.70
	79.5	159.0	120.3
1c	4.08	–	4.95
	69.1	156.7	113.8
1d	4.01	–	5.11
	74.6	156.3	113.3
1e	4.12	–	5.02
	80.4	151.9	111.4

The most important NMR data of **1a–e** are collected in Table 1. The chemical shifts of the bridgehead atoms and the

[*] Prof. Dr. H. Meier, Dr. H. Detert, Dr. C. Anthony-Mayer
Institut für Organische Chemie der Universität
J.-J.-Becherweg 18–22, D-W-6500 Mainz (FRG)

neighboring olefinic CH groups depend markedly on the size of the corresponding ring in the bicycle.[13]

Received: January 13, 1992 [Z 5117 IE]
German version: *Angew. Chem.* **1992**, *104*, 755

CAS Registry numbers:
1a, 140465-17-4; **1b**, 40164-27-0; **1c**, 140465-22-1; **1d**, 7092-03-7; **1e**, 140465-23-2; **2**, 140465-18-5; **3**, 140465-19-6; **4**, 140465-20-9; **5**, 148465-21-0; **6**, 67959-50-6; **7**, 25533-77-1.

[1] J. Bredt, *Justus Liebigs Ann. Chem* **1924**, *437*, 1–13.
[2] Reviews: a) G. Szeimies, *Reactive Intermediates Vol. 3*, Plenum, New York, **1983**, pp 299–366; b) K. J. Shea, *Tetrahedron*, **1980**, *36*, 1683–1715; c) R. Keese, *Angew. Chem.* **1975**, *87*, 568–578; *Angew. Chem. Int. Ed. Engl.* **1975**, *14*, 528–538; G. Köbrich, *ibid.* **1973**, *85*, 494–503 and **1973**, *12*, 464–473.
[3] H. Meier, *Adv. Strain Org. Chem.* **1991**, *1*, 215–272.
[4] C. B. Quinn, J. R. Wiseman, *J. Am. Chem. Soc.* **1973**, *95*, 1342–1343.
[5] Cf. Y. Chiang, A. J. Kresge, P. A. Walsh, *J. Org. Chem.* **1990**, *55*, 1309–1310.
[6] Cf. H. Meier, H. Petersen, *Synthesis* **1978**, 596–598.
[7] 4-Cyclooctyn-1-ol can be prepared analogously with better yields from cyclooctan-5-ol-1-one [6].
[8] L. Ng, K. D. Jordan, A. Krebs, W. Rüger, *J. Am. Chem. Soc.* **1982**, *104*, 7414–7416.
[9] A. Krebs, H. Colberg, *Chem. Ber.* **1980**, *113*, 2007–2014.
[10] H. Spang, M. Hanack, *Chem. Ber.* **1980**, *113*, 2025–2028.
[11] Cf. W. J. Mijs, K. S. de Vries, J. G. Westra, H. A. Angad Gaur, J. Schmidt, J. Vriend, *Recl. Trav. Chim. Pays-Bas* **1968**, *87*, 580–584.
[12] M. Hanack, W. Spang, *Chem. Ber.* **1980**, *113*, 2015–2024; M. Hanack, C. E. Harding, J. L. Deroque, *ibid.* **1972**, *105*, 421–433.
[13] Cf. the data of the corresponding carbocycles: K. B. Becker, *Helv. Chim. Acta* **1977**, *60*, 81–93.

A Binary Quinone Receptor

By *Christopher A. Hunter** and *Duncan H. Purvis*

The photosynthetic reaction centers of purple bacteria contain two quinone binding sites separated by approximately 12 Å.[1] This binary quinone complex functions as a gate between the one-electron chemistry of photoinduced electron-transfer and the two-electron chemistry required to generate stable reduced products.[2] In this communication, we report a supramolecular assembly which has a similar structure and may therefore be capable of performing a similar function.

We recently reported the synthesis of a macrocyclic receptor **1** (Scheme 1), which complexes *p*-benzoquinone by means of H-bonding and π–π interactions (Fig. 1).[3] In addition to the cyclic dimer **1** the reaction also yielded the cyclic tetramer **2** and the [2]-catenane **3**.[4] If 2,6-pyridinedicarbonyl dichloride is used instead of isophthaloyl dichloride in the final step, the cyclic dimer **4** and the cyclic tetramer **5** result (Scheme 1).[5] Catenated products were also obtained, but these have not yet been characterized.

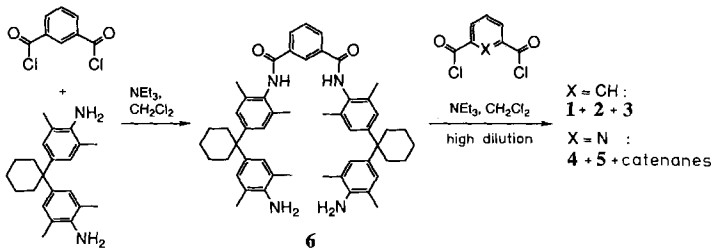

Scheme 1. Synthesis of the macrocyclic receptors.

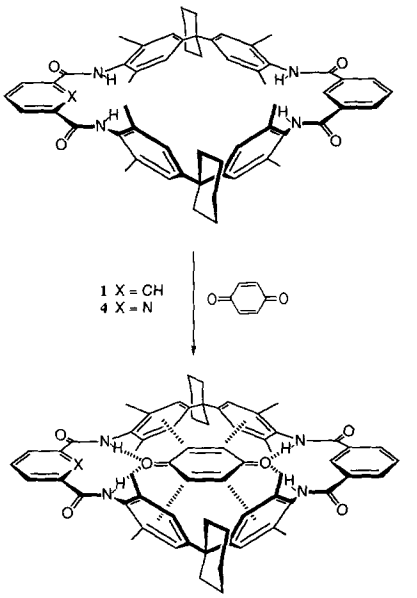

Fig. 1. Complexation of *p*-benzoquinone by **1** and **4**. Intermolecular H-bonds and π–π interactions are shown as dashed lines.

The properties of the cyclic dimer **4** are similar to those of the parent compound **1**: both form 1:1 complexes with *p*-benzoquinone (Fig. 1, Table 1).[6] In contrast, the cyclic tetramers **2** and **5** show very different behavior. The ^{1}H NMR spectrum of **2** is very similar to the spectra of **1** and **6** which suggests that **2** adopts an "open" conformation such as that shown in Figure 2. In contrast, the ^{1}H NMR spectrum of **5** differs significantly from the spectrum of the corresponding dimer **4**. The isophthaloyl signals of **5** are shifted significantly relative to corresponding signals of **4** (Fig. 3). The signals due to the aromatic protons on one side of the ring are shifted upfield which suggests that these protons lie over the face of another aromatic ring. The signal due to the isophthaloyl amide protons is shifted downfield which suggests that these protons are involved in H-bonding. However, the chemical shifts of the pyridyl and diaryl protons of

Table 1. Association constants for *p*-benzoquinone in $CDCl_3$ [M^{-1}] [a].

Compound	K_1	K_2
1	1200	–
2	<1	–
4	1800	–
5	14 [b]	28 [b]

[a] All values are the average of at least five measurements. Errors are ±10%. [b] These values are microscopic association constants which have been corrected for statistical effects. K_1 is half of the observed value and K_2 is twice the experimentally determined value, since in the absence of any cooperativity K_1(observed) = 4 K_2(observed). Errors are ±50% [12].

[*] Dr. C. A. Hunter,[+] D. H. Purvis
Department of Chemistry, University of Otago
P.O. Box 56, Dunedin (New Zealand)
[+] Current Address:
Department of Chemistry, The University
GB-Sheffield S3 7HF (UK)

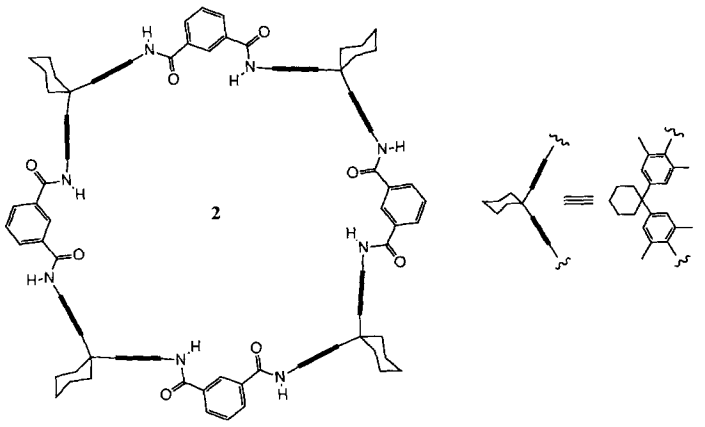

Fig. 2. The open conformation adopted by **2**.

5 are essentially identical to those of **4**. This suggests that these parts of the molecule adopt the same conformation in both compounds, and that they do not interact with the isophthaloyl groups. Thus the two isophthaloyl groups in **5**

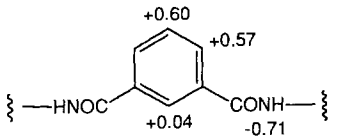

Fig. 3. The changes in ^{1}H NMR δ chemical shifts of the isophthaloyl signals of **5** relative to the corresponding signals of **4**.

must interact with each other, leading to a "folded" conformation (Fig. 4), which is stabilized by two H-bonds and an offset π-stacking interaction.[7]

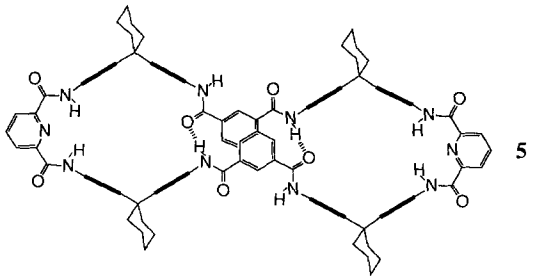

Fig. 4. The folded conformation adopted by **5**.

^{1}H NMR relaxation times provide further evidence for the folded structure of **5** in Figure 4. The pyridine and diaryl protons in **4**, **5**, and **6** all relax at similar rates. However, the T_1 values for the isophthaloyl protons are significantly shorter in **5**, which indicates that these protons are close in space and relax each other. Because of the symmetry of this system, it is not possible to observe this relaxation directly through NOEs.

Molecular mechanics studies of the conformational preferences of the individual subunits provide a clue as to the origin of the difference between **2** and **5** (Fig. 5).[8] The 2,6-pyridyl derivative prefers conformation A which is stabilized by attractive electrostatic interactions between the amide protons and the pyridine nitrogen atom. In conformations B and C, there are unfavorable electrostatic interactions between the pyridine nitrogen and the carbonyl oxygen atoms. In contrast, the lowest energy arrangement for the isophthaloyl derivative is conformation B. These conformational preferences would lead to an open conformation for **2** and a folded conformation for **5** in agreement with the ^{1}H NMR data. Hamilton et al. have recently used a similar effect to control the conformation of 2,6-diacylaminopyridines.[9]

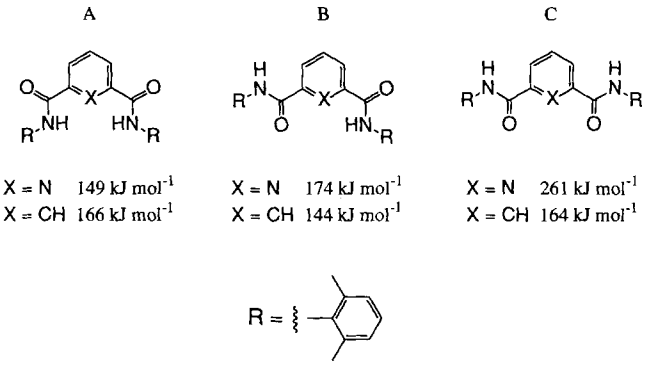

Fig. 5. Conformational preferences of the individual subunits of **2** and **5**. The energies were calculated with the CHARMm force field [8].

These conclusions were tested by subjecting **5** to a NOESY experiment. Figure 6 shows NOESY *f*2 traces through the signals due to the amide protons. NOEs observed in the isophthaloyl subunits are consistent with a type B conformation (Figs. 5 and 6b). In contrast, the signal due to the pyridyl amide protons did not give NOEs to any other aromatic protons which is consistent with a type A conformation (Figs. 5 and 6a).[10] These results provide further evidence for the folded structure of **5** in Figure 4.

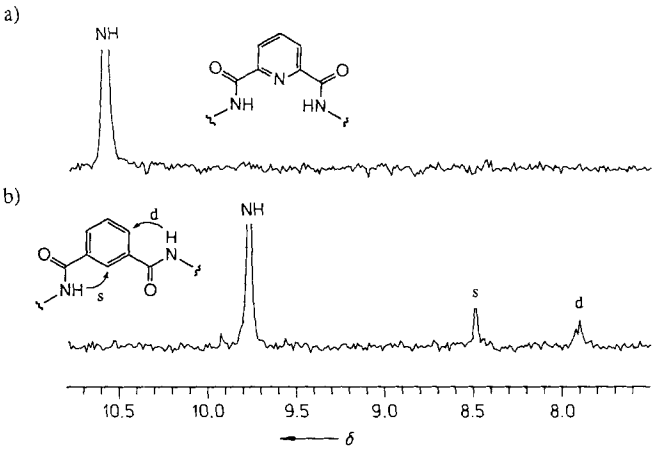

Fig. 6. *f*2 Traces from the 300 MHz NOESY spectrum of **5** in CD_2Cl_2. Interactions leading to NOEs are illustrated on the relevant structures. a) *f*2 Trace through the signal due to the pyridyl amide protons. b) *f*2 Trace through the signal due to the isophthaloyl amide protons.

If **5** does adopt the folded conformation, then it should have two cavities available for the complexation of *p*-benzoquinone. Addition of *p*-benzoquinone to a solution of **5** in $CDCl_3$ caused large changes in the chemical shifts of some of the signals in the ^{1}H NMR spectrum. An exact titration confirmed that **5** binds two molecules of benzoquinone. The

association constants were determined using nonlinear curve-fitting (Fig. 7, Table 1).[11] The titration data in Figure 7b demonstrates that the two binding events are not identical, and the association constants in Table 1 show that there is positive cooperativity in this system.[12] This is a weak allosteric effect and leads to an enhancement of the second association constant by a factor of 2.[12, 13] The benzoquinone signal experiences a large upfield shift on complexation indicating that benzoquinone is in a similar environment to that found in the complexes formed with **1** and **4**.[3]

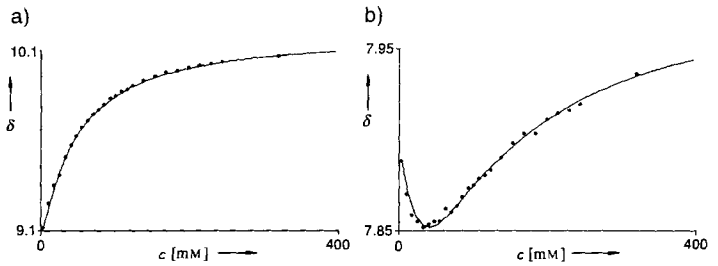

Fig. 7. Titration of *p*-benzoquinone with **5**. The lines were generated by computer-assisted curve-fitting; c = concentration of *p*-benzoquinone. a) Change in chemical shift of the signal due to the pyridyl amide protons. b) Change in chemical shift of the signal due to the isophthaloyl amide protons.

In contrast, addition of a large excess of quinone to a solution of **2** in $CDCl_3$ caused no change in the ^1H NMR spectrum. This confirms that **2** does indeed adopt an open conformation and so cannot complex quinone.

The titration curves in Figure 7 suggest a molecular basis for the observed cooperativity. As far as the pyridyl ends of the molecule are concerned, the first binding resembles the second, producing a simple saturation curve. These NMR signals experience a large downfield shift indicative of H-bond formation. However, the isophthaloyl signal shows quite different behavior. The binding of the first quinone causes an upfield shift of the signal due to the amide protons suggesting a decrease in the extent of H-bonding. The binding of the second quinone causes a large downfield shift indicating an increase in the extent of H-bonding.[14]

These results are consistent with the binding mechanism shown in Figure 8. Complexation of the first molecule of quinone causes a conformational change in **5** so that it can form four H-bonds with the quinone. The conformational change in one of the binding sites pulls the isophthaloyl groups apart and disrupts the intramolecular H-bond in the second binding site. Thus the second quinone molecule does not have to compete with a strong internal H-bond and is complexed more readily. The energy required to effect these conformational changes and break the intramolecular H-bonds would account for the lower association constants observed for **5** as compared with **1** and **4**.

Macrocycle **5** reproduces some of the essential features found in biological macromolecules: 1) The macrocycle folds into a well-defined three-dimensional structure as a result of noncovalent interactions. 2) This folding generates two cavities for complexing substrates. 3) Allosteric interactions make the second binding even more favorable than the first.

These results demonstrate that the conformational preferences of individual subunits can be used to control three-

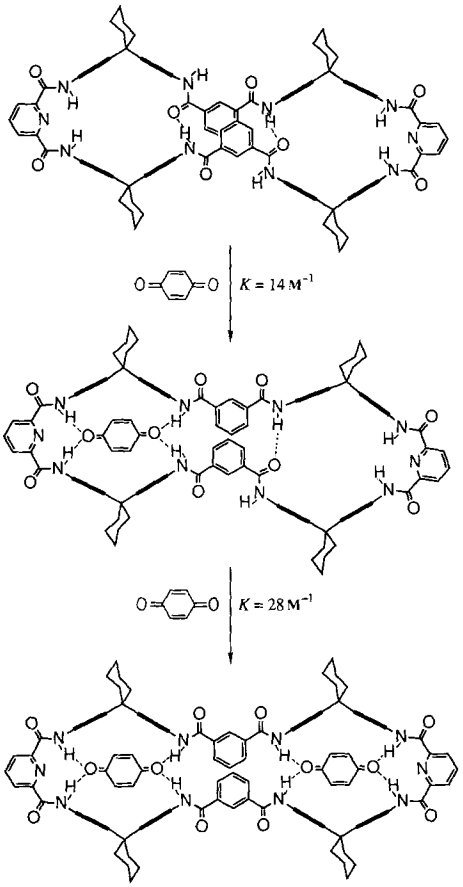

Fig. 8. Complexation of *p*-benzoquinone by **5**. The association constants are microscopic association constants. H-bonds are marked as dashed lines. The dotted line in the 1:1 complex represents a weak H-bond.

dimensional structure and folding in such systems. This should prove useful in the design of future receptors. In the system described here, two quinones are bound in close proximity in an arrangement which is very similar to that found in the quinone-binding domains of the photosynthetic reaction centers of purple bacteria.[1] Similar functional properties may result.

Received: December 27, 1991 [Z 5092 IE]
German version: *Angew. Chem.* **1992**, *104*, 779

CAS Registry numbers:
1 · benzoquinone (1:1), 135328-04-0; **2**, 141062-46-6; **4**, 141062-47-7; **4** · benzoquinone (1:1), 141087-97-0; **5**, 141062-48-8; **5** · benzoquinone (1:2), 141062-49-9; **5** · benzoquinone (1:1), 141062-50-2; **6**, 141062-51-3; isophthaloyl chloride, 99-63-8; diamine (Scheme 1), 22657-66-5; 2,6-pyridinedicarbonyl chloride, 3739-94-4.

[1] a) H. Michel, O. Epp, J. Deisenhofer, *EMBO J.* **1986**, *5*, 2445; b) J. P. Allen, G. Feher, T. O. Yeates, H. Komiya, D. C. Rees, *Proc. Natl. Acad. Sci. USA* **1988**, *85*, 8487.
[2] a) A. R. Crofts, C. A. Wraight, *Biochim. Biophys. Acta* **1983**, *726*, 149; b) J. Deisenhofer, H. Michel, *Angew. Chem.* **1989**, *101*, 872; *Angew. Chem. Int. Ed. Engl.* **1989**, *28*, 829; c) R. Huber, *ibid.* **1989**, *101*, 849 and **1989**, *28*, 848; d) G. Feher, J. P. Allen, M. Y. Okamura, D. C. Rees, *Nature* **1989**, *339*, 111.
[3] C. A. Hunter, *J. Chem. Soc. Chem. Commun.* **1991**, *749*.
[4] C. A. Hunter, *J. Am. Chem. Soc.*, in press.
[5] All new compounds gave satisfactory spectroscopic and FAB mass spectrometric data.
[6] A porphyrin-based quinone receptor has been reported; Y. Aoyama, M. Asakawa, Y. Matsui, H. Ogoshi, *J. Am. Chem. Soc.* **1991**, *113*, 6233.
[7] C. A. Hunter, J. K. M. Sanders, *J. Am. Chem. Soc.* **1990**, *112*, 5525.

[8] Energy minimizations were carried out with the CHARMm force field (B. R. Brooks, R. E. Bruccoleri, B. D. Olafson, D. J. States, S. Swaminathan, M. Karplus, *J. Comput. Chem.* **1983**, *4*, 187). Solvent was not included. In our hands, this force field failed to reproduce experimental observations for large supramolecular systems due to inadequacies in the treatment of intermolecular forces [4, 7]. However, for relatively small molecules such as those in Figure 5, the force field seems to give results which are reliable at least in a qualitative sense.

[9] S. J. Geib, S. C. Hirst, C. Vincent, A. D. Hamilton, *J. Chem. Soc. Chem. Commun.* **1991**, 1293.

[10] The pyridyl and isophthaloyl protons relax at different rates. The possibility that this effect causes the lack of cross-peaks to the pyridyl amide signal cannot be ruled out.

[11] H. L. Anderson, C. A. Hunter, M. N. Meah, J. K. M. Sanders, *J. Am. Chem. Soc.* **1990**, *112*, 5780.

[12] Because of the large number of variables which must be determined by computer-assisted curve-fitting for this system, the errors in the absolute values of the association constants are large (±50%). However, Hill plots (A. V. Hill, *J. Physiol. London* **1910**, *40*, IV) of the titration data gave slopes of 1.1 to 1.2 confirming that there is some positive cooperativity.

[13] For other examples of artifical allosteric systems see J. Rebek, Jr., T. Costello, J. Marshall, R. Wattley, R. C. Gadwood, K. Onan, *J. Am. Chem. Soc.* **1985**, *107*, 7481; P. D. Beer, *J. Chem. Soc. Chem. Commun.* **1988**, *52*; C. A. Hunter, P. Leighton, J. K. M. Sanders, *J. Chem. Soc. Perkin Trans. 1* **1989**, *547*; H.-J. Schneider, D. Ruf, *Angew. Chem.* **1990**, *102*, 1192; *Angew. Chem. Int. Ed. Engl.* **1990**, *29*, 1159; R. P. Sijbesma, R. J. M. Nolte, *J. Am. Chem. Soc.* **1991**, *113*, 6695.

[14] Changes in the geometry of the offset π-stacking interaction may also contribute to the change in the chemical shift of the signal due to the isophthaloyl amide protons.

3,4-Dihydroisocoumarins, a New Class of Ant Trail Pheromones**

By *Hans Jürgen Bestmann*, Friedrich Kern, Doris Schäfer,* and *Matthias Christian Witschel*

Trail pheromones are mainly used by ants for marking the trail between the feeding place and the nest. Until now they have been found mostly in the venom and Dufour glands of the animals, and have been identified as alcohols, aldehydes, esters, nitrogen heterocycles, and terpenoid compounds.[1] The most common ant genera in Germany are *Formica* and *Lasius*, which belong to the Formicinae subfamily (Hymenoptera, Formicidae). Their trail pheromones have hardly been studied at all up to now.[2, 3] They are, however, of general interest, since *Formica* species are important from an entomological viewpoint in many biotopes, and several species of *Lasius* constitute insect pests for humans.

In the species we have studied, unlike other subfamilies, the trail pheromone is found in the hindgut (rectal sac),[1] which has been analyzed by us for the first time. Since the biologically active substance is present only in picogram quantities, identification and structure elucidation were only possible by GC-MS analysis using a solid-phase sampler,[4] and by comparison of mass spectra and GC retention times with those of synthetic material. For the formicine ant, *Lasius niger*, the GC-MS data indicated the possible presence of a 3,4-dihydro-8-hydroxytrimethylisocoumarin with a methyl group in the 3-position of the lactone ring. Compounds **5**, **6**, and **7** were therefore synthesized. The preparation of the 3,4-dihydroisocoumarins proceeded according to Scheme 1, starting from the readily available, substituted 2-methoxybenzoic acids **1**.

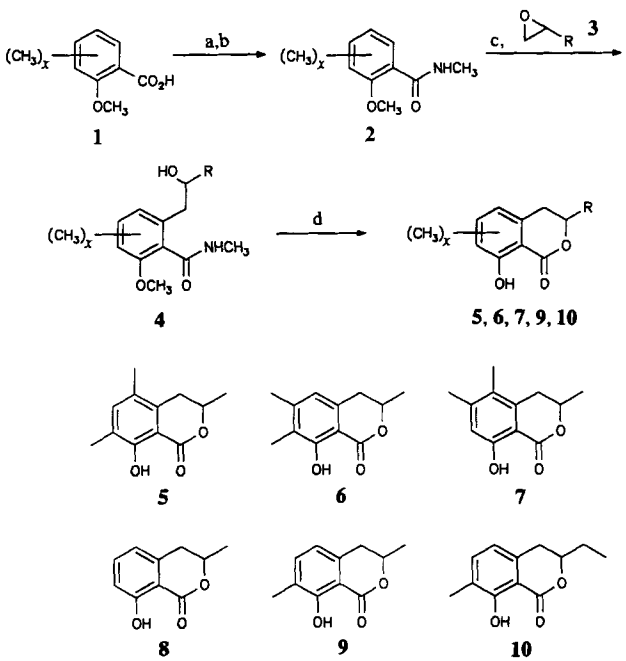

Scheme 1. a) $SOCl_2$; b) NH_2CH_3/H_2O, 0 °C; c) 2.4 equiv. *s*BuLi/TMEDA, THF, −78 °C, 4 h, then epoxide **3**/THF, −78 °C → room temperature, 12 h; d) 5 equiv. BBr_3/CH_2Cl_2, −78 °C → room temperature, 12 h, HCl workup, SiO_2 chromatography, Et_2O/PE (1/1).

These were converted into the N-methylamides **2**, which were then lithiated in the *ortho* position with *s*BuLi/*N*,*N*,*N*′,*N*′-tetramethylethylenediamine (TMEDA) at −78 °C.[5, 6] Reaction of the lithiation product with the corresponding epoxide **3** gave adduct **4**, and subsequent ether cleavage and lactonization with BBr_3[7] led, after column chromatography (SiO_2, Et_2O/petroleum ether (PE) = 1/9), to the 3,4-dihydroisocoumarins **5**, **6**, and **7** (purity by GC >98%) in 10–15% overall yield. When enantiomerically pure epoxides were used, the individual enantiomers could also be obtained, without racemization (*ee* > 95%).

A comparison of the mass spectra (Table 1) of **5**, **6**, and **7** showed characteristic differences caused by *ortho* effects[8] on the arene. The mass spectrum of synthetic **5** was identical with that of the natural product (IV in Fig. 1). In a biotest,[2] **5** triggered trail-following behavior at concentrations of

Table 1. Selected physical data for **5**–**7**, **9** and **10**.

(*R*)-**5**: $[\alpha]_D^{20}$ −104 (*c* = 1.35, $CHCl_3$); R_F = 0.50 (Et_2O/PE = 1/1); m.p. = 111–112 °C; IR (GC): $\tilde{\nu}$ [cm^{-1}] = 1701(C = O); ^{1}H NMR (400 MHz, $CDCl_3$, TMS): δ = 1.54 (d, 3H), 2.16 (s, 3H), 2.22 (s, 3H), 2.69 (dd, 1H), 2.91 (dd, 1H), 4.66 (m, 1H), 7.16 (s, 1H), 11.22 (s, 1H); MS (70 eV): *m*/*z* 206 (M^+, 100%), 188 (M^+-H_2O, 19), 177 (23), 173 (188−CH_3, 25), 162 (M^+-CH_3CHO, 20), 145 (14), 134 (14).

6: Oil, MS (70 eV): *m*/*z* 206 (100%), 188 (27), 177 (10), 173 (40), 162 (26), 145 (11), 134 (6).

7: Oil, MS (70 eV): *m*/*z* 206 (100%), 188 (17), 177 (13), 173 (1); 162 (17), 145 (4), 134 (18).

9: M.p. = 84–86 °C; MS (70 eV): *m*/*z* 192 (M^+, 100%), 174 (41), 163 (18), 159 (23), 148 (35).

10: Oil, MS (70 eV): *m*/*z* 206 (M^+, 100%), 188 (46), 173 (27), 159 (25), 149 (18), 148 (22).

[*] Prof. Dr. H. J. Bestmann, Dipl.-Biol. F. Kern, Dipl.-Chem. D. Schäfer, Dipl.-Chem. M. C. Witschel
Institut für Organische Chemie der Universität Erlangen-Nürnberg
Henkestrasse 42, D-W-8520 Erlangen (FRG)

[**] Pheromones, Part 86. This research was supported by the Deutsche Forschungsgemeinschaft and the Volkswagen Stiftung. We thank Prof. U. Maschwitz (Frankfurt) for the use of his ant colony and Prof. I. Hasenfuss (Erlangen) for the identification of the ant species. – Part 85: H. J. Bestmann, W. Caihong, C. Rehefeld, F. Kern, B. Leinemann, *Angew. Chem.* **1992**, *104*, 353–354; *Angew. Chem. Int. Ed. Engl.* **1992**, *31*, 330–331.

500 pg/trail. Biological selectivity tests were carried out with both enantiomers of **5**. When trails of the two enantiomers were offered to the ants, the animals always preferred the (*R*) enantiomer, and we therefore assign the (*R*) configuration to the natural product. We found additional isocoumarins in the rectal sacs of several *Formica* species. The monomethyl compound **8** (Mellein)[9] was identified from the red wood ant *Formica rufa*, and it led to trail-following behavior in the biotest.

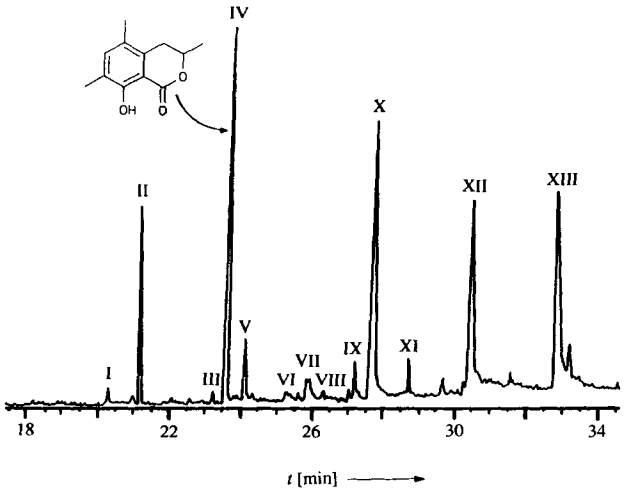

Fig. 1. Reconstructed total ion current chromatogram of forty rectal sacs of the formicine ant *L. niger*. GC-MS combination: Finnigan MAT 90 with Varian GC 3400, carrier gas He 1 mL min^{-1}, EI source 70 eV. Solid-phase sampler without splitting, fused silica capillary column (25m x 0.22mm) with SE-52 coating. Temperature program: 4 min 60 °C, 6 °C min^{-1} to 260 °C. I dodecanoic acid, II dodecyl acetate, III heptadecane, IV 3,4-dihydro-8-hydroxy-3,5,7-trimethylisocoumarin, V tetradecanoic acid, VI isopropyl tetradecanoate, VII octadecane, VIII hexadecanol, IX hexadecenoic acid, X hexadecanoic acid, XI isopropyl hexadecanoate, XII octadecenoic acid, XIII tricosane.

Mellein **8** and compound **5** were also found in *Formica fusca*. However, in this species, trail following could not be induced either by glandular extracts or by the synthetic compounds. In *Formica sanguinea* both the dimethyl derivative **9** and the 3-ethyl-7-methyldihydroisocoumarin occur. Here, too, neither these compounds nor the gland extracts stimulate specific behavior. The syntheses of **9** and **10** were carried out analogously to those of **5**, **6**, and **7**.

Electroantennograms (EAG) of ants have been reported in the literature only very rarely,[10, 11] and never in connection with and chemical–analytical studies. We have carried out electrophysiological tests on the species described, and have compared the results with those of the behavioral tests (Table 2).

All the isocoumarins found in the hindguts of the animals are active in the corresponding EAG, even those of *Formica fusca* and *Formica sanguinea*, for which the chemical signals alone did not induce trail-following behavior. The 8-hydroxydihydroisocoumarins found in various species are active interspecifically in the EAG, although the species-specific compounds have the highest biological activity. Dihydroisocoumarins from other species cannot, however, induce trail-following behavior in the biotest. In *Lasius niger* both (*R*)-**5** and (*S*)-**5** display electrophysiological activity, although the (*R*) enantiomer is the more active of the two, in accordance with the biotest.

Table 2. Components of hindguts of various Formicinae and their biological activity in the EAG and the trail-following test. (+ indicates biologically active, – biologically inactive).

Species	Biologically active components of the hindguts	EAG	Trail-following test
Lasius niger	3,4-Dihydro-8-hydroxy-3,5,7-trimethylisocoumarin(**5**)	+	+
Formica rufa	3,4-Dihydro-8-hydroxy-3-methylisocoumarin (Mellein, **8**)	+	+
Formica fusca	3,4-Dihydro-8-hydroxy-3,5,7-trimethylisocoumarin(**5**)	+	–
	3,4-Dihydro-8-hydroxy-3-methylisocoumarin (Mellein, **8**)	+	–
Formica sanguinea	3,4-Dihydro-8-hydroxy-3,7-dimethylisocoumarin (**9**)	+	–
	3,4-Dihydro-8-hydroxy-3-ethyl-7-methylisocoumarin(**10**)	+	–

The comparison between EAG responses and the behavioral test shows that at biologically relevant concentrations, the receptors located on the antennae are capable even of stereospecific differentiation. This stereospecificity in the primary process of signal uptake is augmented by the fact that in signal processing by the central nervous system, only the signal pattern (information) arising from the pheromone of the correct species will lead to a specific behavior pattern. We assume that the lack of behavioral response to the EAG-active compounds **9** and **10** in *Formica fusca* and *Formica sanguinea* is due to a requirement for additional behavioral rituals, or because chemical components from other glands are absent.

Received: January 15, 1992 [Z 5121 IE]
German version: *Angew. Chem.* **1992**, *104*, 757

CAS Registry numbers:
5, 141249-37-8; (*R*)-**5**, 141249-38-9; (*S*)-**5**, 141249-39-0; **6**, 141249-40-3; **7**, 141249-41-4; **8**, 480-33-1; **9**, 139958-92-2; **10**, 141249-42-5.

[1] B. Hölldobler, E. O. Wilson, *The Ants*, Springer, Berlin, **1990**, pp. 266–276.
[2] W. Hangartner, *Z. Vgl. Physiol.* **1967**, *57*, 103–136.
[3] S. Huwyler, K. Grob, M. Visconti, *J. Insect Physiol.* **1975**, *21*, 299–304.
[4] E. D. Morgan, L. J. Wadhams, *J. Chromatogr. Sci.* **1972**, *10*, 528–529.
[5] N. S. Narasimhan, B. H. Bhide, *Tetrahedron* **1971**, *27*, 6171–6176.
[6] E. J. Corey, J. Kang, *Tetrahedron Lett.* **1982**, *23*, 1647–1650.
[7] J. F. W. McOnie, M. L. Watts, D. E. West, *Tetrahedron* **1968**, *24*, 2289–2292.
[8] H. Schwarz, *Top. Curr. Chem.* **1978**, *73*, 231–265.
[9] We thank Prof. K. Mori (Univ. of Tokyo) for samples of Mellein.
[10] T. L. Payne, M. S. Blum, R. M. Duffield, *Ann. Entomol. Soc. Am.* **1975**, *68(2)*, 385–386.
[11] N. A. Andryszak, T. L. Payne, J. C. Dickens, J. C. Moser, R. W. Fischer, *J. Entomol. Sci.* **1990**, *25(4)*, 593–600.

Book Reviews are written by invitation from the editor. Suggestions for books to be reviewed and for book reviewers are welcome. Publishers should send brochures or (better) books to the following address: Redaktion Angewandte Chemie, Postfach 101161, W-6940 Weinheim, Federal Republic of Germany. The editor reserves the right of selecting which books will be reviewed. Uninvited books not chosen for review will not be returned.

Physical Chemistry from Ostwald to Pauling. The Making of a Science in America. By *J. W. Servos*. Princeton University Press, Princeton, NJ, 1990. XXIII, 402 pp. hardcover $ 49.95.—ISBN 0-691-08566-8

Physical chemistry is not a particularly easy subject to define. In fact, it is difficult to go beyond the obvious and rather vague assertion that physical chemistry is a discipline that is sandwiched somewhere between physics and chemistry. But where physics and chemistry end and physical chemistry takes over has never been adequately defined and probably never can be. In spite of this, however, it cannot be denied that this discipline is now firmly entrenched as a key part of chemistry, and that since the 1930s it has come to be regarded by most chemists as the foundation for all of chemistry. Physical chemistry provides the theoretical underpinning of chemistry; its laws characterize the behavior of a vast array of chemical systems. Its many striking successes have been reflected in the steady growth of the discipline since its initial coalescence in the 1880s. With hindsight, it can now be seen that the emergence of physical chemistry was inevitable. In 1786 the German philosopher Immanuel Kant had suggested that the amount of actual sience in any discipline could be represented by the amount of mathematics that it contained. Perhaps not surprisingly, he concluded that the chemistry of his day would not qualify as one of the natural sciences. We have come a long way since this remark was made. The ever increasing use of mathematics in chemistry over the last two centuries has resulted in chemistry as a whole—and physical chemistry in particular—becoming a highly mathematized discipline. One sign of the inexorable trend towards mathematization has been the establishment of journals devoted to ever more mathematically orientated chemistry. As examples, mention might be made of the *Zeitschrift für Physikalische Chemie* (1887), the *Journal of Physical Chemistry* (1896), the *Journal of Chemical Physics* (1933), *Theoretica Chimica Acta* (1962), and the *Journal of Mathematical Chemistry* (1987).

The book by John Servos traces the development of physical chemistry for the first fifty years of its existence as an organized and separate discipline, that is, it covers the period from the 1880s through to the mid 1930s. The author's prime focus is the emergence of the new discipline on the North American continent. The story of the transmission of physical chemistry from its European homeland to the New World is painstakingly chronicled. It is a story that is not without irony, for, as we all know, that transmission was so effective that ultimately the United States was to eclipse Europe in physical chemistry. The pivotal figure in the establishment of the discipline in America was the German founding father of physical chemistry, the genial and dynamic Wilhelm Ostwald, whose life and times are richly documented in this book. Over a period of some 17 years Ostwald hosted a total of 44 American students in his laboratories at the University of Leipzig. When these returned home they were in many instances to exert tremendous influence, for Ostwald's students included some of the most illustrious names in American chemistry, such as the bonding theorist Gilbert N. Lewis and the Nobel Prize winning experimentalist Theodore W. Richards. Most of them were to eventually occupy powerful positions at prestigious institutions such as Harvard and Yale Universities and the Massachusetts Institute of Technology (MIT).

From Chapter 3 onward the book examines some of the major consequences of the very rapid growth of physical chemistry in the New World during the early part of the twentieth century. As might be anticipated, not all was roses, and strains inherent in the fabric of the discipline began to reveal themselves, and in some cases opened up into yawning chasms. As the author aptly puts it, physical chemistry was beginning to resemble the Holy Roman Empire with its constellation of duchies and principalities that were no longer parts of a functional whole. One rancorous difference of philosophy occurred between the proponents of an ever greater mathematization of the subject and those who felt that mathematics was alien to chemistry. Two former Ostwald students typified the battlelines that were drawn. Arthur A. Noyes at MIT was an enthusiast for all things mathematical, and selected his co-workers on the basis of their grounding in mathematics and physics, whereas Wilder D. Bancroft at Cornell University had a distinct distaste for mathematics, and maintained that physics was no more than "chemistry pure and simple". In spite of such differences, however, both enjoyed successful careers in their respective ways. Noyes was responsible for the construction of the first American institution dedicated to physical chemistry at MIT, which was to become one of only two or three in the world that shaped the contours of the discipline in the early twentieth century. Bancroft was the founder and editor of the *Journal of Physical Chemistry*, became a leading supporter of, and wrote the first monograph on, the Phase Rule of J. Willard Gibbs, and was elected President of the American Chemical Society. Another of the results of the rapid evolution of the field was the marked trend towards fragmentation that became especially evident in research activities. Whereas the pioneers had been jacks of all trades, their successors became increasingly specialized, almost to the point where different sub-disciplines of physical chemistry came to be jealously guarded fiefdoms. The emergence of chemical physics in the late 1920s and early 1930s represented yet another parting of the ways, though in the event it proved to be less traumatic than it might have been. This was largely because the two major American protagonists, Robert S. Mulliken and Linus Pauling, were not given to adversarial tactics, preferring instead a more emollient approach that certainly helped to heal the rift that had arisen between physicists and physical chemists. Their great merit was to present chemical bonding theory in a manner that was both readily understandable to chemists and consistent with quantum mechanics. In performing this signal service to all chemists they accomplished one of the truly great feats of twentieth century chemistry.

All of the above history, and much more, is explored in meticulous detail in this book, In fact, the author presents us with such a mine of information that one is tempted to dip into it time and again. It is not surprising that it took the author some ten years to compile all this material. The book is very well written and the author is to be congratulated on a job well done. I predict that this work will become a classic of its kind, and will remain an important source of reference on the early development of physical chemistry for many years to come. If I have any criticism of this book, it would concern the organization of the abundant material it contains. At times I found it difficult to locate specific facts and information on the lives of the physical chemists it covers. Their lives and their various contributions to physical chemistry tend to be discussed in several different chapters. I would have preferred each of the major figures such as Gilbert N. Lewis and Linus Pauling to have been treated in easy-to-find chapters. However, I would not wish to harp on this minor criticism, for the book as a whole more than compensates us for the time spent reading it. I recommend that this work be read by all who wish to learn something of the origins of physical chemistry in the New World.

Dennis H. Rouvray
Department of Chemistry
University of Georgia
Athens, Georgia (USA)

Chaotic Evolution and Strange Attractors. By *D. Ruelle*. Cambridge University Press, Cambridge (UK), 1989. VIII, 96 pp., paperback £ 8.95.—ISBN 0-521-36830-8.

The author of this little book is an internationally recognized expert in the theory of complex dynamic systems, especially of turbulence phenomena. In it he summarizes a series of lectures that he delivered in 1987 at the Accademia dei Lincei in Rome. The book is divided into two parts. The first describes the phenomenon of turbulence and discusses some of its characteristics, taking low-dimensional chaotic attractors as an example. Here the author is on familiar ground. Deterministic chaos—a class of irregular states of complex dynamic systems that are extremely sensitive to changes in the initial conditions—has become such a popular area of study during the last five years that every scientist has at least heard of it. The author deals in depth with the fundamental question of how it is possible to conclude, from an irregular time-series of recorded data, that the phenomenon being observed is the result of a chaotic attractor and not of accidental fluctuations. He also introduces the concept of fractal dimensions, which is essential for an understanding of chaotic dynamics.

The second part of the book is concerned with deterministic chaos as viewed from the standpoint of the ergodic theory. Here the author moves to the frontier of present knowledge, as this is one of his specialist topics of research. This inevitably involves a detailed discussion of measurement theory, the mathematical basis of which is far from simple. In developing a description of chaotic dynamics the characteristic exponents are of fundamental importance, and these are directly related to the dimensionality and entropy of the attractors. In the final section the author deals with another topic that is currently much discussed in specialist circles, the phenomenon of "resonances" in dynamic systems, which are caused by singularities in the complex representation of the frequency spectrum. They are directly related to the relaxation behavior of the system as a function of time. As the author himself rightly points out in summarizing his conclusions, the relationship between theory and the treatment of experimental data is covered too briefly in this review. Moreover, this is a field of research that has undergone great developments in the last decade. Still, what more can one expect from a little book of only about a hundred pages?

In it the author gives a very concise and well written summary of the present state of knowledge on the theory of deterministic chaos. It can be recommended to all scientists with an appropriate background and the necessary mathematical knowledge. However, it is not an introduction to this field. Chemists and physicists without previous knowledge who wish to learn about complex dynamic systems should read other texts. There is no lack of suitable introductions to the subject.

Peter Schuster
Institut für Theoretische Chemie
der Universität Wien (Austria)

The Chemical Synthesis of Peptides. (International Series of Monographs on Chemistry, Vol. 23.) By *J. Jones*. Oxford Science Publications, Clarendon Press, Oxford, 1991. IX, 228 pp., hardcover £ 35.00.—ISBN 0-19-855643-8

The author of this book has estimated that about 5000 people are now engaged in peptide research. The growing importance of peptide chemistry is further underlined by the fact that the number of publications each year in this field has now increased to well over a thousand, and the upward trend is continuing. Starting from the fundamental studies of the structure and synthesis of peptides by the German Nobel prizewinner Emil Fischer, scientific activity in the area of peptide synthesis spans nearly a century. Important milestones in this development include the first laboratory synthesis of a peptide hormone by Vincent du Vigneaud in 1953 (see pp. 115–119 of this book), and ten years later Bruce Merrifield's experimental realization of the ingenious idea of carrying out a peptide synthesis on a polymeric support (pp. 132–156). Many different types of apparatus for synthesizing peptides are now commercially available, and their operation is almost fully automated. This situation, and the more recent application of the DNA recombination technique to peptide synthesis, often convey to outsiders the impression that the problem of synthesizing peptides is completely solved and now belongs to the category of routine methods. That this is a serious misconception is convincingly argued by the author of this book.

The nine-page general introduction explains clearly why synthetic peptides are needed, how structure-activity studies are used to develop peptides for medical purposes, and the advantages of developing peptide chemistry in conjunction with the DNA recombination technique. Furthermore, it should be noted that of the 59 peptide pharmaceutical agents listed in the "red book" in 1990, 29 are produced by chemosynthesis and only nine by modern genetic engineering methods.

The first part of the book deals with the basic principles and the chemistry of peptide synthesis, and the newcomer will undoubtedly regard this as the most important part; it is pleasing that the mechanistic aspects are adequately covered here. In a skillful didactic presentation of material that is expertly chosen from the large fund of information on synthetic methods, the reader is equipped with the essential basic knowledge. The chapter on "Residue-specific Considerations" not only deals with side-chain protection in trifunctional amino acids, but also gives valuable advice on appro-

priate tactics for syntheses using particular building units, and includes a page and a half on the use of enzymes in peptide synthesis.

In the second and third parts the author discusses examples which illustrate the considerable difficulties involved in the strategy of peptide synthesis, and which show that a single generally applicable method does not exist. All the known variants have their advantages and disadvantages, and in the end the success or failure of a synthesis is determined by experience and skill. While not disputing the fact that the Merrifield method has made a very important contribution to progress in the field of peptides and proteins, the author emphatically warns the reader against having too high expectations of this strategy. This is illustrated by a quotation from the sales literature for a commercial synthesizer: "You don't have to be an expert to synthesize a peptide... Simply enter your sequence, ...push 'Start Synthesis', and walk away."

To summarize, the book offers a critical and up-to-date account of the chemical principles of peptide synthesis, and by limiting the subject matter it has been kept very compact. Inevitably a few topics are omitted; for example, the discussion of the Leuchs anhydrides contains no reference to so-called UNCAs. The bibliographies given at the end of each chapter and section are expertly selected, and Appendix B gives a useful further list of references. In Appendix A the many abbreviations are clearly explained. The subject index appears to contain an adequate selection of keywords, but, as in nearly all books, it does not exploit the full potential.

The book is a valuable aid for the newcomer to chemical methods of peptide synthesis, although by its nature it requires the reader to have a basic knowledge of organic chemistry. Its main attraction is that practically every chapter is packed with a wealth of useful detail, a fact that even the specialist will only come to appreciate after studying it closely.

Hans-Dieter Jakubke
Fachbereich Biowissenschaften
der Universität Leipzig (FRG)

Microscale Techniques for the Organic Laboratory. By *D. W. Mayo, R. M. Pike, S. S. Butcher* and *P. K. Trumper*. Wiley, Chichester, 1991. XVIII, 285 pp., paperback £ 19.20.—ISBN 0-471-62192-7

A significant difficulty that arises in the training of chemistry students is making the transition from techniques suitable for working with relatively large quantities of substances, as already learned, to those needed for carrying out reactions with semi-micro and micro quantities. The failures that so often result would be less serious if, during their basic or advanced practical work, students could learn the rules for working successfully with small quantities of substances. This is the problem that the authors have addressed in the book reviewed here. Under the motto "smaller is better", they have based their discussion on experience gained during a program that has run for about ten years in their own teaching departments. The term "microscale" here refers to quantities in the millimole range, i.e., up to about 200 mg. Practice in using such small amounts of substances has other advantages as well as teaching students to work with special care: it reduces the cost of chemicals, and leads to increased safety, improved air quality in the laboratory, and (of ever growing importance) a reduction in waste disposal problems.

The book is divided into seven chapters. Following a short general introduction and some comments about safety in the laboratory, the authors introduce the apparatus needed for microscale reactions and the basic working techniques. Next comes a short chapter on methods for determining physical properties. An appropriate amount of space is then devoted to methods for isolating and purifying organic compounds, which often determine the difference between success and failure when working with small quantities; all the most important techniques are covered (extraction, distillation, crystallization, and the various forms of chromatography—thin layer, column, gas, and HPLC). The last two chapters deal with the techniques and theoretical background needed for spectroscopic characterization of the compounds that have (hopefully) been isolated by the foregoing methods. Of these two, the chapter on IR spectroscopy is very thorough and detailed, whereas the treatment of NMR spectroscopy is rather cursory. This traditional preference for IR spectroscopy in teaching students does not really imply that IR spectra contain more information for the identification of organic compounds (the authors' remarks on this point are surely not meant to be taken too seriously); it is based rather on the fact that an IR spectrum can be recorded quickly and cheaply, and the student can easily learn the technique.

The main strength of this book lies in the many useful ideas and tips that are included, providing information that is essential for working with microscale quantities. One is reminded here that chemistry is not only a science, but also a craft (and sometimes an art). Thus the book contains much advice that is relatively simple, but not immediately obvious to the student: for example, on how to transfer a small quantity of a substance from one vessel to another. It also describes forms of apparatus that are impressive and of interest for use in the research laboratory, such as a rotating band distillation column, driven by a magnetic stirrer, for separating liquids on the milliliter scale (also used as a cover illustration for the book). The presentation aspects of the book are also pleasing; it is practically free of printing errors and factual inaccuracies, the numerous figures are all of good quality, and the price is not too high. It can therefore be recommended without hesitation as a basis for student practical classes, and will also provide research chemists with many useful ideas.

Norbert Krause
Institut für Organische Chemie
der Technischen Hochschule Darmstadt (FRG)

Houben-Weyl. Methoden der Organischen Chemie. Band E19c: Carbokationen, Carbokation-Radikale. Series Editors: *K. H. Büchel, J. Falbe, H. Hagemann, M. Hanack, D. Klamann, R. Kreher, H. Kropf, M. Regitz* and *E. Schaumann*. Volume Editor: *M. Hanack*. Thieme, Stuttgart, 1990. XVII, 550 pp., hardcover DM 720.00.—ISBN 3-13-219804-8

As the third of the volumes on reactive intermediates in the Houben-Weyl series, that on carbocations and carbocation radicals has now appeared. Following the volume by P. Vogel that was published in 1985, and several review articles covering the field in varying degrees of detail, it was now appropriate to collect together the latest knowledge in a single volume. The introduction (Lenoir, Siehl; 73 pp.) starts with a short historical outline, then describes the preparation of cations in the gas phase and in solution. All the commonly used, and also the more rarely used, methods are described and explained, supported by literature references. Several diagrams showing apparatus for generating cations are in-

cluded, so that the non-specialist too is given some insight into the complexities of this field. Methods for detecting and studying cations are described, devoting special attention and an appropriately large amount of space to NMR spectroscopy, which is the most important method. It is pleasing to find that, as a general principle, efforts have been made to link the experimental data to quantum mechanical calculations (IGLO or geometric optimization methods). In this connection, however, it is regrettable that the theoretical methods have not been given a separate chapter. Also, experience has shown that ab-initio calculations offer an extremely useful and precise tool for determining the structures of carbocations. Apart from this, the introductory chapter is very appropriate as a readily understandable overview for the beginner, as well as giving the specialist a survey of the latest research position.

The main part of the volume covers all the theoretically conceivable forms of carbocations. After dealing with carbocations that are only of theoretical interest, the discussion moves on to the carbocation radicals that are important in preparative electrochemistry. In the chapter on preparative methods for these (Subramanian; 20 pp.), detailed laboratory recipes for syntheses under electrolytic conditions are given, supplemented by extensive tables. 1-Alkenyl cations are treated in great detail (Hanack, Subramanian; 154 pp.); the authors are the leading workers in this area. The next chapter (Lenoir, Siehl; 157 pp.) deals with classical cations having coordination number 3, including alkyl-, cycloalkyl- and heteroatom-substituted cations, as well as aromatic, homoaromatic and special types of destabilized cations; here again there is an emphasis on the preparative aspects. The authors have collected together a remarkable number of reactions that proceed via carbocations as intermediates, in a presentation that includes numerous tables and selected examples of synthetic methods.

Next there is a short chapter (Siehl, Lenoir; 28 pp.) on hypercoordinated non-classical cations. The authors have been remarkably successful in showing the relationship to synthetic chemistry, despite the fact that these species are usually only mentioned in passing as "exotic molecules". The last two chapters are concerned with di- and polycations (Siehl, Lenoir; 14 pp.) and with carbocations in organometallic compounds (Lenoir, Siehl; 3 pp.).

The general subject index is very scanty (5 pp.), making it difficult to search for particular compounds and methods. Moreover, the system used in the formula index is unnecessarily complicated, causing problems when one is searching for compounds. An alphabetical arrangement or a listing according to increasing number of carbon atoms would have made things much easier. Many of the cations have come to be generally known by trivial names; such an excellent book as this should, in my opinion, have been provided with a comprehensive keyword index.

In conclusion I might mention a few unsightly errors. The Coates cation appears in two figures (one below the other) with the different systematic names "Pentacyclo-[4.3.0.$0^{2,9}$.$0^{3,5}$.$0^{4,8}$]non-9-yl-Kation" and "Pentacyclo-[3.3.1.$0^{2,4}$.$0^{3,7}$.$0^{6,8}$]non-9-yl-Kation". This appears not to be an accidental error, since it is stated that the Coates cation is formally a polycyclic derivative of the bicyclo[2.2.1]hept-2-en-7-yl cation. Unfortunately the representations of the trishomoaromatic cations are all incorrect at the critical positions. The equations for the reactions leading to the formation of the bishomoaromatic 7-norbornenyl and 7-norbornadienyl cations are also incorrect. The "λ" nomenclature caused me a certain amount of difficulty when I came across it for the first time, and was unable to find the explanation even after a lengthy search. Also it takes a little time to get used to the names 1-methylethyl cation (instead of 2-propyl cation) and 1-methylpropyl cation (instead of 2-butyl cation). The convention of showing the cationic center in bold type is a useful aid to understanding, but has not been applied consistently. Instead of the adjective "quantenmechanisch" it would be more correct to write "quantenchemisch", since even ab-initio calculations rely on assumptions and approximations, and therefore fall short of exact quantum mechanics. The individual chapters are divided up in a way that is very confusing. It would have been desirable to keep to a uniform system, and to severely limit the number of different levels of sub-headings. The figures are up to the usual high standard found in Houben-Weyl. In a volume containing over 3000 structural formulas, one can excuse the few isolated errors—the vast majority of the formulas are correct. By bringing together a great wealth of data and presenting the information in a clearly understandable form, the authors have succeeded in producing a comprehensive work of reference that will be a valuable aid to everyone concerned with carbocations. Furthermore, the superb compilation of carbocation reactions will be of great value to the synthetic chemist. The inclusion of the rather theoretically and mechanistically orientated topic of carbocations within the Houben-Weyl series, which is usually associated mainly with preparative organic chemistry, has proved highly successful.

Peter Buzek, Paul von Ragué Schleyer
Institut für Organische Chemie
der Universität Erlangen-Nürnberg (FRG)

Chirality – From Weak Bosons to the α-Helix. Edited by *R. Janoschek*. Springer, Berlin, 1991. XI, 246 pp., hardcover DM 168.00.—ISBN 3-540-33920-4

It is hard to think of a property more fundamental, more ubiquitous, more fascinating than the one that gives rise to the distinction between an object and its mirror image. That property is handedness, or chirality, and it arises whenever an object is not invariant under improper rotation. Such an object must then necessarily exist in two, and only two, isometric but nonsuperposable forms, one "right-handed" and the other "left-handed". Chirality, in its many and varied manifestations, permeates all branches of the natural sciences and of the arts. The present volume is a collection of articles designed to provide an interdisciplinary overview of a small part of this vast subject. Considering the range of subject material covered, the authors have succeeded remarkably well in meeting their objective, that of writing "for anybody with a sound scientific education", and "not [just] for specialists in their respective fields of research".

The discovery, in 1956, that parity is not conserved for the weak interactions governing β-decay has led to our present-day understanding that matter is inherently chiral at the most fundamental level. In the introductory chapter of this collection, Latal describes the nature of elementary particles, develops the Dirac equation and the theoretical basis for the idea that particles and antiparticles possess opposite helicities (as in left-handed electrons and neutrinos, and right-handed positrons and antineutrinos), and shows how the unified theory of electromagnetic and weak forces (involving weak neutral bosons) leads to the prediction of parity-violating effects in atoms. Thus, all atoms are in principle optically active, although the effect is tiny and has so far been observed only in heavy atoms (e.g., Pb, Bi). Translated from the

atomic to the molecular level, the parity-violating weak neutral current perturbation lifts the degeneracy of space-inverted enantiomers. The energy difference is only approximately 10^{-17} kJ mol^{-1}, and corresponds to an excess of just *one* molecule of D- or L-alanine in a racemic mixture of 10^{17} alanine molecules in thermodynamic equilibrium at terrestial temperatures. Ab initio calculations indicate that the predominant isomer has the L configuration. Janoschek argues that this minuscule bias, appropriately amplified, is responsible for the fact that all metabolically functional biopolymers are monochiral, both at the monomer level (L-α-amino acids, D-sugars) and in the helical polymer conformations (right-handed polypeptide α-helix, B-DNA), i.e., that the monochirality of the molecules of life has its origins in the systematic chiral bias of the elementary particles. Various amplification mechanisms are described in support of this thesis. However, the reader is cautioned that "any hypothesis on long term processes such as homochirality evolution will most probably remain experimentally unproven for ever."!

After a brief discussion of Kauzmann's "principle of pairwise interactions", Derflinger gets to the heart of his subject: a vigorous critique of the theory of chirality functions developed by Ruch and Schönhofer that focuses on the concept of "qualitative completeness". He thus revives a controversy that had erupted briefly in the pages of *Theoretica Chimica Acta* in 1978. Because only one side of the story is told in this chapter, the reader needs to be made aware of two rebuttals, neither of them cited here, by Ruch (*Theor. Chim. Acta* **1978**, *49*, 107) and by Mead (*Theor. Chim. Acta* **1980**, *54*, 165). The discussion of two other controversial concepts, "qualitative supercompleteness" and "hyperchirality", is equally partisan in tone. The chapter concludes with a description of a method for enumerating enantiomeric pairs.

Snatzke reports on various methods that are employed to specify the sense of helicity in molecules, points out ambiguities (a short path of a three-dimensional curve can be approximated by either a right- or a left-handed helix), and discusses rules designed to correlate the absolute structures (configurations) of chiral chromophores with the signs of appropriately chosen circular dichroism bands. Surprisingly, there is no reference to the excellent review on helical molecules in organic chemistry by Meurer and Vögtle (*Fortschr. Chem. Forsch.* **1985**, *127*, 1). The theme of absolute configuration is also featured in a chapter by Kratky, in which anomalous dispersion of X-rays is described as the method, pioneered by Bijvoet, used to determine the sense of chirality of molecules in crystals with respect to a macroscopic (absolute) reference frame.

The need for enantiomeric purity is particularly acute in pharmacology and medicinal chemistry. This explains why four of the ten essays in this collection are devoted to strategies for the production of enantiomerically enriched (and, in the limit, enantiopure) compounds. Faber and Griengl describe the use of enzymes as efficient, cheap, and highly enantioselective biocatalysts in the preparation of optically active alcohols, amines, and acids (e.g., enzymatically catalyzed asymmetric reductions of ketones and hydrolyses of *meso* diesters). Winterfeldt distinguishes, and illustrates with examples, three general methods for achieving enantiomeric purity: by resolution of racemates, by reactions whose educts are enantiopure natural products, and by enantioselective reactions or asymmetric syntheses. Brunner discusses the use of chiral transition metal complexes as catalysts in asymmetric syntheses (e.g., hydrogenation of olefins with Rh complexes of Diop). Strategies for the separation of enantiomers by liquid column chromatography are the subject of a chapter by Lindner. The nature of chiral recognition between the mobile and stationary phases determines resolution efficiency; column packings are classified, and compared, according to type: derivatives of biopolymers (e.g., microcrystalline triacetylcellulose), chiral synthetic polymers (e.g., Okamoto's helical poly(trityl methacrylate)), and chiral monomers (e.g., cyclodextrin derivatives).

Although it would be asking too much to expect complete coverage of all aspects of this subject, given its enormous scope, it was nevertheless disappointing to find no mention of topological chirality (the chirality of trefoil knots, catenanes composed of orientated rings, Möbius ladders, and so forth) in synthetic and naturally occuring molecules. I was not able to make much sense of the essay by S. Hoffmann, which I found to be intellectually impenetrable. Most texts of this nature are plagued by errors, and the present volume is no exception (e.g., on p. 171 the "symmetry elements" of ethylene are given as "3σ, $3C_{2v}$ and i"). Despite such shortcomings, however, this volume deserves to be read by anyone interested in this important topic.

Kurt Mislow
Department of Chemistry
Princeton University, Princeton NJ (USA)

Wood and Cellulosic Chemistry. Edited by *D. N. S. Hon* and *N. Shiraishi*. Marcel Dekker, New York, 1991. VIII, 1020 pp., hardcover $ 234.00.—ISBN 0-8247-8304-03

Wood is one of the most important renewable raw materials and energy media. The growth of wood in forests makes a significant contribution to reducing the amount of carbon dioxide in the atmosphere. The carbon dioxide produced from fossil and living carbon sources by burning and respiration can, over long periods, be transformed back into organic compounds. For this reason alone, it is clear that wood chemistry and the use of wood as a chemical raw material is currently of great importance.

Research in wood chemistry now involves many different fields of science, and the published results are often widely scattered; surveys that aim to bring together this knowledge in an ordered way are therefore very useful. The book reviewed here is largely successful in achieving that objective.

The authors, 18 Japanese and four American scientists, are all recognized experts in their fields. The book is divided into three main sections, containing 21 chapters altogether. Part 1, "Structure and Chemistry", starts from the structure and mode of formation (lignification) of the woody tissue of the cell wall in plants, and goes on to describe in turn the chemical properties of each of the wood constituents that are bound together in the natural polymer structure—cellulose, hemicellulose, lignin, and substances present in the wood. Separate chapters are devoted to the chemistry of the bark, and to the chemical characterization of wood and its constituents. This part could have been even further improved by devoting a separate chapter to the biochemistry of wood formation.

In Part 2, "Degradation", some of the chapters deal with topics that have not previously been treated in monograph form, such as coloration and discoloration, and the photochemistry of wood. The degradation of wood by chemical, microbiological, enzymic, and pyrolytic mechanisms is described in a detailed and highly informative way. However, it is disappointing that this part does not also deal with the gasification and liquefaction of wood.

Part 3, "Modification and Utilization", discusses the chemical basis for modifying the properties of wood and cellulose so as to broaden their areas of use, both as constructional materials and as chemical raw materials. The main areas considered are the chemical modification of wood and cellulose, the plastification of wood, wood-polymer composites, and adhesives for wood. There is also a chapter (unfortunately rather too brief) on the use of wood and cellulose as sources of chemicals and energy.

Considered as a whole, the work offers a very good, up-to-date, and in some parts detailed survey of the specialized subject of wood and cellulose chemistry. The large number of authors has resulted in some unavoidable overlapping. A particularly useful feature is the large number of literature references given at the end of each chapter; there is, however, a very marked preponderance of Japanese publications. The book can be recommended for everyone in research and teaching who seeks an up-to-date account of the present state of knowledge regarding the chemistry of renewable raw materials, natural polymers, wood, and cellulose.

Otto Wienhaus
Institut für Pflanzenchemie und Holzchemie
der Technischen Universität Dresden
Abteilung Forstwirtschaft, Tharandt (FRG)

Vitamin C: Its Chemistry and Biochemistry. By *M. B. Davies, J. Austin,* and *D. A. Partridge.* Royal Society of Chemistry, Cambridge, 1991. 154 pp., paperback £ 13.50. ISBN 0-85186-333-7

An up-to-date and compact treatise on various aspects of ascorbic acid, this important vitamin, is most welcome, particularly in view of the discrepancy between the biological importance and the limited amount of sound knowledge available, and because of widespread interest on the part of the general public and in the marketplace. The back cover announces this book as just that: the "first" to provide an in-depth, interdisciplinary study of this essential and fascinating compound.

Well, the reader gets only some of this: there is a nice and coherent presentation of the history of scurvy and of the discovery of vitamin C, with due emphasis on Szent-György and on Haworth, with related stories providing good reading (Chapters 2 and 3). Chapter 4 describes the synthesis and manufacture, which, with a yearly output of more than 40000 tonnes, is certainly of quantitative interest. In this chapter one already begins to wonder about the overall scheme of the book, since at the end there is a lengthy section on further chemical reactions that ascorbate can enter into, but without offering a clue as to why this would be of interest.

Chapter 5 is on the biochemistry, and the bottom line is that many actions are being discussed here and there, but there is still much confusion. This is well illustrated by the detailed description of some metabolic pathways, such as the mitochondrial respiratory chain, in lengthy sequences of reactions but only few, if any, clear statements of how ascorbate is chemically involved. AFR, presumably an abbreviation for the ascorbate free radical, is included but not really explained. The few words about the interactions between tocopherol and ascorbate do not reflect current knowledge in this area. Similar comments apply to Chapter 6, on medical aspects: while generally satisfactory, the presentation sometimes doesn't quite make it to the point; I had trouble, for example, trying to understand the passage on page 99 on "vegetarians being in rude health, ascorbutically speaking"(?). The author of this part of the book may not have been from the medical profession, judging from the way some diseases were described. Chapter 7, on inorganic and analytical aspects, was more within the field of expertise, but here the inclusion of four pages on vitamin B_{12} in atomic detail left the reader perplexed, because the connection to the topic, namely vitamin C, was not made clear.

In summary, the book of about 150 pages is attractive initially, but, as even the authors say, the field is still mysterious in several ways. The bibliography could have included some of the more recent literature, e.g. the book for the layman by Linus Pauling ("How to Live Longer and Feel Better"), and the "Handbook of Vitamins" by Machlin. Also, one might disagree that the latest conference of the New York Academy of Sciences on Vitamin C was a "Third World Conference".

Helmut Sies
Institut für Physiologische Chemie
der Universität Düsseldorf (FRG)

Ion Exchangers. Edited by *K. Dorfner.* de Gruyter, Berlin, 1991. XXXI, 1495 pp., hardcover DM 680.00.—ISBN 3-11-010341-9

A whole generation of chemists received their first initiation into the subject of ion exchangers from Dorfner's slim volume entitled "Ionenaustauscher". A much weightier book, "Ion Exchangers", has now appeared. In this a team of authors under Dorfner's guidance has covered all the most important aspects of ion exchangers in a single volume of about 1500 pages.

An introduction to the basic principles of ion exchange is followed by several contributions dealing comprehensively with the synthesis of ion exchangers. Here it is pleasing to note that due importance has been given to synthetic organic ion exchange resins, the most commercially important group of materials. All the important areas of industrial application are competently described by experts; these range from conventional water treatment processes to the applications of ion exchangers and polymeric adsorbers in biotechnology. The contribution by Sherrington on the influence of the structure of the polymer on the reactivities of the functional groups is especially worth reading, despite being relegated to an inconspicuous position in the last part of the book. Also there is a short but highly informative section which surveys the literature on ion exchangers in general, and describes the use of computer-based information retrieval methods. All the contributions include many references to original papers. There is an appendix containing an index of commercially available ion exchangers, and the book is completed by a useful subject index.

Published work up to the mid-eighties is covered in considerable detail, but later results have only rarely been included. The editor has been remarkably successful in avoiding overlapping of subject matter; where this has been allowed to occur, it makes it much easier to read a particular article without needing to know the contents of the previous one. There is a certain amount of inconsistency in the nomenclature and units, but it could not have been avoided, and this reviewer did not find it troublesome. The print is clear and legible, and the tables, formulas, figures, and flow diagrams are mainly clear and informative.

However, the frequent careless errors are a nuisance, of which the following are two examples. In the tables on pages 96 and 1297, which are largely identical in content, we

find on the one hand $-N_3^+R$ and Ba^+, and on the other hand $-NH^2$ and $-SO_3^+$. In the lower equation on page 1008 none of the three structural formulas is shown correctly. One could go on at some length listing the mistakes, and unfortunately they often distract the reader's attention from the discussion. A second edition of the book would benefit greatly from more attention being given to such details.

Who ought to buy this book? The high price will certainly deter individuals from buying it privately. However, the new "Dorfner" should be available in all libraries where there is a need for an expert overview of the many different aspects of ion exchangers.

Werner Strüver
Bayer AG
Leverkusen (FRG)

The Kaiser's Chemists. Science and Modernization in Imperial Germany. By *J. A. Johnson*. University of North Carolina Press, Chapel Hill (USA), 1990. X, 279 pp., hardcover $ 39.95.—ISBN 0-8078-1902-6

Under the attractive title "The Kaiser's Chemists", J. A. Johnson here presents a study in scientific history, with particular emphasis on the difficult period of evolution in the politics and organization of science that led up to the founding of the three Kaiser-Wilhelm Institutes (for chemistry, for physical chemistry and electrochemistry, both at Berlin-Dahlem, and for coal research at Mülheim). Based on very thorough studies of original source material, the author provides detailed insights into the events before and during the formation and building of these institutes for basic chemical research, and into the relevant social history. The outstanding role of Emil Fischer comes repeatedly to the fore. The triumvirate of Emil Fischer, Wilhelm Ostwald, and Walter Nernst initiated the first moves towards setting up an imperial institute for chemistry, in analogy to the institute for physics and technology, but this objective then changed due to the influences of many different social forces and needs, with the result that the three institutes named above were already set up even before World War I. Leading German chemists in universities, technical colleges, and the chemical industry were concerned that the dominant world position of German chemistry, both in research and in industry, should be maintained and reinforced by setting up new institutes of this kind. The most important aim was to push forward developments in analytical, inorganic and physical chemistry, and in biochemistry. As neither the Prussian state nor the Reich were prepared to bear much of the cost that would be incurred in setting up these institutes, it was necessary to find sponsors with the required capital resources from within the economy. How the proponents went about this task, the many different interests that were brought together from different sides to support these projects, the role played by the Prusso-German bureaucracy and by Kaiser Wilhelm II through the "Kaiser-Wilhelm-Gesellschaft zur Förderung der Wissenschaften"—all this is described in detail, put into context, and carefully analyzed by Johnson. The institutional innovation process in German science is considered within the context of the "conservative modernization" that was taking place at that time, with the aim of increasing the might of the Kaiser's Germany. With the start of the First World War, chemical research and technology became closely bound up with military interests. This cooperation focussed on the objectives of developing raw materials resources, and producing substitute materials and chemicals for use in war (Fritz Haber). Chemists in universities, technical colleges, the Kaiser-Wilhelm Institutes, and the chemical industry contributed much to prolonging the war that could not be won. In an epilogue the author traces the subsequent fate of some of these chemists in the post-war period. The balance-sheet is dreadful: Emil Fischer's suicide in 1919; Fritz Haber and Richard Willstätter went into exile in 1934 and 1939 respectively; Walther Nernst retired from scientific work in 1933 as a protest against Nazism. The tragedies of German history in the first half of this century are reflected in the personal stories of many of these chemists.

In summary, there is no doubt that in this book the American science historian Johnson has made a valuable and profound contribution to understanding the history of German science in the first two decades of this century.

Alfred Neubauer
Berlin (FRG)

Biocoordination Chemistry: Coordination Equilibria in Biologically Active Systems. (Inorganic Chemistry Series; Series Editor: J. Burgess). Edited by *K. Burger*. Ellis Horwood, Chichester, 1990. ix, 349 pp., hardcover $ 90.00.—ISBN 0-13-179912-6.

This multiauthored text deals with the coordination chemistry of kinetically labile complexes of biological interest, amino acids, peptides, carbohydrates, nucleic acid bases, nucleosides, and nucleoside monophosphates. Such molecules are potential ligands, and a knowledge of their interactions with metal ions is crucial to studies of the role of metal ions and metal complexes in biology.

The first chapter (Noszal) deals with the acid-base properties of bioligands and, in conjunction with Burger's introduction, provides a good general background to the topic. The broad area of complexes of amino acids is discussed by Kiss in an admirable manner, and the chapter will be very useful to anyone wishing to learn about the solution chemistry of complexes of these ligands. Metal complexes of peptides and their derivatives are covered by Sovago in a good discussion of the field.

The chapter on thermodynamic and kinetic aspects of metalloenzymes and metalloproteins (Hirose and Kidani) deals with carbonic anhydrase, carboxypeptidase, Cu–Zn-superoxide dismutase, human transferrin, and ovatransferrin. This chapter seems a little out of place in this volume but provides interesting reading.

It is pleasant to see a chapter on metal complexes of carbohydrates (Burger and Nagy). This has been a somewhat neglected area, and a comprehensive review of carbohydrate complexes has not previously been available, although various aspects of the topic have been covered. Sawyer's 1964 review (*Chem. Rev., 64*, 633) lists 140 references, and the present discussion covers the literature to 1990. The article should help to stimulate further interest in the area.

The final chapter (Lonnberg) deals with proton and metal ion interactions with nucleic acid bases, nucleosides and nucleoside monophosphates. Owing to the vital role of nucleic acids in molecular biology this has become one of the most extensively studied areas of bioinorganic chemistry. For someone seeking an introduction to the area this chapter will be very useful.

The book is well produced with clear diagrams and tables. The literature citations are somewhat eccentric, and I see no very clear reason for the adoption of, for example, "70 Cl", standing for Clelland's publication in 1970. The book sum-

marizes in one volume much of the current literature on the solution chemistry of bioligands with metal ions, which is normally only available in multivolume works such as Sigel's "Metal Ions in Biological Systems" or in the primary literature. It will be a useful reference text for all those having interests in the chemistry of metal complexes in solution. Those seeking structural and spectroscopic data will have to look elsewhere.

Robert W. Hay
Chemistry Department
University of St. Andrews (UK)

Photochromism. Molecules and Systems. (Series: Studies in Organic Chemistry, Vol. 40.) Edited by *H. Dürr* and *H. Bouas-Laurent*. Elsevier, Amsterdam, 1990. XXII, 1068 pp., hardcover HFl 580.00.—ISBN 0-444-87432-1

This book is a collection of review articles by various authors on different aspects of photochromism. It should therefore be regarded less as a textbook than as a general overview, with the emphasis on recent developments in photochromism. It is intended mainly for the specialist, but is also suitable for those coming to this field for the first time.

The monograph begins with a general introduction by H. Dürr, after which comes a survey by G. Gauglitz of the physics and chemistry of photochromic systems. These two articles form important introductions for the non-specialist who wishes to learn about the area, and also for advanced students with an interest in the subject. For the latter, the "Glossary of Terms" at the end of the book will further contribute to a better understanding, and it should also help to bring some standardization of the terminology used in photochemistry. These introductions are followed by the core part of the book, consisting of chapters dealing with photochromic effects resulting from different types of reactions, such as *E–Z* isomerizations of double bonds, electrocyclic reactions, cycloadditions, tautomerism, and photodissociation processes. Next come chapters on photochromism in biological systems, on medium effects, on the use of silver salts in phototropic glasses, and on applications of photochromism. These chapters, which are the work of a large numer of expert authors, include competent treatments of all the most important aspects of photochromism, especially recent developments.

The monograph is very comprehensive and packed with information, consisting of 1068 closely printed pages. One can expect it to remain the standard work on photochromism for some time to come, and it is also a veritable mine of information for chemists, physical chemists, and physicists. However, it can be criticized on a few points. The subject index is very sparse, which is regrettable, as it means that specific information can only be extracted with difficulty. Also, in the bibliographies included with each chapter it would have been desirable, when citing papers in journals that are not readily accessible, to list not only the original reference but also the *Chemical Abstracts* entry. Nevertheless, this attempt at a review of the literature on photochromism can be described as very successful on the whole, and everyone working in the area of photochemistry should have the book close at hand.

Heinz Langhals
Institut für Organische Chemie
der Universität München (FRG)

Registered names, trademarks, etc. used in this journal, even when not marked as such, are not to be considered unprotected by law.

© VCH Verlagsgesellschaft mbH, D-W-6940 Weinheim, 1992. – Printed in the Federal Republic of Germany by Konrad Triltsch Druck- und Verlagsanstalt Würzburg.

All rights reserved (including those of translation into foreign languages). No part of this issue may be reproduced in any form — by photoprint, microfilm, or any other means — nor transmitted or translated into a machine language without written permission from the publishers. Only single copies of contributions, or parts thereof, may be made for personal use. This journal was carefully produced in all its parts. Nevertheless, authors, editors, and publisher do not warrant the information contained therein to be free of errors. Readers are advised to keep in mind that statements, data, illustrations, procedural details, or other items may inadvertently be inaccurate.

Valid for users in the USA: The appearance of the code at the bottom of the first page of an article (serial) indicates the copyright owner's consent that copies of the article may be made for personal or internal use, or for the personal or internal use of specific clients. This consent is given on the condition, however, that the copier pay stated per-copy fee through the Copyright Clearance Center, Inc. (CCC), for copying beyond that permitted by Sections 107 or 108 of the U.S. Copyright Law. This consent does not extend to other kinds of copying, such as copying, for general distribution, for advertising or promotional purposes, for creating new collective works, or for resale. For copying from back volumes of this journal see 'Permissions to Photo-Copy: Publisher's Fee List' of the CCC.

Editorial office: Postfach 10 11 61, D-W-6490 Weinheim, Federal Republic of Germany, Telephone (06201) 60 23 15, Telex 465 516 vchwh d, Telefax (06201) 602 328, E-Mail Z16@DHDURZ2 *in* Earn Bitnet.

Editor: *Peter Gölitz*

Associate editors: *R. H. Schmidt-Radde, K. J. Schneider, A. Stimson.* **Editorial assistant:** *E. Schweikart*

Publishers: VCH Verlagsgesellschaft mbH. (Managing Directors: *Hans Dirk Köhler, Dr. Karlheinz Köpfer*), Pappelallee 3, W-6940 Weinheim, Federal Republic of Germany.

Advertising office (Advertising Manager: *R. J. Roth*): Postfach 10 11 61, D-W-6940 Weinheim, Federal Republic of Germany, Telephone (0 62 01) 60 61 36, Telex 467 155, Telefax (0 62 01) 606 156.

ANGEWANDTE CHEMIE
International Edition in English
Volume 31 · Number 7
July 1992
Pages 805–930

Nuclear Magnetic Resonance Fourier Transform Spectroscopy (Nobel Lecture)**

By Richard R. Ernst*

Introduction

The world of the nuclear spins is a true paradise for theoretical and experimental physicists. It supplies, for example, most simple test systems for demonstrating the basic concepts of quantum mechanics and quantum statistics, and numerous textbook-like examples have emerged. On the other hand, the ease in handling nuclear spin systems predestines them for the testing of novel experimental concepts. Indeed, the universal procedures of coherent spectroscopy have been developed predominantly within nuclear magnetic resonance (NMR) and have found widespread application in a variety of other fields.

Several key experiments of magnetic resonance have already been honored by Nobel prizes in physics, starting with the famous molecular-beam experiments by Isidor I. Rabi[1–3] acknowledged in 1944, followed by the classical NMR experiments by Edward M. Purcell[4] and Felix Bloch,[5, 6] honored with the 1952 prize, and the optical detection schemes by Alfred Kastler,[7] leading to a prize in 1966. Some further Nobel prize winners in Physics have been associated in various ways with magnetic resonance: John H. Van Vleck developed the theory of dia- and paramagnetism and introduced the moment method into NMR; Nicolaas Bloembergen had a major impact on early relaxation theory and measurements; Karl Alex Müller contributed significantly to electron paramagnetic resonance; Norman F. Ramsey is responsible for the basic theory of chemical shifts and J couplings; and Hans G. Dehmelt developed pure nuclear quadrupole resonance.

But not only for physicists is nuclear magnetic resonance of great fascination. More and more chemists, biologists, and medical doctors discover NMR spectroscopy, not so much for its conceptual beauty but for its extraordinary usefulness. In this context, a great number of magnetic resonance tools have been invented to enhance the power of NMR in view of a variety of applications.[8–15] This Nobel lecture provides a glimpse behind the scenes in an NMR toolmaker's workshop.

Nuclear spin systems possess unique properties that predestine them for studies of molecules:

1) The atomic nuclei serving as sensors are extremely well localized, with a diameter of a few femtometers, and can report on local affairs in their immediate vicinity. It is thus possible to explore molecules and matter in great detail.

2) The interaction energy of the sensors with the environment is extremely small, less than 0.2 J mol^{-1}, corresponding to the thermal energy at 30 mK. The monitoring of molecular properties is thus virtually perturbation-free. Nevertheless, the interaction is highly sensitive to the local environment.

3) Information on the structure of molecules can be obtained from nuclear pair interactions: Magnetic dipole–dipole interactions provide distance information, while scalar J couplings allow one to determine dihedral angles.

At first glance, it may be astonishing that it is possible to accurately determine internuclear distances by radio frequencies with wavelengths $\lambda \approx 1$ m, since this seemingly violates the quantum mechanical uncertainty relation, $\sigma_q \cdot \sigma_p \geq \hbar/2$, with the linear momentum $p = 2\pi\hbar/\lambda$, as it applies to scattering experiments or to a microscope. It is important that in magnetic resonance the geometric

[*] Prof. Dr. R. R. Ernst
Laboratorium für Physikalische Chemie der Eidgenössischen Technischen Hochschule
ETH-Zentrum, CH-8092 Zurich (Switzerland)

[**] Copyright © The Nobel Foundation 1992. – We thank the Nobel Foundation, Stockholm, for permission to print this lecture.

information is encoded in the spin Hamiltonian, $\mathscr{H} = \mathscr{H}(q_1, \ldots, q_k)$, where q_k is the nuclear coordinates. An accurate structure determination, therefore, boils down to an accurate energy measurement that can be made as precise as desired, provided that the observation time t is extended according to $\sigma_E \cdot t \geq \hbar/2$. An upper limit of t is in practice given by the finite lifetime of the energy eigenstates due to relaxation processes. Thus, the accuracy of NMR measurements is not restricted by the wavelength but rather by lifetimes limited by relaxation processes.

The information content of a nuclear spin Hamiltonian and the associated relaxation superoperator of a large molecule, for example a protein, is immense: It is possible to determine the frequencies of the chemical shifts of hundreds of spins in a molecule to an accuracy of 16–18 bits. Internuclear distances for thousands of proton pairs can be measured to about 0.1 Å. Several hundred dihedral angles in a molecule can be determined with an uncertainty of less than 10°.

The weakness of the nuclear spin interactions, so far described as an advantage, leads on the other hand to severe problems in detection. Large numbers of spins are required to discriminate the weak signals from noise. Under optimum conditions with modern high-field NMR spectrometers, 10^{14}–10^{15} spins of one kind are needed to detect a signal within a measurement time of one hour. The low signal-to-noise ratio is the most limiting handicap of NMR. Any increase by technical means would significantly extend the possible range of NMR applications.

This clearly defines the two goals that had to be achieved during the past three decades to promote NMR as a practical tool for molecular structure determination: 1) Optimization of the signal-to-noise ratio; 2) Development of procedures to cope with the enormous amount of inherent information on the molecule under investigation.

One-Dimensional Fourier Transform Spectroscopy

A major improvement in the signal-to-noise ratio of NMR spectra was achieved in 1964 by the conception of Fourier transform (FT) spectroscopy. The basic principle—parallel data acquisition, leading to the multiplex advantage—was applied already by Michelson in 1891 in optical spectroscopy[16] and explicitly formulated by Fellgett in 1951.[17] However, the approach used in optics, spatial interferometry, is unsuited for NMR spectroscopy, since an interferometer with the necessary resolution would require a pathlength of at least 3×10^8 m.

Weston A. Anderson at Varian Associates in Palo Alto was experimenting in the early sixties with a mechanical multiple-frequency generator, the "wheel of fortune", which was conceived to simultaneously excite the spin system with N frequencies, in order to shorten the performance time of an experiment by a factor N, by recording the response of N spectral elements in parallel.[18] It was soon recognized that more elegant solutions were needed for commercial success.

Numerous possibilities are conceivable for the generation of a broad-band frequency source that allows the simultaneous irradiation of all of the spins of a spin system. We mention four schemes: 1) Radio-frequency pulse excitation, 2) stochastic random noise excitation, 3) rapid scan excitation, 4) excitation by a computer-synthesized multiple-frequency waveform. For each method, a different type of data processing is required to derive the desired NMR spectrum.

The application of radio-frequency (rf) pulse excitation was suggested by Weston A. Anderson to the author for a detailed experimental study in 1964.[19–21] The experiment is outlined in Figure 1. To the sample that is polarized in a static magnetic field along the z-axis, an rf pulse is applied

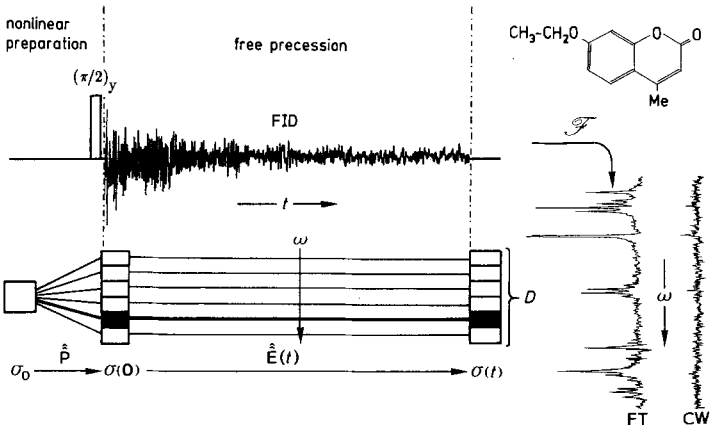

Fig. 1. Schematic representation of pulse FT spectroscopy illustrated by the 60 MHz ^{1}H NMR spectrum of 7-ethoxy-4-methylcoumarin[22]. An initial $(\pi/2)_y$ rf pulse, represented by the rotation superoperator $\hat{\hat{P}}$, excites the transverse magnetization $\sigma(0)$ from the equilibrium state σ_0. Free precession of all coherences in parallel under the evolution superoperator $\hat{\hat{E}}(t)$ leads to the final state $\sigma(t)$. Detection with the detection operator D produces the FID shown (sum of 500 scans) which, after Fourier transformation $\mathscr{F}$ provides the spectrum FT. For comparison, a continuous-wave (CW) spectrum is shown which was also recorded in 500 s under identical conditions.

Richard R. Ernst, born in 1933 in Winterthur, Switzerland, studied chemistry from 1952 to 1956 at the Eidgenössische Technische Hochschule in Zurich (ETH-Z). He worked on his Ph.D. from 1957 to 1962 in the field of NMR spectroscopy under the direction of Professors Hans Primas and Hans H. Günthard. In 1963 he went to Varian in Palo Alto. Five years later he returned to the ETH-Z as Privatdozent for physical chemistry. He became assistant professor in 1970, associate professor in 1972, and full professor in 1976. His many honors include the Gold Medal of the Society of Magnetic Resonance in Medicine (1983), the Ampère Prize (1990), the Wolf Prize for Chemistry (Jerusalem, 1991) and the 1991 Nobel Prize in Chemistry. He is a member of numerous scientific societies and on the editorial boards of many journals. His area of research is the development and application of NMR and ESR spectroscopic methods.

along the y-axis that rotates the magnetization vectors $\boldsymbol{M}_k$ of all spins I_k by $\pi/2$ into an orientation perpendicular to the static field. In the arrow notation[23] with the acting operator, here a $(\pi/2)_y$ rotation, on the top of the arrow this is expressed by Equation (1). The subsequent free induction

$$M_{kz} \xrightarrow{(\pi/2)_y} M_{kx} \tag{1}$$

decay (FID) consists of the superposition of all eigenmodes of the system. The operator D of an observable is used to detect the signal that is Fourier-transformed to separate the different spectral contributions. Figure 1 shows an early example of FT NMR spectroscopy on the sample 7-ethoxy-4-methylcoumarin for which 500 FIDs were coadded and Fourier-transformed to produce the FT spectrum shown.[22] A continuous wave (cw) spectrum obtained by the slow passage through the frequency range was recorded in the same total time of 500 s and is also shown in Figure 1 for comparison of the signal-to-noise ratios.

To please the more mathematically inclined reader, the experiment can also be expressed by the evolution of the density operator $\boldsymbol{\sigma}(t)$ under the preparation superoperator $\hat{\hat{P}} = \exp\{-i\hat{\hat{F}}_y\pi/2\}$ and the evolution superoperator $\hat{\hat{E}}(t) = \exp\{-i\hat{\hat{\mathscr{H}}}t - \hat{\hat{\Gamma}}t\}$. The superoperator $\hat{\hat{F}}_y$ is defined by $\hat{\hat{F}}_y\, A = [F_y, A]$ with $F_y = \sum_k I_{ky}$ where I_{ky} is a component angular momentum operator of spin k. $\hat{\hat{\mathscr{H}}}$ is the Hamiltonian commutator superoperator, $\hat{\hat{\mathscr{H}}}A = [\mathscr{H}, A]$ and $\hat{\hat{\Gamma}}$ is the relaxation superoperator. The expectation value $\langle \boldsymbol{D} \rangle(t)$ of the observable operator D is then given by Equation (2), where $\boldsymbol{\sigma}_0$ represents the density operator of the spin system in thermal equilibrium.

$$\langle \boldsymbol{D} \rangle(t) = \mathrm{Tr}\{\boldsymbol{D}\hat{\hat{E}}(t)\,\hat{\hat{P}}\boldsymbol{\sigma}_0\} \tag{2}$$

The reduction in performance time for *one* spectrum is determined by the number of spectral elements N, that is, the number of significant points in the spectrum, roughly given by $N = F/\Delta f$, where F is the total width of the frequency range and Δf a typical linewidth of a signal. A corresponding increase in the signal-to-noise ratio of $\sqrt{N}$ per unit time can be obtained by coadding an appropriate number of FID signals originating from a repeated pulse experiment. The gain in signal-to-noise can be appreciated from Figure 1.

It has been known for a long time that the frequency response function (spectrum) of a linear system is the Fourier transform of the impulse response (FID). This was already implicitly evident in the work of Jean Baptiste Joseph Fourier who in 1822 investigated the heat conduction in solid bodies.[24] In 1957 Lowe and Norberg proved this relation to hold also for spin systems despite their strongly nonlinear response characteristics.[25]

Stochastic testing of unknown systems by white random noise was proposed in the forties by Norbert Wiener.[26] One could say that the color of the output noise carries the spectral information on the investigated system. The first applications of random noise excitation in NMR spectroscopy were proposed independently by Russel H. Varian[27] and by Hans Primas[28, 29] for broad-band excitation and broad-band decoupling, respectively. The first successful experiments using random noise irradiation led to heteronuclear "noise decoupling",[30, 31] a method that proved to be essential for the practical success of ^{13}C NMR spectroscopy in chemical applications.

In 1970, Reinhold Kaiser[32] and the author[33] independently demonstrated stochastic resonance as a means to improve the signal-to-noise ratio of NMR experiments by broad-band irradiation. Here, the computed cross-correlation function (3) of the input noise $n_i(t)$ and the output noise

$$c_1(\tau) = \overline{n_o(t)\, n_i(t-\tau)} \tag{3}$$

$n_o(t)$ is equivalent to the FID of pulse FT spectroscopy. This is illustrated in Figure 2 for fluorine resonance of 2,4-difluorotoluene. A binary pseudo-random sequence with a

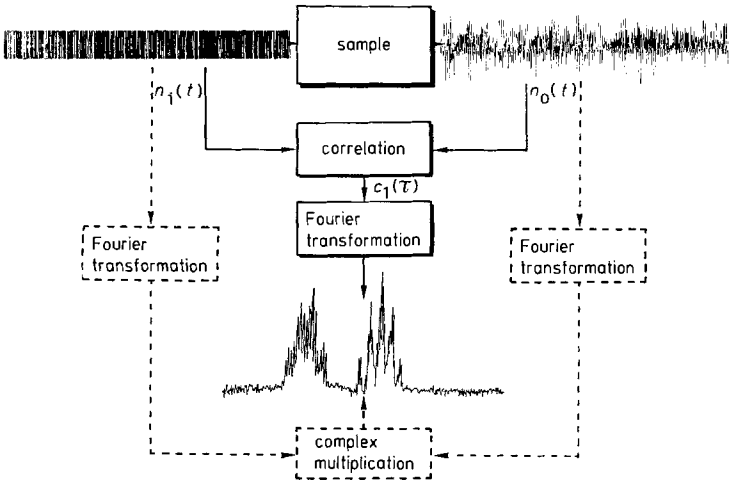

Fig. 2. Schematic representation of stochastic resonance illustrated by the 56.4 MHz ^{19}F NMR spectrum of 2,4-difluorotoluene [33]. Excitation with a binary pseudo-random sequence $n_i(t)$ 1023 points in length generates the response $n_o(t)$. Cross-correlation of the two signals produces $c_1(\tau)$ which, after Fourier transformation, delivers the spectrum shown. In an alternative procedure, which has actually been used in this case, the individual Fourier transforms of $n_i(t)$ and $n_o(t)$ are computed, and the complex conjugate $\mathscr{F}\{n_i(t)\}^*$ is multiplied by $\mathscr{F}\{n_o(t)\}$ to obtain the same spectrum.

maximal white spectrum is used for excitation. Its advantages are the predictable spectral properties and the constant rf power. The low peak-power puts less stringent requirements on the electronic equipment. Disadvantages arise from the simultaneous irradiation and detection which can lead to line-broadening effects absent in pulse FT spectroscopy in which perturbation and detection are separated in time. A further disadvantage, when real random noise is used, is the probabilistic nature of the response which requires extensive averaging to obtain a stable mean value. Higher order correlation functions, such as (4) allow also the

$$c_3(\tau_1,\tau_2,\tau_3) = \overline{n_o(t)\, n_i\,(t-\tau_1)\, n_i\,(t-\tau_2)\, n_i\,(t-\tau_3)} \tag{4}$$

characterization of nonlinear transfer properties of the investigated system.[26] This has been exploited extensively by Blümich and Ziessow for NMR measurements.[34, 35]

A third approach, rapid scan spectroscopy, initially proposed by Dadok and Sprecher,[36] achieves a virtually simul-

taneous excitation of all spins by a rapid sweep through the frequency range.[37, 38] The resulting spectrum is strongly distorted, but can be corrected mathematically because of the deterministic nature of the distortions. Correction amounts to convolution with the signal of a single spin measured under identical conditions or simulated on a computer. An example is given in Figure 3. It is interesting to note how similar a rapid scan spectrum is to an FID except for the successively increasing oscillation frequency.

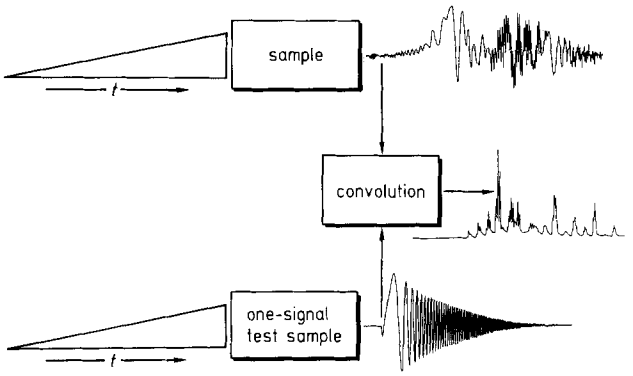

Fig. 3. Schematic representation of rapid scan spectroscopy. The highly distorted sample spectrum obtained by a rapid sweep of the frequency during the time t can be corrected by convolution with the equally sweep-distorted spectrum of a one-signal test sample.

Finally, it is possible by computer synthesis to compute an excitation function with a virtually arbitrary excitation profile. This was originally utilized for decoupling purposes by Tomlinson and Hill,[39] but is also the basis for composite pulse excitation schemes that have proved to be very powerful.[40, 41]

Among the broad-band excitation techniques, pulse excitation is the only one that allows for a rigorous analytical treatment irrespective of the complexity of the spin system. It does not lead to any method-inflicted line broadening as in stochastic resonance nor to correction-resistant signal distortions as in rapid scan spectroscopy of coupled spin systems.[38] Pulse FT spectroscopy is conceptually and experimentally simple, and last but not least, it can easily be expanded and adapted to virtually all conceivable experimental situations. Measurements of relaxation times, for example, require jut a modified relaxation-sensitive preparation sequence, such as a $\pi-\pi/2$ pulse pair of T_1 measurements[42] and a $\pi/2-\pi$ pulse pair for T_2 measurements.[43] Also the extension to the investigation of chemical exchange using the saturation-transfer experiment of Forsén and Hoffman[44] is easily possible.

It should be mentioned at this point that pulse NMR experiments were suggested already by Felix Bloch in 1946 in his famous paper,[6] and the first time-domain magnetic resonance experiments were performed in 1949 by H. C. Torrey[45] and, in particular, by Erwin L. Hahn,[46-48] who may be regarded as the true father of pulse spectroscopy. He invented the spin-echo experiment[46] and devised extremely important and conceptually beautiful solid-state experiments.[49, 50]

Pulse FT spectroscopy has not only revolutioned high-resolution liquid-state NMR spectroscopy, but it has unified NMR methodology across all fields, from solid-state resonance, through measurements of relaxation times, to high-resolution NMR, with numerous spillovers also into other fields such as ion cyclotron resonance,[51] microwave spectroscopy,[52] and electron paramagnetic resonance.[53] It also provided the germ for the development of multidimensional NMR spectroscopy.

Two-Dimensional Fourier Transform Spectroscopy

As long as purely spectroscopic measurements are made for the determination of the eigenfrequencies or normal modes of a system, one-dimensional (1D) spectroscopy is fully adequate. In NMR spectroscopy, this applies to the measurement of the chemical shifts that characterize the local chemical environment of the different nuclei. However, no information can be obtained in this manner on the spatial relationships between the observed nuclei.

There are two important pair interactions in nuclear spin systems, the scalar through-bond electron-mediated spin-spin interaction (J coupling) and the through-space magnetic dipole–dipole interaction (Fig. 4). The J coupling is described by the scalar term $\mathcal{H}_{kl} = 2\pi J_{kl} \boldsymbol{I}_k \boldsymbol{I}_l$ in the spin Hamiltonian. It is responsible for the multiplet splittings in high-resolution spectra of liquids. Under suitable conditions, it can lead to an oscillatory transfer of spin order between the two spins $\boldsymbol{I}_k$ and $\boldsymbol{I}_l$. The magnetic dipole–dipole interaction D_{mn}, on the other hand, is represented by a traceless tensor of second rank. Its average in isotropic solution is zero, and it can lead to signal splitting only in anisotropic media. However, its time modulation causes relaxation processes also in isotropic solution that are responsible for a multiexponential recovery of the spins to thermal equilibrium after a perturba-

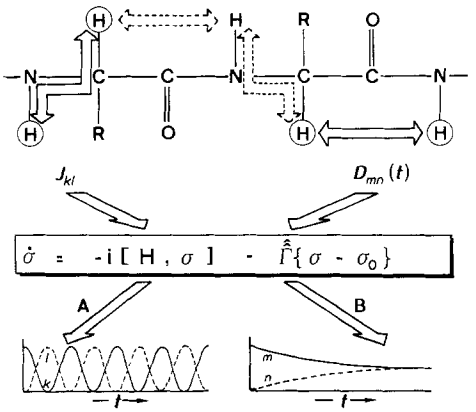

Fig. 4. The two pair-interactions relevant in NMR spectroscopy. The through-bond scalar J_{kl} coupling contributes to the Hamiltonian and leads to a coherent transfer (A) of spin order between spins I_k and I_l. The time-modulated through-space dipole–dipole interaction $D_{mn}(t)$ causes multiexponential cross relaxation (B) between spins I_m and I_n. The two interactions allow a sequential assignment of the resonances of neighboring spins in the peptide fragment shown and the determination of structure parameters. The three-bond J coupling is a measure for the dihedral angle about the central bond, the dipole–dipole interaction for internuclear distances.

tion. Knowledge of these interactions allows one to deduce geometric relations in the molecule in solution[54, 55] and arrangements of atoms in solids. In the optimum case, a complete three-dimensional structure of a molecule can be deduced.[56]

Although these interactions affect 1D spectra, special techniques are needed for their measurement. In the approximation of a linear response, it is impossible by first principles to distinguish two independent signals from a doublet caused by a spin–spin interaction. Experiments to explore the nonlinear response properties of nuclear spin systems have been known since the fifties. In saturation studies with strong rf fields several spins belonging to the same coupled spin system are excited simultaneously yielding multiple-quantum transitions that contain connectivity information.[57] Particularly fruitful were double- and triple-resonance experiments in which two or three rf fields are applied simultaneously, resulting in decoupling and spin-tickling effects.[58–60]

The early multiple-resonance experiments have in the meantime been replaced by multidimensional experiments. Pair interactions among spins are most conveniently represented in terms of a correlation diagram as shown in Figure 5. This suggests the recording of a "two-dimensional spectrum" that establishes such a correlation map of the corresponding spectral features. The most straightforward approach may be a systematic double-resonance experiment whose result can be respresented as an amplitude $S(\omega_1,\omega_2)$ which depends on the frequencies ω_1 and ω_2 of the two applied rf fields.[8, 58]

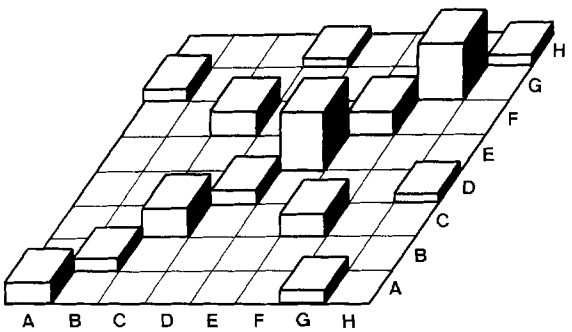

Fig. 5. Schematic correlation diagram for the representation of pair interactions of nuclear spins.

A new approach to measuring two-dimensional (2D) spectra was proposed by Jean Jeener in 1971.[61] He suggested a 2D FT experiment consisting of two $\pi/2$ pulses with a variable time t_1 between the pulses and the time variable t_2 measuring the time elapsed after the second pulse as shown in Figure 6; this is an expansion of the principles illustrated in Figure 1 (see also fig. 10a). Measuring the response $s(t_1,t_2)$ of the two-pulse sequence which is Fourier-transformed with respect to both time variables produces a two-dimensional spectrum $S(\omega_1, \omega_2)$ of the desired form.[62, 63]

This two-pulse experiment by Jean Jeener is the progenitor of a whole class of 2D experiments[8, 63] which can also easily be expanded to multidimensional spectroscopy. Each 2D experiment, as shown in Figures 6 and 7, starts with a preparation pulse sequence $\hat{\hat{P}}$, which excites coherences, that is, coherent superpositions represented by the density operator $\sigma(0)$, that are allowed to precess for an evolution time t_1 under the evolution superoperator $\hat{\hat{E}}(t_1)$. During this period, the coherences are frequency-labeled, so to speak. The subsequent mixing sequence $\hat{\hat{R}}$ performs a controlled transfer of coherence to different nuclear spin transitions that evolve during the detection period as a function of t_2 under the evolution superoperator $\hat{\hat{E}}(t_2)$. Detection is performed with the detection operator $\boldsymbol{D}$ in analogy to Figure 1, leading to Equation (5).

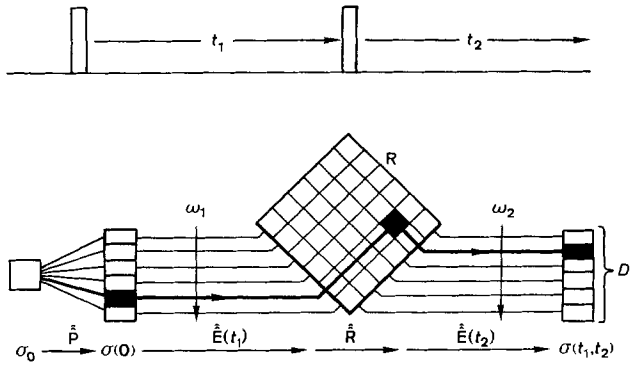

Fig. 6. Schematic representation of a 2D experiment, here with a simple two-pulse sequence. The first pulse excites coherences that precess during t_1 and are transferred by the second pulse to different transitions where the coherences continue to precess with a new frequency. The 2D spectrum obtained by a 2D Fourier transformation of $\langle \boldsymbol{D} \rangle(t_1, t_2)$ is a visual representation of the transfer matrix R.

$$\langle \boldsymbol{D} \rangle(t_1,t_2) = \mathrm{Tr}\{\boldsymbol{D}\hat{\hat{E}}(t_2)\hat{\hat{R}}\hat{\hat{E}}(t_1)\hat{\hat{P}}\sigma_0\} \quad (5)$$

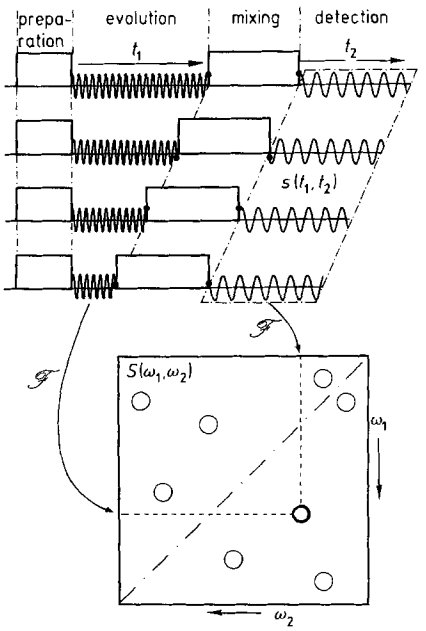

Fig. 7. Schematic representation of a general 2D experiment consisting of preparation, evolution, mixing, and detection periods. The duration t_1 of the evolution period is varied systematically from experiment to experiment. The resulting signal $s(t_1, t_2) \propto \langle \boldsymbol{D} \rangle(t_1, t_2)$ is Fourier-transformed in two dimensions to produce the 2D spectrum $S(\omega_1,\omega_2)$.

It is not sufficient to perform a single two-pulse experiment. To obtain the necessary data $\langle \boldsymbol{D} \rangle(t_1,t_2)$ to compute a 2D spectrum $S(\omega_1,\omega_2)$, it is required to systematically vary t_1 in a series of experiments and to assemble a 2D data matrix that is then Fourier-transformed in two dimensions as is indicated schematically in Figure 7. The resulting 2D spectrum correlates the precession frequencies during the evolution period with the precession frequencies during the detection period, and is a vivid and easily interpretable representation of the mixing process. Diagonal and cross peaks are measures for the elements of the transfer matrix of the mixing pulse sequence in Figure 6.

Among the numerous transfer processes that can be represented in this manner, the most important ones are[8] 1) the scalar J coupling leading to 2D correlation spectroscopy abbreviated as COSY, 2) internuclear cross relaxation leading to 2D nuclear Overhauser effect spectroscopy abbreviated as NOESY, and 3) chemical exchange leading to 2D exchange spectroscopy abbreviated as EXSY.

The COSY transfer, which proceeds through J coupling, is truly a quantum mechanical effect that does not find a satisfactory classical explanation. By means of a single $(\pi/2)_x$ rf mixing pulse, as in Figure 6, it is possible to transfer coherence of spin k, which is antiphase with respect to spin l and represented in the density operator by the operator term $2\boldsymbol{I}_{ky}\boldsymbol{I}_{lz}$ into coherence of spin l, which is antiphase with respect to spin k, represented by $-2\boldsymbol{I}_{kz}\boldsymbol{I}_{ly}$ (6), whereby each

$$2\boldsymbol{I}_{ky}\boldsymbol{I}_{lz} \xrightarrow{(\pi/2)_x} -2\boldsymbol{I}_{kz}\boldsymbol{I}_{ly} \tag{6}$$

factor of the product spin-operator can be considered to be rotated by $\pi/2$ about the x-axis. Antiphase coherence of the type $2\boldsymbol{I}_{ky}\boldsymbol{I}_{lz}$ is only formed during the evolution period when there is a direct spin–spin coupling between the spins I_k and I_l (7). This implies that in a two-dimensional correlation

$$\boldsymbol{I}_{kx} \xrightarrow{2\pi J_{kl}\boldsymbol{I}_{kz}\boldsymbol{I}_{lz}t_1} \boldsymbol{I}_{kx}\cos(\pi J_{kl}t_1) + 2\boldsymbol{I}_{ky}\boldsymbol{I}_{lz}\sin(\pi J_{kl}t_1) \tag{7}$$

spectrum there are cross peaks only between directly coupled spins (as long as the approximation of weak coupling holds). It is obvious from Equation (7) that there is no net coherence transfer, e.g. $\boldsymbol{I}_{kx} \rightarrow \boldsymbol{I}_{lx}$, and the cross-peak integral must disappear. In other words, there is an equal number of cross-peak multiplet lines with positive and negative intensity.

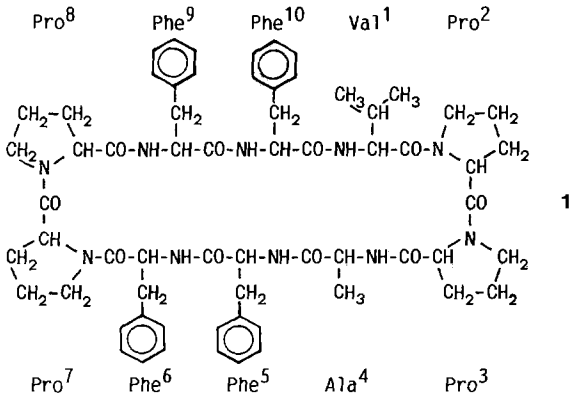

1

A COSY spectrum, such as the one shown in Figure 8 for the cyclic decapeptide antamanide (**1**) can be used to find pairs of spins belonging to the same coupling network of an amino acid residue in the molecule. All intense cross peaks

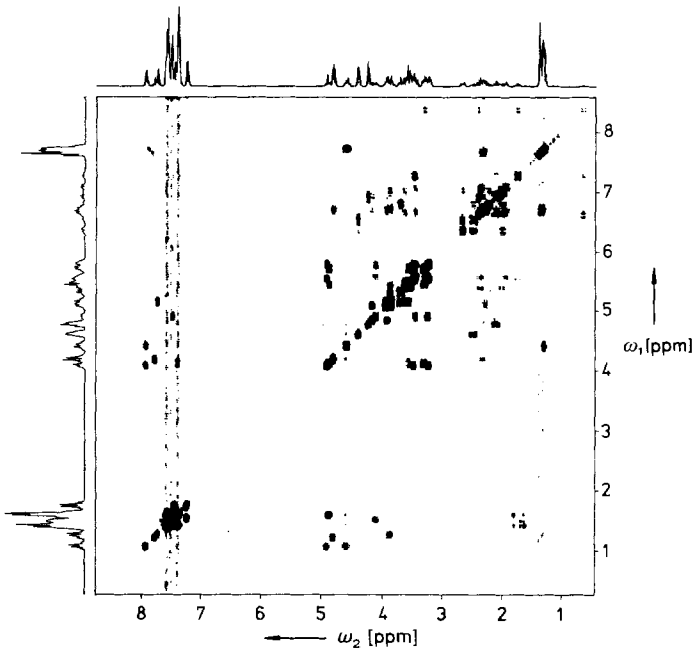

Fig. 8. Phase-sensitive 400 MHz ^{1}H COSY spectrum of antamanide (**1**) in chloroform (at 250 K) in a contour-line representation. Positive and negative contours are not distinguished. The spectrum was recorded by Dr. Martin Blackledge.

arise from couplings over two and three bonds that allow, first of all, the assignment of the pairs of NH and $C_\alpha H$ along the polypeptide backbone (backbone protons), as indicated by C in Figure 9 for the six amino acid residues with NH protons. In addition, it is also possible to assign the protons in the side chains.

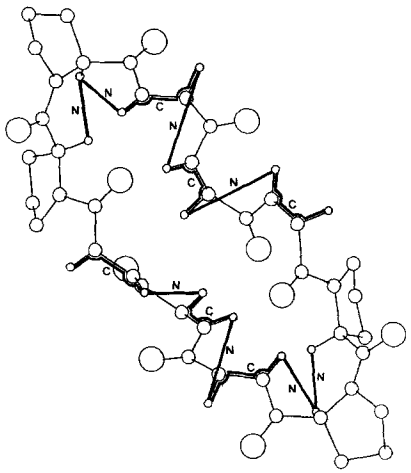

Fig. 9. Assignment of the protons of the backbone of antamanide (**1**) by the combination of COSY (C) and NOESY (N) cross peaks. The missing NH protons in the four proline residues break the chain of sequential C–N connectivities.

The transfers of NOESY and EXSY experiments involve incoherent, dissipative processes that bring the system back to equilibrium in an exponential or multiexponential manner after an initial perturbation. They require an extended mixing time during which the random processes are given a chance to occur. Both processes can be investigated with the same three-pulse scheme (Fig. 10b).[8, 64–67] The mixing period is bracketed by two $\pi/2$ pulses that transform coherence into static spin-order and back into coherence. The exchange processes transfer the spin order between different spins or between different chemical species, respectively. This type of transfer can be understood on the basis of classical kinetic models. The resulting 2D spectrum represents a kinetic matrix with cross-peak intensities proportional to the exchange rate constants of pseudo-first-order reactions.

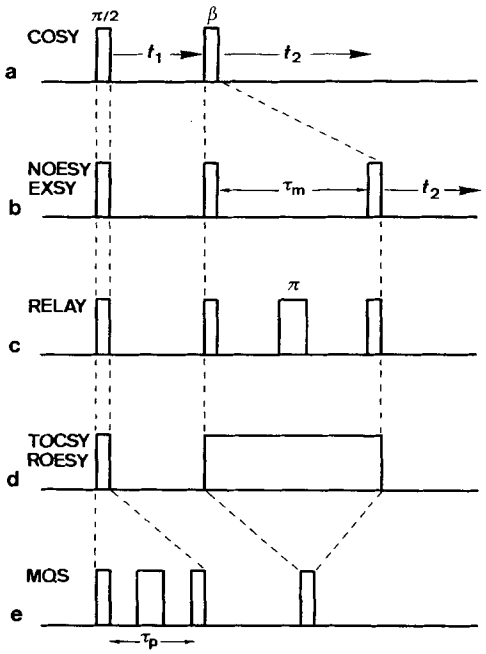

Fig. 10. Pulse sequences for some of the most useful homonuclear 2D experiments: a) COSY, b) NOESY or EXSY, c) relayed COSY, d) TOCSY or ROESY in the rotating coordinate system, e) multiple-quantum spectroscopy.

For the NOESY transfer, the exchange rate constants are given by the cross-relaxation rate constants, which are due to magnetic dipole–dipole interactions, and are proportional to $1/r_{kl}^6$ for nuclear pairs I_k and I_l, and depend on the correlation time τ_c of the tumbling of the molecules in solution. The distance dependence can be used to measure relative or, if τ_c is known, absolute distances in molecules. The NOESY cross peaks thus allow the identification of neighboring protons in a molecule—important, for example, in identifying protons that belong to adjacent amino acid residues in peptides.

A NOESY spectrum of antamanide (**1**) is given in Figure 11. The sequential backbone protons of adjacent amino acid residues with NOESY cross peaks are marked in Figure 9 with N. It is seen in Figure 9 that these together with the protons with *J*- cross peaks from the COSY spectrum (Fig. 8) form two unbroken chains of connectivities that can be used for the identification of the backbone protons. The two chains are not joined because of the absence of NH protons in the four proline residues. The general assessment procedure of proton resonance frequencies based on COSY and NOESY spectra has been established by Wüthrich and his research group.[56]

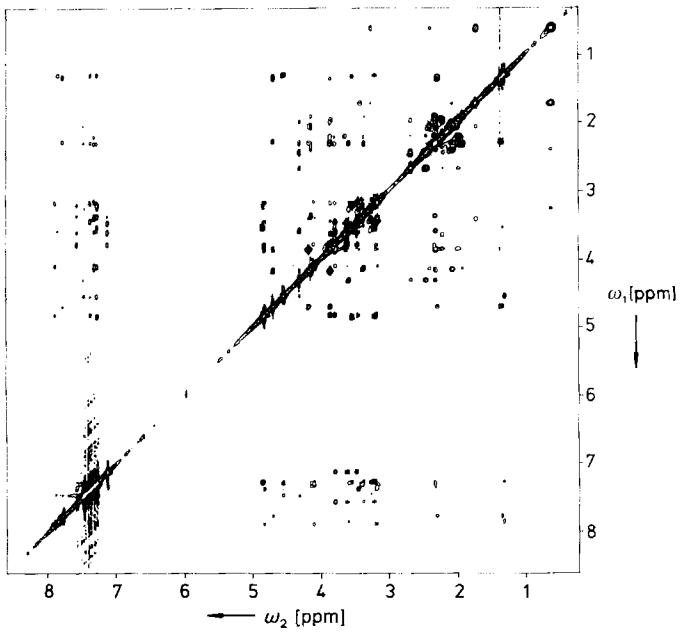

Fig. 11. 400 MHz ^{1}H NOESY spectrum of antamanide (1) in chloroform (at 250 K) in a contour-line representation. The spectrum was recorded by Dr. Martin Blackledge.

Based on a complete or partial set of assigned resonances, it is then possible to deduce information on the molecular structure. Each NOESY cross-peak intensity provides an internuclear distance that can be used in a manual or computerized process to construct a molecular model compatible with the experimental data. In this process it is also possible to employ scalar coupling constants extracted from COSY-type spectra (most conveniently from E. COSY spectra, as mentioned later). According to the Karplus relations,[54] there is a relation between vicinal coupling constants and dihedral angles. Ingenious computer procedures to determine molecular structures based on NMR data were first developed by Kurt Wüthrich and his research team and tested on a large number of small to medium-size proteins.[56, 68–71] At present, mainly two computer algorithms for the structure determination are in use—the distance–geometry algorithm[72, 73] and modifications of it, and the restrained molecular-dynamics algorithm,[74, 75] again with many variations. The structural problem in antamanide (**1**) will be discussed later, as it involves intramolecular dynamic processes that complicate the situation.

Cross peaks in a NOESY-type exchange spectrum can also originate from chemical exchange; the three-pulse experiment of Figure 10b is indeed well suited for the investigation of chemical exchange networks.[64, 65, 76] A distinction of the two types of signals is not possible by inspection of a single 2D spectrum. However, variable-temperature studies are often conclusive. At sufficiently low temperatures

at which chemical exchange becomes slow, only NOESY cross peaks should remain. The two types of signals may also be distinguished in experiments with rotating coordinate systems as mentioned in the next section.

The ^{13}C NMR spectrum of a mixture of *cis*- and *trans*-decalin in Figure 12 is typical for a spectrum showing chemical exchange. The spectrum gives evidence of the well-known

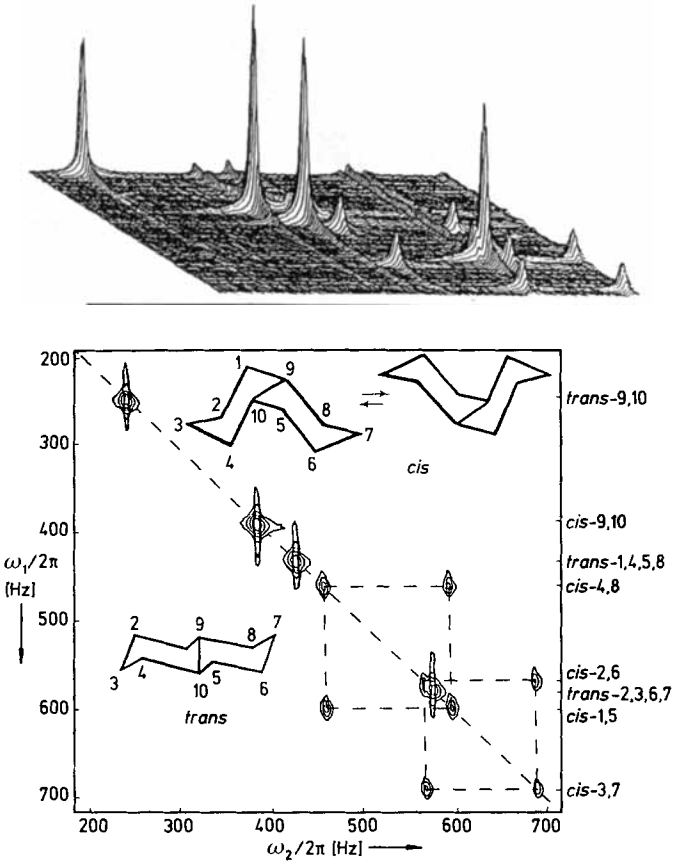

Fig. 12. 2D ^{13}C EXSY spectrum of a mixture of *cis*- and *trans*-decalin recorded at 22.5 MHz and 241 K [76]. Top: Three-dimensional representation (stacked plot). Bottom: A contour-line representation with the assignment of the peaks.

conformational stability of *trans*-decalin, whereas for *cis*-decalin four pairs of carbon spins are involved in a conformational exchange process, giving raise to two pairs of cross peaks.[76]

Modified Two-Dimensional FT-NMR Experiments

Starting from the two prototypical 2D FT NMR experiments, numerous modified, expanded, and improved experiments have been suggested. Many of them have found a place in the arsenal of routine methods for the NMR spectroscopist. A first category of experiments, represented in the upper part of Figure 13, causes extended correlation through two or more transfer steps: Relayed correlation experiments involve two-step correlation, and total correlation spectroscopy (TOCSY) multiple-step correlation. The latter experiment leads to the important class of rotating frame experiments, including rotating frame Overhauser effect spectroscopy (ROESY) an alternative to NOESY. Finally

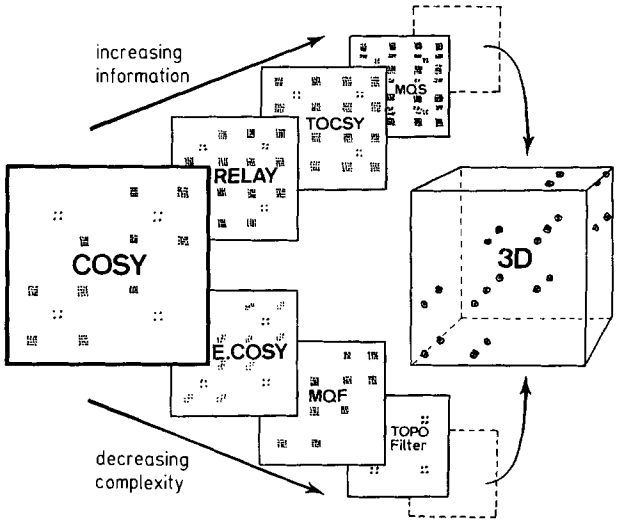

Fig. 13. Extensions of the standard COSY experiment. Relayed correlation, total correlation spectroscopy (TOCSY), and multiple-quantum spectroscopy (MQS) increase the information content, while exclusive correlation (E. COSY), multiple-quantum filtering (MQF), and spin-topology filtration reduce the complexity. Both avenues can lead to three-dimensional spectroscopy.

also multiple-quantum spectroscopy allows one to investigate connectivity in spin systems. A second class of experiments attempts the simplification of spectra by exclusive correlation (E. COSY), multiple-quantum filtering, and spin-topology filtration.

Relayed Correlation

In a standard COSY experiment, coherence is transferred exclusively between two directly coupled spins by means of a single mixing pulse. By a sequence of two $\pi/2$ pulses, as in Fig. 10c, it is possible to effect a transfer of coherence across two sequential couplings from spin I_k to spin I_l through the relay spin I_r.[77, 78] For the relation in (8), $J_{kr}t_1 = J_{kr}\tau_m = J_{rl}\tau_m = 1/2$ is assumed.

$$\begin{aligned} I_{kz} &\xrightarrow{(\pi/2)I_{ky}} I_{kx} \xrightarrow{2\pi J_{kr}I_{kz}I_{rz}t_1} 2I_{ky}I_{rz} \xrightarrow{(\pi/2)(I_{kx}+I_{rx})} \\ -2I_{kz}I_{ry} &\xrightarrow{2\pi J_{kr}I_{kz}I_{rz}\tau_m + 2\pi J_{rl}I_{rz}I_{lz}\tau_m} 2I_{ry}I_{lz} \xrightarrow{(\pi/2)(I_{rx}+I_{lx})} -2I_{rz}I_{ly} \end{aligned} \quad (8)$$

During the extended mixing period τ_m, it is thus necessary to refocus the antiphase character of the I_r spin coherences with respect to spin I_k and create antiphase character with respect to spin I_l to allow for a second transfer by the second mixing pulse. Relayed correlation is useful whenever the resonance of the relay spin I_r cannot be identified unambiguously. With a relay experiment it is then nevertheless possible to assign spins I_k and I_l to the same coupling network (e.g. belonging to the same amino acid residue in a polypeptide chain). It is usually advantageous to refocus the effects of the chemical shift precession during the mixing period by incorporating a central π pulse as shown in Figure 10c.

Relayed coherence transfer is illustrated by 300 MHz ^1H NMR spectra of the linear nonapeptide buserilin, pyro-Glu-His-Trp-Ser-Tyr-D-Ser-Leu-Arg-Pro-$NHCH_2CH_3$. Figure 14a shows a (double-quantum filtered) COSY spec-

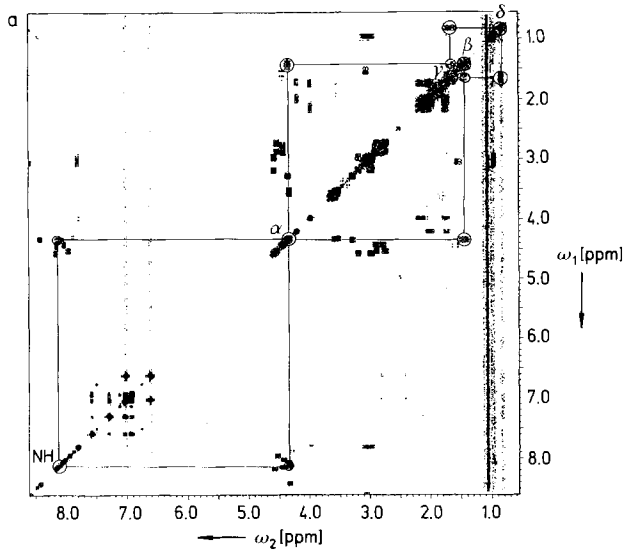

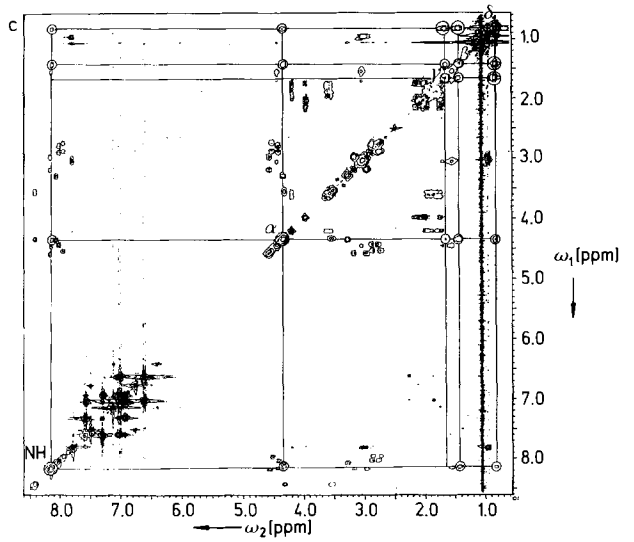

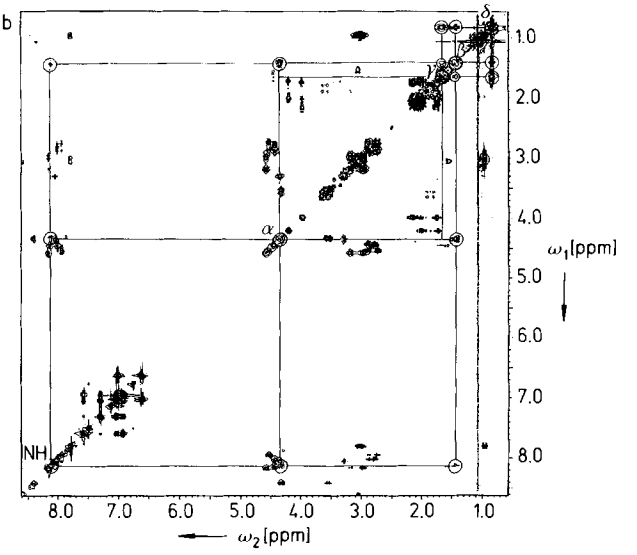

Fig. 14. 300 MHz correlation spectra of the nonapeptide buserilin in dimethyl sulfoxide (DMSO). Phase-sensitive spectra with equal representation of positive and negative contours are shown. The resonance connectivities and the positions of the NH, $C_\alpha H$, $C_\beta H$, $C_\gamma H$, and $C_\delta H$ diagonal peaks are indicated for the leucine residue [79]. a) Double-quantum filtered COSY spectrum with the sequence from Figure 18. b) Relayed COSY spectrum with the sequence from Figure 10c and $\tau_m = 25$ ms. c) TOCSY spectrum with the sequence from Figure 10d, $\tau_m = 112$ ms, and an MLEV-17 pulse sequence applied during τ_m.

trum and Figure 14b the corresponding relayed COSY spectrum.[79] In both spectra, the resonance connectivities for the leucine residue are marked. It is evident that in the COSY spectrum only nearest neighbor protons are connected by cross peaks: NH–$C_\alpha H$, $C_\alpha H$–$C_\beta H^{1,2}$, $C_\beta H^{1,2}$–$C_\gamma H$, and $C_\gamma H$–$(C_\delta H_3)^{1,2}$. On the other hand, in the relayed COSY spectrum, also the next-nearest neighbors NH–$C_\beta H^{1,2}$ and $C_\beta H^{1,2}$–$(C_\delta H_3)^{1,2}$ are connected. The third pair of relayed cross peaks, $C_\alpha H$–$C_\gamma H$, is weak because of the high multiplicity of the $C_\gamma H$ resonance and is not visible in the contour representation of Figure 14b. Similar relayed cross peaks can be found for the other amino acid residues.

Rotating Frame Experiments

By means of an extended mixing pulse sequence, transfer of coherence over an arbitrary number of steps is possible in principle. In particular, continuous wave irradiation leads to the mixing of all eigenmodes of a spin system and correspondingly to transfers of coherence between all of them. This is exploited in total correlation spectroscopy (TOCSY) with the sequence shown in Figure 10d. All spins belonging to the same J-coupling network can be identified with TOCSY.[80, 81] The accurate matching of the precession frequencies of the various spins in the presence of a radio frequency field is crucial in enabling an efficient transfer of coherence. Either very strong radio-frequency fields or specially designed pulse sequences are needed for this purpose.[81] Coherence transfer is possible when the effective average magnetic field strengths B_k^{eff} in the rotating frame are equal to within a J-coupling constant, $|\gamma(B_k^{eff} - B_l^{eff})| < |2\pi J_{kl}|$, corresponding to a strong coupling case in the rotating frame.

The TOCSY experiment is of interest for the assignment of proton resonances to individual amino acid residues in a protein. Of particular value is that its transfer rate is enhanced by a factor of 2 in comparison to COSY or relayed transfer experiments in the laboratory frame.[80] Another property is that, because of the presence of a radio-frequency field, in-phase coherence transfer is possible (9), leading to in-phase cross-peak multiplet structures.

$$I_{kx} \xrightarrow{2\pi J_{kl} I_k I_l \tau_m} I_{lx} \qquad (9)$$

A TOCSY spectrum of buserilin is included in Figure 14c for comparison with the relayed and standard COSY spectra depicted. Again three-step transfers $C_\alpha H$–$(C_\delta H_3)^{1,2}$ and even four-step transfers NH–$(C_\delta H_3)^{1,2}$ are visible here. Some expected cross peaks involving $C_\gamma H$ are missing as before because of the extensive multiplet structure of $C_\gamma H$.

The elimination of the chemical shift precession by the rf irradiation leads not only to the coherent transfer through the J-coupling network, but also to an incoherent transfer of spin order through transverse cross-relaxation. The transverse cross-relaxation terms are, in principle, always present.

However, strong differential chemical shift precession of spin pairs normally causes a quenching of the transfer in the sence of first-order perturbation theory. In the presence of a strong rf field, this quenching is no longer operative and transverse cross-relaxation occurs. This is the transfer mechanism of the rotating frame Overhauser effect spectroscopy (ROESY) experiment.[82]

ROESY has similar properties as NOESY but differs in the dependence of the cross-relaxation rate constant Γ_{kl} on the correlation time τ_c of the molecular rotational motion that modulates the internuclear dipole–dipole interaction responsible for cross-relaxation [cf. (10) and (11) where the spectral density J is defined by (12)]. As usual, ω_0 is the

$$\Gamma_{kl}^{NOE} = \frac{\gamma^4\hbar^2}{10 r_{kl}^6}\left(\frac{\mu_0}{4\pi}\right)^2\left[-\frac{1}{2}J(0) + 3J(2\omega_0)\right] \quad (10)$$

$$\Gamma_{kl}^{ROE} = \frac{\gamma^4\hbar^2}{10 r_{kl}^6}\left(\frac{\mu_0}{4\pi}\right)^2\left[J(0) + \frac{3}{2}J(\omega_0)\right] \quad (11)$$

$$J(\omega) = \frac{2\tau_c}{1 + (\omega\tau_c)^2} \quad (12)$$

Larmor frequency of the two nuclei with the internuclear distance r_{kl}. Equations (10) and (12) imply that Γ_{kl}^{NOE} changes sign for an intermediate correlation time τ_c of $(5/4)^{1/2}\ \omega_0^{-1}$; that is, the cross-relaxation rate becomes small in the neighborhood of this condition. Depending on the viscosity of the solvent and the resonance frequency ω_0, this occurs for globular molecules within a range of molecular mass of 500–2000 Da. Γ_{kl}^{ROE}, on the other hand, is less sensitive to τ_c and remains positive for any molecular mass. The ROESY experiment is therefore of advantage for molecules of intermediate size.

In addition, the different sensitivity of NOE and ROE to τ_c allows one to deduce information on intramolecular mobility by comparison of the two measurements.[83]. An advantage of ROESY over NOESY experiments is that the cross-peak amplitude is negative, while the simultaneously occurring cross peaks due to chemical exchange are positive and allow for an easy distinction as long as the signals do not overlap.

It should be recognized that in the rotating frame coherence transfer through J couplings and cross relaxation occurs simultaneously, whereby TOCSY cross peaks are positive and ROESY cross peaks appear with negative amplitude. This complicates the 2D spectra and calls for separation procedures. The suppression of the coherent transfer through J couplings (TOCSY) is easy, because it is only necessary to mismatch the condition $|\gamma(B_k^{eff} - B_l^{eff})| < |2\pi J_{kl}|$, for example by a slight frequency offset in the presence of not-too-strong rf fields. The cross-relaxation rates are much less sensitive to such a mismatch and a clean ROESY spectrum results.

Obtaining a clean TOCSY spectrum is more demanding because relaxation cannot easily be manipulated. A technique was proposed by C. Griesinger,[84] which relies on a combination of Equations (10) and (11) to set the average cross-relaxation rate constant to zero [Eq. (13)]. A suitable weighting factor p can be found whenever $\Gamma_{kl}^{NOE} < 0$, that is, for sufficiently large molecules with $\tau_c > (5/4)^{1/2}\ \omega_0^{-1}$. This requires the magnetization to move on a trajectory that spends a fraction p of time along the z-axis and a fraction $(1\text{-}p)$ in the transverse plane. For $\tau_c \to \infty$, one finds $p = 2/3$ for $\bar{\Gamma}_{kl} = 0$. A suitable pulse sequence, a modification of an MLEV-17 spin-locking sequence, has been proposed in ref.[84].

$$\bar{\Gamma}_{kl} = p\Gamma_{kl}^{NOE} + (1-p)\Gamma_{kl}^{ROE} \stackrel{!}{=} 0 \quad (13)$$

Another optimized sequence, called "Clean CITY", was developed by J. Briand.[85] A clean TOCSY spectrum of bovine pancreatic trypsin inhibitor (BPTI) using the Clean CITY sequence is compared in Figure 15 with a conventional TOCSY spectrum to demonstrate the efficient suppression of the (negative) ROESY peaks.

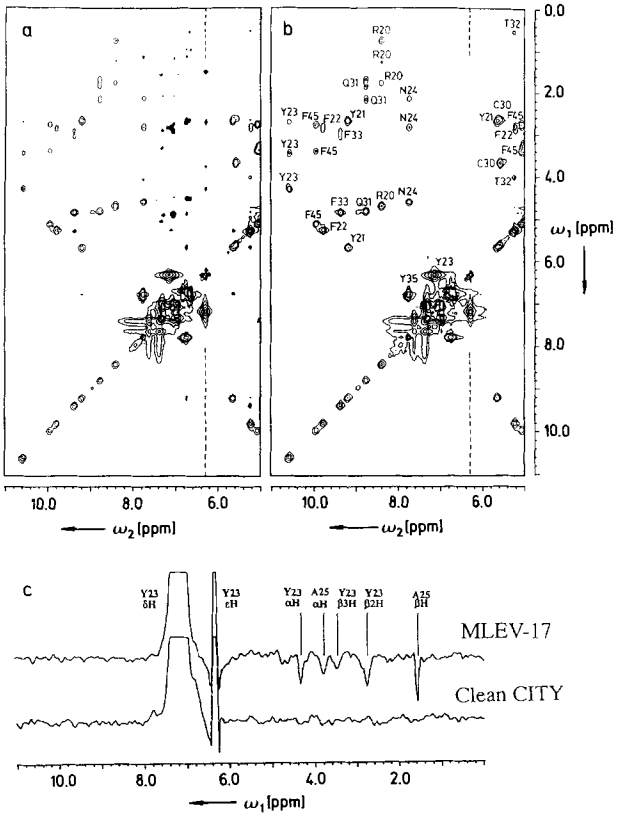

Fig. 15. Phase-sensitive 300 MHz ^{1}H TOCSY spectra of a 15 mM sample of bovine pancreatic trypsin inhibitor in D_2O recorded with a mixing time of 69 ms [85]. a) Mixing process with the MLEV-17 pulse sequence. Negative peaks are shown by contours filled in black. b) Mixing process with the Clean CITY pulse sequence. c) Cross sections along ω_1 through the diagonal peak of Tyr^{23} εH at $\omega_2 = 6.33$ ppm in the spectra a) and b) (marked with broken lines).

Multiple-Quantum Spectroscopy

In the spectroscopy, in general, only those transitions are directly observable for which the observable operator has matrix elements not equal to zero, leading to the so-called allowed transitions. For magnetic resonance in strong magnetic fields with weak cw perturbation or with a free induc-

tion decay in the absence of rf, the observable operator of the transverse magnetization $F_x = \sum_k I_{kx}$ has matrix elements only between eigenstates of the Hamiltonian differing in the magnetic quantum number M by ± 1. Thus single-quantum transitions are the allowed transitions, while multiple-quantum transitions with $|\Delta M| > 1$ are forbidden. Multiple-quantum transitions can, however, be induced by strong cw rf fields that cause a mixing of states[8, 57] or by a sequence of at least two rf pulses (Fig. 10e).[8, 63, 86, 87] Observation is possible again in the presence of a strong rf field[8, 57] or after a further detection pulse.[8, 63, 86, 87]

For spin systems with $I = 1/2$, multiple-quantum transitions invariably involve several spins, and multiple-quantum spectra contain information on the connectivity of spins within the J-coupling network in analogy to 2D correlation spectra. In particular, the highest order transition allows one to determine the number of coupled spins. Relaxation rate constants of multiple-quantum coherences are dependent on the correlation of the random perturbations affecting the spins involved and provide information on motional processes.[88].

A simple instructive example of a 2D double-quantum spectrum is given in Figure 16 to demonstrate the use of multiple-quantum transitions for the assignment of resonances.[89] Along ω_1, double-quantum transitions and along ω_2 single-quantum transitions are displayed for the six-spin system of $[D_3]$3-aminopropanol $DOCH_2CH_2CH_2ND_2$. In general, there are three categories of double-quantum transitions:

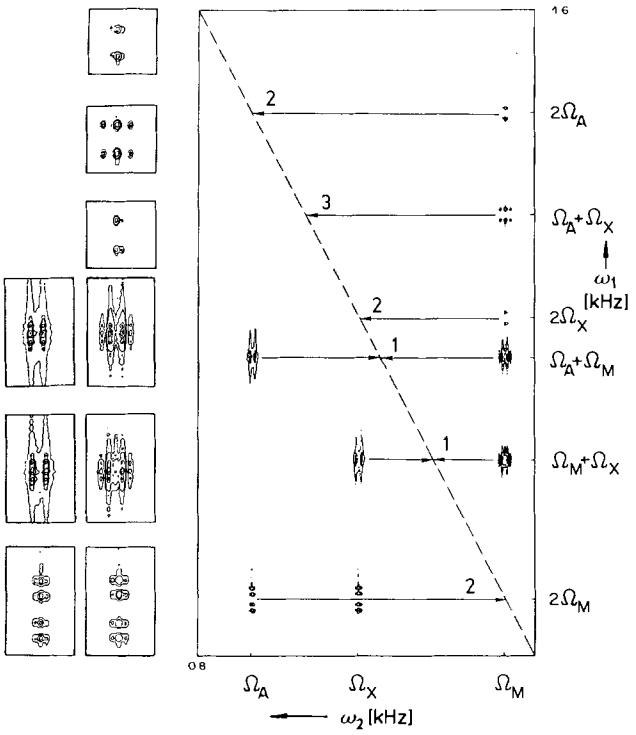

Fig. 16. 90 MHz 2D ^{1}H correlation spectrum of $[D_3]$3-amino-propanol with double-quantum transitions along ω_1 and single-quantum transitions along ω_2. The three types of double-quantum transitions mentioned in the text are indicated. Enlargements of all cross peaks are shown on the left. The spectrum is shown in an absolute value representation (from ref. [89]).

1) Double-quantum transitions involving two directly coupled spins. They lead to pairs of cross peaks displaced symmetrically from the double-quantum diagonal ($\omega_1 = 2\omega_2$) with ω_2 coordinates corresponding to the Larmor frequencies of the two spins (e.g. $\omega_1 = \Omega_A + \Omega_M$, $\Omega_M + \Omega_x$).

2) Double-quantum transitions involving two magnetically equivalent spins. They lead to one or more cross peaks at an ω_1 frequency that intersects the double-quantum diagonal at the ω_2 frequency corresponding to the common Larmor frequency of the two spins (e.g. $\omega_1 = 2\Omega_A$, $2\Omega_M$, $2\Omega_x$, although the spins are magnetically equivalent only within experimental accuracy).

3) Double-quantum transitions involving two remotely coupled spins. They lead to single cross peaks at an ω_1 frequency that intersects the double quantum diagonal at ω_2 equal to the mean of the two Larmor frequencies (e.g. $\omega_1 = \Omega_A + \Omega_x$). These cross peaks carry information identical to that in relayed correlation spectra.

For the practical application it is essential that a multiple-quantum spectrum never contains an array of strong diagonal peaks. It should be mentioned that a beautiful and useful form of a double-quantum experiment is the 2D INADEQUATE spectroscopy proposed by Bax, Freeman, and Kempsell.[90, 91] There, only type 1 peaks can arise.

The methods mentioned so far produce additional cross peaks that provide information not accessible with the standard COSY and NOESY experiments. In the following, techniques are discussed that lead to simplified spectra which may facilitate their interpretation.

Multiple-Quantum Filtering

Selective filtering can be achieved by exciting multiple-quantum coherence, selecting a particular quantum order, and reconverting the selected order into observable magnetization. Depending on the selected order, this leads to multiple-quantum filtering of various orders. The spin-system-selective effect relies on coherence transfer selection rules that limit the allowed transfers for weakly coupled spins:[8, 92]

1) It is impossible to excite p quantum coherence in spin systems with less than p-coupled spins $I = 1/2$.

2) For the appearance of a diagonal peak of spin I_k in a p-quantum-filtered COSY spectrum, the spin I_k must be directly coupled to at least $p - 1$ further spins.

3) For the appearance of the cross peaks between spins I_k and I_l in a p-quantum-filtered COSY spectrum, both spins must simultaneously be coupled to at least $p - 2$ further spins.

Violations of these coherence transfer selection rules occur for strong coupling and for certain special relaxation situations.[93].

In Figure 17, the effect of four-quantum filtering on various four-spin systems is demonstrated. The sample consists of a mixture of the five compounds *trans*-phenylcyclopropanecarboxylic acid (K_4), DL-isocitric acid-lactone ($P_{3,1}$), 1,1-dichloroethane (S_4), 2-chloropropionic acid (C_4), and D-saccharic acid-1,4-lactone (L_4) with the coupling topologies indicated in Scheme 1.[94]

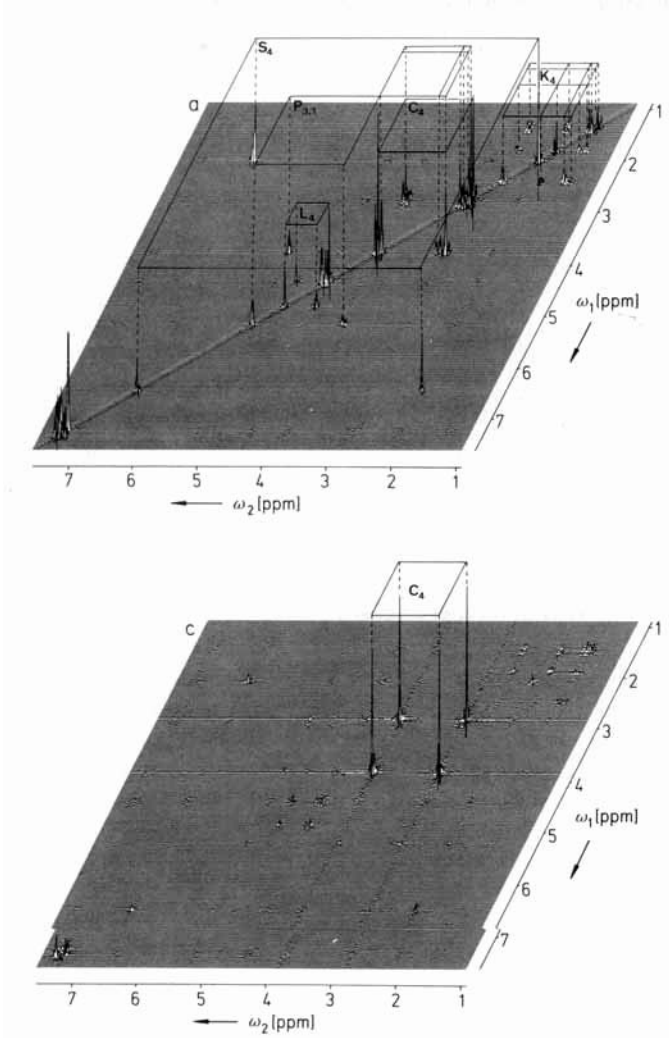

Figure 17a shows a conventional (double-quantum-filtered) COSY spectrum of the mixture, while in Figure 17b the corresponding four-quantum-filtered spectrum is reproduced. The filtering effect can easily be understood based on the given rules and the coupling topologies shown in Scheme 1. The interpretation is left to the reader. Only cross peaks of the molecule with K_4 topology and diagonal peaks of molecules with $P_{3,1}$, S_4, and K_4 topologies remain.

Technically, multiple-quantum filtering exploits the characteristic dependence of a multiple-quantum coherence transfer on the rf phase of the acting pulse sequence.[8, 92, 95, 96] Let us assume a transfer of coherence $c_{p1}(t)$ by a unitary transformation $\boldsymbol{U}(0)$, representing a particular pulse sequence, to coherence $c_{p2}(t)$, where p_1 and p_2 are the orders of

$$c_{p1}(t) \xrightarrow{\boldsymbol{U}(0)} c_{p2}(t) \tag{14}$$

coherence. All rf pulses in the sequence are now phase-shifted by Φ, leading to $\boldsymbol{U}(\Phi)$. Then it can be shown that the resulting coherence $c_{p2}(t)$ is phase-shifted by $(p_2 - p_1)\Phi$. The

$$c_{p1}(t) \xrightarrow{\boldsymbol{U}(\Phi)} c_{p2}(t)\, e^{i(p2-p1)\Phi} \tag{15}$$

phase shift is therefore proportional to the change in coherence order ($\Delta p = p_2 - p_1$). After a series of experiments are performed in which the phase Φ is incremented in regular

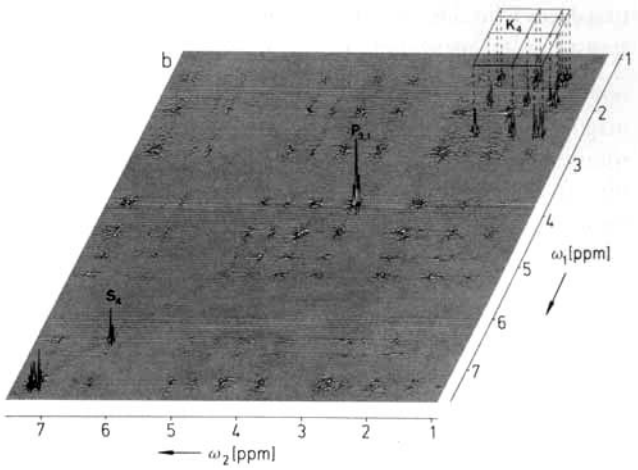

Fig. 17. Multiple-quantum-filtered and spin-topology-filtered 300 MHz ^{1}H COSY spectra of a mixture of the compounds from Scheme 1 containing four-spin systems. a) Double-quantum-filtered spectrum obtained with the pulse sequence from Figure 18. b) Four-quantum-filtered spectrum obtained with the pulse sequence from Figure 18. c) C_4 spin-topology-filtered spectrum obtained with the pulse sequence from Figure 19 (from ref. [94]).

intervals $2\pi/N$ from 0 to $2\pi(N-1)/N$, it is possible to select for a particular Δp by computing the corresponding Fourier coefficient of Δp: Let $s(t,\Phi)$ be the recorded signal of an experiment with phase shift Φ, then we obtain the filtered signal according to (16). The required number of increments

$$s(t, \Delta p) = \sum_{k=0}^{N-1} s(t, 2\pi k/N)\, e^{\frac{-i2\pi k \Delta p}{N}} \tag{16}$$

N of the phase Φ depends on the number of values of Δp that have to be discriminated.[96] It is obvious that unless the initial order of coherence p_1 is known, no particular order of

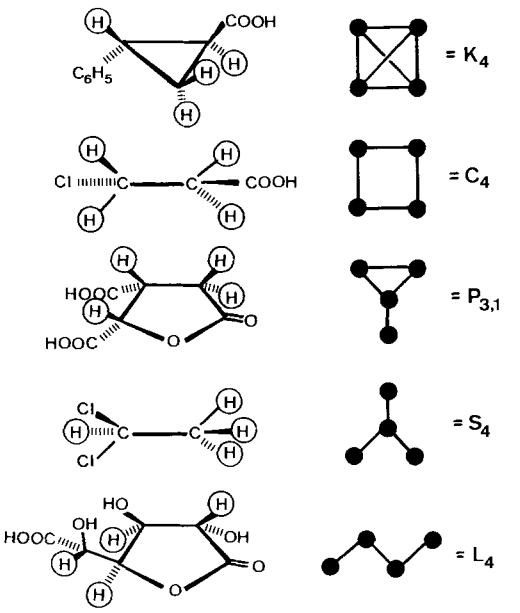

Scheme 1. The compounds used for the spectra in Figure 17 and their spin-coupling topologies.

coherence p_2 can be filtered out in this manner. Most conventiently the initial state is selected to be in thermal equilibrium with $p_1 = 0$. Then, the entire pulse sequence preceding the point at which a coherence order should be selected must be phase-cycled. For multiple-quantum-filtered COSY experiments, this leads to the pulse sequence shown in Figure 18.

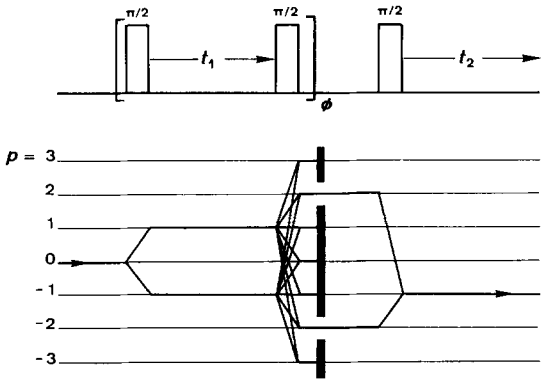

Fig. 18. Pulse sequence for a multiple-quantum-filtered COSY experiment with the coherence transfer diagram for double-quantum filtering. The phase ϕ is incremented systematically in a set of N experiments and the resulting experimental results are combined according to Eq. (16).

Obviously, multiple-quantum-filtering and phase-cycling require N-times more experiments. However, no information is lost, since in each term of Equation (16) just the phase factor is compensated, and identical signals are coadded for the relevant pathways. Thus the longer performance time is refunded in terms of an increased signal-to-noise ratio.

Spin-Topology Filtration

It is may be desirable to enhance the filtering effect illustrated in Figure 17 and to select individual spin coupling topologies. Indeed it is possible to design extended pulse sequences, in combination with multiple-quantum filtration, that are tailor-made for specific spin coupling topologies.[94, 97, 98] A pulse sequence built into a 2D COSY experiment, that is selective for cyclic C_4 spin coupling topologies is depicted schematically in Figure 19. If this pulse sequence is applied to the mixture of compounds with four-spin systems (Scheme 1), the 2D spectrum of Figure 17c is obtained. It shows efficient suppression of all other spin systems. It should be noted, however, that the situation is here rather ideal. Often, these filters do not perform as well because their design relies on all non-zero spin couplings being equal. In

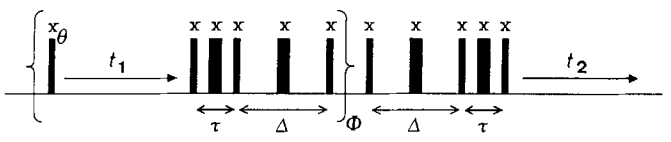

Fig. 19. Pulse sequence for C_4 spin-topology filtration consisting of $\pi/2$ and π pulses. The delays are adjusted to $\tau = 1/(8J)$ and $\Delta = 1/(2J)$, where J is the uniform J-coupling constant. ϕ is phase-cycled for four-quantum selection and θ for the suppression of axial peaks [94].

reality, there are weak and strong couplings that cannot be characterized by topological considerations alone. Often also the intensities of signals decrease during the extended pulse sequences due to relaxation. This limits the practical usefulness of these methods.

Exclusive Correlation Spectroscopy

Multiple-quantum filtering suppresses not only diagonal and cross peaks in 2D spectra but also changes the sign pattern in the cross-peak multiplet structure. By appropriate combination of differently multiple-quantum-filtered 2D spectra, it is possible to simplify the multiplet structure by reducing the number of multiplet components. Exclusive correlation spectroscopy (E. COSY), proposed by O. W. Sørensen, eliminates all multiplet components from a COSY spectrum except for those belonging to pairs of transitions with an energy level in common.[99-101] In practice, it is not necessary to combine multiple-quantum-filtered spectra literally, but it is possible to coadd directly the experimental results from a phase cycle with the appropriate weighting factors.

Figure 20 shows schematically the combination of cross-peak multiplets connecting two spins, I_1 and I_2, in a three-spin system after double- and triple-quantum filtering. The remaining pattern consists of two basic squares with side lengths equal to the active coupling constant J_{12} responsible for the coherence transfer. The displacement vector between the two squares is given by the two passive couplings J_{13} and J_{23} to the third (passive) spin. It should be mentioned that this multiplet structure is identical to the one obtained by a COSY experiment with a mixing pulse with an extremely small flip angle.[102]

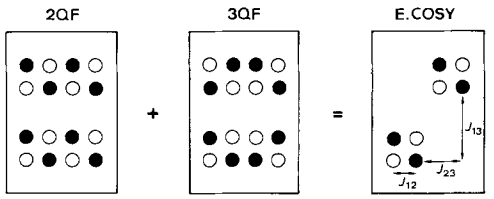

Fig. 20. E. COSY experiment to simplify the multiplet structure of cross peaks. The double-quantum- and the triple-quantum-filtered cross peaks between spins I_1 and I_2 of a three-spin system are combined to produce an E. COSY pattern. Positive and negative multiplet components are distinguished by empty and filled circles.

E. COSY is of practical use whenever the cross-peak multiplet structure must be analyzed for the determination of J-coupling constants. This can be done conveniently by hand by measuring the displacement of peripheral multiplet components[101] or by a recursive contraction procedure on a computer.[103]

Heteronuclear Two-Dimensional Experiments

In addition to the homonuclear 2D experiments discussed so far, at least as many heteronuclear experiments have been

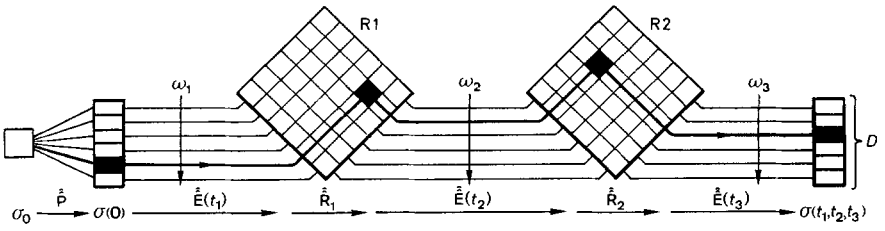

Fig. 21. Schematic representation of a 3D NMR experiment as an extension of Figures 1 and 6. Three evolution periods with the time variables t_1, t_2, and t_3 are separated by two transfer or mixing processes with the transfer matrices R1 and R2. A 3D experiment can be conceived as the contraction of two 2D experiments.

proposed and introduced to the repertoire of routine spectroscopic methods. Of greatest practical importance are heteronuclear shift correlation spectra which correlate the chemical shifts of directly bonded or remotely connected heteronuclei.[104, 105] In this context, so-called inverse detection experiments are of particular interest. Here proton I-spin coherence is observed in t_2 while spin coherence of a less sensitive, less abundant S nucleus evolves in t_1.[104] The most efficient pulse sequences create heteronuclear two-spin coherence that evolves in t_1 and that acquires the frequency information of the S-spin resonance.[106] Also in the heteronuclear environment, relayed coherence transfer[78] as well as experiments in the rotating frame[107] are important. Spin filtering is used for multiplicity selectivity, that is, for distinguishing S spins coupled to one, two, or three I spins,[108] and in the form of J filtering for the distinction of one-bond and multiple-bond couplings.[109] This enumeration of heteronuclear experiments is by no means exhaustive.

Three-Dimensional Fourier-Transformation Spectroscopy

No new principles are required for the development of 3D NMR spectroscopy, which is just a logical extension of 2D NMR spectroscopy. Instead of a single mixing process which relates two frequency variables, two sequential mixing processes relate three frequencies: the original frequency ω_1, the relay frequency ω_2, and the detection frequency ω_3, (Fig. 21). In this sense a 3D experiment can be considered as the combination of two 2D experiments. Obviously a very large number of possible 3D experiments can be conceived. However, only few of them have proved to be indispensible so far.[110–118]

Two applications of the 3D spectroscopy concept have emerged: 1) 3D correlation and 2) 3D dispersion spectroscopy (see also Fig. 13). Three-dimensional correlation is of importance in homonuclear experiments. It has been mentioned that the assignment procedure in biomolecules requires a COSY-type and a NOESY-type 2D spectrum. The two 2D experiments could be contracted into one 3D experiment, combining a J-coupling-mediated transfer and a cross-relaxation transfer. A 3D COSY–NOESY spectrum possesses the advantage that the entire assignment process can be carried out with a single homogeneous data set.[115, 116] It also incorporates redundant information that allows cross checks of the assignments. For obtaining quantitative information, however, 3D spectra are less suited, since all peak intensities are products of two transfer coefficients that are sometimes difficult to separate.

A 3D ROESY–TOCSY spectrum of the linear nonapeptide buserilin is shown in Figure 22 (vf. Fig. 14)[116] A ROESY instead of a NOESY sequence is required for buserilin, as it is a molecule of intermediate size for which the NOE intensities are small. The TOCSY step has the advantage that chains of multiple-step cross peaks extend to nuclei in the side chains are obtained thus facilitating the identification of the amino acid residues.

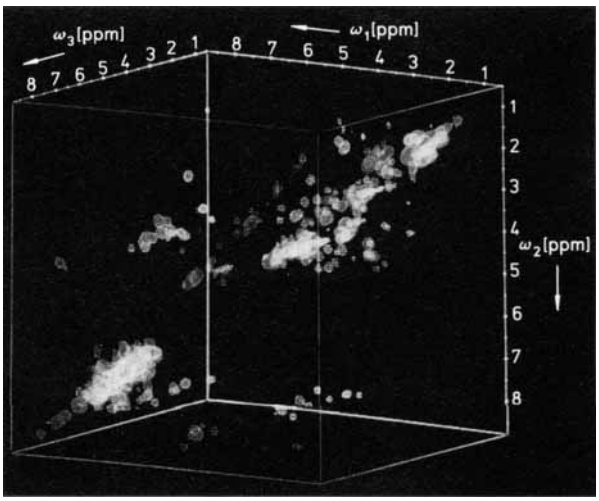

Fig. 22. 3D representation of a 300 MHz 3D homonuclear ROESY–TOCSY spectrum of buserilin in [D_6]DMSO photographed from a computer screen [116].

It should be recognized that recording a 3D spectrum is considerably more time-consuming than two 2D spectra, since two time parameters, t_1 and t_2, must be incremented independently, requiring a 2D array of experiments. Thus the question arises of when it is worth the effort to record a 3D spectrum. This question has been discussed in numerous publications.[116, 119, 120]

Let us consider a particular cross peak in a 3D spectrum that correlates the coherences $\{tu\}$ in the ω_1, $\{rs\}$ in the ω_2 and $\{pq\}$ in the ω_3 dimension. Its intensity is determined by the following product (17) of matrix elements in the eigen-

$$Z_{\{pq\}\{rs\}\{tu\}} = D_{qp} R^{(2)}_{\{pq\}\{rs\}} R^{(1)}_{\{rs\}\{tu\}} (\hat{\hat{P}}\sigma_0)_{tu} \qquad (17)$$

basis of the unperturbed Hamiltonian $\mathcal{H}_0$.[116] A nonvanishing intensity establishes a two-step correlation $\{tu\}$–$\{rs\}$–$\{pq\}$.

The 3D experiment can be compared with two 2D experiments that employ the mixing processes $\hat{\hat{R}}^{(1)}$ and $\hat{\hat{R}}^{(2)}$, re-

spectively. The corresponding intensities are expressed by (18) and (19). If in the 2D spectra the two relevant peaks

$$Z^{(1)}_{\{rs\}\{tu\}} = D^{(1)}_{sr} R^{(1)}_{\{rs\}\{tu\}} (\hat{\hat{\mathbf{P}}}\,\boldsymbol{\sigma}_0)_{tu} \tag{18}$$

$$Z^{(2)}_{\{pq\}\{rs\}} = D_{qp} R^{(2)}_{\{pq\}\{rs\}} (\hat{\hat{P}}^{(2)}\boldsymbol{\sigma}_0)_{rs} \tag{19}$$

with intensities $Z^{(1)}_{\{rs\}\{tu\}}$ and $Z^{(2)}_{\{pq\}\{rs\}}$ can be identified, possibly in crowded regions, the two-step correlation, represented by a 3D peak, could also be established based on the two 2D spectra $\{tu\}-\{rs\}$ and $\{rs\}-\{pq\}$. Provided that $Z_{\{pq\}\{rs\}\{tu\}} \neq 0$ is true, the intensities $Z^{(1)}_{\{rs\}\{tu\}}$ and $Z^{(2)}_{\{pq\}\{rs\}}$ are different from zero when in addition $D^{(1)}_{sr} \neq 0$ and $(\hat{\hat{\mathbf{P}}}^{(2)}\boldsymbol{\sigma}_0)_{rs} \neq 0$ hold. This implies that the relay transition $\{rs\}$ must be excited in the preparation state $P^{(2)}$ and detectable by the observable $D^{(1)}$. For allowed one-spin single-quantum coherences, this condition is fulfilled for single-pulse excitation and direct detection. On the other hand, forbidden multiple-spin single-quantum coherences (combination lines) and multiple-quantum coherences can neither be excited by a single nonselective pulse nor directly detected. Such coherences regularly occur in the ω_2 dimension of a 3D spectrum. The excitation and indirect detection of these coherences in 2D experiments requires special pulse sequences for excitation and detection.

In conclusion, the two constituent 2D experiments deliver the same information on the spin system as the 3D spectrum, provided that 1) the relevant frequencies in the ω_2 dimension of the 3D spectrum can be excited and detected in the 2D experiments, and 2) the cross peaks are not hidden by spectral overlap and can be identified in the 2D spectra. The first condition is normally not severe, as the 2D experiments can be modified for excitation and detection of forbidden transitions whenever required. On the other hand, the limited resolving power of 2D spectra is the most important motivation for justifying 3D (and possibly higher dimensional) spectroscopy.

Because the gain in resolution justifies 3D spectroscopy, it may be worthwhile to introduce a third frequency axis just for resolution purposes, rather than combining two processes relevant for the assignment requiring high resolution in all three dimensions. It is then possible to choose the extent of 3D resolution arbitrarily and optimize the performance time of the 3D experiment. To spread a 2D spectrum into a third dimension, homonuclear or heteronuclear transfers can be used. Heteronuclear one-bond transfers are far more efficient, however, because the strong heteronuclear one-bond couplings prevent leakage to further spins. This allows an efficient transfer, virtually without loss of magnetization. In addition, nuclei like ^{13}C and ^{15}N exhibit large ranges of chemical shifts with high resolving power. The principle of spreading is represented graphically in Figure 23.

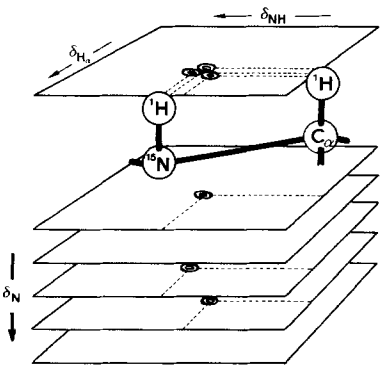

Fig. 23. 3D resolution of a 2D ^1H NMR spectrum by ^{15}N resonance spreading. The NH–$C_\alpha H$ cross peaks are displaced in a third dimension by the corresponding ^{15}N chemical shifts.

A 3D ^{15}N-spread TOCSY spectrum of ribonuclease A is shown in Figure 24. Heteronuclear spreading requires usually

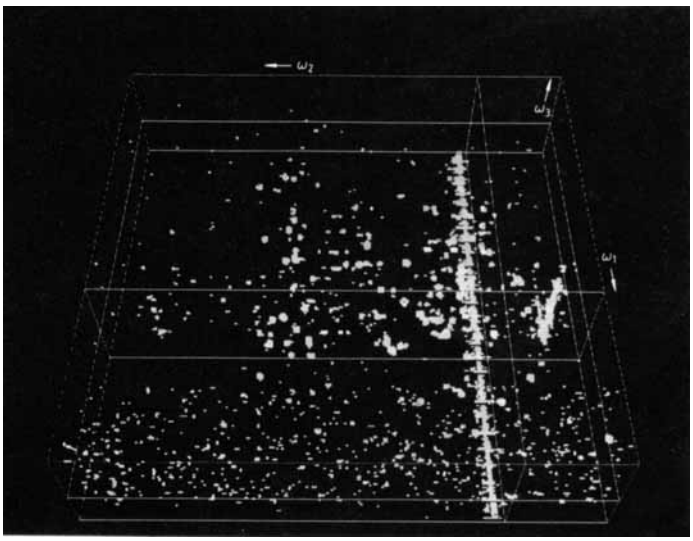

Fig. 24. 3D ^{15}N-spread 600 MHz ^1H TOCSY spectrum of ^{15}N-labeled ribonuclease A in water. The 3D spectrum shows the ^{15}N resonances along the ω_2-axis. The spectrum was recorded by C. Griesinger with the pulse sequence from Figure 25 and processed by S. Boentges. The sample was provided by Prof. S. Benner, ETH Zurich.

isotopic labeling of the molecule. In this case, ribonuclease A was grown in an *E. coli* medium containing ^{15}N-labeled nutrients. The spectrum was obtained with the pulse sequence from Figure 25. Initially proton coherence is excited and

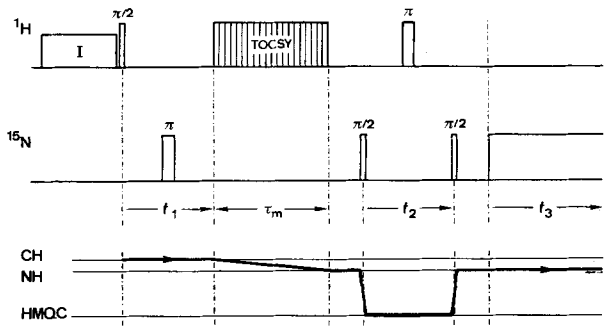

Fig. 25. Pulse sequence for recording a 3D ^{15}N-spread TOCSY spectrum. After presaturation of the water resonance (I), the proton resonances are excited and precess during t_1. After the homonuclear TOCSY transfer from the CH to the NH protons, the coherence is converted into heteronuclear multiple-quantum coherence (HMQC) that evolves during t_2 and acquires ^{15}N shift information. After reconversion to proton coherence, the NH resonances are detected during t_3 under ^{15}N decoupling.

precesses during t_1 under ^{15}N refocusing by the applied π pulse. During the mixing time τ_m, coherence transfer from other protons to the NH protons is effected in the rotating

frame by the application of a TOCSY multiple-pulse sequence. The NH coherence is then converted into ^{15}NH heteronuclear multiple-quantum coherence (HMQC) which precesses during t_2 and acquires ^{15}N resonance information (under proton refocusing). After reconversion into NH proton coherence, detection follows during t_3 under ^{15}N decoupling. For a complete assignment of the proton resonances a ^{15}N-spread NOESY spectrum is required in addition.

The step to 4D spectroscopy[121] is a logical one: In 2D experiments, spins are pairwise correlated, for example NH and $C_\alpha H$ protons. Three-dimensional dispersion uses either ^{15}N or $^{13}C_\alpha$ resonance for spreading the resonances of NH or $C_\alpha H$, respectively. In a 4D experiment, both spreading processes are applied simultaneously (Scheme 2). The order

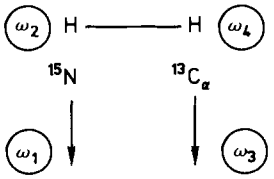

Scheme 2. Double spreading in 4D experiments.

of the frequencies in the actual experiment is a matter of convenience. Normally, the detection frequency ω_4 refers to proton spins for sensitivity reasons. In most cases, the two spreading coordinates are rather coarsely digitized to limit the performance time, just enough to achieve separation of peaks overlapping in the 2D spectrum. Often 8 to 32 points in each of the two dimensions are sufficient.

Molecular Dynamics Investigated by NMR

The molecular structures determined by NMR spectroscopy in solution, by X-ray diffraction in single crystals, or by other means are invariably motionally averaged structures, whereby the averaging process is strongly dependent on the measurement technique. To interpret experimentally determined structures, some knowledge of the motional properties of the molecule is in fact indispensible. Molecular dynamics is also relevant for its own sake, in particular for the understanding of reactivity and interaction with other molecules. In many cases, active sites in a molecular pocket are only accessible due to the flexibility of the molecule itself.

The characterization of the motional properties of a molecule is orders of magnitude more difficult than the description of an averaged molecular structure. While $3N-6$ coordinates are sufficient to fix a structure containing N atoms, the characterization of molecular dynamics requires $3N-6$ variances of the intramolecular coordinates, $(3N-6)(3N-5)/2$ covariances, and the same number of auto- and cross-correlation functions, respectively. In addition, also higher order correlation functions are needed for a more refined description of dynamics. In practice, a sufficient number of observables is never available for a full description of dynamics. In this sense, the study of dynamics is an open-ended problem.

Numerous techniques are available for obtaining data on dynamics: Debye–Waller factors in X-ray diffraction give hints on the variances of the nuclear coordinates, however, without a measure for the time scale. Inelastic and quasi-elastic neutron scattering deliver correlation functions, but without a reference to the structure. Fluorescence depolarization allows one to determine the motional correlation function of fluorescent groups, such as tyrosine residues in proteins. Ultrasonic absorption gives an indication of the frequencies of the dominant motional modes, but again without a structural reference.

NMR spectroscopy is more universally applicable to motional studies than most of the other techniques. The range of correlation times τ_c that can be covered by various NMR methods is enormous, from picoseconds to seconds and more (Scheme 3).

$1\text{ s} < \tau_c$:	Real-time monitoring after initial perturbation
$10\text{ ms} < \tau_c < 10\text{ s}$:	2D exchange spectroscopy (EXSY)
$100\ \mu\text{s} < \tau_c < 1\text{ s}$:	Lineshape analysis, exchange broadening, and exchange narrowing
$1\ \mu\text{s} < \tau_c < 10\text{ ms}$:	Measurements of relaxation time $T_{1\varrho}$ in the rotating frame
$30\text{ ps} < \tau_c < 1\ \mu\text{s}$:	Measurements of relaxation time T_1 in the laboratory frame
$\tau_c < 100\text{ ps}$:	Averaged parameter values

Scheme 3. NMR methods for the determination of motional correlation times τ_c.

Except for slow motions on a time scale of a millisecond or more for which lineshape analysis, saturation transfer experiments, and 2D exchange studies can be performed, many dynamics studies by NMR rely on measurements of relaxation times. The various relaxation parameters, such as the longitudinal relaxation time T_1, the transverse relaxation time T_2, the rotating-frame relaxation time $T_{1\varrho}$, and cross-relaxation rate constants Γ_{kl} depend on the correlation time τ_c of the underlying random process.

The following discussion shall be restricted to a recent study of the intramolecular dynamics in antamanide (**1**)[83, 122, 123] (see Figs. 8, 9, 11). Antamanide is an antidote for toxic components of the mushroom *Amanita phalloides*. Astonishingly, the antidote is a component of the same mushroom. Indications have been found in early ultrasonic absorption studies[124] that the peptide ring seems to undergo a conformational exchange process with a frequency of about 1 MHz. In the course of extensive investigations of antamanide by Kessler's research group,[125] it has also been noticed that the distance constraints obtained from NMR measurements could not be fitted by a single conformation. In our laboratory Martin Blackledge performed rotating-frame relaxation measurements and localized a hydrogen-bond exchange process with an activation energy of about 20 kJ mol^{-1} and a lifetime of 25 μs at room temperature (unpublished results, see also ref.[126]). With a new dynamic structure determination procedure called MEDUSA,[123] the conformational space of antamanide was investigated more systematically than ever before. 1176 feasible low-energy structures were found. They were combined in dynamically interconverting pairs in an attempt to fulfill all experimental

constraints including NOE distance constraints, J-coupling angular constraints, and specific information on hydrogen-bond dynamics. A large set of feasible structural pairs were constructed. Many pairs are compatible with the experimental data within experimental accuracy. For a more restrictive description of the dynamic system of antamanide, additional and more accurate experimental data is required. Figure 26 shows, as an example, the dynamic pair of structures that fits the experimental data best so far. The two interconverting structures differ primarily in the hydrogen bonds Val^1NH–Phe^9O and Phe^6NH–Ala^4O, which exist only in one of the two conformations (**II**), and in the torsional angles ϕ_5 and ϕ_{10}.

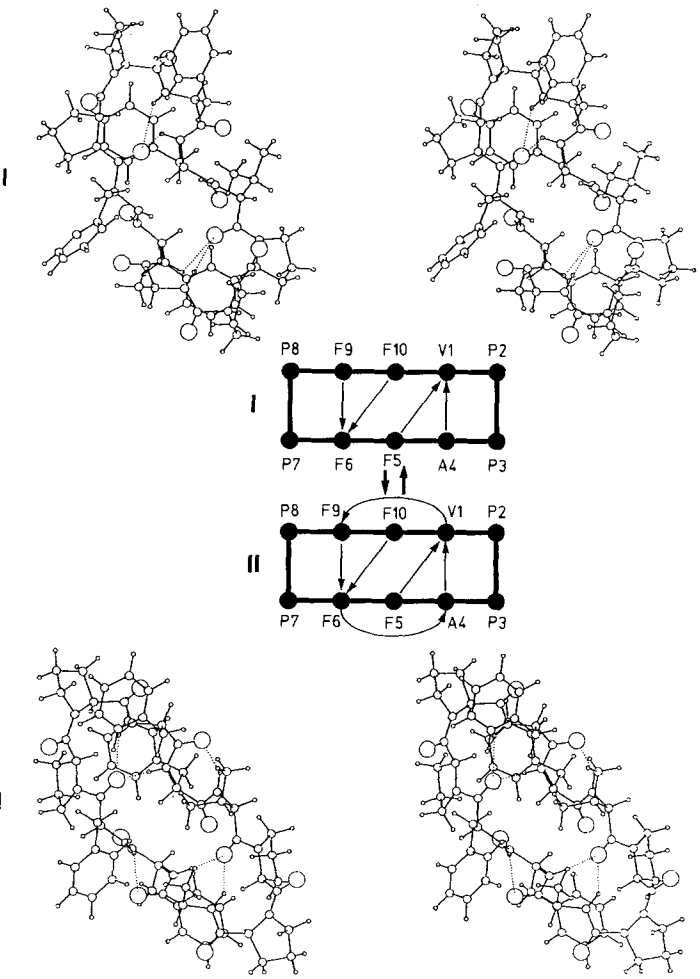

Fig. 26. Pairs of conformers of antamanide that fulfill the experimentally determined structural constraints. The two pairs are shown as stereoplots as well as in abstract form. In the former, hydrogen bonds are indicated by broken lines, in the latter by arrows pointing towards the hydrogen-bonded oxygen atom. The C–C bonds about which the torsion angles ϕ_5 and ϕ_6 are defined are indicated by heavy lines. ϕ_5 is in the lower and ϕ_{10} in the upper half of the stereoplots. (from ref. [123]).

A second study concentrated on the dynamics of ring puckering of the four proline residues in antamanide.[122] The conformation of the five-ring systems can be determined from the dihedral angles χ_1, χ_2 and χ_3 which in turn can be deduced from the vicinal proton–proton J-coupling constants using the Karplus relations.[54] The relevant coupling constants (21 per residue) were determined from E. COSY spectra. Based on these measurements, a model was constructed for each of the proline residues by least-squares fitting. It was found that for Pro^3 and Pro^8 a good fit can be obtained with a single rigid conformation, while for Pro^2 and Pro^7 two rapidly exchanging conformations were required to reduce the fitting error to within an acceptable range. At the same time, measurements of the ^{13}C relaxation time confirmed that Pro^3 and Pro^8 are rigid, while Pro^2 and Pro^7 show dynamic behavior with correlation times between 30 and 40 ps. This implies that the dynamics of the peptide ring and the proline ring are not correlated and proceed on entirely different time scales. The two exchanging conformations found for Pro^2 are shown in Figure 27. It is seen that the conformational changes resemble the up and down movements of the "flap of the envelope" (C_γ).

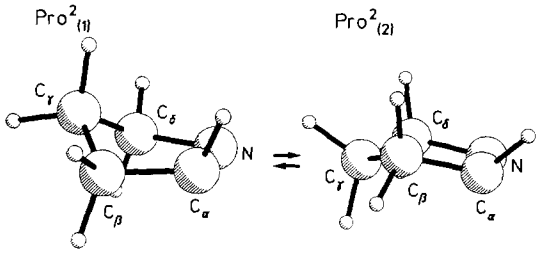

Fig. 27. The two experimentally determined conformations of the amino acid residue Pro^2 in antamanide (**1**) (see ref. [122]).

Magnetic Resonance Fourier Imaging

Magnetic resonance imaging (MRI) has had an enormous impact on medical diagnosis and has rapidly become a powerful routine tool. The basic procedure for recording a 2D or 3D NMR image of an object is attributed to Paul Lauterbur.[127] A magnetic field gradient, applied along different directions in space in a sequence of experiments, produces projections of the nuclear spin density of the object onto the direction of the gradient. From a sufficiently large set of such projections it is possible to reconstruct an image of the object, for example, by filtered backprojection in analogy to X-ray tomography.

A different approach is directly related to 2D and 3D FT spectroscopy. Frequency encoding of the three spatial dimensions is achieved by a linear magnetic field gradient applied successively along three orthogonal directions for the durations t_1, t_2, and t_3, respectively, in a pulse FT experiment.[128] In full analogy to 3D spectroscopy, the time parameters t_1 and t_2 are incremented in regular intervals from experiment to experiment. The recorded signal $s(t_1, t_2, t_3)$ is Fourier-transformed in three dimensions to produce a function $S(\omega_1,\omega_2,\omega_3)$ which is equivalent to a 3D spatial image when the spatial information is decoded using the relations $x = \omega_1/g_x$, $y = \omega_2/g_y$, and $z = \omega_3/g_z$ with the three field gradients g_x, g_y, and g_z. The procedure is illustrated in Figure 28 for two dimensions.

In a further refinement, proposed by Edelstein et al.,[129] the time variables t_1 and t_2 are replaced by variable field

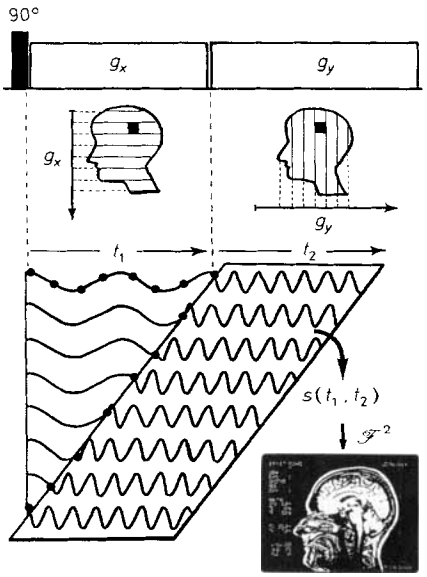

Fig. 28. Schematic representation of Fourier NMR imaging, here shown in two dimensions. Two orthogonal gradients (g_x, g_y) are applied during the t_1 and t_2 periods of a 2D experiment. A 2D Fourier transformation of the data set $s(t_1, t_2)$ produces a 2D image of the investigated subject (R.R.E.).

gradient strengths g_x and g_y applied during a constant evolution time. With regard to the accumulated phase [Eq. (20)] it

$$\gamma = x\, g_x\, t_1 + y\, g_y\, t_2 + z\, g_z\, t_3 \qquad (20)$$

is immaterial whether the evolution time or the field gradients are varied. However, keeping the time t_k constant eliminates undesired relaxation effects.

In medical imaging, 3D experiments have a natural justification, although it is sometimes simpler to apply selective excitation techniques to select a 2D slice through the object to be imaged.[130] Even extensions to higher dimensions are quite realistic. In a fourth dimension, for example, chemical shift information can be accommodated.[131] Also 2D spectroscopic information could be combined with three spatial dimensions, leading to a 5D experiment. No limitations seem to exist for human imagination. However, the practical limits will soon be reached when the required performance times are also taken into consideration.

Conclusion

I am not aware of any other field of science outside of magnetic resonance that offers so much freedom and opportunities for a creative mind to invent and explore new experimental schemes that can be fruitfully applied in a variety of disciplines. NMR spectroscopy is intellectually attractive because the observed phenomena can be understood based on a sound theory, and almost all conceits can also be tested by easy experiments. At the same time, the practical importance of NMR is enormous and can justify much of the playful activities of an addicted spectroscopist.

Most of the credit for the inspiration and execution of the work described should go to my teachers Hans Primas and Hans H. Günthard, to my supervisor Weston A. Anderson, to the inspirator Jean Jeener, and to my co-workers (in more or less chronological order): Thomas Baumann, Enrico Bartholdi, Robert Morgan, Stefan Schäublin, Anil Kumar, Dieter Welti, Luciano Müller, Alexander Wokaun, Walter P. Aue, Jiri Karhan, Peter Bachmann, Geoffrey Bodenhausen, Peter Brunner, Alfred Höhener, Andrew A. Maudsley, Kuniaki Nagayama, Max Linder, Michael Reinhold, Ronald Haberkorn, Thierry Schaffhauser, Douglas Burum, Federico Graf, Yongren Huang, Slobodan Macura, Beat H. Meier, Dieter Suter, Pablo Caravatti, Ole W. Sørensen, Lukas Braunschweiler, Malcolm H. Levitt, Rolf Meyer, Mark Rance, Arthur Schweiger, Michael H. Frey, Beat U. Meier, Marcel Müri, Christopher Councell, Herbert Kogler, Roland Kreis, Norbert Müller, Annalisa Pastore, Christian Schönenberger, Walter Studer, Christian Radloff, Albert Thomas, Rafael Brüschweiler, Herman Cho, Claudius Gemperle, Christian Griesinger, Zoltan L. Mádi, Peter Meier, Serge Boentges, Marc McCoy, Armin Stöckli, Gabriele Aebli, Martin Blackledge, Jacques Briand, Matthias Ernst, Tilo Levante, Pierre Robyr, Thomas Schulte-Herbrüggen, Jürgen Schmidt and Scott Smith. I would also like to thank my technical staff, Hansruedi Hager, Alexandra Frei, Janos A. Deli, Jean-Pierre Michot, Robert Ritz, Thomas Schneider, Markus Hintermann, Gerhard Gucher, Josef Eisenegger, Walter Lämmler and Martin Neukomm; my secretary Irène Müller; and several research groups with which I had the pleasure to collaborate, first of all the research group of Kurt Wüthrich and the group of Horst Kessler. I am grateful for support in the early days from Varian Associates and more recently from the Swiss Federal Institute of Technology, the Swiss National Science Foundation, the Kommission zur Förderung der Wissenschaftlichen Forschung, and last but not least from Spectrospin AG.

Received: January 30, 1992 [A 870]
German version: *Angew. Chem.* **1992**, 104, 817

[1] I. I. Rabi, *Phys. Rev.* **1937**, *51*, 652.
[2] I. I. Rabi, J. R. Zacharias, S. Millman, P. Kusch, *Phys. Rev.* **1938**, *53*, 318; I. I. Rabi, S. Millman, P. Kusch, J. R. Zacharias, *ibid.* **1939**, *55*, 526.
[3] J. M. B. Kellogg, I. I. Rabi, N. F. Ramsey, J. R. Zacharias, *Phys. Rev.* **1939**, *55*, 318; *ibid.* **1939**, *56*, 728; *ibid.* **1940**, *57*, 677.
[4] E. M. Purcell, H. G. Torrey, R. V. Pound, *Phys. Rev.* **1946**, *69*, 37.
[5] F. Bloch, W. Hansen, M. E. Packard, *Phys. Rev.* **1946**, *69*, 127.
[6] F. Bloch, *Phys. Rev.* **1946**, *70*, 460.
[7] J. Brossel, A. Kastler, C. R. Hebd. Seances Acad. Sci. **1949**, *229*, 1213; A. Kastler, *J. Phys. Radium* **1950**, *11*, 255.
[8] R. R. Ernst, G. Bodenhausen, A. Wokaun, *Principles of NMR in One and Two Dimensions*, Clarendon Press, Oxford, **1987**.
[9] A. Bax, *Two-Dimensional NMR in Liquids*, Delft University Press, Reidel, Dortrecht, **1982**.
[10] Attur-ur Rahman, *Nuclear Magnetic Resonance, Basic Principles*, Springer, New York, **1986**.
[11] N. Chandrakumar, S. Subramanian, *Modern Techniques in High-Resolution FT-NMR*, Springer, New York, **1987**.
[12] H. Friebolin, *Ein- und zweidimensionale NMR-Spektroskopie*, VCH, Weinheim, **1988**; *Basic One- and Two-Dimensional NMR Spectroscopy*, VCH, Weinheim, **1991**.
[13] G. E. Martin, A. S. Zektzer, *Two-Dimensional NMR Methods for Establishing Molecular Connectivity*, VCH, Weinheim, **1988**.
[14] J. Schraml, J. M. Bellama, *Two-Dimensional NMR Spectroscopy*, Wiley Interscience, New York, **1988**.
[15] *Pulse Methods in 1D and 2D Liquid-Phase NMR* (Ed.: W. S. Brey), Academic Press, New York, **1988**.
[16] A. A. Michelson, *Philos. Mag. Ser. 5* **1981**, *31*, 256; A. A. Michelson, *Light Waves and Their Uses*, University of Chicago Press, Chicago, **1902**.
[17] P. Fellgett, Dissertation, Cambridge University, **1951**; P. Fellgett, *J. Phys. Radium* **1958**, *19*, 187.
[18] *Varian Associates Magazine* **1979**, *24*, (7), 11; *IEEE Center for the History of Electrical Engineering Newsletter* **1990**, (24), 2.
[19] R. R. Ernst, W. A. Anderson, *Rev. Sci. Instrum.* **1966**, *37*, 93.
[20] R. R. Ernst, *Adv. Magn. Reson.* **1966**, *2*, 1.
[21] W. A. Anderson, R. R. Ernst, US-A 3475680 (Impulse Resonance Spectrometer Including a Time Averaging Computer and a Fourier Analyzer), **1969** (submitted May 26, 1965).

[22] R. R. Ernst in *The Applications of Computer Techniques in Chemical Research*, The Institute of Petroleum, London, **1972**, p. 61.
[23] O. W. Sørensen, G. W. Eich, M. H. Levitt, G. Bodenhausen, R. R. Ernst, Prog. Nucl. Magn. Reson. Spectrosc. **1983**, *16*, 163.
[24] J. B. J. Fourier, *Theorie analytique de la chaleur*, Firmin Didot, Père et fils, Paris, **1822**.
[25] I. J. Lowe, R. E. Norberg, *Phys. Rev.* **1957**, *107*, 46.
[26] N. Wiener, *Mass. Inst. Technol. Res. Lab. Radiation Rep.* **1942** (V) 16 S; *Nonlinear Problems in Random Theory*, Wiley, New York, **1958**.
[27] R. H. Varian, US-A 3287629 (Gyromagnetic Resonance Methods and Apparatus), **1966** (submitted August 29, 1956).
[28] H. Primas, *Helv. Phys. Acta* **1961**, *34*, 36.
[29] R. R. Ernst, H. Primas, *Helv. Phys. Acta* **1963**, *36*, 583.
[30] R. R. Ernst, *J. Chem. Phys.* **1966**, *45*, 3845.
[31] R. R. Ernst, *Mol. Phys.* **1969**, *16*, 241.
[32] R. Kaiser, *J. Magn. Reson.* **1970**, *3*, 28.
[33] R. R. Ernst, *J. Magn. Reson.* **1970**, *3*, 10.
[34] D. Ziessow, B. Blümich, *Ber. Bunsenges. Phys. Chem.* **1974**, *78*, 1169; B. Blümich, D. Ziessow, *J. Chem. Phys.* **1983**, *78*, 1059.
[35] B. Blümich, *Bull. Magn. Reson.* **1985**, *7*, 5.
[36] J. Dadok, R. F. Sprecher, *J. Magn. Reson.* **1974**, *13*, 243.
[37] R. K. Gupta, J. A. Ferretti, E. D. Becker, *J. Magn. Reson.* **1974**, *13*, 275.
[38] J. A. Ferretti, R. R. Ernst, *J. Chem. Phys.* **1976**, *65*, 4283.
[39] B. L. Tomlinson, H. D. W. Hill, *J. Chem. Phys.* **1973**, *59*, 1775.
[40] M. H. Levitt, R. Freeman, *J. Magn. Reson.* **1979**, *33*, 473.
[41] M. H. Levitt, *Prog. Nucl. Magn. Reson. Spectrosc.* **1986**, *18*, 61.
[42] R. L. Vold, J. S. Waugh, M. P. Klein, D. E. Phelps, *J. Chem. Phys.* **1968**, *48*, 3831.
[43] R. Freeman, H. D. W. Hill in *Dynamic NMR Spectroscopy* (Eds.: L. M. Jackman, F. A. Cotton), *Academic Press*, New York, **1975**, S. 131.
[44] S. Forsén, R. A. Hoffman, *J. Chem. Phys.* **1963**, *39*, 2892.
[45] H. C. Torrey, *Phys. Rev.* **1949**, *75*, 1326; *ibid.* **1949**, *76*, 1059.
[46] E. L. Hahn, *Phys. Rev.* **1949**, *76*, 145.
[47] E. L. Hahn, *Phys. Rev.* **1950**, *80*, 297.
[48] E. L. Hahn, *Phys. Rev.* **1950**, *80*, 580.
[49] M. Emshwiller, E. L. Hahn, D. Kaplan, *Phys. Rev.* **1960**, *118*, 414.
[50] S. R. Hartmann, E. L. Hahn, *Phys. Rev.* **1962**, *128*, 2042.
[51] M. B. Comisarow, A. G. Marshall, *Chem. Phys. Lett.* **1974**, *25*, 282; *ibid.* **1974**, *26*, 489.
[52] J. C. McGurk, H. Mäder, R. T. Hofmann, T. G. Schmalz, W. H. Flygare, *J. Chem. Phys.* **1974**, *61*, 3759.
[53] For example, M. K. Bowman in *Modern Pulsed and Continuous-Wave Electron Spin Resonance* (Eds.: L. Kevan, M. K. Bowman), J. Wiley, New York, **1990**, p. 1.
[54] M. Karplus, *J. Chem. Phys.* **1959**, *30*, 11.
[55] J. H. Noggle, R. E. Schirmer, *The Nuclear Overhauser Effect*, Academic Press, New York, **1971**.
[56] K. Wüthrich, *NMR of Proteins and Nucleic Acids*, Wiley Interscience, New York, **1986**.
[57] S. Yatsiv, *Phys. Rev.* **1952**, *113*, 1522.
[58] W. A. Anderson, R. Freeman, *J. Chem. Phys.* **1962**, *37*, 85.
[59] R. Freeman, W. A. Anderson, *J. Chem. Phys.* **1962**, *37*, 2053.
[60] R. A. Hoffman, S. Forsén, *Prog. Nucl. Magn. Reson. Spectrosc.* **1966**, *1*, 15.
[61] J. Jeener, *Ampère International Summer School* (Basko Polje, Yugoslavia) **1971**, unpublished.
[62] R. R. Ernst, *VIth International Conference on Magnetic Resonance in Biological Systems* (Kandersteg, Switzerland) **1974**, unpublished.
[63] W. P. Aue, E. Bartholdi, R. R. Ernst, *J. Chem. Phys.* **1976**, *64*, 2229.
[64] J. Jeener, B. H. Meier, R. R. Ernst, *J. Chem. Phys.* **1979**, *71*, 4546.
[65] B. H. Meier, R. R. Ernst, *J. Am. Chem. Soc.* **1979**, *101*, 6641.
[66] S. Macura, R. R. Ernst, *Mol. Phys.* **1980**, *41*, 95.
[67] Anil Kumar, R. R. Ernst, K. Wüthrich, *Biochem. Biophys. Res. Commun.* **1980**, *95*, 1.
[68] M. P. Williamson, T. F. Havel, K. Wüthrich, *J. Mol. Biol.* **1985**, *182*, 295.
[69] A. D. Kline, W. Braun, K. Wüthrich, *J. Mol. Biol.* **1986**, *189*, 377.
[70] B. A. Messerle, A. Schäffer, M. Vasák, J. H. R. Kägi, K. Wüthrich, *J. Mol. Biol.* **1990**, *214*, 765.
[71] G. Otting, Y. Q. Qian, M. Billeter, M. Müller, M. Affolter, W. J. Gehring, K. Wüthrich, *EMBO J.* **1990**, *9*, 3085.
[72] T. F. Haveland, K. Wüthrich, *Bull. Math. Biol.* **1984**, *46*, 673.
[73] W. Braun, N. Gō, *J. Mol. Biol.* **1985**, *186*, 611.
[74] R. Kaptein, E. R. P. Zuiderweg, R. M. Scheek, R. Boelens, W. F. van Gunsteren, *J. Mol. Biol.* **1985**, *182*, 179.
[75] G. M. Clore, A. M. Gronenborn, A. T. Brünger, M. Karplus, *J. Mol. Biol.* **1985**, *186*, 435.
[76] Y. Huang, S. Macura, R. R. Ernst, *J. Am. Chem. Soc.* **1981**, *103*, 5327.
[77] G. W. Eich, G. Bodenhausen, R. R. Ernst, *J. Am. Chem. Soc.* **1982**, *104*, 3731.
[78] P. H. Bolton, G. Bodenhausen, *Chem. Phys. Lett.* **1982**, *89*, 139.
[79] The spectra were recorded by C. Griesinger; see R. R. Ernst, *Chimia* **1987**, *41*, 323.
[80] L. Braunschweiler, R. R. Ernst, *J. Magn. Reson.* **1983**, *53*, 521.
[81] D. G. Davis, A. Bax, *J. Am. Chem. Soc.* **1985**, *107*, 2821.
[82] A. A. Bothner-By, R. L. Stephens, J. Lee, C. O. Warren, R. W. Jeanloz, *J. Am. Chem. Soc.* **1984**, *106*, 811.
[83] R. Brüschweiler, B. Roux, M. Blackledge, C. Griesinger, M. Karplus, R. R. Ernst, *J. Am. Chem. Soc.* **1992**, *114*, 2289.
[84] C. Griesinger, G. Otting, K. Wüthrich, R. R. Ernst, *J. Am. Chem. Soc.* **1988**, *110*, 7870.
[85] J. Briand, R. R. Ernst, *Chem. Phys. Lett.* **1991**, *185*, 276.
[86] S. Vega, T. W. Shattuck, A. Pines, *Phys. Rev. Lett.* **1976**, *37*, 43.
[87] S. Vega, A. Pines, *J. Chem. Phys.* **1977**, *66*, 5624.
[88] A. Wokaun, R. R. Ernst, *Mol. Phys.* **1978**, *36*, 317.
[89] L. Braunschweiler, G. Bodenhausen, R. R. Ernst, *Mol. Phys.* **1983**, *48*, 535.
[90] A. Bax, R. Freeman, S. P. Kempsell, *J. Am. Chem. Soc.* **1980**, *102*, 4849.
[91] A. Bax, R. Freeman, S. P. Kempsell, *J. Magn. Reson.* **1980**, *41*, 349.
[92] U. Piantini, O. W. Sørensen, R. R. Ernst, *J. Am. Chem. Soc.* **1982**, *104*, 6800.
[93] N. Müller, G. Bodenhausen, K. Wüthrich, R. R. Ernst, *J. Magn. Reson.* **1985**, *65*, 531.
[94] C. Radloff, R. R. Ernst, *Mol. Phys.* **1989**, *66*, 161.
[95] A. Wokaun, R. R. Ernst, *Chem. Phys. Lett.* **1977**, *52*, 407.
[96] G. Bodenhausen, H. Kogler, R. R. Ernst, *J. Magn. Reson.* **1984**, *58*, 370.
[97] M. H. Levitt, R. R. Ernst, *Chem. Phys. Lett.* **1983**, *100*, 119.
[98] M. H. Levitt, R. R. Ernst, *J. Chem. Phys.* **1985**, *83*, 3297.
[99] C. Griesinger, O. W. Sørensen, R. R. Ernst, *J. Am. Chem. Soc.* **1985**, *107*, 6394.
[100] C. Griesinger, O. W. Sørensen, R. R. Ernst, *J. Chem. Phys.* **1986**, *85*, 6837.
[101] C. Griesinger, O. W. Sørensen, R. R. Ernst, *J. Magn. Reson.* **1987**, *75*, 474.
[102] A. Bax, R. Freeman, *J. Magn. Reson.* **1981**, *44*, 542.
[103] B. U. Meier, R. R. Ernst, *J. Magn. Reson.* **1988**, *79*, 540.
[104] A. A. Maudsley, R. R. Ernst, *Chem. Phys. Lett.* **1977**, *50*, 368.
[105] G. Bodenhausen, R. Freeman, *J. Magn. Reson.* **1977**, *28*, 471.
[106] L. Müller, *J. Am. Chem. Soc.* **1979**, *101*, 4481.
[107] M. Ernst, C. Griesinger, R. R. Ernst, W. Bermel, *Mol. Phys.* **1991**, *74*, 219.
[108] M. H. Levitt, O. W. Sørensen, R. R. Ernst, *Chem. Phys. Lett.* **1983**, *94*, 540.
[109] H. Kogler, O. W. Sørensen, G. Bodenhausen, R. R. Ernst, *J. Magn. Reson.* **1983**, *55*, 157.
[110] H. D. Plant, T. H. Mareci, M. D. Cockman, W. S. Brey, *27th Experimental NMR Conference* (Baltimore, MA, USA), **1986**.
[111] G. W. Vuister, R. Boelens, *J. Magn. Reson.* **1987**, *73*, 328.
[112] C. Griesinger, O. W. Sørensen, R. R. Ernst, *J. Magn. Reson.* **1987**, *73*, 574.
[113] C. Griesinger, O. W. Sørensen, R. R. Ernst, *J. Am. Chem. Soc.* **1987**, *109*, 7227.
[114] H. Oschkinat, C. Griesinger, P. Kraulis, O. W. Sørensen, R. R. Ernst, A. M. Gronenborn, G. M. Clore, *Nature* **1988**, *332*, 374.
[115] G. W. Vuister, R. Boelens, R. Kaptein, *J. Magn. Reson.* **1988**, *80*, 176.
[116] C. Griesinger, O. W. Sørensen, R. R. Ernst, *J. Magn. Reson.* **1989**, *84*, 14.
[117] E. R. P. Zuiderweg, S. W. Fesik, *Biochemistry* **1989**, *28*, 2387.
[118] D. Marion, P. C. Driscoll, L. E. Kay, P. T. Wingfield, A. Bax, A. M. Gronenborn, G. M. Clore, *Biochemistry* **1989**, *28*, 6150
[119] S. Boentges, B. U. Meier, C. Griesinger, R. R. Ernst, *J. Magn. Reson.* **1989**, *85*, 337.
[120] O. W. Sørensen, *J. Magn. Reson.* **1990**, *89*, 210.
[121] L. E. Kay, G. M. Clore, A. Bax, A. M. Gronenborn, *Science* **1990**, *249*, 411.
[122] Z. L. Mádi, C. Griesinger, R. R. Ernst, *J. Am. Chem. Soc.* **1990**, *112*, 2908.
[123] R. Brüschweiler, M. Blackledge, R. R. Ernst, *J. Biomol. NMR* **1991**, *1*, 3.
[124] W. Burgermeister, T. Wieland, R. Winkler, *Eur. J. Biochem.* **1974**, *44*, 311.
[125] H. Kessler, M. Klein, A. Müller, K. Wagner, J. W. Bats, K. Ziegler, M. Frimmer, *Angew. Chem.* **1986**, *98*, 1030; *Angew. Chem. Int. Ed. Engl.* **1986**, *25*, 997; H. Kessler, A. Müller, K. H. Pook, *Liebigs Ann. Chem.* **1989**, 903; H. Kessler, J. W. Bats, J. Lautz, A. Müller, *Liebigs Ann. Chem.* **1989**, *913*; J. Lautz, H. Kessler, W. F. van Gunsteren, H. J. Berendsen, R. M. Scheek, R. Kaptein, J. Blaney, *Proc. 20th Eur. Pept. Symp.* **1989**, 438 (Eds. G. Jung, E. Bayer).
[126] R. R. Ernst, M. Blackledge, S. Boentges, J. Briand, R. Brüschweiler, M. Ernst, C. Griesinger, Z. L. Mádi, T. Schulte-Herbrüggen, O. W. Sørensen in *Proteins, Structure, Dynamics, Design* (Eds.: V. Renugopalakrishnan, P. R. Carey, I. C. P. Smith, S. G. Huang, A. C. Storer), ESCOM, Leiden, **1991**.
[127] P. C. Lauterbur, *Nature* **1973**, *242*, 190.
[128] Anil Kumar, D. Welti, R. R. Ernst, *J. Magn. Reson.* **1975**, *18*, 69.
[129] W. A. Edelstein, J. M.S. Hutchison, G. Johnson, T. W. Redpath, *Phys. Med. Biol.* **1980**, *25*, 751.
[130] P. Mansfield, A. A. Maudsley, T. Baines, *J. Phys. E 9*, **1976**, 271.
[131] P. C. Lauterbur, D. M. Kramer, W. V. House, C.-N. Chen, *J. Am. Chem. Soc.* **1975**, *97*, 6866.

Ion Channels for Communication Between and Within Cells (Nobel Lecture)**

By Erwin Neher

The fundamental signal mechanisms for communication between cells of the nervous system were known around 1970. Hodgkin and Huxley[1] had already provided the basis for an understanding of the nerve action potential in 1952. The concept of chemical transmission at synapses had also been experimentally verified by detailed studies on excitatory and inhibitory postsynaptic potentials (see B. Katz[2] for a concise description of the electrical signals in nerve and muscle). The question of the molecular mechanisms underlying these signals was still open, however. Hodgkin and Huxley used the concept of voltage-operated gates for a formal description of conductance changes, and by 1970 the terms Na channel and K channel were used frequently (see review by Hille[3]), although no direct evidence for the existence of channels was available from biological preparations. This was different in the case of artificial membranes. Müller and Rudin[4] introduced 'black-lipid membranes' as experimental model systems, which in many respects resemble the bimolecular lipid membrane of living cells. These membranes are rather good insulators. However, when they are doped with certain antibiotics or proteins they become electrically conductive. R. C. Bean et al.[5] and Hladky and Haydon[6] showed that some of these dopants induce discrete, step-like changes in conductance when they are added in trace amounts. All the evidence suggested that the changes observed in the conductance represent the insertion of single pore-like structures into the membranes.

Similar measurements on biological membranes were not possible at the time, since the methods available for recording currents in living cells typically had background noise levels higher by about a factor of a hundred than the 'single-channel currents' observed in bilayers (see Fig. 1). Indirect methods, however, provided strong evidence that channels similar in conductance to those in artificial membranes should be operative in nerve and muscle cells. Early attempts to count the number of Na channels by tetrodotoxin binding indicated that the contribution of a single channel to Na conductance might be as much as 500 pS. Later, the technique of noise analysis[7, 8] provided more accurate numbers. Anderson and Stevens[9] estimated the conductance contribution of single acetylcholine-activated channels (ACh channels) at the frog neuromuscular junction to be 32 pS. This is close to the conductance of single gramicidin channels as measured by Hladky and Haydon.[6] Thus, it was very tempting to think about better methods for recording currents from biological preparations. There was good reason to hope that an improved technology would reveal a whole 'microcosmos' of electrical signals in a multitude of electrically and chemically excitable cell types. In this lecture I will give a short account of our joint effort to solve this problem, and then focus on further developments to which the solution of the problem led. Bert Sakmann, in the second lecture,[10] will present some of the detailed knowledge that high-resolution current recording provides access to.

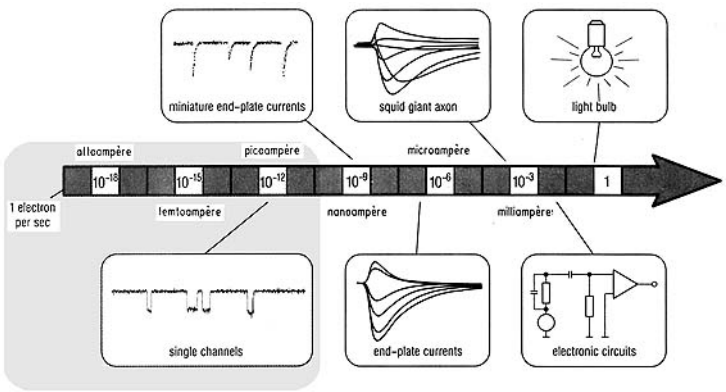

Fig. 1. A graphical representation of the quantity 'current' on a logarithmic scale with representative examples of current signals or current-carrying elements from electronics and biology. The shaded region is that which was dominated by background noise before the development of the patch clamp technique.

Rationale for Using 'Patch Pipettes'

A basic limitation for any current measurement, disregarding instrumentation noise, is the 'Johnson' or thermal noise of the signal source, which for a simple resistor is given by $\sigma_n = \sqrt{4kT\Delta f/R}$ where σ_n is the root-mean-square deviation of the current, k is the Boltzmann constant, T the absolute temperature, Δf the measurement bandwidth, and R the resistance. From this, it is clear that the internal resistance of a signal source (or, more generally, the complex impedance) should be very high for low-noise current recording. Specifically, to record a current of 1 pA at a bandwidth of 1 kHz with 10% accuracy, the internal resistance of the signal source should be about 2 GΩ or higher. We now know that the input resistances of small cells can be as high as that. But early in the seventies the conventional microelectrode techniques required large cells for reliable current measurements, and these typically had input resistances in the range 100 kΩ to 50 MΩ. Thus, it seemed impossible to reach the required resolution with standard techniques and standard preparations. What was required, was a smaller signal source.

With these considerations in mind, we directed our efforts to isolate a small patch of membrane for the purpose of the electrical measurement. I had gained experience with suction pipettes being placed onto the surface of cells for local current measurement in H. D. Lux's laboratory in Munich, where I did my doctoral thesis. Such pipettes had been used before in various contexts for either stimulation of cells or for current measurements.[11–15] It was clear to us, that they should be good tools for single-channel measurements, if

[*] Prof. Dr. E. Neher
Max-Planck-Institut für Biophysikalische Chemie
Postfach 2841, D-W-3400 Göttingen (FRG)

[**] Copyright © The Nobel Foundation 1992. – We thank the Nobel Foundation for permission to print this lecture.

only the 'pipette-to-membrane seal' could be made good enough. The impedance of the patch itself should be higher than required, even for a patch as large as 10 μm in diameter. An incomplete seal, however, is 'seen' by the measuring amplifier in parallel to the patch, and its noise is superimposed onto the patch signal.

Early Single-Channel Measurements

When Bert Sakmann and I started measurements by placing pipettes onto the surface of denervated muscle fibers, we soon realized that it was not so easy to obtain a satisfactory 'seal'. Although Bert Sakmann was very experienced in enzymatically treating cell surfaces through his work in B. Katz's laboratory, and although the work of Katz and Miledi[7] and our own voltage-clamp measurements had shown that denervated muscle should have an appropriate density of diffusely dispersed ACh channels, our initial attempts failed. Our seal resistances were just about 10–20 MΩ, two orders of magnitude lower than desired. However, by reducing the pipette size, and by optimizing its shape we slowly arrived at a point where signals emerged from the background—first some characteristic noise, later on blips which resembled square pulses, as expected. In 1976 we published recordings[16] which, with good confidence, could be interpreted as single-channel currents (see Fig. 2). The fact that similar recordings could be obtained both in our Göttingen laboratory and in Charles F. Stevens' laboratory at Yale, (where I spent parts of 1975 and 1976), gave us confidence that they were not the result of some local demon, but rather signals of biological significance. The square-wave nature of the signals was proof of the hypothesis that channels in biological membranes open and close stochastically in an all-or-none manner. For the first time one could watch conformational changes of biological macromolecules in situ and in real time. However, the measurement was far from perfect. There still was excessive background noise, concealing small and more short-lived contributions of other channel types. Besides, the amplitudes of single-channel currents had a wide distribution, since the majority of channels were located under the rim of the pipette, such that their current contributions were recorded only partially.

We made many systematic attempts to overcome the seal problem (manipulating and cleaning cell surfaces, coating

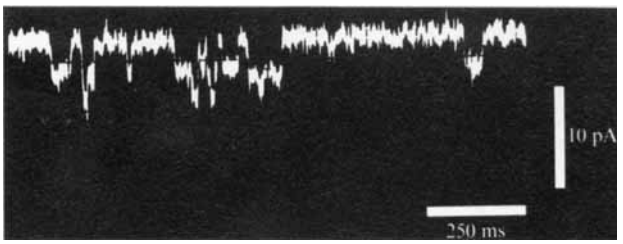

Fig. 2. Early single-channel currents from denervated frog (*Rana pipiens*) cutaneous pectoris muscle. The pipette contained 0.2 μM suberoyldicholine, an analogue of acetylcholine which induces very long-lived channel openings. Membrane potential −120 mV; temperature 8 °C (from [16]).

pipette surfaces, reversing charges on the glass surface etc.) with little success. Nevertheless, some important properties of single channels could be elucidated in the years 1975 to 1980.[17–21]

By about 1980 we had almost given up our attempts to improve the seal, when we noticed by chance, that the seal suddenly increased by more that two orders of magnitude when slight suction was applied to the pipette. The resulting seal was in the gigaohm range, the so-called 'gigaseal'. It turned out that a gigaseal could be obtained reproducibly when suction was combined with some simple measures to provide for clean surfaces, such as using a fresh pipette for each approach and using filtered solutions. The improved seal resulted in much improved background noise.[26] Fortunately, Fred Sigworth had just joined the laboratory. With his experience in engineering he improved the electronic amplifiers to match the advances in recording conditions. Thus, several types of ion channels could rapidly be characterized at good amplitude and time resolution (Fig. 3).

Unexpected Benefits

Solving the seal problem turned out not only to be a matter of improving the electrical recording, but also of providing useful tools for manipulating patches and small cells. Although the physical nature of the 'Gigaseal' is still unknown, we soon realized that it provides not only electrical stability but also a tight mechanical connection between the measuring glass pipette and the membrane. Owen Hamill and Bert Sakmann,[24] simultaneously with Horn and Patlak,[25] found that patches could be removed from cells, by

Erwin Neher, born on March 20, 1944 in Landsberg/Lech, Germany, studied physics at the Technischen Universität München (TUM) and the University of Wisconsin, USA. In 1970 he received his doctorate under the direction of H. D. Lux at the Max-Planck-Institut (MPI) für Psychiatrie and the TUM. After three years as Wissenschaftlicher Assistent at the MPI für Psychiatrie he moved to the MPI für biophysikalische Chemie in Göttingen. He obtained his Habilitation in 1980 in the Faculty of Physics at the Universität Göttingen and has been director at the MPI für biophysikalische Chemie since April 1983. Many distinctions have been conferred on him among them the Nernst-Haber-Bodenstein Prize of the Bunsen-Gesellschaft für Physikalische Chemie (1977), the Gottfried-Wilhelm-Leibniz Prize of the Deutsche Forschungsgemeinschaft (1986), and the Nobel Prize for medicine and physiology (1991). He is member of several academics, including the National Academy of Sciences of the USA and the Akademie der Wissenschaften zu Göttingen.

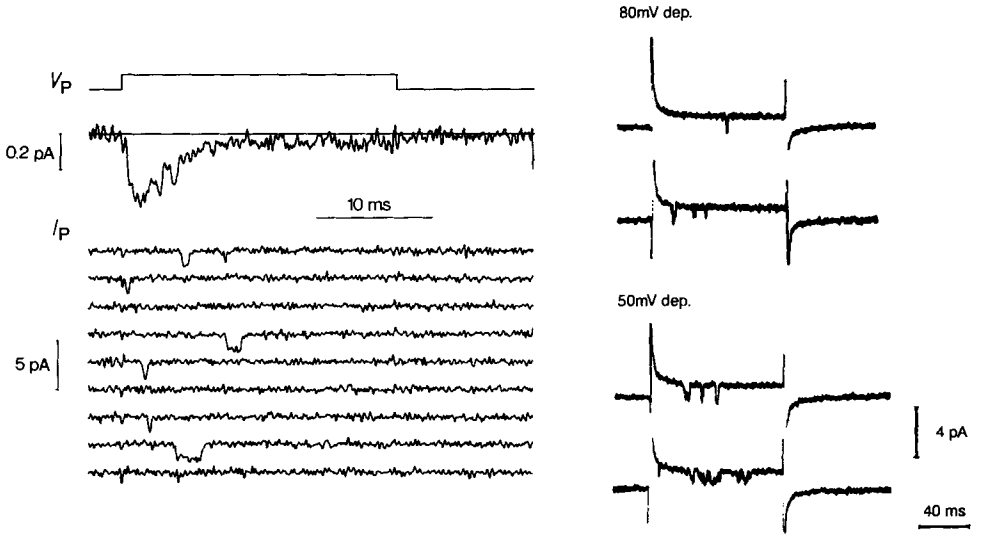

Fig. 3. Early recordings of voltage-activated single channels. The left side shows Na channels (adapted from [22]). The top trace is the voltage protocol. The second trace shows the average response from 300 voltage pulse depolarizations, and the following traces give examples of individual responses. It is seen that in some – but not in all – traces there are individual openings (downward deflection) of Na channels. The patch was hyperpolarized by 30 mV with respect to the rest potential and stimulated with depolarizing pulses of 40 mV. The right side shows individual Ca-channel currents (adapted from [23]). Depolarizing pulses (dep.) as indicated were given from normal resting potential. The pipette contained isotonic Ba solution. Single channel responses are seen superimposed onto a residual capacitive and leak artifact. In the left panel these artifacts were digitally subtracted.

simply withdrawing the pipette. This results in 'excised patches', which are accessible for solution changes from both sides. Alternatively, a patch can be ruptured by a short pulse of suction or voltage without loss of the glass-to-membrane seal. Thus, an electrical connection is established between measuring pipette and cell, with the pipette-cell assembly well insulated against the outside bath. This configuration was termed 'whole-cell recording'. Figure 4 gives a schematic representation of the different procedures and resulting configurations.[26]

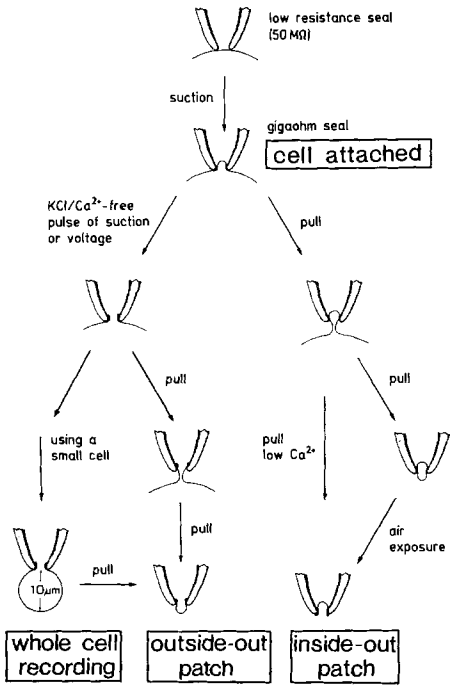

Fig. 4. Schematic representation of the procedures that lead to the different patch clamp configurations (from [26]).

Whole-cell recording is very similar to conventional microelectrode impalement, with, however, some important differences:

1. The leak between cell interior and bath is extremely small, such that this form of penetration is tolerated by cells as small as red blood cells.[27]

2. The electrical access resistance is low (1–10 MΩ) in comparison to that of impalement electrodes (typically 20–100 MΩ for small cells). Thus, voltage-clamp conditions are achieved easily without feedback circuits and additional electrodes, if small cells are used (membrane resistance 100 MΩ–10 GΩ).

3. There is rapid diffusional exchange and equilibration between patch pipette and cell.[28, 29] This provides control over the composition of the medium inside the cell. A cell can easily be loaded with ions, chelators, secondary messengers, fluorescent probes etc., simply by including these substances in the measuring pipette. However, this exchange also implies that the internal milieu is disturbed, and that signaling cascades may be disrupted (see below).

With these properties, 'whole-cell recording' evolved to be the method of choice for recording from most cell-culture preparations and from acutely dissociated tissues. Many cell types, particularly small cells of mammalian origin, became accessible to biophysical analysis for the first time through whole-cell recording, since they would not tolerate multiple conventional impalements. Individual current types could be separated through control of solution composition on both sides of the membrane[30] (see Fig. 5 for an example of whole-cell Ca-channel currents). This development shifted the emphasis of electrophysiological studies away from large-celled preparations, which usually were of invertebrate origin, towards mammalian and human cell types. In the first half of 1981, just before we first published a whole-cell characterization of a small mammalian cell (bovine adrenal chromaffin cells) only five out of fourteen voltage-clamp

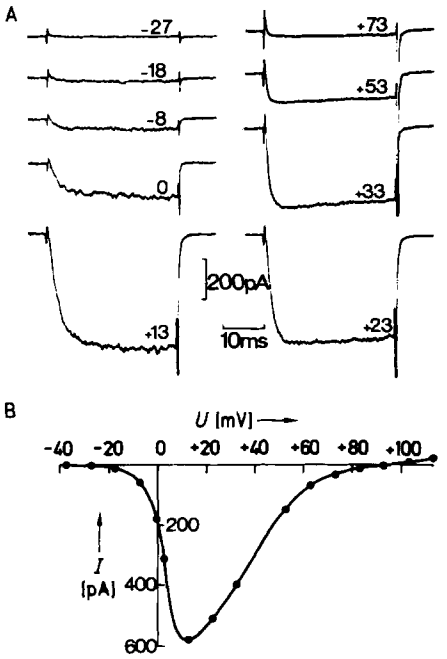

Fig. 5. Whole-cell membrane currents in chromaffin cells bathed in isotonic Ba solution plus 20 $\mu g\,mL^{-1}$ TTX (tetrodextrin). The membrane potential was stepped to values as indicated from a holding potential of −67 mV. The pipette solution contained mainly CsCl and TEA (tetraethylammonium ions). With this solution composition the currents flowing are predominantly carried by Ca channels. Part B shows the current-voltage relationship (from [30]). U = membrane potential, I = plateau current.

studies in the Journal of Physiology were performed on cells of mammalian origin. The first 1991 issue of the same journal alone contained ten voltage-clamp studies on mammalian cells, none on invertebrates, and all using either the whole-cell or single-channel recording techniques.

Disturbing Secondary Messenger Equilibria

All measurement techniques have to deal with a conflict with respect to their objectives. In some instances, one wants to observe a process, disturbing it as little as possible; in other instances one would like to obtain quantitative data under as much experimental control as possible. The two aims are, of course, mutually exclusive. The cell-attached measurement comes close to the first ideal, since it leaves the cell largely intact, and allows one to observe channels open and close, or to record action potentials extracellularly.[31] Excised patches constitute the other extreme, where membrane patches are removed from their natural environment for optimal control of solution composition on both sides of the membrane. The whole-cell recording method is at an intermediate position in this respect. It does provide excellent control over membrane potential, if cells smaller than 20 μm in diameter are used. However, the chemical composition of the internal medium is neither undisturbed, nor is it under good control. We found that small mobile ions typically exchange by diffusion between pipette and cell in a few seconds (for cells of approximately 15 μm diameter and pipettes of 2–5 MΩ resistance). Molecules of intermediate size, like secondary messengers, typically 'wash-out' or 'load' into cells within 10 seconds to a minute, and small regulatory proteins may take several minutes and longer for complete equilibrium.[29]

In retrospect, it seems fortunate that we started our measurements with ACh channels and Na channels, which happen to be relatively robust with regard to diffusible regulatory components. Thus, we initially avoided complications of 'channel modulation'. However, when switching to channels which now are known to be subject to modulation by secondary messengers, G proteins and phosphorylation (such as Ca channels), we soon realized that channel activity would disappear rapidly as a result of the perturbation imposed by the measurement, both in 'whole-cell' and, more so, in excised-patch measurements.[30] Such 'washout' had been observed earlier in studies on dialyzed giant neurones.[32] The prototype of a channel modulated by an intracellular secondary messenger, the Ca-activated K^+ channel was characterized by Alain Marty in 1981. These early studies already showed the ambivalent nature of the new tools: On the one hand there was the advantage of control over intracellular calcium to elucidate the mechanism of Ca modulation. On the other hand there was the loss of cellular function due to the loss of regulators, which at that time were unknown. Subsequently, ingenious use of these tools by many laboratories has revealed a whole network of interactions between channels, secondary messengers, G proteins, and other regulatory proteins (see review by Hille[34]). In order to uncover this network it was necessary not only to record electrically from cells, but also to control or change systematically the concentrations of secondary messengers.[33,35–37] Later on it became possible to impose step-like changes in regulators using caged compounds,[38] or to load cells with fluorescent indicator dyes[39] and regulatory proteins.[40]

All this was made possible by utilizing diffusional exchange between patch pipette and cell or by exposing the cytoplasmic surface of excised patches. Later, ways were found to avoid the adverse effects of 'washout' by making the patch selectively permeable to small ions.[41,42] This technique, at present, seems to be the least invasive method to study the functioning of small cells.

An Electrophysiological Approach to the Study of Secretion

An outstanding property of an electrical measurement with a gigasealed pipette is its high sensitivity. This can be used not only to record currents, but also to study the membrane electrical capacitance, which is a measure of cell surface area. It had been observed before, that membrane capacitance increases under conditions where massive exocytosis of secretory vesicles is expected to occur. Presumably, this is due to the incorporation of vesicular membrane into the plasma membrane.[43,44] The low background noise of the gigaseal measurement made it possible to resolve area changes which result from the exocytotic fusion of single vesicles. This was shown by Neher and Marty[45] for exocytosis from chromaffin cells of the adrenal medulla and by Fernandez, Neher, and Gomperts[46] for secretion of histamine from rat peritoneal mast cells. In the latter case, the granules are somewhat larger, leading to well-

resolved step-like increases in capacitance (see Fig. 6). These records show that capacitance measurement is a *high-resolution* technique. The figure also shows, however, that capacitance is not a very *specific* measure for secretion. This is evident from the fact that there is a continuous, smooth decrease in capacitance before exocytotic events show up. We found[47] that the rate of this decrease depends on the concentration of free intracellular calcium $[Ca]_i$, and that it has many properties expected for pinocytosis.

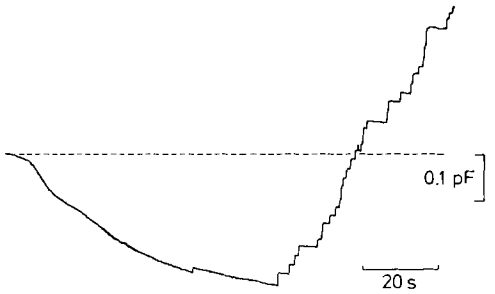

Fig. 6. High-resolution capacitance recording during the onset of a mast cell degranulation. Whole-cell recording from a rat peritoneal mast cell with a pipette containg 20 μM GTP-γ-S. Initially the capacitance slowly decreased, probably due to retrieval of very small pinocytotic vesicles. After some delay degranulation started, leading to a step-like increase in capacitance, each step representing fusion of a single granule (adapted from [47]).

We used capacitance measurement together with current recording and microfluorimetry using the indicator dye (fura-2) to simultaneously study, in a single cell, changes in $[Ca]_i$ and secretion at subsecond time resolution. We were surprised to find quite different effectiveness of regulators of secretion in different cell types (Fig. 7). For chromaffin cells, which in many respects resemble neurons, the classical role of calcium as prime regulator of secretion was fully confirmed.[49] In mast cells, however, which are not electrically excitable, changes in calcium concentration (in the physiological range) had little effect. Ca-independent secretion had been described in a number of inexcitable cell types.[50–52] But for us, who were used to working with electrically excitable cells, it was a shock not to be able to elicit secretion with an intracellular solution buffered to about 1 μM free calcium. Initially, we hypothesized, that the whole-cell configuration resulted in a loss of Ca-dependent regulators by washout – in analogy to early work on muscle contraction in skinned fibers. Later, we learned that cells in the whole-cell recording configuration were still able to secrete, in response to GTP-γ-S, a nonhydrolyzable analogue of GTP.[46] With this response in hand, it was possible to show that calcium, although not able to elicit secretion by itself, was still effective in accelerating an ongoing secretory response. There was no indication of a loss of a Ca-regulator; rather it appeared that the GTP-γ-S stimulus primed the cell to render it more Ca-sensitive.[53]

GTP-γ-S nonspecifically activates intracellular signal pathways, most prominently the dual-signal pathway.[54–55] Using the repertoire of patch clamp methods Penner[56] was able to show that various external secretagogues, which are known to also activate the dual-signal pathway, lead to a characteristic pattern of secretion. This is accompanied by

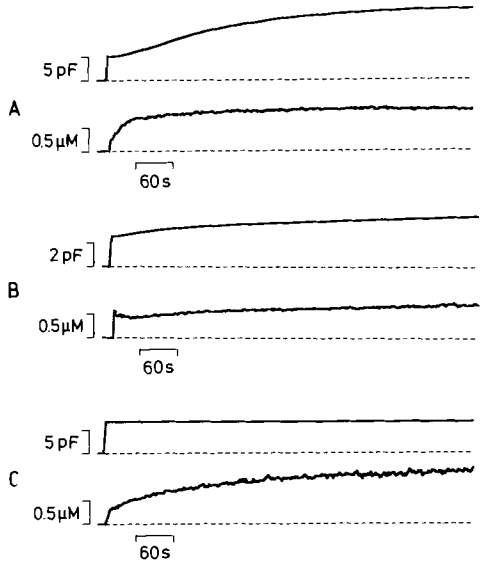

Fig. 7. Different effectiveness of intracellular free calcium in inducing a capacitance increase. Part A represents a measurement from a bovine chromaffin cell. The traces represent the time courses of capacitance (top) and free calcium concentration (bottom; measured by fura-2 fluorescence) following a whole-cell penetration. The concentration of calcium rapidly rises, since the pipette was filled with a Ca-EGTA (EGTA = ethylene glycol-bis(β-aminoethyl ether)-*N*,*N*,*N*',*N*'-tetraacetic acid) mixture adjusted for free calcium of approximately 1 μM. On the capacitance trace the step at the beginning (≈6 pF) represents the initial capacitance of the cell, which becomes 'visible' at the moment of 'break in'. Capacitance then rises about two to threefold due to exocytosis. Part B shows a similar measurement on a pancreatic beta cell, with only little capacitance increase, and part C shows the complete lack of response in a rat peritoneal mast cell (from [48]).

IP_3-induced Ca release from intracellular stores (IP_3 = insitol tris(phosphate). Combining the fura-2 technique with patch clamping one can study the temporal relationship between this prominent transient Ca signal and secretion. In spite of the modulatory effect of calcium described above it was found that there is no strict correlation. The secretory response very often starts well after the peak of the Ca signal. Also, the Ca peak can be abrogated by including EGTA in the patch pipette without drastic effects on secretion (Fig. 8). Phenomenologically this can be explained by the fact that the Ca peak occurs very early at a time when the above-mentioned priming effect of a chemical stimulus has not yet occurred. A sustained phase of increased calcium, which very often follows the Ca-release peak, is more efficient in accelerating secretion, however, since it is more appropriately timed. In terms of molecular mechanisms, the priming is likely to represent the activation of protein kinase C.[56, 58] Additionally, it has been shown that there is another G-protein-mediated pathway, which links a hormonal stimulus to secretion.[56, 59] This link is sensitive to pertussis toxin, and to intracellular application of cAMP.[56]

Our studies on mast cells (see review by Penner and Neher[60]) have taught us that secretory control is not necessarily dominated by calcium, but that rather it involves a meshwork of interacting secondary messenger pathways. In neurons, it appears that changes in calcium[61] or calcium plus voltage[62] largely determine the kinetics of fast secretory events. However, there is increasing evidence that other secondary messengers are responsible for plastic changes in synaptic signals, possibly by regulating the availability of vesicles for secretion.[63] Unfortunately nerve terminals are

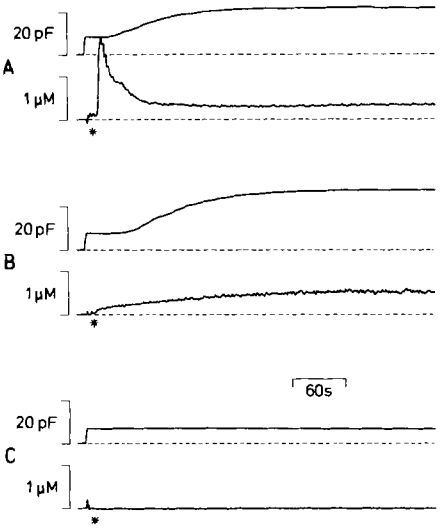

Fig. 8. Responses of mast cells to stimulation by the secretagogue compound 48/80 under different Ca-buffering conditions. The individual panels show combined capacitance calcium (fura-2) measurements similar to those of Figure 7. Panel A shows the 'unbuffered' case. No Ca-buffer was added to the pipette (except for 100 μM fura-2). A Ca transient developed in response to stimulation (asterisk). Secretion typically proceeded mainly during the falling phase of the Ca transient or following it. In panel B an EGTA/Ca mixture (10 mM) was added to the pipette which suppressed the transient, and fixed the Ca concentration to the range 200–500 nM. Nevertheless, secretion proceeded with a time course similar to case A. In panel C 10 mM EGTA was added to clamp calcium to low values. This suppressed both the Ca signal and the secretory response (from [57]).

usually not accessible to the kind of biophysical investigations as described here. However, recent studies on neurosecretory cells reveal new details on the kinetics of Ca-induced secretion.[49, 64–66] They promise to allow a differentiation between the exocytotic event per se and some of the other steps in the life cycle of a secretory vesicle. Together with the ability to control secondary messengers such studies may soon lead to a better understanding of exocytosis and of the molecular processes that direct a vesicle to its site of action.

I am deeply indebted to my teacher in electrophysiology, H. D. Lux, who focused the young physics student's mind onto ion channels, and taught me to use microscopic tools. Superb working facilities in Göttingen were provided by H. Kuhn, O. D. Creutzfeldt, and T. Jovin, who established a Young Investigators Laboratory for Bert Sakmann, F. Barrantes, and myself where we could independently pursue our goals. In more recent years my work was generously supported by a Leibniz Award of the Deutsche Forschungsgemeinschaft.

Received: January 16, 1992 [A 866 IE]
German version: *Angew. Chem.* **1992**, *104*, 837

[1] A. L. Hodgkin, A. F. Huxley, *J. Physiol.* **1952**, *117*, 500–544.
[2] Sir Bernard Katz, *Nerve, Muscle, and Synapse*, McGraw-Hill, New York, **1966**.
[3] B. Hille, *Prog. Biophys. Mol. Biol.* **1970**, *21*, 1–32.
[4] P. Müller, D. O. Rudin, *J. Theor. Biol.* **1963**, *4*, 243–280.
[5] R. C. Bean, W. C. Shepherd, H. Chan, J. T. Eichler, *J. Gen. Physiol.* **1969**, *53*, 741–757.
[6] S. B. Hladky, D. A. Haydon, *Nature (London)* **1970**, *225*, 451–453.
[7] B. Katz, R. Miledi, *J. Physiol.* **1972**, *224*, 665–700.
[8] E. Neher, C. F. Stevens, *Annu. Rev. Biophys. Bioeng.* **1977**, *6*, 345–381.
[9] C. R. Anderson, C. F. Stevens, *J. Physiol.* **1973**, *235*, 655–691.
[10] B. Sakmann, *Angew. Chem.* **1992**, *104*, 844–856; *Angew. Chem. Int. Ed. Engl.* **1992**, *31*, 830–841.
[11] F. H. Pratt, J. P. Eisenberger, *Am. J. Physiol.* **1919**, *49*, 1–54.
[12] A. Strickholm, *J. Gen. Physiol.* **1991**, *44*, 1073–1087.
[13] K. Frank, L. Tauc in *The Cellular Function of Membrane Transport* (Ed.: J. Hoffman), Prentice Hall, Engleweood Cliffs, NJ, USA, **1963**.
[14] E. Neher, H. D. Lux, *Pflügers Arch.* **1969**, *311*, 272–277.
[15] H. M. Fishman, *Proc. Natl. Acad. Sci. USA* **1973**, *70*, 876–879.
[16] E. Neher, B. Sakmann, *Nature (London)* **1976**, *260*, 799–802.
[17] E. Neher, J. H. Steinbach, *J. Physiol.* **1978**, *277*, 153–176.
[18] B. Sakmann, *Fed. Proc.* **1978**, *37*, 2654–2659.
[19] B. Sakmann, G. Boheim, *Nature (London)* **1978**, *282*, 336–339.
[20] F. Conti, E. Neher, *Nature (London)* **1980**, *285*, 140–143.
[21] B. Sakmann, J. Patlak, E. Neher, *Nature (London)* **1980**, *286*, 71–73.
[22] F. J. Sigworth, E. Neher, *Nature (London)* **1980**, *287*, 447–449.
[23] E. M. Fenwick, A. Marty, E. Neher, *J. Physiol.* **1981**, *319*, 100P–101P.
[24] O. P. Hamill, B. Sakmann, *J. Physiol.* **1981**, *312*, 41P–42P.
[25] R. Horn, J. Patlak, *Proc. Natl. Acad. Sci. USA* **1980**, *77*, 6930–6934.
[26] O. P. Hamill, A. Marty, E. Neher, B. Sakmann, F. J. Sigworth, *Pflügers Arch.* **1981**, *391*, 85–100.
[27] O. P. Hamill in *Single Channel Recording* (Eds.: B. Sakmann, E. Neher), Plenum Press, New York, **1983**, pp. 451–471.
[28] A. Marty, E. Neher in *Single Channel Recording* (Eds.: B. Sakmann, E. Neher), Plenum Press, New York, **1983**, pp. 107–122.
[29] M. Pusch, E. Neher, *Pflügers Arch.* **1988**, *411*, 204–211.
[30] E. M. Fenwick, A. Marty, E. Neher, *J. Physiol.* **1982**, *331*, 599–635.
[31] E. M. Fenwick, A. Marty, E. Neher, *J. Physiol.* **1982**, *331*, 577–597.
[32] P. G. Kostyuk, *Neuroscience* **1980**, *5*, 945–959.
[33] A. Marty, *Nature (London)* **1991**, *291*, 497–500.
[34] B. Hille, *Q. J. Exp. Physiol.* **1989**, *74*, 785–804.
[35] M. Kameyama, J. Hescheler, F. Hofmann, W. Trautwein, *Pflügers Arch.* **1986**, *407*, 123–128.
[36] R. Penner, G. Matthews, E. Neher, *Nature (London)* **1988**, *334*, 499–504.
[37] E. E. Fesenko, S. S. Kolesnikov, A. L. Lyubarsky, *Nature (London)* **1985**, *313*, 310–313.
[38] M. Morad, N. W. Davies, J. H. Kaplan, H. D. Lux, *Science (Washington, D.C.)* **1988**, *241*, 842–844.
[39] W. Almers, E. Neher, *FEBS Lett.* **1985**, *192*, 13–18.
[40] J. Hescheler, M. Kameyama, W. Trautwein, *Pflügers. Arch.* **1986**, *407*, 182–189.
[41] M. Lindau, J. M. Fernandez, *Nature (London)* **1986**, *319*, 150–153.
[42] R. Horn, A. Marty, *J. Gen. Physiol.* **1988**, *92*, 154–159.
[43] L. A. Jaffe, S. Hagiwara, R. T. Kado, *Dev. Biol.* **1978**, *67*, 243–248.
[44] T. J. Gillespie, *Proc. R. Soc. London B* **1979**, *206*, 293–306.
[45] E. Neher, A. Marty, *Proc. Natl. Acad. Sci. USA* **1982**, *79*, 6712–6716.
[46] J. M. Fernandez, E. Neher, B. D. Gomperts, *Nature (London)* **1984**, *312*, 453–455.
[47] W. Almers, E. Neher, *J. Physiol.* **1987**, *386*, 205–217.
[48] R. Penner, E. Neher, *J. Exp. Biol.* **1988**, *139*, 329–345.
[49] G. J. Augustine, E. Neher, *J. Physiol.* **1992**, *450*, 247–271.
[50] R. J. Haslam, M. L. Davidson, *FEBS Lett.* **1984**, *174*, 90–95.
[51] R. I. Sha'afi, J. R. White, T. P. F. Molski, J. Shefcyk, M. Volpi, P. H. Naccache, M. B. Feinstein, *Biochem. Biophys. Res. Commun.* **1983**, *114*, 638–645.
[52] F. Di Virgilio, D. P. Lew, T. Pozzan, *Nature (London)* **1984**, *310*, 691–693.
[53] E. Neher, *J. Physiol.* **1988**, *395*, 193–214.
[54] S. Cockcroft, B. D. Gomperts, *Nature (London)* **1985**, *314*, 534–536.
[55] M. J. Berridge, R. F. Irvine, *Nature (London)* **1989**, *341*, 197–205.
[56] R. Penner, *Proc. Natl. Acad. Sci. USA* **1988**, *85*, 9856–9860.
[57] E. Neher, R. Penner in *Molecular Mechanisms in Secretion* (Eds.: N. A. Thorn, M. Treiman, O. H. Petersen), Munksgaard, Copenhagen, **1988**, pp. 262–270.
[58] A. S. Heiman, F. T. Crews, *J. Immunol.* **1985**, *134*, 548–554.
[59] B. D. Gomperts, M. M. Barrowman, S. Cockcroft, *Fed. Proc.* **1986**, *45*, 2156–2161.
[60] R. Penner, E. Neher, *Trends Neural Sci.* **1989**, *12*, 159–163.
[61] G. J. Augustine, M. P. Charlton, S. J. Smith, *Annu. Rev. Neurosci.* **1987**, *10*, 633–693.
[62] H. Parnas, J. Dudel, I. Parnas, *Pflügers Arch.* **1986**, *406*, 121–130.
[63] R. Llinas, J. A. Gruner, M. Sugimori, T. L. McGuiness, P. Greengard, *J. Physiol.* **1991**, *436*, 257–282.
[64] P. Thomas, A. Suprenant, W. Almers, *Neuron* **1990**, *5*, 723–733.
[65] N. F. Lim, M. C. Nowycky, R. J. Bookman, *Nature (London)* **1990**, *344*, 449–451.
[66] M. Lindau, E. L. Stuenkel, J. J. Nordmann, *Biophys. J.* **1992**, *61*, 19–30.

Elementary Steps in Synaptic Transmission Revealed by Currents through Single Ion Channels (Nobel Lecture)

By Bert Sakmann*

Introduction

The plasma membrane of a cell separates its interior from the extracellular environment and from other cells and acts both as a diffusional barrier and as an electrical insulator. This allows differentiation of cells with specialized functions. Coordinated behavior of multicellular organisms requires exchange of signals between individual cells. Because the signal must be transferred from one cell to another, it must occur by a mechanism that allows it to traverse the insulating cell membrane. Signalling occurs in various ways via specific receptors on the receiving cells and subsequent generation of a transmembrane signal. The nervous system connects cells in a very specific way and signal transmission between individual cells takes place at contacts, called synapses, that are anatomically and functionally highly specialized.

Synaptic signal transmission is used preferentially for rapid communication between cells of the nervous system and those cells of peripheral organs which are responsible for sensory transduction and for the generation of secretory and motor activity.[1, 2] Synaptic transmission includes a chemical step, where the signalling substance, called a transmitter, is released very locally from the "sending", presynaptic cell and then acts transiently on receptors of the "receiving", postsynaptic cell. The receptor is part of an ion channel and mediates, upon occupation by the transmitter, a brief flux of ions across the postsynaptic membrane generating a change in the postsynaptic membrane potential.

The signal that actually initiates the cellular response of the postsynaptic cell is the flux of ions across the postsynaptic membrane. The size, duration and direction of this ion flux, as well as the nature of the ions traversing the postsynaptic membrane, determines whether this response will either activate voltage-sensitive membrane conductances and initiate action potentials, or instead reduce the cells electrical activity. The cellular response may also be determined by a change in the intracellular ion concentrations, in particular the concentration of calcium ions, which act as a second messenger for many cellular responses like contraction or secretion.

The neuromuscular junction is often thought of as a prototypical synapse. At the neuromuscular junction the nerve terminal of a motoneuron releases acetylcholine (ACh) and generates end-plate potentials (EPPs), which in turn activate voltage-sensitive conductances to transmit excitation into other parts of the muscle fiber.[1] The current flow across the end-plate, induced by the release of packets of ACh, results from the superposition of many small individual "elementary" events[3] and there is ample evidence that postsynaptic potentials in other synapses are also generated by the superposition of elementary events.

This article describes the properties of elementary currents underlying postsynaptic potentials as well as their molecular determinants. The focus is primarily on the properties of elementary currents mediating neuromuscular transmission. The neuromuscular junction is the synapse characterized best, both functionally and in its molecular constituents, and most of the techniques for recording single channel currents were developed with the muscle fiber preparation. It has turned out that, apart from important details, a comparable behavior of elementary currents is observed for other transmitter-activated postsynaptic potentials, particularly those activated by glycine, γ-aminobutyric acid (GABA), glutamate and serotonin. These transmitters mediate 'rapid' synaptic transmission in the central nervous system (CNS) and produce postsynaptic potentials lasting milliseconds to hundreds of milliseconds.

Elementary Events

End-plate current noise: The notion of "elementary events" was introduced by B. Katz and R. Miledi when they observed "membrane noise" during recording of membrane depolarization induced by addition of ACh to neuromuscular end-plates of frog skeletal muscle.[3] They suggested that the increase in noise associated with depolarization is the result of the independent superpostion of elementary events generated by random activation of individual acetylcholine receptors (AChRs), each activation causing a minute depolarization.

The size of the conductance change generating an elementary event derived from such noise measurements, assuming a pulse-shaped change in conductance, were estimated to be of the order of 30 to 50 picosiemens (pS) with a duration of only a few milliseconds.[3, 4] This means that the amplitude of an elementary current would be of the order of 3–5 picoamperes (pA). This amplitude is about two to three orders of magnitude smaller than what could be resolved by the intracellular recording techniques available at the time.[5]

Current noise in extrasynaptic muscle membrane: ACh sensitivity is restricted, in normal muscle fibers, to a very small area of the muscle which is located underneath the nerve terminal. Following chronic denervation of skeletal muscle, effected by severing the motor nerve, the entire muscle becomes ACh supersensitive.[6] It is now known that this is due to the incorporation of newly synthesized ACh receptors into the extrasynaptic surface membrane of muscle fibers. Using noise analysis of ACh-activated currents we estimated the average increase in conductance underlying elementary events in denervated frog muscle fibers to be about 20 pS.[7]

[*] Prof. Dr. B. Sakmann
Max-Planck-Institut für medizinische Forschung
Abteilung Zellphysiologie
Jahnstrasse 29, D-W-6900 Heidelberg (FRG)

[**] Copyright © The Nobel Foundation 1992. – We thank the Nobel Foundation, Stockholm for permission to print this lecture.

The size of the elementary current in denervated fibers was thus smaller (about 60% of normal). The average duration of the elementary event was, however, 3 to 5 times longer than that of elementary events in the end-plate.

Elementary End-Plate Currents are Pulse Shaped

Solving the background noise problem: Denervated, supersensitive frog muscle fibers were thus the preparation of choice for developing methods for recording from single channels and for investigating the basic properties of ion channels by direct measurement of elementary events. The key for the reduction of background noise in the relevant frequency range (up to 1 kHz) was to restrict the measurement to a small membrane area of about 10 μm^2 and to isolate this membrane patch electrically from the rest of the cell membrane by sealing the narrow tip (1 - 3 μm) of the glass pipette tightly onto the membrane ("Gigaseal", Neher, 1991).[5] Pressing the pipette against a normal muscle fiber resulted in seal resistances of less that 1 MΩ and often damaged the fiber. The sealing problem was solved by exposing the fiber to mild enzymatic treatment, which freed muscle fibers from their covering connective tissue and the basal membrane, thus exposing the bare sarcolemma,[8] and by polishing the tip of the pipette with a small heating filament.[9] When the polished tip of the patch pipette was pressed gently against the bare sarcolemmal membrane of single fibers, secured mechanically by a glass hook, seal resistances of 50 to 150 MΩ were obtained. The membrane potential of the fiber was set locally, close to the membrane patch from which the patch current was recorded, by a conventional voltage clamp amplifier with two intracellular microelectrodes (Fig. 1 A).

Single channel currents: Using these precautions to obtain adequately high seal resistances (> 50 MΩ) and using suberoyldicholine, an agonist causing ACh receptors to open for longer periods, we were able to record current blips from denervated frog muscle fibers which were pulse-shaped, and which had many of the hallmarks of the elementary events that had been inferred from noise analysis of ACh-activated currents.[10] Square-shaped currents were also recorded from denervated rat muscle. They were similar to those obtained from denervated frog muscle, and in both preparations the directly measured amplitudes of elementary events agreed reasonably well with the estimated size derived from fluctuation analysis of macroscopic voltage clamp currents.[11]

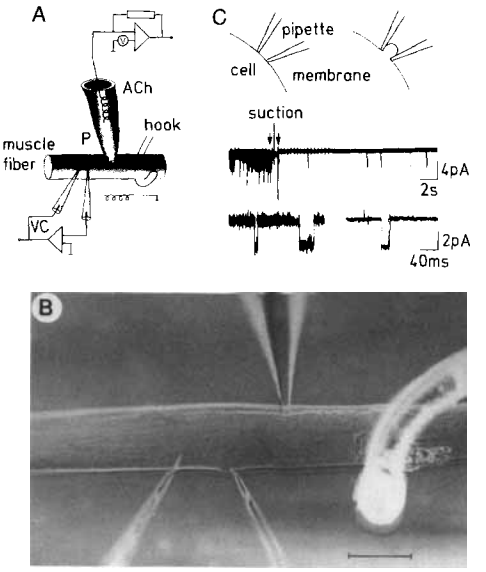

Fig. 1. Recording from a patch of end-plate membrane. A) Schematic diagram of muscle fiber with tip of patch pipette sealed against the cleaned surface of a single muscle fiber. The pipette is filled with extracellular solution and the pipette potential is held isopotential with the extracellular solution by means of feedback circuit. The fiber's membrane potential is clamped to a command value by a two microelectrode voltage clamp amplifier and two intracellular microelectrodes. Patch pipette contains in addition low concentration of acetylcholine (ACh). B) Disjunction of nerve terminal from muscle fiber. Photomicrograph of a single frog muscle fiber with bare end-plate after removal of the nerve terminal. The tip of the patch pipette is touching the end-plate (light streak). Two intracellular microelectrodes are used to locally clamp the membrane potential of the fiber. A glass hook, seen on the right hand side, secures the fiber mechanically. Calibration bar is 50 μm. C) Single channel current recording with seal resistances in the MΩ and GΩ range, respectively. Schematic drawing on top shows the formation of high-resistance seal by application of negative pressure ("suction") to pipette interior. Traces represent records, at two time scales, of elementary end-plate currents from the same membrane patch before (left) and after (right) application of negative pressure to the pipette interior ("suction") which increase the seal resistance of the pipette-membrane contact from 150 MΩ to 60 GΩ [12].

Disjunction of the neuromuscular synapse: To relate the properties of elementary currents to synaptic transmission at the end-plate of *normal* muscle fibers, it was necessary to compare the properties of elementary events with those of miniature end-plate currents (MEPCs). To place the tip of the patch pipette onto the end-plate, the neuromuscular junction must be visible and the nerve terminal, which covers the

Bert Sakmann, born on June 12, 1942, in Stuttgart, studied medicine at the universities of Tübingen, Freiburg, Berlin, Paris, and Munich. From 1968 to 1970 he worked a medical assistant at the Universität München and at the Max-Planck-Institut (MPI) für Psychiatrie in Munich with O. D. Creutzfeldt. After a period with B. Katz at University College London, he obtained his doctorate in 1974 at the Medizinische Fakultät Göttingen, and continued his work at the MPI für Biophysikalische Chemie in Göttingen with O. D. Creutzfeldt. He completed his Habilitation in 1982 and three years later became Director of the Abteilung Zellphysiologie des MPI für medizinische Forschung in Heidelberg. Since 1990 he has also been member of the Fakultät für Theoretische Medizin der Universität Heidelberg. Among his many honors are the Nernst-Haber-Bodenstein prize of the Bunsen-Gesellschaft für Physikalische Chemie 1977, the Gottfried-Wilhelm-Leibniz prize of the Deutsche Forschungsgemeinschaft 1986, and the Nobel prize for Medicine and Physiology 1991.

end-plate in normal fibers, must be removed from the end-plate. This is most easily accomplished by a localized application of collagenase, followed by a gentle stream of Ringer's solution delivered from a pipette with a small (100 μm) tip opening. This procedure resulted in single muscle fiber preparations with their end-plates freely accessible (Fig. 1 B).

Elementary end-plate currents: The elementary events recorded from the end-plate membrane (elementary end-plate current) were about 50% larger in amplitude, but considerably shorter in duration than those measured in the extrasynaptic membrane, as already expected from the fluctuation analysis of ACh-activated currents in normal and denervated fibers.[7] The measurements demonstrated that the elementary end-plate current is a square pulse-like event allowing passage of small cations like Na^+, K^+ or Cs^+ at a very high rate (10^7–10^8 s^{-1}), thus suggesting that these currents reflect the opening of water-filled pores across the membrane.[10]

Some basic properties of end-plate channels became apparent only at this improved resolution, which resulted from the reduction in background noise by establishment of pipette-membrane seals with resistances in the range of several GΩ.[12] Using freshly pulled pipettes and applying slight negative pressure to the pipette interior, thereby pulling the patch of membrane underneath the tip opening into the pipette tip, a molecular contact between the glass and the plasma membrane was established which increased the seal resistance from 50–150 MΩ to 1–100 GΩ. Consequently, the amplitude of the background noise was reduced and rim currents[9] were almost absent (Fig. 1 C). The reduced background noise allowed us to perform recordings of elementary end-plate currents with a band width of up to 10 kHz and to examine quantitatively the fine details of elementary end-plate currents that became apparent at this resolution.

Unitary conductance of the open end-plate channel: Recordings of elementary end-plate currents (Fig. 2 A) indicated that the end-plate channel exists in only two conductance states: either the channel is closed, when there is no agonist occupying the binding site(s), or it is fully open, when the binding site(s) are occupied. The distribution of the amplitudes of a large number of elementary end-plate currents can fitted to a single Gaussian curve (Fig. 2 B) where the remaining variance in the amplitude distribution is mostly due to the remaining background noise of the recording. This confirmed the initial inference that end-plate channels prefer two conductance states, fully closed and fully open (schematic diagram, Fig. 2 A).

Time course of channel closed-open transitions: The time course of the single channel current reports structural transitions of a single macromolecule in real time. An obvious question therefore is whether the time course of the *transition* between the open and closed channel states is measurable (Fig. 2 C): We superimposed the time course of the leading or trailing edge of a single channel current on that of the step response of the recording system. Since no difference was detected, the time course of single channel currents must have been limited by the frequency response of the recording system. The time constant of the channel transition from the closed to the open states is thus less than 10 μs.

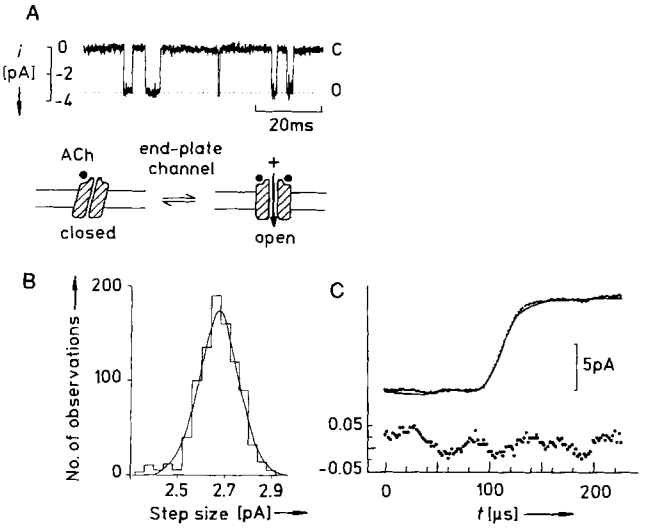

Fig. 2. Elementary end-plate currents. A) Trace of elementary end-plate currents from rat muscle activated by acetylcholine (ACh). Membrane potential was −70 mV. The schematic drawing under the current trace illustrates the opening and closing of an end-plate channel by transmitter binding and unbinding to recognition site on the end-plate channel. The channel is closed in the resting state and is open when two agonist binding sites are occupied by ACh molecules. B) Distribution of elementary end-plate current amplitudes, activated by 200 nM ACh in frog muscle. Histogram is fitted to a Gaussian curve with mean amplitude of 2.69 ± 0.10 pA. C) End-plate channels open rapidly to a unitary conductance. Upper traces show superposition of leading edges of elementary end-plate current (points) and of record of step-test pulse (continuous line, after amplitude scaling) to measure the frequency response of the recording system. Relative difference between the two aligned recordings is shown by open circles (bottom).

Observing the same channel repeatedly: To resolve elementary end-plate currents the concentration of ACh or a related agonist like suberoyldicholine in the pipette, was low (usually below 0.5 μM) to ensure that the opening of end-plate channels was infrequent and individual openings were clearly separated from each other (Fig. 2 A). This implied however that one could not be sure that successive elementary end-plate currents reflect the opening of the same individual end-plate channel, since it is likely that several channels are present in the membrane patch under investigation. In the presence of higher agonist concentrations (for acetylcholine > 5 μM) we found that elementary currents appear in long bursts of several hundreds of milliseconds duration. The reason for the occurrence of current bursts is that the channel can adopt, in addition to the "resting closed" state, an additional, kinetically distinct, closed state designated as "desensitized closed" state. This state is almost absorbing and channels isomerize only occasionally back to the open or "resting closed" states. When this happens the same channel switches back and forth between its "resting closed" and the "open" state repeatedly before it enters again the desensitized closed state[13] thus allowing the observation of several openings and closures of the *same* individual channel. The fact that the amplitude of the elementary currents during such an epoch did not change and that the average durations

of end-plate current were essentially independent of ACh concentration supported the two-state reaction scheme to explain the current recording shown in Figure 2A.

Elementary Steps in Neuromuscular Transmission

Minature end-plate currents and elementary end-plate currents: An obvious question related to the function of the end-plate channel in synaptic transmission is that of the relation between the size and duration of the elementary end-plate currents and that of the synaptic currents. In other words, how is the time course of the end-plate currents related to the gating properties of the end-plate channel?

A simple way to reconstruct the decay of a miniature end-plate current (MEPC), the signal transmitted across the neuromuscular junction following the release of a single vesicle of transmitter, is to align several hundreds of thousands of elementary end-plate currents at their leading edge and superimpose them. The hypothesis behind this procedure is that, following the release from a presynaptic vesicle, the concentration of ACh in the synaptic cleft rises very rapidly (in less than 1 ms) to saturate ACh receptors, and then rapidly decays again to negligible values.[14] If the ACh concentration transient in the cleft is very brief in comparison to the average duration of elementary end-plate currents then the decay of PEPCs would reflect the distribution of the durations of elementary end-plate currents after removal of ACh. In Figure 3 individual elementary end-plate currents are aligned at their leading edges (Fig. 3A). The current generated by superposition of 1000 elementary end-plate currents has a peak of 4.7 nA and decays with a time constant of 2.7 ms (Fig. 3B). These values are similar to those of MEPCs recorded from rat muscle end-plates. This suggests that a single MEPC, which reflects a quantal conductance increase of approximately 50 nS, is generated by the almost simultaneous opening of about one thousand end-plate channels (each with 50 pS conductance), and that the decay of MEPCs is determined to a first approximation, by the average duration of the elementary end-plate currents.

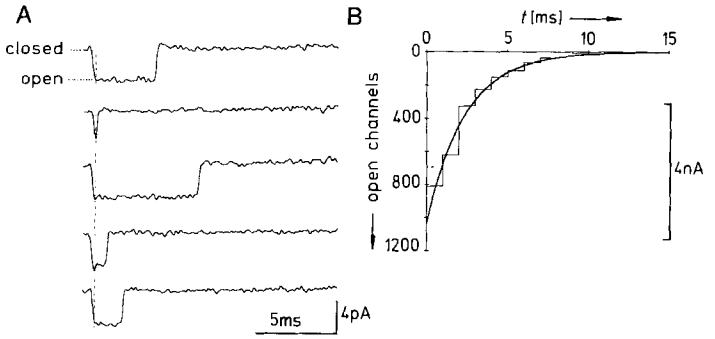

Fig. 3. Elementary end-plate current durations determine the shape of miniature end-plate currents. A) Records of elementary end-plate currents activated by 200 nM ACh in rat muscle fiber aligned at their leading edges to illustrate variation in duration of elementary end-plate currents. B) Average of 1000 superimposed elementary end-plate currents. Individual elementary end-plate currents were digitized and idealized by time course fitting[15] and then digitally superimposed at their leading edges as illustrated in Figure 3A. The continuous line superimposed on the histogram represents single exponential with decay time constant of 2.7 ms.

Elementary currents reflect bursts of single channel openings: The time course of elementary end-plate currents is more complicated in shape than expected from a channel that switches between an open and a single closed state as assumed in Figure 2A. Most elementary end-plate currents, when examined at high time-resolution, are interrupted by very short gaps (Fig. 4a, B), i.e. the current returns transiently to the base line.[15, 16] This behavior is observed in almost all the transmitter- and voltage-gated ion channels investigated so far. In the case of the end-plate channel it reflects the fact that, when the receptor has bound ACh, the channel opens and closes several times before the agonist dissociates from the receptor. The scheme shown in Figure 2A is intended only to illustrate the basic principle of structural transitions of the channel and assumes only one open and one closed channel state. In reality, however, a reaction scheme consistent with the experimental observations involves several closed and open states. The observed behavior of the current during a single elementary event is in fact predicted by a reaction involving transition of the closed, resting receptor to the open state via an intermediate closed state.[17]

Plausible reaction scheme for end-plate channel activation: We investigated the fine structure of these brief transitions for end-plate channels in collaboration with D. Colquhoun. Using the tools of probability theory,[18] it was possible to derive the minimum number of states the channel can adopt and also the rates of transition from one state to another.[15] At least five kinetically distinct states (Fig. 4C) could be discriminated from the measurement of both the open and

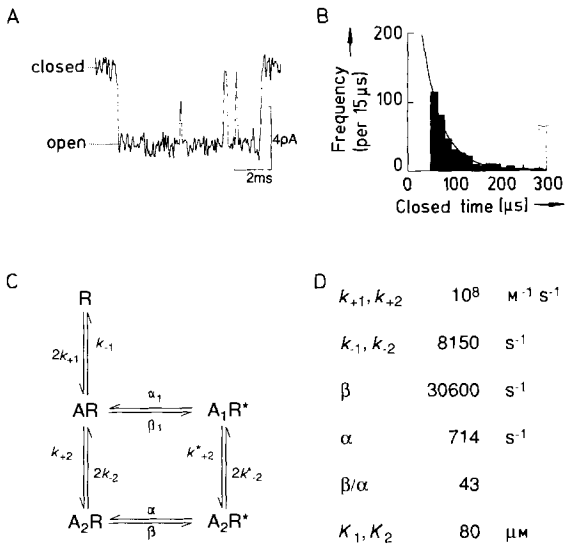

Fig. 4. Reaction scheme for end-plate channel activation by ACh. A) Record of elementary end-plate current activated by suberoyldicholine, an agonist of acetylcholine, to illustrate burst-like appearance of elementary end-plate currents. Note unresolved brief closure. B) Distribution of durations of brief closures measured during elementary end-plate currents. Continuous line represents an exponential curve with decay time constant of 39 µs. C) Reaction scheme for interaction of ACh (A) and end-plate channel (R) comprising five kinetically different states. Conducting states are marked by an asterisk. D) Derived rate constants for interaction of ACh and end-plate channel for the reaction scheme shown in Figure 4C from [15].

closed time distributions at low concentrations of several agonists, and the derived reaction rates satisfactorily described the time interval distributions. It represents a scheme for the gating of the end-plate channel by ACh during normal neuromuscular transmission and is a modification of the scheme proposed initially by Del Castillo and Katz.[19] It comprises a resting, unligated state and four ligated states, two of which are open states. The derived microscopic rate constants (Fig. 4D), which describe the transitions between the various states of the end-plate channel, indicate that the probability of the open channel occurring at high ACh concentrations during neuromuscular transmission (higher than 100 μM) is close to unity. This implies that ACh acts on the end-plate channel as a highly effective transmitter with high efficacy. When an ACh receptor is doubly ligated the equilibrium between the open and the closed states is shifted almost completely to the open state, indicating that the end-plate channel is very effective in rapidly passing current through the end-plate.

Isoforms of End-plate Channels

When recording postsynaptic currents in muscle fibers from young animals we found, in collaboration with H. Brenner, that there is a marked change in the decay time course of MEPCs during postnatal development. This reflects a switch of the functional properties of end-plate channels during this time. Up to postnatal day 8 (P8), the decay of the MEPCs is slower that that of MEPCs recorded in the adult muscle. During the period of P7 to P15 the MEPC decays are described best by the sum of two exponentials; in contrast, after P21 the MEPCs decay equally as fast as in adult fibers.[20, 21] The molecular basis for this difference in synaptic currents is shown in Figure 5. Two classes of elementary currents are recorded from muscle fibers at early postnatal stages. Mammalian skeletal muscle expresses two isoforms of end-plate channels which mediate different elementary end-plate currents,[22] differing both in amplitude and average duration. The expression of these channel isoforms is developmentally regulated. At early stages of development, in the uninnervated muscle, a fetal type of channel with lower conductance and longer average durations of elementary currents predominates. Following innervation a fetal isoform is replaced by the mature adult isoform which has a higher conductance and elementary currents of a shorter duration. Following denervation the fetal isoform is expressed again, suggesting that skeletal muscle expresses a mosaic af AChR channel isoforms and that the composition of this mixture of channel isoforms is under neuronal control (see Sakmann et al. 1992[23] for review).

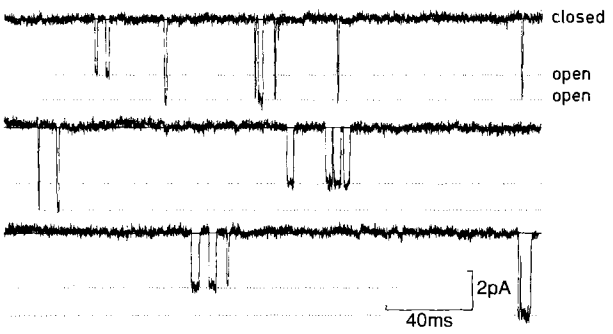

Fig. 5. Two classes of elementary end-plate currents. Record of single channel currents activated by 0.5 μM ACh in postnatal (P8) rat muscle fiber. Two classes of elementary currents, with different amplitudes and average durations, are observed in this patch. The elementary currents with the larger amplitude correspond to end-plate currents observed in adult fibers (> P21), whereas elementary currents of smaller amplitude correpond to those seen predominantly at early postnatal stages (< P8) or in fetal muscle.

Molecular Determinants of Channel Function

Identification of some of the molecular determinants of AChR channel function was achieved using patch clamp techniques and the tools of molecular biology. Biochemical work on *Torpedo* electroplax had shown that the AChR channel is assembled in a pseudosymmetric fashion from several subunits where each subunit contributes to the formation of the channel (see review by Karlin,[24]). In addition it had been demonstrated that recombinant AChR channels can be reconstituted in a functional form in a host membrane by injecting the RNAs that encode constituent subunits into the cytoplasm of *Xenopus laevis* oocytes (see review by Miledi et al.[25]). Following the isolation of the genes encoding the subunits of *Torpedo* electroplax and skeletal muscle AChRs, in vitro synthesized RNAs could be used to direct the synthesis of wild type and mutagenized recombinant AChR channels (see review by Numa[26]). Whole-cell current measurements from oocytes, expressing recombinant AChR channels, though important in showing that only certain subunit combinations would assemble to functional AChR channels, lacked the details necessary to demonstrate the similarity of recombinant and native AChRs or to draw conclusions on more specific structure-function relations. To relate functional properties of native AChRs to structural data, single channel conductance measurements on recombinant AChRs were required.

Because the oocyte plasma membrane is ensheathed by a vitelline membrane, the access of patch pipette tips to the plasma membrane is prevented. The vitelline layer may, however, be removed and the bare oocyte membrane expressed without damaging it, by brief exposure of the oocyte to a strongly hypertonic potassium solution. Oocytes then shrink away from the covering vitelline layer, which can be mechanically removed, leaving the bare plasma membrane.[27] This procedure enabled us to combine single channel conductance measurements with recombinant DNA techniques to identify structural determinants of AChR channel function. Two problems which are closely interrelated – the elucidation of the molecular basis of end-plate channel isoforms and the identification of structural determinants of the channels inner wall – were resolved in collaboration with a group of molecular biologists from S. Numa's laboratory and with V. Witzemann.

Recombinant AChR channel subtypes: The molecular distinction between the two isoforms of the end-plate channel (Fig. 5) was clarified as a result of experiments where the

cRNAs of the five muscle subunits were injected into oocytes, resulting in the functional expression of two AChR isoforms. Following the injection of cNARs encoding the α-, β-,γ-, and δ- or alternatively the α-, β-, δ-, and ε-subunits, two functionally different recombinant channel isoforms were generated (Fig. 6A, B). In their functional properties the two recombinant AChR isoforms resembled closely the two native AChR isoforms observed in muscle membrane.[28] Both the amplitude of single channel currents recorded from oocytes and their average duration (Fig. 6C) were similar to elementary currents observed in bovine or rat skeletal muscle.[28-30] Thus, it seems that native channel

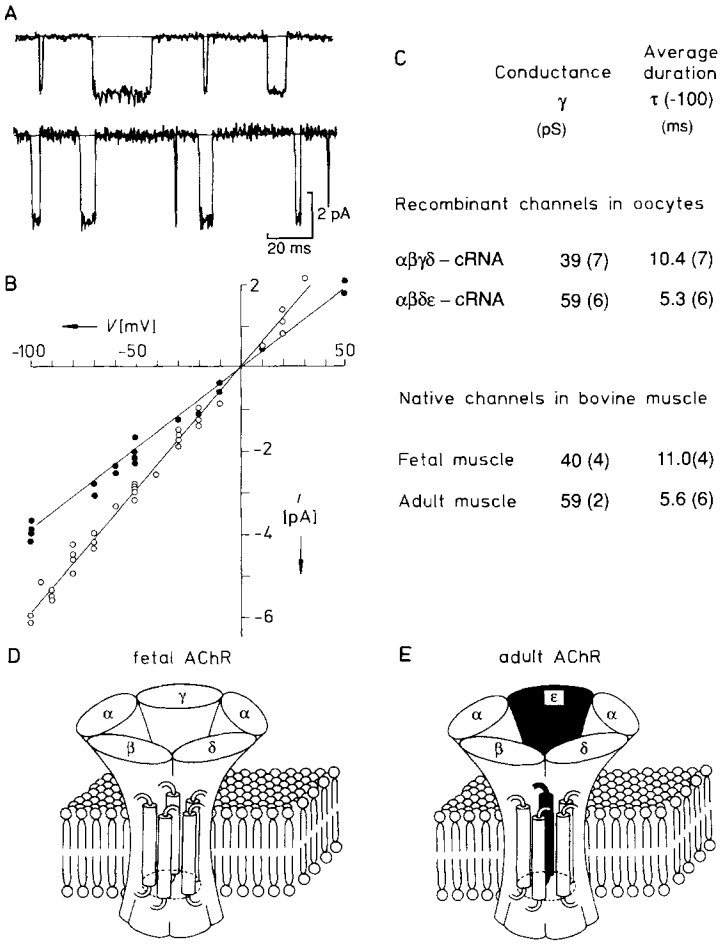

Fig. 6. End-plate channel isoforms are specified by differences in subunit composition. A, B) Single-channel currents and conductance mediated by recombinant AChR channels expressed in *Xenopus* oocytes previously injected with cRNAs encoding the subunit combinations α-, β-, γ- and δ- (upper trace and filled symbols) and α-, β-, δ- and ε-subunits of bovine muscle AChR (lower trace and open symbols). C) Conductance and average open times of two isoforms of recombinant and native AChR channels from bovine skeletal muscle (modified from [28]). D, E) Schematic diagram of the subunit composition of end-plate channel subtypes in fetal and adult skeletal muscle. The structure of the AChR is schematically drawn according to Unwin [31]

isoforms reflect differences in subunit composition of the channel, in the case of the AChR channel an exchange between the γ- and ε-subunit is the molecular difference between the two channel subtypes (Fig. 6D, E).

Differential regulation of γ- and ε-subunits genes: The molecular mechanism underlying the switch in end-plate channel properties effected by the exchange of constituting subunits is a postnatal switch in the expression of the genes encoding the γ- and ε-subunit. Northern blot analysis of total RNAs from muscle at different postnatal ages shows that a reciprocal change in the level of γ- and ε-subunit-specific mRNAs occurs during postnatal development.[32, 33] This differential regulation depends on differences in the regulatory sequences of the γ- and ε-subunit genes and their different responsiveness to neural and myogenic factors.[30, 34, 35] Since in most cells, including neurons, channel isoforms are expressed which often are colocalized in a mosaic-like manner, the regulation of the abundance of channel isoforms by differential expression of subunit genes may be one mechanism by which long-term ("plastic") changes in chemical and electrical excitability can occur (see review by Sakmann et al.[23]).

Molecular determinants of ion transport: The work of Hille and co-workers[36] had indicated that the end-plate channel is a cation-selective pore with a channel constriction of about 6 Å in diameter. The first insight into the molecular determinants of ion transport of the AChR was obtained following the identification of sequence domains in each subunit that may participate in forming the wall of the channel. Conventional whole-cell current measurements from *Xenopus* oocytes, co-injected with wild type and mutagenized AChR subunit specific cRNAs, gave only inconclusive results with respect to the involvement of particular subunit domains.[37] Subunit-specific differences in gating and conductance of various channel isoforms were however detected by single channel conductance measurements from isolated membrane patches where the ion composition and concentration on both membrane faces could be varied.[12] These advantages were exploited to localize functionally important domains in AChR subunits.

Hybrid channels and chimeric subunits: The gating and conductance of recombinant AChR channels assembled from homologous subunits of different species like *Torpedeo californica* and calf (*bos taurus*) depends on the particular combination of subunits cRNAs coinjected.[38] The δ-subunits of bovine muscle and of *Torpedo* electroplax AChR confer slightly different conductances to the hybrid channels when assembled together with α-, β- and γ-subunits of either species.[39] This observation was exploited to construct various chimeric subunits from bovine and *Torpedo* AChR δ-subunits (Fig. 7A, B). Conductance measurements on the recombinant channels carrying different chimeric δ-subunits (Fig. 7C) identified a domain designated as the M2 transmembrane segment to be important for conferring differences in conductance.[39] The most conspicuous difference in the aligned amino acid sequences was in the number of charged amino acids in the extracellular bend bordering the M2 segment (Fig. 7D).

The channels mouths and walls probed by conductance measurements of mutant channels: To precisely locate those amino acids important for ion transport and selectivity we investigated the effect of point mutations in the M2

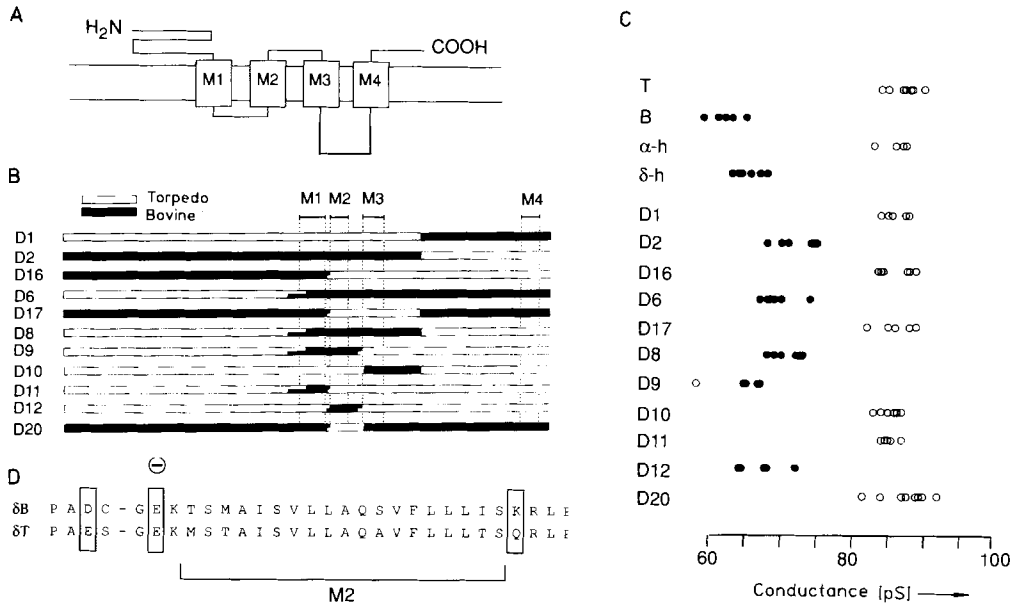

Fig. 7. Localization of M2 segment by single channel conductance measurements of recombinant AChR channels carrying different chimeric δ-subunit constructs. A) Schematic drawing of assumed transmembrane folding of AChR subunits as suggested from hydropathy analysis. N- and C-terminal ends are extracellular. B) Chimeric δ-subunit constructs derived from *Torpedo californica* electroplax and bovine skeletal muscle AChR δ-subunits. C) Single channel conductances of recombinant AChR channels carrying chimeric δ-subunits as shown in Figure 7C (α-h and δ-h represent hybrid channels where α- or δ-subunits were exchanged.) T and B refer to *Torpedo* or bovine muscle wild-type channels respectively. D) Comparison of amino acid sequence of δ-subunits from bovine muscle and *Torpedo* electroplax AChR in their M2 transmembrane segment (single letter code). Note difference in charged amino acids in M2–M3 bend (modified from [39]).

transmembrane segment and the adjacent bends on the con ductances of the mutant channels. Four amino acid positions, homologous in each subunit, were identified where amino acids are localized which are important for cation transport through the open channel and for its selectivity between monovalent cations.

Anionic rings: The M2 transmembrane regions, identified by mapping with chimeric δ-subunits, show a conspicuous clustering of charged amino acids bordering the M2 transmembrane segment in each of the subunits (Fig. 8A). By introducing point mutations at these positions, which changed the charge of the amino acid side chains, we found that largely the net number of negative charges, irrespective in which subunit the mutation was introduced, determines the channel conductance. This suggested that the charged amino acids of the participating subunits present in the bends bordering the M2 segment (Fig. 8A) form three ring-like structures at the extra- and intracellular mouths of the channels, respectively.[40,41]

Channel selectivity: To localize positions where amino acid side chains form the channel wall and in particular those amino acids that form the narrow portion of the channel, we investigated the functional properties of recombinant AChR channels mutagenized within the M2 transmembrane segment. This narrow portion is often referred to as the channel's "Selectivity filter", suggesting that here the interaction of transported ions, and their water shells, with the channels inner wall determines which ions may pass and which may not (see review by Hille[36]). To map amino acids which could be involved in this interaction, the conductances of mutant channels for several cations of different size and mobility were measured (Fig. 8B). These measurements indicated that a major determinant of ion selectivity resides in the residues located in M2 at a position close to the position of the amino acids forming the "intermediate" anionic ring (Fig. 8A). The channel conductance is altered by introducing amino acids with side chains of different bulkiness at this position. Side chains like valine that have larger volumes reduce the conductance, while side chains with smaller volumes increase the conductance.[42] The effect of these point mutations depends on the size and mobility of the ion used to measure the conductance (Fig. 8C), the effects being larger for Cs^+ than for Na^+.[43]

A simple model of the AChR selectivity filter: Single channel conductance measurements on hybrid AChR channels carrying chimeric subunits thus identified the M2 transmembrane segment as one determinant contributing to the formation of the channel's inner wall. Point mutational analysis refined the mapping and identified four positions in each subunit where amino acid side chains are likely to interact with permeating cations. A working hypothesis would be to assume that cations accumulate at the channel's extra- and intracellular mouths because of electrostatic attraction by the negative charges provided by the three anionic rings, whereas anions are excluded because of electrostatic repulsion. The selection between monovalent cation is predominantly due to "sieving" at the narrowest part of the channels constriction, which is formed by amino acid side chains containing hydroxyl groups.

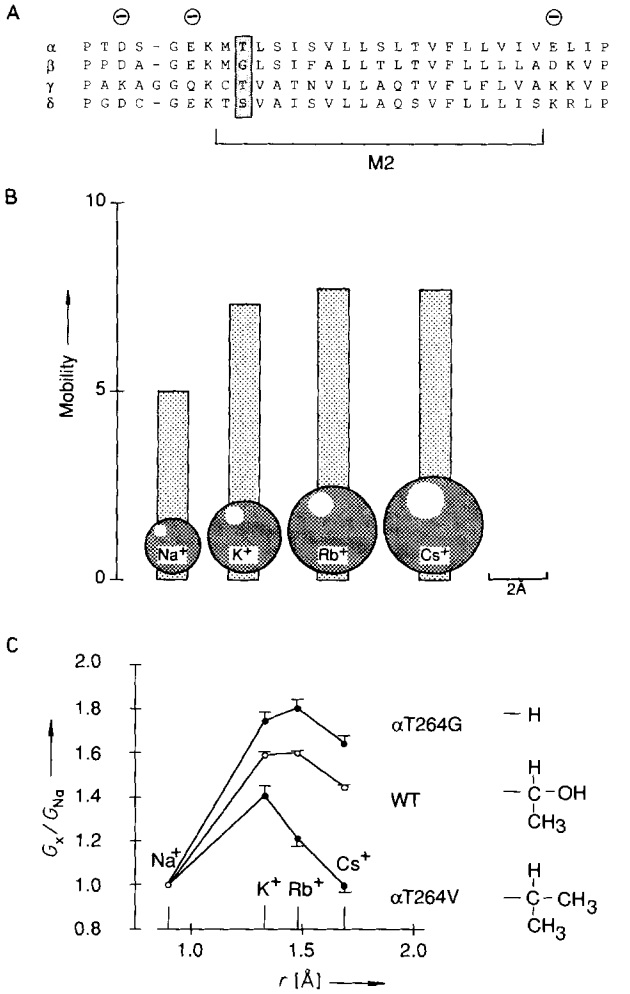

Fig. 8. Localization of selectivity filter of AChR channel by single-channel conductance measurements of recombinant AChR channels carrying mutations in the M2 transmembrane segment. A) Sequence alignment of α-, β-, γ- and δ-subunits of rat muscle AChR in the M2 transmembrane segment and adjacent bends (single letter code). The location of clusters of charged amino acids forming anionic rings at the channels mouths, as identified in *Torpedo* AChRs, are indicated by minus signs above the sequences. The amino acids forming the intermediate anionic ring are located in between those forming the intracellular ring (left) and the extracellular ring (right). The location of amino acids forming the constriction is indicated by the shaded box. B) Schematic representation of sizes and mobility of cations (modified from [44]) used to probe determinants of AChR channel conductance and selectivity. The scale on the left-hand side represents ion mobility $[10^{-4}\,cm\,s^{-1}/(V\,cm^{-1})]$. C) Conductance ratios of wild type (WT) and mutant channels carrying mutations in the cytoplasmic part of the α-subunit M2 segment (indicated by shaded box in A), where a threonine residue is replaced either by a valine (αT264V) or a glycine (αT264G) residue, for different size of cations (modified from [43]).

Ion Channels Mediating Rapid Synaptic Transmission between Neurons

Synapses in the central nervous system (CNS) operate with transmitters which are different from those in peripheral synapses, the most common ones being glycine, GABA, glutamate and serotonin. Moreover CNA synapses fall into two categories, either excitatory or inhibitory. The work of Eccles and his collaborators[45] showed that synaptic communication in the CNS as in the periphery, is mediated by ionic currents that flow across the postsynaptic membrane, generating excitatory or inhibitory postsynaptic potentials (EPSPs and IPSPs). Depending on which ions carry the postsynaptic currents, the respective transmitters are classified as excitatory or inhibitory. Glutamate, serotonin and ACh activate cation currents, carried mostly by Na^+ and K^+ and to a smaller extent by Ca^{2+} under physiological conditions. GABA and glycine activate anion currents, carried under physiological conditions by Cl^-. To characterize the elementary currents underlying postsynaptic potentials in the CNS we initially used isolated neurons obtained from fetal brain, which were kept under cell culture conditions, and which express receptor channels that can be activated by CNS transmitters.

Elementary currents activated by glycine and GABA: An important feature of signal integration in the CNS is the occurrence of postsynaptic inhibition between neurons. This occurs when the electrical activity of a neuron is reduced by IPSPs, which are largely mediated by the transmitters glycine or GABA, which cause an increase in the permeability of the postsynaptic cell to chloride ions. To find out whether ion channels mediate this increase in Cl^- conductance we measured the elementary currents activated by glycine or GABA in neurons isolated from fetal spinal cord and brain. They were freed from their extracellular coats during the isolation procedure and readily allowed the sealing of a pipette tip onto their plasma membrane (Fig. 9A).

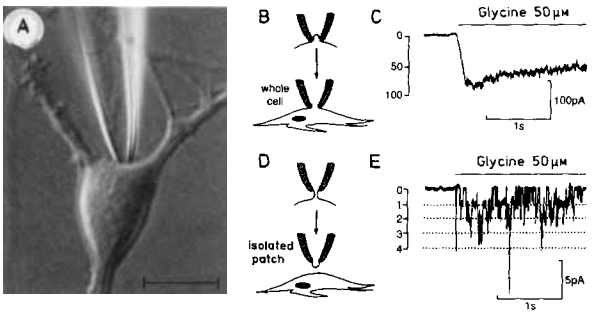

Fig. 9. Noisy whole-cell and square-shaped pulsed elementary currents activated by glycine in isolated neurons kept in tissue culture. A) Photomicrograph of cell body of a cultured neuron and tip of patch pipette touching cell membrane. Calibration bar is 10 μm. B) Schematic diagram of recording configuration to measure whole-cell current from an isolated neuron. C) Record of whole-cell current in response to application of inhibitory transmitter glycine. Note noisy trace during glycine-activated current. Scale on the left refers to number of open channels. D) Schematic diagram of recording configuration to measure elementary currents from outside-out patch, isolated from neuronal cell body. E) Recording of elementary currents in response to glycine application to outside-out membrane patch. Scale refers to number of open channels (modified from [46]).

For the characterization of the ionic requirements and the pharmacology of the currents activated by inhibitory transmitters the "whole-cell" configuration (Fig. 9B) was used, allowing the current through the entire cell membrane to be monitored. Figure 9C illustrates the activation of a membrane current of several hundred pA in a spinal neuron in response to the application of glycine. The current trace becomes "noisy" during glycine-activated current, but elementary currents are not resolvable. Following isolation of an "outside-out" patch (Fig. 9D) the application of glycine at the same concentration activates a much smaller average current, of only a few pA. The superposition of square-

shaped elementary currents is now clearly detectable (Fig. 9E), suggesting that glycine-activated whole-cell currents are generated by the superposition of elementary currents of unitary amplitude and varying duration. The size of glycine-activated elementary currents is in the same range as that of elementary end-plate currents, indicating that CNS transmitters also act by opening ion channels.

Coactivation of GlyR and GABAR channels: Most neurons isolated from fetal CNS have both glycine- and GABA-activated whole-cell currents which are carried by Cl^-. The respective ion channels (GlyR- and GABA-channels) were often co-localized in the same membrane patch (Fig. 10A, B), and their properties were studied by recording single channel currents.

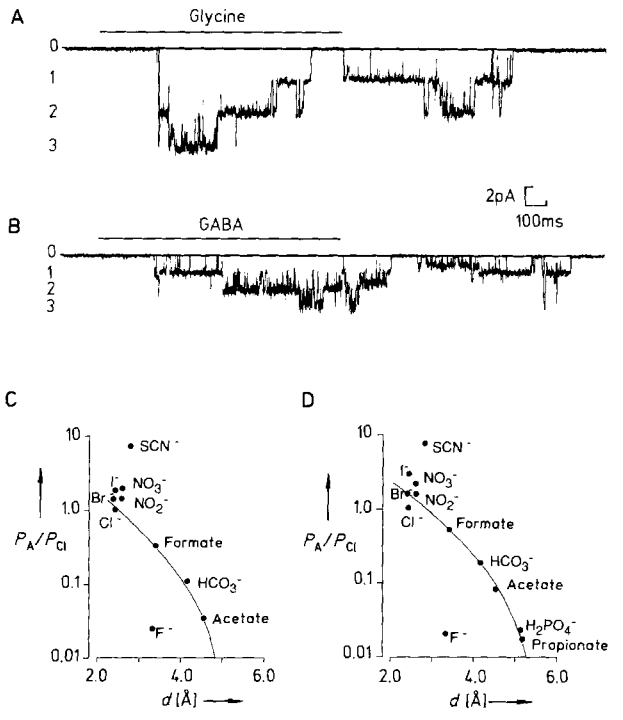

Fig. 10. Coactivation of GlyR and GABAR-channels. A) Single-channel currents activated by glycine in an outside-out patch of mouse spinal neuron. Several GlyR channels are activated in this patch as indicated by scale on left hand side, and elementary GlyR channel currents are superimposed. B) Single-channel currents activated by γ-aminobutyric acid (GABA) in the same patch as shown in Figure 10A. Superposition of elementary currents indicates the presence of several GABAR channels in this patch. C, D) Diameter of narrow part of GlyR and GABAR channels, mapped by reversed potential measurements under biionic conditions with chloride versus inorganic or organic anions of different size. Extrapolated diameters (Stokes diameters) d of constriction of GlyR and GABAR channels are very similar, between 4.8 and 5.4 Å (from [48]).

The GlyR and GABAR channels are different molecular entities[47] which share many functional properties. By measuring the reversed potentials under biionic conditions using different permeant inorganic and organic anions, the diameter of the narrow region of GlyR and GABAR channels was found to be between 4.8 and 5.4 Å at its constriction[48] (Fig. 10C, D). This is comparable to the size of the constriction of the end-plate channel (see review by Hille[36]). The results suggest, in conjunction with structural information obtained from the elucidation of the amino acid sequences of the GlyR and GABAR subunits, that transmitter gated channels are operating according to common principles, possibly being derived from common ancestors (see review by Betz[47]).

Conductance substates of channels activated by CNS transmitters: The elementary currents activated by glycine or GABA are square-shaped pulse events, but in contrast to what we had expected initially, both transmitters opened channels which may adopt several conductance states. Several of these substates are common to both channels; however, the most frequently occurring "main" conductance states are different.[48,49] Glutamate, the major excitatory transmitter in the CNS, also activates elementary currents in the pA-range which fall into several amplitude classes, indicating that glutamate receptor (GluR) channels also adopt substates.[50-52] So far the mechanisms and the possible functional significance of conductance substates remain poorly understood. The analysis of recombinant channels indicates that the receptor channels gated by the major CNS transmitters GABA, glycine and glutamate can show a wide functional diversity. This is probably due to the expression of numerous subunits, which may form both homo- as well as hetero-oligomeric isoforms of channels with subunit-specific properties.[53] A possible, but so far unproven hypothesis would be that channel subtypes are co-localized in the postsynaptic membrane in a mosaic-like fashion and that this may be a prerequisite for the alteration of synaptic effectiveness by changes in the composition of isoforms of the receptor mosaic.

Postsynaptic Currents in Brain Slices

It is important to characterize those receptor channel isoforms that actually mediate postsynaptic potentials in neurons of clearly defined pathways in the intact CNS. In cell culture the cellular identity of isolated neurons is rather ill-defined, and these neurons lack their natural neighbors with which they form specific synapses. Therefore the brain slice technique, pioneered by P. Andersen, was modified to perform whole-cell and single-channel current measurements from neurons in situ, to characterize the quantal conductance changes leading to EPSPs and IPSPs, and the elementary currents underlying them.

Sealing of patch pipettes onto neurons in brain slices: The procedure that allowed us to use patch pipettes for whole-cell and single-channel conductance measurements on neurons in brain slices consisted of a modification of the procedure developed for exposing the end-plates of single skeletal muscle fibers. Initially we used local application of collagenase; however, we found later that a gentle stream of extracellular solution, directed towards the surface of the slice (Fig. 11A), was sufficient to expose the cell body of visually identified neurons (Fig. 11B, C) in almost any part of the brain or spinal cord for recording with patch pipettes.[54]

Quantal transmission in CNS synapses: The recording of stimulated IPSCs from granule cells of the dentate gyrus, as well as the recording of elementary currents from outside-

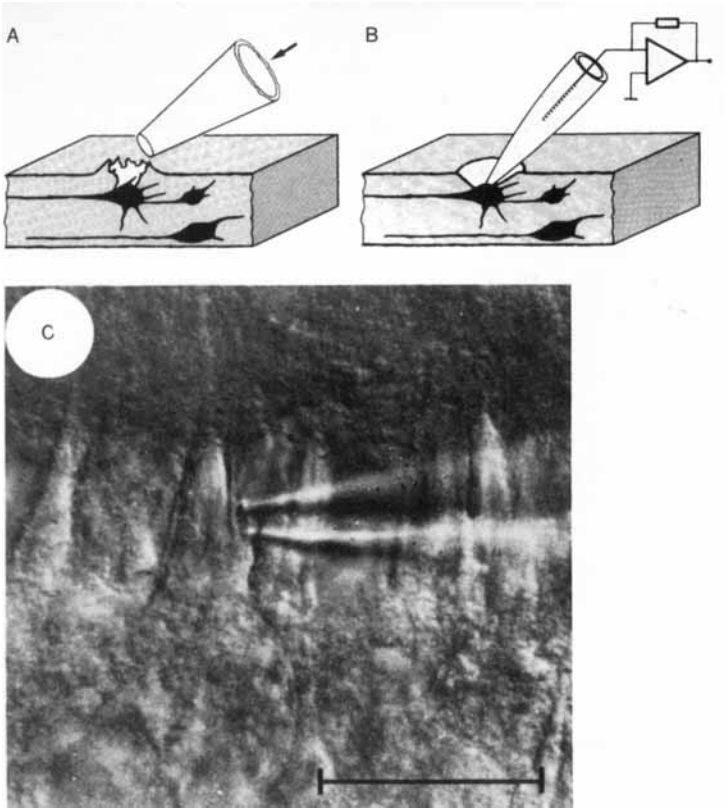

Fig. 11. Exposure of CNS neurons in brain slices for current recording with patch pipettes. A) Schematic drawing of the procedure used to expose the soma of individual neurons in brain slices. The tissue covering the cell body is removed by a gentle stream of extracellular solution delivered from a small pipette. B) Tip of patch pipette is sealed onto exposed cell body. C) Photomicrograph of exposed soma of hippocampal pyramidal neuron in rat brain slice. The tip of the pipette used to deliver a stream of extracellular solution is visible on the right side. Calibration bar is 20 μm. (Modified from [54]).

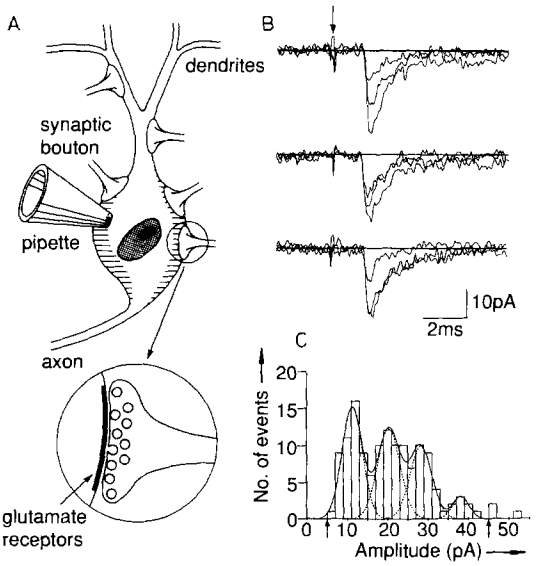

Fig. 12. Excitatory postsynaptic currents in CNS neurons mediated by glutamate acting on glutamate receptors. A) Schematic diagram of whole-cell recording of excitatory postsynaptic currents (EPSCs) from a neuron in the brain slice, where glutamate is released from vesicles to act on postsynaptic glutamate receptors (GluR). B) Examples of stimulated EPSCs mediated by glutamate acting on GluR channels of the AMPA/KA subtype. Time of electrical stimulus delivered to a neighboring neuron is indicated by arrow. Three responses are superimposed in each set of traces to illustrate the fluctuation in peak amplitude of EPSCs in response to constant stimulus. Three uppermost traces correspond to one, two and three quantal events, respectively. C) Amplitude distribution of stimulus evoked EPSCs. Peaks in this distribution indicate that EPSCs are quantal in nature with a quantal change in conductance of the order of 100 pS (from [59]).

out patches, demonstrated the quantal nature of IPSCs mediated by GABA, and showed that the magnitude of the change in conductance occurring during a quantal IPSCs is relatively small (of the order of 100–200 pS). This suggested that only a small number (20 to 40) of postsynaptic GABAR channels are activated by the release of a quantum of transmitter. According to model calculations of the size and time course of IPSCs it appears that the small number of activatable GABAR channels in a single synaptic bouton is the major determinant of this small quantal conductance change.[55–57]

The recording of stimulated EPSCs from neurons where synaptic knobs are located at or close to the cell body, such as in stellate cells in layer IV of visual cortex (Fig. 12A) or in pyramidal cells of the hippocampal CA3 region where mossy fiber terminals form synapses on the shaft of the apical dendrite also demonstrated the quantal nature of EPSCs mediated by glutamate acting on postsynaptic glutamate receptor (GluR) channels of the AMPA subtype.[58, 59] EPSCs are also characterized by a small quantal change of conductance on the order of 100–200 pS (Fig. 12B, C), which most likely also reflects a small number of activated channels.

Gating of GluR channels in CNS synapses: In central synapses the time course of the change in transmitter concentration following axonal release is not known, as is also the case with the density or the kinetic properties of the receptor channels. If the transmitter disappears rapidly from the synaptic cleft, the decay of EPSCs or IPSCs would reflect the distribution of elementary current durations after removal of the transmitter. Alternatively, the decay could reflect desensitization of postsynaptic receptors in the presence of a sustained level of transmitter in the synaptic cleft. To measure the gating properties of postsynaptic receptor channels in the CNS we used a method that allows brief agonist applications to outside-out membrane patches[60] isolated from neurons in an anatomically clearly-defined region of the brain (Fig. 13A, B).

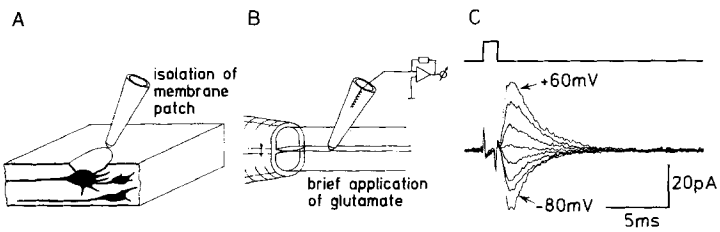

Fig. 13. Characterization of native GluR-channels in CNS neurons of brain slice. A) Schematic diagram of the isolation of outside-out patch from the soma of a neuron in brain slice. B) Schematic diagram of method of brief agonist application to outside-out patch. The tip of the patch pipette, sealed by outside-out patch, is brought close to the opening of a double-barreled application pipette delivering two solutions, one with control solution, the other containing in addition 1 mM L-glutamate. The pipette is moved briefly by 10–20 μm by means of a Piezo-element to expose patch to a pulse of glutamate. C) Family of currents in response to glutamate application to membrane patch isolated from a rat hippocampal cell at different membrane potentials (at 20 mV intervals). Duration of glutamate application is 1 ms as indicated in upper trace. Current rises rapidly (less than 1 ms) to peak. Decay constant of current following removal of glutamate is 2–3 ms.

The experiments showed that although closure of GluR channels by desensitization is fast, it is considerably slower than closure of channels to the resting state following removal of agonist (Fig. 13C).[61] It is, in particular, slower than the decay of EPSCs, for example from excitatory synapses on stellate cells,[59] suggesting that, at least in these cells, the decay of the fast EPSCs reflects predominantly the closure of GluR channels from the open to the resting closed state following rapid removal of transmitter from the synaptic cleft. This implies that glutamate is present only very briefly in the synpatic cleft (less than 1 ms) and that EPSCs are mediated by a GluR channel subtype characterized by short average duration of elementary currents. In spite of this some desensitization of GluR channels may still occur, even during a single EPSC.[62]

Molecular determinants of GluR-channel function: To find out whether the occurrence of functional GluR channel subtypes which mediate rapid synaptic currents is based on the assembly of native channels from different subunit combinations, which may confer different properties to the assembly, we compared, in collaboration with P. Seeburg, the functional properties of native and recombinant GluR channels. Recombinant GluR channels were assembled from different subunits of the AMPA receptor subunit family[63, 64] guided by the pattern of subunit genes which are co-expressed in different parts of the brain.[65]

Comparison of the functional properties of recombinant homomeric and heteromeric GluR channels suggested that properties like the rectification of channel conductance and divalent permeability are dominated by the presence of a particular (GluR-B) subunit in native GluR channels.[66] This dominance was traced to a single amino acid in the putative M2 transmembrane segment.[67–69] The almost ubiquitous expression of the GluR-B subunit gene in CNS most likely determines the conductance properties and the low Ca^{2+} permeability of native GluR channels mediating fast EPSCs. Its differential expression is likely to determine differences in the Ca^{2+} permeability of native GluR channels in different cell types, for example of the cerebellum.[70] In addition to the differential expression of the GluR-B subunit gene an additional mechanism seems to operate in regulating the properties of native GluR channel isoforms. The GluR-B subunit is found in two isoforms differing only by a single amino acid in the M2 transmembrane segment (Fig. 14A–C). The two subunit isoforms confer different conductance properties on heteromeric channels. The difference is most likely due to the editing of the mRNA specific (for the) GluR-B subunit.[71]

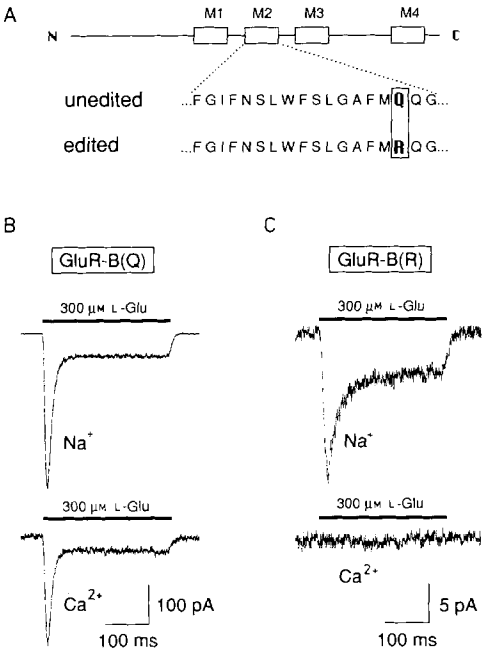

Fig. 14. Characterization of recombinant GluR-channel subtypes expressed in host cell. A) Differences in amino acid sequence of GluR-channel subunits in M2 transmembrane segment of GluR-B subunit. Box indicates amino acid present at Q/R site in the two isoforms of this subunit, GluR-B(Q) and GluR-B(R). The presence of arginine at this site is the consequence of mRNA editing. B) Functional properties of recombinant GluR-channels assembled from unedited GluR-B(Q) subunits. Inward current activated by glutamate is carried both by Na^+ and Ca^{2+}. C) Functional properties of recombinant GluR channels assembled from edited GluR-B(R) subunits. In the presence of high extracellular Na^+ concentrations an inward current is activated, whereas with high extracellular Ca^{2+} concentration no inward current is observed (modified from [68]).

Outlook

Patch clamp techniques are now well established and routinely applied in combination with other techniques like recombinant DNA or fluorimetric techniques to characterize molecular details of the events underlying synaptic signaling between cells. Through the measurement of elementary currents, the biophysical interpretation of the electrical signals which underlie rapid cellular communication across synapses has been simplified and can be partly understood in molecular terms. At the same time single channel conductance measurements have provided evidence for numerous isoforms of receptor channels, as well as for voltage and secondary messenger-gated channels; however the significance of this finding remains to be elucidated regarding synaptic communication in the CNS. It seems that the characterization of the various types of ligand- and voltage-gated ionic channels on the extensive dendritic trees of CNS neurons is necessary for an understanding of their integrative function, i.e. the generation of patterns of electrical activity resulting from IPSPs and EPSPs from many synaptic inputs. Equally important will be the characterization of the ionic channels responsible for the electrical activity of nerve terminals. Patch pipettes could provide the resolution necessary to study the electrical signals in nerve terminals and dendrites. This seems to be a prerequisite if one wishes to understand how changes in synaptic transmission may contribute to changes in funtional connectivity of neuronal pathways during normal and pathological states.

I am greatly indebeted to my teachers in physiology, Otto Creutzfeldt and Bernard Katz, and to the Max-Planck-Gesellschaft for providing ideal research conditions. During the last five years I was supported by the Leibniz Programm of the Deutsche Forschungsgemeinschaft and by an award of the Fondation Louis Jeantet, Geneva.

Received: January 16, 1992 [A 868 IE]
German version: *Angew. Chem.* **1992**, *104*, 844

[1] B. Katz, *Nerve, Muscle and Synapse*. McGraw-Hill, New York, **1966**.
[2] B. Katz, *The release of neural transmitter substances*, The Sherrington Lectures X, Liverpool University Press, **1969**.
[3] B. Katz, R. Miledi, *J. Physiol.* **1972**, *224*, 665.
[4] C. R. Anderson, C. F. Stevens, *J. Physiol.* **1973**, *235*, 655.
[5] E. Neher, in *Les Prix Nobel en 1991*, The Nobel Foundation, Stockholm, **1992**; *Angew. Chem.* **1992**, *104*, 837–843; *Angew. Chem. Int. Ed. Engl.* **1992**, *31*, 824–829.
[6] J. Axelson, S. Thesleff, *J. Physiol.* **1959**, *147*, 178.
[7] E. Neher, B. Sakmann, *J. Physiol.* **1976**, *253*, 705.
[8] W. Betz, B. Sakmann, *J. Physiol.* **1973**, *230*, 673.
[9] E. Neher, B. Sakmann, J. H. Steinbach, *Pflügers Arch.*, **1978**, *375*, 219.
[10] E. Neher, B. Sakmann, *Nature (London)* **1976**, *260*, 799.
[11] B. Sakmann, *Fed. Proc.*, **1978**, *37*, 2654.
[12] O. P. Hamill, A. Marty, E. Neher, B. Sakmann, F. Sigworth, *Pflügers Arch.* **1981**, *391*, 85.
[13] B. Sakmann, J. Patlak, E. Neher, *Nature (London)* **1980**, *286*, 71.
[14] K. L. Magleby, C. F. Stevens, *J. Physiol.* **1972**, *223*, 173.
[15] D. Colquhoun, B. Sakmann, *J. Physiol.* **1985**, *369*, 501.
[16] D. Colquhoun, B. Sakmann, *Nature (London)* **1981**, *294*, 464.
[17] D. Colquhoun, A. G. Hawkes, *Proc. R. Soc. London B* **1977**, *199*, 231.
[18] D. Colquhoun, A. G. Hawkes, *Phil. Trans. R. Soc. B* **1982**, *300*, 1.
[19] J. Del Castillo, B. Katz, *Proc. R. Soc. London B* **1957**, *146*, 369.
[20] B. Sakmann, H. R. Brenner, *Nature (London)* **1978**, *276*, 401.
[21] A. Michler, B. Sakmann, *Dev. Biol.* **1980**, *80*, 125.
[22] O. P. Hamill, B. Sakmann, *Nature (London)* **1981**, *294*, 462.
[23] B. Sakmann, V. Witzemann, H. Brenner in *Fidia Research Foundation Neuroscience Award Lectures, Vol 6*. Raven Press, New York, **1992**, pp. 53–103.
[24] A. Karlin, *Harvey Lect. Ser.* **1991**, *85*, 121.
[25] R. Miledi, I. Parker, K. Sumikawa in *Fidia Research Foundation Neuroscience Award Lectures, Vol. 3*. Raven Press, New York, **1989**, pp. 57–90.
[26] S. Numa, *Harvey Lect. Ser.* **1989**, *83*, 121.
[27] C. Methfessel, V. Witzemann, T. Takahashi, M. Mishina, S. Numa, B. Sakmann, *Pflügers Arch.* **1986**, *407*, 577.
[28] M. Mishina, T. Takai, K. Imoto, M. Noda, T. Takahashi, S. Numa, C. Methfessel, B. Sakmann, *Nature (London)* **1986**, *321*, 406.
[29] V. Witzemann, B. Barg, Y. Nishikawa, B. Sakmann, S. Numa, *FEBS Lett.*, **1987**, *223*, 104.
[30] V. Witzemann, E. Stein, B. Barg, T. Konno, M. Koenen, W. Kues, M. Criado, M. Hofmann, B. Sakmann, *Eur. J. Biochem.* **1990**, *194*, 437.
[31] N. Unwin, *Neuron*, **1989**, *3*, 665.
[32] V. Witzemann, B. Barg, M. Criado, E. Stein, B. Sakmann, *FEBS Lett.* **1989**, *242*, 419.
[33] V. Witzemann, H. R. Brenner, B. Sakmann, *J. Cell Biol.* **1991**, *114*, 125.
[34] M. Numberger, I. Dürr, W. Kues, M. Koenen, V. Witzemann, *EMBO J.*, **1991**, *10*, 2957.
[35] V. Witzemann, B. Sakmann, *FEBS Lett.*, **1991**, *282*, 259.
[36] B. Hille, *Ionic Channels of Excitable Membranes*, Sinauer Associates Inc., Sunderland, MA, USA, **1984**.
[37] M. Mishina, T. Tobimatsu, K. Imoto, K. Tanaka, Y. Fujita, K. Fukada, M. Kurasaki, H. Takahashi, Y. Morimoto, T. Hirose, S. Inayama, T. Takahashi, M. Kuno, S. Numa, *Nature (London)* **1985**, *313*, 364.
[38] B. Sakmann, C. Methfessel, M. Mishina, T. Takahashi, T. Takai, M. Kurasaki, K. Fukuda, S. Numa, *Nature (London)* **1985**, *318*, 539.
[39] K. Imoto, C. Methfessel, B. Sakmann, M. Mishina, Y. Mori, T. Konno, K. Fukuda, M. Kurasaki, H. Bujo, Y. Fujita, S. Numa, *Nature (London)* **1986**, *324*, 670.
[40] K. Imoto, C. Busch, B. Sakmann, M. Mishina, T. Konno, J. Nakai, H. Bujo, Y. Mori, K. Fukuda, S. Numa, *Nature (London)* **1988**, *335*, 645.
[41] T. Konno, C. Busch, E. von Kitzing, K. Imoto, F. Wang, J. Nakai, M. Mishina, S. Numa, B. Sakmann, *Proc. R. Soc. London B 244*, **1991**, 69.
[42] A. Villarroel, S. Herlitze, M. Koenen, B. Sakmann, *Proc. R. Soc. London B.* **1991**, *243*, 69.
[43] A. Villarroel, B. Sakmann, *Biophys. J.* **1992**, *62*, 196.
[44] P. W. Atkins, M. J. Clugston, *Principles of Physical Chemistry*, Pitman Publishing, London, **1983**.
[45] J. C. Eccles, in *Les Prix Nobel en 1963*, The Nobel Foundation, Stockholm, **1963**, pp. 261–283; *Angew. Chem.* **1964**, *76*, 674–681.
[46] B. Sakmann, O. P. Hamill, J. Bormann, *J. Neural Transm. Suppl.* **1983**, *18*, 83.
[47] H. Betz, *Biochemistry* **1990**, *29*, 3591.
[48] J. Bormann, O. P. Hamill, B. Sakmann, *J. Physiol.* **1987**, *385*, 243.
[49] O. P. Hamill, J. Bormann, B. Sakmann, *Nature (London)* **1983**, *305*, 805.
[50] P. Ascher, L. Nowak, *J. Physiol.* **1988**, *399*, 227.
[51] S. G. Cull-Candy, M. M. Usowicz, *Nature (London)* **1987**, *325*, 525.
[52] C. E. Jahr, C. F. Stevens, *Nature (London)* **1987**, *325*, 522.
[53] T. A. Verdoorn, A. Draguhn, S. Ymer, P. H. Seeburg, B. Sakmann, *Neuron*, **1990**, *4*, 919.
[54] F. A. Edwards, A. Konnerth, B. Sakmann, T. Takahashi, *Pflügers Arch.* **1989**, *414*, 600.
[55] B. Sakmann, F. Edwards, A. Konnerth, T. Takahashi, *Q. J. Exp. Physiol.* **1989**, *74*, 1107.
[56] F. A. Edwards, A. Konnerth, B. Sakmann, with an appendix by C. Busch, *J. Physiol.* **1990**, *430*, 213.
[57] C. Busch, B. Sakmann in *The Brain. Cold Spring Harbor Symp. Quant. Biol.* **1990**, *55*, 69–80.
[58] P. Jonas, B. Sakmann, *J. Physiol.* **1992**, in press.
[59] P. Stern, F. A. Edwards, B. Sakmann, *J. Physiol.* **1992**, 427, 449; P. Jonas, B. Sakmann, *ibid.* **1992**, *446*, 515 P.
[60] C. Franke, H. Hatt, J. Dudel, *Neurosci. Lett.* **1987**, *77*, 199.
[61] D. Colquhoun, P. Jonas, B. Sakmann, *J. Physiol.*, (1992) in press.
[62] L. O. Trussell, G. D. Fischbach, *Neuron*, **1989**, *3*, 209.
[63] M. Hollmann, A. O'Shear-Greenfield, W. Rogers, S. Heinemann, *Nature (London)* **1989**, *342*, 643.
[64] K. Keinänen, W. Wisden, B. Sommer, P. Werner, A. Herb, T. A. Verdoorn, B. Sakmann, P. H. Seeburg, *Science (Washington, D.C.)* **1990**, *249*, 556.
[65] B. Sommer, K. Keinänen, T. A. Verdoorn, W. Wisden, N. Burnashev, A. Herb, M. Köhler, T. Takagi, B. Sakmann, P. H. Seeburg, *Science (Washington, D.C.)* **1990**, *249*, 1580.
[66] M. Hollmann, M. Hartley, S. Heinemann, *Science (Washington, D.C.)* **1991**, *252*, 851.
[67] T. A. Verdoorn, N. Burnashev, H. Monyer, P. H. Seeburg, B. Sakmann, *Science (Washington, D.C.)* **1991**, *252*, 1715.
[68] R. I. Hume, R. Dingledine, S. Heinemann, *Science (Washington, D.C.)* **1991**, *253*, 1028.
[69] N. Burnashev, H. Monyer, P. H. Seeburg, B. Sakmann, *Neuron* **1992**, *8*, 189.
[70] A. Khodorova, N. Burnashev, *J. Physiol.* **1991**, 446, 516 P.
[71] B. Sommer, M. Köhler, R. Sprengel, P. H. Seeburg, *Cell*, **1991**, *67*, 11.

Soft Matter (Nobel Lecture)**

By Pierre-Gilles de Gennes*

What do we mean by soft matter? Americans prefer to call it "complex fluids". This is a discouraging expression, but it does indeed incorporate two of the major features:

1) **Complexity.** We may, in a certain primitive sense, say that modern biology has proceeded from studies on simple model systems (bacteria) to complex multicellular organisms (plants, invertebrates, vertebrates...). Similarly, from the explosion of atomic physics in the first half of this century, one of the outgrowths is soft matter, based on polymers, surfactants, liquid crystals, and colloidal grains.

2) **Flexibility.** I like to explain this through one early polymer experiment, which was initiated by the Indians of the Amazon basin. They collected the sap from the hevea tree, put it on their feet and let it "dry" for a short time whereby they had boots. From a microscopic point of view, the starting point is a set of independent, flexible polymer chains. The oxygen in the air forms a few bridges between the chains, and this results in a spectacular change: We shift from a liquid to a network structure which can resist tension—what we now call a **rubber** (in french: caoutchouc, a direct transcription of the Indian word). What is striking about this experiment, is the fact that a very mild chemical action induces a drastic change in mechanical properties: a feature typical of soft matter.

Of course, with some other polymer systems we tend to build more rigid structures. An important example is an enzyme. This is a long sequence of amino acids, which folds up into a compact globule. A few of these amino acids play a vital role; they form the "active site" which is built to perform a specific form of catalysis (or recognition). An interesting question (raised long ago by Jacques Monod) is the following: We have a choice of twenty amino acids at each point in the sequence, and we want to build a receptor site in which the active units are positioned in space in some strict way. We cannot just put these active units next to one another, because, if linked directly, they would not realize the correct orientations and positions. So, in between two active units, we need a "spacer", a sequence of amino acids which has enough variability to allow a good relative positioning of the active sites at both ends of the spacer. Monod's question was: What is the minimum length of spacers?

It turns out that the answer is rather exactly defined.[1] The magic number is 13 or 14. With less than 13 units, you will not usually succeed in getting the desired conformation, whereas with more than 14 units, you will have many sequences with can adopt it. The argument is primitive: It takes into account excluded volume effects, but it does not recognize the need for a stable enzyme—namely that the interior should be built preferably with hydrophobic units, while the outer surface must be hydrophilic. However, my guess is that this cannot change the magic number by much more than one unit. Indeed, when we look at the spacer sizes in a simple globular protein like myosin, we see that they are not far from the magic number.

Let us return now to **flexible polymers** in solution and sketch some of their strange mechanical properties. One beautiful example is the four-roller experiment set up by Andrew Keller and his co-workers.[2] In this experiment, a dilute solution of coils is subjected to a purely longitudinal shear. If the exit trajectory is well chosen (in the symmetry plane of the exit channel), the molecules are stressed for long periods. What is found is that, if the shear rate $\dot{\gamma}$ exceeds a certain threshold value $\dot{\gamma}_c$, an abrupt transition takes place, and the medium becomes birefringent. This is what I called a "coil–stretch transition".[3] When the shear begins to open the coil, it offers more grip to the flow, and opens even more... leading to an abrupt transition. Here, we see another fascinating aspect of soft matter—the amazing coupling between mechanics and conformations. Indeed, Keller showed that the chains break rather quickly (at shear rates $\dot{\gamma} > \dot{\gamma}_c$), and do so very near to their midpoint—a spectacular result.

Another interesting feature of dilute coils is their ability to reduce the losses in turbulent flows. This is currently called the Toms effect, although in actual fact, it was discovered even before Toms by Karol Mysels.[4] Together with M. Tabor, we tried to work out a scaling model of coils in a turbulent cascade,[5] but our friends in mechanics think that it is not realistic. Time will tell which answer is correct.

I have talked a lot about poylmers, let me now switch to **surfactants**—molecules with two parts, a polar head which likes water, and an aliphatic tail which hates water. Benjamin Franklin performed a beautiful experiment, using surfactants: On a pond at Clapham Common, he poured a small amount of oleic acid, a natural surfactant which tends to form a dense film at the water–air interface. He measured the volume required to cover all the pond and since he knew the area, he was able to calculate the height of the film—something like three nanometers in our current units. This was (to my knowledge) the first measurement of the size of molecules. Nowadays, when we are spoilt with exceedingly complex toys, such as nuclear reactors or synchrotron sources, I particularly like to describe experiments of this Franklin style to my students.

Surfactants allow us to protect a water surface and to generate beautiful **soap bubbles**, which delight our children. Most of our understanding of these soap bubbles is due to a remarkable team: Mysels, Shinoda, and Frankel who wrote *the* book on this subject.[6] Unfortunately this book is now very hard to find; I very much hope that it will be reprinted.

Long ago Françoise Brochard, Jean-François Lennon, and I[7] became interested in some *bilayer* systems, in which we have two sheets of surfactant, each pointing towards the neighboring water. A related (although more complex) sys-

[*] Prof. P.-G. de Gennes
Collège de France
11, Place Marcelin-Berthelo, F-75231 Paris Cedex 05 (France)
or
Ecole Supérieure de Physique et
de Chimie Industrielles de la Ville de Paris (ESPCI)
10, Rue Vauquelin, F-75231 Paris Cedex 05 (France)

[**] Copyright © The Nobel Foundation 1992. We thank the Nobel Foundation, Stockholm, for permission to print this lecture.

tem of this type is a red blood cell. For many years it has been known that, when observed under phase contrast, these cells *flicker*. It was sometimes believed that this flicker reflected an instability of a living system under nonequilibrium conditions. Actually it is much simpler: The essential property of insoluble bilayers is that they optimize their area at fixed surfactant number. Thus the energy remains stationary with respect to area, and the surface tension vanishes. This means that the fluctuations in shape of these deflated cells or "vesicles" are huge; the flicker is just an example of Brownian motion for a very flexible object. What Jean-François had done was to measure space–time correlations for the flicker. Françoise then showed that they could be understood from a model containing no surface tensions, but instead only curvature energies plus viscous forces—another good example of soft matter.

This was, in fact, one of the starting points for many studies on surfactant bilayers (pioneered by W. Helfrich) and, on a more formal side, on random surfaces (especially with D. Nelson). One of the great successes in this field has been the invention of the "sponge phase" of **microemulsions**.[8, 9] More generally, it is amusing to learn from these people that there is some overlap in thought between the highbrow string theories and the descriptions of soaps!

Let me now move to another corner in our garden, **liquid crystals**. Here, I must pay tribute first to two great pioneers: 1) Georges Friedel, who was the first to understand exactly what a liquid crystal is and what the main types are, and 2) Charles Frank, who (following some early work of Oseen) constructed the elastic theory of nematics, and described also a number of their topological defects ("disclinations"). Here I will only cover smectics. Observing certain defects ("focal conics") in smectics, Friedel was able to prove that the structure must be a set of liquid, equidistant, deformable layers.[10] From observations at the 100 μm scale, he was thus able to infer the correct structure at the 10 Å scale—an amazing achievement.

Smectics bring me naturally to another important feature of complex fluids, namely that nowadays it is sometimes possible *to create new forms of matter*. The sponge phase mentioned above was an example. Another striking case was the creation of **ferroelectric smectics** by R. B. Meyer (in Orsay, ca. 1975). He thought about a certain molecular arrangement with chiral molecules which should automatically generate a phase (the "C phase") carrying a non O electric dipole. Within a few months, our local chemists had produced the right molecule, and the first liquid ferroelectric was born![11] These materials have already become very important for display purposes; they commute 10^3 times faster than the nematics in our wristwatches.

Another case of far less importance, however amusing, concerns "ferro-smectic" materials constructed by M. Veyssié and P. Fabre. The starting point is a water-based ferrofluid, which is a suspension of very fine magnetic particles. (Ferrofluids were invented long ago by R. Rosensweig, and have amazing properties.) **Ferro-smectic materials** are a type of club sandwich formed from bilayer| ferrofluid| bilayer|... If a system like this is subjected to a magnetic field $\vec{H}$, it is happier when $\vec{H}$ is parallel to the layers. It is then interesting to observe the sandwich (with a polarizing microscope) in the frustrated situation where $\vec{H}$ is perpendicular to the layers. At very low fields, nothing is seen. However, beyond a certain weak threshold $\vec{H}_c$, figures like flowers grow in the field.[12] We understand this as a two-step process: a) Just above threshold there is a chemical undulation instability; b) later, focal conics appear with a basic size imposed by the original undulation, but also with smaller conics (which are required to fill space correctly). This "club sandwich" is reacting to rather weak magnetic fields (ca. 30 Gauss).

Let me mention yet another new animal: the **Janus grains**, first made by C. Casagrande and M. Veyssié. Like god Janus who had two faces, the grains have two sides, one apolar and the other polar. Thus they have certain features in common with surfactants. There is, however, an interesting difference if we consider the films which they make; for instance, at a water–air interface. A dense film of a conventional surfactant is quite impermeable. On the other hand, a dense film of Janus grains always has some interstices between the grains, and allows for chemical exchange between the two sides: that is, "the skin can breathe". This may possibly be of some practical interest.

The first technique used to make the Janus grains was based on spherical particles half embedded in a plastic and silanated on the accessible side.[13] This produces only microquantities of material. A group at Goldschmidt research developed a much cleverer pathway: The starting point is a collection of *hollow* glass particles (which are commercially

Pierre-Gilles de Gennes was born in Paris in 1932. From 1955 to 1959 he was a research engineer at the Atomic Energy Center (Saclay), where he completed his doctorate on neutron scattering and magnetism under the supervision of A. Abragam and J. Friedel in 1957. After a postdoctoral year with C. Kittel at Berkeley in 1959, he became assistent professor in Orsay in 1961, and soon started research on superconductors and later (1968) on liquid crystals. In 1971 he accepted a professorship at the Collège de France, where his attention turned to polymer physics. Starting in 1980 he became interested in interfacial problems, in particular the wetting and adhesion phenomena. Among the many honors he has received are the Ampère prize of the French Academy of Science, the Harvey and Wolf prizes (both from Israel), and the Nobel prize for Physics. He is member of several societies, including the French Academy of Sciences and the National Academy of Sciences of the USA.

available). There the outer surface is hydrophobized, and finally the particles are crushed! The resulting platelets are hydrophilic on one side and hydrophobic on the other. They are irregular but can be produced in tons.

I would now like to consider the style of soft-matter research. One of the most important features is the possibility of carrying out very simple experiments in the spirit of Benjamin Franklin. Let me mention two examples. The first concerns the **wetting** of fibers. Usually a fiber after being dipped in a liquid, shows a string of droplets, and thus, for some time, people thought that most common fibers were nonwettable. F. Brochard analyzed theoretically the equilibria on curved surfaces, and suggested that in many cases we should have a wetting film on the fiber, in between the droplets. J. M. di Meglio and D. Queré established the existence, and thickness of the film in a very elegant way.[14] They created a pair of neighboring droplets, one small, one large and showed that the small one emptied slowly into the big one (corresponding to the capillarity). By measuring the speed of the process, they could determine the thickness of the film which lies on the fiber and connects the two droplets; the Poiseuille flow rates in the film are very sensitive to thickness.

Another elegant experiment in wetting concerns the collective modes of a contact line, the edge of a drop standing on a solid. If one distorts the line by some external means, it returns to its equilibrium shape with a relaxation rate dependent upon the wavelength of the distortion, which we wanted to study. But how could we distort the line? I thought of very complex tricks, using electric fields from an evaporated metal comb, or other, even worse procedures. However, Thierry Ondarcuhu came up with a simple method. First he prepared the unperturbed contact line L by putting a large droplet on a solid. Then he dipped a fiber in the same liquid and obtained (from the Rayleigh instability) a very periodic string of drops. Subsequently, he laid the fiber on the solid, parallel to L, and generated a line of droplets on the solid. Finally he pushed the line L (by tilting the solid) until L touched the droplets; then coalescence took place, and he had a single, wavy line on which he could measure relaxation rates.[15].

I have emphasized experiments more than theory. Of course we need some theory when thinking of soft matter. In fact some amusing theoretical analogies sometimes arise between soft matter and other fields. S. F. Edwards is responsible for one important example.[16] He showed a beautiful correlation between the conformations of a flexible chain and the trajectories of a nonrelativistic particle, the statistical weight of the chain corresponding to the propagator of the particle. In the presence of external potentials, both systems are governed by exactly the same Schrödinger equation! This observation has been the key to all later developments in polymer statistics.

Another amusing analogy relates the smectic A phases to superconductors. This was discovered simultaneously by the late W. McMillan (a great scientist, whom we all miss) and by ourselves. Later, it was exploited artistically by T. Lubensky et al.[17] Here again, we see a new form of matter being created! We knew that type II superconductors let in the magnetic field in the form of quantized vortices. The analogy here is a smectic A phase into which we add chiral solutes. These play the role of the field. In some favorable cases, as predicted in 1988 by Lubensky, this may generate a smectic phase drilled by screw dislocations, the so-called A* phase. This was discovered experimentally only one year later by Pindak and coworkers[18]—a beautiful feat.

Let me now end this sentimental journey into soft matter, with a brief mention of my companions. Some were met along the way, like Jean Jacques, a great creator of liquid crystals, and Karol Mysels, the undisputed master of surfactant science. Some others were with me all the way: Henri Benoit and Sam Edwards, who taught me polymer science; Jacques des Cloizeaux and Gérard Jannink, who have produced a highly theoretical book on this subject. Finally an inner core of fellow travelers, over all forms of land and sea: Phil Pincus, Shlomo Alexander, Etienne Guyon, Madeleine Veyssié, and last but not least, Françoise Brochard, sans laquelle les choses ne seraient que ce qu'elles sont.

The final lines are not mine; they relate to an experiment on soft matter (taken from Eugène Boudin a French painter of the 18th century) which is shown in the figure below. No conclusion could be more appropriate.

Received: January 31, 1992 [A 873 IE]
German version: *Angew. Chem.* **1992**, *104*, 856

La Souffleuse de Savon.
Amusons-nous. Sur la terre et sur l'onde Malheureux, qui se fait un nom! Richesse, Honneurs, faux éclat de ce monde, Tout n'est que boules de savon.[*]

[*] The portrait of the lady blowing soap bubbles is inscribed: "Have fun on sea and land. Unhappy it is to become famous. Riches, false glitters of this world, All is but soap bubbles."

[1] For a recent copy of this work see *Introduction to Polymer Dynamics* (Lezione Lincei), Cambridge Univ. Press, Cambridge, England, **1990**, Chapter 2.
[2] J. A. Odell, A. Keller in *Polymer-flow Interactions* (Ed.: I. Rabin), Am. Inst. Phys., New York, **1985**; A. Keller, J. Odell, *Colloid Polym. Sci*, **1985**, *263*, 181.
[3] P. G. de Gennes, *J. Chem. Phys.* **1974**, *60*, 5030.
[4] For a historical review: K. Mysels, *Chem. Eng. Prog. Symp.* **1971**, *67*, 45.
[5] M. Tabor, P. G. de Gennes, *Europhys. Lett.* **1986**, *2*, 519, P. G. de Gennes *Physica* **1986**, *140 A*, 9.
[6] K. Mysels, K. Shinoda, S. Frankel, *Soap Films*, Pergamon, London, **1959**.
[7] F. Brochard, J. F. Lennon, *J. Phys.(Paris)* **1976**, *36*, 1035.
[8] G. Porte, J. Marignan, P. Bassereau, R. May, *J. Phys. (Paris)* **1988**, *49*, 511.
[9] D. Roux, M. E. Cates in *Proc. 4th Nishinomya-Yukawa Symp.*, Springer, Heidelberg, **1992**, in press.
[10] G. Friedel, *Ann. Phys.* **1922**, *18*, 273.
[11] R. B. Meyer, L. Liebert, L. Strzelecki, P. Keller, *J. Phys. Lett.* **1975**, 69.
[12] P. Fabre, C. Casagrande, M. Veyssié, V. Cabuil, R. Massart ("Ferrosmectics: A New Magnetic and Mesomorphic Phase"), *Phys. Rev. Lett.* **1990**., *64*, 539.
[13] C. Casagrande, M. Veyssié, *C. R. Acad. Sci. (Paris)*, **1988**, *306 II*, 1423; C. Casagrande, P. Fabre, M. Veyssié, E. Raphaël, *Europhys. Lett.* **1989**, *9*, 251.
[14] J. M. di Meglio, *C. R. Acad. Sci. (Paris)* **1986**, *303 II*, 437.
[15] T. Ondarcuhu, M. Veyssié, *Nature* **1991**, *352*, 418.
[16] S. F. Edwards, *Proc. Phys. Soc. (London)* **1965**, *85*, 613.
[17] S. R. Renn, T. Lubensky, *Phys. Rev. A* **1988**, *38*, 2132.
[18] J. W. Goodby, M. A. Waugh, S. M. Stein, E. Chin, R. Pindak, J. S. Datel, *J. Am. Chem. Soc.* **1989**, *111*, 8119.

VCH Index Library

The electronic version can be read by all MS-DOS compatible computers. It is accessed by the Search module of the Literature Management Program VCH-Biblio.

ANGEWANDTE CHEMIE
A Journal of the Gesellschaft Deutscher Chemiker
International Edition in English

30 Year Index of Reviews
– in print or on diskette –

The reviews in Angewandte Chemie are amongst the most often cited chemical publications of each year. Many have become classics of the chemical literature. For thirty years they have been available in English as well as German. The 30 year review index now celebrates this anniversary by facilitating access to these important documents of the rapid development of our discipline. The index—both a chemical dictionary and a history book—offers you:

1. A list of all authors, indicating the main author and the title of the review.
2. A subject index giving the main author.
3. Both indexes provide complete information on date of issue and first and last page numbers of the German and English editions.

The electronic version of the index is available on 5¼" and 3½" diskettes.

The price of the index is DM 98.00, $ 64.00 or £ 37.00. Please order by telephone or in writing to **VCH, Software und Datenbanken, Postfach 10 11 61, D-W-6940 Weinheim, Tel. 0 62 01/6 02-2 71, Telefax 0 62 01/6 02-3 28.**

Cyclodextrins, Off-the-Shelf Components for the Construction of Mechanically Interlocked Molecular Systems

By *J. Fraser Stoddart**

If any one theme is beginning to dominate the development of synthetic chemistry these days, it must surely be self-assembly.[1] The spread of this concept, though somewhat belated, into all branches of chemistry is mainly due to the rapidly accelerating growth and acceptance of supramolecular chemistry.[2] Long before chemists were thinking and practicing their own brands of chemistry beyond the molecule with wholly synthetic systems, nature had been extolling the virtues of molecular recognition in the production of sophisticated molecular and supramolecular arrays with linked form and function.

If one class of compound has provided the bridge between the worlds of natural und unnatural hosts, it has been the cyclodextrins—or CDs as insiders call them. Yet, even as they enter their second century[3a] of cultivation by chemists, they continue to fascinate the chemical community.[3b] The reasons are quite simple: They are aesthetic molecules, and they lend themselves to novel experiments. The recent reports[4–7] from four research laboratories in four different countries of the self-assembly of CDs into [2]rotaxanes and polyrotaxanes (Fig. 1) serve to remind us all that there is still a lot of innovation to be forged in and around CDs in the coming one-hundred years.

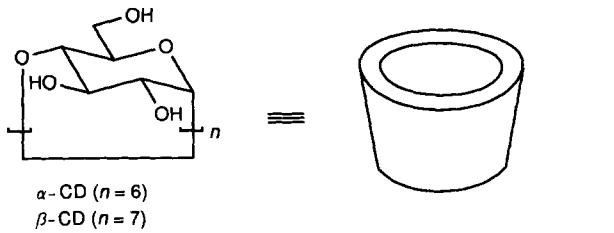

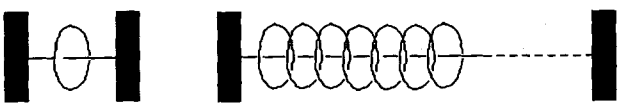

Fig. 1. Schematic representation of α-cyclodextrin (α-CD) and β-cyclodextrin (β-CD) (top), a [2]rotaxane (bottom left), and a polyrotaxane (bottom right).

The self-assembly of the [2]rotaxane–metal complexes with α-CD, described by Wylie and Macartney[4] from Queen's University, Kingston, Ontario (Canada), happens (Scheme 1) irrespective of the order of the addition of the components—the α-cyclodextrin, the 1,1″-(α,ω-alkanediyl)-bis(4,4′-bipyridinium) bromide, and the precursor for the $[Fe(CN)_5(OH_2)]^{3-}$ stoppers, solid $Na_3[Fe(CN)_5NH_3] \cdot 3H_2O$,—to an aqueous reaction mixture. Indeed, the [2]rotaxane is formed even when α-CD is added to the dumbbell-shaped component, $[(NC)_5Fe\{bpy(CH_2)_nbpy\}Fe(CN)_5]^{4-}$. This infers a slow dissociation of one of the $[Fe(CN)_5]^{3-}$ stoppers, formation of a semirotaxane, $[\{bpy(CH_2)_nbpy \cdot \alpha\text{-CD}\}Fe(CN)_5]^-$, and its subsequent rapid recomplexation by $[Fe(CN)_5(OH_2)]^{3-}$ to give the [2]rotaxane. Evidence for the formation of a [2]rotaxane is provided by the ^1H NMR spectra, in which the signals of the symmetry-related protons of the $[bpy(CH_2)_nbpy]^{2+}$ unit are split by the end-to-end asymmetry of the trapped α-CD ring. It is very likely that a family of such [2]rotaxanes will now emerge, since the 4,4′-bipyridine thread can be replaced by pyrazine and other stoppers such as $[M(CN)_5]^{n-}$ and $[M(NH_3)_5]^{m+}$ ions with redox-active d^6 metal (M) centers like Co, Ru, Os, and Fe are conceivable.[1,7]

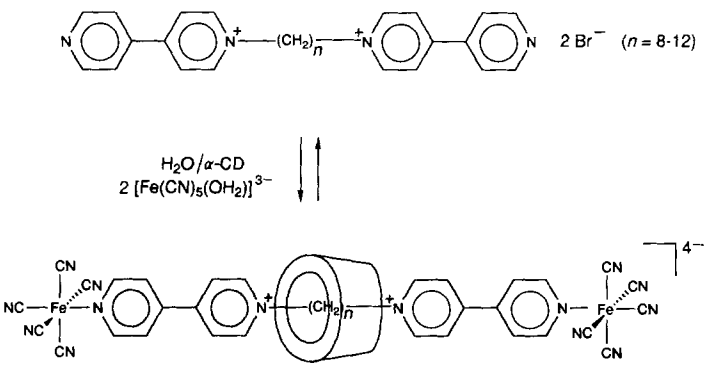

Scheme 1. The [2]rotaxane–metal complex of Wylie and Macartney [4].

The self-assembly of the asymmetric zwitterionic [2]rotaxanes incorporating α-cyclodextrin announced towards the end of last year by Isnin and Kaifer[5] from the University of Miami in Florida (USA), demonstrates a beautifully simple and logical step-by-step approach to what are really quite complicated compounds (Scheme 2). Because alkyldimethyl(ferrocenylmethyl)ammonium cations are known to interact with α-CD and β-CD through their alkyl groups and ferrocene subunits, respectively, the alkyl chain was terminated with carboxyl groups: **1**, $n = 7$; **2**, $n = 11$. Although their binding to α-CD is now pH dependent (for **1** · α-CD $K_a = 425\ M^{-1}$ at pH 2.6; $K_a = 71\ M^{-1}$ at pH 8.0), both are bound in water. The subsequent capping of the carboxyl groups is achieved with potassium 5-amino-2-naphthalenesulphonate with the water-soluble catalyst 1-[3-(dimethylamino)propyl]-3-ethylcarbodiimide hydrochloride (EDC) to promote amide bond formation. In both cases, the isomeric zwitterionic [2]rotaxanes **3a**, **b** and **4a**, **b** can be isolated from the reaction mixtures in 15% yield. The iso-

[*] Prof. J. F. Stoddart
School of Chemistry, The University of Birmingham
Edgbaston, Birmingham B15 2TT (UK)

 © VCH Verlagsgesellschaft mbH, W-6940 Weinheim, 1992 0570-0833/92/0707-0846 $ 3.50+.25/0

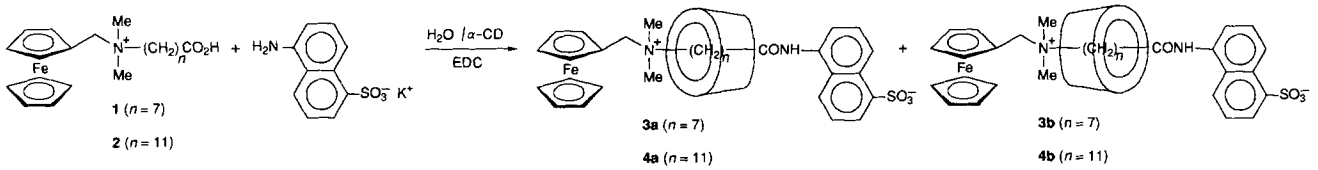

Scheme 2. The zwitterionic [2]rotaxanes of Isnin and Kaifer [5].

mers have since been separated,[8] and the relative orientations of the α-CD ring on the asymmetric dumbbell-shaped component have been established: One isomer is stable but the other one unthreads slowly! Again, the authors recognize the generality of their self-assembly procedure and anticipate the production of "a diversity of rotaxane structures having threaded cyclodextrins."

The isomer phenomenon literally takes on a further dimension in polyrotaxanes, for which the view is growing[8] that CDs might thread under conditions of equilibrium control with alternating orientations, wherein adjacent rings are matched head-to-head, tail-to-tail in order to optimize hydrogen bonding between the neighboring CD units.

In the knowledge[9] that chains of poly(ethyleneglycol) (PEG) thread α-CD beads like a necklace, Harada, Li, and Kamachi[6] at Osaka University in Japan have now succeeded in capping the chain ends of a poly(ethyleneglycol)diamine (PEG-DA; M_w 3450) with dinitrophenyl stoppers. The reaction was carried out in a solution of the PEG-BA in dimethylformamide (DMF) saturated with α-CD and laced with a gross excess (46 mol equiv) of 2,4-dinitrofluorobenzene. After an extensive purification procedure, full characterization of the product, which was obtained in high yield (60%), indicated average molecular weights of 23200 (by ^{1}H NMR) and 26400 (by UV) commensurate with the respective threading of 20 and 23 α-CD rings per polyrotaxane molecule (Fig. 2). This type of molecular structure conjures up the image of a molecular abacus[10] in terms of both structure and dynamics.

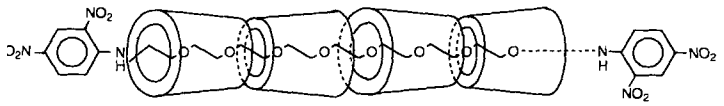

Fig. 2. Schematic representation of the polyrotaxane [6] constructed by Harada et al. by the threading of a poly(ethyleneglycol)diamine (PEG-DA) chain with α-cyclodextrin "beads" and coupling with dinitrophenyl (DNP) stoppers.

Quite independently, Wenz and Keller,[7] working at the Max-Planck-Institut für Polymerforschung in Mainz (Germany), have demonstrated the threading of CD molecules onto two polymer chains (Scheme 3): poly(iminoundecamethylene) **5a** with a $P_n = 43 \pm 5$ and poly(iminotrimethyleneiminodecamethylene) **5b** with a $P_n = 23 \pm 2$. Both ^{1}H NMR spectroscopy and viscosity measurements revealed that, whereas α-CD threads onto **5a** within a couple of hours, it takes over a week for **5b** to receive its full complement of α-CD rings in aqueous solution. Although equilibrium dialysis of **5a** · $(\alpha\text{-CD})_n$ into its separate components was over within 15 hours, dissociation of **5b** · $(\alpha\text{-CD})_n$ was far from complete after two weeks. When **5b** · $(\alpha\text{-CD})_n$ was treated with nicotinoyl chloride to introduce at least two hydrophilic nicotinoyl blocking groups at arbitrary positions along the poly(iminooligomethylene) chain, a polyrotaxane of M_w 55000 ± 5000 (determined by laser light scattering) was isolated with an average of 37 α-CD rings permanently threaded on to the chain.

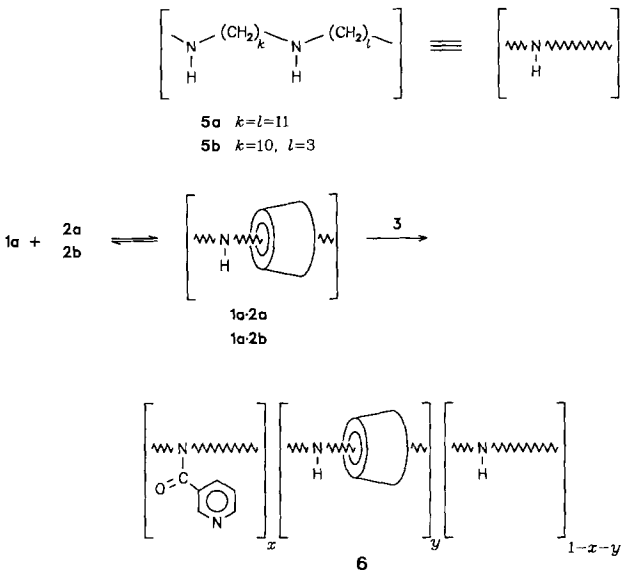

Scheme 3. The [2]rotaxanes and the polyrotaxane of Wenz and Keller [7].

These exciting developments surrounding the CDs[11] have been going on against a background of activity in other laboratories on wholly synthetic rotaxanes[12–15] and polyrotaxanes.[16] Self-assembly is the unifying concept in the construction of all these mechanically interlocked molecular systems. As we begin to comprehend the rules of the game for different systems in a range of media, our fundamental understanding of molecular recognition benefits by leaps and bounds. Applications will begin to surface on a somewhat longer time-scale. Suffice it to say at present that there are high hopes for the advent of new materials with both novel forms and functions.

German version: *Angew. Chem.* **1992**, *104*, 860

[1] D. Philp, J. F. Stoddart, *Synlett*, **1991**, 445.
[2] J.-M. Lehn, *Angew. Chem.* **1988**, *100*, 91; *Angew. Chem. Int. Ed. Engl.* **1988**, *27*, 89; *ibid.* **1990**, *102*, 1347 and **1990**, *29*, 1304.
[3] a) J. F. Stoddart, *Carbohydr. Res.* **1989**, *192*, xii; b) W. Saenger, *Angew. Chem.* **1980**, *92*, 343; *Angew. Chem. Int. Ed. Engl.* **1980**, *19*, 344.
[4] R. S. Wylie, D. H. Macartney, *J. Am. Chem. Soc.* **1992**, *114*, 3136.
[5] R. Isnin, A. E. Kaifer, *J. Am. Chem. Soc.* **1991**, *113*, 8188.
[6] A. Harada, J. Li, M. Kamachi, *Nature* **1992**, *356*, 325.
[7] G. Wenz, B. Keller, *Angew. Chem.* **1992**, *104*, 201; *Angew. Chem. Int. Ed. Engl.* **1992**, *31*, 197.
[8] See the comments in an article by R. Dagani, *Chem. Eng. News*, **1992**, *70* (15) 39.

[9] A. Harada, M. Kamachi, *J. Chem. Soc. Chem. Commun.* **1990**, 1322; see also *Macromolecules* **1990**, *23*, 2821.
[10] M. V. Reddington, A. M. Z. Slawin, N. Spencer, J. F. Stoddart, C. Vicent, D. J. Williams, *J. Chem. Soc. Chem. Commun.* **1991**, 630.
[11] For examples of comb-shaped rotaxane polymers containing noncovalently bound CDs in the side chains, see M. Born, H. Ritter, *Makromol. Chem. Rapid Commun.* **1991**, *121*, 471.
[12] J. F. Stoddart in *Host-Guest Molecular Interactions—From Chemistry to Biology* (*Ciba Found. Symp. No. 158*), Wiley, Chichester, **1991**, p. 5.
[13] P. L. Anelli, N. Spencer, J. F. Stoddart, *J. Am. Chem. Soc.* **1991**, *113*, 5131.
[14] P. R. Ashton, M. Grognuz, A. M.Z. Slawin, J. F. Stoddart, D. J. Williams, *Tetrahedron Lett.* **1991**, *32*, 6235.
[15] P. L. Anelli, P. R. Ashton, R. Ballardini, V. Balzani, M. Delgado, M. T. Gandolfi, T. T. Goodnow, A. E. Kaifer, D. Philp, M. Pietraszkiewicz, L. Prodi, M. V. Reddington, A. M.Z. Slawin, N. Spencer, J. F. Stoddart, C. Vicent, D. J. Williams, *J. Am. Chem. Soc.* **1992**, *114*, 193.
[16] Y. X. Shen, H. W. Gibson, *Macromolecules*, **1992**, *25*, 2058.
[17] After completion of this article a *lipophilic* [2]rotaxane was described (that reported by Wylie and Macartney is *hydrophilic*); G. Wenz, E. van der Bey, L. Schmidt, *Angew. Chem.* **1992**, *104*, 758; *Angew. Chem. Int. Ed. Engl.* **1992**, *31*, 783.

Protein Engineering: Modified Hemoglobin as a Blood Substitute

By *Timm-H. Jessen* and *Rolf Hilgenfeld**

A few years ago, the use of gene technology for modifying and redesigning proteins in order to improve their properties ("protein engineering"[1]), enjoyed generous support by national and international programs. This enthusiasm appears to be gradually waning—today's buzzwords are different ones, such as glycobiology and nanotechnology. And indeed, it seems that some protagonists in the field of protein engineering promised more than they have been able to deliver, at least in the short term. The design of enzymes tailored to fit the requirements for the catalysis of organic reactions with the desirable high stereoselectivity has up to now only been successful in exceptional cases. This is not surprising since our understanding of the relationship between the structure of proteins and their function is still rather limited. While the rapid and spectacular successes, with the exception of a few washing powder proteases, were to a large extent not achieved, protein engineering has now entered a phase of consolidation, during which realistic questions can be treated in a sound scientific manner—and not surprisingly, the fruits of the work are slowly beginning to ripen. This is particularly evident for proteins that are employed as therapeutics, where properties can be adjusted by genetic modification to meet the requirements more effectively. Thus the period of time after injection before human insulin takes effect can be significantly shortened by the specific exchange of certain amino acid residues.[2] Other modifications of the hormone lead to a prolonged activity, thereby reducing the number of injections necessary per day[3]. This, of course, should make life easier for diabetics.

For the rational design of such amino acid exchanges, a precise knowledge of the three-dimensional structure of the protein is necessary. This can be achieved in some cases (for small proteins) by NMR techniques, and in general, by protein crystallography. Thus, the X-ray structure analysis of hemoglobin determined by M. Perutz et al. (MRC, Cambridge)[4] formed the basis for the modification of this blood protein by genetic engineering as reported recently in *Nature* by K. Nagai et al. (MRC), together with reseachers from Somatogen (Boulder, Colorado).[5] With this modified hemoglobin an effective, and at the same time safe, blood substitute seems at last to be within reach after decades of intensive research.

Hemoglobin is crucial for the transport of oxygen in the body. Enclosed in the red blood cells, the protein is supplied with oxygen in the lungs, and delivers it to the respiratory cycle in the capillaries of the tissue. Hemoglobin consists of 2 α and 2 β polypeptide chains ($\alpha_2\beta_2$ tetramer), each including a protoporphyrin IX (the heme) with a Fe^{2+} ion. Local variations in the partial pressure of the gas, allosteric effectors, as well as the cooperativity of the tetramer modulate the oxygen affinity of the hemoglobin in an ideal way.[6] Since hemoglobin is a vital constituent of the blood, its application as a blood substitute seemed logical. There has always been a need for such a substitute in the face of problems associated with blood transfusions (availability, matching of blood groups, and storage stability); however, in recent years this need has become urgent as a result of the emergence of pathogenic viruses.[7]

Since, however, the use of hemoglobin as a blood substitute is not free of problems, other completely different approaches have also been considered. Synthetic oxygen carriers have been developed from perfluorohydrocarbons, which when applied as an emulsion can bind oxygen in quantities proportional to its partial pressure. The low viscosity of the emulsions, as well as the potential to utilize them in cases in which religion prohibits blood transfusions, increased the attractiveness of this approach.[8] At present perfluorooctylbromide is undergoing clinical trials and shows fewer of the potential problems of this class of substitutes—low oxygen capacity, immunogenicity, hepatotoxicity, and insufficient storage stability.[9]

The majority of the research approaches, however, are based on the hemoglobin molecule itself. Already in 1916 an intravenous infusion of a hemoglobin solution was carried out on humans.[10] Hemoglobin can be obtained from erythrocytes whose expiry date has already passed. During the purification process the complete removal of the cell membrane (stroma) must be carried out very carefully because it can induce a strong immune reaction.[11] Even hemoglobin itself shows this immunogenic behavior if it is present in

[*] Dr. R. Hilgenfeld, Dr. T.-H. Jessen
Hoechst Aktiengesellschaft
Postfach 800320
D-W-6230 Frankfurt 80 (FRG)

large amounts in the plasma instead of in the red blood cells. With the use of hemoglobin from cattle or pigs as a blood substitute the danger of immunotoxicity could be considerably greater.[12]

Hemoglobin can only fulfill its physiological task within the erythrocytes. Only there is 2,3-diphosphoglycerate (DPG) present, the essential allosteric effector for controlling oxygen delivery to the tissues.[13] Also, it is only within the erythrocytes that the concentration of hemoglobin is high enough to ensure the stability of the tetramer. These circumstances cause a fatal synergism as soon as hemoglobin is free in the plasma: its oxygen affinity is so high that the tissue is not supplied with enough oxygen, the oxygenated form of hemoglobin readily decomposes in dilute solution to $\alpha\beta$ dimers,[6] and these are so small (molecular weight of 32 kD) that they are excreted by the kidneys. In large quantities the $\alpha\beta$ dimers can cause severe damage to this organ.[14] Therefore, the efforts to use hemoglobin as a blood substitute have concentrated on its encapsulation in liposomes,[15] as well as on modifications of the protein, which stabilize the structure of the tetramer and at the same time reduce its oxygen affinity. Up to now, chemical crosslinking of the subunits by glutaric or fumaric acid derivatives has been the most successful strategy.[16] However, low yield and purity of the modified hemoglobins, insufficient cooperativity and product stability, as well as problems in clinical trials, have so far limited this approach.[9]

Since the end of the 1970s hemoglobin has also been a focus of genetic engineering. While initially α and β chains were expressed separately, the expression of a fully functional human hemoglobin is nowadays possible in *E. coli* and yeast, as well as in transgenic mice and pigs.[17] Of course, these recombinant hemoglobins cannot be used in unmodified form as blood substitutes, since just like the protein isolated from erythrocytes they display too high an oxygen affinity in the absence of 2,3-diphosphoglycerate and dissociate into dimers. Both problems have now been solved by the researchers at the MRC and Somatogen by using a genetic approach.[5] The *C* terminus of one of the two α chains, in the three-dimensional structure close to the *N* terminus of the other α polypeptide chain, was linked to the latter by a glycine residue. Fortunately this fusion did not cause a substantial reduction of the cooperativity, but it prevented the dissociation into dimers and thus led to a prolonged in vivo half-life of the hemoglobin. Furthermore, the β108 Asn → Lys mutation, which had been found in a naturally occurring hemoglobin with reduced oxygen affinity (hemoglobin Presbyterian),[18] was introduced into the β gene, and thus the oxygen affinity of the recombinant product was indeed reduced. Tests on rats and dogs have so far been very promising.[5]

It is difficult to judge whether the researchers at Somatogen and MRC have taken the lead in the race for an efficient and safe blood substitute with their work. It definitely is a race: at least seven companies are carrying out intensive research and development work in this field in an effort to be the first suppliers on the world market, which is estimated to be worth some 10 billion dollars. Because of this keen competition, very little information is published. This results in some rumor mongering; for example, there have been suspicions about cases of kidney failure in volunteers following the administration of unmodified hemoglobin as recently as 1978 when much was already known about the dangers associated with this approach.[19] To put a stop to such practices and create a greater openness the FDA (Food and Drug Administration) called a meeting of the leading companies and research groups almost two years ago. This resulted in an acknowledged catalogue of requirements that potential blood substitutes must fulfill before they can undergo clinical testing. Somatogen has now met the demand for greater openness with its publication in *Nature*; it remains to be seen whether the genetically modified hemoglobin, which was so successful in animals, will pass the clinical examination.

German version: *Angew. Chem.* **1992**, *104*, 862

[1] R. Hilgenfeld in *Biotechnology Focus 2*: (Eds.: R. K. Finn, P. Präve), Hanser, München, **1990**, p. 135.

[2] J. Brange, U. Ribel, J. F. Hansen, G. Dodson, M. T. Hansen, S. Havelund, S. G. Melberg, F. Norris, K. Norris, L. Snel, A. R. Sorensen, H. Q. Voigt, *Nature* **1988**, *333*, 679.

[3] H. Berchtold, A. Liesum, M. Dörschug, K. Geisen, U. Grau, P. Habermann, R. Obermeier, D. Schwabe, G. Seipke, L. Vertesy, R. Hilgenfeld in *Insulin Receptor and Insulin Action – Molecular and Clinical Aspects* (Eds.: E. Bonora, M. Gigolini, P. Moghetti, G. Zoppini), Verona, **1990**, p. 24.

[4] G. Fermi, M. Perutz, M. Shaanan, R. Fourme, *J. Mol. Biol.* **1984**, *175*, 159.

[5] D. Looker, D. Abbott-Brown, P. Cozart, S. Durfee, S. Hoffmann, A. J. Mathews, J. Miller-Roehrich, S. Shoemaker, S. Trimble, G. Fermi, N. Komiyama, K. Nagai, G. L. Stetler, *Nature* **1992**, *356*, 258.

[6] H. F. Bunn, B. G. Forget, *Hemoglobin: Molecular, Genetic and Clinical Aspects*, Saunders, Philadelphia, **1986**; G. K. Ackers, H. R. Halvorson, *Proc. Natl. Acad. Sci. USA* **1974**, *71*, 4312.

[7] *Blood Substitutes* (Ed.: K. C. Lowe), VCH, Weinheim, **1988**.

[8] T. Mitsuno, H. Ohyanagi, R. Naito, *Ann. Surg.* **1982**, *195*, 60.

[9] S. J. Urbaniak, *Brit. Med. J.* **1991**, *303*, 1348.

[10] A. N. Sellards, G. R. Minot, *J. Med. Res.* **1916**, *34*, 469.

[11] S. F. Rabiner, J. R. Helbert, H. Lopes, L. H. Friedman, *J. Exp. Med.* **1967**, *126*, 1127.

[12] N. Yoshioka, M. Z. Atassi, *Biochem. J.* **1986**, *234*, 441; T. M. S. Chang, *Transfus. Med. Rev.* **1989**, *3*, 213.

[13] Bovine hemoglobin, whose oxygen affinity is not modulated by DPG, is an exception [7]. This may be the reason for the development of this variant as a blood substitute by Biopure Inc. (Boston Massachusetts).

[14] H. F. Bunn, W. T. Esham, R. W. Bull, *J. Exp. Med.* **1969**, *129*, 909; H. F. Bunn, J. H. Jandl, *ibid.* **1969**, *129*, 925.

[15] R. Rabinovici, A. S. Rudolf, F. S. Ligler, T. L. Yue, G. Feuerstein, *Circ. Shock* **1990**, *32*, 1.

[16] E. Bucci, A. Razynska, B. Urbaitis, C. Fronticelli, *J. Biol. Chem.* **1989**, *264*, 6191; S. R. Snyder, E. V. Welty, R. Y. Walder, L. A. Williams, J. A. Walder, *Proc. Natl. Acad. Sci. USA* **1987**, *84*, 7280; L. R. Manning, S. Morgan, R. C. Beavis, B. T. Chait, J. M. Manning, J. R. Hess, M. Cross, D. L. Currell, M. A. Marini, R. M. Winslow, *ibid.* **1991**, *88*, 3329.

[17] S. J. Hoffman, D. L. Looker, J. M. Roehrich, P. E. Cozart, S. L. Durfee, J. L. Tedesco, G. L. Stetler, *Proc. Natl. Acad. Sci. USA* **1990**, *87*, 8521; M. Wagenbach, K. O'Rourke, L. Vitez, A. Wieczorek, S. Hoffman, S. Durfee, J. Tedesco, G. Stetler, *Bio/Technology* **1991**, *9*, 57; R. R. Behringer, T. M. Ryan, M. P. Reilly, T. Asakura, R. D. Palmiter, R. L. Brinster, T. M. Townes, *Science* **1989**, *245*, 971; *Genet. Technol. News.* **1992**, *12* (3), 8.

[18] W. F. Moo-Penn, J. A. Wolff, G. Simon, M. Vacek, D. L. Jue, M. H. Johnson, *FEBS Lett.* **1978**, *92*, 53.

[19] E. Parry in [7], p. 37.

A Safe Synthesis of Diphosphazenium Salts

By *Reinhard Link* and *Reinhard Schwesinger**

Recently we published a short communication entitled "Stable Phosphazenium Ions in Synthesis—an Easily Accessible, Extremely Reactive "Naked" Fluoride Salt".[1] A procedure for the synthesis of the cation **1** was given with nitromethane as solvent. Although conclusive information is not yet available, there is some indication that nitromethane might be explosive in connection with Lewis acids or amines.[2] We therefore recommend the following procedure for production of the **1**-BF_4, the precursor of the fluoride salt.

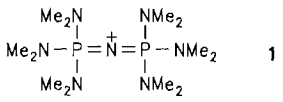

1

1-BF_4: A finely ground mixture of NH_4Cl (17.83 g, 0.333 mol) and NaCl (50 g) together with PCl_5 (208.5 g, 1.00 mol) was heated at reflux in 300 mL $POCl_3$ with vigorous stirring, until the gas evolution (HCl) ceased (ca. 2 h). The solvent was removed by distillation, and the residue was dried under high vacuum at 20 °C, then taken up in 300 mL of dry chlorobenzene. Dimethylamine (360 g, 8.00 mol, free of primary amines and dried over Na_2O) was then passed into the mixture at −20 °C (delivery tube above the solution). After the reaction mixture had been stored at 20 °C for 7 d, a solution of $NaBF_4$ (36.7 g, 0.333 mol) in 500 mL of water was added to the mixture with stirring. (Caution: The solution may contain traces of hexamethylphosphoric triamide. The organic phase was removed and the aqueous phase extracted once more with 50 mL chlorobenzene. The combined organic layers were concentrated in vacuum. The residue was dried in a high vacuum and recrystallized from water. For the subsequent reaction to give **1**-F, **1**-BF_4 was recrystallized from THF (800 ml) and dried under a high vacuum. Yield 103 g (72%); m.p. 260 °C (decomp.). Correct elemental analysis (C,H,N). ^1H NMR (250 MHz, $CDCl_3$, 30 °C, TMS): $\delta = 2.69$ (m).

Received: May 2, 1992
German version: *Angew. Chem.* **1992**, *104*, 864

CAS Registry numbers:
1-BF_4, 137334-98-6; PCl_5, 10026-13-8; dimethylamine, 124-40-3.

[*] Priv.-Doz. Dr. R. Schwesinger, Dipl.-Chem. R. Link
Institut für Organische Chemie und Biochemie der Universität
Albertstrasse 21, D-W-7800 Freiburg (FRG)

[1] R. Schwesinger, R. Link, G. Thiele, H. Rotter, D. Honert, H.-H. Limbach, F. Männle, *Angew. Chem.* **1991**, *103*, 1376; *Angew. Chem. Int. Ed. Engl.* **1991**, *30*, 1372.
[2] L. Roth, U. Weller, *Gefährliche Chemische Reaktionen*, ecomed Verlagsgesellschaft mbH, Landsberg, **1982**.

 © *VCH Verlagsgesellschaft mbH, W-6940 Weinheim, 1992* *0570-0833/92/0707-0850 $ 3.50+.25/0*

Communications may be submitted in English *or* in German. Further details regarding the submission of communications can be found in the "Notice to Authors" reproduced in the January issue of the journal. Copies thereof may be obtained from the editorial office upon request.

Reaction of Heterodinuclear μ-Ethynediyl Complexes Containing Palladium and Platinum: Multiple and Successive Insertion of Isocyanides

By *Kiyotaka Onitsuka, Takashi Joh,* and *Shigetoshi Takahashi**

Extensive studies have been made on the insertion of isocyanide into M–C bonds of various transition metal complexes.[1] Some transition metal complexes such as $[Ni(CO)_4]$, $[Co_2(CO)_8]$,[2] and Ni^{II} compounds[3, 4b] catalyze the polymerization of isocyanide; however, living polymerization is quite rare.[4]

We previously reported on the selective insertion of two molecules of aryl isocyanides into just one of the two Pd–C bonds of μ-ethynediyldipalladium complexes[5] and on the syntheses of heterodinuclear μ-ethynediyl complexes containing palladium and platinum.[6] We have now examined the reactivity of μ-ethynediyl-PtPd complexes toward isocyanides, and observed that multiple and successive insertions of isocyanides occur at the Pd–C bonds. The heterodinuclear complex **1a**, on treatment with 2 equivalents of phenyl isocyanide in THF under reflux, gave an orange, air-stable complex (**2a**) in 94% yield. The characterization by spectroscopic analyses[7] indicated that complex **2a** was a double-insertion product formed by the selective insertion of two molecules of the isocyanide into the Pd–C bond of **1a**. Similarly, *p*-nitrophenyl isocyanide and *p*-tolyl isocyanide reacted with **1a** to give double-insertion products **2b** and **2c**, respectively.

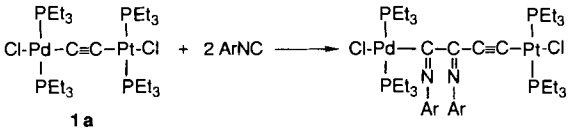

When **1a** was treated with 10 equivalents of phenyl isocyanide under the same conditions, no isocyanide was recovered and an oligomeric complex (**3**) was obtained. The average molecular weight of **3** was determined to be 1850 by vapor pressure osmometry (in benzene), which corresponds to the product derived from one molecule of **1a** and ten molecules of phenyl isocyanide. In the ^1H NMR spectrum the ratio of aromatic protons on PhNC to aliphatic protons on triethylphosphine indicated the same composition for **3**. The IR spectrum of **3** showed absorptions at 2085 cm^{-1} ($\nu_{C\equiv C}$) and at 1640 cm^{-1} ($\nu_{C=N}$); the latter absorption is characteristic of isocyanide polymers.[2, 8] In the ^{31}P NMR spectrum two singlets at δ 18.8 and 21.8 were observed, the latter of which appeared with satellite signals (J = 2350 Hz) due to coupling with the ^{195}Pt nucleus. In general, the spectra of **3** are very similar to those of **2a** (Table 1).

Table 1. Selected spectral data for **1a**, **2a**, **3**, and **7**.

Complex	IR [cm^{-1}]		^{31}P NMR [δ value]	
	$\nu_{(C\equiv C)}$	$\nu_{(C=N)}$	P on Pd	P on Pt ($^1J(^{195}Pt,P)$)
1a	–	–	22.8	19.6 (2518 Hz)
2a	2090	1575	18.7	21.6 (2331 Hz)
3	2085	1640	18.8	21.8 (2350 Hz)
7	2090	1640	17.6	21.0 [a]

[a] The coupling constant could not be determined exactly because of broadening of the signal.

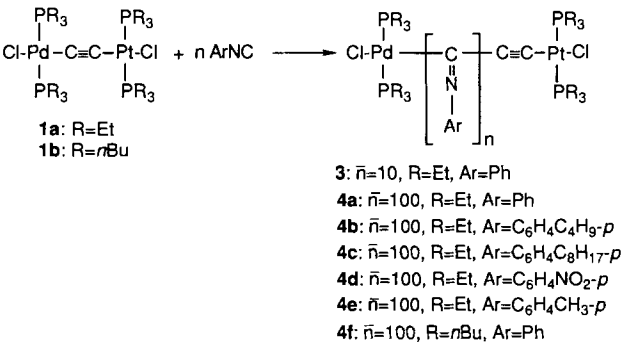

On treatment of **1a** with 100 equivalents of phenyl isocyanide under reflux in THF for 20 h a yellow polymer (**4a**) was obtained in 92% yield. The IR spectrum of **4a** exhibited an absorption at 1660 cm^{-1} ($\nu_{C=N}$), but unfortunately **4a** was insoluble in organic solvents and further characterization was not possible. Hence, **1a** was treated with 100 equivalents of aryl isocyanides containing a long alkyl chain such as an *n*-butyl or *n*-octyl group to afford soluble polymers **4b** and **4c**. The IR and NMR spectra of **4b** and **4c** showed that they have the proposed structures, and gel permeation chromatography (GPC) analyses with polystyrene standards indicated a very narrow distribution of molecular weight $\bar{M}_w/\bar{M}_n = 1.02$ ($\bar{M}_n = 13000$) for **4b** and 1.01 ($\bar{M}_n = 17000$) for **4c**. Thus, the reactions appear to be living polymerizations.

Complex **1a** also catalyzes the living polymerization of aryl isocyanides other than phenyl isocyanide. Similar treatment of **1a** with *p*-nitrophenyl isocyanide and *p*-tolyl isocyanide afforded polymers **4d** and **4e**, respectively. Complex **1b** bearing a tributylphosphine ligand reacted with phenyl isocyanide to give polymer **4f**. On the other hand, alkynepalladium complexes **5** did not yield any polymeric products but only the single-insertion complexes **6**, even when treated with

[*] Prof. Dr. S. Takahashi, Dipl.-Chem. K. Onitsuka, Dr. T. Joh
The Institute of Scientific and Industrial Research
Osaka University
Ibaraki, Osaka 567 (Japan)

 © VCH Verlagsgesellschaft mbH, W-6940 Weinheim, 1992 0570-0833/92/0707-0851 $ 3.50+.25/0

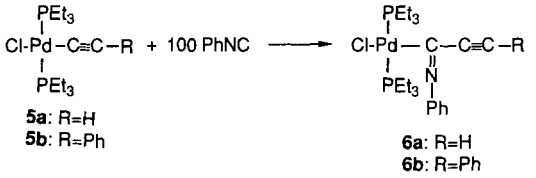

100 equivalents of phenyl isocyanide, which implies that the platinum moiety in complex **1** plays a very important role in the multiple insertion of isocyanides.

Finally, that the reaction of **1a** with isocyanides is a living polymerization has been demonstrated by several experiments. Complexes **2a** and **3** also initiate the polymerization of isocyanides. For example, complex **2a** was treated with 100 equivalents of phenyl isocyanide under reflux in THF to yield polymer **4a** quantitatively, and the reaction of **3** with 10 equivalents of *p*-tolyl isocyanide afforded a soluble block co-oligomer **7** whose structure has been identified by ^1H and ^{31}P NMR spectra.

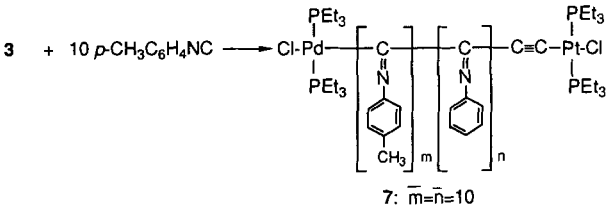

7: $\bar{m}=\bar{n}=10$

Very recently a living polymerization of alkyl isocyanides with $[\{(\eta^3\text{-}C_3H_5)Ni(OC(O)CF_3)\}_2]$ as catalyst was reported.[4b] The polymers produced in this case, however, have a rather broad distribution of molecular weight ($\bar{M}_w/\bar{M}_n = 1.1-1.6$). Our catalysts are active for aryl isocyanides and yield polymers with a narrow molecular weight distribution. All the complexes **2** and the oligo- and polyisocyanide complexes **3**, **4**, and **7** have the active end-group $Pd(PR_3)_2Cl$. They are thus still "living" and able to undergo further insertion of isocyanides. Hence, these complexes as well as complex **1** provide a novel system for the living polymerization of isocyanides and give polymers designed in terms of molecular weight, composition and sequence.

Received: January 2, 1992 [Z 5104 IE]
German version: *Angew. Chem.* **1992**, *104*, 893

CAS Registry numbers:
1a, 141399-20-4; **1b**, 141399-21-5; **2a**, 141399-23-7; **2b**, 141399-24-8; **2c**, 141399-25-9; **5a**, 141399-26-0; **5b**, 55801-97-3; **6a**, 141399-22-6; **6b**, 135757-36-7; PhNC, 931-54-4; *p*-$C_4H_9C_6H_4NC$, 141399-15-7; *p*-$C_8H_{17}C_6H_4NC$, 141399-16-8; *p*-$O_2NC_6H_4NC$, 1984-23-2; *p*-$CH_3C_6H_4NC$, 7175-47-5.

[1] See, for example: a) Y. Yamamoto, H. Yamazaki, *Coord. Chem. Rev.* **1972**, *8*, 225; b) P. M. Treichel, *Adv. Organomet. Chem.* **1973**, *11*, 21; c) E. Singleton, E. H. Oosthuizen, *ibid.* **1983**, *22*, 209.
[2] Y. Yamamoto, T. Takizawa, N. Hagihara, *Nippon Kagaku Zasshi* **1966**, *87*, 1355.
[3] W. Drenth, R. J. M. Nolte, *Acc. Chem. Res.* **1979**, *12*, 30.
[4] a) Y. Ito, E. Ihara, M. Murakami, *J. Am. Chem. Soc.* **1990**, *112*, 6446; b) T. J. Deming, B. M. Novak, *Makromolecules* **1991**, *24*, 6043.
[5] K. Onitsuka, H. Ogawa, T. Joh, S. Takahashi, Y. Yamamoto, H. Yamazaki, *J. Chem. Soc. Dalton Trans.* **1991**, 1531.
[6] K. Onitsuka, T. Joh, S. Takahashi, *Bull. Chem. Soc. Jpn.*, **1992**, *65*, 1179.
[7] Spectral data for **2a**: For IR and ^{31}P NMR data see Table 1; FAB-MS: *m/z* 1076; ^{13}C NMR: $\delta = 195.02$ (s, ≡C-*C*(= NPh)-), 158.24 (s, -*C*(=NPh)-Pd), 99.09 (t, $^2J(P,C) = 14$ Hz, Pr-*C*≡C) with attendant satellite peaks ($^1J(^{195}Pt,C) = 1439$ Hz), 98.46 (s, Pt-C≡*C*) with attendant satellites ($^2J(^{195}Pt,C) = 408$ Hz).
[8] F. Millich, R. G. Sinclair, *J. Polym. Sci. Part C* **1968**, *22*, 33.

Three-Dimensional Structure of an Unsymmetrical Proton–Electron Transfer System Containing a Disulfide Bond: The Bis(4-hydroxyphenyl)disulfide–Benzoquinone Complex**

By *Kenichi Sugiura, Jiro Toyoda, Hiroshi Okamoto, Kaoru Okaniwa, Tadaoki Mitani, Atsushi Kawamoto, Jiro Tanaka,* and *Kazuhiro Nakasuji**

The hydrogen-bonded charge-transfer (CT) complex, 1,4-benzoquinhydrone, has recently been found to undergo a new phase transition, a cooperative proton–electron transfer (PET), under high pressure.[1] The final state is characterized as the molecular assembly of hydrogen-bonded neutral radicals.[2] Such a transition can be analyzed by measuring the pressure dependence of the O–H and C=O stretching frequencies. In order to obtain a new PET system under milder physical conditions, we synthesized the extended conjugated quinhydrones, 1,5-dihalo-2,6-naphthoquinhydrones, which actually responded to applied pressure.[2] We now report the new component molecules, the bis(hydroxyphenyl)systems connected by the disulfide bond. Bis(4-hydroxyphenyl)disulfide **4** produces an unsymmetrical PET system with three-dimensional structure.

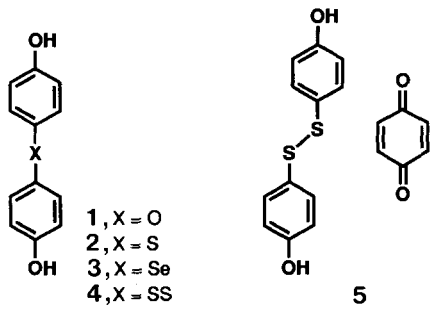

One of the strategies for the design of new PET systems is the substitution of the quinone and hydroquinone skeletons with donor and acceptor groups to make use of the captodative effect in stabilizing the final neutral radicals.[3] However, the attempts to prepare such modified quinhydrones were unsuccessful.[4] In order to develop unsymmetrical PET systems, we designed and synthesized the proton–electron donors **1**–**4**,[5] which are composed of two phenol moieties connected by oxygen, sulfur, selenium, or a disulfide bond. These compounds show the following characteristics: 1) The exchange reactions can be suppressed by the chalcogen atoms, and 2) the twist of the chalcogen–phenyl units affects the crystal packing. The properties of compounds **1**–**4** related to hydrogen bonding and the CT interaction were investigated. The acid dissociation constants K_a of the phenol moi-

[*] Prof. Dr. K. Nakasuji, Dr. J. Toyoda, Dr. H. Okamoto, Prof. Dr. T. Mitani,
Institute for Molecular Science
Myodaiji, Okazaki 444 (Japan)
K. Sugiura, K. Okaniwa,
Department of Structural Molecular Science
Graduate University for Advanced Studies
Myodaiji, Okazaki 444 (Japan)
Dr. A. Kawamoto, Prof. Dr. J. Tanaka
Department of Chemistry, Faculty of Science
Nagoya University
Chikusa-ku, Nagoya 464 (Japan)

[**] This work was supported by a Grant-in-Aid for Scientific Research on Priority Areas (No. 03214103) from the Ministry of Education, Science and Culture, Japan.

ety increase in the order of **1** < **2** ≈ **3** < **4**, as shown in Table 1. This order is consistent with the total electronic effects arising from the inductive and resonance effects of the chalcogen atoms on the phenol moiety.[6] The acidity of **1** is nearly same as that of hydroquinone. Interestingly, the difference between the first and second acid dissociation constants of **2**–**4** are larger than that of **1**. The larger ΔpK_a values indicate that in the S- and Se-bridged molecules the dissociation of the second proton is not as facile as in the O-linked derivatives, since the negative charge in the higher homologues is more delocalized. The electron donor abilities were estimated from the values of the CT transition energies with tetracyanoethylene (TCNE) in acetonitrile (Table 1). These energy values suggest that the donors **1** and **4** are worse donors, and **2** and **3** better donors than hydroquinone.

Table 1. Logarithmic dissociation constants pK_a [a] and CT transition energies E [b] for **1**–**4** and hydroquinone (HQ).

	pK_{a_1}	pK_{a_2}	ΔpK_a	E [eV]
1	11.1	11.2	0.1	2.27
2	10.5	10.9	0.4	2.06
3	10.5	11.0	0.5	2.05
4	10.0	10.5	0.5	2.49
HQ	11.1	11.6	0.5	2.11

[a] The acid dissociation constants were determined potentiometrically with 0.1 N standardized sodium hydroxide solution. The temperature was maintained at 25.0 ± 0.1 °C, and the ionic strength was adjusted to 0.10 M with $NaClO_4$. [b] The charge-transfer transition energies were determined with tetracyanoethylene in acetonitrile.

CT complexes of these donors with various quinone-type acceptors were prepared. The 1:1 CT complex **5** arising from **4** and 1,4-benzoquinone was the only one to form single crystals, specifically, large, cubic, black single-crystals with the dimensions 5 × 5 × 5 mm^3.[7] The crystal structure analysis and the spectroscopic data show that this complex is a unique hydrogen-bonded CT complex (Fig. 1 a).[8] As shown in Figure 1 b, the hydroxyphenyl moiety of **4**, benzoquinone, and the next hydroxyphenyl moiety of **4** are joined by hydrogen bonds. The hydrogen-bonded units are connected by disulfide bonds to form a zigzag chain. In addition, the hydrogen-bonded units stack with a donor–acceptor–donor type of CT interaction to form linear ribbons extended in the [1,1,0] or [1,−1,0] direction (Fig. 1 c). In the crystal, such ribbons are piled alternately with reference to the c axis making a three-dimensional molecular structure (Fig. 1 a, c).

The bond lengths of the benzoquinone component of **5** and uncomplexed benzoquinone differ by only ±0.07 Å.[9] The IR stretching frequencies of **5** ν(C=O) and ν(O–H) (1637 and 3213 cm^{-1}, respectively) are very close to those of benzoquinhydrone (1633 and 3227 cm^{-1} for the average values of monoclinic and triclinic forms of benzoquinhydrone measured in this work).[11] The diheral angle and the S–S bond length for the donor component **4** in **5** are 88° and 2.032 Å, respectively.[12] These data reflect the nonionic nature of **5**. The lowest energy band in the solid-state electronic absorption spectrum for the complex is at 2.28 eV and can be assigned to the CT transition between the hydroxyphenyl moiety and benzoquinone. The intensity of the polarized reflection spectra was largest along the c axis, which is the stacking direction of the donor–acceptor–donor arrangement in the linear ribbons. The transition energy of **5** is higher than that of benzoquinhydrone (2.06 eV). This is consistent with the lower donor ability of **4** relative to hydroquinone, as was measured above. Under high pressure (40 kbar), the OH stretching band in the IR spectrum shifted from 3213 cm^{-1} to 3080 cm^{-1}, and a new band appeared at 2640 cm^{-1}. The CO stretching band also shifted from 1637 cm^{-1} to 1617 cm^{-1}, and an additional band at 1578 cm^{-1} appeared.

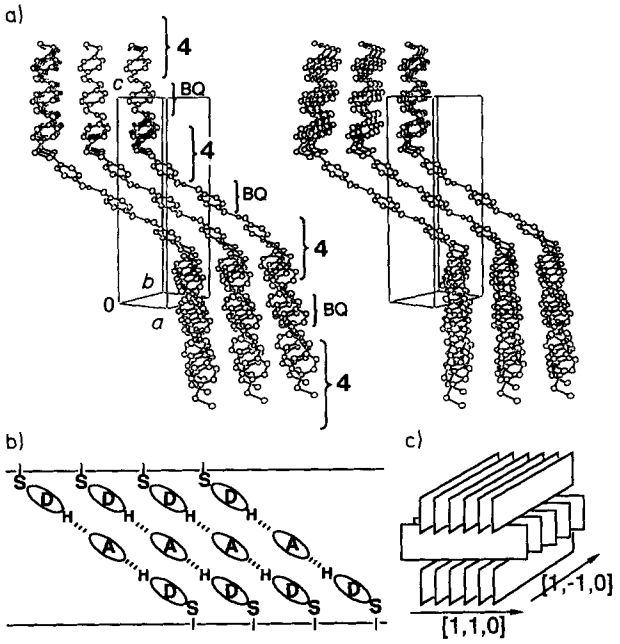

Fig. 1. The crystal structure of **5**. a) Stereoplot showing a section of the molecular packing; BQ = benzoquinone. b) Schematic representation of a linear ribbon. c) Schematic representation of the three-dimensional structure.

Thus, we could show that **5** displays a pressure-dependent IR spectrum. This system should still be characterized in detail on the molecular level. Our next step toward new PET systems will be chemical modification to enhance the electron-donor ability and/or the proton-donor ability in these unsymmetrical PET systems.

Received: January 16, 1992 [Z 5126 IE]
German version: *Angew. Chem.* **1992**, *104*, 877

CAS Registry numbers:
1, 1965-09-9; **2**, 2664-63-3; **3**, 141982-42-5; **4**, 15015-57-3; **5**, 141982-43-6; **1** · TCNE, 141982-44-7; **2** · TCNE, 141982-45-8; **3** · TCNE, 141982-46-9; **4** · TCNE, 141982-41-0; HQ, 123-31-9; HQ · TCNE, 41959-85-7.

[1] a) T. Mitani, G. Saito, H. Urayama, *Phys. Rev. Lett.* **1988**, *60*, 2299–2302; b) T. Mitani, *Mol. Cryst. Liq. Cryst.* **1989**, *171*, 343–355.
[2] K. Nakasuji, K. Sugiura, T. Kitagawa, J. Toyoda, H. Okamoto, K. Okaniwa, T. Mitani, H. Yamamoto, I. Murata, A. Kawamoto, J. Tanaka, *J. Am. Chem. Soc.* **1991**, *113*, 1862–1864.
[3] a) H. G. Viehe, Z. Janousek, R. Merenyi, L. Stella, *Acc. Chem. Res.* **1985**, *18*, 148–154.
[4] For the preparation of quinones and hydroquinones with captodative substituents see: T. Kitagawa, J. Toyoda, K. Nakasuji, H. Yamamoto, I. Murata, *Chem. Lett.* **1990**, 897–900. So far no quinhydrone-type CT complexes have been obtained from these modified components.
[5] a) J. H. Burckhalter, F. H. Tendick, E. M. Jones, W. F. Holcomd, A. L. Rawline, *J. Am. Chem. Soc.* **1946**, *68*, 1894–1901; b) S. Oae, M. Yoshihara, W. Takagi, *Bull. Chem. Soc. Jpn.* **1967**, *40*, 951–958; c) H. M. Leichester, *Org. Synth. Coll. Vol. 2*, 238–240; d) S. Oae, M. Yoshihara, *Bull. Chem. Soc. Jpn.* **1968**, *41*, 2082–2086.
[6] C. Hansch, A. Leo, R. W. Taft, *Chem. Rev.* **1991**, *91*, 165–195.
[7] Equimolar amounts of **4** and benzoquinone were dissolved in anhydrous benzene and the solution was allowed to evaporate slowly.
[8] Crystal data were collected on a Rigaku AFC-5R diffractometer with $Cu_{K\alpha}$ radiation (graphite monochromator). The structure was solved by the Monte-Carlo directed method with aid of the MULTAN-78 program system and refined on F^2 by a full-matrix least-squares techniques with ana-

lytical absorption correction. Crystal data are as follows: $C_{18}H_{14}O_4S_2$, monoclinic, $C_{2/c}$, $a = 6.636$, $b = 9.758$, $c = 24.510$ Å, $\beta = 90.29°$, $V = 1587.1$ Å^3, $Z = 4$, $R = 0.035$. The mean interplanar distance between the hydroxyphenyl moiety and benzoquinone skeleton was 3.13 Å, and the O···O distance in the hydrogen bonds was 2.743(2) Å. Further details of the crystal structure investigation are available on request from the Director of the Cambridge Crystallographic Data Centre, University Chemical Laboratory, Lensfield Road, GB-Cambridge CB21EW (UK), on quoting the full journal citation.

[9] The bond lengths of benzoquinone itself [10] and of the benzoquinone components in **5** are: a) C=C bonds 1.334, 1.327; b) C–C bonds 1.474, 1.479; c) C=O bonds 1.222, 1.228.

[10] F. van Bolhuis, C. T. Kiers, *Acta Crystallogr. Sect. B* **1978**, *34*, 1015–1016.

[11] K. Kubinyi, G. Keresztury, *Spectrochim. Acta Part A* **1989**, *45*, 421–429.

[12] a) A. Hordvik, *Acta Chem. Scand.* **1966**, *20*, 1885–1891; b) J. D. Lee, M. W. R. Bryant, *Acta Crystallogr. Sect. B* **1969**, *25*, 2094–2101; c) M. Aida, C. Nagata, *Theor. Chim. Acta* **1986**, *70*, 73–80.

Structures of Two Highly Reactive Intermediates upon $LiAlH_4$ Reduction in the Solid State and in Solution: $[(Me_3Si)_2NAlH_3Li \cdot 2Et_2O]_2$ and $[(Me_3Si)_2N]_2AlH_2Li \cdot 2Et_2O$ **

By *Andreas Heine* and *Dietmar Stalke**

Lithium aluminum hydride $LiAlH_4$ is a versatile reducing and hydrogenating reagent in both inorganic and organic synthesis.[1, 2] Although more than 60 functional groups are known to react with $LiAlH_4$, very little is known of the reactive intermediates involved in these syntheses. We report here the isolation of the intermediates **1** and **2**.

$$HN(SiMe_3)_2 + LiAlH_4 \longrightarrow \underset{\mathbf{1}}{1/2\,[(Me_3Si)_2NAlH_3Li \cdot 2Et_2O]_2}$$

$$\xrightarrow[-H_2]{+HN(SiMe_3)_2} \underset{\mathbf{2}}{[(Me_3Si)_2N]_2AlH_2Li \cdot 2Et_2O} \xrightarrow[-H_2]{+2\,HN(SiMe_3)_2}$$

$$\underset{\mathbf{3}}{[(Me_3Si)_2N]_3Al} + LiN(SiMe_3)_2$$

The overall reaction to form the trisubstituted aluminum compound **3**[3, 4] proceeds stepwise, whereby the reactive mono-substituted intermediate **1** and the disubstituted intermediate **2** can be isolated. Although the isolation of **1** and **2** does not necessarily prove that these compounds are intermediates in the reaction pathway suggested above, this is, however, chemically plausible. $LiAlH_4$ was allowed to react with hexamethyldisilylamine in diethyl ether. The reaction mixture was stirred for 24 h at room temperature and filtered, whereupon crystals of **1** were obtained after 3 d at −35 °C. The crystals, were directly mounted onto the diffractometer from mother-liquor at ca. −50 °C, thus permitting an X-ray structure analysis. At approximately −30 °C the colorless crystals start to "effervesce" and turn into a white insoluble powder. We assume that they lose hydrogen. **1** (Fig. 1) is a dimer in the solid state.[5] The aluminum atoms in the central eight-membered $Al_2H_4Li_2$ ring are each coordinated by three hydrogen atoms and a $N(SiMe_3)_2$ ligand. The lithium atoms form two bridges between the two $(Me_3Si)_2NAlH_3$ units via Li–H contacts. Each of them is also coordinated to two ether molecules. The average Li–H

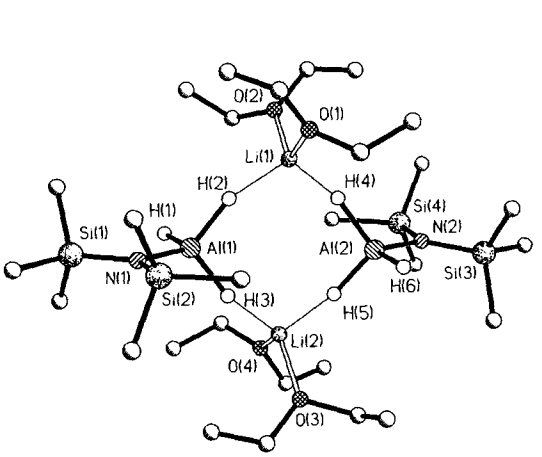

Fig. 1. Structure of the reactive intermediate $[(Me_3Si)_2NAlH_3Li \cdot 2Et_2O]_2$. Selected distances [pm] and angles [°]: Al1-H2 163(4), Al1-H3 158(4), Al2-H4 166(4), Al2-H5 161(4), Al1-H1 158(5), Al2-H6 161(4), Li1-H2 181(4), Li1-H4 174(4), Li2-H3 180(4), Li2-H5 176(4), Al1-N1 185.5 (3), Al2-N2 186.0(3), average Li-O 193.1(8), average Si-N 171.3(3), average H-Al-H 107(2), average H-Li-H 107(2), average Al-H-Li 157(3), average Si-N-Si 125.6(2), average Al-N-Si 117.2(2).

distance in **1** is 177.7 pm and therefore significantly shorter than in solid LiH (204.0 pm)[6] or even $LiAlH_4$ (188–216 pm).[7] To our knowledge, a shorter Li–H contact has only been found (168 and 192 pm, determined by X-ray structure analysis) in $[t\mathrm{Bu}_3\mathrm{AlHLi}]_2$.[8] The shortest Li–H contact (159.6 pm) is found by spectroscopic techniques in molecular LiH.[9] The average Al–H distance of 161.0 pm is in good agreement with the values quoted in the literature.[8, 10–12] Addition of $HN(SiMe_3)_2$ to $LiAlH_4$ in diethyl ether and subsequent refluxing for 3 h followed by stirring for 12 h at room temperature leads to formation of the disubstituted intermediate **2**. Crystals were grown in good yield at −18 °C. Under these conditions the reaction is stopped after substitution of two equivalents of bis(trimethylsilyl)-amine rather than allowing the trisubstituted product **3** to be formed. Crystals of **2** were mounted on the diffractometer at ca. −10 °C and started to effervesce above +5 °C. Presumably they also lose hydrogen. Figure 2 shows the monomeric structure of **2** in the solid state. The most striking feature is the central AlH_2Li four-membered kite-shaped ring, in which the lithium atom bridges the two aluminum-bound hydrogen atoms. The bond angles show that **2** has a relatively strained structure. The average H–Al–H bond an-

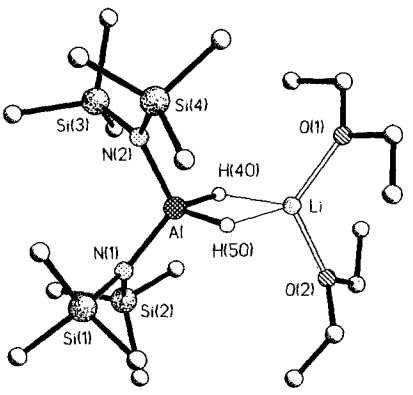

Fig. 2. Structure of the intermediate $[(Me_3Si)_2N]_2AlH_2Li \cdot 2Et_2O$. Selected distances [pm] and angles [°]: Al-H40 162(2), Al-H50 155(2), Li-H40 189(2), Li-H50 197(2), average Li-O 194.4(6), Al-N1 186.7(3), Al-N2 185.7(2), average Li-H50-Al 96(1), Li-H40-Al 96 (1), H40-Li-H50 74(1), O1-Li-O2 120.6(3), N1-Al-N2 117.5(1).

[*] Dipl.-Chem. A. Heine, Dr. D. Stalke
Institut für Anorganische Chemie der Universität
Tammannstrasse 4, D-W-3400 Göttingen (FRG)

[**] This work was supported by the Fonds der Chemischen Industrie.

gle in **2** (94.3°) is 12.9° smaller than that in **1** (107.2°). The average H–Li–H angle (73.6°), however, is even 33.8° smaller than that in **1** (107.4°). The intramolecular bridging of the lithium atom leads to a longer Li–H distance (average 193.3 pm; but 177.7 pm in **1**), which is comparable to the distance in $LiAlH_4$.[7] The hydrogen atoms are forced close together to the transannular distance of 233.1 pm. Despite this steric strain the molecule does not dissociate in solution. The ^{7}Li-NMR spectrum of **2** shows a ^1J(Li,H) coupling constant of 10.5 Hz (Fig. 3). This is in good agreement with

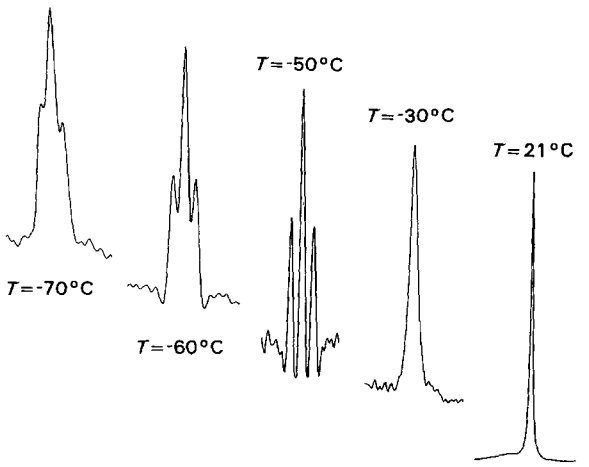

Fig. 3. Experimental ^{7}Li-NMR spectra of **2** at various temperatures. The chemical shift at −50 °C is 0.4, the coupling constant ^1J(Li,H) 10.5 Hz.

the only other known ^1J(Li,H) coupling (8.4 Hz) detected in the ^{1}H/^{7}Li-NMR spectra of [Cp*IrH$_3$Li(pmdeta)] (pmdeta = $(Me_2NCH_2CH_2)_2NMe$).[13] This supports our suggestion[14] that there is more covalent character in bonds to lithium than was previously considered likely. In **2** the ^{7}Li-^{1}H coupling is only resolvable in the temperature window −30 °C to −70 °C. Outside this window the triplet structure of the signal is lost (Fig. 3), at higher temperatures as a result of exchange and at lower temperatures probably as a result of ^{7}Li quadrupole effects. The coupling could not be verified in the ^{1}H-NMR experiment because the hydride signals are too broad. Furthermore, the ^1J(Li,H) coupling could not be observed in **1** at any temperature between room temperature and −120 °C in [D$_8$]toluene. **1** is fluctional in solution.This fluctionality could indicate a monomer/dimer equilibrium superposed on a μ_1 and/or μ_2 and/or μ_3 hydride bridging exchange.

Experimental

1: $HN(SiMe_3)_2$ (7 mL, 33.3 mmol) was added over 8 h to a suspension of $LiAlH_4$ (1.26 g, 33.3 mmol) in diethyl ether (30 mL). The mixture was stirred for 24 h at room temperature. Subsequent filtration furnished a clear solution, storage of which at −35 °C afforded colorless crystals after about one week. ^{1}H NMR ([D$_8$]toluene, ca. 25 °C): $\delta = 0.35$ (s, 36H of $SiMe_3$), 1.08 (t, 24H of CH_2CH_3), 3.35 (q, 16H of CH_2CH_3); ^{7}Li NMR ([D$_8$]toluene, ca. 25 °C): $\delta = -0.37$.

2: A solution of $HN(SiMe_3)_2$ (8 mL, 38.1 mmol) in diethyl ether (20 mL) was added to a suspension of $LiAlH_4$ (0.71 g, 18.7 mmol) in diethyl ether (20 mL). The mixture was stirred for 12 h at room temperature, After the precipitate was filtered off, colorless crystals separated from the clear solution after several days at −18 °C. ^{1}H NMR ([D$_8$]toluene, ca. 25 °C): $\delta = 0.47$ (s, 36H of $SiMe_3$), 0.94 (t, 12H of CH_2CH_3), 3.19 (q, 8H of CH_2CH_3); ^{7}Li NMR ([D$_8$]toluene, ca. 25 °C): $\delta = 0.31$, (−50 °C): 0.4, ^1J(Li,H) = 10.5 Hz; IR: $\tilde{\nu}$ (AlH) = 1754 cm^{-1} (s).

Received: January 25, 1992 [Z 5148 IE]
German version: *Angew. Chem.* **1992**, *104*, 941

CAS Registry numbers:
1, 141612-14-8; **2**, 141634-70-0; $HN(SiMe_3)_2$, 999-97-3; $LiAlH_4$, 16853-85-3.

[1] N. N. Greenwood, A. Earnshaw, *Chemistry of the Elements*, 1st Edit., Pergamon, Oxford, **1984**, p. 256ff; *Chemie der Elemente*, 1st Edit., VCH, Weinheim, **1988**, p. 282ff.
[2] E. Wiberg, E. Amberger, *Hydrides of the Elements of the Main Groups I-IV*, Elsevier, Amsterdam, **1971**, p. 381ff.
[3] J. Pump, E. G. Rochow, U. Wannagat, *Angew. Chem.* **1963**, *8*, 375; *Angew. Chem. Int. Ed. Engl.* **1963**, *2*, 264.
[4] G. M. Sheldrick, W. S. Sheldrick, *J. Chem. Soc. A.* **1969**, 2279.
[5] Crystal data: **1**: $C_{28}H_{82}Li_2N_2O_4Al_2Si_4$, $M = 691.2$, monoclinic, space group $P2_1/c$, $a = 21.157(4)$, $b = 9.387(2)$, $c = 24.983(5)$ Å, $\beta = 95.71(3)°$, $V = 4937$ Å^3, $Z = 4$, $\varrho_{calcd} = 0.930$ Mg m^{-3}, $F(000) = 1536$, $\lambda = 0.71073$ Å, $T = 153$ K, $\mu(Mo_{K\alpha}) = 0.328$ mm^{-1}. Data were collected on a Siemens-Stoe AED using an oil-coated rapidly-cooled crystal of dimensions 0.5 × 0.4 × 0.2 mm by the $2\theta/\omega$ method ($8° \leq 2\theta \leq 50°$). Of a total of 8921 collected reflections, 8643 were unique and 5201 were employed in structure refinement [$(F > 3\sigma(F))$, data-to-parameter ratio 12.8:1]. The structure was solved by direct methods and refined by full matrix least squares to R and R_w values of 0.070 and 0.069, respectively. **2**: $C_{20}H_{58}LiN_2O_2AlSi_4$, $M = 505.0$, triclinic, space group $P\bar{1}$, $a = 11.225(4)$, $b = 11.416(5)$, $c = 14.460(3)$ Å, $\alpha = 90.15(3)$, $\beta = 100.64(5)$, $\gamma = 112.07(2)°$, $V = 1682(3)$ Å^3, $Z = 2$, $\varrho_{calcd} = 0.997$ Mg m^{-3}, $F(000) = 560$, $\lambda = 0.71073$ Å, $T = 153$ K, $\mu(Mo_{K\alpha}) = 0.219$ mm^{-1}. Data were collected on a Siemens-Stoe AED using an oil-coated rapidly-cooled crystal of dimensions 0.5 × 0.4 × 0.2 mm by the $2\theta/\omega$ scan method ($8° \leq 2\theta \leq 58°$). Of 11310 collected reflections, 8893 were unique and 5793 were employed in the structure refinement ($F > 4\sigma(F)$, data-to-parameter ratio 19.6:1). The structure was solved by direct methods and refined by full-matrix least squares to R and R_w values of 0.055 and 0.058, respectively. In both cases the program used was the SHELXTL-Plus, PC version. All hydrogen atoms were located in a difference Fourier map and were refined using a riding model with common refined U values for chemically equivalent atoms. The terminal hydrogen atoms were refined freely in both structures. Further details of the crystal structure investigations are available on request from the Director of the Cambridge Crystallographic Data Centre, University Chemical Laboratory, Lensfield Road, GB-Cambridge CB2 1EW (UK), on quoting the full journal citation.
[6] E. Zintl, A. Harder, *Z. Phys. Chem. B* **1935**, *28*, 478.
[7] N. Sklar, B. Post, *Inorg. Chem.* **1969**, *6*, 669.
[8] W. Uhl, *Z. Anorg. Allg. Chem.* **1989**, *570*, 37.
[9] K. P. Huber, G. Herzog, *Spectra of diatomic molecules*, 4. Constants of diatomic molecules, Van Nostrand Reinhold, New York, **1979**, p. 382f.
[10] J. L. Atwood, D. C. Hrneir, R. D. Rogers, J. A. K. Howard, *J. Am. Chem. Soc.* **1981**, *103*, 6787.
[11] A. Almenningen, G. A. Anderson, F. R. Forgaard, A. Haaland, *Acta Chem. Scand.* **1972**, *26*, 2315.
[12] J. W. Lauher, D. Dougherty, P. J. Herley, *Acta Crystallogr. Sect. B* **1979**, *35*, 1454.
[13] T. M. Gilbert, R. G. Bergmann, *J. Am. Chem. Soc.* **1985**, *107*, 6391.
[14] D. Stalke, U. Klingebiel, G. M. Sheldrick, *J. Organomet. Chem.* **1988**, *344*, 37.

Total Synthesis of the Carbohydrate Fragments of Esperamicin A_1**

By *K. C. Nicolaou** and *David Clark*

Esperamicin A_1[1] (**1**) is one of the most prominent members of the naturally occurring enediyne anticancer antibiotics.[2] In this communication, we report the total synthesis of both its carbohydrate chains **2** and **3**[3] (Scheme 1) in their

[*] Prof. Dr. K. C. Nicolaou, D. Clark
Department of Chemistry, The Scripps Research Institute
10666 N. Torrey Pines Road, La Jolla, CA 92037 (USA)
and
Department of Chemistry, University of California
San Diego, La Jolla, CA 92093 (USA)

[**] We express our many thanks to Dr. Dee Huang and Dr. Gary Siuzdak of The Scripps Research Institute for their excellent assistance with the NMR and mass spectra. This work was financially supported by the National Institutes of Health and The Scripps Research Institute.

optically active forms and in protected versions suitable for an eventual total synthesis of the natural product.

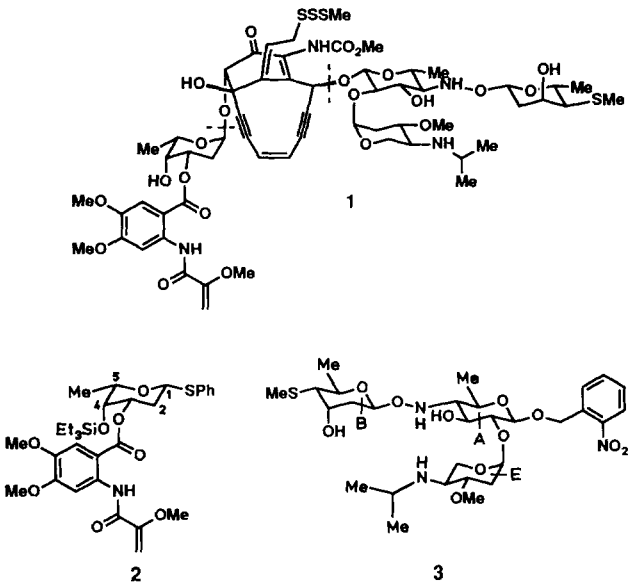

Scheme 1. The structures of esperamicin A_1 (**1**) and the carbohydrate fragments **2** and **3**.

Scheme 2 depicts the synthesis of fragment **2** starting with the readily available **4** and **7**. Methyl-α-L-fucopyranoside (**4**)[4] was regioselectively converted into intermediate **5**[5] by sequential reaction with carbonyldiimidazole and thiocarbonyldiimidazole. This protected compound was deoxygenated at the 2 position and transformed into **6** by means of Hanessian[6] phenylthioglycosidation and base-induced carbonate removal. The other requisite coupling partner, **8**, was prepared from 4,5-dimethoxyanthranilic acid (**7**) by reaction with phthaloyl chloride followed by treatment with oxalyl chloride. For the coupling of compounds **6** and **8** a cyclic tin dialkoxide derivative was prepared from **6** and then stirred with **8** in the presence of Et_3N. After silylation of the remaining 4-hydroxyl group, compound **9** was obtained regioselectively. Hydrazine-induced removal of the phthaloyl group from **9** smoothly gave the free amine **10**, which was condensed with acid chloride **11**[7] in the presence of Et_3N to afford the desired target **2** (Table 1).

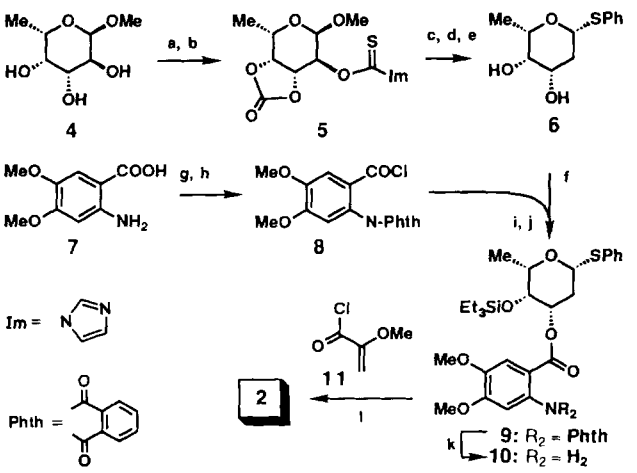

Scheme 2. Synthesis of esperamicin A1 carbohydrate chain **2**. Reagents and conditions: a) 2.5 equiv 1,1'-carbonyldiimidazole, CH_3CN, reflux, 2 h, 76%; b) 1.3 equiv 1,1'-thiocarbonyldiimidazole, CH_3CN, 25 °C, 2 h, 80%; c) 2.0 equiv nBu_3SnH, azobisisobutyronitrile (AIBN, cat.), toluene/dimethoxyethane (DME) (1:1), 110 °C, 1 h, 84%; d) 5.0 equiv $PhSSiMe_3$, 3.0 equiv ZnI_2, 1.2 equiv nBu_4NI, 1,2-dichloroethane, 2.5 h, 70 °C; e) 0.05 equiv NaH, THF/ethylene glycol (20:1), 25 °C, 2 h, 63% for d and e; f) 1.2 equiv nBu_2SnO, MeOH, 65 °C, 1.5 h then solvent exchange with anhydrous THF; g) 1.1 equiv phthaloyl chloride, 2 equiv Et_3N, THF, 25 °C, 2 h, 50%; h) 1.2 equiv oxalyl chloride, CH_2Cl_2/dimethyl formamide (DMF) (100:1), 25 °C, 0.5 h; i) 1.5 equiv **8**, 2.0 equiv Et_3N, THF, 25 °C, 0.75 h, 65% for h and i. j) 1.2 equiv Et_3SiOTf, 1.5 equiv 2,6-lutidine, CH_2Cl_2, 0 °C, 0.2 h, 100%; k) 2.0 equiv hydrazine, 1.0 equiv AcOH, MeOH/CH_2Cl_2 (5:1), 25 °C, 5 h, 83%; l) 3.0 equiv **11** [7], 5.0 equiv Et_3N, THF, 25 °C, 85%.

Table 1. Selected physical properties and spectral data of compounds **2** and **3**.

2: $R_f = 0.35$ (silica gel, 5% ethyl acetate in benzene); $[\alpha]_D^{26} = -166$ ($c = 0.42$, $CHCl_3$); ^1H NMR (500 MHz, C_6D_6): $\delta = 11.96$ (s, 1H, NH), 8.63 (s, 1H, aromatic H), 7.50–7.48 (m, 2H, SPh), 7.47 (s, 1H, aromatic H), 7.32–7.28 (m, 2H, SPh), 7.26–7.22 (m, 1H, SPh), 5.77 (d, $J = 5.4$ Hz, 1H, on C-1), 5.49 (d, $J = 2.5$ Hz, 1H, vinyl H), 5.40 (ddd, $J = 12.6$, 4.5, 2.5 Hz, 1H, on C-3), 4.58 (d, $J = 2.5$ Hz, 1H, vinyl H), 4.45 (q, $J = 6.5$ Hz, 1H, on C-5) 4.11 (br.m, 1H, on C-4), 3.99 (s, 3H, OCH_3), 3.87 (s, 3H, OCH_3), 3.83 (s, 3H, OCH_3), 2.81 (ptd, $J = 12.6$, 12.6, 5.4 Hz (pt = pseudotriplet), 1H, H_{ax} on C-2), 2.03 (dd, $J = 12.6$, 4.5 Hz, 1H, H_{eq} on C-2), 1.24 (d, $J = 6.5$ Hz, 3H, on C-6), 0.90 (t, $J = 7.9$ Hz, 9H, $SiCH_2CH_3$), 0.58–0.52 (m, 6H, $SiCH_2CH_3$); ^{13}C NMR (125 MHz, C_6D_6): $\delta = 167.0$, 161.0, 154.5, 154.0, 144.0, 137.2, 135.1, 128.9, 126.9, 112.3, 107.4, 103.8, 90.6, 83.9, 71.5, 70.5, 67.9, 56.1, 56.0, 30.2, 17.1, 6.9, 5.2; IR ($CDCl_3$): $\tilde{\nu}_{max} = 3262$, 2955, 2875, 1682, 1594, 1518, 1464, 1308, 1252, 1212, 1155, 1088, 1057, 1037, 1006, 734 cm^{-1}; HRMS calcd. for $C_{31}H_{43}O_8NSSi$ (M^+Cs^+) 750.1533, found 750.1536; correct C,H,N,S,Si analyses.

3: $R_f = 0.20$ (silica gel, 50% acetone in dichlormethane); $[\alpha]_D^{26} = -42.3$ ($c = 0.104$, $CHCl_3$); ^1H NMR (500 MHz, C_6D_6) [a]: $\delta = 8.12$ (d, $J = 7.8$ Hz, 1H, aromatic H), 7.71 (d, $J = 8.1$ Hz, 1H, aromatic H), 7.20 (dd, $J = 7.8$, 7.5 Hz, 1H, aromatic H), 6.70 (dd, $J = 8.1$, 7.5 Hz, 1H, aromatic H), 6.01 (br., 1H, E-1), 5.78 (br., 1H, ONH) (the signal of the second NH group was not observed), 5.36 (d, $J = 15.5$ Hz, 1H, nitrobenzyl-CH_2), 5.08 (d, $J = 15.5$ Hz, 1H, nitrobenzyl-CH_2), 5.03 (dd, $J = 10.1$, 1.8 Hz, 1H, B-1), 4.49 (d, $J = 7.8$ Hz, 1H, A-1), 4.26 (dd, $J = 9.7$, 9.3 Hz, 1H, A-3), 4.08 (dd, $J = 9.3$, 7.8 Hz, 1H, A-2), 4.04 (dd, $J = 11.2$, 9.4 Hz, 1H, E-5), 3.83 (dd, $J = 11.2$, 4.7 Hz, 1H, E-5), 3.70 (ddd, $J = 9.5$, 9.3, 4.2 Hz, 1H, E-3), 3.63 (q, $J = 6.3$ Hz, 1H, B-5), 3.61 (m, 1H, B-3), 3.56 (dq, $J = 9.5$, 6.2 Hz, 1H, A-5), 3.14 (s, 3H, OCH_3), 2.89 (ddd, $J = 9.4$, 9.3, 4.7 Hz, 1H, E-4), 2.65 (septet, $J = 6.3$ Hz, 1H, $NCHMe_2$), 2.49 (ddd, $J = 12.5$, 4.2, 2.2 Hz, 1H, E-2 eq), 2.20 (dd, $J = 9.7$, 9.5 Hz, 1H, A-4), 2.10 (ddd, $J = 13.1$, 3.2, 1.8 Hz, 1H, B-2 eq), 2.00 (dd, $J = 10.5$, 2.4 Hz, 1H, B-4), 1.70 (ddd, $J = 12.5$, 9.5, 3.5 Hz, 1H, E-2 ax), 1.44 (s, 3H, SCH_3), 1.39 (ddd, $J = 13.1$, 10.1, 3.2 Hz, 1H, B-2 ax), 1.36 (d, $J = 6.2$ Hz, 1H, B-3-OH), 1.10 (d, $J = 6.3$ Hz, 3H, B-6), 1.07 (d, $J = 6.2$ Hz, 3H, A-6), 0.91 (d, $J = 6.3$ Hz, 3H, $CHMe_2$, 0.85 (d, $J = 6.3$ Hz, 3H, $CHMe_2$); ^{13}C NMR (125 MHz, C_6D_6): $\delta = 147.3$, 135.5, 133.4, 129.4, 127.5, 124.6, 101.9, 100.0, 98.9, 78.1, 77.8, 72.1, 69.5, 68.9, 68.8, 67.5, 64.9, 63.8, 57.0, 55.9, 55.7, 46.8, 35.8, 34.5, 24.7, 23.0, 20.0, 17.6, 13.3; IR($CHCl_3$): $\tilde{\nu}_{max} = 3444$, 2966, 2925, 1526, 1446, 1341, 1305, 1154, 1064, 1015, 990, 960 cm^{-1}; HRMS calcd. for $C_{29}H_{47}O_{11}N_3S$ (M^+Cs^+) 778.1986, found 778.1986

[a] The rings in **3** are denoted by A, B, E. Thus E-2eq stands for the equatorial H on C-2 in ring E.

Scheme 3 summarizes the construction of the trisaccharide **3**. The *o*-nitrobenzyl glycoside **12**[8] was coupled with the glycosyl fluoride **13**[9] to afford disaccharide **14** stereoselectively (α:β anomers, ca. 3:1). The carbonate function of **14** was selectively removed under basic conditions, leading to diol **15**. The hydroxy ketone **16**, obtained from diol **15**,[10] was coupled with the hydroxylamine derivative **17**[11] under acidic conditions, furnishing after silylation trisaccharide **18**.[12] The aryl ester function of **18** was removed with diisobutylaluminum hydride giving **19**, which was treated with thiocarbonyldiimidazole to afford thionoimidazolide **20**. Thermolysis of **20** led, as anticipated,[11] to thioimidazolide **21** by a [3,3]sigmatropic rearrangement. Generation of thiol **22** from **21** by exposure to NaSEt followed by reaction with excess methyl iodide led to the thiomethyl derivative **23**. Selective desilylation of the enol group led to the corresponding carbonyl compound, which was reduced stereoselectively

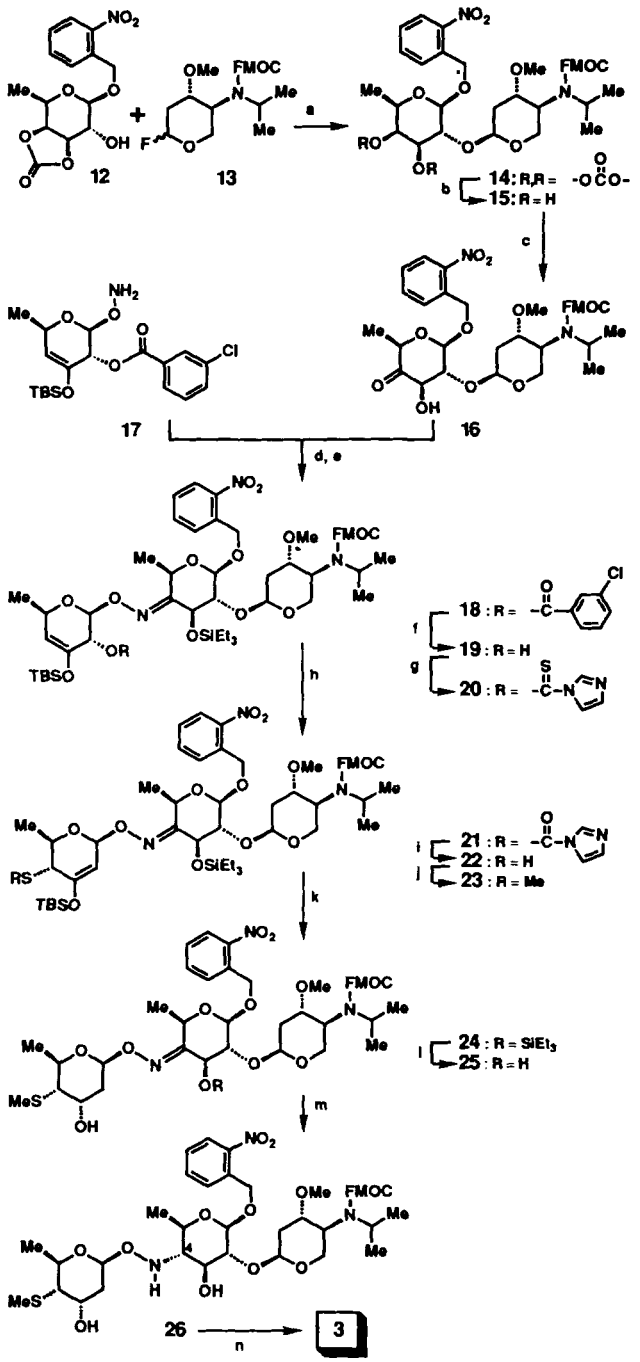

Scheme 3. Total synthesis of esperamicin A1 carbohydrate fragment **3**. Reagents and conditions: a) 1.35 equiv **13**, 1.0 equiv **12** [8], 2.5 equiv $AgClO_4$, 2.5 equiv $SnCl_2$, 4 Å, molecular sieves, THF, $-78 \rightarrow -20\,^{\circ}C$, 7 h, ($\alpha:\beta \approx 3:1$); b) 0.04 equiv NaH, THF/ethylene glycol (20:1), 25 °C, 0.5 h, 60% for a and b; c) 1.0 equiv nBu$_2$SnO, MeOH, reflux, 1.2 h then 1.0 equiv nBu$_3$SnOMe, 1.0 equiv Br_2, CH_2Cl_2, 25 °C, 76%; d) 0.1 equiv pyridinium *para*-toluenesulfonate, 1.5 equiv **17** [11], benzene, 25 °C, 3 h, 70%; e) 1.2 equiv Et_3SiOTf, 1.5 equiv 2,6-lutidine, CH_2Cl_2, $0 \rightarrow 25\,^{\circ}C$, 0.5 h, 100%; f) 3.0 equiv iBu$_2$AlH, CH_2Cl_2, $-78\,^{\circ}C$, 0.5 h, 95%; g) 3.0 equiv 1,1'-thiocarbonyldiimidazole, CH_3CN, 25 °C, 1.5 h, 86%; h) toluene, 100 °C, 1 h, 100%; i) 1.0 equiv NaSMe, 40 equiv EtSH, CH_2Cl_2, 25 °C, 1.5 h, 95%; j) 50 equiv MeI, 2.5 equiv iPr$_2$EtN, CH_2Cl_2, 25 °C, 1 h, 90%; k) 5.0 equiv AcOH, 1.0 equiv nBu$_4$NF, THF, $-40 \rightarrow 0\,^{\circ}C$, then 3.0 equiv K-selectride, DME/THF (7:1), $-78\,^{\circ}C$, 0.7 h, 67%; l) excess HF · py, CH_2Cl_2/THF (7:1), $-20 \rightarrow 0\,^{\circ}C$, 3 h, 85%; m) 13 equiv $NaBH_3CN$, 13 equiv $BF_3 \cdot OEt_2$, CH_2Cl_2/THF/Et_2O (2:1:1), $-60 \rightarrow -40\,^{\circ}C$, 2 h, 90% (**26**:epi-**26** ≈ 2:1); n) THF/Et_2NH (1:1), 25 °C, 2 h, 81%. FMOC = fluorenylmethoxycarbonyl, TBS = tBuMe$_2$Si.

with K-selectride to afford the desired hydroxy compound **24**. Desilylation of **24** with HF · py gave the hydroxy oxime **25**. The C=N bond of **25** was reduced with $NaBH_3CN$ providing the desired product **26** together with its C4 epimer.[13] Finally, chromatographically purified **26** was deprotected to the targeted trisaccharide chain **3** (Table 1).

Received: January 31, 1992 [Z 5162 IE]
German version: *Angew. Chem.* **1992**, *104*, 926

CAS Registry numbers:
1, 99674-26-7; **2**, 141805-51-8; **3**, 141805-52-9; **4**, 14687-15-1; **5**, 141805-53-0; **6**, 141805-54-1; **7**, 5653-40-7; **8**, 141805-55-2; **9**, 141805-56-3; **10**, 141805-57-4; **11**, 84537-07-5; **12**, 132938-43-3; ; **13**, 141805-58-5; **14**, 141805-59-6; **15**, 141805-60-9; **16**, 141805-61-0; **17**, 126900-87-6; **18**, 141805-62-1; **19**, 141805-63-2; **20**, 141865-64-3; **21**, 141805-65-4; **22**, 141805-66-5; **23**, 141805-67-6; **24**, 141823-81-6; **25**, 141823-82-7; **26**, 141823-83-8; C4 epimer of **26**, 141900-21-2.

[1] J. Golik, J. Clardy, G. Dubay, G. Groenewold, H. Kawaguchi, M. Konishi, B. Krishnan, H. Ohkuma, K. Saitoh, T. W. Doyle, *J. Am. Chem. Soc.* **1991**, *109*, 3461; J. Golik, G. Dubay, G. Groenewold, H. Kawaguchi, M. Konishi, B. Krishnan, H. Ohkuma, K. Saitoh, T. W. Doyle, *J. Am. Chem. Soc.* **1987**, *109*, 3462.

[2] For a review on the chemistry and biology of the enediyne antibiotics, see: K. C. Nicolaou, W.-M. Dai, *Angew. Chem.* **1991**, *103*, 1453; *Angew. Chem. Int. Ed. Engl.* **1991**, *30*, 1387.

[3] For previous syntheses of systems related to the esperamicin A_1 trisaccharide chain **3**, see: a) R. L. Halcomb, M. D. Wittman, S. H. Olson, S. J. Danishefsky, J. Golik, H. Wong, D. Vyas, *J. Am. Chem. Soc.* **1991**, *113*, 5080; b) D. Yang, S.-H. Kim, D. Kahne, *ibid.* **1991**, *113*, 4715.

[4] U. Zehavi, N. Sharon, *J. Org. Chem.* **1972**, *37*, 2141.

[5] All new compounds exhibited satisfactory spectral and analytical and/or exact mass data. The yields given refer to spectroscopically and chromatographically homogeneous materials.

[6] S. Hanessian, Y. Guidon, *J. Carbohydr. Res.* **1980**, *86*, C3.

[7] E. Wenkert, M. E. Alonso, B. L. Buckwalter, E. L. Sanchez, *J. Am. Chem. Soc.* **1983**, *105*, 2021.

[8] K. C. Nicolaou, E. P. Schreiner, W. Stahl, *Angew. Chem.* **1991**, *103*, 566; *Angew. Chem. Int. Ed. Engl.* **1991**, *30*, 585.

[9] Prepared by the method previously described: K. C. Nicolaou, R. D. Groneberg, N. A. Stylianides, T. Miyazaki, *J. Chem. Soc. Chem. Commun.* **1990**, 1275.

[10] S. David, A. Thieffry, *J. Chem. Soc. Perkin Trans. 1* **1979**, 1568.

[11] K. Nicolaou, R. D. Groneberg, *J. Am. Chem. Soc.* **1990**, *112*, 4085.

[12] In this reaction a single geometrical isomer about the oxime –C=N– bond was obtained; however, its configuration remains unassigned.

[13] The assignment of the configuration at C-4 for compound **26** was based on the observed coupling constants for H-4 ($J_{3,4} = 9.5$; $J_{4,5} = 9.6$ Hz; 500 MHz, $CDCl_3$, $\delta = 2.21$), which indicate a diaxial relationship of this proton with its two neighboring protons. The epimer of **26** exhibited a doublet at $\delta = 2.99$ for H-4 ($J_{4,5} = 4.7$ Hz).

A New Strategy for Solid-Phase Synthesis of *O*-Glycopeptides**

By *Tim Bielfeldt, Stefan Peters, Morten Meldal, Klaus Bock,* and *Hans Paulsen**

In recent years glycoproteins have become a focus of attention because of their wide-ranging biochemical functions.[1] They participate in the recognition and defense mechanisms of cells to a large extent.[2] A recent finding is that leukozytes interact with endothel cells through the mediation of the receptors of the LEC–CAM (lectin cell adhesion molecules) family.[3] Parts of glycoproteins containing saccharide and peptide residues are interesting with respect

[*] Prof. Dr. H. Paulsen, Dipl.-Chem. T. Bielfeldt, Dipl.-Chem. S. Peters
Institut für Organische Chemie der Universität
Martin-Luther-King-Platz 6, D-W-2000 Hamburg 13 (FRG)
Dr. M. Meldal, Prof. Dr. K. Bock
Department of Chemistry, Carlsberg Laboratory
Gamle Carlsberg Vej 10, DK-2500 Copenhagen Valby (Denmark)

[**] This work was supported by the Studienstiftung des Deutschen Volkes and the Stiftung Stipendien-Fonds des Verbandes der Chemischen Industrie.

to the function of these segments and the specificity of their further biosynthesis.[4] The isolation of such glycopeptides from natural sources is often difficult. As a rule they are more accessible through chemical synthesis. In an *O*-glycopeptide synthesis, a building block that contains an α-glycosidic bond to an acetylated 2-acetamido-2-deoxy-D-galactopyranose (GalNAc) residue at the hydroxyl group of threonine (Thr) or serine (Ser) is synthesized first for the process in solution, as well as for that in the solid state.[5] The amino acid preferentially contains the orthogonal protecting group pattern fluoren-9-ylmethoxycarbonyl (Fmoc)/*tert*-butyl (*t*-Bu)[6] or Fmoc/pentafluorophenyl (Pfp).[7] This building block containing a saccharide residue can be inserted into a peptide chain in any desired position in a normal solid-phase peptide synthesis.[8]

The recovery of the glycosidic amino acid, however, requires a number of steps. To establish the α-glycosidic bond of GalNAc to Thr or Ser, the only possible glycosyl donor is 2-azido-2-deoxy-D-galactose.[9] The transformation into the activated ester of the amino acid then follows after reduction and other steps. We have now developed a new strategy that shortens the synthesis of *O*-glycopeptides drastically. The glycoside synthesis with the 2-azido-2-deoxy-D-galactose donor is carried out directly with the activated ester of the amino acid. Thus a suitable building block containing 2-azido-2-deoxy-D-galactose is obtained in one step and can be utilized directly for peptide synthesis in the solid phase. Peptides carrying α-glycosidically linked 2-azido-2-deoxy-D-galactose residues at any desired site can be prepared by this route. The transformation of the azido groups into acetamido functions can take place after completion of the peptide chain on the solid support. The deacetylation of all sugar residues is also possible on the polymer-bound peptide. In the last step the final glycopeptide is cleaved off from the resin.

The new procedure is realized as follows. The amino acid derivatives **2** and **3** are glycosylated with halide **1**[10] in the presence of $Ag_2CO_3/AgClO_4$ to **4** and **5**.[11] The stereoselectivity $\alpha:\beta$ is 14:1 for Thr and 6:1 for Ser, which is higher than for other amino acid derivatives.[6] Although the acidic function of the glycosyl amino acids is strongly activated by the Pfp residue, the products can be purified by reversed phase (RP)-HPLC with acetonitrile/water (RP-18, 7 μm) without hydrolysis, even in gram quantities (yield: 78% for Thr, 70% for Ser). The glycosides **4** and **5** are characterized by ^{1}H NMR spectroscopy and FAB-MS.[12] They are stable as solids at −20 °C and therefore have good storage properties.

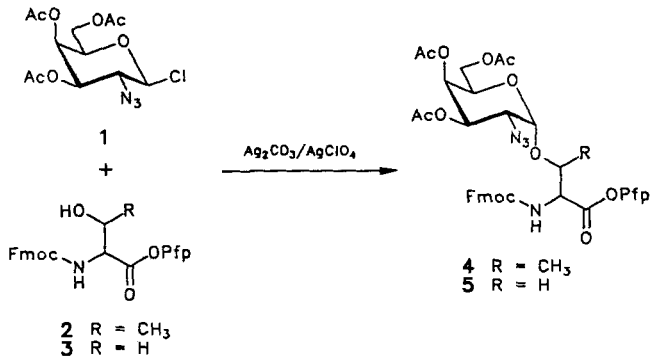

The activated esters **4** and **5** can be used in the solid-phase synthesis directly. Polydimethylacrylamide (P)[13] to which norleucine (Nle) has been attached as internal standard and 5-(4-aminomethyl-3,4-dimethoxyphenoxy)valeric acid as acid-labile peptide amide linker (PAL)[5d,e,14] is employed as resin. On this the stepwise construction of the peptide is performed. The Fmoc cleavage is always carried out with 50% morpholine in DMF (*N*,*N*-dimethylformamide).[15] All *non*-glycosylated amino acids are coupled as 3,4-dihydro-4-oxo-1,2,3-benzotriazin-3-yl (Dhbt) esters.[16] When the glycosylated building blocks **4** or **5** are employed with the Pfp residue, 3,4-dihydro-3-hydroxy-4-oxo-1,2,3-benzotriazine (Dhbt-OH) is added to increase the rate of coupling, probably through the reacylation to the corresponding Dhbt activated esters. This addition has another advantage: it makes the progress of the coupling reaction visible through the yellow color[16,17] caused by ion pairing between Dhbt-OH and free amino groups of the resin. The reaction is complete when the yellow color disappears. The hydroxyl groups of the *non*-glycosylated Thr or Ser residues are protected as *tert*-butyl ether. In the last step of the glycopeptide synthesis, the *N*-terminus is acylated with acetanhydride (Ac_2O) in DMF (1:7), since *N*-acetyl glycopeptide amides are desired. The polymer-bound glycopeptides **6** and **7** were constructed by this method.

In one step on the resin, all azido groups present in **6** and **7** were reduced simultaneously with thioacetic acid and transformed into *N*-acetyl groups, as shown in Scheme 1. The crux of the transformation is the use of multiply distilled thioacetic acid of high purity (GC > 99%). There are then

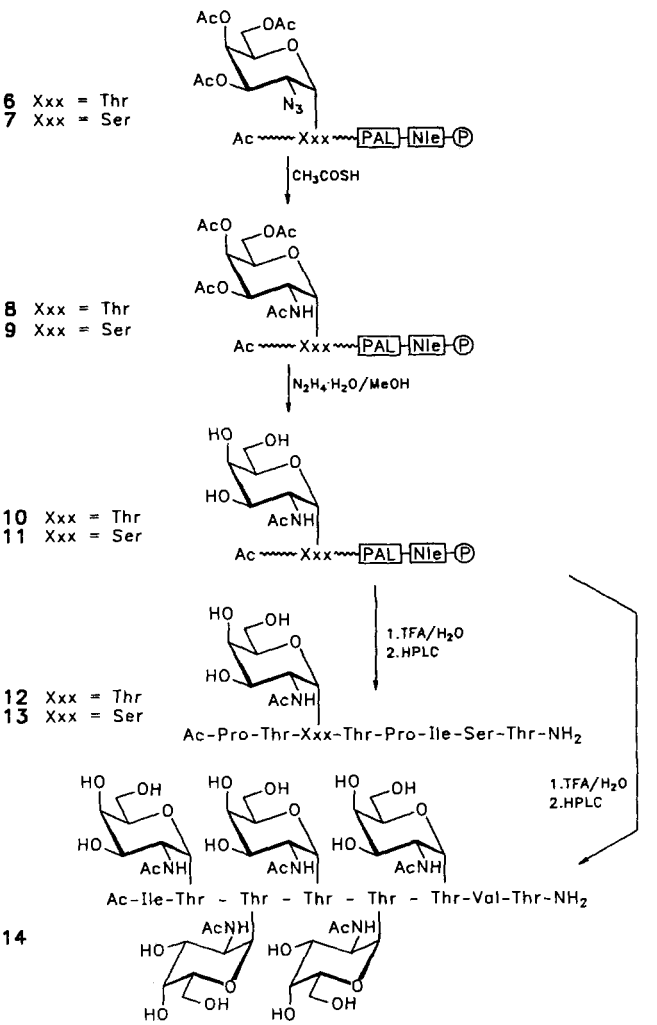

Scheme 1. Glycopeptide solid phase synthesis of the compounds **12**, **13**, and **14**. ~~ = peptide chain; other abbreviations are explained in the text.

no side reactions, and the reaction is complete after 48 h. It was followed by IR spectroscopy by observing the complete disappearance of the azido absorption band at $\tilde{\nu} = 2117\ cm^{-1}$ (KBr windows). At the end the resin-bound **8** and **9** were treated with hydrazine hydrate in methanol (1:7) for about 6 h,[5d-f, 17, 18] which deacetylated all sugar residues to **10** and **11**. The cleavage of the synthesized glycopeptides was achieved in 2 h with 95% aqueous trifluoroacetic acid (TFA). The *N*-acetyl glycopeptide amides **12** and **13** were then purified by RP-HPLC and were identical with those prepared along other routes.[19]

Alternatively, the new procedure can be used in a multiple-column or a fully automatic peptide synthesizer.[17, 20] The multiple column process is preferable when several peptide sequences with few sugar residues are required. For example, besides others the glycopeptides **12** and **13** were synthesized[8, 19] and could be obtained pure in high yields of 77% and 72%.[21] In a fully automatic peptide synthesizer the complex structure of **14** with five vicinal sugar residues was synthesized. In this case the peptide synthesis was observed photometrically and could be controlled by the disappearance of the yellow color of the Dbht-OH salt.[17, 20] In the synthesis of the *penta*-glycosylated octapeptide, the reduction of the azido groups and the deacetylation of the carbohydrates also was achieved without difficulty, and **14** was isolated pure in yields of 40%.[21] The ^1H NMR, FAB-MS, and amino acid analysis data are in accord with the structure.[22] This example serves to illustrate the power of the new method. Peptides **12**, **13**, and also **14** are partial structures of the repeating unit of human intestinal mucin,[23] and should be tested for the specificity of the glycosyl transferases.

Received: January 25, 1992 [Z 5150 IE]
German version: *Angew. Chem.* **1992**, *104*, 881

CAS Registry numbers:
1, 67817-37-2; **2**, 86061-06-5; **3**, 86061-05-4; **4**, 141462-10-4; **5**, 141462-11-5; **12**, 137816-32-1; **13**, 137816-56-9; **14**, 141462-18-2; CH_3COSH, 507-09-5.

[1] a) H. Kunz, *Angew. Chem.* **1987**, *99*, 297–311; *Angew. Chem. Int. Ed. Engl.* **1987**, *26*, 294–308; b) H. Paulsen, *ibid.* **1990**, *102*, 851–867 or **1990**, *29*, 823–839.
[2] J. Montreuil, *Adv. Carbohydr. Chem. Biochem.* **1980**, *37*, 157–223.
[3] a) J. L. Winkelhake, *Glycoconjugate J.* **1991**, *8*, 381–386; b) T. A. Springer, *Nature* **1990**, *346*, 425–434.
[4] I. Brockhausen, G. Möller, G. Merz, K. Adermann, H. Paulsen, *Biochemistry* **1990**, *29*, 10206–10212.
[5] a) H. Paulsen, G. Merz, U. Weichert, *Angew. Chem.* **1988**, *100*, 1425–1427; *Angew. Chem. Int. Ed. Engl.* **1988**, *27*, 1365–1367; b) H. Paulsen, G. Merz, S. Peters, U. Weichert, *Liebigs Ann. Chem.* **1990**, 1165–1173; c) B. Lünning, T. Norberg, C. Rivera-Baeza, T. Tejbrant, *Glycoconjugate J.* **1991**, *8*, 450–455; d) E. Bardají, J. L. Torres, P. Clapés, F. Albericio, G. Barany, R. E. Rodríguez, M. P. Sacristán, G. Valencia, *J. Chem. Soc. Perkin Trans. 1* **1991**, 1755–1759; e) F. Filira, L. Biondi, F. Cavaggion, B. Scolaro, R. Rocchi, *Int. J. Pept. Protein Res.* **1990**, *36*, 86–96; f) F. Filira, L. Biondi, B. Scolaro, M. T. Foffani, S. Mammi, E. Peggion, R. Rocchi, *Int. J. Biol. Macromol.* **1990**, *12*, 41–49.
[6] H. Paulsen, K. Adermann, *Liebigs Ann. Chem.* **1989**, 751–769.
[7] a) M. Meldal, K. J. Jensen, *J. Chem. Soc. Chem. Commun.* **1990**, 483–485; b) A. M. Jansson, M. Meldal, K. Bock, *Tetrahedron Lett.* **1990**, *31*, 6991–6994; c) M. Meldal, K. Bock, *ibid.* **1990**, *31*, 6987–6990; d) K. J. Jensen, M. Meldal, K. Bock, *Peptides 1991*, Proc. 12th Am. Pept. Symp., in press.
[8] S. Peters, T. Bielfeldt, M. Meldal, K. Bock, H. Paulsen, *Tetrahedron Lett.* **1991**, *32*, 5067–5070.
[9] H. Paulsen, *Angew. Chem.* **1982**, *94*, 184–201; *Angew. Chem. Int. Ed. Engl.* **1982**, *21*, 155–173.
[10] H. Paulsen, A. Richter, V. Sinnwell, W. Stenzel, *Carbohydr. Res.* **1978**, *64*, 339–364.
[11] I. Schön, C. Kisfaludy, *Synthesis* **1986**, 303–305.
[12] **4**: $[\alpha]_D^{22} = +39.8$ ($c = 1.0$ in chloroform); m.p. 78 °C; ^1H NMR (400 MHz, C_6D_6, 27 °C, TMS): $\delta = 7.58$–7.14 (4m, 8H; arene H), 5.96 (d, $^3J = 8.5$ Hz, 1H; Thr-NH), 5.59 (dd, 1H; H4), 5.48 (dd, $^3J(3,4) = 3.0$ Hz, 1H; H3), 5.02 (d, $^3J(1,2) = 3.5$ Hz, 1H; H1), 4.72 (m, 1H; Thr-CHα), 4.48 (dd, $^2J = 10.5$ Hz, $^3J = 4.0$ Hz, 1H; Fmoc-CH_2-a), 4.37 (dd, $^3J = 3.5$ Hz, 1H; Fmoc-Ch_2-b), 4.24 (m, 1H; Thr-CHβ), 4.15–3.98 (m, 4H; Fmoc-CH, H5, 2 × H6), 3.62 (dd, $^3J(2,3) = 11.0$ Hz, 1H; H2), 1.72, 1.66 (2s, 9H; 3 × $COCH_3$), 1.13 (d, $^3J = 6.5$ Hz, 3H; Thr-CHγ). FAB-MS: *m/z* 821.2 ($M+1$) (calcd for $C_{37}H_{33}F_5N_4O_{12}$: $M_r = 820.2$). – **5**: $[\alpha]_D^{22} = +77.8$ ($c = 1.0$ in chloroform); m.p. 73 °C; ^1H NMR (400 MHz, $CDCl_3$, 27 °C, TMS): $\delta = 7.78$–7.29 (4m, 8H; arene H), 6.03 (d, $^3J = 8.4$ Hz, 1H; Ser-NH), 5.46 (dd, 1H; H4), 5.31 (dd, $^3J(3,4) = 3.0$ Hz, 1H; H3), 5.01 (d, $^3J(1,2) = 3.6$ Hz, 1H; H1), 4.96 (m, 1H; Ser-CHα), 4.48 (m, 2H; Fmoc-CH_2), 4.34 (dd, $^2J = 11.2$ Hz, $^3J = 3.4$ Hz, 1H; Ser-CHβ-a), 4.26 (t, 1H; Fmoc-CH), 4.18 (t, 1H; H5), 4.10 (dd, $^3J = 3.8$ Hz, 1H; Ser-CHβ-b), 4.08 (dd, $^2J(6a,b) = 11.0$ Hz, $^3J(5,6a) = 6.0$ Hz, 1H; H6a), 4.03 (dd, $^3J(5,6b) = 7.6$ Hz, 1H, H6b), 3.72 (dd, $^3J(2,3) = 11.0$ Hz, 1H; H2), 2.16, 2.07, 1.98 (3s, 9H, 3 × $COCH_3$). FAB-MS: *m/z* 807.3 ($M+1$) (calcd for $C_{36}H_{31}F_5N_4O_{12}$: $M_r = 806.2$).
[13] E. Atherton, C. J. Logan, R. C. Sheppard, *J. Chem. Soc. Perkin Trans. 1* **1981**, 538–546.
[14] a) F. Albericio, N. Kneib-Cordonier, S. Biancalana, L. Gera, R. J. Masada, D. Hudson, G. Barany, *J. Org. Chem.* **1990**, *55*, 3730–3743; b) H. Dürr, A. G. Beck-Sickinger, G. Schnorrenberg, W. Rapp, G. Jung, *Int. J. Pept. Protein Res.* **1991**, *38*, 146–153.
[15] P. Schultheiß-Reimann, H. Kunz, *Angew. Chem.* **1983**, *95*, 64; *Angew. Chem. Int. Ed. Engl.* **1983**, *22*, 62.
[16] E. Atherton, J. L. Holder, M. Meldal, R. C. Sheppard, R. M. Valerio, *J. Chem. Soc. Perkin Trans. 1* **1988**, 2887–2894.
[17] L. R. Cameraon, J. L. Holder, M. Meldal, R. C. Sheppard, *J. Chem. Soc. Perkin Trans. 1* **1988**, 2895–2901.
[18] a) H. Kunz, H. Waldmann, *Helv. Chim. Acta* **1985**, *68*, 618–622; b) H. Kunz, S. Birnbach, *Angew. Chem.* **1986**, *98*, 354–355; *Angew. Chem. Int. Ed. Engl.* **1986**, *25*, 360.
[19] S. Peters, T. Bielfeldt, M. Meldal, K. Bock, H. Paulsen, *J. Chem. Soc. Perkin Trans. 1*, **1992**, 1163–1171.
[20] a) A. Holm, M. Meldal, *Peptides 1988* (Eds.: G. Jung, E. Bayer), Proc. 20th Eur. Pept. Symp. de Gruyter, Berlin, **1989**, p. 208–210; b) A. Dryland, R. C. Sheppard, *Tetrahedron* **1988**, *44*, 859–876.
[21] The yields are calculated on the degree of loading of the resin and the degree of coupling of the first amino acid. Both were determined by quantitative amino acid analysis with Nle as internal standard.
[22] **14**: $[\alpha]_D^{22} = +113.7$ ($c = 1.0$ in water); FAB-MS: *m/z* 1893.9 ($M+1$) (calcd for $C_{77}H_{132}N_{14}O_{40}$: $M_r = 1892.9$).
[23] J. R. Gum, J. C. Byrd, J. W. Micks, N. W. Toribara, D.T.A. Lamport, Y. S. Kim, *J. Biol. Chem.* **1989**, *264*, 6480–6487.

Deuterium-Induced Phase Transition of an Organic Metal—An Unusual Isotope Effect**

By *Siegfried Hünig,* Klaus Sinzger, Martina Jopp, Dagmar Bauer, Werner Bietsch, Jost Ulrich von Schütz,* and *Hans Christoph Wolf*

In this report the extreme sensitivity[1] of the metallic conductivity of 2-(Me_2-DCNQI)$_2$Cu (DCNQI = *N*,*N*′-dicyanoquinonediimine) to minor structural changes is demonstrated in a striking manner. Whereas the conductivity of the copper salt of non-deuterated 2,5-Me_2-DCNQI increases as the temperature is lowered (to 0.45 K) and reaches 500 000 $S\,cm^{-1}$ at 10 K, the partially or fully deuterated derivative switches from quasi three-dimensional behavior with $\sigma \approx 10^3\ S\,cm^{-1}$ at room temperature to quasi one-dimensional conduction below the transition temperature T_{M-I}. As a result, σ changes by about eight orders of magnitude within a few K.

[*] Prof. Dr. S. Hünig, Dipl.-Chem. K. Sinzger, M. Jopp
Institut für Organische Chemie der Universität
Am Hubland, D-W-8700 Würzburg (FRG)
D. Bauer, Dipl.-Phys. W. Bietsch, Dr. J. U. von Schütz,
Prof. Dr. H. C. Wolf
3. Physikalisches Institut der Universität
Pfaffenwaldring 57, D-W-7000 Stuttgart (FRG)

[**] This research was supported by the Fonds der Chemischen Industrie, the Volkswagen Stiftung, and the Deutsche Forschungsgemeinschaft (SFB 329).

Systematic studies have shown that all of the copper–radical-anion salts **1** derived from 2,5-disubstituted DCNQIs with the combination of substituents $R^1 = R^3$ and $R^1 \neq R^3 = CH_3$, OCH_3, Cl, Br, I crystallize in the same space group, $I4_1/a$, and demonstrate metallic conductivity at least at room temperature.[2] Starting with about 200–1000 $S\,cm^{-1}$ (at room temperature) the conductivity increases steadily with cooling. If the substitution pattern of **1** is determined primarily by the small substituents Cl and Br, then a phase transition to a metal-like semiconductor (for definition see ref.[3]) takes place at $T_{M-I} = 160-230\,K$; the large substituents OCH_3 and I guarantee metallic conductivity down to the lowest temperatures.

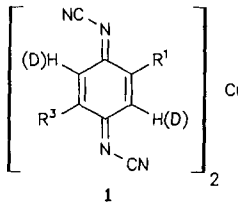

1

	R^1	R^3	H/D	T_{M-I} [K]
1a	CH_3	CH_3	H	–
1b	CH_3	CD_3	H	58
1c	CD_3	CD_3	H	73
1d	CD_3	CD_3	D	82
1e	CH_3	Br	H	160
1f	Br	Br	H	160

For this class of materials it is already known that continuous cooling leads to increased compression of the *c* axis of the crystal lattice (for **1a** a total of 2%), while the *a* axis is lengthened minimally (for **1a** about 0.09%).[4, 5] The associated flattening of the nearly tetrahedral coordination of the ligands to copper (enlargement of the coordination angle α; cf. Fig. 1) splits the t_{2g} set of copper 3d orbitals, which are degenerate for ideal tetrahedral coordination, as a result of the reduction in symmetry from T_d towards D_{2d}.[6] When the coordination angle α exceeds a critical threshold (127–128°),[6] the crystal undergoes a phase transition recognizable by an additional discontinuous compression of the *c* axis.[4, 5]

Recently a sevenfold super-diamond structure was revealed for the DCNQI–copper salts.[7a] Closer examination of a super-adamantane unit in the direction of stacking (Fig. 2) shows that the DCNQI stacks associated with four neighboring stacks of copper atoms form a super helix of seven intertwined single helices,[7b] whose spacing in the direction of stacking has the value of the cell constant *c*.

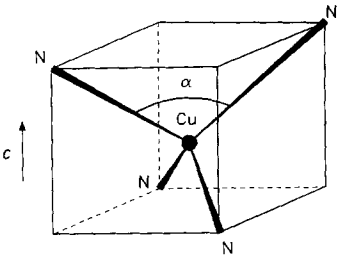

Fig. 1. Coordination geometry of the Cu central atom of the salts (2,5-R^1,R^3-DCNQI)$_2$Cu. N represents the cyano N atoms of the ligands.

The channel formed by the helices is filled by the DCNQI substituents R^1 and R^3; their size thus determines the distance between the individual helices. For the previously described structural type, a direct relationship between the cell constants *a* and *c* and the crucial coordination angle α can be deduced.[8] Combinations of smaller substituents (R^1 = Cl, Br; R^3 = Cl, Me, Br) allow a phase transition; combinations of large substituents (R^1 = I, MeO; R^3 = Cl, Me, Br, I, MeO) prevent one. Thus there is a three-dimensional cooperative interaction of the partners, whose effect on the conductivity is produced by a collective of an "infinite" number of "layers" (DCNQIs).[9]

A thorough analysis of these relationships[8, 10] showed that **1a** occupies a special position. Although the van der Waals volume of the CH_3 group (21.7 $Å^3$) is substantially less than that of Br (25.1 $Å^3$),[11] **1a** (CH_3/CH_3) does not undergo a phase transition until the lowest temperatures, in constrast to **1e** (CH_3/Br) and **1f** (Br/Br). On the contrary, its conductivity increases markedly until 0.45 K[12] and reaches 500000 $S\,cm^{-1}$ at 10 K[13] (cf. Fig. 3). This unexpected stability of **1a** is attributed to the low LUMO energy ($\varepsilon_{LUMO} = -2.42$ eV) and the enhanced donor strength of the n electron pair of the CN group ($\varepsilon_{\sigma n} = -14.51$ eV) relative to **1e** ($\varepsilon_{LUMO} = -2.64$ eV, $\varepsilon_{\sigma n} = -14.64$ eV) and **1f** ($\varepsilon_{LUMO} = -2.85$ eV, $\varepsilon_{\sigma n} = -14.77$ eV.[10]

If all of these explanations are correct, then substituents with electronic properties similar to those of methyl groups but with a smaller volume may possibly trigger a phase transition upon cooling. Both the electronic and the spacial prerequisites are met by CD_3 groups, whose volume at 70 K is about 1.0–1.5% less than that of CH_3 groups.

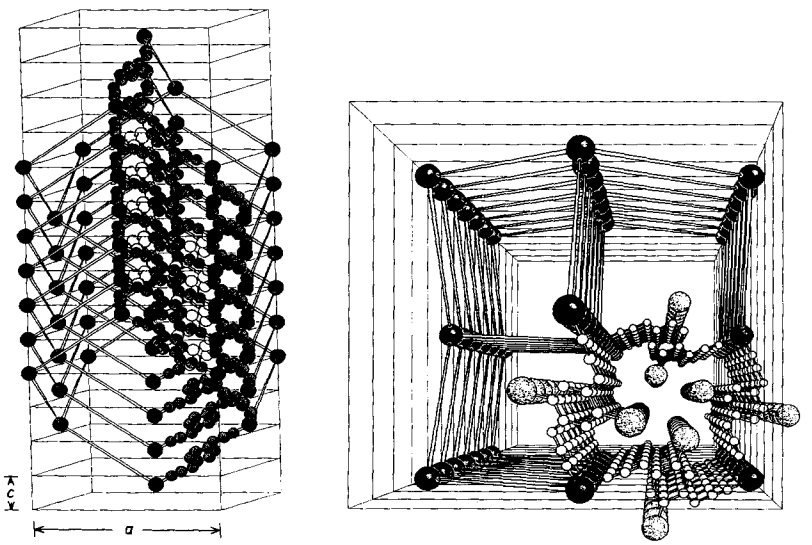

Fig. 2. Sevenfold adamantane super-structures in the crystal lattice of (2,5-R^1,R^3-DCNQI)$_2$Cu (space group $I4_{1/a}$). Cu ions take the place of adamantane C atoms and are connected to each other through the ligands. In both figures three-fourths of the ligands between the copper ions are represented by lines. (SCHAKAL 88B/V16). Left: Side view perpendicular to the direction of stacking. The substituents R^1 and R^3 are not shown. Right: Perspective view in the direction of stacking. The substituents R^1 and R^3 fill the channels.

 © VCH Verlagsgesellschaft mbH, W-6940 Weinheim, 1992 0570-0833/92/0707-0860 $ 3.50+.25/0

As a result of the lower zero-point energy, the mean as well as the maximum C–D bond length is less than the comparable values for a C–H bond in the *gas phase*, 0.15% and 0.37%, respectively.[14] Correspondingly, the molar volume of *liquid* CD_4 relative to CH_4 at 100 K is about 1% less;[15] the volume of the unit cell in the *crystalline* state at 70 K is approximately 1.5% less.[16] As the following literature examples show deuteration of the methyl groups in **1a** should result in only minimal *quantitative* changes. H/D exchange in *crystalline* organic charge-transfer (CT) complexes shifts the transition temperature of the structural phase transition from +0.75 K[17] to −15 K.[18] For deuterated superconductors of the BEDT–TTF type an increase in the critical temperatures by 0.28 K to 0.6 K[19] is observed; however, for deuterated $(TMTSF)_2ClO_4$ a decrease of 0.13 K[20] is noted.

In contrast, we report here a dramatic *qualitative* effect, that is, a phase transition from metallic to semiconducting behavior induced by deuteration. Such a phenomenon due to a secondary deuterium isotope effect has not been reported so far.

As is evident from Figure 3, the introduction of deuterium to just one CH_3 group in **1a** ($CH_3/CH_3/H_2$) giving **1b** ($CH_3/CD_3/H_2$) induces a phase transition at 58 K. The two CD_3 groups in **1c** ($CD_3/CD_3/H_2$) trigger this conversion already at 73 K. Even the substitution of the two hydrogen atoms on the ring in **1c** by deuterium to **1d** ($CD_3/CD_3/D_2$) shifts the phase-transition temperature by another 9 K to 82 K.[21] The resulting phase transitions are unusually sharp: The conductivity drops off by a factor of 10^6–10^8 (!) within 1–2 K.[22]

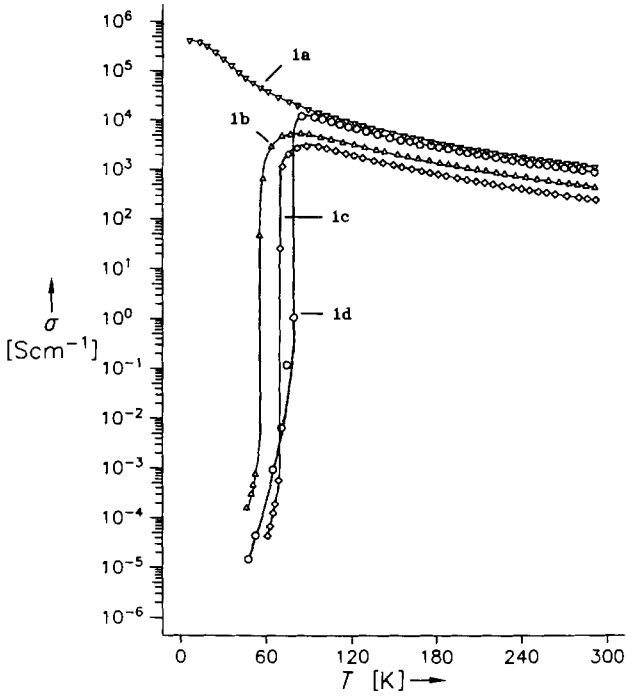

Fig. 3. Temperature dependence of the conductivity σ of **1a** ($CH_3/CH_3/H_2$), **1b** ($CH_3/CD_3/H_2$), **1c** ($CD_3/CD_3/H_2$), and **1d** ($CD_3/CD_3/D_2$) (four-point measurements on single crystals[23].)

The phase transition of the deuterated Cu salts can also be proved by electron spin resonance spectroscopy: Below the phase-transition temperature a relatively narrow ESR signal ($\Delta B_{pp} \approx 2 \cdot 10^{-3}$ T) is observed, whose intensity increases drastically with decreasing temperature. The behaviour of other DCNQI–Cu salts is quite different. Whereas the line width of the ESR signal observed for non-deuterated systems increases upon warming from low temperature to T_{M-I} (increase of the three-dimensional movement of the electrons), the line width for the deuterated copper salts is practically constant below T_{M-I}; this supports the assumption of a transition from three-dimensional to an extremely one-dimensional behavior.[24] Despite its high static susceptibility,[*] this signal is not detectable in the metallic region. Because of the three-dimensional movement of the electrons, the spin-orbit coupling leads to extreme line widths.[25]

Apparently **1a** is protected only minimally from a phase conversion by the electronic properties mentioned. Thus slight changes cause the phase transition in the dimensionality of the movement of the electrons. Besides the deuteration described here, the same effect is induced by applying pressure to **1a**.[12, 26] Even 110 bar produces a sharp phase transition at 47 K (or 400 bar at 76 K). The conductivity drops sharply by at least a factor of 10^4, analogous to the observations for the deuterated systems (Fig. 4).[12]

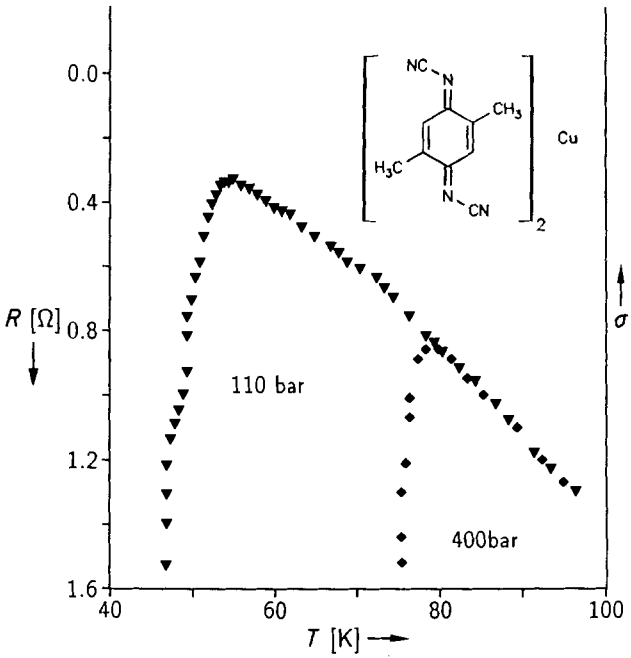

Fig. 4. Pressure dependence of the conductivity of **1a**[12].

Besides the somewhat smaller volume of the CD_3 group, its different rotational barrier could be significant. Studies of crystals of several deuterated compounds (CD_3CO_2Li,[27] CD_3NO_3,[28] and $CD_3C_6D_5$[28, 29]) by inelastic neutron scattering show a marked decrease in the tunnel splitting and thus an increase in the rotation barriers relative to those of the corresponding protonated systems. As a consequence, the motion of the deuterated methyl groups is frozen even at higher temperatures. One argument against this interpretation of our results is that for the reported activation energies at 500–800 K[30] due to intra- and intermolecular hindrance,[31] the motion of the methyl groups of the non-deuterated copper salt **1a** would be too slow at the finite

[*] Note added in proof: At exactly T_{M-I} the static susceptibility exhibits a step in intensity by 1.5×10^{-6} emu g^{-1} to increase considerably with lower temperatures. At 7 K a pronounced peak occurs due to magnetic ordering.

temperature to prevent a phase transition. Further experiments should clarify the situation.

Received: February 13, 1992 [Z 5188 IE]
German version: *Angew. Chem.* **1992**, *104*, 896

CAS Registry numbers:
1a, 103420-86-6; **1b**, 141636-02-4; **1c**, 141636-05-7; **1d**, 141636-07-9; **1e**, 112019-20-2; **1f**, 111958-83-9.

[1] J. U. von Schütz, H. Rieder, H. C. Wolf, H. Meixner, S. Hünig, *Synth. Met.* **1991**, *42*, 1761.
[2] Reviews: a) S. Hünig, P. Erk, *Adv. Mater.* **1991**, *3*, 225–236; b) S. Hünig, *Pure Appl. Chem.* **1990**, *62*, 395–406.
[3] J. S. Miller, A. J. Epstein, *Angew. Chem.* **1987**, *99*, 332–339; *Angew. Chem. Int. Ed. Engl.* **1987**, *26*, 287–293.
[4] R. Moret, *Synth. Met.* **1988**, *27*, B 301–B 307.
[5] a) H. Kobayashi, R. Kato, A. Kobayashi, T. Mori, H. Inokuchi, *Solid State Commun.* **1988**, *65*, 1351–1354; b) A. Kobayashi, T. Mori, H. Inokuchi, R. Kato, H. Kobayashi, *Synth. Met.* **1988**, *27*, B 275–B 280; c) S. Kagoshima, N. Sugimoto, R. Kato, H. Kobayashi, A. Kobayashi, *ibid.* **1991**, *41–43*, 1835–1838.
[6] a) A. Kobayashi, R. Kato, H. Kobayashi, T. Mori, H. Inokuchi, *Solid State Commun.* **1987**, *64*, 45–51; b) H. Kobayashi, R. Kato, A. Kobayashi, T. Mori, H. Inokuchi, Y. Nishio, K. Kajita, W. Sasaki, *Synth. Met.* **1988**, *27*, A 289–A 297; c) R. Kato, H. Kobayashi, A. Kobayashi, *J. Am. Chem. Soc.* **1989**, *111*, 5224–5232.
[7] a) O. Ermer, *Adv. Mater.* **1991**, *3*, 608–611. b) Similar helix structures have been described for other super-diamond lattices: O. Ermer, L. Lindenberg, *Chem. Ber.* **1990**, *123*, 1111.
[8] An exact evaluation of these new structural considerations and their implications for the discussion of phase behavior will be published shortly.
[9] For properties induced by collectives of molecules see: F. M. Menger, *Angew. Chem.* **1991**, *103*, 1104; *Angew. Chem. Int. Ed. Engl.* **1991**, *30*, 1086.
[10] P. Erk, H. Meixner, T. Metzenthin, S. Hünig, U. Langohr, J. U. von Schütz, H.-P. Werner, H. C. Wolf, R. Burkert, H. W. Helberg, G. Schaumburg, *Adv. Mater.* **1991**, *3*, 311–315.
[11] A. Bondi, *J. Phys. Chem.* **1964**, *68*, 441–451. The special position of **1a** is even more apparent by application of these newer van der Waals volumes (K. Sinzger, *Dissertation*, Universität Würzburg, **1992**).
[12] S. Tomic, D. Jérome, A. Aumüller, P. Erk, S. Hünig, J. U. von Schütz, *J. Phys. C: Solid State Phys.* **1988**, *21*, L 203–L 207.
[13] A. Aumüller, P. Erk, G. Klebe, S. Hünig, J. U. von Schütz, H.-P. Werner, *Angew. Chem.* **1986**, *98*, 759–761; *Angew. Chem. Int. Ed. Engl.* **1986**, *25*, 740.
[14] L. S. Bartell, K. Kuchitsu, R. J. deNeui, *J. Chem. Phys.* **1961**, *35*, 1211–1218.
[15] S. Fuks, J.-C. Legros, A. Bellemans, *Physica* **1965**, *31*, 606–612.
[16] S. C. Greer, L. Meyer, *J. Chem. Phys.* **1970**, *52*, 468–469.
[17] J. R. Cooper, J. Lukatela, M. Miljak, J. M. Fabre, L. Giral, E. Aharon Shalom, *Solid State Commun.* **1978**, *25*, 949–954.
[18] N. S. Dalal, L. V. Haley, D. J. Northcott, J. M. Park, A. H. Reddoch, J. A. Ripmeester, D. F. Williams, *J. Chem. Phys.* **1980**, *73*, 2515–2517.
[19] a) C.-P. Heidmann, K. Andres, D. Schweitzer, *Physica* **1986**, *143B*, 357–359; b) K. Oshima, H. Uruyama, H. Yamochi, G. Saito, *J. Phys. Soc. Jpn.* **1988**, *57*, 730–733.
[20] H. Schwenk, E. Hess, K. Andres, F. Wudl, E. Aharon-Shalom, *Phys. Lett. A* **1984**, *102*, 57–60.
[21] The syntheses will be reported elsewhere. All new compounds provided the expected spectroscopic and analytical data. The extent of deuteration was determined by ^{1}H NMR spectroscopy (250 MHz) and confirmed by mass spectrometry. **1b** (D_3: > 99.5%); **1c** (D_6: > 99.5%); **1d** (D_6: > 99.5%; D_2: 97.3%).
[22] A careful analysis of the IR data of **1d** (C. Pecile, personal communication) conducted parallel to the measurements described here also demonstrated the phase transition. We thank Prof. Pecile for the results and for providing us with 100 mg of **1d** for comparison.
[23] All four-point measurements with $T\downarrow$ and $T\uparrow$ were repeated a number of times on various samples.
[24] J. U. von Schütz, unpublished.
[25] J. U. von Schütz, H.-P. Werner, H. C. Wolf, A. Aumüller, P. Erk, S. Hünig, *Proc. 23th Congr. Ampere Magn. Rson.* **1986**, 158–159.
[26] First results of the X-ray structure analysis on a single crystal (R. Bau, T. Metzenthin, unpublished results) and on powder (E. Tillmanns, unpublished results: **1a**: $a = 21.607(1)$, $c = 3.8823(6)$ Å, $V_C = 1812.5$ Å^3; **1c**: $a = 21.628(2)$, $c = 3.8730(6)$ Å, $V_C = 1811.7$ Å^3) indicate a minimal shortening of the cell constant c for the deuterated compounds even at room temperature. Even the pressure-dependent structural investigations of **1a** point to an increased compressability in the direction of stacking[4].
[27] A. Heidemann, H. Friedrich, E. Günther, W. Häusler, *Z. Phys. B: Condens. Matter* **1989**, *76*, 335–344.
[28] a) D. Cavagnat, A. Magerl, C. Vettier, I. S. Anderson, *Phys. Rev. Lett.* **1985**, *54*, 193–196; b) D. Cavagnat, A. Magerl, C. Vettier, S. Clough, *J. Phys. C: Solid State Phys.* **1986**, *19*, 6665–6672; c) D. Cavagnat, A. Magerl, C. Vettier, S. Clough, *J. Phys.: Condens. Matter* **1989**, *1*, 10047–10051.
[29] W. Müller-Warmuth, R. Schüler, M. Prager, A. Kollmar, *J. Magn. Reson.* **1979**, *34*, 83–95.
[30] a) U. Langohr, *Dissertation*, Universität Stuttgart, **1991**; b) M. Schlingmann, *Diplomarbeit*, Universität Stuttgart, **1989**.
[31] a) J. U. von Schütz, H. C. Wolf, *Z. Naturforsch. A* **1972**, *27*, 42–50; b) J. U. von Schütz, F. Noack, *ibid.* **1972**, *27*, 645–651; c) J. U. von Schütz, unpublished.

Doubly Bridged Prismane and Dewar Benzene Intermediates in an Unusual Photochemical Rearrangement of Tricyclic Phthalic Esters**

By *Rolf Gleiter** and *Björn Treptow*

Dedicated to Professor Günther Maier on the occasion of his 60th birthday

Irradiation of alkylbenzenes in solution at wavelengths higher than 250 nm usually yields a positional isomerization of the alkyl groups.[1] To rationalize this phenomenon, it is assumed that valence bond isomers of benzene, such as benzvalene, Dewar benzene, and prismane are short-lived intermediates. The involvement of such isomers has been inferred from isotopic labeling experiments.[1] Possible ring transposition processes that give rise to apparent 1,2 and 1,3 shifts are shown schematically in Scheme 1.

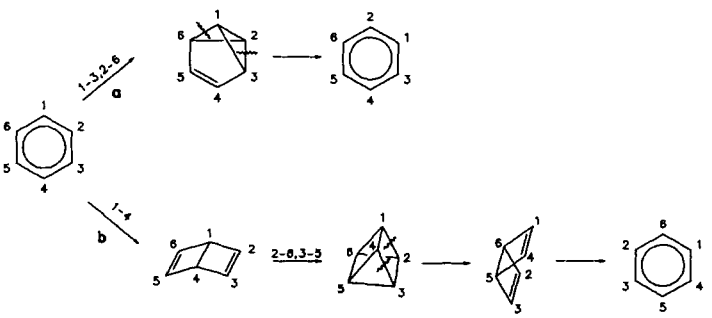

Scheme 1. Proposed rearrangements that proceed via valence isomers of benzene as intermediates.

Two motives prompted us to study the mechanism of the light-induced ring transposition in benzene: 1) We thought that the tethering of neighboring centers in a benzene derivative might stabilize one of the intermediates, and 2) we hoped by this "rope trick" to generate those doubly bridged Dewar benzenes and/or prismanes which were not available to date.[2]

We started our investigations with the doubly bridged Dewar benzene derivatives **1**, which could be obtained easily from cyclic alkynes and dimethyl acetylenedicarboxylates.[2, 3] Ir-

[*] Prof. Dr. R. Gleiter, Dipl.-Chem. B. Treptow
Organisch-chemisches Institut der Universität
Im Neuenheimer Feld 270, D-W-6900 Heidelberg (FRG)

[**] We are grateful to the Volkswagen-Stiftung, the Deutsche Forschungsgemeinschaft, the Fonds der Chemischen Industrie, and the BASF AG (Ludwigshafen) for financial support.

radiation of **1** at wavelengths above 295 nm yielded exclusively the isomeric phthalic ester derivatives **3** (Scheme 2). No trace of the prismanes **2** could be detected, nor was there any hint of a photochemical equilibrium between **1** and **3**. Excitation by the unfiltered light from a high-pressure Hg lamp afforded the isomeric terephthalic esters **4b–4d**. In the case of **3a** no rearranged product was obtained.

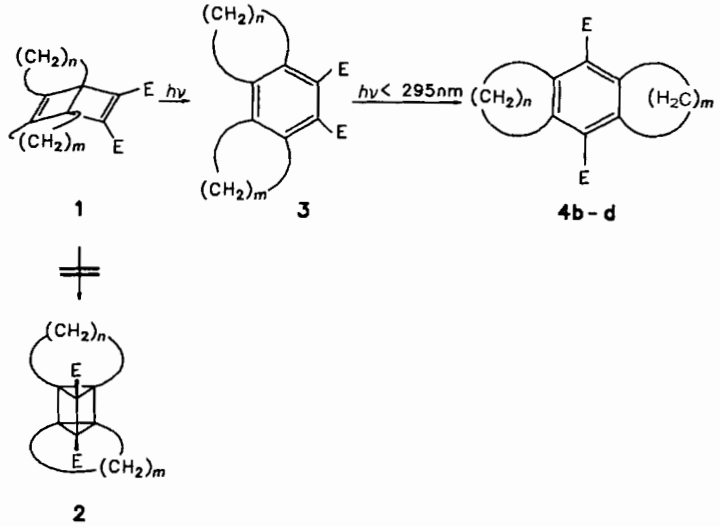

Scheme 2. Rearrangements of **1** on irradiation with light with $\lambda > 295$ nm. **a**: $n,m = 4$; **b**: $n,m = 5$; **c**: $n,m = 6$; **d**: $n = 4$, $m = 5$; E = COOMe.

These unexpected results were an impetus for closer investigation. At first we confined our further studies to **3b** because it was the most readily accessible[2] and gave the highest yields of **4b**. A change of the wavelength to 282 nm afforded two other compounds, prismane **5b** and Dewar benzene **6b**. They were unequivocally identified by their ^{1}H NMR, ^{13}C NMR, and UV spectra (see Table 1). They proved to be direct precursors to **4b**, as irradiation converted them rapidly and quantitatively into **4b**.

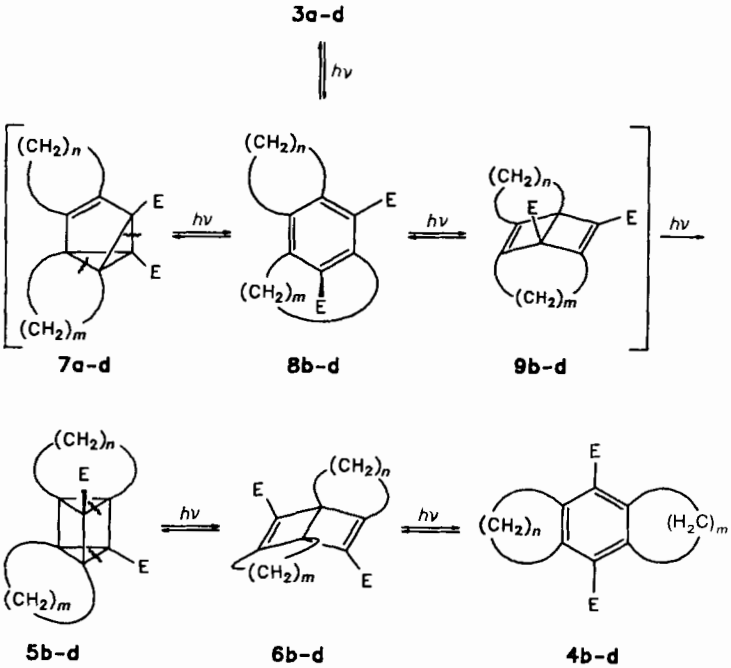

Scheme 3. Sequence of reactions for the rearrangements of **3b–d** to **4b–d**.

Table 1. Selected spectral data of **1a, d, 3a, d, 4b, c, d, 5b**, and **6b, c**.

1a: ^{1}H NMR (200 MHz, $CDCl_3$): $\delta = 3.79$ (s, 6H), 2.4–1.0 (m, 16H); ^{13}C NMR (50.32 MHz, $CDCl_3$): $\delta = 163.8, 150.3, 139.1, 57.6, 52.4, 27.0, 25.2, 24.5, 23.3$; UV/VIS (acetonitrile): λ_{max}[nm] (lgε) = 188 (4.23), 235 sh (3.67); correct C,H,O analysis.

1d: ^{1}H NMR (300 MHz, $CDCl_3$): $\delta = 3.78$ (s, 3H), 3.77 (s, 3H), 2.35–2.25 (m, 2H), 2.2–1.1 (m, 16H); ^{13}C NMR (75.47 MHz, $CDCl_3$): $\delta = 163.3, 163.25, 150.4, 149.3, 143.5, 141.4, 62.7, 54.5, 51.6, 51.55, 31.1, 28.8, 28.1, 27.7, 27.65, 26.5, 24.4, 24.2, 22.9$; high-resolution MS: m/z ($M^{\oplus} - CH_3OH$) calcd: 284.1413, found: 284.1386

3a: colorless crystals, m.p. 148–150 °C; ^{1}H NMR (200 MHz, $CDCl_3$): $\delta = 3.83$ (s, 6H), 2.78 (t, ^3J(H,H) = 6.0 Hz, 4H), 2.57 (t, ^3J(H,H) = 6.1 Hz, 4H), 1.9–1.6 (m, 8H); ^{13}C NMR (50.32 MHz, $CDCl_3$): $\delta = 169.9, 139.3, 133.1, 130.1, 52.8, 28.4, 27.7, 23.3, 23.0$; UV/VIS (acetonitrile): λ_{max}[nm] (lgε) = 213 (4.4), 245 sh (3.45), 287 (2.85); correct C,H,O analysis.

3d: colorless crystals, m.p. 86 °C; ^{1}H NMR (300 MHz, $CDCl_3$): $\delta = 3.83$ (s, 6H), 2.85–2.7 (m, 8H), 1.9–1.5 (m, 10H); ^{13}C NMR (75.47 MHz, $CDCl_3$): $\delta = 169.8, 169.3, 145.3, 138.4, 136.7, 133.3, 129.4, 129.2, 52.2, 52.1, 31.5, 31.3, 28.6, 27.9, 27,9, 27.2, 26.2, 23.0$; UV/VIS (acetonitrile): λ_{max}[nm] (lgε) = 216 (4.59), 252 sh (3.79), 288 (3.31); correct C,H,O analysis.

4b: colorless needles, m.p. 149 °C; ^{1}H NMR (300 MHz, $CDCl_3$): $\delta = 3.87$ (s, 6H), 2.7–2.55 (m, 8H), 1.9–1.7 (m, 4H), 1.7–1.5 (m, 8H); ^{13}C NMR (75.47 MHz, $CDCl_3$): $\delta = 171.1, 137.2, 134.4, 51.9, 32.3, 31.8, 27.2$; UV/VIS (acetonitrile): λ_{max}[nm] (lgε) = 208 (4.27), 230 sh (3.70), 282 (3.06); high-resolution MS: m/z ($M^{\oplus}$) calcd: 330.1831, found: 330.1826; correct C,H,O analysis.

4c: colorless needles, m.p. 169 °C; ^{1}H NMR (200 MHz, $CDCl_3$): $\delta = 3.88$ (s, 6H), 2.7–2.6 (m, 8H), 1.8–1.6 (m, 8H), 1.45–1.25 (m, 8H); ^{13}C NMR (50.32 MHz, $CDCl_3$): $\delta = 171.1, 135.5, 135.3, 51.8, 31.0, 29.2, 26.1$; UV/VIS ($CH_2Cl_2$): λ_{max}[nm] (lgε) = 206 (4.62), 230 sh (3.91), 280 (3.19); high-resolution MS: m/z ($M^{\oplus}$) calcd: 358.2144, found: 358.2150.

4d: colorless crystals, m.p. = 118–119 °C; ^{1}H NMR (200 MHz, $CDCl_3$): $\delta = 3.88$ (s, 6H), 2.7–2.55 (m, 8H), 1.85–1.5 (m, 10H); ^{13}C NMR (50.32 MHz, $CDCl_3$): $\delta = 170.8, 137.2, 134.8, 131.0, 52.0, 32.2, 31.8, 27.4, 26.7, 22.4$; UV/VIS (acetonitrile): λ_{max}[nm] (lgε) = 206 (4.59), 228 sh (3.94), 282 (3.29); correct C,H,O analysis.

5b: ^{1}H NMR (300 MHz, $CDCl_3$): $\delta = 3.68$ (s, 6H), 2.5–2.35 (m, 2H), 2.25–2.1 (m, 2H), 2.0–1.1 (m, 16H); ^{13}C NMR (75.47 MHz, $CDCl_3$): $\delta = 170.5, 56.0, 54.5, 50.8, 48.4, 32.3, 28.6, 27.9, 24.5, 24.2$; UV/VIS (*n*-pentane): λ_{max}[nm] (lgε) = 203 (3.85), 270 sh (2.85); high-resolution MS: m/z ($M^{\oplus}$) calcd: 330.1831, found: 330.1827.

6b: ^{1}H NMR (300 MHz, $CDCl_3$): $\delta = 3.71$ (s, 6H), 2.9–2.7 (m, 2H), 2.5–2.35 (m, 2H), 2.1–1.4 (m, 16H); ^{13}C NMR (75.47 MHz, $CDCl_3$): $\delta = 173.9, 164.2, 134.6, 59.3, 50.8, 31.2, 30.9, 27.9, 27.3, 27.2$; UV/VIS (*n*-pentane): λ_{max}[nm] (lgε) = 218 (4.17), 270 sh (3.47); high-resolution MS: m/z ($M^{\oplus}$) calcd: 330.1831, found: 330.1819

6c: ^{1}H NMR (300 MHz, $CDCl_3$): $\delta = 3.71$ (s, 6H), 3.0–2.8 (m, 2H), 2.4–2.15 (m, 4H), 2.15–1.3 (m, 18H); ^{13}C NMR (75.47 MHz, $CDCl_3$): $\delta = 174.2, 164.1, 136.8, 60.3, 50.7, 30.4, 27.3, 26.6, 25.9, 24.6, 24.2$; high-resolution MS: m/z ($M^{\oplus}$) calcd: 358.2144, found: 358.2169

For the mechanism of the complete photochemical rearrangement we assume that the benzvalene derivative **7b**, [5]metacyclophane **8b**, and Dewar benzene **9b** serve as additional intermediates. We account for the almost complete conversion of **3b** into **4b** through this complex series of rearrangements as follows: As a result of the short 1,3 bridge, **8b** is extremely bent thus generating considerable strain,[4] which under the given conditions can be relieved either by the back reaction or in several steps via the prismane **5b** to **4b**. The back reaction is usually invoked to explain the transformation of [5]metacyclophanes to 1,2-bridged arenes, although benzvalene intermediates have not yet been observed directly.[5] In our particular case, **8b** can also follow the photochemically allowed sequence in Scheme 3 to yield the relaxed terephthalic ester derivative **4b**. It is noteworthy that the geometry of both Dewar benzene **9b** and prismane **5b** is already inherent in the assumed unsymmetric boat conformation[6] of **8b**. The driving force in this series is the irreversibility of prismane formation (**9b** → **5b**). The interaction of the carbomethoxy groups with the cyclopropane portion of the prismane in **5b** stabilizes the distal bonds,[7] thus allowing fragmentation only to **6b**,

which in turn isomerizes immediately to **4b**. This was corroborated by the fact that irradiation of **5b** did not give rise to any of its precursors but afforded exclusively **4b**. A similar argument can be considered for the decomposition of **7b**. The C–C bond linking the carbomethoxy groups in the bicyclobutane moiety is destabilized for the same reason as above (in this case the interaction is with two vicinal groups), so cleavage of this bond leading to [5]metacyclophane **8b** is kinetically favored over the back reaction, which affords the thermodynamically more stable **3b**.

The postulated intermediates **7b**, **8b**, and **9b** have not yet been detected. We attribute this both to their low equilibrium concentrations and their increased reactivity. As already mentioned, **3a** did not undergo this rearrangement. Even with extended irradiation times and shorter wavelengths (254 nm) only a slow polymerization was observed, probably because the potential [4]metacyclophane **9a** does not exist under the given conditions. All efforts to isolate a [4]metacyclophane derivative have failed so far because of its enormous strain energy.[8, 9] In our case we assume that the path leading to **4a** is interrupted at the second step (**7a** → **8a**). Further evidence for benzvalene **7d** and [6]metacyclophane **8c** was obtained from the fact that **3c** and **3d** did afford their respective terephthalic ester isomers **4c** and **4d**. However, under identical conditions as those used for **4b**,[10] the yields of both **4c** (30% after 12 h) and **4d** (24% after 12 h) were considerably smaller. Because the equilibrium concentration was lower, **5c** could only be identified in the reaction mixture by the typical δ value for the protons of the methoxy groups in the ^{1}H NMR spectrum. In the case of **4d**, none of the intermediates could be fully characterized for the same reason. The reduced rate in both cases can be explained

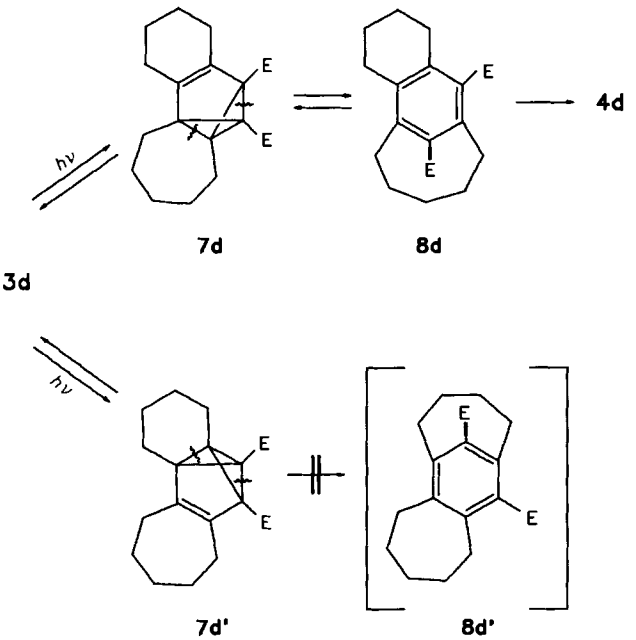

Scheme 4.

by the postulated intermediates. Firstly, [6]metacyclophane **8c** is distinctly more stable[11] than the lower homologue **8b**, and the strain releasing steps (**8c** → **5c** → **4c**) are thus less forceful. Secondly, it is noteworthy that the conversion of **3d** to **4d** occurred at about half the rate of that of **3b** to **4b** (52% after 12 h). A plausible explanation is given in Scheme 4.

Whereas in the case of **3b** two identical benzvalene intermediates afford **8b**, only the path via **7d** is possible for **3d**, since the path via **7d'** would lead to a highly strained [4]metacyclophane **8d'**. A steric factor (tethering of neighboring centers) is necessary, because irradiation of unsubstituted phthalic ester does not yield terephthalic ester. In conclusion, a tuned interplay of steric and electronic effects is responsible for the creation of doubly bridged prismanes with C_2 symmetry from tricyclic phthalic ester derivatives. Experiments in which the ester groups are substituted by different functions are currently in progress to substantiate the electronic argument.

Received: January 13, 1992 [Z 5119 IE]
German version: *Angew. Chem.* **1992**, *104*, 879

CAS Registry numbers:
1a, 141634-78-8; **1b**, 130434-04-7; **1c**, 130434-06-9; **1d**, 141634-79-9; **3a**, 51037-17-3; **3b**, 130434-08-1; **3c**, 130434-09-2; **3d**, 141634-80-2; **4b**, 141634-81-3; **4c**, 141634-82-4; **4d**, 141663-42-5; **5b**, 141663-43-6; **5c**, 141663-44-7; **5d**, 141663-45-8; **6b**, 141634-83-5; **6c**, 141634-84-6; **6d**, 141634-85-7.

[1] Reviews: D. Bryce-Smith, A. Gilbert in *Rearrangements in Ground and Excited States*, (Ed.: P. de Mayo), Academic Press, New York, **1980**, Vol. 3 p. 349; P. A. Wender, T. W. von Geldern in *Photochemistry in Organic Synthesis* (Ed.: J. D. Coyle), The Royal Society of Chemistry, **1986**, p. 226.
[2] R. Gleiter, B. Treptow, *Angew. Chem.* **1990**, *102*, 1452; *Angew. Chem. Int. Ed. Engl.* **1990**, *29*, 1427.
[3] H. Hogeveen, D. M. Kok in *The Chemistry of Triple-Bonded Functional Groups, Suppl. C, Part 2* (Eds.: S. Patai, Z. Rappoport), Wiley, Chichester, **1983**, Chap. 23 and references cited therein.
[4] J. W. van Straten, W. H. de Wolf, F. Bickelhaupt, *Tetrahedron Lett.* **1977**, 4667; L. W. Jenneskens, F. J. J. de Kanter, L. A. M. Turkenburg, H. J. R. de Boer, W. H. de Wolf, F. Bickelhaupt, *Tetrahedron* **1984**, *40*, 4401.
[5] L. W. Jenneskens, H. J. R. de Boer, W. H. de Wolf, F. Bickelhaupt, *J. Am. Chem. Soc.* **1990**, *112*, 8941.
[6] For an X-ray structure of a [5]metacyclophane see: L. W. Jenneskens, J. C. Klamer, H. J. R. de Boer, W. H. de Wolf, F. Bickelhaupt, C. H. Stam, *Angew. Chem.* **1984**, *96*, 236; *Angew. Chem. Int. Ed. Engl.* **1984**, *23*, 238.
[7] H. Irngartinger, D. Kallfass, E. Litterst, R. Gleiter, *Acta Crystallogr.* **1987**, *C 43*, 266; R. Hoffmann, *Tetrahedron Lett.* **1970**, 2907; H. Günther, *ibid.* **1970**, 5173.
[8] L. A. M. Turkenburg, J. W. van Straten, W. H. de Wolf, F. Bickelhaupt, *J. Am. Chem. Soc.* **1980**, *102*, 3256; G. B. M. Kostermans, M. Hogenbirk, L. A. M. Turkenburg, W. H. de Wolf, F. Bickelhaupt, *ibid.* **1987**, *109*, 2855.
[9] G. B. M. Kostermans, P. van Dansik, W. H. de Wolf, F. Bickelhaupt, *J. Am. Chem. Soc.* **1987**, *109*, 7887; *J. Org. Chem.* **1988**, *53*, 4531.
[10] All irradiations were carried out in a 250 mL vessel at 10 °C under argon with a Phillips HPK 125 W lamp. Concentrations: 0.003 mol L^{-1} in diethyl ether.
[11] S. Hirano, H. Hara, T. Hiyama, S. Fujita, H. Nozaki, *Tetrahedron* **1975**, *31*, 2219.

Template-Controlled Organization of a Fluoride Surface—An Analogue of a Crown Ether in the Reaction of $[\{(\eta^5\text{-}C_5Me_5)TiF_3\}_2]$ with Sodium Fluoride**

By *Herbert W. Roesky,* Mansoreh Sotoodeh,* and *Mathias Noltemeyer*

Dedicated to Professor Klaus Weissermel on the occasion of his 70th birthday

So far in studies concerning molecular recognition, host molecules were applied whose receptor surface comprises almost exclusively oxygen, sulfur, nitrogen, and/or phospho-

[*] Prof. Dr. H. W. Roesky, Dipl.-Chem. M. Sotoodeh, Dr. M. Noltemeyer
Institut für Anorganische Chemie der Universität
Tammannstrasse 4, D-W-3400 Göttingen (FRG)

[**] This work was supported by the Deutsche Forschungsgemeinschaft, the Volkswagen-Stiftung, and the Fonds der Chemischen Industrie.

rus atoms.[1-3] For this, the receptor structures were predetermined and could be open, half-open, or closed. We report here a new class of nucleophilic host systems with a "fluoride surface", which forms in a template-controlled manner.

The reaction of $[Cp^*TiCl_3]$ ($Cp^* = \eta^5$-C_5Me_5)[4] with AsF_3 leads to the dimer $[(Cp^*TiF_3)_2]$[5] **1** by chlorine–fluorine exchange. Compound **1** reacts with NaF in MeCN to give **2**.

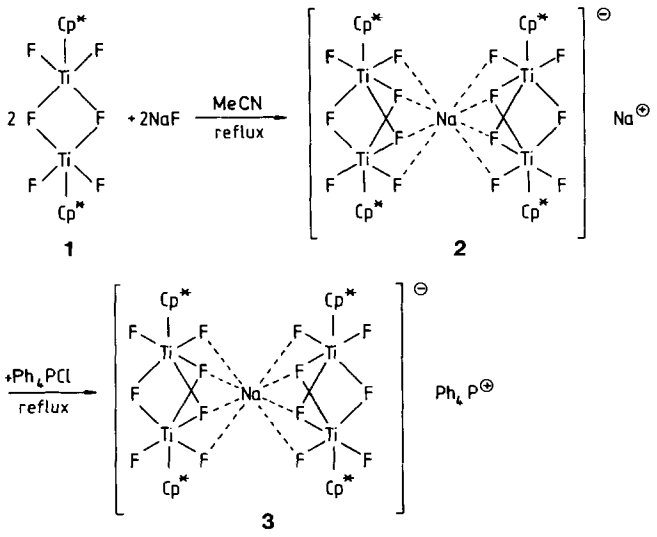

A third fluoride bridge is formed between the titanium atoms by the incorporation of a fluoride ion in **1**. In the salt **2**, one of the two sodium ions is complexed by two $[(Cp^*TiF_3)_2F]^-$ fragments in such a way that a fluoride surface forms at this sodium ion. By this complexation the two sodium ions become distinguishable. With tetraphenylphosphonium chloride only one sodium ion can be exchanged, and thus $Ph_4P[\{(Cp^*TiF_3)_4F_2\}Na]$ (**3**) is obtained. The nature of the wrapping of the Na^+ ion by two $[(Cp^*TiF_3)_4F_2]^-$ fragments is similar to that in $[Na([12]crown\text{-}4)_2]^+$.[6]

In order to find out whether the starting compound can differentiate between different cations, the corresponding reactions were carried out. We observed that LiF did not react, CsF led to insoluble polymeric products, and KF[7] behaved like NaF.

Indications of the stoichiometric composition of **3** were obtained from the elemental analysis and the ^{1}H NMR spectrum. Whereas the FD mass spectrum only shows the $[Ph_4P]^+$ fragment [*m/z* 339 with 100% intensity],[8] in the ^{1}H NMR spectrum the Ph and the Cp* protons are observed in the integration ratio 1:3.

The details of the structure of compound **3** were obtained from a single-crystal X-ray structure analysis (Fig. 1).[9] The Ti atoms are coordinated in a distorted octahedral fashion. The Na atom is surrounded by eight F atoms, and the Na–F distances [237.8(4) to 253.1(5) pm] lie within the values for ionic compounds[10] (ionic radii: Na^+ 116 pm for coordination number (CN) 8; F^- 128 pm for CN 2, 131 pm for CN 4). The Ti1–Ti2 distance [308.4(2) pm] within the dimeric fragment is ca. 20 pm shorter than the Ti–Ti distance in **1** [329.9(3) pm]. The deviations from the average plane of the four F atoms are ±48 and ±49 pm (the angle between the planes is 7.3°).

The selective cationic exchange in the reactions **1** → **3** allows the conclusion that corresponding reactions occur more frequently in organometallic or even inorganic fluorides.

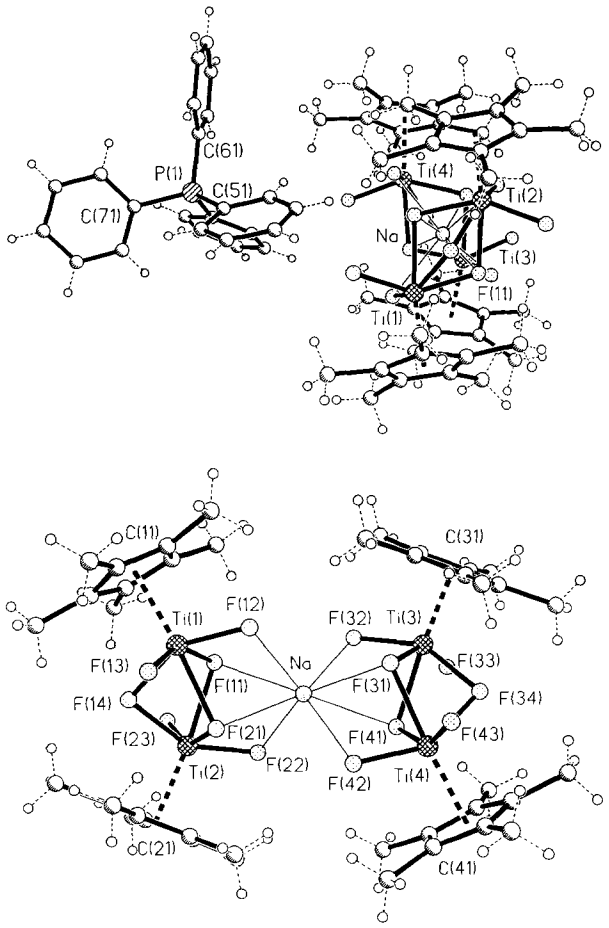

Fig. 1. Crystal structure of **3**. Above: total molecule, below: structure of anion. Selected distances [pm] and angles [°]: Ti(1)-F(12) 186.3(3), Ti(1)-F(21) 221.0(3), Ti(1)-F(11) 199.7(4), Ti(1)-F(13) 183.6(4), Ti(1)-F(14) 202.0(4), Ti(2)-F(11) 221.3(3), Ti(2)-F(22) 186.5(4) Ti(2)-F(23) 184.0(4), Ti(2)-F(14) 202.0(4), Ti(2)-F(21) 199.3(3), Ti(1)-Ti(2) 308.4(2); Ti(1)-F(11)-Ti(2) 94.1(1), Ti(1)-F(14)-Ti(2) 99.4(1), Ti(1)-F(21)-Ti(2) 94.3(1), F(11)-Ti(1)-F(14) 74.1(1), F(11)-Ti(2)-F(14) 69.6(1).

Experimental Procedure

1 (0.5 g, 2.1 mmol) and NaF (0.1 g, 2.1 mmol) were heated to reflux in MeCN (30 mL). After 3 h an orange suspension was formed. For the completion of the reaction it was stirred for a further 3 h at the same temperature. The mixture was allowed to cool and then solid Ph_4PCl (0.2 g,0.6 mmol) was added. The resultant suspension was refluxed and after 30 min the orange solid dissolved. The reflux was continued for a further 3 h, and the reaction mixture was then allowed to cool. The precipitated NaCl was then removed by filtration.

After concentration of the solution to 10 mL and cooling to −5 °C **3** was obtained as orange crystals. Yield 0.4 g, m.p. 230 °C. ^{1}H NMR($CDCl_3$): δ = 1.96 (s), 7.4–8.0 (m); ^{19}F NMR($CDCl_3$): δ = 100 (s), 1 D–MS(70 eV): *m/z* 339 (Ph_4P, 100%); correct elemental analysis (C, H, P, Na).

Received: February 12, 1992 [Z 5185 IE]
German version: *Angew. Chem.* **1992**, *104*, 869

CAS Registry numbers:
1, 141585-08-2; **2**, 141585-09-3; **3**, 141585-11-7; **3** · 3 MeCN, 141585-12-8; NaF, 7681-49-4; KF, 7789-23-3; $[(EtMe_4C_5)TiF_3]_2$, 141585-13-9; $[\{[(EtMe_4C_5)TiF_3]_4F_2\}K]Ph_4P$, 141585-15-1; LiF, 7789-24-4; CsF, 13400-13-0.

[1] F. Vögtle, E. Weber, *Host-Guest Complex Chemistry/Macrocycles*, Springer, Berlin, **1985**; L. F. Lindoy, *The Chemistry of Macrocyclic Ligand Complexes*, Cambridge University Press, Cambridge, **1989**.

[2] For the formation of complexes from anions and inorganic host compounds see: A. Müller, M. Penk, R. Rohlfing, E. Krickemeyer, J. Döring, *Angew. Chem.* **1990**, *102*, 927; *Angew. Chem. Int. Ed. Engl.* **1990**, *29*, 926; X. Yang, C. B. Knobler, M. F. Hawthorne, *ibid.* **1991**, *103*, 1519 and **1991**, *30*, 1507.

[3] For the formation of complexes from anions in anions see: A. Müller, E. Krickemeyer, M. Penk, R. Rohlfing, A. Armatage, H. Bögge, *Angew. Chem.* **1991**, *103*, 1720; *Angew. Chem. Int. Ed. Engl.* **1991**, *30*, 1674; A. Müller, Nature **1991**, *352*, 115.
[4] G. H. Llinás, M. Mena, F. Palacios, P. Royo, R. Serrano, *J. Organomet. Chem.* **1988**, *340*, 37.
[5] M. Sotoodeh, H. W. Roesky, M. Noltemeyer, unpublished.
[6] E. Mason, H. A. Eick, *Acta Crystallogr. Sect. B* **1982**, *38*, 1821.
[7] $Ph_4P[\{[(\eta^5\text{-}EtMe_4C_5)TiF_3]_4F_2\}K]$ is obtained from KF, $[(\eta^5\text{-}EtMe_4C_5)TiF_3]$, and Ph_4PCl. The quality of the crystals was not sufficient for a refinement of the structure.
[8] FD and FAB mass spectra gave no indication of the $[\{(Cp^*TiF_3)_4F_2\}Na]^-$ fragment.
[9] Crystallographic data of **3**·3 MeCN (M_r=1484.0): triclinic, space group $P\bar{1}$; $a = 1257.9(1)$, $b = 1690.2(2)$, $c = 1838.4(3)$ pm, $\alpha = 90.46(1)$, $\beta = 90.67(2)$, $\gamma = 98.40(1)°$, $V = 3.8662(8)$ nm^3, $Z = 2$, $\rho_{calcd} = 1.275$ g cm^{-3}, crystal size $0.6 \times 0.8 \times 0.8$ mm^3, Siemens-Stoe-AED2 four-circle diffractometer, 11296 reflections of $2\theta = 7.0°$ to $45.0°$ ($Mo_{K\alpha}$; $\lambda = 71.073$ pm), 10066 independent reflections and 7209 with ($F > 3.0\,\sigma(F)$) for the refinement (SHELXTL Plus, PC version): $R = 0.069$, $R_w = 0.079$, $w^{-1} = \sigma^2(F) + 0.0008\,F^2$. Further details of the crystal structure investigation may be obtained from the Fachinformationszentrum Karlsruhe, Gesellschaft für wissenschaftlich-technische Information mbH, D-W-7514 Eggenstein-Leopoldshafen 2 (FRG) on quoting the depository number CSD-56295, the names of the authors, and the journal citation.
[10] P. W. Atkins, *Physical Chemistry*, 4 ed., Oxford University Press, Oxford, **1990**, p. 959.

Synthesis of Isocyanate-Substituted Allenes and 1,3-Butadienes by [3,3] Sigmatropic Rearrangements**

By *Klaus Banert** and *Stefan Groth*

In honor of the 100th birthday of Walter Reppe

Allyl cyanates of type **2** are considered possible intermediates in the thermal decomposition of thiatriazoles **1** to isocyanates **3**.[1] However, since intermediates **2** have not yet been proved, a reaction path via heterocycles **4** cannot be discounted.[2]

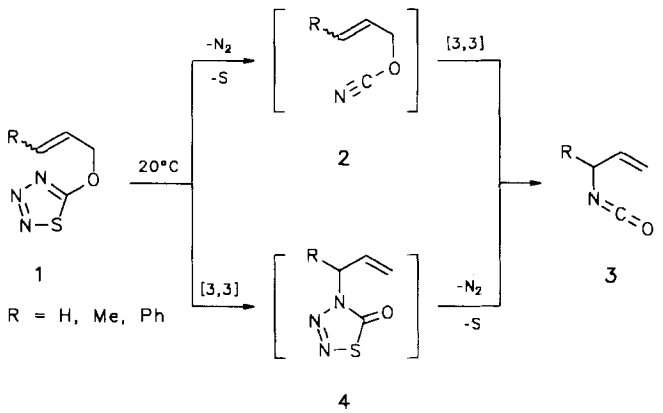

We report here the first direct, spectroscopic observation of a [3,3] sigmatropic cyanate → isocyanate rearrangement; the reactions provide the novel allenyl isocyanates **9** (Scheme 1), the isocyanate-substituted 1,3-butadienes **23** and **27**, as well as the previously unknown thiatriazolones **13** and **15**.

The carbonic acid derivative **6**, readily available from propargyl alcohol **5a**, was treated with sodium azide furnishing heterocycle **7a**. This compound can be isolated and sublimed (**safety shield!**), but it decomposes in solution even at room temperature almost quantitatively to allenylisocyanate **9a**. The decomposition of **7a** in the presence of H_2S led to

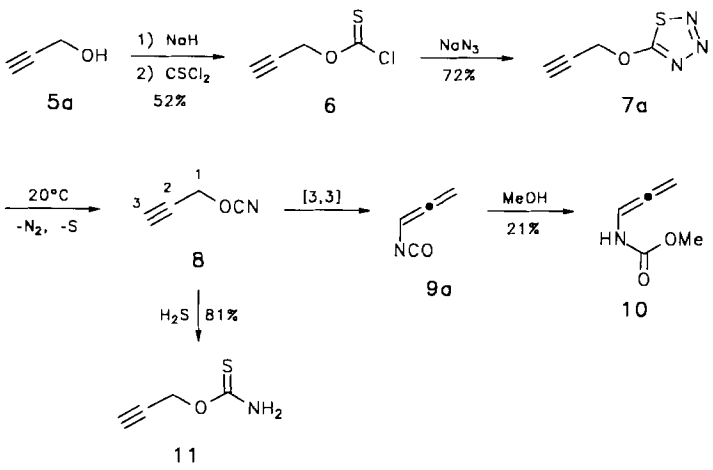

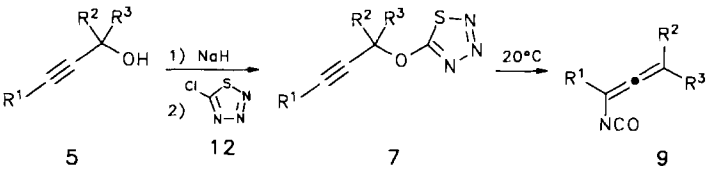

Scheme 1. **a**, $R^1 = R^2 = R^3 = H$; **b**, $R^1 = R^2 = H$, $R^3 = Me$ (yield **7b** 61%, **9b** 56%); **c**, $R^1 = R^2 = H$, $R^3 = n\text{-}C_5H_{11}$ (**7c** 69%, **9c** 67%); **d**, $R^1 = H$, $R^2 = R^3 = Me$ (**7d** 34%, **9d** 47%); **e**, $R^1 = Me$, $R^2 = R^3 = H$ (**7e** 67%, **9e** 38%).

the trapping product **11**. When the conversion **7a** → **9a** was followed by NMR spectroscopy, signals of the intermediate **8** were observed (Table 1). The maximum proportion of the short-lived, quasi-stationary intermediate **8** in the reaction mixture was only 5%.

Thiatriazoles **7** can be prepared in a new one-step procedure from the propargyl alcohols **5b–e** by treatment with sodium hydride followed by chlorothiatriazole **12**.[3] The allenyl isocyanates resulting from the decomposition of **7** are not all equally stable: **9a** can only be handled in solution, whereas **9c** can be isolated and distilled under vacuum. Compounds **9** undergo reactions typical of isocyanates such as the nucleophilic addition **9a** → **10**.[4] Thus the allenyl isocyanates are distinguished from the allenyl isothiocyanates prepared only recently,[5] which react with nucleophiles to form heterocyclic products.

The decomposition of **7d** gives not only the main product **9d**, but from a parallel reaction also thiatriazolone **13**, which is less volatile than **9d** and thus easy to separate. Because compound **13** is stable at room temperature it cannot be a precursor for **9d**. Another novel thiatriazolone, **15**, can be synthesized in one step from allyl alcohol **14** by successive treatment with sodium hydride and **12**. The structural assignment was also supported by ^{15}N NMR spectroscopy (Table 1). Product **15** is a distillable liquid, which upon prolonged heating at 100 °C can be decomposed into carbonyl sulfide and an equilibrium mixture of the azides[6] **16** and **17**, as well as nitrogen, sulfur, and isocyanate **18**.[7] The high thermal stability of **15** makes the reaction path **1** → **4** → **3** seem unlikely, and together with the direct proof of **8** lends support to the sequence **1** → **2** → **3**.

[*] Doz. Dr. K. Banert, Dipl.-Chem. S. Groth
Fachbereich 8, Organische Chemie II der Universität-Gesamthochschule Adolf-Reichwein-Strasse, D-W-5900 Siegen (FRG)

[**] Rearrangement Reactions, Part 2. This research was supported by the Deutsche Forschungsgemeinschaft and the Fonds der Chemischen Industrie. – Part 1: [5].

Table 1. Selected physical data for compounds **6**, **7a**, **8**, **9a**, **10**, **11**, **15**, **23**, **25**, **27** [a].

6: light yellow liquid, lachrymator, b.p. 41 °C/8 Torr; ^{1}H NMR: δ = 2.66 (t, ^4J = 2.4 Hz, 1H; H-3), 5.12 (d, ^4J = 2.4 Hz, 2H; H-1); ^{13}C NMR: δ = 63.34 (t, J = 156 Hz; C-1), 74.83 (dt, J = 51, 8 Hz; C-2), 77.73 (dt, J = 256, 4 Hz; C-3), 185.58 (s; S=C-Cl)

7a: colorless, explosive crystals, m.p. 66 °C; ^{1}H NMR: δ = 2.72 (t, ^4J = 2.4 Hz, 1H; H-3), 5.26 (d, ^4J = 2.4 Hz, 2H; H-1); ^{13}C NMR: δ = 62.18 (td, J = 157, 4 Hz; C-1), 74.61 (dt, J = 51, 8 Hz; C-2), 77.89 (dt, J = 256, 4 Hz; C-3), 185.06 (s; S-C=N)

8: ^{1}H NMR (CD_3CN): δ = 3.34 (t, ^4J = 2.5 Hz, 1H; H-3), 5.01 (d, ^4J = 2.5 Hz, 2H; H-1)

9a: ^{1}H NMR: δ = 5.28 (d, ^4J = 6.2 Hz, 2H; H-3), 6.06 (t, ^4J = 6.2 Hz, 1H; H-1); ^{13}C NMR: δ = 83.53 (td, J = 170, 6 Hz; C-3), 90.36 (dt, J = 193, 9 Hz; C-1), 124.10 (br.s; NCO), 207.00 (s; C-2); IR (CCl_4): $\tilde{\nu}$[cm^{-1}] = 2258 (NCO); GC-MS: m/z 81 ($M^{\oplus}$, 71%), 53 (98), 26 (100)

10: colorless, sublimable crystals, m.p. 74 °C; ^{1}H NMR (C_6D_6): δ = 3.34 (s, 3H; CH_3), 4.95 (d, ^4J = 6.5 Hz, 2H; H-3), 5.76 (br.s, 1H; NH), 6.86 (br.m, 1H; H-1); ^{13}C NMR (C_6D_6): δ = 52.17 (q, J = 147 Hz; CH_3), 85.65 (t, J = 168 Hz; C-3), 96.03 (d, J = 183 Hz; C-1), 154.10 (s; CO), 201.61 (s; C-2)

11: colorless oil; ^{1}H NMR: δ = 2.55 (t, ^4J = 2.2 Hz, 1H; H-3), 5.05 (d, ^4J = 2.2 Hz, 2H; H-1), 6.49 (br.s, 2H; NH_2); ^{13}C NMR: δ = 50.32 (td, J = 154, 4 Hz; C-1), 75.68 (dd, J = 253, 4 Hz; C-3), 77.11 (dt, J = 50, 8 Hz; C-2), 191.19 (s; S=C-N); IR (CCl_4): $\tilde{\nu}$[cm^{-1}] = 1083, 1286, 3305 (H-C≡C)

15: pale yellow liquid, b.p. 51.5 °C/0.012 Torr; ^{1}H NMR: δ = 1.77 (br.s, 3H; CH_3), 1.81 (br.s, 3H; CH_3), 4.72 (d, ^3J = 7.4 Hz, 2H; H-1), 5.39 (t sept, ^3J = 7.4, ^4J = 1.5 Hz; H-2); ^{13}C NMR: δ = 18.02 (q; CH_3), 26.60 (q; CH_3), 44.51 (t; C-1), 116.36 (d; C-2), 140.18 (s; C-3), 171.11 (s; CO); ^{15}N NMR: δ = −140.17 (s; N-4), −18.77 (s; N-2), 36.47 (s; N-3); IR (CCl_4): $\tilde{\nu}$[cm^{-1}] = 1683 (CO); MS: m/z 171 ($M^{\oplus}$, 5%), 69 (68), 68 (100), 41 (92)

23: colorless liquid, b.p. 31 °C/68 Torr; ^{1}H NMR: δ = 4.93 (s, 1H; H-1), 5.03 (s, 1H; H-1), 5.27 (d, ^3J = 10.5 Hz, 1H; H-4), 5.48 (d, ^3J = 17.0 Hz, 1H; H-4), 6.33 (dd, ^3J = 17.0, ^3J = 10.5 Hz, 1H; H-3); ^{13}C NMR: δ = 110.70 (t, J = 161 Hz; C-1), 115.63 (dd, J = 162, 156 Hz; C-4), 124.4 (br.s; NCO), 133.34 (d, J = 158 Hz; C-3), 136.19 (s; C-2); IR (CCl_4): $\tilde{\nu}$[cm^{-1}] = 2270 (NCO); GC-MS: m/z 95 ($M^{\oplus}$, 100%), 67 (49), 42 (74)

25: colorless, explosive crystals; ^{1}H NMR: δ = 5.29 (s); ^{13}C NMR: δ = 62.31 (t, J = 157 Hz; CH_2), 81.52 (s; -C≡), 185.57 (s; S-C=N)

27: ^{1}H NMR: δ = 5.12 (d, ^2J = 0.8 Hz, 2H), 5.36 (d, ^2J = 0.8 Hz, 2H); ^{13}C NMR (C_6D_6): δ = 109.25 (t, J = 163 Hz; C-1), 125.21 (br.s; NCO), 133.38 (s; C-2); IR ($CHCl_3$): $\tilde{\nu}$[cm^{-1}] = 2266 (NCO); GC-MS: m/z 136 ($M^{\oplus}$, 100%), 68 (38), 42 (88), 40 (66)

[a] NMR spectra in $CDCl_3$ (unless specified otherwise); ^{1}H NMR at 80, 200, and 400 MHz; ^{13}C NMR at 100.6 and 50.3 MHz; ^{15}N NMR at 40.5 MHz, CH_3NO_2 as external standard; GC-MS at 70 eV.

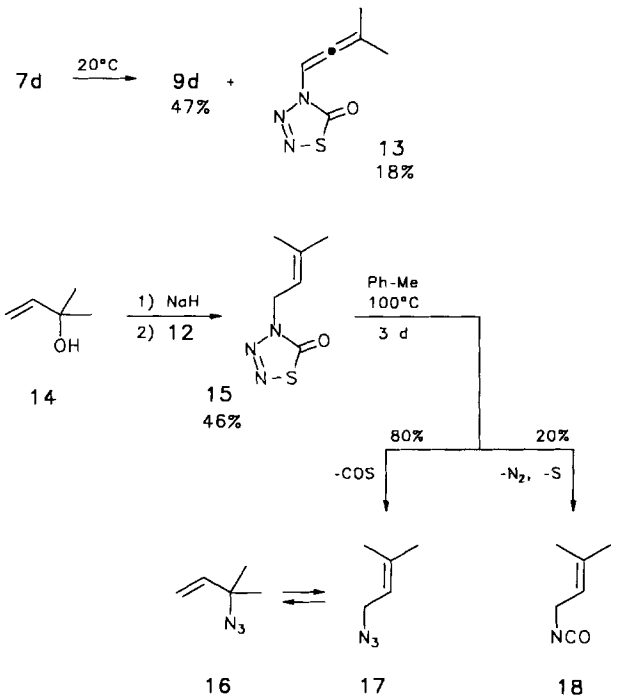

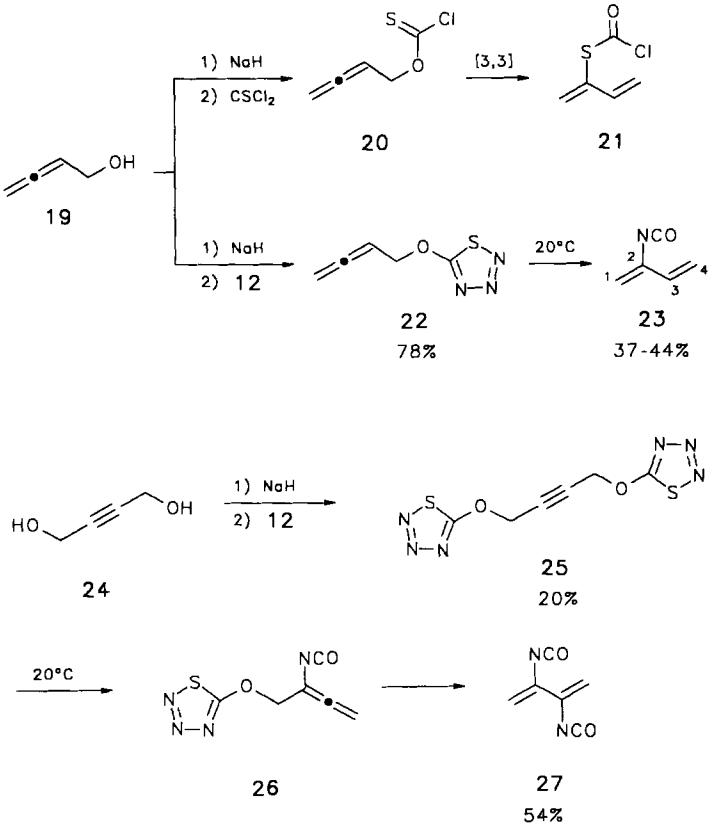

Not only propargyl precursors but also 2,3-butadienyl compounds are suited for rearrangements directing an isocyante function to a vinylic position. Alcohol **19**[8] was allowed to react with sodium hydride and **12** providing thiatriazole **22** which decomposes to **23**. This one-step synthesis of **22** is not only more convenient, it succeeds where the two-step alternative fails. The carbonic acid derivative **20** is not an appropriate precursor for **22** as it isomerizes to **21** during its preparation from **19**. The thiatriazole **25** obtained from **24** decomposes with loss of nitrogen and sulfur to **27** by a double [3,3] sigmatropic rearrangement. This reaction can be followed by NMR spectroscopy giving evidence of intermediate **26**. In contrast to compound **23**, a distillable liquid, **27** can be handled at room temperature only in solution.

These isocyanate-substituted allenes and 1,3-butadienes may find use as synthetic building blocks as well as applications in macromolecular chemistry.

Experimental Procedure

Thiatriazoles **7b–e**, **22**: A solution of the appropriate alcohol (20 mmol) in Et_2O (20 mL) was added dropwise to a suspension of sodium hydride (0.53 g, 22 mmol) in water-free Et_2O (20 mL) at 0 °C. The mixture was stirred at room temperature for 16 h (3 d for **5d** → **7d**), and was then added dropwise under argon to a solution of **12**[3] (2.92 g, 24 mmol) in Et_2O (50 mL) cooled to −5 to −10 °C. The resulting mixture was stirred at −10 °C for 3 h. All subsequent operations were carried out at temperatures ≤0 °C. The reaction mixture was poured into ice water (100 mL). The organic phase was washed thoroughly with ice water and dried over $MgSO_4$. Et_2O, unreacted alcohol, and excess **12** were removed at 10 Torr and then at 0.001 Torr.

Isocyanates **9b–e**, **23**: Solutions of the appropriate thiatriazole in water-free Et_2O, benzene, chloroform, acetonitrile, or CCl_4 were stirred at room temperature for 5–16 h (3–6 d for **7d** → **9d**) and then recondensed at 0.001 Torr. Depending on the volatility and stability of the product, the solution was concentrated under vacuum or the isocyanate was distilled.

15: Compound **14** was treated with sodium hydride and **12** according to the procedure previously described . After the solution of the product was dried over $MgSO_4$, all the volatile compounds were removed at 10 Torr/20 °C.

Received: February 1, 1992 [Z 5164 IE]
German version: *Angew. Chem.* **1992**, *104*, 865

CAS Registry numbers:
5a, 107-19-7; **5b**, 2028-63-4; **5c**, 818-72-4; **5d**, 115-19-5; **5e**, 764-01-2; **6**, 141461-89-4; **7a**, 141461-90-7; **7b**, 141483-78-5; **7c**, 141462-03-5; **7d**, 141462-04-6; **7e**, 141462-05-7; **8**, 135013-47-7; **9a**, 141461-91-8; **9b**, 141462-06-8; **9c**, 141462-07-9; **9d**, 141462-08-0; **9e**, 141462-09-1; **10**, 141461-92-9; **11**, 141461-93-0; **12**, 88892-85-7; **13**, 141461-94-1; **14**, 115-18-4; **15**, 141461-95-2; **17**, 72422-42-5; **18**, 1611-61-6; **19**, 18913-31-0; **20**, 141461-96-3; **21**, 141461-97-4; **22**, 141461-98-5; **23**, 141461-99-6; **24**, 110-65-6; **25**, 141462-00-2; **26**, 141462-01-3; **27**, 141462-02-4.

[1] C. Christophersen, A. Holm, *Acta Chem. Scand.* **1970**, *24*, 1512–1526.
[2] A. Holm, *Adv. Heterocycl. Chem.* **1976**, *20*, 145–174.
[3] E. Lieber, C. B. Lawyer, J. P. Trivedi, *J. Org. Chem.* **1961**, *26*, 1644–1646.
[4] The formation of isocyanurates is also a characteristic reaction of isocyanates. For example, in the presence of CsF/perhydrodibenzo-18-crown-6/toluene, **9b** trimerizes to a colorless solid, m.p. 66 °C (pentane), yield 73%.
[5] K. Banert, H. Hückstädt, K. Vrobel, *Angew. Chem.* **1992**, *104*, 72–74; *Angew. Chem. Int. Ed. Engl.* **1992**, *31*, 90–92.
[6] A. Gagneux, S. Winstein, W. G. Young, *J. Am. Chem. Soc.* **1960**, *82*, 5956–5957.
[7] F. W. Hoover, H. S. Rothrock, *J. Org. Chem.* **1964**, *29*, 143–145.
[8] L. Brandsma, H. D. Verkruijsse, *Synthesis of Acetylenes, Allenes and Cumulenes*, Elsevier, Amsterdam, **1981**, p. 188.

Material Properties and Purity of C_{60}**

By *Harald Werner, Daniela Bublak, Ulrich Göbel, Bettina Henschke, Wolfgang Bensch,* and *Robert Schlögl**

Since the production of larger amounts of fullerenes has become possible by means of an electric arc,[1, 2] interest in this new allotropic form of carbon has grown by leaps and bounds.[3] The availability of C_{60} with reproducible quality and the knowledge of the material properties of C_{60} in the solid state are important for reliable research results as well as potential technical applications. C_{60} forms van der Waals crystals with a face-centered cubic structure.[5, 6] Foreign atoms can be deposited in the interstices giving the crystal superconducting properties, for example.[7] Fullerenes can be considered molecular analogues of the microporous carbon materials, which because of their large inner surfaces are used as adsorbents.[8] For the application, storage, and production of fullerenes it is crucial to know if this allotropic form of carbon is also able to absorb substances from the environment and thus change the properties of the crystals.

An indication of such effects is, for example, the fact that we and others have found the experimentally determined densities of the crystals to be too great (1.72–1.78 $g cm^{-3}$).[4, 6, 9] (The density obtained from the X-ray crystal structure analysis of C_{60} is only 1.68 $g cm^{-3}$.) The reports of paramagnetic behavior,[10] paramagnetic impurities,[11] and an "excess" paramagnetism[12] for pure C_{60} are also remarkable. There are several reports of presumed changes in the crystal structure of C_{60} upon recrystallization[13] and the formation of adducts with donor solvents.[3b, 14] Fullerene oxides with an epoxide structure can be obtained from dissolved fullerenes in the presence of oxygen and light[15] or by reaction with oxygen-transfer reagents.[16] In ultrahigh vacuum (UHV) films of C_{60} react below room temperature with low abundancies of oxygen to give carbon dioxide.[17] Evidence of stable adducts of fullerenes and OH or $(CH_2)_x$ ($x = 1-7$) was provided by mass spectrometry.[18]

All these reports point to the relevance of the analogy of fullerenes and active charcoal, and provide reasons for investigating of the material properties of "pure"[19] C_{60}. Possible impurites are solvent and/or components of the air. The following experiments prove their presence in crystalline powders of C_{60}.

Figure 1 shows powder diffraction diagrams of samples of C_{60} treated in different ways. Only the sublimed sample provides a diffractogram that matches the diffraction pattern simulated from the single-crystal data.[6] Positions, intensi-

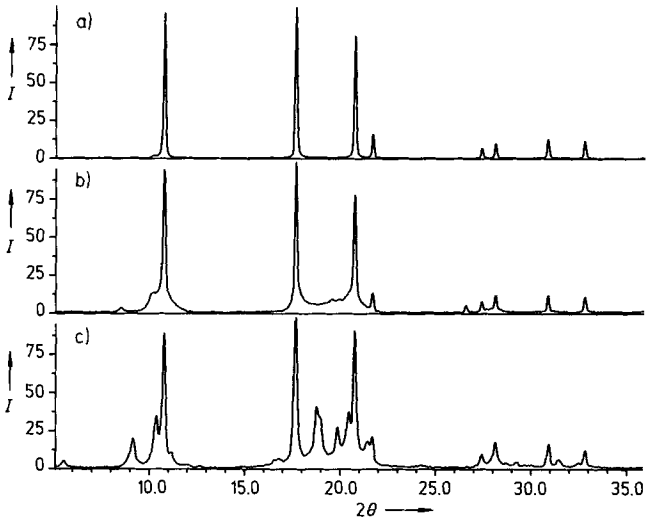

Fig. 1. X-ray powder diffraction patterns of analytically pure (C 99%) samples of C_{60}. The measurements were conducted in sealed capillaries under argon in focussing Bragg-Brentano geometry with monochromated copper radiation. a) After sublimation, b) recrystallized from benzene, c) recrystallized from toluene. The sublimation was carried out in a quartz tube at 1×10^{-7} mbar and 900 K. I = relative intensity.

ties, and widths of the additional reflections of the recrystallized samples correlate with the amount of solvent detected by IR spectroscopy. The position of the main reflections (face-centered cubic lattice with a=1415.2 pm) differs only slightly for the various samples. The additional reflections indicate the formation of partially long range-ordered solvent adducts.

By rigorous drying of the samples under vacuum (10^{-3} mbar at about 350 K, the solvent can be removed until no C–H stretching bands remain in the IR spectrum. However, absorptions in the fingerprint region at 1627, 1537,[20] and especially at 1384 cm^{-1} arise.

The band at 1384 cm^{-1} is intense for sublimed samples and becomes the strongest band in the spectrum when the sample is stored with exposure to light and air; no other absorptions arise, and the C_{60} bands do not change appreciably. The position and the isolated appearance of this band could indicate the formation of a C–O single bond similar to those found in aryl ethers. The X-ray structure analysis of a single crystal obtained by sublimation clearly showed electron density maxima outside the perimeter of C_{60}; these were assigned to statistically occupied oxygen positions distributed over eight hexagonal surfaces.[6]

The presence of paramagnetic impurites in extremely varying concentrations was established by EPR spec-

[*] Prof. Dr. R. Schlögl, Dipl.-Chem. H. Werner, D. Bublak, Dipl.-Chem. U. Göbel, Dipl.-Chem. B. Henschke, Dr. W. Bensch
Institut für Anorganische Chemie der Universität
Niederurseler Hang, D-W-6000 Frankfurt 50 (FRG)

[**] This research was supported by the Fonds der Chemischen Industrie, the Hermann-Willkom-Stiftung, and the Max-Planck-Gesellschaft. We thank Prof. G. Quinkert and Prof. H. Bock for their help in measuring the IR and EPR spectra, respectively.

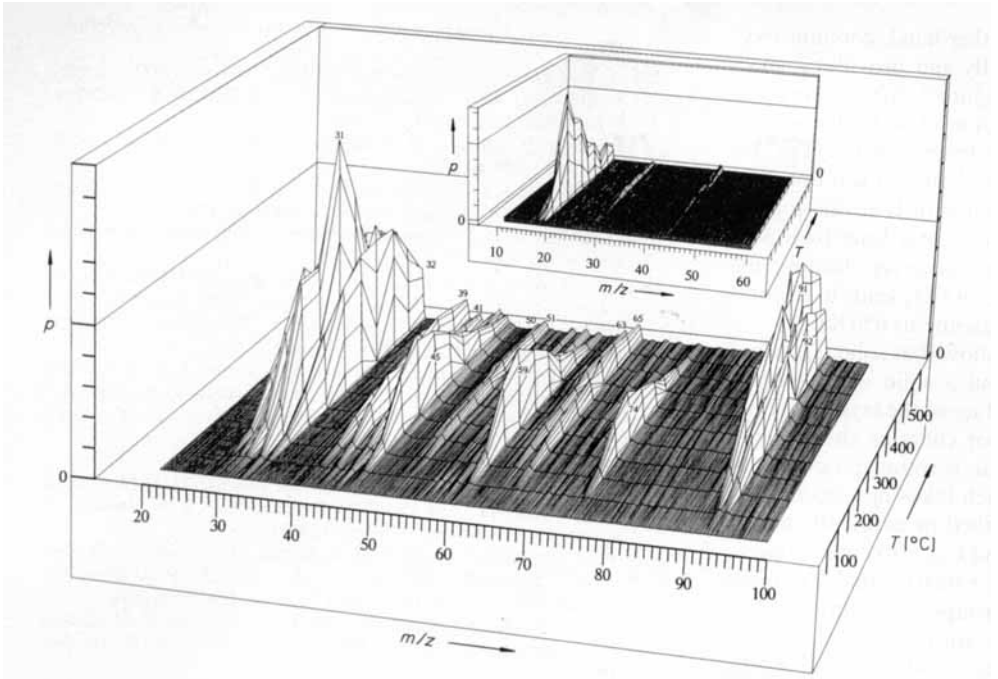

Fig. 2. Summary of the temperature-programmed decomposition experiments followed by mass spectrometry with recrystallized (large picture) and sublimed (small picture) C_{60}. p = pressure in arbitrary units.

troscopy. The parameters of the spectra[22] show that the signals can hardly be attributed to an intrisic spin density[12] of pure C_{60}; rather they indicate paramagnetic impurities that apparently can be removed efficiently but not completely by sublimation.

More detailed information about the nature of the trace impurites is obtained from thermal degradation experiments in UHV.[23] The analysis can be conducted to be either bulk specific or surface sensitive by varying the rate of heating between 1 $K s^{-1}$ and 10 $K s^{-1}$. In Figure 2 the bulk desorption of a C_{60} sample recrystallized from toluene is compared to that of a sublimed sample. Only water and traces of CO_2 and CO were released from the sublimed material at 500 K; no water but oxygen and numerous organic fragments escaped from the recrystallized material in two temperature regions at 523 K and 723 K. The analysis of the peak profile in Figure 2 reveals two series of fragments assigned to diethyl ether (*m/z* 27, 28, 29, 31, 45, 59, 74) and toluene (*m/z* 39, 51, 65, 91, 92). Neither CO nor CO_2 were detected in any significant amounts. Ether had been used to wash the crystals and was apparently incorporated in the crystals in the same way as the actual solvent had been, though the latter escapes primarily at higher temperatures. The high temperatures required for desorption point to considerable binding energies in the van der Waals crystal. It is certainly plausible that these impurites could affect the lattice dynamics of the crystals.[4, 5, 10]

The release of a substantial amount of molecular oxygen from the crystals containing solvent takes place at a different temperature (670 K) than the release of the organic impurities. The oxygen in the crystal is present in a form that does not lead to the oxidation of C_{60} upon thermal activation. This finding is in agreement with the observed stability of molecular C_{60} to oxidation.[3b, 16] Comparison of the oxygen desorption data with the IR spectra reveals that the intensity of the band at 1384 cm^{-1} does not correlate with the amount of liberated oxygen. If the oxygen actually arises from the compound that produces this IR band, then it either reacts in the sublimed material with hydrogen also present[21] to form water, or it binds with the substrate. In material containing solvent the single atoms of oxygen react to give O_2, but never form CO_2. This is in accord with earlier oxidation experiments,[24] in which formation of CO_2 was first observed above 700 K in diluted oxygen.

Desorption experiments with rapid heating rates provide a complementary picture. The data for the sublimed material (a–c) and the recrystallized material (d–f) are summarized in Figure 3. The desorption of toluene (not shown) exhibits the same pattern as seen in Figure 2. The differences in the desorption behavior originate in the various reaction kinetics of oxygen and not from experimental artifacts.

Figure 3a verifies that untreated C_{60} indeed releases molecular oxygen in two temperature ranges, possibly implying that the oxygen is located at different depth (subsurface and bulk) in the crystal. The desorption is complete after

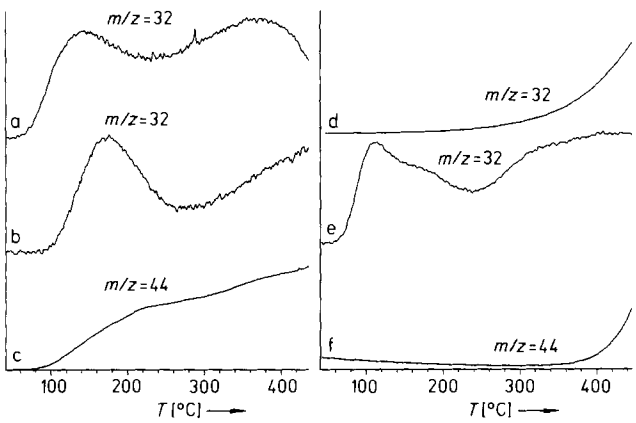

Fig. 3. Temperature profiles of selected mass spectral signals from desorption experiments with crystalline powders of C_{60} after various pretreatments. a)–c) Sublimed material, d)–f) solvent recrystallized and dried C_{60}. See text for details.

the sample is heated once, but oxygen can be readsorbed by treatment of the sample with 200 mbar of O_2 for 2 h at 300 K (Fig. 3b). Thus even the most pure material takes up oxygen from the air or from impure inert gas. Storage under 1 mbar of O_2 for 48 h leads to surface oxidation, as demonstrated by the formation of CO_2 (Fig. 3c); this behavior agrees with the known spectral data.[17]

Recrystallized material, on the other hand, contains oxygen in another binding state initially and provides a spectrum (Fig. 3d) similar to that in Figure 2. After desorption of the solvent, at least from the regions close to the surface, the sample can be loaded like the sublimed material (Fig. 3e) and is then sensitive to oxidation. Spectrum 3f was obtained from a sample that was treated analogously to the sample that provided spectrum 3b and shows that brief treatment with O_2 does not cause oxidation; however, heating the sample under a low partial pressure of CO_2 leads to dissolution in the bulk (decrease in the baseline to 650 K).

In summary, these experiments show that solid C_{60} is not an inert van der Waals crystal, but a solid with complex reaction behavior. The internal surface of the crystal is either saturated with solvent molecules or contains chemisorbed atoms of oxygen. This matches the sorption properties of active charcoal, the surface of which takes up organic substances and/or oxygen in chemisorbed or covalently bound forms.[8] The characteristics of solid C_{60} also correspond to those of a single fullerene molecule, which is capable of binding a large variety of functional groups on its surface.[3b]

The interaction of oxygen atoms with C_{60} can be of various strengths. We identified an epoxide-like binding as the weakest; it can be converted by tempering (sublimation) into a stronger binding mode (aryl ether). These two types of binding differ in their IR data and in their behavior in thermal desorption; their existence is suggested by the data from mass spectrometry, the ESR signals, and the results of single-crystal X-ray diffraction experiments. These oxygen adducts differ markedly from those that produce CO_2 upon thermal decomposition; this latter type forms only slowly on the crystal surface with exclusion of light and moisture and apparently gives rise to the precursor for the total oxidation[17, 18] of C_{60}. The existence of chemically activated oxygen should be taken into account in considering the behavior of C_{60} under catalytically oxidizing conditions.

The differing desorption behavior of the solvents ether and toluene suggests that an intrinsic characteristic of C_{60} is its ability to enter into specific electronic interactions; however, only experiments with thin films can eliminate possible topochemical effects superimposed on this intrinsic property. Until now we have consciously conducted our investigations to avoid a photochemically assisted adsorption—even in the dark the effects of small amounts of foreign atoms are complex enough.

Received: March 31, 1992 [Z 5271 IE]
German version: *Angew. Chem.* **1992**, *104*, 909

CAS Registry numbers:
C_{60}, 99685-96-8; $C_{60} \cdot XO_2$, 141849-16-3; Et_2O, 60-29-7; toluene, 108-88-3.

[1] W. Krätschmer, L. D. Lamb, K. Fostiropoulos, D. R. Huffman, *Nature* **1990**, *347*, 354; R. Ettl, I. Chao, F. Diederich, R. L. Whetten, *ibid.* **1991**, *353*, 149. We used a direct current arc with approximately 1.5 kW power and cooled the entire apparatus with a water-jacket. A continuous flow of helium at a total pressure of 140 mbar proved to be advantageous. An air-tight apparatus (leakproof under static high vacuum) and pure helium are extremely important for respectable yields. The crude extract, obtained in a maximum of 15% yield, was separated by chromatography (in the dark, eluting with toluene) into C_{60}, C_{70}, and higher fullerenes. The purity of the fractions was determined by UV/VIS spectroscopy. This highly sensitive method showed that at this point there is only an insignificant amount of fullerene oxide.[15,16] Conventional elemental analysis showed about 99% C and less than 1% H.

[2] H. W. Kroto, J. R. Heath, S. C. O'Brien, R. F. Curl, R. E. Smalley, *Nature* **1985**, *318*, 162; H. Kroto, *Science* **1988**, *242*, 1139.

[3] a) H. W. Kroto, *Angew. Chem.* **1992**, *104*, 113; *Angew. Chem. Int. Ed. Engl.* **1992**, *31*, 111; b) H. Schwarz, *ibid.* **1992**, *104*, 301 and **1992**, *31*, 293.

[4] D. R. Huffman, *Phys. Today* **1991**, *44* (11), 22.

[5] P. A. Heiney, J. E. Fischer, A. R. McGhie, W. J. Romanow, A. M. Denenstein, J. P. McCauley, Jr., A. B. Smith III, *Phys. Rev. Lett.* **1991**, *66*, 2911.

[6] H. Werner, W. Bensch, R. Schlögl, *Solid State Commun.* **1992**, in press.

[7] K. Holczer, O. Klein, S. M. Huang, P. B. Kauer, K. J. Fu, R. L. Whetten, F. Diederich, *Science* **1991**, *252*, 1154.

[8] R. C. Bansal, J. B. Donnet, F. Stoeckli, *Active Carbon*, Marcel Dekker, New York, **1988**, p. 335.

[9] H. D. Beckhaus, C. Rüchardt, M. Kao, F. Diederich, C. S. Foote, *Angew. Chem.* **1992**, *104*, 69; *Angew. Chem. Int. Ed. Engl.* **1992**, *31*, 63.

[10] C. S. Yannoni, R. D. Johnson, G. Meijer, D. S. Bethune, J. R. Salem, *J. Phys. Chem.* **1991**, *95*, 9.

[11] R. C. Haddon, L. F. Schneemeyer, J. V. Waszczak, S. H. Glarum, R. Tycko, G. Dabbagh, A. R. Kortan, A. J. Muller, A. M. Mujsce, M. J. Rosseinsky, S. M. Zahurak, A. V. Makhija, F. A. Thiel, K. Raghavachari, E. Cockayne, V. Elser, *Nature* **1991**, *350*, 46.

[12] P. M. Allemand, G. Srdanov, A. Koch, K. Khemani, F. Wudl, Y. Rubin, F. Diederich, M. M. Alvarez, S. J. Anz, R. L. Whetten, *J. Am. Chem. Soc.* **1991**, *113*, 2780; P. N. Keizer, J. R. Morton, K. F. Preston, A. K. Sudgen, *J. Phys. Chem.* **1991**, *95*, 7117.

[13] D. Heymann, J. C. Stormer, M. L. Pierson, *Carbon* **1991**, *29*, 1053.

[14] O. Ermer, *Helv. Chim. Acta.* **1991**, *74*, 1339; S. M. Gorun, K. M. Creegan, R. D. Sheerwood, D. M. Cox, V. W. Day, C. S. Day, R. M. Upton, C. E. Briant, *J. Chem. Soc. Chem. Commun.* **1991**, 1556.

[15] K. M. Creegan, J. L. Robbins, W. K. Robbins, J. M. Millar, R. D. Sherwood, P. J. Tindall, D. M. Cox, J. P. Mc Cauley, Jr., D. R. Jones, T. T. Gallagher, A. M. Smith III, *J. Am. Chem. Soc.* **1992**, *114*, 1103.

[16] Y. Elemes, S. K. Silverman, C. Sheu, M. Kao, C. S. Foote, M. M. Alvarez, R. L. Whetten, *Angew. Chem.* **1992**, *104*, 364; *Angew. Chem. Int. Ed. Engl.* **1992**, *31*, 351.

[17] G. H. Kroll, P. J. Benning, Y. Chen, T. R. Ohno, J. H. Weaver, L. P. F. Chibante, R. E. Smalley, *Chem. Phys. Lett.* **1991**, *181*, 112.

[18] J. M. Wood, B. Kahr, S. A. Hooke II, L. Dejarme, R. G. Cooks, D. Ben-Amotz, *J. Am. Chem. Soc.* **1991**, *113*, 5907.

[19] Our freshly recrystallized C_{60} [1] showed four IR bands at 1429, 1184, 577, 528 cm^{-1} and one ^{13}C NMR signal in solution at $\delta = 143$ [3a] with a signal-to-noise ratio of 270.

[20] The band at 1627 cm^{-1} was assigned to a skeletal vibration of the aromatic system that is intensified by oxygen;[16] the band at 1537 cm^{-1} is also described in the literature[4,21] and may be due to a C–H vibration of the $(CH_2)_x$ derivatives [18] present in trace amounts. This band is found only in dry samples. The accompanying C–H stretching vibration can be suppressed.[21]

[21] H. Gaber, R. Hiss, H.-G. Busmann, J. V. Hertel, *Verh. Dtsch. Phys. Ges.* **1992**, *3*, 763.

[22] Several samples of nominally pure C_{60} were examined by EPR spectroscopy in the solid state at 200 K. The intensities correspond to spin densities of up to $N \times 10^{-6}$ per C atom, the linewidth B is given in Gauss. The following values for N, g, and B were obtained: Sublimed sample (N=25, g=2.00007, B=4.3), recrystallized sample (N=125, g=2.00211, B=0.90), a mixture of C_{60} and 10% C_{70} (N=125, g=2.00187, B=1.3), sublimation residue (N=1600, g=2.00262, B=0.58).

[23] U. Göbel, W. Bensch, R. Schlögl, *J. Anal. Chem.* **1992**, in press. For the measurements, 10 mg of the crystalline powder was heated on a preheated stainless steel substrate in UHV (1×10^{-9} mbar) with a linear temperature program. The mass spectra of the desorbed material (Balzers QMG 112 quadropole mass spectrometer) were corrected for the background signals. For technical reasons the background signal at m/z 2 is so intense that hydrogen desorption cannot be observed with certainty.

[24] H. Werner, U. Tegtmeier, J. Blöcker, D. Herein, R. Schlögl, T. Schedel-Niedrig, M. Keil, A. M. Bradshaw, *Chem. Phys. Lett.* **1992**, in press.

Enantioselective Synthesis of the Antidepressant Rolipram by Michael Addition to a Nitroolefin

By *Johann Mulzer,* Ralf Zuhse,* and *Ralph Schmiechen*

Chirally branched pyrrolidones like Rolipram **1a** are highly active antidepressants with novel postsynaptic modes of action.[1] The advantages of Rolipram over conventional antidepressants are the low required dosage (3×0.75 mg per day) and the absence of uncomfortable and sometimes even dangerous anticholinergic side effects like dryness of mouth,

[*] Prof. Dr. J. Mulzer, Dr. R. Zuhse
Institut für Organische Chemie der Freien Universität
Takustrasse 3, D-W-1000 Berlin 33 (FRG)
Dr. R. Schmiechen
Forschungslaboratorium der Schering AG, Berlin

sight problems, and cardiotoxicity. The pharmacological activity depends on the R group and the absolute configuration; for **1a** the (*R*)-(−) enantiomer is the more effective.

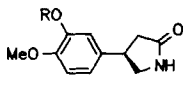

(*R*)-**1a**, R=cyclopentyl (Rolipram)
(*R*)-**1b**, R=benzyl
(*R*)-**1c**, R=H

The known syntheses[2] are limited to the preparation of racemates, which are then separated into the enantiomers by chromatography. We describe here the first enantioselective synthesis of each enantiomer of **1a–c** in multigram quantities. Since by Williamson etherification (*R*)-**1c** can be converted to a variety of ethers, this is a key compound in the series. The main preparative problem is the introduction of the chiral center in the aminocarboxylic acid **2**. Among the numerous possibilities (for example, alkylation of a chiral enolate, Claisen or [2,3] sigmatropic rearrangement, opening of an epoxide with a cuprate etc.) we considered the Michael addition of chiral enolate **4** to ω-nitrostyrene **3** to be especially convenient (Scheme 1).[3] As shown in Scheme 2, aldehyde

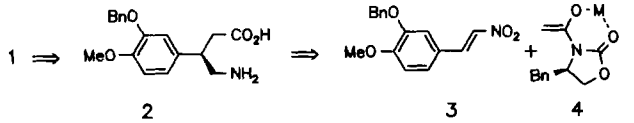

2 **3** **4**

Scheme 1. Retrosynthetic analysis of **1**.

5[4] was converted into nitrostyrene **6** and allowed to react with the enolate (*R*)-**4** of *N*-acetyloxazolidone **8**.[5] Compound **7** and its C(3′) diastereomer were produced in a ratio of 94:6 (analysis by HPLC and ^{13}C NMR spectroscopy). After a single recrystallization from methanol, **7** was 99+ % diastereomerically pure.[6] The conversion of **7** into (*R*)-**1c** was achieved in one step by catalytic hydrogenation,[7] via the intermediates **2b** and (*R*)-**1b**, which were not isolated. Compound **1c** was alkylated with cyclopentylbromide fur-

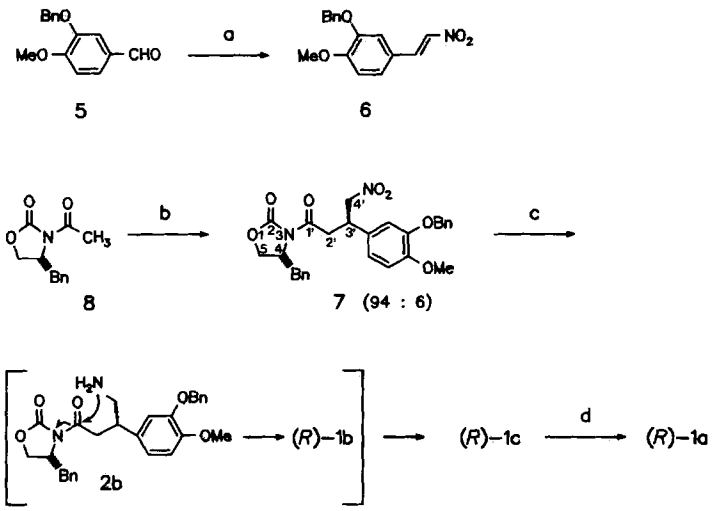

5 **6**

8 **7** (94 : 6)

2b

Scheme 2. Synthesis of (*R*)-**1a** (Rolipram). a: CH_3NO_2, NH_4OAc, HOAc, reflux, 73%; b: 1) $NaN(SiMe_3)_2$, THF, 2) **6**, 65% after recrystallization; c: H_2, Raney nickel, EtOAc/EtOH (1:1), 3 bar, 22 °C, 20 h, 72%; d: $C_6H_{11}Br$, NaH, THF, reflux, 60%.

nishing **1a**. Since the enantiomer of **8** is also available, the (*S*) series is equally accessible.

The stereochemical course of the addition of **4** to **3** follows the model proposed previously by Seebach et al. for the addition of enamines to nitrostyrenes[8] which is based on the following assumptions: 1. The formal double bonds are *syn* oriented as in **9**/**10**. 2. The donor (NR_2) and acceptor functions (NO_2) are as close to each other as possible, leading to a preference for the reactive intermediate **10** over **9**. Our example deviates significantly from the Seebach model, since instead of an enamine a chiral, metalated O,N-acetal[9] **4** is used. As part of an imide unit the amino function of **4** is a weaker donor than the enolate oxygen. Of the possible reactive intermediates **11** and **12** the latter appears to be favored, in analogy to Seebach's findings. This means, however, that it is not so much the donor effect of the enamine nitrogen that matters for the diastereoselectivity of the addition, but rather its *syn* orientation to the nitroolefin unit. A pericyclic shift of the metal cation to the nitro group as required in the Zimmerman–Traxler mechanism of the aldol addition[10] does not appear to play a role because of the unfavorable ring size (eight-membered ring). The high stereoselectivity in the formation of **7** is also noteworthy, since enolates of type **4** which have no substituents on the C atom, do not react stereoselectively in, for example, aldol additions.[11]

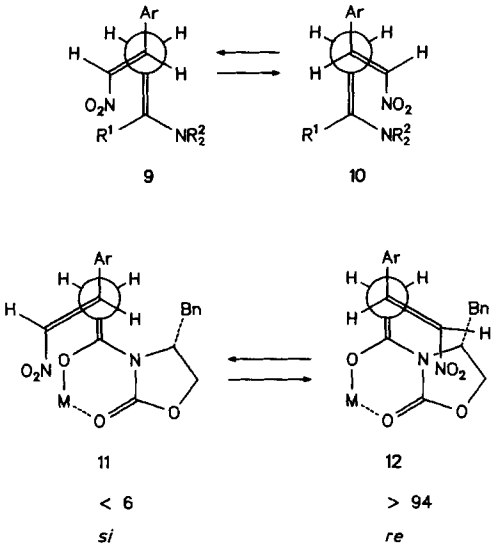

9 **10**

11 **12**

< 6 > 94

si *re*

Received: February 1, 1992 [Z 5165 IE]
German version: *Angew. Chem.* **1992**, *104*, 914

[1] H. H. Schneider, R. Schmiechen, M. Brenzinski, J. Seidler, *Eur. Pharmacol.* **1986**, *127*, 105–115.
[2] J. Crossland, *Drugs of the future* **1988**, *13*, 38–41.
[3] After the completion of our work Evans' oxazolidinones were used in Michael additions, however, with completely different substitution patterns: D. A. Evans, M. T. Bilodeau, T. C. Somers, J. Clardy, D. Cherry, Y. Kato, *J. Org. Chem.* **1991**, *56*, 5750–5752.
[4] C. Schöpf, L. Winterhalder, *Liebigs. Ann. Chem.* **1940**, *544*, 62–71.
[5] Compound **8** was prepared according to the literature procedure for *N*-acyloxazolidinones: D. A. Evans, A. E. Weber, *J. Am. Chem. Soc.* **1986**, *108*, 6757–6761.
[6] Analytical data for (4*S*, 3′*R*)-3-[3-(3-benzyloxy-4-methoxyphenyl)-4-nitrobutyryl]-4-benzyl-2-oxazolidinone **7**: M.p. 153 °C; $[\alpha]_D^{20} = -28.05$ ($c = 2.3$ in chloroform); ^1H NMR (250 MHz, $CDCl_3$, 25 °C, TMS): $\delta = 2.72$ (dd, $J_{vic} = 9$ Hz, $J_{gem} = 13.5$ Hz, 1H; -CH*H*Ph), 3.22 (dd, $J_{vic} = 3.8$ Hz, $J_{gem} = 13.5$ Hz, 1H; -CH*H*Ph), 3.27 (dd, $J_{vic} = 6.3$ Hz,

J_{gem} = 17.5 Hz, 1H; H 2'), 3.47 (dd, J_{vic} = 7.5 Hz, J_{gem} = 17.5 Hz, 1H; H 2'), 3.82 (s, 3H; -OCH_3), 3.95–4.10 (m, 1H; H 3'), 4.06–4.14 (m, 2H; H 5), 4.45–4.59 (m, 1H; H 4), 4.53 (dd, J_{vic} = 7.9 Hz, J_{gem} = 13 Hz, 1H; H 4'), 4.65 (dd, J_{vic} = 7.5 Hz, J_{gem} = 13 Hz, 1H; H 4'), 5.16 (s, 2H; -OCH_2Ph), 6.80–6.88 (m, 3H; arene-H), 7.14–7.50 (m, 10H; arene-H); ^{13}C NMR (63 MHz, CDCl3, 25 °C): δ = 37.70, 38.64, 39.13 (-CH_2Ph, C2' and C3'), 55.00, 55.94, (C4 and -OCH_3), 66.31 (C-5), 71.23 (-OCH_2Ph), 79.60 (C4'), 112.20, 113.90, 120.40, 127.35, 127.50, 127.84, 128.47, 128.90, 129.28, 130.80, 134.96, 136.83, 148.31, 149.46 (arene-C), 153.30 (C1'), 170.04 (C2). IR (KBr): $\tilde{\nu}$ [cm^{-1}] = 1785vs, 1700s, 1550s; MS (80 eV): *m/z* 504 (2%, M^+), 457 (3), 281 (3), 238 (4), 91 (100, $C_7H_7^+$), 65 (5).

[7] Analytical data for (4*S*)-4-(3-hydroxy-4-methoxyphenyl)-2-pyrrolidone **1c**: M.p. = 126 °C; $[\alpha]_D^{20}$ = −36.7 (*c* = 1.8 in chloroform); ^{1}H NMR (250 MHz, $CDCl_3$, 25 °C, TMS): δ = 2.47 (dd, J_{vic} = 9.4 Hz, J_{gem} = 16.5 Hz, 1H; -C*H*HCO), 2.70 (dd, J_{vic} = 8.4 Hz, J_{gem} = 16.5 Hz, 1H; -CH*H*CO), 3.39 (dd, J_{vic} = 7.5 Hz, J_{gem} = 8.5 Hz, 1H; -C*H*HNH), 3.61 (quint, *J* = 8.5 Hz, 1H; H 4), 3.72 (dd, J_{vic} = J_{gem} = 8.5 Hz, 1H; -CH*H*NH), 3.89 (s, 3H; -OCH_3), 5.94 (s, 1H; -NH), 6.38 (s, 1H; -PhO*H*), 6.69–6.86 (m, 3H; arene-H); ^{13}C NMR (63 MHz, DMSO, 25 °C): δ = 37.93 (C5), 40.49 (C4), 48.80 (C3), 55.71 (-OCH_3), 112.39, 114.12, 117.27, 135.60, 146.34, 146.54 (arene-C), 176.02 (-CO); IR (KBr): $\tilde{\nu}$ [cm^{-1}] = 3260br m, 1685vs, 1520s, 1445m, 1295m, 1280m, 1240m, 1055m, 1030m. MS (80 eV): *m/z* 207 (55%, M^+), 150 (100), 135 (40).

[8] D. Seebach, J. Golinski, *Helv. Chim. Acta* **1981**, *65*, 1413–1423; S. J. Blarer, W. B. Schweizer, D. Seebach, *ibid.* **1982**, *65*, 1637–1654.

[9] D. A. Evans in *Asymmetric Synthesis Vol. 3* (Ed.: J. Morrison), Academic Press, New York, **1984**, p. 1

[10] H. E. Zimmerman, M. D. Traxler, *J. Am. Chem. Soc.* **1956**, *79*, 1920–1923.

[11] D. A. Evans, J. Bartoli, T. L. Shih, *J. Am. Chem. Soc.* **1981**, *103*, 2127–2129; D. A. Evans, E. B. Sjogren, J. Bartoli, R. L. Dow, *Tetrahedron Lett.* **1986**, *27*, 4957–4960; D. A. Evans, J. S. Clark, R. Metternich, V. J. Novak, G. S. Sheppard, *J. Am. Chem. Soc.* **1990**, *112*, 866–868.

The Benzene Ring as Dienophile in an Intramolecular [4+2] Cycloaddition: Degenerate Rearrangement of 7,8-Benzobicyclo[4.2.2]deca-2,4,7,9-tetraene**

By *Wolfram Grimme,* Thomas Grommes, Wolfgang R. Roth,** and *Rolf Breuckmann*

The π bonds of benzene rings can—at higher temperatures—participate in pericyclic reactions. Besides the well-known Claisen rearrangement,[1] a sigmatropic hydrogen shift[2] and several electrocyclic ring openings[3] involving benzene π bonds have been described. Benzene also functions as diene in some [4+2] cycloadditions.[4] Here we report the first case of a [4+2] cycloaddition in which one of the π bonds of a benzene ring reacts as dienophile.[5]

We chose an intramolecular cycloaddition for the investigation of the role of benzene as dienophile, because this reaction proceeds even with weakly reactive dienophiles for entropy reasons. Moreover, because the cycloaddition at the benzene ring is endothermic and easily reversible, its detection requires a molecule which yields a Diels–Alder intermediate that can return to two different products.

The 7,8-benzobicyclo[4.2.2]deca-2,4,7,9-tetraene **1a** fulfills these prerequisites: The diene bridge is spatially close to the benzene π bond of the bicycle, and the symmetrical cycloadduct **2a** can return to the aromatic state along two paths (formation of **1a** or **3a**). The intramolecular [4+2] cycloaddition with participation of the benzene ring results

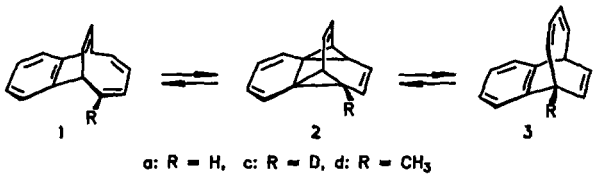

a: R = H, c: R = D, d: R = CH_3

in the degenerate rearrangement **1a** ⇌ **3a**, which can be observed only in the substituted compounds **1c, d**.

A high-yielding synthesis for the already known hydrocarbon **1a**[6] was developed, which also gave access to targeted substituted derivatives (Scheme 1). Under irradiation buta-

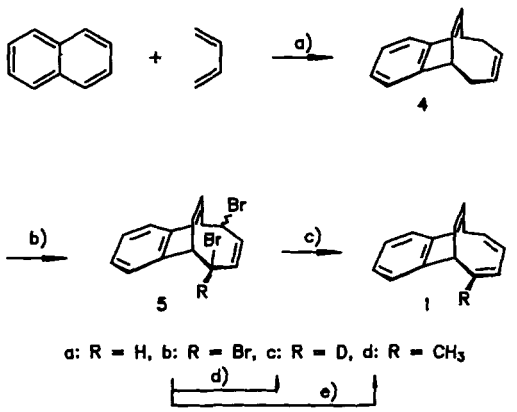

a: R = H, b: R = Br, c: R = D, d: R = CH_3

d) e)

Scheme 1. a) Benzene, *hv* (lamp Q 1200 Hanau), 140 h, 12%. b) CCl_4, 1,3-dibromo-5,5-dimethylhydantoin, 1.6 equiv, 80 °C, 2 h, 72%. c) Dimethylformamide, Zn, 10 equiv, sonation, 7 h, 81%. d) 1) THF, *n*-butyllithium, 1.1 equiv, −78 °C, 10 min; 2) D_2O, 30 equiv, −78 °C to 20 °C, 70%. e) 1) THF, *n*-butyllithium, 1.1 equiv, −78 °C, 10 min; 2) methyl iodide, 4 equiv, −78 °C to 20 °C, 20%.

diene added to naphthalene to afford the [4+4] cycloadduct **4**,[7] which was doubly or triply brominated with 1,3-dibromo-5,5-dimethylhydantoin in the planarizable allylic positions. The 1:1 mixture of **5a** and **5b** obtained was debrominated with zinc, and the products separated by flash chromatography (silica gel, cyclohexane). After halogen–metal exchange with *n*-butyllithium, the bromide **1b** yielded the bicycle **1c, d** deuterated or methylated in position 2 on treatment with D_2O or methyl iodide.

A prior investigation had shown that the thermolysis of **1a** leads to *cis*-4b,8a-dihydrophenanthrene;[8,9] therefore the attempt to detect the rearrangement **1c** ⇌ **3c** had to be performed close to the activation threshold for this thermolysis. Bicycle **1c** (97% D_1) in the gas phase was heated to 235 °C for 93 h, and the crude product was then dehyrogenated with 2,3-dichloro-5,6-dicyano-1,4-benzoquinone (DDQ) in CCl_4. The excess DDQ was reduced with cyclohexa-1,4-diene, and the product filtered through silica gel. Separation by gas chromatography furnished the benzobicyclic isomers and phenanthrene in the ratio 3:1. The ^{1}H NMR spectrum of the benzobicyclic isomers revealed a 1:1 mixture of **1c** and **3c** with 81% D_1 deuteration. The [4+2] cycloaddition with the benzene ring as dienophile therefore takes place under the chosen conditions, and leads to the equilibrium distribution of the marked isomers.

The phenanthrene obtained is 64% monodeuterated according to the mass spectrometric analysis, and its ^{1}H NMR spectrum shows that 60% of the deuterium atoms are situated in positions 9 and 10. When the preequilibrium **1c** ⇌ **3c** is considered, these values are in accord with the previously

[*] Prof. Dr. W. Grimme, Dr. T. Grommes
Institut für Organische Chemie der Universität
Greinstrasse 4, D-W-5000 Köln 41 (FRG)
Prof. Dr. W. R. Roth, R. Breuckmann
Fakultät für Chemie der Universität
Postfach 102148, D-W-4630 Bochum 1 (FRG)

[**] This work was supported by the Fonds der Chemischen Industrie.

proposed mechanism[8] for the formation of dihydrophenanthrene from **1a**, in which a 1,5-shift of the etheno bridge is followed by electrocyclic ring opening and new ring formation. This mechanism would yield, after subsequent dehyrogenation, phenanthrene with 72% deuteration (D_1), in which half the deuterium atoms occupy positions 9 and 10.

The kinetic parameters of the rearrangement of the benzobicyclo[4.2.2]decatetraene skeleton were determined for the 1-methyl compound **3d** from an analysis by gas chromatography. **3d** was obtained analogously to **1a**, from butadiene and 1-methylnaphthalene. The primary photoaddition occurs here at both rings of naphthalene, and when the synthesis sequence is complete, **3d** must be separated from its 3′-positional isomer by gas chromatography. Important physical data for the new compounds are collated in Table 1.

Table 1. Some physical data for the compounds **1b–d**, **3d**, and **4a**. ^{1}H NMR spectra at 80 (**1b**, **4a**) or 300 MHz in $CDCl_3$. ^{13}C NMR spectra at 75.5 MHz in $CDCl_3$. Mass spectra at 70 eV. Satisfactory elemental analyses were obtained for **1b**, **1d**, and **3d**.

1b: M.p. 70 °C; ^{1}H NMR: $\delta = 7.26$-6.98 (m, 4H), 6.45-6.10 (m, 2H), 5.98 (m, 2H), 5.57-5.13 (m, 1H), 4.36 (m, 1H), 3.89 (m, 1H); MS: *m/z* 260 ($M^{\oplus}$, ^{81}Br, 5%), 258 ($M^{\oplus}$, ^{79}Br, 6%), 179 ($M^{\oplus}$-Br, 100), 178 ($M^{\oplus}$-HBr, 86)

1c: M.p. 110 °C; ^{1}H NMR: $\delta = 7.21$-7.05 (AA′BB′, 4H), 6.36-6.23 (m, 1H), 5.92 (m, 2H), 5.68-5.59 (m, 2H), 4.02-3.82 (m, 2H); MS: *m/z* 181 ($M^{\oplus}$, 69%), 180 ($M^{\oplus}$-H, 100), 179 ($M^{\oplus}$-D, 90), 166 ($M^{\oplus}$-CH_3, 30)

1d: M.p. 67 °C; ^{1}H NMR: $\delta = 7.25$-7.10 (pseudo-AA′BB′, 4H), 6.22-6.16 (m, 1H), 6.00-5.88 (m, 2H), 5.59-5.51 (m, 2H), 3.86-3.81 (m, 1H), 3.7 (m, 1H), 2.19 (d, $^4J = 1.3$ Hz, 3H); ^{13}C NMR: $\delta = 152.28$, 138.25, 136.79, 126.76, 126.53, 125.58, 123.33, 122.61, 120.91, 119.33, 45.69, 39.83, 29.21; MS: *m/z* 194 ($M^{\oplus}$, 28%), 179 ($M^{\oplus}$-CH_3, 100), 128($C_{10}H_8^{\oplus}$, 7)

3d: M.p. 90 °C; ^{1}H NMR: $\delta = 7.32$-7.18 (m, 3H), 7.12-7.09 (m, 1H), 6.35-6.28 (m, 1H), 5.89-5.82 (m, 2H), 5.68-5.53 (m, 3H), 3.91-3.89 (m, 1H), 1.69 (s, 3H); ^{13}C NMR: $\delta = 149.04$, 141.26, 140.37, 135.55, 128.99, 126.77, 126.56, 125.77, 123.61, 122.35, 122.30, 119.37, 40.21, 38.97, 27.00; MS: *m/z* 194 ($M^{\oplus}$, 20%), 179 ($M^{\oplus}$-CH_3, 100), 165 ($M^{\oplus}$-C_2H_5, 63)

4a: M.p. 115 °C; ^{1}H NMR: $\delta = 7.18$ (AA′BB′, 4H), 6.22 (m, 2H), 5.07 (m, 2H), 3.61 (m, 2H), 2.76 (m, 4H); MS: *m/z* 182 ($M^{\oplus}$, 4%), 128 ($C_{10}H_8^{\oplus}$, 100)

The advantage of determining the kinetics of the rearrangement **3d** → **1d** by gas chromatography in the gas phase is offset by the loss of degeneracy. The more complex course of the reaction is shown in Scheme 2. Of the methyl-*cis*-

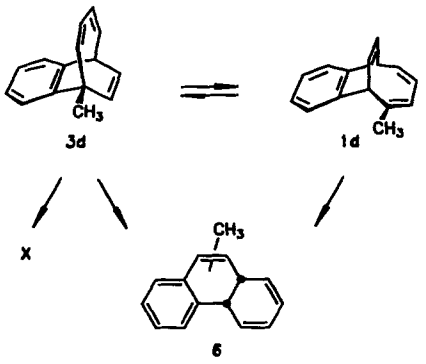

Scheme 2. Formation of the methyldihydrophenanthrene derivatives **6**.

4b,8a-dihydrophenanthrene derivatives **6**, the isomer substituted at position 9 or 10 forms over 50%; moreover, **3d** yields an unknown product **X** in small amounts. As the thermolysis of the starting compounds **3d** and **1d** shows, **6** is formed from both, whereas **X** is derived only from **3d**.

The activation parameters of the pertinent Diels–Alder reaction were found for the gas-phase thermolysis in the temperature range between 231 and 301 °C with already described apparatus and techniques.[10] The simulated reaction course of Scheme 2 was fitted to the data in Table 2 by using a Simplex routine for the optimization.[11]

Table 2. Data for the thermolysis of **3d**.

T [°C]	*t* [s]	**3d** [%]	**1d** [%]	**6** [%]	**X** [%]
231.13	0	98.131	1.317	0.551	0.000
	21900	73.503	19.126	6.299	1.073
	82200	35.102	46.013	16.180	2.704
	103800	28.156	50.472	18.302	3.071
240.27	0	97.703	1.575	0.722	0.000
	8300	77.338	16.151	5.488	1.024
	16700	61.925	27.064	9.358	1.652
	22200	53.686	32.766	11.540	2.008
	34200	39.955	42.120	15.302	2.623
251.63	0	97.517	1.822	0.661	0.000
	3000	79.408	14.316	5.282	0.994
	5900	65.864	23.633	8.863	1.641
	12900	42.721	39.144	15.366	2.769
	18400	31.085	46.637	18.882	3.397
260.39	0	96.754	2.215	0.793	0.238
	1100	84.182	10.827	4.106	0.885
	3100	65.996	23.199	9.075	1.730
	7000	40.985	39.797	16.267	2.951
	10500	28.982	47.797	19.852	3.717
	13300	20.773	52.494	22.617	4.116
	16900	15.561	55.291	24.669	4.479
271.23	0	95.338	3.115	1.235	0.312
	900	73.708	17.449	7.300	1.543
	2100	52.727	31.069	13.622	2.582
	4200	31.359	44.399	20.372	3.870
	6000	21.019	50.486	24.073	4.422
	8500	13.476	54.249	27.347	4.928
	10500	10.163	55.379	29.313	5.144
280.77	0	92.386	5.003	2.110	0.502
	990	53.710	29.772	13.767	2.751
	2090	31.312	43.136	21.232	5.320
	3090	20.153	49.500	25.460	4.887
	4190	13.210	52.567	28.897	5.326
	5190	10.231	53.475	30.641	5.653
290.73	0	87.835	7.799	3.520	0.846
	800	38.849	37.653	19.631	3.867
	1600	18.794	48.442	27.507	5.258
	2400	11.480	51.326	31.328	5.867
	3200	7.834	51.816	34.123	6.226
	4100	7.162	50.208	36.204	6.425
301.14	0	79.578	12.629	6.340	1.455
	700	20.641	46.252	27.560	5.548
	1400	9.567	49.776	34.202	6.455
	2100	7.324	47.933	37.857	6.886

Since the analysis was performed only for **3d**, the resulting activation parameters in Table 3 have a statistical significance only for the reaction **3d** → **1d**;[12] the quoted errors represent a 95% confidence limit.

Table 3. Activation parameters for the thermal rearrangement of **3d** and **1d** in the gas phase (see Scheme 2).

Reaction	E_a [kcal mol^{-1}]	log *A*	$\Delta H^{\neq}$ (265 °C) [kcal mol^{-1}]	$\Delta S^{\neq}$ (265 °C) [cal mol^{-1} K^{-1}]
3d → **1d**	41.2 ± 0.5	12.83 ± 0.2	40.1 ± 0.5	−3.0 ± 0.9
1d → **3d**	43.0	12.81	41.9	−3.0
3d → **6**	43.3	13.28	42.2	−0.9
1d → **6**	41.1	11.20	40.0	−10.4
3d → **X**	46.6	13.85	45.5	1.7

The activation parameters of Table 3 yield a Gibbs activation energy for the rearrangement **3d** → **1d** at 35 °C of $\Delta G^{+} = 41.1$ kcal mol^{-1}; they are valid for the rate-determining step of the reaction, the cycloaddition **3d** → **2d**. The corresponding rearrangements in the parent compound bicyclo[4.2.2]decatetraene and some derivatives take place at this temperature with Gibbs activation energies of 22.3 to 24.2 kcal mol^{-1}.[13] Here the replacement of an olefinic double bond by a π bond of a benzene ring thus increases the Gibbs activation energy by about 18 kcal mol^{-1}. In earlier investigations of pericyclic reactions, such an exchange led to an increase of only about 11 kcal mol^{-1}.[3] Apparently the transition state to the strained cycloadduct **2** in the reaction studied here lies very late on the reaction coordinate and is reached only after substantial loss of resonance energy in the benzene ring.

Received: February 12, 1992 [Z 5181 IE]
German version: *Angew. Chem.* **1992**, *104*, 867

CAS Registry numbers:
1a, 19660-93-6; **1b**, 141510-09-0; **1c**, 141510-10-3; **1d**, 141510-11-4; **3d**, 141510-12-5; **4a**, 141510-13-6; **5a**, 141510-07-8; **5b**, 141510-08-9; **6**, 141510-14-7

[1] L. Claisen, O. Eisleb, *Justus Liebigs Ann. Chem.* **1913**, *401*, 21–119; for a review, see S. J. Rhoads, N. R. Raulins in *Organic Reactions*, *Vol. 22* (Ed.: W. G. Dauben), Wiley, New York, **1974**, p. 1–252.
[2] W. R. Roth, *Tetrahedron Lett.* **1964**, 1009–1013.
[3] a) E. Vogel, D. Wendisch, W. R. Roth, *Angew. Chem.* **1964**, *76*, 432–433; *Angew. Chem. Int. Ed. Engl.* **1964**, *3*, 442–443; b) W. Grimme, J. Lex, T. Schmidt, *ibid.* **1987**, *99*, 1277–1279 and **1987**, *26*, 1268–1270; c) T. Grommes, Dissertation, Universität Köln, **1991**.
[4] a) R. G. Miller, M. Stiles, *J. Am. Chem. Soc.* **1963**, *85*, 1798–1800; b) R. S. H. Liu, *ibid.* **1968**, *90*, 215–216; c) E. Ciganek, *Tetrahedron Lett.* **1967**, 3321–3325.
[5] The [4+2] cycloaddition of some electron-poor dienes to the central bond of benzocyclopropene is known: a) S. Korte, Dissertation, Universität Köln, **1968**; b) J. C. Martin, J. M. Muchowski, *J. Org. Chem.* **1984**, *49*, 1040–1043; c) R. Neidlein, L. Tadesse, *Helv. Chim. Acta* **1988**, *71*, 249–253.
[6] E. Vedejs, R. A. Shepherd, *Tetrahedron Lett.* **1970**, 1863–1864.
[7] K. Kraft, G. Koltzenburg, *Tetrahedron Lett.* **1967**, 4723–4728.
[8] L. A. Paquette, J. C. Stowell, *Tetrahedron Lett.* **1970**, 2259–2262.
[9] E. Vedejs, *Tetrahedron Lett.* **1970**, 4963–4966.
[10] W. Grimme, L. Schumachers, W. R. Roth, R. Breuckmann, *Chem. Ber.* **1981**, *114*, 3197–3208.
[11] S. N. Deming, S. L. Morgan, *Anal. Chem.* **1973**, *45*, 278A.
[12] J. A. Nelder, R. Mead, *Comput. J.* **1965**, *7*, 308.
[13] a) R. T. Seidner, N. Nakatsuka, S. Masamune, *Can. J. Chem.* **1970**, *48*, 187–192; b) H. D. Carnardi, P. Hildenbrand, J. Richter, G. Schröder, *Justus Liebigs Ann. Chem.* **1978**, 2074–2087.

Photoselective Processes in Cyclooctasulfur Layers: Desorption versus Polymerization**

By *Jens Geyer, Heinrich Stülpnagel,* and *Klaus Rademann**

The photolysis of cyclooctasulfur has been studied at various temperatures and wavelengths. To the known photochemistry of sulfur under the influence of UV light in the 250–400 nm range belongs the appearance of sulfur radicals during the irradiation and polymerization of S_8.[1–6] We report here the dependence of the polymerization of sulfur on the wavelength of irradiating light. A central, unprecedented observation, however, is that desorption of a thin cyclooctasulfur layer is stimulated by light ($\lambda = 255$ nm) in high vacuum. As a result of the observed dependence of desorption rate on light intensity, a purely thermal desorption process at a wavelength of 255 nm can be rejected.

The sulfur layer ($d = 100$ to 700 nm) was generated in a high-vacuum apparatus ($p = 4 \times 10^{-6}$ to 1×10^{-7} mbar) by directing a beam of S_8 molecules onto a polycrystalline gold surface ($T = +20$ to -50 °C). This is a component of the probe of the quartz microbalance that monitors the layer's thickness.

The sulfur condenses as a supercooled liquid that precipitates in the form of droplets[7, 8] above -35 ± 2 °C, regardless of the substrate studied (quartz glass, corundum, gold, stainless steel). Below this temperature a continuous film forms because the supercooled sulfur melt is present as a glass.[9] Previously glass transition temperatures for sulfur of -29 °C[10] and -30 °C[11] were reported.[12]

For the sulfur layer consisting of droplets, an activation enthalpy of 68 kJ mol^{-1} for the evaporation could be calculated from the dependence of the thermal desorption rate on temperature (Ford and La Mer[13] report an enthalpy of evaporation of 78 kJ mol^{-1} for a supercooled sulfur melt). Thermal desorption could not be observed below -36 °C for the continuous glasslike film.

For the droplet film (cf. [7,8]) light-induced desorption was detected for the first time (Fig. 1). The wavelength dependence of this desorption was studied at 255, 328, 382, 436, 545, and 656 nm. The maximum desorption rate (calculated with refererence to the radiative power per surface area) was found at 255 nm (see Experimental). Studies on supercooled sulfur melts by UV spectroscopy were hitherto unknown. Absorption measurements for S_8 in solution such as those of Steudel et al.[14] reveal a double maximum in the range 250–280 nm.

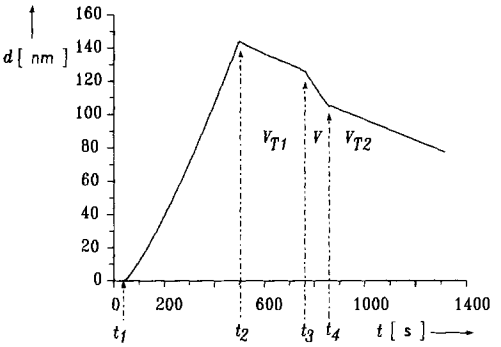

Fig. 1. Growth of the film thickness d with time on adsorption and thermal/light-induced desorption for a S_8 droplet film. $\lambda = 255$ nm, substrate temperature = 0 °C, $p = 4 \times 10^{-6}$ mbar. Desorption rates: $V_{T1} = 61 - 10^{-3}$ nm s^{-1} before irradiation, $V = 215 \times 10^{-3}$ nm s^{-1} during irradiation, $V_{T2} = 59 \times 10^{-3}$ nm s^{-1} after irradiation. t_1: effusive molecular beam source opened, t_2: molecular beam source closed, t_3: UV lamp on, t_4: UV lamp off.

To solve the question whether the desorption of sulfur by UV irradiation at $\lambda = 255$ nm is a purely thermal phenomenon, the dependence of the rate of light-induced desorption on light intensity was investigated. If the influence of the light is exclusively due to a warming of the sulfur film, the dependence of the light-induced desorption rate (V_L) on light intensity should be described by Arrhenius's law; the relationship between light intensity and increase in temperature

[*] Priv. Doz. Dr. K. Rademann, J. Geyer
FB 14, Physikalische Chemie der Universität
Hans-Meerwein-Strasse, D-W-3550 Marburg (FRG)
H. Stülpnagel
Max-Planck-Institut für Quantenoptik
D-W-8046 Garching (FRG)

[**] This work was supported by the Deutsche Forschungsgemeinschaft and the German–Israeli Foundation (GIF).

is required.[15] V_L depends on the temperature as well as the light intensity, but this fact alone does not prove that the desorption is caused exclusively by a local warming of the sulfur layer. A mechanism with a primary electronic step followed by a temperature-dependent reaction step could also be implicated.[16]

A representative experimental curve (Fig. 2), recorded at a substrate temperature of $-24\,^{\circ}C$ (for which the thermal desorption rate $V_T < 1 \times 10^{-3}$ nm s^{-1}) and showing the dependence of V_L on the light intensity, reveals a linear relationship. In addition the calculated course for a purely thermal

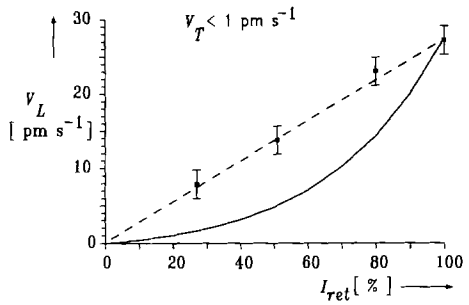

Fig. 2. Dependence of the light-induced desorption rate V_L on light intensity I_{rel} at a substrate temperature T of $-24\,^{\circ}C$; $\lambda = 255$ nm, $p = 4 \times 10^{-6}$ mbar; V_T is the rate of the thermal desorption without any light-induced desorption. The solid line shows the curve calculated from the Arrhenius equation for a purely thermal desorption mechanism.

desorption is superimposed on the graph. The highest value of the intensity (100%) was used in the calculation of V_T according to Arrhenius's law. Likewise, a linear relationship is found at higher temperatures (up to $0\,^{\circ}C$) and therefore at considerably higher V_T (Fig. 3). However, the measurement of V_L is hampered by the rapid increase in thermal desorption with increasing temperature.

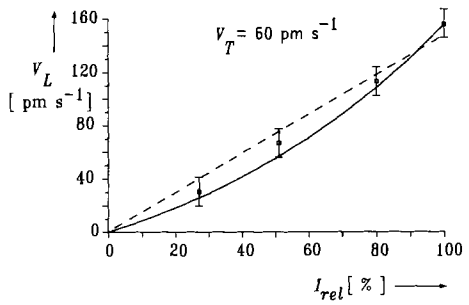

Fig. 3. Dependence of the light-induced desorption rate V_L on light intensity at a substrate temperature T of $\pm 0\,^{\circ}C$; $\lambda = 255$ nm, $p = 4 \times 10^{-6}$ mbar; V_T is the rate of the thermal desorption without any light-induced desorption. The solid line shows the curve calculated from the Arrhenius equation for a purely thermal desorption mechanism.

V_L was also determined at the wavelengths 328 and 382 nm. The following differences with respect to $\lambda = 255$ nm (for the same radiative power per surface area) were discovered: a) V_L is significantly smaller at higher wavelengths (Fig. 4);[17] b) after a short irradiation period, V_T has distinctly diminished from its value before the irradiation (Fig. 4) and c) the homogeneous glasslike film (irradiated at $-43\,^{\circ}C$) is no longer destroyed by heating, or at least only at temperatures higher than $-36\,^{\circ}C$ (cf. [9]). The observations mentioned under b) and c) suggest that the known light-induced polymerization of sulfur is taking place. This supposition is confirmed by solubility studies in CS_2: in contrast to the nonirradiated film, the irradiated sulfur layer dissolves only partially. At $\lambda = 328$ nm the polymerization is more pronounced than at $\lambda = 382$ nm, and at 418 and 437 nm no polymerization can be detected.

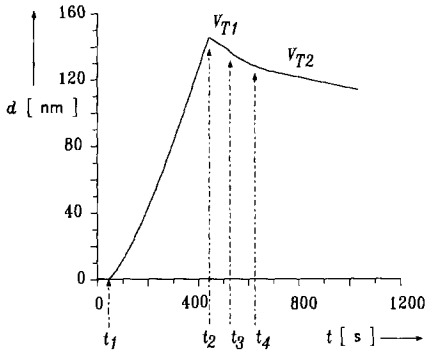

Fig. 4. Growth of the film thickness d with time on adsorption and thermal/light-induced desorption for a S_8 droplet film. $\lambda = 328$ nm, substrate temperature $= 0\,^{\circ}C$, $p = 3 \times 10^{-6}$ mbar. Desorption rates: $V_{T1} = 97$–10^{-3} nm s^{-1} before irradiation, $V_{T2} = 59 \times 10^{-3}$ nm s^{-1} after irradiation. t_1: effusive molecular beam source opened, t_2: molecular beam source closed, t_3: UV lamp on, t_4: UV lamp off. During the irradiation the desorption rate is not constant.

Polymerization is also noticeable for irradiation with light of wavelength 255 nm, but to a distinctly smaller extent than at $\lambda = 328$ or 382 nm. The behavior of the dependence of the light-induced desorption on wavelength, on the other hand, is the reverse: at 255 nm substantially more desorption takes place (a ten- to twentyfold increase in desorption rate) than at 328 or 382 nm.

Experimental Equipment

UV light source: Xe high-pressure lamp from Oriel, 1000 W, model 6271. Radiative power at the substrate's surface: 4–20 mW cm^{-2} at 328 and 382 nm, measured with a Radiometer Rj7100 from Laser Precision Corp., probe Rj P735.

Interference filters: reflection interference filter $\lambda_{max} = 255$ nm, $T_{max} = 79.0\%$, full width at half maximum (FWHM) = 8.9 nm; Transmission interference filter $\lambda_{max} = 328$ nm, $T_{max} = 52.0\%$, FWHM = 5.5 nm; $\lambda_{max} = 382$ nm, $T_{max} = 32.5\%$, FWHM = 8.0 nm; $\lambda_{max} = 436$ nm, $T_{max} = 48.0\%$, FWHM = 21.0 nm; $\lambda_{max} = 545$ nm, $T_{max} = 61.5\%$, FWHM = 20.5 nm; $\lambda_{max} = 656$ nm, $T_{max} = 57.0\%$, FWHM = 20.0 nm.

Monitor of film thickness: Type E5550 from Plano W. Plannet GmbH, Marburg; resolution 0.1 nm, surface area of probe 28 mm^2, temperature control from $+120$ to $-100\,^{\circ}C$.

Vacuum chamber and pumping system: Length of chamber 800 mm, diameter 160 mm, pump stand EXT 100/200 from Edwards.

Effusive molecular beam source: 40 cm long quartz tube, heated by water circulation, filled with α-S_8 (99.999% from Aldrich), inner diameter 20 mm, diameter of the sealable aperture 4 mm, distance from substrate about 50 mm, temperature $+20$ to a maximum of $+79\,^{\circ}C$, corresponding to an α-S_8 equilibrium vapor pressure of 1.1×10^{-3} mbar (at $+79\,^{\circ}C$). The proportion of S_8 rings in the vapor over the subliming S_8 is over 99% [18].

Received: February 19, 1992 [Z 5195 IE]
German version: *Angew. Chem.* **1992**, *104*, 894

[1] Although light-induced polymerization has been known for a long time, the existence of radicals was only proven beyond doubt in recent years by electron spin resonance spectroscopy [3,6].
[2] R. Steudel, *Top. Curr. Chem.* **1982**, *102*, 149.
[3] S. R. Elliot, *J. Phys. (Paris)* **1981**, *42*, 387.
[4] R. Steudel, G. Holdt, A. T. Young, *J. Geochem. Res.* **1986**, *91*, 4971.
[5] E.-M. Strauss, R. Steudel, *Z. Naturforsch. B* **1987**, *42*, 682.

[6] R. Steudel, J. Albertsen, K. Zink, *Ber. Bunsenges. Phys. Chem.* **1989**, *93*, 502, and references cited therein.
[7] S. Hamada, Y. Nakazava, T. Shirai, *Bull. Chem. Soc. Jpn.* **1970**, *43*, 3096.
[8] The size of the droplets varies from less than 1 μm to about 100 μm, depending on the duration of vaporization, and increases with progressive adsorption. They have a low viscosity and can be easily moved on the substrate surface.
[9] On warming to over −33 °C the nonirradiated film tears irreversibly and the droplet layer is formed.
[10] P. Mondrian-Monval, *Ann. Chim.* **1939**, *3*, 5.
[11] A. V. Tobolsky, W. MacKnight, R. B. Beevers, V. D. Gupta, *Polymer* **1963**, *4*, 423.
[12] Here, however, sulfur from a melt obtained by temperature shock is used, which also contains, besides S_8 rings, *catena*-polysulfur (μ-sulfur) and other allotropes.
[13] G. P. Ford, V. K. La Mer, *J. Am. Chem. Soc.* **1950**, *72*, 1959.
[14] R. Steudel, D. Jensen, P. Göbel, P. Hugo, *Ber. Bunsenges. Phys. Chem.* **1988**, *92*, 118.
[15] Note that to report the light-induced desorption rate V_L, the thermal desorption rate V_T was subtracted from the total desorption rate after the UV lamp was switched on ($V = V_L + V_T$), because except at low temperatures, thermal desorption plays a role in addition to light-induced desorption.
[16] In this context a study of the composition, structure, and energy of the desorbed particles would be interesting. Our preliminary investigations by mass spectrometry suggest that S_2 and S_6 are the desorbing species. A photolytic cleavage of S_8 rings into smaller fragments was discussed by Steudel et al. [6].
[17] The light-induced desorption rate V_L at 328 and 382 nm was not sufficiently large to permit a study of its dependence on light intensity.
[18] J. Berkowitz in *Elemental Sulfur* (Ed.: B. Meyer), Wiley, New York, **1965**, p. 152.

A Structurally Distorted Ligand in an Electron-Deficient Dizirconocene Cation: Unusual 1,2- and 1,1-Dimetallioalkenes**

By *Andrew D. Horton** and *A. Guy Orpen*

Formally 14-electron d^0 complexes $[Cp'_2MR]^+$ (M = Ti, Zr, Hf, Th) relieve coordinative unsaturation at the metal atom by unusual bonding interactions with the ligand R or a labile counteranion. Examples of such interactions include $X\text{–}CH_n \cdots M$ (X = C,[1] Si,[2] B,[3] M[4]), Si–Cl ··· M,[5] and multiple-bond ··· M.[2c, 6] Related α-[7] and β-C–H ··· M[8] agostic interactions may play an important role in the stereoselective alkene insertion. In exploring whether the chemistry of electrophilic $[(C_5Me_5)_2ZrR]^+$ species as agents for RC≡CH oligomerization[2c] could be extended to less crowded C_5H_5 analogues, we have observed formation of electron-deficient binuclear zirconocene cations, which contain unusual bridging hydrocarbon ligands. We report here the first highly distorted planar 1,2-dimetallioalkene complex containing two transition metal fragments, which also contains a μ-alkynyl ligand.

Cationic $[(C_5Me_5)_2ZrR]^+$ complexes are catalytically more active and lead to a higher degree of RC≡CH oligomerization than their neutral scandium analogues.[2c] We postulated that this tendency might be further accentuated if sterically less bulky η^5 ligands were employed as catalysts, since such cations in comparison with C_5Me_5 complexes show increased reactivity with terminal alkynes (e.g. double insertion).[6c] Unexpectedly, the reaction of excess *t*BuC≡CH with a 1:1 mixture of $[Cp_2ZrMe_2]$ and $[PhMe_2NH][BPh'_4]$ (to generate unstable $[Cp_2ZrMe(NMe_2Ph)][BPh'_4]$; Ph′ = 4-$C_6H_4F$) at −30 °C affords, on warming to 25 °C, only a few equivalents of $H_2C{=}C(t\text{Bu})C{\equiv}Ct\text{Bu}$ and unreacted alkyne. If the reaction is monitored by NMR spectroscopy the formation of a single organometallic product **1**, and 0.5 equiv of unreacted $[PhMe_2NH]^+$ is observed. Yellow crystals of **1**-BPh'_4 (80% yield) were obtained from the reaction of a 2:1 ratio of zirconocene and "H^+", and excess alkyne [Eq. (a)].

$$2\,[Cp_2ZrMe_2] + [PhMe_2NH][BPh'_4] + m\ t\text{BuC}{\equiv}\text{CH} \xrightarrow[-30 \rightarrow +25\,^\circ\text{C}]{C_6H_5Br} \quad \text{(a)}$$

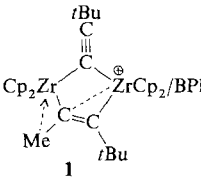

$$\mathbf{1}\text{–}BPh'_4 + NMe_2Ph + 2\,CH_4 + H_2C{=}C(t\text{Bu})Me + n\,H_2C{=}C(t\text{Bu})C{\equiv}C(t\text{Bu})$$

The elemental analysis, ^1H and ^{13}C NMR spectroscopy, and the formation of a 2:1:1 mixture of Cp_2ZrCl_2, *t*BuC≡CH, and *cis*-MeHC=CH(*t*Bu), respectively, on addition of HCl to **1** in C_6D_5Br, all suggest that **1** contains two $[Cp_2Zr]$ fragments with *t*BuCC and MeCC*t*Bu ligands. The NMR spectra indicate that the *t*BuCC and MeCC*t*Bu ligands are situated in the equatorial plane between the Cp ligands; the existence of agostic C–H ··· Zr bonding between the methyl group and the Zr atom is, however, only partially supported by the NMR data (^1H NMR: $\delta = -0.30$; ^{13}C NMR: $\delta = -14.6$; $^1J(CH) = 128$ Hz).[8]

The X-ray structure analysis of **1**-BPh'_4[9] shows that the *tert*-butylalkynyl and the alkenediyl ("μ-alkyne") bridging ligands in the binuclear cation are equatorial with respect to the coordination at the Zr centers (Fig. 1). In contrast to the normal, symmetrical, planar structure of 1,2-dimetallioalkenes,[10] the C2–C3 double bond (1.336(14) Å) in **1** has slid relative to the Zr ··· Zr vector so as to bring C2 in contact with Zr2 (Zr2–C2 = 2.486(13) Å). The electron deficiency

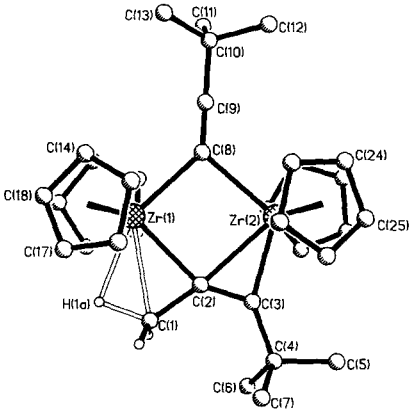

Fig. 1. Structure of the cation **1** (hydrogen atoms, except for those on C(1), omitted for clarity). Selected distances [Å] and angles [°]: C(1)-C(2) 1.513(19); C(3)-C(4) 1.554(16); C(8)-C(9) 1.224(21); C(9)-C(10) 1.516(21); Zr(1) ··· Zr(2) 3.485(2); Zr(1)-C(8) 2.289(14), Zr(2)-C(8) 2.399(12); C(2)-Zr(1)-C(8) 88.7(4); C(2)-Zr(2)-C(8) 83.5(4); C(1)-C(2)-C(3) 125.9(11); Zr(1)-C(2)-Zr(2) 91.8(4); C(2)-C(3)-C(4) 128.0(11); Zr(1)-C(8)-Zr(2) 96.0(6); Zr(1)-C(8)-C(9) 136.6(9); Zr(2)-C(8)-C(9) 127.4(9); C(8)-C(9)-C(10) 177.5(16).

[*] Dr. A. D. Horton
Koninklijke/Shell-Laboratorium, Amsterdam (Shell Research B.V.)
P.O. Box 3003, NL-1003 AA Amsterdam (The Netherlands)
Dr. A. G. Orpen
School of Chemistry
University of Bristol
GB-Bristol BS8 1TS (UK)

[**] According to the rules for IUPAC nomenclature all radicals and substituents with a metal center as a binding site have the suffix -io (see *Nomenclature of Inorganic Chemistry* (Ed.: G. J. Leigh), Blackwell, Oxford, **1990**, p. 274, Table IX). Therefore, alkenes with two Cp_2RZr substituents are described as dimetallioalkenes.

at Zr1 for the rather weak Zr1–C2 bond of 2.365(11) Å (Zr2–C3 = 2.168(12) Å) is partially compensated by the agostic coordination[2b, 8, 11] of C1–H1A to Zr1 (Zr1–C1 = 2.616(14) Å, Zr1–H1A = 2.27(15) Å), and by the slightly stronger bonding of the μ-alkynyl ligand to Zr1. The alkynyl bridge is slightly asymmetric with the Zr1–C8 bond approximately 0.11 Å shorter than Zr2–C8. The deformation of the 1,2-dimetallioalkene is also shown by the Zr1-C2-C1 and Zr2-C3-C4 angles of 81.6(7) and 145.0(8)°, respectively.

Although the general structural features and bonding parameters for the μ-alkyne interaction with Zr2 are similar to those for the Zr complexes, $[Cp_2Zr(\mu\text{-CCPh})\{\mu\text{-MeCCPh}\}AlMe_2]$[12] and $[Cp_2Zr(\mu\text{-Cl})\{\mu\text{-Me}_3SiCCPh\}AlMe_2]$,[13] recently reported by Erker et al., the asymmetric bonding of the bridging ligands at the metal center in **1** cannot be ascribed to different affinities of the two metals to the ligands, as might be invoked for the Zr–Al complexes. The asymmetric coordination of the MeCC*t*Bu ligand in **1** reduces the electronic unsaturation at Zr2 and also relieves the steric congestion at Zr2 caused by the *t*Bu and Cp ligands. This allows agostic bonding at Zr1, by permitting a closer approach of the methyl group (C1).

Sterically less crowded alkynes, RC≡CH (R = *i*Pr, *n*Pr, 4-tolyl), react with $[Cp_2ZrMe_2]/[PhMe_2NH][BPh'_4]$ (2:1 ratio) at −30 °C to give blue microcrystalline complexes **2**-BPh'_4 (≥70% yield) [Eq. (b)]. If a 1:1 ratio of zirconocene/"H$^+$" is used, identical products are obtained, and, in contrast to the reaction with *t*BuC≡CH, no alkyne oligomers are formed under any conditions. The NMR spectra and the formation of $D_2C{=}C(R)Me$ and CH_3D on treatment of **2a–c** with D_2O show that the complexes **2** contain μ-methyl and μ-alkenylidene ligands which bridge the two Cp_2Zr fragments. The unprecedented alkenylidene unit bridging between two d^0 transition metals has been confirmed by the characteristic C_α and C_β resonance frequencies (e.g. **2a**: δ = 304.9 and 159.1, respectively).[14] Through the μ-alkenylidene coordination the bridging methyl group (**2a**: ^{1}H NMR: $\delta = -1.15$; ^{13}C NMR: δ = 55.7) adopts a bent bonding mode ($\sphericalangle$Zr–C–Zr < 180°) as reflected in the low ^1J(C,H) value of 110 Hz for the methyl group.[15] Since the signals for the protons of the Cp ligands in **2a** and **2b** have identical chemical shifts, and those for the carbon atoms nearly identical shifts ($\Delta\delta$ = 0.1–0.3), it is suggested that the $[Cp_2Zr]$ fragments are relatively symmetrically bridged. This conclusion is supported (more tenuously) by the lack of NMR evidence for an agostic interaction with the alkyl groups of the alkylidene ligands.

$$2\,[Cp_2ZrMe_2] + [PhMe_2NH][BPh'_4] + 2\,RC{\equiv}CH \xrightarrow[-30 \rightarrow +25\,^\circ C]{C_6H_5Br} \quad (b)$$

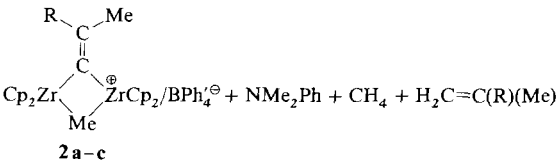

2a–c

R = *i*Pr (**2a**), *n*Pr (**2b**), 4-Tolyl (**2c**)

Possible mechanisms for the formation of **1** and **2a–c** are presented in Scheme 1. The likely first step is the alkyne insertion in "$[Cp_2ZrMe(NMe_2Ph)]^+$", to give alkenyl complexes **3**.[2b, 6c, 16] Rapid σ-bond metathesis with the alkyne then liberates $H_2C{=}C(R)Me$ (proven by NMR spectroscopy)

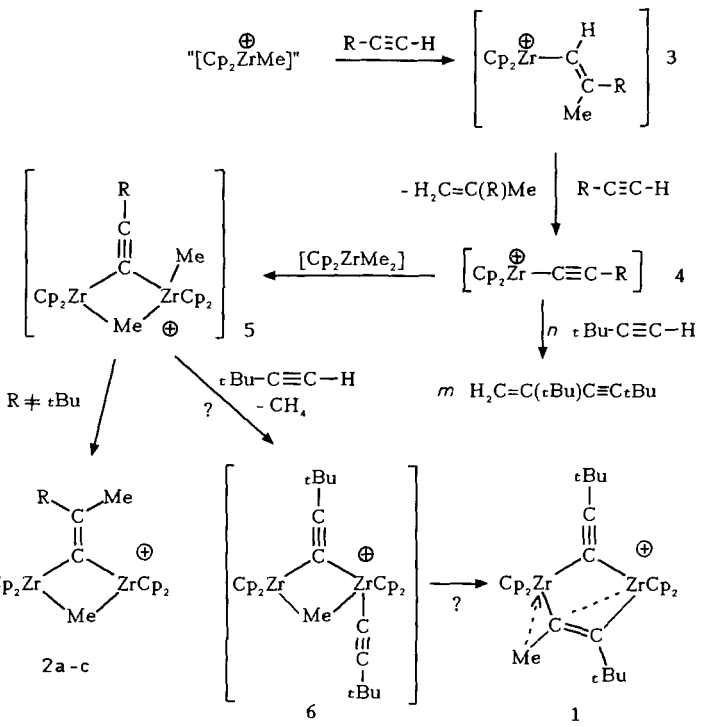

Scheme 1. Possible reaction mechanism for the formation of **1** and **2a–c**. **a**, R = *i*Pr; **b**, R = *n*Pr; **c**, R = 4-tolyl.

and affords the transient alkynyl complex **4**, related to the known $[(C_5Me_5)_2Zr\{C{\equiv}CtBu\}(thf)]^+$.[2c] Trapping of the unsaturated complex **4**[17] by the Lewis base $[Cp_2ZrMe_2]$ may then give a transient dizirconocene intermediate, possibly the μ-alkynyl μ-methyl complex **5**.[4] The rapid insertion of the alkynyl triple bond into a Zr–Me bond in **5** (R ≠ *t*Bu)[18] leads to the μ-alkenylidene complexes **2a–c**. Such insertion appears to be sterically unfavorable for **5** (R = *t*Bu). The formation of **1** may, instead, involve a sterically less demanding σ-bond metathesis reaction between a further molecule of *t*BuC≡CH and a Zr–Me group in **5**, to afford a Zr_2 intermediate with a methyl and two alkynyl ligands, for example, **6** in Scheme 1. "Reductive elimination" of methyl and alkynyl groups[12] in the hypothetical compound **6** could then lead to a MeCC*t*Bu ligand with the required *cis* geometry as found in **1**. Attempts to distinguish these from other possible mechanisms for the formation of **1** and **2a–c** are in progress.

The remarkable sensitivity of these reactions to the steric bulk of both the substituents at the alkyne and cyclopentadienyl ligand is reflected in the selective formation of the catalytically inactive compounds **1** and **2a–c**, in contrast to the catalytic RC≡CH oligomerization observed in reactions of the sterically more crowded $[(C_5Me_5)_2ZrMe]^+$.[2c] Our results suggest that the deactivation of electrophilic d^0 catalysts, by the formation of inactive binuclear compounds,[11b, 19] may also be important in alkene polymerization catalysis, especially when less bulky ligands offer less steric protection to the active species.

Experimental Procedure

1-BPh'_4: A solution of *t*BuC≡CH (0.40 mL, 3.3 mmol) in C_6H_5Br (4 mL) at −30 °C was added to a stirred mixture of $[(C_5H_5)_2ZrMe_2]$ (200 mg, 0.80 mmol) and $[PhMe_2NH][B(4\text{-}C_6H_4F)_4]$ (200 mg, 0.39 mmol). The instantaneously formed purple suspension gave a yellow solution on warming to 25 °C for 5 min. The product was precipitated with hexane, recrystallized from CH_2Cl_2/hexane solution, and dried in vacuum affording pure **1**-BPh'_4 (335 mg, 2 crops; 83%).

2a-BPh$'_4$: Addition of a solution of *i*PrC≡CH (0.30 mL, 3.0 mmol) in C_6H_5Br (6 mL) at −30 °C to a stirred mixture of $[(C_5H_5)_2ZrMe_2]$ (200 mg, 0.80 mmol) and $[PhMe_2NH][B(4\text{-}C_6H_4F)_4]$ (200 mg, 0.39 mmol), followed by warming to 25 °C, resulted in the deposition of a blue microcrystalline solid. Addition of hexane, followed by the recrystallization of the recovered solid from CH_2Cl_2/hexane, and drying in vacuo, afforded pure **2a**-BPh$'_4$ (265 mg; 70%). Compounds **2b**-BPh$'_4$ and **2c**-BPh$'_4$ were obtained analogously; **2b**-BPh$'_4$ contains 10% of cocrystallizing $[(Cp_2Zr)_2(\mu\text{-Me})\{\mu\text{-C}=\text{C}(n\text{Pr})\text{CH}=\text{C}(n\text{Pr})(\text{Me})\}]^+$ (shown by NMR spectroscopy and by the formation of $H_2C=C(n\text{Pr})CH=C(n\text{Pr})(Me)$ with H^+), formed by insertion of *n*PrC≡CH into **3b**; low solubility prevented recrystallization of **2c**-BPh$'_4$. Selected ^{1}H NMR data for cations (also see text). (300 MHz, CD_2Cl_2, 25 °C): **1**: δ = 6.09, 5.92 (s, 10H; C_5H_5), 1.49, 1.29 (s, 9H; CMe_3). ($C_2D_2Cl_4$, 25 °C): **2a**: δ = 6.54 (s, 20H; C_5H_5), 0.82 (d, 6H; $CHMe_2$), 0.39 (s, 3H; C=C(*i*Pr)(*Me*)), −0.18 (sep, 1H; $CHMe_2$). **2b**: δ = 6.54 (s, 20H; C_5H_5), 1.26 (m, 2H; $CH_2CH_2CH_3$), 0.85 (t, 3H; $CH_2CH_2CH_3$), 0.47 (s, 3H; C=C(*n*Pr)(*Me*)), 0.44 (m, 2H; $CH_2CH_2CH_3$), −1.14 (s, 3H; μ-Me). **2c**: δ = 6.63, 6.29 (s, 10H; C_5H_5), −1.10 (s, 3H; μ-Me). Selected ^{13}C NMR data (75.43 MHz, CD_2Cl_2, −30 °C): **1**: δ = 232.5 ($MeCCCMe_3$), 145.9, 127.2 ($CCCMe_3$ or $MeCCCMe_3$), 111.2, 107.9 (C_5H_5), 107.2 ($CCCMe_3$ or $MeCCCMe_3$), 41.7, 29.6 (CMe_3), 29.2, 28.5 (CMe_3). ($C_2D_2Cl_4$, 0 °C): **2a**: δ = 114.2, 113.9 (C_5H_5), 36.7 ($CHMe_2$), 20.4 ($CHMe_2$), 17.6 (C=C(*i*Pr)(*Me*)). **2b**: δ = 306.9 (*C*=C(*n*Pr)(Me)), 153.9 (C=*C*(*n*Pr)(Me)), 114.1, 114.0 (C_5H_5), 56.6 (q, ^1J(C,H) = 109 Hz; μ-Me).

Received: January 30, 1992 [Z 5159 IE]
German version: *Angew. Chem.* **1992**, *104*, 912

CAS Registry numbers:
1, 141847-81-6; **2a**, 141847-83-8; **2b**, 141847-85-0; **2c**, 141847-87-2; $[Cp_2ZrMe_2]$, 12636-72-5; $[PhMe_2NH][B(4\text{-}C_6H_4F)_4]$, 136763-54-7; *t*BuC≡CH, 917-92-0; *i*PrC≡CH, 598-23-2; *n*PrC≡CH, 627-19-0; 4-tolyl−C≡CH, 766-97-2.

[1] G. G. Hlatky, H. W. Turner, R. R. Eckman, *J. Am. Chem. Soc.* **1989**, *111*, 2728.
[2] a) J. J. Eisch, A. M. Piotrowski, S. K. Brownstein, E. J. Gabe, F. L. Lee, *J. Am. Chem. Soc.* **1985**, *107*, 7219; b) A. D. Horton, A. G. Orpen, *Organometallics* **1991**, *10*, 3910; c) A. D. Horton, *J. Chem. Soc. Chem. Commun.* **1992**, 185.
[3] X. Yang, C. L. Stern, T. J. Marks, *J. Am. Chem. Soc.* **1991**, *113*, 3623.
[4] X. Yang, C. L. Stern, T. J. Marks, *Organometallics* **1991**, *10*, 840.
[5] A. D. Horton, A. G. Orpen, *Organometallics* **1992**, *11*, 1193.
[6] a) Z. Lin, J.-F. Le Marechal, M. Sabat, T. J. Marks, *J. Am. Chem. Soc.* **1987**, *109*, 4127; b) A. D. Horton, J. H. G. Frijns, *Angew. Chem.* **1991**, *103*, 1181; *Angew. Chem. Int. Ed. Engl.* **1991**, *30*, 1152; c) A. D. Horton, A. G. Orpen, *Organometallics* **1992**, *11*, 8.
[7] a) H. Krauledat, H.-H. Brintzinger, *Angew. Chem.* **1990**, *102*, 1459; *Angew. Chem. Int. Ed. Engl.* **1990**, *29*, 1412; b) W. E. Piers, J. E. Bercaw, *J. Am. Chem. Soc.* **1990**, *112*, 9406; c) P. Corradini, G. Guerra, *Prog. Polym. Sci.* **1991**, *16*, 239.
[8] R. F. Jordan, P. K. Bradley, N. C. Baenziger, R. E. La Pointe, *J. Am. Chem. Soc.* **1990**, *112*, 1289.
[9] **1**-BF$'_4$: $C_{57}H_{57}BF_4Zr_2$, M_r = 1011.3, triclinic, space group $\bar{P}1$ (No. 2), a = 12.695(3), b = 12.982(5), c = 15.652(5) Å, α = 86.28(3), β = 70.52(2), γ = 77.28(3), V = 2372(1.3) Å^3, Z = 4, ϱ = 1.41 gcm^{-3}, λ = 0.71069 Å, $\mu(Mo_{K\alpha})$ = 4.8 cm^{-1}, $F(000)$ = 1776, T = 200 K; R = 0.079, R_w = 0.069, S = 1.71 for 3889 independent absorption corrected intensities with $I > 2\sigma(I)$ and $4.0 < \theta < 50.0°$. Further details of the crystal structure investigation are available on request from the Director of the Cambridge Crystallographic Data Centre, University Chemical Laboratory, Lensfield Road, GB-Cambridge CB2 1EW (UK) on quoting the full journal citation.
[10] a) R. S. Dickson, G. N. Pain, *J. Chem. Soc. Chem. Commun.* **1979**, 277; b) C.-L. Lee, C. T. Hunt, A. L. Balch, *Inorg. Chem.* **1981**, *20*, 2498.
[11] D. J. Crowther, N. C. Baenziger, R. F. Jordan, *J. Am. Chem. Soc.* **1991**, *113*, 1455.
[12] G. Erker, M. Albrecht, C. Krüger, S. Werner, *Organometallics* **1991**, *10*, 3791.
[13] G. Erker, R. Zwettler, C. Krüger, R. Noe, S. Werner, *J. Am. Chem. Soc.* **1990**, *112*, 9620.
[14] a) T. Yoshida, E. Negishi, *J. Am. Chem. Soc.* **1981**, *103*, 1276; b) V. C. Gibson, G. Parkin, J. E. Bercaw, *Organometallics* **1991**, *10*, 220.
[15] a) M. A. Busch, R. Harlow, P. L. Watson, *Inorg. Chim. Acta* **1987**, *140*, 15; b) S. L. Buchwald, E. A. Lucas, W. M. Davis, *J. Am. Chem. Soc.* **1989**, *111*, 397; c) R. M. Waymouth, B. D. Santasiero, R. J. Coots, M. J. Brownikowski, R. H. Grubbs, *ibid.* **1986**, *108*, 1427.
[16] The related complex, $[Cp_2Zr\{CH=C(t\text{-Bu})(Me)\}(thf)]^+$, is slowly formed (85%, 25 °C, 18 h) on reaction of $[Cp_2ZrMe(thf)]^+$ with *t*BuC≡CH.
[17] Catalysis by **4** (R = *t*Bu), by analogy to C_5Me_5 chemistry [2c], affords some $H_2C=C(t\text{Bu})C\equiv Ct\text{Bu}$ (**1** and **2** show no catalysis), before trapping by $[Cp_2ZrMe_2]$ occurs.
[18] D. Afzal, C. M. Lukehart, *Organometallics* **1987**, *6*, 546.
[19] J. C. W. Chien, A. Razavi, *J. Polym. Sci. Part A Polym. Chem.* **1988**, *26*, 2369.

The Crystal Structure of $[(Pyrene^{\bullet-})\{Na^+[(C_2H_5)_2O]\}]$: A Model for Stacked Radical Anion Salts**

By *Wolfgang Jost, Martin Adam, Volker Enkelmann,* and *Klaus Müllen**

The crystallographic description of the ions generated by reduction of aromatic hydrocarbons is generally limited to diamagnetic species.[1-3] Structures of paramagnetic radical anions[4-6] are scarcely known, whereas the radical cation salts[7] of aromatic hydrocarbons, which are easily accessible through electrocrystallization, have been intensively studied. The latter form electrically conducting crystals with stacked structures, and since the charge transport occurs in the direction of the crystal axis, they serve as models for one-dimensional electrical conductors. In our search for corresponding radical anion salts we have now prepared the title compound and characterized it by X-ray structural analysis.

Reduction of pyrene (202 mg, 10^{-3} mol) by sodium in 20 mL of ether at 193 K for twelve hours yielded a deep red solution that contains red needles. The solution was warmed to 298 K and then slowly cooled over 24 h to 253 K. Dark crystals with a metallic luster formed and were stable at room temperature under an inert atmosphere.

The crystal structure analysis revealed the composition as $[(pyrene^{\bullet-})\{Na^+[(C_2H_5)_2O]\}]$ (**1**).[8] As can be seen in Figure 1, a stacked structure is formed in which the pyrene units are tilted away from each other at an angle of 59.6(3)° along the *a* axis. In the cavity generated thereby is situated a sodium cation, which is coordinated to the oxygen atom of the ether molecule at a distance of 2.24(1) Å. Approximately symmetrical to this bond on either side are two contacts of

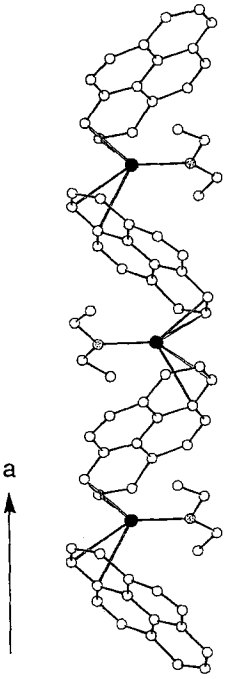

Fig. 1. Section of the polymeric structure of **1** showing the stacking of the pyrene units along the *a* axis. Sodium ions are represented as black spheres, O atoms as dotted spheres, and C atoms as open spheres. For distances and angles, see text.

[*] Prof. Dr. K. Müllen, Dipl.-Chem. W. Jost, Dipl.-Chem. M. Adam, Priv.-Doz. Dr. V. Enkelmann
Max-Planck-Institut für Polymerforschung
Ackermannweg 10, D-W-6500 Mainz (FRG)

[**] This work was supported by the Deutsche Forschungsgemeinschaft.

2.62(2) and 2.79(2) Å to the neighboring pyrene units. Characteristically, the shortest distances are found between counterion and those pyrene carbon atoms that display the highest spin density in the ESR spectrum of the pyrene radical cation.[9]

This structure may be described as a polymeric contact ion pair with a zigzag arrangement of the π electron system. A sodium ion coordinates to every adjacent pair of pyrene rings and has a remarkably small solvation sheath of only one ether molecule. In contrast, the magnesium derivative of an anthracene radical anion[4] is constructed from monomeric contact ion pairs with three solvent molecules and an anthracenide unit. A polymeric anion structure has been described for the diamagnetic sodium fluorenide–bis(tetramethylenediamine); however, here the zigzag aggregation is stabilized by the chelate effect through the nitrogen bases.[10-11] The present radical ion structure, therefore, has no precedent.

A comparison of the crystal structures of pyrene radical anions and radical cations[7] shows that both salts form polymeric stacked structures, but whereas in the anion each pyrene unit is singly charged, in the cation mixed valences are present in which the charge is spread over several units, enabling a high mobility of charge carriers. Adjacent rings in the stacks of the radical cation salts are arranged with very small distances of about 3.2–3.3 Å between them, and the carbon atoms with the highest electron density are in direct contact.

In **1**, a direct orbital overlap is not achieved, which can be readily attributed to the known tendency of small alkali counterions to overlap with conjugated anionic systems[12] and to the mutual coulombic repulsion between the π electron systems. Any potential charge transport will thus be influenced by considerable Coulombic effects, and an electrical conduction in such structures is not anticipated.

Received: February 14, 1992 [Z 5190IE]
German version: *Angew. Chem.* **1992**, *104*, 883

CAS Registry numbers:
1, 141462-76-2; pyrene, 129-00-0.

[1] K. Müllen, *Chem. Rev.* **1984**, *84*, 603–646.
[2] M. Rabinovitz, *Top. Curr. Chem.* **1984**, *146*, 101–169.
[3] a) W. N. Setzer, P. von R. Schleyer, *Adv. Organomet. Chem.* **1985**, *24*, 353–451; b) *ibid.* **1987**, *27*, 169–278.
[4] In 1,4-dimethylanthracenemagnesium–tris(tetrahydrofuran) a contact ion pair is present: B. Bogdanovic, N. Janke, C. Krüger, R. Mynott, K. Schlichte, U. Westeppe, *Angew. Chem.* **1985**, *97*, 972–974; *Angew. Chem. Int. Ed. Engl.* **1985**, *24*, 960–962.
[5] In $[(\text{fluorenone}^{\bullet-})\{\text{Na(dme)}_2\}]_2$ a dimeric contact ion pair of an arene containing a heteroatom is observed: H. Bock, H.-F. Herrmann, D. Fenske, H. Goesmann; *Angew. Chem.* **1988**, *100*, 1125–1127; *Angew. Chem. Int. Ed. Engl.* **1988**, *27*, 1067–1069.
[6] In $[(\text{biphenyl}^{\bullet-})(M^{+}_{solv.})]$(M = Na, K, Rb) the counterion is completely surrounded by polyether units: a) J. J. Mooij, A. A. K. Klaasen, E. De Boer, H. M. L. Degens, T. E. M. van der Hark, J. H. Noordik, *J. Am. Chem. Soc.* **1976**, *98*, 680–685; b) J. H. Noordik, J. Schreuers, E. De Boer, R. O. Gouid, J. J. Mooij, *J. Phys. Chem.* **1978**, *82*, 1105–1110; c) J. H. Noordik, P. T. Beurskens, T. E. M. van der Hark, J. N. M. Smits, *Acta Crystallogr. Sect. B* **1979**, *35*, 621–624.
[7] V. Enkelmann in *Polynuclear Aromatic Compounds* (Ed.: L. B. Ebert) (*Adv. Chem. Ser.* **1988**, *217*, 177–200).
[8] Enraf-Nonius CAD4 diffractometer ($Cu_{K\alpha}$ radiation, graphite monochromator, $\lambda = 1.5404$ Å), $C_{20}H_{20}ONa$, orthorhombic crystals of space group $Pna2_1$, $a = 13.689(2)$, $b = 15.120(4)$, $c = 7.829(2)$ Å, $V = 1620.4$ Å^3, $Z = 4$, $T = 195$ K, $\rho_{calcd} = 1.227$ g cm^{-1}, $\mu = 7.77$ cm^{-1}, 1217 reflections, 623 observed reflections, ($I > 3\sigma_I$). Solution by direct methods (MULTAN), empirical absorption correction. In the last full-matrix refinement the calculated H atoms in riding mode were provided with isotropic, and C, Na, and O with anisotropic temperature coefficients ($R = 0.089$, $R_w = 0.088$ for $w = 1$ and 199 parameters). Further details of the crystal structure investigation may be obtained from the Fachinformationszentrum Karlsruhe, Gesellschaft für wissenschaftlich-technische Information mbH, D-W-7514 Eggenstein-Leopoldshafen 2 (FRG) on quoting the depository number CSD-56294, the names of the authors, and the journal citation.
[9] C. Schnieders, K. Müllen, *Tetrahedron* **1984**, *40*, 1701–1711.
[10] S. Corbelin, J. Kopf, W. Weiss, *Chem. Ber.* **1991**, *124*, 2417–2422.
[11] A structural analogy to the "perimeter system" (see ref. [10]) reveals the linear 1.3-diphenyllithium–diethylether: G. Boche, H. Etzrodt, M. Marsch, W. Massa, G. Baum, H. Dietrich, W. Mahdi, *Angew. Chem.* **1986**, *98*, 84–85; *Angew. Chem. Int. Ed. Engl.* **1986**, *25*, 104–105.
[12] G. D. Stucky in *Polyamine-Chelated Alkali Metal Compounds* (Ed.: A. W. Langer) (*Adv. Chem. Ser.* **1974**, *130*, Chap. 3).

P-Functionalization of the Tetraphosphacubane System**

By *Manfred Birkel, Joachim Schulz, Uwe Bergsträsser,* and *Manfred Regitz**

Dedicated to Professor Fritz Bickelhaupt on the occasion of his 60th birthday

Reactivity studies on the tetraphosphacubane **2** have not been possible so far since this was only accessible in low yield by the thermal cyclotetramerization of tBu–C≡P.[1] This situation suddenly changed with its selective production from the phosphaalkyne dimeric complex **1**[2] by the removal of the zirconium fragment with hexachloroethane,[3] so that we can now report here for the first time the functionalization of the heteroatoms in **2**.

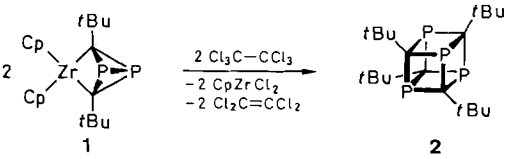

1 **2**

To our knowledge for other cubanes comparable with **2** (Sn–Ph,[4] Si–tBu,[5] Al[6] in place of C–tBu) no reactions are known in which the pentacyclic framework is retained. The participation of the lone pair on the phosphorus atom on the σ P/C framework bond reduces the nucleophilicity at the heteroatom,[7] so that reactions only occur with strong electrophiles and occasionally also only under drastic reaction conditions; the thermally stable tetraphosphacubane can withstand these.

Whereas methyl iodide is not suitable for the quaternization of **2**, the phosphonium triflate **3** (95%) is obtained smoothly with methyl trifluromethylsulfonate; even a large excess of the methylation reagent does not lead to a multiple reaction. Also with twice the molar quantity of nonacarbonyl diiron only one $[Fe(CO)_4]$ fragment is bound to form the complex **4** (56%).

If the NMR data of the cage atoms of **2**[8] are compared with those of **3** and **4** (Table 1), then the signals of the carbon atoms are shifted to lower field and those of the phosphorus

[*] Prof. Dr. M. Regitz, Dipl.-Chem. M. Birkel, Dr. J. Schulz, Dipl.-Chem. U. Bergsträsser
Fachbereich Chemie der Universität
Erwin-Schrödinger-Strasse, D-W-6750 Kaiserslautern (FRG)

[**] Organophosphorus compounds, part 57. This work was supported by the Volkswagen-Stiftung and the Fonds der Chemischen Industrie. Part 56: T. Wettling, U. Bergsträsser, M. Regitz, *J. Chem. Soc. Chem. Commun.* **1992**, in press.

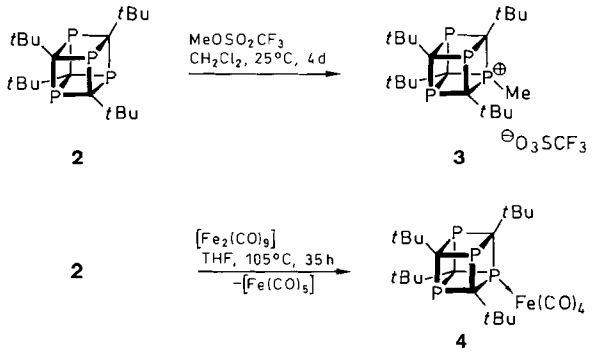

atoms are shifted to higher field (the exception is the fourfold bound phosphorus atom of **4**). The interactions of the lone pair at the P atom with the σ P/C bond,[7] characteristic for **2** and responsible for the extreme positions of the ^{13}C and ^{31}P resonance signals, occur in almost the same way only for a carbon atom as well as its $\lambda^3\sigma^3$-P neighbors. The tetracarbonyl iron complex was additionally confirmed by crystal structure analysis;[9] the molecule has *m* symmetry (Fig. 1).

As in **2**, the inner cyclic C–P–C bond angles in **4** are on average 3° smaller than in the cubane,[10] which naturally results in an opening of the P–C–P angle (Fig. 1). The increase of the exocyclic angles P1–C1–C11 (≡P1–C1′–C11′) and P1–C3–C31 (131.1(3) and 132.5(4)°, respectively, cf. **2**: 122°[11]) is noteworthy, which is almost certainly due to the steric interaction between *t*Bu groups and the [Fe(CO)$_4$] fragment.[11] This effect probably prevents a multiple complexation.

Table 1. Some selected physical data of the tetraphosphacubanes **3**–**11** [a,b].

3: Colorless crystals, m.p. 200 °C (decomp., from dichloromethane at −30 °C); ^{13}C NMR: $\delta = -25.2$ (dq, $^3J(P,C) = 29.0$ Hz, $^1J(P,C) = 6.9$ Hz, 1 framework C), 8.3 (d, $^1J(P,C) = 40.0$ Hz, 3 framework C), 23.5 (d, $^1J(P,C)$, = 19.0 Hz, P-CH_3), 120.2 (q, $^1J(C,F) = 318.0$ Hz, CF_3); ^{31}P NMR: δ =132.8 (s,1P), 213.0 (s, 3P)

4: Yellow crystals, m.p. 210 °C (decomp., from THF at −30 °C); ^{13}C NMR: $\delta = -25.0$ (m, 1 framework C), 2.8 (m, 3 framework C), 213.3 (d, $^2J(P,C) = 13.0$ Hz, CO); ^{31}P NMR: $\delta = 220.5$ (s, 3P), 258.0 (s, 1P)

5: Colorless crystalline powder, m.p. 205 °C (decomp., after washing with dichloromethane); ^1H NMR: $\delta = 1.1$ (s, broad, *t*Bu); ^{31}P NMR: $\delta = -10.6$ (s, 2P), −9.6 (s, 2P)[c]

6 [d]: Colorless crystals, m.p. 182 °C (from pet. ether 30–75 °C at −78 °C); ^{13}C NMR: $\delta = 45.2$ (t, $^1J(P,C) = 40.0$ Hz, 2 framework C), 85.2 (t, pseudo-t, $^1J(P,C) = 27.7$, 5.0 Hz, $^3J(P,C) = 5.0$ Hz, 2 framework C); ^{31}P NMR: $\delta = -18.6$ (s, 2P), −4.7 (s, 2P)

7: Colorless crystals, m.p. 181 °C (from pet. ether 30–75 °C at −30 °C); ^{13}C NMR: $\delta = 40.5$ (t, $^1J(P,C) = 32.5$ Hz, 2 framework C), 78.0 (t, pseudo-t, $^1J(P,C) = 26.1$, 5.4 Hz, $^3J(P,C) = 5.4$ Hz, 2 framework C), 161.8 (d, $^3J(P,C)$ = 45.6 Hz, N=CH); ^{31}P NMR: δ =13.0 (s, 2P), 32.9 (s, 2P)

8: Pale yellow crystals, m.p. 286 °C (from diethyl ether at −30 °C); ^{13}C NMR: δ =75.2 (dq, $^1J(P,C)$ =12.2 Hz, $^3J(P,C) = 3.0$ Hz, 1 framework C), 56.0 (d, pseudo-q, $^1J(P,C) = 29.0$, 4.6 Hz, $^3J(P,C) = 4.6$ Hz, 3 framework C; ^{31}P NMR: $\delta = 41.0$ (s with Se satellites, $^1J(P,Se) = 866$ Hz, 3P), −45.2 (s, 1P)

9: Colorless crystalline powder, m.p. 220 °C (decomp., after washing with pentane); ^1H NMR: δ =1.50 (s, *t*Bu); ^{13}C NMR: $\delta = 29.5$ [m, $C(CH_3)_3$], 45.5 [m, $C(CH_3)_3$], 111.2 (m, framework C); ^{31}P NMR: $\delta = -8.6$

10 [d]: Yellow-brown crystals, m.p. 250 °C (decomp., from diethyl ether at −78 °C); ^{13}C NMR: $\delta = -25.0$ (m, 2 framework C), 42.7 (d, $^1J(P,C)$ = 38.4 Hz, 6 framework C); ^{31}P NMR: δ =1.8(s, 2P), 118.0 (s, 6P)

11[d]: Yellow crystals, m.p. 195 °C (decomp., from pet. ether 30–75 °C at −78 °C); ^{13}C NMR: $\delta = -24.5$ (m, 2 framework C), 34.2 (d, $^1J(P,C)$ = 36.3 Hz, 6 framework C), 150.2 (d, $^3J(P,C) = 48.0$ Hz, N=CH); ^{31}P NMR: δ =71.5 (s, 2P), 140.7 (s, 6P)

[a] ^1H NMR (90 or 400 MHz, TMS), ^{13}C NMR (100.6 MHz, TMS), and ^{31}P NMR spectra (80.8 MHz, 85% H_3PO_4) in $CDCl_3$. [b] ^1H NMR data for *t*Bu groups were reported only for **5** and **9**; for all other cubanes they are in agreement with the given structure. The same is true for the ^{13}C NMR signals of the *t*Bu groups of **3**, **4**, and **6**–**11**. [c] Due to the low solubility in the usual solvents no ^{13}C NMR spectrum could be recorded. [d] In the mass spectrum (70 eV) a peak occrs for the molecular ion.

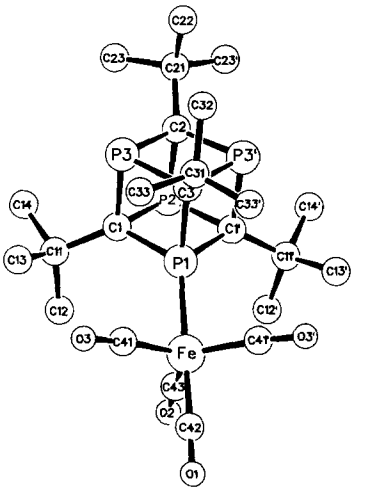

Fig. 1. Crystal structure of **4**. Selected bond distances [Å] and angles [°]: P1-Fe 2.235(2), P1-C1 1.884(4), P2-C1 1.879(4), P3-C1 1.881(4), P2-C2 1.866(6), P3-C2 1.872(4), P1-C3 1.865(5), P3-C3 1.883(4); C1-P1-Fe 127.7(1), C3-P1-C1 87.3(2), C2-P3-C1 86.9(2), C3-P3-C2 86.5(2), P3-C3-P3′ 93.1(2), P3-C1-P1 92.5(2), C11-C1-P1 131.1(3), C11-C1-P3 119.9(3), C21-C2-P2 122.6(4), P3-C3-P1 93.1(2), C31-C3-P3 118.0(2), C1-P2-C1′ 87.4(2), C3-P1-Fe 126.2(2), C2-P2-C1 87.1(2), C3-P3-C1 86.9(2), P3-C2-P3′ 93.7(3), P2-C1-P1 92.8(2), P3-C1-P2 92.6(2), C11-C1-P2 118.6(3), P3-C2-P2 93.3(2), C21-C2-P3 122.9(3), C31-C3-P1 132.5(4), C1-P1-C1′ 86.7(2).

Double functionalization at the phosphorus atom of **2** occurs upon reactions with tetrachloro-*o*-benzoquinone,[12] methyl azide, and 1-diazo-2,2-dimethylpropane. These afford cubanes, which apart from unchanged $\lambda^3\sigma^3$ phosphorus atoms still have phosphorane (**5**, 95%) and iminophosphorane units (**6**, **7**, each 85%). The Staudinger reaction (→ **6**) is successful only at higher temperature.[13] In no case does an excess of reagent lead to further oxidative reactions.

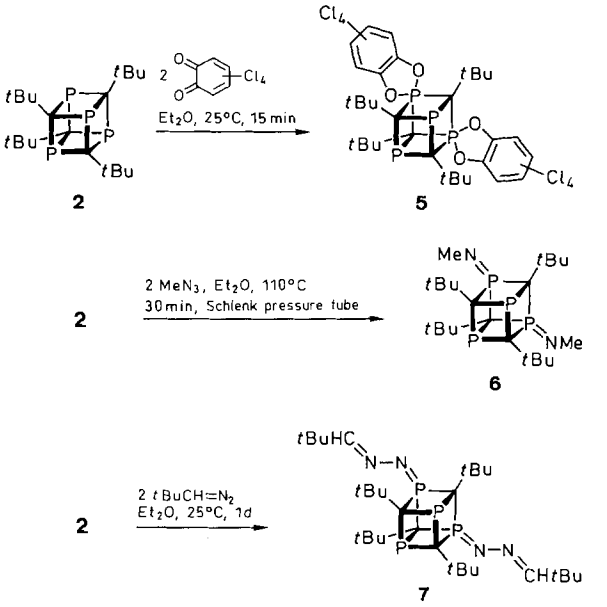

If the ^{13}C and ^{31}P NMR data of the cage atoms of **5**–**7** are compared with those of **2**,[1] **3**, and **4**, respectively (Table 1), then the resonance signals now clearly lie no longer at extreme values, a tendency, which continues with higher degrees of functionalization.

The highest degree of functionalization at the tetraphosphacubane system is achieved by the introduction of elements of Group 16: heating of **2** with an excess of selenium at 110 °C only led to the tris(selenoxo)tetraphosphacubane **8** (90%), however, the reaction of **2** with four equivalents of bis(trimethylsilyl)peroxide afforded the tetraoxide **9** (90%).[14]

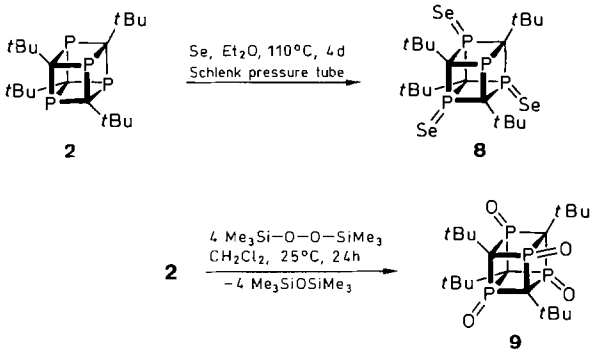

2 **8** **9**

The nonfunctionalized phosphorus atom in **8** resonates at $\delta = -45.2$, whereas the ylidic P atoms absorb at $\delta = 41.0$. A crystal structure analysis confirms the structure of **8** (Fig. 2).[9] The distortion from ideal cubic geometry with an

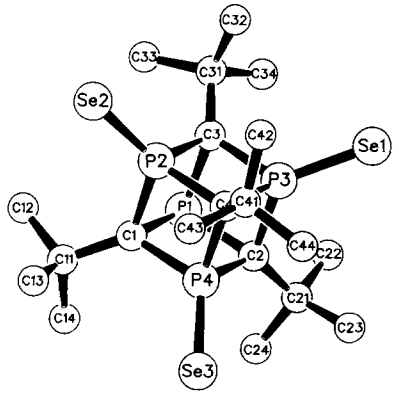

Fig. 2. Crystal structure of **9**. Selected bond distances [Å] and angles [°]: Se1-P3 2.066(3), Se3-P4 2.056(3), P1-C2 1.913(1), P2-C1 1.850(1), P2-C4 1.860(1), P3-C2 1.843(1), P4-C1 1.872(1), P4-C4 1.860(1), Se2-P2 2.056(3), P1-C1 1.914(1), P1-C3 1.901(1), P2-C3 1.856(1), P3-C3 1.863(1), P3-C4 1.859(1), P4-C2 1.828(1); C3-P1-C2 87.1(4), C3-P1-C1 86.7(4), C1-P1-C2 87.2(5), C1-P2-C3 89.9(5), C1-P2-C4 89.5(5), C3-P2-C4 88.7(4), C3-P3-C2 90.3(4), C3-P3-C4 88.5(4), C2-P3-C4 88.6(5), C1-P4-C2 91.1(5), C1-P4-C4 88.8(5), C2-P4-C4 88.9(5).

angle opening at the carbon atoms of only 1.2° (the angle at the phosphorus is correspondingly smaller) is not very large in comparison to that of the tetraphosphacubane **2** (4.4°!)[1] The exocyclic P–C–C bond angles at the nonoxidized phosphorus atom are reduced relative to those in **2** (122°)[1] by 4° to 118°. This is the reason why despite an excess of the oxidation reagent [in contrast to the introduction of oxygen (→ **9**) or sulfur[14]] the fourth phosphorus atom retains its $\lambda^3\sigma^3$ character.

The tetraoxide **9** shows high symmetry which is also illustrated by the small number of lines in the ^1H, ^{13}C, and ^{31}P NMR spetra (Table 1). The chemical shifts of the framework atoms (^{13}C NMR: $\delta = 111.2$; ^{31}P NMR $\delta = -8.6$) prove that the original donor phosphorus atoms in **2**[7] now have acceptor properties.

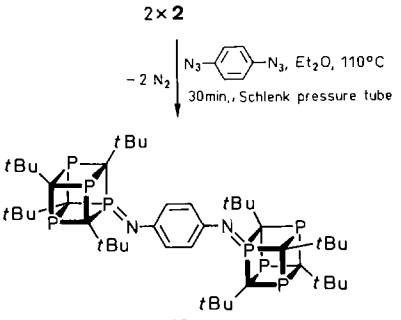

10

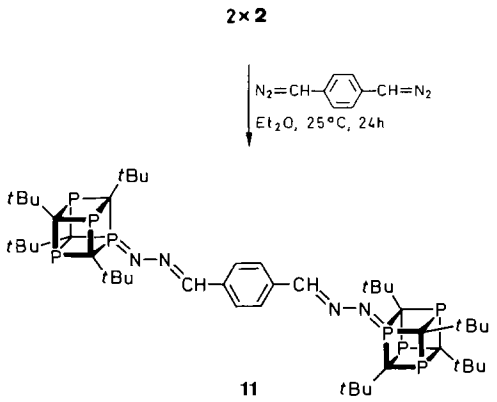

11

Two tetraphosphacubane **2** units can be coupled by a double Staudinger reaction with 1,4-diazidobenzene at 110 °C, whereby the phenylene-bridged bis(iminophosphorane) **10** (62%) is formed. Analogous coupling of **2** by twofold phosphazine formation with 1,4-bis(diazomethyl)-benzene affords **11** (52%).

Elemental composition as well as the NMR data (Table 1) prove the constitution of **10** and **11**. Noteworthy in both cases is the high field position of the framework carbon atoms in the ^{13}C NMR spectra, which without exception have $\lambda^3\sigma^3$ phosphorus atoms as neighboring atoms ($\delta = -25.0$ and -24.5, respectively; cf. with **3** and **4**)

Experimental Procedure

All reactions were carried out under argon in Schlenk tubes. Solvent, reaction temperature, and duration can be taken from the appropriate reaction equations. The reactions were monitored by ^{31}P NMR spectroscopy. After concentration, the residues were taken up in pentane and further purified as described in Table 1.

Received: January 28, 1992 [Z 5153 IE]
German version: *Angew. Chem.* **1992**, *104*, 870

CAS Registry numbers:
2, 121097-72-1; **3**, 141556-31-2; **4**, 141556-38-9; **5**, 141556-32-3; **6**, 141556-33-4; **7**, 141556-34-5; **8**, 141583-48-4; **9**, 141556-35-6; **10**, 141556-36-7; **11**, 141556-36-7; **11**, 141556-37-8; $[Fe_2(CO)_9]$, 15321-51-4; $MeOSO_2CF_3$, 333-27-7; MeN_3, 624-90-8; *t*-BuCH=N_2, 762-64-1; Se, 7782-49-2; Me_3Si-O-O-$SiMe_3$, 5796-98-5; *o*-$N_3C_6H_4N_3$, 2294-47-5; *o*-N_2=CHC_6H_4CH=N_2, 4054-70-0; tetrachloro-*o*-benzoquinone, 2435-53-2.

[1] T. Wettling, J. Schneider, O. Wagner, C. G. Kreiter, M. Regitz, *Angew. Chem.* **1989**, *101*, 1035–1037; *Angew. Chem. Int. Ed. Engl.* **1989**, *28*, 1013–1014.

[2] P. Binger, B. Biedenbach, C. Krüger, M. Regitz, *Angew. Chem.* **1987**, *99*, 798–799; *Angew. Chem. Int. Ed. Engl.* **1987**, *26*, 764–765.
[3] T. Wettling, B. Geißler, R. Schneider, S. Barth, P. Binger, M. Regitz, *Angew. Chem.* **1992**, *104*, 761; *Angew. Chem. Int. Ed. Engl.* **1992**, *31*, 758.
[4] H. Schumann, H. Benda, *Angew. Chem.* **1968**, *80*, 846; *Angew. Chem. Int. Ed. Engl.* **1968**, *7*, 813.
[5] M. Baudler, G. Scholz, K.-F. Tebbe, M. Feher, *Angew. Chem.* **1989**, *101*, 352–354; *Angew. Chem. Int. Ed. Engl.* **1989**, *28*, 339–341.
[6] A. H. Cowley, R. A. Jones, P. R. Harris, D. A. Atwood, L. Contreras, C. J. Burek, *Angew. Chem.* **1991**, *103*, 1164–1166; *Angew. Chem. Int. Ed. Engl.* **1991**, *30*, 1143–1145.
[7] R. Gleiter, K.-H. Pfeifer, M. Baudler, G. Scholz, T. Wettling, M. Regitz, *Chem. Ber.* **1990**, *123*, 757–760.
[8] ^{13}C NMR: $\delta = -29.1$; ^{31}P NMR: $\delta = +257.4$[1].
[9] Crystal structure analyses (Enraf-Nonius CAD4 diffractometer, monochromatic $Mo_{K\alpha}$ radiation, Full matrix refinement): **4** ($C_{24}H_{36}FeO_4P_4$, $M = 512.4$): monoclinic, space group $P2_1/m$ (No. 11), $a = 10.101(2)$, $b = 13.442(2)$, $c = 10.581(1)$ Å; $\beta = 105.09(1)°$; $V = 1378.1$ Å^3; $\rho_{calcd} = 1.361$ g cm^{-3}; $\mu = 8.0$ cm^{-1}; $Z = 2$; 2842 reflections measured in a hemisphere, of which 2349 were observed with $I > 2\sigma(I)$, $2.0 < \theta < 25.0°$; 219 variables; $R = 0.0537$, $Rw = [\Sigma w \Delta^2 F / w F_0^2]^{1/2} = 0.0649$;. maximum shift/error ratio 1.18. **8** ($C_{20}H_{36}P_4Se_3$, $M = 637.3$): orthorhombic, space group $P2_12_12_1$ (No. 19), $a = 11.270(2)$, $b = 21.882(3)$, $c = 10.791(2)$ Å; $V = 2661.2$ Å^3, $\rho_{calcd} = 1.591$ g cm^{-3}; $\mu = 43.5$ cm^{-1}; $Z = 4$, 2933 independent reflections measured, of which 2196 were considered in the refinement with $I > 2\sigma(I)$; 25 reflections in the range $2.0 < \theta < 25.0°$ served for the determination of the unit cell. Number of parameters 292; $R = 0.0621$; $Rw = [\Sigma w \Delta^2 F / w F_0^2]^{1/2} = 0.0519$; maximum shift/error ratio 0.701. Further details of the crystal structure investigation may be obtained from the Fachinformationszentrum Karlsruhe, Gesellschaft für wissenschaftlich-technische Information mbH, D-W-7514 Eggenstein-Leopoldshafen 2 (FRG) on quoting the depository number CSD-56059, the names of the authors, and the journal citation.
[10] E. B. Fleischer, *J. Am. Chem. Soc.* **1964**, *86*, 3889–3890.
[11] The bending away of the equatorial CO groups at the iron is probably due to the same reason: Fe–C41–O3 (≡Fe–C41'–O3') 174.0(4), Fe–C43–O2 173.7(6)°; as expected the angle Fe–C42–O1 is 179.9(0)°.
[12] Double [4+1] cycloaddition onto **2** is also achieved with azodicarboxylate; for this, the O=C–N=N unit of the latter reacts as a hetero-1,3-diene: pale yellow crystals, m.p. 189° (decomp.): ^{13}C NMR: $\delta = 47.4$ (m, 2 framework C), 68.5 (m, 2 framework C); ^{31}P NMR: $\delta = -10.3$ (s, broad, 2P), -6.7 (s, 2P).
[13] The more electrophilic *p*-tosylazide adds even at room temperature to the monotriazene [colorless crystals, m.p. 187 °C (decomp.)]. In $CDCl_3$ at the same temperature it decomposes slowly with loss of N_2 to the *p*-tosyliminotetraphosphacubane [colorless crystals, m.p. 211 °C; ^{31}P NMR: $\delta = 37.4$ (1P), 141.2 (3P)].
[14] The reaction of **2** with sulfur (in the presence of triethylamine), in which one to four thioxo groups can be introduced depending on the stoichiometry will be the subject of a future report.

Pronounced Conformational Changes in Sixfold Nitrogen-Functionalized Metacyclophanes: Syntheses and Crystal Structures of Two 1,10-Diaza[11]metacyclophanes**

By *J. Jens Wolff,* Stephen F. Nelsen, Douglas R. Powell,* and *Bernhard Nuber*

Many metacyclophanes are strained molecules that have received widespread attention.[1] For steric reasons, the central six-membered ring is forced into a boat conformation, particularly by small bridges. Therefore, many cyclophanes have not been prepared by direct annelation of the bridge, but by ring contraction, rearrangement of bridges, or formation of the benzene ring in the final step.[1] We and others have found the benzene core of tris(donor)-substituted 1,3,5-trinitrobenzene derivatives **1** to be strongly distorted into boat[2a–b, 3] or twist boat[2a–c] forms, mainly for electronic reasons. This propensity for bending could be put to advantage for the facile construction of sixfold nitrogen-functionalized metacyclophanes **3**. They would also be frozen in a boat form for steric resons, unlike compounds of type **1**, which exist as an interconverting mixture of boat and twist-boat forms in solution.[2c] Reduction of the nitro groups in **3**, however, should eliminate the electronic bias for a bent conformation, and **4** should be a strained molecule with an essentially planar benzene ring.[1] As a derivative of hexaaminobenzene, **4** should be easily oxidized and would yield stable cations on appropriate substitution.[4, 5] In this paper, we report on the preparations of **3a** and **4a**, as well as their X-ray crystallographic characterization.

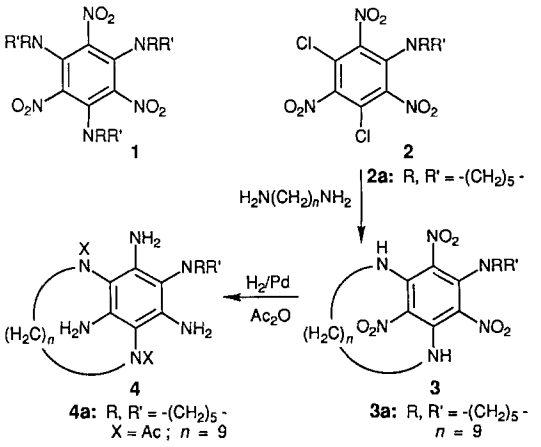

By nucleophilic aromatic substitution of halogen in **2a** with 1,9-nonanediamine, metacyclophane **3a** was obtained in a surprisingly high yield of 67%, without use of special dilution procedures. By this method, a wide range of compounds of type **3** may be synthesized.[6] The X-ray analysis for **3a** (Fig. 1) yields a highly deformed central six-membered ring, adopting a nearly ideal[7] boat conformation; the sum of absolute dihedral angles[8] within the ring is 169.8(1.0)°. To our knowledge, this is the highest amount of distortion found in experimentally accessible cyclophanes and compounds of type **1**. The average length of 1.446(13) Å for the endocyclic C–C bonds is markedly larger than the expected value for benzene derivatives (1.39–1.40 Å); the exocyclic C–N bonds, however, are markedly shortened. For comparison, measured C–N bond lengths for hexakis(dimethylamino)benzene[5] are 1.440, and 1.480 Å for 1,3,5-trinitrobenzene;[9] the corresponding averaged C–N bond lengths in **3a** are 1.311(9) and 1.381(9) Å, respectively. A description of the electronic structure of **3a** is therefore weighted in favor of a [6]radialene form. An additional contribution from a quinoid resonance form is implied by the strong bond-length alternation within the ring: the bonds between C2 and C3, and C5 and C6 are shorter than the other C–C bonds by about 0.03 Å; C1–N1 is shorter than the other C–N(amino) bonds by 0.01 Å. In agreement, the piperidine nitrogen (N1) is planar (the average bond angle α_{av} is 120.0(8)°), and the

[*] Dr. J. J. Wolff
Organisch-chemisches Institut der Universität
Im Neuenheimer Feld 270, D-W-6900 Heidelberg (FRG)
Prof. Dr. S. F. Nelsen, Dr. D. R. Powell
Department of Chemistry, University of Wisconsin, Madison, WI (USA)
Dr. B. Nuber
Anorganisch-chemisches Institut der Universität Heidelberg

[**] Structures of Tris(Donor)-Tris(Acceptor)-Substituted Benzenes, Part 4. This work was supported by Prof. Dr. R. Gleiter (Heidelberg), Deutsche Forschungsgemeinschaft (through SFB 247), and the National Institutes of Health (GM 29549). J. J. W. thanks the Alexander-von-Humboldt-Foundation for a Feodor-Lynen, and the Fonds der Chemischen Industrie for a Liebig fellowship. We would also like to thank the referees for helpful comments. – Part 3: [2a].

two six-membered rings are not twisted relative to each other in order to achieve maximum quinoid donor–acceptor conjugation to the nitro group in *para* position (N4). The nitrogen atoms within the bridge are also in a planar environment. The double-bond character of these short C–N bonds will contribute to the increase in the barrier for ring inversions of the bridge and the unsaturated ring: on the NMR time scale at 298 K the molecule shows neither ring inversion of the "benzene" core – in contrast to **1** – nor ring flip of the cyclophane bridge[10] (in contrast to all-carbon bridged unfunctionalized cyclophanes[1]).

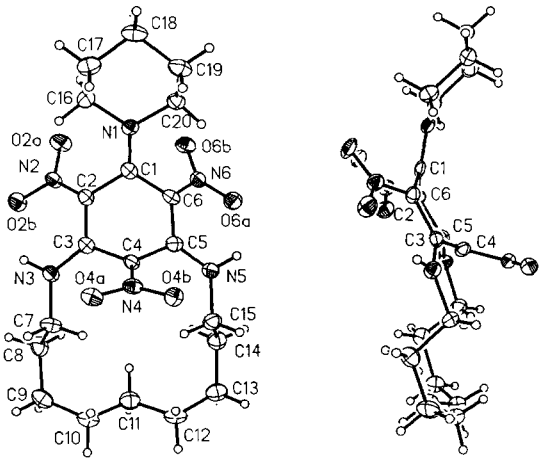

Fig. 1. Two ORTEP views of **3a**; the cosolvating dichloromethane molecules have been omitted for clarity. Selected bond lengths [Å], angles, and dihedral angles [°]: C1-C2 1.463(6), C2-C3 1.429(5), C3-C4 1.456(6), C4-C5 1.447(5), C5-C6 1.423(5), C6-C1 1.459(5), C1-N1 1.304(5), C3-N3 1.316(5), C5-N5 1.313(5), C2-N2 1.373(5), C4-N4 1.385(3), C6-N6 1.386(4); C1 → C3 115.7(3), C2 → C4 114.8(4), C3 → C5 117.5(3), C4 → C6 114.5(3), C5 → C1 116.4(3), C6 → C2 113.8(3); C1 → C4 − 0.5(4), C2 → C5 − 40.0(4), C3 → C6 37.2(5), C4 → C1 5.6(5), C5 → C2 − 44.8(4), C6 → C3 41.7(3).

The semiquantitative "cyanine concept"[11] for systems that evade aromaticity on electronic grounds (Jahn–Teller type distortions) predicts the decomposition of the benzene ring in **3** into two trimethine cyanine subunits. This pattern is frequently encountered in polyamino-substituted benzene dications,[5, 12] and leads to rings in a twist conformation with four short and two long bonds. However, a cross-conjugated quinone with two short and four long bonds is found in **3a** rather than one (at least formally) positively and one negatively charged trimethine cyanine unit, which might be expected in analogy to known structures. A twist conformation is not accessible to **3a** for steric reasons, which may explain the different behavior.[13]

Cyclophane **3a** was reduced catalytically, and the air-sensitive hexaaminobenzene derivative **4** thus formed was protected as its diacetate **4a**. Reduction of the nitro groups restores the aromatic system: **4a** (Fig. 2) contains a "normal" benzene ring with small deviations from planarity (sum of the absolute dihedral angles is 25.3(3.4)°). Nearly two thirds of this torsion is due to the relief of steric congestion resulting from the amino groups and the piperidine ring: the highest values for dihedral angles are found around the C1–C2 and C1–C6 bonds (Fig. 2). For the same reason, the piperidine nitrogen is in an almost planar environment ($\alpha_{av} = 118.3(1.5)°$), and the piperidine ring adopts a position perpendicular to the benzene nucleus. In agreement, the rotation of the piperidine ring around the C–N bound in **4a** is frozen on the NMR time scale at room temperature.[14]

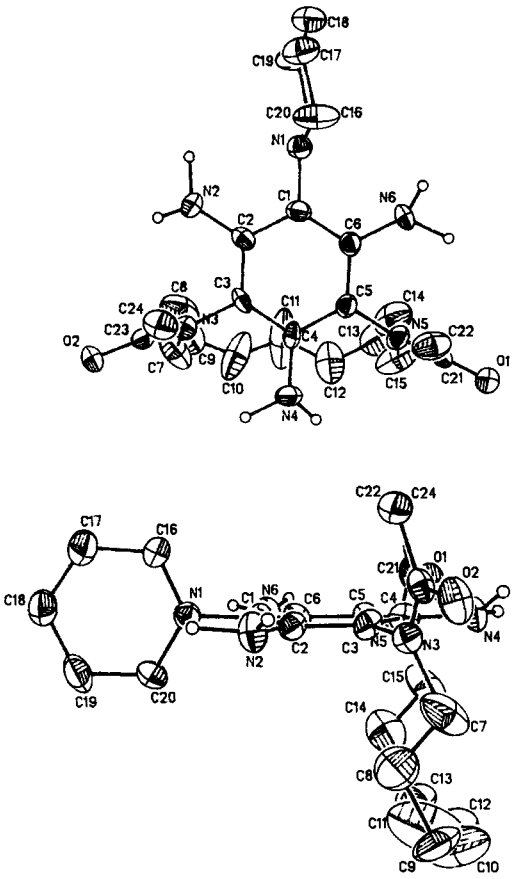

Fig. 2. Two ORTEP views of **4a**; the cosolvating, twofold disordered dichloromethane molecule has been omitted for clarity. Selected bond lengths [Å], angles, and dihedral angles [°]: C1-C2 1.398(15), C2-C3 1.431(16), C3-C4 1.397(13), C4-C5 1.407(14), C5-C6 1.428(16), C6-C1 1.397(14); C1-N1 1.454(15), C3-N3 1.440(13), C5-N5 1.437(12), C2-N2 1.389(13), C4-N4 1.399(15), C6-N6 1.386(14); C1 → C3 117.8(9), C2 → C4 123.0(9), C3 → C5 117.1(10), C4 → C6 121.5(8), C5 → C1 119.2(9), C6 → C2 120.9(11); C1 → C4 − 2.5(15), C2 → C5 − 2.8(14), C3 → C6 3.3(14), C4 → C1 1.7(14), C5 → C2 −7.3(14), C6 → C3 7.7(14).

Both **3a** and **4a** crystallize with inclusion of methylene chloride; cocrystals are often formed with compounds of type **1**.[2a] Work on cosolvates[15] of **1**, **3**, and **4** is in progress.

Experimental Procedure

All new compounds gave correct microanalytical data for C, H, N, Cl.

2a: From 1,3,5-trichloro-2,4,6-trinitrobenzene[16] by reaction with piperidine; m.p. = 196–197 °C (corr.). ^{1}H NMR ($CDCl_3$, 270 MHz): δ = 1.58 (br. m, 6H), 3.06 (br. m, 4H); ^{13}C NMR ($CDCl_3$, 68 MHz): δ = 23.18, 25.80, 52.10, 122.19, 140.58, 142.89, 145.93.

3a: Within two days a solution of 1,9-nonanediamine (395 mg, 2.50 mmol) and dry ethyldiisopropylamine (700 mg, 5.42 mmol) in dry CH_2Cl_2 (40 mL) was added under nitrogen to a stirred, refluxing solution of **2a** (902 mg, 2.47 mmol) in CH_2Cl_2 (300 mL). Heating was continued under reflux for 6 days. After workup, chromatography on basic alumina yielded cyclophane **3a** as a bright yellow powder; m.p. 250–251 °C (decomp., corr.) (740 mg, 1.64 mmol, 66.5%); ^{1}H NMR (CD_2Cl_2, 270 MHz): δ = 1.18–1.50 (m, 10H), 1.63–1.78 (m, 6H), 1.94 (br. m, 4H), 3.40 (ddt, J = 9.5, 14.2, 7.9 Hz, 2H), ca. 3.60 (br. m, 4H), 3.66 (dddd, J = 2.4, 5.9, 8.0, 14.0 Hz, 2H), 10.38 (br.d, J = 7.7 Hz, 2H); ^{13}C NMR (CD_2Cl_2, 68 MHz): δ = 22.23, 23.52, 25.16, 25.72, 26.03, 28.38, 48.55, 55.75, 103.82, 114.15 (double intensity), 152.13 (double intensity), 158.46. X-ray analysis: A yellow prism (0.20 × 0.30 × 0.50 mm) was grown from CH_2Cl_2. $C_{20}H_{30}N_6O_6 \cdot 2CH_2Cl_2$ (620.4); triclinic, $P\bar{1}$, a = 11.121(3), b = 11.560(5), c = 12.817(3) Å; α = 100.34(3), β = 103.12(2), γ = 113.87(2)°, Z = 2; $\varrho_{(calcd)}$ = 1.474 g cm^{-3}. Absorption coefficient = 4.342 mm^{-1}. $F(000)$ = 648. Diffractometer: Siemens P3f, $Cu_{K\alpha}$, −165(2) °C, highly oriented graphite crystal monochromator; 2θ range: 4.0–114.0°, scan type: Wyckoff, scan speed: variable 2.00–12.00° min^{-1} in ω; range: 0.40° (ω). 4194 reflections collected, 3779 independent (R_{int} = 0.0410), 3779 observed ($F > 4.0\sigma(F)$); no absorption correction. Solution by direct methods (Siemens SHELXTL PLUS

(VMS)[17]), full-matrix least-squares refinement. Hydrogen atoms: riding model, isotropic U. Weighting scheme: $\omega^{-1} = \sigma^2(F) + 0.0006F^2$; 345 parameters refined; final R indices (observed and all data): 0.00675 ($R_w = 0.00820$), Gof: 2.38, largest and smallest difference peak (residual electron density primarily around the CH_2Cl_2 molecules): 0.63 and -0.94 eÅ^{-3}.[18].

4a: A suspension of **3a** (300 mg, 0.666 mmol) in ethyl acetate (15 mL) was hydrogenated over 10% Pd/C (100 mg) for 5 days at 65 °C. Acetic anhydride (0.5 mL) was added, and the mixture filtered after 15 min. Chromatography on basic alumina gave the diacetate **4a** (202 mg, 0.454 mmol, 68%); m.p. 290–295 °C (decomp.); ^{1}H NMR ($CDCl_3$, 300 MHz): $\delta = 1.00-1.28$ (m, 8H), 1.33–1.58 (m, 8H), 1.67 (br. s, 4H), 1.93 (s, 6H), 3.01 (m, 4H), 3.66 (centered m, 4H), 3.74 (br. s, 2H), 4.02 (br. s, 4H), ^{13}C NMR ($CDCl_3$, 75.5 MHz): $\delta = 21.46$, 24.21, 25.10, 25.49, 25.94 (double intensity), 27.76, 27.80, 43.69, 50.97, 51.05, 105.02, 114.94, 138.55, 142.95, 173.55. – X-ray analysis: Colorless prisms were grown from CH_2Cl_2/light petroleum by the vapor diffusion technique, and a crystal of $0.15 \times 0.20 \times 0.25$ mm was selected. Slow evaporation of the cosolvating dichloromethane was observed. $C_{24}H_{40}N_6O_2 \cdot CH_2Cl_2$ (529.6); triclinic, $P\bar{1}$, $a = 10.82(1)$, $b = 10.99(1)$, $c = 13.21(1)$ Å; $\alpha = 94.6(7)$, $\beta = 103.28(7)$, $\gamma = 105.10(7)°$, $Z = 2$; $\varrho_{(calcd)} = 1.21$ gcm^{-3}. Absorption coefficient = 0.25 mm^{-1}, $F(000) = 568$. Diffractometer: Syntex R3, $Mo_{K\alpha}$, 25 °C, 2θ range: 3.0–43.0°, scan type: ω. 3403 reflections collected; 1750 with $F > 2.5\sigma(F)$; empirical absorption correction (5 reflections $9.5 < 2\theta < 38.5°$, transmission min. 0.79, max. 1.00). Solution by direct methods (Siemens SHELXTL PLUS (VMS) [17]), full-matrix least-squares refinement. Hydrogen atoms: riding model, isotropic U. 354 parameters refined; R indices (observed data): 0.095 ($R_w = 0.082$), Gof: 3.44, largest and smallest difference peak: 0.38 and -0.29 eÅ^{-3}. The crystal decomposed slightly during the measurement. [18].

Received: February 25, 1992 [Z 5209 IE]
German version: *Angew. Chem.* **1992**, *104*, 899

CAS Registry numbers:
2a, 141510-04-5; **3a**, 141510-05-6; **4a**, 141510-06-7; $H_2N(CH_2)_9NH_2$, 646-24-2.

[1] P. M. Keehn, S. M. Rosenfeld, *Cyclophanes*, Academic Press, New York, **1983**; *Top. Curr. Chem.* **1983**, *113*; ibid. **1983**, *115*; F. Vögtle, *Cyclophanchemie*, Teubner, Stuttgart, **1990**; F. Bickelhaupt, *Pure Appl. Chem.* **1990**, *62*, 373; L. W. Jenneskens, H. J. R. DeBoer, W. H. Wolf, F. Bickelhaupt, *J. Am. Chem. Soc.* **1990**, *112*, 8941 and references cited therein. For the synthesis of pyridino-metacyclophanes by coupling reactions with di-Grignard reactions, see: K. Tamao, S. Kodama, T. Nakatsuka, Y. Kiso, M, Kumada, *ibid.* **1975**, *97*, 4405.

[2] a) J. J. Wolff, S. F. Nelsen, D. R. Powell, *J. Org. Chem.* **1991**, *56*, 5908; b) J. J. Wolff, S. F. Nelsen, P. A. Petillo, D. R. Powell, *Chem. Ber.* **1991**, *124*, 1719; c) J. J. Wolff, S. F. Nelsen, D. R. Powell, J. M. Desper, *ibid.* **1991**, *124*, 1727.

[3] J. M. Chance, B. Kahr, A. B. Buda, J. S. Siegel, *J. Am. Chem. Soc.* **1989**, *111*, 5940.

[4] See for example: D. A. Dixon, J. C. Calabrese, R. L. Harlow, J. S. Miller, *Angew. Chem.* **1989**, *101*, 81; *Angew. Chem. Int. Ed. Engl.* **1989**, *28*, 92 and references cited therein.

[5] J. M. Chance, B. Kahr, A. B. Buda, J. P. Toscano, K. Mislow, *J. Org. Chem.* **1988**, *53*, 3226.

[6] Monoalkylamines, e.g., 2,2-dimethylpropyl-, *iso*-propyl-, and *tert*-butylamine, have also been used successfully for the synthesis of **2** and **3** in comparable yields (J. J. Wolff, I. Bolocan, unpublished results).

[7] An ideal boat form requires two internal torsional angles of α, two of $-\alpha$, and two of 0°.

[8] Instead of calculating angles between planes defined by ring carbon atoms (see, e.g., G. Maas, J. Fink, H. Wingert, K. Blatter, M. Regitz, *Chem. Ber.* **1987**, *120*, 819) we have used the sum of absolute torsional angles as a single parameter to characterize the amount of ring distortion [2a]. An exponential correlation exists [2c] between the averaged C-C bond length within the ring and the sum of the dihedral angles, which also holds in the case of **3a**.

[9] T. S. Choi, J. E. Abel, *Acta Crystallogr. Sect. B* **1972**, *28*, 193.

[10] The protons for the methylene groups next to all amino nitrogen atoms are diastereotopic.

[11] S. Dähne, F. Moldenhauer, *Prog. Phys. Org. Chem.* **1985**, *15*, 1 and literature cited therein.

[12] See, for example: K. Elbl, C. Krieger, H. A. Staab, *Angew. Chem.* **1986**, *98*, 1024; *Angew. Chem. Int. Ed. Engl.* **1986**, *25*, 1023; J. S. Miller, D. A. Dixon, J. C. Calabrese, C. Vazquez, P. J. Krusic, M. D. Ward, E. Wasserman, R. L. Harlow, *J. Am. Chem. Soc.* **1990**, *112*, 381; H. A. Staab, J. Hofmeister, C. Krieger, *Angew. Chem.* **1991**, *103*, 1003; *Angew. Chem. Int. Ed. Engl.* **1991**, *30*, 1030; H. Bock, K. Ruppert, C. Näther, Z. Havlas, *ibid.* **1991**, *103*, 1194 and **1991**, *30*, 1180. The first experimental evidence for cyanine structures in charged polyamino benzene derivatives is found in H. Köhler, G. Scheibe, *Z. Anorg. Allg. Chem.* **1956**, *285*, 221.

[13] Investigations on the electronic situation in **1** and **3** by computational methods will be pusblished elsewhere.

[14] The ^{13}C NMR spectrum shows that all carbon atoms of the pipridine ring are nonequivalent, whereas the benzene ring has C_s symmetry (four signals). Hence, the piperidine ring undergoes fast ring inversion, but the flip of the cyclophane bridge and the rotation of the piperidine ring around the C-N bond is slow.

[15] For cosolvates, see M. C. Etter, S. M. Reutzel, *J. Am. Chem. Soc.* **1991**, *113*, 2586 and references cited therein; E. Weber, S. Finge, I. Csöregh, *J. Org. Chem.* **1991**, *56*, 7281; *Top. Curr. Chem.* **1987**, *140*; *ibid.* **1988**, *149*.

[16] P. Engelbertz (Chemische Fabrik Griesheim), D.R.P. 767510, **1936**; *Chem. Abstr.* **1955**, *49*, 14803d; M. E. Hill, F. Taylor, Jr., *J. Org. Chem.* **1960**, *25*, 1037.

[17] G. M. Sheldrick, SHELXTL PLUS, Versions 4.2 (**3a**) and 3.4 (**4a**); Siemens Analytical X-ray Instruments, Madison, WI, **1990**, and Nicolet Instrument Corporation, **1988**, respectively.

[18] Further details of the crystal structure determinations are available on request from the Fachinformationszentrum Karlsruhe, Gesellschaft für wissenschaftlich-technische Information mbH, D-W-7514 Eggenstein-Leopoldshafen 2, on quoting the depository number CSD-56231, the names of the authors, and the journal citation.

Dynamic Motion in $[HFe(CO)_4]^-$ Ions as Observed by Mössbauer Spectroscopy—Evidence for Hydride "Tunneling"**

By *Gary J. Long,* Fernande Grandjean,* and *Kenton H. Whitmire*

Solution[1–3] and solid-state[4–8] MAS ^{13}C NMR spectroscopy (MAS = *M*agic *A*ngle *S*pinning) as well as Mössbauer spectroscopy,[9–11] have proven useful methods in revealing molecular dynamics in organometallic compounds and clusters. Herein, we report the first study of the dynamic motion of the iron atom in several salts containing the $[HFe(CO)_4]^-$ anion by Mössbauer spectroscopy. Hanson and Whitmire[8] have found that MAS ^{13}C NMR spectra of **1** and **2** show dynamic exchange of the axial and equato-

$[(Ph_3P)_2N][HFe(CO)_4]$ **1** $[Et_4N][HFe(CO)_4]$ **2**

rial carbonyl ligands in $[HFe(CO)_4]^-$. This exchange may result from either a Berry pseudorotation[12] or, perhaps more likely, from "tunneling" of the hydrido ligands within the anion ("tunneling" here refers to a change of position not to the tunnel effect in quantum chemistry). These authors reported an activation energy of 29 ± 3 kJ mol^{-1} for the axial–equatorial exchange in **2**. The displacement of the iron atom as determined by Mössbauer spectroscopy provides strong support for the existence of hydride tunneling in the anion.

The Mössbauer spectra at 78 K[13] of **1**, **2**, and the $[Me_4N]^+$ salt **3** are all very similar and show a single quadrupole doublet. In contrast the Mössbauer spectra at 295 K[14]

$[Me_4N][HFe(CO)_4]$ **3**

[*] Prof. G. J. Long
Department of Chemistry
University of Missouri-Rolla
Rolla, MO 65401 (USA)
Prof. F. Grandjean
Institut de Physique, B5, Université de Liège (Belgium)
Prof. K. H. Whitmire
Rice University, Texas (USA)

[**] This work was supported by the Petroleum Research Fund, administered by the American Chemical Society, and a NATO Cooperative Scientific Research Grant (No. 86/685).

are quite different; **1** exhibits a quadrupole doublet, **2** exhibits a highly broadened absorption profile, and **3** gives no observable absorption spectrum at this temperature. The logarithm of the area beneath the absorption bands plotted against temperature (Fig. 1) reveals a departure from the expected linear behavior of the Debye model[10] above ca. 240 K for **1**, above ca. 220 K for **2**, and above ca. 180 K for **3**. The very small areas under the absorption bands, and hence recoil-free fractions, observed at higher temperatures, result from a motion of the iron atom. In the case of **2**, the temperature at which the onset of this motion occurs is coincident with the coalescence temperature for the signals of the equatorial and axial carbonyl ligands in the MAS ^{13}C NMR spectrum.[8] Unfortunately, the solid-state structures of **2**[8] and **3** are unknown, but the structure determination[15] of **1** at room temperature reveals that the $[HFe(CO)_4]^-$ ion has a structure which is intermediate between a hydride face-capped tetrahedron and a trigonal bipyramid in which the hydride occupies an axial position.

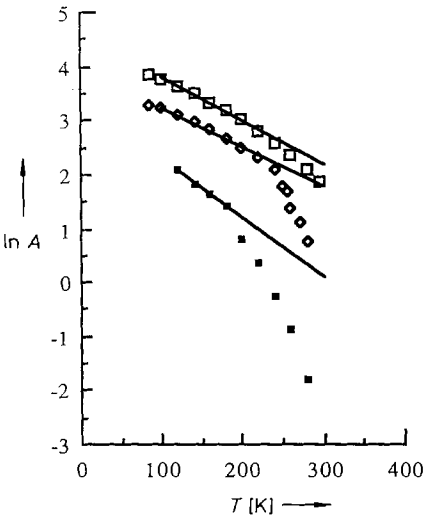

Figure 1. The temperature dependence of the logarithm of the area under the absorption band for **1** (□), **2** (◇), and **3** (■). The logarithmic scale has not been normalized and hence the relative values for the different compounds are arbitrary.

The dynamics of the iron motion, as reflected in the temperature dependence of the logarithm of the area under the absorption bands in the Mössbauer spectrum, may be treated in a fashion similar to that used to understand hydride diffusion in niobium.[16] The temperature dependence of the recoil-free fraction, which is proportional to the area under the absorption band, may be written as Equation (1), where

$$f_{eff}(T) = f_{vib}(T) f_{str}(T) \quad (1)$$

$f_{vib}(T)$ is the normal recoil-free fraction arising from lattice vibrations and $f_{str}(T)$ accounts for the loss of the area under the absorption band due to the local displacement of the iron center during the dynamic process. The magnitude of the dynamic displacements expected for the iron atom, f_{str}, is given by Equation (2), where k is the wavenumber of the

$$f_{str} = \exp(-k^2 \langle u^2 \rangle_{str}/3) \quad (2)$$

14.4 keV γ-ray and $\langle u^2 \rangle_{str}$ is the mean-square displacement of the iron atom. The linear behavior of the Debye model (see Fig. 1), between 85 and 240 K for **1**, 85 and 220 K for **2**, and 85 and 180 K for **3**, yields the Debye temperatures, θ_D, given in Table 1. This table also includes the effective recoil mass M_{eff}, which may be obtained from the temperature dependence of the isomer shift, and the resulting Mössbauer temperature.[10] The observed values of these parameters are

Table 1. Lattice properties of $[HFe(CO)_4]^-$ salts **1**–**3** derived from the Mössbauer spectra.

Salt, cation	**1**, $[(Ph_3P)_2N]^+$	**2**, $[Et_4N]^+$	**3**, $[Me_4N]^+$
Fe displacement [Å] [a]	0.11	0.26	0.34
ΔE_{act} [kJ mol^{-1}]	[b]	29.2	9.7
$d\ln A/dT$ [K^{-1}] [c]	-8.20×10^{-3}	-7.40×10^{-3}	$-1.10 \times 10.^{-2}$
θ_D [K]	129	135	111
$d\delta/dT$ [mm s^{-1} K^{-1}]	-3.98×10^{-4}	-3.79×10^{-4}	-3.84×10^{-4}
M_{eff} [g mol^{-1}]	108	125	112
θ_M [K]	81	109	83

[a] Determined at 280 K. [b] Too few data points were available to obtain a reliable value. [c] A = area under the absorption bands (Fig. 1).

characteristic of organoiron compounds.[10] At higher temperatures $f_{vib}(T)$ can be calculated from the straight lines in Figure 1. The values of $f_{str}(T)$ and $\langle u^2 \rangle_{str}$ may be obtained from Equations (1) and (2), in conjunction with the measured area under the absorption band and the calculated $f_{vib}(T)$. The resulting root-mean-square iron displacements at 280 K are given in Table 1. In **2**,[15] the Fe–$C_{carbonyl}$ distance is approximately 1.7 to 1.8 Å, and hence the displacement of the iron atom observed at 280 K represents about 15% of the bond length. If we assume similar Fe–$C_{carbonyl}$ lengths in **1** and **3**, a very reasonable assumption, then the corresponding values would be 6 and 20%, respectively. The displacements of the iron atoms observed in **2** and **3** are far larger than would be expected for a Berry pseudorotation and strongly support the hypothesis of tunneling of the hydride ion between the faces of the tetrahedral or pseudotetrahedral $[Fe(CO)_4]$ moiety. This was proposed earlier by Hanson and Whitmire[8] on the basis of their MAS ^{13}C NMR results. A similar "tetrahedral tunneling" mechanism was proposed for the non-quantum mechanical tunneling of hydrido ligands without motion of the other ligands in several octahedral dihydridoiron complexes with phosphorus ligands.[17]

If we assume that the displacement of the iron atom is induced by the hydride tunneling, the change of $\langle u^2 \rangle_{str}$ with temperature[18] is proportional to $\exp(-\Delta E_{act}/k_B T)$, where ΔE_{act} is the activation energy for the displacement of the iron atom and hence for the tunneling. The corresponding activation energies for **2** and **3**, which were obtained from Figure 2, are given in Table 1. The activation energy of 29.2 kJ mol^{-1} for **2** is identical to the value determined from ^{13}C NMR spectroscopy,[8] but substantially smaller than those reported for the octahedral dihydroiron complexes.[17] The very large observed displacement of the iron atom strongly supports a hydride tunneling in preference to the alternate Berry pseudorotation[12] as the mechanism which exchanges the axial and equatorial carbonyl ligands in the solid state. We propose that, simultaneously with the tunneling of the hydrido ligand, the iron atom moves to one of the four apexes of a smaller, perhaps distorted, tetrahedron imbedded within the pseudotetrahedral environment of the carbonyl ligand.

For **2**, the shape of the absorption bands gradually changes from a narrow symmetric quadrupole doublet (85 K)[13] to a broad absorption band (295 K),[14] a broadening which can

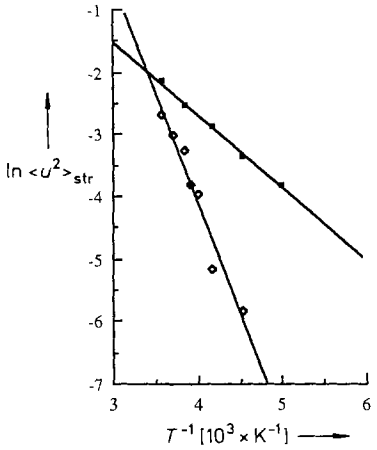

Figure 2. The logarithm of the mean square displacement of the iron atoms versus the reciprocal of the temperature for **3** (■) and **2** (◇).

be attributed to the previously discussed dynamic process. This behavior corresponds to a distinct increase in the symmetry of the electronic arrangement about the iron center, presumably because the hydride tunneling averages the electric field gradient at the iron center to zero. Thus it is possible to use the Tjon–Blume[19] model to fit the observed broadening of the absorption bands in the Mössbauer spectrum. The logarithm of the resulting rate of the dynamic process, versus the inverse temperature, gives an activation energy of 27 ± 3 kJ mol^{-1} for **2**. This value agrees rather well with the 29 kJ mol^{-1} obtained above, especially when one considers that the values are obtained in a completely different fashion. We are currently studying other salts of $[HFe(CO)_4]^-$ in an effort to understand the way in which different cations influence the tunneling process. Furthermore inelastic neutron scattering experiments with deuterated $[HFe(CO)_4]^-$ are planned.

Experimental Procedure

Compounds **1**, **2**, and **3** have been prepared by modifications of previously published procedures. [8, 20] The Mössbauer spectra were recorded as described earlier and the isomer shifts are reported relative to α-iron foil at room temperature. [11]

Received: January 14, 1992 [Z 5118 IE]
German version: *Angew. Chem.* **1992**, *104*, 891

CAS Registry numbers:
1, 56791-54-9; **2**, 25879-01-0; **3**, 63814-56-2; $[HFe(CO)_4]^-$, 18716-80-8.

[1] P. Meakin, E. L. Muetterties, J. P. Jesson, *J. Am. Chem. Soc.* **1972**, *94*, 5271.
[2] P. Meakin, J. P. Jesson, F. N. Tebbe, E. L. Muetterties, *J. Am. Chem. Soc.* **1971**, *93*, 1797.
[3] J. P. Jesson, P. Meakin, *J. Am. Chem. Soc.* **1973**, *95*, 1344.
[4] S. Aime in *The Time Domain in Surface and Structural Dynamics* (Eds.: G. J. Long, F. Grandjean), Kluwer, Dordrecht, **1988**, pp. 65–80.
[5] H. W. Spiess, R. Grosescu, U. Haeberlen, *Chem. Phys.* **1974**, *6*, 226.
[6] H. Dorn, B. E. Hanson, E. Motell, *Inorg. Chim. Acta* **1981**, *54*; L71.
[7] B. E. Hanson, E. C. Lisic, J. T. Petty, G. A. Iannaconne, *Inorg. Chem.* **1986**, *25*, 4062.
[8] B. E. Hanson, K. H. Whitmire, *J. Am. Chem. Soc.* **1990**, *112*, 974.
[9] F. Grandjean in *The Time Domain in Surface and Structural Dynamics*, (Eds.: G. J. Long, F. Grandjean), Kluwer, Dordrecht, **1988**, p. 287.
[10] R. D. Ernst, D. R. Wilson, R. H. Herber, *J. Am. Chem. Soc.* **1984**, *106*, 1646; R. H. Herber in *Chemical Mössbauer Spectroscopy* (Ed.: R. H. Herber), Plenum, New York, **1984**, pp. 199.
[11] F. Grandjean, G. J. Long, C. G. Benson, U. Russo, *Inorg. Chem.* **1988**, *27*, 1524.
[12] R. S. Berry, *J. Chem. Phys.* **1960**, *32*, 933.
[13] At 78 K, the isomer shifts are −0.169, −0.165, and −0.165 mm s^{-1}, the quadrupole splittings are 1.33, 1.38, and 1.33 mm s^{-1}, and the linewidths are 0.24, 0.26, and 0.27 mm s^{-1} for **1**, **2**, and **3**, respectively.
[14] At 295 K, the isomer shifts are −0.256 and −0.240 mm s^{-1}, the quadrupole splittings are 1.14 and 0.72 mm s^{-1}, and the linewidths are 0.27 and 1.3 mm s^{-1} for **1** and **2**, respectively. At 280 K, the isomer shift is −0.235 mm s^{-1}, the quadrupole splitting is 0.74 mm s^{-1}, and the linewidth is 0.32 mm s^{-1} for **3**.
[15] M. B. Smith, R. Bau, *J. Am. Chem. Soc.* **1973**, *95*, 2388.
[16] R. Wordel, F. E. Wagner, *J. Less-Common Met.* **1987**, *129*, 27.
[17] P. Meakin, E. L. Muetterties, J. P. Jesson, *J. Am. Chem. Soc.* **1973**, *95*, 75.
[18] P. Raj, A. Sathyamoorthy, *J. Less-Common Met.* **1987**, *129*, 251.
[19] J. A. Tjon, M. Blume, *Phys. Rev.* **1968**, *163*, 456.
[20] R. B. King, *Organometallic Syntheses, Vol. I*, Academic Press, New York, **1965**, p. 96.

Molecular Modeling of the Class I Human Histocompatibility Molecule HLA-A2 Presenting an Allele-Specific Nonapeptide from Influenza Matrix Protein**

By *Norbert Zimmermann, Olaf Rötzschke, Kirsten Falk, Didier Rognan, Gerd Folkers, Hans-Georg Rammensee,* and *Günther Jung**

Dedicated to Professor Dietrich Brandenburg on the occasion of his 60th birthday

MHC Class I proteins (*M*ajor *H*istocompatibility *C*omplex) are found on the surface of most human cells. In the immune system their function is to present fragments of proteins of the inside of the cell in an antigen binding pocket to the killer cell receptor. Fragments of endogenous proteins (self peptides) are processed and presented when the cell is healthy. If the cell is attacked by viruses, the cytotoxic T-lymphocytes (CTLs or killer cells) recognize the fragments of foreign viral proteins (CTL epitopes) in the MHC antigen binding pocket and destroy the affected cell. The X-ray crystal structure analysis of the human class I histocompatibility antigen HLA-A2[1] shows an antigen binding site composed of two parallel α-helical domains α_1 and α_2, which are connected with a central antiparallel β-sheet. This forms a deep groove with six prominent pockets, the function of which is thought to be the binding of amino acid side chains of antigenic peptides. Furthermore, the residual electron density found in the peptide binding cleft is assumed to be a mixture of peptides cocrystallized with HLA-A2.

Recently, we found allele-specific oligopeptide motifs by sequencing of self-peptides eluted from MHC I proteins.[2] Alignment of viral proteins with the dominant hydrophobic anchor residues at positions 2, 6, and 9 of the HLA-A2 self-peptides suggested that the nonapeptide GILGFVFTL (from influenza matrix protein) was a candidate for a naturally processed antigenic peptide (Table 1). This nonapeptide was used to model a MHC peptide complex based on the

[*] Prof. Dr. G. Jung, Dipl.-Chem. N. Zimmermann
Institut für Organische Chemie der Universität
Auf der Morgenstelle 18, D-W-7400 Tübingen (FRG)
O. Rötzschke, K. Falk, Priv.-Doz. Dr. H.-G. Rammensee
Max-Planck-Institut für Biologie, Abteilung Immungenetik
Corrensstrasse 42, D-W-7400 Tübingen (FRG)
Dr. D. Rognan, Prof. Dr. G. Folkers
Department Pharmazie der Eidgenössischen Technischen Hochschule, ETH-Zentrum
Clausiusstrasse 25, CH-8092 Zürich (Switzerland)

[**] This work was supported by the Deutsche Forschungsgemeinschaft (SFB 323 and 120).

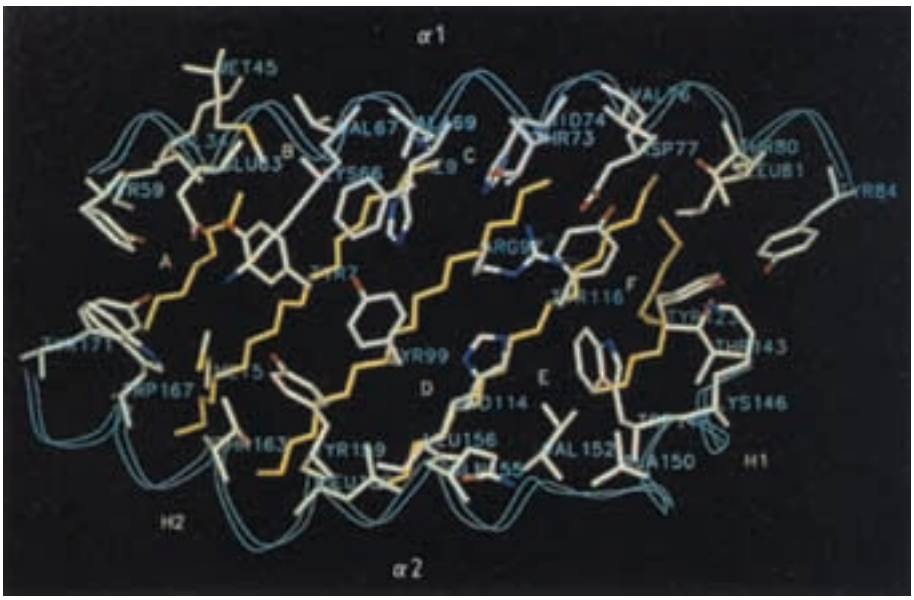

Fig. 1. The HLA-A2 peptide binding site consists of the two α-helical subsites α_1 and α_2 (shown in light blue), and a central antiparallel β-sheet (shown in yellow). All solvent-accessible side chains are indicated by colors typical for those atoms. Prominent binding pockets for antigen side chains are indicated with the letters A to F [1].

subsites derived from the crystal structure of HLA-A2.[1] A molecular dynamics simulation (over 28 ps) in aqueous solution[3–5] was performed to examine the stability and mobility of the constructed complex and to find out the potential recognition sites of the T-cell receptor (TCR).

Starting from the minimized β-sheet conformation for the influenza epitope, we first modeled the hydrophobic interactions of the dominant anchor positions (Ile2 and Leu9), corresponding to the B and F pockets of the HLA-A2 structure (Figures 1–3).[1] Ile2 is located in the hydrophobic B pocket and is surrounded by the allele-specific Met45, Val67, and Phe9 residues. The side chain of Leu9 was modeled in the F pocket of the HLA-A2 molecule, which is bordered by the hydrophobic residues Trp147 and Ile124. The carboxylate function of the *C*-terminus of the antigen Leu9 was docked next to the positively charged Lys146, which is highly exposed and leads from the α-helical "rim" directly towards the binding groove. Strikingly, Lys146 is the only positively charged amino acid in the HLA-A2 binding site which is *not* neutralized with a negatively charged side chain to form a stable salt bridge, as is normally found in globular proteins. Therefore Lys146 is usually predestined to anchor the *C*-termini of the antigenic nonapeptides.[6] In addition, Lys146 is well conserved in both human and mouse MHC class I molecules and could serve as a common binding residue for the charged *C*-termini of T-killer cell epitopes.

Table 1. The HLA-A2 restricted peptide motif as analyzed from the sequencing of HLA-A2 bound self-peptides [2]. Corresponding nonapeptides from protein sequences of viral origin are shown in comparison. The influenza matrix protein sequence most probably represents the natural epitope and was therefore chosen for modeling.

Residue positions	1	**2**	3	4	5	6	7	8	**9**		
Corresponding HLA-A2-pockets[a]		"B"				"D"		"F"			
Dominant anchor residues		**L**							**V**		
Strong		**M**		**E** **K**		**V**		**K**	**L**		
Weak	I L F K M Y V		A Y F P M S R	G P D T	I K Y N G F V H	I L T	A Y H	E S			
	Reported epitopes aligned [b]									Protein source	Ref.
	I	L	K	E	P	V	H	G	V	HIV reverse transcriptase 476–484	[9]
	G	I	L	G	F	V	F	T	L	Influenza matrix protein 58–66	[10]

[a] Pockets "A"–"F", see Figure 1. [b] Alignment on anchor position 2 (Ile, Leu, Met).

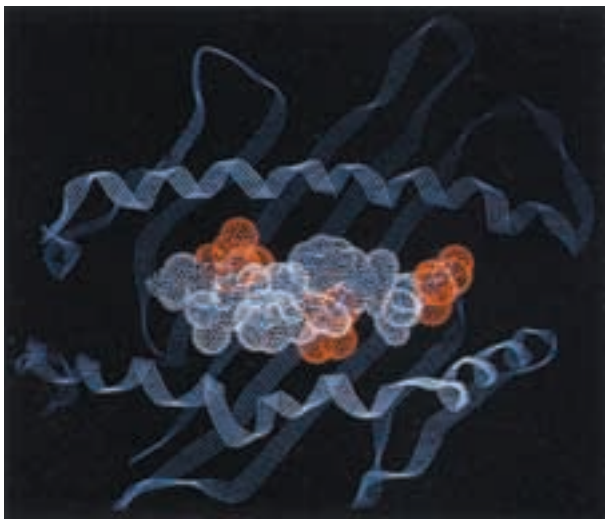

Fig. 2. The nonapeptide CTL epitope GILGFVFTL from influenza matrix protein was modeled into the binding groove of HLA-A2 and additionally minimized as an initial conformation for molecular dynamics simulation. The backbone of the HLA-A2 molecule is shown as a white ribbon while the CTL antigen (with prominent anchor residues Ile2, Val6, and Leu9) is shown as a dotted van der Waals surface (in red).

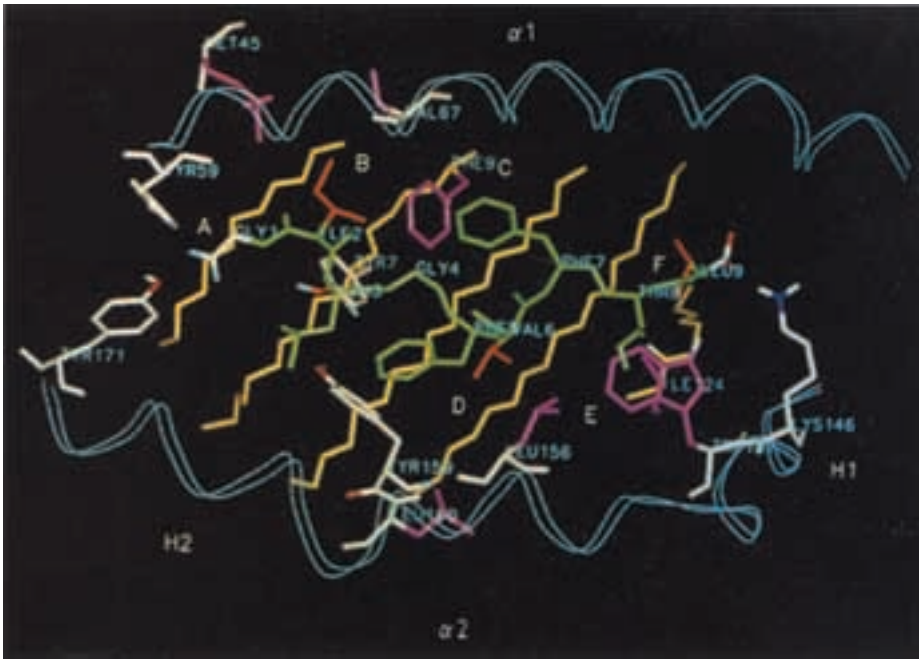

Fig. 3. The detailed model of the complex between HLA-A2 and the GILGFVFTL peptide shows the essential interactions between the prominent HLA binding sites and the CTL epitope. The conserved Ile2, Val6, and Leu9 side chains of the antigen (shown in red) are inserted in pockets B, D, and F, respectively (shown in purple). Pockets C and E remain free. The Leu9 carboxyl group interacts with Lys146, the *N*-terminal amino group with Tyr59 and 171.

According to the results from sequencing self peptides,[2] positions 7 and 8 in the HLA-A2 peptide binding motif are variable. The backbone and side chains of the corresponding Phe7 and Thr8 residues of the influenza epitope were modeled with respect to the minimum interaction energy for optimized hydrogen bonds and van der Waals contacts.

Val6 is an auxiliary anchor residue which was modeled into the hydrophobic D pocket of HLA-A2.[1] This pocket is surrounded by the side chains of Leu156, Leu160, and the rings of Tyr159 and Tyr99, in agreement with a strong peak of residual electron density in this region.[1, 6a] The backbone of the nonconserved residues Phe5, Gly4, and Leu3 has to adopt an extended conformation with a kink between the residues 4 and 5, because the overall length of the peptide's backbone is too long to connect the conserved anchors Ile2 and Val6 with their corresponding pockets (B and D) directly. The conformation of the peptide within this region also corresponds well to the shape of the residual electron density.[1] For this reason, this extended and most exposed part of the antigen should be able to bind to the T-cell receptor (TCR).

The variable, positively charged *N*-terminus of the GILGFVFTL antigen was modeled into the pocket A, forming a hydrogen bond network between the conserved HLA amino acid residues Tyr7, Tyr59, Tyr159, and the variable Tyr171. The pocket A is large enough to accomodate bulky amino acid side chains.

The first conformation of the molecular dynamics simulation was extracted at 1 ps in order to check abrupt changes in geometry due to inappropriate van der Waals interactions resulting from docking before reaching the equilibrium. No significant alteration of the system was observed. The analysis of the trajectories and the energy values of the complex did not show any principle deviation from the proposed nonapeptide–HLA-A2 binding interactions.

As an alternative to the *extended* antigen conformation, we tried to simulate GILGFVFTL in an *α-helical* conformation in the HLA-A2 binding pocket according to published models and suggestions.[7] However, the α-helical conformations neither fitted with the observed shape of the residual electron density,[1] nor did they agree with the geometry of the binding pocket of HLA-A2. The antigen in the α-helical conformation was modeled in such a way that the residues Ile2, Val6, and Leu9 pointed towards the binding pocket and were placed in the hydrophobic pockets as effectively as possible, whereas the three bulky Phe5, Phe7, and Leu3 "epitope residues" pointed towards the TCR recognition site. However, in all the molecular dynamics simulations with α-helical conformations we observed a progressive shift of the antigen out of the binding pocket, suggesting that peptide antigens in α-helical conformations are not able to bind efficiently to the HLA-A2.

In the molecular dynamics simulation with the *extended* conformation of the antigen, both the *C*- and *N*-terminal electrostatic anchor positions 1 and 9 and also the hydrophobic antigen anchors of the side chains in the positions 2, 6, and 9 remain stable with respect to their positions from the crystal structure analysis (Fig. 4), whereas residues 3 to 5,

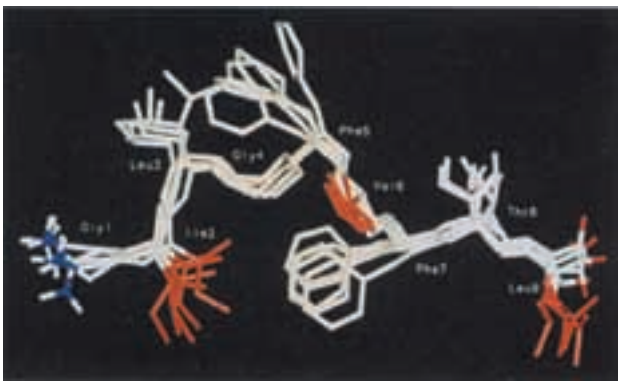

Fig. 4. Overlay of five potential energy minimum conformations of CTL epitope at 1, 7, 12, 14, and 28 ps of molecular dynamics simulation. The RMS deviation between the initial conformation and the molecular dynamics simulation snapshots equates to 0.81, 0.65, 0.81, 1.02, and 0.88 Å for the antigen and to 2.09, 2.09, 2.26, 2.52, and 2.66 Å for the whole HLA-A2 antigen complex.

which point towards the T-cell receptor show the expected greater mobility. Two relevant motions observed during the simulation of the HLA-A2 antigen system seemed to be remarkable (Fig. 5a,b): i) The side chain of Leu9 moves towards the middle of the pocket F, a position which is obviously energetically more favorable and also in agreement with the maximum residual electron density at this location.[1] ii) The salt bridge between Glu63 and Lys66 breaks after about 7 ps, following which Glu63 interacts with the polar backbone atoms of Ile2 and Gly1 (12 ps) and finally docks at the charged *N*-terminus of the antigen, forming a hydrogen bond network together with the conserved Tyr residues of the A pocket (28 ps). The loop region between the two α-helical HLA subsites H1 and H2 of the α_2 domains at position Ala150 represents the most exposed point of the HLA structure. This region, in combination with the Gly162 loop, could be responsible for TCR recognition of peptide-loaded MHC molecules.

a)

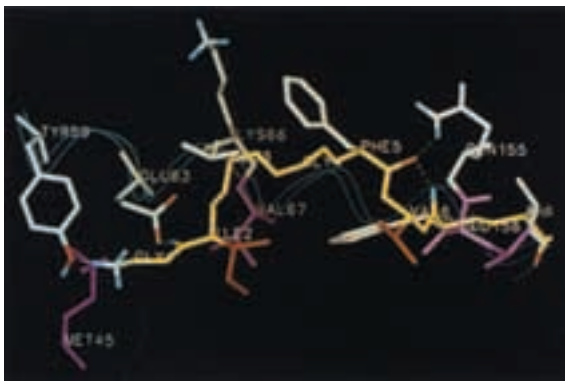

b)

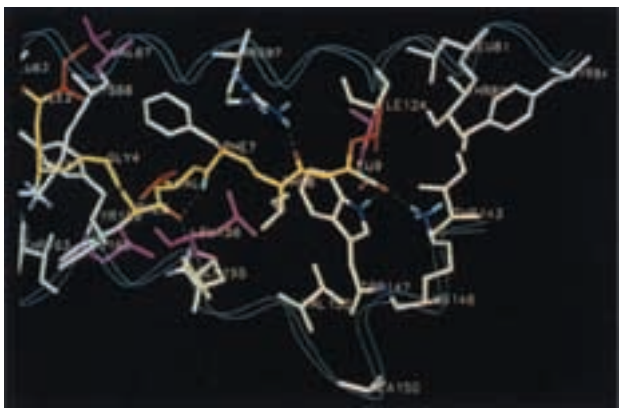

Fig. 5. 12 ps snapshot of molecular dynamics simulation. a) The *N*-terminal amino group of the CTL epitope interacts with Tyr59. Hydrogen bonds are formed between the carbonyl group of Phe5, the Gln155 side chain and the HN proton of Phe7. The antigen backbone is shown in yellow while the B and D pockets are indicated in purple. b) The *C*-terminal carboxyl group of the CTL epitope shows a hydrogen bond network between the positively charged Lys146 residue and Trp147. The carboxyl group of Thr8 is hydrogen-bonded to Arg97.

Summarizing the modeling procedure: Our model of the HLA-A2 antigen complex is in full agreement with the experimental results for HLA-A2[1, 2] and HLA-B27[6] peptide complexes. The maxima of the residual electron density found at the beginning and end of the HLA-antigen binding position reflect the electrostatically fixed *N*- and *C*-termini of the bound antigens. Additionally, the geometry, charges, and the residual electron density peaks of the HLA-A2 pockets A, B, D, and F[1] fit precisely with the prominent anchor residues of our HLA-A2 restricted peptide motif.[2] The charged termini of the antigen in our model are in suitable positions to interact with polar (Tyr59 and Tyr171 at *N*-terminus) and charged (Lys146 at *C*-terminus) HLA amino acid residues at the extreme end of the cleft. Also, all important anchor binding sites are either conserved or at least allele specific in the HLA system. Furthermore, the structure of the antigen backbone between Val6 and Ile2 of the influenza epitope corresponds to the shape of the residual electron density found in this region.[1] Finally, the total length of residual electron density between the *N*- and *C*-terminal link[6] is in agreement with an extended nonapeptide conformation, which is consistent with the length of the self peptides sequenced in our laboratories.[2]

Molecular dynamics investigations of the HLA-A2 antigen complex in aqueous solution revealed the stability of the modeled antigen binding sites and also indicated possible TCR binding sites. Our model, fully supported by experimental results,[2, 6] appears to serve as a basis for site-directed mutagenesis and for labeling experiments, with which the proposed interactions could be confirmed and which should be beneficial for the development of drugs and synthetic vaccines[8] targeted for specific interaction with MHC class I molecules.

Received: December 19, 1991 [Z 5082 IE]
German version: *Angew. Chem.* **1992**, *104*, 928

CAS Registry number:
GILGFVFTL, 141368-69-6.

[1] M. A. Saper, P. J. Bjorkman, D. C. Wiley, *J. Mol. Biol.* **1991**, *219*, 277–319.

[2] K. Falk, O. Rötzschke, S. Stefanović, G. Jung, H.-G. Rammensee, *Nature* **1991**, *351*, 290–296.

[3] Interactive model building was done with the program package SYBYL 5.4 (Tripos, St. Louis, MO, USA) running on a VAX 3500 connected with Evans & Sutherland PS390 and PS350 graphic terminals. Minimization and dynamics simulation of the generated structures was performed with the AMBER 3.0 software [3b] installed on a CONVEX C220 vector computer. For analysis of the generated trajectories from molecular dynamics simulation, we used the animation program ADAPTU [3c] also linked to the Evans & Sutherland graphic stations; b) S. J. Weiner, P. A. Kollman, D. A. Case, C. Singh, C. Ghio, G. Allagona, S. Profeta, P. Weiner, *J. Am. Chem. Soc.* **1984**, *106*, 765–784; c) M. Krug, G. Folkers, *J. Mol. Graphics* **1991**, 119–121.

[4] The three-dimensional HLA-A2 crystal structure at 2.6 Å [1] was retrieved from the Brookhaven Protein data base (F. C. Bernstein, T. F. Koetzle, G. J. B. Williams, E. F. Meyer, Jr., M. D. Brice, J. M. Rodgers, O. Kennard, T. Shimanouchi, M. Tasumi, *J. Mol. Biol.* **1977**, *112*, 535–542, file 3HLA). Due to limited computer resources, only the α_1 and α_2 domains of HLA-A2 from Gly1 to methylamidated Thr182 were taken into account for calculations. In order to simulate the HLA-A2 antigen complex in a waterlike solvent environment, we first minimized the HLA-A2 crystal structure using the AMBER united atom force field for proteins and the TIP3P water model for solvent simulation. A water shell consisting of 1728 water molecules was generated around the HLA solute. Since every single water molecule was calculated explicitly, the dielectric constant during the simulation was set to 1.0. The parameters of 1,4 nonbonding atoms were scaled to 8.0 for Lennard–Jones and 2.0 for electrostatic interactions in order to reproduce "big AMBER" parameters [7]. The partial charge of the oxygen atom in the TIP3P water (Monte Carlo water shell) was set to −0.66. All water molecules more than 5 and less than 1.5 Å from the solute were discarded from the system. After 200 steps of steepest descent minimization a 2000 step minimization according to the conjugate gradient method resulted in a suitable structure ready for docking the influenza epitope GILGFVFTL. Docking was performed interactively, utilizing special SYBYL functions to obtain the optimal HLA-A2 antigen interaction energies, distances, and torsion angles.

[5] In order to examine the stability and mobility of the constructed MHC antigen complex, we performed a 28 ps molecular dynamics simulation in aqueous solution. After minimizing the complex with the protocol [4], Newtons equations of motion were integrated for more than 5000 atoms at a time step of 1 fs, also with AMBER united-atom force field parameters and TIP3P water conditions. Nonbonded interactions were calculated with a residue-based cutoff distance of 10 Å. The list of nonbonding pairs

of atoms was updated every 100 integration steps. Initial random velocity setup of the system was taken from a Maxwell distribution at $T = 300$ K. The simulation temperature was kept constant by coupling the system to a simulated heat bath, rescaling the velocities with a temperature relaxing time of $t = 0.4$ ps. Coordinates and energies were stored on disk after every 100 integrations steps (0.1 ps) resulting in 284 distinct conformations. Evolution of the system's potential energy shows equilibrium conditions after about 14 ps. Extracted conformations were additionally energy minimized to remove the kinetic energy of the system.

[6] a) Nevertheless, as shown in a previous modeling study docking a nonapeptide into the binding cleft of HLA-B27 [6b], there is a certain probability to dock residue 3 into pocket D. However, that docking scheme does not agree with our sequencing results for HLA-A2. Residue 3 of the peptide antigen is not conserved and therefore not predestined for docking in the hydrophobic D pocket. Further modeling studies with different docking schemes may reveal the location of antigen residue 6 more precisely. b) After preparation of this manuscript similar interactions were found modeling a nonapeptide into the binding site of HLA-B27: D. R. Madden, J. C. Gorga, J. L. Strominger, D. C. Wiley, *Nature* **1991**, *353*, 321–325.

[7] a) D. Rognan, M. J. Reddehase, U. H. Koszinowski, G. Folkers, *Proteins* **1992**, *13*, 70–85; b) M. Del Val, H. Volkner, J. B. Rothbard, S. Jonjic, M. Messele, J. Schickedanz, M. J. Reddehase, U. H. Koszinowski, *J. Virol.* **1988**, *62*, 3965–3972; c) M. J. Reddehase, J. B. Rothbard, U. H. Koszinowski, *Nature* **1989**, *337*, 651–653.

[8] K. Deres, H. Schild, K.-H. Wiesmüller, G. Jung, H.-G. Rammensee, *Nature* **1989**, *342*, 561–564.

[9] B. D. Walker, C. Flexner, K. Birch-Limberger, L. Fischer, T. J. Paradis, A. Aldovini, R. Young, B. Moss, R. T. Schooly, *Proc. Natl. Acad. Sci. USA* **1989**, *86*, 9514–9518.

[10] F. Gotch, A. McMichael, J. Rothbard, *J. Exp. Med.* **1988**, *168*, 2045–2057.

Detection of Subpicomole Levels of Compounds Containing Hydroxyl and Amino Groups with the Fluorogenic Reagent, 2-Naphthoylimidazole**

By *Norihiro Ikemoto, Lee-Chiang Lo,* and *Koji Nakanishi**

Highly sensitive methods for the identification of natural products such as oligosaccharides have become increasingly important with the advances in the biosciences. A commonly employed strategy is HPLC analysis following derivatization with a chromophore. Among the various chromophores used to derivatize amino and/or hydroxyl groups,[1] benzoylation[2, 3] has attracted attention because of the strong UV absorbance of the chromophore, ease of derivatization, and stability of the derivatives. The 2-naphthoate chromophore,[4] however, not only possesses these attributes but also exhibits fluorescence, a feature that dramatically enhances sensitivity. To demonstrate the advantages of using this chromophore, we have investigated its application to sugar analysis.

Most methods for compositional analysis of oligosaccharides involve derivatization of the monosaccharides obtained after acid hydrolysis.[3, 5] In the present microscale method, this derivatization scheme consists of a reduction/naphthoylation sequence (Scheme 1, bottom), which was performed on an artificial mixture of nine monosaccharides most commonly encountered in bioconjugates. The resulting alditol pernaphthoates have UV maxima at 234 nm and possess large ε values (in acetonitrile): 254000 for hexanaphthoates and 220000 for pentanaphthoates, that is, 43000 per naphthoate chromophore, a value three times larger than that of the benzoate. Furthermore, the naphthoates exhibit strong fluorescence at 374 nm upon irradiation at 234 nm, which enhances the sensitivity of detection.

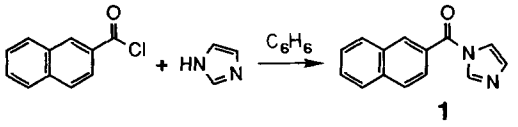

aldoses $\xrightarrow{NaBH_4}$ alditols $\xrightarrow[CH_3CN]{1,\ DBU}$ alditol pernaphthoates $\Rightarrow$ HPLC

Scheme 1. Preparation of naphthoyl imidazole (**1**) and the derivatization/analysis scheme. DBU = 1,8-diazabicyclo[5.4.0]undec-7-ene.

The microscale naphthoylation reaction was performed with 2-naphthoylimidazole (**1**, Scheme 1 top) prepared according to a procedure given for cinnamoylimidazole;[6] the latter reagent has proven to be an excellent reagent for the microscale acylation of acyclic polyols.[7] The pernaphthoylation of alditols and other natural products[8] on a 10 nmol scale occurred rapidly and completely, and only minimal amounts of reagent-derived impurities were formed; in contrast, reactions with 2-naphthoyl chloride, pyridine, and dimethylaminopyridine (DMAP) were slower, required heating, and yielded more extraneous impurity peaks. Prepurification of samples of biological origin prior to derivatization and HPLC analysis minimizes the contaminants of biological origin that may have similar spectroscopic characteristics. Figure 1 shows the chromatogram with about 0.4 pmol of sample injected and monitored with a fluorescence detector (see Experimental). The nine alditol naphthoate derivatives are well resolved on a silica gel column. The absence of incomplete derivatization products in the chromatogram indicates high conversion at the 10 nmol scale.[9] The detection limit is about 0.1 pmole (signal-to-noise ratio S/N $\approx$ 5). Because of the high absorption coefficient of 2-naphthoates and multiple derivatization on each

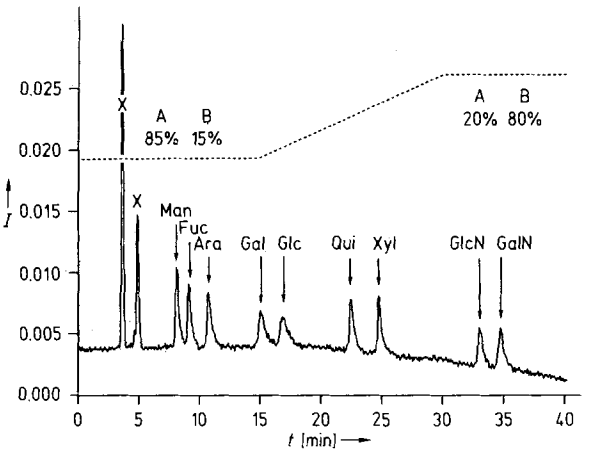

Fig. 1. Chromatogram of ca. 0.4 pmole of pernaphthoate derivatives of mannitol, fucitol, arabitol, dulcitol, sorbitol, quinovitol, xylitol, glucosaminitol, and galactosaminitol (X represents reagent-derived impurities). Solvent A: 0.025% 2-propanol/dichloromethane. Solvent B: 4% acetonitrile/0.025% 2-propanol/dichloromethane. Flow rate: 1 mL min^{-1}. Column: YMC silica gel (4.6 × 250 mm^2, 5 μm). Absorption at 234 nm, Emission intensity I at 374 nm.

[*] Prof. K. Nakanishi, N. Ikemoto, L. Lo
Department of Chemistry
Columbia University
New York, NY 10027 (USA)

[**] This work was supported by National Institutes of Health grants (GM 34509 to KN and 5F32CA08972 to NI). We thank Shaman Pharmaceuticals, Inc. for the use of their fluorescence detector and Bristol-Myers Squibb Company for the use of their beam condenser for CD measurements.

sugar, high sensitivity can still be achieved with UV detection (down approximately to the 1 pmole level, S/N ≈ 2), although it is an order of magnitude less sensitive than fluorescence detection.

Although alditol benzoates have been reported to show poor separation with reverse phase HPLC,[3] the alditol naphthoates could be well separated by normal phase HPLC. Diastereomers differing by one stereocenter, for example, sorbitol/mannitol/dulcitol, xylitol/arabitol, fucitol/quinovitol, and glucosaminitol/galactosaminitol are all well resolved. The amino alditols galactosaminitol and glucosaminitol are retained more strongly by the column than the oxygen sugars and are eluted last. In addition to their higher sensitivity of detection, the good HPLC separation of these 2-naphthoate derivatives offers an important advantage over the use of the benzoate chromophore.

When two or more 2-naphthoate chromophores are present in chiral compounds, exciton coupling interactions are often observed by circular dichroic spectroscopy (CD).[10] The resulting CD curve not only reflects the stereochemistry of the molecule but can be used as an additional handle for structural identification. With the use of a CD beam condenser and a microcell (100 μL, 1 cm), compounds bearing 2-naphthoate chromophores have yielded distinct CD spectra with 50 pmole of sample; ten times more sample is required with a regular CD cell (1 mL, 1 cm).

In conclusion, the advantages of the 2-naphthoate chromophore are evident in the ease of derivatization, the high sensitivity of detection, the good chromatographic behavior, and the possibility of further CD characterization.

Experimental Procedure

Preparation of **1**: Imidazole (0.71 g) was suspended in benzene (40 mL) and cooled to 8 °C. A solution of 2-naphthoyl chloride (1.0 g) in benzene (10 mL) was added dropwise over 10 min, and the mixture stirred for 1 h at room temperature. The reaction mixture was filtered through Celite and lyophilized to afford the product (1.2 g, quantitative).

Mannose, fucose, arabinose, galactose, glucose, quinovose, xylose, glucosamine hydrochloride, and galactosamine hydrochloride (5 μmol each) were stirred for 2 h at room temperature with $NaBH_4$ (10 mg) in water (1 mL). The reaction was quenched with aqueous HCl, and the resulting mixture evaporated six times with methanol. An aliquot (10 nmol of each sugar) was stirred in acetonitrile (0.2 mL) with **1** (10 μmol) and DBU (10 μmol) for 2 h at room temperature. After quenching with water, an aliquot (2 nmol) was evaporated in a silanized test tube. The residue was dissolved in dichloromethane, and aliquots were injected for HPLC analysis [11] (Perkin-Elmer Series 4 Liquid Chromatograph and 7500 Data Station, Shimadzu RF-551 Fluorescence HPLC Monitor).

Received: January 11, 1992 [Z 5115 IE]
German version: *Angew. Chem.* **1992**, *104*, 918

CAS Registry numbers:
1, 141903-34-6; imidazol, 288-32-4; mannose, 3458-28-4; fucose, 2438-80-4; arabinose, 147-81-9; galactose, 59-23-4; glucose, 50-99-7; quinovose, 7658-08-4; xylose, 58-86-6; glucosamine hydrochloride, 66-84-2; galactosamine hydrochloride, 1772-03-8; 2-naphthoyl chloride, 2243-83-6.

[1] T. J. Bruno, P. D. N. Svoronos, *CRC Handbook of Basic Tables for Chemical Analysis*, CRC, Boca Raton, FL, USA, **1989**, p. 118, and references cited therein.
[2] P. F. Daniel, D. F. De Feudis, I. T. Lott, R. H. McCluer, *Carbohydr. Res.* **1981**, *97*, 161.
[3] N. Jentoft, *Anal. Biochem.* **1985**, *148*, 424.
[4] J. Golik, H.-W. Liu, M. Dinovi, J. Furukawa, K. Nakanishi, *Carbohydr. Res.* **1983**, *118*, 135.
[5] K. Kakehi, S. Honda in *Analysis of Carbohydrates by GLC and MS* (Eds.: C. J. Beirmann, G. D. McGinnis), CRC, Boca Raton, FL, USA, **1989**, p. 43, and references cited therein.
[6] G. R. Schonbaum, B. Zerner, M. L. Bender, *J. Biol. Chem.* **1961**, *236*, 2930.
[7] P. Zhou, N. Berova, K. Nakanishi, M. Knani, M. Rohmer, *J. Am. Chem. Soc.* **1991**, *113*, 4040.
[8] Smaller scale reactions (<0.5 nmol), HPLC separation and CD measurements have been successfully carried out with different series of compounds containing hydroxyl groups of biological origin.
[9] The isolated yield was ca. 32% when naphthoylation was performed at the smaller 0.6 nmol scale.
[10] N. Harada, K. Nakanishi, *Circular Dichroic Spectroscopy: Exciton Coupling in Organic Stereochemistry*, University Science Books, Mill Valley, CA, USA, **1983**, p. 38.
[11] If desired, a prepurification step with C18 cartridges may be added to remove the very polar reagent-derived impurities. See [3].

Tetramethyl-*ortho*-quinodimethane, First Member of a Family of Custom-Tailored Cheletropic Spin Traps for Nitric Oxide**

By *Hans-Gert Korth**, *Keith U. Ingold**, *Reiner Sustmann*, *Herbert de Groot*, and *Helmut Sies*

Nitric oxide, •NO, has been shown to be an intra- and intercellular signal molecule; it regulates vascular tone, is a messenger molecule in the central nervous system, and mediates cytotoxicity of macrophages (see reviews[1–4]). Even if •NO is not itself the "Endothelium Derived Relaxing Factor" (EDRF),[5] it certainly appears to be the active agent released by the EDRF. Nitric oxide also plays an important role in air pollution arising from photochemical and/or combustion processes. Because of the well-recognized importance of •NO, some rather sensitive methods have been developed for its identification and quantitation,[4] for example, the spectrophotometrically monitored •NO-induced conversion of oxyhemoglobin (HbO_2) to methemoglobin (MetHb) [Eq. (a)], monitoring its vasorelaxant activity on arterial segments, and in the gas phase, its chemiluminescent reaction with ozone [Eq. (b)].

$$HbO_2 + {}^{\bullet}NO \longrightarrow MetHb + NO_3^- \qquad (a)$$

$$O_3 + {}^{\bullet}NO \longrightarrow O_2 + {}^{\bullet}NO_2^{*} \longrightarrow {}^{\bullet}NO_2 + h\nu \qquad (b)$$

Nevertheless, despite all this effort there is as yet no method that, even in principle, would be suitable for monitoring •NO production continuously, both *in time and in space*, in cell cultures, perfused organs, and living organisms. The most attractive route to this objective appeared to be a chemical reaction by which •NO (itself a persistent radical) could be converted into a persistent nitroxide radical. The

[*] Dr. H.-G. Korth, Prof. Dr. R. Sustmann
Institut für Organische Chemie der Universität – Gesamthochschule, Universitätsstrasse 5, D-W-4300 Essen 1 (FRG)
Prof. Dr. K. U. Ingold
Steacie Institute for Molecular Sciences, National Research Council of Canada, Ottawa, Ontario K1A0R6 (Canada)
Priv. Doz. Dr. H. de Groot, Prof. Dr. H. Sies
Institut für Physiologische Chemie I der Universität Düsseldorf (FRG)

[**] Issued as NRCC No. 33282. We thank Dr. J. C. Scaiano, Ottawa, for a sample of **3** which permitted the initial experiment to be carried out, Prof. A. L. J. Beckwith, Canberra, for a sample of TMIO, and Ms L. Hughes, Ms P. Lommes, and Mr. J.-F. Wang for valuable experimental help. One of us (K. U. I.) wishes to thank the Alexander-von-Humboldt-Stiftung for an Award which gave him both the leisure and the incentive to think about the ways in which nitric oxide might be trapped and imaged in biological systems.

latter could be monitored, quantitated, and imaged by electron spin resonance (ESR) spectroscopy.

Conventional nitrone and nitroso spin traps have proved to be essentially useless as traps for 'NO.[6] This is hardly surprising in view of the very low reactivity of 'NO towards molecules in their ground (singlet electronic) states.

It is well known that 'NO reacts rapidly with carbon-centered radicals to form nitroso compounds[8] [Eq. (c)] and that nitroso compounds are good spin traps for carbo-centered radicals[9] [Eq. (d)].

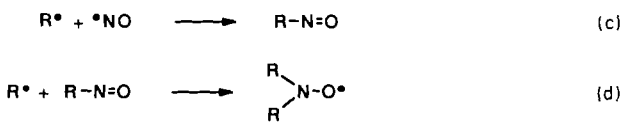

Conceptually, therefore, a biradical reacting in a cheletropic manner would be an effective 'NO trap, and indeed triplet biradicals have been trapped by 'NO and have formed cyclic nitroxide radicals[10] [Eq. (e)].

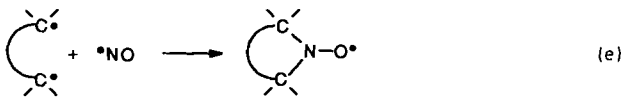

Unfortunately, biradicals with a structure suitable for 'NO trapping are inherently short-lived, with lifetimes generally shorter than 1 μs.[11] Furthermore, they react very rapidly with oxygen.[11, 12]

A double carbon-centered "*biradical equivalent*" was obviously required. This equivalent must react rapidly and efficiently with 'NO to form a persistent, cyclic dialkylnitroxide, but it must not react (at a significant rate) with O_2. Furthermore, the basic structure of the biradical equivalent should be able to be readily elaborated. Such elaboration is necessary so that specific 'NO traps can be synthesized which would be, for instance, water- or lipid-soluble, excluded from or able to pass through cell membranes, or anchored to the surface of a membrane or within the membrane. A family of such 'NO traps would allow the detailed ESR imaging in time and space of 'NO formation under physiological conditions.

1,2-Bis(*exo*-isopropylidene)cyclohexa-3,5-diene (=7,7,8,8-tetramethyl-*o*-quinodimethane) (**1**) seemed likely to meet the foregoing criteria. This compound has lived up to our hopes of creating a custom-tailored double (cheletropic) spin trap for 'NO; that is, it reacts efficiently with 'NO to produce the expected 1,1,3,3-tetramethylisoindolin-2-oxyl radical (TMIO) (**2**). We have therefore christened it NOCT-1 (*N*itric *O*xide *C*heletropic *T*rap 1). Nitroxide **2** is a radical eminently suitable for quantitative ESR measurements since it is completely stable at ambient temperatures and can be synthesized as a pure compound.[13]

The *o*-quinodimethane **1** was synthesized by photodecarbonylation of 1,1,3,3-tetramethyl-2-indanone (**3**) in pentane, hexane, or acetonitrile solution[14] [Eq. (f)].

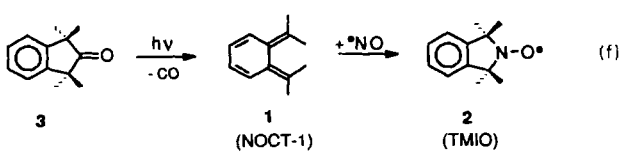

The *o*-quinodimethane **1** is a rather short-lived intermediate (half-life at 20 °C about 9 min[15]), which was not, therefore, separated from the reaction mixture.[16] Fortunately, separation proved unnecessary because the unchanged ketone **3** and the major photolysis product, *o*-isopropyl-α-methylstyrene, were both inert toward 'NO.

On mixing a cold, dilute (approximately 10^{-3} M) deoxygenated solution of **1** in an organic solvent with dilute (10^{-2}–4×10^{-5} M) deoxygenated solutions of 'NO (in the same organic solvent), the characteristic three-line ESR spectra arising from two different nitroxide radicals were produced "instantaneously" (i.e., within the time required to start the recording; ca. 1 min). Comparison with the ESR spectrum of authentic **2**[13] under identical conditions proved that one spectral component was indeed due to **2**, since it exhibited exactly the same nitrogen hyperfine splittings and *g* values in the various solvents (e.g., $a_N = 1.452(3)$ mT, $a_{^{13}C} = 0.630(5)$ mT ($4\ ^{13}C$), $g = 2.00589(1)$ in acetonitrile; 14 °C). Thus, 'NO has been trapped according to Equation (f).[17] The second nitroxide signal displayed the characteristic features ($a_N = 2.712(5)$ mT, $a_{^{13}C} = 0.77(1)$ mT ($1\ ^{13}C$), $g = 2.00565(1)$) of an alkoxynitroxide radical. We tentatively assign this spectrum to the nitroxide radical **4**, which would imply that $^{\bullet}NO_2$[18] has also been trapped by **1** [Eq. (g)].

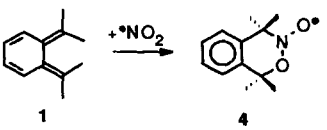

We next employed **1** to monitor 'NO formation by cultured liver macrophages, the *Kupffer cells*. The Kupffer cells were isolated by collagenase perfusion of the liver from male Wistar rats as described previously.[19, 20] In a first series of experiments, approximately 1.5×10^{-7} moles of **1** in 0.2 mL of CH_3CN were injected directly into the buffer solution above the Kupffer cells.[21] After incubation at 37 °C for times between 5 and 60 min, the medium was extracted with 0.8 mL of *n*-hexane, the hexane layer transferred into an ESR quartz tube, and the oxygen removed by bubbling with argon. From all solutions we detected the characteristic ESR signals of **2** (Fig. 1).[22] Despite the relatively unfavorable conditions of this experiment, which arise from the short lifetime of **1** and its negligible solubility in water, the very fact that we could easily detect signals due to **2** shows that we are dealing with a very effective and rapidly reacting cheletropic trap for 'NO. After 30 min[22] the total yield of nitroxide **2** in hexane was about 0.025 nmol,[23] which, in view of the known rate of production of 'NO by Kupffer cells under these conditions (approximately 0.40 nmol per tube in 30 min),[21] implies that we had succeeded in trapping about 6% of the 'NO produced.[24]

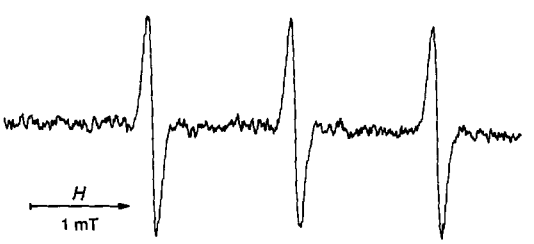

Fig. 1. ESR spectrum (9.5 GHz, *n*-hexane, 14 °C) of **2** obtained after 30 min incubation of Kupffer cells in the presence of **1**.

In a second series of experiments, the same quantity of **1** was added to about 1 mL of *n*-hexane, which was then floated on the aqueous buffer above the cells. The cells were incubated for the same periods of time, and although the $^{\bullet}NO$ had to diffuse through the water layer (ca. 2 mm) to reach **1** in the hexane layer, the ESR spectra characteristic of **2** were obtained, but considerably weaker than in the first series.

Because of its specific physical and chemical properties, NOCT-1 (**1**) is certainly not a practical reagent for monitoring $^{\bullet}NO$ production in biological systems under physiological conditions. However, our intention was simply to show that $^{\bullet}NO$ is trapped by **1** and hence that **1** provides a reasonable basis for the development of a family of structurally related NOCTs. We can safely assume that a water-soluble and longer lived NOCT would be more suitable for $^{\bullet}NO$ monitoring under cell-culture conditions. Such modifications of NOCT-1 are currently being synthesized and evaluated.

In these cell culture experiments, **1** traps $^{\bullet}NO$ and yields a characteristic nitroxide ESR spectrum, although oxygen is necessarily also present. Kinetic experiments show that the lifetime of **1** is not affected by molecular oxygen, solvent polarity, or pH.[25] Of course, even if **1** were to react with $O_2^{\bullet-}$, $HO^{\bullet}$, or any other form of "active oxygen", the product(s) will be ESR silent. The only exceptions to this rule are the $^{\bullet}NO$ and $^{\bullet}NO_2$ radicals.

Received: January 17, 1992 [Z 5127 IE]
German version: Angew. Chem. **1992**, *104*, 915

CAS Registry numbers:
1, 66042-30-6; NO, 10102-43-9.

[1] R. F. Furchgott, P. M. Vanhoutte, *FASEB. J.* **1989**, *3*, 2007–2018.
[2] S. Moncada, R. M. J. Palmer, E. A. Higgs, *Biochem. Pharmacol.* **1989**, *38*, 1709–1715.
[3] L. J. Ignarro, *Biochem. Pharmacol.* **1991**, *41*, 485–490.
[4] E. Noack, M. E. Murphy in *Oxidative Stress: Oxidants and Antioxidants* (Ed.: H. Sies), Academic Press, New York, **1991**, pp. 445–489.
[5] For a summary of the evidence that $^{\bullet}NO$ is the EDRF see [4]. For evidence that NO^- may also be a physiologically important form of EDRF see: M. E. Murphy, H. Sies, *Proc. Natl. Acad. Sci. USA* **1991**, *88*, 10860–10864. For a summary of the evidence that $^{\bullet}NO$ may not be the EDRF see S. S. Greenberg, D. E. Wilcox, G. M. Rubanyi, *Circ. Res.* **1990**, *67*, 1446–1452; A. F. Varin, *FEBS Lett.* **1991**, *289*, 1–34.
[6] C. M. Arroyo, M. Kohno, *Free Radical Res. Commun.* **1991**, *14*, 145–155. Although this paper reports formation of an adduct radical from ^{15}NO and $(CH_3)_3CNO$ i.e. $(CH_3)_3CN(^{\bullet}O)^{15}NO$, such radicals are unknown [7]. Furthermore, to account for the complex ESR spectrum that was obtained, Arroyo and Kohno assumed that the adduct radical exists in two forms with different nitrogen hyperfine splittings for each form! Since the two forms are shown as resonance structures this cannot be true. It would appear that the overall chemistry of the $^{\bullet}NO + (CH_3)_3CNO$ reaction must be quite complex.
[7] A. R. Forrester, *Landolt-Börnstein, New Series, Magnetic Properties of Free Radicals, Vol. 9, Part c1, Vol. 17, Part d1, d2* (Eds.: H. Fischer, K. H. Hellwege), Springer, Berlin, **1979**, **1989**.
[8] Y. Rees, G. H. Williams, *Adv. Free-Radical Chem.* **1969**, *3*, 199–230; M. Györ, A. Rockenbauer, F. Tüdös, *Tetrahedron Lett.* **1986**, *27*, 3759; A. Rockenbauer, M. Györ, F. Tüdös, *ibid.* **1986**, *27*, 3363, 3421, 3425, 4795.
[9] Reviews: M. J. Perkins, *Adv. Phys. Org. Chem.* **1980**, *17*, 1–64; E. G. Janzen, L. D. Haire in *Advances in Free Radical Chemistry, Vol. 1* (Ed.: D. D. Tanner), Jai Press, Greenwich, CT, USA, **1990**; G. M. Rosen, E. Finkelstein, *Adv. Free Radical Biol. Med.* **1985**, *1*, 345–375.
[10] P. Maruthamuthu, J. C. Scaiano, *J. Phys. Chem.* **1978**, *82*, 1588–1590.
[11] J. C. Scaiano, E. A. Lissi, M. V. Encina, *Rev. Chem. Intermed.* **1978**, *2*, 139–196; J. C. Scaiano, *Acc. Chem. Res.* **1982**, *15*, 252–258.
[12] W. Adam, S. Grabowski, W. R. Marshall, *Acc. Chem. Res.* **1990**, *23*, 165–172.
[13] P. G. Griffiths, G. Moad, E. Rizzardo, D. H. Solomon, *Aust. J. Chem.* **1983**, *36*, 397–401.
[14] J. E. Starr, R. H. Eastman, *J. Org. Chem.* **1966**, *31*, 1393–1402.
[15] V. Wintgens, J. C. Netto-Ferreira, H. Casal, J. C. Scaiano, *J. Am. Chem. Soc.* **1990**, *112*, 2363–2367; K. Kamal de Fonseka, J. J. McCullough, A. J. Yarwood, *J. Am. Chem. Soc.* **1979**, *101*, 3277–3282.
[16] **1** was detected by low-temperature (−40 °C) ^1H NMR spectroscopy (300 MHz, CD_3CN, TMS), from the signals of its olefinic protons at $\delta = 6.00$ (dd, $J = 7.8$, 3.2 Hz) and 6.85 (dd, $J = 7.8$, 3.2 Hz), which decayed at room temperature in agreement with the reported liftime [15]. The concentration of **1** after 1 h irradiation of a 5.3×10^{-2} mol L^{-1} solution of **3** in CD_3CN was about 7×10^{-4} mol L^{-1}, and that of *o*-isopropyl-α-methylstyrene about 1.0×10^{-2} mol L^{-1}.
[17] Further evidence that **1** represents the active trap was given by experiments where $^{\bullet}NO$ solutions were mixed with solutions of **1** which had been stored for different periods (1–60 min) at room temperature. The intensity of the ESR signal decreased with increasing storage time of the **1**, as expected in view of the known lifetime [15] of **1**.
[18] The formation of $^{\bullet}NO_2$ in these solutions by reaction of $^{\bullet}NO$ with traces of oxygen and/or disproportionation cannot be excluded. It may also be formed by reaction of $^{\bullet}NO$ with **2**. Separate experiments have shown that **2** does react with excess $^{\bullet}NO$ or $^{\bullet}NO_2$ but quite a large excess of these compounds is necessary for a complete suppression of the ESR signals. In contrast, the ESR signals due to alkoxynitroxide **4** are efficiently destroyed by $^{\bullet}NO$ or $^{\bullet}NO_2$.
[19] B. Rymsa, H. D. Becker, W. Lauchart, H. de Groot, *Res. Commun. Chem. Pathol. Pharmacol.* **1990**, *68*, 263–266.
[20] J.-F. Wang, P. Komarov, H. Sies, H. de Groot, *Biochem. J.* **1991**, *279*, 311–314.
[21] The Kupffer cells were cultured in tubes (5.5 cm^2, Nunc) with RPMI 1640 medium supplemented with 20% (v/v) heat-inactivated fetal-calf serum in a humidified CO_2/air (1/19) atmosphere at 37 °C. After 30 h the cells were pretreated for 18 h with lipopolysaccharides (10 mg mL^{-1}) and with Hank's balanced salt solution, pH 7.4, supplemented with 10 mM glucose and 20 mM Hepes. 1 mM L-arginine was added prior to incubation at 37 °C. Each culture tube contained approximately 7×10^4 Kupffer cells which, under these conditions, released $^{\bullet}NO$ at a rate of 11.6 nmol h^{-1}(10^6 cells)$^{-1}$.
[22] The ESR signal intensity decreased for incubation times longer than 30 min, probably because **2** reacts with excess $^{\bullet}NO$ [18].
[23] Determined by double integration of the ESR signal and comparison with a calibrated spin standard.
[24] A degradation of the ESR signal by a possible reaction of **2** with excess **1** can be excluded on the basis of separate experiments where varying amounts of **1** were added to a solution of pure **2**. If L-arginine is replaced by N^G-nitro-L-arginine the production of $^{\bullet}NO$ by the Kupffer cells in inhibited [20]. In agreement, no ESR signals were detected from parallel experiments in which 0.1 mM N^G-nitro-L-arginine had been added to the cell culture prior to addition of **1**.
[25] R. R. Milburn, NRCC, Ottawa, unpublished results.

Multidentate Macrocyclic Lewis Acids: Release of "[12] Mercuracarborand-4" from Its Iodide Complex and the Structure of Its Tetra(tetrahydrofuran) Dihydrate Complex**

By *Xiaoguang Yang, Stephen E. Johnson, Saeed I. Khan,* and *M. Frederick Hawthorne**

While simple Lewis acids have been used to mediate a wide variety of C–C-bond-forming reactions,[1] multidentate Lewis acids, that is, those with several electrophilic centers, offer the possibility of specific substrate binding accompanied by catalysis with high chemo- and stereoselectivities. Moreover, anion complexation by multifunctional electrophiles is of vital importance to the areas of molecular recognition, enzyme modeling, homogeneous catalysis, and ion transport.[2] Although the complexation of electrophilic guest species has been intensively studied for the last twenty years,[3] anion inclusion complexes had generally been limited to those species in which macrocyclic ammonium salts[4] serve as host molecules for simple anions. More recently, however, several

[*] Prof. Dr. M. F. Hawthorne, Dr. X. Yang, Dr. S. E. Johnson, Dr. S. I. Khan
Department of Chemistry and Biochemistry
University of California
Los Angeles, California 90024 (USA)

[**] This work was supported by the National Science Foundation.

multidentate Lewis acids have been reported which can function as host molecules.[5–8] In a new vein, we recently reported the chloride and iodide complexes of the novel macrocyclic tetradentate Lewis acid, [12]mercuracarborand-4(**1**).[9] The synthesis and reactivity of this novel host molecule and the molecular structure of its tetra(tetrahydrofuran)dihydrate complex are described herein.

The synthesis of **1** was achieved in 80% yield by the reaction of $\mathbf{1}\cdot I_2Li_2$ with two equivalents of AgOAc in ethanol at room temperature [Eq. (1)]. The ^1H, ^{13}C, and ^{11}B NMR

$$[(C_2B_{10}H_{10}Hg)_4I_2]Li_2 \xrightarrow[-2\,AgI,\ -2\,LiOAc]{2\,AgOAc} cyclo\text{-}\left(-C\!-\!C\!-\!Hg-\right)_4 \quad (1)$$

$\mathbf{1}\cdot I_2Li_2$ — **1**

spectra of **1** were nearly identical with those of the halide complexes of **1**.[9] No resonance signals for the AcO^- groups were observed, and all the spectroscopic data confirmed that the tetrameric structure of **1** was preserved following the removal of iodide ions from $\mathbf{1}\cdot I_2Li_2$. The ^{199}Hg NMR spectrum of **1** exhibited a broad solvent-dependent signal at $\delta = -1305$ in THF and $\delta = 1205$ in acetone. The solvent and concentration dependence of ^{199}Hg NMR chemical shifts are well documented. The sensitivity of $\delta(^{199}Hg)$ to solvent identity has been ascribed to coordination phenomena.[10] The fact that the chemical shifts of the halide ion complexes of **1** are both solvent and concentration independent[9] suggests that the halide ion complexes of **1** have no vacant coordination sites suitable for solvent coordination. Thus, the solid-state structures[9] with mercury coordinated in a nonlinear fashion are present in solution.

A single crystal of $\mathbf{1}\cdot(THF)_4\cdot 2H_2O$ grown from THF and hexane was selected for the X-ray diffraction study (Fig. 1).[11] The framework of the molecule **1** consists of four

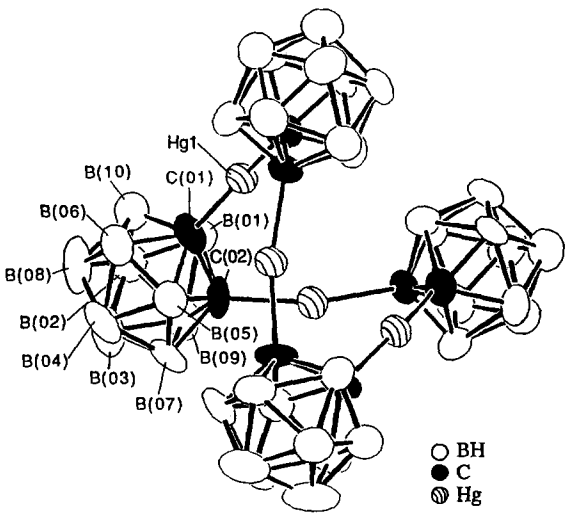

Fig. 1. Structure of the framework of $\mathbf{1}\cdot(THF)_4\cdot 2H_2O$ (ORTEP, with hydrogen atoms, H_2O and THF molecules removed for clarity). Atoms labeled are in the x, y, and z positions of the unit cell; all other atoms are generated by S_4 symmetry of the tetramer. For bond lengths and angles see text.

divalent 1,2-$C_2B_{10}H_{10}$ cages linked by the C vertices to four Hg atoms giving a cyclic tetramer. The complex has crystallographically imposed S_4 symmetry, and the four Hg atoms are approximately in a butterfly configuration. Two disordered water molecules related by the S_4 symmetry reside within the host molecule, although no significant interaction was observed between the frameworks of the host molecules and these water molecules.

Each Hg atom in **1** links carbon atoms of two carborane icosahedra (both Hg–C distances are the same 2.09(2) Å). The Hg-C-C angles are 120.3(13)° and the C-Hg-C angles are 167.7(8)°. The distance between the adjacent mercury atoms is 3.654 Å. The dihedral angle Hg-C-C-Hg is 20(2)° which is significantly larger than those found in $\mathbf{1}\cdot ClLi$ (0.0°) and $\mathbf{1}\cdot I_2(AsPh_4)_2$ (5.3 (10)°). The coordination about the Hg atom in $\mathbf{1}\cdot(THF)_4\cdot 2H_2O$ is more nearly linear, and the Hg···Hg distances are shorter than in the halide ion complexes.[9] The Hg-C-C angles are quite similar to those observed in $[(C_2B_{10}H_{11})_2Hg]\cdot(Et_2O)_2$[12] (118.3(3)°) and $[(C_6H_4Hg)_3]$[13] (average 120(3)°), both of which have linear mercury coordination. It is also noteworthy that the mercury atoms are bent away from the cavity present in $\mathbf{1}\cdot(THF)_4\cdot 2H_2O$, while the mercury atoms of the tetramer in $\mathbf{1}\cdot ClLi$ and $\mathbf{1}\cdot I_2(AsPh_4)_2$ are displaced toward the cavity.[9] This flexibility allows the framework **1** to bind donor solvents (e.g. THF) located outside the cavity through its Lewis-acidic mercury atoms. The C-Hg-O angles between the framework **1** and the bound THF molecules are each 95.2(7)°, and each THF molecule is directed away from the center of the cavity. The Hg–O distance is 2.65(2) Å, which is significantly shorter than the Hg–O distances observed in other ether or THF adducts of diorganomercury compounds. The Hg–O distance is 3.050(3) Å in $[(C_2B_{10}H_{11})_2Hg]\cdot(OEt_2)_2$[12] and 2.776 to 3.052 Å in the DME adduct (DME = 1,2-dimethoxyethane) of a macrocyclic mercuric hexafluoroglutarate.[6e]

The solution behavior of **1** in [D_6]acetone at 25 °C was investigated with ^{199}Hg NMR spectroscopy.[14] The observed broad signal may be due to the presence of a variety of conformations of solvated **1** species produced by the rotation of carborane cages as shown in Scheme 1. The incre-

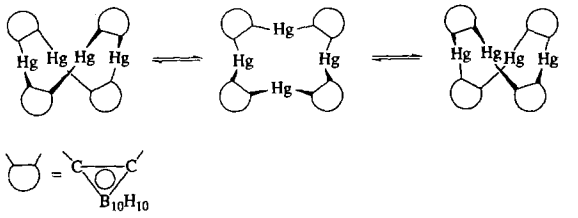

Scheme 1.

mental addition of nBu_4NI to a [D_6]acetone solution of **1** results in the formation of $\mathbf{1}\cdot I^-$ and $\mathbf{1}\cdot I_2^{2-}$ in accord with Equation 2 and as demonstrated by the ^{199}Hg NMR spectra

$$\mathbf{1} \overset{I^-}{\rightleftharpoons} \mathbf{1}\cdot I^- \overset{I^-}{\rightleftharpoons} \mathbf{1}\cdot I_2^{2-} \quad (2)$$

shown in Figure 2. The discrete signals observed here are unique, which means that exchange of I^- among **1**, $\mathbf{1}\cdot I^-$, and $\mathbf{1}\cdot I_2^{2-}$ is not fast on the NMR time scale. In the cases of 1,2-phenylenemercury dichloride and $HgCl_2$, the addition of cloride anion shifted the ^{199}Hg resonance signal down field, and only a single resonance signal was observed[6a, 15] even though more than one species was believed to be present in the solution. When more than two equivalents of tetra-*n*-butylammonium iodide were added to the [D_6]acetone solution of **1**, no further change in the spectrum was observed,

proving that **1**, in agreement with the solid-state structure of $\mathbf{1} \cdot I_2^{2-}$,[9b] is not capable of hosting more than two iodide ions. We thus suggest that the solid-state structure of $\mathbf{1} \cdot I_2^{2-}$ is largely maintained in solution. In contrast to this result, the linear mercuric ion derivatives $Hg(CN)_2$ and HgX_2 co-precipitate with MX (M = Na, K, Rb; X = Cl, Br, I) to from salts with mixed cyanohalogenomercurate ions in which each mercury atom is surrounded by four halide ions in addition to linear bonding to CN^- or X^-.[16]

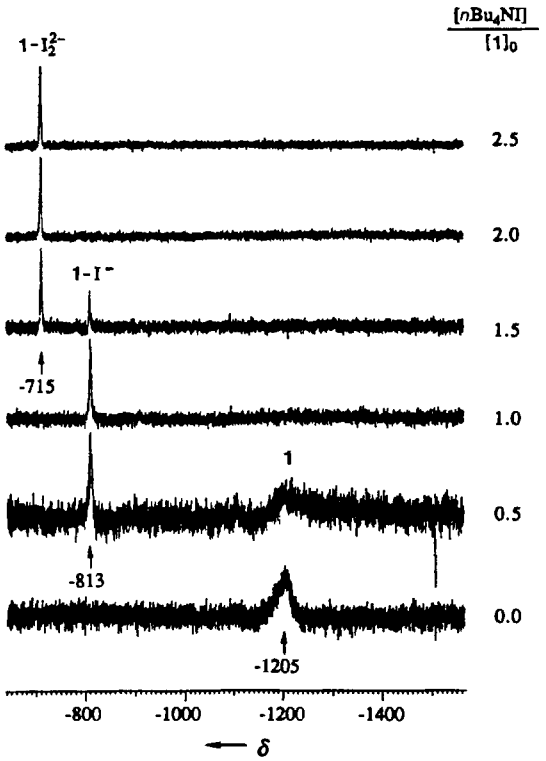

Fig. 2. ^{199}Hg NMR spectra of **1** (0.073 M) in [D$_6$]acetone at 25 °C and the spectra with the sequential addition of tetra-*n*-butylammonium iodide. For details of the measurements see Experimental Procedure and ref. [14].

The synthesis of **1** could only be achieved by the extraction of the halide ions from $\mathbf{1} \cdot I_2Li_2$ or $\mathbf{1} \cdot ILi$ with AgOAc. The reaction of chloride or bromide ion complexes of **1** with AgOAc resulted in incomplete extraction of the halide ions and a low yield of **1**. Longer reaction times permit the destructive oxidation of B–H bonds by Ag^+ ions. The reaction of $\mathbf{1} \cdot I_2Li_2$ or $\mathbf{1} \cdot ILi$ with $AgNO_3$ leads to a nitrate ion complex of **1**. We have previously mentioned[9a] that the efficient synthesis of $\mathbf{1} \cdot X_nLi_n$ (X = Cl, Br, $n = 1$; X = I, $n = 1, 2$) must be due to a template effect in which the halide ion serves as the template, since a trimeric structure is stereochemically more attractive than the tetramer. Indeed, the reaction of *closo*-[1,2-Li_2-1,2-$C_2B_{10}H_{10}$] with $Hg(OAc)_2$ produced a cyclic trimer $[(C_2B_{10}H_{10}Hg)_3]$, [9]mercuracarborand-3, which also binds halide ions and is under investigation.

In summary, the first macrocyclic host molecule with four Lewis acid centers has been synthesized and structurally characterized as its tetra(tetrahydrofuran) dihydrate complex. The demonstrated ability of this host molecule acting as a Lewis acid to bind halide ions as well as nucleophilic organic species promises to find wide application throughout chemistry.

Experimental Procedure

1: $\mathbf{1} \cdot I_2Li_2$ (10 g, 6.1 mmol) in ethanol (50 mL) was treated with AgOAc (2.14 g, 12.8 mmol) at room temperature, and a yellow precipitate immediately formed. After five minutes, the mixture was filtered, the solvent removed, and the residue recrystallized from diethyl ether to give **1** in 80% yield. $\mathbf{1} \cdot (THF)_4 \cdot 2H_2O$ forms on recrystallization from THF/H_2O/hexane; m.p. > 300 °C.

1: ^1H NMR (200 MHz, [D$_6$]acetone, 25 °C): $\delta = 1.0-3.0$ (B–H). ^{13}C NMR (50 MHz, [D$_6$]acetone, 25 °C, decoupled) $\delta = 93$ (carborane-C), signals due to ether and ethanol. ^{11}B NMR (160 MHz, [D$_6$]acetone, 25 °C, $BF_3 \cdot Et_2O$ external, decoupled) $\delta = 0.8, -6.0, -7.6, -9.6$. ^{199}Hg NMR (89.6 MHz, 0.25 M in [D$_6$]acetone, 25 °C, external standard 1.0 M PhHgCl in [D$_6$]DMSO: chemical shift $\delta = -1187$[17] upfield from neat Me_2Hg, decoupled) $\delta = -1205$. IR (KBr): $\tilde{\nu}$ [cm^{-1}] (KBr) = 2556 (B–H).

Received: January 27, 1992 [Z 5152 IE]
German version: *Angew. Chem.* **1992**, *104*, 886

CAS Registry numbers:
1, 138233-74-6; $\mathbf{1} \cdot (THF)_4 \cdot 2H_2O$, 141955-38-6; $\mathbf{1} \cdot I_2Li_2$, 138233-76-8.

[1] For example, see a) E. J. Corey, T.-P. Loh, *J. Am. Chem. Soc.* **1991**, *113*, 8966; b) M. Kuroki, T. Watanabe, T. Aida, S. Inoue, *ibid.* **1991**, *113*, 5903; c) D. Kaufmann, R. Boese, *Angew. Chem.* **1990**, *102*, 568; *Angew. Chem. Int. Ed. Engl.* **1990**, *29*, 545; d) K. Narasaka, N. Iwasawa, M. Inoue, T. Yamada, M. Nakashima, J. Sugimori, *J. Am. Chem. Soc.* **1989**, *111*, 5340.

[2] a) M. T. Reetz, C. M. Niemeyer, K. Harms, *Angew. Chem.* **1991**, *103*, 1515; *Angew. Chem. Int. Ed. Engl.* **1991**, *30*, 1472; b) M. T. P. Viet, V. Sharma, J. D. Wuest, *Inorg. Chem.* **1991**, *30*, 3026; c) V. Rotello, J. Hong, J. Rebek, Jr., *J. Am. Chem. Soc.* **1991**, *113*, 9422; d) ref. [4–9].

[3] a) D. J. Cram, *Science* **1983**, *219*, 1177; b) F. Vögtle, E. Weber, *Host-Guest Complex Chemistry/Macrocycles*, (Eds.: F. Vögtle, E. Weber), Springer, Berlin, **1985**; c) L. F. Lindoy, *The Chemistry of Macrocyclic Ligands*, Cambridge University Press, Cambridge, **1989**.

[4] a) C. H. Park, H. E. Simmons, *J. Am. Chem. Soc.* **1968**, *90*, 2431; b) R. A. Bell, G. G. Christoph, F. R. Fronczek, R. E. March, *Science* **1975**, *190*, 151; c) F. Vögtle, H. Sieger, M. M. Müller in [3b] pp. 319–373, and references therein d) B. Dietrich, J.-M. Lehn, J. Guilhem, C. Pascard, *Tetrahedron Lett.* **1989**, 4125; e) W. B. Farnham, D. C. Roe, D. A. Dixon, J. C. Calabrese, R. C. Harlow, *J. Am. Chem. Soc.* **1990**, *112*, 7707; f) Y. Murakami, J. Kikuchi, T. Ohno, T. Hirayama, Y. Hisaeda, H. Nishimura, J. Snyder, K. Steliou, *ibid.* **1991**, *113*, 8229.

[5] a) M. Newcomb, J. H. Horner, M. T. Blanda, P. J. Squattrito, *J. Am. Chem. Soc.* **1989**, *111*, 6294; b) M. Newcomb, M. T. Blanda, *Tetrahedron Lett.* **1988**, *29*, 4261; c) M. Newcomb, A. M. Madonik, M. T. Blanda, J. K. Judice, *Organometallics* **1987**, *6*, 145; d) K. Jurkschat, H. G. Kuivila, S. Liu, J. A. Zubieta, *ibid.* **1989**, *8*, 2755; e) K. Jurkschat, A. Rühlemann, A. Tzschach, *J. Organomet. Chem.* **1990**, *381*, C53; f) M. Fujita, J. Yazaki, K. Ogura, *Tetrahedron Lett.* **1991**, *32*, 5589.

[6] a) J. D. Wuest, B. Zacharie, *Organometallics* **1985**, *4*, 410; b) A. L. Beauchamp, M. J. Olivier, J. D. Wuest, B. Zacharie, *J. Am. Chem. Soc.* **1986**, *108*, 73; c) J. D. Wuest, B. Zacharie, *ibid.* **1985**, *107*, 6121; d) *ibid.* **1987**, *109*, 4714; e) F. Nadeau, M. Simard, J. D. Wuest, *Organometallics* **1990**, *9*, 1311; f) J. P. Fackler, Jr., R. A. Kresinski, *ibid.* **1991**, *10*, 3392; g) V. B. Shur, I. A. Tikhonova, A. I. Yanovsky, Yu. T. Struchkov, P. V. Petrovskii, S. Yu. Panov, G. G. Furin, M. E. Vol'pin, *J. Organomet. Chem.* **1991**, *418*, C29.

[7] a) M. E. Jung, H. Xia, *Tetrahedron Lett.* **1988**, *29*, 297; b) K. Tamao, T. Hayashi, Y. Ito, M. Shiro, *J. Am. Chem. Soc.* **1990**, *112*, 2422.

[8] a) H. E. Katz, *Organometallics* **1987**, *6*, 1134; b) *J. Am. Chem. Soc.* **1986**, *108*, 7640; c) *ibid.* **1985**, *107*, 1420; d) *J. Org. Chem.* **1989**, *54*, 2179; e) K. Narasaka, H. Sakurai, T. Kato, N. Iwasawa, *Chem. Lett.* **1990**, 1271; f) Y. Chujo, I. Tomita, T. Saegusa, *Macromolecules* **1990**, *23*, 687.

[9] a) X. Yang, C. B. Knobler, M. F. Hawthorne, *Angew. Chem.* **1991**, *103*, 1519; *Angew. Chem. Int. Ed. Engl.* **1991**, *30*, 1507, b) *J. Am. Chem. Soc.* **1992**, *114*, 380.

[10] R. J. Goodfellow in *Multinuclear NMR* (Ed.: J. Mason), Plenum, New York, **1987**, pp. 563–589.

[11] Crystallographic data for $\mathbf{1} \cdot (THF)_4 \cdot 2H_2O$: $C_{24}H_{76}B_{40}Hg_4O_6$, $M = 1697.64$, tetragonal, space group $I4_1/a$, $a = 22.902(1)$, $c = 11.242(1)$ Å, $V = 5896.66$ Å^3, $Z = 4$(1/4 of the tetramer + THF + 1/2 water molecule per asymmetric unit), $\varrho_{calcd} = 1.91$ g cm^{-3}, $T = 25$ °C, absorption coefficient $\mu = 104.17$ cm^{-1}. Data were collected on a Huber diffractometer, using $Mo_{K\alpha}$ radiation ($\lambda = 0.71073$ Å), to a maximum $2\theta = 50°$ for the range $0 \le h \le 28$, $0 \le k \le 28$, $0 \le l \le 15$, giving a total of 2604 unique reflections, of which 1686 reflections with $I > 3\sigma(I)$ were retained for structure analysis. The intensity data were corrected for Lorentz polarization, and absorption effects were applied with the transmission factor ranging from 0.82 to 0.96. The structure was solved by heavy-atom methods. All non-hydrogen atoms were refined anisotropically. The final discrepancy index was $R = 0.064$, $R_w = 0.079$ ($w = 1/\sigma^2(F_0)$) for 1686 independent re-

flections with $I > 3\sigma(I)$. $\Delta\varrho_{max} = 4.22$ Å^{-3} in the final difference Fourier syntheisis (located close to the Hg atom). Hydrogen atoms of the water molecules were not included in the refinement. Further details of the crystal structure investigation may be obtained from the Fachinformationszentrum Karlsruhe, Gesellschaft für wissenschaftlich-technische Information mbH, D-W-7514 Eggenstein-Leopoldshafen 2 (FRG), on quoting the depository number CSD-56190, the names of the authors, and the jornal citation.

[12] X. Yang, S. E. Johnson, C. B. Knobler, M. F. Hawthorne, unpublished.

[13] D. S. Brown, A. G. Massay, D. A. Wickens, *Acta. Crystallogr. Sect. B* **1978**, *34*, 1695.

[14] The ^{199}Hg NMR spectra were recorded at 25 °C with a Bruker 500 spectrometer at 89.6 MHz by using broad-band decoupling. External standard: 1.0 M PhHgCl [D_6]DMSO (chemical shift $\delta = -1187$ relative to neat Me_2Hg). A 0.073 M solution of **1** in [D_6]acetone was used in the study of the exchange of iodide with **1**.

[15] P. D. Godfrey, M. L. Heffernan, D. F. Kerr. *Aust. J. Chem.* **1964**, *17*, 701.

[16] a) G. Thiele, K. Brodersen, H. Frohring, *Z. Naturforsch. B.* **1981**, *36*, 180; b) F. H. Kruse, *Acta Crystallogr.* **1963**, *16*, 105.

[17] M. A. Sen, N. K. Wilson, P. D. Ellis, J. D. Odom, *J. Magn. Reson.* **1975**, *19*, 323.

Synthesis, Structure, and Bonding of $[CpCoW_2(OCH_2tBu)_6]$, and Comments on the Combining Properties of CO and CpCo**

By *Malcom H. Chisholm*, Victor J. Johnston, Odile Eisenstein,* and *William E. Streib*

The isolobal analogy and the frontier molecular orbital (FMO) approach are valuable in providing insight into the bonding in organometallic compounds, and they aid in the strategic synthesis of new molecules.[1] The recent report[2] of the preparation and structure of $[Cp^*_2Co_2]$ ($Cp^* = \eta^5$-C_5Me_5) prompts us to report our synthesis and characterization of the title compound **1**, and also to comment on the interesting analogy with the CO-bridged complex **2**[3] that arises from the isolobal relationship between CO and CpCo.

$[CpCoW_2(OCH_2tBu)_6]$ **1** $[W_2(\mu\text{-CO})(OtBu)_6]$ **2**

The reaction between the Jonas compound[4] $[CpCo(C_2H_4)_2]$ and $[W_2(OCH_2tBu)_6(py)_2]$ (py = pyridine)[5] in hydrocarbon solvents at 25 °C gives rise to the formation of **1** in about 50% isolated yield as dark green crystals. The ^{1}H and ^{13}C NMR spectra of **1** in C_6D_6 are consistent with the molecular structure found in the solid state by single-crystal X-ray crystallography.[6] The molecular structure of **1** is shown in Figure 1.

The W_2O_6 skeleton of **1** is essentially identical to that of **2**. The bonding in **2** was previously examined by Fenske–Hall MO calculations[7] and analyzed by the FMO approach wherein the MOs of the $(HO)_2W(\mu\text{-}OH)_2W(OH)_2$ fragments were made to interact with the MOs of CO (Fig. 2).[3b] The

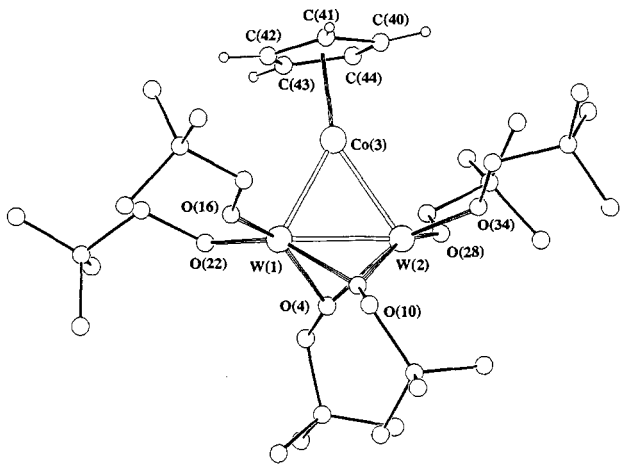

Fig. 1. Crystal structure of **1**. Selected distances [Å]: W-W 2.504(2), Co-W(1) 2.281(4), Co-W(2) 2.340(4), W-$O_{terminal}$ 1.89(2), W-$O_{bridging}$ 2.06(2). The last two distances are average values.

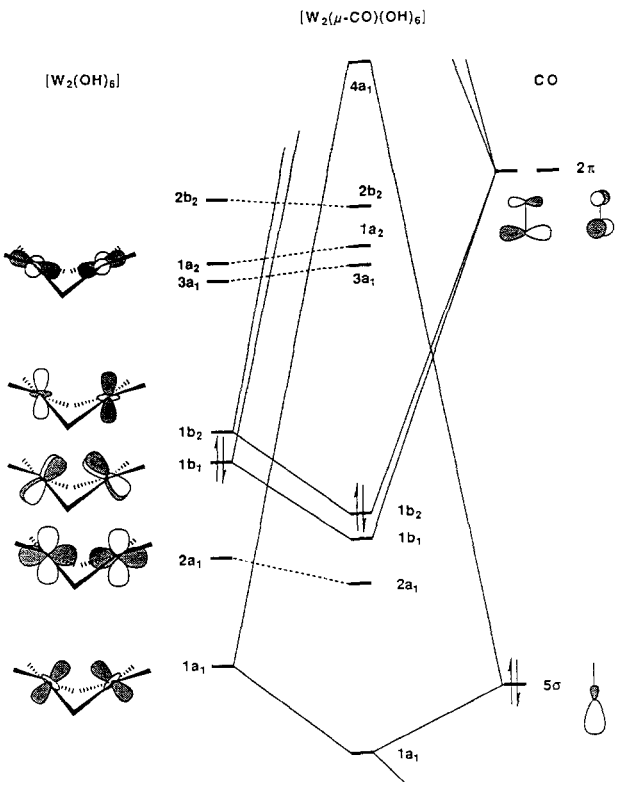

Fig. 2. MO diagram showing the formation of the hypothetical $[W_2(\mu\text{-}CO)(OH)_6]$ molecule from the interactions of the MOs of the fragments $(HO)_2W(\mu\text{-}OH)_2W(OH)_2$ (left) and CO (right). The HOMO is indicated by the pair of arrows.

MOs of **1** have been similarly constructed by the combination of the MOs of the $(HO)_2W(\mu\text{-}OH)_2W(OH)_2$ and CpCo fragments (Fig. 3).[8] The main difference between the bonding in **1** and **2** involves their HOMOs; for **1** this is a Co–(W-W) nonbonding MO whereas in **2** it is a metal-to-carbon bonding MO ($Md\pi \rightarrow CO\pi^*$).

The similarities in the bonding in **1** and **2** which arise from the isolobal nature of CO and CpCo are shown in Scheme 1. Both CO and CpCo have an *a* and an *e* set of orbitals with a total electron count of two. However, the relative energies

[*] Prof. M. H. Chisholm, Dr. V. J. Johnston, Dr. W. E. Streib
Department of Chemistry and Molecular Structure Center
Indiana University, Bloomington, IN 47405 (USA)
Dr. O. Eisenstein
Laboratoire de Chimie Théorique
Bâtiment 490, Centre de Paris-Sud, F-91450 Orsay (France)

[**] This work was supported by the Department of Energy, Office of Basic Sciences, Chemistry Division. O. E. acknowledges support from the Centre National de la Recherche Scientifique and the National Science Foundation for her residence at Indiana University.

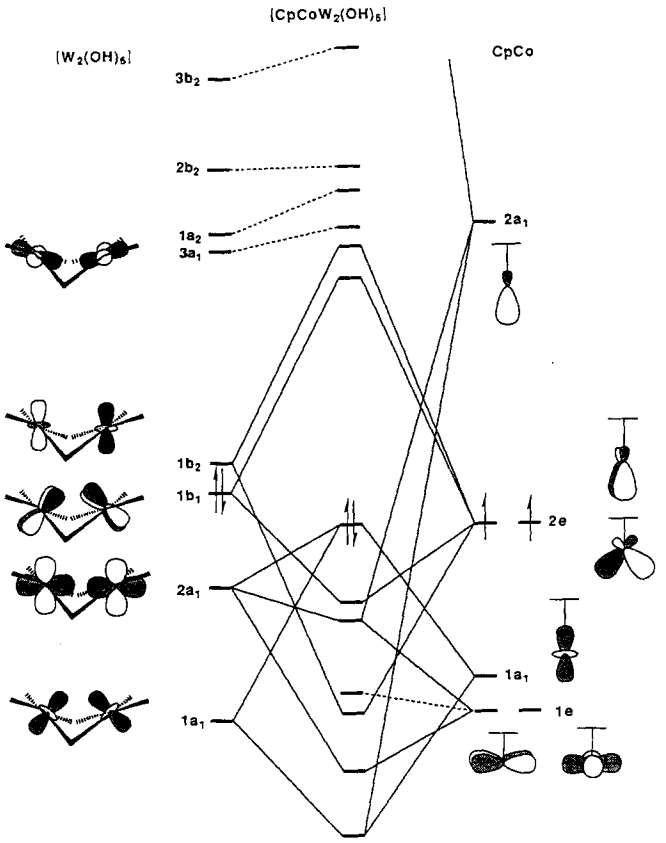

Fig. 3. MO diagram showing the formation of the hypothetical $[CpCoW_2(OH)_6]$ molecule from the interaction of the MOs of the fragments CpCo (right) and $W_2(OH)_6$ (left). The HOMO is indicated by the pair of arrows.

of these sets are inverted. For CO the *a* orbital is the 5σ MO, the lone pair centered on carbon, while for CpCo the *a* orbital is the high-lying valence hybrid orbital of an ML_3 fragment. From the frontier orbitals shown in Scheme 1 we can readily anticipate the bonding in a hypothetical linear [CpCo(CO)] molecule,[9] a spin triplet with a formal Co–CO $\sigma^2\pi^2$ double bond. In the linear $[Cp_2Co_2]$ dimer the relative

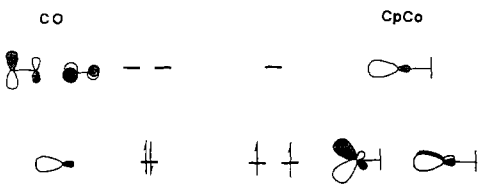

Scheme 1.

energies of the σ and π bonding MOs would need to be determined from a calculation. However, from the observed short Co–Co distance[2] it is not unreasonable to formulate a Co–Co double bond arising from four electrons distributed in a σ,π orbital set. Given the observed paramagnetism,[2] a simple one-electron MO description is not valid, since configuration interactions must also be considered.[10] The isolobal analogy and FMO approach are also useful in considering the hypothetical $(CO)_2$ dimer. The initial approach of two CO molecules to give a linear OCCO molecule would lead to repulsive interactions since both σ and σ^* orbitals will be occupied.[1b] However, at short C–C distances the π bonding MO resulting from the interaction of the in-phase CO π^* MOs would fall below the σ^* MO, again leading to a σ, π orbital set occupied by four electrons. In the dianion, $(OCCO)^{2-}$, which has a short C–C distance, there is a formal C–C $\sigma^2\pi^4$ triple bond. In coordination chemistry the $(OCCO)^{2-}$ anion is stabilized by the presence of cations in the lattice[11] or by complexation to a transition metal as an alkyne after the reductive coupling of two carbonyl ligands.[12]

In summary, we have prepared the cluster $[CpCoW_2(OCH_2tBu)_6]$ (**1**) and have noted its structural similarity to $[W_2(\mu\text{-}CO)(OtBu)_6]$ (**2**). The isolobal nature of CpCo and CO leads to interesting analogies in their combinations as illustrated by **1**, **2**, [CpCo(CO)], $[Cp^*_2Co_2]$, and $(OCCO)^{2-}$. The frontier MOs of $[W_2(OR)_6]$ molecules, either in their unbridged ground-state geometries or in bridged excited states, should make them versatile templates for the synthesis of a wide variety of heterometallic clusters, just as it has for the binding of unsaturated hydrocarbon fragments.[13]

Experimental Procedure

All manipulations were performed under a nitrogen atmosphere using dry, oxygen-free solvents. Starting materials were prepared by the literature methods cited.

1: $[W_2(OCH_2tBu)_6(py)_2]$ (1.015 g, 0.97 mmol), $[CpCo(C_2H_4)_2]$ (200 mg, 1.11 mmol) and hexane (20 mL) were stirred at 25 °C for 2 days. The volatiles were removed on the vacuum line, and **1** (480 mg, 0.48 mmol, 49 %) was recrystallized from dimethoxyethane at −20 °C. Correct C,H analysis.

^1H NMR (C_6D_6, 25 °C, 300 MHz): $\delta = 4.68$ (5H;Cp), 4.49 (d, $J(H,H) = 10.2$ Hz, 4H; OCH_2CMe_3), 4.27 (d, $J(H,H) = 10.2$ Hz, 4H; OCH_2CMe_3), 4.17 (s, 4H; OCH_2CMe_3), 1.16 (s, 36H; OCH_2CMe_3), 0.94 (s, 18H; OCH_2CMe_3); $^{13}C\{^1H\}$ NMR (C_6D_6, 25 °C, 75 MHz): $\delta = 80.8$ (5C; Cp), 85.7 (4C; OCH_2CMe_3), 84.4 (2C; OCH_2CMe_3), 34.3 (OCH_2CMe_3), 27.0 (OCH_2CMe_3).

Received: January 23, 1992 [Z 5143 IE]
German version: *Angew. Chem.* **1992**, *104*, 889

CAS Registry numbers:
1, 141805-49-4; $[W_2(OCH_2tBu)_6(py)_2]$, 88608-50-8; $[CpCo(C_2H_4)_2]$, 69393-67-5; $[CpCoW_2(OH)_6]$, 141805-50-7; $[W_2(\mu\text{-}CO)(OH)_6]$, 103671-08-5.

[1] a) R. Hoffmann, *Angew. Chem.* **1982**, *94*, 725; *Angew. Chem. Int. Ed. Engl.* **1982**, *21*, 711; b) T. A. Albright, J. K. Burdett, M. H. Whangbo, *Orbital Interactions in Chemistry*, Wiley, New York, **1985**; c) F. G. A. Stone, *Angew. Chem.* **1984**, *96*, 85; *Angew. Chem. Int. Ed. Engl.* **1984**, *23*, 89; d) K. P. Hall, D. M. P. Mingos, *Prog. Inorg. Chem.* **1984**, *32*, 237.

[2] J. J. Schneider, R. Goddard, S. Werner, C. Krüger, *Angew. Chem.* **1991**, *103*, 1145; *Angew. Chem. Int. Ed. Engl.* **1991**, *30*, 1124.

[3] a) M. H. Chisholm, D. M. Hoffman, J. C. Huffman, *Organometallics* **1985**, *4*, 986; b) P. J. Blower, M. H. Chisholm, D. L. Clark, B. W. Eichhorn, *ibid.* **1986**, *5*, 2125.

[4] K. Jonas, E. Deffense, D. Habermann, *Angew. Chem.* **1983**, *95*, 729; *Angew. Chem. Int. Ed. Engl.* **1983**, *22*, 716; *Angew. chem. Suppl.* **1983**, 1005.

[5] M. Akiyama, M. H. Chisholm, F. A. Cotton, M. W. Extine, D. A. Haitko, D. Little, P. E. Fanwick, *Inorg. Chem.* **1979**, *18*, 2321.

[6] Crystal structure analysis of **1**. Cell constants at −173 °C: $a = 18.811(2)$, $b = 21.288(3)$, $c = 20.854(3)$, $\beta = 97.65(1)$, monoclinic space group $P2_1/n$; $Z = 8$, $\mu = 60.98\ cm^{-1}$ (an analytical correction was applied), 5831 data with $I \geq 3\sigma(I)$, 384 variables, $R = 0.065$, $R_w = 0.066$. Further details of the crystal structure investigation are available on request from the Fachinformationszentrum Karlsruhe, Gesellschaft für wissenschaftlich-technische Information mbH, D-W-7514 Eggenstein-Leopoldshafen 2 (FRG), on quoting the depository number CSD-56329, the names of the authors, and the journal citation.

[7] M. B. Hall, R. F. Fenske, *Inorg. Chem.* **1972**, *11*, 768.

[8] The basis function used in the MO calculation of $[CpCoW_2(OH)_6]$ were the default values supplied with the Fenske–Hall program, see: F. Herman, S. Skillman, *Atomic Structure Calculations*, Prentice-Hall, Englewood Cliffs, N. J., USA. **1963**; B. E. Bursten, R. F. Fenske, *J. Chem. Phys.* **1977**, *67*, 3138; B. E. Bursten, R. J. Jensen, R. F. Fenske, *ibid.* **1978**, *68*, 3320. For consistency, the calculation of $[W_2(\mu\text{-}CO)(OH)_6]$ was repeated using these basis functions.

[9] P. Hofmann, M. Padmanabhan, *Organometallics* **1983**, *2*, 1273; T. Ziegler, V. Tschinke, L. Fan, A. D. Beche, *J. Am. Chem. Soc.* **1989**, *111*, 9177.

 © VCH Verlagsgesellschaft mbH, W-6940 Weinheim, 1992 0570-0833/92/0707-0897 $ 3.50+.25/0

[CpCoCO] has also been proposed as a reactive intermediate, see: W.-S. Lee, H. H. Brintzinger, *J. Organomet. Chem.* **1977**, *127*, 87.
[10] a) M. B. Hall, *Polyhedron* **1987**, *6*, 679; b) A paper has recently appeared in this journal entitled "The Electronic Structure of $[(\eta^2\text{-}C_5H_5)_2Co_2]$: A Comment on the Existence of a Complex with an Unsupported Co–Co Double Bond", H. B. Abrahamson, G. P. Niccolai, D. M. Heinekey, C. P. Casey, B. E. Bursten, *Angew. Chem.* **1992**, *104*, 464; *Angew. Chem. Int. Ed. Engl.* **1992**, *31*, 471.
[11] a) J. Liebig, *Justus Liebigs Ann. Chem.* **1834**, *11*, 182; b) E. Weiss, W. Büchner, *Helv. Chim. Acta* **1963**, *46*, 1121; W. Büchner, *ibid.* **1963**, *46*, 2111.
[12] R. N. Vrtis, C. P. Rao, S. Warner, S. J. Lippard, *J. Am. Chem. Soc.* **1988**, *110*, 2669; R. N. Vrtis, S. Liu, C. P. Rao, S. G. Bott, S. J. Lippard, *Organometallics* **1991**, *10*, 275.
[13] a) General review: M. H. Chisholm, D. L. Clark, M. J. Hampden-Smith, D. Hoffman, *Angew. Chem.* **1989**, *101*, 446; *Angew. Chem. Int. Ed. Engl.* **1989**, *28*, 432. b) ethene: R. H. Cayton, S. T. Chacon, M. H. Chisholm, J. C. Huffman, *Angew. Chem.* **1990**, *102*, 1056; *Angew. Chem. Int. Ed. Engl.* **1990**, *29*, 1026; c) allene: R. H. Cayton, S. T. Chacon, M. H. Chisholm, M. J. Hampden-Smith, J. C. Huffman, K. Folting, P. Ellis, B. A. Higgins, *ibid.*, **1989**, *101*, 1547 and **1989**, *29*, 1523; S. T. Chacon, M. H. Chisholm, K. Folting, J. C. Huffman, M. J. Hampden-Smith, *Organometallics* **1991**, *10*, 3722; d) butadiene: M. H. Chisholm, J. C. Huffman, E. A. Lucas, E. B. Lubkovsky, *Organometallics* **1991**, *10*, 3424; e) α,β-unsaturated ketones: M. H. Chisholm, E. A. Lucas, A. C. Sousa, J. C. Huffman, *J. Chem. Soc. Chem. Commun.* **1991**, 847.

Synthetic Chain-Substituted Phospholipids: Ion Transport Across Their Bilayer Membranes**

By *Fredric M. Menger** and *Patricia Aikens*

Nature has established the means to control, according to conditions, passive diffusion through its membranes. For example, membranes of cold-water marine life are endowed with high levels of "fluidizing" lipids (i.e. polyunsaturates). Control of permeability is also important to drug delivery systems based on lipid membranes with defined leakage rates.[1] Thus, one would wish to examine, systematically, the effect of lipid structure on permeability. The opportunity to do so presented itself after we synthesized a series of phospholipids for calorimetric and film studies.[2, 3] The new lipids possessed 18-carbon chains bearing alkyl substituents of varying size, location, and number. Two examples of such distearoylphosphatidylcholines (with a self-explanatory nomenclature) are shown in Scheme 1. With this set of lipids

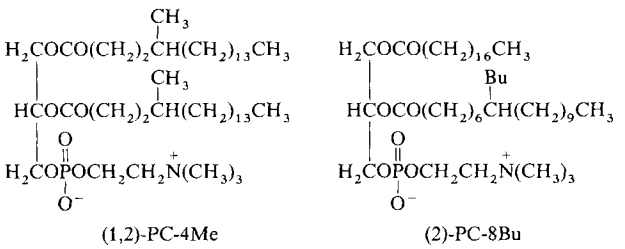

Scheme 1. Two examples of phospholipids with branched chains.

in hand, we were able to examine ion flux through their bilayer membranes. As will be described shortly, alkyl branching disrupts the packing of the lipid chains that reside in a more-or-less parallel array within the membrane. The disruption facilitates the passage of ions in a manner dependent on the size and location of the alkyl substituents.

Ion flux was monitored by the same method described in previous work on synthetic ion channels.[4] A branched phospholipid and a fluorescent dye[5] were co-sonicated in a weak buffer (pH = 7.7, 0.1 M KCl).[6] This created unilamellar vesicles with dye both on the inside and outside. The latter was removed by gel filtration. When the external pH was abruptly lowered to 6.7, protons migrated into the vesicles and protonated the dye, thereby eliminating its fluorescence. According to quasi-elastic light scattering, the vesicles had diameters of 35 ± 5 nm.

Typical plots of fluorescence against time for the parent distearoylphosphatidylcholine (DSPC) and the branched (1,2)-PC-8Me are given in Figure 1. In agreement with previous results of Clement and Gould,[7] the fluorescence decreases in a biphasic manner upon HCl addition to the external water. The initial drop in fluorescence corresponds to an electrically uncompensated diffusion of protons into the vesicles.[8] Inward proton flow, which was too fast to measure conventionally, creates a transmembrane potential that drives the ensuing slower step, the outward diffusion of potassium ions. As potassium ions depart, protons are allowed, on a one-to-one basis, further entry.[9] The initial electrical potential is thereby maintained. Although K^+ flux is known to be orders of magnitude slower than H^+ flux,[10] the difference is mitigated by our operating with 0.1 M KCl and pH = 7 and, therefore, with a 10^6 excess of potassium ions over protons.

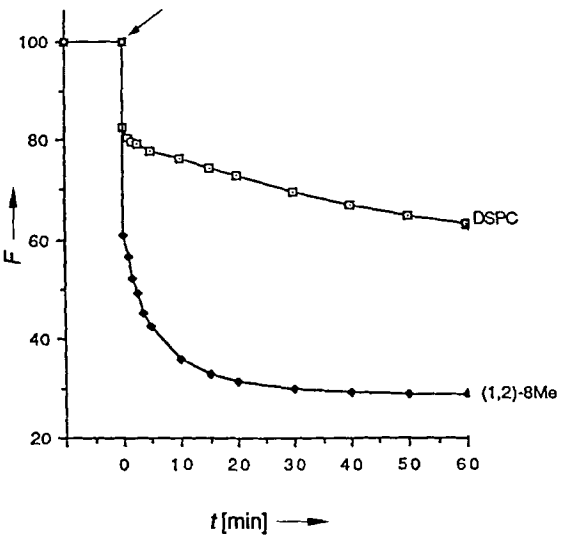

Fig. 1. Fluorescence vs. time graph after HCl was added to vesicles containing a pH-sensitive dye. Plots show how the presence of methyl groups at position 8 of the chains enhances the entry of protons relative to unbranched DSPC. The process is biphasic (the initial fluorescence decrease being too fast to measure by conventional means).

Since outward K^+ flow is a first-order process under our conditions, plots of $\log[F - F_\infty]$ against time are linear [Figs. 2–4]. The intercepts represent the maximum proton-induced potential permitted by a particular membrane. Subsequent K^+ exodus occurs with rates given by the slopes of the plots. Our library of synthetic lipids was sufficiently diverse that we could readily compare systems below and above their phase transition temperature T_c.

[*] Prof. F. M. Menger, P. Aikens
Department of Chemistry
Emory University
Atlanta, GA 30322 (USA)

[**] This work was supported by the National Institutes of Health.

Figure 2 gives the transport data at 20 °C (below T_c) for DSPC and three lipids alkylated at the 4-position.[11] The intercepts show that the extent of proton entry is modestly dependent on the size of the substituent at position 4. Branching may spread the head-group region, thus permitting entry of water and an increase in the membrane's dielectric constant.[12] A greater electrical potential and concomitant proton entry is, therefore, possible. Alternatively, the substituents may thicken the membrane (in the order Bu > Et > Me > H) and thus enhance its ability to tolerate uncompensated proton flux.

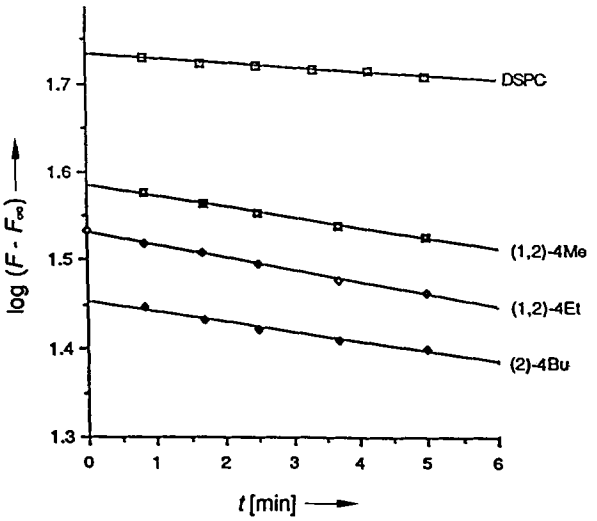

Fig. 2. Comparison of proton entry rates through vesicles composed of three branched lipids and the unbranched DSPC. $T < T_c$. F_∞ = fluorescence at $t \rightarrow \infty$.

The slopes of the four plots in Figure 2 are all similar. Branching clearly has little effect on K^+ exit rates when the membranes are in their gel state. Apparently, no potassium-conducting "channels" are formed across the membrane despite the one or two alkyl substituents per lipid that presumably disrupt the side-by-side packing within the bilayer.

Figure 3 reveals an additional point about vesicle permeability as a function of structure. Methyl substitution at positions 8 and 10 is seen to enhance K^+ flux substantially (15- and 18-fold relative to DSPC), whereas no such effect was observed for substitution at positions 4 and 16. The simplest explanation relates to the fact that our operating temperature of 20° fell below the T_c values of 30.1° and 26.9° for (1,2)-PC-4Me and (1,2)-PC-16Me, respectively. In contrast, the 8-Me and 10-Me derivatives, with T_c values less than 0°, existed in the fluid state. Thus, a locus-sensitive T_c translates directly into a locus-sensitive K^+ flux.[13] This behavior is consistent with an enhanced H^+ and K^+ flux observed when dipalmitoylphosphatidylcholine vesicles were warmed from 32° to the T_c of 42°. Thus, in order to improve membrane permeability, one can either heat or alkylate. As discussed in detail previously,[2, 3] conformational perturbations near the middle of the chain have a particularly potent effect on several membrane properties; permeability must now be added to the list.

A series of lipids with substituents at C8 were examined at 20° where they all existed in their fluid state (Fig. 4). Rates

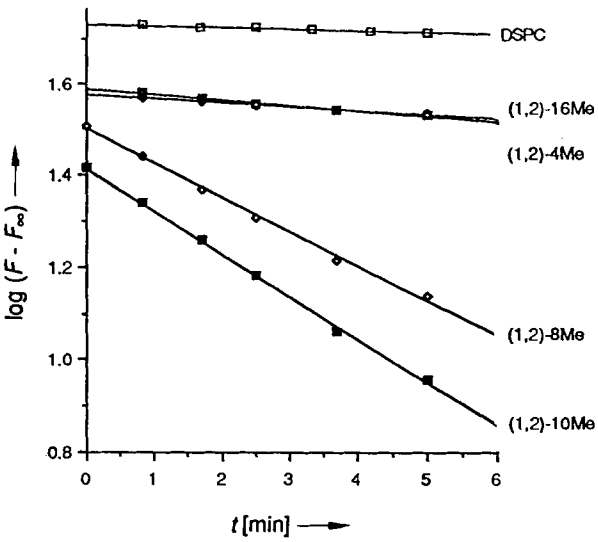

Fig. 3. Dependence of proton entry rates on the location of methyl groups attached to the lipid chains.

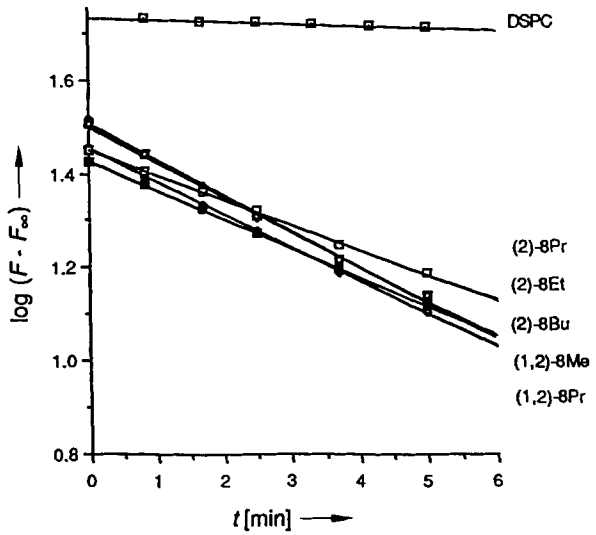

Fig. 4. Dependence of proton entry rates on the size and number of substituents at position 8. $T > T_c$.

of ion flux, although much faster than that of DSPC, are within experimental error of each other regardless of substituent size or number. Rotational disorder induced by alkylation at the critical middle section of the lipid promotes ion movement as does a simple phase transition. The two processes would seem, therefore, to have a common molecular basis.

Received: January 13, 1992 [Z 5116 IE]
German version: *Angew. Chem.* **1992**, *104*, 919

[1] G. Gregoriadis, *Liposomes as Drug Carriers: Recent Trends and Progress*, Wiley, Chichester, England, **1988**.
[2] F. M. Menger, M. G. Wood, Jr., Q. Z. Zhou, H. P. Hopkins, J. Fumero, *J. Am. Chem. Soc.* **1988**, *110*, 6804.

[3] F. M. Menger, M. G. Wood, Jr., S. Richardson, Q. Z. Zhou, A. R. Elrington, M. J. Sherrod, *J. Am. Chem. Soc.* **1988**, *110*, 6797; see also the review F. M. Menger, *Angew. Chem.* **1991**, *103*, 1104; *Angew. Chem. Int. Ed. Engl.* **1991**, *30*, 1086.
[4] F. M. Menger, D. S. Davis, R. A. Persichetti, J.-J. Lee, *J. Am. Chem. Soc.* **1990**, *112*, 2451.
[5] The dye was the trianion of 8-hydroxy-1,3,6-pyrenetrisulfonic acid ($pK_a = 7.2$; $\lambda_{abs.} = 460$ nm, $\lambda_{em.} = 510$ nm).
[6] All vesicle preparations contained 10% anionic distearoylphosphatidic acid to inhibit vesicle aggregation.
[7] N. R. Clement, J. M. Gould, *Biochemistry* **1981**, *20*, 1534.
[8] G. Krishnamoorthy, P. C. Hinkle, *Biochemistry* **1984**, *23*, 1640.
[9] D. W. Deamer, J. W. Nichols, *J. Membr. Biol.* **1989**, *107*, 91.
[10] S. Grzesiek, N. A. Dencher, *Biophys. J.* **1986**, *50*, 265.
[11] T_c values refer to lamellar phases[2] and thus are only qualitatively applicable to small unilamellar vesicles.
[12] D. S. Cafiso, *J. Bioenerg. Biomembr.* **1987**, *19*, 444.
[13] K. Elamrani, A. Blume, *Biochim. Biophys. Acta* **1983**, *727*, 22.

The Pyrolysis of Tetranitromethane in the Gas Phase

By *Hans Bock** and *László Zanathy*

$C(NO_2)_4$, a colorless liquid boiling at 126 °C, contains more than 65% by weight of oxygen and thus represents one of the most oxygen-rich methane derivatives. In addition to its use as a nitration reagent,[1a] therefore, it serves as an additive to propellants and explosives.[1b,c] For this reason, we became interested in its thermal decomposition in the gas phase,[2] which like all compounds with a tendency to explode such as alkyl azides,[3a] diazo alkanes,[3b,c] or even the shock-sensitive S_4N_4,[3d] can be investigated without risk under nearly unimolecular conditions with photoelectron (PE)-spectroscopy in the gas phase[3e] (Fig. 1).

The ionization pattern of $C(NO_2)_4$, whose gas-phase structure exhibits the rather rare symmetry S_4 determined by electron diffraction[4a] (cf. Fig. 1, upper left), shows six bands with maxima at 12.6, 13.3, 14.32, 17,6, and 18.6 in the intensity ratio 4:6:1:1:4:4. They can be assigned by Koopman's correlation, $IE_n^V = -\varepsilon_j^{AM\,1}$, with eigenvalues calculated with AM 1, to altogether 20 radical cation states of the irreducible representations, $\Gamma_{red} = 5a + 5b + 5e$. Accordingly, the low-energy bands correspond to four oxygen lone-pair ionizations, and the second one to four with dominant n_O contributions as well as three of the σ_{CNO} type.[4b] The geometry-optimized AM 1 calculations reproduce the S_4 structure, yield a heat of formation $\Delta H_f^{AM\,1} = +420\ kJ\,mol^{-1}$, and suggest a charge distribution >C(+0.02)–N(+0.46)–O(−0.23) with partial positive charges at the N centers.[4c]

The temperature-dependent PE spectra[5] of $C(NO_2)_4$, recorded in 30 K intervals (Fig. 1), prove that the decomposition starts at a furnace temperature of 520 K and is complete at 610 K (Scheme 1). The decomposition products, identified unequivocally by their needle-like ionization patterns, are exclusively $^{\bullet}NO_2$, $^{\bullet}NO$, CO_2, and above 580 K, CO; neither O_2 nor N_2 form.

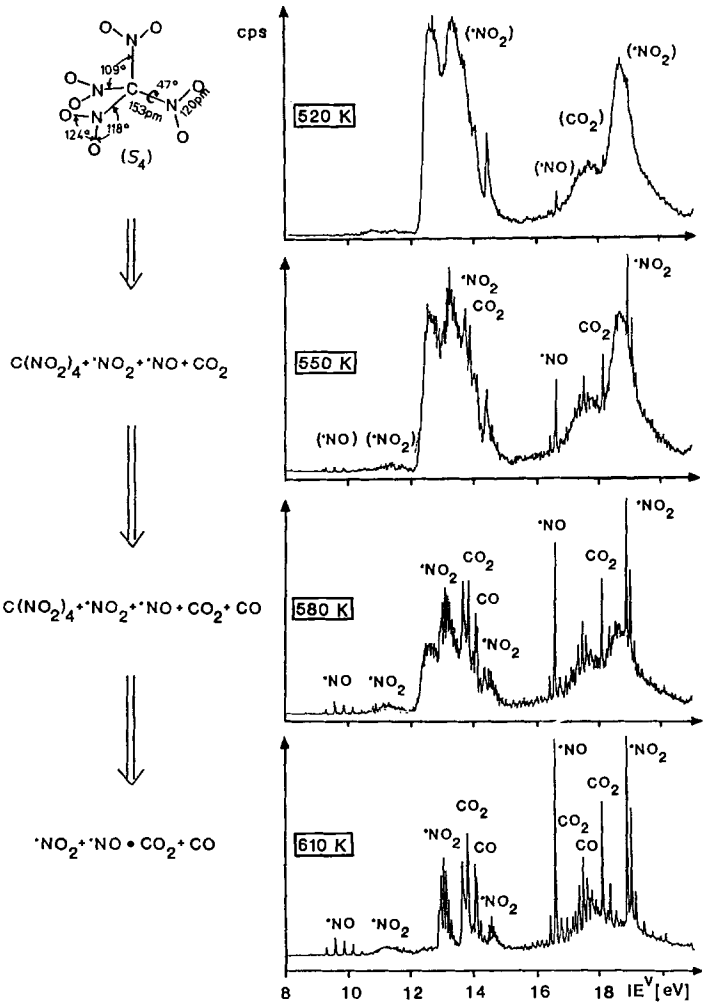

Fig. 1. He(I)PE spectra of tetranitromethane on heating in a flow tube at 10^{-4} mbar to 520, 550, 580, and 610 K (cf. text); cps = counts per second.

The temperature dependence of the $C(NO_2)_4$ decomposition under nearly unimolecular conditions (Fig. 1) suggests a possible microscopic pathway (Scheme 2).

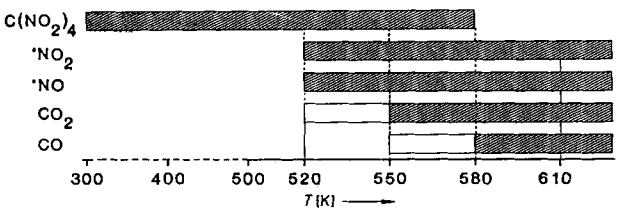

Scheme 1. Temperature dependence of the product distribution of the $C(NO_2)_4$ pyrolysis at 10^{-4} mbar.

For a discussion of the $C(NO_2)_4$ pyrolysis pathway it must be pointed out that none of the postulated intermediates can be detected, even on decomposition in the internal furnace of the high-performance PE spectrometer,[5a] and therefore their half-lives $t_{1/2}$ must be below 10^{-4} s. The dissociation into $^{\bullet}NO_2$ and trinitromethyl radicals assumed as the initial (Scheme 2) is in accord with the unimolecular decomposition proven in a helium flow experiment.[2] The activation enthalpy for the $^{\bullet}NO_2$ elimination from the energy-rich

[*] Prof. Dr. H. Bock, Dr. L. Zanathy[+]
Institute of Inorganic Chemistry of the University
Niederurseler Hang, D-W-6000 Frankfurt am Main (FRG)
[+] Permanent address: Institute of General and Inorganic Chemistry
Eötvös University
Pazmany setany 2,H-1518 Budapest (Hungary)

[**] Gas-phase Reactions, Part 90. The project has been supported by the Deutsche Forschungsgemeinschaft, the Deutsche Akademische Austauschdienst, the state of Hesse and the Fonds der Chemischen Industrie. Part 89: [3b].

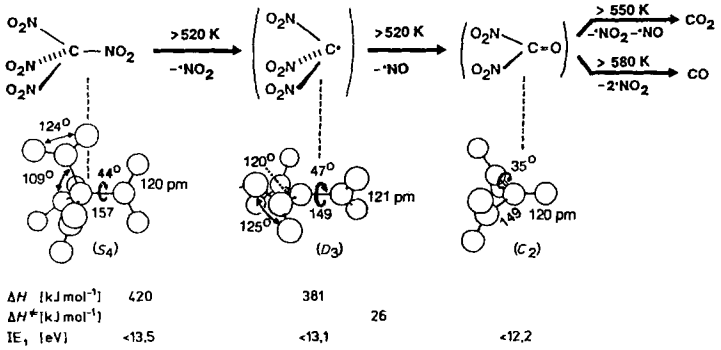

Scheme 2. Proposal for a sequence of steps in the $C(NO_2)_4$ pyrolysis (boldface arrows: PES analysis), supported by AM 1 calculations (cf. text).

$C(NO_2)_4$ estimated by geometry-optimized AM 1 calculations[4c, 7a] is smaller than the kinetically determined one[2] and agrees well with the lower decomposition temperature of only 520 K[7b] observed under the different conditions selected. For the trinitromethyl radical, an enthalpy of formation of 381 kJ mol^{-1} is predicted, as well as a planar D_{3h} structure.[7c] An additional reaction channel in which, after the isomerization $(O_2N)_3C{-}NO_2 \rightarrow (O_2N)_3C{-}ONO$, ·NO is first eliminated to form a $(O_2N)_3CO$· radical can be excluded due to the high isomerization enthalpy predicted by AM 1 calculations (> 500 kJ mol^{-1}[7d]). A subsequent ·NO elimination to form $(O_2N)_2C{=}O$ is postulated as second step (Scheme 2); this second intermediate is also not observed by PE spectroscopy despite its favorable enthalpy of formation and its low first ionization energy estimated by geometry-optimized AM 1 calculations. Nevertheless, among all speculative precursors it best rationalizes the formation of the final products CO_2 and CO in different reaction channels above 500 K and 580 K (Scheme 1 and 2), because not even traces of O_2 or N_2 can be detected.

In addition, the thermal decomposition of gaseous tetranitromethane under reduced pressure has been investigated at solids such as silver wool or charcoal [Eq. (a)] as well as in cothermolyses with added organic compounds.[8a]

$$C(NO_2)_4 \xrightarrow[600\ K]{[Ag]_x} {\cdot}NO_2 + CO_2 + {\cdot}NO + (CO) \qquad (a)$$
$$C(NO_2)_4 \xrightarrow[300\ K]{[C]_x} CO_2 + {\cdot}NO$$

According to the PES band intensities (cf. Fig. 1), only about one third of the ·NO observed in the gas-phase thermolysis is generated at silver wool heated to a furnace temperature of 600 K, in addition to $\cdot NO_2$ and CO_2 as well as traces of CO, a result that indicates a preceding chemisorption at the silver surface. The largest differences are found for the reaction at activated charcoal:[5b] Decomposition takes place already at room temperature, and the only gaseous products formed are ·NO as well as small amounts of CO_2. This suggests coal nitration and oxidation, which are supported by the deflagration of the resulting solid product observed on heating it to 350 K in an additional desorption attempt. A gas-phase nitration could be accomplished by cothermolysis with dimethylamine above 600 K [Eq. (b)].[5b]

$$(H_3C)_2NH \xrightarrow[600\ K]{C(NO_2)_4} (H_3C)_2N{-}NO_2 \qquad (b)$$

Outside the oven-zone, yellow crystals precipitate at the wall of the reaction tube. They are identified as dimethylnitramine by their melting point of 58 °C[8a, b] and their ^{1}H NMR spectrum (CD_3OD/TMS, δ = 2.66 (s)[8b, c]).

The reactive nitration reagent $C(NO_2)_4$ thus belongs to the few compounds, which like azadicarbonitrile ($\rightarrow N_2 + NCCN$[9a]), methyl azide ($\rightarrow N_2 + H_2 + HCN$[2a]) or tetracyano-*para*-benzoquinone ($\rightarrow 2\,CO + 2\,NC{-}C{\equiv}C{-}CN$[9b]) completely decompose on heating into thermodynamically favorable, gaseous components [Eq. (c)]. The reaction energy set free and the simultaneous volume increase, therefore, advise a careful handling.[1b, c]

$$C(NO_2)_4 \xrightarrow{>550\ K} 2\,{\cdot}NO_2 + 2\,{\cdot}NO + CO_2 \qquad (c)$$
$$C(NO_2)_4 \xrightarrow{>580\ K} 3\,{\cdot}NO_2 + {\cdot}NO + CO$$

The thermal decompositions of organic nitro compounds R–NO_2 and R–ONO, which can be investigated without risk under the conditions selected here,[5] provide interesting information. As a striking example, the chemical activation (cf. [3a]) of the propanal generated by thermolysis of allyl nitrite via ·NO elimination is quoted,[10] which decomposes to $H_2C{=}CH_2 + CO$ already 400 K below its decarbonylation temperature. The investigations will therefore be continued with other methane derivatives such as $HC(NO_3)_2$ or $H_2C(NO_2)_2$.[8a]

Received: January 30, 1992 [Z 5157 IE]
German version: *Angew. Chem.* **1992**, *104*, 884

CAS Registry numbers:
$C(NO_2)_4$, 509-14-8; $C(NO_2)_3$, 7408-95-9; $CO(NO_2)_2$, 141556-29-8; NO_2, 10102-44-0; NO, 10102-43-9; CO_2, 124-38-9; CO, 630-08-0.

[1] a) Cf. for example, O. V. Schick, G. Apel, H. G. Padeken, H. H. Schwarz, A. Segnitz, *Methoden Org. Chem. (Houben-Weyl), 4th ed. 1952–*, Vol. X/1 (Nitrogen compounds I, Part 1), G. Thieme, Stuttgart, **1971**, p. 9 ff. b) The Chemical Abstracts Indexes 1967–1991 contain a total of 54 relevant quotations. c) Cf. for example M. I. Trtanj, Z. B. Maksimovic, A. A. Vlakov, V. N. Djakovic, *J. Hazard Mater.* **1988**, *19*, 161, and references quoted therein.

[2] J. M. Sullivan, A. E. Axworthy, *J. Phys. Chem.* **1966**, *70*, 3366, have determined a unimolecular first-order decomposition for $C(NO_2)_4$ using a helium-fed flow reactor, $k_1 = 10^{17.53} \exp(-40.875/RT)\ s^{-1}$. Because of the high Arrhenius factor and the activation energy of 41 ± 1 kcal mol^{-1}, the dissociation $(O_2N)_3C{-}NO_2 \rightarrow (O_2N)_3C{\cdot} + {\cdot}NO_2$ has been proposed as the rate-determining step.

[3] a) H. Bock, R. Dammel, *Angew. Chem.* **1987**, *99*, 518; *Angew. Chem. Int. Ed. Engl.* **1987**, *26*, 504; b) H. Bock, B. Berkner, B. Hierholzer, D. Jaculi, *Helv. Chim. Acta* **1992**, *75*, in press; c) H. Bock, G. Tschmutowa, H.-P. Wolf, *J. Chem. Soc. Chem. Commun.* **1986**, 1068; d) H. Bock, B. Solouki, H.-W. Roesky, *Inorg. Chem.* **1984**, *24*, 4425; e) Review: H. Bock, B. Solouki, S. Aygen, M. Bankmann, O. Breuer, S. Mohmand, H. Müller, P. Rosmus, B. Roth, J. Wittmann, H.-P. Wolf, *J. Mol. Struct.* **1988**, *173*, 31.

[4] a) N. I. Sadova, N. I. Popik, L. V. Vilkow, *J. Mol. Struct.* **1976**, *31*, 399. b) The AM 1 calculations provide as eigenvalues $-\varepsilon_I^{AM\ 1}$ (eV) for the radical cation states with the following predominant contributions: $n_O \approx 13.5$ (9e, 9a, 9b) und ≈ 14.3 (8a, 7e, 7a); $\sigma_{CNO} \approx 13.6$ (8b, 8e) and ≈ 15.2 (7a) as well as $\pi_{NO} \approx 19.8$ (6e, 6a, 6b) and ≈ 20.9 (5e, 5b, 5a). c) Additional AM 1 results: $\Delta H_f^\circ = 402$ kJ mol^{-1}; $d_{CN} = 157$ pm, $d_{NO} = 120$ pm, ∢NCN 109°, ∢CNO 118°, ∢ONO = 124°; $q_c = +0.02$, $q_N = +0.46$, $q_O = -0.24$ and −0.23.

[5] The pyrolyses have been carried out in two different experimental arrangements: a) Decomposition in the short-pathway pyrolysis furnace of the high-performance PES spectrometer Leybold Heraeus UPG 200 (H. Bock, B. Solouki, *Angew. Chem.* **1981**, *93*, 431; *Angew. Chem. Int. Ed. Engl.* **1981**, *20*, 432), in which the distance between the end of the oven-zone and the target chamber is only 2 cm. The molybdenum tube, heated both by resistance wiring and by electron bombardement is loosely filled with quartz wool. b) External pyrolyses in a quartz reaction tube, heated by a hinged furnace and connected to the spectrometer by a glass joint, which is also loosely filled by either quartz wool, silver wool, or charcoal (STREM

Activated Carbon 06-0050) between quartz wool stoppers. The charcoal is activated in the reaction tube by passing a stream of H_2 at 870 K over it for 3 h. All PE spectra have been calibrated by the needle-like $^2P_{3/2}$ ionization bands of Xe ([6]: 12.13 eV) and Ar ([6] 15.76 eV).

[6] Cf. for example, K. Kimura, S. Katsumata, Y. Achiba, T. Yamazaki, S. Iwata, *Handbook of He (I) Photoelectron Spectra of Fundamental Organic Molecules*, Halstead Press, New York, **1981**.

[7] a) The AM 1 estimate of the activation enthalpy is based on the following approximations: σ_{CN} bond is elongated in steps of 5 pm under full geometry optimization of the remaining molecular skeleton, but without CI refinement. b) For seven thermal fragmentations of various molecules under the same reaction conditions, the linear regression $\Delta H^{\neq}$ (kJ mol^{-1}) = 387 + 0.797 I_D [K] results from the experimentally determined decomposition temperature T_D and the calculated activation enthalpies $\Delta H^{\neq}$ (O. M. Nefedov, V. A. Korolev, L. Zanathy, B. Solouki, H. Bock, *Mendeleev Commun.* **1992**, 67; $\sigma = 0.948$). For $T_D = 550$ K a value $\Delta H^{\neq} \approx 44$ kJ mol^{-1} is obtained. c) Further AM 1 results: $d_{NO} = 121$ pm, charge distribution: >C(−0.02)–N(+0.51)–O(−0.25). d) For an estimate of the isomerization barrier, the angle CNO of 118° at one nitro group [4] was contracted in steps of 6° and each the remaining molecular skeleton completely geometry-optimized. For ∢CNO = 102° the CN bond lengths are stretched only by $\Delta d_{CN} \approx 30$ pm, but the enthalpy difference is already $\Delta\Delta H_f^0 = +506$ kJ mol^{-1}. In addition, the isomerization might be sterically hindered. e) Further AM 1 results (cf. Scheme 2): $d_{NO} = 121$ pm, charge distribution in $(O_2N)_2C=O$: O(−0.11) = C(+0.30)–N(+0.43)–O(−0.27).

[8] a) L. Zanathy, unpublished results; b) W. D. Emmons, J. P. Freeman, *J. Am. Chem. Soc.* **1955**, *77*, 4387; m.p. 57–58 °C; c) A. H. Lamberton, O. Sutherland, J. E. Thorpe, H. M. Yusuf, *J. Chem. Soc. B* **1986**, 6.

[9] a) H. Bock, R. Dammel, P. Lorenzak, C. Wentrup, *Z. Naturforsch. B* **1990**, *45*, 59; b) H. Bock, R. Baur, K. Oswald, unpublished; cf. Ph.D. thesis R. Baur, University of Frankfurt, **1991**.

[10] Cf. for example, W. S. Chin, C. Y. Mok, H. H. Huang, *J. Am. Chem. Soc.* **1990**, *112*, 2053; *J. Electron. Spectrosc. Relat. Phenom.* **1991**, *57*, 213.

[11] Note added in proof (May 24, 1992): The thermolysis of tetranitromethane has also been performed with largely comparable results by L. K. Koo, W. S. Chin, C. Y. Mok, H. H. Huang (personal communication, C. Y. Mok; cf. also *Bull Singapore Nat. Inst. Chem.* **1990**, *18*, 21). For a structurally characterized intermediate of the nitration of naphthalene by tetranitromethane, see L. Eberson, M. P. Hartshorn, F. Radner, W. T. Robinson, *J. Chem. Soc. Chem. Commun.* **1992**, 566.

from the corresponding serine *O*-glycopeptides but lacks the anomeric oxygen atom (i.e., the compounds contain a shortened side chain).

The reaction was performed by treatment of the glycosyl bromides **1**–**3** with the urethane-protected dehydroalanine derivatives[6] **4**–**9** with addition of $Bu_3SnH/\alpha,\alpha'$-azobisisobutyronitrile (AIBN) according to Scheme 1 and gave yields of up to 73% (Table 1).[5, 7, 8] Starting materials and

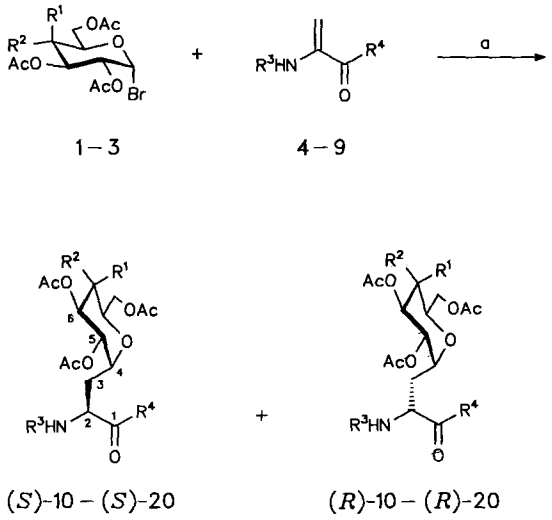

Scheme 1. Synthesis of *C*-glycosides **10**–**20** by free radical addition of glycosyl bromides to dehydroalanine derivatives. (*S*) and (*R*) refer to the configuration at C2. **1**: R^1 = OAc, R^2 = H; **2**: R^1 = H, R^2 = OAc; **3**: R^1 = H, R^2 = *O*-(2,3,4,6-tetra-*O*-acetyl-β-D-galactopyranosyl); **4**; R^3 = Fmoc, R^4 = OBzl; **5**: R^3 = Z, R^4 = OBzl; **6**: R^3 = Boc, R^4 = OBzl; **7**: R^3 = Fmoc, R^4 = Phe-OBzl; **8**: R^3 = Fmoc, R^4 = D-Phe-OBzl; **9**: R^3 = Fmoc-Pro, R^4 = Ala-OBzl. (a) Bu_3SnH, AIBN, dry toluene, 50–65 °C (see experimental procedure). For abbreviations, see Table 1.

Synthesis of *C*-Glycopeptides via Free Radical Addition of Glycosyl Bromides to Dehydroalanine Derivatives**

By *Horst Kessler**, *Valentin Wittmann*, *Matthias Köck*, and *Matthias Kottenhahn*

Dedicated to Professor Ernst Bayer on the occasion of his 65th birthday

Glycoproteins are widely distributed in living organisms and their carbohydrate part plays a fundamental role in many processes of molecular recognition.[1, 2] The oligosaccharide side chain influences the conformation and solubility of proteins and can prohibit proteolytic cleavage.[3] In most cases the sugar residues form an *N*-glycosidic bond to asparagine or an *O*-glycosidic bond to hydroxy-containing amino acids. Unusual and more stable linkages between carbohydrates and peptides are important for an understanding of the mutual interactions between both moieties.

We now report the facile synthesis of *C*-glycopeptides via free radicals according to the tin-hydride procedure of Giese et al.[4] This new class of compounds[5] is formally derived

[*] Prof. Dr. H. Kessler, Dipl.-Chem. V. Wittmann, Dipl.-Chem. M. Köck, Dr. M. Kottenhahn
Organisch-chemisches Institut der Technischen Universität München
Lichtenbergstrasse 4, D-W-8046 Garching (FRG)

[**] This work was supported by the Fonds der Chemischen Industrie and the Deutsche Forschungsgemeinschaft. V. W., M. K., and M. K. thank the Fonds der Chemischen Industrie for doctoral fellowships.

reagents were mixed synchronously after they had been warmed to the reaction temperature. The sugars dehalogenated at C1 could be isolated as side products. Slow addition of a solution of Bu_3SnH and AIBN in toluene to the reaction mixture resulted in reduced yields. As expected,[9] the products are exclusively (>97%) α-configurated at the "anomeric center" in the case of the monosaccharides **1** and **2**. Only small amounts of β-*C*-glycosides were formed when lactosyl bromide (**3**) was used (12% when reacting with **4**, 4% with **5**). In contrast to the high diastereoselectivity at the sugar, the hydrogen atom transfer to C2 of the amino acid yields mixtures of epimers. The diastereomeric ratios vary depending on the protecting group at the *N*-terminus of the amino acid. The best selectivity (3.8:1 in favor of the (2*S*)-epimer) is obtained with Boc-ΔAla-OBzl (**6**). The epimeric mixtures can be separated by HPLC. After the removal of the urethane group, gram-scale separation is possible by chromatography on a silica gel column.

To examine the possiblity of higher distereoselectivity through chirality in the dehydroamino acid building block, the enantiomeric dipeptides **7** and **8**, as well as the tripeptide **9**, were used. In all cases, even lower selectivity was observed (Table 1). In addition, the use of α,β-unsaturated carb*amides* results in lower chemical yields. For electronic reasons,[10] addition to a second dehydroalanine unit occurs (e.g., with Fmoc-ΔAla-D-Phe-OBzl (**8**) a single diastereomer of **21**[11] is

Table 1. Results of free-radical addition of glycosyl bromides **1**–**3** to dehydroalanine derivatives **4**–**9** according to Scheme 1. Abbreviations: Fmoc = 9-fluorenylmethoxycarbonyl, Z = benzyloxycarbonyl, Boc = *tert*-butyloxycarbonyl, ΔAla = dehydroalanine, TA-gal = *C*-(2,3,4,6-tetra-*O*-acetyl-D-galactopyranosyl)-α(1 → 3), TA-glc = *C*-(2,3,4,6-tetra-*O*-acetyl-D-glucopyranosyl)-α(1 → 3), HA-lac = *C*-(2,3,6,2′,3′,4′,6′-hepta-*O*-acetyl-D-lactosyl)-α(1 → 3).

Bromide	Dehydroalanine Derivative		Product [a]		Yield [b]	*S*:*R* [c]
1	Fmoc-ΔAla-OBzl	**4**	Fmoc-Ala(TA-gal)-OBzl	(*S*)-**10**/(*R*)-**10**	65%	2.5:1
1	Z-ΔAla-OBzl	**5**	Z-Ala(TA-gal)-OBzl	(*S*)-**11**/(*R*)-**11**	60%	2.4:1
1	Boc-ΔAla-OBzl	**6**	Boc-Ala(TA-gal)-OBzl	(*S*)-**12**/(*R*)-**12**	61%	3.8:1
2	Fmoc-ΔAla-OBzl	**4**	Fmoc-Ala(TA-glc)-OBzl	(*S*)-**13**/(*R*)-**13**	73%	2.6:1
2	Z-ΔAla-OBzl	**5**	Z-Ala(TA-glc)-OBzl	(*S*)-**14**/(*R*)-**14**	55%	2.3:1
2	Boc-ΔAla-OBzl	**6**	Boc-Ala(TA-glc)-OBzl	(*S*)-**15**/(*R*)-**15**	65%	3.8:1
3	Fmoc-ΔAla-OBzl	**4**	Fmoc-Ala(HA-lac)-OBzl	(*S*)-**16**/(*R*)-**16**	55%	(1.9:1)
3	Z-ΔAla-OBzl	**5**	Z-Ala(HA-lac)-OBzl	(*S*)-**17**/(*R*)-**17**	13%	(3.2:1)
1	Fmoc-ΔAla-Phe-OBzl	**7**	Fmoc-Ala(Ta-gal)-Phe-OBzl	(*S*)-**18**/(*R*)-**18**	45%	1.6:1
1	Fmoc-ΔAla-D-Phe-OBzl	**8**	Fmoc-Ala(TA-gal)-D-Phe-OBzl	(*S*)-**19**/(*R*)-**19**	23%	≥ 2.0:1
1	Z-Pro-ΔAla-Ala-OBzl	**9**	Z-Pro-Ala(TA-gal)-Ala-OBzl	(*S*)-**20**/(*R*)-**20**	40%	1.0:1

[a] (*S*) and (*R*) correspond to the configuration at C2 of the glycosidized amino acid. The products were characterized by ^{1}H and ^{13}C NMR spectroscopy and FAB-MS. [b] Overall yields of the α anomers after chromatography on silica gel. With the exception of two cases (12% for **16**, 4% for **17**), no β anomer could be detected (limit of detection <3%). [c] Isomeric ratios were determined by integration of corresponding signals in the ^{1}H NMR spectra or the HPLC chromatograms. The configuration at C2 was not assigned for compounds **16** and **17** (see text).

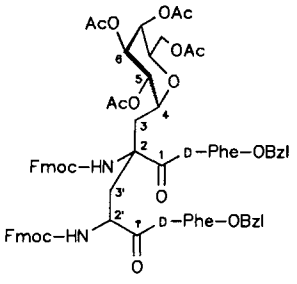

21

obtained in 53% yield). The higher stereoselectivity can be understood by the principle of double stereodifferentiation.[12]

The determination of the absolute configuration at C2 of the amino acids was carried out by NMR spectroscopy of the conformationally restricted lactones **24**, **25**, and **26** (see Scheme 3) and subsequent refinement by molecular dynamics calculations. The lactones were prepared in three steps starting from the corresponding *C*-glycosyl alanine derivatives (*S*)-**15**, (*R*)-**15**, and (*S*)-**12** (Scheme 2). The assignment of proton and carbon atoms was performed by COSY and HMQC[13] spectra. A mixture of [D_6]DMSO/$CDCl_3$ was used in the ratio 1:2 for the lactones **24** and **26** but 1:1.4 for lactone **25**. Pure [D_6]DMSO could not be used because of overlap in the ^{1}H NMR spectrum. An HMBCS–270 experiment[14] confirmed the cyclization to the δ-lactone ($^3J_{C1,H5}$). ^{1}H,^{1}H coupling constants were extracted from 1D spectra after apodization. The interproton distances were obtained from 500 MHz ROESY spectra[15] with a mixing time of 150 ms. Using these data we could assign both diastereotopic protons at C3. A qualitative inspection of the

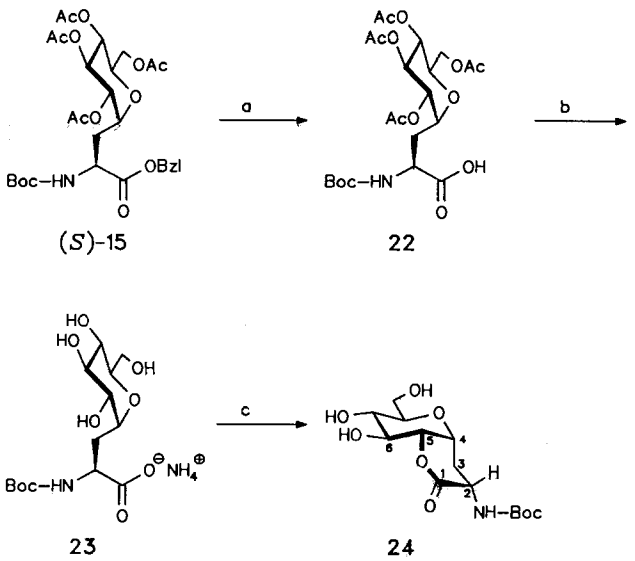

(*S*)-**15** **22** **23** **24**

Scheme 2. Typical reaction sequence illustrated for the synthesis of compound **24**. The lactones **25** and **26** were obtained analogously from coumpounds (*R*)-**15** and (*S*)-**12**, respectively. a) H_2, 10% Pd-C, MeOH, room temperature, 1 h; b) NH_3, MeOH, room temperature, 14 h; c) *N*-ethyl-*N*′-(*N*″,*N*″-dimethylaminopropyl)carbodiimide (EDCI), 1-hydroxybenzotriazole (HOBT), dimethylacetamide (DMA)/THF (1:1), room temperature, 14 h. Quantitative yields were obtained for all three reaction steps.

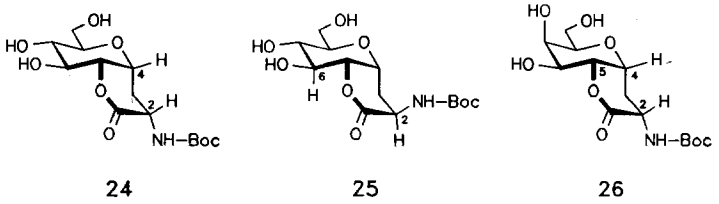

24 **25** **26**

Scheme 3. Formulas of the lactones **24**–**26** synthesized to assign the absolute configuration at C2.

ROESY spectra allows for discrimination between lactones **24** and **25**; a cross peak is observed between H2 and H4 for **24** but between H2 and H6 for **25**. This proves the assignment of the absolute configuration (2*S*) for **24** but (2*R*) for **25**, as shown in Figure 1.

To refine the structures, restrained MD simulations (Discover[16]) were performed by using the interproton distances (25 distances for compound **24** and 16 distances for **25**).[17] The calculated structures (Fig. 1) are in agreement with all measured distances and coupling constants (Table 2). The simulation was then continued for 300 ps without restraints

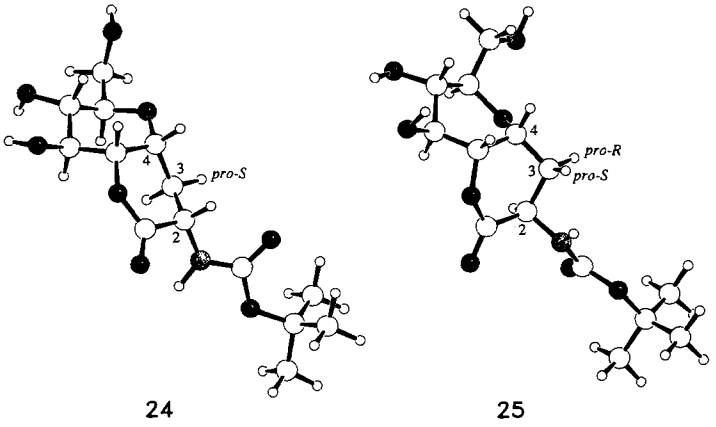

24 25

Fig. 1. MD structures of the lactones **24** and **25**. Oxygen atoms are filled, and nitrogen atoms are stippled.

and exhibited the stability of the obtained structures. To prove the configuration at C2, a calculation under identical conditions but with exchanged starting configurations was performed. As expected, considerable deviations from the interproton distances obtained from NMR spectroscopy were observed. In lactone **26**, which stems from the galactose series, strong ROEs from H2 to H4 and H5 are observed, proving the (2*S*) configuration as in **24**. Again, additional evidence is provided by the $^1H,^1H$ coupling constants (Table 2). The absolute configurations of the lactosyl compounds **16** and **17** were not determined but assumed to be the (2*S*) epimers from analogy with the main products. Transformation of the *C*-glycosides (*S*)-**12** and (*S*)-**15** into (*S*)-**10**, (*S*)-**11**, (*S*)-**18**, (*S*)-**19**, and (*S*)-**13**, (*S*)-**14**, respectively, indicates the natural (2*S*) configuration at the amino acids for all other major products.

Table 2. Selected $^1H,^1H$ coupling constants for compounds **24**–**26**.

^3J(H,H)	2,3(*pro-R*)	2,3(*pro-S*)	4,3(*pro-R*)	4,3(*pro-S*)
24	13.1	6.5	9.4	6.6
25	6.6	12.1	4.3	3.7
26	12.7	7.6	5.7	8.1

The procedure described here yields nonnatural *C*-glycosyl amino acids and *C*-glycosyl peptides in one step with high diastereoselectivity at the anomeric center, from readily available starting materials. The products exhibit high chemical stability, are suitable as potential glycosidase inhibitors, and provide a method to improve pharmaco kinetic properties of peptides.

General procedure

The protected dehydroamino acid is dissolved in dry toluene (about 0.1 M) together with 1.2–2 equivalents of glycosyl bromide and warmed to approximately 60 °C. Bu_3SnH (1.2–2 equiv) and catalytic amounts of AIBN are added under nitrogen or argon.

After completion of the reaction (monitored by TLC), the solvent is evaporated, the residue dissolved in acetonitrile and extracted three to five times with hexane to remove the tin compounds. The acetonitrile is evaporated, and the remaining oil purified by silica gel chromatography. The products are distereomeric mixtures of L- and D-amino acids.

Received: January 27, 1992 [Z 5151 IE]
German version: *Angew. Chem.* **1992**, *104*, 874

CAS Registry numbers:
1, 3068-32-4; **2**, 572-09-8; **3**, 4753-07-5; **4**, 141665-73-8; **5**, 59524-07-1; **6**, 94882-75-4; **7**, 141665-74-9; **8**, 141665-75-0; **9**, 141665-76-1; (*S*)-**10**, 141665-77-2; (*R*)-**10**, 141665-91-0; (*S*)-**11**, 141665-78-3; (*R*)-**11**, 141665-92-1; (*S*)-**12**, 141665-79-4; (*R*)-**12**, 141665-93-2; (*S*)-**13**, 141684-32-4; (*R*)-**13**, 141645-94-3; (*S*)-**14**, 141665-80-7; (*R*)-**14**, 141665-95-4; (*S*)-**15**, 141665-81-8; (*R*)-**15**, 141665-96-5; (*S*)-**16**, 141684-33-5; (*R*)-**16**, 141665-97-6; (*S*)-**17**, 141665-82-9; (*R*)-**17**, 141665-98-7; (*S*)-**18**, 141665-83-0; (*R*)-**18**, 141725-28-2; (*S*)-**19**, 141725-27-1; (*R*)-**19**, 141725-29-3; (*S*)-**20**, 141665-84-1; (*R*)-**20**, 141725-30-6; **21**, 141665-85-2; **22**, 141665-86-3; **23**, 141665-87-4; **24**, 141665-88-5; **25**, 141665-89-6; **26**, 141665-90-9.

[1] J. Montreuil in *Comprehensive Biochemistry, Vol. 19 BII* (Eds.: A. Neuberger, L. L. van Deenen), Elsevier, Amsterdam, **1982**, p. 1–189.
[2] N. Sharon, H. Lis, *Chem. Eng. News* **1981**, *59* (13), 21–44.
[3] a) K. Olden, J. B. Parent, S. L. White, *Biochem. Biophys. Acta* **1982**, *650*, 209–232; b) K. Olden, B. A. Bernard, M. J. Humphries, T.-K. Yeo, K.-T. Yeo, S. L. White, S. A. Newton, H. C. Bauer, J. B. Parent, *Trends Biochem. Sci.* **1985**, *10*, 78–82.
[4] a) B. Giese, J. Dupuis, *Angew. Chem.* **1983**, *95*, 633-634; *Angew. Chem. Int. Ed. Engl.* **1983**, *22*, 622–623; b) B. Giese, J. Dupuis, M. Leising, M. Nix, H. J. Lindner, *Carbohydr. Res.* **1987**, *171*, 329–341; c) B. Giese, T. Linker, R. Muhn, *Tetrahedron* **1989**, *45*, 935–940.
[5] M. Kottenhahn, Dissertation, Universität Frankfurt, **1989**. The synthesis of similar compounds has been described recently: G. Simchen, E. Pürkner, *Synthesis* **1990**, 525–527; L. Colombo, G. Casiraghi, A. Pittalis, G. Rassu, *J. Org. Chem.* **1991**, 56, 3897–3900.
[6] M. J. Miller, *J. Org. Chem.* **1980**, *45*, 3131–3132.
[7] V. Wittmann, Diplom thesis, Universität Frankfurt, **1990**.
[8] For example (*S*)-**15**: $[\alpha]_D^{22} = 50.6$ ($c = 1$, $CDCl_3$); FAB-MS: *m/z* 610 ($M + H^{\oplus}$); ^1H NMR (250 MHz, $CDCl_3$, 300 K, TMS): $\delta = 7.42-7.32$ (m, 5H, C_6H_5), 5.35 (d, 1H, NH), 5.20 (dd, 1H, H-6), 5.30–5.14 (m, 2H, CH_2-Ph), 5.02 (dd, 1H, H-5), 4.96 (dd, 1H, H-7), 4.46 (m, 1H, H-2), 4.35 (ddd, 1H, H-4), 4.21 (dd, 1H, H-9b), 3.95 (dd, 1H, H-9a), 3.85 (ddd, 1H, H-8), 2.24 (ddd, 1H, H-3b), 2.08 (ddd, 1H, H-3a), 2.10–2.00 (4 s, 12H, OAc), 1.42 (s, 9H, Boc); J(NH,2) = 7.2, J(4,5) = 5.3, J(5,6) = 8.7, J(6,7) = 7.4, J(7,8) = 8.6, J(8.9a) = 2.7, J(8,9b) = 4.8, J(9a,9b) = 12.2 Hz; ^{13}C NMR (62.5 mHz, $CDCl_3$, 300 K): δ = 171.4, 170.6, 169.8, 169.4, 169.3, 154.9 (C=O), 135.0, 128.6, 128.5, 128.3 (C_6H_5), 80.1 (CMe_3), 69.9 (C-8), 69.8 (C-6), 69.5 (C-5), 68.7 (C-4), 67.9 (C-7), 67.3 (CH_2-Ph), 61.5 (C-9), 50.5 (C-2), 28.2 (C-3 and $C(CH_3)_3$), 20.6 (4(CO)CH_3).
[9] B. Giese, *Angew. Chem.* **1989**, *101*, 993–1004; *Angew. Chem. Int. Ed. Engl.* **1989**, *28*, 969–980.
[10] a) B. Giese, *Radicals in Organic Synthesis: Formation of Carbon-Carbon Bonds*, 1st ed., Pergamon, Oxford, **1986**, p. 7–10; b) *Angew. Chem.* **1983**, *95*, 771–782; *Angew. Chem. Int. Ed. Engl.* **1983**, *22*, 753–764.
[11] **21**: FAB-MS: *m/z* 1425.5 ($M + H^{\oplus}$); ^1H NMR (500 MHz, $CDCl_3$, 300 K, TMS): δ = 8.12 (d, 1H, Phe-NH), 7.70–7.10 (m, 36H, arenes), 7.05 (d, 1H, Phe-NH), 6.97 (s, 1H, NH), 5.73 (d, 1H, NH), 5.23–5.13 (m, 4H, 2 CH_2-Ph), 5.09 (dd, 1H, H-7), 5.04 (dd, 1H, H-5), 4.93 (dd, 1H, H-6), 4.90, 4.64 (each ddd, 2H, each Phe-H-α), 4.33, 3.85 (each m, 2H, Fmoc-CH_2), 4,27, 3.92 (each m, 2H, Fmoc-CH_2), 4.25 (ddd, 1H, H-4), 4.12 (dd, 1H, H-9b), 4.06 (ddd, 1H, H-2'), 4.05, 3.94 (each m, 2H, each Fmoc-H-9), 3.74 (dd, 1H, H-9a), 3.30 (ddd, 1H, H-8), 3.10, 2.91 (each dd, 2H, Phe-H-β), 3.08, 3.00 (each dd, 2H, Phe-H-β), 2.62 (dd, 1H, H-3'b), 2.42 (dd, 1H, H-3b), 2.30 (dd, 1H, H-3'a), 1.94 (dd, 1H, H-3a), 2.07–1.94 (4 s, 12H, OAc); ^{13}C NMR (125 MHz, $CDCl_3$, 300 K): δ = 172.5, 172.3, 172.2, 170.7, 169.9, 169.7, 169.6, 169.5, 155.9, 155.4 (C=O), 143.8–119.8 (arenes), 68.5 (C-8), 67.8 (C-4, C-5, CH_2-Ph), 67.3 (C-6, CH_2-Ph), 67.2 (C-7), 67.1 (2 Fmoc-CH_2), 61.2 (C-9), 60.8 (C-2), 54.9, 53.9 (each Phe-C-α), 51.2 (C-2'), 47.0, 46.8 (each Fmoc-C-9), 40.8 (C-3'), 37.4, 36.7 (each Phe-C-β), 32.5 (C-3), 20.9–20.6 (4 (CO)CH_3).
[12] S. Masamune, W. Choy, J. S. Petersen, L. R. Sita, *Angew. Chem.* **1985**, *97*, 1–31; *Angew. Chem. Int. Ed. Engl.* **1985**, *24*, 1–30.
[13] A. Bax, S. Subramanian, *J. Magn. Reson.* **1986**, *67*, 565–569.
[14] H. Kessler, P. Schmieder, M. Köck, M. Kurz, *J. Magn. Reson.* **1990**, *88*, 615–618.
[15] a) A. A. Bothner-By, R. L. Stevens, J. Lee, C. D. Warren, R. W. Jeanloz, *J. Am. Chem. Soc.* **1984**, *106*, 811–813; b) H. Kessler, C. Griesinger, R. Kerssebaum, K. Wagner, R. R. Ernst, *ibid.* **1987**, *109*, 607–609; c) C. Griesinger, R. R. Ernst, *J. Magn. Reson.* **1987**, *75*, 261–271.
[16] A. T. Hagler in *The Peptides, Vol. 7* (Eds.: S. Udenfriend, J. Meienhofer, V. Hruby), Academic Press, Orlando, Fl, USA, **1985**, p. 214–296.
[17] Restrained MD simulations in vacuum were performed over 150 ps. The time step for the integration of Newton's equations of motion was 1.0 fs. The starting structures were built interactively with INSIGHT. To take into account errors in the ROESY cross-peak intensities and for the interconversion into distanes, 5% were subtracted from the lower and added to the upper bounds. The simulations were performed for 5 ps at 1000 K, then for 10 ps at 500 K, and finally for an additional 135 ps at 300 K. Only the last 100 ps were used for analysis.

A Rh^I-Centered Cage Compound with Selective Catalytic Properties**

By *Hein K. A. C. Coolen, Piet W. N. M. van Leeuwen,* and *Roeland J. M. Nolte**

The development of synthetic catalysts that function according to the principles of enzymatic catalysis is a topic of great current interest. In the last decade examples of such systems—also called synzymes—have been reported.[1] Their number, however, is still limited. Taking nature as a guide, one can design a synzyme by combining a synthetic host molecule with an organic or inorganic catalyst. The objective is to bind a substrate selectively in the host and to achieve catalysis by positioning it in the correct orientation relative to the catalytic center.

In this communication we describe a cage compound with a Rh^I center, which preferentially binds allyldihydroxybenzenes and converts them into the corresponding styrenes and propyl derivatives by isomerization and hydrogenation of the allyl function. The frame of the cage is formed by the cleft molecule **1a**, which can bind catechol and resorcinol.[2] Binding in **1** occurs by π–π stacking and by hydrogen bonding interactions (Fig. 1). The catalytic center of the cage

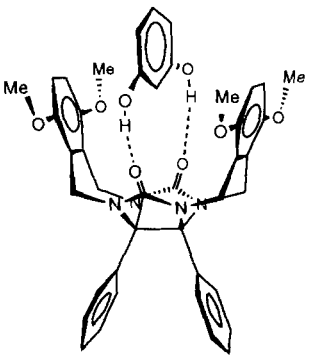

Fig. 1. Structure of the complex of **1a** with resorcinol.

compound is a triphenylphosphite–rhodium complex. The complex $[RhH(CO)\{P(OPh)_3\}_3]$ catalyzes hydroformylation and isomerization reactions.[3] We recently found that $[RhH\{P(OPh)_3\}_4]$ is an isomerization as well as a hydrogenation catalyst. We have succeeded in positioning these complexes above the cavity of compound **1** to form a substrate-selective catalyst.

Synthesis of the cage compound starts from the known diphenylglycoluril derivative **1b**.[4] Double ring-closure of **1b** with two equivalents of *para*-methoxymethyloxybenzylamine[5] in acetonitril resulted in the basket-shaped compound **2b** (71%). Acidic cleavage of the methoxymethyl protecting group in **2b** followed by reaction with $ClP(OPh)_2$ in dichloromethane yielded the bis(triarylphosphite) ligand **2c** in 94% yield. Compound **2c** was fully characterized by elemental analysis and spectroscopic methods (Table 1).

Addition of an equimolar amount of $[Rh(CO)_2(acac)]$ to a solution of **2c** in chloroform resulted in the quantitative exchange of the two carbonyl ligands in the rhodium complex for the phosphites of **2c** and the formation of cage complex **3a**. Cage compound **3b** was prepared in a similar way by using $[Rh(CO)_2(dbm)]$ (Hdbm = dibenzoylmethane)[6]. Space-filling models show that compounds of

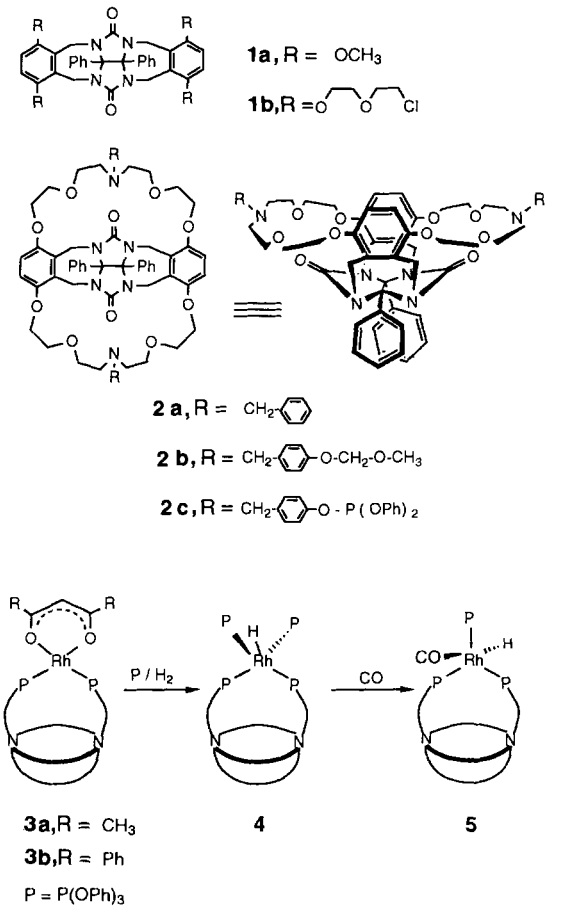

type **3** can exist in different conformations, prescribed by the square-planar coordination of the metal in combination with the rigidity of the spacers. In complex **3a** the acetylacetonate

Table 1. Physical properties of the new compounds. Ar = aryl. Correct C,H,N analyses.

2c: Yield: 94%; ^{31}P NMR (80 MHz, $CDCl_3$, 25 °C, $(MeO)_3PO$): $\delta = 125.9$; ^1H NMR (200 MHz, $CDCl_3$, 25 °C, TMS): $\delta = 7.37-7.07$ (m, 38 H; ArH), 6.70 (s; 4H), 5.66 (d, $^2J(H,H) = 16$ Hz, 4H; Ar-CH*H*-N), 4.23–4.06 (m, 4H; N-CH_2-Ar), 3.94–3.67 (m, 28 H; -CH_2O, Ar-C*H*H-N), 2.88 (t, $^2J(H,H) = 5.6$ Hz, 8H; -CH_2-N); IR (CsI): $\tilde{\nu}$ [cm^{-1}] = 1712 (N-C(O)-N), 1197 (P-O-Ph), 504 ($P(OR)_3$); MS (FAB, *m-nitrobenzyl alcohol*): *m/z* 1522 ($M^+ + H$).

3a: Yield after isolation: 85%; ^{31}P NMR (80 MHz, $CDCl_3$, 25 °C, $(MeO)_3PO$): $\delta = 121.4, 121.3, 121.2, 120.2$ (d, $^1J(Rh,P) = 304$ Hz); ^1H NMR (200 MHz, $CDCl_3$, 25 °C, TMS): $\delta = 7.33-7.00$ (m br, 38 H; ArH), 6.67–6.63 (m br, 4H; ArH), 5.65 (d, $^2J(H,H) = 16$ Hz, 4H; Ar-CH*H*-N), 5.07 (s, 1H; Me-C-C*H*-C-Me), 4.11–3.50 (m br, 32H; N-CH_2-Ar, -CH_2-O, Ar-C*H*H-N), 2.88–2.75 (m br, 8H; -CH_2N), 1.51–1.50 (m, 6H; -CH_3); IR(CsI): $\tilde{\nu}$ [cm^{-1}] = 1715 (N-C(O)-N), 1580 (C-C, diketone), 1197 (P-O-Ph), 596 (diketone).

3b: Yield after isolation: 85%; ^{31}P NMR (80 MHz, $CDCl_3$, 25 °C, $(MeO)_3PO$): $\delta = 120.7$, 120.5, 119.1 (d, $^1J(Rh,P) = 304$ Hz); ^1H NMR (200 MHz, $CDCl_3$, 25 °C, TMS): $\delta = 7.56-6.92$ (m br, 48 H; ArH), 6.64–6.49 (m br, 5 H; ArH, Ar-C-C*H*-C-Ar), 5.64 (d, $^2J(H,H) = 16$ Hz, 4H; Ar-CH*H*-N), 4.07–3.62 (m br, 32H; N-CH_2Ar, -CH_2-O, Ar-C*H*H-N), 2.95–2.63 (m br, 8H; -CH_2-N); IR (CsI): $\tilde{\nu}$ [cm^{-1}] = 1712 (N-C(O)-N), 1542 (C-O, diketone), 1194 (P-O-Ph), 592 (diketone).

[*] Prof. Dr. R. J. M. Nolte, H. K. A. C. Coolen
Nijmegen SON Research Center
University of Nijmegen
Toernooiveld, NL-6525 ED Nijmegen (The Netherlands)
Prof. Dr. P. W. N. M. van Leeuwen
Koninklijke/Shell-Laboratorium, Amsterdam (The Netherlands)

[**] We thank Shell Research B.V. for the grant that made this research possible.

ligand can be *above*, *in*, *partially in*, or *next to* the cavity. In line with this, the ^{31}P NMR spectrum of **3a** shows four doublets at 120.2, 121.2, 121.3, and 121.4 ($J_{Rh,P} = 304$ Hz); the intensity ratio varies with conditions. With more bulky substituents R the diketonate ligand does not fit *inside* the cavity. Therefore, in the ^{31}P NMR spectrum of **3b** only three doublets at $\delta = 119.1$, 120.5, and 120.7 ($J_{Rh,P} = 304$ Hz) are observed. Compounds **3a** and **b** can be isolated by precipitation in hexane (Table 1).

The binding properties of cage complex **3b** were evaluated by monitoring the shift of various cage and guest signals in ^1H NMR titrations.[7] A titration with resorcinol gave an association constant of $K_a = 2850 \pm 300\,M^{-1}$, in good agreement with the value measured for the reference compounds **1a** ($K_a = 2600 \pm 400\,M^{-1}$)[2] and **2a** ($K_a = 2900 \pm 300\,M^{-1}$)[8]. In the case of catechol it was not possible to observe a shift directly because of serious overlap of signals. The association constant for this guest was therefore determined in a competition experiment with resorcinol. The value found, $K_a = 200 \pm 100\,M^{-1}$, is also comparable with that of the binding of catechol in **1a** ($K_a = 60 \pm 10\,M^{-1}$)[2] and in **2a** ($K_a = 70 \pm 30\,M^{-1}$).[8]

Addition of a small excess of $P(OPh)_3$ to **3** in chloroform in the presence of H_2 afforded the hydrido complex **4**. The phosphites in this compound surround the Rh center tetrahedrally, and the hydride is positioned along one of the trigonal axes.[3c, 9] The two P atoms of the $P(OPh)_3$ ligands on the one hand and those of ligand **2c** on the other have almost the same δ and $J_{Rh,P}$ values. Therefore, the $^{31}P\{^1H\}$ NMR spectrum of **4** exhibits one doublet at δ=127.6 with some second order features ($J_{Rh,P} = 229$ Hz) (Fig. 2, left). Because of this nonequivalence combined with the fact that two pairs of faces of the tetrahedron are unequal, the doublet of quintets of the hydride signal in the high-field ^1H NMR spectrum ($\delta = -11.0$, $J_{P,H} = 44$ Hz) is broadened (Fig. 2, right). Even when a large excess of free $P(OPh)_3$ is present, no phosphorus signal of uncoordinated phosphite groups of **2c** was observed. This demonstrates the strong chelate effect of **2c**.[10]

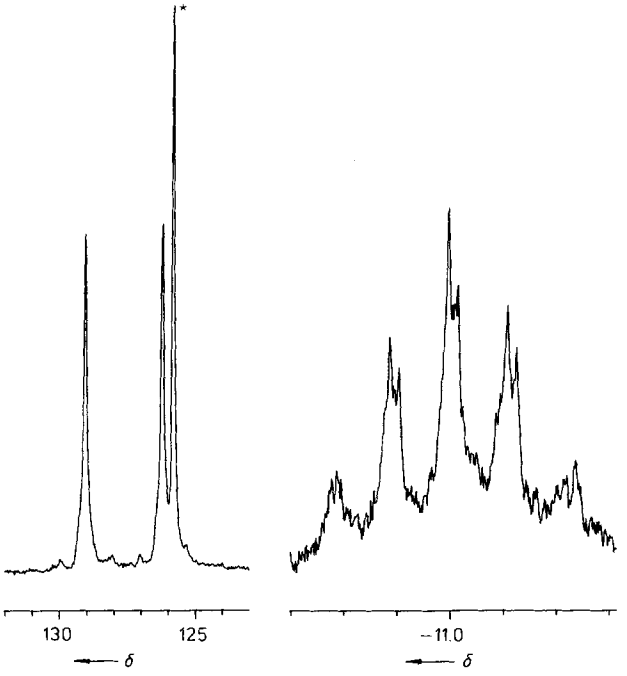

Fig. 2. Left: The $^{31}P\{^1H\}$ NMR spectrum of **4**. The signal marked with an asterisk is due to free $P(OPh)_3$. Right: The hydride region of the ^1H NMR spectrum of **4**.

Bubbling CO through a solution of **4** in chloroform gave the carbonyl hydride cage complex **5**. Compound **5** could also be obtained directly by treating **3a** or **3b** with a mixture of CO and H_2 in the presence of a small excess of $P(OPh)_3$. The model compound $[RhH(CO)\{P(OPh)_3\}_3]$ has a trigonal bipyramidal structure and exhibits only one doublet in its ^{31}P NMR spectrum, because of the equivalence of the P atoms and the very small *cis* P–H coupling.[3c] In the case of cage complex **5**, the $^{31}P\{^1H\}$ NMR spectrum showed a complex doublet at $\delta = 138.6$ ($J_{Rh,P} = 239$ Hz). We attribute this complexity to the nonequivalence of the P atoms in **5**.

Under Ar (1 atm) and in the presence of a small excess of $P(OPh)_3$ a solution of **5** in $CHCl_3$ is able to isomerize an equimolar amount of 4-allylcatechol (**6**)[11] to the corresponding *cis*- and *trans*-methylstyrenes in a ratio of about 1:3. Allylbenzene showed a much lower reactivity under the same conditions (monitored by ^1H NMR spectroscopy; Fig. 3). In two hours 68% of the allylcatechol had been

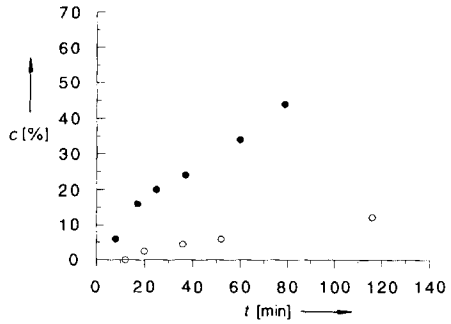

Fig. 3. The isomerization of 4-allylcatechol (●) and allylbenzene (○) in separate experiments by **5**.

converted, while in the same period only 12% of the allylbenzene had reacted. The conversion of 4-allylcatechol starts immediately, whereas for allylbenzene an induction period of about 10 min is observed. In accordance with the literature,[3e] we assume that the actual catalyst is the hydride **4**. This catalyst is probably generated by the substrate itself: in the first step the propylenic substituent displaces the CO ligand. This explains the induction time of the reaction with the nonbinding substrate. From these results we conclude that the isomerization preferentially takes place *inside* the cavity of **5**.

In order to decide whether the reaction is truly catalytic and to exclude possible electronic effects of the substituents on the substrate we carried out a competition experiment with **4** and a fourfold excess of substrates **6**–**8** in chloroform.

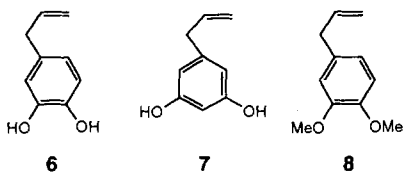

6 **7** **8**

Substrate **8** is not bound in the cavity of **2**. The association constants for **6** and **7**[12] in **2a** were measured by ^1H NMR titrations to be $K_a = 90 \pm 20\,M^{-1}$ and $K_a = 2200 \pm 200\,M^{-1}$, respectively. Under a hydrogen atmosphere ($pH_2 = 1.2$ atm) the substrates were completely converted into products, mainly the propyl derivatives. The conversion and

product formation was followed by gas chromatography. A clear correlation was observed between the rate of conversion and the association constant of the substrate: $t_{1/2}$ of the conversion for **7**, **6**, and **8** amounted to 5, 10, and 38 min, respectively. In individual experiments under the same conditions, substrates **6**–**8** were each converted by $[RhH\{P(OPh)_3\}_4]$ at approximately the same rate ($t_{1/2}$ = 25 min). From these results we conclude that the reaction of the bound substrate is accelerated by **4**, whereas that of the nonbound is delayed.

The fact that **4** can still react with **8** suggests that the rhodium center in the cage complex is not completely shielded from the solution. Work is now in progress to functionalize the top part of **4** with a cap, which may further improve the selectivity of the catalyst.

Received: January 24, 1992 [Z 5147IE]
German version: *Angew. Chem.* **1992**, *104*, 906

[1] a) D. R. Benson, R. Valentekovich, F. Diederich, *Angew. Chem.* **1990**, *102*, 213; *Angew. Chem. Int. Ed. Engl.* **1990**, *29*, 191; b) D. J. Cram, P. Y.-S. Lam, S. P. Ho, *J. Am. Chem. Soc.* **1986**, *108*, 839; c) K. D. Cramer, S. C. Zimmerman, *ibid.* **1990**, *112*, 3680; d) M. W. Hosseini, A. J. Blacker, J.-M. Lehn, *ibid.* **1990**, *112*, 3896; e) J. T. Groves, L. A. Baron, *ibid.* **1989**, *111*, 5442; f) E. Anslyn, R. Breslow, *ibid.* **1989**, *111*, 8931; g) F. Diederich, H.-D. Lutter, *ibid.* **1989**, *111*, 8438.

[2] R. P. Sijbesma, A. P. M. Kentgens, R. J. M. Nolte, *J. Org. Chem.* **1991**, *56*, 3199.

[3] a) A. M. Trzeciak, J. J. Ziolkowski, *J. Mol. Catal.* **1983**, *19*, 41; b) *ibid.* **1986**, *34*, 213; c) A. M. Trzeciak, J. J. Ziolkowski, S. Aygen, R. van Eldik, *ibid.* **1986**, *34*, 337; d) A. M. Trzeciak, *J. Organomet. Chem.* **1990**, *390*, 105; e) A. M. Trzeciak, J. J. Ziolkowski, *J. Mol. Catal.* **1988**, *43*, 335.

[4] J. W. H. Smeets, R. P. Sijbesma, L. van Dalen, A. L. Spek, W. J. J. Smeets, R. J. M. Nolte, *J. Org. Chem.* **1989**, *54*, 3710.

[5] *para*-Methoxymethyloxybenzylamine was prepared by reaction of *para*hydroxybenzonitrile with chlorodimethyl ether (F. R. van Heerden, J. J. van Zyl, G. J. H. Rall, E. V. Brandt, D. G. Roux, *Tetrahedron Lett.* **1978**, 661) followed by reduction with AlH_3 (N. M. Yoon, H. C. Brown, *J. Am. Chem. Soc.* **1968**, *90*, 2927.)

[6] $[Rh(CO)_2(dbm)]$ was prepared from $RhCl_3 \cdot 3H_2O$ and dibenzoylmethane in DMF: Yu. S. Varshavskii, T. G. Cherkasova, *Russ. J. Inorg. Chem.* **1967**, *12*, 899.

[7] J. Granot, *J. Magn. Reson.* **1983**, *55*, 216.

[8] R. P. Sijbesma, R. J. M. Nolte, *J. Org. Chem.* **1991**, *56*, 3122.

[9] This structure has also been found for the phosphine derivative $[RhH(PPh_3)_4]$; see: J. J. Levison, S. D. Robinson, *J. Chem. Soc. Chem. Commun.* **1968**, 1405; M. R. McLean, R. C. Stevens, R. Bau, T. F. Koetzle, *Inorg. Chim. Acta.* **1989**, *166*, 173.

[10] C. G. Spike, R. W. Parry, *J. Am. Chem. Soc.* **1953**, *75*, 2726.

[11] 4-Allylcatechol was obtained by demethylation of eugenol: R. E. Ireland, D. M. Walba, *Org. Synth.* **1977**, *56*, 44.

[12] 5-Allylresorcinol was obtained by the Pd-catalyzed coupling of allylbromide to the Grignard compound of 5-chloro-1,3-dimethoxybenzene followed by demethylation of the product with AlI_3.

Scavenger Templates: Synthesis and Electrospray Mass Spectrometry of a Linear Porphyrin Octamer**

By *Sally Anderson, Harry L. Anderson,* and *Jeremy K. M. Sanders**

Recently we described how cyclic porphyrin oligomers can be assembled with amine ligands as templates and demonstrated two complementary roles for a template.[1] A positive template brings together two reactive ends of a single molecule, encouraging intramolecular cyclization, while a negative template holds the ends apart, inhibiting intramolecular cyclization and so encouraging intermolecular reaction (Fig. 1). Here we report a new role for positive templates:

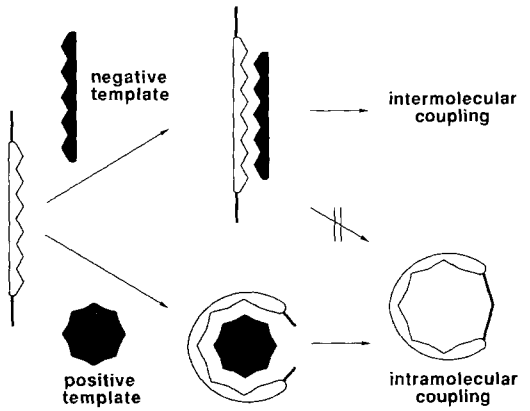

Fig. 1. The use of positive and negative templates to control the outcome of a reaction.

they can scavenge the cyclizable material in a complex mixture and so facilitate the synthesis of linear oligomers.[2] We start by outlining the idea of scavenger templates in general terms and then illustrate its application with the remarkably efficient synthesis of linear porphyrin octamer **1a** from the linear dimer **3a** via linear tetramer **2a**. We also demonstrate

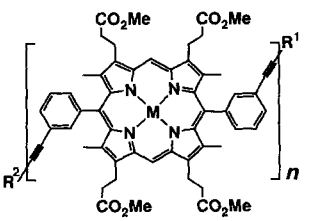

1: $n = 8$ **a**: $R^1 = R^2 = SiMe_3$
2: $n = 4$ **b**: $R^1 = H$, $R^2 = SiMe_3$
3: $n = 2$ **c**: $R^1 = R^2 = H$

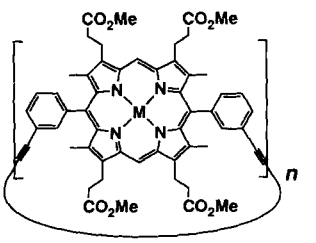

4: $n = 2$ $M = Zn, H_2$
5: $n = 4$

the use of electrospray mass spectrometry (ES-MS)[3] to determine the size and the purity of these molecules, which are otherwise rather difficult to characterize.

A common approach to the building-up of linear oligomers is to deprotect one end of a doubly protected oligomer containing n monomer units and couple it to give a fully protected oligomer containing $2n$ units. The cycle can be repeated as required. Partial deprotection gives a statistical mixture of fully protected, monoprotected, and fully deprotected compounds, which creates difficulty in the coupling step: fully protected material is inert, so it does not need to be separated before coupling, but fully deprotected material can couple with monoprotected material, leading to a new reactive oligomer and ultimately to a complex mixture. Conventionally this problem is avoided by separation of doubly deprotected material before coupling, but separation becomes more difficult with longer oligomers and so limits the chain length that can be achieved.

Scavenger templates overcome this problem by preventing fully deprotected molecules from undergoing bimolecular

[*] Dr. J. K. M. Sanders, S. Anderson, Dr. H. L. Anderson
Cambridge Centre for Molecular Recognition
University Chemical Laboratory
Lensfield Road, Cambridge CB2 1EW (UK)

[**] This work was supported by the Science and Engineering Research Council (UK), Rhône-Poulenc-Rorer Ltd., and Magdalene College Cambridge.

reactions (Fig. 2): the template accelerates their cyclization; thus they do not survive long enough under the coupling conditions to react with monoprotected material. The separation can now be postponed until after coupling, when it becomes easier because the desired linear compound is twice as massive as the starting material and the cyclic by-product. Any positive template could, in principle, be used as a scavenger template, so the concept could have wide application. For example, it should be possible to use alkali metal cations as scavenger templates for the synthesis of linear oligoethylene glycols.

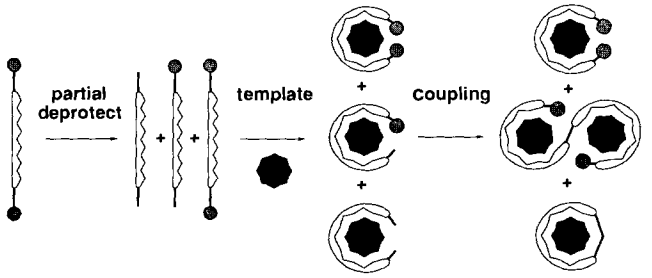

Fig. 2. A scavenger template induces molecules with two reactive end groups to cyclize intramolecularly, so allowing efficient coupling of monoprotected material. Hatched circles represent protecting groups.

Our scavenger-templated synthesis of butadiyne-linked linear porphyrin octamer **1a** involves two cycles of deprotection and Glaser coupling, beginning with linear porphyrin dimer **3a**.[4] In each cycle, tetrabutylammonium fluoride (TBAF) in chloroform was used to remove trimethylsilyl (TMS) protecting groups from the alkynyl substituents on the porphyrins. This deprotection was most efficient with free-base porphyrins, and was followed by metalation with zinc and templated Glaser coupling. After coupling, the zinc was removed with methanolic trifluoroacetic acid (TFA) to facilitate separation of the products.

4,4'-Bipyridyl (bpy) is an efficient template closing linear porphyrin dimer Zn_2-**3c** to cyclic dimer Zn_2-**4**,[4] and can thus be used as a scavenger template in the synthesis of linear tetramer. Half the protecting groups were removed from linear dimer H_4-**3a** with one equivalent of TBAF to give a statistical distribution of dimers, H_4-**3a**, **b**, and **c**. This mixture was treated with zinc acetate to yield Zn_2-**3a**, **b**, and **c** and then subjected to Glaser coupling in the presence of a sixfold excess of bpy. There were just three components in the resulting mixture: cyclic dimer **4**, linear dimer **3a**, and linear tetramer **2a**, the latter being relatively easy to isolate in good purity (Fig. 3). By contrast, in the absence of the bpy template a complex mixture formed, and clean linear tetramer was difficult to isolate in significant yields. Conversions and isolated yields for all reactions are given in Table 1.[5]

Table 1. Product yields [%] in the presence and absence of scavenger templates [a].

Reactant	Template	H_4-**3a**	H_4-**4**	H_8-**2a**	H_8-**5**	H_{16}-**1a**
H_4-**3a**	bpy	25 (20)	24 (15)	48 (29)	2	0
H_4-**3a**	–	25	7	30	10	0
H_8-**2a**	H_2-**6**	–	–	25 (16)	25 (13)	50 (15)
H_8-**2a**	–	–	–	25	17	36 (0)

[a] Overall yields for deprotection, metalation, coupling, and dematalation. Yields are from ^{1}H NMR analysis of crude reaction mixtures [5], except for those in parentheses, which are for recrystallized isolated material.

The second cycle of scavenger templating converted linear porphyrin tetramer into linear porphyrin octamer: *meso*-tetra-4'-pyridylporphyrin (H_2-**6**) is an excellent positive template for the cyclization of fully deprotected linear tetramer, giving more than 90% conversion to cyclic tetramer,[6] so it

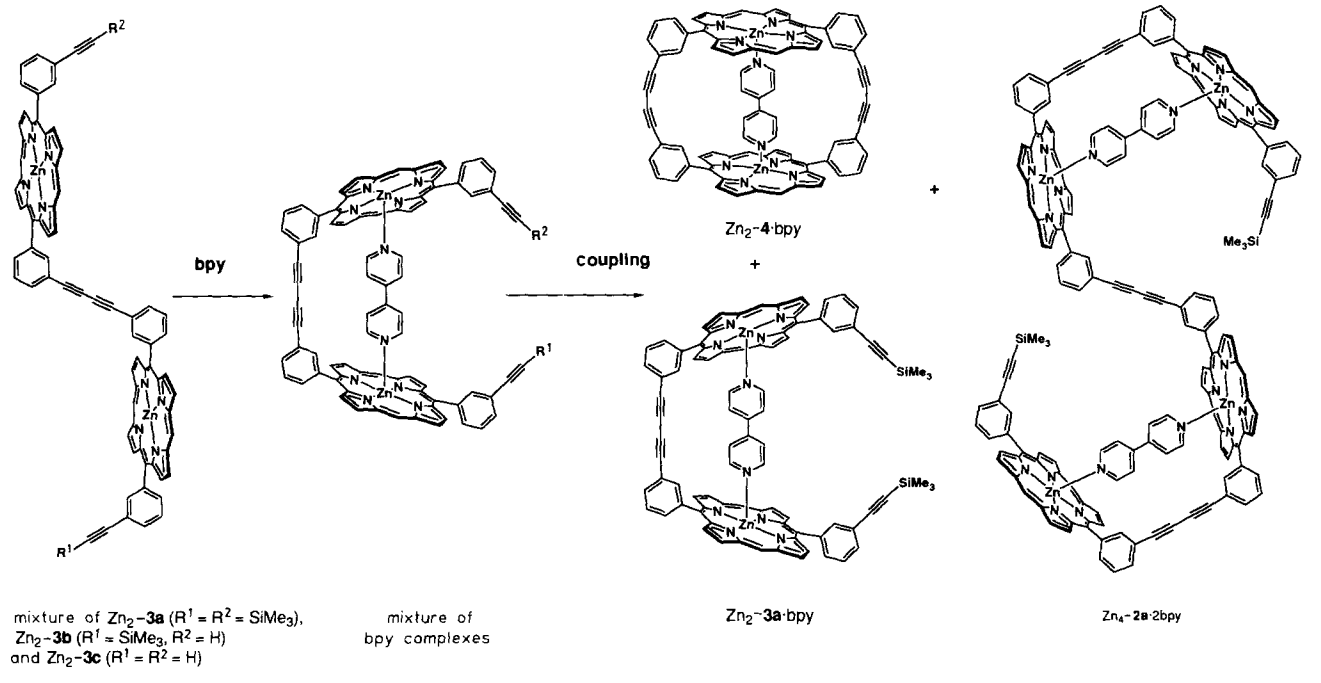

Fig. 3. 4,4'-Bipyridyl (bpy) as a scavenger template in the synthesis of linear tetramer. Zn_4-**2a** · 2 bpy. All porphyrin side chains have been omitted for clarity.

 © VCH Verlagsgesellschaft mbH, W-6940 Weinheim, 1992 0570-0833/92/0707-0908 $ 3.50+.25/0

should be an efficient scavenger template for the synthesis of linear octamer **1a** (Fig. 4). Half the protecting groups were removed from linear tetramer H_8-**2a**, and the resulting mixture was metalated with zinc and then coupled in the presence of excess H_2-**6**. After coupling there were just three chromatographically distinct components in the mixture: linear tetramer **2a**, cyclic tetramer **5**, and linear octamer **1a**. Again, in the absence of template an intractable mixture containing higher oligomers resulted (see Table 1). ^{1}H NMR analysis of the crude mixture containing the template showed the presence of 25 ± 5% cyclic tetramer, so essentially all the monodeprotected material (50% with respect to starting material) must have been converted into linear octamer because no other product was detected. This is the theoretical maximum yield. However the isolated yield of pure recrystallized material was much smaller, reflecting the difficulty of separating linear octamer from cyclic tetramer even in this relatively simple mixture. Nevertheless, there are two advantages of using a scavenger template in this type of reaction: the crude yield of coupled product is increased, but just as importantly, the number of by-products which interfere with separation is greatly reduced.

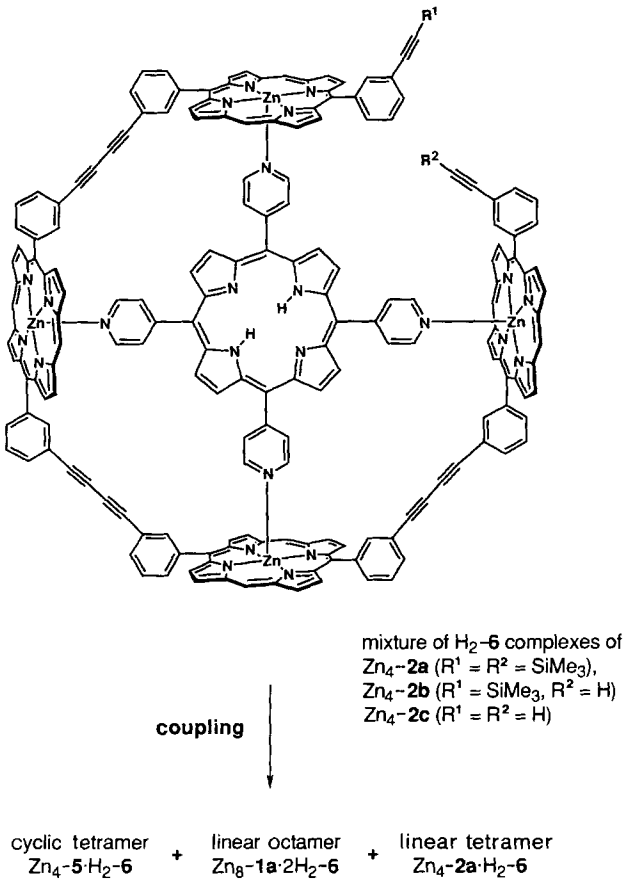

Fig. 4. Tetrapyridyl porphyrin H_2-**6** as a scavenger template in the synthesis of linear octamer Zn_8-**1a** · $2H_2$-**6**. All porphyrin side chains have been omitted for clarity.

Our cyclic porphyrin oligomers have characteristic ^{1}H NMR spectra, but the linear oligomers all have very small similar ^{1}H NMR spectra, making the analysis of mixtures with more than two linear oligomers unsatisfactory. The smaller oligomers give molecular ion peaks in their positive ion FAB mass spectra, but for tetramers only very weak molecular signals are obtained, and when the number of porphyrin units is further increased, no signal is observed. We therefore turned to electrospray mass spectrometry (ES-MS) which has been very successful with a range of large molecules.[7, 8] The compound is dissolved in a suitable solvent and protonated at several sites before injection into the spectrometer and volatilization.[9]

Linear tetramer H_8-**2a** (3783 Da) gave an electrospray mass spectrum with peaks due to the addition of three, four, and five protons: $[H_8\text{-}\mathbf{2a}\text{-}H_3]^{3+}$ (m/z 1262), $[H_8\text{-}\mathbf{2a}\text{-}H_4]^{4+}$ (m/z 947), and $[H_8\text{-}\mathbf{2a}\text{-}H_5]^{5+}$ (m/z 758). Cyclic tetramer gave peaks due to $[H_8\text{-}\mathbf{5}\text{-}H_3]^{3+}$ (m/z 1213) and $[H_8\text{-}\mathbf{5}\text{-}H_4]^{4+}$ (m/z 910). If cyclic oligomers only gave molecular ions with one proton per porphyrin, their spectra would be independent of ring size. This result, however, shows that less protonated molecular ions can be detected, thus allowing different cyclic oligomers to be distinguished. Octamer H_{16}-**1a** gave the spectrum shown in Figure 5. Peaks are observed for the addition of four to nine protons to the octamer, corresponding to a molecular weight of 7421 Da for the most abundant isotope of the neutral molecule. The distribution of ions suggests that the porphyrin units are far enough apart that protonation of each unit occurs independently: perhaps surprisingly, there is no apparent preference for $[H_{16}\text{-}\mathbf{1a}\text{-}H_4]^{4+}$, which would correspond to protonation of alternate units.

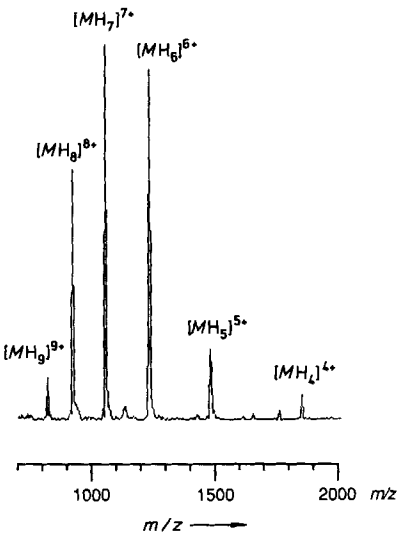

Fig. 5. Electrospray mass spectrum of linear octamer H_{16}-**1a**.

The use of scavenger templates can in principle be applied to the synthesis of any linear oligomer containing an even number of units, provided an effective template can be found that induces cyclization of any doubly deprotected starting material. This leaves the monodeprotected molecule to couple only with itself and hence form the required longer oligomer. The length of oligomer accessible by this method is limited only by our ingenuity in devising suitable templates and the ease with which the final products can be separated.

Experimental Procedure

Linear tetramer H_8-**2a**: Half the protecting groups were removed from H_4-**3a** (250 mg, 127 μmol) with TBAF (1 M in THF, Aldrich), by titrating a solution of the free base porphyrin in $CHCl_3$ (85 mL, 1.5 mM in porphyrin units in $CHCl_3$) with fluoride until about 50% of the TMS groups had been removed, which generally required about one equivalent of TBAF. The reaction was followed by monitoring the ratio of the intensities of the acetylene C–H ($\nu = 3303\ cm^{-1}$) and C = O ($\nu = 1732\ cm^{-1}$) absorptions with FT-IR. The mixture was passed through a short silica column, and then metalated with excess zinc acetate in chloroform refluxing. For the Glaser coupling, a solution of the zinc porphyrins in dichloromethane (500 mL, 0.5 mM per porphyrin unit) was treated with CuCl (1.50 g, 60 equiv), *N,N,N',N'*-tetramethylethylenediamine (2.30 mL, 60 equiv) in the presence of bpy (119 mg, 760 μmol) and stirred in dry air until coupling was complete (monitored by thin-layer chromatography, 15–30 min). The mixture was washed with water, demetalated by treatment with methanolic TFA (10%), washed with water, and concentrated. H_8-**2a** was isolated from the reaction mixture by flash column chromatography and recrystallized from $CHCl_3$/MeOH. Yield: 70 mg (29%). ^1H NMR (400 MHz, $CDCl_3$): $\delta = -2.50$ (s, 8H), 0.26 (s, 18H), 2.53 (s, 48H), 3.10 (br.t, 32H), 3.63 (set of very close singlets, 48H), 4.33 (br.t, 32H), 7.60–8.30 (m, 32H), 10.26 (s, 8H). IR ($CHCl_3$): $\tilde{\nu}$ [cm^{-1}] = 3303 (C-H), 1732 (C = O). UV/VIS (CH_2Cl_2): λ_{max} [nm] = 332, 410, 507, 540, 574, 625 nm. FAB-MS *m/z* 3783 (M^+), 1892 (M^{2+}). Yield of H_4-**5**: 36 mg (15%) and of reclaimed H_4-**3a**: 51 mg (20%).

Linear octamer H_{16}-**1a**: H_8-**2a** (170 mg, 45 μmol) was partly deprotected and coupled in the presence of a sixfold excess of H_2-**6** according to the procedure described above. The resulting mixture was washed, demetalated and chromatographed, and the products were recrystallized from $CHCl_3$/MeOH. Octamer: Yield: 25 mg (15%). ^1H NMR (250 MHz, $CDCl_3$): $\delta = -2.50$ (s, 16H), 0.25 (s, 18H), 2.49 (s, 96H), 3.12 (br.s, 64H), 3.61 (m, 96H), 4.32 (br.s, 64H), 7.68–8.23 (m, 64H), 10.25 (s, 16H). IR ($CHCl_3$): $\tilde{\nu}$ [cm^{-1}] = 1732 (C = O). UV/VIS (CH_2Cl_2): λ_{max} [nm] = 332, 411, 506, 539, 574, 625. ES$^+$-MS: *m/z* 825 ($[MH_9]^{9+}$), 928 ($[MH_8]^{8+}$), 1061 ($[MH_7]^{7+}$), 1237 ($[MH_6]^{6+}$), 1485 ($[MH_5]^{5+}$), 1856 ($[MH_4]^{4+}$). Yield: cyclic tetramer: 22 mg (13%); reclaimed starting material: 28 mg (16%).

Received: January 20, 1992
Revised version: March 17, 1992 [Z 5133/5134 IE]
German version: *Angew. Chem.* **1992**, *104*, 921

CAS Registry numbers:
H_{16} **1a**, 141753-10-8; H_8 **2a**, 141753-12-0; H_4 **3a**, 141709-04-8; H_4 **3c**, 141709-05-9; Zn_2 **3c**, 141709-06-0; Zn_2 **3c**·bpy, 141709-07-1; Zn_2 **4**·bpy, 130829-48-0; H_4 **4**, 130858-12-7; H_8 **5**, 141753-11-9; H_2 **6**, 16834-13-2; bpy, 553-26-4.

[1] H. L. Anderson, J. K. M. Sanders, *Angew. Chem.* **1990**, *102*, 1478; *Angew. Chem. Int. Ed. Engl.* **1990**, *29*, 1440.
[2] These template roles are all types of kinetic template effect—see D. H. Busch, N. A. Stephenson, *Coord. Chem. Rev.* **1990**, *100*, 119.
[3] J. B. Fenn, M. Mann, C. K. Meng, C. M. Whitehouse, *Science* **1989**, *246*, 64.
[4] The protected linear porphyrin dimer H_4-**3a** was prepared by Glaser coupling of partly deprotected monomer. The metalated linear dimer Zn_2-**3c** gives a 1:1 complex with 4,4'-bipyridyl (bpy) (formation constant $\approx 10^6\ M^{-1}$ in $CDCl_3$); the guest in this complex slowly exchanges between excess host molecules on the ^1H NMR chemical-shift time scale at room temperature. The binding of bpy to linear dimer is much stronger than to monomer, but is about 100 times weaker than the binding to cyclic dimer, Zn_2-**4**, presumably because the linear molecule is more flexible. Bpy is a good template for the closure of linear dimer; in the absence of bpy, coupling of Zn_2-**3c** gives 19% conversion to cyclic dimer Zn_2-**4**, whereas with bpy the yield rises to 85%. This result supports the idea that bpy traps the linear intermediate in the formation of cyclic dimer Zn_2-**4** from monomer [1].
[5] These conversions were determined by ^1H NMR spectroscopy of reaction mixtures and are accurate to ±5%. Spectra of pure cyclic oligomers were subtracted from the spectra of the reaction mixtures to determine the proportion of each cyclic component. The relative amounts of the linear components were then estimated from the integration ratios of the difference spectra.
[6] S. Anderson, H. L. Anderson, J. K. M. Sanders, unpublished results.
[7] G. J. Van Berkel, S. A. McLuckey, G. L. Glish, *Anal. Chem.* **1991**, *63*, 1098.
[8] F. Bitsch, C. O. Dieterich-Buchecker, A.-K. Khémiss, J.-P. Sauvage, A. Van Dorsselaer, *J. Am. Chem. Soc.* **1991**, *113*, 4023.
[9] ES-MS was carried out with a VG BIO Q electrospray mass spectrometer. Compounds were injected as approximately 0.1 mM solutions in methanol containing 0.2 vol.-% TFA.

Stereocontrolled Construction of 6 · 5 · 6 and 5 · 5 · 6 Ring Systems by Radical Tandem Cyclization**

By *Uwe Albrecht, Rudolf Wartchow,* and *H. M. R. Hoffmann**

Dedicated to Professor Ekkehard Winterfeldt on the occasion of his 60th birthday

We have devised radical cyclizations,[1] which afford bicyclic and tricyclic pyranofurans and furanofurans in a chemo- and diastereoselective fashion. Reaction of *N*-iodosuccinimide (NIS) and 1,5-hexadiyn-3-ol (**1**) or 1-hexen-5-yn-3-ol (**2**) with 2,3-dihydrofuran and Δ^2-dihydropyran gave

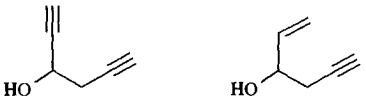

1 **2**

functionalized cyclic α-alkoxy-β-iodo ethers[2, 3] (Scheme 1). In studying radical-initiated cyclizations of these compounds we had to find experimental conditions that allowed us to handle sensitive starting materials and products. To this end, two sets of experimental conditions were investigated in detail.

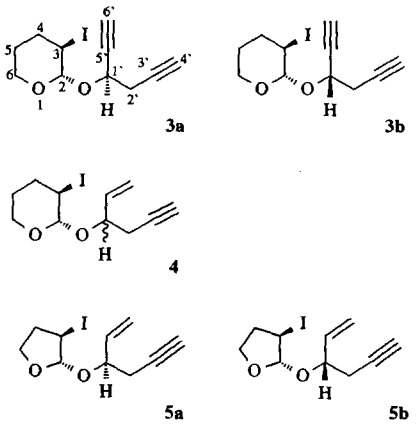

Scheme 1. Synthesized monocyclic iodoacetals. Compounds **3** were obtained in yields of 50–64%, **4** in 81%, and **5** in 66%. Iodoacetal **4** was obtained as a 1:1 mixture of diastereomers.

Cyclization of diastereomerically pure **3a** induced by BEt_3–oxygen[4] gave a mixture of isomeric bicyclic vinyl iodides **6a**(*E*:*Z* = 1:9) in satisfactory yield and under mild conditions (30–55 °C; Scheme 2). Iodine-free *exo* methylene acetal **7a**, formed as a by-product (5%), could be separated from the iodine-containing products by chromatography (petroleum ether/$CHCl_3$). The selective formation of **6a** and

[*] Prof. H. M. R. Hoffmann, Dr. U. Albrecht
Institut für Organische Chemie der Universität
Schneiderberg 1B, D-W-3000 Hannover (FRG)
Dr. R. Wartchow
Institut für Anorganische Chemie der Universität
Callinstrasse 9, D-W-3000 Hannover

[**] We thank Ulrike Eggert for experimental contributions and the Fonds der Chemischen Industrie for support of this work.

7a proved to be markedly dependent on temperature. At elevated temperatures (80–100 °C) complicated product mixtures arose.

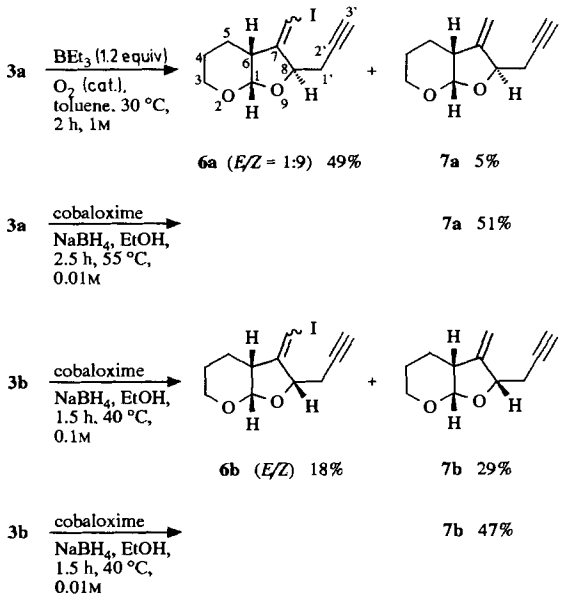

Scheme 2. Monocyclizations of diynes 3. The concentrations given refer to the starting materials.

Similarly, both **3a** and **3b** were monocyclized with cobaloxime under hydrogen-atom-transfer conditions,[2] giving **7a** and **7b**, respectively (Scheme 2). The formation of vinyl iodide **6b** implicates competing intermolecular iodine-atom-transfer,[5] and was favored at higher concentrations of the starting material (0.1 vs. 0.01 M). A second cyclization of the intermediate vinyl radical, for example 6-*endo*-digonal,[6] was not observed; apparently the activation energy required is prohibitively high.

Unlike diynes **3a** and **3b**, the enynes **4** and **5** underwent tandem cyclizations (Scheme 3). The construction of the two ring junctions proceeded stereo- and regioselectively, giving a series of 1,9-*cis*-, 3,8-*trans*-fused tricycles (for numbering of atoms see Scheme 3). The cyclization of **4** with BEt_3 under an argon atmosphere was noticeably very sluggish. Only in the presence of catalytic amounts of oxygen (brief displacement of the argon atmosphere) did the cyclization proceed satisfactorily. Isolation and purification of the tricycles required several chromatographic separations.

Characteristic spectroscopic data of the tricycles are the coupling constants for the 3,8 *trans*- ($^3J = 10$ Hz) and 1,9 *cis*-oriented protons ($^3J = 4-6$ Hz). The structures and relative configurations of **8a**, **8b**, and **12** were further corroborated by X-ray crystallography (Fig. 1).[7]

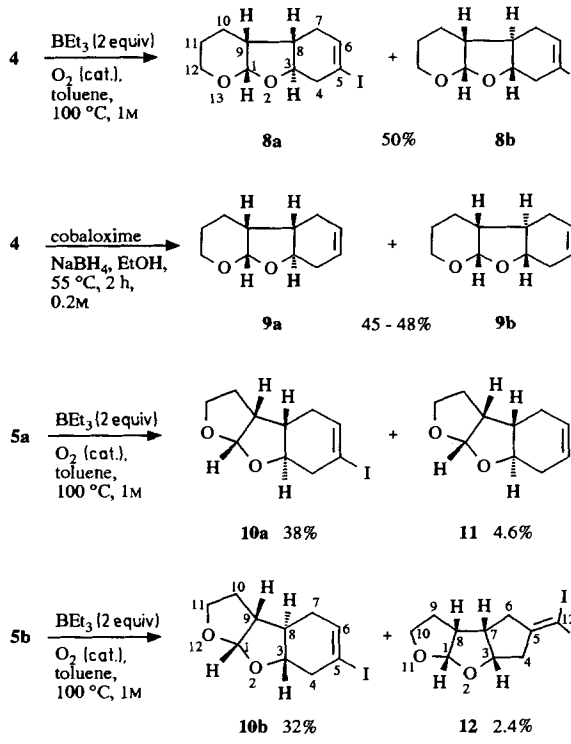

Scheme 3. Stereocontrolled tandem cyclizations of compounds **4** and **5**. The concentrations given refer to starting materials.

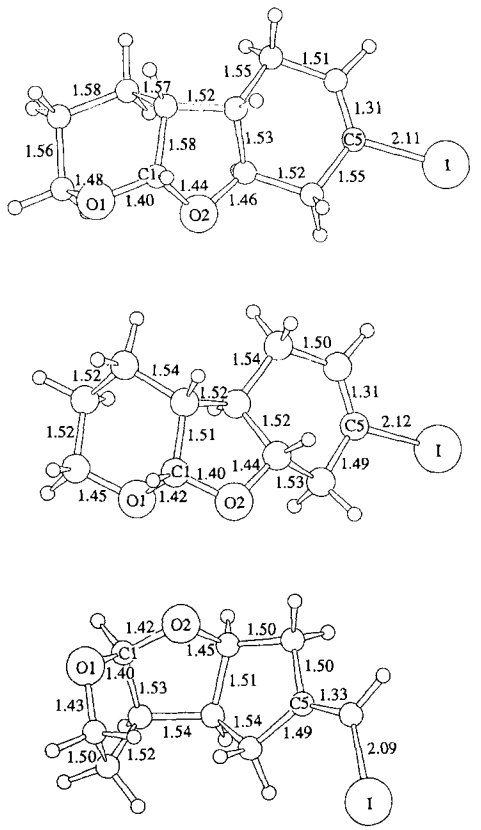

Fig. 1. Crystal structures of **8a** (top), **8b** (middle), and **12** (bottom) (SCHAKAL).

A priori, a 3-oxahex-5-enyl radical generated from **5a** or **5b** can cyclize either via a chair or a boat transition state. In studying carbohydrate systems and changing the configuration of an appendant homoallyl side chain, RajanBabu observed that a boat transition state is feasible provided that the chair alternative is destabilized by an unfavorable eclipsing interaction.[8]

In our investigations, diastereomer **5a** apparently cyclizes preferentially via the chair transition state, in which the methylene group and neighboring propargyl group are transoid. As a consequence, the two hydrogen atoms at C-4 and C-5 are *trans* in tricycle **10a** (numbering in Scheme 4).

The stereochemistry of the formation of **10a** is the "normal" one, and has often been observed in closure to many types of [3.3.0]bicycles.[1]

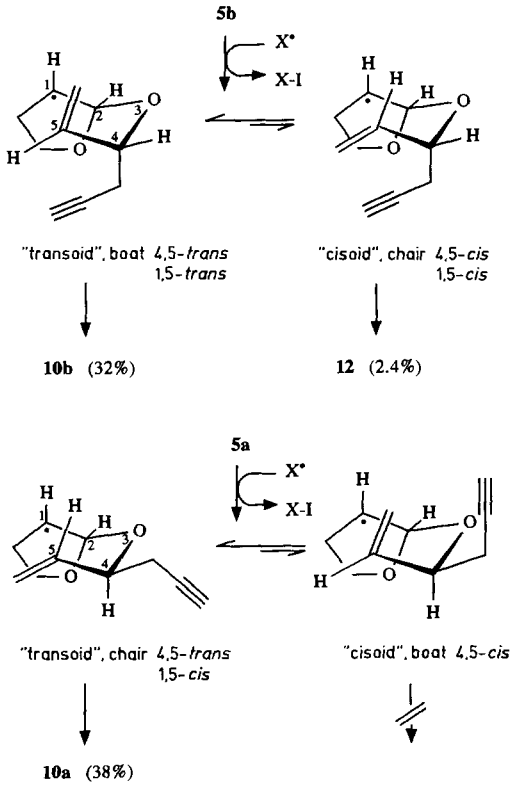

Scheme 4. Transoid versus cisoid transition states (X• = radical initiator).

On the other hand, the stereochemistry of tricycle **10b** from **5b** is "abnormal", since formation of **10b** requires a boat transition state. If the 3-oxahex-5-enyl radical generated from **5b** adopts the chairlike transition state, the propargyl group and methylene group are in a less favorable eclipsing or cisoid arrangement. Upon ring closure the H atoms on C-4 and C-5 are then necessarily *cis*. A priori, the radical chain reaction can continue with an *endo*cyclic or an *exo*-cyclic ring closure. In this case, the 5-*exo*-digonal closure is faster, as usual, and *cis-syn-cis* dioxatriquinane **12** is isolated as a minor by-product. Formation of **12** may be ascribed to the "kinetic error" of the generation of radical **13**, in which all four substituents of the central tetrahydrofuran moiety are placed on the same face of the ring. The formation of **12**

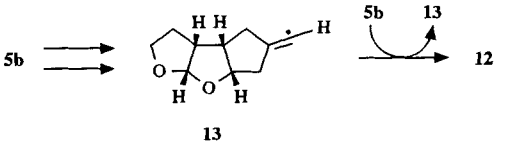

(Fig. 1) complements the well-known Curran synthesis of *cis-anti-cis* fused triquinanes.[9] With regard to entropy and enthalpy, the formation of the open, basketlike triquinane **12** from monocycle **5b** is remarkable. The product ratio **10b**:**12** = 13:1 corresponds to a preference of the boat transition state by 1.5 kcal mol^{-1}.

If the sequential cyclization of iodo-substituted enyne **4** is conducted at lower temperatures (0–40 °C, BEt_3 method), the second ring closure does not occur, and mainly monocyclization products are formed. Tandem cyclizations were usually carried out at 100 °C (Scheme 3). Only the reaction mediated by cobaloxime/$NaBH_4$ **4** → **9a** + **9b** succeeded under milder conditions (55 °C). Thus, the cyclization sequence is also chemoselective in that the triple bond does not take part in an initial 6-*exo*-digonal cyclization,[1] but later in an unexpected 6-*endo*-digonal ring closure. *Endo*-digonal closure to *trans*-fused bicyclo[4.3.0]nonane derivatives is "tolerated" at higher temperature, because the normally favored 5-*exo*-digonal closure would have to produce a high-energy, *trans*-fused bicyclo[3.3.0]octane system.

Experiments have shown that the replacement of the Bu_3SnH/azobis(isobutyronitrile) (AIBN) method with the BEt_3–oxygen method or cobaloxime-mediated hydrogen-atom-transfer has been instrumental in effecting the double cyclization. Our results demonstrate the power of radical reactions in organic synthesis with respect to multiple formation of carbon–carbon bonds and to chemo-, regio-, and diastereocontrol. The usual preference for the formation of *cis*-perhydroindane[10] is negated by the proclivity of the C-4 propargyl group to adopt a transoid conformation with respect to the neighboring methylene group (Scheme 4). The formation of tricycle **10b** implicates a preferred boat transition state with a pseudoaxial propargyl side chain. To our knowledge, these double cyclizations are the first examples in which a favorable formation of a five-membered ring has been coupled with the less favored formation of a *trans*-fused six-membered ring. The previously unknown 6-*endo*-digonal closure is possible, because the potentially faster 5-*exo*-digonal mode is prevented by ring strain.

Experimental Procedure

The cyclization precursors were prepared as follows: A solution of NIS (1.2 equiv) and the alcohol component [11,12] (1.2 equiv) in CH_2Cl_2 was cooled to −30 °C. The cyclic enol ether was added dropwise, and the resulting mixture was cooled to −70 °C, stirred, and allowed to reach room temperature over 15 h. After aqueous workup, chromatography (silica gel) furnished functionalized monocyclic acetals **3**–**5** (Scheme 2). The products were obtained as mixtures of the diastereomers (1:1), which, except for compound **4**, could be separated.

Cobaloxime-induced cyclization; typical procedure: To a solution of **3b** (200 mg, 0.65 mmol) in abs EtOH (5.6 mL) was added solid $NaBH_4$ (50 mg, 1.3 mmol) and 10 N NaOH (0.1 mL, 10 mmol). Argon was passed through the solution, and several portions of finely powdered cobaloxime (14.6 mg, 0.033 mmol) were added over 1.5 h at 40 °C. The solvent was removed on a rotary evaporator, and after addition of water (10 mL), the product was extracted with Et_2O (3 × 10 mL). The combined organic phases were washed with water (5 mL), brine (5 mL), and dried ($MgSO_4$). After removal of the solvent, the resulting oily residue was chromatographed (silica gel, Et_2O/petroleum ether, 1:10). Iodine-free bicycle **7b** (34 mg, 29%) was separated from vinyl iodide **6b** [36 mg, 18%, (*E*/*Z*) (not assigned), 2:1] by repeated chromatography (petroleum ether/$CHCl_3$). **6b** (major isomer): ^{1}H NMR (200 MHz, $CDCl_3$): δ = 6.28 (m, 1H, *exo*-CH_2), 5.25 (d, ^3J = 4 Hz, 1H, H-1), 4.42 (m, 1H, H-8), 3.89 (m, 1H, H_a-3), 3.73 (m, 1H, H_b-3), 2.77–2.58 (m, 3H), 2.21 (br m, 1H), 2.09 (t, ^4J = 2.5 Hz, H-3'), 1.67–1.24 (m, 4H, H-4/H-5). **6b** (minor isomer): ^{1}H NMR (200 MHz, $CDCl_3$): δ = 6.13 (dd, ^4J = 2 Hz, ^4J = 2 Hz, 1H, *exo*-CH_2), 5.24 (d, ^3J = 4 Hz, 1H, H-1), 4.56 (m, 1H, H-8), 3.92 (m, 1H, H_a-3), 3.50 (m, 1H, H_b-3), 3.20 (ddd, J = 17 Hz, J = 2 Hz, ^4J = 2 Hz, 1H, H_a-1'), 2.79 (ddd, J = 17 Hz, J = 10 Hz, ^4J = 2.5 Hz, 1H, H_b-1'), 2.73 (m, 1H, H-6), 2.09 (dd, ^4J = 2.5 Hz, ^4J = 2.5 Hz, 1H, H-3'), 1.99–1.37 (m, 4H, H-4/H-5). **7b**: ^{1}H NMR (200 MHz, $CDCl_3$): δ = 5.29 (m, 1H, H_a-*exo*-CH_2), 5.12 (d, ^3J = 4 Hz, 1H, H-1), 5.02 (m, 1H, H_b-*exo*-CH_2), 4.68 (m, 1H, H-8), 3.85 (dm, 1H, H_a-3), 3.41 (dd, J = 11.8 Hz, J = 11 Hz, J = 2 Hz, 1H, H_b-3), 2.73 (m, 1H, H-6), 2.63 (ddd, J = 8 Hz, J = 7 Hz, ^4J = 2.5 Hz, 2H, H-1'), 2.06 (dd, ^4J = 2.5 Hz, ^4J = 2.5 Hz, 1H, H-3'), 2.12–1.32 (m, 4H, H-4/H-5); ^{13}C NMR ($CDCl_3$): δ = 149.63 (s, C-7), 105.43 (t, *exo*-CH_2), 100.79 (d, C-1), 81.47 (s, C-2'), 79.34 (d, C-8), 69.77 (d, C-3'), 64.45 (t, C-3), 43.07 (d, C-6), 27.21, 22.45, 20.45 (t, C-4, C-5, C-1').

BEt_3/O_2-induced cyclization; typical procedure: A well-dried 10 mL two-necked flask equipped with reflux condenser, $CaCl_2$ tube, and septum was charged with a solution of **5b** (700 mg, 2.39 mmol) in abs toluene (2.4 mL) and heated to 100 °C. A solution of BEt_3 (1 M in hexane, 3.6 mL, 1.5 equiv) was slowly added by syringe over 15 min, and the reaction was monitored by thin-layer chromatography. After the reaction mixture was stirred for 45 min, a further portion of BEt_3 (0.5 equiv) was added. After complete reaction (ca. 2.5 h) the solvent was evaporated, and the oily residue was chromatographed (silica gel, Et_2O/petroleum ether, 1:6), giving three fractions. F1 and F2 were purified by further chromatography (petroleum ether/$CHCl_3$); F3 contained mainly the iodine-free tricycle derived from **10b** and impurities, and was not characterized further). Recrystallization of **10b** from Et_2O/petroleum ether afforded colorless crystals, 223 mg (32%), m.p. 90 °C. ^{1}H NMR (200 MHz, $CDCl_3$): δ = 6.33 (m, 1H, H-6), 5.69 (d, 1H, J = 5.8 Hz, H-1), 4.03 (m, 1H, H_a-11), 3.85 (ddd, 1H, J = 12 Hz, 8 Hz, 5 Hz, H_b-11), 3.53 (ddd, 1H, J = 10 Hz, 10 Hz, 6 Hz, H-3), 2.96 (dm, 1H, H_a-4), 2.71 (m, 1H, H_b-4), 2.45 (m, 2H, H-9, H_a-7), 2.13–1.82 (m, 2H, H_b-7, H_a-10), 1.72 (m, 1H, H_b-10), 1.48 (m, 1H, H-8); ^{13}C NMR ($CDCl_3$): δ = 136.81 (d, C-6), 109.05 (d, C-1), 92.34 (s, C-5), 78.42 (d, C-3), 66.88 (t, C-11), 47.74, 43.41 (d, C-8/9), 45.48, 32.88, 30.58 (t, 3C). NOE effects: H-8 with H_a-7 (5.9%), H_b-4 (4.4%), H_b-11 (5.4%); H-3 with H-9 (2.1%), H_a-4 (4.4%), H-1 (3.9%); H-9 with H_a-10 (10.4%), H-1 (5.3%), H-3 (2.4%); H-1 wih H-3 (3.4%), H-9 (5.2%). Recrystallization of **12** (F2) (Et_2O/petroleum ether) afforded colorless crystals, 17 mg (2.4%), m.p. 71 °C. ^{1}H NMR (200 MHz, $CDCl_3$): δ = 5.96 (m, 1H, H-12), 5.68 (d, ^3J = 4.5 Hz, H-1), 4.63 (dt, 1H, J = 6 Hz, 2 Hz, H-3), 4.04–1.70 (m, 10H); ^{13}C NMR ($CDCl_3$): δ = 153.57 (s, C-5), 110.98 (d, C-1), 85.13 (d, C-12), 70.21 (d, C-3), 69.02 (t, C-10), 46.18, 43.66 (d, C-7/8), 40.51, 37.20, 27.78 (t, 3C).

Received: January 22, 1992 [Z 5142 IE]
German version: *Angew. Chem.* **1992**, *104*, 903

[1] Most recent reviews on radical reactions: C. P. Jasperse, D. P. Curran, T. L. Fevig, *Chem. Rev.* **1991**, *91*, 1237; W. B. Motherwell, D. Crich, *Best Synthetic Methods. Free Radical Chain Reactions in Organic Synthesis*, Academic Press, London, **1991**. See also B. Giese, *Radicals in Organic Synthesis: Formation of Carbon–Carbon Bonds*, Pergamon, Oxford, **1986**; D. P. Curran, *Synthesis* **1988**, 417, 489; M. Ramaiah, *Tetrahedron* **1987**, *43*, 3541; D. J. Hart, *Science* **1984**, *223*, 883; *Houben-Weyl Methoden der Organischen Chemie*, Band E 19a (Eds.: M. Regitz, B. Giese), Thieme, Stuttgart, **1989**.

[2] K. Last, H. M. R. Hoffmann, *Synthesis* **1989**, 901, and references therein.

[3] J. Thiem, H. Karl, J. Schwentner, *Synthesis* **1978**, 696.

[4] Y. Ichinose, S. Matsunaga, K. Fugami, K. Oshima, K. Utimoto, *Tetrahedron Lett.* **1989**, *30*, 3155.

[5] Atom-transfer-cyclization of iodo-substituted alkynes: D. P. Curran, M.-H. Chen, D. Kim, *J. Am. Chem. Soc.* **1989**, *111*, 6265.

[6] A 5-(π-*endo*)-*exo*-dig cyclization was also not observed. The transformation of an acyclic vinyl radial **A** into a monocyclic vinyl radical **B** has been predicted to be favorable: D. Crich, S. M. Fortt, *Tetrahedron Lett.* **1987**, *28*, 2895.

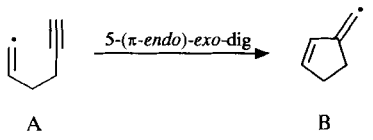

[7] Further details of the crystal structure investigation are available on request from the Director of the Cambridge Crystallographic Data Centre, University Chemical Laboratory, Lensfield Road, GB-Cambridge, CB2 1EW (UK).

[8] T. V. RajanBabu, *Acc. Chem. Res.* **1991**, *124*, 139; calculations and theoretical predictions: D. C. Spellmeyer, K. N. Houk, *J. Org. Chem.* **1987**, *52*, 595; for discussions of the chair transition state see A. L. J. Beckwith, C. H. Schiesser, *Tetrahedron* **1985**, *41*, 3925.

[9] D. P. Curran in *Advances in Free Radical Chemistry, Vol. 1* (Ed.: D. Tanner), JAI, Greenwich, **1990**, p. 121; D. P. Curran, M.-H. Chen, *Tetrahedron Lett.* **1985**, *26*, 4991.

[10] For another radical-induced construction of *trans*-hydrindanes see S. Satoh, M. Sodeoka, H. Sasai, M. Shibasaki, *J. Org. Chem.* **1991**, *56*, 2278.

[11] F. Sondheimer, Y. Amiel, Y. Gaoni, *J. Am. Chem. Soc.* **1962**, *84*, 270. Thanks to a number of procedural improvements [13] the yield of **1** was increased from 54% to 72%.

[12] A. Viola, J. H. MacMillan, *J. Am. Chem. Soc.* **1991**, *90*, 6141. The yield of **2** was increased from 56% to 83% [13].

[13] U. Albrecht, Ph.D. Thesis, University of Hannover, **1991**.

Novel Iron Carbonyl Telluride Clusters: Synthesis and Characterization of $[Fe_5Te_4(CO)_{14}]^{2-}$ and $[Fe_8Te_{10}(CO)_{20}]^{2-}$ **

By *Lisa C. Roof, William T. Pennington,* and *Joseph W. Kolis**

The molecular chemistry of polyselenides and polytellurides is currently receiving much attention because of the novel coordination properties of the molecules[1], as well as their use as starting materials for new solid-state materials.[2]

Recently we have been studying the reactions of polychalcogenides with transition metal carbonyls and have found that they can react through an internal redox reaction to give a variety of novel products.[3] Electrons are transferred from the zero-valent metal center to the polychalcogenide ion. This results in the oxidative decarbonylation of the metal and reductive cleavage of the chalcogenide chain. While polysulfides and polyselenides can induce complete oxidative decarbonylation, producing high-valent metal centers,[4] polytellurides only seem to oxidize metals to the +I or +II state. Metal–metal bonds can also form, leading to clusters, as in the reaction of Te_4^{2-} with $[W(CO)_6]$ which affords $[\{W(CO)_3\}_6(Te_2)_4]^{2-}$.[5]

We decided to study the reactions of polytellurides with iron pentacarbonyl since previous work has shown that iron carbonyl telluride chemistry is extremely rich.[6] Here we report two examples of this internal redox reaction with the synthesis and characterization of two new iron carbonyl tellurides, namely $[Fe_5Te_4(CO)_{14}]^{2-}$ (**1**) and $[Fe_8Te_{10}(CO)_{20}]^{2-}$ (**2**).

When a fivefold excess of $[Fe(CO)_5]$ is allowed to react with $(Ph_4P)_2Te_4$ in dimethylformamide (DMF) at 85 °C, **1** is formed in reasonable yield as the Ph_4P^+ salt [Eq.(a)].

$$5\,[Fe(CO)_5] + (Ph_4P)_2Te_4 \longrightarrow \underset{(Ph_4P)_2\text{-}\mathbf{1}}{(Ph_4P)_2[Fe_5Te_4(CO)_{14}]} + 11\,CO \qquad (a)$$

The X-ray crystal structure analysis showed that the dark brown crystalline product[7] contains a central $Fe(CO)_2$ fragment, which is bonded to two $[Fe_2Te_2(CO)_6]$ "butterflies" (Fig. 1). The geometry about the central iron can be described as distorted octahedral with a bond angle of 160.7(2)° for Te(2)-Fe(1)-Te(2a). The Te(1)–Te(2) distance is 3.152(2) Å, similar to that in other metal complexes with a butterfly structure.[8]. For Te–Te distances of this length a certain degree of bonding interaction has been proposed,[9] but it may be more accurate to view this short bonding distance as arising from the oxidative addition of the original Te–Te bond to the central iron atom Fe(1). Therefore each tellurium atom is formally assigned a −II oxidation state, the central iron atom +II, and each butterfly iron atom +I. Metal–metal bonds and 3 COs complete the 18e count for the butterfly iron atoms. The Fe(2)–Fe(3) distance is 2.592(4) Å, and the Fe(2)–Te(2) distance is 2.573(4) Å, which are similar to those in other iron telluride compounds with butterfly structures.[6d, 8] Iron chalcogen butterfly structures are well known,[6, 8, 10] and the first, $[Fe_2S_2(CO)_6]$, was reported in 1958.[10a] Since then their reactions have been studied thoroughly.[8, 9, 11]

[*] Prof. J. W. Kolis, L. C. Roof, W. T. Pennington
Department of Chemistry
Clemson University
Clemson, SC 29634 (USA)

[**] This work supported by the National Science Foundation (Grant # CHE-9102548). J. W. K. acknowledges a fellowship from the Alfred P. Sloan Foundation.

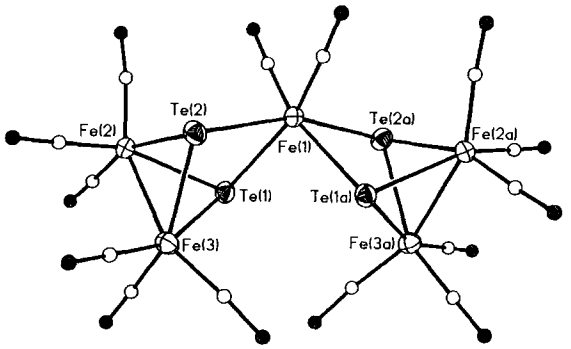

Fig. 1. Structure of **1** in crystals of $(Ph_4P)_2$-**1**. (ORTEP, thermal ellipsoids with 35% probability). Selected distances [Å] and angles [°]: Te(1)-Te(2) 3.152(2), Fe(2)-Fe(3) 2.592(4), Fe(2)-Te(2) 2.573(4), Fe(2)-Te(1) 2.588(3), Fe(1)-Te(2) 2.585(2), Fe(1)-Te(1) 2.675(3); Te(2)-Fe(1)-Te(2a) 160.7(2), Te(1)-Fe(1)-Te(1a) 100.0(1), Te(2)-Fe(1)-Te(1) 73.6(1), Te(2a)-Fe(1)-Te(1a) 73.6(1).

If the reaction is carried out with only a threefold excess of $[Fe(CO)_5]$, compound **2** is formed. A possible balanced reaction is given in Equation (b). Like **1**, product **2** can be isolated as a dark brown crystalline product with Ph_4P^+ as a

$$8\,[Fe(CO)_5] + 3\,(Ph_4P)_2Te_4 \longrightarrow (Ph_4P)_2[Fe_8Te_{10}(CO)_{20}] + 2\,(Ph_4P)_2Te + 20\,CO \quad (b)$$

$(Ph_4P)_2$-**2**

counterion (Fig. 2).[7] The dianion contains two $[Fe_4Te_4(CO)_{10}]$ cubane units connected by a central Te_2^{2-} ligand. The Te_2^{2-} fragment links the two cubes by bonding in

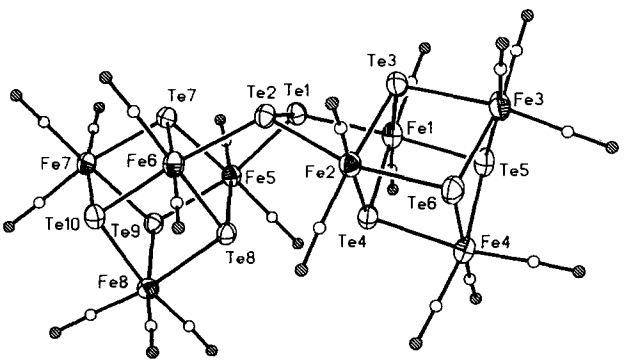

Fig. 2. Structure of **2** in crystals of $(Ph_4P)_2$-**2**. (ORTEP, thermal ellipsoids with 35% probability). Selected distances [Å] and angles [°]: Te(1)-Te(2) 2.828(1), Fe(1)-Te(1) 2.622(2), Te(2)-Fe(2) 2.616(2), Fe(1)-Te(4) 2.587(2), Fe(1)-Te(5) 2.589(2), Fe(4)-Te(4) 2.652(2), Fe(4)-Te(5) 2.630(2), Fe(2)-Te(3) 2.626(2), Fe(2)-Te(6) 2.590(2), Fe(3)-Te(3) 2.643(2), Fe(3)-Te(6) 2.641(2), Fe(1)-Te(3) 2.637(2), Fe(4)-Te(6) 2.615(2), Fe(2)-Te(4) 2.615(2), Fe(3)-Te(5) 2.626(2); Fe(6)-Te(2)-Fe(2) 120.4(1), Fe(6)-Te(2)-Te(1) 101.8(1), Fe(2)-Te(2)-Te(1) 99.3(1), Fe(1)-Te(1)-Fe(5) 123.0(1), Fe(1)-Te(1)-Te(2) 99.9(1), Fe(5)-Te(1)-Te(2) 98.0, Fe(1)-Te(5)-Fe(4) 99.5(1), Te(3)-Fe(3)-Te(6) 80.4(1).

η^2 fashion by donation of lone pair electrons to iron atoms in opposite corners of one face of each cube. The Te(1)–Te(2) bond length (2.828(1) Å) is in the usual range for a Te–Te bond in a metal cluster.[5, 6d] The Fe–Te distances average 2.62(2) Å, and the angles are between 80.4(1)° and 99.5(1)°, so the cubes are only slightly distorted despite the presence of the transannular ditelluride fragment. This is different from the previously reported $[Fe_4Te_4(TePh)_4]^{3-}$ which contains angles varying from 60.2° to 118°.[12] Each iron atom is in an octahedral environment, and has a complete 18e count through bonding with the appropriate number of COs. The dihedral angle between the two cubes is 123.3°.

The chemistry of iron–sulfur cubanes is well investigated because of their presence in the active sites of many enzymes.[13] The neutral parent cubanes $[Fe_4(CO)_{12}(\mu_3\text{-}E)_4]$ (E = S, Se) were structurally characterized in 1982,[14] and several iron–telluride cubanes have also been characterized;[12, 15] however, the type of bridging in **2** is entirely unprecedented. The formation of the neutral cubane $[Fe_4Te_4(CO)_{12}]$ from the dimerization of $[Fe_2(Te_2)(CO)_6]$ has been reported, but this molecule was never structurally characterized.[6b]

Both **1** and **2** are formed by the mild pyrolysis of $[Fe(CO)_5]$ and Te_4^{2-} in DMF. In addition, conversion of **1** to **2** can be achieved by adding elemental Te (4 equiv) to the solution of **1** before workup [Eq. (c)]. This conversion has been monitored in solution by IR spectroscopy and is quite clean. The

$$\underset{\mathbf{1}}{[Fe_5Te_4(CO)_{14}]^{2-}} + 4\,Te \longrightarrow \underset{\mathbf{2}}{[Fe_8Te_{10}(CO)_{24}]^{2-}} \quad (c)$$

CO–Fe–Te system is obviously very versatile, and other intermediate species have been observed in solution. Thus we have shown that neutral $[Fe(CO)_5]$ can be oxidized by polytelluride chains to form very unusual clusters containing reduced tellurides and iron atoms in the +I and +II state.

Experimental Procedure

$(Ph_4P)_2$-**1**: In a typical reaction, $(PPh_4)_2Te_4$ [16] (0.500 g, 0.420 mmol) and $[Fe(CO)_5]$ (0.27 mL, 2.05 mmol) in DMF (10 mL) were stirred at 85 °C for 24 h. The resulting brown solution was filtered, layered with ether (10 mL), and stored at 4 °C for 24 h. After the brown powder that formed was removed by filtration, the solvent was removed under vacuum. The brown oil was redissolved in CH_2Cl_2 (10 mL). Slow addition of ether (5 mL) and storage at 4 °C for 24 h produced a dark brown crystalline product. Yield: 33%. Satisfactory C,H analysis. IR (CH_2Cl_2): $\tilde{\nu}$ [cm^{-1}] = 2025(w), 2006(s), 1975(s), 1936(m).

$(Ph_4P)_2$-**2**: The compound was prepared in an analogous way to $(Ph_4P)_2$-**1**. The only changes were that less $[Fe(CO)_5]$ (0.15 mL, 1.14 mmol) was added and the reaction was stirred for 12 h at 85 °C. Yield: 27%. Satisfactory C,H analysis. IR (CH_2Cl_2): $\tilde{\nu}$ [cm^{-1}] = 2027(s), 2015(m), 1977(s), 1916(w).

Received: January 15, 1992 [Z 5122 IE]
German version: *Angew. Chem.* **1992**, *104*, 924

CAS Registry numbers:
$(Ph_4P)_2$-**1**, 141903-14-2; $(Ph_4P)_2$-**2**, 141903-16-4; $[Fe(CO)_5]$, 13463-40-6; $(Ph_4P)_2Te_4$, 96220-73-4; Te, 13494-80-9.

[1] a) M. A. Ansari, J. A. Ibers, *Coord. Chem. Rev.* **1990**, *100*, 223; b) M. G. Kanatzidis, *Comments Inorg. Chem.* **1990**, *10*, 161.
[2] a) R. C. Haushalter, C. M. O'Conner, J. P. Haushalter, A. M. Umarji, G. K. Shenoy, *Angew. Chem.* **1984**, *96*, 147; *Angew. Chem. Int. Ed. Engl.* **1984**, *23*, 169; b) M. L. Steigerwald, *Chem. Mater.* **1989**, *1*, 52; c) M. L. Steigerwald, C. E. Rice, *J. Am. Chem. Soc.* **1988**, *110*, 4228; d) S. C. Lee, R. H. Holm, *Angew. Chem.* **1990**, *102*, 868; *Angew. Chem. Int. Ed. Engl.* **1990**, *29*, 840.
[3] J. W. Kolis, *Coord. Chem. Rev.* **1990**, *105*, 195, and references therein.
[4] a) S. C. O'Neal, J. W. Kolis, *J. Am. Chem. Soc.* **1988**, *110*, 1971; b) S. C. O'Neal, W. T. Pennington, J. W. Kolis, *Inorg. Chem.* **1989**, *28*, 2780.
[5] L. C. Roof, W. T. Pennington, J. W. Kolis, *J. Am. Chem. Soc.* **1990**, *112*, 8172.
[6] a) D. A. Lesch, T. B. Rauchfuss, *Inorg. Chem.* **1981**, *20*, 3583; b) L. E. Bogan, Jr., D. A. Lesch, T. B. Rauchfuss, *J. Organomet. Chem.* **1983**, *250*, 429; c) P. Mathur, B. H. S. Thimmappa, A. L. Rheingold, *Inorg. Chem.* **1990**, *29*, 4658; d) B. W. Eichhorn, R. C. Haushalter, *ibid.* **1990**, *29*, 728.
[7] Intensity measurements were made at ambient temperature (21 ± 1 °C) on a Nicolet R3mV diffractometer with graphite-monochromated $Mo_{K\alpha}$ radiation (λ = 0.71073 Å). ω-scans, $2\theta \leq 45.0°$, Data were corrected for Lorentz and polarization effects and for absorption (empirical correction).

Crystal data: $(Ph_4P)_2$-**1**, monoclinic, $C2/c$, $a = 14.968(3)$ Å, $b = 20.232(4)$ Å, $c = 22.336(5)$ Å, $\beta = 106.41(2)°$, $V = 6488(2)$ Å^3, $Z = 4$, $\varrho_{calcd} = 1.90$ g cm^{-3}, $\mu(Mo_{K\alpha}) = 2.97$ mm^{-1} (transmission factors: 0.84–1.00). Refined using 2792 observed reflections $[I > 3\,\sigma(I)]$ to $R(F_o) = 0.0734$ and $R_w(F_o) = 0.0851$. All non-hydrogen atoms were refined anisotropically with observed reflections per parameter = 7.086. For $(Ph_4P)_2$-**2**, triclinic, $P\bar{1}$, $a = 13.037(3)$ Å, $b = 14.913(3)$ Å, $c = 24.041(4)$ Å, $\alpha = 76.70(2)°$, $\beta = 86.90(2)°$, $\gamma = 66.75(2)°$, $V = 4176(2)$ Å^3, $Z = 2$, $\varrho_{calcd} = 2.36$ g cm^{-3}, $\mu(Mo_{K\alpha}) = 4.89$ mm^{-1} (transmission factors: 0.58–1.00). Refined using 8609 observed reflections $[I > 3\,\sigma(I)]$, to $R(F_o) = 0.0423$, and $R_w(F_o) = 0.0539$. The carbon atoms of the cation were refined istropically and all other heavy atoms anisotropically, hydrogen atoms were not located, observed reflections per parameter = 11.74. Further details of the crystal structure investigations may be obtained from the Fachinformationszentrum Karlsruhe, Gesellschaft für wissenschaftlich-technische Information mbH, W-7514 Eggenstein-Leopoldshafen 2 (FRG) on quoting the depository number CSD-56092, the names of the authors, and the journal citation.

[8] a) D. A. Lesch, T. B. Rauchfuss, *Organometallics* **1982**, *1*, 499; b) P. Mathur, D. Chakrabarty, Md. M. Hossain, *J. Organomet. Chem.* **1991**, *401*, 167; c) P. Mathur, I. J.Mavunkel, A. L. Rheingold, *J. Chem. Soc. Chem. Commun.* **1989**, 382.

[9] L. E. Bogan, T. B. Rauchfuss, A. L. Rheingold, *J. Am. Chem. Soc.* **1985**, *107*, 3843.

[10] a) W. Hieber, J. Gruber, *Z. Anorg. Allg. Chem.* **1958**, *296*, 91; b) C. F. Campana, F.-Y.-K. Lo, L. F. Dahl, *Inorg. Chem.* **1979**, *18*, 3060.

[11] a) V. W. Day, D. A. Lesch, T. B. Rauchfuss, *J. Am. Chem. Soc.* **1982**, *104*, 1290; b) P. Mathur, V. D. Reddy, *J. Organomet. Chem.* **1990**, *385*, 363; c) D. Seyferth, R. S. Henderson, L.-C.Song, *Organometallics* **1982**, *1*, 125; d) K. S. Bose, E. Sinn, B. A. Averill, *ibid.* **1984**, *3*, 1126.

[12] W. Simon, A. Wilk, B. Krebs, G. Henkel, *Angew. Chem.* **1987**, *99*, 1039; *Angew. Chem. Int. Ed. Engl.* **1987**, *26*, 1009.

[13] Recent reviews: a) R. H. Holm, S. Ciurli, J. A. Weigel, *Prog. Inorg. Chem.* **1990**, *38*, 1; b) D. Coucouvanis, *Acc. Chem. Res.* **1991**, *24*, 1.

[14] L. L. Nelson, F. Y.-K. Lo, A. D. Rae, L. F. Dahl, *J. Organomet. Chem.* **1982**, *225*, 309.

[15] a) W. Bronger, M. Kimpel, D. Schmitz, *Angew. Chem.* **1982**, *94*, 562; *Angew. Chem. Int. Ed. Engl.* **1982**, *21*, 544; b) P. Barbaro, A. Bencini, I. Bertini, F. Briganti, S. Midollini, *J. Am. Chem. Soc.* **1990**, *112*, 7238.

[16] a) J. C. Huffman, R. C. Haushalter, *Z. Anorg. Allg. Chem.* **1984**, *518*, 203; b) R. G. Teller, R. C. Krause, R. C. Haushalter, *Inorg. Chem.* **1983**, *22*, 1809.

The Total Synthesis of (±)-Mitomycin K**

By *John W. Benbow, Gayle K. Schulte,* and *Samuel J. Danishefsky**

The mitomycins and related aziridine-containing alkaloids have enjoyed remarkable longevity as systems of great fascination to chemists.[1, 2] Continuing interest in this family of compounds arises from the clinical importance of at least one member (mitomycin C) as an anticancer agent,[3] and from the novel structures wherein a confluence of potentially labile functionality is maintained, in metastable form, in a small molecular array.[2] Many laboratories have concerned themselves with the isolation,[1, 4] structure proof,[5] chemistry,[6] crystallography,[7] synthesis,[8] and bioorganic chemistry[9] of various mitomycins.

Not the least fascinating type of mitomycin is exemplified by mitomycin K (**1**), in which the methylene group in the 9 position constitutes still another locus of potential structural vulnerability, not present in the more traditional congeners (cf. *N*-methylmitomycin A (**2**)).

Though total syntheses of the more prevalent mitomycins of the type **2** have been accomplished by Kishi et al. and by Fukuyama et al.,[8e–h] to date no total synthesis directed toward a mitomycin of the type **1** has been registered. Such compounds are of particular interest to us from the standpoint of the mechanism of their bioactivation.[9] In principle,

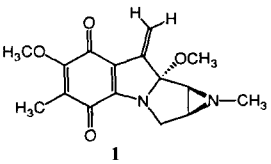

1

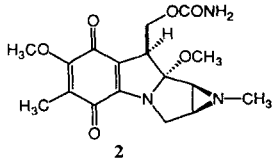

2

it is possible that the presence of the vinylquinone unit confers electrophilicity on these systems even in the absence of reductive activation.[10]

A photochemical route to the framework of the mitomycins (cf. **3** → **4**) has recently been reported.[11] We now describe the total synthesis of (±)-mitomycin K (**1**). While compound **4** contains a significant portion of the mitomycin K structure, some rather challenging and novel chemistry was required to achieve the synthesis of **1**.

Rapid progress was, at first, impeded by our inability to functionalize the C1-C2 double bond of **4** in a constructive fashion.[12] We anticipated[13] that the site of unsaturation in the corresponding conjugated lactam, **5**, could be more generally exploited. Accordingly, compound **4** was oxidized (PDC)[14] to afford a 65% yield of the imide **5**.[15] Indeed, reaction of **5** with (phenylthio)methyl azide[16] at 80 °C gave a 90% yield of the triazoline **6**. The latter underwent reduction with L-Selectride to afford a 77% yield of the hydroxyl compound **7**.[15]

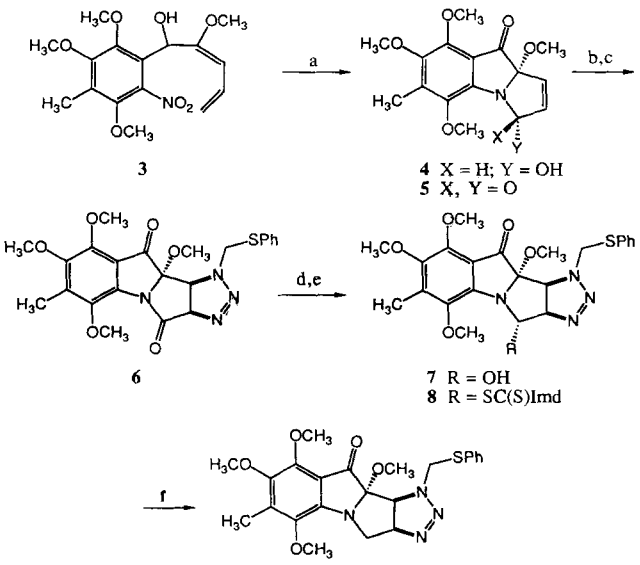

3 — **4** X = H; Y = OH; **5** X, Y = O — **6** — **7** R = OH; **8** R = SC(S)Imd — **11**

Scheme 1. a) *hv*, $\lambda = 350$ nm, THF (45%). b) PDC, Celite, CH_2Cl_2 (65%). c) $PhSCH_2N_3$, PhH, 80 °C (90%). d) L-Selectride (1.25 equiv), THF, −78 °C (77%). e) 1,1'-Thiocarbonyldiimidazole (5 equiv), 4-dimethylaminopyridine (DMAP) (1 equiv), CH_2Cl_2, 35 °C (65%). f) Bu_3SnH (1.70 M), azodiisobutyronitrile (AIBN), PhH, 80 °C (63%). Imd = imidazole.

[*] J. W. Benbow and S. J. Danishefsky
Department of Chemistry
Yale University
225 Prospect Street, New Haven, CT 06511 (USA)
G. K. Schulte
Center for Chemical Instrumentation, Yale University

[**] This research was supported by PHS Grant CA28824. NMR spectra were recorded at the Northeast Regional NSF/NMR Facility at Yale Univeristy, which was supported by NSF Chemistry Division Grant CHE7916210. An NIH Postdoctoral Fellowship to J. W. B. (Grant CA08907-02), is gratefully acknowledged.

Reaction of **7** with 1,1'-thiocarbonyldiimidazole in the presence of DMAP afforded the thiothioxo compound **8**[15] in 65% yield.[17] The curious transformation of **7** → **8** presumably proceeds through rearrangement of the initial thioxo compound into the corresponding thioester. The latter apparently undergoes acyl exchange under the conditions of the reaction to produce **8**. The structure of **8** was secured by an X-ray crystal structure of compound **9** (Fig. 1).[18] Compound **9** was an intermediate in a route which evaluated the possibility of aziridine formation prior to the reduction at C3.[19] However, Barton reduction[20] of **9** led to the allylic amine **10** by a fragmentation pathway.

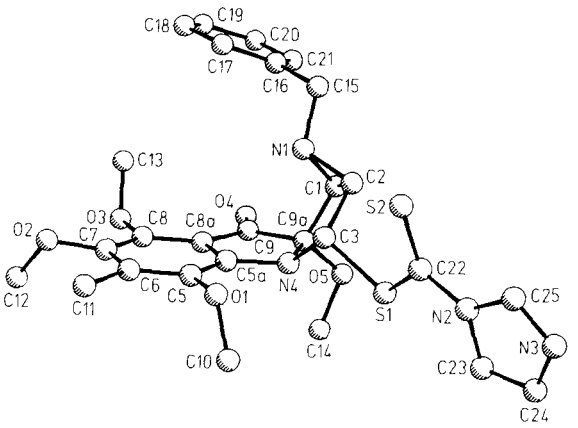

Fig. 1. Crystal structure of **9** (PLUTO).

Given the propensity of β-aziridino radicals toward fragmentation, the deoxygenation of a triazoline substrate was investigated. Fortunately, reductive cleavage of the imidazoledithiocarboxyl unit of **8** could be carried out through the agency of tri-*n*-butyltinhydride, thereby affording the deoxygenated compound **11** (63% yield).

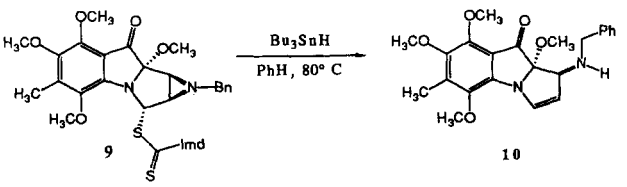

Scheme 2. Bn = CH_2Ph.

Photolytic decomposition of the triazoline unit was accomplished (48% yield) by irradiation at 254 nm (Vycor filter).[13] The resultant (phenylthio)methylaziridine **12** when subjected to the action of Raney Nickel in acetone, was converted (70% yield) to the *N*-methylaziridine derivative **13** (Scheme 3). To the best of our knowledge, this represents the first application of (phenylthio)methylazide for the synthesis of *N*-methylaziridines.

The program for installation of C10 began by reaction of **13** with trimethylsilylmethyllithium.[21] This reaction proceeded quite cleanly to give rise to a 90% yield of adduct **14**,[15] apparently as a single stereoisomer. Reaction of **14** with silver(II) picolinate[22] afforded, in low yield, the very interesting compound **15**, which is formally a trimethylsilanol addition product of mitomycin K. In the last step of the synthesis, quinone **15** responded to the action of PPTS in methylene chloride to provide an 81% yield of racemic mitomycin K. The infrared, ^1H NMR, and ^{13}C NMR spectra of racemic synthetic mitomycin K (m.p. 123–125 °C) were identical with those from a sample procured by partial synthesis via naturally occurring *N*-methylmitomycin A.[23]

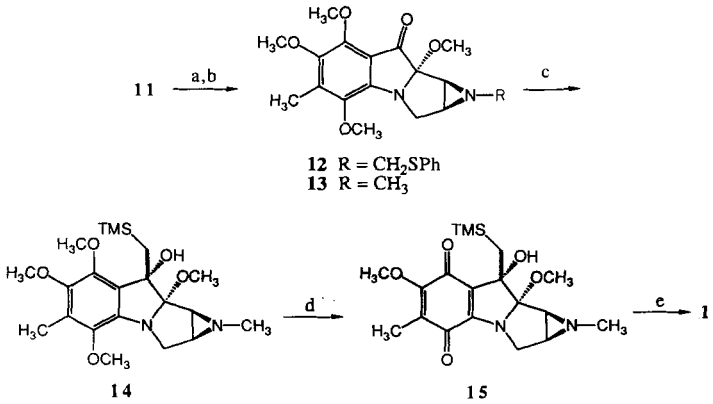

Scheme 3. a) 254 nm Hg lamp/Vycor filter, PhH in quartz tube (48%). b) Raney Nickel, acetone, 60 °C (70%). c) Trimethylsilylmethyllithium (15 equiv), THF, −10 °C (90%). d) Silver(II) picolinate (6 equiv), NaOAc (10 equiv), CH_3CN/H_2O (8–16%). e) Pyridinium *p*-toluenesulfonate (PPTS), CH_2Cl_2 (81%).

Future research will be directed toward improvements in the yields in this rather concise synthesis. Also of value would be insights into the chemical stability of mitomycin K. Studies pertaining to the mode in which mitomycin K is activated for covalent attachment to its biological receptors are envisioned.

Received: January 11, 1992 [Z 5113 IE]
German version: *Angew. Chem.* **1992**, *104*, 934

[1] a) R. Sugawara, T. Hata, *J. Antibiot. Ser. A.* **1956**, *9*, 147; b) S. Wakaki, H. Marumo, K. Tomioka, Y. Mimiru, E. Kato, H. Konada, S. Kudo, Y. Fujimoto, *Antibiot. Chemother. (Basel 1954–70)*, **1958**, *8*, 288.

[2] a) W. A. Remers, *The Chemistry of Antitumor Antibiotics*, Wiley, New York, **1979**, and references therein; b) W. A. Remers, B. S. Iyengor, *Recent Progress in the Chemical Synthesis of Antibiotics* (Eds.: G. Lukacs, M. Chao) Springer, Berlin, **1990**, pp. 415–445.

[3] a) B. A. Chabner, J. M. Collins, *Cancer Chemotherapy Principles and Practice*, Lippencott, Philadelphia, **1990**; b) S. K. Carter, S. T. Crooke, *Mitomycin C Current Status and New Developments*, Academic Press, New York, **1979**.

[4] Porfiromycin: C. DeBoer, A. Dietz, N. E. Lummus, G. M. Savage, *Antimicrobial Agents Annual 1960*, Plenum, New York, **1961**, pp. 17–22. Mityromycin: D. V. Lefemine, M. Dann, F. Barbatschi, W. K. Hansmann, V. Zbinovsky, P. Moonikendan, J. Adam, N. Bohonos, *J. Am. Chem. Soc.* **1962**, *84*, 3184; M. Kono, M. Kasai, K. Shirahata, N. Hirayama, *J. Antibiot.* **1991**, *44*, 309. Isomitomycin A and albomitomycin A: M. Kono, Y. Saitoh, K. Shiriahata, Y. Arai, S. Ishii, *J. Am. Chem. Soc.* **1987**, *109*, 7224. Decarbamoyldehydromitomycins (including mitomycin K): C. Urakawa, H. Tsuchiya, K.-I. Nakano, *J. Antibiot.* **1981**, *34*, 243. C. Urakawa, H. Tsuchiya, K.-I. Nakano, N. Nakamura, *ibid.* **1981**, *34*, 1152.

[5] Mitomycin A: J. S. Webb, D. B. Cosulich, J. H. Mowat, J. B. Patrick, R. B. Broschard, W. E. Meyer, R. P. Williams, C. F. Wolf, W. Fulmor, C. Pidacks, *J. Am. Chem. Soc.* **1962**, *84*, 3184, 3187. Gross structure of mitomycin B: S. Kinoshita, K. Vzu, K. Nakano, M. Shimizu, T. Takahashi, *J. Med. Chem.* **1971**, *14*, 103.

[6] a) C. L. Stevens, K. G. Taylor, M. E. Munk, W. S. Marshall, K. Noll, G. F. Shah, L. G. Shah, K. Uzu, *J. Med. Chem.* **1964**, *8*, 1; b) W. A. Lown, G.

Weir, *Can. J. Chem.* **1978**, *56*, 296; c) M. Tomasz, *Chem.-Biol. Interact.* **1976**, *13*, 89; d) J. B. Patrick, R. P. Williams, W. E. Meyer, W. Fulmor, D. B. Cosulich, R. W. Broschard, J. S. Webb, *J. Am. Chem. Soc.* **1964**, *86*, 1889; e) W. G. Taylor, W. A. Remers, *Tetrahedron Lett.* **1974**, 2483; f) W. G. Taylor, W. A. Remers, *J. Med. Chem.* **1975**, *18*, 307; g) S. Kinoshita, K. Uzu, K.-I. Nakano, M. Shimizu, T. Takahashi, *ibid.* **1971**, *14*, 104.

[7] a) A. Tulinsky, *J. Am. Chem. Soc.* **1962**, *84*, 3188; b) A. Tulinsky, J. H. van de Hende, *ibid.* **1967**, *89*, 2907; c) R. Yahashi, I. Matsubara, *J. Antibiot.* **1976**, *29*, 104; d) R. Yahashi, I. Matsubara, *ibid.* **1978**, *31*, 6. e) N. Hirayama, K. Shirahata, *Acta Crystallogr. Sect B* **1987**, *43*, 555.

[8] For representative synthetic efforts see: a) S. Danishefsky, E. M. Berman, M. Ciufolini, S. J. Etheredge, B. F. Segmuller, *J. Am. Chem. Soc.* **1985**, *107*, 3891; b) K. J. Shaw, J. R. Luly, H. Rapoport, *J. Org. Chem.* **1985**, *50*, 4515; c) J. Rebek, Jr., S. H. Shaber, Y.-K. Shue, J.-C. Gehret, S. Zimmermann, *ibid.* **1984**, *49*, 5164; d) R. W. Franck, *Fortschr. Chem. Org. Naturst.* **1979**, *38*, 4. For the only total syntheses, see: e) F. Nakatsubo, T. Fukuyarna, A. J. Cocuzza, Y. Kishi, *J. Am. Chem. Soc.* **1977**, *99*, 8115; f) T. Fukuyama, F. Nakatsubo, A. J. Cocuzza, Y. Kishi, *Tetrahedron Lett.* **1977**, 4295; g) L. Yang, T. Fukuyama, *J. Am. Chem. Soc.* **1987**, *109*, 7881; h) L. Yang, T. Fukuyama, *ibid.* **1989**, *111*, 8303.

[9] a) W. Szybalski, V. N. Iyer, *Fed. Proc.* **1964**, *23*, 946; b) R. W. Franck, M. Tomasz, *Chemistry of Antitumor Agents* (Ed.: D. E. V. Wilman) Blackie & Sons, Glasgow, **1990**, pp. 379–393; c) S. J. Danishefsky, M. Ciufolini, *J. Am. Chem. Soc.* **1984**, *106*, 6424; d) M. Egbertson, S. J. Danishefsky, *ibid.* **1987**, *109*, 2204; e) H. Kohn, N. Zein, *ibid.* **1983**, *105*, 4105; f) K. Bean, H. Kohn, *J. Org. Chem.* **1985**, *50*, 293; g) M. Tomasz, R. Lipman, B. F. McGuinness, K. Nakanishi, *J. Am. Chem. Soc.* **1988**, *110*, 5892; h) M. Tomasz, R. Lipman, D. Chowdary, J. Pawlek, G. L. Verdine, K. Nakanishi, *Science* **1987**, *235*, 1204; i) B. F. McGuinness, R. Lipman, K. Nakanishi, M. Tomasz, *J. Org. Chem.* **1991**, *56*, 4826; j) Y. P. Hong, H. Kohn, *ibid.* **1991**, *56*, 6479.

[10] It is conceivable that an appropriate biological nucleophile could undergo a 1,6 Michael addition to the quinone via the exocyclic defin. Subsequent expulsion of the methoxyl group at C9a would provide the corresponding C10-substituted mitosene and provide net activation of mitomycin K without initial activation.

[11] K. F. McClure, J. W. Benbow, S. J. Danishefsky, G. K. Schulte, *J. Am. Chem. Soc.* **1991**, *113*, 8185.

[12] Compound **4** was resistant to standard conditions for reductive amination ($NaCNBH_3$), and attempts to convert the alcohol into a substrate suitable for deoxygenation (i.e. an SPh or OC(S)R group) proceeded with a concommitant loss of the methoxyl group at C9a and formation of pyrrole. Osmylation of the olefin unit was successful and stereospecific. However, the resultant diol with the $1\beta,2\beta$ configuration (as was shown in the antipode) was not suitable for conversion into the required $1\beta,2\beta$-aziridine linkage.

[13] The photolytic conversion of trizolines into aziridines has been reported: a) G. J. Sinta, R. W. Franck, R. J. Kempton, *J. Org. Chem.* **1974**, *39*, 3739; b) P. Scheiner, *Tetrahedron* **1968**, *24*, 2757.

[14] E. J. Corey, J. W. Suggs, *Tetrahedron Lett.* **1975**, 2647; E. J. Corey, G. Schmidt, *ibid.* **1979**, 399.

[15] All new compounds gave appropriate ^1H NMR, ^{13}C NMR, and IR spectra as well as satisfactory data from high-resolution mass spectrometry and/or elemental analyses.

[16] B. M. Trost, W. H. Pearson, *J. Am. Chem. Soc.* **1981**, *103*, 2483; B. M. Trost, R. A. Kunz, *J. Org. Chem.* **1974**, *39*, 2648.

[17] Similar rearrangements of thioxocarbonates have been reported: a) H. R. Al-Kazimi, D. S. Tarbell, D. Plant, *J. Am. Chem. Soc.* **1955**, *77*, 2479; b) A. Schönberg, L. Vargha, *Ber. Dtsch. Ges. Chem.* **1930**, *63*, 178.

[18] Crystal data of **9**: triclinic, space group $P\bar{1}$ (No. 2), $a = 11.754(2)$, $b = 24.35(1)$, $c = 9.982(3)$ Å, $\alpha = 101.00(3)°$, $\beta = 100.76(2)°$, $\gamma = 86.66(3)°$, $v = 2755(2)$ Å^3, $Z = 4$; $D_{calc} = 1.332$ g cm^{-3}; $\mu(Cu_{K\alpha}) = 20.72$ cm^{-1}. Intensity data were collected on a Rigaku AFC5S diffractometer using $Cu_{K\alpha}$ radiation (graphite monochromator $\lambda = 1.54178$ Å). A crystal with dimensions $0.25 \times 0.25 \times 0.15$ mm was used. The structure was solved with SHELXS86 direct methods and refined with a full-matrix least-squares technique to $R = 0.070$, $R_w = 0.088$, and $S = 2.81$ for 5013 independent reflections ($2\theta \leq 114°$, $I \geq 3\sigma(I)$). Further details of the crystal structure investigation are available on request from the Director of the Cambridge Crystallographic Data Centre, University Chemical Laboratory, Lensfield Road, GB-Cambridge CB2 1EW (UK), on quoting the full journal citation.

[19] The *N*-benzyl analogue of triazoline **6** was prepared by treatment of **5** with benzylazide. Reduction of the carbonyl group followed by derivatization with 1,1'-thiocarbonyldiimidazole provided **9**. The details of this sequence will be addressed in a subsequent paper.

[20] H. R. Barton, S. W. McCombie, *J. Chem. Soc. Perkin Trans. 1* **1975**, 1574.

[21] a) D. J. Ager, *Synthesis* **1984**, 384; b) D. J. Peterson, *J. Org. Chem.* **1968**, *33*, 780.

[22] K. Kloc, J. Mlochowski, L. Syper, *Chem. Lett.* **1980**, 725.

[23] M. Egbertson, *Part I: Studies Concerning the Reductive Activation of Mitomycins*, Ph.D. Dissertation, Yale University, **1989**.

Supramolecular Self-Assemblies of Two-Directional Cascade Molecules: Automorphogenesis**

By *George R. Newkome,* Charles N. Moorefield, Gregory R. Baker, Rajani K. Behera, Gregory H. Escamillia,* and *Mary J. Saunders*

Molecular self-assembly has fundamental ramifications for our understanding of the origin of life,[1] as well as utilitarian applications in material and polymer sciences.[2] Nature provides examples of self-assembly,[3–5] and recent synthetic efforts, in particular by Lehn, et al.,[6] have resulted, for example, in self-recognizing structures termed helicates. In the broad domain of supramolecular chemistry, which is concerned with structures of higher complexity arising from noncovalent, intermolecular interactions,[7] molecular automorphogenesis[8] is the construction of molecules by self-assembly of complementary shapes. By designing and controlling molecular topology for the purpose of self-assembly, a supramolecular automorphogenesis is possible at the next level. This report describes the preparation of a synthetic nonnatural example of a novel automorphogenic suprastructure possessing helical and ribbonlike morphologies.

Our investigation into control over molecular topology and molecular recognition was prompted initially by an interest in controlling the preorganization of specifically designed macromolecules (dendrimers, arborols).[9] The initially chosen sequence[10] utilized carbon as the branching center and involved the amidation of alkyl-substituted methanetricarboxylates (triester)[11] with tris(hydroxymethyl)-aminomethane (Tris). Since the infrastructure of the product resembled architecturally the Leeuwenberg model[12] for trees and the terminal groups consisted of alcohols, we described these molecules as arborols.[10] Others used the term dendrimers for such compounds.[9]

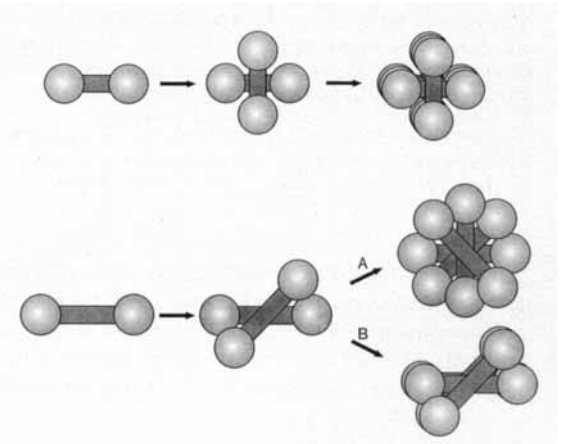

Fig. 1. Postulated stacking arrangements for dumbbell-shaped arborols. Top: orthogonal stacking of the alkane arborols. Bottom: non-orthogonal relationships between adjacent molecules of alkyne arborols lead to **A** helical structures, or **B** ribbon structures.

[*] Prof. G. R. Newkome, Dr. C. N. Moorefield, Dr. G. R. Baker, Dr. R. K. Behera, G. H. Escamillia, Dr. M. J. Saunders
Center for Molecular Design and Recognition
Department of Chemistry—SCA 228
University of South Florida, Tampa, FL 33620-5250 (USA)

[**] Chemistry of Micelles, Part 16. We thank Dr. Robert Potter and Dr. Neil Neuberger for their timely advice. This work was supported by the National Science Foundation [DMR 86-00929, 89-06792 (GRN); DCB 88-02011 (MJS)], the donors of the Petroleum Research Fund (administered by the American Chemical Society), the Florida High Technology and Industry Council, and the USF Central Florida Regional Data Center for the aquisition of CHARMm. Part 15: G. R. Newkome, G. R. Baker, R. K. Behera, A. L. Johnson, C. N. Moorefield, C. D. Weis, W.-J. Cao, J. K. Young, *Synthesis* **1991**, 839.

Dumbbell-shaped poly(amidoalcohol)s were prepared[13] possessing two spherical head groups (each containing nine hydroxyl moieties) connected by a two-directional core. Characterization of specific arborols (i.e., [9]-10-[9]) revealed their ability to form thermally reversible, aqueous gels,[13, 14] which were postulated to arise from the propensity of the dumbbells to stack in an orthogonal fashion, thereby forming a tightly packed supramolecular, rod-shaped assembly by self-recognition (see Fig. 1). The resultant rods possessed a uniform diameter of ca. 35 Å, determined by electron microscopy (see Fig. 2a).

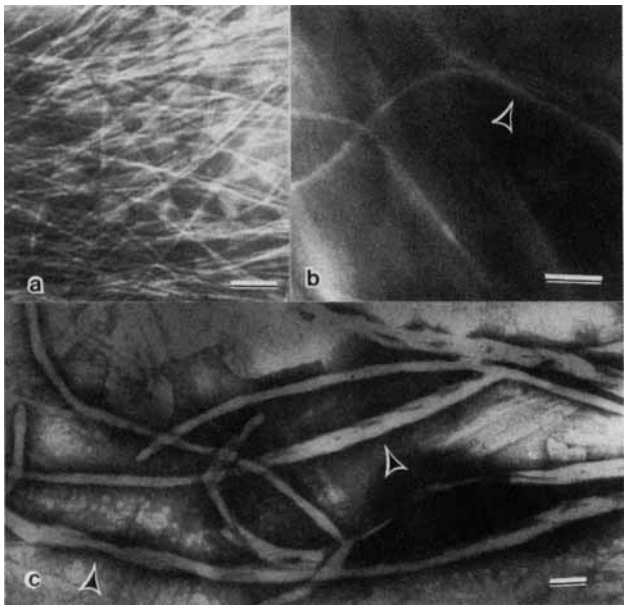

Fig. 2. Electron micrographs of gels of [9]-10-[9] arborol [14] and **4**, negatively stained with 2% phosphotungstic acid and viewed at 50 kV on a Hitachi H 500. a) High magnification (200000 ×) of [9]-10-[9] arborol. Note individual strands of uniform diameter (35 Å), which do not aggregate and remain discrete; bar represents 500 Å). b) Comparably high magnification (220000 ×) of arborol **4** showing individual strands of 30–40 Å and initial associations (arrow) of single polymers; bar represents 500 Å. c) Low magnification of **4** (70000 ×) showing supramolecular associations into large ropelike structures of 300–600 Å diameter. Note twisting "ropes" at arrows; bar represents 1000 Å.

It was postulated that modification of the alkyl chain connecting the two spheres to include a central alkyne moiety, and subsequent polymerization of the *preorganized* stacked cores would lead to a polyacetylene within a hydrophilic sheath creating "molecular wires". Thus, arborol **4** (Fig. 3)

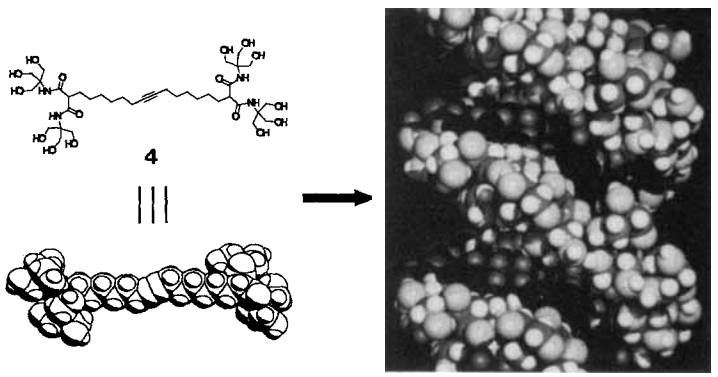

Fig. 3. Formula of arborol **4** and CPK representations of a single molecule and the proposed helical aggregation.

was deemed to possess the structural features necessary for gelation.[14] Incorporation of the alkyne core was accomplished by preparation of the known diol, tetradec-7-yne-1,14-diol (**1**),[15] which was subsequently converted into the corresponding bis(methanesulfonic) ester (**2**: 92%) by treatment with methanesulfonyl chloride and Et_3N in CH_2Cl_2. Characteristic ^{13}C NMR resonances for CH_3 ($\delta = 37.1$) and CH_2O ($\delta = 70.0$), as well as peaks at $\delta = 18.3$ ($C{\equiv}CCH_2$) and 79.9 ($C{\equiv}C$), and the ^1H NMR spectrum ($\delta = 4.17$; t, CH_2O, $J = 6.3$ Hz; 2.96; s, CH_3) supported the structure. Treatment of the dimesylate with triethyl methanetricarboxylate and K_2CO_3 in dimethylformamide (DMF) afforded hexaester **3** (82%). Conversion was evidenced by the classic OCH_2CH_3 patterns in both the ^1H and ^{13}C NMR spectra ($\delta = 1.50$, t, OCH_2CH_3, $J = 7.2$ Hz; 4.25, q, OCH_2CH_3, $J = 7.2$ Hz, and 13.6, OCH_2CH_3; 61.7, OCH_2CH_3). Additional peaks expected in the ^{13}C NMR spectrum: $\delta = 18.4$ ($C{\equiv}CCH_2$), 30.1 ($CH_2C(CO_2Et)_3$), 65.5 ($C(CO_2Et)_3$), 80.0 ($C{\equiv}C$), and 167.2 ($C{=}O$). Finally, treatment of the hexaester with Tris and K_2CO_3 in dimethylsulfoxide (DMSO) afforded the desired alkyne arborol **4** (38%) through amidation and decarbalkoxylation.[14] The structure was supported by ^{13}C NMR resonance signals at $\delta = 18.3$ ($C{\equiv}CCH_2$), 24.1, 28.5, and 28.9 [$CH_2(CH_2)_3CH_2$], 30.2 (CH_2CH), 54.1 (CH), 60.1 (CH_2OH), 62.2 (NHC), 80.2 ($C{\equiv}C$), and 171.0 ($C{=}O$), as well as the disappearance of peaks attributed to the ester groups. Also, characteristic signals at $\delta = 3.75$ (br. s, CH_2OH) and 3.10 (t, CH, $J = 7.1$ Hz) were recorded in the ^1H NMR spectrum.[16]

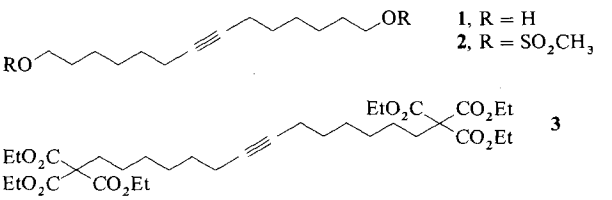

Upon dissolution of **4** in water, the desired self-assembly resulted in gelation.[17] The similarity of the synthesis of arborol **4** and the known saturated arborols[13, 14] dictates that the supramolecular arrangements should be structurally related. The predominant forces driving aggregation presumably involve hydrogen bonding of the hydrophilic spheres and lipophilic interactions between the backbones of the rodlike interiors. The linear rigidity of the alkyne units of arborol **4** limits the compressibility of the hydrocarbon backbone and disfavors the nearly orthogonal criss-cross stacking observed previously[14] for the saturated alkane arborols. Electron micrographs of gelled arborol **4** revealed the presence of single-stranded, rod-shaped structures (Fig. 2b). These single-stranded aggregations self-replicate as demonstrated by formation of higher order aggregates possessing helical morphologies. Figure 2c shows the growth of helical supramolecular structures with regularly repeating twists and diameters approaching 600 Å. These helical suprastructures were not observed for the saturated arborols possessing the less rigid alkyl backbones; therefore, the linear alkyne spacer probably induces a nonorthogonal ($<90°$) stacking, in which two or more molecules define the helical relationship (Fig. 1, bottom: path A). These coiled or twisted structures possess grooves where other aggregates may interact and become intertwined (see Fig. 3, right). Ribbonlike structures are also possible from a scissorlike stacking (Fig. 1, bottom: path B). Molecular modeling calculations[18] support the postulated stacking arrangements shown in Figures 1 and 3.[19]

Further understanding of the molecular interactions will permit chemical reactions and molecular inclusions within the lipophilic domain. The proposed association of these dumbbell-shaped monomers into helical filaments is similar to the assembly of actin monomers (G-actin) into microfilaments (F-actin). Actin filaments similarly bundle to form supramolecular structures such as stress fibers, acrosomal processes, microvilli, and belt desmosomes. The closest parallel may be to actin "cables" described from the Characean algae,[20] which are tightly associated stable actin bundles.

Received: July 10, 1991
Revised: February 10, 1992 [Z 4788 IE]
German version: *Angew. Chem.* **1992**, *104*, 901

CAS Registry numbers:
1, 127999-18-2; **2**, 141823-98-5; **3**, 141823-99-6; **4**, 141807-83-2; CH_3SO_2Cl, 124-63-0; $HC(CO_2Et)_3$, 6279-86-3; Tris, 77-86-1.

[1] H. Kuhn, J. Waser, *Angew. Chem.* **1981**, *93*, 495–515; *Angew. Chem. Int. Ed. Engl.* **1981**, *20*, 500–520.
[2] H. Ringsdorf, B. Schlarb, J. Venzmer, *Angew. Chem.* **1988**, *100*, 117–162; *Angew. Chem. Int. Ed. Engl.* **1988**, *27*, 113–158.
[3] W. Saenger, *Principles of Nucleic Acid Structure*, Springer, New York, **1984**.
[4] A. Klug, *Angew. Chem.* **1983**, *95*, 579–596; *Angew. Chem. Int. Ed. Engl.* **1983**, *22*, 565–582.
[5] R. Jaenicke, *Angew. Chem.* **1984**, *96*, 385–402; *Angew. Chem. Int. Ed. Engl.* **1984**, *23*, 395–413.
[6] J.-M. Lehn, J.-P. Souvage, J. Simon, R. Ziessel, C. Piccini-Leopardi, G. Germain, J.-P. Declercq, M. van Meersche, *Nouv. J. Chim.* **1983**, *7*, 413; J.-M. Lehn, A. Rigault, J. Siegel, J. Harrowfield, B. Chevrier, D. Moras, *Proc. Natl. Acad. Sci. USA* **1987**, *84*, 2565; J.-M. Lehn, A. Rigault, *Angew. Chem.* **1988**, *100*, 1121; *Angew. Chem. Int. Ed. Engl.* **1988**, *24*, 1095.
[7] J.-M. Lehn, *Angew. Chem.* **1988**, *100*, 91–116; *Angew. Chem. Int. Ed. Engl.* **1988**, *27*, 89–112.
[8] J.-M. Lehn, *Angew. Chem.* **1990**, *102*, 1347–1362; *Angew. Chem. Int. Ed. Engl.* **1990**, *29*, 1304–1319.
[9] More recent reviews: K. Krohn in *Organic Synthesis Highlights* (Ed.: J. Mulzer), VCH, Weinheim/New York, **1991**, p. 378; Y.-X. Chen, *Youji Huaxue* **1990**, *10*, 289; D. A. Tomalia, A. M. Naylor, W. A. Goddard, III; *Angew. Chem.* **1990**, *102*, 119–157; *Angew. Chem. Int. Ed. Engl.* **1990**, *29*, 138–175, and references cited therein.; S. Shinkai, *Kagaku* **1987**, *42*, 74.
[10] G. R. Newkome, Z.-Q. Yao, G. R. Baker, V. K. Gupta, *J. Org. Chem.* **1985**, *50*, 2003.
[11] G. R. Newkome, G. R. Baker, *Org. Prep. Proc. Int.* **1986**, *18*, 117.
[12] F. Hallé, R. A. A. Oldeman, P. B. Tomlinson, *Tropical Trees and Forests: An Architectural Analysis*, Springer, Berlin, **1982**.
[13] G. R. Newkome, G. R. Baker, M. J. Saunders, P. S. Russo, V. K. Gupta, Z.-q. Yao, J. E. Miller, K. Bouillon, *J. Chem. Soc. Chem. Commun.* **1986**, 752.
[14] G. R. Newkome, G. R. Baker, S. Arai, M. J. Saunders, P. S. Russo, K. J. Theriot, C. N. Moorefield, J. E. Miller, T. R. Lieux, M. E. Murray, B. Phillips, L. Pascal, *J. Am. Chem. Soc.* **1990**, *112*, 8458.
[15] N. Jayasuriya, S. Bosak, S. L. Regen, *J. Am. Chem. Soc.* **1990**, *112*, 5844.
[16] Because the arborol **4** is hygroscopic, the corresponding acetate was prepared [14] and analyzed.
[17] Gels were formed by adding arborol **4** (100 mg) to H_2O (1.00 mL) and heating the mixture to obtain a clear solution, followed by cooling to 25 °C.
[18] Molecular modeling and minimizations were performed on a Silicon Graphics 4D/50GT workstation using QUANTA/CHARMm software, version 3.0 (Polygen Corporation, 200 Fifth Avenue, Waltham, MA, USA, **1990**).
[19] Four molecules were arranged in the stacking pattern of interest, either scissorlike or helical; CHARMm images were used to simulate an infinite aggregate. Energy minimization (root mean square deviation <0.001) of these starting structures was followed by a burst of molecular dynamics (2000 steps, 1000 K) to generate new randomized structures for subsequent minimization. This process should avoid the local minima problem common to molecular mechanics minimizations. Both stacking arrangements possess an intermolecular separation between alkynes of ca. 4.7 Å. A comparison of the calculated energies of four individual molecules ca. 20 Å apart versus that of either a helical or ribbon arrangement showed the stacks to be ca. 60 kcal mol^{-1} lower in energy.
[20] T. D. Pollard, J. A. Cooper, *Ann. Rev. Biochem.* **1986**, *55*, 987–1035; M. P. Sheets, J. A. Spudich, *Nature* **1983**, *303*, 31–35.

The Reaction of Unactivated Cobalt Powder with Iodophosphoranes. The Synthesis of $[Co(PMe_3)_2I_3]$ and the Isolation of the "Frozen Transition-State" Complex $[(nBu_3PI)_2(\mu\text{-}I)][(nBu_3PI)(\mu\text{-}I)CoI_3]$

By *Charles A. McAuliffe*, Stephen M. Godfrey, Anthony G. Mackie,** and *Robin G. Pritchard*

In an earlier communication we reported a novel synthesis of transition-metal phosphane complexes by the reaction of coarse-grain metal powders and phosphoranes R_3PX_2, exemplified by $[Mn(PPhMe_2)I_2]$, $[Fe(PPhMe_2)_3Br_2]$, and $[Ni(PMe_3)_2I_3]$. This reaction route clearly has extensive applications, for not only are known complexes produced, but novel isomers of existing complexes and complexes in which the central metal atom is in a rare oxidation state are also obtained.[1]

We have established that the nature of the product is dependent on the metal and both the R and X substituents at the phosphorus atom. This is clearly shown in the reactions which we report here between cobalt powder and the phosphoranes Me_3PI_2 and nBu_3PI_2.

The reactions were carried out by mixing the coarse-grain (20–100 μm) cobalt powder with the phosphoranes (1:2 molar ratio) under anhydrous conditions in diethyl ether under argon (see Experimental Procedure). In the case of Me_3PI_2 a dark green powder forms. As shown in Equation (a), in addition to complex **1** elemental iodine is formed, which could be determined quantitatively by spectrophotometry.

$$Co + 2\,Me_3PI_2 \longrightarrow \underset{\mathbf{1}}{[Co(PMe_3)_2I_3]} + 1/2\,I_2 \qquad (a)$$

Recrystallization of **1** from diethyl ether produced dark green needles, which were suitable for an X-ray structure analysis.[2] The crystal structure of **1** is shown in Figure 1.

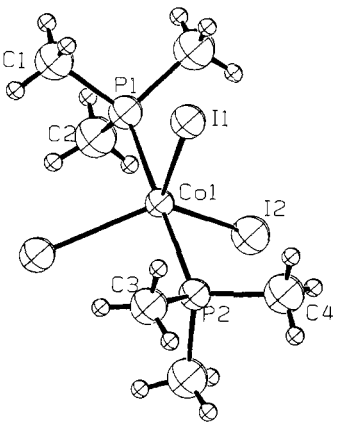

Fig. 1. Structure of **1** (PLUTO). Atoms I(2), Co(1), P(1), P(2), C(1) and C(3) lie on a mirror plane. Selected bond lengths [Å] and angles [°]: I(1)-Co(1) 2.555(1), I(2)-Co(1) 3.543(2), Co(1)-P(1) 2.285(5), Co(1)-P(2) 2.277(4), P(1)-C(1) 1.83(1), P(1)-C(2) 1.83(1), P(2)-C(3) 1.81(2), P(2)-C(4) 1.81(1); I(1)-Co(1)-I(1) 118.17(8), I(1)-Co(1)-I(2) 120.91(4), I(1)-Co(1)-P(1) 90.08(7), I(2)-Co(1)-P(1) 90.0(1), I(2)-Co(1)-P(2) 89.0(1), P(1)-Co(1)-P(2) 179.0(2).

[*] Prof. Dr. C. A. McAuliffe, A. G. Mackie, S. M. Godfrey, Dr. R. G. Pritchard
Department of Chemistry
University of Manchester Institute of Science and Technology
GB-Manchester, M60 1QD (UK)

Examples of trigonal bipyramidal cobalt(III) complexes containing tertiary phosphane ligands are known[3–6] but they are rare and are difficult to synthesize. In fact, apart from a rather low-precision X-ray study of $[Co(PEt_3)_2Cl_3]$[4] the cobalt(III) trigonal-bipyramidal phosphane complex described here represents the first such complex that has been characterized by X-ray crystallography. It has also been reported that the cobalt(II) phosphane complex $[Co(PMe_3)_2I_2]$ cannot be oxidized by iodine to produce the cobalt(III) complex **1**;[5] therefore the synthesis of **1** here must arise from the mechanistic pathway of this novel reaction route. Finally, it is also notable that this cobalt(III) complex is obtained in essentially quantitative yield, and no Co(II) species is produced.

In contrast, the reaction of two equivalents of nBu$_3$PI$_2$ with cobalt powder does not produce a conventional metal phosphane complex. The complex **2**[2] (formula $[Co(n\text{-}Bu_3P)_3I_8]$) is the only product we isolated either by carrying

$[(n\text{Bu}_3\text{PI})_2(\mu\text{-I})][(n\text{Bu}_3\text{PI})(\mu\text{-I})\text{CoI}_3]$ **2**

out the reaction at room temperature or at 60 °C. The structure of **2** (Fig. 2) clearly gives some insight into the mechanism of the reaction of iodophosphoranes with metal powders; it represents a "snapshot" of a metal phosphane complex created by the degradation of the phosphorane. The

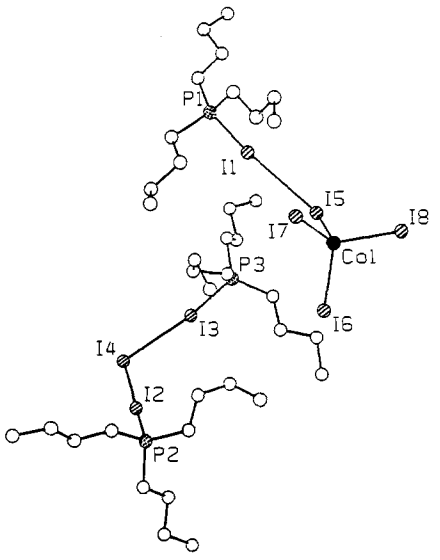

Fig. 2. Structure of **2**. Selected bond lengths [Å] and angles [°]: I(1)-P(1) 2.37(3), I(2)-P(2) 2.37(3), I(3)-I(4) 3.62(1), I(3)-P(3) 2.37(3), I(6)-Co(1) 2.58(2), I(8)-Co(1) 2.69(2), I(1)-I(5) 3.66(1), I(2)-I(4) 3.42(1), I(5)-Co(1) 2.66(2), I(7)-Co(1) 2.59(2); I(5)-I(1)-P(1) 164.9(9), I(4)-I(2)-P(2) 177.8(8), I(6)-Co(1)-I(5) 110.5(6), I(7)-Co(1)-I(6) 109.9(8), I(8)-Co(1)-I(6) 108.1(7), I(7)-Co(1)-I(5) 110.0(7), I(8)-Co(1)-I(5) 109.3(7), I(8)-Co(1)-I(7) 109.0(6).

structures of **1** and **2** also illustrate the subtle dependence on the nature of the phosphorane: Me_3PI_2 produces **1**, whereas nBu$_3$PI$_2$ produces **2**.

The "frozen transition state" represented by **2** shows that only one iodine atom has been abstracted from each phosphorane by the cobalt and no Co–P bonds are formed, which contrasts vividly with the reaction of Co with Me_3PI_2 [Eq. (a), Fig. 1].

There are two discrete fragments in the structure of **2**; the first contains a CoI_4^{2-} moiety bound to a Ph_3PI^+ fragment. This clearly shows that an iodine atom is abstracted from nBu$_3$PI$_2$: the I–I distance in the phosphorane (3.66 Å) is considerably lengthened, but it is still within the range of usual I–I bond lengths when compared to the sum of the van der Waals radii of two iodine atoms.[7–12] There is also a commensurate lengthening of the Co–I bond (2.640 Å) compared with the three terminal Co–I bonds (2.583–2.601 Å). The second fragment of the structure of **2** shows two nBu$_3$PI units linked by an iodine bridge and, once again, this gives some insight into the reaction mechanism for the metal-phosphorane reactions, which are summarized in Equations (b) (not stoichiometric) and (c).

$$n\text{Bu}_3\text{PI}_2 + \text{Co} \longrightarrow [(n\text{Bu}_3\text{PI})(\mu\text{-I})\text{CoI}_3]^- + n\text{Bu}_3\text{PI}^+ \quad \text{(b)}$$

$$n\text{Bu}_3\text{PI}^+ + n\text{Bu}_3\text{PI}_2 \longrightarrow [(n\text{Bu}_3\text{PI})_2(\mu\text{-I})]^+ \quad \text{(c)}$$

If nBu$_3$PI$_2$ and Co[13] are allowed to react in a 1:1 molar ratio, this gives essentially the same product **2**, identified by IR and UV/VIS spectroscopy. However, some new unidentified peaks were present, which suggested the presence of a small amount of impurity. Additionally the compound was contaminated by excess Co which could clearly be seen in the final product.

The complex **2** was not formed from the reaction[13] of nBu$_3$P, Co, and I_2. Instead, a brown oily product formed after approximately six days in dry diethyl ether and was isolated from the reaction mixture. The elemental analysis of this product suggested a compound of formula $[Co(n\text{-}Bu_3PI_2)_2]$; the ^{31}P NMR chemical shift ($\delta = 100.8$) and a Raman absorption band at 205 cm^{-1} indicate the presence of a P–I bond. Interestingly, concentration of the filtrate after the removal of the brown product resulted in the formation of an oily green product whose VIS spectrum is very similar to that of **2**.

The apparently strange connectivity of the atoms in **2** is easily rationalized if the environment of the iodine atoms are considered. Three of these centers (I1, I2, and I3) possess close-to-linear stereochemistry indicating a +I or "metal-like" oxidation state. The angles (101.2, 79.3°) at the other two nonterminal iodine atoms (I4, I5) indicate a normal −I oxidation state for bridging iodo ligands. An overall charge of −1 is thus assigned to the cobalt-containing assembly, of **2** and of +1 to the assembly with three catenated iodines.

In conclusion, these results illustrate the subtlety of the reaction between cobalt metal and iodophosphoranes R_3PI_2. A simple change in the alkyl substituents at the phosphorus atom yields quite different products. The isolation of the frozen transition-state complex gives an insight into the mechanistic pathway of this type of reaction, which halts at **2** when R is nBu, but goes to completion when R is Me to yield a rare example of a pentacoordinate cobalt(III) phosphane complex, **1**.

Experimental Procedure

Strictly anhydrous and anaerobic conditions (argon) were maintained throughout the reactions. **1** and **2** were prepared by the reaction of coarse-grain cobalt powder (20–100 μ) and the appropriate phosphorane (1:2 molar ratio) in dry diethyl ether. Reaction times were approximately 15d at room temperature or 5d under reflux at 60 °C in sealed tubes. In the reaction of $2\,Me_3PI_2$ with Co, a green powder resulted, which was recrystallized from diethyl ehter to produce analytically pure **1**. Dark green-black crystals, m.p. 150 °C, correct elemental analysis (C, H, I).

The low frequency Raman spectrum of **1** was difficult to record because of decomposition of the sample in the laser beam. However, bands were observed at 766, 670 cm^{-1}, ν(P–C) and 126 cm^{-1}, ν(Co–I); unequivocal assignment of a band to ν(Co–P) was not possible. The IR spectrum in the higher frequency region only exhibited bands due to the various stretching, bending, and rocking

vibrations of the methyl groups. The $^{31}P\{H\}$ NMR spectrum of **1** in $CDCl_3$ exhibited only a single extremely broad peak covering the entire spectrum and was essentially meaningless. The VIS spectrum of **1** (2.49×10^{-4} M in diethyl ether) showed the expected bands for a structure with D_{3h} symmetry of electronic ground state $(e'')^4(e')^2(a_1')^0$. Bands were observed at $\lambda \approx 340$ nm, $\varepsilon_{max} \approx 7000$, $P(\sigma) \rightarrow a_1^1$; $\lambda = 390$ nm, $\varepsilon_{max} = 3534$, $e'' \rightarrow a_1^1$; $\lambda = 457.8$ nm, $\varepsilon_{max} = 6611$, $I(\pi) \rightarrow e^1$; $\lambda = 587.2$ nm, $\varepsilon_{max} = 6902$, $P(\sigma) \rightarrow e^1$. The intense color of the complex, and hence high extinction coefficient, are due primarily to the charge-transfer (ligand $\rightarrow$ metal) transitions at $\lambda = 587.2$ nm and 340 nm.

2: In the reaction of $2\,nBu_3PI_2$ with Co, the tube containing the reaction mixture was removed from reflux after approximately 3d and left to stand at room temperature. After a further day green-blue crystals were isolated and identified as **2**. M.p. 82–85 °C, correct elemental analysis (C, H, I, P, Co).

The low frequency Raman spectrum of **2** showed bands at 208 cm^{-1}, ν(P–I) and 142 cm^{-1}, ν(Co–I). A weak band at 113 cm^{-1} is tentatively assigned to ν(I–I). The IR spectrum in the high-frequency spectral region exhibited bands due to various C–C and C–H vibrations, which were generally identical to those observed in the parent phosphorane, nBu_3PI_2. The $^{31}P\{H\}$ NMR spectrum of **2** in $CDCl_3$ showed two signals in approximately 2:1 ratio. The stronger signal occurred at $\delta = 98.3$ and by comparison to the phosphorane nBu_3PI_2, which dissociates in solution, can be assigned to the nBu_3PI^+ ion. This resonance signal is therefore assigned to the cation $[nBu_3P\text{-}I\text{-}I\text{-}I\text{-}PnBu_3]^+$. The weaker signal occurred at $\delta = -94.3$ and is assigned to the anion $[I_3Co\text{-}I\text{-}I\text{-}PnBu_3]^-$. The VIS spectrum of **2** (1.10×10^{-3} M in diethyl ether) showed two bands close together at $\lambda = 715.8$ and 671.1 nm assignable to the transition $^4A_2 \rightarrow 4\pi(P)$ om the tetrahedral Co(II) species. ε_{max} for this transition was calculated to be about 838. However, this could not be experimentally verified since the solution decolorized noticeably during the recording of the spectrum presumably due to the unstability of the complex.

Received: November 26, 1991
Revised: March 17, 1992 [Z 5035 IE]
German version: *Angew. Chem.* **1992**, *104*, 932

CAS Registry numbers:
1, 141903-43-7; **2**, 141903-44-8; Co, 7440-48-4; Me_3PI_2, 98026-25-6; nBu_3PI_2, 21473-75-6.

[1] S. M. Godfrey, D. G. Kelly, A. G. Mackie, P. P. Matear, C. A. McAuliffe, R. G. Pritchard, S. M. Watson, *J. Chem. Soc. Chem. Commun.* **1991**, 1447.
[2] Crystal data for **1**: $C_6H_{18}CoI_3P_2$, $M_r = 591.8$, orthorhombic, space group *Pnma*, $a = 10.217(4)$, $b = 11.184(2)$, $c = 14.252(4)$ Å, $V = 1629$ Å^3, $Z = 4$, $\varrho_{calcd.} = 2.413$ Mgm^{-3}, $Mo_{K\alpha}$ radiation ($\lambda = 0.71069$ Å), crystal dimensions $0.3 \times 0.2 \times 0.2$ mm^3, 1680 reflections were collected on a Rigaku AFC6S diffractometer yielding 1095 observed ($I > 3\sigma(I)$). The structure was solved by standard heavy-atom techniques and refined by full-matrix least-squares (TEXSAN) to final $R = 0.032$, $R_w = 0.036$. – Crystal data for **2**: $C_{36}H_{81}CoI_8P_3$, $M_r = 1681.1$, monoclinc, space group $P2_1/c$, $a = 14.873(2)$, $b = 30.243(5)$, $c = 13.107(2)$ Å, $\beta = 92.72(2)°$, $V = 5888.5$ Å^3, $Z = 4$, $\varrho_{calcd} = 1.90$ Mgm^{-3}, $Mo_{K\alpha}$ radiation ($\lambda = 0.71069$ Å); crystal dimensions $0.1 \times 0.2 \times 0.2$ mm^3. 4651 reflections were measured with a Nicolet R3m/V diffractometer yielding 835 observed [$I \geq 3\sigma(I)$]. The structure was solved by standard heavy-atom techniques and refined by full-matrix least-squares (SHELX-76) to a final $R = 0.082$, $R_w = 0.099$. Iodine atoms were subjected to anisotropic refinement, remaining atoms were treated isotropically with hydrogen atoms ignored. Further details of the crystal structure investigation are available on request from the Director of the Cambridge Crystallographic Data Centre, University Chemical Laboratory, Lensfield Road, GB-Cambridge CB2 1EW (UK), on quoting the full journal citation.
[3] K. A. Jensen, C. K. Jorgensen, *Acta Chem. Scand.* **1965**, *19*, 451.
[4] W. K. P. Van Enckevort, H. M. Hendricks, P. T. Beurskens, *Cryst. Struct. Commun.* **1977**, *6*, 531.
[5] W. Levason, J. S. Ogden, M. D. Spicer, *Inorg. Chem.* **1989**, *28*, 2128.
[6] W. Levason, M. D. Spicer, *J. Chem. Soc. Dalton Trans.* **1990**, 719.
[7] Some I–I distances [Å]: I_2 2.67,[8] Ph_3P–I–I 3.2,[9] tBu_3P–I–I 3.32,[10] Ph_3As–I–I 3.0,[11] $[(PPh_3I)_2I_3]I_3^*$ 2.82–3.50,[12] $(PPh_3I)I_3^*$ 2.86–3.74. [12] Van der Waals radius 4.3[7]. The compounds marked with an asterisk contain several I–I linkages of different lengths.
[8] F. A. Cotton, G. Wilkinson, *Advanced Inorganic Chemistry*, 5th ed. Wiley-Interscience, New York, **1988**.
[9] S. M. Godfrey, D. G. Kelly, A. G. Mackie, C. A. McAuliffe, R. G. Pritchard, S. M. Watson, *J. Chem. Soc. Chem. Commun.* **1991**, 1163.
[10] W. W. du Mont, M. Batcher, S. Pohl, W. Saak, *Angew. Chem.* **1987**, *99*, 945; *Angew. Chem. Int. Ed. Engl.* **1987**, *26*, 912.
[11] C. A. McAuliffe, B. Beagley, G. A. Gott, A. G. Mackie, P. P. MacRory, R. G. Pritchard, *Angew. Chem.* **1987**, *99*, 237; *Angew. Chem. Int. Ed. Engl.* **1987**, *26*, 264.
[12] F. A. Cotton, P. Kibala, *J. Am. Chem. Soc.* **1987**, *109*, 3309.
[13] We are grateful to a referee who requested that we carry out these additional experiments prior to publication.

Synthesis and Structure of $Al(OAr^*)_3$ ($Ar^* = 2,6\text{-}tBu_2\text{-}4\text{-}MeC_6H_2$): The First Three-Coordinate Homoleptic Aluminum Aryloxide**

By *Matthew D. Healy* and *Andrew R. Barron**

The tendency towards the maximization of a metal's coordination number by associating to give aggregates containing tetrahedral and octahedral centers is ubiquitous in the chemistry of metal alkoxide and aryloxide compounds.[1] However, the use of 2,6-di-*tert*-butyl-substituted aryloxides has enabled the isolation of a number of monomeric homoleptic aryloxide compounds, $M(OAr)_x$, in which the metal center is in a low coordination environment,[2] and often a low oxidation state.[3] All attempts[4, 5] to prepare a three-coordinate homoleptic aluminum aryloxide compound have been consistently unsuccessful, including resorting to such extreme reaction conditions as thermolysis of $AlEt_3$ in neat 2,6-di-*tert*-butyl-4-methylphenol, HOAr* ($Ar^* = 2,6\text{-}tBu_2\text{-}4\text{-}MeC_6H_2$).[5b] In each case only the bis(aryloxide) compounds, $AlR(OAr^*)_2$, could be isolated. These results suggested perhaps that steric constraints preclude the formation of the *tris*(aryloxide) complex, in contrast to the thiolate analogue.[6] However, we are now able to communicate that $Al(OAr^*)_3$ can be readily prepared by the reaction of HOAr* with $LiAlH_4$.

The reaction of $LiAlH_4$ with three molar equivalents of HOAr* in Et_2O affords a mixture of $Li(OAr^*)(OEt_2)$[7] and **1** [Eq. (a)]. Compound **1** may readily be isolated by fractional crystallization from Et_2O as a moderately air-sensitive colorless crystalline solid.

$$LiAlH_4 + 3\,HOAr^* \xrightarrow{Et_2O} \underset{\mathbf{1}}{AlH(OAr^*)_2(OEt_2)} + Li(OAr^*)(OEt_2) + 3\,H_2 \qquad (a)$$

The room temperature ^1H NMR spectrum of **1** contains peaks due to the aryloxide substituent and coordinated Et_2O only (see Experimental Procedure). However, at -52 °C an additional broad resonance is observed ($\delta = 4.53$), which we assign to the proton of an aluminum hydride.[8] The IR spectrum of **1** shows the presence of a sharp band at 1896 cm^{-1} indicative of a terminal Al–H group.[9] All spectroscopic and analytical data are therefore consistent with the structure as shown in Scheme 1.

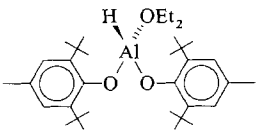

1

Scheme 1.

The interaction of **1** with a further equivalent of HOAr* in refluxing toluene allows the isolation of $Al(OAr^*)_3$ (**2**) in quantitative yield [Eq. (b)], as a moisture-sensitive colorless crystalline solid.

$$\underset{\mathbf{1}}{AlH(OAr^*)_2(OEt_2)} + HOAr^* \xrightarrow[-\,Et_2O]{\text{toluene},\ \Delta} \underset{\mathbf{2}}{Al(OAr^*)_3} + H_2 \qquad (b)$$

[*] Prof. Dr. A. R. Barron, M. D. Healy
Department of Chemistry, Harvard University
Cambridge, MA 02138 (USA)

[**] This work is supported by the Aluminum Research Board.

The ^1H and $^{13}C\{^1H\}$ NMR spectra of **2** show resonances due only to the aryloxide substituents, while the $^{27}Al\{^1H\}$ NMR contains a single resonance ($\delta = 3.2$). Although this ^{27}Al NMR signal is in a region normally associated with six-coordinate aluminum centers,[9] it follows the general trend observed for monomeric three-coordinate aryloxide derivatives: $R_2Al(OAr^*)$ compounds have $\delta(^{27}Al)$ resonance, signals around 190, while those for $RAl(OAr^*)_2$ are found at about 100 ppm.[5c] The medium-resolution mass spectrum (70 eV, EI) of **2** exhibits a parent ion (m/z 684) consistent with a monomeric structure in the gas phase. Compound **2** is also monomeric in the solid state, as evident from an X-ray crystal structure analysis.[10]

The molecular structure of **2** (Fig. 1) consists of discrete molecules with no unusual intermolecular distances. The aluminum is three-coordinate trigonal planar [Σ O-Al-O = 359.9(3)°]. The average Al–O distance and Al-O-C angle are 1.648(7) Å and 177.2(5)°, respectively. The arene rings form

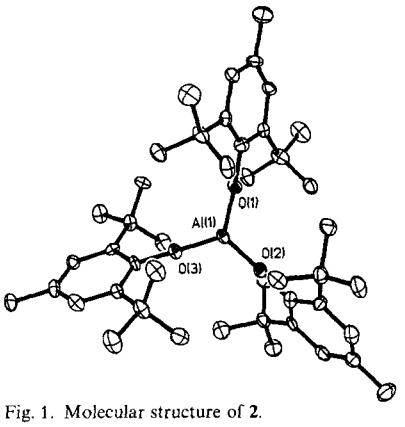

Fig. 1. Molecular structure of **2**.

a propeller-like arrangement around the aluminum, and are canted approximately 56° from the AlO_3 plane. Two molecules of the solvent of recrystallization, CH_2Cl_2, are present in the asymmetric unit. The short Al–O distances are undoubtedly a consequence of three factors. First, the aluminum atom is sp^2 hybridized, whereas sp^3 hybridization is observed in the more common four-coordinate complexes. Second, there is increased s character in the Al–O bond as a result of the near linear Al–O–C bond angle. Third, a $p\pi$–$p\pi$ interaction is present between the vacant Al $3p_z$ orbital (z perpendicular to the AlO_3 plane) and the lone pairs on the aryloxide oxygen centers. This latter interaction may also account for the highly shielded aluminum center, as evident from the upfield resonance signal in the ^{27}Al NMR spectrum.

Experimental Procedure

1: To a suspension of $LiAlH_4$ (5.00 g, 0.125 mol) in Et_2O (400 mL) at −78 °C was added solid HOAr* (82.50 g, 0.375 mol). **Caution:** hydrogen gas is liberated. The reaction mixture was slowly warmed to room temperature and stirred for 12 h. Filtration, followed by fractional crystallization allows for the isolation of **1**. Note that compound **1** is more soluble in Et_2O than $Li(OAr^*)(OEt_2)$ and is thus the second compound to crystallize. Isolated yield: ca. 70%; m.p. 136–140 °C; ^1H NMR (250 MHz, C_6D_6, TMS ext.): $\delta = 7.22$ (4H, s, C_6H_2), 3.68 (4H, m, OCH_2), 2.30 (6H, s, CH_3), 1.59 (36H, s, $C(CH_3)_3$), 0.64 (6H, m, OCH_2CH_3); at −52 °C, $\delta = 4.53$ (br, s, Al-H); $^{13}C\{^1H\}$ NMR (100 MHz, C_6D_6, TMS ext.): $\delta = 154.21$ (O-C), 138.80 (*o*-C), 126.48 (*m*-CH), 126.28 (*p*-C), 66.06 ($O-CH_2$), 35.39 [$C(CH_3)_3$], 31.89 [$C(CH_3)_3$], 21.36 (CH_3), 11.67 (OCH_2CH_3); $^{27}Al\{^1H\}$ NMR (78 MHz, C_6H_5Me, $[Al(H_2O)_6]^{3+}$ ext.) $\delta = 59$ ($w_{1/2} = 5470$ Hz); IR (KBr, Nujol): $\tilde{\nu}$ [cm^{-1}] = 1896 (s), 1460 (vs), 1421 (s), 1387 (m), 1318 (w), 1258 (s), 1203 (m), 1147 (w), 1124 (w), 1088 (m), 1022 (m), 994 (m), 953 (w), 901 (s), 899 (m), 793 (m), 763 (m), 722 (w), 692 (m).

2: To a toluene solution of **1** (4.00 g, 7.40 mmol) was added HOAr* (1.63 g, 7.41 mmol). The reaction mixture was heated at reflux for 12 h. **Caution:** hydrogen gas is liberated. The solution was then cooled, the solvent removed under vacuum, and the residue crystallized from pentane (−20 °C). Crystals suitable for X-ray analysis were obtained from CH_2Cl_2 solution. Yield: ca. 90%; m.p. 116–124 °C; ^1H NMR (250 MHz, C_6D_6, TMS ext.): $\delta = 7.11$ (2H, s, C_6H_2), 2.19 (3H, s, CH_3), 1.51 (18H, s, $C(CH_3)_3$); $^{13}C\{^1H\}$ NMR (100 MHz, C_6D_6, TMS ext.): $\delta = 151.71$ (O-C), 138.51 (*o*-C), 128.64 (*m*-C), 126.77 (*p*-C), 35.45 [$C(CH_3)_3$], 32.49 [$C(CH_3)_3$], 21.25 (CH_3); $^{27}Al\{^1H\}$ NMR (78 MHz, C_6H_5Me $[Al(H_2O)_6]^{3+}$ ext.) $\delta = 3.2$ ($w_{1/2} = 585$ Hz); IR (KBr, Nujol): $\tilde{\nu}$ [cm^{-1}] = 1422 (s), 1390 (m), 1363 (m), 1295 (m), 1265 (s), 1209 (m), 1184 (w), 1157 (w), 1125 (m), 1081 (w), 1026 (w), 977 (s), 941 (m), 909 (w), 889 (w), 859 (m), 810 (w), 802 (w), 768 (m), 727 (w), 659 (m), 634 (w).

Received: January 15, 1992 [Z 5124 IE]
German version: *Angew. Chem.* **1992**, *104*, 939

CAS Registry numbers:
1, 141635-57-6; **2**, 141635-58-7; **2**·$2CH_2Cl_2$, 141635-59-8; $LiAlH_4$, 16853-85-3.

[1] D. C. Bradley, *Adv. Chem Ser.* **1959**, *23*, 10.
[2] a) R. A. Anderson, G. E. Coates, *J. Chem. Soc. Dalton Trans.* **1972**, 2153; b) A. G. Goel, R. C. Mehrotra, *Indian J. Chem. Sect. A.* **1978**, *16*, 428; c) P. B. Hitchcock, M. F. Lappert, A. Singh, *J. Chem. Soc. Chem. Commun.* **1983**, 1499; d) P. B. Hitchcock, M. F. Lappert, R. G. Smith, *Inorg. Chim. Acta* **1987**, *27*, 183; e) J. Calabrese, M. A. Cushing, Jr., S. D. Ittel, *Inorg. Chem.* **1988**, *27*, 867; f) H. A. Stecher, A. Sen, A. L. Rheingold, *ibid.* **1988**, *27*, 1132; g) M. F. Lappert, A. Singh, R. G. Smith, *Inorg. Synth.* **1990**, *27*, 164; h) K. H. Whitmire, H. W. Roesky, S. Brooker, G. M. Sheldrick, *J. Organomet. Chem.* **1991**, *402*, C4.
[3] B. Çetinkaya, I. Gümrükçü, M. F. Lappert, J. L. Atwood, R. D. Rogers, M. J. Zaworotko, *J. Am. Chem. Soc.* **1980**, *102*, 2089; M. Scholz, M. Noltemeyer, H. W. Roesky, *Angew. Chem.* **1989**, *101*, 1419; *Angew. Chem. Int. Ed. Engl.* **1989**, *28*, 1383.
[4] a) M. D. Healy, D. A. Wierda, A. R. Barron, *Organometallics* **1988**, *7*, 2543; b) M. D. Healy, J. W. Ziller, A. R. Barron, *J. Am. Chem. Soc.* **1990**, *112*, 2949.
[5] a) M. Skowronska-Ptasinska, K. B. Starowieyski, S. Pasynkiewicz, M. Carewska, *J. Organomet. Chem.* **1978**, *160*, 403; b) A. P. Streve, R. Mulhaupt, W. Fultz, J. Calabrese, W. Robbins, S. D. Ittel, *Organometallics* **1988**, *7*, 409; c) R. Benn, E. Janssen, H. Lehmkuhl, A. Rufinska, K. Angermund, P. Betz, R. Goddard, C. Krüger, *J. Organomet. Chem.* **1991**, *411*, 37.
[6] K. Ruhlandt-Senge, P. P. Power, *Inorg. Chem.* **1991**, *30*, 2633.
[7] B. Çetinkaya, I. Gümrükçü, M. F. Lappert, J. L. Atwood, R. Shakir, *J. Am. Chem. Soc.* **1980**, *102*, 2086.
[8] A. R. Barron, G. Wilkinson, *Polyhedron* **1986**, *5*, 1897.
[9] A. W. Apblett, A. C. Warren, A. R. Barron, *Chem. Mater.* **1992**, *4*, 167.
[10] X-ray structure analysis of **2**·$2CH_2Cl_2$: space group $P\bar{1}$, $a = 12.903(9)$, $b = 13.911(8)$, $c = 16.201(9)$ Å, $\alpha = 99.71(5)$, $\beta = 103.16(5)$, $\gamma = 114.63(6)°$, $V = 2457(3)$ Å^3, $\rho_{calcd} = 1.155$ g cm^{-3}, $\mu(Mo_{K\alpha}) = 0.295$ mm^{-1}, 6348 unique reflections, 3758 observed ($I > 6\sigma(I)$), $R = 0.083$, $R_w = 0.085$. Further details of the crystal structure investigation may be obtained from the Fachinformationszentrum Karlsruhe, Gesellschaft für wissenschaftlich-technische Information mbH, D-W-7514 Eggenstein-Leopoldshafen 2 (FRG) on quoting the depository number CSD-56189, the names of the authors, and the journal citation.

Efficient Synthesis of Nanoscale Macrocyclic Hydrocarbons**

By *Jeffrey S. Moore** and *Jinshan Zhang*

Structurally well-defined macrocycles[1] have long attracted the interest of many research groups, especially those studying recognition and selective complexation.[2] Our in-

[*] Prof. J. S. Moore, J. Zhang
The Willard H. Dow Laboratories, The University of Michigan
Ann Arbor, MI 48109-1055 (USA)

[**] Nanoarchitectures, Part 2. This research was supported in part by the Donors of the Petroleum Research Fund, administered by the American Chemical Society. J. S. M. wishes to thank the 3M company for support through their awards program for untenured faculty. We also thank Prof. Steven Dierker for stimulating discussions regarding this work. – Part 1: [5].

terest in these compounds is as a class of large molecular building blocks[3] that can be used to assemble new materials by a "modular" approach. Rigid toroids constructed from phenylacetylene monomers are ideally suited for this since both the position and orientation (*endo* vs. *exo*) of pendant groups are well defined. Here we describe the efficient synthesis of very large macrocyclic hydrocarbons having internal diameters up to 22 Å.

Our synthesis involves macrocyclization[4] of α,ω-unsymmetrically difunctionalized phenylacetylene sequences. We recently described an efficient preparation of these oligomers in which the chain length, the sequence order of monomers, and end-group functionality can be precisely controlled.[5] These sequences are cyclized by intramolecular palladium-catalyzed coupling[6] by slow addition of the oligomer to solution of the active catalyst. As shown in Scheme 1, both the products with six (**1**) and twelve (**2**) arene units were obtained in high yield (75% and 70%, respectively). In each case, only a single cyclic product was observed. The *tert*-butyl groups were required to maintain adequate solubility. Molecular models show that the inner diameter (hydrogen to hydrogen) of **1** is 8.4 Å while that of **2** is slightly greater than 22 Å. The high yields and absence of other cyclic products for these large ring systems are probably a consequence of the assembly of the rigid,[7] α,ω-difunctionalized sequences prior to the cyclization reaction.

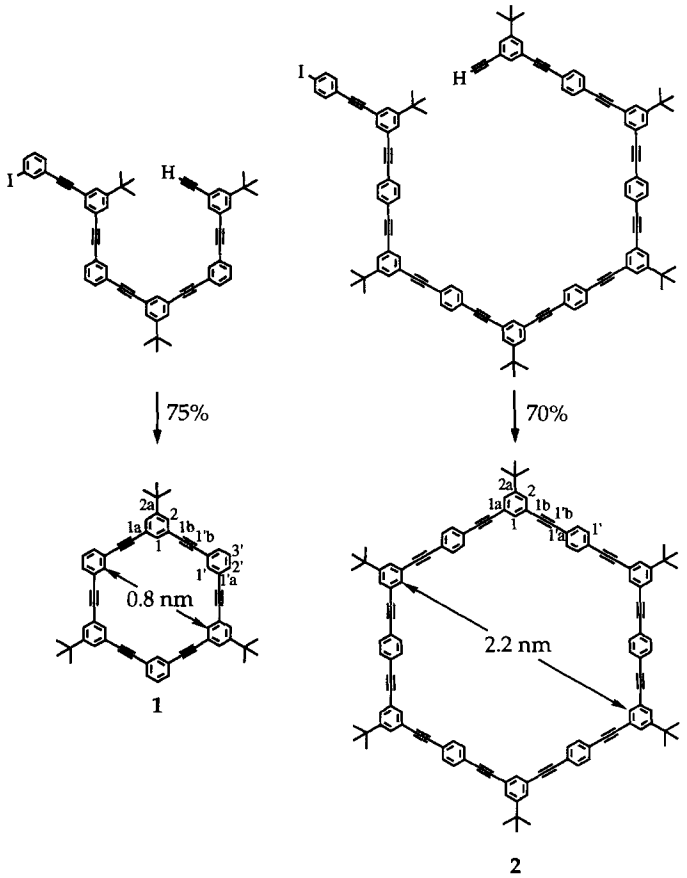

Scheme 1. Synthesis of nanoscale macrocyclic hydrocarbons. Reaction conditions: $[Pd(dba)_2]$, PPh_3, CuI, triethylamine, 70 °C.

There are a number of advantages in using preassembled sequences to synthesize large cyclic structures. The method we describe here should be compared to the more common approach used to prepare macrocycles which involves oligomerization and cyclization in the same reaction flask (i.e. "one-pot" process). Although the one-pot reaction can potentially generate products in a single step, the yield depends strongly on ring size.[4b] As an example, the one-pot synthesis of the parent coumpound of **1** proceeds in only 4.6% yield.[1b] The overall yield for **1** by our route including the synthesis of sequence is nearly an order of magnitude higher. Besides giving low yield, the one-pot process is also limited to products of certain structural types. For example, only cyclic geometries that result from a single type of monomer can easily be realized. Thus, toroidal hydrocarbon **2** could not be prepared from a one-pot reaction but instead would require prior synthesis of the *meta–para* dimer. For these same reasons, products with specific placement of functional groups are not easily prepared by the one-pot process. However, cyclization of a properly functionalized sequence will provide macrocycles with groups positioned according to the sequence order of monomers. The arrangement of *tert*-butyl groups on alternate rings in **1** illustrates this point. Finally, we have recently shown that high yields of large three-dimensional cage molecules can be realized by double cyclization of branched sequences.[8] These structures could probably not be realized using the one-pot approach.

The efficient cyclizations described here, in combination with our phenylacetylene sequence synthesis, offer enormous possibilities for preparing large and well-defined organic structures. The geometric possibilities that can be obtained by cyclization of sequences of phenylacetylene monomer units (combinations of 60°, 120°, and 180° angles) are essentially any framework that lies on the trigonal lattice. Table 1 shows the number of unique planar cyclic geometries that can be obtained from sequences containing three to ten phenylacetylene units.[9] These molecular frameworks should be useful for constructing novel mesogens or building blocks for self-assembled monolayers or rationally designed organic crystals.

Table 1. Relationship between monomer units to be linked and the resulting structure.

Number of monomer units [a]	3	4	5	6	7	8	9	10
Number of possible cyclic geometries [b]	1	1	1	4	5	16	37	120

[a] Monomers are *ortho*-, *meta*-, and *para*-phenylacetylenes. [b] Defined as a "closed path" on a two-dimensional trigonal lattice.

Experimental Procedure

2: A septum-stoppered flask charged with $[Pd(dba)_2]$ [10] (0.15 g, 0.26 mmol), triphenylphosphine (0.41 g, 1.56 mmol), copper(I) iodide (0.05 g, 0.26 mmol) was evacuated and back-filled with nitrogen. Anhydrous triethylamine (75 mL) was added, and the solution was heated to 70 °C. The α-iodo-ω-ethynyl-dodecameric sequence (0.50 g, 3.0 mmol) was taken up in a mixture of triethylamine (25 mL) and benzene (25 mL) and added to the catalyst by a syringe pump at a rate of 2.5 mL h^{-1}. At the end of the addition, the solution was stirred at 90 °C for another five h and then diluted with dichloromethane. The solution was washed with 1 N aqueous HCl, brine, and water and dried over sodium sulfate. After the solvent was removed the residue was purified by flash chromatography (eluting with CH_2Cl_2) and recrystallized (first from $MeOH/CH_2Cl_2$, then toluene) to afford a colorless crystalline solid (**2**) in 70% (0.324 g).

Characterization data for (**2**): ^1H NMR (200 MHz, $[D_6]$benzene): $\delta = 7.84$ (t, $J = 1.3$ Hz, 1H, H-C1), 7.67 (d, $J = 1.3$ Hz, 2H, H-C2), 7.42 (s, 4H, H-C1'), 1.10 (s, 9H, $(CH_3)_3C$-); ^{13}C NMR (90 MHz, $CDCl_3$): $\delta = 151.8$ (C2a), 132.4 (C1), 131.6 (C1'), 128.7 (C2), 123.1 (C1a and C1'a), 91.0 (C≡C), 89.2 (C≡C), 34.7 $(CH_3)_3C$-, 31.2 $(CH_3)_3C$-; MS (FAB) m/z 1539 $[(M + H)]^{\oplus}$. Correct elemental analysis.

Characterization data for **1**: ^{1}H NMR (200 MHz, [D$_6$]benzene): δ = 8.09 (t, J = 1.6 Hz, 1H, H-C1'), 7.98 (t, J = 1.4 Hz, 1H, H-C1), 7.70 (d, J = 1.4 Hz, 1H, H-C2), 7.42 (dd, J = 1.6, 7.9 Hz, 2H, H-C2'), 6.86 (t, J = 7.9 Hz, 1H, H-C3'), 1.10 (s, 9H, (CH_3)$_3$C-); ^{13}C NMR (75 MHz, $CDCl_3$): δ = 151.7 (C2a), 135.3 (C1'), 132.4 (C 1), 131.0 (C 2'), 128.6 (C 2), 128.4 (C3'), 123.6 (C1'a), 123.1 (C1a), 89.8 (C≡C), 88.6 (C≡C), 34.8 (CH_3)$_3$C-), 31.1 (CH_3)$_3$C-); HR MS (70 eV, EI) m/z $C_{60}H_{48}$: calc. 768.3756, found 768.3774. Correct elemental analysis. Crystals of **1** have not provided useful diffraction data.

Received: February 5, 1992 [Z 5168 IE]
German Version: *Angew. Chem.* **1992**, *104*, 873

CAS Registry numbers:
1, 141928-18-9; **2**, 141903-36-8; **3**, 141903-37-9; **4**, 141903-38-0.

[1] For examples of macrocyclic hydrocarbons see: a) Annulenes: I. D. Campbell, G. Eglinton, W. Henderson, R. A. Raphael, *J. Chem. Soc. Chem. Commun.* **1966**, 87–89; b) H. A. Staab, K. Neunhoeffer, *Synthesis* **1974**, 424; c) Coronaphenes: F. Diederich, H. A. Staab, *Angew. Chem.* **1978**, *90*, 383–385; *Angew. Chem. Int. Ed. Engl.* **1978**, *17*, 372–374; d) F. Vögtle, K. Kadei, *Chem. Ber.* **1991**, *124*, 903–907; e) K. Kadei, F. Vögtle, *ibid.* **1991**, *124*, 909–913; f) Cyclynes: A. de Meijere, F. Jaekel, A. Simon, H. Borrmann, J. Köhler, D. Johnels, L. T. Scott, *J. Am. Chem. Soc.* **1991**, *113*, 3935–3941.

[2] For example: a) T. W. Bell, F. Guzzo, M. G. B. Drew, *J. Am. Chem. Soc.* **1991**, *113*, 3115–3122; b) T. W. Bell, A. Firestone, *ibid.* **1986**, *108*, 8109–8111; c) R. C. Helgeson, J.-P. Mazaleyrat, D. J. Cram, *ibid.* **1981**, *103*, 3929–3931; d) G. R. Newkome, H.-W. Lee, *ibid.* **1983**, *105*, 5956–5957; e) J. L. Toner, *Tetrahedron Lett.* **1983**, *24*, 2707–2710; f) J. E. B. Ransohoff, H. A. Staab, *ibid.* **1985**, *26*, 6179–6182; g) M. Dobler, M. Dumic, M. Egli, V. Prelog, *Angew. Chem.* **1985**, *97*, 793–795; *Angew. Chem. Int. Ed. Engl.* **1985**, *24*, 792–794.

[3] A "nanoscale structural unit" was recently described: T. H. Webb, C. S. Wilcox, *J. Org. Chem.* **1990**, *55*, 363–365.

[4] For reviews on macrocyclization see: a) L. Rossa, F. Vögtle, *Top. Curr. Chem.* **1983**, *113*, 1–86; b) L. Mandolini *Adv. Phys. Org. Chem.* **1986**, *22*, 1–110.

[5] J. Zhang, J. S. Moore, Z. Xu, R. Aguirre, *J. Am. Chem. Soc.* **1992**, *114*, 2273–2274.

[6] a) K. Sonogashira, Y. Tohda, N. Hagihara, *Tetrahedron Lett.* **1975**, 4467–4470; b) L. Cassar, *J. Organomet. Chem.* **1975**, *93*, 253–257; c) H. A. Dieck, R. F. Heck, *ibid.* **1975**, *93*, 259–263.

[7] For a discussion of the advantages of rigid structural units in the synthesis of large rings see reference [4a].

[8] Z. Wu, J. S. Moore, unpublished results.

[9] Combinatorial analysis was used to enumerate planar cyclic geometries derived from sequences of *ortho*-, *meta*-, and *para*-phenylacetylene monomers. This was accomplished by performing a systematic n-step walk on a two-dimensional trigonal lattice. As an example, the four isomers that can be obtained from sequences containing six monomer units are shown below.

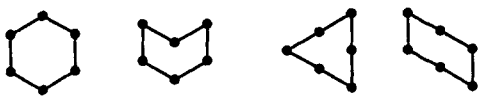

[10] M. F. Rettig, P. M. Maitlis, *Inorg. Synth.* **1977**, *17*, 134–137.

Generalized Edshammar Polyhedra for the Description of a Family of Solid-State Structures

By *Sven Lidin*,* *Thomas Popp*, *Mehmet Somer*, and *Hans Georg von Schnering*

In compounds with the general composition M_nX_p with $n \gg p$, component X, which can be a single atom, ion, or molecule, must build discrete units which are to a certain extent embedded in a continuous medium M. The coordination number (CN) of X is always n/p times that of M: CN(X) = n/p CN(M). Hence when CN(M) is high, CN(X) will be very large and the subsequent coordination polyhedra will also be correspondingly large. Here we would like to introduce a new class of space-filling polyhedra which can be utilized in describing structures in which a small number of linear molecules, large atoms, or large ions are coordinated by many monoatomic units. These polyhedra are obtained by the successive interpenetration of cubes along a threefold axis.

First we would like to consider the condensation of two cubes to form a structural unit having common corners. This can be achieved in five different ways, as shown in Figure 1 a–e. The first four cases yield nothing significantly new. They are generated by fusing one, two, four, or eight corners of each cube, leading to shared corners, edges, faces, and finally to a complete overlap. In contrast, the fifth possibility (Fig. 1e) is of greater interest. In this situation, the cubes are interpentrated so that three corners of each cube are fused together.

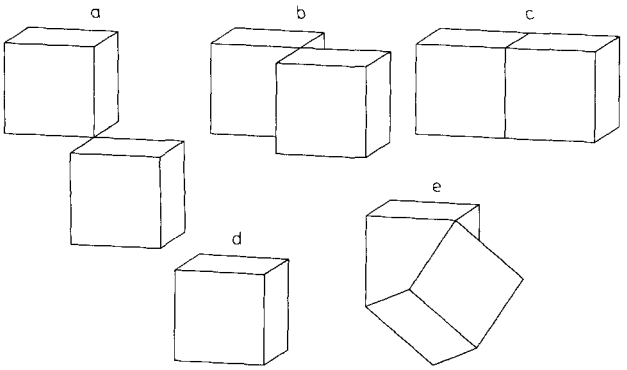

Fig. 1. Two cubes with a) one, b) two, c) four, d) eight, e) three common corners.

A corner of each cube now lies inside the other cube and a structure emerges that is reminiscent of a body-centered cube (bcc). However, the centering is far from perfect; the enclosed point is located closer to the position (1/3, 1/3, 1/3) than to the position (1/2, 1/2, 1/2) of the surrounding cube. The original cubes each possess eight corners, thus sixteen in total. After condensation, only thirteen corners are available. Of these thirteen, two are enclosed by eleven, thus building a new space-filling polyhedron, the Edshammar polyhedron,[11] which will be denoted henceforth by the symbol ^{11}E and the configuration 4^63^6 (Fig. 2a).

The latter designation indicates that the polyhedron is assembled from six squares and six triangles.[12] Certainly this process can be extended further. The condensation of three cubes along a common threefold axis leads to a polyhedron

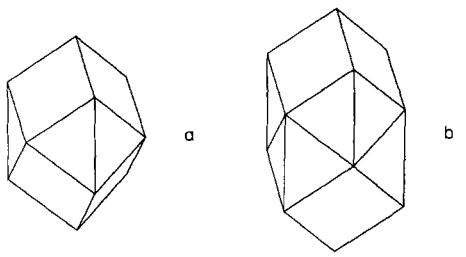

Fig. 2. a) The Edshammar (^{11}E) polyhedron. b) The ^{14}E polyhedron.

[*] Dr. S. Lidin
Dept. Inorganic Chemistry 2
Chemical Centre, P.O. Box 124
S-22100 Lund (Schweden)
Dr. T. Popp, Dr. M. Somer, Prof. Dr. H. G. von Schnering
Max-Planck-Institut für Festkörperforschung, Stuttgart

with fourteen corners, ^{14}E, having the configuration $4^6 3^{12}$ (Fig. 2b). These polyhedra can be described quite generally with the symbol $^{5+3n}$E and the configuration $4^6 3^{6(n-1)}$ where n is the number of cubes involved in the construction of the polyhedron. These polyhedra are either combinations of hexagonal prisms and cubes (odd n, Fig. 3a) or hexagonal prisms and trigonal bipyramids (even n, Fig. 3b).

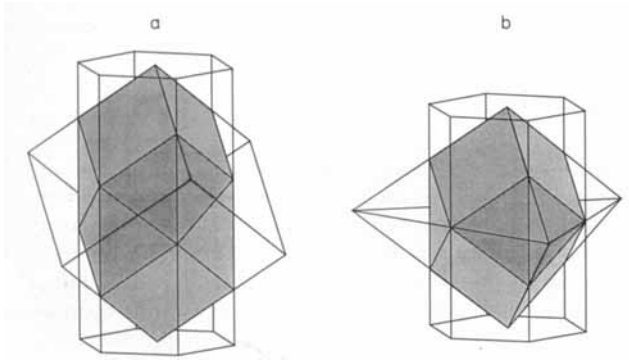

Fig. 3. a) The ^{14}E polyhedron as a combination of cube and hexagonal prism. b) The ^{11}E polyhedron as a combination of trigonal bipyramid and hexagonal prism.

The symmetry of the polyhedra changes with the number n (or the number of corners). When n is odd, $\bar{3}$m symmetry is present, whereas when n is even, the symmetry is $\bar{6}$m2. With increasing n, the polyhedra become more and more tube-shaped. Through a distortion in the direction of the threefold axis, the larger polyhedra like ^{14}E or ^{17}E can be adjusted to coordinate spherical or roughly spherical units (the core).

All the polyhedra of the type $^{5+3n}$E are space-filling. Layers can be constructed by packing the polyhedra perpendicular to the threefold axis whereby the faces of the neighboring hexagonal prisms then coincide. Such layers have a rippled surface (Fig. 4), which is characteristic for a simple packing of cubes perpendicular to the [111] direction.

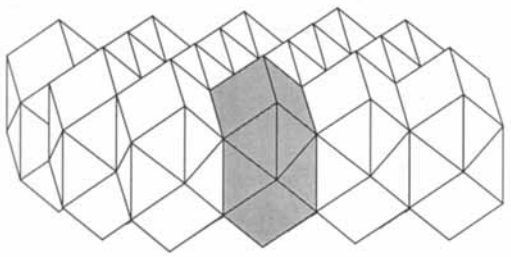

Fig. 4. A close-packed layer of ^{14}E polyhedra.

These layers can now be stacked in a space-filling manner. The stacking of layers of polyhedra consisting, for example, of ^{14}E with alternate layers of cubes or another polyhedra is also possible because they all show the same surface. Actually in nature, very many different stacking structures occur, especially structures where layers derived from $^{5+3n}$E polyhedra alternate with layers made up of cubes.

If these polyhedra are used to describe clusters with $5 + 3n$ atoms on the corners, a maximum of n structural units Z can be enclosed. These units Z may be defects (□), or one or more atoms isolated from one another or linked together. The composition of such a cluster can be formulated as $^{5+3n}EZ_n$ where n indicates how many corners of the original cubes lie in the cavity of the polyhedron.

If the clusters are close packed in solid state then their corners are common to several clusters. Thus the stoichiometric number N of corners is reduced. In a packing of cubes, every corner has the value $N = 1/8$ because it belongs simultaneously to eight cubes, ^{8}E. For the whole cube, N is equal to $8/8 = 1$. In a close packing of ^{11}E polyhedra (Fig. 5), two types of corner atoms exist, namely five corner atoms of type I and six corner atoms of type II, each of which are common to five and six ^{11}E polyhedra respectively: $N_I = 1/5$, $N_{II} = 1/6$; that is, $N(^{11}\text{E-packing}) = 5/5 + 6/6 = 2$. Thus in general for close packings of $^{5+3n}$E polyhedra, $N = n$ is valid.

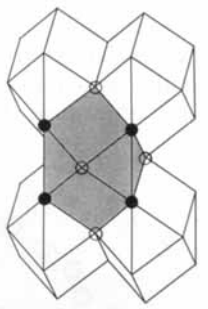

Fig. 5. Close-packing of Edshammar polyhedra. The positions of type I corners are indicated by open circles, type II by filled circles.

The positions of the corners of the polyhedron can be derived directly from the condensation process. The (idealized) polyhedron obtained initially is characterized by two different edge lengths. These edges become closer in length, if the polyhedron is compressed along the threefold axis, or stretched in the plane perpendicular to the threefold axis (Fig. 6). A measure of distortion can be determined from the ratio of the length of the polyhedron along the threefold axis to the length of the orthogonal face diagonal of the "square" face of the polyhedron. This internal axial ratio (c/a) indicates the extent of distortion.

Aside from the states with idealized positions (edges unequal in length, Fig. 6, left) and with identical edge lengths (Fig. 6, center), there are other c/a ratios with special significance. For example, through further compression of the ^{11}E polyhedron, the distance from the center to the two corners on the threefold axis will be the same as the distance from the center to the three corners lying on the (orthogonal) mirror plane. This state ($c/a = 1.154$) is often preferred when a single atom is coordinated by an ^{11}E polyhedron. Table 1 lists the corner positions for these three distinct states.

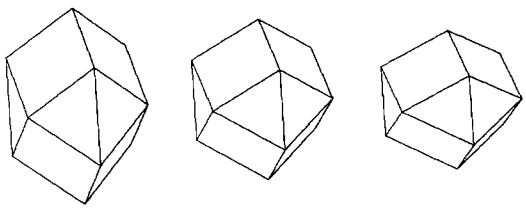

Fig. 6. Edshammar polyhedra. Left: the idealized polyhedron, $\mathbb{P}_{id}$. Center: the polyhedron with identical edge lengths, $\mathbb{P}_{ec}$. Right: the polyhedron with nearly equal distances to the center, $\mathbb{P}_{ez}$.

Table 1. The corner positions of the Edshammar (^{11}E) polyhedron for the three distinct states, $\mathbb{P}_{id}$ ($c/a = 1.633$), $\mathbb{P}_{ee}$ ($c/a = 1.333$), $\mathbb{P}_{ez}$ ($c/a = 1.155$). The relative Cartesian coordinates are given with the threefold axis as z-axis.

x	y	$z(\mathbb{P}_{id})$	$z(\mathbb{P}_{ee})$	$z(\mathbb{P}_{ez})$
0.000	0.000	0.000	0.000	0.000
−0.816	0.000	0.577	0.471	0.408
0.408	0.707	0.577	0.471	0.408
0.408	−0.707	0.577	0.471	0.408
0.816	0.000	1.155	0.943	0.816
−0.408	0.707	1.155	0.943	0.816
−0.408	−0.707	1.155	0.943	0.816
−0.816	0.000	1.732	1.414	1.225
0.408	0.707	1.732	1.414	1.225
0.408	−0.707	1.732	1.414	1.225
0.000	0.000	2.309	1.886	1.633

In the case of a ^{14}E polyhedron with $c/a = 1.836$, all the corners fall exactly on the positions of a body-centered cubic lattice (bcc), thus building a perfectly spaced substructure of this lattice type (Fig. 7). A considerable number of compounds are known having an axial ratio near this value. Table 2 contains the corner positions for the idealized state, for that with identical edges, and for the bcc state. The most important features of the polyhedra with $1 \leq n \leq 5$ are summarized in Table 3.

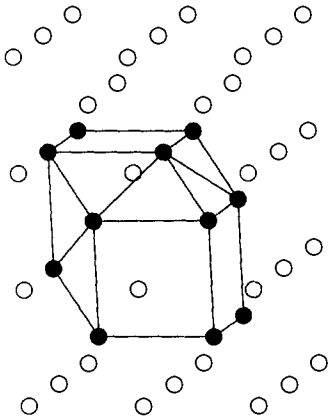

Fig. 7. The ^{14}E polyhedron as a perfectly spaced substructure of the bcc lattice.

Table 2. The corner positions of the ^{14}E polyhedron for the three distinct states, $\mathbb{P}_{id}$ ($c/a = 2.041$), $\mathbb{P}_{ee}$ ($c/a = 1.836$), $\mathbb{P}_{ez}$ ($c/a = 1.1667$). The relative Cartesian coordinates are given with the threefold axis as z-axis.

x	y	z ($\mathbb{P}_{id}$)	z ($\mathbb{P}_{bcc}$)	z ($\mathbb{P}_{ee}$)
0.000	0.000	0.000	0.000	0.000
−0.816	0.000	0.577	0.577	0.471
0.408	0.707	0.577	0.577	0.471
0.408	−0.707	0.577	0.577	0.471
0.816	0.000	1.155	1.155	0.943
−0.408	0.707	1.155	1.155	0.943
−0.408	−0.707	1.155	1.155	0.943
−0.816	0.000	1.732	1.443	1.414
0.408	0.707	1.732	1.443	1.414
0.408	−0.707	1.732	1.443	1.414
0.816	0.000	2.309	2.020	1.886
−0.408	0.707	2.309	2.020	1.886
−0.408	−0.707	2.309	2.020	1.886
0.000	0.000	2.886	2.597	2.357

Table 3. Some important features of the polyhedra. The number of corners corresponds to the coordination number of the whole enclosed structural unit (core). Q is the ratio of the stoichiometric number N to the enclosed core.

Polyhedron	Corners $(5+3n)$	Q	Symmetry	c/a $\mathbb{P}_{id}$	c/a $\mathbb{P}_{ee}$
Cube, ^{8}E	8	1:1	$\bar{3}$m	1.225	1.225
Edshammar-Polyhed. ^{11}E	11	2:1	$\bar{6}$m2	1.633	1.333
^{14}E	14	3:1	$\bar{3}$m	2.041	1.667
^{17}E	17	4:1	$\bar{6}$m2	2.449	2.000
^{20}E	20	5:1	$\bar{3}$m	2.858	2.333

As already mentioned, all the polyhedra of this class are space-filling, also in combination with other polyhedra. Thus the number of possible combinations appears infinitely large, and in addition, the cubes may be empty or occupied by an atom. Indeed we have been successful in finding a multitude of different examples which occur in compounds that exist. In the simplest case only cubes are present. These can all be identical as in CsCl or Po (centered or empty), or several different types can be present like in $Ca(UO_2)O_2$. However, here we want to limit the discussion to structures involving larger polyhedra. Our main focus is directed at binary and ternary alkali metal compounds and a few other systems. Zintl phases, especially, seem to form structures that are based on generalized Edshammar polyhedra. Hyde and Andersson refer to the Edshammar polyhedron to describe the structures of $IrAl_3$ (Na_3As type), LaF_3, and Cu_3P. In these structures, layers of filled ^{11}E polyhedra alternate with layers of empty ^{8}E polyhedra. The composition E_3Z (3:1) results from $^{11}EZ_2$ with $N_1 = 2$ and $Z = 1/2$, as well as $^{8}E\square_1$ with $N_2 = 1$; thus $N_1 + N_2 = 3$ and $Z = 1$. The Na_3As structure type is widespread among alkali metal pnictides. The phosphides, arsenides, and antimonides of lithium, sodium, and potassium show this structure type. Other examples include the bismuthides of sodium, potassium, and rubidium, as well as Rb_3As. In Table 4, the c/a ratios of the ^{11}E polyhedra observed in these compounds are compared to those of the ideal polyhedron (see above), the polyhedron with identical edges, and the polyhedron with nearly equal distances to the center ($\mathbb{P}_{id}$, $\mathbb{P}_{ee}$, and $\mathbb{P}_{ez}$, respectively). In these compounds c/a is close to the value for $\mathbb{P}_{ez}$, as expected for a single-atom core.

Table 4. Axial ratios of the Edshammar polyhedron, ^{11}E, in compounds having the Na_3As type of structure. The c/a ratio is 1.633 for $\mathbb{P}_{id}$, 1.333 for $\mathbb{P}_{ee}$, and 1.155 for P_{ez}.

Comp.	c/a	Ref.	Comp.	c/a	Ref.
Li_3P	1.185	[7]	K_3As	1.179	[9]
Li_3As	1.188	[7]	K_3Sb	1.183	[10]
Li_3Sb	1.288	[7]	K_3Bi	1.180	[7]
Na_3P	1.177	[7]	Rb_3As	1.182	[8]
Na_3As	1.177	[7]	Rb_3Bi	1.180	[11]
Na_3Sb	1.182	[7]	LaF_3	1.355	[12]
Na_3Bi	1.181	[7]	$IrAl_3$	1.187	[13]
K_3P	1.177	[8]			

The Edshammar polyhedron (^{11}E) also occurs in other combinations. In the crystal structures of $Li_{13}Si_4$[4] and Li_7Sn_2, the framework is formed from zigzag chains of ^{11}E and ^{8}E polyhedra. These structures can be derived from the Na_3As type by a mirror operation.[3]

The system obtained by an alternating packing of layers of ^{14}E and ^{8}E polyhedra is especially interesting. In this arrangement three distinctly different compositions can be distinguished (Table 5).

Table 5. Structures derived from combinations of various polyhedra.

Comp.	Polyhedron	Core	c/a	Ref.
K_4BeP_2	^{14}E	BeP_2	1.876	[14]
	cube	–	1.110	
UO_2F_2	^{14}E	–	1.537	[15]
	cube	U	0.910	
K_4BeAs_2	^{14}E	$BeAs_2$	1.892	[16]
	cube	–	1.124	
Na_4HgP_2	^{14}E	HgP_2	1.911	[17]
	cube	–	0.997	
K_4ZnP_2	^{14}E	ZnP_2	1.923	[17]
	cube	–	1.019	
K_4CdP_2	^{14}E	CdP_2	1.976	[17]
	cube	–	1.025	
K_4HgP_2	^{14}E	HgP_2	1.979	[17]
	cube	–	1.055	
$Li_{14}Si_6$	^{14}E	Si_2	1.703	[18]
	cube	Li	1.209	
Li_5Sn_2	^{14}E	Sn_2	1.756	[19]
	cube	Li	1.238	
Li_5Tl_2	^{14}E	Tl_2	1.815	[20]
	cube	Li	1.228	
K_5CuSb_2	^{14}E	$CuSb_2$	2.060	[21]
	cube	K	1.291	
Li_8Pb_3	^{14}E	Pb_2	1.835	[22]
	cube	Li	1.224	
	cube	Pb	1.224	
	cube	Li	1.224	
$Li_{13}Sn_5$	^{14}E	Sn_2	1.812	[23]
	cube	Li	1.226	
	^{14}E	Sn_2	1.812	
	cube	Li	1.221	
	cube	Sn	1.195	
	cube	Li	1.221	
Li_9Ge_4	^{14}E	Ge_2	1.719	[24]
	cube	Li	1.052	
	Edshammar	Ge_2	1.495	
	cube	Li	1.052	
Na_9Sn_4	^{14}E	Sn_2	1.465	[25]
	cube	Li	1.048	
	Edshammar	Sn_2	1.578	
	cube	Li	1.048	
K_5CuAs_2	^{17}E	$CuAs_2$	–	[26]
	cube	K	–	

Li_5Sn_2 is an example of such a compound where both the ^{14}E and ^{8}E polyhedra is filled (the ^{14}E polyhedron with Sn_2 dumbbells and the ^{8}E polyhedron with Li atoms). The structure of compounds of the K_4BeX_2 type have already been described in terms of ^{14}E polyhedra.[6] For example in the structure of K_4BeP_2, the ^{8}E polyhedra are empty while the ^{14}E polyhedra are filled by the linear 16-electron anion $[BeP_2]^{4-}$. Finally in the case of UO_2F_2, the ^{14}E polyhedra are empty and the ^{8}E polyhedra filled, a relatively unusual situation. A list of compounds which can be described on the basis of various combinations of polyhedra is given in Table 5. Remarkable is the dependence of the coordination on the c/a value. For all the polyhedra, it seems that its particular ideal c/a value is an upper limit (Table 5).

This method of describing crystal structures offers a simple way to understand the coordination for a great number of compounds that were previously classified under the "irregular" category. This method also allows for the prediction of structures. The Zintl-Klemm rule indicates which compositions are possible. If such a composition is known, only a few spatial arrangements are possible. For example, for the hexagonal structure of K_4BeSb_2, whose single-crystal structure has not been fully determined, three arrangements can be predicted: a close packing of ^{17}E polyhedra, a layered structure composed of ^{14}E polyhedra and empty cubes, or a packing consisting of ^{11}E polyhedra and filled cubes. The combination with ^{11}E polyhedra can be excluded because of size restrictions; the $BeSb_2$ unit is too voluminous for the cavity of such a small polyhedron. The two remaining possibilities differ in symmetry and unit cell parameters; the X-ray powder diffraction pattern is in accord with a close packing of ^{17}E polyhedra. Similar investigations are currently being conducted for the compounds Na_5Pb_2, Na_9Pb_4, $Na_{13}Pb_5$,[27] and Na_5Pb.[28] The positions of the Hg and Pb atoms have already been established while those for the Na atoms are still unknown.

Received: December 27, 1991
Revised: May 7, 1992
German version: *Angew. Chem.* **1992**, *104*, 936

[1] L.-E. Edshammar, *X-Ray Studies on Binary Alloys of Aluminium with Platinum Metals*, Dissertation, University of Stockholm **1969**.
[2] A. F. Wells, *Structural Inorganic Chemistry*, Oxford University Press, Oxford, **1984**, p. 71–72
[3] B. Hyde, S. Andersson, *Inorganic Crystal Structures*, Wiley, New York, **1989**.
[4] U. Frank, W. Müller, H. Schäfer, *Z. Naturforsch. B* **1975**, *30*, 10–13.
[5] U. Frank, W. Müller, H. Schäfer, *Z. Naturforsch. B* **1975**, *30*, 6–9.
[6] M. Somer, M. Hartweg, K. Peters, T. Popp, H. G. von Schnering, *Z. Anorg. Allg. Chem.* **1991**, *595*, 217–223.
[7] E. Zintl, G. Brauer, *Z. Phys. Chem. Abt. B* **1937**, *37*, 323.
[8] G. Gnutzmann, F. W. Dorn, W. Klemm, *Z. Anorg. Allg. Chem.* **1961**, *309*, 210.
[9] F. W. Dorn, W. Klemm, S. Lohmeyer, *Z. Anorg. Allg. Chem.* **1961**, *309*, 204.
[10] F. W. Dorn, W. Klemm, *Z. Anorg. Allg. Chem.* **1961**, *309*, 189.
[11] G. Gnutzmann, W. Klemm, *Z. Anorg. Allg. Chem.*, **1961**, *309*, 181.
[12] A. Zalkin, D. H. Templeton, T. E. Hopkins, *Inorg. Chem.* **1966**, *5*, 1466.
[13] L.-E. Edshammar, *Acta Chem. Scand.* **1967**, *21*, 1104.
[14] M. Somer, H. Hartweg, K. Peters, H.-G. von Schnering, *Z. Krist. Allorg.* **1990**, *192*, 263–264.
[15] W. H. Zachariasen, *Acta Cryst. Allorg.* **1948**, *1*, 277.
[16] M. Somer, H. Hartweg, K. Peters, H.-G. von Schnering, *Z. Krist. Allorg.* **1990**, *192*, 265–266.
[17] B. Eisenmann, M. Somer, *Z. Naturforsch. B* **1989**, *44*, 1228–1232.
[18] H.-G. von Schnering, R. Nesper, K.-F. Tebbe, J. Curda, *Z. Metallkd.* **1980**, *71*, 357.
[19] U. Frank, W. Müller, H. Schäfer, *Z. Naturforsch. B*, **1975**, *30*, 1.
[20] J. Stöhr, H. Schäfer, *Z. Naturforsch. B*, **1979**, *34*, 653.
[21] G. Savelsberg, H. Schäfer, *Z. Naturforsch. B*, **1979**, *34*, 771.
[22] A. Zalkin, W. J. Ramsey, D. H. Tempelton, *J. Phys. Chem.* **1956**, *60*, 1275.
[23] U. Frank, W. Müller, *Z. Naturforsch. B* **1975**, *30*, 316.
[24] V. Hopf, H. Schäfer, A. Weiss, *Z. Naturforsch. B* **1970**, *25*, 653.
[25] W. Müller, K. Volk, *Z. Naturforsch. B* **1978**, *33*, 275.
[26] B. Eisenmann, J. Klein, M. Somer, *J. Alloys Compd.*, in press.
[27] N. E. Weston, D. P. Shoemaker, *Acta Crystallogr.* **1957**, *10*, 775.
[28] G. J. Lamprecht, L. Dicks, P. Crowther, *J. Phys. Chem.* **1968**, *72*, 1439.

 © VCH Verlagsgesellschaft mbH, W-6940 Weinheim, 1992 0570-0833/92/0707-0927 $ 3.50+.25/0

Book Reviews are written by invitation from the editor. Suggestions for books to be reviewed and for book reviewers are welcome. Publishers should send brochures or (better) books to the following address: Redaktion Angewandte Chemie, Postfach 101161, W-6940 Weinheim, Federal Republic of Germany. The editor reserves the right of selecting which books will be reviewed. Uninvited books not chosen for review will not be returned.

Maximum Entropy in Action. Edited by *B. Buck* and *V. A. Macaulay*. Oxford Science Publications/Clarendon Press, Oxford, 1991. XXVII, 220 pp., hardcover £ 15.00.—ISBN 0-19-853963-0

The purpose of this book is to explain and promote the use of the maximum entropy method, a principle that can be applied to such widely different areas of science as image processing, spectra processing, direct methods of X-ray structural analysis, and statistical thermodynamics. As scientists tend to be polarized into enthusiastic proponents of MEM and skeptics, the appearance of this book is especially welcome. It is based on a series of lectures given by recognized experts during the summer of 1989 in the Physics Department of Oxford University. This has resulted in some lack of uniformity between the individual contributions, and in a few instances of repetition in the introductions; on the other hand, it means that the book is quite up-to-date.

The eight chapters are preceded by the editors' introduction, which gives a brief survey of the information theory approach to entropy (Shannon, 1948) and its relationship to Bayes's probability calculation method (Jaynes, 1959). As mathematical formulas are almost entirely avoided here, the level is suitable for any scientist with broad interests.

In the first chapter ("Of Maps and Monkeys") G. J. Daniell describes the reconstruction of distributions (maps) from sets of measurements that are incomplete or distorted. Examples include one-dimensional NMR spectra, electron density distributions obtained from X-ray scattering data, or images built up from neutron distributions in a Tokamak machine. Bayes's probability theory and the principle of maximizing the Shannon entropy are used to determine the most probable distribution that is consistent with the incomplete experimental data. As well as explaining the theoretical advantages of MEM, its practical superiority to Fourier transformation (FT) is impressively demonstrated for the example of a truncated free induction decay (FID) curve. Unfortunately, however, the example given is based only on a normal FT (with zero-filling but without apodization), which is less suitable for comparison purposes.

The second chapter (J. Skilling) is concerned with two-dimensional image analysis. A mathematically abstract formulation of Bayes's probability theory is used to calculate the probability of an image in order to make it consistent with an incomplete set of experimental data (in this example a γ-ray image of a thyroid gland). The author also describes how a priori knowledge that is already available can be incorporated into the image; thus, in the example of the thyroid gland it was specified that the contrasts (due to differences in the concentration of the γ-emitter) must not be too great. When this image blurring effect (preblur) is taken into account one does, in fact, obtain a better image. Unfortunately, in this example the author fails to compare the technique with Fourier methods that have undergone a corresponding optimization. This is not surprising, however, since one reads in the introductory paragraphs of this chapter that "... MEM is not just a good technique for data analysis from imperfect data, it is *the* technique."

In the third chapter P. Hore deals with one- and two-dimensional NMR experiments. Here the Messianic style of the previous two chapters is mercifully absent, and we have an objective discussion of such matters as resolution enhancement, signal-to-noise enhancement, and truncation of the FID. This is followed by examples in which spectral distortion effects already known to be present (e.g., mixing of the phases in 2D NMR spectroscopy, and offset effects in rotating frame imaging) are eliminated. Lastly the author describes extensions of the algorithm that are specific to NMR, allowing for the presence of negative peaks in the spectrum.

The fourth chapter (S. Davis et al.) is closely related to the preceding one. It contains examples of the analysis of NMR spectra that consist of only a few broad signals (e.g., polymer spectra), followed by Raman spectra and magic angle spinning (MAS) NMR spectra. It is interesting to see how information that one already has about the spectrum, such as the theoretical intensity distribution of rotation side-bands in an MAS spectrum, can be incorporated into the MEM algorithm. However, the example in which an ad hoc modification is introduced into the definition of the Shannon entropy, leading to meaningless spectral constructions, is hardly of more than academic interest.

In the fifth chapter G. A. Cottrell describes some further applications in the reconstruction of one- and two-dimensional distributions, with examples from high energy physics. He gives an impressive account of how the density distribution of neutrons in a neutron beam can be obtained from only 12 centered projections (by using classical "projection reconstruction" methods). In this case it was important to achieve good resolution at the edges of the image (where the intrinsic resolution given by the method of measurement was poor), since the neutrons in this edge region cause damage to the tube wall.

The next two chapters are concerned with certain fundamental topics in theoretical physical chemistry. The sixth chapter (A. J. M. Garrett) has the title "Macroirreversibility and Microreversibility Reconciled", while in the seventh S. F. Gull discusses "Some Misconceptions about Entropy". In the treatment of one-dimensional Brownian motion at the end of the latter article, the topic is extended to include non-equilibrium thermodynamics, providing further confirmation of the impressively wide scope of the entropy maximization principle.

In the eighth article G. Bricogne describes how MEM can be used to improve direct methods of crystal structure analysis. The determination of electron density distributions from scattering data is a classic case of incomplete experimental data, since the X-ray reflections contain no phase information. Direct methods attempt to extract the phase information from a statistical analysis of the peak intensities that can be measured. MEM offers an algorithm for deriving phase information that is considerably better than conventional methods, such as that based on the Edgeworth series. It seems likely that by also using chemical knowledge (for

example, the information that two atoms cannot lie one above the other) one can obtain an improvement over the "random atom model" used in the direct method.

The lack of uniformity, and the inevitable repetitions resulting from the lack of coordination between the individual contributions, cannot detract significantly from the generally very positive impression given by this book, which includes research results extending up to 1991. This fascinating universal concept opens up many new possibilities for the analysis of spectra, images, and X-ray scattering data. Several of the authors extol the virtues of the method too enthusiastically for this reviewer's taste; an extreme example of this tendency was an article in *The Times* (London, 1984), in which it was claimed that MEM analysis would make it possible to record ^{13}C NMR spectra at natural abundance on living animals. However, this is rectified by other chapters that present an objective appraisal. The figures, text, and mathematical formulas are all of an exemplary standard. Because of the wide range of aspects covered in this book, it can be thoroughly recommended, not only for spectroscopists, "imagers", and X-ray crystallographers, but also for all readers with interests in physical chemistry or information science.

Christian Griesinger
Institut für Organische Chemie
der Universität Frankfurt/Main (FRG)

An Introduction to Ultrathin Organic Films from Langmuir–Blodgett to Self-Assembly. By *A. Ulman*. Academic Press, New York, 1991. XIII, 442 pp., hardcover $ 65.00.—ISBN 0-12-708230-1

In an article in the journal *Science* in 1936, Irving Langmuir addressed the following words to the international scientific community: "Today... I propose to tell you of a real two-dimensional world in which phenomena occur that are analogous to those described in 'Flatland'. I plan to tell you about the behavior of molecules and atoms that are held at the surface of solids and liquids." One could hardly have a more comprehensive, and at the same time precise, statement of what research in the area of ultrathin organic films is about. No doubt that is why Abraham Ulman has chosen to preface his book with this quotation from Langmuir who, in collaboration with Kathleen Blodgett, developed the Langmuir–Blodgett (LB) technique.

Most of those engaged in research on ultrathin organic films are either chemists or physicists, and it is to these that Ulman's book is directed. In 440 pages the author introduces readers to a field that has developed at a remarkable rate during the last 15 years. This development stems to a large extent from the elegant experiments carried out by Hans Kuhn in the mid-sixties. Those experiments established the basic principles of a supramolecular architecture, and made it possible to position molecules and monomolecular films with separations of the order of 50 Å with a precision better than 5 Å. At that time the experiments confirmed Foerster's prediction of a transfer of energy from a donor dye molecule to a nearby acceptor dye molecule; nowadays they form part of the practical laboratory training of advanced students.

Ulman's book consists of five parts as follows:

1) Techniques for characterizing the intrinsic properties of films and the properties of their surfaces. Here the author describes most of the analytical methods used, starting with the measurement of thickness by ellipsometry, and continuing through scattering techniques for determining the structures of films, to surface characterization techniques such as contact angle measurements, and the most recently developed imaging techniques such as scanning tunneling microscopy and atomic force microscopy. Only a few methods are not mentioned; one of these is the vibrating quartz crystal technique for measuring the mass of material deposited on a surface.

2) Preparing monomolecular films and transfering them onto solid supports (Langmuir–Blodgett films). Here "film balance" techniques are described, whereby molecules are spread on the surface of a liquid to form a monomolecular layer, which is subsequently compressed into a close-packed state, and this film is then transfered onto a solid support. This section also describes the preparation of substrate surfaces, the transfer process, and the types of materials that have so far been used to make Langmuir–Blodgett films. Ulman attempts to relate the molecular structures, transfer conditions, and substrate properties to the properties of the resulting films, so far as this is possible from the details given in the original papers. The types of amphiphiles discussed include both substances of low molecular mass and polymers.

3) Preparing monomolecular and multimolecular films by self-assembly (SA) techniques (chemi- and physisorption). In this section Ulman draws a rather arbitrary (but, nevertheless, commonly accepted) distinction between LB films and those described here. The term "self-assembly" is meant to imply that the molecules spontaneously form an ordered structure on the surface of the substrate. In contrast to the LB technique, no film balance is needed; instead, the adsorption takes place directly from the solution. The focus of interest is therefore the kinetic aspects, which are here discussed in detail. The cost of the apparatus needed to lay down a monomolecular film by this method is considerably less than with the LB technique. However, if one wishes to build up multimolecular films the choice of compounds that can be used is severely limited, since the bonding between successive layers is usually covalent.

4) Model calculations for monomolecular film systems. In this short section the author outlines the current position regarding the theoretical description of two-dimensional molecular aggregates. It becomes apparent that methods for calculating or predicting the properties of these complex systems are still at an early stage of development. The dilemma is that the results obtained using simplified models are of doubtful value, whereas the established methods cannot be applied to systems with such a large number of degrees of freedom.

5) Potential applications of ultrathin films. This section reviews the importance of ultrathin films for materials science. Although at present (October 1991) there are only two commercial products on the market that are based on LB or SA films, there is an enormous amount of scientific and industrial interest in these systems. The most promising forms of supramolecular architecture are the polar film systems, which have applications in nonlinear optics and as pyroelectric detectors for infrared radiation. Other potential fields of application are in photoresists or electronresists, in sensors, in optical data storage, in gas separation, in friction reduction, and in conducting films.

The book is essentially what its title promises: an introduction. It includes about 1900 references to original papers and reviews. The literature coverage extends to the end of 1989, and is quite comprehensive. However, contrary to what one might expect from the title, Ulman restricts the discussion to Langmuir–Blodgett and self-assembly systems. Other important types of layered films, such as self-supporting (e.g., liquid crystalline) films, films consisting of lipid

double layers, or films prepared by spin-coating or vapor deposition techniques, are not mentioned. Also the subject index is definitely a weak point, as it is neither sufficiently comprehensive nor suitably constructed to do justice to the contents. Often it is easier to locate a topic by searching for the relevant chapter in the contents list. Despite these criticisms, the book can be recommended to everyone who seeks an up-to-date survey of the area of LB and SA films, but does not expect to find here a work of reference providing a detailed solution to every problem—the field of ultrathin films is still too new for that.

Gero Decher
Institut für Physikalische Chemie
der Universität Mainz (FRG)

Inorganic Biochemistry of Iron Metabolism. (Ellis Horwood Series in Inorganic Chemistry). By *R. R. Crichton*. Ellis Horwood, New York, 1991. 263 pp., hardcover $85.95.—ISBN 0-13-728742-9

Although it is well known that iron is essential for virtually all forms of life, there are still many unanswered questions concerning the metabolism of the metal. In this book, Professor Crichton provides a useful survey of current understanding, with the first nine chapters dealing with the topics of general iron biochemistry, iron uptake, transport, storage and homeostasis, and then iron imbalance and its effects in relation to human health treated in the last three chapters. The area the book covers is so vast that it is impossible to provide precise details of all the known and postulated biochemical pathways involved in iron metabolism within the book's 263 pages. Instead the author has furnished us with an excellent bibliography which reflects his wide reading in the field, and upon which he draws frequently within the text, making this an invaluable source-book. There are one or two places where this system falls down, such as in the discussion of hemoprotein structures in Chapter 2, where it is not made clear which references relate to the protein structures discussed, but in general the references are helpful and up-to-date, which will be appreciated by the intended readership of researchers and advanced students.

A much more serious problem occurs in the first chapter, where the relevant inorganic chemistry of iron is considered. Unfortunately the very first page contains much which is simply wrong. It is well-known that iron(III), for example, can have coordination numbers greater than the maximum of six suggested. It is also inadvisable to describe a five-coordinate stereochemistry as octahedral! For any worker not familiar with ligand field therory, the account of "weak- and strong-field ligands", and the unwise attempt to describe them simultaneously in terms of the "soft/hard principle", will probably leave him bewildered. Those who are used to such approaches are probably best advised to treat this first page as an unfortunate misinterpretation of the theory and ignore it completely.

The chapters that deal more with the microbiology and biochemistry involved in metabolic processes may seem hard to digest for chemists, at least on a first reading. However, for those interested in understanding iron metabolism such topics are an essential part. Professor Crichton is obviously quite at home with many of these areas, and his straightforward style helps in leading us through some of the more involved chapters, such as those on "Microbial iron and intracellular release" (Ch. 3) and "Iron assimilation in plants and fungi" (Ch. 4).

The chapter on "Intracellular iron storage" (Ch. 8) is perhaps somewhat shorter than would be expected in view of the author's involvement in this field, but it is here more than anywhere else that Professor Crichton's often anecdotal style comes to the fore. I doubt that any British scientist could suppress a smile when reading the implied comparison between the contemporaneous Oxford chemists who have been dubbed "Iron Lady" in recognition of their rather different achievements.

The book ends with a consideration of the clinical aspects of iron imbalance. The problems of anemia and iron overload are described with their medical consequences. Then the roles iron plays in mechanisms of oxidative damage, which may lead to a variety of medical conditions, such as inflammatory arthritis, induced by the presence of unwanted free radicals, are discussed. Finally, the possible relationship between iron imbalance and infection is considered.

In summary, this book provides a useful addition to the existing literature. It is a readable account of a large and complicated subject and will provide researchers with many useful literature sources. The author's statement in his preface that his long association with iron has not bred contempt "but rather an increasing wonder at what iron, associated with low molecular weight and protein ligands, and often with metal and other nonmetal cofactors, can do in biological systems", is evident from the text. Although the book may raise more questions than it can answer, we are left with a clear idea about where our problems in understanding iron metabolism lie, and also how these problems have been approached to date.

A. K. Powell
School of Chemical Sciences
University of East Anglia, Norwich (UK)

Registered names, trademarks, etc. used in this journal, even when not marked as such, are not to be considered unprotected by law.

© VCH Verlagsgesellschaft mbH, D-W-6940 Weinheim, 1992. – Printed in the Federal Republic of Germany by Konrad Triltsch Druck- und Verlagsanstalt Würzburg.

All rights reserved (including those of translation into foreign languages). No part of this issue may be reproduced in any form — by photoprint, microfilm, or any other means — nor transmitted or translated into a machine language without written permission from the publishers. Only single copies of contributions, or parts thereof, may be made for personal use. This journal was carefully produced in all its parts. Nevertheless, authors, editors, and publisher do not warrant the information contained therein to be free of errors. Readers are advised to keep in mind that statements, data, illustrations, procedural details, or other items may inadvertently be inaccurate.

Valid for users in the USA: The appearance of the code at the bottom of the first page of an article (serial) indicates the copyright owner's consent that copies of the article may be made for personal or internal use, or for the personal or internal use of specific clients. This consent is given on the condition, however, that the copier pay stated per-copy fee through the Copyright Clearance Center, Inc. (CCC), for copying beyond that permitted by Sections 107 or 108 of the U.S. Copyright Law. This consent does not extend to other kinds of copying, such as copying, for general distribution, for advertising or promotional purposes, for creating new collective works, or for resale. For copying from back volumes of this journal see 'Permissions to Photo-Copy: Publisher's Fee List' of the CCC.

Editorial office: Postfach 10 11 61, D-W-6490 Weinheim, Federal Republic of Germany, Telephone (06201) 60 23 15, Telex 465 516 vchwh d, Telefax (06201) 602 328, E-Mail Z16@DHDURZ2 in Earn Bitnet.

Editor: *Peter Gölitz*

Associate editors: *R. H. Schmidt-Radde, K. J. Schneider, A. Stimson.* **Editorial assistant:** *E. Schweikart*

Publishers: VCH Verlagsgesellschaft mbH. (Managing Directors: *Hans Dirk Köhler, Dr. Karlheinz Köpfer*), Pappelallee 3, W-6940 Weinheim, Federal Republic of Germany.

Advertising office (Advertising Manager: *R. J. Roth*): Postfach 10 11 61, D-W-6940 Weinheim, Federal Republic of Germany, Telephone (0 62 01) 60 61 36, Telex 467 155, Telefax (0 62 01) 606 156.

ANGEWANDTE CHEMIE
International Edition in English
Volume 31 Number 8
August 1992
Pages 931–1100

Preparation and Properties, Reactions, and Applications of Radialenes

By Henning Hopf* and Gerhard Maas*

Dedicated to Professor Günther Maier on the occasion of his 60th birthday

Radialenes are alicyclic compounds in which every ring atom is sp^2-hybridized and carries an exocyclic C–C double bond. Because of their unusual topology and electronic structures these hydrocarbons have aroused the interest of both preparative chemists and theoreticians. Although considerable progress has been achieved recently, directed and efficient syntheses of these molecules remain a challenge. The study of their chemical behavior offers vast opportunities. Very recently materials scientists have become interested in these unusual compounds in their search for organic conductors and ferromagnets.

1. Introduction: Nomenclature and Structural Variety

The all-*exo*-methylenecycloalkanes **1**–**4** represent the first members of a homologous series of compounds with the general formula C_nH_n. In contrast to their constitutional isomers with endocyclic, linearly conjugated double bonds such as benzene and cyclooctatetraene, the radialenes possess an uninterrupted cyclic arrangement of cross-conjugated π systems. They are hence closely related to the so-called dendralenes,[1] acyclic and cyclic cross-conjugated polyenes derived from 3-methylene-1,4-pentadiene (**5**).

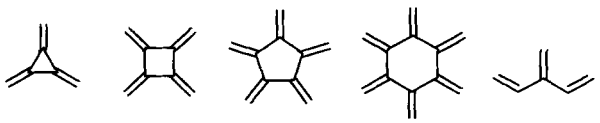

1 **2** **3** **4** **5**

[*] Prof. Dr. H. Hopf
Institut für Organische Chemie der Technischen Universität
Hagenring 30, D-W-3300 Braunschweig (FRG)
Prof. Dr. G. Maas
Fachbereich Chemie der Universität
Erwin-Schrödinger-Straße, D-W-6750 Kaiserslautern (FRG)

Radialenes are a relatively recent class of compounds.[2, 3] Hexaethylidenecyclohexane was the first reported example: its synthesis was published in 1961.[4] The first [3]radialene, triisopropylidenecyclopropane was described in 1965.[5] Among the parent systems, **1** was prepared in 1965,[6] **2** in 1962,[7] and for **4** three independent syntheses were reported in 1977/78.[8–10] Whereas [5]radialene **3** has evaded preparation so far, a derivative has been obtained as recently as 1986.[11] Of course, the radialenes—and the cross-conjugated systems in general (e.g. dendralenes[1] and fulvenes)—have always been overshadowed by the linearly conjugated polyenes and the arenes in preparative and industrial organic chemistry. However, in recent years interest in this class of compounds has increased significantly because new methods of synthesis make radialenes more accessible, and they are potential candidates for the construction of organic conductors and ferromagnets. Meanwhile enough information on synthesis and the chemical, physical, and structural properties of the radialenes has accumulated to justify a compact overview over this group of compounds.[12]

The highly symmetrical structure of **1**–**4** suggested by their constitutional formulas is not only aesthetically appealing but also stimulates the fantasy of the chemist. It is thus not surprising that the search for a fitting trivial name for

 © *VCH Verlagsgesellschaft mbH, W-6940 Weinheim, 1992* *0570-0833/92/0808-0931 $ 3.50+.25/0*

these regular structures with the double bonds "radiating" from the central ring led to the name "radialene(s)".[2] Although this term was coined originally for the hexamethylenecyclohexane **4**,[3] it was quickly adopted for the whole series. To differentiate between its various members, the number of the exocyclic[*] double bonds was put in parentheses in front of the word radialene ([*n*]radialene: $n = 3$:**1**, 4:**2**, 5:**3**, 6:**4** etc.)

The fate of trivial names is that their use is not exactly defined and can hence cover a considerable range of meanings. Thus nowadays molecular frameworks that only show a more or less pronounced topological resemblance to the hydrocarbons **1**–**4** are often also called radialenes. This approach originates from a proposal by Hart[13] to call all ring systems—including condensed, polycyclic, and heterocyclic ones—with the highest possible number of exocyclic double bonds radialenes. Thus the so-called naphtharadialene **6**,[13] which has been postulated as a reactive intermediate (covered in more detail in Section 2.5), contains only sp^2-hybridized ring atoms, but does not consist exclusively of exocyclic methylene groups. In "furano-" (**7**[14, 15]) and "thiophenoradialene" (**8**[15]) the maximum number of exocyclic double bonds is present; however, the cyclic array of π electrons found in [5]radialene **3** is interrupted by the presence of a ring heteroatom. The presence of the maximum number of exocyclic double bonds and the structural element of a cross-conjugated π system is a common feature of all the compounds **6**–**8**.

The radialene terminology becomes entirely unsatisfactory for the polyalkylidene heterocycles **9**–**13**, which are lacking the typical cross-conjugated π systems. A relationship to the radialenes may at best be postulated for the 1,4-diboracyclohexane derivative **12** ($R = NPh_2$) and for the 1,3-diboracyclopentane **13** because of the double-bond character of the B–N bond ($> B-\ddot{N} < \leftrightarrow > \ddot{B}=\overset{+}{N} <$).

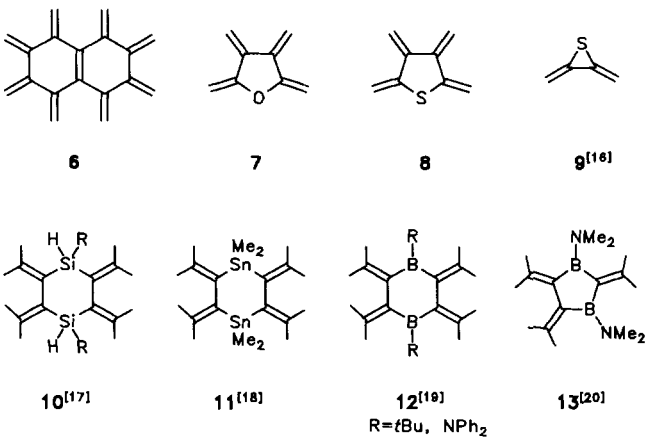

A concise definition of the term "radialene" is thus indispensable. Although molecules of this type are evidently amenable to IUPAC nomenclature, the further use of the term radialene, which so vividly conveys the molecular structure, appears desirable. As is obvious in many other areas of

[*] A class of compounds that contains exclusively "exocyclic" double bonds again gives us cause to point out that the prefix *exo* in this context is not only misleading but incorrect. Double bonds within ring systems can either be part of the ring, that is, both sp^2-hybridized carbon atoms are ring atoms (in that case one is dealing with an *endo*cyclic double bond), or the double bond is located as a substituent outside the ring (i.e., it is *exo*cyclic). In the past A. von Baeyer preferred to call this bonding situation *a*cyclic (A. von Baeyer, *Ber. Dtsch. Chem. Ges.* **1894**, *27*, 436–454). For the case discussed here in which only one olefinic carbon atom is part of the ring, and the other one is located outside it, he proposed the term *semi*cyclic. The resistance towards this (in our view very) convincing proposal could not be overcome, although another attempt to popularize it has been made (G. Zinner, *Chem. Ztg.* **1985**, *109*, 436). We hence yield to the present usage of the term exocyclic.

Henning Hopf was born in 1940 in Wildeshausen/Lower Saxony, Germany. After studying chemistry at Göttingen University (B.Sc. 1963), the University of Wisconsin in Madison, USA, (M.Sc. 1965, Ph.D. 1967 with H. L. Goering), and spending postdoctoral years at Marburg and later Karlsruhe with H. Musso he completed his habilitation in 1972. In 1975 he accepted a position as associate professor at Würzburg University, and in 1978 became full professor of chemistry and director of the Institute of Organic Chemistry at the Technical University of Braunschweig, where he is still working. His research, for which he has received several awards, for instance a Karl Winnacker Scholarship and the prize of the Akademie der Wissenschaft zu Göttingen, concentrates on one hand on the preparation of all types of highly unsaturated hydrocarbons and the study of their chemical and spectroscopic properties, and on the other on the study of the mechanisms of high-temperature pyrolyses of hydrocarbons.

G. Maas, born in 1949 in Riegelsberg, Sarre, Germany, studied chemistry at the Saarbrücken and Heidelberg universities (Diplom 1971) and received his Ph.D. degree at Saarbrücken in 1974 with M. Regitz. From 1974 to 1976 he was Justus-von-Liebig scholar at the newly founded University of Kaiserslautern, and after a postdoctoral year with P. J. Stang at Salt Lake City (USA) he completed his habilitation in 1982 in Kaiserslautern. In 1986 he became assistant professor and in 1992 extraordinary professor at Kaiserslautern. His fields of interest are reactive intermediates, in particular carbenes, transition-metal-catalyzed decompositions of diazo compounds, the use of resonance-stabilized cations in synthesis, organosilicon chemistry, electron-rich allenes, as well the X-ray structural analysis of molecular compounds.

chemistry as well, the continuously growing structural complexity has led to steadily increasing nomenclature problems, and—in turn—to a rich trivial nomenclature.[2] Very likely, one will be forced to include the latter into the official IUPAC rules one day. Since it is also likely that the chemical significance of the radialenes will grow, we would like to present some proposals for their nomenclature without aiming at completeness. To begin with, we propose to employ the radialene nomenclature rather restrictively in order not to jeopardize its descriptiveness and simplicity of use. There is ample precedent for this approach in organic chemical nomenclature, as illustrated by trivial names such as prismanes, rotanes, asteranes, fenestranes, etc.

We thus propose the following definition:

Radialenes are alicyclic compounds in which all ring atoms are sp^2-hybridized and carry—as far as possible[21]—exocyclic carbon–carbon double bonds.

To number the various carbon atoms of a radialene we propose to differentiate between an "inner" and an "outer" ring; the numbering is continued at the periphery after the inner ring atoms have been counted. This principle is illustrated by formula **14** for [3]radialene. For substituents the usual IUPAC rules apply. Thus hydrocarbon **15** is termed 4,4-diethyl-5,5-dimethyl[3]radialene, and the dichloro compound **16** is called 4,4-dichloro[3]radialene. Analogously, the ester **17** is 5-methoxycarbonyl-7,7-dimethyl-[4]radialene. If diastereomers are encountered, the usual *E*/*Z* nomenclature is employed; for example, derivative **18** is (5*E*,6*Z*)-5-ethoxycarbonyl-6-methyl[4]radialene, **19** (5*Z*,8*Z*)-5-cyano-6,6,8-trimethyl[4]radialene, and **20** (7*E*,6*Z*)-7-bromo-6-formyl-6-methyl[5]radialene. Whereas for hydrocarbons like **21** the conventional nomenclature is more convenient (tetrakis(ethenylidene)cyclobutane), we prefer the radialene name for **22** (4,4,5,5,6,6-hexaethynyl[3]radialene), a possible building block for novel carbon networks. Needless to say, radialenes may be part of bi- or polycyclic structures. This is illustrated by the hydrocarbon **23**, for which again, however, a designation along conventional lines (tetramethylenecyclopropylidene) seems preferable to its designation as a radialene.

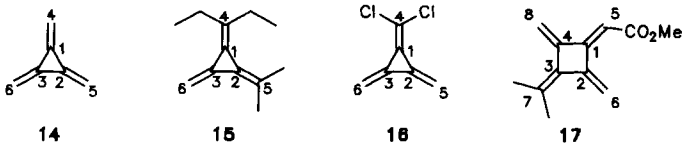

14 **15** **16** **17**

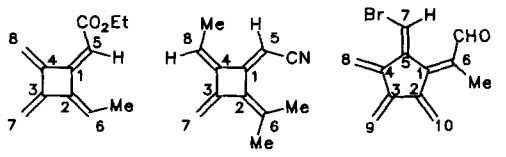

18 **19** **20**

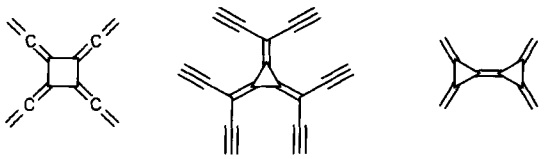

21 **22** **23**

A certain family relationship exists between the [*n*]radialenes and the bicyclic polyenes **24**, **25** ([2.2.1]hericene[22]), and **26** ([2.2.2]hericene), which recently have been discussed comprehensively by P. Vogel.[23] The element of π cross-conjugation has been lost in these systems; instead they are interesting model compounds for the study of homoconjugation and hyperconjugation effects in 1,3-dienes.

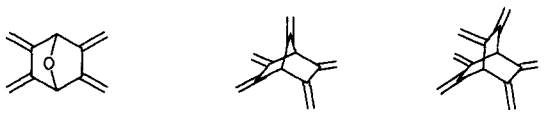

24 **25** **26**

Certain valence-structure formulas of benzo-condensed derivatives of **1**–**4** also suggest a radialene topology. Because of the extended delocalization of the π electrons in the aromatic sextet, such systems (e.g., alkylidenecyclopropparenes,[24] benzocyclobutarenes, perylene, triphenylene, trimethyleneindane and its derivatives) basically may not be considered as radialenes. On the other hand, the thiophene condensed compounds **27**[25] and **28**,[26] which are isoelectronic with perylene, may certainly be regarded as true [6]radialenes, if one takes into account the double-bond fixation that has been observed for **28** by X-ray structural analysis.

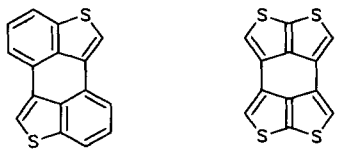

27 **28**

Radialenes whose methylene groups have been replaced partially or fully by heteroatoms, as in **29**–**35**, may be looked upon as heteroanalogs of the radialenes; **29**, for example, would be trisoxa[3]radialene. However, for the (still unknown) carbonyl compounds **29** and **30** and related systems the term "oxocarbons"[27] has been so firmly established, that we propose not to change it.

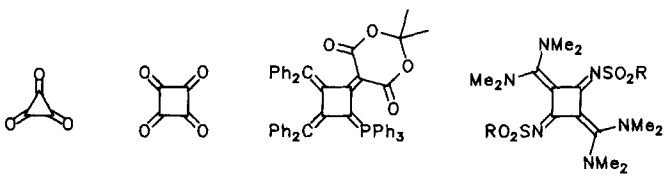

29 **30** **31**[28] **32**[29]

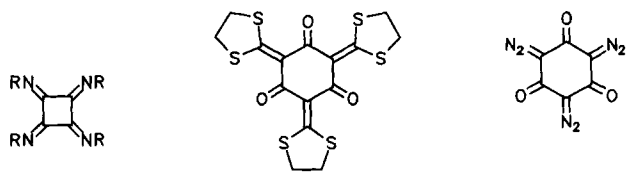

33[30] **34**[31] **35**[32]

Consequently, the oxocarbons as well as sulfur, nitrogen, and other heteroanalogous compounds derived therefrom (including only partially substituted radialenes) are beyond the scope of this review.

2. Methods of Preparation

Altogether one still gains the impression that the directed synthesis of the [*n*]radialenes is not a trivial affair, especially not if the control of the stereochemistry of the exocyclic double bonds is also desired. It therefore comes as no surprise that the vast majority of the known radialene derivatives carries two identical substituents at the exterior carbon atoms. Two general synthetic strategies dominate: on the one hand, olefin-forming reactions at an already existing cycloalkane skeleton, and on the other, thermal and metal-induced cyclooligomerization reactions of suitable [*n*]cumulenes. The latter method has turned out to be the more variable and successful one so far, although it (still) cannot compete in product selectivity with the former (see Sections 2.2 – 2.4). In the following sections we shall discuss the various syntheses of the different radialenes separately.

2.1. [3]Radialenes

The parent compound is accessible by classical olefin-forming elimination reactions from appropriately substituted cyclopropanes (Scheme 1). The low (at best fair) yields are

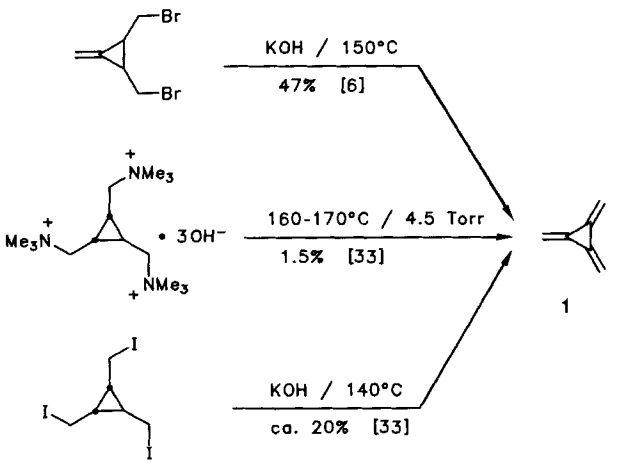

Scheme 1. Synthetic approaches to [3]radialene (**1**). In all cases the product was collected at −78 °C.

not surprising in view of the rather drastic reaction conditions, as well as the high propensity of **1** to undergo polymerization (in the presence of oxygen,[33b] in CCl_4 at 0 °C, and on warming the vapor to room temperature[6]). An attempt to prepare hexaphenyl[3]radialene by threefold HBr elimination from tris(bromodiphenylmethyl)cyclopropane failed because this precursor could not be obtained.[34]

R. West et al. have developed the chemistry of [3]radialenes with quinoid substituents, as illustrated by the synthesis of tris(4-oxo-2,5-cyclohexadienylidene)cyclopropane **38**.[35] At first all chlorine substituents of the trichlorocyclopropenyl cation are successively replaced by 4-hydroxyaryl groups. The salt **36** thus formed is next deprotonated to the diaryl(oxocyclohexadienylidene)cyclopropane **37**, which is finally oxidized to the [3]radialene derivative **38**. The se-

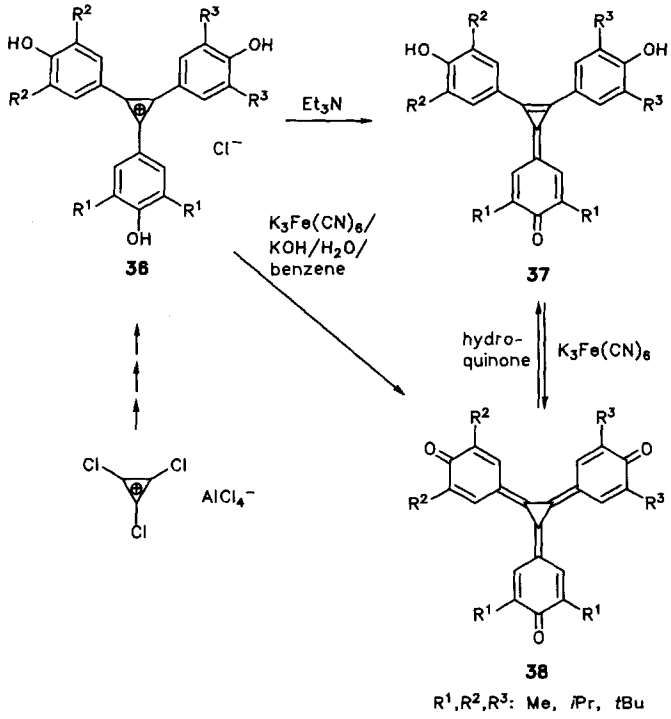

Scheme 2. [3]Radialene with quinoid substituents.

quence **36** → **37** → **38** may also be carried out as a one-pot process. The stability of the deeply colored products increases with growing steric shielding of the carbonyl groups. Thus the methyl derivative ($R^1 = R^2 = R^3 = Me$) has been shown to exist only in solution, whereas the all-*tert*-butyl compound is stable in air up to 250 °C.

By analogous routes [3]radialenes with other quinoid substituents have been prepared, for example, **39**,[36] **40**,[37] **41**,[38] **42**,[39] and **43**.[40] In contrast to the other compounds, **43** decomposes readily to form unidentified products; it was hence characterized only in solution.

By a related synthetic method [3]radialenes that carry—besides the two quinoid substituents—a methylene group with two electron-accepting substituents[41] have also been prepared. The golden-yellow dicyanomethylenebis(4-oxo-2,5-cyclohexadienylidene)cyclopropane **44** (Scheme 3) is a case in point.

An oxidation reaction also constitutes the key step in the preparation of hexacyano[3]radialene **46** and hexakis(methoxycarbonyl)[3]radialene **47**.[42] In this synthesis the dianions **45**,[43] which are readily accessible from tetrachlorocyclopropene and malononitrile and malonic ester, respectively, are oxidized in two successive one-electron steps (Scheme 4). Whereas **47** forms stable yellow crystals, it is difficult to obtain **46** in pure from. Freshly synthesized samples are radiant yellow, but turn brown on contact with air and blue when treated with several solvents. Both KBr and NaI reduce **46** to the radical anion and the dianion **45**.

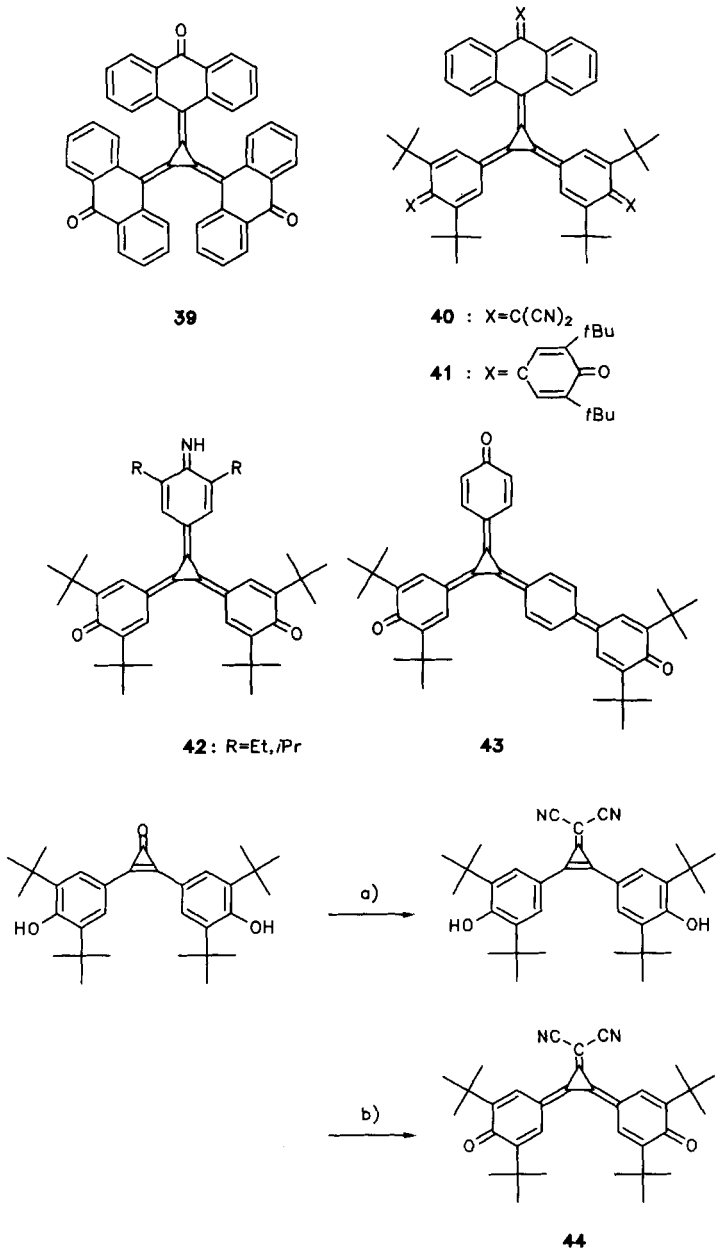

Scheme 3. Synthesis of the [3]radialene **44**. a) $CH_2(CN)_2$, Ac_2O, reflux, β-alanine; b) $K_3[Fe(CN)_6]/H_2O/OH^-/CHCl_3$.

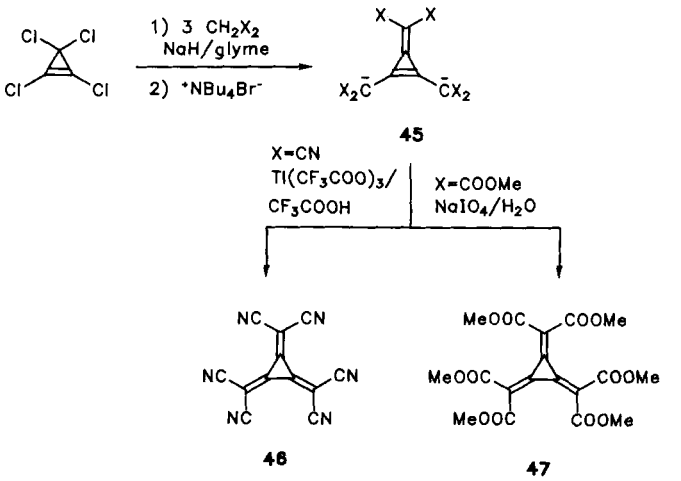

Scheme 4. Synthesis of hexacyano- (**46**) and hexakis(methoxycarbonyl)-[3]radialene (**47**).

The blue radialene **48** may be prepared from hexachlorocyclopropane. Although structurally related to **39**, it constitutes an electron-rich [3]radialene.[44]

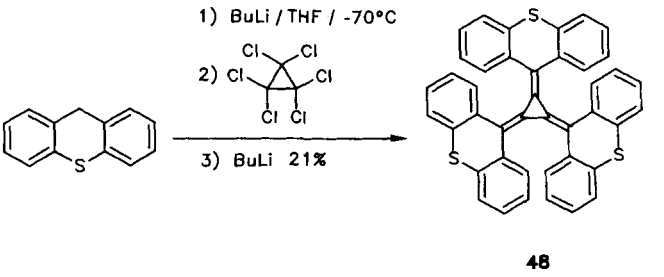

The [3]radialenes discussed so far were prepared from substituted three-membered rings; we now want to discuss methods in which the radialene is formed during the cyclopropane-forming step. Cyclopropanation of a butatriene by an alkylidenecarbene or -carbenoid intermediate, for example **49**, constituted the first synthesis of a [3]radialene by Köbrich et al.[5] (**50**, Scheme 5). The yield is very small though (about 17%), one reason being that the cyclopropanation takes place preferentially at the outer double bonds of the butatriene. This approach has not as yet been generalized. The attempt to cyclopropanate tetra(*tert*-butyl)butatriene with isopropylidenecarbene failed, most likely because of the steric shielding of the cumulene system.[45]

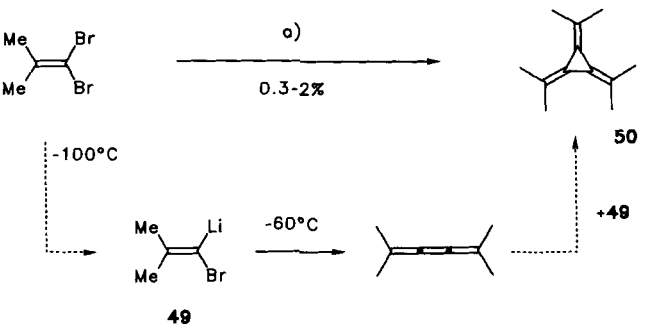

Scheme 5. Synthesis of the [3]radialene **50** and likely intermediates. a) 1) *n*BuLi (1.25 equiv)/THF/−110 °C; 2) −110 °C → −65 °C; 3) *n*BuLi (0.75 equiv).

Copper and nickel carbenoids, which may also be obtained from 1,1-dihaloalkenes, can cyclooligomerize directly to provide radialenes. For example, the lithium cuprate **51** yields the [3]radialene **52** (black-red crystals with a metallic luster). However, the main product of this reaction is the butatriene **53**. If other Cu^I salts are employed for cuprate formation ($CuI \cdot PBu_3$, $CuBr \cdot Me_2S$, CuCN), **53** is produced almost exclusively at the expense of the radialene.[46] As shown by a control experiment, the mechanism of formation of **52**—in contrast to the reaction course summarized in Scheme 5—is very likely not the cyclopropanation of **53**.

Unlike **51**, the cuprate derived from 1,1-dibromo-2-methylpropene does not form a [3]radialene, but rather [4]- and [5]radialenes (Section 2.2). Likewise, the cyclooligomerization of the analogous nickel carbenoids is very strongly substituent-dependent (Scheme 6). Sterically demanding

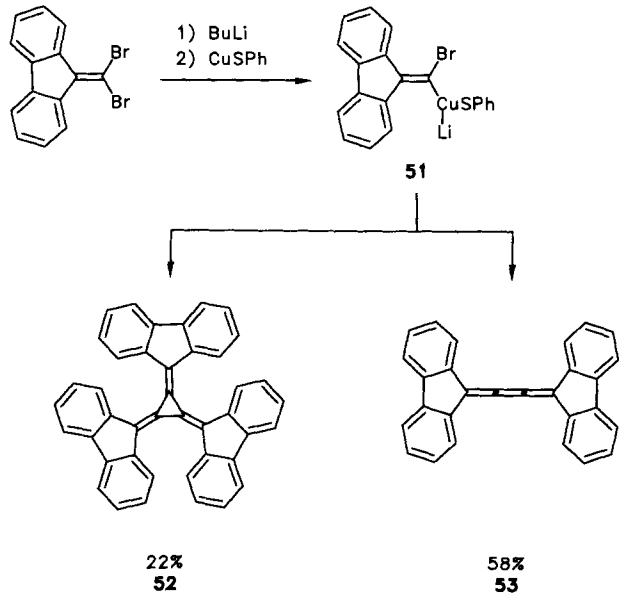

substituents suppress the formation of the higher radialenes and favor [3]radialene production (**52**, **54**–**56**[47a]). Even tris-(2-adamantylidene)cyclopropane may be prepared by this route (with a yield of 64%![47b])

hexadiyne in good overall yield, can also be performed readily. An elegant, although probably not an everyday method for the synthesis of **2** is provided by the thermal [4 + 2] cycloreversion of **60**. [4]Radialene may be kept for extended periods of time in dilute solutions at −78 °C under exclusion of air. At room temperature dimerization sets in rather quickly in solution, and exothermic polymerization took place during an attempt to isolate neat **2**. Towards oxygen the compound is also very sensitive.

Some substituted [4]radialenes have been prepared from cyclobutane precursors as well. Fourfold deprotonation of the tetrakis(4-pyridinio)cyclobutane **61a** yields the highly symmetrical [4]radialene **62a** in a single step as red, poorly soluble crystals[52] (Scheme 8). The presence of the ethoxycarbonyl group at the pyridine nitrogen atom is a prerequisite for the success of this synthesis. This is illustrated by the observation that the deprotonation of the salt **61b** under concomitant dehydrogenation leads to the cyanine **63** or the dication **64**, depending on the reaction conditions. The radialene **62b** could only be generated from **64** by electrochemical reduction.[53] On fourfold deprotonation of **61b** with sodium hydride in dimethylacetamide under exclusion of oxygen, a red solution is formed, which according to its absorption spectrum very probably also contains the radialene. When air is admitted the color immediately changes to blue, and **64** is formed.[53]

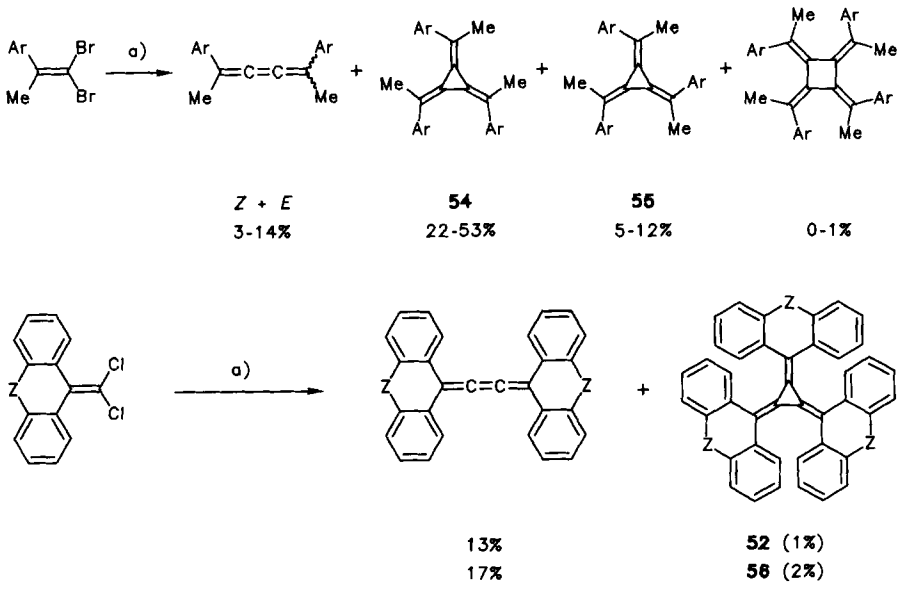

Scheme 6. [3]Radialenes by cyclotrimerization of nickel carbenoids. a) Activated nickel (5–10 equiv), THF, sonication. Ar = C_6H_5, 4-ClC_6H_4, 4-CNC_6H_4; Z = CH_2, O.

2.2. [4]Radialenes

In the same manner in which [3]radialene **1** is obtained from functionalized three-membered ring compounds, cyclobutane derivatives serve as starting materials for [4]radialene (**2**). In fact, all presently known syntheses of **2** employ cyclobutane precursors as starting materials (Scheme 7). Whereas the fourfold β-elimination in **57** is unsatisfactory, HBr elimination from **58** is preparatively useful, especially in its gas-phase variant.[48] The 1,4-dehalogenation of **59**, which in turn may be prepared from 1,5-

The synthetic potential of bis(alkylidene)cyclobutanediones and tris(alkylidene)cyclobutanones for preparing [4]radialenes is amply illustrated by the transformation of **65** and **66** into the four- to sevenfold phenyl-substituted radialenes **67**–**69** and **70**, **71**[54] (Scheme 9). In view of the simplicity of the synthetic steps it is surprising that this route has not been used more often so far. Octaphenyl[4]radialene could not be prepared by this approach, though (see below).[54]

A bis(ethyne) variant of the reductive 1,4-dehalogenation **59** → **2** is provided by the transformation of **73** into **74**.[55] The precursor **73** may be readily prepared from **72** by a

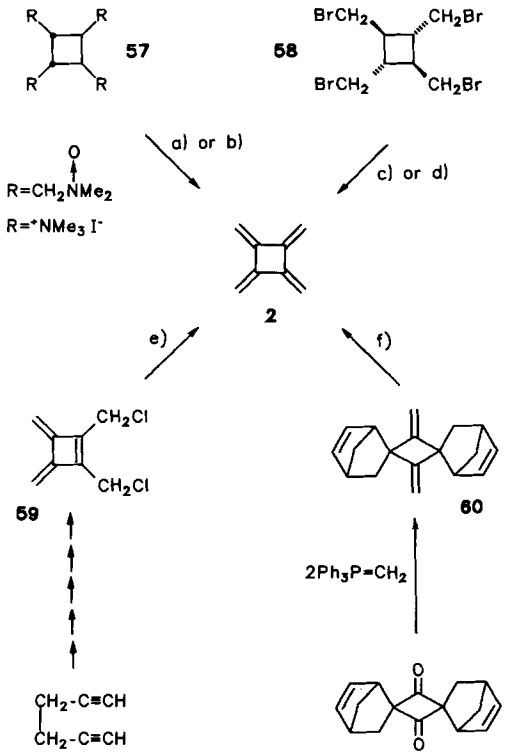

Scheme 7. Preparation of [4]radialene **2**. a) 250 °C, vacuum, 1–2% [7]; b) 115 °C; **2** isolated impure [7]; c) NaOEt, EtOH, 0 °C, > 50% [7]; d) KOH, 150 °C [48, 49]; e) Zn, $BuOCH_2CH_2OCH_2CH_2OBu$, 50 °C, 77% [50]; f) 680 °C, 5×10^{-5} Torr (flash vacuum pyrolysis), 65% [51].

palladium-catalyzed C–C coupling reaction (Scheme 10). Moreover, this method seems to offer many opportunities to vary substituents.

5,6,7,8-Tetravinyl[4]radialene **76** owes its existence to a rather unusual series of steps (Scheme 11). It is formed from the tricyclic cyclobutadiene derivative **75** by consecutive elec-

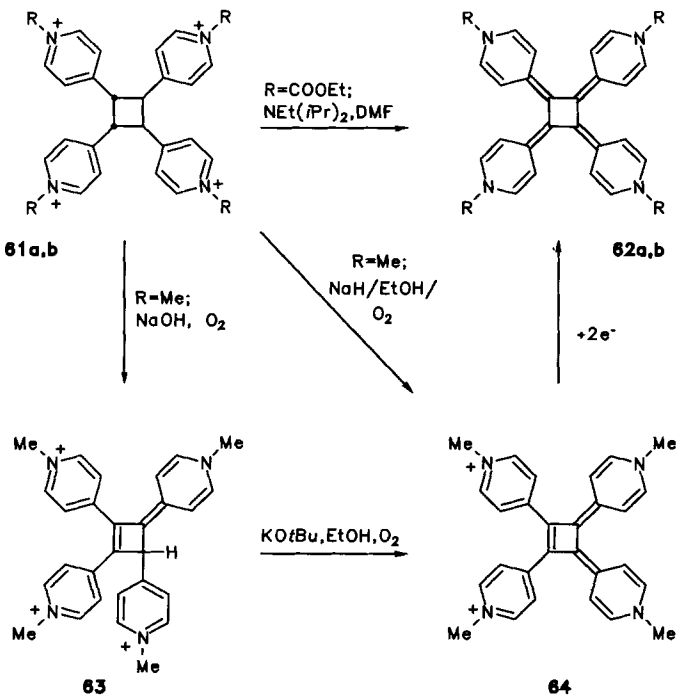

Scheme 8. Preparation of substituted [4]radialenes by elimination reactions. **61a**, **62a**: R = COOEt; **61b**, **62b**: R = Me, DMF = *N*,*N*-dimethylformamide.

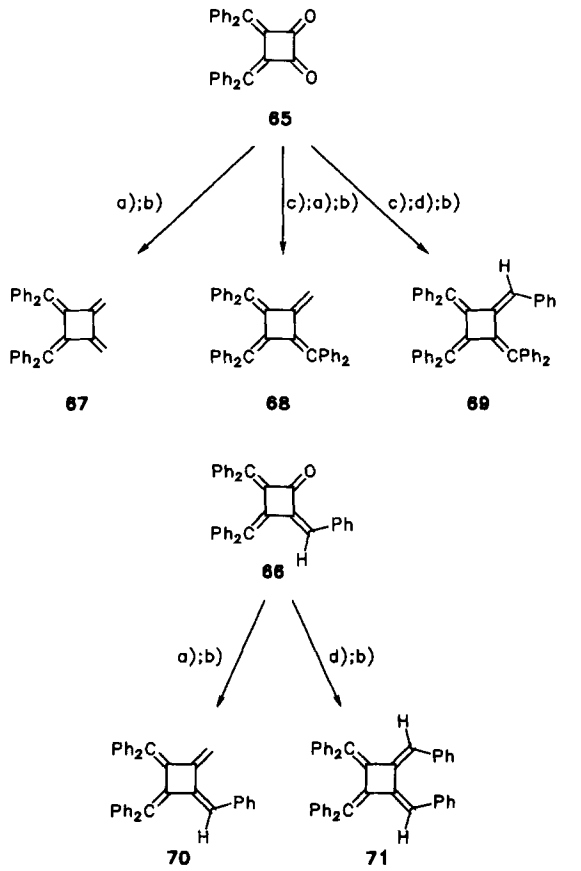

Scheme 9. Synthesis of [4]radialenes from the alkylidenecyclobutanones **65** and **66**. a) MeMgI; b) PBr_3 · pyridine; c) $Ph_2C{=}C{=}O$, Δ; d) $PhCH_2MgCl$.

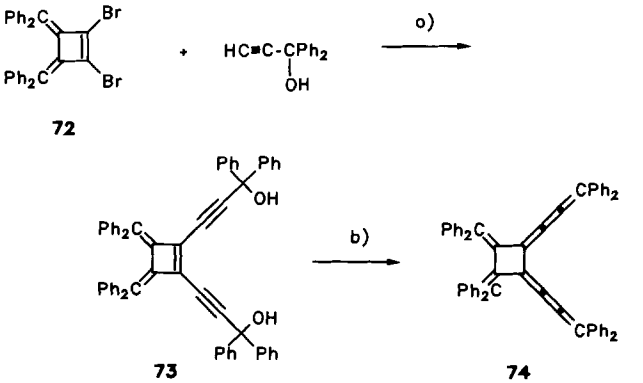

Scheme 10. Synthesis of the [4]radialene **74**. a) $[PdCl_2(PPh_3)_2]$, CuI, Et_3N, 95 °C; 73%. b) $SnCl_2 \cdot 2\,H_2O$, HCl, ether, −50 °C; 68%.

trocyclic ring openings of the two cyclooctatriene rings. Since **76** starts to polymerize slowly under the conditions of its formation, it could not be isolated in pure form. Its structure was established by NMR spectroscopy.[56]

If the thermal [2 + 2] cyclodimerization of allenes is taken as model, the higher [*n*]cumulenes should be ideal precursors for [4]radialenes, especially since butatrienes and their higher homologs are known today in considerable number.[57] However, the parent compound has already been a disappointment. On thermal activation butatriene does not dimerize to **2**, but provides, inter alia, 1,5-cyclooctadiyne.[58] Silyl-, stannyl- and germyl-substituted butatrienes do not undergo any thermal dimerization whatsoever.[59] Two re-

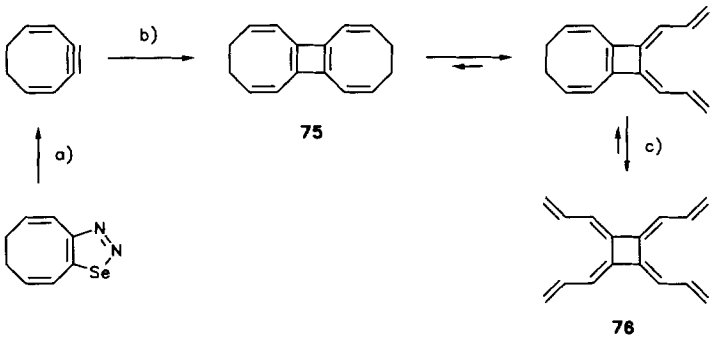

Scheme 11. Synthesis and valence isomerization of 5,6,7,8-tetravinyl[4]-radialene **76**. a) Cu powder, 180 °C; b) chloroform, $t_{1/2}$ (27 °C) = 2 h; c) several days.

ports describing thermal dimerization of butatriene derivatives to [4]radialenes had to be corrected after an X-ray structural analysis of the products was carried out. Thus the cumulenes **77**[60] (on irradiation in the solid state) and **78**[61] (thermally) do not dimerize via their central double bond but by way of their terminal C=C bond, to provide a head-to-tail dimer in the former, and a head-to-head dimer in the latter case.

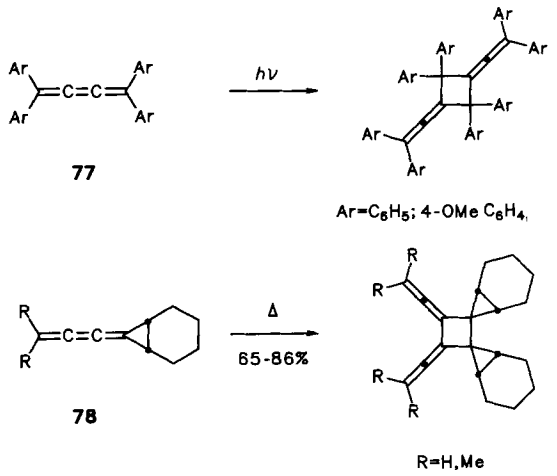

Acyclic butatrienes apparently only dimerize thermally to [4]radialenes if they carry electron-accepting substituents. This is at least borne out by the successful syntheses of **79**[62] (100 °C, 49%), **80**[63] (150 °C, 25%), and **81**[64] (110–120 °C, solid state, 75%) from the corresponding [3]cumulenes.

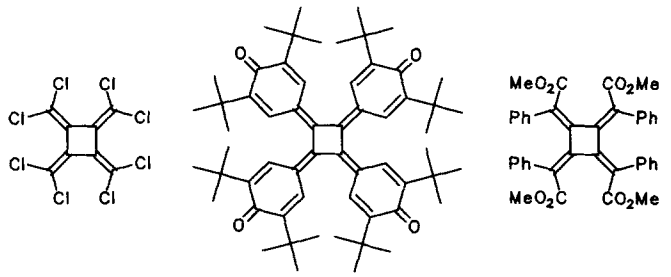

The thermal activation of [4]- and [5]cumulenes (Scheme 12) leads to radialenes in some cases (**83**,[65] **84**[66,67]); in others different cyclodimers are obtained (**82**[68], **85**[61,69]). The reasons for this divergent behavior are unclear, especially since the changes in the substituents of **82** and **83** appear to be marginal at first glance.

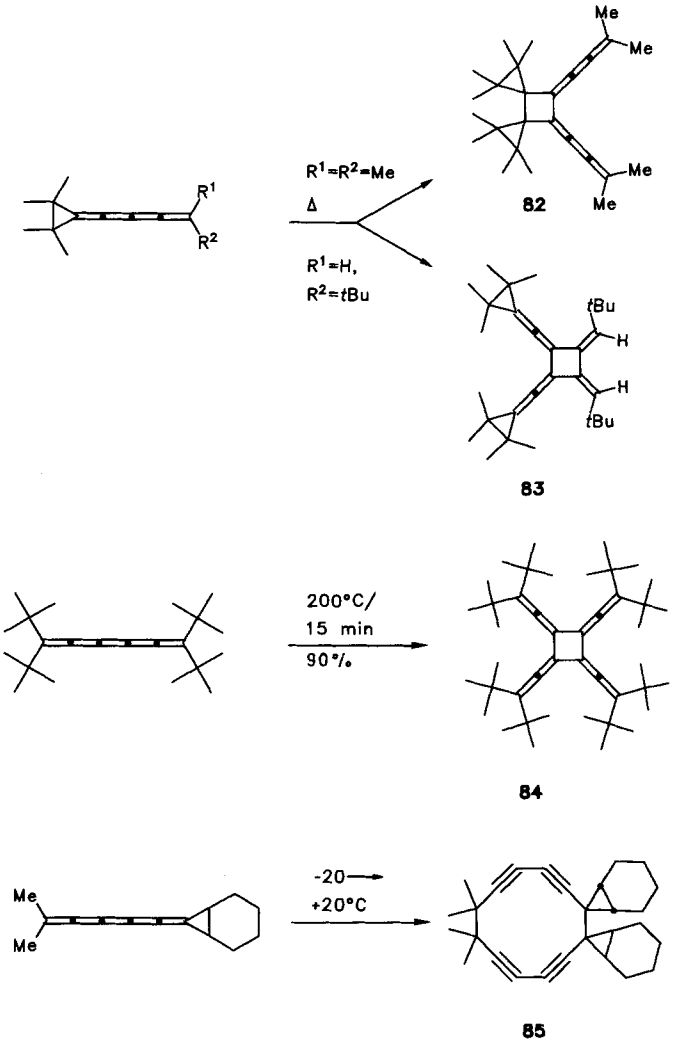

Scheme 12. Radialenes by thermal dimerization of [4]- and [5]cumulenes.

Cyclic 1,2,3-trienes show a behavior as complex as that of their acyclic counterparts. The smallest cyclic [3]cumulene isolated so far, 1,2,3-cyclononatriene, polymerizes when its solutions are concentrated.[70] 1,2,3-Cycloheptatriene, generated as a reactive intermediate, does not dimerize thermally to the corresponding [4]radialene,[71] but does so in the presence of Ni^0 as will be shown below. On the other hand irradiation of [10](9,10)anthracenophane-4,6-diyne (**86**) quantitatively yields the [4]radialene derivative **88**. It is safe to assume that its formation rests on the dimerization of the 1,2,3-cyclooctatriene **87** produced as an intermediate.[72]

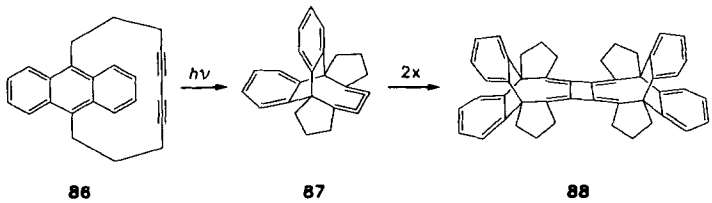

A completely unexpected observation was made when the (1-diazo-2-oxoalkyl)silanes **89** were decomposed either photochemically or in the presence of transition-metal catalysts; the tricyclic [4]radialenes **92** were produced as the sole products.[73] Presumably the silaheterocycles **90** and **91** are passed en route as shown in Scheme 13. The 1,3-dioxa-2-sila-4,5,6-cycloheptatriene **91** could at least be trapped as a [2 + 4] cycloadduct with furan.

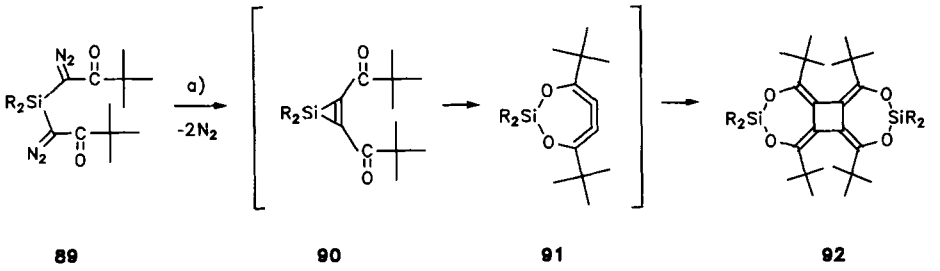

89 **90** **91** **92**

Scheme 13. Postulated intermediates during the formation of the [4]radialenes **92** from **89** (R = Me, *i*Pr). a) Catalysis by either CuO_3SCF_3 or $Pd(OAc)_2$; R = Me: 38–40%; R = *i*Pr: 5–9%).

West et al.[74] opened up a new, efficient, and apparently widely applicable route to [4]radialenes with the Ni^0-catalyzed dimerization of **93** to **80**, (R = *t*Bu, Z = C=O), which was first imitated in the conversion of **94** to **95** (R = Me, Z = CMe_2).[75] Depending on the nature of the substituent(s) of the [3]cumulene the following catalyst systems were shown to be particularly effective: $[Ni(CO)_2(PPh_3)_2]$, $[Ni(PPh_3)_4]$ (usually produced in situ by reduction of $[NiBr_2(PPh_3)_2]$), and $[Ni(cod)_2]$ (cod = 1,5-cyclooctadiene). Conditions and yields for the conversion **93** → **80** are as follows: $[Ni(PPh_3)_2(CO)_2]$ (5 mol%), benzene, 80 °C, 4 h, 95%; $[Ni(PPh_3)_4]$ (20 mol%), benzene, 80 °C, 18 h, 50%; for the purely thermal cyclodimerization the yield is 25% (see above).

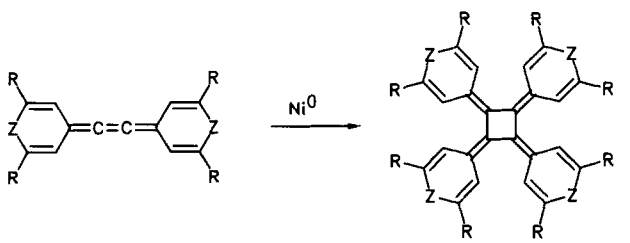

93 **80**
94 **95**

Under the influence of Ni^0 even butatriene derivatives dimerize which cannot be thermally induced to form [4]radialenes, for example, 1,2,3-cycloheptatriene (**96** → **97**[76]) and tetramethylbutatriene.[77, 78]

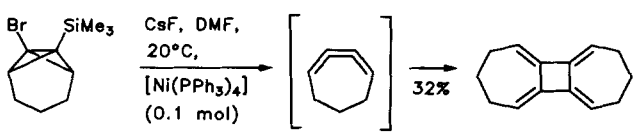

96 **97**

In the latter case a delicate balance exists between cyclodimerization and cyclotrimeriziation. Whereas both $[Ni(PPh_3)_4]$ and $[Ni(CO)_2(PPh_3)_2]$ invariably lead to mixtures in which the [6]radialene predominates,[77] with $[Ni(cod)_2]$ as the catalyst the choice of the solvent alone can determine whether the [4]- or [6]radialene is the major product[78] (Scheme 14, Table 1). A spotlight on the mecha-

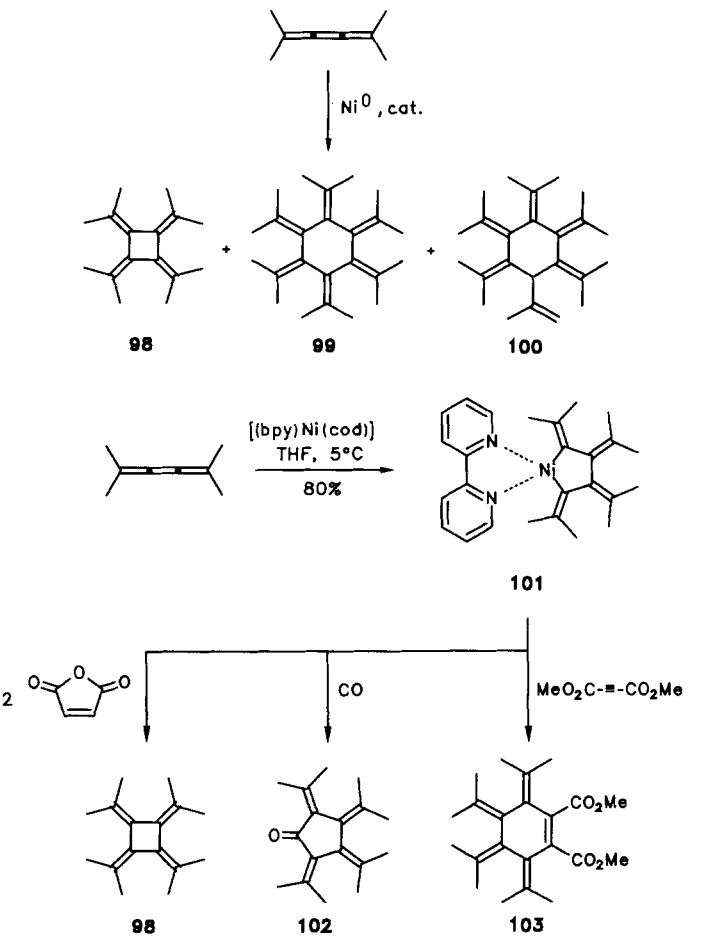

98 **99** **100**
101
98 **102** **103**

Scheme 14. Ni^0-mediated cyclooligomerization of tetramethylbutatriene.

Table 1. Reaction conditions and yields for the Ni^0-catalyzed cyclooligomerization of tetramethylbutatriene to **98**–**100**.

Ni^0 catalyst	Solvent	*T* [°C]	Yield [%]		
			98	**99**	**100**
$[Ni(PPh_3)_4]$	benzene	50	7	–	19
$[Ni(PPh_3)_4]$	DMF	50	2	14	12
$[Ni(CO)_2(PPh_3)_2]$	benzene	80	7	2	30
$[Ni(cod)_2]$	toluene	20	–	–	–
$[Ni(cod)_2]$	DMF	20	–	–	–

nism of the reaction is provided by the 1:1 reaction of tetramethylbutatriene with [(bpy)Ni(cod)] (bipy = 2,2'-bipyridine).[79] Under these conditions the metallacycle **101** is isolated, from which octamethyl[4]radialene **98** is formed in high yield by reductive elimination of the metal atom. Replacing the nickel atom by CO (→**102**) or acetylene dicarboxylate (→**103**) is also possible. Products of type **102** ("6-oxa[5]radialenes") are occasionally also formed during the $[Ni(PPh_3)_2(CO)_2]$-catalyzed cyclodimerization of higher cumulenes (see below). Synthesis and reactivity of the nickel heterocycle **101** support the reaction mechanism shown in Scheme 15[77b] for the Ni^0-initiated cyclodimerization and cyclotrimerization of [3]cumulenes.

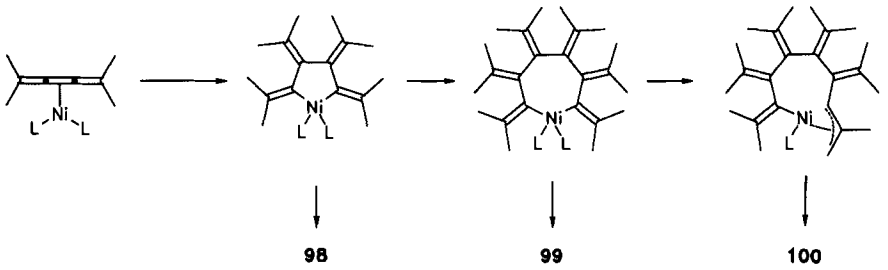

Scheme 15. Mechanistic details of the Ni-mediated cyclooligomerization of [3]cumulenes. L = PPh_3, $PnBu_3$.

The regioselectivity of the Ni^0-initiated cyclodimerization of the hexapentaenes strongly depends on the type of substituents present, as is the case for the thermal variant (Scheme 16[55, 67, 80]). A steric influence is undeniable here. Thus the tetra-*tert*-butyl derivative exclusively dimerizes via its central double bond (although **104** is obtained more efficiently by the purely thermal dimerization, see above), whereas the sterically less demanding substituents allow the dimerization to take place at the lateral sp–sp double bond. Whether in this case the head-to-head (**105**) or the head-to-tail dimer (**106**) is produced, appears again to be a question of the steric circumstances. The formation of the oxaradialene **107** evidently only occurs with those cumulenes for which the radialene formation requires forcing reaction conditions.

A logical extension (Iyoda et al.[77]) of the cyclodimerization of butatrienes shown in Scheme 14 has considerably extended the preparative possibilities of radialene synthesis. In this approach 2,3-dihalo-1,3-butadienes or 1,4-dichloro-2-butynes are dehalogenated with Ni^0 complexes to the corresponding butatrienes, and the latter transformed by the same nickel complexes to [4]- and [6]radialenes, respectively. This one pot variant, in which the cumulene is generated in situ and subsequently cyclooligomerized, provides far better yields than the process shown in Scheme 14. Yields and product ratios depend critically on the nature of the Ni^0 catalyst, the solvent, and the kind of halogen substituent of the substrate.[77b] For example, best results for the preparation of **98** were obtained when 3,4-dibromo-2,5-dimethyl-2,4-hexadiene is treated in THF with a catalyst generated in situ from $[NiBr_2(PPh_3)_2]/Et_4NI/Zn$ (0.5:2:5; 72% **98**, 1% **99**, 7% **100**). On the other hand, with $[Ni(PPh_3)_4]$ (67 mol%), prepared in situ from $[NiBr_2(PPh_3)_2]/Zn/PPh_3$ the same diene in DMF mainly yielded the [6]radialene (5% **98**, 63% **99**).

Iyoda's method has also been employed to synthesize several new peralkylated [4]radialenes.[77b] Very electron-rich [4]radialenes are available by this route as well.[81–84] Thus the purple–brown tetrakis(1,3-dithiol-2-ylidene)cyclobutane **110** has been prepared by both cyclodimerization of **108**[81] and cyclization of **109**[82] (Scheme 17).

1,1-Dibromoalkenes may also serve as precursors for [4]radialenes. However, the success of the Ni^0-initiated (for

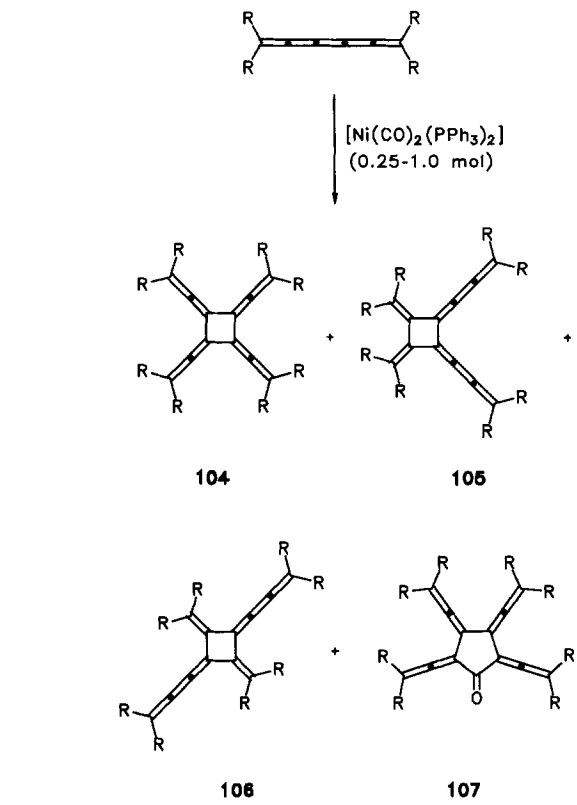

R,R	Aryl,Aryl	*t*Bu,*t*Bu			
Products	**105**	**107,104**	**106**	**106**	**104,107**

Scheme 16. Ni^0-mediated cyclooligomerization of [5]cumulenes.

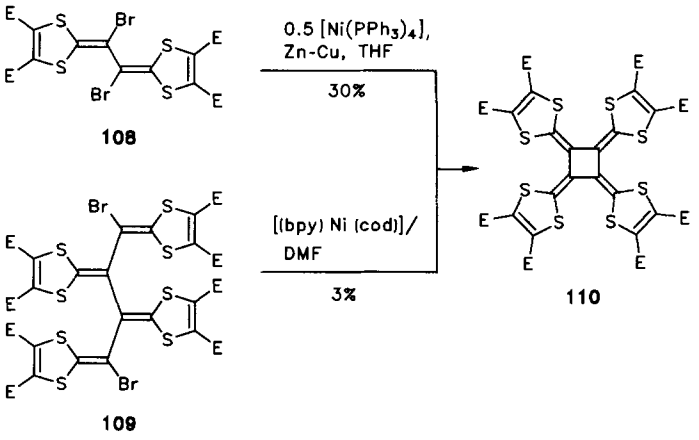

Scheme 17. Preparation of electron-rich [4]radialenes. E = COOMe.

mal) cyclotetramerization is only fair at best.[47, 77b] More suitable starting materials are the lithium bis(1-bromoalkenyl)cuprates. Depending on the Cu^{I} compound and the molar ratios, the thermal decomposition of these carbenoids leads to their (formal) dimers, cyclotetramers, and cyclopentamers (Scheme 18). This is the only known method for the preparation of octaphenyl[4]radialene (**112**).[85] Considerable amounts of tetraphenylbutatriene **111** are also formed (the

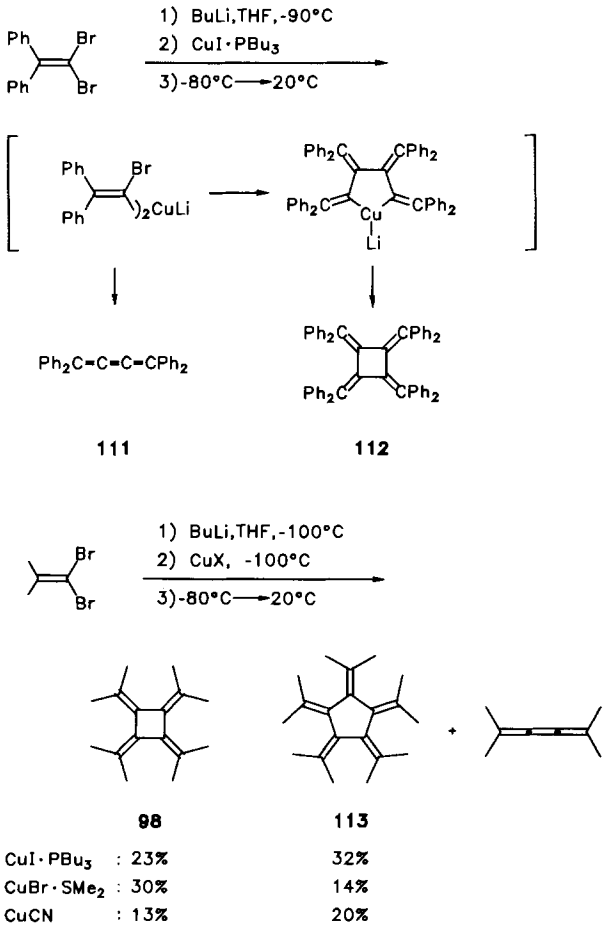

Scheme 18. The copper carbenoid route to [4]- and [5]radialenes.

Ni^{0}-catalyzed dimerization of **111** could not be achieved[77b]. When 1,1-dibromo-2-methylpropene is the starting material, the formation of octamethyl[4]radialene (**98**) competes with that of decamethyl[5]radialene (**113**).[86]

2.3. [5]Radialenes

The parent compound **3** is still unknown. Several attempts to prepare it either in analogy to [4]radialene by multiple β-elimination of suitably functionalized cyclopentane derivatives[87] or by a retro-Diels–Alder decomposition[88] have failed so far. The first derivative, decamethyl[5]radialene (**113**), has been synthesized by the formal cyclopentamerization of nickel[47] or copper carbenoids (Scheme 18).[86] However, the scope of this method for the preparation of other [5]radialenes appears to be limited, since with growing size of the substituents [4]- and [3]radialenes become the preferred reaction products.[47] The preparation of pentakis(1,3-benzodithiol-2-ylidene)cyclopentane (**114**) starting from **108** has also been accomplished.[89]

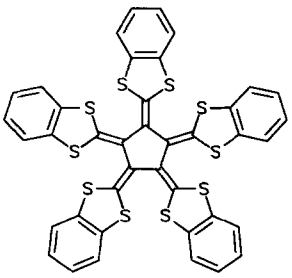

114

2.4. [6]Radialenes

Hexaethylidenecyclohexane **117** (all-*E*-7,8,9,10,11,12-hexamethyl[6]radialene) is regarded as the first [*n*]radialene to be reported in the chemical literature. It was prepared in 1961 by treatment of the hexachloride **115** or the hexabromide **116** with magnesium in methanol.[4, 90]

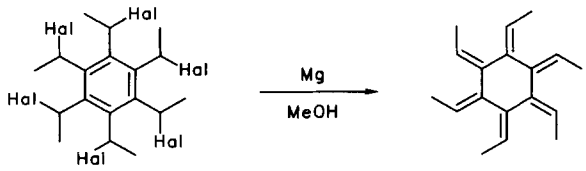

115: Hal = Cl
116: Hal = Br

117

Since for the generation of the hydrocarbon six halogen–carbon bonds have to be cleaved, the isolated yields of **117** (ca. 30%) are acceptable. If, instead of **116**, the corresponding hexabromohexa-*n*-propylbenzene derivative is employed, the hexaethyl[6]radialene (hexapropylidenecyclohexane) corresponding to **117** is isolated.[91] According to the authors[91] the hexaalkyl[6]radialenes prepared by this

route are stereochemically homogeneous and exist in the shown "waterwheel" configuration. Whereas the latter has been confirmed for **117** by an X-ray structural analysis (see Section 3.1), the question whether other diasteromers are also formed in the above elimination reactions should be reinvestigated with the more sensitive analytical techniques of today. This aspect would also be of interest in view of the conformation and configuration of the substrates and the reaction mechanism. Finally, the generalization of this altogether very convenient method is desirable. The hexaalkyl[6]radialenes are stable solids, which may be sublimed and manipulated in the presence of air.

This behavior contrasts strongly with that of the parent hydrocarbon [6]radialene (**4**), for which in short succession several methods of preparation were published (Scheme 19).[8, 9, 10] While the thermal isomerization of 1,5,9-

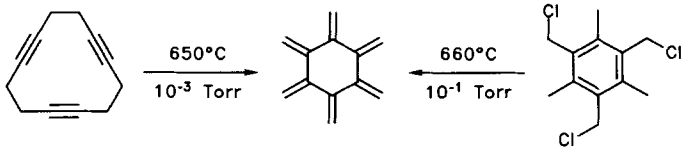

118 **4** **119**

Scheme 19. Preparation of [6]radialene **4**.

cyclododecatriyne **118** to **4**[8, 92] has negligible practical importance because of the difficulties in obtaining the starting material **118**, the thermal dehydrochlorination of the commercially available 2,4,6-tris(chloromethyl)mesitylene, a process discovered practically simultaneously by two research groups,[9, 10] constitutes a preparatively useful method. Since reproducible yields of up to 48% are obtained, **4** has become the starting material for other transformations, which will be reported in Chapter 4.3.[93]

The thieno-condensed [6]radialenes **27**[25] and **28**[26] have already been mentioned in the Introduction. Benzene[1,2-*c*:3,4-*c'*:5,6-*c'*]trithiophene (**121**), which may be prepared from hexakis(bromomethyl)benzene (**120**) by conventional transformations[94] (DDQ = 2,3-dichloro-5,6-dicyano-*p*-benzoquinone), belongs to the same class of compounds.

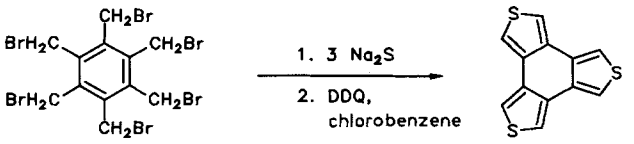

120 **121**

In spite of the successes already mentioned (see Scheme 14, preparation of **99**), the formation of [6]radialene derivatives[77-79] by Ni^0-catalyzed trimerization of [3]cumulenes is at present only of limited practical importance. Although experimentally this route is undemanding, its scope has not been investigated, and it suffers form lack of selectivity and the formation of secondary products (hydrocarbon **100** in the above case). Whether Iyoda's in situ method (see above, Section 2.2), which allows the preparation of permethyl[6]radialene from 3,4-dibromo-2,5-dimethyl-2,5-hexadiene in excellent yields (63%),[77b] can be developed further remains to be seen. Sobering is the observation that the diiodide **122** cannot be converted to the hydrocarbon **123**,[77] but

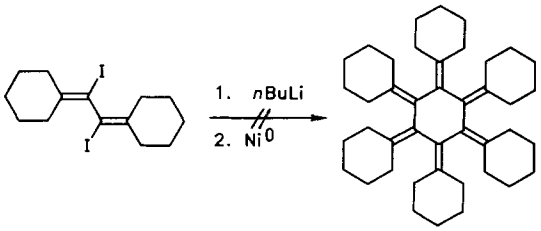

122 **123**

stimulating the fact that the dibromide **108**, which has already been mentioned several times, may be trimerized with $[Ni(PPh_3)_4]$/Zn–Cu in DMF in acceptable yields (35%) to hexakis(methoxycarbonyl)hexakis(1,3-dithiol-2-ylidene)-cyclohexane (**124a**).[96] The benzo-annelated derivative **124b** was prepared by an analogous route and indeed in 72% yield.[96]

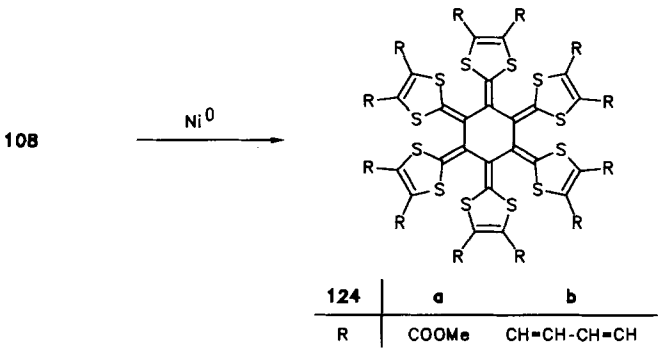

124	**a**	**b**
R	COOMe	CH=CH-CH=CH

2.5. Higher Radialenes

The chapter of the "higher" radialenes practically constitutes an empty page at the present time, since radialenes with a larger "circumference" than the six-membered ring are

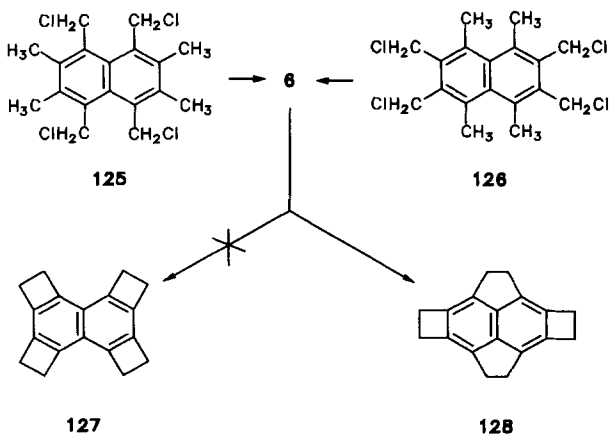

125 **126**

127 **128**

Scheme 20. Generation of naphtharadialene **6**.

unknown. Hart's „naphtharadialene"[13, 97] (1,2,3,4,5,6,7,8-octamethylene-9,10-didehydrodecalin, **6**) still counts as the sole representative of this group of radialenes; it is formed as a reactive intermediate by thermal gas phase dehydrochlorination at 620 °C and 10^{-4} Torr from either the tetrachloride **125** or its isomer **126** (Scheme 20). Evidence for the intermediate generation of **6** may be seen in the isolation of **128**, which is produced as the stable final product in ca. 15% yield in these pyrolyses. Since it was impossible to distinguish between **128** and the also conceivable isomeric hydrocarbon **127** by spectroscopic methods, the structure of **128** had to be secured by X-ray structural analysis.

3. Structure, Bonding, and Spectroscopic Properties

3.1. Structure and Bonding

According to electron diffraction measurements[98] as well as IR and Raman spectra,[99] [3]radialene **1** is a planar molecule with D_{3h} symmetry (see Section 3.3). From the vibrational spectra D_{4h} symmetry is derived for [4]radialene **2**.[49] The molecular symmetry and the conformation of the central ring for substituted radialenes may be inferred from a remarkably large number of crystal structure analyses (Table 2).

In hexamethyl[3]radialene the D_{3h} symmetry of the parent system is not noticeably perturbed. [4]Radialenes possess a planar cyclobutane ring as long as there is no steric strain between substituents. If this is the case, however, a more or less pronounced folding of the four-membered ring is caused, and the $>CR_2$ groups point alternately "up" and "down". The also conceivable structure of a planar ring with a propeller-type substituent arrangement has not been encountered as yet. So far for [5]- and [6]radialenes with the exception of the special case **28**, only structures are known in which steric hindrance between the substituents does not allow a planar radialene skeleton. The chair-type conformation of the sterically hardly hindered hexakis(ethylidene)cyclohexane seems to indicate that the parent molecule **4** prefers this conformation as well.

The high molecular symmetry of substituted radialenes in many cases may be inferred from their NMR, IR, and Raman spectra. An exception is provided, for example, by hexakis(methoxycarbonyl)[3]radialene, whose IR and Raman spectra indicate that the molecule—unlike the hexacyano derivative—does not have D_{3h} symmetry.[42]

The lengths of the exo- and endocyclic bonds of [4]radialenes and higher radialenes correspond to the values normally encountered for C=C and $C_{sp^2}-C_{sp^2}$ bonds, respectively. The endocyclic bonds in [3]radialene and its hexamethyl derivative show the expected shortening to approximately 1.45 Å, an effect which is also reproduced by ab initio calculations.[104, 105] The cyclic arrangement of the π systems of the radialenes led to early speculations on whether in these molecules a stabilizing or destabilizing cyclic electron delocalization was present as encountered in the annulenes. Numerous theoretical investigations involving especially π resonance energies (calculated according to different approaches[106]), total π-electron density indexes,[107] and the absolute and relative hardness[108] as criteria have been concerned with this problem. One result from these studies is that all radialenes are nonaromatic. The occurrence of localized endocyclic single bonds and exocyclic double bonds, as indicated by many calculations[109] as well as structural studies, in addition to the nonplanarity of the substituted higher radialenes clearly speak against the delocalization of the π-electron density.

The introduction of trigonal centers into three-membered rings leads to a pronounced increase in strain energy, whereas in the higher membered ring only small effects are observed.[110] A quantitative comparison of the parent compounds **1**–**4** has hitherto been impossible because of lack of experimentally determined thermochemical data. Only for **1** has an enthalpy of formation $\Delta H_f^0 = 396.12$ kJ mol^{-1} been determined from the fragmentation pattern of the molecular ion $\mathbf{1}^+$ generated by photoionization or electron impact (EI). From this value a strain energy of 226.3 kJ mol^{-1} could be derived,[111] a number which is 56 kJ mol^{-1} smaller than the one estimated from the increase in strain energy when going

Table 2. Structural data for radialenes [a].

Radialene	Molecular symmetry [b]	Ring conformation (folding angle [°])	Bond lengths [Å] [c] endocyclic	exocyclic	Ref.
[3]radialene (**1**)	D_{3h}		1.453(20) [d]	1.343(20) [d]	[98]
hexamethyl-[3]radialene (**50**)	(C_2) [e]		1.451(11) [d]	1.333(1) [d]	[100]
octamethyl-[4]radialene (**98**)	(D_{2d})	puckered	1.500(2)–1.512(8)	1.325(2)–1.339(2)	[78]
97	C_i	planar	1.484(2), 1.492(2)	1.326(2), 1.326(2)	[76]
83	C_{2v}	planar	[f]	1.29(2), 1.30(2)	[65b]
106 (R,R = 1,1,3,3-tetramethyl-2-indanylidene)	C_i	planar			[67]
octachloro-[4]radialene (**79**)	C_2 (D_{2d})	puckered (26.5)	1.466(5), 1.494(7)	1.326(5), 1.329(5)	[101]
heptaphenyl-[4]radialene (**69**)	–	puckered [g] (19.2)	1.478–1.505	1.351–1.359	[102]
octaphenyl-[4]radialene (**112**)	(D_{2d})	puckered (34.7)	1.504 [d]	1.347 [d]	[85]
81		puckered [h] (37.4)	1.494(4)–1.499(4)	1.334(4)–1.342(3)	[64]
110	(D_{2d}) [i]	puckered (19.1)			[81a]
92 (R = Me)	C_2	puckered (35.0)	1.494(3), 1.508(4)	1.324(3), 1.326(3)	[73a]
decamethyl-[5]radialene (**113**)	(C_2)	half-chair	1.496 [d]	1.349 [d]	[86]
dodecamethyl-[6]radialene (**99**)	C_i (D_{3d})	chair	1.504(2)–1.509(3)	1.339(2)–1.344(2)	[78]
hexakis(benzothiol-2-ylidene)cyclohexane	–	twist-boat [j]	1.49 [d]	1.34 [d]	[96]
hexakis(ethylidene)-cyclohexane (**117**)	(S_6)	chair	1.493(3)–1.495(2)	1.332(3)–1.337(3)	[103]
28	C_i	planar	1.439–1.452	1.363–1.376	[25]

[a] Obtained by crystal structure analyses; data for **1** from gas-phase electron diffraction. [b] The crystallographic symmetry is given; symbols in parentheses indicate an approximate, but noncrystallographic symmetry. The bond geometry of **1** has been derived with the assumption of D_{3h} symmetry. [c] Standard deviations are in parentheses. [d] Averaged values. [e] Deviations of the methyl carbon atoms from the least-squares plane for all C atoms are small (0.006–0.05 Å). [f] C_{allene}-C_{alkene} 1.50(2) Å; C_{allene}-C_{allene} 1.624(5) Å; C_{alkene}-C_{alkene} 1.596(5) Å. [g] Torsion angles $R_2C{=}C{-}C{=}CR_2$: −54.6, 41.7, −18.1, 27.7°. [h] Torsion angles $R_2C{=}C{-}C{=}CR_2$: 65.6° (averaged). [i] Ester groups not included. [j] This form is modified on heating (79 °C, xylene) into another one, in which the cyclohexane is likely to have a chair conformation.

from cyclopropane to methylenecyclopropane and assuming that this effect is additive when introducing the second and third double bond.[112]

3.2. Electronic Spectra

The long-wave UV absorption maxima of the parent compounds **1** and **2** (Table 3) show a pronounced bathochromic shift relative to the maximum for 1,2-dimethylenecyclopropane (λ_{max} = 232 nm) and 1,2-dimethylenecyclobutane (λ_{max} = 248 nm), respectively. This corresponds to the influence of extended conjugation known from linear polyenes. In a qualitative way the differences mentioned may be rationalized by a PMO model (PMO = *P*erturbational *M*olecular *O*rbital), in which the π MOs of **1** and **2** are obtained by a linear combination of the π MOs of an s-*cis*-butadiene and an ethylene unit (→**1**) and two s-*cis*-butadiene units (→**2**);[23] for quantitative calculations of the electronic transitions in radialenes see [3, 113]. The short-wavelength absorption maximum of [6]radialene points towards a chair conformation of the molecule, in which extended conjugation between the π systems is impossible.

Table 3. UV absorption maxima of radialenes **1**, **2** and **4**, and long-wavelength absorption maxima of some substituted radialenes with extended π conjugation.

Radialene	Solvent	λ_{max} [nm] (lg ε)	Ref.
1	gas phase	289 (3.97 ± 0.09)	[114]
2	ethanol	208 (4.70 [a]), 263 (3.84), 271 (3.90), 281 (3.84), 296 (3.62)	[7]
4	hexane	220	[9]
38 (R = *t*Bu)	benzene	685 (4.68)	[35a]
39	chloroform	850 (4.18)	[36]
44	benzene	609 (4.80), 640 (sh, 4.25)	[41a]
45a	chloroform	557 (4.35)	[52]
52	CH_2Cl_2	615 (4.72), tailing up to 800 nm	[46]
80	cyclohexane	595 (4.35)	[63]
95	cyclohexane	496 (4.34)	[75]

[a] For the determination of the extinction coefficient, see ref. [7].

The UV spectra of the permethylated radialenes are very similar to those of the parent systems if one takes the bathochromic shift caused by the alkyl groups into account. As can be seen from Figure 1 the longest wavelength absorption maximum is shifted to shorter wavelengths with growing ring size. By extension of the π conjugation the longest wavelength absorption maxima may be shifted very far into the visible region. Several examples illustrating this point are given in Table 3.

The photoelectron spectra of **1**[114] and **2**[48] as well as those of the permethylated derivatives of [3]-,[115] [4]-,[116] and [6]radialene[117] have been measured and the electronic configurations of the various molecular ions have been assigned on the basis of MO calculations. Of importance for the ease of oxidation to the radical cation (cf. Section 4.5) is the observation that the substitution of the H atoms in [4]radialene by eight methyl groups causes a decrease of the first vertical ionization potential from 8.35 to 7.30 eV.

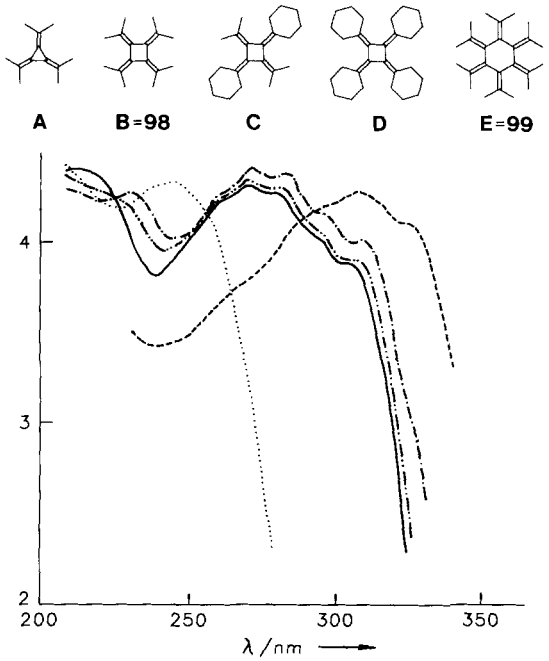

Fig. 1. Electronic spectra of peralkylated radialenes (from [77b]). – – –**A**, —**B**, – · · · · –**C**, – · – · –**D**, · · ·**E**.

3.3. IR and Raman Spectra

The IR and Raman spectra of **1**,[99b] **2**, and [D_8] **2**[49] as well as of octachloro[4]radialene[118] have been analyzed carefully. From these data the molecular symmetry of **1** and **2** could be established unequivocally. For **79** the solution spectra are compatible with D_{2d} symmetry, from which the molecule deviates only slightly in the crystalline state (see Table 2). Table 4 summarizes the C=C stretching modes and their assignments for **1**, **2**, **79**, and several peralkylated radialenes.[77b] The symmetrical stretching modes, which in the Raman spectra are observed at highest frequencies, are

Table 4. Intensity and assignment of C=C stretching modes in some radialenes.

Radialene		Symmetry	$\tilde{\nu}$ [cm^{-1}] [a, b]	
	1	D_{3h}	Raman [c]: IR [d]:	1800 (vs, A_1' (p)), 1620 (vs, E'(dp)) 1634 (w)
	2	D_{4h}	Raman [e]: IR [e]:	1681 (vw, A_{1g}(p)), 1662 (w, B_{1g}(dp)) –
	98	D_{2d}	Raman: IR:	1707 (vs, A_1 (p)), 1662 (m, B_2 (dp)), 1650 (s, E (dp)) 1658, 1645
		C_{2v}	Raman: IR:	1695 (vs), 1652 (m), 1647 (m), 1638(s) 1658, 1654, 1640
	79	D_{2d}	Raman [f]: IR [f]:	1610 (B_2 or E (dp)), 1596 (E or B_2 (dp)) 1611 (s), 1595 (vs)
	99	D_{3d}	Raman: IR:	1650 (vs, A_{1g} (p)), 1637 (s, E_g (dp)) 1639 (vw)

[a] Abbreviations: vs = very strong, s = strong, m = medium, w = weak, vw = very weak; p = polarized, dp = depolarized. [b] All spectra were measured for KBr pellets, unless stated otherwise. [c] Liquid, −65 °C. [d] Gas phase, room temperature. [e] Polycrystalline solid, −190 °C. [f] In CCl_4.

IR inactive for the examples shown. The high frequency of the symmetrical C=C valence vibration for **1** is found in the typical range for methylenecyclopropanes and dimethylenecyclopropanes (see for example reference [5b]). In [4]radialene this vibration is registered at only slightly higher frequency than that of alkenes of the general structure $R_2C{=}CH_2$ (1680–1630 cm^{-1}).

3.4. NMR Spectra

NMR spectroscopic data characterize the radialenes as typical alkenes (Table 5). Thus the exocyclic protons of **1**, **2**, and **4** appear at practically the same chemical shifts as those of ethylene. It is immediately obvious that there is no ring current effect—another indication that a cyclic delocalization of π electrons does not exist in the radialenes. In the ^{13}C NMR spectra of the parent molecules **2** and **4** the ring carbon atoms are shifted downfield by $\Delta\delta = 47$ and 35 relative to the shift of the exocyclic carbon atoms. The chemical shifts, however, do not differ very much from those of methylenecyclobutane ($\delta = 148.8$ and 105.2) and methylenecyclohexane ($\delta = 149.2$ and 106.9).[119] The substitution of the olefinic hydrogen atoms by methyl groups results in the typical substituent effects—deshielding of α- and shielding of β-carbon atoms. Both effects, though, are considerably less pronounced in the permethylated radialenes than in simple alkenes.

Table 5. ^1H and ^{13}C NMR chemical shifts of radialenes (in $CDCl_3$ or CCl_4).

Radialene	$\delta(^1H)$ $=CH_2$ or $=C(CH_3)_2$	$\delta(^{13}C)$ $C_{ring} = C_{exo}$		Ref.
[3]radialene **1**	5.24			[33b]
[4]radialene **2**	5.05 [a]	148.5	101.7	[50]
[6]radialene **4**	5.30	145.0	110.0 [b, c]	[9, 10]
hexamethyl-[3]radialene **50**	1.99			[5b]
octamethyl-[4]radialene **98**	1.80	138.3	115.6	[77b]
97	5.75 (=CH)	142.0	118.6	[76]
octaphenyl-[4]radialene **112**		139.3	132.0	[85]
decamethyl-[5]radialene **113**		138.6	122.6	[11]
dodecamethyl-[6]radialene **99**	1.63	136.8	122.6	[77b]

[a] 5.19 [7]. [b] $J(C,H) = 159$ Hz. [c] In $[D_8]$THF.

4. Reactivity

In Section 2 we mentioned the extreme sensitivity of the parent systems **1**,[6, 33b] **2**,[7, 50] and **4**[9] towards molecular oxygen (formation of oxygen-containing polymers) as well as their high thermal lability. Radialene **1** polymerizes in CCl_4 already at 0 °C, **2** undergoes dimerization in ethanol at 20 °C, and microcrystalline **4** may decompose violently even at 20 °C. Up to now, these unpleasant properties have greatly discouraged efforts to study the reactivity of these radialenes in a broad and systematic manner (perhaps with the exception of **4**), and have nearly completely precluded their use as building blocks in organic synthesis. The more highly substituted the radialenes are, the more stable they become; permethylated radialenes can be considered as perfectly stable under normal conditions (perhaps with the exception of the moderately oxygen-sensitive hexamethyl[3]radialene[5]).

Radialenes **1**, **2**, and **4** have in common a relative stability towards dilute mineral acids and strong bases. Their chemical behavior is dominated by addition of electrophiles and cycloaddition of electron-poor components; some differences exist, however, in the outcome of these reactions.[120] In the following, we shall discuss the characteristic reactions of the individual classes of radialenes separately, and then turn our attention to the interesting redox properties of functionalized radialenes.

4.1. Reactions of [3]Radialenes

On catalytic hydrogenation of [3]radialene (**1**) with Pd/C, ring-opening occurs and a mixture of 3-methylpentane and 3-methyl-2-pentene is formed. With a $Rh{-}Al_2O_3$ catalyst, a small amount of all-*cis*-1,2,3-trimethylcyclopropane was obtained besides the alkane mentioned and isomeric C_6H_{12} alkenes.[33b] The reaction with $PdCl_2 \cdot 2\,PhCN$ yields a sparingly soluble, structurally unidentified complex having the composition $C_6H_6Cl_2Pd$.[33b] No further reactions of **1** appear to be known.

When hexamethyl[3]radialene **50** is dissolved in trifluoroacetic acid, cation **129** is formed, which has been characterized by its electronic spectrum ($\lambda_{max} = 480$ nm).[121] In this respect, **50** resembles hexamethyl[6]radialene (see Section 4.3). With tetracyanoethylene (TCNE), **50** forms the [2 + 2] cycloadduct **130**; as intermediate, a violet-blue charge-transfer complex can be observed.[5b]

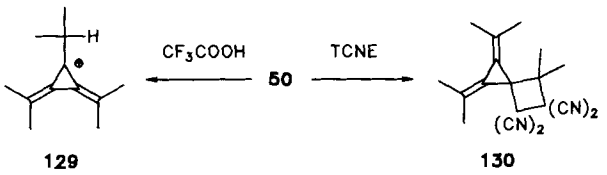

129 **130**

4.2. Reactions of [4]Radialenes

Among all radialenes reported so far, [4]radialene (**2**) is the most thoroughly studied, because of its comparably easy preparation (Scheme 7, Section 2.2) and its convenient manipulation. This hydrocarbon can be kept for an unlimited time at −78 °C, and because of its high volatility it can be easily transferred and dosed by the usual high-vacuum techniques.[7, 50]

As a twofold diene system, **2** lends itself as a component for repetitive Diels–Alder additions, and in their pioneering papers in the early sixties, Griffin and Peterson already reported [2 + 4] cycloaddition reactions with **2**.[7] Thus, [4]radialene reacts with TCNE as a dienophile to give the 1:1 adduct **131a** (0 °C, ethanol, 50% yield), and with *N*-phenylmaleimide; **131b** is obtained analogously (25 °C, 100%).

The 2:1 addition resulting in the tricyclic cyclobutadiene derivatives **132a** and **132b** is not observed. Even the more reactive dienophiles "*N*-phenyltriazolinedione" (4,5-dihy-

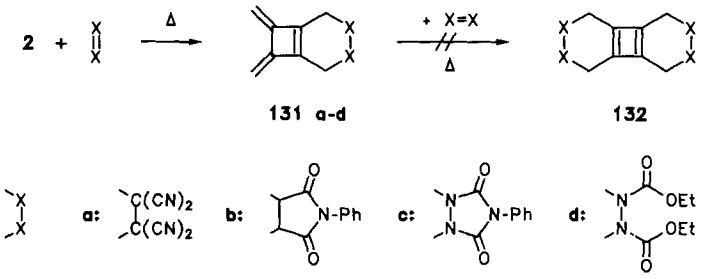

dro-4-phenyl-3*H*-1,2,4-triazol-3,5-dione, NPTD) and diethyl azodicarboxylate at −78 °C cannot overcome the activation barrier presented by the antiaromatic character of **132**, and the cycloaddition reaction again stops at the stage of **131 d** (90%) and **131 c** (46%), respectively.[50] When the temperature is raised to 20 °C, a reaction channel is opened for **2** that has already been observed at its original preparation, namely, a dimerization resulting in cyclooctadiene derivative **134**.

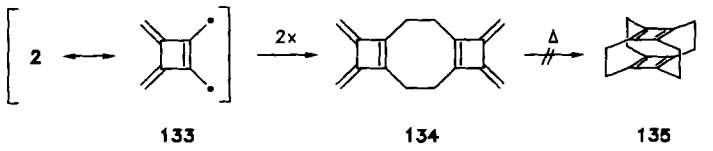

The latter reaction represents a formal [4 + 4] cycloaddition that is symmetry-forbidden as a concerted process. It is probably a stepwise, radical process[50] originating from the resonance structure **133**. Gas phase pyrolysis of **134** at 220 °C leads back to **2**;[87] the desired intramolecular cycloaddition yielding the [2.2.2.2]cyclobutadienophane **135** is avoided, presumably for the same reasons which explain the failure of **131** to act as a diene in the (intermolecular) Diels–Alder reaction.

Another type of cycloaddition, carbene addition to **2**, has provided a simple connection between the chemistries of radialene and rotane.[122] With dichlorocarbene ($:CCl_2$), generated from chloroform by the Makosza method, a product mixture is obtained in pentane (2 h, room temperature, 74% yield), from which the two bisadducts **136** (33%) and **137** (41%) can be isolated by chromatography.

When the product mixture is treated again with dichlorocarbene, trisadduct **138** (X = Cl, 54%) and octachloro[4]-rotane (**139**, X = Cl, 30%) are obtained; the alternating arrangement of the CCl_2 groups in **139** has been established by an X-ray crystal structure analysis.[122] Addition of dibromocarbene ($:CBr_2$) to **2** is not only distinctly slower, but it also stops at the stage of **136** and **137** (X = Br in both cases), apparently for steric reasons. Therefore, it is not surprising that methylene transfer to **2** with diazomethane/copper(I) chloride yields **138** and **139** (X = H in both cases). It should be mentioned, however, that better preparations of these hydrocarbons exist.[123]

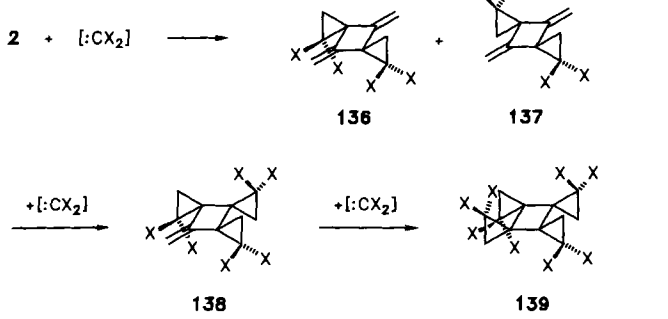

Hydrochlorination and hydrobromination (−78 °C, ether), as well as addition of bromine (−20 °C, CCl_4) were the first ionic reactions of **2** described.[50] These reactions, which yield trisadducts **140** (X = Cl: 68%; X = Br: 50%) and **141**

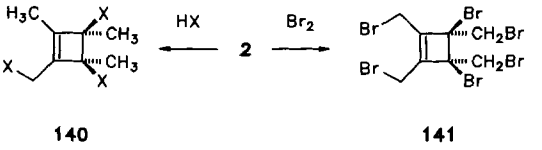

(68%) in good yields, can be interpreted as a 1,4-addition to one of the two 1,3-butadiene subsystems of **2**, followed by two 1,2-addition reactions. As expected, these polyhalogenated cyclobutenes undergo thermal isomerization to the corresponding butadienes by an electrocyclic ring-opening reaction.[50]

The high reactivity of **2** in solution or in the pure state contrasts with its high thermal stability in the gas phase: the tetraene survives flash pyrolysis in a quartz tube unchanged up to 850 °C! A transformation starts only at temperatures above 880 °C, from which mainly styrene (ca. 60%) and small quantities of phenylacetylene, *o*-xylene, toluene, and benzene are obtained. No mechanistic details of these far-reaching reorganizations of the carbon framework of **2** are known.[50]

Octamethyl[4]radialene (**98**) behaves towards TCNE analogously to the parent system **2** by readily yielding a Diels–Alder adduct of type **131 a**. Similarly, the corresponding 1:1 product **142** results from the reaction with NPTD, but in addition a 2:1 adduct is obtained that has the betaine-type constitution **143** according to an X-ray structural analysis.[78]

Another surprising result is provided, when **98** is treated with the cobalt complex **144**, since a catalytic rearrangement of **98** to 2-isopropenyl-1,3-diisopropyl-5-methylbenzene (**146**) is observed, rather than the expected exchange of the ethylene ligand. Whereas no intermediates for the conversion of **98** into **146** have been detected in toluene at 60 °C, the complex **145** is isolated when the reaction is carried out in THF at the same temperature, and it is considered as an intermediate of this very far-reaching isomerization.[124]

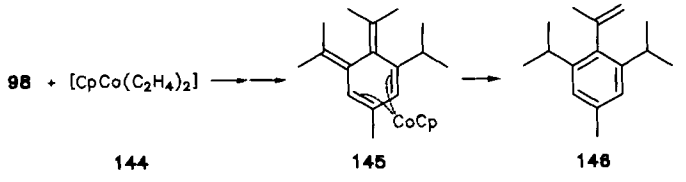

The highly functionalized [4]radialene **92** also displays a variety of partly surprising reactions. Hydrolytic cleavage of the silyl enol ether functionalities in an alkaline medium yields the all-*trans*-tetrapivalolylcyclobutane **147**, whereas acid catalysis leads to the pentacyclic polyether **148**, presumably via the all-*cis* isomer of **147**.[73a]

4.3. Reactions of [5]- and [6]Radialenes, and Higher Radialenes

Except for some findings such as the isomerization of the naphtharadialene **6** to **128** (Section 2.5), studies of the chemical behavior of the higher homologues of **2** have so far been limited to the [6]radialenes. Not very surprisingly, most results have been acquired for the easily accessible and stable alkyl derivatives of [6]radialene, for example **117**.

Just like [4]radialene (**2**), **117** is susceptible to ionic addition and (presumably concerted) [2 + 4] cycloaddition reactions (Scheme 22). In a reversal of its mode of formation, **117** is converted into hexabromide **116** quantitatively by addition of bromine.[4, 90, 126] The transformation may be formu-

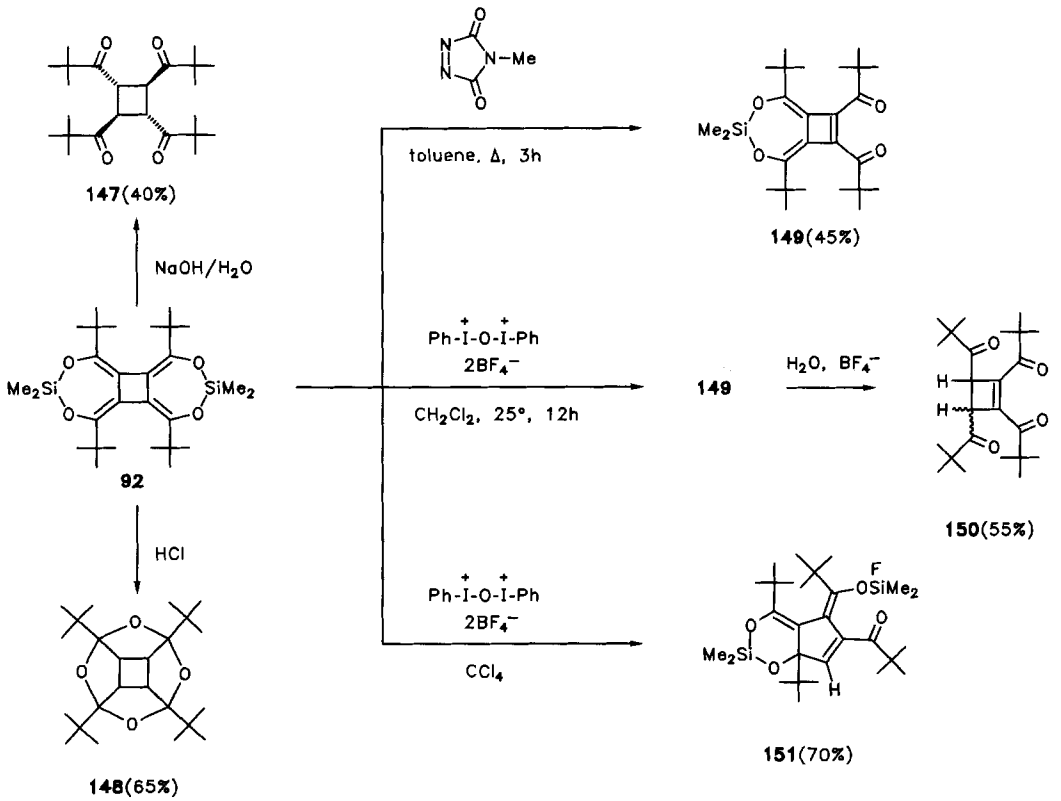

Scheme 21. Reactions of the electron-rich [4]radialene **92**.

Not surprisingly in view of its nonplanar diene units, **92** does not undergo [4 + 2] cycloaddition with *N*-methyltriazolinedione. Instead oxidative desilylation takes place to form **149**. Not unexpectedly, a repetition of this transformation, which would convert **149** into a cyclobutadiene, does not occur. The same oxidative desilylation of **92** also takes place with iodonium salt $(Ph\text{-}I^+\text{-}O\text{-}I^+\text{-}Ph) \cdot 2\ BF_4^-$ in dichloromethane, this time followed by a desilylation to yield **150**. Surprisingly, the bicyclic compound **151**, identified by an X-ray structural analysis, is obtained when the reaction is carried out in tetrachloromethane. Although the mechanistic details are not known, an impurity always present in the reagent seems to account for the reorganization of the molecular framework of **92** and formal addition of HF.[125]

lated as a sequence of 1,4-additions; this reaction mode also prevails on addition of hydrogen chloride or bromide to give **152** and **153**, respectively.[90] In highly acidic solutions (H_0 ranging from -5 to -7), the monoprotonated form of **117** is generated.[3] Diels–Alder reaction with **117** initially yields products **154**, which in principle can undergo a second cycloaddition to afford either angularly annelated (*meta*-type) or linearly annelated (*para*-type) 2:1 adducts.

Experimentally, various dienophiles—including *p*-benzoquinone, dimethyl acetylenedicarboxylate, acrylates, acryl- and crotonaldehyde,[127] besides the compounds shown in Scheme 22—lead only to the linear 2:1 cycloaddition products **155**. Monoadducts **149** most often cannot be isolated,[128] which is attributed at least in part to the reaction conditions applied. Under the harsh conditions originally used (reflux-

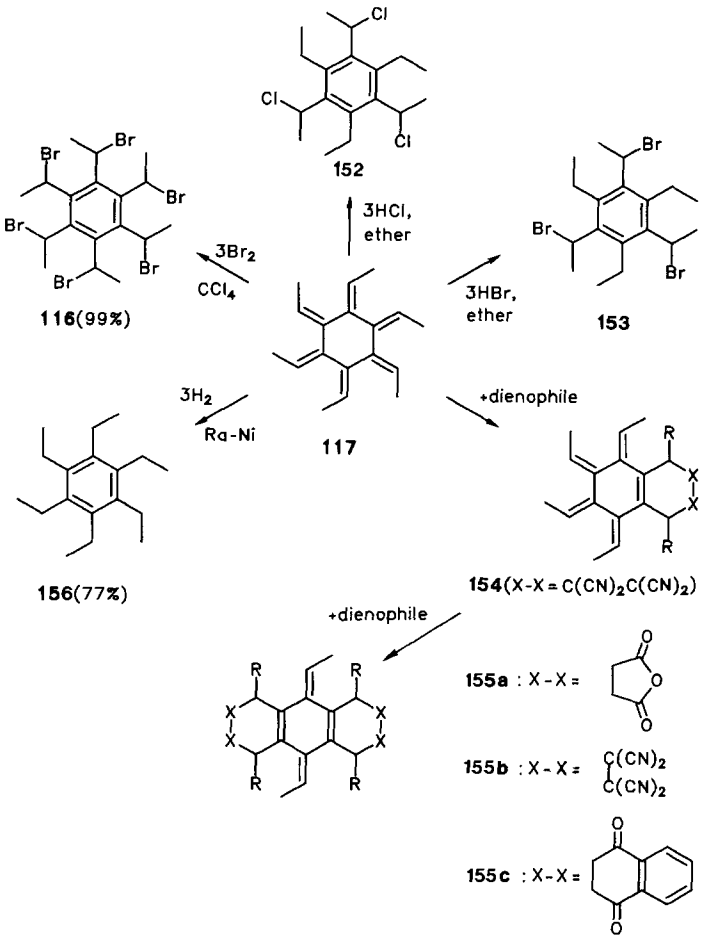

Scheme 22. Addition reactions with hexamethyl[6]radialene (117). Yields [%]: **155a**, 80; **155b**, 76; **155c**, 30. Ra-Ni = Raney nickel.

ing xylene, extended reaction times), only polymer resins were obtained,[90] whereas in low-boiling solvents (ether, tetrahydrofuran, benzene), the expected adducts were formed normally in good yield.[127, 128] Polymer formation is likely to be attributed to the fact that 2:1 adducts **155**, the linear rather than the angularly annelated constitution of which has been established both by spectroscopic methods and chemically,[129] are *p*-quinodimethane derivatives; the tendency of the parent *p*-xylylene to undergo oligomerization and polymerization is well known.[130] The absence of *o*-quinodimethane derivatives resulting from the *meta* addition mode is probably due to steric hindrance between the substituents. Addition reactions of hexaethyl[6]radialene (hexapropylidenecyclohexane) are analogous to those of **117**; however, since they proceed more slowly, 1:1 adducts such as **154** can be isolated without difficulty.[91] Catalytic hydrogenation of **117** yields hexaethylbenzene (**156**), as expected.[90]

The reactions of the sterically unbiased [6]radialene (**4**) are very similar to those of **117**. Hydrogenation leads to hexamethylbenzene,[8, 10] addition of dimethyl acetylenedicarboxylate yields **157**,[9] and an isomer mixture of **158** is obtained from the reaction with fumaroyl chloride followed by methanolysis.[9, 131] In contrast, the sterically shielded double bonds of dodecamethyl[6]radialene (**99**) are unreactive towards dienophiles, even towards the extremely strong dienophile NPTD.[78]

The reaction of **117** with tris(acetonitrile)tricarbonyl-

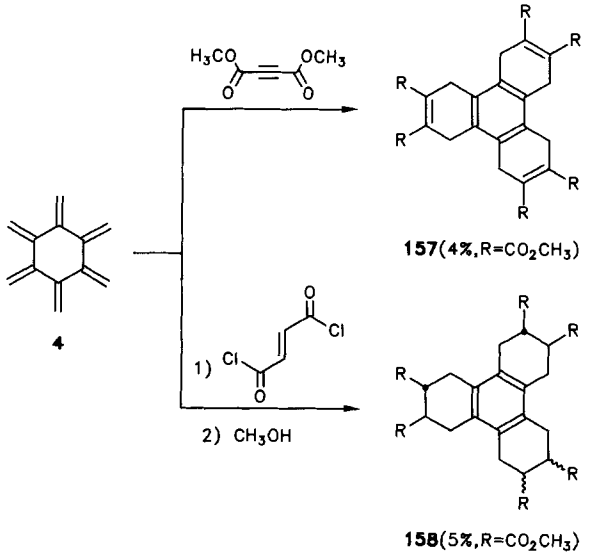

chromium in dioxane at ambient temperature produces **160** in good yield, and not the expected chromium complex **159**. The identity of the product, which is derived from the radialene by a twofold 1,5-H shift, has been established by X-ray structural analysis.[132]

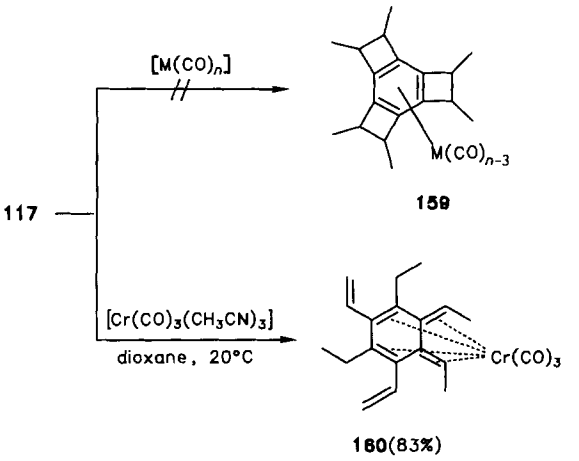

The tris(thiophene) compound **121** seems to be the only more complex [6]radialene that has aroused closer attention. Protonation with fluorosulfonic acid generates a dication with the structure **162a** or **162b**,[94] presumably via the monocation **161**, which is not observed.

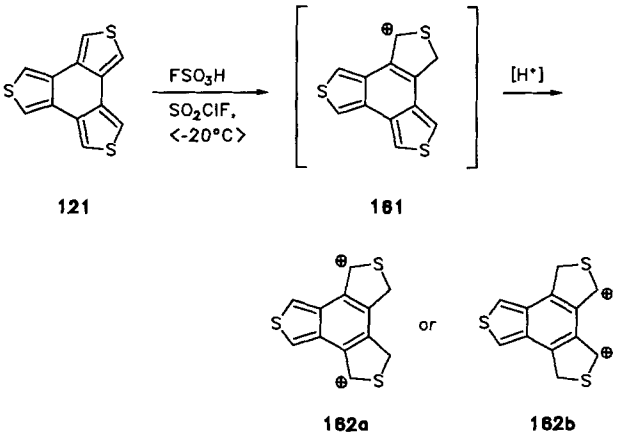

4.4. Redox Properties of Radialenes

Because of their cross-conjugated π system, the radialenes represent multistep redox systems; this feature has been investigated more intensively than any other aspect of their chemical reactivity. The ease of generating individual reduced or oxidized species and their stability depend on both the substituents at the radialene framework and the possibility of generating a planar π system in which the charge(s) can be delocalized as far as possible.

Thus, the parent compounds **1**, **2**, and **4** have been transformed by photoionization into the molecular cations in the gas phase (Section 3.2), but no electrochemical redox reactions in solution are known. For octamethyl[4]radialene (**98**) the first vertical ionization potential is significantly lower than for **2** (Section 3.2), and as expected, **98** is more easily oxidized to the radical cation. However, the kinetic instability of the radical ions in solution at room temperature is indicated by the irreversibility of both the oxidation step (+1.3 V vs. saturated calomel electrode (SCE)) and the reduction step (−2.6 V)[116] in the cyclic voltammogram. Nevertheless, the radical anion and the radical cation have been generated under the conditions indicated in Scheme 23

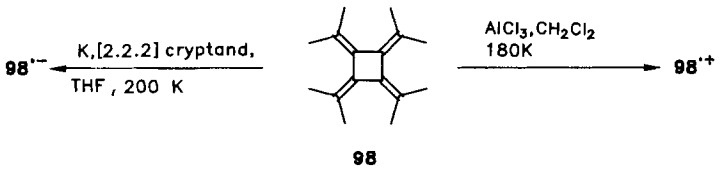

Scheme 23. Oxidation and reduction of **98**.

and have been characterized by their nearly congruent ESR and ^{1}H electron nuclear double resonance (ENDOR) spectra.[116, 133]

The stability of the radical cations of peralkylated [3]radialenes is similar to that of **98**. For example, the radical cation of hexamethyl[3]radialene (**50**) has been generated in an organic glass by γ irradiation, whereas the radical cation of tris(2-adamantylidene)cyclopropane is formed irreversibly under the conditions of cyclic voltammetry.[47b]

The ability of substituents to stabilize individual redox species is illustrated for substituted [4]radialenes in Table 6. The possibilities range from the as yet unknown, extremely electron-poor octacyano[4]radialene (**163**), whose dianion has been isolated as a stable tetrabutylammonium salt, to the electron-rich [4]radialenes tetrakis(1,4-dihydropyridin-4-ylidene)- and tetrakis(1,3-dithiol-2-ylidene)cyclobutane, which can donate up to four electrons. In between is the five-step redox system of **95**, for which fully reversible one-electron transfers between the dianion and the dication can be realized. Only in the case of **62a** is the stepwise oxidation to the cyclobutadiene **62aD** bearing four cationic substituents fully reversible (Scheme 24). In the redox equilibrium **62aC** ⇄ **62aD**, the radical trication dominates (> 99.99%); this species as well as the dication **62aB** (a squaric acid derivative) most likely represent fully delocalized systems.

Acceptor-substituted radialenes in general can be reduced easily to the radical anion and the dianion. Typical examples

Table 6. Observed redox stages of substituted [4]radialenes A (• = initial charge state of the radialene; the numbers are the potentials in volt versus Ag/AgCl. Figures in parentheses indicate irreversible electron transfer steps.

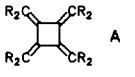

CR_2		charge state: −2	−1	±0	+1	+2	+3	+4	Ref.
$C(CN)_2$	163	1.25[a]							[134]
CH_2	2	[b]			[c]				
CMe_2	98			(−2.6)[a]	(1.3)[a]				[116]
	80		−0.35	−0.05					[63]
	95		−2.11	−1.64	+0.62	+0.67			[75]
	62b				−0.68[d]	−0.73[d]	(+0.26)		[52b]
	62a				+0.12[d]	+0.08[d]	+0.88	+1.39	[52b]
	164				+0.20[d]	+0.24[d]	(+0.98)	(+1.30)	[81a]
	110				+0.65[d]	+0.70[d]	(+1.29)	(+1.79)	[81a]

[a] Potential vs. SCE. [b] The dianion was generated by twofold deprotonation of 1,2-dimethyl-3,4-dimethylencyclobutene with *n*-BuLi/TMEDA. Electron-transfer processes seem to occur beside other reactions on trapping with methyl iodide. [135] No electrochemical transformations of 2^{2-} into **2** or vice versa are known. [c] Determined by PE spectroscopy. [d] The first oxidation step of the radialene is a two-electron transfer.

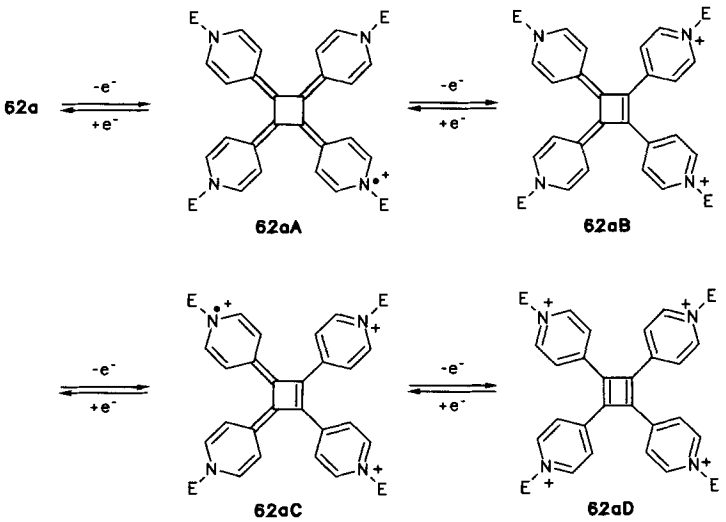

Scheme 24. Radialene **62a** as a fully reversible, five-step redox system. E = COOEt.

are represented by [3]radialenes **46** and **47** (see below), tris(9-fluorenylidene)cyclopropane (**52**; two reversible one-electron reductions: $E_{1/2}$ vs. Ag/AgCl: −0.27 and −0.75 V[46]), the West type [3]radialenes bearing *para*-quinoid substituents such as **38**–**44**, and the [4]radialene **80**. The latter compounds normally display two well-defined, reversible one-electron steps (exception: two-electron reduction of **40**[37]); the first reduction step occurs at relatively high (positive) potential.[37–40, 41a, 41c, 63, 136, 137] In agreement with theoretical predictions,[138] these radialenes therefore represent strong electron acceptors. If one takes into account the

potentials of the two reduction steps, they represent oxidizing reagents which, in general, range between chloroanil and DDQ.[139] It is therefore no surprise that the tris(oxocyclohexadienylidene)cyclopropanes **38** are reduced by hydroquinone to the bis(4-hydroxyaryl)cyclopropanes **37** in a reversal of their original synthesis (see Scheme 2). The analogous reduction of the anthraquinone derivative **39**, however, requires Sn/HCl.[36]

Many of the radical anions of radialenes bearing *para*-quinoid substituents are persistent in solution (THF, dichloromethane) and have been characterized by their ESR spectra.[37–39, 41a, 41c, 63, 137, 140] Since the two-step reduction process may be accompanied by a striking color change, these systems have been proposed as candidates for use in electrochromic displays.[41c]

Hexacyano[3]radialene (**46**) is a very strong electron acceptor,[141] which is reduced to $\mathbf{46}^{\bullet-}$ and $\mathbf{46}^{2-}$ extremely easily (see Section 2.1). A number of salts containing the radical anion $\mathbf{46}^{\bullet-}$ have been isolated. Typically, the radical anion is obtained form the dianion $\mathbf{46}^{2-}$ by one-electron oxidation, but under certain conditions, complex salts containing both $\mathbf{46}^{\bullet-}$ and $\mathbf{46}^{2-}$ are also formed[142] (Scheme 25). In contrast to **46**, hexakis(methoxycarbonyl)[3]radialene (**47**) can be prepared without difficulty; on reduction with iodide, radical anion $\mathbf{47}^{\bullet-}$ is passed as a short-lived intermediate.[142]

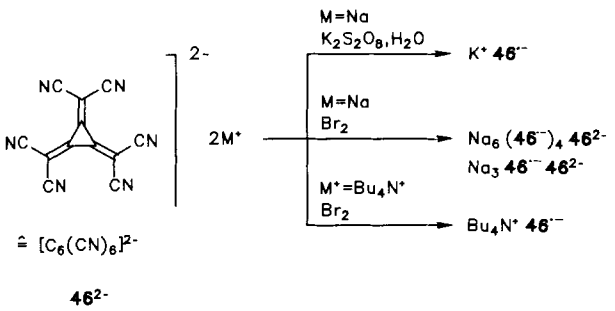

Scheme 25. One-electron oxidation of the dianion of **46**. a) Recrystallization from ethanol.

Focusing on electron-rich radialenes, Yoshida et al. have investigated those containing sulfur as the donor atom.[87] In the homologous series of the radialenes bearing 1,3-dithiol-2-ylidene units, large differences in the electrochemical oxidation behavior have been observed (Tables 6 and 7), the most remarkable feature being the apparent four-electron oxidation step of the [5]radialene **114**. Oxidation of the [3]radialene **48** with $Tl(CF_3COO)_3$ leads via $\mathbf{48}^{\bullet+}$ (detection in the ESR spectrum) to the isolable dicationic salt $\mathbf{48}^{2+} \cdot 2\ CF_3COO^-$, which has a singlet ground state and a thermally accessible triplet state only 0.07 eV above the singlet state.[141, 142]

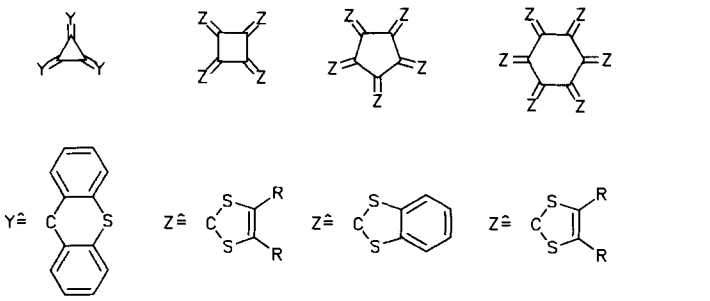

Table 7. Oxidation potentials of some electron-rich radialenes (in volt vs. Ag/AgCl, solvent dichloromethane. Figures in parentheses indicate irreversible steps in the cyclic voltammogram.)

Compound	E_1	E_2	E_3	Ref.
44	+0.67	+0.80		[44]
110	see Table 6			
164	see Table 6			
114		+0.36 [a]		[89b]
124a [b]	+0.73	(+0.89)	(+1.13) [c]	[96]
123b [a, b]	+0.43	(+0.65)	(+0.81) [c]	[96]

[a] In benzonitrile; apparent four-electron transfer. [b] Modification containing twist-boat conformation of the six-membered ring. [c] Two-electron transfer.

5. Radialenes as Building Blocks for Organic Conductors and Organic Ferromagnets

Among organic materials displaying metallic conductivity, molecular π donor–acceptor complexes, whose prototype is the system TTF · TCNQ (TTF = tetrathiafulvalene, TCNQ = tetracyanoquinomethane), must be named first alongside radical cation salts of type D_mX_n (D = donor, X = charge-compensating closed-shell anion, $m > n$), some of which even have superconducting properties.[143] The high conductivities of these systems are not reached, however, when electron-rich radialenes (Table 6) are used as the donor components. The charge-transfer (CT) complex **164** · $(TCNQ)_2$ has a specific electrical conductivity (compressed pellet, room temperature) of 0.032 S cm^{-1},[81a] while that of the complex formed from **164'** and four TCNQF (TCNQF = tetracyanotetrafluoroquinodimethane) units is 0.075 S cm^{-1}.[84] Single crystals of these complexes have not been obtained so far.[89a] The [3]radialene **48** and the [6]radialene **124b** do not form CT complexes with the common electron acceptors.

The perchlorate and hexafluorophosphate salts of the radical cation of **164** (benzo-1,3-dithiol-2-ylidene instead of 1,3-dithiol-2-ylidene) have been obtained as very small single crystals by electrocrystallization. Their electrical conductivity at room temperature is 1 S cm^{-1}, but the temperature dependency is characteristic of semiconductors.[89a]

Since the radialenes used have nonplanar structures (see Section 3.1), the somewhat disappointing results obtained so far are not unexpected. Hopes for higher conductivities rest upon the CT complexes or radical cation salts of the as yet unknown tris(1,3-dithiol-2-ylidene)cyclopropane, which is expected to be a planar compound. The [6]radialenes **27**[125] and **28**[126] should also be ideal donor components. They form complexes with iodine, and a close similarity between perylene and **27** exists as regards the conductivity and low stability. The specific electrical conductivity of the 1:1 complex of **28** and iodine is relatively high (0.11 S cm^{-1}[126]).

The quest for ferromagnetic molecular solids[144] is currently being pursued actively in several research groups. The first organometallic complex exhibiting ferromagnetism, $[Fe^{III}(C_5Me_5)_2]^{\bullet+}$ $[TCNE]^{-}$, has been reported only recently.[146, 147] Ferromagnetic coupling in a molecular solid is essentially equivalent to stabilization of a triplet state. Several models have been suggested to achieve this property.[147c] McConnell in 1967[148] proposed as candidates those ionic charge-transfer complexes built up in alternating chains of radical cation donors and radical anion acceptors, in which either the donor or the acceptor has a neutral triplet ground state; back charge-transfer would then mix some triplet character in the ground state, leading to ferromagnetic coupling of the spins of adjacent ions.

An extension and generalization of McConnell's model was put forward by Miller and Epstein.[145, 147c] They stated that "assuming the electron-transfer excitation arises form the partially occupied molecular orbital (POMO), to achieve ferromagnetic coupling in a molecular solid via the McConnell mechanism a stable radical (neutral, cations/anions, or ions with small diamagnetic counterions) must possess a degenerate POMO that is not half-filled, and the lowest excited state formed via virtual charge transfer (retro or forward) possesses the same spin multiplicity and mixed with the ground state."[147c] The degeneracy of the further orbitals may be accidental or imposed by symmetry; in the latter case, the doubly degenerate POMOs require the symmetry D_{2d} or C_3 or that of a higher point group for the species bearing the unpaired electron(s).

Within this conceptual framework, radialene-containing CT complexes have also been investigated. The DuPont group has used the (diamagnetic[149]) radical anion $\mathbf{46}^{\bullet-}$ to prepare 1:1 CT complexes with organometallic cations such as $[Fe^{III}(C_5Me_5)_2]^{\bullet+}$,[150] $[Fe^{III}(C_5Me_4H)_2]^{\bullet+}$,[151] $[Os(C_5Me_5)_2]^{\bullet+}$,[152] and $[(\eta^6\text{-}C_6Me_3H_3)M]^{\bullet+}$ (M = Fe, Ru);[153] however, none of those complexes displayed ferromagnetism.

Several electron-donating radialenes with an odd-fold symmetry axis have been envisaged as components of organic ferromagnets: hexakis(dimethylamino)[3]radialene, tris(1,3-dithiol-2-ylidene)cyclopropane, the [3]radialene **48**, and the [5]radialene **114**. Whereas the two first-mentioned radialenes are still unknown and **48** does not form donor-acceptor complexes, the complexes of **114**, whose dication is a ground-state triplet, with several strong acceptors do not have the 1:1 stoichiometry required[147b, c] for alternating $D^{\bullet+}A^{\bullet-}D^{\bullet+}A^{\bullet-}\cdots$ linear chains according to the McConnell model for ferromagnetism.[89b] Thus, the temperature-dependent variation of the paramagnetic susceptibility in the solid complexes **114** · 2 DDQ and **114** · 4 TCNQF indicated a weak antiferromagnetic interaction between the radical components. The complex **114** · $(\mathbf{46})_2$, on the other hand, is diamagnetic.[89b]

Breslow's adaptation of the McConnell model aimed at the use of antiaromatic dications with triplet ground states. In that case, a forward charge transfer $D^{\bullet+}A^{\bullet-} \rightarrow D^{2+}A^{2-}$ is required.[154] Donor-acceptor complexes $\mathbf{165}^{\bullet+} \cdot \mathbf{46}^{\bullet-}$ and $\mathbf{166}^{\bullet+} \cdot \mathbf{46}^{\bullet-}$ were prepared.[155] The hexacyano[3]radialene radical anion was chosen as the acceptor not only to match the redox potentials of the components but also in the hope that it would help to preserve the C_3 symmetry of the donor ions in the crystal structure of the complex, since the donor dication is in a triplet ground state only due to its threefold symmetry axis. However, both complexes showed antiferromagnetic, not ferromagnetic, ordering.

The hexaaminobenzene derivative **167** reacts with $\mathbf{46}^{\bullet-}$ to form the ionic complex $\mathbf{167}^{2+} \cdot \mathbf{46}^{2-}$.[156] In contrast to **165** and **166**, dication $\mathbf{167}^{2+}$ has a singlet ground state; however,

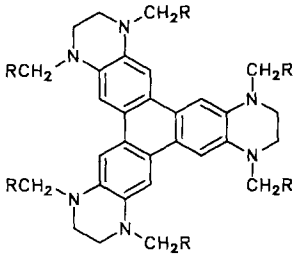

165 : R = CF_3
166 : R = CHF_2

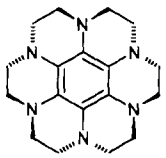

167

its temperature-dependence of the magnetic susceptibility differs from that of other essentially diamagnetic complexes with the same dication by a pronounced upturn of the magnetic susceptibility above about 150 K. This behavior, which in combination with results of ESR measurements suggests the presence of a thermally populated triplet excited-state species beside excited triplet $\mathbf{167}^{2+}$, is not yet understood in detail. The failure to generate ferromagnetism in the radialene-based (as well as in other) materials may have a number of causes;[145, 147b, 147c, 155] their enumeration is beyond the intention of this review. Suffice it to say that promising concepts for building organic ferromagnets do exist, but that the search must go on for appropriate building blocks, and these include novel radialenes as donor or acceptor components.

6. Outlook

Thanks to the considerable progress which has been made in the radialene area especially very recently, this class of highly unsaturated compounds is about to relinquish the status of exotic molecules. As we have shown above, the parent radialenes as well as their alkyl and aryl derivatives can often be obtained by simple and efficient syntheses. Structural and spectroscopic properties of the radialenes are now known, and even theoreticians devote time to them.

On the other hand, the lack of general and versatile syntheses for radialenes bearing functional groups suitable for further transformations, especially acyl-substituted radialenes, and the absence of diastereoselective syntheses (see Introduction) still constitute the major shortcomings in preparative radialene chemistry.

As for the chemical reactivity of the radialenes, the general behavior has emerged, but large gaps can still be located. For example, by virtue of their polyolefinic character the radialenes should be interesting objects for photochemical investigations; however, there are hardly any reports on the photochemistry of radialenes. One of the exceptions is a surprising

sensitized photooligomerization of **117** (Scheme 26) that may probably be taken as a first hint that radialenes can be the building blocks for polymers. According to the molecular weight determination, a hexamer is formed, which has been assigned structure **168**.[157] No products of a "vinylic polymerization" are formed when **117** is heated in the presence of radical initiators or on exposure of γ radiation.

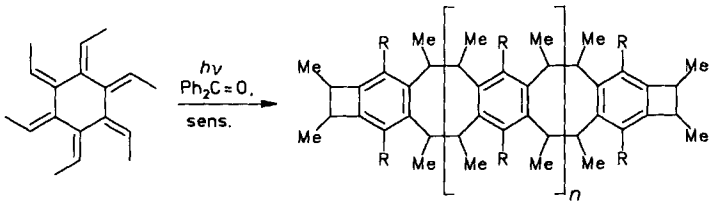

117 **168**

Scheme 26. R = Et, CH_2=CH, CHMeCHMe (as bridge between two aryl rings); sens. = sensitizer.

Some radialenes may also be suitable ligands for novel transition metal complexes; the few experiments described so far represent but a modest beginning.

For highly unsaturated compounds, the question of toxicity and especially of cancerogenic potential must usually be answered. In view of the novelty of this substance class, it comes as no surprise that the data are scarce. At least it has been established that hexamethyl[6]radialene (**117**) is not carcinogenic.[158]

Our expectations on the usefulness of radialenes in materials sciences are positive but not overly optimistic. As we have shown in Section 5, radialenes have not yet been successful as building blocks of organic conductors and ferromagnets. Investigations on the structural motives responsible for the assemblage of low-dimensional molecular crystals of organometallic donor-acceptor complexes are still in their infancy,[153, 159, 160] and among the radialenes, only the radical anion and dianion of hexacyano[3]radialene have been used. Further research on this topic could provide results on which the design of tailor-made complexes with defined magnetic, electrical, and optical properties can be based. Will radialenes ever find an application in practical displays, will they become building blocks of organic conductors (eventually superior to other organic metals) or ferromagnets? Answers to such questions cannot be given at present; since numerous promises to produce radialene-based "new materials" have not been fulfilled in the past, the general attitude tends to be pessimistic. However, we consider it most desirable, particularly under these auspices, to do fundamental research on these highly unsaturated cross-conjugated π-electron systems.

Our own research on radialenes has been supported by the Deutsche Forschungsgemeinschaft, the Fonds der Chemischen Industrie, and the Volkswagenstiftung. We are very grateful to BASF AG, Degussa, Hoechst AG, and Baeyer AG for providing us with financial support and chemicals. The names of our co-workers, to whom we express here our sincere thanks for their efforts in a not always facile research area (e.g., experiments with often small quantities of highly reactive and highly sensitive compounds), are found in the references. Our thanks also go to Martin Vogtherr, who has undertaken the laborious task of drawing the formulas.

Received: January 17, 1992 [A 874 IE]
German version: *Angew. Chem.* **1992**, 104, 953

[1] H. Hopf, *Angew. Chem.* **1984**, *96*, 947–958; *Angew. Chem. Int. Ed. Engl.* **1984**, *23*, 948–960.
[2] The name was originally proposed by J. R. Platt during a Gordon Conference and subsequently introduced by E. Heilbronner into the chemical literature; cf. [3] and A. Nickon, E. F. Silversmith, *Organic Chemistry: The Name Game*, Pergamon, New York, **1987**, p. 84.
[3] E. Weltin, F. Gerson, J. N. Murrell, E. Heilbronner, *Helv. Chim. Acta* **1961**, *44*, 1400–1413.
[4] H. Hopff, A. K. Wick, *Helv. Chim. Acta* **1961**, *44*, 19–24.
[5] a) G. Köbrich, H. Heinemann, *Angew. Chem.* **1965**, *77*, 590; *Angew. Chem. Int. Ed. Engl.* **1965**, *4*, 594; b) G. Köbrich, H. Heinemann, W. Zündorf, *Tetrahedron* **1967**, *23*, 565–584.
[6] E. A. Dorko, *J. Am. Chem. Soc.* **1965**, *87*, 5518–5520.
[7] G. W. Griffin, L. I. Peterson, *J. Am. Chem. Soc.* **1962**, *84*, 3398–3400; **1963**, *85*, 2268–2273.
[8] A. J. Barkovich, E. S. Strauss, K. P. C. Vollhardt, *J. Am. Chem. Soc.* **1977**, *99*, 8321–8322.
[9] P. Schiess, M. Heitzmann, *Helv. Chim. Acta* **1978**, *61*, 844–847; cf. P. Schiess, M. Heitzmann, S. Rutschmann, R. Stäheli, *Tetrahedron Lett.* **1978**, 4569–4572.
[10] L. G. Harruff, M. Brown, V. Boekelheide, *J. Am. Chem. Soc.* **1978**, *100*, 2893–2894; cf. R. Gray, L. G. Harruff, J. Krymowski, J. Peterson, V. Boekelheide, *ibid.* **1978**, *100*, 2892–2893.
[11] M. Iyoda, H. Otani, M. Oda, Y. Kai, Y. Baba, N. Kasai, *J. Chem. Soc. Chem. Commun.* **1986**, 1794–1796.
[12] A tabular summary of the [*n*]radialenes that have been prepared prior to 1970 may be found in B. S. Thyagarajan, *Intra-Sci. Chem. Rep.* **1970**, *4*, 42–47. As part of a review of the [l.m.n]hericenes P. Vogel has recently also compared these hydrocarbons with the [*n*]radialenes **1**–**4**; cf. [23].
[13] H. Hart, A. Teuerstein, M. Jeffares, W.-J. Hukung, D. L. Ward, *J. Org. Chem.* **1980**, *45*, 3731–3735.
[14] a) J. Jullien, J. M. Pechine, F. Perez, J. J. Piade, *Tetrahedron Lett.* **1980**, *21*, 611–612; b) W. S. Trahanovsky, T. J. Cassady, *J. Am. Chem. Soc.* **1984**, *106*, 8197–8201.
[15] N. Münzel, K. Kesper, A. Schweig, H. Specht, *Tetrahedron Lett.* **1988**, *29*, 6239–6242.
[16] W. Ando, Y. Haniu, T. Takata, *Tetrahedron Lett.* **1981**, *22*, 4815–4816.
[17] A. Maercker, F. Brauers, W. Brieden, B. Engelen, *J. Organomet. Chem.* **1989**, *377*, C45–C51.
[18] A. Maercker, F. Brauers, W. Brieden, M. Jung, H. D. Lutz, *Angew. Chem.* **1988**, *100*, 413–414; *Angew. Chem. Int. Ed. Engl.* **1988**, *27*, 404–405.
[19] A. Maercker, W. Brieden, T. Schmidt, H. D. Lutz, *Angew. Chem.* **1989**, *101*, 477–479; *Angew. Chem. Int. Ed. Engl.* **1989**, *28*, 477–478.
[20] M. Enders, A. Krämer, H. Pritzkow, W. Siebert, *Angew. Chem.* **1991**, *103*, 80–81; *Angew. Chem. Int. Ed. Engl.* **1991**, *30*, 84–85.
[21] This restriction includes the naphtharadialene **6**, but excludes compounds like 3,4,5,6-tetrakis(alkylidene)cyclohexene.
[22] The name "hericene" has been proposed by P. Vogel instead of the term bicyclo[l.m.n]radialene introduced by H. Hart. According to our definition Hart's proposal is invalid, cf. [23].
[23] P. Vogel in *Advances in Theoretically Interesting Molecules Vol. 1* (Ed.: R. P. Thummel), JAI Press, Greenwich, CT, USA, **1989**, p. 201.
[24] B. Halton, P. J. Stang, *Acc. Chem. Res.* **1987**, *20*, 443–448.
[25] F. Wudl, R. C. Haddon, E. T. Zellers, F. B. Bramwell, *J. Org. Chem.* **1979**, *44*, 2491–2493.
[26] Y. Kono, H. Miyamoto, Y. Aso, T. Otsubo, F. Ogura, T. Tanaka, M. Sawada, *Angew. Chem.* **1989**, *101*, 1254–1255; *Angew. Chem. Int. Ed. Engl.* **1989**, *28*, 1222–1224.
[27] *Oxocarbons* (Ed.: R. West), Academic Press, New York **1980**; G. Seitz, *Nachr. Chem. Tech. Lab.* **1980**, *28*, 804–807.
[28] R. F. C. Brown, F. W. Eastwood, G. D. Fallon, L. LaVecchia, K. Schank, *Aust. J. Chem.* **1989**, *42*, 451–457.
[29] R. Neidlein, U. J. Klotz, *Arch. Pharm. (Weinheim)* **1985**, *318*, 92–94.
[30] a) G. Seitz in *Oxocarbons* (Ed.: R. West), Academic Press, New York, **1980**, p. 30; b) K. Hesse, S. Hünig, H. J. Bestmann, G. Schmid, E. Wilhelm, G. Seitz, R. Matusch, K. Mann, *Chem. Ber.* **1982**, *115*, 795–797, and references cited therein.
[31] N. Kimura, W. H. Watson, J. Nakayama, *J. Org. Chem.* **1980**, *45*, 3719–3721.
[32] H. Balli, V. Müller, A. Sézen-Gezgin, *Helv. Chim. Acta* **1978**, *61*, 104–107.
[33] a) P. A. Waitkus, L. I. Peterson, G. W. Griffin, *J. Am. Chem. Soc.* **1966**, *88*, 181–183; b) P. A. Waitkus, E. B. Sanders, L. I. Peterson, G. W. Griffin, *ibid.* **1967**, *89*, 6318–6327; J. L. Laseter, A. Manmade, P. A. Waitkus, G. W. Griffin, *Spectrochim. Acta Part A*, **1971**, *27*, 741–745.

[34] I. A. D'yakonov, E. M. Kharicheva, V. A. Pankova, *Zh. Org. Khim.* **1969**, *5*, 85–91; *Chem. Abstr.* **1969**, *70*, 87087a.
[35] a) R. West, D. C. Zecher, *J. Am. Chem. Soc.* **1967**, *89*, 152–153; b) *ibid.* **1970**, *92*, 155–161.
[36] J. L. Benham, R. West, J. A. T. Norman, *J. Am. Chem. Soc.* **1980**, *102*, 5047–5053.
[37] D. E. Wellman, R. West, *J. Am. Chem. Soc.* **1984**, *106*, 355–360.
[38] D. E. Wellman, K. R. Lassila, R. West, *J. Org. Chem.* **1984**, *49*, 965–971.
[39] L. A. Wendling, R. West, *J. Org. Chem.* **1978**, *43*, 1577–1580.
[40] L. A. Wendling, R. West, *J. Org. Chem.* **1978**, *43*, 1573–1577.
[41] a) K. Komatsu, R. West, D. Beyer, *J. Am. Chem. Soc.* **1977**, *99*, 6290–6296; b) R. West, D. Beyer, K. Komatsu, US-A 4133821, **1979**; *Chem. Abstr.* **1979**, *90*, 205790n; c) K. Takahashi, M. Ogiyama, *Chem. Lett.* **1991**, 129–132.
[42] T. Fukunaga, M. D. Gordon, P. J. Krusic, *J. Am. Chem. Soc.* **1976**, *98*, 611–613; J. Mirek, A. Buda, *Z. Naturforsch. A.* **1984**, *39*, 386–390.
[43] T. Fukunaga, *J. Am. Chem. Soc.* **1976**, *98*, 610–611.
[44] T. Sugimoto, Y. Misaki, T. Kajita, T. Nagatomi, Z. Yoshida, J. Yamauchi, *Angew. Chem.* **1988**, *100*, 1129–1131; *Angew. Chem. Int. Ed. Engl.* **1988**, *27*, 1078–1080.
[45] H. D. Hartzler, *J. Am. Chem. Soc.* **1971**, *93*, 4527–4531.
[46] M. Iyoda, H. Otani, M. Oda, *Angew. Chem.* **1988**, *100*, 1131–1132; *Angew. Chem. Int. Ed. Engl.* **1988**, *27*, 1080–1081.
[47] a) M. Iyoda, A. Mizusuna, H. Kurata, M. Oda, *J. Chem. Soc. Chem. Commun.* **1989**, 1690–1692; b) K. Komatsu, H. Kama, K. Takeuchi, *Abstr. Pap. 61st Annu. Meet. Chem. Soc. Jpn.*, Tokyo, **1991**, p. 1061.
[48] T. Bally, U. Buser, E. Haselbach, *Helv. Chim. Acta.* **1978**, *61*, 38–45.
[49] F. A. Miller, F. R. Brown, K. H. Rhee, *Spectrochimica Acta Part A* **1972**, *28*, 1467–1478.
[50] L. Trabert, H. Hopf, *Liebigs Ann. Chem.* **1980**, 1786–1800.
[51] M. C. Lasne, J. L. Ripoll, J. M. Denis, *Tetrahedron*, **1981**, *37*, 503–508.
[52] a) M. Horner, S. Hünig, *Angew. Chem.* **1977**, *89*, 424–425; *Angew. Chem. Int. Ed. Engl.* **1977**, *16*, 410–411; b) M. Horner, S. Hünig, H. U. Reissig, *Liebigs Ann. Chem.* **1983**, 658–667.
[53] M. Horner, S. Hünig, *Liebigs Ann. Chem.* **1983**, 642–657.
[54] K. Tanaka, F. Toda, *Tetrahedron Lett.* **1980**, *21*, 2713–2716.
[55] M. Iyoda, Y. Kuwatani, M. Oda, *J. Am. Chem. Soc.* **1989**, *111*, 3761–3762.
[56] a) H. Meier, T. Echter, O. Zimmer, *Angew. Chem.* **1981**, *93*, 901–902; *Angew. Chem. Int. Ed. Engl.* **1981**, *20*, 865–867; b) T. Echter, H. Meier, *Chem. Ber.* **1985**, *119*, 182–197.
[57] Syntheses of [*n*]cumulenes: a) H. Hopf, *The Chemistry of Ketenes, Allenes and Related Compounds Part 2* (Ed.: S. Patai), Wiley, Chichester, **1980**, Chapter 20; b) M. Murray, *Methoden Org. Chem. (Houben-Weyl)*, 4th ed. Vol. V/2a, **1977**, p. 963.
[58] E. Kloster-Jensen, J. Wirz, *Helv. Chim. Acta.* **1975**, *58*, 162–177.
[59] P. J. Stang, M. R. White, *J. Am. Chem. Soc.* **1981**, *103*, 5429–5433.
[60] Z. Berkovitch-Yellin, M. Lahav, L. Leiserowitz, *J. Am. Chem. Soc.* **1974**, *96*, 918–920.
[61] M. Kaftory, I. Agmon, M. Ladika, P. J. Stang, *J. Am. Chem. Soc.* **1987**, *109*, 782–784.
[62] B. Heinrich, A. Roedig, *Angew. Chem.* **1968**, *80*, 367–368; *Angew. Chem. Int. Ed. Engl.* **1968**, *7*, 375–376.
[63] S. K. Koster, R. West, *J. Chem. Soc. Chem. Commun.* **1971**, 1380; *J. Org. Chem.* **1975**, *40*, 2300–2306.
[64] F. W. Nader, C.-D. Wacker, H. Irngartinger, U. Huber-Patz, R. Jahn, H. Rodewald, *Angew. Chem.* **1985**, *97*, 877–878; *Angew. Chem. Int. Ed. Engl.* **1985**, *24*, 852–853.
[65] a) P. J. Stang, A. E. Learned, *J. Chem. Soc. Chem. Commun.* **1988**, 301–307; b) A. E. Learned, A. M. Arif, P. J. Stang, *J. Org. Chem.* **1988**, *53*, 3122–3123.
[66] a) H. D. Hartzler, *J. Am. Chem. Soc.* **1971**, *93*, 4527–4531; b) H. D. Hartzler, US-A 3363011, **1968**; *Chem. Abstr.* **1968**, *68*, 59167s.
[67] M. Iyoda, M. Oda, Y. Kai, N. Kanehisa, N. Kasai, *Chem. Lett.* **1990**, 2149–2152.
[68] S. Basak, S. Srivastava, W. J. LeNoble, *J. Org. Chem.* **1987**, *52*, 5095–5099; W. J. LeNoble, S. Basak, S. Srivastava, *J. Am. Chem. Soc.* **1981**, *103*, 4638–4639.
[69] A product analogous to **85** has been observed in the Cu(I)-catalyzed dimerization of tetramethylhexapentaene: L.T. Scott, G. J. DeCicco, *Tetrahedron Lett.* **1976**, 2663–2666; C. Santiago, K. N. Houk, G. J. DeCicco, L. T. Scott, *J. Am. Chem. Soc.* **1978**, *100*, 692–696.
[70] R. O. Angus, Jr., R. P. Johnson, *J. Org. Chem.* **1984**, *49*, 2880–2883.
[71] H.-G. Zoch, G. Szeimies, R. Römer, G. Germain, J.-P. Declerq, *Chem. Ber.* **1983**, *116*, 2285–2310.
[72] a) T. Inoue, T. Kaneda, S. Misumi, *Tetrahedron Lett.* **1974**, 2969–2992; b) T. Hayashi, N. Mataga, T. Inoue, T. Kaneda, M. Irie, S. Misumi, *J. Am. Chem. Soc.* **1977**, *99*, 523–526.
[73] a) A. Fronda, G. Maas, *Angew. Chem.* **1989**, *101*, 1750–1752; *Angew. Chem. Int. Ed. Engl.* **1989**, *28*, 1663–1665; b) A. Fronda, F. Krebs, B. Daucher, T. Werle, G. Maas, *J. Organomet. Chem.* **1992**, *424*, 253–272.
[74] L. Hagelee, R. West, J. Calabrese, J. Norman, *J. Am. Chem. Soc.* **1979**, *101*, 4888–4892.
[75] B. Hagenbruch, K. Hesse, S. Hünig, G. Klug, *Liebigs Ann. Chem.* **1981**, 256–263.
[76] S. Hashmi, K. Polborn, G. Szeimies, *Chem. Ber.* **1989**, *122*, 2399–2401.
[77] a) M. Iyoda, S. Tanaka, M. Nose, M. Oda, *J. Chem. Soc. Chem. Commun.* **1983**, 1058–1059; b) M. Iyoda, S. Tanaka, H. Otani, M. Nose, M. Oda, *J. Am. Chem. Soc.* **1988**, *110*, 8494–8500.
[78] G. Wilke, *Angew. Chem.* **1988**, *100*, 189–211; *Angew. Chem. Int. Ed. Engl.* **1988**, *27*, 185–206.
[79] L. Stehling, G. Wilke, *Angew. Chem.* **1985**, *97*, 505–506; *Angew. Chem. Int. Ed. Engl.* **1985**, *24*, 496–497.
[80] M. Iyoda, Y. Kuwatani, M. Oda, Y. Kai, N. Kanehisa, N. Kasai, *Angew. Chem.* **1990**, *102*, 1077–1079; *Angew. Chem. Int. Ed. Engl.* **1990**, *29*, 1062–1064.
[81] a) T. Sugimoto, H. Awaji, Y. Misaki, Z. Yoshida, Y. Kai, H. Nakagawa, N. Kasai, *J. Am. Chem. Soc.* **1985**, *107*, 5792–5793; b) Z. Yoshida, Jpn. Kokai Tokkyo Koho JP 61/254582 A2, **1986**; *Chem. Abstr.* **1987**, *106*, 196433t.
[82] Y. Misaki, Y. Matsumura, T. Sugimoto, Z. Yoshida, *Tetrahedron Lett.* **1989**, *30*, 5289–5292.
[83] If the cyclodimerization of **108** is carried out in the presence of CO, the corresponding tetrakis(1,3-dithiol-2-ylidene)cyclopentanone is formed: T. Sugimoto, Y. Misaki, Y. Arai, Y. Yamamoto, Z. Yoshida, Y. Kai, N. Kasai, *J. Am. Chem. Soc.* **1988**, *110*, 628–629.
[84] T. Sugimoto, H. Awaji, I. Sugimoto, Y. Misaki, Z. Yoshida, *Synth. Met.* **1987**, *19*, 569–572.
[85] M. Iyoda, H. Otani, M. Oda, Y. Kai, Y. Baba, N. Kasai, *J. Am. Chem. Soc.* **1986**, *108*, 5371–5372.
[86] M. Iyoda, H. Otani, M. Oda, Y. Kai, Y. Baba, N. Kasai, *J. Chem. Soc. Chem. Commun.* **1986**, 1794–1796.
[87] L. Trabert, H. Hopf, unpublished.
[88] Private communication, Prof. Dr. E. Haselbach (Fribourg).
[89] a) Z. Yoshida, T. Sugimoto, *Angew. Chem. Adv. Mater.* **1988**, *100*, 1633–1637; *Angew. Chem. Int. Ed. Engl. Adv. Mater.* **1988**, *100*, 1573–1577; b) T. Sugimoto, Y. Misaki, Z. Yoshida, J. Yamauchi, *Mol. Cryst. Liq. Cryst.* **1989**, *176*, 259–268; c) T. Sugimoto, Y. Misaki, Y. Arai, Y. Yamamoto, Z. Yoshida, Y. Kai, N. Kasai, *J. Am. Chem. Soc.* **1988**, *110*, 628–629.
[90] H. Hopff, A. K. Wick, *Helv. Chim. Acta* **1961**, *46*, 380–386.
[91] H. Hopff, A. Gati, *Helv. Chim. Acta* **1965**, *48*, 1289–1296; H. Hopff, A. Gati, *ibid.* **1965**, *48*, 437–443.
[92] For proposals on the reaction mechanism of the remarkable **118** → **4** isomerization, see W. V. Dower, K. P. C.Vollhardt, *Tetrahedron* **1986**, *42*, 1873–1881; H. Hopf, D. Gottschild, W. Lenk, *Isr. J. Chem.* **1985**, *26*, 79–87.
[93] Reference [10] presents other routes leading to **4**, which, however, without exception cannot compete with the method described in Scheme 19 as regards availability of the starting material **119**, yield, purity of product, and (relatively low) pyrolysis temperature are concerned.
[94] H. Hart, M. Sasaoka, *J. Am. Chem. Soc.* **1978**, *100*, 4326–4327; vgl. L.-T. W. Lin, H. Hart, *J. Org. Chem.* **1984**, *49*, 1027–1030.
[95] This compound is interesting from another viewpoint, though: by catalytic hydrogenation it can be converted into all-*trans*-1,2,3,4,5,6-hexaisopropylcyclohexane, a cyclohexane derivative with all its substituents in axial positions: Z. Goren, S. E. Biali, *J. Am. Chem. Soc.* **1990**, *112*, 893–894.
[96] T. Sugimoto, Y. Misaki, T. Kajita, Z. Yoshida, Y. Kai, N. Kasai, *J. Am. Chem. Soc.* **1987**, *109*, 4106–4107.
[97] H. Hart, M. Jeffares, A. Teuerstein, D. L. Ward, *J. Am. Chem. Soc.* **1978**, *100*, 8012–8013.
[98] E. A. Dorko, J. L. Hencher, S. H. Bauer, *Tetrahedron* **1968**, *24*, 2425–2434.
[99] a) J. C. Burr, Jr., E. A. Dorko, J. A. Merritt, *J. Chem. Phys.* **1966**, *45*, 3877–3879; b) K. H. Rhee, F. A. Miller, *Spectrochim. Acta Part A* **1971**, *27*, 1–10; c) E. A. Dorko, R. Scheps, S. A. Rice, *Z. Phys. Chem. (Munich)* **1974**, *78*, 568–571.
[100] H. Dietrich, *Acta Crystallogr. Sect. B* **1970**, *26*, 44–53.
[101] F. P. van Remorrtere, F. B. Boer, *J. Am. Chem. Soc.* **1970**, *92*, 3355–3360.
[102] H. Hart, D. L. Ward, K. Tanaka, F. Toda, *Tetrahedron Lett.* **1982**, *23*, 2125–2128.
[103] W. March, J. D. Dunitz, *Helv. Chim. Acta* **1975**, *58*, 707–712.
[104] a) M. Said, D. Maynau, J.-P. Malrieu, M.-A. Garcia Bach, *J. Am. Chem. Soc.* **1984**, *106*, 571–579; b) A. Banks, G. J. Mains, C. W. Bock, M. Trachtman, P. George, *J. Mol. Struct.* **1979**, *56*, 267–275.
[105] The shortening of the endocyclic C–C bond of [3]radialene by 0.03–0.05 Å compared to [4]radialenes (see Table 2) is equivalent to the difference between the average bond lengths of cyclopropane and cyclobutane: F. H. Allen, S. Bellard, M. D. Brice, B. A. Cartwright, A. Doubleday, H. Higgs, T. Hummelink, B. G. Hemmelink-Peters, O. Kennard, W. D. S. Motherwell, J. R. Rodgers, D. G. Watson, *Acta Crystallogr. Sect. B* **1979**, *35*, 2331–2339; F. H. Allen, *ibid.* **1984**, *40*, 64–72. The shortening of the bond lengths of the three-membered ring of [3]radialene compared to cyclopropane (1.510 Å) is caused by conjugation and the difference in hybridization: F. H. Allen, *ibid.* **1981**, *37*, 890–900.

[106] a) M. J. S. Dewar, G. J. Gleicher, *J. Am. Chem. Soc.* **1965**, *87*, 692–696; b) M. J. S. Dewar, C. De Llano *ibid.* **1969**, *91*, 789–795; c) B. A. Hess, Jr., L. J. Schaad, *J. Org. Chem.* **1972**, *37*, 4179–4184; d) W. C. Herndon, M. L. Ellzey, Jr., *Tetrahedron Lett.* **1974**, 1399–1402; cf. W. C. Herndon, *Pure Appl. Chem.* **1980**, *52*, 1459–1469; e) J. Aihara, *J. Am. Chem. Soc.* **1976**, *98*, 2750–2758; cf. J. Aihara, *Bull. Chem. Soc. Jpn.* **1975**, *48*, 517–520; f) I. Gutman, S. Bosanac, *Tetrahedron* **1977**, *33*, 1809–1812; g) I. Gutman, M. Milun, N. Trinajsti'c, *J. Am. Chem. Soc.* **1977**, *99*, 1692–1704; h) S. El-Basil, *Int. J. Quantum Chem.* **1981**, *19*, 593–609; i) Y. Jiang, H. Zhang, *Theor. Chim. Acta* **1989**, *75*, 279–297; j) H. Kolmar, *J. Am. Chem. Soc.* **1979**, *101*, 4832–4840; k) A. Moyano, J. C. Paniagua, *J. Org. Chem.* **1986**, *51*, 2250–2257.

[107] J. Aihara, *Bull. Chem. Soc. Jpn.* **1980**, *53*, 1751–1752.

[108] Z. Zhou, R. G. Parr, *J. Am. Chem. Soc.* **1989**, *111*, 7371–7379.

[109] [3]Radialene: N. C. Baird, M. J. S. Dewar, *J. Am. Chem. Soc.* **1987**, *89*, 3966–3970; E. A. Castro, M. Fernández, *Z. Phys. Chem. (Leipzig)* **1981**, *262*, 83–89; reference [104]. [4]Radialene: G. Buemi, *Z. Phys. Chem. (Munich)* **1980**, *119*, 1–21. [5]Radialene: D. A. Bochvar, E. G. Gal'pern, *Izv. Akad. Nauk SSSR, Ser. Khim.* **1976**, 655–656 (engl. 639–640); G. Buemi, *Bull. Chem. Soc. Jpn.* **1980**, *53*, 3344–3355. Different radialenes: M. J. S. Dewar, G. J. Gleicher, *J. Am. Chem. Soc.* **1965**, *87*, 692–696; M. Kowalewski, A. Goliebiewski, *Acta Phys. Pol.* **1969**, *35*, 585–594; V. Buss, H.-D. Försterling, *Tetrahedron* **1973**, *29*, 3001–3009.

[110] K. B. Wiberg in *The Chemistry of the Cyclopropyl Group Part 1* (Ed.: Z. Rappoport), Wiley, Chichester, **1987**, Chapter 1.

[111] T. Bally, H. Baumgärtel, U. Büchler, E. Haselbach, W. Lohr, J. P. Maier, J. Vogt, *Helv. Chim. Acta* **1978**, *61*, 741–753.

[112] There are some reservations concerning the experimentally determined value of ΔH_f^0 (**1**), since the structures of the fragment ions $C_4H_4^+$ and $C_2H_2^+$ have possibly been assigned incorrectly: J. F. Liebman, A. Greenberg in *The Chemistry of the Cyclopropyl Group Part 2* (Ed.: Z. Rappoport), Wiley, Chichester, **1987**, Chapter 18.

[113] a) E. Heilbronner, *Theor. Chim. Acta* **1966**, *4*, 64–68; b) G. Favini, G. Buemi, *Theor. Chim. Acta* **1972**, *24*, 61–70; c) C. Sieiro, C. Ponce, *An. Quim.* **1976**, *72*, 201–205; d) G. Buemi, *Z. Phys. Chem. (Munich)* **1980**, *119*, 1–21; cf. G. Buemi, *Bull. Chem. Soc. Jpn.* **1980**, *53*, 3344–3355; e) P. Rancurel, B. Huron, L. Praud, J. P. Malrieu, G. Berthier, *J. Mol. Spectrosc.* **1976**, *60*, 259–276.

[114] T. Bally, E. Haselbach, *Helv. Chim. Acta* **1978**, *61*, 754–761; vgl. E. A. Dorko, R. Scheps, S. A. Rice, *J. Phys. Chem.* **1974**, *78*, 568–571.

[115] T. Bally, E. Haselbach, *Helv. Chim. Acta* **1975**, *58*, 321–333.

[116] H. Bock, G. Rohn, *Helv. Chim. Acta* **1991**, *74*, 1221–1232. See also H. Bock, G. Rohn, *ibid.* **1992**, *75*, 160–169 for analogous investigations with octaphenyl[4]radialene.

[117] G. Rohn, Dissertation, Universität Frankfurt, **1990**.

[118] a) F. A. Miller, *Appl. Spectrosc.* **1975**, *29*, 461–469; b) D. H. Finseth, F. A. Miller, *J. Raman Spectrosc.* **1976**, *4*, 245–252.

[119] H.-O. Kalinowski, S. Berger, S. Braun, *^{13}C-NMR-Spektroskopie*, Thieme, Stuttgart, **1984**.

[120] Based on qualitative HOMO/LUMO estimates it has been proposed that [4]radialene **2** should react with either electron-poor or electron-rich partners. The latter type of reaction has apparently not been observed so far. Cf. S. Inagaki, K. Iwase, *Nouv. J. Chimie* **1983**, *8*, 73–77.

[121] T. Bally, E. Haselbach, Z. Lanyiova, P. Baertschi, *Helv. Chim. Acta* **1978**, *61*, 2488–2502.

[122] L. Trabert, H. Hopf, D. Schomburg, *Chem. Ber.* **1981**, *114*, 2405–2414.

[123] a) J. M. Denis, P. Le Perchec, J. M. Conia, *Tetrahedron* **1977**, *33*, 399–408; b) L. Fitjer, *Angew. Chem.* **1976**, *88*, 804–805; *Angew. Chem. Int. Ed. Engl.* **1976**, *15*, 763–764.

[124] L. Stehling, G. Wilke, *Angew. Chem.* **1988**, *100*, 575–577; *Angew. Chem. Int. Ed. Engl.* **1988**, *27*, 571–572.

[125] A. Fronda, Dissertation, Universität Kaiserslautern, **1991**.

[126] H. Hopff, A. K. Wick, *Helv. Chim. Acta* **1960**, *43*, 1473–1481.

[127] H. Hopff, G. Kormany, *Helv. Chim. Acta* **1963**, *46*, 2533–2538.

[128] A repetition of the reaction between **117** and tetracyanoethylene in dichloromethane at room temperature provided the mono adduct **154** in 91% yield: C. Rücker, D. Lang, J. Sauer, H. Friege, R. Sustmann, *Chem. Ber.* **1980**, *113*, 1663–1690.

[129] H. Hopff, G. Kormany, *Helv. Chim. Acta* **1965**, *48*, 437–443.

[130] W. F. Gorham, *J. Polym. Sci. Polym. Chem. Ed.* **1966**, *4*, 3027–3039.

[131] The adducts **157** and **158** must have been formed via *meta*-type addition modes (see above). Their very low yields may be rationalized by assuming that the linearly annelated 2:1 intermediates of type **155**, which are probably produced as main products in this case as well, and which now do not carry reactivity-reducing substituents at their exocyclic double bonds, polymerize quickly and completely under the reaction conditions: see references [8, 9, 130]

[132] M. Yalpani, R. Benn, R. Goddard, G. Wilke, *J. Organomet. Chem.* **1982**, *240*, 49–57.

[133] The agreement of the ESR spectrum of **98**$^{\cdot-}$ and the ENDOR spectrum of **98**$^{\cdot+}$ is experimental proof of the π alternation predicted by HMO theory for the even-membered radialenes.

[134] T. A. Blinka, R. West, *Tetrahedron Lett.* **1983**, *24*, 1567–1568.

[135] W. D. Thorstad, N. S. Mills, D. Q. Buckelew, L. S. Govea, *J. Org. Chem.* **1989**, *54*, 773–776.

[136] K. Komatsu, R. West, *J. Chem. Soc. Chem. Commun.* **1976**, 570–571.

[137] J. L. Benham, R. West, *J. Am. Chem. Soc.* **1980**, *102*, 5054–5058.

[138] According to HMO calculations these compounds have extremely low-lying LUMOs [36].

[139] The potential for the reduction to the radical anion lies between that of chloranil and that of DDQ; for the second reduction step it normally is less negative than that of DDQ (exceptions: **42**, **80**). See for example references [37, 41a, 137].

[140] R. West, D. C. Zecher, S. K. Koster, D. Eggerding, *J. Org. Chem.* **1975**, *40*, 2295–2299.

[141] The adiabatic electron affinity as well as the LUMO energy of [3]radialene and its di-, tetra- and hexacyano derivatives have been determined by MNDO calculations: J. Mirek, A. Buda, *Z. Naturforsch. A* **1984**, *39*, 386–390.

[142] The very small zero-field splitting parameter D (0.7 mT), which has been derived from the low temperature ESR spectrum, demonstrates that the two unpaired electrons are widely separated from each other.

[143] a) *The Physics and Chemistry of Low Dimensional Solids* (Ed.: L. Alcácer), *NATO ASI Ser. Ser. C* **1980**, *56*. b) D. O. Cowan, A. Kini, L.-Y. Chiang, K. Lerstrup, D. R. Talham, T. O. Poehler, A. N. Bloch, *Mol. Cryst. Liq. Cryst.* **1982**, *86*, 1–26; c) F. Wudl, *Acc. Chem. Res.* **1984**, *17*, 227–232; d) J. M. Williams, M. A. Beno, H. H. Wang, P. C. W. Leungt, T. J. Emge, U. Geiser, K. D. Carlson, *Acc. Chem. Res.* **1985**, *18*, 261–267.

[144] A molecular solid has been defined as a solid consisting of "low molecular weight molecules or ions that do not possess extended covalent bonding in the solid state. However, shorter than van der Waals separations may be present in the solid"; see reference [145], footnote 17.

[145] J. S. Miller, A. J. Epstein, *J. Am. Chem. Soc.* **1987**, *109*, 3850–3855.

[146] a) J. S. Miller, J. C. Calabrese, R. W. Bigelow, A. J. Epstein, J. H. Zhang, W. M. Reiff, *J. Chem. Soc. Chem. Commun.* **1986**, 1026–1028; b) J. S. Miller, J. C. Calabrese, H. Rommelmann, S. R. Chittapeddi, J. H. Zhang, W. M. Reiff, A. J. Epstein, *J. Am. Chem. Soc.* **1987**, *109*, 769–781.

[147] a) J. S. Miller, A. J. Epstein, W. M. Reiff, *Isr. J. Chem.* **1987**, *27*, 363–373; b) J. S. Miller, A. J. Epstein, W. M. Reiff, *Acc. Chem. Res.* **1988**, *21*, 114–120; c) J. S. Miller, A. J. Epstein, W. M. Reiff, *Chem. Rev.* **1988**, *88*, 201–220; d) G. T. Yee, J. M. Manriquez, D. A. Dixon, R. S. McLean, D. M. Groski, R. B. Flippen, K. S. Narayan, A. J. Epstein, J. S. Miller, *Adv. Mater.* **1991**, *3*, 309–311; e) J. M. Manriquez, G. T. Yee, R. S. McLean, A. J. Epstein, J. S. Miller, *Science* **1991**, *252*, 1415–1417.

[148] H. McConnell, *Proc. R. A. Welch Found. Conf. Chem. Res.* **1967**, *11*, 144.

[149] The salt Me_4N^+ **46**$^{\cdot-}$ undergoes a structural and magnetic phase transition at 364 K; in the low-temperature phase, strong antiferromagnetic coupling occurs, but the high-temperature phase is paramagnetic: S. C. Abrahams, H. E. Bair, F. J. DiSalvo, P. Marsh, L. A. Deuring, *Phys. Rev. B Condens. Matter* **1984**, *29*, 1258–1262; cf. S. C. Abrahams, P. Marsh, L. A. Deuring, *Acta Crystallogr. Sect. B* **1988**, *44*, 263–271.

[150] J. H. Zhang, W. M. Reiff, J. S. Miller, *Hyperfine Interact.* **1988**, *42*, 1099–1102.

[151] J. S. Miller, D. T. Glatzhofer, D. M. O'Hare, W. M. Reiff, A. Chakraborty, A. J. Epstein, *Inorg. Chem.* **1989**, *28*, 2930–2939.

[152] D. O'Hare, J. C. Green, T. P. Chadwick, J. S. Miller, *Organometallics* **1988**, *7*, 1335–1342.

[153] M. D. Ward, *Organometallics* **1987**, *6*, 754–762. These complexes are described as "superionic donor–acceptor complexes with nominally doubly charged ($D^{2-}A^{2+}$) ground states and ($D^{\cdot-}A^{\cdot+}$) excited states".

[154] a) R. Breslow, B. Jaun, R. Klutz, C.-Z. Xia, *Tetrahedron* **1982**, *38*, 863–867; b) R. Breslow, *Mol. Cryst. Liq. Cryst.* **1985**, *125*, 261–267.

[155] T. J. LePage, R. Breslow, *J. Am. Chem. Soc.* **1987**, *109*, 6412–6421.

[156] J. S. Miller, D. A. Dixon, J. C. Calabrese, C. Vazquez, P. J. Krusic, M. D. Ward, E. Wasserman, R. L. Harlow, *J. Am. Chem. Soc.* **1990**, *112*, 381–398.

[157] O. A. Yuzhakova, I. V. Isakov, E. E. Rider, G. N. Gerasimov, A. D. Abkin, *Vysokomol. Soedin Ser. B.* **1977**, *19*, 431–435; *Chem. Abstr.* **1977**, *87*, 85322a.

[158] H. Druckrey, C. Landschütz, *Z. Krebsforsch.* **1969**, *73*, 87–88.

[159] M. D. Ward, P. J. Fagan, J. C. Calabrese, D. C. Johnson, *J. Am. Chem. Soc.* **1989**, *111*, 1719–1732.

[160] D. O'Hare, J. Brookes, D. J. Watkin, *J. Mater. Chem.* **1991**, *1*, 691–697.

Nitrido Complexes of Transition Metals

By Kurt Dehnicke,* and Joachim Strähle

In the past decade new syntheses and numerous structural determinations have enlivened studies in the still relatively young field of nitrido-transition-metal complexes. Aside from the terminal function of the nitrido ligand M≡N:, this group also occurs as linear μ_2-bridging ligand in symmetric and asymmetric coordination; examples are known with almost right-angled bridge function; and, finally, it also functions as μ_3-bridging ligand. Accordingly, the fresh impulses given to synthetic chemistry by nitrido complexes are also many-sided: such complexes are used, inter alia, for the preparation of phosphaniminato and thionitrosyl complexes as well as for the synthesis of metallaheterocycles of the type MN_3S_2 and MN_3P_2 with delocalized π-systems. In technetium chemistry complexes with terminal nitrido group are employed as radiopharmaceuticals, and, owing to the strong *trans* influence of the M≡N: group, nitrido complexes of molybdenum are suitable as catalysts in olefin metathesis. Finally, nitrido complexes are also of wide interest in theoretical studies.

1. Introduction

The following article surveys the development of the chemistry of nitrido complexes containing transition metal–nitrogen multiple bonds. It constitutes an updated continuation of our previous review article published in 1981.[1] Up to that time only complexes with the terminal nitrido ligand **A** and complexes with linear asymmetric and symmetric bridges **B** and **D**, respectively, were known, while in the meantime complexes containing bent bridges **E** with bond angles as small as 91.3° have been synthesized, and in many cases the unusual T-shaped bridge arrangement **F** in trinuclear complexes with metal–metal bonds could also be prepared. Scheme 1 gives an overview of the hitherto established bonding functions of the nitrido-ligand.

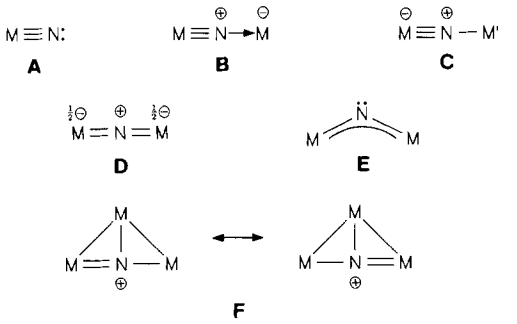

Scheme 1. Bond functions of the nitrido ligand demonstrated so far. **A** = terminal, **B** = asymmetric, linear bridge of the donor-acceptor type, **C** = asymmetric linear bridge with covalent bond, **D** = symmetric, linear bridge, **E** = bent bridge, **F** = T-shaped arrangement.

Nitrido-complexes have also been treated in detail by Nugent and Mayer[2] in a monograph on Metal-Ligand Multiple Bonds. The present article does not deal with nitrido-complexes with interstitial N-atoms, as met with, e.g., in $NEt_4[FeRu_3N(CO)_{12}]$[3] or $[(Ph_3PAu)_5N]^{2+}$.[4]

2. New Synthetic Strategies

2.1. Reactions with the Bromide of Millon's Base

Dominant among the new methods for the synthesis of nitrido-transition-metal complexes are the reactions of metal halides with nitride transfer reagents, which represent ligand exchange reactions. One such reagent is Millon's base, $[Hg_2N]OH$, which is readily accessible in anhydrous form,[5] and despite its polymeric structure and consequent sparing solubility is astonishingly reactive. For example, the bromide of this base reacts with tungsten hexachloride in boiling carbon tetrachloride with formation of the binuclear μ-nitrido-complex $[W_2NCl_9]$[7] [Eq. (1), Scheme 2 (top)], which upon heating furnishes $WNCl_3$,[1] a compound also accessible via other routes [Eq. (2)].

$$2WCl_6 + [Hg_2N]Br \longrightarrow [W_2NCl_9] + HgCl_2 + HgClBr \quad (1)$$

$$[W_2NCl_9] \xrightarrow{130\,^\circ C} WNCl_3 + WCl_6 \quad (2)$$

The halide nitrides can be separated from the accompanying mercury halides by heating in vacuo. In this way, starting from the metal pentachlorides, the chloride nitrides of molybdenum(v) and tungsten(v) were also obtained for the first time [Eq. (3), M = Mo, W].[8, 9]

$$[MCl_5]_2 + [Hg_2N]Br \longrightarrow [M_2NCl_7] + HgCl_2 + HgClBr \quad (3)$$

This reaction can also be extended to the synthesis of bromide nitrides. Thus, on heating tungsten hexabromide with $[Hg_2N]Br$ in dibromomethane, $WNBr_3$ is smoothly obtained,[10] from tungsten pentabromide the corresponding $[W_2NBr_7]$,[10] (Scheme 2, below) and from molybdenum tetrabromide the nitrido complex of tetravalent molyb-

[*] Prof. Dr. K. Dehnicke
Fachbereich Chemie der Universität
Hans-Meerwein-Strasse, D-W-3550 Marburg/Lahn (FRG)
Prof. Dr. J. Strähle
Institut für Anorganische Chemie der Universität
Auf der Morgenstelle 18, D-W-7400 Tübingen 1 (FRG)

denum[10] [Eq. (4)]. All these reactions proceed almost quantitatively and are thus also suitable for the synthesis of ^{15}N-labeled complexes.[7]

$$2MoBr_4 + [Hg_2N]Br \longrightarrow [Mo_2NBr_5] + 2HgBr_2 \quad (4)$$

According to the IR spectra and magnetic susceptibilities the halide nitrides are coupled both via nitrido- as well as via halogeno-bridges, whereby high M–N bond orders are realized even in the case of compounds with bent M–N–M bridges (Scheme 2).

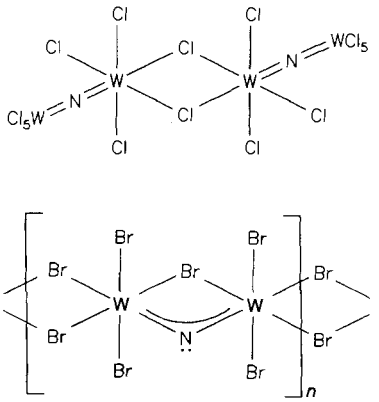

Scheme 2. Schematic structure of the compounds $[\{W_2NCl_9\}_2]$ (top) and $[\{W_2NBr_7\}_n]$ (bottom).

The complex $[Mo_2NCl_7]$, obtainable by reaction (3), can be oxidized with chlorine in $POCl_3$ to give the mixed valent Mo^V/Mo^{VI} chloride nitride $[Mo_2NCl_8]$, which can be converted by reaction with tetraphenylphosphonium chloride into $(PPh_4)_2[\{Mo_2NCl_9\}_2]$.[11] The structure of the anion

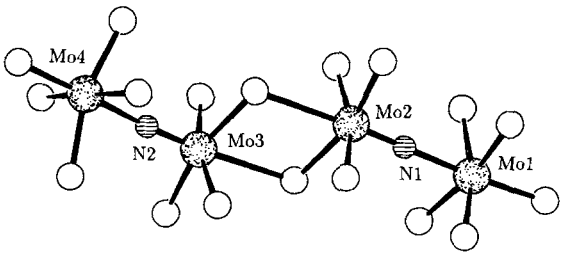

Fig. 1. Structure of the anion $[\{Mo_2NCl_9\}_2]^{2-}$. The white spheres are Cl atoms

(Fig. 1) compares with that of the $[\{W_2NCl_9\}_2]$ molecule, however the Mo–N–Mo bridge with Mo–N distances of 167 and 212 pm is markedly asymmetric.[11] The anion can therefore be regarded as a donor–acceptor complex of $[MoNCl_4]^-$ and $MoCl_5$. Indeed, it can be readily prepared from these components in dichloromethane.[11]

Also $[W_2NCl_7]$ can be oxidized with chlorine to the mixed valent complex $[W_2NCl_8]$, which, unlike $[Mo_2NCl_8]$ reacts with PPh_4Cl with formation of the dianion $[W_2NCl_{10}]^{2-}$.[9] A crystal structure analysis of the $AsPh_4^+$ salt[12] revealed eclipsed arrangement of the equatorial chlorine atoms and a linear W–N–W axis with W–N distances of 171 and 203 pm, consistent with the formulation $W{\equiv}N^{\oplus}{-}W^{\ominus}$. Unclear is which of the two tungsten atoms is pentavalent; possibly it is the one with the short W–N bond, since with d^1 configuration one has to reckon with Jahn–Teller stabilization which can be effective along the fourfold axis. Consistent with this is the conspicuously short W–W distance of 373.3 pm, which is significantly shorter than in W–N–W bridged tungsten(VI) complexes such as $[WNCl_3 \cdot POCl_3]_4 \cdot 2POCl_3$[1] with W–W distances of 386.0 pm. A W–W distance of 372.8 pm analogous to that in the $[W_2NCl_{10}]^{2-}$ ion was also found in the tetrameric anion of $(NHMe_3)_2[\{WO_2Cl_2(H_2O)\}_4] \cdot 2H_2O$ in which tungsten(V) and tungsten(VI) atoms are likewise coupled via linear W–O–W bridges.[13]

Kurt Dehnicke was born in 1931 in Köln. He studied chemistry from 1950 to 1955 in Leipzig and was awarded his doctorate in 1957 at Stuttgart for research on boron trifluoride adducts of amino acids under the supervision of J. Goubeau. In 1965 he habilitated in inorganic chemistry with work on the chemistry of compounds containing electropositive chlorine. Two years later he accepted a position as professor at the University of Marburg. In 1989 he was awarded the Wilhelm Klemm Prize of the German Chemical Society. His main areas of research are transition-metal complexes with metal–nitrogen multiple bonds, alkyne complexes of transition metals in high oxidation states, and polyselenido and polytellurido complexes.

Joachim Strähle, born 1937 in Dresden, studied chemistry in Stuttgart from 1958 to 1963, and was awarded his doctorate in 1965 for research on metal azide halides and metal nitride halides under the supervision of K. Dehnicke. After three years with G. Brauer in Freiburg and five years with H. Bärnighausen in Karlsruhe (introduction to crystal structure analysis) he habilitated in 1973 with a treatise on the synthesis and crystal structures of metal–nitrogen compounds. In the same year he took up an appointment at the University of Tübingen as Head of the Department of Inorganic Structural Chemistry. As successor to W. Rüdorff (1975) he has occupied the chair for Inorganic Chemistry I at Tübingen since 1976. The areas of research carried out by his group concerned the synthesis and crystal structure analysis of mixed transition metal gold clusters, coordination compounds with nitrogen donor ligands, and metal fluoride nitrides.

2.2. Reactions with $N(SiMe_3)_3$ and with $N(SnMe_3)_3$

Silylated and stannylated amines, even though infrequently used, are very efficient nitride transfer reagents. Tris(trimethylsilyl)amine reacts with tungsten hexachloride in the cold to give very pure $[W_2NCl_9]$ [Eq. (5)], at room temperature to give $WNCl_3$[14] [Eq. (6)].

$$2\,WCl_6 + N(SiMe_3)_3 \xrightarrow{T<20\,^{\circ}C} [W_2NCl_9] + 3\,ClSiMe_3 \quad (5)$$

$$WCl_6 + N(SiMe_3)_3 \xrightarrow{T\approx 20\,^{\circ}C} WNCl_3 + 3\,ClSiMe_3 \quad (6)$$

There are indications that the reactions (5) and (6) proceed with stepwise cleavage of trimethylchlorosilane. In the case of $[MoNCl_4]^-$ the reaction stops at the first substitution step. The reaction product $[MoNCl_3\{N(SiMe_3)_2\}]^-$ can be isolated as the tetraphenylphosphonium salt[15] (Fig. 2). Besides the very short Mo–N distance of the nitrido ligand (164.8 pm), which corresponds to a Mo≡N triple bond, the Mo–N bond of the amido ligand (193.7 pm) also has a remarkable amount of π-bond character. Accordingly the geometry around the nitrogen atom N1 is planar (Scheme 3).

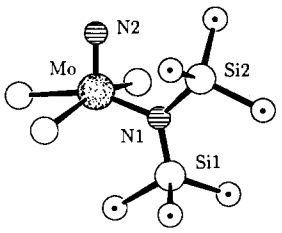

Fig. 2. Structure of the anion $[MoNCl_3\{N(SiMe_3)_2\}]^-$. The white spheres attached to the Mo atom are Cl atoms, the spheres with central dots and attached to the Si atoms are C atoms of the methyl groups.

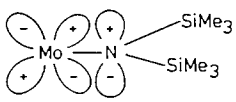

Scheme 3. Planar environment at the N atom of the amido ligand due to partial π-bonding of the Mo–N bond.

The metal–nitrogen bond has even more π-bond character in the monomeric nitreno-complex[*] $[Cl_3V^{\ominus}{\equiv}N^{\oplus}{-}SiMe_3]$ (obtainable via an alternative route from VCl_4 and Me_3SiN_3) with a V–N–Si bond angle of 177.5° and very short V–N bond length of 159 pm, corresponding to a V≡N triple bond.[16]

The $[W_2NCl_9]$ complex accessible via reaction (5) reacts with tetraphenylphosphonium chloride with formation of $[W_2NCl_{10}]^-$, in which, as in $[W_2NCl_{10}]^{2-}$[9, 12] eclipsed arrangement of the equatorial chlorine atoms is observed[14] (Fig. 3).

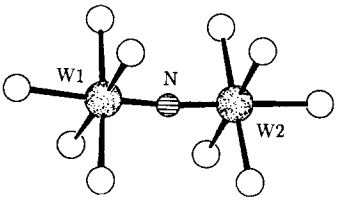

Fig. 3. Structure of the anion $[W_2NCl_{10}]^-$. The white spheres are Cl atoms.

Other than in the $[W_2NCl_{10}]^{2-}$ ion the two tungsten atoms are now coupled via an almost symmetrical nitrido bridge with a W–N–W bond angle of 173° and W–N distances of 179 and 188 pm, corresponding approximately to double bonds. The marked *trans* influence of the nitrido ligand, expressed in the 9 pm longer W–Cl distances in comparison to the usual W–Cl bond lengths in *cis* position. Similar conditions are found in the anion of $(PMe_3Ph)_2[Ta_2OCl_{10}]$,[17] which is isoelectronic with the $[W_2NCl_{10}]^-$ ion. Here the Ta–Cl distances $Ta{-}Cl_{ax}/Ta{-}Cl_{eq}$ (ax = axial, eq = equatorial) differ by only 4 pm because of the smaller *trans* influence of the oxo ligand of the Ta–O–Ta bridge.[17]

In dichloromethane solution the $[W_2NCl_{10}]^-$ ion slowly decomposes with cleavage of tungsten hexachloride and formation of the trinuclear μ-nitrido complex $[W_3N_2Cl_{14}]^{2-}$[18] [Eq. (7)].

$$2[W_2NCl_{10}]^- \longrightarrow [W_3N_2Cl_{14}]^{2-} + WCl_6 \quad (7)$$

The structure analysis shows an almost linear arrangement of the skeletal atoms and eclipsed position of all twelve equatorial chlorine atoms (Fig. 4). The W–N distances at the central tungsten atom W2 (207 pm) compare very closely with the value expected for single bonds, whereas the other two W–N distances (184 pm) can be regarded almost as double bonds. The reason for the relatively long W–N bonds at the central tungsten atom might be due to the competition of the two N atoms for the electrons of the d_{z^2} orbital.

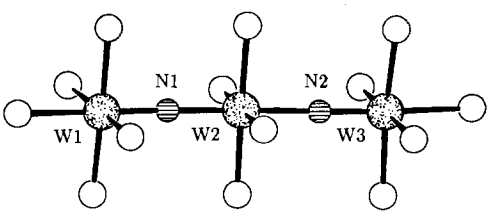

Fig. 4. Structure of the anionic μ-nitrido complex $[W_3N_2Cl_{14}]^{2-}$. The white spheres are Cl atoms.

If one of the chlorine atoms in $[W_2NCl_9]$ is substituted by the bidentate chelate ligand of the dichlorophosphate ion an unusual bridging of the W–N–W axis with simultaneous narrowing of the W–N–W bond angle to 166.2°[19] occurs (Fig. 5).

[*] In this article, complexes with linear $M{\equiv}\overset{\ominus}{N}{-}\overset{\oplus}{X}$ arrangement (sp-hybridized N atom) are designated as nitreno complexes, those with bent M=N̈-X arrangement (sp^2-hybridized N atom) as imido complexes [1].

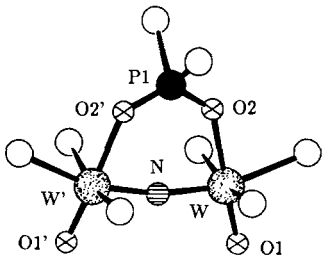

Fig. 5. Structure of the anion $[Cl_3OWNWOCl_3(O_2PCl_2)]^{2-}$. The white spheres are Cl atoms, the crossed spheres O atoms, the black sphere a P atom.

An even smaller M–N–M bond angle of 128° is found in the structure of the cyclic complex $[\{Cp^*TaN(Cl)\}_3]$ ($Cp^* = C_5Me_5$) forming an almost planar six-membered Ta_3N_3 ring, and which can be regarded to a first approximation as triazatritantalabenzene[20] (Fig. 6). The Ta–N

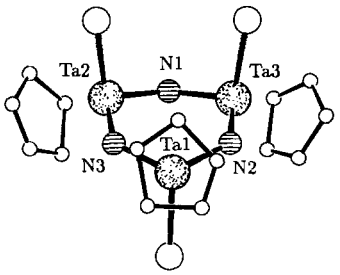

Fig. 6. Structure of the benzene-analogous nitrido complex $[\{Cp^*TaN(Cl)\}_3]$. For clarity, the methyl groups attached to the Cp* ligand have been omitted. The C atoms are depicted as small white spheres, the Cl atoms as large white spheres.

distances vary only very little in the range from 184 to 191 pm, corresponding approximately to Ta=N double bonds, if one regards the value of 185 pm in the anion of $(NH_4)_3[Br_5Ta{=}N{=}TaBr_5]$[1] as reference.

The compound was obtained in the form of shiny yellow crystals upon reaction of $[Cp^*TaCl_4]$ and $N(SnMe_3)_3$ at 50 °C in toluene[20] [Eq. (8)]. The corresponding methyl compound $[\{Cp^*TaN(CH_3)\}_3]$ is formed upon ammonolysis of $[Cp^*TaMe_4]$[21] [see Eq. (12)].

$$3[Cp^*TaCl_4] + 3N(SnMe_3)_3 \longrightarrow [\{Cp^*TaN(Cl)\}_3] + 9Me_3SnCl \quad (8)$$

The unusual stability of benzene-analogous cyclic trimers of metal nitrides had been predicted shortly beforehand by R. Hoffmann et al.[22] (see Section 6).

2.3. Reactions with Ammonia

Reactions of metal halides with ammonia generally lead to mixtures of substances owing to the formation of ammonium halide as by-product. Thus, for example, ammonolysis of niobium pentabromide leads to a mixture of amido- and imido-derivatives and NH_4Br, and, upon heating at 220 °C simultaneous sublimation of the ammonium bromide and formation of a bromide nitride $[Nb_6Br_9N_7]$ of unknown structure occurs.[23] To overcome this problem a new synthetic strategy was developed in which the ammonium halide itself is used as reactant. In this way it was possible to synthesize the binuclear μ-nitrido-complexes $(NH_4)_3[Nb_2NBr_{10}]$ [Eq. (9)], $(NH_4)_3[Ta_2NI_{10}]$ and $(NH_4)_3[W_2NBr_{10}]$ [Eq. (10)] by reaction with the pentahalides of niobium and tantalum as well as with tungsten hexabromide at temperatures between 300 and 420 °C.[24]

$$2NbBr_5 + 4NH_4Br \longrightarrow (NH_4)_3[Nb_2NBr_{10}] + 4HBr \quad (9)$$

$$6WBr_6 + 14NH_4Br \longrightarrow 3(NH_4)_3[W_2NBr_{10}] + 20HBr + N_2 \quad (10)$$

According to the crystal structure analysis of $(NH_4)_3[Nb_2NBr_{10}]$ the anion has D_{4h} symmetry and a linear, symmetrical nitrido bridge with Nb–N distances of 184.5 pm, as would be expected for double bonds.[24]

Roesky et al. overcame the problems of the ammonolysis of metal halides in another way when they treated the trimethyl derivative $[Cp^*Ti(CH_3)_3]$ with ammonia, and were able to prepare a titanium imide nitride in good yields according to Equation (11) via elimination of methane.[25]

$$3[Cp^*Ti(CH_3)_3] + 4NH_3 \longrightarrow [\{Cp^*Ti(NH)\}_3N] + 9CH_4 \quad (11)$$

According to the structure analysis the nitrido-ligand N1 links all three titanium atoms, while the imido ligands form μ_2-bridges between the Ti-atoms[25] (Fig. 7). The Ti–N1 distances of 191 pm indicate a small amount of π-bonding character.

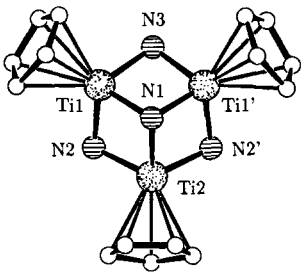

Fig. 7. Structure of the imidonitrido complex $[\{Cp^*Ti(NH)\}_3N]$. For clarity the methyl groups attached to the Cp* ligand and the H atoms at the imido groups have been omitted.

The previously mentioned $[\{Cp^*TaN(CH_3)\}_3]$ could be obtained in a similar way from $[Cp^*Ta(CH_3)_4]$ and excess ammonia in benzene at 20 °C[21] [Eq. (12)].

$$[Cp^*Ta(CH_3)_4] + NH_3 \longrightarrow \tfrac{1}{3}[\{Cp^*TaN(CH_3)\}_3] + 3CH_4 \quad (12)$$

The binuclear μ-nitridoosmium(IV) complex $[(NH_3)_5Os{-}NOs(NH_3)_5]Cl_5 \cdot H_2O$ is formed in astonishingly good yields in a strongly exothermic reaction upon treatment of solid $(NH_4)_2[OsCl_6]$ with hydrazine hydrate.[26] The reaction in-

volves disproportionation of hydrazine into N_2 and NH_3, so that it can be formulated as in Equation (13).

$$2(NH_4)_2[OsCl_6] + 14NH_3 + H_2O \longrightarrow [Os_2N(NH_3)_{10}]Cl_5 \cdot H_2O + 7NH_4Cl \quad (13)$$

Owing to the strong *trans* effect of the nitrido ligand of the linear Os–N–Os bridge, the *trans* NH_3-ligands can be readily replaced, so the complex can serve as starting material for the synthesis of complexes of the type $[X(NH_3)_4OsNOs(NH_3)_4X]Cl_5$.[26] Interestingly, reaction (13) takes another course if the components are allowed to react with each other in the reversed order. Addition of solid $(NH_4)_2[OsCl_6]$ to hydrazine hydrate then leads to formation of the dinitrogen complexes $[Os(NH_3)_5(N_2)]Cl_2$ and $[Os(NH_3)_4(N_2)_2]Cl_2$.[26]

A similar result as depicted in Equation (13) is observed however in the albeit experimentally more time-consuming reaction of $(NH_4)_2[OsCl_6]$ with concentrated aqueous ammonia at 150 °C in a Carius tube. After 9 days the μ-nitrido complex $[Os_2N(NH_3)_8Cl_2]Cl_3 \cdot 2H_2O$ was obtained.[27]

The result of the reaction of $(t\text{BuCH}_2)_3\text{Ta}{=}\text{CH}t\text{Bu}$ with ammonia at room temperature in benzene[28] [Eq. (14)] is

$$(t\text{BuCH}_2)_3\text{Ta}{=}\text{CH}t\text{Bu} \xrightarrow{NH_3} \tfrac{1}{5}[\{(t\text{BuCH}_2)_2\text{TaN}\}_5] + 2\text{CMe}_4 \quad (14)$$

most remarkable. The product crystallizes from toluene together with one coordinated NH_3 molecule and with the composition $[\{(t\text{BuCH}_2)_2\text{TaN}\}_5] \cdot NH_3 \cdot 2C_7H_8$; a crystal structure analysis indicated the unusual T-shaped coupling of three of the five nitride groups and two μ_2-nitrido bridges with a very small bond angle of 98°[28] (Fig. 8).

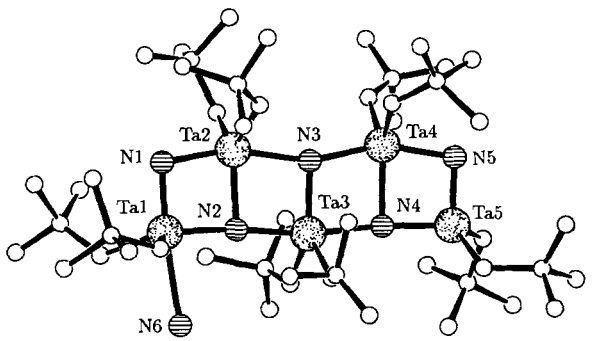

Fig. 8. Structure of $[\{(t\text{BuCH}_2)_2\text{TaN}\}_5] \cdot NH_3$. The white spheres are C atoms.

The Ta_5N_5 skeleton is almost planar; it is best formulated as in Scheme 4. The edge-sharing Ta_2N_2 units reproduce the coupling motif of cubic TaN, into which the compound can be converted by heating at 820 °C.[28]

For further details on the T-shaped coupling of metal atoms and on nitrido bridges with very small bond angles, see also Section 3.4.

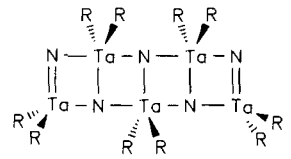

Scheme 4. Schematic representation of the Ta_5N_5 framework in $[\{(t\text{BuCH}_2)_2\text{TaN}\}_5]$.

2.4. Reactions with Nitrogen Trichloride

Reactions with nitrogen trichloride do not present any danger when carried out in CCl_4 solution; their use for the synthesis of nitrido complexes is, however, somewhat limited, but in the few cases where they can be used they are very efficient. Aside from the previously described synthesis of $[ReNCl_4]$ from $ReCl_5$[1] and the reaction of $MoCl_5$ with NCl_3, which led to $[MoNCl_4]_2$,[29] none of the known metal chlorides was found to react with NCl_3.

In contrast, reactions of the hexacarbonyls of molybdenum and tungsten with excess nitrogen trichloride led in almost quantitative yields to the synthetically very useful *N*-chloronitreno complexes [Eq. (15), M = Mo, W].[30, 31] The *N*-bound chlorine atom in these compounds has a marked ($\delta+$)-character. Thermolysis accordingly leads with cleavage of chlorine to the chloride nitrides $MNCl_3$[30, 31] [Eq. (16)].

$$2[M(CO)_6] + 4NCl_3 \longrightarrow [\{Cl_4M{\equiv}N\text{-}Cl\}_2] + N_2 + Cl_2 + 12CO \quad (15)$$

$$[\{Cl_4M{\equiv}N\text{-}Cl\}_2] \longrightarrow 2MNCl_3 + 2Cl_2 \quad (16)$$

To our knowledge this is the most efficient entry to the chloride nitrides $MoNCl_3$ and $WNCl_3$, which in turn are the most important starting substances in the complex chemistry of the nitrides of molybdenum and tungsten.

The partial positive character of the *N*-bound Cl atom is also manifested in the capability of the pentachloro derivative $[Cl_5W{\equiv}N\text{-}Cl]^-$ as PPh_4^+ salt to bind a chloride ion[32] (Fig. 9). The chloride ion coordinates with formation of a linear Cl_3-bridge between two anions.

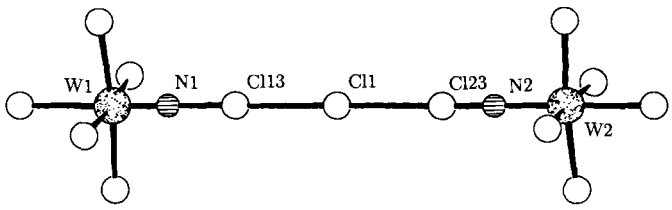

Fig. 9. Structure of the binuclear *N*-chloronitrene complex with the bridging chloride ion $[\{Cl_5W(NCl)\}_2Cl]^{3-}$.

2.5. Oxidation of Coordinated NH_3-Ligands

An elegant entry to nitrido complexes of osmium and chromium was opened up by the reaction of strong oxidizing agents such as cerium(IV)[33] [Eq. (17)] or sodium hypochlorite[34] [Eq. (18)] with complexes containing NH_3 ligands.

Reaction (17) corresponds to an oxidation of the osmium atom from +III to +VI, reaction (18) to an oxidation of the chromium atom from +III to +V. In exactly the same way it was also possible to synthesize the first nitrido complexes of manganese(V), namely [MnN(ttp)] and [MnN(oepMe$_2$)] [ttp = 5,10,15,20-tetra-*p*-tolylporphyrinate(2−); (oepMe$_2$)$^{2-}$ = α-γ-dimethyl-α-γ-dihydrooctaethylporphyrinate].[35, 36]

$$[Os(NH_3)_6]^{3+} + 3Ce^{4+} + H_2O \longrightarrow [:N{\equiv}Os(NH_3)_4(OH_2)]^{3+} + 3Ce^{3+} + 2H^+ + NH_4^+ \quad (17)$$

$$[Cr(ttp)(OH)(NH_3)] + OCl^- \longrightarrow [:N{\equiv}Cr(ttp)] + Cl^- + 2H_2O \quad (18)$$

According to crystal structure analyses the metal atoms in the porphyrinato complexes are fivefold coordinated, with extremely short M≡N: distances of 156.5 pm in the case of the chromium complex[37] and 151.2 pm in the case of the manganese complex.[36] Upon chlorination of the NH_3 ligand in the phthalocyaninatomanganese complex [(NH_3)Mn(OH)pc] with elemental chlorine, which leads according to Equation (19) to the corresponding nitridomanganese(V) complex, intermediary formation of the *N*-chloronitreno complex [(ClN)Mn(pc)] with manganese(IV) is assumed.[38]

$$2[(H_3N)Mn(pc)(OH)] + 2Cl_2 \longrightarrow 2[:N{\equiv}Mn(pc)] + 2H_2O + 4HCl \quad (19)$$

2.6. Thermolysis and Photolysis of Azido Complexes

The chemistry of coordinated azide groups was reviewed in 1985.[39] Many of the known decomposition reactions of azides, which lead to nitrido complexes, are thermally induced.[1, 39] The conversion of an azido ligand M−N_3 into a nitrido ligand M≡N: via N_2-cleavage is accompanied by a two-step oxidation of the metal atom. The formation of the nitrido complex [$MoN(N_3)$(dppe)$_2$][40] (dppe = $Ph_2PCH_2CH_2PPh_2$) observed in the reaction of [$Mo(N_2)_2$(dppe)$_2$] with trimethylsilyl azide would therefore suggest [$Mo(N_3)_2$(dppe)$_2$] as being the initial product. In the nitrido complex the Mo–N distance to the nitrido ligand (179 pm) is remarkably long; it corresponds almost to a double bond.[40]

In the synthesis of the corresponding tungsten complex [$WN(N_3)$(dppe)$_2$], the authors found evidence of a radical reaction following previous replacement of N_2 by Me_3SiN_3.[41]

The synthesis of *trans*-[$MoN(N_3)$(depe)$_2$] (depe = $Et_2PCH_2CH_2PEt_2$) starting from *trans*-[$Mo(N_2)_2$(depe)$_2$] proceeds analogously; however, in this case, formation of the linearly bridged, trinuclear complex [{$MoN(N_3)$(depe)$_2$}$_2$$MoN(N_3)_2$] with a bond angle of 156.3° at the central molybdenum(V) atom is also observed (Scheme 5).[42] The terminal Mo≡N: bond (167 pm), as expected, is somewhat shorter than the Mo^{IV}≡N bridge-bond length (170 pm).

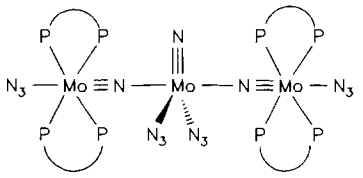

Scheme 5. Schematic representation of the linearly bridged, trinuclear complex [{$MoN(N_3)$(depe)$_2$}$_2$$MoN(N_3)_2$].

Cyclovoltammetric measurements show a reversible one-electron reduction of the molybdenum(V) atom with a potential ($E^{0\prime}$) of −2.10 V relative to ferrocenium/ferrocene in THF solution.[42]

Thermolysis of the tetraazidepyridine complex of molybdenum leads to the corresponding monomeric triazidonitrido complex with fivefold coordinated molybdenum atom[43] [Eq. (20)], whereas reaction of the tetrachloroterpyridyl

$$[Mo(N_3)_4(py)_2] \longrightarrow [MoN(N_3)_3(py)] + N_2 + py \quad (20)$$

complex with trimethylsilyl azide leads, after partial Cl/N_3 exchange, to the azido-chloro-nitrido complex [$MoN(N_3)_2$Cl(terpy)][44] [Eq. (21)]. In this complex, the

$$[MoCl_4(terpy)] + 3Me_3SiN_3 \longrightarrow [MoN(N_3)_2Cl(terpy)] + N_2 + 3ClSiMe_3 \quad (21)$$

molybdenum has an unusual pentagonal-bipyramidal environment with the chloro ligand in the axial position[44] (Fig. 10).

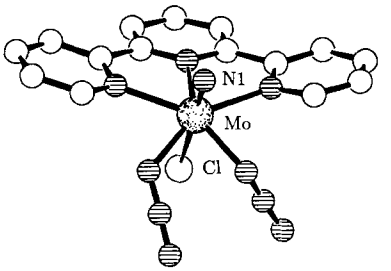

Fig. 10. Structure of the nitrido complex [$MoN(N_3)_2$Cl(terpy)]. With exception of the atom labeled as Cl, all white spheres are C atoms.

The nitridoniobium(V)-complex [{$NbNCl_2 \cdot SMe_2$}$_n$] could be prepared in a corresponding way by reaction of trimethylsilyl azide with the niobium(III) complex [$Nb_2Cl_6(SMe_2)_3$].[45] Osmium(IV) complexes can also be readily oxidized with trimethylsilyl azide to give nitridoosmates(VI), as shown by the example in Equation (22) (L = PPh_3).[46]

The origin of the $[Ph_3PNH_2]^+$ ion can be explained by hydrolysis of the $SiMe_3NPPh_3$ formed at the same time by Staudinger reaction.

Addition of $(NEt_2H_2)[S_2P(OMe)_2]$ to a mixture of [$MoCl_3(thf)_3$] and trimethylsilyl azide leads to formation of orange-brown crystals of the tetrameric complex [{$Mo^VN[S_2P(OMe)_2]_2$}$_4$], the sole example of a square Mo_4N_4 unit with four symmetric Mo=N=Mo bridges.[47] The Mo–N bond distances are, within statistical deviation, equal and with a value of 186.5 pm correspond very well with the value ex-

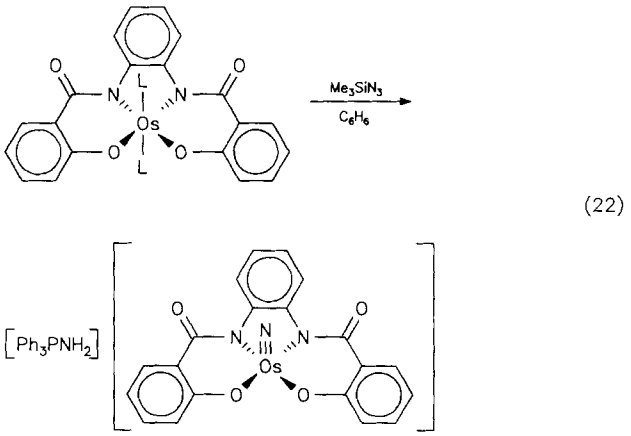

(22)

pected for double bonds. Consistent with this finding, the observed ferromagnetism is explained in terms of a superexchange mechanism.[47]

The photolytic decomposition of a chromium azide was first described in 1981.[48] Irradiation of azido-*N*,*N*'-ethylenebis(salicylaldiminato)chromium(III) with light of wavelength 320 nm smoothly furnished a nitrido chromium(v) complex[48] [Eq. (23)].

$$[Cr(N_3)(salen)] \cdot 2H_2O \xrightarrow{h\nu} [CrN(salen)]\ H_2O + N_2 + H_2O \qquad (23)$$

Later, Groves et al. obtained by photolysis of the azido-tetra-*p*-tolylporphyrinatochromium(III) complex in CH_2Cl_2 solution the corresponding nitrido complex of pentavalent chromium in which, according to the crystal structure analysis, the chromium is fivefold coordinated and the nitrido ligand is in the apical position.[37] In an analogous way azidometal(III)porphyrins of chromium, manganese and iron were also converted into the corresponding nitrido complexes [MN(ttp)],[49] and from [Cr(N$_3$)(bpb)] [bpb = 1,2-bis[2-pyridinecarboxamido(2−)]benzene] the nitrido complex [CrN(bpb)] was obtained.[50]

2.7. Reactions with Trithiazyl Chloride

Some nitrido complexes are best prepared by reaction of metal chlorides with the readily accessible trithiazyl chloride $(NSCl)_3$. Initially, chlorothionitreno complexes are formed in which the $[\ddot{N}{=}\ddot{S}{-}Cl]^{2-}$ ligand, which does not exist in the free state, is bound at the metal atom with linear arrangement of the elements M–N–S as $M{=}\overset{\ominus}{N}{=}\overset{\oplus}{\ddot{S}}{-}Cl$.[51] An example is provided by the reaction with tungsten hexachloride[52] [Eq. (24)].

$$2WCl_6 + \tfrac{2}{3}(NSCl)_3 \longrightarrow [\{Cl_4W(NSCl)\}_2] + 2Cl_2 \qquad (24)$$

Some of the initially formed chloronitreno complexes furnish the corresponding nitrido complexes under gentle, thermally-induced conditions [Eq. (25–27)].[53, 54]

$$[\{Cl_4Mo(NSCl)\}_2] \xrightarrow{130\,^\circ C} 2MoNCl_3 + 2SCl_2 \qquad (25)$$

$$PPh_4[Cl_5Mo(NSCl)] \xrightarrow[CH_2Cl_2]{20\,^\circ C} PPh_4[MoNCl_4] + SCl_2 \qquad (26)$$

$$[(Cl_3PO)ReCl_4(NSCl)] + AsPh_4Cl \xrightarrow[CH_2Cl_2]{20\,^\circ C} AsPh_4[ReNCl_4] + POCl_3 + SCl_2 \qquad (27)$$

Reduction of the chlorothionitreno complex used as educt in Equation (27) with triphenylphosphane leads in good yields to a nitridorhenium(v) complex[55] [Eq. (28)].

$$2[(POCl_3)ReCl_4(NSCl)] + 9PPh_3 \longrightarrow 2[ReNCl_2(PPh_3)_2] + 3PPh_3Cl_2 + 2PPh_3S + 2POCl_3 \qquad (28)$$

This complex had already been prepared earlier by Chatt et al. by reaction of $Na[ReO_4]$ with hydrazine dihydrochloride in the presence of PPh_3;[56] according to the structure analysis[57] the rhenium atom is fivefold coordinated with a coordination geometry between trigonal-bipyramidal and tetragonal-pyramidal. In contrast, the corresponding nitrido complex with the less bulky dimethylphenylphosphane, $[ReNCl_2(PMe_2Ph)_3]$, contains sixfold coordinated rhenium with one of the chloro ligands *trans* to the nitrido group.[58]

In attempts at the transhalogenation of the chlorothionitreno complexes of molybdenum and tungsten with trimethylbromosilane only $[WCl_4(NSCl)]$ could be converted into the bromo complex $[WBr_4(NSBr)]$, whereas the molybdenum compound reacted smoothly and quantitatively with formation of $MoNBr_3$[59] [Eq. (29)]. Reaction (29) opens up a simple preparative entry to $MoNBr_3$ compared to the synthesis from $MoBr_4$ and iodine azide.[1]

$$[\{MoCl_4(NSCl)\}_2] + 10BrSiMe_3 \longrightarrow 2MoNBr_3 + S_2Br_2 + Br_2 + 10ClSiMe_3 \qquad (29)$$

The transhalogenation of $[\{Cl_4Mo(NSCl)\}_2]$ with sodium fluoride in acetonitrile solution in the presence of [15]crown-5 as phase transfer reagent at 80 °C also led to a nitrido complex[60] [Eq. (30)].

$$[\{MoCl_4(NSCl)\}_2] + 12NaF + 2[15]crown\text{-}5 \xrightarrow{80\,^\circ C} [Na([15]crown\text{-}5)]_2[(MoNF_4)_2] + 2SF_2 + 10NaCl \qquad (30)$$

The compound crystallizes as ion triplet (Fig. 11), in which the sodium atoms coordinated fivefold by the crown ether molecules form short Na···F contacts to the axially arranged F atoms of the $[(MoNF_4)_2]^{2-}$ ion.

The Na···F distances of 234 pm are only slightly longer than in the sodium fluoride structure (230.7 pm). The molybdenum atoms of the anion are coupled via asymmetric fluoro bridges with Mo–F distances of 198 and 245 pm, whereby the long Mo–F bond is a result of the strong *trans* influence of the terminal nitrido ligands. The small Mo–F–Mo bridge angle of 109° is unusual, since up to now only bridging angles

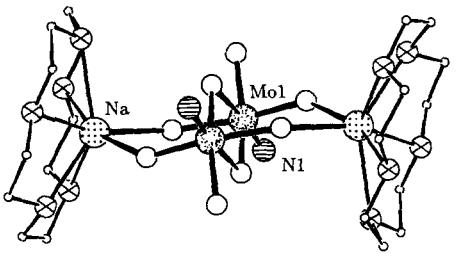

Fig. 11. Structure of the ion triple $[Na([15]crown-5)]_2[(MoNF_4)_2]$. The white spheres are F atoms, the smaller white spheres C atoms, and the crossed white spheres O atoms.

between 132° and 180° have been observed for fluorides of 4d and 5d metals.[61]

2.8. Direct Syntheses from the Elements

Kniep et al. were able to prepare the ternary nitrido complexes $Li_6[MN_4]$ (M = Cr, Mo, W)[62] and $Ba_3[MN_4]$ (M = Mo, W)[63] from the elements by high-temperature syntheses; the complexes were obtained as pale yellow to reddish-brown, moisture-sensitive single crystals. According to the crystal structure analyses only slightly distorted $[MN_4]^{6-}$ tetrahedra are present, in which the bond lengths (M = Cr, 176–178 pm; M = Mo, 185–189 pm; M = W, 189–193 pm) have marked π-bond character.

2.9. Special Synthetic Methods

The $[VNCl_3]^-$ ion, isoelectronic with the $VOCl_3$ molecule, is obtained upon reaction of $[Ph_3PNPPh_3]Cl$ with $[Cl_3V{\equiv}N\text{-}SiMe_3]$ in dichloromethane[64] [Eq. (31)].

The V≡N bond (6.9 $N\,cm^{-1}$) has an equally large valence force constant as the V≡O bond in the $VOCl_3$ molecule.[64]

$$[Ph_3PNPPh_3]Cl + Cl_3VNSiMe_3 \longrightarrow [Ph_3PNPPh_3][VNCl_3] + ClSiMe_3 \quad (31)$$

Also the reactions of $Cl_3VNSiMe_3$ with bases such as 2,2′-bipyridyl (bpy), pyridine (py) or quinuclidine (quin) lead to a cleavage of chlorotrimethylsilane and formation of the complexes $[VNCl_2(bpy)]$,[64] $[VNCl_2(py)_2]$[65] and $[VNCl_2(quin)_2]$, respectively.[65]

On the other hand, the trimethylsilylimido complexes $[MCl_2(NSiMe_3)L_3]$ (M = Mo, W; L = phosphane) and $[WCl_2(NSiMe_3)_2L]$ show no tendency to be converted into the corresponding nitrido complexes.[66] The pyridine complex $[VNCl_2(py)_2]$ (Fig. 12) is also formed upon heating the cyclothiazeno complex $[\{VCl(N_3S_2)(Py)_2\}_2]$ in toluene.[67] According to crystal structure analyses the $[VNCl_2(py)_2]$ complexes are stacked into columns via alternating long $V{\equiv}N\cdots V{\equiv}N$ bridges with V–N distances of 160 and 256 pm.[65, 67]

With bulky amino bases such as quinuclidine, monomeric, readily soluble complexes with fivefold coordination at the

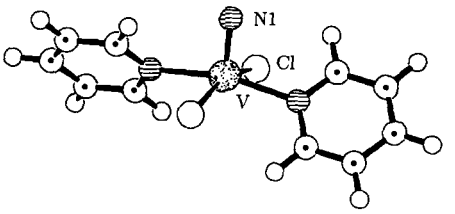

Fig. 12. Structure of the complex $[VNCl_2(pyridine)_2]$. The white spheres are Cl atoms, the smaller white spheres H atoms, and the spheres with central dot C atoms.

vanadium atom are formed. The V≡N distance of 157 pm in $[VNCl_2(quin)_2]$ corresponds to a triple bond.[65]

The reaction of molybdenum(II) benzoate with trimethylsilyl azide in the presence of PPh_4Cl led in an unexpected redox reaction with participation of the solvent dichloromethane to the azidochloronitrido complex $[\{MoN(N_3)_3Cl\}_2]^{2-}$[68] [Eq. (32)].

$$[Mo_2(O_2CPh)_4] + 2PPh_4Cl + 4CH_2Cl_2 + 8Me_3SiN_3 \longrightarrow (PPh_4)_2[\{MoN(N_3)_3Cl\}_2] + 4Me_3SiOC(O)Ph + 2C_2H_4Cl_2 + 4Me_3SiCl + 2N_2 \quad (32)$$

In contrast to the monomeric structure of the tetraazidonitrido complex $[MoN(N_3)_4]^-$,[69, 70] the chloro derivative $[MoN(N_3)_3Cl]_2^{2-}$ is coupled via the α-N-atoms of two azido groups to give a centrosymmetric dimer with Mo–N distances of 208 and 260 pm[68] (Fig. 13). The long Mo–N

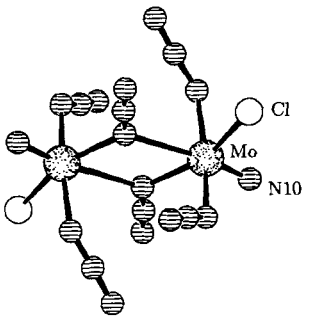

Fig. 13. Structure of the anion $[\{MoN(N_3)_3Cl\}_2]^{2-}$.

distance is in the *trans* position to the terminal nitrido ligand, whose Mo≡N distance of 164 pm corresponds to a triple bond.

A surprising redox reaction also forms the basis of a new alternative method for the synthesis of the nitrido complex $[\{MoNCl_3 \cdot POCl_3\}_4]$, which was obtained by heating the phosphoryl trichloride solvate $[MoCl_5 \cdot OPCl_3]$ with urea in boiling carbon tetrachloride[71] [Eq. (33)].

$$4[MoCl_5 \cdot OPCl_3] + 2OC(NH_2)_2 \longrightarrow [\{MoNCl_3 \cdot OPCl_3\}_4] + 2CO + 8HCl \quad (33)$$

Surprisingly, the elimination of $PhSO_2Cl$ from the nitreno complex $[Cl_4Mo{=}NSO_2Ph]$ also takes place in reverse to the

electrophilic addition of $PhSO_2Cl$ to the nitrido function (cf. Section 3.2) upon reaction with $[Ph_3PNPPh_3]Cl$ in dichloromethane[72] [Eq. (34)].

$$[MoCl_4(NSO_2Ph)] + 2[Ph_3PNPPh_3]Cl \longrightarrow [Ph_3PNPPh_3]_2[MoNCl_5] + PhSO_2Cl \quad (34)$$

An unusual entry to a nitridotungsten complex was found upon attempting to prepare an amidinato complex from tungsten hexachloride and *N,N,N'*-tris(trimethylsilyl)benzamidine[73] [Eq. (35)].

$$WCl_6 + [Ph-C(NSiMe_3)N(SiMe_3)_2] \longrightarrow [WNCl_3 \cdot NC-Ph] + 3\,ClSiMe_3 \quad (35)$$

Whereas numerous metal halides react with the silylated benzamidine to give amidinato complexes of type **G**,[74]

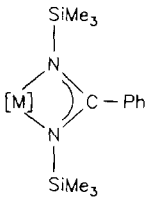

G

reaction (35) does not stop at this stage but leads, with further cleavage of $ClSiMe_3$ and formation of benzonitrile, to the nitridotungsten complex, which crystallizes as the tetramer.[73] The acetonitrile solvate $[WNCl_3 \cdot NCCH_3]$, which was obtained by reaction of tris(trimethylsilyl)amine with the *N*-chloronitrenotungsten complex, also crystallizes as the tetramer[75] [Eq. (36)].

$$3[WCl_4(NCl)(CH_3CN)] + N(SiMe_3)_3 \longrightarrow 3[WNCl_3 \cdot NCCH_3] + \tfrac{1}{2}N_2 + 1\tfrac{1}{2}Cl_2 + 3\,ClSiMe_3 \quad (36)$$

With an original metathetic reaction of *tert*-butylcarbonitrile and $[(tBuO)_3W{\equiv}W(OtBu)_3]$ leading to cleavage of the W≡W bond, Schrock et al. were able to prepare at one and the same time a nitrido complex and a carbyne complex of tungsten(VI)[76] [Eq. (37)].

$$tBu-C{\equiv}N + [(tBuO)_3W{\equiv}W(OtBu)_3] \longrightarrow [(tBuO)_3W{\equiv}N] + [(tBuO)_3W{\equiv}CtBu] \quad (37)$$

According to the crystal structure analysis the nitrido complex contains W≡N–W chains with markedly alternating W–N bond lengths[77] (Fig. 14). The corresponding molybdenum compound has a comparable structure with Mo–N distances of 166 and 286 pm.[78]

The rare trigonal-bipyramidal coordination was previously only observed in the structure of the trinuclear

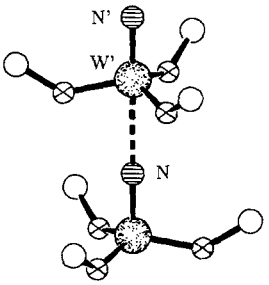

Fig. 14. Section of the polymeric structure of $[(tBuO)_3W{\equiv}N]$. The white spheres are C atoms, the crossed spheres O atoms. For clarity, the methyl groups of the *t*Bu residue have been omitted.

nitrenonitrido complex $CPh_3^+[Ph_3C-N{\equiv}WCl_4(\mu\text{-}F)WNCl_2(\mu\text{-}F)Cl_4W{\equiv}N\text{-}CPh_3]^-$ (Fig. 15), and in the structure of the trinuclear molybdenum complex $[\{\mu\text{-}MoN(N_3)_2\}\{NMo(N_3)(depe)_2\}_2]$[42] already described in Section 2.6.

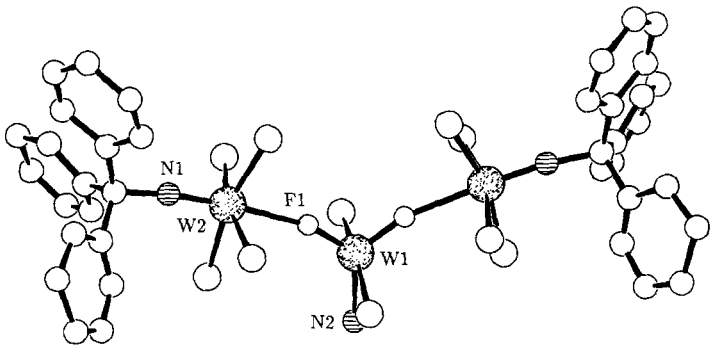

Fig. 15. Structure of the anion $[WNF_2Cl_2(Cl_4WNCPh_3)_2]^-$. The smaller white spheres which bridge two W atoms are F atoms; the larger white spheres attached to the W atoms are Cl atoms. The white spheres which are coordinated to the N atoms are C atoms of the triphenylmethyl groups.

Reactions of *tert*-butyl isocyanate with the dioxo complexes $[RuO_2Cl_3]^-$ and $[MO_2Cl_4]^{2-}$ (M = Ru, Os) in the form of their tetraphenylphosphonium salts in boiling acetonitrile led to some surprising results. The air-stable nitrido complexes $PPh_4[MN(tBuNC(O)NtBu)Cl_2]$ are formed which contain a *N,N'*-ureato(2–)-chelate ligand[80]

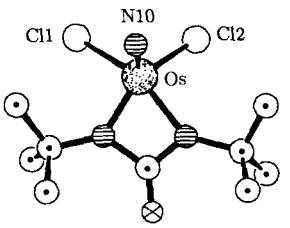

Fig. 16. Structure of the anion $[OsN(tBuNC(O)NtBu)Cl_2]^-$. The spheres with central dot are C atoms, the crossed spheres O atoms.

(Fig. 16). The formation of the ureato ligand most likely proceeds via an imido complex as intermediate [Eq. (38)].

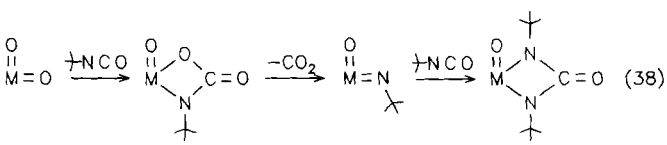

(38)

The ureato complex can subsequently react with a further molecule of *tert*-butyl isocyanate to give an imido complex, from which the nitrido ligand is finally formed by elimination of 2-methylpropene and HCl[80] [Eq. (39)].

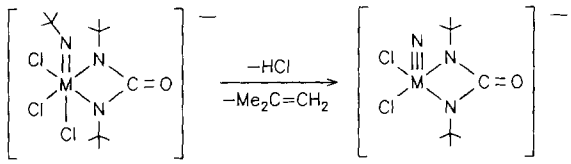

(39)

3. Chemical Reactions of the Nitrido Complexes

Many of the chemical reactions dealt with here lead with retention of the nitrido function to novel nitrido derivatives so they are also to be grouped under the heading of new synthetic routes. In other reactions the nitrido function itself serves as reactive group, and enables the synthesis, in particular, of new metallaheterocycles.

3.1. Addition of Lewis Bases

The uncomplexed halide nitrides, such as $MoNCl_3$, $WNCl_3$, $ReNCl_3$, $MoNBr_3$, and $WNBr_3$, despite their polymeric structures, have Lewis acidity. They react with various Lewis bases with formation of well-defined donor-acceptor complexes. Of the uncomplexed halide nitrides, the only compound crystallographically characterized is $MoNCl_3$, which forms $[MoNCl_3]_4$ units in the lattice; these are associated via chloro bridges $MoCl_2Mo$ to form a layer lattice.[81] In reactions with Lewis bases the formation of tetrameric molecular structures $[MNCl_3 \cdot D]_4$ (D = donor molecule) is preferred. Since all halide nitrides MNX_3 can form tetrameric units with Lewis bases, these compounds presumably have the same structure as $MoNCl_3$.

In the reaction of $WNCl_3$ with hydrogen azide as Lewis base only every second tungsten atom coordinates with the α-N-atom of HN_3. This leads to only some of the chloro bridges of $WNCl_3$ being ruptured, and a band structure results[82] (Fig. 17).

Upon coordination with trichloroacrylonitrile a degradation of the polymeric structure of $MoNCl_3$ down to a dimeric unit occurs, and terminal nitrido ligands result[83] (Fig. 18).

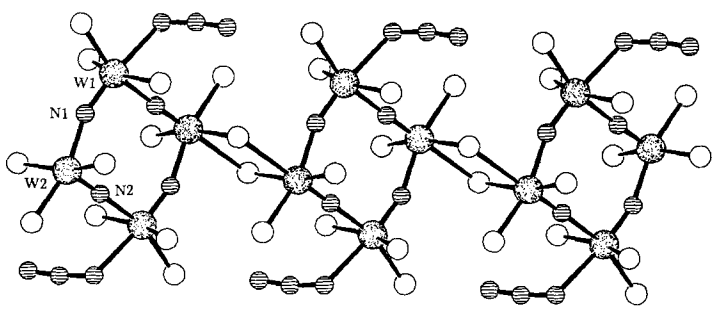

Fig. 17. The coupling of the tetrameric complex $[\{WNCl_3 \cdot 0.5HN_3\}_4]$.

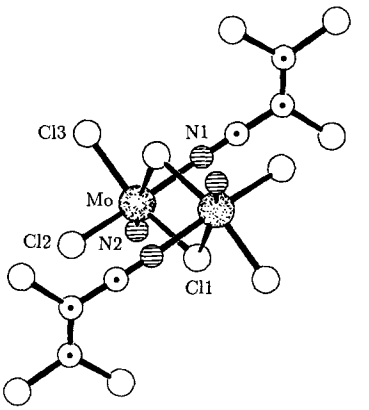

Fig. 18. Structure of the dimeric complex $[\{MoNCl_3 \cdot NCC_2Cl_3\}_2]$. The white spheres are Cl atoms, the spheres with central dot C atoms.

The Mo–Cl distances of 240.7 and 276.0 pm in the $MoCl_2Mo$ bridges are markedly different, the long Mo–Cl distance being determined by the *trans* influence of the nitrido ligand.

Bifunctional donor solvents suitable for chelation, such as dimethoxyethane, lead in the reaction with $MoNCl_3$ to monomeric complexes which are readily soluble in organic solvents (Fig. 19). The Mo–O bond to the O atom, which is

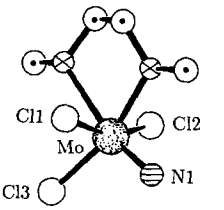

Fig. 19. Structure of $[MoNCl_3(MeOC_2H_4OMe)]$. The spheres with central dot are C atoms, those that are crossed O atoms.

in the *trans* position to the nitrido ligand, is long (247 pm) because of the *trans*-influence, whereas the Mo–O bond length of the *cis* O-atom is 215 pm.[84] Polymers with attached $MoNCl_3$ units can be obtained if the polymer bears, e.g., bipyridyl residues as functional groups[85] (Scheme 6).

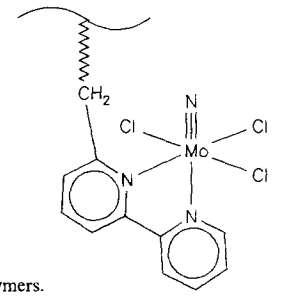

Scheme 6. $MoNCl_3$ moieties bound to polymers.

Reaction of the halide nitrides with anionic bases leads finally to the known monomeric complex ions $[MNX_4]^-$[11] with C_{4v} symmetry and with the M≡N group in the axial position. The absence of association of the $[MNX_4]^-$ ions is,

on the one hand, a result of the repulsive negative charge, but also a result of the frequently employed counterions PPh_4^+ or $AsPh_4^+$, which because of their bulkiness counteract an association. However, if instead, one uses the $[Cl_3PNPCl_3]^+$ ion, then also $[MoNCl_4]^-$ ions can stack in columns[86] (Fig. 20).

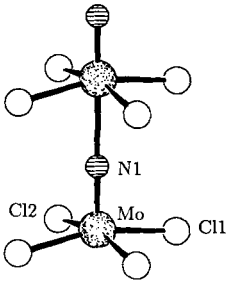

Fig. 20. Section of the chain structure of $[MoNCl_4]^-$.

The long Mo–N bond (243 pm), however, corresponds to only a very weak interaction.

Especially interesting is the acceptor behavior of the binuclear nitridoporphyrinatoiron complex $[Fe_2N(tpp)_2]$ (H_2tpp = 5,10,15,20-tetraphenylporphine), which according to the EPR spectrum has an A_1-ground state with two equivalent iron centers of formal oxidation state $Fe^{+3.5}$.[87] Addition of one mole of pyridine leads to non-equivalence of the two iron atoms, indicating an Fe^{IV} center with coordinated pyridine and coordination number six and an Fe^{III} center with coordination number five. Equivalence of the two iron centers occurs again only at high pyridine concentrations.[87] At low temperatures even an O_2 molecule can add to $[Fe_2N(tpp)_2]$,[88] whereby, according to the ^{57}Fe-Mössbauer spectra, the two iron atoms become non-equivalent again. The formation of the 1:1 adduct, which however can only be described as a weak interaction,[88] could be demonstrated by an EPR spectrometric titration.

The electronic properties of the complex $[Fe_2N(tpp)_2]$ are similar to those of complexes of the type $[Fe_2N(pc)_2]$ (H_2pc = phthalocyanine)[89] (see also Section 6). These complexes can easily be oxidized with bromine, trifluoroperoxoacetic acid or nitric acid to the air-stable radical cations $[Fe_2N(pc)_2]^+$ with Fe^{IV}-centers.[89] Like the corresponding porphyrinato derivatives[90] they serve as model substances for the mode of action of hydroperoxidase enzyme.[91]

3.2. Addition of Lewis Acids

The addition of Lewis acids to nitrido complexes has hitherto attracted relatively little interest. In all known examples the addition takes place at the nitrido ligand. Already known for some time are addition reactions of boron trihalides to rhenium(V) complexes which lead to complexes of the type $[X_2Re{\equiv}N{-}BY_3(PEt_2Ph)_3]$ (X = Cl, Br; Y = F, Cl, Br).[92] Later, the corresponding methylphosphane derivative $[Cl_2Re{\equiv}N{-}BCl_3(PMe_2Ph)_3]$ was crystallographically characterized.[93] According to the crystallographic analysis the structural group $Re{\equiv}N{-}BCl_3$, as in the analogous nitreno

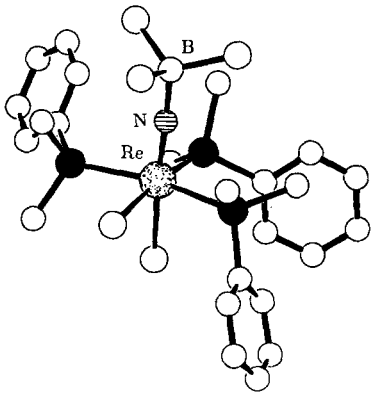

Fig. 21. Structure of the borylnitrene complex $[Re(NBCl_3)Cl_2(PMe_2Ph)_3]$. The white spheres which are coordinated to the B and Re atoms are Cl atoms; the white spheres coordinated to the black P atoms are C atoms.

complexes $M{\equiv}N{-}R$,[1,2] is linear with sp-hybridized N atom (Fig. 21).

The addition of the BCl_3 molecule causes a stretching of the Re–N bond length from 166 pm in the nitrido complex $[ReNCl_2(PMe_2Ph)_3]$ with terminal $Re{\equiv}N$ group[58] to 173 pm.[93] At the same time the *trans*-influence of the $NBCl_3$ ligand—compared to the nitrido ligand—decreases very strongly, as evidenced by the difference in the Re–Cl bond lengths between *cis* and *trans* Re–Cl bonds, which is only 4 pm in the boryl complex, whereas in the nitrido complex a difference of 20 pm was found.[58]

A much smaller tendency for the addition of boron trihalides is observed in the case of the nitridorhenium(VI) complexes. Whereas BCl_3 adds neither to $[ReNCl_4]^-$ nor to $[ReNBr_4]^-$, with boron tribromide a stable adduct is obtained. It is formed upon transhalogenation of the chloro complex with excess boron tribromide.[94] [Eq. (40)].

$$3\,AsPh_4[ReNCl_4] + 7\,BBr_3 \longrightarrow 3\,AsPh_4[Br_4Re{\equiv}N{-}BBr_3] + 4\,BCl_3 \qquad (40)$$

Above 200 °C the bromo complex loses BBr_3 leading to formation of $AsPh_4[ReNBr_4]$.[94]

Despite the weakening of the Re–N bond by the addition of the boron trihalides, a shift of ν(ReN) to shorter wavelengths is generally observed in the IR spectra. Thus, this band changes its position from 1099 cm^{-1} in the spectrum of $AsPh_4[ReNBr_4]$ to 1170 cm^{-1} after addition of BBr_3.[94] The effect is due to a vibrational coupling with the B–N stretching vibration, which in turn has a long-wave shift.

The electrophilic attack of the triphenylcarbonium ion on the nitrido function of molybdenum, tungsten and rhenium complexes leads to the synthesis of imido complexes [Eq. (41)].

$$M{\equiv}N{:} + CPh_3^+ \longrightarrow [M{\equiv}N{-}CPh_3]^+ \qquad (41)$$

First examples of such syntheses were found by Chatt et al. on using as starting material the dithiocarbaminato complexes $[MoN(S_2CNMe_2)_3]$ and $[ReN(S_2CNMe_2)_2(PMe_2Ph)]$.[95] The structure analysis of the molybdenum complex $[Mo(NCPh_3)(S_2CNMe_2)_3][BF_4]$ threw light on the

pentagonal-bipyramidal coordination at the molybdenum atom with the Mo≡N-CPh_3 group in the axial position.[95]

Also other electrophilic reagents such as PhCOCl, Ph-SO_2Cl, ArSCl, ArCl and $R_3O^+BF_4^-$ react in a similar way at the nitrido function[95] (Ar = aryl, R = Me, Et).

Of importance is the activation of nitrogen and its transfer to olefins in the reaction of nitrido-porphyrinato (por) complexes of manganese by reaction with trifluoroacetic anhydride. An electrophilic addition takes place at the nitride-nitrogen with formation of a 'nitrenoid'-manganese-porphyrinate[96] [Eq. (42)]. This can then react in a second step with olefins to give aziridines[96] [Eq. (43)].

$$[(por)Mn{\equiv}N{:}] + O(COCF_3)_2 \longrightarrow [(por)Mn{\equiv}N\text{-}C(O)CF_3]^+[CF_3CO_2]^- \quad (42)$$

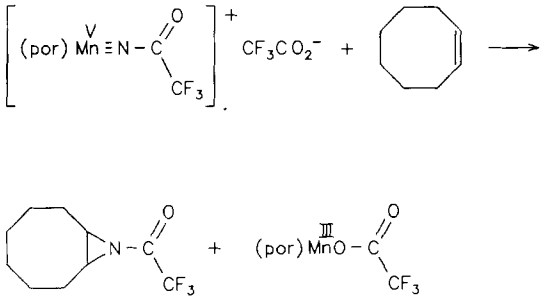

(43)

Reaction (43) can be regarded as the aza-analogous epoxidation of olefins. Kinetic studies have shown that the previous reaction (42) depends very strongly on the basicity of the porphyrinato group and on the steric conditions at the Mn≡N function.[97]

More complicated is the reaction of $CPh_3^+BF_4^-$ with the chloronitridotungstate $AsPh_4[WNCl_4]$, which is accompanied by a partial Cl/F exchange that leads to a trinuclear nitrenonitrido complex $CPh_3^+[Ph_3C\text{–}N{\equiv}WCl_4(\mu\text{-}F)\text{-}WNCl_2(\mu\text{-}F)Cl_4W{\equiv}N\text{–}CPh_3]^-$ (Abb. 15) [Gl. (44)], associated via the two F atoms.[79]

$$3[WNCl_4]^- + 3CPh_3BF_4 \longrightarrow CPh_3^+[(WNF_2Cl_2)(Cl_4WNCPh_3)_2]^- + 2BF_3 + [BF_4]^- + 2Cl^- \quad (44)$$

A surprising result was observed in the reaction of $[Cl_3PNPCl_3]Cl$ with $WNCl_3$, in which initially the expected chloronitrido complex was formed; however, this slowly rearranges in a secondary reaction to a phosphoraniminato complex[98] [Eq. (45)].

$$[Cl_3PNPCl_3]Cl + WNCl_3 \longrightarrow [Cl_3PNPCl_3][WNCl_4] \longrightarrow [Cl_5\overset{\ominus}{W} = \ddot{N}\text{–}\overset{\oplus}{P}(Cl_2)\text{-}\ddot{N}{=}PCl_3] \quad (45)$$

Also this reaction can be regarded as electrophilic attack of one of the P atoms of the cation at the nitrido ligand. The atoms of the W–N–P–N–P chain of the phosphoraniminate are almost coplanar, and the P–N bonds, the lengths of which differ only slightly, point to a through conjugation of this chain[98] (Fig. 22).

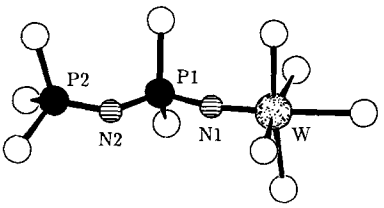

Fig. 22. Structure of the phosphoraniminato complex $[Cl_5WNP(Cl_2)NPCl_3]$. The white spheres are Cl atoms.

The phosphoraniminato ligand $[P_2N_2Cl_5]^-$, unknown in the free state, is isoelectronic with the molecular phosphazene P_2ONCl_5, which also has a planar atomic skeleton and comparable bonding parameters.[99]

Addition of molybdenum pentachloride to the chloronitridomolybdates $[MoNCl_4]^-$ and $[MoNCl_4]^{2-}$ leads to the formation of μ-nitrido-complexes. Whereas the complex $[Mo_2NCl_9]^-$ with Mo^V and Mo^{VI} centers formed with $[MoNCl_4]^-$ contains a highly asymmetric $Mo^{VI}{\equiv}N\text{–}Mo^V$ bridge (see Fig. 1), the spectroscopic findings for the $[Mo_2NCl_9]^{2-}$ ion accessible from $[MoNCl_4]^{2-}$ indicate presence of largely symmetric $Mo^V{=}N{=}Mo^V$ bridges[100] (Scheme 7).

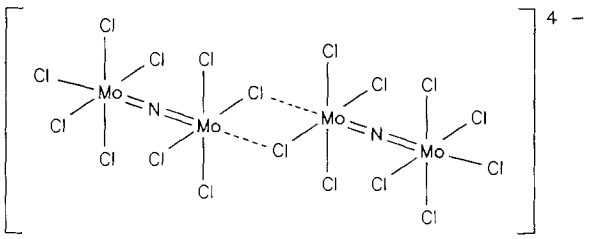

Scheme 7. The Structure of $[Mo_2NCl_9]^-$ units associated to dimers.

Similarly, structures associated to dimers are also found in the case of the previously mentioned $[W_2NCl_9]$ (Section 2.2), as also in the case of the $[Nb_2OCl_9]^-$ ion isoelectronic with $[Mo_2NCl_9]^{2-}$.[101]

A nitrido bridge Re≡N–Au is formed between two different metal atoms upon addition of the AuCl molecule accessible from [Au(CO)Cl] to the nitrido function of $[Cl_2Re{\equiv}N(PMe_2Ph)_3]$.[102] As the crystal structure analysis shows, the resulting μ-nitrido complex $[Cl_2Re{\equiv}N\text{–}AuCl(PMe_2Ph)_3]$ has a structure analogous to that of $[Cl_2Re{\equiv}N\text{-}BCl_3(PMe_2Ph)_3]$[93] with the metallanitrene function in *trans*-position to a Cl ligand and meridional arrangement of the phosphane ligands.[102] Whereas the formation of this complex is to be regarded as addition of AuCl to the nitrido function, the complex $[(Me_3SiO)_3V{\equiv}N\text{-}Pt(Me)(PEt_3)_2]$ prepared by Doherty et al.[103] by reaction of $[(Me_3SiO)_3V{\equiv}N\text{-}SiMe_3]$ with $[FPtMe(PEt_3)_2]$, despite an analogous atomic sequence in the bridge V≡N-Pt (compared to Re≡N-Au), is a metallanitreno complex.

The remarkable bond relationship of the β-N-atom of the covalently bound azido ligand of $[W(N_3)Cl_5]$ to the nitride function of $WNCl_3$ can also be regarded as addition of a Lewis acid[104] [Eq. (46); here, both the formal charges as well as the chlorine atoms are omitted].

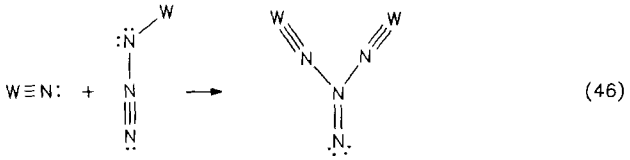

(46)

In the presence of tetraphenylarsonium chloride this reaction leads to the μ-isotetrazenido(4−) complex of tungsten(VI) [Eq. (47)].

$$2\,AsPh_4Cl + WNCl_3 + [W(N_3)Cl_5] \longrightarrow (AsPh_4)_2[Cl_5W(\mu\text{-}N_4)WCl_5] \quad (47)$$

The $[N_4]^{4-}$ ligand couples the two tungsten atoms via short W–N bonds (average length 164 pm) and two relatively long N–N bonds (149 pm)[104] (Fig. 23).

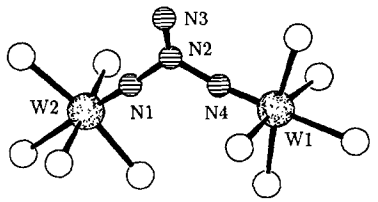

Fig. 23. Structure of the μ-isotetrazenido(4−) complex $[Cl_5W(\mu\text{-}N_4)WCl_5]^{2-}$. The white spheres are Cl atoms.

The long N–N bonds signal the ready thermal cleavability of nitrogen. The $[N_4]^{4-}$ bridge ligand can derive from the deprotonated, unknown isotetrazene, which is isoelectronic with urea and with the well-characterized tetrazene, $H_2NN{=}NNH_2$.[105]

3.3. Substitution Reactions

Starting materials for ligand exchange reactions which proceed with retention of the nitrido function are mostly chloronitrido complexes in which the Cl ligands can, by suitable choice of reaction partners, be partially or completely substituted. We shall now describe some typical examples from the wide spectrum of preparative possibilities.

A suitable reagent for the preparation of fluoronitrido complexes is anhydrous silver fluoride in acetonitrile. Treatment of the chloronitrido complex with this reagent leads to the formation of extremely moisture-sensitive fluoronitrido silver complexes in the form of their readily soluble acetonitrile solvates[106] [Eq. (48)].

$$MoNCl_3 \quad CH_3CN + 4\,AgF \xrightarrow{CH_3CN} [Ag(CH_3CN)_2][MoNF_4] + 3\,AgCl \quad (48)$$

Also alkali-metal fluorides such as NaF or KF can be used for the fluorination if the reactions are carried out in acetonitrile in the presence of suitable crown ethers. The fluoronitrido metalates are formed in which their cations form ion pairs or triplets owing to the anisotropic coordination by the crown ether molecules. An example is reaction (49), which goes to completion very rapidly at room temperature.[107]

$$[WCl_4(NCl)] + 5\,KF + [18]\text{crown-6} \longrightarrow [K([18]\text{crown-6})][WF_5(NCl)] + 4\,KCl \quad (49)$$

The positively charged Cl atom on the nitreno ligand is not exchanged (Fig. 24).

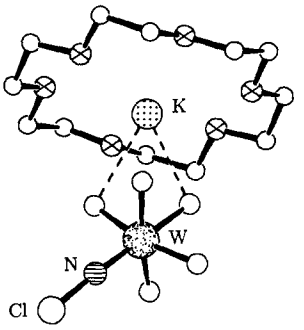

Fig. 24. Structure of the ion pair $[K([18]\text{crown-6})][F_5W(NCl)]$. Crossed spheres are O atoms, smaller white spheres in the crown ether C atoms. The white spheres which are bound directly to the W atom are F atoms.

A crystallographically characterized ion triplet is shown in Figure 11. Occasionally chloride nitrides have also been allowed to react with elemental fluorine, whereby the nitrido function remains intact despite the drastic reaction conditions. Thus, reaction of $ReNCl_4$ with fluorine yields mainly red $[ReNF_4 \cdot ReF_5(NCl)]$[109] [Eq. (50)] besides small amounts of yellow crystals of $ReNF_4$, which is also accessible from ReF_6 and trimethylsilyl azide.[108]

$$2\,ReNCl_4 + 8\,F_2 \longrightarrow [ReNF_4 \cdot ReF_5(NCl)] + 7\,ClF \quad (50)$$

The two Re components are coupled by an asymmetric fluorine bridge with Re–F distances of 188 and 228 pm, respectively[109] (Fig. 25).

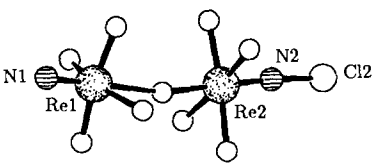

Fig. 25. Structure of the molecular complex $[ReNF_4 \cdot Re(NCl)F_5]$. With exception of the labeled Cl2 atom, white spheres are F atoms.

The long Re1–F bond is in the *trans*-position to the nitrido ligand $[{\equiv}N{:}]^{3-}$, which therefore exercises a much larger *trans* influence than the nitreno ligand $[{\equiv}N\text{-}Cl]^{2-}$. The short

Re2–F bond remains almost unaltered compared to the free molecule $[ReF_5(NCl)]$.[108]

A Cl/Br ligand exchange can generally be achieved quite readily with the help of trimethylsilyl bromide, especially if the chloro ligands are complexochemically enfeebled by excess negative charges [Eq. (51), M = Mo, W].[110]

$$[MNCl_4]^- + 4\,BrSiMe_3 \longrightarrow [MNBr_4]^- + 4\,ClSiMe_3 \quad (51)$$

Occasionally ethyl bromide is also suitable for ligand exchange; however, longer reaction times of up to eight days are required[111] [Eq. (52)].

$$AsPh_4[RuNCl_4] + 4\,EtBr \xrightarrow[80\,^\circ C]{CH_3CN} AsPh_4[RuNBr_4] + 4\,EtCl \quad (52)$$

Nitrido derivatives of molybdenum and tungsten with alkoxy ligands can be prepared by reaction of the *tert*-butyloxy derivatives obtainable from the metathetic reaction (37) with alcohols bearing sterically less demanding residues R[76, 77] [Eq. (53)].

$$[(t\mathrm{BuO})_3M{\equiv}N{:}] + 3\,ROH \longrightarrow [(RO)_3M{\equiv}N{:}] + 3\,t\mathrm{BuOH} \quad (53)$$

The complex $[NBu_4][OsN(OSiMe_3)_4]$,[112] readily accessible by reaction of $[NBu_4][OsNCl_4]$ with $NaOSiMe_3$, has proven to be an excellent starting material for the synthesis of organo-substituted nitridoosmium(VI) complexes. Alkylmagnesium and -aluminum compounds with $R = CH_3$, CH_2Ph, CH_2CMe_3, and CH_2SiMe_3 are suitable as alkylating reagents.[112] The crystal structure analysis of $[NBu_4][OsN(CH_2SiMe_3)_4]$ shows the anion in a slightly distorted C_4 symmetry with the nitrido ligand in the apical position (Os≡N = 163 pm) and the methylene C atoms in the basal plane (Os–C = 212–214 pm).[113]

Attempts to prepare anionic nitrido complexes $[(t\mathrm{BuO})_4M{\equiv}N{:}]^-$ starting from the chloronitridometalates (M = Mo, W) were unsuccessful owing to the bulkiness of the organic residues. Instead, these reactions proceed according to Equation (54).[114] In contrast, no problems were encountered in the synthesis of the corresponding anionic phenolato complexes[114] [Eq. (55)].

$$PPh_4[MNCl_4] + 3\,NaO\,t\mathrm{Bu} \longrightarrow [(t\mathrm{BuO})_3M{\equiv}N{:}] + PPh_4Cl + 3\,NaCl \quad (54)$$

$$PPh_4[MNCl_4] + 4\,NaOPh \longrightarrow PPh_4[(PhO)_4M{\equiv}N{:}] + 4\,NaCl \quad (55)$$

Attempts to convert the chloride nitrides into alkoxidonitrido complexes with alcohols led, even in the presence of bases, via loss of the nitrido group to formation of homoleptic alkoxido complexes. If diols are used as reactants, trischelates of molybdenum(VI) can be obtained[114] [Eq. (56)].

$$MoNCl_3 + 3\,HO{-}CH_2{-}CH_2{-}OH \xrightarrow{DBU} [Mo(OCH_2CH_2O)_3] + 3\,DBU \cdot HCl + NH_3 \quad (56)$$

DBU = 1,8-diazabicyclo[5.4.0]undec-7-ene

By comparison, the reactions of thiophenolates with nitridorhenium(V) complexes present no problems. Thus, complexes of the type $[ReNCl_2(PR_3)_n]$ ($PR_3 = PPh_3$, $n = 2$ or PMe_2Ph, $n = 3$) react with 1,3,5-triisopropylthiophenol (Htipt) in the presence of triethylamine smoothly according to Equation (57),[115] and with sodium thiophenolate according to Equation (58) to give the thiophenolato complexes.[115]

$$[ReNCl_2(PR_3)_n] + 2\,Htipt \xrightarrow{NEt_3} [ReN(tipt)_2(PR_3)_n] + 2\,HCl \quad (57)$$

$$[ReNCl_2(PR_3)_n] + 4\,Na(tipt) \xrightarrow{THF} Na_2[ReN(tipt)_4] \cdot 2THF + 2\,NaCl + n\,PR_3 \quad (58)$$

In some cases substitution reactions can also be achieved by exploiting the chelate effect of neutral multidentate donor molecules. Thus, $AsPh_4[ReNCl_4]$ reacts with 2,2′-dipyridyl in dichloromethane solution via exchange of a chloride to give the uncharged molecular complex $[ReNCl_3(bpy)]$[116] [Eq. (59)], while reaction of $[OsNCl_4]^-$ with the tridentate chelate terpyridyl in boiling acetone even leads to the cationic nitrido complex $[OsN(terpy)Cl_2]^+$[117] [Eq. (60)].

$$[ReNCl_4]^- + bpy \longrightarrow [ReNCl_3(bpy)] + Cl^- \quad (59)$$

$$[OsNCl_4]^- + terpy \longrightarrow [OsN(terpy)Cl_2]^+ + 2\,Cl^- \quad (60)$$

Other than in the terpyridyl complex $[MoNCl(N_3)_2(terpy)]$,[44] in which the nitrido ligand is in the *cis*-position to the terpyridyl chelate ligand (Fig. 10), in the osmium complex the nitrido ligand is in the *trans*-position to the N atom of the central terpyridyl ring[117] (Fig. 26). This leads to an

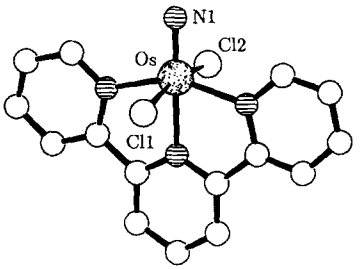

Fig. 26. Structure of the cation $[OsNCl_2(terpy)]^+$. With exception of the labeled Cl atoms, white spheres are C atoms.

enormous stretching of this Os–N bond by 85 pm compared to the two other Os–N distances to the terpyridyl ligand.[117] As in other d^2-configurated complexes with π-bound ligands[118] the nitridoosmium complex is also diamagnetic, corresponding to a marked energetic separation of the d-orbitals according to $d_{xy} < d_{xz}, d_{yz}$.[117]

Also the μ-nitridoruthenium complex $K_3[Ru_2NCl_8(H_2O)_2]$ can be converted in a slow reaction, via replacement of the chloro ligands by ethylenediamine, into the cationic complex $[Ru_2N(en)_5]Cl_5 \cdot H_2O$[119] (Fig. 27). The bridging of the two ruthenium atoms by one of the ethylenediamine chelates leads to only a slight bending of the Ru–N–Ru bond angle to 174.6°.

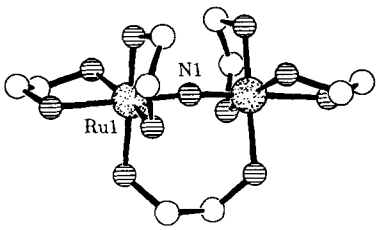

Fig. 27. Structure of the cationic μ-nitrido complex $[Ru_2N(en)_5]^{5+}$. White spheres are C atoms.

Substitution of the chlorine atoms of the polymeric chloride nitrides $MoNCl_3$ and $WNCl_3$ by sterically demanding diphenylamido groups led to the first monomeric molecular nitrido complexes with four-coordination at the metal atom[120] [Eq. (61)]. The steric requirements of the NPh_2

$$MNCl_3 + 3\,LiNPh_2 \xrightarrow{THF} [MN(NPh_2)_3] + 3\,LiCl \qquad (61)$$

groups lead to a structural peculiarity: whereas in all other nitrido complexes the large π-electron density of the M≡N: bond leads to :N≡M–X bond angles which are larger than those of the regular geometric arrangement, the N≡Mo–N bond angles in the structure of $[MoN(NPh_2)_3]$ (100.5°) are

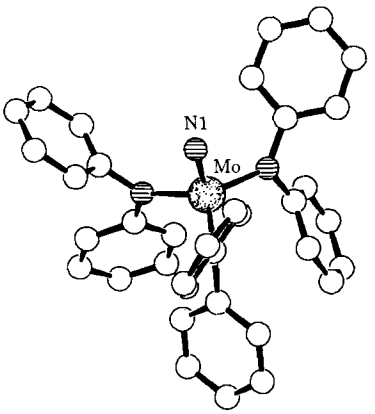

Fig. 28. Structure of the diphenylamidonitrido complex $[MoN(NPh_2)_3]$. The white spheres are C atoms. One N atom is masked by a phenyl ring.

smaller than the ideal tetrahedral angle, while the bond angles N–Mo–N (114.9–119.6°) are correspondingly larger than the tetrahedral angle[120] (Fig. 28). The Mo≡N bond length (163.4 pm), however, remains unaltered.

In the case of nitrido complexes whose nitrido function is not sensitive towards proton-active reagents such as water, alcohols etc., there are far more numerous possibilities for derivatization by substitution of the halogeno ligands. This is true in particular for the nitrido complexes of technetium and osmium.

Thus, e.g., reaction of $AsPh_4[OsNCl_4]$ with sodium cyanide in THF/methanol furnishes the mixed complex $[OsN(CN)_4(OH)]^{2-}$ in which the OH^- ligand is *trans* to the nitrido ligand.[121]

Owing to the strong *trans* effect of the Os–N group, the OH^- ligand is readily replaced by CN^- when the complex is treated with excess sodium cyanide, thus affording the pentacyanonitrido complex $[OsN(CN)_5]^{2-}$.[121]

The structure of the cyano complex corresponds entirely to that of the long-known $[OsNCl_5]^{2-}$ ion;[122] the *trans* influence of the nitrido ligand is reflected in the long Os–C bond to the *trans* CN^- ligand, which, with 235 pm, is 27 pm longer than the Os–C distances of the equatorially arranged cyano ligands.[121] In solution at room temperature the complex shows an intense phosphorescence at 550 nm upon excitation with light of wavelength 300–400 nm.[121]

The remarkable inertness of the nitrido function in technetium complexes towards proton-active reagents permits a wide variety of substitution reactions. Starting materials for this purpose are frequently the readily accessible nitrido complexes $AsPh_4[TcNCl_4]$ with C_{4v} symmetry of the $[TcNCl_4]^-$ anion[123] or $[TcNCl_2(PPh_3)_2]$ with trigonal-bipyramidal geometry at the technetium atom and *trans* arrangement of the phosphane ligands. The structure of this molecular complex was first elucidated only recently[124] (Fig. 29).

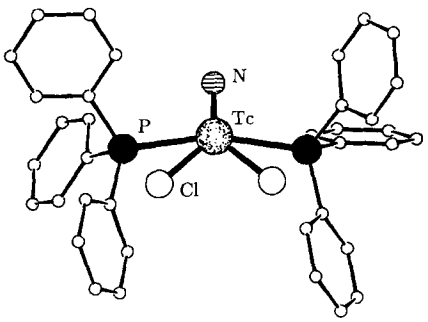

Fig. 29. Structure of the nitrido complex $[TcNCl_2(PPh_3)_2]$. The C atoms are scaled down.

Thus, for example, cyclam (Scheme 8) reacts with $[TcNCl_2(PPh_3)_2]$ smoothly according to Equation (62) with displacement of the two phosphane ligands and one chloro ligand and formation of a cationic complex.[125]

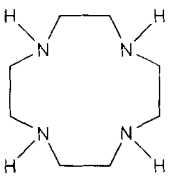

Scheme 8. The cyclam ligand.

$$[TcNCl_2(PPh_3)_2] + cyclam \longrightarrow [TcNCl(cyclam)]^+Cl^- + 2\,PPh_3 \qquad (62)$$

With the cyclam derivative 1,4,8,11-tetraazacyclotetradecane-5,7-dione (H_2L), substitution with elimination of HCl already takes place at 40 °C in CH_2Cl_2/EtOH [Eq. (63)].

$$[TcNCl_2(PPh_3)_2] + H_2L + 3\,H_2O \longrightarrow [TcN(L)(H_2O)]\cdot 2\,H_2O + 2\,HCl + 2\,PPh_3 \qquad (63)$$

In $[TcN(L)(H_2O)] \cdot 2H_2O$ the technetium is surrounded in a distorted octahedral fashion by the four equatorially arranged N atoms of the cyclam ligand (distances Tc–NH 213 pm, Tc–N 205 pm) as well as axially by the nitrido ligands (Tc≡N 161 pm) and the O atom of the water molecule. Owing to the strong *trans* influence of the nitrido ligand the aqua ligand is only very loosely bound.[125]

Also other proton-active chelating reagents such as dithiacarbamide or azomethine derivatives react with $[TcNCl_2(PPh_3)_2]$ in a very similar way with elimination of HCl. Thus, the reactions with the carbamide derivatives H_2L^3 and HL^2 in boiling benzene lead to the molecular

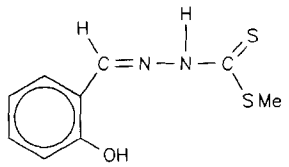

(H_2L^3)

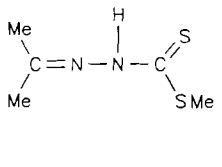

(HL^2)

complexes $[TcNL^3(PPh_3)]$ [Eq. (64)] and $[TcN(L^2)_2]$ [Eq. (65)], respectively.[126]

$$[TcNCl_2(PPh_3)_2] + H_2L^3 \longrightarrow [TcNL^3(PPh_3)] + PPh_3 + 2HCl \quad (64)$$

$$[TcNCl_2(PPh_3)_2] + 2HL^2 \longrightarrow [TcN(L^2)_2] + 2PPh_3 + 2HCl \quad (65)$$

In these two complexes the technetium is surrounded in a distorted tetragonal-pyramidal fashion, with the nitrido ligand in the apical position[126] (Fig. 30).

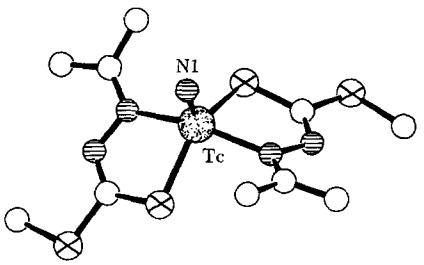

Fig. 30. Structure of the dithiocarbamido complex $[TcN(Me_2CNNC(S)SMe)_2]$. The white spheres are C atoms, the crossed spheres S atoms.

Analogous results could be achieved with the tridentate chelating reagent H_2ecbap (Scheme 9) in methanol[127] [Eq. (66)].

$$[TcNCl_2(PPh_3)_2] + H_2ecbap \longrightarrow [TcN(ecbap)(PPh_3)] + PPh_3 + 2HCl \quad (66)$$

The tridentate ligand coordinates with the ligator atoms ONO as rigid planar group[127] (Fig. 31).

The chloronitrido complexes of technetium, $[TcNCl_4]^-$ and $[TcNCl_5]^{2-}$, are suitable for substitution reactions even

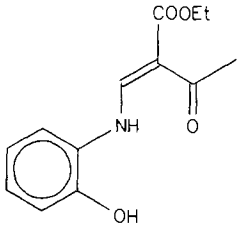

Scheme 9. Structural formula of the tridentate ligand H_2ecbap (*N*-(2-ethoxycarbonyl-3-oxobut-1-en(1)yl)-2-aminophenol, non-IUPAC name).

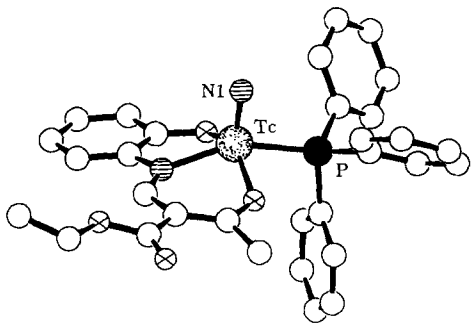

Fig. 31. Structure of the nitrido complex $[TcN(ecbap)(PPh_3)]$. The white spheres are C atoms, the crossed spheres O atoms.

in aqueous medium, since, in each case, the nitrido ligand is insensitive to hydrolysis. This could be exploited in the remarkable synthesis [Eq. (67)] of the nitridooxotechnetium complex coupled via oxo- and oxalato bridges[128] (Fig. 32).

$$4AsPh_4[TcNCl_4] + 6H_2C_2O_4 + 2H_2O \xrightarrow{H_2O/acetone} (AsPh_4)_4[Tc_4N_4O_2(C_2O_4)_6] + 16HCl \quad (67)$$

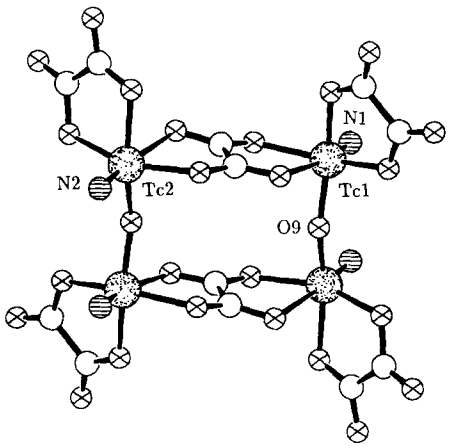

Fig. 32. Structure of the tetranuclear nitrido complex $[Tc_4N_4O_2(C_2O_4)_6]^{4-}$. The white spheres are C atoms, the crossed spheres O atoms.

With hydrogen peroxide it was even possible to synthesize the first nitridoperoxo complex[129] [Eq. (68)].

$$2Cs_2[TcNCl_5] + 5H_2O_2 \longrightarrow 2Cs[TcNCl(O_2)_2] + 6HCl + 2CsCl + 2H_2O \quad (68)$$

In this reaction the substitution is accompanied by an oxidation of the technetium from Tc^{VI} to Tc^{VII}. The structure of the anion (Fig. 33) can be best described in terms of a

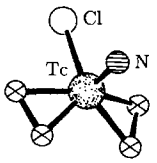

Fig. 33. Structure of the nitridoperoxo complex $[TcNCl(O_2)_2]^-$. The crossed spheres are O atoms.

distorted pentagonal pyramid,[129] but to a first approximation also in terms of a pseudotetrahedral arrangement.

In contrast, the substitution reactions of the $[TcNCl_4]^-$ ion are more frequently accompanied by a reduction of the technetium to Tc^V. Examples are the reaction with 8-quinolinethiol, which leads to the molecular complex $[TcN(C_9H_6NS)_2]$ with fivefold coordinated technetium atom[130] or the reaction with 1,1-dicyanoethene-2,2-diselenolate $[(NC)_2C=CSe_2]^{2-}$, in which the technetium(V) complex $[TcN(Se_2C=C(CN)_2)_2]^{2-}$ with tetragonal-pyramidal coordination is formed. The chelate ligands bound via their selenium atoms are arranged equatorially, whereas the nitrido ligand occupies an apical position.[131]

3.4. Redox Reactions

Investigations of redox reactions of nitrido complexes, particularly of molybdenum, have attracted special attention in model concepts concerning natural N_2-assimilation. The molybdenum atom participates in redox processes from the N_2-fixation at the metal center through to the nitrido complex Mo≡N:.[132, 133] Electron transfer reactions of nitridoosmium complexes have recently also gained importance.

The nitridomolybdenum(VI) complex $[MoNCl_4]^-$ can be readily converted into the corresponding molybdenum(V) complex in CH_2Cl_2 solution even with iodide as reducing agent[134] [Eq. (69)]. According to the crystal structure anal-

$$2\,PPh_3Me[MoNCl_4] + 3[PPh_3Me]I \longrightarrow 2[PPh_3Me]_2[MoNCl_4] + [PPh_3Me]I_3 \quad (69)$$

ysis the $[MoNCl_4]^{2-}$ ion retains the C_{4v} symmetric structure of the $[MoNCl_4]^-$ ion. The Mo–N bond length remains virtually unchanged (163.4 pm), whereas the Mo–Cl distances, owing to the higher negative charge of the ion, are 5.5 pm longer than in the singly charged ion. This bonding situation is also reflected in the results of the EPR spectrum, in which the $g_\perp$ parameter with a value of 1.984(1) is significantly lower than in the corresponding oxomolybdenum(V) compounds, and can be interpreted as an expression of the strong Mo≡N π bond.[134]

On the other hand, the sterically very crowded thioarene complex $[ReN(tipt)_4]^{2-}$ (tipt = 2,4,6-triisopropylbenzenethiolate) can be oxidized very easily with atmospheric oxygen to the corresponding rhenium(VI) complex $[ReN(tipt)_4]^-$.[135]

The reduction of $MoNCl_3$ in THF solution also proceeds with retention of the tetrameric structural unit of the solvates of $MoNCl_3$, as has been demonstrated crystallographically, e.g., with the dibutyl ether solvate $[MoNCl_3 \cdot OBu_2]_4$.[136] Upon reaction of $[MoNCl_3 \cdot thf]_4$ with an equivalent amount of sodium naphthalide in the presence of [15]crown-5 the tetrameric molybdenum(V) complex $[\{MoNCl_3 \cdot thf\}_4]^{4-}$ could be isolated[137] [Eq. (70)].

$$[\{MoNCl_3 \cdot thf\}_4] + 4NaC_{10}H_8 + 2([15]crown\text{-}5) + 4THF \longrightarrow [Na([15]crown\text{-}5)Na(thf)]_2[\{MoNCl_3 \cdot thf\}_4 \cdot 2THF + 4C_{10}H_8 \quad (70)$$

The compound is an ionic ensemble which is formed by direct contacts of chlorine atoms of the complex anion $[\{MoNCl_3 \cdot thf\}_4]^{4-}$ each with two differently associated sodium ions[137] (Fig. 34).

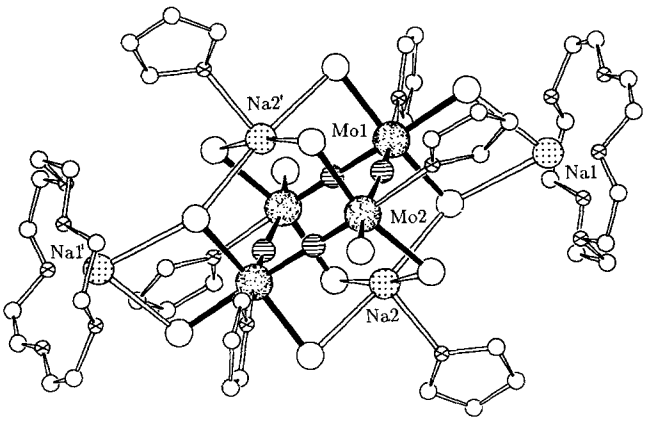

Fig. 34. Structure of the ionic ensemble $[\{Na([15]crown\text{-}5)Na(thf)\}_2][\{MoNCl_3 \cdot thf\}_4]$. The large white spheres are Cl atoms, the small white spheres C atoms, the crossed spheres O atoms.

The sodium ions Na1 are, on the one hand, each coordinated by five O atoms of the crown ether molecule, and, on the other, by two chlorine atoms of the tetrameric anion, so a coordination number seven results for these sodium ions. The sodium ions Na2 are square-pyramidally coordinated, namely by four chlorine atoms, which form the pyrimid base, while the apical position is occupied by the O atom of a tetrahydrofuran molecule.

The Mo–N distances in the $[\{MoNCl_3 \cdot thf\}_4]^{4-}$ ion can, as in the comparable molecular complexes, be interpreted as triple and single bonds. However, from the EPR spectrum, in comparison to the spectrum of the $(PPh_3Me)_2[MoNCl_4]$ complex with monomeric anion, a doubling of the orbital moment can be concluded. This is a result of the weakening of the Mo≡N bond, which is determined by the bridging function of the nitrido ligand.[137]

The unusual tetranuclear tungsten complex, $[W_4N_4(NPh_2)_6(OC_4H_9)_2]$,[120] is formed under reducing conditions in the reaction of $WNCl_3$ with $LiNPh_2$ [cf. Eq. (61)] in the presence of butyllithium in THF. According

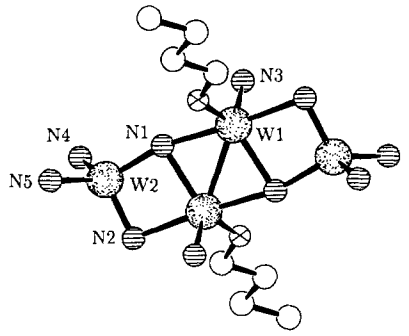

Fig. 35. Arrangement of the framework atoms of the complex $[W_4N_4(NPh_2)_6(OC_4H_9)_2]$ without phenyl groups of the amido ligands. White spheres are C atoms, crossed spheres O atoms.

to the crystal structure analysis[120] (Fig. 35) the two tungsten atoms W1 and W2 are coupled one under the other via a W–W single bond (253.5 pm) (corresponding to d^1 configuration). The two remaining tungsten atoms have the oxidation number +VI; they are coupled via two unusual nitrido bridges (N1 and N2) with the W–W dumbbell. The nitrido ligand N2 has a W–N–W bond angle of only 91.3°, the smallest such angle observed so far. The nitrido ligand N1 has a T-shaped bridging function, which has already been observed occasionally. The bonding situations are best formulated as in Scheme 10.

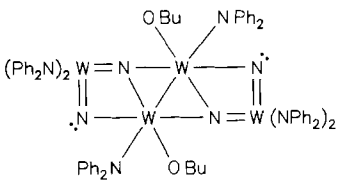

Scheme 10. Bond situation in $[W_4N_4(NPh_2)_6(OBu)_2]$ (schematic).

Other complexes with the T-shaped bridging ligand are shown in Scheme 11.

In all these cases we have complexes in which the μ_3-N ligand couples metal atoms, which, in turn, form metal–metal bonds. An exception is the pentameric complex $[(t\mathrm{BuCH_2})_2\mathrm{TaN}]_5$[28] (cf. Section 2.3).

$[Mo_4(\mu_3\text{-}N)_2(\mu_2\text{-}O\mathit{i}Pr)_2(O\mathit{i}Pr)_{10}]$[138]

$[Mo_3(\mu_3\text{-}N)(O)(CO)_4(\eta\text{-}C_5H_5)_3]$[139]

$(PPh_4)_2[W_3(\mu_3\text{-}N)(O)(\mu_2\text{-}NCl)Cl_9]_2$[9]

Scheme 11. Complexes with nitrido ligands which form T-shaped bridges.

The previously mentioned complex $[AsPh_4]_2[OsN(CN)_4(OH)]$[121] (cf. Section 3.3) has proven to be a strong oxidizing agent in flash photolysis experiments with laser excitation of 355 nm. The self-quenching process of the excited state can be formulated as in Equation (71).[121]

$$[Os^{VI}{\equiv}N]^* + [N{\equiv}Os^{VI}] \longrightarrow [Os{\equiv}N\cdots N{\equiv}Os] \longrightarrow 2[Os^{V}{\equiv}N] \quad (71)$$

The cationic nitridoosmium(VI) complex $[OsN(terpy)Cl_2]^+$ can also be very readily reduced electrochemically through four oxidation states to give the amminoosmium(II) complex[117] [Eq. (72)], which is easily oxidized by atmospheric oxygen to the cationic complex $[Os^{III}(NH_3)(terpy)Cl_2]^+$.[117]

$$[OsN(terpy)Cl_2]^+ + 4e + 3H^+ \longrightarrow [Os(NH_3)(terpy)Cl_2] \quad (72)$$

3.5. Nitrides as Educts for the Synthesis of Phosphoraniminato Complexes

Phosphoraniminato complexes are compounds containing the ligand $[NPR_3]^-$ **H**, which is isoelectronic with compounds of the type OPR_3 **I**, and thus far could not been observed as uncoordinated ion.

H **I**

The known phosphoraniminato complexes of various transition metals which were discussed in detail in a recent review[140] contain the structural group $MNPR_3$, mainly in a linear arrangement (**J**); but M–N–P angles of up to 130° are also known (**K**).

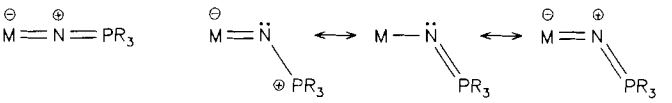

J **K**

Reactions of nitrido complexes with phosphanes are often suitable for their syntheses; these are interpreted as nucleophilic attack of the phosphorus atom at the nitrido ligand[141] (Scheme 12).

$$M{\equiv}N{:} + {:}PR_3 \longrightarrow \overset{\ominus}{M} = \overset{\oplus}{N} = PR_3$$

Scheme 12. Nucleophilic attack of the P atom at the nitrido ligand.

The phosphorus atom is oxidized (change in oxidation state by two), the metal correspondingly reduced.

More recent examples for the phosphoraniminato complexes accessible in this way are the reactions of $ReNCl_4$ with triphenylphosphane to give $[(Ph_3P)Cl_4Re(NPPh_3)]$,[116] the formation of $PPh_4[MoCl_5(NPCl_3)]$ from $PPh_4[MoNCl_4]$ and PCl_3/PCl_5,[142] and the reaction of $MoNCl_3$ with trimethylphosphane in CH_2Cl_2, which already takes place at room temperature[143] [Eq. (73)].

$$Mo^{VI}NCl_3 + 4PMe_3 \longrightarrow [Mo^{IV}(NPMe_3)Cl_2(PMe_3)_3]Cl \quad (73)$$

The Mo–N–P bond angle in the structure of the first cationic phosphoraninimato complex (167.6°)[143] corresponds to that in the most frequently observed structure type **J**.[140]

On prolonged standing in CH_2Cl_2 solution, this Mo^{IV} complex undergoes a remarkable transformation; besides the bis(trimethylphosphane)iminium ion, a μ-nitridomolybdenum(IV) complex is formed[143] [Eq. (74)]. In the structure

$$2[Mo(NPMe_3)Cl_2(PMe_3)_3]Cl \longrightarrow [Me_3PNPMe_3]^+[\{MoCl_3(PMe_3)_2\}_2N]^- + 2PMe_3 \quad (74)$$

of the anion (Fig. 36) the Mo–N–Mo axis is almost symmetrical and nearly linear (bond angle 175.3°).[143]

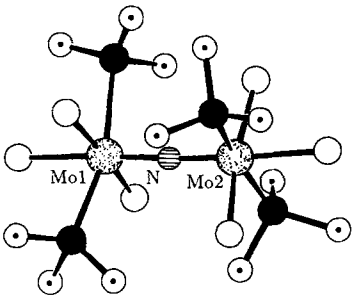

Fig. 36. Structure of the anionic μ-nitrido complex $[\{MoCl_3(PMe_3)_2\}_2N]^-$. The white spheres are Cl atoms, the black spheres P atoms, the spheres with central dot C atoms.

Cyclic metallaphosphazenes could be prepared in good yields for the first time by reaction of bis(aminodiorganophosphane)iminium chloride with the chloride nitrides $MoNCl_3$ or $WNCl_3$[144, 145] [Eq. (75)]. Crystal structure investigations of the acetonitrile solvates revealed the presence of almost planar MN_3P_2 rings with delocalized P–N bonds.[145, 146] Still unclear is whether the nitrogen of the ammonium chloride that is formed stems from the metal chloride nitride or from an amino function of the iminium ion. The synthesis of the cyclotungstaphosphazene $Cl_3\overline{WNPPh_2NPPh_2N}$ starting from tungsten hexachloride and $[H_2NPPh_2NPPh_2NH_2]Cl$, which leads to elimination of HCl, would suggest that it originates from the $MNCl_3$ component.[146]

$MNCl_3 + [H_2NPR_2NPR_2NH_2]Cl \longrightarrow$ 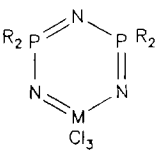 $+ NH_4Cl$ (75)

(M = Mo, W)

The formation of bis(phosphane)iminium ions from phosphoraniminato complexes was previously only observed on starting from a molybdenum complex with *cis* phosphoraniminato ligands[147] [Eq. (76)].

$$cis\text{-}[MoCl_4(NPPh_3)_2] \longrightarrow [Ph_3PNPPh_3]^+[MoNCl_4]^- \quad (76)$$

A further example of a cationic phosphoraniminato complex could be prepared by reaction of the terpyridyl complex *trans*-$[Os^{VI}(terpy)Cl_2N]Cl$ with triphenylphosphane [Eq. (77)] and was crystallographically characterized as the PF_6^- salt.[148]

$$[Os^{VI}(terpy)Cl_2N]^+ + PPh_3 \longrightarrow [Os^{IV}(terpy)Cl_2(NPPh_3)]^+ \quad (77)$$

In this case the Os–N–P bond angle of 132.5° lies at the lower limit of the previously known values. Only in the complex [Mo(NO)(NPMePh$_2$)(dttd)] [dttd = 2,3,8,9-dibenzo-1,4,7,10-tetrathiadecane(2−)] is it somewhat smaller (129.7°).[149] Also remarkable is the length of the Os–N bond of 209 pm,[148] which corresponds to a single bond.

3.6. Nitrides as Educts for the Synthesis of M–N–S Sequences

Some nitrido complexes can be converted by reaction with elemental sulfur or with S_2Cl_2 into thionitrosyl complexes [Eq. (78), (79)]. Suitable educts are dithiocarbamato complexes of molybdenum $[MoN(S_2CNR_2)_3]$ with sevenfold coordinated molybdenum atom as well as nitrido complexes of rhenium and osmium.[150]

$$[MoN(S_2CNR_2)_3] + \tfrac{1}{8}S_8 \longrightarrow [Mo(NS)(S_2CNR_2)_3] \quad (78)$$

$$[ReNCl_2(PR_3)_3] + \tfrac{1}{2}S_2Cl_2 \longrightarrow [Re(NS)Cl_3(PR_3)_2] + PR_3 \quad (79)$$

According to structural investigations the thionitrosyl ligand is bound in linear arrangement $\overset{\ominus}{M}=\overset{\oplus}{N}=S$ with the metal center (for a review see Ref. [151]).

The reaction of $ReNCl_4$ with tetrasulfur tetranitride leads to an interesting product. Initially, a chloro-bridged polymerized product $[ReCl_2(NS)(NSCl)]_\infty$ is formed which can be resolved with tetraphenylarsonium chloride in dichloromethane to give the dianion $[ReCl_4(NS)(NSCl)]^{2-}$.[152] According to the structural analysis (Fig. 37) the anion contains both a thionitrosyl as well as a chlorothionitrene ligand[152] (cf. also Section 2.7).

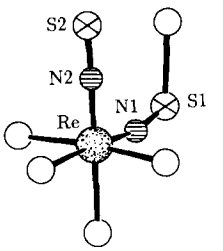

Fig. 37. Structure of the anionic chlorothionitrenethionitrosyl complex $[Cl_4Re(NSCl)(NS)]^{2-}$. The white spheres are Cl atoms.

Also remarkable is the reaction of molybdenum chloride nitride with trithiazyl chloride, which is in equilibrium with its monomer in solution. A cyclothiazenomolybdenum

derivative [Eq. (80)] is formed whose chloro bridges are detached with tetraphenylphosphonium chloride to give the monomeric anionic derivative[153] [Eq. (81)].

$$2\,MoNCl_3 + 4{:}N{\equiv}S\text{-}Cl \longrightarrow [\{Cl_3Mo(N_3S_2)\}_2] + 2\,Cl_2 \quad (80)$$

$$[\{Cl_3Mo(N_3S_2)\}_2] + 2\,PPh_4Cl \longrightarrow 2\,PPh_4[Cl_4Mo(N_3S_2)] \quad (81)$$

According to the crystal structure analyses of the $AsPh_4^+$ salt[154] and the PPh_4^+ salt,[155] which are not isotypic, the

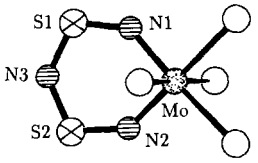

Fig. 38. Structure of the anion $[MoCl_4(N_3S_2)]^-$. The white spheres are Cl atoms.

molybdenum atom is component of a planar six-membered MoN_3S_2 ring (Fig. 38), whose S–N distances are almost equal in length and can be described in terms of delocalized π-bonds.

For a review of ring compounds of this type see Ref. [156].

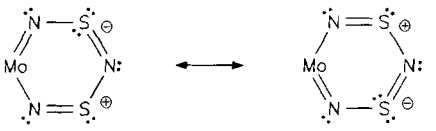

Scheme 13. Resonance structures of the planar six-membered MoN_3S_2 ring.

4. NMR Spectroscopic Investigations

Very little has been reported in the past few years concerning NMR spectra of nitrido complexes. ^{95}Mo-NMR spectra disclose a wide range of the values of the chemical shift through its dependence on the coordination number, on the electronegativity of the ligands, and on the charge of the complexes[157] (Table 1).

Table 1. Chemical shifts δ and line widths b of nitrido complexes [157] in ^{95}Mo-NMR spectra [a].

Compound	δ	b [Hz]
$[MoN(S_2CNMe_2)_3]$	−121	40
$[MoN(S_2CNEt_2)_3]$	−103	40
$[MoN(OtBu)_3]$	55	40
$MoNCl_3$ [b]	952	80
$PPh_4[MoNCl_4]$	1106	<20
$(PPh_4)_2[MoNCl_5]$	395	50

[a] Measurements in CH_2Cl_2, external standard 2 M $Na_2[MoO_4]$ in D_2O, pH 11. [b] Solution in acetonitrile. The complex $[\{MoNCl_3 \cdot CH_3CN\}_4]$ is formed in this solvent.

The largest deshielding is observed in the $[MoNCl_4]^-$ ion with fivefold coordinated molybdenum, the least deshielding in $[MoN(S_2CNMe_2)_3]$ with coordination number seven.

^{15}N-NMR investigations have been carried out on a few nitrido complexes of molybdenum, tungsten, and rhenium[7, 158, 159] (Table 2). Also these measurements show a

Table 2. ^{15}N-NMR data of nitrido complexes.

Complex	Solvent	δ [a]	Ref.
$[ReCl_2(^{15}N)(PnPrPh_2)_2]$	CH_2Cl_2	85.8	[158]
$[ReCl_2(^{15}N)(PMe_2Ph)_3]$	CH_2Cl_2	68.2	[158]
$[ReCl(^{15}N)(dppe)_2]Cl$ [b]	CH_2Cl_2	67.1	[158]
$[Mo(^{15}N)(S_2CNEt_2)_3]$	CH_2Cl_2	40.0	[158]
trans-$[MoCl(^{15}N)(dppe)_2]$	THF	166.8	[159]
trans-$[MoBr(^{15}N)(dppe)_2]$	THF	190.6	[159]
$[W_2(^{15}N)Cl_9 \cdot CH_3CN]$	CD_2Cl_2	211.2	[7]
$[\{W(^{15}N)Cl_3 \cdot CH_3CN\}_4]$	CD_2Cl_2	222.7	[7]
$PPh_4[W(^{15}N)Cl_4]$	CH_2Cl_2	258.8	[7]
$PPh_4[W_2(^{15}N)Cl_{10}]$	CH_2Cl_2	251.0	[7]

[a] Chemical shifts relative to nitromethane. [b] dppe = $Ph_2PCH_2CH_2PPh_2$.

strong dependence of the values of the chemical shift on the coordination number at the metal center and on the type of ligands. The strongest shielding is experienced by the nitrido ligand in the complex $[Mo(^{15}N)(S_2CNEt_2)_3]$ with sevenfold coordinated molybdenum atom, which has its complete equivalent in the large extent of the shielding of the ^{95}Mo nucleus in this compound (see above). The N-nuclei of the nitrido ligands in the tungsten compound are the most strongly deshielded. Tungsten is thus a particularly strong π-electron acceptor towards the nitrido ligand, as is also reflected in the IR spectra by very short wave W–N stretching frequencies and correspondingly large valence force constants. Thus, e.g., in the ions $[MNCl_4]^-$ an M–N valence force constant of 8.00 N cm^{-1} is calculated for M = Mo and of 8.15 N cm^{-1} for M = W.[7]

5. Catalytic Activity of Nitrido Complexes

Nitridomolybdenum(VI) complexes such as $[MoNCl_3(OPPh_3)_2]$ or $[NBu_4][MoNCl_4]$ together with ethylaluminum chloride as cocatalyst are very efficient catalysts for olefin metathesis.[160] For example, pent-2-ene is rapidly converted into but-2-ene and hex-3-ene [Eq. (82)], whereby the high

$$\underset{(46\%)}{2\,CH_3\text{-}CH{=}CH\text{-}C_2H_5} \rightleftharpoons \underset{(27\%)}{CH_3\text{-}CH{=}CH\text{-}CH_3} + \underset{(27\%)}{C_2H_5\text{-}CH{=}CH\text{-}C_2H_5} \quad (82)$$

initial rate of the reaction is impressive. It is assumed that the course of the olefin metathesis proceeds via the initial formation of a carbene complex. An organylation of the $MoNCl_3$ precatalyst followed by α-H-elimination with reduction to an active carbenenitridomolybdenum(IV) complex fragment is conceivable as catalyst formation reaction[160] [Eq. (83)].

$$[Mo^{VI}NCl_3(OPPh_3)_2] + (2 + x)C_2H_5AlCl_2 \longrightarrow [Mo^{IV}N(CHCH_3)Cl \cdot xC_2H_5AlCl_2] + 2[Cl_3Al \leftarrow OPPh_3] + C_2H_6 \quad (83)$$

This assumption is supported by the isolation of the carbeneoxotungsten complex $[\{WO(CHCMe_3)(PMe_3)Cl_2\}_2]$, which likewise catalyzes the olefin metathesis, albeit less efficiently.[161]

On the basis of theoretical considerations R. Taube and K. Seyferth came to the conclusion that the strong π-donor action of the nitrido ligand favors the form **M** of the carbene complex with d^2_{xy} configuration over the form **L**, which is

L **M**

essential for the subsequent reaction with the olefin.[162] This can then lead via the intermediate step of a metallacycloalkane to the metathesized olefin.[162]

The nitrido complexes, which have hitherto only been little exploited for catalytic purposes obviously present a challenge for the future. Whereas the development of homogeneous catalysts based on oxo complexes, for which $[CH_3ReO_3]$ is mentioned as key substance, has already led to excellent results in the metathesis of functionalized olefins,[164] in olefin epoxidation with H_2O_2[165] or even in the olefin synthesis from aldehydes, cyclic ketones etc.,[166] the catalytic potential of nitrido complexes still awaits recognition. Optimism accrues from a comparison of oxo function and imido function, which are isolobal (Scheme 14).

$$M=\ddot{O} \longleftrightarrow \overset{\ominus}{M}\equiv\overset{\oplus}{O}:$$

$$M=\ddot{N}-R \longleftrightarrow \overset{\ominus}{M}\equiv\overset{\oplus}{N}-R$$

Scheme 14. Comparison of the isolobal oxo and imido ligands.

Carbenimido complexes such as $[Mo(NtBu)(CHtBu)(OR_2)]$[167] ($R = CH(CF_3)_2$), like oxo complexes, have also proven to be effective as catalysts in olefin metathesis. Recently, the catalytic activity in the metathesis of terminal and functionalized olefins of a carbyneruthenium complex, $[Ru(CtBu)(CHtBu)(OR_2)]$[168] ($R = C(Me)(CF_3)_2$) was reported on for the first time. Since the carbyne function is isolobal with the nitrido ligand (Scheme 15), correspondingly modified properties are also to be expected for nitrido complexes. The above mentioned examples are a good indication of this being the case.

$$M\equiv C-R \longleftrightarrow M\equiv N:$$

Scheme 15. Comparison of the isolobal carbyne and nitrido ligands.

6. Bonding Situations in Multinuclear Nitrido Complexes

As has already been shown, binuclear, oligomeric chain or ring-shaped as well as polymeric complexes can be formed by the bridging function of the nitrido ligand. The nitrido bridge can be symmetrical or asymmetrical, linear or bent (see Scheme 1).

R. Hoffmann et al. have devoted several studies to the bonding situations in multinuclear complexes with nitrido bridges[22, 169, 170] and have examined the geometric and electronic properties using extended Hückel MO calculations. They also compare the nitrido bridges with fluoro, oxo-, and carbido-bridges.

In the case of binuclear porphyrin-analogous model complexes $[(N_4)Fe\text{-}X\text{-}Fe(N_4)]$ with X = O, N, C, the calculations[169] show that when X = O two and when X = N one d electron of the Fe ions is located in antibonding Fe–X–Fe orbitals. Due to a bending of the bridge the orbitals of these electrons are energetically lowered, but at the same time an occupied non-bonding level is slightly raised. This indicates that a bent oxo bridge leads to an energetically more favorable situation, whereas in the case of the nitrido bridge the lowering of the only singly occupied antibonding orbital cannot compensate the opposing effect in the non-bonding MO, so that the frequently observed linear arrangement is preferred. However, the calculated bending of Fe–O–Fe bridge is in fact only observed when this is stereochemically allowed. Thus, the oxo bridge is linear for example in the phthalocyaninato complex [(pc)Fe-O-Fe(pc)].

In the carbido complex $[(N_4)Fe{=}C{=}Fe(N_4)]$ the antibonding Fe–C–Fe MOs are unoccupied, so a linear bridge results, as is found in [(tpp)Fe=C=Fe(tpp)][171] and [(pc(Fe=C=Fe(pc)].[172] Naturally, the Fe–X bond strength increases with decreasing number of antibonding electrons. Hence, the strongest Fe–X bond is found in the carbido bridge.

In binuclear complexes the symmetrical M=N=M bridge with equal M–N distances is preferred, whereas in polymeric and most of the oligomeric nitrido complexes the nitrido bridges $M\equiv\overset{\oplus}{N}-\overset{\ominus}{M}$ are, as a rule, asymmetrical. In addition, a pyramidalization of the equatorial plane L_nM ($n = 3, 4$) formed by the central metal atom and the *cis* oriented ligands occurs.

R. Hoffmann et al.[170] show, in the case of complexes with a d^0- or d^1-electron configuration at the central atom, that this is the result of a second-order Jahn–Teller effect, in which, due to a HOMO-LUMO interaction, the HOMO is lowered with respect to its energy and the LUMO is raised. The HOMO-LUMO interaction is thereby all the more stronger the smaller the energy difference between the two MOs. This increases with increasing electronegativity of the bridge ligand X, so that also the asymmetry of the bridge decreases along the series X = C, N, O, F. This is confirmed by structure analyses. Fluoro bridges are usually symmetric, nitrido bridges, on the other hand, asymmetric. Polynuclear complexes with carbido bridges have so far not been synthesized. Here, highly asymmetric bridges should occur.

Since the highest occupied MOs are two degenerate M–X π-orbitals, the gain in energy by the second-order Jahn–Teller effect leads in the first instance to a strengthening of

the π-bond, whereas the M–X σ-bond is influenced only slightly. Rather it stabilizes the symmetrical bridge bonding.

In the case of the hitherto unknown polymeric nitrido complexes with two or more free d-electrons on the transition metal, according to calculations symmetrical nitrido bridges should occur, since here the antibonding M–N π* levels are filled and the Jahn–Teller effect cannot be effective.

Similarly as in the case of the polymeric nitrido complexes $[MNL_3]_n$ and $[MNL_4]_n$, a second-order Jahn–Teller effect also leads in the case of tetrameric complexes to stabilization of the less symmetric structure with alternating M–N distances. Calculations show, in the case of the model compound $[\{MoNCl_3(OH_2)\}_4]$ an energy gain of about 193 kJ mol^{-1} on going from the complex with symmetrical nitrido bridges to the complex with alternating Mo–N distances, in which the weakly bound aqua ligands are then arranged *trans* to the Mo≡N triple bond.

In the transition from a nitrido bridge to an oxo- or fluoro bridge the extent of distortion decreases with increasing electronegativity of the bridge ligand, since the energy difference between HOMO and LUMO increases and therefore the second-order Jahn–Teller effect becomes weaker. $[NbF_5]_4$ has indeed symmetrical fluoro bridges. Likewise, in the cyclic tetrameric phosphazenes $[PNX_2]_4$ the corresponding orbitals are energetically so different that no second-order Jahn–Teller effect occurs, thus explaining the equalized P–N bond distances.[122]

Interesting is a comparison of the polynuclear nitrido complexes and linear and cyclic $(CH_2)_n$ polyenes.[122] It emerges that the known nitrido complexes are related to the polyene analogues polyacetylene, allyl and pentadienyl cation and cyclooctatetraene. This structural relationship is explained by the similarity of the π-systems, which is evident in particular in nitrido complexes, since the difference in electronegativity between metal and bridging N atom is small.

Thus, it appears that binuclear nitrido complexes with symmetrical nitrido bridges correspond to the allyl system. Trinuclear complexes such as $[W_3N_2Cl_{14}]^{2-}$[118] containing the structural group W≡N-W-N≡W are comparable with the pentadienyl cation, $[\{MoNCl_3\}_4]$[81] corresponds to cyclooctatetraene, and the polymeric nitrido complexes $[ReNCl_4]_n$,[173] $[MoNCl_4^-]_n$[86] and $[(RO)_3WN]_n$[77] have alternating M–N distances, as is the case in polyacetylene.

The most interesting conclusion which R. Hoffmann et al.[122] drew from the comparison of multinuclear nitrido complexes with organic polyenes was the prediction that a cyclic, trimeric nitrido complex $[\{L_nMN\}_3]$ ought to be stable and in analogy to benzene should presumably have equal M–N distances.

A little later Roesky et al.[120] then synthesized the nitrido complex $[\{Cp^*TaN(Cl)\}_3]$, which can be regarded as triazatritantalabenzene, and shows almost equal Ta–N distances of 184 and 191 pm.

Mononuclear complexes MNL_4 almost always have a tetragonal-pyramidal structure. Exceptions are provided by the complexes $[WNCl_2F_2]^-$[179] and $[TcNCl_2(PPh_3)_2]$[124] with trigonal-bipyramidal structure and the nitrido ligand in equatorial position. In this connection, R. Hoffmann et al.[170] investigated the question of a change in structure in the sense of a Berry pseudorotation. The calculations show that the tetragonal-bipyramidal structure with the nitrogen atom in the apical position is only about 12–13 kJ mol^{-1} more stable than the trigonal-bipyramidal alternative. This explains why, for example, steric effects such as are effected by the phosphane ligands in $[TcNCl_2(PPh_3)_2]$,[124] can stabilize the trigonal-bipyramidal arrangement.

For a trigonal bipyramid with the N atom in the axial position there is likewise a local minimum, which however lies at higher energy than in the case of the equatorial arrangement.

A pseudorotation should, according to calculations, be easily possible in the case of a d^0–d^2 electron configuration of the metal; in the case of d^3–d^7 electron configuration it is symmetry forbidden.

7. Outlook

Nitrogen is an extremely versatile element, which, owing to its manifold bonding and coordination possibilities, also promises a diversified chemistry in the future. Thus, the chemistry of the nitrido complexes has developed extensively in the past few years. This is due in the first instance to the many new synthetic methods which have opened up entries to nitrogen compounds. It is expected that this development will continue in the coming years, since the known synthetic methods are still not exhausted and surely new ones will be added. Possibly also new nitrido complexes of the previously little investigated main group elements will be found. Also in the area of catalysis it can be expected that nitrido complexes will find application as effective catalysts. Finally, the search for preceramic materials will give new impetus to the chemistry of the nitrides of main and sub-group elements.

We thank the Deutsche Forschungsgemeinschaft and the Verband der Chemischen Industrie for generous support of our work. Thanks are also due to our co-workers for their enthusiastic and invaluable cooperation. We also thank Mrs. E. Niquet for preparing the SCHAKAL diagrams.

Received: December 30, 1991 [A 869 IE]
German version: *Angew. Chem.* **1992**, *104*, 978

[1] K. Dehnicke, J. Strähle, *Angew. Chem.* **1981**, *93*, 451–464; *Angew. Chem. Int. Ed. Engl.* **1981**, *20*, 413–426.
[2] W. A. Nugent, J. M. Mayer, *Metal-Ligand Multiple Bonds*, Wiley, New York, **1988**.
[3] D. E. Fjare, W. L. Gladfelter, *J. Am. Chem. Soc.* **1984**, *106*, 4799–4810.
[4] A. Grohmann, J. Riede, H. Schmidbaur, *Nature* **1990**, *345*, 140–141.
[5] W. Rüdorff, K. Brodersen, *Z. Anorg. Allg. Chem.* **1953**, *274*, 323–340.
[6] K. Brodersen, H.-J. Becher, *Chem. Ber.* **1956**, *89*, 1487–1495.
[7] T. Godemeyer, K. Dehnicke, E. Fluck, *Z. Anorg. Allg. Chem.* **1988**, *565*, 41–46.
[8] T. Godemeyer, K. Dehnicke, *Z. Anorg. Allg. Chem.* **1988**, *558*, 114–118.
[9] D. Fenske, T. Godemeyer, K. Dehnicke, *Z. Naturforsch. B* **1988**, *43*, 12–20.
[10] T. Godemeyer, K. Dehnicke, *Z. Anorg. Allg. Chem.* **1988**, *566*, 77–82.
[11] T. Godemeyer, F. Weller, K. Dehnicke, D. Fenske, *Z. Anorg. Allg. Chem.* **1987**, *554*, 92–100.
[12] F. Weller, W. Liebelt, K. Dehnicke, *Z. Anorg. Allg. Chem.* **1982**, *484*, 124–130.
[13] Y. Jeannin, J.-P. Launnay, J. Livage, A. Nel, *Inorg. Chem.* **1978**, *17*, 374–378.
[14] T. Godemeyer, A. Berg, H.-D. Gross, U. Müller, K. Dehnicke, *Z. Naturforsch. B* **1985**, *40*, 999–1004.

[15] D. Fenske, A. Frankenau, K. Dehnicke, *Z. Anorg. Allg. Chem.* **1989**, *574*, 14–20.
[16] E. Schweda, K. D. Scherfise, K. Dehnicke, *Z. Anorg. Allg. Chem.* **1985**, *528*, 117–124.
[17] F. A. Cotton, R. C. Najjar, *Inorg. Chem.* **1981**, *20*, 1866–1869.
[18] T. Godemeyer, K. Dehnicke, D. Fenske, *Z. Naturforsch. B* **1985**, *40*, 1005–1009.
[19] I. Sens, U. Müller, R. Wollert, K. Dehnicke, unpublished.
[20] H. Plenio, H. W. Roesky, M. Noltemeyer, G. M. Sheldrick, *Angew. Chem.* **1988**, *100*, 1377–1378; *Angew. Chem. Int. Ed. Engl.* **1988**, *27*, 1330–1331.
[21] M. M. B. Holl, M. Kersting, B. D. Pendley, P. T. Wolczanski, *Inorg. Chem.* **1990**, *29*, 1518–1526.
[22] R. A. Wheeler, R. Hoffmann, J. Strähle, *J. Am. Chem. Soc.* **1986**, *108*, 5381–5387.
[23] L. Maya, *Inorg. Chem.* **1987**, *26*, 1459–1462.
[24] M. Hörner, K.-P. Frank, J. Strähle, *Z. Naturforsch. B* **1986**, *41*, 423–428.
[25] H. W. Roesky, Y. Bai, M. Noltemeyer, *Angew. Chem.* **1989**, *101*, 788–789; *Angew. Chem. Int. Ed. Engl.* **1989**, *28*, 754–755.
[26] P. A. Lay, H. Taube, *Inorg. Chem.* **1989**, *28*, 3561–3564.
[27] S.-H. Kim, B. A. Moyer, S. Azan, G. M. Brown, A. L. Olins, D. P. Allison, *Inorg. Chem.* **1989**, *28*, 4648–4650.
[28] M. M. B. Holl, P. T. Wolczanski, G. D. Van Duyne, *J. Am. Chem. Soc.* **1990**, *112*, 7989–7994.
[29] W. Liebelt, K. Dehnicke, *Z. Naturforsch. B* **1979**, *34*, 7–9.
[30] A. Frankenau, K. Dehnicke, *Z. Naturforsch. B* **1989**, *44*, 493–494.
[31] A. Görge, K. Dehnicke, D. Fenske, *Z. Naturforsch. B* **1988**, *43*, 677–681.
[32] A. Görge, U. Patt-Siebel, U. Müller, K. Dehnicke, *Z. Naturforsch. B* **1988**, *43*, 1633–1638.
[33] J. D. Buhr, J. R. Winkler, H. Taube, *Inorg. Chem.* **1980**, *19*, 2416–2425.
[34] J. W. Buchler, C. Dreher, K.-L. Lay, A. Raap, K. Gersonde, *Inorg. Chem.* **1983**, *22*, 879–884.
[35] J. W. Buchler, C. Dreher, K.-L. Lay, *Z. Naturforsch. B* **1982**, *37*, 1155–1162.
[36] J. W. Buchler, C. Dreher, K.-L. Lay, Y. J. A. Lee, W. R. Scheidt, *Inorg. Chem.* **1983**, *22*, 888–891.
[37] J. T. Groves, T. Takahashi, W. M. Butler, *Inorg. Chem.* **1983**, *22*, 884–887.
[38] H. Grunewald, H. Homborg, *Z. Naturforsch. B* **1990**, *45*, 483–489.
[39] J. Strähle, *Comments Inorg. Chem.* **1985**, *4*, 295–321.
[40] J. R. Dilworth, P. L. Dahlstrom, J. R. Hyde, J. Zubieta, *Inorg. Chim. Acta* **1983**, *71*, 21–28.
[41] P. C. Bevan, J. Chatt, J. R. Dilworth, R. A. Henderson, G. J. Leigh, *J. Chem. Soc. Dalton Trans.* **1982**, 821–824.
[42] D. L. Hughes, M. Y. Mohammed, C. J. Pickett, *J. Chem. Soc. Dalton Trans.* **1990**, 2013–2019.
[43] E. Schweda, J. Strähle, *Z. Naturforsch. B* **1981**, *36*, 662–665.
[44] J. Beck, E. Schweda, J. Strähle, *Z. Naturforsch. B* **1985**, *40*, 1073–1076.
[45] L. G. Hubert-Pfalzgraf, G. Aharonian, *Inorg. Chim. Acta* **1985**, *100*, L21–L22.
[46] C. J. Barner, T. J. Collins, B. E. Mapes, B. D. Santarsiero, *Inorg. Chem.* **1986**, *25*, 4322–4323.
[47] M. E. Noble, K. Folting, J. C. Huffman, R. A. D. Wentworth, *Inorg. Chem.* **1982**, *21*, 3772–3776.
[48] S. I. Arshankow, A. L. Poznjak, *Z. Anorg. Allg. Chem.* **1981**, *481*, 201–206.
[49] J. W. Buchler, C. Dreher, *Z. Naturforsch. B* **1984**, *39*, 222–230.
[50] C.-M. Che, J.-X. Ma, W.-T. Wong, T.-F. Lai, C.-K. Poon, *Inorg. Chem.* **1988**, *27*, 2547–2548.
[51] K. Dehnicke, U. Müller, *Comments Inorg. Chem.* **1985**, *4*, 213–228.
[52] U. Kynast, U. Müller, K. Dehnicke, *Z. Anorg. Allg. Chem.* **1984**, *508*, 26–32.
[53] U. Kynast, K. Dehnicke, *Z. Anorg. Allg. Chem.* **1983**, *502*, 29–34.
[54] U. Müller, W. Kafitz, K. Dehnicke, *Z. Anorg. Allg. Chem.* **1983**, *501*, 69–78.
[55] H. G. Hauck, P. Klingelhöfer, U. Müller, K. Dehnicke, *Z. Anorg. Allg. Chem.* **1984**, *510*, 180–188.
[56] J. Chatt, C. D. Falk, G. J. Leigh, R. J. Paske, *J. Chem. Soc. A* **1969**, 2288–2293.
[57] R. J. Doedens, J. A. Ibers, *Inorg. Chem.* **1967**, *6*, 204–210.
[58] E. Forsellini, U. Casellato, R. Graziani, L. Magon, *Acta Crystallogr. Sect. B* **1982**, *38*, 3081–3083.
[59] K. Hösler, K. Dehnicke, *Z. Anorg. Allg. Chem.* **1987**, *554*, 108–112.
[60] K. Völp, K. Dehnicke, D. Fenske, *Z. Anorg. Allg. Chem.* **1989**, *572*, 26–32.
[61] A. F. Wells, *Structural Inorganic Chemistry*, Clarendon, Oxford, **1984**.
[62] A. Gudat, S. Haag, R. Kniep, A. Rabenau, *Z. Naturforsch. B* **1990**, *45*, 111–120.
[63] A. Gudat, P. Höhn, R. Kniep, A. Rabenau, *Z. Naturforsch. B* **1991**, *46*, 566–572.
[64] K. D. Scherfise, K. Dehnicke, *Z. Anorg. Allg. Chem.* **1986**, *538*, 119–122.
[65] S. C. Critchlow, M. E. Lerchen, R. C. Smith, N. M. Doherty, *J. Am. Chem. Soc.* **1988**, *110*, 8071–8075.
[66] J. D. Lichtenhan, S. C. Critchlow, N. M. Doherty, *Inorg. Chem.* **1990**, *29*, 439–442.
[67] W. Willing, R. Christophersen, U. Müller, K. Dehnicke, *Z. Anorg. Allg. Chem.* **1987**, *555*, 16–22.
[68] K. Jansen, J. Schmitte, K. Dehnicke, D. Fenske, *Z. Anorg. Allg. Chem.* **1987**, *522*, 201–209.
[69] K. Dehnicke, J. Schmitte, D. Fenske, *Z. Naturforsch. B* **1980**, *35*, 1070–1074.
[70] J. Beck, J. Strähle, *Z. Anorg. Allg. Chem.* **1987**, *554*, 50–60.
[71] T. Ernst, A. El-Kholi, U. Müller, K. Dehnicke, *Z. Anorg. Allg. Chem.* **1988**, *566*, 7–17.
[72] H. W. Roesky, J. Sundermeyer, J. Schimkowiak, P. G. Jones, M. Noltemeyer, T. Schroeder, G. M. Sheldrick, *Z. Naturforsch. B* **1985**, *40*, 736–739.
[73] C. Ergezinger, A. El-Kholi, U. Müller, K. Dehnicke, *Z. Anorg. Allg. Chem.* **1989**, *568*, 55–61.
[74] K. Dehnicke, *Chem.-Ztg.* **1990**, *114*, 295–304.
[75] A. Görge, U. Patt-Siebel, U. Müller, K. Dehnicke, *Z. Naturforsch. B* **1989**, *44*, 903–910.
[76] R. R. Schrock, M. L. Listemann, L. G. Sturgeoff, *J. Am. Chem. Soc.* **1982**, *104*, 4291–4293.
[77] M. H. Chisholm, D. M. Hoffmann, J. C. Huffman, *Inorg. Chem.* **1983**, *22*, 2903–2906.
[78] D. M.-T. Chan, M. H. Chisholm, K. Folting, J. C. Huffman, N. S. Marchant, *Inorg. Chem.* **1986**, *25*, 4170–4174.
[79] D. Fenske, R. Kujanek, K. Dehnicke, *Z. Anorg. Allg. Chem.* **1983**, *507*, 51–58.
[80] W.-H. Leung, G. Wilkinson, B. Hussain-Bates, M. B. Hursthouse, *J. Chem. Soc. Dalton Trans.* **1991**, 2791–2794.
[81] J. Strähle, *Z. Anorg. Allg. Chem.* **1970**, *375*, 238–254; *ibid.* **1971**, *380*, 96.
[82] I. Walker, J. Strähle, P. Ruschke, K. Dehnicke, *Z. Anorg. Allg. Chem.* **1982**, *487*, 26–32.
[83] A. Khabou, K. Dehnicke, K. Findeisen, D. Fenske, *Z. Naturforsch. B* **1988**, *43*, 1616–1620.
[84] E. Rentschler, K. Dehnicke, unpublished.
[85] N. Ueyama, H. Zaima, H. Okada, A. Nakamura, *Inorg. Chim. Acta* **1984**, *89*, 19–23.
[86] U. Patt-Siebel, A. Khabou, U. Müller, K. Dehnicke, *Z. Anorg. Allg. Chem.* **1989**, *569*, 91–96.
[87] L. A. Bottomley, B. B. Garrett, *Inorg. Chem.* **1982**, *21*, 1260–1263.
[88] D. F. Bocian, E. W. Findsen, J. A. Hofmann, Jr., G. A. Schick, D. R. English, D. N. Hendrickson, K. S. Suslick, *Inorg. Chem.* **1984**, *23*, 800–807.
[89] B. J. Kennedy, K. S. Murray, H. Homborg, W. Kalz, *Inorg. Chim. Acta* **1987**, *134*, 19–21.
[90] D. R. English, D. N. Hendrickson, K. S. Suslick, *Inorg. Chem.* **1985**, *24*, 121–122; *ibid.* **1983**, *22*, 367–368.
[91] W. D. Hewson, L. P. Hager in *The Porphyrines, Vol. VIII* (Ed.: D. Dolphin), Academic, New York, **1979**, p. 295.
[92] J. Chatt, B. T. Heaton, *J. Chem. Soc. A* **1971**, 705–707.
[93] R. Dantona, E. Schweda, J. Strähle, *Z. Naturforsch. B* **1984**, *39*, 733–735.
[94] W. Kafitz, F. Weller, K. Dehnicke, *Z. Anorg. Allg. Chem.* **1982**, *490*, 175–181.
[95] M. W. Bishop, J. Chatt, J. R. Dilworth, P. Dahlstrom, J. Hyde, J. Zubieta, *J. Organomet. Chem.* **1981**, *213*, 109–124.
[96] J. T. Groves, T. Takahashi, *J. Am. Chem. Soc.* **1983**, *105*, 2073–2074.
[97] L. A. Bottomley, F. L. Neely, *J. Am. Chem. Soc.* **1988**, *110*, 6748–6752.
[98] U. Müller, U. Patt-Siebel, A. Khabou, K. Dehnicke, E. Fluck, *Chem.-Ztg.* **1987**, *111*, 371–372.
[99] H. R. Allcock, N. M. Tollefson, R. A. Arcus, R. R. Whittle, *J. Am. Chem. Soc.* **1985**, *107*, 5166–5177.
[100] J. Schmitte, K. Dehnicke, *Z. Naturforsch. B* **1986**, *41*, 793–795.
[101] E. Hey, F. Weller, K. Dehnicke, *Z. Anorg. Allg. Chem.* **1983**, *502*, 45–54.
[102] G. Beuter, U. Englert, J. Strähle, *Z. Naturforsch. B* **1988**, *43*, 145–148.
[103] N. M. Doherty, S. C. Chritchlow, *J. Am. Chem. Soc.* **1987**, *109*, 7906–7908.
[104] W. Massa, R. Kujanek, G. Baum, K. Dehnicke, *Angew. Chem.* **1984**, *96*, 149; *Angew. Chem. Int. Ed. Engl.* **1984**, *23*, 149.
[105] N. Wiberg, H.-W. Häring, S. K. Vasisht, *Z. Naturforsch. B* **1979**, *34*, 356–357; M. Veith, G. Schlemmer, *Z. Anorg. Allg. Chem.* **1982**, *494*, 7–19.
[106] H. Stenger, Dissertation, Universität Marburg, **1991**.
[107] H. Stenger, K. Dehnicke, W. Hiller, *Z. Naturforsch. B*, in press.
[108] J. Fawcett, R. D. Peacock, D. R. Russell, *J. Chem. Soc. Dalton Trans.* **1987**, 567–571.
[109] W. Kafitz, K. Dehnicke, E. Schweda, J. Strähle, *Z. Naturforsch. B* **1984**, *39*, 1114–1117.
[110] K. Dehnicke, unpublished.
[111] D. Collison, C. D. Garner, F. E. Mabbs, T. J. King, *J. Chem. Soc. Dalton Trans.* **1981**, 1820–1824.
[112] P. A. Belmonte, Z.-Y. Own, *J. Am. Chem. Soc.* **1984**, *106*, 7493–7496.
[113] P. A. Shapley, Z.-Y. Own, J. C. Huffman, *Organometallics* **1986**, *5*, 1269–1271.

[114] S. Buth, S. Wocadlo, B. Neumüller, F. Weller, K. Dehnicke, *Z. Naturforsch. B* **1992**, *47*, 706–712.
[115] P. J. Blower, J. R. Dilworth, *J. Chem. Soc. Dalton Trans.* **1985**, 2305–2309.
[116] K. Dehnicke, H. Prinz, W. Kafitz, R. Kujanek, *Liebigs Ann. Chem.* **1981**, 20–27.
[117] D. W. Pipes, M. Bakir, S. E. Vitols, D. J. Hodgson, T. J. Meyer, *J. Am. Chem. Soc.* **1990**, *112*, 5507–5512.
[118] H. H. Thorp, J. Van Houten, H. B. Gray, *Inorg. Chem.* **1989**, *28*, 889–892.
[119] W. P. Griffith, N. T. McManus, A. C. Skapski, *J. Chem. Soc. Chem. Commun.* **1984**, 434–435.
[120] Z. Gebeyehu, F. Weller, B. Neumüller, K. Dehnicke, *Z. Anorg. Allg. Chem.* **1991**, *593*, 99–110.
[121] C.-M. Che, M. H.-W. Lam, T. C. W. Mak, *J. Chem. Soc. Chem. Commun.* **1989**, 1529–1531.
[122] D. Bright, J. A. Ibers, *Inorg. Chem.* **1969**, *8*, 709–716.
[123] J. Baldas, J. F. Boas, J. Bonnyman, G. A. Williams, *J. Chem. Soc. Dalton Trans.* **1984**, 2395–2400.
[124] M. J. Abrams, S. K. Larsen, S. N. Shaikh, J. Zubieta, *Inorg. Chim. Acta* **1991**, *185*, 7–15.
[125] A. Marchi, R. Rossi, L. Magon, A. Duatti, U. Casellato, R. Graziani, M. Vidal, F. Riche, *J. Chem. Soc. Dalton Trans.* **1990**, 1935–1940.
[126] A. Marchi, A. Duatti, R. Rossi, L. Magon, R. Pasqualini, V. Bertolasi, V. Ferreti, G. Gilli, *J. Chem. Soc. Dalton Trans.* **1988**, 1743–1749.
[127] U. Abram, S. Abram, R. Münze, E.-G. Jäger, J. Stach, R. Kirmse, G. Admiraal, P. T. Beurskens, *Inorg. Chim. Acta* **1991**, *182*, 233–238.
[128] J. Baldas, S. F. Colmanet, M. F. Mackay, *J. Chem. Soc. Dalton Trans.* **1988**, 1725–1731.
[129] J. Baldas, S. F. Colmanet, M. F. Mackay, *J. Chem. Soc. Chem. Commun.* **1989**, 1890–1891.
[130] J. Baldas, J. Bonnyman, G. A. Williams, *Inorg. Chem.* **1986**, *25*, 150–153.
[131] U. Abram, S. Abram, J. Stach, W. Dietzsch, W. Hiller, *Z. Naturforsch. B* **1991**, *46*, 1183–1187.
[132] E. I. Stiefel, *Progr. Inorg. Chem.* **1977**, *22*, 1–223.
[133] J. Chatt, J. R. Dilworth, R. L. Richards, *Chem. Rev.* **1978**, *78*, 589–625.
[134] J. Schmitte, C. Friebel, F. Weller, K. Dehnicke, *Z. Anorg. Allg. Chem.* **1982**, *495*, 148–156.
[135] P. J. Blower, J. R. Dilworth, *J. Chem. Soc. Dalton Trans.* **1985**, 2305–2309.
[136] U. Müller, R. Kujanek, K. Dehnicke, *Z. Anorg. Allg. Chem.* **1982**, *495*, 127–134.
[137] R. Figge, C. Friebel, U. Patt-Siebel, U. Müller, K. Dehnicke, *Z. Naturforsch. B* **1989**, *44*, 1377–1384.
[138] M. H. Chisholm, K. Folting, J. C. Huffman, J. Leonelli, N. S. Marchant, C. A. Smith, L. C. E. Taylor, *J. Am. Chem. Soc.* **1985**, *107*, 3722–3724.
[139] N. D. Feasey, S. A. R. Knox, A. G. Orpen, *J. Chem. Soc. Chem. Commun.* **1982**, 75–76.
[140] K. Dehnicke, J. Strähle, *Polyhedron* **1989**, *8*, 707–726.
[141] D. Pawson, W. P. Griffith, *J. Chem. Soc. Dalton Trans.* **1975**, 417–423.
[142] I. Schmidt, U. Kynast, J. Hanich, K. Dehnicke, *Z. Naturforsch. B* **1984**, *39*, 1248–1251.
[143] V. C. Gibson, D. N. Williams, W. Clegg, *J. Chem. Soc. Chem. Commun.* **1989**, 1863–1864.
[144] H. W. Roesky, K. V. Katti, U. Seseke, H. G. Schmidt, E. Egert, R. Herbst, G. M. Sheldrick, *J. Chem. Soc. Dalton Trans.* **1987**, 847–849.
[145] M. Witt, H. W. Roesky, *Polyhedron* **1988**, *8*, 1736–1741.
[146] H. W. Roesky, K. V. Katti, U. Seseke, M. Witt, E. Egert, R. Herbst, G. M. Sheldrick, *Angew. Chem.* **1986**, *98*, 447–448; *Angew. Chem. Int. Ed. Engl.* **1986**, *25*, 477–478.
[147] K. Hösler, K. Dehnicke, unpublished; cited in Ref. [140].
[148] M. Bakir, P. S. White, A. Dovletoglou, T. J. Meyer, *Inorg. Chem.* **1991**, *30*, 2836–2838.
[149] D. Sellmann, J. Keller, M. Moll, C. F. Campana, M. Haase, *Inorg. Chim. Acta* **1988**, *141*, 243–251.
[150] M. W. Bishop, J. Chatt, J. R. Dilworth, *J. Chem. Soc. Dalton Trans.* **1979**, 1–5.
[151] H. W. Roesky, K. K. Pandey, *Adv. Inorg. Chem. Radiochem.* **1983**, *26*, 337–356.
[152] J. Anhaus, Z. A. Siddiqi, H. W. Roesky, J. W. Bats, Y. Elerman, *Z. Naturforsch. B* **1985**, *40*, 740–744.
[153] U. Kynast, E. Conradi, U. Müller, K. Dehnicke, *Z. Naturforsch. B* **1984**, *39*, 1680–1685.
[154] J. Anhaus, P. G. Jones, M. Noltemeyer, W. Pinkert, H. W. Roesky, G. M. Sheldrick, *Inorg. Chim. Acta* **1985**, *97*, L7–L9.
[155] H. Wadle, E. Conradi, U. Müller, K. Dehnicke, *Z. Naturforsch. B* **1986**, *41*, 429–435.
[156] H. W. Roesky in *Rings, Clusters and Polymers of Main Group and Transition Elements* (Ed.: H. W. Roesky), Elsevier, Amsterdam, **1989**.
[157] M. Minelli, C. G. Young, J. H. Enemark, *Inorg. Chem.* **1985**, *24*, 1111–1113.
[158] J. R. Dilworth, S. Donovan-Mtunzi, C. T. Kan, R. L. Richards, J. Mason, *Inorg. Chim. Acta* **1981**, *53*, L161–L162.
[159] S. Donovan-Mtunzi, R. L. Richards, J. Mason, *J. Chem. Soc. Dalton Trans.* **1984**, 1329–1332.
[160] K. Seyferth, R. Taube, *J. Organomet. Chem.* **1982**, *229*, C19–C23.
[161] J. H. Wengrovius, R. R. Schrock, M. R. Churchill, J. R. Missert, W. J. Youngs, *J. Am. Chem. Soc.* **1980**, *102*, 4515–4516.
[162] R. Taube, K. Seyferth, *J. Organomet. Chem.* **1983**, *249*, 365–369.
[163] W. A. Herrmann, *Angew. Chem.* **1988**, *100*, 1269–1286; *Angew. Chem. Int. Ed. Engl.* **1988**, *27*, 1297–1314.
[164] W. A. Herrmann, W. Wagner, U. N. Flessner, U. Volkhardt, H. Komber, *Angew. Chem.* **1991**, *103*, 1704–1706; *Angew. Chem. Int. Ed. Engl.* **1991**, *30*, 1636–1638.
[165] W. A. Herrmann, R. W. Fischer, D. W. Marz, *Angew. Chem.* **1991**, *103*, 1706–1709; *Angew. Chem. Int. Ed. Engl.* **1991**, *30*, 1638–1641.
[166] W. A. Herrmann, M. Wang, *Angew. Chem.* **1991**, *103*, 1709–1711; *Angew. Chem. Int. Ed. Engl.* **1991**, *30*, 1641–1643.
[167] G. Schoettel, J. Kress, J. A. Osborn, *J. Chem. Soc. Chem. Commun.* **1989**, 1062–1063.
[168] R. Toreki, R. R. Schrock, *J. Am. Chem. Soc.* **1990**, *112*, 2448–2449.
[169] K. Tatsumi, R. Hoffmann, *J. Am. Chem. Soc.* **1981**, *103*, 3328–3341.
[170] R. A. Wheeler, M.-H. Whangbo, T. Hughbanks, R. Hoffmann, J. K. Burdett, T. A. Albright, *J. Am. Chem. Soc.* **1986**, *108*, 2222–2236.
[171] V. L. Goedken, M. R. Deakin, L. A. Bottomley, *J. Chem. Soc. Chem. Commun.* **1982**, 607–608.
[172] G. Rossi, V. L. Goedken, C. Ercolani, *J. Chem. Soc. Chem. Commun.* **1988**, 46–47.
[173] W. Liese, K. Dehnicke, I. Walker, J. Strähle, *Z. Naturforsch. B* **1979**, *34*, 693–696.

In Vitro Selection of Specific Ligand-binding Nucleic Acids**

By Michael Famulok* and Jack W. Szostak*

In vitro selection is a method that allows the simultaneous screening of very large numbers of nucleic acid molecules for a wide range of properties from binding characteristics to catalytic properties; moreover, the isolation of the very rare functional molecules becomes possible. Binding sites between proteins and nucleic acids, for example, have been evaluated by this methodology in order to gain information about protein/nucleic acid interactions. Structure and function of catalytic RNA ("ribozymes") has been studied by in vitro selection and has led to new ribozymes with improved catalytic function. Substrate specificity of catalytic RNA has been changed and has led to a ribozyme that cleaves DNA. Other applications include the isolation of nucleic acids that bind specifically to small organic molecules and of RNA molecules that form triple helices with double-stranded DNA. In this article we discuss the background, design, and results of in vitro genetic experiments, which bridge biochemical/molecular biological and organic chemical approaches to molecular recognition.

1. Introduction

The rational design of nucleic acids with tertiary structures complementary to a given chemical structure is currently unattainable because it requires not only the ability to predict the three-dimensional structure corresponding to a given sequence, but also the ability to anticipate changes in structure that might occur upon ligand binding. The design of nucleic acid structures complementary to ligands of unknown structure is, by the very nature of the problem, impossible. Nevertheless, it is now possible to routinely isolate DNA and RNA molecules that bind tightly and specifically to a wide range of ligands, including proteins, other nucleic acids, and small organic molecules. This development is the result of new techniques that sidestep the whole issue of design by allowing the isolation of very rare molecules with specified ligand-binding properties from extremely large pools of random sequence nucleic acids.[1] These in vitro selection methods were recently developed independently in several different laboratories for a wide range of applications, from the evaluation of protein binding sites on nucleic acids, to the study of the structure and function of catalytic RNAs.

The methodology is conceptually straigthforward: first, a large library of completely random oligodeoxynucleotides, or a library of degenerate oligodeoxynucleotides containing as many variants as possible of a sequence of interest, is generated by chemical synthesis.[2] If desired, this library of DNA sequences may be converted into a library of RNA sequences by in vitro transcription. The pool is then subjected to selection steps that will result in enrichment of the molecules of interest. Since only a very small fraction of the random or degenerate sequences will be functional, complete purification in one step is not usually possible. The pool of molecules resulting from each selection step is therefore amplified so that further enrichment of the functional molecules can be achieved in additional selection cycles. Amplification is achieved through the polymerase chain reaction (PCR),[3] or in a transcription-based step. Successive selection and amplification cycles result in an exponential increase in the abundance of functional sequences, until they dominate the population (Scheme 1).

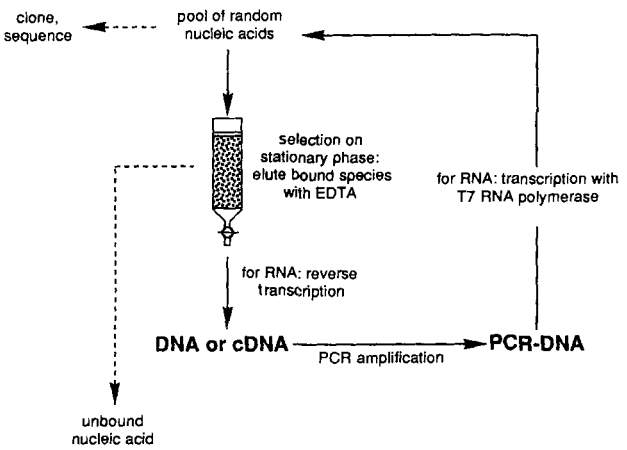

Scheme 1. Selection for ligand-binding RNA molecules by means of affinity chromatography. For the selection of DNA sequences, reverse transcription and transcription are not needed, but asymmetric PCR or single-strand purification is required to prevent combination of complementary strands into inactive duplex DNA.

In vitro selection can be applied to the analysis of known nucleic acid sequences; for example, it provides a rapid way of identifying important residues that cannot be changed without loss of function, whether in a protein binding site on a DNA molecule, or in an RNA catalyst. However, this method can also be applied to more difficult problems, such as the isolation of novel nucleic acid molecules that bind very specifically to targets ranging from small organic molecules to large regulatory proteins. The de novo isolation of functional sequences with catalytic activity is an even bigger challenge currently being addressed in several laboratories.

[*] Dr. M. Famulok
Institut für Biochemie der Universität München
c/o Max-Planck-Institut für Biochemie
Am Klopferspitz 18a, D-W-8033 Martinsried (FRG)
Prof. J. Szostak
Department of Molecular Biology, Wellman-9
Massachusetts General Hospital
Boston, MA 02114 (USA)

[**] Important technical terms have been explained in a glossary in Section 5.

An immediate advantage of in vitro selection over standard in vivo genetic methods is that the selection conditions, binding specificity, or the reactions for which catalysis is to be selected are independent of any constraints imposed by cellular physiology. Another major advantage of in vitro selection is that pools as large as 10^{15} different species, or even larger, can be screened for functional sequences, greatly increasing the likelihood of generating at least one molecule with the desired properties.

2. Design of In Vitro Selection Experiments

An in vitro selection experiment may begin with either completely random sequences, or with a library of partially randomized sequences.

Partial randomization would normally be applied to the analysis of the structure of a known functional sequence, or to the isolation of a variant sequence with altered properties. A certain percentage of random nucleotides may be incorporated into part or all of the sequence to be studied, or alternatively a short region of a longer, defined sequence may be completely randomized. In either case, a family of closely related sequences is created (Scheme 2).

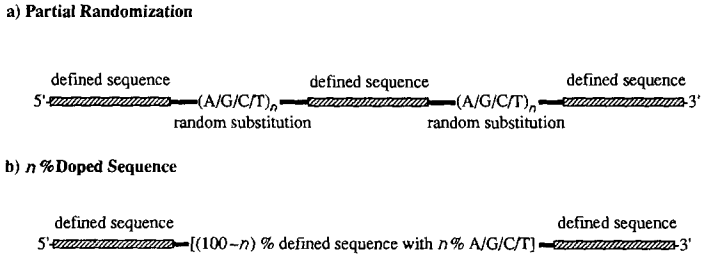

Scheme 2. Examples of partially randomized sequences: a) Partial sequences within a defined nucleic acid sequence are substituted by completely randomized short sections. b) The nucleic acid sequence is synthesized so that a certain percentage of nucleotides is randomly introduced in a defined sequence. In principle this describes the synthesis of a sequence of nucleic acids with an extremely high mutation rate.

After the selection of a functional pool, comparative sequence analysis allows the identification of positions that can be classified as a) variable, and thus not necessary for the selected function, b) highly conserved, which indicates their functional importance, c) covarying with another position, which indicates an interaction between these positions.

The de novo isolation of nucleic acid receptors with specificity for particluar biomolecules or small substrates requires a large initial library of completely random sequences, flanked by defined primer binding sites that allow the amplification of the selected molecules (Scheme 3).

Scheme 3. Schematic representation of synthetic DNA oligonucleotides designed for transcription into a library of RNA molecules containing random sequence inserts.

In order to maximize the probability of the presence of substrate-specific tertiary structures, the general strategy is to start with a pool of maximum complexity.[4] With automated oligonucleotide synthesis,[5] a complexity of roughly $10^{13}-10^{15}$ different DNA molecules can be generated.[6, 7] Principles for the design of in vitro selection experiments and pool syntheses have been described.[8]

3. Applications

3.1. Selection for DNA Protein Recognition

The first report of the in vitro selection of random DNA sequences came from Oliphant et al.,[9] who performed affin-

Michael Famulok, born in 1960 in Fulda, Germany, studied chemistry at the University of Marburg from 1981 to 1989), where he obtained his Ph.D. in 1989 with Prof. G. Boche. In 1989 and 1990 he did postdoctoral work with Prof. J. Rebek, Jr. at the Massachusetts Institute of Technology, in the field of molecular recognition by abiotic receptor molecules. Thereafter he joined Prof. J. W. Szostak as postdoc. (1990–1992) to study in vitro selection. He is now completing his Habilitation at the Department of Biochemistry, University of Munich. His research interests are the molecular recognition of ligands by nucleic acids and nucleic acid catalysis.

Jack W. Szostak was born in 1952 in London, England. He attended McGill University in Montreal, Canada, from 1968 to 1972, where he received his B. Sc. His Ph.D. work (1972–1977) was carried out at Cornell University in the laboratory of Prof. Ray Wu. After postdoctoral work there, he moved to the Dana-Farber Cancer Institute and Harvard Medical School as an Assistant Professor, where he worked on recombination and chromosome structure. He is now Professor of Genetics at Harvard University and Massachusetts General Hospital in Boston. His research interests concentrate on the structure and function of RNA enzymes and the origin of life.

ity chromatography of random DNA sequences; however, the selection steps were carried out one after the other, without amplification. The analysis of the selected sequences was done by ligation into a plasmid, transformation, and cloning. Thus, the system can be described as in vitro selection/in vivo amplification. This selection system was applied to the isolation of DNA sequences that bind to the protein GCN4, a transcriptional activator protein that binds within the promotor region of many yeast genes coding for enzymes required for amino acid biosynthesis. A sequence of nine base pairs was thought to be important for GCN4 binding. To examine the details of the site specificity and the role of flanking nucleotides, a randomized 23 nucleotide region of DNA was synthesized, flanked on each side by different restriction sites. Single-stranded DNA was synthesized chemically and used as a template to make radioactive double-stranded DNA (dsDNA), which then was selected on GCN4-derivatized agarose in the presence of a carrier DNA. Bound DNAs were then eluted, digested with restriction enzyme, and subjected to three more cycles of chromatographic selection. After the final selection, 0.01% of the input-DNA was recovered. Cloning and sequencing revealed that 40 out of 43 clones contained the symmetric sequence TGA(C/G)TCA; six of these seven bases were present in the three other clones. Such a high degree of conservation indicates that the most significant GCN4/DNA-contacts are likely to occur in this region.

The first experiment to combine in vitro selection and in vitro amplification was reported in 1989 by Kinzler and Vogelstein, who selected for DNA sequences that contained binding sites for the transcription factor TFIIIA.[10a] Instead of synthetic random DNA, they used highly fragmented human DNA as the source of their initial pool; this DNA was derivatized with restriction site linkers to facilitate subsequent cloning and sequence analysis. Selection for DNA fragments containing binding sites was achieved by immunoprecipitation of protein–DNA complexes with anti-TFIIIA antibodies; the selected DNA was then amplified by PCR. By comparison of the sequences of the selected molecules a consensus binding site could be identified. In similar experiments the binding site of the human GL1 zinc-finger protein was determined.[10b]

A system for the selection of protein-binding DNA molecules based solely on in vitro techniques and synthetic DNA was described by Thiesen and Bach.[11] As a model protein for their studies they used a fragment of the DNA-binding human transcription factor SP1. The chemically synthesized DNA pool contained twelve random nucleotides flanked by defined primer binding sites. Double-stranded DNA was synthesized by PCR, incubated with the SP1 fragment, and the DNA–protein complexes were bound to nitrocellulose filters. A related oligonucleotide with defined SP1 binding sites was used for comparison and competition-binding assays. Bound DNAs were eluted with a zinc-chelator that denatures the zinc-finger domains of the SP1 protein, and the recovered DNA was amplified by PCR.[12] After five cycles of selection, 19 out of 20 cloned oligoucleotides showed binding to SP1. The relative affinities of some of these DNAs were tested in the presence of competitor DNA by bandshift electrophoresis. Two sequences, S2 and S3, showed up to ten times tighter binding than the known binding site used as competitor DNA. Sequencing of several cloned DNAs revealed striking sequence similarities. Some selected binding sequences differed in only one base from the SP1 consensus sequence GGGGCGGGGC. S2 and S3, the sequences with the highest affinity to SP1, showed mutations in three different positions.

3.1.1. Characteristics of Binding by Basic Helix-Loop-Helix Proteins to DNA

A third variation on the theme of DNA–protein recognition was reported by Blackwell and Weintraub,[13] who used cycles of in vitro selection and PCR amplification as above, but avoided the labor of cloning and sequencing many individual selected DNAs by simply sequencing the entire pool of DNA molecules as a mixture. Blackwell and Weintraub studied the DNA-binding sequence of several basic helix-loop-helix (bHLH) proteins, such as MyoD. The bHLH proteins are a family of transcriptional activators containing a conserved set of basic amino acids that are important for DNA recognition and are immediately adjacent to a region thought to form a helix-loop-helix (HLH) structure involved in oligomerization.[14] MyoD is responsible for the induction of muscle-specific genes in muscle cells, while other bHLH proteins induce different sets of tissue-specific genes in other tissues.[15] However, MyoD and all other known bHLH proteins bind in vitro to the consensus DNA sequence CANNTG.[16]

To see whether the different in vivo effects of these proteins might be due to differences in their DNA binding specificities, Blackwell and Weintraub performed a series of in vitro selection experiments. A pool of synthetic DNA molecules was generated containing the CANNTG consensus, in which the two central and several flanking positions were completely randomized. This mixture of DNA sequences was incubated with the protein (MyoD, E2A, E52, or heterooligomers of these proteins), and DNA–protein complexes were isolated by the electrophoresis mobility shift assay. After PCR amplification of the recovered DNA, the final pool of DNA was sequenced as a pool without prior cloning. This technique saves much time and effort, because it provides the possibility of reading out any bases that are required for specific recognition in addition to the defined CANNTG sequence directly from the sequencing gel.[17] The defined bases serve to ensure that the protein is similarly aligned on each DNA molecule. Unimportant bases or bases that are not involved in base-specific interactions remain as a mixture in the pool, and show up as a mixture in the sequencing ladder. This rapid analysis method enables the easy screening of mutant proteins generated by in vitro translation for any changes in their binding behavior. On the other hand, sequencing a mixture of sequences rather than individual clones means that some information may be lost if a pool contains different sequences that bind equally well.

3.1.2. In Vitro Selection Involving Immunoprecipitation

The purification of DNA–protein complexes by immunoprecipitation was used as an in vitro selection system by

Pollock and Treisman.[18] The great advantage of this approach is that the protein whose binding site is being defined need not be available in pure form. These authors used cell extracts as a source of the transcription factor SRF (serum response factor) and an in vitro translation system as a source of the *fos* oncoprotein. The selection strategy was similar to that used in the experiments described above: a 26 base region of randomized DNA was flanked by 25 nucleotide (nt) primer binding sites. The crude extract was incubated with the DNA pool and a competitor DNA (to decrease the formation of nonspecific complexes with pool DNA), whereupon the SRF- or *fos*-DNA complexes were isolated with SRF- or *fos*-specific antibodies. Bound DNA was purified, PCR-amplified, and reselected; after several cycles individual molecules were cloned and sequenced.

This approach will be particularly useful for the study of DNA-binding proteins that require post-translational modification or association with other proteins for correct DNA recognition. In such cases, protein obtained from bacterial over-expression systems may give misleading results. The ability to use material obtained by in vitro translation means that the effect of mutations in the protein on the DNA-binding specificity will be much easier to study, since mutant proteins can now be generated entirely in vitro (by PCR mutagenesis of a cloned gene, followed by in vitro transcription and in vitro translation).

3.2. In Vitro Selection for RNA Molecules for Protein Recognition

Protein binding sites on DNA are relatively simple to define since most DNA regulatory elements conform to the well-defined structures of the B-type double helix. In contrast, protein recognition mechanisms of RNA can make use of structural features found in the primary, secondary, or tertiary structure of the RNA. Detailed knowledge of the structural requirements can sometimes be achieved by means of phylogenetic studies, if sufficient sequence data exist.[19] Covariations may be found that allow conclusions to be drawn about the secondary or tertiary structure of the binding site. However, if there is insufficient variation between the available sequences, it will not be possible to deduce the relevant structure. Computer-generated secondary structures of RNA may be helpful in such analyses, but often fail to predict functionally important structures.[20] The Rev protein is an example: sequenced HIV isolates showed only very slight variation in the region of the Rev binding site, and several different foldings of the sequence were possible. In such cases, in vitro selection may be an excellent method of obtaining functional sequences that are sufficiently divergent for interesting structural information to be extracted by comparative sequence analysis.

3.2.1. The Rev Binding Site

The Rev protein of HIV and other closely related retroviruses mediates the transport of the mRNAs for *gag*, *pol*, end *env* from the nucleus to the cytoplasm in infected cells and is therefore essential for the replication of these viruses.[21] Rev binds within a 66 nucleotide (66 nt) long segment in the mRNA to be transported; however, the exact location and structure of the binding site were controversial.[22] Bartel et al. used an in vitro selection approach to address these issues.[23]

To avoid the selection of completely unrelated structures that happen to bind to the protein, the 66 base Rev binding element was not completely randomized; rather, the pool was synthesized so that 65% of the bases would be wild type, 30% not wild type, and 5% deleted. This degree of degeneracy was chosen so that nucleotides that played an important role in the binding site could be recognized as being conserved, while unimportant positions would vary extensively. Moreover, it was hoped that interacting bases could be recognized by covariation. The synthetic DNA template was amplified by PCR and then used to generate an RNA pool by in vitro transcription with T7 RNA polymerase. Selection was carried out by purification of RNA protein complexes on nitrocellulose filters. Bound RNA was eluted and amplified by reverse transcription to generate cDNA, followed by PCR amplification of the DNA and T7 transcription to regenerate an RNA pool. In order to measure the average affinity of the pool RNA for Rev, relative to the wild type binding sequence, a limiting amount of Rev was incubated with an excess of a mixture of pool RNA and a shorter wild type RNA. The partitioning of Rev protein between the two RNAs showed that the final selected pool (generated by three rounds of selection and amplification) actually bound Rev three times better than the wild-type RNA and 460 times better than the initial degenerate pool.

Cloning of 31 sequences from the final pool gave 18 monoclonal RNAs that bound as well or better to Rev than wild type RNA. One sequence showed 10 times better binding than the wild type. All of the conserved bases were found in two segments (U45 to G53 and C65 to A75). These segments represent the core of the Rev binding site; they pair with each other to form a stem-bulge-stem secondary structure (Scheme 4).

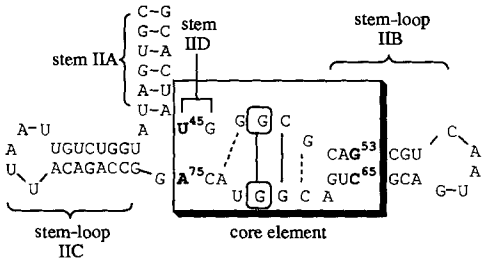

Scheme 4. Secondary structure of the 66 nucleotide long Rev responsive element, as determined by comparative sequence analysis of selected Rev binding RNAs. The boxed area shows the binding motif for the Rev recognition. The G:G base pair is indicated by the circles.

Seven out of the ten bases in the bulged region are highly conserved, indicating essential RNA–RNA or RNA–protein contacts. Further analysis of covariation G48 and G71 suggested that the formation of a nonstandard G48:G71 base pair was very important for Rev recognition. A single G → A substitution in either one of these positions dramatically reduces Rev binding, whereas the A:A double mutation fully

restores binding. This result leads to the conclusion that the bases of the base pair are not recognized by Rev directly. Although A:A and G:G are able to form isosteric base pairs,[24] they are completely different in the geometry of accessible hydrogen-bond donors and acceptors. Presumably, the geometry of the sugar–phosphate backbone is changed by the purine:purine pair and this change—or one of its consequences—is recognized by Rev.

3.2.2. Variation of the RNA Binding Sequence of T4 DNA Polymerase

The DNA polymerase of bacteriophage T4 (gp43) binds to a 36 nt sequence within its own mRNA and represses its own translation.[25a] Part of this region is a helix of five base pairs closed by a loop of eight nucleotides[26] (Scheme 5).

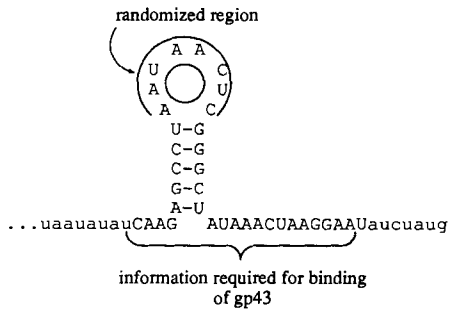

Scheme 5. The 36 nucleotide long RNA binding site for the T4 DNA polymerase (gp 43). In the stem-loop structure shown here eight nucleotides of the loop were randomized.

In order to determine the roles of the loop bases in DNA–polymerase binding, Tuerk and Gold randomized the 8 nt wild-type sequence of the loop and selected for functional sequences.[25b]

The synthesis of the 110 base template was carried out by ligation of three synthetic oligonucleotides, one of which contained the randomized sequence. A pool of 4^8 (=65536) different RNA molecules was generated by T7 transcription, and then subjected to four cycles of selection for DNA–polymerase binding by retention of RNA–protein complexes on nitrocellulose filters. After reverse transcription of the eluted RNA, PCR amplification, and transcription, the enriched RNA pool was used as the input for the next cycle of selection.[27] After the fourth selection/amplification cycle, no further change in the binding behavior of the remaining RNA with respect to wild-type RNA was observed. Two sequences predominated in the selected pool: the wild-type sequence AAUAACUC; and one other, AGCAACCU, which differs from the wild type at four positions. The four mutations are located in the part of the loop adjacent to the stem, and could allow the stem to be extended by two additional base pairs. The complexes of the two variants with T4 DNA polymerase exhibited the same dissociation constants ($K_d = 4.8 \times 10^{-9}$) in filter-binding assays. It is not yet clear if the protein binds equally well to two different structures, or if the two different sequences are able to form very similar tertiary structures in some unknown way.

3.3. Recognition of Double-stranded DNA(dsDNA) by RNA

Single-stranded DNA and RNA can bind to DNA duplexes in the major groove, and can recognize specific sequences through the formation of T–AT and C^+–GC base triples. In order to explore more fully the rules of duplex DNA recognition, Pei et al.[28] used in vitro selection to isolate RNA sequences that could bind to a polypurine:polypyrimidine duplex DNA. The target duplex was attached to a thiol-Sepharose support through a disulphide linkage. Control experiments showed that an oligonucleotide complementary to the polypurine sequence was retained by the derivatized column matrix under high salt conditions, and was eluted under low salt conditions. A library of RNA molecules containing a random sequence region of 50 nts flanked by defined primer binding sites was then subjected to five cycles of selection for binding to the duplex DNA column. Any RNAs that might have bound to the thiol-Sepharose support itself were removed by negative selection on underivatized thiol-Sepharose. Sequencing of 17 clones from the final selected pool showed that most of these clones contained extensive polypyrimidine tracts that could be aligned with the sequence of the target duplex to form the expected T-AT and C^+-GC base triples. Surprisingly, many of the selected sequences contained "mismatched" base triples, or even substantial insertions of six to eight bases. Further selection experiments of this nature may clarify or expand the rules for the formation of stable triplex structures.

3.4. Structure and Function of Catalytic RNAs

The group I intron found within the pre-ribosomal RNA of *Tetrahymena* catalyzes its own removal to generate mature rRNA.[29] The first step in this self-splicing reaction consists of an S_N2 attack by the 3′-OH group of a free guanosine on the phosphate at the 5′-exon–intron junction. The phosphodiester bond between the intron and the 5′-exon is broken, and a new bond is formed between the guanosine and the intron. The 3′-OH group at the end of the 5′-exon then carries out a similar nucleophilic attack on the 3′-end of the intron. The intron is released and the two exon segments are ligated.[30] The structure of this RNA catalyst, its substrate-binding properties, and its mechanism of catalysis have been the subject of extensive experimentation over the last decade; in vitro selection promises to be quite useful in the study of this and other ribozymes.

3.4.1. Structure of the Tetrahymena ribozyme

Much of our knowledge of the structure of the *Tetrahymena* ribozyme has been deduced from a comparative analysis of the sequences of over 100 group I introns. This approach has been extraordinarily fruitful in providing evidence for the detailed secondary and tertiary structures of this RNA enzyme. Nevertheless, the phylogenetic approach is entirely dependent upon the availability of suitably divergent sequences. In order to avoid this limitation, Green

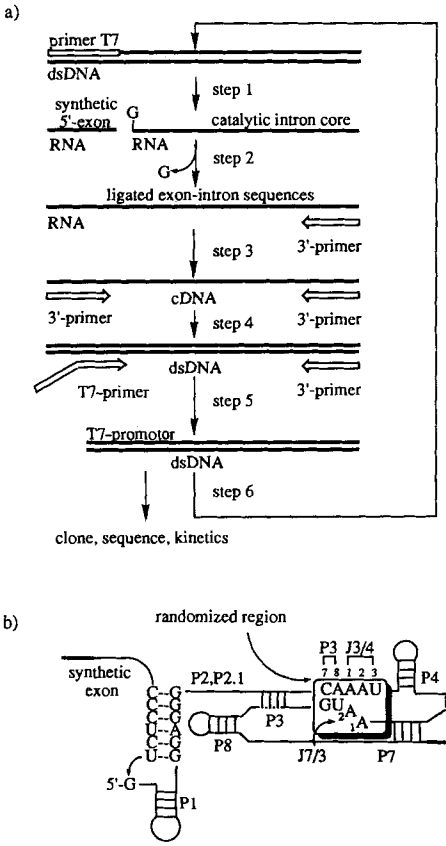

Scheme 6. a) Schematic representation of the selection strategy for the determination of functionally important interactions in the *Tetrahymena* ribozyme. Step 1: Transcription of double-stranded DNA (dsDNA) with T7 RNA polymerase. Step 2: Only the catalytically active variants can ligate the 5'-exon to the core. Step 3: Reverse transcription of ligated and unligated RNAs. Step 4: PCR amplification of the ligated exon–intron sequences, which have the 3'- and 5'-primer binding sites. Step 5: Nested PCR regenerates the starting intron sequence. Step 6: Return to Step 1 for the next selection cycle. b) The five and four nucleotide region that was randomized within the catalytic portion of the ribozyme. The annealing sequence of the synthetic exon is also shown.

et al.[31] have analyzed a derivative of the *Tetrahymena* ribozyme by in vitro selection.

The selection procedure was based on the reverse of the cleavage reaction catalyzed by the ribozyme. A ribozyme was generated that corresponds to the product of the first splicing step, that is, the 5'-exon has been removed and the guanosine substrate covalently bound to the intron. The addition of a synthetic 5'-exon then allows reversal of the reaction: the exon becomes joined to the intron with concomitant release of free guanosine (Scheme 6).

The selection scheme takes advantage of the fact that exon ligation introduces new, unique sequences, which can be used as a primer binding site for PCR amplification; thus, only molecules which have taken part in a catalytic event can subsequently be amplified. After the initial PCR amplification of ligated RNAs, a second round of PCR is used to regenerate the starting intron sequence, including the guanosine that was cleaved during catalysis. In vitro transcription then regenerates RNA sequences that can be used in the next round of selection.

Two segments of four and five nucleotides within the wild-type intron, suspected on the basis of previous evidence to interact with one another,[32] were randomized.[33] Since the entire intron sequence was too long to synthesize chemically, the pool was generated by PCR amplification of a plasmid template by using primers containing the randomized sequences. After the pool of 4^9 (= 262144) different variants had been subjected to three cycles of selection and amplification, it showed half the control activity of the wild-type intron. Cloning of individual variants of the selected pool gave the wild-type sequence as the most common. In the remaining sequences, some positions were invariant, while others were quite variable. Two interesting positions did vary, but in a correlated manner; this suggests that these positions interact strongly with each other. With this information, hypotheses[34] about tertiary interactions between bases in the investigated region could be tested.

3.5. Selection for Altered Catalytic Properties

Robertson and Joyce recently reported an in vitro selection system for group I introns, similar to that described in the preceding section, but designed to select for variants with altered catalytic function.[35] Scheme 7 shows the selection strategy.

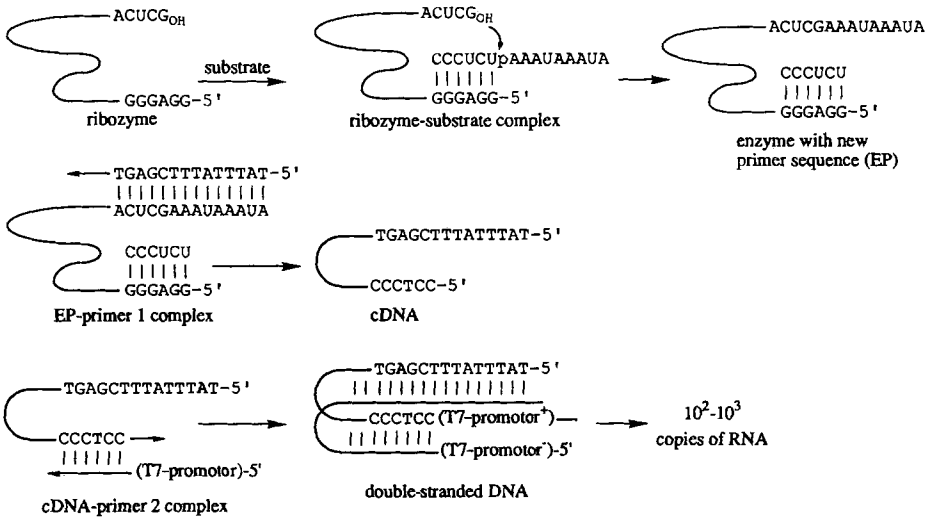

Scheme 7. Strategy of selection for the isolation of variants of the *Tetrahymena* ribozyme. DNA oligonucleotides were employed as substrates. The experiment was designed so that those forms of the ribozyme that could react best with the DNA substrate were selected.

The reaction being used can be viewed as the reverse of the second step of self-splicing (exon ligation). An added oligonucleotide, representing the ligated exons, is attacked by the 3'-OH of the ribozyme, which results in cleavage of the oligonucleotide and ligation of the 3'-half of the oligonucleotide to the ribozyme itself. This new 3'-sequence is only added to catalytically active variants of the ribozyme, and hence the complementary primer used to initiate reverse transcription can hybridize only to active molecules. The resulting cDNA is converted into dsDNA with a second primer; however, this DNA is not amplified by PCR, but amplification occurs as a result of the transcription step, during which T7 RNA polymerase synthesizes many copies of RNA from each DNA template. Although Robertson and Joyce attempted to select for a ribozyme variant that would preferentially cleave DNA rather than RNA, it appears that they have primarily obtained variants that have increased activity with both RNA and DNA substrates. Nevertheless, their approach is readily adaptable to selection over many sequential cycles, and the resulting ability to "evolve" novel ribozyme activities promises to be extremely interesting.

Self-replicating RNA molecules are thought to have played an important role in the early evolution of life.[36] The group I introns are of interest in this regard, because the chemistry of self-splicing is quite similar to the chemistry of existing RNA polymerases, although the substrates differ substantialy. Indeed, the catalytic abilities of the group I ribozymes have been used to demonstrate primitive replication like reactions.[37] Further modification of these ribozymes will be required to generate an RNA enzyme capable of efficiently and accurately copying another RNA molecule. In the absence of sufficient information to permit the rational design of such an RNA enzyme, the in vitro selection approach seems the most likely to lead to progress in this area.

3.6. Molecular Recognition of Small Substrates by Nucleic Acids

Ribozymes, like protein enzymes, have binding clefts and pockets that can very specifically recognize substrates.[38] The guanosine binding site in the *Tetrahymena* ribozyme[39] is an example of such substrate recognition, while interactions between drugs and DNA[40] and salt bridges between arginine and the phosphate backbone[24] are other examples of more or less sequence-specific nucleic acid/ligand interactions. The relative paucity of examples of small molecule recognition by nucleic acids has left open the question whether this sort of molecular recognition is general. The ability of nucleic acids to recognize small organic and even abiotic molecules has been addressed by in vitro selection experiments, as has the related but more subtle question of the probability of finding a sequence capable of such recognition in a pool of random sequences.

3.6.1. Selection for Substrate-Specific RNA Receptors

Ellington and Szostak used a completely random sequence of 100 base pairs, flanked by primer binding sites and the T7 promotor (see Scheme 3) for the selection of RNA receptors.[41] The pool contained more than 10^{13} different RNA molecules, which is larger than the number of possible antibodies in the mouse ($10^9 - 10^{10}$).[42] Affinity chromatography was used to select for RNA molecules capable of binding to dye molecules **1**–**3** covalently linked to agarose (Scheme 8). Such columns are commonly used for the purification of dehydrogenases by affinity chromatography because the dyes mimic the structure of NAD^+ and other cofactors.[43] The dyes are aromatic systems with many hydrogen-bond donors and acceptors and charged groups, all of which would seem to provide opportunities for strong interactions with RNA (Scheme 8).

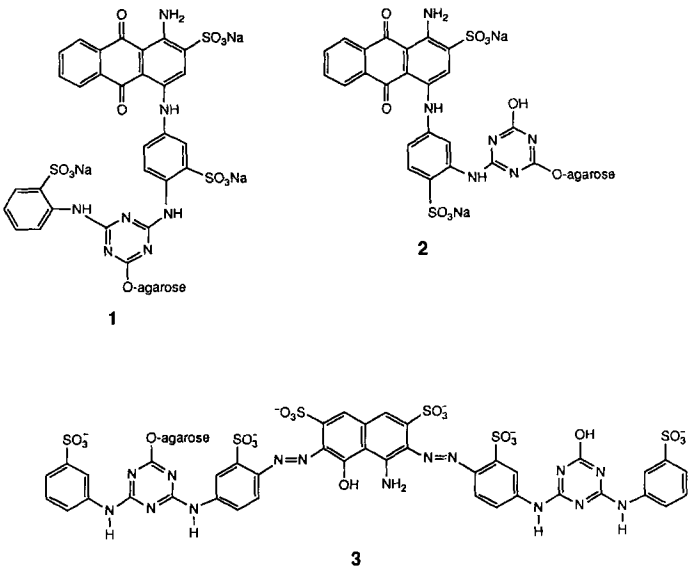

Scheme 8. Structures of dye molecules used for the selection of specifically binding RNA molecules. **1**: cibacron blue 3G-A, **2**: reactive blue 4, **3**: reactive green 19.

Because bivalent cations can help RNA to fold into defined three-dimensional structures, the RNA pool was loaded onto each column in a buffer containing Mg^{2+} ions, and unbound species were washed off with the same buffer. Bound species were then eluted with ethylenediamine tetraacetic acid (EDTA) and amplified. After the first few rounds of selection, only a small fraction of the RNA was recovered in the EDTA wash, however, after five cycles of selection approximately 50% of the input RNA bound to the column and was recovered in the EDTA elution step. The total enrichment for binding molecules over the five cycles of selection was between 10^8 and 10^{10}. Dissociation constants for dye binding were determined by analytical affinity chromatography and found to be between 500 μM and 10 μM.

The pool of selected RNAs contained both dye-specific molecules and molecules that bound to agarose itself rather than to the dye ligand. The dye-specific RNA molecules bind only to the dyes with which they were selected[44] (Table 1).

The specificity observed in this study is remarkable because of the structural similarity of dyes **1** and **2**. In fact, the RNA-receptors show higher specificity than many proteins for these ligands.[45]

Table 1. Specificity of the binding of dye-specific RNAs on agaroses derivatized with dyes.

ararose derivatized with	RNA selected on dyes 1	2	3	oligo (dT)
	[% bound]			
1	63	1	1	6
2	8	85	1	5
3	7	1	73	6
oligo (dT)	7	7	4	61

To define the substrate-binding site on particular RNAs, templates for two of the clones were synthesized with a large number of mutations (85% wild type, 5% of each non-wild-type base, see Scheme 2b) and used to make new degenerate RNA pools, which were then reselected for dye-binding. Alignment of the sequences of the newly selected clones revealed conserved regions; these apparently represent the binding site. For the RNA that binds cibacron blue (**1**) these sequences could potentially form a stem–bulge–stem structure (Scheme 9).

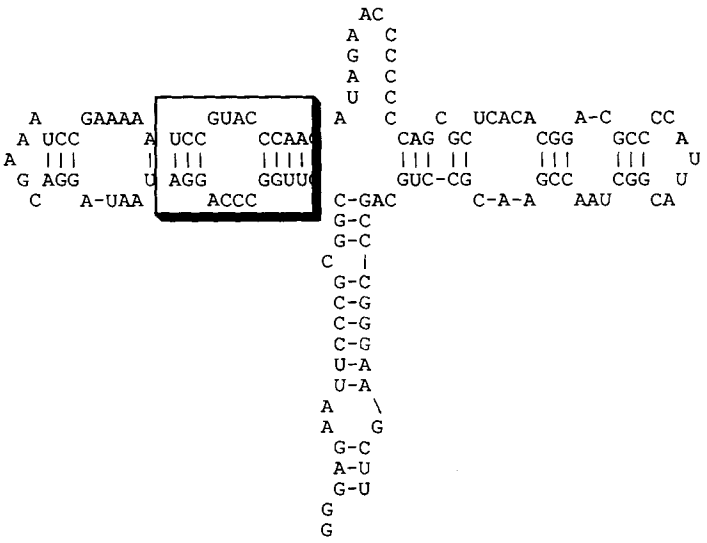

Scheme 9. Possible secondary structure of the reactive blue 4-binding RNA B4-25. The sequences in the boxed area were conserved between functional variants of B4-25, and were also found in an independent clone (B4-45).

Can the method described here also be applied for smaller molecules that have fewer potential interaction sites? We have recently obtained an RNA pool that was selected on agarose derivatized with D-tryptophan. Remarkably, the binding of this pool is stereospecific[46]—the pool binds to D- but not to L-tryptophan agarose or other substrates. Analytical affinity chromatography of one clone revealed a K_D of 18 μM. This clone binds to L-tryptophan agarose with a K_D of greater than 12 mM, corresponding to a difference in the relative binding energies of $\Delta\Delta G = 3.8$ kcal mol^{-1}.

The finding that many RNA sequences are able to distinguish between **1** and **2** or between D- and L-tryptophan agarose shows that binding pockets similar to those found in proteins have been selected. Furthermore, many different sequence "solutions" exist for the problem of recognizing a particular structure.

All of the experiments described above were done with pools of RNA molecules. RNA, as opposed to DNA, was chosen because the existence of tRNA and RNA enzymes proves that RNA is capable of forming the complex three-dimensional structures required for molecular recognition. However, single-stranded DNA differs from RNA only in the lack of 2′-hydroxyls and in the presence of a 5-methylated version of uracil (i.e., thymidine), and so might also be capable of folding into complex shapes that can recognize other molecules. Selection experiments similar to those described above have recently been done with pools of single-stranded DNA molecules.[47] The pools were generated and amplified by asymmetric PCR, in which one primer acts more efficiently than the other; the result is an excess of one strand over its complement. Single-stranded DNAs that were able to bind to and discriminate between the various dye-agaroses described above were readily obtained. Interestingly, an RNA version of one of these DNA sequences did not bind its cognate dye-agarose, which suggests that RNA and DNA versions of the same sequence are nonequivalent in terms of molecular recognition.

4. Summary and Future Directions

We have discussed a number of applications of in vitro selection, ranging from the determination of protein binding sites on DNA and RNA, to the selection of improved and altered ribozymes and the synthesis and evaluation of novel nucleic acid receptors. In view of the tremendous effort that has gone into the design of molecules capable of molecular recognition,[48] it is perhaps ironic that the methods of molecular biology now allow the facile isolation of nucleic acids with just such properties, but without any knowledge on the part of the experimenter of the structure of these molecules or of how they bind and recognize their ligands. Pharmacological applications of these techniques are easy to imagine[49, 50] and it seems quite plausible that short oligonucleotides that inhibit the action of important proteins by binding could be isolated.[51]

Perhaps one of the most interesting scientific questions can now be approached: can RNAs or DNAs, selected for binding to ligands that mimic the transition state of a chemical reaction,[52] generate novel biocatalysts, similar to catalytic antibodies.[53] There exists thus the potential of finding chemical reactions experimentally that can be catalyzed by RNA (or DNA). This endeavour could help to test the plausibility of theories in which primitive life forms developed a complex metabolism based on RNA catalysis.[54]

5. Glossary

cDNA: short for "complementary DNA"; single-stranded DNA that has been synthesized by the reverse transcription of an RNA template.

Electrophoresis Mobility Shift Assay (EMSA) and band-shift electrophoresis: methods to detect the binding of a ligand (usually a protein or peptide) to a nucleic acid. Binding of the ligand influences the mobility of the polynucleotide in

the electric field; the nucleic acid migrates more slowly in the gel when bound to the ligand.

Env, gag, and pol: viral genes that are responsible for the replication of retroviruses; *env* encodes for the outer virus shell, *gag* the virus capsid, and *pol* the reverse transcriptase.

fos oncoprotein: the gene product of *fos*, an oncogene of the mouse osteosarcoma virus. It is a 55 kDa phosphoprotein and is found in the nucleus. *Fos* acts as a transcriptional activator for several growth factors and helps initiate their transcription by forming heterodimers with proteins such as the oncoprotein *jun*. The role of the *fos* oncoprotein in these regulatory processes is not yet understood in full detail (see, for example, M. J. Bishop, *Cell* **1985** *42*, 23).

Immunoprecipitation: a technique for the rapid isolation and purification of a target antigen in mixtures of proteins. The technique uses polyclonal or monoclonal immunoglobulins (Igs) that bind specifically to the protein of interest. The antibody/antigen complex is precipitated by binding to a secondary reagent, such as an anti-antibody coupled to a carrier matrix. Immunoprecipitation is extremely selective and sensitive: as little as 100 pg of a radiolabeled protein can be detected. Target proteins are normally precipitated from radiolabeled cell extracts (see, for example, D. J. Anderson, G. Blobel, *Methods Enzymol.* **1983**, *96*, 111).

In vitro translation: mRNAs that have been generated by in vitro transcription or have been extracted from mammalian cells can be translated in cell-free extracts to generate their encoded proteins (see for example, P. A. Krieg, D. A. Melton *Nature* **1984**, *308*, 203.).

Phylogenetic studies: phylogeny is the relationship between individuals, species, or population as a reflection of their evolutionary history. In phylogenetic studies, classifications are made on the basis of evolutionary similarities or differences, for example in DNA sequences, and relationships established.

Polymerase chain reaction (PCR): a technique that allows the amplification of DNA sequences. Applications range from genetics and disease diagnosis to forensic science. The key tool in PCR is the heat-stable DNA polymerase from the microorganism *Thermus aquaticus*, Taq–DNA polymerase. This enzyme has its optimal activity at 72 °C, but is stable at temperatures as high as 95 °C. A PCR cycle consists of three stages (see Scheme 10): a) Denaturation of double-stranded DNA into the two single strands (94 °C). b) Annealing of the primer sequences to the single-stranded templates. Primer binding sites have to be at least 18–20 bases long, but can be much longer. Depending on the length of the primer binding site, the annealing temperature can range from 40–60 °C. Primers are added to the PCR mix in large excess over the template. c) Synthesis of the complementary strands by Taq-DNA polymerase at 72 °C.

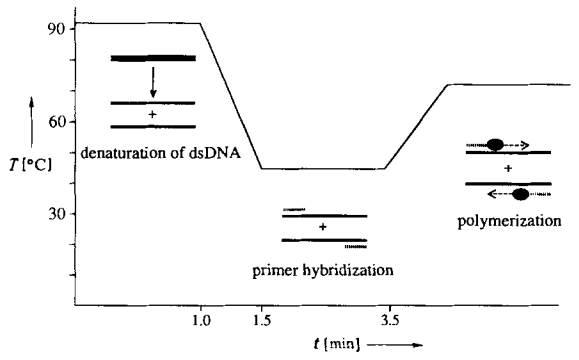

Scheme 10.

Every PCR cycle doubles the amount of template that was generated in the cycle before. After 20 PCR cycles ideally $2^{20} = 1{,}048{,}576$ copies of the input template are generated (for a brief and illustrative discussion of PCR, see H. Zinke, G. Gassen, Angew. Chem. **1990**, *102*, A–292; see also a) J. L. Marx, *Science* **1988**, *240*, 1408; b) K. B. Mullis, *Sci. Am.* **1990**, *262*, no. 4, p. 56; c) H. Ibelgaufts: *Lexikon Zytokine*, Medikon Verlag, München, **1992**, p. 66 ff.)

Serum Response Factor (SRF): a transcription factor that binds to the *c-fos* Serum Response Element (SRE), a multifunctional regulatory region of the *c-fos* promotor that responds to a variety of inducers (see: C. Norman, M. Runswick, R. M. Pollock, R. Treisman *Cell* **1988**, *55*, 989).

Zinc finger: a structural motif in various eukaryotic transcriptional regulatory proteins. Zinc fingers are about 30 amino acids in length. The motif contains histidine and cysteine residues whose side chains serve as ligands for a tetrahedrally coordinated Zn^{2+} ion. For specific DNA binding, several zinc finger domains within the protein chain are required. In the protein TFIIIA, for example, are about ten zinc fingers (see for example, helix-turn-helix, zinc finger, and leucine zipper motifs for eukaryotic transcriptional regulatory proteins: K. Struhl, *Trends Biochem. Sci. 14*, 137–140).

We are grateful to Hoechst AG and the Fonds der Chemischen Industrie (Liebig Stipend to M. F.) for the generous support of our work. We thank our co-workers and colleagues, David Bartel, Andrew Ellington, Rachel Green, Anusch Peyman, Mandana Sassanfar, and Charles Wilson for their contributions and discussions, and Jon Lorsch for help in writing the glossary.

Received: December 27, 1991 [A 875IE]
German version: *Angew. Chem.* **1992**, *104*, 1001

[1] a) For a short discussion see: R. Lewin, *New Sci.* **1990**, *128*, 8. Dezember 1990, p. 30; b) J. W. Szostak, *Trends Biochem. Sci.* **1992**, *17*, 89.

[2] Even in a very good library of, for instance, 100 base-pair random sequences, only a small fraction of possible sequences are in fact present in the pool. That is not a result of the inefficiency of the chemical oligonucleotide synthesis: to have all possible permutations of a 100 base random sequence present in the pool, $4^{100} = 10^{60}$ different molecules would have to be made. This corresponds to no less than 10^{38} kg of DNA. At present automated oligonucleotide synthesis allows a complete coverage of all possible sequence permutations of 25 bases or less.

[3] a) K. B. Mullis, F. A. Faloona, *Methods Enzymol.* **1987**, *155*, 335; b) T. J. White, N. Arnheim, H. A. Ehrlich, *Trends Genet.* **1989**, *5*, 185.

[4] At first sight, this idea seems to oppose the general direction of modern organic chemistry, where unique products are highly disirable. Here, the more different molecules we generate during the synthesis, the better. However, it is clear that clean reaction steps with as high yields as possible are necessary to maximize the yield of synthetic DNA. In the future, new methods for oligonucleotide synthesis that lead to very clean products, such as developed by Noyori et al., could prove to be very useful: Y. Hayakawa, S. Wakabayashi, H. Kato, R. Noyori, *J. Am. Chem. Soc.* **1990**, *112*, 1691; Y. Hayakawa, H. Kato, T. Nobori, R. Noyori, J. Imai, *Nucleic Acids Res. Symp. Ser.* **1986**, *17*, 97; Y. Hayakawa, H. Kato, M. Uchiyama, H. Kajino, R. Noyori, *J. Org. Chem.* **1986**, *51*, 2400. In addition, it may be desirable to use sequences as long as 400–1000 bases in length. Such sequences cannot be generated chemically, but could be accessible if defined restriction sites are built into the random oligonucleotides, to allow the ligation of several fragments. (D. P. Bartel, M. Famulok, J. W. Szostak, unpublished.)

[5] J. W. Engels, E. Uhlmann, *Angew. Chem.* **1989**, *101*, 733; *Angew. Chem. Int. Ed. Engl.* **1989**, *28*, 716.

[6] D. P. Bartel, M. Famulok, R. Green, J. W. Szostak, unpublished.
[7] One of the main problems in the synthesis of longer sequences (150–200 bases) is the increasing depurination that occurs with increasing chain length. (G. Remaud, X.-X. Zhou, J. Chattopadhyaya, M. Oivanen, H. Lönnberg, *Tetrahedron* **1987**, *43*, 4453; see also C. Tamm, E. Hodes, E. Chargaff, *J. Biol. Chem.* **1952**, *195*, 49; C. Tamm, H. Shapiro, R. Lipshitz, E. Chargaff, *ibid.* **1953**, *203*, 673). This can lead to branching of the DNA strand during the subsequent synthesis steps or to chain termination. Branched oligonucleotides are not amplifiable by PCR. One possibility for minimizing depurination is the use of the aprotic Lewis acid BF_3-methanol complex instead of the protic acid $Cl_2CHCOOH$ or Cl_3COOH, normally used to remove the dimethoxytrityl protecting group. (M. Mitchell, *Nucleic Acids Res.* **1990**, *18*, 5321).
[8] R. Green, A. D. Ellington, D. P. Bartel, J. W. Szostak, *Methods* **1991**, *27*, 5.
[9] a) A. R. Oliphant, K. Struhl, *Methods Enzymol.* **1987**, *155*, 568; b) *Nucleic Acids Res.* **1988**, *16*, 7673; c) A. R. Oliphant, C. J. Brandl, K. Struhl, *Mol. Cell. Biol.* **1989**, *9*, 2944.
[10] a) K. W. Kinzler, B. Vogelstein, *Nucleic Acids Res.* **1989**, *17*, 3645; b) *Mol. Cell. Biol.* **1990**, *10*, 634.
[11] a) H.-J. Thiesen, C. Bach, *Nucleic Acids Res.* **1990**, *18*, 3203; b) H.-J. Thiesen in *Immunological Methods* (Eds.: I. Lefkovits, B. Perris), Academic Press, Orlando, FL, USA, **1990**, pp. 61–75.
[12] This in vitro selection approach was called the "Target Detection Assay" or TDA.
[13] T. K. Blackwell, H. Weintraub, *Science* **1990**, *250*, 1104.
[14] P. Donner, I. Greiser-Wilke, K. Moelling, *Nature* **1982**, *296*, 262; R. N. Eisenman, C. Y. Tachibana, H. D. Abrams, S. R. Hann, *Mol. Cell. Biol.* **1985**, *5*, 114.
[15] R. L. Davis, P.-F. Cheng, A. B. Lassar, H. Weintraub, *Cell* **1990**, *60*, 733.
[16] C. Murre, P. Schonleber McCaw, H. Vaessin, M. Caudy, L. Y. Jan, Y. N. Jan, C. V. Cabrera, J. N. Buskin, S. D. Hauschka, A. B. Lassar, H. Weintraub, D. Baltimore, *Cell* **1989**, *58*, 537.
[17] This technique was referred to as "Selected And Amplified Binding sites" or "SAAB".
[18] R. Pollock, R. Treisman, *Nucleic Acids Res.* **1990**, *18*, 6197.
[19] a) C. R. Woese, R. Gutell, R. Gupta, H. F. Noller, *Microbiol. Rev.* **1983**, *47*, 621; b) M. Levitt, *Nature* **1969**, *224*, 759.
[20] Structural stability per se is not necessarily a criterion for evolutionary conservation, because unproductive foldings can be lower in energy than productive secondary structures.
[21] a) M. H. Malim, J. Hauber, S.-Y. Le, J. V. Maizel, B. R. Cullen, *Nature* **1989**, *338*, 254; b) B. K. Felber, M. Hadzopoulou-Cladaras, C. Cladaras, T. Copeland, G. N. Pavlakis, *Proc. Natl. Acad. Sci. USA* **1989**, *86*, 1495; c) M. Emerman, R. Vazeux, K. Peden, *Cell* **1989**, *57*, 1155; d) M.-L. Hammarskjöld, J. Heimer, B. Hammarskjöld, I. Sangwan, L. Albert, D. Rekosh, *J. Virol.* **1989**, *63*, 1959.
[22] a) M. H. Malim, L. S. Tiley, D. F. McCarn, J. R. Rusche, J. Hauber, B. R. Cullen, *Cell* **1990**, *60*, 675; b) S. Heaphy, C. Dingwall, I. Ernberg, M. J. Gait, S. M. Green, J. Karn, A. D. Lowe, M. Singh, M. A. Skinner, *ibid.* **1990**, 685; c) S. M. Holland, N. Ahmad, R. K. Maitra, P. Wingfield, S. Venkatesan, *J. Virol.* **1990**, *64*, 5966.
[23] D. P. Bartel, M. L. Zapp, M. R. Green, J. W. Szostak, *Cell*, **1991**, *67*, 529.
[24] a) W. Saenger, *Principles of Nucleic Acid Structure*, Springer, New York, **1984**; b) .
[25] a) M. Andrake, N. Guild, T. Hsu, L. Gold, C. Tuerk, J. Karam, *Proc. Natl. Acad. Sci. USA* **1988**, *85*, 7942; b) C. Tuerk, L. Gold, *Science* **1990**, *249*, 505.
[26] Bacteriophage RB69 contains a stemloop indentical to the T4 structure in the related ribosome binding site of its DNA-polymerase gene: C. Tuerk, S. Eddy, D. Parma, L. Gold, *J. Mol. Biol.* **1990**, *213*, 749.
[27] The authors named this method „SELEX" (Systematic Evolution of Ligands by Exponential Enrichment).
[28] D. Pei, H. D. Ulrich, P. G. Schultz, *Science* **1991**, *253*, 1408.
[29] T. R. Cech, *Angew. Chem.* **1990**, *102*, 761; *Angew. Chem. Int. Ed. Engl.* **1990**, *29*, 759.
[30] a) T. R. Cech, A. J. Zaug, P. J. Grabowski, *Cell* **1981**, *27*, 487; b) K. Kruger, P. J. Grabowski, A. J. Zaug, J. Sands, D. E. Gottschling, T. R. Cech, *ibid.* **1982**, *31*, 147; c) T. R. Cech, *Science* **1987**, *236*, 1532; d) *Gene* **1988**, *73*, 259; e) N. R. Pace, T. L. Marsh, *Orig. Life Evol. Biosphere* **1985**, *16*, 97.
[31] R. Green, A. D. Ellington, J. W. Szostak, *Nature* **1990**, *347*, 406.
[32] Phylogenetic comparisons of some group I introns show an interesting potential covariation: in 32 out of 35 group I introns, base pair 7 in the P3-stem (P3-7) is G-C, the second base in the region that connects P3 with P7 (J3/7–2) is A and the connecting region contains three bases. In the three remaining group I introns, P3-7 is G-C, J3/7–2 either U or G and J3/4 contains only two bases. On the basis of such phylogenetic data it seems plausible that nucleotides in this region interact with each other. S. Couture, A. D. Ellington, J. A. Doudna, R. Green, M. Hanna, U. Pace, J. Rajagopal, J. W. Szostak, *J. Mol. Biol.* **1990**, *215*, 345.
[33] J. M. Burke, M. Belfort, T. R. Cech, R. W. Davies, R. J. Schweyen, D. A. Shub, J. W. Szostak, H. F. Tabak, *Nucleic Acids Res.* **1987**, *15*, 7217.
[34] a) F. Michel, E. Westhof, *J. Mol. Biol.* **1990**, *216*, 585; b) F. Michel, A. D. Ellington, S. Couture, J. W. Szostak, *Nature* **1990**, *347*, 578.
[35] a) D. L. Robertson, G. F. Joyce, *Nature* **1990**, *344*, 467; b) G. F. Joyce in *RNA: Catalysis, Splicing and Evolution* (Eds.: M. Belfort, D. Shub), Elsevier, Amsterdam, **1977**, p. 83.
[36] a) See ref. [30c]; b) P. A. Sharp, *Cell* **1985**, *42*, 397; c) G. F. Joyce, *Nature* **1989**, *338*, 519. See also: d) M. Famulok, J. S. Nowick, J. Rebek, Jr., *Acta Chim. Scand.* **1992**, *46*, 315; e) A. D. Ellington, *Methods Enzymol.*, in press; f) A. Terfort, G. von Kiedrowski, *Angew. Chem.* **1992**, *104*, 626; *Angew. Chem. Int. Ed. Engl.* **1992**, *31*, 654, and references cited therein.
[37] a) J. A. Doudna, J. W. Szostak, *Nature* **1989**, *339*, 519; b) J. A. Doudna, S. Couture, J. W. Szostak, *Science* **1991**, *251*, 1605; c) T. R. Cech, *Nature* **1989**, *339*, 507.
[38] a) J. A. Latham, T. R. Cech, *Science* **1989**, *245*, 276; b) D. W. Celander, T. R. Cech, *Biochemistry* **1990**, *29*, 1355.
[39] F. Michel, M. Hanna, R. Green, D. P. Bartel, J. W. Szostak, *Nature* **1989**, *342*, 391.
[40] F. Takusagawa, M. Dabrow, S. Neidle, H. M. Berman, *Nature* **1982**, *296*, 406.
[41] A. D. Ellington, J. W. Szostak, *Nature* **1990**, *346*, 818.
[42] J. Klein, *Immunology: The Science of Self-Nonself Discrimination*, Wiley, New York, **1982**, S. 219.
[43] a) S. T. Thompson, K. H. Cass, E. Stellwagen, *Proc. Natl. Acad. Sci. USA* **1975**, *72*, 669; b) C. R. Lowe, M. Glad, P.-O. Larsson, S. Ohlson, D. A. P. Small, T. Atkinson, K. Mosbach, *J. Chromatogr.* **1981**, *215*, 303; c) K. Schneider, M. Pinkwart, K. Jochim, *Biochem. J.* **1983**, *213*, 391; d) C. V. Stead, *J. Chem. Technol. Biotechnol.* **1987**, *37*, 55.
[44] For the selected RNA molecules the term "aptamer" was coined (from the Latin "aptus" = to fit).
[45] a) A. Ashton, G. M. Poyla, *Biochem. J.* **1978**, *175*, 501; b) Y. D. Clonis, C. R. Lowe, *ibid.* **1980**, *191*, 247.
[46] M. Famulok, J. W. Szostak, *J. Am. Chem. Soc.* **1992**, *114*, 3990.
[47] A. D. Ellington, J. W. Szostak, *Nature* **1992**, *355*, 850.
[48] See for example: a) J. M. Lehn, *Angew. Chem.* **1990**, *102*, 1347; *Angew. Chem. Int. Ed. Engl.* **1990**, *29*, 1304; b) J. Rebek, Jr., *ibid.* **1990**, *102*, 1347, and **1990**, *29*, 245; c) H.-J. Schneider, *ibid.* **1991**, *103*, 1419 and **1991**, *30*, 1417.
[49] M. L. Riordan, J. C. Martin, *Nature* **1991**, *350*, 442.
[50] J. Abelson, *Science* **1990**, *249*, 488.
[51] The use of unmodified oligonucleotides would have to be restricted to extracellular applications because of the problem of cell permeation.
[52] a) L. Pauling, *Am. Sci.* **1948**, *36*, 51; b) W. P. Jencks, *Catalysis in Chemistry and Enzymology*, McGraw-Hill, New York, **1969**; c) P. A. Bartlett, C. K. Marlowe, *Biochemistry* **1983**, *22*, 4618.
[53] a) K. D. Janda, D. Schloeder, S. J. Benkovic, R. A. Lerner, *Science* **1988**, *241*, 1188; b) P. G. Schultz, *Angew. Chem.* **1989**, *101*, 1336; *Angew. Chem. Int. Ed. Engl.* **1989**, *28*, 1283; c) P. G. Schultz, R. A. Lerner, S. J. Benkovic, *Chem. Eng. News* **1990**, *68*, no. 22, 26.
[54] a) See Ref. [36b]; b) L. E. Orgel, *J. Theor. Biol.* **1986**, *123*, 127.

On Quantifying Chirality

By Andrzej B. Buda, Thomas Auf der Heyde, and Kurt Mislow*

Since Pasteur's epochal discoveries a century and a half ago, the concept of chirality has continued to play a central role in chemistry and biochemistry. Can chirality be measured? It has long been known that molecular chirality can be given a quantitative meaning through functions specifically parametrized to match the magnitude of pseudoscalar observables. However, chirality is a property that is independent of its physical and chemical manifestations: for a system to be chiral, all that is required is the absence of improper rotations in the symmetry group of the system. This being the case, how can chirality be measured if the "system" is an abstract geometric figure, for example, a scalene triangle in the plane or an asymmetric tetrahedron in three-dimensional space? How does chirality vary as a function of pure shape? In this review we describe recent efforts designed to answer these and related questions.

1. Introduction

1-Stearoyl-2,3-dipalmitoylglycerin (**1**) exemplifies a class of enantiomerically pure triglycerides that exhibit no measurable optical activity in the visible and ultraviolet regions.[1] This result is readily understandable because the fatty acid residues in the 1- and 3-positions are "very similar... and hence the asymmetry of the molecule is very slight".[1b] Similar reasoning underlies the assertion that enantiomerically pure 7-methyl-[1-^{14}C]-tridecane (**2**) "would have zero rotation within experimental error on the most sensitive polarimeter now available".[2]

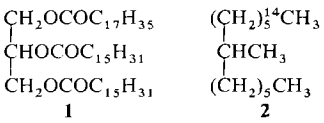

1

2

These examples, in which the "very slight" asymmetry in the structures of **1** and **2** is obviously the root cause for the observed optical inactivity of the samples, show that it is natural to attach a quantitative meaning to the chirality of molecular structures, and that the degree of chirality is manifested in the magnitudes of appropriate observables.[3, 4] By extension, it is possible to rank the chirality of closely related structures,[3] and to speak, for example, of 6-methyl-[1-^{14}C]-undecane and 8-methyl-[1-^{14}C]-pentadecane as being "more" and "less" chiral than **2**, respectively, with reference both to their molecular structures and to their chiroptical properties.[5]

In this review we explore some of the ways in which the chirality of molecular structures, more specifically of their geometric representations, may be placed on a quantitative basis. For the purposes of our discussion, we take the position that chirality is an inherent molecular property,[6] and we neglect problems arising from the parity-violating energy differences between enantiomers.[7, 8]

[*] Prof. K. Mislow, Dr. A. B. Buda
Department of Chemistry, Princeton University
Princeton, NJ 08544-1009 (USA)
Dr. T. Auf der Heyde
Department of Chemistry, University of the Western Cape
Bellville 7530 (South Africa)

2. Measures of Geometric Chirality

2.1. From Abbé Haüy to Lord Kelvin

The story that culminates in Pasteur's momentous discovery of April 1848—the correlation of crystalline hemihedry with optical activity in the tartrates—begins with the observation of hemihedral facets in quartz ("quartz plagièdre") by Abbé René Just Haüy, the founder of modern crystallography.[9a] Following Biot's observation that the plane of linearly polarized light is rotated by passage through quartz and through certain organic liquids and solutions, Herschel[9b] recognized that hemihedry in quartz leads to the existence of two kinds of crystals, left-handed and right-handed, and that there is a causal relationship between the handedness of the crystals and their sense of optical rotation. Herschel's findings and concurrent studies by Biot and Fresnel prepared the ground for Pasteur's discovery[10] and for his demonstration that the optical activity of tartaric acid is a manifestation of molecular chirality ("dissymétrie moléculaire").[11]

From its historic roots in nineteenth-century science to the present day, chirality in chemistry has been associated with crystals and molecules. However, chirality is a general attribute of objects or figures, and does not depend for its definition on any connection to the material world and to the natural sciences, even though this connection is of the greatest importance.[12] It was left for Lord Kelvin to formulate a definition of chirality that gives explicit expression to the inherently abstract nature of the concept: "I call any geometrical figure, or group of points, *chiral*, and say it has *chirality*, if its image in a plane mirror, ideally realized, cannot be brought to coincide with itself."[13] Chirality is thus defined as the absence of reflection symmetry. As a property, it is attributable to objects regardless of whether they are models of molecules.

2.2. Classification of Chirality Measures

2.2.1. Degree of Chirality

We define as the "degree of chirality" of an object the value of a real-valued, continuous function that is zero

if, and only if, the object is achiral.[14] The degree of chirality is the measure of an absolute quantity, and its value is therefore the same for both enantiomorphs of the measured object.

In addition, like measures of symmetry for convex sets,[15] the degree of chirality of geometric figures should also be similarity invariant, because the chirality of such objects is measured by shape and not by size, and invariance under similarity transformations eliminates the factor of size.[16] Normalization of the function then renders it dimensionless in the interval [0, 1]. Thus, we see no reason for not applying measures of chirality to geometric figures as well as to geometric models of molecules and molecular ensembles.

2.2.2. *Classes of Measures for Chirality*

We recognize two general classes of measures: in the first, the degree of chirality expresses the extent to which a chiral object (or "chiroid"[13]) differs from an achiral reference object, while in the second it expresses the extent to which two enantiomorphs differ from one another. In chirality measures of the first kind the question to be answered is: how dissimilar are the chiroid and its achiral reference object? In chirality measures of the second kind (or "overlap measures") the question is: how dissimilar are the two enantiomorphs of a chiroid? The underlying concept is that of a "distance" measured between a chiral and an achiral object or between two enantiomorphous objects.[17] The following example may serve to illustrate the distinction between the two classes.

Consider a tetrahedron K and an achiral polyhedron P inscribed in K. Let $[K]$ and $[P]$ denote the volumes of the corresponding polyhedrons, and let P_{max} denote the inscribed polyhedron for which $R = [P]/[K]$ is at a maximum. Under this limiting condition, P_{max} fills K to its maximum capacity, that is, the unfilled volume of K is at a minimum. Clearly, K is achiral if, and only if, $P_{max} = K$ so that $R = 1$; otherwise K is chiral. The function $f(K) = \max_{P} \{[P]/[K]\}$ defined on the class of tetrahedrons then is a measure that is unity only for achiral tetrahedrons. Thus $\chi(K) = 1 - f(K)$, which expresses

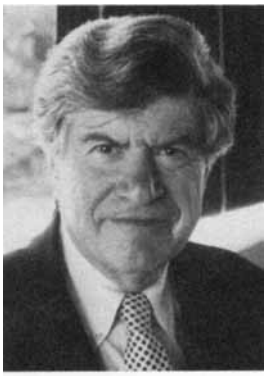

Kurt Mislow was born in Berlin, Germany, in 1923. He obtained his B. S. degree at Tulane University (1944) and his Ph.D. at the California Institute of Technology (1947) with Linus Pauling. In 1964, after 17 years on the faculty of New York University, he joined Princeton University as the first incumbent of the Hugh Stott Taylor Chair of Chemistry. A member of the National Academy of Sciences and a Fellow of the American Academy of Arts and Sciences, he has been a Guggenheim Fellow twice, an Overseas Fellow of Churchill College at the University of Cambridge, a Fairchild Distinguished Scholar at Caltech, and has received numerous honors and awards, including the first Prelog medal of the ETH, Zürich, in 1986. Now Professor Emeritus at Princeton, he is continuing his exploration of stereochemical theory.

Andrzej B. Buda, born in Krosno, Poland, in 1953, studied chemistry at the Jagiellonian University in Kraków, where he received his Master's degree in 1977 and Ph.D. in 1982 with J. Mirek. After a year with E. Ōsawa in Hokkaido University, as a Fellow of the Japanese Ministry of Education, he returned to Kraków and was appointed Assistant Professor at the Jagiellonian University (1984–1986). In 1986 he joined K. Mislow's group at Princeton as a visiting research scientist, and in 1987 he went to the University of California at Los Angeles, where he was visiting scholar with K. N. Houk. He returned to Princeton in 1988, where he was appointed as a Research Staff Member. His scientific interests include dynamic stereochemistry, mechanisms of organic reactions, and electronic effects in nucleic bases during interactions of DNA with proteins, metals, and metal complexes.

Thomas Auf der Heyde was born in East London, South Africa, in 1958 and studied chemistry at the University of Cape Town (UCT), where be obtained his Ph.D. with L. R. Nassimbeni in 1988. Concomitant with his studies he worked as a research assistant to D. A. Thornton at UCT (1979–1980) and served as Lecturer in chemistry at the University of the Western Cape (UWC), where he is now an Associate Professor. While working for his Ph.D., he spent some months in 1984 and 1986 as a pre-doctoral fellow with H.-B. Bürgi in Berne, Switzerland. During a sabbatical/study-leave from mid-1989 to mid-1991 he spent six months with H.-B. Bürgi, four with F. H. Allen at the Cambridge Crystallographic Data Centre, and twelve in Princeton, working with his present co-authors. The dynamic stereochemistry of metal complexes remains the focus of his research interests.

the degree of chirality of K as a deviation from the achiral reference polyhedron P, is seen to be a measure of the first kind.

For a related measure of the second kind, consider again a tetrahedon K and its enantiomorph, K'. When K and K' are overlapped, $K^* = K \cap K'$ is a polyhedron inscribed in K and K'. Let K^*_{max} denote the intersection for which $R = [K^*]/[K]$ is at a maximum. Under this limiting condition, K^*_{max} fills K to its maximum capacity, and K is achiral if, and only if, $K^*_{max} = K$. The degree of chirality of K is now given by $\chi(K) = 1 - f(K)$, where $f(K) = \max_{K^*} \{[K^*]/[K]\}$, and where $\chi(K)$ expresses the extent to which K and K' differ from one another.[18]

The results for the two measures are the same if, and only if, $K^*_{max} = P_{max}$. In both systems, $f(K)$ cannot become zero (i.e., $\chi(K) \neq 1$), because it is always possible to inscribe an achiral polyhedron within any tetrahedron, or to overlap partially any pair of enantiomorphous tetrahedrons.

In Sections 2.3 and 2.4 we review salient results of work carried out at Princeton. We selected the tetrahedron as the principal target in our investigation of geometric chirality measures because of the historic role of the asymmetric (irregular) tetrahedron in stereochemistry.[19] At the focus of our investigation was the question: what is the most chiral tetrahedron? Evidently the answer would have to depend on the measure employed. As a first exploratory step we therefore applied several measures to the scalene triangle, whose special position as the asymmetric simplex in the Euclidean plane (E^2) parallels that of the asymmetric tetrahedron in three-dimensional space (E^3). The results of our quest for the most chiral triangle are described in the next section.

2.3. In Search of the Most Chiral Triangle

Section 2.3.2 describes two chirality measures of the first kind—those that express the "distance" of a chiral triangle from an achiral one[20]—while Section 2.3.3 describes two chirality measures of the second kind—those that express the "distance" between two enantiomorphous triangles.[21] But first we must provide a brief outline of symmetry and chirality in E^2; this is the subject of Section 2.3.1.

2.3.1. Chirality in the Euclidean Plane

Chirality is an extrinsic property; that is, its existence depends on the dimension of the space in which the object is embedded. Thus, objects that are enantiomorphs in E^n are superposable by proper rotations in E^{n+1}; for example, a scalene triangle is a chiroid in E^2 but not in E^3. There are two classes of point groups in E^2, cyclic (C_n) and dihedral (D_n). Figures in E^2 are chiral if, and only if, they belong to C_n, and achiral if, and only if, they belong to D_n. All chiroids in E^2 except those belonging to C_1 (the asymmetric group) have rotational symmetry with respect to a point at the center. A figure in E^2 that is symmetric with respect to inversion through a point is said to possess centric symmetry; centric symmetry is therefore the special case of rotational symmetry for which n is even. If, and only if, the figure is symmetric with respect to reflection through a line (axial symmetry), it belongs to D_n and is therefore achiral; if $n > 1$ the figure also has rotational symmetry. Accordingly, scalene, isosceles, and equilateral triangles belong to C_1, D_1, and D_3, respectively.

In chemistry, idealized models of chiral molecules distributed in monolayers or adsorbed on surfaces[22] are also said to possess "two-dimensional chirality".[23]

2.3.2. Deviation from Achirality

2.3.2.1. Geometric Chirality Products

In 1890, only 16 years after van 't Hoff's and LeBel's revolutionary proposals to extend the structural formulas of chemistry into three-dimensional space,[19] Guye[24] introduced the first algebraic function designed to correlate a pseudoscalar property, the optical rotation, with the molecular structure of a chiroid. Appropriately called "produit d'asymétrie", this was the first example of a chirality function in chemistry.[25] According to Guye, the chirality product P for a tetrahedral coordination skeleton, in which the bond angles subtended by the central carbon atom remain those of the regular tetrahedron (the "α-constraint", where α is the tetrahedral angle), is defined by Equation (a), where d_i is the distance of the molecular center of mass of the ith of six planes defined by each of the six edges and the center of the tetrahedron.

$$P(d) = \prod_{i=1}^{6} d_i \qquad \text{(a)}$$

$P(d)$ may also be expressed by Equation (b), where m_1, m_2, m_3, and m_4 are four masses at the vertices of the tetrahedron, separated by four distances, l_1, l_2, l_3, and l_4, from the central carbon atom.[26] If the four point-masses in Guye's model are taken to be all the same, then Equation (b) reduces to Equation (c), where $c = \left[\left(\sin\frac{\alpha}{2}\right)\Big/4\right]^6$.

$$P(m, l) = \left(\frac{\sin\frac{\alpha}{2}}{\sum_{i=1}^{4} m_i}\right)^6 \prod_{i>j}^{1-4} (m_i l_i - m_j l_j) \qquad \text{(b)}$$

$$P(l) = c \prod_{i>j}^{1-4} (l_i - l_j) \qquad \text{(c)}$$

$P(l)$ is a function of geometry alone and vanishes in all cases but one, that of the asymmetric tetrahedron. Geometric chirality products such as $P(l)$, which express the shape of geometric chiroids, are fully in accord with Ruch's theory.[27, 28] Thus, imagine a regular tetrahedron **t**, with center-to-vertex distances r, inscribed within a tetrahedron **T** whose chirality is given by $P(l)$, so that the center of **t** coincides with the center of **T** and the r's of **t** are coextensive with the l's of **T**. Because **t** is inscribed within **T**, $l - r \geq 0$. The four line segments, $l - r$, are therefore the geometric equivalents of ligands on a T_d permutation skeleton. Ruch[28b] had previously likened the ligand parameters λ to the diameters of spheres centered at the vertices of an achiral permutation

skeleton. The present construct, with $\lambda = l - r$, evokes a similar image.[29, 30]

These and related functions can also be rendered similarity invariant. However, the complexity of the resulting polynomials obscures basic features that are easily seen in the far more tractable polynomials of chirality products for triangles. A chirality product $P(e)$ for triangles [Equation (d)], where a, b, and c are the lengths of the sides, is not subject to the two-dimensional analog of the α-constraint, which is the constraint that none of the internal angles in the triangle can exceed $2\pi/3$ radians. Thus, Equation (d) encompasses all possible shapes of a triangle. In contrast, because of the α-constraint, Equations (a)–(c) cannot accommodate chiral tetrahedrons with C_2 or D_2 symmetry.

$$P(e) = (a - b)(b - c)(c - a) \qquad \text{(d)}$$

Division by abc transforms $P(e)$ into a similarity invariant function, $\chi(e)$ [Eq. (e)], which is bounded, normalized, and dimensionless in the interval $[-1, 1]$, and whose absolute value yields the degree of chirality for any triangle of defined shape.

$$\chi(e) = (1 - b/a)(1 - c/b)(1 - a/c) \qquad \text{(e)}$$

The shapes of triangles may be represented by points in an xy coordinate system in which side c opposite vertex C of a triangle ABC coincides with the x axis, and in which the center of c is fixed at the origin, with $c = 1$ so that the coordinates of A, B, and C are (1/2, 0), (−1/2, 0), and (x, y), respectively (Fig. 1). Accordingly, the coordinates of C define the shape of the triangle. We shall adhere to the labeling convention in Figure 1 throughout the following discussion.

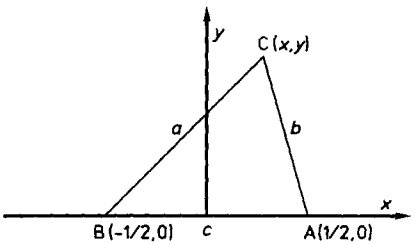

Fig. 1. Coordinate system and labeling convention for the shape space of triangles, in which a, b, and c, in that order, are arranged in a clockwise manner.

Points in the xy plane that represent isosceles triangles lie on one of three nodal curves, depending on whether $a = b$ [$x = 0$], $a = c$ [$(x + 1/2)^2 + y^2 = 1$], or $b = c$ [$(x - 1/2)^2 + y^2 = 1$]. Figure 2 shows two of the nodal curves as semicircles with radius $c = 1$, centered at $(-1/2, 0)$ and $(1/2, 0)$, that intersect the third nodal curve, the y axis, at $(0, \sqrt{3}/2)$, the point that represents the equilateral triangle. The three nodal curves divide the xy plane into six regions, each of which represents all chiral (scalene) triangles that have in common a given inequality of sides. The six regions fall into two sets representing enantiomorphous triangles: $\{c < a < b,\ a < b < c,\ b < c < a\}$ and $\{a < c < b,\ b < a < c,\ c < b < a\}$. However, because the shape of each scalene triangle is represented in three regions, and its enantiomorph in the other three, the six regions may be reduced to two, for example, those in which c is taken to be the longest side. All triangular shapes are then accommodated, without redundancy, within two regions, $a \leq b \leq c$ and $b \leq a \leq c$. In Figure 2 these regions are contained within a gothic arch whose apex is at $(0, \sqrt{3}/2)$ and which is bounded on two sides by arcs that belong to the two nodal semicircles and on the third by the x axis.[31] All isosceles triangles with $a = c$ or with $b = c$ are represented by points on the two arcs, while those with $a = b$ are represented by points on the y axis. All points that lie on the x axis represent degenerate triangles, that is, triangles whose three vertices are collinear and which are therefore excluded from the set of triangles under consideration. The shape space within the gothic arch is thus bounded on all three sides, but it is not closed at $y = 0$.

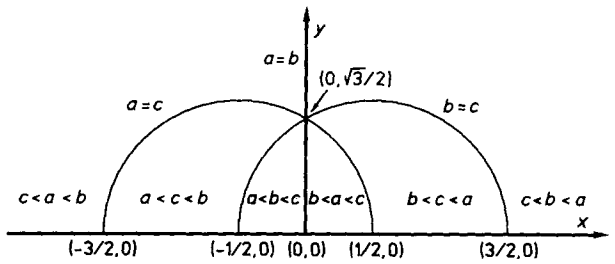

Fig. 2. The regions of shape space labeled according to the convention in Figure 1.

The dependence of $\chi(e)$ on triangular shape was explored by examining the behavior of the function as x varies for a given value of y within the bounds of the two arcs. Since $c = 1$, this corresponds to an examination of $\chi(e)$ as a function of triangular shape for all triangles with a given area $y/2$.

Figure 3 displays plots of $\chi(e)$ vs. x, computed for selected values of the altitude y. For each of the two enantiomorphous sets of triangles, $a < b < c$ and $b < a < c$, all values of $\chi(e)$ have the same sign, positive and negative, respectively, regardless of triangular shape. Within the conceptual framework developed by Ruch and coworkers,[28] $\chi(e)$ may therefore be characterized as a homochirality func-

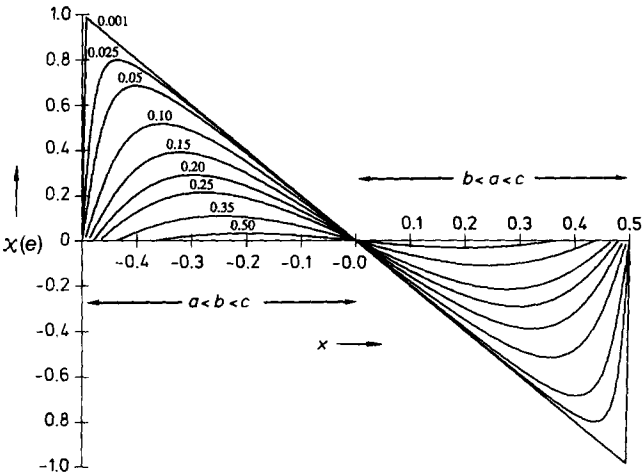

Fig. 3. Calculated plots of the chirality product $\chi(e)$ for triangles vs. x for the unique regions $\{a < b < c, b < a < c\}$ and several values of the altitude y. The altitudes are indicated by the numbers above the curves.

tion: the two sets are mutually heterochiral, all triangles within a given set are homochiral (i.e., chirally related), and the boundary between and around the two sets represents the set of achiral triangles.

For each value of y, $\chi(e)$ assumes a maximum value, χ_{max}, which is the same in magnitude but oppositely signed for the two sets. It is obvious on inspection of Figure 3 that with decreasing values of y, χ_{max} increases in magnitude and at the same time is shifted in the direction of the bounds at $x = \pm 1/2$. In the limit of $y = 0$, c is made up of two segments, a and b, so that $\chi(e) = -2x$ in the interval $(-1/2, 1/2)$. Thus $\chi(e)$ in the limit of $y = 0$ becomes a measure of one-dimensional chirality.

The magnitude of χ_{max} is negligible for values of y greater than 0.5, and becomes significant only for triangles that are extremely flat (i.e., for values of y close to zero) and extremely skewed (i.e., for values of x close to $\pm 1/2$). Within this domain, as the triangle becomes more chiral and more skewed, the vertex (C) representing the triangle with χ_{max} shifts towards the arched borders of the shape space. In the limit of $x = \pm 1/2$ and $\chi_{max} = \mp 1$, vertex C coincides with vertex A or vertex B. The most chiral triangle is therefore one that is infinitely flat and skewed, with an altitude y that is arbitrarily close to zero. Thus, paradoxically, the most chiral triangle is infinitely close to an achiral one.

2.3.2.2. *Symmetry Coordinates*

The problem of quantifying the distortion of a chemical molecule from a more symmetrical reference structure has been addressed by Murray-Rust, Bürgi, and Dunitz,[32] who set out to attach a quantitative meaning to statements of the type "the molecule has approximate T_d symmetry". In terms of their method, a given nuclear configuration is represented by a point in a multidimensional space spanned by a set of symmetry coordinates $\mathbf{S}_i$ for the more symmetric reference structure. The coordinates of the representative point are given by displacements along the $\mathbf{S}_i$'s, which are linear combinations of the internal coordinates that transform according to the irreducible representations of the molecular point group $\mathbf{G}$ of the reference structure; the origin of the space represents that reference structure. The magnitudes of these displacements then serve as the basis for quantifying the deformation of the observed configuration away from the reference structure.

This method is readily adapted to the problem of estimating degrees of chirality for triangles. A "conformation space" spanned by symmetry coordinates may be constructed, in which the choice of the three internal angles α, β, and γ as a basis set ensures similarity invariance, so that each point in this space represents the shape of a triangle, regardless of size. The achiral reference group, $\mathbf{G} = D_3$, is a two-dimensional group that is isomorphic with C_{3v}, in that the three σ_v elements in E^3 correspond to lines of reflection in E^2. The internal coordinates α, β, and γ transform as $A_1 + E$; three symmetry coordinates derived by standard methods[33] may be chosen as in Scheme 1, where Δ refers to the deviation from the angles in the reference structure, the equilateral triangle. However, the positive and negative deviations of the angles in the A_1 representation cancel out, since their sum must always remain zero. The conformation space of triangles is therefore adequately represented in terms of just the E coordinates.

$$\mathbf{S}_1(A_1) = (1/\sqrt{3})(\Delta\alpha + \Delta\beta + \Delta\gamma)$$
$$\mathbf{S}_{2a}(E) = (1/\sqrt{6})(2\Delta\gamma - \Delta\beta - \Delta\alpha)$$
$$\mathbf{S}_{2b}(E) = (1/\sqrt{2})(\Delta\beta - \Delta\alpha)$$

Scheme 1. Symmetry coordinates of the conformation space for triangles.

A projection of this space onto the plane defined by $\mathbf{S}_{2a}$ and $\mathbf{S}_{2b}$ is shown in Figure 4. The lines RP, PQ, and QR

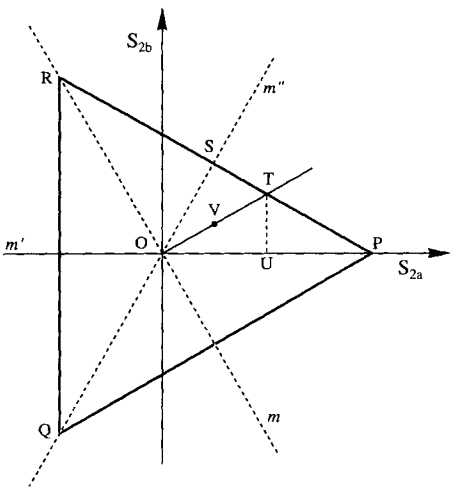

Fig. 4. Diagram of the conformation space for triangles. The dimensions of $\mathbf{S}_{2a}$ and $\mathbf{S}_{2b}$ are any angular measures. The space has symmetry $3m$, with O as the point of threefold rotation, and m, m', m'' representing the lines of reflection. Section OSP corresponds to one of the six asymmetric units. The significance of points S, T, U, and V is discussed in the text.

form the boundaries of the space and correspond to degenerate triangles with $\alpha = 0°$, $\beta = 0°$, and $\gamma = 0°$, respectively; the corners Q, R, and P correspond to degenerate triangles with $\alpha = 180°$, $\beta = 180°$, and $\gamma = 180°$, respectively. As in Section 2.3.2.1, degenerate triangles are excluded from the set of triangles under consideration. The space has symmetry $3m$; the point of threefold rotation, O, represents the equilateral triangle, while the three lines of reflection, m, m', and m'', which correspond to the coordinates $(\mathbf{S}_{2b} = -\sqrt{3}\ \mathbf{S}_{2a})$, $\mathbf{S}_{2b} = 0$, and $(\mathbf{S}_{2b} = \sqrt{3}\ \mathbf{S}_{2a})$, respectively, map isosceles triangles with $\alpha = \gamma$, $\alpha = \beta$, and $\beta = \gamma$, respectively. The points of intersection of these "achiral coordinates" with PQ, QR, and RP(S) represent degenerate triangles with $\alpha = \gamma = 90°$, $\alpha = \beta = 90°$, and $\beta = \gamma = 90°$, respectively. The three achiral coordinates divide the conformation space into six asymmetric units that correspond to the six permutations of α, β, and γ; for example, all triangles in asymmetric unit OSP have $\gamma \geq \beta \geq \alpha$, all triangles in asymmetric unit ORS have $\beta \geq \gamma \geq \alpha$, etc. In contrast to the shape space of triangles in Figure 2, all six asymmetric units in the conformation space of Figure 4 map triangles with the same handedness.[34]

A given chiral triangle is represented by a point C that lies in a general position—that is, not on any of the special positions mapped by the achiral coordinates—within any one of

the six equivalent asymmetric units. The degree of chirality of such a triangle is then gauged by the distance of C from the *nearest* point on an achiral coordinate. Since each asymmetric unit is bordered by two achiral coordinates, there will in general be two distances (d_1 and d_2) that need be considered. For example, in the asymmetric unit OSP the distances to the coordinates m' and m'' are $d_1 = (1/\sqrt{2})(\Delta\beta - \Delta\alpha)$ and $d_2 = (1/\sqrt{2})(\Delta\gamma - \Delta\beta)$, respectively. The degree of chirality **d** of the triangle is defined as the shorter of the two distances, that is, $\mathbf{d} = \min\{d_1, d_2\}$.

The location of the representative point for the most chiral triangle is obtained as follows. Consider, for example, the asymmetric unit OSP (Fig. 4): line OT (which corresponds to all triangles with $\beta = 60°$) is the bisector of angle SOP, and thus represents all geometries that are equidistant from the two achiral coordinates bordering this unit. The projections from point T onto the achiral coordinates are the suprema for perpendicular distances that can be realized within this asymmetric unit, and hence represent the upper bound for the displacement from achirality. It follows that the most chiral triangle corresponds to a point that is arbitrarily close to T, in other words, to a triangle that is infinitely flat and approachable only as a limit, with one angle of 60° (β), another (α) that is arbitrarily close to 0°, and a third (γ) that is arbitrarily close to 120°. The displacements d_1 and d_2 from U (the representative point for a triangle with $\alpha = \beta = 30°$ and $\gamma = 120°$) and S (see above) to T are given by the line segments $UT = (1/\sqrt{2})(\Delta\beta - \Delta\alpha)$ and $ST = (1/\sqrt{2})(\Delta\gamma - \Delta\beta)$, respectively, and are the same in magnitude. In both cases the displacement is accompanied by a total absolute angular change of 60°, with $d_1 = d_2 = \mathbf{d} = (1/\sqrt{2})(60°) \approx 42.4°$. This value defines the least upper bound (i.e. supremum) for **d** in the conformation space for triangles and allows normalization of **d** to the interval [0, 1].

It needs to be emphasized that the search for the point farthest from the achiral reference point and from the achiral boundaries, that is, for the point that is representative of the most chiral triangle, is not limited to the conformation space shown in Figure 4. For example, in the region of the shape space in Figure 2 that is labeled $b < a < c$, the point that is farthest from the achiral boundaries defined by $a = b$ and $a = c$ is located on the x axis, at (1/4, 0), and is representative of a degenerate triangle whose ratio of sides is 1:3:4. The most chiral triangle, which is arbitrarily close to this point, therefore differs in shape from the triangle close to T in Figure 4. As this example demonstrates, the shape of an extremal object given by a chirality measure of the first kind depends on the particular representation of the object space.

2.3.3. *Nonsuperposability of Enantiomorphs*

2.3.3.1. *Common Volumes*

This method was illustrated in section 2.2.2. by the example of overlapped tetrahedrons. Let T' denote the enantiomorph of a triangle T, taken to be a convex set with interior points, and let $T^* = T \cap T'$ denote the intersection resulting from the overlap of the two triangles in E^2. The problem of finding the most chiral triangle now becomes one of determining the conditions under which T^* assumes its maximum value, T^*_{max}. An analytical solution to this problem is far from trivial, considering the innumerable arrangements that are possible when two enantiomorphous triangles are superimposed; a priori, all that can be said is that T^*_{max} must be a polygon with 3, 4, 5, or 6 sides. Fortunately the problem becomes amenable to solution thanks to a theorem proved by Giering[35] that maximal overlap obtains only if both of two conditions are met: a) T^* must be axially symmetric, and b) the edges of T^* must be segments of all six sides of the two overlapped triangles. A measure of chirality that is in harmony with Giering's conditions is $\chi(T) = 1 - f(T)$, with $f(T) = \max_{T^*}\{[T^*]/[T]: T^* \text{ is axially symmetric and } T^* \subset T\}$ where $[T]$ and $[T^*]$ denote the areas of the corresponding polygons. The function $f(T)$ is similarity invariant, normalized in the interval [0, 1], and $f(T) = 1$ if, and only if, T is achiral.

To find the value of $\chi(T)$ for the most chiral triangle, that is, the supremum of the function, requires as a first step the systematic investigation of each class of polygonal intersections. Because Giering's second condition requires the edges of T^*_{max} to be segments of all six sides of the two overlapped triangles, triangular intersections are ipso facto excluded for all chiral triangles. Furthermore, it can be shown[21b] that only quadrilateral and pentagonal intersections, with a shared angle and a shared side, respectively, need be considered as candidates for $f(T)$. This analysis leads to Equation (f) for the unique geometry of a triangle T, with a given c/b or a given α, that corresponds to the lowest value of $f(T)$ for all possible intersections of T and its enantiomorph under conditions of maximal overlap, and to Equation (g) for the corresponding measure. In both equations, b and c are the two sides of T whose ratio is closest to unity and $b \leq c$, α is the angle subtended by vertex A (opposite side a), and for α the limits $1/2 \leq \cos\alpha < 1$ hold.

$$c/b = \sqrt{2\cos\alpha} \tag{f}$$

$$f(T) = \frac{2}{1 + \sqrt{2\cos\alpha}} \tag{g}$$

The value of $f(T)$ for the most chiral (i.e., least achiral) triangle obtains when $\alpha = 0$. It follows that the supremum of $\chi(T)$ can only be approached as a limit. At this limit, $c/b = \sqrt{2}$ [Eq. (f)], $f(T) = 2/(\sqrt{2}+1) \approx 0.828$,[36] and $\chi(T) = 1 - f(T) \approx 0.172$. The most chiral triangle is therefore infinitely flat, with an altitude h arbitrarily close to zero and with $c/b = \sqrt{2}$ and $a/b = \sqrt{2} - 1$ in limit $h = 0$. At the supremum the triangle would be completely flattened into a straight-line segment.

The small limiting value of $\chi(T)$ is particularly noteworthy, for it shows that the area of *any* triangle can be covered to the extent of *at least* 82.8% by overlapping the triangle with its mirror image in E^2.

2.3.3.2 *Hausdorff Distances*

The array of nuclear positions in a rigid molecular model may be represented by a discrete set of points in E^3. The

Hausdorff distance[37a] between sets is therefore a natural choice for a measure of chirality.

Consider two nonempty and bounded sets Q and Q'. Let $\delta(Q,q')$ denote the shortest distance between a fixed point $q' \in Q'$ and set Q; similarly, let $\delta(Q',q)$ denote the shortest distance between a fixed point $q \in Q$ and set Q'. Let $\rho(Q,Q') = \sup_{q' \in Q'} \delta(Q,q')$ and $\rho(Q',Q) = \sup_{q \in Q} \delta(Q',q)$. Then the Hausdorff distance between Q and Q' is given by $h(Q,Q') = h(Q',Q) = \max\{\rho(Q,Q'); \rho(Q',Q)\}$.[37b] If Q and Q' are geometric objects or sets of points in Euclidean space, the value of $h(Q,Q')$ depends on the relative orientations of Q and Q', and by varying the position of one with respect to the other by translation–rotations, it is possible to alter, and ultimately to minimize, $h(Q,Q')$ to $h_{min}(Q,Q')$, corresponding to the position of optimal superimposition.

Let Q' be the mirror image of Q. Then we define a similarity invariant Hausdorff chirality measure, $f(Q)$ [Eq. (h)], where $d(Q)$, the "diameter" of Q, is the maximum distance that can be realized between any two points of Q.

$$f(Q) = \frac{h_{min}(Q,Q')}{d(Q)} \qquad \text{(h)}$$

This function is normalized in the interval [0, 1] and it is zero if, and only if, Q is achiral.[38, 39]

Because the Hausdorff chirality measure for triangles is similarity invariant, the longest side can be assigned unit length without loss of generality. Hence, $f(Q) = h_{min}(Q,Q')$. Like other chirality measures of the second kind, the Hausdorff measure is combinatorial in character, that is, it requires an analysis of many different superimpositions of a given triangle T and its mirror image T'. In our approach to this problem[21c] we have resorted to a numerical analysis, in which a multidimensional hypersurface is explored in search of the global minimum corresponding to $h_{min}(Q,Q')$. The triangles are represented as physical objects in E^3 consisting of unit masses centered at the three vertices. A given triangle Q is placed with its center of mass (i.e., its centroid) at the origin of the Cartesian coordinate system, with the principal axes of inertia aligned along the axes of the coordinate system; this is done by diagonalizing the tensor of inertia and then using the eigenvectors to construct a rotational matrix for the triangle. The largest eigenvalue of the tensor of inertia is assigned to the z axis so that Q is located in the xy plane. This position of Q in the coordinate system is kept fixed throughout the minimization.

The superimposition of Q and Q' involves two variables, u and w, that describe the translation of Q' in the xy plane along the x and y axes, and a third, θ, that describes rotation about the z axis. Accordingly, $f(Q) = \min_{u,w,\theta} \{h(Q,Q',u,w,\theta)\}$. Rotations and translations of Q' relative to Q are carried out until $f(Q)$ is minimized as a function of u, w, and θ by the Broyden–Fletcher–Goldfarb–Shanno (BFGS) procedure.[40] In this manner, $f(Q)$ can be calculated for any given Q.

We showed in Section 2.3.2.1 that all chiral triangular shapes are represented in a construction in which two vertices, A and B, are located at (1/2, 0) and (−1/2, 0), respectively, while the third, C(x,y), maps into one of the two heterochiral regions labeled $a < b < c$ and $b < a < c$ in Figure 2. The most chiral triangle, corresponding to the supremum of $f(Q)$, must be located within one of these regions, and its enantiomorph within the other. We therefore explored the $a < b < c$ region by the grid method in a search for $\max\{f(Q) \equiv f(x,y)\}$. The results, displayed in Figure 5,

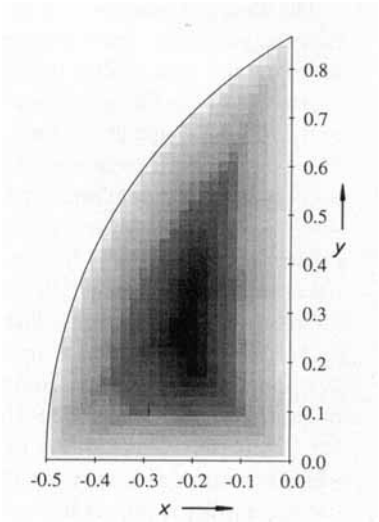

Fig. 5. Density plot of the Hausdorff chirality measure for triangles, evaluated on a 0.02 unit grid along the x and y axes. The values of the function are represented by different shadings: darker shadings indicate higher values. The shape space is the same as the region labeled $a < b < c$ in Figure 2.

show that there is only one relatively flat maximum located in the central portion of the region. Maximization by the BFGS procedure locates the point in the region with the largest value of $f(x,y)$. This point corresponds to the most chiral triangle: $f(x,y) \approx 0.196$, $\alpha \approx 21.5°$, $\beta \approx 44.2°$, $\gamma \approx 114.3°$. Orientations of Q' relative to Q that correspond to optimal overlap for this triangle are shown in Figure 6. Our calculations show that in all three orientations a line of reflection passes through the region of overlap, but that this line does not pass through the origin of the coordinate sys-

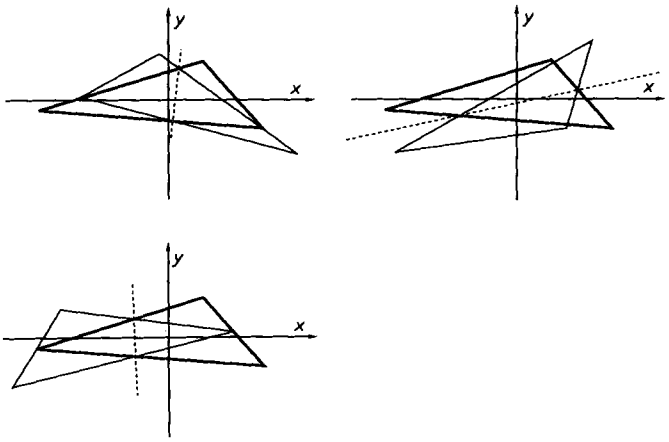

Fig. 6. Optimized orientations of Q' relative to Q for the most chiral triangle according to the Hausdorff measure, as determined by distances between vertices. The position of Q (heavy lines) in the xy plane remains fixed, with the centroid at the origin. The regions of overlap are axially symmetric. Lines of reflection are dashed. Degrees of chirality $f(Q)$ are 0.196 (top, left), 0.197 (top, right), 0.201 (bottom), that is, they are identical within the error limits of the calculation.

tem; the significance of this observation will be discussed in Section 2.3.4.

2.3.4. A Comparison of the Results

The principal conclusion of this study is that each chirality measure yields a different answer to the question: what is the shape of the most chiral triangle? Although three of the measures yield as the most chiral triangle one that is infinitely flat,[41] the shape at the limit differs with each measure. Thus, where both measures of the first kind described in Section 2.3.2 yield an ultimate triangle with the same ratio of sides (1:1:0), the ratios of internal angles are different (0°:0°:180° and 0°:60°:120°), and where the ratios of internal angles are the same (0°:0°:180°), the ratios of sides are different (1:1:0 and 1:3:4). The overlap measure described in Section 2.3.3.1 yields a triangle whose ratio of sides, $1:1/\sqrt{2}:(1-1/\sqrt{2})$, differs from that given by both measures in Section 2.3.2. As for the Hausdorff measure (Section 2.3.3.2), it is evident a priori that the most chiral triangle, which corresponds to $\max\{h_{min}(Q, Q')\}$, cannot be infinitely flat—as in fact it proves not to be—because, under conditions of optimal overlap, two infinitely flat enantiomorphous triangles are arbitrarily close to superposition and $h_{min}(Q,Q')$ is hence arbitrarily close to zero.

That triangular shape and degree of chirality depend on the measure may be further illustrated by the example of the most chiral right triangle (Table 1). According to the overlap measure described in Section 2.3.3.1, the shape of this triangle is given by $\arccos 2^{-1/3} \approx 37.5°$ and its degree of chirality by $(2^{1/3}-1)/(2^{1/3}+1) \approx 0.115$.[21a] Within the shape space defined by the gothic arch of Figures 2 (and 5), all right triangles are represented by points on a circle of radius 1/2 that is centered at (0, 0).[20a] The maximum degrees of chirality on this locus are 0.074 and 0.141 for the chirality product and the Hausdorff measure, respectively, and the corresponding shapes of the right triangles are given by $\alpha \approx 18.8°$ and 35.2°, respectively. In Figure 4, the most chiral right triangle in the asymmetric unit OSP lies at point V; according to this measure, the degree of chirality is $(1/\sqrt{2})(30°) \approx 21.2°$ and $\alpha = 30°$.[20b] Table 1 lists the degrees of chirality of the most chiral right triangles as fractions of the supremum on the values of the four measures. The four measures also yield different degrees of chirality for the right triangle with α fixed at 30° (Table 1).

Table 1. Comparison of four independent chirality measures for two defined right triangles.

Measure [Section]	Most chiral right triangle			Right triangle with $\alpha = 30°$	
	α	χ[a]	Rel. χ[b]	χ[a]	Rel. χ[b]
geometry [2.3.2.1]	18.8°	0.074	0.074	0.057	0.057
symmetry [2.3.2.2]	30.0°	0.500	0.500	0.500	0.500
overlap [2.3.3.1]	37.5°	0.115	0.669	0.073	0.423
Hausdorff [2.3.3.2]	35.2°	0.141	0.719	0.106	0.541

[a] Degree of chirality. [b] Degree of chirality relative to that of the most chiral triangle.

A fifth function, $\chi(\theta) = \sin 4\theta$, where θ is one of the acute angles in a right triangle, also meets all the conditions required of a chirality measure. This function achieves its maximum at $\theta = 22.5°$, while $\chi = 0.866$ for $\theta = 30°$; these values are to be compared with the corresponding entries in Table 1. The special significance of this function lies in the fact that it is one of a family of chirality measures that take the form $\chi(\theta) = \sin n\theta$ and that are continuous, normalized in the interval $[1, -1]$, oppositely signed for enantiomorphous objects, and that vanish if, and only if, the objects are achiral. For example, consider an array of two line segments of equal lengths, joined at their midpoints by a third line segment of finite length that is normal to both and that serves as an axis of rotation. The chirality of this array is a function of the torsion angle θ subtended by the two lines,[42] and its measure is $\chi(\theta) = \sin\theta$ if the lines are oriented and $\chi(\theta) = \sin 2\theta$ if they are not;[43] the latter may also be taken as a measure of helicity if one of a skew pair of nonoriented lines is the tangent of a cylindrical helix and the other is collinear with the screw axis.[42, 44]

The present work has revealed that the two overlap measures (Section 2.3.3) share at least two significant characteristics. First, according to the Hausdorff measure, the union of Q and Q' under conditions of optimal overlap is axially symmetric (Fig. 6). This meets the first of Giering's two conditions that were applied to the common volume measure (Section 2.3.3.1), which states that optimal overlap obtains only if the intersection, and hence the union, are axially symmetric. Our results suggest that *the union $K \cup K'$ of any object or set K and its mirror image K' is achiral under conditions of optimal overlap*. Further support for this conjecture comes from the results of the study reported in Section 2.4.2.

Second, in neither one of the two measures are the centroids of the two enantiomorphous triangles coincident under conditions of optimal overlap. In the case of the Hausdorff measure, because the line of reflection does not pass through the origin where the centroid of Q is located (see Fig. 6), it immediately follows that the centroid of Q' does not lie on the origin. In the case of the common volume measure, it is easily shown that for quadrilateral and pentagonal intersections of T and T' (with a shared angle and a shared side, respectively) the centroids do not lie on the line of reflection of T^*. In both measures, the centroids coincide only if the triangle is achiral.

2.4. In Search of the Most Chiral Tetrahedron

The construction of chirality measures for tetrahedrons is substantially more complex than that for triangles. First, while two independent parameters, for example two internal angles, suffice to define the shape of a triangle, five such parameters are required for a tetrahedron. Second, while C_1 is the only chiral group possible for triangles, three such groups (C_1, C_2, D_2) need to be considered for tetrahedrons.[45] We have therefore limited ourselves to the design of two measures, one of each kind.[21c] Sction 2.4.1 describes preliminary results obtained by use of the method of symme-

try coordinates, chosen because of its relationship to crystallographic analyses.[32] The Hausdorff measure described in Section 2.4.2 was chosen for several reasons. First, this measure is far easier to implement computationally than measures based on the fraction of overlapping volumes. Second, as noted before, the Hausdorff distance between sets of points in enantiomorphous geometric figures may be taken as an expression of the corresponding distance between nuclear positions of enantiomeric molecules—in contrast to measures based on overlapping volumes, which require the assumption of a uniform and continuous distribution of points within the model rather than the physically more realistic localization of matter in discrete regions. Finally, by use of the Hausdorff measure it may be possible, through the incorporation of chemical or physical parameters, to forge a connection to the world pseudoscalar observables.

2.4.1. Deviation from Achirality

Deformations of tetrahedral frameworks of carbon, specifically methane and the $C(C)_4$ fragment of neopentane, have received some attention in the past.[46] In all of these cases the focus was on the flattening of the T_d framework to a rectangular-planar (D_{2h}) or square-planar (D_{4h}) conformation. The former deformation may take place by means of a digonal twist involving two opposite edges, maintaining the D_2 symmetry of the tetrahedron, while the latter involves a compression along a C_2 axis that maintains D_{2d} symmetry.

Luef et al.[46c] used the symmetry coordinate approach to analyze angular distortions at the central carbon atom of the $C(C)_4$ fragment in some substituted spiro[4.4]nonanes. By contrast, we chose to describe the shape of a general tetrahedron by the set of twelve facial angles, three subtended at each vertex; the choice of this basis set ensures similarity invariance. Each angle may be denoted by a set of three numbers that specify the vertices that form it; for example, $\theta 123$ is the angle subtended at vertex 2 by vertices 1 and 3. For each angle we list the three vertices in an anticlockwise sense. This basis set transforms as $A_1 + E + T_2$. The six-dimensional conformation space for the tetrahedron may therefore be broken down into three subspaces of dimensionality one, two, and three, whose symmetries are 1, $3m$, and $\bar{4}3m$, respectively. The symmetry coordinates are given explicitly in Scheme 2.

As in the case of the triangles (Section 2.3.2.2), displacements along $\mathbf{S}_1$ will always be zero, since the sum of the angles for each face must always be 180°. Consequently we need only consider the E and T_2 subspaces of the conformation space. Moreover, for these spaces the value of the ideal facial angle (60°) cancels out in the expressions for the symmetry coordinates, so that the deviations (Δ) may be dropped, giving rise to the simplified expressions listed above.

We can probe the shape of the E subspace by holding displacements along the T_2 symmetry coordinates fixed at zero—as they would be for tetrahedrons with D_2 symmetry, for example—and then considering the maximal displacements that are possible ablong $\mathbf{S}_{2a}$ and $\mathbf{S}_{2b}$ (Fig. 7). The reaches of the E subspace that are available to such tetrahedrons are limited by the geometrical restrictions on the values that the facial angles can adopt. For example. a positive displacement along $\mathbf{S}_{2a}$ maps a compression of the tetrahedron along the C_2 axis passing through edges 12 and 34 that maintains D_{2d} symmetry: its maximum is reached when the edges become coplanar, that is, when angle $\theta 132$ (and the symmetry-equivalent angles $\theta 241$, $\theta 314$, and $\theta 423$) becomes 90°. A negative displacement maps a stretch along the same axis: its maximal value is reached when $\theta 132$ is 0°, that is, when the edges have been stretched apart to infinity. In the limit, these two conformations correspond to flattened (D_{4h}) and linear ($D_{\infty h}$) degenerate tetrahedrons, represented in Figure 7 by points Y and P respectively. Coordinate $\mathbf{S}_{2a}$ hence constitutes an achiral coordinate (m'). Two further such coordinates (lines m'' and m in Fig. 7) that map compressions and stretches along the other C_2 axes can be found

$$
\begin{aligned}
\mathbf{S}_1(A_1) &= (1/\sqrt{12})(\Delta\theta 132 + \Delta\theta 213 + \Delta\theta 321 + \Delta\theta 241 + \Delta\theta 124 \\
&\quad + \Delta\theta 412 + \Delta\theta 314 + \Delta\theta 431 + \Delta\theta 143 + \Delta\theta 423 + \Delta\theta 342 \\
&\quad + \Delta\theta 234) \\
\mathbf{S}_{2a}(E) &= (1/\sqrt{24})(2\Delta\theta 132 - \Delta\theta 213 - \Delta\theta 321 + 2\Delta\theta 241 - \Delta\theta 124 \\
&\quad - \Delta\theta 412 + 2\Delta\theta 314 - \Delta\theta 431 - \Delta\theta 143 + 2\Delta\theta 423 - \Delta\theta 342 \\
&\quad - \Delta\theta 234) \\
&= (3/\sqrt{24})(\theta 132 + \theta 241 + \theta 314 + \theta 423 - 240°) \\
\mathbf{S}_{2b}(E) &= (1/\sqrt{8})(\Delta\theta 213 - \Delta\theta 321 + \Delta\theta 124 - \Delta\theta 412 + \Delta\theta 431 - \Delta\theta 143 \\
&\quad + \Delta\theta 342 - \Delta\theta 234) \\
\mathbf{S}_{3a}(T_2) &= (1/\sqrt{24})(2\Delta\theta 132 - \Delta\theta 213 - \Delta\theta 321 + 2\Delta\theta 241 - \Delta\theta 124 \\
&\quad - \Delta\theta 412 - 2\Delta\theta 314 + \Delta\theta 431 + \Delta\theta 143 - 2\Delta\theta 423 + \Delta\theta 342 \\
&\quad + \Delta\theta 234) \\
&= (3/\sqrt{24})(\theta 132 + \theta 241 - \theta 314 - \theta 423) \\
\mathbf{S}_{3b}(T_2) &= (1/\sqrt{24})(2\Delta\theta 321 - \Delta\theta 132 - \Delta\theta 213 + 2\Delta\theta 143 - \Delta\theta 314 \\
&\quad - \Delta\theta 431 - 2\Delta\theta 412 + \Delta\theta 241 + \Delta\theta 124 - 2\Delta\theta 234 + \Delta\theta 423 \\
&\quad + \Delta\theta 342) \\
&= (3/\sqrt{24})(\theta 321 + \theta 143 - \theta 412 - \theta 234) \\
\mathbf{S}_{3c}(T_2) &= (1/\sqrt{24})(2\Delta\theta 213 - \Delta\theta 321 - \Delta\theta 132 + 2\Delta\theta 342 - \Delta\theta 234 \\
&\quad - \Delta\theta 423 - 2\Delta\theta 431 + \Delta\theta 143 + \Delta\theta 314 - 2\Delta\theta 124 + \Delta\theta 412 \\
&\quad + \Delta\theta 241) \\
&= (3/\sqrt{24})(\theta 213 + \theta 342 - \theta 431 - \theta 124)
\end{aligned}
$$

Scheme 2. Symmetry coordinates of the conformation space for tetrahedrons.

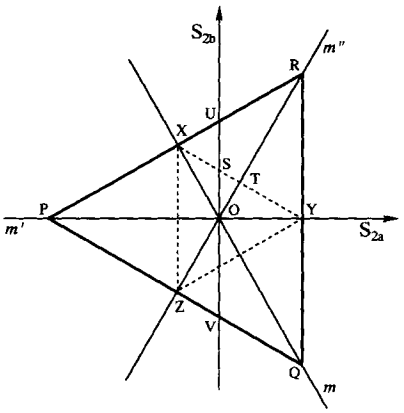

Fig. 7. Triangular *E*-subspace (PQR) of the conformation space for tetrahedrons. Lines m, m', and m'' are mirror lines, and the origin O represents a point of threefold rotation; the symmetry of the space is $3m$. ORX demarcates one of six asymmetric units, within which line OU maps D_2 tetrahedrons of increasing degrees of chirality. Triangle YZX traces the tetrahedral distortions that are mapped by the edges of the octahedral faces ABC of the T_2 subspace (Fig. 9). In terms of this construction, YZX can be visualized as one octahedral face, where m, m', and m'' represent mirror planes, point O a threefold axis, and section OTX an asymmetric unit.

displaced 120° and 240° from S_{2a}. The shape of the resulting two-dimensional conformation space is triangular ($3m$ symmetry), as it was in the case of the triangles (Fig. 4). Positive and negative displacements along S_{2b} map clockwise and anticlockwise digonal twists of edges 12 and 34 about their C_2 axis, such that the facial angle $\theta 132$ remains constant at 60°, with no attendant flattening or compression along this C_2 axis. Accordingly, the limiting conformations are rectangular-planar (D_{2h}) with edges in the ratio $1:\sqrt{3}$ (points U and V in Fig. 7). Similar coordinates for twists about the other two C_2 axes may be found displaced by 120° and 240°, but these are not illustrated in Figure 7. The edges of the subspace map degenerate tetrahedrons whose vertices are coplanar—when they are not colinear, as at the points P, Q, and R. Thus, segement RX, for example, maps the transformation of a linear ($D_{\infty h}$, point R) to a rectangular-planar (D_{2h}, point U) and finally a square-planar (D_{4h}, point X) degenerate tetrahedron; segment XP traces the reverse distortion.

By analogy to the triangles, the most chiral tetrahedron with D_2 symmetry will lie on the angle bisector between two adjacent achiral coordinates. When we consider the asymmetric unit ORX, for example, line OU is the bisector of the angle subtended by OR and OX, and the most chiral tetrahedron is situated at the point U. But, as before, the dimensionality reduces by one when this point is reached, so that the most chiral D_2 tetrahedron may once again be approached only as a limit. This limit takes the form of a planar rectangle whose sides are in the proportions $1:\sqrt{3}$, thereby yielding angles of 30°, 60°, and 90° in each of the four faces (Fig. 8, left). As was the case for the triangle, point U is displaced from the nearest achiral points on m and m'' by $d_1 = d_2 = \mathbf{d} = (1/\sqrt{2})(30°) \approx 42.4°$; this value once again defines the least upper bound, and allows for normalization of **d** to the interval [0,1].

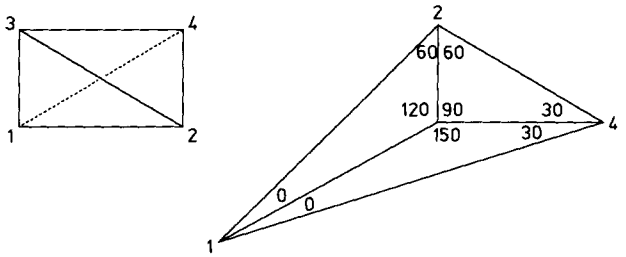

Fig. 8. Left: illustration of the limiting conformation for the most chiral D_2 tetrahedron with facial angles 30°, 60°, 90° according to the measure in Section 2.4.1. Right: schematic diagram of the limiting conformation for the most chiral C_1 tetrahedron, showing the limits to the values of the facial angles (see [47]). The representative point for this tetrahedron is situated at S in the E subspace (Fig. 7) and on the edge of AE in the T_2 subspace (heavy dot, Fig. 9).

As mentioned earlier, a displacement from the origin of the E subspace along S_{2b} int he direction of point U corresponds to a digonal twist of the tetrahedron about a C_2 axis; in other words, the more twisted the tetrahedron, the greater its degree of chirality. This result certainly makes intuitive sense in the extreme case of an infinitesimal deformation away from T_d symmetry: a tetrahedron with this symmetry is achiral, while one with even a miniscule twist of two opposite edges would be chiral; and the greater the twist, the greater the degree of chirality might appear to be. The result for the most chiral D_2 tetrahedron simply carries this reasoning to its logical extreme, and the apparently counterintuitive answer—that the most chiral tetrahedron is infinitely close to an achiral object—is a consequence of the fact that this method cannot deal with the collapse in dimensionality that occurs at the extreme.

For any tetrahedron whose displacement along S_{3a}, S_{3b}, or S_{3c} (Scheme 2) is not zero, the position of its representative point in the T_2 subspace will also need to be considered. The shape of this space will once again be determined by geometrical constraints that exist in tetrahedrons. Because of the tetrahedral symmetry of the subspace ($\bar{4}3m$), it might be supposed that its shape would be similarly tetrahedral. However, it turns out[21c] that the conformation space has an octahedral shape that can be viewed as constructed from a tetrahedron whose four vertices have been truncated at the midpoint of each edge (Fig. 9). In order to be consistent with its symmetry, the space may be imagined as a two-colored octahedron, with adjacent faces differently colored. In the context of such a perspective, the twofold axes of the subspace are visualized as the C_2 axes of a tetrahedron the midpoints of whose edges—bisected by the C_2 axes—represent the outer limits of the subspace. The mutually orthogonal symmetry coordinates spanning the space are coincident with these twofold axes: displacements along S_{3a}, S_{3b}, and S_{3c} map distortions of the tetrahedron that maintain C_{2v} symmetry. Similarly, the tetrahedron's C_3 axes are symbolized by the threefold axes of the colored subspace; these are coordinates along which real tetrahedrons with C_{3v} symmetry are found. Each pair of opposite faces of this octahedron maps either infinitely stretched tetrahedrons with three vertices coplanar and the fourth at an infinite distance (but possibly within the plane of the others), or infinitely flattened tetrahedra in which the fourth vertex is found within the triangular plane formed by the remaining three. For example, the face bound by the maximal positive displacements along each of S_{3a}, S_{3b}, and S_{3c} (face ABC in Fig. 9)

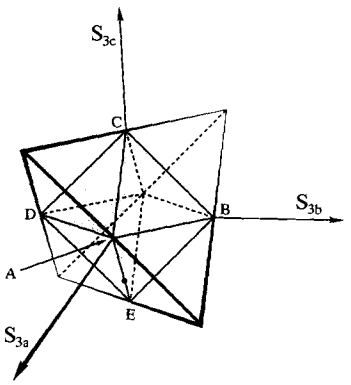

Fig. 9. Octahedral T_2 subspace of the conformation space for tetrahedrons. The symmetry coordinates may be thought of as the C_2 axes of a regular tetrahedron, and the octahedral subspace (shaded) can be constructed by truncating each of the vertices at the midpoints of the edges. In order to represent the $\bar{4}3m$ symmetry of the space, the octahedron must be viewed as two-colored, so as to yield adjacent faces with different colors. Each pair of opposite octants together contains six asymmetric units.

maps all degenerate tetrahedrons for which vertex 4 lies within the triangular plane formed by vertices 1, 2, and 3, while the face opposite it maps all those in which vertex 4 is at an infinite perpendicular distance to this plane.

Tetrahedral distortions that are mapped by the edges of the octahedral face ABC in the T_2 conformation space are represented in the E subspace by the edges of triangle YZX (Fig. 7). Each of the other octahedral edges map onto this triangle in a similar way, so that triangle YZX may be visualized as any one of the octahedral faces. In terms of this construction, mirror lines m, m', and m'' then represent the mirror planes (achiral coordinates) of the T_2 conformation space, which, together with the threefold axis through the center of the face (emerging perpendicularly from point O), define six asymmetric units in each octant of the octahedron. One such asymmetric unit is given by the section OTX (Fig. 7). However, since we are dealing with a two-color octahedron, opposite octants are not symmetry-equivalent. This implies that each such pair of octants *in combination* contains six asymmetric units, and each asymmetric unit takes the shape of a body constructed by joining two trigonal pyramids at a common vertex (which, in this case, is situated at the origin of the space). Depending on whether a particular tetrahedron is flattened or stretched along the C_3 axis, it will be represented in one or the other "half" of the asymmetric unit.

The representative point in T_2 space for the most chiral tetrahedron will have to be situated on the perimeter of the space (on one of the faces), since any position closer to the origin will also bring this point into closer proximity with the mirror planes that span the space and that intersect at the origin. Hence, with reference to the asymmetric unit OTX, when triangle YZX is viewed as a face of the T_2 conformation space, it will be obvious that the most chiral tetrahedron will once again be situated on the angle bisector (OU) between the coordinates m and m''. Point S is now seen to correspond to a point on one of the octahedral edges, at the outermost reaches of the subspace. Not unexpectedly, this yields a degenerate tetrahedron, which in this case is both planar and infinitely skewed. Figure 8 (right) illustrates this degenerate (C_1) tetrahedron schematically, while Figure 9 shows where in the T_2 subspace its representative point would be located.[47] In terms of this construction, triangle YZX could represent either face ABE, or face ADE (corner points are named in corresponding order). Note that each octahedral edge contains two such points, the total of 24 corresponding to the 24 possible permutations of the labels in the schematic illustration of the most chiral tetrahedron (Fig. 8). Point S is displaced by a distance $d_1 = d_2 = \mathbf{d} = (1/\sqrt{14})(15°) \approx 56.1°$ from its nearest achiral neighbors in the five-dimensional space spanned by the E and T_2 symmetry coordinates. This value again allows for normalization to the range [0, 1]. In terms of this approach, the most chiral D_2 tetrahedron ($\mathbf{d} = (1/\sqrt{2})(30°) \approx 42.4°$) is seen to be about 76% as chiral as the most chiral C_1 tetrahedron.

2.4.2. *Nonsuperposability of Enantiomorphs*

The Hausdorff chirality measure for tetrahedrons, $f(Q)$ as defined in Equation (h), like that for triangles (Section 2.3.3.2), requires a numerical analysis of many different superimpositions of a tetrahedron Q and its mirror image Q'. Each tetrahedron is represented as a physical object consisting of unit masses centered at the four vertices. A given Q is placed with its center of mass at the origin of the Cartesian coordinate system and the principal axes of inertia are aligned along the axes of the coordinate system. The enantiomorph Q' is generated by inversion of Q through the origin. The position of Q remains fixed throughout the calculations and the position of Q' is varied in relation to it.

For a tetrahedron, as for any object embedded in E^3, the value of $h(Q,Q')$ depends on six variables; three of them, u, v, and w, describe translations of Q' along the x, y, and z axes, respectively, and three others, ϕ, θ, and ω, define rotations around those axes. Determination of $f(Q)$ thus becomes a typical problem of searching for a global minimum on the multidimensional hypersurface and can be addressed by standard computational means, such as the BFGS procedure[40] that was successfully employed in the search for the most chiral triangle. This procedure is used to minimize $h(Q,Q')$ as a function of u, v, w, ϕ, θ, and ω [Eq. (i)], where $d(Q)$ is defined as in Equation (h).

$$f(Q) = \frac{\min\limits_{u,v,w,\phi,\theta,\omega} \{h(Q,Q',u,v,w,\phi,\theta,\omega)\}}{d(Q)} \qquad \text{(i)}$$

While all triangular shapes are uniquely represented by points within the two-dimensional shape space depicted in Figure 2, the shape space for tetrahedrons requires five dimensions. This space may be partitioned into asymmetric units in each of which every tetrahedral shape, without exclusions, is uniquely represented by exactly one point. However, asymmetric tetrahedrons, unlike asymmetric triangles, are chirally connected.[39] It follows that the set of points that represents achiral tetrahedra does not bisect an asymmetric unit into two heterochiral regions. Although an asymmetric unit in the shape space of tetrahedrons can be partitioned into two subsets, each of them containing the representation of one enantiomorph, one cannot assign a common sense of handedness to members of these subsets. This is in contrast to the regions in Figure 2, each of which represents a set of homochiral triangles (Section 2.3.2.1). The same applies to chiral tetrahedrons with C_2 or D_2 symmetry, since such figures can be continuously deformed into asymmetric (C_1) shapes.[48]

The shape space of a general tetrahedron with vertices A, B, C, and D is defined as follows. First, because $f(Q)$ is similarity invariant, the size of the tetrahedron can be constrained by setting one edge (AB) equal to unity, without loss of generality. All other edges are constrained to be no longer than AB, so that $d(Q) = 1$. Let Z denote the intersection of two unit spheres centered at A, $(x + 0.5)^2 + y^2 + z^2 = 1$, and at B, $(x - 0.5)^2 + y^2 + z^2 = 1$. To satisfy the constraint on length specified above, the other two vertices, C and D, must also belong to Z. Every tetrahedron can be oriented in the Cartesian coordinate system in such a way that if two vertices (A and B) are placed on the xy plane, the other two vertices (C and D) are located in a second plane, parallel to the xy plane and at some height h above it. Figure 10 depicts Z truncated on the positive side of the z axis by that second

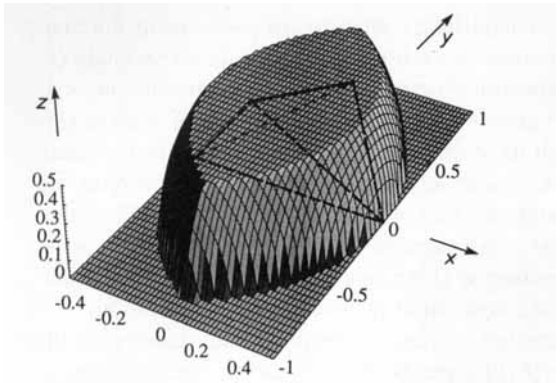

Fig. 10. Intersection of two unit spheres centered at (-0.5, 0, 0) and (0.5, 0, 0) and truncated by a plane parallel to the xy plane that intersects the z axis at 0.5. This defines a domain that contains the vertices of a general tetrahedron ABCD with vertices A and B at the centers of the spheres and C and D located in the plateau at $z = 0.5$.

plane, while Figure 11 shows the projection along the z axis of the same truncated intersection. At any particular height h, $0 < h \leq \sqrt{3}/2$, the plateau consists of the intersection Δ of two overlapping circles $(x + 0.5)^2 + y^2 = 1 - h^2$ and $(x - 0.5)^2 + y^2 = 1 - h^2$. Both C and D are contained in Δ. To eliminate redundancies in Δ, C is restricted to the quadrant of Δ that is bounded by the positive segments of the x and y axes, D is restricted to the intersection of Δ and a circular domain bounded by a circle $(x - x_C)^2 + (y - y_C)^2 = 1$ (see Fig. 11), and the y coordinate of D is lim-

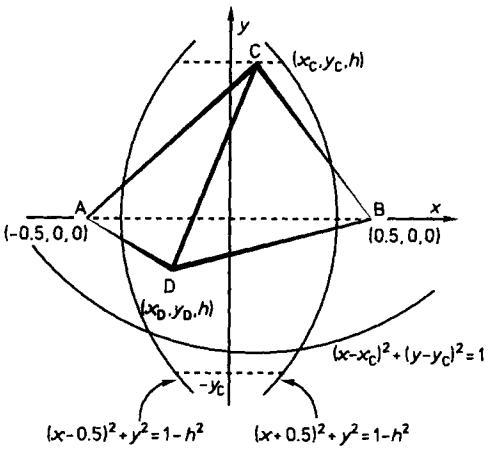

Fig. 11. Projection of Figure 10 along the z axis.

ited to the interval $y_C > y_D \geq -y_C$. The shape of a tetrahedron is therefore fully defined by a set of at most five shape coordinates (h, x_C, y_C, x_D, y_D); the actual number of independent parameters is a function of the tetrahedron's symmetry.

For any D_2 tetrahedron, symmetry requires that the lengths of the AB and CD edges both equal unity. From this constraint it follows that the shape of such a tetrahedron is fully determined by just two independent variables, h and x_C. To find the most chiral D_2 tetrahedron, $\mathbf{Q}_a$, therefore requires locating the point in the asymmetric unit that corresponds to $f(\mathbf{Q}_a) = \max \{f(Q_a) \equiv f(h, x_C)\}$. This two-dimentional space is easily explored by the grid method, and calculations show that there is only one maximum within the asymmetric unit. This maximum, localized by the BFGS procedure, corresponds to the most chiral D_2 tetrahedron, $f(\mathbf{Q}_a) = 0.221$, whose faces have internal angles of 35.1°, 60.5°, and 84.4°. Figure 12 shows three optimal overlaps of

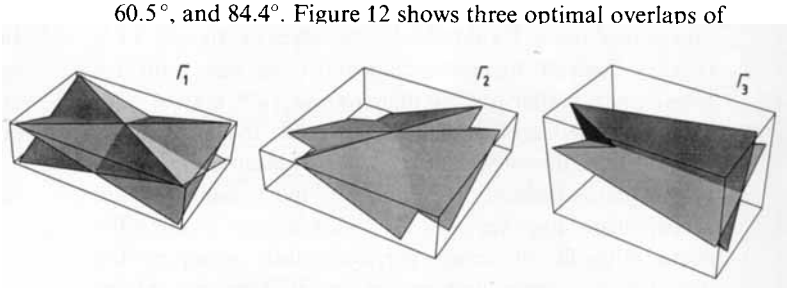

Fig. 12. Unions (Γ) of the most chiral D_2 tetrahedron, $\mathbf{Q}_a$, and its enantiomorph, $\mathbf{Q}'_a$, according to the Hausdorff measure. Γ_1 has D_{2h} symmetry. Γ_2 and Γ_3 have D_{2d} symmetry. The shape of each union is visualized by two interpenetrating solid tetrahedrons, although their Hausdorff chirality measures are determined by the distances between vertices.

$\mathbf{Q}_a$ with its mirror image $\mathbf{Q}'_a$ that are characterized by the same value of $f(\mathbf{Q}_a)$ but that differ in the geometry of the union, $\Gamma_a = \mathbf{Q}_a \cup \mathbf{Q}'_a$. One union, Γ_1, has D_{2h} symmetry with the three twofold axes of $\mathbf{Q}_a$ collinear with the three symmetry-related twofold axes of $\mathbf{Q}'_a$, while the other two, Γ_2 and Γ_3, have D_{2d} symmetry and can be obtained from Γ_1 by 90° rotations of $\mathbf{Q}'$ around one of the three axes.[49]

While C_2 symmetry does not require the CD edge to be equal in length to AB, vertices C and D must be related to each other by a twofold axis that is perpendicular to the xy plane and that passes through the origin of the coordinate system. The shape of a C_2 tetrahedron is therefore fully determined by a set of three independent variables, h, x_C, and y_C. The most chiral C_2 tetrahedron, $\mathbf{Q}_b$, localized by the BFGS procedure, has $f(\mathbf{Q}_b) = 0.252$; its shape is characterized by internal angles $\theta 312 = 45.6°$, $\theta 132 = 34.7°$, $\theta 134 = 38.0°$, and $\theta 314 = 83.4°$, with the C_2 axis bisecting edges 12 and 34. As in the case of $\mathbf{Q}_a$, our calculations show that there are three different unions, $\Gamma_b = \mathbf{Q}_b \cup \mathbf{Q}'_b$, that are characterized by the same value of $f(\mathbf{Q}_b)$; one of the three has C_{2v} symmetry with the twofold axes of the enantiomorphs collinear and their centroids superposed, while the other two have C_s symmetry.

For C_1 symmetry there are no constraints, so that all five independent shape variables must be taken into account in the search for the most chiral C_1 tetrahedron, $\mathbf{Q}_c$. The Monte Carlo procedure was used initially to search the asymmetric unit for regions characterized by high values of $h(Q,Q')$, and the final search by use of the BFGS method localized the point corresponding to $\mathbf{Q}_c$, $f(\mathbf{Q}_c) = 0.255$. The shape of $\mathbf{Q}_c$ differs only slightly from that of $\mathbf{Q}_b$. Once again, the same value of $f(\mathbf{Q}_c)$ is represented by more than one union, $\Gamma_c = \mathbf{Q}_c \cup \mathbf{Q}'_c$, all with C_s symmetry.

Our calculations provide strong support for the conjecture (Section 2.3.4) that the union of an object and its mirror image is achiral under conditions of optimal overlap. Furthermore, the observed trend of an increase in $f(\mathbf{Q})$ with a decrease in symmetry parallels results obtained by the method of symmetry coordinates (Section 2.4.1).

3. Other Chirality Measures

Our efforts to develop measures of chirality, described in Sections 2.3 and 2.4, grew from the seeds of ideas that were planted in 1976.[3] The last few years have witnessed a resurgence of interest in this subject, and in what follows we select for discussion several studies that were carried out independently of, and contemporaneously with, our own, and that illustrate the great variety of approaches that may be employed.

3.1. Kuz'min's Method

As discussed in Section 2.3.2.1, the chirality product of a molecular model, as conceived by Guye[24, 26] and by Ruch et al.,[27, 28] is a product of differences between appropriately chosen ligand parameters. This function, which vanishes for achiral objects, is a chirality measures of the first kind. It is therefore of interest to note that a product function recently developed by Kuz'min et al.[50] is a chirality measure of the second kind.

In Kuz'min's scheme, the model of a molecule, M, is represented by a rigid body consisting of a set of point masses, m_i. This object is placed with its center of mass at the origin of a reduced system of coordinates, with the principal axes of inertia aligned along the axes of a Cartesian coordinate system. If M has a plane of symmetry, the center of mass must lie in that plane, which also contains two of the principal axes of inertia, and if M has an axis of symmetry of any order, the center of mass must lie on that axis, which is also one of the principal axes of inertia.[51] If, in such a coordinate system, a rotation–reflection (improper rotation) operation, S_n, is performed on M, then S_n can be a symmetry or covering operation only if M is achiral; if M is chiral, S_n will generate the nonsuperposable enantiomorph, M'. The degree of chirality of M can therefore be gauged by some function of r_i, the distance between corresponding points m_i and m_i' in M and M'. Keeping in mind the expression for moments of inertia, Kuz'min has defined a function of r_i as the "level of dissymmetry", LD [Eq. (j)].

$$LD = \sum_i m_i r_i^2 \qquad (j)$$

Thus, LD $\neq 0$ if M is chiral, and the larger the value of LD, the greater the degree of chirality of M.

Each S_n performed on M, except for S_2 (central inversion), generates the three LD's that correspond to the three improper rotation axes aligned along the principal axes of inertia. For example, pure reflection, S_1, generates $LD^{S_1^x}$, $LD^{S_1^y}$, and $LD^{S_1^z}$. The exception is LD^{S_2}. The "dissymmetry function", DF, defined as the geometric mean of the ten LD's that result from operations ranging from S_1 to S_6, is expressed in Equation (k), where LD_n for $n = 1, 4$, and 6 stands for $(LD^{S_n^x})$ $(LD^{S_n^y})$ $(LD^{S_n^z})$, and, for $n = 2$, $LD_2 = LD^{S_2}$.

$$DF = [(LD_1)(LD_2)(LD_4)(LD_6)]^{1/10} \qquad (k)$$

The reason for truncating the DF at LD_6 is based on the practical consideration that compounds whose symmetry is S_n with $n > 6$ are quite rare, but Equation (k) could always be expanded to include LD_n's with $n > 6$ should the need arise. Kuz'min et al. have reported several chemical applications of their function.[52]

A limitation on the applicability of Kuz'min's approach that is significant in principle, though not in practice, arises from the fact that in spherical tops all three principal moments of inertia are equal, and the choice of the three principal axes of inertia is therefore rendered arbitrary.[51] As a consequence, the approach fails with objects having T, O, or I symmetry.[50b] Similar limitations apply to symmetric tops. It must also be borne in mind that the numerical values of the LD's, and hence of the DF's, are obtained by computational methods that do not entail optimization of the relative spatial positions of the enantiomorphs. One constraint imposed by the method is that the centers of masses of the enantiomorphs are both located at the origin of the reduced system of coordinates. However, as was noted in section 2.3.4, according to either the Hausdorff or the common volume measure, the centroids of enantiomorphous triangles do not coincide under conditions of optimal overlap. This observation suggests the possibility that optimal overlap may not be achieved under the constraints imposed in Kuz'min's method.

3.2. Hel-Or's Method

The difference in behavior between chiral and achiral two-dimensional objects under rotation is the basis for an attempt by Hel-Or et al.[53] to develop a measure of chirality. In E^2 a statically achiral object under rotation about a point on the mirror line acquires "dynamic chirality" and exists in two enantiomorphous states that are characterized by the sense of rotation, clockwise or anticlockwise.[54] The two states are symmetry-equivalent and therefore exhibit the same scalar properties. On the other hand, a statically chiral object under rotation exists in two states that are characterized by the fixed sense of chirality of the object combined with the sense of rotation. These two states are symmetry-nonequivalent and may be expected in general to exhibit different scalar properties. The difference in scalar properties, zero for rotating achiral objects and nonzero for rotating chiral objects, might therefore be taken as the basis for a chirality measure of the first kind.

The computational scheme invented by Hel-Or et al. to actualize this difference may be illustrated by the following example. Imagine two objects, an achiral one shaped like the capital letter M and a chiral one shaped like the capital letter F, embedded in a plane full of tiny two-dimensional particles. When rotated in the plane about a point on its mirror line, the M-shaped object will scoop up the same number of particles whether the rotation is clockwise or anticlockwise. In contradistinction, the F-shaped object will scoop up more particles when rotated in one direction than in the other. The difference in collected particles after rotation, appropriately normalized, gauges the chirality of M and F. For the enantiomorph of F in E^2, the measure is the same in magnitude but opposite in sign. Note that, as this example demonstrates, the difference between chiral and achiral objects is discussed by comparison of their states before and after (not

during) the rotation; what is gauged is therefore static rather than dynamic chirality.

An interesting comparison with our work is possible through an analysis of L-shaped objects in which the ratio of legs, a/b, is allowed to vary. The chirality of such an object in E^2 achieves its maximum somewhere within the achiral bounds of $a/b = 1$ and a/b (or b/a) $= 0$, and in Hel-Or's computational scheme this maximum is located in the neighborhood of $a/b = 0.5$.[53a] If we think of the L-shaped object as a right triangle lacking a hypotenuse, we find that a value of about 0.5 as a ratio of sides falls well within the range of values (0.34–0.76) calculated for the most chiral right triangle by the five independent measures discussed in Section 2.3.4.

As regards applications to chemistry,[53b] stringent limitations are placed on molecular representations because Hel-Or's measure works only for simply connected binary shapes,[53a] such as the M-, F-, and L-shaped objects discussed above. More significant in our view is the fact that this measure is incapable of "telling right from left" whenever enantiomorphous shapes are chirally connected;[28b] as noted above,[38] a chiral zero is bound to occur in such a case and corresponds to a chiral object collecting the same number of particles under clockwise and anticlockwise rotations. However, chirality is a symmetry property, and a measure of chirality can therefore be zero if, and only if, the object is achiral. Because this condition is not always fulfilled, Hel-Or's measure fails to qualify as a measure of chirality in the general case.

3.3. Mezey's Method

A chirality measure of the first kind has been devised by Mezey[55] and is based on his approach to molecular shape analysis.[17b] The measure requires the assessment of shape chirality in an object at various levels of resolution. For example, consider three closed curves in the plane ("Jordan curves") J_1, J_2, and J_3, within the interiors of which are inscribed "interior filling animals", $A(J,n)$ (Fig. 13).[56] Figure 13 shows several stages in the stepwise increase in resolution. At the lowest levels the results are clearly unsatisfactory: for $n = 3$ all three curves are approximated by the same $A(J,3)$ even though the curves are all different, and for $n = 5$ all three curves are approximated by chiral $A(J,5)$'s even though J_3 is achiral. However, with an increase in n and progressively higher levels of resolution, the shape of the perimeter of $A(J,n)$ is increasingly constrained to approximate the shape of the surrounding curve. Mezey has shown that for each chiral curve there exists a critical level of resolution that is defined by a finite cell number, n_0, the "chirality index", above which all interior filling animals are chiral.[57] The chirality index then becomes an inverse measure of the chirality of the curve, in the sense that the more pronounced the chirality of the shape, the lower the requisite minimum level of resolution and hence the smaller the value of n_0.

The upper and lower bounds of n_0 are well defined. The upper bound, $n_0 = \infty$, obtains only for achiral Jordan curves, for example J_3 in Figure 13, since the number of cells of the interior filling animal exceeds any finite threshold. The lower bound, $n_0 = 4$, corresponds to the perimeter J_4 of

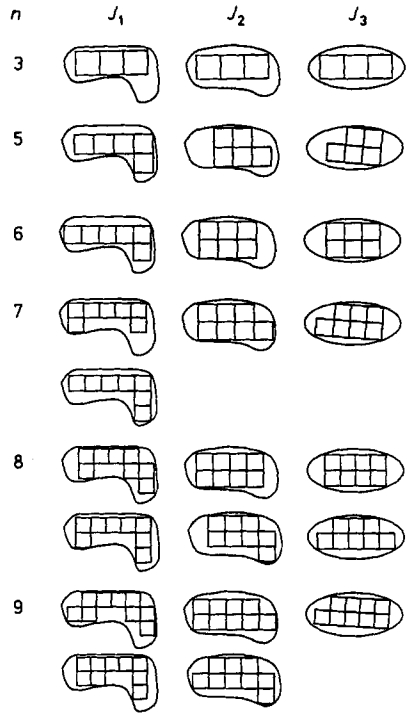

Fig. 13. The n-cell interior filling animals of three curves, J_1, J_2, and J_3, for selected values of n. Curves J_1 and J_2 are chiral, whereas ellipse J_3 is achiral (adapted from [55b]).

"Tippy", the 4-cell animal with C_2 symmetry, since no achiral $A(J,n)$ with $n > 4$ can be inscribed in J_4.[55d] On this basis a "degree of chirality", $\chi(J)$, may be defined [Eq. (l)] whose bounds, 0 and 1, correspond to the upper and lower limits of n_0, respectively.

$$\chi(J) = \frac{1}{n_0 - 3} \qquad \text{(l)}$$

The function $\chi(J)$ is unique among the chirality measures discussed in this review because n_0 can only assume integral values and $\chi(J)$ is therefore not continuous.[58]

The technique for shape characterization described for curves in E^2 is easily extended to three-dimensional bodies; the role of animals are now played by polycubes—cubes joined to one another by shared faces—and the chirality of boundary surfaces are now assessed by the use of interior filling polycubes.[55b, c] All else remains the same, and Equation (l) still applies: as before, the outer bounds on the chirality index are $n_0 = \infty$ for achiral bodies and $n_0 = 4$ for the three-dimensional analog of "Tippy", that is, the C_2-symmetric polycube with $n = 4$.

The concept underlying Mezey's measure is appealing, but there remains the problem of implementation. While the upper and lower bounds of n_0 are well defined, how are the numerical values of n_0, and hence of the degree of chirality, determined in the general case? As a specific example, consider a comparison of J_1 and J_2 in Figure 13: on visual inspection the chirality of J_1 seems more evident than that of J_2; stated differently, the shape of J_2 seems closer to that of the achiral ellipse J_3 than the shape of J_1. Accordingly, the chirality of J_1 should manifest itself at a lower level of resolution than that of J_2, and one would therefore be justified

in expecting a smaller value of n_0 for J_1 than for J_2. In harmony with this qualitative visual ranking, Harary and Mezey have asserted[55b] that $n_0 = 8$ and 15 for J_1 and J_2, respectively. However, this assertion is unsupported by any evidence that all interior filling animals with $n > 8 (J_1)$ and $n > 15 (J_2)$ are chiral. Indeed, the value of n_0 in the general case is a priori unknown, and the levels of resolution that need to be tested before such evidence can be supplied in order to determine n_0 with complete confidence are therefore also a priori unknown. In practice, of course, one can get around this difficulty by setting some upper limit—chosen arbitrarily or on some extraneous grounds, such as computational convenience—to the level of resolution, and then estimating some confidence level for the resulting numerical value of n_0.

4. Scope and Limitations of Chirality Measures

We have seen that there are many ways to approach the problem of quantifying chirality, and that there is great diversity among individual chirality measures. In this section we offer some remarks on the general applicability of these measures.

4.1. Characteristics of the Two Classes

We shall show that chirality measures of the first kind, which depend on the quantification of deviations from achirality, are severely limited in scope because of the need for an achiral reference object. We begin our analysis with examples taken from the realm of chemistry.

In keepint within the spirit of Kelvin's definition (Section 2.1), our discussion so far has focused on applications of chirality measures to geometric objects. As chemists we naturally entertain the hope that such objects might also serve as iconic models[59] of molecules, but geometric objects are rigid entities and thus are limited to the representation of rigid or quasi-rigid[60] structures. Yet there is no dearth of nonrigid (i.e., flexible or fluxional) molecules, whose portrayal by the point group formalism on the fast-exchange time scale "at the very least is a step removed from reality".[61] For such molecules, "dynamic models"[62] in the form of reaction graphs or supergroups[63] are the more appropriate representations.[64] While overlap measures are not affected by molecular nonrigidity—for every chiral structure in conformation space there exists a corresponding enantiomorph—serious difficulties are introduced in the choice of an achiral reference structure for chirality measures of the first kind. These difficulties become acute when "chemical achirality"[65] refers to an achiral ensemble composed of chiral molecules—dubbed "molecular Euclidean rubber gloves"[66]—that undergo rapid enantiomerization *exclusively* through chiral pathways;[67] they become insuperable when the structures to be modeled exhibit topological chirality.

Structures are said to be topologically chiral if the molecular graphs of their enantiomorphs are nonhomeotopic, that is, if they cannot be interconverted by continuous deformations in E^3.[66, 68, 69] Examples are the Simmons–Paquette K_5 molecule,[70] Walba's 3- and 4-rung THYME Möbius ladders,[71] Sauvage's catenane composed of two interlocked oriented rings[72] and his molecular trefoil knot,[73] and the DNA knots and linked loops that are among the subjects of "biochemical topology".[74] It follows that such molecular graphs are incapable of attaining rigidly achiral presentations by continuous deformations in E^3,[75] in contradistinction to the graphs of molecular "Euclidean rubber gloves".[76] The absence of homeotopic achiral comparison standards for intrinsically achiral graphs that have topologically chiral embeddings (e.g., Sauvage's trefoil knot) and the absence of *any* achiral comparison standards for intrinsically chiral topological embeddings (e.g. Walba's 3-rung THYME Möbius ladder) means that the corresponding continuous chirality functions cannot attain a value of zero. It follows that chirality measures of the first kind are ruled out for topologically chiral structures. In contrast, the absence of an achiral zero has no effect on the general applicability of chirality measures of the second kind, since all conceivable conformations (presentations) of molecules with topologically chiral embeddings are matched by their enantiomorphs and may thus be assigned degrees of chirality by such measures.[77] It is clear that this conclusion is general and applies not only to molecules but also to abstract objects regardless of whether they are models of molecules.[78]

While measures of the second kind therefore have a significantly broader range of application than those of the first kind, they too have their limitations. Thus, in measures of common volumes (Sections 2.2.2 and 2.3.3.1) the intersection of the enantiomorphous objects must have the same dimension as the objects themselves; if this condition is not fulfilled, the measures cannot be applied. For example, the degree of chirality of one-dimensional figures in E^3 (e.g. Möbius ladders, knots, rigid helices) or in E^2 (e.g. triangles with no interior points, spirals), or of two-dimensional figures in E^3 (e.g. Möbius strips) cannot be determined by these measures. However, the Hausdorff measure is not limited in the same way; for this reason, and because it is applicable to continuous sets as well as to sets of discrete points, the Hausdorff chirality measure has emerged as the general method of choice for the quantification of chirality.

4.2. Dependence of Ranking on Measure

Molecules may be unambiguously ranked as relatively "more" or "less" chiral according to an agreed criterion,[3] but the ranking depends on the nature of the chosen criterion. The same applies to the ranking of abstract geometric figures. For example, consider two right triangles, A and B, with $\alpha = 18.8°$ and $30°$, respectively, and their degrees of chirality χ as calculated by various measures. According to the measure described in Section 2.3.2.1, A ($\chi = 0.074$) is more chiral than B ($\chi = 0.057$) (see Table 1), whereas according to the measure described in Section 2.3.2.2, B ($\chi = 0.500$) is more chiral than A ($\chi = 18.8/60 = 0.313$). Such reversals in the rank ordering of chiral figures are direct consequences of differences in the functions that express the degree of chirality; see also Section 2.3.4. In short, *the ranking of objects according to degree of chirality generally depends on the particular function that is chosen as the chirality measure.*

From all that has been said, it should be abundantly clear that there is no unique answer to the question: what is the shape of the most chiral member in a given class of objects. Nevertheless, it seems reasonable to assume that, regardless of which measure is chosen, maximal chirality of an object is attainable in general only when all constraints on the shape of the object are relaxed. The evidence so far fully supports this assumption. Thus, for each of the four independent measures in Section 2.3, the degree of chirality of the most chiral right triangle is less than that of the most chiral general triangle (Table 1). As another example, according to each of the two independent measures in Section 2.4, the degree of chirality of the most chiral tetrahedron increases with a decrease in symmetry from D_2 to C_1. The last result suggests that *the most chiral figure (object) in E^n is invariably the least symmetric.*

5. Summary and Future Prospects

Every geometric figure—and every rigid molecular model—is either chiral or achiral, and no figure is both; the set of all figures is thus partitioned into two disjoint, complementary subsets.[5,8] Nevertheless, within the domain of chiroids it is possible to measure degrees of chirality and to rank chiroids as "more" or "less" chiral, depending on the measure. As we have defined them, chirality measures are real-valued and continuous functions that are zero if, and only if, the object is achiral and that should ideally be similarity invariant. We find that these measures fall into two categories: those that gauge the extent to which a chiroid differs from an achiral reference object (measures of the first kind) and those that gauge the extent to which two enantiomorphs differ from one another (measures of the second kind).

In this review we have described some of the many chirality measures that might in principle be devised. Our principal conclusions are that measures of the second kind have, in general, a significantly wider range of application than those of the first kind, that chirality rank depends on the measure, that the bounds of each chirality measure are dictated by the nature of the function so that the shape of the most chiral object in a given class differs from measure to measure, that maximum chirality is associated with minimum symmetry, and that the union of an object and its mirror image is achiral under conditions of optimal overlap.

Efforts to quantify chiral shapes have so far been limited to geometric figures and to rigid models of molecules; future work might be devoted to broadening the scope of these studies by addressing related problems in dynamic and topological chirality. Beyond this, there remains the daunting challenge of bridging the gap between the results of chiral shape analysis and the world of experimental observables. There has been no shortage of precedent for this type of correlation: beginning with Guye's "produit d'asymétrie" in 1890 and continuing to the present day, great ingenuity has been expended in the design of chirality functions to model pseudoscalar physical and chemical properties. Although these models have so far found rather limited utility, it may not be naive to expect that the type of approach described in this review will eventually prove useful in correlating molecular shape with properties arising from molecular chirality.

We thank Victor Klee (Seattle) and Paul Mezey (Saskatoon) for helpful discussions, Viktor Kuz'min (Odessa) for permission to cite unpublished results from his laboratory, and the National Science Foundation (U.S.A.) for support of this work. T. Auf der Heyde thanks the University of the Western Cape for leave of absence, and the Foundation for Research Development (South Africa) for financial assistance.

Received: January 13, 1992 [A 872 IE]
German version: *Angew. Chem.* **1992**, *104*, 1012

[1] a) E. Baer, H. O. L. Fischer, *J. Biol. Chem.* **1939**, *128*, 463, 475; H. O. L. Fischer, E. Baer, *Chem. Rev.* **1941**, *29*, 287; b) W. Schlenk, Jr., *Angew. Chem.* **1965**, *77*, 161; *Angew. Chem. Int. Ed. Engl.* **1965**, *4*, 139; c) *J. Am. Oil Chemists' Soc.* **1965**, *42*, 945.

[2] J. D. Morrison, H. S. Mosher, *Asymmetric Organic Reactions*, Prentice Hall, Englewood Cliffs, **1971**, p. 5.

[3] "An Epistemological Note on Chirality": K. Mislow, P. Bickart, *Isr. J. Chem.* **1976/77**, *15*, 1. In this paper we pointed out that it is "permissible to speak of degrees of chirality, and to compare molecules or molecular ensembles by the use of expressions such as 'more' or 'less' chiral or achiral."

[4] In addition to optical rotatory power (rotationai strength), chiral discriminations between enantiomers or between enantiotopic groups may also be expressed on the scale of a numerically valued variable. These discriminations result from the differential interaction of enantiomers or of enantiotopic groups (which are necessarily incorporated in an achiral molecule) with a chiral environment (reagent, solvent, surface, field, etc.); examples include different reaction rates with a chiral reagent (e.g. an enzyme), NMR chemical shift differences in a chiral solvent or in the presence of a chiral shift reagent, and different rates of elution from a chiral column. Symmetry arguments suffice to explain the existence of chiral discriminations, but separate theoretical models appropriate to each type of observation are required to account for their magnitude and direction. For partial overviews, see S. F. Mason, *Molecular Optical Activity and the Chiral Discriminations*, Cambridge University Press, Cambridge, **1982**; *Asymmetric Synthesis Vol. 1: Analytical Methods* (Ed.: J. D. Morrison), Academic Press, New York, **1983**; *Chiral Liquid Chromatography* (Ed.: W. J. Laugh), Chapman and Hall, New York, **1989**.

[5] Even if all three compounds are to all appearances optically inactive (i.e., "crypto-active" [1c]), the model still demands different levels of optical activity below the operational null [3].

[6] In this view, enantiomers are time-dependent molecular states with very long tunneling times, that is, kinetically stable states and therefore individually (separately) observable. Beginning with Hund's "Paradoxon der optischen Isomeren" [F. Hund, *Z. Phys.* **1927**, *43*, 805], the quantum-mechanical treatment of molecular structure has raised issues that profoundly affect theories of molecular chirality. Most notable among these is the radical proposition, advanced by Woolley, that if nuclear and electronic motions are not separated (i.e., in the absence of the Born-Oppenheimer approximation), *isolated* molecules in stationary (time-independent) quantum states are spherically symmetric and thus lack all of the features that are associated with molecular shape, including chirality. However, the question becomes moot if the model of the molecule is based on observations of bulk matter, that is, of molecules in a many-body environment. See "Quantum Theory and Molecular Structure": R. G. Woolley, *Adv. Phys.* **1976**, *25*, 27; "Must a Molecule Have a Shape?": R. G. Woolley, *J. Am. Chem. Soc.* **1978**, *100*, 1073; "Natural Optical Activity and the Molecular Hypothesis": R. G. Woolley, *Struct. Bonding (Berlin)* **1982**, *52*, 1. For commentary on these ideas, see, inter alia, L. D. Barron, *J. Am. Chem. Soc.* **1979**, *101*, 269; C. Trindle, *Isr. J. Chem.* **1980**, *19*, 47; P. Claverie, S. Diner, *ibid.* **1980**, *19*, 54; R. A. Harris, L. Stodolsky, *J. Chem. Phys.* **1981**, *74*, 2145; A. Julg, *Croat. Chem. Acta* **1984**, *57*, 1497; S. J. Weininger, *J. Chem. Educ.* **1984**, *61*, 939; P. Claverie, G. Jona-Lasinio, *Phys. Rev. A* **1986**, *33*, 2245; B. R. Fischer, P. Mittelstaedt, *Phys. Lett. A* **1990**, *147*, 411.

[7] The parity-violating weak neutral current perturbation lifts the degeneracy of space-inverted enantiomers, for example, D- and L-alanine; an *exact* degeneracy exists only between a chiral molecule and its mirror image composed of antiparticles, such as D-alanine and L-"anti"-alanine or D-"anti"-alanine and L-alanine. Barron [8a] has emphasized that this parity-violating energy difference, which is of the order of 10^{-18} kcal mol^{-1}, obtains only for systems whose sense of chirality is invariant to time reversal, that is, for systems that are able to support time-even pseudoscalar observables. As he has noted, the helical sense of a spinning sphere that is translating along its spin axis, or of a circularly polarized photon or a longitudinally polarized electron, is also invariant to time (i.e., motion) reversal. In contrast, the sense of chirality of a cone spinning about but not translating along its axis is reversed by time reversal.

[8] a) L. D. Barron, *Mol. Phys.* **1981**, *43*, 1395; *Chem. Phys. Lett.* **1981**, *79*, 392; *ibid.* **1986**, *123*, 423; *Chem. Soc. Rev.* **1986**, *15*, 189; *J. Am. Chem. Soc.*

1986, *108*, 5539; *Biosystems* **1987**, *20*, 7; L. D. Barron in [55a], p. 1; b) L. D. Barron, *Molecular Light Scattering and Optical Activity*, Cambridge University Press, Cambridge, **1982**.

[9] R. J. Haüy, *Traité de minéralogie*, Vol. I, Louis, Paris, **1801**, p. 193; Vol. II, pp. 60–65 and 413–414; Vol. V, plates XIX and XL; b) J. F. W. Herschel, *Trans. Cambridge Philos. Soc.* **1822**, *1*, 43.

[10] a) L. Pasteur, *Ann. Chim. Phys.* **1848**, *24*, 442; *ibid.* **1850**, *28*, 56; *ibid.* **1853**, *38*, 437; "De la Dissymétrie Moléculaire": L. Pasteur, *Leçons de Chimie Professées en 1860*, Lib. Hachette, Paris, **1861**, pp. 1–48; b) For a historical overview, see S. H. Mauskopf, *Trans. Am. Philos. Soc.* **1976**, *66*, 1; G. L. Geison, J. A. Secord, *Isis* **1988**, *79*, 6.

[11] According to a principle attributed to F. E. Neumann [A. V. Shubnikov, V. A. Koptsik, *Symmetry in Science and Art*, Plenum, New York, **1974**, p. 334; J. D. Donaldson, S. D. Ross, *Symmetry and Stereochemistry*, John Wiley, New York, **1972**, p. 132], the properties of a system are invariant with respect to its symmetry operations. In a famous aphorism by Curie [P. Curie, *J. Phys. Theor. Appl. Ser. 3*, **1894**, *3*, 393], "c'est la dissymétrie qui crée le phénomène," that is, observable phenomena result from a lowering of the symmetry (desymmetrization) of the system. Thus, all manifestations of chirality originate from a single source: the absence of improper rotations in the symmetry group that describes the system under observation.

[12] The classic text by Gardner [a) M. Gardner, *The Ambidextrous Universe*, Basic Books, New York, **1964**; 2nd ed.: Charles Scribner, New York, **1979**, b) *The New Ambidextrous Universe*, 3rd ed., Freeman, New York, **1990**] remains the premier popularization of the left-right dichotomy in Nature.

[13] W. T. Kelvin, *Baltimore Lectures on Molecular Dynamics and the Wave Theory of Light*, C. J. Clay, London, **1904**, pp. 439, 618–619; see also L. L. Whyte, *Nature (London)* **1957**, *180*, 513; *ibid.* **1958**, *182*, 198; *Leonardo* **1975**, *8*, 245. From Kelvin's definition it follows that the chirality of an object is a function of the object's *shape*. Thus, to achieve chirality it is not sufficient to assign different labels to parts of an achiral object. For example, an irregular tetrahedron is chiral, but a regular tetrahedron in which the four different vertices are distinguished by different indices (labels) is not.

[14] Any function that does not satisfy this conditio sine qua non fails to qualify as a measure of chirality. An egregious example is a recently proposed "chirality measure" [D. Avnir, A. Y. Meyer, *J. Mol. Struct. (Theochem)* **1991**, *226*, 211] that gives "chirality values" for achiral halogenated normal alkanes: not only are these values not zero but they are even higher than the "chirality values" of the corresponding chiral halogenated alkanes!

[15] B. Grünbaum, *Proc. Symp. Pure Math. Am. Math. Soc.* **1963**, *7*, 233.

[16] In geometry, similarity is an equivalence relation among figures that preserves shape. See H. S. M. Coxeter, *Introduction to Geometry*, 2nd ed., Wiley, New York, **1969**.

[17] a) This includes objects that are models of molecules. b) On the related subject of "molecular similarity", see "A Review and Examination of the Mathematical Spaces Underlying Molecular Similarity Analysis": M. A. Johnson, *J. Math. Chem.* **1989**, *3*, 117; *Concepts and Applications of Molecular Similarity*, (Eds.: M. A. Johnson, G. M. Maggiora), Wiley-Interscience, New York, **1990**; "The Degree of Similarity of Three-dimensional Bodies: Application to Molecular Shape Analysis": P. G. Mezey, *J. Math. Chem.* **1991**, *7*, 39; see also "Similarity and Complexity of the Shapes of Square-Cell Configurations": F. Harary, P. G. Mezey, *Theor. Chim. Acta* **1991**, *79*, 379.

[18] a) The "common volume" measure of chirality exemplified here is a straightforward extrapolation of Kitaigorodskii's proposal [A. I. Kitaigorodskii, *Organic Chemical Crystallography*, Consultants Bureau, New York, **1961**, p. 230] that the resemblance in the shapes of two molecular models M and M' may be gauged by superimposition of M on M' in such a way that the nonoverlapping volumes equal some minimum value Δ: "If the overlapping volumes add up to τ, then $\varepsilon = 1 - \Delta/\tau$ is the degree of molecular isomorphism". If M and M' denote enantiomorphous chiroids, the fraction of nonoverlapping volumes under conditions of maximal overlap beomes a measure of the degree of chirality. b) See also B. Chion, J. Lajzerowicz, D. Bordeaux, A. Collet, J. Jacques, *J. Phys. Chem.* **1978**, *82*, 2682; G. Gilat, L. S. Schulman, *Chem. Phys. Lett.* **1985**, *121*, 13; G. Gilat, *J. Phys. A.: Math. Gen.* **1989**, *22*, L545; *Found. Phys. Lett.* **1990**, *3*, 189; A. Y. Meyer, W. G. Richards, *J. Comput. Aided Mol. Des.* **1991**, *5*, 427.

[19] a) J. H. van 't Hoff, *Voorstel tot uitbreiding der tegenwoordig in de scheikunde gebruikte structuur-formules in de ruimte*, J. Greven, Utrecht **1874**; *Arch. Néerl. Sci. Exactes Nat.* **1874**, *9*, 445; *Bull. Soc. Chim. Fr.* **1875**, *23*, 295; *La Chimie dans l'Espace*, P. M. Bazendijk, Rotterdam, **1875**; b) J. A. LeBel, *Bull. Soc. Chim. Fr.* **1874**, *22*, 337; see also D. F. Larder, *J. Chem. Educ.* **1967**, *44*, 661; J. Weyer, *Angew. Chem.* **1974**, *86*, 604; *Angew. Chem. Int. Ed. Engl.* **1974**, *13*, 591; *van 't Hoff-LeBel Centennial*, (Ed.: O. B. Ramsay): (ACS Symp. Ser. **1975**, *12*).

[20] a) A. B. Buda, T. P. E. Auf der Heyde, K. Mislow, *J. Math. Chem.* **1991**, *6*, 243; b) T. P. E. Auf der Heyde, A. B. Buda, K. Mislow, *ibid.* **1991**, *6*, 255.

[21] a) A. B. Buda, K. Mislow, *J. Mol. Struct. (Theochem)* **1991**, *232*, 1; b) *Elemente der Mathematik* **1991**, *46*, 65; c) A. B. Buda, T. P. E. Auf der Heyde, K. Mislow, unpublished.

[22] N. G. Harvey, D. Mirajovsky, P. L. Rose, R. Verbiar, E. M. Arnett, *J. Am. Chem. Soc.* **1989**, *111*, 1115; H. M. McConnell, V. T. Moy, *J. Phys. Chem.* **1988**, *92*, 4520; G. A. Somorjai, *ibid.* **1990**, *94*, 1013.

[23] Two-dimensional chirality has also served as a teaching tool in stereochemistry: C. E. Wintner, *J. Chem. Educ.* **1983**, *60*, 550.

[24] P.-A. Guye, *C. R. Hebd. Seances Acad. Sci.* **1890**, *110*, 714.

[25] In considering a formula that might relate optical rotation to parameters (κ) associated with the ligands attached to the "asymmetric carbon atom," Crum Brown [A. Crum Brown, *Proc. R. Soc. Edinburgh* **1890**, *17*, 181] independently concluded that "we may presume that it contains the product of the differences of the κ's."

[26] P.-A. Guye, *C. R. Hebd. Seances Acad. Sci.* **1893**, *116*, 1378, 1451, 1454.

[27] Ruch et al. [28] have defined a function $\chi(\lambda)$ with reference to a model in which a set of n ligands is partitioned among the n sites of an achiral permutation skeleton, such as a regular tetrahedron, and in which λ is a transferable, ligand-specific, scalar parameter with a physical dimension, for example polarizability, or with geometrical properties.

[28] a) E. Ruch, I. Ugi, *Theor. Chim. Acta* **1966**, *4*, 287; E. Ruch, A. Schönhofer, I. Ugi, *ibid.* **1967**, *7*, 420; E. Ruch, A. Schönhofer, *ibid.* **1968**, *10*, 91; E. Ruch, *ibid.* **1968**, *11*, 183; E. Ruch, I. Ugi, *Top. Stereochem.* **1969**, *4*, 99; E. Ruch, A. Schönhofer, *Theor. Chim. Acta* **1970**, *19*, 225; E. Ruch, *Acc. Chem. Res.* **1972**, *5*, 49; A. Mead, E. Ruch, A. Schönhofer, *Theoret. Chim. Acta* **1973**, *29*, 269; b) E. Ruch, *Angew. Chem.* **1977**, *89*, 67; *Angew. Chem. Int. Ed. Engl.* **1977**, *16*, 65; see also I. Ugi, *Chimia* **1965**, *19*, 89; I. Ugi, *Z. Naturforsch. B* **1965**, *20*, 405; J. H. Brewster, *Top. Stereochem.* **1967**, *2*, 1; C. A. Mead, *Top. Curr. Chem.* **1974**, *49*, 1; R. B. King, *J. Math. Chem.* **1988**, *2*, 89, and references cited therein; *ibid.* **1991**, *7*, 69; R. B. King in [55a], p. 131; G. Derflinger in *Chirality – From Weak Bosons to the α-Helix*, (Ed.: R. Janoschek) Springer, Berlin, **1991**, p. 34.

[29] Only five tetrahedral symmetries, T_d, C_{3v}, C_{2v}, C_s, and C_1 are possible for $P(I)$ under the α-constraint. These are the same five symmetries that result from different ligand partitions on a regular tetrahedral permutation skeleton.

[30] In a construct used by Boys to model optical rotatory power [S. F. Boys, *Proc. R. Soc. London A*, **1934**, *144*, 675], four spheres are brought into mutual contact so that their centers form the vertices of a tetrahedron, the length of each edge of which is equal to the sum of the radii of two spheres. Boys remarked that the variables "were termed the radii of repulsion of the radicals, but rather than representing any exact physical quantity they must be regarded more as parameters used to express the shape of the molecule". For any given symmetry, this shape is obviously different from that of Ruch's model in which the same four spheres are centered at the vertices of a regular tetrahedron; the shape of this model is given by a different chirality product.

[31] Gothic arches based on the same geometric design can be found in windows of the cathedral of Reims built during 1211–1221. See B. Artmann, *The Mathematical Intelligencer* **1991**, *13*, 44.

[32] P. Murray-Rust, H. B. Bürgi, J. D. Dunitz, *Acta Crystallogr. Sect. B34* **1978**, 1787, 1793; *Acta Crystallogr. Sect. A35*, **1979**, 703.

[33] F. A. Cotton, *Chemical Applications of Group Theory*, 3rd ed., Wiley-Interscience, New York, **1990**; S. F. A. Kettle, *Symmetry and Structure*, Wiley, New York, **1985**.

[34] This difference arises from the labeling convention adopted in Figure 1. Consider, for example, applying the labels a, b, and c to the sides of a given scalene triangle, with $a < b < c$. When the labels a and b are transposed, the sense of cyclic directionality (orientation) of the labels is reversed. Therefore, in order to preserve the same orientation of labels for both inequalities, $a < b < c$ and $b < a < c$, as required by the convention, enantiomorphs of the triangle will have to be considered. The two segments of the shape space (Fig. 2) in which the representative points for the enantiomorphs will be found hence represent enantiomorphous triangles labeled in the same sense.

[35] O. Giering, *Elemente der Mathematik* **1967**, *22*, 5.

[36] The same bound was found by Nohl [W. Nohl, *Elem. Math.* **1962**, *17*, 59] for centric convex sets in E^2, with equality for a special class of parallelograms, and by Bondensen and Dou [A. Bondensen, J. Dou, *Crux Mathematicorum*, **1989**, (3), pp. 78–87], who proved that any triangular piece of paper of area 1 can be folded once so that, when placed on a table, it will cover an area of less than $2 - \sqrt{2}$. We are grateful to Professor J. C. Fisher (Regina) for drawing our attention to this proof.

[37] a) F. Hausdorff, *Set Theory*, transl. by J. R. Aumann et al., Chelsey, New York, **1957**, pp. 166–168. b) The following formulation of Hausdorff's definition was suggested to us by Professor V. Klee (Seattle). The Hausdorff distance $h(Q,Q')$ between sets Q and Q' is the smallest number δ that has the following two properties: 1) each spherical ball of radius δ centered at any point of Q contains at least one point of Q'; 2) each spherical ball of radius δ centered at any point of Q' contains at least one point of Q.

[38] Rassat [A. Rassat, *C.R. Acad. Sci. Ser. 2* **1984**, *299*, 53] has proposed a classification of geometric figures A as right- or left-handed, depending on which of two Hausdorff distances, $h_{min}(A,B)$ or $h_{min}(A,B')$ in our notation, is the smaller, where B and B' are the enantiomorphs of an arbitrarily chosen reference figure (such as a chiral tetrahedron). If A is achiral, $\delta h_{min} = h_{min}(A,B) - h_{min}(A,B') = h_{min}(A,B) - h_{min}(A',B) = 0$, where A' is

the mirror image of A. However, δh_{min} may also zero if A is chiral. Such "chiral zeros" are bound to occur whenever two enantiomorphs are chirally connected [28b, 39]. In such a case it is difficult to see how Rassat's scheme can be of any use in assigning a sense of chirality to A, since nothing less than a change to a different set of arbitrarily chosen reference enantiomorphs is required to lift the "cryptochirality" [3] of A. It follows from the existence of chiral zeros that the achirality of A is a sufficient but not a necessary condition for $\delta h_{min} = 0$, and that δh_{min} is therefore in general unsuitable as a chirality measure.

[39] Asymmetric tetrahedrons, in Ruch's simile [28b], are potato-like, since an asymmetric tetrahedron (or any four points asymmetrically distributed in E^3) and its mirror image are chirally connected. That is, connecting paths exist by which the enantiomorphs can be interconverted by continuous deformation without ever passing through an achiral shape. An important corollary follows: *concepts like "left-handed" and "right-handed" with reference to asymmetric tetrahedra are meaningless.* Indeed, because the tetrahedron is the simplex in E^3, every such classification is meaningless (or at best arbitrary) for any object in E^3 in the absence of well-defined constraints. In contrast, all scalene triangles are partitioned into heterochiral sets (Section 2.3.2.1).

[40] W. H. Press, B. P. Flannery, S. A. Teukolsky, W. T. Vetterling, *Numerical Recipes*, Cambridge University Press, Cambridge, **1986**. See also C. G. Broyden, *J. Inst. Math. Its Appl.* **1970**, *6*, 222; R. Fletcher, *Comput. J.* **1970**, *13*, 317; B. Goldfarb, *Math. Comput.* **1970**, *24*, 23; D. F. Shanno, *ibid.* **1970**, *24*, 647.

[41] An extremal triangle corresponding to the supremum of the functions described in Sections 2.3.2.1, 2.3.2.2, and 2.3.3.1 does not exist, and is only approached in the limit. This finding is consistent with the noncompactness of the space of similarity invariant triangles. Grünbaum [15] has pointed out that the space of similarity invariant convex sets is noncompact; see also B. A. deValcourt, *Isr. J. Math.* **1966**, *4*, 65. Thus, the range of measures defined on such sets is bounded but may not be closed, and it follows that the bounds of the measures may not be attainable.

[42] T. Damhus, C. E. Schäffer, *Inorg. Chem.* **1983**, *22*, 2406.

[43] These measures are qualitatively correlated to the rotational strength, as given by the coupled oscillator model [8b], of a system consisting of two diatomic molecules arrayed as described above; homonuclear molecules are then modeled by nonoriented lines and heteronuclear molecules by oriented lines.

[44] A different measure of helicity is given by the volume of a cylinder on the surface of which is inscribed one complete turn of a helical thread [J. H. Brewster, *Top. Curr. Chem.* **1974**, *47*, 29]. If L denotes the height of the cylinder, that is, the pitch of the helix, and D the length of the thread, then, according to Brewster's analysis, the volume of the cylinder is at a maximum when $L = D/\sqrt{3}$. Maximum helicity is therefore achieved when the angle of rise is $\arcsin 3^{-1/2} \approx 35.3°$.

[45] Of the five chiral subsymmetries of T_d, two (C_3 and T) cannot be realized by a tetrahedron [V. Prelog, G. Helmchen, *Helv. Chim. Acta* **1972**, *55*, 2581].

[46] a) R. Hoffmann, R. W. Alder, C. F. Wilcox, Jr., *J. Am. Chem. Soc.* **1970**, *92*, 4992; b) J. B. Collins, J. D. Dill, E. D. Jemmis, Y. Apeloig, P. von R. Schleyer, R. Seeger, J. A. Pople, *ibid.* **1976**, *98*, 5419; c) W. Luef, R. Keese, H. B. Bürgi, *Helv. Chim. Acta* **1987**, *70*, 534; d) G. Erker, R. Zwettler, C. Krüger, R. Noe, S. Werner, *J. Am. Chem. Soc.* **1990**, *112*, 9620.

[47] Edge AE of the T_2 conformation space maps degenerate tetrahedrons for which, first, vertex 1 is infinitely far from vertices 2, 3, and 4 (face ABE in Fig. 9), and, second, vertex 3 is contained within the tetrahedral face formed by vertices 1, 2, and 4 (face ADE).

[48] If the constraints of D_2 or C_2 symmetry are not relaxed, interconversion of enantiomorphs unavoidably requires passage through an achiral shape. The set of achiral shapes then constitutes a boundary that separates two heterochiral classes, and it becomes possible to describe such tetrahedrons as "left-handed" or "right-handed" with reference to an arbitrarily chosen coordinate system. See also [39].

[49] Rotation about the third axis yields a union that corresponds to a local minimum with a much larger value of $h(Q,Q')$ (0.44).

[50] a) V. E. Kuz'min, I. B. Stel'makh, *Zh. Strukt. Khim.* **1987**, *28*, 45, 50; V. E. Kuz'min, I. B. Stel'makh, *Dokl. Akad. Nauk SSSR* **1989**, *307*, 150; L. A. Kutulya, V. E. Kuz'min, I. B. Stel'makh, I. B. Nemchenok, T. V. Khandrimailova, *Zh. Obshch. Khim.* **1990**, *60*, 737; b) V. E. Kuz'min, et al., *J. Phys. Org. Chem.*, in press.

[51] L. D. Landau, E. M. Lifschitz, *Course of Theoretical Physics Vol. 1: Mechanics*, 3rd ed., Pergamon Press, Oxford, **1976**.

[52] For details, see [50]. Note that the work reported in our review describes a minor modification [50b] of the earlier approach in [50a].

[53] a) "How to tell Right from Left": Y. Hel-Or, S. Peleg, H. Zabrodsky, *Proc. IEEE Comput. Vision Pattern Recognition* **1988**, 304; b) Y. Hel-Or, S. Peleg, D. Avnir, *Langmuir* **1990**, *6*, 1691.

[54] Dynamic chirality in E^2 cannot be invariant to time reversal because, to achieve invariance, a third spatial dimension is needed for the required translation along the spin axis [7].

[55] a) *New Developments in Molecular Chirality*, (Ed.: P. G. Mezey), Kluwer, Dordrecht, **1991**; b) F. Harary, P. G. Mezey in [55a], p. 241; c) P. G. Mezey in [55a], p. 257; d) P. G. Mezey, *J. Math. Chem.*, in press.

[56] A lattice "animal" is a graph consisting of n square cells that are joined to one another by shared edges. The number of animals with intrinsically different (i. e., symmetry-nonequivalent) shapes is 1, 1, 2, 5, and 12 for $n = 1, 2, 3, 4$, and 5, respectively. Among the five animals with four cells, two are chiral, and among the twelve animals with five cells, six are chiral. An n-cell animal $A(J,n)$ inscribed in a Jordan curve J is said to be "interior filling" if, and only if, no animal of the same cell size and with more than n cells can be inscribed in J [55b].

[57] Let $a(J)$ denote the interior area of any chiral Jordan curve J. There exists a maximal achiral subset S of J whose area, $a(S)$, can be inscribed in J. Since J is chiral, some area, $a(J) - a(S)$, must be left over. By sufficiently reducing the size of the cells, interior filling animals $A(J,n \geq n_0)$ can therefore always be generated whose areas $a(A)$ are larger than $a(S)$, that is, $a(J) \geq a(A) > a(S)$. It follows that all such animals are chiral [55d].

[58] Kelvin's definition of chirality (Section 2.1), when analyzed from an algebraic point of view, also implicitly contains a proposition for a noncontinuous measure of chirality, $k(Q)$. This can be paraphrased as follows: if any geometrical figure or set of points, Q, can be brought to coincide with its mirror image, then $k(Q) = 0$ (object is not chiral); otherwise $k(Q) = 1$ (object is chiral). The implications of this "black-and-white" or binary approach to chirality have been discussed *in* [3].

[59] "The Hierarchy of Models in Chemistry": C. Trindle, *Croat. Chem. Acta* **1984**, *57*, 1231; "Models and Modeling in Theoretical Chemistry": J. Tomasi, *J. Mol. Struct. (Theochem)* **1988**, *179*, 273.

[60] We refer here to structures whose nuclei undergo small-amplitude librations about well-defined equilibrium positions.

[61] E. L. Muetterties, *Inorg. Chem.* **1965**, *4*, 769. See also F. A. Cotton, J. W. Faller, A. Musco, *J. Am. Chem. Soc.* **1968**, *90*, 1438; F. A. Cotton, *Acc. Chem. Res.* **1968**, *1*, 257.

[62] "Molecular Machinery in Organic Chemistry": K. Mislow, *Chemtracts Org. Chem.* **1989**, *2*, 151.

[63] a) Molecular symmetry (permutation–inversion) groups ["The Symmetry Groups of Non-rigid Molecules": H. C. Longuet-Higgins, *Mol. Phys.* **1963**, *6*, 445; see also "Symmetry beyond Point Groups in Molecular Spectroscopy": J. T. Hougen, *J. Phys. Chem.* **1986**, *90*, 562; "Self-Inverse and Non-Self-Inverse Degenerate Isomerizations": J. G. Nourse, *J. Am. Chem. Soc.* **1980**, *102*, 4883]; b) isometric groups ["Isometric Groups and Chirality of Nonrigid Molecules: A Generalization of Kelvin's Theorem": H. Frei, Hs. H. Günthard, *Chem. Phys.* **1976**, *15*, 155; see also "The Isometric Group of Nonrigid Molecules": H. Frei, A. Bauder, Hs. H. Günthard, *Top. Curr. Chem.* **1979**, *81*, 1]; c) chemical identity groups ["A Group Theoretical Analysis of Conformational Flexibility": J. Dugundji, J. Showell, R. Kopp, D. Marquarding, I. Ugi, *Isr. J. Chem.* **1980**, *20*, 20; see also I. Ugi, J. Dugundji, R. Kopp, D. Marquarding: *Perspectives in Theoretical Stereochemistry* (*Lect. Notes Chem.* **1984**, *36*) Chapters I, VI].

[64] The time-average symmetry, as given by the molecular symmetry (MS) group [63a], may sometimes be isomorphic to the point group of an intuitively appealing time-average structure at the fast exchange limit, as in the case of NH_3 (D_{3h}) or cyclohexane (D_{6h}). However, such convenient coincidences cannot always be counted on. For example, the MS groups of ethane and PF_5 appropriate to the fast exchange limit are isomorphic to $D_3 \times D_3$ (order 36) and $S_5 \times S_2$ (order 240), respectively. Neither group corresponds to the symmetry of any conceivable conformation of these molecules [J. Reisse, R. Ottinger, P. Bickart, K. Mislow, *J. Am. Chem. Soc.* **1978**, *100*, 911].

[65] As defined by Ugi et al. [63c], a molecule is "chemically achiral" if each momentary geometry of the molecule can be superposed on its mirror image by using the rotations, translations, *and* intramolecular motions that can occur under the given observation conditions. Chemical achirality is thus a special case of "stochastic achirality" [3].

[66] D. M. Walba in [55a], p. 119.

[67] a) *meso*-Biphenyls/internal rotation: K. Mislow, *Science (Washington, D.C.)* **1954**, *120*, 232; K. Mislow, R. Bolstad, *J. Am. Chem. Soc.* **1955**, *77*, 6712; K. Mislow, *Introduction to Stereochemistry*, Benjamin, New York, **1965**, pp. 91–93; see also G. W. Wheland, *Advanced Organic Chemistry*, 3rd ed., Wiley, New York, **1960**, p. 278ff.; b) molecular propellers/two-ring flip: D. Gust, K. Mislow, *J. Am. Chem. Soc.* **1973**, *95*, 1535; K. Mislow, *Acc. Chem. Res.* **1976**, *9*, 26; R. Glaser, J. F. Blount, K. Mislow, *J. Am. Chem. Soc.* **1980**, *102*, 2777; c) molecular gears/correlated rotation: W. D. Hounshell, C. A. Johnson, A. Guenzi, F. Cozzi, K. Mislow, *Proc. Natl. Acad. Sci. USA* **1980**, *77*, 6961; A. Guenzi, C. A. Johnson, F. Cozzi, K. Mislow, *J. Am. Chem. Soc.* **1983**, *105*, 1438; d) phosphoranes/Berry pseudorotation: E. L. Muetterties, *Inorg. Chem.* **1967**, *6*, 635; see also K. Mislow, *Acc. Chem. Res.* **1970**, *3*, 321.

[68] "Stereochemical Topology": D. M. Walba in *Chemical Applications of Topology and Graph Theory*, (Ed.: R. B. King), Elsevier, Amsterdam, **1983**, p. 17; "Topological Stereochemistry": D. M. Walba, *Tetrahedron* **1985**, *41*, 3161; "Topological Stereochemistry: Knot Theory of Molecular Graphs": D. M.Walba in *Graph Theory and Topology in Chemistry*. (Eds.: R. B. King, D. H. Rouvray), Elsevier, Amsterdam, **1987**, p. 23.

[69] On the subject of topological chirality, see also: a) J. Simon, *Topology* **1986**, *25*, 229; J. Simon in *Graph Theory and Topology in Chemistry*. (Eds.: R. B. King, D. H. Rouvray), Elsevier, Amsterdam, **1987**, p. 43; J. Simon,

J. Comput. Chem. **1987**, *8*, 718; b) E. Flapan in *Graph Theory and Topology in Chemistry* (Eds.: R. B. King, D. H. Rouvray) Elsevier, Amstedam **1987**, p. 76; E. Flapan, *Pacific J. Math.* **1987**, *129*, 57; E. Flapan in [55a], p. 209; c) K. C. Millett, *Croat. Chem. Acta* **1986**, *59*, 669; *J. Comput. Chem.* **1987**, *8*, 536; K. C. Millett in [55a], p. 165.

[70] H. E. Simmons III, J. E. Maggio, *Tetrahedron Lett.* **1981**, *22*, 287; L. A. Paquette, M. Vazeux, *ibid.* **1981**, *22*, 291.

[71] D. M. Walba, R. M. Richards, R. C. Haltiwanger, *J. Am. Chem. Soc.* **1982**, *104*, 3219; D. M. Walba, J. D. Armstrong III, A. E. Perry, R. M. Richards, T. C. Homan, R. C. Haltiwanger, *Tetrahedron* **1986**, *42*, 1883.

[72] D. K. Mitchell, J.-P. Sauvage, *Angew. Chem.* **1988**, *100*, 965; *Angew. Chem. Int. Ed. Engl.* **1988**, *27*, 930.

[73] C. O. Dietrich-Buchecker, J.-P. Sauvage, *Angew. Chem.* **1989**, *101*, 192; *Angew. Chem. Int. Ed. Engl.* **1989**, *28*, 189; see also C. O. Dietrich-Buchecker, J. Guilhem, C. Pascard, J.-P. Sauvage, *ibid.* **1990**, *102*, 1202 and **1990**, *29*, 1154; J.-P. Sauvage, *Acc. Chem. Res.* **1990**, *23*, 319.

[74] S. A. Wasserman, N. R. Cozzarelli, *Science (Washington, D.C.)* **1986**, *232*, 951.

[75] This conclusion is valid regardless of whether such graphs are "intrinsically achiral", that is, topologically equivalent (homeomorphic) to achiral embeddings in E^3 (as is the case with knots and links, all of which are homeomorphic to unknotted and unlinked rings), or "intrinsically chiral", that is chiral in all embeddings (like Möbius ladders with an odd number of differentiated rungs). See [66] and [69b].

[76] These graphs *can* attain rigidly achiral presentations by continuous deformation in E^3, even if the presentations correspond to conformations that are unrealistic from a chemical point of view: questions of internal energy are totally disregarded. For example, in the enantiomerization of asymmetric phosphoranes [67d], a planar molecular graph is required for achiral Pabcde.

[77] The sharp differentiation between the two classes of chirality measures confirms that "it is good not to forget the distinction between metrical chirality and the deeper topological chirality" [12b, p. 163].

[78] In this connection we need to comment on an intriguing notion by Walba that classes of molecular graphs may be ranked "by degree of chirality, from most chiral to least chiral" [66]. Walba's "topological hierarchy of molecular chirality" consists of six classes, "three resolvable and three non-resolvable." In our view, the energetics of racemization have no bearing on the degree of chirality of the molecule undergoing racemization, and Walba's scheme may therefore be reduced to four classes: molecular graphs that are topologically and intrinsically chiral, topologically chiral and intrinsically achiral, topologically achiral with no rigidly achiral presentations (e.g. the knot known as 8_{17} [69b], a "topological rubber glove" [66] that has not yet been realized at the molecular level), and topologically achiral with rigidly achiral presentations (all formally achiral molecules, as well as formally chiral molecules such as Nabc, Cabcd, and "molecular Euclidean rubber gloves"). Whatever the merits of this classification might be, Walba's ranking is not a numerical function and is therefore not a measure of chirality.

ANGEWANDTE CHEMIE
A Journal of the Gesellschaft Deutscher Chemiker

Reviews planned or recently published

The Enchanting Alkaloids of Yuzuriha
C.H. Heathcock

Transition Structures of Hydrocarbon Pericyclic Reactions
K.N. Houk, Y. Li, J. D. Evanseck

Natural Products as Probes of Cellular Function
S.L. Schreiber, M.K. Rosen

Synthetic Approaches towards Molecular and Polymeric Carbon
F. Diederich, Y. Rubin

Cubanes: Starting Materials for the 1990s and the New Century
P.E. Eaton

Optically Anomalous Crystals
B. Kahr, J.M. McBride

Chemistry and Biology of the Enediyne Anticancer Antibiotics
K.C. Nicolaou, W.M. Dai

Scanning Tunnel Microscopy and Atomic Force Microscopy in Organic Chemistry
J. Frommer

Synchotron X-Ray and Neutron Diffraction Studies in Solid-State Chemistry
A.K. Cheetham, A.P. Wilkinson

What subscribers and authors have to say about Angewandte Chemie:

Jean-Marie Lehn, Université Louis Pasteur, Strasbourg:

"I consider Angewandte Chemie as one of the top not only chemical but scientific journals... It presents the highly effective combination of well chosen, exciting and thorough review articles, reflecting timely topics that cover a very broad range in science, with short but informative communications reporting specific advances of particular interest for chemistry. It is also carefully produced and nicely presented, which adds to the reading pleasure."

VCH

Special Rate for ACS members: US$ 165.00
US$ 190.00 (air mail)*

To subscribe please call 1-800-422-8824

Annual subscription rate 1992 for institutions: US$ 581.00 (air mail)*

Peptide Nucleic Acids (PNAs)—Unusual Properties of Nonionic Oligonucleotide Analogues

By *Chris Meier*, and *Joachim W. Engels**

There is no molecule more important in the molecular processes in living systems than the DNA double helix. All fundamental functions of life are established by this molecule: the storage, the transfer (replication), as well as the translation (expression) of the genetic information. This is based on the order of only four constituents (nucleosides): deoxyadenosine (dA), deoxyguanosine (dG), thymidine (T), and deoxycytidine (dC). Two nucleosides, dA and T, as well as dG and dC, form Watson–Crick base pairs by association through hydrogen bonds which leads to a double helix in the case of the polymer DNA. For many years the DNA double helix has been a main research topic for chemists because of its uniqueness and importance, as well as its relatively simple construction.

Single-stranded nucleic acids of $n = 3-100$ nucleosides are called oligonucleotides **1** (Scheme 1). Oligomers such as **1** with a defined sequence may be prepared synthetically.

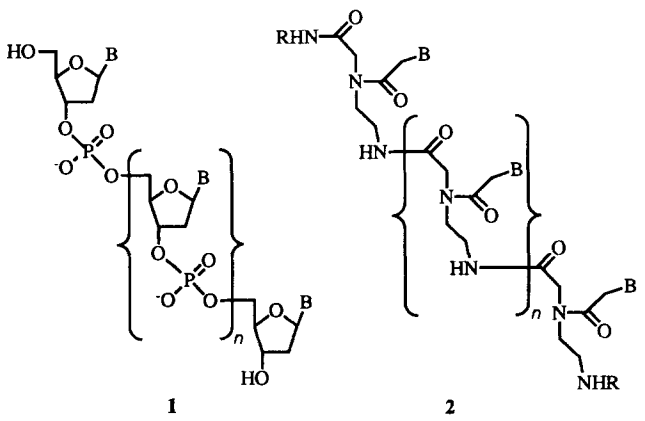

Scheme 1. **2a**, $n = 6$; **2b**, $n = 8$; **2c**, $n = 10$.

They serve as models of the DNA double helix because of their ability to form complementary sequences with oligonucleotides under formation of relatively short double helices, and their physical and biological characteristics are studied. Noncovalent and reversible binding of synthetic oligonucleotides **1** is not restricted to oligomers bearing deoxyriboses (DNA) but is also possible with ribose-containing oligonucleotides (RNA) under duplex formation as well as with a complementary sequence in an intact DNA double helix under triple helix formation.[1] The fact that an oligonucleotide with a definite sequence of 17 nucleosides (17mer oligonucleotide) would find statistically only one exact complementary sequence within the human genome shows the enormous potential of synthetic oligonucleotides. The facile access to **1** as well as several applications (e.g., the application as primers or starter oligonucleotides for the polymerase chain reaction (PCR) amplification technique) were made possible by the introduction of automated oligonucleotide synthesis.[2]

It is not surprising that a new application of oligonucleotides has been recently explored: the development of pharmaceuticals as gene blockers where either the DNA double helix (triple helix formation) or mRNA (double helix formation, antisense approach) are the targets for binding.[3, 4] The advantage of these concepts over present methodologies is obvious. Several regions of the genome of a virus or a cancer cell must be transcribed into mRNA and expressed as proteins for the duplication of these organisms. Many protein molecules are produced from one mRNA copy. If one is able to inhibit the transcription process by triple helix formation or to bind the mRNA copy by an antisense oligonucleotide with a complementary sequence, it could be possible to treat diseases on the DNA or RNA level and not by inhibition of proteins (enzyme blockers). For this purpose unmodified oligonucleotides are not applicable because of their instability to oligonucleotide-degrading enzymes (endo- and exonucleases) and their bad membrane permeation properties. In order to increase nuclease stability as well as improve transport behavior, several modifications were introduced. As analogues of the sugar/phosphate backbone mono- or dithiophosphate, methylphosphonate, phosphotriester oligonucleotides, and nonphosphate nonionic analogues like formacetal-, carbamate-, sulfoxido-, and sulfone-linked species were intensively studied.[5]

A total turn away from this concept of substituting the phosphodiester linkage by isosteric groups was published recently by Egholm, Burchardt, Nielsen, and Berg.[6a, b] They made use of a widely distributed natural polymer as a backbone analogue—the peptides: Taking a monomeric building block that consisted of an amino acid (2-aminoglycine) bearing the nucleobase (thymine) attached with a defined spacer (methylenecarbonyl), they polymerized this monomer according to the Merrifield method of peptide synthesis and obtained a peptide nucleic acid (PNA, **2**; Scheme 1).[6c] The monomeric building block **3** used in the Merrifield synthesis was prepared as follows: Thymine **4** was treated with α-bromomethylacetate **5** in DMF in the presence of potassium carbonate followed by aqueous saponification and DCC-mediated esterification with pentafluorophenol (Pfp) to yield α-thyminylpentafluorophenylacetate **6**. Nucleophilic substitution of **6** by *N*-(*N'*-Boc-aminoethyl)glycine (*N'*-BocAeg, **7**)/triethylamine in DMF and subsequent esterification (Pfp/DCC) gave the Pfp-active ester **3** (Boc-Taeg-OPfp) of the monomer (Scheme 2). **3** was oligomerized under conditions of the "single-coupling protocol"[7] in 30% DMF/methylene chloride on a 4-methylbenzhydrylamino solid support. The yield per step was determined by quantitative ninhydrin analysis (>99%). The cleavage of **2** from the solid support was achieved by treatment with anhydrous HF.

This approach, amazingly simple upon first glance, has some advantages over the applications of modified oligonu-

[*] Prof. Dr. J. W. Engels, Dr. C. Meier
Institut für Organische Chemie der Universität
Niederurseler Hang 29, D-W-6000 Frankfurt/Main 50 (FRG)

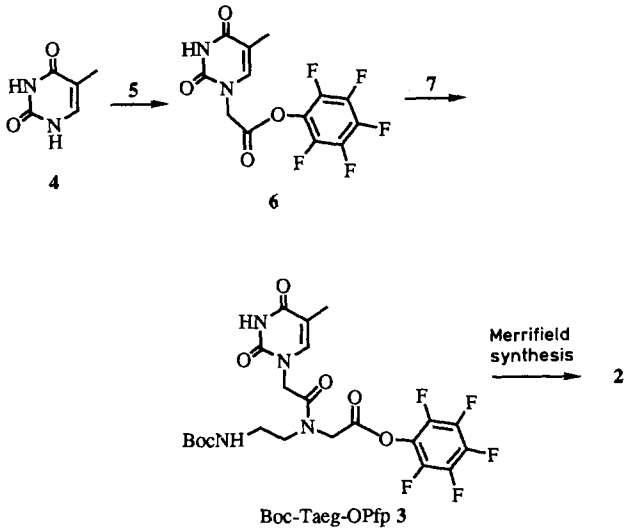

Scheme 2. **5** = methyl α-bromoacetate, **7** = *N*-(*N'*-Boc-aminoethyl)glycine. For details of the synthesis of **2** see text.

cleotides studied so far. Nonionic oligonucleotides are stable to nucleases. In aqueous medium, complexes of nonionic species with unmodified oligonucleotides are much more stable than their ionic counterparts. It is possible to synthesize larger amounts of PNAs **2** according to the Merrifield methodology while the synthesis of modified oligonucleotides is limited by the capacities of the oligonucleotide synthesizers. The synthetic method for PNAs may also allow access to not only PNAs with an achiral peptide backbone but also those with a chiral backbone. The controlled introduction of stereochemistry into methylphosphonates, phosphotriesters, and phosphothioates[8] has been achieved only in the last case. Stereochemical nonuniform products result in complex, not verifiable hybridization properties. In addition, the flexibility of the described peptide backbone is significantly less than that of a phosphodiester backbone because of the two amide bonds per monomeric unit. A disadvantage of PNAs **2** is perhaps the limited membrane transport relative to oligonucleotides because of the lack of active transport mechanisms. The metabolic pathways of **2** inside cells are also not known.

The authors used molecular modeling in their selection of the described monomeric building block. A monomer with six bonds (2-aminoglycine) as well as a spacer with two bonds separating the nucleobase from the backbone fulfilled the requirements for the optimal binding of **2** to a B-DNA single-strand oligonucleotide with formation of a double helix. These structural requirements were proposed recently by Weller et al. independently from the work of Nielsen et al.[9] In Weller's studies, also based on molecular modeling, the formation of helical peptide structures with simultaneous base stacking is clearly dependent on the monomer size.[9] The calculated optimal distances are not surprising, however, because these are also found in a natural DNA strand (see Scheme 1). Nielsen et al. synthesized hexa-, octa-, and decamers (**2a**, **2b**, and **2c**, respectively) of the thymine-containing monomer. **2a–c** were capped at the *C*-terminus by a lysine residue to avoid self-association. This would also increase the interaction (attractive effects) with an unmodified oligonucleotide, because at physiological pH value the amino group of the lysine side chain is protonated. Modifications at the *N*-terminus are possible as was shown by the introduction of the intercalator acridine. As in analogous compounds acridine causes an increase in association with single- or double-stranded DNA.

Some very astonishing results were obtained from the binding studies. The hybrid of the lysine–thymine decamer PNA **2c** with a dA decamer has an extremely high melting point T_m of 72 °C (ca. 50 °C higher than the T_m value of a dA/T decamer hybrid)! Additionally, the increase of the T_m value of 10 °C per monomer unit is unusually high. As expected, the T_m value dropped by the same value when mismatches were introduced. The introduction of acridine at the *N*-terminus caused an increase of the T_m value by 13 °C. One has to wonder if electrostatic interactions coupled with the formation of hydrogen bonds provide sufficient explanation for these observations or if other unnoticed contributions are responsible for these enormous hybridization capabilities. On the other hand, the hybridization of oligo(dA) with oligo(T) has always been exceptional, and one should wait for sequence-specific studies.

Another interesting feature of **2c** was revealed in hybridization studies with a DNA double strand containing a T_{10}/dA_{10} fragment. It seemed that lysine–thymine$_{10}$ PNA **2c** displaced the T_{10} strand from the complementary dA_{10} strand and did not form a triple helix as one might have expected and as the authors had originally intended.[6a] This conclusion was convincingly supported by enzymatic and chemical degradation experiments.

Despite these positive properties of PNAs **2** described for the first time by Nielsen et al., the results pose other questions that are important for the use of **2** as antisense oligonucleotide analogues with mRNA as target. First of all there is the question of the binding properties of a 17mer PNA that are essential for a sequence-specific recognition. A rough extrapolation of the T_m value of the 10mer would result a value of approximately 140 °C for the 17mer. Thus it is difficult to consider a reversible binding at body temperature. Additionally, there is the question if such an oligomer would be able to bind specifically to a complementary sequence. Even eight (!) mismatches in the 17mer do not reduce the T_m value to below body temperature (37 °C). In UV titration experiments of the formed duplexes the authors found a 2:1 ratio of PNA:DNA. This puzzling result points to the possible formation of a triple helix. Another question is how an oligomer designed for DNA would behave with RNA as a result of the different structural types of these molecules. The former shows a B-DNA type conformation whereas the latter has an A-DNA type conformation. Are the PNAs able to allow the conformational changes necessary? The stability of **2** to nucleases is obvious, but what about its stability to proteases or peptidases? Investigations of the use of PNAs instead of backbone-modified oligonucleotides may give new exciting results. Small changes in the natural phosphate/sugar backbone (methylphosphonates or phosphothioates) cause great changes in the hybridization properties of oligonucleotides. However, the results presented by Nielsen et al. suggest that extensive modifications may change the hybridization capabilities in an apparently more controllable fashion. The paper points out one thing very clearly: the search for new DNA analogues as antisense reagents sup-

plies new, surprising, and unpredictable insights on the interaction of these compounds with unmodified oligonucleotides. The data presented also show that computer modeling is a helpful tool in the design of new DNA analogues.

German version: *Angew. Chem.* **1992**, *104*, 1039

[1] H. E. Moser, P. B. Dervan, *Science* **1987**, *238*, 645–650; P. A. Beal, P. B. Dervan, *ibid.* **1991**, *251*, 1360–1363.
[2] M. H. Caruthers, *Science* **1985**, *230*, 281–285; J. Engels, E. Uhlmann, *Angew. Chem.* **1989**, *101*, 733–751; *Angew. Chem. Int. Ed. Engl.* **1989**, *28*, 716–734.
[3] J. Engels, *Nachr. Chem. Tech.* **1991**, *39*, 1250, and literature cited therein.
[4] One should keep in mind the successful regulation of gene expression in tomatoes: P. Eckes, *Angew. Chem.* **1992**, *104*, 182; *Angew. Chem. Int. Ed. Engl.* **1992**, *31*, 175, and literature cited therein.
[5] E. Uhlmann, A. Peyman, *Chem. Rev.* **1990**, *90*, 544–584.
[6] a) M. Egholm, O. Burchardt, P. E. Nielsen, R. Berg, *Science* **1991**, *254*, 1497–1500; b) *J. Am. Chem. Soc.* **1992**, *114*, 1895–1897; c) Other authors have designed peptides as analogues of the backbone of DNA/RNA; however, none of the derivatives examined showed hybridization properties: H. De Koning, U. K. Pandit, *Rec. Trav. Chim.* **1971**, *91*, 1069; J. D. Buttrey, A. S. Jones, R. T. Walker, *Tetrahedron* **1975**, *31*, 73–75.
[7] R. B. Merrifield, *Angew. Chem.* **1985**, *97*, 801; *Angew. Chem. Int. Ed. Engl.* **1985**, *24*, 799.
[8] W. Stec, A. Grajkowski, M. Koziolkiewicz, B. Uznanski, *Nucleic Acids Res.* **1991**, *19*, 58883–58888.
[9] D. D. Weller, D. T. Daly, W. K. Olson, J. E. Summerton, *J. Org. Chem.* **1991**, *56*, 6000–6006; S.-B. Huang, J. S. Nelson, D. D. Weller, *ibid.* **1991**, *56*, 6007–6018.

Synthetic Models for Iron–Oxygen Aggregation and Biomineralization

By *Karl S. Hagen**

Iron, the most abundant transition element in the earth's crust, plays a major role in biological systems primarily because of its rich redox chemistry, and to a lesser extent the structural and magnetic properties of its various mineral forms. A streamlined biological apparatus for handling free iron is imperative, since free Fe(II) ions will react with dioxygen to form highly reactive and destructive radicals, whereas uncomplexed Fe(III) ions form insoluble iron hydroxide under physiological conditions. The iron-storage protein ferritin, made up of 24 subunits forming a shell approximately 70 Å in diameter which can contain up to 4500 iron atoms, is primarily responsible for solubilization and storage of excess Fe(III).[1] The structure of the hydroxo(oxo)iron core of ferritin is not well-defined and is variable in composition. The best information is obtained under low phosphate concentrations for which considerable long-range order, resembling that of the mineral ferrihydrite, is detected by X-ray diffraction and electron microscopy. The variable phosphate component in the core is thought not to play a dominant structural role, although phosphate may play a significant role in binding to isolated iron ions, small aggregates, or the surface of large crystallites.

Iron oxides have a rich mineral chemistry, and more than twenty years ago stable, soluble nanoparticles averaging 70 Å in diameter were prepared by hydrolytic polymerization of iron(III).[2] Yet the chemistry of molecular iron–oxygen clusters has been dominated by the fundamental oxo-bridged diiron(III) unit[3] and the trinuclear basic iron carboxylates. The crystal structure determination in 1981 of a binuclear iron–oxygen species in hemerythrin and the discovery of related oxo-bridged bimetallic centers in other proteins has revived the study of iron–oxygen chemistry. An extensive chemistry of binuclear model complexes has been developed, and larger Fe_4, Fe_6, Fe_{11}, and Fe_{16} aggregates,[4] predominantly ligated by bridging carboxylato ligands, have been characterized.

However, the precipitation process of iron hydroxide oxides remains ill-defined, and unlike the rich polyoxoanion chemistry of early transition metal ions, no molecular polyiron(III) species containing only aqua, hydroxo, or oxo ligands has been crystallized. The inability of high-spin Fe^{III} ions to strongly polarize and stabilize terminal oxo ligands favors the uncontrolled growth of polyiron complexes. Therefore the formation of molecular aggregates necessarily relies on multidentate or bulky organic capping ligands. A few model studies of the basic aggregation process are now available to aid our understanding of the molecular basis of polymer growth. This report highlights the advances in this field culminating in a recent report in this journal[11] on the largest polyiron aggregates isolated and crystallographically characterized to date.

The electronic spectroscopy of ferritin indicates octahedral coordination about the high-spin iron(III) ions. Therefore aggregates are best conceptualized as a construction of FeL_6 octahedra which share vertices, edges, or faces (L = H_2O, OH^-, O^{2-}, phosphate, or donor atoms from amino acid side chains). The $Fe_2(\mu\text{-O})$ unit in **1**[3] has the simplest structure in which two octahedra share a vertex at oxygen.[*] Dibridged cores $Fe_2(\mu\text{-OR})_2$ as in **2**[3b] (where

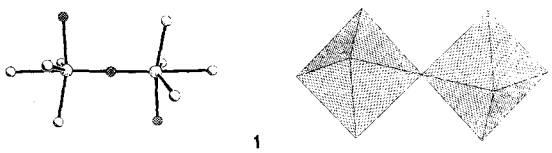

1

[*] Prof. K. S. Hagen
Department of Chemistry, Emory University
1515 Pierce Drive, Atlanta, GA 30322 (USA)

[*] In the structures of **1**–**11** depicted here, only the central skeletons of the polyiron compounds are shown for reasons of clarity. Atom representations are: Fe dotted, O cross-hatched, (carboxylate O atoms in **9** are white), N partially shaded circles. The same perspectives are presented for ball-and-stick and polyhedral drawings except for those of **5** where orthogonal views are depicted.

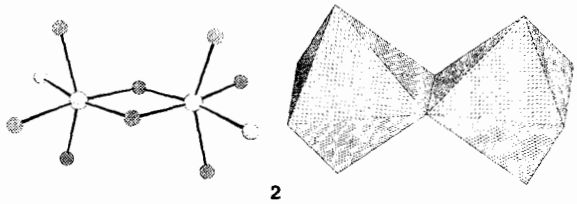

2

R = H or alkyl or aryl groups) are also known. The only structurally characterized trinuclear iron complex without carboxylate bridges contains the planar $Fe_3O_2(OH)$ core in **3**[5] in which tetradentate ligands block all but two coordination sites at the octahedral iron center. Use of tridentate

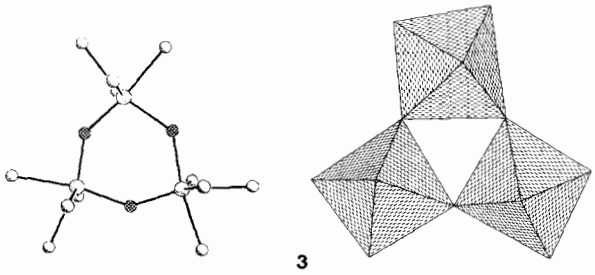

3

facially coordinating ligands affords the "three-dimensional" core $Fe_4O_2(OR)_4$ in compounds of type **4** in which a fourth octahedron caps the three octahedra arranged like

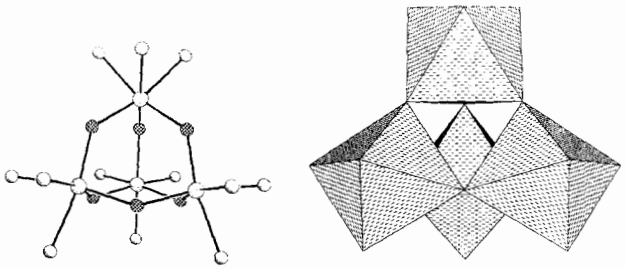

4

those in **3**.[6] This core may be prepared by the hydrolysis of [Fe(tacn)Cl_3] (tacn = 1,4,7-triazacyclononane). Further hydrolysis affords the octanuclear Fe–O aggregate

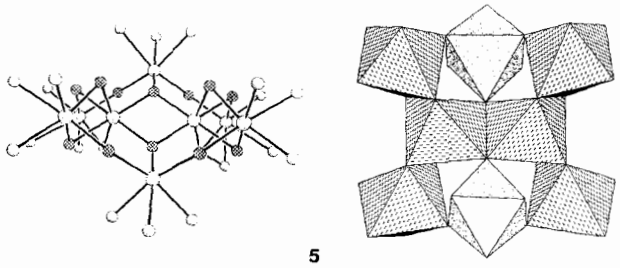

5

$[Fe_8O_2(OH)_{12}]^{8+}$ in **5**[7a] which, for the first time, contains two discrete layers of close-packed ligand atoms (O and N) with Fe(III) ions in octahedral holes. This is also the first compound containing the Fe_3O unit which does not have bridging carboxylate groups.

Subsequent growth in iron–oxygen aggregates can be viewed either from variation in the role of bridging oxo ligands or increasing nuclearity. An example of the former is the introduction of the μ_4-O unit as in the $[Fe_8(\mu_4\text{-}O)(\mu_3\text{-}O)_4]^{14+}$ core in **6**.[7b] This results in a compact core with four

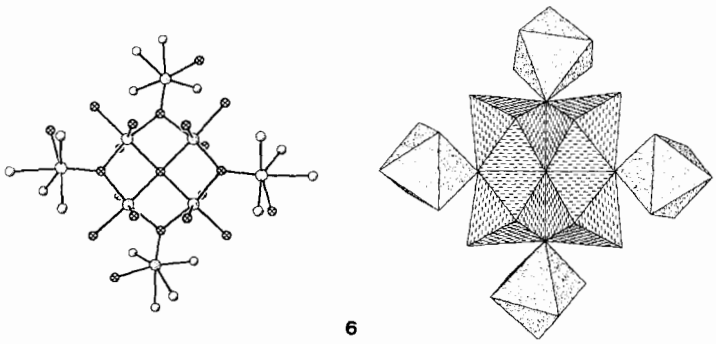

6

central octahedra sharing a common vertex and each sharing two edges with neighbors. This central core is a fragment of the alkoxido(oxo)hexaferrate $[Fe_6(\mu_6\text{-}O)(\mu\text{-}OR)_{12}(OR)_6]^{2-}$ in **7**,[7b] a structural motif common to early transition-metal polyoxoanions.[8] The next step in polyoxoanion growth is a

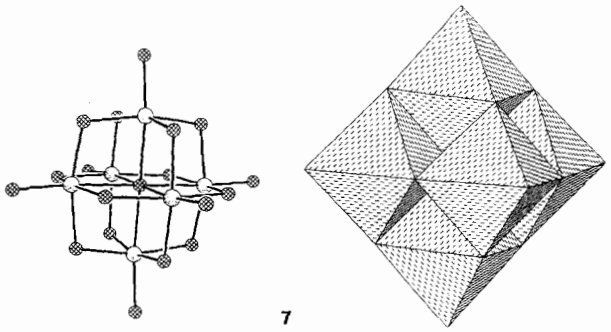

7

fusion of two hexametalates to the decametalates, $[M_{10}O_{28}]^{n-}$, a fragment of which is seen in the hexairon oxo alkoxide, $[Fe_6(\mu_4\text{-}O)_2(\mu\text{-}OR)_8(OR)_4(tren)_2]^{2+}$ **8**[7c] (tren = tris(2-aminoethyl)amine). The coordination of terminal amine ligands has presumably prevented the full decametalate structure from forming.

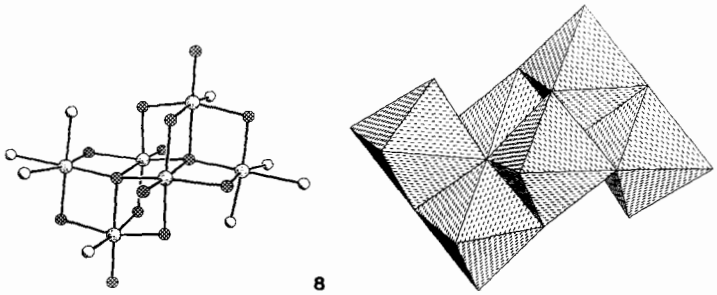

8

An example of Fe–O aggregates with higher nuclearity is the carboxylate $[Fe_{11}O_6(OH)_6(O_2CPh)_{15}]$ shown in **9**.[4a] The bidentate carboxylate ligands dictate the overall geome-

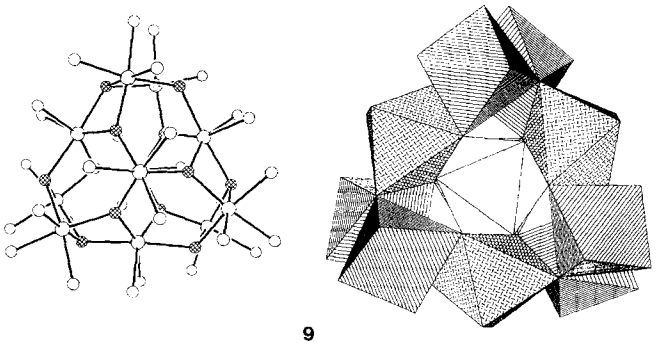

9

try and prevent layered structures from forming. Such aggregates may represent the structures of amorphous iron oxides which are present in ferritin and a prerequisite for subsequent nucleation and crystal growth.[10] The largest iron–oxygen aggregates crystallized to date are **10** and **11** (H_3heidi = $N(CH_2COOH)_2(CH_2CH_2OH)$).[11] They are excellent models for the incipient stages of the biomineralization of layered iron oxides. The Fe_7O_{12} cores are clearly

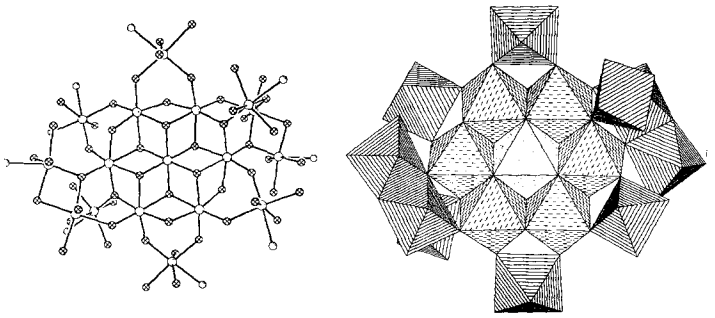

10

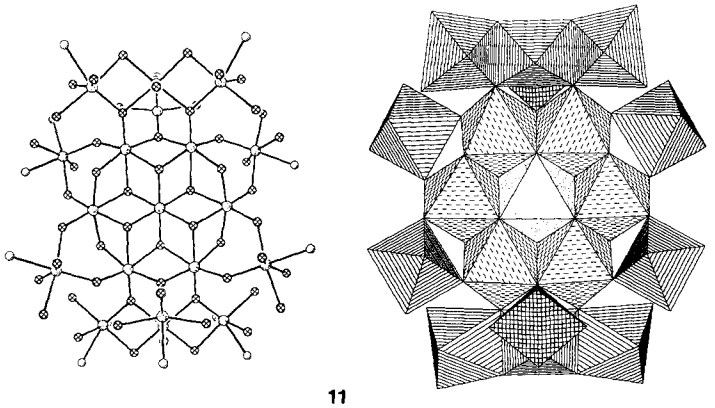

11

$[Fe_{17}(\mu_3\text{-}O)_4(\mu_3\text{-}OH)_6(\mu\text{-}OH)_{10}(heidi)_8(H_2O)_{12}]^{3+}$ **10**
$[Fe_{19}(\mu_3\text{-}O)_6(\mu_3\text{-}OH)_6(\mu\text{-}OH)_8(heidi)_{10}(H_2O)_{12}]^{+}$ **11**

fragments of the layered AX_2 structural type and are surrounded by less highly structured shells made up of eight and ten iron atoms capped and bridged by the tetradentate ligand heidi.

These synthetic models shed light on two basic aggregation processes: the formation of soluble aggregates with high nuclearity related to well-defined polyoxometalates of the early transition metals, and the formation of insoluble layered minerals such as goethite. They lay the groundwork for the synthesis of models of technologically important iron(II) oxides[12a] and the mixed-valence mineral magnetite, which has recently been synthesized in ferritin.[12b]

German version: *Angew. Chem.* **1992**, *104*, 1036

[1] *Biomineralization: Chemical and Biochemical Perspectives* (Eds.: E. S. Mann, J. Webb, R. J. P. Williams), VCH, Weinheim, **1989**, Chap. 9 and 10.

[2] a) T. G. Spiro, S. E. Allerton, J. Renner, A.Terzis, R. Bils, P. Saltmann, *J. Am Chem. Soc.* **1966**, *88*, 2721–2726; b) S. E. Allerton, J. Renner, S. Colt, P. Saltman, *ibid.* **1966**, *88*, 3147–3148.

[3] a) K. S. Murray, *Coord. Chem. Rev.* **1974** *12*, 1; b) D. M. Kurtz, Jr., *Chem. Rev.* **1990**, *90*, 585–606.

[4] a) S. J. Lippard, *Angew. Chem.* **1988**, *100*, 353–371; *Angew. Chem. Int. Ed. Engl.* **1988**, *27*, 344–361; b) J. B. Vincent, G. L. Olivier-Lilley, B. A. Averill, *Chem. Rev.* **1990**, *90*, 1447–1467.

[5] $[Fe_3O_2(OH)(tren)_3]^{4+}$: K. S. Hagen, V. S. Nair, unpublished.

[6] Examples: $[Fe_4L_2O_2(OH)_2]$, L = 2-hydroxy-5-methyl-1,3-xylylenediaminetetraacetate: a) B. P. Murch, P. D. Boyle, L. Que, Jr., *J. Am. Chem. Soc.* **1985**, *107*, 6728; b) B. P. Murch, F. C. Bradley, P. D. Boyle, V. Papaefthymiou, L. Que, Jr. *ibid.* **1987**, *109*, 7993–8003; c) $[Fe_4O_2(OH)_4(tacn)_4]^{4+}$: from $[Fe(tacn)Cl_3]$: S.Drueke, K. Wieghardt, B. Nuber, J. Weiss, E. L. Bominaar, A. Sawaryn, H. Winkler, A. X. Trautwein, *Inorg. Chem.* **1989**, *28*, 4477–4483; from $[Fe(tacn)_2]^{2+}$: K. S. Hagen, unpublished.

[7] a) $[Fe_8(tacn)_6(\mu_3\text{-}O)_2(\mu_2\text{-}OH)_{12}]^{8+}$: K. Wieghardt, K. Pohl, I. Jibril, G. Huttner, *Angew. Chem.* **1984**, *96*, 66–67; *Angew. Chem. Int. Ed. Engl.* **1984**, *23*, 77–78. b) $[Fe_8O_5(O_2CMe)_8(tren)_4]^{6+}$ and $[Fe_6O_2(OMe)_{12}(tren)_2]^{2+}$: K. S. Hagen, V. S. Nair, *Inorg. Chem.*, submitted.

[8] a) $[Fe_6O((OCH_2)_3CCH_3)_6]^{2-}$: K. Hegetschweiler, H. Schmalle, H. M. Streit, W. Schneider, *Inorg. Chem.* **1990**, *29*, 3625–3627; b) $[Fe_6O(OCH_3)_{18}]^{2-}$: K. Hegetschweiler, H. Schmalle, H. M. Streit, V. Gramlich, H.-U. Hund, I. Erni, *ibid.* **1992**, *31*, 1299–1302.

[9] Reviews: a) M. T. Pope, *Heteropoly and Isopoly Oxometalates*, Springer, New York, **1983**; b) V. W. Day, W. G. Klemperer, *Science* **1985**, *228*, 533–541; c) M. T. Pope, A. Müller, *Angew. Chem.* **1991**, *103*, 56–70; *Angew. Chem. Int. Ed. Engl.* **1991**, *30*, 34–48.

[10] a) *Biomineralization: Chemical and Biochemical Perspectives* (Eds.: S. Mann, J. Webb, R. J. P. Williams), VCH, Weinheim, 1989., b) L. Addadi, S. Weiner, *Angew. Chem.* **1992**, *104*, 159–176; *Angew. Chem. Int. Ed. Engl.* **1992**, *31*, 153–169.

[11] S. L. Heath, A. K. Powell, *Angew. Chem.* **1992**, *104*, 191–192; *Angew. Chem. Int. Ed. Engl.* **1992**, *31*, 191–193.

[12] a) R. F. Ziolo, E. P. Giannelis, B. A. Weinstein, M. P. O'Horo, B. N. Ganguly, V. Mehrotra, M. W. Russell, D. R. Huffman, *Science* **1992**, *257*, 219–223; b) F. C. Meldrum, B. R. Heywood, S. Mann, *ibid.* **1992**, 257, 522–523.

Artificial Replication Systems

By *Siegfried Hoffmann**

"It has not escaped our notice that the specific pairing we have postulated immediately suggests a possible copying mechanism for the genetic material"—rarely has anything fascinated Science as much as the "hallowed" structure of DNA, born in that classical understatement of Watson and Crick, but also of Franklin and Wilkins. From the chemical side, however, the euphoria was mingled with a little melancholy and dismay. The chemists had loved proteins too much to be able to devote due attention to the nucleic acids. Schrödinger's "aperiodic crystal", which revealed in its enchanting statics a wealth of dynamics inconceivable before its discovery (Fig. 1), had, beginning with Miescher and Altmann, remained largely the domain of nonchemists and chemical outsiders.[1]

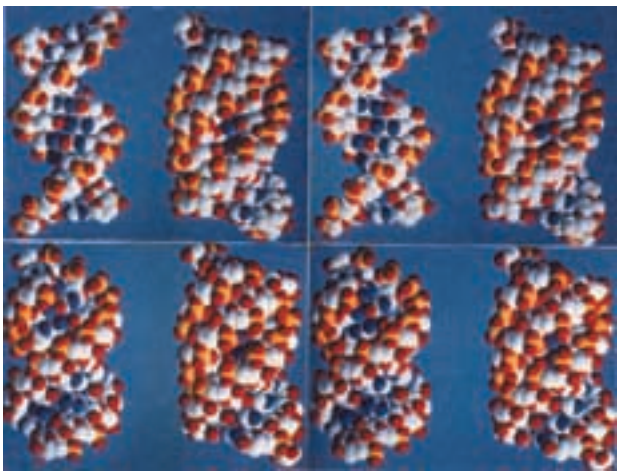

Fig. 1. Stereo representations of DNA and RNA duplex and triplex systems. (Top: DNA; bottom: RNA. Left triplex, right duplex).

Todd sought to answer for chemistry in a landmark appeal: "The use of one molecule as a template to guide and facilitate the synthesis of another...has not hitherto been attempted in laboratory synthesis, although it seems probable that it is common in living systems. It represents a challenge which must, and surely can, be met by organic chemistry".[2] And the grand concept indeed appeared to be portentous. Quite soon, Schramm et al.[3] aroused enthusiasm with the "nonenzymatic synthesis of polysaccharides, nucleosides and nucleic acids, and the origin of self-replicating systems". There it stood, diagnosed by hybridization techniques and portrayed by electron microscopy; the first nucleic acid to be generated in vitro, in the form of a polyadenylic acid, and, of course, the first attempt at an artificial matrix reaction, the polycondensation of uridylic acid onto the orienting $(A)_n$ matrix. Was this the breakthrough that would lead chemistry not only into the wonderland of biology, but also rapidly to ordered macromolecular organizations in its own dominions?

[*] Professor Dr. S. Hoffmann
Institut für Biochemie der Universität Halle-Wittenberg
Weinbergweg 16a, D-O-4050 Halle (FRG)

Schramm's dramatic experiments had to push the natura standards optimized by evolution back into the high erro phase of a prebiotic beginning. Purely artificial template experiments that evaluated all the interactive possibilities of both covalent and noncovalent nature, however, were devoid of even this possible relationship to evolutionary development. The first great "chemical" departure into the temptations of such matrix reactions[4] ran aground on innumerable difficulties. The dominant element in scientific progress came to be not the tremendous variety of chemical matrices and the distant aim of building systems capable of self-replication. Rather, fascination with the effortless elegance of the natural prototypes stimulated the vanguards of chemistry and biology in their campaign of molecular penetration of biological systems. Rapid scientific breakthroughs were achieved which had never been thought possible. The golden age of molecular biology had begun.[4]

Oparin and Haldane's heirs, Eigen and Kuhn, gave these events a time perspective, and with their "information" also described the vector of the "Grand Process" of evolution.[5] With this, however, a multitude of rival problems, which had been simmering in the collective unconscious, resolved themselves out of the complexity of the original goals of template experiments. Self-replication, mutation, and metabolism (as prerequisites for selection) made up the list of criteria; through these, information and its origin, evaluation, processing, and optimization had governed the evolutionary history of prebiotic and biotic systems.

In connection with Spiegelman's initial experiments, Eigen and Schuster, Joyce, and others attempted to "bring to life" the theoretical premises behind the laboratory realities of enzyme-catalyzed RNA replication and evolution experiments. Orgel's groups, by contrast, exerted themselves to transform diverse matrix relationships into artificial, enzyme-free nucleic acid formation.[5] When Altman and Cech raised RNA to the throne of an archaic informational and functional omnipotence—confirming earlier speculations by Crick, Orgel, and Woese—it amounted to a late justification of the toil and trouble of this "nucleic acids first" route. "A tRNA looks like a nucleic acid doing the job of a protein", Crick once observed. Now, self-splicing RNA complexes, polymerase activities, ribozymes and hypothetical RNAsomes afforded unusual insights into the genotypical and (!) phenotypical complex behavior of a single nucleic acid species.[6] And with the supposedly greater understanding of this "RNA-world", fresh impetus was given even to the purely chemical approaches, once so promising and now almost forgotten. As "bioid" successors to Decker, these now attempted to work through evolutionary conceptions in classical chemical systems. Once again—but more strongly and at a higher level—a "Kuhn" period of divergent evolution of matrix approaches between molecular biology and classical chemistry had begun.

Three self-replicating systems are representative and exemplary for the wealth of variety of this creative outburst, and clarify, with their different degrees of abstraction, one of the dynamic scientific peripheries of our times (Fig. 2–

 © VCH Verlagsgesellschaft mbH, W-6940 Weinheim, 1992 0570-0833/92/0808-1013 $ 3.50+.25/0

4).[7-9] Through elucidation of the static and dynamic principles of replicative information systems, all three endeavor to gain insight into both the transitional stages between chemical and biological evolution and the possibilities of artificial development of their chemical duplication.

After innumerable attempts to explain the matrix relationships of mono- and oligonucleotides to orienting and catalytic oligo- and polynucleotide templates, here, first, are two self-replicating nucleic acid models (Fig. 2): a DNA-analogous hexamer system by von Kiedrowski et al.[8a, c-f] and an RNA-analogous tetrameric assembly from the Orgel group.[8b] The earlier of these, in concept and realization,

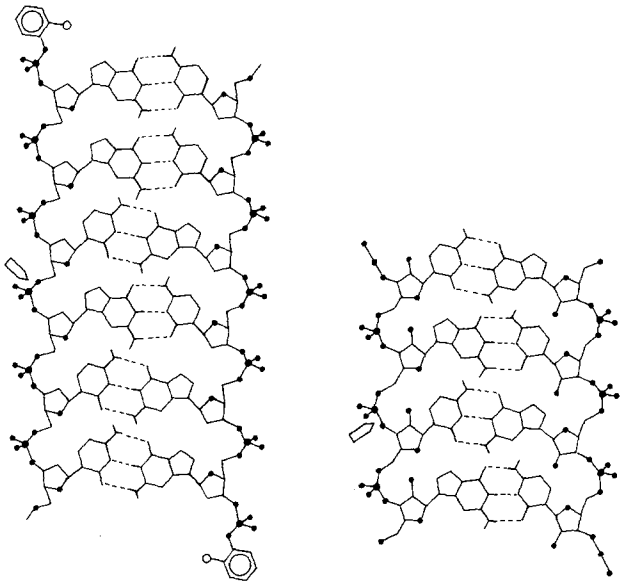

Fig. 2. Self-replicative oligonucleotide matrix systems with self-complementary G/C sequences developed by Kiedrowski et al. (left) and Zielinski and Orgel (right). The bond formed in ligation (carbodiimide method) is marked with an arrow. Left: hexa(3'-deoxyribo)nucleotide matrices with 3'-5'-phosphoester [8a] or 3'-5'-phosphoamidate bonds [8e] in the ligation region; other sugars are 3'-5'-phosphoester linked; 5'-hydroxy groups are alkyl-protected, 3'-phosphate residues are protected as 2-chloro-1-phenoxy derivatives. Right: tetranucleoside triphosphoamidate matrices with 3'-amino-3'-deoxyriboses and 3'-azido modification of the sugar moiety in the 3'-position [8b].

was von Kiedrowski's first successful model hexadeoxyribonucleotide duplex,[8a] which became a leitmotif in the detailed treatment of growth kinetics, and anticipated later self-replicating "minimal systems" in many ways (Fig. 3). By using the ligation of oligonucleotides, he exploited their higher cooperativity to attain increased stability of the matrix duplex and the ternary formation complex. The choice of a palindromic system reduced the complexity of biological replication experiments to a simplified kinetic measurement of its identical (since self-complementary) matrix components. In this way he could obtain direct proof for self-replication, demonstrating the autocatalytic behavior of his system. The surprising square root law of matrix growth kinetics with its ideal case of a parabolic reaction course, derived from the hexadeoxynucleotide duplex, confirmed slightly later by the Zielinski-Orgel system,[8b] and finally also verified in the Rebek dimer assembly,[9, 8d-f] was recognized as autocatalytic system behavior of self-replicative oligonucleotide templates under isothermal conditions. Lat-

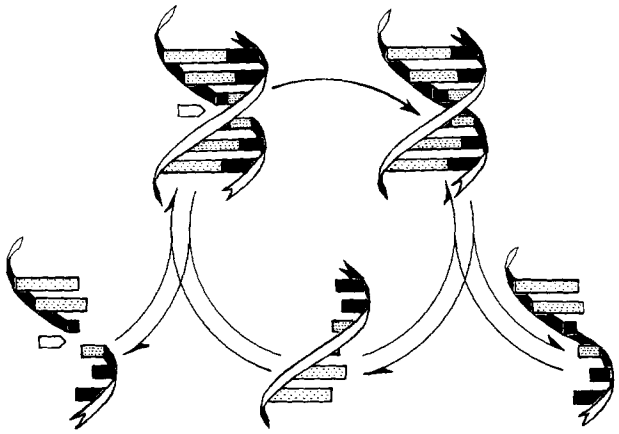

Fig. 3. Self replication diagram for an autocatalytic matrix synthesis, modified from ref. [8f].

er functional and reactive refinements overcame the difficulties remaining in the first approach,[8a] in which the autocatalytic reaction channel was too heavily disguised by the noninstructed, spontaneous synthesis. A hexameric system constructed from two trimeric blocks by phosphoamidate coupling reveals sigmoidal growth behavior and stands out for its extraordinary "autocatalytic efficiency".[8e, f]

The patterns of autocatalysis with respect to parabolic and exponential reaction courses can by now be derived from the thermodynamic and kinetic data of the matrix partners and their reactivities. The findings closely affect the conclusions of Eigen's evolution experiments concerning the decision criteria for mutant selection and coexistence, and offer quite new views, with "autocatalytic co-operation" between competitive species.[8, 9] Basic questions of prebiotic behavior patterns can for the first time become the object of detailed experimental study, separate from "enzyme-catalyzed" evolution experiments with RNA and DNA systems. While studying more complex autocatalysis patterns, von Kiedrowski et al.—extremely aptly—diagnosed modulation of molecular recognition as an operational deficit of earlier self-replicating artificial nucleic acid systems with regard to exponential reaction courses, and identified it as an ideal aim for future models. On its way to the nucleoprotein system, evolution must have had a similar view of the problem when, in Lucretius's "eternal game"[5a] (Fig. 5), it endowed nucleic acids, which are somewhat inefficient in this respect, with proteins experienced in phase and domain regulation control to achieve an ideal milieu for directing modulations of recognition.

Matrix growth kinetics as known for oligonucleotides are followed even by a drastically abstracted artificial replication system developed by Rebek's group (Fig.4). After all that has gone before, this seems to augur a fresh departure for the far horizons of artificial chemical evolution systems. The dimer assembly developed from host-guest relationships combines the interactive and cognitive possibilities of native nucleic acid matrices with the more general biopolymer relationships of the amide bond formation involved in the matrix reactions.[9] When Rebek et al., who have in the meantime sought to stimulate the competition and selection behavior of their self-replicating species by "chemical" mutations, state that one of their main aims is artificial peptide

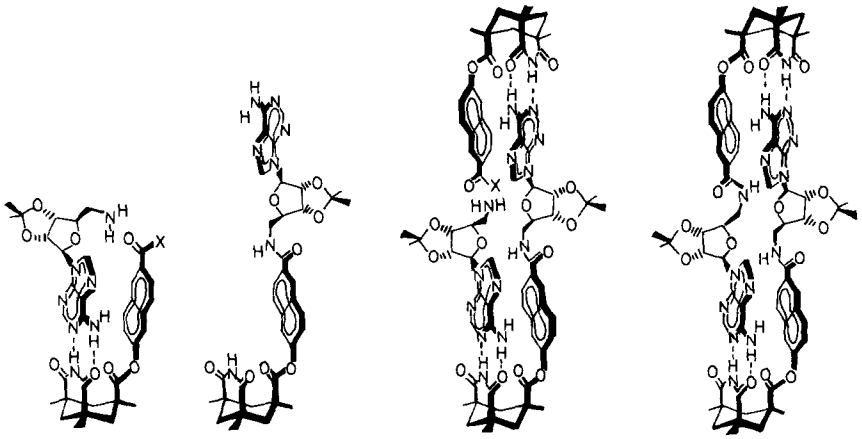

Fig. 4. Self-replicating matrix system of Rebek et al. [9]; the acyl component of the ligation bond is activated in various manners.

synthesis on a nucleic acid matrix, it is slightly reminiscent of the very beginnings. Long before computer simulations fitted protein β-pleated sheets snugly into the minor groves of DNA duplexes and shallow grooves of RNA duplexes to allow modeling of early stages of nucleation of the nucleoprotein system with the mutual polymerase activities for the two grand partner structures,[5i-k] Todd had already—along with his "template"-vision—suggested hypothetical peptide syntheses as one of his "Perspectives in Organic Chemistry". He proposed that the amino acid building blocks of the nascent peptide chain might be activated as common "mixed anhydrides" of the nucleic acid phosphates, and suitably localized stereoelectronically by the orienting matrix—an early view of evolution, developed by human rationality,[2] without regard for the actual biological complexity.

It is, indeed, just this complexity which for today's chemistry provides provocation and stimulation, intimidation and temptation, love, hate and fate together. The systems presented here still remain utterly outclassed by even the most primitive life forms, such as RNA-viruses. The possibility of describing natural selection behavior according to quasi-species distributions in the extreme multidimensionalities of sequence spaces is, for artificial systems, at best a very distant utopia. However, independently of the respective chemical character, basic patterns of autocatalytic activities once again make the original image of that "notionally reduplicative" DNA double helix the center of hopeful expectations. With all its early primitivity, but also with its promising inherent potential of "minimal models of self-replication", chemistry is throwing down the gauntlet to biological complexity in what must be the most decisive region of evolutionary formative processes, and in doing so is gaining new qualities.

Kuhn divergences generate a tremendous number of new matrix and replication variations,[10] and from this breadth develop an impressive depth of impending convergences. The successors to elite nucleic acid templates were surprisingly the apparently simplified amidinium–carboxylate matrices.[8a, 10f] However, in the attempt to simplify generalizing principles as far as possible, the desirable operational modes, astoundingly, become accessible. The dramatically abstracted amidinium–carboxylate systems, which nevertheless cover certain aspects of complex protein–nucleic acid interactions, prove to be susceptible to modulation of molecular recognition and even delight their examiners with exponential growth kinetics. Detailed aspects, such as the possibilities of coordination in native nucleic acid assemblies, make themselves independent in helicates whose structures reflect the relationship between our life process and its basic matrices. Matrix studies of triplex systems (cf. Fig. 1) model possible regulation strategies of nucleic acid organization and at the same time bridge the gap to basic, hysteretic mechanisms of information processing in more highly condensed systems. The paths of chemistry—from the chemical bond to the chemical system, from molecularity to supramolecularity, from statics to dynamics—are united with the spatial–temporal coherences of phase and domain regulations from physics in the asymmetries and nonlinearities of the "Life Sciences",[11] affording processes which are stabilized by their own dynamics. From the earliest preludes (Fig. 5) to the unknown intimacies of nucleation of the nucleoprotein system, up to today's complex evolutionary character, only the half-way adequate complexity of the scientific approach might provide sufficient simulation potential to approximate the Grand Process.

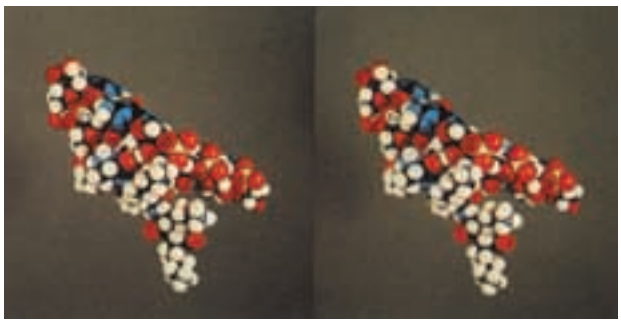

Fig. 5. Quacumque inter se possent congressa creare—Lucretius. (Translation: Whatever they would be able to do stems from their coming together.) [5a]

And finally, there is also the "evolution" of an individual scientific life's work,[12] which itself follows decisive stages of the Grand Process: the exploration of early chemical requirements, the development of prebiotic ligand systems, the fixation into the ordered structures of "inorganic" matrix patterns and, finally, the liberation of their inherent wealth of design and information into the order–disorder dialectics of today's nucleoprotein system. Using basic hexose structures, the actual successes of evolution, a never attempted, or perhaps

only forgotten, "evolutionary step" is now taking place—once again in the area of replicative nucleic acid systems.

But this is another whole story—and another great game.

Angew. Chem. **1992**, *103*, 1032

[1] Routes to the replicative double helix: a) F. Miescher, "On the chemical composition of pyocytes", *Hoppe-Seyler's med. Untersuchungen,* **1871**; F. Miescher, *Die histochemischen and physiologischen Arbeiten* (Ed.: F. C. W. Vogel), Leipzig, **1897**; b) R. Altmann, *Arch. Anat. Phys. Phys. Abt.* **1889**; R. Altmann, *Die Elementarorganismen,* Veit, Leipzig, **1890**; c) E. Schrödinger, *What is life?,* Cambridge Univ. Press, New York, **1944**; d) J. D. Watson, F. H. C. Crick, *Nature* **1953**, *171*, 737; e) F. H. C. Crick, J. D. Watson, *Proc. R. Soc. London [Ser. A]* **1954**, *223*, 80.

[2] A. Todd in *Perspectives in Organic Chemistry* (Ed.: A. Todd), Interscience, New York, **1956**, p. 245.

[3] G. Schramm, H. Grötsch, W. Pollmann, *Angew. Chem.* **1962**, *74*, 53; *Angew. Chem. Int. Ed. Engl.* **1962**, *1*, 1.

[4] On the matrix problem: a) W. Kern, H. Kämmerer, *Chem. Ztg.* **1967**, *91*, 73; b) H. Kämmerer, *ibid.* **1972**, *96*, 7; c) J. H. Winter, *Angew. Chem.* **1966**, *78*, 887; *Angew. Chem. Int. Ed. Engl.* **1966**, *5*, 862; d) S. Hoffmann, *Molekulare Matrizen (I Evolution, II Proteine, III Nucleinsäuren, IV Membranen)*, Akademie-Verlag, Berlin, **1978**; *Z. Chem.* **1979**, *19*, 241.

[5] Views of evolution: a) T. Lucretius Carus, *De rerum natura.* Weidmann, Leipzig, **1795**; b) A. I. Oparin, *The Origin of Life on Earth,* Academic Press, New York, **1957**; *Origin of Life*, Moscow, **1924**; c) J. B. S. Haldane, *The Cause of Evolution*, Longman, New York, **1932**; d) M. Eigen, *Naturwissenschaften* **1971**, *58*, 465; *Stufen zum Leben*, Piper, München, **1987**; *Cold Spring Harbor Symp. Quant. Biol.* **1987**, *LII*, 307; *Chem. Scr.* **1986**, *26 B*, 13; *Ber. Bunsenges. Phys. Chem.* **1985**, *89*, 658; M. Eigen, P. Schuster, *Naturwissenschaften* **1977**, *64*, 541; *ibid.* **1978**, *65*, 7; e) P. Schuster, *Physica* **1986**, *22 D*, 100; *Chem. Scr.* **1986**, *26 B*, 27; in *Darwin Today* (Eds.: E. Geissler, W. Scheler), Akademie-Verlag, Berlin, **1983**, p. 151; f) H. Kuhn, *Angew. Chem.* **1972**, *84*, 838; *Angew. Chem. Int. Ed. Engl.* **1972**, *11*, 798; in *Darwin Today* (cf. e), p. 271; g) G. F. Joyce, *Nature* **1989**, *338*, 217; *Cold Spring Harbor Symp. Quant. Biol.* **1987**, *LII*, 41; h) L. E. Orgel, *ibid.* 9; *J. Theor. Biol.* **1986**, *123*, 127; *Folia Biol. (Praha)* **1983**, *29*, 65; i) C. W. Carter, J. Kraut, *Proc. Natl. Acad. Sci. USA* **1974**, *71*, 283; k) G. M. Church, J. L. Sussman, S.-H. Kim, *Proc. Natl. Acad. Sci. USA* **1977**, *74*, 1458; l) P. Decker, *Orig. Life* **1975**, *6*, 211; *Angew. Chem. Nachr. Chem. Tech.* **1975**, *23*, 165; *J. Mol. Evol.* **1974**, *4*, 49; m) S. Hoffmann in *Darwin Today* (cf. e), p. 193; cf. [4d].

[6] On the "RNA-world": a) S. Altman, *Angew. Chem.* **1990**, *102*, 735; *Angew. Chem. Int. Ed. Engl.* **1990**, *29*, 707; b) T. R. Cech, *ibid.* 745 and 716; cf. also [5d-i].

[7] a) L. E. Orgel, R. Lohrmann, *Acc. Chem. Res.* **1974**, *7*, 368; R. Lohrmann, L. E. Orgel, *J. Mol. Biol.* **1980**, *142*, 555; T. Inoue, L. E. Orgel, *Science* **1983**, *219*, 859; T. Inoue, G. F. Joyce, K. Grzeskowiak, L. E. Orgel, J. M. Brown, C. B. Reese, *J. Mol. Biol.* **1984**, *178*, 669; C. B. Chen, T. Inoue, L. E. Orgel, *ibid.* **1985**, *181*, 271; A. W. Schwartz, L. E. Orgel, *Science* **1985**, *228*, 585; O. L. Acevedo, L. E. Orgel, *Nature* **1986**, *321*, 790; S. L. Miller, L. E. Orgel, *The Origins of Life on Earth*, Prentice Hall, Englewood Cliffs, N.Y., USA, **1974**; cf. also [5h]; b) R. Naylor, P. T. Gilham, *Biochemistry* **1966**, *5*, 2723. Most recent review: L. E. Orgel, *Nature* **1992**, *358*, 203.

[8] a) G. von Kiedrowski, *Angew. Chem.* **1986**, *93*, 932; *Angew. Chem. Int. Ed. Engl.* **1986**, *25*, 932; b) W. S. Zielinski, L. E. Orgel, *Nature* **1987**, *327*, 346; c) G. von Kiedrowski, B Wlotzka, J. Helbing, *Angew. Chem.* **1989**, *102*, 1259; *Angew. Chem. Int. Ed. Engl.* **1989**, *28*, 1235; d) G. von Kiedrowski in *40 Jahre Fonds der Chemischen Industrie, 1950–1990*, VCI-Verlag, Frankfurt, **1990**; e) G. von Kiedrowski, B. Wlotzka, J. Helbing, M. Matzen, S. Jordan, *Angew. Chem.* **1991**, *103*, 456, 1066; *Angew. Chem. Int. Ed. Engl.* **1991**, *30*, 423; 892; f) G. von Kiedrowski, J. Helbing, B. Wlotzka, S. Jordan, M. Mathen, T. Achilles, D. Sievers, A. Terfort, B. C. Kahrs, *Nachr. Chem. Tech. Lab.* **1992**, *40*, 578; cf. also [10a].

[9] T. Tjivikua, P. Ballester, J. Rebek, Jr., *J. Am.Chem. Soc.* **1990**, *112*, 1249; J. Rebek, Jr., *Angew. Chem.* **1990**, *102*, 261; *Angew. Chem. Int. Ed. Engl.* **1990**, *29*, 245; J. S. Nowick, Q. Feng, T. Tjivikua, P. Ballester, J. Rebek, Jr., *J. Am. Chem. Soc.* **1991**, *113*, 8831; V. Rotello, J.-I. Hong, J. Rebek, Jr., *ibid.* **1991**, *113*, 9422; J.-I. Hong, Q. Feng, V. Rotello, J. Rebek, Jr., *Science* **1992**, *255*, 849. Latest papers: Q. Feng, T. K. Park, J. Rebek, Jr., *ibid.* **1992**, *256*, 1179; T. K. Park, Q. Feng, J. Rebek, Jr. *J. Am. Chem. Soc.* **1992**, *114*, 4529.

[10] On the "Kuhn divergences" of the matrix systems: a) amidinium carboxylate matrices: A. Terfort, G. von Kiedrowski, *Angew. Chem.* **1992**, *104*, 626; *Angew. Chem. Int. Ed. Engl.* **1992**, *31*, cf. also [8f]; b) helicates: J.-M. Lehn, A. Rigault, *Angew. Chem.* **1988**, *100*, 1121; *Angew. Chem. Int. Ed. Engl.* **1988**, *27*, 1059; W. Zarges, J. Hall, J.-M. Lehn, C. Bolm, *Helv. Chim. Acta* **1991**, *74*, 1843; A. F. Williams, C. Piguet, G. Bernardinelli, *Angew. Chem.* **1991**, *103*, 1530; *Angew. Chem. Int. Ed. Engl.* **1991**, *30*, 1490; E. C. Constable, *ibid.* **1991**, *103*, 1482 and **1991**, *30*, 1450; c) Triplexes: K. J. Luebke, P. B. Dervan, *J. Am. Chem. Soc.* **1989**, *111*, 8733; on triplexes in connection with molecular hysteresis cf.: E. Neumann, A Katchalsky, *Proc. Natl. Acad. Sci. USA* **1972**, *69*, 993; A. Katchalsky, E. Neumann, *Int. J. Neurosci.* **1972**, *3*, 175; E. Neumann, *Angew. Chem.* **1973**, *85*, 430; *Angew. Chem. Int. Ed. Engl.* **1973**, *12*, 356; W. Guschlbauer, *Encycl. Polymer Sci. Eng.* **1988**, *12*, 699; in *Dynamic Aspects of Conformation Changes in Biological Macromolecules* (Ed.: C. Sadron), Reidel, Dordrecht, Holland, **1973**; S. Hoffmann, W. Witkowski in *Mesomorphic Order in Polymers and Polymerization in Liquid Crystalline Media* (Ed.: A. Blumstein), *Am. Chem. Soc. Symp.-Ser.* **1978**, *74*, 178.

[11] "Life sciences"-views: a) cf. [12]; b) H. Ringsdorf, B. Schlarb, J. Venzmer, *Angew. Chem.* **1988**, *100*, 117; *Angew. Chem. Int. Ed. Engl.* **1988**, *27*, 113; M. Ahlers, W. Müller, A. Reichert, H. Ringsdorf, H. Venzmer, *ibid.* **1990**, *102*, 1310 bzw. **1990**, *29*, 1269; c) J.-M. Lehn, *ibid.* **1988**, *100*, 91 and **1988**, *27*, 89; *ibid.* **1990**, *102*, 1347 and **1990**, *29*, 1304; *Science* **1985**, *227*, 849; d) D. Seebach, *Angew. Chem.* **1990**, *102*, 1363; *Angew. Chem. Int. Ed. Engl.* **1990**, *29*, 1320; e) H. Frauenfelder, *Ann. N. Y. Acad. Sci.* **1987**, *504*, 151; in *Structure and Dynamics of Nucleic Acids, Proteins and Membranes* (Eds.: E. Clementi, S. Chin), Plenum, New York, **1986**, p. 169; f) S. Hoffmann in *Chirality – From Weak Bosons to the α-Helix* (Ed.: R. Janoschek), Springer, Berlin, **1991**, p. 205.

[12] A. Eschenmoser, *Angew. Chem.* **1988**, *100*, 5; *Angew. Chem. Int. Ed. Engl.* **1988**, *27*, 5; Nachr. Chem. Tech. Lab. **1991**, *39*, 795; *Nova Acta Leopold.* **1992**, *NF67/281*, 201; A. Eschenmoser, M. Dobler, *Helv. Chim. Acta* **1992**, *75*, 218; cf. also: G. Quinkert, *Nachr. Chem. Tech. Lab.* **1991**, *39*. 788.

Communications may be submitted in English *or* in German. Further details regarding the submission of communications can be found in the "Notice to Authors" reproduced in the January issue of the journal. Copies thereof may be obtained from the editorial office upon request.

Molecular Recognition of Primary Amines by Three-Point Binding with Boron-Containing Host Molecules**

By *Manfred T. Reetz,* Christof M. Niemeyer, Marcus Hermes,* and *Richard Goddard*

Host molecules capable of showing pronounced molecular recognition of primary amines RNH_2 have not been synthesized to date.[1, 2] Crown ethers, for example, form only weak and unselective interactions with amines.[1] The corresponding ammonium ions $RNH_3^{\oplus}$ are bound more strongly by suitable crown ethers, but generally the degree of selectivity here is also quite low.[1] The latter is hardly surprising because the $RNH_3^{\oplus}$/crown ether complexes, which are held together by hydrogen bonds, are structurally so arranged that the groups R are too remote from the framework of the host molecule.[3, 4] The formation of adducts with Lewis acids,[5] for example with trialkyl boranes leading to reversible formation of adducts $R_3N \cdot BR'_3$,[6] is a quite different type of amine complexation. The dissociation constants of these equilibria depend, among other factors, on the number and size of the groups R in the amine.

We describe here a new concept in molecular recognition in which host molecules containing a Lewis acid metal center[2b, 4, 7] and at least two donor sites selectively bind primary amines via three-point binding (Scheme 1). If the amine RNH_2 forms a reversible dative bond with the metal center, it takes on the character of an ammonium ion. This should permit the formation of hydrogen bonds with the donor positions situated spatially nearby, thereby leading to synergistic effects.

To test this concept experimentally we synthesized the boron-containing crown ethers **1**–**3**[8] and allowed them to react with the amines **4**–**8**. Treatment of host **2b**, for example, with a stoichiometric amount of benzylamine **4** in dichloromethane leads to a spontaneous reaction with formation of the adduct **9**. Especially the ^{11}B and ^{13}CNMR spectra indicate the existence of a dative B–N bond and formation of hydrogen bonds between the amine hydrogen atoms and the crown ether.[9] Only the secondary amine **8** appears to be an exception, since the ^{13}CNMR signals of the crown ether carbon atoms do not indicate any participation in the sense of hydrogen bonds.

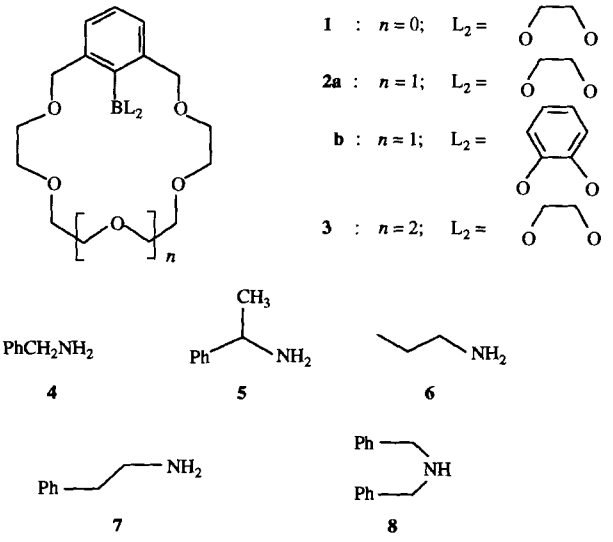

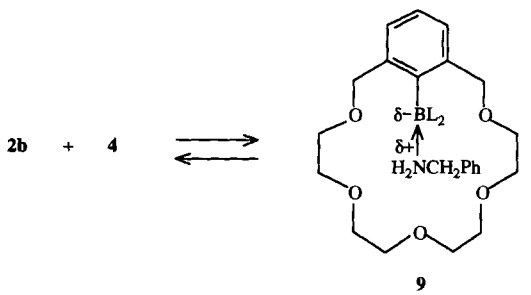

The crystal structure analysis[10] of the host/guest molecule **9** provides conclusive proof of the postulated three-point binding (Fig. 1, left). In particular, the space-filling representation[11] (Fig. 1, right) shows the strong embracement of the guest by the host. Figure 1 (right) suggests the possibility of a high degree of molecular recognition with respect to different amines RNH_2. In 1:1:1 competition experiments with the host **2b** and two different amines at room temperature, the ratio of the two possible host/guest compounds is not easy to determine by NMR spectroscopy because of rapid exchange processes. However, the ratio could be measured at −30 °C by integration of the appropriate ^1HNMR signals. Accordingly, the host **2b** shows a very

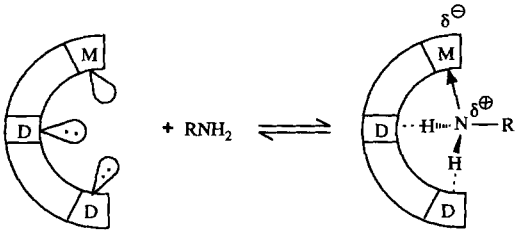

Scheme 1. Molecular recognition of amines by three-point binding.

[*] Prof. Dr. M. T. Reetz, Dipl.-Chem. C. M. Niemeyer, M. Hermes, Dr. R. Goddard
Max-Planck-Institut für Kohlenforschung
Kaiser-Wilhelm-Platz 1, D-W-4330 Mülheim an der Ruhr (FRG)

[**] This work was supported by the Deutsche Forschungsgemeinschaft (Leibniz program) and the Fonds der Chemischen Industrie.

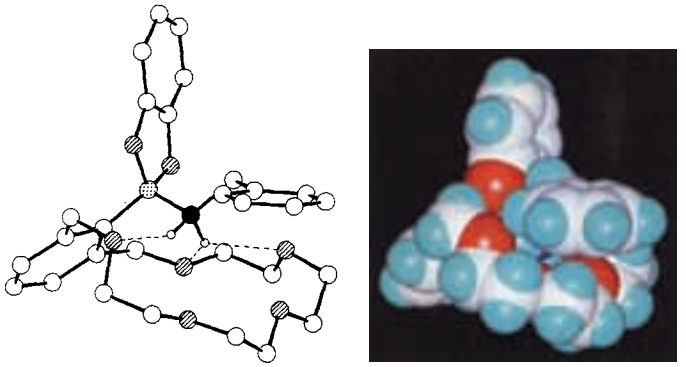

Fig. 1. Left: Crystal structure of **9**; boron, dotted; carbon: white; oxygen: hatched; nitrogen: black (only hydrogen atoms attached to nitrogen are shown). Right: space-filling portrayal of **9** [11]. Carbon: white; oxygen: red; nitrogen: dark blue; hydrogen: light blue; boron: concealed.

sensitive response to steric factors. For example, in the case of benzylamine/methylbenzylamine or benzylamine/dibenzylamine pairs (**4**/**5** or **4**/**8**), benzylamine is bound exclusively. Of particular significance is the selectivity in the competition between two α-unbranched primary amines, for example, **6** versus **4** and **7** versus **4**. (**4** vs. **5** = >98:<2; **4** vs. **8** = >98:<2; **6** vs. **4** = 90:10; **7** vs. **4** = 80:20.)

Synergism as the result of three-point binding could also be demonstrated with the hosts **1**, **2a**, and **3**. The binding constants K for the reaction of these hosts with benzylamine **4** were determined by the NMR titration method[12] at room temperature.[13] The data collected in Table 1 point to a distinct dependence of the values of K on the ring size of the crown ether (cf. positions 1–3). In fact, when the existence of

Table 1. Binding constants K for the equilibrium host + benzylamine $\overset{K}{\rightleftharpoons}$ host/benzylamine at 23 °C in CCl_4.

Position	Host	K
1	**1**	795
2	**2a**	30
3	**3**	6
4	phenylboronic acid glycol ester/ benzo[18]crown-6	1.3
5	phenylboronic acid glycol ester	0.3

a three-point interaction is assumed, Corey–Pauling–Koltun (CPK) models show that benzylamine fits distinctly better into the smaller crown ether. To what extent preorganization[1] also plays a role cannot be answered at present, because the conformation of the neutral host molecule is unknown. Control experiments with phenylboronic acid glycol ester as the host (Table 1; position 5) and phenylboronic acid glycol ester/benzo[18]crown-6 as the host system[14] (position 4) are also revealing: although the boron centers of the respective boronic acid esters are sterically less shielded than in the hosts **1**–**3**, the binding constants K are considerably *smaller*. This result also shows that the boron compounds **1**–**3** are not conventional Lewis acids.[5,6]

Finally, several experiments were conducted with anhydrous ammonia. For example, the host **2b** reacts with NH_3 to form the adduct **10**, in which strong four-point binding may be operative. The ammonia molecule is not displaced by the addition of a 100% excess of benzylamine. The binding constants for the reaction of ammonia with the hosts **2a** (K = 310) and **3** (K = 27) at room temperature demonstrate that NH_3 is actually bound more strongly than benzylamine (**2a**: K = 30; **3**: K = 5.8) or *n*-propylamine (**2a**: K = 132; **3**: K = 7.6). This observation is in contrast to that for conventional boron compounds such as $(CH_3)_3B$ which bind ammonia *less* strongly than they do primary amines.[6]

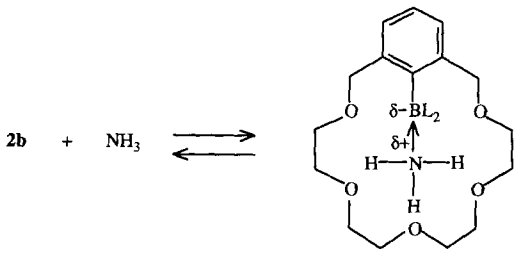

10

The selectivities described here are without precedence in molecular recognition. All experimental findings are in agreement with the synergism outlined in Scheme 1. It remains to be seen whether a high degree of enantioselective recognition is possible for racemic amines on the basis of chiral hosts containing boron or other σ-bound metal centers.

Received: February 12th, 1992 [Z 5182 IE]
German version: *Angew. Chem.* **1992**, *104*, 1053

CAS Registry numbers:
1, 139719-98-5; **1** · **4**, 141928-11-2; **2a**, 139719-99-6; **2a** · **4**, 141902-94-5; **2b**, 136426-46-5; **2b** · **5**, 141902-90-1; **2b** · **6**, 141902-91-2; **2b** · **7**, 141902-92-3; **2b** · **8**, 141902-93-4; **3**, 139720-00-6; **3** · **4**, 141902-95-6; **4**, 100-46-9; **5**, 98-84-0; **6**, 107-10-8; **7**, 64-04-0; **8**, 103-49-1; **9**, 141902-87-6; **9** · 0.5 C_7H_8, 141902-88-7; **10**, 141902-89-8; phenylboronic acid glycol ester · **4**, 97376-88-0.

[1] See, for example: F. Vögtle, *Supramolekulare Chemie*, Teubner, Stuttgart, **1989**; *Supramolecular Chemistry*, Wiley, Chichester, England, **1991**; H.-J. Schneider, *Angew. Chem.* **1991**, *103*, 1419–1439; *Angew. Chem. Int. Ed. Engl.* **1991**, *30*, 1417; J.-M. Lehn, *ibid.* **1988**, *100*, 92–116 and **1988**, *27*, 90; D. J. Cram, *ibid.* **1988**, *100*, 1041–1052 and **1988**, *27*, 1009; J. Rebek, Jr., *ibid.* **1990**, *102*, 261–272 and **1990**, *29*, 245.

[2] a) The complexation of amino-substituted heterocycles has been reported frequently [1]; see also J. C. Adrian, Jr., C. S. Wilcox, *J. Am. Chem. Soc.* **1991**, *113*, 678–680; J. D. Kilburn, A. R. MacKenzie, W. C. Still, *ibid.* **1988**, *110*, 1307–1308; K. S. Jeong, T. Tjivikua, A. Muehldorf, G. Deslongchamps, M. Famulok, J. Rebek, Jr., *ibid.* **1991**, *113*, 201–209; b) Compounds with two zinc-containing porphyrin rings form complexes with diamines: H. L. Anderson, C. A. Hunter, M. N. Meak, J. K. M. Sanders, *J. Am. Chem. Soc.* **1990**, *112*, 5780–5789; S. Kugimiya, *J. Chem. Soc. Chem. Commun.* **1990**, 432–434.

[3] J. Goldberg in *Crown ethers and Analogs* (Eds.: S. Patai, Z. Rappoport), Wiley, Chichester, England, **1989**, p. 359.

[4] Boron-containing host molecules of type **1**–**3** bind amines and alcohols simultaneously with formation of supramolecular complexes: M. T. Reetz, C. M. Niemeyer, K. Harms, *Angew. Chem.* **1991**, *103*, 1517–1519; *Angew. Chem. Int. Ed. Engl.* **1991**, *30*, 1474.

[5] *Comprehensive Coordination Chemistry, Vols. 1–7* (Eds.: G. Wilkinson, R. D. Gillard, J. A. McCleverty), Pergamon, Oxford, **1987**.

[6] H. C. Brown, *Boranes in Organic Chemistry*, Cornell University Press, Ithaca, USA, **1972**, p. 58–64; see also K. Maruoka, S. Nagahara, H. Yamamoto, *J. Am. Chem. Soc.* **1990**, *112*, 6115–6117.

[7] Other metal-containing macrocycles as host molecules [1,5]: A. R. van Doorn, M. Bos, S. Harkema, J. van Eerden, W. Verboom, D. N. Reinhoudt, *J. Org. Chem.* **1991**, *56*, 2371–2380; C. E. Osterberg, A. M. Arif, T. G. Richmond, *J. Am. Chem. Soc.* **1988**, *110*, 6903–6904; M. T. Blanda, J. H. Horner, M. Newcomb, *J. Org. Chem.* **1989**, *54*, 4626–4636.

[8] a) The synthetic principle has been described previously [4]; cf. M. Skowronska-Ptasinska, V. M. L. J. Aarts, R. J. M. Egberink, J. van Eerden, S. Harkema, D. N. Reinhoudt, *J. Org. Chem.* **1988**, *53*, 5484–5491; b) Alternative synthesis: S. M. Tuladhar, C. D'Silva, *Tetrahedron Lett.* **1992**, *33*, 265–268.

[9] The ^{11}B NMR signal (CD_2Cl_2, BF_3-etherate as external standard) of the host **2b** ($\delta = 30$) is shifted upfield ($\delta = 9$) by the addition of benzylamine. In the ^{13}C NMR spectrum of the adduct **9**, the signals of the benzylic C atoms, for example, are shifted down field, cf. [4].

[10] Crystallographic data for **9** · 0.5 toluene ($C_{29}H_{36}BNO_7 \cdot 0.5C_7H_8$, M_r 567.5): triclinic, space group $P\bar{1}$ [no. 2], $a = 10.648(1)$, $b = 11.760(1)$, $c = 13.755(2)$ Å, $\alpha = 67.66(1)$, $\beta = 73.60(1)$, $\gamma = 87.29(1)°$, $Z = 2$, $\rho_{calcd} = 1.24$ g cm^{-3}, $\mu(Mo_{K\alpha}) = 0.80$ cm^{-1}. Measurements were made with an Enraf–Nonius CAD4 diffractometer ($Mo_{K\alpha}$ radiation, $= 0.71069$ A, graphite monochromator, $T = 297$ K); 9275 reflections, 8825 independent, 5907 with $I > 2\sigma(I)$ considered as observed. Solution by direct methods and refinement with SHELX-76, $R = 0.074$, $R_w = 0.094$ ($w = 1/\sigma^2(F)$); all non-hydrogen atoms isotropic; hydrogen atoms attached to N and O atoms localized and refined (isotropic), the others calculated and fixed. Further details of the crystal structure determination are available on request from the Fachinformationszentrum Karlsruhe, Gesellschaft for wissenschaftlich-technische Information mbH, D-W-7514 Eggenstein-Leopoldshafen 2 (FRG), on quoting the depository number CSD-56138, the names of the authors, and the full journal citation.

[11] For the generation of the space-filling presentation given in Figure 1, the crystallographic data were employed on a Silicon Graphics computer.

[12] The equilibrium constants were obtained mathematically by a nonlinear two parameter fit of chemical shift (δ) and the logarithm of the binding constants ($\lg K$) according to the method of least squares. We thank Dr. H.-J. Buschmann, Textilforschungsanstalt Krefeld, for providing a computer program to evaluate the titration results.

[13] In a typical titration experiment 500 µL of a 0.15 M solution of the host in CCl_4 (with 5 vol.% C_6D_6) was prepared, and various equivalents of benzylamine stock solution (in the same solvent mixture) added in portions. Eight measurements were made in the range guest:host = 0.2–6. The duration of the experiments did not exceed 2 h, because in some cases slow deborylation of the host molecule was observed with a large excess of amine after ca. 6 h. The values of K given arise from the shifts of the ^{1}H NMR signals of the glycol units attached to boron. Inaccuracies arise in particular in the determination of the concentration of the host. An uncertainty of ±5% leads to a maximum derivation of ±10% in $\lg K$.

[14] The ammonia–borane adduct $H_3N \cdot BH_3$ forms complexes with various crown ethers: H. Shahriari-Zavereh, J. F. Stoddart, M. K. Williams, B. L. Allwood, D. J. Williams, *J. Inclusion Phenom.* **1985**, *3*, 355–377.

Effect of Torsional Strain and Electrostatic Interactions on the Stereochemistry of Nucleophilic Additions to Cyclohexanone and Related Systems**

By *Yun-Dong Wu, Kendall N. Houk,** and *Michael N. Paddon-Row**

Recently, Frenking, Köhler, and Reetz[1] offered a frontier molecular orbital rationalization of the well-known preference for small nucleophiles to attack cyclohexanones from the axial direction.[2] We show here that the torsional effects identified by Felkin et al.[3] provide an explanation not only of the stereoselectivity of nucleophilic addition to cyclohexanone, but to other cyclic ketones as well. The LUMO extensions identified by Frenking et al. are a simple consequence of the geometry of the transition structure, and are maximized in the direction *trans* to the bond best eclipsed with the C–O π orbitals. In addition, we show that electrostatic interactions can also have a profound effect on stereoselectivity when polar substituents are present.[4, 5]

[*] Prof. Dr. K. N. Houk, Prof. Dr. Y.-D. Wu
Department of Chemistry and Biochemistry
University of California, Los Angeles
Los Angeles, CA 90024 (USA)
Prof. Dr. M. N. Paddon-Row
Department of Organic Chemistry
University of New South Wales, Kensington NSW, 2033 (Australia)

[**] This work was supported by the U.S. National Science Foundation and the Australian Research Council. We thank the Pittsburgh Supercomputer Center for a grant of computing time.

Kobayashi et al. observed that nucleophilic additions to 1,3-dioxan-5-one (**1**) occur more by axial attack than those to cyclohexanone, while nucleophilic additions to 1,3-dithian-5-one (**7**) proceed predominantly by equatorial attack.[6, 7] These results were rationalized by Felkin's torsional effects based on structural features of these ketones,[8] an interpretation which was supported by force-field modeling of the transition state.[4b, c]

We have now calculated the axial and equatorial transition structures for the reactions of lithium hydride with **1** and **7**. The structures were fully optimized with the 3-21G or the 3-21G* (d orbitals on sulfur) basis set,[9] and the energies were further evaluated with MP2/6-31G*(sp)[10] calculations (Table 1).

Table 1. Absolute [Hartree] and relative energies [kcal mol^{-1}] of the transition structures of the reactions of 1,3-dioxan-5-one (**1**), 1,3-dithian-5-one (**7**), and cyclohexanone with lithium hydride.

	Theoretical level [a]	axial E	equatorial E	$E_{(rel)}$ [b]
1	3-21G//3-21G	385.36311	385.36494	−1.1
	6-31G*//3-21G	387.52178	387.52010	1.1
	6-31G*//6-31G*	387.52748	387.52596	1.0
	MP2/6-31G*//3-21G	388.57545	388.57784	−1.5
7	3-21G*//3-21G*	1027.819891	1027.83148	−7.9
	6-31G*//3-21G*	1032.83476	1032.84559	−6.8
	MP2/6-31G*//3-21G*	1033.79098	1033.80353	−7.9
Cyclohexanone	3-21G//3-21G	314.15521	314.15372	0.9
	6-31G*//3-21G	315.90968	315.90700	1.7
	MP2/6-31G*//3.21G	316.88236	316.88028	1.3

[a] The 6-31G* basis set here is the 6-31G* with a set of diffuse s and p orbitals on the hydride ion. [b] Always based on the transition structure of the axial attack.

Figure 1 shows the optimized structure of **1**, and axial and equatorial transition structures (**3** and **5**, respectively) for LiH addition. The six-membered ring of **1** is quite flat, as indicated by a flap angle of 156° and a ring O-C-C-C dihedral angle of 27°. The corresponding values for cyclohex-

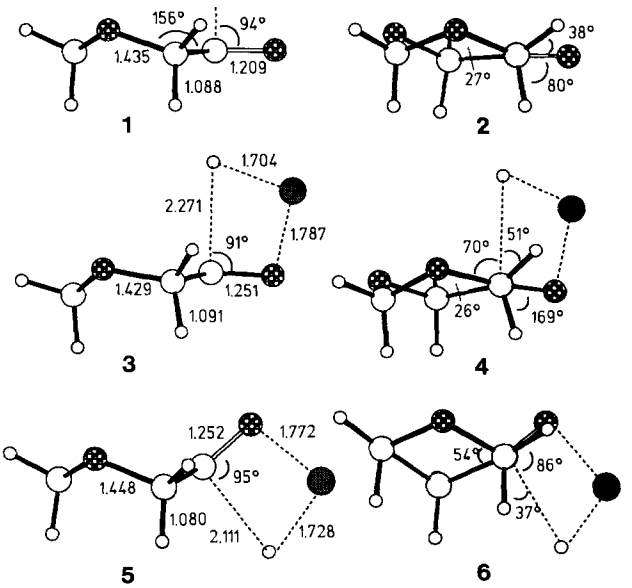

Fig. 1. Calculated structures of 1,3-dioxan-5-one (**1**), the axial (**3**) and equatorial (**5**) transition structures of the addition of lithium hydride to **1**, and Newman projections of the same structures (**2**, **4**, and **6**, respectively) along the C4–C5 bonds. Important structural parameters are also shown.

anone are 130° and 54°, respectively.[4a] This flattening is caused by the short ring O–C bonds. The axial transition structure **3** achieves a staggered conformation about the C4–C5 bond without ring distortion. However, a partially eclipsed arrangement of the substituents exists in the equatorial transition structure **5** despite major ring distortions, as indicated by a 27° increase in the ring O-C-C-C dihedral angle.

The structures of **7** and the axial (**9**) and equatorial (**11**) transition structures for LiH addition are given in Figure 2. The long S–C bonds and small C-S-C angles cause the six-membered ring to be significantly puckered (flap angle 120°, S-C-C-C dihedral angle 68°. As a result, the O=C–C–H_{eq}

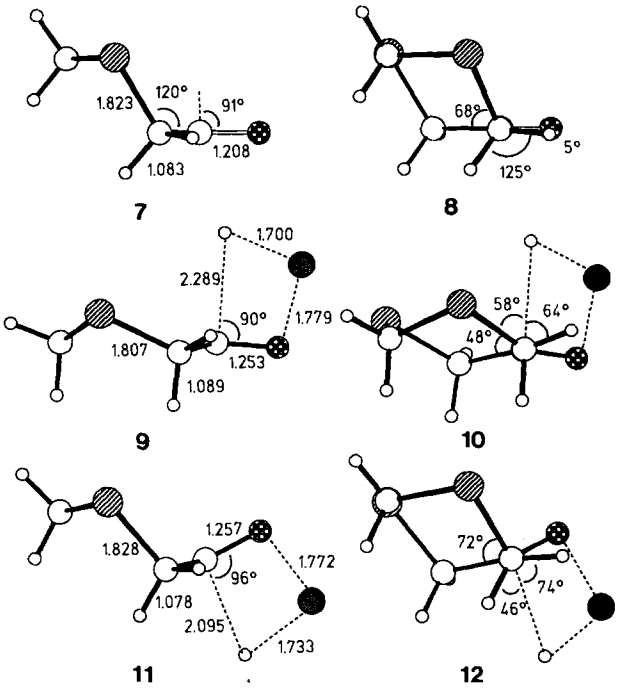

Fig. 2. Calculated structures of 1,3-dithian-5-one (**7**), the axial (**9**) and equatorial (**11**) transition structures of the addition of lithium hydride to (**7**), and Newman projections of the same structures (**8**, **10**, and **12**, respectively) along the C4–C5 bonds. Important structural parameters are also shown.

moiety is distorted on the opposite face (compare to **1**). This calculated structure is very similar to the crystal structure of 2-phenyl-1,3-dithian-5-one determined by X-ray structural analysis.[8] While there is no ring distortion in the equatorial transition structure, significant ring flattening occurs in the axial transition structure, as indicated by a 20° decrease in the S-C-C-C dihedral angle.

Removal of LiH from the transition structures and recalculation of energies of the isolated distorted ketones provides a qualitative estimate of the ring strain contribution to stereoselectivity (see below).[1, 4] The ketone moiety of **3** is 2.5 kcal mol^{-1} more stable than that of **5**, reflecting the lack of distortion in **3**. The ketone moiety in the axial transition structure **9** is less stable than that in equatorial transition structure **11** by 1.2 kcal mol^{-1}, reflecting the ring distortion in **9**.[11]

Why are the axial transition structures calculated (see Table 1) for the reactions of **1** and **7** with LiH to be disfavored by 1.5 and 8 kcal mol^{-1}, respectively? There is significant electrostatic repulsion between the negative hydride ion and the lone pairs of the respective oxygen and sulfur atoms in the axial transition structures: the hydridic hydrogen atom is quite negatively charged (H, −0.5 e, 6-31G*(sp)); the H^-–O distances in **3** (and the H^-–S distances in **9**) are only about 3.3 Å; a simple Coulomb's Law calculation using point charge interactions (− 0.6 e on O) gives repulsion of about 3 kcal mol^{-1} for each H^-–O interaction. Therefore, significant electrostatic repulsions are expected in the axial transition structures. These electrostatic interactions are less significant with lithium aluminum hydride in solution, and the axial addition to **1** becomes favorable. In the case of **7**, both torsional and electrostatic effects work against the axial addition, resulting in a large preference for the equatorial addition. For the reaction of 2-phenyl-1,3-dithian-5-one,[6] the two observed products are both likely to be derived from an equatorial attack of the nucleophile, the major transition state having the phenyl substituent equatorial and the less populated transition state having it axial. The degree of stereoselectivity is roughly equal to the relative stability of the two conformations of the reactant.[12]

Electrostatic effects of the type involved here have also been shown for other cases. We proposed that electrostatic effects cause stereochemical variations in nucleophilic additions to cyclohexanone and acetaldehyde derivatives with polar substituents.[4a, 5c] For example, a fluorine substituent at C3 of cyclohexanone causes increased axial attack of the nucleophile due to increased positive charge at the C3 position, which gives stabilizing coulombic interactions with the nucleophile approaching from the axial direction.[13]

It is necessary to reiterate our version of the Felkin torsional strain theory[3] for the preference of axial addition to cyclohexanone by small nucleophiles,[4] as Frenking et al. misinterpreted our argument.[1] For equatorial addition, in order to form an ideal staggered transition structure, ring strain would have to be introduced; to reduce or avoid this ring strain, the equatorial transition structure is forced to adapt a partially eclipsed conformation. The overall result is a balance between the two types of strain. For the cyclohexanone–LiH reaction, calculations give an ideal staggered axial transition structure (**13**) but a partially eclipsed equatorial transition structure (**14**) in which the ring strain is largely avoided,[14] but only at the expense of eclipsing strain involving the attacking nucleophile.[15]

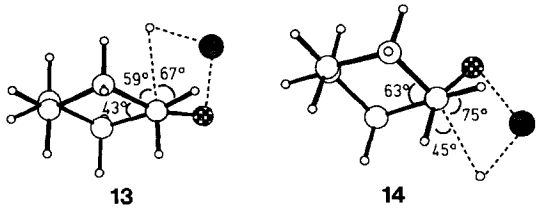

Torsional effects and orbital interactions are not mutually exclusive. Earlier, we described the secondary orbital interactions which cause the attack of nucleophiles, radicals, and electrophiles on unsaturated centers to occur in a staggered fashion with respect to allylic bonds.[16] The LUMO extensions in cyclohexanone identified by Frenking et al. are a direct consequence of geometrical distortion. As shown in Scheme 1, the LUMO interacts with the most eclipsed allylic bond in an antibonding fashion. This leads to an extension of the LUMO in the direction *trans* to the allylic bond. In cyclohexanone, the ring distortion causes the C–H bond to

be more eclipsed with the π orbitals (≮ O-C-C-H, 115°) than the C–C bond is (≮ O-C-C-C, 127°), resulting in orbital distortion in the axial direction.[1, 17] On the other hand, ring distortions in dithianone and in benzocycloheptenone are opposite to that in cyclohexanone.[18] This geometrical distortion causes equatorial orbital extension,[19] and equatorial addition of hydride ion is favored.[18]

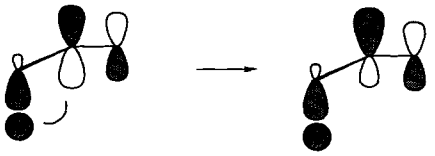

Scheme 1. The antibonding interaction indicated (left) leads to the extension of the LUMO in the direction *trans* to the allylic bond (right).

What role, if any, do orbital interactions involving the antiperiplanar C–O, C–S, C–C, and C–H bonds have?[20] The β C–O or β C–S bonds in the axial transition structures are about 0.02 Å shorter than the corresponding bonds in the equatorial transition structures. However, the C–C bonds in the axial transition structure of the cyclohexanone–LiH reaction are also shorter by about 0.02 Å. These bond length variations reflect the geometrical differences in the axial and equatorial transition structures, and do not support the argument of significant differences in hyperconjugative interactions by antiperiplanar C–O, C–S, C–C, and C–H bonds.

In summary, we demonstrate that torsional strains, and electrostatic effects in the presence of polar substituents, are most responsible for the stereoselectivity of nucleophilic additions to cyclohexanone and related systems. Orbital interactions due to the inherent difference in C–C, C–H, C–O, and C–S bonds are less important. We also point out that LUMO extension and small pyramidalizations of sp^2 centers[4a] are a direct consequence of geometrical distortions.

Received: December 16, 1991
Revised: June 3, 1992 [Z 5074 IE]
German version: *Angew. Chem.* **1992**, *104*, 1087.

[1] G. Frenking, K. F. Köhler, M. T. Reetz, *Angew. Chem.* **1991**, *103*, 1167; *Angew. Chem. Int. Ed. Engl.* **1991**, *30*, 1146.
[2] J. R. Boone, E. C. Ashby, *Top. Stereochem.* **1979**, *11*, 53.
[3] a) M. Cherest, H. Felkin, *Tetrahedron Lett.* **1968**, 2201, 2205; b) N. T. Anh, *Top. Curr. Chem.* **1980**, *88*, 145.
[4] a) Y.-D. Wu, J. A. Tucker, K. N. Houk, *J. Am. Chem. Soc.* **1991**, *113*, 5018; b) Y.-D. Wu, K. N. Houk, *ibid.* **1987**, *109*, 908; c) K. N. Houk, Y.-D. Wu in *Stereochemistry of Organic and Bioorganic Transformations* (Eds.: W. Bartmann, K. B. Sharpless), VCH, Weinheim, **1987**, pp. 247–260; d) Y.-D. Wu, K. N. Houk, B. M. Trost, *J. Am. Chem. Soc.* **1987**, *109*, 5560; e) Y.-D. Wu, K. N. Houk, J. Florez, B. M. Trost, *J. Org. Chem.* **1991**, *56*, 3656.
[5] a) S. S. Wong, M. N. Paddon-Row, *J. Chem. Soc. Chem. Commun.* **1990**, 456; b) *ibid.* **1991**, 327; c) *Aust. J. Chem.* **1991**, *44*, 765; d) Y.-D. Wu, Ph.D. Thesis, University of Pittsburgh, **1986**.
[6] Y. M. Kobayashi, J. Lambrecht, J. C. Jochims, U. Burkert, *Chem. Ber.* **1978**, *111*, 3442; J. C. Jochims, Y. Kobayashi, E. Skrzelewski, *Tetrahedron Lett.* **1974**, 571, 575.
[7] See also: T. Terasama, T. Okada, *J. Chem. Soc. Perkin Trans. 1* **1978**, 1252.
[8] Y. M. Kobayashi, Y. Iitaka, *Acta Crystallogr. Sect. B* **1977**, *33*, 923.
[9] The calculations were performed with the GAUSSIAN 90 program; M. J. Frisch, M. Head-Gordon, G. W. Trucks, J. B. Foresman, H. B. Schlegel, K. Raghavachari, M. A. Robb, J. S. Binkley, C. Gonzalez, D. J. Defrees, D. J. Fox, R. A. Whiteside, R. Seeger, C. F. Melius, J. Baker, R. L. Martin, L. R. Kahn, J. J. P. Stewart, S. Topiol, J. A. Pople, Gaussian Inc., Pittsburgh, PA, USA, **1990**.
[10] A set of diffuse s and p orbitals was added to the hydride ion.
[11] The 6-31G* and MP2/6-31G* energies of the ketone moieties are (in Hartree): 379.51067 and 380.54766 in **3**; 379.50198 and 380.54374 in **5**; 1024.82766 and 1025.76654 in **9**; 1024.82760 and 1025.76839 in **11**.
[12] R. J. Abraham, W. A. Thomas, *J. Chem. Soc.* **1965**, 335.
[13] A thorough discussion can be found in [4a]. Frenking et al. [1] suggested a change in 2s(C) coefficient in the C-O π* orbital by a 3-F substituent at C3 to be responsible for the increased axial addition, although the change is very small.
[14] The energy difference between the cyclohexanone moiety in the two cyclohexanone–LiH transition structures is basis set dependent. It is 0.0, 0.8, −0.3, and 0.2 kcal mol^{-1} with the 3-21G, 6-31G*//3-21G, MP2/6-31G*//3-21G, and MP3/6-31G*//3-21G calculations. Similar basis set dependence is also found for dioxanone and dithianone systems and for relative energies of transition structures.
[15] This strain can be roughly estimated by the calculations on the transition structure of acetone–LiH reaction. A 15° rotation of the two methyl groups away from the transition structure position in either direction causes about 1 kcal mol^{-1} increase in energy.
[16] P. Caramella, N. G. Rondan, M. N. Paddon-Row, K. N. Houk, *J. Am. Chem. Soc.* **1981**, *103*, 2438.
[17] J. Klein, *Tetrahedron Lett.* **1983**, *24*, 4307; O. Eisenstein, J. Klein, J.-M. Lefour, *Tetrahedron* **1979**, *25*, 225.
[18] D. Mukherjee, Y.-D. Wu, F. R. Fronczek, K. N. Houk, *J. Am. Chem. Soc.* **1988**, *110*, 3328.
[19] Y. Kurita, C. Takayama, *Tetrahedron Lett.* **1990**, *46*, 3789.
[20] A. S. Cieplak, *J. Am. Chem. Soc.* **1981**, *103*, 4540; A. S. Cieplak, B. D. Tait, C. R. Johnson, *ibid.* **1989**, *111*, 8447.

The Reaction of $[Cp_2^+Nb_2(B_2H_6)_2]$ ($Cp^+ = \eta$-$EtMe_4C_5$) with Sulfur: Stabilization of the Tetrathioborato Ligand in Novel Sulfido Niobium Clusters

By *Henri Brunner, Günther Gehart, Bernd Nuber, Joachim Wachter,** and *Manfred L. Ziegler*

The structural chemistry of binary boron–sulfur compounds is characterized by the formation of rings either in isolation or linked to chains, in which boron usually has the coordination number three.[1] In contrast the coordination number four is not often found. Tetrathioborates with corner-linked BS_4 tetrahedra occur in the layer structures of heavy metal thioborates.[1] However, monomeric $M[H_nB(SH)_{4-n}]$ ($n = 0-3$) compounds could only be proven by spectroscopy in solution in the form of their alkali metal salts because they are easily polymerized.[2] Hitherto tetrathioborates have not been observed as ligands in organometallic chemistry. Herein we report the first tridentate, triply bridging tetrathioborato ligand.

The surprisingly stable diboranato complex **1** was chosen as the starting material. The synthesis of **1** had been mentioned previously ten years ago, however, without specific details being given.[3] We have have recently studied **1** systematically with regard to its method of formation, structure, and spectroscopic properties.[4] The two (unstable in the free state) B_2H_6 dianions, which are arranged as bridges perpendicular to the (formal) Nb–Nb double bond are characteristic of **1**. The reaction of **1** with sulfur in decane at 170 °C affords the neutral, diamagnetic complex **2** in yields of up to 26%. The boiling temperature of *o*-xylene (144 °C)

[*] Dr. J. Wachter, Prof. Dr. H. Brunner, G. Gehart
Institut für Anorganische Chemie der Universität
Universitätsstrasse 31, D-W-8400 Regensburg (FRG)
Dr. B. Nuber, Prof. Dr. M. L. Ziegler (deceased)
Anorganisch-chemisches Institut der Universität
Im Neuenheimer Feld 270, D-W-6900 Heidelberg (FRG)

is the lowest temperature at which **2** is still formed. However, under these conditions the preparation of complex **3** (20–45% yield) predominates, which differs from **2** in that it contains an additional S atom. Elemental analyses and FD mass spectra strongly indicate the stoichiometry $[Cp_3^+Nb_3S_nBH]$ ($n = 7$ and 8, respectively) of **2** and **3**. The IR spectra show weak absorptions at 2560 (**2**) and 2550 cm^{-1} (**3**); ν_{SH} bands of diorganoborosulfanes occur in a similar region of the spectrum.[5] The ^1H NMR spectra provide interesting information about the different symmetry characteristics of **2** and **3**: whereas all Cp^+ ligands are equivalent in **2**, they are split in a ratio of 2:1 in **3**. The ^{11}B NMR spectrum of **2** shows a sharp signal at $\delta = 1.9$ ($h_{1/2} = 20$ Hz)[6] and thus lies in a similar region ($\delta = -0.6$) as that observed for $[B(SH)_4]^-$.[2]

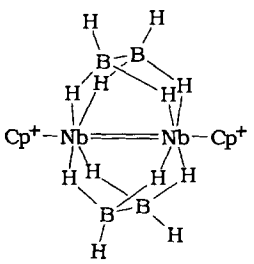

1

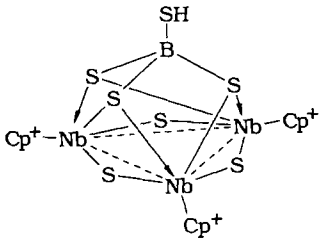

2

A crystal structure analysis has so far only been carried out for **2**[7] (Fig. 1), and this shows that the molecule consists of an equilateral Nb_3 triangle whose edges are spanned by the corners of a BS_4 tetrahedron. The sulfido ligands bridge

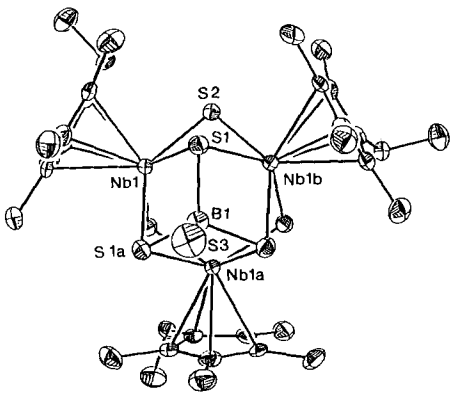

Fig. 1. Structure of **2** (ORTEP). Selected distances [Å] and angles [°]: Nb1-S1 2.554(4), Nb1-S2 2.396(4), Nb1-Nb1a 3.157(3), S1-B1 1.929(10), S3-B1 1.884(22); S1-Nb1-S1a 72.5(1), S1-Nb1-S2 80.7(1), Nb1-S1-Nb1-b 76.5(1), Nb1-S2-Nb1b 82.7(1), Nb1-S1-B1 90.8(5), S1-B1-S1a 102.8(7), S1-B1-S3 115.5(6).

the Nb–Nb edges on the "underside" of the molecule. The threefold metal-substituted ligand which is derived from $B(SH)_4^-$ is bound to the Nb_3 unit with normal Nb–S distances (average 2.554(4) Å). In contrast the Nb–S distances to the S^{2-} bridges are approximately 0.16 Å shorter. They are also shorter than the values found so far in cyclopentadienylsulfidoniobium complexes.[8] Whereas the average B–S distances are similar to those found in BS_4 tetrahedra, the angles at B1 differ from ideal tetrahedral angles by $\pm 6°$. The localization of the proton on S3 is not possible because of a disorder about the threefold axis through B1–S3. The organization of the molecules in the columnlike unit cell (c is almost 100 Å!) to give layers is peculiar. These layers are built up from BS_4 tetrahedra which lie opposite one another in such a way that the B1–S3 vectors are arranged parallel to the threefold axis and all the S3 atoms are in the same plane. Disordered solvent molecules (Et_2O) are situated approximately in this same layer (Fig. 2). The shortest intermolecular contacts between non-hydrogen atoms of the single molecules are not less than 4.0 Å.

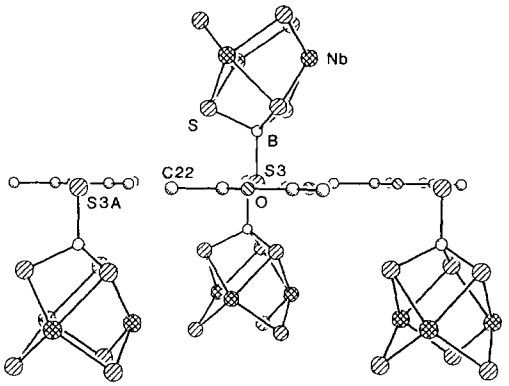

Fig. 2. Section of the unit cell of **2** with the view perpendicular to the trigonal axis. Symmetry related molecules lying opposite each other are shown without the Cp^+ ligands; the distorted ether molecules are shown in the side view. Selected distances: S3···S3A 6.98, S···C22 4.02, S3···C22 4.67 Å.

The tridentate tetrathioborato ligand of **2** acts as a 12e donor, and when the 30e of the cyclopentadienyl and sulfido ligands as well as the 2e of the Nb_3^{13+} core are added, a total of 44 valence electrons is obtained for **2**. Thus, **2** is isoelectronic with $[Cp_3^*Nb_3(\mu\text{-}Cl)_3(\mu\text{-}O)_3]^+$ ($Cp^* = C_5Me_5$),[9] which above all has an effect on the Nb–Nb bonds: from the MO calculations carried out for $[Cp_3^*Re_3(\mu\text{-}O)_6]^{2+}$[10] it was deduced that the cluster orbital with the lowest energy ($1a_1'$ symmetry) is of a strongly bonding character and should be delocalized over the Nb three-membered ring. Its occupation with the two electrons of the Nb_3^{13+} core leads to the formation of equal M–M bonds of the formal bond order 2/3. This is indicated by the Nb–Nb distances of 3.157(3) Å which are between bonding and nonbonding interactions.[9, 12]

The structure of **3** remains unclear. If the framework of **2** is considered as a basis for that of **3**, the eighth S atom must be arranged in such a way that only two Cp^+ ligands are equivalent. μ_3-S or S_2 ligands in all their varieties of coordination could then be conceivable, such as in multinuclear cyclopentadienylsulfidoniobium complexes.[8] Attempts to interconvert **2** and **3** by the directed removal and addition of sulfur, respectively, have so far been unsuccessful.

Experimental Procedure

The violet solution obtained from **1** (391 mg, 0.72 mmol) and S_8 (372 mg, 1.45 mmol) in decane (50 mL) was refluxed for 15 h, whereby the color of the solution had already changed to red-brown after 1 h. The decane was then distilled off and the residue was taken up in toluene and the suspension was filtered over SiO_2. The red filtrate was subsequently chromatographed on SiO_2 (column 30 × 3 cm). A series of small quantities of firstly an unknown compound, then **3** (15%), and **2** (18–26%) were eluted with a toluene/pentane mixture (3:1). Recrystallization was achieved from Et_2O (**2**) or Et_2O/pentane 10:1 (**3**) and this afforded analytically pure substances (correct C, H, S analyses). **2**: ^1H NMR (250 MHz, $CDCl_3$): $\delta = 1.13$ (t, $^3J(H,H) = 7.6$ Hz, 9H; CH_3), 2.11 (s, 36H; CH_3), 2.48 (q, $^3J(H,H) = 7.6$ Hz, 6H; CH_2); FD-MS (toluene) m/z 962.6 ($M^{\oplus}$); **3**: ^1H NMR (250 MHz, $CDCl_3$): $\delta = 1.13$ (t, $^3J(H,H) = 7.6$ Hz, 3H; CH_3), 1.14 (t, $^3J(H,H) = 7.6$ Hz, 6H; CH_2), 2.09 (s, 12H; CH_3), 2.10 (s, 12H; CH_3), 2.20 (s, 6H; CH_3), 2.18 (s, 6H; CH_3), 2.44 (q,

^3J(H,H) = 7.6 Hz, 4H; CH_2), 2.58 (q, ^3J(H,H) = 7.6 Hz, 2H; CH_2); FD-MS (toluene): m/z 994.1 ($M^{\oplus}$).

Received: December 2, 1991 [Z 5046 IE]
German version: *Angew. Chem.* **1992**, *104*, 1096

CAS Registry numbers:
1, 141903-35-7; **2**, 141928-15-6; **2** · Et_2O, 141928-16-7; **3**, 141928-17-8.

[1] B. Krebs, *Angew. Chem.* **1983**, *95*, 113; *Angew. Chem. Int. Ed. Engl.* **1983**, *22*, 113.
[2] H. Binder, H. Loos, K. Dermentzis, H. Borrmann, A. Simon, *Chem. Ber.* **1991**, *124*, 427; K. Wolfer, Dissertation, Universität Stuttgart, **1985**.
[3] J. E. Bercaw in *Comprehensive Organometallic Chemistry*, *Band 3* (Eds.: G. Wilkinson, F. G. A. Stone, E. W. Abel) Pergamon, New York, **1982**, p. 765, cited as a personal communication; V. C. Gibson, J. E. Bercaw, W. J. Burton, Jr., R. D. Sanner, *Organometallics* **1986**, *5*, 972.
[4] H. Brunner, G. Gehart, W. Meier, J. Wachter, B. Wrackmeyer, B. Nuber, M. L. Ziegler, *J. Organomet. Chem.*, in press.
[5] H. Vahrenkamp, *J. Organomet. Chem.* **1971**, *28*, 181; W. Siebert, E. Gast, F. Riegel, M. Schmidt, *ibid.* **1975**, *90*, 13.
[6] We thank Prof. Dr. B. Wrackmeyer, Universität Bayreuth, for carrying out the ^{11}B NMR measurement.
[7] **2** crystallized in the form of dark red, very small octahedral crystals which contained half a molecule of ether per formula unit. The systematic absences $-h+k+l = 3n$ for (h,k,l) and $l = 6n$ for (001) and the number of the formula units to be expected led to the rhombohedral space group $R\bar{3}c(D3d/6)$. The lattice constants were refined on the basis of 18 reflections ($4.0 < 2\theta < 23°$) $a = 12.08(1)$, $c = 99.77(6)$ Å, $\gamma = 120°$, $V = 12608.5$ Å^3; $Z = 12$. Syntex-R3 diffractometer $Mo_{K\alpha}$, $3.0 < 2\theta < 46.0°$; 4223 measured reflections of which 1359 with $I < 2.5\sigma(I)$ were used for the refinement. Patterson and Fourier methods, anisotropic refinement up to $R = 0.062$, $R_w = 0.047$. Further details of the crystal structure investigation may be obtained from the Fachinformationszentrum Karlsruhe, Gesellschaft für wissenschaftlich-technische Information mbH, D-W-7514 Eggenstein-Leopoldshafen 2 (FRG) on quoting the depository number CSD-56281, the names of the authors, and the journal citation.
[8] H. Brunner, W. Meier, J. Wachter, B. Nuber, M. L. Ziegler, *J. Organomet. Chem.* **1990**, *381*, C7.
[9] F. Bottomley, S. Karslioglu, *Organometallics* **1992**, *11*, 326.
[10] W. A. Herrmann, R. Serrano, M. L. Ziegler, H. Pfisterer, B. Nuber, *Angew. Chem.* **1985**, *97*, 50; *Angew. Chem. Int. Ed. Engl.* **1985**, *24*, 50.
[11] P. Hofmann, N. Rösch, H. R. Schmidt, *Inorg. Chem.* **1986**, *25*, 4470.
[12] F. Bottomley, P. N. Keizer, P. S. White, K. F. Preston, *Organometallics* **1990**, *9*, 1916; M. D. Curtis, J. Real, *Inorg. Chem.* **1988**, *27*, 3176.

Palladium-Catalyzed C-H Activation of Methoxy Groups: A Facile Synthesis of Substituted 6*H*-Dibenzo[*b*,*d*]pyrans**

By *Gerald Dyker**

Transition metal catalyzed reactions have proved themselves particularly efficient in the synthesis of annelated ring systems.[1] Palladium-catalyzed coupling reactions of aryl halides with alkenes,[2] alkynes,[3] and, intramolecularly, with arenes,[4] have been well characterized and have found numerous applications in organic synthesis. In several cases, domino processes have been observed, in which polycyclic products are formed from several molecules of simple synthetic building blocks.[5] We now report a new domino coupling reaction, where for the first time a palladium-catalyzed CH-activation at a methoxy group occurs.

ortho-Iodoanisole **1** is condensed with palladium catalysis to give a 90% yield of the substituted 6*H*-dibenzo[*b*,*d*]pyran **2**, a colorless, crystalline solid (m.p. 135°C).[6] In order to investigate the generality of this annelation, and to clarify the regiochemical course of the reaction, a series of readily available 1-iodo-2,*n*-dimethoxybenzenes ($n = 3-6$)[7] were transformed under the reaction conditions described above (Scheme 1). In the case of 1-iodo-2,3-dimethoxybenzene (**3**),

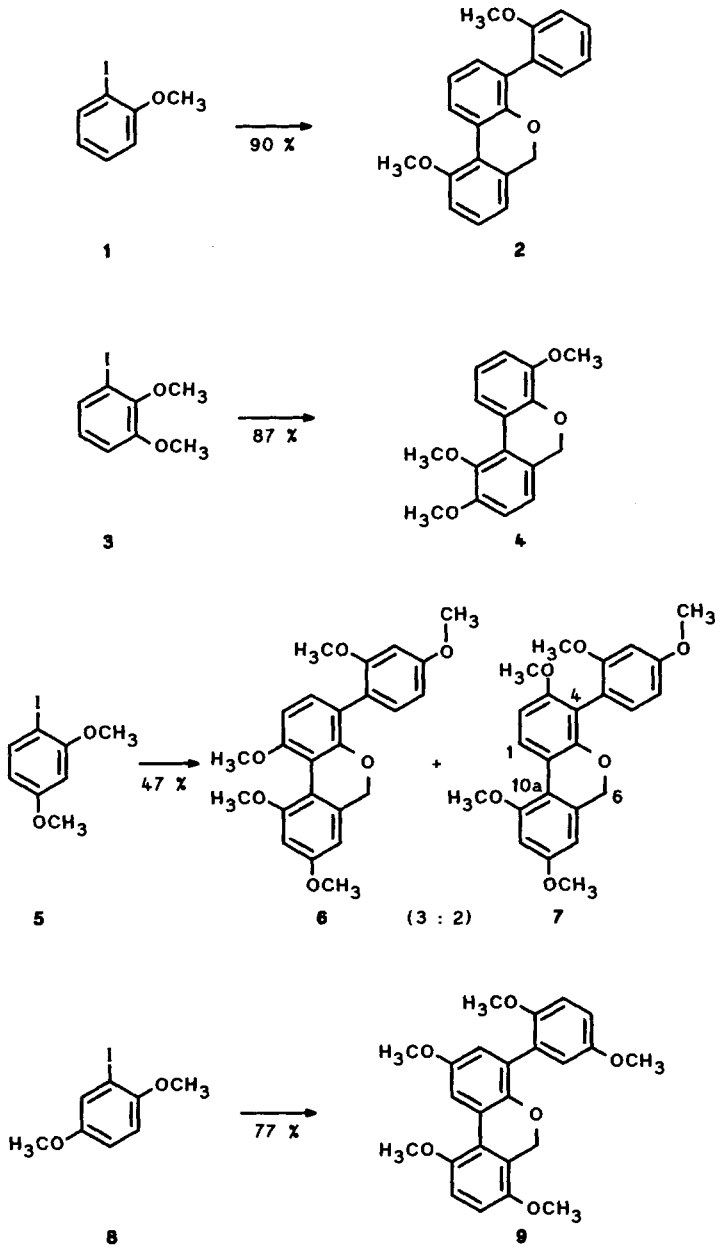

Scheme 1. Synthesis of dibenzopyrans **2**, **4**, **6**, **7**, and **9**. Reaction conditions: 4 mol% $Pd(OAc)_2$, K_2CO_3, nBu_4NBr, dimethylformamide, N_2, 3 d, 100 °C.

the condensation product **4** was obtained (87% yield, m.p. 119°C), which originates from only two molecules of the starting compound. Clearly, a crucial position for the third condensation step is blocked.

1-Iodo-2,4-dimethoxybenzene (**5**), on the other hand, affords a 47% yield of the regioisomeric annelation products **6** and **7** in a 3:2 ratio (71% yield with respect to unrecovered

[*] Dr. G. Dyker
Institut für Organische Chemie der Technischen Universität
Hagenring 30, D-W-3300 Braunschweig (FRG)

[**] Transition metal catalyzed annelation reactions, Part 2. This work was support by the Fonds der Chemischen Industrie with a Liebig Scholarship, and by Bayer AG, Monheim, with chemicals and glassware. Part 1: G. Dyker, *Tetrahedron Lett.* **1991**, *32*, 7241–7242.

starting material). A pure sample of **7** was obtained after several recrystallizations from ether/pentane to constant melting point (m.p. 162–163°C). Because of the C4–C1′ chirality axis, the methylene protons of the CH_2-6 group in the pyran ring of **7** are diastereotopic, and give rise to an AB signal in the ^1H NMR spectrum (geminal coupling constant 12.9 Hz). The ^1H NMR spectrum of **6** reveals only a singlet corresponding to two protons for this methylene group. Since the methoxy group in position 3 is absent in **6**, the C4–C1′ axis is not a chirality element in this molecule, due to the reduced steric hindrance on the NMR timescale. The methylenoxy bridge on the C10a–C10b axis ought to lead to a reduction in the atropic isomerization threshold,[4, 8] relative to the analogous di-*ortho*-substituted, but unbridged derivative.

Condensation of 1-iodo-2,5-dimethoxybenzene (**8**) leads regioselectively to **9** as the sole product isomer, in 77% yield (m.p. 134–135°C). Reaction of 1-iodo-2,6-dimethoxybenzene returns only the starting material, in 95% yield. A coupling product could not be detected. It is possible that stabilized palladium complexes are formed which lead to interruption of the catalytic cycle, and this is currently being investigated.[9]

By using the condensation reaction of **1** as an example, a possible mechanism has been developed which is in accord with the experimental findings (Scheme 2). The decisive reaction step is suggested to be the cyclometallation of the aryl Pd^{II} iodide **10** to the five-membered ring compound **11**, involving an intramolecular C-H activation[10]. Pd^{IV} complexes as additional reactive intermediates are an interesting explanation both for this reaction step and for the formation of **12** from **11**. Recently, evidence that the oxidative addition of Pd^{II} compounds to C–H and C–halogen compounds proceeds via Pd^{IV} intermediates with subsequent reductive elimination to the Pd^{II} complexes (i.e. Pd^{II}–Pd^{IV}–Pd^{II} cycles) has been documented in detail.[11]

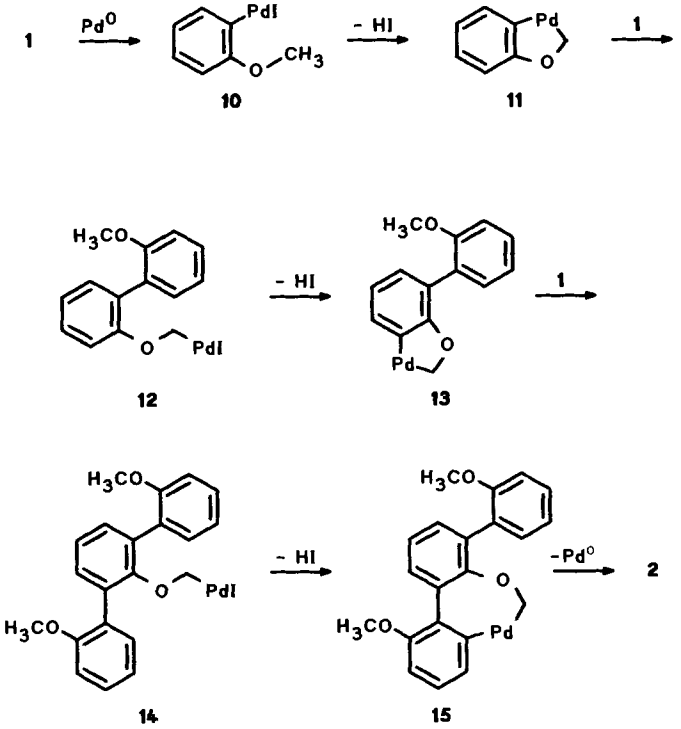

Scheme 2. Possible reaction mechanism for the domino coupling reaction of **1** to afford **2**.

The cyclometallation of **12** with dehydrohalogenation ought, by contrast, to yield a five-membered ring (**13**). Repeated addition of **1** to give the symmetric intermediate **14**, cyclometallation to the heptacyclic compound **15**, and subsequent reductive elimination lead to the condensation product **2**.

The C-H activation of methoxy groups described here represents a new reaction principle for palladium-catalyzed processes. The simple and efficient synthesis of substituted 6*H*-dibenzo[*b*,*d*]pyrans is the first application. The intramolecular palladium-catalyzed C-H activation of other neighboring groups is one target of our continuing studies, as is the development of cross couplings based on this reaction principle.

Experimental Procedure

A mixture of 2 mmol of **1**, **3**, **5**, or **8**, 0.08 mmol of $Pd(OAc)_2$, 8 mmol of K_2CO_3, and 2 mmol of nBu_4NBr in 10 mL of dimethylformamide was stirred for 3 d at 100 °C under nitrogen in a closed flask. After addition of 50 mL of water, the mixture was extracted three times with ether, the organic phase filtered through silica gel, and the solvent removed by evaporation. The products were isolated by flash chromatography (silica gel, petroleum ether/ether, 4/1), and crystallized from ether/pentane.

Selected spectroscopic and analytical data:[6]

2: ^1H NMR (400.1 MHz, $CDCl_3$, TMS): δ = 3.78 (s, 3H; 2′-OCH_3), 3.92 (s, 3H; 10-OCH_3), 4.93 (s, 2H; H-6), 6.75 ("d", "J" = 7.4 Hz, 1H; H-7), 6.93 ("d", "J" = 8.3 Hz, 1H; H-9), 6.98 ("d", "J" = 8.5 Hz, 1H; H-3′), 7.01 (m, 1H; H-5′), 7.10 ("t", "J" = 7.7 Hz, 1H; H-2), 7.20 (dd, ^3J = 7.5, ^4J = 1.7 Hz, 1H; H-3), 7.22 ("t", "J" = 7.9 Hz, 1H; H-8), 7.26 (m, 1H; H-6′), 7.33 (m, 1H; H-4′), 8.39 (dd, ^3J = 7.9, ^4J = 1.7 Hz, 1H; H-1); ^{13}C NMR (100.6 MHz, $CDCl_3$): δ = 55.57 (q; OCH_3), 55.62 (q; OCH_3), 68.85 (t; C-6), 110.89 (d; C-3′), 111.34 (d; C-9), 117.17 (d; C-7), 119.24 (s; C-10a), 120.41 (d; C-5′), 121.08 (d; C-2), 122.32 (s; C-10b), 127.42 (s; C-4), 127.68 (s; C-1′), 128.05 (d; C-1), 128.32 (d; C-8), 128.67 (d; C-4′), 130.52 (d; C-3), 131.40 (d; C-6′), 135.03 (s; C-6a), 152.77 (s; C-4a), 156.61 (s; C-10), 157.00 (s; C-2′).

4: ^1H NMR (400.1 MHz, $CDCl_3$, TMS): δ = 3.73 (s, 3H; OCH_3), 3.89 (s, 3H; OCH_3), 3.90 (s, 3H; OCH_3), 5.00 (s, 2H; H-6), 6.85 (d, ^3J = 8.2 Hz, 1H; H-8), 6.89 (dd, ^3J = 8.0, ^4J = 1.4 Hz, 1H; H-3); 6.90 (d, ^3J = 8.2 Hz, 1H; H-7), 7.01 (t, ^3J = 8.0 Hz, 1H; H-2), 8.08 (dd, ^3J = 8.0, ^4J = 1.4 Hz, 1H; H-1).

6: ^1H NMR (400.1 MHz, $CDCl_3$, TMS): δ = 3.76 (s, 3H), 3.82 (s, 3H), 3.83 (s, 3H), 3.89 (s, 3H), 3.94 (s, 3H), 4.76 (s, 2H; H-6), 6.38 (d, ^4J = 2.4 Hz, 1H), 6.52–6.56 (m, 3H), 6.74 (d, ^3J = 8.6 Hz, 1H; H-2), 7.15 (d, ^3J = 8.6 Hz, 1H; H-3), 7.16 (d, ^3J = 8.2 Hz, 1H; H-6′).

7: ^1H NMR (400.1 MHz, $CDCl_3$, TMS): δ = 3.76 (s, 3H), 3.77 (s, 3H), 3.82 (s, 3H), 3.84 (s, 3H), 3.91 (s, 3H), 4.85 (d, ^2J = 12.9 Hz, 1H; H_A-6), 4.88 (d, ^2J = 12.9 Hz, 1H; H_B-6), 6.28 (d, ^4J = 2.4 Hz, 1H), 6.50 (d, ^4J = 2.4 Hz, 1H), 6.55–6.60 (m, 2H; H-3′, H-5′), 6.70 (d, ^3J = 8.9 Hz, 1H; H-2), 7.12 (d, ^3J = 8.1 Hz, 1H; H-6′); 8.26 (d, ^3J = 8.9 Hz, 1H; H-1).

9: ^1H NMR (400.1 MHz, $CDCl_3$, TMS): δ = 3.75 (s, 3H), 3.76 (s, 3H), 3.77 (s, 3H), 3.83 (s, 3H), 3.87 (s, 3H), 5.02 (s, 2H; H-6), 6.78 (d, ^3J = 9.0 Hz, 1H), 6.79 (d, ^4J = 3.1 Hz, 1H; H-3), 6.82–6.94 (m, 4H), 8.02 (d, ^4J = 3.1 Hz, 1H; H-1).

Received: March 26, 1992 [Z 5263 IE]
German version: *Angew. Chem.* **1992**, *104*, 1079

CAS Registry numbers:
1, 529-28-2; **2**, 141957-81-5; **3**, 25245-33-4; **4**, 141957-82-6; **5**, 20469-63-0; **6**, 141957-83-7; **7**, 141957-84-8; **8**, 25245-35-6; **9**, 141957-85-9; $Pd(OAc)_2$, 3375-31-3.

[1] B. M. Trost, *Science* **1991**, *254*, 1471–1477.
[2] R. F. Heck, *Org. React. (N.Y.)* **1982**, *27*, 345–390.
[3] S. Takahashi, Y. Kuroyama, K. Sonogashira, N. Hagihara, *Synthesis* **1980**, 627–630.
[4] G. Bringmann, R. Walter, R. Weirich, *Angew. Chem.* **1990**, *102*, 1006–1019; *Angew. Chem. Int. Ed. Engl.* **1990**, *29*, 977–991.
[5] a) M. Catellani, G. P. Chiusoli, M. Costa, *Pure Appl. Chem.* **1990**, *62*, 623–630; b) W. Tao, L. J. Silverberg, A. L. Rheingold, R. F. Heck, *Organometallics* **1989**, *8*, 2550–2559; c) O. Reiser, M. Weber, A. de Meijere, *Angew. Chem.* **1989**, *101*, 1071–1072; *Angew. Chem. Int. Ed. Engl.* **1989**, *28*, 1037–1038.

[6] The new compounds **2**, **4**, **7**, and **9** were fully characterized by spectroscopic methods (IR, UV, ^{1}H NMR, ^{13}C NMR, MS) and by elemental analysis. All the NMR signals of **2** were assigned from 2D NMR spectra (H,H-COSY, C,H-COSY, COLOC); NMR data were obtained for **6** (for selected data see *Experimental Procedure*).
[7] a) H. D. Empsall, P. N. heys, B. L. Shaw, *J. Chem. Soc. Dalton Trans.* **1978**, 257–262 (Iodolysis of aryllithium compound); b) R. C. Larock, L. W. Harrison, *J. Am. Chem. Soc.* **1984**, *106*, 42118–4227.
[8] G. Bringmann, H. Reuscher, *Tetrahedron Lett.* **1989**, *30*, 5249–5252.
[9] Our own findings prove that 1-iodo-2,6-dimethoxybenzene reacts in the presence of styrene to form 2,6-dimethoxystilbene in 91% yield as product of the Heck reaction and is therefore certainly not inert under the reaction conditions.
[10] A. D. Ryabov, *Chem. Rev.* **1990**, *90*, 403–424.
[11] A. J. Canty, *Acc. Chem. Res.* **1992**, *25*, 83–90.

Carbene Osmium Complexes by Double Metalation of Alkoxylalkyl- and Aminoalkylphosphanes**

By *Helmut Werner,* Birgit Weber, Oliver Nürnberg,* and *Justin Wolf*

Dedicated to Professor Ekkehard Winterfeldt on the occasion of this 60th birthday

Since the first synthesis of a carbene metal complex by Fischer and Maasböl,[1] a wide variety of substrates have been employed to generate metal-bound carbenes.[2] In the extensive literature, however, there is no single report to date which illustrates that a compound of the general composition $[L_nM{=}CHX]$ (X = OR, NR_2, etc.) is formed from a suitable precursor CH_3X and a transition metal compound. We report here[3] that such a conversion succeeds with high efficiency with osmium as the metal center if the CH_3O or CH_3N group to be metalated is part of an alkoxylalkyl- or aminoalkylphosphane molecule.

Recently, we described that $[RuCl_2(PPh_3)_3]$ reacts with alkoxyalkylphosphane **1** by ligand exchange to give the octahedral complex $[RuCl_2(\eta^2\text{-}\mathbf{1})_2]$. If the osmium complex **2**[5] is treated with **1** under similar conditions (benzene, 80 °C, 45 h), a small amount of a yellow solid is isolated with a composition corresponding to **3a** [Eq. (a)]. Because of the

$$[OsCl_2(PPh_3)_3] \;\xrightarrow[C_6H_6,\ \Delta,\ 45\ h]{\mathbf{1}}\; [OsCl_2(=CHOCH_2CH_2P\mathit{i}Pr_2)(\eta^2\text{-}\mathbf{1})] \quad \text{(a)}$$

2 **3a**

$\mathbf{1} = \mathit{i}Pr_2PCH_2CH_2OMe$

unsatisfactory yield of **3a** (16%), we attempted to prepare this complex directly from $OsCl_3 \cdot 3H_2O$ and **1**. This reaction provided almost quantitatively (80% yield with regard to $OsCl_3 \cdot 3H_2O$) a lemon-yellow crystalline product **3b** with the same analytical composition as **3a** [Eq. (b)]. The ^{1}H NMR

$$OsCl_3{\cdot}3H_2O \;\xrightarrow[\mathit{i}PrOH,\ \Delta,\ 2\ d]{\mathbf{1}}\; [OsCl_2(=CHOCH_2CH_2P\mathit{i}Pr_2)(\eta^2\text{-}\mathbf{1})] \quad \text{(b)}$$

3b

[*] Prof. Dr. H. Werner, Dipl.-Chem. B. Weber, Dipl.-Chem. O. Nürnberg, Dr. J. Wolf
Institut für Anorganische Chemie der Universität
Am Hubland, D-W-8700 Würzburg (FRG)

[**] This work was supported by the Deutsche Forschungsgemeinschaft (SFB 347), the Fonds der Chemischen Industrie, and Degussa AG.

spectra of both compounds, **3a** and **3b**, reveal a signal in the low-field region which is split due to P–H coupling into a doublet at $\delta = 15.50$ and 15.46, respectively, thus indicating the presence of a =CHOR unit.[2c,6] In the ^{13}C NMR spectrum of **3b** a signal at $\delta = 247.33$ characteristic of a carbene moiety appears in a position very similar to that of cyclic oxycarbene complexes with the structural unit $Os{=}\overline{CCH_2CH_2CH(R)O}$.[7] The ^{31}P NMR spectra of both **3a** and **3b** show two doublets with a small P–P coupling which confirms the *cis* position of the two phosphorus atoms. These and other selected spectroscopic data for the new compounds are summarized in Table 1.

Table 1. Selected spectroscopic data (without ^{1}H and ^{13}C NMR data for the CH_2 and *i*Pr groups). ^{1}H NMR spectra at 400 MHz (at 60 MHz for **3a** only), ^{13}C NMR spectra at 100.6 MHz (at 22.5 MHz for **10** only), ^{31}P NMR spectra at 162.0 MHz for **3b** and **5**, at 36.2 MHz for **3a**, **8**, **9**, and **10**.

3a: ^{1}H NMR ($CDCl_3$): $\delta = 15.50$ (d, J(PH) = 4.0 Hz, Os=CH), 3.80 (s, OCH_3); ^{31}P NMR ($CDCl_3$): $\delta = 15.37$ and -19.00 (both d, J(PP) = 10.3 Hz)

3b: ^{1}H NMR (C_6D_6): $\delta = 15.46$ (d, J(PH) = 3.6 Hz, Os=CH), 3.79 (s, OCH_3); ^{13}C NMR ($CDCl_3$): $\delta = 247.33$ (t, J(PC) = 17.05 Hz, Os=C), 59.80 (s, OCH_3); ^{31}P NMR ($CDCl_3$): $\delta = 20.95$ (d, J(PP) = 10.1, $J(^{187}Os^{31}P) = 266$ Hz), -15.13 (d, J(PP) = 10.1, $J(^{187}Os^{31}P) = 228$ Hz)

5: ^{1}H NMR ($CDCl_3$): $\delta = 13.14$ (d, J(PH) = 4.2 Hz, Os=CH), 3.23, 2.80, and 2.40 (each s, NCH_3); ^{13}C NMR ($CDCl_3$): $\delta = 212.99$ (d, J(PC) = 7.6 Hz, Os=C), 50.59 and 49.69 (both s, NCH_3); ^{31}P NMR ($CDCl_3$): $\delta = 16.33$ (d, J(PP) = 7.3, $J(^{187}Os^{31}P) = 280$ Hz), -18.95 (d, J(PP) = 7.3, $J(^{187}Os^{31}P) = 274$ Hz)

8: ^{1}H NMR (C_6D_6): $\delta = 3.41$ (s, OCH_3); ^{13}C NMR (C_6D_6): $\delta = 185.25$ (s, CO_2Me), 55.03 (s, OCH_3); ^{31}P NMR (C_6D_6): $\delta = 2.75$ (s)

9: IR (KBr): $\tilde{\nu}$[cm^{-1}] = 1915 (OsCO), 1710 (CO_2Me, free), 1615 (CO_2Me, coord.); ^{1}H NMR ([D$_8$]toluene): $\delta = 3.53$ and 3.52 (both s, OCH_3); ^{31}P NMR ($CDCl_3$): $\delta = 24.80$ and 9.59 (both d, J(PP) = 290.2 Hz)

10: ^{1}H NMR ([D$_8$]toluene, 60 °C): $\delta = 7.38$ and 6.95 (both m, C_6H_5), 3.52 (s, OCH_3), 2.64 (t, J(PH) = 5.9 Hz, Os=C*H*Ph); ^{13}C NMR (C_6D_6): $\delta = 297.11$ (t, J(PC) = 22.0 Hz, Os=*C*=CHPh), 109.31 (t, J(PC) = 6.1 Hz, Os=C=*C*HPh), 53.25 (s, OCH_3); ^{31}P NMR ([D$_8$]toluene): $\delta = 2.56$ (s) at 40 °C; $\delta = 9.51$ and -2.93 (both d, J(PP) = 332 Hz) at -80 °C.

The stereochemistry of **3b** is established by the X-ray structure analysis.[8] It confirms (Fig. 1) that one of the alkoxyalkylphosphane ligands is converted by double metalation of the methoxy group into a carbene unit, which is

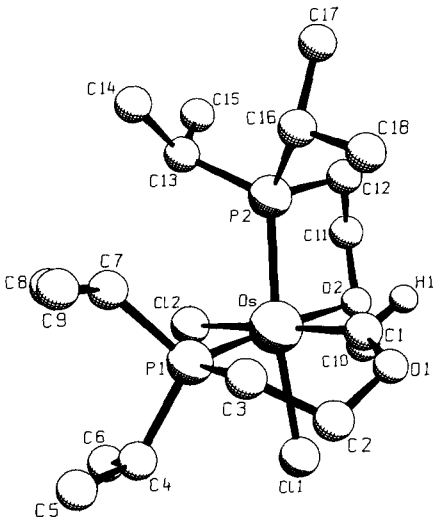

Fig. 1. Crystal structure of **3b**. Selected bond distances [Å] and angles [°]: Os-C1 1.83(1), Os-P1 2.256(3), Os-P2 2.336(3), Os-Cl1 2.466(4), Os-Cl2 2.495(3), Os-O2 2.297(8), C1-O1 1.34(1), C2-O1 1.42(2); P1-Os-O2 176.5(3), P2-Os-Cl1 167.3(1), C1-Os-Cl2 167.4(3), Os-C1-O1 138.8(9).

 © VCH Verlagsgesellschaft mbH, W-6940 Weinheim, 1992 0570-0833/92/0808-1025 $ 3.50+.25/0

part of a six-membered chelate ring system. The intact alkoxyalkylphosphane ligand is coordinated to the metal center at P and O. The Os–C1 distance is significantly shorter than that in related carbene osmium complexes such as $[OsCl(=CH_2)(NO)(PPh_3)_2]$ (1.92(1) Å) and $[OsCl_2(=CHPh)(CO)(PPh_3)_2]$ (1.94(1) Å),[6] both of which also contain two phosphane ligands.

For $[OsCl_2(=CHOCH_2CH_2PiPr_2)(\eta^2\text{-}1)]$ there are three more possible stereoisomers besides **3b**—**A**, **B**, and **C** which are all chiral (Scheme 1). The question of which of the isomers **A**, **B**, or **C** corresponds to the complex **3a** is still open. Remarkably, in the single crystal of **3b** used for the X-ray structural analysis only one enantiomer is present, which according to the designation for octahedral complexes not containing two cisoid bidentate or three bidentate ligands has the *A* configuration (corresponding to the *S* configuration for tetrahedral compounds).[9] The enantiomeric purity of the crystal could be due to packing effects or, alternatively, could originate from the mechanism of the reaction of $OsCl_3 \cdot 3H_2O$ with **1**. We assume that the formation of **3a** and **3b** occurs via hydridometal intermediates, and that an insertion of the metal into the C–H bond of a OCH_3 group is the primary step. In this context we note that in the reaction of the olefin iridium compound $[IrCl(C_8H_{14})_2]_2$ with **1**, the metallated hydridoiridium complex $[IrHCl(CH_2OCH_2CH_2PiPr_2)(\eta^2\text{-}1)]$ is formed nearly quantitatively.[10]

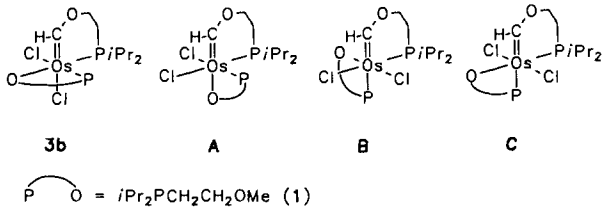

Scheme 1.

The reaction of $OsCl_3 \cdot 3H_2O$ with aminophosphane **4** proceeds in moderate yield (40–50%) to the carbene complex **5**, and that of **2** with **4** in good yield (70–75%). In the reaction of $OsCl_3 \cdot 3H_2O$ with **4**, several by-products are formed which could not as yet be completely separated from **5**. By comparing the ^1H, ^{13}C, and ^{31}P NMR data of **5** and **3b** we conclude that the compounds are structurally related.

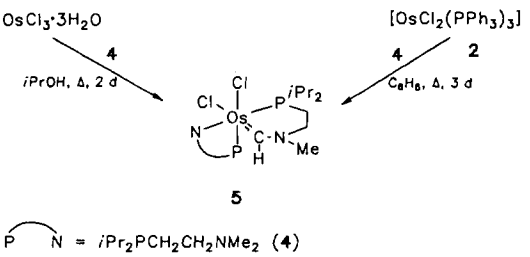

Scheme 2.

An osmium complex of the general type $[OsCl_2(\eta^2\text{-}iPr_2P\text{-}Y)_2]$ (Y = heteroatom unit), originally expected as the product of the reaction of **2** and **1**, is accessible with the methyloxycarbonylphosphane **6**. Compound **8** is isolated in 90% yield after a mixture of **7**[11] and **6** in hexane is heated at 110 °C for 4 h (Scheme 3). Surprisingly, the reaction of **8** with CO leads to a monocarbonyl and not to a dicarbonyl metal complex (isolated yield of **9**: 77%); the reaction of **8** and phenylacetylene affords vinylidene–osmium derivative **10** quantitatively. The Os=C distance in **10** is 1.802(6) Å, comparable with the Os=C bond length in **3b**.[3]

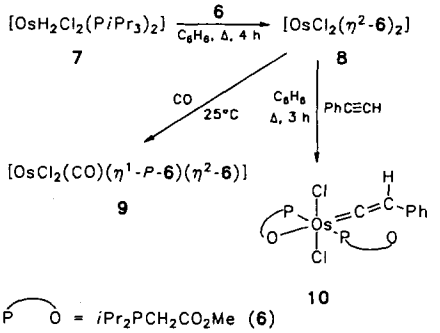

Scheme 3.

In toluene at room temperature compound **10** exists in two rapidly converting isomeric forms as is apparent from the broadening of the ^1H NMR signals. The free energy of activation $\Delta G^{\neq}$ for the "open-and-close mechanism" (i.e. the simultaneous cleavage and formation of one Os–O bond) is 53 kJ mol^{-1} (T = 288 K).[12] The carbonyl complex was found to be rigid at room temperature on the NMR timescale; owing to the large P–P coupling (290 Hz) of the signals in the ^{31}P NMR spectrum there is no doubt that the two nonequivalent phosphane ligands are *trans* to each other.[13]

Experimental Procedure

3b: A suspension of 413 mg (1.18 mmol) of $OsCl_3 \cdot 3H_2O$ in 20 mL of 2-propanol was treated with 870 µL (4.70 mmol) of **1** and heated for 48 h at reflux. After the solution was cooled, it was concentrated to 2 mL, and 25 mL of ether was added. The yellow solid that precipitated was filtered off and recrystallized twice from methanol/ether. A second fraction of **3b** was isolated from the filtrate; yield 576 mg (80%); m.p. 132 °C.

5: A solution of 214 mg (0.37 mmol) of **2** in 10 mL of benzene was treated with 234 µL (1.10 mmol) of **4** and heated for 72 h under reflux. After the solution was cooled, the solvent was removed and the brown oily residue stirred with 10 mL of hexane to give a pale yellow solid; yield 166 mg (71%) m.p. 176 °C.

8: A suspension of 119 mg (0.20 mmol) of **7** in 15 mL of hexane was treated dropwise with 120 µL (0.61 mmol) of **6** and heated for 4 h at 110 °C in a sealed tube. After the solution was cooled, orange crystals started to precipitate. To enhance the precipitation, the reaction mixture was concentrated to 2 mL. The orange crystalline solid was filtered off and washed with ether; yield 118 mg (90%); m.p. 69 °C.

10: A solution of 93 mg (0.145 mmol) of **8** in 5 mL of benzene was treated with 32 µL (0.29 mmol) of phenylacetylene and heated for 3 h at reflux. After the solution was cooled, the solvent was removed and the residue stirred with a small amount of hexane to give a salmon-colored solid; yield 103 mg (96%); m.p. 154 °C.

Received: March 12, 1992 [Z 5236 IE]
German version: *Angew. Chem.* **1992**, *104*, 1079

[1] E. O. Fischer, A. Maasböl, *Angew. Chem.* **1964**, *76*, 645; *Angew. Chem. Int. Ed. Engl.* **1964**, *3*, 580.
[2] a) K. H. Dötz, H. Fischer, P. Hofmann, F. R. Kreissl, U. Schubert, K. Weiss, *Transition Metal Carbene Complexes*, Verlag Chemie, Weinheim, **1983**, Chap. 1; b) *Advances in Metal Carbene Chemistry* (Ed.: U. Schubert) (*NATO ASI Ser. Ser. C* **1989**, *269*); c) P. J. Brothers, W. R. Roper, *Chem. Rev.* **1988**, *88*, 1293–1326.
[3] B. Weber, Diplomarbeit, Universität Würzburg, **1992**.
[4] H. Werner, A. Stark, M. Schulz, J. Wolf, *Organometallics* **1992**, *11*, 1126–1130.

[5] P. R. Hoffman, K. G. Caulton, *J. Am. Chem. Soc.* **1975**, *97*, 4221–4228.
[6] a) M. A. Gallop, W. R. Roper, *Adv. Organomet. Chem.* **1986**, *25*, 121–198; b) W. R. Roper, *J. Organomet. Chem.* **1986**, *300*, 167–190.
[7] H. Werner, W. Knaup, M. Schulz, *Chem. Ber.* **1991**, *124*, 1121–1125.
[8] Crystals from methanol/diethyl ether (1:5); crystal size $0.1 \times 0.2 \times 0.4$ mm; orthorhombic, space group $P2_12_12_1$ (No. 19); $Z = 4$; $a = 10.459(2)$, $b = 14.232(3)$, $c = 15.925(3)$ Å, $V = 2370.4$ Å^3, $\rho_{calcd} = 1.71$ g cm^{-3}; max. $2\theta = 52°$ ($Mo_{K\alpha}$, $\lambda = 0.70930$ Å, graphite monochromator, $\omega/2\theta$-scan, $T = 293$ K); 2645 independent reflections, 1645 observed [$F_o > 3\sigma(F_o)$], Lorentz, polarization, and empirical absorption corrections ($\mu = 57.4$ cm^{-1}, Ψ-scan method, min. transmission 88.2%); Patterson method (SHELXS 86), refinement with program package SDP (Enraf–Nonius). The hydrogen atoms were calculated for ideal geometry by the riding method and included in the final refinement (full-matrix least-squares); $R = 0.045$, $R_w = 0.049$; reflex/parameter ratio 7.32; residual electron density $+1.56/-0.91$ eÅ^{-3}. The absolute configuration at the osmium center was determined after the anomalous dispersion had been taken into account. For the other enantiomer $R = 0.060$ and $R_w = 0.069$. Further details of the X-ray structure analysis are available on request from the Fachinformationszentrum Karlsruhe, Gesellschaft for wissenschaftlich-technische Information mbH, D-W-7514 Eggenstein-Leopoldshafen 2 (FRG), on quoting the depository number CSD-56271, the names of the authors, and the journal citation.
[9] T. E. Sloan in *Top. Stereochem.* (Ed.: G. L. Geoffroy), **1981**, *12*, 1–36.
[10] M. Schulz, Ph.D. Thesis, Universität Würzburg 1991.
[11] M. Aracama, M. A. Esteruelas, F. J. Lahoz, J. A. Lopez, U. Meyer, L. A. Oro, H. Werner, *Inorg. Chem.* **1991**, *30*, 288–293.
[12] For further examples see: A. Bader, E. Lindner, *Coord. Chem. Rev.* **1991**, *108*, 27–110.
[13] a) P. Braunstein, D. Matt, Y. Dusausoy, *Inorg. Chem.* **1983**, *22*, 2043–2047; b) E. Lindner, U. Schober, R. Fawzi, W. Hiller, U. Englert, P. Wegner, *Chem. Ber.* **1987**, *120*, 1621–1628.

Double Open-Edged P_{10} Dihydrofulvalene as a 16-Electron Donor Ligand**

By *Otto J. Scherer,* Bernd Höbel,* and *Gotthelf Wolmershäuser*

Since the discovery of the stabilization of P, As, and several other P_n and As_n molecules by complexation approximately 20 years ago, it has become clear—especially in very recent times—that no limit has yet been placed on the structural variety of such acyclic, cyclic, and polycyclic P_n and As_n ligands.[1] Whereas theory predicts polycyclic molecules as being the most stable isomers for P_5 to P_{11},[2] the *cyclo*-E_n molecules (E = P, As; $n = 4–6$), isovalent with the carbocyclic $(CH)_n$ π systems, can also be stabilized by coordination.[1]

Starting from **1** and E_4 (E = P, As) we have now been able to synthesize E_n building blocks of this type, namely, P_{10} and As_{10} (structure type **B**). These are analogous to the dihydrofulvalene **A** and are coordinated in an open-edged form as ligand in the tetranuclear rhodium complexes **2** [Eq.(a)].

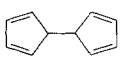

A ($C_{10}H_{10}$)

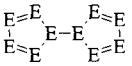

B (E_{10}; E = P, As)

Complexes **2a**, **b** form black crystals which can be handled in air for a short time. These crystals dissolve well in hexane and are even more soluble in benzene and dichloromethane.

$$[Cp''Rh(CO)_2]\ \mathbf{1} \xrightarrow[190\,°C,\ 3\ h]{E_4,\ decalin} \begin{matrix}[(Cp''Rh)_2(E_5\text{–}E_5)(RhCp'')_2]\quad \mathbf{2a, b}\\ +\\ [\{(Cp''Rh)(\mu,\eta^2\text{:}\eta^2\text{-}E_2)\}_2]\quad \mathbf{3a, b}\end{matrix} \qquad (a)$$

a: E = P, **b**: E = As; Cp'' = 1,3-tBu$_2$C$_5$H$_3$

The X-ray structure analysis[3] (Fig. 1) shows that the polycyclic Rh_4P_{10} framework of **2a** is centrosymmetric and also that the all-phophorus analogue of dihydrofulvalene P_{10}[4] (structure type **B**) is arranged so that the Rh atoms can achieve the 18 valence electron configuration; formally, Rh 2 receives the four π electrons of the double bonds P2–P 3 and P 4–P 5 [2.143(2) and 2.148(2) Å, respectively], and Rh 1 has the pair of nonbonding electrons on P 1 at its disposal, as well as a bonding electron pair as a result of the opening (oxidative addition) of the P 3–P 4 edge [2.624(2) Å]. Thus,

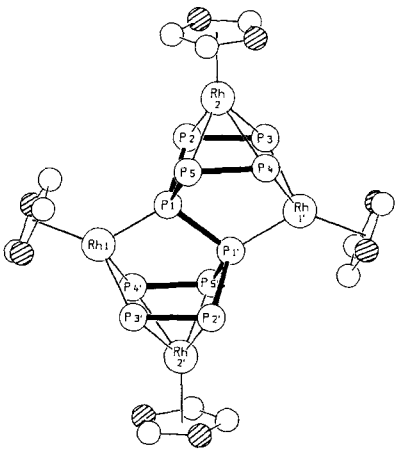

Fig. 1. Crystal structure of **2a**. Selected bond lengths [Å] and bond angles [°]: P1-P1' 2.184(2), P1-P2 2.192(1), P1-P5 2.193(1), P2-P3 2.143(2), P4-P5 2.148(2), P3 ··· P4 2.624(2), Rh1-P1 2.209(1), Rh1-P3' 2.329(1), Rh1-P4' 2.325(1), Rh2-P2 2.406(1), Rh2-P3 2.435(1), Rh2-P4 2.443(1), Rh2-P5 2.401(1), Rh1-Cp'' (center) 1.95, Rh2-Cp'' (center) 1.90; P1'-P1-P2 101.7(1), P1'-P1-P5 102.2(1), P1'-P1-Rh1 111.0(1), P2-P1-P5 91.2(1), P1-P2-P3 100.2(1), P2-P3-P4 96.7(1), P3-P4-P5 96.9(1), P4-P5-P1 99.5(1), P3-Rh1'-P4 68.6(1), P3-Rh2-P4 65.1(1), Rh1'-P3-Rh2 112.6(1), Rh1'-P4-Rh2 112.4(1), P1-P2-Rh2 93.5(1), P1-P5-Rh2 93.6(1), P2-Rh2-P5 81.4(1). ⊘ = CtBu.

P_{10} functions as a 16-electron donor ligand. The structure of the [Rh 2,P 3,P 2,P 5,P 4,Rh 1'] fragment differs only slightly from the analogously constructed binuclear complex **4**[5] (for **2a** one has to imagine that P 2 is connected to P 5, Fig. 1). The Rh 1–P 1 distance (2.209(1) Å) is similar to the Rh–P

$[Cp'Rh(\mu,\eta^4\text{:}\eta^1\text{:}\eta^1\text{-}P_4)Rh(CO)Cp']$ **4**, Cp' = C_5Me_4Et $\quad$ $[(Ph_3P)_2Rh(\mu\text{-}Cl)]_2$ **5**

$[\{CpCr(CO)_2\}_5(P_{10})]$ **6**, Cp = C_5H_5 $\quad$ BaP_{10} **7** $\quad$ Cu_4SnP_{10} **8**

distances of 2.200(2) and 2.213(2) Å found in the binuclear complex **5**.[6] The average value of the P–P distances (2.17 Å) in **2a** is significantly shorter than that for the same distances

[*] Prof. Dr. O. J. Scherer, Dipl.-Chem. B. Höbel, Dr. G. Wolmershäuser[+]
Fachbereich Chemie der Universität
Erwin-Schrödinger-Strasse, D-W-6750 Kaiserslautern (FRG)

[+] X-ray structure analyses

[**] This work was supported by the Fonds der Chemischen Industrie. We thank Johnson Matthey, Reading, England, for their generous loan of $RhCl_3$.

in complex **6** (2.22 Å), the polycyclic P_{10} framework of which is constructed from a P_7 norbornane with a P_2 bridge and one terminal P atom.[7] The P_{10} ion in the polyphosphide **7** [$\bar{d}$(P–P) = 2.21 Å] forms the two-dimensional infinite polyanion $^2_\infty[P^{2-}_{10}]$ by the linkage of pentagons of phosphorus atoms arranged in tubes in one direction;[8] the polyphosphide **8** [$\bar{d}$(P–P) = 2.18 Å] has a P^{6-}_{10} framework with a structure analogous to adamantane.[9] The four-membered rings Rh 2-P 2-P 1-P 5 (sum of angles = 359.7°) and Rh 2-P 3-Rh 1′-P 4 (358.7°) in **2a** are almost planar. The plane P 3-P 4-P 5-P 2 is almost parallel with the C_5 plane of the Cp″ ligand at Rh 2 (deviation 1.1°), whereas for the P 1′-P 3-P 4 plane and the C_5 plane of the Cp″ ligand at Rh 1′ the deviation is greater (5.6°).

The structure of the P_{10} framework of **2a** was also established from an analysis of the P,P-COSY 45 NMR spectrum.[10] According to the most recent theoretical studies[2b] the P_8 cuneane framework with a P_2 bridge is considered to be the most stable framework for the calculated P_{10} isomers. All indications from the X-ray structure data[3] obtained for **2b** were in agreement with an As_{10} framework analogous to the P_{10} ligand of **2a**.[11] To our knowledge neither the polyarsenide ions corresponding to the polyphosphides **7** and **8** nor other As^{n-}_{10} polyarsenide ions are known.

For the E_4 unit of the complexes **3a, b** we propose a $(\mu, \eta^2{:}\eta^2\text{-}E_2)_2$ ligand, which has already been confirmed by X-ray structure analyses.[12]

Experimental Procedure

2a, 3a: A solution of P_4 (1.5 g, 12.1 mmol) in decalin (75 mL) was allowed to react with **1** (1.04 g, 3.09 mmol) and the mixture was stirred under reflux for 3 h. After the removal of the solvent in vacuum the dried residue was transferred to a column (20 × 1.5 cm) packed with Al_2O_3 (3% H_2O) and petroleum ether. With petroleum ether/toluene (10:1) a yellow-orange fraction was obtained from which **3a** (47 mg, 4.5%) was isolated as an orange powder. With petroleum ether/toluene (1:1) pure **2a** (384 mg, 35%) was eluted, which after recrystallization from hexane gave black, rectangular crystals.

2b, 3b: 200 mL of a boiling solution of As_4 in decalin (about 12 mg As_4 per mL, ca. 8 mmol) was allowed to react with **1** (1.1 g, 3.27 mmol). The reaction and work up was carried out analogously to **2a, 3a**. With petroleum ether/toluene (10:1) a violet fraction was eluted from which **3b** (280 mg, 20%) was isolated as a brown powder. A 5:1 mixture of the same solvents led to a beige-brown fraction which after the removal of the solvent in vacuum afforded brown $[Cp''_2Rh_2As_6]$ (53 mg, 3%) [13]. With a 1:1 mixture a red-brown fraction was eluted from which pure **2b** (517 mg, 34%) could be isolated. After recrystallization from benzene thin, black, diamond-shaped crystals were obtained.

Received: March 6, 1992 [Z 5228 IE]
German version: *Angew. Chem.* **1992**, *104*, 1042

CAS Registry numbers:
1, 142039-96-1; **2a**, 142039-97-2; **2b**, 142039-99-4; **3a**, 142039-98-3; **3b**, 142040-00-4; $[Cp''_2Rh_2As_6]$, 142040-01-5; P_4, 12185-10-3; As_4, 12187-08-5.

[1] Recent review: O. J. Scherer, *Angew. Chem.* **1990**, *102*, 1137–1155; *Angew. Chem. Int. Ed. Engl.* **1990**, *29*, 1104–1122.

[2] a) R. O. Jones, D. Hohl, *J. Chem. Phys.* **1990**, *92*, 6710–6721; b) R. O. Jones, G. Seifert, *J. Chem. Phys.*, **1992**, *96*, 7564–7572.

[3] **2a**: triclinic, space group $P\bar{1}$, $a = 11.219(8)$, $b = 14.816(10)$, $c = 10.152(8)$ Å, $\alpha = 102.02(4)$, $\beta = 111.45(4)$, $\gamma = 83.39(5)°$, $Z = 1$, 5728 independent reflections ($Mo_{K\alpha}$: $1.5° \le \theta \le 25°$), of which 5351 were observed with $I \le 2\sigma(I)$; $R = 0.038$, $R_w = 0.049$. Solution and refinement carried out with the SHELXS-86 and SHELX-76 programs. For **2b** so far no single crystals suitable for a complete X-ray analysis have been obtained. All the crystals investigated only gave very weak X-ray reflections. In addition there were ambiguities with the determination of the Laue group and space group, combined with problems with twinning and the superstructure. Further details of the crystal structure investigation may be obtained from the Fachinformationszentrum Karlsruhe, Gesellschaft für wissenschaftlich-technische Information mbH, D-W-7514 Eggenstein-Leopoldshafen 2 (FRG) on quoting the depository number CSD-56601, the names of the authors, and the journal citation.

[4] Cf. with $(\dot{C}R)_4\dot{E}\text{-}\dot{E}(R\dot{C})_4$, E = P: F. Mathey, *Chem. Rev.* **1988**, *88*, 429–453; E = As: A. J. Ashe III, W. M. Butler, T. R. Diephouse, *Organometallics* **1983**, *2*, 1005–1008.

[5] O. J. Scherer, M. Swarowsky, G. Wolmershäuser, *Angew. Chem.* **1988**, *100*, 738–739; *Angew. Chem. Int. Ed. Engl.* **1988**, *27*, 694–695.

[6] M. D. Curtis, W. Butler, J. Greene, *Inorg. Chem.* **1978**, *17*, 2928–2931.

[7] L. Y. Goh, R. C. S. Wong, E. Sinn, *J. Chem. Soc. Chem. Commun.* **1990**, 1484–1485.

[8] H. G. von Schnering, G. Menge, *Z. Anorg. Allg. Chem.* **1982**, *491*, 286–294.

[9] J. W. Hönle, H. G. von Schnering, *Z. Kristallogr.* **1980**, *153*, 339–350; cf. with $P_{10}R_6$: M. Baudler, L. de Riese-Meyer, C. Wiaterek, *Z. Naturforsch. B.* **1989**, *44*, 375–380.

[10] AA′A″A‴BB′B″B‴CC′XX′YY′ Spin system (≙ P2P5P5′P2′P3P4P4′P3′ P1P1′Rh1Rh1′Rh2Rh2′ in Figure 1). δ(P2P5P5′P2′) ≈ −160 (m, 4P), δ(P3P4P4′P3′) ≈ 53 (m, 4P), δ(P1P1′) ≈ 280 (m, 2P). A simulation of the spectra is reserved for future studies. Cross-signals: P2P5P5′P2′ × P3P4P4′P3′ and P1P1′. We thank Priv.-Doz. Dr. J. Hahn, Cologne, for recording the COSY spectrum. ^{31}P NMR (162 MHz, C_6D_6, 85% H_3PO_4 ext.): **3a**: $\delta = 76.6$ (t, 4P), $^1J(Rh,P) = 26.7$ Hz. ^{1}H NMR (400 MHz, C_6D_6, C_6D_5H as internal standard) **2a**: $\delta = 1.31$ (s, 36H), 1.66 (s, 36H), 4.81 (s, br. 4H), 4.93 (s, br. 2H), 5.79 (s, br. 4H), 5.86 (s, br. 2H); **2b** $\delta = 1.28$ (s, 36H), 1.61 (s, 36H), 4.66 (s, br. 4H), 4.81 (s, br. 2H), 5.66 (s, br. 4H), 5.83 (s, br. 2H); **3a** $\delta = 1.38$ (s, 36H), 4.92 (s, br. 4H), 5.14 (s, br. 2H); **3b** $\delta = 1.30$ (s, 36H), 4.80 (s, br. 4H), 5.00 (s, br. 2H).

[11] EI-MS Spectrum (70 eV), *m/z* 1870 ($M^{\oplus}$, 0.2%) 1570 ($[Cp''_4Rh_4As_6]^+$, 0.6%), 1420 ($[Cp''_4Rh_4As_4]^+$, 69%), 1243 ($[Cp''_3Rh_4As_4]^+$, 18%), 1140 ($[Cp''_3Rh_3As_4]^+$, 1.4%), 1065 ($[Cp''_2Rh_3As_3]^+$, 13%), 1010 ($[Cp''_2Rh_2As_6]^+$, 1.6%), 990 ($[Cp''_3Rh_3As_2]^+$, 29%), 935 ($[Cp''_2Rh_2As_5]^+$, 4%), 860 ($[Cp''_2Rh_2As_4]^+$, 100%), 785 ($[Cp''_2Rh_2As_3]^+$, 3.3%), 710 ($[Cp''_2Rh_2As_2]^+$, 25%), 682 ($[Cp''Rh_2As_4]^+$, 4.4%), 430 ($[Cp''RhAs_2]^+$, 4.4%), 355 ($[Cp''RhAs]^+$, 1.3%, 300 (As_4^+, 8.3%) as well as other fragments.

[12] a) O. J. Scherer, M. Swarowsky, G. Wolmershäuser, *Angew. Chem.* **1988**, *100*, 423–424; *Angew. Chem. Int. Ed. Engl.* **1988**, *27*, 405–406; b) M. E. Barr, L. F. Dahl, *Organometallics* **1991**, *10*, 3991–3996; c) O. J. Scherer, K. Pfeiffer, G. Heckmann, G. Wolmershäuser, *J. Organomet. Chem.*, **1992**, *425*, 141–149.

[13] For this molecule we propose a structure analogous to $[Cp^*_2Co_2As_6]$ with a single open-edged As_6 Dewar benzene ligand [12c].

Stepwise Synthesis of Binuclear Photoactive Complexes with a Bridging 3,4-Dihydroxyphenylterpyridine Ligand**

By *Christine A. Howard* and *Michael D. Ward**

The ability of polypyridyl complexes of ruthenium(II) to act as photosensitizers is well established.[1] Recently attention has turned to the incorporation of 'light-harvesting' ruthenium centers into large molecular assemblies containing covalently attached quenching groups, so that energy or electron transfer from the chromophore to the accepting group is intramolecular and not dependent on collision of the two species in solution.[2] These covalently attached quenching groups may be organic electron donors or acceptors such as phenothiazines[3] or viologens,[4, 5] energy-accepting groups such as anthracene,[3] or inorganic complexes such as $[Ni(cyclam)]^{2+}$.[6] One aim of this type of work is the synthesis of large molecular assemblies—photochemical devices—which mimic biological photosynthesis by efficient intramolecular transfer of energy from the excited state 'antenna' to a reaction center. The reaction center then uses the energy in a catalytic process. Despite this interest, synthetic methods for the preparation of heteropolynuclear complexes incorporating photoactive groups are scarce.

The successful synthesis of multicomponent supramolecular assemblies of this type may be achieved by the *stepwise*

[*] Dr. M. D. Ward, C. A. Howard
School of Chemistry, Cantock's Close
GB-Bristol BS8 1TS (UK)

[**] This work was in part supported by the Nuffield Foundation. We thank Dr. J. Maher for assistance with the EPR spectroscopy and Dr. M. Murray for the two-dimensional NMR spectra.

synthesis of heteropolynuclear complexes with a 'complexes as ligands' approach, in which a metal complex is prepared which contains a vacant, externally directed binding site. A second complex fragment may then be attached to the vacant site, allowing the stepwise buildup of polynuclear species from individual building blocks whose properties are known. We have recently prepared some derivatives of $[Ru(bpy)_3]^{2+}$ (bpy = 2,2'-bipyridine) containing externally directed pyridyl or phenol ligands for this purpose.[5] We now wish to describe the synthesis of **4**, a derivative of $[Ru(terpy)_2]^{2+}$ (terpy = 2,2':6',2''-terpyridine), in which the terpy ligand has a 3,4-dihydroxyphenyl substituent, and the syntheses and properties of binuclear complexes **5** and **6** prepared by subsequent attachment of a second metal center to the catechol binding site.

The key component in these syntheses is the ligand 3,4-dimethoxyphenylterpyridine (**2**), prepared in 42% yield by reaction of **1** with *N*-[2-(2-pyridyl)-2-oxoethyl]pyridinium iodide in the presence of ammonium acetate and refluxing glacial acetic acid (Scheme 1) in a standard Kröhnke-type pyridine synthesis.[7] The ligand was purified by isolation as

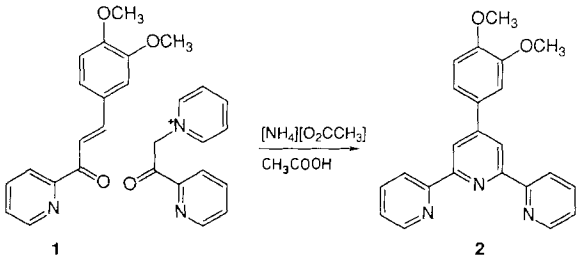

Scheme 1. The synthesis of 3,4-dimethoxyphenylterpyridine (**2**) is carried out in glacial acetic acid under reflux.

its Fe^{II} complex and subsequent demetalation,[8] followed by recrystallization from ethanol.[9] Chalcone **1** was in turn prepared in 63% yield by condensation of 2-acetylpyridine with 3,4-dimethoxybenzaldehyde in aqueous ethanol/KOH at room temperature. Reaction of **2** with $[Ru(terpy)Cl_3]$ in ethylene glycol at reflux followed by addition of aqueous KPF_6 gave the mixed-ligand complex **3** in 75% yield; it was purified by chromatography on silica with an acetonitrile/aqueous KPF_6 mixture as eluent. Reaction of **3** with BBr_3 in CH_2Cl_2 at room temperature[10] resulted in near-quantitative removal of the methoxy protecting groups, thus unmasking the secondary catechol binding site *after* initial formation of the ruthenium complex **3**.

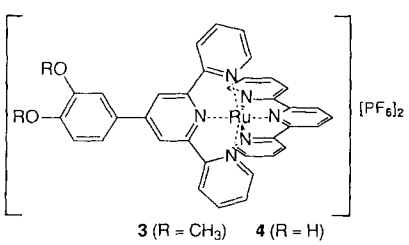

3 (R = CH_3) **4** (R = H)

The binuclear ruthenium complex **5** was prepared by reaction of **4** with $[Ru(bpy)_2Cl_2]$, under the same conditions as required for the formation of the analogous mononuclear complex $[Ru(bpy)_2(sq)]^+$ (sq = the monoanionic semiquinone ligand arising from one-electron oxidation of catechol)[11] followed by precipitation with KPF_6. Complex **5** was obtained in 40% yield after purification by preparative thin-layer chromatography (TLC) on alumina plates with acetonitrile/toluene (2:1) as eluent. As in $[Ru(bpy)_2(sq)]^+$, the catecholate ligand oxidizes to the semiquinone oxidation state on exposure to air: **5** therefore contains a trication and is paramagnetic; the EPR spectrum shows a single, sharp resonance at $g = 2.00$. This precludes its characterization by

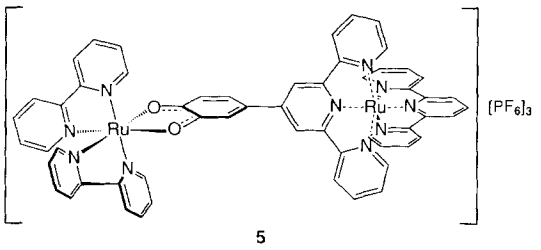

5

NMR spectroscopy, but its fast atom bombardment (FAB) mass spectrum shows a peak centered at m/z 1088 which corresponds to the mass of the binuclear cation of **5** and has the appropriate isotopic pattern.

A cyclic voltammogram of **5** (Fig. 1) shows that all three redox processes are reversible ($\Delta E_p = 60-90$ mV at scan rates up to 500 mVs^{-1}; $i_{p,a} \approx i_{p,c}$). The first two processes

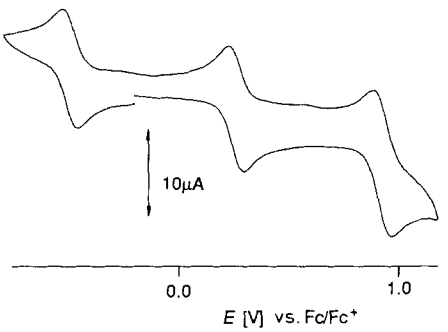

Fig. 1. Cyclic voltammogram **5** in CH_3CN at a scan rate of 0.2 Vs^{-1}.

($E_{1/2} = -0.51$ and $+0.26$ V vs. ferrocene/ferrocenium (Fc/Fc^+)) correspond respectively to the catecholate/semiquinone and semiquinone/benzoquinone redox couples of the bridging ligand. The analogous ligand-based redox processes in $[Ru(bpy)_2(sq)]^+$ are also reversible and occur at -0.69 and $+0.16$ V (vs. Fc/Fc^+);[12] the shifts of 100–200 mV of these waves to more positive potentials in **5** may be simply ascribed to the presence of a second cationic metal center nearby, which electrostatically destabilizes the oxidized forms of the catecholate. The third process ($E_{1/2} = +0.94$ V vs. Fc/Fc^+) has no counterpart in the voltammogram of $[Ru(bpy)_2(sq)]^+$, and is assigned to the Ru^{II}/Ru^{III} couple of the bis(terpyridyl)ruthenium center (the redox potential of $[Ru(terpy)_2]^{2+}$ under the same conditions was $+0.90$ V vs. Fc/Fc^+).

Part of the UV/VIS spectrum of complex **5** is shown in Figure 2, which compares the spectrum of **5** with the sum of the spectra of the mononuclear counterparts $[Ru(bpy)_2(sq)]^+$ and $[Ru(terpy)_2]^{2+}$ at the same concentration. There is a significant increase in the width of the metal-to-ligand charge transfer (MLCT) band at 480 nm, but the biggest difference

is in the Ru^{II}–semiquinone MLCT band. In $[Ru(bpy)_2(sq)]^+$ this occurs at 889 nm ($\varepsilon = 6400\ dm^3mol^{-1}cm^{-1}$); in **5** it has shifted to 967 nm and become about three times more intense ($\varepsilon = 20000\ dm^3mol^{-1}cm^{-1}$), indicating that the semiquinone fragment in **5** is a better electron acceptor than that in $[Ru(bpy)_2(sq)]^+$ due to its attachment to the $[Ru(terpy)_2]^{2+}$ fragment (i.e. a simple substituent effect).

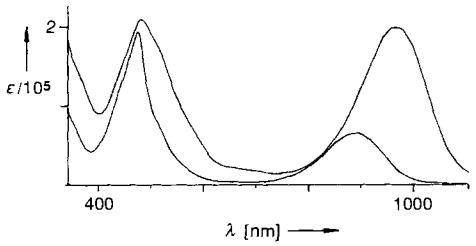

Fig. 2. UV/VIS spectrum of **5** in CH_3CN (upper trace) and the sum of the spectra of $[Ru(bpy)_2(sq)][PF_6]$ and $[Ru(terpy)][PF_6]_2$ at the same concentration (lower trace).

The binuclear Ru–Pd complex **6** was prepared by reaction of **4** with one equivalent of $[Pd(bpy)Cl_2]$ and three equivalents of KOH in methanol at room temperature under N_2 (Scheme 2). The resulting purple precipitate was purified (30% final yield) by preparative TLC on alumina plates with acetonitrile/toluene (2:1) as eluent. In **6**, as in the mononuclear analogue [Pd(bpy)(cat)][12] (cat = dianion of catechol), the catecholate ligand does not oxidize. The ^1H NMR spectrum shows eighteen signals in the region of the aromatic protons; these were assigned[13] with the help of a two-dimensional COSY spectrum and by comparison of the spectrum with the spectra of **4** and [Pd(bpy)(cat)]. The FAB mass spectrum shows a peak centered at *m/z* 936, which corresponds to the mass of the binuclear cation and has the appropriate isotopic pattern.

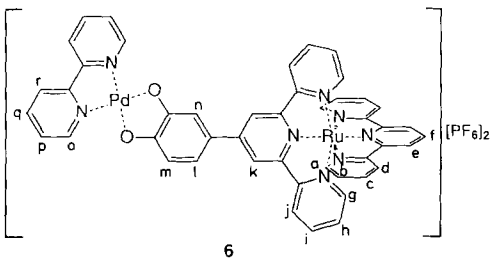

Scheme 2. The letters correspond to the labeling of the protons that was used for the assignment of the ^1H spectrum [13].

The cyclic voltammogram shows an irreversible oxidation at +0.18 V vs. Fc/Fc^+, which is characteristic of the [Pd(bpy)(cat)] fragment,[12, 14] and a reversible oxidation at +0.93 V vs. Fc/Fc^+ corresponding to the Ru^{II}/Ru^{III} couple. The UV/VIS spectrum of **6** is shown in Figure 3, which compares the spectrum of **6** with the sum of the spectra of the mononuclear counterparts $[Ru(terpy)_2]^{2+}$ and [Pd(bpy)(cat)] at the same concentration. The most striking difference is in the ligand-to-ligand charge transfer (LLCT) band (catecholate–bipyridine). In [Pd(bpy)(cat)] this absorption occurs at $\lambda_{max} = 535$ nm ($\varepsilon = 1300\ dm^3mol^{-1}cm^{-1}$); in **6** this band has moved only slightly ($\lambda_{max} = 524$ nm) but has increased in intensity by over an order of magnitude ($\varepsilon = 19000$), resulting in a beautiful and very strong wine-red color in solution. The catecholate fragment in **6** is evidently more electron-rich than the catecholate in [Pd(bpy)(cat)]; this may be ascribed to the fact that it is attached to the π-acidic terpyridine ligand, which contains electron density accepted from the ruthenium ion, and is in interesting contrast to the apparently enhanced electron-accepting nature of the semiquinone fragment in **5**.

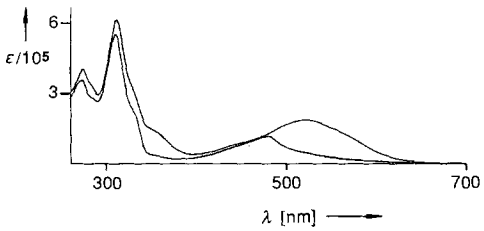

Fig. 3. UV/VIS spectrum of **6** in dimethylformamide (upper trace) and the sum of the spectra of [Pd(bpy)(cat)] and $[Ru(terpy)_2][PF_6]_2$ at the same concentration (lower trace).

The LLCT excited state of [Pd(bpy)(cat)] is quenched by triplet O_2 in solution giving singlet O_2.[15] Since singlet O_2 reacts with 2,2,6,6-tetramethyl-4-piperidinol to give a stable nitroxide radical, the efficiency of the production of singlet O_2 under irradiation may be determined. This is achieved by measuring the intensity of the EPR signal of the nitroxide radical as a function of irradiation time in an O_2-saturated solution of the palladium complex to which 2,2,6,6-tetramethyl-4-piperidinol has been added.[12] Comparison of [Pd(bpy)(cat)] with **6** showed that **6** is about 50% more efficient as a photocatalytic producer of singlet O_2.

In conclusion, we have developed a straightforward new method for the stepwise synthesis of polynuclear complexes which contain a $[Ru(terpy)_2]^{2+}$ chromophore. Unmasking the second coordination site after formation of the first complex allows the efficient, unambiguous preparation of heterobinuclear complexes with strong electronic interactions between the two fragments.

Received: February 4, 1992 [Z 5167 IE]
German version: *Angew. Chem.* **1992**, *104*, 1077

[1] A. Juris, V. Balzani, F. Barigeletti, S. Campagna, P. Belser, A. von Zelewsky, *Coord. Chem. Rev.* **1988**, *84*, 85.
[2] V. Balzani, F. Scandola, *Supramolecular Photochemistry*, Ellis Horwood, Chichester, **1991**.
[3] T. J. Meyer, *Pure. Appl. Chem.* **1990**, *62*, 1003, and references cited therein.
[4] B. P. Sullivan, H. Abruna, H. O. Finklea, D. J. Salmon, J. K. Nagle, T. J. Meyer, H. Sprintschnik, *Chem. Phys. Lett.* **1978**, *58*, 389.
[5] M. A. Hayes, C. A. Meckel, E. Schatz, M. D. Ward, *J. Chem. Soc. Dalton Trans.* **1992**, 703.
[6] E. Kimura, S. Wada, M. Shionoya, T. Takahashi, Y. Iitaka, *J. Chem. Soc. Chem. Commun.* **1990**, 397.
[7] F. Kröhnke, *Synthesis* **1976**, 1.
[8] E. C. Constable, M. D. Ward, S. Corr, *Inorg. Chim. Acta* **1988**, *141*, 201.
[9] All new compounds were satisfactorily characterized on the basis of NMR spectroscopy, mass spectrometry, and elemental analysis.
[10] J. F. W. McOmie, M. L. Watts, D. E. West, *Tetrahedron* **1968**, *24*, 2289.
[11] M. Haga, E. S. Dodsworth, A. B. P. Lever, *Inorg. Chem.* **1986**, *25*, 447.
[12] K. H. Puthraya, T. S. Srivastava, *Polyhedron* **1985**, *4*, 1579.
[13] **6**: ^1H NMR (400 MHz, CD_3CN, TMS): $\delta = 6.65$ (d, $J = 8.1$ Hz, 1H; H_m), 7.12 (td, $J = 5.6$, 1.2 Hz, 2H; H_b), 7.19 (td, $J = 5.6$, 1.2 Hz, 2H, H_h), 7.27 (d, $J = 2.3$ Hz, 1H; H_n), 7.29 (dd, $J = 5.6$, 0.7 Hz, 2H, H_d), 7.32 (dd, $J = 8.1$, 2.3 Hz, 1H; H_l), 7.49 (d, $J = 5.6$ Hz, 2H; H_j), 7.73 (m, 2H; H_p), 7.91 (m, 4H; $H_c + H_i$), 8.24 (m, 4H; $H_q + H_r$), 8.38 (t, $J = 8.2$ Hz, 1H; H_f), 8.49 (d, $J = 7.8$ Hz, 2H; H_g), 8.64 (d, $J = 7.8$ Hz, 2H; H_a), 8.70 (m, 2H; H_o), 8.74 (d, $J = 8.3$ Hz, 2H; H_e), 8.90 (s, 2H; H_k).
[14] S. S. Kamath, V. Uma, T. Srivastava, *Inorg. Chim. Acta* **1989**, *166*, 91.
[15] Y. Lion, M. Delmelle, A. Van de Vorst, *Nature* **1976**, *263*, 442; Y. Lion, E. Gandin, A. Van de Vorst, *Photochem. Photobiol.* **1980**, *31*, 305.

Tetraphosphafulvalene Dianions: Isoelectronic Species of Tetrathiafulvalene Dications

By *Nicole Maigrot, Louis Ricard, Claude Charrier,* and *François Mathey**

Recently, we described the synthesis of the first tetraphosphafulvalenes.[1] Our ultimate aim was to prepare charge-transfer (CT) complexes of the tetrathiafulvalene–tetracyanoquinodimethane type and to study their electrical conductivity. However, for this purpose tetraphosphafulvalenes themselves are useless since they incorporate four pyramidal phosphorus atoms that prevent the stacking of such species. We report herein the selective cleavage of the four exocyclic P–C bonds, a crucial step for the formation of tetraphosphacycles which can be stacked.

The reaction of the octaphenyl derivative **1** with an excess of lithium or potassium in THF at room temperature afforded a single phosphorus-containing product **2** (Scheme 1). The

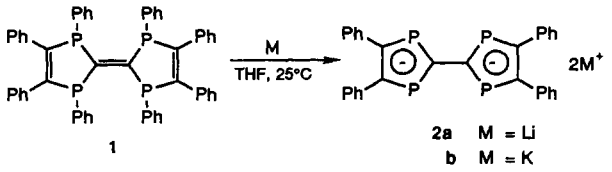

Scheme 1. M is added in excess.

resonance frequency for **2** in the ^{31}PNMR spectrum ($\delta \approx 170$) lies in the same range as those of 1,3-diphospholide ions.[2] We were able to obtain crystals of **2b** suitable for an X-ray structural analysis from a mixture of ether and 1,2-dimethoxyethane[3] (Fig. 1). The two diphospholyl rings are coplanar (maximum deviation 0.010(3) Å) and aromatic. The length of C1–C1′ bond that links the two five-membered rings [1.482(5) Å] corresponds to a normal single bond between two sp^2 hybridized carbon atoms. The P–C bonds are between 1.748(3) and 1.761(3) Å long and are thus similar in length to those found in the lithium phospholide Li(tmeda)PC$_4$Me$_4$.[4] The C3–C4 bond (1.401(4) Å) is longer than a localized C=C bond; however, it is similar in length to the corresponding bond in the previously mentioned lithium phospholide.[4] The most intriguing feature of this structure is the position of the potassium ions relative to the central tetraphosphafulvalene unit. Instead of pentahapto coordination of the metal as in Li(tmeda)PC$_4$Me$_4$,[4] the potassium ions in **2b** are shared by the two 1,3-diphospholyl units. These are positioned on both sides of the cycle at a distance of 2.82 Å and can be viewed as bis η^2-coordinated to the two P2–C1 and the two P5–C1 bonds. The K–P distances are close to the sum of the covalent radii (K + P = 3.37 Å). If we consider a K$_2$(dme)$_4$ unit (dme = dimethoxyethane) sandwiched between two tetraphosphafulvalene planes, in addition to the four "terminal" oxygen atoms, two oxygen atoms of two DME molecules (022,022*) bridge the two potassium ions so that each of the potassium ions is heptacoordinated (Fig. 2). The dianion contains a center of symmetry, and the ions are arranged in infinite chains produced by translation of the unit cell along the *b* axis of the crystal.

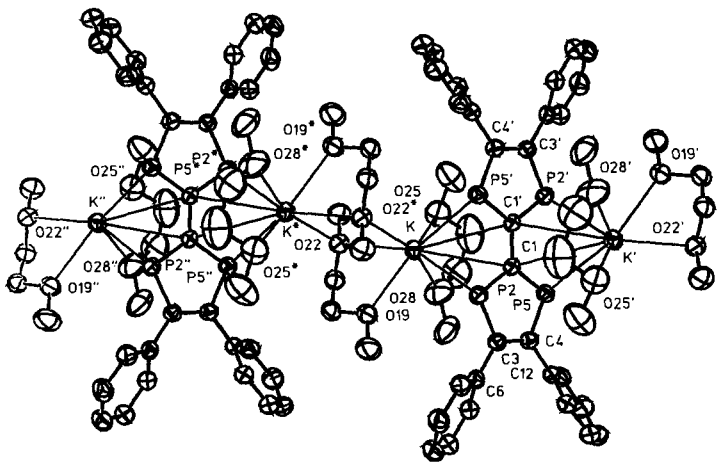

Fig. 1. Crystal structure of **2b** [3]. Ellipsoids are scaled to enclose 50% of the electronic density. Hydrogen atoms are omitted for clarity. Important bond distances [Å] and angles [°]: K-K′ 4.604(1), K-P2 3.267(1), K-P5 3.393(1), C1-C1′ 1.482(5), C1-P2 1.748(3), C1-P5 1.753(3), P2-C3 1.761(3), C3-C4 1.401(4), C4-P5 1.761(3); P2-K-P5 60.51(2), C1-C1′-P2 123.7(3), C1-C1′-P5 121.1(3), P2-C1-P5 115.2(1), K-P2-C1 82.7(1), K-P2-C3 120.2(1), C1-P2-C3 96.3(1), P2-C3-C4 116.1(2), C3-C4-P5 116.3(2), K-P5-C1 81.5(1), K-P5-C4 122.2(1), C1-P5-C4 96.1(1).

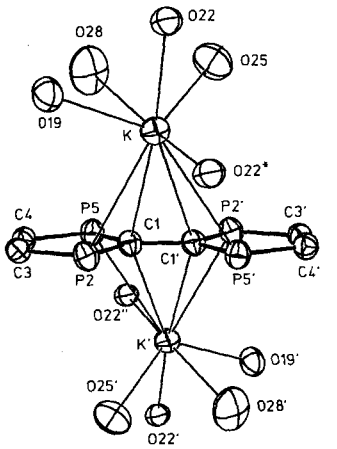

Fig. 2. The coordination sphere of a potassium ion in a crystal of **2b**.

The reaction of **2a** with an excess of sulfur led to the expected lithium tetrakis(dithiophosphinate) **3**[5] (Scheme 2) whose structure was established by X-ray crystal structure analysis[6] (Fig. 3). Both the aromaticity of the rings and the

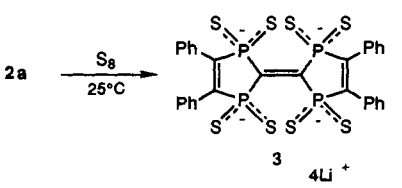

Scheme 2. Sulfur is added in excess.

planarity of the whole tetraphosphafulvalene unit in **3** are lost and the central C1–C1′ bond clearly has double-bond character. Two tetrahedral trisaqua acetonato lithium ions and one doubly charged di-μ^2-aqua-tetrakis-η^1-aqua dilithium ion serve as the counter ions.

[*] Prof. Dr. F. Mathey, N. Maigrot, Dr. L. Ricard, Dr. C. Charrier
Laboratoire de Chimie du Phosphore et des Métaux de Transition
UM 13 C.N.R.S., DCPH, Ecole Polytechnique
F-91128 Palaiseau Cedex (France)

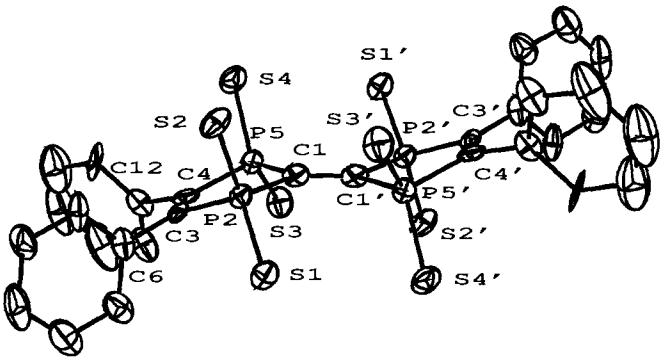

Fig. 3. Crystal structure of **3** [4]. Ellipsoids are scaled to enclose 50% of the electronic density. Hydrogen atoms are omitted for clarity. Important bond distances [Å] and angles [°]: S1-P2 1.977(5), S2-P2 1.993(5), S3-P5 1.957(5), S4-P5 2.003(5), P2-C1 1.89(1), P2-C3 1.82(1), P5-C1 1.85(1), P5-C4 1.81(1), C1-C1' 1.34(2), C3-C4 1.33(1), C4-C12 1.51(2), C3-C6 1.49(2); S1-P2-S2 118.8(2), S1-P2-C1 111.7(4), S1-P2-C3 107.9(4), S2-P2-C1 112.3(4), S2-P2-C3 106.3(4), C1-P2-C3 97.4(5), S3-P5-S4 117.2(2), S3-P5-C1 113.2(4), S3-P5-C4 107.1(5), S4-P5-C1 113.0(4), S4-P5-C4 105.9(4), C1-P5-C4 98.1(5), P2-C1-P5 106.7(6), P2-C1-C1' 123.7(8), P5-C1-C1' 129.5(8), P2-C3-C4 116.9(9), P2-C3-C6 116.8(7), C4-C3-C6 126.0(1), P5-C4-C3 117.7(9), P5-C4-C12 118.3(8), C3-C4-C12 124.0(1). The four phosphorus atoms and the C1-C1' double bond are coplanar. The dihedral angle between this plane and the P2-C3-C4-P5 mean plane is 20.37 ± 0.58°.

Additional characterization of **2a** was provided by its reaction with (η^5-cyclopentadienyl)(η^6-*p*-xylene)iron hexafluorophosphate.[7] The resulting η^5-complex **4**[8] is very sensitive toward oxidation, but it could be characterized after chelation with the [W(CO)$_4$] fragment (→ 5) (Scheme 3).[9]

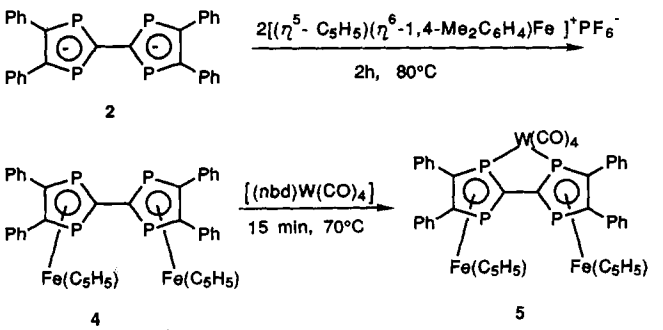

Scheme 3. nbd = norbornadiene.

Dianions such as **2** are isoelectronic with tetrathiafulvalene dications. We are currently studying the electrochemistry of **2**.

Experimental Procedure

2a: The P–Ph bonds of tetraphosphafulvalene **1** (810 mg, 1 mmol) were cleaved under an argon atmosphere by stirring with lithium containing 1% of sodium (47 mg, 6.6 mmol) in freshly distilled dry THF (15 mL). The cleavage was complete after 3 h. The phenyllithium by-product was destroyed by addition of anhydrous NH_4Cl (200 mg, 4 mmol).

2b was prepared by stirring the tetraphosphafulvalene **1** (470 mg, 0.55 mmol) with potassium (150 mg, 3.8 mmol) in freshly distilled dry DME (10 mL). The reaction was complete after 3 h. The phenylpotassium by-products formed insoluble polymers which were eliminated by filtration under an argon atmosphere. The solution was concentrated (5 mL) and 5 mL of dry ether was added. Pale yellow crystals of **2b** were obtained after one week at −18 °C.

3: To the solution of **2a** was added an excess of sulfur (270 mg, 8.4 mmol). The reaction mixture was stirred for 15 min and filtered. The solvent was evaporated and the residue extracted with 4 × 30 mL of diethyl ether. The evaporation of ether yielded a pasty yellow residue which was crystallized from acetone. Yield 35%.

4: To a solution of dianion **2a** was added [Cp(η^6-1,4-$Me_2C_6H_4$)Fe]PF_6 (820 mg, 2.3 mmol). The reaction mixture was heated at 80 °C for 2 h, concentrated to 5 mL, and quickly chromatographed on a silica gel column (20 g, l = 8 cm, ∅ = 26 mm) with dichloromethane as eluent. After evaporation of the solvent, the product was again chromatographed on silica gel (100 g, l = 21 cm, ∅ = 36 mm) with hexane/toluene (50/50) as eluent. A deep red crystalline product was obtained. Yield 30%. Compound **4** proved to be unstable on standing and in solution.

5: Crude **4** was allowed to react in situ with [(nbd)W(CO)$_4$] (700 mg, 2.1 mmol). The reaction mixture was heated at 70 °C for 15 min. After concentration to 5 mL, the solution was quickly chromatographed on silica gel (20 g, l = 8 cm, ∅ = 26 mm) with toluene as eluent. After evaporation, the residue was once more chromatographed on silica gel (100 g, l = 21 cm, ∅ = 36 mm) with toluene as eluent. A red-orange crystalline compound was thus obtained in 34% yield.

Received: March 2, 1992 [Z 5221 IE]
German version: *Angew. Chem.* **1992**, *104*, 1082

CAS Registry numbers:
1, 114862-89-4; **2a**, 142397-60-2; **2b**, 142397-59-9; **2b** · 4 DME, 142397-69-1; **3**, 142397-61-3; **3** · 9 H_2O · 2 MI_2CO, 142397-66-8; **4**, 142397-67-9; **5**, 142397-68-0; [(η^5-C_5H_5)(η^6-1,4-$Me_2C_6H_4$)Fe]PF_6, 34978-37-5; (nbd)W(CO)$_4$, 12129-25-8.

[1] N. Maigrot, L. Ricard, C. Charrier, F. Mathey, *Angew. Chem.* **1988**, *100*, 997; *Angew. Chem. Int. Ed. Engl.* **1988**, *27*, 950.

[2] A. H. Cowley, S. W. Hall, *Polyhedron* **1989**, *8*, 849; R. Bartsch, J. F. Nixon, *Polyhedron* **1989**, *8*, 2407; N. Maigrot, L. Ricard, C. Charrier, F. Mathey, *Angew. Chem.* **1990**, *102*, 575; *Angew. Chem. Int. Ed. Engl.* **1990**, *29*, 534.

[3] X-ray structure determination of **2b**: Crystals of **2b**, $C_{46}H_{60}K_2O_8P_4$ were grown at −18 °C from ether/dimethoxyethane. Data were collected at −150 ± 0.5 °C with an Enraf–Nonius CAD4 diffractometer. The crystal structure was solved and refined using the Enraf–Nonius Molen package. The compound crystallizes in space group $P\bar{1}$, a = 10.047(1), b = 10.999(1), c = 12.409(2) Å, α = 77.53(1), β = 87.11(1), γ = 69.91(1)°; V = 1257.1(3) Å^3; Z = 1; ϱ_{calcd} = 1.246 g cm^{-3}; $Cu_{K\alpha}$ radiation (λ = 1.54184 Å), graphite monochromator; μ = 33.0 cm^{-1}; F(000) = 498. A total of 5033 unique reflections were recorded in the range $2° \le 2\theta \le 150.0°$ of which 1164 were considered as unobserved ($F^2 < 3.0\sigma(F^2)$), leaving 3869 for solution and refinement. Twenty-six of the thirty independent atoms in the molecule were solved by direct methods. The hydrogen atoms were included as fixed contributions in the final stages of least-squares refinement while using anisotropic temperature factors for all other atoms. A non-Poisson weighting scheme was applied with a p factor of 0.08. R = 0.055, R_w = 0.082, GOF = 1.67.

[4] T. Douglas, K. H. Theopold, *Angew. Chem.* **1989**, *101*, 1394; *Angew. Chem. Int. Ed. Engl.* **1989**, *28*, 1367.

[5] **3**: ^{31}PNMR ([D$_6$]acetone): δ = 60.5; ^{13}CNMR: δ = 144.1 (m, C$_1$), 136.2 (*pseudo* t, C$_3$, C$_4$); MS: *m/z* 696 (M − 2S, 7%), 664 (M − 3S, 21%), 632 (M − 4S, 31%).

[6] X-ray structure determination for **3**: Crystals of **3**, $[C_{30}H_{20}P_4S_8]^{4-}[Li_2(H_2O)_6]^{2+}[Li(H_2O)_3C_3H_6O]_2^+ \cdot C_3H_6O$ were grown at −18 °C from acetone. Data were collected at 20 ± 1 °C on an Enraf–Nonius CAD4 diffractometer. The crystal structure was solved and refined using the Enraf–Nonius supplied SDP package. The compound crystallizes in space group $P\bar{1}$, a = 9.419(1), b = 11.419(1), c = 14.848(2) Å, α = 96.78(1), β = 100.56(1), γ = 95.50(1)°; V = 1547.66(63) Å^3; Z = 1; ϱ_{calcd} = 1.265 g cm^{-3}; $Mo_{K\alpha}$ radiation (λ = 0.71073 Å), graphite monochromator; μ = 4.29 cm^{-1}; F(ooo) = 616. A total of 3762 unique reflections were recorded in the range $2° \le 2\theta \le 44.0°$ of which 2203 were considered as unobserved ($F^2 < 3.0\sigma(F^2)$), leaving 1559 for solution and refinement. The structure was solved by direct methods, yielding a solution for the whole anion. The hydrogen atoms were not included and anisotropic temperature factors were used for all atoms. A non-Poisson weighting scheme was applied with a p factor of 0.08. R = 0.063, R_w = 0.077, GOF = 1.35. Further details of the crystal structure investigations may obtained from the Fachinformationszentrum Karlsruhe, Gesellschaft für wissenschaftlich-technische Information mbH, D-W-7514 Eggenstein-Leopoldshafen 2 (FRG) on quoting the depository number CSD-56244), the names of the authors, and the journal citation.

[7] A similar reaction with phospholide anions yields monophosphaferrocenes: R. M. G. Roberts, A. S. Wells, *Inorg. Chim. Acta* **1986**, *112*, 171.

[8] **4**: ^{31}PNMR (CD_2Cl_2): δ = 2.3; MS: *m/z* 746 (*M*, 40%), 745 (*M* − H, 100%).

[9] Compound **5** is a pure stereoisomer but its stereochemistry is unknown. ^{31}PNMR (CD_2Cl_2): AA'XX': δ_A 50.1, δ_X −33.8, $^1J_{(PA-W)}$ = 249 Hz; ^{13}C NMR: 78.2 (s, Cp), 98.4 (m, $P_2C{=}CP_2$), 99.2 (s, Ph-*C*-P_A), 110.0 (*pseudo* t, Ph-*C*-P_X), 127.4, 127.6 (2s, *para* CH), 128.1, 128.3 (2s *meta* CH), 131.0, 131.7 (2s, *ortho* CH), 136.1, 139.2 (2 *pseudo* t, C *ipso*), 195.8 (t, $^2J_{(C-P)}$ = 8 Hz, CO *ax*), 204.1 (*pseudo*-t, CO *eq*); MS: *m/z* 746 (M − W(CO)$_4$, 30%), 745 (M − W(CO)$_4$-H, 59%), 744 (M − W(CO)$_4$-2H, 100%).

Diacetoneglucose as Auxiliary Group for the Asymmetric Hetero-Diels–Alder Reaction with Nitrosoalkenes**

By *Thomas Arnold, Beate Orschel,* and *Hans-Ulrich Reissig**

Dedicated to Professor Ekkehard Winterfeldt on the occasion of his 60th birthday

In our search for efficient optically active auxiliaries for the asymmetric hetero-Diels–Alder reaction,[1] we recently came across diacetoneglucose (DAG-H, **1**). With this easily accessible[2] and cheap sugar derivative,[3] enol ethers and allenyl ethers can be readily prepared, which undergo cycloaddition reactions with nitrosoalkenes[4] in high diastereomeric excesses. The resulting optically active dihydro-1,2-oxazines attract much attention as a versatile building blocks in synthesis.[5]

Enol ethers **3** and **5** were prepared from the allyl ethers **2** and **4**, respectively, which can be readily obtained from **1** and the appropriate allyl halide under phase-transfer conditions[6] (Scheme 1). $[Fe(CO)_5]$-catalyzed isomerization[7]

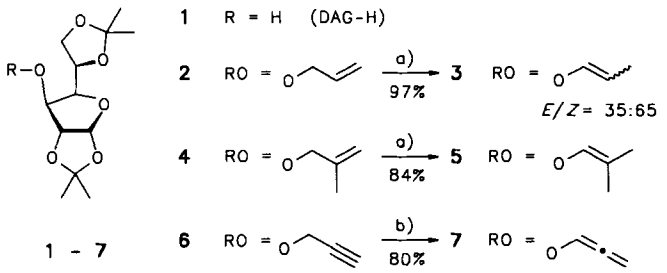

Scheme 1. Compound **2** from **1** and allyl bromide according to [6]; **4** analogously from **1** and 3-chloro-2-methyl-1-propene (KOH, [18]crown-6, THF, 20 °C, 3 days), 63%; **6** from **1** and propargyl bromide (NaOH, nBu$_4$NI, THF, 20 °C, 4 days), 92%; a) $[Fe(CO)_5]$ (0.12 or 0.20 equiv, xylene, 135 °C, 8 or 15 h); b) KOtBu (1.75 equiv, toluene, 110 °C, 1 h).

gave the enol ethers **3** and **5** in satisfactory overall yields. A disadvantage, however, is the E/Z mixture of **3** that forms with this catalyst, but the isomers can be at least partially separated by chromatography.[8] The optically active allene derivative **7** can be obtained from the propargyl ether **6** through standard procedures without difficulty.[9]

The highly reactive nitrosoalkenes **9a–c** were generated in situ from the α-halooximes **8a–c** with sodium carbonate.[4] Scheme 2 summarizes the trapping reactions for **9** with the 1-propenyl ethers (*Z*)-**3**/(*E*)-**3**. In each of these exploratory experiments, the ethers were used as a mixture with varying Z/E ratios (Table 1), and the products were the dihydro-1,2-oxazines **10a–c** and **11a–c**. It is important that the (*E*)-enol ether reacts considerably faster than the (*Z*)-enol ether with **9** (see Table 1).[10] Therefore, for an appropriate **9**/**3** ratio, (*Z*)-**3** can be recovered in highly enriched form and again treated with **9** in a second cycle. Thus a confident assignment of the isolated dihydrooxazines **10** and **11** to *cis*/*trans* isomeric cycloadducts or diastereomers with respect to the auxiliary is possible.[11] In Scheme 2 only the major diastereomers of **10** and **11** are presented.

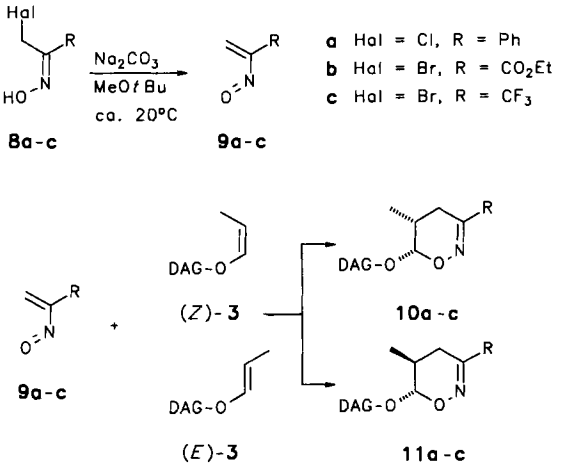

Scheme 2. Asymmetric [4 + 2] cycloadditions of nitrosoalkenes **9** with (*Z*)-**3**/(*E*)-**3** (for an experimental procedure see [1e]). **a**, Hal=Cl, R=Ph; **b**, Hal=Br, R=CO_2Et; **c**, Hal=Br, R=CF_3.

Table 1. Diastereomeric ratios (dr) in reactions of (*Z*)-**3**/(*E*)-**3** with nitrosoalkenes to give dihydro-1,2-oxazines **10**/**11**.

(*Z*)-**3**/(*E*)-**3**	**9**	yield [%]	**10**	**11**
20:80	**a**	52	2:0	98:0
94:6	**a**	54	73:19	8:0
			dr = 79:21/ > 95:5	
92:8	**b**	33	61:14	25:0
			dr = 81:19/ > 95:5	
70:30	**c**	65	76:6	16:2
			dr = 93:7/ ≈ 90:10	

The cycloadditions of the nitrosoalkenes **9a–c** with (*Z*)-**3** proceed with good diastereoselectivity (dr = 79:21 to 93:7, see Table 1). The selectivity increases with increasing reactivity of the heterodiene (**9a** < **9b** < **9c**).[12] The reactions of the (*E*)-enol ether (*E*)-**3** with **9a** and **9b** yields the dihydrooxazines **11a** and **11b**, respectively, in diastereomerically pure state, whereas with **9c** the minor isomer of **11c** constitutes 10% of the product mixture. Therefore, as in earlier examples,[1e] the substantially more reactive (*E*) olefin shows a distinctly higher selectivity than the (*Z*) olefin; only with **9c** are the diastereomeric ratios of **10** and **11** approximately equal. The selectivity of the reaction between isobutenyl ether (**5**) and nitrosostyrene (**9a**), which forms dihydrooxazine **12**, lies between that of (*Z*)-**3** and (*E*)-**3**.

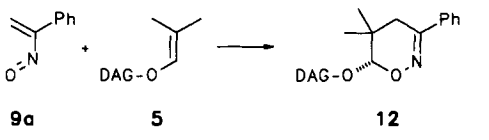

dr = 88:12, 60%

The absolute configurations given for **10**, **11**, and **12** are based on a crystal structure analysis[13] of the major diastereomer of **10a**, which was obtained pure after chromatography (m.p. 106–109 °C, $[\alpha]_D^{20}$ +57.7, c=1.00 in $CHCl_3$). That the configurations of **10a** and **11a** must be different at C5 of the heterocycle, and thus the same at C6 because of the stereospecific course of the cycloaddition,[10] follows from the hydrogenolysis of these cycloadducts. In

[*] Prof. Dr. H.-U Reissig, Dipl.-Ing. T. Arnold, Dipl.-Ing. B. Orschel Institut für Organische Chemie der Technischen Hochschule Petersenstrasse 22, D-W-6100 Darmstadt (FRG)

[**] This work was supported by the Deutsche Forschungsgemeinschaft, the Fonds der Chemischen Industrie, and the Vereinigung von Freunden der Technischen Hochschule Darmstadt.

this reductive nitrogen transposition,[14] the *cis* adduct **10a** yields the primary amine (*R*)-**13** ($[\alpha]_D^{20}$ +15.5, *c*=2.00 in $CHCl_3$), whereas **11a** affords the enantiomer (*S*)-**13** ($[\alpha]_D^{20}$ −15.9, *c* = 1.11 in $CHCl_3$). The enantiomeric excess of (*R*)-**13** was determined to be >90% by NMR spectroscopy, with the aid of a shift reagent.

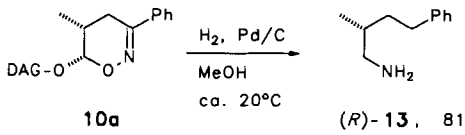

10a (*R*)-**13**, 81%

Our results show that predominantly or exclusively the *Si* side (with reference to C1) of the enol ether is attacked by **9a**. For (*E*)-**3** this means that a back side approach to the reactive conformation **A** and a front side approach to **B** (Scheme 3) must be considered above all others. Although in **B** the diastereotopic sides of the olefin should be more clearly differentiated, reactive conformation **A** may also be plausible, because here the repulsion between the dioxolane group at C4 and the propenyl unit is less than in **B**.[15] Besides, the cycloaddition will profit from a stronger electronic activation of the double bond in the s-cisoid conformation **A**.[16] The difference in the sides in **A**, however, is less pronounced, in particular if an *exo* transition state is involved.[17] Nevertheless, the back side of **A** should be more "open" to attack than the front side.[18]

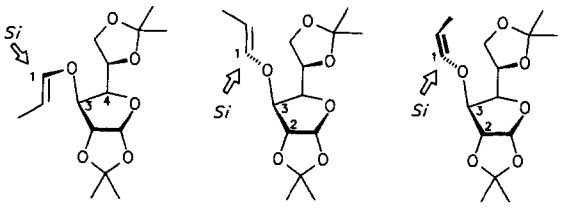

A C-1/O cisoid C-1/O/C-3/C-4 *anti*

B C-1/O transoid C-1/O/C-3/C-2 *anti*

C C-1/O *gauche* C-1/O/C-3/C-2 *anti*

Scheme 3. Reactive conformations **A**–**C** of (*E*)-**3** and (*Z*)-**3**.

For (*Z*)-**3** a similar consideration of models is even more difficult, but a reactive conformation corresponding to **A** is hardly feasible. In retrospect, the results can be explained with a *gauche* conformation **C**, in which the propenyl unit is turned slightly forward, and a front side attack of **9a**. The lower selectivity of (*Z*)-**3** might be due to the poorer differentiation between the sides in **C** or the participation of other reactive conformations.

The mechanistic interpretation proposed for (*E*)-**3** can also be applied to the allene derivative **7** (Scheme 4), which yields the labile primary adducts **14** with the nitrosoalkenes **9a** and **9c** (dr about 90:10). These alkenes are transformed into the stable conjugated 6*H*-1,2-oxazines **15**, which after chromatography are obtained diastereomerically pure in good overall yields. The assignment of the configuration at C6 is based on the results with the enol ether **3**, but mainly on the transformation of **15**, R=Ph, into the primary amine **13**. Here the first step can be assumed to be a hydrogenation of the CC double bond from the side opposite to the bulky DAG group. The intermediate is probably **10a**. The optical rotation of **13** ($[\alpha]_D^{20}$ +12.4, *c* = 2.00 in $CHCl_3$), which corresponds to an enantiomeric excess of about 80%, shows that the asymmetric induction in this hydrogen addition is good, but not perfect.

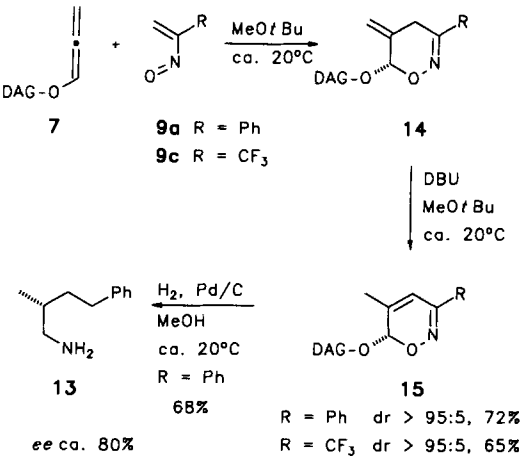

Scheme 4. Reactions of **9** with the allenyl ether **7**. DBU = diazabicycloundecene.

The results presented here demonstrate that using the cheap diacetoneglucose as optically active auxiliary[20] gives surprisingly high diastereoselectivities in hetero-Diels–Alder reactions. The enol ethers and the allene derivative containing this group are expected to gain in general significance (e.g., for other cycloadditions or reactions with electrophiles); furthermore, the optically active dihydro-1,2-oxazines obtained here are interesting intermediates, as exemplified by the synthesis of the primary amines (*R*)-**13** and (*S*)-**13** in high enantiomeric purity.

Received: January 17, 1992
Revised version: April 4, 1992 [Z 5130 IE]
German version: *Angew. Chem.* **1992**, *104*, 1084

CAS Registry numbers:
1, 582-52-5; **2**, 20316-77-2; **3**, *E* isomer, 142435-23-2; **3**, *Z* isomer, 142435-25-4; **4**, 20771-02-2; **5**, 20771-03-3; **6**, 67441-18-3; **7**, 142363-22-2; **8a**, 21572-32-7; **8b**, 73472-94-3; **8c**, 117341-57-8; **9a**, 61145-11-7; **9b**, 87497-88-9; **9c**, 142363-32-4; **10a**, 142363-23-3; **10b**, 142363-28-8; **10c**, 142363-29-9; **11a**, 142435-24-3; **11b**, 142435-26-5; **11c**, 142435-27-6; **12a**, 142363-24-4; **13**, 142363-25-5; **14a**, 142363-26-6; **14c**, 142363-30-2; **15a**, 142363-27-7; **15c**, 142363-31-3.

[1] Recent review: a) D. L. Boger, S. N. Weinreb, *Hetero Diels–Alder Methodology in Organic Synthesis*, Academic Press, New York, **1987**; Diels–Alder reactions with inverse electron demand with optically active enol ethers: b) G. H. Posner, D. G. Wettlaufer, *Tetrahedron Lett.* **1986**, *27*, 667–670; c) A. Choudhury, R. W. Franck, R.-B. Gupta, *ibid.* **1989**, *30*, 4921–4924; d) J.-E. Bäckvall, F. Rise, *ibid.* **1989**, *30*, 5347–5348; e) application of terpene auxiliaries for nitrosoalkene cycloadditions: T. Arnold, H.-U. Reissig, *Synlett* **1990**, 514–516; f) S. E. Denmark, C. B. W. Senanyahe, G. D. Ho, *Tetrahedron* **1990**, *46*, 4857–4876; g) S. E. Denmark, M. E. Schute, *J. Org. Chem.* **1991**, *56*, 6738–6739; h) V. Prapansiri, E. R. Thornton, *Tetrahedron Lett.* **1991**, *32*, 3147–3150.

[2] 1 is commercially available or can be easily prepared in a one-step reaction: K. P. R. Kartha, *Tetrahedron Lett.* **1986**, *27*, 3415–3416, and references cited therein.

[3] Short review on the use of sugar derivatives as auxiliaries for asymmetric synthesis: H.-U. Reissig, *Angew. Chem.* **1992**, *104*, 295–297; *Angew. Chem. Int. Ed. Engl.* **1992**, *31*, 288–290; for one of this report's aspects see also P. Cintas, *Tetrahedron* **1991**, *47*, 6079–6111.

[4] For nitrosoalkenes and their cycloadditions, see a) review: T. L. Gilchrist, *Chem. Soc. Rev.* **1983**, *12*, 53–73; [1a], p. 261–267; b) C. Hippeli, H.-U. Reissig, *Liebigs Ann. Chem.* **1990**, 217–226; c) R. Zimmer, H.-U. Reissig, *ibid.* **1991**, 553–562; d) R. Zimmer, H.-U. Reissig, *J. Org. Chem.* **1992**, *57*, 339–347.

[5] a) C. Hippeli, R. Zimmer, H.-U. Reissig, *Liebigs Ann. Chem.* **1990**, 469–474; b) C. Hippeli, H.-U. Reissig, *ibid.* **1990**, 475–481, and references cited therein.

[6] M. Bessodes, J. Shamsazar, K. Antonakis, *Synthesis* **1988**, 560–562.

[7] R. Damico, *J. Org. Chem.* **1968**, *33*, 1550–1556. *E*/*Z* mixtures are also obtained with the expensive Wilkinson catalyst ([1e]).
[8] With an iridium(I) catalyst, (*E*)-enol ethers are reported to be selectively accessible. (D. Baudry, E. Ephritikhine, H. Felkin, *J. Chem. Soc. Chem. Commun.* **1978**, 694–695). However, the allyl ether **2** could not yet be isomerized under these conditions.
[9] Cf. the synthesis of methoxyallene: S. Hoff, L. Brandsma, J. F. Arens, *Recl. Trav. Chim. Pays-Bas* **1968**, *87*, 916–924.
[10] On this point see H.-U. Reissig, C. Hippeli, T. Arnold, *Chem. Ber.* **1990**, *123*, 2403–2411.
[11] The isomeric ratios refer to the crude products and were determined by ^1H and ^{13}C NMR spectroscopy (±5% error). The quoted yields refer to purified products after chromatography and, if possible recrystallization. Satisfactory elemental analyses and the expected spectral data were obtained for all compounds.
[12] With increasing electron-withdrawing property of group R, the LUMO energy of the nitrosoalkenes decreases (H.-U. Reissig, unpublished MNDO calculations) and the reactivity toward electron-rich olefins increases; see also [4d].
[13] We thank Prof. Dr. H. J. Lindner (Technische Hochschule Darmstadt) for the structure determination. Details will be published in a full paper.
[14] For details on the mechanism of this six-step transformation, which most probably proceeds with retention of configuration at the nonparticipating stereogenic center, see [5b].
[15] Similar preferential conformations were found by X-ray analysis for 3-*O*-alkylated diacetoneglucose derivatives (for example, I. W. Krajewski, P. Głuzinski, Z. Urbanczyk-Lipkowska, A. Banaszek, K. Vangehr, P. Luger, *Carbohydr. Res.* **1984**, *125*, 203–216). We thank one referee for this hint and other critical comments.
[16] See D. Bond, P. von R. Schleyer, *J. Org. Chem.* **1990**, *55*, 1003–1013, and references cited therein.
[17] Whether an *exo* or an *endo* transition state is involved in these cycloadditions cannot be deduced from the products. Earlier studies on a model compound ([10]) indicate that an *exo* transition state should dominate. An *endo* approach to the nitrosoalkenes should, however, result in a greater side differentiation. For a similar discussion see [1f].
[18] Fixation of the conformation by Lewis acids, as discussed for similar auxiliaries [19], should not play a role here, because even the sodium ions present exert no influence: If Et*i*Pr$_2$N is used as base to generate **9a**, similar diastereomeric ratios are obtained from (*Z*)/(*E*)-**3** for **10a**/**11a** as when Na_2CO_3 is used as base.
[19] For the use of similar sugar auxiliaries for the Diels–Alder reaction with acrylates, see H. Kunz, B. Müller, D. Schanzenbach, *Angew. Chem.* **1987**, *99*, 269–271; *Angew. Chem. Int. Ed. Engl.* **1987**, *26*, 267–269; T. K. M. Shing, P. Lloyd-Williams, *J. Chem. Soc. Chem. Commun.* **1987**, 423–424; W. Stähle, H. Kunz, *Synlett* **1991**, 260–262; R. Nougier, J.-L. Gras, B. Giraud, A. Virgili, *Tetrahedron Lett.* **1991**, *32*, 5529–5530.
[20] Other examples with remarkable selectivities: U. Gerlach, S. Hünig, *Angew. Chem.* **1987**, *99*, 1323–1325; *Angew. Chem. Int. Ed. Engl.* **1987**, *26*, 1283–1285; H. Kunz, J. Mohr, *J. Chem. Soc. Chem. Commun.* **1988**, 1315–1317; R. O. Duthaler, A. Hafner, M. Riediker, *Pure Appl. Chem.* **1990**, *62*, 631–642; P. Duhamel, J. Jamal Eddine, J. Y. Valnot, *Tetrahedron Lett.* **1987**, *28*, 3801–3804; L. Duhamel, P. Angibaud, J. R. Desmur, J. Y. Valnot, *Synlett* **1991**, 807–808.

A One-Pot Synthesis of Ketones and Aldehydes from Carbon Dioxide and Organolithium Compounds**

By *Guido Zadel* and *Eberhard Breitmaier**

Dedicated to Professor Ernst Bayer on the occasion of his 65th birthday

Besides the old textbook examples such as the carboxylation of Grignard compounds to carboxylic acids,[1] and the Kolbe–Schmitt conversion of phenol to salicylic acid,[2] there are only a few more recent preparative applications of carbon dioxide;[3] one is the introduction of a carbamate protecting group to nitrogen heterocycles.[4]

We report here a new method of synthesizing ketones and aldehydes from carbon dioxide, in which CO_2 (**1**) reacts as an electrophile with an alkyllithium compound R^1Li **2a**. If after

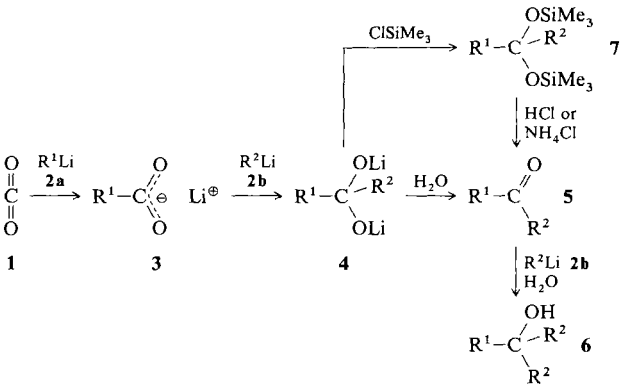

the excess carbon dioxide is removed, another alkyllithium compound R^2Li **2b** or lithium hydride (**2b**, R = H) is added in aprotic media (Table 1) and the reaction mixture is hydrolyzed, for example with aqueous hydrochloric acid or ammonium chloride, then symmetric ($R^1 = R^2$) or unsymmetric ketones **5** or aldehydes (**5**, R = H) are formed.

Table 1. Results of the syntheses of ketones and aldehydes.

Starting materials		Results		Conditions	
R^1 in **2a**	R^2 in **2b**	product	yield [%][a]	solvent	workup
Ph	prop-2-enyl	**5a**	78	ether	Me_3SiCl
*t*Bu	Ph	**5b**	92(83)	pentane, ether	NH_4Cl
*t*Bu	2-pyridyl	**5c**	65(54)	pentane, THF	HCl
Ph	[b]	**5d**	88	ether	Me_3SiCl
Ph	2-furyl	**5e**	68(44)	ether	Me_3SiCl
3-pyridyl	Bu	**5f**	58	ether, hexane	HCl
1-naphthyl	Ph	**5g**	88	THF, ether	NH_4Cl
cyclohexyl	Me	**5h**	93(37)	THF	HCl
Ph	Ph	**5i**	89	ether	HCl
Bu	H	**5j**	54	hexane	Me_3SiCl
3-pyridyl	H	**5k**	72	1,2-dimethoxyethane	HCl
mesityl	H	**5l**	45	1,2-dimethoxyethane	Me_3SiCl
*t*Bu	H	**5m**	51	pentane	Me_3SiCl
cyclopropyl	H	**5n**	43	THF	Me_3SiCl

[a] The values in parentheses refer to the results from the addition of **2b** before **2a**.
[b] 2-Tetrahydrofuryl.

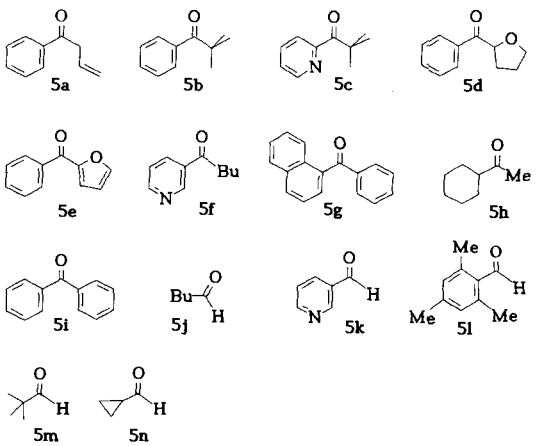

[*] Prof. E. Breitmaier, Dipl.-Chem. G. Zadel
Institut für Organische Chemie und Biochemie der Universität
Gerhard-Domagk-Strasse, D-W-5300 Bonn (FRG)

[**] This research was supported by the state of Nordrhein-Westfalen and the Fonds der Chemischen Industrie.

Besides the ketones or aldehydes, the tertiary alcohols **6** may be isolated before the reaction has gone to completion. They arise during the alkaline hydrolysis by addition of the alkyllithium compound **2b**, present in excess, to the already formed ketone **5**. If a series of samples are taken from an equimolar mixture of phenyllithium (**2b**, R^2 = Ph) and lithium-2,2-dimethylpropanoate (**3**, R^1 = *t*Bu, prepared in situ from 2-chloro-2-methylpropane, lithium, and carbon dioxide), and the concentrations of pivalophenone (**5b**), 2,2-dimethyl-1,1-diphenylpropanol (**6**, R^1 = *t*Bu, R^2 = phenyl), and pivalic acid are measured, it is apparent that the yield of ketone increases with time (Table 2). After the reaction is complete, tertiary alcohols **6** are formed only if more R^2Li is added during the workup (Table 2, last line). This experiment also supports the reaction sequence that Gilman et al.[3c] sketched out for the reaction of phenyllithium with carbon dioxide to give benzophenone: CO_2 (**1**) adds to the first alkyllithium compound **2a**; the resulting lithium carboxylate **3** reacts with the second alkyllithium compound **2b** or with lithium hydride (**2b**, R^2 = H) to give the dilithiated acetal or ketal **4**; hydrolysis leads to ketone (or aldehyde) **5**.

Table 2. Product distribution (GC analysis) as related to the reaction time for the reaction of **3**, R^1=*t*Bu, and **2b**, R^2=Ph, with workup in concentrated ammonium chloride solution.

Reaction time at reflux [h]	Products [%] ketone	alcohol	acid
0.5	29	25	44
1	32	25	41
2	37	26	35
3	55	16	26
4	63	10	22
5	70	7	19
10	91	0	7
24	92	0	6
24 [a]	53	33	7

[a] After 24h, 1 equiv **2b**, R^2 = Ph, was added.

The undesired formation of alcohols can be suppressed if the dilithiated acetals **4** are converted into the trimethylsilylacetals **7** by treatment with chlorotrimethylsilane. Compounds **7** are then hydrolyzed with aqueous hydrochloric acid.

The reaction lends itself to the synthesis of ketones and aldehydes with almost any substitution pattern, even those that are accessible conventionally only with difficulty. ^{13}C-labeled ketones and aldehydes can be prepared (from ^{13}C carbonate). Varying the reaction conditions according to Table 2 also opens the way to specific tertiary alcohols.

Experimental Procedure

Ketones and aldehydes: Dried powdered CO_2 (**1**, 132 g) was suspended in approximately 50 mL of solvent (Table 1) under argon in an apparatus with an additional gas inlet into the reaction mixture. A solution of the alkyllithium compound **2a** (0.05 mol) in 30 mL of solvent was cooled to −40 °C and added dropwise over 10 min; the reverse procedure leads primarily to symmetric ketones. After all the CO_2 had reacted or gone into solution, the reaction mixture was stirred for 1 h at −10 °C, heated 10 to 15 min at reflux, and then flushed free of CO_2 with argon (monitored with $Ba(OH)_2$).

Ketones: The reaction mixture was cooled to 0 °C, a solution of the alkyllithium compound **2b** (0.06 mol, 1–1.5 M solution) was added dropwise over 1 min, and the reaction mixture was then heated at reflux for 5 h (suspensions were heated for 10 to 24 h). The extent of reaction can be monitored titrimetrically according to ref.[5].

In situ variation: Alternatively, alkyllithium **2b** was prepared in situ by the addition of the haloalkane (0.06 mol) to lithium (0.06 mol, 0.48 g) over 30 min; the reaction mixture was heated for 5 to 10 h as previously described.

Aldehydes: After all of the CO_2 had been removed (monitored with $Ba(OH)_2$; metal hydrides and CO_2 form explosive mixtures![6]), the reaction mixture was cooled to −40 °C, and lithium hydride (**2b**, R^2=H, 0.065 mol, 0.48 g) was added. The reaction mixture was carefully allowed to warm to room temperature and then stirred for 12 h, or in the case of slower reactions, heated for 12 to 24 h at reflux.

Workup: The reaction mixture was pipetted in 2 mL aliquots into cold hydrochloric acid (1 N, 130 mL) or into saturated aqueous NH_4Cl solution (50 mL) for the hydrolysis. (The reversed procedure leads to the tertiary alcohols.) Alternatively, the reaction mixture was cooled to 0 °C and treated with chlorotrimethylsilane (15 mL). The reaction mixture was warmed and then quenched with hydrochloric acid (1 N, 50 mL) (Table 1). For both methods of hydrolysis the phases were separated, and the aqueous phase was extracted with ether. The collected organic phases were washed with NaCl solution, dried over $MgSO_4$, filtered, and distilled or recrystallized. The purity and identity of the known carbonyl compounds (Table 2) were determined by gas chromatography and ^1H NMR spectroscopy.

Received: February 25, 1992 [Z 5210 IE]
German version: *Angew. Chem.* **1992**, *104*, 1070

CAS Registry numbers:
5a, 6249-80-5; **5b**, 938-16-9; **5c**, 31595-32-1; **5d**, 141957-79-1; **5e**, 2689-59-0; **5f**, 1701-72-0; **5g**, 642-29-5; **5h**, 823-76-7; **5i**, 119-61-9; **5j**, 110-62-3; **5k**, 500-22-1; **5l**, 487-68-3; **5m**, 630-19-3; **5n**, 1489-69-6; CO_2, 124-38-9; PhLi, 591-51-5; *t*BuLi, 594-19-4; 3-pyridyl Li, 60573-68-4; 1-naphthyl Li, 14474-59-0; cyclohexyl Li, 10074-42-7; BuLi, 109-72-8; mesityl Li, 5806-59-7; cyclopropyl Li, 3002-94-6; prop-2-enyl Li, 3052-45-7; 2-pyridyl Li, 17624-36-1; 2-furyl Li, 2786-02-9; MeLi, 917-54-4; LiH, 7580-67-8; 2-tetrahydrofuryl Li, 141957-80-4.

[1] V. Grignard, *Ann. Chim. Ser. 7* **1901**, *24*, 433.
[2] H. Kolbe, E. Lautemann, *Justus Liebigs Ann. Chem.* **1860**, *113*, 125; R. Schmitt, DRP 29939, **1884**.
[3] a) F. Bodroux, *C. R. Hebd. Seances Acad. Sci.* **1903**, *137*, 710; b) *Bull. Soc. Chim. Fr.* **1904**, *31*(3), 24; c) H. Gilmann, P. R. Van Ess, *J. Am. Chem. Soc.* **1933**, *55*, 1258; d) D. Seyferth, R. Spohn, *ibid.* **1969**, *91*,6192; e) L. Garnier, Y. Rollin, J. Perichon, *J. Organomet. Chem.* **1989**, *367*, 347.
[4] A. R. Katritzky, M. Black, W.-Q. Fan, *J. Org. Chem.* **1991**, *56*, 5045.
[5] F. C. Watson, J. F. Eastham, *J. Organomet. Chem.* **1967**, *9*, 165.
[6] G. Barbaras, G. D. Barbaras, A. E. Finholt, H. J. Schlesinger, *J. Am. Chem. Soc.* **1948**, *70*, 877.

The Pentagonal Bipyramid as Fundamental Structure for Compounds with the Coordination Number Seven**

By *Ali-Reza Mahjoub, Thomas Drews,* and *Konrad Seppelt**

Tetrahedrons and octahedrons are the commonest polyhedral shapes for molecules with the coordination numbers 4 and 6.[1] In the case of coordination number 5 the principle geometry is the trigonal bipyramid, at least for homoleptic compounds. Here, however, it must be borne in mind that a square-pyramidal structure often has only marginally higher energy, which leads to the known intramolecular rearrangements.[2] A molecule AB_7 has three potential ideal geometries: the pentagonal bipyramid, (1:5:1 structure), the capped octahedron (1:3:3 structure), and the capped trigonal prism (1:4:2 structure) (Fig. 1). The theoretical treatment of this structural problem—considering the electrostatic ligand repulsions as the only determining factor—shows that the 1:3:3 structure is energetically most favorable, followed by the 1:4:2 and 1:5:1 structures.[3] This theoretical study, however, also reveals that these three structures inter-

[*] Prof. Dr. K. Seppelt, Dipl.-Chem. A.-R. Mahjoub, T. Drews
Institut für Anorganische und Analytische Chemie der Freien Universität
Fabeckstrasse 34–36, D-W-1000 Berlin 33 (FRG)

[**] This work was supported by the Deutsche Forschungsgemeinschaft and the Fonds der Chemischen Industrie.

convert through changes in angles almost without activation energy, and the pentagonal bipyramid and the capped trigonal prism are saddle points only a little higher on the energy surface.[3]

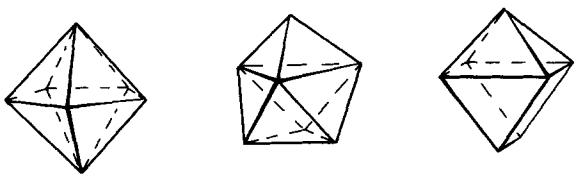

Fig. 1. The three polyhedrons of homoleptic compounds with coordination number 7 that are lowest in energy: pentagonal bipyramid (left), capped octahedron (center), capped trigonal prism (right).

A very small selection of compounds with the coordination number 7 are known whose structures are minimally affected by other effects. If the choice is limited to compounds of the main group elements to minimize the influence of d orbitals, and if, moreover, complications due to nonbonding electron pairs and lattice energy are to be avoided, the only remaining possibility is IF_7. In the gaseous state this is, without doubt, pentagonal bipyramidal,[4] although the structural data is imprecise. In particular, the important question of whether this homoleptic molecule has strict D_{5h} symmetry or whether it shows certain systematic deviations (puckering) cannot be answered at present. The electron diffraction data suggest a nonideal structure. The structure of IF_7 in the crystal has likewise not been unambiguously elucidated. In the solid state a complicating factor is the plastic phase containing disordered molecules, which transforms into an ordered phase only at $-120\,^{\circ}C$.[5]

We set ourselves the goal of solving the structural problem of substances with coordination number 7 by looking at tellurium compounds, of which TeF_7^- is already known.[6] The possible distortion of a fundamental structure by interionic interactions was to be decreased by the use of the large $(CH_3)_4N^+$ ion as counterion. The existence of $(CH_3)_4N^+TeF_7^-$ was demonstrated by the ^{125}Te and ^{19}F NMR spectra in CH_3CN.[6c, d] However, since all seven fluorine atoms are magnetically equivalent, the molecule is fluctional in solution. Studies with vibrational spectroscopy suggest, in analogy to IF_7, a pentagonal bipyramidal structure.[6c, d]

Large single crystals of $(CH_3)_4N^+TeF_7^-$, prepared from $(CH_3)_4N^+F^-$ and TeF_6, are easily grown, but are severely disordered because of the almost spherical shape of cation and anion.[7] This disorder can be restricted to (parts of) the anion by particularly slow crystal growth. The crystal structure analysis shows very clearly the presence of a pentagonal bipyramidal structure with shorter axial Te–F bond lengths than equatorial ones, but also the distinct distortion of the equatorial flourine atoms from a perfect planar arrangement (Fig. 2). The fourfold disorder of these fluorine atoms throws doubt on their positions; thus an equatorial fluorine atom in Figure 1 represents only the electron density of 21/4 electrons in the vicinity of the 52 electrons of the tellurium atom.

To prove conclusively the important statement on nonplanarity of the equatorial positions in the pentagonal bipyramid, the system was modified. Substituted tellurium(VI) fluorine compounds such as CH_3OTeF_5,[8] *trans*-[9] and *cis*-$(CH_3O)_2TeF_4$,[8] $(CH_3)_2NTeF_5$,[10] *cis*-$[(CH_3)_2N]_2TeF_4$,[10] $F_5Te(O)_nTeF_5$ ($n=1$,[11] 2[12]), and TeF_5Cl[13] were also allowed to react with $(CH_3)_4N^+F^-$ [Eq. (a) and (b)]. In two cases ^{19}F and ^{125}Te NMR spec-

$$CH_3OTeF_5 + F^- \longrightarrow CH_3OTeF_6^- \xrightarrow{25\,^{\circ}C} CH_3F + TeF_5O^- \qquad (a)$$

$$trans\text{-}(CH_3O)_2TeF_4 + F^- \longrightarrow trans\text{-}(CH_3O)_2TeF_5^- \xrightarrow{>0\,^{\circ}C} \text{decomposition} \qquad (b)$$

troscopy revealed sevenfold coordination. In all other cases only decomposition to TeF_5^-, TeF_7^-, and $TeOF_5^-$ was observed.

In the ^{125}Te NMR spectrum the anion $CH_3OTeF_6^-$ shows coupling to six equivalent fluorine atoms as well as to three protons; therefore this anion is also fluxional (Fig. 3). Because of the distortion of the high symmetry by the methoxy group, the compound $(CH_3)_4N^+CH_3OTeF_6^-$ crystallizes without disorder or twinning (Fig. 4). The methoxy group is

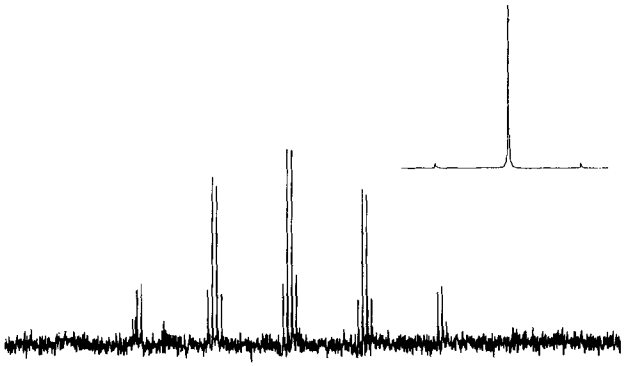

Fig. 3. ^{125}Te NMR spectrum of the $CH_3OTeF_6^-$ ion in CH_3CN at $-10\,^{\circ}C$. $\delta = -332.8$. The inset shows the ^{19}F NMR spectrum.

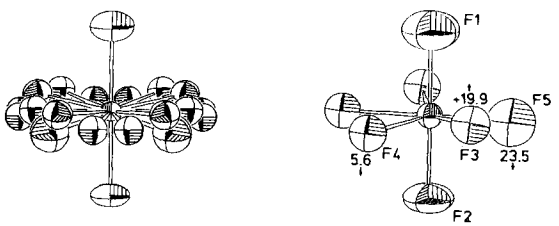

Fig. 2. Crystal structure of the TeF_7^- ion. Left: fourfold disordered model; right: one possible arrangement. Te–F1 178.8(16), Te–F2 179.1(17), Te–F3 186.1(21), Te–F4 183.2(20), Te–F5 190.3(39) pm. The numbers at the equatorial fluorine atoms give the distance in pm from the ideal equatorial plane.

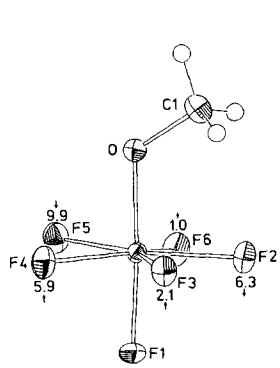

Fig. 4. Crystal structure of the $CH_3OTeF_6^-$ ion. The numbers at the equatorial fluorine atoms give the distance in pm from the ideal equatorial plane. Te–F1 182.2(3), Te–F2 190.9(2), Te–F3 192.3(2), Te–F4 191.2(2), Te–F5 190.5(2), Te–F_6 191.6(2), Te–O 185.8(3) pm; O-Te-F1 176.7(1), Te-O-C1 121.7(3)°.

in an axial position, in complete accord with the electron pair repulsion model: this position enables better space filling. The deviation of the O-Te-F_{ax} angle of 180 °C can, without doubt, be explained by the bent structure of the methoxy group. Again the equatorial Te–F bonds are longer than the axial bond, and the equatorial fluorine atoms lie distinctly off the ideal plane. This structural analysis is precise enough for the latter statement to be valid.

The crystal structure analysis of *trans*-$(CH_3O)_2TeF_5^-$ shows the oxygen atoms in the biaxial position (Fig. 5), as expected from the preceding discussion. Interestingly, in the solid state the anion occurs in both the *syn* and the *anti* conformation with respect to the methoxy groups. In both cases the equatorial fluorine atoms deviate from the ideal plane, and in slightly different ways, influenced here also by the orientation of the methoxy groups. The latter also determine the deviation from linearity of the vertical axis of the molecule.

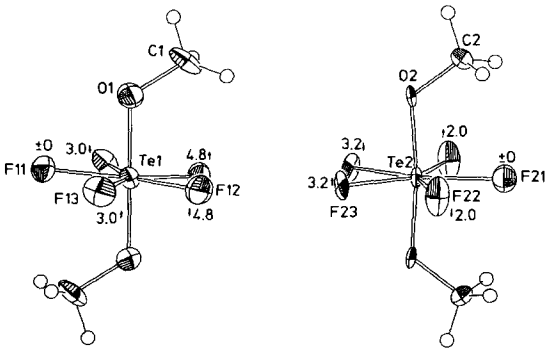

Fig. 5. Crystal structure of the two *trans*-$(CH_3O)_2TeF_5^-$ ions. The numbers at the equatorial fluorine atoms give the distance in pm from the ideal equatorial plane. Left: Te1–F11 192.1(5), Te1–F12 191.8(3), Te1–F13 192.6(3), Te1–O1 187.2(4) pm; O1-Te1-O1′ 180.6(2), Te1-O1-C1 119.6(4)°. Right: Te2–F21 196.3(4), Te2–F22 193.5(3) Te2–F23 194.0(3), Te2–O2 184.7(4) pm, O2-Te2-O2′ 172.8(2), Te2-O2-C2 124.1(3)°.

For *trans*-$(CH_3O)_2TeF_5^-$ it is not possible to prove that the anion is fluctional from NMR spectroscopy, because all fluorine atoms are equivalent by symmetry, if free rotation about the tellurium–oxygen bond is assumed.

The following preliminary structural principles for compounds with coordination number 7 can be deduced:

1) The fundamental structure of a homoleptic compound with coordination number 7 is the pentagonal bipyramid in which the bonds to the axial substituents are shorter than those to the equatorial ones. In the case of nonidentical ligands, smaller substituents take up equatorial positions.

2) When identical or very similar substituents are present, the pentagonal bipyramid is never rigid, with the exception of IOF_6^-: in this case the oxygen atom avoids an equatorial position because of the substantial double-bond character of the iodine–oxygen bond and therefore hinders the intramolecular exchange processes.[7]

3) An ideal pentagonal bipyramid is never achieved. That is, as a result of the repulsion among the spatially confined equatorial positions, this part of the molecule is distorted from planarity. The slightly greater repulsive energy of a pentagonal bipyramid compared with that of the capped octahedron can thus be accommodated while the highest symmetry is still approximately maintained. The highest possible symmetry has the arrangement that requires the fewest parameters to describe it: an (ideal) pentagonal bipyramid requires two, a capped octahedron five, and a capped trigonal prism five. As the highest symmetric arrangement is also the commonest for compounds with 5 (trigonal bipyramid) and 8 (square Archimedean antiprism[7]) as coordination number, this construction principle seems to be general.

Experimental Procedure

TeF_6, CH_3OTeF_5 [8], *trans*- [9] or *cis*-$(CH_3O)_2TeF_4$ [8], were condensed into a Teflon FEP tube that contained $(CH_3)_4N^+TeF^-$ [14] partly dissolved in CH_3CN. Crystals of $(CH_3)_4N^+F_7^-$ were obtained by heating to +40 °C and slow cooling over weeks to −18 °C. $(CH_3)_4N^+CH_3OTeF_6^-$ was dissolved at room temperature and cooled to −18 °C within a few hours to prevent decomposition. $(CH_3)_4N^+$-*trans*-$(CH_3O)_2TeF_5^-$ crystallizes from relatively concentrated solutions in the form of large, rectangular, colorless crystals. In each case a suitable crystal was placed on a CAD-4 diffractometer ($Mo_{K\alpha}$, graphite monochromator) with a special apparatus [15].

$(CH_3)_4N^+TeF_7^-$: $a = 894.7(1)$, $c = 623.1(1)$ pm, $V = 498.8 \times 10^6$ pm^3, −158 °C. *P4/nmm* (no. 129), $Z = 2$. In the range $2° < \theta < 35°$, 2479 measured reflections ($\pm h$, $+k$, $+l$, ω-2θ scan), 652 independent reflections, 620 reflections with $F \geq 3\sigma(F)$, $\mu = 31.49$ cm^{-1}, full matrix, equatorial fluorine atoms isotropic, fourfold disordered, other atoms anisotropic. SHELXS, $R = 0.062$, $Rw = 0.046$. The calculation with the twinning program SFLS [16] (*Pmmn*, no. 59) with remaining twofold disorder according to the twinning law (010)(−100)(001) yields no other results. For other physical properties see ref. [5c,d].

$(CH_3)_4N^+CH_3OTeF_6^-$: $a = 853.4(2)$, $b = 628.7(2)$, $c = 2002.5(7)$ pm, $\beta = 94.25(2)°$, $V = 1071.4 \times 10^6$ pm^3, −154 °C, $P2_1/c$, $Z = 4$. In the range $2° < \theta < 25°$, 2125 measured reflections, ω-θ scan, $\pm h$, $+k$, $+l$, 1870 independent reflections, 1621 reflections with $I \geq 3\sigma(I)$, $\mu = 29.2$ cm^{-1}, full matrix, SHELXS, $R = 0.027$, $Rw = 0.020$, all atoms anisotropic. ^{19}F NMR (CH_3CN): $\delta = 14.2$, singlet; ^{125}Te NMR: $\delta = -332.8$, (H_6TeO_6/H_2O), $J(Te,F) = 2630$ Hz, septet, $J(Te,H) = 148$ Hz, quartet. Raman (cryst.) $\tilde{\nu}$[cm^{-1}] = 956(s), 950(s), 846(w), 760(w), 760(vs), 674(w)m 630(w), 597(s), 581(w, Sch), 566(w), 527(w), 458(m), 379(m), 325(w), 206(w); IR (Nujol): $\tilde{\nu}$ [cm^{-1}] = 1229, 1014(w), 955(m,Sch), 947(s), 842(m), 630(m), 459(m) cm^{-1}.

$(CH_3)_4N^+$-*trans*-$(CH_3O)_2TeF_5^- \cdot 2CH_3CN$: $a = 1448.1(4)$, $b = 1764.5(3)$, $c = 2693.9(9)$ pm, $V = 6883.3 \times 10^6$ pm^3, −145 °C, *Ibca* (no. 73), $Z = 16$. In the range $2° < \theta < 25°$, 4774 measured reflections, 2996 independent reflections, 2702 reflections with $F \geq 3\sigma(F)$, $\mu = 31.49$ cm^{-1}, full matrix, SHELXS, $R = 0.044$, $Rw = 0.035$, all atoms anisotropic. ^{19}F NMR (CH_3CN): $\delta = 10.3$, singlet; ^{125}Te NMR: $\delta = -304.3$, $J(Te,F) = 2422$ Hz, sextet, $J(Te,H) = 148$ Hz, septet.

Further details of the crystal structure investigation may be obtained from the Fachinformationszentrum Karlsruhe, Gesellschaft für wissenschaftlich-technische Information mbH, D-W-7514 Eggenstein-Leopoldshafen 2 (FRG) on quoting the depository number CSD-56260, the names of the authors, and the journal citation.

Received: February 28, 1992 [Z 5215 IE]
German version: *Angew. Chem.* **1992**, *104*, 1047

CAS Registry numbers:
$(CH_3)_4N^+TeF_7^-$, 135912-45-7; $(CH_3)_4N^+CH_3OTeF_6^-$, 141927-97-1; $(CH_3)_4N^+$-*trans*-$(CH_3O)_2TeF_5^- \cdot 2CH_3CN$, 141903-67-5; CH_3OTeF_5, 28926-86-5; *cis*-$(CH_3O)_2TeF_4$, 29073-80-1; *trans*-$(HO)_2TeF_4$, 53108-94-4; *trans*-$(CH_3O)_2TEF_4$, 55056-70-7.

[1] Recently the knowledge has been growing that this sometimes is not valid for octahedral symmetry. [$W(CH_3)_6$] is trigonal-prismatic: A. Haaland, A. Hammel, K. Ryptal, H. V. Holden, *J. Am. Chem. Soc.* **1990**, *112*, 4547–4549. For a discussion of the structure of CrF_6: C. J. Marsden, P. P. Wolynec, *Inorg. Chem.* **1991**, *30*, 1681–1682; E. G. Hope, W. Levason, J. S. Ogden, *ibid.* **1991**, *30*, 4873–4874.

[2] R. S. Berry, *J. Chem. Phys.* **1960**, *32*, 933–938.

[3] D. Kepert, *Inorganic Stereochemistry*, Springer, Berlin, **1982**.

[4] W. J. Adams, H. B. Thompson, L. S. Bartell, *J. Chem. Phys.* **1970**, *53*, 4040–4046.

[5] R. D. Burbank, F. N. Bensey, *J. Chem. Phys.* **1957**, *27*, 981–982; R. D. Burbank, *Acta Crystallogr.* **1962**, *15*, 1207–1215; *ibid.* **1963**, *16*, 700–701; J. Donohue, *J. Chem. Phys.* **1959**, *30*, 1618–1619.

[6] a) E. L. Muetterties, *J. Am. Chem. Soc.* **1957**, *79*, 1004; b) H. Selig, S. Sarig, S. Abramovitz, *Inorg. Chem.* **1974**, *13*, 1508–1511; c) K. O. Christe, J. C. P. Sanders, G. J. Schrobilgen, W. W. Wilson, *J. Chem. Soc. Chem. Commun.* **1991**, 837–840; d) A.-R. Mahjoub, K. Seppelt, *ibid.* **1991**, 840–841.

[7] This phenomenon is notorious for the tetramethylammonium ion and also causes problems in the structural analysis of $(CH_3)_4N^+IOF_6^-$ and $(CH_3)_4N^+IF_8^-$; see [6d] and K. O. Christe, D. Dixon, A.-R. Mahjoub, J. C. P. Sanders, G. J. Schrobilgen, K. Seppelt, W. W. Wilson, *J. Am. Chem.*

Soc., in press; A. R. Mahjoub, K. Seppelt, *Angew. Chem.* **1991**, *103*, 844–845; *Angew. Chem. Int. Ed. Engl.* **1991**, *30*, 876–878.
[8] A. Cluston, R. D. Peacock, J. W. Fraser, *J. Chem. Soc. Chem. Commun.* **1970**, 1197.
[9] *trans*-$(HO)_2TeF_4$, prepared according to B. Pötter, D. Lentz, H. Pritzkow, K. Seppelt, *Angew. Chem.* **1981**, *93*, 1095–1096; *Angew. Chem. Int. Ed. Engl.* **1981**, *20*, 1036–1037, was methylated with CH_2N_2 in ether. Colorless liquid, yield quantitative, m.p. 32 °C; ^{1}H NMR: δ = ^{19}F NMR: δ = 62.6, ^{125}Te NMR: $\delta = -77.5$; J(HF) = 1.7, J(TeH) = 148, J(TeF) = 3672 Hz; Raman (fl.): 3031(m), 2965(s), 2908(w), 2854(m), 1461(w), 1379(w), 1299(w), 1216(vw), 117(w), 1002(w), 733(m), 681(w), 620(vs), 577(s), 386(w), 362(w), 313(m), 293(m), 241(w) cm^{-1}. IR (fl.) 3015(m), 2959(s), 2919(w), 2848(w), 1452(s), 1223(w), 996(vs), 901(w), 676(vs), 641(s), 585(w) cm^{-1}.
[10] J. W. Fraser, R. D. Peacock, P. M. Watkins, *J. Chem. Soc. Chem. Commun.* **1967**, 1248.
[11] A. Engelbrecht, W. Loreck, W. Nehoda, *Z. Anorg. Allg. Chem.* **1968**, *360*, 88–97; H. Bürger, *ibid.* **1968**, *360*, 97–104.
[12] K. Seppelt, D. Nöthe, *Inorg. Chem.* **1973**, *12*, 2727–2730.
[13] J. W. Fraser, R. D. Peacock, P. U. Watkins, *J. Chem. Soc. Chem. Commun.* **1968**, 1257.
[14] W. W. Wilson, K. O. Christe, J. Feng, R. Bau, *J. Am. Chem. Soc.* **1990**, *112*, 7619–7625.
[15] M. Veith, H. Bärnighausen, *Acta Crystallogr. Sect. B 30*, **1974**, 1806–1821; H. Schumann, W. Genthe, E. Hahn, M. B. Hossein, D. von der Helm, *J. Organomet. Chem.* **1986**, *299*, 67–85.
[16] H. Bärnighausen, *Z. Kristallogr.* **1985**, *170*, 5–6; M. Eitel, Dissertation, Universität Karlsruhe, **1985**.

Semiconductor-Catalyzed Photoaddition of Cyclic Enol Ethers to 1,2-Diazenes**

By *Ronald Künneth, Christian Feldmer,* and *Horst Kisch**

Suspensions of inorganic semiconductors such as TiO_2 and CdS have in recent years found increased application as photocatalysts in the synthesis of organic compounds. Potentially useful preparative reactions include oxidations,[1] reductions,[2] cyclodimerizations,[3] and isomerizations,[4] which usually lead to known products. We now show that ZnS and CdS powder photocatalyze the linear addition of cyclic enol ethers to 1,2-diazenes to afford hitherto unknown hydrazine derivatives.

On irradiation ($\lambda \geq 290$ nm) of a suspension of ZnS in a solution of 1,2-diphenyldiazene and 3,4-dihydro-2*H*-pyran (3,4-DHP) in methanol, the initially deep orange mixture decolorizes completely. The major reaction is an addition of 3,4-DHP to the diazene, in which the hydrazines **1** are formed (Scheme 1). Only after 20% conversion can 1,2-diphenylhydrazine be detected as minor product. As soon as all the 1,2-diphenyldiazene has been converted, the dehydrodimerization of the excess 3,4-DHP starts with simultaneous hydrogen evolution, in analogy to the known reaction of 2,5-dihydrofuran (2,5-DHF).[5] In addition the product **1a** decomposes on longer exposure times. The yield of **1a**, determined by HPLC at the end of the reaction, is 65%, but after isolation and two recrystallizations it decreases to 30%. When the reaction is performed without addition of ZnS, only a *cis/trans* isomerization of the diazene component takes place.

Analogous to 1,2-diphenyldiazene, 1,2-di-*p*-tolyldiazene and 1-*tert*-butyl-2-phenyldiazene react to form the adducts **1b** and **1c**, respectively. When 3,4-DHP is replaced by 2,3-dihydrofuran or 2,5-DHF, **1d** is isolated in 20% yield. According to HPLC, linear addition products are also obtained with 4,7-dihydro-1,3-dioxepin and cyclohexene. However, if 4,5-dihydro-2-methylfuran is used, 1,2-diphenylhydrazine forms as major product beside traces of the addition product. Saturated ethers like THF or 1,4-dioxane, on the other hand, are completely inert and induce no reaction.

The structure of the products is deduced from mass spectrometric data, as well as one- and two-dimensional ^{1}H and ^{13}C NMR spectra (see Table 1). The ^{13}C NMR signals of the enol ether group in **1a** have typical chemical shifts (δ = 148.3, 99.2); the coupling of the protons at C5 (for numbering see Scheme 1) with those on C1 and C4 are obtained unambiguously from the ^{1}H–^{1}H COSY spectra, which show that the new C-N bond is formed regioselectively at the C1 position of the substrate R_3H. Furthermore, in the reaction of 1-*tert*-butyl-2-phenyldiazene the addition of 3,4-DHP occurs regioselectively at the phenyl-substituted nitrogen atom; this follows from the chemical shift of the NH protons (δ = 3.17). In **1a**, **1b**, and **1c** the resonance signal of this proton is in the δ range of 5.35 to 5.62.

Table 1. Selected NMR and IR data and yields of **1a**–**1d**.

	1a	**1b**	**1c**	**1d**
δ (^{13}C NMR) [a]				
C1	51.2	51.7	58.7	64.0
C2	99.2	99.8	102.3	97.0
C3	148.3	148.1	145.7	150.7
C4	64.4	64.8	64.6	71.9
C5	26.8	26.7	26.9	
δ (^{1}H NMR) [b]				
NH	5.62	5.35	3.17	5.47
IR				
ν(N-H) [c]	3328	3288	3286	3290
ν(O-C=C) [c]	1636	1640	1641	1601
Yields [d]				
ZnS	65	60	60	55
CdS	70	44	65	75

[a] $CDCl_3$, 67.7 MHz. [b] $CDCl_3$, 270 MHz. [c] In cm^{-1}. [d] Yields in %; determination by HPLC.

For all described reactions, CdS can also be used instead of ZnS as heterogeneous catalyst. Since CdS absorbs visible light sufficiently ($\lambda_{bg} \geq 516$ nm), a tungsten lamp ($\lambda \geq 350$ nm) was employed for the irradiation in this case. Within 48 h about 10 mmol of 1,2-diphenyldiazene was converted in the presence of 2 mmol CdS.[6]

The reaction presented here can be explained with the simplified catalytic cycle sketched in Scheme 2. The electron promoted to the conduction band by irradiation of the semiconductor (e^-) drifts to the surface and reduces the diazene to the hydrazyl radical (R^1–$\dot{N}$–NH–R^2). In accord with this step are the findings that protic solvents are essential for the reaction, that the reduction of water is inhibited by the pres-

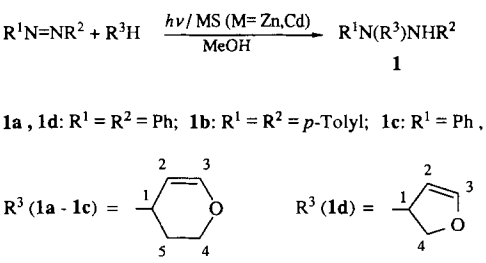

Scheme 1.

[*] Prof. Dr. H. Kisch, Dipl.-Chem. R. Künneth, Dipl.-Chem. C. Feldmer Institut für Anorganische Chemie der Universität Erlangen-Nürnberg Egerlandstrasse 1, D-W-8520 Erlangen (FRG)

[**] Heterogeneous Photocatalysis, Part 10. Part 9: H. Kisch, G. Twardzik, *Chem. Ber.* **1991**, *124*, 1161–1162.

ence of the diazene, and that 1,2-di-*p*-tolyldiazene, which is more difficult to reduce, reacts more slowly than 1,2-diphenyldiazene. The hole in the valence band (h^+) that is created at the same time oxidizes the ether via an intermediate radical cation to an allyl-stabilized radical $^{\bullet}R^3$. Recombination of R^1–$\dot{N}$–NHR^2 with $^{\bullet}R^3$ affords the final product **1**. The intermediacy of the radical $^{\bullet}R^3$ is deduced from the formation of the dehydrodimers R^3–R^3 as side products. Regioisomeric products, which could arise from the allyl rearrangement of the dihydropyranyl radical, have not been detected.

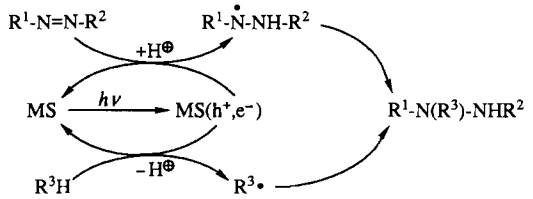

M= Zn, Cd

Scheme 2. Postulated photocatalysis cycle.

The proposed mechanism is supported by the irradiation ($\lambda \geq 290$ nm) of a dilute solution of 1,2-diphenyldiazene and benzophenone in 3,4-DHP. This reaction also affords the addition product **1a** regioselectively in a yield of 30% according to HPLC. In the excited triplet state, benzophenone, which functions as sensitizer in this system, abstracts an H atom from 3,4-DHP.[7] The benzhydryl radicals that result react with 1,2-diazenes to afford the corresponding hydrazyl radicals,[8] which recombine with the dihydropyranyl radicals to form **1a**.

The overall reaction corresponds to an addition of an allylic C–H bond of a cyclic enol ether to a diazene group, a reaction type that was hitherto known only for electron-poor diazenes like azodicarboxylic acid esters.[9] Thus, we have shown for the first time that two different organic substrates can be coupled to form a linear addition product on the irradiated surface of a semiconductor.

Experimental Procedure

All manipulations were conducted under an inert atmosphere of N_2 with dry, N_2-saturated solvents. ZnS and CdS were prepared according to [10] and [11]. General procedure: 1,2-diphenyldiazene (0.5 g, 2.74 mmol), ZnS (0.5 g, 5.13 mmol), 3,4-DHP (3.00 mL, 33.2 mmol), and MeOH (85.0 mL) or 1,4-dioxane/H_2O (70.0/15 mL) were suspended in an ultrasound bath in a Pyrex immersion lamp apparatus for 15 min and thereafter irradiated with a Hg high-pressure lamp (Phillips HPK 125 W) until no more diazene could be detected by thin-layer chromatography (about 15 h). ZnS was filtered off, and evaporation to dryness (25 °C) yielded a yellow oil. **1a** and **1d**: white solids after two recrystallizations from MeOH (yield: 30 and 20% respectively); **1b** and **1c**: after column chromatography (Al_2O_3/petroleum ether) **1b** was isolated (40%) as a pale yellow oil that yields a white solid on crystallization from petroleum ether (10%). **1c** is isolated as colorless oil (30%).

Received: March 10, 1992 [Z 5233 IE]
German version: *Angew. Chem.* **1992**, *104*, 1102

CAS Registry numbers:
1a, 142065-25-4; **1b**, 142040-07-6; **1c**, 142040-03-7; **1d**, 142040-04-8; 3,4-DHP, 110-87-2; 4,5-DHF, 1191-99-7; PhN=NPh, 103-33-3; *p*-tolyl N=N *p*-tolyl, 501-60-0; PhN=N*t*Bu, 1775-83-3.

[1] M. A. Fox, *Top. Curr. Chem.* **1987**, *142*, 71–99.
[2] A. J. Frank, Z. Goren, I. Willner, *J. Chem. Soc. Chem. Commun.* **1985**, 1029–1030; T. Shiragami, C. Pac, S. Yanagida, *J. Phys. Chem.* **1990**, *94*, 504–506.
[3] A. M. Draper, M. Ilyas, P. de Mayo, V. Ramamurthy, *J. Am. Chem. Soc.* **1984**, *106*, 6222–6230; H. Al-Ekabi, P. de Mayo, *J. Org. Chem.* **1987**, *52*, 4756–4759.
[4] S. Yanagida, K. Mizumoto, C. Pac, *J. Am. Chem. Soc.* **1986**, *108*, 647–654; P. de Mayo, G. Wenska, *J. Chem. Soc. Chem. Commun.* **1986**, 941–942.
[5] a) J. Bücheler, N. Zeug, H. Kisch, *Angew. Chem.* **1982**, *94*, 792–793; *Angew. Chem. Int. Ed. Engl.* **1982**, *21*, 777; b) N. Zeug, J. Bücheler, H. Kisch, *J. Am. Chem. Soc.* **1985**, *107*, 1459–1465; c) S. Yanagida, T. Azuma, Y. Midori, C. Pac, H. Sakurai, *J. Chem. Soc. Perkin Trans. 2* **1985**, 1487–1493.
[6] a) This corresponds to the conversion of 3.6 monolayers of 1.2-diphenyldiazene per hour, if it is assumed that a monolayer consists of 10^{14} particles cm^{-2}; for ZnS (see Experimental Procedure) 2.2 monolayers per hour; see L. P. Childs, D. F. Ollis, *J. Catal.* **1980**, *66*, 383–389. The specific surface area determined by N_2 adsorption for CdS and ZnS is 120 and 100 m^2g^{-1}, respectively. b) We thank Prof. Dr. G. Emig, University of Erlangen-Nürnberg, for these measurements.
[7] This was also observed in the system benzaldehyde/3,4-DHP: A. G. Griesbeck, S. Stadtmüller, *J. Am. Chem. Soc.* **1990**, *112*, 1281–1283.
[8] P. S. Engel, W.-X. Wu, *J. Am. Chem. Soc.* **1989**, *111*, 1830–1835.
[9] G. O. Schenck, H. Formanek, *Angew. Chem.* **1958**, *70*, 505; R. C. Cookson, I. D. R. Stevens, C. T. Watts, *Chem. Commun.* **1965**, 259–260; G. Ahlgren, *Tetrahedron Lett.* **1974**, 2779–2782.
[10] A. Kurian, C. V. Suryanarayana, *J. Appl. Electrochem.* **1972**, *2*, 223–229.
[11] W. Hetterich, H. Kisch, *Chem. Ber.* **1989**, *122*, 621–627.

Bis(trisyl)oxadiborirane**

By *Peter Paetzold,* Laurence Géret-Baumgarten,* and *Roland Boese*

Dedicated to Professor Hermann Stetter on the occasion of his 75th birthday

As ab initio calculations show,[1] the diboriranes **1a**–**4a** (R = R′ = H) have a tendency to contract the B–B distance and open the H-B-B angle with increasing electronegativity of Y. This behavior is similar to that of the corresponding heterocyclopropanes and disiliranes.

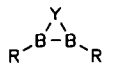

1, Y = BR′
2, Y = CR_2'
3, Y = NR′
4, Y = O

In the case of the azadiborirane **3**, experimental crystal structure determinations are only available for two derivatives with amino groups bonded to boron.[2, 3] Since the electronic effect of these substituents is strong, a comparison with theoretical predictions makes little sense. An alkyl derivative (**3b**, R = R′ = *t*Bu) proved to be disordered in the crystal.[4] We have now prepared the first oxadiborirane, title compound **4b**, by initially converting the chloroborane **5** into the diboryl oxide **6** [Equation (a)] and, subsequently, **6** into **4b** through reduction with Na/K alloy [Equation (b)].

The colorless crystalline product **4b** shows only one NMR signal in C_6D_6 for each of the atoms H, B, and C.[5] For the structure of the parent compound **4a** determined by ab initio methods, an NMR shift of $\delta(^{11}B) = 67.0$ has been calculat-

[*] Prof. P. Paetzold, L. Géret-Baumgarten
Institut für Anorganische Chemie der Technischen Hochschule Templergraben 55, D-W-5100 Aachen (FRG)
Dr. R. Boese
Institut für Anorganische Chemie der Universität-Gesamthochschule Universitätsstrasse 5–7, D-W-4300 Essen (FRG)

[**] Trisyl = tris(trimethylsilyl)methyl.

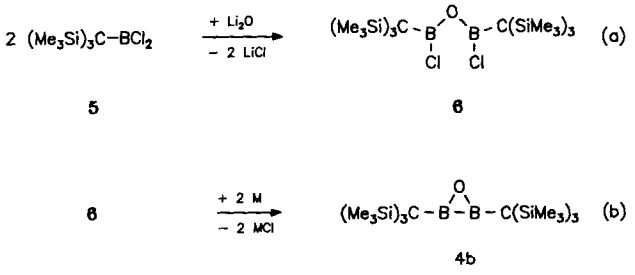

ed[6] by the IGLO method, which agrees well with the measured value for **4b** of 65.7. The X-ray crystal structure analysis of **4b**[7] confirms the three-membered ring structure with an almost linear C–B–B′–C′ moiety (Fig. 1). The O atoms are disordered about the crystallographic C_2 axis and are therefore found with half the electron density on each side of the B–B′ bond. This disorder leads to centrosymmetry, which—as the isotropic dislocation parameters show—is strictly valid for the $C(SiMe_3)_3$ groups. The same parameters indicate such a strong displacement of the ring atoms out of the ring plane that an exact description of the ring geometry becomes impossible.

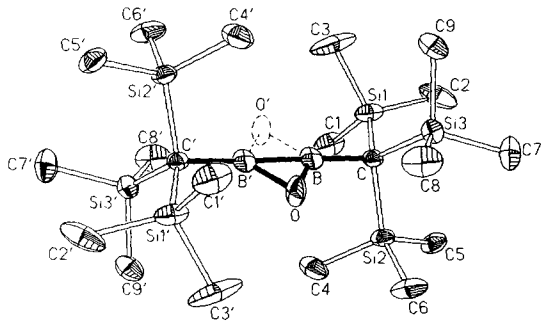

Fig. 1. Molecular structure of **4b** in the solid state. The ellipsoids correspond to 50% probability of electron occupation, hatched and unhatched atoms are equivalent by crystallographic centrosymmetry, the disordered oxygen atom is drawn as an ellipse with dashed outline, and the hydrogen atoms are omitted for clarity. Selected distances [Å] and angles [°] (standard deviations in parentheses): B-B′ 1.601(7), B-O 1.545(5), B′-O 1.510(6), B-C 1.544(4); O-B-B′ 57.4(3), B-O-B′ 63.2(3), C-B-O 120.2(3), C-B-B′ 177.7(3).

In spite of disorder in the region of the B–B′ bond, this bond length can be determined with satisfactory accuracy to 1.60 Å. It is almost as short as the B–B bond in anion **A** (1.58 Å; R = $SiMe_3$),[8] which is—to our knowledge—the shortest B–B bond measured up to now. It is noteworthy, in

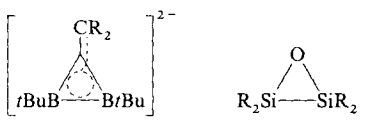

A **B**

this context, that B–B bond lengths are scattered over a wide range; the B7–B8 distance in $B_{10}H_{14}$ of 2.01 Å,[9] for example, is still considered bonding. The B–B bond distance calculated for **4a** of 1.594 (3-21G) or 1.562 Å (MP2/6-31G*[6]) is close to that measured for **4b**. Theory[1] draws a picture of a diborane(2), RB=BR, that is bridged by an O atom in analogy to an olefin bonded side-on by a transition metal ("σ-bridged π bonding"). In oxadisilirane **B** (R = Mes), which is related to three-membered rings of type **4** through the diagonal relationship in the periodic system, a Si–Si distance of 2.23 Å is found,[10] which is closer in length to a double bond than to a single bond, each of these bond lengths being found in a typical range, in contrast to B–B bonds. Certainly, the short B–B and Si–Si distances of oxadiborirane and oxadisilirane can also be accurately described by a model with bent bonds and no π interaction.[11] The remarkably long B–O distances of 1.545 and 1.510 Å in **4b** do not agree well with those calculated for **4a** (1.409[1] or 1.403 Å[6]) and prove to be drastically longer than the 1.32 Å measured for the open-chain compound, $(RO)_2B–B(OR)_2$ ($(RO)_2$ = $–OCMe_2–CMe_2O–$), that can be used for comparison. Because of the disordered O atoms, the C-B-B′ and B-B′-C′ angles of **4b** (177.7 and 182.3°, respectively) can only be compared with the values of 173.9°[1] and 175.2°[6] calculated for **4a**, insofar as these angles accurately reflect the tendency toward linearization of the chain R–B–B–R on passing from **1** to **4**; the corresponding angles for unknown three-membered ring compounds of type **1** where R = R′ are expected to be 150°.

The oxadiborirane **4b** proves to be quite inert. In contrast to the azadiboriridine **3b** (R = R′ = *t*Bu), it reacts neither with CO,[12] nor with RN_3 (R = Pr, Bu),[13] BH_3,[14] or EtB≡N*t*Bu,[15] and not even with alkynes RC≡CR (R = Et, Me_3Si), whose reaction with the B–B bond of diborane(4) derivatives is considered typical. It is inert even towards O_2 and H_2O. Attempts to cleave the O atom reductively with phosphanes PR_3 (R = Me, Ph) as acceptors left **4b** intact. The only reaction that we could find for **4b** is the oxidative addition of formic or acetic acid in the ratio 1:1 according to Equation (c), in which the crystalline products **7a**, **b** are ob-

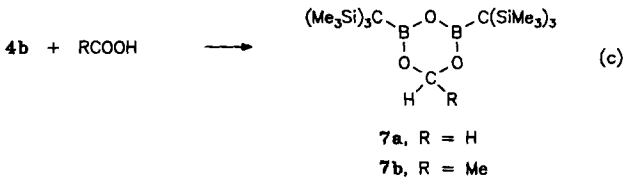

7a, R = H
7b, R = Me

tained in yields of 82 or 71%, respectively.[16] Unexpectedly, not the acidic proton, but the carboxyl C atom is oxidizing.

Experimental Procedure

Bis[chloro{tris(trimethylsilyl)methyl}boryl] oxide **6**: Li_2O (0.17 g) was added to a solution of **5** (3.57 g) [17] in THF (30 mL). The mixture was stirred for 10 h at room temperature before the solvent was removed in vacuo, the residue dissolved in pentane (20 mL), and LiCl filtered off. At −80°C **6** crystallized (3.10 g, 95%, m.p. 198°C) [18]. The same product was obtained with a similar procedure from **5** and $NaOSiMe_3$ in the ratio 2:1 (75%).

Bis[tris(trimethylsilyl)methyl]oxadiborirane **4b**: A solution of **6** (3.10 g) in hexane (30 mL) was heated under reflux in the presence of Na/K alloy (3 mL) for 10 h. The excess alloy and alkali-metal salts were filtered off, and the filtrate was evaporated to dryness. Sublimation at 120°C/0.005 Torr afforded **4b** (1.55 g, 57%, m.p. 242°C).

Received: March 27, 1992 [Z 5268 IE]
German version: *Angew. Chem.* **1992**, *104*, 1071

CAS Registry numbers:
4b, 142066-17-9; **6**, 142066-18-0; **7a**, 142066-16-8; **7b**, 142066-19-1; HCO_2H, 64-18-6; $MeCO_2H$, 64-19-7.

[1] C. Liang, L. C. Allen, *J. Am. Chem. Soc.* **1991**, *113*, 1878–1884; Calculations with the 3-21G basis set.
[2] F. Dirschl, E. Hanecker, H. Nöth, W. Rattay, W. Wagner, *Z. Naturforsch. B* **1986**, *41*, 32–37.

[3] K.-H. van Bonn, P. Schreyer, P. Paetzold, R. Boese, *Chem. Ber.* **1988**, *121*, 1045–1057.
[4] R. Boese, B. Kröckert, P. Paetzold, *Chem. Ber.* **1987**, *120*, 1913–1915.
[5] **4b**: NMR (C_6D_6): $\delta(^1H) = 0.29$; $\delta(^{11}B) = 65.7$; $\delta(^{13}C) = 4.33$(q); according to experience the signal for the B-bonded C atoms is broad and was not resolved.
[6] We thank P. von R. Schleyer and M. Bühl, Universität Erlangen, for the calculations with the 6-31G* basis set at MP2 level, which they completed for us before the paper of Allen et al. [1] appeared.
[7] Crystal data of **4b**: $a = 16.033(3)$, $b = 8.906(2)$, $c = 23.781(4)$ Å, $\beta = 109.06(1)°$, $V = 3209.5(1.0)$ Å^3, $T = 103$ K, $Z = 4$, $\rho_{calcd} = 1.036$ g cm^{-3}, $C2/c$ (no. 15); Nicolet R3m/V diffractometer; $\mu(Mo_{K\alpha}) = 2.6$ cm^{-1}; range $3 \leq 2\theta \leq 40°$; 2098 independent reflections, 1798 of which observed with $F_0 \geq 4\sigma(F)$; anisotropic temperature factors for non-hydrogen atoms; 163 refined parameters; $R = 0.0424$, $R_w = 0.0520$. Further details of the crystal structure investigation may be obtained from the Fachinformationszentrum Karlsruhe, Gesellschaft für wissenschaftlich-technische Information mbH, D-W-7514 Eggenstein-Leopoldshafen 2 (FRG) on quoting the depository number CSD-320470, the names of the authors, and the journal citation.
[8] H. Meyer, G. Schmidt-Lukasch, G. Baum, W. Massa, A. Berndt, *Z. Naturforsch. B* **1988**, *43*, 801–806.
[9] J. S. Kasper, C. M. Lucht, D. Harker, *Acta Crystallogr.* **1950**, *3*, 436–455.
[10] H. B. Yokelson, A. J. Millevolte, G. R. Gillette, R. West, *J. Am. Chem. Soc.* **1987**, *109*, 6865–6866.
[11] J. A. Boatz, M. S. Gordon, *J. Phys. Chem.* **1989**, *93*, 3025–3029.
[12] H. Nötz, *Z. Naturforsch. B* **1984**, *39*, 1463–1466.
[13] P. Paetzold, B. Redenz-Stormanns, R. Boese, *Angew. Chem.* **1990**, *102*, 910–911; *Angew. Chem. Int. Ed. Engl.* **1990**, *29*, 900–903.
[14] P. Paetzold, B. Redenz-Stormanns, R. Boese, M. Bühl, P. von R. Schleyer, *Angew. Chem.* **1990**, *102*, 1059–1060; *Angew. Chem. Int. Ed. Engl.* **1990**, *29*, 1059.
[15] P. Paetzold, B. Redenz-Stormanns, R. Boese, *Chem. Ber.* **1991**, *124*, 1435–2441.
[16] **7a**: m.p. = 228 °C (from pentane); NMR (C_6D_6): $\delta(^1H) = 0.30$ (s, 54H), 4.85 (s, 2H); $\delta(^{11}B) = 32.7$; $\delta(^{13}C) = 5.1$(q), 84.3(t). – **7b**: m.p. = 142 °C (from pentane); NMR (C_6D_6): $\delta(^1H) = 0.27$ (s, 54H), 1.54 (d, 3H), 4.12 (q, 1H); $\delta(^{11}B) = 32.3$; $\delta(^{13}C) = 4.2$(q), 30.5(q), 89.3(d).
[17] S. S. Al-Juaid, C. Eaborn, M. N. A. El-Kheli, P. B. Hitchcock, P. D. Likiss, M. E. Molla, J. D. Smith, J. A. Zora, *J. Chem. Soc. Dalton Trans.* **1989**, 447–452.
[18] **6**: NMR (C_6D_6): $\delta(^1H) = 0.32$(s); $\delta(^{11}B) = 40.4$; $\delta(^{13}C) = 5.2$(q), 19.4(s).

troscopy shows only the intense $S_0 \rightarrow S_2$ transition. Likewise, normally no information can be gleaned from fluorescence spectroscopy about the energetic situation of S_1 in long-chain polyenes such as β-carotene.

Experiments showed that shorter polyenes containing fewer than nine double bonds generally fluoresce from the first singlet state S_1, a state forbidden for absorption, whereas longer carotenoids containing more than eight π bonds, such as β-carotene, show an anti-Kasha emission from the S_2 state.[11] We now report the synthesis of novel, modified carotenoids with nine and eleven π bonds, for which dual fluorescence (that is, emission from the S_1 and the S_2 state) occurs, and thus the energetic level of S_1 can be determined at least approximately.

In the planning of the synthesis of modified, sufficiently photostable carotenoids, we were first guided by the idea of substituting the saturated ethano fragments in lycopene by conjugatively stabilizing carbonyl groups (oxalyl fragments). To achieve this we linked two C_4 end components with a C_n central component (dialdehydes **1**–**4**) according to the synthesis principle $C_4 + C_n + C_4 = C_{n+8}$. As shown in Figure 1, the diones **7**–**10** and the tetrones **11**–**14** can be obtained in this way (Table 1). Whereas the color of the diones **7**–**10**

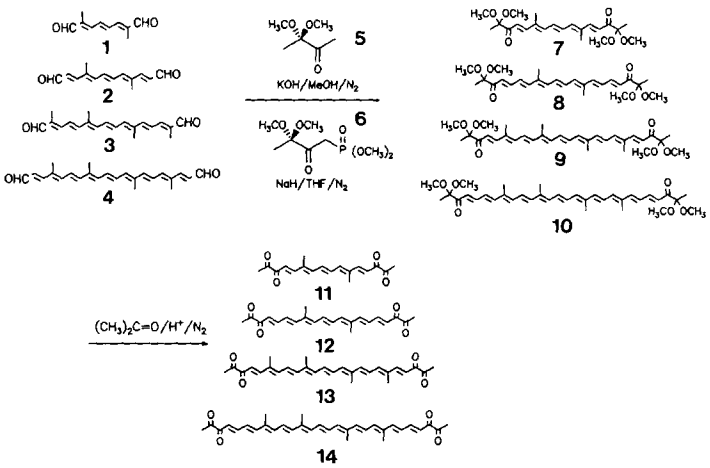

Fig. 1. The synthesis of tetramethoxydiapocarotenediones **7**–**10** and diapocarotenetetrones **11**–**14**. Compounds **5** or **6** may be used to provide the carbonyl groups.

Dual Fluorescence of Novel Modified Carotenoids**

By *Hans Bettermann,* Martin Bienioschek, Hans Ippendorf,* and *Hans-Dieter Martin**

Carotenoids are counted among the most important and also most numerous naturally occurring chromophores.[1, 2] In the photosynthesis of higher plants, algae, and bacteria they assume a dual role: a) they absorb energy as accessory pigments (antenna function); thus they aid in energy transfer and b) they quench the triplet state of various chlorophylls or remove reactive or excited oxygen species.

The key to the understanding of the energy transfer processes in carotenoids is a knowledge of their lowest excited states, in particular the states S_1 (2^1A_g), S_2 (1^1B_u), and T_1 (C_{2h} symmetry assumed). Unfortunately little is known about the energy of S_1 and T_1, in spite of intensive spectroscopic investigations:[3–10] conventional absorption spec-

[*] Dr. H. Bettermann, Dipl.-Chem. M. Bienioschek
Institut für Physikalische Chemie und Elektrochemie der Universität
Universitätsstrasse 1, D-W-4000 Düsseldorf (FRG)
Prof. Dr. H.-D. Martin, Dipl.-Chem. H. Ippendorf
Institut für Organische Chemie und Makromolekulare Chemie der Universität Düsseldorf

[**] Chromophoric Systems, Part 5. This work was supported by the Deutsche Forschungsgemeinschaft, the Fonds der Chemischen Industrie and BASF AG. Part 4: H.-D. Martin, T. Werner, *J. Mol. Struct.*, **1992**, *266*, 91–96.

Table 1. Selected physical data of **6**–**14** [a].

6: MS(70 eV): m/z 209 (M^+)

7: M.p. 174 °C, MS(70 eV): m/z 392 (M^+), UV/VIS($CHCl_3$): λ[nm](ε) = 409 (64000), 433 (63500)

8: M.p. 157 °C, MS(70 eV): m/z 444 (M^+), UV/VIS($CHCl_3$): λ[nm](ε) = 457 (79000), 484 (73000)

9: M.p. 204 °C, MS(70 eV): m/z 524 (M^+), UV/VIS($CHCl_3$): λ[nm](ε) = 499 (99800), 530 (85900)

10: M.p. 216 °C, MS(70 eV): m/z 576 (M^+), UV/VIS($CHCl_3$): λ[nm](ε) = 515 (119000), 555 (87500)

11: M.p. 197 °C, MS(70 eV): m/z 300 (M^+), UV/VIS($CHCl_3$): λ[nm](ε) = 442 (36900), 468 (33800)

12: M.p. 190 °C, MS(70 eV): m/z 352 (M^+), UV/VIS($CHCl_3$): λ[nm](ε) = 488 nm (59700), 510 (60900)

13: M.p. 217 °C, MS(70 eV): m/z 432 (M^+), UV/VIS($CHCl_3$): λ[nm](ε) = 532 (85300), 555 (80800)

14: M.p. 240 °C, MS(70 eV): m/z 484 (M^+), UV/VIS($CHCl_3$): λ[nm](ε) = 549 (112000), 580 (110000)

[a] All compounds have the correct elemental analysis. The compounds were purified by column chromatography, and their purity tested by thin-layer chromatography.

varies from yellow to dark red, the tetrones **11**–**14** are orange to reddish blue. The photostability of the diones **7**–**10** at radiant flux densities in the order of 10^{22} photons $cm^{-2}s^{-1}$ is good enough for spectroscopic studies (see Experimental), but the tetrones **11**–**14** proved unexpectedly to be not persistent enough under the same conditions. In the following, therefore, the results of fluorescence spectroscopy on diones **8** and **9** will be described in detail.

In the absorption spectra of unsubstituted all-*trans* polyenes, or those with identical substituents as end groups, the visible transition with lowest energy is the $S_0 \rightarrow S_2$ band, since the $S_0 \rightarrow S_1$ transition is symmetry forbidden and therefore cannot be detected in conventional absorption spectroscopy. The S_1 state of all-*trans* polyenes (point group C_{2h}), like the ground state, belongs to the symmetry species A_g. This was confirmed by two-photon spectroscopy.[10] The substitution of terminal double bonds in polyenes by carbonyl groups changes the position of the absorption bands by only a few nanometers. The additional $n \rightarrow \pi^*$ states cannot influence the fluorescence because, as experience shows, they are substantially more hypsochromic (about 300–400 nm).

Figure 2 shows the absorption spectra of compounds **8** and **9** in chloroform at room temperature. That the vibronic structure of the $S_0 \rightarrow S_2$ absorption band arises from at least two vibrational progressions follows from the second derivative. However, only the C–C stretching vibrational progressions (**8**: 1218 cm^{-1}, **9**: 1172 cm^{-1}) are unambiguously determinable. The two clearly visible vibronic bands in the spectrum of **8** are assigned to the transitions $0 \rightarrow 1$ (484 nm, 20640 cm^{-1}) and $0 \rightarrow 2$ (457 nm, 21856 cm^{-1}); the $0 \rightarrow 0$ transition lies at 19422 cm^{-1} (515 nm). This is in accord with the position of the origin of the fluorescence ($0 \rightarrow 0$ transition) of **8** and the only slight shift of the $0 \rightarrow 0$ transition in absorption and fluorescence for carotenoids such as β-carotene.[11] Also in agreement with the origin of the fluorescence spectrum to be discussed later, the first visible vibronic transition in the spectrum of compound **9** at 18868 cm^{-1} (530 nm) is, however, assigned to the $0 \rightarrow 0$ transition of the C–C stretching vibrational progression.

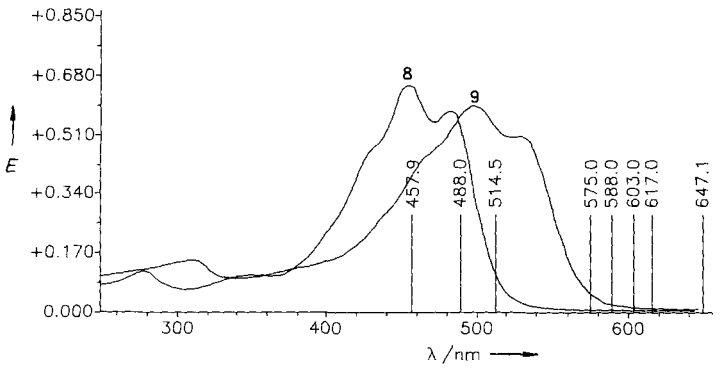

Fig. 2. Absorption spectra of compounds **8** (8.2×10^{-6} M) and **9** (6×10^{-6} M), dissolved in chloroform. E = extinction.

Figure 3 shows the fluorescence spectra of **8** and **9**. Each have two fluorescence maxima (**8**: 18492 cm^{-1}, 540 nm and 13600 cm^{-1}, 735 nm; **9**: 17492 cm^{-1}, 571 nm and around 13500 cm^{-1}, 740 nm). The less intense fluorescence signals overlap with the Raman signals of the solvent and the substance under investigation. The two maxima are the result of different emission transitions. The maximum at higher energy is assigned to the $S_2 \rightarrow S_0$ emission and that at lower energy to the $S_1 \rightarrow S_0$ emission. This dual fluorescence is supported by the following findings:

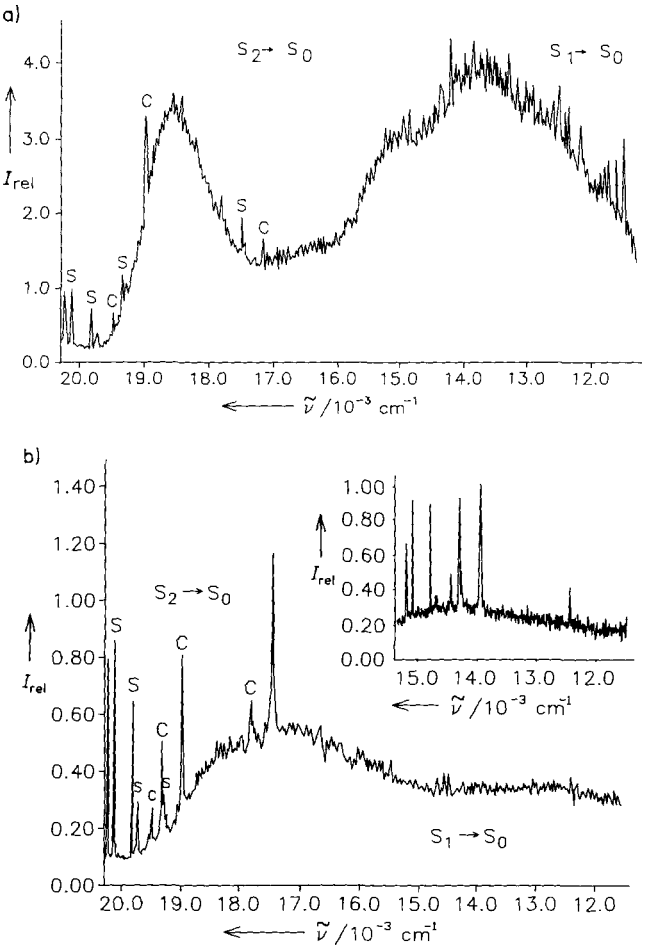

Fig. 3. Fluorescence spectra of **8** (a) and **9** (b) in chloroform (10^{-5} M, excitation wavelength λ_{ex} = 488.0 nm). C: Raman signals of the compound under investigation; S: Raman signals of the solvent. The inset in (b) shows the $S_1 \rightarrow S_0$ fluorescence of **9** in chloroform (10^{-3} M) after excitation with a krypton ion laser (λ_{ex} = 647.1 nm)

- On excitement with frequencies smaller than the $S_0 \rightarrow S_2$ absorption, the fluorescence at lower energy can be observed separately. If **8** is excited with light of wavenumbers 17391 (575), 17007 (588), 16584 (603), and 16207 cm^{-1} (617 nm), the red-shifted luminescence band appears, irrespective of the energy of the excitation irradiation. This proves that the fluorescence is from a single state. Likewise **9** shows one luminescence on excitement beyond the $S_0 \rightarrow S_2$ absorption band determined from the UV/VIS spectrum; its maximum lies at approximately 14000 cm^{-1} (714 nm; inset in Fig. 3b). The Raman signals in the spectra of both compounds show a distinct resonance enhancement, which confirms the direct excitement into the S_1 state.
- For small concentrations (10^{-7}–10^{-8} M) the long-wavelength emission band is missing. This concentration dependence indicates that the two fluorescence emissions do not proceed from the same excited state. The nonlinear concentration dependence of the ratio of the two emission bands excludes the simultaneous presence of excimer and monomer fluorescence. Presumably the different concentration dependence of the $S_1 \rightarrow S_0$ and $S_2 \rightarrow S_0$ fluorescence is attributable to different intermolecular radiationless deactivation.

The $S_2 \rightarrow S_0$ fluorescence band of **8** does not show the mirror image of the $S_0 \rightarrow S_2$ absorption band. This points to different geometries for the S_0 and S_2 states. The $0 \rightarrow 0$ transition of the $S_2 \rightarrow S_0$ fluorescence is found in the range 19200–19500 cm^{-1} (520–512 nm), while the $0 \rightarrow 0$ transition of the $S_1 \rightarrow S_0$ fluorescence can be assigned to the band at 16200 cm^{-1} (617 nm) on the grounds of the fluorescence excitation spectra.

The origins ($0 \rightarrow 0$ transitions) of the $S_2 \rightarrow S_0$ and the $S_1 \rightarrow S_0$ fluorescence of compound **9** are estimated to be 19000 ± 200 and 15200–15400 cm^{-1}, respectively.

Dual fluorescence in linear conjugated polyenes was hitherto observed only for all-*trans*-tetradecaheptaene[11] and fucoxanthin (nine conjugated π bonds).[12] In condensed phases the long-chain polyenes show $S_2 \rightarrow S_0$ fluorescence preferentially, whereas $S_1 \rightarrow S_0$ emission occurs for short-chain polyenes. This general observation is related to the exponential decay of the nonradiative deactivation rate when the $S_1 \rightarrow S_2$ energy difference increases.[13] For short-chain polyenes with smaller $S_1 \rightarrow S_2$ energy differences (e.g., 4900 cm^{-1} for dodecahexaene[11]), predominantly the $S_1 \rightarrow S_0$ fluorescence is observed.

Known compounds that emit from an S_1 and an S_2 state mostly have a large energy difference between these two states (e.g., 14000 cm^{-1} for azulene[14]). The dual fluorescence observed here for compound **8**, which has a small $S_1 \rightarrow S_2$ energy difference (3000–3300 cm^{-1}) is precisely for this reason very remarkable.

In the longer chain carotenoid **9** the $S_1 \rightarrow S_2$ difference was measured to be 3400–4000 cm^{-1}. This is in accord with the fact that $\Delta E(S_2\text{–}S_1)$ increases with increasing chain length.[11] Since for β-carotene (eleven π bonds) $\Delta E(S_2\text{–}S_1)$ is not known exactly, but is thought—not uncontested—to lie at approximately 3500 cm^{-1},[15] it is interesting to note that the carotenoid **9** (likewise containing eleven π bonds) yields an experimental value in this range.

Experimental Procedure

The emission spectra were generated with excitation from an argon ion laser (488.0 nm, 250 mW), a krypton ion laser (647.1 nm, 300 mW), and a dye laser (Rhodamin 6G, 575, 588, 603, and 617 nm), and measured with a grating spectrometer (Jarrell-Ash, model 25-400; Czerny-Turner double monochromator, 1 m focal length; Peltier-cooled photomultiplier RCA C31034 combined with a photon counter [16]). The measurements were performed with a constant mechanical slit width. The spectral slit width was 9 cm^{-1} (488.0 nm) and 6 cm^{-1} (647.1 nm). The spectra were recorded with a scan speed of 300 $cm^{-1}min^{-1}$ (100 $cm^{-1}min^{-1}$ for excitement with the dye laser) at a step size of 2.25 cm^{-1} (1 cm^{-1} for excitement with the krypton ion laser and the dye laser).

The samples were measured in a rotating cuvette to avoid local heating by the focused laser beam [17]. Since the path of the focused beam was tangential to the inner wall of the cuvette, the fluorescence signals could not be reabsorbed. The luminescence was observed at an angle of 90° to the excitation beam. The signal detection and processing was computer-controlled [18]. The spectra were corrected as follows:

- At the same time that the data was recorded, a photodiode measured the laser power to make fluctuations visible.
- The spectra were corrected to account for the spectral sensitivity curve of the monochromator/detector system.
- The decrease in intensity of the exciting light due to the absorption by the sample solution was compensated by normalization of the spectra with a Raman signal of the solvent.

To monitor the photochemical stability of the samples, UV/VIS spectra were recorded before and after each measurement on a diode-array spectrophotometer (Hewlett-Packard, Model 8452A). After 30 min irradiation (λ_{ex} = 488.0 nm, 250 mW, 10^{-5} M solution) the photochemical conversion was 4%.

Received: February 28, 1992 [Z 5218 IE]
German version: *Angew. Chem.* **1992**, *104*, 1073

CAS Registry numbers:
1, 5056-17-7; **2**, 53163-53-4; **3**, 502-70-5; **4**, 34561-05-2; **5**, 21983-72-2; **6**, 141903-39-1; **7**, 141290-97-3; **8**, 141290-93-9; **9**, 141290-92-8; **10**, 141903-40-4; **11**, 141290-96-2; **12**, 141903-41-5; **13**, 141290-91-7; **14**, 141903-42-6.

[1] N. I. Krinsky, M. M. Mathews-Roth in *Carotenoids, Chemistry and Biology* (Ed.: R. F. Taylor), Plenum Press, New York, **1989**.
[2] W. Vetter, G. Englert, N. Rigassi, U. Schwieter in *Carotenoids*, (Ed.: O. Isler), Birkhäuser, Basel, **1971**.
[3] T. Gillbro. R. J. Cogdell, *Chem. Phys. Lett.* **1989**, *158*, 312.
[4] S. L. Bondarev, S. M. Bachilo, S. S. Dvornikov, S. A. Tikhomirov, *J. Photochem. Photobiol. A* **1989**, *46*, 315.
[5] R. J. Trash, H. Fang, G. E. Leroi, *Photochem. Photobiol.* **1979**, *29*, 1049.
[6] N. E. Binnie, L. V. Haley, J. A. Koningstein, *Chem. Phys. Lett.* **1985**, *120*, 564.
[7] H. Hashimoto, Y. Koyama, *Chem. Phys. Lett.* **1989**, *163*, 251.
[8] T. Noguchi, S. Kolaczkowski, C. Arbour, S. Armaki, G. H. Atkinson, H. Hayashi, M. Tasumi, *Photochem. Photobiol.* **1989**, *50*, 603.
[9] G. R. Holtom, W. M. McClain, *Chem. Phys. Lett.* **1976**, *44*, 436.
[10] B. S. Hudson, B. E. Kohler, K. Schulten in *Excited States, Vol. 6* (Ed.: E. C. Lim), Academic Press, New York, **1982**.
[11] R. Snyder, E. Arvidson, C. Foote, L. Harrigan, R. L. Christensen, *J. Am. Chem. Soc.* **1985**, *107*, 4117; S. A. Cosgrove, M. A. Guite, T. B. Burnell, R. L. Christensen, *J. Phys. Chem.* **1990**, *94*, 8118.
[12] A. P. Shreve, J. K. Trautman, T. G. Owens, A. C. Albrecht, *Chem. Phys.* **1991**, *154*, 171.
[13] R. Englman, J. Jortner, *J. Mol. Phys.* **1970**, *18*, 145.
[14] M. Beer, H. C. Longuet-Higgins, *J. Chem. Phys.* **1955**, *23*, 1390.
[15] R. J. Thrash, H. Fang, G. E. Leroi, *J. Chem. Phys.* **1977**, *67*, 5930.
[16] E. J. Darland, J. E. Hornschuh, C. G. Enke, G. E. Leroi, *Anal. Chem.* **1979**, *51*, 245.
[17] W. Kiefer, *Appl. Spectrosc.* **1974**, *28*, 115.
[18] W. Rauch, K. Kelbert, H. Bettermann, *Rev. Sci. Instrum.* **1988**, *59*, 376.

Ten-Membered Ring Enediynes with Remarkable Chemical and Biological Profiles**

By *K. C. Nicolaou*, Erik J. Sorensen, Robert Discordia, Chan-Kou Hwang, Robert E. Minto, Kamal N. Bharucha,* and *Robert G. Bergman**

We report the synthesis and study of a novel series of ten-membered ring enediynes[1, 2] with geminal dimethyl groups flanking the enediyne moiety as protecting devices.[3] These compounds, which are analogues of more complex anticancer antibiotics, exhibit novel rates of cycloaromatization and DNA-cleaving properties.

The critical steps in the synthesis of molecules **2**–**4** (Scheme 1) from dialdehyde **1**[4] are illustrated in Scheme 1; additional details of the synthesis and characterization will be provided in the full account of this work. The configurations of the conformationally rigid compounds **2** and **3** were assigned by NMR spectroscopy with chiral shift reagents and confirmed by X-ray crystallographic analysis of the *trans* isomer **2** (Fig. 1).

Molecular modeling studies suggested a nearly orthogonal arrangement of the two carbonyl groups in dione **4**, an inference supported by its IR spectrum, which showed a C=O band at $\tilde{\nu}_{max} = 1708$ cm^{-1} (see Table 1). The ^1H NMR spec-

[*] Prof. Dr. K. C. Nicolaou, E. J. Sorensen, Dr. R. Discordia, Dr. C.-K. Hwang
Department of Chemistry, The Scripps Research Institute
10666 North Torrey Pines Road, La Jolla, CA 92037 (USA)
and
Department of Chemistry, University of California,
San Diego, La Jolla, CA 92093 (USA)
Prof. Dr. R. G. Bergman, R. E. Minto, Dr. K. N. Bharucha,
Department of Chemistry, University of California
Berkeley, CA 94720 (USA)

[**] We thank Drs. Raj Chadha, Dee H. Huang and Gary Siuzdak of The Scripps Research Institute for their assistance with X-ray crystallography, NMR spectroscopy, and mass spectrometry, respectively. R.E.M. thanks the Natural Sciences and Engineering Research Council (Canada). This work was financially supported by the National Institutes of Health (GM-45312 to R.G.B. and CA-46446 to K.C.N.

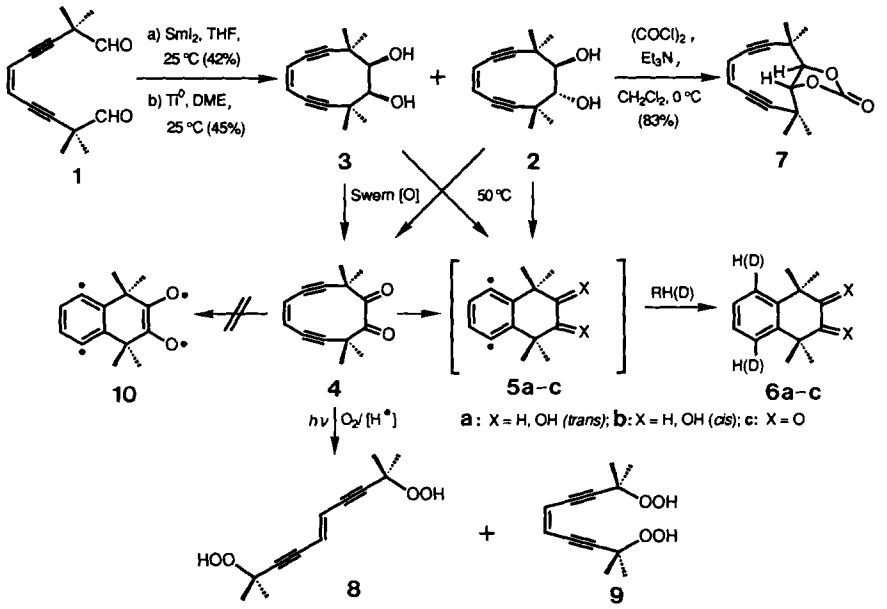

Scheme 1. Synthesis and chemistry of ten-membered ring enediynes **2**–**4**. Under reaction conditions a, **2** and **3** were formed in a 20:1 ratio; under reaction conditions b (slow addition of **1** to Ti°), in a 1:2.6 ratio. For important data of compounds **2**–**4** and **7** see Table 1.

trum of **4** is temperature dependent and suggests that an exchange process involving interconversion of two degenerate ring conformations occurs. Two sharp resonances for the methyl groups at $\delta = 1.62$ and 1.43 observed below $-60\,^{\circ}C$ coalesced to a singlet at $-3.0\,^{\circ}C$. An Arrhenius plot provided $\Delta H^{\neq} = 12.9\ kcal\,mol^{-1}$ and $\Delta S^{\neq} = +3.2\ cal\,K^{-1}\,mol^{-1}$ as thermodynamic parameters for this interconversion.

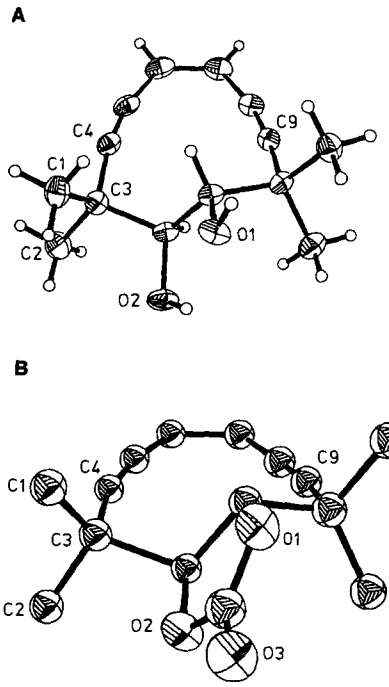

Fig. 1. ORTEP representation of compounds **2** (A) and **7** (B). The C4–C9 distances are 3.422 and 3.424 Å, respectively.

Thermal cycloaromatization of **2** at temperatures ranging from ambient to 105 °C in 1,4-cyclohexadiene/THF gave 50–75% isolated yields of **6a**. In [D_8]THF, a mixture of [D_2]**6a** (55%) and products resulting apparently from coupling with solvent-derived radicals (45%) were formed. The rate laws of this reaction were found to be first order in **2** and independent of the solvent, concentration of **2**, and concentration of hydrogen atom donor ($\Delta H^{\neq} = 30.2\ kcal\,mol^{-1}$ and $\Delta S^{\neq} \approx 9.7\ cal\,K^{-1}mol^{-1}$ temperature range 60–105 °C). Interestingly, the *cis* isomer **3** cyclized faster in [D_8]toluene ($t_{1/2} \approx 4$ h at 50 °C) than the *trans* isomer **2** ($t_{1/2} \approx 22$ h at 50 °C); **6a** was obtained in 49% yield in both cases. Significantly higher temperatures (75–100 °C) were required to convert dione **4** to the bicyclic aromatic diketone **6a**. CIDNP (Chemically Induced Dynamic Nuclear Polarization) was observed when the cyclization of **2** was carried out in the probe of an NMR spectrometer between 70 and 100 °C in [D_8]THF, [D_6]acetone, or [D_3]MeCN. Kaptein's rules[5] suggest that **2** cyclizes via singlet diradical **5a**, in agreement with earlier results for acyclic enediyne systems.[6]

Carbonate **7**, a crystalline solid (Fig. 1 B), interested us since we expected the second ring to act as a "locking device" that would prevent cycloaromatization. Indeed **7** proved to be completely stable at 100 °C for several hours.

Dione **4** was subjected to UV irradiation in the presence of 1,4-cyclohexadiene in an attempt to generate the oxygen-

Table 1. Selected physical and spectroscopic data of compounds **2**–**4**, and **7**.

2: $R_f = 0.42$ (30% ether in petroleum ether; SiO_2); m.p. 100 °C (decomp.); IR($CHCl_3$) $\tilde{\nu}_{max} = 3500, 3025, 2400, 2280, 1650\ cm^{-1}$; ^1H NMR (500 MHz, $CDCl_3$): $\delta = 5.79$ (s, 2 H olefinic H), 4.03 (s, 2H, C*H*OH), 2.83 (br. s, 2H, O*H*), 1.31 (s, 6H, CH_3), 1.12 (s, 6H, CH_3); ^{13}C NMR (125 MHz, $CDCl_3$) $\delta = 122.5, 107.4, 82.7, 76.8, 38.2, 26.5, 18.4$; HRMS: *m/z* calcd for $C_{14}H_{18}O_2Na(M + Na)$ 241.1205, found 241.1212

3: $R_f = 0.40$ (30% ether in petroleum ether; SiO_2); m.p. 90 °C (decomp.); IR($CHCl_3$) $\nu_{max} = 3500, 3015, 2125, 1602\ cm^{-1}$; ^1H NMR (500 MHz, $CDCl_3$) $\delta = 5.81$ (s, 2H, olefinic H), 4.00 (br. d, 1H, C*H*OH), 3.38 (dd, $J = 13.5, 3.9$ Hz, 1H, C*H*OH), 2.94 (d, $J = 13.5$ Hz, 1H, O*H*), 1.84 (br. s, 1H, O*H*), 1.38 (s, 6H, CH_3), 1.32 (s, 3H, CH_3), 1.31 (s, 3H, CH_3); HRMS: *m/z* calcd for $C_{14}H_{18}O_2Na$ (M+Na) 241.1205, found 241.1205

4: $R_f = 0.20$ (petroleum ether; SiO_2); 35–51% yield; IR (neat) $\tilde{\nu}_{max} = 2984, 2937, 2197, 1708\ cm^{-1}$; ^1H NMR (500 MHz, $CDCl_3$) $\delta = 5.79$ (s, 2H, olefinic H), 1.55 (br.s, 12H, CH_3); ^{13}C NMR (125 MHz, $CDCl_3$) $\delta = 200.9, 122.8, 101.6, 85.8, 43.2, 25.1$; HRMS: *m/z* calcd for $C_{14}H_{14}O_2(M)$, 241.0994, found 241.0995

7: $R_f = 0.35$ (5% ether in petroleum ether); 83% yield; m.p. = 132–134 °C; IR($CHCl_3$) $\tilde{\nu}_{max} = 2978, 2924, 2197, 1805\ cm^{-1}$; ^1H NMR (500 MHz, $CDCl_3$) $\delta = 5.87$ (s, 2H, olefinic H), 4.64 (s, 2H, 2 C*H*OC), 1.43 (s, 6H, CH_3), 1.24 (s, 6H, CH_3); ^{13}C NMR (125 MHz, $CDCl_3$) $\delta = 154.0, 123.0, 103.2, 84.4, 84.0, 36.3, 26.1, 18.4$; HRMS: *m/z* calcd for $C_{15}H_{16}O_3Na$ (M + Na) 267.0997, found 267.0988, HRMS: *m/z* calcd for $C_{15}H_{16}O_3H$ (M+H) 245.1178, found 245.1170

and carbon-centered "multiple warhead" tetraradical **10**, a potentially powerful species for DNA damage. In the event, however, none of the products expected to arise from **10** were formed. Instead, the two novel dihydroperoxides **8** and **9** were isolated in 22 and 10% yield, respectively. The same transformations were also effected, although less cleanly, by thermolysis in the presence of hydrogen atom donors. Quite intriguing is the possibility of the intermediacy of a dioxetene[7] which is presumed to eject the equivalent of ethenedione,[8] perhaps as two carbon monoxide molecules.[9]

Compounds **2** and **3** caused significant DNA cleavage when incubated with φX174 supercoiled DNA at pH 8.5 and 50 °C (Fig. 2). Interestingly, dione **4** caused only slight DNA damage under the same conditions, whereas hydroperoxides **8** and **9** showed, as expected, quite strong DNA-cleaving activities. Based on the chemistry of these systems we presume that whereas the ten-membered ring enediynes **2** and **3** may exert their DNA-cleaving power by cyclization to an aromatic diradical, the open-chain enediynes **8** and **9** may operate by an entirely different mechanism involving the generation of oxygen-centered radicals.

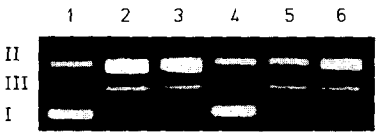

Fig. 2. Interaction of supercoiled DNA with enediynes **2**–**4**, **8**, and **9**. φX174 DNA was incubated for 48 h at 50 °C with the enediynes in buffer (50 mM Tris-HCl, pH 8.5) and analyzed by electrophoresis (1% agarose gel, ethidium bromide stain). Lane 1: DNA control; Lane 2: DNA + *cis* diol **3** (5000 μM); Lane 3: DNA + *trans* diol **2** (5000 μM); Lane 4: DNA + dione **4** (5000 μM); Lane 5: DNA + *trans* enediyne **8** (5000 μM); Lane 6: DNA + *cis* enediyne **9** (5000 μM). I–III stand for form I, form II, and form III DNA, respectively.

The described chemistry demonstrates a highly convergent route to conjugated cyclic enediynes, some fascinating stereochemical effects of rigid ten-membered ring systems, the introduction of new "locking devices" to stabilize labile enediynes, and the DNA-cleaving action of a number of new enediynes.

Received: March 19, 1992 [Z 5250 IE]
German version: *Angew. Chem.* **1992**, *104*, 1094

[1] For recent reviews, see: K. C. Nicolaou, W.-M. Dai, *Angew. Chem.* **1992**, *103*, 1453; *Angew. Chem. Int. Ed. Engl.* **1991**, *30*, 1387; M. D. Lee, G. A. Ellestad, F. B. Borders, *Acc. Chem. Res.* **1991**, *24*, 235.

[2] For the design and synthesis of the first monocyclic ten-membered ring enediynes with DNA-cleaving properties, see: K. C. Nicolaou, G. Zuccarello, Y. Ogawa, E. J. Schweiger, T. Kumazawa, *J. Am Chem. Soc.* **1988**, *110*, 4866; K. C. Nicolaou, Y. Ogawa, G. Zuccarello, H. Kataoka, *ibid.* **1988**, *110*, 7247.

[3] For a theoretical discussion of the effect of substituents at the bridge connecting enediyne moiety, see: J. P. Snyder, *J. Am. Chem. Soc.* **1990**, *112*, 5267.

[4] Dialdehyde **1** was prepared by two methods starting from either 2,2-dimethyl-1,3-propanediol or methyl acetoacetate and (*Z*)-1,2-dichloroethene.

[5] R. Kaptein, *J. Chem. Soc.* **1971**, 732.

[6] T. P. Lockhart, R. G. Bergman, *J. Am Chem. Soc.* **1981**, *103*, 4091.

[7] A similar dioxetene system has been previously postulated: N. J. Turro, V. Ramamurthy, K.-C. Liu, *J. Am. Chem. Soc.* **1976**, *98*, 6758.

[8] The existence of ethenedione is debatable; see: M. B. Rubin, A. Patyk, W. Sander *Tetrahedron Lett.* **1988**, *29*, 6641; D. M. Birney, J. A. Berson, *Tetrahedron*, **1986**, *42*, 1561; G. P. Raine, H. F. Schaefer, R. C. Haddon, *J. Am. Chem. Soc.* **1983**, *105*, 194 and references cited therein.

[9] For references on the photochemistry of α-diketones, see: M. B. Rubin, *Fortschr. Chem Forsch.* **1969**, *13*, 251; G. E. Gream, J. C. Paice, C. C. R. Ramsay, *Austr. J. Chem.* **1967**, *20*, 1671.

Kinetics of Hydride Transfers from CH, SiH, GeH, and SnH Groups to Carbenium Ions**

By *Herbert Mayr** and *Nils Basso*

Dedicated to Professor George A. Olah on the occasion of his 65th birthday

Hydrides of the group IV elements are important hydrogen sources in radical and ionic reductions.[1–4] While homolytic fissions of these element–hydrogen bonds have been studied intensively,[5] the current kinetic data on ionic hydride-transfer reactions[6–8] do not allow a direct comparison of the reactivity of these compounds toward hydride acceptors. We now report on the kinetics of the reactions of triphenylmethane and of trisubstituted germanes and stannanes with diarylcarbenium ions, and we compare these data with the recently published rate constants for the hydride abstractions from silanes.[6] Because of the huge differences in reactivity, not all experiments could be carried out with the same hydride acceptor; We used linear free energy relationships for a quantitative comparison of these reducing agents.

The recently described photometric method for determining the kinetics of the reactions of diarylcarbenium ions with silanes[6d] was also employed here for the investigation of element hydrides with the general formula HER_3. Since the nature of the counterion (trifluoromethanesulfonate (OTf^-) or $TiCl_5^-$) was found not to affect the rates of the reactions of the bis-*para*-methoxy-substituted benzhydryl cation (p-$MeOC_6H_4)_2CH^+$ with tributylgermane and triphenylstannane, we conclude that under the selected reaction conditions, the counterion is not involved in the rate-determining step, as previously reported for silanes (Scheme 1).

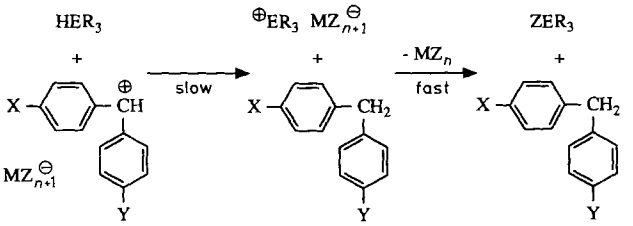

Scheme 1.

In analogy to the reactions of diarylcarbenium ions with alkenes, the reactions of free and paired carbenium ions have identical rates, resulting in a second-order rate law [Eq. (a)], where $[Aryl_2CH^+]$ is the sum of the concentrations of free and paired carbenium ions.

$$d[Aryl_2CH^+]/dt = -k_2[Aryl_2CH^+][HER_3] \quad (a)$$

When the rate constants listed in Table 1 are plotted against the rate constants of the reference reaction previously used, $Aryl_2CH^+$ + 2-methyl-1-pentene,[9] almost parallel lines are obtained (Fig. 1), indicating that the relative reac-

[*] Prof. Dr. H. Mayr,[+] Dipl.-Ing. N. Basso
Institut für Chemie der Medizinischen Universität
Ratzeburger Allee 160, D-W-2400 Lübeck (FRG)
[+] New address:
Institut für Organische Chemie der Technischen Hochschule
Petersenstrasse 22, D-W-6100 Darmstadt (FRG)

[**] This work work was supported by the Deutsche Forschungsgemeinschaft and the Fonds der Chemischen Industrie.

Table 1. Rate constants of the reactions of *p,p'*-substituted benzhydryl cations (*p*-XC_6H_4)(*p*-YC_6H_4)CH^+ (counterion MZ_{n+1}^-) with element hydrides HER_3 in CH_2Cl_2 at $-70\,^\circ C$.

HER_3	X	Y	MZ_{n+1}^-	k_2 [$M^{-1}s^{-1}$]	ΔH^* [$kJmol^{-1}$]	ΔS^* [$Jmol^{-1}K^{-1}$]	Lit.
$HCPh_3$	Cl	Cl	$GaCl_4^-$	6.57×10^{-3}	37.9	−97	
$HSiPh_3$	OMe	OMe	OTf^-	6.52×10^{-2}			[6d]
	OMe	Me	$TiCl_5^-$	2.22			[6d]
	OMe	H	$TiCl_5^-$	8.27	22.2	−115	[6d]
	OPh	H	$TiCl_5^-$	4.52×10^{1}			[6d]
	Me	Me	$TiCl_5^-$	3.47×10^{2}			[6d]
$HSinBu_3$	OMe	OMe	$TiCl_5^-$	4.30			[6d]
	OMe	OPh	$TiCl_5^-$	2.15×10^{1}			[6d]
	OMe	Me	$TiCl_5^-$	1.22×10^{2}			[6d]
	OMe	H	$TiCl_5^-$	3.85×10^{2}			[6d]
$HGePh_3$	OMe	OMe	$TiCl_5^-/OTf^-$	1.59			
	OMe	H	$TiCl_5^-$	1.14×10^{2}			
	OPh	H	$TiCl_5^-$	5.86×10^{2}			
	Me	Me	$TiCl_5^-$	2.96×10^{3}			
$HGenBu_3$	NMe_2	NMe_2	OTf^-	8.8×10^{-6}	51.2	−86	
	OMe	OMe	$TiCl_5^-/OTf^-$	3.19×10^{2}			
	OMe	OPh	$TiCl_5^-$	2.11×10^{3}			
	OMe	Me	$TiCl_5^-$	4.57×10^{3}			
	OMe	H	$TiCl_5^-$	2.8×10^{4}			
$HSnPh_3$	NMe_2	NMe_2	OTf^-	1.01×10^{-4}	38.2	−130	
	OMe	OMe	$OTf^-/TiCl_5^-$	1.13×10^{2}			
	OMe	OPh	$TiCl_5^-$	2.65×10^{2}			
	OMe	Me	$TiCl_5^-$	1.78×10^{3}			
	OMe	H	$TiCl_5^-$	4.98×10^{3}			
$HSnnBu_3$	NMe_2	NMe_2	OTf^-	4.22×10^{-2}	37.2	−85	

tivities of these element hydrides are almost independent of the electrophilicities of the hydride abstractors (constant selectivity relationship according to Ritchie).[9c, 10] Intersections of these lines may be observed, however, when a very wide range of reactivity is considered: The bis(*para*-dimethylaminophenyl)carbenium ion (*p*-$Me_2NC_6H_4)_2CH^+$, which is 5 to 10 orders of magnitude less electrophilic than the other carbenium ions examined in this study, reacts 11.5 times more slowly with $HGenBu_3$ than with $HSnPh_3$, while $HGenBu_3$ is three to eight times more reactive than $HSnPh_3$ toward the carbenium ions shown in Figure 1.

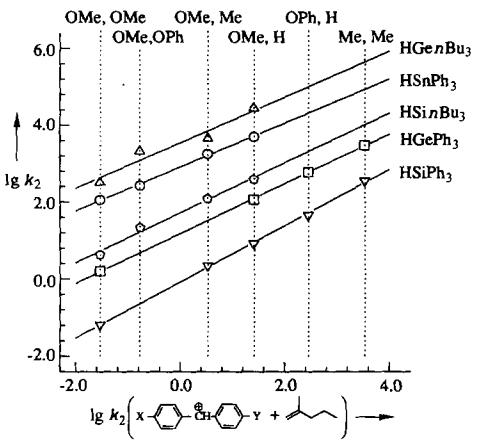

Fig. 1. Correlation of the reactivities (CH_2Cl_2, $-70\,^\circ C$) of substituted diarylcarbenium ions (*p*-XC_6H_4)(*p*-YC_6H_4)CH^+ (*para* substituents X and Y on the upper edge of the graph) versus several hydride donors HER_3 and 2-methyl-1-pentene (reference reaction [9c]).

When these small differences in slopes are neglected, a reactivity scale of hydride donors can be given, which is conveniently based on the reactivities toward the mono-*para*-methoxy-substituted benzyhydryl cation $AnPhCH^+$ (An = *p*-$MeOC_6H_4$) (Table 2). The k_2 value for $HSnnBu_3$ is calculated from the relative reactivities of $HSnnBu_3$ and $HSnPh_3$ toward (*p*-$Me_2NC_6H_4)_2CH^+$. The corresponding rate constant for $HCPh_3$ is derived from the relative reactivities of $HCPh_3$ (Table 1) and $HSiPh_3$ toward (*p*-$ClC_6H_4)_2CH^+$. The latter value, $\lg k_2[HSiPh_3 + (p\text{-}ClC_6H_4)_2CH^+, 70\,^\circ C] = 5.39$, is extrapolated from the correlation of $\lg k_2$ ($HSiPh_3$) with pK_{R^+} of the particular hydride abstractors.[6d]

Table 2 indicates that the decrease of the enthalpy of homolytic bond dissociation (C − H ≳ Si − H > Ge − H > Sn − H) is associated with an acceleration of the hydride and of the hydrogen radical abstractions. Whereas in radical reactions the triphenyl-substituted compounds are generally somewhat more reactive than the trialkyl-substituted ones, in ionic reactions the ratio $k_2(HEBu_3)/k_2(HEPh_3)$ grows with the size of the core atom from less than 1 for HCR_3 to a value of approximately 400 for $HSnR_3$. This trend may be explained by the decreasing ability of the phenyl group to donate π electrons as the size of the central atom increases. The considerably greater influence of the nature of the core atom on the rates of the ionic reactions (compared with the radical reactions) may be caused by the decrease of the ionization potential in the series $R_3C^\bullet$ to $R_3Sn^\bullet$ as well as by a more productlike transition state of the ionic reactions.

Table 2. Comparison of the rates of hydride abstractions to the rates of H$^\bullet$ abstraction from HER_3 and the corresponding bond dissociation energies (BDE).

	R	HER_3			
		HCR_3	$HSiR_3$	$HGeR_3$	$HSnR_3$
k_2(AnPhCH$^+$) [a]	*n*Bu		3.9×10^{2}	2.8×10^{4}	(2×10^{6}) [b]
	Ph	(2×10^{-7}) [b]	8.3	1.1×10^{2}	5.0×10^{3}
	k_{Bu}/k_{Ph}	<1 [c]	4.7×10^{1}	2.5×10^{2}	$\approx4.2\times10^{2}$
k_2(tBuO$^\bullet$) [d]	*n*Bu	2.7×10^{5}	5.7×10^{6} [e]	8.0×10^{7}	2.2×10^{8}
	Ph	2.6×10^{6}	1.1×10^{7}	8.9×10^{7}	4.0×10^{8}
	k_{Bu}/k_{Ph}	0.1	0.5	0.9	0.5
BDE	*n*Bu	390 [f]	377 [g]	346 [h]	308 [i]
[$kJmol^{-1}$]	Ph	339 [j]	≈356 [k]	336 [h]	

[a] This work; determined at 203 K. [b] Extrapolated, see text. [c] Approximation based on the different stabilization of carbenium ions by phenyl and alkyl substituents. [d] Determined at 300 K; ref. [11a]. [e] Et_3SiH. [f] Me_3CH, ref. [11b]. [g] Et_3SiH, ref. [11c]. [h] Ref. [11d]. [i] Ref. [11c]. [j] Ref. [11e]. [k] K. B. Clark, D. Griller, National Research Council of Canada, personal communication.

Received: March 5, 1992 [Z 5227 IE]
German version: *Angew. Chem.* **1992**, *104*, 1103

[1] General reviews: a) *Reduction* (Ed.: R. L. Augustine), Dekker, New York, **1968**; b) M. Hudlicky, *Reductions in Organic Chemistry*, Horwood, Chichester, **1984**; c) A. Hajós, *Methoden Org. Chem. (Houben-Weyl)* 4th ed. 1952–, Vol. IV/1d, **1981**, pp. 1–486; d) F. G. A. Stone, *Hydrogen Compounds of the Group IV Elements*, Prentice Hall, New York, **1962**.

[2] Silanes: a) D. N. Kursanov, Z. N. Parnes, *Russ. Chem. Rev. (Engl. Transl.)* **1969**, *38*, 812; b) F. A. Carey, *Intra-Sci. Chem. Rep.* **1973**, *7*, 55; c) D. N. Kursanov, Z. N. Parnes, N. M. Loim, *Synthesis* **1974**, 633; d) Y. Nagai, *Org. Prep. Proced. Int.* **1980**, *12*, 13; e) E. Keinan, *Pure Appl. Chem.* **1989**, *61*, 1737; f) E. W. Colvin, *Silicon Reagents in Organic Synthesis*, Academic Press, London, **1988**; g) S. Pawlenko, *Methoden Org. Chem. (Houben-Weyl)* 4th ed. 1952–, Vol. XIII/5, **1980**, pp. 350–360.

[3] Germanes: a) D. Quane, R. S. Bottei, *Chem. Rev.* **1963**, *63*, 403; b) G. Bähr, H.-O. Kalinowski, *Methoden Org. Chem. (Houben-Weyl)* 4th ed. 1952–, Vol. XIII/6, **1978**, pp. 61–67.

[4] Stannanes: a) R. K. Ingham, S. D. Rosenberg, H. Gilman, *Chem. Rev.* **1960**, *60*, 459; b) H. G. Kuivila, *Synthesis* **1970**, 499; c) W. P. Neumann, *ibid.* **1987**, 665; d) M. Pereye, J.-P. Quintard, A. Rahm, *Tin in Organic Synthesis*, Butterworth, Londen, **1987**; e) I. Omae, *Organotin Chemistry*, Elsevier, Amsterdam, **1989**; f) *Chemistry of Tin* (Ed.: P. G. Harrison),

Blackie & Son, Glasgow, **1989**; g) G. Bähr, S. Pawlenko, *Methoden Org. Chem. (Houben-Weyl)* 4th ed. 1952–, Vol. XIII/6, **1978**, pp. 451–470.
[5] a) J. M. Kanabus-Kaminska, J. A. Hawari, D. Griller, C. Chatgilialoglu, *J. Am. Chem. Soc.* **1987**, *109*, 5267; b) M. Lesage, J. A. Martinho Simoes, D. Griller, *J. Org. Chem.* **1990**, *55*, 5413; c) P. Arya, C. Samson, M. Lesage, D. Griller, *ibid.* **1990**, *55*, 6248; d) M. Ballestri, C. Chatgilialoglu, K. B. Clark, D. Griller, B. Giese, B. Kopping, *ibid.* **1991**, *56*, 678; e) U. Müller, E. Popowski, *Z. Phys. Chem. (Leipzig)* **1990**, *271*, 703; f) J. Lusztyk, B. Maillard, D. A. Lindsay, K. U. Ingold, *J. Am. Chem. Soc.* **1983**, *105*, 3578; g) J. Lusztyk, B. Maillard, S. Deycard, D. A. Lindsay, K. U. Ingold, *J. Org. Chem.* **1987**, *52*, 3509; h) K. U. Ingold, J. Lusztyk, J. C. Scaiano, *J. Am. Chem. Soc.* **1984**, *106*, 343; i) C. Chatgilialoglu, K. U. Ingold, J. C. Scaiano, *ibid.* **1981**, *103*, 7739; j) J. O. Metzger, *Methoden Org. Chem. (Houben-Weyl)* 4th ed. 1952–, Vol. E XIXa, Part 1, **1989**, p. 91; k) C. Chatgilialoglu, *Acc. Chem. Res.* **1992**, *25*, 188.
[6] Silanes: a) J. Chojnowski, W. Fortuniak, W. Stanczyk, *J. Am. Chem. Soc.* **1987**, *109*, 7776; b) J. Chojnowski, L. Wilczek, W. Fortuniak, *J. Organomet. Chem.* **1977**, *135*, 13; c) F. A. Carey, C.-L. Wang Hsu, *ibid.* **1969**, *19*, 29; d) H. Mayr, N. Basso, G. Hagen, *J. Am. Chem. Soc.* **1992**, *114*, 3060.
[7] Stannanes; a) J. Lusztyk, E. Lusztyk, B. Maillard, K. U. Ingold, *J. Am. Chem. Soc.* **1984**, *106*, 2923; b) J.-P. Quintard, M. Pereye, *Bull. Soc. Chim. Fr.* **1972**, *5*, 1950; c) A. J. Leusink, H. A. Budding, W. Drenth, *J. Organomet. Chem.* **1968**, *13*, 163; d) A. J. Leusink, H. A. Budding, W. Drenth, *ibid.* **1967**, *9*, 295; e) G. L. Grady, J. R. Saucier, W. J. Foley III, D. J. O'Hern, W. J. Weidmann, *ibid.* **1972**, *35*, 307; f) D. D. Tanner, H. K. Singh, *J. Org. Chem.* **1986**, *51*, 5182.
[8] Hydrocarbons: a) N. Deno, G. Saines, M. Spangler, *J. Am. Chem. Soc.* **1962**, *84*, 3295; b) M. M. Kreevoy, I.-S. H. Lee, *ibid.* **1984**, *106*, 2550; c) D. Ostovic, I.-S. H. Lee, R. M. G. Roberts, M. M. Kreevoy, *J. Org. Chem.* **1985**, *50*, 4206; d) M. M. Kreevoy, D. Ostovic, I.-S. H. Lee, D. A. Binder, G. W. King, *J. Am. Chem. Soc.* **1988**, *110*, 524; e) M. M. Kreevoy, A. T. Kotchevar, *ibid.* **1990**, *112*, 3579; f) A. Ohno, T. Shio, H. Yamamoto, S. Oka, *ibid.* **1981**, *103*, 2045; g) A. van Laar, H. J. van Ramesdonk, J. W. Verhoeven, *Recl. Trav. Chim. Pays-Bas* **1983**, *102*, 157; h) T. T. Romoff, N. S. Sampson, P. van Eikeren, *J. Org. Chem.* **1987**, *52*, 4454; i) J. W. Bunting, M. A. Luscher, *Can. J. Chem.* **1988**, *66*, 2524; j) J. W. Bunting, M. M. Conn, *ibid.* **1990**, *68*, 537; k) M. Ishikawa, S. Fukuzumi, *J. Chem. Soc. Chem. Commun.* **1990**, 1353; l) S. J. Hannon, T. G. Traylor, *J. Org. Chem.* **1981**, *46*, 3645; m) T. G. Traylor, G. S. Koermer, *ibid.* **1981**, *46*, 3651.
[9] H. Mayr, R. Schneider, C. Schade, J. Bartl, R. Bederke, *J. Am. Chem. Soc.* **1990**, *112*, 4446; b) H. Mayr, *Angew. Chem.* **1990**, *102*, 1415; *Angew. Chem. Int. Ed. Engl.* **1990**, *29*, 1371; c) H. Mayr, R. Schneider, U. Grabis, *J. Am. Chem. Soc.* **1990**, *112*, 4460.
[10] a) C. D. Ritchie, *Acc. Chem. Res.* **1972**, *5*, 348; b) C. D. Ritchie, *Can. J. Chem.* **1986**, *64*, 2239.
[11] a) C. Chatgilialoglu, K. U. Ingold, J. Lusztyk, A. S. Nazran, J. C. Scaiano, *Organometallics* **1983**, *2*, 1332; b) D. F. McMillen, D. M. Golden, *Annu. Rev. Phys. Chem.* **1982**, *33*, 493; c) D. Griller, D. D. M. Wayner, *Pure Appl. Chem.* **1989**, *61*, 717; d) K. B. Clark, D. Griller, *Organometallics* **1991**, *10*, 746; e) F. G. Bordwell, J.-P. Cheng, G.-Z. Ji, A. V. Satish, X. Zhang, *J. Am. Chem. Soc.* **1991**, *113*, 9790.

[RuO(dppz)(tpy)]$^{2+}$: a DNA Cleavage Agent with High DNA Affinity**

By *Nishi Gupta, Neena Grover, Gregory A. Neyhart, Weigen Liang, Phirtu Singh*, and *H. Holden Thorp**

The development of new DNA cleavage agents is of interest for the designing of synthetic restriction enzymes,[1] for an understanding of the structure of DNA,[2] and for pharmaceutical applications.[3] We have recently directed our efforts at investigating functional metal complexes that initiate DNA cleavage by unusual mechanisms,[4] and have reported efficient cleavage of DNA by the dicationic complex **1**[5] (bpy = 2,2′-bipyridine, tpy = terpyridine). **1** was generated via oxidation of **2** [Eqs. (a) and (b)].[6]

$$\underset{\mathbf{2}}{[Ru^{II}OH_2(bpy)(tpy)]^{2+}} \rightleftharpoons [Ru^{III}OH(bpy)(tpy)]^{2+} + e^- + H^+ \quad (a)$$

$$[Ru^{III}OH(bpy)(tpy)]^{2+} \rightleftharpoons \underset{\mathbf{1}}{[Ru^{IV}O(bpy)(tpy)]^{2+}} + e^- + H^+ \quad (b)$$

The DNA cleavage with **1** can be effected either stoichiometrically by addition of **1** to the DNA or electrocatalytically by application of a potential of 0.8 V to a solution of DNA and **2**.[5] In attempts to increase the binding affinity of these agents, we have now prepared the dicationic complex **3** (dppz = dipyridophenazine, see Scheme 1).

$[RuOH_2(dppz)(tpy)]^{2+}$ **3** $[Ru(bpy)_2(dppz)]^{2+}$ **4**

The planar dppz ligand imparts high DNA affinity to the complex **4**.[7] Studies with topoisomerase showed that **4** unwinds DNA by 30°, strongly implicating an intercalative binding mode. Complex **4** has very attractive photophysical properties, but does not exhibit DNA cleavage reactivity. Complex **3** also exhibits a high DNA affinity while retaining the DNA cleavage reactivity of the $Ru^{II}OH_2/Ru^{IV}O$ functionality. Furthermore, the X-ray crystal structure of this complex shows extensive π-stacking of the planar dppz ligand (see Fig. 3), which may provide insight into the high DNA affinity of dppz complexes.

Reaction of $Ru(tpy)Cl_3$ with dppz in the presence of triethylamine affords the complex [RuCl(dppz)(tpy)]Cl. Treatment of an aqueous solution of this complex with $AgClO_4$ leads to the precipitation of **3**-$(ClO_4)_2 \cdot H_2O$, in the form of black crystals suitable for X-ray structure analysis. The complex exhibits a typical $Ru^{II} \rightarrow py(\pi^*)$ metal-ligand charge transfer (MLCT) absorption band with $\lambda_{max} = 482$ nm ($\varepsilon = 12000\ M^{-1}cm^{-1}$). In aqueous solution, the complex is oxidized sequentially to the dicationic Ru^{IV} complex [Eqs. (c) and (d)].

$$\mathbf{3} \rightleftharpoons [Ru^{III}OH(dppz)(tpy)]^{2+} + e^- + H^+ \quad (c)$$

$$[Ru^{III}(dppz)(tpy)]^{2+} \rightleftharpoons \underset{\mathbf{5}}{[Ru^{IV}O(dppz)(tpy)]^{2+}} + e^- + H^+ \quad (d)$$

At pH 7, $E_{1/2}(Ru^{III}/Ru^{II}) = 0.56$ V and $E_{1/2}(Ru^{IV}/Ru^{III}) = 0.62$ V (SCE), compared to 0.49 V and 0.62 V in the case of the complex **2**.[6] The pK_a value of the aqua ligand in **3** is 8.6 compared to a pK_a of 9.7 in **2**.[6] The structure of **3** is shown in Figure 1.[8] The coordination about the Ru center is very similar to that in both $[Ru^{II}OH_2(tmen)(tpy)]^{2+}$ (tmen = *N*,*N*,*N*′,*N*′,-tetramethylethylenediamine)[9] and **2**.[10] Thus, incorporation of the strongly intercalating dppz ligand has not altered the electronic properties of the $Ru^{II}OH_2$ functionality that are vital to the DNA cleavage reactivity.

Complex **3** binds very strongly to DNA. We have determined the binding constants for a series of complexes related to **2** using an electrochemical method based on the cyclic voltammetric currents for the Ru^{III}/Ru^{II} redox pairs of the complexes with and without DNA.[9] When the complex is

[*] Prof. H. H. Thorp, Dr. N. Gupta, N. Grover, Dr. G. A. Neyhart, W. Liang, Dr. P. Singh
Department of Chemistry
North Carolina State University
Raleigh, NC 27695 (USA)

[**] This work was supported by the National Science Foundation (Presidential Young Investigator Award), the David and Lucile Packard Foundation (Fellowship in Science and Engineering), and the North Carolina Biotechnology Center. Helpful discussions with Prof. M.-H. Whangbo are gratefully acknowledged.

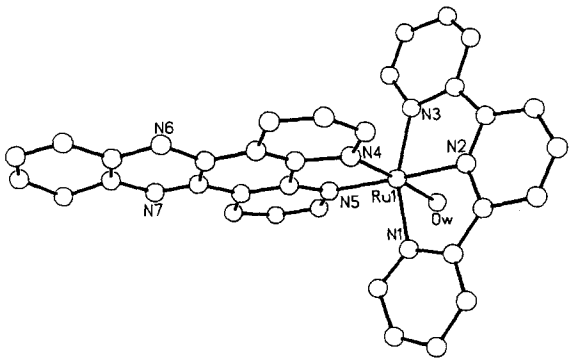

Fig. 1. Structure of **3** in the crystal (counterion ClO_4^-). Hydrogen atoms have been omitted for clarity; unlabeled atoms are carbon. Selected bond lengths [Å] and angles [°]: Ru-N1 2.047(29), Ru-N2 1.998(20), Ru-N3 2.039(28), Ru-N4 2.022(26), Ru-Ow 2.168(24), N1-Ru-N3 159.3(9), N4-Ru-Ow 174.4(8).

bound to DNA, a decrease in current is observed because the diffusion coefficient of the bound complex is much smaller than the diffusion coefficient of the free complex; the binding constant can therefore be determined using equations developed by Bard et al.[11] As a result of the change in diffusion coefficient, a drop in current as a function of added DNA is observed, as shown for **2** ($K_b = 15000\ M^{-1}$) in Figure 2a. For complex **3**, the drop in current is so rapid that a binding constant cannot be determined (Fig. 2a). In addition, the binding is also too strong for determining K_b by equilibrium dialysis, even at a buffer ionic strength of 50 mM.[12] Based on the electrochemical and equilibrium dialysis experiments, we can estimate a lower limit of $K_b \geq 10^6\ M^{-1}$ for the complex **3**.[7]

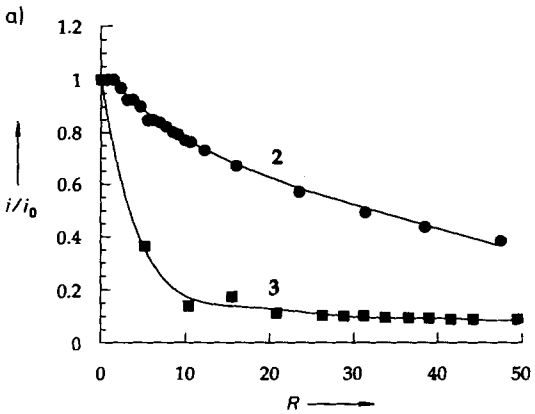

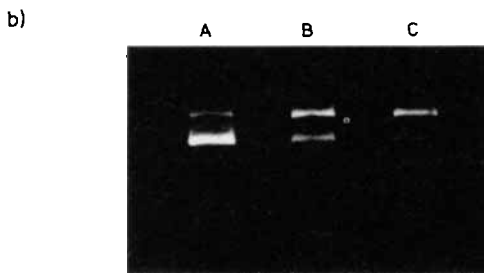

Fig. 2. a) Plots of voltammetric current for **2** (●) and **3** (■) as a function of the DNA concentration. R = [DNA-nucleotide phosphate]/[Ru complex]. i_0 Current measured in the absence of DNA; i current measured after addition of DNA. b) 1% Agarose gel showing the results of electrophoresis of supercoiled ϕX174 DNA (A) alone, (B) after electrolysis at 0.8 V for 3 h in the presence of 40 mM **2**, (C) after electrolysis at 0.8 V for 10 h with 40 mM **3**.

Identical observations were made in the equilibrium dialysis of **4**, and the same conclusions were drawn.[7] However, with the present complex, rapid conversion of superhelical DNA (form I) into circular DNA with single strand breaks ("nicked circular DNA" form II) occurs upon incubation of the DNA with **5** (data not shown). Indeed, optical spectroscopy shows that the dppz ligand dramatically increases the efficiency of the thermal reaction. Under identical conditions, the reaction of calf thymus DNA with **1** is 85% complete after 6.5 min, while the reaction of **5** with calf thymus DNA is 85% complete in 10 s.[13] This increased efficiency of the stoichiometric reaction is no doubt a result of the high affinity of the dppz ligand for the DNA. Cleavage is also realized upon electrolysis of the DNA at 0.8 V in the presence of **3** (Fig. 2b). The longer electrolysis time required for **3** results from the effect of the high binding affinity on the rate of oxidation of **3** to **5** and is not related to the efficiency of the cleavage reaction itself, as we have discussed in detail in Ref. [9]. Complex **3** is not as effective a photophysical probe as **4**, because replacement of a pyridine ligand by an aqua ligand apparently deactivates the MLCT excited state quite efficiently.

Some insight into the high binding affinity of dppz complexes can be gained from consideration of the X-ray crystal structure of **3**. There are two unique Ru centers (Ru1 and Ru2) that are related to the other two Ru centers by an inversion center. In the pair Ru1 and Ru1′, it is evident that ring α (the nitrogen ring) of the Ru1-complex is stacked directly above the ring β of the Ru1′ complex and vice versa.

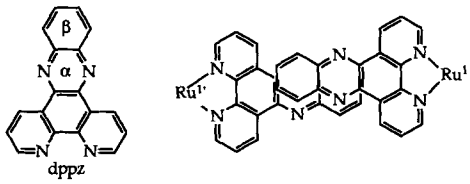

Scheme 1. Superposition of two molecules of **3**.

The distance between the ring planes of the two ligands is 3.51 Å, similar to the base-pair stacking distance in DNA[14] and the intercalator-base pair stacking distance in crystal

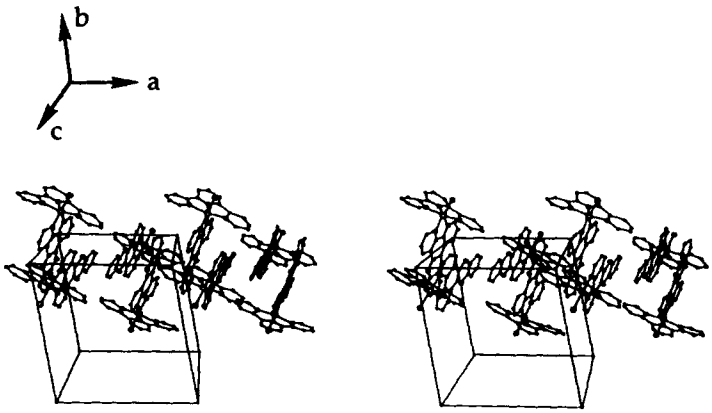

Fig. 3. Stereodiagram of the packing of **3** in the crystal. ClO_4^- counterions and hydrogen atoms are omitted for clarity.

structures of oligonucleotide-intercalator complexes.[15] A similar two-ring overlap pattern has been observed in the case of stacked acridine orange intercalators in the crystal structure of a Pt complex attached to the acridine intercalator by a long alkyl linker.[16] An infinite π-stacking interaction therefore exists throughout the crystal, as illustrated in the stereodiagram in Figure 3. Thus, it appears that the dppz ligand has an innate propensity for π-stacking that is no doubt responsible for the high DNA binding affinity of **3** and **4**. Observations of π-stacking interactions in the crystal structures of more conventional organic intercalators such as acridine orange[16] and phenanthridinium salts[17] are common.

Received: December 10, 1991;
revised: February 28, 1992 [Z 5065 IE]
German version: *Angew. Chem.* **1992**, *104*, 1058

CAS Registry numbers:
3, 142260-91-1; **4**, 87564-74-7.

[1] J. K. Barton, *Science (Washington D.C.)* **1986**, *233*, 727; P. B. Dervan, *ibid.* **1986**, *232*, 464.
[2] T. D. Tullius, B. A. Dombroski, *Science (Washington, D.C.)* **1985**, 235, 679; A. M. Burkhoff, T. D. Tullius, *Nature (London)* **1988**, *331*, 455; A. M. Burkhoff, T. D. Tullius, *Cell (Cambridge Mass.)* **1987**, *48*, 935.
[3] S. M. Hecht, *Acc. Chem. Res.* **1986**, *19*, 83; J. Stubbe, J. W. Kozarich, *Chem. Rev.* **1987**, *87*, 1107; K. Nagai, B. J. Carter, J. Xu, S. M. Hecht, *J. Am. Chem. Soc.* **1991**, *113*, 5099.
[4] W. A. Kalsbeck, N. Grover, H. H. Thorp, *Angew. Chem.* **1991**, *104*, 1525; *Angew. Chem. Int. Ed. Engl.* **1991**, *30*, 1517.
[5] N. Grover, H. H. Thorp, *J. Am. Chem. Soc.* **1991**, *113*, 7030.
[6] K. J. Takeuchi, M. S. Thompson, D. W. Pipes, T. J. Meyer, *Inorg. Chem.* **1984**, *23*, 1845.
[7] A. E. Friedman, J.-C. Chambron, J.-P. Sauvage, N. J. Turro, J. K. Barton, *J. Am. Chem. Soc.* **1990**, *112*, 4960.
[8] $C_{33}H_{25}N_7O_{10}Cl_2Ru$: triclinic, $P\bar{1}$, $a = 15.882(11)$ Å, $b = 15.952(9)$ Å, $c = 16.283(9)$ Å, $\alpha = 105.75(4)°$, $\beta = 94.80(5)°$, $\gamma = 101.15(5)°$, $V = 3855(4)$ Å^3, $\rho_{calcd} = 1.44$ g cm^{-2}, $\mu(Mo_{K\alpha}) = 8.42$ cm^{-1}. The structure was solved by the Patterson method. Block-diagonal least-squares refinement yielded $R = 0.1074$ and $R_w = 0.1520$ for 3854 reflections with $I \geq 2\sigma(I)$ measured on a Nicolet P3/F diffractometer up to $2\theta = 43°$ at 25 °C ($Mo_{K\alpha}$, $\lambda = 0.71073$ Å). Two molecules coupled via an inversion center are present in the crystal. The high value for R is partly a result of the large number (106) of non-hydrogen atoms refined, but primarily a result of disorder in the ClO_4^- counterions. Correct C,H,N analysis. Further details of the crystal structure investigation are available on request from the Fachinformationszentrum Karlsruhe, Gesellschaft für wissenschaftlich-technische Information mbH, D-W-7514 Eggenstein-Leopoldshafen 2 (FRG), on quoting the depository number CSD-56384, the names of the authors, and the journal citation.
[9] N. Grover, N. Gupta, P. Singh, H. Thorp, *Inorg. Chem.* **1992**, *31*, 2014.
[10] W. Seok, Ph.D. Thesis, University of North Carolina at Chapel Hill, **1988**.
[11] M. T. Carter, M. Rodriguez, A. J. Bard, *J. Am. Chem. Soc.* **1989**, *111*, 8901.
[12] Equilibrium dialysis was performed according to: A. M. Pyle, J. P. Rehmann, R. Meshoyrer, C. V. Kumar, N. J. Turro, J. K. Barton, *J. Am. Chem. Soc.* **1989**, *111*, 3051.
[13] Complex **5** was prepared by electrolysis of **3** at 0.8 V in phosphate buffer (pH 7). $[RuO(bpy)(tpy)]^{2+}$ was prepared as described in Ref. [9]. Rate data were measured by optical spectroscopy at $\lambda = 406$ nm, where the kinetics of oxidation by $Ru^{IV}O^{2+}$ are known to be first-order [5]. Experimental conditions for the kinetic measurements: 0.8 mM DNA, 0.08 mM $Ru^{IV}O^{2+}$, 50 mM phosphate buffer, pH 7. The change in absorption with time can described in terms of a first order rate equation. The measurements were carried out on a Cary 14 spectrometer. The experimental conditions for electrocatalytic cleavage were identical to those described in Ref. [5]. None of the cleavage results is affected upon treatment with base.
[14] L. Stryer, *Biochemistry*, Freeman, New York, **1988**, p. 76.
[15] A. H.-J. Wang, J. Nathans, G. van der Marel, J. H. van Boom, A. Rich, *Nature* (London) **1978**, *276*, 471; A. H.-J. Wang, G. J. Quigley, A. Rich, *Nucleic Acids Res.* **1979**, *6*, 3879.
[16] B. E. Bowler, K. J. Ahmed, W. I. Sundquist, L. S. Hollis, E. E. Whang, S. J. Lippard, *J. Am. Chem. Soc.* **1989**, *111*, 1299.
[17] M. Cory, D. D. McKee, J. Kagan, D. W. Henry, J. A. Miller, *J. Am. Chem. Soc.* **1985**, *107*, 2528.

Empty Octahedral Hexazirconium Clusters with Only Ten Electrons, $[Zr_6X_{14}(PR_3)_4]$**

By *F. Albert Cotton,* Xuejun Feng, Maoyu Shang,* and *William A. Wojtczak*

The existence of compounds comprised of octahedral Zr_6 clusters with bridging halogen atoms on all edges and one additional bond to each zirconium atom along a four-fold axis of the $[Zr_6X_{12}]$ unit was first reported many years ago.[1] Several years later it was realized[2] that these compounds, all prepared by high-temperature reactions, contain an additional atom (e.g. Be, B, C, N, and even a transition metal atom) in the center of the octahedron. The idea then took hold[3] that the central atom, and the electrons it could contribute to the Zr_6 cluster bonding, were essential to the stability of such $[Zr_6X_{12}]X_6$ systems. However, the report[4] in 1988 of $[Zr_6Cl_{12}(PMe_2Ph)_6]$, which was made in an entirely different way, at low temperature and in solution, showed that an empty cluster with 12 electrons can be stable. We are still seeking a better preparative method for such compounds, and in the course of doing so, we have found that empty Zr_6 clusters with even fewer electrons (ten) can be prepared. Herein we report on the results of the crystal structure analyses and the $^{31}P\{^1H\}$-NMR spectra of the new clusters **1**–**4**, as well as on SCF-Xα-SW molecular orbital calculations on the model compound $[Zr_6Cl_{14}(PH_3)_4]$.

$[Zr_6Cl_{14}(PMe_3)_4] \cdot 2CH_2Cl_2$ **1** $[Zr_6Cl_{14}(PEt_3)_4] \cdot 2CH_2Cl_2$ **2**
$[Zr_6Cl_{14}(PPr_3)_4] \cdot 2C_6H_6$ **3** $[Zr_6Br_{14}(PMe_3)_4] \cdot 2CH_3CN$ **4**

The new compounds **1**–**4** were synthesized by reduction of ZrX_4 (X = Cl or Br) with two equivalents of $(n\text{-}C_4H_9)_3SnH$[5] in benzene (CH_2Cl_2 for **1**). The reduction was allowed to proceed for a period of 36 h, during which time a dark colored precipitate collected on the bottom of the reaction vessel. The addition of one equivalent of phosphane immediately solubilized the precipitate, furnishing a deep-red solution, which afforded very air- and moisture-sensitive crystals upon layering. The $^{31}P\{^1H\}$-NMR spectrum of dissolved crystals of **2** shows a singlet at $\delta = 21.27$ ($\Delta\nu_{1/2} = 31.4$ Hz at 20 °C, 81 MHz). The singlet shifts downfield by $\Delta\delta \approx 1$ over the temperature range −40 °C to 60 °C, which is consistent with weak temperature-dependent paramagnetism arising from a diamagnetic ground state having some access to a paramagnetic excited state at higher temperature. This will be discussed further in the context of our theoretical calculations. The direction of the peak shift is undoubtedly dependent on the particular spin transfer mechanism. The ^1H-NMR spectrum of **2** shows two broad peaks corresponding to protons of the ethyl group of the bound phosphane ligand and gives no indication of the existence of a hydridic proton within the cluster; however, the line-broadening effect arising from the weak paramagnetism of the compound precludes any definitive statement in this regard.

The compounds **1**–**4** were characterized by X-ray crystallography,[6] pertinent crystallographic parameters are listed

[*] Dr. F. A. Cotton, Dr. X. Feng, Dr. M. Shang, W. A. Wojtczak
Department of Chemistry and
Laboratory for Molecular Structure and Bonding
Texas A & M University
College Station, TX 77843 (USA)

[**] This work was supported by the Robert A. Welch Foundation (Grant No. A 494). We thank Mrs. Bo Hong for her assistance with the temperature-dependent ^{31}P-NMR spectra and Dr. P. Kibala for helpful suggestions regarding the preparative scheme.

Table 1. Crystallographic data of the clusters **1**–**4**.

	1	**2**	**3**	**4**
Formula	$C_{14}H_{40}Cl_{18}Zr_6P_4$	$C_{26}H_{64}Cl_{18}Zr_6P_4$	$C_{48}H_{96}Cl_{14}Zr_6P_4$	$C_{16}N_2H_{42}Br_{14}Zr_6P_4$
Space group	$P2_1/n$ (No. 14)	*Pbca* (No. 61)	$P\bar{1}$ (No. 2)	*P4/mnc* (No. 128)
a [Å]	11.153(2)	12.127(3)	12.636(6)	13.523(2)
b [Å]	11.053(4)	21.794(5)	13.653(2)	13.523(3)
c [Å]	20.676(6)	23.022(4)	11.540(2)	15.476(2)
α [°]	90.00	90.00	95.34(1)	90.00
β [°]	103.43(2)	90.00	96.64(2)	90.00
γ [°]	90.00	90.00	93.58(3)	90.00
V [Å^3]	2479(1)	6084(2)	1963(1)	2830.3(8)
Z	2	4	1	2
Data with $F_o^2 > 3\sigma(F_o^2)$	2727	3097	3210	771
No. of refined parameters	250	209	325	51
R	0.0379	0.0669	0.0686	0.0544
R_w	0.0494	0.101	0.0874	0.0686

in Table 1, important molecular dimensions in Table 2. Figure 1 shows a molecule of **1** as viewed along its Cl_t–Zr_{ax} bond. It should be noted that all hydrogen atoms of **1** were found from a Fourier map that followed the anisotropic refinement of the non-hydrogen atoms. The hydrogen atoms (including the hydrogens on the CH_2Cl_2 of crystallization were positionally refined with fixed thermal parameters of 1.3 B_{eqv} of the corresponding carbon atom. Compound **1** resides on a crystallographic inversion center in the monoclinic space group $P2_1/n$. In order to determine whether adequate electron density exists at the center of the Zr_6 cluster to support the hypothesis that *any* atom is there, we attempted to refine a hydrogen atom with fixed coordinates at (0,0,0). The thermal parameter of the aforementioned hydrogen atom grew very large after only a few refinement cycles by the least-square method ($B > 50$ Å^2).

Table 2. Selected distances [Å] and angles [°] for clusters **1**–**4**. X_t = terminal halogen atom, X_b = bridging halogen atom (X = Cl, Br). The terminal halogen atoms are bound to the Zr atoms designated as Zr_{ax}.

	1 [a]	**2** [b]	**3**	**4**
Zr_{eq}–Zr_{eq}	3.301 [6] [c]	3.304 [1]	3.319 [6]	3.356 (2) [d]
Zr_{ax}–Zr_{eq}	3.354 [8]	3.357 [3]	3.367 [3]	3.411 (1)
Zr_{ax}–X_b	2.573 [8]	2.562 [5]	2.572 [2]	2.705 (1)
Zr_{eq}–X_b	2.556 [9]	2.553 [7]	2.557 [8]	2.692 [8]
Zr–P	2.757 [6]	2.789 [6]	2.796 [6]	2.777 (5)
Zr_{ax}–X_t	2.495 (2)	2.501 (3)	2.486 (4)	2.677 (3)
Zr_{eq}–X_b–Zr_{ax}	81.8 [1]	82.2 [2]	82.2 [1]	78.55 (5)
Zr_{eq}–X_b–Zr_{eq}	80.2 [2]	80.5 [2]	80.7 [4]	76.94 (5)
Zr_{ax}-Center	2.4083 (6)	2.411 (1)	2.415 [1]	2.451 (2)
Zr_{eq}-Center	2.334 [8]	2.3366 [5]	2.346 [1]	2.373 (1)

[a] Data collection conducted at −75 °C. [b] Data collection conducted at −60 °C. [c] Square brackets denote mean deviation from the unweighted arithmetic mean; each is given for the last significant figure. [d] Parantheses denote esd of an individual value.

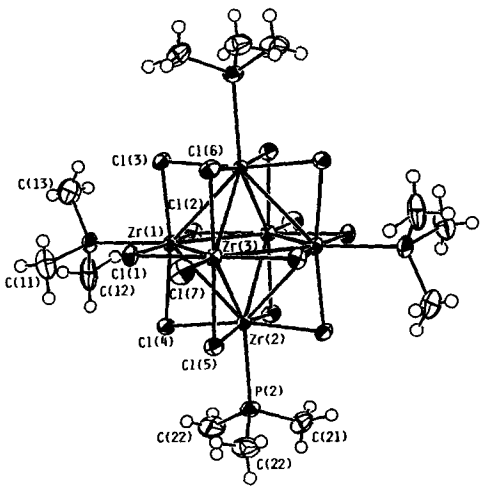

Fig. 1. **1** viewed along the Zr_{ax}–Cl_t bond. Hydrogen atoms have been given arbitrary thermal parameters and heavy atoms are represented by their ellipsoids at the 50% probability level.

The two distinct sets of Zr–Zr bond lengths (eq–eq, ax–eq) in the $[Zr_6X_{14}(PR_3)_4]$-type clusters suggest that a small but real tetragonal distortion exists, in which the Zr_{ax}–Zr_{eq} bond lengths are longer than the Zr_{eq}–Zr_{eq} bond lengths. This phenomenon has been observed previously[7] in solid-state clusters of the composition $[Zr_6X_{14}Z]^{n+}$ and may be attributed to the chemical inequality of the Zr_{ax} and Zr_{eq}, positions resulting from the disparate electron donor ability of the terminal ligands. The bromo complex, **4**, contains slightly longer Zr–Zr bonds than its chloro analogue. This trend has also been observed in the edge-sharing bioctahedral complexes of the elements of group IV and has been attributed to greater ligand–ligand repulsive forces of the larger halogen atoms.[8] The Zr–Zr bond lengths of the compounds **1** to **3** lie in the range 3.167–3.450 Å recently reported for centered zirconium hexanuclear clusters, with cluster based electron counts between twelve and eighteen, that were obtained by dissolution of solid-state phases.[9] Further comparison between our clusters **1**–**4** and those just mentioned is unjustified, since large differences exist with respect to ligand environments, electron counts, and the presence of interstitial atoms.

Our ten-electron clusters can, however, be compared with the twelve-electron cluster **5**.[4] The average Zr_{eq}–Zr_{eq} bond

$[Zr_6Cl_{12}(PMe_2Ph)_6]$ **5**

length of 3.319(6) Å in **3** is 0.096(9) Å longer than the Zr–Zr distance in **5**. The lengthening of the Zr-Zr-bond is not surprising, considering that removal of two electrons that are Zr_6 core bonding from the t_{1u} HOMO of **5** is required for formation of the ten-electron cluster **3** (cf. **8** in Fig. 2). The commensurate enlargement of the Zr_6 cage in **3** can be gauged from the Zr_{eq}–Center radius of 2.346(1) Å, compared to 2.279(2) Å in **5**. The degree of bond lengthening is small, since the bond order changes only from 0.5 (**5**) to 0.42 (**3**), respectively.

$[Zr_6Cl_{14}(Ph_3)_4]$ **6** $[Zr_6Cl_{14}(Ph_3)_4H]$ **7** $[Zr_6Cl_{12}(Ph_3)_6]$ **9**

Molecular orbital calculations were carried out by the SCF-X_α-SW method for the C_{4v}-symmetric clusters **6** and **7**. The latter compound was assumed to be structurally the same as the former except for having a hydrogen atom at its center. For comparison, a compound of similar structure (D_{3d} symmetry) but with twelve metal cluster electrons, **8**,[4] was also calculated. Figure 2 shows the MO diagram for the upper valence orbitals in these molecules. For all three molecules, the MOs in the energy range between −9 and −11 eV are mostly metal-ligand(terminal) bonding, while the higher energy orbitals are predominantly metal-metal

bonding and accommodate all metal cluster electrons. The $7a_1$ orbital in **7** provides the bonding between the metal atoms and the centered atom and is correlated to the $18a_1$ orbital in **6**, as indicated by the asterisks in Figure 2. Three pairs of nearly degenerate MOs in **8** (right-hand column in Fig. 2), each of which correlates to a level of *t*-symmetry of the octahedral $Zr_6Cl_{12}P_6$ framework, are labeled accordingly. Upon lowering the symmetry to C_{4v}, the levels are split.

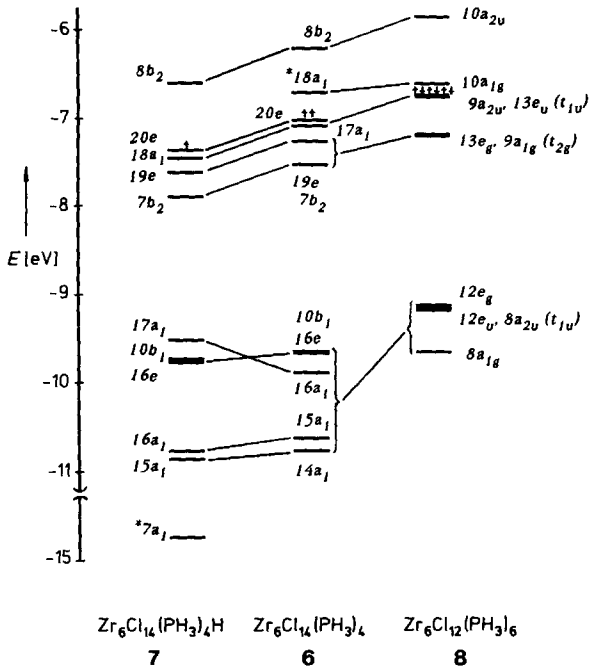

Fig. 2. Molecular orbital diagram of the upper valence orbitals for **6**–**8**.

According to the electronic structures shown in Figure 2, the compound we are concerned with $(Zr_6Cl_{14}(PH_3)_4)$ should be strongly paramagnetic, whether it contains a hydrogen atom at the center or not. Paramagnetism is absolutely unavoidable in the case of the hydrogen-centered model compound **7** since it contains an odd number of electrons. However, as indicated by the $^{31}P\{^1H\}$-NMR spectra recorded at various temperatures, compound **2** exhibits only very weak temperature-dependent paramagnetism, which suggests that it should have a closed-shell electronic configuration in the ground state. Thus, the possibility that the compound has a centered hydrogen atom can be eliminated. The NMR result shows that the calculation for **6** has not correctly predicted the exact ordering of the closely-spaced MOs in the HOMO-LUMO region (middle column of Fig. 2). This is not surprising in view of the very similar energies of the $17a_1$, $20e$ and $18a_1$ orbitals. The calculation may have overestimated the metal-ligand(terminal) antibonding contribution in the $18a_1$ orbital (see Fig. 3, left). Orbitals of the same character in other systems such as $[Zr_6Cl_{18}]^{4-}$,[10, 11] have been found to be much lower than the t_{2g} level. Noticing also the strong metal-metal bonding character with the d_{z^2} orbitals of all metal atoms pointing towards the center of the Zr_6 cage, it is then possible that the $18a_1$ orbital actually lies lower than the $17a_1$ orbital. Furthermore, if there is a larger splitting between the $17a_1$ and the $20e$ orbitals, there could be a closed-shell electronic configuration with the $17a_1$ and $20e$ orbitals as the HOMO and LUMO, respectively. The $17a_1$ and $20e$ orbitals have the same metal-metal bonding character (Fig. 3, right). The splitting between the two is caused by differences in metal-ligand(terminal) antibonding character of the orbitals. In the $17a_1$ orbital, the antibonding is between the metal atoms and the chlorine atoms, while in the $20e$ orbital it is between the metal and the phosphorus atoms. Because of this, the other possibility of a closed shell configuration by reversing the order of these two orbitals seems unlikely.

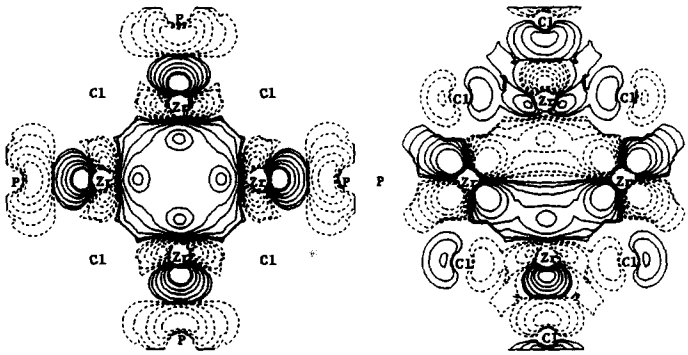

Fig. 3. Molecular orbital contour plots for the $18a_1$ orbital (left) and the $17a_1$ orbital (right) of **6**.

We are currently attempting to synthesize other hexanuclear clusters, for example, $[Zr_6Cl_{12}L_6]$, as well as investigating other synthetic routes for clusters of elements of Group IV.

Experimental

All operations were carried out under an argon atmosphere using standard vacuum-line and Schlenk techniques. The solvents were freshly distilled under nitrogen from the appropriate drying reagent and the reactants were used as received from the supplier.

Synthesis of **1**–**4**: ZrX_4 (X = Cl, 0.466 g, 2.0 mmol; X = Br, 0.822 g, 2.0 mmol) was reduced with $(nC_4H_9)_3SnH$ (1.05 mL, 4.0 mmol) in 20 mL of benzene (20 mL of CH_2CL_2 for **1**) for 36 h. The resulting red-brown precipitate (dark blue for X = Br) was washed with two 10-mL portions of fresh solvent to remove excess $(nC_4H_9)_3SnH$, followed by addition of 20 mL of fresh solvent. One equivalent of PR_3 (R = Me; 0.20 mL, 2.0 mmol, R = Et; 0.29 mL, 2.0 mmol, R = Pr; 0.40 mL, 2.0 mmol) was added dropwise. The precipitate was solubilized immediately, producing a deep-red/brown solution. The benzene was removed from **2** and **4** under vacuum, and CH_2Cl_2 and CH_3CN were added, respectively. The solutions were filtered through 2 cm of Celite and layered with 25 mL of hexane (for **1**, **2**, and **3**) and 25 mL of Et_2O for **4**. Red crystals separated out within one to two weeks. The yields of crystalline material isolated ranged from 10–20% for **1**–**4**.

2: $^{31}P\{^1H\}$ NMR (CH_3CN/[D_6]benzene, 81 MHz): δ = 20.97, 21.08, 21.20, 21.33, 21.46, 21.58, 21.69 ($\Delta\nu_{1/2}$ = 31.4 Hz), 21.83, 21.95, 22.08(s) (from −40 to 50 °C in 10° intervals). ^1H NMR (CD_3CN, 25 °C, measuring range: δ = 20–30, 200 MHz): δ = 1.20 (br., $-CH_3$), 2.17 (br., $-CH_2$).

4: $^{31}P\{^1H\}$ NMR (CH_3CN/[D_6]benzene, 81 MHz): δ = −2.27 (s, $\Delta\nu_{1/2}$ = 25.2 Hz, 21 °C).

Received: February 10, 1992 [Z 5179 IE]
German version: *Angew. Chem.* **1992**, *104*, 1117.

CAS Registry numbers:
1, 142438-18-4; **2**, 142438-19-5; **3**, 142457-03-2; **4**, 142438-21-9; **6**, 142438-23-1; **7**, 142438-22-0; **8**, 142438-24-2.

[1] J. D. Corbett, R. L. Daake, K. R. Poeppelmeier, D. H. Guthrie, *J. Am. Chem. Soc.* **1978**, *100*, 652.

[2] R. P. Ziebarth, J. D. Corbett, *J. Am. Chem. Soc.* **1985**, *107*, 4571.
[3] T. Hughbanks, G. Rosenthal, J. D. Corbett, *J. Am. Chem. Soc.* **1988**, *110*, 1511.
[4] F. A. Cotton, P. A. Kibala, W. J. Roth, *J. Am. Chem. Soc.* **1988**, *110*, 298.
[5] We have also found that under slightly less reducing conditions square pyramidal pentanuclear clusters of the composition $[Zr_5X_{12}(PR_3)_5]$ are formed. These will be described in detail at a later date.
[6] Further details of the crystal structure investigations are available on request from the Fachinformationszentrum Karlsruhe, Gesellschaft für wissenschaftlich-technische Information mbH, D-W-7514 Eggenstein-Leopoldshafen 2 (FRG), on quoting the depository number CSD-56200, the names of the authors, and the journal citation.
[7] R. P. Ziebarth, J. D. Corbett, *J. of Solid State Chem.* **1989**, *80*, 56.
[8] F. A. Cotton, M. Shang, W. A. Wojtczak, *Inorg. Chem.* **1991**, *30*, 3670.
[9] F. Rogel, J. D. Corbett, *J. Am. Chem. Soc.* **1990**, *112*, 8198.
[10] J. D. Smith, J. D. Corbett, *J. Am. Chem. Soc.* **1985**, *107*, 5704.
[11] R. P. Ziebarth, J. D. Corbett, *J. Am. Chem. Soc.* **1988**, *111*, 3272.

An Organometallic Analogue of the "Criss-Cross" Cycloaddition Reaction**

By *Colleen Kelley, Lisa A. Mercando, Michael R. Terry, Noël Lugan, Gregory L. Geoffroy,* Zhengtian Xu,* and *Arnold L. Rheingold*

Azines have been known since 1917[1] to undergo consecutive [3 + 2] cycloaddition reactions with 1,3-dipolarophiles to give bicyclic products having fused five-membered rings [Eq. (a)], a transformation that is commonly known as the criss-cross reaction.[2] Electron-rich azines typically require

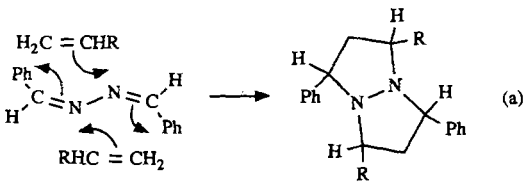

electron-deficient alkenes as partners and often need elevated temperatures and prolonged reaction times. In contrast, azines with electron-withdrawing CF_3 substituents react with a variety of substrates, including electron-rich olefins.[2, 3] We report herein the first examples of organometallic analogues of this criss-cross cycloaddition involving benzalazine and vinylidene or carbyne complexes.

It has been found that the ethylidyne complexes **1** undergo deprotonation to form the new vinylidene complexes **2**.

$[Cp(CO)_2M{\equiv}C{-}CH_3]BCl_4$ **1** $[Cp(CO)_2M{=}C{=}CH_2]$ **2**

a, M = Mn; **b**, M = Re

This deprotonation may be accomplished by treating complexes **1** with Et_3N, although the rhenium complex **1b** is sufficiently acidic to deprotonate spontaneously upon dissolution in CH_2Cl_2 or THF. Vinylidene complexes analogous to **2a, b** with organic substituents on the β-carbon are known,[5] but the unsubstituted derivatives **2a, b** have not been previously described. However, **2a** has been proposed as a reaction intermediate.[6] The complexes **2a, b** have been spectroscopically characterized, but they cannot be isolated since upon warming to 22 °C they rapidly decompose, with formation of the μ-vinylidene complexes $[\{Cp(CO)_2M\}_2(\mu\text{-}C{=}CH_2)]$.[6, 7] Consequently, they must be generated and studied at low temperature.

The criss-cross cycloaddition product **3b** was formed upon addition of benzalazine to the vinylidene complex **2b** [Eq. (b)]. IR monitoring indicates a clean transformation without

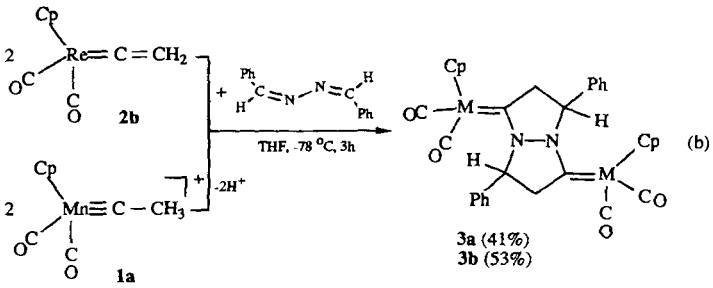

detectable by-products, and **3b** was isolated as a solid and was spectroscopically characterized. A similar reaction occurs between the carbyne complex **1a** and *two* equivalents of benzalazine to give the analogous product **3a**, with the second benzalazine equivalent necessary to deprotonate the intermediate formed between **1a** and the azine. The ORTEP drawing of **3a** (see Fig. 1[8]) shows the fused five-membered rings to be nearly planar [max. deviation = 0.17 Å at C(20)] as is the entire bridging ligand (dihedral angle [C(15)-N(1)-N(2)-C(17)]-[C(20)-N(1)-N(2)-C(18)] = 171.5°). The Mn–

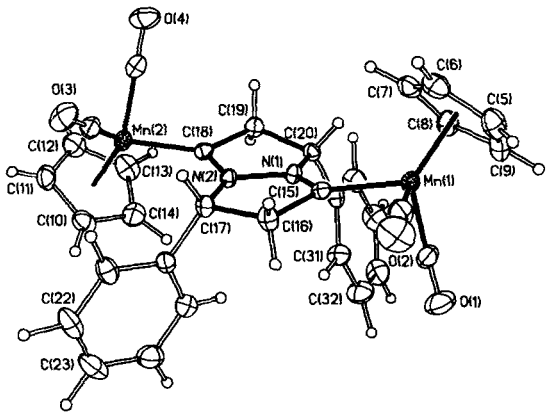

Fig. 1. An ORTEP drawing of **3a**. Selected bond lengths [Å]: Mn(1)-CP(1), 1.791(4); Mn(2)-Cp(2), 1.782(4); Mn(1)-C(15), 1.945(3); Mn(2)-C(18), 1.936(3); N(1)-N(2), 1.438(3); N(1)-C(20), 1.472(4); N(1)-C(15), 1.312(4); N(2)-C(17), 1.473(4); N(2)-C(18), 1.306(4).

C(carbene) bond lengths of 1.945(3) and 1.936(3) Å lie in the typical range.[9] The planes defined by the carbene carbon atoms and their attached carbon and nitrogen substituents do not bisect the CO–Mn–CO angle, as often found for $[Cp(CO)_2Mn{=}CRR']$ carbene complexes,[9] but instead

[*] Prof. G. L. Geoffroy, Dr. C. Kelley, L. A. Mercando, M. R. Terry
Department of Chemistry, The Pennsylvania State University, University Park, PA 16802 (USA)
Dr. N. Lugan
Laboratoire de Chimie de Coordination du CNRS, Toulouse (France)
Z. Xu, Prof. A. L. Rheingold
Department of Chemistry, University of Delaware, Newark, DE (USA)

[**] This work was supported by the Office of Basic Energy Sciences, U.S. Department of Energy, and a NATO Cooperative Research Grant.

appear to be oriented so as to minimize steric interactions. The two benzylic carbons of the bridging organic ligand are both chiral, and thus the molecule could be present as a pair of enantiomers or in the *meso* form. However, NMR data indicates only the formation of a single spectroscopically detectable stereoisomer, and the crystal structure shows it to be the *RR*/*SS* pair with the two phenyl groups on the same side of the fused five-membered rings.

The reaction mechanism proposed for the formation of **3b** resembles that which has been established for organic analogues of this criss-cross reaction[2] (Scheme 1). The α-

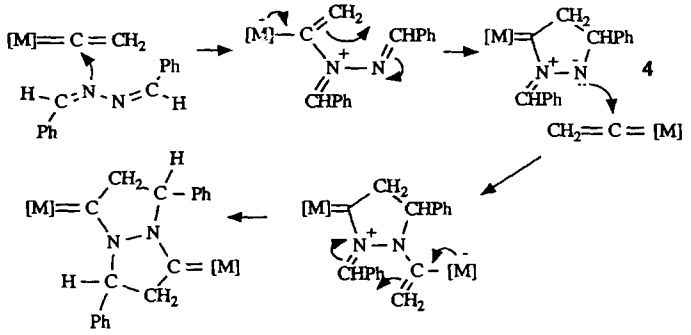

Scheme 1. Proposed mechanism for the formation of **3b**; [M] = $Cp(CO)_2Re$.

carbon of vinylidene complexes is known to be electrophilic,[5] and the cycloaddition reaction is most likely initiated by addition of the azine nitrogen to this carbon in **2b**. Cyclization then ensues to give **4**, an organic analogue of which is known.[3a] Addition of the nucleophilic nitrogen of **4** to a second equivalent of **2b** with subsequent cyclization would give **3b**. The carbyne complex **1a** is believed to react in a similar fashion but with deprotonation of the methyl substituent occurring *after* the initial addition of the azine nitrogen to the carbyne carbon.[10]

Vinylidene complex **2b** also undergoes [2 + 2] cycloaddition with PhN=CHPh to give the carbene complex **5b** [Eq. (c)], a reaction which has precedent in the cycloaddition of

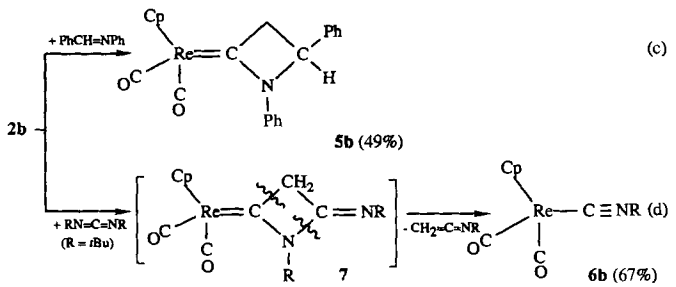

imines with vinylidene iron complexes.[11] A novel transformation of vinylidene complexes is that with **2b** and *t*BuN=C=N*t*Bu to form the isocyanide complex **6b** [Eq. (d)].[12] This reaction represents a net metathesis of the vinylidene C=C bond with the N=C bond of the carbodiimide and may proceed via the intermediate carbene complex **7**, which could undergo a retro-cycloaddition to give the observed products. For the addition of $C_6H_{11}N{=}C{=}NC_6H_{11}$ to $[(CO)_5Cr{=}C(OH)CH_3]$, in which a chromium analogue of **7** could be isolated, a vinylidene complex was proposed as intermediate.[13]

The above reactions demonstrate that the vinylidene complex **2b** is a highly reactive species, and in particular the criss-cross cycloaddition with benzalazine indicates that this complex is a potent 1,3-dipolarophile which should be capable of undergoing cycloadditions with a variety of other substrates. Interestingly, the manganese vinylidene complex **2a** does not readily react with benzalazine and *t*BuN=C=N*t*Bu, implying a decreased electrophilicity of the vinylidene α-carbon in **2a** compared to that in the rhenium complex **2b**. However, the much more electrophilic carbyne complex **1a** does react rapidly with each of these substrates to give, after treatment with Et_3N, the analogous complexes **3a**, **5a**, and **6a**. Thus, in the manganese reactions deprotonation must be accomplished after substrate addition, but in the rhenium case it occurs before addition.

Experimental

Dissolution of $[Cp(CO)_2Re{\equiv}CCH_3][BCl_4]$ in CH_2Cl_2 at −50 °C gave immediate deprotonation to yield gaseous HCl (the vapors turned litmus paper red) and complex **2b**, (detected by IR). A two-fold excess of benzalazine was added, the mixture was stirred for 1 h at 0 °C, the solvent was removed under vacuum, and the residue was chromatographed on neutral alumina to afford a yellow band of PhCH=NN=CHPh [eluent: CH_2Cl_2/hexane (1:1)] as well as a yellow band of **3b** [eluent: CH_2Cl_2/hexane (3:1); 53% yield]. To prepare **3a**, a two-fold excess of benzalazine was added to a −50 °C THF solution of $[Cp(CO)_2Mn{\equiv}CCH_3]BCl_4$, and the solution was stirred at −50 °C for 3 h followed by warming to 22 °C and evaporation of solvent under vacuum to afford a red oil which was chromatographed on neutral alumina to give first a yellow band of PhCH=N−N=CHPh [eluent: CH_2Cl_2/pentane (1:1)] followed by a yellow band of **3a** (eluent: 100% CH_2Cl_2; 41% yield). **2a**: IR (CH_2Cl_2, ca. −50 °C): $\tilde{\nu}$ [cm^{-1}] = 1998, 1935 (CO), 1623 (C=C); **2b**: IR (CH_2Cl_2, ca. −50 °C): $\tilde{\nu}$ [cm^{-1}] = 1990, 1915 (CO), 1629 (C=C); ^1H NMR (300 MHz, CD_2Cl_2, −10 °C): δ = 2.32 (s, 2H, CH_2), 5.48 (s, 5H, Cp). **3a**: ^1H NMR (300 MHz, C_6D_6, 25 °C): δ = 7.38-6.99 (Ph), 5.34 (dd, J = 10.2, 2.4 Hz, C*H*Ph), 4.03 (s, Cp), 3.34 (dd, 1H, J = 18.4, 10.2 Hz, CH_2), 3.10 (dd, J = 18.4, 2.4 Hz, CH_2). $^{13}C\{^1H\}$ NMR (75.5 MHz, CD_2Cl_2, 25 °C): δ = 245.5 (Mn = C), 233.95, 232.89 (CO), 140.6-126.8 (Ph), 84.0 (Cp), 66.25 (*C*HPh), 59.26 (CH_2). IR (CH_2Cl_2): $\tilde{\nu}$ [cm^{-1}] = 1926, 1858 (CO). MS (FAB): m/z = 612 ($M^{\oplus}$). **3b**: ^1H NMR (300 MHz, C_6D_6, 25 °C): δ = 7.8-6.7 (Ph), 4.91 (s, 5H, Cp), 4.03 (dd, J = 7.5, 2.4 Hz, C*H*Ph), 1.85 (dd, 1H, J = 16.6, 7.5 Hz, CH_2), 1.81 (dd, 1H, J = 16.6, 2.4 Hz, CH_2). $^{13}C\{^1H\}$ NMR (75.5 MHz, CD_2Cl_2, 25 °C): δ = 228.3 (Re = C), 206.9, 206.5 (CO), 148.2-125.9 (Ph), 87.5 (Cp), 38.3 (*C*HPh), 22.6 (CH_2). IR (CH_2Cl_2): $\tilde{\nu}$ [cm^{-1}] = 1926, 1847 (CO).

Received: January 24, 1992 [Z 5146 IE]
German version: *Angew. Chem.*, **1992**, *104*, 1066

CAS Registry numbers:
1a, 81616-28-6; **1b**, 141902-81-0; **2a**, 141902-82-1; **2b**, 141902-83-2; **4a**, 141902-84-3; **4b**, 141902-85-4; **5a**, 83111-32-4; **5b**, 141902-86-5; $[Cp(CO)_2Mn{\equiv}CCH_3]BCl_4$, 59831-16-2; $[Cp(CO)_2Re{\equiv}CCH_3]BCl_4$, 141902-80-9; $PhCH{=}NCH_3$, 622-29-7; *t*BuN=C=NBu*t*, 691-24-7; benzalazine, 588-68-1.

[1] J. R. Bailey, N. H. Moore, *J. Am. Chem. Soc.* **1917**, *39*, 279; J. R. Bailey, A. T. McPherson, *ibid.* **1917**, *40*, 1322.
[2] A. Padwa, *1,3-Dipolar Cycloaddition Chemistry*, Wiley, New York, **1984**; T. Wagner-Jauregg, *Synthesis* **1976**, 349.
[3] A. G. Gieren, P. Narayanan, K. Burger, W. Thenn, *Angew. Chem.* **1974**, *86*, 482; *Angew. Chem. Int. Ed. Engl.* **1974**, *13*, 475; O. Nuyken, G. Maier, K. Burger, *Makromol. Chem.* **1988**, *189*, 2245; *ibid.* **1989**, *190*, 623; K. Burger, F. Hein, *Justus Liebigs Ann. Chem.* **1982**, 853; K. Burger, H. Schickaneder, F. Hein, A. Gieren, V. Lamm, H. Engelhard, *ibid.* **1982**, 845; K. Burger, W. Thenn, R. Rauh, H. Schickaneder, A. Gieren, *Chem. Ber.* **1975**, *108*, 1460.
[4] E. O. Fischer, G. Z. Besl, *Z. Naturforsch. B* **1979**, *34*, 1186; E. O. Fischer, R. L. Clough, P. Stückler, *J. Organomet. Chem.* **1976**, *120*, C6.
[5] a) M. I. Bruse, *Chem. Rev.* **1991**, *91*, 197; b) M. I. Bruce, A. G. Swincer, *Adv. Organomet. Chem.* **1983**, *22*, 59.
[6] K. Folting, J. C. Huffman, L. N. Lewis, K. G. Caulton, *Inorg. Chem.* **1979**, *18*, 3483; B. E. Boland-Lussier, M. R. Churchill, R. P. Hughes, A. L. Rheingold, *Organometallics* **1982**, *1*, 628.
[7] The new compound $[Cp(CO)_2Re]_2(\mu\text{-}C{=}CH_2)$ [IR (CH_2Cl_2): $\tilde{\nu}$ [cm^{-1}] = 1977(w), 1948(s), 1900(s) (CO)] is similar to $[\{Cp(CO)_2Re\}_2(\mu\text{-}C{=}CHPh)]$: N. E. Kolobova, A. B. Antonova, O. M. Khitrova, M. Y. Antipin, Y. T. Struchkov, *J. Organomet. Chem.* **1977**, *137*, 69.

 © VCH Verlagsgesellschaft mbH, W-6940 Weinheim, 1992 0570-0833/92/0808-1054 $ 3.50+.25/0

[8] $C_{32}H_{26}Mn_2N_2O_4$: triclinic, $P\bar{1}$, $a = 10.652(5)$, $b = 10.870(3)$, $c = 13.199(6)$ Å, $\alpha = 75.97(3)$, $\beta = 67.85(3)$, $\gamma = 82.54(3)°$, $V = 1372.0(9)$ Å^3, $Z = 4$, $R(F) = 0.0391$, $T = 297$ K.. Further details of the crystal structure investigation are available upon request from the Director of the Cambridge Crystallographic Data Centre, University Chemical Laboratory, Lensfield Road, GB-Cambridge CB21EW (UK), on quoting the full journal citation.

[9] K. H. Dötz, H. Fischer, P. Hoffmann, F. R. Kreissl, U. Schubert, K. Weiss, *Transition Metal Carbene Complexes*, Verlag Chemie, Weinheim, **1983**.

[10] For related reactions of **1a** see: B. Handwerker, K. E. Garrett, K. L. Nagle, G. L. Geoffroy, A. L. Rheingold, *Organometallics* **1990**, *9*, 1562; H. Fischer, C. Troll, *J. Organomet. Chem.* **1992**, *427*, 77.

[11] A. G. M. Barrett, J. Mortier, M. Sabat, M. A. Sturgess, *Organometallics* **1988**, *7*, 2553; A. G. M. Barrett, M. A. Sturgess, *J. Org. Chem.* **1987**, *52*, 3940; *Tetrahedron Lett.* **1986**, *27*, 3811.

[12] G. W. Harris, J. C. A. Boeyens, N. J. Coville, *J. Organomet. Chem.* **1983**, *255*, 87.

[13] K. Weiss, E. O. Fischer, J. Müller, *Chem. Ber.* **1974**, *107*, 3548.

Spirocyclization of a Stable Phosphaalkyne with Aluminum Trichloride—Key Reaction for the Production of Triphospha Dewar Benzene Derivatives**

By *Bernhard Breit, Uwe Bergsträsser, Gerhard Maas,* and *Manfred Regitz**

Dedicated to Professor Günter Maier on the occasion of his 60th birthday

The organometallic chemistry of phosphaalkynes received considerable impetus from cyclooligomerization reactions, in which their metal complex fragments were incorporated into the products.[1] Significant milestones along this route include the cyclodimerization of *tert*-butylphosphaacetylene **5** to give the 1,3-diphosphacyclobutadiene complexes **1** (e.g., with cyclopentadienylrhodium[2] or -cobalt fragments[3]), the unusual linkage of **5** to the tricyclic zirconium complex **2**,[4] and finally the cyclotrimerization of **5** to give the molybdenum compound **3** of 1,3,5-triphosphabenzene,[5] as well as the Dewar isomer **4** with vanadium as the central metal atom.[6] Whereas in the case of **2** the true phosphaalkyne dimer was used successfully as a building block for cyclic phosphorus–carbon compounds,[7] cleavage reactions of the metal complex fragments of the other complexes have so far been unsuccessful.

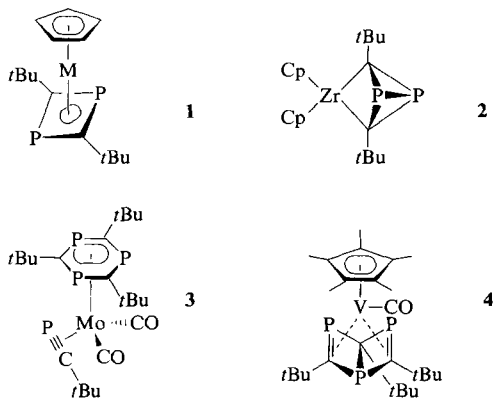

Herein we report for the first time a spirocyclotrimerization of the phosphaalkyne **5**[8] in the presence of aluminum trichloride. In dichloromethane this reaction occurs highly selectively (≥95%) in a 3:1 molar ratio and gives betaine **8** with the incorporation of the Lewis acid. First indications of a cyclooligomerization were provided by the ^{1}H NMR spectrum, which showed three different *tert*-butyl groups (Table 1), and the ^{31}P NMR spectrum, in which the three observed absorptions lie at completely different δ values

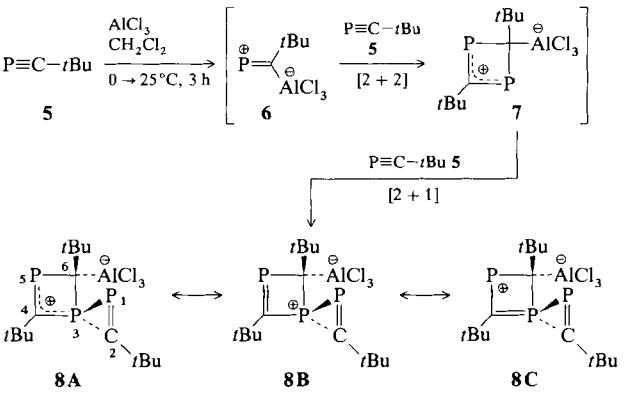

[Table 1; $\delta = -80.1$ (P3), 261.4 (P1), 417.9 (P5)]. The two latter absorptions indicate that the reaction product still has

Table 1. Selected physical data for the spirocyclic betaine **8** as well as for the tetracycles **12** and **13** [a].

8; ^{1}H NMR: $\delta = 1.34$ (dd, ^4J(P,H) = 0.7, 0.8 Hz, 9H, *t*Bu), 1.43 (d, ^4J(P,H) = 1.2 Hz, 9H, *t*Bu), 1.59 (pseudo-t, ^4J(P,H) = 0.9 Hz, 9H, *t*Bu); ^{13}C NMR: $\delta = 31.9$ (s, C(CH_3)$_3$), 33.8 (pseudo-t, ^3J(P,C) = 9.2 Hz, C(CH_3)$_3$), 34.9 (dd, ^3J(P,C) = 12.2 Hz, ^4J(P,C) = 12.5, 4.5 Hz, C(CH_3)$_3$), 41.1 (d, ^2J(P,C) = 8.4 Hz, *C*(CH_3)$_3$), 43.6 (pseudo-t, ^2J(P,C) = 2.0 Hz, *C*(CH_3)$_3$), 48.1 (d, ^2J(P,C) = 3.0 Hz, *C*(CH_3)$_3$), 202.9 (d, ^1J(P,C) = 65.4 Hz, P = C), 245.9 (dd, ^1J(P,C) = 68.2, 81.7 Hz, P = C); ^{31}P NMR: $\delta = -80.1$ (d, ^1J(P,P) = 214.5 Hz, P3), 261.4 (dd, ^1J(P,P) = 214.5 Hz, ^3J(P,P) = 18.0 Hz, P1), 417.9 (d, ^3J(P,P) = 18.0 Hz, P5).

12; ^{1}H NMR: $\delta = 0.96$ (s, 9H, *t*Bu), 1.40 (d, ^4J(P,H) = 0.9 Hz, 9H, *t*Bu), 1.43 (d, ^4J(P,H) 1.5 Hz, 9H, *t*Bu), 1.58 (pseudo-t, ^4J(P,H) = 1.4 Hz, 9H, *t*Bu); ^{13}C NMR: $\delta = 31.9$ (dd, ^3J(P,C) = 15.1 Hz, ^4J(P,C) = 6.0 Hz, C(CH_3)$_3$), 32.6 (pseudo-t, ^3J(P,C) = 10.1 Hz, C(CH_3)$_3$), 33.1 (pseudo-t, ^3J(P,C) = 14.6 Hz, C(CH_3)$_3$), 34.7 (s, C(CH_3)$_3$), 36.7 (d, ^2J(P,C) = 12.1 Hz, *C*(CH_3)$_3$), 36.9, 38.2, 40.8 (each m, each *C*(CH_3)$_3$), 42.1, 58.2 (each m, C2/C3), 96.7 (m, C5), 211.6 (m, C8); ^{31}P NMR: $\delta = -160.0$ (pseudo-quintet, ^2J(P,P) = 32.9, 16.6 Hz, ^3J(P,P) = 13.2 Hz, P4), 111.5 (d, pseudo-t, ^2J(P,P) = 33.1, 32.9, 16.6 Hz, P1), 134.3 (ddd, ^1J(P,P) = 264.8 Hz, ^2J(P,P) = 33.1, 19.8 Hz, P6), 417.1 (d, pseudo-t, ^1J(P,P) = 264.8 Hz, ^3J(P,P) = 13.2 Hz, P7); MS(70 eV): *m/z* 401 ($M^{\oplus}$ + H, 20%), 355 ($M^{\oplus}$ − 3 Me, 5), 300 ($M^{\oplus}$ − *t*BuCP, 10), 262 ($M^{\oplus}$ − 2 *t*BuC, 25), 200 ($M^{\oplus}$ − 2 *t*BuCP, 8), 169 ($M^{\oplus}$ − 2 *t*BuCP, −P, 100).

13: ^{1}H NMR: $\delta = 1.00$, 1.17, (each s, each 9H, *t*Bu), 1.43 (d, ^4J(P,H) = 2.0 Hz, 9H, *t*Bu), 1.80 (s, 9H, *t*Bu); ^{13}C NMR: $\delta = 29.9$ (d, ^3J(P,C) = 8.4 Hz, C(CH_3)$_3$), 31.3 (s, C(CH_3)$_3$), 31.6 (d, ^3J(P,C) = 11.4 Hz, C(CH_3)$_3$), 33.9 (d, ^3J(P,C) = 6.1 Hz, C(CH_3)$_3$), 36.5 (pseudo-t, ^2J(P,C) = 20.6 Hz, *C*(CH_3)$_3$), 37.0 (d, ^2J(P,C) = 9.2 Hz, *C*(CH_3)$_3$), 39.1 (pseudo-t, ^2J(P,C) = 12.2 Hz, C(CH_3)$_3$), 41.0 (pseudo-t, ^2J(P,C) = 16.0 Hz, *C*(CH_3)$_3$), 60.1 (pseudo-t, ^1J(P,C) = 34.3 Hz, C2), 64.2, 89.3 (each m, C5/C6), 224.3 (pseudo-t, ^1J(P,C) = 54.2 Hz, C8); ^{31}P NMR: $\delta = -174.4$ (d, ^1J(P,P) = 83.0 Hz, P3 or P4), −147.3 (ddd, ^1J(P,P) = 83.0 Hz, ^2J(P,P) = 31.2, 16.6 Hz, P3 or P4), 64.6 (d, ^2J(P,P) = 31.2 Hz, P1), 399.0 (s, P7); MS(70 eV): *m/z* 401 ($M^{\oplus}$ + H, 45%), 300 ($M^{\oplus}$ − *t*BuCP, 10), 262 ($M^{\oplus}$ − 2 *t*BuC, 62), 200 ($M^{\oplus}$ − 2 *t*BuCP, 22), 169 ($M^{\oplus}$ − 2 *t*BuCP, −P, 100).

[a] ^{1}H (90 or 400 MHz, TMS), ^{13}C (100.6 MHz, TMS), and ^{31}P NMR spectra (80.8 MHz, 85% H_3PO_4) in CD_2Cl_2 for **8**, in C_6D_6 for **12**, **13**.

[*] Prof. Dr. M. Regitz, Dipl.-Chem. B. Breit, Dipl.-Chem. U. Bergsträsser, Prof. Dr. G. Maas
Fachbereich Chemie der Universität
Erwin-Schrödinger-Strasse, D-W-6750 Kaiserslautern (FRG)

[**] Phosphorus Compounds, Part 58. This work was supported by the Volkswagen-Stiftung and the Fonds der Chemischen Industrie. Part 57: M. Birkel, J. Schulz, U. Bergsträsser, M. Regitz, *Angew. Chem.* **1992**, *104*, 870; *Angew. Chem. Int. Ed. Engl.* **1992**, *31*, 879.

two phosphaalkene units;[9] the relatively high-field position of the third phosphorus signal (P3) lies approximately in the range of phosphirenium ions.[10] The signals due to the heteronuclei P1 and P3 are each split by a $^1J(P,P)$ coupling of 214.5 Hz to give doublets, which indicates that they are direct neighbors; P1 has an additional P,P coupling of 18.0 Hz, and this splits the resonance signal of P5.

Finally characteristic low-field absorptions for two phosphaalkyne carbons occur in the ^{13}C NMR spectrum of **8** at $\delta = 202.9$ and 245.9, which have $^1J(P,C)$ couplings (Table 1). The signal for the C6 atom in the four-membered ring cannot be observed. This has to be considered as good evidence for the C6 atom being a direct neighbor of the aluminum atom.[11]

The final confirmation of the constitution of the phosphaalkyne/aluminum trichloride compound **8** was achieved by an X-ray crystal structure analysis (Fig. 1).[12] The bond

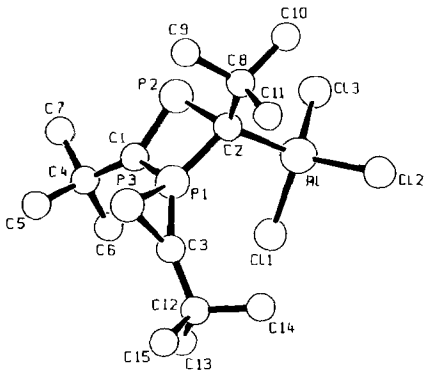

Fig. 1. Structure of **8** (SCHAKAL plot). Selected distances [Å] and angles [°]: P1-C1 1.77(1), P1-C2 1.80(1), P2-C1 1.70(1), P2-C2 1.91(1), C2-Al 2.02(1), P1-P3 2.108(4), P1-C3 1.74(1), P3-C3 1.68(1); C1-P1-C2 90.8(5), P3-P1-C1 122.8(4), P3-P1-C2 128.1(4), P3-P1-C3 50.8(3), C1-P1-C2 90.8(5), C1-P1-C3 131.6(5), C2-P1-C3 133.0(5), P1-P3-C3 53.3(3), P1-C3-P3 75.9(4), P1-C2-P2 85.0(5), C2-P2-C1 89.4(5), P2-C1-P1 93.1(5). Torsion angles [°]: C1-P1-C2-P2 9.4(4), C1-P2-C2-P1 −9.7(4), C2-P2-C1-P1 9.9(4), C2-P1-C1-P2 −10.5(5), P3-P1-C1-C4 −54.0(1.1), C3-P1-C1-C4 10.3(1.2). The second independent molecule is different from the one depicted here especially with regard to the torsion angles in the four-membered ring (which are 1.2–1.4° smaller than the ones given above) as well as the bonds C1–C4, C2–Al, and C3–C12.

lengths P2–C1 (1.70 Å) and P1–C1 (1.77 Å) justify the formulation of the key product **8** as the resonance hybrid **8B** ↔ **8C** with an almost delocalized P=C bond and positive charge on the heteroatom in accordance with **8A**. Both values for the bond lengths are above the average values for open-chain phosphaalkenes (1.67 Å[13]), but are a long way from being within the range of single P–C bonds. The four-membered ring is no longer planar (see torsion angles in the legend to Fig. 1). The P3–C3 distance is within the expected range (1.68 Å); for the $W(CO)_5$ complex of a 2*H*-diphosphirene the P=C bond length was found to be 1.634 Å,[14] and for a 1*H*-diphosphirene with a donor substitutent at the phosphaalkyne unit it was 1.702 Å.[15]

With regard to the mechanism it may be assumed that the title reaction is initiated by the addition of the Lewis acid at the carbon atom of the phosphaalkyne **5** (→ **6**) in keeping with the polarization of the P≡C bond.[16] Starting from **6** the [2+2] cycloaddition of a second equivalent of the phosphaalkyne **5** occurs to give the dimeric complex **7**,[17] in which the phosphorus has electrophilic character. The final [2+1] cycloaddition with the third equivalent of **5** leads to the formation of the product (→ **8**).

If the aluminum chloride substituent in betaine **8** is removed by the addition of the Lewis base dimethyl sulfoxide, the spirocyclic $\lambda^5\sigma^4,\lambda^3\sigma^2$ diphosphete **9** is generated, which cannot be isolated. Even at −45 °C (CH_2Cl_2) after the P–P bond breakage in the diphospirene ring, **9** rearranges to the 1,3,5-triphospha Dewar benzene **10**, which also cannot be isolated. If the phosphaalkyne **5** is added as a trapping

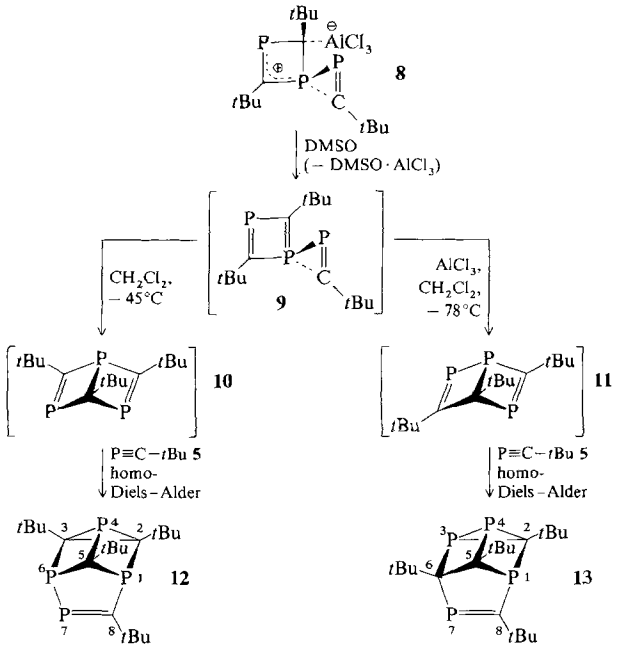

reagent for **10** before the release of **9**, the tetraphosphatetracycle **12** (37%) is formed by a homo-Diels–Alder reaction. However, with an excess of aluminum trichloride, and at −78 °C (CH_2Cl_2), the same experiment leads to the constitutional isomer **13** (38%). Under these conditions the rearrangement of **9** occurs with the breakage of the P–C bond to give the 1,2,5-triphospha Dewar benzene **11**, which is also trapped by a homo-Diels–Alder reaction (→ **13**). The role of the aluminum chloride (or its DMSO adduct) during the rearrangement reaction at present remains unexplained. Both processes are highly selective and allow the desired formation of the hitherto unknown phosphaalkyne cyclotetramers.

In the ^1H NMR spectra of **12** and **13** the signals for four *t*Bu groups are found for each compound. These signals are partly split by $^4J(P,H)$ couplings of 0.9–2.0 Hz (Table 1). The position and splitting of the ^{31}P NMR resonance signals of the two isomers prove the constitutions; for **12** the high-field position of the phosphorus atom P4 of the three-membered ring at $\delta = -160.0$[18] as well as the low-field absorption of P7 ($\delta = 417.1$) are characteristic. The latter resonance signal is split by $^1J(P,P)$ coupling of 264.8 Hz, which also occurs for P6 ($\delta = 134.3$). Naturally for P1 ($\delta = 111.5$) three $^2J(P,P)$ couplings (33.1, 32.9, 16.6 Hz) are found. In **13** the resonance signals $\delta = -174.4$ and −147.3 [$^1J(P,P) = 83.0$ Hz] are assigned to the diphosphirane unit.[18] The $\lambda^3\sigma^2$ phosphorus atom P7 ($\delta = 399.0$) is not coupled with another heteronucleus. P1 ($\delta = 64.6$) shows only one $^2J(P,P)$ coupling of 31.2 Hz. The position and splitting of the carbon resonance signals in the ^{13}C NMR spectra (Table 1) are in agreement with the structures **12** and **13**.

Chemically the existence of the P=C bond of **13** can be proven by the reaction with mesitylnitriloxide. The regio- and stereospecific [3 + 2] cycloaddition affords quantitatively crystalline **14** [colorless crystals with m.p. 184°C (from *n*-pentane)]. The break up of the phosphaalkene unit in **13** is indicated by the considerable high-field shift of the absorption of P7 in the ^{31}P NMR ($\delta = 75.6$) as well as of C8 in the ^{13}C NMR spectrum ($\delta = 108.6$, ^1J(P,C) = 53.4, 37.4 Hz).

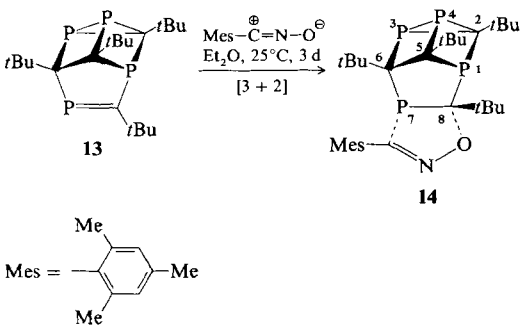

The crystal structure analysis[12] confirms the constitution of the cycloadduct **14** (and thus also the precursor **13**) (Fig. 2). The P–C distances in the polycycle are worthy of note, since they vary greatly between 1.807 (P2–C4) and 1.927 Å (P4–C2).

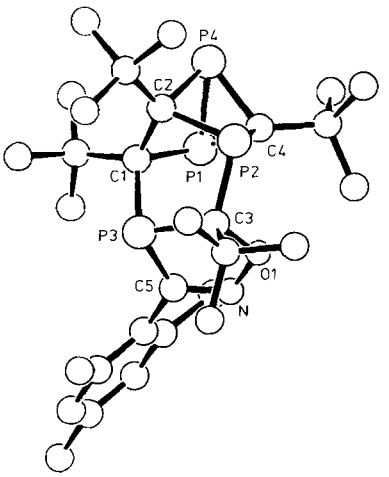

Fig. 2. Structure of **14** (SCHAKAL plot). Selected distances [Å] and angles [°]: P4-P1 2.179(3), P3-C1 1.886(7), C2-C1 1.596(9), P2-C4 1.807(7), P3-C5 1.854(7), N-C5 1.261(8), P4-C2 1.927(7), P2-C3 1.895(7); O1-C3 1.960(8), P1-C1 1.914(7), O1-N 1.396(7), P1-C4 1.845(7), P4-C4 1.866(7), P2-C2 1.876(7), P3-C3 1.836(7); C1-P1-P4 81.4(2), C4-P1-C1 95.5(3), C3-P2-C4 103.9(3), C2-P4-P1 78.2(2), P3-C1-P1 115.1(3), C2-C1-P3 106.6(4), P4-C4-P1 71.9(3), P4-C2-P2 88.4(3), C1-C2-P4 98.4(4), C4-P1-P4 54.5(2), C2-P2-C4 83.2(3), C3-P2-C2 101.2(3), C3-P3-C1 98.0(3), C4-P4-P1 53.6(2), C2-P4-C4 80.2(3), C2-C1-P1 95.1(4), P2-C4-P1 111.8(4), P4-C4-P2 92.4(3), C1-C2-P2 103.3(4), P3-C3-P2 106.9(3).

Experimental Procedure

8: To a suspension of aluminum trichloride (0.67 g, 5.0 mmol) in dichloromethane (5 mL) a solution of the phospaalkyne **5** (1.50 g, 15.0 mmol) [8] in dichloromethane (5 mL) was added dropwise and stirred at 0 °C (air and moisture exclusion). After 1 h the solution was allowed to warm to 25 °C and stirred for a further 2 h. The solution was concentrated under vacuum at 25 °C/10^{-3} mbar, whereby **8** remained as a spectroscopically pure (^{31}P NMR) red-brown oil. Yield after recrystallization from toluene: 2.06 g (95%) yellow crystals; m.p. 134 °C (decomp).

12: To a solution of betaine **8** (1.47 g, 3.4 mmol) in dichloromethane (10 mL) the phosphaalkyne **5** (0.34 g, 3.4 mmol) [8] and dimethyl sulfoxide (0.80 mL, 11.3 mmol) each in dichloromethane (5 mL) were added dropwise one after the other and stirred at −45 °C (air and moisture exclusion). Over a period of 6 h the mixture was allowed to warm up to 25 °C and then stirred for a further 18 h after which it was concentrated under vacuum at 25 °C/10^{-3} mbar. Extraction of the residue with *n*-pentane (5 × 10 mL) and concentration of the solution afforded spectroscopically pure (^{31}P NMR) **12** as a red oil. Yield: 0.50 g, (37%). Middle-pressure chromatography on silica gel with *n*-pentane was possible but with large losses of the product.

13: To a solution of betaine **8** (1.16 g, 2.7 mmol) and aluminum chloride (0.59 g, 4.4 mmol) in dichloromethane (10 mL), the phosphaalkyne **5** (0.26 g, 2.6 mmol) [8] and dimethyl sulfoxide (0.62 mL, 8.7 mmol) each in dichloromethane (5 mL) were added dropwise one after the other and stirred at −78 °C (air and moisture exclusion). Workup as for **12** afforded **13** as a yellow oil. Yield: 0.39 g (38%). Column chromatography on silica gel (inert gas) with *n*-pentane is possible, but involves great losses.

Received: January 29, 1992
Revised: May 11, 1992 [Z 5156 IE]
German version: *Angew. Chem.* **1992**, *104*, 1043

CAS Registry numbers:
5, 78129-68-7; **8**, 141957-89-3; **12**, 141957-86-0; **13**, 141957-87-1; **14**, 141957-88-2; $\overset{\oplus}{\text{Mes}}\text{C}\equiv\text{N}\overset{\ominus}{\text{O}}$, 2904-57-6.

[1] Reviews: a) J. F. Nixon, *Chem. Rev.* **1988**, *88*, 1327–1362; b) M. Regitz, P. Binger, *Angew. Chem.* **1988**, *100*, 1541–1565; *Angew. Chem. Int. Ed. Engl.* **1988**, *27*, 1484–1508; c) *Multiple Bonds and Low Coordination in Phosphorus Chemistry* (Eds.: M. Regitz, O. J. Scherer), 1. ed., Thieme, Stuttgart, **1990**; d) P. Binger in [1c], pp. 90–111.

[2] P. B. Hitchcock, M. J. Maah, J. F. Nixon, *J. Chem. Soc. Chem. Commun.* **1986**, 737–738.

[3] P. Binger, R. Milczarek, R. Mynott, M. Regitz, W. Rösch, *Angew. Chem.* **1986**, *98*, 645–646; *Angew. Chem. Int. Ed. Engl.* **1986**, *25*, 644–645.

[4] P. Binger, B. Biedenbach, C. Krüger, M. Regitz, *Angew. Chem.* **1987**, *99*, 798–799; *Angew. Chem. Int. Ed. Engl.* **1987**, *26*, 764–765.

[5] A. R. Barron, A. H. Cowley, *Angew. Chem.* **1987**, *99*, 956; *Angew. Chem. Int. Ed. Engl.* **1987**, *26*, 907–908.

[6] R. Milczarek, W. Rüsseler, P. Binger, K. Jonas, K. Angermund, C. Krüger, M. Regitz, *Angew. Chem.* **1987**, *99*, 957–958; *Angew. Chem. Int. Ed. Engl.* **1987**, *26*, 908–909.

[7] See for example, P. Binger, T. Wettling, R. Schneider, F. Zurmühlen, U. Bergsträsser, J. Hoffmann, G. Maas, M. Regitz, *Angew. Chem.* **1991**, *103*, 208–211; *Angew. Chem. Int. Ed. Engl.* **1991**, *30*, 207-210.

[8] Synthese of **5** in [1c], p. 59–63.

[9] For the ^{31}P NMR-absorption see K. Karaghiosoff [1c], pp. 463–471.

[10] K. S. Fougers, H. Hogeveen, R. F. Kingma, *Tetrahedron Lett.* **1983**, *24*, 643–646; S. Lochschmidt, F. Mathey, A. Schmidpeter, *ibid.* **1986**, *27*, 2635–2638; S. A. Weisman, S. G. Baxter, *ibid.* **1990**, *31*, 819–822.

[11] This phenomenon was also observed for structurally similar cyclobutadiene/aluminum trichloride complexes; D. S. B. Grace, H. Hogeveen, P. A. Wache, *Tetrahedron Lett.* **1976**, *17*, 123-126.

[12] Crystal structure analysis (diffractometer: Enraf-Nonius CAD4, $Mo_{K\alpha}$ radiation, full-matrix refinement) **8**: $C_{15}H_{27}AlCl_3P_3$, M_r=433.7; orthorhombic, space group $P2_12_12_1$; a=14.619(3), b=17.029(7), c=17.682(13) Å, $\alpha=\beta=\gamma=90°$; ρ_{calcd}=1.31 g cm^{-3}, Z=8 (two independent molecules); crystal size 0.45 × 0.4 × 0.7 mm^3, 4739 symmetry-independent reflections in the range $2.0 \geq \theta \geq 26.0°$ were measured, correction for the loss of intensity (up to 6.7% on three control reflections); absorption correction (μ=6.7 cm^{-1}); 3144 reflections with $I \geq 2\sigma(I)$, 397 variables, positions of the H atoms were calculated in staggered conformations and included in the refinement. R=0.0745, $R_w=(\sum w\Delta^2 F/\sum wF_0^2)^{1/2}$=0.0647, residual electron density 0.67 e Å^{-3}. The absolute configuration of **8** could not be determined (no changes of the R values for the structure with opposite absolute configuration). **14**: $C_{30}H_{47}NOP_4$; monoclinic, space group $P2_1/c$ (no. 14); a = 13.865(5), b = 12.971(5), c = 17.971(12) Å, β = 106.5(3)°, ρ_{calcd} = 1.20 g cm^{-3}, Z = 4; crystal size 0.25 × 0.19 × 0.25 mm^3, 4854 symmetry-independent reflections in the range $2.0 \geq \theta \geq 26.0°$ were measured; 3499 reflections with $I \geq 2\sigma(I)$, 325 variables, H atoms were not included in the refinement. R = 0.0887, $R_w = (\sum w\Delta^2 F/\sum wF_0^2)^{1/2}$ = 0.0986; the difference-Fourier synthesis on the basis of the valid structural model shows a maximum of 0.46 e Å^{-3} and a minimum −0.32 e Å^{-3}. Further details of the crystal structure investigation may be

obtained from the Fachinformationszentrum Karlsruhe, Gesellschaft for wissenschaftlich-technische Information mbH, D-W-7514 Eggenstein-Leopoldshafen 2 (FRG) on quoting the depository number CSD-56023, the names of the authors, and the journal citation.
[13] R. Appel in [1c], p. 160.
[14] O. Wagner, G. Maas, M. Regitz, *Angew. Chem.* **1987**, *99*, 1328–1330; *Angew. Chem. Int. Ed. Engl.* **1987**, *26*, 1257–1259.
[15] E. Niecke, R. Streubel, M. Nieger, D. Stalke, *Angew. Chem.* **1989**, *101*, 1708–1710; *Angew. Chem. Int. Ed. Engl.* **1989**, *28*, 1673–1675.
[16] See for example M. Regitz, *Chem. Rev.* **1990**, *90*, 191–213.
[17] Isolable compounds of the type **7** are known in carbon chemistry. They are formed from the cyclodimerization of but-2-yne with aluminum halides (P. B. J. Driessen, H. Hogeveen, *J. Organomet. Chem.* **1978**, *156*, 265–278) or by oxidative ring opening of tetra-*tert*-butyltetrahedrane (G. Maier, R. Emrich, K.-D. Malsch, K.-A. Schneider, M. Nixdorf, H. Imgartinger, *Chem. Ber.* **1985**, *118*, 2798–2810); in the latter case they have the character of homocyclopropenylium ions.
[18] F. Mathey, *Chem. Rev.* **1990**, *90*, 997–1025.

Cyclopentadienyl Cobalt Complexes of Cobaltapentalenes: Products Formed by Reaction of (μ-Cyclopentadienylidene) Cobalt Complexes with Silylalkynes**

By *Hubert Wadepohl,* Wolfgang Galm, Hans Pritzkow,* and *Andreas Wolf*

Dedicated to Professor Wolfgang Beck on the occasion of his 60th birthday

Coupling reactions of metal-carbene complexes with alkynes are very important in chemical syntheses.[1] Depending on the isolobal character of the relevant metal fragment, metallacyclobutenes **A** or η^3-vinylcarbene complexes **B** are postulated as intermediates in these mechanistically still largely unexplained reactions.[2] In the Dötz reaction[3] (that is, the reaction of certain Fischer carbenes with alkynes) **B** or an η^1-vinylcarbene complex **C** derived from the latter is carbonylated by a CO ligand. The resulting vinylketene complex can then react further, depending on the starting materials and the reaction conditions, to form one of numerous possible types of products. Carbene complexes of the Schrock type react with alkynes—with the insertion of the alkynes into the M=C bonds—only as far as stage **C**.[4]

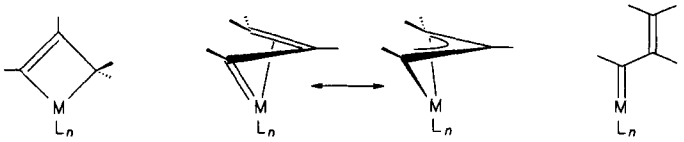

A B C

The μ-cyclopentadienylidene dicobalt complexes **1** can be described by the limiting structures **D** (carbene complex) and **E** (zwitterion).[5] With alkynes they do not react by insertion of the alkyne into the Co2–C1 bond.

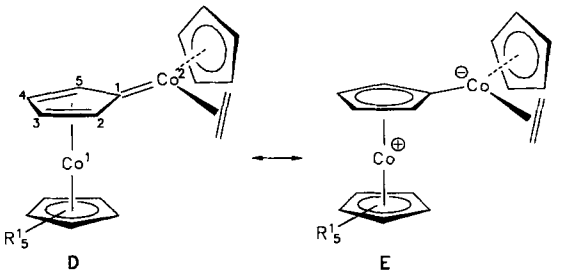

D E

1a, R^1 = H
1b, R^1 = Me
1c, R^1_5 = Me_4Et

Turquoise **1a** decomposes in the presence of but-2-yne, hex-3-yne, bis(*tert*-butyl)acetylene, diphenylacetylene, or bis(benzo-1,2-dioxaborolyl)acetylene at temperatures above 50 °C after a short time to form dark products that could not be characterized. Bis(trimethylsilyl)acetylene **2a**, on the other hand, reacts readily with the complexes **1** at 45 °C in a very unusual reaction to form the binuclear complexes **4** with a cobaltabicyclic ring system as ligand (Scheme 1). With

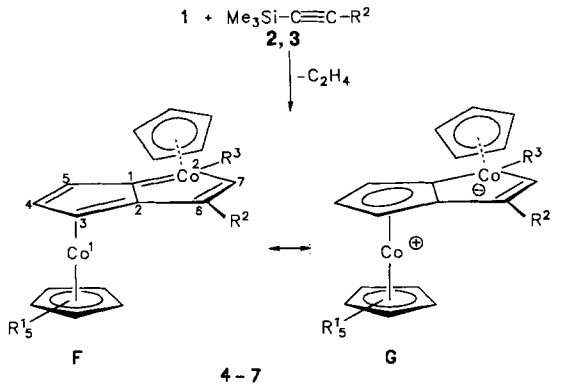

F 4–7 G

Scheme 1. **2a**, R^2 = $SiMe_3$; **2b**, R^2 = $SiEt_3$; **2c**, R^2 = $SiMe_2tBu$; **3**, R^2 = *t*Bu; **4a**, R^1 = H, R^2 = R^3 = $SiMe_3$; **4b**, R^1 = Me, R^2 = R^3 = $SiMe_3$; **4c**, R^1_5 = Me_4Et, R^2 = R^3 = $SiMe_3$; **5a**, R^1 = H, R^2 = $SiEt_3$, R^3 = $SiMe_3$; **5a'**, R^1 = H, R^2 = $SiMe_3$, R^3 = $SiEt_3$; **6a**, R^1 = H, R^2 = $SiMe_2tBu$, R^3 = $SiMe_3$; **6a'**, R^1 = H, R^2 = $SiMe_3$, R^3 = $SiMe_2tBu$; **7a**, R^1 = H, R^2 = *t*Bu, R^3 = $SiMe_3$.

bis(triethylsilyl)acetylene, **1a** does not react under similar conditions; decomposition occurs above 60 °C. The unsymmetrically substituted bis(silyl)alkynes **2b, c** react with **1a** to give nonseparable mixtures of the stereoisomers **5a**, **5a'** and **6a**, **6a'**, respectively. In both cases smaller amounts of the complex **4a** with two trimethylsilyl groups in the cobaltabicyclic system are also formed. Only the product **7a** with the trimethylsilyl group on the cobalt atom is obtained regioselectively from **1a** and **3**.

The constitution of the novel blue-violet binuclear complexes **4–7** can be derived from the NMR spectra.[6] The singlet resonance signals displaced far downfield (δ = 9.9–11.1) for the metal-enyl hydrogen atom 7-H as well as the broadened downfield ^{29}Si NMR signals ($\delta \approx 30$–40) of the silyl groups on the cobalt atoms are especially characteristic. ^{13}C NMR signals for the quaternary carbon atoms C1 bound to the cobalt atom are not observed at all. The "car-

[*] Priv.-Doz. Dr. H. Wadepohl,[+] Dr. W. Galm, Dr. H. Pritzkow, Dipl.-Chem. A. Wolf
Anorganisches Chemisches Institut der Universität
Im Neuenheimer Feld 270, D-W-6900 Heidelberg (FRG)
[+] Current address:
University of Oxford, Inorganic Chemistry Laboratory
South Parks Road, Oxford OX1 3QR (UK)

[**] This work was supported by the Deutsche Forschungsgemeinschaft (Sonderforschungsbereich 247 of the Universität Heidelberg) and by the Fonds der Chemischen Industrie.

bene" carbon atoms are not detectable in the starting materials **1** either.[5, 7]

The complexes **4**–**7** can be described by limiting structures such as **F** with η^4-bonding of the metallabicyclic ring system to the $CpCo^1$ group ($Cp = \eta^5$-C_5H_5) as well as by zwitterionic formulations such as **G**. In the latter case the bicyclic system should be η^5-coordinated to the $[CpCo]^+$ group. A charge separation such as in **G** then appears to be energetically favorable if at the same time partial structures that resemble the cobaltocenium cation are possible. This becomes clear, for example, in **1** (limiting structures **D**↔**E**) and the mononuclear complexes $[(C_5R_5)Co$(acenaphthylene)] (**8**, R = H, Me),[8] both of which should be formulated

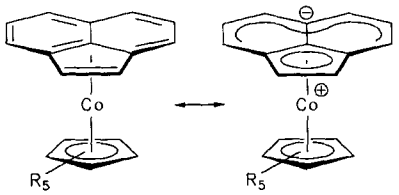

8a, R=H
8b, R=Me

with considerable zwitterionic contributions. **4**–**7** are related to π complexes of pentalene (**H**) on the one hand and to π complexes of dihydropentalenyl (**I**) on the other by the isolobal series $CpCoR \leftrightarrow d^7\text{-}ML_4 \leftrightarrow CH$ and $[CpCoR]^- \leftrightarrow d^8\text{-}ML_4 \leftrightarrow CH_2$ respectively. To our knowledge, at the present time only the latter are known, however, they have η^5-dihydropentalenyl ligands.[9]

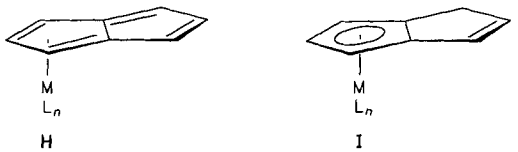

H I

Insight into the bonding is provided by an X-ray structural analysis of **4c**.[10] The carbacyclic five-membered ring of the cobaltapentalene ligand is bonded through all five carbon atoms to the $[(\eta^5\text{-}C_5Me_4Et)Co]$ fragment (Fig. 1). The bond between Co1 and C1, which is slightly displaced (0.07 Å) from the C2-C3-C4-C5 plane, is, at 2.206(6) Å, longer than the bonds between Co1 and the carbon atoms C2–C5. This indicates a transition to the η^4-coordination, as is also found for the cyclopentadienylidene ligand in the binuclear complexes of type **1** (d(Co1–C1) = 2.186(6) (**1a**[11]), 2.204(5) Å (**1b**[11]), d(Co1-C2 to C4) = 1.98–2.04 and 1.99–2.06 Å (**1b**). It is striking that, in the planar CoC_4 five-membered ring, both of the endocyclic Co–C bonds starting from Co2 are very short and almost equal in length (1.88 Å). This value is comparable to the bond lengths Co2–C1 in **1** (**1a**: 1.866(6) Å,[11] **1b**: 1.872(5) Å[11]). The length of formal Co–C(sp^2) single bonds, for example in the cobaltacyclopentadienes (cobaltoles) $[(\eta\text{-}C_5H_4R)(PPh_3)Co(C_4H_4)]$ (R = H, COOMe),[12] lies between 1.93 and 1.95 Å. The C6–C7 bond is shorter than the remaining C–C bonds in the cobaltapentalene. Overall, the structural data indicate that several limiting structures such as **F** and **G** have to be taken into account in a qualitative description of the bonding in the dicobalt complexes **4**–**7**.

Compared to the extremely air- and moisture-sensitive starting compounds **1**, **4**–**7** are much less reactive. They are

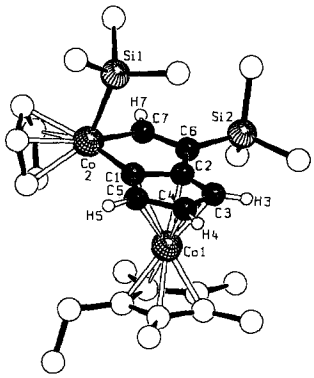

Fig. 1. Molecular structure of **4c**. Hydrogen atoms of the Cp, CH_3, and C_2H_5 groups are not shown. Selected bond lengths [Å] and angles [°] with standard deviations given in parentheses: Co1-C1 2.206(6), Co1-C2 2.106(6), Co1-C3 2.007(7), Co1-C4 1.981(7), Co1-C5 2.049(6), Co2-Si1 2.281(2), Co2-C1 1.883(6), Co2-C7 1.877(7), C1-C2 1.462(8), C1-C5 1.433(8), C2-C3 1.410(9), C2-C6 1.459(8), C3-C4 1.428(10), C4-C5 1.410(10), C6-C7 1.379(9); C5-C1-C2 105.0(5), C2-C1-Co2 114.7(4), C1-C2-C3 109.1(5), C1-C2-C6 113.6(5), C2-C3-C4 107.9(6), C3-C4-C5 107.9(6), C1-C5-C4 109.9(6), C1-Co2-C7 81.9(3), Co2-C7-C6 122.0(5), C2-C6-C7 107.7(5), C5-C1-Co2 140.2(5).

only moderately air-sensitive, can be chromatographed on silica gel, and can be distilled or sublimed without decomposition under vacuum (oil pump) at about 100 °C. They do not react with CO, even under pressure (30 bar, room temperature). The high stability of the cobaltabicyclic system is also shown by the fact that hydrogenation of the formal C6–C7 double bond over a Pd/C catalyst is not possible (1 bar H_2, room temperature).

The mechanism of formation of **4**–**7** can only be surmised at the present time. We believe that oxidative addition of the silylalkyne to the electron-rich Co2 in **1** is probably one of the first reaction steps.[13] The σ-alkynyl group that is thus formed could attack the cyclopentadienylidene ligand at C2, from which a [1,3] hydride shift to the enylic position (C7) would be possible.

Experimental

1b: A solution of [Cp*Co(cyclopentadiene)] (580 mg, 2.33 mmol) [14] and $[CpCo(C_2H_4)_2]$ (440 mg, 2.44 mmol) [15] in petroleum ether (ca. 40 mL) was transferred to a 250 mL reaction flask, a slight vacuum was applied, and the solution was left to stand at room temperature. The flask was flushed daily with argon and slightly re-evacuated. After four days the deep-green reaction solution was decanted off from the crude product which was recrystallized from toluene at −20 °C. Yield 230 mg (25%) of dark-green **1b**. M.p. 152 °C; correct C,H analysis.

^{1}H NMR (200 MHz, [D$_8$]toluene) δ = 1.2 (m, 2H, C_2H_4), 1.40 (s, 15H, Cp*), 3.0 (m, 2H, C_2H_4), 3.49 (br.s, 2H, CH), 3.85 ("t", 2H, CH), 4.67 (s, 5H, Cp); ^{13}C{^{1}H} NMR (50 MHz, [D$_8$]toluene, assignment by J-modulation test) δ = 9.8 (C_5Me_5), 31.7 (C_2H_4), 79.4 (CH), 84.0 (Cp), 85.4 (CH), 90.7 (C_5Me_5); MS (EI, 70 eV) m/z 382 (10 [$M - C_2H_4$]$^+$), 260 (16, [Cp*Co(C_5H_6)]$^+$), 259 (100, [Cp*CoCp]$^+$), 258 (23, [Cp*Co(C_5H_4)]$^+$), 189 (18, [Cp_2Co]$^+$), 133 (8, [Cp*-2H]$^+$), 124 (18, [CpCo]$^+$), 59 (6, Co$^+$).

1c: Preparation from [(C_5Me_4Et)Co(cyclopentadiene)] [14] and $[CpCo(C_2H_4)_2]$ analogous to **1b** (yield 55%).

4a: A solution of **1a** (400 mg, 1.2 mmol) and **2a** (200 mg, 1.2 mmol) in toluene (20 mL) was heated in a slight vacuum for three hours at 45 °C. After the reaction solution was concentrated by evaporation to about 5 mL, the solution was chromatographed on silica gel (eluent toluene). After the solvent was removed from the violet eluate, 440 mg (78% yield) of solid **3a** was isolated. Correct C,H analysis; MS (EI, 70 eV) m/z 482 (32, M^+), 409 (8, [M − $SiMe_3$]$^+$), 285 (42, [M − $SiMe_3$ − CpCo]$^+$), 189 (42, [Cp_2Co]$^+$), 124 (12, [CpCo]$^+$), 73 (30, [$SiMe_3$]$^+$).

4b: is obtained in a similar manner to **4a**, from **1b** and **2a** (yield 69%).

4c: A solution of **1c** (650 mg, 1.5 mmol) and **2a** (280 mg, 1.6 mmol) in toluene (40 mL) was heated in a slight vacuum for five hours at 60 °C. After the reaction mixture was concentrated to 5 mL by evaporation, the solution was chromatographed twice on silica gel (eluent toluene). After the solvent was removed

from the violet eluate, 680 mg (80% yield) of pure **3c** was obtained and was recrystallized from cyclopentane at −78 °C; yield 590 mg (69%); m.p. 124–126 °C, correct C,H analysis; MS (EI, 70 eV) *m/z* 566 (46, M^+), 493 (14, $[M - SiMe_3]^+$), 442 (13, $[M - CoCp]^+$), 369 (100, $[M - CoCp - SiMe_3]^+$), 273 (19, $[(C_5Me_4Et)CoCp]^+$).

5a, **5a′** (mixture of isomers): obtained similarly to **4a**, from **1a** and **2b**; yield 68% (mixture of **5a**, **5a′** and a small amount of **4a**).

6a, **6a′** (mixture of isomers): obtained similarly to **4a**, from **1a** and **2c**: yield 82% (mixture of **6a**, **6a′** and a small amount of **4a**).

7a: obtained similarly to **4a** from **1a** and **3** (yield 83%).

Received: February 13, 1992 [Z 5187 IE]
German version: *Angew. Chem.* **1992**, *104*, 1050

CAS Registry numbers:
1a, 106250-11-7; **1b**, 141982-09-4; **1c**, 141982-10-7; **2a**, 14630-40-1; **2b**, 23183-97-3; **2c**, 107474-01-1; **3**, 14630-42-3; **4a**, 141982-11-8; **4b**, 141982-12-9; **4c**, 141982-18-5; **5a**, 141982-13-0; **5a′**, 141982-14-1; **6a**, 141982-15-2; **6a′**, 141982-16-3; **7a**, 141982-17-4; $C_5Me_5CoC_5H_6$, 141982-19-6; $C_5Me_4EtCoC_5H_6$, 141982-20-9; $C_5H_5Co(C_2H_4)_2$, 69393-67-5.

[1] J. P. Collman, L. S. Hegedus, J. R. Norton, R. G. Finke, *Principles and Applications of Organotransition Metal Chemistry*, University Science Books, Mill Valley, **1987**, chap. 16.
[2] P. Hofmann, M. Hämmerle, *Angew. Chem.* **1989**, *101*, 940–942; *Angew. Chem. Int. Ed. Engl.* **1989**, *28*, 908, and references cited therein.
[3] K. H. Dötz, *Angew. Chem.* **1975**, *87*, 672–673; *Angew. Chem. Int. Ed. Engl.* **1975**, *14*, 644; *ibid.* **1984**, *96*, 573–594 and **1984**, *23*, 587.
[4] R. R. Schrock, *Acc. Chem. Res.* **1979**, *12*, 98–104.
[5] H. Wadepohl, H. Pritzkow, *Angew. Chem.* **1987**, *99*, 132–134; *Angew. Chem. Int. Ed. Engl.* **1987**, *26*, 127.
[6] ^{1}H NMR (200 MHz, C_6D_6) **4a**: $\delta = 0.09$ (s, 9H, $SiMe_3$), 0.35 (s, 9H, $SiMe_3$), 4.26 (t, 1H, CH), 4.33 (s, 5H, Cp(Co1)), 4.62 (dd, 1H, CH), 4.78 (dd, 1H, CH), 4.85 (s, 5H, Cp(Co2)), 11.00 (s, 1H, CH); **4b**: $\delta = 0.11$ (s, 9H, $SiMe_3$), 0.38 (s, 9H, $SiMe_3$), 1.42 (s, 15H, Me), 3.91 (t, 1H, CH), 4.18 (d, 1H, CH), 4.36 (dd, 1H, CH), 4.93 (s, 5H, Cp), 10.95 (s, 1H, CH); **4c**: $\delta = 0.12$ (s, 9H, $SiMe_3$), 0.39 (s, 9H, $SiMe_3$), 0.72 (t, 3H, CH_2CH_3), 1.43 (d, 6H, CH_3), 1.47 (d, 6H, CH_3), 2.05 (q, 2H, CH_2CH_3), 3.93 (t, 1H, CH), 4.20 (d, 1H, CH), 4.40 (d, 1H, CH), 4.94 (s, 5H, Cp), 10.96 (s, 1H, CH); **5a**: $\delta = 0.08$ (s, 9H, $SiMe_3$), 0.44 (q, 6H, $Si(CH_2CH_3)_3$), 1.19 (t, 9H, $Si(CH_2CH_3)_3$), 4.27 (t, 1H, CH), 4.36 (s, 5H, Cp), 4.65 (d, 1H, CH), 4.77 (d, 1H, CH), 4.83 (s, 5H, Cp), 11.01 (s, 1H, CH); **5a′**: $\delta = 0.35$ (s, 9H, $SiMe_3$), 0.56 (q, 6H, $Si(CH_2CH_3)_3$), 1.05 (t, 9H, $Si(CH_2CH_3)_3$), 4.25 (t, 1H, CH), 4.34 (s, 5H, Cp), 4.63 (d, 1H, CH), 4.83 (d, 1H, CH), 4.86 (s, 5H, Cp), 11.06 (s, 1H, CH); **6a**: $\delta = 0.03$ (s, 9H, $SiMe_3$), 0.39 (s, 6H, $SiMe_2$), 1.11 (s, 9H, *t*Bu), 4.28 (t, 1H, CH), 4.37 (s, 5H, Cp), 4.58 (d, 1H, CH), 4.76 (d, 1H, CH), 4.80 (s, 5H, Cp), 11.11 (s, 1H, CH); **6a′**: $\delta = 0.12$ (s, 9H, $SiMe_3$), 0.31 (s, 6H, $SiMe_2$), 0.99 (s, 9H, *t*Bu), 4.27 (t, 1H, CH), 4.34 (s, 5H, Cp), 4.59 (d, 1H, CH), 4.78 (d, 1H, CH), 4.81 (s, 5H, Cp), 11.08 (s, 1H, CH); **7a**: $\delta = 0.11$ (s, 9H, $SiMe_3$), 1.34 (s, 9H, *t*Bu), 4.26 (t, 1H, CH), 4.36 (s, 5H, Cp), 4.49 (d, 1H, CH), 4.78 (d, 1H, CH), 4.86 (s, 5H, Cp), 9.94 (s, 1H, CH); ^{13}C{^{1}H} NMR (50 MHz, C_6D_6) **4a**: $\delta = 0.23$ ($SiMe_3$), 6.99 ($SiMe_3$), 81.63 (Cp), 87.15 (Cp), 68.32 (CH), 77.13 (CH), 83.56 (CH), 79.29 (C7), 141.93 (C), 222.25 (C); **4c**: $\delta = 1.85$ ($SiMe_3$), 7.05 ($SiMe_3$), 9.70 (CH_3), 9.83 (CH_3), 14.41 (CH_3), 18.96 (CH_2), 71.65 (CH), 79.95 (CH), 86.14 (Cp), 86.73 (CH), 90.02 (CH), 90.49 (C), 91.51 (C), 96.13 (C), 138.68 (C), 162.10 (C), 219.94 (C); **7a**: $\delta = 7.03$ ($SiMe_3$), 31.15 (CCH_3), 36.05 (CCH_3), 68.81 (CH), 76.83 (CH), 79.15 (C7), 81.48 (Cp), 83.05 (CH), 87.13 (Cp), 146.47 (C), 219.15 (C); ^{29}Si{^{1}H} NMR (40 MHz, C_6D_6, INEPT) **4a**: $\delta = -15.00$, 30.2 (br); **5a**: $\delta = -7.1$, 30.6 (br); **5a′**: $\delta = -15.1$, 38.5 (br); **7a**: $\delta = 29.5$ (br).
[7] This can presumably be attributed to relaxation effects due to coupling with the ^{59}Co nucleus.
[8] K. Jonas, *J. Organomet. Chem.* **1990**, *400*, 165–184.
[9] a) T. J. Katz, M. Rosenberger, *J. Am. Chem. Soc.* **1963**, *85*, 2030–2031; b) T. J. Katz, J. J. Mrowca, *J. Am. Chem. Soc.* **1967**, *89*, 1105–1111.
[10] Monoclinic, space group $P2_1/a$, $a = 14.336(10)$, $b = 15.493(8)$, $c = 14.658(10)$ Å, $\beta = 113.64(5)°$, $V = 2982$ Å^3, $Z = 4$, Stoe–Siemens four-circle diffractometer ($Mo_{K\alpha}$ radiation, graphite monochromator, ω-scan, $3° < 2\theta < 50°$, empirical absorption correction), 2875 independent reflections with $(I > 2\sigma(I))$, all non-hydrogen atoms anisotropic, all H-atoms of the cobaltapentalene localized in difference Fourier syntheses and refined isotropically $R = 0.054$; $R_w = 0.054$, $w^{-1} = (\sigma^2(F) + 0.0003\,F^2)$ (SHELX-76 [G. M. Sheldrick, University of Cambridge 1976]). Further details of the crystal structure investigation may be obtained from the Fachinformationszentrum Karlsruhe, Gesellschaft for wissenschaftlich-technische Information mbH, D-W-7514 Eggenstein-Leopoldshafen 2 (FRG) on quoting the depository number CSD-56207, the names of the authors, and the journal citation.
[11] H. Wadepohl, W. Galm, H. Pritzkow, A. Wolf, unpublished.
[12] H. Yamazaki, Y. Wakatsuki, *J. Organomet. Chem.* **1984**, *272*, 251–263.
[13] The substitution of the ethylene ligand in **1** can take place dissociatively or associatively. An η^2-alkyne complex would be a possible, but not a necessary intermediate stage. With $Me_3SnC_2SnMe_3$ as ligand there is evidence for such a complex. However, with this alkyne **1** does not react to form a complex of the type **4** (A. Wolf, Diplomarbeit, Universität Heidelberg, **1991**).
[14] W. Galm, Dissertation, Universität Heidelberg, **1990**.
[15] K. Jonas, C. Krüger, *Angew. Chem.* **1980**, *92*, 513–531; *Angew. Chem. Int. Ed. Engl.* **1980**, *19*, 520; K. Jonas, E. Deffense, D. Habermann, *ibid.* **1983**, *95*, 729 and **1983**, *22*, 716; *Angew. Chem. Suppl.* **1983**, 1005–1016.

Synthesis of (2-Arylindol-3-yl)acetamides as Probes of Mitochondrial Steroidogenesis—A New Mechanism for $GABA_A$ Receptor Modulation**

By *Alan P. Kozikowski,* Dawei Ma, Elena Romeo, James Auta, Vissilios Papadopoulos, Gulia Puia, Erminio Costa*, and *Alessandro Guidotti*

Binding studies,[1] molecular biological studies,[2] and steroid biosynthesis studies[3] have revealed the presence in the central nervous system (CNS) of a structurally and functionally distinct class of benzodiazepine binding sites located on the outer mitochondrial surface. These receptors bind benzodiazepines and non-benzodiazepine derivatives such as imidazopyridines (Alpidem) and other ligands including the endogenous peptide DBI. This peptide is present in the peripheral and CNS cells that contain this mitochondrial receptor[4]; it binds with high affinity (10^{-8} M) and stimulates mitochondrial steroidogenesis in vitro.[5] In order to adhere to the classical nomenclature that names a receptor from the endogenous ligand, we have termed this receptor the mitochondrial DBI receptor (MDR).[5] This MDR is thus to be distinguished from the neuronal benzodiazepine binding sites located predominantly on the extracellular domain of the type A receptor for γ-aminobutyric acid ($GABA_A$ receptor), sites which when occupied serve to modulate the GABA-dependent conformational transitions in the associated chloride ion channel.[6]

Neurosteroid precursors are synthesized in mitochondria under the regulation of the mitochondrial benzodiazepine receptors. The glial cells probably constitute the most important steroidogenic cells in the brain, and evidence indicates that they produce pregnenolone and perhaps[7] dehydroepiandrosterone sulfate, 3α-hydroxy-5α-pregnan-20-one (3α-OH-DHP), and 3α,21-dihydroxy-5α-pregnan-20-one (THDOC).[4] These steroids bind with high affinity to sites probably located on the transmembrane domain of the heterooligomeric integral membrane protein functioning as the $GABA_A$ receptor, thereby modulating the responsiveness of the $GABA_A$ receptor. These MDR receptors would therefore appear to offer an intriguing new, but indirect, pharmacological approach to modulation of the $GABA_A$ receptor complex (Fig. 1).

At present, the isoquinolinecarboxamide PK11195 is the only compound known to possess high affinity for the MDR without binding to other known neurotransmitter recep-

[*] Prof. A. P. Kozikowski, Dr. D. Ma
Neurochemistry Research, Mayo Clinic Jacksonville
4500 San Pablo Road, Jacksonville, FL 32224 (USA)
E. Romeo, M. D., Dr. J. Auta, Dr. V. Papadopoulos, Dr. G. Puia, E. Costa, M. D., A. Guidotti, M. D.
Fidia-Georgetown Institute for the Neurosciences
[**] This work was supported by the Fidia Research Foundation.

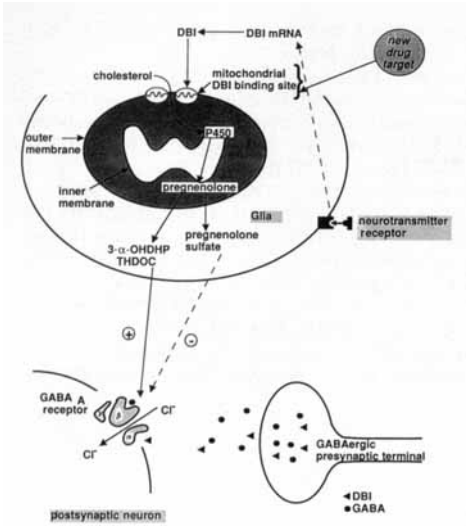

Fig. 1. Modulation of GABAergic function by neurosteroids.

tors.[8] This compound, however, fails to cause marked behavorial effects in rats,[9] probably because either it acts as a partial agonist of the MDR, or it has some other action in the biosynthesis or release of neurosteroids. In an effort to discover agonists that exhibit high affinity and selectivity for these mitochondrial receptors, thereby permitting the determination of their role and therefore the role of steroidogenesis in CNS function, we have synthesized a novel class of (3-indolyl)acetamides possessing these desired properties.

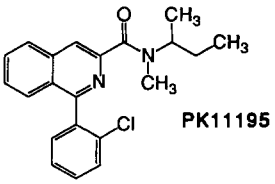

Of the many diverse (2-arylindol-3-yl)acetamides we prepared molecule **1a**, possessing a 2-*para*-fluorophenyl substituent and two *n*-hexyl substituents on the amide nitrogen atom, proved to be one of the most potent and efficacious. This compound was readily prepared by a five-step protocol (Scheme 1). The starting keto acid was obtained from the CN^--catalyzed addition of *p*-fluorobenzaldehyde to acrylonitrile,[10] followed by hydrolysis of the nitrile group. Next, the acid was transformed into the amide via its mixed anhydride (Scheme 1a), and the oxoamide was treated with phenylhydrazine to furnish the corresponding hydrazone. A Fischer indole synthesis promoted by zinc chloride[11] then gave crystalline **1a** in an overall yield of 70% (Scheme 1b). Compound **1a** has a K_i value of 4.4 ± 0.15 nM for the MDR as measured by the displacement of [^{3}H]4′-chlorodiazepam from rat cerebellar glial cell membranes, and a K_i value of 5.0 ± 1.6 nM as measured by the displacement of [^{3}H]PK11195. Compound **1b**, an analogue of **1a** with a chloride substituent on the indole unit, has a K_i value of 2.3 ± 0.9 nM for the MDR, whereas analogue **1c** lacking halogens has a K_i value of 9.7 ± 0.6 nM. In order to gain further insights as to the structural characteristics of these molecules relevant to their high affinities for the MDR, we also synthesized inter alia two conformationally rigid analogues of **1c**. In these molecules the amide group is linked either to the *ortho* position of the phenyl substituent (**2**) or to the 4 position of the indole ring (**3**) (Scheme 2). Syntheses of

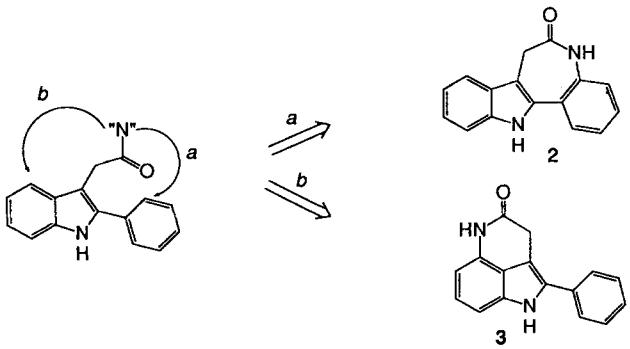

Scheme 2. Two possibilities for fixing the conformation of (2-phenylindol-3-yl)acetamides.

2 and **3** are presented in Scheme 3. Compound **2** was prepared by Fischer indole synthesis of the γ-oxolactam **4**, which is readily obtained from naphthoquinone by reaction with sodium azide in sulfuric acid followed by catalytic hydrogenation in analogy to ref. [12]. Analogue **3** was available from indole **5**, which was prepared according to the Bergman

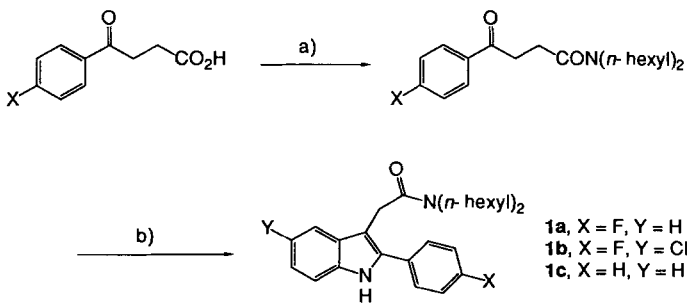

Scheme 1. Synthesis of the MDR-selective (2-arylindol-3-yl)acetamides by the Fischer indole reaction. a) EtOCOCl, Et_3N, THF, −40 °C → −20 °C, 30 min, addition of HN(*n*-hexyl)$_2$, → room temperature (RT). b) 1. *p*-$YC_6H_4NHNH_2$, 100 °C, 30 min; 2. $ZnCl_2$, 170 °C, 5 min (65–85% overall).

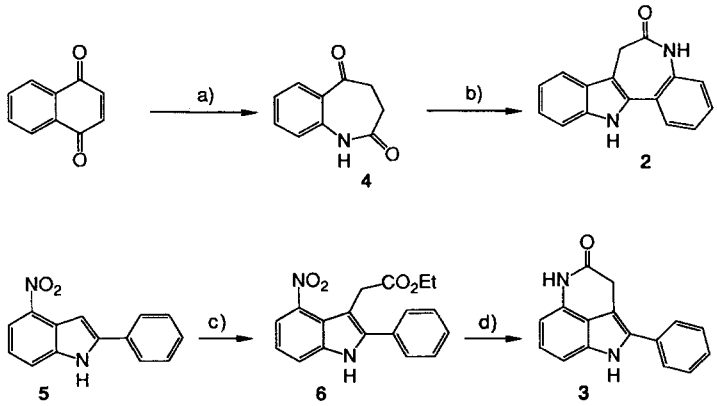

Scheme 3. Synthesis of conformationally rigid analogues of the MDR-selective (2-phenylindol-3-yl)acetamide **1c**. a) 1. NaN_3, H_2SO_4, 0 °C → 10 °C, 3 d; 2. Pd/C, 1 atm H_2, $CHCl_3$ (9% overall). b) 1. $PhNHNH_2$, benzene, reflux, 30 min; 2. $ZnCl_2$, 170 °C, 5 min (85%). c) 1. $H_2C{=}NMe_2^+Cl^-$, CH_2Cl_2; 2. Me_2SO_4, NaCN, MeOH, RT, 18 h (57% overall); 3. HCl, EtOH, H_2O, reflux, 18 h (87%). d) 1. 1 atm H_2, Pd/C, EtOH (96%); 2. toluene, reflux, 72 h (69%).

protocol.[13] **5** was converted to its gramine derivative and then to the 3-indolylacetonitrile by reaction with dimethyl sulfate and sodium cyanide. The nitrile was converted in turn to ethyl ester **6** and the nitro group reduced to an amine group by hydrogenation over Pd/C. Heating the aminoindole derivative in toluene at reflux then furnished the required lactam **3**. In our experiments neither **2** nor **3** was capable of displacing the binding of [^{3}H]4′-chlorodiazepam, thus suggesting the importance of other conformations of the amide unit to MDR affinity.[14]

Further details of the biological properties of the new ligands **1** will be reported separately. We wish to note here, however, that **1a** failed to bind to a wide variety of other receptor systems[15] thus establishing its selectivity, and moreover, electrophysiological experiments failed to show any direct action on GABA-gated chloride ion currents in cortical neurons.[16] Furthermore, **1a** was found to produce an increase in pregnenolone formation in glial cells[3] with an EC_{50} of about 3 nM. In behavioral experiments with rats, compound **1a** was found to increase the number of entries and the time spent in the open arms of the elevated plus maze[17] in a dose-dependent fashion (0.57 to 1.1 $\mu mol\,kg^{-1}$), allowing the conclusion that such compounds can reduce fear of novelty (neophobia) without causing sedation.

In summary, the novel, structurally simple, and readily modifiable 3-indolylacetamides[18] reported herein may herald a new direction in the development of modulators of GABAergic receptor function by binding to MDR with stimulation of neurosteroid production. These compounds are of added interest in view of a recent report that pregnenolone and steroids metabolically derived from it possess memory-enhancing effects.[19]

Received: March 17, 1992 [Z 5243 IE]
German version: *Angew. Chem.* **1992**, *104*, 1092

[1] C. Braestrup, R. F. Squires, *Proc. Natl. Acad. Sci. USA* **1977**, *74*, 3805.
[2] R. Sprengel, P. Werner, P. H. Seeburg, A. G. Mukhin, M. R. Santi, D. R. Grayson, A. Guidotti, K. E. Krueger, *J. Biol. Chem.* **1989**, *264*, 20415.
[3] K. E. Krueger, V. Papadopoulos, *J. Biol. Chem.* **1990**, *265*, 15015.
[4] E. Costa, A. Guidotti, *Life Sci.* **1991**, *49*, 325.
[5] P. Guarneri, V. Papadopoulos, B. Pan, E. Costa, *Proc. Natl. Acad. Sci. USA* **1992**, *89*, 5118.
[6] a) E. Costa, *Neuropsychopharmacology* **1991**, *4*, 225; b) R. W. Olsen, A. J. Tobin, *FASEB J.* **1990**, *4*, 1469.
[7] V. Papadopoulos, P. Guarneri, K. Krueger, A. Guidotti, E. Costa, *Proc. Natl. Acad. Sci. USA* **1992**, *89*, 5113.
[8] a) G. Le Fur, N. Vaucher, M. L. Perrier, A. Flamier, J. Benavides, C. Renault, M. C. Dubroeucq, C. Guérémy, A. Uzan, *Life Sci.* **1983**, *33*, 449. b) The imidazopyridine Alpidem shows high affinity for MDR but also binds to $GABA_A$ receptors (K_d = 50 nM); S. Z. Langer, S. Arbilla, S. Tan, K. G. Lloyd, P. George, J. Allen, A. E. Wick, *Pharmacopsychiatry* **1990**, *23*, 103.
[9] a) J. J. Benavides, F. Guilloux, D. E. Allam, A. Uzan, J. Mizoule, C. Renault, M. C. Dubroeucq, C. Guérémy, G. Le Fur, *Life Sci.* **1984**, *34*, 2613; b) S. Pellow, S. E. File, *ibid.* **1984**, *35*, 229.
[10] H. Stetter, *Angew. Chem.* **1976**, *88*, 695; *Angew. Chem. Int. Ed. Engl.* **1976**, *15*, 639.
[11] R. L. Shriner, W. C. Ashley, E. Welch, *Org. Syn. Coll. Vol.* **1955**, *3*, 725.
[12] S. Rossi, M. Micheli, M. Giannotti, A. Salvatori, *Gazz. Chim. Ital.* **1981**, *111*, 365.
[13] J. Bergman, P. Sand, *Tetrahedron* **1990**, *46*, 6085.
[14] Very likely, the conformation of the phenyl substituent as well as the nature of the *N*-alkyl groups also contribute to MDR affinity. Molecular modeling methods are currently being used to develop a receptor map for the MDR.
[15] Compound **1a** failed to displace [^{3}H]baclofen from $GABA_B$ receptors, [^{3}H]spiperone from dopamine and 5-HT_1 receptors, [^{3}H]ketanserin from 5-HT_2 serotonin receptors, [^{3}H]glycine, [^{3}H]MK-801, and [^{3}H]AMPA from glutamate receptors, [^{3}H]naloxone and [^{3}H]3-PPP from opiate and sigma receptors, [^{3}H]L-365,260 from choleocystokinin receptors, and [^{125}I]pindolol from β-adrenergic receptors.
[16] G. Puia, M. R. Santi, S. Vicini, D. B. Pritchett, R. H. Perdy, S. M. Paul, P. H. Seeburg, E. Costa, *Neuron* **1990**, *4*, 759.
[17] S. E. File, S. Pellow, *Br. J. Pharmacol.* **1985**, *86*, 729.
[18] All compounds were characterized by ^{1}H NMR, ^{13}C NMR, and IR spectroscopy as well as elemental analysis or high-resolution mass spectrometry. For example, **1a**: M.p. 97–98 °C; ^{1}H NMR ($CDCl_3$, 300 MHz): δ = 8.14 (s, 1H; NH), 7.65 (d, J = 7.7 Hz, 1H), 7.54 (m, 2H), 7.32 (d, J = 7.6 Hz, 1H), 7.08–7.20 (m, 4H), 3.84 (s, 2H; CH_2CO), 3.29 (t, 2H; NCH_2), 3.17 (t, 2H; NCH_2), 1.37–1.45 (m, 4H), 1.09–1.22 (m, 10H), 1.03 (m, 2H), 0.85 (t, 6H); ^{13}C NMR ($CDCl_3$, 75.46 MHz): δ = 170.6, 162.6 (d, J = 246.6 Hz; CF), 136.0, 134.6, 130.1 (d, J = 7.9 Hz), 129.1, 129.0, 122.6, 120.1, 119.6, 116.1 (d, J = 21.6 Hz), 110.8, 107.3, 48.3, 46.3, 31.7, 31.6, 30.9, 29.1, 27.8, 26.8, 26.5, 22.7, 22.6, 14.1, 14.0; IR (KBr): $\tilde{\nu}$[cm^{-1}] = 3198, 2953, 1620 (C = O), 1501, 1458, 1224; MS (15 eV): m/z 436 (M^+), 407, 294, 251, 224, 196, 147, 128, 85; correct C,H,N analysis.
[19] J. F. Flood, J. E. Morley, E. Roberts, *Proc. Natl. Acad. Sci. USA* **1992**, *89*, 1567.

Dependence of the Reactivity of Ag and Ni Clusters Deposited on Solid Substrates on the Cluster Size

By *C. N. Ramachandra Rao*,* *Venugopal Vijayakrishnan*, *Asok Kumar Santra*, and *Menno W. J. Prins*

The structure and properties of metal clusters are currently subjects of intense research.[1] Many fundamental aspects of metal clusters need to be understood, such as the dependence of the metallicity of the clusters on the size. Another important question, the variation of the reactivity of the metal clusters with size, has been examined in studies on alkali metal clusters in the gas phase.[2] We are interested in investigating how the reactivity of transition metal clusters deposited on solid substrates varies with cluster size, since such a study is relevant to heterogeneous catalysis. For this purpose we have examined the interaction of O_2 with Ag clusters deposited on graphite as well as the interaction of H_2S and CO with Ni clusters deposited on graphite or Al_2O_3 by employing X-ray and UV photoelectron spectroscopy (XPS and UPS). We have also employed Bremsstrahlung isochromat spectroscopy (BIS) and Auger electron spectroscopy for the characterization of the clusters. This study has revealed that the cluster size strongly determines the reactivity of Ag clusters towards O_2 and of the Ni clusters towards H_2S and CO, that is, the cluster size indeed plays an important role in heterogeneous reactions.

Ag and Ni were deposited on the solid substrate in situ at room temperature under ultrahigh vacuum (UHV) conditions in the preparation chamber (base pressure ca. 10^{-10} Torr) of the electron spectrometer (VG-ESCA3 Mk II). The metals were vaporized by means of resistive heating of high purity samples wound around a tungsten filament as described elsewhere.[3] Polycrystalline graphite was annealed at 600 K and sputtered with 6 kV Ar ions to produce an amorphous surface and remove the surface contaminants. The Al_2O_3 substrate was prepared in situ by surface oxidation of a pure Al foil in the preparation chamber. The final oxide film was approximately 20 Å thick. Charging effects of the Al_2O_3 film were marginal and were corrected for. We quantified the sizes of the clusters by comparing the intensity of the signal for the transitions of the metal core level I_M (Ag,

[*] Prof. Dr. C. N. R. Rao, V. Vijayakrishnan, A. K. Santra, M. W. J. Prins [+]
Solid State and Structural Chemistry Unit
and CSIR Centre of Excellence in Chemistry
Indian Institute of Science, Bangalore, 560 012 (India)
[+] Permanent address: University of Nijmegen (The Netherlands)

$3d_{5/2}$; Ni $2p_{3/2}$) to the intensity of the signal for transitions of the core level of the support I_S (S 1s for graphite and O 1s for Al_2O_3). The surface coverage θ, estimated by the method of Carley and Roberts,[4] was 4.8×10^{13} and 6.3×10^{13} atoms per cm^2, respectively, for the smallest of clusters of Ag and Ni studied. These values correspond to a mean cluster radius of 5–9 Å as estimated by the method of Wertheim and Di-Cenzo.[5] The clusters were exposed to purified O_2, CO, or H_2S in the preparation chamber (1 Langmuir = 10^{-6} Torr s).

We examined the variation of the shift in the Ag $3d_{5/2}$ binding energy ΔE (relative to 368.2 eV, the value for bulk silver) with the cluster size (or I_{Ag}/I_C) before studying the interaction of O_2 with the clusters. The results (Fig. 1 top) show that ΔE increases markedly with the decrease in the cluster size, especially when $I_{Ag}/I_C < 3$. The value of ΔE for the smallest Ag cluster is approximately 0.6 eV; the kinetic energy of the Auger electrons [Ag ($M_4N_{45}N_{45}$) line] at this cluster size also shifts by −1.2 eV relative to the value of silver metal. The marked change in ΔE occurring around $I_{Ag}/I_C \approx 3.0$ indicates a stage at which metallic screening

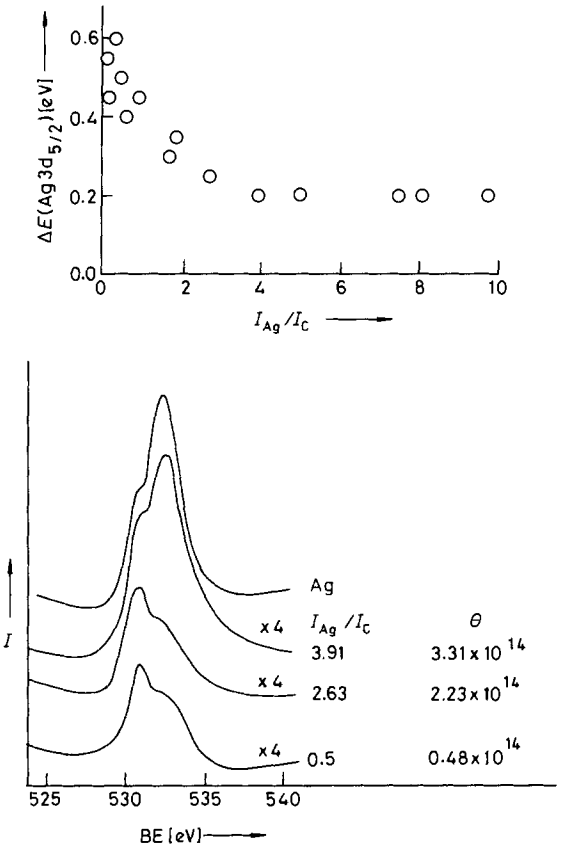

Fig. 1. Top: Variation in the shift of $3d_{5/2}$ binding energy of Ag clusters deposited on graphite relative to the bulk metal with I_{Ag}/I_C. Bottom: Change in the O 1s spectra of Ag clusters exposed to 500 L O_2 at 80 K. I = relative intensity, θ = surface coverage, number of atoms per cm^2.

becomes negligible. The variation of ΔE in Figure 1 is therefore a manifestation of the metal–insulator transition that occurs with decreasing cluster size. We have obtained further confirmation of such a transition by BIS measurements which show the emergence of new states close to the Fermi energy E_F with increase in cluster size.

In Figure 1 bottom, typical O 1s spectra of Ag clusters exposed to 500 L O_2 at 80 K are shown. We see that the intensity of the O 1s signal at 530.5 eV attributed to dissociated atomic oxygen (O) decreases with increase in cluster size relative to the signal due to molecular oxygen (O_2) (532.5 eV). We verified that the 532.5 eV feature was not due to OH species. On bulk Ag, the adsorbed oxygen species at 80 K is known to be predominently O_2.[6, 7] It appears that small clusters favor dissociation of O_2. The proportion $O:O_2$ on large clusters ($I_{Ag}/I_C > 3$) is close to that on bulk Ag. Furthermore, the temperature dependence of the intensity ratio of the O 1s signals $I(530)/I(532)$, that is, the ratio $O:O_2$, is dependent on cluster size. $I(530)/I(532)$ is temperature independent between 80 and 300 K for small values of I_{Ag}/I_C but shows a marked dependence for the bulk silver metal as well as for large clusters. This interaction of O_2 with Ag dependent on cluster size is remarkable.

The interaction of H_2S with Ni clusters deposited on graphite shows a definite size dependence. H_2S adsorbed on Ni clusters or bulk Ni at 80 K (500 L) gives rise to two signals at 164.5 eV and 162.0 eV due to H_2S and S^{2-}, respectively. When the temperature is increased to 150 K, the major sulfur species is S^{2-} in all the cases, but the ratio of H_2S to S^{2-} shows a temperature dependence which varies with cluster size. In Figure 2 we have plotted the intensity ratio of the signals for the core-level transitions $I_{S^{2-}}(T)/I_{S^{2-}}(300)$ versus temperature for different cluster size.

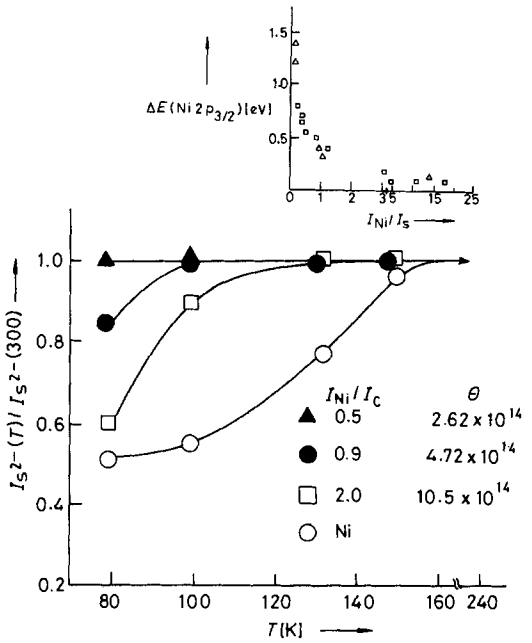

Fig. 2. Variation of the normalized intensities of the signals for the core-level transitions of S^{2-} with temperature for different sizes of Ni clusters deposited on graphite (for θ see Fig. 1). The inset shows the variation in the shift of the $2p_{3/2}$ binding energy of Ni clusters relative to the bulk metal with I_{Ni}/I_S. □ = Nickel on graphite; △ = nickel on Al_2O_3.

The inset shows the variation of the shift in the Ni $2p_{3/2}$ binding energy relative to the value for bulk nickel (852.9 eV). This demonstrates how metallic screening decreases with the decrease in cluster size, especially when $I_{Ni}/I_C \leq 1$. For the smallest clusters we examined, the kinetic energy of the Auger electrons [Ni ($L_3M_{45}M_{45}$) line] decreases by −1.4 and −2.8 eV (relative to the bulk metal) on graphite and Al_2O_3,

respectively. From Figure 2 we see that when the clusters are small ($I_{Ni}/I_C < 1$), the proportion of S^{2-} is essentially independent of temperature, but the temperature dependence becomes more marked with the increase in the cluster size. This observation suggests that on small Ni clusters, H_2S dissociates to the maximum extent possible even at the lowest temperature, whereas in the case of larger clusters, the extent of dissociation is dependent on temperature.

We have studied the interaction of carbon monoxide on Ni clusters deposited onto an Al_2O_3 substrate by means of He II UPS. Figure 3 shows the difference spectra of CO absorbed on Ni clusters of different sizes.

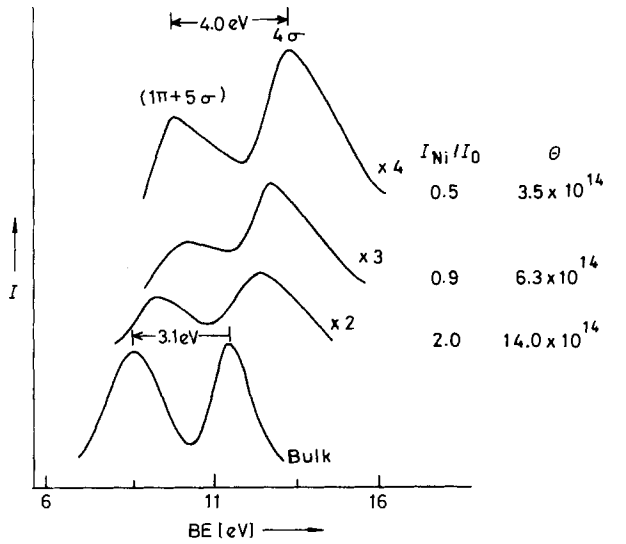

Fig. 3. He II difference spectra of CO adsorbed (at 50 L) on Ni clusters (Al_2O_3 substrate) for various cluster sizes. The asymmetry of the bands arises because of the low intensity of the signal and the background signal due to the Al_2O_3 support.

A shift in the Co valence band closer to the E_F is evident with increasing cluster size. This shift is due to the increasing relaxation of the highest excited states of the CO molecule which depends on the density of Ni clusters and therefore on their size. More importantly, the size of the separation between the $(1\pi + 5\sigma)$ and the 4σ bands of the adsorbed CO varies with the cluster size. On bulk nickel this is around 3 eV. The separation increases with the decrease in the cluster size reaching a value of ≈ 4.0 eV for the smallest cluster size we studied ($I_{Ni}/I_O \approx 0.5$). We consider this to be due to the weakening of the C–O bond as a result of the increasing interaction between CO and Ni with decreasing cluster size.[8]

The present investigation shows that small clusters of Ag and Ni are more reactive than the bulk metal, a conclusion that finds support from an earlier study on the chemisorption of Cl_2 on Cu, Ag, and Pt clusters[9, 10] and of CO on Pt clusters.[11] What is noteworthy in the present study is that the dependence of reactivity on cluster size becomes marked at a stage where metallic screening becomes weak, signifying the onset of a metal–insulator transition. The cluster regime where the reactivity is enhanced seems to correspond to one where the clusters are not really metallic. This observation is of relevance to heterogeneous catalysis in which the metals dispersed on oxide supports generally consist of clusters of 100–200 atoms.

Received: January 20, 1992 [Z 5135 E]
German version: *Angew. Chem.* **1992**, *104*, 1110

[1] T. P. Martin, T. Bergmann, T. Lange, *J. Phys. Chem.* **1991**, *95*, 6421.
[2] M. A. El-Sayed, *J. Phys. Chem.* **1991**, *95*, 3898.
[3] V. Vijayakrishnan, C. N. R. Rao, *Surf. Sci Lett.* **1991**, *255*, L516.
[4] A. F. Carley, M. W. Roberts, *Proc. R. Soc. London Ser. A*, **1978**, *363*, 403.
[5] G. K. Wertheim, S. B. DiCenzo, *Phys. Rev. B.* **1988**, *37*, 374.
[6] M. K. Rajumon, K. Prabhakaran, C. N. R. Rao, *Surf. Sci. Lett.* **1990**, *233*, L237.
[7] C. N. R. Rao, K. Prabhakaran, M. K. Rajumon, *Rev. Solid. State Sci.*, **1990**, *4*, 843.
[8] C. N. R. Rao, G. Ranga Rao, *Chem. Phys. Lett.*, **1988**, *146*, 557.
[9] R. C. Baetzold, *J. Am. Chem. Soc.* **1981**, *103*, 6116.
[10] R. C. Baetzold, *Inorg. Chem.* **1982**, *21*, 2189.
[11] M. Grunze, *Chem. Phys. Lett.* **1978**, *58*, 409.

A Simple Method for the Replacement of the OH Group in Free Carboxylic Acids by the Phosphonium Ylide Group**

By *Hans Jürgen Bestmann,** *Roman Dostalek,* and *Bernd Bauroth*

Bis(trimethylsilyl)methylenetriphenylphosphorane **3**[1] can be prepared readily and in larger amounts[2] from the reaction of the monosilylated ylide **1**[1, 2] with trimethylbromo- or -iodosilane **2** to the corresponding salt of **3** followed by deprotonation, best conducted with sodium(bistrimethylsilyl)amide.[3] The oxidation of **3** with the adduct of ozone and triphenylphosphite, **4**, leads to bistrimethylsilylketone **5**.[4]

We have now treated **3** with the free carboxylic acids **6** and observed that acyl ylides **9** are formed besides hexamethyl-

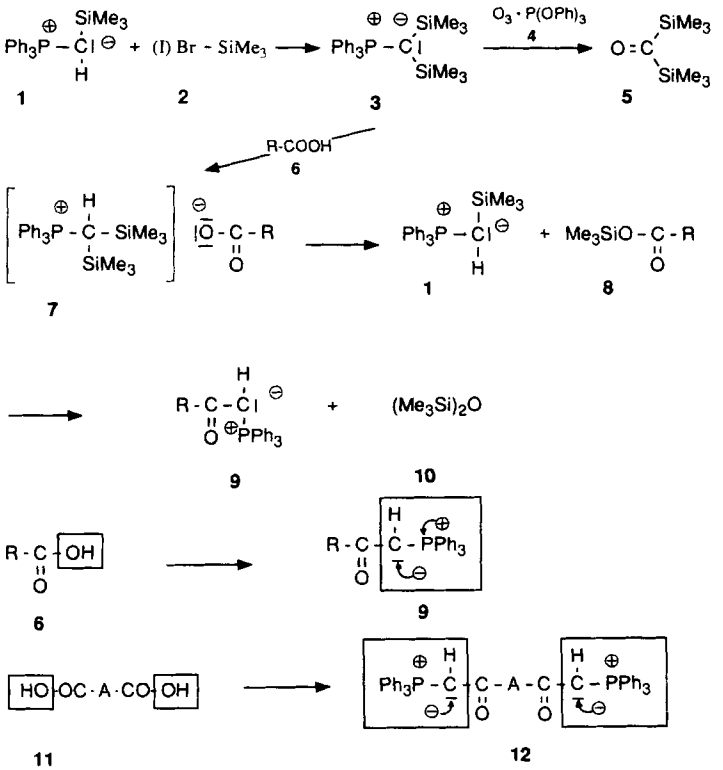

[*] Prof. Dr. H. J. Bestmann, Dr. R. Dostalek, Dipl.-Chem. B. Bauroth
Institut für Organische Chemie der Universität Erlangen-Nürnberg
Henkestrasse 42, D-W-8520 Erlangen (FRG)

[**] This research was supported by the Volkswagen Stiftung.

disiloxane (**10**). We assume that the phosphonium salts **7** arise primarily from **3** and **6**. The carboxylate anion desilylates the phosphonium ion leading to **1** and the trimethylsilyl ester **8**, which react to give **9** and **10**.[2]

The reaction thus allows the replacement of the OH group of the free carboxylic acid by the ylide function in a one-pot procedure without the initial preparation of an acid chloride, a thiol ester,[5] or an acylimidazole.[6] Dicarboxylic acids **11** are converted to bisacyl ylides **12**. Free amino acids may also be employed in the reaction as shown in Table 1. This method allows access to α-aminoacyl ylides such as **9k** and **9l** for the first time. Reactions with *O*-protected tartaric acids and monomethyl ester tartrate derivatives lead to undefined elimination products.

Table 1. Monoacyl ylides **9** [a] and bisacyl ylides **12** [a] prepared from monocarboxylic acids **6** and dicarboxylic acid **11**, respectively.

	R (**6**/**9**) or A (**11**/**12**)	Yield (**9**/**12**) [%]	M.p. **9**/**12** [°C]
a	C_2H_5	85	221
b	n-C_5H_9	76	178–185 (*Z*)
c	n-C_7H_{13}	81	155
d	c-C_6H_{11}	65	157
e	*t*Bu	68	175–177
f	C_6H_5	62	176
g	1,4-$(CH_3O)_2C_6H_3$	65	142–144
h	3,4,5-$(CH_3O)_3C_6H_2$	74	158
i	1,4-$(NO_2)_2C_6H_3$	55	153–155
j	o-IC_6H_4	75	133–136
k	H_2N-CH_2	79	140–143
l	$CH_3-CH-NH_2$	66	170–173 (*Z*) [b]
m	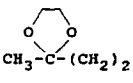	78	118–119
n	[c]	62	241 (*Z*)
o	$(CH_2)_2$	71	232
p	$(CH_2)_4$	52	205
q		78	178–218 (*Z*)
r [7]		61	198–200 (*Z*)
s	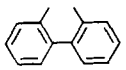	75	217–221 (*Z*)

[a] All new compounds **9** and **12** provided correct elemental analyses and clean spectra. Our data for known compounds are identical to those in the literature. [b] $[\alpha]_D = +18.4$ ($c = 1.6$ in CH_2Cl_2). [c] Treated with oxalic acid.

Compound **9l** (prepared from alanine and **3**) is attacked by Boc anhydride **13** (Boc = *tert*-butoxycarbonyl) at the amino group (98% yield); the subsequent reaction with benzaldehyde **14** provides the *N*-Boc-protected merucathinone **15** in 88% yield. The preparation of the free base (isolated as the oxalate) from **15** is known.[8] It is a component of Catha edulis Forsk., a wide-spread drug in Yemen and eastern

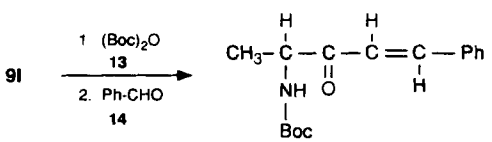

15

Africa.[9] The measurements of the optical rotation of **15** provided an *ee* of 78.5% (in comparison to the literature value[8]: *ee* ≧ 98%). A determination of the enantiomeric excess of **9k** by means of ^1H NMR spectroscopy with shift reagents did not succeed. Thus we could not prove if the partial racemization occurred in the reaction of alanine with **3** or in the Wittig reaction.

To test the synthetic potential of the bisacyl ylides **12**, compound **12q**, prepared from (*Z*)-1,2-cyclopropane dicarboxylic acid, was oxidized with singlet oxygen.[10] The resulting spirobicyclic cyclopentenedione derivative **16**, produced in 40% unoptimized yield, was treated with dimethylbutadiene **17**. The formation of the product **18** demonstrated the dienophilic character of **16**. A potential application of **16** is in the synthesis of prostaglandins with a spirocyclic cyclopentane ring.

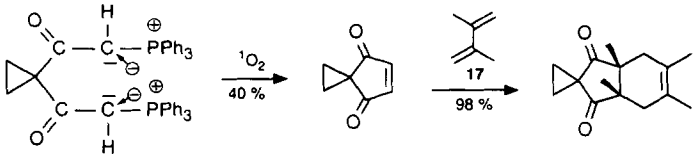

12q **16** **18**

Experimental Procedure

9, **12**: 30 mmol of bis(trimethylsilyl)methylenetriphenylphosphorane **3** was dissolved in 120 mL of THF. 30 mmol of the appropriate monocarboxylic acid **6** or 15 mmol of the dicarboxylic acid **11** were added to the solution at room temperature. The reaction mixture was stirred for 30 min at room temperature and then heated at reflux for ca. 3–4 d. After the reaction was complete, the solvent was removed under aspirator pressure. The residue was recrystallized from ethyl acetate or toluene (diethyl ether was added if necessary). Addition of diethyl ether to the mother liquor allowed the isolation of a second fraction, which in the most cases is only slightly impure.

Received: February 5, 1992 [Z 5169 IE]
German version: *Angew. Chem.* **1992**, *104*, 1062

CAS Registry numbers:
1, 3739-97-7; **2** (Br), 2857-97-8; **2** (I), 16029-98-4; **3**, 36050-78-9; **4**, 29855-83-8; **5**, 42606-61-1; **6a**, 79-09-4; **6b**, 109-52-4; **6c**, 111-14-8; **6d**, 98-89-5; **6e**, 75-98-9; **6f**, 65-85-0; **6g**, 2785-98-0; **6h**, 118-41-2; **6i**, 610-28-6; **6j**, 88-67-5; **6k**, 56-40-6; **6l**, 56-41-7; **6m**, 4388-57-2; **7a**, 141980-83-8; **7b**, 141957-57-5; **7c**, 141957-58-6; **7d**, 141957-59-7; **7e**, 141957-60-0; **7f**, 141957-61-1; **7g**, 141957-62-2; **7h**, 141957-63-3; **7i**, 141957-64-4; **7j**, 141957-65-5; **7k**, 141957-66-6; **7l**, 141957-67-7; **7m**, 141957-69-9; **7n**, 141957-70-2; **7o**, 141957-71-3; **7p**, 141957-72-4; **7q**, 141957-73-5; **7r**, 141957-75-7; **7s**, 141957-76-8; **8a**, 16844-98-7; **8b**, 26429-16-3; **8c**, 25435-96-5; **8d**, 69435-89-8; **8e**, 37170-49-3; **8f**, 2078-12-8; **8g**, 141957-48-4; **8h**, 25432-43-3; **8i**, 141957-49-5; **8j**, 59147-01-2; **8k**, 5269-37-4; **8l**, 5269-38-5; **8m**, 85877-53-8; **8n**, 18294-04-7; **8o**, 40309-57-7; **8p**, 18105-31-2; **8q**, 56407-76-2; **8r**, 141957-77-9; **8s**, 141957-78-0; **9a**, 19753-66-3; **9b**, 41693-11-2; **9c**, 41692-90-4; **9d**, 17615-02-0; **9e**, 26487-93-4; **9f**, 859-65-4; **9g**, 141957-50-8; **9h**, 122682-77-3; **9i**, 141957-51-9; **9j**, 141957-52-0; **9k**, 141957-53-1; **9l**, 141957-54-2; **9m**, 141957-55-3; **10**, 107-46-0; **11n**, 144-62-7; **11o**, 110-15-6; **11p**, 124-04-9; **11q**, 598-10-7; **11r**, 73875-01-1; **11s**, 482-05-3; **12n**, 56849-14-0; **12o**, 101305-47-9; **12p**, 41726-56-1; **12q**, 141957-45-1; **12r**, 141957-46-2; **12s**, 141957-47-3; **13**, 24424-99-5; **14**, 100-52-7; **15**, 142035-21-0; **16**, 141404-45-9; **17**, 513-81-5; **18**, 141957-44-0; $P(OPh)_3$, 101-02-0.

[1] H. Schmidbaur, H. Stühler, W. Vornberger, *Chem. Ber.* **1972**, *105*, 1084–1086.
[2] H. J. Bestmann, A. Bomhard, R. Dostalek, R. Pichl, R. Riemer, R. Zimmermann, *Synthesis*, in press.
[3] H. J. Bestmann, O. Vostrowsky, W. Stransky, *Chem. Ber.* **1976**, *109*, 1694–1700.
[4] A. Ricci, M. Fiorenza, A. Degl'Innocenti, G. Seconi, P. Dembech, K. Witzgall, H. J. Bestmann, *Angew. Chem.* **1985**, *97*, 1068–1069; *Angew. Chem. Int. Ed. Engl.* **1985**, *24*, 1068.

 © VCH Verlagsgesellschaft mbH, W-6940 Weinheim, 1992 0570-0833/92/0808-1065 $ 3.50+.25/0

[5] H. J. Bestmann, B. Arnason, *Chem. Ber.* **1962**, *95*, 1513–1527. H. J. Bestmann, *Angew. Chem.* **1965**, *77*, 651–666; *Angew. Chem. Int. Ed. Engl.* **1965**, *4*, 645; H. J. Bestmann, R. Zimmermann, *Fortschr. Chem. Forsch.* **1971**, *20*, 28–40.
[6] H. J. Bestmann, N. Sommer, H. A. Staab, *Angew. Chem.* **1962**, *74*, 293.
[7] We thank Prof. Dr. E. Vogel, (Cologne), for providing cycloheptatriene-1,6-dicarboxylic acid.
[8] J. P. Wolf, H. Pfander, *Helv. Chim. Acta* **1986**, *69*, 1498–1504.
[9] J. P. Wolf, H. Pfander, *Helv. Chim. Acta* **1986**, *69*, 918–926, and references cited therein.
[10] C. W. Jefford, G. Barchietto, *Tetrahedron Lett.* **1977**, *51*, 4531–4534.
[11] **16**: yellow crystals, m.p. 112 °C; ^{1}H NMR: δ = 1.60 (s, 4H), 7.41 (s, 2H); ^{13}C NMR; δ = 17.77, 31.25, 148.40, 201.74; IR: $\tilde{\nu}$ [cm^{-1}] = 1705 (C = O); MS: *m/z* 122 ($M^{\oplus}$).
[12] **18**: B.p.$_{0.005}$ 82–85 °C (Kugelrohr), ^{13}C NMR: δ = 19.00, 25.34, 37.84, 46.34, 125.95, 215.11; IR: $\tilde{\nu}$ [cm^{-1}] = 1710 (C = O); MS: *m/z* 204 ($M^{\oplus}$).
[13] Cf. R. Noyori, M. Suzuki, *Angew. Chem.* **1984**, *96*, 854–882; *Angew. Chem. Int. Ed. Engl.* **1984**, *23*, 847.

Inhibition of the [2+2+2] Cyclization by the Formation of Chelates: Alkyne and Vinylidene Complexes with Cyclopentadienylcobalt(I)**

By *Holger Butenschön*,* *Ralf T. Kettenbach*, and *Carl Krüger*

The reactivity of cyclopentadienylcobalt(I) complexes as well as many of their derivatives substituted on the cyclopentadienyl ligand has been investigated intensively, particularly with regard to the cyclotrimerization of alkynes to arenes and also their [2+2+2] cocyclization with a large variety of other unsaturated substrates.[1] With the use of $\eta^{5:1}$-[(phosphinoalkyl)cyclopentadienyl]cobalt(I) chelate complexes such as **1** and **4** these reactions are almost completely prevented by the phosphinoalkyl groups.[2] We have now found that this is a good precondition for obtaining alkyne complexes with cyclopentadienylcobalt(I) fragments which for the first time also contain alkynes whose triple bond is arranged terminally. Furthermore, with the formation of the previously unknown cyclopentadienyl-vinylidene cobalt(I) complexes a reaction type hitherto not observed for cyclopentadienylcobalt(I) compounds has become possible.[3] The vinylidene complex **8** is available in just a few steps in high yield (Scheme 1).

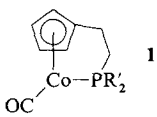

1

Since the carbonyl complexes **1** (R′ = Ph, *i*Pr, *t*Bu) readily available from the reaction of lithium [phosphinoethyl]-cyclopentadienides with [ICo(CO)$_4$][4] have proven to be not very reactive,[2] the corresponding ethene complex **4** was prepared according to the method of Kölle et al.[5] For this the anion **2**[2] was treated with cobalt(II)chloride to give the paramagnetic dimer **3** (74%). Treatment of a solution of **3**

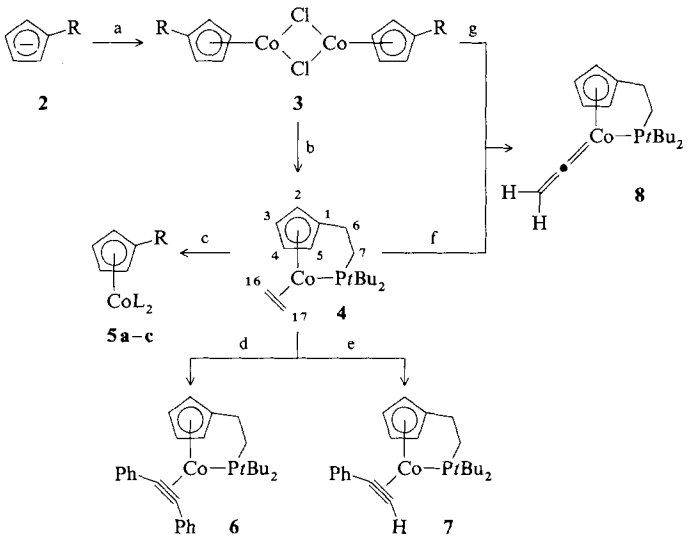

Scheme 1. R=$CH_2Ch_2PtBu_2$; a) $CoCl_2$, THF, −30 → 20 °C, 20 min, then 20 °C, 1 h, 74%; b) 1% Na/Hg, ethene, THF, −55 °C, 1 h, 93%; c) L_2, THF, 20 °C, **5a**: L_2 = cycloocta-1,5-diene, 4 d, 82%, **5b**: L_2 = 1,2-bis(diisopropylphosphino)ethane, 40 h, 93%, **5c**: L_2 = 2,2′-bipyridyl, 18 h, 88%; d) diphenylethyne, THF, 20 °C, 14 h, 83%; e) phenylethyne, THF, 0 °C, 14 d, 98%; f) ethyne, pentane, 20 °C, 18 h, 20%; g) 1% Na/Hg, ethyne, THF, −50 °C, 1 h, then 20 °C, 2 h, 88%.

and introduction of ethene afforded compound **4** in 93% yield (red-black crystals, m.p. 115 °C, spectroscopic data see Table 1). The ^{1}H NMR spectrum of **4** is temperature dependent and indicates a hindered rotation of the ethene ligand about the metal–olefin axis. The activation energy of **4** is 62 kJ mol^{-1} estimated from the coalescence temperature. It lies within the range also observed for the barrier to rotation of other ethene complexes.[6]

All spectroscopic data are in complete agreement with the structure of **4**. The mass spectrum of **4** is only slightly different from that of **1** (R′ = *t*Bu) since the ethene and CO ligands, respectively, (both *m/z* 28) are the first to be lost, in both cases the same fragment ions are formed. The crystal structure of **4** is shown in Figure 1.[7] The cobalt atom is in a distorted trigonal-planar environment if the centers of the Cp (D1) and C_2H_4 ligands (D2) as well as the P atom are considered as coordination sites. The dihedral angles C1-C6-C7-P (36°) and C6-C7-P-Co (29°) indicate a torsion of the ethene bridge by which the formation of tetrahedral angles at C6 [110.6(2)°] and C7 [110.9(2)°] is made possible. The distance from the cobalt atom to the carbon atom C1 [2.057(3) Å] is only slightly shorter than the distance to the other C atoms of the cyclopentadienyl ligand, probably because of the chelate bridge.

Compound **4** is significantly more reactive than **1** (R′ = *t*Bu). Ligand exchange reactions with bidentate ligands at 20 °C with the loss of ethene lead to the chelate complexes **5** in high yields. In these complexes the di-*tert*-butylphosphinoethyl substituent of the cyclopentadienyl ligand is no longer bound to the cobalt atom (^{31}P NMR). Compound **5a**

[*] Priv.-Doz. Dr. H. Butenschön[+], Dr. R. T. Kettenbach, Prof. Dr. C. Krüger
Max-Planck Institut für Kohlenforschung
Kaiser-Wilhelm-Platz 1, D-W-4330 Mülheim an der Ruhr 1 (FRG)
[+] New address:
Universität – Gesamthochschule
Fachbereich 9, Organische Chemie
Postfach 100127, D-W-5600 Wuppertal 1 (FRG)

[**] This work was supported by the Fonds der Chemischen Industrie. H. B. thanks the Verband der Chemischen Industrie for a Liebig-Stipendium, R. T. K. the Max-Planck-Gesellschaft for a doctoral stipend. We thank the director of the Max-Planck-Institut für Kohlenforschung, Prof. Dr. G. Wilke, for his supporting interest.

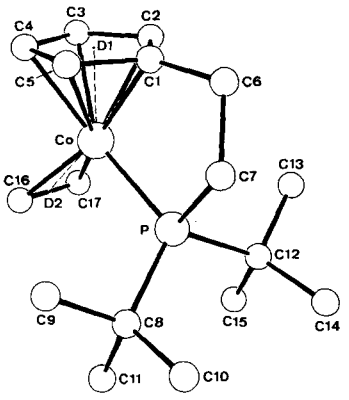

Fig. 1. Crystal structure of **4**. Selected distances [Å] and angles [°]: Co-D1 1.700(3), Co-D2 1.882(3), Co-P 2.200 (1), Co-C1 2.057(3), Co-C2 2.082(3), Co-C3 2.073(3), Co-C4 2.095(3), Co-C5 2.093(3), Co-C16 2.008(3), Co-C17 2.007(3), P-C7 1.856(3), C1-C6 1.496(4), C6-C7 1.524(4), C16-C17 1.396(5); C17-Co-C16 40.7(1), P-Co-D2 104.6(1), P-Co-D1 121.1(1), D2-Co-D1 134.3(1), C7-P-Co 102.3(1), C6-C1-C5 125.4(3), C7-C6-C1 110.6(2), C6-C7-P 110.9(2) [7].

had previously been obtained by the irradiation of **1** (R′ = *t*Bu) in cycloocta-1,5-diene in 42% yield.[2]

Whereas the η^2-alkyne complex **6** was obtained in only 39% yield by the reaction of **1** (R′ = *t*Bu) with diphenylethyne under photochemical conditions, **4** afforded **6** in 83% yield at 20 °C with the loss of ethene. Compound **4** reacts with phenylethyne at 0 °C to give the η^2-alkyne complex **7** (98%), which is the first cyclopentadienylcobalt(I) complex of an alkyne with a terminal triple bond. Unexpectedly, the reaction of the ethene complex **4** with ethyne at 20 °C does not yield the η^2-ethyne complex but **8**, the first vinylidene complex of a cyclopentadienylcobalt(I) compound,[8] in 20% yield. The identity of **8** was confirmed from the spectroscopic data; the chemical shift of the vinylidene carbon atom C10 (δ = 303.7) is particularly characteristic for the compound. Analogously to the formation of other vinylidene complexes it may be assumed that the η^2-ethyne complex occurs as an intermediate during the formation of **8**.[8] [(Phosphinoalkyl)cyclopentadienyl]vinylidene cobalt(I) complexes such as **8** are interesting as precursors for the rare cobalt–carbene complexes, which should be accessible by addition of nucleophiles.[8] To make this preparation feasible in worthwhile quantities, firstly higher yields from the preparation of the vinylidene complexes were necessary. In order to achieve this the synthetic route was shortened. Thus, the dimer **3** was not initially converted into the ethene complex **4** but was immediately treated with sodium amalgam and ethyne to give **8** (yield 88%). As a result **8** is available in amounts which allow further investigations, especially on the formation of cobalt–carbene complexes. At present we are investigating whether **7** can also be rearranged in order to establish whether the method can be extended to the synthesis of substituted vinylidene complexes.

Table 1. Spectroscopic data of the compounds **4**, **5b**,**c**, **7**, and **8** [a].

4: ^{1}H NMR (400 MHz, 300 K, [D$_8$]toluene): δ = 1.06 (d, 18H, CH$_3$, $^3J_{P,H}$ = 11.4 Hz), 1.81 (m, 2H, 6-H), $^3J_{P,H}$ = 19.0 Hz), 1.87 (m, 4H, 7-H, 16-H or 17-H, $^2J_{P,H}$ = 7.0 Hz), 2.27 (m, 2H, 16-H or 17-H, $\sum J_{16,17}$ = 9.0 Hz), 3.50 + 5.39 [AA′BB′ system, 4H, 2(5)-H, 3(4)-H, $\sum J_{2(5),3(4)}$ = 4.0 Hz]; (400 MHz, 353 K, [D$_8$]toluene): δ = 1.09 (d, 18H, CH$_3$, $^3J_{P,H}$ = 11.4 Hz), 1.84 (m, 2H, 6-H), 1.97 (m, 2H, 7-H), 2.02 (m, 4H, 16-H, 17-H), 3.46 + 5.38 [AA′BB′ system, 4H, 2(5)-H, 3(4)-H].

5b: ^{1}H NMR (200 MHz, [D$_8$]THF): δ = 1.04 (dd, 6H, 11-H, $^3J_{10,11}$ = 6.8 Hz, $^3J_{P2,H}$ = 5.2 Hz), 1.10 (d, 18H, 9-H, $^3J_{P1,H}$ = 10.5 Hz), 1.12 (dd, 6H, 12-H, $^3J_{10,12}$ = 7.1 Hz, $^3J_{P2,H}$ = 6.8 Hz), 1.26 (d, 4H, 13-H, $^2J_{P2,H}$ = 9.5 Hz), 1.57 (m, 2H, 6-H or 7-H, $J_{P1,H}$ = 3.8 Hz), 1.94 (dsept, 4H, 10-H, $^2J_{P2,H}$ = 8.6 Hz), 2.52 (m, 2H, 6-H or 7-H), 4.37 + 4.42 [AA′BB′ system, 4H, 2(5)-H, 3(4)-H].

5c: ^{1}H NMR (200 MHz, [D$_8$]THF): δ = 1.01 (d, 18H, CH$_3$, $^3J_{P,H}$ = 10.4 Hz), 1.72 (m, 2H, 6-H or 7-H), 2.70 (m, 2H, 6-H or 7-H), 4.50 + 4.59 [AA′BB′ system, 4H, 2(5)-H, 3(4)-H, $\sum J_{2(5),3(4)}$ = 3.8 Hz], 6.71 (ddd, 2H, 11-H, $^3J_{11,12}$ = 6.4 Hz), 7.30 (ddd, 2H, 12-H, $^3J_{12,13}$ = 8.6 Hz), 7.46 (ddd, 2H, 13-H), 10.20 (2H, 10-H, $^3J_{10,11}$ = 6.4 Hz).

7: IR (KBr): $\tilde{\nu}$ = 1748 cm^{-1} (s, C≡C); ^{1}H NMR (400 MHz, [D$_8$]THF): δ = 1.03 (d, 9H, CH$_3$, $^3J_{P,H}$ = 11.8 Hz), 1.33 (d, CH$_3$, $^3J_{P,H}$ = 11.8 Hz), 2.06 (m, 2H, 6-H), 2.29 (m, 2H, 7-H), 3.72 (s, 1H, 2-H or 5-H), 3.76 (s, 2-H or 5-H), 4.98 (s, 1H, CCH), 5.31 (s, 1H, 3-H or 4-H), 5.99 (s, 1H, 3-H or 4-H), 7.08 (t, 1H, *para*-H), 7.23 (t, 2H, *meta*-H), 7.38 (d, 2H, *ortho*-H); ^{13}C NMR (100.6 MHz, [D$_8$]THF): δ = 25.9 (dt, C-6), 29.5 (dq, C-9 or C-11), 30.1 (dq, C-9 or C-11), 35.4 (d, C-8 or C-10), 35.5 (d, C-8 or C-10), 38.0 (dt, C-7), 77.3 (dd, C-2 or C-5), 77.9 (dd, C-12), 78.1 (dd, C-3 or C-4), 80.6 (dd, C-3 or C-4), 84.0 (dd, C-2 or C-5), 87.4 (d, C-1), 111.5 (d, C-1), 125.6 (dd, C-17), 128.2 (dd, C-16), 131.5 (dd, C-15), 134.0 (d, C-14); ^{31}P NMR (81 MHz, [D$_8$]THF): δ = 97.3; MS (70 eV) m/z (%) 398 (31) [$M^{\oplus}$], 296 (100), 240 (46), 184 (50), 59 (11).

8: IR ([D$_8$]THF): $\tilde{\nu}$ = 1606 cm^{-1} (m, vinylidene C=C); ^{1}H NMR (400 MHz, [D$_8$]THF): δ = 1.33 (d, 18H, CH$_3$, $^2J_{P,H}$ = 12.6 Hz, 2.08 (m, 2H, 6-H, $^3J_{6,7}$ = 7.4 Hz, $^3J_{P,H}$ = 19.3 Hz), 2.09 (d, 2H, 10-H, $J_{P,H}$ = 9.6 Hz), 2.80 (m, 2H, 7-H, $^2J_{P,H}$ = 7.8 Hz), 4.49 [m, 2H, 2(5)-H or 3(4)-H, $\sum J_{2(5),3(4)}$ = 3.8 Hz], 5.03 [m, 2H, 2(5)-H or 3(4)-H]; ^{13}C NMR (100.6 MHz, [D$_8$]THF): δ = 25.8 (dt, C-6), 30.1 (dq, C-9), 36.6 (d, C-8), 41.0 (dt, C-7), 80.0 [d, C-2(5)], 81.6 [d, C-3(4)], 106.2 (dt, C-11), 112.3 (d, C-1), 303.7 (d, C-10); ^{31}P NMR (81 MHz, [D$_8$]THF): δ = 111.7; MS (70 eV): m/z (%) 322 (14) [$M^{\oplus}$], 296 (51), 254 (13), 240 (47), 184 (100), 137 (44), 59 (33), 57 (16).

[a] All new compounds were completely characterized by spectroscopy (^{1}H, ^{13}C, ^{31}P NMR, IR) and spectrometry (MS, and high-resolution MS) as well as by correct elemental analyses.

Experimental Procedure

All operations were carried out under argon.

3: In a Schlenk tube with a magnetic stirring bar, a solution of **2** (1.95 g, 15.1 mmol) in THF (120 mL) which had been previously cooled to −30 °C was added to cobalt(II) chloride (7.35 g, 30.1 mmol). The red suspension was stirred for 20 min, during which time its temperature warmed from −30 °C to 20 °C and subsequently for a further hour at 20 °C. The THF was removed under vacuum, the residue taken up in diethyl ether (2500 mL), and filtered through a P4 frit (under an argon atmosphere). The red-violet ether solution was cooled to −78 °C for the crystallization. This afforded **3** (7.33 g, 11.4 mmol, 73%) as black-violet plates, m.p. 192 °C (decomp).

4: In a 1000 mL three-necked flask with gas inlet tube, magnetic stirrer and two gas inlets with taps, ethene is introduced into a solution of (6.8 g, 10.2 mmol) **3** in THF (400 mL) at −55 °C. After 10 min, sodium amalgam (301.5 g, 1%, 152 mmol Na) was pipetted into the cooled, red-violet solution. The mixture was stirred for 1 h and warmed to 20 °C. The mud-brown mixture was filtered through a P4 frit, the red filtrate was concentrated to 20 mL and cooled to −78 °C. This afforded **4** (6.15 g, 19 mmol, 93%) as red-black crystals, m.p. 115 °C (decomp).

Received: February 12, 1992 [Z 5183 IE]
German version: *Angew. Chem.* **1992**, *104*, 1052

CAS Registry numbers:
2, 141847-73-6; **3**, 141847-74-7; **4**, 141847-75-8; **5a**, 131377-63-4; **5b**, 141847-78-1; **5c**, 141847-79-2; **6**, 131377-62-3; **7**, 141847-76-9; **8**, 141847-77-0; $CoCl_2$, 7646-79-9; cycloocta-1,5-diene, 111-78-4; 2,2′-bipyridyl, 366-18-7; 1,2-bis-(diisopropylphosphino)ethane, 87532-69-2; diphenylethyne, 501-65-5; phenylethyne, 536-74-3; ethyne, 74-86-2.

[1] a) N. E. Schore, *Chem. Rev.* **1988**, *88*, 1081–1119; b) K. P. C. Vollhardt, *Angew. Chem.* **1984**, *96*, 525–541; *Angew. Chem. Int. Ed. Engl.* **1984**, *23*, 539–556; c) H. Bönnemann, *Angew. Chem.* **1985**, *97*, 264–279; *Angew. Chem. Int. Ed. Engl.* **1985**, *24*, 248–262.

[2] R. T. Kettenbach, H. Butenschön, *New J. Chem.* **1990**, *14*, 599–601.

[3] Cf. C. Bianchini, M. Peruzzini, F. Zanobini, *Organometallics* **1991**, *10*, 3415–3417; C. Bianchini, M. Peruzzini, A. Vacca, F. Zanobini, *ibid.* **1991**, *10*, 3697–3707.

[4] M. Tasi, T. Ranga, G. Pályi in *Organometallic Syntheses, Vol. 4* (Eds.: R. B. King, J. J. Eisch), Elsevier, New York, **1988**, p. 262.

[5] U. Kölle, F. Khouzami, B. Fuss, *Angew. Chem.* **1982**, *94*, 132–133; *Angew. Chem. Int. Ed. Engl.* **1982**, *21*, 131–132; *Angew. Chem. Suppl.* **1982**, 230–240.

[6] J. W. Faller, *Adv. Organomet. Chem.* **1977**, *16*, 211–239 and references cited therein. It is worth mentioning that (η^5-cyclopentadienyl)(η^2-ethene)-(triphenylphosphane)cobalt(I) did not show any rotation of the ethene lig-

and for NMR measurements up to 55°; cf. E. R. Evitt, R. G. Bergman, *J. Am. Chem. Soc.* **1980**, *102*, 7003–7011.

[7] Crystal structure analysis of **4** ($C_{17}H_{30}CoP$, $M_r = 324.3$): crystal size $0.14 \times 0.32 \times 0.39$ mm^3, dark red, monoclinic, space group $P2_1/n$ [no. 14], $Z = 4$, $a = 8.619(1)$, $b = 13.571(1)$, $c = 14.346(1)$ Å, $\beta = 93.86(1)°$, $V = 1674.3$ Å^3, $\rho_{calcd} = 1.29$ g cm^{-3}, $\mu = 11.03$ cm^{-1}, $\lambda = 0.71069$ Å, $F(000) = 696\,e$, Enraf-Nonius CAD4 diffractometer, measurement temperature 20 °C, measurement method ω-2θ, $Mo_{K\alpha}$ radiation, $[(\sin\theta)/\lambda]_{max} = 0.65$ Å^{-1}, 4134 measured reflections $[\pm h, +k, +l]$, 3813 independent reflections ($R_{int} = 0.01$), of which 3057 were observed [$I > 2\sigma(I)$], 172 refined parameters, solution of the the structure by heavy atom method, H atom positions calculated ($U_{iso} = 0.05$ Å^2), $R = 0.040$, $Rw = 0.048$ [$w = 1/\sigma^2(Fo)$], EOF = 1.8, maximum residual electron density 0.37 eÅ^{-3}. Further details of the crystal structure investigation may be obtained from the Fachinformationszentrum Karlsruhe, Gesellschaft for wissenschaftlich-technische Information mbH, D-W-7514 Eggenstein-Leopoldshafen 2 (FRG) on quoting the depository number CSD-56206, the names of the authors, and the journal citation.

[8] M. I. Bruce, *Chem. Rev.* **1991**, *91*, 197–257, and references cited therein.

Reduction of Dispersed Indigo Dye by Indirect Electrolysis**

By *Thomas Bechtold,* Eduard Burtscher,* Angelika Amann*, and *Ortwin Bobleter*

The reduction of indigo, which is insoluble in water and alkaline solution, to the disodium salt of leuco-indigo, which is soluble in alkaline solution, is crucial to the application of indigo as a textile dye. This reduction is carried out in alkaline media with an excess of the reducing agent with a sufficiently negative redox potential. Because of the economic importance of this dye technology, a multitude of reducing agents have been examined (for instance, $Na_2S_2O_4$, sulfinic acid derivatives, organic hydroxycarbonyl compounds).[1] The reducing agents currently in use have the disadvantage of not being reversible, that is, the reducing agents cannot be recovered and the process baths cannot be recycled. Numerous mediators for the indirect electrochemical reaction of organic substances in homogenous solvent system have been described.[2] Investigations of reversible reducing agents led to the development of a procedure for indirect electrolysis: Coordination compounds of iron(II) and iron(III) salts and triethanolamine (TEA), which are stable in alkaline medium, were employed as mediators for the reduction of dispersed systems.[3]

Triethanolamine can form complexes with iron(II) as well as iron(III) ions in aqueous alkaline solvent systems that are stable enough,[4] so that iron concentrations up to 0.1 mol L^{-1} in aqueous sodium hydroxide ($c = 1$ mol L^{-1}) are possible. As was previously shown with cyclic voltammetry, a reversible charge transfer to the complexes can be achieved on HMDE electrodes (HMDE = hanging mercury drop electrode).[5] The cathodic peak potential E_{pc} of the coordination compounds for the transition Fe^{II}/Fe^{III} in aqueous alkaline solution is -1055 mV (vs. Ag/AgCl/3 mol L^{-1} KCl).

With this reversible redox system as a mediator, the finely dispersed indigo dye can be reduced by indirect electrolysis. The course of the reaction is summarized along the lines of the reaction model for the direct electrochemical reduction of anthraquinone-2-sulfonate[6] in Scheme 1.

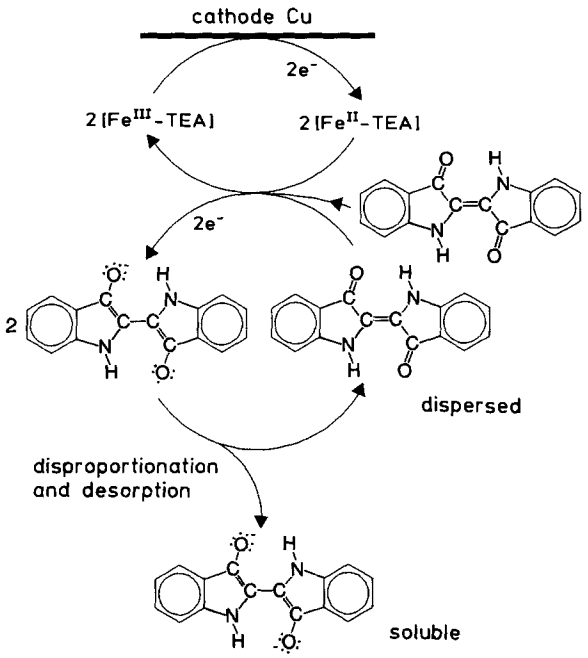

Scheme 1. Course of the indirect electrochemical reduction of finely dispersed indigo with triethanolamine–iron coordination compounds in dilute sodium hydroxide solution.

The triethanolamine–Fe^{III} complexes generated in situ are reduced at the cathode (-1050 to -1100 mV vs. Ag/AgCl/3 mol L^{-1} KCl) to the corresponding Fe^{II} complexes. Since the reduction potential of the Fe^{II} complexes is low enough for a reduction of indigo, one electron is transferred from the Fe^{II} complex to the surface of the dispersed dye particle. The dye radical anion formed initially disproportionates with formation of leuco-indigo dianions, which are soluble in alkaline solution, and reoxidized indigo molecules. The dianion is desorbed from the surface of the dye particle and goes into solution. Whereas indigo is colored blue in the oxidized form, the reduced form provides yellow solutions with an absorption maximum at 410 nm. The extent of reaction can be followed either by photometric methods, or the indirect electrolysis can be monitored by a redox titration of the electrolyte with $K_3[Fe(CN)_6]$. The results of the potentiometric analyses are presented in Figure 1. The complete reduction of the dye is evident after electrolysis for 130 to 150 min.

The increase in the amount of dye dianions ($E = -710$ mV vs. Ag/AgCl/3 mol L^{-1} KCl) with increasing electrolysis times and the increase of the potential to the redox potential of the Fe^{II}/Fe^{III} complexes after complete reduction of the dispersed indigo are clearly recognizable. The current yields calculated from the experimental data are around 50–55%. It is important in estimating the current yields to take into account that the experiments were conducted in an electrolysis cell under air. Back-oxidation processes on the liquid–air interface thus lead to an apparent reduction of the current yield. Control experiments were

[*] Dr. T. Bechtold, Dr. E. Burtscher, A. Amann, Prof. O. Bobleter
Institut für Textilchemie und Textilphysik der Universität Innsbruck
Höchsterstrasse 73, A-6850 Dornbirn (Austria)

[**] This research was supported by the Fonds zur Förderung der Wissenschaftlichen Forschung (Austria) and the Verein zur Förderung der Forschung und Entwicklung in der Textilwirtschaft Vorarlberg.

conducted in the absence of dye in the same electrolysis cell in which the current yields had been determined by a manganometric titration of the Fe^{II} ions produced; current yield in the range of 80–90% were obtained without inert gas atmosphere. The concentration of the reduced mediator at the time of the measurements was thus approximately 0.008 mol L^{-1}, which corresponds to 60–70% of the starting complex (0.012 mol L^{-1}).

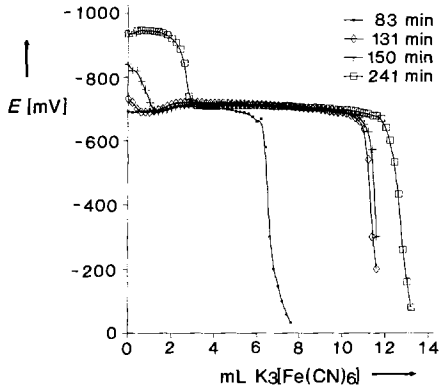

Fig. 1. Titration curves of the potentiometric determination of the extent of reaction with 0.01 mol L^{-1} $K_3[Fe(CN)_6]$. Samples: 5 mL catholyte at four different reaction times.

The solutions obtained after the complete reduction of indigo can be used directly for textile dyeing processes. Experiments with cotton textiles gave comparable results in terms of the depth and location of color to those obtained with the use of conventional reduction agents such as $Na_2S_2O_4$.

Experimental Procedure

For the preparation of 1 L of electrolyte, iron(III) sulfate (6 g, 0.012 mol) was dissolved in about 100 mL of water and treated with a mixture of triethanolamine (40 g, 0.268 mol), NaOH (10 g, 0.25 mol), and 50 mL of water. After the iron(III) hydroxide that had initially precipitated had dissolved, water was added to make a total volume of 1000 mL. The solution was filtered (0.45 μm membrane filter) to remove small amounts of undissolved hydroxides. The mediator solution thus obtained was used as both catholyte (ca. 950 mL) and anolyte (ca. 50 mL). To the catholyte solution was added indigo (5 g, 0.019 mol, technical grade, BASF) and a dispersion agent (0.5 g naphthalenesulfonic acid condensation product, Setamol WS, BASF). The electrolysis was conducted in a cylindrical cell at room temperature; the anode and the cathode were separated by a ceramic diaphragm.

The cathode was a Cu electrode with a surface of 500 cm^2; a stainless steel wire with a surface of 6 cm^2 served as the anode. The cathodic potential was regulated from −1050 to −1100 mV vs. Ag/AgCl/3 mol L^{-1} KCl, in order to avoid the undesired formation of hydrogen. The current density at the start of the electrolysis was 1 mA cm^{-2} and decreased as the reaction proceeded to 0.4 mA cm^{-2}. The catholyte solution was stirred with a magnetic stirrer. The concentration of sodium hydroxide in the anolyte was kept constant by addition of sodium hydroxide solution.

Received: February 20, 1992 [Z 5199 IE]
German version: *Angew. Chem.* **1992**, *104*, 1046

[1] U. Baumgarte, *Melliand Textilber.* **1987**, *68*, 189–195, 276–280.
[2] E. Steckhan, *Angew. Chem.* **1986**, *98*, 681–699; *Angew. Chem. Int. Ed. Engl.* **1986**, *25*, 693.
[3] T. Bechtold, E. Burtscher, D. Gmeiner, O. Bobleter, *Melliand Textilber.* **1991**, *72*, 50–54.
[4] M. Kunaszewska, *Rocz. Chem.* **1973**, *47*, 683–691.
[5] T. Bechtold, E. Burtscher, D. Gmeiner, O. Bobleter, *J. Electroanal. Chem. Interfacial Electrochem.* **1991**, *306*, 169–183.
[6] S. I. Bailey, *Chem. Aust.* **1982**, *50*, 202–204.

$C_{36}H_{36}$—Tetrahedral Clamping of Four Benzene Rings in a Spherical Hydrocarbon Framework

By *Fritz Vögtle,* Jens Gross, Christian Seel,* and *Martin Nieger*

Molecules with a spherical shape and a closed surface are of topical interest: the first preparation of fullerenes has rapidly led to the development of a new field of science;[1] guests encapsulated in the interior of carcerands are totally isolated from the environment, and thus are considered to be in a new state of matter;[2] and aesthetically appealing platonic hydrocarbons like dodecahedrane continue to present a challenge for synthetic chemists.[3] Our intention was to synthesize, based upon experiences in cyclophane and host/guest chemistry,[4] a nearly spherical hydrocarbon as a potential π ligand with a largely (but not completely) closed surface and intramolecular cavity.

Starting from dimethyl 5-methylisophthalate (**1**),[5] the key compound **4** for the cyclization reaction is available in six steps. Bromination with *N*-bromosuccinimide (NBS) (a in Scheme 1), phosphorylation (b), and threefold Wittig reaction (c) with the trialdehyde **2**[6] lead to the "tristilbene" **3** as a mixture of isomers. These are converted into the

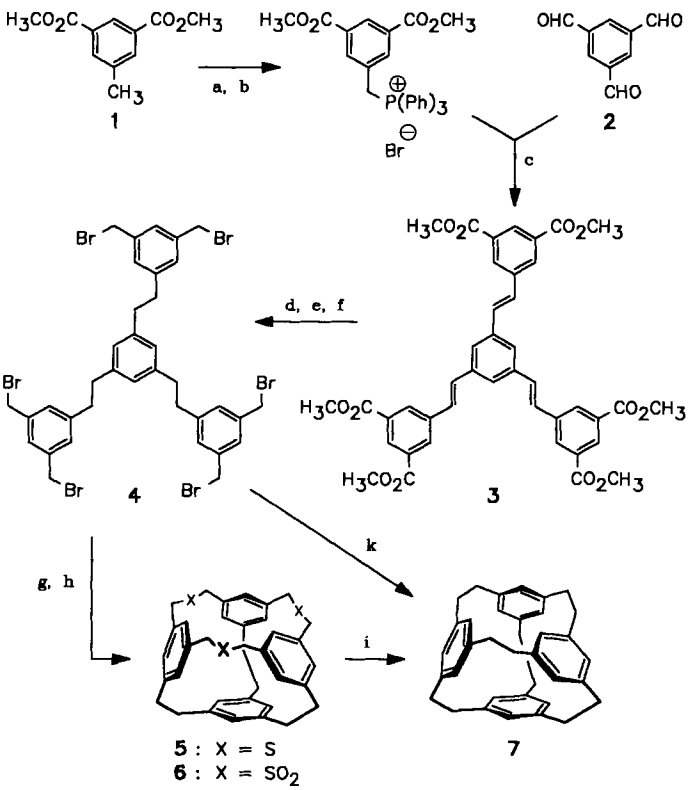

Scheme 1. a) NBS, azobisisobutyronitrile (AIBN), CH_2Cl_2, *hv*, reflux, 69%; b) PPh_3, $CHCl_3$, 2 h reflux, 99%; c) Li, MeOH/THF, argon, 12 h at room temperature, 64%; d) 3 bar H_2, Pd/C (5%), toluene, 99%; e) $LiAlH_4$, THF, argon, 2 h reflux, then Ac_2O, 4 h reflux, 89%; f) HBr/acetic acid (30%), 8 h at 60 °C, 77%; g) dilution principle, 3 equiv $Na_2S \cdot 9H_2O$, 20 equiv Cs_2CO_3, benzene/EtOH (1:1), argon, 16 h reflux, 18%; h) 12 equiv *m*-chloroperoxybenzoic acid, $CHCl_3$, 24 h at room temperature, 73%; i) 10^{-2} Torr, 570 °C, 45%; k) dilution principle, 15 equiv PhLi, THF/ether, argon, 8 h at room temperature; 11%.

[*] Prof. Dr. F. Vögtle, Dr. C. Seel, Dipl.-Chem. J. Gross
Institut für Organische Chemie und Biochemie der Universität
Gerhard-Domagk-Strasse 1, D-W-5300 Bonn 1 (FRG)
Dr. M. Nieger
Institut für Anorganische Chemie der Universität Bonn

hexabromide **4** by hydrogenation (d), reduction of the ester and acetylation (e), and treatment with hydrogen bromide/acetic acid (f). The well-established sulfide cyclization reaction with sodium sulfide[4a] provides the macrotricyclic phane **5** in 18% yield (g). The pyrolytic desulfurization reaction (SO_2 extrusion) (i)[7] of the trisulfone **6**, which is easily available by oxidation (h), leads to the heptacyclic hydrocarbon **7** in amounts of 25 mg.[8] However, the threefold intramolecular Wurtz coupling of **4** with phenyllithium (k) turned out to be the better alternative since twice the amount of **7** can be synthesized more conveniently and in less time.

The high symmetry of the spheriphane **7**, a tetramer of 1,3,5-trimethylenebenzene, is proved by spectroscopy: The ^{1}H NMR spectrum shows only one signal for the aromatic and benzylic protons, respectively, and the ^{13}C NMR spectrum has only three signals.[9] Even at temperatures lower than $-90\,^\circ$C the molecular skeleton is flexible enough not to hinder the twisting of the ethano bridges about the C_3 symmetry axes, so no splitting of the signals is observed.[10]

The X-ray structure analysis of the 1:1 adduct of chloroform and **7** exhibits (exclusively)[11] a *P*-helical conformation of the spherical molecular framework (Fig. 1).[12] The

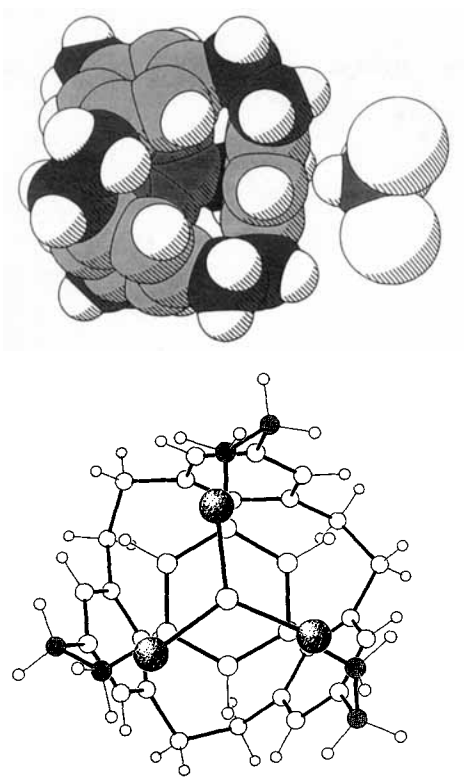

Fig. 1. Crystal structure of the 1:1 adduct of chloroform and **7**. Top: This perspective shows the coordination of the chloroform molecule to one of the benzene rings and the compact shape of the spheriphane. Bottom: Looking at the $CHCl_3$ molecule along the symmetry axis reveals the chiral twist of the hydrocarbon skeleton. The carbon atoms of three ethano bridges are hatched to elucidate the *P* helix.

centroids of the four benzene rings form a tetrahedron slightly compressed (4 pm) along the C_3 symmetry axis. The radius of the intramolecular cavity is 284 pm (average distance of the arene centroids from the center of the molecule; taking the van der Waals radii into account, the value is about 114 pm), and thus there is enough space for the inclusion of metal cations like Ag^+[13] and Ga^+.[14] (For comparison, the radii of C_{60} and dodecahedrane are approximately 351 pm[15] and 216 pm,[16] respectively.) The "windows" on the surface formed by [2.2.2]metacyclophane subunits are 386 pm in diameter (about 180 pm in consideration of the van der Waals radii). The solvent molecule lies on the symmetry axis and is bound by attractive hydrogen–π interactions to one of the benzene rings.[17] The ideal distance between the $CHCl_3$ carbon atom and the arene centroid in the chloroform–benzene complex has been calculated to be 336 pm.[18] In the adduct of **7** this value is distinctly shorter: only 323 pm (227 pm for the $CHCl_3$ hydrogen atom). The chlorine atoms are placed in a nearly eclipsing position above the quarternary carbon atoms; the deviation is 5.9° (Fig. 1 bottom).

In complexation experiments with silver triflate (trifluoromethanesulfonate) in THF a 1:1 complex precipitated readily.[19] The colorless solid is insoluble in solvents of low polarity like dichloromethane but dissociates into its components in methanol/dichloromethane mixtures. In contrast to this, the silver triflate complexes of [2.2.2]paracyclophane[13a] and [2$_6$](1,2,4,5)cyclophane (deltaphane)[13b] are readily soluble in chloroform and THF. The structure of $7 \cdot AgO_3SCF_3$ could not be determined spectroscopically, so it is uncertain if the cation is inside the cavity or faces one of the [2.2.2]metacyclophane windows as in the deltaphane complex.[20]

Attempted dehydrogenation of **7** with palladium/charcoal (10%) at 500 °C did not lead to significant reaction, whereas dehydrogenations at higher temperatures as well as treatment in an $AlCl_3$/NaCl melt at 140 °C caused decomposition.[21] Reduction reactions with platinum as a catalyst in dioxane/ethyl acetate (2:1) yield derivatives of **7** with successively hydrogenated benzene rings up to perhydrogenated $C_{36}H_{60}$.

The new synthetic strategy allows the preparation of similar concave hydrocarbons with larger molecular frameworks by use of longer bridges or building blocks containing more arene units. Such molecules are of interest as potential host compounds with hydrophobic cavities.[22]

Received: February 17, 1992 [Z 5194 IE]
German version: *Angew. Chem.* **1992**, *104*, 1112

[1] W. Krätschmer, L. D. Lamb, K. Fostiropoulos, D. R. Huffman, *Nature* (London) **1990**, *347*, 354–358; R. F. Curl, R. E. Smalley, *Sci. Am.* **1991**, *265* (10), 32–41; *Spektrum d. Wissenschaft* **1991**, No. 12, pp. 88–98; H. W. Kroto, *Angew. Chem.* **1992**, *104*, 113–133; *Angew. Chem. Int. Ed. Engl.* **1992**, *31*, 111–131; H. Schwarz, *ibid.* **1992**, *104*, 301–305, and **1992**, *31*, 293–298, and references cited therein.

[2] M. E. Tanner, C. B. Knobler, D. J. Cram, *J. Chem. Soc.* **1992**, *57*, 40–46, and references cited therein.

[3] R. Pinkos, J.-P. Melder, H. Prinzbach, *Angew. Chem.* **1990**, *102*, 102–105; *Angew. Chem. Int. Ed. Engl.* **1990**, *29*, 92–95; L. A. Paquette, *Chem. Rev.* **1989**, *89*, 1051–1065, and references cited therein.

[4] a) F. Vögtle, *Cyclophan-Chemie*, Teubner, Stuttgart, **1990**; b) F. Vögtle, *Supramolecular Chemistry*, Wiley, Chichester, **1991**.

[5] M. M. E. Grysziewicz-Trochimovsky, W. Schmidt, O. Grysziewicz-Trochimovsky, *Bull. Soc. Chim. Fr.* **1948**, 593–597.

[6] W. Ried, F.-J. Königstein, *Chem. Ber.* **1959**, *92*, 2532–2542; H.-E. Högberg, O. Wennerström, *Acta Chem. Scand.* **1982**, *B36*, 661–667.

[7] A. Dohm, F. Vögtle, *Top. Curr. Chem.* **1991**, *161*, 69–106.

[8] $R_f = 0.5$ (petroleum ether 40–60/CH_2Cl_2 2:1); m.p. > 350 °C; IUPAC name: heptacyclo[13.13.2^{1,15}.2^{8,22}.1^{3,27}.1^{6,10}.1^{13,17}.1^{20,24}]hexatriaconta-1,3(33),6,8,10(34),13,15,17(35),20,22,24(36),27-dodecaene; "semitrivial name": hexaethylentetra(1,3,5-benzene).

[9] Spectroscopical data of $7 \cdot CHCl_3$: ^{1}H NMR (250 MHz, $CDCl_3$): $\delta = 6.47$ (s, 12H; Ar-H), 2.89 (s, 24H; CH_2); ^{13}C NMR (62.89 MHz, $CDCl_3$): $\delta = 138.67$ (12C; Ar-C), 126.48 (12C; Ar-CH), 33.25 (12C; CH_2); MS (70 eV): *m/z* 468.2831 (M^+, 100%, calc.: 468.2817), 234 (M^{2+}, 16).

[10] THF had to be used as solvent in the low-temperature experiments, since the solubility of **7** in dichloromethane and chloroform is very poor below $-10\,^\circ$C.

[11] It is possible that the crystal analyzed was picked out of a conglomerate of crystals of both enantiomeric conformations.
[12] Crystal structure data for **7**: $C_{36}H_{36} \cdot CHCl_3$, colorless crystals, rhombohedral, space group $R\bar{3}$ (No. 146); $a = 932.4(1)$ pm, $\alpha = 100.80(1)°$; $V = 761.1(2) \times 10^6$ pm^3; $Z = 1$; $\rho_{calc.} = 1.281$ g cm^{-1}; $Mo_{K\alpha}$ ($\lambda = 0.71071$ Å); $\mu(Mo_{K\alpha}) = 0.325$ mm^{-1}; $F(000) = 310$; $T = 193$ K; crystal dimensions: $0.45 \times 0.50 \times 0.55$ mm^3; CAD4 diffractometer (Enraf-Nonius); $4° < 2\theta < 50°$; hkl range: $-11 \le h \le 10$; $-11 \le k \le 10$, $0 \le l \le 11$; 1670 measured, unique reflexes, 1646 with $|F| > 3\sigma(F)$. The structure was solved using direct methods and refined with SHELXTL-Plus: $R = 0.022$ ($R_w = 0.024$, $w^{-1} = \sigma^2(F) + 0.0001\,F^2$), non-H atoms refined anisotropically, H atoms localized by difference-electron-density determination and refined with a riding model. The absolute structure was determined by η refinement, $\eta = 1.11(9)$. Further details of the crystal structure investigations are available on request from the Fachinformationszentrum Karlsruhe, Gesellschaft für wissenschaftlich-technische Information mbH, D-W-7514 Eggenstein-Leopoldshafen 2 (FRG), on quoting the depository number CSD-56227, and the full journal citation.
[13] In alkene–silver complexes the bond length is between 240 and 260 pm [see c)]. Examples of such Ag complexes: a) J.-L. Pierre, P. Baret, P. Chautemps, M. Armand, *J. Am. Chem. Soc.* **1981**, *103*, 2986–2988; C. Cohen-Addad, P. Baret, P. Chautemps, J.-L. Pierre, *Acta Crystallogr. Sect. C* **1983**, *39*, 1346–1349; b) H. C. Kang, A. W. Hanson, B. Eaton, V. Boekelheide, *J. Am. Chem. Soc.* **1985**, *107*, 1979–1985; c) J. E. McMurry, G. J. Harley, J. R. Matz, J. C. Clardy, J. Mitchell, *ibid.* **1986**, *108*, 515–516.
[14] a) H. Schmidbaur, R. Hager, B. Huber, G. Müller, *Angew. Chem.* **1987**, *99*, 354–356; *Angew. Chem. Int. Ed. Engl.* **1987**, *26*, 338–340; b) C. Elschenbroich, J. Schneider, M. Wünsch, J.-L. Pierre, P. Baret, P. Chautemps, *Chem. Ber.* **1988**, *121*, 177–183.
[15] J. M. Hawkins, A. Meyer, T. A. Lewis, S. Loren, F. J. Hollander, *Science* **1991**, *252*, 312–313.
[16] J. C. Gallucci, C. W. Doecke, L. A. Paquette, *J. Am. Chem. Soc.* **1986**, *108*, 1343–1344.
[17] We recently reported on a similar interaction between acetonitrile and a macrobicyclic host molecule: R. Berscheid, M. Nieger, F. Vögtle, *J. Chem. Soc. Chem. Commun.* **1991**, 1364–1366.
[18] W. L. Jorgensen, D. L. Severance, *J. Am. Chem. Soc.* **1990**, *112*, 4768–4774.
[19] Correct C,H,Ag-analysis.
[20] In the deltaphane and [2.2.2]paracyclophane complexes the anion is coordinated to the silver ion. In the case of the complex of **7** the low solubility might be caused by the naked triflate anion if the Ag^+ ion is encapsulated inside the cavity.
[21] Investigations with mass spectrometry indicate the formation of naphthalene, anthracene, and phenanthrene derivatives.
[22] We have already synthesized heteroanalogous spheriphanes containing three ether or amino bridges, respectively, and will report on them elsewhere.

Diastereoselective Synthesis of Substituted Cyclohexadienes from Enantiomerically Pure Tricarbonyl(2-phenyl-4,5-dihydrooxazole)chromium Complexes**

By *Ernst Peter Kündig,* Alberto Ripa,* and *Gérald Bernardinelli*

The one-pot transformation of arenes into regio- and stereoselectively *trans*-disubstituted dihydroarenes can be carried out efficiently via the readily accessible $Cr(CO)_3$ complexes.[1, 2] Absolute stereochemical control would be highly desirable in order to extend the synthetic utility of this transformation. We here show that this can be realized.

Chiral 4,5-dihydrooxazoles have been used extensively in asymmetric synthesis.[3] Meyers et al. reported the sequential addition of a nucleophile and an electrophile to naphthalene[4a–d] and pyridine derivatives[4e, f] activated by σ-bound chiral 4,5-dihydrooxazoles. While this constitutes a useful methodology and provides access to regio- and stereoselectively substituted dihydronaphthalene and dihydropyridine derivatives, extension to benzene and its derivatives failed.[5]

Recently, we found that the tricarbonyl(2-phenyl-4,5-dihydrooxazole)chromium complex **1** undergoes regioselective *ortho*-addition of C-nucleophiles under lithium coordination control.[6] Subsequent reactions of the anionic intermediate *rac*-**2** with primary C-electrophiles yielded the regio- and stereoselectively substituted cyclohexadienes *rac*-**3** or *rac*-**4**, the distribution of which strongly depended on the electrophile and on the reaction conditions (Scheme 1).[7]

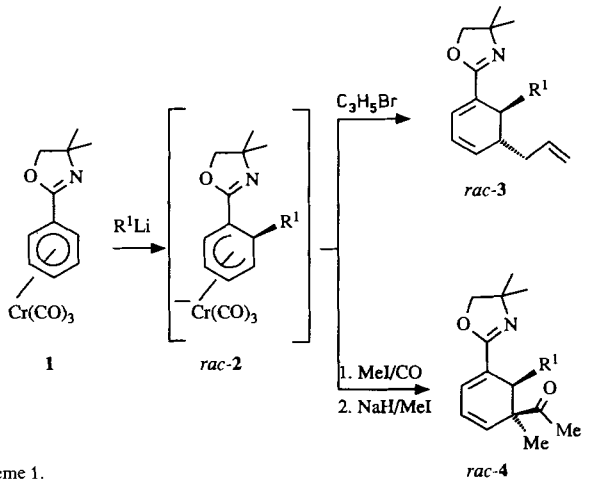

Scheme 1.

An asymmetric version of this methodology was conceived based on a chiral dihydrooxazole. We anticipated that the addition of a C-nucleophile could be preferentially directed to one of the resulting diastereotopic *ortho* positions of the complexed arene.[8] The data reported here confirm this hypothesis and show that the absolute configuration of the two new stereogenic centers can be easily controlled with the enantiomerically pure complexes **5** and **6** derived from L-valinol and L-*tert*-butylglycinol.[9]

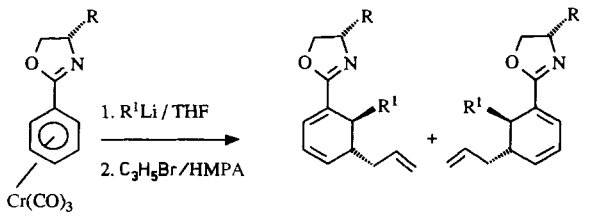

Scheme 2. R^1 = alkyl, vinyl, phenyl; HMPA = hexamethylphosphoric triamide.

Low-temperature sequential addition of alkyl-, vinyl-, or phenyllithium and allyl bromide to **5** or **6** afforded the cyclohexadienes **7** and **8** (Scheme 2, Table 1). MeLi (→**7a**, **8a**), *n*BuLi (→**7b**, **8b**) and vinyl lithium (→**7c**, **8c**) added to **5**

[*] Prof. Dr. E. P. Kündig, Dr. A. Ripa
Departement de Chimie Organique, Université de Genève
30 Quai Ernest Ansermet, CH-1211 Genève 4 (Switzerland)
Dr. G. Bernardinelli
Laboratoire de Crystallographie, Université de Genève

[**] We thank the Swiss National Foundation for support of this work.

with the same high level of diastereoselectivity (up to 92% *de*), whereas PhLi gave a ca. 4:1 mixture of **7d** and **8d**.[10]

The already high diastereoselectivity could be further improved with complex **6**, which contains a sterically more demanding dihydrooxazole group. MeLi (→**7e**, **8e**) and *n*BuLi (→**7f**, **8f**) afforded a single detectable diastereoisomer; and PhLi (→**7g**, **8g**) also added with considerably improved selectivity.[10]

Table 1. Sequential diastereoselective addition of organolithium reagents and allyl bromide to complexes **5** and **6**.

R	R^1Li	Product 7, 8	Yield [%] [a]	7:8 [b]
*i*Pr	MeLi	**a**	61	96:4
*i*Pr	*n*BuLi [c]	**b**	54	95.5:4.5
*i*Pr	VinylLi [d, e]	**c**	48	95.5:4.5
*i*Pr	PhLi [f]	**d**	60	81:19
*t*Bu	MeLi	**e**	69	≥99:1
*t*Bu	*n*BuLi	**f**	62	≥99:1
*t*Bu	PhLi [f]	**g**	51	95.5:4.5

[a] Ketone products were also formed in 10–25% yield; see Ref. [7]. [b] Determined by 400-MHz ^{1}H NMR and HPLC. [c] Reaction run in THF/toluene (1:10) at −90 °C. [d] Generated in situ from MeLi and tetravinyltin. [e] Reaction run at −90 °C. [f] Reaction run in THF/toluene (1:5) at −80 °C.

The same level of asymmetric induction by the two auxiliaries was obtained in the tandem addition of MeLi and MeI, followed by a second alkylation with MeI. This afforded **9a** (R = *i*Pr) and **9b** (R = *t*Bu) in 54 and 58% yield, and with 90 and 98% *de*, respectively (Scheme 3).

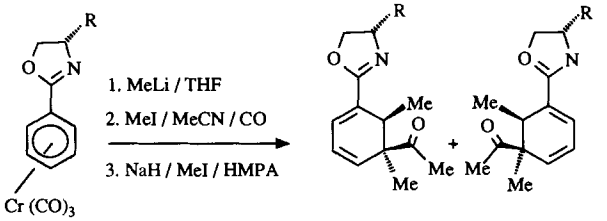

5, 6	[%]	9a-b		10a-b
5, 9a, 10a: R = *i*Pr	54	95	:	5
6, 9b, 10b: R = *t*Bu	58	>99	:	1

Scheme 3. HMPA = hexamethylphosphoric triamide.

The result of a single-crystal X-ray analysis of **9a** is shown in Figure 1.[11] It establishes the relative configuration of the two new stereogenic centers with respect to that of the auxiliary. For a mechanistic interpretation (see Scheme 4) let us

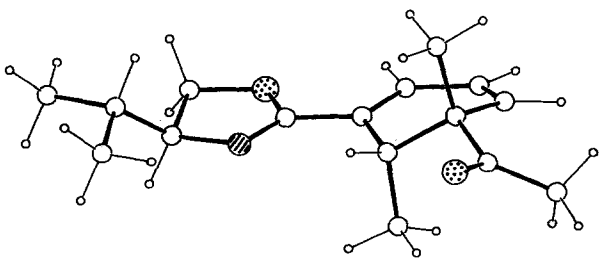

Fig. 1. Crystal structure of **9a**. Dotted spheres are O, shaded N, white C, and small white H atoms.

first consider the two rotamers. Models, and, more definitively, the X-ray structure of **5**, show that in the *syn*-rotamer the isopropyl group is located far away from the [Cr(CO)$_3$] group. There is no steric interaction between these two fragments and it is therefore unlikely that one of the rotamers of **5** and **6** is strongly favored. In fact, the X-ray structure of **5** shows the presence of both the *syn*- and the *anti*-rotamer in the unit cell (ratio 1:1).[12] Next we recall that it is well documented that nucleophiles add to the *exo* face of arene tricarbonyl chromium complexes[1c, 2, 13] and that both imine and oxazoline groups very efficiently direct nucleophiles to the *ortho*-position of the arene.[4, 6, 7] Based on these observations, we assume that lithium coordination to the nitrogen atom precedes nucleophilic addition as shown in Scheme 4.[14] Product stereochemistry then reflects a transi-

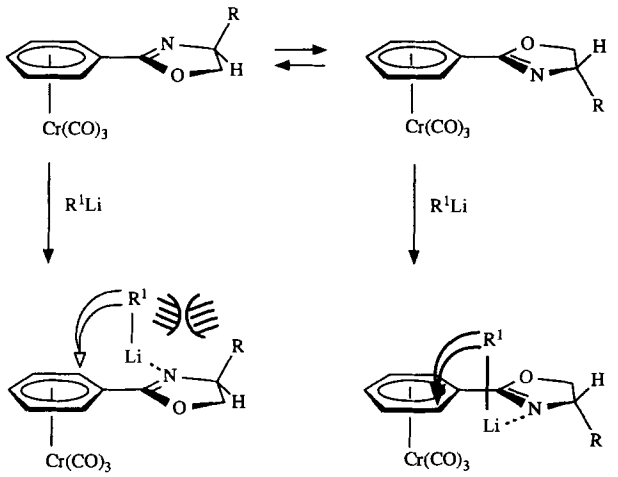

Scheme 4. Left: Coordination controlled by the Li atom in the *anti*-rotamer; right: in the *syn*-rotamer.

tion state in which the R substituent of the chiral auxiliary is *syn* to the metal fragment. In the *anti* rotamer, the lithium coordination controlled addition of the C-nucleophile would lead to a very congested transition state because of strong steric interactions between the R and R^1 groups (as usual, the organolithium reagents are represented as monomers, even though aggregates may be the reacting species[15]). These interactions become more important with the size of R, and this readily accounts for the higher induction by the *tert*-butyldihydrooxazole in **6** compared to the isopropyl analogue **5**.

In conclusion, the first examples of a highly regio- and diastereoselective introduction of two or three C substituents across a benzene double bond have been achieved via the combined activation of the arene by σ-bound and π-bound groups.

Experimental

7e: To a stirred solution of complex **6** (63 mg, 0.186 mmol) in 1.9 mL of dry THF was added dropwise MeLi (133 μL of a 1.67 M ether solution, 0.223 mmol, 1.2 equiv.) at −90 °C under N_2. The solution was slowly warmed to −78 °C (3 h) and dry HMPA (323 μL) and allyl bromide (161 μL, 10 equiv., distilled from P_2O_5) were added. The solution was slowly warmed to room temperature and stirred for about 15 h. Excess of electrophile and THF were evaporated in vacuo. The residue was dissolved in ether (30 mL) and washed with water (2 × 10 mL), and brine (10 mL). The combined aqueous phases were extracted with ether (3 × 10 mL). The combined organic phases were dried ($MgSO_4$), exposed to sunlight until colorless (decomplexation), filtered through celite, and evaporated. Flash-chromatography (SiO_2, hexane:ether 3:1) afforded 33.2 mg of **7e** (69%) ^{1}H NMR (400 MHz, $CDCl_3$, 25 °C, TMS) δ = 0.89 (s;

9H; $C(CH_3)_3$), 1.03 (d, $^3J(H,H) = 7.3$ Hz, 3H; CH_3), 1.89–2.03 (m, 1H; CH), 2.07–2.17 (m, 2H; CH_2), 2.87 (bq, $^3J(H,H) = 7.3$ Hz, < 1 Hz, 1H; CH), 3.91 (dd, $^3J(H,H) = 6.7$, 10 Hz, 1H; CH), 4.08–4.18 (m, 2H; CH_2), 4.91–5.03 (m, 2H; $=CH_2$), 5.69–5.80 (m, 1H; =CH), 5.94 (dd, $^3J(H,H) = 5.5$, 9.6 Hz, 1H; =CH), 5.99 (dd, $^3J(H,H) = 5.1$, 9.6 Hz, 1H; =CH), 6.56 (d, $^3J(H,H) = 5.1$ Hz, 1H; =CH); IR (CH_2Cl_2): $\tilde{\nu}$[cm^{-1}] = 1650, 1612; MS (70 eV): *m/z* 259 ($M^{\oplus}$, 20%), 218 ($M^{\oplus} - C_3H_5$, 100); $[\alpha]_D^{20} = -512.4$ (*c* = 0.835, $CHCl_3$).

9a: A pressure resistant Schlenk tube was used for this reaction. To a stirred solution of complex **5** (78.7 mg, 0.2419 mmol) in 2.5 ml of dry THF was added dropwise MeLi (177 μL of a 1.62 M solution, 0.290 mmol, 1.2 equiv.) at −90 °C under N_2. The solution was slowly warmed to −78 °C over a period of 3 h. MeI (150 μL, 10 equiv., distilled from P_2O_5) and dry MeCN (2.5 mL) were added and the mixture cooled to liq. N_2 temperature. The reaction vessel was evacuated, warmed to −78 °C and further reaction carried out under CO (4 bar). The solution was slowly warmed to room temperature and stirred for about 15 h. Volatiles were removed in vacuo. The residue was dissolved in dry THF (8 mL), cooled to −78 °C and cannulated into a dispersion of NaH (29 mg of a 60% oil dispersion, 3 equiv., prewashed with dry pentane) in dry THF (2 mL) at the same temperature. After 30 minutes MeI (10 equiv.) and dry HMPA (420 μL) were added. The temperature was brought to 20 °C over a 4 h period. After work-up, flash-chromatography (SiO_2, hexane:ether = 2:1 to 1:2) afforded 34.2 mg (54%) of **9a**. M.p. 71 °C; ^1H NMR (200 MHz, $CDCl_3$, 25 °C): $\delta = 0.86$ (d, $^3J(H,H) = 6.7$ Hz, 3H; CH_3), 0.88 (d, $^3J(H,H) = 6.8$ Hz, 3H; CH_3), 0.96 (d, $^3J(H,H) = 6.8$ Hz, 3H; CH_3), 1.23 (s, 3H; CH_3), 1.80–2.00 (m, 1H; CH), 2.21 (s, 3H; CH_3), 3.07 (q, $^3J(H,H) = 6.7$ Hz, 1H; CH), 3.97–4.30 (m, 3H; CH, CH_2), 6.01 (dd, $^3J(H,H) = 5.4$, 9.8 Hz, 1H; =CH), 6.37 (bd, $^3J(H,H) = 9.8$ Hz, 1H; =CH), 6.59 (bd, $^3J(H,H) = 5.4$ Hz, 1H; =CH); IR (CH_2Cl_2): $\tilde{\nu}$[cm^{-1}] = 1707 (C=O); MS (70 eV): *m/z* 218 ($M^{\oplus} - C_2H_3O$, 47%), 133 (100); $[\alpha]_D^{20} = -316.8$ (*c* = 1.12, $CHCl_3$). The diastereomeric ratio **9a**:**10a** was determined by HPLC analysis of the crude mixture (Silica-spheri 5 μm, 250 × 10 mm column; hexane:AcOEt = 3:1, 5 ml min^{-1}; UV detector at 280 nm); R_t = 8 min (**9a**) and 10 min (**10a**).

Received: March 9, 1992 [Z 5230 IE]
German version: *Angew. Chem.* **1992**, *104*, 1115

[1] a) E. P. Kündig, D. P. Simmons, *J. Chem. Soc. Chem. Commun.* **1983**, 1320; b) E. P. Kündig, *Pure Appl. Chem.* **1985**, *57*, 1855; c) E. P. Kündig, A. F. Cunningham, Jr., P. Paglia, D. P. Simmons, *Helv. Chim. Acta* **1990**, *73*, 386; d) E. P. Kündig, M. Inage, G. Bernardinelli, *Organometallics* **1991**, *10*, 2921.

[2] For a recent review of reactions of [areneCr(CO)$_3$] complexes see: M. F. Semmelhack in *Comprehensive Organic Synthesis, Vol. 4* (Eds.: B. M. Trost, I. Fleming), Pergamon, Oxford, **1991**, p. 517.

[3] For a review, see: a) K. A. Lutomski, A. I. Meyers in *Asymmetric Synthesis, Vol. 3* (Asymmetric Synthesis via Chiral Oxazolines), Academic Press, New York, **1984**, p. 213; b) C. Bolm, *Angew. Chem.* **1991**, *103*, 556; *Angew. Chem. Int. Ed. Engl.* **1991**, *30*, 542; Biaryl synthesis: c) A. I. Meyers, J. R. Flisak, R. A. Aitken, *J. Am. Chem. Soc.* **1987**, *109*, 5446; d) A. I. Meyers, A. Meier, D. J. Rawson, *Tetrahedron Lett.* **1992**, *33*, 853; Michael addition: e) A. I. Meyers, M. Shipman, *J. Org. Chem.* **1991**, *56*, 7098; Claisen rearrangements; f) M. J. Kurth, O. H. W. Decker, H. Hope, M. D. Yanuck, *J. Am. Chem. Soc.* **1985**, *107*, 443; g) M. J. Kurth, O. H. W. Decker, *J. Org. Chem.* **1985**, *50*, 5769; Diels-Alder reactions: h) C. Kouklovsky, A. Pouilhes, Y. Langlois, *J. Am. Chem. Soc.* **1990**, *112*, 6672; i) Y. Langlois, A. Pouilhes, *Tetrahedron: Asymmetry* **1991**, *2*, 1223.

[4] a) A. I. Meyers, B. A. Barner, *J. Am. Chem. Soc.* **1984**, *106*, 1865; b) A. I. Meyers, G. P. Roth, D. Hoyer, B. A. Barner, D. Laucher, *ibid.* **1988**, *110*, 4611; c) D. J. Rawson, A. I. Meyers, *J. Org. Chem.* **1991**, *56*, 2292; d) A. J. Robichaud, A. I. Meyers, *ibid.* **1991**, *56*, 2607, and references cited therein; e) A. I. Meyers, N. R. Natalee, D. G. Wettlaufer, *Tetrahedron Lett.* **1981**, *22*, 5123; f) A. I. Meyers, N. R. Natale, *Heterocycles* **1982**, *18*, 13.

[5] 2-Phenyl-4,5-dihydrooxazoles undergo *ortho* lithiation when treated with organolithium reagents. See: M. Reuman, A. I. Meyers, *Tetrahedron* **1985**, *41*, 837. *o*-Alkoxy- or *o*-fluorophenyldihydrooxazoles undergo *ortho* nucleophilic aromatic substitution: a) A. I. Meyers, R. Gabel, E. D. Mihelich, *J. Org. Chem.* **1978**, *43*, 1372; b) A. I. Meyers, B. E. Williams, *Tetrahedron Lett.* **1978**, *3*, 223.

[6] E. P. Kündig, D. Amurrio, R. Liu, A. Ripa, *Synlett* **1991**, 657.

[7] E. P. Kündig, G. Bernardinelli, R. Liu, A. Ripa, *J. Am. Chem. Soc.* **1991**, *113*, 9676.

[8] *Ortho* regio- and diastereoselective additions of *t*BuLi to enantiomerially pure and racemic chirally substituted [(benzene)Cr(CO)$_3$] complexes have been reported: a) J. Blagg, S. G. Davies, C. L. Goodfellow, K. H. Sutton, *J. Chem. Soc. Perkin Trans. 1* **1990**, 1133; b) J. A. Heppert, J. Aubé, M. E. Thomas-Miller, M. L. Milligan, F. Takusagawa, *Organometallics* **1990**, *9*, 727.

[9] These complexes were prepared in three steps from L-valinol and L-*tert*-butylglycinol in 53 and 47% yield, respectively. See also [6].

[10] The lower diastereoselectivity of phenyllithium addition compared to alkyllithium addition may reflect the lower degree of aggregation of PhLi in THF and its resulting higher reactivity. See: L. M. Jackman, L. M. Scarmoutzos, *J. Am. Chem. Soc.* **1984**, *106*, 4627.

[11] Crystallographic data for **9a**: Yellow crystals were grown from MeOH solution. $C_{16}H_{23}NO_2$, $M_r = 261.4$, orthorhombic $P2_12_12_1$, $a = 7.3362(12)$, $b = 7.5273(10)$, $c = 27.700(6)$, based on 20 reflections ($19° < 2\theta < 35°$), $V = 1529.6(5)$ Å^3, $Z = 4$, $F(000) = 568$, $\mu = 0.069$ mm^{-1}. Intensity data were collected at room temperature on a Philips PW 1100 diffractometer with $Mo_{K\alpha}$ radiation ($\lambda = 0.71069$ Å), $4° < 2\theta < 48°$, 1424 unique reflections measured. Structure solved by direct methods [16], other calculations were made using the XTAL system [17]. Full matrix refinement (172 parameters). All coordinates of the H atoms were calculated. Final *R* factor was 0.067 ($\omega R = 0.034$, $\omega = 1/\sigma^2(Fo)$) for 916 observed reflections ($|F_o| > 4\sigma(F_o)$). Further details of the crystal structure investigation are available on request from the Director of the Cambridge Crystallographic Data Center, University Chemical Laboratory, Lensfield Road, GB Cambridge CB2 1EW (UK), on quoting the full journal citation.

[12] Details of the X-ray structure analysis of **5** will appear in a future full paper.

[13] M. F. Semmelhack, H. T. Hall, R. Farina, M. Yoshifuji, G. Clark, T. Bargar, K. Hirotsu, J. Clardy, *J. Am. Chem. Soc.* **1979**, *101*, 3535.

[14] A π-facial coordination of the incoming nucleophile has been proposed to explain the diastereofacial selectivity of nucleophilic additions to chiral 2-alkenyl- and 2-naphthyldihydrooxazoles derived from L-valinol and L-*tert*-butylglycinol [3e, 4c]. This mode of addition could not account for the high diastereoselectivity observed in the reactions reported here.

[15] For a recent article on organolithium aggregation, see: G. Fraenkel, A Chow, W. R. Winchester, *J. Am. Chem. Soc.* **1990**, *112*, 6190.

[16] P. Main, S. J. Fiske, S. E. Hull, L. Lessinger, G. Germain, J.-P. Declerq, M. M. Woolfson, *A System of Computer Programs for the Automatic Solution of Crystal Structures from X-Ray Diffraction Data*, Universities of York, England, and Louvain-la-Neuve, Belgium **1987**.

[17] *XTAL 3.0 User's Manual* (Eds.: S. R. Hall, J. M. Stewart, Universities of Western Australia and Maryland, **1987**.

Strain-Activated Formation of a Triple-Layered Phane**

By *Henning Hopf,* Bernhard Witulski, Peter Bubenitschek,* and *Peter G. Jones*

The ease with which [2.2]paracyclophane and its homologues with more than two bridges undergo cycloadditions, substitutions, and rearrangements is strongly dependent upon how much strain is released in these processes.[1, 2] One strain-relieving reaction was reported in 1966 in which the parent hydrocarbon [2.2]paracyclophane was isomerized with a Lewis acid to [2.2]metaparacyclophane.[3] This type of reaction was shown in the following years to be typical also for cyclophanes with multiple bridges.[1, 4] In a study designed to accomplish an analogous isomerization with [2.2](2,5)furanoparacyclophane (**1**), we were surprised to observe that in the presence of Lewis acids (MX_n) this heterophane gave a dimer in good yield that rearranged to the triple-layered structure **5**, identified by spectroscopic (see *Experimental Procedure*) and X-ray crystallographic data.[5] Aluminum chloride or titanium chloride in dichloromethane at 0 °C afforded the best yields (60 and 64%, respectively), whereas milder acids such as zinc(IV) chloride and ether–boron tri-

[*] Prof. Dr. H. Hopf, Dipl.-Chem. B. Witulski
Institut für Organische Chemie der Technischen Universität
Hagenring 30, D-W-3300 Braunschweig (FRG)
Dipl.-Chem. P. Bubenitschek, Prof. Dr. P. G. Jones
Institut für Anorganische und Analytische Chemie
der Technischen Universität Braunschweig

[**] Cyclophanes, Part 37. This work was supported by the Fonds der Chemischen Industrie, the BASF Aktiengesellschaft, and the Deutsche Forschungsgemeinschaft.–Part 36: H. Hopf, T. Laue, M. Zander, *Angew. Chem.* **1991**, *103*, 441–442; *Angew. Chem. Int. Ed. Engl.* **1991**, *30*, 432–433.

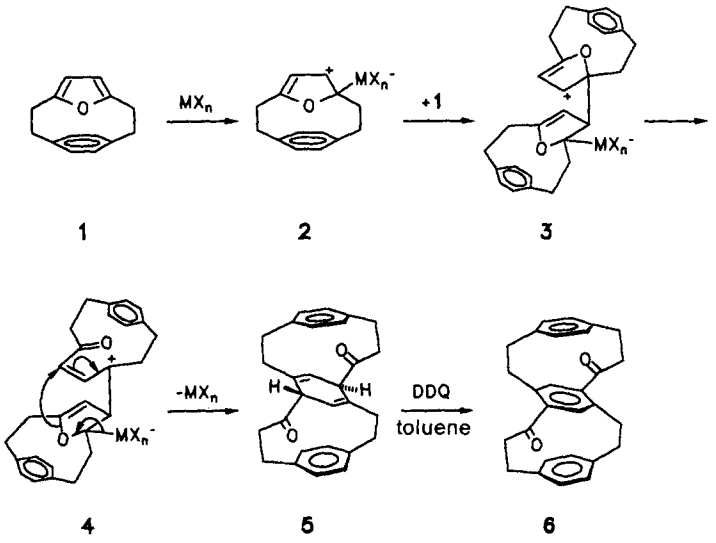

Scheme 1. A possible mechanism for the Lewis acid catalyzed formation of **5** from **1**.

fluoride failed to cause dimerization; instead the starting material **1** could be recovered unchanged.[6]

The central 1,4-cyclohexadiene moiety of **5** is predisposed to aromatization, which can be induced by heating (110 °C, 5 h) with 2,3-dichloro-5,6-dicyano-1,4-benzoquinone (DDQ) to produce the triple-layered arene **6** (yield 50%, unoptimized). Definitive proof for the structure of **6** was obtained from the X-ray structure analysis[5] seen in Figure 1.

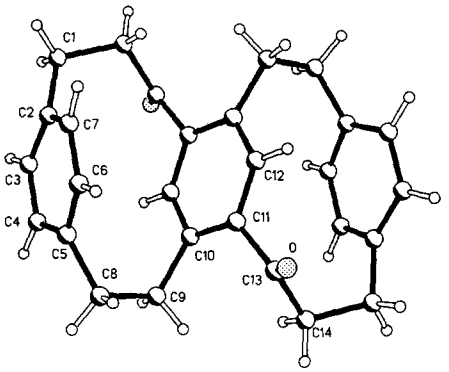

Fig. 1. The crystal structure of **6**. The radii are arbitrary. Only the asymmetric unit is numbered. This numbering system was also used in the assignment of the NMR signals of **5** and **6**.

A mechanism for this novel reaction, which builds layered compounds, is unknown; the sequence of steps proposed in Scheme 1, however, seems plausible at present:[7] initial activation of furan **1** with the Lewis acid leads to complex **2**. Electrophilic attack of this complex on a second molecule of **1** results in a dimer **3** that then releases its internal strain by undergoing ring opening to complex **4**. Subsequent loss of the catalyst molecule and further release of strain (opening of the "lower" phane system) give rise to the stabilized product **5**. The importance attached to stress reduction in this interpretation of the mechanism[5] gains support from the observation that 2,5-dimethylfuran, serving as an "unstrained half" of **1**, gave no identifiable products under our experimental conditions.[8]

Additional studies should show whether the reaction described here can be used as a general method for synthesizing multilayered compounds by starting from precursors containing appropriately substituted furan units as reaction initiators.[7] In all events, diketones **5** and **6** offer readily accessible starting materials for triple-layered systems

Experimental Procedure

5: A solution of **1** (500 mg, 2.5 mmol) [9] in dichloromethane (20 mL) was added dropwise to a cooled (0 °C) suspension of $AlCl_3$ (340 mg) in dry dichloromethane (70 mL) and the mixture stirred for 5 h at 0 °C. Next, the mixture was diluted with 1 N HCl (30 mL), extracted with dichloromethane, washed until neutral, and dried with magnesium sulfate. The solvent was removed and the product mixture purified by column chromatography (SiO_2, dichloromethane); fraction 1: 50 mg (10%) **1**, fraction 2: 320 mg (64%) **5**. Physical and spectroscopic data: m.p. 276 °C (colorless needles from $CHCl_3$/pentane); IR (KBr): $\tilde{\nu}$[cm^{-1}] = 3020 (w), 2975 (m), 2935 (m), 2849 (m), 1691 (s), 1507 (m), 1432 (m), 1346 (m), 1161 (m), 1082 (s), 1041 (m), 895 (m), 848 (m), 814 (s); ^{1}H NMR (400.1 MHz, $CDCl_3$, internal TMS): δ = 6.90 (s, 2H), 6.81 (AB pattern, J = 7.9 Hz, 1H, arene H), 6.69 (AB pattern, J = 7.9 Hz, 1H, arene H), 4.31 (s, 1H, 12-H), 3.09 (s, 1H, 11-H), 2.92–2.73 (m, 3H), 2.48 (ddd, J_1 = 13.3, J_2 = 10.7, J_3 = 4.6 Hz, 1H), 2.32 (m, 1H), 2.11 (m, 2H), 1.96 (m, 1H, 1-CH_2, 8-CH_2, 9-CH_2, 14-CH_2); ^{13}C NMR (100.6 MHz, $CDCl_3$): δ = 211.0 (br.s, C13), 140.5 (s), 138.9 (s), 130.4 (s, C2, C5, C10), 129.9 (d), 129.6 (d), 128.4 (d), 128.0 (d, C3, C4, C7, C6), 123.7 (br.d., C12), 54.4 (d, C11), 43.9 (t, C14), 40.0 (t, C9), 32.9 (t), 32.7 (t, C1, C8).

6: A solution of **5** (200 mg, 0.51 mmol) in dry toluene (50 mL) was added to DDQ (347 mg, 1.53 mmol), and the reaction mixture was heated for 5 h at 110 °C. After the solvent was removed, the residue was dissolved in dichloromethane and filtered through alumina III/N. Separation by column chromatography [alumina III/N, dichloromethane/hexane: 6/6 (v/v)] yielded 110 mg of **6** (50%) [5]. Physical and spectroscopic data: m.p. > 300 °C (colorless prisms from $CHCl_3$/pentane); IR (KBr): $\tilde{\nu}$[cm^{-1}] = 3017 (m), 2973 (m), 2953 (m), 2944 (m), 2930 (s), 2859 (m), 2835 (m), 1681 (s), 1650 (m), 1643 (m), 1502 (m), 1444 (s), 1439 (s), 1427 (m), 1377 (m), 1332 (m), 1228 (m), 1177 (s), 1096 (m), 1050 (s), 924 (s), 888 (s), 807 (s), 724 (m); ^{1}H NMR (200.1 MHz, CD_2Cl_2, internal TMS: δ = 6.90–6.7 (br.m, 4H, outer benzene rings), 4.92 (s, 1H, 12-H), 3.0–2.7 (br.m, 8H, -CH_2-). The width of the signal in the ^{1}H NMR spectrum is an indication of the mobility of the rings in **6**, a subject for future study.

Received: February 10, 1992 [Z 5178 IE]
German version: Angew. Chem. **1992**, *104*, 1068

CAS Registry numbers:
1, 5040-51-7; **5**, 141902-96-7; **6**, 141928-12-3; aluminum trichloride, 7446-70-0; titanium tetrachloride, 7550-45-0.

[1] Review: J. Kleinschroth, H. Hopf, *Angew. Chem.* **1982**, *94*, 485–496; *Angew. Chem. Int. Ed. Engl.* **1982**, *21*, 469–480; compare A. F. Mourad, J. Kleinschroth, H. Hopf, *ibid.* **1980**, *92*, 388–389 bzw. **1980**, *19*, 389–390.

[2] H. Hopf, C. Marquard in *Strain and Its Implications in Organic Chemistry* (Eds.: A. de Meijere, S. Blechert), Kluver, Dordrecht, **1989**, pp. 297–332.

[3] D. J. Cram, R. C. Helgeson, D. Lock, L. A. Singer, *J. Am. Chem. Soc.* **1966**, *88*, 1324–1325.

[4] H. Hopf, A. F. Mourad, *Chem. Ber.* **1980**, *113*, 2358–2371; cf. K. Broschinski, Dissertation, Braunschweig, **1984**, and unpublished results.

[5] Crystal structure data: 5 at −95 °C: Monoclinic, $P2_1/n$, a = 598.9(2), b = 2011.3(5), c = 868.6(2) pm, β = 105.31(2)°, V = 1.0091 nm^3, Z = 2, $2\theta_{max}(Mo_{K\alpha})$ = 50°, R = 0.046, R_w = 0.047 for 1132 reflections with $F > 4\sigma(F)$. **6** at −95 °C: Monoclinic, $P2_1/n$ a = 960.1(3), b = 668.8(2), c = 1546.7(3) pm, β = 93.00(2)°, V = 1.0034 nm^3, Z = 2, $2\theta_{max}(Mo_{K\alpha})$ = 55°, R = 0.041, R_w = 0.048 for 1653 reflections with $F > 4\sigma(F)$. The molecules **5** and **6** show crystallographic inversion symmetry. Further details of the crystal structure investigations may be obtained from the Fachinformationszentrum Karlsruhe, Gesellschaft for wissenschaftlich-technische Information mbH, D-W-7514 Eggenstein-Leopoldshafen 2 (FRG) on quoting the depository number CSD-56344, the names of the authors, and the full journal citation.

[6] Besides the quoted yields of **5**, 10% of the starting material **1** was recovered in the $AlCl_3$-catalyzed reaction and 18% in the $TiCl_4$-catalyzed reaction. Unlike BF_3 and $SnCl_4$, $SnCl_4 \cdot HCl$ did catalyze the dimerization of **1**, although it also yielded an HCl-addition product with **5**, whose structure is not yet known.

[7] For a summary of conventional methods for synthesizing multilayered cyclophanes see S. Misumi in *Cyclophanes* (Eds.: P. M. Keehn, S. Rosenfeld), Academic Press, New York, **1983**, pp. 573–628.

[8] The formation of dimer and trimer compounds with totally different structures from [6]cyclophanes in the presence of sulfuric acid was briefly described in Y. Tobe, M. Jimbo, K. Kobiro, K. Kakiuchi, *J. Org. Chem.* **1991**, *56*, 5241–5243; cf. Y. Tobe, A. Takemura, M. Jimbo, T. Takahashi, K. Kobiro, K. Kakiuchi, *J. Am. Chem. Soc.* **1992**, *114*, 3479–3491.

[9] D. J. Cram, G. R. Knox, *J. Am. Chem. Soc.* **1961**, *83*, 2204–2205.

Nitrocalix[4]arenes as Molecules for Second-Order Nonlinear Optics**

By *Erik Kelderman, Lode Derhaeg, Gerard J. T. Heesink, Willem Verboom, Johan F. J. Engbersen, Niek F. van Hulst, Andre Persoons,* and *David N. Reinhoudt**

Organic molecules with π electron systems and unsymmetric charge distributions are promising for use in nonlinear optics (NLO), for example for frequency-doubling of laser light and electro-optic switching.[1-3] In the molecules investigated so far the "NLO-phore", that is the structural unit responsible for the nonlinear optical properties, consists of one single π electron system with one or more electron donors and/or acceptors (D-π-A molecules). Extension of the conjugated system increases the nonlinear hyperpolarizability β, but unfortunately this is accompanied by a shift of the charge-transfer absorption band (CT band) to longer wavelength, thereby restricting the applicability in frequency-doubling.[1-5] Here we describe a novel class of compounds which combine more D-π-A systems resulting not only in an increased hyperpolarizability, and dipole moment, but also in a shift of the CT bands to shorter wavelengths.

Calix[4]arenes are cyclophanes that consist of four phenol moieties connected by methylene bridges.[6] Functionalization of these phenols allows the combination of four D-π-A units within a single calix[4]arene molecule. These calix[4]arenes can be present in four idealized conformations[6-9] with different relative orientations of the intramolecular NLO-phores (Scheme 1).

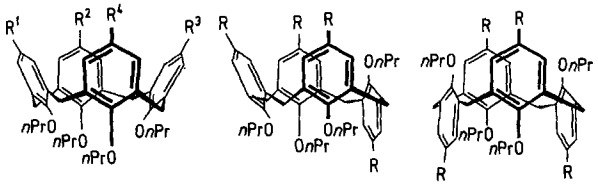

cone | *paco* | *1,3-alternate*

1a, $R^1=R^2=R^3=R^4=t$Bu
1b, $R^1=R^2=R^3=R^4=NO_2$
1c, $R^1=R^2=R^3=R^4=H$
4, $R^1=NO_2$ $R^2=R^3=R^4=H$
5, $R^1=R^3=NO_2$ $R^2=R^4=H$
6, $R^1=R^2=NO_2$ $R^3=R^4=H$

2a, R = *t*Bu
2b, $R=NO_2$

3a, R = *t*Bu
3b, $R=NO_2$

Scheme 1.

In the *cone* conformer (e.g. **1**) the four oxygen atoms of the phenol hydroxyl groups are all on the same side of the calix, whereas in the partial cone (*paco*) conformer (e.g. **2**) only three are. The *1,2-* and *1,3-alternate* conformers (e.g. **3**) have idealized point and radial symmetry, respectively. The different conformers are not interconvertible[7b] when the hydroxyl groups are alkylated by groups larger than 2-hydroxyethyl.[10] *n*-Propylation of *para-tert*-butylcalix[4]arene[6] in *N,N*-dimethylformamide (DMF) at room temperature for 5 days with sodium hydride as a base afforded only **1a** in 93% yield. However, when the reaction was carried out in refluxing benzene with potassium *tert*-butoxide as a base, a 1:1 mixture of **2a** and **3a** in an overall yield of 70% was obtained. The *paco* (**2a**) and *1,3-alternate* conformers (**3a**) could be isolated by crystallization of the crude mixture from chloroform/methanol and chloroform/hexane, respectively. Subsequent *ipso* nitration[11] of **1a**–**3a** afforded the desired tetranitrocalix[4]arenes **1b**–**3b** in 70% yield. The mononitro- **4**, 5,17-dinitro- **5**, and the 5,11-dinitrocalix[4]arene **6** were obtained by reaction of tetrapropoxycalix[4]arene[12] **1c** with nitric acid in dichloromethane and subsequent separation of the mixture of nitrocalix[4]arene products by column chromatography.

To determine the influence of the different orientations of the D-π-A dipoles in the tetranitrocalix[4]arenes[13] on the hyperpolarizability β we have studied the *cone*, *paco*, and the *1,3-alternate* conformers **1b**, **2b**, and **3b**, respectively, by electric field induced second harmonic generation (EFISH).[14] The data obtained for **1b**–**3b** are summarized in Table 1.

Table 1. Hyperpolarizability in the direction of the field-induced *z* axis β_z, dipole moment μ, and the wavelength of the longest wavelength absorption for the nitrocalix[4]arenes **1b**–**6** and the reference compounds **7** and **8**.

	$\beta_z \times 10^{30}$ [esu]	μ [D]	λ_{max} [nm]
1b	30	13.8	291
2b	27	6.7	291
3b	0	0	291
4	16	4.5	308
5	15	7.8	302
6	20	8.7	307
7	12	4.6	302
8	–	–	288

Compound **1b** has a β_z value of 30×10^{-30} esu, about 30% of the value of the reference compound 4-methoxy-4′-nitrostilbene (MONS),[14a] which has a more extended π system. Moreover **1b** has a large dipole moment of 13.8 D. The *paco* conformer **2b** also has a comparably high β_z value, but its dipole moment is only 6.7 D. As expected, the centrosymmetric *1,3-alternate* conformer **3b** exhibits no frequency-doubling of 1064 nm laser light (Nd:YAG laser).

In order to examine whether the β_z values of the four individual D-π-A units are additive, we synthesized a series of *cone* nitrocalix[4]arenes besides **1b** with NO_2 groups in various numbers and positions (**4**, **5**, and **6**) and compared their β values and UV spectra with the reference compounds 4-nitroanisole (**7**) and 2,6-dimethyl-4-nitro-1-*n*-propoxybenzene (**8**).[3,15] The β_z value of the mononitrocalix[4]arene **4** is slightly greater than that of 4-nitroanisole (**7**). Surprisingly, 5,17-dinitrocalix[4]arene **5** has almost the same β_z value. The conformational flexibility of the four aromatic rings in the *cone* conformers and the intramolecular repulsion of the charged D-π-A systems might explain the relatively low β_z value of **5**. In addition, the local field factor $F(\omega)$, which describes the influence of the electrostatic field in the neigh-

[*] Prof. Dr. Ir. D. N. Reinhoudt, Drs. E. Kelderman, Dr. W. Verboom, Dr. J. F. J. Engbersen
Laboratory of Organic Chemistry
University of Twente
P.O. Box 217, NL-7500 AE Enschede (The Netherlands)
Ir. G. J. T. Heesink, Dr. N. F. van Hulst
Laboratory of Optoelectronics and Applied Physics
University of Twente, Enschede (The Netherlands)
Drs. L. Derhaeg, Prof. Dr. A. Persoons
Department of Chemistry, University of Leuven (Belgium)

[**] This investigation was supported by the Netherlands Foundation of Chemical Research (SON) and the Foundation for Fundamental Material Research (FOM) with financial aid from the Netherlands Organization for Scientific Research (NWO). We wish to thank J. M. Visser, J. L. M. Vrielink, T. W. Stevens, and A. M. Montanaro-Christenhusz for recording the IR, UV-VIS, and mass spectra and for performing the elemental analyses.

borhood of the NLO-phore on β [Eq. (a)], is expected to be lower for two cofacial D-π-A aromatic rings.[1, 2] In Equation (a), $\Delta\mu$ is the difference between the dipole moment in the ground and first excited state and f is the oscillator strength of the CT band. 5,11-Dinitrocalix[4]arene **6**, on the other hand, has a slightly higher β_z value than **5**. This may be due to a more parallel and noncofacial orientation of the D-π-A moieties in **6**. The larger dipole moment of 8.7 D, possibly due to reduced dipole-dipole repulsion in **6**, lends further support.

$$\beta_{CT} = \frac{3e^2\hbar^2 F(\omega) f \Delta\mu}{2m} \qquad \text{(a)}$$

From these results it can be concluded that the D-π-A moieties in the calix[4]arenes **1b** and **4**–**6** do not behave as completely independent NLO-phores. This is also in line with the UV spectra. The λ_{max} values of the nitrocalix[4]arenes **1b** and **4**–**6** show a remarkable trend when compared to the reference compound 2,6-dimethyl-4-nitro-1-*n*-propoxybenzene (**8**). The longest wavelength band of **4** (λ_{max} = 308 nm) is shifted bathochromically by 20 nm relative to that of **8** (λ_{max} = 288 nm). This difference must be due to interactions with the other aromatic rings of the calix[4]arene. Remarkably, with increasing numbers of nitro substituents, the λ_{max} values for the CT band of the nitrocalix[4]arenes in the cone conformation decrease slightly, whereas the μ values and the β_z values increase. A λ_{max} of shorter wavelength indicates a more restricted electron transfer from the ground state to the first excited state ($F(\omega)$). According to Equation (a), a lower $F(\omega)$ will cause the β_z value to decrease, and this effect may contribute to the nonlinear increase of β_z with an increase in the number of strong dipoles in a calix[4]arene molecule.

The large dipole moment of **1b** (13.8 D) in combination with the preorganized framework of the four NLO-phores can be used to orient **1b** in a polymeric methylmethacrylate (PMMA) matrix by corona-poling with a strong DC electrical field.[16] For a film with 4.5 wt % of **1b** the degree of orientation[17] $\cos^3\theta$ obtained was 0.28, whereas a similar film with 2 wt % of poled *N*,*N*-dimethylaminonitrostilbene (DANS) gave the much lower $\cos^3\theta$ value of 0.02 under identical conditions. In Equation (b), N is the density of molecules with nonlinear optical properties in the film, and F is the local field factor.[18]

$$\langle\cos^3\theta\rangle = \frac{2d_{33}}{NF\beta_z} \qquad \text{(b)}$$

The NLO efficiences d_{33} of poled films with 4.5 and 25 wt % of **1b** were initially 0.21 and 1.1 pmV^{-1}, respectively. Measurements over a period of two months showed a decrease of the d_{33} value to 60% of the initial value, that is to 0.13 and 0.65 pmV^{-1}, respectively. These values were attained in about one week and did not change thereafter. For comparison, the d_{33} of a film with 2 wt % of DANS had decreased to 30% of the initial value of 0.21 pmV^{-1} after one week and was inactive after one month.[19]

The high stability of the film of **1b** is probably a result of the bulkiness of the calix[4]arene skeleton, the restricted rotation of the individual D-π-A moieties, and the complexation of the methyl groups of the polymer backbone with this molecule.

In conclusion, this new class of NLO compounds possesses a unique combination of four nonconjugated D-π-A dipoles in one molecule. These compounds combine high β_z, and μ values with relatively low λ_{max} values. The low λ_{max} values make them suitable for frequency-doubling 820 nm emission from diode lasers to blue laser light at 410 nm.[4, 5] The high μ value of the tetranitrocalix[4]arene **1b** enables a high degree of orientation upon poling in a polymeric matrix. Further functionalization leading to extended π electron systems with high β_z values and the synthesis of polymerizable calixarenes with high dipole moments are currently under investigation.

Experimental Procedure

All new compounds were fully characterized by ^{1}H and ^{13}C NMR spectroscopy, mass spectroscopy, elemental analysis, UV-VIS and IR spectroscopy.

General procedure for *ipso* nitration of the *tert*-butylcalix[4]arenes **1a**, **2a**, and **3a**: To a solution of calix[4]arene **1a**, **2a**, and **3a** (3.00 mmol) in a mixture of CH_2Cl_2 (30 mL) and glacial acetic acid (30 mL) was aded 100% HNO_3 (10 mL, ca. 240 mmol) at 0 °C. The reaction mixture was stirred at room temperature until the black–purple color had discharged and subsequently poured into water (200 mL). The aqueous layer was extracted with CH_2Cl_2 (2 × 50 mL). The combined organic layers were washed with water (2 × 50 mL), dried over $MgSO_4$, and concentrated. Recrystallization of the crude reaction products from methanol gave analytically pure compounds.

^{1}H NMR spectroscopic data of **2b** and **3b** (conditions: 250 MHz, $CDCl_3$, 25 °C, TMS): **2b**: δ = 8.23, 8.15 (s, 4H; ArH), 7.89, 7.11 (d, 4H, J = 2.7 Hz; ArH), 4.1–3.3 (m, 16H; $ArCH_2Ar$ and OCH_2), 2.2–1.8 (m, 8H; CH_2CH_3), 1.2–1.1 (m, 9H; CH_3), 0.62 (t, 3H, J = 7.5 Hz; CH_3). **3b**: δ = 7.96 (s, 8H; ArH), 3.80 (t, 8H, J = 7.3 Hz; OCH_2), 3.74 (s, 8H; $ArCH_2Ar$), 2.0–1.9 (m, 8H; CH_2CH_3), 1.05 (t, 12H; CH_3).

Procedure for nitration of calix[4]arene **1c**: To a solution of **1c** (1 g, 1.7 mmol) in a mixture of CH_2Cl_2 (100 mL) and acetic acid (4 mL) was added 65% nitric acid (1 mL, 25 mmol, 15 equiv) whereupon the mixture was stirred for 0.5 h at room temperature. The reaction was stopped by the addition of water (100 mL), and the product mixture was extracted with CH_2Cl_2 (3 × 25 mL). The combined organic layers were washed with water (3 × 25 mL), saturated sodium bicarbonate solution (3 × 25 mL), and water (3 × 25 mL), dried over $MgSO_4$, and concentrated. The reaction mixture consisted mainly of mononitrocalix[4]arene **4** (30%) and traces of 5,17-dinitrocalix[4]arene **5** and 5,11-dinitrocalix[4]arene **6**. The same reaction with **1c** for 3 h afforded **5** and **6** in 30% and 10% yields, respectively. The products were separated by column chromatography SiO_2/CH_2Cl_2.

4: M.p. 192–193 °C; ^{1}H NMR: δ = 7.25 (s, 2H; ArH-NO_2), 7.0–6.8 (m, 6H; ArH), 6.22 (s, 3H; ArH), 4.47 and 3.20 (ABq, 4H, J = 13.7 Hz; $ArCH_2Ar$), 4.42 and 3.16 (ABq, 4H, J = 13.5 Hz; $ArCH_2Ar$), 4.0–3.7 (m, 8H; OCH_2), 2.0–1.8 (m, 8H; CH_2CH_3), 1.1–0.9 (m, 12H; CH_3), ^{13}C NMR: δ = 161.2, 157.0, 155.6 (s, ArC-O), 142.4 (s, ArC-NO_2), 76.8, 76.5, 76.4 (t, OCH_2), 30.9, 30.8 (t, $ArCH_2Ar$), 23.2, 22.9 (t, CH_2CH_3), 10.4, 10.3, 10.0 (q, CH_3).

5: M.p. 185–186 °C; ^{1}H NMR: δ = 7.42 (s, 4H; ArH), 6.74 (s, 6H; ArH), 4.47 and 3.25 (ABq, 8H, J = 13.7 Hz; $ArCH_2Ar$), 4.0–3.8 (m, 8H; OCH_2), 2.0–1.8 (m, 8H; CH_2CH_3), 1.2–0.9 (m, 12H; CH_3); ^{13}C NMR: δ = 161.7, 156.1, 142.3, 136.1, 134.0 (s, ArC), 128.7, 123.2, 122.9 (d, ArC), 77.1, 76.7 (t, OCH_2), 30.8 (t, $ArCH_2Ar$), 23.1, 22.9 (t, CH_2CH_3), 10.1, 10.0 (q, CH_3).

6: M.p. 151–152 °C; ^{1}H NMR: δ = 7.5–7.4 (m, 4H; ArH-NO_2), 6.6–6.5 (m, 6H; ArH), 4.6–4.4 and 3.3–3.1 (3 ABq, 8H, J = 13.7 Hz; $ArCH_2Ar$), 4.0–3.7 (m, 8H; OCH_2), 1.9–1.8 (m, 8H; CH_2CH_3), 1.0–0.9 (m, 12H; CH_3); ^{13}C NMR: δ = 162.2, 156.4 (s, ArC-O), 142.5 (s, ArC-NO_2), 31.1, 30.8 (t, $ArCH_2Ar$), 23.3, 23.2 (t, CH_2CH_3), 10.3, 10.2 (q, CH_3).

The EFISH measurements are described in ref. [14].

Poled films were prepared in a clean room facility with dust class 1000 and at 20 °C and 5% humidity. A solution of **1b** (4.5 wt %)/PMMA (M = 33000) in chloroform was spun on pyrex glass yielding thin films with thicknesses in the range of 0.25–1 μm. The film was orientated by corona-poling with a field of 8 kV at 110 °C for 15 min and allowed to cool to room temperature while the high voltage was maintained. The SHG efficiency of the film was measured at 1064 nm against a sample of α-quartz as reference to determine the absolute d_{33} value.

Received: February 12, 1992 [Z 5173 IE]
German version: *Angew. Chem.* **1992**, *104*, 1107

[1] D. J. Williams, *Angew. Chem.* **1984**, *96*, 637; *Angew. Chem. Int. Ed. Engl.* **1984**, *23*, 6.
[2] *Nonlinear Optical Properties of Organic Molecules and Crystals, Vol. 1, 2* (Eds.: D. S. Chemla, J. Zyss), Academic Press, Orlando, FL, USA, **1987**.
[3] L.-T. Cheng, W. Tam, G. R. Meredith, G. L. J. A. Rikken, E. W. Meijer, *Proc. SPIE Int. Soc. Opt. Eng.* **1989**, *1147*, 61.
[4] S. Nijhuis, G. L. J. A. Rikken, E. E. Havinga, W. ten Hoeve, E. W. Meijer, *J. Chem. Soc. Chem. Commun.* **1990**, 1093.

[5] E. G. J. Staring, G. L. J. A. Rikken, C. J. E. Seppen, S. Nijhuis, A. H. J. Venhuizen, *Adv. Mater.* **1991**, *3*, 401.
[6] a) C. D. Gutsche, *Calixarenes*, The Royal Chemical Society, Cambridge, **1989**; b) *Calixarenes, A Versatile Class of Macrocyclic Compounds* (Eds.: J. Vicens, V. Böhmer), Kluwer, Dordrecht, **1991**; c) C. D. Gutsche, L.-G. Lin, *Tetrahedron* **1986**, *42*, 1633.
[7] J.-D. van Loon, A. Arduini, L. Coppi, W. Verboom, A. Pochini, R. Ungaro, S. Harkema, D. N. Reinhoudt, *J. Org. Chem.* **1990**, *55*, 5639, and references cited therein.; b) L. C. Groenen, J.-D. van Loon, W. Verboom, S. Harkema, A. Casnati, R. Ungaro, A. Pochini, F. Ugozzoli, D. N. Reinhoudt, *J. Am. Chem. Soc.* **1991**, *113*, 2385.
[8] K. Iwamoto, K. Araki, S. Shinkai, *J. Org. Chem.* **1991**, *56*, 4955.
[9] L. C. Groenen, B. H. M. Ruël, A. Casnati, P. Timmerman, W. Verboom, S. Harkema, A. Pochini, R. Ungaro, D. N. Reinhoudt, *Tetrahedron Lett.* **1991**, *32*, 2675.
[10] The recently synthesized *cone* conformers of tetrakis(2-hydroxyethyl)calix[4]arenes isomerize slowly to the *paco* conformer in a DMF solution at room temperature.
[11] W. Verboom, A. Durie, R. J. M. Egberink, Z. Asfari, D. N. Reinhoudt, *J. Org. Chem.* **1992**, *57*, 1313.
[12] The tetrapropoxycalix[4]arene **1c** could be obtained exclusively in the *cone* conformation in 80% yield by reaction of calix[4]arene [6c] with 1-iodopropane in NaH/DMF at room temperature for 20 h. With somewhat different reaction conditions Shinkai et al. [8] found a mixture of *cone* and *paco* conformers of which the latter is the major isomer. For a general study in which the possible factors are discussed that determine the ultimate conformation of tetra-*O*-alkylated calix[4]arenes see ref. [9].
[13] From here on the prefix "tetrapropoxy" is omitted from the calix[4]arene to improve readability.
[14] a) L. Derhaeg, C. Samyn, A. Persoons in *Organic Molecules for Nonlinear Optics and Photonics* (Eds.: J. Messier, F. Kazjar, P. Prasad), Kluwer, Dordrecht, **1991**, p. 177; b) E. Kelderman, W. Verboom, J. F. J. Engbersen, S. Harkema, G. J. T. Heesink, E. Lehmusvaara, N. F. van Hulst, D. N. Reinhoudt, L. Derhaeg, A. Persoons, *Chem. Mater.*, **1992**, *4*, 626.
[15] *Standard Ultraviolet Spectra Collection* (Sadler Research Laboratories, Division of Bio-Rad Laboratories), Researchers, Editors & Publishers, USA, **1980**.
[16] a) M. A. Montazawi, A. Knoesen, S. T. Kowel, B. G. Higgens, A. Dienes, *J. Opt. Soc. Am.* **1989**, *6*, 733; b) J.-R. Li, H. J. Wintle, *J. Appl. Phys.* **1989**, *65*, 4617.
[17] K. D. Singer, J. E. Sohn, S. J. Lalama, *Appl. Phys. Lett.* **1986**, *49*, 248.
[18] The local field factor ($F = 2.5$) was determined from refractive index measurements ($n = 1.45$) on the film. Because of the low dispersion of the material, the refractive indices at both wavelengths are approximately equal. The number density of the film with 4.5 wt% of **1b** is about $4.5 \times 10^{-25}\ m^{-3}$.
[19] Hampsch et al. measured a d_{33} value of $0.4\ pm\ V^{-1}$ for a film with 4.5 wt% of DANS; this is in good agreement with our results. H. L. Hampsch, Jianyang, G. K. Wong, J. M. Torkelson, *Macromolecules* **1990**, *23*, 30640.

[{Cp*Cr(μ_3-H)}$_4$]—a Paramagnetic Chromium Hydride with a Cubane Structure**

By *Robert A. Heintz, Brian S. Haggerty, Hong Wan, Arnold L. Rheingold*, and *Klaus H. Theopold**

During the course of our exploration of paramagnetic organometallic complexes of chromium(III)[1] many attempts at preparing hydride complexes have come to naught. However, we have now discovered a novel class of electron-deficient alkylchromium(II) compounds, which undergo efficient hydrogenolysis to yield unusual paramagnetic chromium hydrides.[2] Herein we report the synthesis, structural characterization, and some unusual magnetic properties of the latter.[3]

Addition of two equivalents of Li[HB*s*Bu$_3$] to a solution of [(Cp*CrCl$_2$)$_2$] (Cp* = C$_5$Me$_5$) in THF yielded the reduction product [{Cp*Cr^{II}(μ-Cl)}$_2$] (**1**) instead of the desired complex [{Cp*Cr^{III}(H)Cl}$_2$]. Alerted to the stability of this rather simple starting material for organometallic compounds with divalent chromium,[4] we found that **1** may also be prepared in reasonable yield (65%) directly from Cp*Li and CrCl$_2$ (Scheme 1). The X-ray crystal structure determination revealed that **1** is a dinuclear complex with pseudo C_{2v} symmetry and a Cr–Cr distance of 2.642(2) Å. The effective magnetic moment (μ_{eff}) of this compound is temperature dependent and gradually rises to 2.0 μ_B per dimer at room temperature, consistent with some degree of metal–metal bonding.

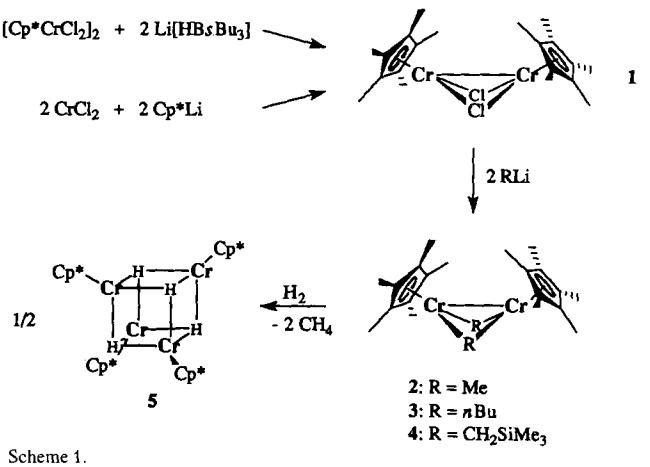

Scheme 1.

Complex **1** was easily alkylated and thereby yielded a series of extremely electron-deficient alkylchromium(II) complexes of the type [Cp*Cr(μ-R)]$_2$ **2**–**4** (Scheme 1). The methyl complex **2** was structurally characterized by X-ray diffraction. As expected, the substitution of the 3-center/4-electron chloride bridges with the 3-center/2-electron methyl bridges causes a dramatic decrease in the Cr–Cr distance (2.263(3) Å).[5] The greater strength of the metal–metal interaction is also evident in the magnetic behavior of **2**; μ_{eff} for the dinuclear complex only reaches 0.92 μ_B at room temperature. Finally, the muted reactivity of the compound supports the presence of a strong metal–metal bond. Complex **2** is thermally stable up to 100 °C in solution and does not react with ethylene under mild conditions; although **2** is eventually cleaved by bis(dimethylphosphino)ethane (dmpe) to produce the known [Cp*Cr(dmpe)CH$_3$],[1b] the reaction is very slow (several hours at room temperature). **2** is one of the few chromium(II) complexes thought to exhibit multiple Cr–Cr bonds despite the absence of binucleating ligands akin to carboxylates.[6]

In our experience alkylchromium(III) complexes have largely resisted hydrogenolysis; in contrast **2** reacted slowly with H_2 at room temperature to generate methane and a black paramagnetic precipitate. Elemental analysis and IR spectroscopy of the solid indicated the presence of Cp* ligands. Well-formed crystals of this material were eventually grown from hot toluene; however, only a rough crystal structure could be obtained due to disorder that likely resulted from an unresolvable superlattice.[7] This problem was finally overcome when the EtMe$_4$C$_5$ ligand was used instead

[*] Prof. Dr. K. H. Theopold, R. A. Heintz, B. S. Haggerty,
Prof. Dr. A. L. Rheingold
Department of Chemistry and Biochemistry
University of Delaware
Newark, DE 19716 (USA)
H. Wan
Department of Physics and Astronomy, University of Delaware (USA)

[**] This work was supported by the National Science Foundation (CHE-9096251) and the University of Delaware. We thank Prof. H. Hope (University of California at Davis) for obtaining a low-temperature X-ray diffraction data set of [{Cp*Cr(μ_3-H)}$_4$], and Prof. G. Hadjipanayis (University of Delaware) for the use of his SQUID.

of Cp*. The result of an X-ray structure determination is shown in Figure 1;[8] the products of the hydrogenation of **2** and **2'** (with $EtMe_4C_5$ ligand) are tetranuclear chromium hydrides of the formulas $[\{Cp^*Cr(\mu_3\text{-}H)\}_4]$ (**5**) and $[\{(\eta^5\text{-}EtMe_4C_5)Cr(\mu_3\text{-}H)\}_4]$ (**5'**), respectively (the heavy atom cores of **5** and **5'** were essentially identical). Each molecule of **5'** has a crystallographic mirror plane passing through the positions of the atoms Cr2, Cr3, H2, and H3. The basic framework of the complex is an essentially regular cube, whose corners are occupied alternately by Cr and H atoms. The average Cr–Cr distance of 2.715 Å is long by comparison to those of the complexes **2** and **1**; the distribution of the sixteen available d-electrons over six equal metal–metal interactions probably precludes significant multiple metal–metal bonding. The Cr–Cr distance is also greater than the Co–Co distance in the isostructural complex $[\{CpCo(\mu_3\text{-}H)\}_4]$ (2.467 Å).[9] This "saturated" complex has been assigned a metal–metal single bond[10] and thus **5'** (and **5**) may best be described as lacking metal–metal bonds. The hydride ligands were located by the X-ray structure analysis and their positions refined. While X-ray structural parameters of hydrogen atoms are of necessity uncertain, there is no doubt that the hydride ligands are capping the four faces of the Cr_4 tetrahedron.

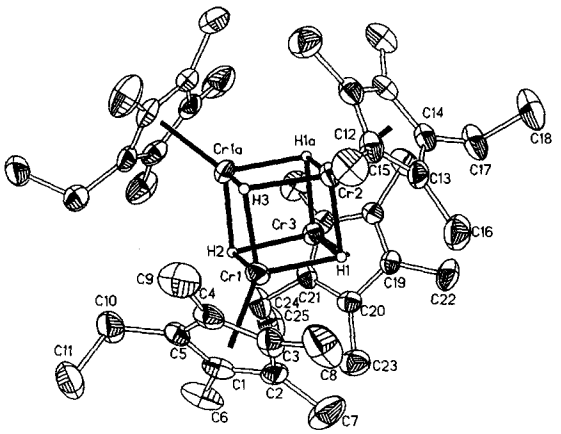

Fig. 1. The molecular structure of $[\{(EtMe_4C_5)Cr(\mu_3\text{-}H)\}_4]$ (**5'**). Selected distances [Å] and angles [°]: Cr1-Cr1a 2.722(2), Cr1-Cr2 2.715(1), Cr1-Cr3 2.716(2), Cr2-Cr3 2.703(2), average Cr-H 1.969 (1.894–2.014), average Cr-C 2.267; average H-Cr-H 92.7 (88.9–94.3).

Mindful of the extreme variability of metal–metal distances in polynuclear chromium compounds and the ongoing discussion of Cr–Cr bonding in such complexes,[6b] we have investigated the magnetic behavior of **5**. Figure 2 depicts the results of measurements of the magnetic susceptibility of complex **5** with a Faraday balance. Somewhat surprisingly, the complex exhibits almost ideal Curie-type paramagnetism.[11] The effective magnetic moment is constant from room temperature down to 15 K ($\mu_{eff} = 5.7\ \mu_B$, or 2.85 μ_B per chromium atom). This value is ambiguous: it can either be interpreted as resulting from complete lack of any exchange interaction between the four Cr^{II} ions ($S = 1$, spin-only moment 2.83 μ_B) or as μ_{eff} of a complex with a ground state of high spin multiplicity ($S = 2$, augmented by an orbital contribution) caused by accidental degeneracy of MOs. Evidence for the latter, more probable, explanation was provided by saturation magnetization measurements[12] on **5** at high magnetic field ($H < 55$ kOe) and $T = 4.0$ K. Under these conditions, the magnetic moment of the sample, induced by aligning all of the spin moments, was that expected for a system of four unpaired electrons per Cr_4 molecule.

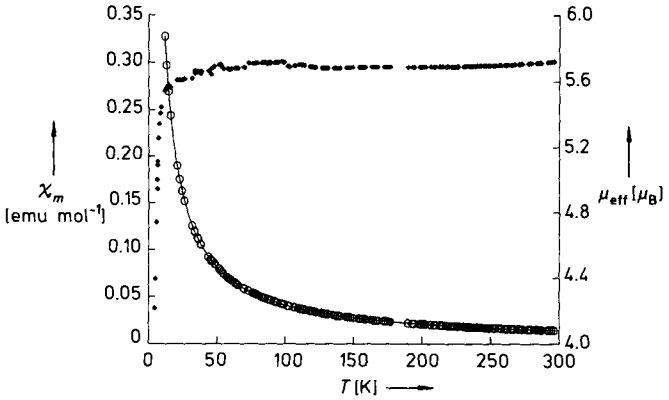

Fig. 2. Temperature dependence of the molar magnetic susceptibility (χ_m, corrected for diamagnetism and temperature-independent paramagnetism, open circles) and the effective magnetic moment (μ_{eff} per Cr_4 cluster, filled squares) of **5**. The line represents the fit of χ_m data with the Curie–Weiss law [11].

The electronic spectrum of the **5** is dominated by a very intense absorption below 400 nm; in addition, there are two discernable shoulders of much lower extinction at approximately 480 and 980 nm. While the low solubility of **5** precludes characterization by NMR spectroscopy in solution, its analogue **5'** exhibits a distinct ^1H NMR spectrum in C_6D_6 attributable to the $EtMe_4C_5$ moiety ($\delta = 7.9$ (6H), 7.2 (6H), 3.4 (2H), 1.1 (3H), full width at half-maximum (fwhm): 18–65 Hz); the resonance signals are broad but are still within the normal range of chemical shifts. To our surprise, even a ^{13}C NMR spectrum of **5'** exhibiting the seven expected resonance signals could be obtained ($\delta = 119.7$, 114.7, 111.0, 94.0, 91.7, 84.5, 37.9). Various attempts to record mass spectra of **5** (EI, FAB, laser desorption) yielded only spectra with the fragmentation patterns of the known $[\{Cp^*Cr(\mu_3\text{-}O)\}_4]$;[13] the considerable air-sensitivity of **5** and **5'** probably explains this observation. To enable the assignment of any Cr–H vibrations in the IR spectrum, $[D_4]$ **5** and $[D_4]$ **5'** were prepared; however, the largely featureless solid-state IR spectra of the deuterides do not differ significantly from those of the hydrides. Corroborating evidence for the presence of hydrido ligands in **5**, **5'** came from protonation reactions of these complexes. Addition of an excess of gaseous HCl to solutions of **5'** liberated 5.9 equivalents of H_2 (measured with a Töpler pump) leaving a quantitative yield of $[\{(EtMe_4C_5)Cr^{III}Cl_2\}_2]$. Two equivalents of H_2 were formed in the apparent oxidation of four Cr^{II} ions to Cr^{III} ions, and the additional H_2 presumably resulted from proton–hydride combination. Complex **5** could not be reduced even in the presence of a mixture of potassium metal and the [222] cryptand;[14] however, **5** is rapidly oxidized by air and by $AgBF_4$. None of the compounds reported herein catalyze the polymerization of ethylene in homogeneous solution. Further experiments are under way in our laboratory.

The chemistry of paramagnetic organometallic chromium compounds now encompasses hydrides too. We are investigating their range of stability, physical properties, and reactivity characteristics.

Experimental Procedure

1: Cp*Li (1.0 g, 7.0 mmol) was added to a stirred suspension of $CrCl_2$ (0.87 g, 7.7 mmol) in 50 mL of THF. After the mixture was stirred for 12 hours the

solvent was evaporated, and the residue was extracted with pentane. Concentration and cooling of the green–brown solution to −30 °C yielded 1.01 g of **1** (2.27 mmol, 65%). ^{1}H NMR (C_6D_6): δ = 10.8 (br s); IR (KBr): $\tilde{\nu}$[cm^{-1}] = 2959 sh, s), 2909 (s), 2857 (s), 1441 (m), 1377 (s), 1069 (w), 1022 (m), 799 (w), 523 (w); correct elemental analysis for $C_{20}H_{30}Cl_2Cr_2$.

2: 2.0 equivalents of MeLi (1.4 M in Et_2O) were added to a THF solution of **1** (prepared in situ as above). Evaporation of THF and extraction with pentane gave a brown solution, which was filtered and concentrated. Cooling to −30 °C for approximately 15 h yielded 0.85 g of **2** (2.1 mmol, 60%). ^{1}H NMR (C_6D_6): δ = 14.9 (br s, 3H), 2.51 (s, 15H); IR (KBr): $\tilde{\nu}$[cm^{-1}] = 2960 (sh, s), 2909 (s), 2857 (s), 1435 (m), 1375 (s), 1165 (w), 1111 (w), 1022 (w), 937 (m), 824 (w), 475 (w); correct elemental analysis for $C_{22}H_{36}Cr_2$.

5: A solution of **2** (0.80 g, 2.0 mmol) in pentane (50 mL) was placed in a 500 mL flask fitted with a needle valve. The solution was degassed and the flask backfilled with H_2 (1 atm). After the mixture was stirred at room temperature for 6 days, the solution was filtered to yield a black solid **5**, which was washed with pentane and dried (0.51 g, 0.68 mmol, 68%). IR (KBR): $\tilde{\nu}$[cm^{-1}] = 2982 (m), 2903 (s), 2852 (s), 1435 (m), 1370 (s), 1020 (m), 550 (s), correct elemental analysis for $C_{40}H_{64}Cr_4$.

Received: February 21, 1992 [Z 5201 IE]
German version: *Angew. Chem.* **1992**, *104*, 1100

[1] a) K. H. Theopold, *Acc. Chem. Res.* **1990**, *23*, 263; b) B. J. Thomas, S. K. Noh, G. K. Schulte, S. C. Sendlinger, K. H. Theopold, *J. Am. Chem. Soc.* **1991**, *113*, 893; c) S. K. Noh, R. A. Heintz, B. S. Haggerty, A. L. Rheingold, K. H. Theopold, *ibid.* **1992**, *114*, 1892.

[2] Other chromium hydrides: a) E. O. Fischer, W. Hafner, *Z. Naturforsch. B* **1955**, *10*, 140; b) J. L. Petersen, R. K. Brown, J. M. Williams, *Inorg. Chem.* **1981**, *20*, 158; c) M. Y. Darensbourg, R. Bau, M. W. Marks, R. R. Burch, Jr., J. C. Deaton, S. Slater, *J. Am. Chem. Soc.* **1984**, *104*, 6961; d) G. S. Girolami, J. E. Salt, G. Wilkinson, M. Thornton-Pett, M. B. Hursthouse, *ibid.* **1983**, *105*, 5954; e) F. A. Van-Cattledge, S. D. Ittel, J. P. Jesson, *Organometallics* **1985**, *4*, 18; f) E. Thaler, K. Folting, J. C. Huffman, K. G. Caulton, *Inorg. Chem.* **1987**, *26*, 374; paramagnetic hydrides: g) J. E. Bercaw, H. H. Brintzinger, *J. Am. Chem. Soc.* **1969**, *71*, 7301; h) J. R. Sanders, *J. Chem Soc. Dalton Trans.* **1973**, 748; i) J. Müller, H. Dorner, G. Huttner, H. Lorenz, *Angew. Chem.* **1973**, *85*, 1117; *Angew. Chem. Int. Ed. Engl.* **1973**, *12*, 1005; j) M. Gargano, P. Giannocaro, M. Rossi, G. Vasopollo, A. Sacco, *J. Chem. Soc. Dalton Trans.* **1975**, 9; k) I. H. Elson, J. K. Kochi, *J. Am. Chem. Soc.* **1975**, *97*, 1262; l) S. G. Shore, W.-L. Hsu, M. R. Churchill, C. Bueno, *ibid.* **1983**, *105*, 655; m) M. L. Luetkens, Jr., J. C. Huffman, A. P. Sattelberger, *ibid.* **1983**, *105*, 4474; n) E. Samuel, J. F. Harrod, *ibid.* **1984**, *106*, 1859; o) P. Mura, A. Segre, *Angew. Chem.* **1986**, *98*, 453; *Angew. Chem. Int. Ed. Engl.* **1986**, *25*, 460; p) P. Mura, *J. Am. Chem. Soc.* **1986**, *108*, 351; q) P. Mura, A. Segre, S. Sostero, *Inorg. Chem.* **1989**, *28*, 2853; r) B. Hessen, F. van Bolhuis, J. H. Teuben, J. L. Petersen, *J. Am. Chem. Soc.* **1988**, *110*, 295; s) C. Bianchini, F. Laschi, D. Masi, C. Mealli, A. Meli, F. M. Ottaviani, D. M. Proserpio, M. Sabat, P. Zanello, *Inorg. Chem.* **1989**, *28*, 2552.

[3] Further details of the synthesis, structural characterization, and reactivity of the chromium(II) complexes used as precursors (i.e. **1**–**4**) will be published later.

[4] "[CpCrCl]$_n$" is thought to be formed upon reduction of [(CpCrCl$_2$)$_2$] with Zn, but it apparently disproportionates rapidly to [Cp_2Cr] and $CrCl_2$; J. Heck, presented at the IXth FECHEM Conference on Organometallic Chemistry, Heidelberg, Germany, July 14–19, **1991**.

[5] a) S. K. Noh, S. C. Sendlinger, C. Janiak, K. H. Theopold, *J. Am. Chem. Soc.* **1989**, *111*, 9127, and references therein. b) A detailed theoretical study of this effect in Cr(III) chemistry has been made; C. Janiak, J. Silvestre, K. H. Theopold, *Inorg. Chem.* submitted.

[6] a) F. A. Cotton, R. A. Walton, *Multiple Bonds Between Metal Atoms*, Wiley, New York, **1982**, p. 178 f; b) J. J. H. Edema, S. Gambarotta, *Comments Inorg. Chem.* **1991**, *11*, 195.

[7] Crystal data for **5**: dark brown, M_r = 752.9, triclinic, $P\bar{1}$, a = 10.617(5), b = 10.845(17), c = 17.895(17) Å, α = 83.00(3), β = 82.53(3), γ = 67.33(2)°, V = 1879.3(8) Å^3, Z = 2. Axial photographs taken along the c axis revealed interlayer streaks suggesting the presence of a superlattice. Attempts to determine the relationship of the superlattice to the one reported were unsuccessful. The intensity of the reflections defining the superlattice were orders of magnitude weaker than the sublattice data. Solution and refinement of the sublattice data was terminated due to extreme light-atom disorder. However, a tetrahedral Cr_4 core with Cr–Cr distances of 2.61–2.74 Å was unambiguous.

[8] Crystal data for **5'**: $C_{44}H_{72}Cr_4$, dark brown, M_r = 809.0, orthorhombic, *Pnma*, a = 15.412(4), b = 17.195(4), c = 16.221(3) Å, V = 4298.7(14) Å^3, Z = 4, ρ_x = 1.250 g cm^{-3}, $R(F)$ = 0.0494 for 1958 observed ($3\sigma F_0$) data, max. 2θ = 45°. Further details of the crystal structure investigation are available on request from the Director of the Cambridge Crystallographic Data Centre, University Chemical Laboratory, Lensfield Road, GB-Cambridge CB2 1EW, on quoting the full journal citation.

[9] G. Huttner, H. Lorenz, *Chem. Ber.* **1975**, *108*, 973.

[10] R. Hoffmann, B. E. R. Schilling, R. Bau, H. D. Kaesz, D. M. P. Mingos, *J. Am. Chem. Soc.* **1978**, *100*, 6088.

[11] The susceptability data was fitted with a Curie-Weiss expression (χ_m = [C/(T-θ)] + TIP). C = 4.081, θ = −0.8 K, TIP = 750 × 10^{-6} emu mol^{-1}.

[12] R. L. Carlin, *Magnetochemistry*, Springer, Berlin, **1986**, p. 14 ff.

[13] F. Bottomley, J. Chen, S. M. MacIntosh, R. C. Thompson, *Organometallics* **1991**, *10*, 907.

[14] [222]Cryptand is 1,10-diaza-4,7,13,16,21,24-hexaoxabicyclo[8.8.8]hexacosane.

A Short Diastereoselective Entry to Indole Alkaloids of the Corynanthe Type by the Intramolecular Ene Reaction**

By *Lutz F. Tietze** and *Jürgen Wichmann*

Dedicated to Professor Ekkehard Winterfeldt on the occasion of his 60th birthday

Pericyclic reactions, primarily the Diels–Alder reaction,[1] are widely employed in natural product synthesis. The ene reaction[2] has not been utilized to the same extent, possibly because of its higher activation energy. However, much milder reaction conditions have been developed—activation of the enophile by introducing electron-withdrawing groups[3] and the use of Lewis acids[4]—which make the ene reaction very attractive nowadays. Therefore, it is astonishing that this reaction has not been applied to the synthesis of indole alkaloids, which make up an intensively examined field of natural product synthesis.[5] The *trans*-specific formation of six-membered ring systems by intramolecular ene reactions by means of enophiles with two electron-withdrawing groups at the terminal position[3] should provide a short route to indole alkaloids of the corynanthe group according to the retrosynthetic analysis shown for corynantheine (**1**) in Scheme 1.

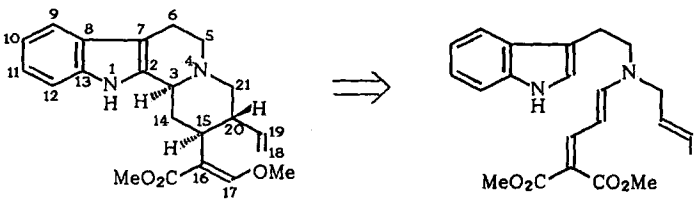

1 **3a**

Scheme 1. Retrosynthesis of corynantheine (**1**).

We report here on a short and highly diastereoselective synthesis of the *trans*-indolo-[2,3-*a*]-quinolizidine framework by a sequential Pictet–Spengler[6] intramolecular ene reaction starting from **3a** and **3b**. Compounds **3** were obtained from **2**[7] by alkylation with 1-bromo-2-butene and 1-bromo-3-methyl-2-butene, respectively (Scheme 2). The one-pot, double cyclization was accomplished without the isolation of intermediates **4** by treatment of **3** with trifluoro-

[*] Prof. Dr. L. F. Tietze, Dr. J. Wichmann
Institut für Organische Chemie der Universität
Tammannstraße 2, D-W-3400 Göttingen (FRG)

[**] Intramolecular Ene and Related Reactions, Part 10. This work was supported by the Fonds der Chemischen Industrie.—Part 9: L. F. Tietze, J. R. Wünsch, *Synthesis*, **1990**, 985.

acetic acid (TFA) followed by $SnCl_4$[8] to give the *trans*-indolo-[2,3-*a*]-quinolizidines **6**. When **3** was allowed to react with only trifluoroacetic acid, **4** was obtained in 63–66% yield. Thus, it was not possible to carry out a double cyclization with a Brønsted or a Lewis acid alone. Surprisingly, $SnCl_4$ was the only one of the common Lewis acids which could promote the intramolecular ene reaction.

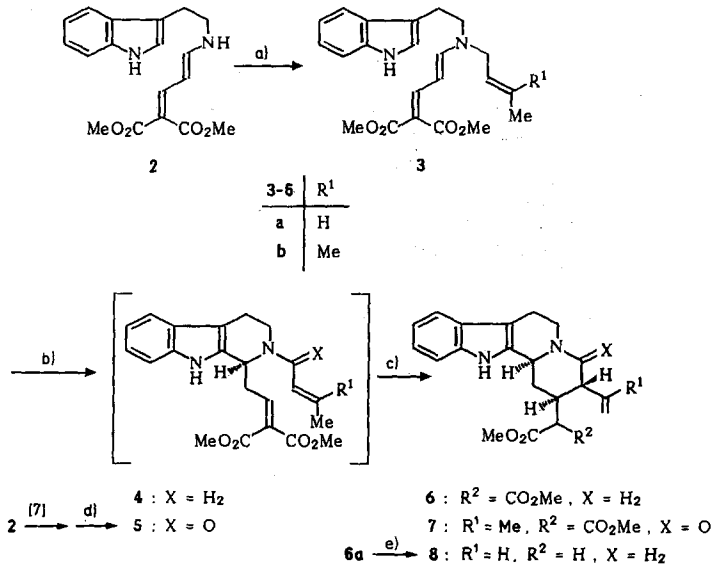

Scheme 2. a) $BrCH_2$–CH=CR^1–Me, $LiNiPr_2$, THF, −78 → 20 °C, 12 h; 60% (**3a**), 76% (**3b**). b) 1.5 equiv TFA, CH_2Cl_2, 20 °C, 24 h. c) 1.2 equiv $SnCl_4$, 20 °C, 24 h; 42% (**6a**), 47% (**6b**). d) Me–R^1CH=CH–COCl, pyridine, CH_2Cl_2, 0 → 20 °C, 12 h; 74% (**5b**). e) LiI · $3H_2O$, Me_2SO, 180 °C, 2.5 h; 65%.

In a similar transformation, **5b**, which was obtained from **2** by cyclization[7] followed by acylation with 3-methylbutenoyl chloride, was converted with $SnCl_2$ into **7** in 65% yield. In contrast, **5a** did not react under these conditions, presumably because of the low energy of the HOMO of the ene moiety.

The intramolecular ene reactions of **4a**, **4b**, and **5b** are highly diastereoselective, leading to only the respective desired diastereomers **6a**, **6b**, and **7** which have the same relative configurations at the stereogenic centers as the corynanthe alkaloids. We assume that the transition structure has an *exo*-*E*(ene)-*anti*-orientation with a chair-type arrangement of the tether as shown in Scheme 3. As pointed out

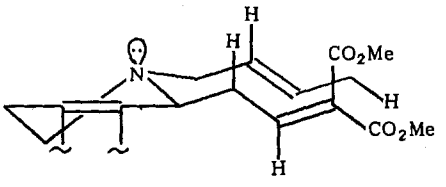

Scheme 3. Postulated transition structure of the intramolecular ene reaction of **4a**.

earlier,[9] the excellent stereocontrol may be a result of the conformation fixed by the 1,3-allylic strain,[10] which is due to the disubstituted enophile terminus (sp^2 geminal effect[3c]).

The configuration and conformation of the compounds **6a**, **6b**, and **7** have been determined by NMR spectroscopy. 3-H of **6a** and **6b** resonates at $\delta = 3.14$ and 3.18, respectively, clearly proving the existence of a *trans*-quinolizidine unit. The axial orientation of 3-H, 15-H, and 20-H in **6a** (and **6b**) can be deduced from the three large couplings of $J = 11-12$ Hz for the signal of 14-H_{ax} at $\delta = 1.72$ (1.64 for **6b**) and from the two large couplings of $J = 11$ Hz for 21-H_{ax} at $\delta = 2.13$ (2.28 for **6b**). A similar argument holds for **7**.

The ene product **6a** was transformed into the known methyl corynantheate (**8**) by demethoxycarbonylation.[11] Compound **8** is an intermediate often used in the synthesis of corynantheine (**1**), dihydrocorynantheine, corynantheol, and dihydrocorynantheol.[5a, 12]

Received: February 20, 1992 [Z 5198 IE]
German version: *Angew. Chem.* **1992**, *104*, 1091

CAS Registry numbers:
2, 142611-08-3; **3a**, 142611-09-4; **3b**, 142611-10-7; **4a**, 142611-11-8; **4b**, 142611-12-9; **5b**, 142611-13-0; **6a**, 142611-14-1; **6b**, 142611-15-2; **7**, 142611-16-3; **8**, 129995-90-0; 1-bromo-2-butene, 4784-77-4; 1-bromo-3-methyl-2-butene, 870-63-3; 3-methyl-2-butenoyl chloride, 3350-78-5.

[1] a) L. F. Tietze, *J. Heterocycl. Chem.* **1990**, *27*, 47; b) S. J. Danishefsky, M. P. De Ninno, *Angew. Chem.* **1987**, *99*, 15; *Angew. Chem. Int. Ed. Engl.* **1987**, *26*, 15; c) T. Kametani, S. Hibino, *Adv. Heterocycl. Chem.* **1987**, *42*, 245–333; d) G. Desimoni, G. Tacconi, A. Barco, G. P. Pollini, *Natural Products Synthesis Through Pericyclic Reactions (ASC Monogr.* **1983**, *180)*; e) J. Sauer, R. Sustmann, *Angew. Chem.* **1980**, *92*, 773; *Angew. Chem. Int. Ed. Engl.* **1980**, *19*, 779.

[2] a) B. B. Snider in *Comprehensive Organic Synthesis, Vol. 5* (Eds.: B. M. Trost, I. Fleming, L. A. Paquette), Pergamon Press, Oxford, **1991**, p. 1; b) D. F. Taber, *Intramolecular Diels-Alder and Alder-Ene Reactions* Springer, Heidelberg, **1984**; c) W. Oppolzer, *Angew. Chem.* **1984**, *96*, 840; *Angew. Chem. Int. Ed. Engl.* **1984**, *17*, 476; d) W. Oppolzer, V. Snieckus, *ibid.* **1978**, *90*, 506 and **1978**, *17*, 476; e) H. M. R. Hoffmann, *ibid.* **1969**, *81*, 597 and **1969**, *8*, 559.

[3] a) L. F. Tietze, U. Beifuss, M. Ruther, *J. Org. Chem.* **1989**, *54*, 3120; b) L. F. Tietze, U. Beifuss, *Liebigs Ann. Chem.* **1988**, 321; c) L. F. Tietze, U. Beifuss, M. Ruther, A. Rühlmann, J. Antel, G. M. Sheldrick, *Angew. Chem.* **1988**, *100*, 1200; *Angew. Chem. Int. Ed. Engl.* **1988**, *27*, 1186; d) L. F. Tietze, U. Beifuss, *ibid.* **1985**, *97*, 1067 and **1985**, *24*, 1042.

[4] a) B. B. Snider, *Acc. Chem. Res.* **1980**, *13*, 426; b) L. F. Tietze, U. Beifuss, *Synthesis* **1989**, 359; c) J. H. Edwards, F. J. McQuillin, *J. Chem. Soc. Chem. Commun.* **1977**, 838; d) H. Felkin, J. D. Umpleby, E. Hagaman, E. Wenkert, *Tetrahedron Lett.* **1972**, 228.

[5] a) I. Ninomiya, T. Naito, O. Miyata, T. Shineda, E. Winterfeldt, R. Freund, T. Ishida, *Heterocycles* **1990**, *30*, 1031; b) W. Benson, E. Winterfeldt, *ibid.* **1981**, *15*, 935; c) *Chem. Ber.* **1979**, *112*, 1913; d) B. Hachmeister, D. Thielke, E. Winterfeldt, *ibid.* **1976**, *109*, 3825; e) E. Winterfeldt, J. M. Nelke, T. Korth, *ibid.* **1971**, *104*, 802.

[6] A. Pictet, T. Spengler, *Chem. Ber.* **1911**, *44*, 2030.

[7] a) P. Rosenmund, M. Hosseini-Merescht, *Tetrahedron Lett.* **1990**, *31*, 647; b) L. E. Overman, A. J. Robichaud, *J. Am. Chem. Soc.* **1989**, *111*, 300; c) E. J. Corey, D. S. Scott, *ibid.* **1973**, *95*, 2303.

[8] All compounds were obtained as racemic mixtures. **6a** (Atom numbering as shown in **1**, H_{eq} = equatorial H): ^{1}H NMR (500 MHz, C_6D_6): $\delta = 1.72$ (pseudo quartet, $J = 11.5$ Hz, 1H, 14-H_{ax}), 2.13 (pseudo t, $J = 11.0$ Hz, 1H, 21-H_{ax}), 2.29 (dddd, $J = 3.0$, 3.5, 11.5, 12.0 Hz, 1H, 15-H), 2.38 (pseudo dt, $J = 4.0$, 11.0 Hz, 1H, 5-H_{ax}), 2.51–2.58 (m, 2H, 6-H_{ax}, 14-H_{eq}), 2.65 (dddd, $J = 4.5$, 10.0, 11.0, 12.0 Hz, 1H, 20-H), 2.74 (m_c, 1H, 5-H_{eq}), 2.85 (dd, $J = 4.5$, 11.0 Hz, 1H, 21-H_{eq}), 2.97 (m_c, 1H, 6-H_{eq}), 3.14 (m_c, 1H, 3-H), 3.16 (s, 3H, OCH_3), 3.38 (s, 3H, OCH_3), 3.89 (d, $J = 3.0$ Hz, 1H, 16-H), 5.07 (dd, $J = 2.0$, 10.0 Hz, 1H, 18-H), 5.21 (dd, $J = 2.0$, 17.0 Hz, 1H, 18-H), 5.40 (pseudo dt, $J = 10.0$, 17.0 Hz, 1H, 19-H), 6.82 (s, 1H, NH), 7.02 (dd, $J = 2.0$, 7.5 Hz, 1H, 9-H), 7.22 (pseudo dt, $J = 2.0$, 7.5 Hz, 1H, 10-H), 7.25 (pseudo dt, $J = 2.0$, 7.5 Hz, 1H, 11-H), 7.56 (dd, $J = 2.0$, 7.5 Hz, 1H, 12-H). – ^{13}C NMR (126 MHz, C_6D_6): $\delta = 22.24$ (C-6), 32.40 (C-14), 40.73 (C-15), 45.12 (C-20), 51.75 (C-16), 52.04 (OCH_3), 52.81 (OCH_3), 53.05 (C-5), 59.71 (C-3), 61.26 (C-21), 108.5 (C-7), 111.5 (C-12), 118.2 (C-18), 118.4 (C-9), 119.6 (C-10), 121.5 (C-11), 127.9 (C-8), 134.8 (C-2), 136.8 (C-13), 138.9 (C-19), 168.9, 170.0 (CO).

[9] L. F. Tietze, M. Ruther, *Chem. Ber.* **1990**, *123*, 1387.

[10] R. W. Hoffmann, *Chem. Rev.* **1989**, *89*, 1841.

[11] A. P. Krappcho, *Synthesis* **1982**, *805*, 893.

[12] a) R. T. Brown, M. F. Jones, M. Wingfield, *J. Chem. Soc. Chem. Commun.* **1984**, 847; b) R. L. Autrey, P. W. Scullard, *J. Am. Chem. Soc.* **1968**, *90*, 4917; c) E. E. van Tamelen, E. G. Wright, *Tetrahedron Lett.* **1964**, 295; d) E. E. van Tamelen, J. B. Hester, *J. Am. Chem. Soc.* **1959**, *81*, 3805.

Synthesis and Structure of a Mononuclear η^2-Hydrazine Complex by Protonation of an $[N_2H_2]^{2-}$ Complex**

By *William J. Evans,* Gabriele Kociok-Köhn,* and *Joseph W. Ziller*

One of the models for the fixation of dinitrogen in biological systems is the coordination of N_2 to a metal center followed by subsequent protonation of the N_2 ligand to give N_2H_x compounds ($x = 1-4$) and ultimately NH_3.[1] Although model complexes of several of these N_2H_x ligands have been characterized,[2] they are generally not prepared by the sequence of protonation reactions thought to occur in the biological systems. We report here a rare example of a structurally characterized η^2-hydrazine complex prepared by protonation of a $(N_2H_2)^{2-}$ complex.

The starting material **1** of the reaction (a) is prepared in quantitative yield by the addition of THF to complex **4**.[3]

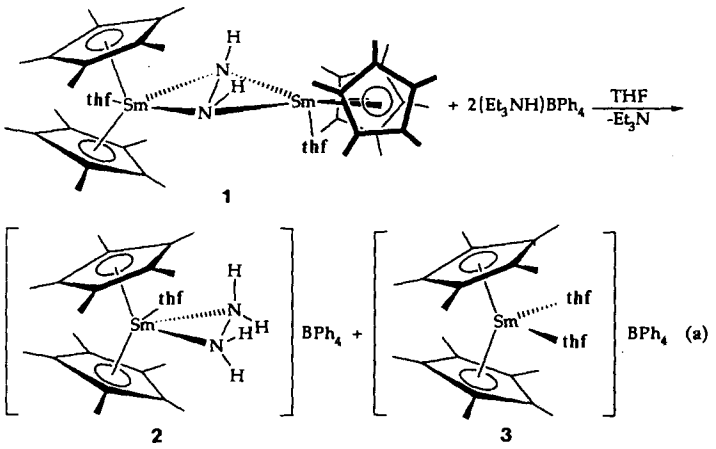

$[\{C_5Me_5)_2Sm\}_2(\mu\text{-}\eta^2\text{:}\eta^2\text{-HNNH})]$ **4**

Complexes **1** and **4**[3] have been characterized by elemental analysis, NMR spectroscopy,[4] and X-ray structural analysis.[5] **1** is unusual in that it retains the overall structure of **4** despite the addition of two THF molecules (Fig. 1); this demonstrates the remarkable ability of the $[(C_5Me_5)_2Sm]_2$ unit to coordinate a variety of ligand sets and sizes.[6]

The reaction of **1** with two equivalents of $(Et_3NH)BPh_4$ in THF leads to the formation of complex **2** with side-on coordination of the hydrazine ligand and to the previously characterized tetrahydrofuran complex **3**[7] [Eq. (a)]. Complex **2** was characterized by elemental analysis, NMR spectroscopy,[4] and X-ray structural analysis (Fig. 2).[5] Apparently, the η^2-hydrazine ligand is strongly attached to the samarium atom, since the ligand remains coordinated when solvent is removed under vacuum from a solution of **2** and also when **2** is recrystallized from THF/toluene. Complex **2** can also be made from **4** and $(Et_3NH)BPh_4$ in toluene. The protonation is reversible in that **2** reacts with $[\{(C_5Me_5)_2Sm(\mu\text{-H})\}_2]$ in hexane to regenerate **4**.

Complex **2** is unusual both with regard to its synthesis and structure. With one exception,[2e] all previously characterized hydrazine complexes were prepared from hydrazine rather than from N_2H_2 metal complexes. In addition, most structurally characterized hydrazine complexes are either $\mu\text{-}\eta^1\text{:}\eta^1\text{-}MNH_2NH_2M$ compounds or mononuclear complexes, MNH_2NH_2.[2b, 8] The exceptions are $[(tripod)Co(\eta^2\text{-}N_2H_4)]^{2+}$ (prepared from $[(tripod)Co(\eta^2\text{-}N_2H_3)]^+$, tripod $= MeC(CH_2PPh_2)_3$),[2e] and $[(C_5Me_5)Me_3W(\eta^2\text{-}H_2NNH_2)]$-OTf (prepared from H_2NNH_2); the structure has been determined but not yet reported.[2a]

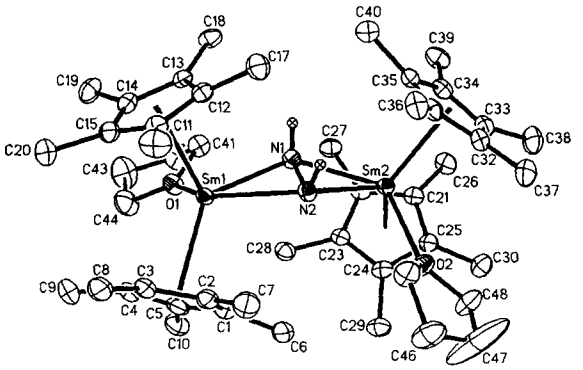

Fig. 1. Crystal structure of **1** (ORTEP) with probability ellipsoids drawn at the 50% level. Selected distances [Å] and angles [°]: Sm1-N1 2.456(4), Sm1-N2 2.413(4), Sm2-N1 2.417(4), Sm2-N2 2.459(4), Sm1-O1 2.522(4), Sm2-O2 2.507(4); Sm-C(ring) average 2.82(4), N1-N2 1.484(6), Cp_1^*(center)-Sm-Cp_2^*(center) average 125.8.

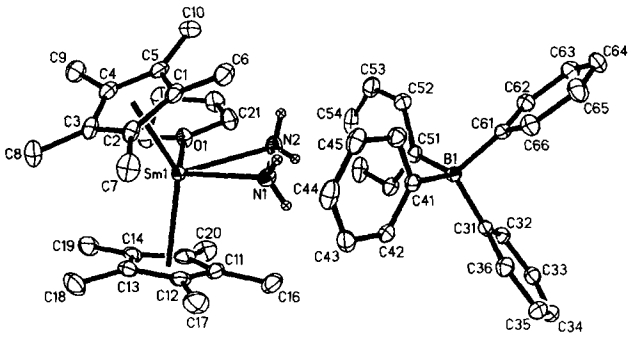

Fig. 2. Crystal structure of **2** (ORTEP) with probability ellipsoids drawn at the 50% level. Selected distances [Å] and angles [°]: Sm1-N1 2.492(2), Sm1-N2 2.523(2), Sm1-O1 2.470(2), N1-N2 1.471(3); Sm1-C(ring) average 2.73(2); Sm1-N1-N2 74.1(1), Sm1-N2-N1 71.8(1), N1-Sm1-N2 34.1(1), N2-Sm1-O1 80.8(1); Cp_1^*(center)-Sm1-Cp_2^*(center) 138.9.

The N–N distances in **1** and **2** (1.484(6) and 1.471(3) Å, respectively) are in the expected range for single bonds.[9] The Sm–N distances in **1** are intermediate between typical Sm–NR_2 and Sm ← NR_3 bond lengths.[10] The longer Sm–N distances in **2** are consistent with Sm ← NR_3 bonds, in which the NR_3 ligand is bound to a cationic samarium center. The hydrogen atoms shown in Figures 1 and 2 were located in both X-ray structural analyses.

The existence of these complexes and the reaction sequence shown in Equation (a) demonstrate that the organolanthanide unit $(C_5Me_5)_2Sm$ provides an interesting metallic environment with which to study transformations of nitrogen-containing substrates relevant to nitrogen fixation.[11] Since no redox chemistry occurs in the Sm^{III} reactions, these organosamarium complexes provide the opportunity to study how protons can be transferred between nitrogen substrates without concomitant redox processes.

Experimental Procedure

Complex **1** was prepared under nitrogen in a glovebox by addition of THF to $[(C_5Me_5)_2Sm]_2(HNNH)$ [3] followed by removal of solvent by rotary evapora-

[*] Prof. W. J. Evans, Dr. G. Kociok-Köhn, Dr. J. W. Ziller
Department of Chemistry, University of California
Irvine, CA 92717 (USA)

[**] This work was supported by the National Science Foundation (USA) and by the Deutsche Forschungsgemeinschaft (postdoctoral fellowship for G. K.-K.).

tion. Complex **2** was prepared by the addition of a suspension of $(Et_3NH)BPh_4$ (75.9 mg, 0.18 mmol, from $(Et_3NH)Cl$ and $NaBPh_4$) in 5 mL of THF to a stirred orange-yellow solution of **1** (90 mg, 0.09 mmol) in 7 mL of THF. The reaction was stirred overnight and the solvent was removed by rotary evaporation to leave a dark orange product. This was washed with 5 mL of toluene to remove oily by-products and left a 2:1 mixture (by NMR spectroscopy of **2** and **3** (110 mg). Complex **2** was separated by recrystallization from THF: toluene (4:1).

Received: March 25, 1992 [Z 5261 IE]
German version: *Angew. Chem.* **1992**, *104*, 1114

CAS Registry numbers:
1, 142509-12-4; **2**, 142509-14-6; **3**, 127914-40-3; **4**, 142509-15-7.

[1] a) G. J. Leigh, *J. Mol. Cat.* **1988**, *47*, 363; b) R. R. Eady, *Adv. Inorg. Chem.* **1991**, *36*, 77.

[2] For example: a) R. R. Schrock, T. E. Glassman, M. G. Vale, *J. Am. Chem. Soc.* **1991**, *113*, 725; b) D. Sellmann, W. Soglowek, F. Knoch, M. Moll, *Angew. Chem.* **1989**, *101*, 1244; *Angew. Chem. Int. Ed. Engl.* **1989**, *28*, 1271; c) R. R. Schrock, A. H. Liu, M. B. O'Regan, W. C. Finch, J. F. Payack, *Inorg. Chem.* **1988**, *27*, 3574; d) J. P. Collman, J. E. Hutchison, M. A. Lopez, R. Guilard, R. A. Reed, *J. Am. Chem. Soc.* **1991**, *113*, 2794; e) S. Vogel, A. Barth, G. Huttner, T. Klein, L. Zsolnai, R. Kremer, *Angew. Chem.* **1991**, *103*, 325; *Angew. Chem. Int. Ed. Engl.* **1991**, *30*, 303; f) D. Sellmann, W. Kern, G. Pöhlmann, F. Knoch, M. Moll, *Inorg. Chim. Acta* **1991**, *185*, 155, and references cited therein; g) G. Huttner, W. Gartzke, K. Allinger, *Angew. Chem.* **1974**, *86*, 860; *Angew. Chem. Int. Ed. Engl.* **1974**, *13*, 822; h) M. R. Churchill, Y.-J. Li, L. Blum, R. R. Schrock, *Organometallics* **1984**, *3*, 109; i) N. Y. Zhu, S. W. Du, X. T. Wu, J. X. Lu, *Angew. Chem.* **1992**, *104*, 83; *Angew. Chem. Int. Ed. Engl.* **1992**, *31*, 87.

[3] W. J. Evans, G. Kociok-Köhn, V. S. Leong, J. W. Ziller, *Inorg. Chem.*, in press.

[4] **1**: ^1H NMR (500 MHz, 25 °C; C_6D_6, 0.032 M): $\delta = 3.48$ (THF), 1.26 (THF), −0.97 (C_5Me_5); ^{13}C NMR: $\delta = 112.9$ (C_5Me_5), 68.0 (THF), 25.6 (THF), 21.4 (C_5Me_5). **2**: ^1H NMR (C_4D_8O): $\delta = 7.12$ (br), 6.79 (t), 6.69 (t, BPh_4), 1.04 (s, C_5Me_5), 0.37 (br, NH); ^{13}C NMR (C_4D_8O): $\delta = 164.9$, 136.9, 125.8, 122.0 (BPh_4), 112.9 (C_5Me_5), 16.2 (C_5Me_5); ^{11}B NMR (C_4D_8O): $\delta = -3.41$.

[5] **1** crystallizes from THF in space group $P2_1/n$ with $a = 14.772(2)$, $b = 11.272(1)$, $c = 31.424(3)$ Å, $\beta = 90.745(9)°$, $V = 5232(1)$ Å^3, $\rho_{calcd} = 1.43$ g cm^{-3}, $Z = 4$. Least-squares refinement of the model based on 8864 reflections ($|F_0| > 3.0\sigma(|F_0|)$) converged to a final $R_F = 0.039$. **2** crystallizes from THF in space group $P2_1/n$ with $a = 11.8026(13)$, $b = 23.010(4)$, $c = 15.486(2)$ Å, $\beta = 91.778(10)°$, $V = 4204(1)$ Å^3, $\rho_{calcd} = 1.33$ g cm^{-3}, $Z = 4$. Least-squares refinement of the model based on 8766 reflections ($|F_0| > 2.0\sigma(|F_0|)$) converged to a final $R_F = 0.027$. Further details of the crystal structure investigation are available on request from the Director of the Cambridge Crystallographic Data Centre, University Chemical Laboratory, Lensfield Road, GB-Cambridge, CB2 1EW (UK), on quoting the full journal citation.

[6] W. J. Evans, T. A. Ulibarri, J. W. Ziller, *J. Am. Chem. Soc.* **1990**, *112*, 2314, and references cited therein.

[7] W. J. Evans, T. A. Ulibarri, L. R. Chamberlain, J. W. Ziller, D. Alvarez, *Organometallics* **1990**, *9*, 2124.

[8] a) D. Sellmann, P. Kreutzer, G. Huttner, A. Frank, *Z. Naturforsch. B* **1978**, *33*, 1341; b) L. Blum, I. D. Williams, R. R. Schrock, *J. Am. Chem. Soc.* **1984**, *106*, 8316.

[9] *Spec. Publ. Chem. Soc.* **1965**, *18*.

[10] W. J. Evans, D. K. Drummond, *J. Am. Chem. Soc.* **1989**, *111*, 3329.

[11] See also [3] as well as a) W. J. Evans, T. A. Ulibarri, J. W. Ziller, *J. Am. Chem. Soc.* **1988**, *110*, 6877; b) K. G. Wang, E. D. Stevens, S. P. Nolan, *Organometallics* **1992**, *11*, 1011.

Reduction of a Boron–Nitrogen 1,3-Butadiene Analogue: Evidence for a Strong B–B π-Bond**

By *Afarin Moezzi, Ruth A. Bartlett,* and *Philip P. Power**

A recurring theme in inorganic and organometallic chemistry is the, often close, structural analogy that is drawn between organic compounds and their inorganic and organometallic counterparts.[1] Perhaps the most well-known case involves the boron–nitrogen compounds which frequently possess physical properties and structures that are very similar to their organic analogues.[2] One illustration of the B–N, C–C relationship involves the diboron species of the general formula $R(R'_2N)BB(NR'_2)R$ (R = alkyl or aryl groups) which may be regarded as substituted 1,3-butadiene analogues.[3–5] Their structures[6, 7] show that the π-interaction is localized exclusively in the B–N bonds and that the B–B bonds are single and ca. 1.7 Å long. Generally, there is a large angle (> 60°) between the coordination planes at the boron atoms, whereas the angle between the boron and nitrogen planes is ca. 0°. Recent work in this laboratory has shown that it is possible to doubly reduce the related tetraaryl diboron species B_2Ar_4 to give the substituted ethene analogue $[B_2Ar_4]^{2-}$, which has a B–B bond length of 1.636(11) Å and an almost planar B_2 (*ipso*-C)$_4$ core.[8] This result is in agreement with an earlier prediction of the existence of a B–B multiple bond in the hypothetical species $[B_2H_4]^{2-}$.[9] In this paper we provide independent evidence for the presence of strong boron–boron double bonds in these dianions via the reduction of the butadiene analogue **1** to give the dianion **2**.

$Ph(Me_2N)BB(NMe_2)Ph$ **1** $[\{(Et_2O)Li\}_2\{Ph(Me_2N)BB(NMe_2)Ph\}]$ **2**

$Br(Me_2N)BB(NMe_2)Br$ **3**

Compound **1**[10] was synthesized by the reaction of **3**[11] with two equivalents of LiPh in hexane. The X-ray crystal structure analyses[6] of **1** and **3** revealed average B–N lengths of 1.399 Å (**1**) and 1.36 Å (**3**) and B–B lengths of 1.714(4) Å (**1**) and 1.682(16) Å (**3**). Moreover, the angles between the planes at the boron atoms are large (88.7° for **1** and 83.7° for **3**). In short, the structures display the features that are consistent with a B–N 1,3-butadiene analogy for **1** and **3**. Reduction of **1** with excess Li powder occurs readily in Et_2O/THF solution, from which red crystals of the product **2** can be obtained after suitable work-up.[12] The X-ray crystal structure[13] of **2** is illustrated in Figure 1. Each asymmetric unit in the cell contains two half molecules, which, therefore, possess a center of inversion. The B_2N_2 (*ipso*-C)$_2$ array is planar and the B–B distances in the molecules are 1.623(8)

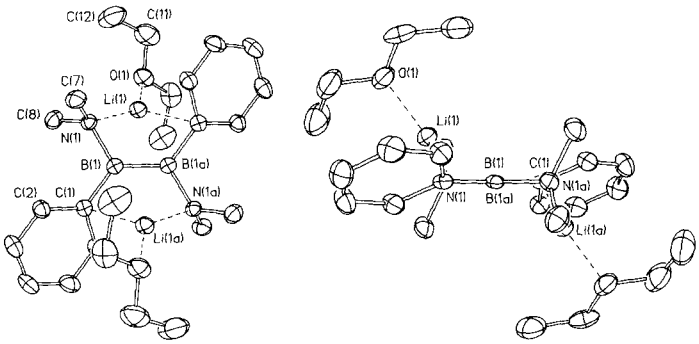

Fig. 1. Two views of one of the molecules of **2**; H atoms are omitted for clarity. Selected distances [Å] and angles [°], with the corresponding parameter for the second molecule in brackets, are: B(1)-N(1) 1.560(5) [1.562(5)], B(1)-B(1a) 1.631(9) [1.623(8)], B(1)-C(1) 1.595(6) [1.591(6)], Li1···O(1) 1.920(7) [1.916(7)], Li1···N(1) 1.978(7) [1.977(7)], Li1a···C(1a) 2.251(7) [2.249(8)], Li(1)···B(1) 2.281(8) [2.251(8)], Li-B(1a) 2.337(8) [2.304(8)]; N(1)-B(1)-C(1) 114.2(3) [114.9(3)], N(1)-B(1)-B(1a) 119.4(4), C(1)-B(1)-B(1a) 126.4(4). Angle between B(1) N(1) C(1) plane and the plane of the C(1) ring = 31.5°.

[*] Professor P. P. Power, A. Moezzi, R. A. Bartlett
Department of Chemistry, University of California
Davis, CA 95616 (USA)

[**] This work was supported by the National Science Foundation and the Petroleum Research Fund.

and 1.631(9) Å, which are significantly shorter than those observed in the precursor. The most important features of the structure, however, are the long B–N bond lengths (1.560(5) and 1.562(5) Å) and the orientation (ca. 90° angle) of the NMe_2 groups with respect to the core, which show that the B–N π-interactions have been destroyed in the reduction process. In effect, the formation of the B–B π-bond proceeds at the expense of B–N π-bond rupture. The solvation of the Li^+ ions by ether, the nitrogen lone pair, and the *ipso* carbon atom also provide impetus for reduction.[14] The ^{11}B-NMR spectrum of **2** displays a broad singlet at $\delta = 33$, whereas the corresponding peak for **1** appears at $\delta = 49.3$. The upfield shift upon reduction is indicative of an increase in the electron density at the boron centers in spite of the elimination of strong π-donation by the NMe_2-substituents. The structural and spectroscopic data thus indicate that the reductive process may be represented schematically as in Scheme 1.[15]

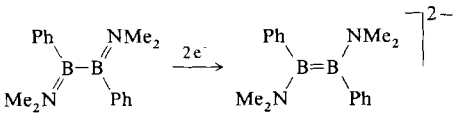

Scheme 1. Schematized reduction.

The electronic absorption spectrum of **2** in Et_2O displays an intense peak at 320 nm. If this is taken to be indicative of the $\pi \rightarrow \pi^*$ transition of the B–B π-bond than an energy difference of ca. 90 kcal mol^{-1} between the π and π^* levels may be estimated. The energy of the π-bond is probably less than half of this value, perhaps in the region of 40 kcal mol^{-1}. If this estimate seems high in view of the ca. 0.09 Å difference between the B–B distances in **1** and **2**, it should be borne in mind that the presence of two negative charges in close proximity may give rise to Coulombic repulsion which lengthens the bond. The B–B distance (1.859(8) Å) found in the compound $[Li_2\{(Me_3Si)_2CB(Mes)(Mes)BC(SiMe_3)_2\}]$,[16] which has a single bond between two negatively charged boron atoms, suggests that B–B π-bond formation results in a shortening of ca. 0.23 Å rather than the 0.09 Å with respect to the precursor **1**. This difference in length which is similar to that observed between H_3CCH_3 (1.54 Å) and H_2CCH_2 (1.34 Å) supports the presence of a strong B–B π-bond.

Experimental

Under anaerobic and anhydrous conditions, a solution of **1** (0.485 g, 1.8 mmol) in diethyl ether (25 mL) and tetrahydrofuran (10 mL) was added dropwise to a suspension of lithium powder (0.07 g, 10 mmol) in diethyl ether (10 mL). Stirring for 3 h at room temperature afforded a deep-red solution. The solvents were removed under reduced pressure and the residue was extracted with diethyl ether (25 mL). Filtration and reduction of the solution volume to 10–12 mL followed by cooling overnight in a freezer (−20 °C) furnished deep-red crystals of **2** in 70% yield (0.54 g). M.p. = 105–110 °C; ^{11}B NMR (96.25 MHz, Et_2O): $\delta = 33$; ^{1}H NMR (300 MHz, C_6D_6): $\delta = 0.99$ (t, 12H), 2.55 (s, 12H), 3.11 (q, 8H), 7.3 (m, 10H), UV/VIS (Et_2O): $\lambda_{max} = 320$ nm.

Received: January 21, 1992 [Z 5140 IE]
German version: *Angew. Chem.* **1992**, *104*, 1075

CAS Registry numbers:
1, 19127-90-3; **2**, 142131-94-0; **3**, 80476-71-7.

[1] F. A. Cotton, G. Wilkinson, *Advanced Inorganic Chemistry*, 4th Edn., Wiley, New York, **1980**. N. N. Greenwood, A. Earnshaw, *Chemistry of the Elements*, Pergamon, Oxford, **1984**.
[2] K. Niedenzu, J. W. Dawson, *Boron Nitrogen Compounds*, Springer, Berlin, **1964**.
[3] H. Nöth, P. Fritz, *Angew. Chem.* **1961**, *73*, 408.
[4] R. J. Brotherton, H. M. Manasevit, A. L. McCloskey, *Inorg. Chem.* **1962**, *1*, 749.
[5] H. Nöth, P. Fritz, *Z. Anorg. Allg. Chem.* **1963**, *324*, 129.
[6] Several structures incorporating the moiety R_2–N–B–B–NR_2 as part of a ring have been published; see for example: M. Hildenbrand, H. Pritzkow, W. Siebert, *Angew. Chem.* **1985**, *97*, 769; *Angew. Chem. Int. Ed. Engl.* **1985**, *24*, 759; H. Krämer, H. Pritzkow, W. Siebert, *ibid.* **1988**, *100*, 963 and **1988**, *27*, 926. The structures mentioned in Ref. [7] and described in the text appear to be the first for acyclic species.
[7] The structures of **1** and **3** have been determined in this laboratory and will be reported elsewhere in the near future. See text for some of the important details.
[8] A. Moezzi, M. M. Olmstead, P. P. Power, *J. Am. Chem. Soc.*, in press. Earlier work by Berndt et al. has shown that it is possible to reduce tetraalkyldiboron species to give the radical anions $[B_2R_4]^{\cdot-}$, H. Klusik, A. Berndt, *Angew. Chem.* **1980**, *93*, 903; *Angew. Chem. Int. Ed. Engl.* **1981**, *20*, 870; A. Berndt, H. Klusik, K. Schlüter, *J. Organomet. Chem.* **1981**, *222*, 25.
[9] E. Kaufmann, P. von R. Schleyer, *Inorg. Chem.* **1988**, *27*, 3987.
[10] A synthesis of this compound is described in Refs. [3] and [4].
[11] H. Nöth, H. Schick, W. Meister, *J. Organomet. Chem.* **1964**, *1*, 401.
[12] Ring compounds that are superficially similar to **2** (e.g. $[\{Li(TMEDA)\}_2$-1,2-$C_4H_4(BNMe_2)_2]$) have been reported. However, they were generated by deprotonation of CH_3 groups bonded to boron and not by reduction of the boron centers: G. E. Herberich, B. Hessler, M. Hostalek, *Angew. Chem.* **1986**, *98*, 637; *Angew. Chem. Int. Ed. Engl.* **1986**, *25*, 642.
[13] Crystal data for **2** at 130 K with $Mo_{K\alpha}$ radiation ($\lambda = 0.71069$ Å): $a = 9.721(3)$, $b = 11.192(3)$, $c = 12.893(4)$ Å, $\alpha = 87.78(3)$, $\beta = 81.30(3)$, $\gamma = 89.41(2)°$, $Z = 2$, triclinic, space group $P\bar{1}$, $\varrho_{calcd} = 1.021$ g cm^{-3}, $V = 1385.5(8)$ Å^3, 2990 unique observed data ($I > 2\sigma(I)$), $R = 0.084$. Data were obtained on a Siemens R3 m/v diffractometer equipped with a locally modified low-temperature device. Further details of the structure investigation may be obtained from the Fachinformationszentrum Karlsruhe, Gesellschaft für wissenschaftlich-technische Information mbH, W-7514 Eggenstein-Leopoldshafen 2 (FRG), on quoting the depository number CSD-56195, the names of the authors, and the journal citation.
[14] The lithium ions also closely approach the boron centers (ca. 2.3 Å) but this 'interaction' may be imposed by the coordination of Li to N and C(*ipso*).
[15] This process may be compared with the two-electron oxidation of $(Me_2N)CC(NMe_2)_2$: H. Bock, K. Ruppert, K. Merzweiler, D. Fenske, H. Goesmann, *Angew. Chem.* **1989**, *102*, 1715; *Angew. Chem. Int. Ed. Engl.* **1989**, *28*, 1684.
[16] M. Pilz, J. Allwohn, P. Willershausen, W. Massa, A. Berndt, *Angew. Chem.* **1990**, *102*, 1084; *Angew. Chem. Int. Ed. Engl.* **1990**, *29*, 1030.

Synthesis of (*R*)- and (*S*)-2-*tert*-Butyl-6-trifluoromethyl-1,3-dioxin-4-ones, Transformations into 3-Hydroxy-3-(trifluoromethyl)alkanoates, and Surprising Differences in the Reactivity of CH_3- and CF_3-Substituted Compounds**

By *Markus Gautschi* and *Dieter Seebach**

For many years[1] we have been engaged in the preparation and investigation of chiral, trifluoromethyl-substituted compounds.[2] Our interest in these systems has grown as we continue to be fascinated by their surprising reactivity, and because we expect that our results will finally lead to a better understanding of inter- and intramolecular interactions of fluoro-substituents in organic compounds. In addition, the reactions we have performed and the compounds we have synthesized during these investigations should find application in the development of new agrochemicals and pharmaceuticals.[3] As in the case of non-fluorinated chiral building-blocks, simple compounds with one, or at most, two stereogenic centers are predicted to have greatest potential.

[*] Prof. Dr. D. Seebach, Dipl.-Chem. M. Gautschi
Laboratorium für Organische Chemie
der Eidgenössischen Technischen Hochschule
ETH-Zentrum, Universitätstrasse 16, CH-8092 Zürich (Switzerland)
[**] Part of the planned Ph.D. thesis by M. G., ETH Zürich

When we attempted to transform the (*S*)- and (*R*)-trifluorohydroxybutanoic acids **1** (Scheme 1), which are accessible on a large scale by separation of the enantiomers,[1a] into the chiral trifluoroacetylacetic acid derivatives **4** and *ent*-**4**, we observed that bromination of the corresponding dioxanones with *N*-bromosuccinimide (NBS),[4] which had been possible in the case of other β-hydroxy acids, was not successful due to the low reactivity of the trifluoromethyldioxanone **2** towards this reagent. On the other hand,

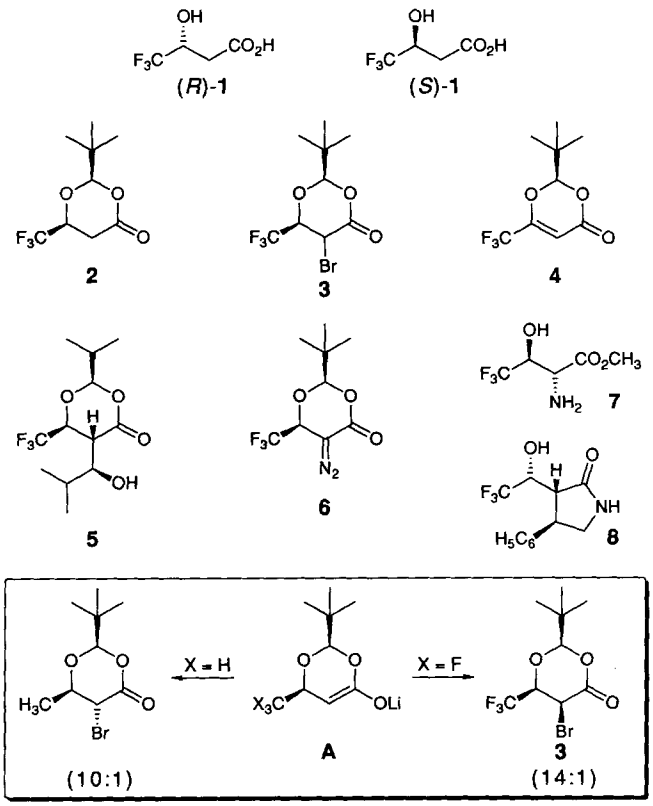

Scheme 1. Starting materials **1** and products from the Li-enolate **A** of **2** [generated using *t*BuLi or $LiN(SiMe_3)_2$(LHMDS), THF, −78 °C] and electrophiles. **2** → **3** → **4**: see *Experimental*.—**5** (m.p. = 123 °C): 66% from **2**, LHMDS (Li hexamethyl disilazamide), 10 Me_2CHCHO, under transacetalization.—**6** (m.p. = 91 °C): 56% from **2**, LHMDS, $TosN_3$.—**7** (m.p. = 117 °C): 57% from **2**, *t*BuLi, Boc-N=N-Boc (*tert*-butoxycarbonyl), then HCl/MeOH, then H_2/PtO_2; comparison with the coupling constants of trifluorothreonine and -*allo*-threonine, respectively [7].—**8** (m.p. = 164 °C, main diastereoisomer): from *ent*-**2**, *t*BuLi, nitrostyrene (95%, 66% ds), then H_2/Raney-Ni/EtOH/70 °C. The assignments of configuration are based on NMR measurements (see *Experimental*).

the 5-bromodioxanone **3**, obtained via bromination of the Li-enolate **A** of **2**,[5] led, on treatment with base, to the desired dioxin-4-one **4** (46%) in contrast to the non-fluorinated analogue[6a] (see Scheme 1 and *Experimental*). The enolate of **2** also reacts with other "fast"[8] electrophiles, see products **5**–**8**. Surprisingly, inversion of the stereochemical course of the bromination is observed on switching from the CH_3- to the CF_3-derivative, the *trans*-configurated CH_3- and the *cis*-configurated CF_3-compounds being formed, respectively (see legend and box in Scheme 1).[6b] The enolate of **2** reacts with both aldehydes (→ **5**) and azodicarboxylate (→ **7**), leading to *trans*-products, whereas with nitrostyrene the *cis*-product results (**8**).

Like non-fluorinated dioxin-4-ones,[9] **4** is an excellent acceptor for cuprates or CuCl-doped Grignard reagents: addition with relative topicity *like* (*trans* to the *tert*-butyl group) occurs, and the 6,6-disubstituted dioxanones **9** are formed. These are transformed, almost quantitatively, into the hydroxytrifluoromethyl-substituted carboxylic esters **10** upon treatment with methanolic HCl (Scheme 2). Up to this point, the CF_3-substituted dioxacyclohexenone behaved in an "inconspicious" manner. Doubly surprising was the reaction with benzylmagnesium chloride (Scheme 3): In essen-

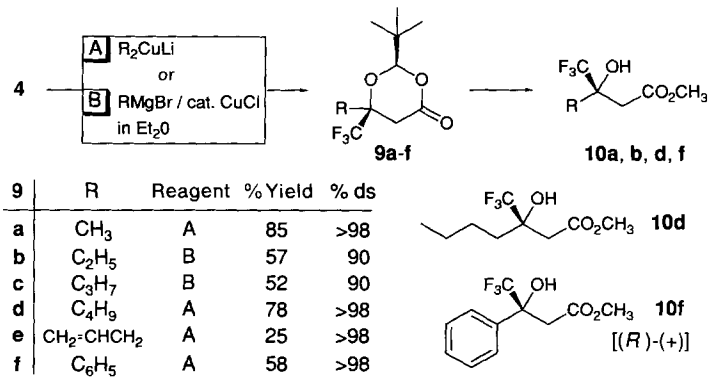

9	R	Reagent	% Yield	% ds
a	CH_3	A	85	>98
b	C_2H_5	B	57	90
c	C_3H_7	B	52	90
d	C_4H_9	A	78	>98
e	CH_2=$CHCH_2$	A	25	>98
f	C_6H_5	A	58	>98

Scheme 2. Reactions of the Michael-acceptor **4**. The yields refer to samples obtained after chromatography performed on the crude products **9** from 5 mmol-scale reactions, the diastereoselectivities were determined by NMR spectroscopy of the crude products; the indicated configuration follows from NOE measurements on **9a** and **9f**, and from a comparison of the $[\alpha]_D^{RT}$ values of the dioxanones **9** (**a**–**e** dextrorotatory, **f** levorotatory, all $c \approx 1$ in EtOH). **9** → **10**: HCl/MeOH/RT (**10a**,**b**,**d** levorotatory, **f** dextrorotatory, $c \approx 1$ in EtOH).

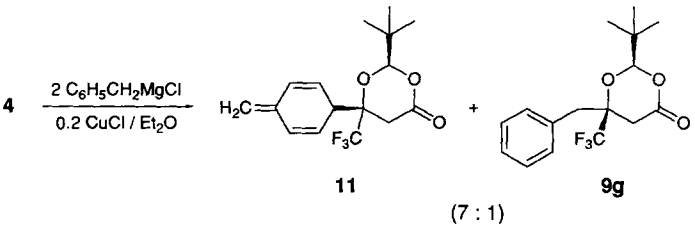

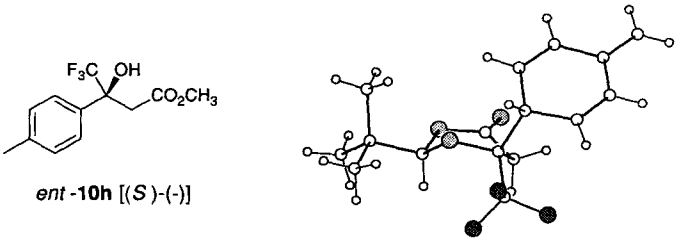

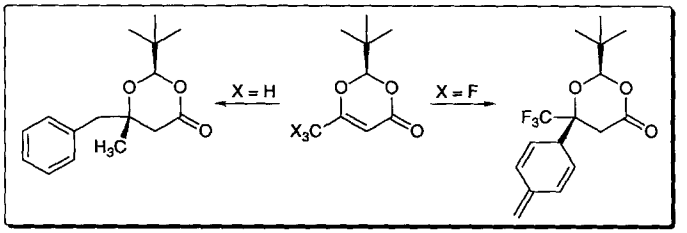

Scheme 3. Reactions of **4** with benzylmagnesium chloride and proof of the structure of **11**. Separation of **11** and **9g** by flash chromatography (SiO_2; pentane/Et_2O 4:1; RT). **9g**: m.p. = 78.5 °C; $[\alpha]_D^{RT}$ +2.8 (c = 1.0, EtOH).—**11**: m.p. = 104 °C; $[\alpha]_D^{RT}$ −131.4 (c = 1.05, EtOH).—*ent*-**10h** (from **11**, MeOH/HCl): 94%, b.p. = 75 °C/0.2 torr; $[\alpha]_D^{RT}$ −8.8 (c = 1.02, EtOH).—The X-ray crystal structure analysis was performed by V. Gramlich, T. Bremi, and F. Kühnle within the crystallography course (WS1991/92) at ETH-Zürich; **11** exists in a boat conformation, which is unusual for dioxanones [10]; further details concerning the crystal structure analysis may be obtained from the Director of the Cambridge Crystallographic Data Centre, University Chemical Laboratory, Lensfield Road, GB-Cambridge CB2 1EW, on quoting the full literature citation of this paper.

tially quantitative yield a 7:1 mixture of the isomers **11** and **9g** is formed (67 and 10% of the pure products were isolated, respectively). The main product turned out to have arisen from a 1,5-addition of the benzylic nucleophile with relative topicity *unlike* (*cis* to the *tert*-butyl group), as proven by aromatization of **11** to *ent*-**10h** and X-ray crystallographic analysis of **11**. For comparison, the non-fluorinated dioxin-4-one (**4**, CH_3 instead of CF_3) was treated with benzylmagnesium chloride under identical conditions. This led to the isolation of 60% "normal" product (**9g**, CH_3 instead of CF_3) and 36% of starting material (see box in Scheme 3).[11] The inversion of the regio- *and* stereochemical course of the reaction on going from the methyl- to the trifluoromethyl-dioxin-4-one must be due to a change in the reaction mechanism.[12] Investigations concerning the mechanism are in progress.

Experimental

3: To a cooled (−78 °C) solution of dioxanone **2** (11.31 g, 50 mmol) in 200 mL THF, under argon, was added 36.2 mL (55 mmol) of a 1.52 M solution of *t*BuLi in hexane such that the reaction temperature did not rise above −70 °C. The yellow enolate solution was added via teflon cannula to a precooled (−78 °C) solution of 2.85 mL (55 mmol) of bromine in 125 mL of THF. Work-up (80 mL sat. aq. NH_4Cl, Et_2O, drying over $MgSO_4$), and recrystallization of the sublimed (60 °C/0.01 torr), crude product (15.15 g, 98%) from pentane, afforded 12.1 g (75%) of **3** as a colorless crystalline solid. M.p. = 82.0–83.5 °C; $[\alpha]_D^{RT}$ −30.5 (c = 1.0, EtOH); ^{1}H NMR (400 MHz, $CDCl_3$, TMS): δ = 1.03 (s, *t*Bu); 4.54 (d, ^3J(H,H) = 5.6 Hz, H-C(5)); 4.71 (dq, ^3J(H,H) = 5.6 Hz, ^3J(H,F) = 5.6 Hz, H-C(6)); 5.29 (s, H-C(2)); the relative configuration was assigned by NMR-comparison with the analogous non-fluorinated *cis*- and *trans*-bromides, as well as with numerous other *cis*/*trans*-isomeric pairs of the same type [6, 9, 13] and by NOE-measurements.

4: To an ice-cold solution of 1.52 g (5 mmol) of dioxanone **3** in 30 mL Et_2O, under argon, was added 1.5 mL (9.6 mmol) of 1,8-diazabicyclo[5.4.0]undec-7-ene (DBU), rapidly. The resulting colorless suspension was stirred for 15 min (0 °C), quenched with 30 mL of 2 M HCl, and then extracted with Et_2O. The combined ethereal extracts were dried ($MgSO_4$) and concentrated. Distillation (bulb to bulb, 30 °C/10 torr) furnished 690 mg (62%) of **4** as a colorless, crystalline solid; m.p. = 32–33 °C; $[\alpha]_D^{RT}$ −141.9 (c = 1.04, $CHCl_3$); IR ($CHCl_3$): $\tilde{\nu}$[cm^{-1}] = 2980 m, 1750 s, 1420 s, 1405 s, 1365 s, 1280 s, 1270 s, 1200 s, 1170 s, 1095 s; ^{1}H NMR (300 MHz, $CDCl_3$, TMS): δ = 1.10 (s, *t*Bu); 5.22 (s, H-C(2)); 5.94 (s, H-C(5)); ^{13}C NMR (75 MHz, $CDCl_3$, TMS): δ = 23.76 (CH_3); 34.70 (C); 98.81 (CH); 108.37 (CH); 117.98 (q, $^1J_{CF}$ = 273.4 Hz); 157.81 (q, $^2J_{CF}$ = 39.0 Hz); 160.24 (CO); ^{19}F NMR (282.2 MHz, $CDCl_3$, TMS): δ = −73.89 (s); MS: m/z 225 ([M + 1]$^{\oplus}$, 0.1), 57 (76); correct C,H,F analysis. Enantiomeric purity of **4** > 99% (GC-analysis, Chrompack CP-Cyclodextrin-β-2,3,6-M-19 WCOT fused silica column, 50 m × 0.25 mm; 1.1 bar H_2, 40 °C, 0.7°/min).

Received: March 10, 1992 [Z 5232 IE]
German version: *Angew. Chem.* **1992**, *104*, 1061

CAS Registry numbers:
2, 131970-17-7; **3**, 142133-95-7; **4**, 142133-96-8; **5**, 142133-97-9; **6**, 142133-98-0; **7**, 142234-99-9; **8**, 142160-15-4; **9a**, 142133-99-1; **9b**, 142134-03-0; **9c**, 142134-04-1; **9d**, 142134-05-2; **9e**, 142134-06-3; **9f**, 142134-07-4; **9g**, 142134-10-9; **10a**, 142134-00-7; **10b**, 142134-08-5; **10d**, 142134-09-6; **10f**, 75369-68-5; *ent*-**10h**, 142134-02-9; **11**, 142134-01-8; Me_2CHCHO, 78-84-2; $TosN_3$, 941-55-9; $PhCH_2MgCl$, 6921-34-2; BOCN=NBOC, 870-50-8; nitrostyrene, 102-96-5.

[1] a) See references [93]–[97] in D. Seebach, *Angew. Chem.* **1990**, *102*, 1363–1409; *Angew. Chem. Int. Ed. Engl.* **1990**, *29*, 1320–1367; b) A. K. Beck, D. Seebach, *Chem. Ber.* **1991**, *124*, 2897–2911.

[2] Review: T. Kitazume, *J. Synth. Org. Chem. Jpn.* **1991**, *49*, 721–736.

[3] J. T. Welch, *Tetrahedron* **1987**, *43*, 3123–3197; J. T. Welch, S. Eswarakrishnan, *Fluorine in Bioorganic Chemistry*, Wiley, New York, **1991**.

[4] A. K. Beck, A. Brunner, V. Montanari, D. Seebach, *Chimia* **1991**, *45*, 379–382, and references cited therein.

[5] For these reactions the enolate was directly generated from **2** using *t*BuLi. This laboratory scale practical method of generating enolates can be applied, in our experience, to many other carbonyl compounds. For a discussion of salt- and amine-free Li-enolates see section 4 (Scheme 10) in D. Seebach, *Angew. Chem.* **1988**, *100*, 1685–1715; *Angew. Chem. Int. Ed. Engl.* **1988**, *27*, 1624–1654.

[6] a) As observed earlier [J. N. Kinkel, U. Gysel, D. Blaser, D. Seebach, *Helv. Chim. Acta* **1991**, *74*, 1622–1635], the HBr-elimination from 5-bromo-1,3-dioxan-4-ones normally does not occur. Under the reaction conditions used for the step **3** → **4**, the nonfluorinated analogue of **3** is mostly decomposed! The increased acidity of H-C(6) in **3**, due to the CF_3-group, must be responsible for this difference in reactivity. b) It is not possible, without further investigations, to explain this inversion. For example, the CF_3-group might interact in a special way with the electrophile (bromine) or lead to a changed reactive conformation of the enolate **A** [compare the discussion in: J. Zimmermann, D. Seebach, T.-K. Ha, *Helv. Chim. Acta* **1988**, *71*, 1143–1155].

[7] C. Scolastico, E. Conca, L. Prati, G. Guanti, L. Banfi, A. Berti, P. Farina, U. Valcavi, *Synthesis* **1985**, 850–855; D. Seebach, E. Juaristi, D. D. Miller, C. Schickli, T. Weber, *Helv. Chim. Acta* **1987**, *70*, 237–261.

[8] Reaction with methyl iodide, allyl- and benzyl bromide only occurs at increased temperature. Yields and selectivities are modest to poor; the *trans*-products predominate.

[9] D. Seebach, J. Zimmermann, U. Gysel, R. Ziegler, T.-K. Ha, *J. Am. Chem. Soc.* **1988**, *110*, 4763–4772; W. Amberg, D. Seebach, *Chem. Ber.* **1990**, *123*, 2429–2438; D. Seebach, U. Gysel, J. N. Kinkel, *Chimia* **1991**, *45*, 114–117.

[10] D. Seebach, B. Lamatsch, R. Amstutz, A. K. Beck, M. Dobler, M. Egli, R. Fitzi, M. Gautschi, B. Herradón, P. C. Hidber, J. J. Irwin, R. Locher, M. Maestro, T. Maetzke, A. Mouriño, E. Pfammatter, D. A. Plattner, C. Schickli, W. B. Schweizer, P. Seiler, G. Stucky, W. Petter, J. Escalante, E. Juaristi, D. Quintana, C. Miravitlles, E. Molins, *Helv. Chim. Acta* **1992**, *75*, 913–934.

[11] "Abnormal products" of type **11** from benzyl-Grignard reagents are well known [M. S. Kharasch, O. Reinmuth, *Grignard Reactions of Nonmetallic Substances*, Prentice-Hall, New York, **1954**; for a more recent example: M. Kato, A. Ouchi, A. Yoshikoshi, *Chem. Lett.* **1984**, 1697–1700].

[12] Nucleophile addition vs. one electron transfer reaction or 1,4-addition vs. 1,2-addition to the enoate system, followed by Cope-rearrangement(s) are two other possible mechanisms.

[13] P. Äyräs, K. Pihlaja, *Tetrahedron* **1973**, *29*, 1311–1316.

Synthesis of Cubane-like and Double Cubane-like Tungsten-Copper-Sulfur Clusters from the "Butterfly" Cluster $[Cu_2S_3W(O)(PPh_3)_3]$**

By *Shaowu Du, Nianyong Zhu, Pengcheng Chen,* and *Xintao Wu**

The tetrathiometalate anions $[MoS_4]^{2-}$ and $[WS_4]^{2-}$, which have proven to be useful and versatile reagents,[1] play a key role in bioinorganic chemistry.[2–3] Since cubane or double cubane-like clusters with cores $\{MoFe_3S_4\}$,[4] $\{NiFe_3S_4\}$[5] and $\{VFe_3S_4\}$,[6] or $\{MoFe_3S_4S_4Fe_3Mo\}$, respectively,[7] have model character for the active sites of some enzymes, they have received much attention. The anion $[MoS_4]^{2-}$ has been claimed to be the most effective antagonist[3] of copper metabolism. Extensive research has been carried out on $[MoS_4]^{2-}/Cu^I$ and $[WS_4]^{2-}/Cu^I$ complexes.[1, 8] The cubane-like series of Mo–Cu–S and W–Cu–S clusters have been completed as $\{M_3CuS_4\}^{5+}$,[9] $\{M_2Cu_2S_4\}^{4+}$,[10] and MCu_3S_3X,[11] in which the first two were synthesized from the homometallic trinuclear clusters $[M_3S_4\{S_2P(OCH_2CH_3)_2\}_4(H_2O)]$[12] and dinuclear complexes $[M_2S_4(SCH_2CH_2S)_2]^{2-}$[13] (M = Mo, W). In this communication, the heterometallic butterfly cluster $[Cu_2S_3W(O)(PPh_3)_3]$ **1**[14] was used as a reactive fragment in the designed synthesis of W–Cu–S clusters, in which the coordinatively unsaturated μ_2-sulfido atoms with lone-pair

[*] Prof. X.-T. Wu, S.-W. Du, N.-Y. Zhu, P.-C. Chen
Fuzhou Laboratory of Structural Chemistry
Fujian Institute of Research on Structure of Matter
Chinese Academy of Sciences
Fuzhou, Fujian 350002 (China)

[**] This research was supported by grants from the Structural Chemistry Research Laboratory of the Fujian Institute of Research on Structure of Matter, Chinese Academy of Sciences and the National Science Foundation of China.

electrons have a high affinity for metal complexes with unsaturated sites or with easily displaceable ligands.

The cubane-like cluster **2** [Eq. (a)] was obtained by reaction of **1** and $[Cu(S_2COEt)]$ in the molar ratio 1:1, while the double cubane-like cluster **3** [Eq. (b)] was isolated from the reaction of equimolar amounts of **1** and $[Cu(SCMe_3)]$. Both compounds were characterized by elemental analysis, IR, UV/VIS spectroscopy, and by a single-crystal X-ray structure analysis.[15]

$$\underset{\mathbf{1}}{[Cu_2S_3W(O)(PPh_3)_3]} + Cu(S_2COEt) \longrightarrow \underset{\mathbf{2}}{[Cu_3S_3W(S_2COEt)(O)(PPh_3)_3]} \quad (a)$$

$$2\underset{\mathbf{1}}{[Cu_2S_3W(O)(PPh_3)_3]} + 2Cu(SCMe_3) \longrightarrow \underset{\mathbf{3}}{[Cu_6S_6W_2(SCMe_3)_2(O)_2(PPh_3)_4]} \quad (b)$$

Possible pathways for the reactions are shown in Scheme 1. Presumably, depending upon the thiolate complex employed, the reaction can proceed in one of two ways: a monodentate thiolate ligand will lead to dimerization of the starting compound to give a double cubane-like cluster; a bidentate dithiolate ligand causes the formation of a cubane-like cluster. This assumption was subsequently confirmed by the synthesis of the clusters $[Cu_3S_3W\{S_2P(OEt)_2\}(O)(PPh_3)_3]$, $[Cu_6S_6W_2(SCH_2CH_2OH)_2(O)_2(PPh_3)_4]$, and $[Cu_6S_6W_2(SCH_2CHMe_2)_2(O)_2(PPh_3)_4]$.

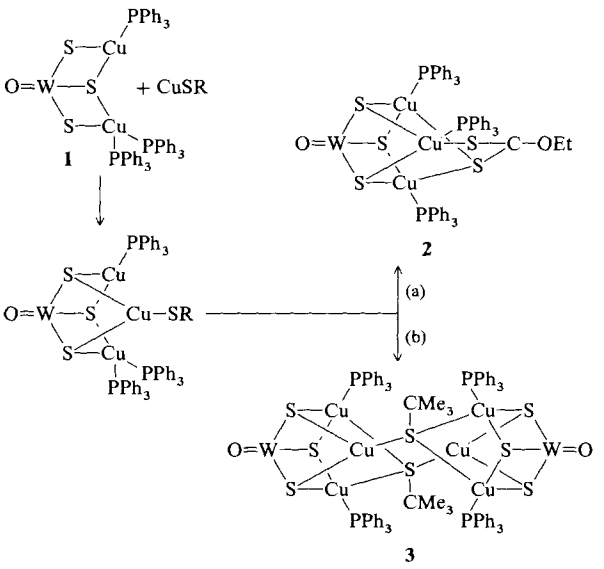

Scheme 1. Possible pathways of the reactions (a) and (b). R = CMe_3, C(S)OEt.

The compound **2** crystallizes in the space group $P\bar{1}$ with two molecules per unit cell. Figure 1 shows one of the two independent molecules. The structure is similar to that of the cluster $[Cu_3S_3W(Cl)(O)(PPh_3)_3]$,[11b] except that the chloride ion is replaced by a triply-bridging bidentate dithiocarbonato ligand $EtOCS_2^-$. The bridging mode of the bidentate dithiocarbonato ligand is unusual.[16] Such bridging is known in the case of thiocarbamates of the type $R_2NC(O)S^-$, e.g. in $[M(Pr_2mtc)]_6$ (M = Cu,[17a] Ag;[17b] Pr_2mtc = *N*,*N*-dipropylmonothiocarbamate), but so far has not been reported for dithiocarbonates(1-) as ligands.[16]

3 crystallizes in the space group $P\bar{1}$ with one molecule per unit cell (Fig. 2). The crystallographic inversion center

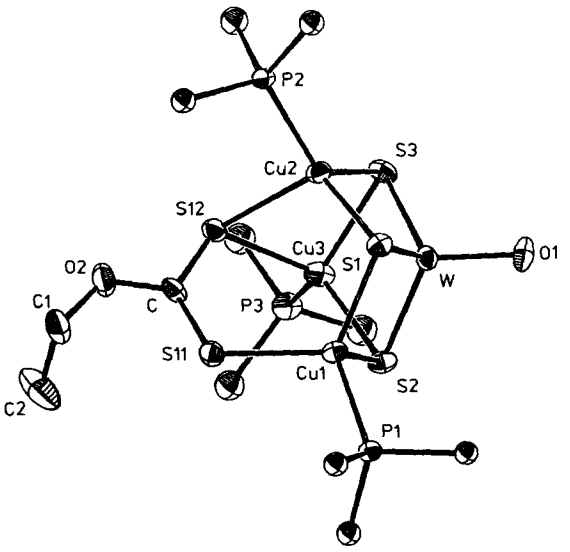

Fig. 1. ORTEP drawing of **2** (thermal ellipsoids at the 30% probability level). Selected bond lengths [Å] and angles [°]: W-Cu(1) 2.798(2), W-Cu(2) 2.721(2), W-Cu(3) 2.736(2), W-S (average) 2.246(3), W-O(1) 1.752(7), Cu(1)-S(1) 2.321(3), Cu(1)-S(2) 2.322(3), Cu(1)-S(11) 2.312(3), Cu(1)-P(1) 2.277(3), Cu(2)-S(1) 2.290(3), Cu(2)-S(3) 2.353(3), Cu(2)-S(12) 2.536(3), Cu(2)-P(2) 2.224(3), Cu(3)-S(2) 2.287(3), Cu(3)-S(3) 2.352(3), Cu(3)-S(12) 2.457(3), Cu(3)-P(3) 2.213(3), S(11)-C 1.67(1), S(12)-C 1.69(1), O(2)-C 1.36(1); S(1)-Cu(1)-S(2) 102.0(1), S(1)-Cu(1)-P(1) 116.7(1), S(3)-Cu(2)-S(12) 89.1(1), S(3)-Cu(2)-P(2) 124.3(1), S(3)-Cu(3)-S(12) 91.0(1), S(3)-Cu(3)-P(3) 124.0(1), Cu(2)-S(12)-Cu(3) 78.5(1).

overlaps the center of the molecule. The molecule consists of two cubane-like $[Cu_3S_3W(SCMe_3)(O)(PPh_3)_2]$ units linked by two triply bridging $SCMe_3$ groups. This kind of μ_3-coordination of Me_3CS^- is rare in organothiolato transition metal complexes.[18] The structure of **3** is similar to that of the double cubane-like cluster $[Cu_2S_8Mo_6(H_2O)_{18}]^{8+}$[19] in which the molybdenum is in a low oxidation state.

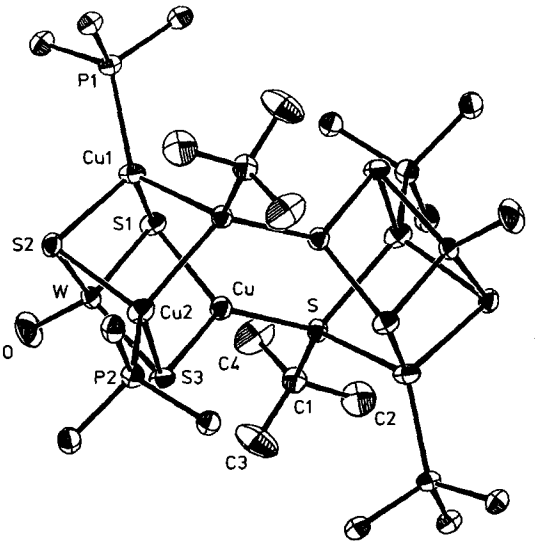

Fig. 2. ORTEP drawing of **3** (thermal ellipsoids at the 30% probability level). Selected bond lengths [Å] and angles [°]: W-Cu 2.682(1), W-Cu(1) 2.7731(9), W-Cu(2) 2.786(1), W-S (average) 2.248(2), W-O(1) 1.695(5), Cu-S 2.207(2), Cu-S(1) 2.249(2), Cu-S(3) 2.247(2), Cu(1)-S(1) 2.348(2), Cu(1)-S(2) 2.391(2), Cu(1)*-S 2.425(2), Cu(1)-P(1) 2.225(2), Cu(2)-S(2) 2.393(2), Cu(2)-S(3) 2.354(2), Cu(2)*-S 2.437(2), Cu(2)-P(2) 2.228(2), S-C(1) 1.861(7); S-Cu-S(1) 125.80(7), S-Cu-S(3) 126.06(7), S(1)-Cu-S(3) 106.74(7).

 © VCH Verlagsgesellschaft mbH, W-6940 Weinheim, 1992 0570-0833/92/0808-1086 $ 3.50+.25/0

Our findings demonstrate once again the high tendency of formation of transition metal-copper-sulfur clusters and their structural variants. The driving force for the reactions studied is the preferred formation of μ_3S compared to μ_2S moieties in the presence of soft metal centers, which corresponds to the formation of the prismane type cage $[CuP(Ph_3)_4(MoOS_3)_2]$ from two halves of it, that means from the butterfly type species $[Cu_2(PPh)_3(MoOS_3)]$.[14] Subunits of M–Cu–S complexes seem to be suitable for the synthesis of various molecular structures. Whereas the synthesis of transition-metal clusters like **2** and **3** with sulfido-bridges by "spontaneous self-assembly" reactions from simple inorganic reagents is highly unlikely, in some cases smaller clusters can be used as building blocks in cluster synthesis.

Experimental

2: A mixture of 0.20 g (0.165 mmol) of **1** and 0.032 g (0.17 mmol) of $Cu(S_2COEt)$—obtained from 2.0 g of CuI in saturated KI solution (30 g KI in 30 mL H_2O) and 1.7 g KS_2COEt (in 10 mL H_2O) as a yellow precipitate, which was washed with saturated KI solution, water, ethanol and ether—was dissolved in 15 mL CH_2Cl_2 and stirred for 3.5 h. The orange reaction solution was then filtered and the filtrate treated with 60 mL diethyl ether. This solution was allowed to stand for about 12 h at ca. 5 °C and 0.15 g of pure red crystals were obtained (yield: 65 %); satisfactory C,H,Cu,P,S analysis.

3: A mixture of 0.20 g (0.165 mmol) of **1** and 0.027 (0.18 mmol) of $Cu(SCMe_3)$—obtained by reaction of 5.0 g $Cu(NO_3)_2 \cdot 3H_2O$ with 5 mL $HSCMe_3$ and 5 mL NEt_3 in 50 mL ethanol as a yellow precipitate, which was washed with ethanol and ether—was dissolved in 30 mL of CH_2Cl_2 and stirred for 25 min. The orange-red solution was filtered and the filtrate was treated with 30 mL of diethyl ether. The filtrate was allowed to stand for ca. 12 h at 5–10 °C, orange crystals were obtained. The orange-red crystals that separated out were recrystallized from 25 mL of CH_2Cl_2 solution by gaseous diffusion of diethyl ether. Yield: 0.10 g (55 %); satisfactory C,H,P,S analysis.

Received: January 30, 1992 [Z 5160 IE]
German version: *Angew. Chem.* **1992**, *104*, 1098

CAS Registry numbers:
1, 125302-32-1; **2**, 142700-17-2; **3**, 142700-18-3.

[1] A. Müller, E. Diemann, R. Jostes, H. Bögge, *Angew. Chem.* **1981**, *93*, 957; *Angew. Chem. Int. Ed. Engl.* **1981**, *20*, 934.
[2] M. P. Coughlan, *Molybdenum and Molybdenum Containing Enzymes*, Pergamon Press, Oxford, **1980**.
[3] C. F. Mills, *Chem. Br.* **1979**, *15*, 512.
[4] a) R. E. Palermo, R. Singh, J. K. Bashkin, R. H. Holm, *J. Am. Chem. Soc.* **1984**, *106*, 2600, and references therein. b) Q.-T. Liu, L.-R. Huang, H.-Q. Liu, X.-J. Lei, D.-X. Wu, B.-S. Kang, and J.-X. Lu, *Inorg. Chem.* **1990**, *29*, 4131, and references therein.
[5] S. Ciurli, S.-B. Yu, R. H. Holm, K. K. P. Srivastava, E. Münck, *J. Am. Chem. Soc.* **1990**, *112*, 8169.
[6] J. A. Kovacs, R. H. Holm, *J. Am. Chem. Soc.* **1986**, *108*, 340; *Inorg. Chem.* **1987**, *26*, 711.
[7] a) T. E. Wolff, J. M. Berg, K. O. Hodgson, R. B. Frankel, and R. H. Holm, *J. Am. Chem. Soc.* **1979**, *101*, 4140. (b) G. Christou, C. D. Garner, F. E. Mabbs, and T. J. King, *J. Chem. Soc. Chem. Commun.* **1978**, 740.
[8] a) Review: S. Sarkar, S. B. S. Mishra, *Coord. Chem. Rev.* **1984**, *59*, 239; b) S. R. Acott, C. D. Garner, J. R. Nicholson, W. Clegg, *J. Chem. Soc., Dalton Trans.* **1983**, 713; c) J. R. Nicholson, A. C. Flood, C. D. Garner, W. Clegg, *J. Chem. Soc., Chem. Commun.* **1983**, 1179; d) C. D. Garner, J. R. Nicholson, W. Clegg, *Acta Crystallogr. Sect. C*, **1983**, *39*, 552.
[9] a) X.-T. Wu, S.-F. Lu, N.-Y. Zhu, Q.-J. Wu, J.-X. Lu, *Inorg. Chim. Acta.* **1987**, *133*, 39; b) S.-F. Lu, N.-Y. Zhu, X.-T. Wu, Q.-J. Wu, J.-X. Lu, *J. Mol. Struc.* **1989**, *197*, 15; c) H.-Q. Zhang, Y.-F. Zheng, X.-T. Wu, J.-X. Lu, *Inorg. Chim. Acta*, **1989**, *156*, 277; d) Y.-F. Zheng, H.-Q. Zhang, X.-T. Wu, J.-X. Lu, *Transition Met. Chem. (London)* **1989**, *14*, 161.
[10] a) N.-Y. Zhu, Y.-F. Zheng, X.-T. Wu, *J. Chem. Soc., Chem. Commun.* **1990**, 780; b) N.-Y. Zhu, R.-C. Wu, X.-T. Wu, *Acta Crystallogr. Sect. C*, **1991**, *47*, 1537.
[11] a) A. Müller, H. Bögge, U. Schimanski, *J. Chem. Soc. Chem. Commun.* **1980**, 91; b) A. Müller, H. Bögge, U. Schimanski, *Inorg. Chim. Acta* **1983**, *69*, 5; c) X.-T. Wu, Y.-F. Zheng, S.-W. Du, *Acta Crystallogr. Sect. C*, **1989**, *45*, 1070; d) X.-T. Wu, Y.-F. Zheng, S.-W. Du, N.-Y. Zhu, *Transition Met. Chem. (London)* **1989**, *14*, 157; e) N.-Y. Zhu, J.-H. Wu, X.-T. Wu, *Acta Crystallogr. Sect. C*, **1991**, *C47*, 856.
[12] a) X.-T. Lin, Y.-H. Lin, J.-L. Huang, J.-Q. Huang, *Kexue Tongbao (Foreign Lang. Ed.)* **1987**, *32*, 810; b) H.-Q. Zhang, Master thesis of Fujian Institute of Research on Structure of Matter, **1989** (Chinese).
[13] W.-H. Pan, T. Chandler, J. H. Enemark, E. I. Stiefel, *Inorg. Chem.* **1984**, *23*, 4265.
[14] A. Müller, U. Schimanski, J. Schimanski, *Inorg. Chim. Acta* **1983**, *76*, L245.
[15] a) **2**: IR (KBr pellet, $\tilde{\nu}$ [cm^{-1}]): δ(C-H) in Ph_3P, 750(s), 745(s), 705(s), 695(vs); bonds due to stretching vibratios of the following type: Cu-P, 525(s), 515(shoulder), 510(s), and 495(s); W-μ_3-S, 440(s); W-O, 930(vs). UV/Vis (in CH_2Cl_2): λ = 286 nm. Crystallographic data: triclinic, space group $P\bar{1}$ (No. 2), a = 12.732(5), b = 22.896(6), c = 10.499(5) Å, α = 99.92(3), β = 109.51(3), γ = 86.86(3)°, V = 2842(2) Å^3, Z = 2; R = 0.049 for 5823 observed reflections with $I > 5\sigma(I)$ and 402 variables [15c]. b) **3**: IR (KBr pellet, $\tilde{\nu}$ [cm^{-1}]): δ(C-H) in Ph_3P, 755(s), 745(vs), 705(shoulder), and 695(vs); bonds due to stretching vibrations of the following type: Cu-P, 530(vs), 510(s), and 500(s); W-μ^3-S, 460(s); W-O: 940(vs). UV/Vis (in CH_2Cl_2): λ = 348 nm. Crystallographic data: triclinic, space group $P\bar{1}$ (No. 2), a = 14.206(2), b = 14.729(3), c = 12.428(2) Å, α = 110.43(1), β = 90.45(1), γ = 62.93(1)°, V = 2134.1(6) Å^3; Z = 1; R = 0.040 for 5998 observed reflections with $I > 3\sigma(I)$ and 460 variables [15c]. c) Further details of the crystal structure investigations are available on request from the Fachinformationszentrum Karlsruhe, Gesellschaft für wissenschaftlich-technische Information mbH, W-7514 Eggenstein-Leopoldshafen 2 (FRG), on quoting the depository number CSD-56196, the names of the authors, and the journal citation.
[16] G. Wilkinson, R. D. Gillard, J. A. McCleverty, *Comprehensive Coordination Chemistry*, Vol. 2, Pergamon, Oxford **1987**, pp. 579–593.
[17] a) R. Hesse, U. Aava, *Acta Chem. Scand.* **1970**, *24*, 1355; b) P. Jennische, R. Hesse, *ibid.* **1971**, *25*, 423.
[18] a) I. G. Dance, *Polyhedron*, **1986**, *5*, 1037; b) P. J. Blower, J. R. Dilworth, *Coord. Chem. Rev.* **1987**, *76*, 121.
[19] T. Shibahara, H. Akashi, H. Kuroya, *J. Am. Chem. Soc.* **1988**, *110*, 3313.

Docking of a Second Functional Protein Layer to a Streptavidin Matrix on a Solid Support: Studies with a Quartz Crystal Microbalance

By *Hiroshi Ebato, James N. Herron, Wolfgang Müller, Yoshio Okahata, Helmut Ringsdorf,** and *Peter Suci*

The specific interaction of streptavidin[1] with biotinylated lipids at the air/water interface leads to the formation of optically anisotropic two-dimensional streptavidin crystals.[2–4] This perfectly ordered matrix of the protein streptavidin, with two of its original four binding sites remaining free, can be functionalized in various ways with biotinylated subunits.[2] Recently, it has been shown by Ward et al. that it is possible to detect the binding of biotinylated moieties to unspecifically adsorbed avidin and streptavidin layers with a quartz crystal microbalance (QCM) for biosensor applications.[5] In the study presented here, the possibility of using a streptavidin film, specifically bound via biotin to a solid support, as a template for docking a second functional protein layer was explored. A quartz crystal microbalance[6] was utilized to study both the interaction of streptavidin with biotinlipid membranes and the docking of biotinylated anti-fluorescyl-antibody fragments (Fab fragments)[7] to streptavidin.

Previous monolayer experiments with biotinlipids at the air/water interface revealed that it is necessary to have sufficient mobility and free space around the biotin headgroups of the lipids for proper binding of the ligand.[3, 4] One would expect, that on a solid support, mobility and access of the

[*] Prof. Dr. H. Ringsdorf, Dipl.-Chem. W. Müller, Dr. P. Suci
Institut für Organische Chemie der Universität
J. J. Becherweg 18–20, D-W-6500 Mainz 1 (FRG)
Dr. J. N. Herron
Department of Pharmaceutics, University of Utah
421 Wakara Way, Salt Lake City, UT 84101 (USA)
Dipl.-Chem. H. Ebato, Prof. Dr. Y. Okahata
Department of Polymer Chemistry, Tokyo Institute of Technology
2-12-1 Ookayama, Meguro-ku, Tokyo 152 (Japan)

biotin headgroups will be even more important and hence biotin lipids with a short (**1**) and a long (**2**) hydrophilic spacer were compared in the studies. For all the experiments presented below, three monolayers of the corresponding lipids mixed with L-α-dipalmitoylphosphatidylethanolamine (L-α-DPPE) in varying amounts were deposited by means of the Langmuir–Blodgett (LB) technique on the gold electrode of a QCM. All measurements with the QCM were performed in buffer solution (50 mmol phosphate, pH = 7.5).

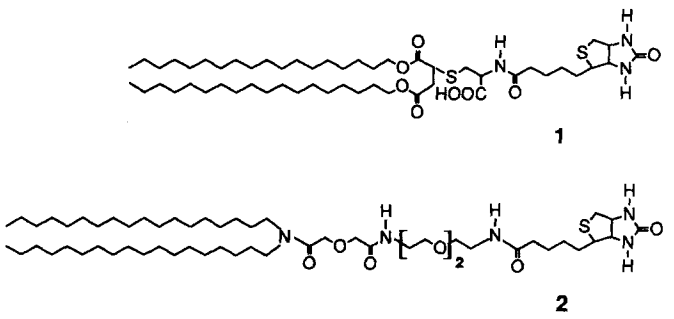

1

2

As expected the spacer length plays an important role in the docking process of streptavidin on solid supports. The frequency change observed with the long spacer lipid **2** (5 mol-% in DPPE[8]; Fig. 1 filled circles) is strongly dependent on the protein concentration up to the saturation of the membrane, which occurs between 2.5×10^{-7} and 3.5×10^{-7} M streptavidin in the buffer solution. The resulting saturation frequency change of 65 Hz is in agreement with the frequency change expected for a monolayer of streptavidin as predicted by the Sauerbrey equation (in air).[9] In contrast to this, for the biotin-free (pure DPPE) membrane and the membrane with 5 mol-% of the short spacer lipid **1**, a maximum frequency change of only 15 Hz is found (Fig. 1 open circles, triangles). With the pure DPPE membrane, a specific interaction with the biotin ligand is excluded, and therefore the frequency changes produced can be assumed to result from nonspecific adsorption of streptavidin to the membrane surfaces. Apparently, sufficient spacer length between the biotin-headgroup and the membrane-forming alkyl chains of the biotinlipids can compensate for the reduced mobility and close packing of the headgroups on the surface and allow proper binding of a streptavidin layer.

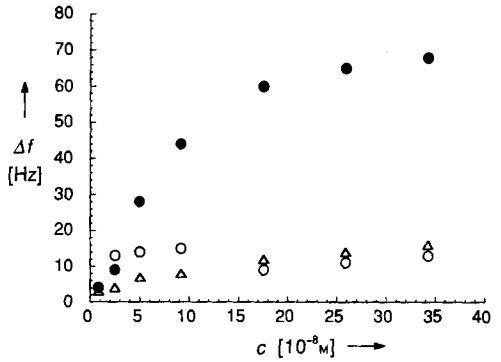

Fig. 1. Interaction of streptavidin with different lipid membranes, measured via the change in resonance frequency Δf of a quartz crystal microbalance as a function of the streptavidin concentration c. ○: pure DPPE membrane; △: DPPE with 5 mol-% of biotinlipid **1**; ●: DPPE with 5 mol-% of biotinlipid **2**.

This is confirmed by experiments to determine the amount of biotinlipid needed for a total protein coverage of the surface in mixed DPPE/**2** layers. It could be shown (Fig. 2) that with approximately 1 mol-% of **2** in the DPPE matrix the saturation frequency change of 65 Hz is already found.

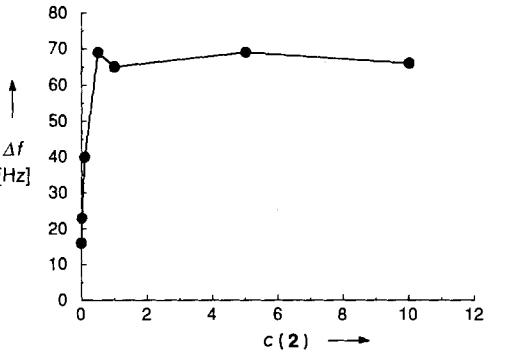

Fig. 2. Dependence of the change in resonance frequency on the content (c in mol-%) of biotinlipid **2** in the membrane.

When the biotinlipid **2** content was increased further no difference in the equilibrium frequency change was observed, even when the content was 10 mol-%, indicating that under these conditions no further protein can be induced to adsorb once the surface is saturated.

The protein used for the docking of a second protein layer to the streptavidin matrix is a Fab fragment of a monoclonal antifluorescyl antibody (clone 4-4-20).[7] Two different biotinylation procedures of the Fab were used: the results presented in Figure 4 were obtained with a Fab fragment biotinylated nonspecifically with an amino-reactive reagent (BioFab) (see *Experimental*); the measurements presented in Figure 5, on the other hand, were performed using a Fab fragment specifically monobiotinylated in the hinge region via a disulfide bridge (Fab') (see *Experimental*). This results in formation of a layer structure (Fig. 3), in which the antigen-binding sites face the adjacent solution.

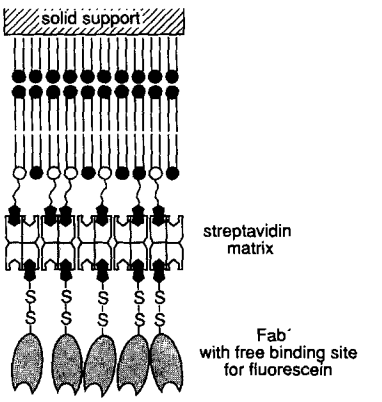

Fig. 3. Schematic representation of the docking of a Fab fragment which was specifically biotinylated in the hinge region to a two-dimensional streptavidin layer. The Fab' layer can serve as a matrix for further binding of fluorescein-containing molecules.

Figure 4 shows the course of the streptavidin interaction with time with a biotinlipid-containing membrane (5 mol-% of lipid **2** in DPPE) before and after addition of the Fab- and BioFab-fragments.

Binding of streptavidin (5×10^{-7} M) to the biotinlipids is very fast and the equilibrium frequency change of 65 Hz described above is reached after six minutes. The streptavidin covered membrane was rinsed with buffer, transferred into a fresh buffer solution and incubated with streptavidin a second time to see whether washing affects the coverage of the surface. No frequency change could be detected during this process, indicating that the streptavidin layer is tightly bound to the membrane surface. The surface was then washed as before and now incubated with non-biotinylated Fab (1.8×10^{-7} M). No significant frequency change was detected indicating no or only a negligible amount of nonspecific adsorption. Thereafter 3.5×10^{-8} M of biotinylated Fab was added to the buffer; this resulted in a slow but significant frequency change reaching saturation at 55 Hz relative to the original saturation frequency change (Fig. 4), pointing to a dense packing of the Fab molecules onto the streptavidin layer, as already shown with ellipsometry measurements at the air/water interface.[10]

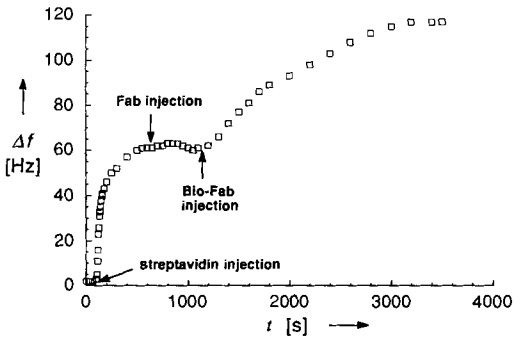

Fig. 4. Course of streptavidin binding with time to a lipid membrane containing 5 mol-% of lipid **2** and interaction of non-biotinylated antifluorescyl-Fab and biotinylated antifluorescyl-Fab with a streptavidin matrix.

It was interesting to see whether the same extent of binding could be attained using the site-specifically monobiotinylated Fab fragment. The results of these docking experiments are presented as a binding curve in Figure 5. This specific

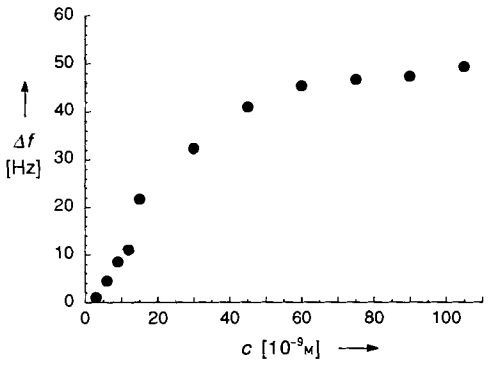

Fig. 5. Binding of a site-specifically monobiotinylated Fab fragment (Fab') to a streptavidin matrix as monitored with the QCM (each symbol represents averaged data of three independent measurements).

interaction leads to an increasing frequency change with increasing Fab' concentration, reaching again a saturation value of 50 Hz for a Fab' concentration of 1×10^{-7} M. As before, the control experiment with non-biotinylated Fab fragment resulted in no detectable frequency change (not shown).

In conclusion it has been shown that the QCM is able to differentiate between specific binding and nonspecific adsorption of streptavidin to different biotinlipid membranes. Employing this first streptavidin layer as a template, docking of monoclonal antibody Fab (biotinylated by two different methods) was followed using the QCM. In general, surface bound, highly organized protein matrices, having a vast variety of binding specificities, can be constructed using this method.

Experimental

The resonance frequency of the quartz crystal of the QCM is sensitive to the mass bound to the surface of the gold electrode, although in liquids the relation between adsorbed mass and frequency change may be quite complex [11]. In air, the frequency change expected from a quantity of adsorbed mass is given by the Sauerbrey equation [9]. Thus, in principle, the QCM technique allows one to quantify the binding process of proteins to various membranes. Furthermore, the course of the interaction with time can be followed in real time. The experimental setup used by us has already been described elsewhere [6]. The crystals used in the experiments had a resonance frequency of 9 MHz.

LB-deposition of the lipid membranes was performed at a speed of 1 cm/min and a surface pressure of 40 mN m^{-1} ($T = 22$ °C) from the solid analogous phase of the lipid monolayer. This resulted in a close packing and low lateral mobility of the lipids on the support. For the mixed membranes (DPPE/biotinlipid) adequate amounts of chloroform solutions of the corresponding lipids were mixed prior to spreading. For the measurements the crystal was immersed in buffer solution (50 mmol phosphate buffer, pH 7.5). The starting frequency (f_0) and the change in resonance frequency of the crystal ($\Delta f = f_0 - f(t)$) was monitored as a function of the protein concentration in the buffer solution.

The nonspecific biotinylation of the Fab fragment was performed with 6-(6-(biotinoyl)amino)-hexanoylamino)hexanoic acid succinimidyl ester (B-1606 Molecular Probes, Inc., Eugene, OR 97402, USA). The selective biotinylation of the Fab' fragment in the hinge region was achieved with *N*-(6-(biotinamidohexyl)-3-(2-pyridyldithio)propionamide (21341 Pierce, Rockford, IL 61105, USA) via formation of a disulfide bridge.

Biotinlipid **1** was synthesized as described earlier [12].

Biotinlipid **2** was synthesized in the following way [13]: 4 g (6.3 mmol) of *N,N*-dioctadecyldiglycolic acid monoamide (DODA-GSA) was refluxed with 1.1 g (6.8 mmol) of carbonyldiimidazole in 30 mL of dry THF for 2 h to yield the corresponding imidazole-active ester. The resulting solution was then added dropwise to a stirred solution of 8 g (54 mmol) of 1,8-diamino-3,6-dioxaoctane in 50 mL of dry THF. The reaction was monitored by TLC ($CHCl_3$/MeOH: 5/1). After completion (20 min), the solvent was evaporated off and the residue taken up in $CHCl_3$, extracted with water to remove the excess of diamine, and purified by chromatography to yield 2.8 g of 1-*N,N*-dioctadecyl-14-amino-5-oxo-3,9,12-trioxa-6-azatetradecanoic acid amide (DODA-EO_2-NH_2). 300 mg (0.39 mmol) of DODA-EO_2-NH_2 and 133 mg (0.39 mmol) of *N*-hydroxysuccinimidobiotin were dissolved in 10 mL of dry DMF and allowed to react at room temperature until no DODA-EO_2-NH_2 could be detected by TLC ($CHCl_3$/MeOH: 10/1). The solvent was removed by evaporation in vacuo; the residue was then taken up in $CHCl_3$ and purified by chromatography to yield 220 mg of pure **2**. Its structure was confirmed by elemental analysis and ^{1}H NMR spectroscopy (400 MHz).

Received: December 27, 1991;
revised: February 20, 1992 [Z 5096 IE]
German version: *Angew. Chem.* **1992**, *104*, 1064

CAS Registry numbers:
1, 122567-70-8; **2**, 142260-90-0; quartz, 14808-60-7; streptavidin, 9013-20-1; DPPE, 923-61-5.

[1] *Methods in Enzymology, Vol. 184* (Eds.: E. A. Bayer, M. Wilchek), Academic Press, San Diego, **1990**, p. 5.
[2] S. A. Darst, M. Ahlers, P. Meller, E. W. Kubalek, R. Blankenburg, H. O. Ribi, H. Ringsdorf, R. D. Kornberg, *Biophys. J.* **1990**, *59*, 387.
[3] M. Ahlers, W. Müller, A. Reichert, H. Ringsdorf, J. Venzmer, *Angew. Chem* **1990**, *29*, 1310; *Angew. Chem. Int. Ed. Engl.* **1990**, *29*, 1269.
[4] a) M. Ahlers, M. Hoffmann, H. Ringsdorf, A. M. Rourke, E. Rump, *Makromol. Chem. Makromol. Symp.* **1991**, *46*, 307; b) M. Ahlers, R. Blankenburg, H. Haas, D. Möbius, H. Möhwald, W. Müller, H. Ringsdorf, H.-U. Siegmund, *Adv. Mat.* **1991**, *3*, 39.

[5] R. C. Ebersole, J. A. Miller, J. R. Moran, M. D. Ward, *J. Am. Chem. Soc.* **1990**, *112*, 3239.
[6] Y. Okahata, H. Ebato, *Anal. Chem.* **1991**, *63*, 203.
[7] J. N. Herron, X.-M. He, L. Mason, E. W. Voss, Jr., A. B. Edmundson, *Proteins* **1989**, *5*, 271.
[8] Since LB-transfer of the homogeneous lipid mixtures was performed in the solid condensed state of the monolayer at 40 mN/m the space required for one lipid molecule is approximately 40 Å^2. 5 mol-% biotinlipid content will thus result in approximately seven biotinlipid molecules on an area convered by two streptavidin molecules (5000 Å^2).
[9] G. Sauerbrey, *Z. Phys.* **1959**, *155*, 206. According to the Sauerbrey equation the change of resonance frequency of a piezo quarz crystal is proportional to the change in mass on the electrode surface. For the crystals used here, calibration revealed that a frequency change of 1 Hz corresponds to a mass increase of 1.05 ± 0.01 ng. The gold electrode has a diameter of 4.5 mm resulting in a sensitive area of 15.9 mm^2. A monolayer coverage with streptavidin (2500 Å^2 per molecule) should thus result in a frequency decrease of 63 Hz. But due to the electrode surface roughness this can only be a rough estimation.
[10] J. N. Herron, W. Müller, M. Paudler, H. Riegler, H. Ringsdorf, P. Suci, *Langmuir* **1992**, *18*, 1413.
[11] a) P. W. Walton, M. E. Butler, M. R. O'Flaherty, *Biochem. Soc. Trans.* **1990**, *19*, 44; b) M. Thompson, U. J. Krull, *Anal. Chem.* **1991**, *63*, 393 A; c) K. K. Kanazawa, J. G. Gordon II, *Anal. Chim. Acta* **1985**, *175*, 99; d) R. Schumacher, *Angew. Chem.* **1990**, *102*, 347; *Angew. Chem. Int. Ed. Engl.* **1990**, *29*, 329; e) R. C. Ebersole, M. D. Ward, *J. Am. Chem. Soc.* **1988**, *110*, 8623.
[12] R. Blankenburg, P. Meller, H. Ringsdorf, C. Salesse, *Biochemistry* **1989**, *28*, 8214.
[13] M. Ahlers, Dissertation, Universität, Mainz, **1990**.

A Remarkable Change in Framework Cation Positions upon Lithium Exchange: the Crystal Structure of $LiMnPO_4(OH)$

By *Miguel A. G. Aranda,* J. Paul Attfield* and *Sebastian Bruque*

In the search for new battery materials, molecular sieves, and ionic conductors and exchangers, reactions involving the insertion or exchange of lithium into the channels or interlamellar spaces of precursor structures are of great interest.[1, 2] We have recently reported the synthesis and structure of a new material, manganese(III) arsenate hydrate $MnAsO_4 \cdot H_2O$,[3] which undergoes a topotactic lithium exchange reaction with solid $LiNO_3$ to give $LiMnAsO_4(OH)$.[4] This reaction is accompanied by an unusual switch in the framework geometry as the Jahn-Teller distortions of the MnO_6 octahedra change although the topology is unaltered. In this communication we describe the analogous lithium exchange reaction of $MnPO_4 \cdot H_2O$ to give $LiMnPO_4(OH)$, which is accompanied by a different, remarkable change in the framework, as the Mn^{3+} cations are displaced to alternative octahedral sites within the $PO_4(OH)$ sublattice.

$LiMnPO_4(OH)$ was prepared in the form of a microcrystalline powder by solid-state reaction of $MnPO_4 \cdot H_2O$ with $LiNO_3$. The use of low temperatures and long reaction times furnished a sufficiently crystalline material for crystal structure determination from laboratory X-ray powder diffraction data to be successful (see *Experimental*). A restrained Rietveld[5] refinement of the $MnPO_5$ framework and the Li position was performed, and although the remaining H atom was not located, bond valence calculations[6] showed that it is attached to O(3), as are those in $MnPO_4 \cdot H_2O$[7] and $LiMnAsO_4(OH)$,[4] confirming the formulation as a phosphate hydroxide rather than as a hydrogen phosphate oxide.

Polyhedral[8] representations of the structures of $MnXO_4 \cdot H_2O$ (X = P, As), $LiMnAsO_4(OH)$ and $LiMnPO_4(OH)$ are shown in Figures 1a, 1b and 1c, respectively.

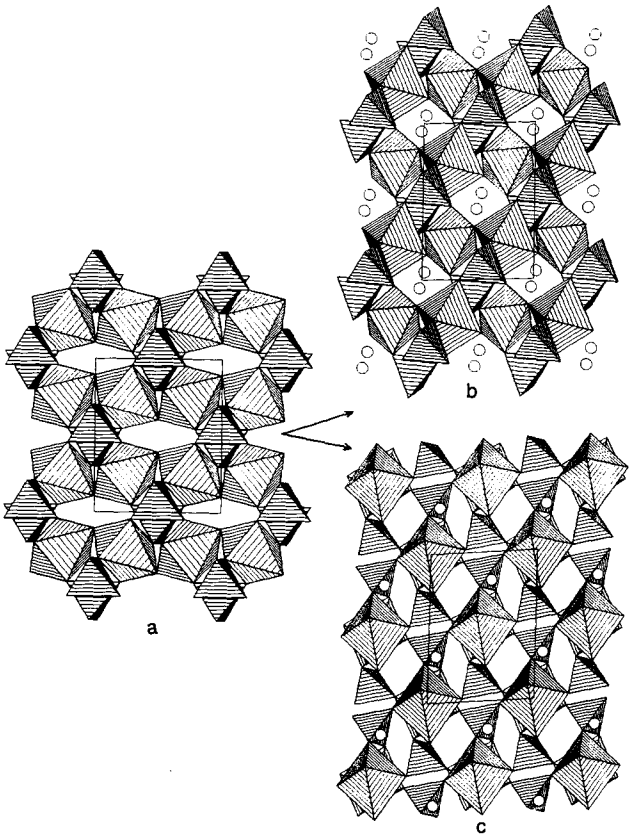

Fig. 1. Polyhedral near-(001) views (*b* axis vertical) of a) $MnXO_4 \cdot H_2O$ (X = P, As), b) $LiMnAsO_4(OH)$, and c) $LiMnPO_4(OH)$ with lithium atoms shown as open circles. Hydrogen atoms are not included.

In the first two structures, the MnO_6 octahedra are linked via opposite vertices by H_2O or OH^- groups to form infinite zigzag chains in the [101] direction that are interconnected by XO_4 tetrahedra, resulting in a three-dimensional framework. This encloses small channels parallel to the *c*-axis into which the hydrogen atoms project in $MnXO_4 \cdot H_2O$ (X = P, As), and in which the lithium ions are located in $LiMnAsO_4(OH)$. In the $LiMnPO_4(OH)$ structure, the MnO_6 octahedra are also linked through opposite vertices by OH^- groups to give infinite zigzag chains, but these now lie in the [001] direction. This structural rearrangement is due to a migration of the manganese atoms from the octahedral sites at 1/4 ,1/4 ,0 and related positions in $MnXO_4 \cdot H_2O$ to alternative octahedral holes in the channels at 0, 0, 0 and equivalent positions. Remarkably, this change in Mn positions results in little change to the cell parameters or the coordinates of the other atoms (Table 1). The two possible octahedral sites in the $MnXO_4 \cdot H_2O$ structure type are shown in Figure 2. The vacant sites in $LiMnPO_4(OH)$ are also connected to form channels in which the lithiums reside, but these run in a [101] direction rather than [001] in the starting material. This re-

[*] Dr. M. A. G. Aranda, Prof. Dr. S. Bruque
Departamento de Química Inorgánica
Universidad de Málaga, Aptd. 59
E-29071 Málaga (Spain)
Dr. J. P. Attfield
Department of Chemistry
University of Cambridge
Lensfield Road, GB-Cambridge CB2 1EW, (U.K.)

Table 1. Results of the refinement of the crystal structure of $LiMnXO_4(OH)$ (X = P, As[4]) in the space group $C\bar{1}$. Edge lengths of the unit cell in Å, angles in degrees.

Cell parameters						
X	*a*	*b*	c	α	*β*	*γ*
P	6.7262(3)	8.1815(3)	7.1230(3)	89.481(3)	117.775(3)	86.389(3)
As	6.8874(5)	8.4326(4)	7.2511(3)	94.213(1)	118.145(2)	86.498(3)

Structural parameters [a]					
Atom	X	*x*	*y*	*z*	B_{iso}[Å^2] [b]
Mn(a)	P	0.0000	0.0000	0.0000	0.16(4)
	As	0.2500	0.2500	0.0000	
Mn(b)	P	0.0000	0.0000	0.5000	0.16
	As	0.7500	0.2500	0.5000	
X	P	0.0238(5)	0.3474(4)	0.2347(5)	1.18(7)
	As	−0.0371(3)	0.4022(2)	0.2391(3)	
O(1a)	P	0.3784(8)	0.2678(6)	−0.1210(8)	0.43(7)
	As	0.4877(11)	0.1838(10)	−0.0560(12)	
O(1b)	P	−0.4660(8)	0.2285(6)	0.6004(8)	0.43
	As	−0.3917(16)	0.2460(10)	0.6574(13)	
O(2a)	P	0.3217(8)	0.0189(5)	−0.3370(9)	0.43
	As	0.3338(15)	0.0025(10)	−0.4123(14)	
O(2b)	P	−0.3075(7)	0.0596(6)	0.9442(7)	0.43
	As	−0.2468(16)	−0.0306(10)	0.8809(15)	
O(3)	P	0.0675(9)	−0.0981(5)	0.2813(9)	0.43
	As	−0.0405(14)	−0.1616(10)	0.2779(16)	
Li	P	0.429(3)	0.189(2)	0.230(3)	2.0
	As	0.021(6)	0.051(4)	0.189(5)	

[a] Sites that are equivalent in the monoclinic $MnXO_4 \cdot H_2O$ structures (X = P, As) are labeled (a) and (b). [b] *B* = isotropic temperature factor.

arrangement of the manganese sublattice results in only slight displacements and distortions of the phosphate groups (Table 1 and Fig. 1c).

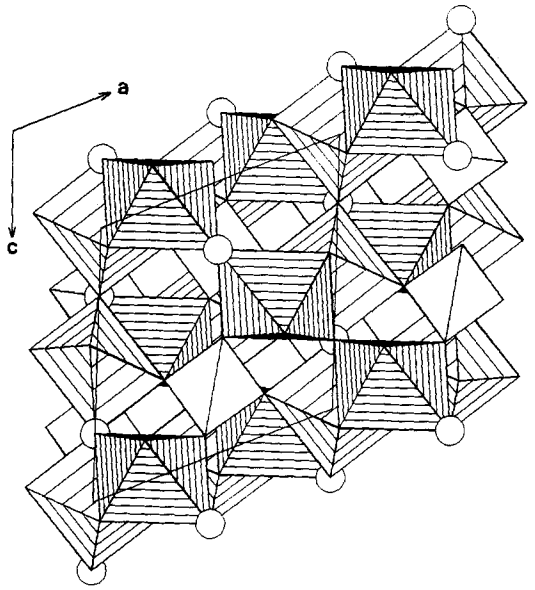

Fig. 2. A polyhedral (010) view showing the Mn sites occupied in the two different structures of $AMnPO_4(OH)$. The MnO_6 octahedra are shaded heavily/lightly for A = H/Li. The XO_4 tetrahedra are unshaded and the oxygens of the water molecules that link the octahedra into chains in both structures are shown as open circles.

Comparison of the bond distances in $MnPO_4 \cdot H_2O$ and $LiMnXO_4(OH)$ (X = P, As) (Table 2) shows a surprising change in the Jahn-Teller distortions of the MnO_6 octahedra that arise from the $t_{2g}^3 e_g^1$ electronic configuration of a high-spin Mn^{III} ion. In $MnPO_4 \cdot H_2O$, the manganese environment shows the well known [4 + 2] elongated tetragonal distortion with four short bonds to phosphate oxygens and two long bonds to the shared water molecules. The Mn atoms in $LiMnAsO_4(OH)$ are [2 + 2 + 2] coordinated with two short and two long Mn–OAs bonds plus two further intermediate Mn–OH bonds (Table 2) due to the previously reported switch in Jahn-Teller modes.[4] In $LiMnPO_4(OH)$, the distortions of the MnO_6 octahedra are intermediate between the [4 + 2] and the [2 + 2 + 2] types. The coordination geometries in the two lithium derivatives are remarkably similar considering that different Mn sites are occupied. In both cases, the Mn–OH bonds have shortened drastically from ca. 2.30 Å in the μ-aqua bridges to ca. 1.98 Å in the μ-hydroxo bridges in the two inequivalent $Mn(a)O_6$ and $Mn(b)O_6$ octahedra. This change decreases the Mn–Mn distance in the chains of octahedra from 3.976 and 4.048 Å in $MnXO_4 \cdot H_2O$ (X = P, As) to 3.561 and 3.636 Å in $LiMnXO_4(OH)$ (X = P, As). The Li^+ ions in $LiMnPO_4(OH)$ are irregularly coordinated in the channels parallel to the [101] direction, with contacts to five arsenate oxygen atoms and one hydroxy oxygen atom; the Li–Li distance is 3.14(3) Å.

Table 2. Mn–O distances [Å] in $MnPO_4 \cdot H_2O$ [7] and $LiMnXO_4(OH)$ (X = P, As [4])

$MnPO_4 \cdot H_2O$		$LiMnXO_4(OH)$	X = P	As
Mn-O(1)	1.886(3)	Mn(a)-O(1a)	2.142(5)	1.908(8)
		Mn(b)-O(1b)	2.292(5)	1.821(9)
Mn-O(2)	1.909(3)	Mn(a)-O(2b)	1.944(5)	2.104(9)
		Mn(b)-O(2a)	1.938(6)	2.168(9)
Mn-O(3)	2.284(3)	Mn(a)-O(3)	1.985(6)	1.966(11)
		Mn(b)-O(3)	1.978(6)	2.026(10)

The different structural changes produced for X = P and As when the $MnXO_4 \cdot H_2O$ compounds undergo lithium exchange under the same reaction conditions to give $LiMnXO_4(OH)$ reflect the size of the channels and differing flexibilities of the XO_4 groups in the starting materials. The arsenic compound, with wider channels, undergoes the exchange reaction without changes in the framework topology, although the switch in the Jahn-Teller modes due to the loss of H^+ from the framework strains the arsenate group.[4] Such strain cannot be tolerated by the phosphate analogue, and the exchange of H^+ for Li^+ is accompanied by a migration of the manganese atoms to a different set of octahedral holes that give a new framework topology, although with similar local coordination geometries, which can more easily accommodate the lithium ions.

Experimental

$MnPO_4 \cdot H_2O$ was synthesized hydrothermally as previously described[9]. An intimate mixture of solid $LiNO_3$ and $MnPO_4 \cdot H_2O$ in a 4:1 molar ratio was heated at 200 °C for 4 weeks in air, and the product was washed with dilute nitric acid and water and dried at 60 °C. Chemical analysis of the yellow-brown residue showed it to be $LiMnPO_4(OH)$. Mn, P, Li and H_2O were analyzed as described elsewhere[4, 10]. Obtained (and calculated for $LiMnPO_4(OH)$) results: Li:P and Mn:P ratios 0.95 (1.0) and 1.02 (1.0), respectively; Mn oxidation state + 3.1 (3.0), and H_2O content ≈5.4% (5.2%).

Structure Determination: X-ray powder diffraction data were collected for $LiMnPO_4(OH)$ (Siemens D501 automated diffractometer, θ–2θ geometry, flat-plate sample, graphite-monochromated $Cu_{K\alpha}$ radiation, $13 < 2\theta < 130$ °C (2θ), step size = 0.02°, counting time per point = 25 s).The pattern was indexed [11] on a *C*-centered triclinic cell similar to that of $LiMnAsO_4(OH)$ (see Table 1) [4]. However, all attempts to refine the crystal structure of $LiMnPO_4(OH)$ by the Rietveld method using the atomic coordinates of $LiMnAsO_4(OH)$ as starting model were unsuccessful. Therefore an ab initio structure solution was attempted with 81 structure factors obtained from a limited data range [$16 < 2\theta < 54°$] using Le Bail's method [12]. The Mn(a) and Mn(b) positions were derived from

a Patterson map and a difference Fourier map revealed the phosphorus position. A trial framework was then constructed from these heavy-atom coordinates and oxygen positions taken from the structure of $LiMnAsO_4(OH)$. Atomic positions, usual profile parameters and isotropic temperature factors were refined using the GSAS program [13] giving a good fit. A difference Fourier map revealed the lithium position, but the hydrogen position was not located. The final refinement with restraints in the P–O bonds (to maintain a reasonable PO_4 geometry) converged at $R_{wp} = 0.079$, $R_p = 0.062$ and $R_F = 0.053$. In this final refinement, the isotropic temperature factors of each type of atoms were constrained to have the same value to avoid correlations. Results of the refinement are given in Table 1. Further details of the crystal structure investigation may be obtained from Fachinformationszentrum Karlsruhe, Gesellschaft für wissenschaftlich-technische Information mbH, D-W-7514 Eggenstein-Leopoldshafen 2 (FRG), on quoting the depository number CS-56 602, the names of the authors, and the journal citation.

Received: February 12, 1992 [Z 5186 IE]
German version: *Angew. Chem.* **1992**, *104*, 1056

[1] D. W. Murphy, P. A. Christian, *Science* **1979**, *205*, 651.
[2] A. Clearfield, *Chem. Rev.* **1988**, *88*, 125.
[3] M. A. G. Aranda, S. Bruque, J. P. Attfield, *Inorg. Chem.* **1991**, *30*, 2043.
[4] M. A. G. Aranda, J. P. Attfield, S. Bruque, *J. Chem. Soc. Chem. Commun.* **1991**, *604*.
[5] H. M. Rietveld, *J. Appl. Crystallogr.* **1969**, *2*, 65.
[6] I. D. Brown, D. Altermatt, *Acta Crystallogr. Section B* **1985**, *41*, 244.
[7] P. Lightfoot, A. K. Cheetham, A. W. Sleight, *Inorg. Chem.* **1987**, *26*, 2544.
[8] R. X. Fischer, *J. Appl. Crystallogr.* **1985**, *18*, 258.
[9] M. A. G. Aranda, J. P. Attfield, S. Bruque, F. Palacio, *J. Mater Chem.* **1992**, *2*, 501.
[10] M. A. G. Aranda, S. Bruque, *Inorg. Chem.* **1990**, *29*, 1334.
[11] P. E. Werner, *Z. Kristallogr.* **1969**, *120*, 375.
[12] A. Le Bail, H. Duroy, J. L. Fourquet, *Mater. Res. Bull.* **1988**, *23*, 447.
[13] A. C. Larson, R. B. Von Dreele, Los Alamos National Lab. Report No. LA-UR-86-748, **1987**.

The ^{31}P-NMR Spectroscopic Determination of the Enantiomeric Excess of Unprotected Amino Acids**

By *Ron Hulst, N. Koen de Vries,* and *Ben L. Feringa**

The increasing use of natural and synthetic amino acids and their derivatives for the modification of proteins and as chiral building blocks or chiral ligands in numerous asymmetric syntheses[1] demands new methodologies for the fast and accurate determination of the enantiomeric excess (*ee*) of these compounds. The enantiomeric purity of amino acids is routinely analyzed by gas or liquid chromatography through the use of chiral stationary phases and various (in situ) derivatizing techniques.[2]. A number of methods exist for the determination of the enantiomeric excess of amino acid derivatives by NMR spectroscopy, employing chiral[3] or achiral[4] derivatizing agents. Similar methods for *free amino acids* are scarce, mainly due to the low solubility in organic solvents[5] or to the lack of proper chiral derivatizing agents. We now report a simple and efficient ^{31}P-NMR method for the determination of the enantiomeric excess of unprotected amino acids which is based on the use of phosphonate **1** as new chiral derivatizing agent.

The reagent **1** is readily prepared from (*S*)-2-butanol and PCl_3.[6] All amino acids examined thus far react with **1** quantitatively in a few hours at room temperature providing phosphonic amides **3**. The formation of diastereomeric phosphonic amides **3** is most conveniently carried out using aqueous ethanolic solutions of amino acids **2** and reagent **1** dissolved in CCl_4 employing triethylamine as base.[7]

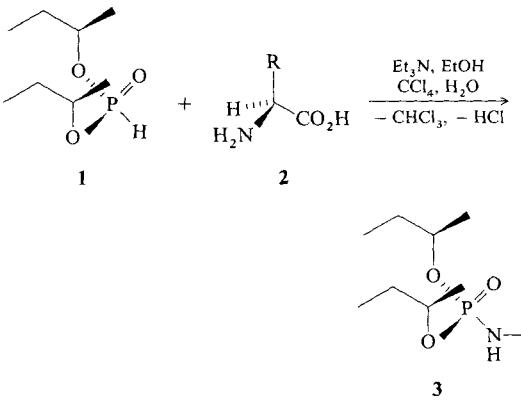

It should be emphasized that aqueous solutions of the amino acids can be analyzed following this methodology and, in particular, by using **1** that no purification of the adducts **3** is necessary, thus allowing rapid *ee* determination. Typical results of the ^{31}P-NMR analyses are summarized in Table 1.

Table 1. ^{31}P-NMR data of the phosphonic amides **3** prepared from amino acids and from chiral amines and alcohols and **1**, recorded in C_6D_6 [a].

Entry	Substrate	δ [b]	$\Delta\delta$ [c]	Peak ratio
1	DL-Ala	6.51	0.099	49.5:50.5
		6.47	0.116	49.5:50.5
2	DL-Phe	5.93	0.025	50:50
		5.91	0.106	50:50
3	DL-Val	6.93	0.069	49.5:50.5
		6.92	0.127	49.5:50.5
4	DL-Try	6.03	0.038	49:51
		6.00	0.091	49:51
5	DL-Ser	6.11	0.079	49.5:50.5
		6.03	0.117	49.5:50.5
6	DL-phenylglycine	5.71	0.098	49.5:50.5
		5.69	0.172	49.5:50.5
7	DL-Tyr	5.65	0.093	49.5:50.5
	DL-Tyr [b]	5.59	0.191	49.5:50.5
8	DL-Cys	5.98	0.087	50:50
		5.98	0.156	50:50
9	DL-Pro	4.63	0.127	49:51
10	DL-α-Me-PG [d]	2.20	0.487	49.5:50.5
11	DL-α-Me-Phe	4.32	0.051	49.5:50.5
12	DL-α-Me-Phe-amide	5.85	0.035	49.5:50.5
13	DL-α-allyl-PG-amide [d]	5.50	0.185	49.5:50.5
14	DL-α-allyl-PG methyl ester [d]	5.48	0.037	49.5:50.5
15	DL-α-phenylethylamine	5.94	0.185	50:50
16	DL-α-phenylethyl alcohol	5.23	0.103	49.5:50.5
17	DL-menthol	5.63	0.127	50:50

[a] In each of the entries 1–8 the first row applies to the diastereomeric separations of **3** with half a molar equivalent of bound water, the second to the diastereomeric separations of **3** after removal of the bound water. [b] Mean of the δ-values of the two diastereomers. [c] Absolute value of the difference in the δ-values of the diastereomers. [d] PG = phenylglycine.

The ^{1}H-decoupled ^{31}P-NMR spectra of **3**, derived from racemic amino acids, show, in all the cases, two well separated singlets corresponding to the two diastereomers. On the

[*] Prof. Dr. B. L. Feringa, R. Hulst
Department of Organic Chemistry, University of Groningen
Nijenborgh 4, NL-9747 AG Groningen (The Netherlands)
Dr. N. K. de Vries
Department of Physical and Analytical Chemistry
DSM Research, Geleen (The Netherlands)

[**] We thank Dr. J. H. Kamphuis and Dr. B. Kaptein for the synthesis of the α-alkylated amino acids.

other hand, a singlet is observed in each case for the enantiomerically pure compounds **3**. Figure 1 shows the ^{31}P-NMR spectra of an amino acid at different *ee* values.

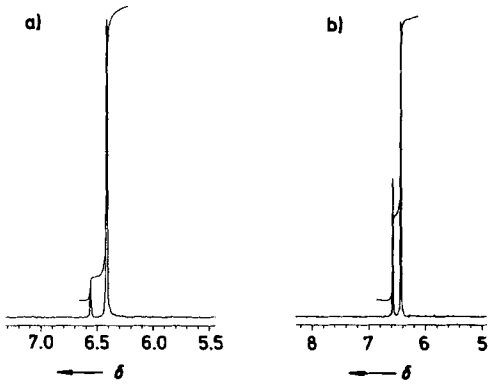

Fig. 1. Noise-decoupled ^{31}P-NMR spectrum of **3** (R = Me) in C_6D_6. a) 82% *ee*. b) 40% *ee* for the (*S*)-enantiomer of **2**.

Though diastereomeric peak separations have also been observed in the ^{1}H-NMR spectra the phosphorus–proton long range coupling gives rise to rather complex spectra.

Phosphonic amides **3** form stable complexes with water, alcohols, and ethyl acetate. After normal workup, 0.5 equivalents of H_2O are complexed which can be removed by heating at 60 °C under high vacuum. Removal of the complexed water results in nearly doubling of the chemical shift differences of the diastereomers of **3** (Table 1).

Some typical results of the *ee* determinations performed on partially enriched compounds are listed in Table 2 together with the *ee*'s determined by the known α-chloropropionyl chloride method[5] and by rotation measurements. These results clearly show that the enantiomeric purities obtained via the different methods are in excellent agreement and that no racemization or kinetic resolution occurs during phosphonic amide formation.

Table 2. Comparison of the *ee* values, those for samples with known enantiomeric composition determined ^{31}P-NMR spectroscopically by rotation [8], and by the α-chloropropionyl chloride method [5] [a].

Entry [b]	Ratio of enantiomers		
	by polarimetry	^{1}H-NMR	^{31}P-NMR
1	76.40:23.60	76.35:23.65	76.40:23.60
2	73.45:26.55	74.10:25.90	74.10:25.90
15	70.80:29.20	70.10:29.90	70.50:29.50

[a] Estimated errors: ^{31}P-NMR 2%, polarimetry 3%, ^{1}H-NMR 2%. [b] Numbering of entries as in Table 1.

1 is not only suitable as derivatizing reagent for the determination of the enantiomeric excess of unprotected amino acids but can also be used in the case of α-alkylated amino acids (Table 1, entries 10–14), amino acid esters and amides, chiral amines, and alcohols. Typical examples are given in Table 1.

The new method has some unique features and several advantages over existing methods. To our knowledge this is the first ^{31}P-NMR method to be reported for the determination of the *ee* of free amino acids using facile in situ derivatization and broad solvent tolerance including aqueous solutions; the chiral derivatizing agent **1** is readily prepared, and excellent results are obtained with α-alkylated amino acids and their derivatives. Furthermore, the method compares favorably with currently available NMR techniques for amino acids in view of the large shift differences and the possibility of using phosphorus nuclei besides other nuclei.

Experimental

(*S,S*)-*O,O*-Di-*s*-butylphosphonate **1** was synthesized according to known literature procedures [6].

Synthesis of phosphonic amide **3**: A suspension of amino acid (1.0 mmol) in Et_3N (0.4 mL), H_2O (0.2 mL) and ethanol (0.5 mL) was cooled to 0 °C and treated dropwise with a solution of the phosphonate **1** (1.15 mmol) in CCl_4 (0.5 mL) and the mixture stirred at 20 °C for 2 h. The reaction was quenched by acidifying the mixture to pH 2 with 10% HCl solution. After extraction of the mixture with EtOAc (3 × 5 mL) the combined EtOAc phases were washed with water (5 mL) and dried (Na_2SO_4). The solvent was then removed by evaporation and the oily residue used as such for the *ee* determination. The phosphonic amides were purified by crystallization from EtOAc/petroleum ether or column chromatography on silica gel, providing white solids or oils.

With other substrates such as amino acid esters, the use of water as cosolvent may be omitted. When alcohols are used, addition of a catalytic amount of *N,N*-dimethylaminopyridine is recommended or alternatively the potassium alkoxides can be used.

The ^{31}P-{^{1}H}-NMR spectra were recorded on a Varian VXR 300 spectrometer operating at 121.42 MHz; the chemical shifts are given relative to those of $(NPCl_2)_3$ (δ = 19.91).

Received: December 27, 1991;
revised: February 18, 1992 [Z 5090 IE]
German version: *Angew. Chem.* **1992**, *104*, 1089

[1] See for example: J. Martens, *Top. Curr. Chem.* **1984**, *125*, 165; D. Seebach, R. Imwinkelried, T. Weber, *Mod. Synth. Methods* **1986**, *4*, 125–129.
[2] V. Schurig, *Kontakte Darmstadt* **1986** (1) 3; R. H. Buck, K. J. Krummen, *J. Chromatogr.* **1987**, *387*, 256; V. Schurig, H.-P. Nowotny, *Angew. Chem.* **1990**, *102*, 969; *Angew. Chem. Int. Ed. Engl.* **1990**, *29*, 939; Y. Okamota, K. Hatada, *J. Chromatogr.* **1986**, *363*, 173; *ibid.* **1987**, *387*, 95; W. A. König, I. Benecke, H. Bretting, *Angew. Chem.* **1981**, *93*, 688; *Angew. Chem. Int. Ed. Engl.* **1981**, *20*, 693.
[3] C. R. Johnson, R. C. Elliott, T. D. Penning, *J. Am. Chem. Soc.* **1984**, *106*, 5019; J. A. Dale, D. L. Dull, H. S. Mosher, *J. Org. Chem.* **1969**, *34*, 254.
[4] B. L. Feringa, B. Strijtveen, R. M. Kellogg, *J. Org. Chem.* **1986**, *51*, 5484; A. Dobashi, N. Saito, Y. Motoyama, H. Hara, *J. Am. Chem. Soc.* **1986**, *108*, 307.
[5] W. H. Kruizinga, J. Bolster, R. M. Kellogg, J. Kamphuis, W. H. J. Boesten, E. M. Meijer, H. E. Schoemaker, *J. Org. Chem.* **1988**, *53*, 1826.
[6] B. L. Feringa, A. Smaardijk, H. Wijnberg, *J. Am. Chem. Soc.* **1985**, *107*, 4798; A. Zwierzak, *Can. J. Chem.* **1967**, *45*, 2501.
[7] J. N. Ji, C.-B. Xue, Q.-W. Chen, Y.-F. Zhao, *Bioorg. Chem.* **1989**, *17*, 434; G.-J. Ji, C.-B. Xue, J.-N. Zeng, L.-P. Li, W.-G. Chai, Y.-F. Zhao, *Synthesis* **1988**, 444.
[8] Materials used for entries 1, 2, and 15 were obtained from Janssen Chimica.

A Diels–Alder Route to [5]- and [6]-Helicenes**

By *Nikolaos D. Willmore, Longbin Liu*, and *Thomas J. Katz**

Before the discovery of the transformation in Scheme 1 (X = H),[1] the only easy route to carbocyclic helicenes was the photocylization of stilbenes,[2] a procedure that suffers two severe limitations: the solutions irradiated must be very dilute,[3] thus restricting the scale on which reactions can be performed, and functional groups that perturb or depopulate the reactive excited state must be absent.[4] The synthesis

[*] Prof. T. J. Katz, N. D. Willmore, Dr. L. Liu
Department of Chemistry
Columbia University
New York, NY, 10027 (USA)

[**] This work was supported in part by the National Science Foundation (NSF DMR87-01968) and by Bristol-Myers Squibb.

of [5]-helicenebis(quinone) **2** according to Scheme 1 is therefore noteworthy because it is very simple, proceeds without irradiation, and affords an interesting functionalized helicene from cheap reagents. The low yield (17%) is inconse

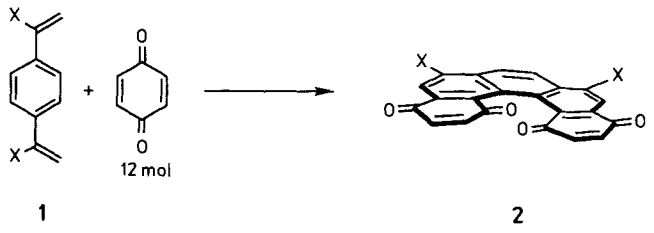

Scheme 1. Synthesis of [5]-helicenes. Reaction conditions: refluxing toluene containing an acidic or basic catalyst.

quential since large quantities of the product are prepared with little effort and little cost. The same cannot be said of the next higher homologue (Scheme 2), for the starting compound 2,7-divinylnaphthalene, unlike *p*-divinylbenzene, is not a cheap commercially available chemical. Its synthesis requires effort,[5] and the low yield of **4** (X = H), found here to be only 6%,[7] is in this case detrimental. We report herein how higher yields can be achieved.

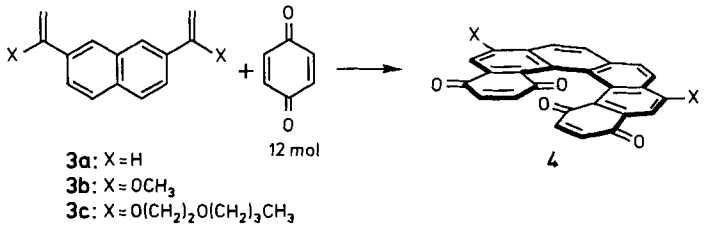

Scheme 2. Synthesis of [6]-helicenes.

This problem is solved by substituting the 1-positions of the vinyl groups in divinylarenes by alkoxyls. Thus, when, for example, X in Scheme 2 is OCH_3, the yield is 47%. When it is $O(CH_2)_2O(CH_2)_3CH_3$, the yield is 45%.[8] No other product is isolated. Accordingly, since bis(enol ethers) are easily synthesized, [6]-helicenes can be prepared in this way in very much larger quantities than by conventional photocyclization of bis(stilbenes). Similar principles apply to [5]-helicenes, the yield in Scheme 1 tripling (to 50%) when X is changed from H to $OC_{12}H_{25}$.[9]

The structures of **2** (X = $OC_{12}H_{25}$), **4b**, and **4c** were determined with the help of spectroscopic data.[10] Of the symmetrical structures for **4b** and **4c** required by the ^1H and ^{13}CNMR's, those with four linearly-fused rings are excluded by the proton spectra, which exhibit, at $\delta > 5$, two pairs of doublets and one singlet, not one pair of doublets and three singlets. For **2** (X = $OC_{12}H_{25}$) the structures with linearly and angularly fused rings are distinguished by the complexity of the resonances of the OCH_2 proton resonances, at *ca.* $\delta = 4.34$. They imply that the ring-system itself is chiral. Similar evidence, confirming structure **4c**, is the splitting of the analogous resonance signals into two clear sets ($\delta = 4.48$ and 4.56).

1 (X is $OC_{12}H_{25}$) was prepared from the corresponding ester and Tebbe's reagent,[11] and **3b** and **3c** according to the procedure shown in Scheme 3. Noteworthy are the syntheses of the enol ethers. While **3b** and **3c** could be made satisfactorily by treating the corresponding acetals with $(CH_3)_3SiOSO_2CF_3$ and $(iPr)_2NEt$ in CH_2Cl_2,[14] we found $(CH_3)_3SiCl$ superior to the silyl triflate because it costs 1/50th as much. The use of benzoic acid plus pyridine was modeled on a method of Newman et al.,[15] while the use of NaI and Et_3N was adopted from methods used to make silyl enol ethers.[16]

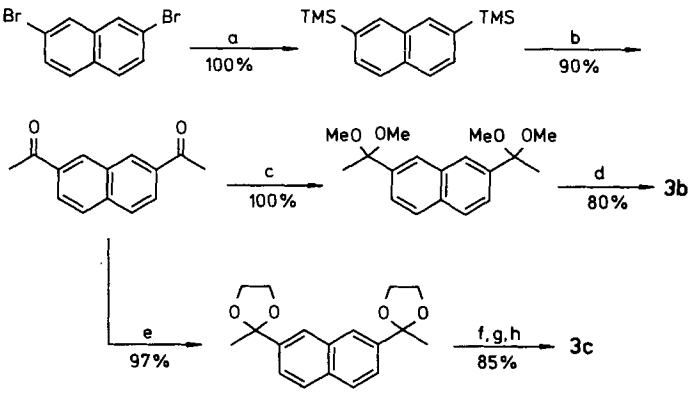

Scheme 3. Synthesis of **3b** and **3c**. Reagents and conditions: a) trimethylsilyl chloride (TMSCl) (3 mol), *n*BuLi (2.75 mol), THF (0.5 M), $-78 \rightarrow -20\,^{\circ}C$; b) $(CH_3CO)_2O$ (2.2 mol), $AlCl_3$ (4.4 mol), CH_2Cl_2, 0 °C [12]; c) $HC(OMe)_3$ (5.5 mol), MeOH (0.5 M), *p*-TsOH (0.1 mol); d) TMSCl (5.4 mol), $PhCO_2H$ (0.1 mol), pyridine (0.7 M), 65 °C, 1 h; e) $(HOCH_2)_2$ (3 mol), *p*-TsOH (0.1 mol), PhH (0.5 M), reflux; f) TMSCl (5.4 mol), NaI (5.4 mol), Et_3N (5.8 mol), CH_3CN (0.5 M), reflux; g) K_2CO_3 (1.6 mol), MeOH (0.25 M), ambient temperature; h) *n*BuBr (4 mol), KOH powder (8 mol), DMSO (0.5 M), ambient temperature, 1.5 h [13].

It is remarkable that of the styrene derivatives used during the past 65 years as diene components of Diels–Alder reactions,[17] only a single example seems to have been the enol ether of an acetophenone.[18, 19] Yet the reactivities of other styrenes are not comparably great. The beneficial effects of alkoxy substitution were seen to disappear when the substituents, instead of being on the double bonds, were on the benzene-rings.[20, 21] This implies that Diels–Alder reactions of acetophenone enol ethers could be especially useful in synthesis. Our findings described illustrate this by showing how the combination of such enol ethers with *p*-benzoquinone can be used to construct helicenes rapidly, on a large scale, without much effort, and in decent yields.

Experimental

4c: Benzoquinone (6.8 g, 63 mmol) and **3c** (2.0 g, 4.8 mmol) in toluene (49 mL) were stirred and refluxed for 48 h under nitrogen (not more than 1 atm). The residue, after removal of solvent, was boiled for one minute with 10% THF in benzene (ca. 100 mL), cooled to room temperature, and passed through a column of silica gel (∅ = 1 inch), using more 10% THF in benzene to wash the product through. Two flash chromatographic separations with this solvent and one with 10% ethyl acetate in benzene furnished 1.4 g (a 45% yield) of pure **4c**, a deep-red solid, m.p. 152–166 °C, soluble in many organic solvents.

Received: March 5, 1992 [Z 5225 IE]
German version: *Angew. Chem.* **1992**, *104*, 1081

[1] L. Liu, T. J. Katz, *Tetrahedron Lett.* **1990**, *31*, 3983. Small amounts of trichloroacetic acid were used as a catalyst.
[2] a) W. H. Laarhoven, W. J. Prinsen, *Top. Curr. Chem.* **1984**, *125*, 63; b) F. B. Mallory, C. W. Mallory, *Organic Reactions Vol. 30* (Ed.: W. G. Dauben), Wiley, New York, **1984** p. 1; c) The method used by D. Bogaert-Verhoogen and R. H. Martin (*Tetrahedron Lett.* **1967**, 3045, was later said by R. H. Martin, *Angew. Chem.* **1974**, *86*, 727; *Angew. Chem. Int. Ed. Engl.*

1974, *13*, 649) to suffer serious limitations. See also, J. Brison, R. H. Martin, *Bull. Soc. Chim. Belg.* **1983**, *92*, 893.
[3] See footnote [3] in Ref. [1].
[4] a) F. B. Mallory, C. W. Mallory, *Organic Reactions, Vol. 30* (Ed.: W. G. Dauben), Wiley, New York, S. 6; b) C. S. Wood, F. B. Mallory, *J. Org. Chem.* **1964**, *29*, 3373 (but see P. H. Gore, F. S. Kamonah, *Synth. Commun.* **1979**, *9*, 377).
[5] From naphthalene-2,7-diol and $(CF_3OSO_2)_2O$ in pyridine ($0 \rightarrow 25\,^{\circ}C$, 45% yield) followed by Stille coupling (68% yield) [6a] with vinyltributyltin [6b]. Alternatively, the diol was converted into the dibromide [6c] and the dibromide into the dialdehyde (*n*BuLi in THF, then DMF). Wittig reaction (*n*BuLi in THF) then gave the divinylnaphthalene in 53% overall yield.
[6] a) A. M. Echavarren, J. K. Stille, *J. Am. Chem. Soc.* **1987**, *109*, 5478; b) D. Seyferth, F. G. A. Stone, *ibid.* **1957**, *79*, 515; c) G. Porzi, C. Consilio, *J. Organomet. Chem.* **1977**, *128*, 95.
[7] The reaction was run for 12 h in refluxing acetic acid (cf. W. Davis, Q. N. Porter, *J. Chem. Soc.* **1957**, 4967). The product was identical with that synthesized in a different way: B. Yang, L. Liu, T. J. Katz, C. A. Liberko, L. L. Miller, *J. Am. Chem. Soc.* **1991**, *113*, 8993.
[8] The reactions were run in toluene with no catalyst, for 66 h with **3b** and for 48 h with **3c**. The red quinone **4b** that does not melt below 255 °C. Unlike **4c**, it is soluble in only few solvents, among them $CHCl_3$ and CH_2Cl_2.
[9] In the experiments with **1** ($X = OC_{12}H_{25}$), basic alumina was used as a catalyst and the reaction time was 62 h. Trichloroacetic acid gave *p*-diacetylbenzene, while if no catalyst was used, the yield was half as great and the product was less pure. The quinone is a bright orange solid, m.p. = 99–100 °C.
[10] **2** ($X = OC_{12}H_{25}$): ^{1}H NMR (400 MHz, $CDCl_3$): $\delta = 0.88$ (m, 6H), 1.27–1.58 (m, 36H), 1.99 (m, 4H), 4.32 (m, 2H), 4.36 (m, 2H), 6.77 (d, $J = 10$ Hz, 2H), 6.88 (d, $J = 10$ Hz, 2H), 7.54 (s, 2H), 8.38 (s, 2H); ^{13}C-NMR (75 MHz): $\delta = 14.1$, 22.7, 29.2, 29.3, 29.6 (m), 31.9, 69.4, 102.7, 122.4, 127.6, 127.7, 129.7, 132.0, 136.1, 139.9, 158.5, 185.3, 186.3; IR ($CDCl_3$): $\tilde{\nu}$[cm^{-1}] = 1654, 1587; HRMS: calcd 706.4233, found 706.4249.
4b: ^{1}H NMR: $\delta = 4.22$ (s, 6H), 6.34 (d, $J = 10.0$ Hz, 2H), 6.79 (d, $J = 10.2$ Hz, 2H), 7.54 (s, 2H), 7.97 (d, $J = 8.7$ Hz, 2H), 8.43 (d, $J = 8.7$ Hz, 2H); ^{13}C NMR: $\delta = 56.6$, 101.4, 122.1, 126.4, 127.2, 127.6, 128.6, 131.2, 133.1, 133.7, 135.7, 140.2, 159.3, 185.1, 185.2; IR: $\tilde{\nu}$[cm^{-1}] = 1658, 1596; HRMS: calcd 448.0947, found 448.0972.
4c: ^{1}H NMR: $\delta = 0.96$ (t, $J = 7.4$ Hz, 6H), 1.45 (m, 4H), 1.66 (m, 4H), 3.64 (t, $J = 6.6$ Hz, 4H), 4.01 (m, 4H), 4.48 (m, 2H), 4.56 (m, 2H), 6.63 (d, $J = 10.2$ Hz, 2H), 6.78 (d, $J = 10.2$ Hz, 2H), 7.53 (s, 2H), 7.96 (d, $J = 8.7$ Hz, 2H), 8.47 (d, $J = 8.6$ Hz, 2H); ^{13}C NMR: $\delta = 13.9$, 19.3, 31.8, 68.8 (two peaks), 71.5, 102.1, 122.2, 126.3, 127.2, 127.6, 128.5, 131.2, 133.1, 133.5, 135.6, 140.2, 158.5, 185.1, 185.2; IR: $\tilde{\nu}$[cm^{-1}] = 1663, 1596; HRMS: calcd 620.2410; found 620.2429.
[11] L. F. Cannizzo, R. H. Grubbs, *J. Org. Chem.* **1985**, *50*, 2386.
[12] a) K. Dey, C. Eaborn, D. R. M. Walton, *Organomet. Chem. Synth.* **1970/71**, *1*, 151; b) A. Sudhakar, T. J. Katz, *J. Am. Chem. Soc.* **1986**, *108*, 179.
[13] R. A. W. Johnstone, M. E. Rose, *Tetrahedron* **1979**, *35*, 2169.
[14] P. G. Gassman, S. J. Burns, *J. Org. Chem.* **1988**, *53*, 5574.
[15] M. S. Newman, M. C. VanderZwan, *J. Org.Chem.* **1973**, *38*, 2910.
[16] P. Cazeau, F. Duboudin, F. Moulines, O. Babot, J. Dunogues, *Tetrahedron* **1987**, *43*, 2075.
[17] a) O. Diels, K. Alder, *Justus Liebigs Ann. Chem.* **1926**, *450*, 237; b) T. Wagner-Jauregg, *Synthesis* **1980**, 769.
[18] a) Y. Kita, H. Yasuda, O. Tamura, Y. Tamura, *Tetrahedron Lett.* **1984**, *25*, 1813; b) Much earlier, K. Alder, H. Niklas, *Justus Liebigs Ann. Chem.* **1954**, *585*, 97, reported that dimethyl diazodicarboxylate with α-methoxystyrene gives a complex adduct resulting from a Diels-Alder followed by an ene-reaction.
[19] Alkoxybutadienes and acyloxybutadienes have been used frequently. See F. Fringuelli, A. Taticchi, *Dienes in the Diels-Alder Reaction*, Wiley, New York, **1990**.
[20] L. Liu, Ph. D. Dissertation, Columbia University, **1991**.
[21] There are many examples of Diels-Alder reactions of stryrenes with alkoxyls on the benze ring: a) W. B. Manning, T. P. Kelly, G. M. Muschik, *J. Org. Chem.* **1980**, *45*, 2535, and related work by Manning's group; b) B. I. Rosen, W. P. Weber, *libid.* **1977**, *42*, 3463; c) V. Bruckner, *Chem. Ber.* **1942**, 75, 2034; d) B. J. F. Hudson, R. Robinson, *J. Chem. Soc.* **1941**, 715.

BOOK REVIEWS

Book Reviews are written by invitation from the editor. Suggestions for books to be reviewed and for book reviewers are welcome. Publishers should send brochures or (better) books to the following address: Redaktion Angewandte Chemie, Postfach 101161, W-6940 Weinheim, Federal Republic of Germany. The editor reserves the right of selecting which books will be reviewed. Uninvited books not chosen for review will not be returned.

Quanta. A Handbook of Concepts. 2nd Edition. By *P. W. Atkins*. Oxford University Press, Oxford, 1991. 434 pp., hardcover £ 50.00.—ISBN 0-19-855572-5; paperback £ 25.00.—ISBN 0-19-855573-3

The reader immediately becomes aware that this is no ordinary textbook when he or she looks for the list of contents and fails to find one. The concepts of quantum mechanics have been subdivided into a large number of easily digestible morsels, ranging in alphabetical order from "Ab initio", through "Frontier orbitals" and "Ligand field theory", to "Zero point energy". The lengths of the articles vary from a few lines (e.g., for "Rydberg level") to several pages (as for "Molecular orbital theory"). Mathematical formulas have been almost entirely excluded from the main text. Where formulas are really unavoidable, as when explaining the terms "Laplacian" and "Overlap integral", they are given in boxes distinguished by coloring. Atkins is well known for his clear didactic presentations and the excellent standard of illustrations in his textbooks, and here again one is not disappointed. The author has a remarkable ability to present complex situations using simple diagrammatic aids. Thus the fundamentals of quantum mechanics are explained mainly in a visual form, which is very appropriate for the chemist accustomed to the diagrammatic language of chemistry (see R. Hoffmann, P. Laszlo, *Angew. Chem.* **1991**, *103*, 1; *Angew. Chem. Int. Ed. Engl.* **1991**, *30*, 1). Cross-references to other articles in the book enable one to quickly read up all the material on a particular subject area. However, some familiarity with the basic language of quantum mechanics would be useful—though not essential—if one is not to lose one's way when searching for information on particular concepts. Finally, a comprehensive index provides a good means of access to the contents of the book.

The paragraphs headed "Further information" at the end of each article are very useful. Instead of a comprehensive bibliography, which can often be quite laborious to search, a short commentary is provided, giving references to material for further reading. This enables readers to search the literature in a way that suits their own level of knowledge.

In this second edition the small errors in the first have been largely eliminated. In the article "Alternant hydrocarbon" propene is wrongly given as an example instead of the allyl radical. The orbital diagrams in the article "Woodward-Hoffmann rules" seem confusing compared with the explanations given in other textbooks. However, the manner of presentation is, in the end, a matter of personal preference.

The standard of production is remarkably good for a book in this price bracket. In this respect it stands out from the flood of books that are poor value for money because the camera-ready texts vary in print quality and layout (a situation that must be blamed not on the authors but on the publishers). Two-color printing is used throughout, but the use of color for emphasis has been applied sparingly. Many of the figures are printed in the broad margin, which makes for an easily readable text and also invites browsing. The book is pleasing to handle and use, both with regard to its outward form and its content.

Although this book is, of course, not a substitute for a textbook on quantum mechanics, it can be strongly recommended as an aid to finding one's way around the field and as a reference manual to use in conjunction with other reading.

Wolfram Sander
Institut für Organische Chemie
der Technischen Universität Braunschweig (FRG)

Chirality and Optical Activity in Organometallic Compounds. Edited by *V. I. Sokolov*. Gordon and Breach, New York, 1990. VIII, 145 pp., hardcover $ 110.00.—ISBN 2-88124-714-1

"Optically active compounds" and "chirality" are terms that were, until not very long ago, associated only with organic chemistry. Only gradually did it come to be appreciated that the principles of asymmetry could be carried over to organometallic compounds, if one surrounded a metal center with chiral organic ligands, or constructed it in such a way as to form a chiral center. The field then developed very rapidly and in many different directions. V. I. Solokov correctly recognized that there was a need for a systematic treatment of the stereochemistry of organometallic compounds. He has restricted his treatment to transition metals, a fact that is not obvious from the title.

The book is divided into four chapters. After an introduction to the basic concepts of chirality in organometallic compounds, a chapter by A. P. Klyagina establishes a relationship between optical activity and electronic structure, based on the theoretical analysis of circular dichroism (CD) spectra. The book concludes with a description of various structural types of chiral and optically active organometallic compounds and their applications in organic synthesis.

Although the theoretical treatment of CD spectra forms an important part of the book, it is a preliminary to the main core, centered on the description of classes of compounds in Chapter 3. It is undoubtedly difficult to make a representative selection from the great wealth of complexes that have a metal atom as a chiral center, but even so, the choice of examples here seems rather strange. Except for the classic example of $[CpMn(NO)(CO)PPh_3][PF_6]$, the opportunity to sketch the historical development of this field of chemistry has been missed, and that would certainly have been useful as an aid to understanding the subject. Instead of this the reader is expected to refer to an inappropriately large number of original papers. Important stereochemical reactions are introduced by means of examples, but tetragonal-pyramidal complexes are treated much too briefly and their intramolecular dynamics are not covered at all. In contrast, planar chiral complexes and chiral metal clusters are treated in great detail.

Applications to organic synthesis have been confined to stoichiometric reactions, which is appropriate since most asymmetric catalysts do not contain organometallic groups. However, at the end of the book is a list, covering 1 ½ pages, of reactions that are catalyzed asymmetrically by optically inactive organometallic compounds. Surely one could have done even better by starting from the phenomenon of optical induction in metal complexes with chiral centers (unfortunately not mentioned), and progressing from this to the transfer of chirality from the optically active ligand of an organometallic catalyst onto the coordination center, and thence to a state-of-the-art analysis of mechanistic studies. This is a case where less quantity would have meant better quality.

Despite these criticisms one should not overlook the fact that the book is a first attempt at a clear and up-to-date presentation of a very heterogeneous body of knowledge (the literature coverage extends up to 1989). The wealth of detailed information that it contains will make it a valuable resource for the specialist.

Joachim Wachter
Institut für Anorganische Chemie
der Universität Regensburg (FRG)

The Green Flame: Surviving Government Secrecy. By *A. Dequasie*. American Chemical Society, Washington, DC (USA), 1991. XII, 220 pp., hardcover $ 22.95.—ISBN 0-8412-1857-9

This is a most unusual and unconventional book that virtually defies categorization. The title refers to the bright green flame that occurs when pyrophoric boron hydrides ignite in air, as well as to the youthful, green naiveté of the scientists and engineers who worked with them, and the cover of the book is quite appropriately colored green. Yet if one is seeking the kind of chemical and technical information contained in such monographs as Alfred Stock's *Hydrides of Boron and Silicon* (Cornell University Press, 1933), William Gerrard's *The Organic Chemistry of Boron* (Academic Press, 1961), William N. Lipscomb's *Boron Hydrides* (W. A. Benjamin, 1963), or Herbert C. Brown's *Boranes in Organic Chemistry* (Cornell University Press, 1972), one will be disappointed. This is not a systematic treatise on boron hydrides, although some of the chemistry of these intriguing compounds is discussed, along with pertinent chemical equations. Rather it is the anecdotal, personal reminiscences of a sexagenarian recalling his activities and adventures as a young (23–29 years old) chemical engineer working from 1953 to 1960 for the U.S. Government on secret research to develop a boron-based jet and rocket super fuel for the Army's Project Hermes and Navy's Project Zip.

The writing career of the author, who received his B.S. in chemical engineering in 1950 from the University of Pittsburgh and who spent the period 1951–1953 as a writer in the U.S. Army Chemical Corps, is as unconventional as this, his third, book. Dequasie's previous books are *The Dragonslayers* (Carlton, 1972), a medieval satire, and *Thirsty* (Walker, 1983), a western novel. In 1983 he received the Medicine Pipe

 © VCH Verlagsgesellschaft mbH, W-6940 Weinheim, 1992 0570-0833/92/0808-1096 $ 3.50+.25/0

Award of the Western Writers of America, of which he is a member. His writing skills are evidenced by the entertaining and easygoing style of his latest book, which, despite the inclusion of many chemical engineering details, is readily accessible to the general reader.

The 13-chapter book begins with the author's acceptance of an assignment on a classified government project without knowing what the job was and having been misled as to where the work was to take place (he thought that he would be employed at Olin Mathieson's Niagara Falls plant, but instead he was assigned to the same company's boron fuels pilot plant at the Malta Rocket Test Station at Malta, New York). Dequasie managed pilot plants and assisted in the design of the first commercial plant until the project, which consumed about a billion dollars (as measured in 1990 dollars) in the construction alone for eight plants was abandoned on August 10, 1959, shortly before production was to begin in earnest. The project was terminated because of excessive costs but primarily because boric oxide, one of the combustion products of boron fuels, is a solid, which caused problems of erosion and deposits in the engines and produced less thrust than if the combustion product were a gas. This unsurmountable defect should have been recognized before the project was even begun.

The boron hydrides not only ignited spontaneously in air, but they possessed nerve-gas toxicity, making gas masks routine equipment for project workers. Boron hydride poisoning, nicknamed "the goodies", was also rumored to cause sterility or impotence. Furthermore, in combination with solvents and other substances, boranes were explosive, and eight persons were killed in explosions during the course of the project. Dequasie strikingly recounts these "hazards at every turn" and other chemical and engineering challenges along with quotidian problems such as testing valves, filling cylinders, changing vacuum pump oil, scaling up reactions, cleaning pots, and dealing with broken pipes, toxic exposures, shock waves, and the like. He also discusses at length after-hours activities such as snowball fights, pinochle and drinking parties, girl-chasing, dating, swimming, fishing, camping, canoeing, hiking, cooking, flying lessons, social clubs, ball games, explorer scout leadership, and bachelor life in general. In his own words, the book is "not a documentary about high-level administrative decisions [but]...the story of the project as lived by front-line, hands-on people." The 56 illustrations consist of snapshots of project workers, plant maps, documents, newspaper articles, scenery, buildings, equipment, airplanes, and even a groundhog. A 10-page (2 columns per page) index adds to the utility of the volume.

As those of us who have worked under government security clearance can testify, work on such projects carried out during the cold war era was complicated by the stringent secrecy imposed by concerns with national security. In keeping with the subtitle of his book, Dequasie fully considers these problems. He makes extensive use of hundreds of newspaper and technical magazine articles and recollections of his project colleagues to reinforce his own memories, and he uses recently declassified documents to, in his own words, "fill in things I had not known." He speculates on the possible existence of spies and sabotage but leaves the ultimate decision about these to the reader.

Although the boron hydrides were an expensive failure as aircraft fuels, this engaging story of the boron fuels project is much more than a history of chemical engineering or a secret government project. It vividly captures the life and vibrancy of an era. It can also serve as a cautionary tale, for Dequasie declares that "today's chemists, engineers, and budding scientists still in school should be aware of the lessons learned by our experience. This book is designed to help others to avoid repeating our mistakes."

George B. Kauffman
California State University, Fresno
Fresno, CA (USA)

Band Theory of Solids. An Introduction from the Point of View of Symmetry. By *S. L. Altman*. Oxford Science Publications/Clarendon Press, Oxford, 1991. XIV, 286 pp., hardcover £ 37.50.—ISBN 0-19-855184-3

In this book S. L. Altman is concerned with the electronic properties of solids, with special reference to symmetry principles. In the preface the author explains that the book is intended partly for solid state physicists; however, he has also aimed to examine chemical aspects of solid state theory and to provide solid state chemists with an introduction to the field. Leaving aside the question of the appropriate readership, the author here offers a survey, written at a very advanced level, of symmetry aspects of the band structures of solids. For solid state physicists at least, the book provides an easier introduction to the subject than, for example, Ziman, Kittel, or Lax. However, the author is perhaps too optimistic in believing that it will find general acceptance among theoretical solid state chemists. In order to reach a quantitative understanding of the symmetry properties of solids and their band structures, it is essential to work through a textbook such as this one. However, in the opinion of this reviewer it is questionable whether chemists will accept this approach. It seems more probable that solid state chemists will look for an easier, qualitative, way into this field, and will be content to leave it at that. Even at this level one can find suitable review articles. Nevertheless, it is to be hoped that in future chemists will become increasingly involved in the area of solids, and will be prepared to acquire the necessary working knowledge.

Altman's book is divided into 14 chapters. At the end of each chapter there are exercise problems, the solutions to which are discussed in detail in the appendix. There are over 80 problems altogether, with a steadily increasing level of difficulty. Nearly all the chapters are well constructed from a learning standpoint, and they enable the reader to get to grips with a field that is by no means easy, and demands some ability to deal with abstract concepts.

Chapter 1 is easily understandable, and explains the basic principles of the model of free electrons in solids. The wave vector $\boldsymbol{k}$ is introduced, and the significance of the Fermi energy and Fermi surface is explained. The density of electronic states and energy bands are also discussed. Chapter 2 gives a very short introduction to the elements of group theory (19 pp.). Unfortunately this part of the book is too brief to meet the needs of an introductory text. The book would be more easily understood by readers who already have some knowledge of group theory. In the opinion of this reviewer, the very condensed introduction to group theory is the only negative aspect of the book. Chapter 3 deals with space groups, covering such important topics as the Bravais lattice and the definition of the Seitz operators for handling point symmetry and translational symmetry in solids. Chapters 4 and 5 then introduce reciprocal lattices, Brillouin zones, and the Bloch functions for solids. The derivation of energy bands from the Bloch functions is also explained. Chapter 6 returns to the theme of Chapter 3 with a discussion of ways of representing space groups. The effects of

 © *VCH Verlagsgesellschaft mbH, W-6940 Weinheim, 1992* *0570-0833/92/0808-1097 $ 3.50+.25/0*

symmetry operations in a space group on the corresponding Bloch functions are discussed in detail. Some applications of this are then described in Chapter 7. Chapter 8 is concerned mainly with energy bands in metals, semiconductors, and insulators, and with how they are affected by the symmetry of the lattice. This general theme is continued in Chapter 9. Chapter 10 describes theoretical methods based on band structure. Regrettably, however, Altman does not go into detail regarding the more recent approaches that are of such great importance for solid state calculations; examples of these are linearized muffin-tin calculations and density functional methods, which in recent years have at last made it possible to handle systems of chemical interest. However, perhaps these topics are outside the scope of an introduction. The remaining four chapters deal with selected subject areas in the general field of condensed matter. Chapter 11 is mainly concerned with lattice vibrations and electrical conductivity, and also touches on electron–phonon coupling. Chapter 12 discusses instabilities and their dependence on characteristic solid-state properties such as dimensionality. Here Altman analyzes the physical causes of the so-called Peierls instabilities. The next chapter looks at analogies between band models and representations of the electronic wave-function in real space. The book ends with a review of surface states and localized defect states.

To summarize, S. L. Altman has here written a very good book on symmetry in solids. The material in the individual chapters is very concentrated, and considerable effort is needed to work through them. The main emphasis is on explaining group theoretical methods, rather than on covering the whole range of potential applications. From the chemistry standpoint, the book will only be of interest to specialists in solid state theory.

Michael C. Böhm
Institut für Physikalische Chemie
der Technischen Hochschule Darmstadt (FRG)

Cytochromes C. Evolutionary, Structural and Physicochemical Aspects. (Springer Series in Molecular Biology). By *G. R. Moore* and *G. W. Pettigrew*. Springer, Berlin, 1990. XVI, 478 pp., hardcover DM 168.00.—ISBN 3-540-50852-X

The book reviewed here is the second monograph written by Moore and Pettigrew on the subject of cytochromes C. The first one, "Cytochromes C. Biological Aspects", was published in 1987 in the same series. Although cytochrome C is only one of many hemoproteins of importance in energy metabolism, it serves here as an example for describing the many different physical methods used to analyze structure and function of hemoproteins. The physicochemical fundamentals of hemoprotein structures and the spectroscopic methods used to determine them, such as NMR, EPR, CD, MCD, fluorescence, phosphorescence, Mössbauer and X-ray spectroscopies, are all described in great detail. Examples of actual results are discussed and summarized in the form of tables. A further chapter lists all the known amino-acid sequences of cytochrome C variants. The molecular geometries and crystal structures are treated in great detail, including variants in which the central atom is changed or the amino-acids are modified. The chapter on evolution includes detailed discussions of the problems of phylogenetic trees, the molecular clock, and the theory of random genetic drift, as well as questions such as that of genus and species in bacteria, or the theory of endosymbionts to explain the formation of mitochondria and chloroplasts. A further chapter deals with the redox potentials of cytochromes C, and here too the explanation of the physicochemical fundamentals is thorough and lucid. The final chapter gives a very detailed and thorough treatment of the question of electron transfer mechanisms.

The authors have shown a commendable awareness of the need to relate the large amount of published work on cytochrome C to the basic physicochemical principles, and to summarize the findings in useful generalizations. The book is intended primarily for specialists, but also provides the less experienced student with the basic knowledge needed to embark on the study of hemoproteins. Consequently it will still remain an up-to-date work of reference ten years hence. The book is indispensable for the libraries of biophysics departments and those engaged in research on energy metabolism.

Bernhard Kadenbach
Fachbereich Chemie
der Universität Marburg (FRG)

Nucleoside Synthesis. Organosilicon Methods. (Ellis Horwood Series in Organic Chemistry.) By *E. Lukevics* and *A. Zablocka*. Ellis Horwood, New York, 1991. 496 pp., hardcover $ 221.95.—ISBN 0-13-812652-6

The chemistry of nucleosides, nucleotides, and nucleic acids is currently a rapidly growing area of research. It soon became clear from studies of the structure and biological function of these natural products that synthetically modified species would have an enormous biological potential. Synthetic analogues of nucleosides, nucleotides, and nucleic acids are nowadays used as antimetabolites in biochemistry and medicine. Examples are antiviral agents such as the nucleoside analogues 3′-azidothymidine (AZT, which has anti-HIV activity) and acyclovir (with anti-Herpes-simplex activity), the antitumor agent 5-fluoridine, and the use of "antisense-RNA" and "antisense-DNA" as gene blockers. Since biologically active nucleoside analogues are now so widely used, methods for synthesizing them are of great importance.

One approach is by chemical modification, using a naturally occurring nucleoside as a precursor. However, the scope for introducing such modifications is rather limited, owing to the lability of the β-glycosidic linkage that is already present. Another method is to build up the aromatic heterocycle by using an *N*-glycosylated derivative as a precursor, but this method can only be considered in special cases because of the considerable amount of synthetic work required. The most important method, and the one that allows most scope for modifications, is the glycosylation of the aglycone component using an appropriate carbohydrate derivative. A special variant of this is the silyl method, in which the glycosylation is carried out using a silylated heterocycle, and this method is the subject of the book reviewed here. The first part of the book is devoted to a thorough discussion of the synthetic aspects, and the second part contains a survey, in the form of tables, of glycosylations that have so far been carried out using a silylated heterocycle (2549 examples in all!). The book is completed by indexes listing the heterocycles and carbohydrate derivatives that are covered, and a bibliography containing 1056 references.

The first part is divided into six chapters. The first of these gives a brief summary of the conventional methods of nucleoside synthesis, including the Hilbert–Johnson method, the Fischer–Helferich method, and the fusion and nitromethane methods. Transglycosylation reactions are also briefly discussed. Surprisingly, however, there is no mention of another modern method whereby the glycosidic linkage is formed from the aromatic heterocycle and the carbohydrate component by a phase transfer reaction in the presence of a base; this is one of the few methods that does not require the use of metal halides as catalysts, which is a crucially important advantage for analogues that are to be used in biological systems. The yields are no worse than with the silyl method. Chapter 1 ends with some examples of nucleoside syntheses in which the heterocycle is built up from *N*-glycosylated carbohydrates. Chapter 2 introduces the method using glycosylation of silylated heterocyclic arenes. First the reagents used for the silylation of the heterocycle are described, followed by a detailed discussion of the possible reaction mechanisms. From this it quickly becomes apparent that the method is closely related to the Hilbert–Johnson method. The mechanisms are also considered from the standpoint of reactions using carbohydrate derivatives (halogenoses on p. 32, and 1-*O*-acyloxy- and 1-*O*-alkyloxy sugars on p. 39). The influences of solvent and of catalyst (e.g., $AlCl_3$, $TiCl_4$, $SnCl_4$, or trimethylsilyltriflate, p. 41) are discussed, as also are the effects of substituents in the heterocycle with regard to the α/β anomer ratio of the glycosidic linkage and the reaction yield. The advantages of the silyl method compared with the conventional glycosylation methods are also explained. Chapter 3 describes various syntheses that lead to modified pyrimidine nucleosides and their aza and deaza analogues, and discusses the factors influencing them. Chapter 4 then gives corresponding data for nucleosides formed from bicyclic heteroarenes, and also deals with the purine nucleosides and their *N*-isomers. Chapter 5 contains a detailed description of nucleosides derived from other heterocyclic bases. These latter three chapters use selected examples to discuss all the factors that influence the course of the reaction. For example, pages 58 and 59 summarize, in the form of text and tables, data on the reaction of a β-D-glucopyranosyl bromide with 2,4-bis(trimethylsilyl)thymine under nine different sets of reaction conditions. Also reactions performed by the silyl method are frequently compared with the conventional methods (e.g., on p. 59). In the glycosylation of bicyclic *N*-heteroarenes (Chapters 4 and 5) one is interested in controlling not only the anomeric configuration but also the regioselectivity in relation to the nitrogen atom of the heterocycle. Ways of achieving this are described using various examples (e.g., p. 174). Chapter 6 adds a brief discussion of methods for synthesizing nucleotides.

I feel that the usefulness of the book could have been improved by a clearer subdivision of the material. It would have been desirable to make a clear distinction between nucleosides containing only a pyrimidine ring and those containing only a purine ring, and to have one chapter dealing with aza, deaza, and *N*-isomeric analogues of pyrimidine and purine nucleosides (see Sections 3.8 and 3.9, and Sections 4.2 to 4.8), together with nucleoside analogues derived from other heterocyclic bases.

The authors have succeeded in their aim of presenting an overview of this variant of the glycosylation method, which has now come very much into favor because it is easy to carry out. This easily readable and well illustrated book is a worthwhile purchase for everyone concerned with the synthesis of nucleoside analogues, as it contains a useful and remarkably comprehensive collection of data on the silyl method. Regrettably, however, the astronomically high price will mean that it reaches only a limited readership.

Chris Meier
Institut für Organische Chemie
der Universität Frankfurt am Main (FRG)

Essential Molecular Biology. A Practical Approach. Vols. 1 and 2. (The Practical Approach Series.) Edited by *T. A. Brown*. IRL Press at Oxford University Press, Oxford, 1991. Vol. 1: XIX, 299 pp., paperback £ 22.50.—ISBN 0-19-963111-7; Vol. 2: XX, 296 pp., paperback £ 22.50.—ISBN 0-19-963113-1

The rapid advances that have occurred in the techniques of molecular biology during the last decade have brought about a quantum leap in virtually every biologically-orientated area of research, especially since the basic techniques of cloning can, in principle, be mastered by anyone. Consequently, there is now a wide and growing demand for introductory textbooks on molecular biological methods that are experimentally orientated and easily understandable. Alongside "Maniatis", the excellently written and well-proven standard work in this field, a crop of new textbooks and manuals is now springing up like mushrooms. The continuing rapid pace of progress, which is also apparent from the growing number of new or modified reagents and techniques, means that these publications will soon become outdated.

In the two volumes reviewed here, which belong to the successful "Practical Approach" series on modern techniques of bioscience, the editor offers another introduction to practical methods in molecular biology, aimed at beginners and non-specialists. Volume 1 ("Molecular Cloning") explains the underlying principles and the basic techniques needed for carrying out experiments on DNA cloning. These include microbiological techniques for handling bacteria and phages, methods for purifying DNA and RNA, analytical and preparative methods for electrophoretic separation of nucleic acids, and procedures for generating, transforming, and selecting recombinant DNA using suitable combinations of cloning vectors and host bacteria. Building on this groundwork, Volume 2 ("Recombinant DNA") gives a comprehensive description of the relevant procedures for genome analysis. After describing the preparation of gene banks in lambda and cosmid vectors or in the form of cDNA, an account is given of the techniques commonly used for investigating the structure of a cloned gene; these include identification by labeling, immobilization, and hybridization of the nucleic acid, multiplication by means of the polymerase chain reaction (PCR), and DNA sequencing by the didesoxy method. Lastly the volume explains procedures for investigating the cellular expression by DNA–protein interactions or RNA transcript analysis.

The background knowledge and practical advice on experimental procedures is generally presented in such a straightforward and detailed way that even lay readers will understand the basis of the techniques, what they aim to achieve, and how they can be adapted to design appropriate experiments for individual scientific problems. Also in many cases the reader is referred to more advanced or specialized techniques. Finally, the beginner will benefit from the valuable expert advice regarding the most suitable materials to work with, and especially from the detailed troubleshooting guidance, since locating potential sources of error often presents difficulties for the inexperienced. Each chapter concludes

with a detailed and well-balanced list of references to more advanced literature.

Apart from the variations in level of treatment and amount of detail that are usual in a multi-author work, the presentation of the subject matter is commendably thorough. Also, from 1991 the volumes in this series have changed their appearance: the layout has been considerably altered to provide a better subdivision of the material and improved clarity. Important statements in the text are shown with emphasis. Experimental procedures are clearly separated from the rest of the text; each includes a list of the materials and reagents needed, safety precautions, cross-references to other related procedures in the same volume, and useful hints regarding special circumstances.

The appendices include a list of some important *E. coli* host strains, culture and buffer media, DNA- and RNA-modifying enzymes, restriction patterns for individual vectors, and addresses of commercial suppliers (although these do not always include those of the parent companies). The appendix listing the various safety points connected with work in molecular biology is *far* too brief to be useful. In contrast to this, there is an excellent appendix containing general information on essential laboratory equipment; this will be especially valuable in helping those who must first decide whether or not their research environment is adequate to allow experimental work in molecular biology.

A picture tells more than a thousand words—this old saying applies especially to "do-it-yourself" introductions aimed at a general readership. Comparing these two volumes with the standard that has been set by "Maniatis" reveals their only serious weakness, namely that figures and sketches are rather infrequent. For example, a reaction sequence involving a steplike or flush scission of DNA is conveyed so much more clearly and succinctly by a small reaction scheme diagram than by a description in words alone, even when the latter uses very descriptive technical terms such as "sticky end" and "blunt end"!

To summarize, these volumes live up to their claim that the reader with no previous experience is led step by step, by means of easily understandable introductory explanations and exact detailed descriptions, into a fascinating new world of experimentation. At this affordable price, therefore, Volume 1 can be recommended for both students and teachers as an accompaniment to a technique-orientated practical course (subject to the reservation mentioned above regarding the scanty provision of diagrams). The two-volume set is recommended for everyone who wishes to become familiar with the experimental methods of recombinant DNA work—and who finds "Maniatis" too expensive or too unwieldy.

Wolf-Dieter Fessner, Matthias Dreyer
Institut für Organische Chemie und Biochemie
der Universität Freiburg (FRG)

Registered names, trademarks, etc. used in this journal, even when not marked as such, are not to be considered unprotected by law.

© VCH Verlagsgesellschaft mbH, D-W-6940 Weinheim, 1992. – Printed in the Federal Republic of Germany by Konrad Triltsch Druck- und Verlagsanstalt Würzburg.

All rights reserved (including those of translation into foreign languages). No part of this issue may be reproduced in any form — by photoprint, microfilm, or any other means — nor transmitted or translated into a machine language without written permission from the publishers. Only single copies of contributions, or parts thereof, may be made for personal use. This journal was carefully produced in all its parts. Nevertheless, authors, editors, and publisher do not warrant the information contained therein to be free of errors. Readers are advised to keep in mind that statements, data, illustrations, procedural details, or other items may inadvertently be inaccurate.

Valid for users in the USA: The appearance of the code at the bottom of the first page of an article (serial) indicates the copyright owner's consent that copies of the article may be made for personal or internal use, or for the personal or internal use of specific clients. This consent is given on the condition, however, that the copier pay stated per-copy fee through the Copyright Clearance Center, Inc. (CCC), for copying beyond that permitted by Sections 107 or 108 of the U.S. Copyright Law. This consent does not extend to other kinds of copying, such as copying, for general distribution, for advertising or promotional purposes, for creating new collective works, or for resale. For copying from back volumes of this journal see 'Permissions to Photo-Copy: Publisher's Fee List' of the CCC.

Editorial office: Postfach 10 11 61, D-W-6490 Weinheim, Federal Republic of Germany, Telephone (06201) 60 23 15, Telex 465 516 vchwh d, Telefax (06201) 602 328, E-Mail Z16@DHDURZ2 in Earn Bitnet.

Editor: *Peter Gölitz*

Associate editors: *R. H. Schmidt-Radde, K. J. Schneider, A. Stimson.* **Editorial assistant:** *E. Schweikart*

Publishers: VCH Verlagsgesellschaft mbH. (Managing Directors: *Hans Dirk Köhler, Dr. Karlheinz Köpfer*), Pappelallee 3, W-6940 Weinheim, Federal Republic of Germany.

Advertising office (Advertising Manager: *R. J. Roth*): Postfach 10 11 61, D-W-6940 Weinheim, Federal Republic of Germany, Telephone (0 62 01) 60 61 36, Telex 4 67 155, Telefax (0 62 01) 606 156.

ANGEWANDTE CHEMIE
International Edition in English
Volume 31 · Number 9
September 1992
Pages 1101–1264

Synthetic Approaches toward Molecular and Polymeric Carbon Allotropes

By François Diederich* and Yves Rubin

Life on earth is based on compounds that have carbon frames and backbones. Today, chemists have added to the world of biomolecules and biopolymers approximately 10^7 different synthetic molecules and polymers, the structures of which also depend on the formation of strong, stable carbon–carbon bonds. Although the stability of carbon–carbon bonds has been recognized for more than a century, the two natural modifications graphite and diamond were, until recently, the only allotropic forms of carbon on earth that were available in macroscopic quantities and were structurally well characterized. With the synthesis of macroscopic quantities of buckminsterfullerene (C_{60}) and the higher fullerenes (C_{70}, C_{76}, C_{78}, etc.) and the exploration of the fascinating properties of these all-carbon spheres, this situation has completely changed. In the coming decades, the design, preparation, and study of novel molecular and polymeric allotropic forms of carbon will be a central topic in chemistry. Research in this area will dramatically advance the fundamental knowledge on carbon-based matter and, as already illustrated by the ongoing work on C_{60}, generate unprecedented technological perspectives. This review surveys synthetic organic-chemical approaches toward the preparation and study of all-carbon molecules and polymers that differ from the familiar networks of graphite and diamond as well as from the fullerenes. We will also discuss the ongoing research on fullerenes with a particular focus on the synthetic approaches to these all-carbon spheres and their transition metal complexes.

1. Introduction

Until recently, graphite and diamond were the only two structurally well characterized carbon allotropes available in macroscopic quantities (Scheme 1). The technological importance of these networks is enormous.[1] Graphite is used as a solid lubricant, in pencils, as a moderator in nuclear reactors, and, most importantly, as a reinforcement material in carbon fiber composites.[2] Diamond is mostly known for its hardness and its high refractive index. It is used in the jewelry industry and in drilling heads for the extraction of crude oil. More recently, diamond thin films have attracted great interest for use in electronic devices and in protective coating of tools and materials.[3, 4] A whole variety of other, yet unprepared all-carbon network polymers have been predicted to exhibit interesting material properties. This was a

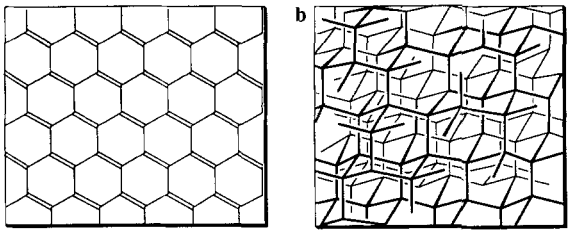

Scheme 1. Network structures of graphite (a) and diamond (b).

[*] Professor Dr. F. Diederich,[+] Dr. Y. Rubin
Department of Chemistry and Biochemistry
University of California
Los Angeles, CA 90024-1569 (USA)
[+] New Address:
Laboratorium für Organische Chemie
ETH-Zentrum
Universitätsstrasse 16, CH-8092 Zürich (Switzerland)

 © VCH Verlagsgesellschaft mbH, W-6940 Weinheim, 1992 0570-0833/92/0909-1101 $ 3.50+.25/0

strong incentive for us to initiate a research program for the synthesis of novel molecular and polymeric forms of carbon.[5-7]

Additional interest in the structures and properties of new carbon allotropes is derived from their potential relevance to combustion processes and soot formation.[8, 9] Also, all-carbon molecules are believed to be present in carbon-rich stars and interstellar dust and, therefore, have been of tremendous interest to astronomers and astrophysicists during the past two decades.[10, 11] Whereas carbon is the fourteenth most abundant element on earth, it has the sixth highest abundance in the cosmos.[12] It is therefore not so surprising that the first preparation of macroscopic quantities of C_{60}, the third allotropic form of carbon, was been reported by a team of astronomers led by Wolfgang Krätschmer and Donald Huffman (see Scheme 2).[13] In 1990, these researchers reported the isolation of C_{60} from soot produced by resistive heating of graphite under an inert atmosphere. The now well-established cagelike structure of C_{60} with the shape of a truncated icosahedron had been predicted in 1985 by Kroto, Smalley, et al. at Rice University to account for the exceptional stability of the C_{60} species in carbon cluster beams produced by the laser vaporization of graphite.[14] In honor of Buckminster Fuller, the American architect renowned for his geodesic domes, these researchers gave the name "buckminsterfullerene" to C_{60}. Although other scientists had previously predicted that C_{60} would be a stable, soccerball-shaped molecule,[5, 15] it was only after the 1985 communication by the group at Rice University that a broad range of chemists and physicists became interested in theoretical calculations to predict the structure and properties of buckminsterfullerene.[11, 16-18] The predicted IR spectrum[19] for C_{60} proved to be crucial to its discovery. When Krätschmer et al. recorded the IR spectrum of their soot, they detected four distinct absorptions at 1429, 1183, 577, and 528 cm^{-1} superimposed on a broad background absorption.[20] A comparison with the frequencies that had been previously calculated for C_{60} (1600 ± 200, 1300 ± 200, 630 ± 100, and $500 \pm 50\ cm^{-1}$) showed that the soot contained significant amounts of this carbon sphere.

Prior to the landmark study on C_{60} by the group at Rice University, experiments in 1984 at Exxon Research Laboratories on the abundances of carbon clusters generated by the laser vaporization of graphite provided the surprising observation that only even-numbered clusters were present in the C_{40} to C_{200} ion range.[21] Kroto, Smalley, et al. explained the abundance of these even-numbered species in 1985 by evoking the formation of an entire family of carbon cages containing a central cavity called the fullerenes.[22] They defined fullerenes as all-carbon molecules with the composition C_{20+2m}, which take the form of hollow closed nets composed of twelve pentagons and m hexagons. The ellipsoidal fullerene C_{70}, initially reported by the Rice University group as the second most prominent carbon cluster besides C_{60},[14] was also found by Krätschmer, Huffman, et al.[13] as the second most abundant carbon cage in their soot. A series of other higher fullerenes have now been isolated and characterized either in pure form[23, 24] or as mixtures.[25, 26] Diederich, Whetten, et al. characterized in pure form the next higher members of the fullerene family beyond C_{60} and C_{70}—the chiral D_2-symmetric molecule C_{76}[23] and the isomeric C_{2v}-C_{78} and D_3-C_{78} molecules (Scheme 2)—and determined their structures by ^{13}C NMR spectroscopy.[24] The ongoing fullerene research has recently been the subject of a

François Diederich was born in Ettelbruck in the Grand-Duchy of Luxembourg on July 9, 1952. He studied chemistry at the University of Heidelberg and obtained his Diplom in 1977 and his doctoral degree in 1979 for work with Heinz A. Staab. After postdoctoral research with Orville L. Chapman at the University of California at Los Angeles from 1979 to 1981, he became a research associate at the Max-Planck-Institut für medizinische Forschung in Heidelberg. Following his Habilitation at the University of Heidelberg in 1985, he joined the faculty at UCLA where he advanced in 1989 to full professor of organic chemistry. Since April 1992, he has been a professor of organic chemistry at the ETH Zürich. He is a recipient of the Otto-Hahn-Medaille of the Max-Planck-Gesellschaft, the Camille Dreyfus Teacher-Scholar Award, and the Arthur C. Cope Scholar Award of the American Chemical Society. His research interests are the chemistry of all-carbon molecules and network polymers, molecular recognition, and the general area of supramolecular chemistry.

Yves Rubin was born on March 9, 1963 in Yverdon, Switzerland. He received his Diplom in chemistry in 1987 from the University of Fribourg with Albert Gossauer and Alexander von Zelewski as thesis advisors. From 1987 to 1991, he was a doctoral student with François Diederich at UCLA, working on syntheses of all-carbon molecules and networks and on the isolation and characterization of fullerenes C_{60}, C_{70}, and C_{84}. After receiving his Ph.D. degree, he became a postdoctoral fellow with Ronald Breslow at Columbia University, working on the development of organic ferromagnets. He won the Saul Winstein Dissertation Award at UCLA and was awarded a postdoctoral fellowship from the Schweizerischen Nationalfonds zur Förderung der wissenschaftlichen Forschung. Since July 1992, he has been an assistant professor of organic chemistry at UCLA and recently received a Dreyfus New Faculty Award. His research interests include the total synthesis of C_{60} and functionalized derivatives and the preparation and study of organic materials.

number of reviews.[11, 16–18] We take a different approach in this article, summarizing synthetic approaches to C_{60} and surveying fullerene transition metal complexes as part of a general chapter on transition metal complexes of all-carbon molecules.

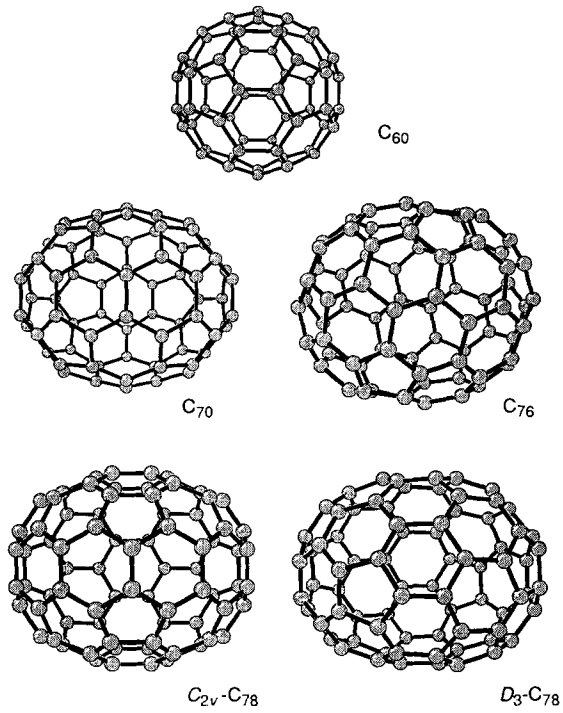

Scheme 2. Molecular structures of the five fullerenes isolated in pure form.

Long before the discovery of C_{60} and the subsequent development of fullerene chemistry, the assembly of carbon atoms into all-carbon molecules and polymers had already been the subject of a large body of experimental and theoretical work. In 1942, Hahn, Strassmann, et al. detected by mass spectrometry the formation of carbon ions from C_1^+ to C_{15}^+ in the vapor obtained by electrical discharge between graphite electrodes.[27] Subsequent mass spectrometric analyses led to the discovery of even larger carbon ions ranging up to C_{21}^+.[28] With the advent of laser vaporization techniques in the early 1980s, all-carbon molecules and ions became the subject of intensive experimental and theoretical studies.[29–33] Molecules and ions of sizes ranging from C_2 to $> C_{600}$ have been detected in the supersonic beams produced by the laser vaporization of graphite[21] and other carbon-rich materials,[34] and a variety of theoretical investigations have been useful in assigning structures to these species. Ion cyclotron resonance experiments have been particularly valuable for generating mass-selected ion beams of significant lifetime, allowing the study of both physical and chemical properties of these ions. Alternatively, the spectral properties of some of the smaller carbon ions produced by the vaporization of graphite or the photolysis of acetylene have been studied in low-temperature matrices. A comprehensive review of the gas-phase and matrix studies on carbon molecules and ions until April 1989 has been provided by Weltner and Van Zee.[29] For the smaller molecules C_2 through C_9,[35] linear chain structures, and for compounds as small as C_3, cyclic structures also have been discussed.[36] The consensus among the theoreticians is that the larger molecules C_{10} through C_{29} should have monocyclic structures, and experimental results could be interpreted consistently with these hypothesized structures.[37] Special stability was predicted by Roald Hoffmann in Extended Hückel calculations for the neutral cycles with $[4n + 2]$ atoms that are aromatic closed-shell systems, such as C_{14}, C_{18}, and C_{22}.[38] Carbon molecules in the range from C_{30} to C_{40} are, by comparison, very reactive.[39] Above C_{40}, fullerene structures become abundant.[40]

A variety of imaginative and practical, as well as impractical, structures can be found in the literature for two-dimensional (2-D) and three-dimensional (3-D) all-carbon networks that differ from graphite and diamond. As early as 1946 in a work on amorphous carbon and carbon combustion, Riley[8, 41] proposed a new 3-D network composed of interconnecting hexaphenylbenzene subunits. A variety of interesting 2-D nets were proposed in 1968 by Balaban et al.[42] Scheme 3 shows two of these interesting structures which, in more recent work by the same author,[12] were complemented with other 2-D and 3-D all-carbon structures. Carbon networks have also been of particular interest to Hoffmann et al.[7, 43] Scheme 3c shows their proposed three-dimensional, possibly metallic net in which infinite polyene chains run along two dimensions with no conjugation in the third dimension.[44, 45]

The most significant early efforts towards the synthesis of all-carbon molecules were initiated in 1981 by Orville Chapman at the University of California, Los Angeles (UCLA). At that time, Chapman was convinced of the high stability of the soccerball structure for C_{60}.[46] These efforts, which extended between 1981 and 1990, are documented in four

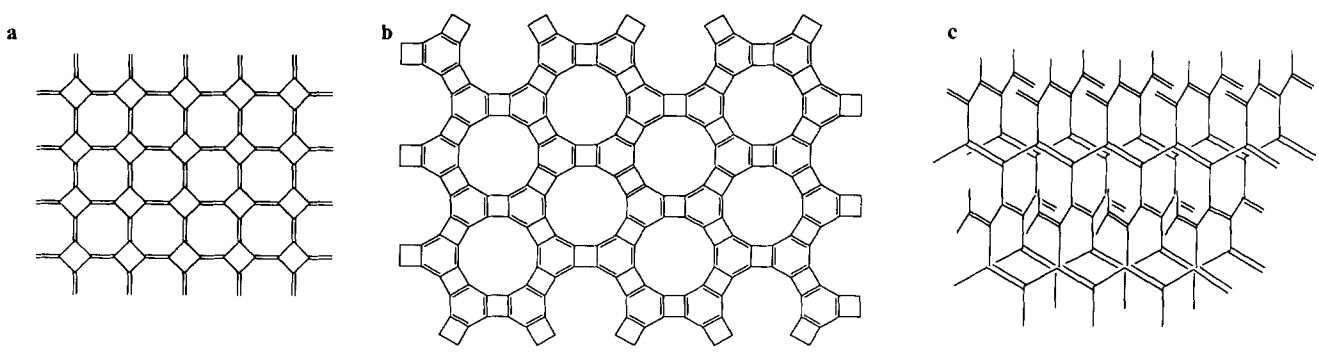

Scheme 3. Representative 2-D (a,b) and 3-D (c) carbon networks. Networks a and b were suggested by Balaban et al. [42], network c by Hoffmann et al. [43].

UCLA Ph.D. theses, and some of the synthetic approaches are discussed below. In 1986, Diederich et al. started a research program exploring the preparation of new carbon allotropes different from the fullerene structures through rational chemical synthesis.[47] This review article gives an overview of the progress in these studies directed to the synthesis of all-carbon rods, rings, nets, and spheres.

2. Polyynes as Precursors to Molecular Carbon Rods

An intriguing aspect of carbon chemistry is the preparation of infinite one-dimensional rods constituted of alkyne units (Scheme 4).[30c] Such infinite linear polyynes, which

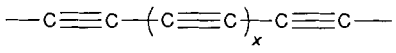

Scheme 4. Infinite one-dimensional polyyne.

have been called "carbyne" or "chaoite",[48,49] are expected to be one-dimensional conductors, and calculations predict an unusual variety of soliton and polaron states.[50] Reports on their preparation are controversial: materials obtained by oxidative polycondensation of acetylenes, dehydrochlorination of polyvinylidene chloride $(CHCl)_x$,[51] or contact heating of pyrolytic graphite at temperatures of 2700–3000 K led only to ill-defined materials with poorly reproducible structural characteristics.[48,52] The stability of carbyne, which is predicted to prefer the acetylenic form $\cdot C-(C\equiv C)_n-C\cdot$ over the cumulenic form $:C=(C=C)_n=C:$,[50] should be substantially affected by chain-to-chain polymerizations, for example Diels–Alder-type cyclizations or $[n+m]$ cycloadditions between cumulene units.[53]

Materials approaching carbyne are the extended linear polyynes incorporating up to 16 conjugated acetylene units prepared by Walton et al.[54] Whereas stable solutions of $H(C\equiv C)_{12}H$ could still be obtained by deprotection of the corresponding bis(triethylsilyl) derivative, the longer polyynes were only stable when protected with two bulky Et_3Si end-groups. When we became interested in a systematic synthetic approach towards linear polyynes $X-(C\equiv C)_x-Y$ with thermally or photochemically removable end-groups X and Y for the generation of unsubstituted C_x species, we found that there were very few procedures for the preparation of such oligomers.[55,56] Long-chain polyynes were usually constructed in tedious stepwise procedures by multiple Cadiot–Chodkiewicz,[57] Eglinton–Glaser,[58] or Hay[59] coupling reactions starting from terminal mono- or diynes. No convenient general method for the preparation of linear polyynes with an odd number of C≡C bonds existed. Therefore, we developed a general method for the preparation of symmetrically and unsymmetrically substituted polyynes starting from readily available 3,4-dichloro-3-cyclobutene-1,2-dione (**1**).[60] As shown in Scheme 5, the new synthetic sequence makes use of the acetylene synthon, 3-cyclobutene-1,2-dione, which readily loses its two carbonyl groups in pyrolytic or photolytic reactions.[61–63]

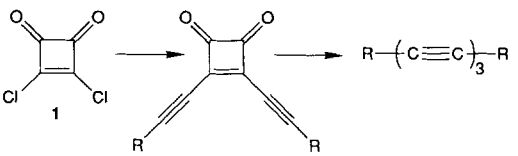

Scheme 5. Synthesis of polyynes with an odd number of C≡C bonds.

Despite the extensive amount of work reported on squaric acid and its derivatives,[61,64,65] no 3,4-dialkynyl-3-cyclobutene-1,2-diones, the key intermediates in the new polyyne synthesis, had previously been prepared. Using organotin[66] and organocopper[67] compounds, we developed two methods to prepare these colored compounds in good to high yields (Table 1).[60,68,69] The structure of the bis(phenylethynyl) derivative **2a** was determined by X-ray crystallography. Since the majority of the 3,4-dialkynyl-3-cyclobutene-1,2-diones showed poor volatility and thermal instability, they could not be subjected to conventional flash vacuum pyrolysis (FVP)[70] for the extrusion of the two carbonyl groups to give the linear polyynes. Therefore, we developed solution-spray flash vacuum pyrolysis (SS-FVP) as a potentially general method for the preparative-scale pyrolysis of thermally sensitive compounds with high molecular

Table 1. Preparation of 3,4-dialkynyl-3-cyclobutene-1,2-diones **2a–g**.

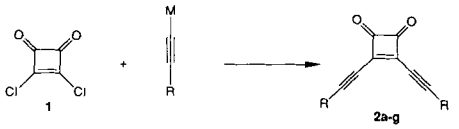

R	Product	Yield [%], m.p., appearance
Tributyltin route (M = $SnBu_3$) [a]		
Ph	**2a**	70, 114–115 °C, orange needles
Ph-C≡C	**2b**	11, >184 °C, deep red crystals
*n*Pr	**2c**	51, yellow oil
Me_3Si	**2d**	30, 95–97 °C, yellow needles
iPr_3Si	**2f**	80, 37–38 °C, yellow needles
Copper acetylide route (M = Cu) [b]		
Me_3Si	**2d**	27
$tBuMe_2Si$	**2e**	68, 57–59 °C, orange crystals
iPr_3Si	**2f**	59
Me_3Si-C≡C	**2g**	26, unstable brown oil

[a] Conditions: $[Pd(PPh_3)_4]$, $ClCH_2CH_2Cl$, 20 °C. [b] Conditions: treatment of alkyne with *n*BuLi, then CuI; then alkynylation of **1** in THF, 20 °C.

Table 2. Preparation of linear polyynes **3a–i** by solution-spray flash vacuum pyrolysis (SS-FVP).

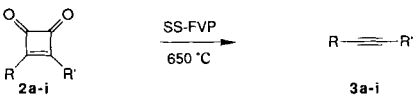

Dione	R	R′	Product (yield [%])
2a	PhC≡C	PhC≡C	**3a** (97)
2b	PhC≡C–C≡C	PhC≡C–C≡C	**3b** (59)
2c	*n*PrC≡C	*n*PrC≡C	**3c** (78)
2d	$Me_3SiC\equiv C$	$Me_3SiC\equiv C$	**3d** (99)
2e	$tBuMe_2SiC\equiv C$	$tBuMe_2SiC\equiv C$	**3e** (99)
2f	$iPr_3SiC\equiv C$	$iPr_3SiC\equiv C$	**3f** (95)
2h	$iPr_3SiC\equiv C-C\equiv C$	$iPr_3SiC\equiv C-C\equiv C$	**3h** (42)
2i	$iPr_3SiC\equiv C$	$Me_3SiC\equiv C$	**3i** (71)

weights.[60] In this procedure, solutions of the 3,4-dialkynylcyclobutene-1,2-diones **2a–i** in benzene were introduced by capillary tubing as aerosols[71] into a hot pyrolysis tube made of quartz glass and filled with quartz rings. The triynes and pentaynes **3a–i** were obtained in good to excellent yields by this method (Table 2). The reaction could even be applied to convert the bis(cyclobutenedione) **4** into the hexayne **5** (31% yield, Scheme 6). As in Fowler's "solvent-assisted sublimation" method,[72] the sublimation of the solid substrate into the gas phase during SS-FVP is assisted by the flash evaporation of benzene.

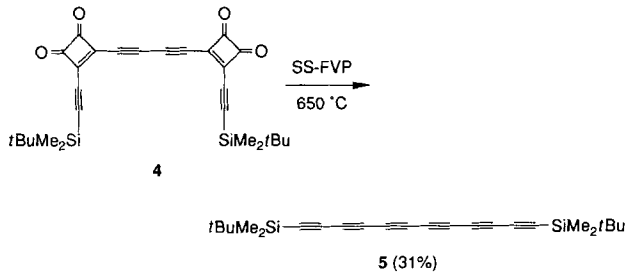

Scheme 6. Preparation of the hexayne **5**.

This new method for the preparation of symmetrically and unsymmetrically protected linear polyynes should greatly facilitate the generation of longer molecular carbon rods through oxidative coupling reactions and provide us with an entry into the study of linear C_x species of various sizes. Also, the topochemical[73] or the thermal polymerization of suitable polyyne derivatives in the solid state could lead to ladder polymers[74] exhibiting, among other characteristics, bulk spin alignment[75] or non-linear optical properties.[76]

3. The Cyclo[*n*]carbons

3.1. Definitions and Structural Predictions

As a first target in our synthetic approach towards all-carbon molecules, we chose the cyclic polyyne C_{18} **6** (Scheme 7).[47] This compound belongs to the novel class of monocyclic molecules which we call the cyclo[*n*]carbons. As in the [*n*]annulenes,[77, 78] *n* defines the number of carbon atoms that are connected to form the monocyclic structure. A distinctive aromatic stabilization might be among the potentially interesting properties of cyclo[18]carbon (**6**), since

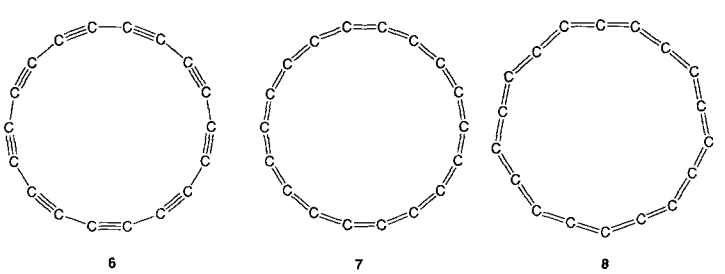

Scheme 7. Calculated structures for C_{18}.

two perpendicular systems of conjugated π orbitals exist, one in-plane and one out-of-plane, with $[4n + 2]$ π-electrons each.

Extended Hückel[38] and semiempirical MNDO calculations[32, 37b] predict an energetic preference for a monocyclic structure of C_{18} over a linear one. These predictions were further refined by ab initio molecular orbital calculations. Interestingly, conflicting results were obtained at different levels of theory.[47, 79a] Results of SCF calculations with a 3-21G or larger basis set suggest that the cyclic acetylenic D_{9h} structure **6** with alternating bond lengths represents the ground state geometry and is more stable than the cumulenic D_{18h} and D_{9h} structures **7** and **8**. However, optimization at the MP2 level including valence electron correlations[79a] produced an opposing prediction and favored the D_{18h} structure **7** over **6** and **8** (Table 3). This discrepancy should eventually be resolved when cyclo[18]carbon is synthesized.[79b]

Table 3. Relative energies, bond lengths, and bond angles of optimized structures **6–8** of cyclo[18]carbon [47, 79a].

Method	Basis set	Structure		
		6	**7**	**8**
Relative Energies [kcal mol^{-1}]				
SCF	3-21G	0.0	53.8	37.6
	[4s3p1d]	0.0	68.7	35.2
	[5s4p3d2f]	0.0	71.5	
36-MP2 [a]	[4s3p1d]	54.6	0.0	108.8
72-MP2 [b]	[5s4p3d2f]	85.7	0.0	
Bond Lengths [Å]				
SCF	3-21G	1.362 (C–C) 1.199 (C≡C)	1.265	1.271
	[4s3p1d]	1.375 (C–C) 1.194 (C≡C)		1.277
36-MP2	[4s3p1d]		1.277	
Bond Angles [°]				
SCF	3-21G	160	160	170.4 149.6
	[4s3p1d]	160		175
36-MP2	[4s3p1d]		160	

[a] Thirty-six valence electrons were correlated.[b] Seventy-two valence electrons were correlated.

A variety of data predict that the cyclic polyyne structure **6** should not have unusual strain-related instability and should be isolable at room temperature. Strain in the monocyclic structures **6–8** results mainly from the distortions of bond angles from the ideal value of 180° to ≈160°. This distortion of the bonding of an acetylenic or allenic C atom requires about 4 kcal mol^{-1}, leading to a predicted total strain of 72 kcal mol^{-1}.[80] Several stable strained cycloalkynes with C≡C–C angles around 160° and even as small as 145.8°[81] have been reported; the reader is referred to excellent reviews on this subject.[82, 83] Finally, a computational assessment of the stability of **6** shows that the energy change for the isodesmic reaction summarized in Equation (a) is

$$\mathbf{6} + 2HC{\equiv}CH \longrightarrow HC{\equiv}C{-}(C{\equiv}C)_7{-}C{\equiv}CH + HC{\equiv}C{-}C{\equiv}CH \quad (a)$$

76 kcal mol^{-1}, far less than the energy of about 130 kcal mol^{-1} required to cleave a C–C single bond joining two acetylene units.

3.2. Synthetic Approaches to Cyclo[18]carbon

The strategies which we pursued to synthesize cyclo[18]carbon were all based on the same retrosynthetic analysis. By oxidative coupling of (*Z*)-3-hexene-1,5-diyne (**9**), Sondheimer and Okamura obtained in 1967 exclusively the yellow trimer **10** (Scheme 8).[84, 85] In analogy, we intended

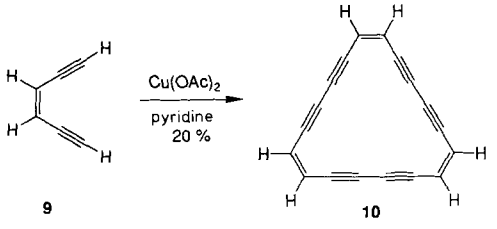

Scheme 8. The Sondheimer synthesis of hexadehydro[18]annulene **10** [84].

to synthesize "hexadehydroannulene" structures similar to **10** but with suitable leaving groups instead of the six peripheral hydrogen atoms. Thus, C_{18} would be generated in the final step of the synthesis by extrusion of the functional groups. The four routes pursued are shown in Scheme 9.

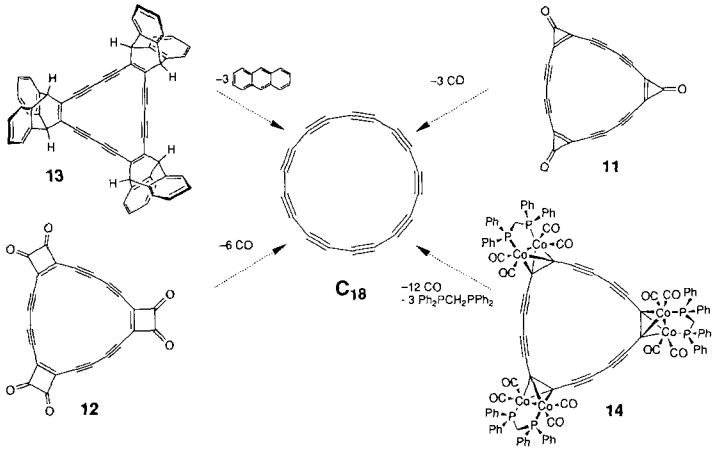

Scheme 9. The four synthetic routes to cyclo[18]carbon (the acetylenic structure **6** is shown).

3.2.1. The Cyclopropenone Route to C_{18}

Cyclopropenones, like 3-cyclobutenediones, are known to eliminate carbon monoxide readily in pyrolytic[62b, 82b] and photolytic processes[63] to form acetylenes. Therefore, one route to C_{18} departed from **15** which, upon oxidative cyclization, could yield **11** and ultimately, by extrusion of three CO molecules, cyclo[18]carbon (Scheme 9). Whereas dialkynylcyclopropenones such as **15**–**17** (Scheme 10) were not

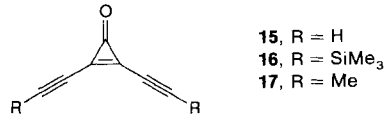

15, R = H
16, R = $SiMe_3$
17, R = Me

Scheme 10. Dialkynylcyclopropenones **15**–**17**.

known,[86] a great variety of other disubstituted cyclopropenones had previously been prepared by the reaction of arenes,[87] alkynes,[88] or alkenes[88, 89] with trichlorocyclopropenylium salts, generated from tetrachlorocyclopropene and a Lewis acid such as aluminum chloride. We hoped to

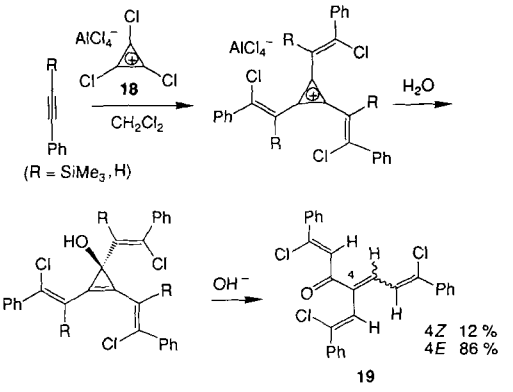

Scheme 11. Reaction of **18** with phenylacetylene derivatives. The dinitrophenylhydrazone derivative of **19** was characterized by X-ray crystallography.

prepare 2,3-dialkynylcyclopropenones in the reaction of alkynyltrimethylsilanes with trichlorocyclopropenylium tetrachloroaluminate (**18**)[90] as the electrophile in analogy to the reaction of alkynyltrimethylsilanes with acyl halides to give alkynylketones.[91] Schemes 11–13 show some of the

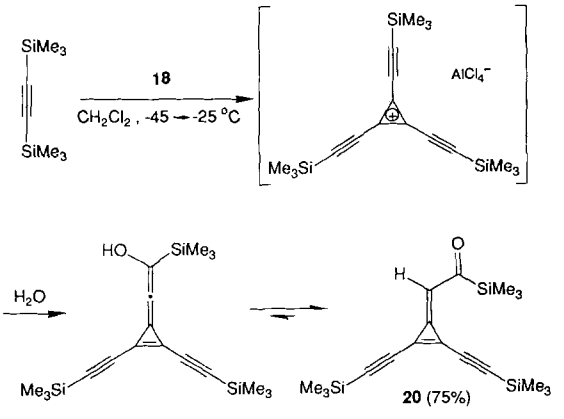

Scheme 12. Reaction of **18** with bis(trimethylsilyl)acetylene.

surprising results obtained in these studies.[68b] The only 2,3-dialkynylcyclopropenone that we were able to prepare was the bis(1-propynyl) derivative **17** (Scheme 13). This compound reacts readily with methanol to give the enediyne **21**.[92]

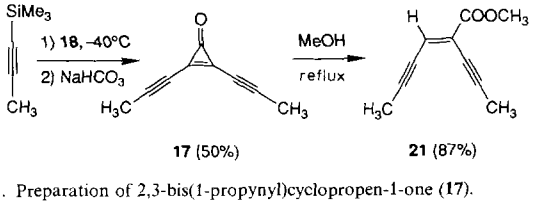

Scheme 13. Preparation of 2,3-bis(1-propynyl)cyclopropen-1-one (**17**).

In a variation of the cyclopropenone route to C_{18}, we tried to obtain the protected derivative **22** which subsequently would be cyclized to the trimer and finally deprotected to give **11** (Scheme 14).[93] As a precursor to **22**, ketal **24** was prepared in nearly quantitative yield from **23**.[94] However, all attempts to transform **24** into **22**[95] led to the opening of the cyclopropene ring.[96]

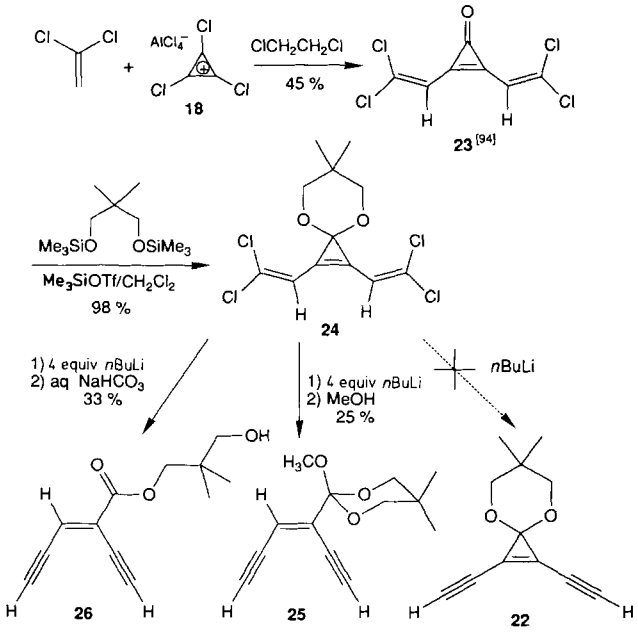

Scheme 14. Attempted preparation of ketal **22**. OTf = OSO_2CF_3.

The cyclopropenone route to cyclo[18]carbon is very short and elegant. However, the chemistry of 2,3-dialkynylcyclopropenones must first be developed before this pathway can be further pursued. At present, the bis(1-propynyl) derivative **17** remains the only known member of this class of compounds.

3.2.2. The 3-Cyclobutene-1,2-dione Route to Cyclo[18]carbon

3.2.2.1. Cyclobutene-Annelated Dehydro[n]annulenes: Surprisingly Stable [4n + 2] and [4n]π Electron Perimeters

The direct approach to **12**, the macrocyclic precursor in the cyclobutenedione route to cyclo[18]carbon (Scheme 9), required the oxidative cyclization of the diethynyl derivative **2j** (Scheme 15). However, all attempts to prepare this compound, for example by deprotection of the silyl-protected derivatives **2d–f**, failed presumably due to the extreme reactivity of **2j** as a Michael acceptor. Instead, the diketal **27** was formed from dione **2e** under unusually forcing conditions.[68b] Compound **27** readily afforded the diethynyl derivative **28**, which was cyclized under Hay coupling[59] conditions to yield the three cyclobutene-fused dehydroannulenes **29–31** in good overall yield.

The comparison of the macrocycles **29–31** and the parent dehydroannulenes **10** and **35** prepared by Sondheimer et al.[84, 97] shows a pronounced effect of the cyclobutene annelation on the structure and reactivity of the macrocycles (Schemes 8, 15, and 16). The oxidative coupling of **9** exclusively led to the formation of the trimer **10**, a planar diatropic highly unstable hexadehydro[18]annulene which explodes at approximately 85 °C. The octadehydro[24]annulene **35**, prepared by dimerization of **34**, is a nonplanar, cyclooctatetraene(COT)-like shaped atropic compound and is also highly unstable, with a tendency to explode upon heating. In

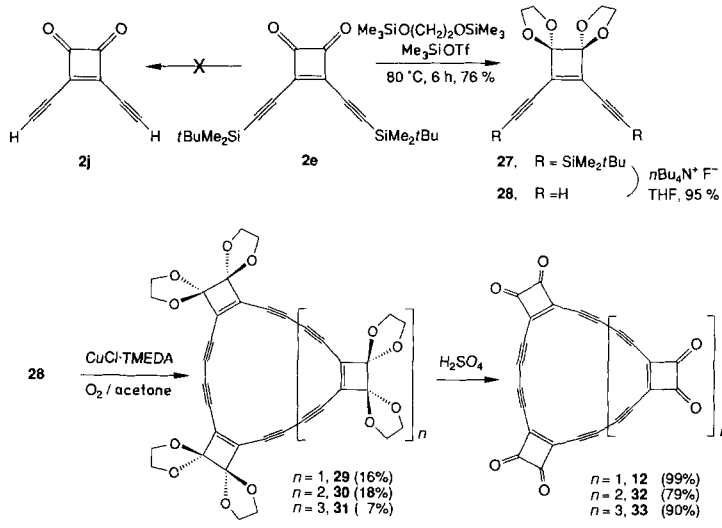

Scheme 15. Synthesis of the carbon oxides **12**, **32**, and **33**.

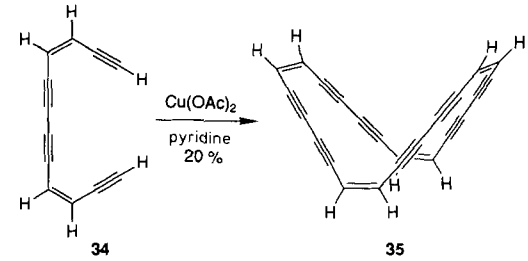

Scheme 16. The Sondheimer preparation of octadehydro[24]annulene **35** [97].

sharp contrast, oxidative coupling of **28** led to the three compounds **29–31**; the tetramer **30** was formed with the best yield. ^{1}H NMR and UV/VIS spectroscopic analysis show that the pale-yellow trimer **29** has a planar diatropic 18 π-electron perimeter and the orange-red tetramer **30** a planar paratropic 24 π-electron perimeter, whereas the bright-yellow pentamer **31** (30 π-electrons) is a conformationally more flexible, atropic system.[68, 98] All three macrocycles are stable compounds at room temperature and when exposed to air. The fusion of cyclobutene rings particularly stabilizes the planar [24]annulene perimeter and is majorly responsible for the preferred formation of tetramer **30** in the oxidative coupling reactions. Investigations on a second series of cyclobutene-fused dehydroannulenes (**36–38**) provided similar results (Scheme 17).[68b]

Computational studies with the MM2 force field[99] and semiempirical AM1[100] molecular orbital calculations reproduce the size and conformational preferences of the macrocycles observed by Sondheimer et al. and by us.[98]

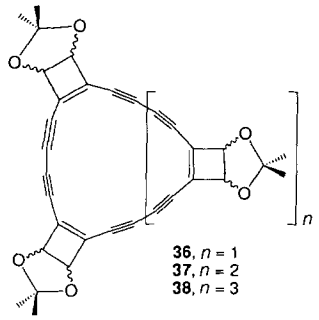

Scheme 17. Dehydroannulenes **36**–**38**.

Some of the computational results are shown in Scheme 18. Steric rather than electronic (e.g. $[4n + 2]$ vs. $[4n]$ π-electrons) factors determine the structural preferences. The calculations show that, with its C=C–C angle α of 125.4°, the parent enediyne **9** is best converted into a planar trimer (ideal angle $\alpha = 120°$) or a nonplanar COT-type tetramer (ideal angle $\alpha \approx 120°$), but not into a planar tetramer with an ideal angle α of 135°. In contrast, the diethynylcyclobutene unit **28**

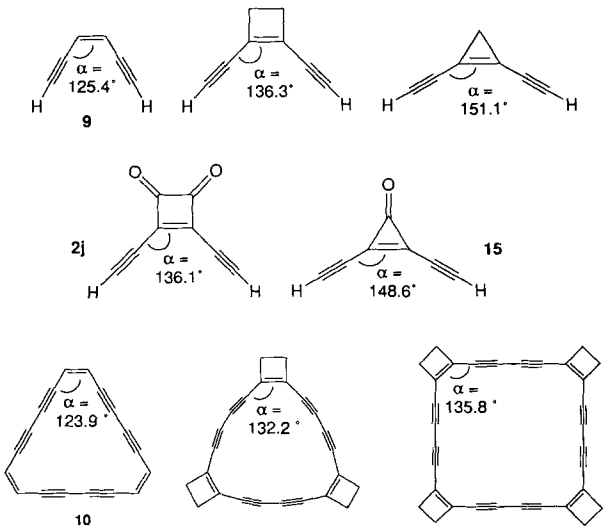

Scheme 18. C=C–C bond angles α at enediyne units calculated by AM1.

with its large C=C–C angle α of 136.1° is accommodated in a nearly strain-free way in the planar tetramer ($\alpha = 135.8°$), whereas its incorporation into the planar trimer **29** generates considerable angle strain and bending of the diacetylene units as is illustrated by the X-ray crystal structure of **12** (Fig. 1).

The increased stability of the cyclobutene-fused derivatives **29**–**31** compared to the parent compounds **10** and **35** is a result of enhanced rigidity of the ring skeleton in the annelated systems. It is well recognized in annulene chemistry that, besides the absence of transannular steric interactions or angle strain, the rigidity of the ring skeleton is an essential structural prerequisite for stability.[101–104] Rigidity and planarity can be imposed on annulene perimeters by annelation to arenes.[105] However, the more effective benzenoid delocalization is superposed on the annulenoid delocalization, and the diatropism of the $[4n + 2]$ π-electron perimeter of the annulene is weakened. In the extreme case of kekulene,[106] a perfectly stable planar molecule with an inner [18]annulene and an outer [30]annulene perimeter, all experimental evidence shows that macrocyclic delocalization is overwhelmed by benzenoid aromaticity.[107] Annulenes can be stabilized without disturbing the macrocyclic delocalization by bridging the perimeter to enforce rigidity and planarity.[108–111] The rigidity of annulenes also increases upon introduction of acetylene units into the π-electron perimeters.[77, 112] Also, a large number of annulenes including the porphyrins and analogues[78, 102, 113, 114] are made planar and stable by the five-membered aromatic heterocycles such as pyrrole and furan that are integrated into the macrocyclic π-electron system.

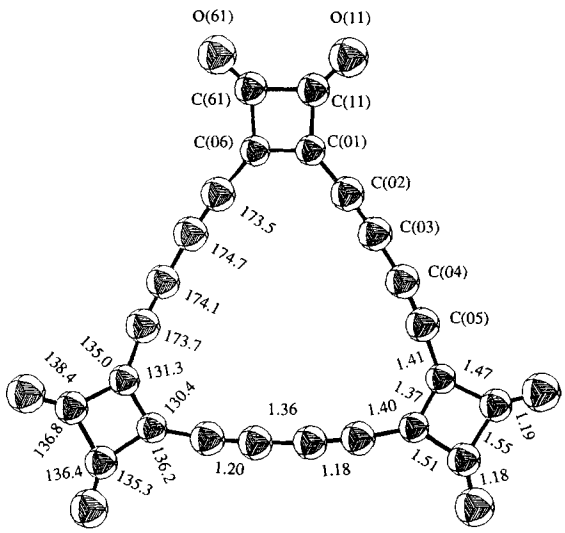

Fig. 1. X-ray crystal structure of the carbon oxide $C_{24}O_6$ **12**. Important distances [Å] and bond angles [°] are noted.

The enhanced kinetic stability of the cyclobutene-fused dehydroannulenes **29**, **30**, **36**, and **37**, compared to the parent systems **10** and **35**, can be explained by the fact that the bending and out-of-plane distortions normally required to reach transition states are energetically more difficult in the former rigid systems.[98, 111] This previously unrecognized stabilization through annelation with small cycloalkenes does not alter the macrocyclic π system. Mills–Nixon effects,[115] that is, the localization of double bonds in aromatic systems as a result of strain caused by annelation to small rings, have not been found to be very effective in benzenoid and annulenoid systems.[116] It will be interesting to see how fusion with small cycloalkenes affects structures and stabilities in other series of annulenes.[117–119]

3.2.2.2. The Higher Carbon Oxides $C_{8n}O_{2n}$: Direct Precursors to Cyclo[n]carbons

The removal of the ketal protecting groups in **29**–**31** to form the corresponding carbon oxides proved to be exceptionally difficult and could only be achieved by dissolution of the compounds in concentrated sulfuric acid.[69] The particular sensitivity of the products formed also required unusual workup conditions. Dilution of the sulfuric acid solu-

tions with water led to instant polymerization of the product. Therefore, the sulfuric acid solutions were extracted with 1,2-dichloroethane and the organic layer neutralized with powdered $CaCO_3$ to give the carbon oxides $C_{24}O_6$ (**12**), $C_{32}O_8$ (**32**), and $C_{40}O_{10}$ (**33**) in high yields. Solutions of these compounds in 1,2-dichloroethane are orange-yellow (**12**), red (**32**), and yellow (**33**). The X-ray crystal structure of oxide **12** was obtained (see Fig. 1) and reveals appreciable strain within the perfectly planar annulene perimeter. The three higher oxides of carbon **12**, **32**, and **33** are extremely sensitive to nucleophiles, which induce polymerization through initial Michael addition. Also, they undergo rapid Diels–Alder reactions with dienes, for example furan, leading to strained derivatives that subsequently polymerize. Although these carbon oxides are stable at room temperature, they explode above 80 °C.

Other oxides of carbon, molecules of the composition C_xO_y, have recently attracted much attention, although the total number of compounds in this interesting class still remains rather small.[120–122] In the series of the linear cumulene-type oxides (C_nO_2),[123], a new stable member with an odd number of carbon atoms, 1,2,3,4-pentatetraene-1,5-dione (O=C=C=C=C=C=O, C_5O_2),[124] has been added to the well known derivatives CO_2 and carbon suboxide C_3O_2. Members of the series with an even number of carbon atoms have long defied experimental detection.[125] Calculations predict that they have a triplet ground state, which would explain the high reactivity of these molecules.[125, 126] The synthesis of the first cumulenic carbon oxide with an even number of C atoms, 1,2,3-butatriene-1,4-dione (O=C=C=C=C=O, C_4O_2), was recently accomplished in an argon matrix[125] as well as in the gas phase.[126] As large molecules of composition C_xO_y, the fullerene oxides have been under intensive investigation. Compound $C_{70}O$, an oxide of D_{5h}-C_{70},[25a] as well as $C_{60}O$[127] are isolated as by-products of the fullerenes when the resistive heating of graphite is done in a He atmosphere containing residual amounts of oxygen. Compound $C_{70}O$ is also formed by burning graphite rods doped with La_2O_3 for the production of endohedral lanthanum compounds.[128] Electrochemical oxidation of C_{60} was reported to generate a mixture of $C_{60}O_n$ ($n = 1-4$).[129] Pure $C_{60}O$ has been prepared by photooxidation of C_{60} in benzene[130] and by reaction of the fullerene with 2,2-dimethyldioxirane.[131] The ^{13}C NMR data of $C_{60}O$ strongly support the epoxide structure **39** over the oxo-bridged annulene structure **40** (Scheme 19).[132] With the further developments in the chemistry of the fullerenes and carbon allotropes in general, we will undoubtedly also see a rapid increase in the number of oxides as well as sulfides[122f, 133] of carbon that are prepared.

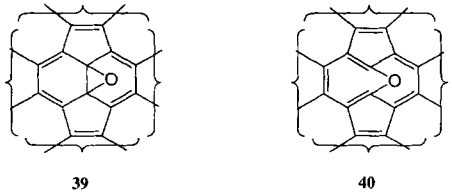

39 **40**

Scheme 19. Epoxide (**39**) and oxo-bridged annulene (**40**) structures for fullerene oxides.

The good availability of gram quantities of **12**, **32**, and **33** now allows systematic investigations of the transformation of these compounds into the cyclocarbons C_{18}, C_{24}, and C_{30}, respectively. Laser desorption Fourier transform (FT) mass spectra of these compounds show a remarkable ease of successive losses of two CO molecules to give C_{18}, C_{24}, and C_{30} ions.[69] Preliminary IR spectroscopic investigations of **12** isolated in a matrix suggest that the photolytic extrusion of six CO molecules from **12** shows promise as a way to prepare isolable quantities of cyclo[18]carbon.[134] Irradiation ($\lambda > 338$ nm) of **12** ($\tilde{\nu}$[C=O] = 1791 cm^{-1}) in a 1,2-dichloroethane glass at 30 K generates quantitatively within six minutes the hexaketene ($\tilde{\nu}$[C=C=O] = 2115 cm^{-1}). Subsequent irradiation at a shorter wavelength ($\lambda > 280$ nm) for three hours leads to complete disappearance of the ketene band and to the build up of the C≡O absorption band at 2137 cm^{-1}. Further experiments on this very promising route are now under way. The significance of the cyclocarbons in the gas-phase formation of fullerenes is described in detail in Section 6.

3.2.3. The Retro-Diels–Alder Route to Cyclo[18]carbon

The hexadehydro[18]annulene **13** (Scheme 9) was chosen as the precursor in our initial approach to cyclo[18]carbon since it should readily lose three anthracene molecules under thermolytic conditions with formation of C_{18}.[47] The macrocyle was assembled starting from anthracene via the bromochloro derivative **41**, a compound previously described by Hart et al. (Scheme 20).[135] Whereas enediynes

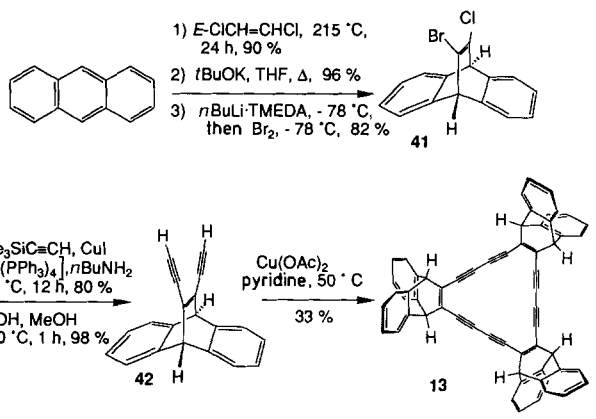

Scheme 20. Preparation of the C_{18} precursor **13**.

fused to cyclobutene rings (e.g. **28**, Scheme 15), are stable at room temperature, crystalline enediyne **42** is very unstable and, in one case, a crystalline sample exploded spontaneously. Oxidative coupling of **42** under Eglinton–Glaser conditions[136] yielded the red cyclic trimer **13** as the only product in 33% yield.

In contrast to **42** and the parent macrocycle **10**, the annelated hexadehydro[18]annulene **13** is an extraordinarily stable compound. It can be recrystallized from boiling pyridine, is stable to air, and can be heated in the solid state under N_2 to 250 °C without appreciable decomposition. It must be assumed that, in addition to the rigidification im-

posed by the annelation (Section 3.2.2.1), the steric shielding of the annulene perimeter by the six benzene rings contributes to the unusual stability of **13** with respect to bimolecular reactions and polymerization. The X-ray crystal structure of **13** (Fig. 2) shows a nearly perfectly planar 18-membered macrocycle. With an average value of 123.3°, the C=C–C angle α in **13** is small and close to the comparable angle in **42** (calculated by MM2: $\alpha = 125°$, AM1: $\alpha = 127°$).[137] As discussed in Section 3.2.2.1, this steric matching between monomer and macrocyclic oligomer explains the preferential formation a cyclic trimer. If ^{1}H NMR chemical shifts are used as a criterion for aromaticity, then **13** is aromatic: the diatropicity of **13** is reflected in the deshielding ($\Delta\delta = 0.75$) of the bridgehead methine protons ($\delta = 5.89$) compared to the methine protons in **42** ($\delta = 5.14$).

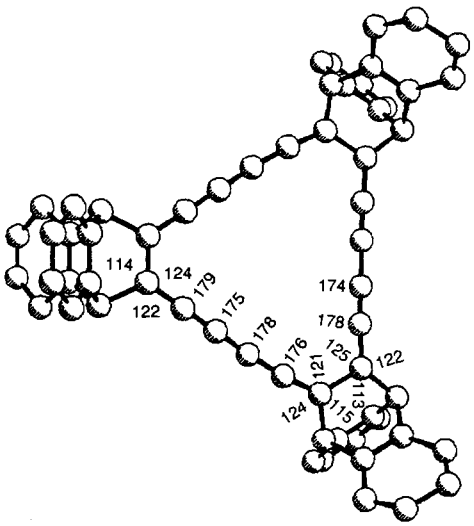

Fig. 2. X-ray crystal structure of the hexadehydro[18]annulene **13**. Important bond angles are noted.

Laser flash heating experiments clearly demonstrated that cyclo[18]carbon can be prepared by the threefold retro-Diels–Alder reaction of **13** (Scheme 9). In these experiments, a thin film of **13** was coated onto a tantalum rod, which in turn was mounted in vacuum within a pulsed He jet nozzle source and molecular beam chamber.[138] Under flash heating with a XeCl laser ($\Delta T \geq 1000$ K), the macrocycle was desorbed and underwent retro-Diels–Alder reactions leading to the successive loss of one, two, and three anthracene units and formation of cyclo[18]carbon. After all of the charged species present in the He-cooled desorption cloud were deviated by an electrical field, the neutral products were detected by resonant two-photon ionization mass spectrometry. Anthracene and cyclo[18]carbon together with cleavage products of **13** with one or two anthracene units still attached were found to be by far the most abundant neutral species in the molecular beam. This clearly shows that, under thermolysis conditions, the retro-Diels–Alder reaction to cyclo[18]carbon is the predominant fragmentation channel of **13**. We have not yet been successful in generating cyclo[18]carbon by this route on a preparative scale: flash vacuum pyrolysis as well as solution-spray flash vacuum pyrolysis of **13** (see Section 2 and Table 2) have so far only afforded anthracene besides polymeric material.

3.2.4. Stable Cobalt Complexes of Cyclo[18]- and Cyclo[24]carbon

The last proposed route to the cyclocarbons involved the preparation of metal complexes of C_{18} and the larger cyclocarbons as direct precursors to the all-carbon molecules.[139] A variety of transition metals form stable complexes with alkynes.[140, 141] The chemistry of metal complexes with strained cycloalkynes and arynes has recently been reviewed.[142] Of particular interest to us was the chemistry of alkyne–dicobalt complexes,[143] since when an alkyne is complexed with $[Co_2(CO)_8]$ the two C≡C–C angles are reduced to a value of $\approx 140°$,[144] and the alkyne can be easily liberated from its complex through oxidation of cobalt,[145, 146] alkyne–ligand exchange,[147] or flash vacuum pyrolysis.[148] Hexacarbonyldicobalt fragments have been used as protecting groups to allow disfavored cyclization reactions to proceed by bending the alkyne moiety, or to stabilize strained alkynes.[146, 149, 150] Thus, the synthesis of cyclo[18]carbon seemed promising along the pathway outlined in Scheme 21.

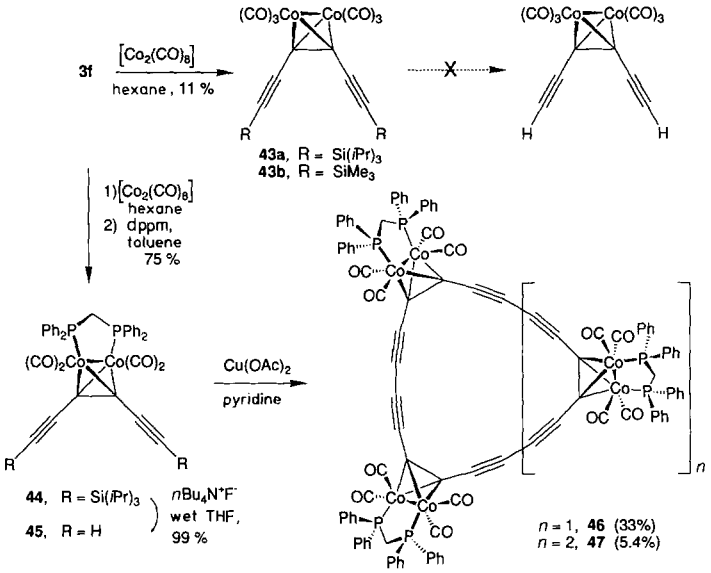

Scheme 21. Synthesis of the cobalt complexes of C_{18} (**46**) and C_{24} (**47**). dppm = Bis(diphenylphosphino)methane.

Reaction of triyne **3f** with $[Co_2(CO)_8]$ afforded as expected the sterically least crowded dicobalt complex **43a** which, however, was found to be rather unstable. Attempts to remove the silyl protecting groups in **43a** with fluoride anion led to complete decomposition of the compound. A similar negative result was obtained with the TMS-derivative **43b** under milder conditions (K_2CO_3, MeOH). Complex **43a** could be stabilized by the bridging ligand dppm,[151] which could be introduced easily[152] to afford the heat and air stable complex **44** (Scheme 21). Complex **44** was then smoothly converted to the 1,3,5-hexatriyne complex **45** which was characterized by X-ray crystallography. Oxidative coupling under high-dilution conditions finally afforded the very stable cobalt complexes of cyclo[18]carbon (**46** = **14**) and cyclo[24]carbon (**47**), both as shiny black needles. The X-ray crystal structure of **46** (Fig. 3) shows

considerable bending of the three butadiyne units within the nearly planar C_{18} ring. With a value of 161°, some of the C≡C–C angles in **46** approach the degree of bending expect-

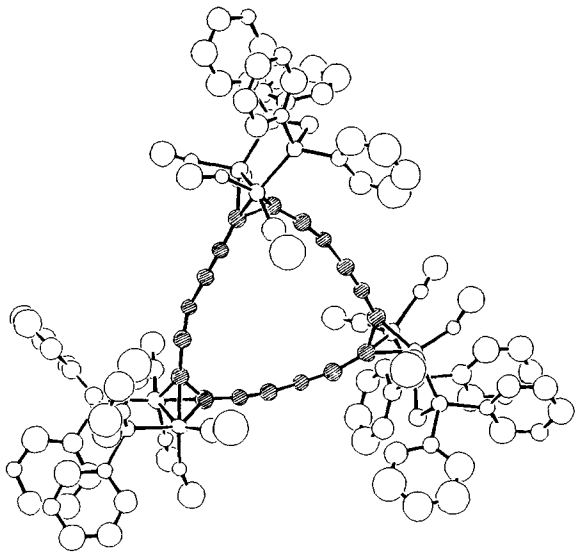

Fig. 3. X-ray crystal structure of the hexacobalt complex **46** of cyclo[18]-carbon. C atoms in the C_{18} ring are represented by shaded spheres.

ed for **6** (Section 3.1). Comparisons between the electronic absorption spectra of monomer **45**, complex **48** with two dicobalt units in direct conjugation (Scheme 22),[139] and the two macrocycles **46** and **47** strongly suggest the presence of cyclic conjugation in the two cyclocarbon complexes.[153]

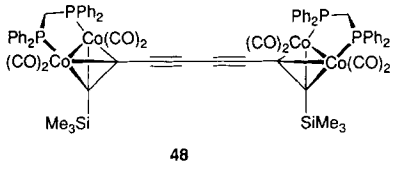

48

Scheme 22. Tetracobalt complex **48**.

Unfortunately, all attempts to free cyclo[18]carbon and cyclo[24]carbon from the coordinating metal atoms in **46** and **47** failed so far, partially because of the stabilization of the complexes by the basic dppm ligands and the extreme shielding of the cobalt atoms by the bulky dppm ligands.

4. Transition Metal Complexes with All-Carbon Ligands

The arrival of fullerenes and the synthesis of other molecular and polymeric carbon allotropes have led to developments in the exciting area of transition metal complexes with all-carbon ligands. Prior to the preparation of cyclocarbon (Section 3.2.4) and fullerene complexes (Section 4.2), a number of stable complexes of small linear carbon units C_x ($x = 2-6$) had already been reported.

4.1. Small All-Carbon Ligands in Organometallic Complexes

We do not consider metal carbides MC_2 (M = Ca, Th, U, Lu, Tb, La), La_2C_3, or $Gd_2Cl_2C_2$ and the covalently bound Be_2C, SiC, and B_4C as carbon–metal complexes.[154, 155] The same holds for the graphite–metal intercalation compounds like C_8K.[154] However, there are a few classes of true organometallic complexes in which all-carbon units act as ligands. Organometallic complexes in which single C atoms are stabilized within a metal carbonyl cluster have become quite common and are called carbidocarbonyl cluster compounds.[156] First reported as a curiosity, they can now be prepared routinely. Besides the complexation of single carbon atoms, the preparation of C_2, C_4, and even C_6 carbidocarbonyl cluster complexes has been reported, and this chemistry has recently been reviewed.[155a, 156–159]

Another type of stable molecular complex with carbon ligands is based on the chemistry of the complex fragments carbyne(nonacarbonyl)tricobalt and alkyne(hexacarbonyl)-dicobalt.[160, 161] The C_2 complex **49** (Scheme 23) was prepared in the reaction of $[Co_2(CO)_8]$ with hexachloroethane or with diiodoethyne.[162] In the C_4 complex **50**, a C≡C unit

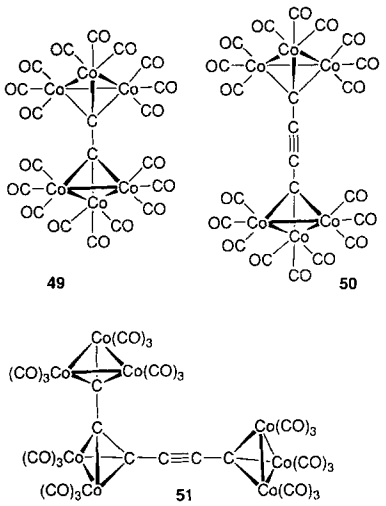

49 **50**

51

Scheme 23. Structures of cobalt complexes with C_2, C_4, and C_6 ligands.

separates the two carbyne(nonacarbonyl)tricobalt moieties.[163a] In the C_6 complex **51**,[163b, c] a butadiyne unit separates the carbyne(nonacarbonyl)tricobalt moieties and, in addition, a hexacarbonyldicobalt unit is capping one of the two C≡C bonds. The C_4 complex **50** and the C_6 complex **51** were not prepared by rational synthesis but rather obtained from the reaction of chloro- or bromomethinyl-(nonacarbonyl)tricobalt with xylene or mesitylene. Alternatively, the C_6 complex **51** was also prepared from hexachlorocyclopropane and $[Co_2(CO)_8]$.[163b]

In another class of complexes of all-carbon ligands, two transition metal atoms are bridged by μ-ethynediyl bridges. Although structures consistent with all three valence bond descriptions (M–C≡C–M, M=C=C=M, and M≡C–C≡M) have been prepared,[164a] most of the complexes contain an μ-C≡C bridge. Examples are [{(CO)$_5$-

$Re\}_2C_2]$,[164b] $[(Cp_2^*Sc)_2C_2]$ ($Cp^* = \eta^5$-C_5Me_5),[164c] $[\{Cp(CO)_2Ru\}_2C_2]$,[164d] and $[\{Cl(PBu_3)_2Pd\}_2C_2]$.[164e] A cumulenic bridge was found by X-ray crystallography in the tantalum complex $[\{(Me_3SiO)_3Ta\}_2C_2]$.[164f] The μ-C_2-bridged dinuclear complexes have been proposed as reactive intermediates in acetylene conversions on heterogenous surfaces and in the Fischer–Tropsch synthesis.[164d,f]

Finally, compounds with metalloids (Ge, Sn, Pb, Sb, As, etc.) flanking small molecular carbon units, for example alkynes, are common. More interesting in this respect are the bis(iodonium) salts **52** and **53**, which can be utilized in preparative conversions as "stabilized" forms of C_2 and C_4 (Scheme 24).[165] Similarly, compound **54** can be viewed as a

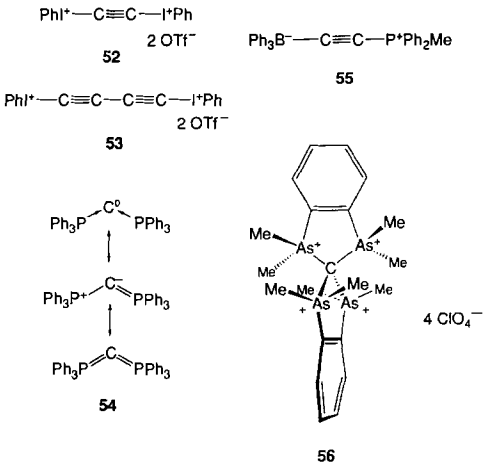

Scheme 24. Carbon complexes of metalloids.

C_1 complex consisting of two donor phosphane units and an electron-accepting carbon atom.[166,167] The stabilization of C_2 in **55** by a donor and an acceptor "ligand" was achieved by Bestmann et al.[166] The tetraarsonium salt **56** incorporating a C_1 unit within a tetrahedral array of positively charged arsenic atoms was prepared by the reaction of CBr_4 with the corresponding ditertiary diarsane ligand.[168]

4.2. Fullerene Transition Metal Complexes

4.2.1. Exohedral Fullerene Complexes

From the moment macroscopic quantities of fullerenes C_{60} and C_{70} became available, the formation of exohedral ("outside the cage") transition metal complexes was pursued. By osmylation, Hawkins et al. prepared the C_{60}–osmium tetraoxide adduct **58** (Scheme 25) and provided unambiguous confirmation of the soccerball structure of C_{60} by X-ray crystallography.[18h,169] Soon after, the preparation and X-ray crystal structure of the platinum derivative **59** was reported.[170a] These structures showed that the free space inside C_{60}, which is available for guest incorporation (Section 4.2.2), has a diameter of approximately 3.5 Å. Both **58** and **59** are formed by attack at one of the reactive C=C bonds in C_{60} found in the center of the pyracylene (**57**) subunits. Six of these reactive double bonds are located in a pseudo-octahedral arrangement on the fullerene surface.

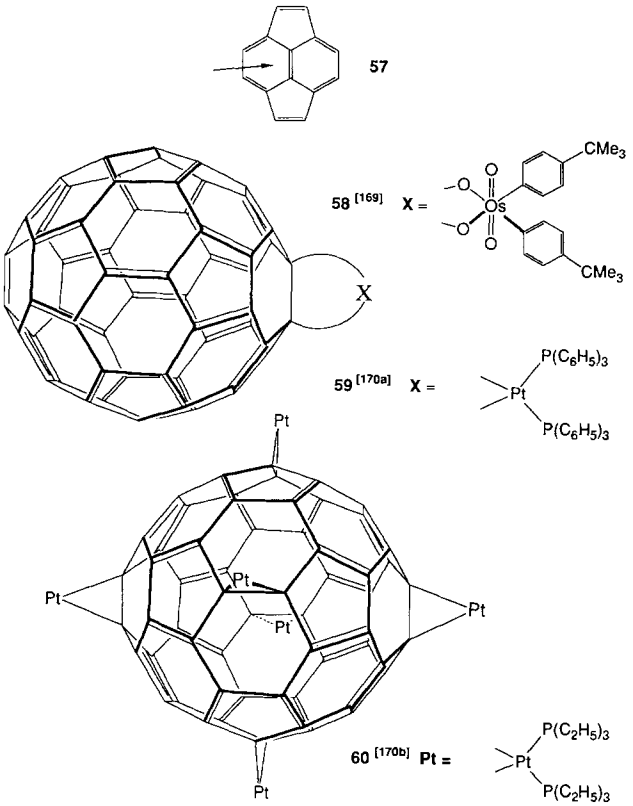

Scheme 25. Transition metal complexes of C_{60} by addition to central pyracylene-type C=C bonds (marked in pyracylene (**57**) with an arrow).

Upon reaction of C_{60} with an excess of $[\{(C_2H_5)_3P\}_4Pt]$ in benzene, the sixfold metallated derivative **60** was obtained and subsequently characterized by X-ray crystallography.[18f,170b,171]

Iridium complexes of both C_{60} and C_{70} have been described[172,173] and the X-ray crystallographic analysis of **61** provided unambiguous confirmation of the ellipsoidal D_{5h}-symmetrical cage structure[173a] shaped like a rugby ball which had previously been assigned to C_{70} based on its ^{13}C NMR spectrum (Scheme 26).[17d,g,18k,174] Similar to **58**–**60**, the metallacycle **61** forms at the reactive pyracylene-type double bond. Two different bonds of this type are present in C_{70}: one on the more curved area of the fullerene cap and one on the flatter central region of the molecule. However, the metallacycle is formed only at the double bond in the more curved region. The binding of the metal is accompa-

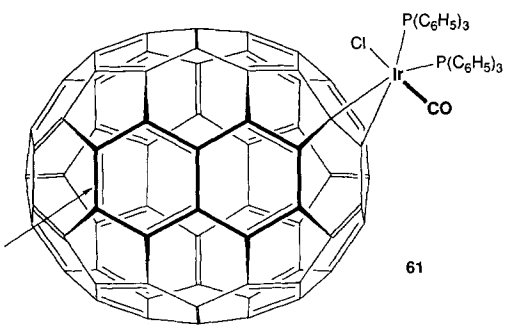

Scheme 26. An iridium derivative of C_{70}[173a]. The less reactive pyracylene-type C=C bond is marked with an arrow.

nied by local distortion; the two carbon atoms involved in the coordination are pulled out from the C_{70} surface. This distortion is energetically more favorable on the more curved cap surface where the sp^2 carbon atoms are significantly rehybridized and more strongly pyramidalized than on the flatter central surface.

In gas-phase studies with an FT mass spectrometer, the formation of the exohedral complex cations $[Ni(C_{60})_2]^+$, presumed to have a metallocene-type structure, and $[MC_{60}]^+$ (M = Fe, Co, Ni, Cu) was observed.[175] In contrast to the endohedral ("inside the cage") complexes discussed in the next section, these ions require relatively little activation energy for loss of the metal from the complex leaving an intact C_{60} species.

In a metalloporphyrin derivative, the fullerene radical anion $C_{60}^{\bullet-}$ was found to act as a very weakly coordinating anion.[176] The reaction of $[Cr^{II}(tpp)]$ (tpp = tetraphenylporphyrin) in THF with a solution of C_{60} in toluene gave purple-black crystals of $[Cr^{III}(tpp)(thf)_2]^+[C_{60}^{\bullet}]^- \cdot thf$. EPR studies in solution demonstrated that the $C_{60}^{\bullet-}$ counterion in the salt is unable to compete with THF for axial ligation to the porphyrinatochromium(III).

4.2.2. Endohedral Fullerene Complexes

It is not difficult to predict that the development of endohedral[177] complexes will become one of the most active areas of fullerene chemistry. Some of the most spectacular discoveries both in terms of basic structural understanding as well as in materials applications may be expected. As early as 1985, Smalley et al. obtained the first mass spectrometric evidence for the gas-phase formation of endohedral metal–fullerene complexes MC_{60} (M = La, K, Cs) by laser vaporization of graphite impregnated with various metal salts.[18a, 178] In contrast to exohedral complexes, the endohedral complexes are quite stable, and substantial amounts of laser energy were required to induce their fragmentation by sequential C_2 losses which eventually led to species such as $C_{36}La^+$, $C_{44}K^+$, or $C_{48}Cs^+$.[178b] The metal ions remain encapsulated in the fragmented carbon shells as long as the latter retain a cage structure that fits the ion size.

Similarly to the first reports on the formation of stable C_{60} with I_h symmetry,[16, 17a, b] the early publications in which postulates for the formation of endohedral complexes were presented triggered some controversy.[179] With the recent isolation[180] of small amounts of soluble endohedral lanthanum and yttrium complexes from soot produced by resistive or arc-heating of graphite doped with La_2O_3 and Y_2O_3, all scepticism has vanished.[180–183] Among the most abundant lanthanum complexes is LaC_{82}, an air- and moisture-stable compound which can be extracted from the soot, together with C_{60} and other uncomplexed higher fullerenes, with solvents like toluene, CS_2, or pyridine. The endohedral complexes LaC_{60}, LaC_{70}, and LaC_{74}, which are also formed, are not extractable with toluene but can be detected in air-stable films obtained by sublimation.[180] Electron paramagnetic resonance[182] as well as X-ray photoemission spectroscopy[181] showed that the central La atom in LaC_{82} has a formal charge of 3 + . The most abundant yttrium derivatives have a similar stoichiometry to those of the lanthanum compounds. Dimetallofullerenes have also been reported: both Y_2C_{82} and La_2C_{80} were extracted as air-stable endohedral complexes from the soot.[181, 183a, b]

The endohedral metal fullerene complexes form in small yield (1–3%)[182] and have not yet been isolated in pure form. Characterization so far has been possible only for mixtures of metallated and free fullerenes. Although the endohedral nature of the complexes is strongly supported by a variety of experimental evidence data such as stability, EPR spectra, and typical fragmentation pattern in the mass spectrum,[180–183] the molecular structures of the encapsulating fullerenes as well the nature of the fullerene–metal ion interactions are not known. Since all endohedral complexes have been isolated in mixtures together with free fullerenes, the formation of saltlike structures like $[LaC_{82}]^+C_{60}^-$ cannot be excluded. Structural assignments[184a–c] currently rely mainly on theoretical predictions made by Manolopoulos and Fowler who combined their very successful search for fullerene geometries based on a spiral algorithm with restricted Hartree–Fock (RHF) ab initio calculations to generate favorable geometries for endohedral fullerene complexes.[184] In addition to a detailed experimental structural analysis, future studies should also provide a more quantitative evaluation of the stability[183b] and chemical reactivity of these fascinating and unprecedented materials.[185]

5. Carbon Networks

As already mentioned in the introduction, a great variety of carbon networks differing from the familiar, naturally occurring diamond and graphite can be written down on paper, and several of them have actually been proposed in published work.[6, 7, 12, 42, 43] However, the preparation of synthetic polymeric modifications of carbon has not received much attention from polymer and organic chemists in the past, which may be explained by the fact that the postulated synthetic networks are thermodynamically less stable than graphite and diamond, leading to the expectation that the unnatural allotropes should undergo facile conversion into the natural allotropes. The ongoing fullerene research clearly shows that, in view of the very high activation barriers required to break stable C–C bonds, such expectations are not justified. The standard heat of formation for crystalline C_{60} was determined as $\Delta H_f^\circ(c) = 544.99\ kcal\,mol^{-1}$.[186] This corresponds to 9.08 kcal mol^{-1} per C atom which compares with the values of 0.0 kcal mol^{-1} for graphite and 0.4 kcal mol^{-1} per C atom for diamond. Despite this large thermodynamic instability, crystalline C_{60} is kinetically a perfectly stable molecule under ambient conditions. By extrapolation, synthetic all-carbon networks for which no facile mechanisms for interconversion into graphite or diamond exist, should also exhibit high kinetic stability.

In our ongoing program[93] to prepare polymeric network allotropes of carbon, we have chosen target compounds according to the following criteria: 1) The network structures should neither be highly strained nor easily interconverted into graphite or diamond, 2) the new compounds should have the potential to exhibit interesting material properties such as electrical conductivity, and 3) promising synthetic routes should be available. The latter criterion includes the

"finite molecular approximation approach to infinite structures",[187] that is, the synthesis and study of monomers, dimers, and higher oligomers from which the properties of extended networks can eventually be extrapolated.

5.1. The Cyclo[*n*]carbons as Precursors to Carbon Networks

The unprecedented electronic structures of the cyclo[*n*]carbons (Section 3.1) make them fascinating target molecules. In addition, some of these C_n rings are precursors to interesting two-dimensional carbon networks. Thus, the controlled oligotrimerization[149b] of cyclo[18]carbon (**6**) should lead to the macromolecular network **62** (Scheme 27).

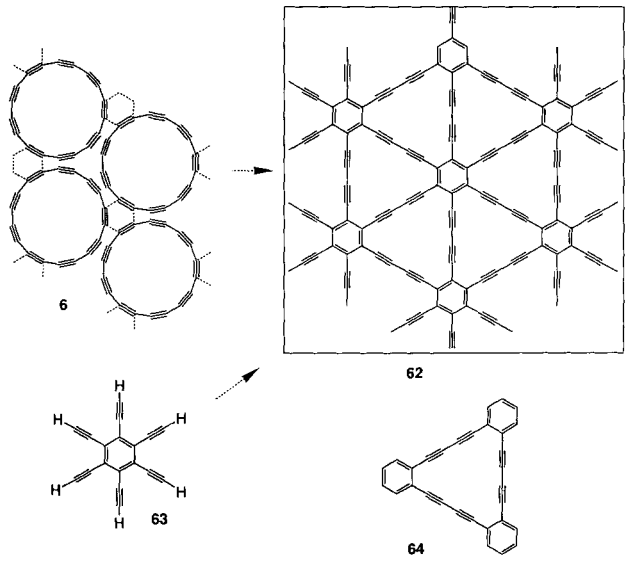

Scheme 27. Synthetic approaches to the planar carbon network **62**. Macrocycle **64** is a model compound for the substructure of **62** and has not yet been synthesized.

Another potential monomeric precursor to **62** is hexaethynylbenzene (**63**), which has been synthesized by Vollhardt et al.[188] The model compound **64** for another substructure in the network remains elusive since Eglinton–Glaser coupling of *o*-diethynylbenzene only leads to a dimer, not a trimer.[136, 189]

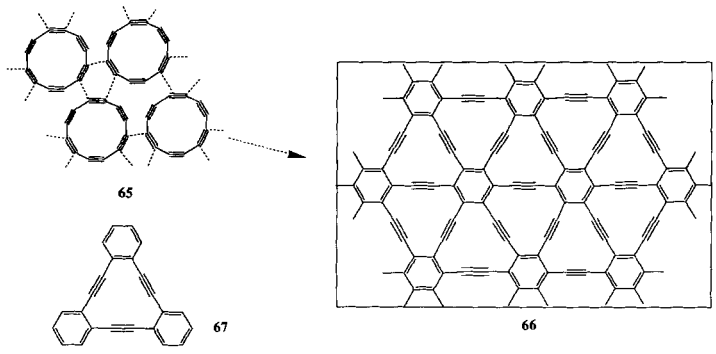

Scheme 28. From cyclo[12]carbon (**65**) to graphyne (**66**). Macrocycle **67** is a known model compound for the substructure of **66**.

The highly strained and presumably highly reactive cyclo[12]carbon (**65**) is a potential monomeric precursor which could undergo a controlled trimerization to yield the 2-D network **66** known as "graphyne" in the literature.[6] The formation energy calculated for **66** in the solid state, 12.4 kcal mol^{-1} per C atom, is quite low. Graphyne has been predicted to be a semiconductor with a large bandgap and to show interesting nonlinear optical properties including large third-order susceptibility.[6] A known stable model for a substructure of **66** is the stable tribenzohexadehydro[12]annulene **67**.[190]

5.2. Two- and Three-Dimensional Carbon Networks Derived from Acyclic Acetylenic Precursors

Two fascinating planar carbon networks, **69** and **70**, characterized by the absence of significant strain in individual angles and bonds may be derived potentially from the monomer "tetraethynylethene" (3,4-diethynyl-3-hexene-1,5-diyne) **68** (Scheme 29). This cross-conjugated molecule was

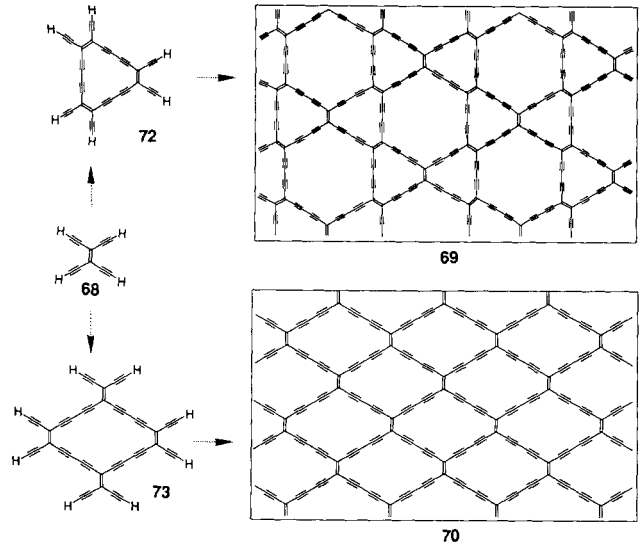

Scheme 29. Planar networks derived from tetraethynylethene **68**.

elusive for many years[191] until its synthesis was accomplished in 1991 (Scheme 30).[192] Its simple IR spectrum is characterized by four major bands which were assigned to the C–H stretch (3307 cm^{-1}), the C≡C stretch (2102 cm^{-1}) and the two coupled C–H deformations (symmetric and antisymmetric, 653 and 632 cm^{-1}, respectively). Recent ab ini-

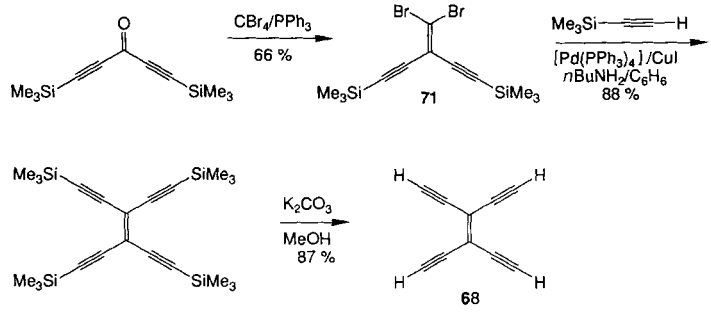

Scheme 30. Synthesis of tetraethynylethene **68**.

tio calculations support this assignment.[193] Rather than attempting to produce solid material with high crystallinity by oxidative coupling of tetraethynylethene, we are currently pursuing synthetic routes via the cyclic hexaethynyl and octaethynyl monomers **72** and **73**, both worthwhile target molecules in their own right.

Another interesting network structure, **74**, is derived from the [3]radialene **75** (Scheme 31), which in turn would be prepared from dibromide **71** following the radialene synthesis starting from 1,1-dibromoolefins described by Iyoda et al.[194]

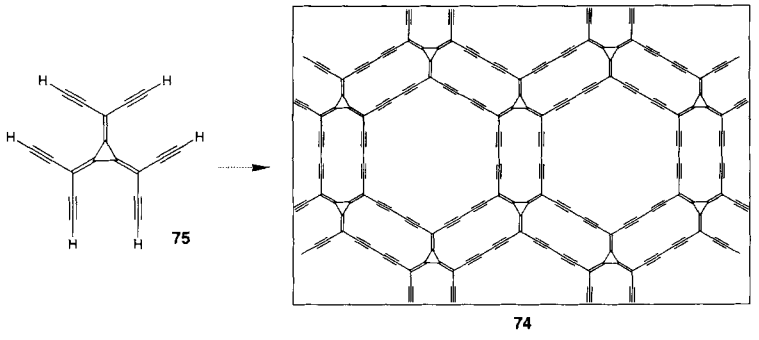

Scheme 31. Planar networks derived from radialene **75**.

The networks **69**, **70**, and **74** represent structures that are under investigation in our laboratory. Undoubtedly, the readers of this article can imagine many more polymeric all-carbon structures that would present true synthetic challenges and may give rise to materials with unusual properties. Among the possible three-dimensional lattices,[6, 7, 12, 42, 43] the "superdiamond" structure **76** is of particular interest since, with its lack of extended acetylenic π conjugation, it can be expected to be quite stable. Several attempts to prepare the monomeric precursor "tetraethynylmethane" **77** (Scheme 32) have not been successful.[44, 195] A

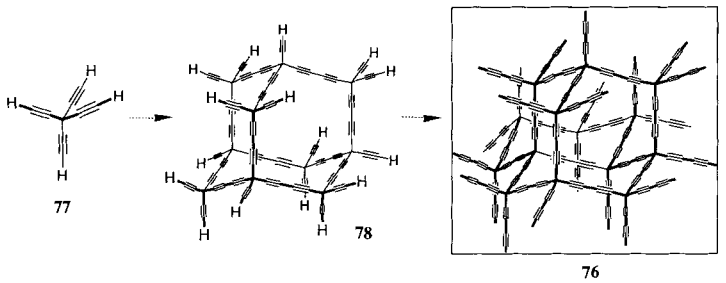

Scheme 32. From tetraethynylmethane **77** to a "superdiamond" network **76**.

number of polyethynyl building blocks are currently being developed as monomers for all-carbon networks or for rigid polymers with a high C:H ratio.[196, 197] The expanded hexadecaethynyladamantane **78** en route to **76** is another interesting target molecule.

Finally, the carbon frame of allene is the monomeric subunit in yet another three-dimensional lattice (Scheme 33). The network **79** was recently proposed by Elguero et al.[198] and is closely related to the structure introduced earlier by

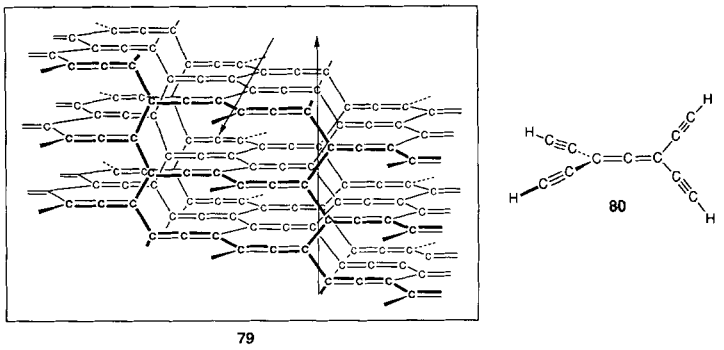

Scheme 33. A three-dimensional allenic carbon network **79**. Arrows indicate the directions of the orthogonal chains of sp^2-hybridized carbon atoms in the lattice [198]. A network similar to **79** can be constructed from tetraethynylallene **80**, yet unknown.

Hoffmann (Scheme 3c). In both systems, orthogonal chains of sp^2 carbon atoms extend across the network; in the earlier structure, these chains are directly interconnected, whereas in **79** they are separated by allenic sp-hybridized carbon atoms. A network related to **79** but derived from the elusive tetraethynylallene **80**[44a] has become of interest to us. The oxidative coupling of monomer **80** could lead to a structure similar to **79** but with butadiyne segments ($-C\equiv C-C\equiv C-$) instead of single bonds between the sp^2 carbon atoms in the orthogonal chains.

6. Toward a Total Synthesis of C_{60}

The greatest preparative challenge in organic chemistry today is the "classical" total synthesis of C_{60}! Since 1981, Chapman and his group at UCLA have explored a variety of synthetic routes to buckminsterfullerene.[46] Among them was the attempted preparation of the soccerball from two halves, each containing 30 of the 60 carbon atoms required (Schemes 34 and 35).[46c] In this approach, the triketone **82** could yield a spherical structure with 60 carbon atoms cor-

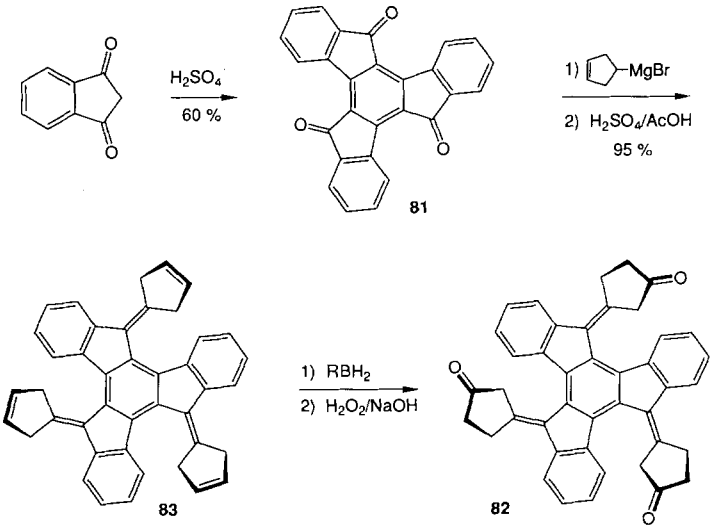

Scheme 34. Synthesis of the triketone **82**, a possible precursor in the [30C + 30C] route to C_{60} [46c, 199]. R = 1,1,2-trimethylpropyl (thexyl). The conversion of **83** to **82** proceeds in low yield.

rectly positioned for closure to C_{60} through a threefold McMurry coupling reaction (Scheme 34). Compound **82**[199] containing six of the twelve five-membered rings in C_{60} was synthesized from 1,3-indanedione in only a few steps via the novel hydrocarbon **83**, a severely distorted nonplanar[200] molecule according to X-ray crystallographic results.[46c]

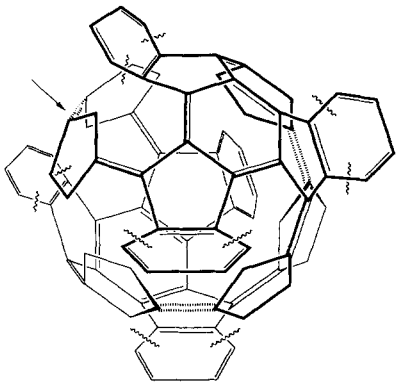

Scheme 35. Assembly of a spherical precursor of C_{60} by threefold McMurry coupling of two molecules of triketone **82**[46c,199]. The arrow indicates the site of the McMurry coupling.

The synthetic route to C_{60} depicted in Schemes 34 and 35 is based on a geometrical [30C + 30C] partition of the carbon sphere. Buckminsterfullerene could also be constructed according to a geometrical [15C + 45C] partition. For such a synthetic approach, compound **84** was prepared as precursor to the C_{45} fragment **85**, which was also obtained in small yield in the condensation reaction (Scheme 36).[201]

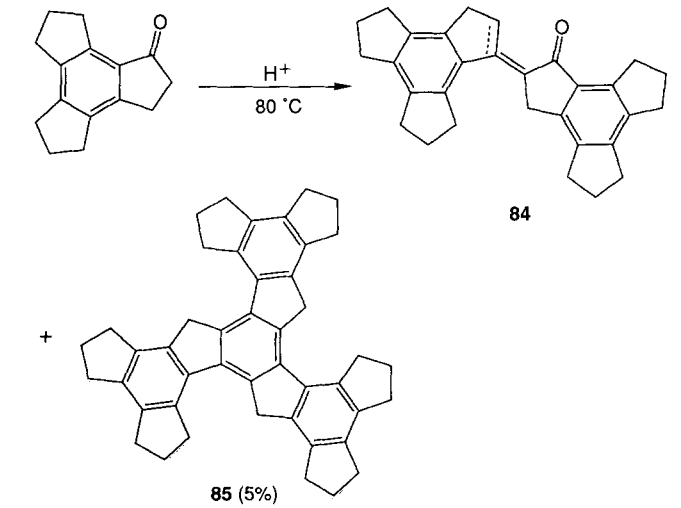

Scheme 36. Synthesis of ketone **84**, a precursor of the C_{45} fragment **85** in a [45C + 15C] approach to C_{60}[201]. The isomer of **84** with an exocyclic double bond is formed in 15% yield, that with an endocyclic double bond (double bond shown as a broken line) in 24% yield.

Are there more facile synthetic approaches to the fullerene framework? The chemistry of the cage hydrocarbons[202] reveals that the hypersurface for rearrangements of $C_{10}H_{10}$ has a minimum for adamantane and the hypersurface for rearrangements of $C_{20}H_{20}$ for dodecahedrane.[203, 204] Could the hypersurface for similar rearrangements of C_{60}, starting from functionalized or hydrogenated spherical or curved molecules with 60 carbon atoms, have a minimum for the soccerball structure of buckminsterfullerene? The removal of functional groups or hydrogen atoms at the end of such a synthesis should not be problematic. Many of the C_{60} derivatives prepared so far lose their functional groups under mild thermolysis conditions to regenerate the intact fullerene.[18i, 131, 205, 206] Therefore, the main question open is to what extent a molecule with 60 carbon atoms must resemble a soccerball to be able to undergo rearrangement into buckminsterfullerene. This question seems intimately connected to the mechanism for the exclusive formation of C_{60} by the Krätschmer–Huffman method in which the C atoms are arranged in the shape of a truncated icosahedron.[36c]

In FT mass spectrometric studies of the cyclocarbons C_{18}, C_{24}, and C_{30}, unexpected and fascinating ion–molecule reactions were observed leading from the all-carbon rings to fullerene ions.[69, 207] Cyclo[30]carbon, generated from the carbon oxide **33**, forms almost exclusively C_{60}: the observed typical fragmentation pattern showing successive losses of C_2 identifies the new ion as a fullerene. The smaller ring C_{24}, obtained from the oxide **32**, undergoes dimerization to C_{48}, followed by trimerization to C_{72} which, upon loss of one C_2 unit, generates almost exclusively fullerene C_{70} and no C_{60}.[207] Although caution is advised in deriving conclusions for syntheses on a preparative scale, the results of these ongoing gas-phase studies suggest that buckminsterfullerene could eventually be prepared by trimerization of suitable molecules with 20 carbon atoms followed by rearrangement and, if necessary, loss of residual functional groups.

Perhaps the best molecule for testing this hypothesis is corannulene (**86**, $C_{20}H_{10}$),[208, 46a] another key substructure of C_{60} in addition to pyracylene (**57**).[209] The connection of three corannulenes to a [0.0.0]corannulenophane would generate a spherical $C_{60}H_{24}$ molecule which could be rearranged and dehydrogenated to produce buckminsterfullerene. Until

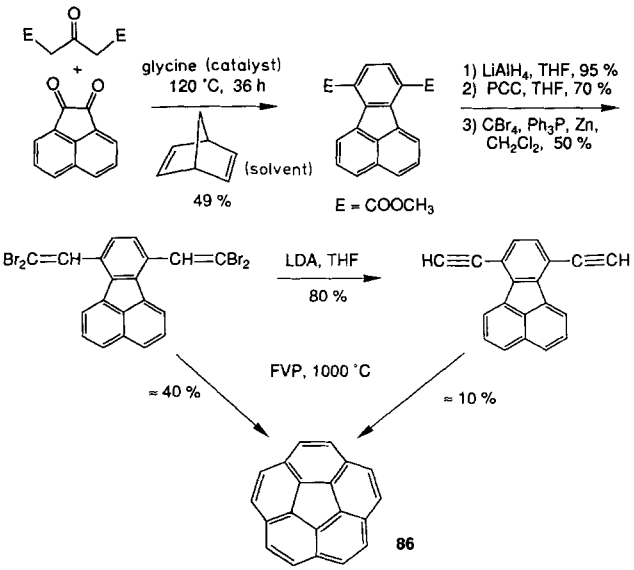

Scheme 37. Corannulene synthesis by Scott et al. [46a, 208b]. PCC = pyridinium chlorochromate, LDA = lithium diisopropylamide. FVP = flash vacuum pyrolysis.

recently, the bowl-shaped corannulene was only available through the remarkable 17-step synthesis (0.40% overall yield) developed in 1966 by Barth and Lawton.[208a] The short and high-yielding new syntheses of corannulene (Schemes 37 and 38), recently developed by Scott et al.[208b] and Siegel et al.,[208c] now open the possibility of testing its potential as a precursor to C_{60}.

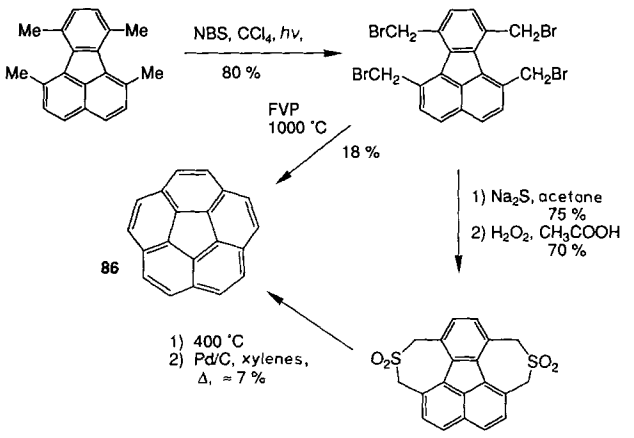

Scheme 38. Corannulene synthesis by Siegel et al. [208c]. NBS = *N*-bromosuccinimide.

7. Preparation of Fullerenes: Resistive versus Arc-Heating of Graphite

Since the discovery made by Krätschmer and Huffman,[13] the methods to prepare and purify fullerenes have been further developed and improved in many research groups. The most popular preparations of C_{60} and the higher fullerenes today are the original resistive heating[13, 210] and the arc-heating of graphite under inert atmosphere.[17a, 205a] A convenient benchtop reactor has been developed for the resistive heating process.[211] In other experiments, macroscopic quantities of the fullerenes have been prepared in oxidizing benzene flames,[212] and recently, by evaporation of graphite or amorphous carbon in a high-frequency oven.[213]

A great variety of chromatographic techniques have been applied to the separation of fullerenes. Good separations of C_{60} and C_{70} are obtained by gravity chromatography on neutral alumina with toluene/hexane solvent mixtures.[214] When this chromatography is done in a Soxhlet apparatus, the solvent quantities needed are reduced and the solvent can be efficiently recycled.[215] Separations of the higher fullerenes have been particularly successful by high-performance liquid chromatography (HPLC) on C18 reversed-phase columns with a diversity of eluents, for example toluene/acetonitrile, toluene/methanol or pure CS_2.[23, 24, 25b, 26] The two most abundant fullerenes, C_{60} and C_{70}, have also been separated on Pirkle columns with hexane as the mobile phase.[216a, b] Successful separations of these two fullerenes have also reported with graphite as the chromatographic support.[216c]

The application of most of the above methods to large-scale separations (> 500 mg) is limited by the low solubility of the fullerenes in the solvent mixtures chosen as eluents. For the separation of larger fullerene quantities, gel permeation chromatography with pure toluene as the mobile phase seems particularly effective.[217] Nonchromatographic methods[218] could provide valuable alternatives for fullerene separations. The preparation and X-ray crystallographic characterization of a 3:1 clathrate between hydroquinone and C_{60} by Ermer suggests the exploration of size-selective clathrate formation as an economic method for bulk separations of fullerenes.[219]

It was quite unexpected to find that the two most common methods for fullerene production, the resistive and arc-heating of graphite, lead to distinctively different product distributions. The soot produced at UCLA by the resistive heating of graphite contains C_{60} ($\approx$65%) and C_{70} ($\approx$30%) as the most prominent components together with approximately 5% of higher fullerenes.[18d] Among the higher fullerenes, chiral D_2-C_{76} is the most abundant[23] followed by the C_{78} and the C_{84} fractions. The C_{78} fraction contains the two isomers C_{2v}-C_{78} and D_3-C_{78} which were separated and isolated in pure form.[24] Very minor fractions that could be isolated comprise the higher fullerenes C_{90} and C_{94}.[25a] A more recent analysis of the fractions of the larger fullerene also indicates formation of C_{96} in quantities similar to those of C_{90} and C_{94}.[220] Fractions of C_{82}, which prefers forming endohedral complexes (Section 4.2.2), and C_{74} are so small that these fullerenes could not be isolated; the formation of minuscule amounts of these carbon spheres is only evident from mass spectrometric studies.[220]

Very different results were obtained by the group of Achiba et al. who produced soot by arc-heating of graphite.[26] These researchers isolated a significant amount of C_{82} and showed by ^{13}C NMR spectroscopy that among several isomers a C_2-C_{82} isomer with 41 independent resonances is the most abundant.[221, 222a] Besides the two isomers of C_{78} found by the UCLA group, Achiba et al. isolated an additional third. This isomer also has C_{2v} symmetry and is the most abundant one in the product mixture.[222b] Interestingly, although the UCLA group did not find this isomer, they predicted it by MM3 calculations to be the most stable one.[24] As an additional difference in the product distribution, arc-heating of graphite seems to produce significantly larger quantities of C_{90} and C_{96}. Also, fullerenes C_{76}, C_{78}, and C_{84} are obtained in similar yield.[26b] Both methods lead to the same C_{84} fraction containing as isolable isomers a D_2- (21 resonances in its ^{13}C NMR spectrum) and a D_{2d}-symmetrical isomer (11 resonances in its ^{13}C NMR spectrum).[222, 223]

All higher fullerenes isolated and characterized by Diederich et al. and Achiba et al. obey the "isolated pentagon" rule,[22, 184, 224] that is, all twelve pentagons are fully annelated by hexagons, yielding corannulene substructures. Therefore, this rule provides a rigorous guidance for identifying stable fullerene structures. The major difference in the product distribution obtained by the resistive and arc-heating methods awaits explanation. It clearly suggests that other processes for fullerene preparation could well lead to other product distributions with higher yields of the very large fullerenes with more than 100 carbon atoms, which so far have been isolated only as mixtures.[25a, c] The origin of the observed product distributions is obviously closely related to

the mechanisms of fullerene formation by resistive or arc-heating of graphite. The elucidation of these mechanisms[11, 17a, 18a, 24, 25a, 184g–i, 225] is one of the most ambitious as well as rewarding intellectual and experimental challenges in fullerene chemistry as well as in carbon chemistry in general.

8. Conclusions

With the spectacular discovery of a method for the bulk preparation of fullerenes by Krätschmer and Huffman, the chemistry and physics of carbon allotropes, which had been pursued in laboratories worldwide since the 1940s, has moved into the center of scientific interest. Efforts to prepare molecular and polymeric carbon allotropes such as the cyclocarbons and the networks discussed in this review are now rapidly expanding in many organic laboratories. As a result, macroscopic quantities of other fascinating synthetic all-carbon structures should soon become available. From this research, major fundamental and technological advances can be expected in the coming years. This optimism is based on the explosive growth of exciting discoveries since the end of 1990 when bulk quantities of the fullerenes became available. Since then, unprecedented structures of carbon-based matter have been explored, extending from the highly symmetrical C_{60} with the shape of a truncated icosahedron[13] to the chiral, doubly helical fullerene C_{76},[23] tubular carbon fibers,[226, 227] and three-dimensional carbon networks displaying the negative curvature of a saddle, instead of the positive curvature of the fullerenes.[228] The synthesis and study of alkali metal doped fullerene superconductors,[18e, 229–231] the preparation of a fulleride-based organic ferromagnet,[232] and the conversion of fullerenes into diamond[233] are only the tip of the iceberg in discoveries with high technological potential.

Several conclusions can be drawn from the ongoing research on fullerenes and other all-carbon molecules and networks. The successful exploration of the chemistry, physics, and materials properties of these compounds requires a highly interdisciplinary approach. Therefore, research in this area contributes to breaking down the artificial barriers of communication between faculty and students in departments and between departments. This way, synthetic chemists may discover techniques familiar to their colleagues in physics, physical chemistry, or material sciences, and test them as new methods to prepare new molecules. Examples for such cross-fertilization are the laser flash heating used for the generation of cyclo[18]carbon by means of the retro-Diels–Alder reaction, and the Krätschmer–Huffman process for fullerene production. The discovery of the latter suggests that other unconventional preparative techniques may be found in interdisciplinary collaborations, and entire classes of new compounds might become accessible by crossing the boundaries of classical synthesis. The ongoing work on synthetic carbon allotropes also sends a strong message to chemists interested in organic synthesis. Organic synthesis and the development of synthetic methodology are alive and well in organic materials sciences. Challenges in this future-oriented field easily rival those in the more established direction of natural product synthesis. Therefore, it is hoped that, in view of the great technological potential of new carbon allotropes, more synthetically oriented chemists will decide to pursue careers in this worthwhile direction.

This work would not have been possible without the generous support of the National Science Foundation and the Office of Naval Research. Additional funding was provided by the Petroleum Research Fund administered by the American Chemical Society, and by NATO and the Grand-Duchy of Luxemburg. Another important factor for the development of this research was the stimulating environment provided by the students and faculty in the Department of Chemistry and Biochemistry at UCLA. We are particularly grateful to Professors Orville Chapman, Ken Houk, and Robert L. Whetten for their continuing interest in this work. We warmly thank Drs. Roland Ettl and Carlo Thilgen, and John Anthony, Armen Boldi, Nancy Goroff, and Sophia Lin for their contributions to the science described in this article. Special thanks go to Dr. Carolyn B. Knobler for providing us with important structural information by solving the X-ray crystal structures of key molecules.

Received: March 13, 1992 [A 877 IE]
German version: *Angew. Chem.* **1992**, *104*, 1123

[1] a) R. E. Kirk, D. F. Othmer, M. Grayson, D. Eckroth, *Kirk-Othmer Encycl. Chem. Technol. 3rd ed. 1978–1984, Vol. 4*, Wiley, New York, **1978**, pp. 556–709; b) B. T. Kelly, *Physics of Graphite*, Applied Science Publishers, New Jersey, **1981**; c) *The Properties of Diamond* (Ed.: J. E. Fields), Academic Press, London, **1979**.

[2] a) *Carbon Fibers and Their Composites* (Ed.: E. Fitzer), Springer, Berlin, **1985**; b) M. C. Reisch, *Chem. Eng. News* **1987**, *65*(5), 9; c) A. M. Thayer, *ibid.* **1990**, *68*(30), 37; d) E. Fitzer, *Carbon* **1989**, *27*, 621; e) J. B. Donnet, R. C. Bansal, *Carbon Fibers*, Dekker, New York, **1984**; f) J. Delmonte, *Technology of Carbon and Graphite Fibre Composites*, Van Nostrand-Reinhold, Princeton, **1981**.

[3] a) P. K. Bachmann, R. Messier, *Chem. Eng. News*, **1989**, *67*(20), 24; b) M. Simpson, *New Sci.* **1988**, *117* (March 10), 50.

[4] Because of advances in diamond-film technology, the magazine *Science* chose diamond in 1990 as the molecule of the year; C_{60} was the runner up; R. L. Guyer, D. E. Koshland, Jr., *Science (Washington D.C.)* **1990**, *250*, 1640. Buckminsterfullerene was finally named molecule of the year by *Science* in 1991 (E. Culotta, D. E. Koshland, Jr., *Science (Washington D.C.)* **1991**, *254*, 1706); this title had already been conferred to C_{60} (and C_{70}) in 1990 by *Angewandte Chemie* (*Angew. Chem.* **1991**, *103*, A-5; *Angew. Chem. Int. Ed. Engl.* **1991**, *30*, A-7).

[5] I. V. Stankevich, M. V. Nikerov, D. A. Bochvar, *Russ. Chem. Rev. (Engl. Transl.)* **1984**, *53*, 640.

[6] R. H. Baughman, H. Eckhardt, M. Kertesz, *J. Chem. Phys.* **1987**, *87*, 6687.

[7] K. M. Merz, Jr., R. Hoffmann, A. T. Balaban, *J. Am. Chem. Soc.* **1987**, *109*, 6742.

[8] H. L. Riley, *J. Chim. Phys. Phys. Chim. Biol.* **1950**, *47*, 565.

[9] a) P. Gerhardt, S. Löffler, K. H. Homann, *Chem. Phys. Lett.* **1987**, *137*, 306; b) H. W. Kroto, *J. Chem. Soc. Faraday Trans.* **1991**, *87*, 2871.

[10] A. E. Douglas, *Nature (London)* **1977**, *269*, 130.

[11] H. W. Kroto, A. W. Allaf, S. P. Balm, *Chem. Rev.* **1991**, *91*, 1213.

[12] A. T. Balaban, *Comput. Math. Applic.* **1989**, *17*, 397.

[13] W. Krätschmer, L. D. Lamb, K. Fostiropoulos, D. R. Huffman, *Nature (London)* **1990**, *347*, 354.

[14] H. W. Kroto, J. R. Heath, S. C. O'Brien, R. F. Curl, R. E. Smalley, *Nature (London)* **1985**, *318*, 162.

[15] a) D. E. H. Jones, *New Sci.* **1966**, *32*, 245; b) E. Osawa, *Kagaku (Kyoto)* **1970**, *25*, 854; c) Z. Yoshida, E. Osawa, *Aromatikkusu* **1971**, p. 174; d) D. A. Bochvar, E. G. Gal'pern, *Dokl. Akad. Nauk SSSR* **1973**, *209*, 610; e) R. A. Davidson, *Theor. Chim. Acta* **1981**, *58*, 193.

[16] a) R. F. Curl, R. E. Smalley, *Science (Washington D.C.)* **1988**, *242*, 1017; b) H. Kroto, *ibid.* **1988**, *242*, 1139.

[17] a) R. F. Curl, R. E. Smalley, *Sci. Am.*, **1991**, *265* (10) 54; b) R. E. Smalley, *Sciences (N. Y.)* **1991**, *31* (March/April), 22; c) J. S. Miller, *Adv. Mater.* **1991**, *3*, 262; d) J. F. Stoddart, *Angew. Chem.* **1991**, *103*, 71; *Angew. Chem. Int. Ed. Engl.* **1991**, *30*, 70; e) F. Diederich, R. L. Whetten, *ibid.* **1991**, *103*,

695 and **1991**, *30*, 678; f) H. Schwarz, *ibid.* **1992**, *104*, 301 and **1992**, *31*, 293; g) H. W. Kroto, *ibid.* **1992**, *104*, 113 and **1992**, *31*, 111.

[18] The March 1992 issue of *Accounts of Chemical Research* reports exclusively on fullerene chemistry: a) R. E. Smalley, *Acc. Chem. Res.* **1992**, *25*, 98; b) J. P. Hare, H. W. Kroto, *ibid.* **1992**, *25*, 106; c) J. E. Fischer, P. A. Heiney, A. B. Smith, III, *ibid.* **1992**, *25*, 112; d) F. Diederich, R. L. Whetten, *ibid.* **1992**, *25*, 119; e) R. C. Haddon, *ibid.* **1992**, *25*, 127; f) P. J. Fagan, J. C. Calabrese, B. S. Malone, *ibid.* **1992**, *25*, 134; g) J. H. Weaver, *ibid.* **1992**, *25*, 143; h) J. M. Hawkins, *ibid.* **1992**, *25*, 150; i) F. Wudl, *ibid.* **1992**, *25*, 157; j) S. W. McElvany, M. M. Ross, J. H. Callahan, *ibid.* **1992**, *25*, 162; k) R. D. Johnson, D. S. Bethune, C.S. Yannoni, *ibid.* **1992**, *25*, 169.

[19] a) D. E. Weeks, W. G. Harter, *J. Chem. Phys.* **1989**, *90*, 4744; b) R. E. Stanton, M. D. Newton, *J. Phys. Chem.* **1988**, *92*, 2141; c) S. J. Cyvin, E. Brendsdal, B. N. Cyvin, J. Brunvoll, *Chem. Phys. Lett.* **1988**, *143*, 377; d) Z. C. Wu, D. A. Jelski, T. F. George, *ibid.* **1987**, *137*, 291.

[20] W. Krätschmer, K. Fostiropoulos, D. R. Huffman, *Chem. Phys. Lett.* **1990**, *170*, 167.

[21] E. A. Rohlfing, D. M. Cox, A. Kaldor, *J. Chem. Phys.* **1984**, *81*, 3322.

[22] R. E. Smalley, cited in: R. M. Baum, *Chem. Eng. News* **1985**, *63*(51), 20.

[23] a) R. Ettl, I. Chao, F. Diederich, R. L. Whetten, *Nature (London)* **1991**, *353*, 149; b) Q. Li, F. Wudl, C. Thilgen, R. L. Whetten, F. Diederich, *J. Am. Chem. Soc.* **1992**, *114*, 3994.

[24] F. Diederich, R. L. Whetten, C. Thilgen, R. Ettl, I. Chao, M. M. Alvarez, *Science (Washington, D.C.)* **1991**, *254*, 1768.

[25] a) F. Diederich, R. Ettl, Y. Rubin, R. L. Whetten, R. Beck, M. Alvarez, S. Anz, D. Sensharma, F. Wudl, K. C. Khemani, A. Koch, *Science (Washington D.C.)* **1991**, *252*, 548; b) J. C. Fetzer, E. J. Gallegos, *J. Polycycl. Arom. Comp.*, **1992**, *2*, 245; c) D. H. Parker, P. Wurz, K. Chatterjee, K. R. Lykke, J. E. Hunt, M. J. Pellin, J. C. Hemminger, D. M. Gruen, L. M. Stock, *J. Am. Chem. Soc.* **1991**, *113*, 7499; d) D. Ben-Amotz, R. G. Cooks, L. Dejarme, J. C. Gunderson, S. H. Hoke, II, B. Kahr, G. L. Payne, J. M. Wood, *Chem. Phys. Lett.* **1991**, *183*, 149; e) H. Shinohara, H. Sato, Y. Saito, M. Takayama, A. Izuoka, T. Sugarawa, *J. Phys. Chem.* **1991**, *95*, 8449; f) L. D. Lamb, D. R. Huffman, R. K. Workman, S. Howells, T. Chen, D. Sarid, R. F. Ziolo, *Science (Washington, D.C.)* **1992**, *255*, 1413; g) B. L. Zhang, C. Z. Wang, K. M. Ito, *Chem. Phys. Lett.* **1992**, *193*, 225; h) C. Smart, B. Eldridge, W. Reuter, J. A. Zimmerman, W. R. Creasy, N. Rivera, R. S. Ruoff, *Chem. Phys. Lett.* **1992**, *188*, 171.

[26] a) K. Kikuchi, N. Nakahara, M. Honda, S. Suzuki, K. Saito, H. Shiromaru, K. Yamauchi, I. Ikemoto, T. Kuramochi, S. Hino, Y. Achiba, *Chem. Lett.* **1991**, 1607; b) K. Kikuchi, N. Nakahara, T. Wakabayashi, M. Honda, H. Matsumiya, T. Moriwaki, S. Suzuki, H. Shiromaru, K. Saito, K. Yamauchi, I. Ikemoto, Y. Achiba, *Chem. Phys. Lett.* **1992**, *188*, 177.

[27] O. Hahn, F. Strassmann, J. Mattauch, H. Ewald, *Naturwissenschaften* **1942**, *36*, 541. We thank Professor R. E. Smalley (Rice University) for bringing this and other early references to our attention through his electronic mail fullerene bibliography.

[28] a) E. Dörnenburg, H. Hintenberger, *Z. Naturforsch. A* **1959**, *14*, 765; b) H. B. Palmer, M. Shelef, in *Physics and Chemistry of Carbon, Vol. 4* (Ed.: J. R. Walker, Jr.), Marcel Deckker, New York, **1967**, S. 85-135.

[29] W. Weltner, Jr., R. J. Van Zee, *Chem. Rev.* **1989**, *89*, 1713.

[30] a) Q. L. Zhang, S. C. O'Brien, J. R. Heath, Y. Liu, R. F. Curl, H. W. Kroto, R. E. Smalley, *J. Phys. Chem.* **1986**, *90*, 525; b) S. H. Yang, C. L. Pettiette, J. Conceicao, O. Cheshnovsky, R. E. Smalley, *Chem. Phys. Lett.* **1987**, *139*, 233; c) J. R. Heath, Q. Zhang, S. C. O'Brien, R. F. Curl, H. W. Kroto, R. E. Smalley, *J. Am. Chem. Soc.* **1987**, *109*, 359; d) S. C. O'Brien, J. R. Heath, R. F. Curl, R. E. Smalley, *J. Chem. Phys.* **1988**, *88*, 220.

[31] a) L. A. Bloomfield, M. E. Geusic, R. R. Freeman, W. L. Brown, *Chem. Phys. Lett.* **1985**, *121*, 33; b) M. E. Geusic, M. F. Jarrold, T. J. McIlrath, R. R. Freeman, W. L. Brown, *J. Chem. Phys.* **1987**, *86*, 3862.

[32] J. Bernholc, J. C. Phillips, *J. Chem. Phys.* **1986**, *85*, 3258.

[33] D. C. Parent, S. W. McElvany, *J. Am. Chem. Soc.* **1989**, *111*, 2393.

[34] H. Y. So, C. L. Wilkins, *J. Phys. Chem.* **1989**, *93*, 1184.

[35] a) J. R. Heath, R. A. Sheeks, A. L. Cooksy, R. J. Saykally, *Science (Washington, D. C.)* **1990**, *249*, 895; b) C. A. Schmuttenmaer, R. C. Cohen, N. Pugliano, J. R. Heath, A. L. Cooksy, K. L. Busarow, R. J. Saykally, *ibid.* **1990**, *249*, 897.

[36] a) W. L. Brown, R. R. Freeman, K. Raghavachari, M. Schlüter, *Science (Washington, D.C.)* **1987**, *235*, 860; b) J. M. L. Martin, J. P. François, R. Gijbels, J. Almlöf, *Chem. Phys. Lett.* **1991**, *187*, 367; c) K. Raghavachari, C. M. Rohlfing, *J. Phys. Chem.* **1992**, *96*, 2463.

[37] a) E. Dörnenburg, H. Hintenberger, J. Franzen, *Z. Naturforsch. A* **1961**, *16*, 532; b) K. S. Pitzer, E. Clementi, *J. Am. Chem. Soc.* **1959**, *81*, 4477; c) N. Fürstenau, F. Hillenkamp, *Int. J. Mass Spectrom. Ion Processes* **1981**, *37*, 135.

[38] R. Hoffmann, *Tetrahedron* **1966**, *22*, 521.

[39] S. Yang, K. J. Taylor, M. J. Craycraft, J. Conceicao, C. L. Pettiette, O. Cheshnovsky, R. E. Smalley, *Chem. Phys. Lett.* **1988**, *144*, 431.

[40] G. von Helden, M.-T. Hsu, P. R. Kemper, M. T. Bowers, *J. Chem. Phys.* **1991**, *95*, 3835.

[41] J. Gibson, M. Holohan. H. L. Riley, *J. Chem. Soc.* **1946**, 456.

[42] A. T. Balaban, C. C. Rentia, E. Ciupitu, *Rev. Roum. Chim.* **1968**, *13*, 231.

[43] a) R. Hoffmann, T. Hughbanks, M. Kertész, P. H. Bird, *J. Am. Chem. Soc.* **1983**, *105*, 4831; b) R. L. Johnston, R. Hoffmann, *ibid.* **1989**, *111*, 810.

[44] a) A. H. Alberts, H. Wynberg, *J. Chem. Soc. Chem. Commun.* **1988**, 748; b) A. H. Alberts in *Integration of Fundamental Polymer Science and Technology – 4* (Eds.: P. J. Lemstra, L. A. Kleintjens), Elsevier Applied Science, London, **1990**, pp. 396–401; c) For another carbon network see H. R. Karfunkel, T. Dressler, *J. Am. Chem. Soc.* **1992**, *114*, 2285.

[45] For a humorous and creative look at carbon allotropes, see: H. Hopf, H. Musso, *Nachr. Chem. Tech. Lab.* **1984**, *32*, 379 (April issue!).

[46] UCLA Ph.D. theses: a) R. H. Jacobson, *"Searching for the Soccer Ball: an Unsuccessful Synthesis of Corannulene"*, **1986**; b) Y. Xiong, *"Part B. Syntheses of [1.1.1]paracyclophane and Other Strained Aromatic Compounds, in Search for the Soccer Ball C_{60}"*, **1987**; c) D. Loguercio, Jr., *"Studies Toward a Convergent Synthesis of C_{60}"*, **1988**; d) D. Shen, *"Approaches to Soccerene (I_h-C_{60}) and Other Carbon Spheres"*, **1990**.

[47] F. Diederich, Y. Rubin, C. B. Knobler, R. L. Whetten, K. E. Schriver, K. N. Houk, Y. Li, *Science (Washington, D.C.)* **1989**, *245*, 1088.

[48] a) A. M. Sladkov, Y. P. Kudryavtsev, *Usp. Khim.* **1963**, *32*, 509; b) A. M. Sladkov, Y. I. Mikulin, *ibid* **1982**, *51*, 736; c) V. M. Mel'nichenko, A. M. Sladkov, Y. N. Nikulin, *Russ. Chem. Rev.* **1982**, *51*, 421; d) A. G. Whittaker, *Nature (London)* **1978**, *276*, 695; e) A. G. Whittaker, *Science (Washington, D.C.)* **1978**, *200*, 763.

[49] First attempts to prepare extended polyynes and carbyne-type material were reported by A. von Baeyer, who started his publication "Über Polyacetylenverbindungen" (*Ber. Dtsch. Chem. Ges.* **1885**, *18*, 674) as follows: "Wenn man sich die Aufgabe stellt Verbindungen zu erzeugen, welche Ketten von reinen Kohlenstoffatomen erhalten. . ."; see also: A. Baeyer, *Ber. Dtsch. Chem. Ges.* **1882**, *15*, 50; *ibid.* **1885**, *18*, 2269.

[50] M. J. Rice, A. R. Bishop. D. K. Campbell, *Phys. Rev. Lett.* **1983**, *51*, 2136.

[51] K. Akagi, M. Nishiguchi, H. Shirakawa, Y. Furukawa, I. Harada, *Synth. Met.* **1987**, *17*, 557.

[52] P. P. K. Smith, P. R. Buseck, *Science (Washington, D.C.)* **1982**, *216*, 984.

[53] P. J. Stang, M. Ladika, *J. Am. Chem. Soc.* **1981**, *103*, 6437.

[54] a) R. Eastmond, T. R. Johnson, D. R. M. Walton, *Tetrahedron* **1972**, *28*, 4601; b) R. Eastmond, D. R. M. Walton, *ibid.* **1972**, *28*, 4591; c) T. R. Johnson, D. R. M. Walton, *ibid.* **1972**, *28*, 5221.

[55] U. Niedballa *Methoden Org. Chem. (Houben-Weyl)*, 4th ed. 1952–, Vol 5/2a (Eds.: E. Müller, O. Bayer), **1977**, pp. 913–962.

[56] a) K. Sonogashira in *Comprehensive Organic Synthesis, Vol 3, Carbon-Carbon σ-Bond Formation* (Eds.: B. M. Trost, I. Fleming, G. Pattenden), Pergamon Press, Oxford, **1991**, pp. 551–561; b) G. Märkl, P. Attenberger, J. Kellner, *Tetrahedron Lett.* **1988**, *29*, 3651.

[57] a) W. Chodkievicz, *Ann. Chim. (Paris)* **1957**, *2*, 819; b) F. Bohlmann, P. Herbst, H. Gleinig, *Chem. Ber.* **1961**, *94*, 948; c) J. A. Miller, G. Zweifel, *Synthesis* **1983**, 128.

[58] a) C. Glaser, *Ann. Chem.* **1870**, *154*, 137; b) G. Eglinton, A. R. Galbraith, *Chem. Ind. (London)* **1956**, 737; c) G. Eglinton, W. McCrae, *Adv. Org. Chem.* **1963**, *4*, 225.

[59] A. S. Hay, *J. Org. Chem.* **1962**, *27*, 3320.

[60] Y. Rubin, S. S. Lin, C. B. Knobler, J. Anthony, A. M. Boldi, F. Diederich, *J. Am. Chem. Soc.* **1991**, *113*, 6943.

[61] a) A. H. Schmidt, *Synthesis* **1980**, 961; b) A. H. Schmidt, W. Ried, *ibid.* **1978**, 1; c) H. Knorr, W. Ried, *ibid.* **1978**, 649; d) A. H. Schmidt, W. Ried, *ibid.* **1978**, 869.

[62] a) H. Meier, *Synthesis* **1972**, 235; b) D. H. Wadsworth, B. A. Donatelli, *ibid.* **1981**, 285.

[63] a) N. Obata, T. Takizawa, *Bull. Chem. Soc. Jpn.* **1977**, *50*, 2017; b) D. C. Zecher, R. West, *J. Am. Chem. Soc.* **1967**, *89*, 153; c) R. Hochstrasser, J. Wirz, *Angew. Chem.* **1989**, *101*, 183; *Angew. Chem. Int. Ed. Engl.* **1989**, *28*, 181; d) D. E. Wellman, K. R. Lassila, R. West, *J. Org. Chem.* **1984**, *49*, 965; e) H. Bock, W. Ried, U. Stein, *Chem. Ber.* **1981**, *114*, 673; f) C. Wentrup, R. Blanch, H. Briehl, G. Gross, *J. Am. Chem. Soc.* **1988**, *110*, 1874; g) O. L. Chapman, K. Mattes, C. L. McIntosh, J. Pacansky, G. V. Calder, G. Orr, *ibid.* **1973**, *95*, 6134; h) D. R. Boate, L. C. Johnston, P. C. Kwong, E. Lee-Ruff, J. C. Scaiano, *ibid.* **1990**, *112*, 8858; i) W. Sander, O. L. Chapman, *Angew. Chem.* **1988**, *100*, 402; *Angew. Chem. Int. Ed. Engl.* **1988**, *27*, 398;

[64] a) L. S. Liebeskind, R. W. Fengl, K. R. Wirtz, T. T. Shawe, *J. Org. Chem.* **1988**, *53*, 2482; b) L. S. Liebeskind, J. Zhang, *ibid.* **1991**, *56*, 6379.

[65] a) M. W. Reed, D. J. Pollart, S. T. Perri, L. D. Foland, H. W. Moore, *J. Org. Chem.* **1988**, *53*, 2477; b) S. L. Xu, M. Taing, H. W. Moore, *ibid.* **1991**, *56*, 6104.

[66] a) W. F. Goure, M. E. Wright, P. D. Davis, S. S. Labadie, J. K. Stille, *J. Am. Chem. Soc.* **1984**, *106*, 6417; b) J. K. Stille, *Angew. Chem.* **1986**, *98*, 504; *Angew. Chem. Int. Ed. Engl.* **1986**, *25*, 508; c) M. W. Logue, K. Teng, *J. Org. Chem.* **1982**, *47*, 2549.

[67] M. W. Logue, G. L. Moore, *J. Org. Chem.* **1975**, *40*, 131.

[68] a) Y. Rubin, F. Diederich, *J. Am. Chem. Soc.* **1989**, *111*, 6870; b) Y. Rubin, C. B. Knobler, F. Diederich, *ibid.* **1990**, *112*, 1607.

[69] Y. Rubin, M. Kahr, C. B. Knobler, F. Diederich, C. L. Wilkins, *J. Am. Chem. Soc.* **1991**, *113*, 495.

[70] a) U. E. Wiersum, *Recl. Trav. Chim. Pays-Bas* **1982**, *101*, 317, 365; b) R.

F. C. Brown, *Pyrolytic Methods in Organic Chemistry, Organic Chemistry Monographs, Vol. 41*, Academic Press, New York, **1980**.
[71] a) M. G. Clancy, D. G. Hawkins, M. M. Hesabi, O. Meth-Cohn, S. Rhouati, *J. Chem. Res. Synop.* **1982**, 78; b) M. G. Clancy, M. M. Hesabi, O. Meth-Cohn, *J. Chem. Soc. Perkin Trans. 1*, **1984**, 429.
[72] J. Magrath, F. W. Fowler, *Tetrahedron Lett.* **1988**, *29*, 2171.
[73] a) G. Wegner, *Z. Naturforsch. B* **1969**, *24*, 824; b) G. Wegner, *Chimia*, **1974**, *28*, 475; c) G. Wegner, *Makromol. Chem.* **1972**, *154*, 35; d) G. Wegner, *Makromol. Chem. Suppl.* **1984**, *6*, 347; e) R. Galli, M. Neuenschwander, P. Engel, *Helv. Chim. Acta* **1989**, *72*, 1324; f) A. Bartlome, U. Stämpfli, M. Neuenschwander, *ibid.* **1991**, *74*, 1264; g) M. Neuenschwander, A. Bartlome, *ibid.* **1991**, *74*, 1489.
[74] a) L. Yu, M. Chen, L. R. Dalton, *Chem. Mater.* **1990**, *2*, 649; b) M. Yamaguchi, K. Torisu, K. Hiraki, T. Minami, *Chem. Letters* **1990**, 2221; c) S. Okada, H. Matsuda, A. Masaki, H. Nakanishi, K. Hayamizu, *ibid.* **1990**, 2213, d) A.-D. Schlüter, *Adv. Mater.* **1991**, *3*, 282.
[75] a) Y. V. Korshak, T. V. Medvedeva, A. A. Ovchinnikov, V. N. Spector, *Nature (London)* **1987**, *326*, 370; b) J. H. Zhang, A. J. Epstein, J. S. Miller, C. J. O'Connor, *Mol. Cryst. Liq. Cryst.* **1989**, *176*, 271; c) D. W. Wiley, J. C. Calabrese, J. S. Miller, *ibid.* **1989**, *176*, 277; d) K. Inoue, N. Koga, H. Iwamura, *J. Am. Chem. Soc.* **1991**, *113*, 9803.
[76] a) D. F. Eaton, *Science (Washington, D.C.)* **1991**, *253*, 281; b) A. W. Olsen, Z. H. Kafafi, *J. Am. Chem. Soc.* **1991**, *113*, 7758; c) P. N. Prasad, D. J. Williams, *Introduction to Nonlinear Optical Effects in Molecules and Polymers*, Wiley, New York, **1991**.
[77] a) F. Sondheimer, *Acc. Chem. Res.* **1972**, *5*, 81; b) P. J. Garratt, *Aromaticity*, Wiley, New York, **1986**; c) P. J. Garratt in *Comprehensive Organic Chemistry, Vol. 1* (Eds.: J. F. Stoddart, D. Barton, W. D. Ollis), Pergamon Press, Elmsford, **1979**, pp. 361–410.
[78] a) N. Jux, P. Koch, H. Schmickler, J. Lex, E. Vogel, *Angew. Chem.* **1990**, *102*, 1429; *Angew. Chem. Int. Ed. Engl.* **1990**, *29*, 1385; b) M. Pohl, H. Schmickler, J. Lex, E. Vogel, *ibid.* **1991**, *103*, 1737 and **1991**, *30*, 1693.
[79] a) V. Parasuk, J. Almlöf, M. W. Feyereisen, *J. Am. Chem. Soc.* **1991**, *113*, 1049; b) A cumulenic D_{5h} geometry in the ground state was calculated for monocyclic C_{10}, J. D. Watts, R. J. Bartlett, *Chem. Phys. Lett.* **1992**, *190*, 19.
[80] S. W. Benson, *Thermochemical Kinetics*, Wiley, New York, **1968**.
[81] a) J. Haase, A. Krebs, *Z. Naturforsch. A* **1972**, *27*, 624; b) A. Krebs, H. Kimling, *Liebigs Ann. Chem.* **1974**, 2074.
[82] a) A. Krebs, J. Wilke, *Top. Curr. Chem.* **1983**, *109*, 189; b) H. Meier, *Synthesis* **1972**, 235; c) R. Gleiter, W. Schäfer, *Acc. Chem. Res.* **1990**, *23*, 371; for recent references on strained cycloalkynes, see: d) X. M. Wang, R. J. Wang, T. C. W. Mak, H. N. C. Wong, *J. Am. Chem. Soc.* **1990**, *112*, 7790; e) W. C. Shakespeare, R. P. Johnson, *ibid.* **1990**, *112*, 8578; f) M. J. Plater, C. W. Rees, A. M. Z. Slawin, D. J. Williams, *J. Chem. Soc. Chem. Commun.* **1990**, 1315; g) R. Gleiter, *Angew. Chem.* **1992**, *104*, 29; *Angew. Chem. Int. Ed. Engl.* **1992**, *31*, 27.
[83] For non-annulenic macrocyclic alkynes, see: a) L. T. Scott, M. J. Cooney, D. W. Rogers, K. Dejroongruang, *J. Am. Chem. Soc.* **1988**, *110*, 7244; b) L. T. Scott, M. J. Cooney, D. Johnels, *ibid.* **1990**, *112*, 4054; c) L. T. Scott, M. Unno, *ibid.* **1990**, *112*, 7823; d) A. de Meijere, F. Jaekel, A. Simon, H. Borrmann, J. Köhler, D. Johnels, L. T. Scott, *ibid.* **1991**, *113*, 3935.
[84] W. H. Okamura, F. Sondheimer, *J. Am. Chem. Soc.* **1967**, *89*, 5991.
[85] H. P. Figeys, M. Gelbcke, *Tetrahedron Lett.* **1970**, 5139.
[86] For the preparation of a monoalkynylcyclopropenone, see: E. V. Dehmlov, *J. Organomet. Chem.* **1966**, *6*, 296.
[87] S. W. Tobey, R. West, *J. Am. Chem. Soc.* **1964**, *86*, 4215.
[88] R. Weiss, H. Kölbl, C. Schlierf, *J. Org. Chem.* **1976**, *41*, 2258.
[89] K. Musigman, H. Mayr, A. de Meijere, *Tetrahedron Lett.* **1987**, *28*, 4517.
[90] D. E. Wellman, K. R. Lassila, R. West, *J. Org. Chem.* **1984**, *49*, 965.
[91] C. Eaborn, D. R. M. Walton, *J. Organomet. Chem.* **1964**, *2*, 95.
[92] K. C. Nicolaou, W.-M. Dai, *Angew. Chem.* **1991**, *103*, 1453; *Angew. Chem. Int. Ed. Engl.* **1991**, *30*, 1387.
[93] Y. Rubin, Ph.D. Dissertation **1991**, UCLA.
[94] S. W. Tobey, (Dow Chemical Company, Midland, MI), US-A *Patent* 3 787 500, **1974**.
[95] a) E. J. Corey, P. L. Fuchs, *Tetrahedron Lett.* **1972**, 3769; b) T. Liese, A. de Meijere, *Chem. Ber.* **1986**, *119*, 2995.
[96] a) D. L. Boger, C. E. Brotherton, *J. Am. Chem. Soc.* **1986**, *108*, 6695; b) M. Isaka, S. Matsuzawa, S. Yamago, S. Ejiri, Y. Miyachi, E. Nakamura, *J. Org. Chem.* **1989**, *54*, 4727; c) D. L. Boger, C. E. Brotherton, G. I. Georg, *Org. Synth.* **1987**, *65*, 32.
[97] R. M. McQuilkin, P. J. Garratt, F. Sondheimer, *J. Am. Chem. Soc.* **1970**, *92*, 6682.
[98] Y. Li, Y. Rubin, F. Diederich, K. N. Houk, *J. Am. Chem. Soc.* **1990**, *112*, 1618.
[99] a) U. Burkert, N. L. Allinger, *Molecular Mechanics*, American Chemical Society, Washington, D.C., **1982**; b) N. L. Allinger, *J. Am. Chem. Soc.* **1977**, *99*, 8127; Quantum Chemistry Program Exchange No. 406.
[100] M. J. S. Dewar, E. G. Zoebisch, E. F. Healy, J. J. P. Stewart, *J. Am. Chem. Soc.* **1985**, *107*, 3902.
[101] M. Gosmann, B. Franck, *Angew. Chem.* **1986**, *98*, 1107; *Angew. Chem. Int. Ed. Engl.* **1986**, *25*, 1100.
[102] a) E. Vogel, W. Haas, B. Knipp, J. Lex, H. Schmickler, *Angew. Chem.* **1988**, *100*, 445; *Angew. Chem. Int. Ed. Engl.* **1988**, *27*, 406; b) W. Haas, B. Knipp, M. Sicken, J. Lex, E. Vogel, *ibid.* **1988**, *100*, 448 and **1988**, *27*, 409; c) E. Vogel, M. Sicken, P. Röhrig, H. Schmickler, J. Lex, O. Ermer, *ibid.* **1988**, *100*, 450 and **1988**, *27*, 411.
[103] S. Nakatsuji, S. Akiyama, M. Nakagawa, *Tetrahedron Lett.* **1976**, 2623.
[104] K. Yamamoto, M. Shibutani, S. Kuroda, E. Ejiri, J. Ojima, *Tetrahedron Lett.* **1986**, *27*, 975.
[105] U. E. Meissner, A. Gensler, H. A. Staab, *Tetrahedron Lett.* **1977**, 3.
[106] H. A. Staab, F. Diederich, C. Krieger, D. Schweitzer, *Chem. Ber.* **1983**, *116*, 3504.
[107] For recent theoretical controversy about the superaromaticity in kekulene, see: a) J. Cioslowski, P. B. O'Connor, E. D. Fleischmann, *J. Am. Chem. Soc.* **1991**, *113*, 1086; b) J. Aihara, *ibid.* **1992**, *114*, 865.
[108] a) E. Vogel, *Pure Appl. Chem.* **1982**, *54*, 1015; b) E. Vogel, *Isr. J. Chem.* **1980**, *20*, 215.
[109] a) V. Boekelheide, *Pure Appl. Chem.* **1975**, *44*, 751; b) V. Boekelheide in *Topics in Nonbenzenoid Aromatic Chemistry, Vol. 1* (Eds.: T. Nozoe, R. Breslow, K. Hafner, S. Ito, I. Murata), Wiley, New York, **1973**, pp. 46–79.
[110] a) J. Ojima, E. Ejiri, T. Kato, S. Kuroda, S. Hirooka, M. Shibutani, *Tetrahedron Lett.* **1986**, *27*, 2467; b) J. Ojima, S. Fujita, M. Matsumoto, E. Ejiri, T. Kato, S. Kuroda, Y. Nozawa, H. Tatamitsu, *J. Chem. Soc. Chem. Commun.* **1987**, 534; c) J. Ojima, E. Ejiri, T. Kato, M. Nakamura, S. Kuroda, S. Hirooka, M. Shibutani, *J. Chem. Soc. Perkin Trans. 1* **1987**, 831.
[111] R. C. Haddon, L. T. Scott, *Pure Appl. Chem.* **1986**, *58*, 137.
[112] M. Nakagawa in *Topics in Nonbenzenoid Aromatic Chemistry, Vol. 1* (Eds.: T. Nozoe, R. Breslow, K. Hafner, S. Ito, I. Murata), Wiley, New York, **1973**, pp. 191–219.
[113] G. Knübel, B. Franck, *Angew. Chem.* **1988**, *100*, 1203; *Angew. Chem. Int. Ed. Engl.* **1988**, *27*, 1170.
[114] a) J. L. Sessler, T. Murai, V. Lynch, M. Cyr, *J. Am. Chem. Soc.* **1988**, *110*, 5586; b) A. K. Burrell, J. L. Sessler, M. J. Cyr, E. McGhee, J. A. Ibers, *Angew. Chem.* **1991**, *103*, 83; *Angew. Chem. Int. Ed. Engl.* **1991**, *30*, 91; c) J. L. Sessler, T. Morishima, V. Lynch, *ibid.* **1991**, *103*, 1018 and **1991**, *30*, 977.
[115] a) W. H. Mills, I. G. Nixon, *J. Chem. Soc.* **1930**, 2510; b) A. Stanger, *J. Am. Chem. Soc.* **1991**, *113*, 8277.
[116] a) B. Halton, *Chem. Rev.* **1973**, *73*, 113; b) Y. Apeloig, D. Arad, *J. Am. Chem. Soc.* **1986**, *108*, 3241; c) R. H. Mitchell, P. D. Slowey, T. Kamada, R. V. Williams, P. J. Garratt, *ibid.* **1984**, *106*, 2431.
[117] a) G. M. Pilling, F. Sondheimer, *J. Am. Chem. Soc.* **1971**, *93*, 1970; b) P. J. Beeby, R. T. Weavers, F. Sondheimer, *Angew. Chem.* **1974**, *86*, 163; *Angew. Chem. Int. Ed. Engl.* **1974**, *13*, 138.
[118] P. J. Garratt, K. P. C. Vollhardt, *Angew. Chem.* **1971**, *83*, 111; *Angew. Chem. Int. Ed. Engl.* **1971**, *10*, 125.
[119] E. Vogel, J. Sombroek, *Tetrahedron Lett.* **1974**, 1627.
[120] a) M. F. D. Steinfatt, *Bull. Soc. Chim. Belge* **1985**, *94*, 85, and references cited therein; b) J. Sauer, B. Schröder, R. Wiemer, *Chem. Ber.* **1967**, *100*, 306; c) J. Sauer, B. Schröder, A. Mielert, *ibid.* **1967**, *100*, 315; d) P. R. Hammond, *Science (Washington D.C.)* **1963**, *142*, 502; e) H. S. Verter, H. Potter, R. Dominic, *J. Chem. Soc. Chem. Commun.* **1968**, 973; f) H. S. Verter, R. Dominic, *Tetrahedron* **1967**, *23*, 3863; g) C. Nallaiah, *ibid.* **1984**, *40*, 4897; h) R. J. Van Zee, G. R. Smith, W. Weltner, Jr., *J. Am. Chem. Soc.* **1988**, *110*, 609.
[121] Reviews on oxocarbons: a) G. Seitz, *Nachr. Chem. Tech. Lab.* **1980**, *28*, 804; b) A. H. Schmidt, *Chem. Unserer Zeit* **1982**, *16*, 57; c) R. West, *Oxocarbons*, Academic Press, New York, **1980**.
[122] Other work on oxocarbons: a) R. West, D. L. Powell, *J. Am. Chem. Soc.* **1963**, *85*, 2577; b) R. West, H. Y. Niu, M. Ito, *ibid.* **1963**, *85*, 2584. c) W. C. Herndon, *J. Mol. Struct. (THEOCHEM)* **1983**, *103*, 219; d) W. Städeli, R. Hollenstein, W. von Philipsborn, *Helv. Chim. Acta* **1977**, *60*, 948; e) S. Skujins, J. Delderfield, G. A. Webb, *Tetrahedron* **1968**, *24*, 4805; f) G. Frenking, *Angew. Chem.* **1990**, *102*, 1516; *Angew. Chem. Int. Ed. Engl.* **1990**, *29*, 1410; g) Q. Chen, S. Liu, J. Zubieta, *ibid.* **1990**, *102*, 100 and **1990**, *29*, 70.
[123] T. Kappe, E. Ziegler, *Angew. Chem.* **1974**, *86*, 529; *Angew. Chem. Int. Ed. Engl.* **1974**, *13*, 491.
[124] a) G. Maier, H. P. Reisenauer, U. Schäfer, H. Balli, *Angew. Chem.* **1988**, *100*, 590; *Angew. Chem. Int. Ed. Engl.* **1988**, *27*, 566; b) F. Holland, M. Winnewisser, G. Maier, H. P. Reisenauer, A. Ulrich, *J. Mol. Spectrosc.* **1988**, *130*, 470.
[125] G. Maier, H. P. Reisenauer, H. Balli, W. Brandt, R. Janoschek, *Angew. Chem.* **1990**, *102*, 920; *Angew. Chem. Int. Ed. Engl.* **1990**, *29*, 905.
[126] D. Sülzle, H. Schwarz, *Angew. Chem.* **1990**, *102*, 923; *Angew. Chem. Int. Ed. Engl.* **1990**, *29*, 908.
[127] J. M. Wood, B. Kahr, S. H. Hoke, II, L. Dejarme, R. G. Cooks, D. Ben-Amotz, *J. Am. Chem. Soc.* **1991**, *113*, 5907.
[128] R. B. Kaner, E. G. Gillan, F. Diederich, C. Thilgen, unpublished results.
[129] W. A. Kalsbeck, H. H. Thorp. *J. Electroanal. Chem. Interfacial Electrochem.* **1991**, *314*, 363.
[130] K. M. Creegan, J. L. Robbins, W. K. Robbins, J. M. Millar, R. D. Sherwood, P. J. Tindall, D. M. Cox, A. B. Smith, III, J. P. McCauley, Jr., D. R. Jones, R. T. Gallagher, *J. Am. Chem. Soc.* **1992**, *114*, 1103.

[131] Y. Elemes, S. K. Silverman, C. Sheu, M. Kao, C. S. Foote, M. M. Alvarez, R. L. Whetten, *Angew. Chem.* **1992**, *104*, 364; *Angew. Chem. Int. Ed. Engl.* **1992**, *31*, 131.

[132] a) E. Vogel, M. Biskup, W. Pretzer, W. A. Böll, *Angew. Chem.* **1964**, *76*, 784; *Angew. Chem. Int. Ed. Engl.* **1964**, *3*, 642; for related discussions, see also: b) R. Arnz, J. W. de M. Carneiro, W. Klug, H. Schmickler, E. Vogel, R. Breuckmann, F.-G. Klärner, *ibid.* **1991**, *103*, 702 and **1991**, *30*, 683.

[133] For recent references on carbon sulfides, see: a) G. Maier, H. P. Reisenauer, J. Schrot, R. Janoschek, *Angew. Chem.* **1990**, *102*, 1475; *Angew. Chem. Int. Ed. Engl.* **1990**, *29*, 1464; b) D. Sülzle, N. Beye, E. Fanghänel, H. Schwarz, *Chem. Ber.* **1989**, *122*, 2411; c) D. Sülzle, H. Schwarz, *ibid.* **1989**, *122*, 1803; d) G. Maier, J. Schrot, H. P. Reisenauer, *ibid.* **1991**, *124*, 2613; e) G. Maier, J. Schrot, H. P. Reisenauer, G. Frenking, U. Jonas, *ibid.* **1992**, *125*, 265; f) X. Yang, T. B. Rauchfuss, S. R. Wilson, *J. Am. Chem. Soc.* **1989**, *111*, 3465.

[134] N. Goroff, O. L. Chapman, F. Diederich, unpublished results.

[135] H. Hart, S. Shamouilian, Y. Takehira, *J. Org. Chem.* **1981**, *46*, 4427.

[136] O. M. Behr, G. Eglinton, A. R. Galbraith, R. A. Raphael, *J. Chem. Soc.* **1960**, 3614.

[137] Y. Li, UCLA, unpublished results.

[138] J. Grotemeyer, U. Boesl, K. Walter, E. W. Schlag, *Org. Mass. Spectrom.* **1986**, *21*, 645.

[139] Y. Rubin, C. B. Knobler, F. Diederich, *J. Am. Chem. Soc.* **1990**, *112*, 4966.

[140] a) W. Bonrath, K. R. Pörschke, G. Wilke, K. Angermund, C. Krüger, *Angew. Chem.* **1988**, *100*, 853; *Angew. Chem. Int. Ed. Engl.* **1988**, *27*, 833; b) G. Peyronel, A. Ragni, E. F. Trogu, *Gazz. Chim. Ital.* **1967**, *97*, 1327; c) M. Green, D. M. Grove, J. A. K. Howard, J. L. Spencer, F. G. A. Stone, *J. Chem. Soc. Chem. Commun.* **1976**, 759; d) N. M. Boag, M. Green, D. M. Grove, J. A. K. Howard, J. L. Spencer, F. G. A. Stone, *J. Chem. Soc. Dalton Trans.* **1980**, 2170; e) K. Nicholas, L. S. Bray, R. E. Davis, R. Pettit, *J. Chem. Soc. Chem. Commun.* **1971**, 608.

[141] For recent references on transition metal alkyne complexes, see: a) D. J. Wink, B. T. Creagan, *J. Am. Chem. Soc.* **1990**, *112*, 8585; b) R. A. Williams, T. P. Hanusa, *ibid.* **1990**, *112*, 2454; c) J. B. Hartung, Jr., S. F. Pedersen, *ibid.* **1989**, *111*, 5468; d) K. Takai, M. Tezuka, Y. Kataoka, K. Utimoto, *J. Org. Chem.* **1990**, *55*, 5310; e) A. Romero, D. Peron, P. H. Dixneuf, *J. Chem. Soc. Chem. Commun.* **1990**, 1410; f) A. Romero, A. Vegas, P. H. Dixneuf, *Angew. Chem.* **1990**, *102*, 210; *Angew. Chem. Int. Ed. Engl.* **1990**, *29*, 215; g) J. Breimair, M. Steinmann, B. Wagner, W. Beck, *Chem. Ber.* **1990**, *123*, 7; h) M. I. Bruce, *Chem. Rev.* **1991**, *91*, 197; i) N. L. Pocard, D. C. Alsmeyer, R. L. McCreery, T. X. Neenan, M. R. Callstrom, *J. Am. Chem. Soc.* **1992**, *114*, 769; j) H. B. Fyfe, M. Mlekuz, D. Zargarian, N. J. Taylor, T. B. Marder, *J. Chem. Soc. Chem. Commun.* **1991**, 188; k) S. J. Davies, B. F. G. Johnson, M. S. Khan, J. Lewis, *ibid.* **1991**, 187; l) D. Schneider, H. Werner, *Angew. Chem.* **1991**, *103*, 710; *Angew. Chem. Int. Ed. Engl.* **1991**, *30*, 700.

[142] M. A. Bennett, H. P. Schwemlein, *Angew. Chem.* **1989**, *101*, 1349; *Angew. Chem. Int. Ed. Engl.* **1989**, *28*, 1296.

[143] a) G. Pályi, F. Piacenti, L. Markó, *Inorg. Chim. Acta Rev.* **1970**, *4*, 109; b) R. S. Dickson, P. J. Fraser, *Adv. Organomet. Chem.* **1974**, *12*, 323.

[144] a) P. H. Bird, A. R. Fraser, D. N. Hall, *Inorg. Chem.* **1977**, *16*, 1923; b) F. Baert, A. Guelzim, *Acta Crystallogr. Sect. B* **1984**, *40*, 590; c) D. Gregson, J. A. K. Howart, *Acta Crystallogr. Sect. C* **1983**, *39*, 1024; d) A. Meyer, A. Gorgues, Y. Le Floc'h, Y. Pineau, J. Guillevic, J. Y. Le Marouille, *Tetrahedron Lett.* **1981**, *22*, 5181; e) P. Galow, A. Sebald, B. Wrackmeyer, *J. Organomet. Chem.* **1983**, *259*, 253.

[145] a) H. Petersen, H. Meier, *Nouv. J. Chim.* **1980**, *4*, 687; b) Y. Shvo, E. Hazum, *J. Chem. Soc. Chem. Commun.* **1974**, 336.

[146] P. Magnus, D. P. Becker, *J. Chem. Soc. Chem. Commun.* **1985**, 640.

[147] G. Cetini, O. Gambino, R. Rossetti, E. Sappa, *J. Organomet. Chem.* **1967**, *8*, 149.

[148] N. T. Allison, J. R. Fritch, K. P. C. Vollhardt, E. C. Walborsky, *J. Am. Chem. Soc.* **1983**, *105*, 1384.

[149] For a general review on organocobalt chemistry in synthesis, see: a) K. M. Nicholas, M. O. Nestle, D. Seyferth in *Transition Metal Organometallics in Organic Synthesis, Vol. II* (Ed.: H. Alper), Academic Press, New York, **1978**; b) K. P. C. Vollhardt, *Angew. Chem.* **1984**, *96*, 525; *Angew. Chem. Int. Ed. Engl.* **1984**, *23*, 539.

[150] For applications of alkyne cobalt carbonyl complexes in synthesis, see: a) P. Magnus, P. A. Carter, *J. Am. Chem. Soc.* **1988**, *110*, 1626; b) M. E. Krafft, *ibid.* **1988**, *110*, 968; c) P. Magnus, D. P. Becker, *ibid.* **1987**, *109*, 7495; d) S. L. Schreiber, M. T. Klimas, T. Sammakia, *ibid.* **1987**, *109*, 5749.

[151] a) P. H. Bird, A. R. Fraser, D. N. Hall, *Inorg. Chem.* **1977**, *16*, 1923; b) B. E. Hanson, J. S. Mancini, *Organometallics* **1983**, *2*, 126; c) *Aldrichimica Acta* **1983**, *16*(4), 80, and references cited therein.

[152] R. S. Dickson, P. J. Fraser, *Adv. Organomet. Chem.* **1974**, *12*, 323.

[153] P. Sautet, O. Eisenstein, E. Canadell, *New. J. Chem.* **1987**, *11*, 797.

[154] F. A. Cotton, G. Wilkinson, *Advanced Inorganic Chemistry*, 5th ed., Wiley, New York, **1988**.

[155] a) M. Tachikawa, E. L. Mutterties, *Prog. Inorg. Chem.* **1981**, *28*, 203; b) J.-F. Halet, D. M. P. Mingos, *Organometallics* **1988**, *7*, 51.

[156] W. A. Herrmann, *Angew. Chem.* **1986**, *98*, 57; *Angew. Chem. Int. Ed. Engl.* **1986**, *25*, 56.

[157] a) P. Chini, G. Longoni, V. G. Albano, *Adv. Organomet. Chem.* **1976**, *14*, 285; b) J. S. Bradley, *ibid.* **1983**, *22*, 1; c) Aumann, R. *Nachr. Chem. Tech. Lab.* **1982**, *30*, 771; d) M. McPartlin, *Polyhedron* **1984**, *3*, 1279.

[158] a) E. H. Braye, L. F. Dahl, W. Hübel, D. L. Wampler, *J. Am. Chem. Soc.* **1962**, *84*, 4633; b) A. Sirigu, M. Bianchi, E. Benedetti, *J. Chem. Soc. Chem. Commun.* **1968**, 468; c) V. G. Albano, M. Sansoni, P. Chini, S. Martinengo, *J. Chem. Soc. Dalton Trans.* **1973**, 651; d) V. G. Albano, P. Chini, G. Ciani, M. Sansoni, D. Strumolo, B. T. Heaton, S. Martinengo, *J. Am. Chem. Soc.* **1976**, *98*, 5027; e) J.-F. Halet, D. G. Evans, D. M. P. Mingos, *ibid.* **1988**, *110*, 87.

[159] a) A. Ceriotti, G. Piro, G. Longoni, M. Manassero, N. Masciocchi, M. Sansoni, *New. J. Chem.* **1988**, *12*, 501; b) A. Ceriotti, G. Longoni, M. Manassero, N. Masciocchi, G. Piro, L. Resconi, M. Sansoni, *J. Chem. Soc. Chem. Commun.* **1985**, 1402; c) A. Ceriotti, A. Fait, G. Longoni, G. Piro, L. Resconi, F. Demartin, M. Manassero, N. Masciocchi, M. Sansoni, *J. Am. Chem. Soc.* **1986**, *108*, 5370; d) A. Ceriotti, A. Fait, G. Longoni, G. Piro, F. Demartin, M. Manassero, N. Masciocchi, M. Sansoni, *ibid.* **1986**, *108*, 8091; e) P. D. Smith, B. R. James, D. H. Dolphin, *Coord. Chem. Rev.* **1981**, *39*, 31.

[160] G. Pályi, F. Piacenti, L. Markó, *Inorg. Chim. Acta Rev.* **1970**, *4*, 109.

[161] R. S. Dickson, P. J. Fraser, *Adv. Organomet. Chem.* **1974**, *12*, 323.

[162] a) G. Bor, L. Markó, B. Markó, *Chem. Ber.* **1962**, *95*, 333; b) B. H. Robinson, W. S. Tham, *J. Organomet. Chem.* **1969**, *16*, P45; c) G. Varadi, G. Pályi, *Inorg. Chim. Acta* **1976**, *20*, L33; d) M. D. Brice, B. R. Penfold, *Inorg. Chem.* **1972**, *11*, 1381.

[163] a) R. J. Dellaca, B. R. Penfold, B. H. Robinson, W. T. Robinson, J. L. Spencer, *Inorg. Chem.* **1970**, *9*, 2204; b) D. Seyferth, R. J. Spohn, M. R. Churchill, K. Gold, F. R. Scholer, *J. Organomet. Chem.* **1970**, *23*, 237; c) R. J. Dellaca, B. R. Penfold, *Inorg. Chem.* **1971**, *10*, 1269.

[164] a) M. H. Chisholm, *Angew. Chem.* **1991**, *103*, 690; *Angew. Chem. Int. Ed. Engl.* **1991**, *30*, 673; b) J. Heidrich, M. Steimann, M. Appel, W. Beck, J. R. Phillips, W. C. Trogler, *Organometallics* **1990**, *9*, 1296; c) M. St. Clair, W. P. Schaefer, J. E. Bercaw, *ibid.* **1991**, *10*, 525; d) G. A. Koutsantonis, J. P. Selegue, *J. Am. Chem. Soc.* **1991**, *113*, 2316; e) H. Ogawa, K. Onitsuka, T. Joh, S. Takahashi, Y. Yamamoto, H. Yamazaki, *Organometallics*, **1988**, *7*, 2257; f) D. R. Neithamer, R. E. LaPointe, R. A. Wheeler, D. S. Richeson, G. D. Van Duyne, P. T. Wolczanski, *J. Am. Chem. Soc.* **1989**, *111*, 9056.

[165] a) P. J. Stang, V. V. Zhdankin, *J. Am. Chem. Soc.* **1990**, *112*, 6437; b) P. J. Stang, A. M. Arif, C. M. Crittell, *Angew. Chem.* **1990**, *102*, 307; *Angew. Chem. Int. Ed. Engl.* **1990**, *29*, 287. Review: P. J. Stang *ibid.* **1992**, *104*, 281 and **1992**, *31*, 274.

[166] H. J. Bestmann, H. Behl, M. Bremer, *Angew. Chem.* **1989**, *101*, 1303; *Angew. Chem. Int. Ed. Engl.* **1989**, *28*, 1219.

[167] a) W. C. Kaska, D. K. Mitchell, R. F. Reichelderfer, *J. Organomet. Chem.* **1973**, *47*, 391; b) H. Schmidbaur, *Angew. Chem.* **1983**, *95*, 980; *Angew. Chem. Int. Ed. Engl.* **1983**, *22*, 907.

[168] R. N. Collinge, R. S. Nyholm, M. L. Tobe, *Nature (London)* **1964**, *201*, 1322.

[169] a) J. M. Hawkins, A. Meyer, T. A. Lewis, S. Loren, F. J. Hollander, *Science (Washington, D.C.)* **1991**, *252*, 312; b) J. M. Hawkins, S. Loren, A. Meyer, R. Nunlist, *J. Am. Chem. Soc.* **1991**, *113*, 7770.

[170] a) P. J. Fagan, J. C. Calabrese, B. Malone, *Science (Washington, D.C.)* **1991**, *252*, 1160; b) P. J. Fagan, J. C. Calabrese, B. Malone, *J. Am. Chem. Soc.* **1991**, *113*, 9408.

[171] a) For the synthesis of the metal-containing C_{60} polymer, $C_{60}Pd_n$, see: H. Nagashima, A. Nakaoka, Y. Saito, M. Kato, T. Kawanishi, K. Itoh, *J. Chem. Soc. Chem. Commun.* **1992**, 377; b) For experimental evidence of the formation of a stable dodecohedral "metallocarbohedrene", $Ti_8C_{12}^+$ in the gase phase, see: B. C. Guo, K. P. Kerns, A. W. Castleman, Jr., *Science (Washington, D.C.)* **1992**, *255*, 1411; for other metallocarbohedrenes $M_8C_{12}^+$ (= V, Cr, Zr, Hf), see: B. C. Guo, S. Wei, J. Purnell, S. Buzza, W. Castleman, Jr., *ibid.* **1992**, *256*, 515.

[172] R. S. Koefod, M. F. Hudgens, J. R. Shapley, *J. Am. Chem. Soc.* **1991**, *113*, 8957.

[173] a) A. L. Balch, V. J. Catalano, J. W. Lee, M. M. Olmstead, S. R. Parkin, *J. Am. Chem. Soc.* **1991**, *113*, 8953; b) A. L. Balch, V. J. Catalano, J. W. Lee, *Inorg. Chem.*, **1991**, *30*, 3980.

[174] a) R. D. Johnson, G. Meijer, J. R. Salem, D. S. Bethune, *J. Am. Chem. Soc.* **1991**, *113*, 3619; b) D. R. McKenzie, C. A. Davis, D. J. H. Cockayne, D. A. Muller, A. M. Vassallo, *Nature (London)* **1992**, *355*, 622.

[175] a) Y. Huang, B. S. Freiser, *J. Am. Chem. Soc.* **1991**, *113*, 9418; b) Y. Huang, B. S. Freiser, *ibid.* **1991**, *113*, 8186; c) L. M. Roth, Y. Huang, J. T. Schwedler, C. J. Cassady, D. Ben-Amotz, B. Kahr, B. S. Freiser, *ibid.* **1991**, *113*, 6298; d) Q. Jiao, Y. Huang, S. A. Lee, J. R. Gord, B. S. Freiser, *ibid.* **1992**, *114*, 2726.

[176] A. Pénicaud, J. Hsu, C. A. Reed, A. Koch, K. C. Khemani, P.-M. Allemand, F. Wudl, *J. Am. Chem. Soc.* **1991**, *113*, 6698.

[177] J. Cioslowski, *J. Am. Chem. Soc.* **1991**, *113*, 4139.

[178] a) J. R. Heath, S. C. O'Brien, Q. Zhang, Y. Liu, R. F. Curl, H. W. Kroto, F. K. Tittel, R. E. Smalley, *J. Am. Chem. Soc.* **1985**, *107*, 7779; b) F. D. Weiss, J. L. Elkind, S. C. O'Brien, R. F. Curl, R. E. Smalley, *ibid.* **1988**, *110*, 4464; c) R. E. Smalley, *Nav. Res. Rev.* **1991**, *43* (III), 3.

[179] a) D. M. Cox, D. J. Trevor, K. C. Reichmann, A. Kaldor, *J. Am. Chem.*

Soc. **1986**, *108*, 2457; b) D. M. Cox, K. C. Reichmann, A. Kaldor, *J. Chem. Phys.* **1988**, *88*, 1588.
[180] Y. Chai, T. Guo, C. Jin, R. E. Haufler, L. P. F. Chibante, J. Fure, L. Wang, J. M. Alford, R. E. Smalley, *J. Phys. Chem.* **1991**, *95*, 7564.
[181] J. H. Weaver, Y. Chai, G. H. Kroll, C. Jin, T. R. Ohno, R. E. Haufler, T. Guo, J. M. Alford, J. Conceicao, L. P. F. Chibante, A. Jain, G. Palmer, R. E. Smalley, *Chem. Phys. Letters,* in press.
[182] R. D. Johnson, M. S. de Vries, J. Salem, D. S. Bethune, C. S. Yannoni, *Nature (London)* **1992**, *355*, 239.
[183] a) M. M. Alvarez, E. G. Gillan, K. Holczer, R. B. Kaner, K. S. Min, R. L. Whetten, *J. Phys. Chem.* **1991**, *95*, 10561; b) H. Shinohara, H. Sato, Y. Saito, M. Ohkohchi, Y. Ando, *ibid.*, **1992**, *96*, 3571; c) For a report on the formation of an endohedral iron complex, FeC_{60}, see: T. Pradeep. G. U. Kulkarni, K. R. Kannan, T. N. Guru Row, C. N. R. Rao, *J. Am. Chem. Soc.* **1992**, *114*, 2272; d) H. Shinohara, H. Sato, M. Ohkohchi, Y. Ando, T. Komada, T. Shida, T. Kato, Y. Saito, *Nature (London)* **1992**, *357*, 52; e) C. S. Yannoni, M. Hoinkis, M. S. de Vries, D. S. Bethune, J. R. Salem, M. S. Crowder, R. D. Johnson, *Science (Washington D.C.)* **1992**, *256*, 1191.
[184] a) P. W. Fowler, D. E. Manolopoulos, *Nature (London)* **1992**, *355*, 428; b) D. E. Manolopoulos, P. W. Fowler, *Chem. Phys. Lett.* **1991**, *187*, 1; c) D. E. Manolopoulos, P. W. Fowler, R. P. Ryan, *J. Chem. Soc. Faraday Trans.* **1992**, *88*, 1225; d) D. E. Manolopoulos, P. W. Fowler, *Chem. Phys. Lett.* **1991**, *187*, 1; e) D. E. Manolopoulos, *J. Chem. Soc. Faraday Trans.* **1991**, *87*, 2861; f) P. W. Fowler, D. E. Manolopoulos, R. C. Batten, *ibid.* **1991**, *87*, 3103; g) D. E. Manolopoulos, P. W. Fowler, *J. Chem. Phys.*, **1992**, *96*, 7603; h) D. E. Manolopoulos, P. W. Fowler, *J. Chem. Phys.* **1992**, in press; i) P. W. Fowler, D. E. Manolopoulos, R. P. Ryan, *J. Chem. Soc. Chem. Commun.* **1992**, 408.
[185] For endohedral rare gas fullerene complexes, see: a) T. Weiske, D. K. Böhme, J. Hrusák, W. Krätschmer, H. Schwarz, *Angew. Chem.* **1991**, *103*, 898; *Angew. Chem. Int. Ed. Engl.* **1991**, *30*, 884; b) M. M. Ross, J. H. Callahan, *J. Phys. Chem.* **1991**, *95*, 5720; c) K. A. Caldwell, D. E. Giblin, C. S. Hsu, D. Cox, M. L. Gross, *J. Am. Chem. Soc.* **1991**, *113*, 8519; d) T. Weiske, J. Hrusák, D. K. Böhme, H. Schwarz, *Chem. Phys. Lett.* **1991**, *186*, 459; e) T. Weiske, T. Wong, W. Krätschmer, J. K. Terlouw, H. Schwarz, *Angew. Chem.* **1992**,*104*, 242; *Angew. Chem. Int. Ed. Engl.* **1992**, *31*, 183; f) T. Weiske, J. Hrusák, D. K. Böhme, H. Schwarz, *Helv. Chim. Acta.* **1992**, *75*, 79.
[186] H. D. Beckhaus, C. Rüchardt, M. Kao, F. Diederich, C. S. Foote, *Angew. Chem.* **1992**, *104*, 69; *Angew. Chem. Int. Ed. Engl.* **1992**, *31*, 63.
[187] a) J. Sauer, *Chem. Rev.* **1989**, *89*, 199; b) M. Shen, H. F. Schaefer, III, C. Liang, J.-H. Lii, N. L. Allinger, P. von R. Schleyer, *J. Am. Chem. Soc.* **1992**, *114*, 497.
[188] R. Diercks, J. C. Armstrong, R. Boese, K. P. C. Vollhardt, *Angew. Chem.* **1986**, *98*, 270; *Angew. Chem. Int. Ed. Engl.* **1986**, *25*, 268.
[189] O. M. Behr, G. Eglinton, I. A. Lardy, R. A. Raphael, *J. Chem. Soc.* **1964**, 1151.
[190] a) H. A. Staab, F. Graf, *Chem. Ber.* **1970**, *103*, 1107; b) H. Irngartinger, L. Leiserowitz, G. M. J. Schmidt, *Chem. Ber.* **1970**, *103*, 1119; c) J. W. Barton, M. K. Shepherd, *Tetrahedron Lett.* **1984**, *25*, 4967; d) J. D. Ferrara, C. Tessier-Youngs, W. J. Youngs, *J. Am. Chem. Soc.* **1988**, *110*, 3326; e) C. Huynh, G. Linstrumelle, *Tetrahedron* **1988**, *44*, 6337.
[191] a) Y. Hori, K. Noda, S. Kobayashi, H. Taniguchi, *Tetrahedron Lett.* **1969**, 3563; b) H. Hauptmann, *Angew. Chem.* **1975**, *87*, 490; *Angew. Chem. Int. Ed. Engl.* **1975**, *14*, 498; c) H. Hopf, M. Kreutzer, *ibid.* **1990**, *102*, 425 and **1990**, *29*, 393; d) H. Hopf, M. Kreutzer, P. G. Jones, *Chem. Ber.* **1991**, *124*, 1471.
[192] Y. Rubin, C. B. Knobler, F. Diederich, *Angew. Chem.* **1991**, *103*, 708; *Angew. Chem. Int. Ed. Engl.* **1991**, *30*, 698.
[193] B. Ma, Y. Xie, H. F. Schaefer, III, *Chem. Phys. Lett.*, **1992**, *191*, 521.
[194] a) M. Iyoda, H. Otani, M. Oda, *Angew. Chem.* **1988**, *100*, 1131; *Angew. Chem. Int. Ed. Engl.* **1988**, *27*, 1080; b) M. Iyoda, H. Otani, M. Oda, Y. Kai, Y. Baba, N. Kasai, *J. Am. Chem. Soc.* **1986**, *108*, 5371; c) For the use of radialene **75** as a precursor to carbon networks see also H. Hopf, G. Maas, *Angew. Chem.* **1992**, *104*, 953; *Angew. Chem. Int. Ed. Engl.* **1992**, *31*, 931.
[195] a) J. A. Kremers, A. H. Alberts, personal communication; b) A. H. Alberts, *Recl. Trav. Chim. Bays-Bas.* **1989**, *108*, 242.
[196] a) T. X. Neenan, G. M. Whitesides, *J. Org. Chem.* **1988**, *53*, 2489; b) T. X. Neenan, M. R. Callstrom, L. M. Scarmoutzos, K. R. Stewart, G. M. Whitesides, V. R. Howes, *Macromolecules* **1988**, *21*, 3525; c) D. R. Rutherford, J. K. Stille, *ibid.* **1988**, *21*, 3530; d) M. R. Callstrom, T. X. Neenan, R. L. McCreery, D. C. Alsmeyer, *J. Am. Chem. Soc.* **1990**, *112*, 4954; e) P. E. Eaton, D. Stössel, *J. Org. Chem.* **1991**, *56*, 5138; f) J. Suffert, R. Ziessel, *Tetrahedron Lett.* **1991**, *32*, 757; g) H. L. Anderson, *ibid,* **1992**, *33*, 1101.
[197] J. S. Moore, Z. Xu, *Macromolecules* **1991**, *24*, 5893.
[198] J. Elguero, C. Foces-Foces, A. L. Llamas-Saiz, (Instituto de Química Médica, Madrid), personal communication. We thank Professor J. D. Dunitz (ETH Zürich) for bringing this structure to our attention.
[199] D. Loguercio, Jr., R. Moss, O. L. Chapman, unpublished results. We warmly thank Professor Orville Chapman (UCLA) for making these results available for publication in this review article.
[200] For recent examples of other nonplanar extended arenes, see: a) K. Yamamoto, T. Harada, Y. Okamoto, H. Chikamatsu, M. Nakazaki, Y. Kai, T. Nakao, M. Tanaka, S. Harada, N. Kasai, *J. Am. Chem. Soc.* **1988**, *110*, 3578; b) K. Yamamoto, Y. Saitho, D. Iwaki, T. Ooka, *Angew. Chem.* **1991**, *103*, 1202; *Angew. Chem. Int. Ed. Engl.* **1991**, *30*, 1173; c) R. A. Pascal, Jr., D. M. Ho, *Tetrahedron Lett.* **1992**, *33*, 13; d) R. A. Pascal, Jr., W. D. McMillan, D. Van Engen, R. G. Eason, *J. Am. Chem. Soc.* **1987**, *109*, 4660.
[201] C. Fabre, A. Rassat, *C. R. Acad. Sci. Paris Ser. 2,* **1989**, *308*, 1223.
[202] *Cage Hydrocarbons* (Ed.: G. A. Olah), Wiley, New York, **1990**.
[203] a) P. von R. Schleyer, *J. Am. Chem. Soc.* **1957**, *79*, 3292; b) P. von R. Schleyer in ref. [202], pp. 1–38.
[204] a) W.-D. Fessner, B. A. R. C. Murty, H. Prinzbach, *Angew. Chem.* **1987**, *99*, 482; *Angew. Chem. Int. Ed. Engl.* **1987**, *26*, 451; b) W.-D. Fessner, B. A. R. C. Murty, J. Wörth, D. Hunkler, H. Fritz, H. Prinzbach, W. D. Roth, P. v. R. Schleyer, A. B. McEven, W. F. Maier, *ibid.* **1987**, *99*, 484 and **1987**, *26*, 452; c) W.-D. Fessner, H. Prinzbach, in ref. [202], pp. 353–405.
[205] Functionalized derivatives of C_{60} for which ready conversion back to the pure carbon sphere was reported under thermolysis or mass spectral conditions: a) R. E. Haufler, J. Conceicao, L. P. F. Chibante, Y. Chai, N. E. Byrne, S. Flanagan, M. M. Haley, S. C. O'Brien, C. Pan, Z. Xiao, W. E. Billups, M. A. Ciufolini, R. H. Hauge, J. L. Margrave, L. J. Wilson, R. F. Curl, R. E. Smalley, *J. Phys. Chem.* **1990**, *94*, 8634; b) F. Wudl, A. Hirsch, K. C. Khemani, T. Suzuki, P.-M. Allemand, A. Koch, G. Srdanov in *Fullerenes: Synthesis, Properties and Chemistry of Large Carbon Clusters* (Eds.: G. S. Hammond, V. J. Kuck), *ACS Symp. Ser.* **1992**, *481*, 161; c) F. N. Tebbe, R. L. Harlow, D. B. Chase, D. L. Thorn, G. C. Campbell, J. C. Calabrese, N. Herron, R. J. Young, Jr., E. Wasserman, *Science (Washington, D.C.)*, **1992**, *256*, 822; d) F. N. Tebbe, J. Y. Becker, D. B. Chase, L. E. Firment, E. R. Holler, B. S. Malone, P. J. Krusic, E. Wasserman, *J. Am. Chem. Soc.* **1991**, *113*, 9900; e) G. A. Olah, I. Bucsi, C. Lambert, R. Aniszfeld, N. J. Trivedi, D. K. Sensharma, G. K. Surya Prakash, *ibid.* **1991**, *113*, 9385; f) H. Selig, C. Lifshitz, T. Peres, J. E. Fischer, A. R. McGhie, W. J. Romanow, J. P. McCauley, Jr., A. B. Smith, III, *ibid.* **1991**, *113*, 5475; g) P. R. Birkett, P. B. Hitchcock, H. W. Kroto, R. Taylor, D. R. M. Walton *Nature (London)* **1992**, *357*, 479.
[206] Other functionalized fullerenes: a) A. Hirsch, Q. Li, F. Wudl, *Angew. Chem.* **1991**, *103*, 1339; *Angew. Chem. Int. Ed. Engl.* **1991**, *30*, 1309; b) J. W. Bausch, G. K. Surya Prakash, G. A. Olah, D. S. Tse, D. C. Lorents, Y. K. Bae, R. Malhotra, *J. Am. Chem. Soc.* **1991**, *113*, 3205; c) T. Suzuki, Q. Li, K. C. Khemani, F. Wudl, Ö. Almarsson, *Science (Washington, D.C.)* **1991**, *254*, 1186; d) P. J. Krusic, E. Wasserman, P. N. Keizer, J. R. Morton, K. F. Preston, *ibid.* **1991**, *254*, 1183; e) J. H. Holloway, E. G. Hope, R. Taylor, G. J. Langley, A. G. Avent, T. J. Dennis, J. P. Hare, H. W. Kroto, D. R. M. Walton, *J. Chem. Soc. Chem. Commun.* **1991**, 966; f) G. A. Olah, I. Bucsi, C. Lambert, R. Aniszfeld, N. J. Trivedi, D. K. Sensharma, G. K. Surya Prakash, *J. Am. Chem. Soc.* **1991**, *113*, 9387.
[207] M. M. Ross, S. McElvany, J. Milliken, N. Goroff, Y. Rubin, F. Diederich, unpublished results.
[208] a) W. E. Barth, R. G. Lawton, *J. Am. Chem. Soc.* **1966**, *88*, 380; *ibid.* **1971**, *93*, 1730; b) L. T. Scott, M. M. Hashemi, D. T. Meyer, H. B. Warren, *ibid.* **1991**, *113*, 7082; c) A. Borchardt, A. Fuchicello, K. V. Kilway, K. K. Baldridge, J. S. Siegel, *ibid.* **1992**, *114*, 1921; d) L. T. Scott, M. M. Hasemi, M. S. Bratcher, *ibid.* **1992**, *114*, 1920.
[209] a) B. M. Trost, G. M. Bright, C. Frihart, D. Britelli, *J. Am. Chem. Soc.* **1971**, *93*, 737; b) G. Schaden, *J. Org. Chem.* **1983**, *48*, 5385; c) B. Freiermuth, S. Gerber, A. Riesen, J. Wirz, M. Zehnder, *J. Am. Chem. Soc.* **1990**, *112*, 738.
[210] a) H. Ajie, M. M. Alvarez, S. J. Anz, R. D. Beck, F. Diederich, K. Fostiropoulos, D. R. Huffman, W. Krätschmer, Y. Rubin, K. E. Schriver, D. Sensharma, R. L. Whetten, *J. Phys. Chem.* **1990**, *94*, 8630; b) R. L. Whetten, M. M. Alvarez, S. J. Anz, K. E. Schriver, R. D. Beck, F. Diederich, Y. Rubin, R. Ettl, C. S. Foote, A. P. Darmanyan, J. W. Arbogast, *Mater. Res. Soc. Symp. Proc.* **1991**, *206*, 639.
[211] A. S. Koch, K. C. Khemani, F. Wudl, *J. Org. Chem.* **1991**, *56*, 4543.
[212] J. B. Howard, J. T. McKinnon, Y. Makarovsky, A. L. Lafleur, M. E. Johnson, *Nature (London)* **1991**, *352*, 139.
[213] M. Jansen, G. Peters, *Angew. Chem.* **1992**, *104*, 240; *Angew. Chem. Int. Ed. Engl.* **1992**, *31*, 223.
[214] a) P.-M. Allemand, A. Koch, F. Wudl. Y. Rubin, F. Diederich, M. M. Alvarez, S. J. Anz, R. L. Whetten, *J. Am. Chem. Soc.* **1991**, *113*, 1050; b) R. Taylor, J. P. Hare, A. K. Abdul-Sada, H. W. Kroto, *J. Chem. Soc. Chem. Commun.* **1990**, 1423.
[215] K. C. Khemani, M. Prato, F. Wudl, *J. Org. Chem.*, **1992**, *57*, 3254.
[216] a) J. M. Hawkins, T. A. Lewis, S. D. Loren, A. Meyer, J. R. Heath, Y. Shibato, R. J. Saykally, *J. Org. Chem.* **1990**, *55*, 6250; b) W. H. Pirkle, C. J. Welch, *ibid.* **1991**, *56*, 6973; c) A. M. Vassallo, A. J. Palmisano, L. S. K. Pang, M. A. Wilson, *J. Chem. Soc. Chem. Commun.* **1992**, 60.
[217] a) M. S. Meier, J. P. Selegue, *J. Org. Chem.* **1992**, *57*, in press; b) A. Gügel, M. Becker, D. Hammel, L. Mindach, J. Räder, T. Simon, M. Wagner, K. Müllen, *Angew. Chem.* **1992**, *104*, 666; *Angew. Chem. Int. Ed. Engl.* **1992**, *31*, 644.
[218] D. M. Cox, R. D. Sherwood, P. Tindall, K. M. Kreegan, W. Anderson,

D. Martella in *Fullerenes: Synthesis, Properties and Chemistry of Large Carbon Clusters* (Eds.: G. S. Hammond, V. J. Kuck), *ACS Symp. Ser.* **1992**, *481*, 117.
[219] O. Ermer, *Helv. Chim. Acta* **1991**, *74*, 1339.
[220] C. Thilgen, F. Diederich, unpublished results. We thank Dr. G. Tschopp and Dr. M. Schär, Ciba-Geigy, Basel, for measuring the matrix-assisted laser desorption time-of-flight mass spectra.
[221] We thank Professor Y. Achiba (Tokyo Metropolitan University) for communicating some of his results to us prior to publication.
[222] K. Kikuchi, N. Nakahara, T. Wakabayashi, S. Suzuki, H. Shiromaru, Y. Miyake, K. Saito, I. Ikemoto, M. Kainosho, Y. Achiba, *Nature (London)* **1992**, *357*, 142.
[223] We thank Professor Y. Achiba (Tokyo Metropolitan University) for communicating their ^{13}C NMR data on C_{84} to us prior to submission.
[224] H. W. Kroto, *Nature (London)* **1987**, *329*, 529.
[225] a) J. M. Hawkins, A. Meyer, S. Loren, R. Nunlist, *J. Am. Chem. Soc.* **1991**, *113*, 9394; b) T.-M. Chang, A. Naim, S. N. Ahmed, G. Goodloe. P. B. Shevlin, (Auburn University), personal communication; c) T. Wakabayahsi, Y. Achiba, *Chem. Phys. Lett.* **1992**, *190*, 465.
[226] a) S. Iijima, *Nature (London)* **1991**, *354*, 56; b) T. W. Ebbesen, P. M. Ajayan, *ibid.* **1992**, *191*, 336.
[227] a) P. Labastie, R. L. Whetten, H.-P. Cheng, K. Holczer, *Chem. Phys. Lett.*, in press; b) J. W. Mintmire, B. I. Dunlap, C. T. White, *Phys. Rev. Lett.*, submitted; c) K. Tanaka, K. Okahara, M. Okada, T. Yamabe, *Chem. Phys. Lett.* **1992**, *191*, 469.
[228] a) T. Lenosky, X. Gonze, M. Teter, V. Elser, *Nature (London)* **1992**, *355*, 333; b) S. Iijima, T. Ichihashi, Y. Ando, *ibid.* **1992**, *356*, 776.
[229] a) A. F. Hebard, M. J. Rosseinsky, R. C. Haddon, D. W. Murphy, S. H. Glarum, T. T. M. Palstra, A. P. Ramirez, A. R. Kortan, *Nature (London)* **1991**, *350*, 600; b) A. R. Kortan, N. Kopylov, S. Glarum, E. M. Gyorgy, A. P. Ramirez, R. M. Fleming, F. A. Thiel, R. C. Haddon, *ibid.* **1992**, *355*, 529.
[230] a) K. Holczer, O. Klein, S.-M. Huang, R. B. Kaner, K. J. Fu, R. L. Whetten, F. Diederich, *Science (Washington, D.C.)* **1991**, *252*, 1154; b) P. W. Stephens, L. Mihaly, J. B. Wiley, S.-H. Huang, R. B. Kaner, F. Diederich, R. L. Whetten, K. Holczer, *Phys. Rev. B: Condens. Matter* **1992**, *45*, 543; c) P. W. Stephens, *Nature (London)* **1992**, *356*, 383.
[231] a) O. Zhou, G. B. M. Vaughan, Q. Zhu, J. E. Fischer, P. A. Heiney, N. Coustel, J. P. McCauley, Jr., A. B. Smith, III, *Science (Washington, D.C.)* **1992**, *255*, 833; b) J. P. McCauley, Jr., Q. Zhu, N. Coustel, O. Zhou, G. Vaughan, S. H. J. Idziak, J. E. Fischer, S. W. Tozer, D. M. Groski, N. Bykovetz, C. L. Lin, A. R. McGhie, B. H. Allen, W. J. Romanow, A. M. Denenstein, A. B. Smith, III, *J. Am. Chem. Soc.* **1991**, *113*, 8537; c) C. Politis, V. Buntar, W. Krauss, A. Gurevich, *Europhys. Lett.* **1992**, *17(2)*, 175.
[232] a) P.-M. Allemand, K. C. Khemani, A. Koch, F. Wudl, K. Holczer, S. Donovan, G. Grüner, J. D. Thompson, *Science (Washington, D.C.)* **1991**, *253*, 301; b) P. W. Stephens, D. Cox, J. W. Lauher, L. Mihaly, J. B. Wiley, P.-M. Allemand, A. Hirsch, K. Holczer, Q. Li, J. D. Thompson, F. Wudl, *Nature (London)* **1992**, *355*, 331.
[233] a) M. N. Regueiro, P. Monceau, J.-L. Hodeau, *Nature (London)* **1992**, *355*, 237; b) see also: R. Meilunas, R. P. H. Chang, S. Liu, M. M. Kappes, *Nature (London)* **1991**, *354*, 271.

A stop-gap solution?

If the latest library copy of Angewandte spends more time off the shelf than on, stop the gap with a personal subscription.

Just call or fax

VCH

USA: Tel. 1-(800) 422-8824; Fax (305) 428-8201
UK: Tel. (0223) 321111, Fax (0223) 313221

Flexible Molecules with Defined Shape—Conformational Design

By Reinhard W. Hoffmann*

Chemists have for a long time considered molecules simply in terms of their constitution. The importance of molecular shape was recognized perhaps for the first time by the semiochemists, who were interested in the interactions of fragrant substances with a receptor. Apart from the case of rigid molecules, our ideas and concepts of molecular shape simply reflect an instantaneous situation, because flexible molecules take advantage of the whole range of conformation that is available to them. Nature frequently utilizes flexible molecules whose conformational space is restricted, in other words, molecules that can adopt only a few preferred conformations. This review discusses some of the principles that nature employs in order to impart a defined shape to flexible molecules. The purposeful application of these principles then allows the conformational design of molecular skeletons.

1. Introduction

The biological activity of many natural and synthetic substances is based on the fact that they bind to a receptor by the interaction of specific functional groups. The receptors have binding sites situated either in a pocket, in a cleft, or on the surface. For optimal binding the functional groups of the active substances complementary to those in the binding site must have or adopt a specific spatial arrangement. In only a few areas of biochemistry does nature use active substances that are predominantly rigid, such as steroids. Often conformationally flexible substances are involved, which nonetheless adopt a specific preferred conformation,[1] in other words, they take on a defined shape. If the preferred conformation of the active substance is also that required by the receptor, then the free energy of binding becomes more favorable in terms of both entropy and enthalpy. On the other hand, the conformational mobility allows the particular substances to diffuse rapidly into and out of the receptor.[1]

The principles according to which nature imparts a defined shape to such molecules while largely preserving their conformational mobility are of interest. In the case of proteins and oligopeptides these principles are generally known: the amide bond in these substances exists in the preferred conformation **1** and has, thanks to the partial double-bond character, a rotation barrier of approximately 20 kcal mol^{-1}.[2]

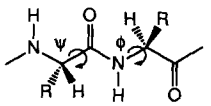

1

Although rotation about the amide bond is certainly still possible, at any given moment the preferred conformation is adopted almost exclusively. Preferred conformations exist also along the other N–C_α (dihedral angle ϕ) and C_α–C=O (dihedral angle ψ) skeletal bonds. Which preferred conformation is adopted in any particular case depends among other things on the nature of the side-chain groups R. It is known, for example, which amino acid sequences result as a rule in the formation of an α helix or a β turn or, again, which are typical of β-sheet structures.[3] In the area of the polypeptides one has therefore a general understanding of how structural elements affect the secondary structure, an understanding that can be utilized in designing peptide-like active substances.[4]

In the case of a biologically active substance that binds to the receptor by a short peptide sequence, it should be irrelevant whether the remainder of the molecular skeleton is a continuation of the peptide chain[1] or has another structure,[5, 6] as long as this produces a specific shape of the overall molecule. Substances such as jaspamide (**2**)[7] or geodiamolide A (**3**)[8] illustrate this clearly.

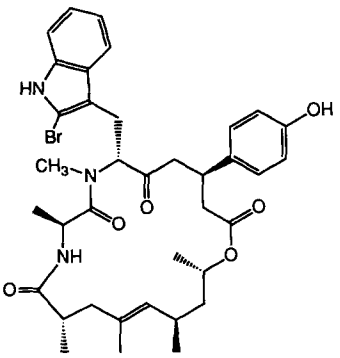

2

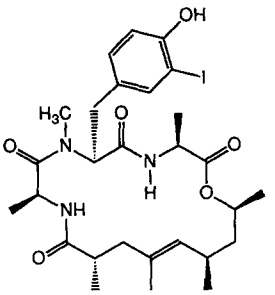

3

It may be concluded that the (propionogenic) partial structures in **2** and **3** derived from the fatty acid metabolism adopt quite specific preferred conformations as a consequence of the existing stereocenters, despite their obviously unrestricted conformational mobility. Chemists dealing with polyketide natural products are of course fully aware of this.[9] The principles illustrated in nature could thus be utilized, and indeed should also be developed further, in order to impart a specific shape to arbitrary molecular skeletons while retaining conformational mobility. These principles are a) the avoidance of g^+g^- interactions[10] and b) the avoidance of allylic 1,3 strain.

[*] Prof. Dr. R. W. Hoffmann
Fachbereich Chemie der Universität
Hans Meerwein Strasse, D-W-3550 Marburg (FRG)

2. g^+g^- Interactions as a Conformation-Determining Factor

The g^+g^- interaction (also termed *syn*-pentane interaction) brings two methyl (alkyl) groups, for example the methyl groups of *n*-pentane (see **4** in Scheme 1) into such spatial proximity as to produce a destabilizing steric interaction. The nature of the interaction is well known in the form

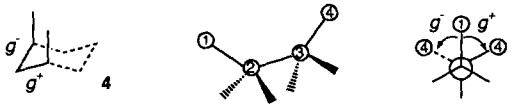

Scheme 1. Left: Conformation of *n*-pentane (**4**) leading to g^+g^- interactions. The cyclohexane ring drawn in dashed lines points out the analogy to 1,3-diaxial interactions. The g^+ and g^- interactions are defined with the help of sawhorse (middle) and Newman projections (right).

of the 1,3-diaxial interaction in cyclohexane derivatives. The term g^+g^- interaction derives from the fact that the conformation of a molecule can be given as a sequence of the dihedral angles of the principal chain. With a dihedral angle of about 60° one has a *gauche* arrangement; with a dihedral angle of +60° one speaks of g^+, with one of −60°, of g^-. A dihedral angle of 180° corresponds to a *trans* arrangement (*t*) of the chain. The sign of the dihedral angle is independent of whether the chain is analyzed from C1 to C4, or vice versa. The arrangement in structure **4** is characterized, when one looks at the principal chain of the molecule, by a g^+ dihedral angle followed by a g^- dihedral angle.

Calculations[11] and experiments[12] show that a 1,3-diaxial interaction of two substitutents on a cyclohexane ring produces a destabilization of approximately 2.6–6.2 kcal mol^{-1}. This would also apply to the *syn*-pentane conformation **4** compared to the all-*trans* chain,[13, 14] if the molecule did not decrease this strain by opening the dihedral angle to 80–95°.[14–17] Nevertheless, the relaxed g^+g^- interaction still produces a destabilization on the order of 1.4–3.0 kcal mol^{-1}.[10, 15, 18] The consequence of this is evident in the partial structures **5** and **6**, which in each case can adopt only two conformations that are free of g^+g^- interactions[9b] (Scheme 2, see also ref.[19, 20]).

The structural elements **5** and **6** are typical of propionogenic natural substances. An evaluation of the X-ray structure analyses of 30 arbitrarily chosen compounds containing the partial structure **5** or **6** showed that in 46 out of 51 of these structural elements the specific conformation adopted

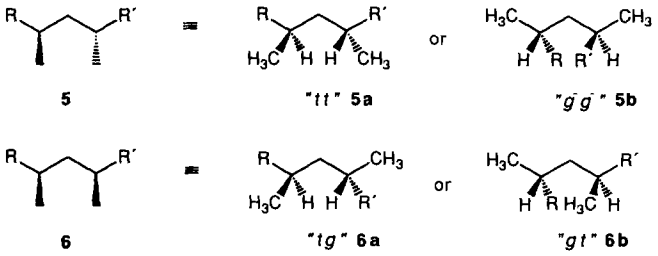

Scheme 2. **5a, b** and **6a, b** are the only conformations of **5** and **6** without g^+g^- interactions.

is one in which the g^+g^- interaction is avoided. This is demonstrated very clearly in the structure of a derivative of bougeanic acid **7**[21] and in the partial structures of ionomycin (**8**)[22] (Fig. 1).

Compounds with the unit **5** thus have a straight main chain (*tt* conformation **5a**, eight of thirteen cases, dihedral angles 170 ± 9°) or more rarely (five of thirteen cases, dihedral angles 68 ± 11°) a doubly bent chain (g^+g^+ or g^-g^- conformation). The unit **6** necessarily leads to a simple bending of the main chain (*tg* conformation, 33 cases, dihedral angles 171 ± 6°; 62 ± 8°). The structural formulas of a number of pheromones suggest that these molecules may have a specific folding pattern despite complete conformational mobility. For example, the shape of lardolure (**9**)[23] may well be essential for its biological signaling action. Epimers of **9**[24] having other preferred conformations of the chain are ineffective.

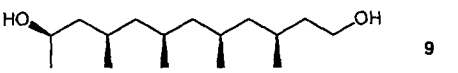

The different preferred conformations of the partial structures **5** and **6** have been known already for a long time from polymer chemistry. **5** corresponds to the repeating unit in syndiotactic polypropylene, which exists either as an all-*trans* chain[25] or as a ttg^+g^+ helix **10**.[26] **6** corresponds to isotactic polypropylene, in which the direction of the chain changes at every other double bond in order to avoid g^+g^- interactions. The resulting $tg^+tg^+tg^+$ conformation likewise leads to a helical structure **11**[27] (Scheme 3).

The stereotriads **A**–**D** frequently occur as structural elements in propionogenic natural substances.[28] Whitesell and Hildebrandt[29] pointed out that these partial structures have quite specific preferred conformations. An inspection

Reinhard W. Hoffmann was born in Würzburg, Germany in 1933. He studied chemistry at the University of Bonn and gained his doctorate in 1958 for research conducted with B. Helferich. After two years as a postdoctorate with G. W. Brindley at the Pennsylvania State University, he became an assistent to G. Wittig at the University of Heidelberg, where he habilitated in 1964. Three years later he was appointed as Dozent at the Technische Hochschule in Darmstadt. He has been professor at the University in Marburg since 1970. At various times he has been a guest professor at the University of Wisconsin, the University of Bern, and the University of California at Berkeley. He is currently interested in developing methods for stereoselective C–C bond formation and exploring their applications in natural products synthesis, as well as generally studying the stereochemistry of reactive organometallic compounds.

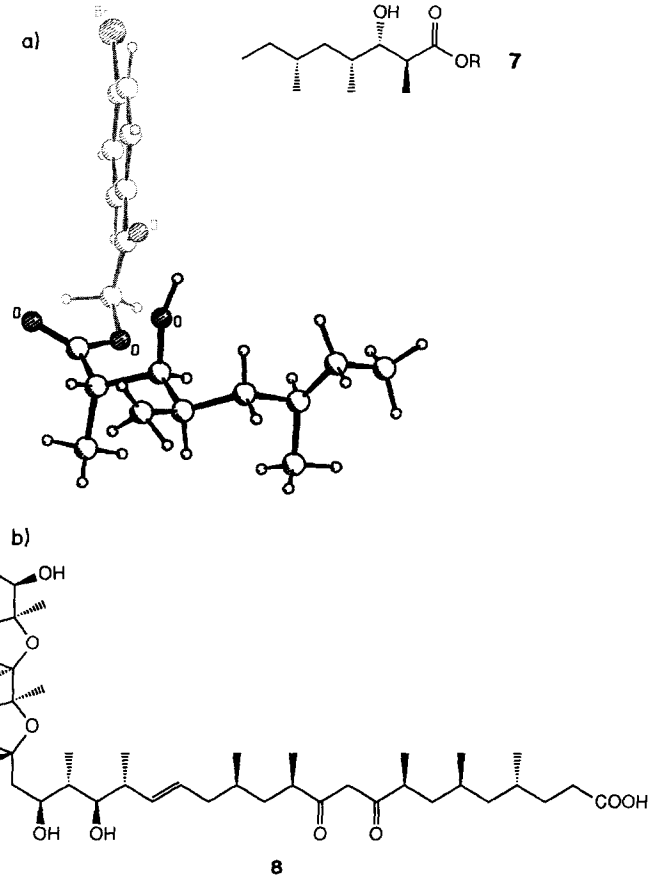

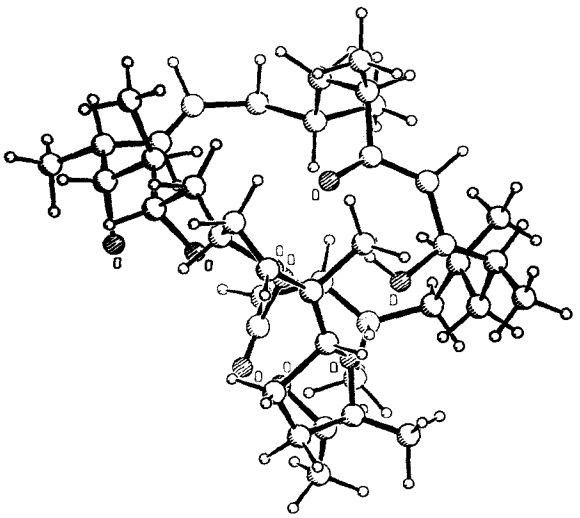

Fig. 1. a) Chemical formula of bougeanic acid **7** and the crystal structure of a derivative (R = $CH_2C(O)C_6H_4Br$). b) Chemical formula of ionomycin (**8**) and the crystal structure of its Ca^{2+} salt. In this and the following figures, the partial structures relevant to the discussion are highlighted in black. The remaining parts of the structures are reproduced in gray.

of the crystal structures of a random selection of 26 compounds with these structural elements show that the conformation of the main chain is again mainly determined by the methyl branchings, as in the case of **5** and **6**. In this respect only the structural types **12** and **13** are significant with regards to conformation. The hydroxyl groups are oriented outward into the free space independent of their relative configuration, even in the case of folded chains, and may interact either intramolecularly or intermolecularly.

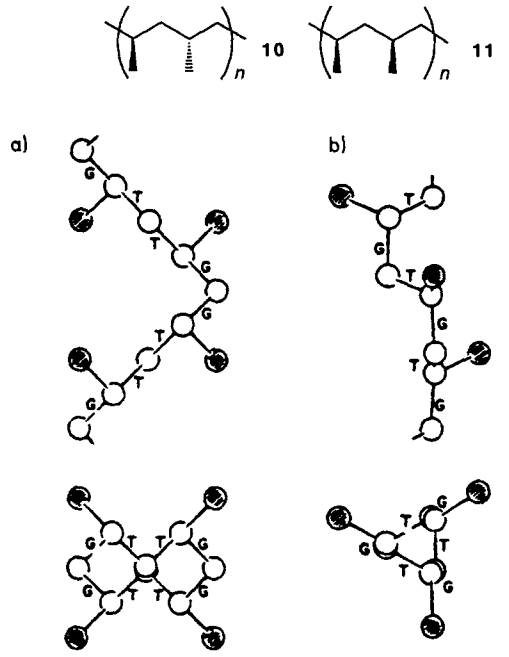

Scheme 3. a) Helical conformation of syndiotactic polypropylene **10** and b) of isotactic polypropylene **11**. T = *trans*, G = *gauche*.

If several hydroxyl groups on the main chain are at the relative positions 1 and 3, the conformation of the main chain can be stabilized additionally by hydrogen bonds if the hydroxyl groups have an appropriate spatial arrangement;[30] see for example the partial structures of rifamycin (**14**)[31] or zincophorin (**15**)[32] (Fig. 2).

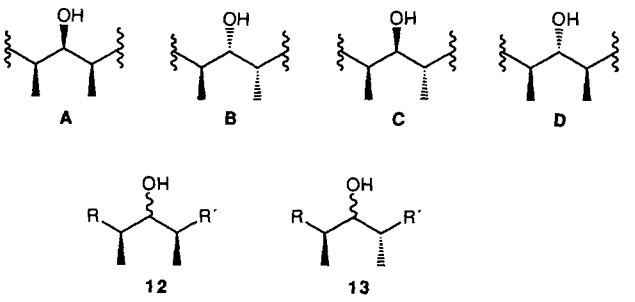

In the area of propionogenic natural substances, compounds are also found in which the conformational mobility of the main chain is restricted, but not suppressed, by a fused six-membered ring, as for example in the partial structures **16** and **17**.

Firl and Kresse et al.[33] showed by NMR investigations on terpenes that for these partial structures the illustrated conformations are largely populated, in other words, exactly those conformations in which a g^+g^- interaction is avoided. Thus, the equatorial (in **16**) or axial (in **17**) position of the substituent R determines the preferred conformation along the C2–C7 bond. This was subsequently discussed in detail also by Kishi et al.[34] and Sih et al.[35] Similar effects were also observed in five-membered ring lactones.[36] Finally, 14 randomly chosen X-ray structure analyses of propionogenic natural substances show that corresponding partial struc-

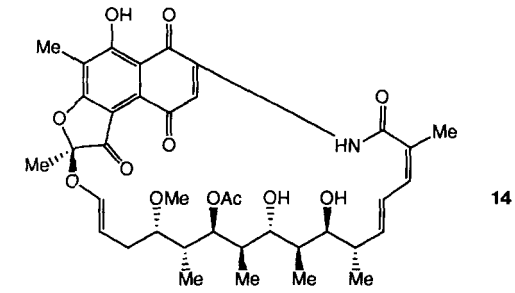

14

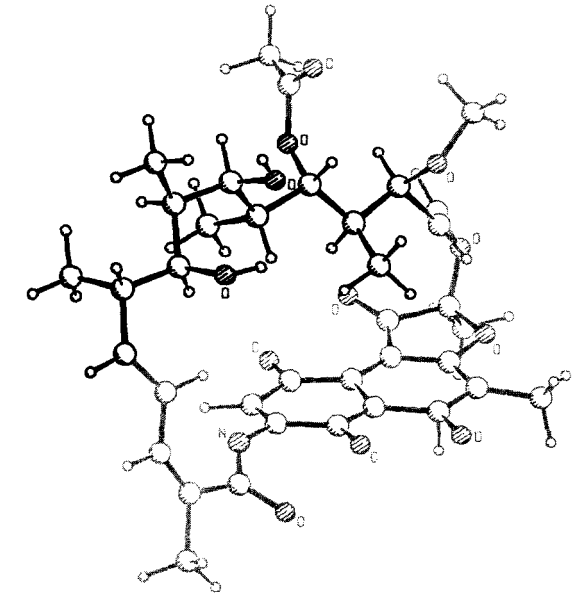

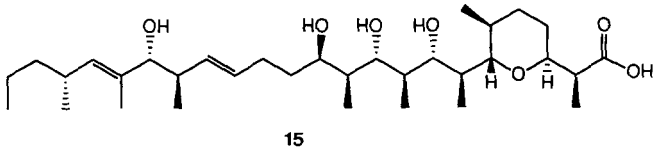

15

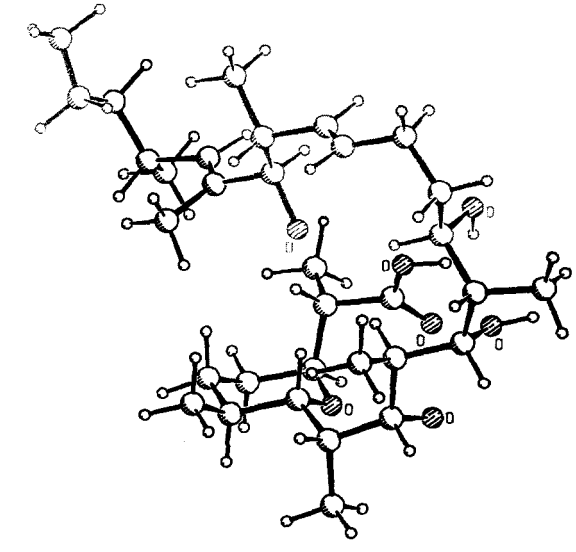

Fig. 2. Because of the appropriate spatial arrangement of OH groups, the conformations of rifamycin S (**14**, top) and zincophorin (**15**, bottom) are additionally stabilized by hydrogen bonds.

tures exist in exactly these conformations. One should keep in mind that, notwithstanding the preference for these conformations, both inversion of six-membered rings and rotation about the exocyclic bonds are fully possible at ambient temperature.

Allinger et al.[37] referred early on to the fact that a branched side chain in an axial position on a six-membered ring, as in **18**, adopts only a single preferred conformation in order to avoid g^+g^- interactions.[38] This arrangement[39] is found for example in the structure of zincophorin,[32] (see Fig. 2 bottom). However, even an unbranched axial side chain can be fixed in space if an equatorial group is present in the adjacent position, as in **19**.[9b] Essentially, this is a

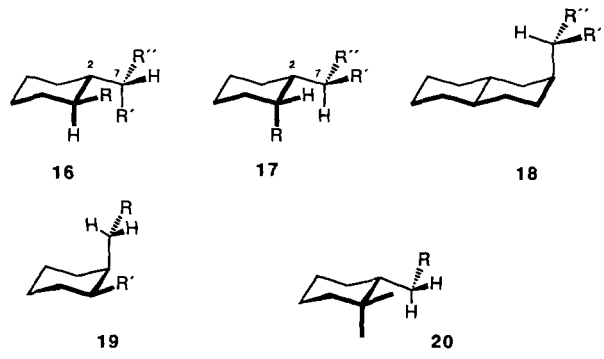

special case of the *gem*-dimethyl effect.[40,41] Likewise, a defined orientation of an unbranched, equatorially situated side chain can be achieved if it is located adjacent to a disubstituted ring position, as in **20**. This relates to structural elements that occur, for example in pederin (**21**),[44] onnamide,[45] mycalamide,[46] and bryostatin.[47] A section of

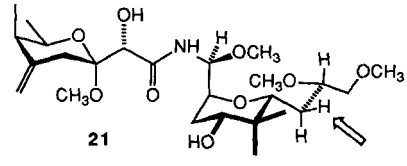

21

the crystal structure of 18-*epi*-benzoylpedamide[48] illustrates this effect clearly (Fig. 3).

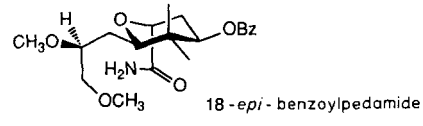

18-*epi*-benzoylpedamide

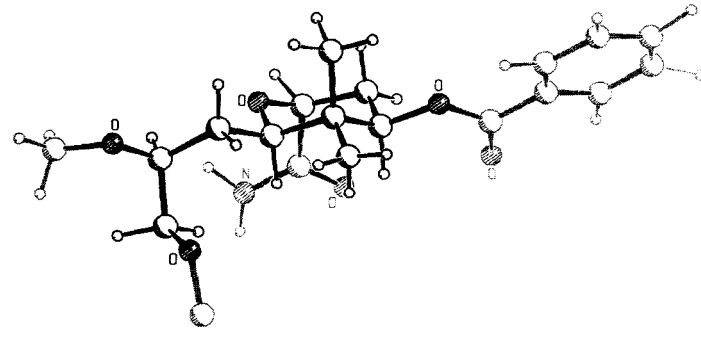

Fig. 3. Chemical formula and crystal structure of 18-*epi*-benzoylpedamide. The orientation of the side chain is dictated by the two neighboring *gem* methyl groups.

In the structures examined hitherto the central atom of the partial structures **5** and **6** was sp^3-hybridized. If it is sp^2-hybridized as in **22**, the central bond angle is larger, so that the methyl groups are better able to avoid one another. An analysis of a small number of randomly selected structures of compounds of type **22** show a broad multiplicity of possible conformations. The number of conformations that can be adopted at room temperature is thus not noticeably restricted by g^+g^- interactions in this type of structure.

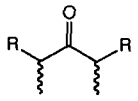

22

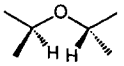

23

If the central atom of the structural units **5** and **6** is an oxygen atom, however, as in **23**, then the shorter C-O-C distances and the smaller C-O-C bond angles mean that g^+g^- interactions become more pronounced. This is reflected, for example, in the preferred conformation of diisopropyl ether **23**.[49]

3. Allylic 1,3 Strain as a Conformation-Determining Factor

Allylic 1,3 strain was defined by Johnson,[50] who stated that in partial structures of the type **24** ($R^Z \neq H$) those conformations in which the groups R and R^Z are coplanar, as in **24a**, are energetically unfavorable. The preferred conformation is **24b**, in which the H-C-C=C-R^Z unit lies in one plane.

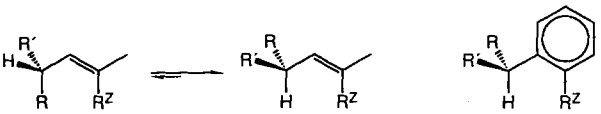

24a **24b** **25**

Recent calculations show[51] that conformation **24b** is almost exclusively populated, and that conformation **24a** is approximately 3.5 kcal mol^{-1} higher in energy. Rotation about the vinylic C–C bond is, however, fully possible at ambient temperatures. Calculations show furthermore that the potential curve for libration of the C=C-C-H dihedral angle ϕ is initially flat and increases more steeply only at $\phi > 35°$. An evaluation of about 50 crystal structures of natural substances and synthetic products with the structural element **24** shows, in agreement with this, that the dihedral angles are uniformly distributed in the range 0–30°. In individual cases values of 40° were obtained, but dihedral angles greater than 44° were not found. If the π bond in **24** is part of an aromatic system, as in **25**, then somewhat larger dihedral angles may be tolerated on account of the longer C=C bond. Values up to 48° have been found.[38, 52]

The partial structure **24** is thus a conformationally flexible element, which exists in a preferred conformation that always produces a bend in the main chain. The resulting change in the direction of the main chain is not identical to that which occurs in compounds with the partial structure **6** as discussed in Section 2.

The conformation-determining action of the allylic 1,3 strain is illustrated, for example, in the compounds stegobinone (**26**) and 1′-*epi*-stegobinone (**27**),[53] of which the former is the sex pheromone of the drugstore beetle, *stegobium paniceum*, whereas the 1′ epimer inhibits the pheromone action (Fig. 4).[54]

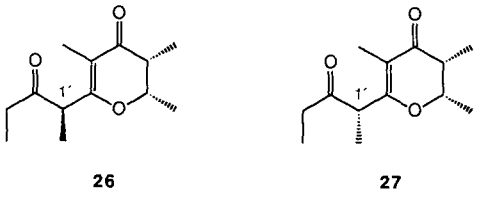

26 **27**

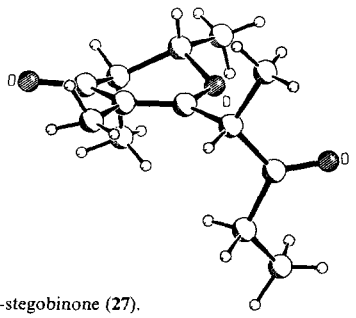

Fig. 4. Crystal structure of 1′-*epi*-stegobinone (**27**).

The configurational change in the transition from **26** to **27** appears at first glance to be only minor. Yet because of the allyl system, the spatial arrangement of the side chain[55] is completely different in the two epimers.[56] 2-Substituted vinyl units located in equatorial positions of six-membered rings, as in **28**, often serve to fix large structural units in natural products in an energetically preferred, spatial arrangement. Such a structural unit is found for example in

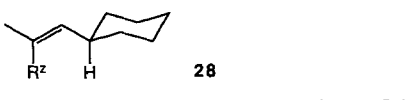

28

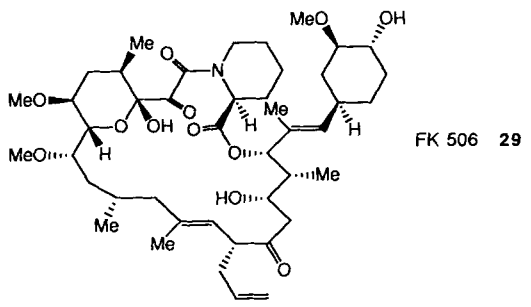

FK 506 **29**

FK 506 (**29**).[57] In **28** the orientations of the substituents on the vinyl group as well as those of all the bonds about the six-membered ring are set by the single preferred conformation of this structural unit.

The phenomenon of allylic 1,3 strain was originally recognized in compounds of type **30**.[50] Here, the ring substituent R prefers to adopt the axial position because of the *Z* orientation of the substituent R^Z. This also applies to amides of the type **31**, due to the double-bond character of the N–CO bond.[58] It has been known and understood for a long time that a ring substituent in the 2 position of *N*-acylpiperidines **31** preferentially adopts an axial arrangement, even if this is offset by a 1,3-diaxial interaction.

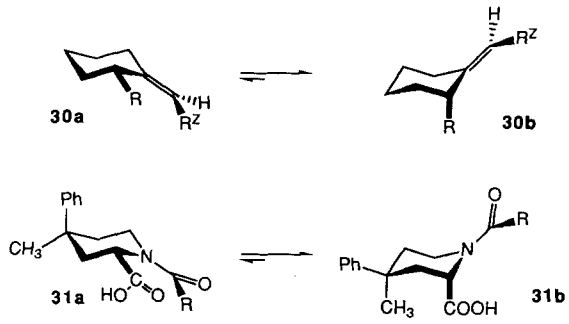

Nature utilizes this effect, as can be seen by a glance at the crystal structure of FK 506 (**29**) (Fig. 5). The COOR substituent on the piperidine ring of **29** is axial, and oriented analogously to that in conformation **31b**. A combination of

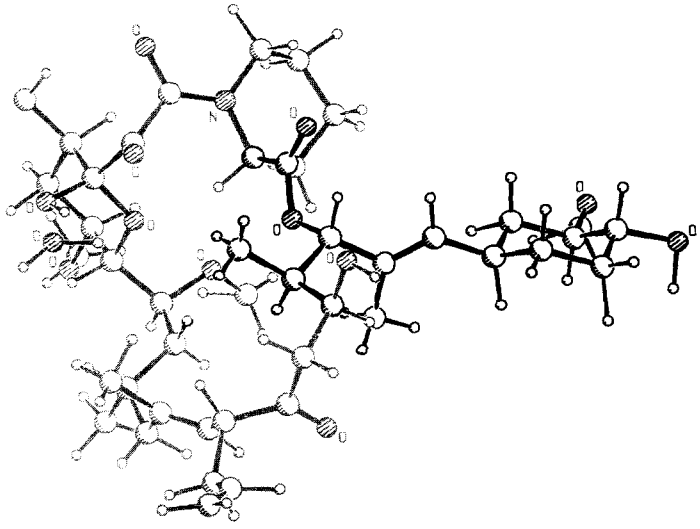

Fig. 5. Crystal structure of FK 506 (**29**). The COOR substituent on the piperidine ring is in the otherwise energetically unfavorable axial position, in order to minimize interactions with the *N*-acyl substituent.

conformational control by allylic 1,3 strain with that produced by methyl substituents (avoidance of g^+g^- interactions) is found for example in the antibiotic M139603 (**32**)

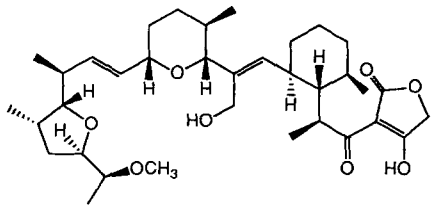

M 139603 **32**

(Fig. 6).[59] One can follow through segment by segment in this structure how the substituents arranged in this particular way favor just the one conformation found in the X-ray crystal structure. Despite total conformational mobility, this conformation causes a 180° bend in the molecular backbone.

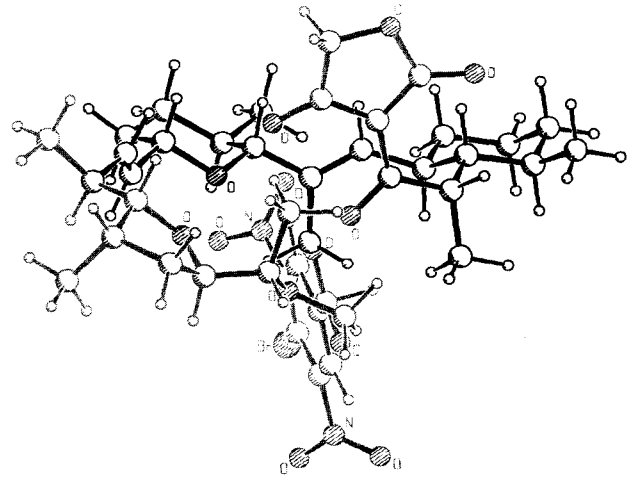

Fig. 6. Crystal structure of the antibiotic M139603 (**32**) as a 4-bromo-3,5-dinitrobenzoate. The conformation is determined by allylic 1,3 strain and the avoidance of g^+g^- interactions (CH_3 groups).

4. Conformational Design of Molecular Skeletons

The goal of molecular design nowadays is frequently the synthesis of a complementary molecule for a receptor, so that this molecule exhibits specific functionalities in a spatial arrangement suitable for binding to the receptor. One of the problems in this connection is finding an appropriate molecular skeleton on which the bonds to the functional groups, for example to a C-NH_2 or C-COOH group (see **33**), not only have the correct spacing but are also vectorially in the correct spatial orientation. The program CAVEAT, developed by P. A. Bartlett et al.[60] (Berkeley) for this purpose, searches all structures stored in the Cambridge Structural Data File for a matching molecular skeleton. In this search it is irrelevant whether the molecular skeleton is rigid or flexible. A recent survey of peptide conformation mimetics[61] shows that up to now mainly rigid molecular skeletons have been tested in order to simulate, for example, a bend in a peptide chain corresponding to a β turn (β-turn mimetics).

An attempt could also be made in this context to connect the necessary functionalities with one another by means of a section from a diamond lattice. Assuming that this would be possible with sufficient spatial agreement, one could design a rigid, polycyclic molecule that would inevitably produce the necessary arrangement of the functional groups in space. By omitting individual skeleton bonds one by one, one would eventually reach the other extreme, namely a completely flexible chain-type molecule, which could of course adopt the desired conformation, but only as one of an almost infinite number of possibilities. The intellectual challenge now is to design, with the aid of principles illustrated in nature or developed by insight and intuition, a completely or overwhelmingly flexible molecular skeleton, which neverthe-

less has the desired conformation as its preferred conformation. For example, the recently described[62] antagonist **34** of *N*-methyl-D-aspartate exhibits (accidentally or intentionally) just such properties, since in **34** the allylic 1,3 strain ensures a specific preferred conformation of the molecular skeleton.

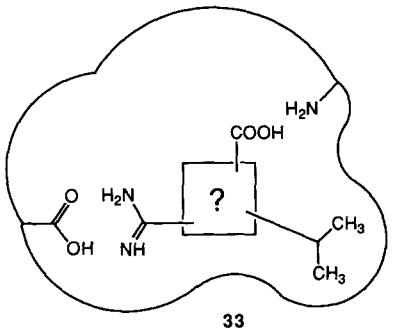

33

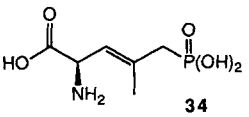

34

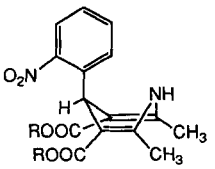

35

Likewise, the nitro group in the *ortho* position of the phenyl substituent in nifedipin (**35**) ensures, due to allylic 1,3 strain, that the phenyl ring is orthogonal to the dihydropyridine ring, an arrangement which is decisive for the pharmacological effect.[63]

4.1. Design of Preferred Conformations of a C_7 Chain; Flexible Building Blocks for Conformational Design

The chemist will be inclined to tackle a complex problem in conformational design stepwise, that is, by considering skeletal segments with specific preferred conformations. These segments could then be assembled like building blocks to form larger, realistic molecular skeletons. One could, for example, consider the C_7 chain of *n*-heptane as a skeletal segment which is long enough to illustrate repeatable units. The conformation of *n*-heptane can be described by a sequence of four dihedral angles. The 13 conformations that are free of g^+g^- interactions (see ref.[17]), as well as those with a partially relaxed g^+g^- interaction are all populated at room temperature.

The conformations of *n*-heptane without g^+g^- interactions can now be depicted on a diamond lattice.[64, 65] Scheme 4 illustrates this on the basis of the molecular skeleton of spirodiadamantane. Those conformations composed of a central *tt*, tg^+, or g^+g^+ unit are shown in separate groups. It becomes apparent that derivatives of spirodiadamantane may serve as rigid models for the conformers of *n*-heptane when a correct spatial arrangement of functional groups along a heptane chain is required.

In addition to the two extreme cases, namely the conformationally fully flexible *n*-heptane of unspecified shape on the one hand, and the completely rigid spirodiadamantane derivative with a fixed, defined shape on the other hand, flexible *n*-heptane skeletons with a defined shape should be able to be constructed according to the principles illustrated by nature (avoidance of g^+g^- interactions). In a first stage the problem can be simplified by fusing a six-membered ring to the C_7 chain. One or two dihedral angles can thus be set in a preferred conformation. Conformational mobility is retained, although restricted, about these intraring bonds as a consequence of the inversion of the six-membered ring, which is in full operation at ambient temperatures. With the fusion of a six-membered ring to the two internal bonds of *n*-heptane, a 1,3 diequatorial arrangement of substituents on the cyclohexane ring corresponds to a central *tt* conformation, and a 1,3 equatorial–axial arrangement to a central *tg* conformation. If further auxiliary substituents are attached to the ring or to positions 2 and 5 on the chain, any of the four arrangements of a C_7 chain with a central *tt* unit, or any of the six arrangements with a central *tg* unit can be rendered to be the preferred conformation (Scheme 5). Calculations with MACROMODEL[66] show that the conformation sought in each case should be populated predominantly.

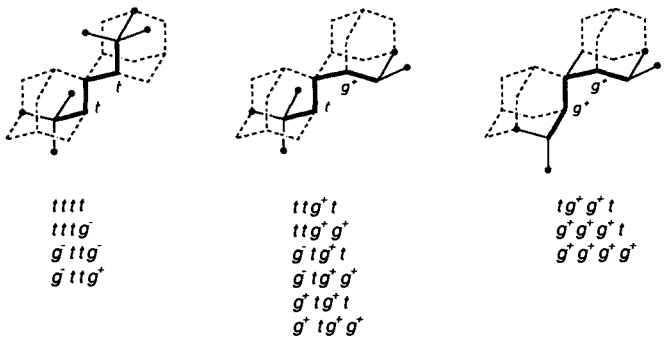

tttt
tttg^-
$g^-tt g^-$
$g^-tt g^+$

ttg^+t
ttg^+g^+
g^-tg^+t
$g^-tg^+g^+$
g^+tg^+t
$g^+tg^+g^+$

tg^+g^+t
$g^-g^+g^+t$
$g^+g^+g^+g^+$

Scheme 4. Conformations of *n*-heptane without g^+g^- interactions superimposed on a diamond lattice.

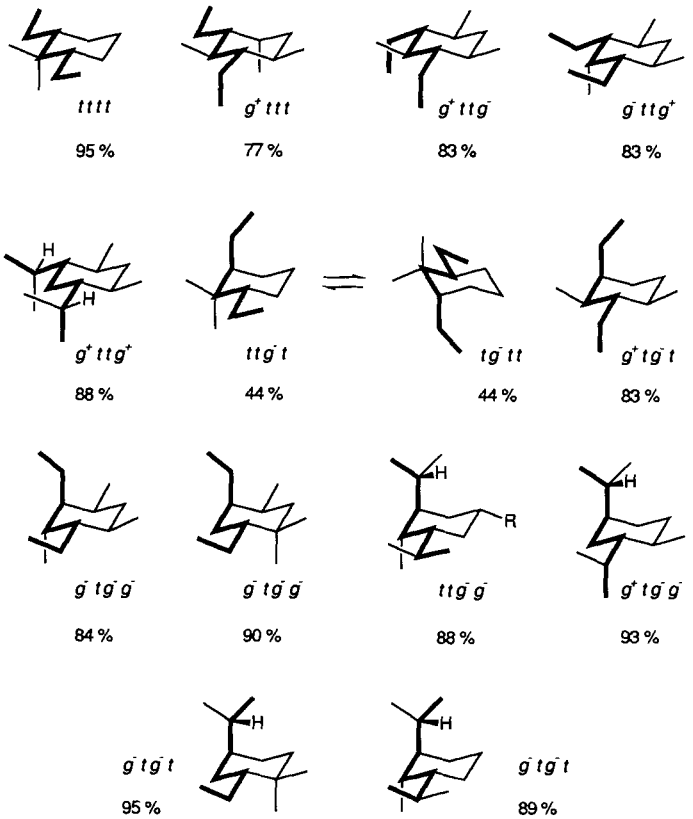

Scheme 5. Fusion of a six-membered ring to *n*-heptane. The 1,3 diequatorial orientation of the substituents on the cyclohexane ring corresponds to a *tt* conformation on the internal bonds of *n*-heptane, the 1,3 equatorial–axial orientation to a *tg* conformation.

Of course, one or both of the outer dihedral angles of the heptane chain can also be fixed in specific preferred conformations by ring fusion. For example, **36** corresponds to a chain with g^+ttg^+ conformation.

Without altering the conformational preference, two further methyl (alkyl) groups may be placed in a strategically correct manner on **36**. In the resultant compound **37**, 13 of the regular conformations of *n*-heptane can be superimposed onto the preferred conformation **37a**. The skeleton **37** thus offers numerous possibilities for spatially stabilizing specific heptane conformations, and this with unrestricted conformational mobility.

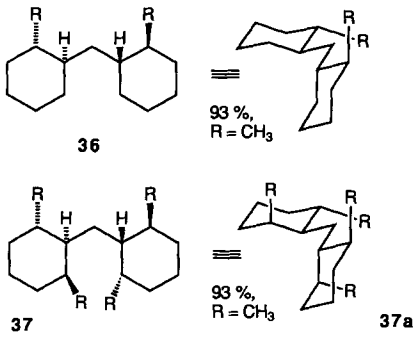

A *gem*-dialkyl substitution offers a further starting point for the conformational fixing of a heptane chain, for example at C4 in **38**. As Alder et al.[67] have pointed out, this means in the first place that the two outer dihedral angles of the C_7 chain prefer a *t* conformation (MACROMODEL calculations show a ca. 86% preference for a *t* conformation). Further methyl substituents, for example in **41**, favor the *ttgt* arrangement **41a** (74%). The isomer **42** on the other hand has, according to MACROMODEL calculations, two sets of similar, roughly equally populated conformations, namely the *tttt* arrangement **42a** and the tg^-g^-t arrangement **42b**.

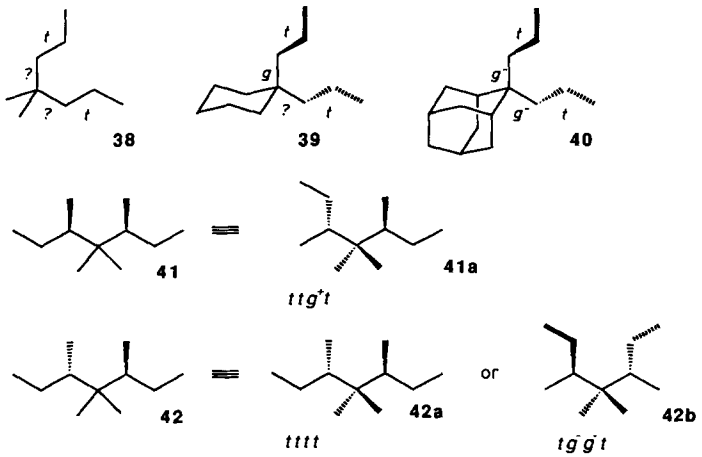

If it is desired to model a heptane chain with a central g^+g^+ (or g^-g^-) conformation, the two geminal methyl groups can be replaced by a six-membered ring, as in **39**. A *g* conformation is thereby imposed on one of the internal bonds of the heptane chain. On account of the rapid inversion of the six-membered ring, a *g* conformation is then effectively preferred for both internal heptane bonds, that is, molecule **39** should exist mainly in the tg^+g^+t conformation (or the enantiomeric tg^-g^-t conformation). This can then be achieved completely by turning to the adamantane derivative **40**. This is a remarkable molecule: on the one hand rotation about all the bonds of the heptane chain is unrestricted, while on the other hand **40** has only one pair of enantiomeric preferred conformations!

The structures shown here model 11 of the 13 regular conformations of an *n*-heptane chain without g^+g^- interactions, such that the desired conformation is the preferred conformation with total or substantial preservation of the conformational mobility.

While as a rule g^+g^- conformations are energetically unfavorable if population of such a conformation chain is desired, this can be achieved by the introduction of a *tert*-butyl substituent on the chain. The molecule **43** might well exist to a large extent in the conformations **43a** and **43b**, which both exhibit a *syn*-pentane interaction.

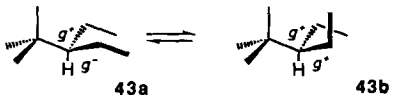

According to DeClercq et al.[68] this "*tert*-butyl anchoring" is one way of populating the otherwise unfavorable g^+g^- conformation of a chain, so that ring-closing reactions of the chain ends are favored.

4.2. Applications of Conformational Design

The shape of a molecule and the associated spatial arrangement of functional groups are particularly important when the molecule is to be bound to another molecule or to ions. For this reason conformational design is currently used primarily in the development of host molecules for ions or amino acids.

Ligand conformation is particularly important in the development of optimum polydentate ligands. The coordination of the ligand is most favorable when its ground-state conformation resembles that in the complex. This can be achieved, for example, by suitably located methyl substituents.

Such conformational design was demonstrated by Still et al.[69] par excellence in the case of a polyether chain. Polyethers have many acceptor positions for hydrogen bonds; they thus have a marked tendency to complex ammonium ions. The polyether **44** may well prefer the $tg^+ttg^+ttg^+$ helical arrangement, which predominates in polyethyleneglycol derivatives,[70] though of course only as one of many other possible conformations. The fusion of six-membered rings as in form **45** specifies in each case two successive *t* arrangements of the main polyether chain. The resulting *t*?*tt*?*tt*? sequence still permits 25 conformations which are up to 3 kcal mol^{-1} higher in energy than the most stable conformation. Only when further methyl substituents are intro-

duced, as in **46**, is a molecule attained with only a single low-energy conformation, since all other conformations have destabilizing g^+g^- interactions. We are thus dealing with a conformationally fully flexible molecule, which nevertheless has only a single helical designer conformation ($g^+ttg^-ttg^+$). As a consequence, **46** exhibits a substantially higher enantioselective recognition of protected amino acids than **45**.[69, 71]

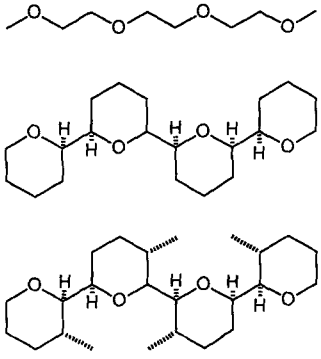

44

45

46

A further example of such a ligand design is provided by a [14]thiacrown-4 for complexing Ni^{2+} (Fig. 7).[72] By means of a geminal dimethyl substitution on the macrocycle **47**, a *trans* conformation of the CC–SC bond in **49** is induced which is also found in complex **48**. The binding constant for Ni^{2+} increases correspondingly by a factor of 50 in the transition from the ligand **47** to **49**.[72]

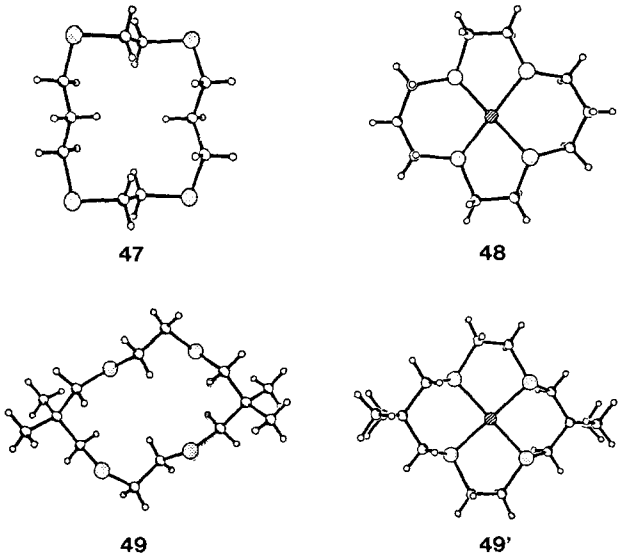

47 **48**

49 **49'**

Fig. 7. Crystal structures of the [14]thiacrown-4 macrocycles **47** and **49** as well as their respective complexes which form upon addition of Ni^{2+}, **48** and **49'**. Hatched spheres are Ni atoms, dotted spheres S atoms.

Molecules with a boomerang shape could also be tailor-made. For example, compound **51** should—by analogy to the investigations carried out by Vögtle et al.[73] on **50**—be even better able to bind thiourea than **50** since the host molecule **51** should spontaneously adopt the optimum conformation for bonding.[74]

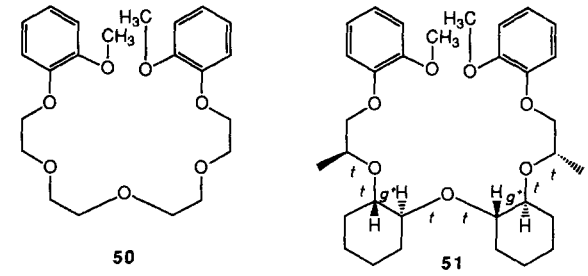

50 **51**

The control of conformer populations by means of avoidance of g^+g^- interactions is just one of the principles that can be applied in conformational design. Flexible structural elements whose shape is determined by allylic 1,3 strain or by the conformational preferences of an amide or urea group,[75] may also be used.

A timely problem is the design and synthesis of chiral ligands for metal-catalyzed reactions. For example, the easily accessible complex **52** would have the disadvantage that the phenyl and methyl groups on the ligand, which should be responsible for asymmetric induction, are not spatially fixed. In other words, many conformations are possible regarding rotation about the indicated bonds. This disadvantage is

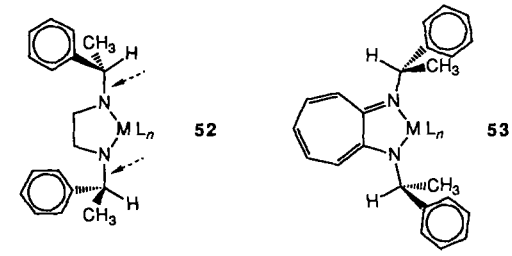

52 **53**

avoided in the complex **53**,[76] since allylic 1,3 strain specifically fixes the phenyl and methyl groups in the ligand to produce a defined chiral environment at the metal center.

5. Summary and Future Prospects

The spatial structure of many polyketide natural substances illustrates the principles that nature employs to impart a defined shape to these molecules while largely retaining conformational flexibility. These principles can be utilized as such or developed further in order to confer by structural modifi-

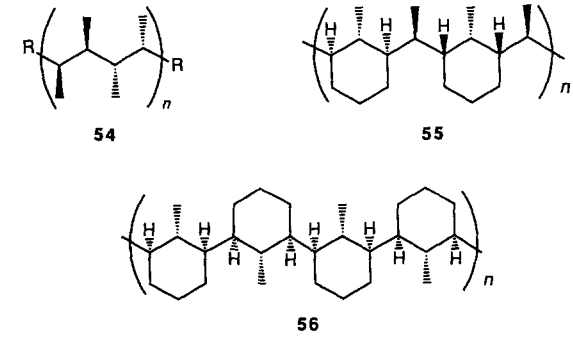

54 **55**

56

cation a definite preferred conformation on a molecular chain (conformational design). If, for example, it is desired to produce a rod-shaped flexible molecule, structures **54** to **56** could be sought.

In the syntheses of such compounds with fairly short chains the problem would be primarily that of stereoselectivity, while in the syntheses of those with longer chains it would that of stereoregular polymerization.[77]

If on the other hand it is desired to construct helical molecular chains, one could seek a steep helix through a $tg^+(tg^+)_n tg^+$ sequence, as in **57**. This would be an isotactic polypropylene reinforced in its conformational preference. A flatter helix would result from a $ttg^+(ttg^+)_n ttg^+$ conformation (cf. ref.[70]). This could be achieved for example with a structure such as **58**.

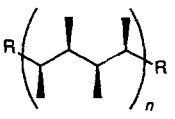

57

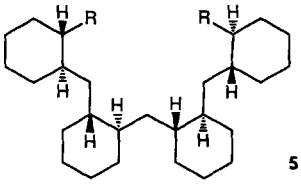

58

The examples given above are obvious solutions, though certainly not the only and perhaps also not the best solutions for the design problems presented. It is clear, however, that high demands will be placed on the art of stereoselective synthesis when such molecules are synthesized. In view of the breathtaking developments in methods and procedures of stereoselective synthesis over the last 15 years, it may be hoped that molecules such as **56** or **57** will soon no longer present insuperable synthetic problems. With further progress in synthesis, efficient conformational design will be able to be performed not only on the computer screen but also in the laboratory as a matter of routine. One will then also be able to answer the question of whether conformationally flexible, biologically active substances hitherto employed by nature have advantages over conformationally rigid, biologically active substances.

The review does not aim to, and certainly is not able to, deal exhaustively with all the possibilities in the conformational design of molecular skeletons. It should, however, indicate above all the relevant principles and provide a stimulus for further thought.

I wish to thank M. Brumm and Dr. T. Sander, Marburg, (FRG), for the results of MACROMODEL calculations reproduced herein. I also wish to thank Prof. G. Frenking, Marburg, for advice regarding technical details.

Received: February 14, 1992 [A 878 IE]
German version: *Angew. Chem.* **1992**, *104*, 1147

[1] a) R. J. P. Williams, *Angew. Chem.* **1977**, *89*, 805; *Angew. Chem. Int. Ed. Engl.* **1977**, *16*, 766; b) H. Kessler, *ibid.* **1982**, *94*, 509 and **1982**, *21*, 512; c) H. Kessler, S. Steuernagel in *Peptide Pharmaceuticals – Approaches to the Design of Novel Drugs* (Ed.: D. Ward), Open University Press, Buckingham, GB, **1991**, p. 18.

[2] K. B. Wiberg, K. E. Laidig, *J. Am. Chem. Soc.* **1987**, *109*, 5935, and references cited therein.

[3] J. S. Richardson, D. C. Richardson, *Principles and Patterns of Protein Conformation* in *Prediction of Protein Structure and the Principles of Protein Conformation* (Ed.: G. D. Fasman), Plenum, New York, **1989**, p. 1.

[4] a) W. F. Degrado, *Adv. Protein Chem.* **1988**, *39*, 51; b) H. Kessler in *Trends in Drug research (Proc. 7th Noordwijkerhout-Camerino Symp.)* (Ed.: H. Timmerman), Elsevier, Amsterdam, **1990**, p. 73.

[5] M. T. Goulet, D. W. Hodkey, *Tetrahedron Lett.* **1991**, *32*, 4627.

[6] D. Boumrah, M. M. Campbell, S. Fenner, R. G. Kinsman, *Tetrahedron Lett.* **1991**, *32*, 7735.

[7] T. M. Zabriskie, J. A. Klocke, C. M. Ireland, A. H. Marcus, T. F. Molinski, D. J. Faulkner, C. Xu, J. C. Clardy, *J. Am. Chem. Soc.* **1986**, *108*, 3123.

[8] W. R. Chan, W. F. Tinto, P. S. Manchand, L. J. Todaro, *J. Org. Chem.* **1987**, *52*, 3091.

[9] a) W. C. Still, P. Hauck, D. Kempf, *Tetrahedron Lett.* **1987**, *28*, 2817: Lasalocid has "particular arrays of chiral centers, which destabilize undesired rotamers of acyclic bonds"; b) W. C. Still, D. Cai, D. Lee, P. Hauck, A. Bernardi, A. Romero, *J. Heterocycl. Chem.* **1987**, *24*, S-33: "The nonligating substituents of monensin are functional and exert their effect by preorganizing the structure to favor the binding conformation"; c) D. A. Evans, R. P. Polniaszek, K. M. DeVries, D. E. Guinn, D. J. Mathre, *J. Am. Chem. Soc.* **1991**, *113*, 7613: "It is noteworthy that *syn*-pentane interactions dictate virtually all acyclic dihedral angle relationships in this region of ferensimycin"; d) P. K. Somers, T. J. Wandless, S. L. Schreiber, *J. Am. Chem. Soc.* **1991**, *113*, 8045: "minimizing gauche butane, $-gauche/+gauche$ (*syn*-pentane), and allylic $A^{1,3}$ strain along the C14-C26 chain results in the local conformation of FK 506 observed in the solid state."

[10] P. W. Smith, W. C. Still, *J. Am. Chem. Soc.* **1988**, *110*, 7917: "These molecules illustrate that the avoidance of g^+g^- interactions can create an efficient mechanism for an acyclic conformational lock and control the geometry of otherwise flexible molecules."

[11] V. J. Klimkowski, J. P. Manning, L. Schäfer, *J. Comput. Chem.* **1985**, *6*, 570.

[12] N. L. Allinger, M. A. Miller, *J. Am. Chem. Soc.* **1961**, *83*, 2145.

[13] a) R. A. Scott, H. A. Scheraga, *J. Chem. Phys.* **1966**, *44*, 3054; b) S. Sykora, *Collect. Czech. Chem. Commun.* **1968**, *33*, 3514.

[14] K. B. Wiberg, M. A. Murcko, *J. Am. Chem. Soc.* **1988**, *110*, 8029.

[15] A. Abe, R. L. Jernigan, P. J. Flory, *J. Am. Chem. Soc.* **1966**, *88*, 631.

[16] J. E. Anderson, K. H. Koon, J. E. Parkin, *Tetrahedron* **1985**, *41*, 561.

[17] M. Saunders, *J. Am. Chem. Soc.* **1987**, *109*, 3150.

[18] S. Tsuzuki, L. Schäfer, H. Goto, E. D. Jemmis, H. Hosoya, K. Siam, K. Tanabe, E. Osawa, *J. Am. Chem. Soc.* **1991**, *113*, 4665.

[19] C. A. Kingsbury, *J. Chem. Educ.* **1979**, *56*, 431.

[20] S. R. Wilson, F. Guarnieri, *Tetrahedron Lett.* **1991**, *32*, 3601.

[21] B. Bodo, W. Trowitzsch-Kienast, D. Schomburg, *Tetrahedron Lett.* **1986**, *27*, 847.

[22] B. K. Toeplitz, A. I. Cohen, P. T. Funke, W. L. Parker, J. Z. Gougoutas, *J. Am. Chem. Soc.* **1979**, *101*, 3344.

[23] K. Mori, S. Kuwahara, *Tetrahedron* **1986**, *42*, 5539.

[24] K. Mori, S. Kuwahara, *Tetrahedron* **1986**, *42*, 5545.

[25] G. Natta, *Angew. Chem.* **1956**, *68*, 393.

[26] G. Natta, M. Peraldo, G. Allegra, *Makromol. Chem.* **1964**, *75*, 215.

[27] G. Natta, P. Corradini, *J. Polym. Sci.* **1959**, *39*, 29.

[28] R. W. Hoffmann, *Angew. Chem.* **1987**, *99*, 503; *Angew. Chem. Int. Ed. Engl.* **1987**, *26*, 489.

[29] J. K. Whitesell, B. Hildebrandt, *J. Org. Chem.* **1985**, *50*, 4975.

[30] a) A. J. Kinneging, V. Mom, F. C. Mijlhoff, G. H. Rennes, *J. Mol. Struct.* **1982**, *82*, 271; b) R. W. Hoffmann, U. Weidmann, *Chem. Ber.* **1985**, *118*, 3980.

[31] M. Brufani, S. Cerrini, W. Fedeli, A. Vaciago, *J. Mol. Biol.* **1974**, *87*, 409.

[32] H. A. Brooks, D. Gardner, J. P. Poyser, T. J. King, *J. Antibiot.* **1984**, *37*, 1501.

[33] J. Firl, G. Kresze, T. Bosch, V. Arndt, *Justus Liebigs Ann. Chem.* **1978**, 87.

[34] M. D. Lewis, Y. Kishi, *Tetrahedron Lett.* **1982**, *23*, 2343.

[35] D. V. Patel, F. VanMiddlesworth, J. Donaubauer, P. Gannett, C. J. Sih, *J. Am. Chem. Soc.* **1986**, *108*, 4603.

[36] a) G. Dana, J. Gharbi-Benarous, J. Vaissermann, M. Philoche-Levisalles, C. Bois, *Tetrahedron* **1988**, *44*, 6357; b) G. Dana, E. Touboul, M. Mellot-Srour, *Tetrahedron* **1992**, *48*, 1617.

[37] N. L. Allinger, J. Allinger, *Structures of Organic Molecules*, Prentice Hall, Englewood Cliffs, NJ, **1965**, p. 101; cf. also O. Golan, Z. Goren, S. E. Biali, *J. Am. Chem. Soc.* **1990**, *112*, 9300.

[38] S. Knapp, T. G. M. Dhar, J. Albaneze, S. Gentemann, J. A. Potenza, D. Holten, H. J. Schugar, *J. Am. Chem. Soc.* **1991**, *113*, 4010.

[39] S. L. Schreiber, Z. Wang, G. Schulte, *Tetrahedron Lett.* **1988**, *29*, 4085.

[40] For references see M. E. Jung, J. Gervay, *J. Am. Chem. Soc.* **1991**, *113*, 224.

[41] It has long been known that an equilibrium mixture of the conformers of a chain is shifted by a *gem*-dialkyl substitution in favor of specific conformations (reactive rotamer effect) [42]. This is reflected in particular in the kinetics of ring-closing reactions [43].

[42] a) T. C. Bruice, U. K. Pandit, *J. Am. Chem. Soc.* **1960**, *82*, 5858; b) E. Riande, J. Guzmán, E. Saiz, J. de Abajo, *Macromolecules* **1981**, *14*, 608; c) P. S. Hillery, L. A. Cohen, *J. Org. Chem.* **1983**, *48*, 3465.

[43] a) R. F. Brown, N. M. van Gulick, *J. Org. Chem.* **1956**, *21*, 1046; b) C. Galli, G. Giovannelli, G. Illuminati, L. Mandolini, *ibid.* **1979**, *44*, 1258; c) R. K. Boeckman, S. S. Ko, *J. Am. Chem. Soc.* **1982**, *104*, 1033; d) D. D. Sternbach, D. M. Rossana, K. D. Onan, *Tetrahedron Lett.* **1985**, *26*, 591; e) W. H. Okamura, M. L. Curtin, *Synlett.* **1990**, *1*, 1.

[44] A. Furusaki, T. Watanabe, T. Matsumoto, M. Yanagiya, *Tetrahedron Lett.* **1968**, 6301.
[45] S. Sakemi, T. Ichiba, S. Kohmoto, G. Saucy, *J. Am. Chem. Soc.* **1988**, *110*, 4851.
[46] N. B. Perry, J. W. Blunt, M. H. G. Munro, L. K. Pannell, *J. Am. Chem. Soc.* **1988**, *110*, 4850.
[47] G. R. Pettit, Y. Kamano, C. L. Herald, M. Tozawa, *J. Am. Chem. Soc.* **1984**, *106*, 6768.
[48] T. M. Willson, P. Kocienski, K. Jarowicki, K. Isaac, P. M. Hitchcock, A. Faller, S. F. Campbell, *Tetrahedron* **1990**, *46*, 1767.
[49] a) N. L. Allinger, M. Rahman, J.-H. Lii, *J. Am. Chem. Soc.* **1990**, *112*, 8293; b) H. Takeuchi, M. Fujii, S. Konaka, M. Kimura, *J. Phys. Chem.* **1987**, *91*, 1015.
[50] F. Johnson, *Chem. Rev.* **1968**, *68*, 375.
[51] J. L. Broeker, R. W. Hoffmann, K. N. Houk, *J. Am. Chem. Soc.* **1991**, *113*, 5006.
[52] T. Imamoto, T. Matsumoto, H. Yokoyama, M. Yokoyama, K. Yamaguchi, *J. Org. Chem.* **1984**, *49*, 1105.
[53] T. Ebata, K. Mori, *Agric. Biol. Chem.* **1990**, *54*, 527.
[54] H. Kodama, K. Mochizuki, M. Kohno, A. Ohnishi, Y. Kuwahara, *J. Chem. Ecol.* **1987**, *13*, 1859.
[55] R. W. Hoffmann, W. Ladner, K. Steinbach, W. Massa, R. Schmidt, G. Snatzke, *Chem. Ber.* **1981**, *114*, 2786.
[56] T. Ebata, K. Koseki, K. Shimazaki, H. Kawakami, T. Chuman, H. Matsushita, K. Mori, *Heterocycles* **1990**, *31*, 581.
[57] H. Tanaka, A. Kuroda, H. Marusawa, H. Hatanaka, T. Kino, T. Goto, M. Hashimoto, *J. Am. Chem. Soc.* **1987**, *109*, 5031.
[58] E. E. Sugg, J. F. Griffin, P. S. Portoghese, *J. Org. Chem.* **1985**, *50*, 5032.
[59] D. H. Davies, E. W. Snape, P. J. Suter, T. J. King, C. P. Falshaw, *J. Chem. Soc. Chem. Commun.* **1981**, 1073.
[60] P. A. Bartlett, G. T. Shea, S. J. Telfer, S. Waterman, *Spec. Publ. R. Soc. Chem. (Molecular Recognition: Chem. Biochem. Probl.)* **1989**, *78*, 182.
[61] G. Hölzemann, *Kontakte (Darmstadt)* **1991**, (1) 3; *ibid.* **1991**, (2), 55.
[62] G. E. Fagg, H.-R. Olpe, M. F. Pozza, J. Baud, M. Steinmann, M. Schmutz, C. Portet, P. Baumann, K. Thedinga, H. Bittiger, H. Allgeier, R. Heckendorn, C. Angst, D. Brundish, J. G. Dingwall, *Br. J. Pharmacol.* **1990**, *99*, 791.
[63] S. Goldmann, J. Stoltefuss, *Angew. Chem.* **1991**, *103*, 1587; *Angew. Chem. Int. Ed. Engl.* **1991**, *30*, 1559.
[64] a) S. A. Babirad, Y. Wang, P. G. Goekjian, Y. Kishi, *J. Org. Chem.* **1987**, *52*, 4825; b) V. Prelog, M. Kovacevic, M. Egli, *Angew. Chem.* **1989**, *101*, 1173; *Angew. Chem. Int. Ed. Engl.* **1989**, *28*, 1147.
[65] For other rigid molecular skeletons see R. N. Warrener, P. Groundwater, I. G. Pitt, D. N. Butler, R. A. Russell, *Tetrahedron Lett.* **1991**, *32*, 1885; K. S. Feldman, Y. B. Lee, *J. Am. Chem. Soc.* **1987**, *109*, 5850.
[66] F. Mohamadi, N. G. J. Richards, W. C. Guida, R. Liskamp, M. Lipton, C. Caufield, G. Chang, T. Hendrickson, W. C. Still, *J. Comput. Chem.* **1990**, *11*, 440.
[67] R. W. Alder, C. M. Maunder, A. G. Orpen, *Tetrahedron Lett.* **1990**, *31*, 6717.
[68] S. Cauwberghs, P. J. DeClercq, *Tetrahedron Lett.* **1988**, *29*, 2493.
[69] T. Iimori, S. D. Erickson, A. L. Rheingold, W. C. Still, *Tetrahedron Lett.* **1989**, *30*, 6947; X. Wang, S. D. Erickson, T. Iimori, W. C. Still, *J. Am. Chem. Soc.* **1992**, *114*, 4128.
[70] T. Miyazawa, K. Fukushima, Y. Ideguchi, *J. Chem. Phys.* **1962**, *37*, 2764.
[71] G. Li, W. C. Still, *J. Org. Chem.* **1991**, *56*, 6964.
[72] J. M. Desper, S. H. Gellman, R. E. Wolf, Jr., S. R. Cooper, *J. Am. Chem. Soc.* **1991**, *113*, 8663.
[73] a) I.-H. Suh, W. Saenger, *Angew. Chem.* **1978**, *90*, 565; *Angew. Chem. Int. Ed. Engl.* **1978**, *17*, 534; b) W. Rasshofer, F. Vögtle, *Tetrahedron Lett.* **1978**, 309.
[74] Compare in this context the preferred conformation of diisopropyl ether [49].
[75] K. Yamaguchi, G. Matsumura, H. Kagechika, I. Azumaya, Y. Ito, A. Itai, K. Shudo, *J. Am. Chem. Soc.* **1991**, *113*, 5474.
[76] G. M. Villacorta, C. P. Rao, S. J. Lippard, *J. Am. Chem. Soc.* **1988**, *110*, 3175; K.-H. Ahn, R. B. Klassen, S. J. Lippard, *Organometallics* **1990**, *9*, 3178.
[77] G. W. Coates, R. M. Waymouth, *J. Am. Chem. Soc.* **1991**, *113*, 6270.

ANGEWANDTE CHEMIE
A Journal of the Gesellschaft Deutscher Chemiker

Reviews planned or recently published

The Enchanting Alkaloids of Yuzuriha
C.H. Heathcock

Transition Structures of Hydrocarbon Pericyclic Reactions
K.N. Houk, Y. Li, J. D. Evanseck

Natural Products as Probes of Cellular Function
S.L. Schreiber, M.K. Rosen

Synthetic Approaches towards Molecular and Polymeric Carbon
F. Diederich, Y. Rubin

Cubanes: Starting Materials for the 1990s and the New Century
P.E. Eaton

Optically Anomalous Crystals
B. Kahr, J.M. McBride

Chemistry and Biology of the Enediyne Anticancer Antibiotics
K.C. Nicolaou, W.M. Dai

Scanning Tunnel Microscopy and Atomic Force Microscopy in Organic Chemistry
J. Frommer

Synchotron X-Ray and Neutron Diffraction Studies in Solid-State Chemistry
A.K. Cheetham, A.P. Wilkinson

What subscribers and authors have to say about Angewandte Chemie:

Jean-Marie Lehn, Université Louis Pasteur, Strasbourg:

"I consider Angewandte Chemie as one of the top not only chemical but scientific journals... It presents the highly effective combination of well chosen, exciting and thorough review articles, reflecting timely topics that cover a very broad range in science, with short but informative communications reporting specific advances of particular interest for chemistry. It is also carefully produced and nicely presented, which adds to the reading pleasure."

VCH

Special Rate for ACS members: US$ 165.00
US$ 190.00 (air mail)*

*To subscribe please call 1-800-422-8824

Annual subscription rate 1992 for institutions: US$ 581.00 (air mail)*

The Organosulfur Chemistry of the Genus *Allium* – Implications for the Organic Chemistry of Sulfur

By Eric Block*

A Cook's tour is presented of the organosulfur chemistry of the genus *Allium*, as represented, inter alia, by garlic (*Allium sativum* L.) and onion (*Allium cepa* L.). We report on the biosynthesis of the *S*-alk(en)yl-L-cysteine *S*-oxides (aroma and flavor precursors) in intact plants and on how upon cutting or crushing the plants these precursors are cleaved by allinase enzymes, giving sulfenic acids—highly reactive organosulfur intermediates. In garlic, 2-propenesulfenic acid gives allicin, a thiosulfinate with antibiotic properties, while in onion 1-propenesulfenic acid rearranges to the sulfine (*Z*)-propanethial *S*-oxide, the lachrymatory factor (LF) of onion. Highlights of onion chemistry include the assignment of stereochemistry to the LF and determination of the mechanism of its dimerization; the isolation, characterization, and synthesis of thiosulfinates which most closely duplicate the taste and aroma of the freshly cut bulb, and additional unusual compounds such as zwiebelanes (dithiabicyclo[2.1.1]hexanes), a bissulfine (a 1,4-butanedithial *S,S'*-dioxide), antithrombotic and antiasthmatic cepaenes (α-sulfinyl disulfides), and *vic*-disulfoxides. Especially noteworthy in the chemistry of garlic are the discovery of ajoene, a potent antithrombotic agent from garlic, and the elucidation of the unique sequence of reactions that occur when diallyl disulfide, which is present in steam-distilled garlic oil, is heated. Reaction mechanisms under discussion include [3,3]- and [2,3]-sigmatropic rearrangements involving sulfur (e.g. sulfoxide-accelerated thio- and dithio-Claisen rearrangements) and cycloadditions involving thiocarbonyl systems. In view of the culinary importance of alliaceous plants as well as the unique history of their use in folk medicine, this survey concludes with a discussion of the physiological activity of the components of these plants: cancer prevention, antimicrobial activity, insect and animal attractive/repulsive activity, olfactory–gustatory–lachrymatory properties, effect on lipid metabolism, platelet aggregation inhibitory activity and properties associated with ajoene. And naturally, comments about onion and garlic induced bad breath and heartburn may not be overlooked.

1. Introduction

We remember the fish which we did eat in Egypt, the cucumbers, melons, leeks, onions and garlic!
Num. 11:4–6

What is more familiar and pleasant to the senses than freshly chopped or sauted garlic, sliced or boiled onions, steaming leeks, finely diced chives, crisp raw scallions, or the delicate shallot? The scents of these commonplace plants brings back memories of mother's kitchen, a favorite restaurant or even a walk through a meadow rich with the aroma of wild onions. The adjectives applied to these plants, zesty, lusty, assertive, piquant, and distinctive, and even the botanical name *Allium*, derived from the Celtic word "all", which means pungent, betray the presence of a host of remarkable flavorants and odorants all having in common one element, sulfur. Many of these flavorful sulfur compounds contain the allyl group, which in turn gets its name from *Allium*. It is the presence of these organosulfur compounds, more than any other attribute, that defines the character of this extraordinary genus. The great American poet Carl Sanburg said: *"Life itself is like an onion; it has a bewildering number of layers. You peel them off, one by one, and sometimes you cry."* The "bewildering number of layers" of the onion has its counterpart in the complex chemistry of this and other alliaceous plants, representing a microcosm of the field of organosulfur chemistry. More specifically, *Allium* chemistry presents us with examples of sulfur compounds with striking physiological activity as well as culinary appeal, reactive organosulfur intermediates with unusual bonding, challenging analytical problems, compounds with chirality at sulfur and other stereochemical features related to the presence of sulfur, novel organosulfur heterocycles with notable spectroscopic properties, redox reactions involving sulfur, as well as processes involving sulfur radicals, sulfur stabilized carbocations, pericyclic reactions, noteworthy rearrangements, and reactions of utility in synthetic organic chemistry.[1]

For twenty-five years I have been exploring the organosulfur chemistry of the genus *Allium*, as represented by garlic (*Allium sativum* L.), onion (*Allium cepa* L.), leek (*Allium ampeloprasum* L. var. porrum), scallion (*Allium fistulosum*), shallot (*Allium ascalonicum* auct.), great-headed ("elephant") garlic (*Allium ampeloprasum* L. var. holmense), wild garlic (*Allium ursinum*), chive (*Allium schoenoprasum* L.), and Chinese chive (*Allium tuberosum* L.) (Fig. 1). When I began this study, much outstanding research had already been done in this area, e.g. as summarized in a review article by Nobel Laureate Arturi Virtanen.[2] As my research proceeded it became clear that there were still significant puzzles remaining to be solved, that these most common plants could teach us much about sulfur chemistry, and that the compounds and mixtures produced when these plants are cut display an even broader range of biological activities than

[*] Professor E. Block
Department of Chemistry
State University of New York at Albany
Albany, NY 12222 (USA)

 © *VCH Verlagsgesellschaft mbH, W-6940 Weinheim, 1992* *0570-0833/92/0909-1135 $ 3.50+.25/0*

earlier suspected. While extracts and potions of garlic and onion have been used for millennia in folk medicine, commercial products derived from these plants are now enjoying growing popular use in many countries. Furthermore, responding to epidemiological evidence that lower cancer risks are associated with increased consumption of alliaceous plants, health organizations have recently targeted garlic and onion as prime candidates for "designer foods" programs, programs to develop new foods that will help prevent cells from becoming cancerous. For all of these reasons a detailed exploration of the organosulfur chemistry of the genus *Allium* seemed justified as well as timely. This review summarizes progress in this field both in my own and other laboratories.[3]

2. Organosulfur Compounds of Intact Plants

Well loved he garleek, oynons, and eek lekes,
and for to drynken strong wyn, reed as blood.

"Canterbury Tales"
Geoffrey Chaucer (1342–1400)

The earliest reports concerning the isolation of organic compounds from garlic (1844, 1892) and onion by Wertheim (1844) and Semmler (1892) in Germany identified diallyl sulfide[4] (corrected in 1892 to the disulfide[5]) and a propenyl propyl disulfide[5] as the principal components of the distilled oils ("ätherische Öle") of garlic and onion, respectively. In the 1940s it became apparent that these and other volatile sulfur compounds were secondary compounds formed by enzymatic action on precursors in the intact bulb. Thus, in 1945, Cavallito et al. in Rennselaer, New York, reported that when garlic cloves were frozen in dry ice, pulverized, and extracted with acetone, "the acetone extracts upon evaporation yielded only minute quantities of residue and no sulfides, indicating the absence of free sulfides in the plant. The [white] garlic powder had practically no odor, but upon addition of small quantities of water, the typical odor was detected and the antibacterial principle (**1**) could be extracted and isolated. This demonstrates that neither **1** nor the allyl sulfides found in "Essential Oil of Garlic" are present as such in whole garlic. When the powder was heated to reflux for thirty minutes with a small volume of 95% ethanol, no activity could be demonstrated by addition of water to the insoluble residue. When, however, a small quantity (1 $mg\,mL^{-1}$) of fresh garlic powder was added to the alcohol insoluble fraction in water (20 $mg\,mL^{-1}$), the activity of the treated sample was shown to be equal to that of the original untreated powder. The 95% ethanol treatment has inactivated the enzyme required for cleavage of the precursor and addition of a small quantity of fresh enzyme brought about the usual cleavage.[6]

Since a strict definition of "essential oil" is "a volatile substance contained in certain aromatic plants that imparts distinctive odor to the plant" and since the volatile substances of the *Allium* spp. are not found in the plant but result from disrupting the plant cells, it is preferable to describe the process leading to a particular *Allium*-derived product, e.g. "steam volatile components" or "head space volatiles".[7]

2.1. Sulfur Amino Acids Secondary Metabolites in *Allium* spp.

Let onion atoms lurk within the bowl
and, scarce suspected, animate the whole.

"Recipe for Salad",
Sydney Smith (1771–1845)

Garlic, onion and other members of the *Allium* spp. contain 1–5% dry weight of nonprotein sulfur amino acid secondary metabolites. Pioneering studies in the 1940s by Stoll and Seebeck in Basel demonstrated that the stable precursor of Cavallito's antibacterial principle of garlic **1** is (+)-*S*-2-propenyl-L-cysteine *S*-oxide (**2**, "alliin").[8] In the intact cell, **2** and related *S*-alk(en)yl-L-cysteine *S*-oxides (aroma and flavor precursors) are located in the cytoplasm and the C–S lyase enzyme allinase in the vacuole.[9] Disruption of the cell results in release of allinase and subsequent α,β-elimination of the *S*-oxides, ultimately affording volatile and odorous low molecular weight organosulfur compounds such as **1** (Scheme 1). Four sulfoxides occur in *Allium* spp.: *S*-2-propenyl-, *S*-(*E*)-1-propenyl-, *S*-methyl- and *S*-propyl-L-cysteine *S*-oxides (**2**, **5**–**7** respectively). Onions contain **5**–**7** while garlic contains **2**, **5**, and **6**.[10–13] The distinctive flavors of the various *Allium* spp. reflect the varying amounts of compounds **2**, **5**–**7**, particularly of **5** ("isoalliin"), which is

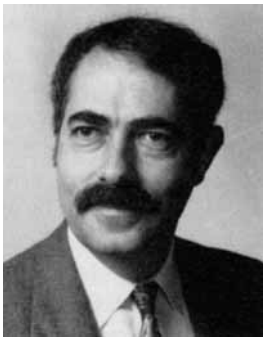

Eric Block, born in 1942 in New York City, studied chemistry at Queens College of the City University of New York. He received his Ph.D. degree from Harvard University, where in the laboratory of Professor E. J. Corey he first developed an interest in organosulfur chemistry, the chemistry of natural products, synthetic methods, and organic reaction mechanisms. In 1967 he joined the faculty at the University of Missouri-St. Louis where he was promoted to Professor. In 1981 he moved to the State University of New York at Albany, serving as Chairman of the Chemistry Department from 1985 to 1991. He has been the recipient of a number of awards and honors including a Guggenheim Fellowship and the ACS Award for Advancement and Application of Agricultural and Food Chemistry; he serves on several journal editorial boards, and has been a visiting professor at Harvard, and the Universities of Illinois-Urbana, Frankfurt, and Bologna. He is an avid photographer and traveler. In his overseas travels he enjoys visiting produce markets to see displays of local Allium species.

Fig. 1. Several plants of the genus *Allium*. a) C. C. Calwer, *Landwirtsch. Pflanzenf.*, Plate 26, Stuttgart, **1852**; b) L. Reichenbach, *Icones Florae Germanicae*, Plate 494, Leipzig, **1848**.

the precursor to the onion lachrymator, and of **2**, which is the precursor to the characteristic allylic compounds of garlic. Also present in *Allium* spp. are 24 γ-glutamyl peptides of sulfur amino acids. These are considered to function as storage compounds of nitrogen and sulfur (precursors to plant chemical defense agents?) and may have a role in the transport of amino acids across cell membranes.[14]

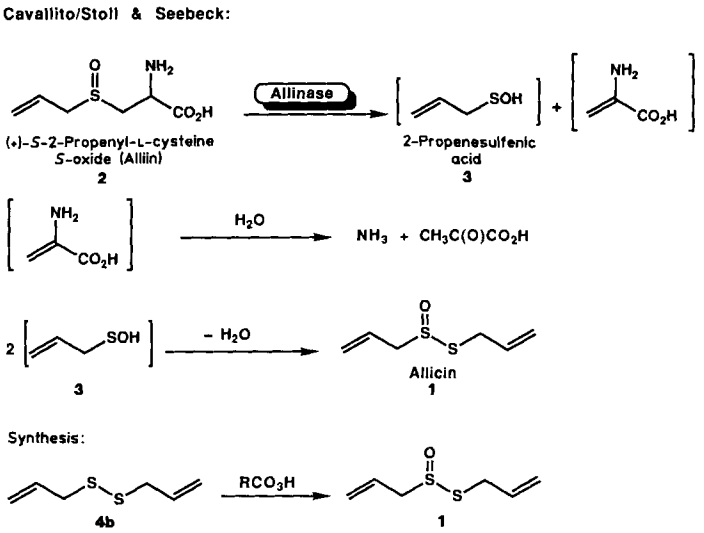

Scheme 1. Cavallito's pioneering discovery and synthesis of allicin **1**, the antibacterial principle of garlic (anticipating subsequent studies by Stoll and Seebeck on the precursor alliin **2**).

Scheme 2 summarizes the proposed biosynthesis of the various *Allium* spp. peptides and aroma precursors based on the results of labeling experiments, in which $^{35}SO_4^{2-}$ was fed to onion plants[15]. By briefly boiling the bulb or homogenizing the plants with alcohol containing limited quantities of water the allinase enzymes can be deactivated, thus permitting analysis of the peptides by HPLC.[12, 16] The sulfate is reduced and assimilated into cysteine in the chloroplasts[17] and then enters the glutathione cycle.[18] Michael addition of γ-glutamylcysteine to methacrylic acid (from valine) can afford γ-glutamyl-*S*-2-carboxypropylcysteine (**8**) which in onion undergoes sequential decarboxylation to give γ-glutamyl-*S*-1-propenylcysteine **e**, oxidation to γ-glutamyl-*S*-1-propenylcysteine *S*-oxide **i**, and cleavage by γ-glutamyl transpeptidase [EC 2.3.2.1] to **5**.[19a] Labeling experiments have established that the precursor **8** is converted into **5** with loss of the 3-*pro-R* hydrogen atom and that the oxidative decarboxylation reaction proceeds with *anti* geometry, analogous to terminal alkene biosynthesis (Scheme 2).[19b] Parallel processes involve Michael addition of glutathione to methacrylic acid giving *S*-2-carboxypropylglutathione **a** followed by conversion of the latter into **8** and methylation of glutathione giving *S*-methylglutathione **b** followed by conversion of the latter into γ-glutamyl-*S*-methylcysteine **f**. The situation with garlic is less clear. γ-Glutamyl-*S*-2-propenylcysteine **c**, formed from **8**, or more likely, from serine and 2-propenethiol by a process not well understood,[20] is converted into γ-glutamyl-*S*-2-propenylcysteine *S*-oxide **g** by an oxidase and is then cleaved by γ-glutamyl transpeptidase to **2**.

It has recently been reported[11] that the concentration of γ-glutamyl-*S*-(*E*)-1-propenylcysteine **e** and γ-glutamyl-*S*-2-propenylcysteine **c**, the dominant γ-glutamyl peptides in homogenates of fresh garlic, decreases markedly when freshly

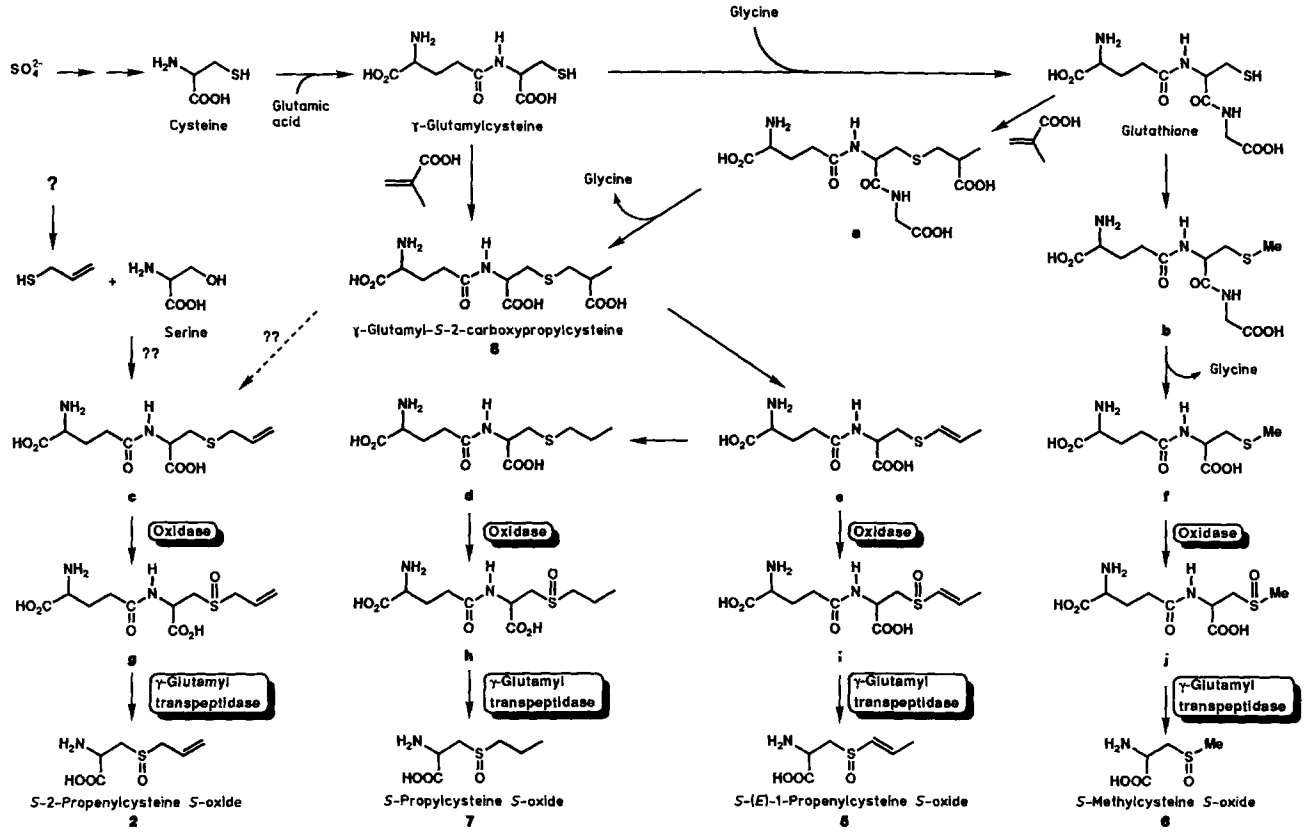

Scheme 2. An overview of biosynthesis from sulfate of the amino acid/peptide precursors to the flavorants and odorants of plants of the *Allium* spp. **a**, **b**, **c**, **e**, **f**, **g**, **i** see text. **d**: γ-glutamyl-*S*-propylcysteine; **h**: γ-glutamyl-*S*-propylcysteine *S*-oxide; **j**: γ-glutamyl-*S*-methylcysteine *S*-oxide.

picked garlic is stored, especially at 4 °C. The consequence of cold storage of garlic is increased production of **5** and therefore low molecular weight organosulfur compounds containing the 1-propenyl group (see Section 5.2.3). A second discovery, recently made in our laboratories is that garlic *grown* in colder climates contains far less **6** than garlic grown in more temperate climates, although levels of precursor compounds, such as γ-glutamyl-*S*-methylcysteine **f**, are normal.[21]

2.2. Allinase Enzymes

Allinases [EC 4.4.1.4] are pyridoxal 5′-phosphate dependent α,β-eliminating lyases which catalyze the decomposition of (+)-*S*-2-propenyl-L-cysteine *S*-oxide (**2**) and other (+)-*S*-alk(en)yl-L-cysteine *S*-oxides to ammonium pyruvate and allicin (**1**) and its homologs (Section 3). Synthetic **2** is racemic at the sulfur atom. The natural (+)-diastereomer (the first acyclic natural product with both an asymmetric carbon and an asymmetric heteroatom) is quantitatively and rapidly converted into **1** by garlic allinase, whereas the (−)-isomer of **2** decomposes much more slowly; derivatives of D-cysteine are completely inactive.[2] Conflicting results have been published in the case of garlic allinase. One group suggests that it is a dimer of molecular mass between 108000 and 111000 and subunit mass 53500 and requires a flavin-coenzyme in addition to pyridoxal 5′-phosphate,[22a] while a second group claims that it is a tetramer with a molecular mass of 180 kDa with subunits of mass 45 kDa.[23] Welsh onion (*Allium fistulosum* L.) allinase is a tetramer with a molecular mass of 220 kDa and subunit mass of 52 kDa and an optimum pH of 7.0.[24] Virtanen reported the purification of an onion allinase which showed maximal activity at pH 7.4.[3h, 8e, 25–27] Recent work suggests that there are *two* different allinase activities in garlic: one is specific for substrates **2** and **5**, has an optimum pH of 4.5, and cleaves 97% of **2**/**5** within 0.5 min at 23 °C; the second is specific for substrate **6**, has an optimum pH of 6.5, and cleaves 97% of **6** within 5 min at 23 °C. Both allinases are irreversibly deactivated at pH 1.5–3 (the pH of the stomach) and >9.[28]

2.3. A Question of Semantics

"What is a natural product?" This question can be raised with regard to all of the organic sulfur compounds that follow allinase-catalyzed release of the sulfenic acids, since none of the subsequently formed compounds occur in the bulb itself nor does their formation require enzyme involvement. On the other hand, volatile thiosulfinates are emitted in the field by *Allium* spp. such as the leek and are the most attractive compounds for predatory insects, e.g. the leek moth, *Acrolepiopsis assectella*.[29] Thus, in a broad sense, thiosulfinates and related secondary products such as disulfides and thiosulfonates can be classified as "natural products".

3. Organosulfur Compounds from Cut *Allium* spp.: Pre-1972 Results

If your Majesties is remembered of it, the Welshmen did good service in a garden where leeks did grow, wearing leeks in their Monmouth caps, which your Majesty know to this hour is an honourable badge of the service. And I do believe your Majesty takes no scorn to wear the leek upon Saint Davy's day.

"Henry V", IV. vii. 100
William Shakespeare (1564–1616)

For the purposes of this review I have chosen to first summarize research on the organosulfur compounds of cut *Allium* spp. prior to 1972, when my contributions first appeared, allowing me to subsequently describe my own work, and recent work of others, in the proper historical perspective. In 1944 a series of notable reports by Cavallito et al.[30] appeared describing the isolation and characterization of allicin (2-propenyl-2-propenethiosulfinate) (**1**),[31] an odoriferous, unstable antibacterial substance ("considerably more bacteriostatic than bactericidal"; "exceptionally sensitive and polymerizes easily ...must be stored at a low temperature"[30]) isolated from cut garlic cloves by extraction with ethanol at room temperature. Decomposition of allicin was said to afford diallyl disulfide as a major breakdown product. Cavallito found that reversal of this decomposition process, e.g. oxidation of diallyl disulfide (**4b**)[32] with peracetic acid, represents the most direct method of synthesizing allicin (Scheme 1).[33, 34] Attempts by Brodnitz et al. in 1971 to determine allicin **1** by GC-MS provided evidence for another more unusual mode of decomposition. A 2.4:1 mixture of two compounds claimed (incorrectly as we shall see below) to be 3-vinyl-3,4-dihydro-1,2-dithiin (**9**) and 3-vinyl-3,6-dihydro-1,2-dithiin (**9a**) were found by GC (Scheme 3).

Brodnitz:

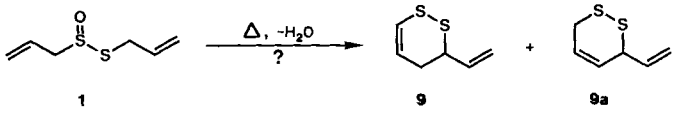

1 **9** **9a**

Scheme 3. Decomposition of allicin **1** in a gas chromatograph according to Brodnitz.

It was suggested that "upon gas chromatography diallyl thiosulfinate undergoes dehydration" affording **9** and **9a**.[35a] At room temperature neat **1** is said to rearrange, affording sulfur dioxide and diallyl mono-, di-, and trisulfide (**4a–c**)[35]. Analytical methods for quantitative allicin determination which rely on GC detection of "**9**" and "**9a**" are still employed[36] even though serious problems exist with this method and more accurate HPLC methods have been developed.

All-S-All **4a** All-S-S-All **4b** All-S-S-S-All **4c**

After the discovery of alliin in garlic, other *S*-alk(en)yl-L-cysteine *S*-oxides such as **5–7** were discovered in other *Allium* spp.[37] Upon cutting the plants, such *S*-oxides (type **a** and **b**) are cleaved by allinase to sulfenic acids, whose condensation could lead to four types of thiosulfinates. These thiosulfinates, and polysulfides derived therefrom, were assumed to be the principle sources of flavor and aroma in *Allium* spp., and were viewed as important taxonomic markers. Indirect methods were used to identify and quantify the various thiosulfinates.

$RS(O)CH_2CH(NH_2)COOH$ **a** $R'S(O)CH_2CH(NH_2)COOH$ **b**

RS(O)SR **c** RS(O)SR′ **d** R′S(O)SR **e** R′S(O)SR′ **f**

One method involved separation of the thiosulfinates by paper chromatography followed by treatment with cysteine to form *S*-alk(en)ylthiocysteines, which in turn were chro-

$RSSCH_2CH(NH_2)COOH/R'SSCH_2CH(NH_2)COOH$

matographed.[38] In this manner the following thiosulfinate profiles were determined (increasing amounts indicated as +, ++, +++): in garlic, MeS(O)SMe **12** (+), MeS(O)SAll **101** (++), MeS(O)SPr **29** (+), AllS(O)SAll **1** (+++), AllS(O)SPr (++), PrS(O)SPr **13** (+); in onion, **13** (++), **29** (+), **12** (+); in Chinese chive, **12** (+++), **101** and **1**.[38] This working group also allowed allinase to react with a mixture of **2** and **6**, and obtained **1**, **12**, and "MeS(O)SAll".[38]

A second method involved "headspace" GC analysis, where it was assumed that the proportion of different alk(en)yl groups in the stable, volatile polysulfide fraction paralleled the relative abundance of the same alk(en)yl groups in the thiosulfinates.[39] It was felt that even if the polysulfides revealed by GC are artifacts of analysis, they are [still] clearly related to *Allium* odors.[39] Although both methods of analysis give data which are generally in agreement with more recent composition profiles, significant errors are apparent (see Section 5.2).

With the development of mass spectrometry, gas chromatography (GC), and IR spectroscopy it was possible in 1956 to identify the following compounds as constituents of raw onion vapor:[40] 1-propanethiol, propanal, dipropyl disulfide, SO_2, H_2S, and a substance of *m/z* 90 (C_3H_6SO), showing loss of OH (*m/z* 73) as well as *m/z* 45. It was assumed, albeit on somewhat feeble grounds, that it could be 3-hydroxypropanethial. In 1961 Virtanen et al. showed[10a] that (+)-*S*-((*E*)-1-propenyl)-L-cysteine *S*-oxide (**5**), present to the extent of ca. 0.2% by weight in the onion, is the precursor of the lachrymatory factor (LF; the *E*-geometry of the 1-propenyl group was later established by NMR spectroscopy).[10a, 12, 41–43] Virtanen also demonstrated that onion allinase converts *S*-methyl- and *S*-propyl-L-cysteine *S*-oxides (**6** and **7**, respectively), present to the extent of ca. 0.005–0.02% by weight in the onion,[44, 45] and *S*-2-propenyl-L-cysteine *S*-oxide (**2**), found in garlic, into the corresponding thiosulfinates **12**, **13**, and **1** via sulfenic acids **10**, **11**, and **3**, respectively (Schemes 4 and 1).[2]

On the basis of the above results, Virtanen formulated the LF as the S–H tautomer (**14a**) of (*E*)-1-propenesulfenic acid rather than the S–OH tautomer **14b** (Scheme 4).[2] The assignment of structure **14a** to the LF was said to be consistent with deuteration studies involving crystallized precursor **5** and a purified onion enzyme preparation. Thus, when the

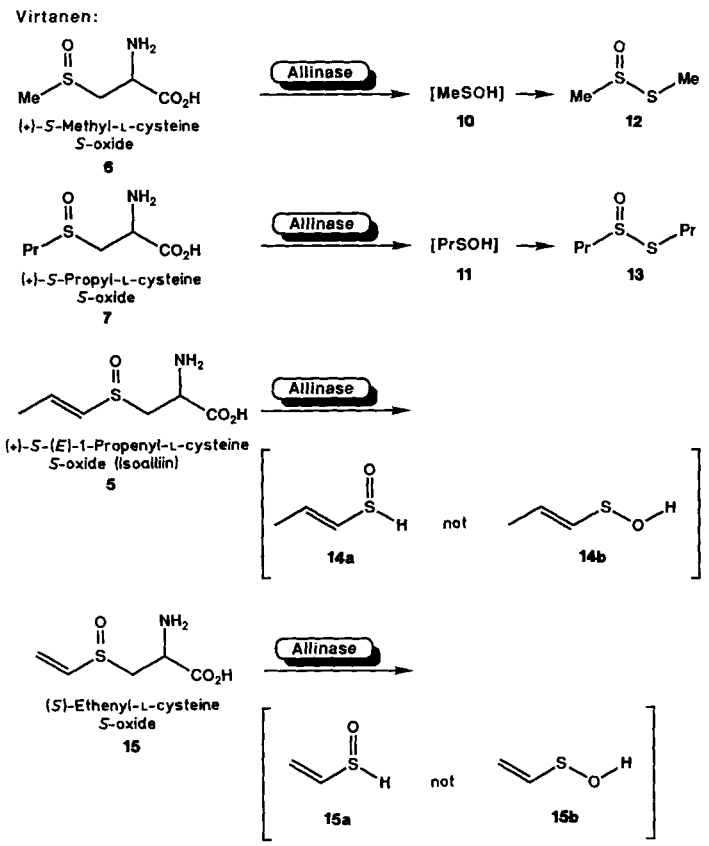

Scheme 4. Virtanen's view of the action of allinase on homologues of alliin **2**. In the case of **6**, **7**, **5**, and **15** they are L-cysteine derivative; **6**, **7**, and **5** are dextrorotatory.

LF is generated in D_2O, its mass spectrum shows a shift in the molecular peak from 90 to 91, indicating a single exchangeable proton. Fragmentation of the normal LF as well as the deuterated LF shows that in both cases an OH fragment is set free. The molecule therefore contains no OH group (the hydrogen of which would be replaced by deuterium in D_2O).[10b] Virtanen raises the perplexing question of why **14a** does not form 1-propenyl 1-propenethiosulfinate analogous to the ready formation of allicin from 2-propenesulfenic acid.[43] He hypothesizes that perhaps 2-propenesulfenic acid disproportionates immediately to 2-propenesulfinic acid and 2-propenethiol, which afford allicin by elimination of water, whereas in **14a** the position of the double bond is a possible stabilizing factor.[2] Virtanen suggests that (*E,Z*)-1-propenyl propyl (and methyl) disulfides, found in *Allium* volatiles and possessing "strong onion-like flavors", might arise from precursor **5** by splitting of a C–S bond, reduction, and coupling with some thiol present when the plants are crushed.[43] Virtanen and Däbritz synthesized the non-natural homolog of **5**, *S*-vinyl-L-cysteine *S*-oxide (**15**) and demonstrated that onion allinase converted it into a lachrymatory substance formulated as ethenesulfenic acid tautomer **15a**, paralleling the conversion of **5** into **14a**.[46]

In 1961, simultaneous with the work of Virtanen, Wilkens of Cornell University isolated by preparative GC the purified LF, which was depicted as propanethial *S*-oxide (**16**; Scheme 5; drawn by him with a linear ketene-like structure $CH_3CH_2CH{=}S{=}O$).[47] Evidence supporting structure **16** included: 1) the presence of strong IR absorption bands at 1113 and 1144 cm^{-1} (S=O region) together with the absence of bands attributable to S–H, O–H, or C=C; 2) ready decomposition of the LF to propanal (suggested to involve the intermediacy of 3-ethyloxathiirane (**17**)) and to a second compound possessing IR bands at 1140 and 1330 cm^{-1} formulated as condensation product 2,4-diethyl-1,3-dithietane 1,3-dioxide (**18a**).[47] Wilkens rationalized the inconsistency between the IR data for **18a**, which showed absorption bands typical of the sulfone stretching modes, and the postulated disulfoxide structure **18a** as due to the proximity of the antipodal sulfinyl groups in this strained-ring structure... postulated to induce a pseudosulfone infrared absorption, which would be of less intensity than that of a true sulfone.[47]

In 1963–1964 the first syntheses of *S*-oxides of thials and thiones (termed *sulfines*) were reported, involving dehydrochlorination of the corresponding sulfinyl chlorides (Scheme 5),[48,49] and evidence was presented for a bent C–S–O group[48,49] (e.g. the methyl groups in Me_2CSO are nonequivalent according to NMR).[48a] In 1971 Brodnitz

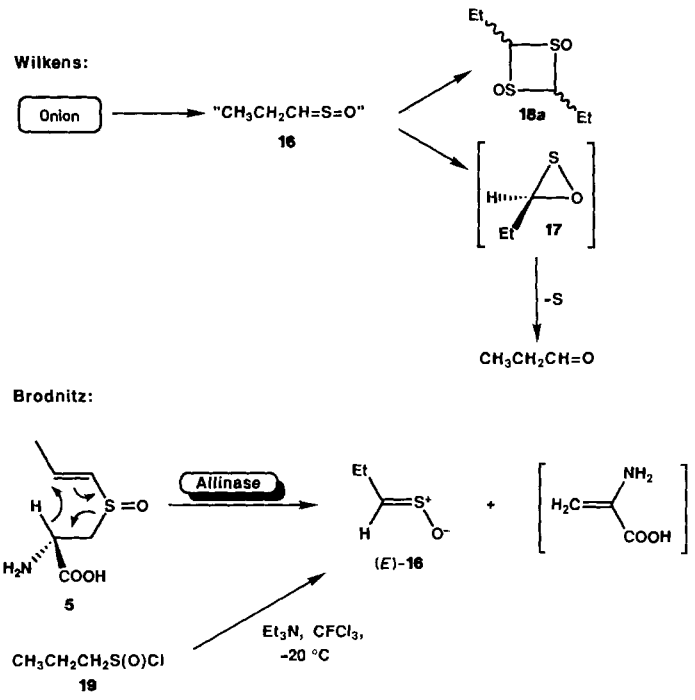

Scheme 5. Contributions by Wilkens and Brodnitz on proposed structure, "biosynthesis" and laboratory synthesis, and mechanisms for desulfurization and dimerization of onion lachrymatory factor (LF).

and Pascale[50] showed that propanethial *S*-oxide (arbitrarily depicted by them as (*E*)-**16**), from dehydrochlorination of propanesulfinyl chloride (**19**), was spectroscopically identical to the natural onion LF. These authors provided the

mechanism for the formation of the LF from its known precursor **5** shown in Scheme 5.[50]

4. Structures of Reactive Organosulfur Compounds Relevant to *Allium* Chemistry

I counted two and seventy stenches,
All well defined, and several stinks.

"Cologne"
Samuel Taylor Coleridge (1772–1834)

4.1. Methyl Methanethiosulfinate, Higher Homologs and Derivatives

Despite the identification of the active agent of garlic as allyl 2-propenethiosulfinate (**1**, allicin), an alkyl alkanethiosulfinate, little systematic information existed in 1970 on the chemistry of this class of compounds, perhaps because of their reputation as malodorous, unstable substances.[51] Thus, in 1970 I undertook a study of the naturally occurring parent member of this family, methyl methanethiosulfinate (**12**).

True to its reputation, methyl methanethiosulfinate (**12**) prepared by careful oxidation of dimethyl disulfide (**20**) with peroxy acids or singlet oxygen,[52, 53] is an unpleasant smelling, reactive and unstable vesicant with the property of readily attaching itself to hair and clothing. Fortunately, **12** proved to have a rich chemistry.[54] Pyrolysis of **12** in the presence of methyl propiolate affords methyl (*E*)-β-(methylsulfinyl)acrylate (**21**) in good yield by a sequence involving cycloelimination to methanesulfenic acid (**10**) and thioformaldehyde (**22**), followed by regiospecific addition of the

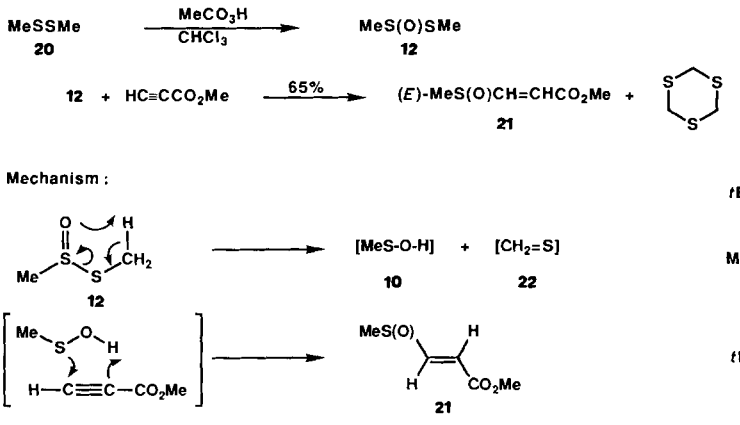

Scheme 6. Methyl methanethiosulfinate decomposes into thioformaldehyde **22** and methanesulfenic acid **10**. The latter can be trapped giving α,β-unsaturated sulfoxides such as **21** in a synthetically useful procedure.

former to the alkyne and trimerization of the latter (Scheme 6). This procedure represents a convenient synthesis of α,β-unsaturated sulfoxides.[54] Both **10** and **22** were subsequently identified by microwave spectroscopy; **10** was shown (see Section 4.3) to have the structure MeS–O–H rather than MeS(O)H.[55] When methyl 2-methyl-2-propanethiosulfinate (**23**) is heated with methyl propiolate, the major product is (*E,E*)-dimethyl-3,3′-sulfinyldiacrylate (**27b**; Scheme 7).[54] Compound **27b** is thought to be formed by a sequence involving generation of 2-methyl-2-propanesulfenic acid (**24**), addition of this to methyl propiolate giving methyl (*E*)-β-*tert*-butylsulfinylacrylate (**26**), elimination of isobutylene from **26** giving α,β-unsaturated sulfenic acid **27a**, and finally addition of **27a** to methyl propiolate. When

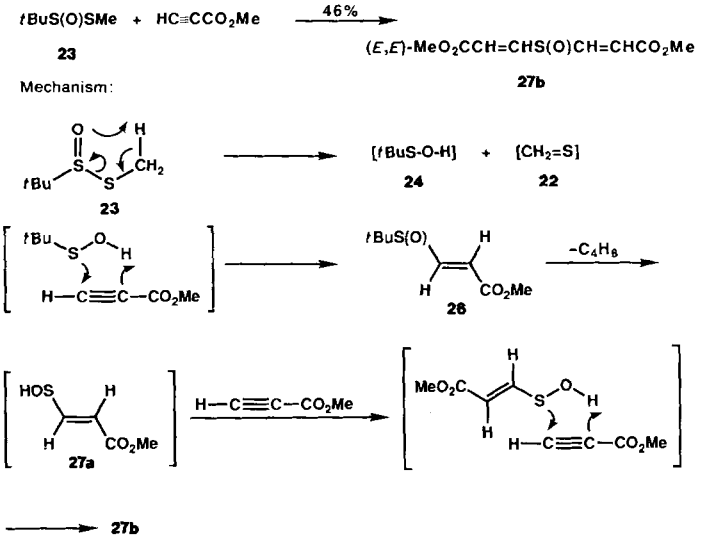

Scheme 7. Alkyl-2-methylpropanethiosulfinates like **23** react with alkynes to furnish adducts which lose isobutylene giving α,β-unsaturated sulfenic acids such as **27a**. These add to a second molecule of alkyne ultimately giving bis(1-alkenyl)sulfoxides such as **27b**.

23 is heated neat at 96 °C for 5 hours, the major product is *tert*-butyl 2-methyl-2-propanethiosulfinate (**25**). Sulfenic acid **24** is suggested to be an intermediate in this reaction, condensing with itself via an acid-catalyzed S_N2-like process or, orbital geometry-permitting, via a five-membered or seven-membered hydrogen bonded transition state (Scheme 8). In these condensation reactions the sulfenic acid functions as both a nucleophile and electrophile. Compound **25** was also

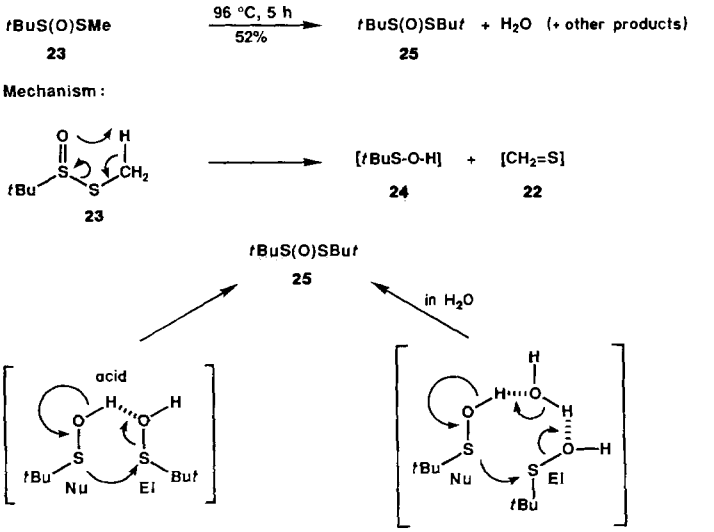

Scheme 8. Upon heating, unsymmetrical alkyl alkanethiosulfinates such as **23** give symmetrical thiosulfinates such as **25** by a mechanism involving sulfenic acids.

found to decompose thermally. When heated in the presence of methyl propiolate it gave the α,β-unsaturated adduct **28b** by way of 2-methyl-2-propanethiosulfoxylic acid (**28a**), a member of a previously unknown class of sulfur acids (Scheme 9).[54b]

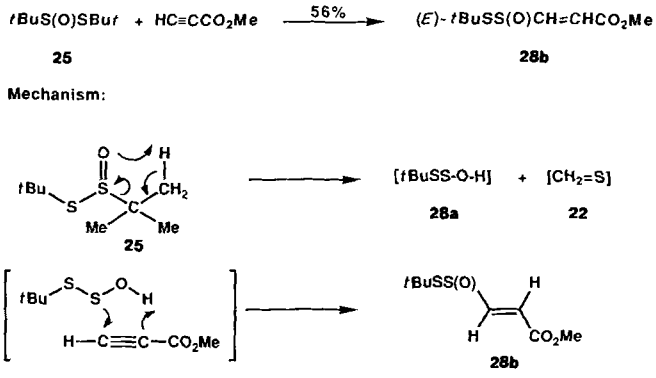

Scheme 9. Formation and trapping of the thiosulfoxylic acid ester **28a**.

The unimolecular decomposition of **12** (cf. Scheme 6) is favored by the weak S–S bond, determined by appearance potential measurements to have a bond energy of 46 ± 4.6 kcal mol^{-1}, comparable to the S–S bond dissociation energy in dimethyl trisulfide, but considerably smaller than that in dimethyl disulfide (75 kcal mol^{-1}).[54f] For comparison the S–S bond energies in phenyl benzenethiosulfinate and diphenyl disulfide are ca. 35 and 65 kcal mol^{-1}, respectively.[56] The thiosulfinate oxygen actively participates in hydrogen bonding, although not quite as strongly as the oxygen in sulfoxides. Using the hydrogen bond strength method,[57] whereby the phenol OH stretching vibration band frequency shift is determined in the presence of oxygen donors, it was demonstrated that **12**, ethyl ethanethiosulfinate (**31**) and dimethyl sulfoxide caused frequency shifts of 278, 308 and 360 cm^{-1}, respectively.[54] Thiosulfinates can be distinguished from sulfoxides by a shift in the position of the S=O stretch in the infrared from 1075–1090 cm^{-1} for the former to 1030–1065 cm^{-1} for the latter.

When **12** and its higher homologs **13** or **31** were mixed, rapid equilibria were established at 25 °C affording in each case statistical mixtures of four thiosulfinates, even after substantial dilution (Scheme 10). The scrambling reaction is catalyzed by acid, inhibited by base or methyl acrylate, and the ESR spectrum shows no evidence of free radical formation. A rapid sulfenic acid–thiosulfinate exchange is postulated. In this reaction the sulfenic acid functions as a nucleophile and as a proton donor. Gas chromatography (GC) using short packed columns (2 m × 3 mm internal diameter) and injection port and column temperatures below 100 °C nicely separates the various thiosulfinates shown in Scheme 10; unique GC-MS data can be obtained for each regioisomer.[54e] As we shall see in Section 5.2.1, the processes of Scheme 10 and methods of isomer separation play an important role in *Allium* chemistry.

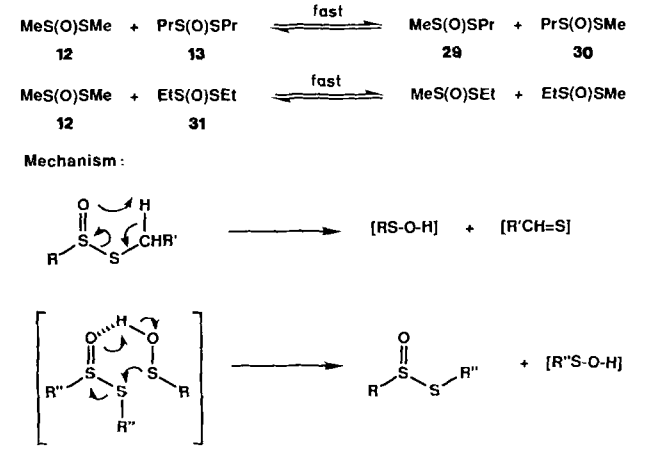

Scheme 10. The exchange reaction of the thiosulfinate pairs **12**/**13** and **12**/**31** involves attack of sulfenic acids on thiosulfinates.

While **12** undergoes ready disproportionation to dimethyl disulfide (**20**) and methyl methanethiosulfonate (**32**, Scheme 11), when **12** is refluxed in benzene with an equivalent of water, 2,3,5-trithiahexane 5-oxide (**33**) is formed in 84% yield. In a similar manner **13** affords 6-ethyl-4,5,7-

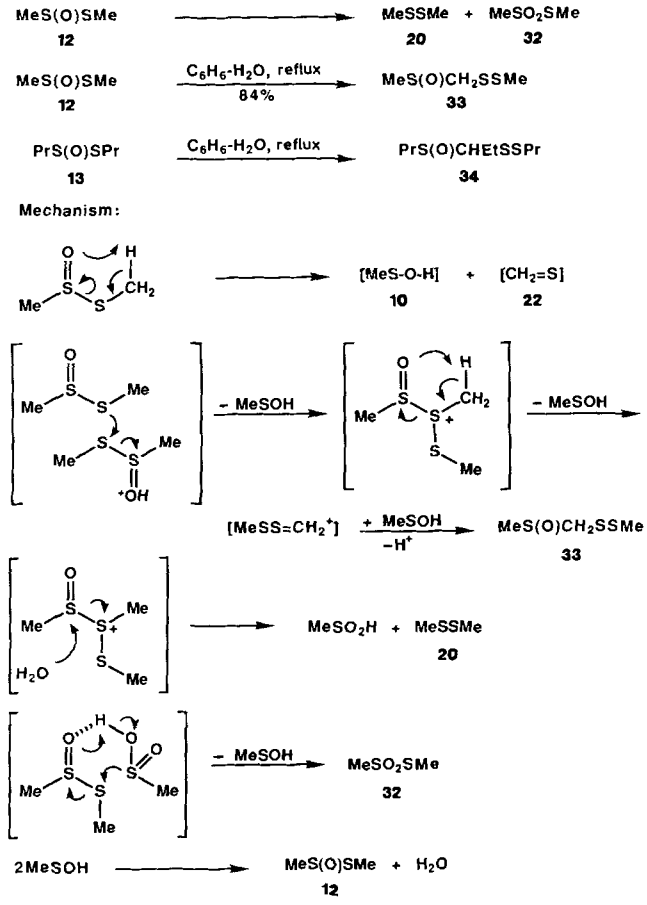

Scheme 11. Rearrangement of the Pummerer-type for the conversion of alkyl alkanethiosulfinates such as **12** and **13** into α-sulfinyl disulfides such as **33** and **34**, respectively. Reaction of sulfinic acids with thiosulfinates leading to alkyl alkanethiosulfonates, e.g. **32**.

trithiadecane 7-oxide (**34**). We had anticipated as long ago as 1973 that the unique combination of functional groups in α-sulfinyl and α-sulfonyl disulfides ought to lead to unusual physiological properties,[54d] a prediction recently borne out with the discovery of structurally analogous antithrombotic and lipoxygenase inhibitory cepaenes in onions (Sec-

tion 5.2.6). In order to account for the formation of **33** from **12**, we postulated the intermediacy of an α-alkyldithiocarbocation in a Pummerer-like reaction (Scheme 11). Solvolysis studies revealed that acyclic α-alkyldithiocarbocations are far less stable than α-alkylthiocarbocations (for example $MeSCH_2Cl$ hydrolyzes 6800 times faster than $MeSSCH_2Cl$.[58] We have suggested that the near 90° C–S–S–C dihedral angle adopted by acyclic disulfides is also favored by acyclic α-alkyldithiocarbocations and that this conformation precludes charge delocalization by the second (distant) sulfur, while at the same time diminishing by inductive effects the electron availability on the first (nearest) sulfur (see Fig. 2).[58] The above solvolysis study is relevant to

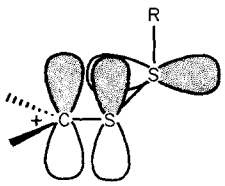

Fig. 2. Postulated conformation of acyclic carbocations containing the S–S–C$^+$ group.

the observation that in the mass spectrum of $MeSCH_2SSMe$, fragmentation to $MeSCH_2^+$/MeSS$^\bullet$ is greatly favored over fragmentation to $MeSSCH_2^+$/MeS$^\bullet$. This observation also proves useful in establishing the structures of "deoxycepaenes" (see Section 5.2.6).

4.2. 1,3-Dithietane *S*-Oxides

The suggestion by Wilkens that the dimer of the onion LF is 2,4-diethyl-1,3-dithietane 1,3-dioxide **18a**[47] piqued our interest in this little studied class of heterocycles. Although derivatives of 1,3-dithietane have been known since 1872, the parent compound **35** was unknown prior to our work. We developed convenient syntheses of **35** and its *S*-oxides (Scheme 12).[59] Thus, treatment of bis(chloromethyl)

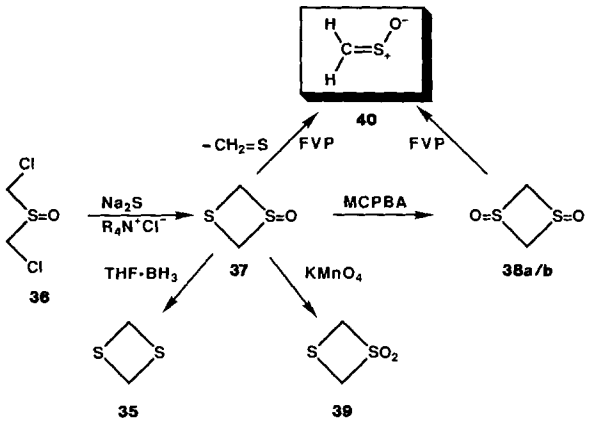

Scheme 12. Synthesis of 1,3-dithietane (**35**) ($\delta_C = 19$), 1,3-dithietane 1-oxide (**37**) ($\delta_C = 53$), 1,3-dithietane 1,3-dioxide (**38a/b**) ($\delta_C = 69$), and 1,3-dithietane 1,1-dioxide (**39**) ($\delta_C = 68$), and pyrolytic conversion of **37** and **38a/b** into sulfine (thioformaldehyde *S*-oxide) (**40**) ($\delta_C = 159$, $\delta_H = 7.73$, 7.84 ($J = 5.5$ Hz)). MCPBA = *m*-chloroperbenzoic acid.

sulfoxide (**36**) with sodium sulfide in the presence of a phase transfer catalyst gave 1,3-dithietane 1-oxide (**37**) in 36% yield as a colorless solid with a garlic like odor. Compound **37** could be reduced with THF · BH_3, giving the parent compound **35** in 70% yield, or oxidized with MCPBA or $KMnO_4$/acetone, giving *cis/trans*-1,3-dithietane 1,3-dioxide (**38a/b**) or 1,3-dithietane 1,1-dioxide (**39**), respectively, in excellent yields. While Wilkens[47] indicated that his LF dimer, formulated as **18a**, had sulfone type IR absorption at 1330 and 1140 cm^{-1}, we found compounds **37** and **38a/b** to have sulfoxide bands in the normal 1100–1035 cm^{-1} region,[1] with additional bands at 1132–1159 cm^{-1}, presumably associated with the four-membered ring. Sulfone **39** showed typical sulfonyl absorption bands[1] at 1393–1315 and 1200–1130 cm^{-1}. Compounds **38a/b** are stable solids melting above 200 °C, in contrast to **18a**, described by Wilkens[47] as an unstable liquid. Flash vacuum pyrolysis (FVP) of **37** and **38a/b** at 350–480 °C gave sulfine **40** (thioformaldehyde *S*-oxide).[59]

4.3. Sulfenic Acids

Sulfenic acids are key enzymatically formed intermediates in *Allium* chemistry. Prior to 1978 it was not known whether the structure of simple sulfenic acids was best represented by RS–O–H (**A**) or RS(O)H (**B**) or an equilibrium involving both forms.[51,60] Isolation proved difficult because of the high reactivity of sulfenic acids as *both* electrophiles and nucleophiles (cf. Scheme 8).[55] Using flash vacuum pyrolysis (FVP) we were able to demonstrate that above 250 °C at 0.1 torr both *tert*-butyl methyl sulfoxide and methyl methanethiosulfinate (**12**) decompose affording methanesulfenic acid (**10**) and isobutylene or thioformaldehyde (**22**), respectively (Scheme 13).

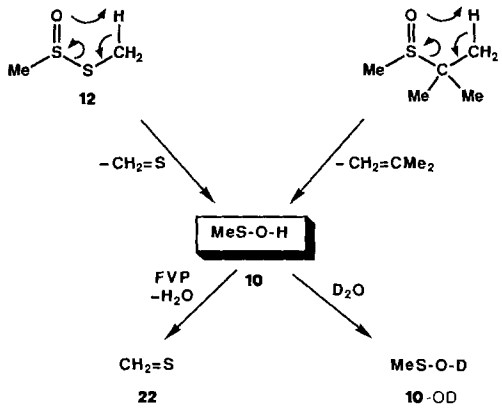

Scheme 13. Generation of methanesulfenic acid (**10**) by FVP methods.

Compound **10** showed a molecular ion at *m/z* 64 when examined using coupled FVP-mass spectrometric analysis. Through coupled FVP-microwave spectroscopic studies of a series of isotopically substituted forms of **10** (^{13}C, CD_3; ^{18}O, OD) its full structure was determined (Fig. 3). Compound **10** contains dicoordinate rather than tricoordinate sulfur (form

A rather than **B**) and a geometry similar to that of H_2S_2 (HSSH angle 90.6°).[61] The structural determination was aided by the finding that **10** readily exchanges with deuterium oxide in the waveguide giving **10**-OD. By means of a tandem pyrolysis experiment it was further demonstrated that **10** undergoes dehydration giving thioformaldehyde (Scheme 13). The half-life of **10** in the gas phase at 0.1 torr and 25 °C is ca. one minute. When condensed at −196 °C **10** could not be recovered on warming in vacuum. Analysis of calculated charge densities. The gas-phase lifetimes of **40** and **22** at room temperature and 30 μm are ca. 30 minutes and 20 seconds, respectively. Compound **40** could be generated at room temperature by fluorodesilylation of (trimethylsilyl)methanesulfinyl chloride (**41**; Scheme 14).[70] Cyclopentadiene was used as an *in situ* trap for **40**. The major cyclopentadiene Diels–Alder adduct of **40**, 2-thiabicyclo-[2.2.1]hept-5-ene *endo*-2-oxide (**42**; 10% of the *exo* isomer was also present) proved to be thermally unstable at room

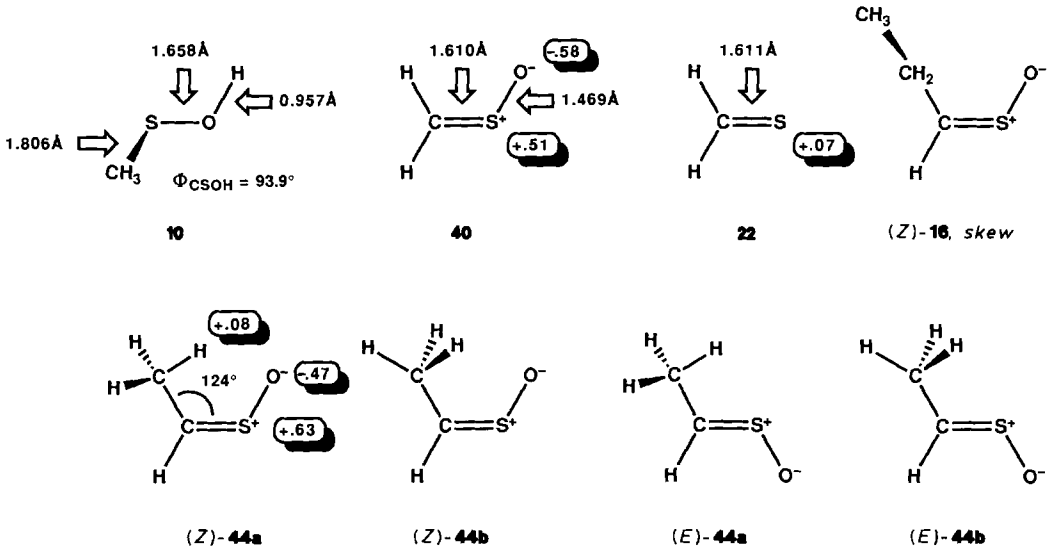

Fig. 3. Structures of methanesulfenic acid (**10**), thioformaldehyde *S*-oxide (**40**), thioformaldehyde (**22**), propanethial *S*-oxide (**16**), and the conformers of ethanethial *S*-oxide (**44**) determined by microwave spectroscopy.

the low-temperature condensate warmed to room temperature revealed the presence of **12**. In the gas-phase experiments we were unable to detect even minor amounts of the tautomer of type **B**. In agreement with our experimental observations, theoretical calculations confirm that CH_3S–O–H and its inorganic homologue H–S–O–H are significantly more stable than their respective isomers $CH_3S(O)H$[62] and $H_2S(O)$.[63] The preference for form **A** rather than **B** has also been found with stable, sterically hindered sulfenic acids.[64] In other relevant work, 1-anthraquinonesulfenic acid, another stable sulfenic acid, has been found to have a pK_a value of 7.51.[65]

4.4. Sulfine (Thioformaldehyde *S*-Oxide)

Like sulfenic acids, sulfines (thiocarbonyl *S*-oxides) are key compounds in *Allium* chemistry. We generated the previously unknown parent sulfine, thioformaldehyde *S*-oxide (**40**), by pyrolysis of 1,3-dithietane 1-oxide (**37**), 1,3-dithietane 1,3-dioxide (**38a/b**; cf. Scheme 12), or methanesulfinyl chloride. Compound **40** was fully characterized by mass spectrometry, microwave, photoelectron, IR and NMR spectroscopy.[66–69] The structures of **40** and, for comparison, thioformaldehyde (**22**) are shown in Figure 3 along with temperature, undergoing a [2,3]-sigmatropic rearrangement to 2-oxa-3-thiabicyclo[3.3.0]oct-7-ene (**43**), a rare example of an isolable sultene (a heterocycle containing an S–O single bond).

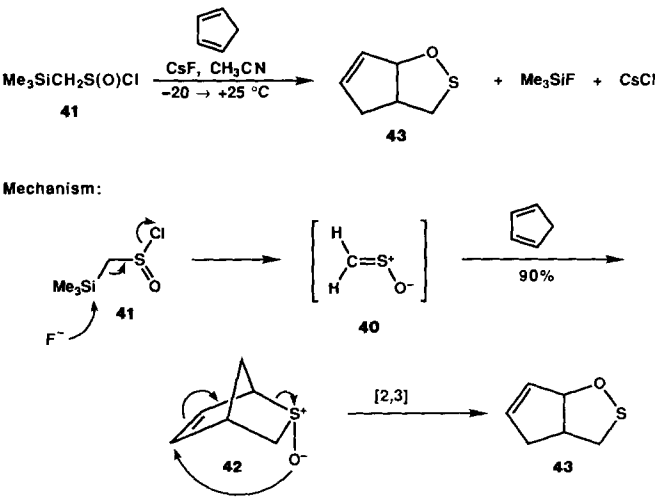

Scheme 14. Generation and Diels–Alder trapping reaction of sulfine **40**, which was generated from **41** by fluorodesilylation. The rearrangement of the primary adduct **42** to led to the **43**.

5. Organosulfur Compounds from Cut *Allium* Spp.: Post-1972 Results

Come, follow me by the smell,
here are delicate onions to sell;
I promise to use you well.
They make the blood warmer,
You'll feed like a farmer;
For this is every cook's opinion,
no savoury dish without an onion;
But, lest your kissing should be spoiled,
Your onions must be thoroughly boiled:
Or else you may spare your mistress a share,
the secret will never be known:
She cannot discover the breath of her lover but think it as sweet as her own.

"Verses for Fruitwomen",
Jonathan Swift (1667–1745)

The work done prior to 1972 suggests that, when *Allium* spp. are cut, highly reactive sulfenic acids and/or sulfines are produced by enzymatic action on precursors in the intact bulb. The main fate of the short-lived sulfenic acids appears to be condensation to form thiosulfinates. The thiosulfinates can then participate in a variety of subsequent reactions which depend on conditions and which afford various types of organosulfur compounds. These compounds can be categorized as headspace volatiles (products formed above cut *Allium* or *Allium* homogenates at room temperature), products formed when the thiosulfinates stand in solution at room temperature, or compounds produced by more vigorous processes such as steam distillation (or decomposition in the injection port of a GC[71]!) (Scheme 15). The volatile, thermally stable compounds are best analyzed by GC or GC-MS while the thermally unstable compounds are preferably isolated/identified by milder chromatographic methods (e.g. HPLC, supercritical fluid chromatography (SFC), or GC under modified injection conditions). In our discussion we will first treat the unique low-temperature volatile onion lachrymatory factor and its dimer, then those thermally unstable constituents of *Allium* homogenates formed in solution, and finally those constituents of headspace volatiles and steam distillates identified primarily by gas chromatography.

5.1. Onion Lachrymatory Factor (LF) and its Dimer

Indeed the tears live in an onion that should water this sorrow.

"Antony and Cleopatra", I. ii. 173
William Shakespeare (1564–1616)

A number of points from the published work on the onion LF required clarification. Assuming that the LF is propanethial *S*-oxide (**16**) as postulated by Wilkens[47] and Brodnitz,[50] how can the exchange of a single proton (from Virtanen's deuteration studies[2]) be rationalized? Is the stereochemistry of the LF indeed *E* (anti)? Is it reasonable to assume that the same enzyme allinase could catalyze *both* the sulfenic acid eliminations of Schemes 1 and 4 as well as Brodnitz's retro-ene mechanism of Scheme 5? These questions will be addressed below.

Extraction of chopped onions at low temperatures with $CFCl_3$ followed by low-temperature vacuum distillation gave the onion lachrymatory factor (LF). The LF was purified by trap-to-trap distillation (−35 to −196 °C) at 0.001 torr. Authentic propanethial *S*-oxide (**16**) and its lower homolog ethanethial *S*-oxide (**44**) were prepared from the reactions of propanesulfinyl chloride (**19**) and ethanesulfinyl chloride (**45**), respectively, with triethylamine.

$$\underset{\mathbf{19}}{CH_3CH_2CH_2S(O)Cl} \longrightarrow \underset{\mathbf{16}}{CH_3CH_2CH{=}S^+{-}O^-}$$

$$\underset{\mathbf{45}}{CH_3CH_2S(O)Cl} \longrightarrow \underset{\mathbf{44}}{CH_3CH{=}S^+{-}O^-}$$

5.1.1. Microwave and NMR Spectroscopic Analysis of Onion LF and Homologs

Mine eyes smell onions; I shall weep anon;
good Tom Drum, lend me a handkercher.

"All's Well That Ends Well", V. iii. 316
William Shakespeare (1564–1616)

Samples of the LF and **44**, prepared as described in Section 5.1, were evaporated at room temperature into a microwave guide. Only the normal isotopic species were used in the analysis of the microwave spectra of **16** and **44**. Structural conclusions for **44** are based upon the assumption that

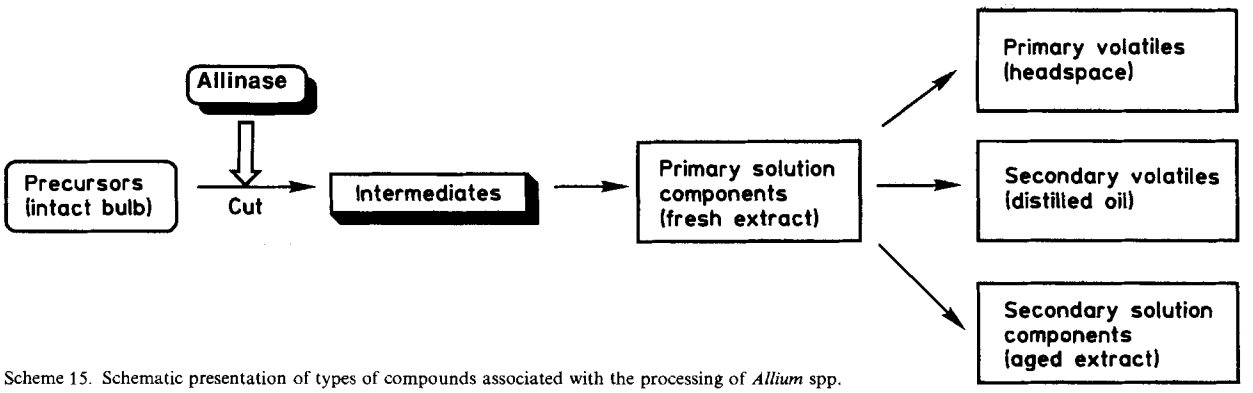

Scheme 15. Schematic presentation of types of compounds associated with the processing of *Allium* spp.

the CHSO framework is identical to that of thioformaldehyde *S*-oxide (**40**) and that the methyl groups are tetrahedral with C–H = 1.093 Å. The structures of (*Z*)-**44** and the onion LF, (*Z*)-**16**, determined by microwave spectroscopy, are given in Figure 3 (also see Section 5.1.4).[72] The *E* (*anti*) isomer of **44** could not be detected by microwave spectroscopy. The dipole moment of (*Z*)-**44** is 3.23(2) D, slightly larger than that determined for **40** (2.994 D). Microwave analysis of **16** is complicated by the fact that internal rotation about the $CH–CH_2$ bond gives this sulfine an additional conformational degree of freedom. Of the four possible conformations/structures for **16**—*Z* skew ((*Z*)-**16a**), *Z cis* ((*Z*)-**16b**), *E* skew ((*E*)-**16a**), and *E cis* ((*E*)-**16b**)—only (*Z*)-**16a** fits the calculated rotational constants and fulfills the heavy-atom nonplanarity implied by the observed constants. Unlike **40**, sulfines **16** and **44** are stable in the wave guide at 0.050 torr and 25 °C. Neither ethenesulfenic acid (**15a**/**15b**) nor (*E*)- or (*Z*)-1-propenesulfenic acid (**14**) could be detected in any of the samples examined by microwave spectroscopy (cf. Scheme 4). As will be detailed in Section 5.3.1, ^{1}H-NMR analysis of the onion LF indicated a *Z*:*E* ratio of 95:5 for **16**. Similar *Z*:*E* ratios were obtained for **44** and other thioaldehyde *S*-oxides.

5.1.2. Determination of the Configuration of Onion LF from the Structures of Cyclopentadiene Diels–Alder Adducts

Determination of the configuration of the onion LF by spectroscopic means requires concentration and, in the case of microwave spectroscopy, vaporization. An alternative approach involves directly trapping the LF with cyclopentadiene at low temperature followed by NMR measurement of the adduct *cis*:*trans* ratio [(**46a** + **46d**):(**46b** + **46c**), Scheme 16]. As we have already mentioned in Section 4.3, sulfine **40** is readily trapped by cyclopentadiene giving thermally labile *endo*-adduct **42** which undergoes a facile [2,3]-sigmatropic rearrangement to **43** even at 0 °C (see Scheme 14).

Adducts **46b** and **46d** were independently synthesized and characterized (Schemes 16 and 17); adduct **46c** could not be prepared.[73] A novel procedure was used to prepare 2-thiabicyclo[2.2.1]hept-5-ene 2,2-dioxide (**47**). Thus, treatment of (trimethylsilyl)methanesulfonyl chloride (**48**) or (trimethylsilyl)methanesulfonic anhydride (**49**) with cesium fluoride and excess cyclopentadiene gave **47** in 64% isolated yield from **48** or 75% isolated yield from **49** by a reaction which must involve thioformaldehyde *S*,*S*-dioxide (**50**, sulfene) as an intermediate.[74] This reaction represents the first instance of Diels–Alder trapping of sulfene.[48b] Compound **47** could also be prepared by oxidizing the unstable adduct **42** of cyclopentadiene and sulfine (**40**) or by oxidation of the known 2-thiabicyclo[2.2.1]hept-5-ene.[75] Sequential treatment of **47** with butyllithium followed by ethyl iodide gave *exo*-3-ethyl-2-thiabicyclo[2.2.1]hept-5-ene 2,2-dioxide (**51a**), which was reduced with lithium aluminum hydride to *exo*-3-ethyl-2-thiabicyclo[2.2.1]hept-5-ene (**52a**) and then oxidized with MCPBA to *exo*-3-ethyl-2-thiabicyclo[2.2.1]hept-5-ene *exo*-2-oxide (**46d**).

A 23:77 mixture of **51a** and its *endo*-isomer (**51b**) could be prepared in 76% yield by treatment of 1-(trimethylsilyl)propanesulfonic anhydride (**53**) with cesium fluoride and excess cyclopentadiene, a reaction which must involve propanethial *S*,*S*-dioxide (**54**) as an intermediate (Scheme 17). When the product from the Diels–Alder reaction of cyclopentadiene with the onion LF or **16**, prepared from propanesulfinyl chloride (**20**), was oxidized with one

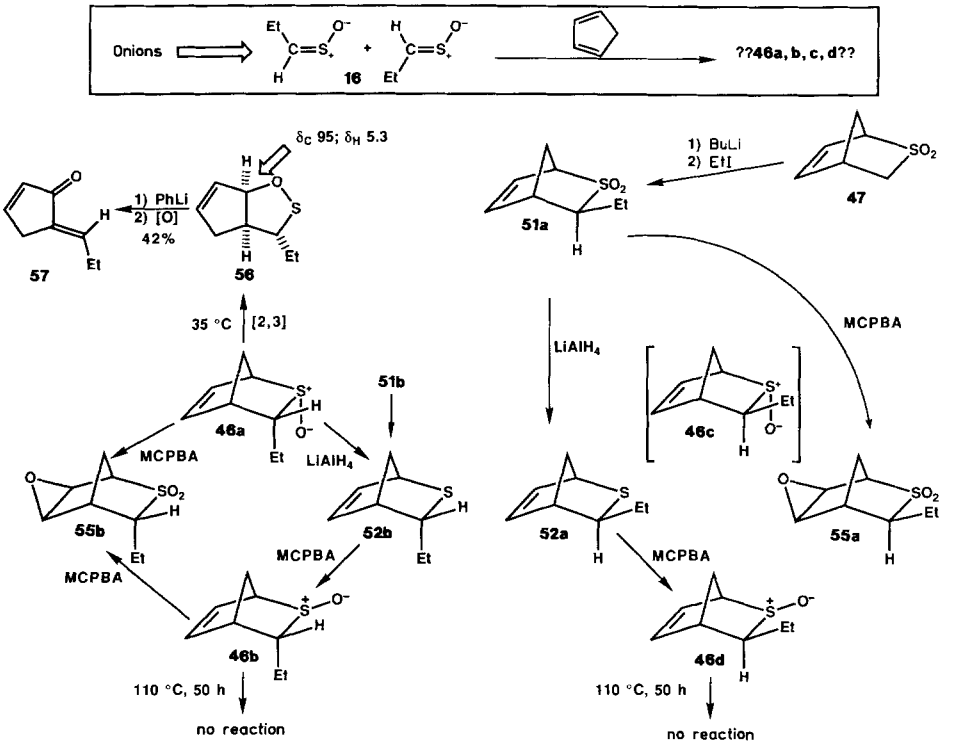

Scheme 16. Cyclopentadiene-LF adducts of type **46**: their synthesis, interconversion, and rearrangement.

equivalent of MCPBA, **51b** could be isolated in 79% yield. Lithium aluminum hydride reduction of the above cyclopentadiene-LF or cyclopentadiene-**16** adduct gave *endo*-3-ethyl-2-thiabicyclo[2.2.1]hept-5-ene (**52b**)[76] which on reoxidation with one equivalent of MCPBA gave *endo*-3-ethyl-2-thiabicyclo[2.2.1]hept-5-ene *exo*-2-oxide (**46b**). Oxidation of **51a** and **51b** with excess MCPBA gave *exo*-5,6-epoxy-*exo*-3-ethyl-2-thiabicyclo[2.2.1]hept-5-ene 2,2-dioxide (**55a**) and *exo*-5,6-epoxy-*endo*-3-ethyl-2-thiabicyclo[2.2.1]hept-5-ene 2,2-dioxide (**55b**), respectively. The structure of **55b** was established by X-ray crystallography.[73, 77a]

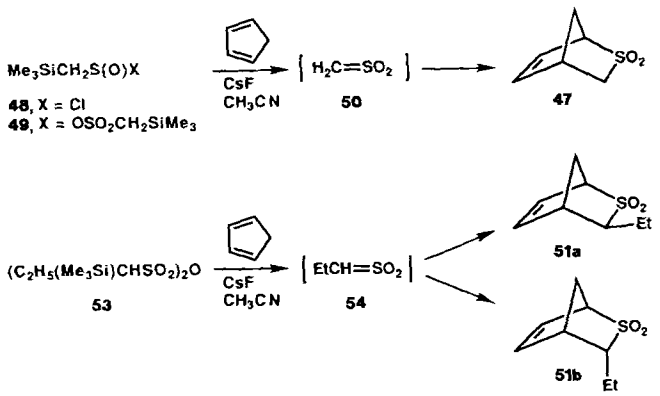

Scheme 17. Synthesis of **47** (64–75% yield) and **51a,b** (76% yield) by trapping of thioformaldehyde *S,S*-dioxide (**50**) and propanethial *S,S*-dioxide (**54**) with cyclopentadiene. The sulfenes are generated by fluorodesilylation.

While compounds **46b** and **46d** were unchanged after refluxing in deuteriotoluene for 50 hours, the adducts of cyclopentadiene with LF or **16** rearranged upon refluxing in methylene chloride for 1.5 hours to give *exo*-4-ethyl-2-oxa-3-thiabicyclo[3.3.0]oct-7-ene (**56**), isolated in 50% yield. The same type of rearrangement was also observed for the adducts of cyclopentadiene with ethanethial *S*-oxide (**44**), and butanethial *S*-oxide.[77a] This novel rearrangement forms the basis for a useful synthesis of 5-alkylidene-2-cyclopentenones, e.g. **57** (Scheme 16).[77a]

When an onion slurry, prepared from frozen chopped onions, was extracted with Freon-11 and the dried extract treated with cyclopentadiene at −78 °C followed by low-temperature concentration, a 15:1 mixture of *endo*-3-ethyl-2-thiabicyclo[2.2.1]hept-5-ene *endo*-2-oxide (**46a**) and *exo,exo*-adduct **46d** could be detected through coincidence of ^{13}C-NMR peaks in the olefinic region with corresponding peaks of authentic samples. We were unable to detect NMR peaks corresponding to *exo,endo*-adduct **46b**. The reason for the absence of **46b** is clear if we assume that formation of *exo*-3-ethyl-2-thiabicyclo[2.2.1]hept-5-ene *endo*-2-oxide (**46c**) is significantly favored by secondary orbital interactions over **46b** and that substantially less **46c** is formed than **46a**. While we could not prepare an authentic sample of **46c**, in the LF-cyclopentadiene adduct mixture we observed several minor unidentified olefinic ^{13}C-NMR signals which disappeared on warming, and could be due to **46c**. We estimate that the concentration of **46c** is less than 5%, reflecting a *Z*:*E* ratio for the LF of at least 95:5, in agreement with the NMR data (see Section 5.3.1).[77b]

5.1.3. *Mechanism for the Formation of Onion LF from (E)-1-Propenesulfenic Acid*

And if the boy have not a woman's gift to rain
a shower of commanded tears,
An onion will do for such a shift,
which in a napkin being close conveyed,
Shall in despite enforce a watery eye.

"The Taming of the Shrew", Introduction, 122.
William Shakespeare (1564–1616)

We examined the pyrolysis of (*E,Z*)-*tert*-butyl-1-propenyl sulfoxide (**58**) and *tert*-butyl-2-vinyl sulfoxide (**59**) with the hope of generating (*E,Z*)-1-propenesulfenic acid (**14b**) and ethenesulfenic acid (**15b**) (which, by analogy with the structure of methanesulfenic acid (**10**), should possess dicoordinate sulfur) and determining the relationship, if any, between these sulfenic acids and propanethial *S*-oxide (**16**) and ethanethial *S*-oxide (**44**), respectively. Both **58** and **59** are efficiently converted by FVP at 250 °C into the respective (*Z*)-sulfines (*Z*)-**16** and (*Z*)-**44**, as characterized by both microwave and NMR spectroscopy (Scheme 18). A 97:3 (*Z*)-

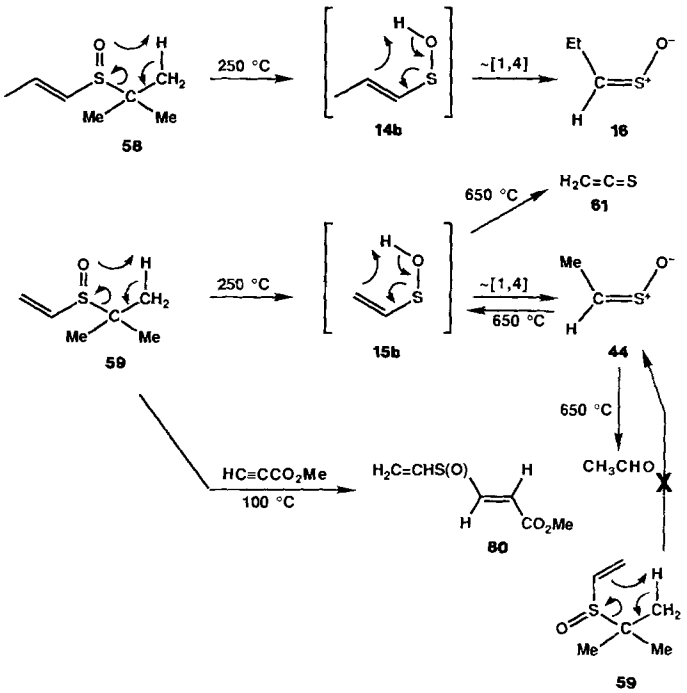

Scheme 18. Flash vacuum pyrolysis of 1-alkenyl *tert*-butyl sulfoxides such as **58** and **59** as a route to 1-alkenesulfenic acids such as **16** and **44**, respectively.

16:(*E*)-**16** ratio and a 95:5 (*Z*)-**44**:(*E*)-**44** ratio was established by ^{1}H-NMR analysis (discussed in Section 5.3.1). Heating a solution of **59** in excess methyl propiolate at 100 °C affords sulfenic acid adduct **60**. Neat **59** decomposes within 4 h at 100 °C to give, among other products, acetaldehyde, which we have separately found to be a major decomposition product of ethanethial *S*-oxide (**44**). Finally, microwave spectroscopic analysis indicates that sulfine **44** decomposes under high-temperature FVP conditions (650–750 °C) to both acetaldehyde and thioketene (**61**).[72]

The above results are most simply explained in terms of a [1,4]-sigmatropic rearrangement of **14b** and **15b** (Scheme 18), a reaction leading to (*Z*)-sulfines. The conversion of **58** via **14b** into **16**, and of **59** via **15b** into **44** finds precedence in the known tautomerism of thioamide *S*-oxides[78] and the isomerization of other α,β-unsaturated sulfenic acids to sulfines.[79] At high temperatures **15b** undergoes unimolecular dehydration to thioketene (**61**), in analogy with the previously noted high-temperature dehydration of methanesulfenic acid (Scheme 13). McLafferty et al. have examined the formation of **15b** and **44** from **59** by tandem FVP and neutralization-reionization mass spectrometry and ab initio calculations.[80] Their studies exclude an alternative retro-ene route from **59** to **2** (Scheme 13) and indicate that **44** is 12 kJ mol^{-1} (2.9 kcal mol^{-1}) more stable than **15b** with a transition state interconversion barrier of 137 kJ mol^{-1} (33 kcal mol^{-1}) and that **15b** has a near-orthogonal geometry with a CSOH dihedral angle of 88°. When **15b**-OD is examined in the mass spectrometer under conditions allowing conversion into **44**, OH loss predominates >2:1 over OD loss.

A mechanism for the genesis of the onion LF from precursor **5** is proposed (Scheme 19). Our mechanism is consistent

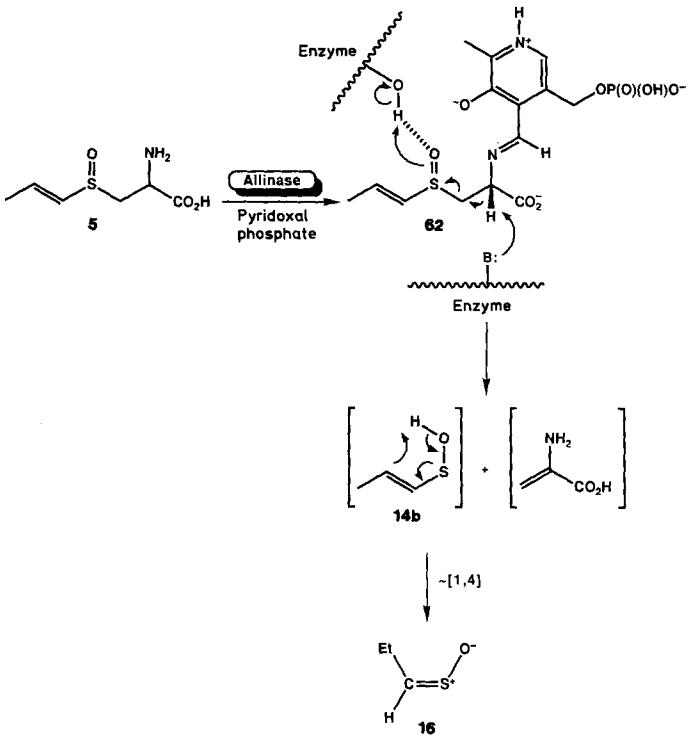

Scheme 19. Mechanism for allinase catalyzed conversion of **5** into the onion LF **16**.

with the deuteration studies of Virtanen if it is assumed that rearrangement of deuterated 1-propenesulfenic acid **14b**-OD precedes electron-impact-induced fragmentation (Scheme 20). Our mechanism also has the advantage of allowing a common mode of enzymatic decomposition for LF precursor **5** and cysteine sulfoxides **2**, **6**, and **7**. The intermediacy of Schiff base **62** is consistent with the requirement for pyridoxal phosphate as a cofactor for the enzymatic reac-

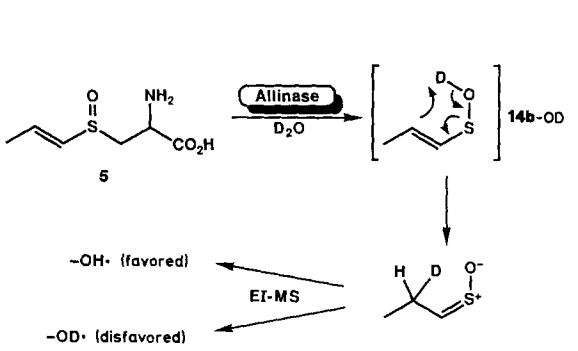

Scheme 20. Mechanisms of the allinase-catalyzed conversion of **5** into LF **16** in the presence of deuterium oxide.

tion[3h, i] and the demonstration that sulfenic acids can be eliminated from related structures (Scheme 21) in vitro at neutral pH and ambient temperatures.[81]

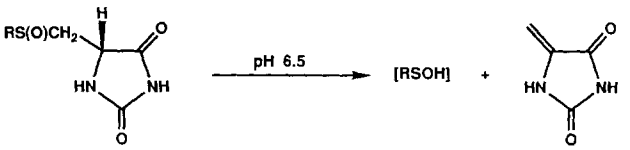

Scheme 21. Formation of sulfenic acids from hydantoins at room temperature in almost pH neutral solution.

5.1.4. The "Syn Effect" of Onion LF and Other Sulfines

While the [1,4]-sigmatropic rearrangements of **14b** to (*Z*)-**16** and **15b** to (*Z*)-**44** are aesthetically appealing and accommodate most observations (Scheme 18), it is curious that (*Z*)-**16** and (*Z*)-**44** are also the predominant products formed upon treatment of propanesulfinyl chloride (**19**) and ethanesulfinyl chloride (**45**), respectively, with triethylamine, reactions that should not involve the intermediacy of **14b** and **15b**! Theoretical calculations were therefore performed to examine the relative energies of the conformers of **44**.[82] Restricted Hartree-Fock calculations on **44** indicate that conformer (*Z*)-**44a** is more stable than conformers (*Z*)-**44b**, (*E*)-**44a**, and (*E*)-**44b** by 0.8, 1.7, and 3.1 kcal mol^{-1}, respectively (Fig. 3). These calculations are in good agreement with microwave spectroscopic studies of **44**-CH_2D ($CH_2DCH{=}S^+{-}O^-$), in which **44a** was the only conformation to be observed. The conformational preference for *Z*-**44a** can be explained in terms of orbital and electrostatic interactions between the terminal oxygen and methyl hydrogens, which are negligible in the (*E*)-form. Calculations indicate substantial negative charge on the sulfine oxygen (Fig. 3). It is suggested that there is an attractive electrostatic interaction between the methyl hydrogens (which according to the calculations bear a positive charge) and the negatively charged oxygen. A σ-type interaction, characterized by the formation of six σ-MOs, of which the HOMO is 1,5-bonding, also favors conformer (*Z*)-**44a**.[82] Both of these types of interactions are missing in the (*E*)-conformers. The general phenomenon of enhanced stability of (*Z*)- or *syn* isomers, the "*syn*-effect", is in fact well known.[82, 83] An important consequence of the above theoretical findings is that alternative routes from **14b** to (*Z*)-**16**, e.g. by protonation of the enolate of the (*E*)-1-propenesulfenate anion, cannot be excluded.

5.1.5. The Hydrolysis of Onion LF

When **16** is allowed to remain in contact with water, sulfur is split off, perhaps initially as HSOH, leaving behind propanal, which readily undergoes aldol condensation. In the medium following hydrolysis of **16**, sulfur is found as the free element as well as (in minor quantities) sulfate and sulfite. Hydrogen sulfide, detected in onion volatiles and presumably a decomposition product of **16**, may be trapped by propanal, forming *cis*- and *trans*-3,5-diethyl-1,2,4-trithiolane (**63**). **63** has likewise been isolated from volatiles of onion and other *Allium* spp. (Scheme 22).[84]

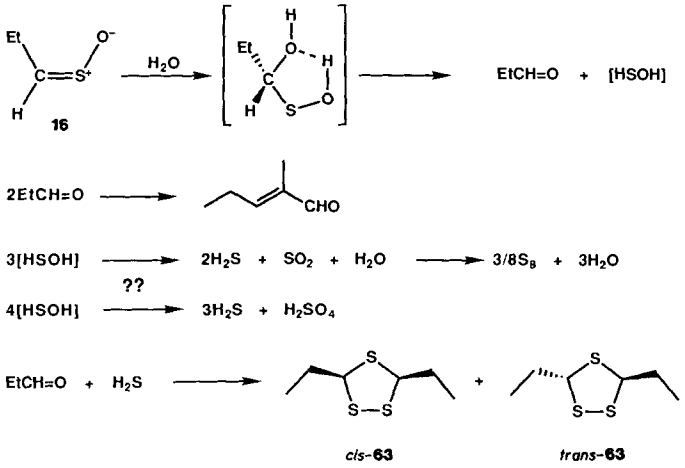

Scheme 22. Hydrolysis of LF **16** and formation of 1,2,4-trithiolanes *cis*- and *trans*-**63**.

5.1.6. The Dimer of Onion LF

As already noted, in 1961 Wilkens reported that the onion LF dimerized, affording a compound claimed to be 2,4-diethyl-1,3-dithietane 1,3-dioxide (**18a**) (cf. Scheme 5).[47] The proposed structure seemed to us to be at odds with the IR spectrum of the dimer, which indicated the presence of a sulfonyl group, and our examination of the IR spectra of authentic *cis*- and *trans*-1,3-dithietane 1,3-dioxide (**38a/b**) (cf. Scheme 12),[59] which failed to show the type of unusual "pseudo-sulfone infrared absorption" proposed by Wilkens to explain the spectrum of **18a**. Furthermore, the stability of the **38a/b** contrasts with the instability of **18a**. Finally, it is mechanistically difficult to reconcile the formation of **18a** from **16** with the reported formation of *trans*-4,5-diphenyl-1,2,3-trithiolane 1,1-dioxide (**65**) from thiobenzaldehyde *S*-oxide (**64**, Scheme 23).[85] In view of the uncertainty about the structure of the LF-dimer we re-examined the self-condensation of **16**.

A sample of **16** from natural or synthetic sources was purified by trap-to-trap distillation at −30 °C, dissolved in about twice its volume of freshly dried benzene and kept in the dark at 3 °C for 7 days. The slightly yellow solution, now devoid of lachrymatory properties, was concentrated in vacuo and the residue subjected to molecular distillation, affording a clear, practically colorless liquid with a strong onion-like odor. Analysis by GC indicated a single major

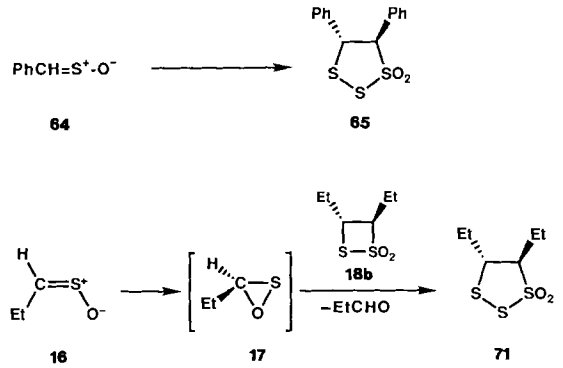

Scheme 23. Formation of 1,2,3-trithiolane 1,1-dioxides **65** and **71** from sulfines **64** and **16**, respectively.

product with retention time slightly longer than that of propyl propanethiosulfonate. High resolution mass spectrometry confirmed the formula $C_6H_{12}S_2O_2$ for the LF dimer. The IR spectrum, showing sulfonyl bands, was very similar to that published by Wilkens.[47] The LF dimer gave a positive thiosulfonate test[86] and absorbed in the UV (EtOH or hexane) at $\lambda_{max} = 280$ (ε 100, sh).[87] Reduction of the compound with $LiAlH_4$ in ether gave 90% (±)-hexane-3,4-dithiol and 10% *meso*-hexane-3,4-dithiol. The above data and the ^1H- and ^{13}C-NMR spectra, discussed in Section 5.3.2, are most consistent with *trans*-3,4-diethyl-1,2-dithietane 1,1-dioxide (**18b**) as the structure of the LF dimer.[88a] Compound **18b** is formed by a process that begins with 1,3-dipolar addition of **16** to itself followed by rearrangement (Scheme 24).[88b] Minor amounts of *cis*-**18b** are also formed.

(*Z,E*)-(Trimethylsilyl)methanethial *S*-oxide (**66**), prepared by treatment of (trimethylsilyl)methanesulfinyl chloride (**41**)

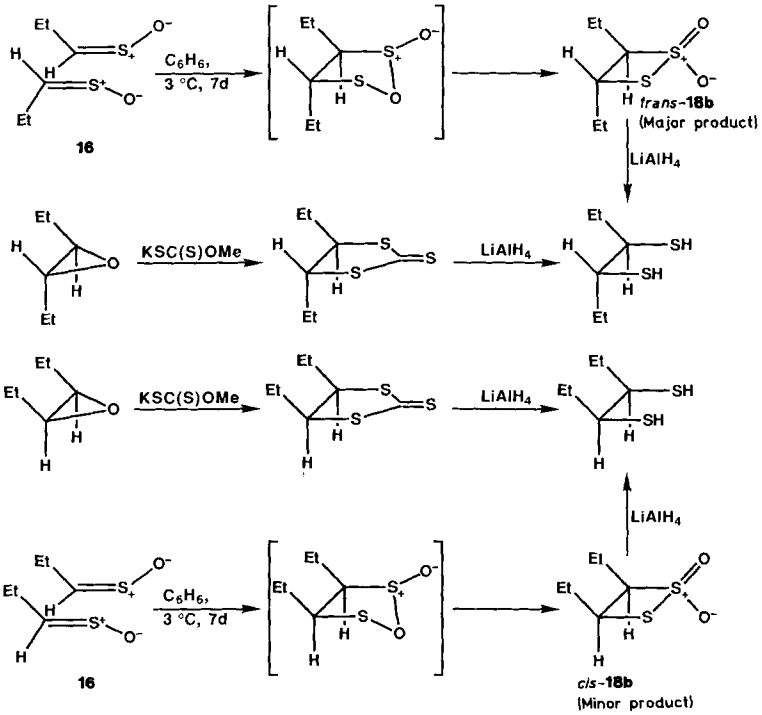

Scheme 24. Mechanism for the dimerization of propanethial *S*-oxide **16** to **18b**.

with one equivalent of triethylamine. also dimerizes on storage at room temperature for several days to afford *trans*-3,4-bis(trimethylsilyl)-1,2-dithietane 1,1-dioxide (**67**) in 42% yield as a colorless, crystalline solid of m.p. 100–101 °C (Scheme 25).[77b, 89] Compound **67** affords (±-1,2-bis-

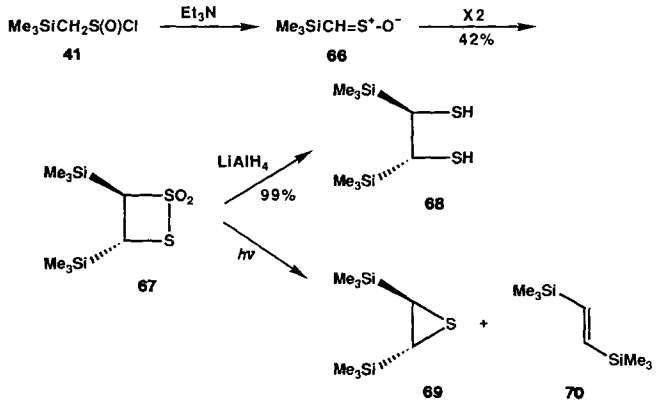

Scheme 25. Synthesis of silylated 1,2-dithietane 1,1-dioxide **67** from (trimethylsilyl)methanethial *S*-oxide (**66**); conversion of **67** into 2,3-bis(trimethylsilyl)thiirane (**69**) and the compounds (±)-**68** and **70** (only the *S,S* forms are shown).

(trimethylsilyl)-1,2-ethanedithiol (**68**) on reduction and *trans*-2,3-bis(trimethylsilyl)thiirane (**69**) and *trans*-1,2-bis(trimethylsilyl)ethene (**70**) on photolysis.[89] In benzene solution, the LF **16** may also undergo unimolecular rearrangement giving oxathiirane **17**, which in turn could donate sulfur to LF dimer **18b** giving *trans*-4,5-diethyl-1,2,3-trithiolane 1,1-dioxide (**71**, Scheme 23).

5.1.7. α-Chloroalkyl Alkanethiosulfonates: By-products in the Synthesis of Onion LF and Other Alkanethial S-Oxides from Alkanesulfinyl Chlorides

In the course of preparing onion LF **16** by treatment of propanesulfinyl chloride (**19**) with triethylamine we noticed the formation of small quantities of 1-chloropropyl propanethiosulfonate (**72**). We found that the formation of α-chloroalkyl alkanethiosulfonates was a general reaction with optimum yields when an alkanesulfinyl chloride was

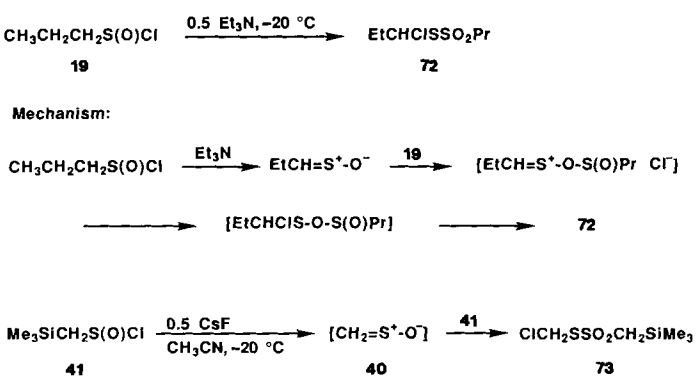

Scheme 26. Synthesis of α-chloroalkyl alkanethiosulfinates such as **72** and **73** from sulfines such as **19** and **41**, respectively.

treated at low temperature with *one-half an equivalent* of triethylamine.[90] Thiosulfonates such as **72** result from reaction of the sulfine, functioning as a nucleophile, with the sulfinyl chloride, functioning as an electrophile (Scheme 26). In support of this mechanism we found that separately generated sulfines react with sulfinyl chlorides forming the expected chlorinated thiosulfonates. If thionyl chloride is substituted for the sulfinyl chloride, the product is a bis(α-chloroalkyl) disulfide. In another variant, we found that slow addition of 0.5 equivalent of cesium fluoride to (trimethylsilyl)methanesulfinyl chloride (**41**) in acetonitrile at −20 °C gave *S*-chloromethyl (trimethylsilyl)methanethiosulfonate (**73**) in nearly quantitative yield. Here the sulfine being trapped is the parent compound **40**.[70] We have recently utilized this reaction to establish the formation of cyclopropanethione *S*-oxide from cyclopropanesulfinyl chloride.[91]

5.2. Organosulfur Constituents of *Allium* Homogenates Separated by HPLC and GC-MS

If Leekes you like but do their smell dis-leeke
Eat Onyuns and you shall not smell the Leeke.
If you of Onyuns would the scent expelle
Eat Garlicke and that shall drowne the Onyun's smelle.
Anonymous

A variety of procedures have been examined for the separation of compounds formed in solution from cut *Allium* spp. The plant can be finely cut using a Waring Blender, a food processor or a tissue homogenizer. While the Waring Blender gives satisfactory results with "softer" plants, garlic and shallot bulbs are best cut first with a food processor followed by a tissue homogenizer. The plant is chopped using a 2:1 water:plant ratio. For the preparation of an *extract*, the homogenate is squeezed through cheese cloth or nylon mesh, saturated with sodium chloride, and shaken twice with dichloromethane, filtering/centrifuging each time. The separated dichloromethane layers are combined, dried and concentrated in vacuo at room temperature and then analyzed by FT-NMR and HPLC and/or GC (with a modified injector; see Section 5.2.1). Supercritical carbon dioxide can also be used as the extraction solvent.[92] For preparation of *a room temperature "steam distillate"*, the above homogenate is subjected to distillation at high vacuum using an oil bath to keep the pot at room temperature. The distillate is collected at −196 °C,[93, 94] saturated with sodium chloride and extracted and analyzed as above. For a particular plant the extract and room-temperature distillate were analytically quite similar (cf. Fig. 4). Although the distillates were generally cleaner with less component isomerization, in some cases more material was lost by distillation than by extraction, or other differences were observed.

5.2.1. Thiosulfinates: Primary Products in Cut Allium spp.

In addition to LF **16**, detected exclusively in the case of the onion but probably formed in other *Allium* spp., the primary

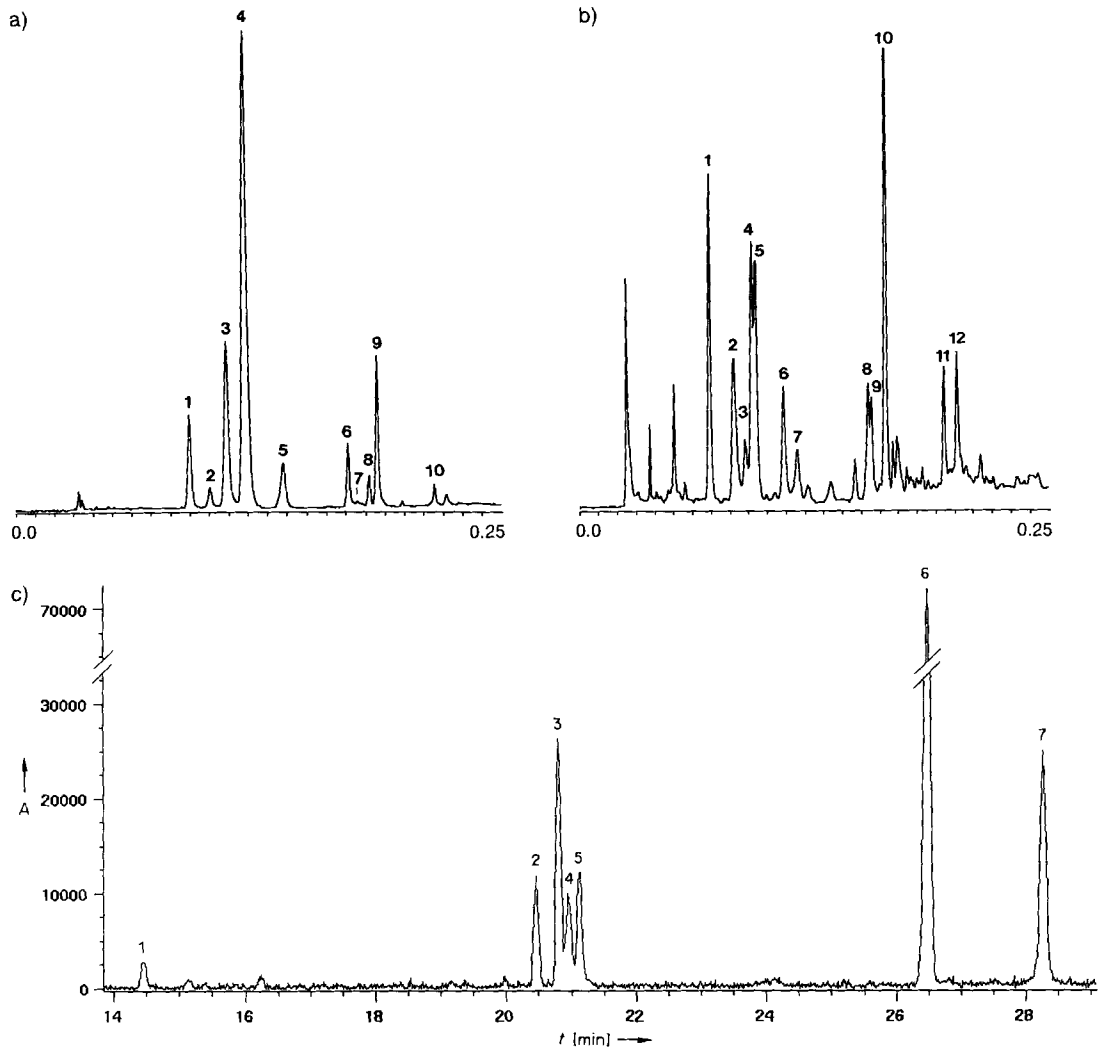

Fig. 4. a) HPLC separation of an extract of store-purchased garlic containing benzyl alcohol as internal standard. Conditions: 250 × 4.6 mm, 5 μm Rainin Microsorb silica gel column, UV detection at 254 nm; 1.6 mL min^{-1}, gradient from 2:98 2-propanol:hexane (10 min hold), to 20:80 during 10 min (5 min hold). Peak identification: 1, (*E*)-**105**, R = All); 2, (*Z*)-**106**, R = All); 3, (*E*)-**106**, R = All); 4, allicin **1**; 5, benzyl alcohol, internal standard; 6, **102**; 7, (*Z*)-**106**, R = Me; 8, (*E*)-**106**, R = Me; 9, **101**, 10, **12** (cf. Schemes 1, 4, 34, and 37). b) HPLC separation of a distillate of white onion (conditions as above). Peak identification: 1, (*E*)-**105**, R = Pr; 2, (*Z*)-**106**, R = Pr; 3, **16**; 4, (*E*)-**106**, R = Pr; 5 (shoulder), **13**; 6, (*E*)-**105**, R = Me; 7, benzyl alcohol, internal standard; 8, **30**; 9, (*Z*)-**106**, R = Me; 10, (*E*)-**106**, R = Me and **29** (overlapping peaks); 11, **123**; 12, **12** (cf. Schemes 4, 5, 10, 37, and 46). c) GC-EI-MS total ion chromatogram of the same sample of white onion as in Figure 4b. A = abundance. Conditions: 30 m × 0.53 mm methyl silicone gum capillary column, cryogenic on-column injection at 0 °C, column programmed from 0–200 °C at 5 °C min^{-1}; column head pressure 34.5 × 10^3 Pa (5 psi), GC-MS transfer line temperature, 100 °C. Peak identification: 1, **12**; 2, **29**; 3, (*E,Z*)-**106**, R = Me; 4, **30**; 5, (*E*)-**105**, R = Me; 6, (*E*)-**106**, R = Pr and *trans*-zwiebelane (**118**); 7, *cis*-zwiebelane (**117**) (cf. Schemes 4, 10 and 37, and Fig. 7).

products detected by HPLC, NMR, and GC-MS from the above procedures are thiosulfinates (Table 1) with negligible di- and polysulfides or thiosulfonates. Together with LF **16**, these thiosulfinates closely duplicate the taste and aroma of the freshly cut *Allium* spp. and serve as progenitors of virtually all of the organosulfur compounds formed in the cut plants. In view of the thermal instability of allicin **1** and other thiosulfinates it is surprising that vacuum "steam distillation" succeeds so well. Room-temperature steam distillation is successful because of the stabilizing effect of water, through hydrogen bonding, on the thiosulfinates; mildly acidic conditions (e.g. pH 2–4) also seem to stabilize thiosulfinates.[28] Since the thiosulfinates are water soluble, the physical laws applied to steam distillation of water-insoluble compounds are not applicable. It is likely that thiosulfinates form azeotropes under our vacuum "steam distillation" conditions.[21b]

Some comments are necessary regarding the "best" chromatographic methods for characterizing and quantifying unstable aroma and taste substances such as thiosulfinates produced on cutting *Allium* spp. Because of their excellent resolving powers, GC and GC-MS have dominated studies on *Allium* headspace volatiles and room-temperature extracts, despite early cautionary notes that many of the compounds seen by GC may be "artifacts of analysis"[39] and that more recent work suggests that equivalent or superior resolution of *Allium* components may be achieved at room temperature using HPLC![95, 96, 121] We have already noted in Section 4.1 that some, but not all, aliphatic thiosulfinates possessing up to eight carbons survive GC analysis using short columns and low injection port and column temperatures.[29, 54e] Unfortunately most studies on *Allium* volatiles employ long, narrow bore capillary columns (e.g. 0.20 mm × 50 m) and/or injection port temperatures as high

Table 1. Relative concentrations of thiosulfinates and other compounds in *Allium* spp. (in mol-% referred to total RS(O)SR′). Data from Ref. [21b,c]. **105** MeCH=CHS(O)SR **106** RS(O)SCH=CHMe

RS(O)SR	Garlic (NY) [b]	Garlic (NY) D [b]	Garlic (NY) R [b, c]	Garlic (S) [b]	Garlic (S)R [b, c]	Garlic (Ind. 1) [b, e]	Garlic (Ind. 2) [b, e]	"Elephant"-garlic [b]	"Elephant"-garlic (NY) D [b]	Wild garlic [b]
12 MeS(O)SMe	–	–	–	2.2	0.9	2	4	10	8.6	20
101 MeS(O)All	2.9	3.0	3.9	18	11	20	27	27	28	34
102 AllS(O)SMe	1.4	1.7	1.6	8.1	7.5	9	11	15	16	16
(*E,Z*)-**106**, R = Me [a]	x	x	x	1.2 [a]	1.9 [a]	1 [a]	1 [a]	3.6 [a]	1.5 [a]	1 [a]
(*E*)-**105**, R = Me	–	–	–	x	0.6	–	–	1.7	x	x
29 MeS(O)SPr	–	–	–	–	–	–	–	–	–	–
30 PrS(O)SMe	–	–	–	–	–	–	–	–	–	–
1 AllS(O)SAll	89	89	79	62	59	64	53	38	43	28
(*E,Z*)-**106**, R = All [a]	5.3 [a]	5.5 [a]	13 [a]	5.9 [a]	18 [a]	3 [a]	3 [a]	4.5 [a]	2.6 [a]	1 [a]
(*E*)-**105**, R = All	1.6	0.8	3.1	2.1	1.6	1	1	0.6	0.6	–
13 PrS(O)SPr	–	–	–	–	–	–	–	–	–	–
(*E,Z*)-**106**, R = Pr [a]	–	–	–	–	–	–	–	–	–	–
(*E*)-**105**, R = Pr	–	–	–	–	–	–	–	–	–	–
16 LF	–	–	–	–	–	–	–	–	–	–
123 Bissulfine	–	–	–	–	–	–	–	–	–	–
117/118 *cis/trans*-Zwiebelane	–	–	–	–	–	–	–	–	–	–
Total-% Allyl	94	95	89	80	78	80	74	61	67	54
Total-% Methyl	2	2	3	16	11	18	24	34	31	45
Total-% 1-Propenyl	3	3	8	4	11	2	2	5	2	1
Total-% Propyl	–	–	–	–	–	–	–	–	–	–
Total-RS(O)SR′ [μmol g^{-1}]	14.3 [f]	7.5 [f]	22.1 [f]	25.6 [f]	20.7 [f]	15.5 [f]	36.5 [f]	5.2 [f]	2.7 [f]	20.8 [g]

RS(O)SR′	Onion (white) [b–d]	Onion (yellow) [b–d]	Shallot [b–d]	Scallion [b–d]	Chive [b–d]	Leek [b–d]	Chinese chive [b–d]
12 MeS(O)SMe	1	14	9	1	1.2	3	74
101 MeS(O)SAll	–	–	–	–	–	–	12
102 AllS(O)SMe	–	–	–	–	–	–	9
(*E,Z*)-**106**, R = Me [a]	34 [a]	25 [a]	15 [a]	18 [a]	4.4 [a]	27 [a]	5 [a]
(*E*)-**105**, R = Me	14	24	9	2.5	1.3	12	–
29 MeS(O)SPr	1	1	1.2	7.5	6.8	5	–
30 PrS(O)SMe	1	1	2.8	7.5	3.8	5	–
1 AllS(O)SAll	–	–	–	–	–	–	–
(*E,Z*)-**106**, R = All [a]	–	–	–	–	–	–	–
(*E*)-**105**, R = All	–	–	–	–	–	–	–
13 PrS(O)SPr	9	13	27	35	57	25	–
(*E,Z*)-**106**, R = Pr [a]	33 [a]	10 [a]	22 [a]	28 [a]	23 [a]	15 [a]	–
(*E*)-**105**, R = Pr	7	12	14	1.5	2.4	8	–
16 LF	+ +	+ +	+ +	+ +	–	+	–
123 Bissulfine	8% TS	0.5% TS	0.2% TS	x	x	x	–
117/118 *cis/trans*-Zwiebelane	29% TS	20% TS	4% TS	8% TS	4% TS	11% TS	–
Total-% Allyl	–	–	–	–	–	–	11
Total-% Methyl	19	33	22	17	9	27	87
Total-% 1-Propenyl	59	47	33	30	19	31	3
Total-% Propyl	22	20	45	53	72	42	
Total-RS(O)SR′ [μmol g^{-1}]	0.20 [f]	0.35 [f, h]	0.25 [f, h]	0.08 [f]	0.26 [f]	0.15 [f, h]	2.0 [f]

[a] Typical *E*:*Z* ratio 2–3:1. [b] by HPLC analysis; [c] by NMR analysis; [d] by GC-MS analysis; [e] Ind. 1 = from farm in mountainous region of India with 22–23 °C average growing temperatures; Ind. 2 = from farm in plains region of India with 30–32 °C average growing temperatures; [f] fresh weight; for comparison, average fresh weight values reported for garlic and elephant garlic by Lawson by extraction are 34 μmol g^{-1} and 11 μmol g^{-1}, respectively; since garlic and elephant garlic contain ca. 60% water, approximate dry weight values are obtained by multiplying fresh weight values by 2.5 [121b]; [g] dry weight; [h] average fresh weight values reported by Lawson for *1-propenyl thiosulfinates* from scallion, shallot, leek, yellow onion, and white onion are 1.65, 1.89, 1.77, 0.50, and 0.40 μmol g^{-1}, respectively [121a]; *, trace level detected; + +, substantial amounts of LF detected; not quantitated due to variable loss on workup; zwiebelanes and bis-sulfine **123** not included in calculation of total number of moles present but indicated as % total thiosulfinates (TS) present; D, distilled then extracted (if not indicated, sample prepared by direct extraction of homogenized plant); R, refrigerated for 8 weeks; S, typical store purchased garlic (Mexican or Californian origin); NY, from farm in upstate New York (average growing temperature 19–22 °C); Total, percent of total thiosulfinates found as allyl-, methyl- 1-propenyl- and propyl group, respectively.

as 280 °C,[71, 92b, 97, 98] conditions which are especially conducive to thiosulfinate decomposition.

Our comparison of the results of both GC and HPLC analyses of fresh extracts and room-temperature distillates of *Allium* spp., using authentic samples of the thiosulfinates thought to be present to evaluate analysis conditions, reveal that *gas chromatography, as typically performed with high injector and column temperatures, presents a highly inaccurate picture of the composition, both of the headspace volatiles as well as of the room-temperature extracts from Allium species.*[21b] Thus, analysis of *Allium* extracts or vacuum distillates by both normal (Si) and reverse phase (C-18) HPLC, using diode-array UV detection, indicate that the predominant constituents are thiosulfinates. *We find no evidence from HPLC for the presence in these samples of the polysulfides claimed by prior GC-MS studies*! Using Si-HPLC, almost all of the thiosulfinates from *Allium* spp. can be separated and quantified using an internal standard.

While some thiosulfinates survive gas chromatography using short columns and low temperatures, these earlier GC analyses frequently suffered from peak broadening and tailing, indicative of partial sample decomposition. We find that

by using a standard polymethylsilicone column (30 m, 0.53 mm internal diameter, "Megabore") with *on-column injection ramped from 0 °C (liquified CO_2 cooling) with a 5 °C min^{-1} temperature injector and column program and a GC-MS transfer line temperature of 100 °C*, nicely resolved, clean GC-MS total ion chromatograms could be obtained for pairs of thermally unstable C_4 regioisomers such as **105**/**106**, R = Me, and **29**/**30**.[21c] While some C_6 compounds

RSS'(O)CH=CHMe	RS(O)SCH=CHMe	MeS(O)SPr	MeSS(O)Pr
105, R = Me	**106**, R = Me	**29**	**30**

could also be resolved under the above conditions, compounds such as PrS(O)SPr **13** required a slower temperature program (2 °C min^{-1}) and higher flow rates or a shorter (15 m) column for analysis. The various allylic thiosulfinates from garlic, such as allicin, could not be satisfactorily analyzed even under the mildest GC conditions.[21c]

The Si-HPLC and cryogenic-injector silicone capillary column GC-MS *Allium* analyses are complementary since the former separates on the basis of polarity and uses UV detection, while the latter separates on the basis of boiling point and uses EI/CI-MS detection. Peaks that are not resolved using one technique can often be separated using the other technique. Furthermore, ion extraction and selective ion MS methods (SIMS) can be employed to resolve overlapping GC peaks, especially when authentic samples are available for calibration purposes. Because of the great thermal instability of allylic thiosulfinates, HPLC represents the preferred method of analysis for garlic, elephant garlic, wild garlic, and Chinese chive extracts. HPLC peaks can also be identified by LC-MS, although the volatility of the C_2 and C_4 components limit the utility of this technique at present.[21b] Representative analyses of *Allium* extracts under our HPLC and GC-MS conditions are shown in Figure 4a–c and Table 1. An important conclusion from these analyses is that *thiosulfonates and di- and polysulfides are not detected in the fresh Allium extracts examined by us*. Thiosulfonates are seen in some samples that have been allowed to stand for some time. These compounds therefore may contribute to the flavor (or off-flavor!) of processed or cooked *Allium* spp.

The *Allium*-derived thiosulfinates are of four types: 1) fully saturated, RS(O)SR' (R,R' = Me or Pr) such as **12**, **13**, **29**, and **30**; 2) mono- or bis-β,γ-unsaturated thiosulfinates AllS(O)SMe **102**, AllSS(O)Me **101** or AllS(O)SAll **1**; 3) mono-α,β-unsaturated thiosulfinates, (*E*)-**105** or (*E,Z*)-**106** (R = Me or Pr); 4) mixed α,β- and β,γ-unsaturated thiosulfonates, (*E*)-**105** or (*E,Z*)-**106**, R = All. Notable in their omission from this listing are the isomeric bis-α,β-unsaturated thiosulfinates, MeCH=CHS(O)SCH=CHMe. These are thought to be formed and to rapidly rearrange; they will be considered separately (see Section 5.2.5). The chemistry of the fully saturated thiosulfinates has already been discussed above (Section 4.1). The chemistry of the other classes of *Allium* thiosulfinates will be considered in Sections 5.2.3 and 5.2.4 following some general observations on thiosulfinates from garlic, wild garlic, elephant garlic, onion, shallot, scallion, chive, leek, and Chinese chive (see Table 1).

5.2.2. *General Observations on Thiosulfinates from Each Allium spp.*

One way to categorize the different *Allium* spp. is by the types of alkyl groups present in the thiosulfinates, or less reliably (using gas chromatography), in derived compounds such as polysulfides. This type of chemotaxonomic information has been used to establish relationships between different members of the *Allium* genus.[39, 99, 100] Only the Chinese chive showed a predominance of *methyl* groups, although all of the *Allium* species examined contain methyl groups.[101] In three of the plants, garlic, elephant garlic, and wild garlic, the *allyl* group is the major alkyl group (Fig. 5). The only

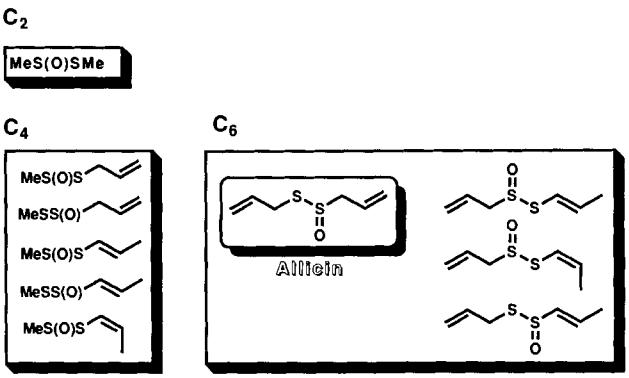

Fig. 5. C_2, C_4, and C_6 thiosulfinates in garlic extracts.

other plant containing detectable quantities of allyl groups is Chinese chive. The *propyl* group is the major alkyl group in chive, scallion, shallot, and leek, and is present in onion. Contrary to earlier reports[3i, 38] but consistent with Lawson's observation[121] the *propyl* group is *absent* in garlic as well as in elephant garlic, wild garlic and Chinese chive, the *1-propenyl* group being present instead. While *all* of the plants contain *1-propenyl* groups, it is the dominant group only in onion (Fig. 6). The total percentage of the 1-propenyl

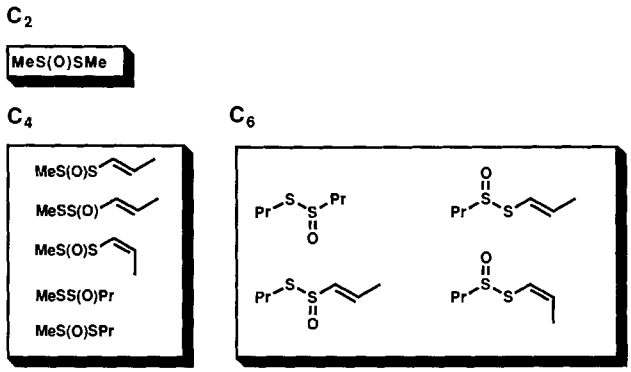

Fig. 6. C_2, C_4, and C_6 thiosulfinates in onion extracts.

group incorporated in onion thiosulfinates, zwiebelanes and bissulfine (e.g. 59% for white onions) is somewhat misleading since the majority of the 1-propenyl group generated as

1-propenesulfenic acid ends up as the LF, which is not included in the calculation because most is lost during analysis. However, in one experiment using ether as solvent to extract white onion, 0.5 $\mu mol\,g^{-1}$ of LF was isolated compared to ca. 0.2 $\mu mol\,g^{-1}$ total thiosulfinate! Small quantities of bissulfine were also found in some of the extracts. When the plant homogenates were allowed to stand in *methanol* for 24 hours before extraction and workup by chromatographic methods, a number of other organosulfur compounds were isolated as described below.

In view of the ephemeral nature of *Allium* thiosulfinates, the significance of the numbers in Table 1 can be questioned both with regard to variation in isolation techniques and in plant specimens. *Allium* homogenates prepared from the trimmed bulbs (garlic, elephant garlic, wild garlic, onion, shallot) or the trimmed plants (scallion, chive, leek, Chinese chive; roots and tips of stalks removed) were typically allowed to stand at room temperature for 30 min and then analyzed after rapid extraction and extract concentration. The analytical results were not altered upon increasing the interval between homogenization and extraction to 6 h. When the homogenate was allowed to stand overnight at room temperature, the only significant change was the disappearance of thiosulfinates of type MeCH=CHS(O)SR **105** (see Section 5.2.5). For quantitative analysis, some variation is seen between different methods of homogenization. Lower yields of thiosulfinates and, in some cases, minor qualitative differences were obtained using distillation rather than extraction methods. Organoleptic evaluation of the room temperature "steam distillate" of the onion indicated that the taste and smell closely duplicate that of the freshly cut plant. Thus, for a given plant sample, reasonable reproducibility is achieved and the analytical data so obtained is relevant to plant flavor.

The situation with regard to the plant specimens is more ambiguous. Thus, the relative percentages for different alkyl groups can vary with the part of the plant, e.g. in Chinese chives the methyl:allyl ratio varies from 71:29 to 36:64 with the leaves, roots, and rhizomes,[102] with the plant variety (e.g. yellow, white or red onion), with the developmental stage[45] and, as we shall discuss below, with the growing and storage conditions.[28c] In particular, we find considerable variation in methyl group percentages between plant samples.

Despite limitations in the reproducibility of the data in Table 1, a number of interesting features can still be noted. The following data, extracted from Table 1 and from more extensive studies, will be considered in more detail in Sections 5.2.3 to 5.2.5:

a) There is excellent qualitative agreement in the thiosulfinate composition of extracted and room temperature "steam-distilled" garlic (see Table 1) and elephant garlic (NY extract not shown).
b) For thiosulfinates of type **106** both *E* and *Z* isomers are found, with *E*:*Z* ratios varying from 9:1 to 1.1:1, with an average value of 2:1. Since pure *E* and *Z* isomers undergo rapid isomerization in solution (see Section 5.2.4) only the *E* + *Z* sum is reported. For thiosulfinates of type **105**, only the *E* isomer is found in plant extracts or distillates. In all but one case, significantly more (*E*,*Z*)-**106** is found than (*E*)-**105**.
c) Store-purchased garlic (origin: Mexico) shows a typical allyl:methyl:1-propenyl ratio of 80:16:4; the ratio of **101**:**102** is 2.2:1.
d) Refrigerated store-purchased garlic shows an allyl:methyl:1-propenyl ratio of 78:11:11; the ratio **101**:**102** is 1.4:1.
e) New York grown garlic (average growing temperature 19–22 °C) shows an allyl:methyl:1-propenyl ratio of 95:2:3; the ratio **101**:**102** is 1.8–2.1:1.
f) Refrigerated New York grown garlic shows an allyl:methyl:1-propenyl ratio of 89:3:8; the ratio **101**:**102** is 2.4:1.
g) Garlic grown in a plains region of India (average growing temperature 30–32 °C) shows an allyl:methyl:1-propenyl ratio of 74:24:2; the ratio **101**:**102** is 2.5:1.
h) Garlic grown in a mountainous region of India (average growing temperature 22–23 °C) shows an allyl:methyl:1-propenyl ratio of 80:18:2; the ratio **101**:**102** is 2.2:1.
i) "Deodorized" garlic[103] shows an allyl:methyl:1-propenyl ratio of 84:11:6 (not listed in Table 1).
j) Store-purchased elephant garlic shows an allyl:methyl:1-propenyl ratio of 61:34:5; the ratio **101**:**102** is 1.8:1.
k) New York grown elephant garlic shows an allyl:methyl:1-propenyl ratio of 67:31:2; the ratio **101**:**102** is 1.8:1.

5.2.3. *Mono- and Bis-β-γ-unsaturated Thiosulfinates and Their Derivatives*

The first thiosulfinate to be discovered was allicin (**1**), so it is appropriate to consider its chemistry first. As already noted, **1** is a colorless, odoriferous, unstable antibacterial substance with a characteristic garlic odor (cf. Section 3).[30] While **1** was first described as being optically inactive[30] recent work suggests that *natural* **1** *is in fact optically active* as determined qualitatively by HPLC with a chiral detector and quantitatively using a polarimeter.[104] Natural **1** shows a specific rotation of $-3.90°$; its optical purity is unknown. Thiosulfinates such as methyl 2-methyl-2-propanethiosulfinate (**23**) have been prepared in optically active form.[105] In the absence of *tert*-butyl or other bulky groups they tend to be optically unstable. If the optical activity of **1** is real, what is its origin? Based on mechanisms suggested above for thiosulfinate formation (Scheme 8), if natural **1** originates from free, achiral 2-propenesulfenic acid (**2**) or its anion, it must also be achiral. On the other hand, if the sulfenic acid remains bound to the allinase via hydrogen bonding (cf. Scheme 19) when it is attacked by a second, free sulfenic acid, asymmetric induction giving optically active **1** is possible.[105b] Further research is necessary to clarify these possibilities.

Decomposition of neat allicin is said to afford sulfur dioxide along with allyl alcohol, dimethyl trisulfide, diallyl mono-, di- and trisulfides (**4a–c**), and allyl methyl di- and trisulfides, while passage through a gas chromatograph is said to furnish a 2.4:1 mixture of 3-vinyl-3,4-dihydro-1,2-dithiin (**9**) and 3-vinyl-3,6-dihydro-1,2-dithiin (**9a**) (Scheme 3).[35a] Thiosulfonates (RSO_2SR'), typically produced along with disulfides upon disproportionation of most thiosulfinates (cf. Scheme 11), were not formed from **1**.

Compounds **9** and **9a** were thought to be dehydration products of **1** formed according to the following equation akin to

$$\underset{\mathbf{1}}{C_6H_{10}S_2O} \longrightarrow \underset{\mathbf{9/9a}}{C_6H_8S_2} + H_2O$$

the formation of 1-propenyl propyl disulfide from propyl propanethiosulfinate (**13**).[35a] (cf. Ref. [35b]). Our investigation of the mechanism of decomposition of **1** was prompted by a collaborative study with M. K. Jain and R. Apitz-Castro on the identity of several antithrombotic substances they had isolated from garlic extracts[106] and it is this work that is presented first. The chromatographic separation of solutions prepared by soaking chopped garlic in methanol afforded allicin (**1**), diallyl di-, tri-, and tetrasulfides (**4b–d**), allyl methyl trisulfide, 2-vinyl-2,4-dihydro-1,3-dithiin (**74**), 3-vinyl-3,4-dihydro-1,2-dithiin (**9**) along with two isomeric polar compounds, showing the greatest antithrombotic activity. The substances were named (*E*)- and (*Z*)-ajoene (based on the Spanish word for garlic, ajo, pronounced "aho"), ultimately characterized as (*E*)- and (*Z*)-4,5,9-trithiadodeca-1,6,11-triene 9-oxide (**75**) (cf. Scheme 31) by spectroscopic and synthetic methods.[107]

The sulfoxide thio-Claisen rearrangement: Two pairs of structures, (*E,Z*)-**75** and (*E,Z*)-4,5,9-trithiadodeca-1,7,11-triene 9-oxide (**76**), seemed compatible with the spectroscopic data for (*E,Z*)-ajoene and we sought syntheses of both. A proposed synthesis of **76** involved oxidation of allyl 3-chloro-1-propenyl sulfide[108] (**77**) to allyl 3-chloro-1-propenyl sulfoxide **78**, displacement of chloride by thioacetate, and hydrolysis of thioacetate to thiolate followed by use of allyl 2-propenethiosulfonate (**79**) to construct the S–S bond (Scheme 27). To our surprise MCPBA oxidation of **77** at 0 °C did not lead to **78** but rather to (*Z*)-2-chloromethyl-4-pentenethial *S*-oxide (**80**) in 90% isolated yield. This sulfine could be converted into 2-methylene-4-pentenal (**81**) by sequential desulfurization with boron trifluoride etherate-mercuric oxide[109] and dehydrochlorination with DBU.[110]

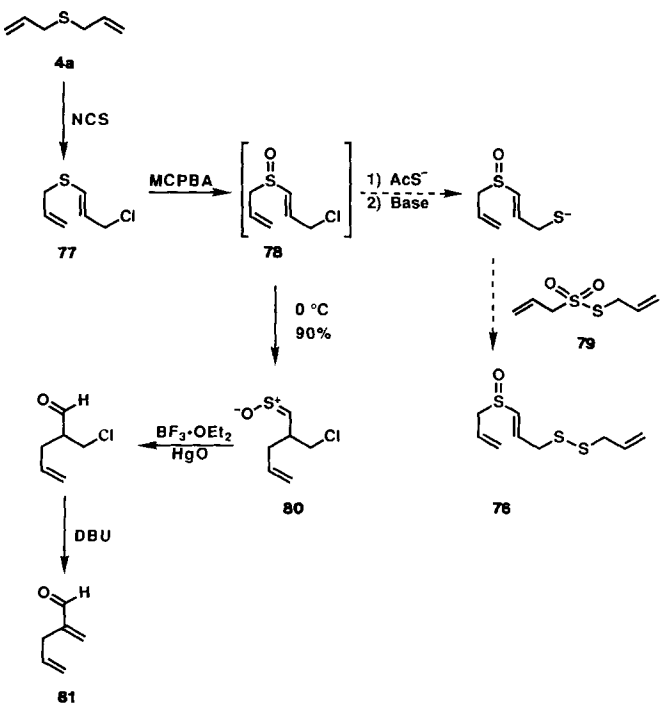

Scheme 27. Discovery of the sulfoxide thio-Claisen rearrangement.

The conversion of **78** into **80** is an example of a sulfoxide-accelerated thio-Claisen rearrangement,[79] a stereospecific [3,3]-sigmatropic process occurring under unusually mild conditions. Additional examples of the sulfoxide thio-Claisen rearrangement include conversion of allyl vinyl sulfoxide (**82**) into lacrymatory (*E,Z*)-4-pentenethial *S*-oxide (**83**; *E,Z* = 5:95) and then aldehyde **84**, of allyl (*E*)-1-propenyl sulfoxide (**85**) into (*E,Z*)-2-methyl-4-pentenethial *S*-oxide (**86**; *E,Z* = 2:98) and then aldehyde **87**, and of allyl 2-methyl-1-propenyl sulfoxide (**88**) into (*E,Z*)-2,2-dimethyl-4-pentenethial *S*-oxide (**89**; *E,Z* = 70:30) and then aldehyde **90** (Scheme 28).[110]

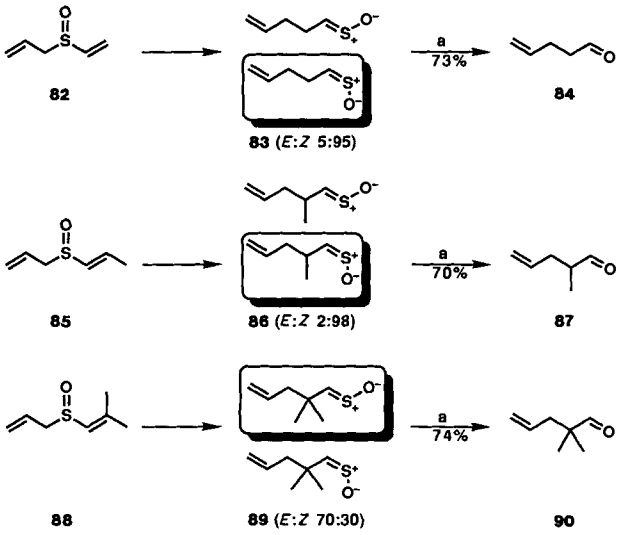

Scheme 28. Examples of the sulfoxide thio-Claisen rearrangement. a: $BF_3 \cdot OEt_2$, HgO.

While the activation enthalpy for the thio-Claisen reaction is typically greater than that for the Claisen rearrangement,[111] the activation energy for the sulfoxide thio-Claisen reaction of allyl vinyl sulfoxide **82** ($\Delta H^{\neq} = 19.32\ kcal\,mol^{-1}$, $\Delta S^{\neq} = -4.3\ cal\,mol^{-1}K^{-1}$) is *lower* than that for the Claisen rearrangement of allyl vinyl ether ($\Delta H^{\neq} = 25.40\ kcal\,mol^{-1}$, $\Delta S^{\neq} = -15.9\ cal\,mol^{-1}K^{-1}$[112]). The sulfoxide thio-Claisen rearrangement, an example of a zwitterion-accelerated Cope process,[113] proceeds with comparable substrates at 23 °C ca. 50 times faster than the thio-Claisen rearrangement under neutral conditions and 39 times faster under acidic conditions. The low $\Delta H^{\neq}$ for this reaction reflects, in part, the low C_{sp^3}–S(O) bond strength (ca. 46 $kcal\,mol^{-1}$ in **82**).

We have noted (Section 5.1.4) that the *Z*-stereochemistry is favored for sulfines. Thus, it is of interest to observe that **88** (and several other similarly substituted 1-alkenyl allyl sulfoxides) prefer the *thermodynamically less stable E-configuration* in the rearranged sulfine **89**. If it is assumed that the sulfoxide thia-Claisen rearrangement involves a pseudo chair transition state then pseudoaxial or pseudoequatorial

orientations are possible for sulfoxide oxygen. For thiane *S*-oxides an axial oxygen orientation is favored *except* when there are substituents at the 3- or 5-positions *cis* to sulfoxide oxygen, such as 3,3-dimethylthiane *S*-oxide where the equatorial/axial oxygen ratio is >95:5.[114] Similar effects should prevail in the sulfoxide thio-Claisen favoring **91a** → (*Z*)-**92** when $R^4 = H$ but favoring **91b** → (*E*)-**92** when $R^4 = Me$ (Scheme 29).[110, 115]

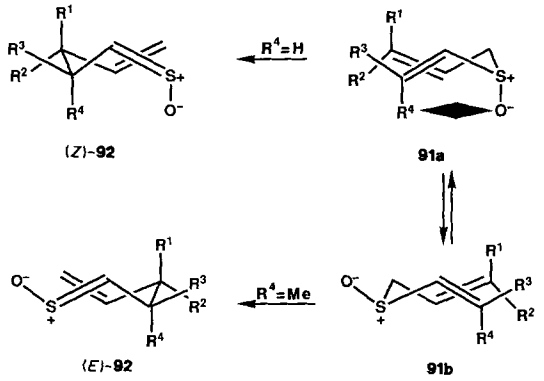

Scheme 29. Steric arrangement of the transition state **91a** ⇌ **91b** for the sulfoxide thio-Claisen rearrangement.

Synthesis of ajoenes, 2-vinyl-2,4-dihydro-1,3-dithiin and 3-vinyl-3,4-dihydro-1,2-dithiin and mechanistic considerations: Our discovery of the significant facilitating effect of the sulfinyl oxygen on the thio-Claisen rearrangement made it apparent that structure **75** (cf. Scheme 31) was to be preferred to **76** for (*E,Z*)-ajoene as there was no indication of rearrangement of this material to a sulfine upon heating. Since allicin (**1**) is the first isolable product formed when garlic is cut, we suspected that **1** might be the immediate precursor of **75**. Indeed, we found that when synthetic **1** was refluxed with 3:2 acetone:water for 4 hours, (*E,Z*)-**75** could be isolated in 34% yield.[107, 116] Other products included 2-vinyl-2,4-dihydro-1,3-dithiin (**74**) and 3-vinyl-3,4-dihydro-1,2-dithiin (**9**), in a 4.4:1 ratio, diallyl di- and trisulfides (**4b** and **4c**), and propene. The structures of **74** and **9** were established by comparison with the known products of the dimerization of thioacrolein (**93**) at −180 °C *which likewise affords* **74** *and* **9** *in a 4.4:1 ratio*. **93** is formed in the flash vacuum pyrolysis of diallyl sulfide (**4a**) (Scheme 30).[117]

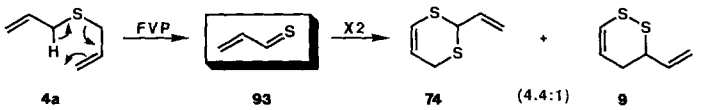

Scheme 30. Dimerization of thioacrolein (**93**) from flash vacuum pyrolysis of diallyl disulfide (**4a**).

The isolation of **74** and **9** as decomposition products of **1** and the identity of the **74**:**9** ratio to that observed upon dimerization of **93** suggests that the first step in the decomposition of **1** involves Cope-elimination to give 2-propenesulfenic acid (**3**) and **93** (Scheme 31). This postulate, which is consistent with our suggestion for the decomposition of methyl methanethiosulfinate (**12**) (Scheme 6), finds additional support in our observation of the characteristic sapphire blue color of **93** when **1** is distilled into a liquid nitrogen cooled trap, and our isolation of ethyl-3,4-dihydro-2*H*-thiopyran-2- (**94**) and -3-carboxylates (**95**) and (*Z*)-ethyl-2-thioformyl-4-pentenoate *S*-oxide (**97**) when solutions of **1** in ethyl acrylate and ethyl propiolate, respectively, are kept overnight at room temperature (Scheme 32).[118] Presumably **97** results from sulfoxide thio-Claisen rearrangement of the initial adduct **96** of ethyl propiolate and **3**. The earlier work of Brodnitz[35a] (Scheme 3) on the decomposition of **1** in a gas chromatograph must be corrected by replacing his incorrect structure **9a** with **74**.

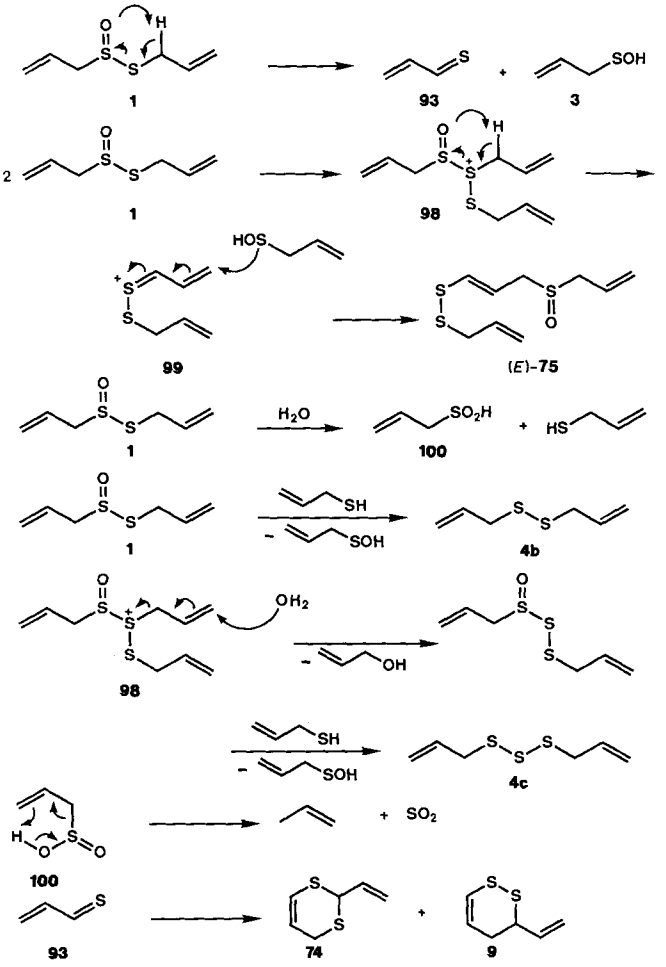

Scheme 31. Mechanism for the decomposition of allicin (**1**) and formation of ajoene (**75**).

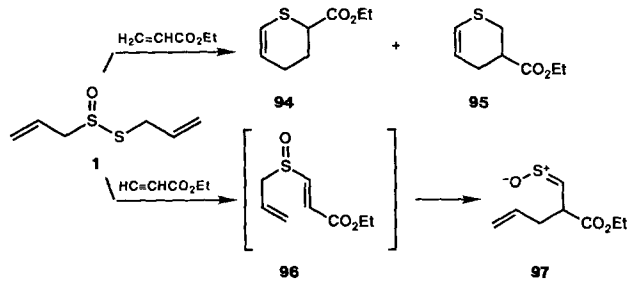

Scheme 32. Trapping of thioacrolein (**93**) (H_2C=CH-CH=S) and 2-propenesulfenic acid (**3**) (H_2C=CH-CH_2SOH) from allicin (**1**) as **94** + **95** and **97**, respectively.

With the mechanism proposed by us for the decomposition of **12** (Scheme 11) as a model, a detailed scheme for the decomposition of allicin **1** can be suggested (Scheme 31). A key step involves *S*-allylthiolation of **1** to give the sulfonium ion **98**, which can: a) undergo β-elimination to give carbocation **99** followed by γ-addition of **3** to give (*E*,*Z*)-**75**; b) undergo S_N2' hydrolysis giving allyl alcohol and then **4c**; c) undergo hydrolysis to 2-propenesulfinic acid (**100**) and **4b**.[119a] Direct hydrolysis of **1** can give **100** and 2-propenethiol. β,γ-Unsaturated sulfinic acids such as **100** are known to readily lose sulfur dioxide by retro-ene type reactions.[119c] A search was made for the presence of allyl 2-propenethiosulfonate (**79**) among the decomposition products of **1**, but none was found. This observation can be rationalized by assuming that the rate of loss of sulfur dioxide from **100** (k_1) is more rapid than its rate of nucleophilic attack on **1** (k_2; Scheme 33).[119d] It is noteworthy that when **1** is dissolved in liquid sulfur dioxide and the solution is allowed to stand at room temperature in a sealed vial, **79** can be isolated in good yield (Scheme 33).[135d] Compound **79**, sometimes referred to as pseudoallicin, has only 50% of the antibacterial activity of alliicin.[120]

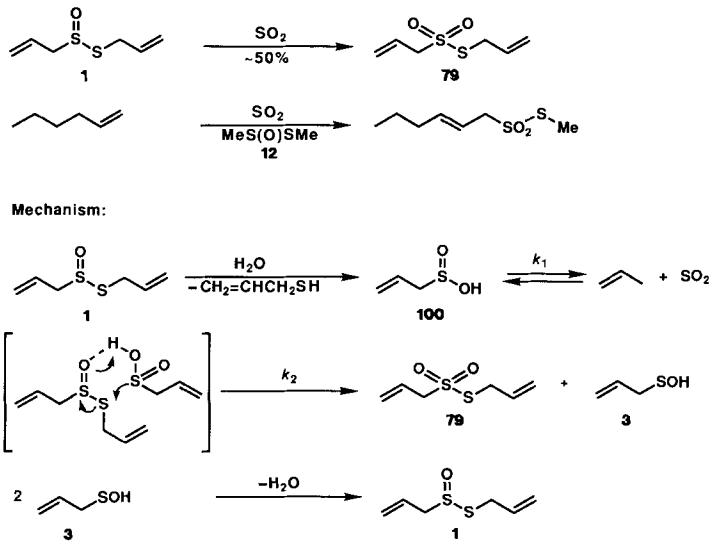

Scheme 33. Formation of allyl 2-propenethiosulfonate (**79**) from allicin (**1**) and sulfur dioxide.

Other allyl thiosulfinates in garlic, elephant garlic, and wild garlic: We have previously noted (Section 2.1) that garlic *grown* in colder climates contains far less (+)-*S*-methylcysteine *S*-oxide (**6**) than garlic grown in more temperature climates.[21] This lower concentration of **6** translates into diminished levels of methyl group-containing thiosulfinates. Thus, some garlic grown in New York State (cooler climate: 19–22 °C average growing temperatures) shows an allyl:methyl:1-propenyl ratio of 94:2:3, which differs dramatically from the more typical ratio of 80:16:4 seen in store-purchased garlic of Mexican origin. A similar but smaller decrease in methyl group levels is seen when the composition of New York State grown elephant garlic (allyl:methyl:1-propenyl ratio of 67:31:2) is compared to that of store-purchased elephant garlic (allyl:methyl:1-propenyl ratio of 62:35:3), grown in a warmer climate. A comparison of samples of Indian garlic obtained from a mountainous area (22–23 °C average) and from an area with a climate averaging 10 °C warmer show a similiar trend: the allyl:methyl ratio is larger for the garlic grown in a cooler climate. Finally, garlic treated to allegedly make it "odorless"[103] also shows a lower relative methyl content (allyl:methyl:1-propenyl ratio of 84:11:6). It can therefore be concluded that when garlic (and elephant garlic) is grown under harsher conditions or treated with certain chemicals the specific enzymes associated with formation or hydrolysis of *S*-methylcysteine *S*-oxide (**6**) are attenuated or destroyed.[21, 28b]

Lawson has observed that γ-glutamyl-*S*-(*E*)-1-propenylcysteine and γ-glutamyl-*S*-2-propenylcysteine (see **e** and **c**, respectively, in Scheme 2), the dominant γ-glutamyl peptides in homogenates of fresh garlic, decrease markedly when freshly picked garlic is refrigerated.[11, 121] This decrease is coupled with a corresponding increase in (+)-*S*-(*E*)-1-propenylcysteine *S*-oxide (**5**) and (+)-*S*-2-propenylcysteine *S*-oxide (**2**), respectively, which in turn afford 1- and 2-propenesulfenic acids. Thus, for store-purchased garlic of Mexican origin the allyl:methyl:1-propenyl ratio of 80:16:4 changes to 78:11:11 after refrigeration for two months; for New York grown garlic the allyl:methyl:1-propenyl ratio of 94:2:3 changes to 90:3:8 after refrigeration for this same period.

In addition to **1** and α,β-unsaturated thiosulfinates, two isomeric thiosulfinates, allyl methanethiosulfinate **101**, and methyl 2-propenethiosulfinate **102**, are important components of some *Allium* homogenates. Interpretation of the data in Table 1 is facilitated if it is recognized that in garlic, thiosulfinates containing only the 1- and 2-propenyl groups are formed *ten times more rapidly* than thiosulfinates containing methyl groups.[122] There would therefore be little 1- or 2-propenesulfenic acid available to condense with the more slowly forming methanesulfenic acid (**10**). A mechanism involving reaction of **10** with allicin **1** (Scheme 34) accommodates the facts that: 1) after **1** is maximally formed in 0.5 min it decreases until the mixed allyl methyl thiosulfinates are maximally formed after 5 min;[122] 2) for each mole of **1** lost, 1.9 moles of mixed allyl methyl thiosulfinates are formed;[122] 3) the **101**:**102** ratio increases to ca. 2:1 after

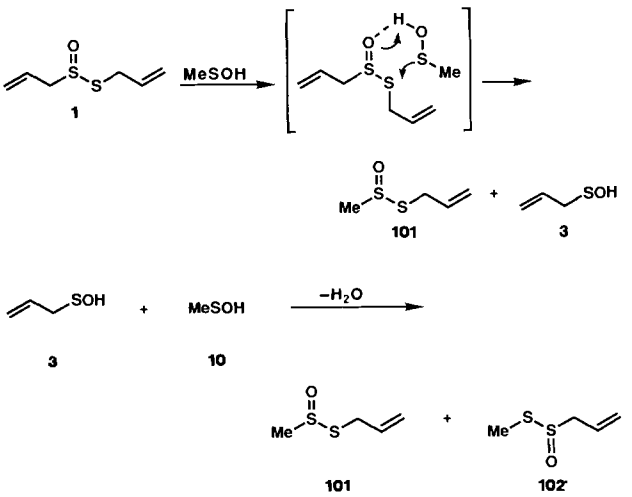

Scheme 34. Formation of allyl methanethiosulfinate (**101**) and methyl 2-propenethiosulfinate (**102**) in garlic.

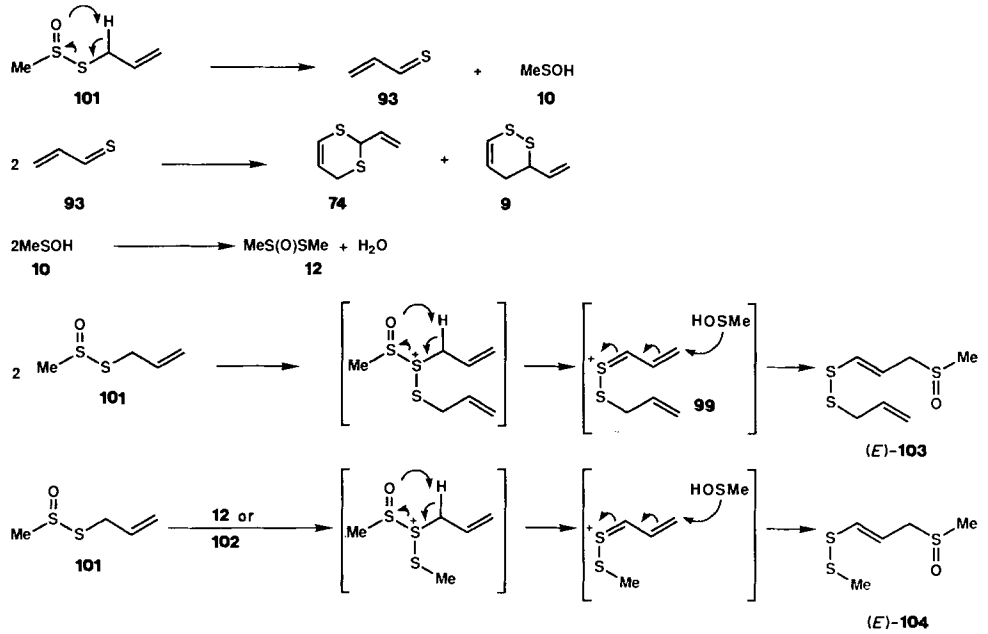

Scheme 35. Formation of methylajoene (**103**) and dimethylajoene (**104**) from allyl methanethiosulfinate **101**.

1–5 min and **101** dominates; 4) when powdered garlic (e.g. alliin/allinase) is added to excess aqueous methyl methanethiosulfinate (**12**), the major product is **102** (Scheme 34).[21a]

Decomposition of an authentic sample of **101** in acetone/water affords **9**, **74**, **12**, **4b**, **4c**, allyl methyl trisulfide and two new polar compounds identified as (*E*,*Z*)-2,6,7-trithiadeca-4,9-diene 2-oxide (**103**, "methyl ajoene") and (*E*,*Z*)-2,3,7-trithiaocta-4-ene 7-oxide (**104**, "dimethyl ajoene") (Scheme 35). Compounds **103** and **104**, thought to be present in low concentrations in garlic extracts, have recently been found in extracts of ramsons or wild garlic (*Allium ursinum*) and are derived from the isomers **101**/**102**, which predominate over allicin **1** in this plant (ratio of **1**:**101**/**102**:**12** is 1.26:0.14:0.01 in garlic and 0.53:0.70:0.27 in ramsons).[123]

After our identification of **74** as one of the antithrombotic components of garlic extracts, the novel use of **74** in a copolymer with *N*-vinylpyrrolidone was described (Scheme 36).[124] This copolymer is proposed as an anti-

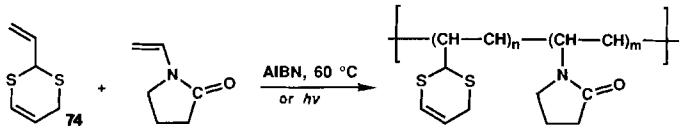

Scheme 36. Copolymer of 2-vinyl-2,4-dihydro-1,3-dithiin (**74**) and *N*-vinyl pyrrolidone [124].

thrombogenic and antibiotic composition for use as a coating for artificial prostheses and implants which remain in contact with blood.

5.2.4. *Mono-α,β-unsaturated Thiosulfinates*

While saturated aliphatic and allylic thiosulfinates have been known for many years, little work has been carried out on α,β-unsaturated thiosulfinates, despite the fact that such compounds are present in onion and garlic extracts and display significant inhibitory activity toward lipoxygenase and cyclooxygenase enzymes.[28, 125] We therefore conducted a systematic study of the natural occurrence, synthesis and properties of these compounds.

Natural occurrence of mono-α,β-unsaturated thiosulfinates: Considerable quantities of α,β-unsaturated thiosulfinates of type (*E*)-**105** (alkyl (*E*)-1-propenethiosulfinate) and (*E*,*Z*)-**106** ((*E*,*Z*)-1-propenyl alkanethiosulfinates, R = Me, Pr, or All) are present in fresh extracts or room-temperature steam distillates of all of the *Allium* spp. examined as noted in Table 1. The thiosulfinates **106** (R = Me, Pr) have been identified in yellow onion extracts by Wagner et al.[150] and by Kawakishi et al.;[149d] Wagner also noted the rapid interconversion of geometric isomers. Lawson reports the presence of **105** and **106** (R = Me and Pr) in scallion, shallot, leek, yellow onion, boiling onion, white onion and red onion[121] and of **105** and **106** (R = Me, All) in garlic, and also comments on the ease of geometric isomerism in **106**.[121b]

Synthesis of mono-α,β-unsaturated thiosulfinates: Synthetic routes to the stereoisomers **105** and **106** (R = Me, Pr, All) are summarized in Scheme 37. One approach involves propyl 1-propynyl sulfide (**108**), available from base-catalyzed isomerization[126] of propyl 2-propynyl sulfide (**107**), as the key intermediate. Lithium aluminum hydride converts **108** into (*E*)-1-propenyl propyl sulfide ((*E*)-**109**) while diisobutylaluminum hydride or trimethoxyaluminum hydride-cuprous bromide[127] converts **108** into (*Z*)-**109**. Lithium-liquid ammonia reduction of (*E*)- and (*Z*)-**109** gives lithium (*E*)- and (*Z*)-1-propenethiolate (**110**), which are treated with the appropriate thiosulfonate to afford alkyl (*E*)- and (*Z*)-1-propenyl disulfides (**111**). Oxidation of (*E*)- and (*Z*)-**111** affords (*E*)-**105**/(*E*)-**106** and (*Z*)-**105**/(*Z*)-**106**, respectively. A second approach to (*E*)- and (*Z*)-1-propenethiolate (**110**) involves lithiation at −110 °C of readily available pure (*E*)- and (*Z*)-1-bromo-1-propene[128, 129] (**112**) followed by treat-

ment of each lithio compound with styrene sulfide. The unique ^{1}H- and ^{13}C-NMR chemical shifts for **105**/**106** are useful[130] in determining the composition of *Allium* extracts.[21, 135a]

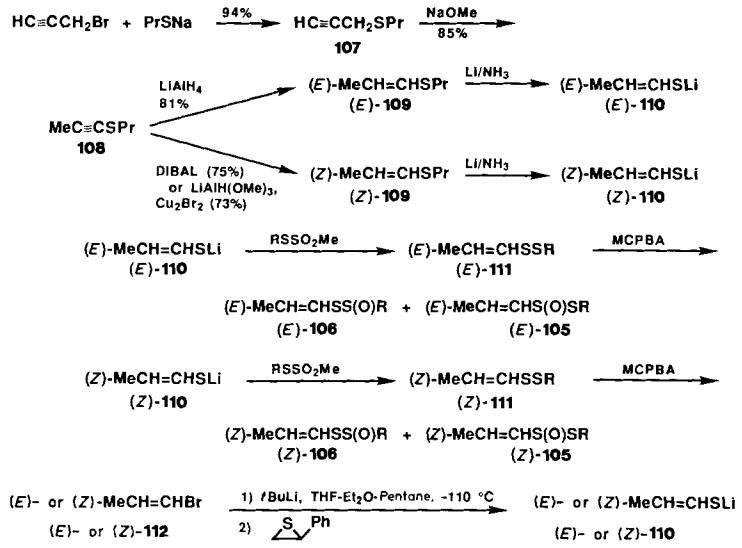

Scheme 37. Synthesis of the α,β-unsaturated thiosulfinates **105** and **106**.

E,Z-Isomerization of mono-α,β-unsaturated thiosulfinates: All attempts to isolate pure samples of (*E*)- or (*Z*)-**106** from mixtures with **105** always led to mixtures of (*E,Z*)-**106**. Furthermore stereochemically pure samples of (*E*)-**105**/(*E*)-**106** or (*Z*)-**105**/(*Z*)-**106** were converted during the course of one hour at 25 °C into (*E*)-**105**/(*E,Z*)-**106** or (*Z*)-**105**/(*E,Z*)-**106**, respectively. This facile isomerization of isomers of **106**, but not **105** or precursor disulfides **111**, can be explained by a [2,3]-sigmatropic rearrangement (Scheme 38) analogous to reactions of allylic sulfoxides or methallyl 2-methyl-2-propenethiosulfinate.[131] This isomerization explains the puzzling observation that although only (+)-*S*-(*E*)-1-propenyl-L-cysteine *S*-oxide (**5**) occurs naturally, affording, it is assumed, only (*E*)-1-propenesulfenic acid ((*E*)-**14b**), both (*E*)- and (*Z*)-**106**, but only (*E*)-**105**, are found in *Allium* extracts and distillates. Compound **105**, of course, is incapable of isomerization by the mechanism of Scheme 38.

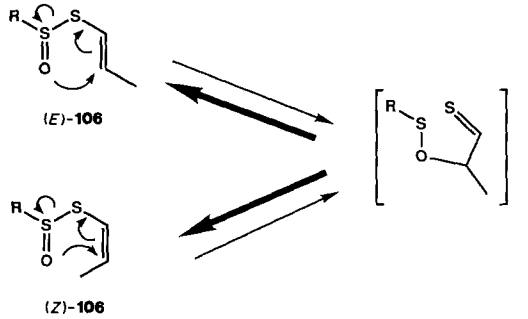

Scheme 38. Interconversion of (*E*)- and (*Z*)-1-propenyl alkanethiosulfinate geometric isomers **106**. The half-life at 25 °C is ca. 1 h.

Oxidation of mono-α,β-unsaturated thiosulfinates: We have examined the oxidation of **105**/**106** as a route to the corresponding thiosulfonates **113**/**114**, of interest as natural products themselves (e.g. methyl (*E*)-propenethiosulfonate, (*E*)-**113**, R = Me, has been isolated from *Allium grayi*)[132] as well as synthetic reagents for preparation of α,β-unsaturated disulfides. "Nucleophilic" oxidation[133] of (*E*)-**105**/(*E*)-**106** or (*Z*)-**105**/(*Z*)-**106** using sodium metaperiodate/acetic acid gave (*E*)-**113**/(*E*)-**114** or (*Z*)-**113**/(*Z*)-**114** (R = Me, Pr, All) with no stereoisomerization (Scheme 39). Unlike (*E*)- and (*Z*)-**106**, stereoisomers of **114** were configurationally stable, showing no tendency to undergo *E,Z*-isomerization. "Electrophilic" oxidation[133] of either (*E*)-**105**/(*E*)-**106** or (*Z*)-**105**/(*Z*)-**106** with MCPBA gave identical 1:1 mixtures of

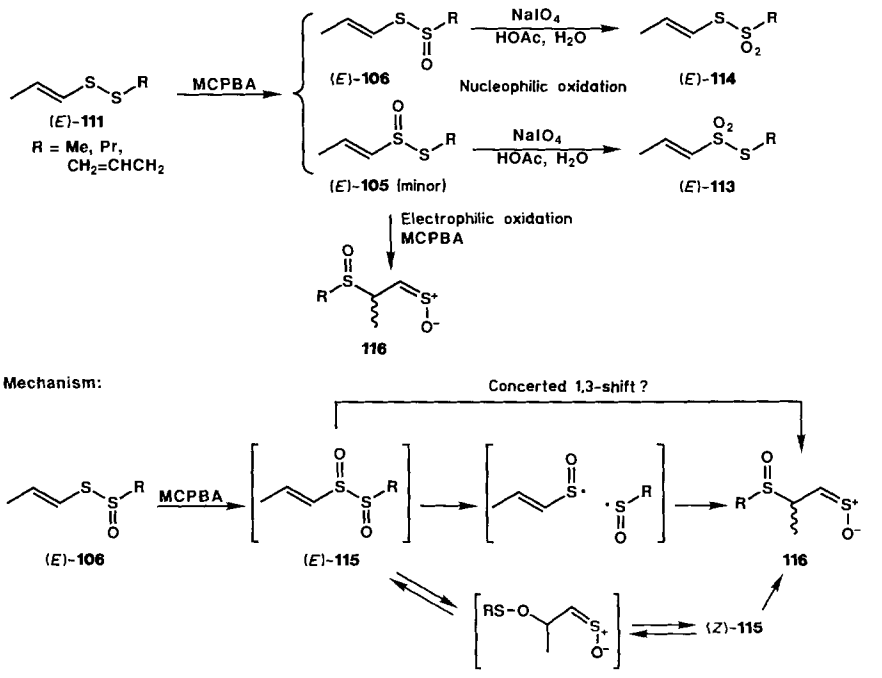

Scheme 39. Nucleophilic and electrophilic oxidation of 1-propenyl alkanethiosulfinates (**106**) and alkyl 1-propenethiosulfinates (**105**) furnishing thiosulfonates **113**/**114** and α-sulfinylsulfines **116**.

compounds characterized as (*Z*)-2-(alkanesulfinyl)propanethial *S*-oxide (*Z*)-**116** (see below for NMR assignment of sulfine stereochemistry as *Z*). We presume that initial oxidation of **105**/**106** gives α-disulfoxide **115**. While **115** could undergo pseudopericyclic[134] rearrangement to **116**, stereochemistry would be expected to be conserved, which is not the case. Therefore either: 1) stereochemistry in **115** is lost through [2,3]-sigmatropic rearrangement (Scheme 39) which is more rapid than pseudopericyclic processes; 2) *two* diastereomers of **115** are formed initially; or 3) a free radical mechanism (Scheme 39) is involved in conversion of **115** into **116**.[135a]

5.2.5. *Bis-α,β-unsaturated Thiosulfinates*

"Is there any point to which you would wish to draw my attention?"
"To the curious incident of the dog in the nighttime."
"The dog did nothing in the nighttime."
"That was the curious incident," remarked Sherlock Holmes.

"Silver Blaze"
Sir Arthur Conan Doyle (1859–1930)

What is unusual about the thiosulfinates isolated from cut *Allium* spp. is the *complete absence* of bis-α,β-unsaturated derivatives, despite the preeminence of the bis-β,γ-unsaturated thiosulfinate allicin (**1**) from garlic and the abundance of mono-α,β-unsaturated thiosulfinates from onion. Our curiousity piqued, we examined synthetic approaches to 1-propenyl 1-propenethiosulfinates. Serendipitously, while these efforts were underway, Professor Hildebert Wagner invited our participation in a study of some unusual organosulfur compounds isolated by his doctoral student, Thomas Bayer.[136] This collaborative study led to some fascinating chemistry, detailed below.

2,3-Dimethyl-5,6-dithiabicyclo[2.1.1]hexane 5-oxides ("zwiebelanes"): Two isomers **117** and **118** (smaller amounts of latter) were isolated as colorless oils of formula $C_6H_{10}OS_2$ following chromatography of onion extracts. Compound **117** showed intense IR bands at 1065 and 1085 cm^{-1} (S=O) and UV $\lambda_{max} = 250$ nm. NMR data for **117** and **118** are discussed in Section 5.3.3. The above spectroscopic data, the chemical shifts in presence of $Eu(fod)_3$ shift reagent and aromatic solvents, as well as the synthetic results described below point to **117** and **118** having the structures (1α,2α,3α,4α,5β)- and (±)-(1α,2α,3β,4α,5β)-2,3-dimethyl-5,6-dithiabicyclo[2.1.1]hexane 5-oxide, respectively (Fig. 7). These two compounds were given the trivial names *cis*- and *trans*-zwiebelane ("zwiebel" is German for onion), respectively.[137] Compounds **117** and **118** have been isolated by us from extracts of shallot, scallion and chive as well. The mixture of **117** and **118** showed a 65–90% inhibition of thrombin-induced TXB_2 biosynthesis in human platelet rich plasma at a concentration of 0.1–1.0 $mg\,mL^{-1}$. Recently, other examples of substituted 5,6-dithiabicyclo[2.1.1]hexanes have been reported.[138]

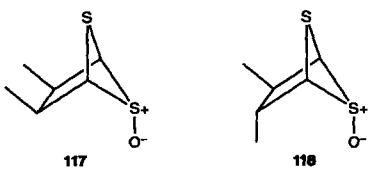

Fig. 7. Isomeric "zwiebelanes" **117** and **118** isolated from onion extracts.

Monooxidation of the isomeric bis(1-propenyl) disulfides: The isomeric bis(1-propenyl) disulfides (*E,E*)-**119** and (*Z,Z*)-**119** were prepared by oxidation of lithium (*E*)- and (*Z*)-1-propenethiolate ((*E*)-**110** and (*Z*)-**110**) while (*E,Z*)-bis(1-propenyl) disulfide ((*E,Z*)-**119**) was prepared by reaction of (*E*)-**110** with (*Z*)-1-propenyl methanethiosulfonate ((*Z*)-**114**) at −78 °C (Schemes 37 and 40).[135d] Compound (*Z*)-**114** can be conveniently synthesized through reaction of (*Z*)-**110** with methanesulfonyl chloride; the latter reagent can also be used for the conversion of (*E*)-**110** and (*Z*)-**110** into (*E,E*)-**119** and (*Z,Z*)-**119**, respectively (Scheme 40).[135c] Isomers of **119** can be separated by preparative HPLC on a C-18 reverse phase column. While (*E,E*)-**119** and (*Z,Z*)-**119** are relatively stable at room temperature, (*E,Z*)-**119** disproportionates on standing to a mixture of all three isomers of **119**.

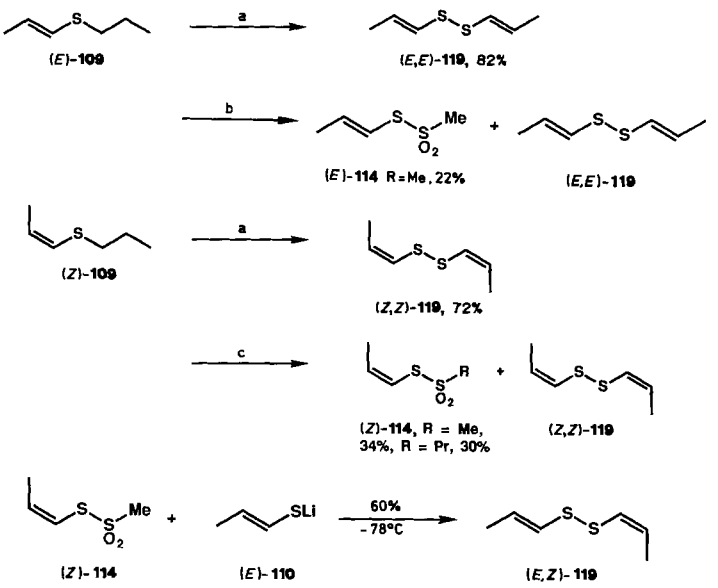

Scheme 40. Synthesis of (*E,E*)-, (*Z,Z*)-, and (*E,Z*)-bis(1-propenyl) disulfide **119**. For the reaction **109** → **110** cf. Scheme 37. a: 1) Li/NH_3; 2) $2\,MeSO_2Cl$, −78 °C; 3) H_2O. b) 1) Li/NH_3; 2) $20\,MeSO_2Cl$, −78 °C; 3) H_2O. c) 1) Li/NH_3; 2) $20\,RSO_2Cl$, −78 °C; 3) H_2O.

Solutions of pure isomers of **119** in $CDCl_3$ at −60 °C were treated with chilled solutions of MCPBA in the presence of one equivalent of anhydrous sodium carbonate. After 5 min the reaction mixture was transferred to an NMR tube cooled to −60 °C and placed in a −60 °C NMR probe. Thus, (*E,E*)-**119** gave (*E*)-1-propenyl (*E*)-1-propenethiosulfinate ((*E,E*)-**120**) (Scheme 41), (*Z,Z*)-**119** gave the (*Z,Z*)-isomer, ((*Z,Z*)-**120**) (Scheme 42), and (*E,Z*)-**119** gave a ca. 2:1 mixture of (*Z*)-1-propenyl (*E*)-1-propenethiosulfinate ((*E,Z*)-**120a**) and (*E*)-1-propenyl (*Z*)-1-propenethiosulfinate ((*E,Z*)-**120b**) (Scheme 43). Qualitative studies indicate that the relative rates of oxidation are (*E,E*)-**119** > (*E,Z*)-**119** > (*Z,Z*)-**119**. Assignment of structures to isomers

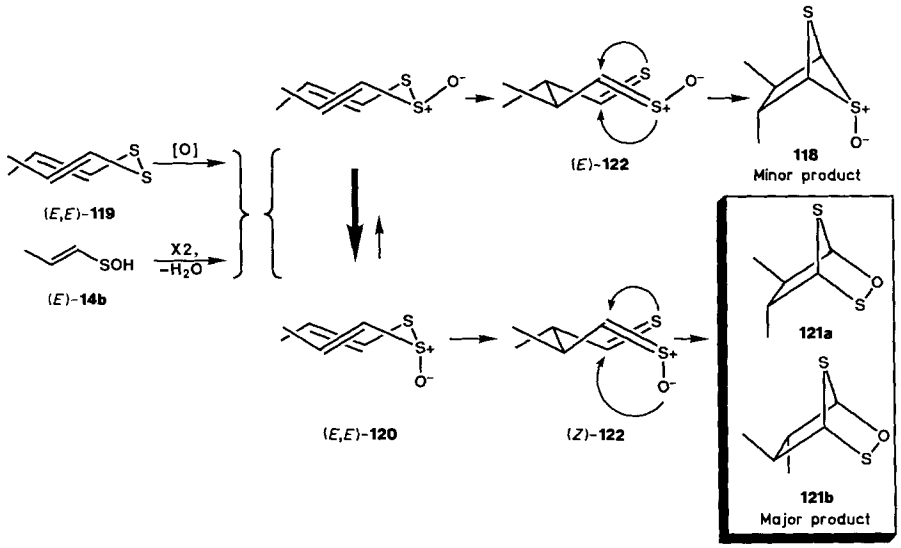

Scheme 41. Oxidation of (*E,E*)-bis(1-propenyl) disulfide (*E,E*)-**119** giving **121a** (via (*E,E*)-**120**). **122** always shown as the (2*S*,3*R*) form.

(*E,Z*)-**120a,b** is based both on kinetic considerations that the disulfide sulfur adjacent to a *cis* double bond is oxidized at a slower rate than the disulfide sulfur adjacent to a *trans* double bond, as well as on careful comparison of the ^{1}H and ^{13}C chemical shift data for thiosulfinates (*E,E*)-**120**, (*Z,Z*)-**120**, (*E,Z*)-**120a,b**, and the methyl 1-propenethiosulfinates (*E*)-**106** and (*Z*)-**106**, R = Me.

Solutions of thiosulfinates (*E,E*)-**120**, (*Z,Z*)-**120**, and (*E,Z*)-**120a,b** in NMR tubes with dioxane as internal standard were warmed to −15 °C. The disappearance of peaks associated with the thiosulfinates was followed with time. The so-determined first order rate constants for disappearance of thiosulfinates at −15 °C are $8.22\times10^{-4}\,s^{-1}$ for (*E,E*)-**120**, $4.13\times10^{-4}\,s^{-1}$ for (*E,Z*)-**120a,b**, and $3.02\times10^{-4}\,s^{-1}$ for (*Z,Z*)-**120**. From the rate data for disappearance (rearrangement) of (*Z,Z*)-**120** we calculate: $E_a = 16\,kcal\,mol^{-1}$, $\Delta H^{\neq} = 15.5\,kcal\,mol^{-1}$, $\Delta S^{\neq} = -15.3\,cal\,mol^{-1}K^{-1}$, and $\Delta G^{\neq} = 19.5\,kcal\,mol^{-1}$, all at 273 K. These values may be compared to those described in Section 5.2.3 for the Claisen and sulfoxide thio-Claisen rearrangements. If the ratio of these rate constants, 2.7:1.4:1, is compared to the analogous ratio for Claisen rearrangement of isomeric 1-propenyl 2-butenyl ethers,[139] it is apparent that the rate ratio for the rearrangement of thiosulfinates is contracted suggesting a more *advanced* transition state than for the Claisen rearrangement. The initial products of rearrangement are a 4.5:1 mixture of *endo*-5-methyl-*exo*-6-methyl-2-oxa-3,7-dithiabicyclo[2.2.1]heptane (**121a**) and its *exo,endo*-isomer **121b** from (*E,E*)-**120** after 3 h at −40 °C, a 27:3:1 mixture of (±)-**118**, **121a** and **121b** from (*Z,Z*)-**120** after 3 h at −40 °C, and a 10:10:1 mixture of **117**, *exo*-5-methyl-*exo*-6-methyl-2-oxa-3,7-dithiabicyclo[2.2.1]heptane (**121c**) and its *endo,endo*-isomer **121d** from (*E,Z*)-**120a,b** after 3 h at −40 °C (Schemes 41–43). Isomers **121** are bicyclic sultenes similar to compounds **43** and **56** (see Sections 4.4 and 5.1.2 and Schemes 14 and 16). Isomers **121** react rapidly with thiophenol giving ring-opened thiolane derivatives.

Mechanistic considerations: We propose that—following the oxidation of (*E,E*)-**119** with *one* equivalent of peroxy acid—the thiosulfinate ((*E,E*)-**120**) oxygen assumes a pseudoaxial orientation for the [3,3]-sigmatropic rearrangement since this orientation is also favored in 1,2-dithiane 1-oxides

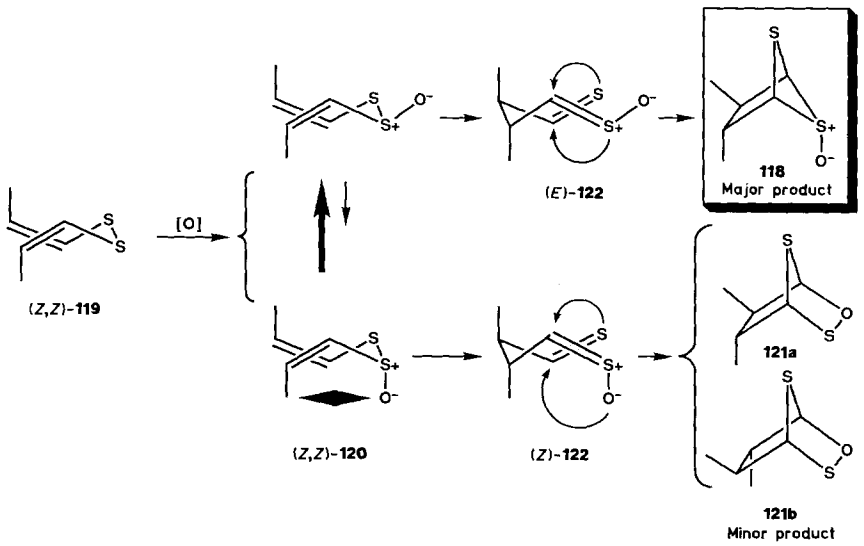

Scheme 42. Oxidation of (*Z,Z*)-bis(1-propenyl) disulfide (*Z,Z*)-**119** giving **118** (via (*Z,Z*)-**120**). **122** always shown as the (2*R*, 3*S*) form.

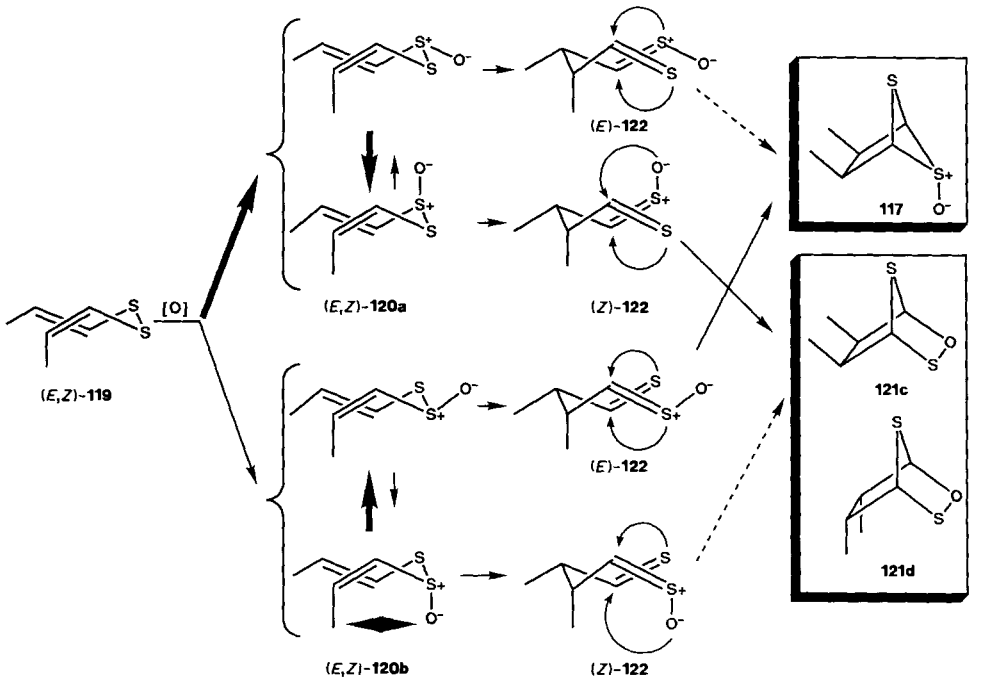

Scheme 43. Oxidation of (*E*,*Z*)-bis(1-propenyl) disulfide (*E*,*Z*)-**119** giving **117** and **121c** (via (*E*,*Z*)-**120a**,**b**). **122** always shown as (*R*,*R*) form.

and in sulfoxide thio-Claisen rearrangements.[115,135b] Rearrangement from this transition state gives (*Z*)-(2*R*,3*S*/2*S*,3*R*)-2,3-dimethyl-1,4-butanedithial *S*-oxide ((*Z*)-**122**), which can assume an appropriate conformation to undergo a very facile intramolecular 1,3-dipolar cycloaddition of the $C{=}S^{+}{-}O^{-}$ group to the C=S function[88b] with formation of **121a,b** (Scheme 41), a structure similar to the well-known 2,5-dimethylthiophene–singlet oxygen adduct[140] and to 5,6-dimethyl-2,3,7-trithiabicyclo[2.2.1]heptane, recently isolated from scallion distillates.[141] Rearrangement of (*E*,*E*)-**120** should be facilitated by the weak S–S bond (the bond dissociation energy would be expected to be quite similar to that of phenyl benzenethiosulfinate, e.g. 35 kcal mol^{-1}). Subsequent cyclization should be aided by the very high reactivity of the thial group of (*Z*)-**122** as a 1,3-dipolarophile.[142] Precedence exists for formation of heterobicyclo[2.2.1]heptanes via intramolecular 1,3-dipolar cycloaddition reactions.[143] On the other hand, on analogous oxidation of (*Z*,*Z*)-**119**, steric effects associated with the *cis* double bonds lead the intermediate to adopt a transition state geometry in which thiosulfinate ((*Z*,*Z*)-**120**) oxygen is pseudoequatorial, resulting in the formation of (*E*)-(2*R*,3*S*/2*S*,3*R*)-2,3-dimethyl-1,4-butanedithial *S*-oxide ((*E*)-**122**), where the (*E*)-geometry of the $C{=}S^{+}{-}O^{-}$ group favors the [2+2] process yielding **118** over the sterically now more difficult 1,3-dipolar cycloaddition (Scheme 42). In the case of (*E*,*Z*)-**119** either pseudoaxial or pseudoequatorial thiosulfinate ((*E*,*Z*)-**120a**, (*E*,*Z*)-**120b**) oxygen transition state geometry is possible with the consequence that the heterobicyclo[2.1.1]hexane and heterobicyclo[2.2.1]heptane systems (**117** and **121c** respectively) are formed in comparable amounts (Scheme 43). While there is variation in the type of ring system formed on monooxidation of (*E*,*E*)-, (*Z*,*Z*)- and (*E*,*Z*)-**119**, there is complete stereoselectivity in carbon–carbon bond formation.[135b]

Problems are encountered in extending the above concepts of the mechanism of the monooxidation of stereoisomers of **119** to reactions that occur when onions are cut. We have shown that zwiebelane **118** originates from (*Z*,*Z*)-**120**. Formation of this latter compound in onion homogenates would require condensation of two molecules of (*Z*)-1-propenesulfenic acid ((*Z*)-**14b**). However, since (*Z*)-(+)-*S*-1-propenyl-L-cysteine *S*-oxide ((*Z*)-**5**) is not found in onions, and the barrier to interconversion of (*E*)- to (*Z*)-1-propenesulfenic acid is anticipated to be substantial (a 33 kcal mol^{-1} activation energy barrier separates ethenesulfenic acid and ethanethial *S*-oxide;[80] a similar barrier should exist for interconversion of (*E*)- and (*Z*)-**14b** by way of LF **16**), it is unlikely that the concentration of (*Z*)-**14b** would suffice for *self condensation* to take place. Furthermore, the detection of substantial amounts of alkyl (*E*)-1-propenethiosulfinates ((*E*)-**105**), *but not a trace of the Z-isomers* in *Allium* spp. extracts, also argues against the formation of significant amounts of (*Z*)-**14b** and thus of (*Z*,*Z*)-**120**. It is possible, under the conditions existing when onions are cut, that **121a** can isomerize to **118** (Scheme 44), and that **117** is similarly formed by isomerization of **121c**. Alternatively, a molecule of (*E*)-**14b** could react with a second molecule of (*E*)-**14b** that is hydrogen bonded to allinase (see Scheme 19; the

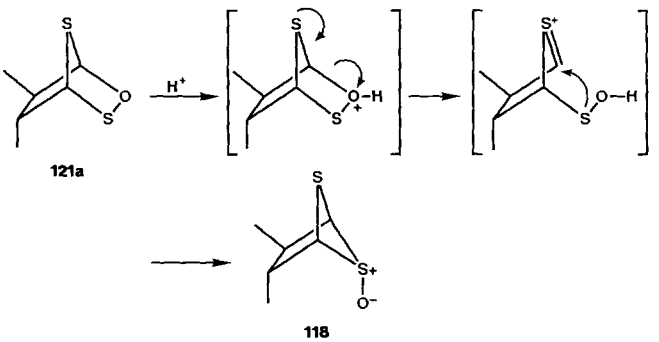

Scheme 44. Possible isomerization of **121a** to **118**.

dimeric/tetrameric structure proposed for allinase is consistent with the presence of more than one sulfenic acid molecule within the enzyme at any given time). The resultant (*E,E*)-**120**, if still associated with the allinase, may undergo a [3,3]-sigmatropic process from a more compact transition state, with the sulfoxide oxygen pseudoequatorial, to give **118**. (*E,Z*)-**120a**, the postulated precursor to **121c**, could be formed in onion homogenates through reaction of (*E*)-**14b** with (*Z*)-**106** (Scheme 45).

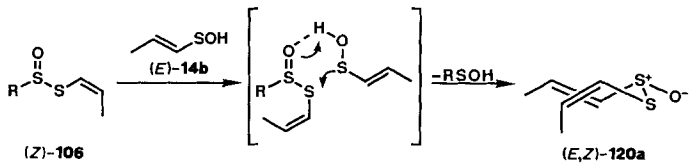

Scheme 45. Reaction of (*E*)-**14b** with (*Z*)-**106** giving (*E,Z*)-**120a**.

(Z,Z)-(±)-2,3-Dimethylbutanedithial S,S'-dioxide: Examination of the ^{1}H-NMR spectrum of onion extracts revealed the presence of a doublet at $\delta = 8.09$ just upfield from the position of the triplet for the methine proton in LF **16** ($\delta = 8.21$), suggesting the natural occurrence of a second sulfine.[77b, 144] Ultimately, compound **123** was isolated as a colorless solid of formula $C_6H_{10}S_2O_2$ which showed absorption bands at 1103 and 1120 cm^{-1} (C=S=O) in the IR spectrum. Sequential treatment of synthetic **123** (see below) with ozone (at −50 °C), H_2O_2/HCOOH and MeOH/H_2SO_4 gave in 88% yield a compound which according to GC-MS and ^{13}C-NMR was identical with an authentic sample of (±)-dimethyl 2,3-dimethylsuccinate ((±)-**124**), but different from an authentic sample of *meso*-**124**, thereby establishing **123** as (*Z,Z*)-(±)-2,3-dimethylbutanedithial *S,S'*-dioxide ((±)-**123**) (Scheme 46). The *Z,Z* arrangement of the CSO

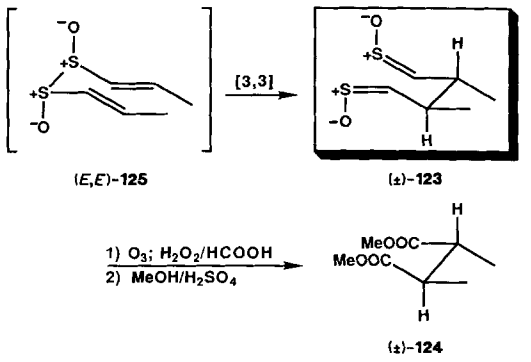

Scheme 46. Proof of structure of bis-sulfine **123** by ozonolysis. **123** and **125** always shown as (*R,R*) form.

group was established by NMR methods similar to those used with **16** (see Section 5.3.1). Compound **123** is unique as the first example of a bis(thial *S*-oxide); so far, also only a single example of a bis(thione *S*-oxide) is known.[145]

Bis-oxidation of bis(1-propenyl) disulfides; mechanistic considerations: The close relationship that **123** bears to intermediate (*Z*)-**122** in Scheme 41 suggests that **123** originates via a novel double sulfoxide-accelerated dithio-Claisen rearrangement of (*E,E*)-bis(1-propenyl) *vic*-disulfoxide ((*E,E*)-**125**) (Scheme 46). Indeed, oxidation of (*E,E*)-**119** with 2.2 equivalents of MCPBA at −60 °C or of (*E,E*)-**120** with one equivalent of MCPBA (Scheme 47) leads to a product identical to **123** isolated from onion extracts.[144] Oxidation of (*E,E*)-**120** should give (*E,E*)-**125** with an *anti* (diaxial) arrangement of the oxygens, which represents an energy minimum according to theoretical calculations on model systems.[146] This geometry of (*E,E*)-**125** correlates with (*Z*)-CSO geometry in **123** (Scheme 47). Compound (*E,E*)-

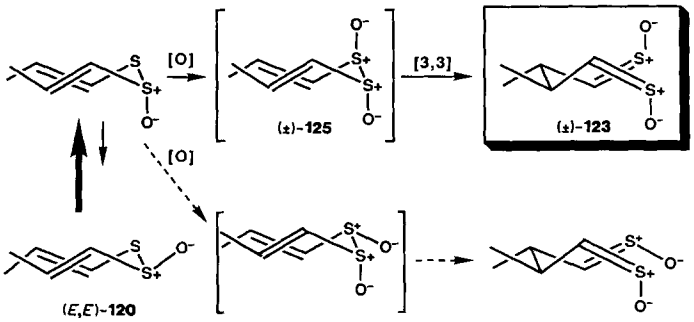

Scheme 47. Oxidation of (*E,E*)-**120** to (±)-**123** (shown as (*S,S*) form).

125 should undergo particularly facile [3,3]-sigmatropic rearrangement due to the weakness of the S–S bond (comparable with the S–S bond in diphenyl *vic*-disulfoxide, i.e. ca. 26 kcal mol^{-1}) as well as the rate-enhancing effect of the two zwitterionic sulfinyl functions.[113] This assumption is in agreement with the observation that (*E,E*)-**125** could not be detected in low-temperature NMR studies[147] of the oxidation of (*E,E*)-**120**. In contrast, to the stereospecificity seen in the oxidation of (*E,E*)-**120** or its precursor (*E,E*)-**119**, oxidation of (*Z,Z*)-**119** with two equivalents of MCPBA gives a 2:1 mixture of (±)-**123** and *meso*-**123** (Scheme 48).[135b] In this case, for the second oxygen to be antiperiplanar to the first, the bis(1-propenyl) *vic*-disulfoxide (*Z,Z*)-**125** would have to assume an open conformation unsuitable for [3,3]-sigmatropic rearrangement, and favoring a homolytic process.[135b]

How is **123** formed in onion extracts? One possibility would involve thioalkylation of (*E*)-**105** (R = Me) giving thiosulfonium ion **126**, which could undergo nucleophilic displacement at the sulfinyl sulfur by (*E*)-1-propenesulfenate (Scheme 49 A). A second possibility would involve "thiophilic" addition of (*E*)-**14b** to **16** (Scheme 49 B; the reverse of *vic*-disulfoxide decomposition,[148] shown in Scheme 49 C) followed by nucleophilic attack of a second molecule of (*E*)-**14b** on *vic*-disulfoxide intermediate **115**. A weakness of both mechanisms is the need for one reactive intermediate ((*E*)-**14b** or its anion) to attack another one (**126** or **115**). An additional problem with the second mechanism is that attack of (*E*)-**14b** on **115** would have to occur more readily than the rate of rearrangement **115** to **116** (see Scheme 39), since the latter is not found in onion extracts.

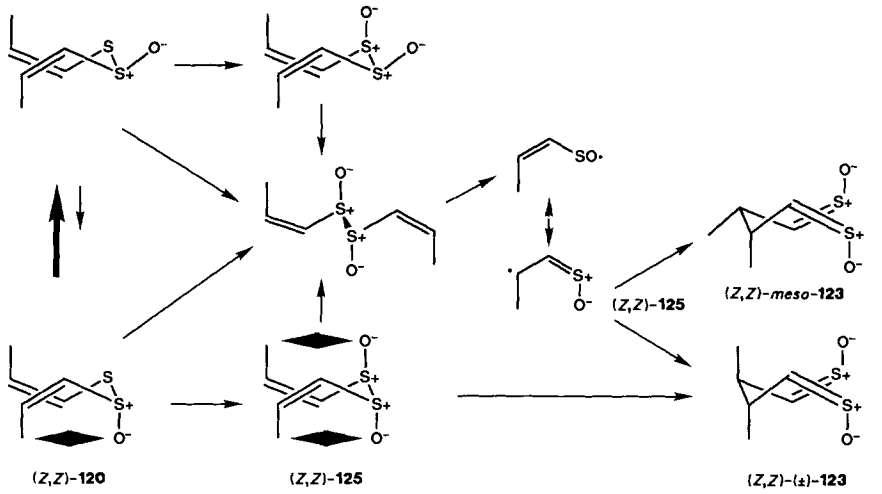

Scheme 48. Oxidation of (*Z*,*Z*)-**120** to (±)-**123** (shown as (*R*,*R*) form) and *meso*-**123**.

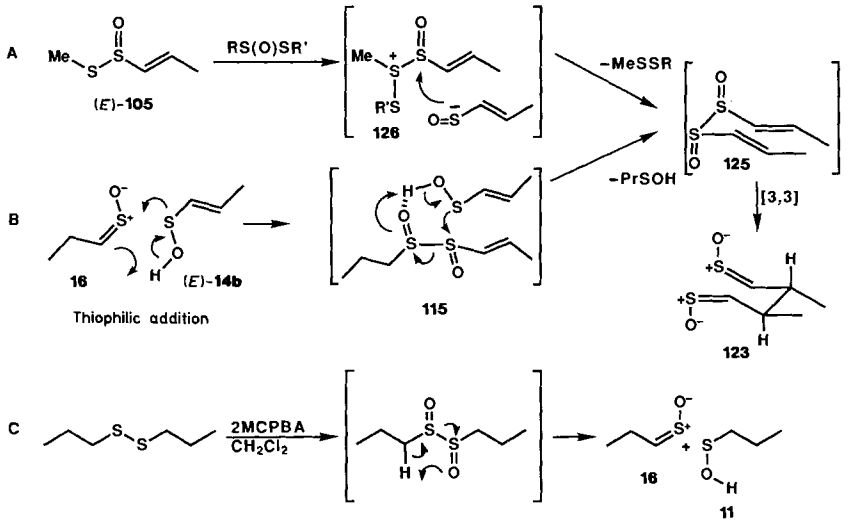

Scheme 49. Proposed mechanisms for formation of bissulfine **123** in onion homogenates. A–C, see text.

5.2.6. Cepaenes

Isolation of cepaenes and mechanisms of formation: In 1988 Kawakishi and Morimitsu identified methyl 1-(methylsulfinyl)propyl disulfide (**127a**, R = R′ = Me) as a new platelet aggregation inhibitor from onion extracts.[149a] Simultaneously, Wagner et al. reported the isolation of diastereomeric pairs 1-((*E*)-1-propenylsulfinyl)propyl propyl disulfide (**127c**) (R = (*E*)-MeCH=CH, R′ = Pr) and 1-((*E*)-1-propenylsulfinyl)propyl (*E*,*Z*)-1-propenyl disulfide (**127d**) (R = (*E*)-MeCH=CH, R′ = (*E*,*Z*)-MeCH=CH) as cyclooxygenase and 5-lipoxygenase inhibitors from onion extracts.[125c, 136] Wagner proposed that the onion α-sulfinyl disulfides be called "cepaenes". Later it was reported that: 1) other cepaenes could be isolated including 1-(methylsulfinyl)propyl (*E*,*Z*)-1-propenyl disulfide (**127b**, R = Me, R′ = (*E*,*Z*)-MeCH=CH);[149b] 2) individual enantiomers of diastereomeric pairs showed only a twofold to fourfold difference in biological activity, contrary to expectations of substantial differences associated with stereospecific enzymatic recognition;[149c] 3) cepaenes display a variety of types of interesting biological activity (see Section 7.3);[125a, b, 149d, 150] 4) by combining fresh onion and garlic juice, various mixed cepaenes, including some with allylic groups, can be prepared.[149d] A mechanism for formation of cepaenes in onion juice is proposed (Scheme 50A).[135c, 144, 149c, d] Precedence for "carbophilic" addition of (*E*)-**14b** to **16** includes addition of thiols to **16** (Scheme 50B)[151] and sulfenic acids to thiones.[152] α-Alkylthiodisulfides ("deoxycepaenes") are found in distilled oils of shallot and scallion, e.g. ethyl-1-(methylthio)propyl disulfide,[95] methyl 1-(methylthio)propyl disulfide, 1-(methylthio)propyl propyl disulfide,[153] 1-(methylthio)-propyl 1-propenyl disulfide, 1-propenyl-1-(propylthio)-propyl disulfide, and 1-propenyl-1-(1-propenylthio)propyl disulfide.[141, 153, 154] It is not known whether these compounds originate via deoxygenation of cepaenes, either in solution or in the inlet of a gas chromatograph, or through entirely different mechanisms.

Synthesis of fully saturated cepaenes: In 1973 we reported that refluxing alkyl alkanethiosulfinates in benzene/water affords α-sulfinyl disulfides, e.g. **33** or **34** (Scheme 11).[54d] The isolated yield of **33** was high, whereas the yield of **34** was quite low. A more efficient synthesis of the saturated cepaenes such as **127a** was developed starting from 1-chloropropanesulfenyl chloride (**128**) via: 1) nucleophilic attack on

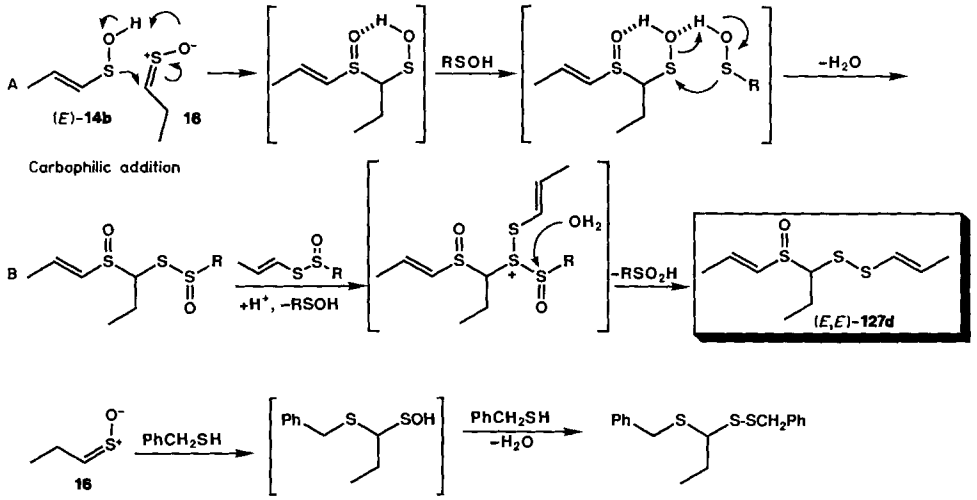

Scheme 50. Proposed mechanism for formation of cepaenes **127** in onion homogenates. A, B see text.

the sulfenyl chloride group by an alkanethiol with formation of an alkyl 1-chloropropyl disulfide; 2) replacement of the α-chloride by thioacetate; 3) hydrolysis and alkylation of the latter giving an alkyl 1-(alkylthio)propyl disulfide; 4) oxidation of the latter to the alkyl 1-(alkylsulfinyl)propyl disulfide **127**, formed as diastereomeric pairs (Scheme 51 A). When methanethiol was used, **128** could be directly converted into methyl 1-(methylthio)propyl disulfide.[155a]

chloride by thioacetate to give **130**; 3) hydrolysis of **130** followed by thioalkylation with an alkyl alkanethiosulfonate to give an alkyl 1-((*E*)- or (*Z*)-1-propenylthio)propyl disulfide; 4) oxidation of the latter to the alkyl 1-((*E*)- or (*Z*)-1-propenylsulfinyl) propyl disulfide diastereomers (Scheme 51 B). An alternative non-stereospecific synthesis of **130** involves addition of one equivalent of HCl to bis(1-propenyl) sulfide followed by displacement of the α-chlo-

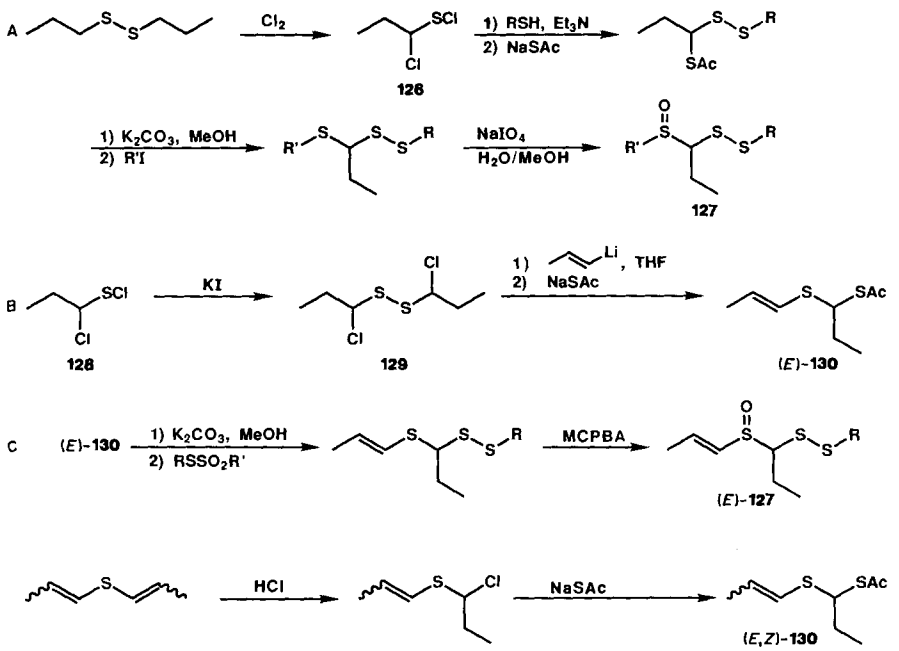

Scheme 51. Synthesis of fully saturated and singly unsaturated cepaenes. A–C see text.

Synthesis of singly unsaturated cepaenes: In the above syntheses, the sulfenyl chloride group becomes the disulfide function of **127** while the α-chloride of **128** becomes the alkylsulfinyl group. The fate of these groups is reversed in a synthesis of singly unsaturated cepaenes, which involves: 1) oxidation of **128** to bis(1-chloropropyl) disulfide (**129**); 2) treatment of **129** with (*E*)- or (*Z*)-1-propenyllithium at low temperature followed by immediate displacement of the α-

rides by thioacetate (Scheme 51 C). 1-(Methylthio)propyl (*E,Z*)-1-propenyl disulfide (a deoxycepaene) has been synthesized from methyl dithiopropionate (Scheme 52).[156]

Synthesis of doubly unsaturated cepaenes: Two novel syntheses of doubly unsaturated cepaenes have been developed. The first involves 3,5-diethyl-1,2,4-trithiolane (**63**), a component of onion oil. Treatment of **63** with (*E*)-1-propenyllithium followed by bis((*E*)-1-propenyl) disulfide ((*E*)-**119**) gives

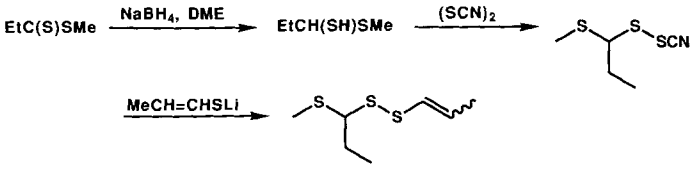

Scheme 52. Synthesis of the deoxycepaene 1-(methylthio)propyl (*E,Z*)-1-propenyl disulfide; total yield 36%.

the deoxycepaenes (*E,E*)-6-ethyl-4,5,7-trithiadeca-2,8-diene (**131**; 31%) and (*E,E*)-6,8-diethyl-4,6,7,9-tetrathiadodeca-2,10-diene (**132**; 16%) (Scheme 53).[135d, 155b] We suggest that the initial product (**133**) from ring-opening of **63** fragments to **134** and propanethial (**135**) at a rate competitive with nucleophilic attack on (*E,E*)-**119** to form **132**. The reverse of the fragmentation reactions, carbophilic addition to **135**, may also take place.

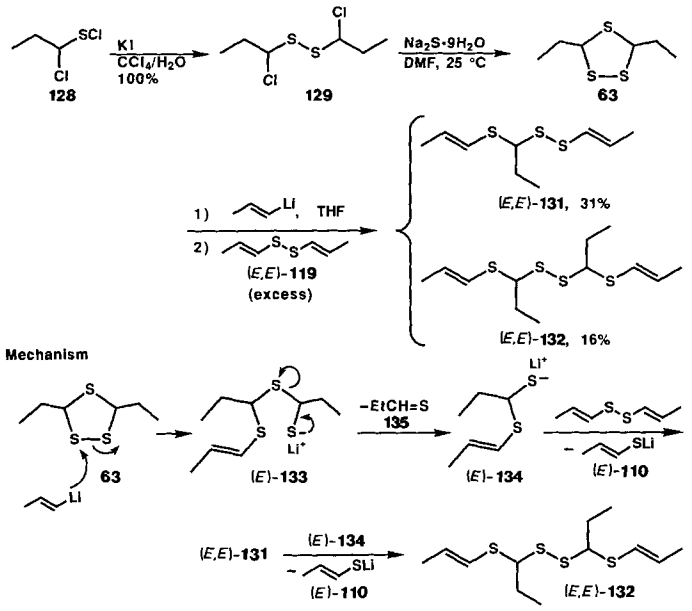

Scheme 53. Synthesis of doubly unsaturated deoxycepaenes **131** and **132** via 3,5-diethyl-1,2,4-trithiolane **63**.

A second synthesis of **131** and **132** also involves fragmentation of α-(alkenylthio)alkanethiolates such as **134** to thials such as **135**. This synthetic route was developed in connection with a study concerning the use of mesyl chloride as an alternative to iodine for stereospecific conversion of (*E*)- or (*Z*)-1-propenethiolate (**110**) into (*E,E*)- or (*Z,Z*)-**119**, respectively (Schemes 37 and 40).[135d] While treatment of (*E*)-**110** (from lithium-ammonia cleavage of (*E*)-**109**) with two equivalents of mesyl chloride gave (*E,E*)-**119** in 82% yield, use of 0.7 equivalents of mesyl chloride led instead to a mixture of (*E,E*)-**131** (27%) and (*E,E*)-**132** (15%). Similarly, while treatment of (*Z*)-**110** (from (*Z*)-**109**) with 2 equivalents of mesyl chloride gave (*Z,Z*)-**119** in 72% yield, use of 0.7 equivalents of mesyl chloride led to a mixture of (*Z,Z*)-**131** (20%) and (*Z,Z*)-**132** (10%). Oxidation of (*E,E*)-**131** with MCPBA led to a 2:1 diastereomeric mixture of the cepaene (*E,E*)-6-ethyl-4,5,7-trithiadeca-2,8-diene 7-oxide **127d** (64%) which could be separated by chromatography. The results in Scheme 54 can be explained by the mechanism shown in Scheme 55.[135d]

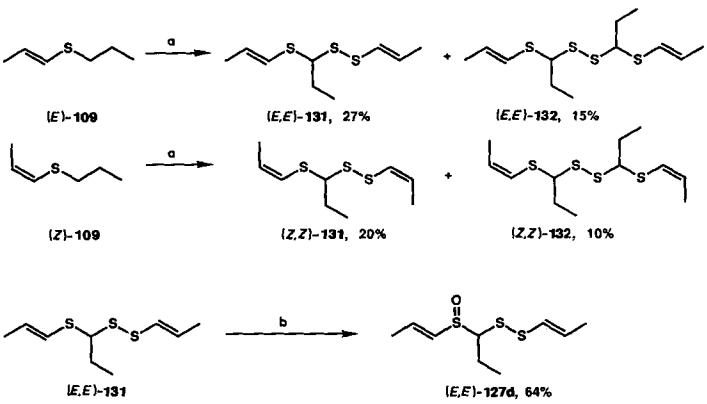

Scheme 54. Synthesis of **131**, **132**, and **127d**. (*E,E*)-**127d** formed as a chromatographically separable 2:1 mixture of diastereomers. a: 1) Li/NH_3; 2) 0.7 $MeSO_2Cl$, −60 °C; 3) −5 °C 1.5 h; H_2O. b) 100% MCPBA, −78 °C, CH_2Cl_2.

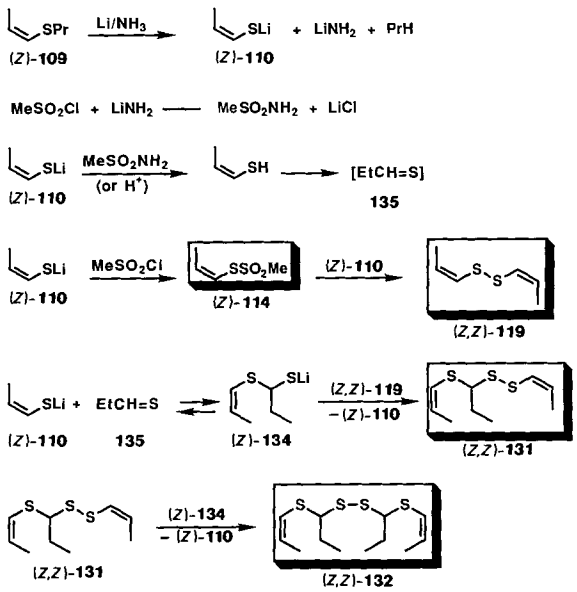

Scheme 55. Mechanism for formation of (*Z,Z*)-**131** and (*Z,Z*)-**132** by reaction of (*Z*)-**110**, obtained by liquid ammonia reduction of (*Z*)-**109**, with mesyl chloride.

5.3. Characterization of Organosulfur Constituents of *Allium* Preparations by Nuclear Magnetic Resonance Spectroscopy

My dear Watson, you see but you do not observe!

Sir Arthur Conan Doyle (1859–1930)

Of the analytical techniques available for the study of such sensitive organosulfur compounds as are associated with *Allium* spp., none is more powerful than NMR spectroscopy. It permits the direct observation of all of the relevant nuclei (H, C, O) at low as well as ambient temperatures. A broad range of chemical shifts are observed, allowing identification of the components of complex mixtures. The configuration

can be determined by analysis of coupling constants, facilitated by two-dimensional NMR methods, and by studying solvent- or reagent-induced chemical shift effects in compounds containing the sulfinyl group. With the more unusual organosulfur components, novel NMR effects abound.

5.3.1. NMR Study of the Onion Lachrymatory Factor (LF) and Related Sulfines

Sulfines (thiocarbonyl *S*-oxides) play an important role in *Allium* chemistry. We have studied the *S*-oxides of ethanethial (**44**), propanethial (**16**), (trimethylsilyl)methanethial (**66**), and 2-(alkanesulfinyl)propanethial (**116**), as well as the bissulfine (±)-2,3-dimethyl-1,4-butanedithial *S,S'-dioxide* (**123**). The stereochemistry about the C=S bonds was established by NMR methods.

The NMR spectrum of onion lachrymatory factor (LF) **16** in $CDCl_3$ shows a downfield methine triplet at $\delta = 8.21$ ($J = 7.81$ Hz), in agreement with the spectrum of **16**, which was prepared from propanesulfinyl chloride (**19**) or by pyrolysis of (*E,Z*)-*tert*-butyl 1'-propenyl sulfoxide (**58**). Examination of the NMR spectrum of the natural **16** in $CDCl_3$ reveals the presence of a second downfield triplet at $\delta = 8.88$ ($J = 8.79$ Hz), with ca. 5% of the area of the triplet at $\delta = 8.21$. This minor triplet, not reported in earlier NMR studies of LF **16**, was found to be present at somewhat lower intensity in the NMR spectrum of synthetic **16**. In C_6D_6, **16** shows downfield triplets at $\delta = 7.61$ (major triplet; $J = 7.82$ Hz) and 8.37 ppm (minor triplet; $J = 8.89$ Hz).[77b, 157]

Thus, the NMR spectrum of **16** reveals a minor triplet $\Delta\delta = 0.67-0.68$ downfield from the major triplet in $CDCl_3$ and $\Delta\delta = 0.77$ downfield from the major triplet in C_6D_6. On using C_6D_6 instead of $CDCl_3$ as solvent, the major triplet was shifted $\Delta\delta = 0.59$, the minor triplet $\Delta\delta = 0.50$ to higher field. From a comparison of this NMR data with NMR data of related structures of the type RCH=N–X (X = OR, NR'R")[158] we concluded that **16** exists as a mixture of *E*- and *Z*-isomers, with the latter dominating. This assignment is consistent with the observation in the nitrogen systems that: 1) protons resonate at lower fields when *syn* than when *anti* to X in RCH=N–X; 2) *anti* protons are shifted further upfield than *syn* protons on changing the solvent from CCl_4 to C_6D_6; and 3) the coupling constant $J_{H_1H_\alpha}$ (e.g. $J_{H_1H_2}$ in **16**) is slightly larger in the *anti* compound than in the *syn* compound.[158] In analogy with the mechanism proposed for the aromatic solvent induced shifts in nitrogen systems[158] and sulfoxides,[73, 159] dipole forces should favor the orientation relative to benzene shown in Figure 8 in which the *anti*-proton in the (*Z*)-isomer (Et) should experience greater shielding than the *syn*-protons (R_2 = H) in the (*E*)-isomer.

Similar conclusions are drawn from consideration of solvent effects on the ^{1}H-NMR spectra of **44**, **66**, **116**, and **123**. In the case of the bissulfine **123** isolated from onion a *Z,Z*-configuration is assumed, since the HC=SO proton is shifted to even lower field ($\delta = 8.09$ in $CDCl_3$, $\delta = 7.06$ in C_6D_6), and this change of solvent influences the chemical shift even more strongly ($\Delta\delta = 1.03$) than in the case of the corresponding proton in (*Z*)-**16**. In the case of the sulfine **116** (R = Me and Pr) a *Z*-configuration is assumed, because of similarity of the chemical shifts of **116** and of (*Z*)-**16** (**116**, R = Me, diastereomer **A**: HC=SO appears as a doublet at $\delta = 8.27$ in $CDCl_3$ and $\delta = 7.19$ in C_6D_6; diastereomer **B**: HC=SO appears at $\delta = 8.44$ in $CDCl_3$ and $\delta = 7.62$ in C_6D_6; very similar effects are seen for the two diastereomers of **116**, R = Pr). Interestingly, in methanethial *S*-oxide (**40**) the chemical shifts of the two protons ($\delta = 7.84$ and 7.73 in $CFCl_3$[68]) are much closer together in value than in the higher homologs, perhaps due to the slight change in HCS angles. It is also of interest to contrast the chemical shift of the *HC*=S proton in 2,2-dimethylpropanethial (*t*BuCH=S)[160] at $\delta = 11.67$ with the chemical shift of this proton in 2,2-dimethylpropanethial *S*-oxide (*t*BuCH=SO) at $\delta = 7.62$ (*Z*)/9.00 (*E*) (all data recorded in $CDCl_3$ as solvent). While the C=S group deshields an attached proton relative to C=O, the C=SO group has the opposite effect!

The ^{13}C-NMR spectra of (*Z*)- and (*E*)-**16** show the resonances for *C*=SO at $\delta = 180.5$ and 184.5, respectively. The minor *E*-isomer shows deshielding at the sp^2-carbon center compared to the major *Z*-isomer. In the case of the sulfine **116** (R = Me or Pr) and the bissulfine **123** in $CDCl_3$, *C*=SO appears at $\delta = 175.92$ (**116**, R = Me), 176.24 (**116**, R = Pr), and 179.6 (**123**), values more consistent with a *Z*- rather than an *E*-configuration. These ^{13}C-NMR values for *C*=SO differ markedly from the value for *HC*=S in 2,2-dimethylpropanethial[160] ($\delta_C = 255.6$).

In the ^{17}O-NMR spectrum the signal for the sulfine oxygen atom of (*Z*)-**16** and (*Z*)-**44** appears at $\delta_O = 196$ and 199, respectively. These values may be compared to the ^{17}O chemical shifts of $SOCl_2$, $(MeO)_2S{=}O^*$, $Me_2S{=}O$, thiane *S*-oxide and thiolane *S*-oxide which have been determined as $\delta_O = 292$, 176, 13, −3, and 15, respectively.[49, 161] The strong deshielding of the oxygen in sulfines compared to that in simple sulfoxides may be a consequence of the enhanced electronegativity of carbon sp^2 orbitals attached to the sulfine sulfur compared to carbon sp^3 orbitals utilized in the sulfoxides, since other sulfinyl compounds containing electronegative substituents on sulfur are also deshielded relative to simple sulfoxides.

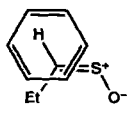

Fig. 8. Aromatic solvent induced shift (ASIS) effects on onion LF (*Z*)-**16**.

5.3.2. NMR Spectroscopy of the Dimer of LF: the Four-Membered Ring Sulfone Effect

The ^{1}H- and ^{13}C-NMR data of the LF dimer **18b** (see Scheme 24) and of the homolog *trans*-3,4-bis(trimethylsilyl)-1,2-dithietane 1,1-dioxide (**67**) (see Scheme 25) clearly indicate the presence of two substantially different, coupled, "CHR" groups, i.e. $-SO_2CHR$ and $-SCHR$. The difference in the δ_c values of the two pairs of methine carbon atoms (e.g. 97.9 and 39.2 in **18b** and 88.4 and 14.8 in **67**) is quite striking. While part of the difference is due to deshielding of the α-sulfonyl carbon atoms of thiosulfonates compared with sulfones,[162] and a vicinal deshielding effect due to the *trans*-ethyl or *trans*-trimethylsilyl groups (e.g. 2-methyloxetane and *cis*- and *trans*-2,3-dimethyloxetane show ^{13}C shifts

for C-2/C-3 at δ_c = 78.3/29.2, 79.6/31.8 and 85.0/37.4, respectively),[163] it is necessary to invoke an unusual deshielding effect characteristic of four-membered ring sulfones[164] to fully explain the magnitude of the difference.

Consider the ^{13}C-NMR shifts of the α-carbon atoms in the three- to six-membered ring sulfur heterocycles thiirane, thietane, thiolane and thiane (with –S– group), which are 18.1, 26.1, 31.7, 29.1. In the analogous sulfoxides (–S(O)–) and sulfones (–S(O_2)–) the values are 33.8, 52.7, 54.3, 49.0 and 31.6, *65.6*, 51.1, 52.6, respectively.[164] Note the downfield shift of the C_α-signal of $\Delta\delta$ = 40 on oxidation of thietane to thietane 1,1-dioxide and the downfield shift of $\Delta\delta$ = 13 in the oxidation of thietane 1-oxide to the 1,1-dioxide. With most sulfide-sulfoxide-sulfone systems, oxidation of a sulfide to a sulfone results in such a downfield shift of only $\Delta\delta$ = 20–25; very little difference is seen in the chemical shifts of the α-carbon atoms in the sulfoxides and sulfones, the latter sometimes even appearing slightly upfield of the former (cf., e.g., the above data for thiolane 1-oxide and 1,1-dioxide). The so-called "four-membered ring sulfone effect" contributes to the above noted differences in the chemical shifts of the methine carbon atoms in the sulfine dimers **18b** and **67**.

The unusual ^{13}C chemical shift effects for thietane 1,1-dioxides and related four-membered rings such as **18b** and **67** are reflected in similar but smaller effects in the ^{1}H and ^{17}O chemical shifts. Thus, unusually deshielded *H*CSO_2 protons are observed in **18b** (δ = 4.35) and **67** (δ = 5.06). The ^{17}O chemical shifts for thiirane, thietane, thiolane and thiane 1,1-dioxide appear at δ_O = 111, *182*, 165, and 142, respectively, once again showing maximum deshielding for the four-membered ring. Compound **18b** shows bands at δ_O = 210 and 243 which is notable for the substantial deshielding seen as well as the fact that *for the first time discrete ^{17}O chemical shifts are observed for nonequivalent sulfone oxygens.*[164] Additional examples of ^{17}O-NMR investigations on sulfones with diastereotopic protons have subsequently appeared in the literature.[165]

5.3.3. *Comparative NMR Spectroscopy of Derivatives of Bicyclo[2.1.1]hexane, 5-Thiabicyclo[2.1.1]hexane, and 5,6-Dithiabicyclo[2.1.1]hexane*

In connection with the identification of the zwiebelanes by ^{1}H- and ^{13}C-NMR spectroscopy, heterobicyclo[2.1.1]-hexanes were sought as model compounds for comparison of coupling constants. While 5-thiabicyclo[2.1.1]hexane (**136a**), its *S*-oxide **136b**, and its *S,S*-dioxide **136c** are known, the symmetry of **136** limits the number of H–H couplings seen. The synthesis of a less symmetrical derivative of **136a**, namely **139a**, was therefore developed (Scheme 56).[166] Exposure of 3-cyclopentenol (**137**) to Mitsunobu thioacetylation conditions affords *S*-3-cyclopentenylthioacetate, which was treated directly with bromine in CCl_4 to give the *trans*-1,2-dibromo derivative **138** in 54% overall yield. Treatment of **138** with KOH in aqueous ethanol at reflux for 90 hours afforded *exo*-2-bromo-5-thiabicyclo[2.1.1]hexane (**139a**) in 40% yield. Compound **139a** was oxidized to the corresponding sulfoxide **139b** and sulfone **139c** with H_2O_2/HOAc/CH_2Cl_2 at 0 °C and at reflux, respectively. Table 2 enables a comparison to be made of the NMR data for zwiebelane **118** with those for model compounds **139a–c**. It is noteworthy that

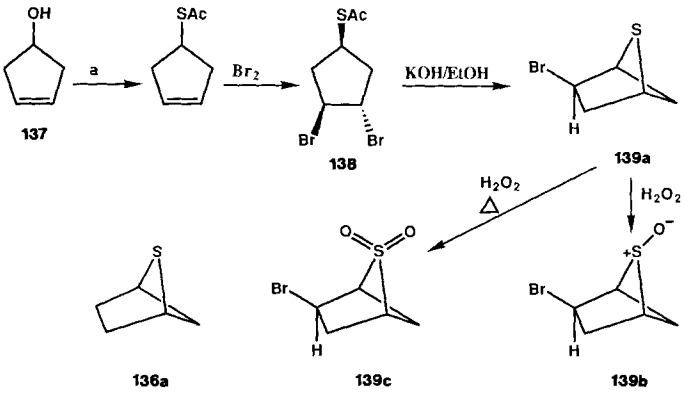

Scheme 56. Synthesis of 2-bromo-5-thiabicyclo[2.1.1]hexane **139a** and its *S*-oxides **139b** and **139c**. a: HSAc, Ph_3P, $EtO_2CN{=}NCO_2Et$.

Tabelle 2. ^{1}H- and ^{13}C-NMR data for compounds **118** and **139a–c**.

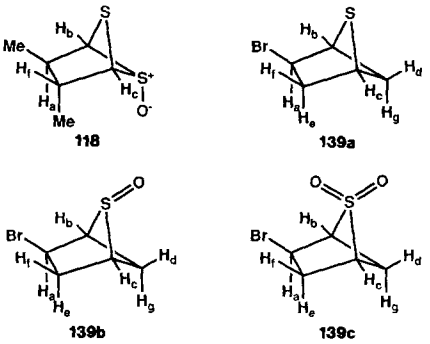

Cpd.		Position a	b	c	d	e	f	g
118	^{13}C	48.0	79.4	77.7			39.4	
	^{1}H	2.33	4.25	4.21			2.85	
	J_{HH}	J_{ab} 1.0 J_{af} 4.0	J_{bc} 6.7	J_{cf} 1.0				
139a	^{13}C	51.1	62.4	54.6	49.0	43.6		
	^{1}H	4.79	3.89	3.80	3.09	2.87	2.53	1.88
	J_{HH}	J_{ab} 2.2 J_{ae} 7.3 J_{af} 2.2	J_{bc} 6.2 J_{bd} 2.2	J_{cd} 2.2 J_{ce} 1.7 J_{cf} 0.7	J_{df} 2.2 J_{dg} 7.5	J_{ef} 13.0		
139b	^{13}C	41.3	68.5	63.0	33.6	22.8		
	^{1}H	4.49	3.88	3.66	1.17	2.97	2.79	1.49
	J_{HH}	J_{ab} 2.2 J_{ae} 7.8 J_{af} 3.2	J_{bc} 6.1 J_{bd} 2.2	J_{cd} 2.2 J_{ce} 2.2	J_{df} 2.2 J_{dg} 12.3	J_{ef} 13.4		
139c	^{13}C	38.3	78.5	72.0	33.6	31.8		
	^{1}H	4.49	4.14	3.98	(2.76)	(2.76)	2.65	1.76
	J_{HH}	J_{ab} 2.3 J_{ae} 10.7 J_{af} 4.6	J_{bc} 6.1	J_{cd} 2.3	J_{df} 2.3 J_{dg} 12.8	J_{ef} 12.8		

the $^4J_{HH}$ bridgehead-bridgehead coupling in **118** (6.7 Hz) is quite similar to that in **139a–c** (6.1 Hz) and that reported for bicyclo[2.1.1]hexane (6.23 Hz).[167] Apparently this large "W" long-range coupling is little affected by the nature of the "spacer atoms" between the CH groups.

5.3.4. *Diastereotopic Effects in Polysulfides*

The diastereotopic character of CH_2 protons in sulfinyl compounds is well known, and leads to complex NMR spectra for compounds such as allicin, alliin, and ajoene. It is less well recognized that the helical geometry of polysulfides can also lead to magnetic nonequivalence of methylene protons or enhancement of this effect in molecules containing other chiral centers. In the case of the ^{1}H-NMR spectra of compounds **140a–c** (Fig. 9) found in the distilled oil of garlic, we find that the $SCH_cCH_aH_bS$ group shows the *largest difference* between H_a and H_b in the case of **140c** ($\delta_a = 3.09$, $\delta_b = 3.17$, $J_{ab} = 14.1$ Hz, $J_{ac} = 8.7$ Hz, $J_{bc} = 6.5$ Hz). The

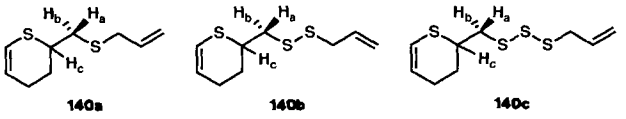

Fig. 9. 3,4-Dihydro-2*H*-thiopyran derivatives **140a–c**.

^{1}H-NMR spectrum of **140a** shows no separation of H_a and H_b while that of **140b** shows a separation of only $\Delta\delta = 0.01$ for these protons.[118]

6. Steam-Distilled Oils

The earliest chemical studies on garlic and onion involved distillation procedures. While the first detailed chemical report of the preparation and analysis of the distilled oil of garlic appeared in 1844,[4] it is likely that many centuries earlier alchemists and pharmacists distilled garlic bulbs to produce potions for a plethora of ailments. Wertheim's 1844 paper attributes garlic's appeal to "the presence of a sulfur-containing, liquid body, the so-called garlic oil. All that is known about the material is limited to some meager facts about the pure product which is obtained by steam distillation of bulbs of *Allium sativum*. Since sulfur bonding has been little investigated so far, a study of this material promises to supply useful results for science." The components of garlic oil, separated by Wertheim by fractional distillation, were described as forms of "allylschwefel", establishing the garlic connection to the common name "allyl". Semmler[5] indicated that the principal constituents of the distilled oils of garlic and onion are, respectively, diallyl disulfide (**4b**) and a compound of formula $C_6H_{12}S_2$, structurally unspecified by him but suggested by others to be allyl propyl disulfide.[168] For the onion oil analysis, 5000 kg of onions were steam distilled, affording only 233 g (0.005%) of oil! Today the steam-distilled oils of garlic and onion are items of commercial importance for use both in food and health products.

6.1. Oil of Garlic

Although distilled garlic oil lacks the antibacterial and antithrombotic activity of the room temperature extract, it possesses equally interesting antitumor and antioxidant properties. Garlic oil and some of its components inhibit lipoxygenase (LO), one of the enzymes involved in arachidonic acid metabolism, which may be related to its antitumor activity and other biological properties. Two observations in particular prompted us to study the effect of heat on garlic oil: 1) Belman and Barany noted that ageing or heating of the garlic oil component allyl methyl trisulfide effected an increased inhibitory activity toward the soybean 15-lipoxygenase (LO) enzyme compared to a freshly synthesized sample;[169] 2) Granroth observed that "diallyl disulfide **4b** is slowly decomposed even at room temperature, and at 100 °C at least 25 reaction products were revealed by gas chromatography, the true number being still greater" and that "allylic compounds may undergo changes upon heating garlic-spiced foods, but the chemistry and possible physiological importance of these changes do not so far appear to have been investigated."[20] Analysis of the thermally more robust heavier compounds in garlic oil by GC and GC-MS suggested the presence of an unusual family of thiaheterocycles and acyclic compounds. The composition and origin of this group of compounds was clarified by examining the behavior of diallyl disulfide upon heating.

We have analyzed distilled garlic oil preparations using the inhibition of soybean lipoxygenase (LO) to determine the compounds responsible for its biological activities. We found that: 1) the LO-inhibitory activity of garlic oil increases upon heating and concentration; 2) GC-MS analysis of garlic oil revealed a group of previously unknown higher boiling cyclic and acyclic organosulfur compounds with two to five sulfur atoms (e.g. **140a–c**, **141a–c**, **142a–f**, Scheme 57); 3) most

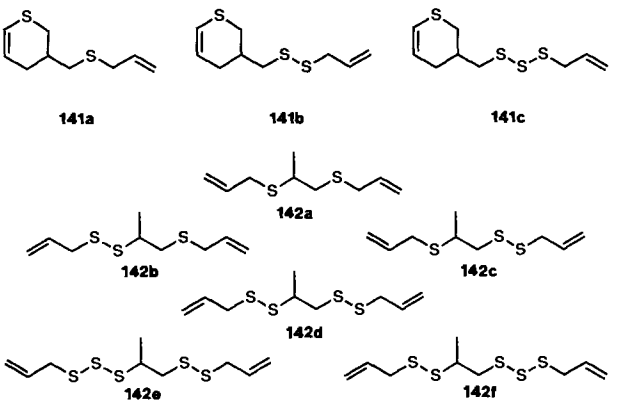

Scheme 57. Higher molecular weight compounds of type **140–142** from the pyrolysis of diallyl disulfide.

of these same compounds are generated upon heating pure samples of diallyl disulfide (**4b**); 4) the formation of these new compounds is best explained by a remarkable sequence involving thermal C–S homolysis of **4b** (rather than S–S homolysis, which only occurs upon photolysis), addition of the allyldithio radical in Markownikoff fashion to **4b**, intramolecular hydrogen atom abstraction-fragmentation of the radical adduct to produce thioacrolein (**93**, Scheme 58), and finally Diels–Alder addition of **93** as a heterodiene to diallyl sulfide (**4a**) and **4b** and dimerization to form **9** and **74** (Scheme 59).[118] The viability of such processes could be independently established using known thermal sources of **93** including allicin (Scheme 32) and diallyl sulfide (in a

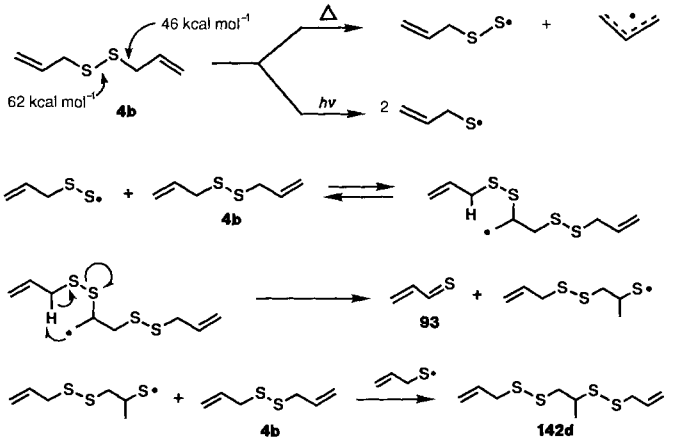

Scheme 58. Mechanism for decomposition of diallyl disulfide (**4b**).

An unexpected dividend to our examination of different thermal sources of **93** was our discovery that one of the most efficient low-temperature sources of **93** is diallyl sulfoxide (**143**)! Thus, when excess **143** is heated at 110 °C with dienophiles such as *N*-phenylmaleimide, dimethyl fumarate or ethyl acrylate, the corresponding thioacrolein Diels–Alder adducts such as **144** can be isolated in good to excellent yields (Scheme 61).[171] We suggest that the sulfur atom of reversibly formed allyl-2-propenesulfenate (**145**) acts as a nucleophile toward a second molecule of **145**, forming thiosulfonium ion **146**, a process similar to that observed with thiosulfinates (Schemes 11 and 31). Hydrolysis of **146** gives allicin **1**, known to be a low-temperature source of **93** (Scheme 32). When garlic oil is examined by HPLC, polysulfides with up to six sulfur atoms (e.g. All_2S_6, **4f**) are

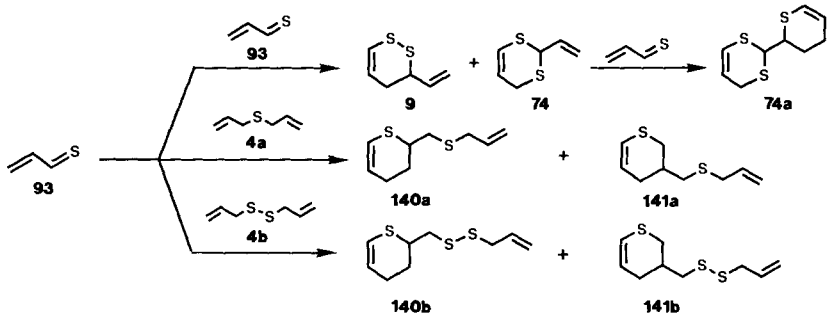

Scheme 59. Diels–Alder reaction of thioacrolein (**93**).

sealed tube; Scheme 60) and by demonstrating by mass spectrometric methods that the C–S and S–S bond dissociation energies in **4b** are 46 and 62 kcal mol^{-1}, respectively.[118] We conclude that the formation of the complex mixture of acyclic and heterocyclic polysulfides in the distilled oil of garlic is a consequence of the action of heat during the distillation process on the allicin and **4b** forming **93** and allyldithio radicals. Obviously any culinary procedure which exposes garlic or garlic-spiced food to heat could also generate the types of compounds described herein with possible health benefits associated with the antioxidant or lipoxygenase-inhibitory activity.[170a]

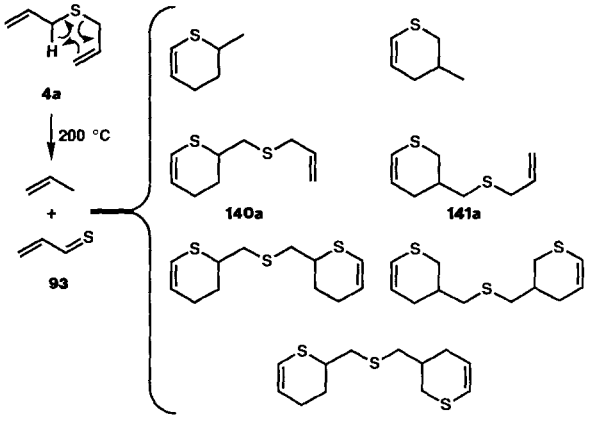

Scheme 60. Sealed tube pyrolysis of diallyl sulfide (**4a**).

found.[170b] These are difficult to detect by GC because of their thermal instability. They may be formed by known sulfur transfer processes from allylic disulfides.[118, 172]

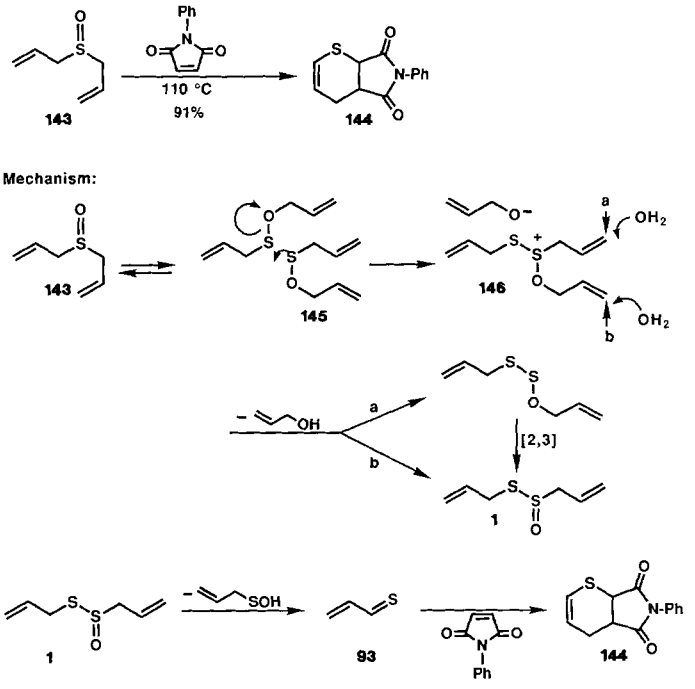

Scheme 61. Pyrolysis of diallyl sulfoxide (**143**) to give thioacrolein **93**; trapped as 3,4-dihydro-2*H*-thiopyran derivative **144**.

6.2. Pyrolysis of Bis(1-propenyl) Disulfide

When a 1% solution of the isomers of bis(1-propenyl) disulfide **119** in benzene is kept at 85 °C for 3 hours two new compounds, identified as *cis*- and *trans*-3,4-dimethyl-2,3-dihydrothiophene-2-thiol (**147a,b**), are formed in a 1:1 ratio in over 85% yield together with minor quantities of 3,4-dimethylthiophene (**148**).[173] Compound **148** was previously observed as the predominant product formed when **119** is heated to 150–200 °C in the presence of $KHSO_4$.[174] Prolonged heating at higher temperatures results in the conversion of **147a,b** into **148** (Scheme 62). All three isomers of **119** lead to the same mixture of **147a,b**; no isomerization from one isomer of **119** to another occurs under pyrolysis conditions. The relative rates of reaction of the three isomers of **119** were found to be *E,Z* > *E,E* > *Z,Z*.

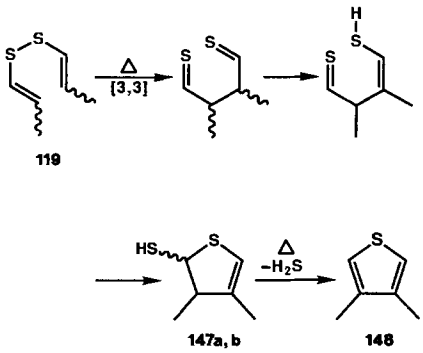

Scheme 62. Dithio-Claisen reaction of bis(1-propenyl) disulfide (**119**) and formation of *cis*- and *trans*-3,4-dimethyl-2,3-dihydrothiophenethiol (**147a,b**) and 3,4-dimethylthiophene (**148**).

Compounds **147a,b** are thought to be formed from **119** via a [3,3]-sigmatropic dithio-Claisen rearrangement[175] followed by thioenolization and intramolecular addition of SH to CH=S (Scheme 62), similarly to cyclizations involving 1,4-diketones. The similarity of the activation parameters for rearrangement of (*Z,Z*)-**119** (E_a = 19 kcal mol^{-1}, $\Delta H^{\neq}$ = 18.3 kcal mol^{-1}, $\Delta S^{\neq}$ = −24.8 cal mol^{-1}K^{-1}, and $\Delta G^{\neq}$ = 27.5 kcal mol^{-1}, all at 373 K)[135a] to the corresponding values for (*Z,Z*)-**120** (Section 5.2.5, cf. Schemes 41–43) suggests a similar mechanism. The absence of interconversion of isomers of **119** under the reaction conditions precludes a homolytic route to **147a,b**. Compounds **147a,b** as well as 2-alkyldithio-3,4-dimethylthiophenes (alkyl = Me or Pr) have been detected in steam-distilled volatiles from scallion and Welsh onion.[141] It is likely that the thiophene **148**, one of the significant contributors to the aroma of garlic, leek, and cooked or fried onion,[176] is formed in these plants from **147a,b** by loss of H_2S, although additional routes to **148** and other dimethylthiophenes are conceivable.

7. Physiological Activity

Belief in the preventive or curative effect of vegetables towards disease has persisted for thousands of years. Garlic, onion, cress, and cabbage are examples. In Eastern Europe and Asia Minor, large amounts of raw onion or garlic are a normal feature of the diet. The science of nutrition has paid little serious attention to these beliefs, since, to some extent, they can be explained on the basis of the vitamins and minerals contained in these vegetables, and because other alleged effects, if they exist, seem to be connected with substances better regarded as drugs than foods.

A. Virtanen (1895–1973)[2]

7.1. Antimicrobial Activity

Since things that here in order shall ensue,
Against all poysons have a secret power.
Peare, garlicke, reddish root, nuts, rape and rue—
But garlicke chiefe; for they that it devoure
May drinke, and care not who their drinke do brewe.
May walk in aires infected, every houre
Sith garlicke them have power to save from death,
Bear with it though it maketh unsavory breath,
And scorne not garlicke, like some that thinke
It only maketh men winke, and drinke—and stinke.

"The Englishman's Doctor"
Sir John Harington (1561–1612) [177a]

Before the availability of modern antibiotics, garlic preparations were widely used in epidemics of typhus, cholera, dysentery, amoebic dysentery, diphtheria, and tuberculosis.[3i] Albert Schweitzer first treated amoebic dysentery in Africa with garlic only.[177b] The antimicrobial effect of allicin is considerable.[122b] It has a growth inhibiting effect on both gram-negative and gram-positive bacteria (e.g. *Streptococci, Staphylococci, Eberthella typhosa, B. dysenteriae, B. enteritidis* and *Vibrio chlorae*) even at a 1:100000 dilution.[33] The antimicrobial effect of methyl methanethiosulfinate (**12**), propyl propanethiosulfinate (**13**), and thiosulfinates found in onion extracts (first noted to be antibacterial by Louis Pasteur![178]) are weaker than allicin **1**.[2, 179, 180] Allicin and garlic extracts show anticandidal and antifungal (e.g. anti-*Cryptococcus neoformans*) activity.[181–183] Garlic bulb volatiles have fungicidal properties[184, 185] which may protect the bulb against invading microorganisms. Diallyl trisulfide, **4c**, a constituent of garlic oil, has been used in China to treat viral infections and cryptococcal meningitis.[186]

7.2. Cancer Preventive Properties

Since the 1957 discovery that ethyl ethanethiosulfinate **31** showed anti-tumor activity, considerable attention has focussed on the cancer preventive properties of *Allium* spp.[186, 187] A fascinating epidemiological study conducted in the People's Republic of China reveals that in a region of China where gastric cancer rates are high, a significant reduction in gastric cancer risk parallels increasing consumption of garlic, scallion, and Chinese chive. Persons in the highest quartile of intake of these plants experienced only 40% of the risk of those in the lowest.[188] Since nitrites have been implicated in gastric cancer, it is relevant that gastric juice nitrite concentrations were lower in individuals consuming garlic compared to those who rarely take garlic; the

reduction of nitrite concentration in gastric juice after introduction of fresh garlic homogenate was significantly larger than that of controls.[189a] It is also known that diallyl disulfide **4b** inhibits in vivo activation of nitrosamines.[189b] Unsaturated polysulfides found in *Allium* spp. inhibit tumor promotion,[187, 190-193] perhaps by enhancing glutathione-dependent detoxification enzymes,[194a, b] and also modulate mutagenesis of aflatoxin B1.[194c] Steam-distilled onion oil, but not garlic oil, can also function as a weak tumor *promoter* as well as antipromoter in 7,12-dimethylbenz[*a*]-anthracene-initiated mouse skin.[195]

7.3. Cardiovascular Effects on Lipid and Arachidonic Acid Metabolism, and Platelet Aggregation Inhibitory Activity

Dietary garlic has a lipid- and cholesterol-lowering effect.[3i, 196] γ-Glutamyl-*S*-alkylcysteines inhibit the blood-pressure regulation hormone.[201a] A detailed mortality study[196b] on patients who had prior heart attacks showed that of those given gelatin capsules containing garlic oil (ca. 6 mg/person/day) high in ajoene (**75**) and dithiins (**9**, **74**)[119b] for three years, there was significant reduction in serum lipids, a 35% reduction in new heart attacks, and a 45% reduction in total deaths compared to those consuming placebo capsules. Allicin (**1**) is a specific inhibitor of acetyl-CoA synthetases from plants[197a] while diallyl disulfide (**4b**) inhibits 3-hydroxy-3-methylglutaryl CoA;[197b] in this manner lipid, cholesterol and fatty acid biosynthesis may be inhibited. The inhibitory effect of garlic and onions on human platelet aggregation has been known for two decades and has been variously attributed to adenosine, allicin **1**, alliin **2**, ajoene **75**, polysulfides (such as **4f**), and vinyl dithiins (e.g. **9** and **74**).[28, 198] The identity of the organosulfur compounds found in the blood or tissues after consumption of the plants remains unknown (apart from the compounds found in breath or sweat after ingestion of garlic). In view of the in vivo findings of Lawson[28] and the observations of Cavallito[30] and Wills[199a] that allicin reacts immediately with the SH-group of free or enzyme-bound cysteine forming *S*-(allylthio)cysteine, it is unlikely that allicin itself is found in blood after consumption of garlic. Indeed *S*-(allylthio)-cysteine may well be responsible for much of the biological effects of garlic within the body.[28a] Several studies indicate that the components of freshly cut garlic[199b] and onion[149] inhibit platelet aggregation and smooth muscle contraction through inhibition of cyclooxygenase and related enzymes. The antiasthmatic effects of onion extracts has been demonstrated; some of the most active components are thiosulfinates and cepaenes. These compounds exert a wide range of pharmacological effects such as inhibition of the cyclooxygenase and lipoxygenase pathways of arachidonic acid metabolism, inhibition of histamine release and leukotriene biosynthesis, prevention of bronchial asthma in guinea pigs after inhalation of allergens and platelet-activating factor, and inhibition of inflammatory cell influx.[125] Allicin is reported to inhibit human platelet aggregation in vitro without affecting cyclooxygenase or thromboxane synthase activity or cyclic AMP levels, possibly by influencing calcium movement.[198a]

7.4. Physiological Activity of Ajoene

Ajoene **75** is cytotoxic toward a tumorgenic lymphoid cell line with an EC_{50} of 12 μM;[200] it shows an IC_{50} of 1.6 μM and 5.1 μM towards the 5-lipoxygenase and cyclooxygenase enzymes, respectively;[201] it synergistically potentiates the antiaggregatory action of prostacyclin, forskolin, indomethacin and dypiridamole on human blood platelets.[106] Administration of **75** to dogs under conditions used in open heart surgery prevents the thrombocytopenia induced by contact of blood with artificial surfaces; it shows excellent activity in preventing the loss of platelets and in increasing the rate of restoration of platelet clotting activity.[202a] Other anticlotting agents (aspirin, heparin) had longer lasting effects and did not protect platelets. Ajoene is thought to inhibit platelet activation by impairing the interaction of fibrinogen receptors on the platelet surface with the rest of the membrane signal transduction system and by affecting the plasma-membrane internal microviscosity.[202b-d] Alternatively, it is suggested that ajoene alters the conformation of a hemoprotein implicated in platelet activation.[203a] Ajoene can also inhibit adhesive interactions of human neutrophiles and consequently effect in vivo superoxide anion formation.[203b] Ajoene possesses significant antifungal activity, inhibiting the growth of *Aspergillus niger, Candida albicans, Paracoccidioides-Brasiliensis*, and *Fusarium* species at concentrations of $< 20\ \mu g\,mL^{-1}$,[204] possibly by damaging the fungal cell walls.[204b] Ajoene inactivates human gastric lipase (HGL), a sulfhydryl enzyme involved in the digestion and adsorption of dietary fats. This observation corroborates previous reports on the ability of garlic to lower triacylglycerol blood levels ("blood thinning" effect of folk medicine).[205] A garlic preparation prepared by dissolving fresh garlic extract in coconut oil (forming ajoene and dithiins[28]) significantly decreases ADP-induced platelet aggregation in volunteers consuming $0.25\ mg\,kg^{-1}$ daily for 4 weeks.[206]

7.5. Acid Reflux Effect

Eat no onions nor garlic, for we are to utter sweet breath.

"A Midsummer Night's Dream"
William Shakespeare (1564-1616)

Anyone who has overindulged in onions is aware of the consequences. Gastroenterologists refer to the effect as "acid reflux and reflux symptoms", e.g. regurgitation of the stomach contents into the esophagus with resultant "heartburn". A more precise physiological description is inappropriate transient lower esophageal sphincter (LES) relaxation, e.g. erratic opening of the valve separating the esophagus from the stomach.[207] Since, as we have already mentioned in Section 7.3, several of the organosulfur compounds formed when onions are cut are potent inhibitors of the cyclooxygenase and lipoxygenase pathways of arachidonic acid metabolism, raw onions may cause heartburn by blocking these pathways.[208] This inhibition might then result, either singly or in combination, in the transient relaxation of the LES as well as injury to the esophageal mucosa.

7.6. Lachrymatory, Olfactory, and Gustatory Characteristics of *Allium* spp.

Provence with her garlic-scented smile.
Rudyard Kipling (1865–1936)

While it is not known precisely how crying is triggered by an onion, it has been suggested that the onion LF, along with other lachrymators such as tear gases, undergo particularly facile reduction by NADPH following reception in a nerve cell membrane.[209] The organoleptic properties of some fresh onion extract and distilled onion oil components have been evaluated by "expert flavorists" who described odor and taste. The "room-temperature steam distillate" of onion, consisting primarily of α,β-unsaturated thiosulfinates, had an odor and taste quite similar to that of fresh onions. Of the isomeric pair (*E*)-**106**, R = Me/(*E*)-**105**, R = Me, the former had a pronounced fresh raw onion or shallot flavor while the latter had more of a cabbage or radish note. The flavor of (*E,Z*)-**106**, R = Pr, is that of green, raw fresh onions. On the other hand, (*E,Z*)-**114**, R = Pr, lacked the fresh raw onion flavor of the thiosulfinates, having more of an oniony, solvent-like flavor. The cepaene (*E,E*)-**127d** had a fruity melon-like flavor combined with a slight fresh onion flavor.[21] Propyl, propenyl di- and trisulfides possess the odor of cooked onions.[176] The threshold (minimal levels for detection in aqueous solutions by taste) range from 5–10 ppb for the thiosulfinates, the deoxycepaenes (*E,E*)- and (*Z,Z*)-**131** and the cepaene **127d** to 0.01–6 ppb for (*Z,Z*)-**119**, Pr_2S_2, MeSSCH=CHMe, and PrSSCH=CHMe, to an amazing level (for one experienced flavorist) of 0.001 ppb for (*E,Z*)-**114**, R = Pr.[21,176]

MeCH=CHSS(O)R
106

MeCH=CHS(O)SR
105

(*E,Z*)-MeCH=CHSSO$_2$R
114

(*E,E*)-MeCH=CHS(O)CHEtSSCH=CHMe
127d

7.7. Bad Breath and Further Negative Effects of Garlic and Other *Allium* spp.

...edit cicutis alium nocentius.[*]
"Episode 3"
Horace (65 B.C.–8 B.C.)

Eating alliaceous plants causes bad breath and perspiration odors. Components of garlic breath and prespiration include: allyl methyl sulfide and disulfide, diallyl sulfide and disulfide, 2-propenethiol, and *p*-cymene and (+)-limonene (present in garlic distilled oils).[210,211] Garlic breath odor comes from the lungs presumably by way of the blood and not solely from particles of garlic retained in the structures about the mouth.[212] After ingestion of 2 g of raw garlic, garlic odor in human urine was said to persist up to 96 hours while exhaled air no longer had an odor after 24 hours.[213a] When garlic is rubbed on the foot, a garlic taste is soon detected.[213b] Presumably fat-soluble allicin is absorbed through the skin (as in the case of dimethyl sulfoxide) into the lymphatic system which carries it intact to the upper part of the body in a medium where no protein or cysteine is present.[213b] In areas where *Allium* spp. grow wild, cows often eat them, causing a bad flavor in milk. A vacuum treatment can remove these sulfur compounds and the bad taste.[20] Studies on nursing mothers have shown that their milk has a more intense odor 2 hours after having ingested garlic. Furthermore it was found that the nursing babies sucked more and ingested more milk when the milk smelled like garlic.[214]

A few individuals have an allergic response, e.g. dermatitis or asthma, to fresh garlic or onions,[215a] diallyl disulfide, allicin or garlic dust.[3i,215] Freshly ground garlic can cause severe dermatitis on prolonged contact with the skin.[216] In a case associated with excessive garlic ingestion, spontaneous spinal epidural hematoma causing paraplegia following a qualitative platelet disorder has been reported.[217] When given orally to laboratory animals, garlic has been noted to cause anemia,[3i] abdominal hemorrhage and death.[187] In mice, allicin (**1**) has an LD_{50} of 60 mg kg^{-1} i.v. and 120 mg kg^{-1} s.c.[30] An occupational hazard associated with sulfur compounds in the perspiration of a garlic lover has been reported.[211]

[*] That wicked garlic, more poisonous than the hemlock.

7.8. Insect and Animal Attractive/Repulsive Effects

Propyl propanethiosulfinate (**13**) has been identified as the most attractive substance from crushed leek for the leek moth, *Acrolepiopsis assectella*; **13** is repellent to *Ephestia kuehniella* (based on our recent analyses of thiosulfinates from leek, this work may require revision!)[29] Allicin, its homologs, and related sulfur compounds are thought to protect *Allium* spp. against pathogens and predators.[10b,14b] Garlic oil components/metabolites diallyl disulfide and trisulfide are toxic to mosquito and other insect larvae at levels of 2 ppm[218] and are repellant to *Ixodes ricinus*, the tick which carries the encephalitis virus.[219] Diallyl disulfide has been employed to drive away crop-damaging birds.[3i]

8. Summary and Outlook

In the fifty years since the discovery of allicin (**1**)[30] much progress has been made in identifying the various unusual organosulfur compounds formed when garlic and onion are cut (Figs. 10 and 11) and in understanding their origin. Despite this progress, many other compounds remain to be identified in *Allium* extracts. For example, application of field desorption mass spectroscopy to the analysis of onion extracts indicates that the heaviest compounds present have masses of m/z = 325–326 and 298–301, corresponding respectively to molecular formulas $C_{12}H_{20}S_4O_2/C_{12}H_{22}S_4O_2$ and $C_{10}H_{18}S_4O_2/C_{10}H_{20}S_4O_2$. Analysis of these extracts by LC-MS indicate the presence of a series of compounds (perhaps a family of homologous isomers?) with masses 324/326 and 298. Possible structures include *S,S'*-dioxides of **132** (Scheme 53) or isomers **149** (Scheme 63), together with ho-

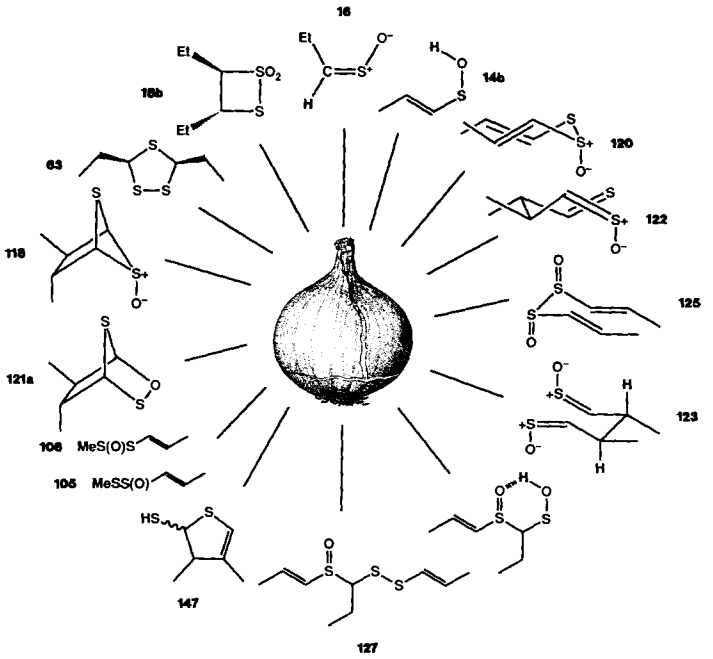

Fig. 10. Collection of some of the principal organosulfur compounds and intermediates associated with onion.

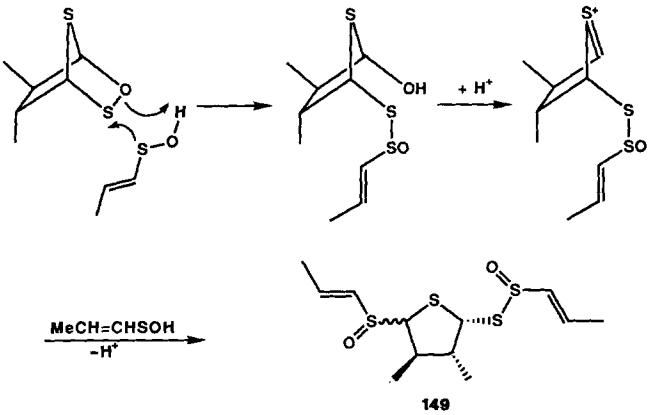

Scheme 63. Possible structure for *m/e* 324 compound (**149**) from onion extracts.

mologs with methyl replacing a 1-propenyl group. Efforts to identify these compounds are underway.

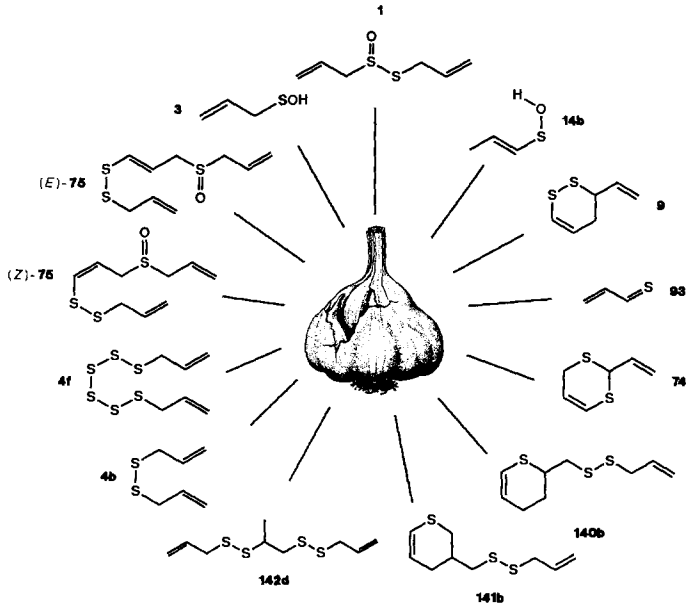

Fig. 11. Collection of some of the principal organosulfur compounds and intermediates associated with garlic.

How might dietary *Allium* spp. benefit us? Consider the following: 1) The *Allium* spp. tissue is not completely crushed when it is eaten, thus allowing a significant portion of the *S*-alk(en)ylcysteine *S*-oxides such as **2**, **5**, **6**, and **7** to pass unchanged into the intestinal tract. While allinases are irreversibly deactivated at the pH of gastric juice, intestinal bacteria have been shown to cleave the sulfoxides, ultimately giving the corresponding disulfides.[10b] 2) Thiosulfinates which have made their way into the stomach may survive the low pH long enough to act on pathogenic microorganisms present. 3) Alk(en)ylthiolation of certain biological SH groups by thiosulfinates, di- or polysulfides or ajoene might be beneficial. For example, "allylthiolation" of thiamine readily occurs affording allithiamine, which is more easily absorbed from the intestine than thiamine.[3i, 38] 4) Disulfides and other sulfur compounds formed from *Allium* spp. are thought to play an important role in the intestinal tract in deactivating nitrites or other environmental toxins. One thing is clear: tracking the metabolic fate of *Allium* spp. organosulfur compounds is both an important and a fertile area for future research.

I am profoundly grateful to my many excellent co-workers and collaborators, whose names appear in the references, for their valuable contributions to the research described herein. I particularly thank S. Naganathan, D. Putman, and S. H. Zhao for their expert assistance in the preparation of this manuscript. I am deeply appreciative for financial support of this work by the National Science Foundation, the American Heart Assocation, the John Simon Guggenheim Foundation, the Petroleum Research Fund, administered by the American Chemical Society, the Herman Frasch Foundation, NATO, Société Nationale Elf Aquitaine, McCormick and Company, Wakunaga Pharmaceutical Company, and the State University of New York at Albany. I thank Dr. Larry Lawson for critically reviewing the entire manuscript and C. T. Ho, W. le Noble, O. Sticher, and L. Lawson for unpublished material.

Received: January 3, 1992 [A 876 IE]
German version: *Angew. Chem.* **1992**, *104*, 1158

[1] For a general overview of organosulfur chemistry, see E. Block, *Reactions of Organosulfur Compounds*, Academic Press, New York, **1978**.
[2] A. I. Virtanen, *Angew. Chem.* **1962**, *74*, 374–382; *Angew. Chem. Int. Ed. Engl.* **1962**, *1*, 299–306.
[3] General reviews on *Allium* chemistry: a) E. Block, *Sci. Am.* **1985**, *252*, 114–119; *Spektrum Wiss.* **1985**, 66–72; b) E. Block, *Lect. Heterocycl. Chem.* **1987**, *9*, 27–31; c) E. Block in *Sulfur-Centered Reactive Intermediates in Chemistry and Biology* (Eds.: C. Chatgilialoglu, D. Asmus), Plenum Press, New York, **1991**, S. 282–289 [NATO Conf. Ser.]; d) E. Block, *Phosphorus, Sulfur, Silicon Relat. Elem.* **1991**, *58*, 3–15; e) G. R. Fenwick, A. B. Hanley, *CRC Crit. Rev. Food Sci. Nutr.* **1985**, *22*, 199–271, 273–377; **1986**, *23*, 1–73; f) J. F. Carson, *Food Rev. Int.* **1987**, *3*, 71–103; g) J. L. Brewster, H. D. Rabinowitch (Eds.), *Onions and Allied Crops*, CRC Press, Boca Raton, **1990**, *Vol. 1–3*; h) J. R. Whitaker, M. Mazelis in *Food Enzymology* (Ed.: P. Fox), Elsevier, London, **1991**, Vol. 1. Ch. 13, pp. 479–498; i) J. R. Whitaker, *Adv. Food. Res.* **1976**, *22*,

73–133; j) H. P. Koch, G. Hahn, *Knoblauch*, Urban & Schwarzenberg, München, **1988**; k) M. K. Jain, C. Scanzello, R. Apitz-Castro, *Chem. Unserer Zeit* **1988**, *22*, 193–200; l) E. Block, S. Naganathan, D. Putman, S.-H. Zhao, *Pure Appl. Chem.* **1993**, in press.

[4] T. Wertheim, *Ann. Chem. Pharm.* **1844**, *22*, 193–200.

[5] F. W. Semmler, *Arch. Pharm.* **1892**, *230*, 434–443, 443–448.

[6] C. J. Cavallito, J. H. Bailey, J. S. Buck, *J. Am. Chem. Soc.* **1945**, *67*, 1032–1033.

[7] K. Knobloch, L. Lawson, *Planta Med.* **1990**, *56*, 246.

[8] a) A. Stoll, E. Seebeck, *Experientia* **1947**, *3*, 114–115; b) A. Stoll, E. Seebeck, *Helv. Chim. Acta* **1948**, *31*, 189–210; c) A. Stoll, E. Seebeck, *ibid.* **1949**, *32*, 197–205; d) A. Stoll, E. Seebeck, *Sci. Pharm.* **1950**, *18*, 61–79; e) A. Stoll, E. Seebeck, *Adv. Enzymol.* **1951**, *11*, 377–400.

[9] J. E. Lancaster, H. A. Collin, *Plant Sci. Lett.* **1981**, *2*, 169–176.

[10] a) A. I. Virtanen, C.-G. Spåre, *Suom. Kemistil. B* **1961**, *34*, 72; *ibid.* **1962**, *35*, 28; b) A. I. Virtanen, *Phytochemistry* **1965**, *4*, 207–228.

[11] L. D. Lawson, Z.-Y. J. Wang, B. G. Hughes, *J. Nat. Prod.* **1991**, *54*, 436–444.

[12] a) M. Mütsch-Eckner, *Ph. D. Thesis*, ETH Zürich **1991**; b) M. Mütsch-Eckner, B. Meier, A. D. Wright, O. Sticher, *Phytochemistry* **1992**, *31*, 2389–2391.

[13] Y. Ueda, M. Sakaguchi, K. Hirayama, R. Miyajima, A. Kimizuka, *Agric. Biol. Chem.* **1990**, *54*, 163–169.

[14] a) T. Kasai, P. O. Larsen, *Prog. Chem. Org. Nat. Prod.* **1980**, *39*, 173–285; b) J. E. Lancaster, M. L. Shaw, *Phytochemistry* **1991**, *30*, 2857–2859.

[15] J. E. Lancaster, M. L. Shaw, *Phytochemistry* **1989**, *28*, 455–460.

[16] S. J. Ziegler, O. Sticher, *Planta Med.* **1989**, *55*, 372–378.

[17] H. Rennenberg, *Phytochemistry* **1982**, *21*, 2771.

[18] J. W. Anderson in *The Biochemistry of Plants*, (Eds.: E. E. Conn, P. K. Stumpf), Academic Press, New York, **1980**, p. 203.

[19] a) R. J. Parry, G. R. Sood, *J. Am. Chem. Soc.* **1989**, *111*, 4514–4515; b) R. J. Parry, F.-L. Lii, *ibid.* **1991**, *113*, 4704–4706.

[20] B. Granroth, *Ann. Acad. Sci. Fenn. Ser. A 2* **1970**, *154*, 1–71.

[21] a) Garlic cloves from two different New York State farms showed concentrations of **6** of 0.08–0.25 mg/g garlic compared to "normal" values of 1–1.6 mg/g garlic. The concentrations of **2** and the *S*-substituted γ-glutamyl cysteines **e**, **f**, and **g** (see Scheme 2) in the New York garlic samples were within the "normal" range. We thank Dr. L. D. Lawson for performing this analysis [21b] (also see Ref. [28b]); b) E. Block, S. Naganathan, D. Putman, S. H. Zhao, *J. Agric. Food Chem.* **1992**, in press; c) E. Block, D. Putman, S. H. Zhao, *ibid.* **1992**, in press.

[22] a) H. Jansen, B. Müller, K. Knobloch, *Planta Med.* **1989**, *55*, 434–439, 440–445; L. P. Nock, M. Mazelis, *Arch. Biochem. Biophys.* **1986**, 248, 27–33; b) H. Jansen, B. Müller, K. Knobloch, *ibid.* **1987**, *53*, 559–562.

[23] A. Rabinkov, M. Wilchek, D. Mirelman, *FASEB J.* **1991**, *5*, 1149.

[24] M. Fujita, M. Endo, M. Sano, *Agric. Biol. Chem.* **1990**, *54*, 1077–1079.

[25] F. P. Kupiecki, A. I. Virtanen, *Acta Chem. Scand.* **1960**, *14*, 1913–1918.

[26] M. Mazelis, L. Crews, *Biochem. J.* **1968**, *108*, 725–730.

[27] S. Schwimmer, *Arch. Biochem. Biophys.* **1969**, *130*, 312–320.

[28] a) L. D. Lawson, D. K. Ransom, B. G. Hughes, *Thromb. Res.* **1992**, *65*, 141–156; b) Lancaster [28c] also suggests that there is a basic difference in the regulation of *S*-methylcysteine *S*-oxide **6** compared with alliin **2**; c) J. E. Lancaster, E. M. Dommisse, M. L. Shaw, *Phytochemistry* **1988**, *27*, 2123–2124.

[29] a) J. Auger, C. Lecomte, E. Thibout, *J. Chem. Ecol.* **1989**, *15*, 1847–1854; b) J. Auger, F. X. Lalau-Keraly, C. Belinsky, *Chemosphere* **1990**, *21*, 837–843; c) J. Auger, E. Thibout, *C. R. Séances Acad. Sci. Ser. III* **1981**, *292*, 217–220; d) J. Auger, E. Thibout, *Can. J. Zool.* **1979**, *57*, 2223–2229.

[30] a) C. J. Cavallito, J. H. Bailey, *J. Am. Chem. Soc.* **1944**, *66*, 1950–1951; b) C. J. Cavallito, J. S. Buck, C. M. Suter, *ibid.* **1944**, *66*, 1952–1954; c) C. J. Cavallito, US-A 2554088, **May 22, 1951**.

[31] Chemical Abstracts names allicin **1** as 2-propene-1-sulfinothioic acid *S*-2-propenyl ester, **12** as methanesulfinothioic acid *S*-methyl ester, and alliin **2** as L-alanine, 3-(2-propenylsulfinyl)-, (*S*)-. As these names are quite cumbersome to use, we employ here the IUPAC nomenclature. Compounds of the type RS(O)SR′ are named according to Rule C-641 as esters of the thiosulfinic acid RS(O)SH. Accordingly, allicin **1** is named *S*-2-propenyl(or *S*-allyl) 2-propenethiosulfinate. (Since only *S*-esters occur here the *S* will be omitted.) This system of nomenclature is preferable to an alternative system where compounds RS(O)SR are named alk(en)yl alk(en)yl′ thiosulfinate with the first group (R) attached to the sulfinyl sulfur and the second ("primed") group (R′) to the sulfenyl sulfur [121].

[32] V. V. Nosyreva, S. V. Amosova, *Zh. Org. Khim.* **1990**, *26*, 1412–1415 (*Engl. Transl.* 1218–1221).

[33] L. V. Small, J. H. Bailey, C. J. Cavallito, *J. Am. Chem. Soc.* **1947**, *69*, 1710–1713.

[34] C. J. Cavallito, L. V. D. Small, US-A 2508745, **May 23, 1950**.

[35] a) M. H. Brodnitz, J. V. Pascale, L. Van Derslice, *J. Agric. Food Chem.* **1971**, *19*, 273–275. b) We suggest that 1-propenyl propyl disulfide is formed from **13** via the intermediacy of **34** (Scheme 11) rather than by a direct dehydration.

[36] K. Saito, M. Horie, Y. Hoshino, N. Nose, E. Mochizuki, H. Nakazawa, M. Fujita, *J. Assoc. Off. Anal. Chem.* **1989**, *72*, 917–920.

[37] a) Alkylcysteine *S*-oxides have been found in other plants [37b] including cabbage [37c], turnip [37d], and *Phaseolus* [37e]; allinase is not always present [42]. Allicin is produced on cutting the Amazonian garlic bush (*Adenocalymma alliaceum*) [37f]. In nature the –SS(O)– and –SSCH=CH– linkages are uncommon. Examples of the former are all cyclic [37g]; examples of the latter include the powerfull antitumor agents esperamycin [37h] and calicheamicin [37i], and compounds from the plants *Agathosma apiculata* [37j], *Azadirachta indica* [37k], and *Ferula assa-foetida* [37l]; b) R. Gmelin, M. N'Galamulume-Treves, G. Höfle, *Phytochemistry* **1980**, *19*, 553–557; c) R. L. M. Synge, J. C. Wood, *Biochem. J.* **1956**, *64*, 252–259; d) C. J. Morris, J. F. Thompson, *J. Am. Chem. Soc.* **1956**, *78*, 1605–1608; e) H. Rinderknecht, D. Thomas, S. Aslin, *Helv. Chim. Acta* **1958**, *41*, 1; f) M. G. Zoghbi, L. R. Ramos, J. G. S. Maia, M. L. Da Silva, A. I. R. Luz, *J. Agric. Food Chem.* **1984**, *32*, 1009–1010; g) A. Kato, M. Numata, *Tetrahedron Lett.* **1972**, 203–206; H. Yanagawa, T. Kato, Y. Kitahara, *ibid.* **1973**, 1073–1075; S. J. Wratten, D. J. Faulkner, *J. Org. Chem.* **1976**, *41*, 2465–2467; G. H. N. Towers, *Phytochemistry* **1990**, *29*, 2901–2904; F. Balza, G. Pattenden, A. J. Shuker, *Tetrahedron Lett.* **1991**, *32*, 6625–6628; h) J. Golik, G. Dubay, G. Groenewold, H. Kawaguchi, M. Konishi, B. Krishnan, H. Ohkuma, K. Saitoh, T. W. Doyle, *J. Am. Chem. Soc.* **1987**, *109*, 3462–3464; i) M. D. Lee, T. S. Dunne, C. C. Chang, G. A. Ellestad, M. M. Siegel, G. O. Morton, W. J. McGahren, D. B. Borders, *ibid.* **1946**, *31*, 3466–3468; j) J. L. B. Smith, D. E. A. Rivett, *Trans. R. Soc. S. Afr.* **1946**, *31*, 111; *Chem. Abstr.* **1946**, *40*, 6752; k) A. M. Mubarak, C. P. Kulatilleke, *Phytochemistry* **1990**, *29*, 3351–3352; M. F. Balandrin, S. M. Lee, J. A. Klocke, *J. Agric. Food Chem.* **1988**, *36*, 1048–1054; l) T. Kajimoto, K. Yahiro, T. Nohara, *Phytochemistry* **1989**, *28*, 1761–1763.

[38] M. Fujiwara, M. Yoshimura, S. Tsuno, *J. Biochem. (Tokyo)* **1955**, *42*, 591.

[39] A. R. Saghir, L. K. Mann, R. A. Bernhard, J. V. Jacobsen, *Proc. Am. Hort. Sci.* **1964**, *84*, 386–398.

[40] a) W. D. Niegisch, W. H. Stahl, *Food. Res.* **1956**, *21*, 657–665; b) Kohmann first identified propanal in onion volatiles: E. F. Kohmann, *Science (Washington D.C.)* **1947**, *106*, 625–627.

[41] a) J. F. Carson, R. E. Lundin, T. M. Lukes, *J. Org. Chem.* **1966**, *31*, 1634–1635; b) J. F. Carson, L. E. Boggs, *ibid.* **1966**, *31*, 2862–2864.

[42] R. Kuttan, N. G. Nair, A. N. Radhakrishnan, T. F. Spande, H. J. Yeh, B. Witkop, *Biochemistry* **1974**, *13*, 4394–4400.

[43] C.-G. Spåre, A. I. Virtanen, *Acta Chem. Scand.* **1963**, *17*, 641–650.

[44] E. J. Matikkala, A. I. Virtanen, *Acta Chem. Scand.* **1967**, *21*, 2891–2893.

[45] J. E. Lancaster, K. E. Kelly, *J. Sci. Food Agric.* **1983**, *34*, 1229–1235.

[46] a) E. Däbritz, A. I. Virtanen, *Chem. Ber.* **1965**, *98*, 781–788; b) E. Däbritz, A. I. Virtanen, *Acta Chem. Scand.* **1964**, *18*, 837–838.

[47] a) W. F. Wilkens: *Ph. D. Thesis*, Cornell University, Ithaca, NY, **1961**; b) W. F. Wilkens, *Cornell Agricultural Experimental Station Memoir*, Ithaca, NY, **Jan. 1964**, 385.

[48] a) W. A. Sheppard, J. Diekmann, *J. Am. Chem. Soc.* **1964**, *86*, 1891–1892; b) J. F. King, R. Rathore in *The Chemistry of Sulphonic Acids, Esters, and their Derivatives* (Eds.: S. Patai, Z. Rappoport), Wiley, New York, **1991**, S. 697–766; c) B. Zwanenburg, *Recl. Trav. Chim. Pays-Bas* **1982**, *101*, 1–26; B. G. Lenz, B. Zwanenburg in *Methoden Org. Chem. (Houben-Weyl), Teil 2, Vol. E11*, Thieme, Stuttgart, **1985**, 911; B. Zwanenburg in *Reviews on Heteroatom Chemistry, Vol. 1* (Eds.: S. Oae), Myo, Tokyo, **1988**, pp. 218–234; d) L. Thijs, B. Zwanenburg, *Recl. Trav. Chim. Pays-Bas* **1964**, *83*, 631–636.

[49] E. Block in *Organic Sulfur Chemistry* (Eds.: R. Kh. Freidlina, A. E. Skorova), Pergamon Press, Oxford, **1981**, pp. 15–34.

[50] M. H. Brodnitz, J. V. Pascale, *J. Agric. Food Chem.* **1971**, *19*, 269–272.

[51] J. L. Kice, *Adv. Phys. Org. Chem.* **1980**, *17*, 65–181.

[52] T. L. Moore, D. E. O'Connor, *J. Org. Chem.* **1964**, *31*, 3587–3592.

[53] a) R. W. Murray, R. D. Smetana, E. Block, *Tetrahedron Lett.* **1971**, 299–302; b) R. W. Murray, S. L. Jindal, *Photochem. Photobiol.* **1972**, *16*, 147–151; c) R. W. Murray, S. L. Jindal, *J. Org. Chem.* **1972**, *37*, 3516–3520.

[54] a) E. Block, *J. Am. Chem. Soc.* **1972**, *94*, 642–644; b) E. Block, *ibid.* **1972**, *94*, 644–645; c) E. Block, S. W. Weidman, *ibid.* **1973**, *95*, 5046–5048; d) E. Block, J. O'Connor, *ibid.* **1973**, *95*, 5048–5051; e) E. Block, J. O'Connor, *ibid.* **1974**, *96*, 3921–3929; f) E. Block, J. O'Connor, *ibid.* **1974**, *96*, 3929–3944.

[55] R. E. Penn, E. Block, L. K. Revelle, *J. Am. Chem. Soc.* **1978**, *100*, 3622–3624.

[56] The increasing bond length in the series ArSSAr, $ArSO_2SAr$, ArS(O)SAr (2.03 Å, 2.09 Å, and 2.108 Å, respectively) parallels the weakening of the S–S bond: C. T. Kiers, A. Vos, *Recl. Trav. Chim. Pays-Bas* **1978**, *97*, 166–170.

[57] J. B. F. N. Engberts, G. Zuidema, *Recl. Trav. Chim. Pays-Bas* **1970**, *89*, 1202.

[58] E. Block, *J. Org. Chem.* **1974**, *39*, 734–736.

[59] a) E. Block, E. R. Corey, R. E. Penn, T. L. Renken, P. F. Sherwin, *J. Am. Chem. Soc.* **1976**, *98*, 5715–5717; b) E. Block, E. R. Corey, R. E. Penn, T. L. Renken, P. F. Sherwin, H. Bock, T. Hirabayashi, S. Mohmand, B. Solouki, *ibid.* **1982**, *104*, 3119–3130.

[60] F. A. Davis, R. L. Billmers, L. A. Jenkins, *J. Org. Chem.* **1986**, *51*, 1033–1040.

[61] G. Winnewisser, M. Winnewisser, W. Gordy, *J. Chem. Phys.* **1968**, *51*, 3465.
[62] F. Turecek, L. Brabec, T. Vondrák, V. Hanus, J. Hájícek, Z. Havlas, *Collect. Czech. Chem. Commun.* **1988**, *53*, 2140–2158; F. Turecek, D. E. Drinkwater, F. W. McLafferty, *J. Am. Chem. Soc.* **1989**, *111*, 7696–7701.
[63] S. Besnainou, J. L. Whitten, *J. Am. Chem. Soc.* **1980**, *102*, 7444–7448.
[64] N. Nakamura, *J. Am. Chem. Soc.* **1983**, *105*, 7172–7173.
[65] J. L. Kice, L. Weclas-Henderson, A. Kewan, *J. Org. Chem.* **1989**, *54*, 4198–4203.
[66] E. Block, R. E. Penn, R. J. Olsen, P. F. Sherwin, *J. Am. Chem. Soc.* **1976**, *98*, 1264–1265.
[67] D. E. Powers, C. A. Arrington, W. C. Harris, E. Block, V. F. Kalasinsky, *J. Phys. Chem.* **1979**, *83*, 1890–1892.
[68] Y. Vallee, J.-L. Ripoll, C. Lafon, G. Pfister-Guillouzo, *Can. J. Chem.* **1987**, *65*, 290–291.
[69] E. Suzuki, R. Ishiguro, F. Watari, *J. Mol. Struct.* **1990**, *238*, 71–77.
[70] E. Block, A. Wall, *Tetrahedron Lett.* **1985**, *26*, 1425–1428.
[71] a) H. Kallio, L. Salorinne, *J. Agric. Food Chem.* **1989**, *38*, 1560–1564; b) H. Kallio, M. Leino, L. Salorinne, *J. High Resolut. Chromatogr.* **1989**, *12*, 174–177.
[72] E. Block, R. E. Penn, L. K. Revelle, *J. Am. Chem. Soc.* **1979**, *101*, 2200–2201.
[73] E. Block, A. Wall, *J. Org. Chem.* **1987**, *52*, 809–818.
[74] E. Block, M. Aslam, *Tetrahedron Lett.* **1982**, *23*, 4203–4206.
[75] C. R. Johnson, J. E. Keiser, J. C. Sharp, *J. Org. Chem.* **1969**, *34*, 860–864.
[76] G. A. Krafft, P. T. Meinke, *Tetrahedron Lett.* **1985**, *26*, 1947–1950.
[77] a) E. Block, A. Wall, J. Zubieta, *J. Am. Chem. Soc.* **1985**, *107*, 1783–1784; b) E. Block, A. A. Bazzi, L. K. Revelle, R. E. Penn, C. Saha, unpublished.
[78] W. Walter, K. Wohlers, *Justus Liebigs Ann. Chem.* **1971**, *752*, 115–135.
[79] a) Y. Makisumi, S. Takada, Y. Matsukara, *J. Chem. Soc. Chem. Commun.* **1974**, 850; b) G. A. Koppel, S. Kukolja, *ibid.* **1975**, 57–58; c) R. Bell, P. D. Cottam, J. Davies, D. N. Jones, *J. Chem. Soc. Perkin Trans. 1* **1981**, 2106–2115; d) R. Bell, P. D. Cottam, J. Davies, D. N. Jones, N. A. Meanwell, *Tetrahedron Lett.* **1980**, *21*, 4379–4382; e) A. Heckel, W. Pfleiderer, *ibid.* **1983**, *24*, 5047–5050.
[80] F. Turecek, F. W. McLafferty, B. J. Smith, L. Radom, *Int. J. Mass Spectrom. Ion Processes* **1990**, *101*, 283–300.
[81] a) S. Tahara, H. Okamura, Y. Miura, J. Mizutani, *Agric. Biol. Chem.* **1979**, *43*, 2017–2020; b) S. Tahara, J. Mizutani, *ibid.* **1979**, *43*, 2021–2028.
[82] E. Block, R. E. Penn, A. A. Bazzi, D. Cremer, *Tetrahedron Lett.* **1981**, *22*, 29–32.
[83] R. Hoffman, R. A. Olofson, *J. Am. Chem. Soc.* **1966**, *88*, 943–946.
[84] H. Kameoka, Y. Demizu, *Phytochemistry* **1979**, *18*, 397–1398.
[85] A. M. Hamid, S. Trippett, *J. Chem. Soc. C* **1968**, 1612–1615.
[86] D. Barnard, E. R. Cole, *Anal. Chim. Acta* **1959**, *20*, 540–547.
[87] L. Field, R. B. Barbee, *J. Org. Chem.* **1969**, *34*, 36–41.
[88] a) E. Block, A. A. Bazzi, L. K. Revelle, *J. Am. Chem. Soc.* **1980**, *102*, 2490–2492; b) An example of *intermolecular* 1,3-dipolar addition of a sulfine to a thione has been described recently: G. Mloston, R. Huisgen, K. Polborn, *Abstracts, 15th International Symposium on the Organic Chemistry of Sulfur*, Caen, France, June 1992, 157.
[89] E. Block, A. Yencha, M. Aslam, V. Eswarakrishnan, J. Luo, A. Sano, *J. Am. Chem. Soc.* **1988**, *110*, 4748–4753.
[90] a) E. Block, A. A. Bazzi, *Tetrahedron Lett.* **1988**, *110*, 4569–4572; b) see also: F. Freeman, M. C. Keindl, *J. Org. Chem.* **1988**, *53*, 2026–2031.
[91] a) E. Block, A. Schwan, D. A. Dixon, *J. Am. Chem. Soc.* **1992**, *114*, 3492–3499.
[92] a) E. M. Calvey, J. M. Betz, J. E. Matusik, K. D. White, E. Block, S. Naganathan, in press; b) N. K. Sinha, D. E. Guyer, D. A. Gage, C. T. Lira, *J. Agric. Food Chem.* **1992**, *40*, 368–372.
[93] J. F. Carson, F. F. Wong, *J. Agric. Food Chem.* **1961**, *9*, 140–143.
[94] For a related example of a steam distillation under reduced pressure see: N. S. A. Edwards, R. D. Gillard, P. W. Groundwater, *Chem. Ind. (London)* **1991**, 763.
[95] J. L.-P. Wu, C.-M. Wu, *J. Chromatogr.* **1981**, *214*, 234–236.
[96] H. Miething, *Dtsch. Apoth.-Ztg.* **1985**, *125*, 2049–2050; *Chem. Abstr.* **1985**, *103*, 187, 210.
[97] a) C. H. Wijaya, H. Nishimura, T. Tanaka, J. Mizutani, *J. Food Sci.* **1991**, *56*, 72–75; b) H. Nishimura, C. H. Wijaya, J. Mizutani, *J. Agric. Food Chem.* **1988**, *36*, 563–566; c) H. Nishimura, K. Fujiwara, J. Mizutani, Y. Obata, *ibid.* **1971**, *19*, 992–994.
[98] a) V. V. Talyzin, V. Y. Anisimova, O. I. Yakovleva, R. V. Golovnya, T. A. Misharina, S. V. Vitt, *Zh. Anal. Khim. (USSR)* **1988**, *43*, 911–916 (Engl. Transl. 718–722); b) T.-H. Yu, C.-M. Wu, Y.-C. Liou, *J. Agric. Food Chem.* **1989**, *37*, 725–730; c) G. Vernin, J. Metzger, D. Fraisse, C. Scharff, *Planta Med.* **1986**, 96–101; d) L. Schreyen, P. Dirinck, F. Van Wassenhove, N. Schamp, *J. Agric. Food Chem.* **1976**, *24*, 336–341.
[99] R. A. Bernhard, *Phytochemistry* **1977**, *9*, 2019–2027.
[100] G. G. Freeman, R. J. Whenham, *J. Sci. Food Agric.* **1975**, *26*, 1869–1886.
[101] H. Iida, S. Hashimoto, M. Miyazawa, H. Kameoka, *J. Food Sci.* **1983**, *48*, 660–661.
[102] I. A. Mackenzie, D. A. Ferns, *Phytochemistry* **1977**, *16*, 763–764.
[103] I. Sakai, *US-A 4933201*, **June 12, 1990**.
[104] B. H. Müller, *Dissertation*, Universität Erlangen-Nürnberg, **1991**.
[105] a) M. Mikolajczyk, J. Drabowicz, *J. Am. Chem. Soc.* **1978**, *108*, 2510–2515; b) Note that in the presence of chiral amines *t*-BuSOH gives chiral *t*BuS(O)S*t*Bu: J. Drabowicz, P. Lyzwa, M. Mikolajczyk, *Phosphorus Sulfur* **1983**, *16*, 267–270.
[106] a) R. Apitz-Castro, S. Cabrera, M. R. Cruz, E. Ledezma, M. K. Jain, *Thromb. Res.* **1983**, *32*, 155–169; b) R. Apitz-Castro, E. Ledezma, J. Escalante, F. M. Pinate, J. Moreno-Rea, G. Carrillo, O. Leal, M. K. Jain, *ibid.* **1986**, *42*, 303–311.
[107] a) E. Block, S. Ahmad, M. K. Jain, R. W. Crecely, R. Apitz-Castro, M. R. Cruz, *J. Am. Chem. Soc.* **1984**, *106*, 8295–8296; b) E. Block, S. Ahmad, J. Catalfamo, M. K. Jain, R. Apitz-Castro, *ibid.* **1986**, *108*, 7045–7055; c) E. Block, S. Ahmad, *US-A 4643994*, **February 17, 1987**; d) E. Block in *Folk Medicine: The Art and the Science* (Ed.: R. P. Steiner), American Chemical Society, Washington, D.C., **1986**, p. 125–137.
[108] a) A. J. Mura, Jr., D. A. Bennett, T. Cohen, *Tetrahedron Lett.* **1975**, 4433–4436; b) E. Vilsmaier, J. Schutz, S. Zimmerer, *Chem. Ber.* **1979**, *112*, 2231–2242.
[109] E. Vedejs, P. L. Fuchs, *J. Org. Chem.* **1971**, *36*, 366–367.
[110] E. Block, S. Ahmad, *J. Am. Chem. Soc.* **1985**, *107*, 6731–6732.
[111] H. Kwart, J. L. Schwartz, *J. Org. Chem.* **1974**, *39*, 1575–1583.
[112] C. J. Burrows, B. K. Carpenter, *J. Am. Chem. Soc.* **1981**, *103*, 6983–6984.
[113] J. R. Hwu, D. A. Anderson, *Tetrahedron Lett.* **1986**, *27*, 4965–4968; J. R. Hwu, D. A. Anderson, *J. Chem. Soc. Perkins Trans. 1* **1991**, 3199–3206.
[114] J. B. Lambert, D. S. Bailey, C. Mixan, *J. Org. Chem.* **1972**, *37*, 377–382.
[115] A. Mukherjee, E. M. Schulman, W. J. le Noble, *J. Org. Chem.* **1992**, *57*, 3120–3126.
[116] a) B. Iberl, G. Winkler, K. Knobloch, *Planta Med.* **1990**, *56*, 202–211; b) with 2-propanol as solvent yields as high as 45% are claimed: B. Iberl, G. Winkler, B. Müller, K. Knobloch, *ibid.* **1990**, *56*, 320.
[117] a) H. Bock, S. Mohmand, T. Hirabayashi, A. Semkow, *Chem. Ber.* **1982**, *115*, 1339–1348; b) E. Vedejs, T. H. Eberlein, D. L. Varie, *J. Am. Chem. Soc.* **1982**, *104*, 1445–1447; c) P. Beslin, *J. Heterocycl. Chem.* **1983**, *20*, 1753–1754.
[118] E. Block, R. Iyer, S. Grisoni, C. Saha, S. Belman, F. P. Lossing, *J. Am. Chem. Soc.* **1988**, *110*, 7813–7827.
[119] a) Lawson finds that **1** from garlic homogenized in water decomposes to the extent of 9% after 24 h at room temperature affording **4c** and **4b** in a 2:1 molar ratio [119b]. He also finds that the half-life of **1** at room temperature is 10 days in 1 mM citric acid (pH 3), 4 days in water, 48 h in MeOH or $CHCl_3$, 3 h in ether, 2 h in hexane and 16 h in the absence of solvent [119b]. On the other hand, Brodnitz reports that *neat* **1** decomposes nearly completely in 20 h at 20 °C giving **4c** and **4b** in a 0.14:1 molar ratio [35a]; b) L. D. Lawson in *Human Medicinal Agents from Plants* (Eds: A. D. Kinghorn and M. Balandarin), American Chemical Society, Washington, D. C., in press; c) E. J. Corey, T. A. Engler, *Tetrahedron Lett.* **1984**, *25*, 149–152; d) recent work indicates that as much as 10% of **79** may in fact be formed from decomposition of **1** (L. D. Lawson, personal communication).
[120] M. A. Belous, I. Y. Postovsskii, *Zh. Obshch. Khim.* **1950**, *20*, 1701–1710; *Chem. Abstr.* **1951**, *45*, 2391.
[121] a) L. D. Lawson, B. G. Hughes, paper presented at the International Joint Symposium, Bonn (FRG), July, 1990; b) L. D. Lawson, S. G. Wood, B. G. Hughes, *Planta Med.* **1991**, *57*, 263–270.
[122] a) L. D. Lawson, B. G. Hughes, *Planta Med.* **1992**, *58*, 345–350; b) B. G. Hughes, L. D. Lawson, *Phytotherapy Research* **1991**, *5*, 154–158.
[123] A. Sendl, H. Wagner, *Planta Med.* **1991**, *57*, 361–362.
[124] R. E. Hermes, *US-A 4917921*, **April 17, 1990**.
[125] a) W. Dorsch, E. Schneider, T. Bayer, W. Breu, H. Wagner, *Int. Arch. Allergy Appl. Immunol.* **1990**, *92*, 39–42; b) H. Wagner, W. Dorsch, T. Bayer, W. Breu, F. Willer, *Prostaglandins, Leukotrienes Essential Fatty Acids* **1990**, *39*, 59–62; c) T. Bayer, H. Wagner, V. Wray, W. Dorsch, *Lancet* **1988**, 906; d) W. Dorsch, H. Wagner, T. Bayer, B. Fessler, G. Hein, J. Ring, P. Scheftner, W. Sieber, T. Strasser, E. Weiss, *Biochem. Pharmacol.* **1988**, *37*, 4479–4485; e) W. Dorsch, B. Adelmann-Grill, T. Bayer, M. Ettl, G. Hein, H. Jaggy, J. Ring, P. Scheftner, H. Wagner, *Allergologie* **1987**, *10*, 316–324; f) W. Dorsch, M. Ettl, G. Hein, P. Scheftner, J. Weber, T. Bayer, H. Wagner, *Int. Arch. Allergy Appl. Immunol.* **1987**, *82*, 535–536; g) W. Dorsch, H. Wagner, T. Bayer, *Allergologie* **1989**, *12*, 388–396; h) W. Dorsch in *Late Phase Allergic Reactions* (Ed.: W. Dorsch), CRC Press, Boca Raton, **1990**, Ch. 32, pp. 325–332.
[126] H. Nishimura, A. Mizuguchi, J. Mizutani, *Tetrahedron Lett.* **1975**, 3201–3202.
[127] P. Vermeer, J. Meijer, C. Eylander, L. Brandsma, *Recl. Trav. Chim. Pays-Bas* **1976**, *51*, 25–27.
[128] T. Hayashi, M. Konishi, Y. Okamoto, K. Kabeta, M. Kumada, *J. Org. Chem.* **1986**, *51*, 3772–3781.
[129] C. E. Fuller, D. G. Walker, *J. Org. Chem.* **1991**, *56*, 4066–4067.
[130] F. Freeman, C. S. Lee, *Magn. Reson. Chem.* **1988**, *26*, 813–816.
[131] J. E. Baldwin, G. Höfle, S. Choi, *J. Am. Chem. Soc.* **1971**, *93*, 2810–2812.
[132] M. Tada, Y. Hiroe, S. Kiyohara, S. Suzuki, *Agric. Biol. Chem.* **1988**, *52*, 2383–2385.
[133] Y. H. Kim, T. Takata, S. Oae, *Tetrahedron Lett.* **1978**, *26*, 2305–2308.
[134] J. A. Ross, R. P. Seiders, D. M. Lemal, *J. Am. Chem. Soc.* **1976**, *98*, 4325–4327.

[135] a) E. Block, S. Naganathan, T. Bayer, unpublished; b) E. Block, S. Naganathan, T. Bayer, unpublished; c) E. Block, D. Putman, H. Gulati, S.-H. Zhao, J. Catalfamo, unpublished; d) E. Block, S.-H. Zhao, *J. Org. Chem.* **1992**, in press.
[136] T. Bayer, *Dissertation*, Universität München, **1988**.
[137] T. Bayer, H. Wagner, E. Block, S. Grisoni, S. H. Zhao, A. Neszmelyi, *J. Am. Chem. Soc.* **1989**, *111*, 3085–3086.
[138] A. Ishii, J. Nakayama, M. Ding, N. Kotaka, M. Hoshino, *J. Org. Chem.* **1990**, *55*, 2421.
[139] P. Vittorelli, H.-J. Hansen, H. Schmid, *Helv. Chim. Acta* **1975**, *58*, 1293–1309.
[140] M. G. Matturro, R. P. Reynolds, *Tetrahedron Lett.* **1987**, *28*, 4981–4984 and references cited therein.
[141] a) M.-C. Kuo, M. Chien, C.-T. Ho, *J. Agric. Food Chem.* **1990**, *38*, 1378–1381; b) M.-C. Kuo, C. T. Ho, *ibid.* **1992**, *40*, 111–117.
[142] R. Huisgen, E. Langhals, *Tetrahedron Lett.* **1989**, *30*, 5369–5372.
[143] a) W. C. Lumma, *J. Am. Chem. Soc.* **1969**, *91*, 2820–2821; b) J. R. Hwu, J. A. Robl, *J. Chem. Soc. Chem. Commun.* **1986**, 704.
[144] E. Block, T. Bayer, *J. Am. Chem. Soc.* **1990**, *112*, 4584–4585.
[145] B. Zwanenburg, A. Wagenaar, L. Thijs, J. Strating, *J. Chem. Soc. Perkin Trans. 1* **1973**, 73–75.
[146] F. Freeman, C. N. Angeletakis, W. J. Pietro, W. J. Hehre, *J. Am. Chem. Soc.* **1982**, *104*, 1161–1165.
[147] P. L. Folkins, D. N. Harpp, *J. Am. Chem. Soc.* **1991**, *113*, 8998–9000.
[148] a) F. Freeman, C. N. Angeletakis, *J. Am. Chem. Soc.* **1981**, *103*, 6232–6235; **1982**, *104*, 5766–6774; **1983**, *105*, 4039–4044; b) F. Freeman, C. Lee, *J. Org. Chem.* **1988**, *53*, 1263–1266; c) F. Freeman, *Chem. Rev.* **1984**, *84*, 117.
[149] a) S. Kawakishi, Y. Morimitsu, *Lancet* **1988**, 330; b) Y. Morimitsu, S. Kawakishi, *Phytochemistry* **1990**, *29*, 3435–3439; c) Y. Morimitsu, S. Kawakishi, *Agric. Biol. Chem.* **1991**, *55*, 889–890; d) Y. Morimitsu, Y. Morioka, S. Kawakishi, *J. Agric. Food Chem.* **1992**, *40*, 368–372.
[150] T. Bayer, W. Breu, O. Seligmann, V. Wray, H. Wagner, *Phytochemistry* **1989**, *28*, 2373–2377.
[151] M. Yagami, S. Kawakishi, M. Namiki, *Agric. Biol. Chem.* **1980**, *44*, 2533–2538.
[152] E. Block, M. Aslam, *Tetrahedron Lett.* **1985**, *26*, 2259–2262.
[153] J. W. Chen, C.-M. Wu, paper presented at the 9th Int. Congr. of Essential Oils, Singapore, **1983**.
[154] H. Naimie, Z. Samek, L. Doleis, Z. ReHacek, *Collect. Czech. Chem. Commun.* **1972**, *37*, 1166–1177.
[155] a) P. Dubs, R. Stüssi, *Helv. Chim. Acta* **1978**, *61*, 2351–2359; b) for related syntheses, see: P. Dubs, M. Joho, *ibid.* **1978**, *61*, 2809–2812.
[156] J. Meijer, P. Vermeer, *Recl. Trav. Chim. Pays-Bas* **1974**, *93*, 242.
[157] E. Block, L. K. Revelle, A. A. Bazzi, *Tetrahedron Lett.* **1980**, *21*, 1277–1280.
[158] a) G. J. Karabatsos, R. A. Taller, *J. Am. Chem. Soc.* **1964**, *86*, 4373–4378; b) G. J. Karabatsos, N. Hsi, *Tetrahedron* **1967**, *23*, 1079; c) G. J. Karabatsos, K. L. Krumel, *ibid.* **1967**, *23*, 1097; d) G. J. Karabatsos, R. A. Taller, *ibid.* **1968**, *24*, 3347; e) G. J. Karabatsos, C. E. Osborne, *ibid.* **1968**, *24*, 3361.
[159] R. R. Fraser, T. Durst, M. R. McClory, R. Viau, Y. Y. Wigfield, *Int. J. Sulfur Chem. Part A* **1971**, *1*, 133–142.
[160] E. Vedejs, D. A. Perry, R. G. Wilde, *J. Am. Chem. Soc.* **1986**, *108*, 2985–2989.
[161] W. G. Klemperer, *Angew. Chem.* **1978**, *90*, 258–271; *Angew. Chem. Int. Ed. Engl.* **1978**, *17*, 246–254.
[162] T. Takata, Y. H. Kim, S. Oae, K. T. Suzuki, *Tetrahedron Lett.* **1978**, 4303–4306.
[163] D. F. Ewing, K. A. Holbrook, R. A. Scott, *Org. Magn. Reson.* **1975**, *7*, 554–556.
[164] a) E. Block, A. A. Bazzi, J. B. Lambert, S. M. Wharry, K. K. Andersen, D. C. Dittmer, B. H. Patwardhan, D. J. H. Smith, *J. Org. Chem.* **1980**, *45*, 4807–4810; b) J. B. Lambert, S. M. Wharry, E. Block, A. A. Bazzi, *ibid.* **1983**, *48*, 3928–3985.
[165] a) T. A. Powers, S. A. Evans, K. Pandiarajan, J. C. N. Benny, *J. Org. Chem.* **1991**, *56*, 5589–5594; b) T. A. Powers, L. G. Pedersen, S. A. Evans, *Phosphorus, Sulfur, Silicon Relat. Elements.* **1991**, *58*, 499–504.
[166] E. Block, S. Naganathan, *Heteroat. Chem.*, in press.
[167] M. Barfield, E. W. Della, P. E. Pigou, *J. Am. Chem. Soc.* **1984**, *106*, 5051–5054.
[168] F. Challenger, D. Greenwood, *Biochem. J.* **1949**, *44*, 87–91.
[169] S. Belman, G. Barany, private communication.
[170] a) Boiling chopped/crushed garlic in water for 20 min in a closed container completely converts **1** into **4b** and **4c**, while in an open container 7% of thiosulfinates are retained but most **4b** and **4c** are evaporated. [119b] Cysteine sulfoxides and γ-glutamylcysteines (see Scheme 2) are the exlusive sulfur compounds found when whole cloves of garlic are cooked under similar conditions. [119b] Stir-frying chopped garlic cloves in hot soybean oil for 1 min retains 16% of **4b** and **4c** in the oil, but no **1**. [119b]; b) L. D. Lawson, Z.-Y. J. Wang, B. G. Hughes, *Planta Med.* **1991**, *57*, 363–370.
[171] E. Block, S.-H. Zhao, *Tetrahedron Lett.* **1990**, *31*, 5003–5006.
[172] R. D. Baechler, J. P. Hummel, K. Mislow, *J. Am. Chem. Soc.* **1973**, *95*, 4442–4444.
[173] E. Block, S.-H. Zhao, *Tetrahedron Lett.* **1990**, *31*, 4999–5002.
[174] H. Boelens, L. Brandsma, *Recl. Trav. Chim. Pays-Bas* **1972**, *91*, 141–145.
[175] a) M. M. Campbell, D. M. Evgenios, *J. Chem. Soc. Perkin Trans. 1* **1973**, 2866; b) F. C. V. Larsson, L. Brandsma, S.-O. Lawesson, *Recl. Trav. Chim. Pays-Bas* **1974**, *93*, 258.
[176] M. Boelens, P.J. de Valois, H. J. Wobben, A. van der Gen, *J. Agric. Food Chem.* **1971**, *19*, 984–991.
[177] a) This is said to be a Rabelaisan verse from the Medical School of Salerno translated by Harington; b) Dr. Simon, *Med. Klin.* **1932**, *3*, 86–87.
[178] L. Pasteur, *Ann. Chim. Phys. Ser. 3* **1858**, *52*, 404–418.
[179] A. I. Virtanen, E. J. Matikkala, *Acta Chem. Scand.* **1959**, *13*, 1898–1900.
[180] N. Didry, M. Pinkas, L. Dubreuil, *Pharmazie* **1987**, *42*, 687–688.
[181] F. Barone, M. Tansey, *Mycologia* **1977**, *69*, 713–824.
[182] L. E. Davis, J.-K. Shen, Y. Cai, *Antimicrob. Agents Chemother.* **1990**, *34*, 651–653.
[183] M. A. Ghannoum, *J. Gen. Microbiol.* **1988**, *134*, 2917–2924.
[184] a) V.-N. Tariq, A. C. Magee, *Mycol. Res.* **1990**, *94*, 617–620; b) R. D. Durbin, T. F. Uchytil, *Phytopathol. Mediterr.* **1971**, *10*, 227–230.
[185] Y. Cai in *Cardiol. Practice* **1991**, June Suppl., p. 11.
[186] A. S. Weisberger, J. Pensky, *Science (Washington, D.C.)* **1957**, *126*, 1112–1115.
[187] a) B. H. S. Lau, P. P. Tadi, J. M. Tosk, *Nutr. Res. (N.Y.)* **1990**, *10*, 937–948; b) J. G. Dausch, D. W. Nixon, *Prev. Med.* **1990**, *19*, 346–361.
[188] a) W. C. You, W. J. Blot, Y. S. Chang, A. Ershow, Z. T. Yang, Q. An, B. E. Henderson, J. F. Fraumeni, Jr., T. G. Wang, *J. Natl. Cancer Inst.* **1989**, *81*, 162–164; b) W. J. Blot in *Accomplishments in Cancer Research 1987* (Eds.: J. G. Fortner, J. E. Rhoads), J. B. Lippincott, Philadelphia, **1987**, pp. 231–239; c) E. Buiatti, W. Blot et al., *Int. J. Cancer* **1989**, *44*, 611–616.
[189] a) M. Xing, W. Mei-ling, X. Hai-xiu, P. Xi-pu, G. Chun-yi, H. Na, F. Mei-yun, *Yingyang Xuebao (Acta Nutr. Sin.)* **1982**, *4*, 53–58; b) C. S. Yang, *Cancer Res.* **1991**, *51*, 1509–1514.
[190] a) S. Belman, J. Solomon, A. Segal, E. Block, G. Barany, *J. Biochem. Toxicol.* **1989**, *4*, 151–160; b) J. P. Perchellet, E. M. Perchellet, S. Belman, *Nutr. Cancer* **1990**, *14*, 183–193.
[191] a) M. Wargovich, *Carcinogenesis (London)* **1987**, *8*, 487–489; b) M. Wargovich, J. C. Woods, L. V. Eng, L. C. Stephens, K. Gray, *Cancer Res.* **1988**, *48*, 6872–6875; c) M. A. Hayes, M. T. Goldbert, T. H. Rushmore, *Carcinogenesis* **1987**, *8*, 1155–1157; d) J. F. Brady, H. Ishizaki, D. Li, C. S. Yang, *Cancer Res.* **1988**, *48*, 5937–5940; e) H. Sumiyoshi, M. Wargovich, *ibid.* **1990**, *50*, 5084–5087.
[192] V. L. Sparnins, G. Barany, L. W. Wattenberg, *Carcinogenesis* **1988**, *9*, 131–134.
[193] L. W. Wattenberg, *Proc. Nutr. Soc.* **1990**, *49*, 173–183.
[194] a) V. A. Gudi, S. V. Singh, *Biochem. Pharmacol.* **1991**, *42*, 1261–1265; A. K. Maurya, S. V. Singh, *Cancer Lett.* **1991**, *57*, 121–129; b) H. J. Prochaska, A. B. Santamaria, P. Talalay, *Proc. Natl. Acad. Sci. USA* **1992**, *89*, 2394–2398; c) P. P. Tadi, *Nutr. Cancer* **1991**, *15*, 87–95.
[195] S. Belman, A. Seilakumar, M. C. Bosland, K. Savarese, R. D. Estensen, *Nutr. Cancer* **1990**, *14*, 141–148.
[196] a) A. Bordia, H. C. Bansal, *Lancet* **1973**, *2*, 1491–1492; A. Bordia, *Am. J. Clin. Nutr.* **1981**, *34*, 2100–2103; b) A. Bordia, *Dtsch. Apoth. Ztg.* **1989**, *129* (Suppl. 15), 16–17; A. Bordia, *Cardiol. Prac.* **1989**, *7* (Suppl. 10), 14; c) K. T. Augusti, P. T. Mathew, *Experientia* **1974**, *30*, 468–470; d) M. F. Kerekes, T. Feszt, *Artery* **1975**, *1*, 325–326; e) R.C. Jain, *Am. J. Clin. Nutr.* **1977**, *30*, 1380–1381; f) Second International Garlic Symposium, in *Die Medizinische Welt* **1991**, Suppl. 7a, pp. 1–50; *Cardiol. Practice* **1991**, June Suppl., pp. 2–19; *Dtsch. Apoth.-Ztg.* **1991**, *131*, Suppl. 24, pp. 1–24.
[197] a) M. Focke, A. Feld, H. K. Lichtenthaler, *FEBS-Lett.* **1990** (14), 106–108; b) R. V. O. Kumar, A. Banerji, C. K. R. Kurup, T. Ramasarma, *Biochim. Biophys. Acta* **1991**, *1078*, 219–225.
[198] a) P. R. Mayeux, K. C. Agrawal, J.-S. H. Tou, B. T. King, H. L. Lippton, A. L. Hyman, P. J. Kadowitz, D. B. McNamara, *Agents Actions* **1988**, *25*, 182–190; b) A. Bordia, *Atherosclerosis (Shannon, Irel.)* **1978**, *30*, 355–360; c) D. J. Boullin, *Lancet* **1981**, 776–777; d) A. N. Makheja, J. Y. Vanderhoek, R. W. Bryant, J. M. Bailey, *Adv. Prostaglandin Thromboxane Res.* **1980**, *6*, 309–312; e) J. Y. Vanderhoek, A. N. Makheja, J. M. Bailey, *Biochem. Pharmacol.* **1980**, *29*, 3169–3173; f) H. Weisenberger, H. Grube, E. Koenig, H. Pelzer, *FEBS-Lett.* **1972** (26), 105–108; g) M. Ali, M. Thomson, M. A. Alnaqeeb, J. M. Al-Hassan, S. H. Khater, S. A. Gomes, *Prostaglandin Leukotriene Essential Fatty Acids* **1990**, *41*, 95–99.
[199] a) E. D. Wills, *Biochem. J.* **1956**, *63*, 514–520; b) J. D. Gaffen, I. A. Tavares, A. Bennett, *J. Pharm. Pharmacol.* **1984**, *36*, 272–274.
[200] K. Scharfenberg, R. Wagner, K. G. Wagner, *Cancer Lett.* **1990**, *53*, 103–108.
[201] a) A. Sendl, G. Elbl, B. Steinke, K. Redl, W. Breu, H. Wagner, *Planta Med.* **1992**, *58*, 1–7; b) H. Wagner, M. Wierer, B. Fessler, *Planta Med.* **1987**, *53*, 305–306.
[202] a) R. Apitz-Castro, E. Ledezma, J. Escalante, F. M. Pinate, J. Moreno-Rea, G. Carrillo, O. Leal, M. K. Jain, *Drug Res.* **1988**, *38*, 901–904; b) F. Rendu, M. K. Jain, D. Daveloose, J. C. Debouzy, R. Apitz-Castro, N.

Bourdeau, S. Levy-Toledano, *Biochem. Pharmacol.* **1989**, *38*, 1321–1328; c) J. C. Debouzy, D. Daveloose, J. M. Neumann, J. Viret, M. Herve, R. Apitz-Castro, *Eur. Biophys. J.* **1989**, *17*, 211–216; d) R. Apitz-Castro, M. K. Jain, F. Bartoli, E. Ledezma, M.-C. Ruiz, R. Salas, *Biochim. Biophys. Acta* **1991**, *1094*, 269–280.

[203] a) M. P. Jamaluddin, L. K. Krishnan, A. Thomas, *Biochem. Biophys. Res. Commun.* **1988**, *153*, 479–486; b) G. F. Sud'ina, A. V. Tatarintsev, A. A. Koshkin, S. V. Zaitsev, N. A. Fedorov, S. D. Varfolomeev, *Biochim. Biophys. Acta* **1991**, *1091*, 257–260.

[204] a) S. Yoshida, S. Kasuga, N. Hayashi, T. Ushiroguchi, H. Matsuura, S. Nakagawa, *Appl. Environ. Microbiol.* **1987**, *53*, 615–617; b) U. P. Singh, V. N. Pandey, K. G. Wagner, K. P. Singh, *Can. J. Bot.* **1990**, *68*, 1354–1356; c) G. Sanblas, F. Sanblas, F. Gil, L. Marino, R. Apitz-Castro, *Antimicrob. Agents Chemother.* **1989**, *33*, 1641–1644.

[205] Y. Gargouri, H. Moreau, M. K. Jain, G. H. de Haas, R. Verger, *Biochem. Biophys. Acta* **1989**, *1006*, 137–139.

[206] a) S. A. Barrie, J. V. Wright, J. E. Pizzorno, *J. Orthomol. Med.* **1987**, *2*, 15–21; b) Lawson suggests that the garlic oil used by Bordia in his extensive clinical studies of lowering of blood lipids [196a] is also rich in **9**, **74**, and **75** [119b].

[207] M. L. Allen, M. H. Mellow, M. G. Robinson, W. C. Orr, *Am. J. Gastroenterol.* **1990**, *85*, 377–380.

[208] E. Block, P. F. Purcell, S. R. Yolen, *Am. J. Gastroenterol.* **1992**, *87*, 679.

[209] K. Wallenfels, W. Ertel, A. Hockendorf, J. Rieser, K. H. Uberschar, *Naturwissenschaften* **1975**, *65*, 459–467.

[210] a) I. Laakso, T. Seppanen-Laakso, R. Hiltunen, B. Mueller, H. Jansen, K. Knobloch, *Planta Med.* **1989**, *55*, 257–261; b) T. Minami, T. Boku, K. Inada, M. Morita, Y. Okazaki, *J. Food Sci.* **1989**, *54*, 763–765; c) T. G. Hartman, J. Lech, R. T. Rosen, *Abstracts, Society of Mass Spectrometrists*, **Mai 1991**, Nashville, TN.

[211] a) A patient who made reproduction antique china dolls complained that whereever she touched the dolls' heads when painting them, black speckles appeared after firing, requiring that those dolls' heads be rejected [211b]. It was determined that the clay was high in iron, the speckles consisted of iron sulfides, and the doll maker ate a great deal of garlic and sweated in her job. Analysis of sweat samples showed the presence of diallyl disulfide, allyl methyl disulfide and dimethyl disulfide. Thus, the mystery was solved and simple solutions, abstinence from garlic or use of latex gloves, proposed. b) C. M. Harris, R. H. Waring, S. C. Mitchell, G. L. Hendry, *Lancet* **1986**, 492–493.

[212] M. A. Blankenhorn, C. E. Richards, *J. Am. Med. Assoc.* **1936**, *107*, 409–410.

[213] a) P. Noether, *Münch. Med. Wochenschr.* **1925**, *72*, 1641–1642; b) L. Lawson, private communication (1992).

[214] J. A. Mennella, G. K. Beauchamp, *Pediatrics* **1991**, *88*, 737–744.

[215] a) J. W. Burks, *Ann. Allergy* **1954**, *12*, 592–596; b) C. Papageorgiou, J. P. Corbet, F. Menezes-Brandao, M. Pecegueiro, C. Benezra, *Arch. Dermatol. Res.* **1983**, *275*, 229–234; c) A. E. Falleroni, C.4R. Zeiss, D. Levitz, *J. Allergy Clin. Immunol.* **1981**, *68*, 156–160.

[216] a) B. Kaplan, M. Schewach-Millet, S. Yorav, *Int. J. Dermatol.* **1990**, *29*, 75–76; b) T. Y. Lee, T. H. Lam, *Contact Dermatitis* **1991**, *24*, 193–196; c) G. Lembo, N. Balato, C. Patruno, L. Auricchio, F. Ayala, *ibid.* **1991**, *25*, 330–331.

[217] K. D. Rose, P. D. Croissant, C. F. Parliament, M. B. Levin, *Neurosurgery* **1990**, *29*, 880–882.

[218] a) S. V. Amonkar, A. Banerji, *Science (Washington, D.C.)* **1971**, *174*, 1343–1344; b) S. V. Amonkar, E. L. Reeves, *J. Econ. Entomol.* **1970**, *63*, 1172–1175.

[219] G. Catar, *Bratisl. Lek. Listy* **1954**, *34*, 1004–1010; *Chem. Abstr.* **1955**, *49*, 2002.

meso Epoxides in Asymmetric Synthesis: Enantioselective Opening by Nucleophiles in the Presence of Chiral Lewis Acids

By *Ian Paterson** and *David J. Berrisford*

It is over a decade since the seminal discovery[1] of the asymmetric epoxidation of allylic alcohols catalyzed by titanium(IV) isopropoxide and tartrate esters. The utility of this transformation is a result of many factors, not least of which is the regio- and stereocontrol possible in the subsequent nucleophilic substitution (opening) reactions of the derived epoxy alcohols. Thus a reaction sequence of asymmetric epoxidation, epoxide opening, and further functionalization allows access to an impressive array of target molecules in enantiomerically pure form. In contrast to the asymmetric epoxidation, the enantioselective epoxidation of nonfunctionalized alkenes[2] is only just emerging as a viable synthetic method. At present, the substrates are limited to certain *cis* alkenes. A less common strategy, but one with considerable merit, is the enantioselective opening[3] of *meso* epoxides by achiral nucleophiles in the presence of chiral Lewis acids (Scheme 1 for $R^1 = R^2$). The metal center of the Lewis acid

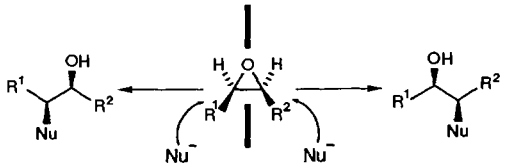

Scheme 1. Enantioselective opening of *meso* epoxides ($R^1 = R^2$).

catalyst or reagent should be able to complex the epoxide oxygen atom, and the ligand environment should allow the discrimination of the formally enantiotopic carbon–oxygen bonds of the epoxide by an appropriate achiral nucleophile. Such a process leads to an enantioselective epoxide-opening reaction. The discrimination of enantiotopic groups[3] remains relatively rare in nonenzymic asymmetric reactions. Scheme 2 shows some examples[4] of the discrimination attainable *without* a nucleophile—using chiral lithium amide bases in the rearrangements of *meso* epoxides to allylic alcohols.

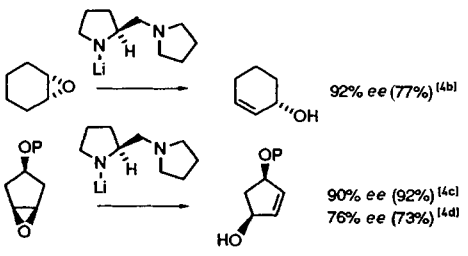

Scheme 2. P = Si*t*BuMe$_2$.

[*] Dr. I. Paterson, Dr. D. J. Berrisford
University Chemical Laboratory
Lensfield Road, GB-Cambridge CB2 1EW (UK)

Enantioselective opening of *meso* epoxides by heteroatom nucleophiles has been investigated previously. Some examples are shown in Scheme 3. Zinc tartrate (10 mol%) promotes the opening of simple epoxides with *n*-butyl thiol and aniline with good enantioselectivity.[5] Copper tartrate is more efficient than zinc tartrate in promoting the reaction of trimethylsilyl azide with epoxides.[5] Diisopinocampheylboron halides also display[6] promising asymmetric induction in their reactions with epoxides to give β-halohydrins. The reagents, derived from either (+) or (−)-α-pinene, are used in stoichiometric quantities at very low temperatures. In certain cases, recrystallization leads to enantiomerially pure product. The combination of various ligands with titanium alkoxides has been explored[7, 8] with trimethylsilyl azide for epoxide opening. A recent refinement[8] is the combination of $TiCl_2(OiPr)_2$ with the sterically demanding di-*tert*-butyl tartrate. In the presence of trimethylsilyl azide and 10 mol% of the titanium catalyst, cyclohexene oxide gives the corresponding β-azido cyclohexanol with 62% *ee*.

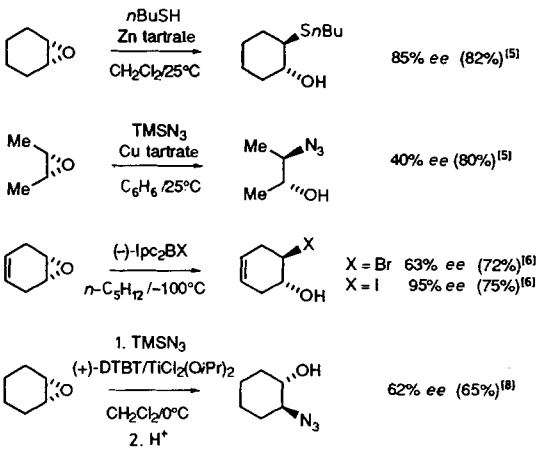

Scheme 3. TMS = trimethylsilyl; Ipc = isopinocamphenyl; DTBT = di-*tert*-butyltartrate.

The methodology described[9] recently by W. A. Nugent at DuPont is a major advance in this area (Scheme 4). A novel chiral zirconium Lewis acid promotes the reaction of trialkylsilyl azide with a range of *meso* epoxides to give the corresponding β-azido alcohols in excellent enantiomeric excess. The catalyst is derived from zirconium *tert*-butoxide and the tetradentate C_3-symmetric ligand **1**. This ligand is readily available from commercial (albeit expensive) starting materials—(*S*)-propene oxide and (*S*)-1-aminopropan-2-ol—with a high diastereomeric excess. Other epoxide/aminoalcohol combinations may also be useful for the preparation of other ligands with C_3 symmetry. In this way the reaction can be optimized for each substrate. Furthermore, **1** is one of the few C_3-symmetric ligands[10, 11] that

 © VCH Verlagsgesellschaft mbH, W-6940 Weinheim, 1992 0570-0833/92/0909-1179 $ 3.50+.25/0

have been designed, synthesized, and successfully employed in asymmetric catalysis. Other reactions[9] may be amenable to catalysis by metal complexes with these or related chiral ligands. The reaction of **1** with $Zr(OtBu)_4$ at room temperature affords complex **2** with the loss of three equivalents of *tert*-butanol. Controlled addition of water to **2** in THF affords complex **3** which may be isolated. The analyses show that this complex contains 0.5 equivalents of *tert*-butanol per equivalent of zirconium. The spectroscopic properties of **3** are complex, and the precise mechanistic details of the catalysis will therefore be difficult to determine. The relative rates of the reactions mediated by the precursor zirconium alkoxide and the new chiral complexes such as **3** have not been reported. It will be interesting to note the rate differences between the titanium and zirconium complexes with identical ligands and to investigate the effect of the ligand structure on the rate as well as the enantioselectivity.

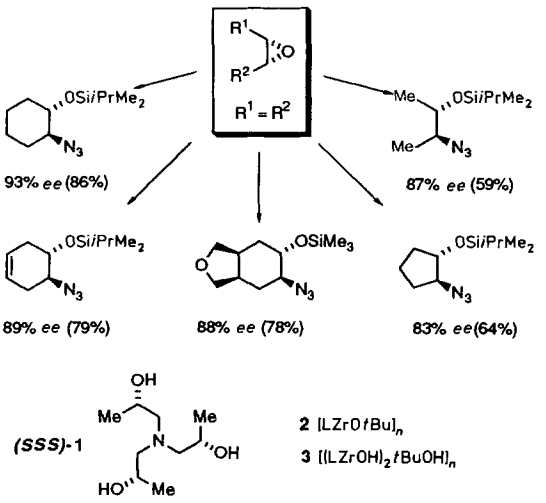

Scheme 4. Synthetic applications of zirconium complex **3**. All reactions were performed in CH_2Cl_2 at 0 °C or room temperature (48 h) with 1.04 equivalents of trialkylsilyl azide/2 mol% $CF_3CO_2SiMe_3$/8 mol% **3**.

The reaction is carried out by combining **3** (8 mol%), trimethylsilyl trifluoroacetate (2 mol%), and a trialkylsilyl azide with the epoxide substrate. The *ee* values of the β-azido alcohols produced are dependent on the bulk of the nucleophilic azide with isopropyldimethylsilyl azide being superior to trimethylsilyl azide. The trimethylsilyl trifluoroacetate is essential for the enantioselectivity. The reaction is simple to carry out, proceeds at either room temperature or 0 °C, and affords excellent yields. Thus the method offers an expeditious route to *threo* amino alcohols. One limitation is the lack of reactivity with highly hindered epoxides such as cyclooctene oxide. New developments are anticipated with the use of other nucleophiles, for example, trimethylsilyl cyanide.

The work of W. A. Nugent addresses one of the major classes of epoxides—symmetrically substituted *cis* epoxides. However, kinetic resolution[12] of racemic *trans* epoxides may also be possible. One of the challenges stemming from the discovery of the asymmetric catalytic epoxidation of nonfunctionalized alkenes is the problem of regiocontrol in the opening of unsymmetrically substituted epoxides. Here too, the opening of epoxides mediated by chiral Lewis acids may be useful in discriminating between the "pseudoenantiotopic" (actually diastereotopic) carbon–oxygen bonds (Scheme 1 for $R^1 \neq R^2$) when there is little, if any, substrate control during epoxide opening.

The Nugent reaction, just as the Sharpless asymmetric epoxidation,[1] utilizes an early transition metal alkoxide as the catalyst precursor. This is further proof, if any is required, of the rewards of searching for new reactivity in this area of the periodic table.

German version: *Angew. Chem.* **1992**, *104*, 1204

[1] T. Katsuki, K. B. Sharpless, *J. Am. Chem. Soc.* **1980**, *102*, 5974; R. M. Hanson, K. B. Sharpless, *J. Org. Chem.* **1986**, *51*, 1922; S. S. Woodard, M. G. Finn, K. B. Sharpless, *J. Am. Chem. Soc.* **1991**, *113*, 106; M. G. Finn, K. B. Sharpless, *ibid.* **1991**, *113*, 113.

[2] W. Zhang, J. L. Loebach, S. R. Wilson, E. N. Jacobsen, *J. Am. Chem. Soc.* **1990**, *112*, 2801; R. Irie, K. Noda, Y. Ito, N. Matsumoto, T. Katsuki, *Tetrahedron Lett.* **1990**, *31*, 7345; W. Zhang, E. N. Jacobsen, *J. Org. Chem.* **1991**, *56*, 2296. See also: C. Bolm, *Angew. Chem.* **1991**, *103*, 414; *Angew. Chem. Int. Ed. Engl.* **1991**, *30*, 403.

[3] Other examples of nonenzymatic selective enantiotopic group transformations: *meso* anhydride → lactone: K. Osakada, M. Obana, T. Ikaria, M. Saburi, S. Yoshikawa, *Tetrahedron Lett.* **1981**, *22*, 4297; acetal → enol: Y. Naruse, H. Yamamoto, *ibid.* **1986**, *27*, 1363; Y. Naruse, T. Esaki, H. Yamamoto, *ibid.* **1988**, *29*, 1417; asymmetric hydrogenation of epoxides: A. S. C. Chan, J. P. Coleman, *J. Chem. Soc. Chem. Commun.* **1991**, 535.

[4] a) J. K. Whitesell, S. W. Felman, *J. Org. Chem.* **1980**, *45*, 755; b) M. Asami, *Chem. Lett.*, **1984**, 829; c) M. Asami, *Tetrahedron Lett.* **1985**, *26*, 5803; d) S. K. Hendrie, J. Leonard, *Tetrahedron* **1987**, *43*, 3289; e) M. Asami, H. Kirihara, *Chem. Lett.* **1987**, 389.

[5] H. Yamashita, T. Mukaiyama, *Chem. Lett.* **1985**, 1643; H. Yamashita, *ibid.* **1987**, 525; *Bull. Soc. Chem. Jpn.* **1988**, *61*, 1213.

[6] N. N. Joshi, M. Srebnik, H. C. Brown, *J. Am. Chem. Soc.* **1988**, *110*, 6246.

[7] M. Enziane, K. I. Sutowardoyo, D. Sinou, *J. Organomet. Chem.* **1988**, *346*, C7; C. Blandy, R. Choukroun, D. Gervais, *Tetrahedron Lett.* **1983**, *24*, 4189.

[8] M. Hayashi, K. Kohmura, N. Oguni, *Synlett* **1991**, 774.

[9] W. A. Nugent, *J. Am. Chem. Soc.* **1992**, *114*, 2768.

[10] C. Bolm, K. B. Sharpless, *Tetrahedron Lett.* **1988**, *29*, 5101; C. Bolm, W. M. Davis, R. L. Halterman, K. B. Sharpless, *Angew. Chem.* **1988**, *100*, 882; *Angew. Chem. Int. Ed. Engl.* **1988**, *27*, 835.

[11] M. J. Burk, R. L. Harlow, *Angew. Chem.* **1990**, *102*, 1511; *Angew. Chem. Int. Ed. Engl.* **1990**, *29*, 1462.

[12] M. Asami, N. Kanemaki, *Tetrahedron Lett.* **1989**, *30*, 2125.

 © VCH Verlagsgesellschaft mbH, W-6940 Weinheim, 1992 0570-0833/92/0909-1180 $ 3.50+.25/0

"Non-Coordinating" Anions: Underestimated Ligands

By *Manfred Bochmann**

The mention of "non-coordinating anions" usually brings to mind complex anions such as BF_4^-, PF_6^- or ClO_4^-, and it is certainly true that in the presence of only relatively weak donor ligands these anions show no noticeable interactions with metal centers. On the other hand, Fischer et al. and Beck et al. pointed out several years ago[1, 2] that coordinatively unsaturated complexes, for example $[CpMo(CO)_3]^+$, coordinate anions such as BF_4^- through fluoride bridges, and it is therefore not surprising that with strongly electrophilic cationic complexes such as $[Cp_2M(CH_3)]^+$ (M = Ti, Zr) fluoride abstraction is a facile process.[3] Even the recently reported very weakly basic anion $[B(OTeF_5)_4]^-$ is still capable of coordinating to metals through O and F bridges and of transferring F_5TeO groups as has been demonstrated, for example, in the synthesis of $Ag[B(OTeF_5)_4]$.[4]

In cases where BF_4^- or PF_6^- prove too reactive, BPh_4^- is often used to advantage because of its well-known stability and low basicity. It is sometimes overlooked, however, that BPh_4^- as a π ligand has been known for a long time, and that it is able to form η^6-arene complexes such as **1** with electron-rich metal centers (Scheme 1). The first complex of this kind

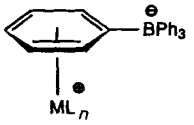

1

Scheme 1. ML_n = CrCp* [5], $Mo(C_7H_7)$ [6], $Mo(CO)_3^-$ [6], CoL_2 (L = pyridine, PMe_3) [7], $Rh[P(OMe)_3]_2$ [8], MCp (M = Fe, Ru) [9a].

$[\{(MeO)_3P\}_2Rh(\eta^6\text{-}C_6H_5BPh_3)]$, was crystallographically characterized as long ago as 1969,[8] and analogous compounds have been described for a number of different transition metals. The complexes are fairly unreactive, and the coordinated phenyl ring is relatively inert towards substitution by other ligands. It appears that in these compounds the coordination of BPh_4^- is stabilized not only by π back-donation but also by electrostatic cation–anion interactions. BPh_4^- is also capable of coordination to two and three metal centers, as was recently shown[9b] for $[\{(C_2H_4)_2Rh\}_2(\eta^6\text{-}Ph_2BPh_2)]^+CF_3SO_3^-$ and $[\{(C_2H_4)_2Rh\}_3(\eta^6\text{-}Ph_3BPh)]^{2+}\text{-}(CF_3SO_3^-)_2$.

Cation–anion interactions have attracted special attention recently, particularly in the case of electron-deficient early transition metal compounds with d^0 electron configurations, since it is now accepted that cationic alkyl complexes of group IV metals represent the catalytically active species in olefin polymerizations with homogeneous Ziegler–Natta catalysts. The coordination of a phenyl ring of BPh_4^- to a d^0 metal center, i.e. without stabilization by back-bonding, was first demonstrated for the zirconium complex **2** using variable-temperature NMR spectroscopy.[10]

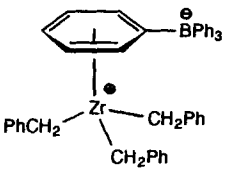

2

In contrast to complexes of type **1** the coordination of the phenyl ring is temperature dependent, and the molecule is fluxional. In spite of this, the BPh_4^- ligand cannot be displaced by electron-rich neutral arenes, an indication for the importance of electrostatic interactions with complexes of this kind.

Horton et al. were able to show that in cationic zirconocene derivatives **3** one of the phenyl groups of BPh_4^- may be coordinated in η^2- or η^3-fashion.[11] Here, too, the anion is fluxional on the NMR time scale, and it is not clear whether the anion interacts with the metal through the π electron system or through some of the hydrogen atoms of the phenyl ring.

For catalytic applications such interactions are highly undesirable. Phenyl coordination as in **2** or **3** may be regarded as the first step towards catalyst deactivation by phenyl group transfer, but metalation of the phenyl ring can also subsequently occur, as in **4**.[12] More stable catalysts with

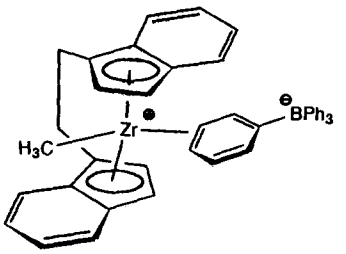

3

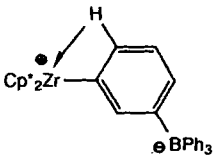

4

significantly higher catalytic activities are obtained if the tendency of the anion towards coordination is reduced, for example by introducing fluoro substituents on the ring. Thus, in the zwitterionic complex **5** recently prepared by Marks et al. metal–aryl interactions are absent, and the anion is bonded through a methyl bridge.[13] On the other Hand, Horton et al. has shown in the case of complex **6** that even the basicity of a C–F bond may be sufficient in certain circumstances to give isolable adducts.[14] As far as is known, only the extremely weakly basic perfluorinated anion $B(C_6F_5)_4^-$ is inert enough for cation–anion interactions

[*] Dr. M. Bochmann
School of Chemical Sciences
University of East Anglia
Norwich NR4 7TJ (UK)

 © VCH Verlagsgesellschaft mbH, W-6940 Weinheim, 1992 0570-0833/92/0909-1181 $ 3.50+.25/0

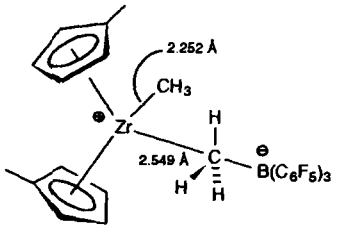

5

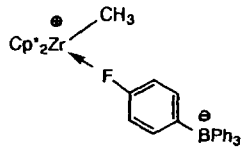

6

to be essentially absent. For example, the crystal structure of 7 shows thorium–fluorine distances which are significantly longer than the sum of the ionic radii.[15] In agreement with this assumption such cationic alkyl complexes with $B(C_6F_5)_4^-$ as the counter ion are highly active polymerization catalysts.

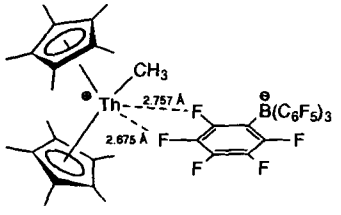

7

Pampaloni et al. have now been able to extend the spectrum of coordination modes of tetraarylborates further by synthesizing $[\{Ph_2B(\eta^6\text{-}C_6H_5)_2\}Nb(C_2Me_2)]$ **8**, the first example of a complex which contains BPh_4^- as a chelating ligand, with two of the phenyl groups η^6-bonded to the metal (Scheme 2).[16] The compound is prepared by thermolysis of $[Nb(C_6H_3Me_3)_2(C_2Me_2)]BPh_4$ in toluene. Judging from the

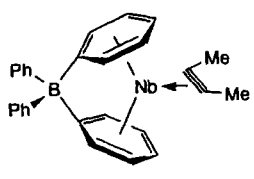

8

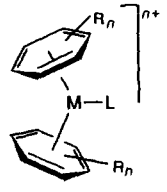

9

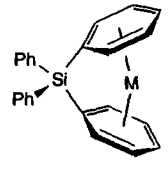

10

Scheme 2. **9**: $n = 0$, M = Zr, Hf, L = PMe_3 [17]; $n = 1$, M = Nb, L = Co [18], M = Nb, L = PEt_3 [19], M = W, L = H [17].

length of the C≡C bond the coordinated butyne acts as an η^2-ligand, and the metal has to be regarded as Nb(I) (d^4). As is the case with complexes of type **1** the phenyl ring coordination in **8** is stabilized by back-bonding; the complex is nonfluxional, and the BPh_4^--ligand cannot be replaced by neutral arenes. Structurally, **8** is related to a series of well-known non-bridged bis(arene) complexes **9**. *Ansa*-arene complexes such as **8** or the silyl-bridged complexes **10** (M = V, Cr) synthesized by Elschenbroich et al.[20] are comparatively rare. The surprising synthesis of **8** demonstrates a coordination mode for tetraarylborates which has apparently not been considered until now and should serve as a precedent for the synthesis of further complexes of this type.

German version: *Angew. Chem.* **1992**, *104*, 1206

[1] K. Richter, E. O. Fischer, C. G. Kreiter, *J. Organomet. Chem.* **1976**, *122*, 187.
[2] W. Beck, K. Schloter, *Z. Naturforsch. B* **1978**, *33*, 1214.
[3] R. F. Jordan, W. E. Dasher, S. F. Echols, *J. Am. Chem. Soc.* **1986**, *108*, 1718; M. Bochmann, L. M. Wilson, *J. Chem. Soc. Chem. Commun.* **1986**, 1610.
[4] P. K. Hurlburt, O. P. Anderson, S. H. Strauss, *J. Am. Chem. Soc.* **1991**, *113*, 6277; D. M. van Seggen, P. K. Hurlburt, M. D. Noirot, O. P. Anderson, S. H. Strauss, *Inorg. Chem.* **1992**, *31*, 1423.
[5] B. J. Thomas, S. K. Noh, G. K. Schulte, S. C. Sendlinger, K. H. Theopold, *J. Am. Chem. Soc.* **1991**, *113*, 893.
[6] M. B. Hossain, D. van der Helm, *Inorg. Chem.* **1978**, *17*, 2893.
[7] L. C. A. de Carvalho, M. Dartiguenave, Y. Dartiguenave, *J. Am. Chem. Soc.* **1984**, *106*, 6848; G. Fachinetti, T. Funaioli, P. F. Zanazzi, *J. Chem. Soc. Chem. Commun.* **1988**, 1100.
[8] M. J. Nolte, G. Gafner, L. M. Haines, *J. Chem. Soc. Chem. Commun.* **1969**, 1406.
[9] a) G. F. Kruger, A. L. du Preez, R. J. Haines, *J. Chem. Soc. Dalton Trans.* **1974**, 1302; R. D. Rogers, D. C. Hrncir, *Acta Crystallogr. Sect. C* **1984**, *40*, 1160; b) M. Aresta, E. Quaranti, A. Albinerti, unpublished.
[10] M. Bochmann, G. Karger, A. J. Jaggar, *J. Chem. Soc. Chem. Commun.* **1990**, 1038.
[11] A. D. Horton, J. H. G. Frijns, *Angew. Chem.* **1991**, *103*, 1181; *Angew. Chem. Int. Ed. Engl.* **1991**, *30*, 1152.
[12] G. G. Hlatky, H. W. Turner, R. R. Eckman, *J. Am. Chem. Soc.* **1989**, *111*, 2728.
[13] X. Yang, C. L. Stern, T. J. Marks, *J. Am. Chem. Soc.* **1991**, *113*, 3623.
[14] A. D. Horton, A. G. Orpen, *Organometallics* **1991**, *10*, 3910.
[15] X. Yang, C. L. Stern, T. J. Marks, *Organometallics* **1991**, *10*, 840.
[16] F. Calderazzo, U. Englert, G. Pampaloni, L. Rocchi, *Angew. Chem.* **1992**, *104*, 1230; *Angew. Chem. Int. Ed. Engl.* **1992**, *31*, 1235. C. J. Schaverien has also observed the coordination of two phenyl rings of a BPh_4^- ligand to a La atom in $[Cp^*\{CH(SiMe_3)_2\}LaBPh_4]$: *Organometallics*, **1992**, *11*, in press.
[17] F. G. N. Cloke, M. L. H. Green, *J. Chem. Soc. Dalton Trans.* **1981**, 1938.
[18] F. Calderazzo, G. Pampaloni, L. Rocchi, J. Strähle, K. Wust, *J. Organomet. Chem.* **1991**, *413*, 91.
[19] J. A. Bandy, K. Prout, F. G. N. Cloke, H. C. de Lemos, J. M. Wallis, *J. Chem. Soc. Dalton Trans.* **1988**, 1475.
[20] C. Elschenbroich, J. Hurley, B. Metz, W. Massa, G. Baum, *Organometallics* **1990**, *9*, 889.

Enantioselective Rhodium(II) Catalysts

By *Henri Brunner**

In the complexes $[M_2(OAc)_4]$ (OAc = CH_3COO) two metal(II) cations are bridged by four acetate anions (Fig. 1). In this highly symmetrical framework four oxygen atoms occupy the corners of two ecliptically arranged squares.[1] The valencies of the two octahedrally coordinated metal atoms perpendicular to these squares are oriented to the inside and to the outside of the $M_2(OAc)_4$ unit. The metal–metal interaction within the $M_2(OAc)_4$ unit depends critically on the electron configuration of the metal atoms.[1] It ranges from a quadruple bond in $[Cr_2(OAc)_4]$ (Cr^{2+} is a d^4 system) to a weak interaction in $[Cu_2(OAc)_4]$ (Cu^{2+} is a d^9 system). Further ligands can be bound, but also catalyses can be carried out at the valencies of the $M_2(OAc)_4$ unit which point outwards.

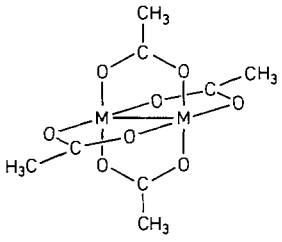

Fig. 1. The structural unit $M_2(OAc)_4$.

$[Rh_2(OAc)_4]$ is a green, air-stable compound, which is soluble in organic solvents with the retention of its dinuclear structure. It is prepared from $RhCl_3$ and HOAc/NaOAc in boiling ethanol.[2] Other carboxylate ions can also be incorporated in place of acetate ions. Anions of fluorinated carboxylic acids afford particularly stable compounds such as $[Rh_2(OOCCF_3)_4]$. $[Rh_2(OAc)_4]$ and its derivatives have for a long time proven valuable as catalysts for carben(oid) reactions, for example, the formation of cyclopropanes from olefins and diazo compounds or the formation of five-membered rings in intramolecular C–H insertions.[3–6] They are also considered to show anti-tumor activity.[1] Recently these dimeric rhodium(II) compounds have created a furore in enantioselective catalysis.

The dimeric rhodium(II) compounds become enantioselective catalysts if they contain optically active ligands. For this the anions of optically active carboxylic acids seemed to be the most appropriate. The complex in which the Rh_2 unit is clamped by four mandelate anions was synthesized and structurally characterized some time ago.[7] As a catalyst, however, this complex results in only small enantiomeric excesses.[8] The reason for this is probably that the asymmetrical centers lie in a plane between the two Rh atoms and are thus too far away from the coordination sites directed to the outside, at which the catalysis occurs. Chiral substituents at the nitrogen atoms of carboxamide anions would be considerably closer to these reaction centers, and indeed on this basis a breakthrough has been achieved recently, which in particular, is linked to the $[Rh_2(5S\text{-mepy})_4]$ complex (Fig. 2). The name of the optically active ligand has, as usual, been abbreviated, and in this case mepy[*] stands for the methyl ester of the pyrrolidone-5-carboxylic acid, which is deprotonated at the nitrogen atom. In the following the complex $[Rh_2(5S\text{-mepy})_4]$ and its "capacity" for enantioselective catalysis are introduced before finally discussing why complexes of the type $[Rh_2(5S\text{-mepy})_4]$ are so successful.

The introduction of carboxamides instead of carboxylates as bridging ligands is achieved by an exchange reaction between $[Rh_2(OAc)_4]$ and the appropriate amides. In this way $[Rh_2(5S\text{-mepy})_4]$ is prepared from methyl (−)-(*S*)-pyrrolidone-5-carboxylate. Similarly, $[Rh_2(5R\text{-mepy})_4]$ is accessible from methyl (+)-(*R*)-pyrrolidone-5-carboxylate so that the catalysts are available in both configurations (5*S* and 5*R*). In $[Rh_2(5S\text{-mepy})_4]$ each rhodium atom is in a square-planar environment in which two O atoms and two N atoms are arranged *cis* to each other (Fig. 2).

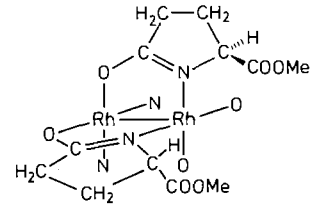

Fig. 2. $[Rh_2(5S\text{-mepy})_4]$. The two amide ligands which are directed downwards and to the rear are incompletely drawn to provide a better overview.

$[Rh_2(5S\text{-mepy})_4]$ was first used for cyclopropanation. Enantioselective cyclopropanation is industrially important since synthetic pyrethroids, which are used as insecticides, contain substituted three-membered rings, whose configuration is crucial for their biological effect.[9] Enantioselective cyclopropanation has tradition. It was this reaction type which in 1966 opened up the field of enantioselective homogeneous catalysis with transition metal complexes. The copper(II) complex of the Schiff base from salicylaldehyde and optically active 1-phenylethylamine at that time reached 6% *ee*.[10] With optimized optically active amines in the salicylaldimine ligands the industrial group headed by Aratani set early records in the 1970s.[11] New aspects were forthcoming with the introduction of the cobalt(II) semicorrin complexes by Pfaltz et al. 1986,[12, 14] and more recently with the bisoxazoline ligands from Masamune et al.[13a, 14] and Evans et al.[13b, 14]

The reaction of styrene with (1*S*,3*S*,4*R*)-menthyl diazoacetate [Eq.(a)] leads to the incorporation of two new stereocenters into the cyclopropane ring. The *cis* and *trans* isomers are formed each consisting of an enantiomeric pair. With the

[*] Prof. Dr. H. Brunner
Institut für Anorganische Chemie der Universität
Universitätsstrasse 31, D-W-8400 Regensburg (FRG)

[*] The acronym mepy has usually been written in capital letters. However, according to the IUPAC rules for nomenclature abbreviations for ligands should be written with small letters.

 © VCH Verlagsgesellschaft mbH, W-6940 Weinheim, 1992 0570-0833/92/0909-1183 $ 3.50+.25/0

$[Rh_2(5S\text{-mepy})_4]$ catalyst 86 % *ee* is achieved in the *cis* series and 48 % *ee* in the *trans* series.[15]

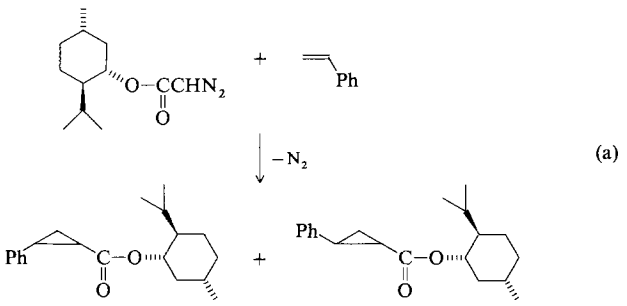

(a)

In the catalysis shown in Equation (a) a double stereoselection is involved. The formation of the new asymmetrical centers in the cyclopropane ring is influenced by the menthyl group contained in the substrate (1*S*,3*S*,4*R*)-menthyl diazoacetate and by the mepy ligand contained in the catalyst. The two influences are referred to as substrate and catalyst control, respectively. With regard to the efficiency it has to be noted that whereas substrate control requires a stoichiometric amount of the reagent, catalyst control requires a substoichiometric amount of the catalyst. For example, in the case of $[Rh_2(5S\text{-mepy})_4]$ a catalyst concentration of 1 mol% is sufficient with respect to the substrates.

The reaction in Equation (a) is controlled mainly by the catalyst; substrate control by the menthyl group plays only a minor role. This is evident from the fact that with the achiral $[Rh_2(OAc)_4]$ catalyst only 9 % *ee* can be achieved for the *cis* product and 13 % *ee* for the *trans* product. Catalysis with $[Rh_2(5S\text{-mepy})_4]$ was extended from styrene to other prochiral olefins for which similar results were obtained.[15]

$[Rh_2(5S\text{-mepy})_4]$ is particularly useful for intramolecular cyclopropanation; in several examples up to 94% *ee* was obtained.[16] Highly substituted cyclopropanes are accessible by this reaction; an example is given Equation (b). With the two enantiomeric catalysts both enantiomeric products can be obtained from the same allyl diazoacetate. For this intramolecular variant the (*Z*) configuration of the olefin proves superior to the (*E*) configuration.

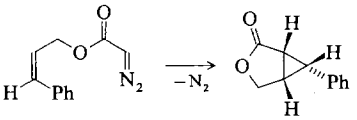

(b)

As mentioned previously, enantioselective cyclopropanation has been known for a long time and there are other efficient catalysts for this reaction apart from dimeric rhodium(II) complexes. This is different to the cyclopropenation of alkynes with diazo compounds. Copper catalysts do not only result in lower enantiomeric excesses but also poor yields, since the high temperatures required for the reaction favor side and consecutive reactions such as the ring opening of the primary products. The improvements brought about by the use of $[Rh_2(5S\text{-mepy})_4]$ (with regard to yield and enantioselectivity) are shown for the cyclopropenation of propargyl methyl ether with a series of diazo esters in Equation (c). For the ethyl ester (R = Et) the enantiomeric excess is 69%, for the *tert*-butyl ester (R = *t*Bu) 78%, and for the (+)-menthyl ester (R = 1*S*,3*S*,4*R*-menthyl) 98%. The yields of the reactions range between 43 and 73%.[17]

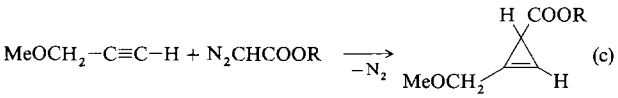

(c)

Metal-catalyzed enantioselective C–H insertions of carbenes have so far not been studied in great detail. Copper catalysts are of no use for this type of reaction, rhodium(II) catalysts, however, allow intramolecular C–H insertions, for example, in the alkyl group of diazoacetates with longer chains. The formation of five-membered rings such as γ-lactones is favored. $[Rh_2(5S\text{-mepy})_4]$ affords 3-methyl-γ-butyrolactone (see [Eq. (d)]) in 91 % *ee* and is thus unprecedented for such reactions.[18]

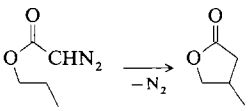

(d)

In order to explain the success of $[Rh_2(5S\text{-mepy})_4]$ a general and a specific argument shall be put forward. Generally for enantioselective catalysts, a reduction of the conformative variety has a favorable effect on the enantioselectivity. In $[Rh_2(5S\text{-mepy})_4]$ at each of the two planes of the Rh_2 unit which point outwards, a chiral framework is built whose rigidity is mainly the result of the incorporation of the amide part into the five-membered ring. In the case of $[Rh_2(5S\text{-mepy})_4]$ special electronic and steric effects are also involved. Model considerations as well as reactivity and selectivity studies show that during the cleavage of nitrogen from the diazo compound a carbene-rhodium complex is formed, whose empty p orbital at the carbene carbon atom can be stabilized by interaction with a polar substituent.[6] Therefore, as shown in Figure 3, the two *cis* ester groups in

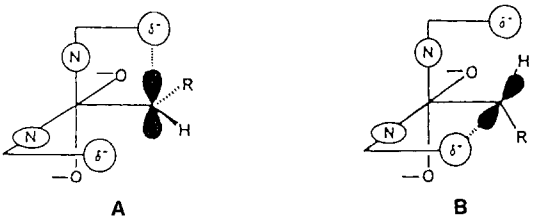

Fig. 3 Carbene ligand at $[Rh_2(5S\text{-mepy})_4]$ stabilized by the polar COOMe substituents.

$[Rh_2(5S\text{-mepy})_4]$ fix the carbene ligand in the positions **A** and **B**, in which the large substituent R of the carbene adopts the less hindered position. The attack of the nucleophile at the conformations **A** and **B** occurs from the rear. The observed stereochemistry of the products can be understood

when the preferred orientation of the reaction partners with their C=C, C≡C, and C–H bonds in the inter- or intramolecular reactions are taken into consideration.

German version: *Angew. Chem.* **1992**, *104*, 1208

[1] F. A. Cotton, R. A. Walton, *Multiple Bonds Between Metal Atoms*, Wiley, New York, **1982**.
[2] G. A. Rempel, P. Legzdins, H. Smith, G. Wilkinson, *Inorg. Synth.* **1972**, *13*, 90.
[3] M. P. Doyle, *Chem. Rev.* **1986**, *86*, 919.
[4] M. P. Doyle, *Acc. Chem. Res.* **1986**, *19*, 348.
[5] G. Maas, *Top. Curr. Chem.* **1987**, *137*, 75.
[6] M. P. Doyle, *Recl. Trav. Chim. Pays-Bas* **1991**, *110*, 305.
[7] P. A. Agaskar, F. A. Cotton, L. R. Falvello, S. Hahn, *J. Am. Chem. Soc.* **1986**, *108*, 1214.
[8] H. Brunner, H. Kluschanzoff, K. Wutz, *Bull. Soc. Chim. Belg.* **1989**, *98*, 63.
[9] D. Arlt, M. Jautelat, R. Lantzsch, *Angew. Chem.* **1981**, *93*, 719; *Angew. Chem. Int. Ed. Engl.* **1981**, *20*, 703.
[10] H. Nozaki, S. Moriuti, H. Takaya, R. Noyori, *Tetrahedron Lett.* **1966**, 5239.
[11] T. Aratani, *Pure Appl. Chem.* **1985**, *57*, 1839.
[12] H. Fritschi, U. Leutenegger, A. Pfaltz, *Angew. Chem.* **1986**, *98*, 1028; *Angew. Chem. Int. Ed. Engl.* **1986**, *25*, 1005.
[13] a) R. E. Lowenthal, A. Abiko, S. Masamune, *Tetrahedron Lett.* **1990**, *31*, 6005; b) D. A. Evans, K. A. Woerpel, M. M. Hinman, *J. Am. Chem. Soc.* **1991**, *113*, 726.
[14] Short review: C. Bolm, *Angew. Chem.* **1991**, *103*, 556; *Angew. Chem. Int. Ed. Engl.* **1991**, *30*, 542.
[15] M. P. Doyle, B. D. Brandes, A. P. Kazala, R. J. Pieters, M. B. Jarstfer, L. M. Watkins, C. T. Eagle, *Tetrahedron Lett.* **1990**, *31*, 6613.
[16] M. P. Doyle, R. J. Pieters, S. F. Martin, R. E. Austin, C. J. Oalmann, P. Müller, *J. Am. Chem. Soc.* **1991**, *113*, 1423.
[17] M. N. Protopopova, M. P. Doyle, P. Müller, D. Ene, *J. Am. Chem. Soc.* **1992**, *114*, 2755.
[18] M. P. Doyle, A. v. Oeveren, L. J. Westrum, M. N. Protopopova, T. W. Clayton, Jr., *J. Am. Chem. Soc.* **1991**, *113*, 8982.

New Impetus for Inorganic Host-Guest Chemistry

By *Hans Reuter**

Exactly 25 years ago the probably coincidental dislodging of a small stone—the synthesis of the first crown ether and the discovery of its coordinating properties[1]—started an avalanche—supramolecular organic chemistry. The rapid development of this field, which reached an all-time high in 1987 with the award of the Nobel Prize in Chemistry to C. J. Pedersen, J.-M. Lehn, and J. Cram, rests on the fact that through it abiotic counterparts to biological processes, for example enzyme catalysis, can be studied. It is therefore not surprising that here a very close interaction between organic chemistry and biochemistry exists and that receptor–substrate interactions are fundamental in supramolecular chemistry.[2]

Under the term supramolecular compounds, as portrayed graphically in Scheme 1, is meant aggregates of two or more different building blocks, stable in solution as well as in the solid state, in which the parts themselves are already compounds with defined physical and chemical properties. Characteristic of this type of host–guest relationship is, first, that the bonding interactions (hydrogen bonds, van der Waals forces) between the partners are so weak that the supermolecule can also dissociate reversibly into its starting compounds again under specific conditions, and second, that the host has a structure that enables it to enclose the guest selectively and securely.

On this point inorganic chemistry need not be modest, since after all, it has dealt with host–guest compounds for more than 150 years. Already in 1826 J. Berzelius[3] described the transformation of ammonium molybdate (**1**) with phosphoric acid (**2**), formulated in Equation (a), in which he obtained a yellow precipitate. Today we know that it must have been the compound **3**, the ammonium salt of 12-molybdatophosphoric acid. The anion of **3** consists of a

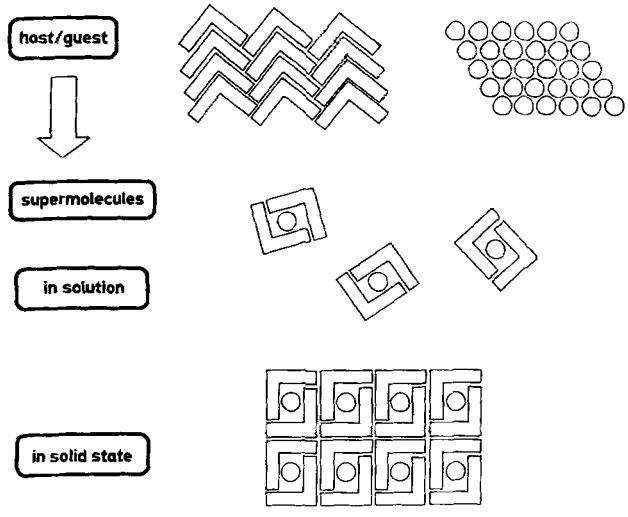

Scheme 1.

shell of twelve $\{MoO_6\}$ octahedrons linked together according to the principle of the α-Keggin structural type, leaving a hole in the middle that accommodates a single phosphorus atom.

$$\underset{\mathbf{1}}{12(NH_4)_2MoO_4} + \underset{\mathbf{2}}{H_3PO_4} \longrightarrow \underset{\mathbf{3}}{(NH_4)_3[(PO_4)Mo_{12}O_{36}]} + 21\,NH_3 + 12\,H_2O \quad \text{(a)}$$

A significant difference between such a compound and the typical supramolecular compounds of organic chemistry, however, lies in the special position of the oxygen atoms of the phosphate group of this heteropolyanion, which are simultaneously components of the host compound. Thus according to the narrow definition of organic chemistry, **3** is strictly speaking not a supramolecular compound. In this case one prefers to call it a molecular material.[4]

[*] Dr. Hans Reuter
Institut für Anorganische Chemie der Universität
Gerhard-Domagk-Strasse 1, D-W-5300 Bonn (FRG)

This rigid distinction is, however, only of secondary importance for the compound class of the heteropolyacids described here,[5] especially since depending on the pH of the solution, the compounds also dissociate again into the starting compounds. The dissociation shows very clearly the influence of the solvent on the formation of such compounds, since—in the sense of the above-mentioned definition—the solvent itself enters more or less strongly into a supramolecular interaction with the two starting materials and thereby influences their reactivity and availability decisively.

Furthermore, this example depicts very clearly another aspect of inorganic host–guest chemistry. The structure of the heteropolyanion can only be explained if the host is built up around the guest in the condensation reaction in solution, a phenomenon known as the *template effect*.

If in a limiting case the interactions between the units in a host–guest complex are extremely weak, the supercomplex may be stable in the crystalline state but dissociate to its individual components in solution, because these enter into significantly stronger interactions with the solvent. Such host–guest complexes existing only in the solid state are termed inclusion compounds or clathrates. A known example from inorganic chemistry is the chlorohydrate $Cl_2 \cdot 7.27\,H_2O$, described in many textbooks.[6]

Although the field of inclusion compounds today is mainly the domain of organic chemistry, there have recently been interesting developments in inorganic chemistry. By far the most remarkable discovery was certainly the compound $CsF \cdot Br_2$,[7] in which the Br_2 dumbbells are only marginally extended and embedded in a tetragonally distorted CsF arrangement of the NaCl structural type.

Another example of recent developments in inorganic clathrates is the compound $Cd(CN)_2 \cdot$ neopentane (**4**).[8] In contrast to the layered structure of $Ni(CN)_2NH_3 \cdot$ benzene,[9] the very first structurally elucidated inclusion compound, the host lattice of $[Cd(CN)_2]$ in **4** is based on a spatial network structure (Fig. 1) in which structural elements such as those in SiO_2 and H_2O modifications are present. Cadmium

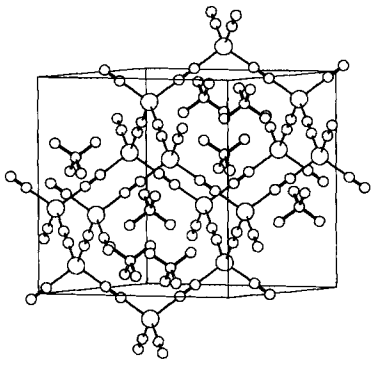

Fig. 1. Section of the crystal structure of $Cd(CN)_2 \cdot$ neopentane (from [8]).

is tetrahedrally surrounded by four cyanide groups, which in turn bridge two metal atoms, building cavities in which stoichiometric amounts of neopentane molecules are enclosed in an ordered fashion. In this compound the relationship between host and guest is thus inverted: the organic molecule no longer constitutes the host; instead the inorganic compound does.

The structural analogy of the two clathrate types introduced here to other AB and AB_2 compounds allows the imagination free rein and now, since this conceptual hurdle has been crossed, the discovery of many original examples of such inorganic host–guest compounds can be predicted.

In contrast to these clathrates, "true" supramolecular inorganic compounds remained unknown for a long time. However, many years ago evidence was found that the large isopolyvanadates can possibly enclose water molecules in the interior of the vanadium–oxygen cage. Nevertheless, it came as a great surprise when Day et al. first showed that these compounds also incorporate organic solvent molecules. In the compound $(Ph_4P)_4[(CH_3CN) \subset V_{12}O_{32}] \cdot 3\,CH_3CN \cdot 4\,H_2O$ (**5**) prepared and studied by X-ray diffraction, the water molecules and three of the four acetonitrile molecules are built into the spaces in the crystal lattice, while the other, as shown in Figure 2, is almost completely immersed (its methyl group projects) in the interior of the $[V_{12}O_{32}]^{4-}$ ion, which is shaped like a basket. Although the distances between the atoms of the guest and the host are very large, and the interactions between them therefore only relatively weak, this "open" aggregate is retained in solution, as proven by NMR spectroscopy.[11]

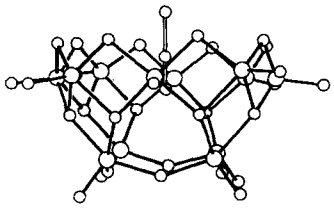

Fig. 2. Crystal structure of the $[V_{12}O_{32}]^{4-}$ ion, showing the incorporated acetonitrile molecule (from [11]).

The astonishment was even greater when a short time later A. Müller et al. proved for the first time with complexes of the type $(NMe_4)_6[(X) \subset V_{15}O_{36}]$ (**6**) that simple ($X = Cl^-$, Br^-) and complex anions ($X = CO_3^{2-}$) can also be incorporated into such polyvanadates.[12] But not only the inclusion of an *anion in an anion* is surprising; the *widely divergent sizes* of the included anions is exceptional. As can be seen from Figure 3, all vanadium atoms of the $[V_{15}O_{36}]^{5-}$ ion of **6** are pentacoordinate; the oxygen atoms are arranged in a square

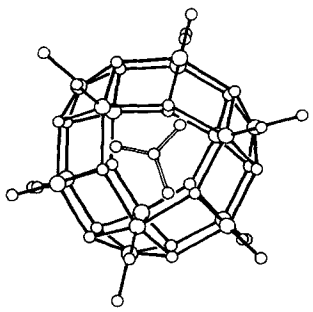

Fig. 3. Crystal structure of the $[V_{15}O_{36}]^{5-}$ ion, showing the included carbonate ion (from [12]).

pyramid around them with the apexes directed outwards. For the first time this basal linkage of the 15 individual polyhedrons leads to a closed structure with a cavity of such dimensions that different sized components can be accommodated.

That in all the previous cases the structure and charge of the guest determined the geometry of the cavity and thereby the constitution of the isopolyvanadate was demonstrated by the same research group only a little later with the complexes $(NEt_4)_6[(ClO_4) \subset V_{22}O_{53}(OH)]$ (**7**) and $(NEt_4)_5[(N_3) \subset V_{18}O_{42}(OH)_2]$ (**8**). In **7** a tetrahedral perchlorate ion guest is present in a $[V_{22}O_{53}(OH)]^{5-}$ host and in **8** a linear azide ion guest in a $[V_{18}O_{42}(OH)_2]^{4-}$ host, which indicates that the formation of the isopolyvanadate shells is controlled by the molecular recognition of the template. Also remarkable is that the two hosts are structurally directly related and that as in the previous cases mixed-valent V^{IV}–V^{V} complexes are involved.[13]

That is not yet the end. In this issue A. Müller et al. describe the compound $(Me_2NH_2)_5(NH_4)[(NH_4Cl)_2 \subset V_{14}O_{22}(OH)_4(H_2O)_2(PhPO_3)_8] \cdot 5H_2O \cdot 4DMF$ (**9**) in which for the first time two anions are simultaneously incorporated in a large cavity divided into two by two coordinatively bound water molecules. The shell of this cage, as depicted in Figure 4, is formed from two half shells in which isopolyvanadate building blocks are linked internally and to one another by phenylphosphonate groups. Furthermore, the

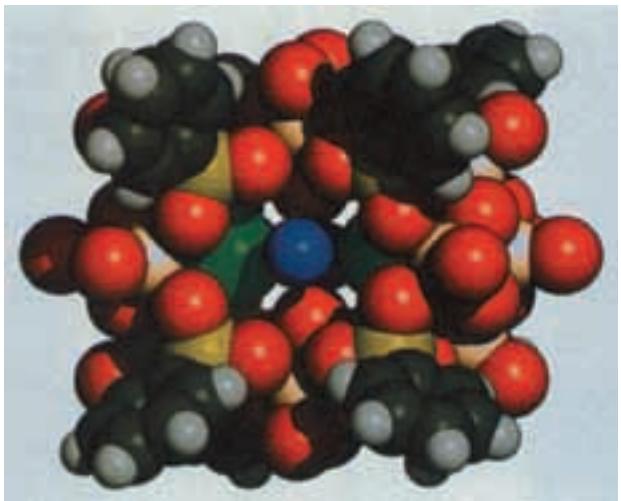

Fig. 4. Crystal structure of the $[V_{14}O_{22}(OH)_4(H_2O)_2(PhPO_3)_8]^{6-}$ ion, showing the incorporated chloride and ammonium ions (from [14]). Color code: V light brown; O red; P yellow; C black; H white; Cl green; NH_4 blue.

cage is formed and polarized by the combination of apolar organic residues (phenyl groups) and polar inorganic ligands (terminal oxygen atoms) in such a way that two niches are created, in which two ammonium ions can be incorporated as in a coronand. The anions (Cl^-) and cations (NH_4^+) are not only approximately as far apart as in the ionic crystal, but also in a square planar environment as there.[14]

It seems to be only a question of time and the dexterity of the preparative chemists until not only single ions, ion pairs, or as in the case of **9**, two-dimensional fragments of ionic crystals will be built into supramolecular inorganic compounds, but also three-dimensional fragments. The inclusion and thus the directed synthesis of nanocrystals would be a good deal closer.

Naturally the hetero- and isopolyacids are in the forefront of the research activities in the search for such supramolecular inorganic compounds, because decades of practical experience is available. But one must not forget that supramolecular effects can also occur in other sectors of inorganic chemistry. Recently we found the first example for the inclusion of ions in organometallic compounds by use of the template effect.[15] In the compound $[(Na) \subset (i\mathrm{PrSn})_{12}O_4(OH)_{24}][Ag_7I_{11}]Cl \cdot 10\,DMSO \cdot H_2O$ (**10**), each atom of the tin–organic cation is surrounded by a distorted octahedron of five oxygen atoms and one isopropyl group. The individual octahedrons are linked to each other as in the γ-Keggin structural type. This produces a cavity in the center that is the right size to take up a sodium ion, which is then coordinated tetrahedrally to four μ_3-O atoms.

The construction and type of octahedron linkage in the cation of **10** might still strongly resemble a heteropolycation surrounded by organic residues, but the supramolecular unit of the compound $(NH_4)_3[(Na) \subset Au_{12}Se_8]$ (**11**), described only recently by S.-P. Huang and M. G. Kanatzidis, bears no trace of similarity to such a structure.[16] In the crystal lattice, besides the ammonium ions, the centrosymmetric $[Au_{12}Se_8]^{4-}$ ions exist in the form of an almost regular cube. The selenium atoms occupy the eight corners, and the gold atoms the centers of the twelve edges. Exactly in the middle of this gold selenide, a sodium atom is situated, forming twelve short distances to gold atoms and eight long distances to selenium atoms (Fig. 5).

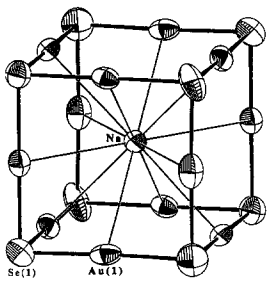

Fig. 5. Crystal structure of the cubic $[Au_{12}Se_8]^{4-}$ ion, showing the included sodium ion (from [16]).

Similarly unusual host–guest relationships are also found in the compound $Ph_4P[\{(\eta^5\text{-}C_5Me_5TiF_3)_4F_2\}Na]$ (**12**), which was recently described by Roesky et al.[17] In **12** two $[(\eta^5\text{-}C_5Me_5TiF_3)_4F_2]^-$ fragments form the nucleophilic host, and its fluoride surface binds the Na^+ ion in a similar way as the oxygen-containing analogues, the crown ethers. The sodium ion is thereby surrounded by eight fluorine atoms.

All these examples show that the inorganic host–guest chemistry is experiencing an upswing. Already the range of isolated observations demonstrates the scope of this field.

German version: *Angew. Chem.* **1992**, *104*, 1210

[1] C. J. Pedersen, *J. Am. Chem. Soc.* **1967**, *89*, 2495, 7017; C. J. Pedersen, H. K. Frensdorff, *Angew. Chem.* **1972**, *84*, 16; *Angew. Chem. Int. Ed. Engl.* **1972**, *11*, 16.

[2] J.-M. Lehn, *Pure Appl. Chem.* **1980**, *52*, 2441; *Science* **1985**, *227*, 849; *Angew. Chem.* **1988**, *100*, 91; *Angew. Chem. Int. Ed. Engl.* **1988**, *27*, 89; *ibid.* **1990**, *102*, 1347 bzw. **1990**, *29*, 1304.
[3] J. Berzelius, *Ann. Phys. (Leipzig)* **1826**, *6*, 369, 380.
[4] Cf. F. Vögtle, *Supramolekulare Chemie*, Teubner, Stuttgart, **1989**, p. 15ff.
[5] On account of the relatively long bonds between the transition metal atoms and the oxygen atoms on the phosphorus atom, an alternative description has also been suggested for this heteropolyanion (C. J. Clark, D. Hall, *Acta Crystallogr. Sect. B* **1976**, *32*, 1545), in which the shell comprises twelve square-pyramidal $\{MoO_5\}$ units linked to each other through their basal oxygen atoms. In this case a further largely isolated phosphate ion is situated in the center of the anion, and a true supramolecular compound is indeed present; for a comprehensive discussion of the bonding, see G. M. Brown, M.-R. Noe-Spirlet, W. R. Busing, H. A. Levy, *Acta Crystallogr. Sect. B* **1977**, *33*, 1038.
[6] K. W. Allen, *J. Chem. Soc.* **1959**, 4131.
[7] D. D. DesMarteau, T. Grelbig, S.-H. Hwang, K. Seppelt, *Angew. Chem.* **1990**, *102*, 1519; *Angew. Chem. Int. Ed. Engl.* **1990**, *29*, 1448.
[8] T. Kitazawa, S. Nishikiori, A. Yamagishi, R. Kuroda, T. Iwamoto, *J. Chem. Soc. Chem. Commun.* **1992**, 413.
[9] H. J. Powell, J. H. Rayner, *Nature* **1949**, *163*, 566.
[10] G. J. Johnson, E. O. Schlemper, *J. Am. Chem. Soc.* **1978**, *100*, 3645.
[11] V. W. Day, W. G. Klemperer, O. M. Yaghi, *J. Am. Chem. Soc.* **1989**, *111*, 5959.
[12] A. Müller, M. Penk, R. Rohlfing, E. Krickmeyer, J. Döring, *Angew. Chem.* **1990**, *102*, 927; *Angew. Chem. Int. Ed. Engl.* **1990**, *29*, 926.
[13] A. Müller, E. Krickmeyer, M. Penk, R. Rohlfink, A. Armatage, H. Bögge, *Angew. Chem.* **1991**, *103*, 1720; *Angew. Chem. Int. Ed. Engl.* **1991**, *30*, 1674.
[14] A. Müller, K. Hovemeier, R. Rohlfing, *Angew. Chem.* **1992**, *104*, 1214; *Angew. Chem. Int. Ed. Engl.* **1992**, *31*, 1192.
[15] H. Reuter, *Angew. Chem.* **1991**, *103*, 1487; *Angew. Chem. Int. Ed. Engl.* **1991**, *30*, 1482.
[16] S.-P. Huang, M. G. Kanatzidis, *Angew. Chem.* **1992**, *104*, 799; *Angew. Chem. Int. Ed. Engl.* **1992**, *31*, 787.
[17] H. W. Roesky, M. Sotoodeh, M. Noltemeyer, *Angew. Chem.* **1992**, *104*, 869; *Angew. Chem. Int. Ed. Engl.* **1922**, *31*, 864.

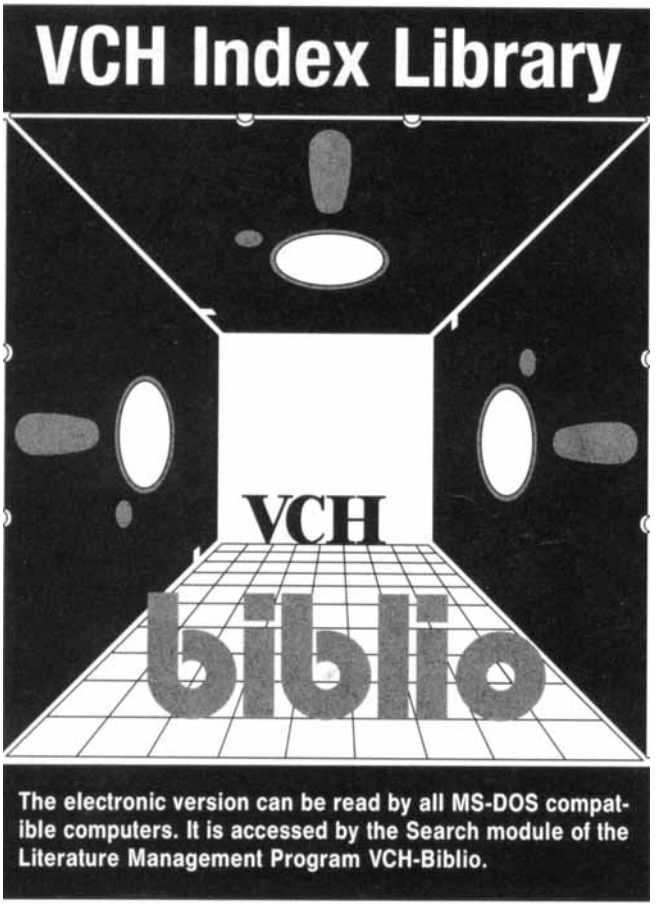

The electronic version can be read by all MS-DOS compatible computers. It is accessed by the Search module of the Literature Management Program VCH-Biblio.

ANGEWANDTE CHEMIE
A Journal of the Gesellschaft Deutscher Chemiker
International Edition in English

30 Year Index of Reviews
– in print or on diskette –

The reviews in Angewandte Chemie are amongst the most often cited chemical publications of each year. Many have become classics of the chemical literature. The 30 year review index was compiled to provide easy access to these important documents of the rapid development of our discipline. The index—both a chemical dictionary and a history book—offers you:

1. A list of all authors, indicating the main author and the title of the review.
2. A subject index giving the main author.
3. Both indexes provide complete information on date of issue and first and last page numbers of the German and English editions.

The electronic version of the index is available on 5¼" and 3½" diskettes and costs DM 98.00 or sFr 96.00 (plus shipping costs). This is your last chance to order a copy of the **printed version.** In order to clear out our warehouse we are selling the remaining lot for the reduced price of DM 48.00, £ 19.00, or sFr 41.00 (plus shipping costs). Please order by telephone or in writing to **VCH, Software und Datenbanken, Postfach 10 11 61, D-W-6940 Weinheim, Tel. 0 62 01/6 02-2 71, Telefax 0 62 01/6 02-3 28. U.S. customers please contact VCH Publishers, Inc., 303 N.W. 12th Avenue, Deerfield Beach, FL 33442-1788; Telephone 1-(8 00) 422-8824; Telefax (305) 428-8201.**

Communications may be submitted in English *or* in German. Further details regarding the submission of communications can be found in the "Notice to Authors" reproduced in the January issue of the journal. Copies thereof may be obtained from the editorial office upon request.

Selective Oxidation of Methane to CO and H_2 over Ni/MgO at Low Temperatures

By *Vasant R. Choudhary**, *Ajit S. Mamman*, and *Subhash D. Sansare*

The energy-efficient conversion of methane (or natural gas) to CO and H_2 (i.e. to syngas, a versatile feedstock for ammonia, methanol, and Fischer–Tropsch synthesis as well as hydrogenation and carbonylation processes) is of great practical importance in the present energy crisis. Selective oxidation of methane to syngas [Eq. (a)] is only mildly exothermic ($\Delta H = -5.4\,\mathrm{kcal\,mol^{-1}}$) and is hence quite

$$CH_4 + 0.5\,O_2 \longrightarrow CO + 2H_2 \qquad (a)$$

promising. However, in this process the formation of CO and H_2 over that CO_2 and H_2O is favored only at high temperatures.[1, 2] The noncatalytic oxidation of methane to syngas[3, 4] at thermodynamic equilibrium is possible only at very high temperatures (>1300 °C) and is thus not employed. Recently, a few studies on the selective, catalytic oxidation of methane to CO and H_2 over $Ln_2Ru_2O_7$ (Ln = lanthanide),[1] $Eu_2Ir_2O_7$, supported transition metal oxides,[5] and Ni/Al_2O_3[2] at >750 °C with the establishment of thermodynamic equilibrium have been described. However, although these catalytic processes display high conversion and selectivity, they are technically difficult to regulate and more hazardous because of the high temperatures required. Since at low temperatures and equilibrium conditions the CO selectivity in the oxidation process is very low,[2] it is essential to operate the process far from the equilibrium with a catalyst showing high activity/selectivity at lower temperatures (<700 °C) and extremely high space velocities (i.e. very low contact times). We report here our preliminary, highly promising results on the oxidative conversion of methane to syngas at atmospheric pressure with a Ni/MgO catalyst and at much lower temperatures. Our system shows high activity/selectivity and efficiency at extremely high flow velocities.

Our results are summarized in Figure 1. The high catalytic activity of both NiO/MgO (Fig. 1a) and the reduced catalyst, Ni/MgO, (Fig. 1b) in the oxidation of methane to syngas (mol ratio H_2/CO 2:1) is evident at lower temperatures (300–700 °C) with high conversion and much higher CO selectivity than that achieved at equilibrium conditions.[2]

[*] Dr. V. R. Choudhary, A. S. Mamman, Dr. S. D. Sansare
Chemical Engineering Division, National Chemical Laboratory
Pune-411 008 (India)

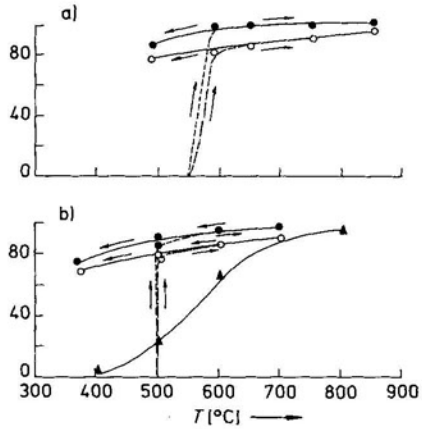

Fig. 1. Effect of temperature on the catalytic activity/selectivity of the catalysts a) NiO/MgO (unreduced) and b) Ni/MgO (reduced). Ni/Mg mol ratio = 3:1, (feedstock: 67 mol% CH_4, 33 mol% O_2, GHSV = $5.2\times10^5\,cm^3g^{-1}h^{-1}$). The ordinates correspond to the conversion of CH_4 (○), the CO selectivity (●), and the CO selectivity under equilibrium conditions (▲) in % [2].

The reaction over NiO/MgO, however, starts at higher temperatures than that over Ni/MgO. The NiO/MgO catalyst was expected to be reduced by the H_2 formed in the reaction at temperatures ≥550 °C. It is interesting to note that not only the unreduced catalyst but also the reduced one showed catalytic activity at temperatures below 500 °C only after they had been used in the reaction at ≥500 °C. This suggests that the active sites responsible for the low-temperature catalytic activity/selectivity may arise from further reduction of the catalyst and/or formation of surface carbon species. The latter was confirmed by O_2 pulse experiments over the used catalysts. Such surface species are probably formed according to Equations (b) and (c). Figure 2 reveals that the cata-

$$2CO \longrightarrow CO_2 + C_{adsorbed} \qquad (b)$$

$$CO + H_2 \longrightarrow H_2O + C_{adsorbed} \qquad (c)$$

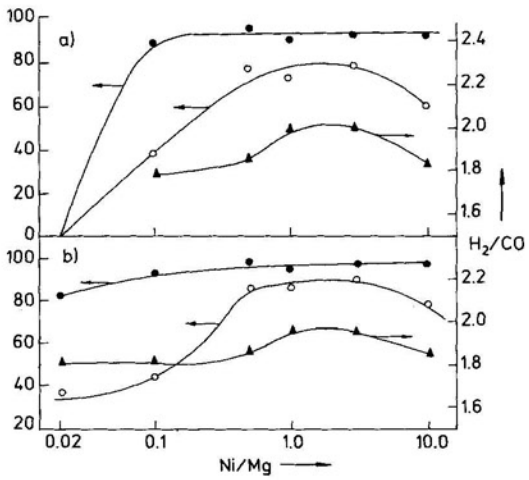

Fig. 2. Effect of the mol ratio Ni/Mg on the catalytic activity/selectivity of Ni/MgO at a) 500 °C and b) 700 °C; (feedstock: 67 mol% CH_4 and 33 mol% O_2, GHSV = $5.2\times10^5\,cm^3g^{-1}h^{-1}$). The ordinates on the left correspond to the conversion of CH_4 (○) and the CO selectivity (●) in %. The ordinates on the right correspond to the mol ratio H_2/CO in the product mixture (▲).

 © VCH Verlagsgesellschaft mbH, W-6940 Weinheim, 1992 0570-0833/92/0909-1189 $ 3.50+.25/0

lyst with an Ni/Mg ratio between 1:1 and 3:1 shows the best performance in this process. This catalyst showed no loss of activity over a period of 20 h.

The influence of gas hourly space velocity (GHSV) of the methane feedstock on the process performance (Fig. 3) can be summarized as following: The conversion passes through a maximum, the CO selectivity increases with increasing GHSV, and H_2/CO ratio decreases with increasing GHSV. The increase in the selectivity of the reaction indicates that it is controlled by kinetics rather than the thermodynamic equilibrium. The production of CO is also much higher (one to three orders of magnitude) than that observed previously.[1, 2, 5]

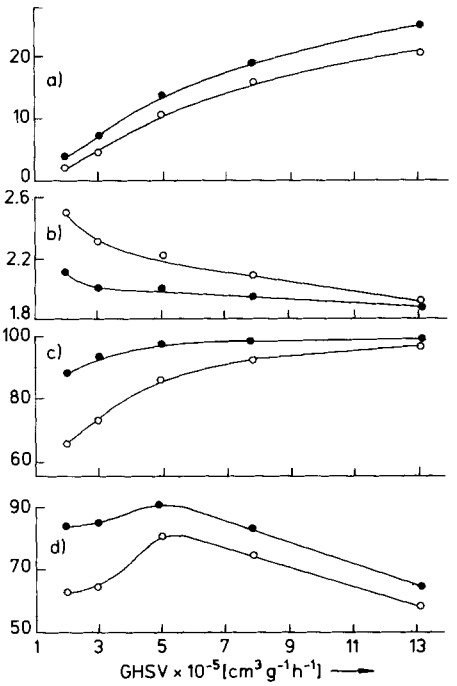

Fig. 3. Influence of the GHSV on catalytic activity/selectivity of Ni/MgO (Ni/Mg ratio ≈ 3:1) at 500 °C (○) and 700 °C (●). The ordinates correspond to the amount of CO formed [mol $g^{-1}h^{-1}$] (a), the mol ratio H_2/CO (b), the CO selectivity [%] (c), and the conversion of CH_4 [%] (d).

Upon addition of steam to the methane feedstock, the H_2/CO and CO_2/CO ratios increased. This indicates the existence of a CO conversion according to Equation (d) which

$$CO + H_2O \rightleftharpoons CO_2 + H_2 \qquad (d)$$

operates parallel to the oxidative methane conversion. Further, the formation of CO and CH_4 in the hydrogenation of CO_2[7] indicates that the back reaction of the CO conversion may operate simultaneously when the methane conversion is conducted at low temperatures.

The negligibly small conversion of methane in its reaction with CO_2 or steam[8] reveals that CO_2 and water are not the reaction intermediates in the process described here, in contrast to high-temperature noncatalytic or catalytic processes.[1-3] In the present case, the direct formation of CO and H_2 from methane may involve its heterolytic dissociation into CH_3^- and H^+, followed by the oxidation of CH_3^- to OCH_3^-, providing H_2, CO, H_2O, and CO_2, similar to the process observed in the oxidation of preadsorbed methane on MgO at low temperatures.[9]

Experimental Procedure

The NiO/MgO catalysts were prepared from a thick paste of thoroughly mixed, finely ground nickel nitrate (GR LOBA), magnesium carbonate (GR LOBA), and deionized water, which was dried and heated in air at 600 °C for 4 h. The treated solid was powdered, pressed without a binding agent, crushed to particles of 22–30 mesh, and calcined in air at 900 °C for 6 h. The catalytic reactions were carried out in a continuous microreactor constructed of quartz (i.d.: 4 mm) containing about 20 mg catalyst which was pretreated in situ at 900 °C in a flow of moisture-free N_2. The reaction temperature was measured with a Chromel-Alumel thermocouple located in the catalyst bed. The reaction was carried out over the catalyst with or without its prereduction by H_2 at 500 °C with a flow (80 cm^3min^{-1}) of 20% H_2 (80% N_2) for 1 h (i.e. over Ni/MgO and NiO/MgO). The water formed in the reaction was condensed from the product gases at 0 °C and measured. The feedstock and products were analyzed by on-line gas chromatography. The C,H, and O balances were within 5%.

Received: February 7, 1992
Revised: March 12, 1992 [Z 5174 IE]
German version: *Angew. Chem.* **1992**, *104*, 1273

[1] A. T. Ashcroft, A. K. Cheetham, J. S. Foord, M. L. H. Green, C. P. Grey, A. J. Murrell, P. D. F Vernon, *Nature* **1990**, *344*, 319–321.
[2] D. Dissanayake, M. P. Rosynek, K. C. C. Kharas, J. H. Lunsford, *J. Catal.* **1991**, *132*, 117–127.
[3] *Encyclopedia of Chemical Technology, Vol. 12* (Eds.: R. E. Kirk, D. F. Othmer), 3rd ed., Wiley Interscience, New York, **1980**, p. 938.
[4] *Ullmann's Encyclopedia of Industrial Chemistry, Vol. A 12*, 5th ed., VCH, Weinheim, **1989**, p. 169.
[5] P. D. F. Vernon, M. L. H. Green, A. K. Cheetham, A. T. Ashcroft, *Catal. Lett.* **1990**, *6*, 181–186.
[6] The mol ratios of the products H_2/CO and CO_2/CO increased from 2.0 to 3.5 and 0.09 to 0.77, respectively, because of the addition of steam to the feedstock in the oxidative methane conversion at 550 °C over Ni/MgO (GHSV = 5.2×10^5 $cm^3g^{-1}h^{-1}$, $CH_4/O_2 = 2:1$ and $H_2O/CH_4 = 1:1$).
[7] In the reaction of CO_2 with H_2 at 500 °C over Ni/MgO (feedstock: 67 mol% H_2, 33 mol% CO_2, GHSV = 5.1×10^5 $cm^3g^{-1}h^{-1}$) the conversion of CO_2 to CO and CH_4 was 10.0 and 15.8%, respectively.
[8] The conversion of methane in its reaction with CO_2 or steam (feedstock: 50 mol% CH_4 and 50 mol% CO_2 or H_2O, GHSV = 5.2×10^5 $cm^3g^{-1}h^{-1}$) at 500 °C over Ni/MgO was less than 1%.
[9] T. Ito, T. Watanabe, T. Tashiro, K. Toi, *J. Chem. Soc. Faraday Trans. 1* **1989**, *85*, 2381–2395.

trans-2-*tert*-Butylcyclohexanol, a Simple Selectively Optimized Cyclohexanol Auxiliary**

By *Peter Esser, Helmut Buschmann, Markus Meyer-Stork*, and *Hans-Dieter Scharf**

Systematic investigation of the asymmetric Paternó–Büchi reaction gave rise to the isoinversion principle,[1] a general chemical selection model. The isoinversion principle, applied to the same reaction, was utilized to develop a model concerning the relation between structure and selectivity in cyclohexanol auxiliaries.[2] As a result of these studies, *trans*-2-*tert*-butylcyclohexanol **1** was derived as a "structurally minimized" cyclohexanol auxiliary with an optimized induction potential. Besides, its two enantiomers can be prepared on a large scale by an economical and simple route.

[*] Prof. Dr. H.-D. Scharf, Dipl.-Chem. P. Esser, Dr. H. Buschmann, M. Meyer-Stork
Institut für Organische Chemie der Technischen Hochschule
Prof.-Pirlet-Strasse 1, D-W-5100 Aachen (FRG)

[**] This work was supported by the Deutsche Forschungsanstalt für Luft und Raumfahrt e.V., Hauptabteilung Energietechnik, Köln, der Deutsche Forschungsgemeinschaft, and the Fonds der Chemischen Industrie. We are grateful to Hüls AG (Marl) for supplying technical 2-*tert*-butylcyclohexanol. We also thank D. Gillmann for the synthetic work and S. Diebel for performing the GC analyses.

The induction potential of *trans*-2-*tert*-butylcyclohexanol **1** is similar to that of 8-phenylmenthol **5**. In this respect, the auxiliary **1** differs considerably from menthol **6** and from *trans*-2-phenylcyclohexanol **7**,[3] as exemplified by the four test reactions shown in Table 1. The *de* values listed in Table 1 were obtained for reactions at the listed temperatures. Temperature optimization according to the inversion principle thus makes it possible to increase the *de* value of the Paternó-Büchi reaction of *trans*-2-*tert*-butylcyclohexanol **1** at 231 K to 96%.

Table 1. Comparison of the diastereoselectivity (*de* values in %) achieved with the auxiliaries R*OH in four test reactions.

	7	**8**	**1**	**5**
R* =	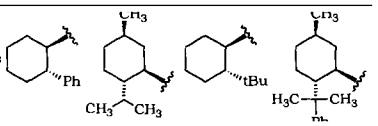			
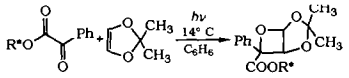	56	58	92	> 96
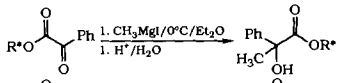	47	26	72	76
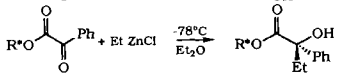	> 96	66	> 96	> 96
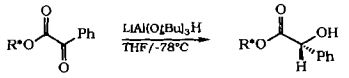	35[a]	15	38	46

[a] While almost complete conversion was attained with the three other auxiliaries, in this case only 50% conversion was reached after the same reaction time (3 h).

Both isomers, (−)-(1*R*,2*S*)- and (+)-(1*S*,2*R*)-2-*tert*-butylcyclohexanol, can be synthesized on a preparative scale from economical starting materials by a simple enzymatic process. The starting material, racemic 2-*tert*-butylcyclohexanol as a mixture of diastereomers in a *cis*/*trans* ratio of 8:2, is a technical product resulting from catalytic hydration of *ortho*-*tert*-butylphenol.[4]

The technically accessible mixture of isomers was oxidized by treatment with sodium dichromate in sulfuric acid solution and then reduced selectively to afford *trans*-2-*tert*-butylhexanol **1**. Recrystallization from *n*-hexane yielded a diastereomerically pure product. **1** may be esterified to form the corresponding acetate **4a**[7] or the chloroacetate **4b**.[8]

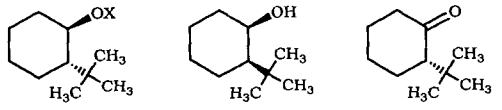

X = H : (−)-**1** (−)-**2** (−)-**3**
X = Ac : (−)-**4a**
X = $ClCH_2CO$: (−)-**4b**

Enzyme-catalyzed esterifications and saponifications of racemic cyclohexanol derivatives have been described a number of times.[9, 10] However, the good enantioselectivity obtained was compromised by low substrate concentration and extended reaction times. The esters were enantioselectively saponified with PLAP (pig liver acetone powder).[11] Because of its ready availability, fresh pig liver was ground, extracted with acetone, and dried for better stability. PLAP-

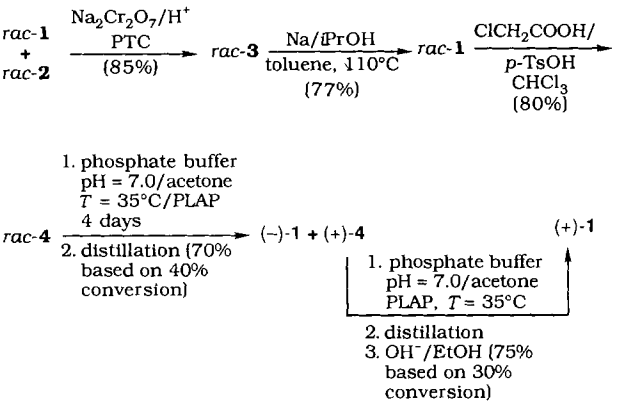

Scheme 1. Synthesis of enantiomerically pure (−)-**1**, starting from a technical racemic mixture of **1** and **2**. PTC = Phase-transfer catalysis.

catalyzed saponification was performed in water/acetone[12] at 35 °C and a pH of 7. A high-capacity buffer eliminated the need for an autoburet. At a pH below 6.5, the reaction rate dropped noticeably, while the enantioselectivity was considerably reduced at a pH above 7.5. The heterogeneous substrate/water/acetone/enzyme system, containing 40 g of PLAP per 900 mL aqueous phase, was saturated with enzyme. It is important to stir this mixture well in order to optimize the reaction rate. The chloroacetate **4b**[9] showed a reaction rate which is ten times greater than that of acetate **4a** and an equal enantioselectivity. The resulting space-time yield is considerable for an enzymatic reaction. For kinetic reasons,[13] the saponification reaction was interrupted at 40% conversion. After the mixture of ester and (−)-(1*R*,2*S*)-2-*tert*-butylcyclohexanol (−)-**1** was extracted from the aqueous phase, enantiomerically pure (−)-**1** was isolated by distillation (chloroacetate) or column chromatography (acetate) and subsequent crystallization from *n*-hexane. The enantioselectivity values are consistent with the active site model by Toone et al.[11c, 14] In addition, the assignment of the enantiomers is consistent with the structure–selectivity model for cyclohexanol auxiliaries[2] and with the stereochemical assignment according to Djerassi et al.[15] The remaining ester, now enriched with (+)-**4**, was saponified again in the same enzymatic system with up to 30% conversion. The resulting enantiomerically pure ester (+)-**4** was saponified and recrystallized from *n*-hexane to yield (+)-(1*S*,2*R*)-2-*tert*-butylcyclohexanol (+)-**1**.

Experimental Procedure

GC: HP 5890 series II, FID detector with HP 3396 A integrator; for chiral GC, Analytik Siemens Sichromat, FID detector with Shimadzu CR3A integrator. NMR, IR, MS, and CH analyses agree with the structure [16].

tert-Butylcyclohexanone **3**: A 3 M solution of *cis*/*trans*-2-*tert*-butylcyclohexanol was oxidized with sodium dichromate in a sulfuric acid solution, according to the procedure outlined in Organikum [5]. Distillation afforded the ketone in 85% yield. B.p. 76 °C/10 Torr.

trans-2-*tert*-Butylcyclohexanol **1**: 154 g (1 mol) of ketone **3** in 440 g of 2-propanol were quickly added to a well agitated, refluxing suspension of sodium sand (128 g) and toluene (4 L) (the quality of the toluene suspension has a decisive influence on the quality of the *trans* selectivity). (Temperature of the oil bath approx. 160 °C.) Initially, the oil bath was removed. After 3 h of stirring at an oil bath temperature of 140 °C, the mixture is allowed to cool. Then 110 g of sodium dihydrogenphosphate in 550 mL water followed by 660 mL of concentrated hydrochloric acid in 2.2 L of water were added. The aqueous phase was extracted with ether. After drying, the solution was concentrated to afford *trans*-2-*tert*-butylcyclohexanol **1** with a *trans* selectivity of more than 90% (GC = HP FFAP 25 m × 0.32 mm, T = 100 °C, 10 min, N_2 = 2 atm). Recrystallization from *n*-hexane gives 120 g (77%) of *trans*-2-*tert*-butylcyclohexanol **1** with more than 99.9% purity.

trans-2-*tert*-Butylcyclohexylchloroacetate **4b**: 468 g (3 mol) of *trans*-2-*tert*-butylcyclohexanol **1** and 283.5 g (3 mol) of chloroacetic acid were esterified azeotropically by adding 0.5 g (2.6 mmol) of *para*-toluenesulfonic acid in chloroform. When no more water was removed, the catalytic acid was washed out with water, aqueous hydrogen carbonate, and again with an aqueous solution.

Distillation of the crude product afforded the ester **4b** in 80% yield. B.p. 60 °C, 0.19 Torr. (*trans*-2-*tert*-Butylcyclohexanol was acylated in 1 M solution with acetic anhydride, a proton-catalyzed reaction which proceeds analogously to the reaction outlined in Organikum [8].) Distillation afforded the ester **4a** in 82% yield. B.p. 78 °C/3 Torr.

(−)-(1*R*,2*S*)-2-*tert*-Butylcyclohexanol (−)-**1**: A 1 L four-necked flask equipped with a glass precision stirrer shaft, an Ultraturraux stirrer, and a pH meter was filled with a solution of 800 mL of water, 110 mL of acetone, 41.4 g of potassium hydrogen phosphate, 22.4 g of potassium dihydrogen phosphate, 0.5 g of albumin, 40 g of PLAP, and 0.5 mol of *trans*-2-*tert*-butylcyclohexylester **4** (99 g acetate **4a** or 116 g chloroacetate **4b**). The reaction solution was thermostatted at 35 °C and a pH of 7.0 ± 0.5 was maintained by occasionally adding NaOH solution. The reaction was halted at 40% conversion (in the case of acetate **4a**, after about 30 days (conversion rate approx. 0.006 mol per day), in the case of chloroacetate **4b**, after about 4 days (conversion rate approx. 0.05 mol per day). The activity of PLAP depends on the charge and on the freshness of the liver used. The reaction solution was extracted with ether, and the extracts were concentrated and distilled (chloroacetate; *trans*-2-*tert*-butylcyclohexanol (−)-**1**, b.p. 88 °C/8 Torr, chloroacetate (+)-**4b**, b.p. 84 °C/0.2 Torr) or separated by chromatography (acetate **4a**) (cyclohexane/ethyl acetate = 9/1). *trans*-2-*tert*-Butylcyclohexanol **1** is highly volatile; it is thus important to distill the solvents at moderate conditions. Crystallization from *n*-hexane afforded (−)-(1*R*,2*S*)-2-*tert*-butylcyclohexanol (−)-**1** in 70% yield, relative to the conversion, and > 99% *ee* (GC: 25 m × 0.25 mm dimethylacetyl-β-cyclodextrin/polysiloxane. T: 60–190 °C (0.5 K min^{-1}, H_2 = 0.8 bar), $[\alpha]_D^{23}$ −41.1 (*c* = 1.1, $CHCl_3$).

(+)-(1*S*,2*R*)-2-*tert*-butylcyclohexanol (+)-**1**: "Oversaponification" was carried out analogously. At another 30% conversion, the reaction is interrupted and the reaction solution was extracted with ether, and the extracts were concentrated and separated by distillation (chloroacetate) or chromatography (acetate). The ester was saponified in ethanol/KOH. After the solution was concentrated, ether/water was added, the aqueous phase extracted, and the combined organic phases dried over magnesium sulfate and evaporated to dryness. The remaining alcohol was recrystallized from *n*-hexane to afford (+)-(1*S*,2*R*)-2-*tert*-butylcyclohexanol (+)-**1** in 75% yield, relative to the conversion.

Received: October 25, 1991
Revised: May 16, 1992 [Z 4987 IE]
German version: *Angew. Chem.* **1992**, *104*, 1254

CAS Registry numbers:
rac-**1**, 67738-25-4; (−)-**1**, 98104-30-4; (+)-**1**, 13492-07-4; **1** (COCOPh), 142864-89-9; **1** [COC(OH)(Ph)CH_3], 142798-14-9; **1** [COC(OH)(Ph)CH_2CH_3], 142798-15-0; **1** [COCH(OH)Ph], 142798-16-1; *rac*-**3**, 13495-19-7; *rac*-**4a**, 142798-19-4; *rac*-**4b**, 142798-18-3; **5** (COCOPh), 88002-15-7; **5** [COC(OH)-(Ph)CH_3], 88292-44-8; **5** [COC(OH)(Ph)CH_2CH_3], 142798-17-2; **5** [COCH-(OH)Ph], 88292-43-7; **6** (COCOPh), 20229-41-8; **6** [COC(OH)(Ph)CH_3], 57133-37-6; **6** [COC(OH)(Ph)CH_2CH_3], 57133-41-2; **6** [COCH(OH)Ph], 25926-70-9; **7** (COCOPh), 136032-07-0; **7** [COC(OH)(Ph)CH_3], 142798-11-6; **7** [COC-(OH)(Ph)CH_2CH_3], 142798-12-7; **7** [COCH(OH)Ph], 109462-87-9.

[1] H. Buschmann, H.-D. Scharf, N. Hoffmann, P. Esser, *Angew. Chem.* **1991**, *103*, 480; *Angew. Chem. Int. Ed. Engl.* **1991**, *30*, 477.
[2] H. Buschmann, H.-D. Scharf, N. Hoffmann, *Tetrahedron Asymmetry* **1991**, *2*, 1429.
[3] a) J. K. Whitesell, J. F. Carpenter, *J. Am. Chem. Soc.* **1987**, *109*, 2839; b) J. K. Whitesell, R. M. Lawrence, H.-H. Chen, *J. Org. Chem.* **1986**, *51*, 4779; c) J. K. Whitesell, J. F. Carpenter, H. K. Yaser, T. Machajewski, *J. Am. Chem. Soc.* **1990**, *112*, 7653; d) J. K. Whitesell, H. K. Yaser, *ibid.* **1991**, *113*, 3626; e) D. Basavaiah, T. K. Bharathi, *Tetrahedron Lett.* **1991**, *32*, 3417; f) A. E. Greene, F. Charbonnier, *J. Am. Chem. Soc.* **1987**, *109*, 4752; g) J. Castro, H. Sörensen, A. Riera, C. Morin, A. Mogano, M. A. Pericàs, A. E. Greene, *ibid.* **1990**, *112*, 9388; h) N. A. Porter, J. K. Kaplan, P. H. Dussault, *ibid.* **1990**, *112*, 1266; i) G. Boireau, A. Deberly, D. Abenhaim, *ibid.* **1988**, *29*, 2175; j) G. Boireau, A. Deberly, *Tetrahedron Asymmetry* **1991**, *2*, 771; k) C. A. Brown, S. Krishnamurty, S. C. Kim, *J. Chem. Soc. Chem. Commun.* **1973**, 391.
[4] O. Werner, N. Rudolf, M. Zur Hausen (Chem. Werke Hüls AG), DE 3401343 A1(Kl. C 07 C35/08), **1985**; *Chem. Abstr.* 104:50586g.
[5] *Organikum*, 18th edition, Deutscher Verlag der Wissenschaften, Berlin, 1990, p. 360.
[6] S. K. Pradhan, *Tetrahedron* **1986**, *42*, 6351.
[7] Ref. [5], p. 403.
[8] Ref. [5], p. 405.
[9] a) K. Laumen, M. P. Schneider, *J. Chem. Soc. Chem. Commun.* **1988**, 598; b) D. H. G. Crout, V. S. B. Goudet, K. Laumen, M. P. Schneider, *ibid.* **1986**, 808; c) K. Laumen, M. P. Schneider, *ibid.* **1986**, 1298; d) K. Laumen, D. Breitgoff, R. Seemayer, M. P. Schneider, *ibid.* **1989**, 148.
[10] a) H. Hönig, P. Seufer-Wasserthal, *Synthesis* **1990**, 1137; b) G. M. Whitesides, C.-H. Wong, *Angew. Chem.* **1985**, *97*, 617; *Angew. Chem. Int. Ed. Engl.* **1985**, *24*, 617; c) G. Langrand, M. Secchi, G. Buono, J. Baratti, C. Triantaphylides, *Tetrahedron Lett.* **1985**, *26*, 1857; d) A. Y. Prah, *Chem. Br.* **1989**, 282; e) C.-S. Chen, C.-J. Sih, *Angew. Chem.* **1989**, *101*, 711; *Angew. Chem. Int. Ed. Engl.* **1989**, *28*, 695; f) H.-J. Altenbach, *Nachr. Chem. Tech. Lab.* **1988**, *36*, 1114; g) H. J. Gais, H. Hemmerle, *Chem. Unserer Zeit* **1990**, *24*, 239; h) R. Seemayer, M. G. Schneider, *Recl. Trav. Chim. Pays-Bas* **1991**, *110*, 171.
[11] a) J. Boutelje, M. Hialmarsson, P. Szmulik, T. Norin, K. Hult, *Stud. Org. Chem.* **1987**, *29*, 361; b) L. M. Zhu, M. C. Tedford, *Tetrahedron* **1990**, *46*, 6587; c) J. B. Jones, *Pure Appl. Chem.* **1990**, *62*, 1445.
[12] a) J. K. Whitesell, R. M. Lawrence, *Chimia* **1986**, *40*, 318; b) A. Schwartz, P. Madan, J. K. Whitesell, R. M. Lawrence, *Org. Synth.* **1990**, *69*, 1.
[13] C.-H. Wong, *Chemtracts Org. Chem.* **1990**, 91.
[14] a) E. J. Toone, M. J. Werth, J. B. Jones, *J. Am. Chem. Soc.* **1990**, *112*, 4946; b) E. J. Toone, J. B. Jones, *Tetrahedron Asymmetry* **1991**, *2*, 207.
[15] C. Djerassi, P. A. Hart, E. J. Wareia, *J. Am. Chem. Soc.* **1964**, *86*, 78.
[16] H. Buschmann, *Dissertation*, Aachen, **1992**.

A Novel Host/Guest System with a Nanometer Large Cavity for Anions and Cations: $[2\,NH_4^+, 2\,Cl^- \subset V_{14}O_{22}(OH)_4(H_2O)_2(C_6H_5PO_3)_8]^{6-}$**

By *Achim Müller*,* *Kai Hovemeier*, and *Ralf Rohlfing*

Dedicated to Professor Wolfgang Beck on the occasion of his 60th birthday

Host/guest chemistry, molecular recognition, and nanotechnology are buzzwords that characterize highly topical fields in chemistry.[1] Whereas the relationship between electrophilic "guest ions", such as alkali metal ions, and nucleophilic "host molecules", such as crown ethers, have been studied intensively for many years, only recently has anionic complex chemistry with electrophilic "hosts" been reported.[1] Polytopic hosts for several cations *and* anions or cation/anion aggregates were hitherto unknown.[2] Such host/guest systems should open new fields of application; with them the cooperative, allosteric, and regulatory effects can be studied as well as the condensation of substrates that are brought into proximity by the host.[1] We have now been able to detect the organization of a large "host"[3] (nanometer dimensions), which is probably the result of a novel synergetic template effect by a cation/anion aggregate. Another unusual feature is the nature of the coupling of the guest(s) to the host.

On reaction of ammonium metavanadate with phenylphosphonic acid and hydrazine hydrate in the presence of dimethylammonium chloride in a 3:1 mixture of water and *N*,*N*-dimethylformamide, the host/guest compound **1** is formed, which has been characterized by elemental analysis, manganometric titration of V^{IV}, IR, Raman and UV/VIS/near IR spectroscopy, magnetochemical measurements, calculations of bond-valence sums,[4] and single crystal X-ray analysis.[5]

$$[(CH_3)_2NH_2]_5[NH_4][2\,NH_4^+, 2\,Cl^- \subset V_{14}O_{22}(OH)_4(H_2O)_2(C_6H_5PO_3)_8] \cdot 5\,H_2O \cdot 4\,(CH_3)_2NCHO \quad \mathbf{1}$$

[*] Prof. Dr. A. Müller, Dipl.-Chem. K. Hovemeier, Dipl.-Chem. R. Rohlfing
Fakultät für Chemie der Universität
Lehrstuhl für Anorganische Chemie I
Postfach 100131, D-W-4800 Bielefeld 1 (FRG)

[**] We thank Dr. H. Bögge for discussions in connection with the X-ray structure analysis.

The anion of **1** (cf. Fig. 1 and the structures of fragments in Fig. 2) lies on a crystallographic center of inversion and (without the phenyl groups) has approximate D_{2h} symmetry. It consists formally of two $\{V_5O_9\}^{3+}$ units (**2**, each with a localized V^V center) and two hypothetical binuclear complexes $[V_2^{IV}O_2(OH)_2(H_2O)(C_6H_5PO_3)_4]^{6-}$ (**3**). Two each of

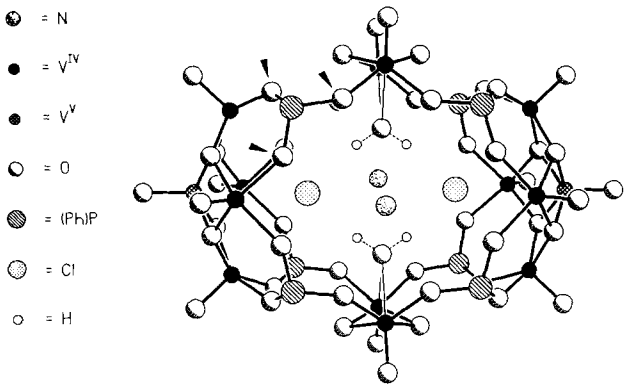

Fig. 1. Structure of the anion in crystals of **1** with illustration of the hydrogen bonds important for the binding of the guest system to the host system, viewed approximately along one of the idealized C_2 axes (characteristic distances [pm]: V-O_{term} 157.8(3)–160.0(2), V^V-O_{br} 185.7(2)–188.8(2), V^{IV}–O_{br} 195.1(2)–198.0(2), V-O(H) 199.9(2)–200.6(3), V-O$(H)_2$ 247.7(3); 252.0(3), P-O 151.6(3)–152.7(2), P-C 179.1(4)–179.9(3); the O atoms of a phosphonate ligand (**6**) are marked by arrows).

components **2** and **3** together form a cavity in which an $(NH_4)_2Cl_2$ ring system (**4**) is enclosed. Unit **2** occurs, for instance, as fragment in the cage system of $[H_4V_{18}O_{42}(X)]^{9-}$ (X = Cl, Br, I),[6] but also in the complex $[V_5O_9Cl(tca)_4]^{2-}$ (tca^- = thiophene-2-carboxylate).[7] The binuclear fragment **3** consists of the central $\{V_2^{IV}O_2(OH)_2(H_2O)\}^{2+}$ group (**5**) and four monodentate phenylphosphonate ligands $[C_6H_5PO_3]^{2-}$ (**6**, Fig. 2a). The V–O distances and results of computations of the bond-valence sums suggest that the three bridging O atoms of **5** are singly and doubly (oxygen atom *trans* to $V{=}O_t$) protonated, which is in accord with the overall charge on the anion of **1**. Because of its open structure, **3** would not be stable as an isolated entity. Stability is, however, expected for the same central unit **5**, but with two bidentate ligands **6**.[8]

The (formal) condensation of the two $\{V_5O_9\}^{3+}$ units (**2**) with two phosphonato complexes **3** to form V_2PO_3 hexagons, which correspond to the M_3O_3 rings of $[H_4V_{18}O_{42}(X)]^{9-}$ (X = Cl, Br, I), produces a cavity with nanometer dimensions (about 1.2 nm between two V^V centers), which is partitioned by two H_2O ligands (Fig. 1).

The novel and almost planar coronand formed from four PO_2 units and four V atoms (formally comparable with a hitherto unknown "[16]crown-8-crown ether"; Fig. 2b,c) occurs twice in **1**. In each of these coronands an ammonium ion is localized at distances from 299 to 366 pm to the eight O atoms. The deviation of the eight O atoms, four P atoms, and also two of the four V atoms and the central N atom from the best plane through the O atoms is maximally 27 pm.

Alternatively, the cavity of the anion of **1** can be visualized as derived from the intact inner spherical shell of $[H_4V_{18}O_{42}(X)]^{9-}$ (X = Cl, Br, I), which has D_{4d} symmetry and the composition $(V_{18}O_{24})$ (Fig. 2d). (This is important for the explanation of the template effect of the chloride ion; see below.) The $V_{18}O_{24}$ shell in which 24 oxygen atoms form a pseudo-rhombicuboctahedron, is divided into two halves

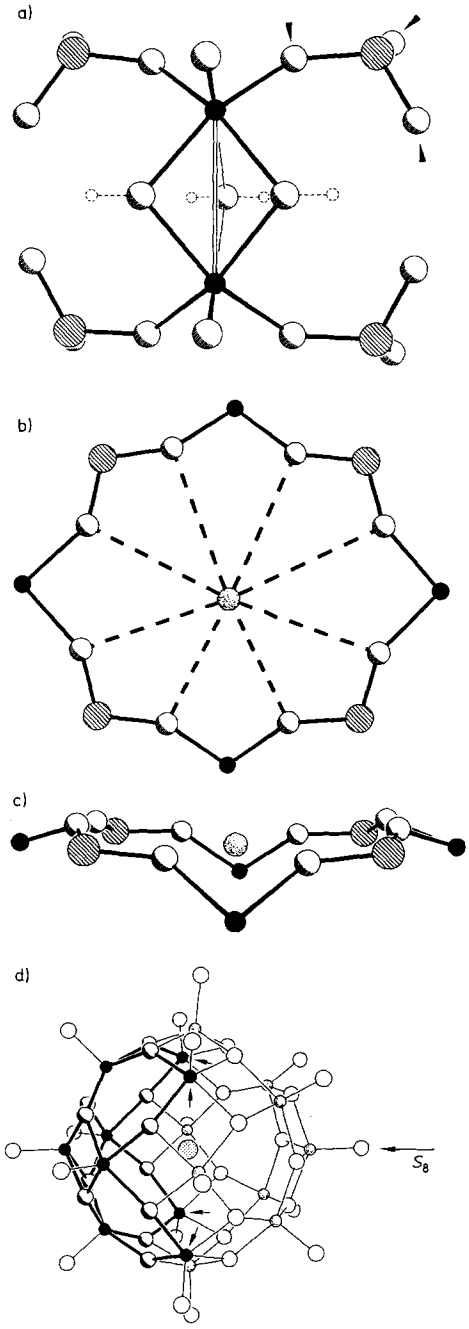

Fig. 2 Important fragments of **1**: a) a hypothetical complex **3** shown perpendicular to the position in Figure 1 (V^{IV}-V^{IV} distance 305 pm; O atoms of one ligand **6** marked by arrows); b) nucleophilic coronand viewed as in Figure 1 and c) perpendicular to that position to illustrate the site of the NH_4^+ ion; d) V_9O_{12} and $V_5P_4O_{12}$ fragment (boldface lines) described as part or half, respectively, of the (inner) $V_{18}O_{24}$ half-shell of $[H_4V_{18}O_{42}(X)]^{9-}$ (X = Cl, Br, I) [6a] (the V atoms of the equator marked by arrows must be replaced by P atoms for the topological generation of the anion of **1**.

as if zipped open along the equator perpendicular to the S_8 axis; four V_3O_3 hexagons are thus retained in each half shell. Then all eight atoms of the equator (marked in Fig. 2d for one half of the shell) that belong to the V_3O_3 hexagons are replaced by the P atoms of **6**. The two substituted half shells visualized in this way are twisted through 45° relative to each other and linked with two units of **5** through eight additional O atoms as shown in Figure 1. The half shells lie symmetrically about the horizontal mirror plane of **1**. The analogy to $[H_4V_{18}O_{42}(X)]^{9-}$ (X = Cl, Br, I) is also obvious in the similar V···Cl distances (from 359 to 376 pm[6a]).

For the twelve localized V^{IV} centers, at least for the $\{V_5O_9\}^{3+}$ fragments at room temperature, magnetic coupling is negligible,[4] as the V^{IV}–V^{IV} distances of 367–369 pm in those fragments are too large. In accord with this the compound is green. Since the two V^{V} centers at the poles are closer to the V^{IV} centers (288–293 pm), a strong antiferromagnetic interaction has to be anticipated for the fully reduced V^{IV}_{14} cluster. The organization of the spins in **1** and the corresponding reduced species is a step towards *supramolecular magneto chemistry*.

The organization of the cluster shell—a novel host—might be directed by two Cl^- ions inducing the generation of two polar $\{V_5O_9\}^{3+}$ fragments,[9] and the two NH_4^+ ions inducing the formation of the two nucleophilic coronands (Fig. 2b,c). Thus the formation of **1** formally corresponds to the linking of nucleophiles and electrophiles, that is, of electronically inverse hosts;[10] four V atoms are thus shared by these different kinds of hosts.

The organization of the central guest system **4** is determined predominantly by electrostatic interactions, since the distances in the planar four-membered rings are comparable to those of the ion lattice of NH_4Cl (Fig. 3). The two encapsulated chloride ions are 475 pm apart (other distances: to the V^{IV} centers 332–363 pm, to the V^{V} center of the $\{V_5O_9\}^{3+}$ fragments 361 pm). In the docking of **4** to the host, besides the already mentioned interactions between the V/O shell fragments and Cl^- ions[10] and between the nucleophilic O functions of the two coronands and the NH_4^+ ions, hydrogen bonds also play a role, because the relevant O–H–Cl arrangement (see Fig. 1) is approximately linear (O···Cl, 311 and 316 pm). In contrast, hydrogen bonds with NH_4^+ are not crucial, because derivatives of **1** can also be synthesized with alkali metal ions. Exchange of the NH_4^+ ion after the assembly of the host system has not yet been achieved. However, analogous systems with alkali metal ions, for example, the host–guest system with the isostructural anion $[2Rb^+, 2Cl^- \subset V_{14}O_{22}(OH)_4(H_2O)_2(C_6H_5PO_3)_8]^{6-}$, can be synthesized. (We will not discuss the crystal structure here because of an unresolved disorder in the cationic lattice.)

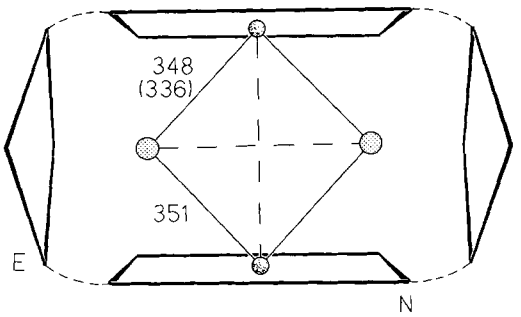

Fig. 3. Host/guest relationships in **1** drawn to scale for the host systems E and N which are perpendicular and electronically inverse to one another: E corresponds to the electrophilic half-shell (see text; the illustrated plane is spanned by four V^{IV} centers), and N corresponds to the nucleophilic coronand plane (the illustrated plane is spanned by four P atoms). Distances in **1** and in the NH_4Cl ionic lattice (in parentheses) in pm.

These results are significant for the following fields: anion–cation separations under physiological conditions,[11] control of oligomer formation from cations and anions and their template function, for example as tips or holes on crystal surfaces with potential relevance for directed prebiotic reactions, and the interaction in confined spaces of simple ion lattices on variation of the interionic distances. With unsymmetric poly/heterotopic hosts that are comparable with **1**, information on the charge separation processes could become available. In order to draw further conclusions, the study of systems[12] with larger ion aggregates as guests would be necessary.[13]

Experimental Procedure

Dimethylammonium chloride (2.04 g, 25.0 mmol) and *N*,*N*-dimethylformamide (30 mL) were added to a solution of NH_4VO_3 (2.92 g, 25.0 mmol) in water (100 mL) at 100 °C in a 300 mL narrow-necked Erlenmeyer flask. Phenylphosphonic acid (1.00 g, 6.3 mmol) was added at 90 °C (color change to orange-red). After reduction with N_2H_5OH (99%, 0.36 mL, 7.5 mmol) the almost black solution was cooled to 65 °C and kept at this temperature for approximately one day. The precipitated green crystals, which weather slowly outside the mother liquor but are soluble in DMF without decomposition, were filtered off. Yield: about 1.2 g (21.3% referred to V).

Received: February 28, 1992 [Z 5219 IE]
German version: *Angew. Chem.* **1992**, *104*, 1214

CAS Registry number:
1, 142581-16-6.

[1] a) J.-M. Lehn, *Angew. Chem.* **1988**, *100*, 91; *Angew. Chem. Int. Ed. Engl.* **1988**, *27*, 89; *ibid.* **1990**, *102*, 1347 and **1990**, *29*, 1304; b) F. Vögtle, *Supramolekulare Chemie*, Teubner, Stuttgart, **1989**; for metal-directed organization in the construction of macromolecular hosts, see also c) Y. Kobuke, Y. Sumida, M. Hayashi, H. Ogoshi, *Angew. Chem.* **1991**, *103*, 1513; *Angew. Chem. Int. Ed. Engl.* **1991**, *30*, 1496.

[2] Recently a cation *and* an anion were complexed for the first time by building a Lewis acidic center into a crown ether: M.T. Reetz, C. M. Niemeyer, K. Harms, *Angew. Chem.* **1991**, *103*, 1515; *Angew. Chem. Int. Ed. Engl.* **1991**, *30*, 1472; for inorganic Lewis acidic host compounds, cf. also X. Yang, C. B. Knobler, M. F. Hawthorne, *ibid.* **1991**, *103*, 1519 and **1991**, *30*, 1507.

[3] The term host/guest system is intended to reflect the structure of the anion of **1**.

[4] Characterization of **1**: IR (KBr, some characteristic bands): $\tilde{\nu}$ [cm^{-1}] = 1652 (s, δ, H_2O and ν, CO), 1466 (m, δ_{as}, CH_3), 1418 (vw, δ_{as}, NH_4^+), 1387 (m, δ_s, CH_3), 1095 (vs, ν_{as}, PO_3), 1017 (s, ν, V^V = O, 996 (vs, ν, V^{IV} = O). Characteristic bands in the Raman spectrum (solid, rotating pellet/ λ_e = 488.0 nm): $\tilde{\nu}$ [cm^{-1}]: 1026(vw, ν_s, PO_3), 996(m, ν, V^{IV} = O); (λ_e = 514.5 nm): $\tilde{\nu}$ [cm^{-1}] = 1025(w,ν_s, PO_3), 993(m, ν, V^{IV}=O). UV/VIS/near IR (in DMF): $\tilde{\nu}$ = 38000 (π(C···C) → π^*(C···C)), 31800, 25100 (π(O) → d(V)-CT, 16300(d(V)) 14400 (intervalence charge transfer). Magnetism (room temperature): μ_{eff}/anion = 6.12 $\mu_B \triangleq \mu_{eff}/V^{IV}$ = 1.77 μ_B. The bond valence sum $\sum\exp(-(R-R_0)/B)$ (R = V–O distance [pm], R_0 = 179 pm, B = 31.9 pm) is 4.94 for the two V^V centers and between 4.04 and 4.18 for the twelve V^{IV} centers (cf. I. D. Brown in *Structure and Bonding in Crystals Vol. II* (Eds.: M. O'Keeffe, A. Nawrotsky), Academic Press, New York, **1981**, p. 1).

[5] **1**: Correct elemental analysis. Crystal structure analysis: $P\bar{1}$, a = 1405.9(4), b = 1473.0(5), c = 1713.1(5) pm, α = 69.32(2), β = 67.37(2), γ = 83.17(3)°, V = 3062.9(16) × 10^6 pm^3, Z = 1, ρ_{calcd} = 1.711 $g cm^{-1}$; solution with direct methods, R = 0.050 for 11203 independent reflections, ($F_0 > 4\sigma(F_0)$). The measured powder diffractogram agrees with the results calculated from the single crystal data. On account of their sensitivity to weathering, the crystals from the mother liquor were embedded in silicon oil and sealed in capillary tube for the measurement, which was performed at −78 °C. Further details of the crystal structure determination may be obtained from the Fachinformationszentrum Karlsruhe, Gesellschaft für wissenschaftlich-technische Information mbH, D-W-7514 Eggenstein-Leopoldshafen 2 (FRG) on quoting the depository number CSD-56243, the names of the authors, and the journal citation.

[6] a) A. Müller, M. Penk, R. Rohlfing, E. Krickemeyer, J. Döring, *Angew. Chem.* **1990**, *102*, 927; *Angew. Chem. Int. Ed. Engl.* **1990**, *29*, 926; b) M. T. Pope, A. Müller, *ibid.* **1991**, *103*, 56 and **1991**, *30*, 34; see also c) W. G. Klemperer, T. A. Marquart, O. M. Yaghi, *ibid.* **1992**, *104*, 51 and **1992**, *31*, 49.

[7] D. D. Heinrich, K. Folting, W. E. Streib, J. C. Huffman, G. Christou, *J. Chem. Soc. Chem. Commun.* **1989**, 1411.

[8] The $C_6H_5PO_3^{2-}$ ligand has already been used for polyoxometalate syntheses; cf. for example: W. S. Kwak, M. T. Pope, P. R. Sethuraman, *Inorg. Synth.* **1990**, *27*, 123.

[9] Cf. a) A. Müller, *Nature* **1991**, *352*, 115; b) A. Müller, E. Krickemeyer, M. Penk, R. Rohlfing, A. Armatage, H. Bögge, *Angew. Chem.* **1991**, *103*, 1720; *Angew. Chem. Int. Ed. Engl.* **1991**, *30*, 1674; c) M. T. Pope, *Nature* **1992**, *355*, 27.

[10] One could expect the generation of a nucleophilic coronand through condensation of RPO_3 groups. The reason for the electronically inverse host behavior of the V/O shell system lies in the (extremely) weak attraction of the central anions by the Lewis acidic $V^{IV/V}$ centers (but simultaneously very weak repulsion by the O atoms of the shell seems to be important, too). EH-SCCC (Extended Hückel–Self Consistent Charge and Configuration) calculations for the anions of the compounds $(PhCH_2NEt_3)_2[V_5O_9Cl(tca)_4]\cdot MeCN$ [7], $(Me_4N)_6[V_{15}O_{36}Cl]\cdot 4H_2O$ (A. Müller, E. Krickemeyer, M. Penk, H.-J. Walberg, H. Bögge, *Angew. Chem.* **1987**, *99*, 1060; *Angew. Chem. Int. Ed. Engl.* **1987**, *26*, 1045), and $K_9[H_4V_{18}O_{42}Cl]\cdot 16H_2O$ [6a] confirm the picture of attractive interactions between electrophilic V centers and Cl^- ions, for example by the significantly reduced negative charge density on the Cl^- ions; for larger systems the interaction per V–Cl vector is extremely weak (corresponding to the larger distance; A. Müller, D. Sölter, unpublished).

[11] A model for the anion paradox in sodium taste reception has been published recently: Q. Ye, G. L. Heck, J. A. DeSimone, *Science* **1991**, *254*, 724.

[12] The term system here refers to a set of elements interacting with one another; the term organization here also represents the construction of a structure or ordered system of elements (atoms) or subsystems (host/guest).

[13] *Addition in the proof*: A very recent publication makes clear that an ion (e.g. Na^+) that, according to the classical view, is predominantly involved in ionic lattice formation can generate environments even from very hard "particles" (e.g. F^-) by template control in discrete molecular systems, as occurs in topologically comparable preorganized hosts such as crown ethers (H. W. Roesky, M. Sotoodeh, M. Noltemeyer, *Angew. Chem.* **1992**, *104*, 869; *Angew. Chem. Int. Ed. Engl.* **1992**, *31*, 864.

The Thermal Conversion of Poly[(silylene)-diacetylene] Metal Oxide Composites: A New Approach to β-SiC–MC Ceramics**

By *Robert Corriu,* Philippe Gerbier, Christian Guérin,* and *Bernard Henner*

Polymers **1** with a regular alternating arrangement of (di)silylene and diacetylene units[1] are interesting because of their charge-transport properties, which are consistent with a delocalization of the π electron density along the main chain, and because of their thermal properties.[1, 2] As summarized in Table 1, their pyrolysis in an argon atmosphere

$$\{(SiR^1R^2)_m(C{\equiv}C{-}C{\equiv}C)\}_n$$

1a, $R^1 = R^2 = CH_3$, $m = 1$
1b, $R^1 = R^2 = C_2H_5$, $m = 1$
1c, $R^1 = R^2 = CH_3$, $m = 2$
1d, $R^1 = CH_3$, $R^2 = C_6H_5$, $m = 1$
1e, $R^1 = R^2 = C_6H_5$, $m = 1$

at 1400 °C affords β-SiC-containing ceramics in high yields.[2, 3] All the silicon present in the organosilyl groups of the starting polymers is found in the ceramic as SiC. In addition, the ceramic chars contain a large excess of free carbon coming in part from the diacetylene units. The carbon content can range from 37.5 to 78.3%,[2–4] depending on the type of groups attached to silicon. Both these observations have been related to the crucial influence of the crosslinking of the polymers through the triple bonds. The polymers are thermally converted into an amorphous matrix of sp^2-hybridized carbon atoms in which the SiC network is formed without loss of volatile organosilicon compounds.[2, 3]

Table 1. Pyrolysis of poly[(silylene)diacetylene]s **1a–e** in an argon atmosphere.

Polymer	Ceramic yield [%]	Composition of the ceramic	C content [%]
1a	85	SiC-4C	54.5
1b	72	SiC-4C	54.5
1c	72	2(SiC)-4C	37.5
1d	87	SiC-9C	73
1e	83	SiC-12C	78.3

Taking advantage of such particular properties, we decided to investigate the use of poly[(silylene)diacetylene]s as reactive wrapping polymers for metal oxide particles. Thermal conversion of the preceramic polymer metal oxide composites should result in the "carboreduction" of the encapsulated oxide and the formation of SiC metal carbide ceramics[5, 6] as shown in Scheme 1 for **1a**. This approach would allow a great deal of flexibility in the preparation of these types of binary ceramics. We wish now to report our preliminary data in this area.

$$4MO_2 + \mathbf{1a} \xrightarrow{\text{Ar, } 210\,^\circ C} 4MO_2 + 3\,\mathbf{1a}' \quad \text{(a)}$$

$$4MO_2 + 3\,\mathbf{1a}' \xrightarrow{\text{Ar, } 450\text{–}700\,^\circ C} 4MO_2 + 3\,(\text{SiC-4C}) \quad \text{(b)}$$

$$4MO_2 + 3\,(\text{SiC-4C}) \xrightarrow{\text{Ar, } 1300\text{–}1400\,^\circ C} 3SiC + 4MC + 8CO \quad \text{(c)}$$

Scheme 1. Formation of SiC–MC ceramics from **1a** metal oxide composites. **1a**′ denotes the crosslinked polymer.

In a typical experiment, for example for SiC–TiC ceramics, a precursor material was formed by dispersing 0.266 g of a finely divided TiO_2 powder[7] in 25 mL of a solution of 0.265 g of the poly[(dimethylsilylene)diacetylene] in THF. The molar ratio TiO_2:polymer was based on the reaction $3\,\mathbf{1a} + 4TiO_2 \rightarrow 3SiC + 4TiC + 8CO$, that is, 4:3. The mixture was treated with ultrasound while the solvent was evaporated under vacuum.[8] A sample of the resulting solid

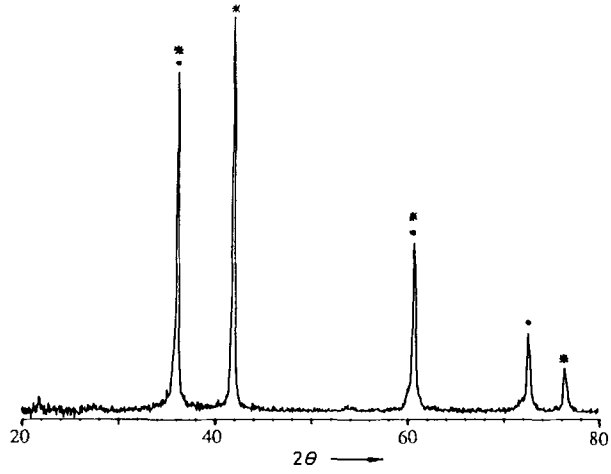

Fig. 1. X-ray powder diffraction diagram of the ceramic obtained by pyrolysis of 3 **1a**–4TiO_2. (● = β-SiC; ⋆ = TiC).

[*] Prof. R. Corriu, P. Gerbier, Prof. C. Guérin, Dr. B. Henner
UM CNRS – Rhône Poulenc – USTL N° 44
Université Montpellier II, Sciences et Techniques du Languedoc
Place E. Sataillon, F-34095 Montpellier Cedex 5 (France)

[**] This work was supported by the Centre National de la Recherche Scientifique, the Ministère de l'Education Nationale, and Rhône-Poulenc. The authors thank Prof. R. Fourcade (Lavoratoire des Agrégats Moléculaires et Matériaux Inorganiques, URA CNRS 79, Université Montpellier II) for X-ray diffraction studies.

was then heated in an aluminum boat in a cylindrical furnace under argon at 1400 °C for 2 h. The solid residue was obtained in 60% ceramic yield[9] (theoretical ceramic yield: 56.4%). The X-ray powder diffraction spectrum shows only lines caused by SiC and TiC[10] (Fig. 1) and provides no evidence of either unreacted TiO_2 or other crystalline complex oxides. As shown in Figure 2, the strong band in the IR spectrum of the solid residue (KBr pellet) centered near 830 cm^{-1}, characteristic of the Si–C stretch,[11] provides further evidence for the formation of β-SiC. Moreover, IR peaks that could be characteristic of the presence of amorphous O-, C-, Si-, and Ti-containing phases are absent in the region 900–1100 cm^{-1}.[12] Peaks that could be due to residual TiO_2 were not observed in the region 200–500 cm^{-1} (polyethylene pellet).

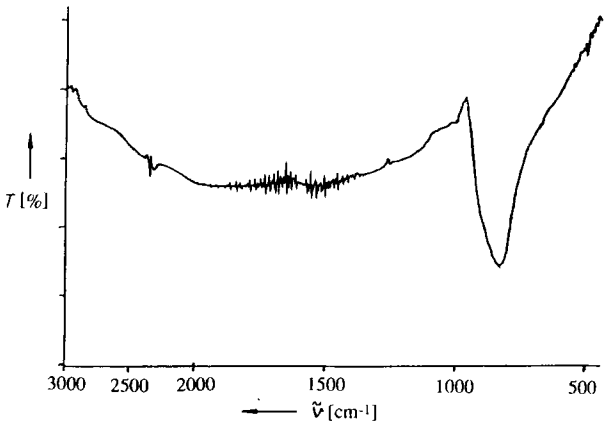

Fig. 2. IR spectrum of the ceramic obtained by pyrolysis of 3 **1a**–4 TiO_2. T = transmittance.

Thermogravimetric (TGA) and differential thermal analysis (DTA) were conducted with a thermogravimetric analyzer interfaced with a mass spectrometer.[13] Total weight loss is about 45–46%, very close to the expected theoretical value of 43.6%. Moreover, the thermograms (Fig. 3) clearly suggest that a three-step reaction takes place when the temperature of the sample is increased up to 1400 °C:

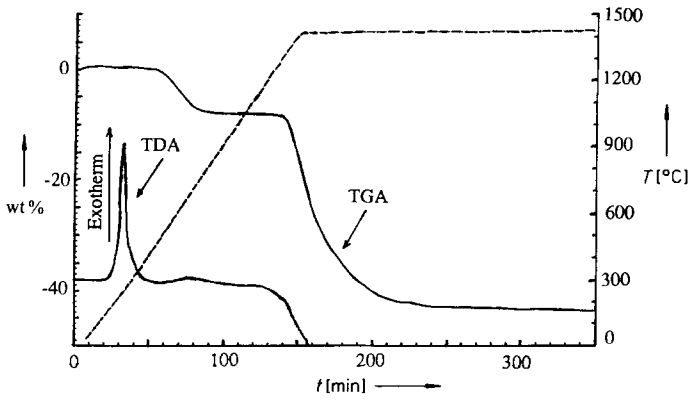

Fig. 3. Pyrolysis of 3 **1a**–4 TiO_2 under argon followed by TGA and TDA. (– – –: temperature in the furnace).

1) Initially, the DTA curve exhibits a strong maximum at about 210 °C, as observed previously for **1a**.[2] The exothermic transformation indicated is related to the thermally induced cross-polymerization through the diacetylene groups [Scheme 1, Eq. (a)]. The presence of TiO_2 has no significant effect on this step.

2) Second, the TGA trace shows an initial weight loss primarily between 500 and 700 °C (versus 400–750 °C for **1a**). The off-gases from the pyrolysis were identified by mass spectrometry as CH_4 and H_2 (Fig. 4). No gaseous silicon-

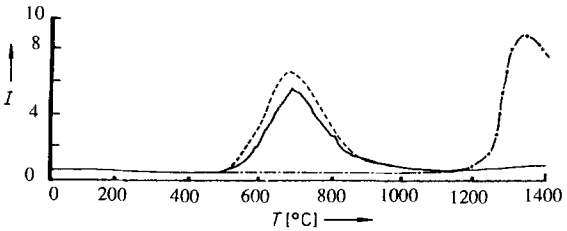

Fig. 4. Pyrolysis of 3 **1a**–4 TiO_2 under argon. Analysis of the volatiles by mass spectrometry. (– – –: CH_4; ——: H_2; –·–·–: CO). I = ion flow (arbitrary units).

containing species were detected. Furthermore, the measured weight loss (8–9%) is quite close to that expected for the thermal decomposition of the starting polymer alone leading to a 3(SiC-4C)–4 TiO_2 material (theoretical yield: 8.5%) [Scheme 1, Eq. (b), and Table 1].

3) Finally, this intermediate material reacts at higher temperatures (1300–1400 °C) with TiO_2 to produce the SiC–TiC ceramic. All the free carbon present is converted into CO and TiC. The weight loss (36%) is consistent with a complete carboreduction of the metal oxide [Scheme 1, Eq. (c)].

Interestingly, the carboreduction starts at a relatively low temperature, namely 1300 °C. As a comparison, TiO_2 is converted by carbon alone at temperatures higher than 1700 °C.[14] The crucial influence of the cross-polymerization of **1a** on the overall yield of the carboreduction of TiO_2 was demonstrated in the following reference reaction. Under similar experimental conditions (1400 °C, 5 h), thermal treatment of TiO_2 with a SiC–4C powder obtained by a separate pyrolysis of **1a** led to a complex residue containing a high percentage of TiO_2 and other oxides besides SiC. This clearly suggests that the ability of the poly[(dimethylsilylene)-diacetylene] **1a** to act as an efficient reagent in carboreduction reactions originates from its conversion into a silylated carbon matrix which coats the TiO_2 particles during the initial stages of the pyrolysis.

The above approach is quite general, and a wide range of binary SiC-MC ceramics can be easily obtained (Tables 2 and 3). Two observations may be summarized: 1) The method can be extended to a number of metal oxides including B_2O_3.

Table 2. Generation of β-SiC metal carbide ceramics from pyrolysis of **1a** metal oxide composites.

Polymer (equiv)	Metal oxide [a] (equiv)	Ceramic yield [%]	Composition of the ceramic [b] (MC [%])
1a (3)	TiO_2 (4)	56	3 SiC-4 TiC (72.7)
1a (3)	ZrO_2 (4)	62	3 SiC-4 ZrC (77.4)
1a (7)	B_2O_3 (8)	35	7 SiC-4 B_4C (44.4)
1a (7)	MoO_3 (8)	59	7 SiC-4 Mo_2C (60.7)
1a (13)	V_2O_5 (8)	52	13 SiC-4 V_4C_3 (64.8)
1a (3)	HfO_2 (4)	71	3 SiC-4 HfC (86.4)
1a (7)	Nb_2O_5 (4)	62	7 SiC-8 NbC (80.5)

[a] Temperatures for carboreduction[14]: TiO_2 (>1700 °C); ZrO_2 (1900–2100); B_2O_3 (2000–2500 °C); MoO_3 (>1600); V_2O_5 (1150–1300); HfO_2 (>1700); Nb_2O_5 (>1600). [b] SiC and metal carbides were characterized by X-ray powder diffraction.

Under similar experimental conditions (1400 °C, 5 h), the pyrolysis of the poly[(dimethylsilylene)diacetylene] metal oxide composites in an argon atmosphere gave high yields of crystalline solid phases that contained the respective metal carbide and SiC. In all cases, the reaction with the metal oxide takes place at lower temperatures than with only carbon. 2) Variation of the poly[(silylene)diacetylene]s allows the modulation of the composition of the final ceramics as summarized for TiO_2 (Table 3). When aryl groups are bonded to the silylene unit, ceramic residues containing higher amounts of TiC result (Table 3, run 3). In contrast, **1c**, a polymer with two dimethylsilylene units, produces a ceramic with a TiC content of 57.1 % (Table 3, run 2).

Table 3. Pyrolysis of poly[(silylene)diacetylene]–TiO_2 composites.

Run	Polymer (equiv)	TiO_2 (equiv)	Ceramic yield [%]	Composition (MC [%])
1	**1a**	(4)	56	3 SiC-4 TiC (72.7)
2	**1c**	(4)	60	6 SiC-4 TiC (57.1)
3	**1e**	(4)	51	SiC-4 TiC (88.9)

Thus, we may expect to prepare a wide range of multiphase ceramics of defined composition. Investigation of the potential of this method and the mechanistic implications are now under progress.

Received: March 17, 1992 [Z 5242 IE]
German version: *Angew. Chem.* **1992**, *104*, 1228

CAS Registry numbers:
SiC, 409-21-2; TiC, 12070-08-5; ZrC, 12070-14-3; B_4C, 12069-32-8; Mo_2C, 12069-89-5; V_4C_3, 12076-63-0; HfC, 12069-85-1; NbC, 12069-94-2.

[1] R. Corriu, C. Guérin, B. Henner, A. Jean, T. Kuhlmann, Fr.-A 05567, **1989**; R. Corriu, C. Guérin, B. Henner, A. Jean, F. Garnier, A. Yassar, *Chem. Mater.* **1990**, *2*, 351; *Organometallics*, **1992**, *11*, 2500.
[2] R. Corriu, C. Guérin, B. Henner, A. Jean, H. Mutin, *J. Organomet. Chem.* **1990**, *396*, C35; *Organometallics*, **1992**, *11*, 2507.
[3] A. Jean, *Ph.D. Thesis*, Université Montpellier, **1991**.
[4] S. Ijadi-Magsoodi, T. J. Barton, *Macromolecules* **1990**, *23*, 4485.
[5] SiC metal carbide ceramics have been recently obtained by the pyrolysis of polycarbosilane metal powder composites: D. Seyferth, N. Bryson, D. P. Workman, C. A. Sobon, *J. Am. Ceram. Soc.* **1991**, *74*, 2687.
[6] For the formation of a SiC-TaC ceramic, see: K. Thorne, E. Liimatta, J. D. Mackenzie, *J. Mater. Res.* **1991**, *6* (10), 2199, and references therein.
[7] TiO_2 particle size: <100 mesh.
[8] K. Su, L. G. Sneddon, *Chem. Mater.* **1991**, *3*, 10.
[9] The pyrolysis experiments were carried out on weighed samples (0.1 to 1 g) of the polymer metal oxide composite which were heated in an aluminum oxide boat (80 × 10 × 10 mm) with a gas-tight aluminium oxide tube (length 100 cm, diameter 30 mm) fitted with glass taps to allow the connection with a vacuum line. The argon flow was maintained at about 50 mL min^{-1}. Experiments were performed in Eurotherm or Carbolite furnaces (heating rate of 10 °C min^{-1} up to 1400 °C; then 5 h at 1400 °C). Ceramic yield = (weight of pyrolysis residue × 100) (weight of pyrolysis carge)$^{-1}$.
[10] SiC and TiC were characterized by X-ray powder diffraction (Phillips diffractometer, $Cu_{K\alpha}$ radiation). The elemental analysis 48.20% Ti and 21.16% Si indicates the SiC–TiC phases to be present in a 3:4 ratio.
[11] See, for example: G. Ramis, P. Quintard, M. Cauchetier, G. Busca, V. Lorenzelli, *J. Am. Ceram. Soc.* **1989**, *72*, 1692.
[12] See, for example: R. Jabra, J. Phalippou, M: Prassas, J. Zarzycki, *J. Chim. Phys. Phys. Chim. Biol.* **1981**, *78*, 777; M. Camblor, A. Corma, A. Martinez, J. Pérez-Pariente, *J. Chem. Soc., Chem. Commun.* **1992**, 589, and references therein.
[13] Simultaneous TGA and TDA analyses were performed in a stream of argon (50 mL min^{-1}) with a Netzsch STA thermogravimetric analyzer interfaced with an Anagas 200 Delsi-Nermag mass spectrometer (heating rate 10 °C min^{-1}). TGA and TDA measurements were conducted with the Netzsch SW-STA-311. 001 software on a HP 9000-300 computer.
[14] P. Pascal, *Nouveau Traité de Chimie Minérale*, Masson, Paris; *Gmelin Handbuch der Anorganischen Chemie*, Springer, Heidelberg.

(Organoarsonato)polyoxovanadium Clusters: Properties and Structures of the V^V Cluster $[V_{10}O_{24}(O_3AsC_6H_4\text{-}4\text{-}NH_2)_3]^{4-}$ and the V^{IV}/V^V Cluster $[H_2\{V_6O_{10}(O_3AsC_6H_5)_6\}]^{2-}$ **

By *M. Ishaque Khan, Yuanda Chang, Qin Chen, Hakon Hope, Sean Parking, D. P. Goshorn*, and *Jon Zubieta**

The chemistry of polyoxovanadium clusters incorporating Group 5 elements has witnessed significant growth in recent years. Arsenic–vanadium clusters exhibit a variety of structural types of considerable topological interest[1, 2] and possess a range of stable cluster oxidation states as well as unusual magnetic properties.[3–6] Furthermore, these heteropolyvanadates exhibit a pronounced tendency to form cage structures which may encapsulate neutral molecules or anions, a feature shared with a number of isopolyanions such as $[V_{18}O_{42}(H_2O)]^{12-}$,[7] $[V_{14}O_{42}(SO_4)]^{8-}$,[5] $[H_4V_{18}O_{42}(X)]^{9-}$ (X = Cl, Br, I),[8–10] and $[V_{12}O_{36}(CH_3CN)]^{4-}$[11] and recently described for $[V_{12}As_8O_{40}(HCO_2)]^{n-}$ (n = 3,5),[3] $[V_{15}As_6O_{42}(H_2O)]^{6-}$,[4] $[V_{14}As_8O_{42}(SO_4)]^{6-}$,[5] and $[V_{14}As_8O_{42}(0.5\,H_2O)]^{4-}$.[6] A related family of (organophosphonato)polyoxovanadium clusters constitutes a new class of layered compounds which can exhibit useful sorptive and catalytic properties,[12–14] while the molecular polyanions $[H_{12}V_{12}O_{24}(O_3PC_6H_5)_8]^{4-}$[15] and $[H_6V_{16}O_{32}(O_3PCH_3)_8]^{8-}$[16] provide examples of structures displaying cage and "tire" structural motifs, respectively. However, in contrast to this rapid development of the arsenic- and (organophosphonato)polyoxovanadium systems, the chemistry of oxovanadium clusters with organoarsonates $RAsO_3^{2-}$ remains relatively unexplored, although one example of a layered structure $[V_2O_4(C_6H_5AsO_3H)] \cdot H_2O$[17] has been described. In this communication, we report two novel polyoxovanadium structural types found in the "oxidized" cluster **1** and the mixed valence cluster **2**. The structures of these clusters illustrate the dramatic influences of small changes in ligand type upon the overall molecular geometry.

$(TBA)_2(NH_4)_2[V_{10}O_{24}(O_3AsC_6H_4\text{-}4\text{-}NH_2)_3]$ **1**
$(TBA)_2[H_2\{V_6O_{10}(O_3AsC_6H_5)_6\}] \cdot 2H_2O$ **2**
TBA = $(n\text{-}C_4H_9)_4N$

Red, parallelepiped crystals of **1** were prepared in approximately 45% yield by heating a mixture of $(NH_4)_2Na_2K_2[V_{10}O_{28}]$, arsanilic acid $4\text{-}NH_2C_6H_4\text{–}AsO(OH)_2$, and (TBA)Br in methanol at reflux for 20 min. X-ray structure analysis of **1**[18] revealed the presence of discrete (TBA) and NH_4^+ ions and a $[V_{10}O_{24}(O_3AsC_6H_4\text{-}4\text{-}NH_2)_3]^{4-}$ ion, whose structure is shown in Figure 1. The overall structure may be described as a $[V_9O_{21}(O_3AsC_6H_4NH_2)_3]^{3-}$ toroid encapsulating a VO_3^- moiety. The toroid consists of three trinuclear $\{V_3O_{13}\}$ units of edge-sharing octahedra with the conventional 60° angle formed by the V centers,[19] which are linked through bridging oxo groups and the arsonato

[*] Prof. J. Zubieta, Dr. M. I. Khan, Y. Chang, Dr. Q. Chen
Department of Chemistry, Syracuse University
Syracuse, NY 13244 (USA)
S. Parkin, Prof. H. Hope
Department of Chemistry, University of California, Davis
Davis, CA 95616 (USA)
Dr. D. P. Goshorn
Exxon Research and Development Co.
Annandale, NJ 08801 (USA)

[**] This work was supported by a grant from the National Science Foundation (CHE9119910 to J. Z.)

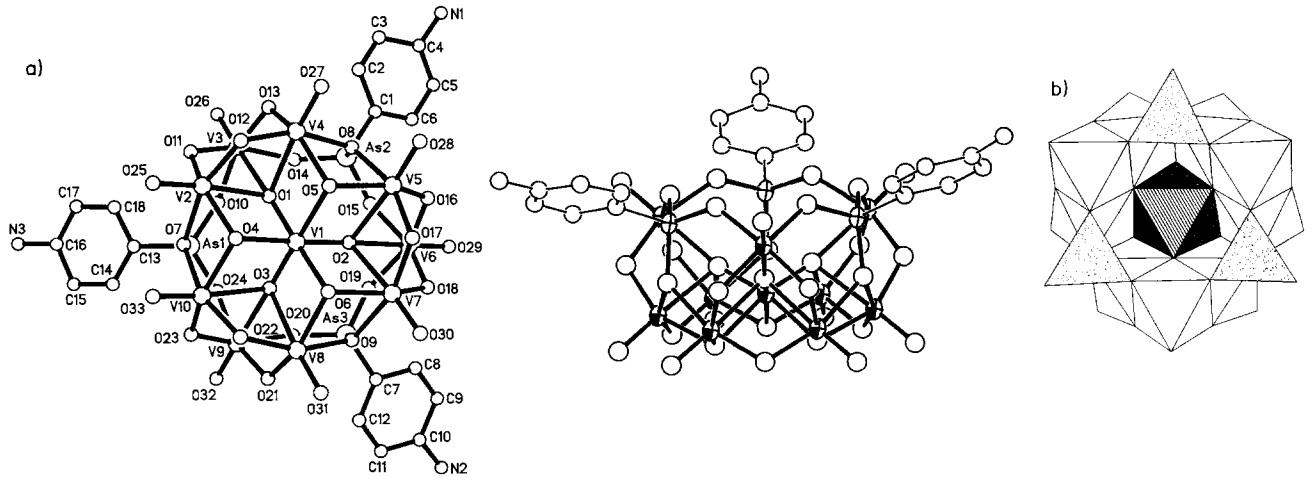

Fig. 1. a) Perspective views of the crystal structure of the anion in **1**. Left: View along the approximate threefold axis of the anion. Right: View perpendicular to this threefold axis. Selected bond lengths [Å] and angles [°]: V(ring)-O(terminal), 1.56(1)–1.61(1); V(ring)-O(μ^2), 1.79(1)–1.86(1); V(ring)-O(μ^3), 1.92(2)–1.99(1); V(ring)-O(μ^4), 2.28(1)-2.33(1); V1-O(μ^3), 2.10(1)–2.20(1); V1-O(μ^4), 1.69(1)–1.71(1); As-O(μ^2), 1.65(2)–1.69(2); As-O(μ^3), 1.72(2)–1.75(2); O1-V1-O6, 166.1(6); O2-V1-O4, 167.1(6); O3-V1-O5, 168.8(6). b) A polyhedral representation of the structure of the anion illustrating the stacking one ring of V octahedra and As tetrahedra, $[V_3(RAsO)_3]^{9+}$, on an Anderson core $[V_7O_{24}]^{13-}$.

ligands. The central vanadium atom V1 is in a highly distorted octahedral environment, in which the metal atom is displaced toward the O1-O2-O3 face; the average V–O(1,2,3) distance is 1.70(2) Å as compared to an average distance of 2.14(2) Å for V–O(4,5,6). This unusual oxometalate arrangement in **1** gives rise to four distinct types of oxo groups: terminal O atoms associated with the V centers of the nine-membered ring, μ^2 oxo groups that bridge V atoms of the $\{V_3O_{13}\}$ units, μ^3 types that link the $\{V_3O_{13}\}$ units to the central vanadium atom, and μ^4 oxo groups which provide both the common vertex for the V octahedra of the trinuclear units and the link to the encapsulated V atom. Each organoarsonate group shares two of its oxygen atoms with vanadium centers of adjacent trinuclear units, while the third is bound to two vanadium centers in neighboring trinuclear units. The anion in **1** exhibits structural features common to polyanions exhibiting a central MO_6 octahedron[20–22] and to ε-Keggin types.[23] The polyhedral representation of Figure 1b clearly shows the relationship of **1** to the Anderson $\{M_7O_{24}\}$ clusters.[23] The structure of the anion in **1** may be best described as a double layer of polyhedra, one layer composed of the $[V_7O_{24}]^{13-}$ Anderson core and the second consisting of a $[V_3(RAsO_3)_3]^{9+}$ ring which rests on one face of the Anderson core.

Complex **1** undergoes a reversible one-electron reduction at -0.54 V to give the green-brown $[V_{10}O_{24}(O_3AsC_6H_4\text{-}4\text{-}NH_2)_3]^{5-}$ which displays a broad EPR signal centered at $g = 1.95$. In contrast, chemical oxidation of **1** with hydrazines results in multiple-electron transfer coupled to proton transfer to give purple solutions of $[V_{10}O_{21}(OH)_3(O_3AsC_6H_4\text{-}4\text{-}NH_2)_3]^{4-}$. Carefully controlled addition of the hydrazine reagents produces anions of intermediate reduction/protonation states. Such multiple electron–proton transfer processes appear to be characteristic of the chemistry of polyvanadates stabilized by organic ligands.[30]

The reaction of $(NH_4)_2Na_2K_2[V_{10}O_{28}]$ with $C_6H_5AsO(OH)_2$ in the presence of (TBA)Br quite unexpectedly resulted in partial reduction to give **2** as bright green crystals in 65% yield. The structure of **2**[24] consists of discrete (TBA) ions and molecular anions of $[H_2\{V_6O_{10}(O_3AsC_6H_5)_6\}]^{2-}$, shown in Figure 2a. Although the numerous examples of arsonatopolyoxovanadates studied to date invariably exhibit spherical or annular structures, similar to that of the anion in **1**, the structure of the anion in **2** consists of a twisted 24-membered ring $\{V_6As_6O_{12}\}$ (Fig. 2b), which is highly distorted by the presence of additional intraring V-O-V and As-O-V bridges; the As-phenyl substituents, the ter-

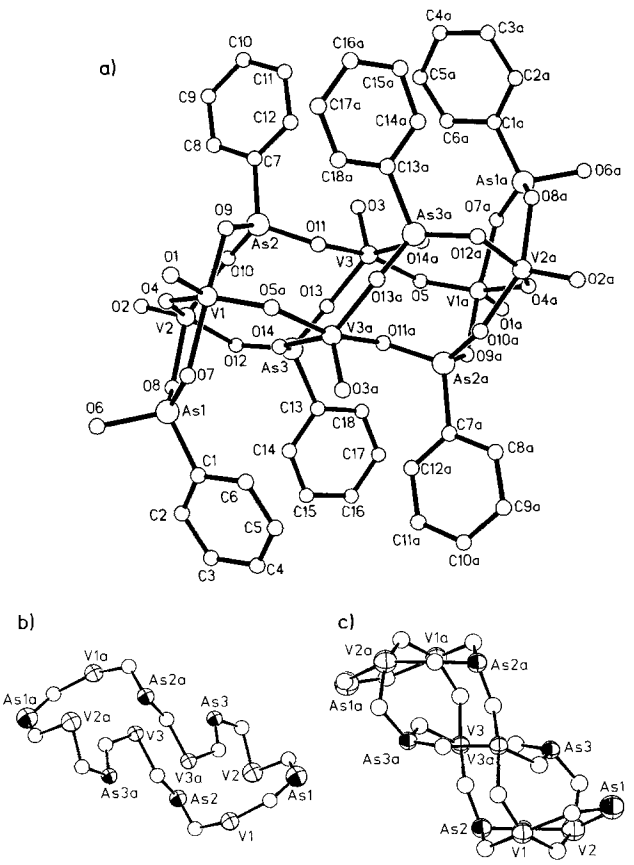

Fig. 2. a) Crystal structure of the anion in **2** (ORTEP). Selected bond lengths [Å]: V1-O1, 1.60(2); V1-O4, 1.97(2); V1-O5, 1.69(2); V1-O7, 2.04(2); V1-O9, 1.94(2); V2-O2, 1.57(3); V2-O4, 1.71(2); V2-O8, 1.98(2); V2-O10, 1.94(2); V2-O12, 1.93(2); V3-O3, 1.59(2); V3-O5, 1.99(2); V3-O11, 2.01(2); V3-O13, 1.99(2); V3-O14, 1.99(2); As1-O6, 1.79(3); all other As-O distances from 1.60(2) to 1.70(2) Å. b) A view of the $\{V_6As_6O_{12}\}$ ring of the anion. c) The stacking of the $\{V_2As_2O_4\}$ rings.

 © VCH Verlagsgesellschaft mbH, W-6940 Weinheim, 1992 0570-0833/92/0909-1198 $ 3.50+.25/0 Angew. Chem. Int. Ed. Engl. 1992, 31, No. 9

minal oxo groups of the vanadium atoms, and the hydroxyl groups of As1 and As1a project from this central ring. Alternatively, the structure may be described in terms of a layer structure of three $\{V_2As_2O_4\}$ rings connected in a stacking fashion by μ^2 oxo groups, as shown in Figure 2c.

The vanadium centers exhibit square-pyramidal geometry with the standard apical disposition of the terminal oxo groups. Each of the organoarsonate groups is bound to two oxygen atoms and contributes to the formation of the $\{V_2As_2O_4\}$ rings, and four of them employ a third oxygen atom to coordinate to an adjacent ring. The remaining two organoarsonate groups participate in the outermost $\{V_2As_2O_4\}$ rings, while the third oxygen atom of each is a terminal ligand. The latter oxygen atoms, O6 and O6a, are protonated. This assignment is based on the fact that the As3–O6 bond is long relative to the value anticipated for a terminal As=O bond, and the location of one peak in the difference electron density maps is consistent with a hydroxyl proton. The overall anionic charge of 2– requires the presence of four V^V and two V^{IV} centers, an assumption confirmed by potentiometric titration. On the basis of valence sum calculations,[25] the reduced sites are identified as V3 and V3a.

The presence of two reduced centers is confirmed by the magnetic properties of **2**. This compound exhibits behavior characteristic of isolated V_2 units. The temperature dependence of the magnetic susceptibility in the range 4.2 to 300 K follows the Bleany–Bowers equation[26] for isolated dimers containing two $S = 1/2$ cations with isotropic g tensors; the susceptibility displays a maximum at 20 K. The susceptibility data are consistent with extremely weak exchange coupling ($2J = -9.1\ cm^{-1}$) within vanadium dimers which are effectively isolated from each other. The magnetic data may be compared to that for $(VO^{2+})_2$ systems in which J ranges from -25 to $-250\ cm^{-1}$.[27] The weak exchange coupling in **2** is similar to that observed for $VO(HPO_4) \cdot 0.5\ H_2O$[28] and $VO(HPO_4) \cdot 2H_2O$,[29] salts which possess building blocks made up of two VO^{2+} units with similar exchange networks. Furthermore, in contrast to **1**, **2** undergoes two successive, facile, and reversible one-electron oxidations at +0.09 and +0.46 V, which is consistent with the presence of two readily oxidized V^{IV} centers. Thus, the cluster possesses magnetic and electron-transfer properties suggestive of a dimer $\{V_2O_4(O_3AsC_6H_5)_2\}$ encapsulated and stabilized by sandwiching between two $\{V_2O_5(O_3AsC_6H_5)_2\}$ fragments. While ligand-free polymetalates undergo almost exclusively cathodic processes, the introduction of organic ligands into the polymetalate framework allows the development of a more extensive electrochemistry by stabilizing a variety of "reduced" and mixed valence clusters with modified electron-storage and proton-transfer properties.[30]

The organoarsonate chemistry of vanadium appears to be remarkably diverse, such that relatively minor changes in substituents can produce dramatic structural differences as exemplified by **1** and **2**. Furthermore, their electrochemical and magnetic properties suggest extensive electron storage and coupled electron–proton transfer in the chemistry of clusters of this type.

Experimental Procedure

1: Under an atmosphere of argon, (TBA)Br (2.58 g, 8 mmol) and arsanilic acid (0.868 g, 4 mmol) were placed in a Schlenk tube fitted with a reflux condenser and were then dissolved in methanol (25 mL). $(NH_4)_2Na_2K_2[V_{10}O_{28}]$ (0.56 g, 0.5 mmol) was added, and the resulting suspension was heated at reflux with stirring for 20 min whereupon a clear red-brown solution was obtained. After the hot solution was filtered and cooled to room temperatue, it was stored at 4 °C for 20 h. Shiny red crystals of **1** were collected in 45% yield. Satisfactory C,H,N-analysis. IR (KBr): $\tilde{\nu}\ [cm^{-1}] = 3456(s), 3365(s), 1624(s), 1591(s), 1500(s), 1479(m), 1457(m), 1307(m), 1181(m), 1092(s), 985(s), 972(vs), 878(s), 790(sh), 733(s), 626(m), 530(m)$; UV/VIS ($CH_3CN$): λ_{max} [nm] ($\varepsilon\ [cm^{-1}M^{-1}]$) = 258 ($6.72 \times 10^4$), 294 (sh). ^{51}V NMR (CH_3CN, $VOCl_3$ standard): $\delta = -499, -507, -533$; electrochemical parameters (10^{-3} M **1**, 10^{-1} M (TBA)PF_6, CH_3CN, ferrocene/ferrocenium standard): -0.54 V (ΔE = 64 mV).

2: A mixture of phenylarsenic acid (0.802 g, 4 mmol), (TBA)Br (2.58 g, 8 mmol), and $(NH_4)_2Na_2K_2[V_{10}O_{28}]$ (0.56 g, 0.5 mmol) in methanol (40 mL) was heated at reflux for 40 min to give a bright green solution. A small amount of insoluble residue was removed by filtration, and the filtrate was evaporated to dryness. The resultant green solid was dissolved in a minimum amount of acetronitrile, carefully layered with 50 mL of pentane, isopropanol, and diethyl ether (1:1:1), and allowed to stand at room temperature for 4 d. Dark green crystals of **2** were isolated in 65% yield. Satisfactory C,H,N-analysis. IR (KBr): $\tilde{\nu}\ [cm^{-1}] = 3058(w), 2962(m), 2874(m), 1482(m), 1440(m), 1382(w), 1094(m), 982(s), 872(vs), 841(vs), 743(s), 691(m), 561(sh), 492(s)$. UV/VIS ($CH_3CN$): λ_{max} [nm] ($\varepsilon\ [cm^{-1}M^{-1}]$) = 240 ($2.25 \times 10^4$), 275 (sh), 368 ($3.30 \times 10^3$), 660 (352); magnetic properties: Bleany–Bowers fit: $\chi_o = -3.74 \times 10^{-4}\ cm^3mol^{-1}$, $C_i = 0.0139\ cm^3K\ mol^{-1}$, $C_d = 0.3036\ cm^3K\ mol^{-1}$, $2J = -9.1\ cm^{-1}$; μ_{eff} = 1.73 μ_B; electrochemical parameters (10^{-3} M **2**), 10^{-1} M (TBA)PF_6, CH_3CN, ferrocene/ferrocenium standard): +0.09 V (ΔE_p = 62 mV), +0.46 V (ΔE_p = 74 mV).

Received: March 11, 1992 [Z 5235 IE]
German version: *Angew. Chem.* **1992**, *104*, 1236

CAS Registry numbers:
1, 142839-60-9; **2**, 142839-67-6; 4-$NH_2C_6H_4$-$AsO(OH)_2$, 98-50-0; $[V_{10}O_{24}(O_3AsO_6H_4\text{-}4\text{-}NH_2)_3]^{5-}$, 142839-61-0; $[V_{10}O_{21}(OH)_3(O_3AsC_6H_4\text{-}4\text{-}NH_2)_3]^{4-}$, 142839-62-1; $(NH_4)Na_2K_2[V_{10}O_{28}]$, 142097-04-9; $C_6H_5AsO(OH)_2$, 98-05-5; $[V_6O_{10}(O_3AsC_6H_5)_6]^{3-}$, 142839-64-3; $[V_6O_{10}(O_3AsC_6H_5)_6]^{3-}$, 142839-63-2.

[1] M. T. Pope, A. Müller, *Angew. Chem.* **1991**, *103*, 56; *Angew. Chem. Int. Ed. Engl.* **1991**, *30*, 34.
[2] A. Müller, J. Döring, M. I. Khan, V. Wittneben, *Angew. Chem.* **1991**, *103*, 203; *Angew. Chem. Int. Ed. Engl.* **1991**, *30*, 210.
[3] A. Müller, J. Döring, H. Bögge, *J. Chem. Soc. Chem. Commun.* **1991**, 273.
[4] A. Müller, J. Döring, *Angew. Chem.* **1988**, *100*, 1789; *Angew. Chem. Int. Ed. Engl.* **1988**, *27*, 1721.
[5] A. Müller, J. Döring, *Z. Anorg. Allg. Chem.* **1991**, *595*, 251.
[6] G. Huan, M. A. Greaney, A. J. Jacobson, *J. Chem. Soc. Chem. Commun.* **1991**, 260.
[7] G. K. Johnson, E. O. Schlemper, *J. Am. Chem. Soc.* **1978**, *100*, 3645.
[8] A. Müller, J. Döring, H. Bögge, E. Krickemeyer, *Chimia* **1988**, *42*, 300.
[9] A. Müller, E. Krickemeyer, M. Penk, H.-J. Walberg, H. Bögge, *Angew. Chem.* **1987**, *99*, 1060; *Angew. Chem. Int. Ed. Engl.* **1987**, *26*, 1045.
[10] A. Müller, M. Penk, R. Rohlfing, E. Krickemeyer, J. Döring, *Angew. Chem.* **1990**, *102*, 927; *Angew. Chem. Int. Ed. Engl.* **1990**, *29*, 926.
[11] V. W. Day, W. G. Klemperer, O. M. Yaghi, *J. Am. Chem. Soc.* **1989**, *111*, 5959.
[12] J. W. Johnson, A. J. Jacobson, W. M. Butler, S. E. Rosenthal, J. F. Brody, J. T. Lewandowski, *J. Am. Chem. Soc.* **1989**, *111*, 381.
[13] M. S. Whittingham, A. J. Jacobson, *Intercalation Chemistry*, Academic Press, New York, **1982**.
[14] A. Clearfield, *Inorganic Ion Exchange Materials*, CRC Press, Boca Raton, FL, USA, **1982**.
[15] G. Huan, V. W. Day, A. J. Jacobson, D. P. Goshorn, *J. Am. Chem. Soc.* **1991**, *113*, 3188.
[16] G. Huan, A. J. Jacobson, V. W. Day, *Angew. Chem.* **1991**, *103*, 426; *Angew. Chem. Int. Ed. Engl.* **1991**, *30*, 422.
[17] G. Huan, J. W. Johnson, A. J. Jacobson, J. S. Merola, *Chem. Mater.* **1990**, *2*, 719.
[18] a) **1**: Monoclinic, space group $P2_1/c$ with $a = 13.081(3)$, $b = 23.018(4)$, $c = 27.561(8)$ Å, $\beta = 101.85(1)°$, $V = 8122(3)$ Å^3, $Z = 4$ (ϱ_{calc} = 1.676 g cm^{-1}; $\mu(Cu_{K\alpha}) = 11.41\ mm^{-1}$), $R = 0.087$ for 5290 reflections with $2\theta < 108.5°$ and $I > 3\sigma(I)$; Siemens P3RA diffractometer with rotating anode, Ni-filtered Cu radiation. The structure was solved using direct methods with the Siemens SHELXTL PLUS package. Further details of the crystal structure investigation may be obtained from the Fachinformationszentrum Karlsruhe, Gesellschaft für wissenschaftlich-technische Information mbH, D-W-7514 Eggenstein-Leopoldshafen 2 (FRG), on quoting the depository number CSD-56316, the names of the authors, and the journal citation.
[19] D. L. Keppert, *The Early Transition Metals*, Academic Press, London, **1972**.
[20] M. T. Pope, *Heteropoly and Isopoly Oxometalates*, Springer, New York, **1983**.
[21] T. J. R. Weakley, *J. Less-Common Met.* **1977**, *54*, 129.
[22] A. Kobayaski, Y. Sasaki, *Chem. Lett.* **1975**, 1123.

[23] M. Ichida, K. Nagai, Y. Sasaki, M. T. Pope, *J. Am. Chem. Soc.* **1989**, *111*, 586.
[24] **2**: Monoclinic, space group $P2_1/c$ with $a = 13.193(2)$, $b = 16.091(4)$, $c = 23.096(5)$ Å, $\beta = 92.96(1)°$, $V = 4896(1)$ Å^3, $Z = 2$ ($\varrho_{calc} = 1.304$ g cm^{-1}; $\mu(Mo_{K\alpha}) = 10.45$ cm^{-1}), $R = 0.069$ for 2067 reflections with $2\theta < 50°$ and $I > 3\sigma(I)$; Rigaku AFC5S diffractometer, graphite monochromated $Mo_{K\alpha}$ radiation. The structure was solved using the direct methods routine of the TEXSAN program package [18b].
[25] I. D. Brown, K. K. Wu, *Acta Crystallogr. Sect. B* **1976**, *32*, 1957.
[26] B. Bleany, K. D. Bowers, *Proc. R. Soc. London. A* **1952**, *214*, 451.
[27] A. P. Ginsberg, E. Koubek, H. J. Williams, *Inorg. Chem.* **1966**, *5*, 1656; A. Syamal, *Coord. Chem. Rev.* **1975**, *26*, 309.
[28] J. W. Johnson, D. C. Johnston, A. J. Jacobson, J. F. Brody, *J. Am. Chem. Soc.* **1984**, *106*, 8123.
[29] G. Villeneuve, K. S. Suh, P. Amoros, N. Casan-Pastor, D. Beltran-Porter, *Chem. Mater.* **1992**, *4*, 108.
[30] Q. Chen, D. P. Goshorn, C. P. Scholes, X.-L. Tan, J. Zubieta, *J. Am. Chem. Soc.* **1992**, *114*, in press.

Novel Polyether Copolymers Consisting of Linear and Dendritic Blocks**

By *Ivan Gitsov, Karen L. Wooley,* and *Jean M. J. Fréchet**

Polyethylene glycols (PEGs), their derivatives and amphiphilic block copolymers have many applications as phase-transfer reagents,[1] as compounds that could potentially encapsulate other materials,[2] and as emulsifying agents.[3] Their properties arise from the existence of both hydrophilic and hydrophobic parts of the macromolecules. In spite of the promising results achieved up to now, the synthesis of novel polymers and copolymers of that type is still of importance due to the high demand for new materials with defined architecture and improved properties.

Recently, the synthesis of novel dendritic polyethers was reported.[4, 5] Because of their dense, but nonentangled structure these dendrimers are expected to impart unusual properties to other polymeric materials when incorporated in the polymer chain. This report explores the incorporation of these highly branched amorphous and hydrophobic dendrimers in a crystalline hydrophilic PEG as well as the properties of the resulting copolymers.

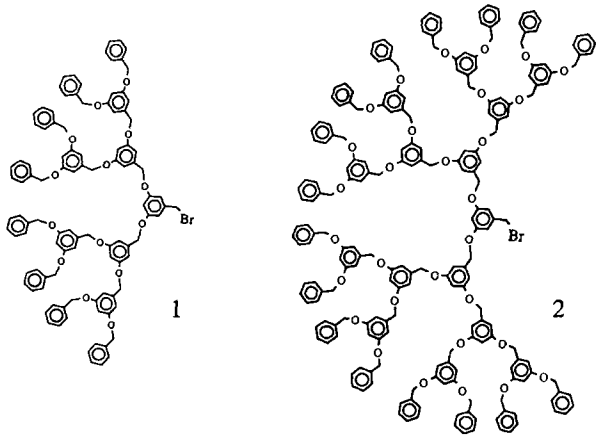

Scheme 1. The dendritic macromolecules employed in the reaction with the polyethylene glycols.

In a first approach PEG copolymers containing dendritic blocks were prepared by capping the ends of α, ω-bifunctional PEGs with dendrimers possessing a reactive functional group at their core. In order to estimate the influence of the size of the dendritic molecule on the reaction yields and the properties of the copolymers that are formed, dendrimers of the third ([G-3]-Br: **1**) and fourth ([G-4]-Br: **2**) generations were used (Scheme 1).

In order to avoid the association of acidic moieties with PEG[6] and the incomplete conversion[1] of some Williamson-type syntheses, the formation of the PEG dianion in situ by reaction with NaH was carried out in the presence of the dendritic bromide (Scheme 2) as described previously for the synthesis of PEG macromers.[7]

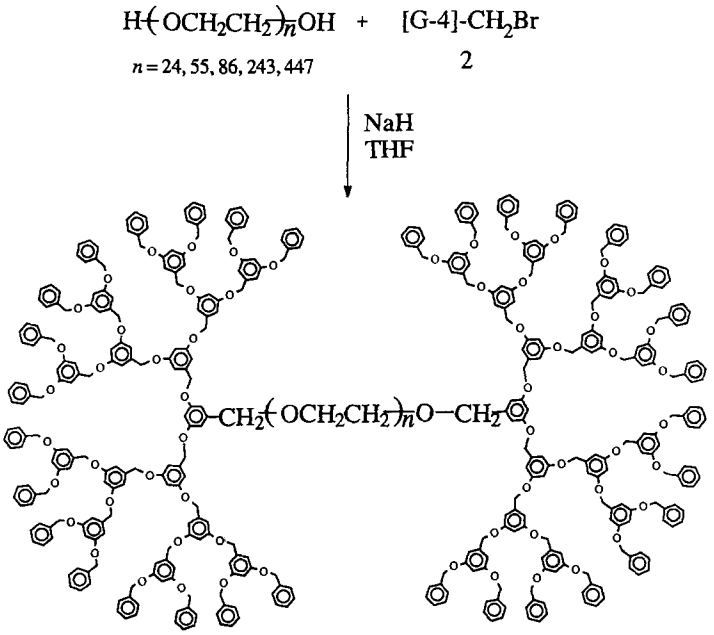

Scheme 2. Synthesis of the copolymers.

In all cases investigated, the end-capping reaction proceeded smoothly at room temperature and was complete within 24 h. The length of the initial PEG block and the size of the dendritic bromide have no influence on the rate of formation of the copolymers. In contrast to the previously reported end-capping reactions of PEGs,[1, 7] the low molar ratio of the dendritic bromides to terminal hydroxyl groups (1.2:1) does not affect the yields, which remain over 90%.

The molecular weights of the starting materials and the resulting block copolymers are listed in Table 1. The molecular weights at the peak apex M_p in the size-exclusion chromatography (SEC) traces are used as characteristic values for each product since they are less affected by low- and high-molecular weight impurities. The molecular weight distribution is calculated as the average of three measurements. It should be noted that most copolymers obtained have narrower molecular weight distributions than the inital PEGs, and all of them have apparent molecular weights lower than the values predicted for triblock copolymers of the type [G-m]-PEG-[G-m] (Table 1, Fig. 1). This difference between calculated and apparent molecular weights increases with the length of the initial PEG block.

[*] Prof. J. M. J. Fréchet, Dr. I. Gitsov, K. L. Wooley
Baker Laboratory, Department of Chemistry
Cornell University
Ithaca, NY 14853-1301 (USA)

[**] Financial support of this project was provided by National Science Foundation (DMR-8913278) and The William and Mary Greve Foundation (fellowship for I.G.).

Table 1. Molecular weights of PEGs H-$(OCH_2CH_2)_n$-OH and their dendritic copolymers as determined by SEC versus PEG standards with narrow molecular distributions (THF, 30 °C, flow rate 1 mL min^{-1}).

initial PEGs			M_p of the dendritic copolymers					
			[G-3] copolymers			[G-4] copolymers		
n	M_p	$\bar{M}_w/\bar{M}_n$	M_p (calc)	M_p (obs)	$\bar{M}_w/\bar{M}_n$	M_p (calc)	M_p (obs)	$\bar{M}_w/\bar{M}_n$
24	1050	1.03	4200	3600	1.02	7600	5500	1.05
23	1700	1.05	3360 [a]	3000	1.03	4980 [a]	3900	1.03
55	2400	1.03	5650	5000	1.01	8950	6400	1.02
56	2500	1.08	4160 [b]	4000	1.03	5780 [b]	4850	1.07
86	3800	1.08	6950	6400	1.05	10350	8000	1.04
243	10700	1.04	13850	12600	1.03	17250	12600	1.04
447	19700	1.11	22850	20300	1.10	26250	22700	1.08

[a] Reaction product of monofunctional lauryl PEG $C_{12}H_{25}(OCH_2CH_2)_{23}$-OH (Brij 35®) and dendritic bromide. [b] Reaction product of monofunctional methyl PEG $CH_3(OCH_2CH_2)_{56}$-OH and dendritic bromide.

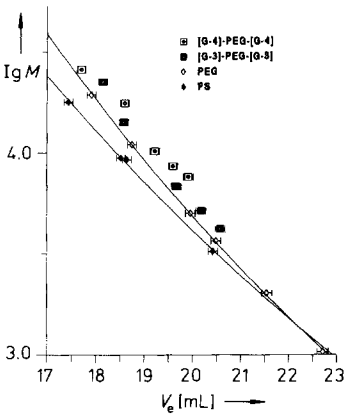

Fig. 1. SEC calibration curves for polystyrene (PS) standards, PEGs with narrow molecular weight distributions, and dendritic triblock copolymers [G]-PEG-[G]. THF, 30 °C, flow rate 1 mL min^{-1}; columns: PLGel 500 Å, 1000 Å, mixed-C.

In order to check the efficiency of the end-capping reaction, experiments with monofunctional PEGs were also performed (Table 1, Fig. 2). It is seen that the end-capping reactions of both mono- and bifunctional PEGs of similar molecular weight with a dendritic bromide proceed to completion. In the SEC traces of the monofunctional PEGs the shoulders at high molecular weights originate most probably from bifunctional impurities in the starting materials. Thus, it may be assumed that the lower values of the apparent molecular weights are caused not by incomplete functionalization (end-capping), but most probably by the smaller size of the resulting dendritic copolymers. A similar behavior was reported for dendritic versus linear macromolecules.[8, 9]

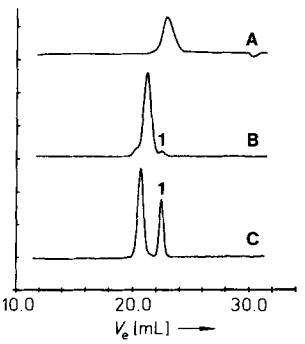

Fig. 2. SEC traces of the initial PEGs. **A**: H-$(OCH_2CH_2)_{24}$-OH, **B**: reaction mixture of H-$(OCH_2CH_2)_{23}OC_{12}H_{25}$ and **1**, **C**: reaction mixture of H-$(OCH_2CH_2)_{24}$-OH and **1**. THF, 30 °C, flow rate 1 mL min^{-1}; columns: PLGel 500 Å, 1000 Å, mixed-C.

Another factor contributing to the differences in the calculated and apparent molecular weights discussed above might be the formation of monomolecular micelles. The calibration curve for PEGs has a more negative slope compared to that for polystyrenes (PS) (Fig. 1), which confirms the well-known fact that the solubility of PEGs in THF decreases as their molecular weight increases. Thus, in copolymers with dendritic and linear blocks, the central PEG block should shrink in THF as its length increases, while the dendritic end blocks would undergo an intramolecular association. Since there are no other reports on copolymers consisting of linear and dendritic blocks, our results are best compared to those obtained for polyethylene oxide–polystyrene block copolymers. Indeed, a similar phenomenon was reported for polystryrene-*b*-polyethylene oxide-*b*-polystyrene.[10] Some authors have predicted a narrowing in the molecular weight distribution of block copolymers undergoing an association of their end groups.[11] However, with the copolymers in this study it would be very difficult to estimate quantitatively the contribution of both factors—collapse of the linear central block in solvents in which the PEGs are not well soluble (THF), and intramolecular association of the dense, hyperbranched endgroups—to the overall decrease in the molecular dimensions of the synthesized copolymers.

In order to gain qualitative information on the possible formation of micelles, we recorded ^{1}H NMR spectra in solvents selective for solubilizing the PEG and dendritic blocks. An interesting phenomenon is observed in [D_8]THF. At room temperature the initial PEG block with molecular weight of 19700 is obviously not soluble. Therefore, only signals for the protons of the groups -CH_2O- (δ = 3.28–3.58) and -CH_2CH_2- (δ = 1.57–1.73) of THF molecules are observed in the spectrum. The integrals of the two signals should be equal, but that of the CH_2CH_2 protons is greater ($I_{CH_2CH_2}:I_{CH_2O}$ = 1.35) due to the different isotopic distributions at the two positions. When the sample in the NMR tube is heated to 50 °C for 15 min, PEG visibly dissolves and the ratio of the integrals is strongly shifted towards the CH_2O protons ($I_{CH_2CH_2}:I_{CH_2O}$ = 0.17). The ^{1}H NMR spectra of dendritic copolymers having the same PEG as above for the central block are not temperature dependent. Theoretically, the ratio of the methylene PEG protons to the protons in the dendritic side-blocks for [G-4]-PEG19700-[G-4] should be equal to 4.84. In $CDCl_3$ the ratio of their integrals is about 4.9, but in [D_8]THF, the values obtained at room temperature and 50 °C are 2.49 and 2.30, respectively, after the integral intensity of solvent protons is subtracted. Thus, it may be assumed that attachment of dendritic blocks to PEG increases its solubility in THF to a certain extent; however, the screening of the PEG core by the dendritic outer shell in the micelles that are formed prevents further solubilization at higher temperatures.

Figure 3 presents the ^{1}H NMR spectra of [G-3]-$(OCH_2CH_2)_{243}$-O-[G-3] in $CDCl_3$ (**A**, both blocks are soluble) and CD_3OD (**B**, the PEG block is selectively soluble). It is noteworthy that while the signal for the methylene PEG protons remains sharp and is only slightly shifted downfield in CD_3OD (from δ = 3.32–3.72 to 3.29–3.70), the signals of the aromatic protons in the dendritic end blocks become very broad (δ = 7.06 ($\Delta\nu$ = 120 Hz), 6.38 (204 Hz), 4.72 (571 Hz) (Fig. 3, **B**.). It is quite surprising that the signals of the [G-3] block are observed, since the corresponding dendritic bromide and its derivatives are not soluble in methanol and consequently not evident in the NMR spectra recorded in

that solvent. The PEG block seems to carry its dendritic counterpart into solution as was observed for G blocks in [D_8]THF. However, the broadness of the signals is evidence of the limited flexibility of the dendritic blocks of the copolymers. When hyperbranched blocks of the next generation are attached to the same bifunctional PEG, the methanol solution of the resulting copolymer is milky and opalescent, and the aromatic signals are not seen in the NMR spectra (Fig. 3, **C**.). A similar behavior and the same values for $\Delta\nu$ are also

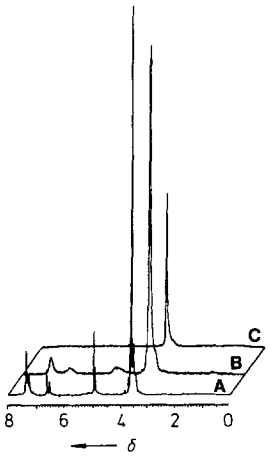

Fig. 3. ^{1}H NMR spectra of [G-3]-$(OCH_2CH_2)_{243}$-O-[G-3] in $CDCl_3$ (**A**), [G-3]-$(OCH_2CH_2)_{243}$-O-[G-3] in CD_3OD (**B**), and [G-4]-$(OCH_2CH_2)_{243}$-O-[G-4] in CD_3OD (**C**). 300 MHz, 22 °C, polymer concentration 1 wt%.

observed for dendritic copolymers of monofunctional PEGs. Thus, it could be assumed that in methanol both di- and triblock copolymers undergo the same type of transformation. Similar phenomena were reported for polystyrene-*b*-polyethylene oxide[12] and other micelle-forming copolymers[13] and were also interpreted as micelle formation. Although additional investigations are necessary to evaluate the number of molecules in the micelles formed, the results of SEC and ^{1}H NMR experiments strongly suggest that in selective and poor solvents the copolymers might undergo different size and shape transitions (Scheme 3).

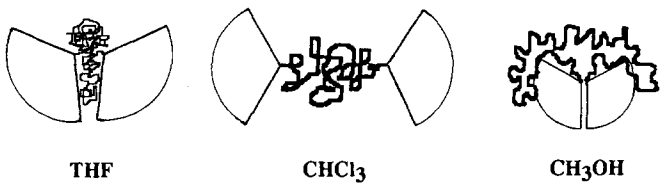

Scheme 3. Left: Collapse of the central PEG block as the length increases. The dendritic G blocks are partially associated. Middle: Both blocks are soluble in the solvent. Right: Collapse and association of G blocks of higher generations. The PEG block expands.

The results show that the relatively bulky dendritic wedges, up to fourth generation, do not affect the reactivity and accessibility of the functional group at the core of the dendritic macromolecules. Thus, novel amphiphilic block copolymers of PEGs having different extents of hydrophobic and hydrophilic character can be formed in a single reaction under mild conditions. The preliminary characterization studies of these products show that they are able to form micelles in solvents in which both blocks are poorly soluble or in which one block is selectively soluble. Further investigations on their properties are in progress.

Experimental Procedure

A typical end-capping reaction was performed as follows: PEG of molecular weight 3800 [$H(OCH_2CH_2)_{86}OH$] (0.031 g, 8.3×10^{-6} mol) and **1** (0.029 g, 1.72×10^{-5} mol), synthesized according to ref. [8], were mixed and dissolved in dry THF (2 mL). To the solution was added NaH (0.001 g, 4×10^{-5} mol), and the reaction mixture was stirred at room temperature under nitrogen for a set time. The conversion was followed by SEC. After the PEG peak in the chromatogram had disappeared, the reaction mixture was filtered and purified by precipitation into acetone/methanol (1:3) and reprecipitation from THF into heptane. Yield: 0.056 g (93%). ^{1}H NMR (300 MHz $CDCl_3$, 22 °C): $\delta = 7.28-7.33$ (m, 80H; H in outer aromatic rings of [G-3]), 6.51–6.62 (m, 42H; H in inner aromatic rings of [G-3]), 4.89, 4.94 (d, 60H; benzylic CH_2 in [G-3]), 3.55–3.73 (m, 344H; CH_2CH_2O in PEG). All other experiments were performed by the same procedure with similar yields.

Received: March 25, 1992 [Z 5260 IE]
German version: *Angew. Chem.* **1992**, *104*, 1282

CAS Registry number:
[G]–PEG[G] (block copolymer), 143104-76-1.

[1] J. M. Harris, M. G. Case, *J. Org. Chem.* **1983**, *48*, 5390 and references therein.
[2] T. K. Khan, R. H. Mobbs, C. Price, J. R. Quintana, R. B. Stubbersfield, *Eur. Polym. J.* **1987**, *23*, 191.
[3] H.-Ba Gia, B. Jérôme, P. Teyssie, *J. Polym. Sci., Polym. Phys Ed.* **1980**, *18*, 2391.
[4] C. J. Hawker, J. M. J. Fréchet, *J. Chem. Soc., Chem. Commun.* **1990**, 1010.
[5] K. L. Wooley, C. J. Hawker, J. M. J. Fréchet, *J. Am. Chem. Soc.* **1991**, *113*, 4252.
[6] J. M. Harris, *J. Macromol. Sci., Rev. Macromol. Chem. Phys. C* **1985**, *25*, 325.
[7] D. Chao, S. Itsuno, K. Ito, *Polym. J.* **1991**, *23*, 1045.
[8] C. J. Hawker, J. M. J. Fréchet, *J. Am. Chem. Soc.* **1990**, *112*, 7638.
[9] A. Morikawa, M. Kakimoto, Y. Imai, *Macromolecules* **1991**, *24*, 3469.
[10] I. Berlinova, N. Vladimirov, I. Panayotov, *Makromol. Chem. Rapid Commun.* **1989**, *10*, 163.
[11] K. Solc, H. G. Elias, *J. Polym. Sci. Polym. Phys. Ed.* **1973**, *11*, 137.
[12] K. Nakamura, R. Endo, M. Takeda, *J. Polym. Sci. Polym. Phys. Ed.* **1976**, *14*, 135.
[13] J. Spévacek, *Makromol. Chem. Rapid Commun.* **1982**, *3*, 697.

Indigoid *para*-Quinodimethanes**

By *Rudolf Gompper,** *Robert Kellner*, and *Kurt Polborn*

Dedicated to Professor Wolfgang Beck on the occasion of his 60th birthday

Indigo and indigoid compounds are important technical dyes because of their applications in coloration, especially in textile dying. The nature of the indigo chromophore was studied intensively and is now well understood.[1b, 2] However, the search for new indigoid compounds continues. The UV/VIS absorption of these systems at very long wavelengths makes them attractive materials for optical data storage,[3, 4] since such materials must absorb in the near-IR (>750 nm). This can be accomplished, for example, by complexation.[5] Alternatively, the indigo chromophore and structurally related chromophores can be fused to π electron systems to produce compounds with the desired bathochromic shift and the stability of the indigoid system. We have succeeded in synthesizing *para*-quinodimethane homologues of this type, **1**–**3**; their absorption is at a consider-

[*] Prof. R. Gompper, Dipl.-Chem. R. Kellner, Dr. K. Polborn
Institut für Organische Chemie der Universität
Karlstrasse 23, D-W-8000 München 2 (FRG)

[**] This research was supported by the Deutsche Forschungsgemeinschaft and the Fonds der Chemischen Industrie.

ably longer wavelength than that of the related vinylogues. For example, the absorption of **3** (λ_{max}(*p*-xylene) = 626 nm) has a wavelength about 100 nm greater than that of **11** (λ_{max}(*p*-xylene) = 528 nm).[6]

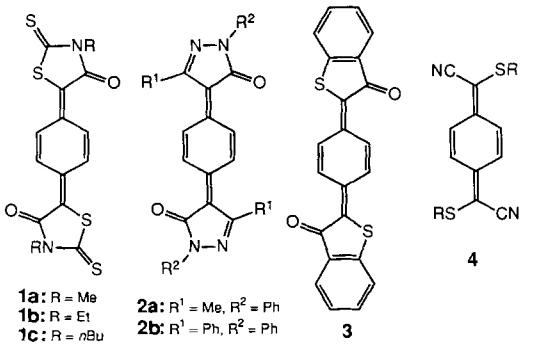

The first *para*-quinodimethane derivatives **4** with the donor(D)–acceptor(A) pattern of the indigo chromophore were reported during the course of our investigations by Iwatsuki et al.[7] ; however, these compounds are quite unstable and not suited for the applications we have in mind. The incorporation of the D-A functional groups into five-membered rings should increase the stability of the compounds and make the chromophore system more similar to that of indigo.

The rhodanines **5** were warmed with cyclohexane-1,4-dione (**6**) in ethanol. This solution was treated with concentrated ammonia followed immediately by a hot saturated solution of aqueous ammonium chloride to give the condensation product **7** (**7a**: m.p. 254–256 °C; λ_{max}(DMSO) = 356 nm (ε = 64600); **7b**: m.p. 280–282 °C; λ_{max}($CHCl_3$) = 357 nm (ε = 74100); **7c**: m.p. 262–264 °C; λ_{max}($CHCl_3$) = 357 nm (ε = 74100). In contrast to **7a–c**, compound **7d** is sufficiently soluble in deuterochloroform at room temperature; its ^{13}C NMR spectrum displays two sets of signals indicating that compounds **7** are mixtures of the (*E*) and (*Z*) isomers.

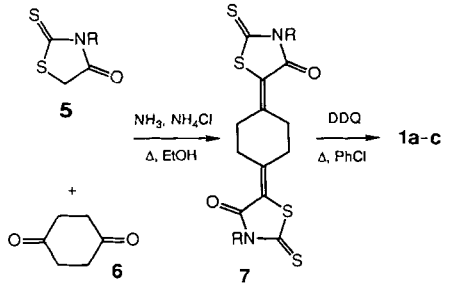

5,7: **a**: R = H ; **b**: R = Me ; **c**: R = Et ; **d**: R = *n*Bu

The dehydrogenation of **7b–d** to the amorphic quinodimethanes **1**, which range in color from dark violet to black (**1a**: m.p. 333–335 °C; λ_{max}($PhNO_2$) = 576 nm (ε = 97700)), was accomplished with an excess of 2,3-dichloro-5,6-dicyano-*p*-benzoquinone (DDQ) in refluxing chlorobenzene. **7a** could not be dehydrogenated to the corresponding quinodimethane with DDQ. In comparison to the birhodanines **8**[8, 9] the quinodimethane homologues **1** absorb at wavelengths about 140 nm longer. The extinction coefficients of **1** are larger than those of **8** (**8**, R = *n*Bu: λ_{max}($PhNO_2$) = 437 nm (ε = 36300), as is generally the case upon extension of the chromophore.

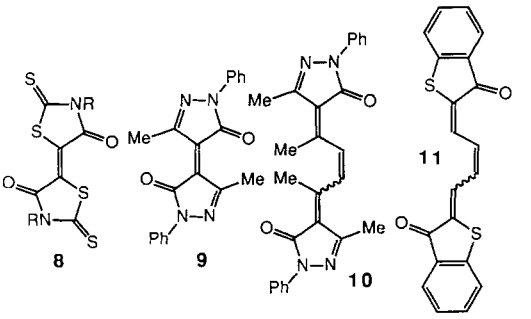

2-Pyrazolin-5-ones **12** reacted with **6** in pyridine in the presence of air to provide phenylenedipyrazoles **13** (**13a**: colorless, crystalline powder, m.p. > 340 °C (decomp); **13b**: m.p. 312–313 °C (decomp); **13c**: yellow, crystalline powder, m.p. 263–265 °C; **13d**: m.p. > 360 °C). The dehydrogenation of these compounds to the dark-blue to black *para*-quinodimethane derivatives **2a,b** proceeded best with DDQ (**2a**: small, dark-blue needles, m.p. 262 °C (decomp); λ_{max}($CHCl_3$) = 705 nm (broad, ε = 5750); λ_{max}(DMF) = 625 nm (ε = 2500), 705 (shoulder, ε = 1800); **2b**: small, black needles, m.p. 297 °C (decomp); λ_{max}(DMF) = 630 nm (broad, ε = 1000)).

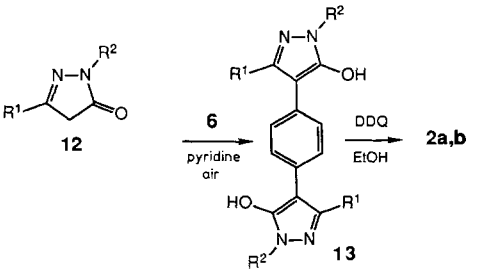

12,13: **a**: R¹ = Me, R² = Ph ; **b**: R¹ = Me, R² = *n*Bu
c: R¹ = Ph, R² = Ph ; **d**: R¹ = Me, R² = CH_2Ph

Alternatively, **13a** can be brominated to **14** with *N*-bromosuccinimide (NBS) and then reduced to **2a** with zinc powder. Treatment of **2a** with bromine regenerated **14** (yellow powder, m.p. 172–173 °C).

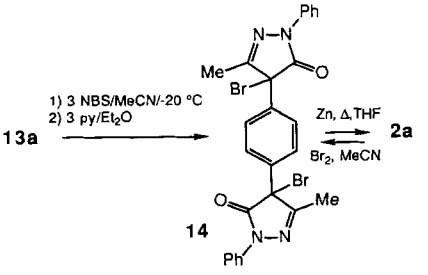

Compound **2a** is the quinodimethane homologue of pyrazole blue (**9**). The insertion of the quinodimethane system (**9** → **2a**) causes a bathochromic shift of the longest wavelength absorption of about 110 nm. In comparison to **10**,[10] the vinylogue of **9** described as red but not more thoroughly

analyzed, compounds **2a,b** absorb at considerably longer wavelengths.

The reaction of oxobenzo[*b*]thiophene (**15**) with **6** in refluxing ethanol in the presence of a mixture of ammonia and ammonium chloride afforded the yellow phenylenebis(hydroxybenzothiophene) **16a** (yellow needles, m.p. 281 °C; λ_{max}(DMSO) = 387 nm (ε = 35 500)). The methylation of the Na salt of **16a** led to **16b** (yellow needles, m.p. 220–221 °C). Dehydrogenation of **16a** with DDQ yielded the new quinodimethane **3** (black microcrystals, m.p. 328 °C; λ_{max}(*p*-xylene) = 626 nm (ε = 57 500)).

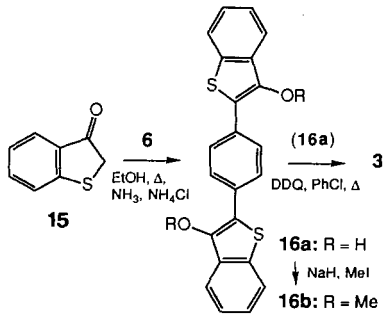

It is typical of the indigoid systems that upon extension of the central π electron system by one or two double bonds, the longest wavelength absorption maximum undergoes a hypsochromic shift,[11–13] rather than a bathochromic one as is seen for the cyanines, merocyanines, and polyenes.[1c, 14] The case is different for **3**, which absorbs at a wavelength 82 nm longer than that of *trans*-thioindigo (λ_{max}(*p*-xylene) = 544 nm[6]).

In cyclovoltammetric studies the quinodimethanes can be reduced reversibly to semiquinodimethanes which can be reduced further reversibly to dianions. Since the difference in potentials for the two redox processes is large enough (>100 mV), two single-electron transfer steps can be observed. The quinodimethanes **2** are somewhat stronger electron acceptors than the quinodimethanes **1**. Interestingly, tetracyanoquinodimethane with E_1 = 0.37 V (in dimethylformamide (DMF)) is only a slightly stronger electron acceptor than **2b** (E_1 = 0.28 V (in DMF)).

We were able to show previously that the dihydropyrazine derivatives **18**, obtained from diketopiperazine, can be treated with 1,3-dithiolium salts to provide tetradonor-substituted 2,5-diazaquinodimethanes **17**.[15] Thus, indigoid 2,5-diazaquinodimethane derivatives **19** should be accessible, for example from the analogous reaction of isatin and **18** RX = MeS. We were not successful with this reaction. The most promising candidates for the production of indigoid diazaquinodimethanes remain compounds related to the violet bis(oxindolylidene)diketopiperazine **21a**,[16] prepared from 1,4-diacetylpiperazine-2,5-dione (**20**) and isatin. We also obtained the violet bis(*N*-methyloxindolylidene)-

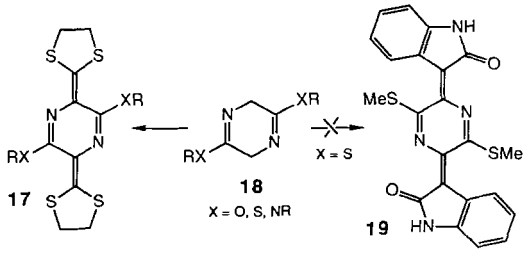

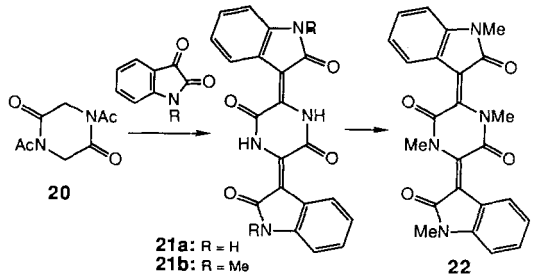

diketopiperazine **21b** (violet powder, m.p. > 360 °C; λ_{max}(solid) = 550 nm; λ_{max}(dimethyl sulfoxide) (DMSO)) = 490 nm (ε = 19 500); λ_{max}(H_2SO_4) = 469 nm) by treating **20** with *N*-methylisatin in DMF in the presence of triethylamine at room temperature. All attempts at converting **21b** into an RO-substituted 2,5-diazaquinodimethane derivative of type **19** failed. The reaction of the Na salt of **21b** with methyl iodide furnished the tetramethyl compound **22** (orange–red needles, m.p. 300 °C (decomp); λ_{max}(solid) = 357 nm; λ_{max}(DMSO) = 359 nm (ε = 24 000); λ_{max}(H_2SO_4) = 442 nm).

The electron spectra of **21a** and **21b** differ only slightly. The "medium effect" known for indigo is remarkably strong here: in the solid phase as a thin layer on a quartz plate **21a** absorbs at a wavelength 54 nm longer than when dissolved in DMSO, for **21b** even 60 nm longer. In contrast, the electron spectra of **22** as a solid (thin layer on a quartz plate) and dissolved in DMSO are almost identical. Yellow **22** absorbs

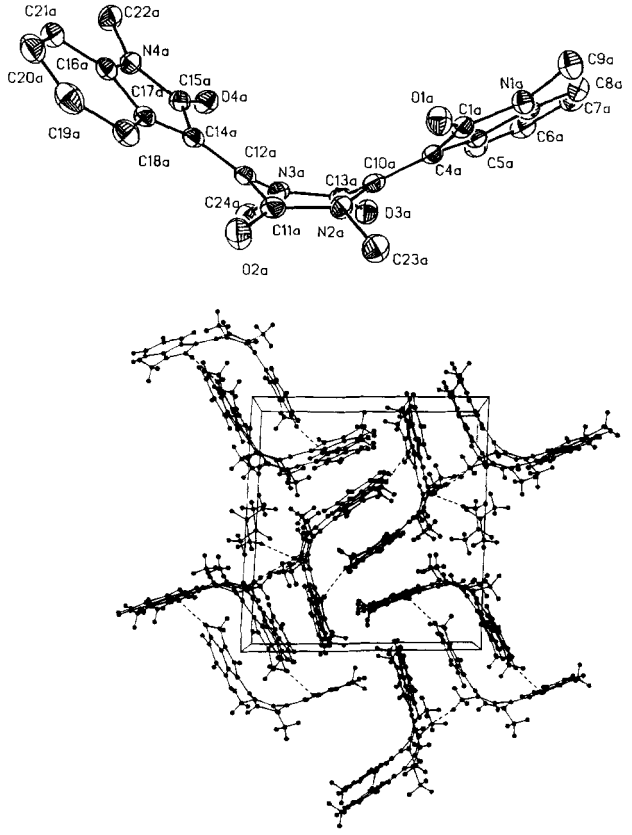

Fig. 1. Top: Crystal structure of **22** (ORTEP)[17]: Selected bond lengths [pm] and angles [°]: O1a-C1a 121.5(6), C1a-N1a 136.9(6), C1a-C4a 149.3(8), C14a-C17a 145.5(7), C4a-C10a 136.7(7), C10a-C13a 149.8(8), C10a-N2a 139.6(6), C13a-O3a 120.9(6), C13a-N3a 136.6(7), C11a-N2a 137.5(7), C23a-N2a 147.5(7); C11a-C12a-C14a 124.0(5), C12a-C14a-C15a 120.7(4), N3a-C12a-C11a 111.9(4), N2a-C11a-C12a 114.2(5), C12a-N3a-C13a 121.1(4), C12a-N3a-C24a 121.0(4), O2a-C11a-C12a 123.5(5). Bottom: Unit cell of **22**.

at a wavelength substantially shorter than **21a,b**. Thus, relative to the absorption maximum of **21b** in the solid state, that of **22** is shifted hypsochromically by 193 nm, in DMSO by 131 nm. The values measured for **21a** and **21b** in sulfuric acid display a slightly negative halochromism relative to those in DMSO; however, **22** shows a strongly positive halochromism. The longest wavelength absorption band of **22** in sulfuric acid is therefore only 27 nm shorter than that of **21b**.

Compound **21a** is planar, whereby intramolecular hydrogen bonds play an important role.[16] On the basis of the similar electron spectra of **21a** and **21b** one may assume that **21b** is also planar. The situation is different for **22**. The X-ray structure analysis reveals that the compound is in a concave "flagpole-boat" conformation (Fig. 1). The unit cell contains four molecules of **22** and two molecules of acetone (solvent). Channels are formed by the meshing of the molecules of **22** that surround the acetone molecules. The compound thus belongs to the group of channel inclusion compounds. Further investigations should show if host **22** is able to accomodate other guest molecules besides acetone.

Experimental Procedure

16a: To a solution of **15** (7.56 g, 50.3 mmol) and **6** (2.80 g, 25 mmol) in 75 mL of ethanol under N_2 were added first 3.50 mL of concentrated aqueous ammonia and then a hot solution of 3.50 g of ammonium chloride in 6 mL of water. The mixture was heated at reflux for 2h. The precipitate was filtered off and treated successively with boiling water, ethanol, and toluene, whereby the residue was vacuum-filtered each time while still hot. The crude product was dried under vacuum, and recrystallized from 75 mL of nitrobenzene. (Purification of the crude product was also possible by extractive recrystallization from toluene.) Yield 5.56 g (59%).

3: A solution of **16a** (2.50 g, 6.68 mmol) and DDQ (10.6 g, 46.5 mmol) in 200 mL of water-free chlorobenzene was heated at reflux for 6h under argon. The solvent was then removed by distillation, and the residue was treated with boiling ethanol and vacuum-filtered while still hot. The product was dried under vacuum and purified by extractive recrystallization from 75 mL of toluene over 27d. Yield 1.66 g (67%).

Received: April 15, 1992 [Z 5306 IE]
German version: *Angew. Chem.* **1992**, *104*, 1222

CAS Registry numbers:
1b, 142868-55-1; **2a**, 142868-60-8; **2b**, 142868-61-9; **3**, 142868-66-4; **5a**, 141-84-4; **5b**, 4807-55-0; **5c**, 7648-01-3; **5d**, 21494-64-4; **6**, 637-88-7; **7a**, 142868-51-7; **7b**, 142868-52-8; **7c**, 142868-53-9; **7d**, 142868-54-0; **12a**, 89-25-8; **12b**, 65156-70-9; **12c**, 4845-49-2; **12d**, 946-23-6; **13a**, 142868-56-2; **13b**, 142868-57-3; **13c**, 142868-58-4; **13d**, 142868-59-5; **14**, 142895-72-5; **15**, 130-03-0; **16a**, 142868-62-0; **16b**, 142868-63-1; **20**, 3027-05-2; **21b**, 142868-64-2; **22**, 142868-65-3; *N*-methylisatin, 2058-74-4.

[1] a) J. Fabian, H. Hartmann, *Light Absorption of Organic Colorants*, Springer, Berlin, **1980**; b) [1a], p. 115; c) [1a], p. 32, 162.
[2] G. Miehe, P. Süsse, V. Kupcik, E. Egert, M. Nieger, G. Kunz, R. Gerke, B. Knieriem, M. Niemeyer, W. Lüttke, *Angew. Chem.* **1991**, *103*, 1008; *Angew. Chem. Int. Ed. Engl.* **1991**, *30*, 964.
[3] a) M. G. Clark, *Chem. Ind. (London)* **1985**, 258; b) E. M. Engler, *Adv. Mater.* **1990**, *2*, 166; c) M. Emmelius, G. Pawlowsky, H. W. Vollmann, *Angew. Chem.* **1989**, *101*, 1475; *Angew. Chem. Int. Ed. Engl.* **1989**, *28*, 1445.
[4] M. Matsuoka, S. H. Kim, T. Kitao, *J. Chem. Soc. Chem. Commun.* **1985**, 1195.
[5] W. Beck, C. Schmidt, R. Wienold, M. Steimann, B. Wagner, *Angew. Chem.* **1989**, *101*, 1532; *Angew. Chem. Int. Ed. Engl.* **1989**, *28*, 1529.
[6] P. Friedländer, F. Risse, *Ber. Dtsch. Chem. Ges.* **1914**, *47*, 1919; see also: M. A. Mostoslavskii, V. A. Izmail'skii, M. M. Shapkina, *Zh. Obshch. Khim.* **1962**, *32*, 1746; *J. Gen. Chem. USSR.* **1962**, *32*, 1731 (Engl. Transl.) [*Chem. Abstr.* **1963**, *58*, 2021f]; G. M. Wyman, W. R. Brode, *J. Am. Chem. Soc.* **1951**, *73*, 1487; H. Meier, W. Lüttke, *Liebigs Ann. Chem.* **1981**, 1303.
[7] S. Iwatsuki, T. Itoh, I. Miyashita, *Macromolecules* **1988**, *21*, 557.
[8] A. Nederlof, *Rec. Trav. Chim. Pays-Bas* **1962**, *81*, 578; *ibid.* **1963**, *82*, 75.
[9] H. Nagase, *Chem. Pharm. Bull.* **1973**, *21*, 279; *ibid.* **1974**, *22*, 505.
[10] G. Westöö, *Acta Chem. Scand.* **1959**, *13*, 679.
[11] M. Klessinger, W. Lüttke, *Tetrahedron* **1963**, *19* (*Suppl. 2*), 315.
[12] D. Leupold, S. Dähne, *Theor. Chim. Acta* **1965**, *3*, 1.
[13] H. Herrmann, W. Lüttke, *Chem. Ber.* **1968**, *101*, 1715.
[14] a) S. S. Malhotra, M. C. Whiting, *J. Chem. Soc.* **1960**, 3812; b) P. Nayler, M. C. Whiting, *ibid.* **1955**, 3037.
[15] R. Gompper, W. Breitschaft, *Angew. Chem.* **1983**, *95*, 727; *Angew. Chem. Int. Ed. Engl.* **1983**, *22*, 717.
[16] A. R. Katritzky, W.-Q. Fan, M. Szajda, Q.-L. Li, K. C. Caster, *J. Heterocycl. Chem.* **1988**, *25*, 591; A. R. Katritzky, W.-Q. Fan, A. E. Koziol, G. J. Palenik, *ibid.* **1989**, *26*, 821.
[17] Crystal structure analysis of **22**: Enraf-Nonius CAD-4 diffractometer, $Mo_{K\alpha}$ radiation, $\lambda = 71.069$ pm, single crystal $0.20 \times 0.27 \times 0.53$ mm^3, $T = 294$K. Crystal data: $M_r = 914.98$, $\rho_{calc} = 1.375$ g cm^{-3}, triclinic, space group $P\bar{1}$ (No. 2), $a = 891.3(2)$, $b = 1526.2(3)$, $c = 1635.9(4)$ pm, $\alpha = 87.29(2)$, $\beta = 84.50(2)$, $\gamma = 86.59(2)°$, $V = 2.2093$ nm^3; $Z = 2$. ω-Data collection: $2\theta = 4-46°$; scan width $0.90° + 0.35\tan\theta$; maximum time for measurement 70s. 5536 symmetry-independent reflections, 4555 with $I > 2\sigma(I)$. Refined parameters 613. Structure solution: SHELXS-86, refinement SHELXTL PLUS. All non-hydrogen atoms were refined anisotropically; full matrix; hydrogen atoms at calculated positions. $R = 0.0645$, $R_w = 0.0534$; maximum residual electron density 0.36 and -0.34 e pm^{-3} 10^6. Further details of the crystal structure investigation may be obtained from the Fachinformationszentrum Karlsruhe, Gesellschaft für wissenschaftlich-technische Information mbH, D-W-7514 Eggenstein-Leopoldshafen 2 (FRG) on quoting the depository number CSD-56379, the names of the authors, and the journal citation.

[Lithium Piperidide–Piperidine]$_4$: Crystal Structure of an Oligomeric 1:1 Lithium Amide–Amine Mixed Complex, an Intermediate in the *N*-Lithiation of Amines**

By *Gernot Boche,* Ira Langlotz, Michael Marsch, Klaus Harms,* and *Norma E. S. Nudelman**

The importance of lithium amides $LiNR^1R^2$ (R^1, R^2 = aliphatic and/or aromatic substituents) in organic synthesis is amply documented by the recent intensive investigations of their structures in the solid state and in solution, and by means of calculations; the same holds for lithium imides $LiN{=}CR^1R^2$.[1-5] There is, however, not much known about lithium amide–amine mixed complexes, although such species are likely to be formed during, for example, the preparation of lithium amides from amines (in excess) with organolithium compounds RLi, or the reactions of lithium amides with CH-acidic compounds R^1H to give R^1Li and amine. Lithium amide–amine complexes are also of special significance in the carbonylation reaction of lithium amides.[6-8] Crystal structure determinations have been performed on the monomeric [Ph(2-Pyr)NLi · HN(2-Pyr)Ph · hmpa] (= pyridyl, hmpa = hexamethylphosphoric triamide), though an extra hmpa donor ligand cocrystallizes,[9] and of the lithiated azomethine *N*-(cyclohexylidene)phenylamine, which crystallizes with diisopropyl amine to give [Ph(*cyclo*-C_6H_9)NLi · HN*i*Pr_2]$_2$.[3c] Very recently the crystal structure of a sodium ketimide that forms "an unexpected complex" with nonmetalated ketimine, [(*t*$Bu_2C{=}NNa)_4$ · (HN=C*t*Bu_2)$_2$], has been published.[10] Here we report on the crystal structure of lithium piperidide (**1**-Li), which crystallizes with piperidine (**1**-H) in a 1:1 ratio (see Fig. 1).[11]

$[H_2\overline{C(CH_2)_4}NLi \cdot H\overline{N(CH_2)_4}CH_2]_4$ [**1**-Li · **1**-H]$_4$

[*] Prof. Dr. G. Boche, I. Langlotz, M. Marsch, Dr. K. Harms
Fachbereich Chemie der Universität
Hans-Meerwein-Straße, D-W-3550 Marburg (FRG)
Prof. Dr. N. E. S. Nudelman
Facultad de Ciencias Exactas y Naturales, Universidad de Buenos Aires, Ciudad Universitaria, Buenos Aires 1428 (Argentina)

[**] We thank Dr. R. Snaith, University Chemical Laboratory, Cambridge, United Kingdom, for very valuable discussions. This work was supported financially by the Deutsche Forschungsgemeinschaft (Sonderforschungsbereich 260) and the Fonds der Chemischen Industrie.

As can be seen from Figure 1, a limited-length "concave" (N4-Li4-N6 144.0(5), Li1-N4-Li4 117.6(4), N1-Li3-N2 143.0(5), Li2-N2-Li3 116.4(3)°) ladder is formed, and only the terminal lithium atoms are complexed. The same structural type was found in model calculations of $[H_2NLi \cdot H_2O]_4$ to be the most stable one; the alternative eight-membered ring structure is 17.1 kcal mol^{-1} higher in energy, while the ladder with H_2O molecules on each lithium atom is 62.9 kcal mol^{-1} less favorable.[15] This reflects the steric

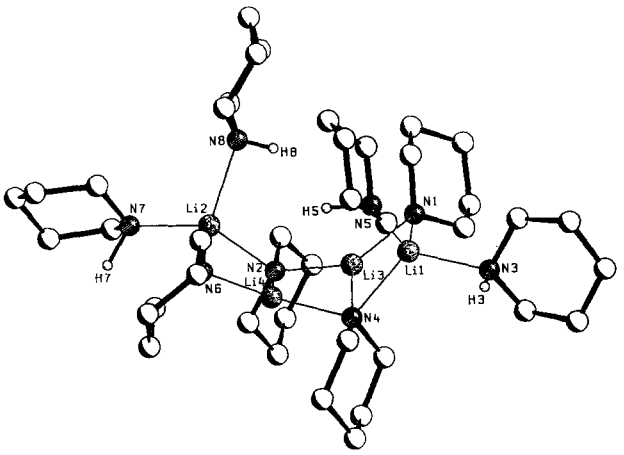

Fig. 1. Crystal structure of [**1**-Li · **1**-H]$_4$ [11]. Selected distances [pm] and angles [°] are: Li2-N2 216.8(12), N2-Li4 207.6(10), Li4-N6 193.3(12), N6-Li2 208.0(12), N2-Li3 203.5(11), Li3-N4 206.1(10), N4-Li4 205.6(10), Li3-N1 195.3(12), N1-Li1 204.1(13), Li1-N4 214.3(11), Li2-N7 210.0(13), Li2-N8 217.2(12), Li1-N3 213.9(13), Li1-N5 221.7(11), N4-N5 347.3(6), N4-H5 333.5(10), N4-N3 369.1(7), N4-H3 383.0(7), N4-N8 531.0(6), N4-H8 471(5), N4-N7 625.9(7), N4-H7 646(5), N2-N8 346.4(6), N2-H8 316(5), N2-N7 369.7(8), N2-H7 408(5), N2-N5 535.3(6), N2-N3 630.4(7), N2-H3 672.3(7), N1-N5 368.0(8), N1-H5 394(5), N1-N3 342.5(6), N1-H3 416.7(6), N1-N8 465.1(8), N1-H8 376(5), N1-N7 695.4(9), N1-H7 759(5), N4-Li4-N6 144.0(5), L1-N4-Li4 117.6(4), Li2-N2-Li3 116.4(4), N1-Li3-N2 143.0(5), Li1-N1-Li3 76.3(5), N1-Li3-N4 107.6(5), Li1-N4-Li3 71.9(4), N1-Li1-N4 101.5(5), N2-Li2-N6 99.1(4), Li2-N6-Li4 77.4(5).

crowding that would exist around the central Li atoms (Li3 and Li4 in the structure of [**1**-Li · **1**-H]$_4$) if ligand molecules (piperidine) were also coordinated there instead of exclusively at the outer Li atoms (Li1 and Li2). The internal ring N2-Li4-N4-Li3 is not planar. N2 and N4 lie 0.19(3) pm below, Li3 (0.19(3) pm) and Li4 (0.18(3) pm) above the best plane. Relatively short (Li3–N1 195.3(12) pm) and long (N1–Li1 204.1(13) pm) bonds are found alternating along the uncomplexed ladder edges (as at N1, for example). The Li3-N1-Li1 angle is 76.3(5); while the N1-Li1-N4 angle is much wider (101.5(5)°). A similar situation holds around Li2 and N6 (see Fig. 1). The internal ring has relatively long bonds (203.5(11) to 207.6(10) pm). The longest Li–N bonds occur at the complexed Li atoms such as Li1: Li1–N4 214.3(11), Li1–N3 213.9(13), and Li1–N5 221.7(11) pm. A similar situation is observed in the structurally related complex $[(H_2\overline{C(CH_2)_3}NLi)_4(tmeda)_2]$ (tmeda = *N*,*N*,*N*′,*N*′-tetramethylethylene diamine), which also has 4 Li:4N donor centers, but a lithium:ligand ratio of 2:1 (furthermore, tmeda is a tertiary amine).[16] The crystal structure of the first oligomeric 1:1 lithium amide–amine mixed complex [**1**-Li · **1**-H]$_4$ therefore fits nicely the experimental and theoretical data so far collected for lithium amide structures.[1, 2] In addition, it is of special interest with regard to the mechanism of the formation of one of the two structural types of lithium amides, the ladders. $(R_2NLi)_n$ rings are formed when R is large or floppy; ladders of medium or long length are observed when R is small or tied together as in the case **1**-Li.[1, 2] Thus, the oligomeric [**1**-Li · **1**-H]$_4$ is almost a long ladder, but not fully; a long ladder would form if all the piperidine molecules were deprotonated: [**1**-Li · **1**-H]$_4$ is an intermediate in the formation of lithium amides from RLi and amines.[17]

Moreover, the crystal structure of [**1**-Li · **1**-H]$_4$ agrees completely with investigations on the carbonylation reactions of lithium amides in solution and with reactivity investigations on them, studied extensively by Nudelman et al.[6–8] Thus, the existence of a 1:1 complex of **1**-Li and **1**-H was concluded from ^{13}C NMR investigations of **1**-Li in THF in the presence of **1**-H. Furthermore, workup of the reaction mixture of **1**-Li (prepared from **1**-H) with CO under different conditions (hydrolysis, deuterolysis, oxidation, and reaction with cyclohexanone) likewise suggested an apparently very stable 1:1 mixed complex of **1**-Li and **1**-H to be the reactive intermediate.[6–8]

Experimental Procedure

Preparation of the crystals of [**1**-Li · **1**-H]$_4$: *n*-Butyllithium (1.00 mmol, 0.63 mL, 1.6 M in hexane) was added to a solution of piperidine (2.00 mmol, 0.17 g) in hexane (0.63 mL) under a nitrogen atmosphere at room temperature. The crystals were formed on cooling the solution to 4 °C. The solvent was removed and the crystals were washed with 2 mL of pentane and dried under vacuum at room temperature. Yield: 91.2 mg (62%); see also ref. [7f].

Received: May 7, 1992 [Z 5329 IE]
German version: *Angew. Chem.* **1992**, *104*, 1239

CAS Registry number:
1, 143268-20-6.

[1] Review: R. E. Mulvey, *Chem. Soc. Rev.* **1991**, *20*, 167–209.
[2] Review: K. Gregory, P. von R. Schleyer, R. Snaith, *Adv. Inorg. Chem.* **1991**, *37*, 47–142.
[3] a) J. H. Gilchrist, D. B. Collum, *J. Am. Chem. Soc.* **1992**, *114*, 794–795; b) P. L. Hall, J. H. Gilchrist, A. T. Harrison, D. J. Fuller, D. B. Collum, *ibid.* **1991**, *113*, 9575–9585, and references cited therein. c) R. A. Wanat, D. B. Collum, G. Van Duyne, J. Clardy, R. T. De Pue, *ibid.* **1986**, *108*, 3415–3422.
[4] D. Sato, H. Kawasaki, I. Shimada, Y. Arata, K. Okamura, T. Date, K. Koga, *J. Am. Chem. Soc.* **1992**, *114*, 761–763, and references cited therein.
[5] L. M. Jackman, L. M. Scarmoutzos, B. D. Smith, P. G. Williard, *J. Am. Chem. Soc.* **1988**, *110*, 6058–6063, and references cited therein.
[6] Review: N. S. Nudelman, *Carbonylation of Main-Group Organometallic Compounds* in *The Chemistry of Double-Bonded Functional Groups* (Ed.: S. Patai), Wiley, Chichester, **1989**, pp. 799–962.
[7] a) N. S. Nudelman, E. S. Lewkowicz, D. G. Pérez, *Synthesis* **1990**, 917–920; b) D. G. Pérez, N. S. Nudelman, *J. Org. Chem.* **1983**, *48*, 133–134; c) J. J. P. Furlong, E. S. Lewkowicz, N. S. Nudelman, *J. Chem. Soc. Perkin Trans 2* **1990**, 1461–1465; d) N. S. Nudelman, D. G. Pérez, *ibid.* **1989**, 931–936; e) V. Rautenstrauch, M. Joyeux, *Angew. Chem.* **1979**, *91*, 73–74; *Angew. Chem. Int. Ed. Engl.* **1979**, *18*, 85; f) D. G. Pérez, N. S. Nudelman, *J. Org. Chem.* **1988**, *53*, 408–413.
[8] N. S. Nudelman, E. Lewkowicz, J. J. P. Furlong, *J. Org. Chem.*, submitted.
[9] D. Barr, W. Clegg, R. E. Mulvey, R. Snaith, *J. Chem. Soc. Chem. Commun.* **1984**, 469–470.
[10] W. Clegg, M. MacGregor, R. E. Mulvey, P. A. O'Neil, *Angew. Chem.* **1992**, *104*, 74–76; *Angew. Chem. Int. Ed. Engl.* **1992**, *31*, 93.
[11] Crystal data for [**1**-Li · **1**-H]$_4$: $(C_{40}H_{84}Li_4N_8)$, orthorhombic space group $Pna2_1$, $a = 22.077(1)$, $b = 12.230(1)$, $c = 16.528(1)$ Å. Data collection with an Enraf-Nonius CAD4 diffractometer, $Cu_{K\alpha}$ radiation, 193 K, 6086 measured reflections, 5578 independent, 4295 observed ($F_o > 4\sigma(F_o)$). Solution and refinement with the Siemens SHELXTL-PLUS package (direct methods) [12–14]. One solvent molecule is twofold disordered (0.54:0.46). Disordered positions have been refined with isotropic temperature factors, the other non-hydrogen atoms anisotropic, hydrogen atoms with common isotropic temperature factors, C-bonded and disordered N-bonded H atoms riding, other N-bonded H atoms have been refined. 477 parameters, $R = 0.0606$, $wR = 0.0491$. An absolute structure could not be determined. Further details of the crystal structure investigation may be obtained from the Fachinformationszentrum Karlsruhe, Gesellschaft für wissenschaftlich-technische Information mbH, D-W-7514 Eggenstein-Leopoldsha-

fen 2 (FRG) on quoting the deposition number CSD 320 464, the names of the authors, and the journal citation.
[12] SHELXTL-PLUS (VMS), Release 4.2, Siemens Analytical Instruments, **1991**.
[13] A. L. Spek, PLATON 88, Program for Geometrical Analysis of Crystal Structures, Utrecht, **1988**.
[14] E. Keller, SCHAKAL-88B, A FORTRAN Program for the Graphic Representation of Molecular and Crystallographic Models, Freiburg, **1988**.
[15] a) D. R. Armstrong, D. Barr, W. Clegg, S. M. Hodgson, R. E. Mulvey, D. Reed, R. Snaith, D. S. Wright, *J. Am. Chem. Soc.* **1989**, *111*, 4719–4727; b) D. R. Armstrong, R. E. Mulvey, G. T. Walker, D. Barr, R. Snaith, W. Clegg, D. Reed, *J. Chem. Soc. Dalton Trans.* **1988**, 617–628.
[16] D. R. Armstrong, D. Barr, W. Clegg, R. E. Mulvey, D. Reed, R. Snaith, K. Wade, *J. Chem. Soc. Chem. Commun.* **1986**, 869–870.
[17] It is probably long lithium amide ladders that precipitate from the solution immediately after the last complexing amine molecules have been lithiated [1, 2].

Interactions Between Acyclic and Cyclic Peralkylammonium Compounds and DNA**

By *Hans-Jörg Schneider** and *Thomas Blatter*

The quantification of electrostatic interactions between DNA[1] and positively charged effectors is as important for an understanding of the biological function of biogenic amines,[2] proteins, and peptides[3] as for the development of cytostatic agents.[4] Polyamines are bound predominantly in the strongly negatively charged larger groove of the double helix by coulombic interactions with the ribose phosphate groups and presumably also by formation of hydrogen bonds with the nucleobases.[5] We hoped to obtain further information on the mechanisms of molecular recognition relevant here by systematic variation of the structure of the polyamine – including hitherto little investigated[5d] peralkylated amines as well as amines conformationally restricted by cyclization. Using the principle of additive increments,[6] with which we have previously found a surprisingly uniform coulombic interaction energy of $\Delta G_{ES} = (5 \pm 1)$ kJ mol^{-1} for each salt bridge (at an ionic strength of about 0) for over 50 synthetic complexes,[6b] we first analyzed known equilibrium constants[7] for complexation of the biogenic amines **1** ($K = 3.2 \times 10^3$ M^{-1}); **2** ($K = 5.8 \times 10^4$ M^{-1}) and **3** ($K = 2.1 \times 10^5$ M^{-1}) with DNA (Scheme 1). When the differences in the number n of the salt bridges formed between N^+ (amine) and P-O$^-$(DNA), as evident from computer-supported molecular modeling,[5c] are taken into account, the following values for the coulombic increment ΔG_{ES} are obtained: **1** ($n = 3$, $\Delta G_{exp} = 20$) 6.7, **2** ($n = 6$, $\Delta G_{exp} = 27$) 4.5, and **3** ($n = 7$, $\Delta G_{exp} = 30$) 4.3 (all ΔG values in kJ mol^{-1}). The average value of 5.2 kJ mol^{-1} for the interaction with DNA lies in the same range as that of all previously analyzed salt bridges,[6] although molecular simulations[5c] indicate the presence of two to three additional N^+-H hydrogen bonds with the nucleobases. The existence of a largely constant bonding increment per N^+ group is in agreement with interactions between the DNA and protonated polyamines[8] and also between polylysine and polynucleotides.[9]

The comparison of the results of measurements on peralkylated polyammonium ions (Scheme 1) with those of the analogous compounds containing protonated nitrogen atoms makes it possible to estimate the contribution of the additional hydrogen bonds present for the protonated compounds in binding to DNA. By analogy to the comparable investigations of Stewart et al. with protonated polyamines,[8] we have used the polyamine concentration level (C_{50}), which leads to a 50% reduction in the fluorescence intensity of the intercalated probe ethidium bromide, as a measure of the interaction with the B-DNA double helix (calf thymus). These C_{50} values provide, at least approximately, a measure of the various equilibrium constants for complexation of the polyamines with the DNA.[8] The affinities of the *alkylated* open-chain compounds observed in this way generally lie only a little lower than those of the correspondingly charged *protonated* compounds (compare, e.g. **4** with **3**). The contribution of hydrogen bonds is therefore almost negligibly small; this result is in agreement with observations on amide hydrogen bridges, which are completely suppressed[11] by protic solvents,[10] especially water. This result does not, however, exclude small differences in selec-

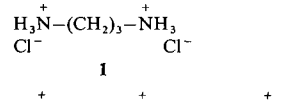

1 **2**

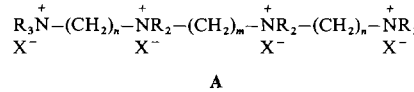

A

	C_{50}	ΔT
A = **3**: $n = 3$, $m = 4$, R = H, X = Cl	1.2	5.2
4: $n = 3$, $m = 4$, R = CH_3, X = I	2.1	5.3
5: $n = 4$, $m = 2$, R = CH_3, X = Br	1.5	11.0
6: $n = 4$, $m = 6$, R = CH_3, X = Br	1.8	7.0
7: $n = 6$, $m = 2$, R = CH_3, X = Br	2.2	7.3
8: $n = 6$, $m = 6$, R = CH_3, X = Br	3.0 ± 1.0	–

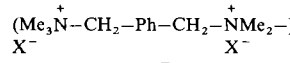

B

	C_{50}	ΔT
B = **9**: Y = $(CH_2)_2$, X = Br	2.5	–
10: Y = $(CH_2)_6$, X = Br	3.0	1.2
11: Y = CH_2–Ph–CH_2, X = Br	2.3	12

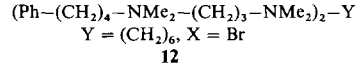

Y = $(CH_2)_6$, X = Br	3.0	1.5

12

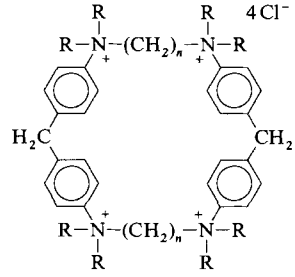

C, R = CH_3

	C_{50}	ΔT
C = **13**: $n = 3$	7.2	2.2
14: $n = 4$	0.27	5.1
15: $n = 5$	8.5	1.4
16: $n = 6$	1.5	3.0
17:	3.4	

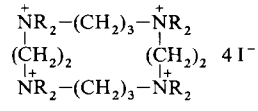

17, R = CH_3

Scheme 1. Structures of the polyamine derivatives **1**–**17** investigated. (C_{50} values of these derivatives with B-DNA (calf thymus) in units of 10^6 M determined by titration with ethidium bromide; changes in the melting point ΔT of DNA complex in °C (with 10^{-6} M polyammonium compound). DNA concentrations correspond in each case to $A_{060} = 0.5$ DNA, 0.01 SHE buffer (9.4 mM NaCl, 10 mM EDTA, 2 mM HEPES (2-[4-(2-hydroxyethyl)-1-piperazino]ethanesulfonic acid), pH 7.

[*] Prof. Dr. H.-J. Schneider, Dipl.-Chem. T. Blatter
Fachrichtung Organische Chemie der Universität des Saarlandes
D-W-6600 Saarbrücken 11 (FRG)

[**] Host-Guest/Supramolecular Chemistry, Part 33. This work was supported by the Deutsche Forschungsgemeinschaft and the Fonds der Chemischen Industrie. Part 32: H.-J. Schneider, I. Theis, *J. Org. Chem.* **1992**, *57*, 3066.

tivity arising from additional hydrogen bridges, for example, by a partial base-selective recognition.

Variation in the alkyl chains in the tetraammonium ions **4** to **12** leads to surprisingly small changes in the C_{50} values (Scheme 1), essentially in agreement with Stewart's results[8] for protonated polyamines. Even the introduction of an arene as spacer between the N^+ groups (**9**–**12**, Scheme 1) leads to similar constants, explicable by four largely undisturbed salt bridges. This obviously is a consequence of the small distance dependence of the coulombic potential, but also the high flexibility of the open-chain compounds.

Macrocyclic peralkylated tetraammonium compounds **13**–**17** can behave quite differently. These compounds display an effect towards DNA that is up to 15 times higher than that for the open-chain analogues (Scheme 1 and 2). (All the

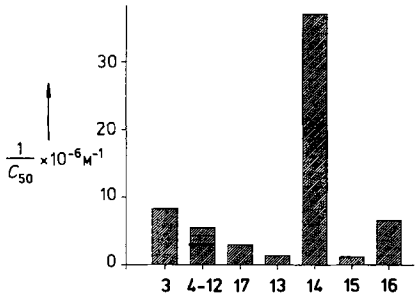

Scheme 2. Affinities of the polyammonium derivatives **3**–**17** for B-DNA (shown as values of $1/C_{50} \times 10^{-6}\,M^{-1}$); the minimum and maximum values for the acyclic compounds **4**–**12** are indicated within the columns.

azoniacyclophanes[12] **13**–**16** employed were obtained by a one-pot cyclization of bistosylated bis(4-aminophenyl) methane with α,ω-dibromoalkanes, and subsequent permethylation after removal of the tosyl groups.[13]). For a given number of N^+ groups, azoniacyclophane **14** shows by far the highest interaction of a tetraamine with DNA that has been seen to date. Also, in contrast to the other cyclophanes, the change in melting point of the DNA complex is markedly higher for **14**, $\Delta T = 5.1\,^{\circ}C$ (Scheme 1).

What are the reasons for the particular high efficiency of an azoniacyclophane? Since the host compound **16**, for example, binds adenosine phosphate by enclosing the nucleobases within the cyclophane cavity with $K = 10^3$ to $10^4\,M^{-1}$,[14] and a larger acridinophane[15] has shown itself to be a potent intercalator[16] (by violation of the "neighbor exclusion" principle[17], according to which the inclusion of further intercalators between neighboring base pairs is not usually possible), an additional contribution to binding of the cyclophane to DNA by intercalation could not be ruled out. To examine this, we have conducted NMR and viscosity measurements, both of which exclude intercalation. Whereas intercalation typically causes shifts in the NMR signals of the intercalate of $\delta = -0.7$,[18] for example, by ring current effects, we have observed maximum differences of $\Delta\delta = 0.02$ for all aromatic protons. Moreover, the cyclophanes show similarly small changes in viscosity ($L/L_0 = 0.95$ to 1.05) with DNA as, for example. the open-chain spermine **3**, whereas intercalators cause considerable increases in viscosity[19] (e.g. for chinacrin: $L/L_0 = 1.16$). Both methods also show the lack of intercalation for the open-chain compounds containing aryl units (**11** and **12**). Electrostatic bonding therefore remains the dominating factor, also for the azoniacyclophanes. Molecular simulation shows that the particularly effective macrocycle **14** finds sufficient space in the large groove of the DNA double helix, thereby permitting predominantly ion-pair contact between the positive $^+$N-C-H protons and the ribose phosphate oxygen atoms.

In summary, the following results have been obtained: 1. Ionic bonding between polyamines and DNA can be described by additive increments of $5 \pm 1\,kJ\,mol^{-1}$ per salt bridge, thereby falling into the general range of numerous inorganic and organic ion pairs. 2. Peralkylated compounds have almost the same affinity for DNA as for example, biogenic amines, whereby the small contribution of hydrogen bonds to the bonding with DNA is also evident here. 3. Relatively rigid azoniacyclophanes show the same or higher affinities, although their arene units do not participate in intercalation.[20]

Received: March 2, 1992 [Z 5262IE]
German version: *Angew. Chem.* **1992**, *104*, 1244

[1] a) W. Saenger, *Principles of Nucleic Acid Structure*. Springer, New York, **1984**; b) G. S. Manning, *Quart. Rev. Biophys.* **1978**, *11*, 179.
[2] C. W. Tabor, H. Tabor, *Annu. Rev. Biochem.* **1984**, *53*, 749.
[3] D. L. Ollis, S. W. White, *Chem. Rev.* **1987**, *87*, 981.
[4] a) *Chemistry and Physics of DNA-Ligand Interaction* (Eds.: N. R. Kallenbach), Adenine Press, Guilderland, NY, USA, **1989**; b) S. Neidle, Z. Abraham, *Crit. Rev. Biochem.* **1984**, *17*, 73.
[5] a) H. R. Drew, R. E. Dickerson, *J. Mol. Biol.* **1981**, *151*, 535; b) S. Jain, G. Zon, M. Sundaralingam, *Biochemistry* **1989**, *28*, 2360; c) L. Stekowski, D. B. Harden, R. L. Wydra, K. D. Stewart, W. D. Wilson, *J. Mol. Recognit.* **1989**, *2*, 158; d) An earlier investigation with DNA and one peralkylated steroid diamine contained no details on the contribution of hydrogen bridge bonds: D. J. Patel, L. L. Canuel, *Proc. Nat. Acad. Sci. USA* **1979**, *76*, 24.
[6] a) H.-J. Schneider, *Angew. Chem.* **1991**, *103*, 1419; *Angew. Chem. Int. Ed. Engl.* **1992**, *30*, 1417; b) H.-J. Schneider, I. Theis, *ibid.* **1989**, *101*, 757 and **1989**, *28*, 753; c) H.-J. Schneider, T. Schiestel, P. Zimmermann, *J. Am. Chem. Soc.*, in press.
[7] W. H. Braunlin, T. J. Strick, M. T. Record, Jr., *Biopolymers* **1982**, *21*, 1301.
[8] a) K. D. Stewart, *Biochem. Biophys. Res. Commun.* **1988**, *152*, 1441; b) K. D. Stewart, T. A. Gray, *J. Phys. Org. Chem.*, in press, references cited therein. (We thank Dr. K. D. Stewart, Burroughs Welcome Co., Research Triangle Park, USA, for a preprint.)
[9] S. A. Latt, M. A. Sober, *Biochemistry* **1967**, *6*, 3293; It is of interest that the association constants ($\lg K$) of polylysine with polynucleotides display a linear increase with the length of the peptide chain, from which a value of $\Delta G \approx 6\,kJ\,mol^{-1}$ per lysine unit can be calculated likewise from the data provided[9] (by extrapolation to zero ionic strength).
[10] W. J. Jorgensen, *Acc. Chem. Res.* **1989**, *22*, 184.
[11] Cf. H.-J. Schneider, R. K. Juneja, S. Simova, *Chem. Ber.* **1989**, *122*, 1211 and unpublished results.
[12] K. Odashima, K. Koga in *Cyclophanes, Vol. 2* (Eds.: P. M. Kehn, S. M. Rosenfeld), Academic Press, New York, **1983**, 629.
[13] H.-J. Schneider, R. Busch, *Chem. Ber.* **1986**, *119*, 747.
[14] H.-J. Schneider, T. Blatter, *J. Am. Chem. Soc.*, in press.
[15] S. C. Zimmerman, C. R. Lamberson, M. Cory, T. A. Fairly, *J. Am. Chem. Soc.* **1989**, *111*, 6805.
[16] J. M. Veal, Y. Li, S. C. Zimmerman, C. R. Lamberson, M. Cory, G. Zon, W. D. Wilson, *Biochemistry* **1990**, *29*, 10918; see also: L. P. G. Wakelin, M. Romanos, T. K. Chen, E. S. Canelaakis, M. J. Waring, *ibid.* **1978**, *17*, 5057.
[17] L. P. G. Wakelin, M. Romanos, T. K. Chen, D. Glaubiger, E. S. Canellakis, M. J. Waring, *Biochemistry* **1978**, *17*, 5057, and references therein.
[18] See, for example, a) S. Chandrasekaran, S. Kusuma, D. W. Boykin, W. D. Wilson, *Magn. Reson. Chem.* **1986**, *24*, 630; b) W. D. Wilson, F. A. Tanious, H.-J. Barton, R. L. Wydra, R. L. Jones, D. W. Boykin, L. Strekowski, *Anti-Cancer Drug Des.* **1990**, *5*, 31.
[19] For example W. A. Denny, *Anti-Cancer Drug Des.* **1989**, *4*, 241.
[20] The C_{50} measurements [8] and the melting point investigations [22] were carried out – as described in the cited references – with calf thymus DNA (average molecular weight 8.9×10^6); for the viscosity [23] and NMR [18] experiments solutions of DNA with $500\,000 < M_r < 800\,000$ (by viscometry [24]) were prepared by ultrasonic treatment. The ionic strength for the C_{50} measurements was 0.01 [17] and should, according to published literature [9,21], only lead to small reductions in the energy of complexation.
[21] a) H.-J. Schneider, R. Kramer, S. Simova, U. Schneider, *J. Am. Chem. Soc.* **1988**, *110*, 6442; b) H.-J. Schneider, I. Theis, *J. Org. Chem.*, **1992**, *57*, 3066.
[22] H. S. Basu, L. J. Marton, *Biochem. J.* **1987**, *244*, 243.
[23] U. Wirth, O. Buchardt, T. Koch, P. E. Nielsen, B. Norden, *J. Am. Chem. Soc.* **1988**, *110*, 932.
[24] a) J. E. Godfrey, *Biophys. Chem.* **1976**, *5*, 285; b) J. Eigner, P. Doty, *J. Mol. Biol.* **1965**, *12*, 549.

A Novel Six-Center Deprotonation–Lithiation Reaction Mechanism Supported by the X-Ray Structure Analysis of a Lithium Carbazolide**

By *Christoph Lambert, Frank Hampel,* and *Paul von Ragué Schleyer**

Although deprotonation–metalation reactions of NH-acidic compounds with LiOR are important in organic chemistry,[1] details concerning the mechanism are scarce. Earlier experimental and theoretical investigations have assumed a four-center transition state (TS) **I**.[2]

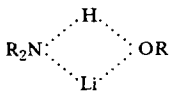

TS, **I**

We propose an alternative *two-step* mechanism, which could occur in cases of similar NH and OH acidities in protic media (Scheme 1). This mechanism involves a precursor

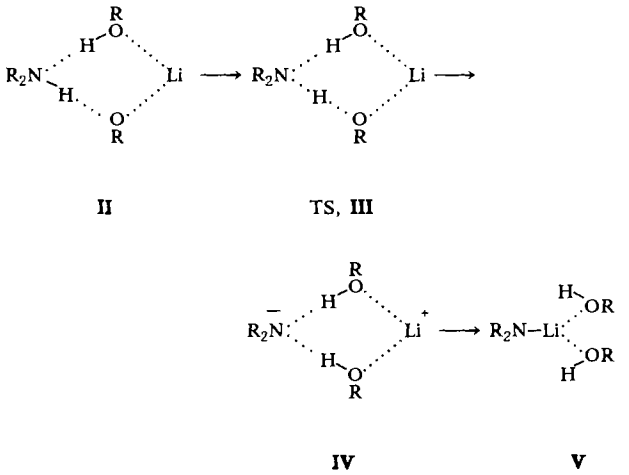

II TS, **III** **IV** **V**

Scheme 1.

complex **II** (comprising the NH compound, the LiOR base, and an additional H-bound ROH solvent molecule), a six-center transition state **III** and a product complex **IV**. No direct Li–N contact is present in the transition state or in these complexes. Evidence for this pathway is given by a single X-ray structure of a lithium carbazolide (**1**,

$[Li(tBuOH)_2 \cdot (thf)_2][cb]$ **1**

Hcb = carbazole) (Fig. 1).[3] This complex was synthesized by deprotonation of carbazole in THF by a mixture of *t*BuOLi/*t*BuOH in THF. While the deprotonation with *n*BuLi in THF yielded a lithiocarbazole dimer,[4] a monomeric species with *t*BuOH as a ligand and without any Li–N contact (*d* Li-N = 3.636 Å) was obtained under the present conditions.

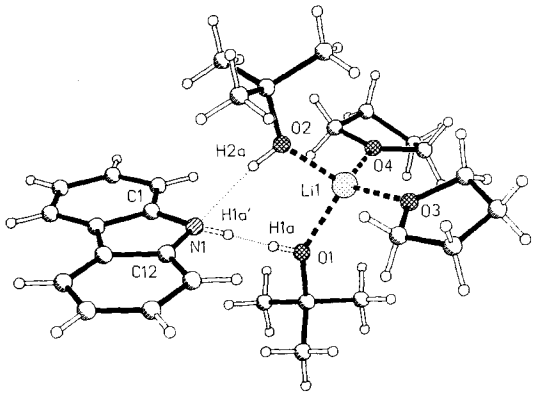

Fig. 1. Structure of **1** in the solid state. Selected bond distances [Å] and angles [°]: Li1-O1 1.924(12), Li1-O2 1.896(10), Li1-O3 1.939(11), Li1-O4 1.929(10), N1-O1 2.727(7), N1-O2 2.770(7), N1-Li1 3.636(10), O2-H2a 0.860(57) N1···H2a 1.913(56), O1-H1a 0.945(120), N1···H1a 1.844(103), N1-H1a' 0.851, O1···H1a' 1.877; O1-Li1-O2 95.8(4), O3-Li1-O4 101.0(4), O1-Li1-O3 111.4(5), O2-Li1-O4 112.7(4), O1-Li1-O4 114.0(7), O2-Li1-O3 112.4(7), Li1-O2-H2a 103.9(4.0), Li-O1-H1a 86.1(8.0), C1-N1-C12 105.7(5), C1-N1-H1a' 120.9, C12-N1-H1a' 125.5, N1-H2a-O2 174.8, N1-H1a-O1 154.4, N1-H1a'-O1 175.4.

The structural analysis of **1** exhibits disorder for a proton undergoing transfer. At 200 K the structure refinement gave ca. 40% occupation probability for the proton site at the carbazole nitrogen (H1a') and about 60% occupation probability for the site at a *tert*-butyl alcohol oxygen atom (H1a). The occupation probabilities correspond to a slightly asymmetric double minimum potential where the ΔG difference of the minima is about -0.4 kcal mol^{-1}. Therefore we reason that the acidity of carbazole and *tert*-butyl alcohol in the solid state must be quite similar. In fact, the differences in acidity are very small in protic media: pK_a (carbazole) = 17.06 in DMSO/H_2O (DMSO = dimethyl sulfoxide);[5] pK_a (*t*BuOH) = 16.54 in EtOH/EtO^-.[6] Hence, complex **1** provides a good structural model for both the precursor complex **II** and the product complex **IV**. The second *tert*-butyl alcohol molecule also incorporated into the structure obviously stabilizes the complexes **II** and **IV** (as well as the assumed transition state **III**) by forming of a six-center hydrogen-bridged arrangement. The X-ray structure supports a model in which hydrogen bonding is not only important in stabilizing anionic centers,[7] but may also be involved in the proton-transfer step. After proton transfer (first step) in solution, a rearrangement (second step) could take place to give an *N*-lithiated carbazole (as in **V**) by a stepwise rather than by a concerted mechanism.

Only a few structures of lithiated NH- or CH-acids complexed with ROH derivatives have been reported.[8] None of these, however, exhibit a partial transfer of the proton to the anionic (lithiated) center. The structure of a water-complexed lithiomalonodinitrile we reported recently[8e] also shows disorder, but this involves an H_2O proton and the ligand, and not the anionic center.

Furthermore, it is interesting that **1** is a solvent-shared ion pair rather than a contact ion pair as commonly observed for lithiated amines.[9] This preference of **1** is noteworthy, since

[*] Prof. Dr. P. von R. Schleyer, Dipl.-Chem. C. Lambert, Dipl.-Chem. F. Hampel
Institut für Organische Chemie der Universität Erlangen-Nürnberg
Henkestrasse 42, D-W-8520 Erlangen (FRG)

[**] This work was supported by the Fonds der Chemischen Industrie and the Deutsche Forschungsgemeischaft. C. L. gratefully acknowledges a scholarship from the Fonds der Chemischen Industrie.

solvent-shared or solvent-separated ion pairs are expected to be less favorable for lithium amides than for lithium-carbon compounds due to the greater electrostatic Li–N interaction (stronger N–Li than C–Li bonding[10]) in amides.[11] Indeed, only few solvent-separated lithium amide structures are known.[12] In all these cases the ion-separation is induced by crown-ether complexation of the Li^+ ion, which is favored entropically over complexation by monodentate ligands like water, alcohols or ethers.[13]

Our direct experimental demonstration of a reaction pathway for proton transfer encourages the search for further examples.

Experimental Procedure

To a solution of 669 mg (4 mmol) carbazole in 4 mL THF a mixture of 2.5 mL (4 mmol) 1.6 M *n*BuLi/hexane and 1.5 mL (16 mmol) *tert*-butyl alcohol in 4 mL THF (the mixture was prepared at 0 °C and contains 1 equivalent *t*-BuOLi) was added dropwise at 0 °C. The colorless solution was stirred at room temperature for 1 day and kept at 5 °C for 1 day and at −18 °C for 1 day, during which time colorless crystals formed.

Received: April 27, 1992 [Z 5324IE]
German version: *Angew. Chem.* **1992**, *104*, 1242

CAS Registry numbers:
1, 143143-34-4; Hcb, 86-74-8; *t*BuOLi, 1907-33-1.

[1] F. Hibbert, *Adv. Phys. Org. Chem.* **1986**, *22*, 113.
[2] a) R. Huisgen, J. Sauer, *Angew. Chem.* **1960**, *72*, 91; b) J. J. Eisch, W. C. Kaska, *J. Org. Chem.* **1962**, *27*, 3745; c) G. Wittig, *Bull. Soc. Chim. Fr.* **1963**, 1352; d) P. West, R. Waack, J. I. Purmont, *J. Organomet. Chem.* **1969**, *19*, 267; e) D. Liotta, M. Saindane, L. Waykole, J. Stephens, J. Grossman, *J. Am. Chem. Soc.* **1988**, *110*, 2667; f) E. Kaufmann, P. von R. Schleyer, *J. Comput. Chem.* **1989**, *10*, 437; g) E. Kaufmann, S. Sieber, P. von R. Schleyer, *J. Am. Chem. Soc.* **1989**, *111*, 121.
[3] Crystal data: $C_{28}H_{44}LiNO_4$, $M = 465.6$, triclinic space group $P\bar{1}$, $a = 10.282(5)$, $b = 11.050(5)$, $c = 14.397(5)$ Å, $\alpha = 71.53(3)$, $\beta = 73.72(3)$, $\gamma = 73.11(4)°$, $V = 1452.3(12)$ Å^3, $Z = 2$, $\varrho_{calc} = 1.065$ Mgm^{-3}, 7967 collected ($3.0° < 2\theta < 55.0°$), 6710 independent, and 2063 observed reflections ($F > 4.0\sigma(F)$), 318 refined parameters, $R = 0.0869$, $wR = 0.0637$; all data were collected on a Nicolet R3m/V diffractometer at 200 K with $Mo_{K\alpha}$ radiation ($\lambda = 0.71073$ Å). The structure was solved with direct methods (SHELXTL + 4.11/V). All non-hydrogen atoms were refined anisotropically, the hydrogen atoms isotropically in fixed positions except H1, H1a', and H2a. H2a and H1a were refined independently and isotropically; H1a' was located from a difference electron density map and refined with fixed isotropic thermal parameters at the located position. Further details of the crystal structure investigation are available on request from the Fachinformationszentrum Karlsruhe, Gesellschaft für wissenschaftlich-technische Information mbH, D-W-7514 Eggenstein-Leopoldshafen 2 (FRG), on quoting the depository number CSD-56397, the names of the authors, and the journal citation.
[4] R. Hacker, E. Kaufmann, P. von R. Schleyer, W. Mahdi, H. Dietrich, *Chem. Ber.* **1987**, *120*, 1533.
[5] R. Gaboriaud, J.-C. Halle, P. Letellier, *Bull. Soc. Chim. Fr.* **1976**, 1093.
[6] W. Reeve, C. M. Erikson, P. F. Aluotto, *Can. J. Chem.* **1979**, *57*, 2747.
[7] S. Buchholz, K. Harms, M. Marsch, W. Massa, G. Boche, *Angew. Chem.* **1989**, *101*, 57; *Angew. Chem. Int. Ed. Engl.* **1989**, *28*, 72.
[8] a) G. Klebe, K. H. Böhn, M. Marsch, G. Boche, *Angew. Chem.* **1987**, *99*, 62; and *Angew. Chem. Int. Ed. Eng.* **1987**, *26*, 78; b) D. Barr, P. R. Raithby, P. von R. Schleyer, R. Snaith, D. S. Wright, *J. Chem. Soc. Chem. Commun.* **1990**, 643; c) D. R. Armstrong, D. Barr, P. R. Raithby, R. Snaith, D. S. Wright, P. von R. Schleyer, *Inorg. Chim. Acta* **1991**, *185*, 163; d) [Lithio-2-mercaptobenzoxazole · MeOH · HMPA]$_2$; M. Davidson, C. P. G. S. Thesis, Cambridge, **1991**; e) C. Lambert, P. von R. Schleyer, U. Pieper, D. Stalke, *Angew. Chem.* **1992**, *104*, 78; *Angew. Chem. Int. Ed. Engl.* **1992**, *31*, 77; f) We recently found a water-complexed lithio-*p*-nitrophenoxide also exhibiting a disorder of the transferred proton: F. Hampel, P. von R. Schleyer, unpublished.
[9] a) K. Gregory, P. von R. Schleyer, R. Snaith, *Adv. Inorg. Chem.* **1991**, *37*, 47; b) R. E. Mulvey, *Chem. Soc. Rev.* **1991**, *20*, 167.
[10] C. Lambert, M. Kaupp, P. von R. Schleyer, *J. Am. Chem. Soc.*, submitted.
[11] a) R. A. Bartlett, H. V. R. Dias, H. Hope, B. D. Murray, M. M. Olmstead, P. P. Power, *J. Am. Chem. Soc.* **1986**, *108*, 6921; b) P. P. Power, *Acc. Chem. Res.* **1988**, *21*, 147.
[12] a) R. A. Bartlett, P. P. Power, *J. Am. Chem. Soc.* **1987**, *109*, 6509; b) G. E. Underiner, R. P. Tan, D. R. Powell, R. West, *ibid.* **1991**, *113*, 8437.
[13] E. Kaufmann, J. Gose, P. von R. Schleyer, *Organometallics* **1989**, *8*, 2577.

Dynamic Proton Exchange in the Hydrogen Dihydroxide Ion $H_3O_2^-$ of the Hydroxosodalite Hydrate $[Na_4(H_3O_2)]_2[SiAlO_4]_6$: ^{1}H MAS NMR Spectroscopic Evidence**

By *Günter Engelhardt,** *Peter Sieger*, and *Jürgen Felsche*

Structure and properties of the hydrogen dihydroxide ion $H_3O_2^-$, that is the monohydrate of the hydroxide ion, $[H–O\cdots H\cdots O–H]^-$, in which OH^- and H_2O can no longer be distinguished, have been of great interest both for theoreticians and also for experimenters in the last 15 years. Optimized structures were proposed by several authors from ab initio calculations, [1–3] and following experimental investigations into the hydration of OH^- in the gas phase[4] performed earlier several papers since 1979 have reported about crystal structures with discrete $H_3O_2^-$ ions (see, e.g., ref. [5–8] and references cited therein). Thus, in compounds of the natrocalcite type[6, 7] as well as in crystalline aqua hydroxo complexes of transition metals with organic ligands[5, 8] an (on average) symmetrical $[H–O\cdots H\cdots O–H]^-$ ion was observed, characteristic of which is a strong central hydrogen bond $O\cdots H\cdots O$ with $O\cdots O$ distances of 2.3–2.6 Å. In these compounds the $H_3O_2^-$ ion is coordinated by neighboring oxygen atoms and/or metal ions[6–8] or bonded to additional H_2O molecules by weak hydrogen bonds.[5]

Ardon and Bino discussed the significance of $H_3O_2^-$ as a bridging ligand in the primary hydrolysis products of metal salts and the possibility of its existence in aqueous solutions of aqua hydroxo complexes.[8] In the same work it is indicated that detailed investigations of the properties of the $H_3O_2^-$ ion can contribute to a deeper understanding of substitution and redox reactions, including enzymatic reactions, in which a hydrogen transfer via H_3O_2 bridges is conceivable. For such considerations apart from the static (or dynamically averaged) crystal structures, as obtained by X-ray or neutron diffraction, information about the dynamic proton exchange and reorientation processes of the $H_3O_2^-$ ion is of particular interest. Such information can be obtained, for example, from ^{1}H NMR spectroscopy, which was already widely used for the characterization of molecular dynamic processes in liquids occurring in a time interval of between approximately 1 s and 10^{-6} s. The investigation of solids however can be complicated by strong signal broadening due to dipole–dipole interactions of neighboring H atoms. This can be avoided (at least partly) by special measurement techniques (e.g. magic angle spinning (MAS), combined rotation and multipulse spectroscopy (CRAMPS)) as well as by the use of samples with only a few H atoms that experience no, or only weak, dipolar coupling. Therefore, as the first step towards the characterization of the dynamics of the $H_3O_2^-$ ion investigations on an isolated $H_3O_2^-$, that is, a $H_3O_2^-$ which is not or only weakly bound to other proton-containing species, would be desirable.

A suitable system for such investigations is sodium hydroxosodalite hydrate $[Na_4(H_3O_2)]_2[SiAlO_4]_6$, which according to the crystal structure recently published by Wiebcke et al.[9] contains discrete $H_3O_2^-$ ions, isolated in the sodalite cages. Figure 1 shows such a sodalite cage ($[4^6 6^8]$ polyhedron) built from alternating SiO_4 and AlO_4 tetrahe-

[*] Dr. G. Engelhardt
Institut für Technische Chemie I der Universität
Pfaffenwaldring 55, D-W-7000 Stuttgart 80 (FRG)
Dipl.-Chem. P. Sieger, Prof. Dr. J. Felsche
Fakultät für Chemie der Universität Konstanz

[**] This work was supported by the Deutsche Forschungsgemeinschaft and the Alfried Krupp von Bohlen and Halbach Stiftung.

dra, from which the sodalite framework is formed by three-dimensional connections with identical cages via four- and six-membered rings. Each cage contains one $H_3O_2^-$ ion and four Na^+ ions tetrahedrally arranged over the six-membered ring windows, the latter are necessary for the charge compensation. Within the Na_4 tetrahedra the $H_3O_2^-$ ions show a six or twelvefold orientational disorder. One of the possible orientations is drawn in Figure 1. The short O2···O2 distance of only 2.36(4) Å in the ion determined from the X-ray diffraction data indicates the existence of a very strong central hydrogen bond, whereas the long H2···O1 and O2···O1 distances of 2.83 and 3.38 Å, respectively, definitely rule out hydrogen bonds between the terminal hydrogen atoms H2 and the framework oxygen atoms O1. Interactions between $H_3O_2^-$ ions in neighboring cages can also be ruled out because of the long distance and the mutual shielding by the Na^+ ions and the cage framework.

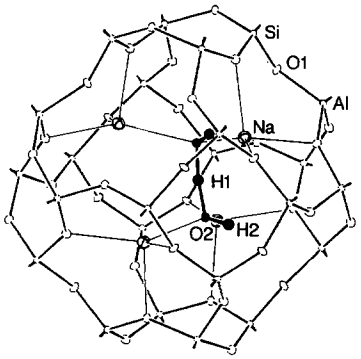

Fig. 1. Structure of $[Na_4(H_3O_2)]_2[SiAlO_4]_6$: $[4^66^8]$ sodalite cage with the $H_3O_2^-$ ion and four Na^+ ions as guest species [9].

A selection of the ^1H MAS NMR spectra of hydroxosodalite hydrate recorded in the temperature range between 365 and 155 K is reproduced in Figure 2. Apart from a sharp signal of an impurity (see below) whose position ($\delta = 5.0$) and line width up to 210 K remains unchanged, the spectra at 365 K and 335 K show only a broad signal at $\delta \approx 5$, superimposed with this sharp signal. With further decrease in temperature two signals at first broad, but up to 210 K becoming significantly narrower, occur at $\delta = -0.1$ and $\delta = 16.3$, which show an integral intensity ratio of 2:1. Thus, the spectra are typical for a dynamic exchange between two chemically nonequivalent kinds of protons occurring in the ratio 2:1; quite similar spectra are observed for analogous dynamic processes in the liquid phase.[10]

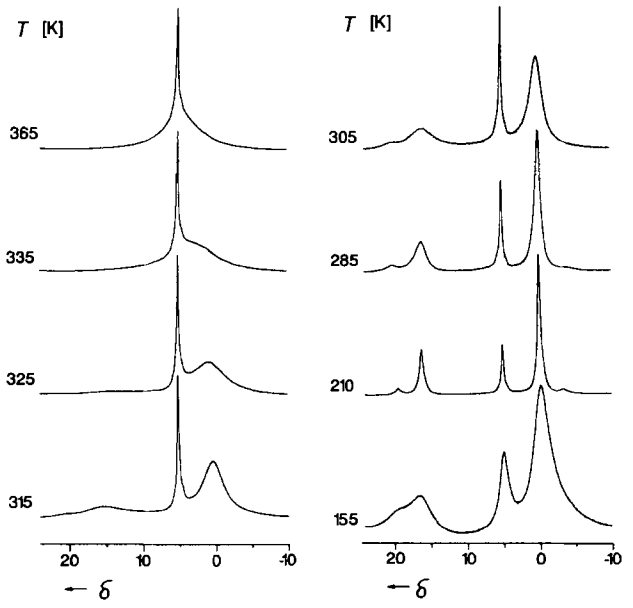

Fig. 2. ^1H MAS NMR spectra of the $H_3O_2^-$ ion in the sodium hydoxosodalite hydrate at several temperatures. The sharp signal at $\delta = 5$ stems from an impurity, the weak signals at $\delta \approx 20$ and $\delta \approx -4$ are spinning side bands.

On the basis of the chemical shifts and the relative intensities the signal at high field must be assigned to the two terminal H atoms H_t and the one at low field to the central H atom H_c of the $(H{-}O\cdots H\cdots O{-}H)^-$ ion.[9] The latter assignment is in excellent agreement with the results from ab initio calculations of the ^1H chemical shift of the free $H_3O_2^-$ ion. According to these calculations the central H atom has a chemical shift of $\delta = 16.3$[11] for a O···O distance of 2.42 Å. Furthermore, the assignment agrees with the linear correlation between OH···O distances and ^1H chemical shifts given by Yesinowski and Eckert.[12] The sharp signal at $\delta = 5.0$ is assigned to H_2O molecules found in small admixtures of hydrosodalite $[Na_3(H_2O)_4]_2[SiAlO_4]_6$, which is difficult to avoid during the preparation of the hyroxosodalite hydrate.[13] The narrow and up to 210 K unchanged line width of this signal shows that these H_2O molecules undergo a rapid dynamic reorientation and do not participate in the exchange process of the $H_3O_2^-$ protons.

Thus, the spectra in Figure 2 reveal unambiguously a dynamic exchange between the two terminal protons H_t and the central proton H_c of the $H_3O_2^-$ ion. On the NMR time scale this exchange occurs rapidly at 365 K (occurrence of only one signal) and becomes slower with decreasing temperature (two signals with decreasing line width). For such a dynamic process the position of the signal for rapid exchange (δ_{ct}) is the weighted population p average value of the positions of the signals at slow exchange: $\delta_{ct} = p_t\delta_t + p_c\delta_c$. With $p_t = 2/3$ and $p_c = 1/3$ $\delta_{ct} = 5.3$ is obtained which is in good agreement with the experimental value. Below 210 K an increasing broadening of all signals is observed (see spectrum at 155 K in Fig. 2), which in all probability is a result of the freezing of the dynamic reorientation of the whole $H_3O_2^-$ ion as well as the H_2O molecules of the impurity in the sodalite cage and the resulting increase of the dipole–dipole interaction of the H atoms.

From the half width $\Delta\nu$ of the signals measured at several temperatures the average life times τ_t and τ_c of the H atoms in the terminal and the central position respectively as well as the rate constants k and the activation energy E_a of the exchange process can be estimated. $\Delta\nu$ must be corrected for the residual line width occurring without exchange, for this the half width (80 Hz) of the signal of the water protons not participating in the exchange at $\delta = 5.0$ was used. For rapid exchange, that is, observation of only one signal $\tau_t = \Delta\nu/(4\pi p_t p_c^2 \Delta\delta^2)$ and $\tau_c = \Delta\nu/(4\pi p_c p_t^2 \Delta\delta^2)$ with $\Delta\delta = \delta_c - \delta_t$ (in Hz) is valid; in contrast, for slower exchange, that is, the occurrence of separate signals for H_t and H_c, $\tau_t = (\pi\Delta\nu_t)^{-1}$ and $\tau_c = (\pi\Delta\nu_c)^{-1}$ is valid.[14] Since the central H atom exchanges with two terminal H atoms, it follows that $\tau_c = \tau_t/2$. The rate constants k for the different temperatures T are given by $k = 2\tau_t^{-1} = \tau_c^{-1}$; from these the activation energy E_a of the proton exchange can be determined from the Arrhenius equation, $k = A \exp(-E_a/RT)$, by plotting lg k over $1/T$ (Fig. 3).

To avoid misrepresentations of the line widths as a result of the dipole–dipole interactions of the H atoms occurring at lower temperatures, only the ^1H MAS NMR spectra of the

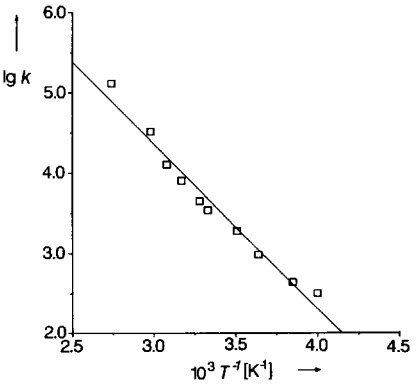

Fig. 3 Arrhenius plot of the rate constants k [s^{-1}] for the proton exchange in the $H_3O_2^-$ ion.

hydroxosodalite hydrate recorded between 365 and 250 K for ten temperatures were included in the evaluation. Average life times τ_c between 7.5×10^{-6} s at 365 K and 3×10^{-3} s at 250 K as well as an activation energy E_a for the exchange process of 39 ± 5 kJ mol^{-1} (estimation of the error according to [14]) were calculated this way. The activation energy lies significantly below the energy required for the dissociation of $H_3O_2^-$ into H_2O and OH^- (100 kJ mol^{-1}), determined experimentally[4] as well as by ab initio calculations.[3] Accordingly, the proton exchange in hydroxosodalite hydrate cannot occur via a complete splitting of the hydrogen bond and subsequent reorientation of the H_2O molecule (Scheme 1 top). Energetically more favorable and in better agreement with the estimated activation energy is the formation of a short-lived intermediate with bifurcated hydrogen bonds. According to ab initio calculations the energy of this intermediate is only 20–40 kJ mol^{-1} above the one of the structure of the $H_3O_2^-$ ion with a linear hydrogen bond.[1, 3] The exchange between terminal and central H atoms could thus occur as shown in Scheme 1 (bottom). Analogous ^{1}H MAS NMR investigations on the hydroxo alumogermanate sodalite hydrate $[Na_4(H_3O_2)]_2[GeAlO_4]_6$ showed that here a dynamic proton exchange within the $H_3O_2^-$ ion also occurs, for which an activation energy of 50 ± 10 kJ mol^{-1} was determined.

Our results show that even without the application of complicated multipulse techniques such as CRAMPS the ^{1}H MAS NMR spectroscopy of solids can produce highly resolved spectra, from whose temperature dependence detailed and selective information about the kinetics and mechanism of dynamic proton exchange and reorientation processes on the time scale of between approximately 10^{-2} and 10^{-6} can be derived. Recent investigations using inelastic and the quasi-elastic neutron scattering[15] showed that faster dynamic reorientation in the ps range, such as those proven for the OH group in the dehydrated hydroxosodalite $[Na_4(OH)]_2[SiAlO_4]_6$,[15, 16] do not occur in the $H_3O_2^-$ ion of the hydroxosodalite hydrate.

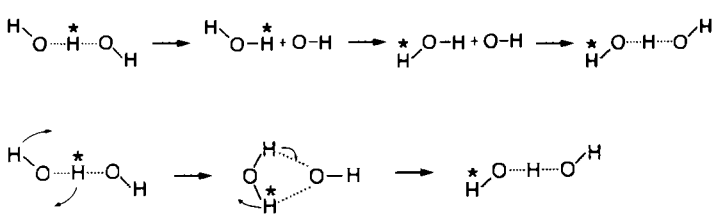

Scheme 1. Improbable (top) and probable (bottom) mechanism of the exchange process in the $H_3O_2^-$ ion.

Experimental Procedure

Crystalline sodium hydroxosodalite hydrate $[Na_4(H_3O_2)]_2[SiAlO_4]_6$ was prepared according to the procedure given in [13] from sintered Kaolin and carbonate-free, 16 M sodium hydroxide solution by hydrothermal synthesis at 623 K and 110 MPa. The crystals (0.5–1 mm) were ground into fine powders prior to NMR study. A microcrystalline powder of sodium hydroxoalumogermanate sodalite hydrate $[Na_4(H_3O_2)]_2[GeAlO_4]_6$ was obtained from GeO_2, γ-Al_2O_3, and carbonate-free, 16 M sodium hydroxide solution at 473 K and a reaction time of 14 days in teflon-coated steel autoclaves. The ^{1}H MAS NMR spectra were recorded at 400.13 MHz with a Bruker MSL-400 NMR spectrometer utilizing a double bearing MAS probe and ZrO_2 rotors with 4 mm diameter. Dry nitrogen was used as bearing and drive gas for the sample rotation, the rotation rate was kept constant at 8 kHz. For each spectrum 16 FIDs were accumulated, the length of pulse was 3 µs (corresponding to a flip angle of 65°), the pulse separation 3 s. The samples were thermostated with the bearing gas and the temperatures were corrected with a calibration curve, which was obtained by the ^{13}C NMR spectra of samarium acetate recorded at identical thermostated conditions and rotation rates [17].

Received: March 21, 1992 [Z 5252 IE]
German version: *Angew. Chem.* **1992**, *104*, 1248

CAS Registry numbers:
$H_3O_2^-$, 12501-19-8; $[Na_4(H_3O_2)]_2[SiAlO_4]_6$, 142810-07-9.

[1] M. D. Newton, S. Ehrenson, *J. Am. Chem. Soc.* **1971**, *93*, 4971.
[2] C. McMichael Rohlfing, L. C. Allen, C. M. Cook, *J. Chem. Phys.* **1983**, *78*, 2598.
[3] J. Gao, D. S. Garner, W. L. Jorgensen, *J. Am. Chem. Soc.* **1986**, *108*, 4784.
[4] P. Kebarle, *Annu. Rev. Phys. Chem.* **1977**, *28*, 445.
[5] K. Abu-Dari, K. N. Raymond, D. P. Freyberg, *J. Am. Chem. Soc.* **1979**, *101*, 3688.
[6] G. Giester, J. Zemann, *Z. Kristallogr.* **1987**, *179*, 431.
[7] G. Chevrier, G. Giester, D. Jarosch, J. Zemann, *Acta Crystallogr Sect. C* **1990**, *46*, 175.
[8] M. Ardon, A. Bino, *Struct. Bonding* (Berlin) **1987**, *65*, 1.
[9] M. Wiebcke, G. Engelhardt, J. Felsche, P. B. Kempa, P. Sieger, J. Schefer, P. Fischer, *J. Phys. Chem.* **1992**, *96*, 392.
[10] K. C. Ramey, J. F. O'Brien, I. Hasegawa, A. E. Borchert, *J. Phys. Chem.* **1965**, *69*, 3418.
[11] C. McMichael Rohlfing, L. C. Allen, R. Ditchfield, *Chem. Phys. Lett.* **1982**, *86*, 380.
[12] J. P. Yesinowski, H. Eckert, *J. Am. Chem. Soc.* **1987**, *109*, 6274.
[13] G. Engelhardt, J. Felsche, P. Sieger, *J. Am. Chem. Soc.* **1992**, *114*, 1173.
[14] G. Binsch in *Dynamic Nuclear Magnetic Resonance Spectroscopy* (Eds.: L. M. Jackman, F. A. Cotton), Academic Press, New York, **1975**, S. 45.
[15] O. Elsenhans, W. Bührer, I. Anderson, J. Nicol, T. Udovic, F. Rieutord, J. Felsche, P. Sieger, G. Engelhardt, unpublished.
[16] W. Bührer, J. Felsche, S. Luger, *J. Chem. Phys.* **1987**, *87*, 2316.
[17] G. C. Campbell, R. C. Crosby, J. F. Haw, *J. Magn. Reson.* **1986**, *69*, 191.

Chelate Complexes of Tripodal, Aliphatic Triisocyanide Ligands**

By *F. Ekkehardt Hahn** and *Matthias Tamm*

For some time we have been occupied with the coordination chemistry of multidentate isocyanides with regard to the preparation of stable hexaisocyanide complexes of ^{99m}Tc as myocardium perfusion agents.[1, 2] Recently we were able to prove that aromatic, tripodal triisocyanides form chelate complexes of the form *fac*-[(triisocyanide)W(CO)$_3$] in spite of the linear M–CNR unit in the metal complex.[3] Depending on the ligand three 18- or 20-membered chelate rings were formed, which rank with the largest ring systems in organometallic compounds. We have now prepared the aliphatic triisocyanide Ctalc **1** and studied its coordination

[*] Prof. Dr. F. E. Hahn, Dipl.-Chem. M. Tamm
Institut für Anorganische Chemie der Freien Universität
Fabeckstrasse 34–36, D-W-1000 Berlin 33 (FRG)

[**] This work was supported by the Deutsche Forschungsgemeinschaft and the Fonds der Chemischen Industrie. We thank the BASF Aktiengesellschaft for a predoctoral grant for M.T.

chemistry. Attempts to obtain chelate complexes with the similar ligand Ntalc **2**, led only to insoluble products. This behavior can be explained by the protonation of the central nitrogen atom[3] or by the formation of polymers as a result of the small number of framework atoms (rings with a maximum size of 12 atoms can be formed). Ctalc **1** can no longer be protonated at the central methine unit, so that the coordination chemistry of aliphatic triisocyanides with a small number of framework atoms can be studied with the preclusion of the protonation of the ligand.

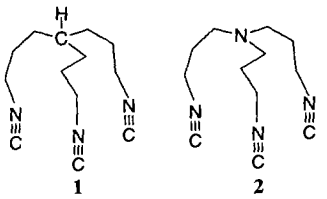

1 **2**

Compound **1** was synthesized according to Scheme 1 and isolated as a colorless oil. It was completely characterized by elemental analyses and IR, ^{1}H, and ^{13}C NMR spectroscopy.[4] The ^{1}H NMR spectrum (400 MHz, in $CDCl_3$) of **1** shows three groups of signals.[4] The protons of the

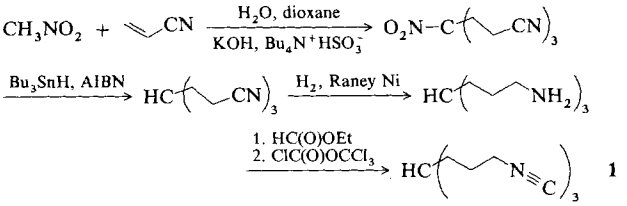

Scheme 1. Synthesis of **1**.

methylene groups next to the isocyanide functions appear as a triplet of triplets at $\delta = 3.41$ by ^{14}N ^{1}H coupling. The signal for the proton of the central methine group and for the protons of the neighboring methylene group form a multiplet at $\delta = 1.45$. The remaining methylene protons appear as a broad multiplet at $\delta = 1.69$. The observed $^2J(^{14}\text{N}\ ^1\text{H})$ coupling in aliphatic isocyanides has already been described.[3, 6] The reaction of **1** with $[(C_7H_8)M(CO)_3]$ (C_7H_8 = cycloheptatriene, M = Cr, W) in CH_2Cl_2 leads to the colorless complexes **3** and **4**.

fac-$[HC(CH_2CH_2CH_2\text{-}NC)_3M(CO)_3]$
3, M = Cr; **4**, M = W

The new compounds were completely characterized by elemental analyses, mass spectrometry, and IR, ^{1}H, and ^{13}C NMR spectroscopy.[5] The ^{1}H NMR spectra for complexes **3** and **4** are very similar to each other but differ appreciably from the spectrum of the free ligand **1** (Fig. 1). In **4** the multiplicity of the signal for the methylene group D was reduced by the coordination of the isocyanide functions to the metal atom from a triplet of triplets in the free ligand to a triplet at $\delta = 3.65$. As expected, the ^{14}N ^{1}H coupling is removed by the coordination of the isocyanide function to the metal center. Hence, also for the signals of the methylene groups C (quint) and B (dt) only the expected $^3J(^1\text{H}\ ^1\text{H})$ coupling patterns are observed. The change of the signal for

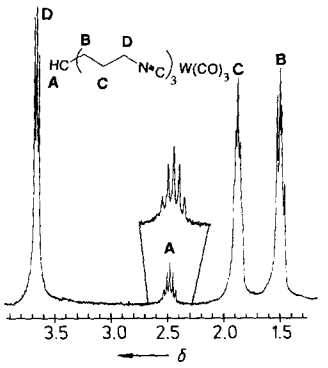

Fig. 1. ^{1}H NMR spectrum (270 MHz, CD_2Cl_2) of **4**.

the proton at the central methine group is the most obvious. It experiences a low-field shift of more than $\Delta\delta = 1$ and appears as a septet at $\delta = 2.48$. To our knowledge the ^{1}H NMR signal of a methine group substituted with three propyl groups has so far never been observed at such low field. From the low-field shift of the signal for the methine group the structure of the presumably isostructural chelate complexes **3** and **4** can be deduced. From previous studies of metal complexes of tripodal ligands with a nitrogen atom as the central framework atom it is known that this atom can adopt the *in*[3, 7] or the *out* configuration.[3] Similar isomers are possible for the coordinated ligand **1** with a central methine unit (Scheme 2).

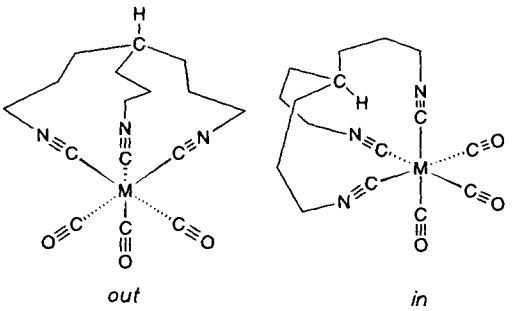

Scheme 2. The *in* and *out* isomers for complexes of the type *fac*-$[HC(CH_2CH_2CH_2\text{-}NC)_3M(CO)_3]$.

The low-field shift of the signal of the methine protons in **3** and **4**[5] can only be explained by the formation of *in* isomers since here the proton of the methine group would penetrate the deshielding region of the anisotropy cone of the NC triple bonds, which leads to the observed low-field shift. In the *out* configuration this proton should not be deshielded and thus its chemical shift approximates that of the free ligand. To gain support for this hypothesis and to show that also aliphatic triisocyanides with a low number of framework atoms can form chelate complexes a structural analysis of **4** was carried out.[8]

Single crystals of **4** were obtained from dichloromethane/hexane (1:1) by slow evaporation of the solvents at room temperature. The X-ray structural analysis shows that the conclusions drawn from the ^{1}H NMR spectrum are correct (Fig. 2 left). The ligand coordinates through three isocyanide groups to the tungsten atom forming three 12-membered chelate rings. Complex **4** and the probably isostructural **3** are the first chelate complexes with aliphatic tripodal triisocyanide ligands.

The quality of the X-ray diffraction data ($2\theta_{max}$ 55° at 100(5) °C) allowed for the determination and refinement

of the positional parameters of H1. Thus, the postulated *in* configuration of the central methine group in **4** was proven unequivocally. The C1–H1 vector points towards the W atom [angle C1-H1-W 177(3)°]. The distances of H1 to the nitrogen atoms lie between 2.69(4) and 2.78(5) Å, the H1–W distance is 3.56(5) Å. These data clearly explain the observed low-field shift of the signal for the methine proton by penetration of this proton into the deshielding region of the anisotropy cone of the NC triple bonds.

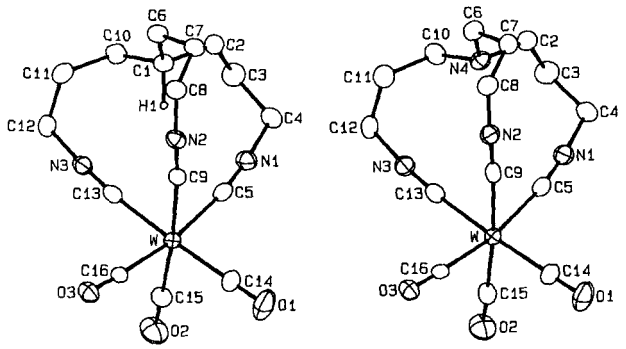

Fig. 2. Crystal structures of **4** (left) and **5** (right) (ORTEP) without hydrogen atoms (with the exception of H1 in **4**). Selected distances [Å] and angles [°] for **4** [**5**]: W-C5 2.138(3) [2.130(4)], W-C9 2.131(3) [2.125(4)], W-C13 2.119(3) [2.114(4)], W-C14 2.005(3) [1.999(4)], W-C15 1.994(3) [1.996(4)], W-C16 1.989(3) [1.983(4)], O1-C14 1.153(4) [1.157(5)], O2-C15 1.158(4) [1.157(5)], O3-C16 1.152(4) [1.160(5)], N1-C5 1.159(4) [1.158(5)], N2-C9 1.151(4) [1.165(5)], N3-C13 1.152(4) [1.157(5)], C1-H1 1.11(5); W-C5-N1 170.3(3) [170.1(3)], W-C9-N2 171.6(2) [171.3(3)], W-C13-N3 174.5(3) [173.6(3)], C5-N1-C4 174.7(3) [174.8(4)], C9-N2-C8 173.4(3) [174.6(4)], C13-N3-C12 174.1(3) [171.6(4)].

The influence on the chemical shift of protons by their interaction with aromatic ring systems have often been described, for example, the marked high-field shift of methine protons in certain cyclophanes.[9] In contrast, we report herein about the induction of a low-field shift, caused by the coordination of the ligand to a metal center and the resulting change of configuration of the ligand.

After we were able to show that also aliphatic tripodal triisocyanides such as **1** can form chelate complexes with only eleven framework atoms, the experiments with the Ntalc **2** ligand were repeated. If a very dilute solution of **2** is allowed to react with $[(C_7H_8)W(CO)_3]$, the polymers[3] originally postulated by us are not formed but a soluble monomeric complex, which was completely characterized. Microanalytical data and ^{1}H NMR and IR spectra[5] indicate the

fac-$[N(CH_2CH_2CH_2\text{-}NC)_3W(CO)_3]$ **5**

formation of complex **5**. This assumption is confirmed by the structural analysis of **5** (Fig. 2 right). This is also a chelate complex with three 12-membered rings. The central nitrogen atom is not protonated, and the ligand adopts the *in* configuration.

The bond parameters for **4** and **5** lie in the expected range. Corresponding parameters in these complexes are identical within the margins of error. The aliphatic triisocyanides are weaker π acceptors than the previously described aromatic triisocyanides.[3] Hence, the W–CN distances are longer than in compounds of the type *fac*[(aromatic triisocyanide)W(CO)$_3$]. The W-C-N angles deviate from linearity by up to 10° whereas the W-C-O angles are almost linear.

With the compounds **3**–**5** it could be shown that also aliphatic triisocyanides with a small number of framework atoms are able to form chelate complexes with low-valent transition metals. In comparison to the aromatic triisocyanides[3] it is noticeable that the marked reduction in the number of framework atoms (from 17 and 19) to 11 does not influence the ability to form chelates.

Received: April 8, 1992 [Z 5293 IE]
German version: *Angew. Chem.* **1992**, *104*, 1218

[1] M. J. Abrams, A. Davison, A. G. Jones, C. E. Costello, H. Pang, *Inorg. Chem.* **1983**, *22*, 2798–2800.
[2] Q.-S. Li, T. L. Frank, D. Franceschi, H. N. Wagner, Jr., L. C. Becker, *J. Nucl. Med.* **1988**, *29*, 1539–1548.
[3] F. E. Hahn, M. Tamm, *Angew. Chem.* **1991**, *103*, 213–215; *Angew. Chem. Int. Ed. Engl.* **1991**, *30*, 203–205; *J. Organomet. Chem.* **1990**, *398*, C19–C21; F. E. Hahn, M. Tamm, A. Dittler-Klingemann, R. Neumeier, *Chem. Ber.* **1991**, *124*, 1683–1686; F. E. Hahn, M. Tamm, *Organometallics* **1992**, *11*, 84–90.
[4] Correct elemental analysis. Selected physical data of **1**: Total yield 31% (based on nitromethane); colorless oil; IR (KBr): $\tilde{\nu}$[cm^{-1}] = 2148 (NC); ^{1}H NMR (400 MHz, $CDCl_3$): δ = 3.41 [tt, $^2J(^{14}N,^1H)$ = 1.6 Hz, $^3J(^1H,^1H)$ = 6.5 Hz, 6H; CH_2NC], 1.69 (m, br, 6H; $CH_2CH_2CH_2$), 1.49–1.43 (m, br, 7H; HC-CH_2 and HC-CH_2); $^{13}C\{^1H\}$ NMR (20.15 MHz, $CDCl_3$): δ = 156.07 (t, $^1J(^{14}N,^{13}C)$ = 5.6 Hz; NC), 41.52 (t, $^1J(^{14}N,^{13}C)$ = 6.7 Hz; CH_2-NC), 35.35 (HC-CH_2), 29.60 (CH_2-CH_2-CH_2), 25.82 (HC-CH_2).
[5] Correct elemental analyses for **3**–**5**. Analytical data: **3**: Yield 23%; colorless crystals; IR (KBr): $\tilde{\nu}$[cm^{-1}] = 2162, 2120 (NC), 1933, 1859 (CO); ^{1}H-NMR (270 MHz, CD_2Cl_2): δ = 3.60 (t, 6H; CH_2NC), 2.43 (septet, 1H; HC-CH_2), 1.82 (quint, 6H; $CH_2CH_2CH_2$), 1.44 (dt, 6H; HC-CH_2); $^{13}C\{^1H\}$ NMR (67.89 MHz, CD_2Cl_2): δ = 206.57 (CO), 151.00 (br, NC), 46.09 (CH_2-NC), 35.49 (HC-CH_2), 34.88 (CH_2-CH_2-CH_2), 25.61 (HC-CH_2).—**4**: yield 13% colorless crystals; IR (KBr): $\tilde{\nu}$[cm^{-1}] = 2167, 2122 (NC), 1930, 1849 (CO); ^{1}H NMR (270 MHz, CD_2Cl_2): δ = 3.65 (t, 6H; CH_2NC), 2.48 (septet, 1H; HC-CH_2), 1.86 (quint, 6H; $CH_2CH_2CH_2$), 1.50 (dt, 6H; HC-CH_2); $^{13}C\{^1H\}$ NMR (67.89 MHz, CD_2Cl_2): δ = 206.57 (CO), 150.78 (br, NC), 46.09 (CH_2-NC), 35.49 (HC-CH_2), 34.87 (CH_2-CH_2-CH_2), 25.60 (HC-CH_2); MS (70 eV): *m/z* 485 ($M^{\oplus}$, 27.3%), 457 ($M^{\oplus}$ – CO, 17.0), 429 ($M^{\oplus}$ – 2CO, 100), 401 ($M^{\oplus}$ – 3CO, 95.5).—**5**: yield 15%; colorless crystals; IR (KBr): $\tilde{\nu}$[cm^{-1}] = 2160, 2115 (NC), 1932, 1854 (CO); ^{1}H NMR (270 MHz, CD_2Cl_2): δ = 3.65 (t, 6H; CH_2NC), 2.47 (t, 6H; NCH_2CH_2), 1.94 (quint, 6H; $CH_2CH_2CH_2$); $^{13}C\{^1H\}$ NMR (67.89 MHz, CD_2Cl_2): δ = 207.40 (CO), 151.78 (br, NC), 56.77 (N-CH_2), 45.18 (CH_2-NC), 28.33 (CH_2-CH_2-CH_2); MS (70 eV): *m/z* 486 ($M^{\oplus}$, 73.6%), 458 ($M^{\oplus}$ – CO, 51.0), 430 ($M^{\oplus}$ – 2CO, 55.9), 402 ($M^{\oplus}$ – 3CO, 100.0).
[6] I. D. Kuntz, P. von R. Schleyer, A. Allerhand, *J. Chem. Phys.* **1961**, *35*, 1533–1534.
[7] F. E. Hahn, S. Rupprecht, K. H. Mook, *J. Chem. Soc. Chem. Commun.* **1991**, 224–225; A. R. Bulls, C. G. Pippin, F. E. Hahn, K. N. Raymond, *J. Am. Chem. Soc.* **1990**, *112*, 2627–2632; T. M. Garrett, T. J. McMurry, M. W. Hossaini, Z. E. Reyes, F. E. Hahn, K. N. Raymond, *ibid.* **1991**, *113*, 2965–2977.
[8] Structure determinations: **4** [**5**]: $C_{16}H_{19}N_3O_3W$ [$C_{15}H_{18}N_4O_3W$], a = 7.974(2) [7.8685(12)], b = 13.588(2) [13.468(3)], c = 8.104(2) [8.1525(11)] Å, β = 99.52(3) [98.501(12)]°, V = 866.0(6) [854.4(5)] Å^3, monoclinic space group $P2_1$[$P2_1$], ρ_{exp} = 1.88 [1.90], ρ_{calcd} = 1.861 [1.890] g cm^{-3}, $Mo_{K\alpha}$ radiation (λ = 0.71073 Å), $\mu(Mo_{K\alpha})$ = 68.29 [69.23] cm^{-1}. 3981 [3015] symmetry-independent reflections (h, ±k, ±l, polar axis), measured at –100(5) °C in the 2θ range 2°–55° [2°–50°]. Solution of the structure in both cases with Patterson methods, refinement of all non-hydrogen atoms with anisotropic thermal parameters. The positional parameters of H1 in **4** were taken from a difference Fourier analysis and refined. All other hydrogen atoms were in calculated positions (d(C–H) = 0.95 Å) with $B_{eq(H)}$ = 1.3 $B_{eq(C)}$. R = 0.0149 [0.0151], R_w = 0.0216 [0.0199] for 3882 [2930] reflections with $F_o^2 \geq 3\sigma(F_o^2)$. The crystallographically correct enantiomer in the chiral space group $P2_1$ was in both cases determined by the refinement of the inverted structrural model; the structural model with the better R value was taken as correct one (difference in the R values 1.8 [1.9]%). Further details of the crystal structure investigation may be obtained from the Fachinformationszentrum Karlsruhe, Gesellschaft für wissenschaftlich-technische Information mbH, D-W-7514 Eggenstein-Leopoldshafen 2 (FRG) on quoting the depository number CSD-56469, the names of the authors, and the journal citation.
[9] R. A. Pascal, Jr., C. G. Winans, D. Van Engen, *J. Am. Chem. Soc.* **1989**, *111*, 3007–3010; R. P. L'Esperance, A. P. West, Jr., D. Van Engen, R. A. Pascal, Jr., *ibid.* **1991**, *113*, 2672–2676.

The Electrochemical Oxidation of [Co^{II}(salen)] in Solvent Mixtures—An Example of a Ladder Scheme with Coupled Electron-Transfer and Solvent-Exchange Reactions**

By *Emerich Eichhorn, Anton Rieker,* and *Bernd Speiser**

Dedicated to Professor Ernst Bayer on the occasion of his 65th birthday

Recently Evans discussed electrode processes[1] in which electron-transfer (E) and chemical (C) reactions are coupled in such a way that a horizontal and vertical formulation of the E and C steps, respectively, leads to a closed, cyclic, so-called square scheme. Fence (more than two oxidation states, two structurally different compounds per oxidation state) and ladder schemes (more than two compounds linked by structural changes, in each case two oxidation states) are extensions of the square scheme. Evans emphasizes that ladder schemes are less common than fence schemes.[2] He quotes a series of systems[3] in which the different charge transfers of the ladder scheme could not be detected separately by experiment.

We now provide an example of a three-rung ladder scheme that we have discovered during a cyclic voltammetric study of *N,N'*-bis(2-hydroxybenzylidene)ethylenediaminatocobalt(II) ([Co(salen)], **1**) in several solvents and solvent mixtures. All electron-transfer reactions can be observed.

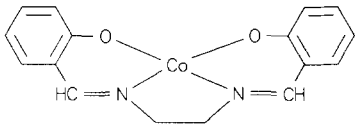

1

Compound **1** is used as oxygen carrier for the oxygenation of organic substrates[4] and is a model compound for enzymes with monooxygenase, dioxygenase, or peroxidase activity. The catalytic function of the oxygen transfer depends strongly on the nature of the solvent.[4, 5]

Earlier work has shown that **1** is oxidized in a relatively fast, quasi-reversible one-electron transfer [Eq. (a)],[6] for which the formal potential E^0 varies strongly with solvent.

$$[Co^{II}(salen)] \underset{}{\overset{e^-}{\rightleftharpoons}} [Co^{III}(salen)]^+ \qquad \text{(a)}$$
$$\mathbf{1} \qquad\qquad \mathbf{2}$$

Complex **1** interacts with the solvent; details, however, have not yet been elucidated. As regards the catalytic reaction, Carter et al.[7] demonstrated that a relationship exists between E^0 and the capacity of **1** to bind oxygen. A knowledge of the structure of each Co complex involved in each solvent and its electrochemistry is essential for the understanding and control of the catalytic reaction, in which the oxidation of **1** to the cationic Co^{III} complex **2** [Equation (a)] possibly also plays a role.[8] In order to define the various complexes in different solvents, we studied the oxidation formulated in Equation (a) at a Pt electrode by cyclic voltammetry.[9]

Both in dimethylformamide (DMF) and pyridine (py) only *one* couple of peaks is observed in the cyclic voltammograms. However, in mixtures of these two solvents three reducible compounds are formed successively on changing from L_1 (DMF) to L_2 (py). This can only be explained if *three* Co^{III} complexes are electroactive (formal potentials E_1^0, E_2^0, and E_3^0 in Scheme 1).

$$\begin{array}{ccc}
\mathbf{1}\cdot 2\,L^1 + 2\,L^2 & \overset{E_1^0}{\rightleftharpoons} & \mathbf{2}\cdot 2\,L^1 + 2\,L^2 + e^- \\
k_1 \Big\| k_{-1}K_1 = \dfrac{k_1}{k_{-1}} & & k_2 \Big\| k_{-2}K_2 = \dfrac{k_2}{k_{-2}} \\
\mathbf{1}\cdot L^1\cdot L^2 + L^1 + L^2 & \overset{E_2^0}{\rightleftharpoons} & \mathbf{2}\cdot L^1\cdot L^2 + L^1 + L^2 + e^- \\
k_3 \Big\| k_{-3}K_3 = \dfrac{k_3}{k_{-3}} & & k_4 \Big\| k_{-4}K_4 = \dfrac{k_4}{k_{-4}} \\
\mathbf{1}\cdot 2\,L^2 + 2\,L^1 & \overset{E_3^0}{\rightleftharpoons} & \mathbf{2}\cdot 2\,L^2 + 2\,L^1 + e^-
\end{array}$$

Scheme 1. Ladder scheme for the oxidation of [Co^{II}(salen)] (**1**) in a mixture of two solvents for two complexed solvent molecules L^1 and L^2, here DMF/pyridine, dichloromethane/pyridine, or acetonitrile/pyridine.

In the quasi-reversible voltammogram in DMF the formal potential is $E_1^0 = -471$ mV vs. ferrocene/ferrocenium (Fc/Fc$^+$). On addition of pyridine (excess of **1** relative to pyridine) the reduction peak splits into peak 1 and peak 2 (Fig. 1a). If complex **1** and pyridine are present in equimolar amounts, the dominant peak is peak 2, and on further addition of pyridine finally only peak 3 is found. With increasing pyridine concentration, at first **2**·2DMF, then **2**·DMF·py, and finally **2**·2py is formed after the electron transfer. These three complexes are reduced at sufficiently different potentials that separate peaks appear in the cyclic voltammograms. The oxidation peak broadens until about a 120-fold excess of pyridine over **1** is reached. Then, like peak 3, it shifts to more negative potentials (in pure pyridine, $E^0 = -871$ mV). This behavior is in fact anticipated for a preequilibrium (defined by K_3 in Scheme 1).[10] Possibly, after the reduction one of the two solvent molecules is cleaved to form the five-coordinate complex.

In DMF/py mixtures the oxidation peaks for the three complexes are not resolved. This is observed when L^1 is CH_2Cl_2 and L^2 is pyridine. The reaction in pure CH_2Cl_2 as solvent is complicated by adsorption phenomena (Fig. 1b). On addition of half an equivalent of pyridine (relative to **1**) the oxidation peak is resolved into two well-defined peaks 1 and 2 of equal intensity. Besides the reduction of the complex containing no pyridine ligands (peak 4), peak 5 appears at approximately -750 mV, which corresponds to the electron transfer to **2**·2py. Its intensity is relatively small, because the concentration of pyridine is still too small to convert all the cobalt(III) complex into **2**·2py. If the concentration of pyridine is increased, reduction peak 4 disappears, and simultaneously peak 2 grows at the expense of peak 1. Although an equimolar amount of pyridine should convert all of **1** to **1**·py·CH_2Cl_2, peak 1 still remains; some of the pyridine is used by the oxidized Co complex to form the bis(pyridine) complex. The equilibrium K_4 thus lies far to the side of **2**·2py. Finally a third oxidation peak (peak 3) forms the signal of a quasi-reversible electron transfer with the now more intense reduction peak 5, which shifts in the negative potential direction towards E_3^0 on increasing the pyridine concentration further. Although CH_2Cl_2 is usually a weak coordinating solvent, a quantitative assessment of the peak shift shows that the equilibrium constant K_3 has a value close

[*] Priv.-Doz. Dr. B. Speiser, Dipl.-Chem. E. Eichhorn, Prof. Dr. A. Rieker
Institut für Organische Chemie der Universität
Auf der Morgenstelle 18, D-W-7400 Tübingen 1 (FRG)

[**] Electrochemistry of Oxygenation Catalysts, Part 1. This work was supported by the Volkswagen-Stiftung (research funds), the state of Baden-Württemberg (graduate scholarship for E.E.), and the Deutsche Forschungsgemeinschaft (Heisenberg Fellowship for B.S.)

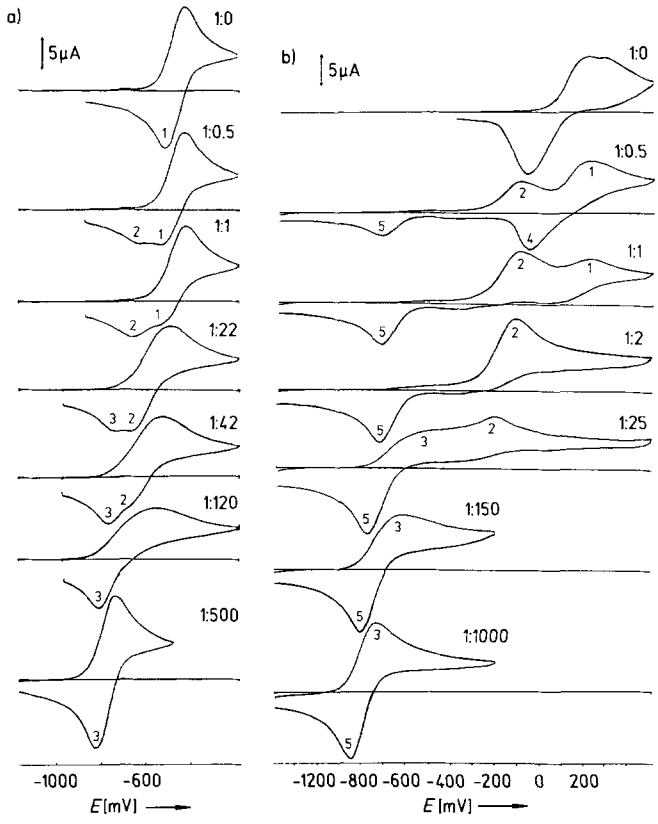

Fig. 1. a) Cyclic voltammograms of **1** in mixtures of DMF and pyridine; potential sweep rate $v = 100\ mVs^{-1}$, $c[\mathbf{1}] = 1.0$ mM; in each case the ratio of the concentrations of **1** to pyridine is given. Top curve: cyclic voltammogram in pure DMF; peak 1: $\mathbf{2}\cdot 2DMF \rightarrow \mathbf{1}\cdot 2DMF$, peak 2: $\mathbf{2}\cdot DMF\cdot py \rightarrow \mathbf{1}\cdot DMF\cdot py$, peak 3: $\mathbf{2}\cdot 2py \rightarrow \mathbf{1}\cdot 2py$. b) Cyclic voltammograms of **1** in mixtures of CH_2Cl_2 and pyridine; potential sweep rate $v = 50\ mVs^{-1}$, $c[\mathbf{1}] = 1.0$ mM; in each case the ratio of the concentrations of **1** to pyridine is given. Top curve: cyclic voltammogram in pure CH_2Cl_2; peak 1: $\mathbf{1}\cdot 2CH_2Cl_2 \rightarrow \mathbf{2}\cdot 2CH_2Cl_2$, peak 2: $\mathbf{1}\cdot CH_2Cl_2\cdot py \rightarrow \mathbf{2}\cdot CH_2Cl_2\cdot py$, peak 3: $\mathbf{1}\cdot 2py \rightarrow \mathbf{2}\cdot 2py$, peak 4: $\mathbf{2}\cdot 2CH_2Cl_2 \rightarrow \mathbf{1}\cdot 2CH_2Cl_2$, peak 5: $\mathbf{2}\cdot 2py \rightarrow \mathbf{1}\cdot 2py$.

to **1**. This points to a weak interaction of the second solvent molecule with the central atom of the Co^{II} complex.

Finally, in the solvent system CH_3CN/pyridine all six electron-transfer reactions could be observed separately (Fig. 2). The voltammogram in CH_3CN shows peaks 1 and 4 (redox reaction at $E_1^0 = -198$ mV). Already on addition of 0.25 equivalents of pyridine to the solution of the cobalt complex in acetonitrile a splitting of the reduction peak can be observed. With increasing pyridine concentration a shoulder grows out of the left flank of the oxidation peak (ratio of complex:py of 1:1). Simultaneously, the reduction of a third Co^{III} species becomes evident. On addition of more pyridine (excess 1:100) a continuous transition of the shoulder into oxidation peak 3 at still more negative potential occurs. Finally, the reduction of only the third species $\mathbf{2}\cdot 2py$ (process with E_3^0) can be observed (peaks 3 and 6).

Results of experiments, in which the potential scan rate v is varied and several successive cycles are recorded, are in accord with the proposed mechanism. A change in v shifts the reduction peak current ratio: increasing v in DMF at a **1**:py ratio of 1:0.5 increases peak 1 relative to peak 2; at higher concentrations of pyridine, peak 2 increases relative to peak 3. Apparently the exchange of DMF for pyridine at the Co^{III} stage takes place relatively slowly. Analogous effects are observed for the other solvent mixtures. If for a *multicycle experiment* the salt $[Co^{III}(salen)]Cl$ is dissolved in DMF and one equivalent of pyridine is added, a mixture of $\mathbf{2}\cdot 2DMF$ and $\mathbf{2}\cdot py\cdot DMF$ results. In such a solution reduction peaks 1 and 2 are observed as expected. On subsequent oxidation exclusively the electron transfer at E_1^0 takes place: at the Co^{II} stage $\mathbf{1}\cdot 2DMF$ forms predominantly because of the small pyridine concentration (equilibrium constant K_1). A second cycle shows only the redox behavior of the bis(dimethylformamide) complex. Ligand exchange reactions are thus very fast for the Co^{II} complexes, but slow for Co^{III} complexes.[11]

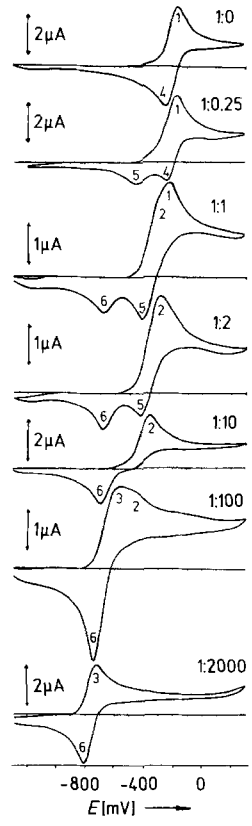

Fig. 2. Cyclic voltammograms of **1** in mixtures of CH_3CN and pyridine; potential sweep rate $v = 50\ mVs^{-1}$, $c[\mathbf{1}] = 0.25$ mM; in each case the ratio of the concentrations of **1** to pyridine is given. Top curve: cyclic voltammogram in pure CH_3CN; peak 1: $\mathbf{1}\cdot 2CH_3CN \rightarrow \mathbf{2}\cdot 2CH_3CN$, peak 2: $\mathbf{1}\cdot CH_3CN\cdot py \rightarrow \mathbf{2}\cdot CH_3CN\cdot py$, peak 3: $\mathbf{1}\cdot 2py \rightarrow \mathbf{2}\cdot 2py$, peak 4: $\mathbf{2}\cdot 2CH_3CN \rightarrow \mathbf{1}\cdot 2CH_3CN$, peak 5: $\mathbf{2}\cdot CH_3CN\cdot py \rightarrow \mathbf{1}\cdot CH_3CN\cdot py$, peak 6: $\mathbf{2}\cdot 2py \rightarrow \mathbf{1}\cdot 2py$.

The results discussed here are important for a detailed description of the catalytic activity of **1**. The redox behavior of the cobalt complex is relatively strongly influenced by variation of the solvent. The observed effect is larger than that of electronically and sterically active substituents on the arene rings of the ligand.[12] The voltammograms show that the change in the formal potential is linked to the change in the coordination sphere of the central atom. This could affect the catalytic activity of **1**, if the substrate for the oxygenation and—as postulated[4]—in some cases also the oxygen to be activated is bound to the complex. Furthermore, the analysis of the proposed exchange equilibria opens the way for an experimental investigation of the primary steps in the catalysis reaction and therefore the preparative oxygenation in the presence of **1**. Preliminary results with substrates such as aromatic amines suggest a connection between the ability of the substrate to expel a solvent molecule from the ligand sphere of cobalt and its tendency to be oxygenated.

Received: February 6, 1992 [Z 5172 IE]
German version: *Angew. Chem.* **1992**, *104*, 1246

CAS Registry numbers:
DMF, 68-12-2; Co^{II}(salen), 14167-18-1; $[Co^{III}(salen)]^+$, 66511-70-4; Pt, 7440-06-4; CH_2Cl_2, 75-09-2; CH_3CN, 75-05-8; pyridine, 110-86-1.

[1] D. H. Evans, *Chem. Rev.* **1990**, *90*, 739–751.
[2] "Ladder schemes.. are probably less common than fences owing to the improbability that the various structurally related species... will have sufficiently different electrochemical behavior to allow voltammetric resolution." [1].
[3] A. M. Bond, F. R. Keene, N. W. Rumble, G. H. Searle, M. R. Snow, *Inorg. Chem.* **1978**, *17*, 2847–2853; A. M. Bond, T. W. Hambley, M. R. Snow, *ibid.* **1985**, *24*, 1920–1928.
[4] T. Matsuura, *Tetrahedron* **1977**, *33*, 2869–2905.
[5] A. Sobkowiak, D. T. Sawyer, *J. Am. Chem. Soc.* **1991**, *113*, 9520–9523.
[6] A. Kapturkiewicz, B. Behr, *Inorg. Chim. Acta* **1983**, *69*, 247–251; *J. Electroanal. Chem.* **1984**, *179*, 187–199.
[7] M. J. Carter, D. P. Rillema, F. Basolo, *J. Am. Chem. Soc.* **1974**, *96*, 392–400.
[8] A. Nishinaga, H. Ohara, H. Tomita, T. Matsuura, *Tetrahedron Lett.* **1983**, *24*, 213–216.
[9] Tetra-*n*-butylammonium hexafluorophosphate as electrolyte in 0.1 M solution; working electrode: Pt disk with an electroactive surface area of $A = 0.065\ cm^2$; Bruker E 310 or Bioanalytical Systems BAS 100 B as function generator and potentiostat; complex concentration approximately 10^{-3} M. All potentials are given relative to the external ferrocene standard in the appropriate solvent or solvent mixture.
[10] R. S. Nicholson, I. Shain, *Anal. Chem.* **1964**, *36*, 706–723.
[11] The quantitative determination of the equilibrium and rate constants will be published elsewhere.
[12] A. Nishinaga, K. Tajima, B. Speiser, E. Eichhorn, A. Rieker, H. Ohya-Nishiguchi, K. Ishizu, *Chem. Lett.* **1991**, 1403–1406.

The Reaction of Tetramesityldisilene with As_4: Synthesis and Structure of a Novel Arsenic–Silicon Tricyclic Ring System**

By *Robin P. Tan, Nadia M. Comerlato, Douglas R. Powell,* and *Robert West**

Dedicated to Professor Ulrich Wannagat on the occasion of his 70th birthday

Tetramesityldisilene, $Mes_2Si{=}SiMes_2$ (Mes = 2,4,6-trimethylphenyl) (**1a**), and other disilenes react with many organic reagents and inorganic elements to form novel heterocyclic compounds.[1, 2] Recently we have been interested in the reactions of disilenes with group 5 elements. With phosphorus in the form of P_4, disilenes react to yield interesting butterfly structures, the 1,3-diphospha-2,4-disilabicyclobutanes,[3] **2a–c** [Eq. (a)]. We now report the results of the reaction of disilene **1a** with arsenic (As_4).

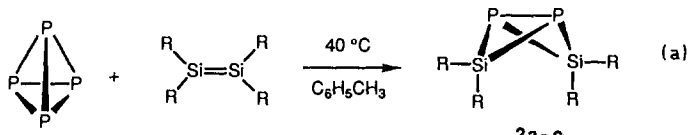

(a)

1a, R = 2,4,6-$Me_3C_6H_2$
1b, R = 2,6-$Me_2C_6H_3$
1c, R = 2,6-Me_2-4-tBuC_6H_2

2a–c

Tetramesityldisilene reacts with As_4 in toluene to give mainly a mixture of 5-(2,2,3,3-tetramesityl-1-arsa-2,3-disilacyclopropyl)-2,2,3,3-tetramesityl-1,4,5-triarsa-2,3-disilabicyclo[2.1.0]pentane (**3**) and 2,2,4,4-tetramesityl-1,3-diarsa-2,4-disilabicyclo[1.1.0]butane (**4**) [Eq. (b)]. Both compounds have been characterized by ^1H and ^{29}Si NMR spectroscopy, mass spectrometry, and elemental analysis. Furthermore,

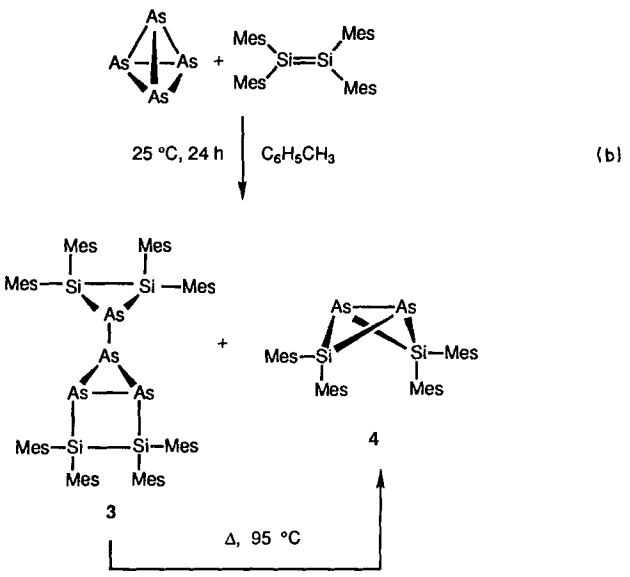

(b)

the structure of **3** has been confirmed by a single-crystal X-ray analysis.[4] The tricyclic structure of **3** is quite remarkable (Fig. 1). This molecule contains: 1) the first example of a 1,2-diarsadisiletane ring, Si_2As_2, 2) the first example of an "open" cyclotriarsane, not incorporated in a cluster, and 3) the first arsadisilirane ring, Si_2As. This reaction also appears to be the first synthesis of a silicon–arsenic compound starting from elemental arsenic.

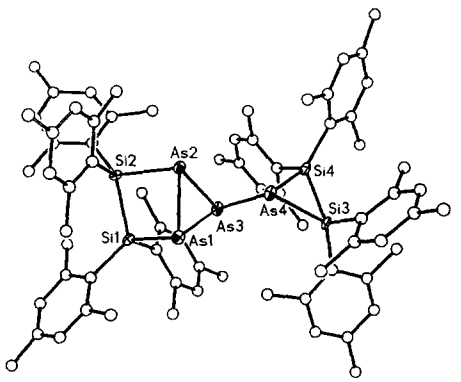

Fig. 1. Crystal structure of **3** (50% thermal ellipsoids for As and Si; hydrogens omitted for clarity). Selected bond lengths [pm] and angles [°]: As1–As2 245.6(3), As2–As3 245.0(3), As1–As3 246.3(3), As3–As4 245.6(3), As1–Si1 245.6(6), As2–Si2 239.2(5), As4–Si3 240.4(6), As4–Si4 240.1(6), Si1–Si2 241.7(7), Si3–Si4 231.5(7); As1–As2–As3 60.3(1), As1–As3–As2 60.0(1), As4–Si4–Si3 61.3(2), As4–Si3–Si4 61.1(2), As1–Si1–Si2 85.2(2), As2–Si2–Si1 90.3(2), As1–As2–Si2 85.7(1), As2–As1–Si1 87.9(1). Dihedral angles between planes: As1, Si1, Si2–As1,As2,Si2 34.6; As1,As2,Si2–As1,As2,As3 112.5; As1,As2,As3–As4,Si3,Si4 149.7.

The $^{29}Si\{^1H\}$ NMR spectrum of **3** shows two signals at $\delta = -6.6$ and -64.0; the latter can be assigned to the silicon atoms within the $AsSi_2$ three-membered ring, since there are several examples of disilacyclopropanes with resonances in this region.[2] The other product from this reaction, **4**, is analogous to the 1,3-diphospha-2,4-disilabicyclo[1.1.0]-butane **2a** obtained from the reaction of tetramesityldisilene

[*] Prof. R. West, Dr. R. P. Tan, N. M. Comerlato, Dr. D. R. Powell
Department of Chemistry, University of Wisconsin–Madison
Madison, WI 53706 (USA)

[**] This research was supported by a grant from the National Science Foundation. N. M. C. thanks the Conselho Nacional de Desenvolvimento Científico e Tecnológico, Brazil, for a fellowship.

with P_4.[3] The ^1H NMR spectrum of **3** is very similar to that of the analogous phosphorus compound. The spectrum shows a total of six signals, corresponding to the two sets of chemically nonequivalent *exo* and *endo* mesityl groups. As expected, the $^{29}Si\{^1H\}$ NMR spectrum of **4** shows a singlet at $\delta = -35.1$.

The diarsadisilabicyclobutane compound **4** can be independently synthesized from compound **3** by heating in toluene at approximately 95 °C. This conversion from **3** to **4** is, however, quite slow; approximately 80% of the dimer is converted to **4** after 30 days of heating[5].

The cyclotriarsane ring is also an unusual structural feature of **3**. The other covalent, main group compounds containing cyclotriarsane rings are polycyclic cluster-type compounds, including a triarsatricycloheptane $As_3C_5H_9$[8] and a series of three heptaarsanes $As_7(MMe_3)_3$ (M = Si, Ge, Sn) with nortricyclene structures, reported by von Schnering et al.[9]

Like the phosphorus bicyclobutanes **2a–c**, compounds **3** and **4** may bind to transition metals, either as ligands or by insertion into the E–E bond (E = As, P). In a first attempt to explore such chemistry, we treated **4** with ethenebis(triphenylphosphine)platinum, which resulted in the formation of an adduct $[Mes_4Si_2As_2Pt(PPh_3)_2]$ [Eq. (c)]. The spec-

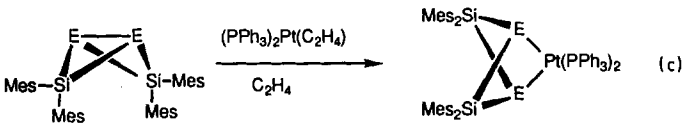

(c)

4, E = As
2a, E = P

5a, E = As
5b, E = P

troscopic properties of this compound are consistent with an asterane-like structure **5a**, entirely analogous to the corresponding compound **5b** formed from the phosphorus bicyclobutane **2a**.[10] In the $^{31}P\{^1H\}$ NMR spectrum of **5a**, the resonance of the phosphorus atoms of the triphenylphosphine groups is observed as a singlet ($\delta = 19.5$) with platinum satellite peaks; the $^1J_{P-Pt}$ coupling constant is equal to 2655 Hz. These values are similar to those of the phosphorus analog **5b** ($\delta = 22.5$, $^1J_{P-Pt} = 2523$ Hz).

Experimental Procedure

3: Tetramesityldisilene (400 mg, 0.93 mmol) was added to 120 mL of a toluene solution of As_4[11] (excess) in a drybox. The solution immediately turned orange. The reaction mixture was left in the box for 24 h, before the toluene was removed under vacuum. The residue was redissolved in toluene and decanted away from excess arsenic, present as a black precipitate. The toluene solvent was then stripped, leaving an orange residue which, according to its ^1H NMR spectrum, is made up of a 3:1 mixture of compounds **3** and **4**. About 10 mL of hexane was added to the residue, and the slurry was stirred for a few minutes. The residue was then transferred to a glass frit and washed with more hexane. The light yellow solid on the glass frit was identified as **3** (200 mg, 32%): m.p. 282–284 °C (decomp); ^1H NMR (200 MHz, C_6D_6): $\delta = 1.99–2.63$ (m, 72H, *o*-CH_3, *p*-CH_3), 6.58, 6.61, 6.65, 6.82 (16H, $C_6H_2Me_3$); $^{29}Si\{^1H\}$ NMR (INEPT, 99.4 MHz, C_6D_6): $\delta = -6.6$, -64.0; MS (FD), *m/z* calcd for $^{12}C_{72}{}^1H_{88}{}^{28}Si_4{}^{75}As_4$ 1364.283, found 1364.3. Correct elemental analysis. The orange mother liquor contained a mixture of **4** and other minor products.

4: Compound **3** (150 mg, 0.11 mmol) in 30 mL of toluene was sealed in a thick-walled glass ampule and heated at 95 °C for 30 d. The solvent was removed under vacuum, and a small amount of hexane was added to the residue. The slurry was stirred and then filtered; the light yellow residue (approximately 20 mg) was identified by ^1H NMR as compound **3**. The solvent from the yellow mother liquor was removed under vacuum, leaving an orange solid that was identified as **4** (126 mg, 85%): ^1H NMR (200 MHz, C_6D_6): $\delta = 2.01$ (s, 6H, *p*-CH_3), 2.05 (s, 6H, *p*-CH_3), 2.43 (s, 12H, *o*-CH_3), 2.77 (s, 12H, *o*-CH_3), 6.35 (s, 4H, $C_6H_2Me_3$), 6.68 (s, 4H, $C_6H_2Me_3$), $^{29}Si\{^1H\}$ NMR (INEPT, 99.4 MHz, C_6D_6): $\delta = -35.1$; MS (30 eV), *m/z* (rel. intensity) 682 (M^+, 94.3), 487 ($M^+ - Mes - As + 1$, 6.3), exact mass calcd for $^{12}C_{36}{}^1H_{44}{}^{28}Si_2{}^{75}As_2$ 682.1413, found 682.1420. Correct elemental analysis.

5a: A solution of **4** (26 mg, 0.038 mmol) in 5 mL of toluene was treated with $[Pt(PPh_3)_2(C_2H_4)]$ (28.4 mg, 0.038 mmol) at room temperature. Upon addition, the solution turned brown. After the solution was stirred overnight, the solvent was removed under vacuum, and a brown solid (**5a**) was obtained (23.8 mg, 45%): ^1H NMR (200 MHz, C_6D_6): $\delta = 2.02$ (s, 6H, *p*-CH_3), 2.21 (s, 6H, *p*-CH_3), 2.63 (brs, 24H, *o*-CH_3), 6.33 (s, 4H, $C_6H_2Me_3$), 6.76 (s, 4H, $C_6H_2Me_3$), 6.80–6.90 (m, 18H, PPh_3), 7.25–7.38 (m, 12H, PPh_3), $^{29}Si\{^1H\}$ NMR (INEPT, 99.4 MHz, C_6D_6): $\delta = -42.7$ (s, $^2J_{Si-Pt} = 116$ Hz); $^{31}P\{^1H\}$ NMR (202.5 MHz): $\delta = 19.5$ (s, PPh_3, $^1J_{P-Pt} = 2655$ Hz). MS (FAB, 3:1 mixture of dithiothreitol and dithioerythritol) calcd maximum mass for the signal for $C_{72}H_{74}Si_2P_2As_2Pt$ 1402.29, found 1401.3 $(M - H)^+$.

Received: May 16, 1992 [Z 5354 IE]
German version: *Angew. Chem.* **1992**, *104*, 1251

CAS Registry numbers:
1a, 143076-87-3; **3**, 143076-88-4; **4**, 143076-89-5; **5a**, 143076-90-8; As_4, 36275-68-0; $[Pt(PPh_3)_2(C_2H_4)]$, 12120-15-9.

[1] R. West, G. R. Gillette, H. B. Yokelson, *Phosphorus, Sulfur and Silicon* **1989**, *41*, 3; R. West, *Novel Silicon Ring Compounds from Disilenes*, in *The Chemistry of Inorganic Ring Systems* (Ed.: M. Steudel), Elsevier, Amsterdam, **1992**, chapter 4, pp. 35–50.
[2] R. P. Tan, G. R. Gillette, D. R. Powell, R. West, *Organometallics* **1991**, *10*, 546.
[3] M. Driess, A. D. Fanta, D. R. Powell, R. West, *Angew. Chem.* **1989**, *101*, 1087; *Angew. Chem. Int. Ed. Engl.* **1989**, *28*, 1038; A. D. Fanta, R. P. Tan, N. M. Comerlato, M. Driess, D. R. Powell, R. West, *Inorganica Chimica Acta*, in press. Similar compounds have been made by another route: M. Driess, H. Pritzkow, M. Reigys, *Chem. Ber.* **1991**, *124*, 193B.
[4] X-ray structure analysis of **3** ($C_{72}H_{88}As_4Si_4$): $M_r = 1365.5$; yellow prisms; (0.1 × 0.1 × 0.2 mm); space group $P2_1/c$ (No. 14); $a = 20.480(4)$, $b = 10.413(2)$, $c = 32.181(6)$ Å, $\beta = 101.03(3)°$; $V = 6736(2)$ Å^3; $Z = 4$; $\rho_{calcd} = 1.346$ g cm^{-3}; $\mu(Cu_{K\alpha}) = 3.322$ mm^{-1}; 6297 independent reflections ($2\theta_{max} = 100°$), 4357 with $F > 3\sigma(F)$ were used for refinement (362 variables); solved by direct methods; As and Si atoms refined anisotropically, C atoms refined isotropically, H atom positions calculated and refined with a riding model. $R = 0.104$ ($R_w = 0.101$, $\omega^{-1} = \sigma^2(F) + 0.0006\,F^2$). Further details of the crystal structure investigation are available on request from the Fachinformationszentrum Karlsruhe, Gesellschaft für wissenschaftlich-technische Information mbH, D-W-7514 Eggenstein-Leopoldshafen 2 (FRG), on quoting the depository number CSD-56479, the names of the authors, and the journal citation.
[5] While this work was under way a 1,3-diarsa-2,4-disilabicyclo[1.1.0]butane, prepared by loss of hydrogen from a 1,3-diarsadisiletane ring, was prepared by Driess et al. (*Angew. Chem.* **1992**, *104*, 449; *Angew. Chem. Int. Ed. Engl.* **1992**, *31*, 460). The only other cyclosilaarsanes which we have found in the literature are the eight-membered ring compound $(Me_2SiAsMe)_4$ [6] and $(Me_2Si)_6As_4$ with an adamantane-like structure [7].
[6] E. W. Abel, J. Crow, *J. Organomet. Chem.* **1969**, *28*, 337.
[7] W. Hönle, H. G. von Schnering, *Z. Naturforsch. B* **1980**, *35*, 789.
[8] G. Thiele, G. Zoubek, H. A. Lindner, J. Ellermann, *Angew. Chem.* **1978**, *90*, 133; *Angew. Chem. Int. Ed. Engl.* **1978**, *17*, 135.
[9] W. Hönle, J. Wolf, H. G. von Schnering, *Z. Naturforsch. B* **1987**, *43*, 219.
[10] A. D. Fanta, M. Driess, D. R. Powell, R. West, *J. Am. Chem. Soc.* **1991**, *113*, 7806.
[11] O. J. Scherer, H. Sitzmann, G. Wolmershäuser, *J. Organomet. Chem.* **1986**, *309*, 77. Slight modification: The metallic arsenic was sublimed at 450 °C instead of 550 °C since pyrex tubing was used. Also, the solvent used was toluene instead of xylene.

Matrix Isolation of Diisocyanogen CNNC**

By *Günther Maier,* Hans Peter Reisenauer, Jürgen Eckwert, Claudia Sierakowski,* and *Thomas Stumpf*

The ambident CN radical **1** can in principle dimerize to cyanogen **2**, isocyanogen **3**, and diisocyanogen **4**. After the initial synthesis of cyanogen **2** in 1815 by Gay-Lussac[1] 173 years passed until a second isomer was prepared.[2] On the

[*] Prof. G. Maier, Dr. H. P. Reisenauer, Dipl.-Chem. J. Eckwert, Dr. C. Sierakowski, Dipl.-Chem. T. Stumpf
Institut für Organische Chemie der Universität
Heinrich-Buff-Ring 58, D-W-6300 Giessen (FRG)

[**] This research was supported by the Fonds der Chemischen Industrie.

basis of NMR[2] and photoelectron (PE)[3] spectroscopic data this compound was assigned the structure of diisocyanogen **4**. However, microwave[4] and infrared spectra[4, 5] soon showed that the new isomer must actually be isocyanogen **3**; in light of these results the PE[6, 7] and NMR spectra[8] were subsequently reinterpreted. If **3** is considerably higher in energy than **2** and only stable for a short time in the gas phase or at low temperature in the condensed phase,[8] then diisocyanogen **4** should have an even higher reactivity, as numerous theoretical studies have predicted.[9–13]

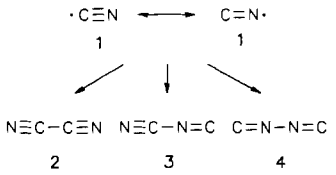

We obtained the first indication of the existence of **4** in our matrix spectroscopic investigations of the thermolysis of norbornadienonazine (**5**).[5] Besides the IR bands of the main product isocyanogen **3** and those of the by-product cyanogen **2**, an additional weak absorption at 1997 cm^{-1} was observed when the products were frozen in an argon matrix at 12 K immediately after passing the pyrolysis zone. This band did not arise when the reaction products were condensed first at 77 K, then evaporated, and isolated in a matrix at 12 K. Thus, this band must be due to a substance that is considerably more reactive than **2** and **3**.

The obvious assignment of this IR absorption at 1997 cm^{-1} to the antisymmetric CN stretching vibration (ν_3) of diisocyanogen **4**, the only IR-active stretching vibration of this linear molecule, is supported by the results of quantum mechanical calculations. If the calculated values are corrected with a suitable scaling factor, namely the mean quotient of the experimental (Ar matrix) and the calculated wavenumbers for the stretching frequency of **2**(ν_3) and **3**(ν_1, ν_2), then the values predicted for **4** (ν_3) are in good agreement with the observed position of the band (AM1: 1992 cm^{-1},[5] SCF/6-31G*: 1973 cm^{-1},[9] MP2/6-31G*: 2027 cm^{-1},[10] MP2/D95: 2048 cm^{-1},[11] ab initio CEPA: 1996 cm^{-1}[13]). The second IR-active fundamental band of **4** (bending, ν_5) is very weak in intensity according to calculations and should be in the far-IR region which we did not record. This band cannot be used for additional support of the assignment.

For unequivocal proof of our claims we not only prepared and isolated **4** in the matrix by independent routes from different precursors, but we also carried out specific isotopic labeling and compared the resulting shifts in the IR band with the theoretical values. Di-*tert*-butylcyclopropenonazine (**6**), accessible by condensation of di-*tert*-butylcyclopropenone with hydrazine dihydrochloride, proved to be a good precursor. The photolysis of **6** in an argon matrix at 12 K with a low-pressure Hg lamp ($\lambda = 254$ nm) causes a clean fragmentation into di-*tert*-butylacetylene, isocyanogen **3** (IR: 2295 cm^{-1}, ν_1; 2054 cm^{-1}, ν_2), and diisocyanogen **4** (IR: 1997 cm^{-1}, ν_3). Cyanogen **2** is not formed in the photolysis of **6**. The ratio of compounds **3**:**4** is estimated at 3:1 from the observed intensities of the bands when the calculated absolute intensities are taken into account.[13] The flash vacuum thermolysis (quartz tube, 600 °C, heating zone 8 × 50 mm) of **6** followed by matrix isolation does not proceed so cleanly. Isocyanogen **3** is the only CN dimer detectable by IR spectroscopy. In addition, the absorption bands of di-*tert*-butylacetylene, isobutene, and propene are observed.

In another approach, tetrabromoformaldazine (**7**) isolated in a matrix was irradiated with a low-pressure Hg lamp ($\lambda = 254$ nm) producing a very small amount of diisocyanogen **4** besides bromocyan and isocyanogen. We have previously observed an analogous photochemical elimination of bromine in the synthesis of isofulminic acid from dibromoformoxime.[14] The dehalogenation of **7** is also possible with potassium metal. Gaseous tetrabromoformaldazine (**7**) at room temperature and low pressure is allowed to pass through a glass tube filled with quartz wool and with a potassium mirror on its surface. When the resulting products are condensed with a large excess of argon on the spectroscopic window at 12 K the bands of of bromocyan, cyanogen **2**, and diisocyanogen **4** are detected by IR spectroscopy, however, not those of isocyanogen **3**.

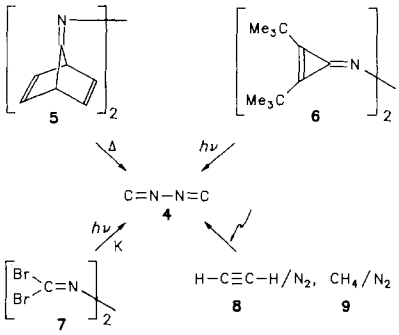

A completely different and convenient access to all three CN dimers is possible from the microwave discharge of mixtures of acetylene **8** and nitrogen. We actually ran preliminary experiments hoping to be able to produce the unknown species diazodicarbon CCNN.[15] In a typical experiment a

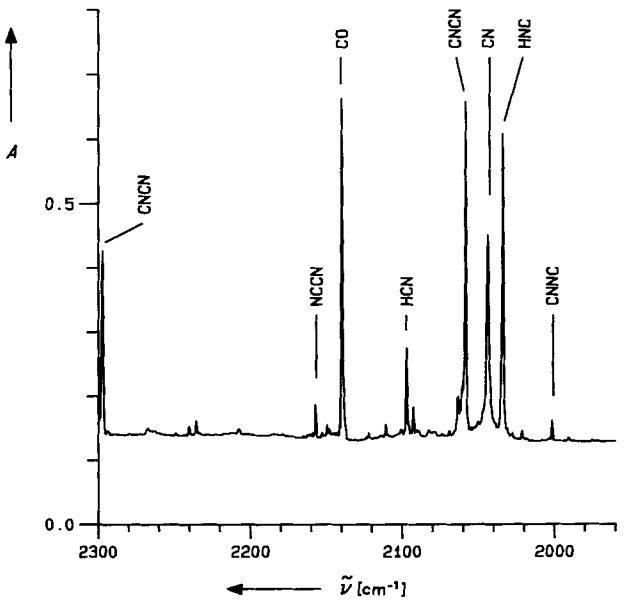

Fig. 1 Section of the FT-IR spectrum of the reaction products resulting from a microwave discharge in a mixture of acetylene and nitrogen (N_2 matrix, C_2H_2:N_2 = 1:500, 12 K).

discharge in a quartz tube (ca. 10×200 mm) through which the gas mixture flowed was maintained by a 2.45 GHz microwave generator. Immediately after the gas mixture passed out of the plasma zone it was frozen at 12 K on the spectroscopic window of the cryostat, and the condensate was examined by UV/VIS and IR spectroscopy. The characteristic IR absorptions, which are shifted roughly three or four wavenumbers relative to those measured in the argon matrix, indicate unequivocally the formation of all three CN dimers (**2**: 2157.0 cm^{-1}, ν_3; **3**: 2296.8 cm^{-1}, ν_1, and 2058.4 cm^{-1}, ν_2; **4**: 2001.3 cm^{-1}, ν_3). Based on the calculated intensities of the IR bands[13] the discharge delivers about 70% cyanogen **2**, 30% isocyanogen **3**, and very little ($\approx 1\%$) diisocyanogen **4**. Thus, this product distribution reflects the differing thermodynamic stabilities of the isomers. Their common precursor is likely to be the CN radical, which can be identified by its characteristic electron spectrum[16] as well as by its IR absorption at 2043.4 cm^{-1}.[16, 17] In addition, the bands of HCN, HNC, NH_3, NH_2, and other species are observed. Discharges in a mixture of methane (**9**) and nitrogen give rise to the same palette of products, although with a higher proportion of hydrogen-containing compounds (HCN, HNC, NH_2, and NH_3), as expected. Apparently the CN dimers are formed from C and N atoms (the connection to prebiotic processes is obvious). It is understandable then why the existence of the molecule actually hoped for, CCNN[15] (from the trapping of C_2 with N_2 molecules), could not be proved.

Isotopic labeling could be carried out easily with the microwave discharge technique. When a 1:1 mixture of $^{15}N_2$ and $^{14}N_2$ with 0.2% acetylene is employed, the nitrogen isotopes are found in a statistical distribution in the CN dimers. Accordingly, the unsymmetrical isocyanogen **3** shows four equally intense IR bands for the ν_1 as well as for the ν_2 stretching vibration. The symmetric diisocyanogen **4**, on the other hand, displays three IR absorptions as expected in the intensity ratio 1:2:1 for the isotopomers $C^{14}N^{14}NC$ (2001.3 cm^{-1}), $C^{15}N^{14}NC$ (1984.6 cm^{-1}), and $C^{15}N^{15}NC$ (1971.2 cm^{-1}), respectively. In other experiments we obtained the doubly ^{15}N-labeled CN dimers **2**, **3**, and **4** by flash pyrolysis of labeled norbornadienonazine **5**.[18] When this precursor is used (without or with double ^{15}N labeling), the observed bands of CNNC **4** are intense enough for the measurement of the $^{13}C^{14}N^{14}NC$ and the $^{13}C^{15}N^{15}NC$ isotopomers in their natural abundance. The vibrational frequency of the ^{13}C-labeled isotopomers may also be obtained by examination of the products arising from microwave discharge in a mixture of $^{13}CH_4$ or $^{13}C_2H_2$ and nitrogen. The wavenumbers of the ν_3 bands of the six observed CNNC isotopomers are compared to the calculated values from ab initio CEPA in Table 1. The good agreement leaves little doubt that our assignment is correct.

Table 1. Antisymmetric stretching frequencies (ν_3) of the observed CNNC isotopomers [cm^{-1}] in argon and nitrogen matrices.

Isotopomer	Experiment	Calculation [a]	
12-14-14-12	Ar: 1997.0 N_2: 2001.3	2019.9	
13-14-14-12	Ar: 1975.3 N_2: 1979.9	1998.0	(1975.3) [b] (1979.8) [c]
13-14-14-13	Ar: – N_2: 1960.1	1978.1	(1955.9) [b] (1960.1) [c]
12-14-15-12	Ar: 1979.9 N_2: 1984.6	2002.7	(1979.9) [b] (1984.5) [c]
12-15-15-12	Ar: 1966.6 N_2: 1971.2	1989.1	(1966.5) [b] (1971.0) [c]
13-15-15-12	Ar: 1944.3 N_2: –	1966.1 [d]	(1944.3) [b] (1948.2) [c]

[a] Ab initio CEPA 1/104 CGTOS[13]. [b] The value in parentheses is scaled with the factor 1997.0/2019.9 = 0.98876. [c] The value in parentheses is scaled with the factor 2001.3/2019.9 = 0.99079. [d] P. Botschwina, personal communication.

The upshot is that diisocyanogen **4** is extremely reactive, but is capable of existence under matrix isolation conditions.

Experimental Procedure

6: A solution of di-*tert*-butylcyclopropenone (6.3 g, 38 mmol) and hydrazine dihydrochloride (2 g, 19 mmol) in 150 mL of methanol was stirred at room temperature for 24 h. After the solvent was removed by rotary evaporation (aspirator pressure), the residue was washed in 150 mL of ether, dissolved in 300 mL of dichloromethane, filtered, and then concentrated to provide di-*tert*-butylcyclopropenonazine dihydrochloride (4.8 g, 12 mmol) as a colorless solid [m.p. 206 °C (decomp); MS (70 eV): *m/z* 328 ($M^{\oplus} - 2HCl$); ^1H NMR (400 MHz, $CDCl_3$): $\delta = 16.2$ (s, 2H), 1.51 (s, 18H), 1.49 (s, 18H); ^{13}C NMR (100 MHz, $CDCl_3$): $\delta = 151.72$ (C=N), 150.87/147.82 (C=C), 33.50/33.14 (CMe_3), 28.44/27.85 (CMe_3); IR (KBr): $\tilde{\nu}$ [cm^{-1}] = 1885 (C=C), 1540 (C=N); UV(C_2H_5OH): end absorption below 300 nm; correct elemental analysis. A suspension of di-*tert*-butylcyclopropenonazine dihydrochloride (516 mg, 1.29 mmol) in 15 mL of water-free THF at −78 °C was treated with a solution of 2.25 mmol of methyllithium in ether. The reaction mixture was stirred for 3 h at −78 °C before the solvent was removed by distillation. The residue was sublimed at 0.01 Torr/80 °C and washed with 1 mL of cold (−30 °C) water-free pentane to furnish **6** (325 mg, 0.99 mmol) as a colorless solid [m.p. 186 °C (decomp); MS (70 eV): *m/z* 328.2890 ($M^{\oplus}$, calc. 328.2870); ^1H NMR ($CDCl_3$): $\delta = 1.28$ (s, 18H), 1.23 (s, 18H); ^{13}C NMR ($CDCl_3$): $\delta = 150.47$ (C=N), 144.42/139.73 (C=C), 32.17/31.69 (CMe_3), 29.19/28.50 (CMe_3); IR (CCl_4): $\tilde{\nu}$ [cm^{-1}] = 1828 (C=C), 1603 (C=N); UV (cyclohexane): λ_{max} [nm] (lg ε) = 228 (4.10); correct elemental analysis.

Received: April 24, 1992 [Z 5321 IE]
German version: *Angew. Chem.* **1992**, *104*, 1287

CAS Registry numbers:
4 (isotopomer 1), 78800-21-2; **4** (isotopomer 2), 142841-29-0; **4** (isotopomer 3), 142841-30-3; **4** (isotopomer 4), 142841-31-4; **4** (isotopomer 5), 142865-92-7; **4** (isotopomer 6), 142865-93-8; **6**, 142841-32-5; 7, 14928-04-2; **8**, 74-86-2; **9**, 74-82-8; N_2, 7727-37-9; di-*tert*-butylcyclopropenone, 19985-79-6; hydrazine dihydrochlorid, 5341-61-7; di-*tert*-butylcyclopropenoazine dihydrochloride, 142841-33-6.

[1] L. J. Gay-Lussac, *Ann. Chim. (Paris)* **1815**, *95*, 175.
[2] T. van der Does, F. Bickelhaupt, *Angew. Chem.* **1988**, *100*, 998–1000; *Angew. Chem. Int. Ed. Engl.* **1988**, *27*, 936–938.
[3] O. Grabandt, C. A. de Lange, R. Mooyman, T. van der Does, F. Bickelhaupt, *Chem. Phys. Lett.* **1988**, *155*, 21–26.
[4] F. Stroh, M. Winnewisser, *Chem. Phys. Lett.* **1989**, *155*, 21–26.
[5] F. Stroh, M. Winnewisser, B. P. Winnewisser, H. P. Reisenauer, G. Maier, S. J. Goede, F. Bickelhaupt, *ibid.* **1989**, *160*, 105–112.
[6] L. S. Cederbaum, F. Tarantelli, H. G. Weikert, M. K. Scheller, H. Köppel, *Angew. Chem.* **1989**, *101*, 770–771; *Angew. Chem. Int. Ed. Engl.* **1989**, *28*, 761–762.
[7] M. K. Scheller, H. G. Weikert, L. S. Cederbaum, F. Tarantelli, *J. Electron. Spectrosc.* **1990**, *51*, 75–89.
[8] S. J. Goede, F. J. J. de Kanter, F. Bickelhaupt, *J. Am. Chem. Soc.* **1991**, *113*, 6104–6107.
[9] M. Sana, G. Leroy, *J. Mol. Struct.* **1981**, *76*, 259–276.
[10] M. T. Nguyen, *Chem. Phys. Lett.* **1989**, *157*, 430–435.
[11] W. B. De Almeida, A. Hinchliffe, *THEOCHEM* **1990**, *65*, 77–87.
[12] K. K. Sunil, J. H. Yates, K. D. Jordan, *Chem. Phys. Lett.* **1990**, *171*, 185–190.
[13] P. Botschwina, P. Sebald, *Chem. Phys.* **1990**, *141*, 311–323.
[14] J. H. Teles, G. Maier, B. A. Hess, Jr., L. J. Schaad, M. Winnewisser, B. P. Winnewisser, *Chem. Ber.* **1989**, *122*, 753–766.
[15] We have not yet found any evidence for the formation of CCNN. For a calculational study concerning this molecule see M. K. Scheller, L. S. Cederbaum, R. Tarantelli, *J. Am. Chem. Soc.* **1990**, *112*, 9484–9490.
[16] G. Herzberg, *Molecular Spectra and Molecular Structure, Vol. 1*, 2nd ed., Krieger Publ., Malabar, FL, USA, **1989**.
[17] D. E. Milligan, M. E. Jacox, *J. Chem. Phys.* **1967**, *47*, 278–285.
[18] We thank Prof. R. Bickelhaupt, Amsterdam, for a sample of this compound.

The Tandem Sakurai–Carbonyl–Ene Reaction: A New and Highly Stereoselective Sequential Transformation and Its Use for the Synthesis of Steroid Derivatives**

By *Lutz F. Tietze** and *Matthias Rischer*

Dedicated to Prof. Dr. Gerhard Quinkert on the occasion of his 65th birthday

The development of new sequential transformations[1] for the construction of organic molecules is of great interest since these procedures often open a short route to a very efficient and stereoselective assembling of complex molecules. In recent years we have elaborated several new sequences such as the tandem Knoevenagel hetero-Diels–Alder,[2] the tandem Knoevenagel–ene reaction,[3] the tandem Knoevenagel–allylsilane cyclization,[4] and the tandem Pictet–Spengler–ene reaction.[1a] In this paper we describe the tandem Sakurai–carbonyl–ene reaction and its use in the diastereoselective synthesis of the enantiomerically pure BCD part of steroids **1** with a methyl group in ring B according to the retrosynthetic scheme **1a** → **4**. In the Sakurai reaction[5] an α,β-unsaturated carbonyl compound reacts with an allylsilane to give a δ,ε-unsaturated carbonyl moiety, which yields a cyclic homoallylic alcohol in an intramolecular carbonyl–ene[6] reaction. Steroids with an additional methyl group at the steroid skeleton often show an increased biological activity; for example 6α-methylprednisolone is a five times more potent antiphlogistic agent than cortisone.[7]

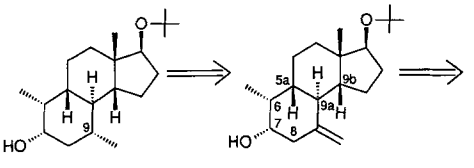

1a
1b: β-CH_3 at C-9

2a
2b: β-CH_3 at C-6, β-OH at C-7
2c: β-OH at C-7

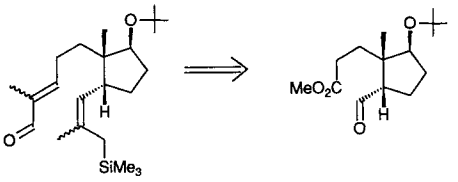

3 **4**

The starting material used for the synthesis of **1a** was the enantiomerically pure aldehyde **4**, which can be obtained from the ketone **5**[8] in a few steps by reduction and ozonolysis. Wittig reaction of **4** with **6**[9] generated in situ gives **8** (**6**, *n*BuLi, THF, −78 °C → 0 °C, 2 h; +**4**, −78 °C → 20 °C, 3 h, 50%, *E*/*Z* = 1:1). Reduction with lithium aluminium hydride (1 equiv, THF, 20 °C; reflux, 30 min, 90%) and oxidation with pyridinium dichromate (1.5 equiv, CH_2Cl_2, 20 °C, 15 h, 87%) afforded the aldehyde **9**, which was treated with **7** to yield **3** (THF, −78 °C → 20 °C, 4 h; HCl, THF, 3 h, 70%, four isomers 1:1:1:0.1).

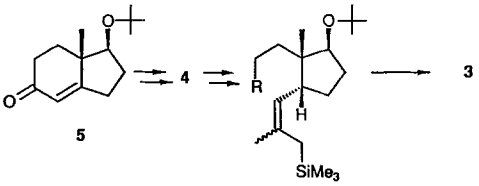

$Ph_3PC(CH_3)CH_2SiMe_3$ **6**
$H_3C(SiMe_3)C{=}NC(CH_3)_3$ **7**

8: R = CO_2Me
9: R = CHO

For the tandem Sakurai–carbonyl–ene reaction of **3**, several Lewis acids were investigated as mediators. The best results could be obtained with trimethylsilyl trifluoromethanesulfonate (TMS-OTf), which in a highly stereoselective fashion led to **2a** as the only cyclized product in 52% yield (1.1 equiv, CH_2Cl_2, −78 °C, 2 h; −30 °C, 2 h). The selectivity in this sequence is quite astounding since a mixture of all four geometrical isomers of **3** was used; we have to assume that the configuration of the double bonds in **3** has no influence on the selectivity of the Sakurai reaction; for the following carbonyl–ene reaction an epimerization of the new stereogenic center, presumably formed nonselectively, in the chain at C6 of the hydrindane 11 must be proposed. However, since the yield of **2a** is not quantitative, it is possible that one or two of the isomers do not cyclize under the reaction conditions. Amazingly, with $EtAlCl_2$ a different stereocontrol was observed; in this case the two diastereomers **2b** and **2c** were formed in a 3:1 ratio in 40% yield. Such a pronounced difference in selectivity with Lewis acids and Me_3SiOTf has recently been described for hetero-Diels–Alder reactions of 1-oxa-1,3-butadienes.[10]

As transition structures for the transformation of **3** into **2a** with Me_3SiOTf, conformations **10a** and **11a** with a chairlike arrangement of the chains and an equatorially oriented carbonyl group is assumed. The use of $EtAlCl_2$ as mediator may force the carbonyl group in the complexes **10b** and **11b** to take up an axial orientation and thus lead to the diastereomers **2b** and **2c**.

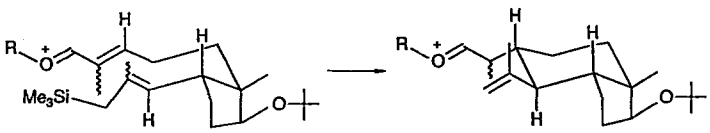

10a: R = $SiMe_3$
10b: R = $AlEtCl_2^-$

11a: R = $SiMe_3$
11b: R = $AlEtCl_2^-$

Homogeneous hydrogenation with $[(Ph_3P)_3RhCl]$ in benzene afforded **1a** as a single isomer in 96% yield. In contrast, with the heterogeneous catalyst $Pd/CaCO_3$ a 3:1 mixture of **1a** and **1b** as well as a small amount of the corresponding ketone was obtained.

The *trans*-axial arrangement of 5a-H, 9a-H, and 9b-H in **2a** could be deduced from the two large coupling constants of J = 12.5 Hz of the signal for 9a-H at δ = 1.53. The equatorial orientation of the hydroxy group at C7 and the axial orientation of the methyl group at C6, each displaying an α-configuration, is clearly seen from the two large couplings (J = 12 Hz) of the signal for 8-H_{ax} at δ = 2.16 and the large (J = 12 Hz) and two small couplings (J = 4.5 Hz) for 7-H at δ = 3.51.

[*] Prof. Dr. L.F. Tietze, Dr. M. Rischer
Institut for Organische Chemie der Georg-August-Universität
Tammannstrasse 2, D-W-3400 Göttingen (FRG)

[**] Intramolecular Ene and Related Reactions, Part 11. This work was supported by the Fonds der Chemischen Industrie. We thank Prof. Dr. R. Wiechert and Dr. G. Sauer, Schering AG, Berlin for a gift of **5**. Part 10: Ref. [1a].

Received: May 9, 1992 [Z 5336]
German version: *Angew. Chem.* **1992**, *104*, 1269

[1] Selected examples of sequential transformations: a) L. F. Tietze, J. Wichmann, *Angew. Chem.* **1992**, *104*, 1091; *Angew. Chem. Int. Ed. Engl.* **1992**, *31*, 1079; b) S. D. Burke, D. N. Deaton, *Tetrahedron Lett.* **1991**, *32*, 4651; J. Mulzer, H. Bock, W. Eck, J. Buschmann, P. Luger, *Angew. Chem.* **1991**, *103*, 450; *Angew. Chem. Int. Ed. Engl.* **1991**, *30*, 414; W. Oppolzer, R. J. De Vita, *J. Org. Chem.* **1991**, *56*, 6256; M. Ihara, M. Suzuki, K. Fukumoto, C. Kabuto, *J. Am. Chem. Soc.* **1990**, *112*, 1164; L. F. Tietze, U. Beifuss, M. Lökös, M. Rischer, A. Göhrt, G. M. Sheldrick, *Angew. Chem.* **1990**, *102*, 545; *Angew. Chem. Int. Ed. Engl.* **1990**, *29*, 527; D. Guay, W. S. Johnson, U. Schubert, *J. Org. Chem.* **1989**, *54*, 4731; I. Patterson, P. A. Craw, *Tetrahedron Lett.* **1989**, *42*, 5799; T. Hudlicky, A. Fleming, L. Radesca, *J. Am. Chem. Soc.* **1989**, *111*, 6691; R. B. Ruggeri, K. F. McClure, C. H. Heathcock, *ibid.* **1989**, *111*, 1530; S. Blechert, *Synthesis* **1989**, 71; W. D. Fessner, C. Grund, H. Prinzbach, *Tetrahedron Lett.* **1989**, *30*, 3133; L. F. Tietze, J. Bachmann, W. Schul, *Angew. Chem.* **1988**, *100*, 983; *Angew. Chem. Int. Ed. Engl.* **1988**, *27*, 971; L. F. Tietze, H. Denzer, X. Holdgrün, M. Neumann, *ibid.* **1987**, *99*, 1309 and *26*, 1295; L. Fitjer, U. Quabeck, *ibid.* **1987**, *99*, 1054 and **1987**, *26*, 1023; D. P. Curran, S. C. Kuo, *J. Am. Chem. Soc.* **1986**, *108*, 1106; G. Stork, P. M. Sher, H. L. Chen, *ibid.* **1986**, *108*, 6384; S. H. Lecker, N. H. Nguyen, K P. C. Vollhardt, *ibid.* **1986**, *108*, 856; C. Bohlmann, R. Bohlmann, E. G. Rivera, C. Vogel, M. D. Manandhar, E. Winterfeldt, *Liebigs Ann. Chem.* **1985**, 1752; G. Quinkert, H. Stark, *Angew. Chem.* **1983**, *95*, 651; *Angew. Chem. Int. Ed. Engl.* **1983**, *22*, 637. Review: L. Tietze, U. Beifuss, *ibid.* **1992**, *104*, in press and **1992**, *31*, in press.

[2] L. F. Tietze, U. Beifuss, in *Comprehensive Organic Synthesis, Vol. 2* (Ed.: B. M. Trost), Pergamon, Oxford, **1991**, p. 369; L. F. Tietze, *J. Heterocyclic Chem.* **1990**, *27*, 47; L. F. Tietze in "Selectivity – a Goal for Synthetic Efficiency" (Eds.: W. Bartmann, B. M. Trost), Verlag Chemie, Weinheim, **1984**, p. 299.

[3] L. F. Tietze, U. Beifuss, U. Ruther, *J. Org. Chem.* **1989**, *54*, 3120.

[4] L. F. Tietze, U. Ruther, *Chem. Ber.* **1990**, *123*, 1387.

[5] A. Hosomi, H. Sakurai, *J. Am. Chem. Soc.* **1977**, *99*, 1673; G. Majetich, J. S. Song, C. Ringgold, G. A. Nemeth, M. G. Newton, *J. Org. Chem.* **1991**, *56*, 3973; D. Schinzer, *Synthesis* **1988**, 263.

[6] B. B. Snider in *Comprehensive Organic Synthesis, Vol. 2* (Ed.: B. M. Trost), Pergamon, Oxford, **1991**, p. 527.

[7] A. R. Daniewski, E. Piotrowska, *Lieb. Ann. Chem.* **1989**, 571.

[8] Z. G. Hajos, D. R. Parrish, *J. Org. Chem.* **1974**, *39*, 1615; U. Eder, G. Sauer, R. Wiechert, *Angew. Chem.* **1971**, *83*, 492; *Angew. Chem. Int. Ed. Engl.* **1971**, *10*, 496.

[9] G. Majetich, M. Behnke, K. Hull, *J. Org. Chem.* **1985**, *50*, 3615.

[10] L. F. Tietze, C. Schneider, *Synlett* **1992**, in press.

Indirect $^{113}Cd,^{14}N$ Spin-Spin Coupling Constants as a Structural Probe of Solid Cadmium Thiocyanate Complexes**

By *Klaus Eichele* and *Roderick E. Wasylishen**

In the past decades the coordination chemistry of ambidentate ligands has seen explosive growth.[1] These ligands are sensitive chemical probes of their environment, and their response to electronic or steric effects is of synthetic and theoretical interest. The thiocyanate ion, in particular, has revealed a fascinating variety of coordination modes. In addition to the terminal *N*- and *S*-bonding modes, five different bridging modes have been established by single crystal X-ray diffraction.[1] Solution NMR studies have not been very informative in characterizing metal thiocyanate complexes. First, the structural integrity of these complexes is frequently lost in solution. Second, indirect spin-spin coupling constants, *J*, between NMR-active metal nuclei and ^{14}N often cannot be measured because of rapid ligand–metal exchange. Furthermore, efficient ^{14}N relaxation by the quadrupolar mechanism generally results in self-decoupling. The observation of $J(^{x}M,^{14}N)$ is important because the magnitude of *J* indicates the mode of bonding and the multiplicity provides information on the number of nitrogen atoms directly bonded to the metal.[2] The present study demonstrates that the aforementioned problems can be overcome, and $^{x}M-^{14}N$ coupling can be observed in solid-state magic-angle spinning (MAS) NMR spectra of the metal nucleus. For this purpose, the cadmium thiocyanate system is of particular interest. The Cd^{2+} ion is an acid of intermediate softness and forms many different linkage isomers with the thiocyanate ligand.[1] Moreover, cadmium, which has two isotopes of nuclear spin $I = \frac{1}{2}$, ^{111}Cd (12.8%) and ^{113}Cd (12.3%), offers the opportunity to use metal NMR to study the metal center directly.[3]

Figure 1 shows the ^{113}Cd CP–MAS NMR (CP = cross polarization) spectrum of a powder sample of tetra-*n*-propylammonium trithiocyanatocadmate(II) (**1**) together with

$(NnPr_4)[Cd(SCN)_3]$ **1**

the relevant part of the crystal structure as reported recently.[4] The central peak with isotropic chemical shift at $\delta = 310.9$ is flanked by several spinning sidebands, the intensity profile of which mimics the overall line shape that one would observe in the absence of MAS. Analysis of the spinning sideband intensities allows the reconstruction of the line shape of a static sample that is defined by the three principal components of the chemical shift tensor.[5] The magnitude of these components describes the dependence of the chemical shift on the orientation of the molecule with respect to the applied magnetic field. In the case of **1**, this orientation dependence is relatively large (components $\delta_{11} = 540$ and $\delta_{22} = \delta_{33} = 196$) and rules out a symmetrical tetrahedral or octahedral structure. This conclusion is in agreement with

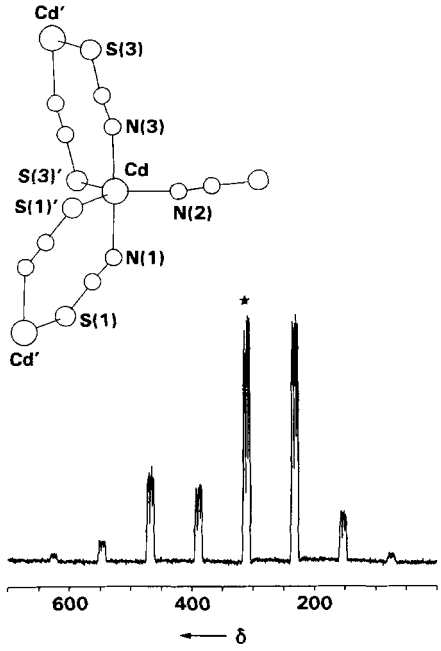

Fig. 1. Top: the relevant part of the crystal structure of **1** as reported in ref. [4]. Bottom: ^{113}Cd CP–MAS NMR spectrum (44.38 MHz) of **1**, obtained at a spinning speed of 3.5 kHz with 90° pulses of 5 μs duration after 9000 scans. The isotropic region is labeled by an asterisk. Chemical shifts are referenced with respect to $Cd(ClO_4)_2 \cdot 6H_2O$.

[*] Prof. Dr. R. E. Wasylishen, Dr. K. Eichele
Department of Chemistry
Dalhousie University
Halifax, N.S., B3H 4J3 (Canada)

[**] This work was supported by the NSERC of Canada. K. E. is grateful for the award of an Izaak Walton Killam Postdoctoral Fellowship.

the reported crystal structure,[4] which indicates a trigonal-bipyramidal ligand arrangement around the cadmium center with a unique nonbridging *N*-bonded thiocyanate group in the equatorial position and four bridging ligands, *N*-bonded to the metal at apical and *S*-bonded at equatorial positions.

The most striking features of the ^{113}Cd CP–MAS NMR spectrum of **1** are the complex multiplets due to ^{113}Cd,^{14}N spin-spin interactions. An expansion of the isotropic region is shown in Figure 2. The slight asymmetry observed in the

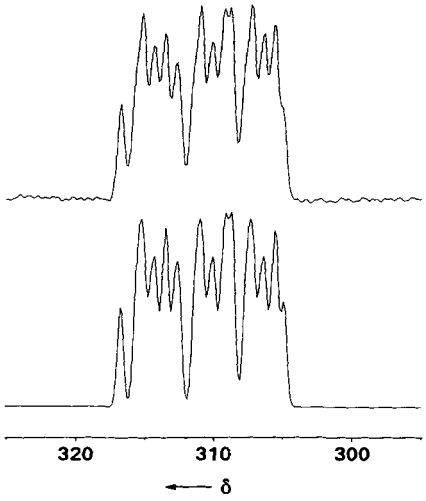

Fig. 2. Expansion of the isotropic region of the ^{113}Cd CP–MAS NMR spectrum displayed in Figure 1. The top trace shows the experimental, the bottom trace the simulated spectrum.

splitting pattern arises because of a breakdown of the high-field approximation for ^{14}N. It indicates that the quadrupolar coupling to the electric field gradient (EFG) causes a significant perturbation on the pure Zeeman energy term. Thus, the ^{14}N spin states are not solely quantized by the external field direction and the orientation dependence of the ^{113}Cd,^{14}N dipolar interaction differs from the usual $(3\cos^2\theta-1)$. As a result, MAS is unable to average the dipolar interaction completely, and the ^{113}Cd NMR frequencies are shifted relative to those in the pure high-field case.[6] A recently developed first-order perturbation approach,[7] for cases where the quadrupolar interaction with the EFG is smaller than the Zeeman interaction, has been successfully applied to analyze the MAS NMR spectrum of spin-$\frac{1}{2}$ nuclei coupled with a quadrupolar nucleus.[8] Application of this approach predicts three nonequidistant lines for ^{113}Cd coupled with one ^{14}N nucleus (Fig. 3), with frequencies $\nu_1 = |J| + d$, $\nu_2 = -2d$, and $\nu_3 = -|J| + d$, with respect to the Larmor frequency of the uncoupled ^{113}Cd nucleus. The residual dipolar coupling d is given by Equation (a)

$$d = -(3D\chi/20Z)(3\cos^2\beta - 1) \quad \text{(a)}$$

where D is the ^{113}Cd,^{14}N direct dipolar coupling constant, χ and Z are the ^{14}N quadrupolar coupling constant and Larmor frequency, respectively, and β is the angle between the Cd–N bond and the largest component of the ^{14}N EFG tensor. The dipolar coupling constant is given by Equation (b). For the case of thiocyanate complexes, the EFG at

$$D = (\mu_0/4\pi)\,\gamma_{Cd}\gamma_N r_{Cd-N}^{-3}(\hbar/2\pi) \quad \text{(b)}$$

^{14}N has been assumed to be axially symmetric.[9] Figure 3 shows, that the parameters J and d are readily obtained from

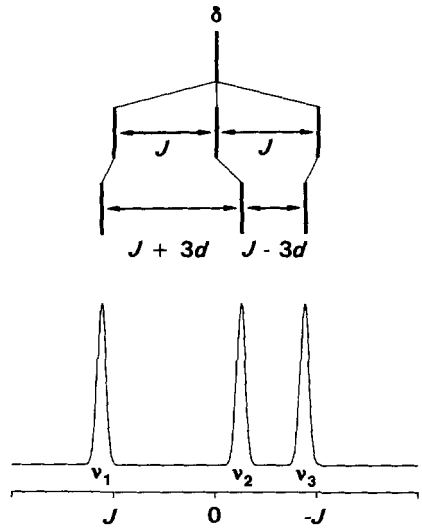

Fig. 3. Schematic representation of the CP–MAS NMR spectrum of ^{113}Cd coupled with one ^{14}N nucleus. Indirect spin-spin coupling results in three equally spaced lines. The perturbation on the ^{14}N spin states due to the quadrupolar interaction (shown here for $\chi < 0$) shifts the lines ν_1, ν_2, and ν_3 by d, $-2d$, and d, respectively, from their unperturbed positions at J, 0, and $-J$.

the separations within the asymmetric triplet. Interaction with a second ^{14}N will further split up each of the three lines into new asymmetric triplets. The simulated spectrum in Figure 2 has been calculated by expanding this simple approach to several ^{14}N nuclei coupled to ^{113}Cd, leading to three sets of values for J (and d): 178 (+ 3.8), 50 (+ 4.7), and 38 Hz (+ 4.2 Hz). As indicated by the multiplicity of this pattern and in agreement with the crystal structure, cadmium is bonded to three nonequivalent nitrogen atoms. Interestingly, $J(^{113}\text{Cd},^{14}\text{N})$ varies over a wide range, suggesting a significant dependence on subtle structural changes. Since the value of 178 Hz represents the largest $J(^{113}\text{Cd},^{14}\text{N})$ reported, it is reasonable to assign this value to the Cd–N2 bond, which shows the shortest reported bond distance, 216.3 pm. The much smaller values for $J(^{113}\text{Cd},^{14}\text{N})$, 50 and 38 Hz, are associated with the considerably longer Cd–N bond distances for Cd–N3, 233.8 pm, and Cd–N1, 236.3 pm. Similar correlations of $J(^{x}\text{M},^{31}\text{P})$ with M–P separations, r_{M-P}, have been reported for metal phosphine complexes.[10]

As indicated above, the parameter d contains information regarding the value of χ and the orientation of the largest principal component of the ^{14}N EFG tensor. Knowledge of the bond lengths leaves d dependent only on χ and β. The ^{13}C CP–MAS NMR spectrum of **1** also exhibits typical asymmetric line shapes characteristic of systems where the high-field approximation breaks down for the ^{14}N nucleus.[11] Combined analysis of the d values from ^{113}Cd and ^{13}C CP–MAS NMR spectra leads to the following values for χ (and β): -2.0 MHz (27°) for N1, -0.9 MHz (10°) for N2, and -1.9 MHz (22°) for N3. The errors in χ and β are estimated to be ± 0.2 MHz and $\pm 5°$, respectively. These values of χ are typical of those derived from nuclear quadrupole resonance (NQR) experiments for other systems containing *N*-coordinated thiocyanate ligands.[9] Noteworthy is the observation that χ for N2 is less than half χ for N1 and N3. The unique value of χ is associated with the nitrogen which exhibits the largest value of J(Cd,N) and the shortest Cd–N separation. The small value of β, 10°, is also consistent with the near linear arrangement of the Cd-N2-C2 moiety.

This analysis of the high-resolution ^{113}Cd CP–MAS NMR spectrum indicates the wealth of information available from such spectra. We have obtained the three principal

components of the ^{113}Cd chemical shift tensor and values of $J(^{113}Cd,^{14}N)$ for the three unique thiocyanate ligands in **1**. The magnitudes of $J(^{113}Cd,^{14}N)$ indicate a strong dependence on Cd–N bond length. Further studies are under way in our laboratory to examine the generality of such relationships in related compounds. In addition, the ^{14}N quadrupolar coupling constants and their respective orientations have been deduced from the ^{113}Cd and ^{13}C CP-MAS NMR spectra. None of this information is available from solution NMR studies of cadmium thiocyanate complexes. The techniques employed in this study should be applicable in characterizing other thiocyanate, cyanate, and selenocyanate complexes containing spin-$\frac{1}{2}$ metal centers.

Received: April 22, 1992 [Z 5316 IE]
German version: *Angew. Chem.* **1992**, *104*, 1263

CAS Registry numbers:
N_2, 7727-37-9; ^{113}Cd, 14336-66-4; **1**, 121163-15-3.

[1] J. L. Burmeister, *Coord. Chem. Rev.* **1990**, *105*, 77-133.
[2] S. J. Blunden, P. A. Cusack, D. G. Gillies, *J. Magn. Reson.* **1984**, *60*, 114-117.
[3] P. D. Ellis, *Science* **1983**, *221*, 1141-1146; M. F. Summers, *Coord. Chem. Rev.* **1988**, *86*, 43-134.
[4] M. Taniguchi, A. Ouchi, *Bull. Chem. Soc. Jpn.* **1989**, *62*, 424-428.
[5] J. Herzfeld, A. E. Berger, *J. Chem. Phys.* **1980**, *73*, 6021-6030.
[6] N. Zumbulyadis, P. M. Henrichs, R. H. Young, *J. Chem. Phys.* **1981**, *75*, 1603-1611; J. G. Hexem, M. H. Frey, S. J. Opella, *ibid.* **1982**, *77*, 3847-3856.
[7] A. C. Olivieri, L. Frydman, L. E. Diaz, *J. Magn. Reson.* **1987**, *75*, 50-62; A. C. Olivieri, *ibid.* **1989**, *81*, 201-205.
[8] D. C. Apperley, H. Bai, R. K. Harris, *Mol. Phys.* **1989**, *68*, 1277-1286; E. Lindner, R. Fawzi, H. A. Mayer, K. Eichele, K. Pohmer, *Inorg. Chem.* **1991**, *30*, 1102-1107; R. Gobetto, R. K. Harris, D. C. Apperley, *J. Magn. Reson.* **1992**, *96*, 119-130.
[9] W. C. Fultz, J. L. Burmeister, C. P. Cheng, T. L. Brown, *Inorg. Chem.* **1981**, *20*, 1734-1738.
[10] P. B. Hitchcock, B. Jacobson, A. Pidcock, *J. Chem. Soc. Dalton Trans.* **1977**, 2038-2042; H. B. Buergi, E. Fischer, R. W.Kunz, M. Parvez, P. S. Pregosin, *Inorg. Chem.* **1982**, *21*, 1246-1256; S. Attar, G. A. Bowmaker, N. W. Alcock, J. S. Frye, W. H. Bearden, J. H. Nelson, *ibid.* **1991**, *30*, 4743-4753.
[11] K. Eichele, R. E. Wasylishen, *Solid State Nucl. Magn. Reson.* in press.

The Structure and Stability Trends of Fluoro(methyl)plumbanes**

By *Martin Kaupp* and *Paul von R. Schleyer**

The dramatic differences in the stability of inorganic and organometallic Pb^{IV} compounds are best exemplified by comparing tetraalkyllead with lead tetrahalides: While Et_4Pb, for example, is a relatively stable compound with (still) considerable industrial use, $PbCl_4$ decomposes even at low temperatures.[1] On the other hand, Et_2Pb is unknown but $PbCl_2$ is perfectly stable. These remarkable differences between inorganic and organometallic compounds are of general importance in the chemistry of the heavy elements in groups 13 and 14 but do not yet seem to be fully understood.[2] We herein present ab initio pseudopotential calculations[3] on the structures of fluoro(methyl)plumbanes **1**–**3** which have the general formula $(CH_3)_nPbF_{4-n}$ ($n = 1-3$), as well as $(CH_3)_4Pb$ and PbF_4, and compare their stabilities with those of the corresponding divalent species $(CH_3)_2Pb$, CH_3PbF, and PbF_2.

$(CH_3)_3PbF$ **1** $(CH_3)_2PbF_2$ **2** CH_3PbF_3 **3**

The optimized geometries[3] of **1**–**3** are shown in Figure 1. The bond angles in all of these unsymmetrically substituted species deviate significantly from idealized tetrahedral values.[4] While the F-Pb-F angles are smaller than 109.5°, the

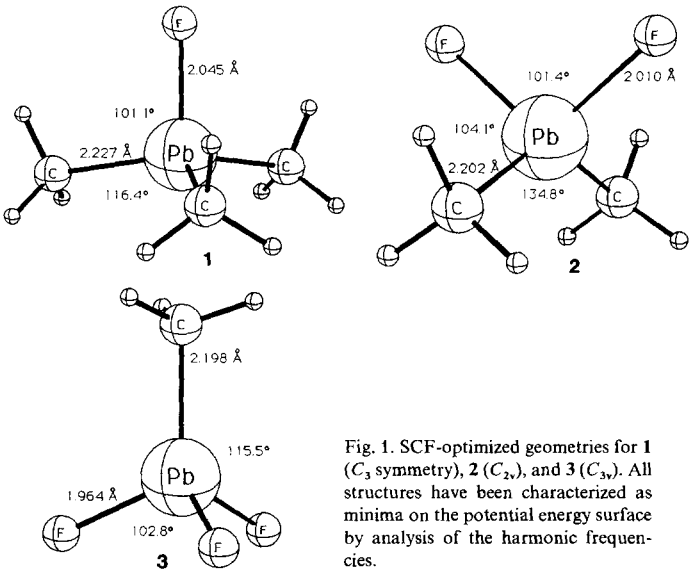

Fig. 1. SCF-optimized geometries for **1** (C_3 symmetry), **2** (C_{2v}), and **3** (C_{3v}). All structures have been characterized as minima on the potential energy surface by analysis of the harmonic frequencies.

C-Pb-C angles are considerably larger. This is most apparent in **2** with its C-Pb-C angle of approximately 135°. Similarly, the C_3Pb unit in **1** approaches planarity. These angle distortions have consequences for the polymeric arrangements found in the solid state: R_3PbX and R_2PbX_2 compounds (R is an alkyl or aryl group, X an electronegative substituent) usually form chain structures of types **4** and **5**, respectively.[1b] Note the almost planar PbR_3 arrangement in **4** (cf. **1**) and the *trans* orientation of the alkyl groups in **5** (cf. **2**). The calculated Pb–C and Pb–F bonds shorten when the number of fluorine substituents is increased,[5] consistent with the results of calculations on the fluoromethanes and -silanes.[6]

Both the distorted bond angles and the contracted bond lengths may be rationalized by hybridization arguments with

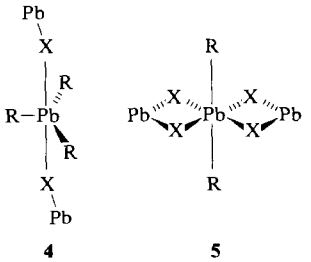

[*] Prof. Dr. P. von R. Schleyer, M. Kaupp
Institut für Organische Chemie I der Universität Erlangen-Nürnberg
Henkestrasse 42, D-W-8520 Erlangen (FRG).

[**] This work was supported by the Deutsche Forschungsgemeinschaft, the Fonds der Chemischen Industrie, the Volkswagen-Stiftung, and Convex Computer Corporation. M. K. acknowledges a Kékulé grant from the Fonds der Chemischen Industrie. We thank Prof. H. Stoll (Stuttgart) for stimulating discussions and for providing unpublished pseudopotentials and basis sets.

nonorthogonal hybrid orbitals.[6a, 7] Figure 2 displays the partial atomic charges on lead, the p:s ratio n of the Pb-sp^n hybridization of the hybrid orbitals used for Pb–C and Pb–F bonding, and the p:s ratio of the average Pb hybridization (Weinhold et al.'s "natural population/hybridization analysis" (NPA)[8] was employed). With increasing fluorine substitution, the positive charge on lead increases, and to the contributions of the p orbitals to the Pb hybrid orbitals and the bonding decrease. The larger contributions of the s orbitals to the bonds lead to the observed bond length contraction. Since the hybrid orbitals directed towards the electronegative fluorine substituents generally exhibit roughly twice as much p character as the hybrids used for Pb–C bonding (Fig. 2), the observed deviations from 109.5° angles follow expectations based on Bent's rule.[9]

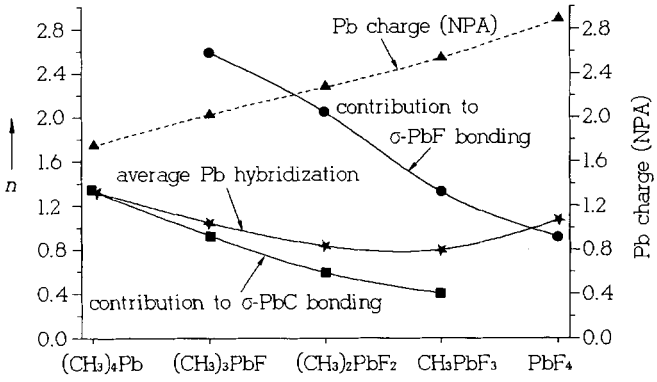

Fig. 2. p:s Ratio n of the Pb-sp^n hybridization (based on "natural population analysis" NPA[7]) and partial atomic charges on lead (NPA[7]) for the homologous series of fluoro(methyl)plumbanes (the average lead NPA hybridization and the p:s ratios of the contributions of the lead hybrid orbitals to the σ-bonding "natural localized MOs" (NLMOs)[7] are given). The differences between the average p:s ratio and the p:s ratio of the lead contributions to the σPb–F bonding NLMOs in PbF_4 are due to small hyperconjugative interactions.

The energies ΔE for the 1,1-elimination of F_2, methyl fluoride, or ethane from these Pb^{IV} compounds (to give Pb^{II} derivatives) are shown in Figure 3. In general, these reactions become less endothermic or more exothermic as the number of fluorine substituents increases. For example,

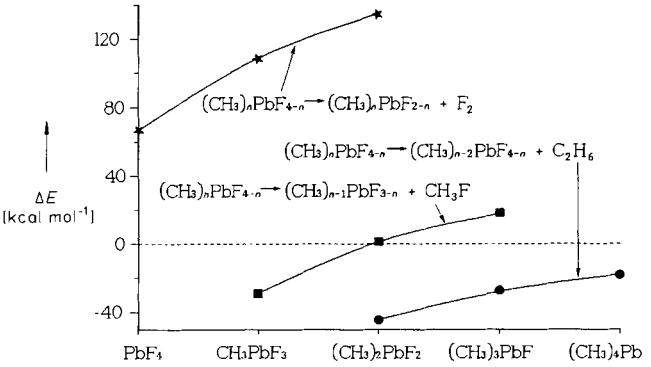

Fig. 3. Calculated energies ΔE [kcal mol^{-1}] for 1,1-elimination reactions (loss of F_2, C_2H_6, or CH_3F, respectively) of substituted Pb^{IV} compounds $(CH_3)_nPbF_{4-n}$ ($n = 0$–4). These reactions convert Pb^{IV} to Pb^{II} compounds. The MP4SDTQ single-point calculations at the SCF-optimized geometries [2,4] (cf. Fig. 1) used the same basis sets employed for the geometry optimizations [2] (the reaction $(CH_3)_4Pb \rightarrow (CH_3)_2Pb + C_2H_6$ was calculated at the MP4SDQ level).

elimination of CH_3F from $(CH_3)_3PbF$ (**1**) is *endothermic*, whereas loss of CH_3F is quite *exothermic* for CH_3PbF_3 (**3**). Obviously, the tetravalent lead compounds are destabilized in this sense by electronegative substituents. As a result, the disproportionation reaction $2\,(CH_3)_2Pb \rightarrow Pb(^3P) + (CH_3)_4Pb$ is exothermic, but the reaction $2\,PbF_2 \rightarrow Pb(^3P) + PbF_4$ is strongly endothermic.[10].

This destabilization of Pb^{IV} compounds by electronegative substituents may also be explained by the hybridization. The increasing metal charge contracts the lead 6s orbitals more strongly than the 6p orbitals.[11] Thus, the already significant differences in the radial extension of s and p orbitals in compounds of heavy main-group elements[7] become even larger. Since efficient hybridization requires the size of the orbitals involved to be similar, electronegative substituents increase the hybridization defects[7] (cf. Fig. 2) which leads to less efficient covalent bonding. A possible gain in ionic bonding contributions in the polyhalo compounds most probably is compensated by the increased electrostatic repulsions between the substituents.

In contrast to these Pb^{IV} compounds, alkanes and silanes are stabilized by geminal fluorine substitution.[6] This was shown to be due to negative hyperconjugation $n(F) \rightarrow \sigma^*(AH, AF)$ (A = C, Si).[6a] Due to less favorable orbital overlap, these hyperconjugative interactions which lead to a delocalization of the electron density do not contribute significantly to the stabilization of multiply fluorosubstituted alkylplumbanes. Preliminary calculations on the corresponding parent compounds (H instead of alkyl) with both quasi-relativistic and nonrelativistic lead pseudopotentials indicate that relativistic effects also contribute to the trends discussed here. We will present more detailed analyses of a larger set of such group 14 derivatives in a the full paper.

Received: April 9, 1992 [Z 5295 IE]
German version: *Angew. Chem.* **1992**, *104*, 1240

CAS Registry numbers:
1, 420-54-2; **2**, 23890-85-9; **3**, 21986-71-0; $(CH_3)_2Pb$, 63588-56-7; CH_3PbF, 142947-24-8; PbF_2, 7783-46-2.

[1] a) F. A. Cotton, G. Wilkinson, *Advanced Inorganic Chemistry*, 5. Ed., Wiley, New York, **1988**. b) P. G. Harrison in *Comprehensive Coordination Chemistry*, Vol. 3, (Ed.: G. Wilkinson), Pergamon, Oxford, **1987**, p. 183.

[2] Schwerdtfeger et al. have recently studied a) organothallium compounds (P. Schwerdtfeger, P. D. W. Boyd, G. A. Bowmaker, H. G. Mack, H. Oberhammer, *J. Am. Chem. Soc.* **1989**, *111*, 15) and b) a series of heavy-element hydrides and halides (P. Schwerdtfeger, G. A. Heath, M. Dolg, M. A. Bennett, *J. Am. Chem. Soc.*, in press.) by pseudopotential calculations.

[3] Full Hartree–Fock gradient geometry optimizations have been carried out with the Gaussian 90 program (Gaussian 90, Revision F, M. J. Frisch, M. Head-Gordon, G. W. Trucks, J. B. Foresman, H. B. Schlegel, K. J. Raghavachari, M. Robb, J. S. Binkley, C. Gonzalez, D. J. DeFrees, D. I. Fox, R. A. Whiteside, R. Seeger, C. F. Melius, J. Baker, L. R. Kahn, J. J. P. Stewart, S. Topiol, J. A. Pople, Gaussian, Inc., Pittsburgh, PA, **1990**). Quasi-relativistic 4-valence-electron pseudopotentials for Pb and C, and a 7-valence-electron pseudopotential for F have been used with double-zeta valence basis sets augmented by d-polarization functions and, in the case of fluorine, by a diffuse sp set (W. Küchle, M. Dolg, H. Stoll, H. Preuss, *Mol. Phys.* **1991**, *74*, 1245. W. Küchle, A. Bergner, M. Dolg, H. Stoll, H. Preuss, to be published. M. Dolg, Ph.D. Thesis, Universität Stuttgart, **1989**. *Gaussian Basis Set for Molecular Calculations* (Ed.: S. Huzinaga), Elsevier, New York, **1984**). M. Kaupp, P. von R. Schleyer, H. Stoll, H. Preuss. *J. Am. Chem. Soc.* **1991**, *113*, 6012). A [4s1p]/(2s1p) basis set was used for hydrogen (T. H. Dunning, H. Hay in *Methods of Electronic Structure Theory* (Modern Theoretical Chemistry, Vol. 3), (Ed.: H. F. Schaefer III), Plenum, New York, **1977**, p. 1). The main geometry parameters calculated for the divalent species are: RPb-C = 2.323 Å, ∢C-Pb-C = 93.0° (Me_2Pb); RPb-C = 2.300 Å, RPb-F = 2.062 Å, ∢C-Pb-F = 92.9° (MePbF); RPb-F = 2.027 Å, ∢F-Pb-F = 95.8° (PbF_2).

[4] See a) P. von R. Schleyer, *Abstract Orgn.* 352, Am. Chem. Soc. Meet. San Francisco, CA, April, **1992**, b) R. Boese, D. Bläser, N. Niederprüm, M.

Nüsse, W. Brett, P. von R. Schleyer, M. Bühl, N. J. R. van E. Hommes, *Angew. Chemie* **1992**, *104*, 356; *Angew. Chem. Int. Ed. Engl.* **1992**, *31*, 314.
[5] Our calculated Pb–F separation in PbF_4 is 1.924 Å; the Pb-C bond length in $(CH_3)_4Pb$ is 2.248 Å (in good agreement with relativistic all-electron calculations and experiment, cf.: J. Almlöf, K. Faegri, Jr., *Theor. Chim. Acta* **1986**, *69*, 438).
[6] a) A. E. Reed, P. von R. Schleyer, *J. Am. Chem. Soc.* **1987**, *109*, 7362; b) D. A. Dixon, *J. Phys. Chem.* **1988**, *92*, 86.
[7] W. Kutzelnigg, *Angew. Chem.* **1984**, *96*, 262; *Angew. Chem. Int. Ed. Engl.* **1984**, *23*, 272; W. Kutzelnigg, *Theochem* **1988**, *169*, 403.
[8] A. E. Reed, R. B. Weinstock, F. Weinhold. *J. Chem. Phys.* **1985**, *83*, 735.
[9] H. A. Bent, *Chem. Rev.* **1961**, *61*, 275.
[10] The MP4 energy for the first reaction is $-18.3\ kcal\,mol^{-1}$, that for the second $+90.0\ kcal\,mol^{-1}$, when corrected for zero-point vibrational energy and for atomic spin–orbit coupling of $Pb(^3P)$ (cf. ref. [11b]). See ref. [2b] for QCISD(T) results on the lead hydrides and fluorides.
[11] a) For a given principal quantum number, orbitals with higher angular momentum quantum number generally are affected less strongly by an increase of the nuclear charge. This is obvious from the spin–orbit-averaged experimental $s \rightarrow p$ excitation energies (ref. [11b]) for Pb^{+1} ($176\ kcal\,mol^{-1}$), Pb^{+2} ($206\ kcal\,mol^{-1}$), and Pb^{+3} ($258\ kcal\,mol^{-1}$). b) C. E. Moore, *Atomic Energy Levels*, Circular Nat. Bur. Standards 467, Washington, **1958**.

$[(\eta^5\text{-Cp})_2Sn(\mu\text{-}\eta^5\text{-Cp})Na \cdot PMDETA]$, a Compound with a Trigonal-Planar "Paddle Wheel" Triorganostannate Ion**

By *Matthew G. Davidson, Dietmar Stalke,* and *Dominic S. Wright**

Recently we have explored the bonding between early main group metals M (alkali or alkaline earth metals) and heavy p-block metals E such as In, Tl (group 3), Sn, Pb (group 4), and Sb, Bi (group 5).[1, 2] The monomeric complex $[Ph_3SnLi \cdot PMDETA]$ (PMDETA = $(Me_2NCH_2CH_2)_2$-NMe) was shown to be the first compound to contain such a bond in the solid state,[1] and the retention of such bonding in solutions of this complex was proved by the first observation of direct $^{119,117}Sn$–^7Li NMR coupling.[1] More recently our efforts have concerned the development of synthetic routes to complexes with M–E bonds (including M = Sn).[2]

Here we report the synthesis of the title compound **1** by the addition of sodium cyclopentadienide (CpNa) to bis(cyclopentadienyl)tin(II)[3] and PMDETA (mol ratio 1:1:1) in THF. Recrystallization of the crude product from toluene gives yellow crystals of **1** (see *Experimental Procedure*), which were investigated by X-ray diffraction.[4]

$[(\eta^5\text{-Cp})_2Sn(\mu\text{-}\eta^5\text{-Cp})Na \cdot PMDETA]$ **1**

Compound **1** is monomeric in solid state (Fig. 1 top). The structure contains an $(\eta^5\text{-Cp})_3Sn$ unit, a "paddle wheel" triorganostannate anion in which one Cp ligand is additionally involved in a $Sn(\mu\text{-}\eta^5\text{-Cp})Na$ bridge. The Sn center is nearly trigonal-planar (average angle Cp_c-Sn-Cp_c, 119.7(1)°, Cp_c = Cp centroid); Sn deviates approximately 0.14 Å from the plane of the three Cp centroids. The overall structure of **1**, and in particular the geometry of its Cp_3Sn unit, can be rationalized in terms of the competition by the Sn and Na centers for the electron density on the $\mu\text{-}\eta^5$-Cp ligand, through the slightly bent $Sn(\mu\text{-}\eta^5\text{-Cp})Na$ bridge (Sn(1)-Cp(A)-Na(1) 172.3(1)°). This competition weakens the interaction of the $\mu\text{-}\eta^5$-Cp contact with the Sn center (Cp(A)–Sn(1) 2.733(1) Å) compared to that between Sn and terminally attached Cp ligands (average value Cp(B,C)–Sn(1), 2.538(1) Å; cf. Sn–Cp, ca. 2.42 Å in $[Cp_2Sn]$[3]).

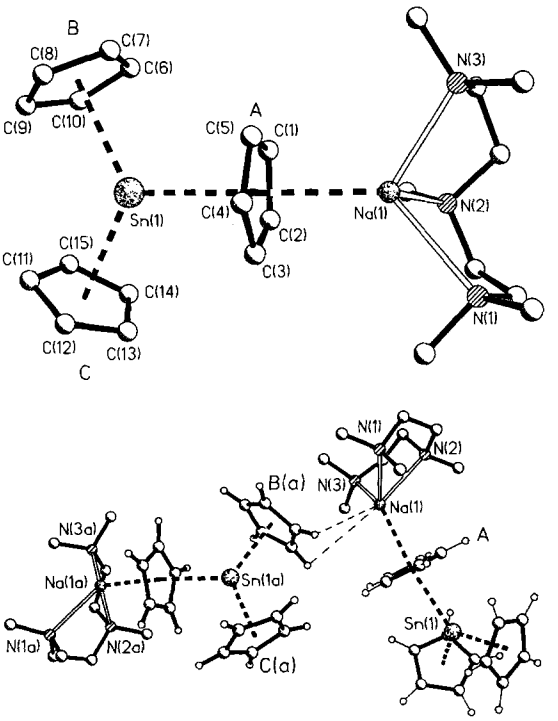

Fig. 1. Top: Crystal structure of **1**. Hydrogen atoms have been omitted for clarity. Selected distances [Å] and angles [°]: Cp(A)-Sn(1) 2.733(1), Cp(B)-Sn(1) 2.551(1), Cp(C)-Sn(1) 2.526(1), Cp(A)-Na(1) 2.550(1); Cp(A)-Sn(1)-Cp(B) 116.3(1), Cp(A)-Sn(1)-Cp(C) 118.9(1), Cp(B)-Sn(1)-Cp(C) 124.0(1), Sn(1)-Cp(A)-Na(1) 172.3(1). Bottom: Crystal packing of **1** determined by intermolecular C–H ··· Na interactions. Selected distances [Å]: H ··· Na 3.148(2), 3.490(2).

The deviation from linearity of the $Sn(\mu\text{-}\eta^5\text{-Cp})Na$ bridge (172.3(1)°) appears to be almost entirely a consequence of crystal packing. The Na–Cp_c vector is almost perpendicular (88.30(1)°) to the plane of the Cp ligand (Cp(A)–Na(1) 2.550(1) Å; cf. $(\mu\text{-}\eta^5\text{-Cp})$–Na in the polymer $[(\mu\text{-}\eta^5\text{-Cp})Na \cdot TMEDA]_\infty$ (TMEDA = $Me_2NCH_2CH_2NMe_2$) ca. 2.65 Å,[5] and Cp*–Na (Cp* = C_5Me_5) in molecular $[Cp^*Na(py)_3]$ (py = pyridine) 2.40 Å[6]). This bending of the $Sn(\mu\text{-}\eta^5\text{-Cp})Na$ bridge is caused by two long-range intermolecular C(H) ··· Na interactions (H ··· Na(1) 3.148(2) and 3.490(2) Å) with the $Na \cdot PMDETA^+$ unit. Thus, the apparently "naked" Na face is further coordinated and, as a result, units of **1** are linked into a polymeric array (Fig. 1 bottom).

Although a number of early main group metal stannates have been structurally characterized, only $[Ph_3SnLi \cdot PMDETA]$ contains a metal–Sn contact.[1] The role of the $\mu\text{-}\eta^5$-Cp ligand in **1** in holding the Sn and Na centers together is comparable with that of bridging heteroatoms (e.g., O, P, Cl) in other stannate complexes, for example O in $[Li(\mu_2\text{-}Ph_2C_6H_3O)_3Sn]$.[7] The planar geometry of the Sn center in **1** is unprecedented in the structures of triorganostannates.

[*] Dr. D. S. Wright, M. G. Davidson
University Chemical Laboratory
Lensfield Road, Cambridge CB2 1EW (UK)
Dr. D. Stalke
Institut für Anorganische Chemie
Tammannstrasse 4, D-W-3400 Göttingen (FRG)

[**] This work was supported by the British Science and Engineering Research Council (D. S. W., M. G. D.), the Associated Octel Co. Ltd., Ellesmere Port (M. G. D.), and the Deutsche Forschungsgemeinschaft (D. S.). We also thank S. Wilkinson (Cambridge) for recording NMR spectra.

All other such complexes, whether separated ions[8] or contact ion pairs are present,[1] have nearly pyramidal stannate ions as a result of the construction of σ bonds with substantial Sn p character and the lone pair on Sn having mainly s character. The geometry of the Sn center in **1** implies a very different use of orbitals than in other stannates.[9]

The title compound **1** is rare among organotin(II) compounds in containing three aromatic ligands π-bonded to Sn. Polymerically linked (μ-η^5-Cp)$_3$SnX units (X = μ-F-BF_3^- and THF) have been seen in the structure of $\{[(\eta^5\text{-Cp})_2\text{Sn}(\mu\text{-}\eta^5\text{-Cp})\text{Sn(thf)}]^+BF_4^-\}_\infty$, produced by the reaction of BF_3 with [Cp_2Sn] in THF (Cp–Sn, ca. 2.29–3.67 Å).[10] In orthorhombic [Cp_2Pb], (μ-η^5-Cp)$_2$(η^5-Cp)Pb units are present within its polymeric zigzag structure[11] (cf. the well-known bent structure of [Cp_2Sn][3]). Interestingly [Cp_2Pb] forms a 1:1 electrolyte in THF.[12] On the basis of our current work, it seems most likely that $[\text{CpPb(thf)}_x]^+[Cp_3Pb]^-$ is present in solution, rather than the suggested $[\text{CpPb}]^+$ and discrete Cp^- ions.[12, 13]

Finally, cryoscopic molecular mass determinations combined with variable-temperature ^{1}H NMR spectroscopy show that **1** is involved in a dissociative equilibrium in aromatic solvents.[14] At room temperature **1** is completely dissociated into $[(\eta^5\text{-Cp})_3\text{Sn}]^-$ and [Na · PMDETA]$^+$ ions. As the temperature is reduced (finally to ca. −80 °C) these ions pair up to give intact **1**. These results illustrate that the paddle wheel $[(\eta^5\text{-Cp})_3\text{Sn}]^-$ ion has a separate existence.

Previous work has concentrated on the reactions of electrophiles such as MeI with [Cp_2Sn].[13, 15] We are currently investigating the addition reactions (which produce mixed-ligand triorganostannates $[Cp_2RSn]^-$) and the substitution reactions (which produce mixed ligand organotin compounds [CpSnR]) of various nucleophiles, such as organolithium compounds, with [Cp_2Sn]. To our knowledge, these are new approaches to triorganostannate complexes and organotin(II) compounds. We are also investigating the use of $[Cp_3Sn]^-$ as a new ligand to other main group metals.

Experimental Procedure

1: CpNa (1.25 mL, 2.0 mol L^{-1} in THF, 2.5 mmol) was added to a solution of [Cp_2Sn] (0.623 g, 2.5 mmol) (preparation ref. [3]) and PMDETA (0.53 mL, 2.5 mmol) in THF (5 mL) at 20 °C under nitrogen. Stirring the reaction mixture (0.5 h) at 20 °C gave an orange-red solution. The THF was removed under vacuum, replaced with toluene (5 mL), and the solution was filtered to remove a faint precipitate. Storage of the orange-red filtrate at 20 °C (48 h) gave air-sensitive, yellow crystals, identified as **1**. First-batch yield 20%, m.p. 93–98 °C to a yellow oil. IR (solid): $\tilde{\nu}$ = 3079, 3061 cm^{-1} (s, ν, C-H, η^5-Cp), disappears upon exposure to air. ^{1}H NMR (25 °C, C_6D_6): δ = 6.00 (s, 15H; η^5- and μ-η^5-CpH; cf. δ = 5.78 (^2J(Sn,H) = 15.7 Hz) in [Cp_2Sn]), 1.80 (s, 15H; CH_3N and $(CH_3)_2N$), 1.65 (s, 8H; $(CH_2)_2$). Correct C, H, N analysis.

Received: April 2, 1992 [Z 5274 IE]
German version: *Angew. Chem.* **1992**, *104*, 1265

CAS Registry numbers:
1, 142981-18-8; CpNa, 4984-82-1; Cp_2Sn, 1294-75-3.

[1] D. Reed, D. Stalke, D. S. Wright, *Angew. Chem.* **1991**, *103*, 1539–1540; *Angew. Chem. Int. Ed. Engl.* **1991**, *30*, 1459–1460.

[2] D. R. Armstrong, M. G. Davidson, D. Moncrieff, D. Stalke, D. S. Wright, unpublished results.

[3] a) E. O. Fischer, H. Grubert, *Z. Naturforsch. B* **1956**, *11*, 423–424; b) A. Almenningen, A. Haaland, T. Motzfeld, *J. Organomet. Chem.* **1967**, *7*, 97–104.

[4] X-ray structure data: $C_{24}H_{38}N_3NaSn$, M = 510.25, monoclinic, space group $P2_1/c$, a = 8.713(2), b = 17.221(3), c = 16.345(3) Å, β = 96.61(3)°, V = 2436.2(8) Å^3, Z = 4, ρ_{calcd} = 1.392 Mg m^{-3}, $F(000)$ = 1056, λ = 0.71073 Å, T = 153 K, $\mu(Mo_{K\alpha})$ = 1.081 mm^{-1}. Data were collected on a Siemens–Stoe AED using an oil-coated, rapidly cooled crystal of dimensions 0.50 × 0.55 × 0.40 mm by the $2\theta/\omega$ method ($8° \le 2\theta \le 60°$). Of a total of 10529 collected reflections, 7091 were unique. The structure was solved by direct methods (SHELXS 92) and refined by full least squares $\sigma_n F^2$ with all data to R_1 and wR_2 values of 0.026 and 0.050, respectively (SHELXL 92); largest difference peak and hole 0.39 and −0.33 eÅ^{-3}, respectively. All hydrogen atoms were located in the difference Fourier map and their positions were refined freely with common refined U values for chemically equivalent atoms. Further details of the crystal structure investigations are available on request from the Director of the Cambridge Crystallographic Data Centre, University Chemical Laboratory, Lensfield Road, GB-Cambridge CB2 1EW (UK), by quoting the full journal citation.

[5] T. Aoyagi, H. M. M. Shearer, K. Wade, G. Whitehead, *J. Organomet. Chem.* **1979**, *175*, 21–31.

[6] G. Rabe, H. W. Roesky, D. Stalke, F. Pauer, G. M. Sheldrick, *J. Organomet. Chem.* **1991**, *403*, 11–19.

[7] G. D. Smith, P. E. Fanwick, I. P. Rothwell, *Inorg. Chem.* **1989**, *26*, 618–620.

[8] T. Birchall, J. A. Vetrone, *J. Chem. Soc. Chem. Commun.* **1988**, 877–879.

[9] MO Calculations are currently being performed on the $[(\eta^5\text{-Cp})_3\text{Sn}]^-$ ion and on models of **1** to probe the nature of the bonding in these.

[10] T. S. Dory, J. J. Zuckerman, C. L. Barnes, *J. Organomet. Chem.* **1985**, *281*, C1–C7.

[11] a) E. O. Fischer, H. Grubert, *Z. Anorg. Allg. Chem.* **1956**, *286*, 237–242; b) C. Panattoni, G. Bombieri, U. Croatto, *Acta Crystallogr.* **1966**, *21*, 823–826.

[12] W. Strohmeier, H. Landsfeld, F. Gernet, *Z. Electrochem.* **1962**, *66*, 823–827.

[13] P. Jutzi, *Adv. Organomet. Chem.* **1986**, *26*, 217–288.

[14] Cryoscopic molecular mass measurements (in benzene) show that two solution species are present over a range of concentrations (n = 0.49 ± 0.02 (0.015 mol L^{-1}); 0.51 ± 0.02 (0.030 mol L^{-1})). ^{1}H NMR spectra of **1** at 25 °C (in $C_6D_5CD_3$) have, apart from signals due to PMDETA, just one sharp signal at δ = 5.97 due to discrete $[(\eta^5\text{-Cp})_3\text{Sn}]^-$ ions. No signals below this could be attributed to CpNa. Reducing the temperature to ca. −40 °C results in the splitting of the η^5-Cp signal. At ca. −80 °C these two resonances are fully resolved at a ratio of 2:1; δ = 6.02 (η^5-Cp, ^2J(Sn, H) = 29.4 Hz), and 6.00 (μ-η^5-Cp, ^2J(Sn, H) = 28.8 Hz).

[15] J. W. Connolly, C. Hoff, *Adv. Organomet. Chem.* **1981**, *19*, 123–153.

Opening of an Aza-*closo*-dodecaborane to an Aza-*nido*-dodecaborate**

By *Franc Meyer, Jens Müller, Peter Paetzold,** and *Roland Boese*

Aza-*closo*-dodecaborane $NB_{11}H_{12}$ is isoelectronic with dicarba-*closo*-dodecaborane $C_2B_{10}H_{12}$.[1] Upon attack by base the icosahedral framework of $C_2B_{10}H_{12}$ is broken down into the open frame of dicarba-*nido*-undecaborate $C_2B_9H_{12}^-$.[2] We wanted to apply this reaction to $NB_{11}H_{12}$. Its N-bound proton is so acidic, however, that it is removed even by a weak base like NEt_3 forming $[HNEt_3][NB_{11}H_{11}]$ **1**.[1] Thus, before the examination of the attack of a base on the NB_{11} framework, it was imperative to protect the N atom by alkylation. The salt **1** was treated with the strong methylating agent methyltriflate, and $MeNB_{11}H_{11}$ **2** was obtained [Eq. (a)]. The three ^{11}B NMR signals of **2**, their intensity ratio of 5:5:1, and the characteristic B–H coupling constant leave no doubt that $NB_{11}H_{12}$ and its methyl derivative are structurally analogous.

$$\underset{\mathbf{1}}{[HNEt_3][NB_{11}H_{11}]} \xrightarrow[-[HNEt_3][O_3SCF_3]]{+MeO_3SCF_3} \underset{\mathbf{2}}{MeNB_{11}H_{11}} \qquad (a)$$

[*] Prof. P. Paetzold, F. Meyer, Dr. J. Müller
Institut für Anorganische Chemie der Technischen Hochschule
Templergraben 55, D-W-5100 Aachen (FRG)

Priv.-Doz. R. Boese
Institut für Anorganische Chemie der Universität-Gesamthochschule
Universitätsstrasse 5-7, D-W-4300 Essen (FRG)

[**] This research was supported by the Deutsche Forschungsgemeinschaft.

Compound **2** adds methanol in the ratio 1:1 and thereby forms the acid $H[MeNB_{11}H_{11}(OMe)]$, which is completely dissociated in dichloromethane solvent in the presence of an excess of methanol. The acid cannot be isolated in a pure form; when solvent is removed under vacuum, the acid decomposes completely to yet-unknown fragments. If the salt $[N(PPh_3)_2]Cl$ is added to a solution of the acid, one obtains product **3** [Eq. (b)], the anion of which is identical to that of the acid as is evident from their identical NMR spectra.

$$2 \xrightarrow{+MeOH} \xrightarrow[-HCl]{+[N(PPh_3)_2]Cl} [N(PPh_3)_2][MeNB_{11}H_{11}(OMe)] \qquad (b)$$

3

The structure of the anion of **3** is derived from the hypothetical *closo*-tridecaborate $B_{13}H_{13}^{2-}$ **A**[3] by removal of the B3 atom. Seven signals are seen in the ^{11}B NMR spectrum with the intensity ratio 1:2:2:2:1:2:1. Thus, three B atoms lie in one mirror plane, namely B2, B12, and B13, and one of these, B2, does not show B–H coupling. The 2D ^{11}B–^{11}B NMR spectrum reflects the connectivity of the B_{12} framework; the lack of a cross peak between B2 and B4/B5 is expected for a B–B bond bridged by an N atom.[4] The $^1H\{^{11}B\}$ NMR spectrum also consists of seven signals of the B-bound H atoms with the intensity ratio 1:1:2:2:2:1:2; they could be assigned with the help of the 2D ^{11}B–^1H NMR spectrum. Of special interest are the atoms B8/B9, each bound to a terminal H atom as well as a bridging H atom, and the atom B2, not bound to any H atom.

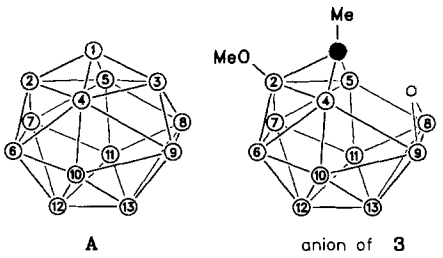

The unequivocal assignment of the spectroscopic data to the structure of the anion of **3** in solution is in agreement with the results of the X-ray structure analysis (Fig. 1).[5]

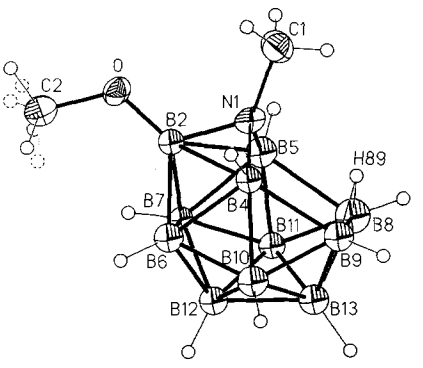

Fig. 1. Crystal structure of the anion of **3**. Selected distances [Å], standard deviations in parentheses: N1-B2 1.490(5), N1-B4 1.520(9), N1-B5 1.604(10), B2-B4 2.004(9), B2-B5 2.107(10), B2-B6 1.813(8), B2-B7 1.814(8), B4-B6 1.910(10), B4-B9 1.969(9), B4-B10 1.852(8), B5-B7 1.863(9), B5-B8 2.053(10), B5-B11 1.724(8), B6-B7 1.797(10), B6-B10 1.782(10), B6-B12 1.788(9), B7-B12 1.740(8), B7-B11 1.774(9), B8-B11 1.714(10), B8-B9 1.819(11), B9-B10 1.766(10), B9-B13 1.727(9), B10-B12 1.755(11), B10-B13 1.820(11), B11-B12 1.837(11), B11-B13 1.791(11), B12-B13 1.821(6), N1-C1 1.464(5); B2-O 1.356(4).

Whereas all 21 of the B–B distances remote from nitrogen fall within the range expected between 1.71 and 1.91 Å, the two distances B4–B9 and B5–B8 in the open pentagon of the cluster, as well as the distances B2–B4 and B2–B5, bridged by the N atom, are all especially long (1.97–2.11 Å). Accordingly, the triangles B2-B4-N and B2-B5-N deviate from equilateral with angles at the N atom of 83.5 and 85.8°, respectively. The further away the cluster faces are from the N atom, the closer they approach regularity.

The *nido* structure found for the anion of **3** is exactly that expected. Removal of the B3 atom from the hypothetical *closo* skeleton **A** eliminates the unfavorable connectivity $k = 6$ of the atoms B4 and B5 in the cluster framework, which means sevenfold coordination when the the *exo* H atoms are also taken into account. Simultaneously, an optimal place is made available for the electronegative N atom in position 1 with $k = 3$. Atoms B8 and B9 attain the connectivity $k = 4$, and are thus able to accommodate a bridging H atom on the mirror plane of the free anion of **3**, whereas all the other B atoms with $k = 5$ are not likely to form H bridges. Two other compounds set the precedent for the *nido* structure found here. One is the compound *nido*-$[(Cp^*Rh)OB_{10}H_8Cl(PMe_2Ph)]$ with the strongly electronegative O atom in position 1, the Rh atom surprisingly in position 8 (transition metals usually prefer positions with higher connectivity), and the ligands Cl and PMe_2Ph in the positions 5 and 9, respectively.[6] In the second example, $[(CpCo)Se_2B_9H_9]$, the Co atom and the two Se atoms occupy the respective positions 4, 1, and 9, so that the Se atoms have a minimum connectivity and the metal atom a maximum. In addition, the metal atom has the Se atoms as desirable neighbors.[7] The *nido* compound $Et_4C_4B_8H_8$ follows the same structural principle, but in this case the B4–B9 bond is opened so that the electronegative C atoms occupy positions 1, 4, 8, and 9 with two of these positions having $k = 3$ and the other two $k = 4$.[8] Other possibilities for obtaining *nido* derivatives of **A** arise from the removal of atom B5, or of B1 with simultaneous opening of the B5–B8 bond.[9]

The structure of the anion of **3** appears to be thermodynamically very stable, since **3** does not react solvolytically with either water or alcohols. The same anion is formed when **2** is treated with LiMe/tmeda, KO*t*Bu/[18]crown-6, or KF/[18]crown-6; however, instead of the base MeO^-, the respective bases Me^-, $tBuO^-$, and F^- are bound in the 2 position.[10] In the formation of these anions, the bridging H atom apparently comes from the formerly terminal position 2, having been displaced by the base. Methanol may also be considered as a source of the μ-H atom. However, in the methanolysis of **2** with CD_3OD no deuterium is transferred to the bridging position. This proves that it is the H atom in the 2 position of **2** that is apparently shifted intramolecularly to the bridging position during the methanolysis, and in addition that this H atom does not undergo exchange with either the excess of methanol or the protons of the medium.

The attack of base on *closo*-$MeNB_{11}H_{11}$ proceeds differently to that on *closo*-$C_2B_{10}H_{12}$. In the case reported, instead of the strongly basic alkoxide, weakly basic alcohol suffices; the twelve-vertex *closo* cluster is not broken down into an eleven-vertex *nido* cluster, but is rather opened to a twelve-vertex *nido* cluster.

Experimental Procedure

2: Methyltriflate (0.46 mL, 4.19 mmol) was added dropwise to a solution of **1** (1.02 g, 4.14 mmol) in 20 mL of CH_2Cl_2 at −50 °C. The reaction mixture was stirred at room temperature for 12h. The solvent was then removed under vacuum and the residue extracted with pentane (3 × 15 mL). The combined

pentane solutions were concentrated to 10 mL and cooled to −40 °C. A colorless solid crystallized (0.28 g, 42%), which sublimed at 20 °C/0.001 Torr.—NMR spectra measured in C_6D_6 at 25 °C; ^{1}H NMR (499.843 MHz, TMS): δ = 1.83 (s, Me), 2.16 (H2–H6), 2.47 (H7–H11), 3.03 (H12), measurement and assignment of the three B–H signals as cross peaks in the 2D ^{11}B–^{1}H NMR spectrum; ^{11}B NMR (160.364 MHz, $Et_2O{\cdot}BF_3$): δ = −11.2 (d, J = 147 Hz, B7–B11, cross peaks in the 2D ^{11}B–^{11}B NMR spectrum with B2–B6 and with B12), −5.1 (d, J = 183 Hz, B2–B6, no cross peak with B12), −0.1 (d, J = 147 Hz, B12).

3: To a solution of **2** (39.0 mg, 0.245 mmol) in 2 mL of CH_2Cl_2 at room temperature was added 0.10 mL of methanol. This mixture was stirred for 30 min and then treated with a solution of $[N(PPh_3)_2Cl]$ (140 mg, 0.256 mmol) in 3 mL of CH_2Cl_2. Pentane was added to the reaction mixture; **3** precipitated and was filtered, washed with pentane three times, and dried. Analytically pure bis(triphenylphosphoranylidene)ammonium [2-methoxy-1-methyl-8,9-μ-hydrodecahydro-1-aza-*nido*-dodecaborate] (**3**) was obtained (175 mg, 98%). Single crystals of **3** were obtained from hexane/dichloromethane at −40 °C. – NMR spectra were measured at 25 °C in $CDCl_3$ (same frequencies and standard as for **2**); ^{1}H{^{11}B} NMR: δ = −3.81 (broad, μ-H8/9), 0.32 (H13), 1.41 (H10/11), 1.52 (H4/5), 1.85 (H6/7), 2.15 (s, 3H, NMe), 2.44 (H12), 3.16 (H8/9), 3.80 (s, 3H, OMe), 7.42–7.68 (30H, Ph), assignment of the *exo* B-H signals as cross peaks in the 2D ^{11}B–^{1}H NMR spectrum; ^{11}B NMR spectrum: δ = −34.7 (d, J = 134 Hz, B13), −18.6 (d, J = 134 Hz, B6/7), −13.4 (d, J = 134 Hz, B4/5), −11.8 (d, J = 134 Hz, B10/11), −8.2 (d, J = 134 Hz, B12), 1.9 (d, J = 147 Hz, B8/9), 9.3 (s, B2), assignment with help of the cross peaks in the 2D ^{11}B–^{11}B NMR spectrum; ^{13}C NMR (125.697 Hz, TMS): δ = 37.7 (NMe), 53.4 (OMe), 126.9 (d, J_{PC} = 108 Hz, *ipso*-C of Ph), 129.6, 132.0, 133.8 (Ph).

Received: April 8, 1992 [Z 5288 IE]
German version: *Angew. Chem.* **1992**, *104*, 1221

CAS Registry numbers:
1, 142581-18-8; **2**, 142581-19-9; **3**·PPN, 142581-21-3; **3**·H$^+$, 142611-00-5; Me$^-$, 15194-58-8; *t*BuO$^-$, 16331-65-0; F$^-$, 16984-48-8.

[1] J. Müller, J. Runsink, P. Paetzold, *Angew. Chem.* **1991**, *103*, 201; *Angew. Chem. Int. Ed. Engl.* **1991**, *30*, 175.
[2] R. A. Wiesboeck, M. F. Hawthorne, *J. Am. Chem. Soc.* **1964**, *86*, 1642–1643.
[3] L. D. Brown, W. N. Lipscomb, *Inorg. Chem.* **1977**, *16*, 2989–2996.
[4] J. Müller, P. Paetzold, R. Boese, *Heteroatom Chem.* **1990**, *1*, 461–465.
[5] Crystal data: a = 18.181[5], b = 9.015(3), c = 24.401(8), $\alpha = \beta = \gamma = 90°$, V = 4000(2) Å^3, Z = 4, ρ_{calc} = 1.413 g cm^{-3}, $Pca2_1$ (No. 29), Nicolet R3m/V; recording temperature 125 K; $\mu(Mo_{K\alpha})$ = 1.6 cm^{-1}; 4465 independent reflections with $3 < 2\theta < 45°$, 3919 of these observed ($F_0 < 4\sigma(F)$); structure solution and refinement with 398 parameters with SHELXTL-PLUS (version 4.2); R = 0.058, R_w = 0.066, $w^{-1} = \sigma^2(F_0) + 0.0015F_0^2$. All H atoms bound to B atoms were located by difference Fourier synthesis and refined with a common isotropic dislocation factor. The H atoms on C2 are disordered; the H atoms on the cation were treated as riding groups. Further details of the crystal structure investigation may be obtained from the Fachinformationszentrum Karlsruhe, Gesellschaft für wissenschaftlich-technische Information mbH, D-W-7514 Eggenstein-Leopoldshafen 2 (FRG) on quoting the depository number CSD-320454, the names of the authors, and the journal citation.
[6] X. L. R. Fontaine, H. Fowkes, N. N. Greenwood, J. D. Kennedy, M. Thornton-Pett, *J. Chem. Soc. Dalton Trans.* **1987**, 2417–2429.
[7] G. D. Friesen, A. Barriola, P. Daluga, P. Ragatz, J. C. Huffmann, L. J. Todd, *Inorg. Chem.* **1980**, *19*, 458–462.
[8] T. L. Venable, R. B. Maynard, R. N. Grimes, *J. Am. Chem. Soc.* **1984**, *106*, 6187–6193.
[9] R. E. Williams in *Electron Deficient Boron and Carbon Clusters*, (Eds.: G. A. Olah, K. Wade, R. E. Williams), Wiley, New York, **1991**, pp. 11–93.
[10] F. Meyer, *Dissertation*, Technische Hochschule Aachen, in preparation.

Chain Elongation of Thiodipeptides with Proteases**

By *Carlo Unverzagt,* Armin Geyer,* and *Horst Kessler**

The thioamide bond is a useful element for the structural variation of biologically active peptides to increase their activity and selectivity. Thiopeptides are attractive as peptidomimetics[1] because of their enhanced stability towards proteases[2] and the conformational changes they induce.[3] Their general application has been, however, prevented by insufficient synthetic availability. The O/S exchange in peptides by Lawesson's reagent[4] or its variants[5] may be selective in cyclic peptides[3, 6b] but its effectiveness is difficult to predict. Only protected dipeptides **1** allow the selective O/S exchange at the amide position (→ **2**) in high yields without affecting urethane or ester groups. Deprotection of thiopeptides **2** generally causes no difficulties.

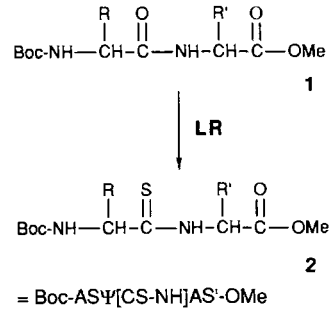

= Boc-ASΨ[CS-NH]AS'-OMe

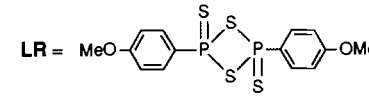

Boc-D-Ala-Ψ[CS-NH]Phe-OMe **2a**

Boc-LeuΨ[CS-NH]Leu-OMe **2b**

Boc-PheΨ[CS-NH]Gly-OMe **2c**

Peptide elongation at the C terminus of thiopeptides by means of classical peptide chemistry fails;[6] instead the activated thiopeptide **3** forms a sulfur-containing heterocycle **4**. These thiazolones **4** are poor acylating agents and are prone to racemization of the two chiral centers. Hence, only few elongations of thiopeptides have been performed with achiral C termini, such as glycine or α-aminobutyric acid.[6]

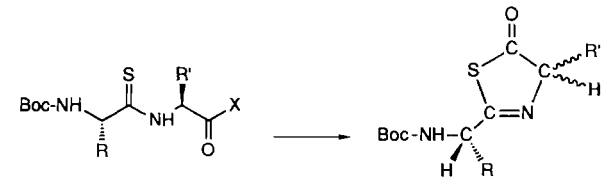

We report here on the enzymatic C-terminal elongation of thiopeptides **2a**, **b** and the N-terminal elongation of the derivative of **2c** deblocked at the N terminus (= **5c**). Subtilisin Carlsberg and subtilisin BPN′ accept **2a–c** as substrates: in 50% dimethylformamide (DMF) the corresponding free carboxylic acids are obtained in almost quantitative yield. Under these conditions proteases do not cleave amide bonds.[7, 8] Proteases can also be used to catalyze the elongation of amino acid esters and peptide esters at their C terminus.[8] We have successfully applied this mild synthetic method to sensitive thiopeptides. The subtilisin BPN′ catalyzed reaction of thiopeptide methyl ester **2a** with leucine amide H-Leu-NH_2 (**5c**) yields mainly the hydrolyzed dipeptide acid (60%) but also the desired tripeptide **6c** (24%) (see Table 1). Obviously the enzyme activates **2a** mildly, thereby allowing the elongation to thiopeptide **6c**, whereas the undesired side product (thiazolone) is not formed. The 250 MHz ^{1}H NMR spectrum of **6c** exhibits a characteristic signal for the thioamide proton at δ = 10.2 and the resonances of all three amino acids. It also proves the sterochemical uniformity of the peptide bond formation.

The yields in the enzymatic peptide elongation of **2a** with H-Leu-NH_2 (**5c**) could be increased with chymotrypsin as a biocatalyst (Table 1). Under the reaction conditions the thiodipeptides are completely converted into **6** by hydrolysis

[*] Dr. C. Unverzagt, Prof. Dr. H. Kessler, Dipl.-Chem. A. Geyer
Organisch-Chemisches Institut
der Technischen Universität München,
Lichtenbergstrasse 4, D-W-8046 Garching (FRG)

[**] This work was supported by the Fonds der Chemischen Industrie, the Deutschen Forschungsgemeinschaft, and the Leonhard-Lorenz-Stiftung.

Table 1. Thiopeptides **6a–g** synthesized with chymotrypsin.

Starting materials [a]	Thiopeptides	Yield [%]
2a + **5a**	Boc-D-AlaΨ[CS-NH]Phe-Val-OAll **6a**	70
2a + **5b**	Boc-D-AlaΨ[CS-NH]Phe-Val-OMe **6b**	49
2a + **5c**	Boc-D-AlaΨ[CS-NH]Phe-Leu-NH_2 **6c**	48
2a + **5e**	Boc-D-AlaΨ[CS-NH]Phe-PheΨ[CS-NH]Gly-OMe **6d**	63
	+ Boc-D-AlaΨ[CS-NH]Phe-(PheΨ[CS-NH]Gly)$_2$-OMe **6e**	8 [b]
2b + **5d**	Boc-LeuΨ[CS-NH]Leu-Phe-NH_2 **6f**	66
2b + **5e**	Boc-LeuΨ[CS-NH]Leu-PheΨ[CS-NH]Gly-OMe **6g**	26

[a] **5a** = H-Val-OAll, **5b** = H-Val-OMe, **5c** = H-Leu-NH_2, **5d** = H-Phe-NH_2, **5e** = H-PheΨ[CS-NH]Gly-OMe. [b] Byproduct in the synthesis of **6d**.

or peptide elongation. Exceptions are the reactions of **2a** + **5c** and **2b** + **5e** in which 46 and 30% of the respective starting peptides were recovered. The results of the enzymatic reactions (Table 1) are not optimized, and yields may be increased by variation of cosolvent, substrate, and enzyme.

When thiopeptides such as **5e** are used as the amino component in peptide couplings, tetrapeptides with alternating thioamide bonds (**6d, g**) are formed. The hexapeptide **6e** containing three thioamide groups was isolated as a byproduct (8%) in the synthesis of **6d**. Apparently some of the amine **5e** dimerized to the tetrapeptide H-PheΨ[CS-NH]Gly-PheΨ[CS-NH]Gly-OMe, which was then preferentially elongated by chymotrypsin to **6e**.

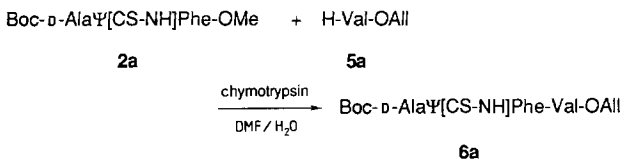

Chymotrypsin cleaves peptides after aromatic amino acids and leucine with high specifity,[8] but does not attack valine esters.[9] Hence, the reaction of thiopeptide **2a** with valine allyl and methyl esters **5a, b** proceeds to thiotripeptides esters. It is remarkable that the slightly larger and more lipophilic allyl ester group in the nucleophile increases the yield by more than 20%. The resulting tripeptides **6a** (70% yield) and **6b** (49% yield) can be deprotected and incorporated into larger fragments. Removal of the allyl ester protecting group in thiotripeptide **6a** under Pd^0 catalysis was not affected by the nucleophilic thioamide sulfur atom (Scheme 1).[10, 11] Subsequent coupling with **7** in the presence of *N'*-(3-dimethylaminopropyl)-*N*-ethylcarbodiimide hydrochloride/1-hydroxybenzotriazole (EDCI/HOBt) gave thiohexapeptide **8** in 85% yield. Deprotection yielded **9** which is presently under investigation in cyclization reactions.

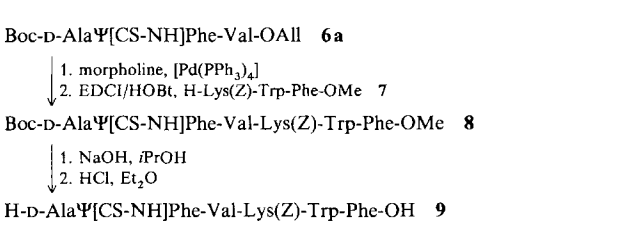

Scheme 1. Reactions sequence starting from thiopeptide **6a**.

The method described here for the enzymatic elongation of thiodipeptides can certainly be applied for the elongation of a number of other amino acids at the *C* terminus. The choice of suitable enzymes and appropriate protecting groups should allow the selective introduction of thioamide bonds in a variety of peptide linkages.

Experimental Precedure

N-tert-Butyloxycarbonyl-D-thioalanyl-L-phenylalanyl-L-valine allyl ester (**6a**): A 500 mg portion (1.37 mmol) of **2a** and 860 mg (5.48 mmol) of **5a** were dissolved in 21.2 mL of DMF/H_2O (1/1) in a plastic vessel. 250 mg of chymotrypsin was added, and the solution was stirred for 48 h. The mixture was concentrated in high vacuum and chromatographed on 30 g silica gel eluting with CH_2Cl_2/MeOH (100/1). Yield 472 mg (70%) **6a**. $[\alpha]_D^{22} = -4.0$ ($c = 1$, MeOH).

Received: March 13, 1992 [Z 5238IE]
German version: *Angew. Chem.* **1992**, *104*, 1231

CAS Registry numbers:
2a, 142765-11-5; **2b**, 128421-81-8; **5a**, 88224-01-5; **5b**, 4070-48-8; **5c**, 687-51-4; **5d**, 5241-58-7; **5e**, 142765-12-6; **6a**, 142765-13-7; **6b**, 142765-14-8; **6c**, 142765-15-9; **6d**, 142765-16-0; **6e**, 142765-17-1; **6f**, 142765-18-2; **6g**, 142765-19-3; **7**, 142765-20-6; **8**, 142765-21-7; **9**, 142765-22-8; chymotrypsin, 9004-07-3; protease, 9001-92-7.

[1] A. F. Spatola in *Chemistry and Biochemistry of Amino Acids, Peptides and Proteins, Vol. 7* (Ed.: B. Weinstein), Marcel Dekker, New York, **1983**, pp. 267–357.
[2] R. E. Beattie, D. T. Elmore, C. H. Williams, D. J. S. Guthrie, *Biochem. J.* **1987**, *245*, 285–288, and references therein.
[3] D. Seebach, S. Y. Ko, H. Kessler, M. Köck, M. Reggelin, P. Schmieder, M. D. Walkinshaw, J. J. Bölsterli, D. Bevec, *Helv. Chim. Acta* **1991**, *74*, 1953–1990; H. Kessler, H. Matter, A. Geyer, H.-J. Diehl, M. Köck, G. Kurz, F. R. Opperdoes, M. Callens, R. K. Wierenga, *Angew. Chem.* **1992**, *104*, 343–345; *Angew. Chem. Int. Ed. Engl.* **1992**, *31*, 328–330.
[4] K. Clausen, M. Thorsen, S.-O. Lawesson, *Tetrahedron* **1981**, *37*, 3635–3639.
[5] a) M. Yokoyama, Y. Hasegawa, H. Hatanaka, Y. Kawazoe, T. Imamoto, *Synthesis* **1984**, 827–829; b) G. Lajoie, F. Lepine, B. Belleau, *Tetrahedron Lett.* **1983**, *24*, 3815–3818; c) H. Davy, *J. Chem. Soc. Chem. Commun.* **1982**, 457–458.
[6] a) O. E. Jensen, A. Senning, *Tetrahedron* **1986**, *42*, 6555–6564; b) D. B. Sherman, A. F. Spatola, *J. Am. Chem. Soc.* **1990**, *112*, 433–441; c) D. W. Brown, M. M. Campbell, M. S. Chambers, C. V. Walker, *Tetrahedron Lett.* **1987**, *28*, 2171–2174.
[7] C. F. Barbas III, J. R. Matos, J. B. West, C. H. Wong, *J. Am. Chem. Soc.* **1988**, *110*, 5162–5166.
[8] H. D. Jakubke in *The Peptides, Vol. 9* (Eds.: S. Udenfriend, J. Meienhofer), Academic Press, London, **1987**, pp. 103–165.
[9] G. Kloss, G. Schroeder, *Hoppe-Seyler's Z. Physiol. Chem.* **1964**, *336*, 248–256.
[10] H. Waldmann, H. Kunz, *Liebigs Ann. Chem.* **1983**, 1712–1725.
[11] H. Kunz, C. Unverzagt, *Angew. Chem.* **1984**, *96*, 426–427; *Angew. Chem. Int. Ed. Engl.* **1984**, *27*, 1697–1699.

2,4-Didehydrophenol—First Proof of a *meta*-Aryne by IR Spectroscopy**

By *Götz Bucher, Wolfram Sander,* Elfi Kraka,* and *Dieter Cremer**

Dedicated to Professor Günther Maier on the occasion of his 60th birthday

Since the pioneering work of Wittig et al.[1] arynes have enjoyed a special status in mechanistic and preparative organic chemistry.[2] This area has received added impetus re-

[*] Prof. W. Sander, Dipl.-Chem. G. Bucher
Institut für Organische Chemie der Technischen Universität
Hagenring 30, D-W-3300 Braunschweig (FRG)

Prof. D. Cremer, Prof. E. Kraka
Department of Theoretical Chemistry, University of Göteborg
Kemigården 3, S-41296 Göteborg (Sweden)

[**] This work was supported by the Deutsche Forschungsgemeinschaft, the Fonds der Chemischen Industrie, the Swedish Natural Science Research Council, and the Nationellt Superdatorcentrum (Linköping, Sweden).

cently from the discovery that derivatives of *p*-dehydrobenzene play an important role in the mechanism of action of the enediyne anticancer agents.[3] Although *o*-dehydrobenzene has been well characterized,[4] unequivocal spectroscopic evidence for *m*- and *p*-dehydrobenzene is lacking. 9,10-Dehydroanthracene is the only derivative of *p*-dehydrobenzene to be characterized by spectroscopy.[5] Both *m*- and *p*-dehydrobenzene have already been investigated by mass spectrometry and UV spectroscopy,[6a, b] but the methods employed did not allow a definite assignment of the UV spectra. Recently, the heats of formation of *o*-, *m*-, and *p*-dehydrobenzene determined by mass spectrometry by measurement of the collision-induced dissociation (CID) were shown to be 106 ± 3, 116 ± 3, and 128 ± 3 kcal mol^{-1}, respectively.[7] According to these results *m*- and *p*-dehydrobenzene should be isolable in a matrix. Ab initio investigations of the dehydrobenzenes have not thoroughly treated *m*- and *p*-dehydrobenzene.[8] The *ortho* isomer has received more attention; its harmonic oscillation frequencies have been determined on the GVB,[9] MP2, and TCSCF levels.[10] Here we report on the first direct IR spectroscopic proof of 2,4-didehydrophenol (**1**), an *m*-dehydrobenzene, by means of matrix isolation.[11, 12]

In connection with our work on the vinylcarbene–cyclopropene rearrangement[13, 14] we also examined 3-carboxy-4-oxo-2,5-cyclohexadienylidene (**2**) and the isotopomer deuterated at the carboxyl group, [D$_1$]**2**. Irradiation of quinone diazide **3**[11] in a matrix with visible light (argon, 10 K, $\lambda > 470$ nm) did not lead to the expected carbene **2**, but rather by cleavage of CO_2 to a new compound, which we identified as aryne **1** (see below). Carbene **2** may be obtained from **3** by narrow-band irradiation ($\lambda = 432 \pm 10$ nm, 90 min) and subsequently investigated by IR and UV/VIS spectroscopy.[15] Proof of the existence of **2** in the matrix was provided by the very characteristic formation of carbonyl oxide **4**[16] in the diffusion-controlled reaction with molecular oxygen.[17] Carbonyl oxide **4** rearranges upon long-wavelength irradiation ($\lambda > 515$ nm) into dioxirane **5**,[18] which is transformed in turn into a lactone[19] when irradiated with blue light ($\lambda > 400$ nm; Scheme 1).

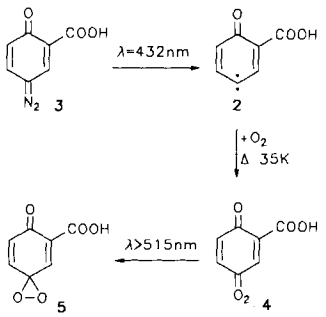

Scheme 1.

A notable feature in the IR spectrum of **2** is the low vibrational frequency of the C4 carbonyl group, which at 1415 cm^{-1} is red-shifted by 82 cm^{-1} relative to the parent compound **6**. This is evidence of the increased importance of the phenoxyl structure **2b** in describing the ground state of **2**. Structure **2b** is presumably stabilized by an intramolecular hydrogen bond. In the UV/VIS spectrum an absorption with a broad and very weak maximum at approximately 600 nm is observed as well as a narrow band with an absorption maximum at 390 nm , both characteristic for a 4-oxo-cyclohexadienylidene structure.[14, 20]

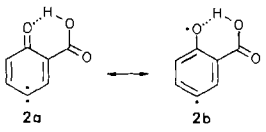

Irradiation of the long-wavelength absorption band of **2** ($\lambda = 575 \pm 10$ nm, 20 min) causes a rapid decarboxylation (intense absorption of CO_2 at 2347 cm^{-1}) and formation of a new compound, **1** (Scheme 2), with intense IR bands at

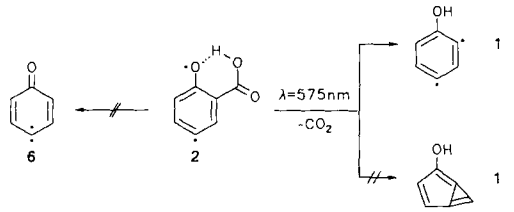

Scheme 2.

3612.0, 1516.3, 641.2, and 518.8 cm^{-1} (Fig. 1, Table 1). The IR bands assigned to **1** disappear upon irradiation with $\lambda > 420$ nm (see below).

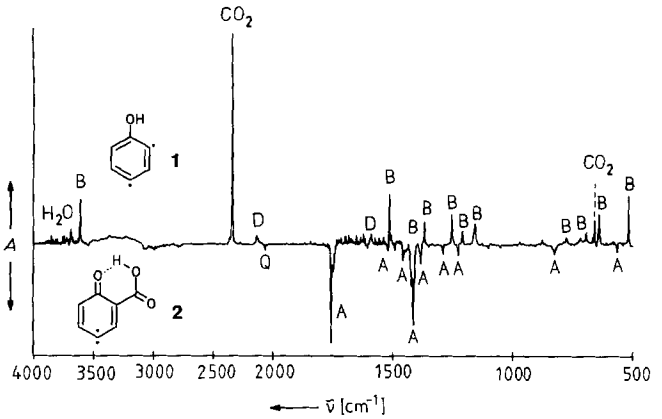

Fig. 1. Difference IR spectrum showing the photochemistry of carbene **2** ($\lambda = 575$ nm, Ar, 10 K). Bottom : bands that disappear upon irradiation; top: bands that arise. A: Carbene **2**, B: dehydrophenol **1**, D: unknown side product, Q: diazide.

The decarboxylation can also be observed in the UV/VIS spectrum: The bands assigned to carbene **2** disappear upon irradiation with $\lambda = 575 \pm 10$ nm, and a new band with a maximum at 344 nm and a shoulder at 356 nm arise.

Under the same conditions other 4-oxo-2,5-cyclohexadienylidenes undergo vinylcarbene–cyclopropene rearrangement to 1,3-bridged cyclopropenes;[13, 14] in our case this is of at most minor importance.[21] Irradiation of [D$_1$]**3**, the derivative of **3** deuterated on the carboxy group, provides a product with absorption bands at 3612.0 and 1157.6 cm^{-1} which are red-shifted relative to the non-deuterated product by 944 and 215 cm^{-1}, respectively. This allows the corresponding assignment of the O–H stretching and the C–O–H deformation vibrations. All the other IR bands show only small deuterium shifts. Analogous bands were observed for phenol at 3623 (− 973) cm^{-1} and 1180 (− 270) cm^{-1}, respectively, indicating the similarity of the hydroxyl groups in the decarboxylated product **1** and in phenol.

Table 1. IR spectroscopic data for 1.

Experiment $\tilde{\nu}$[cm^{-1}]	I [a]	$\tilde{\nu}_i/\tilde{\nu}$ [b]	GVB/6-31G(d,p) $\tilde{\nu}$[cm^{-1}] [c]	I [a]	$\tilde{\nu}_i/\tilde{\nu}$ [b]	Assignment [d]
3612.0	s	0.738	3776	0.85	0.728	ν_{27} (O-H, str.)
			1623	0.26	0.998	ν_{23}
1516.3	s	0.997	1551	0.64	0.998	ν_{22}
1429.0	w	0.982	1409	0.3	0.999	ν_{21}
1368.2	m	0.987	1386	0.46	0.981	ν_{20}
1290.1	w	0.979	1280	0.16	0.990	ν_{19}
1254.9	m	– [e]	1243	1.0	0.982	ν_{18}
1209.1	m	– [e]	1183	0.31	0.979	ν_{17}
1157.6	m	0.814	1117	0.55	0.815	ν_{16} (O-H, def.)
1128.6	vw	– [e]	1074	0.11	1.0	ν_{15}
971.0	w	1.008	979	0.1	1.0	ν_{14}
877.0	w	0.997	905	0.06	1.0	ν_{12}
–			819	0.76	1.0	ν_{10}
–			757	0.32	0.988	ν_9
694.7	m	0.981	–			
641.2	s	1.0	–			
518.8	s	0.984				
–			257	0.43	0.738	ν_1 (O-H, tors.)

[a] Relative intensities. [b] Ratio of the vibration frequencies $\tilde{\nu}_i/\tilde{\nu}$ upon deuteration. [c] Scaling factor 0.9. [d] Approximate assignment based on the positions and the relative intensities of the bands. [e] Because of the large changes in intensities upon deuteration, $\tilde{\nu}_i/\tilde{\nu}$ cannot be determined reliably.

This unequivocal proof of the presence of a hydroxyl group and the absence of a carbonyl group greatly reduces the number of possible structures for **1** with the molecular formula C_6H_4O. Because of the very mild conditions in the synthesis of **1** (irradiation with $\lambda = 575$ nm, 10 K), a rearrangement of the carbon framework or a ring opening can be ruled out. (These would also cause a loss of phenol character.) The remaining reasonable structures are 2,4-didehydrophenol (**1**) and its bicyclic isomer, bicyclo[3.1.0]hexa-1,3,5-trien-1-ol (**1'**) (Scheme 2).

According to calculations (GVB/6-31G(d,p)//HF/6-31G(d,p)), in the singlet ground state the monocyclic biradical structure **1** is 17 kcal mol^{-1} more stable than the bicyclic structure **1'**.[23] In the geometry optimizations with GVB/6-31G(d,p) as well as with MP2/6-31G(d,p), **1'** is converted to **1**, indicating that **1'** most likely does not exist. In the GVB equilibrium geometry of **1** the C_{2v}-symmetric carbon framework of 1,3-didehydrobenzene is only slightly perturbed by the OH substituent (which is also indicated by the small dipole moment of 0.7 D). Thus **1** offers a realistic insight into the bonding relationships in 1,3-didehydrobenzene. **1** is planar, and the OH group points in the direction of the neighboring radical center (Fig. 2). Examination of the calculated electron-density distribution shows that the OH group is held in the plane of the ring by the electrostatic attraction between the partially positively charged H atom and the neighboring radical center.

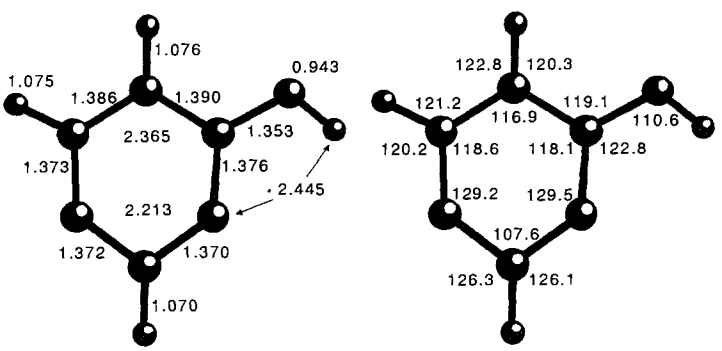

Fig. 2. Structure of 2,4-didehydrophenol (**1**) optimized by GVB/6-31G(d,p). Left, bond lengths [Å], right, bond angles [°].

An assignment of the experimental spectra to **1** or **1'** is possible by comparison with the calculated vibration spectra (Fig. 3). The calculated IR spectrum of **1** (GVB/6-31G(d,p,)) is in full agreement with the measured IR spectrum between 3600 and 800 cm^{-1}; only the bands at 641 and 519 cm^{-1} were not reproduced very well in the calculation. For [D_1]**1** the calculated isotopic shifts of 1027 and 207 cm^{-1} for the O–D stretching and the C–O–D deformation vibrations agree well with the corresponding experimental values (see Table 1).

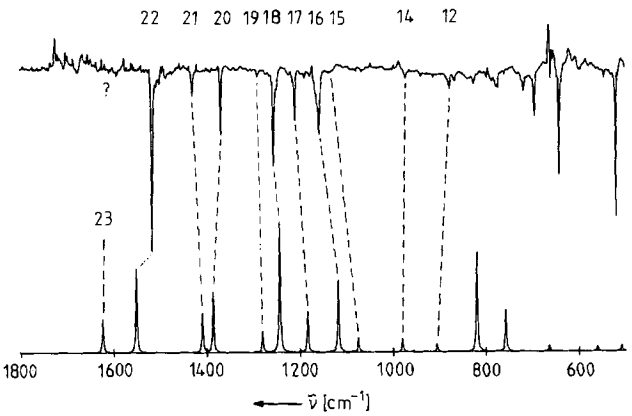

Fig. 3. Correlation between the experimental IR spectrum (top) and that calculated (GVB/6-31G(d,p); bottom). The assignment is only approximate and is based on the comparison of the positions and intensities of the bands. The calculated spectrum has been scaled by a factor of 0.9.

The alternative isomer, bicycle **1'**, can be ruled out by comparison of the experimental and theoretical spectra and by the fact that calculations with neither GVB nor with MP2 indicated its existence. The observed, intense long-wavelength absorption in the UV/VIS spectrum, which is about 80 nm red-shifted relative to the longest wavelength band for phenol, also supports to the diradical structure **1**.[25]

Dehydrophenol **1** is stable to irradiation with $\lambda > 570$ nm, but short-wavelength light ($\lambda > 420$ nm) will convert it into a ketene (IR, Ar, 10 K: $\tilde{\nu}$ = 2138.2 (s), 1419.4 (w), 1046.7 (w), 963.3 (w) cm^{-1}). Upon warming to 30 K in an O_2-doped matrix **1** reacts at a rate comparable to that of carbene **2** to give an oxidation product of unknown composition. Because of the small amount of **3** that could be sublimed into the matrix,[11] the ketene and the oxidation product of **1** could not be characterized further. However, the fast reaction with O_2 is further support for the diradical character of **1**. All experimental and theoretical findings can be explained only with the diradical structure **1**.

Received: March 10, 1992 [Z 5234 IE]
German version: *Angew. Chem.* **1992**, *104*, 1225

CAS Registry numbers:
1, 142746-79-0; **2**, 142746-80-3; **3**, 121-13-1; **4**, 142746-81-4; **5**, 142746-82-5.

[1] G. Wittig, *Naturwiss.* **1942**, 696.
[2] a) C. Grundmann, *Methoden Org. Chem. (Houben-Weyl)*, 4th ed. 1952-, Vol. 5, [Arene und Arine (Ed.: C. Grundmann)], pp. 613–648; b) R. W. Hoffmann, *Dehydrobenzene and Cycloalkynes* in *Organic Chemistry, Vol. 11* (Ed.: A. T. Blomquist), Academic Press, New York, **1967**.
[3] K. C. Nicolaou, W. M. Dai, *Angew. Chem.* **1991**, *103*, 1453; *Angew. Chem. Int. Ed. Engl.* **1991**, *30*, 1387.

[4] a) O. L. Chapman, K. Mattes, C. L. McIntosh, J. Pacansky, G. V. Calder, G. Orr, *J. Am. Chem. Soc.* **1973**, *95*, 6134; b) O. L. Chapman, C. C. Chang, J. Kolc, N. R. Rosenquist, H. Tomioka, *ibid.* **1975**, *97*, 6586; c) C. Wentrup, R. Blanch, H. Briehl, G. Gross, *ibid.* **1988**, *110*, 1874; d) J. G. G. Simon, N. Muenzel, A. Schweig, *Chem. Phys. Lett.* **1990**, *170*, 187; e) J. G. Radziszewski, B. A. Hess, Jr., R. Zahradnik, *J. Am. Chem. Soc.* **1992**, *114*, 52.

[5] O. L. Chapman, C. C. Chang, J. Kolc, *J. Am. Chem. Soc.* **1976**, *98*, 5703.

[6] a) R. S. Berry, J. Clardy, M. E. Schafer, *Tetrahedron Lett.* **1965**, *15*, 1011; b) *ibid.* **1965**, *15*, 1003.

[7] P. G. Wenthold, J. A. Paulino, R. R. Squires, *J. Am. Chem. Soc.* **1991**, *113*, 7414.

[8] J. O. Noell, M. D. Newton, *J. Am. Chem. Soc.* **1979**, *101*, 51.

[9] K. Rigby, I. H. Hillier, M. Vincent, *J. Chem. Soc. Perkin Trans.* **1987**, *2*, 117.

[10] A. C. Scheiner, H. F. Schaefer III, B. Liu, *J. Am. Chem. Soc.* **1989**, *111*, 3118.

[11] An APD closed-cycle helium cryostat was used in the matrix experiments (see ref.[12]). IR spectra were recorded with a Bruker IFS 66 spectrometer between 4000 and 500 cm^{-1} with a resolution of 1 cm^{-1}, UV/VIS spectra with an HP 8452A diode array spectrometer with a resolution of 2 nm. **3** was deposited in the matrix at 25–30 K, the photolyses and the recording of spectra were conducted at 10 K. Because of the low volatility and the low thermal stability of **3** (ref.[24]) only small amounts could be sublimed onto the matrix window. **3**: IR (Ar, 10 K): $\tilde{\nu}$ 2113.6 (s), 2092.9 (w), 2057.2 (vw), 1740.9 (w), 1595.8 (vs), 1564.0 (vw), 1535.1 (w), 1481.1 (m), 1473.3 (s), 1458.4 (w), 1379.3(m), 1335.0 (vw), 1260.3 (vw), 1204.3 (w), 1164.8 (s), 1127.2 (w), 838.9 (vw), 528.9 (vw) cm^{-1} (rel. intensity).

[12] For a description of the apparatus see W. Sander, *J. Org. Chem.* **1989**, *54*, 333.

[13] W. Sander, G. Bucher, F. Reichel, D. Cremer, *J. Am. Chem. Soc.* **1991**, *113*, 5311.

[14] a) G. Bucher, W. Sander, *J. Org. Chem.* **1992**, *57*, 1346; b) G. Bucher, W. Sander, *Chem. Ber.* **1992**, *125*, in press.

[15] **2**: IR (Ar, 10 K): $\tilde{\nu}$ = 1758.3 (vs, 0.994), 1750.1 (m, –), 1523.5 (w, –), 1495.0 (m, 0.998), 1458.9 (w, 0.999), 1422.2 (s, –), 1415.0 (vs, 1.000), 1383.7 (w, 1.000), 1291.6 (w, 1.001), 1228.9 (w, –), 1053.9 (vw, –), 982.6 (vw, –), 826.3 (w, –), 565.0 (vw, 1.000), 542.9 (vw, –) cm^{-1} (rel. intensity, $\tilde{\nu}/\tilde{\nu}_i$); UV/VIS (Ar, 10 K): ca. 600 (vw, br), 390 (m), 316 (s), 306 (s), 236 (vs) nm (rel. intensity).

[16] **4**: IR (Ar, 10 K): $\tilde{\nu}$ = 1772.7 (s), 1766.0 (s), 1607.9 (m), 1601.6 (s), 1598.7 (s), 1583.3 (m), 1578.0 (m), 1573.1 (m), 1406.8 (vs), 1219.3 (m), 1082.4 (s), 888.5 (w), 849.0 (m), 844.2 (m), 658.6 (m), 655.2 (m) cm^{-1} (rel. intensity).

[17] W. Sander, *Angew. Chem.* **1990**, *102*, 362; *Angew. Chem. Int. Ed. Engl.* **1990**, *29*, 344.

[18] **5**: IR (Ar, 10 K): $\tilde{\nu}$ = 1778 (vs), 1674.9 (s), 1657.0 (s), 1633.4 (w), 1405.9 (vs), 1395.2 (vs), 1391.9 (vs), 1321.5 (m), 1271.3 (vw), 1105.0 (m), 1039.0 (m), 1034.1 (m), 989.3 (vw), 953.1 (vw), 864.0 (w), 853.3 (m), 847.6 (m), 804.2 (w), 793.1 (w), 654.2 (m) cm^{-1} (rel. intensity).

[19] Because of the low concentration of **2** and the products of its subsequent reactions in the matrix, it was not possible to characterize unequivocally the isomeric lactones that formed. In the frequency range for carbonyl groups, absorptions were observed at 1783.8 (s, COOH), 1740.4 (s), 1724.5 (s), 1713.4 (s), 1672.9 (m), and 1623.8 (s) cm^{-1}. However, in analogy to the chemistry of *p*-benzoquinone-*O*-oxide, the formation of a 2,5-oxepinedione is expected (for the parent compound: $\tilde{\nu}$(C=O) at 1753 and 1660 cm^{-1}, ref.[13,14,20]).

[20] W. Sander, *J. Org. Chem.* **1988**, *53*, 2091.

[21] In the very slow decarboxylation with red light ($\lambda > 600$ nm) small amounts of an extremely photolabile compound also form with absorption bands between 1700 and 1800 cm^{-1}; this could be the cyclopropene.

[22] a) J. Gebicki, A. Krantz, *J. Am. Chem. Soc.* **1984**, *106*, 8093; b) J. H. S. Green, *J. Chem. Soc.* **1961**, 2236; c) G. T. Reedy, S. Bourne, P. T. Cunningham, *Anal. Chem.* **1979**, *51*, 1535; H. D. Bist, J. C. D. Brand, D. R. Williams, *J. Mol. Spectrosc.* **1967**, *24*, 402.

[23] GVB(1)/6-31G(d,p)//HF/6-31G(d,p) energies [Hartree]: −304.27655 (**1**), −304.248998 (**1'**); GVB(1)/6-31G(d,p): −304.27809 (**1**); RMP2/6-31G(D,p): −305.24500 (**1**). RMP2 and GVB geometries differ only slightly. Thus, the geometry does not depend on the calculational method. This does not hold for the reliable determination of relative energies and the vibration spectrum. In these cases an HF wave-function with corrections for dynamic correlation effects (estimated e.g. with MP2) is not sufficient. The GVB approximation is the simplest multiconfiguration (MC) method that provides a usable description of **1**. More exact data, especially for the low-frequency end of the IR spectrum, could be obtained with a larger MC formulation preferentially along with MP2 in order to account for both statistical and dynamic correlation effects.

[24] A. Rugeddi, *Gazz. Chim. Ital.* **1929**, 13.

[25] According to CNDO/S calculations the UV/VIS band of phenol with the longest wavelength λ_{max} lies at 282 nm, of **1a** at 362 nm. Another band calculated for **1** at λ_{max} = 476 nm is too weak in intensity to be observable under experimental conditions.

Hydride Transfer by Hydrido Transition-Metal Complexes. Ionic Hydrogenation of Aldehydes and Ketones, and Structural Characterization of an Alcohol Complex**

By *Jeong-Sup Song, David J. Szalda, R. Morris Bullock,* Christophe J. C. Lawrie, Mikhail A. Rodkin,* and *Jack R. Norton**

Transfer of hydrogen as a proton (H^+), hydrogen atom ($H^\cdot$), or hydride (H^-) is a decisive step in numerous catalytic and stoichiometric reactions utilizing metal hydrides.[1] The kinetics of proton transfer from metal hydrides[2] to metal-,[3] carbon-,[4] and nitrogen-centered[3] bases have been examined. Quantitative studies of the relative ability of carbonylhydridometal complexes to donate a hydrogen atom to olefins[5] or carbon-centered radicals[5, 6] have recently been reported. However, the little that is known about hydride transfer largely concerns substrates already coordinated to the metal atom.[7–9]

Direct hydride transfer to an uncoordinated substrate appears to be involved in the hydrogenation of sterically hindered olefins by transition-metal hydrides and triflic acid (CF_3SO_3H).[10] Such ionic hydrogenations (the addition to a double bond of H^+ from one source and H^- from another) are common in biological systems,[11] and probably occur in other organometallic reactions, e.g., the hydrogenation of aldehydes and/or ketones by acids and $[Mo_2(CO)_{10}(\mu\text{-H})]^-$,[12] $[Cr(CO)_5H]^-$,[13] $[Ru(bpy)_2(CO)H]^+$ (bpy = 2,2'-bipyridine),[14] $[Cp_2MoH_2]$,[15] or $[Cp_2Ta(CO)H]$.[16] These reactions offer a remarkable instance of kinetic selectivity: the H^+ and H^- are transferred to the same substrate more rapidly than they react with each other to form hydrogen gas.[17–19] In this communication we report on the scope and mechanism of the ionic hydrogenation of aldehydes and ketones by transition-metal hydrides and acids, and on the structure of the hydrogen-bonded alcohol complex that is formed upon hydrogenation of acetone with CF_3SO_3H and the hydrido tungsten complex **1a**.

When a pale yellow CD_2Cl_2 solution of acetone (0.10 M) and **1a** (1.5 equiv.) is treated with CF_3SO_3H (2 equiv.) at room temperature, the color changes to burgundy-red in less than 5 minutes, and the tungsten complex **2** is formed in quantitative (^1H NMR) yield [Eq. (a)]. The proton of the hydroxyl group of **2** gives rise to a doublet (J_{HH} = 7.6 Hz) at δ = 6.29 (^1H NMR in CD_3NO_2), significantly downfield from the position reported for the signal of the hydroxyl proton in the analogous complex with SbF_6 as counterion (δ = 4.90 in CD_3NO_2).[20] This shift suggests formation of hydrogen bond between the triflate anion and the alcohol ligand. A single-crystal X-ray diffraction study[21, 25] of **2** has verified that such a hydrogen bond is present in the solid state (Fig. 1). Especially informative in this connection is the short O···O distance of 2.63(1) Å, similar to the O–H···O distances found in other organometallic complexes that exhibit hydrogen bonding.[22] Only a few other alcohol com-

[*] Dr. R. M. Bullock, Dr. J.-S. Song, Dr. D. J. Szalda[+]
Department of Chemistry, Brookhaven National Laboratory
Upton, NY 11973 (USA)
Prof. J. R. Norton, Dr. C. J. C. Lawrie, Dr. M. A. Rodkin
Department of Chemistry, Colorado State University
Fort Collins, CO 80523 (USA)
[+] Permanent address: Baruch College
New York, NY 10010 (USA)

[**] This work was supported by the U.S. Department of Energy, Division of Chemical Sciences, Office of Basic Energy Sciences (DE-AC02-76CH00016, Brookhaven National Laboratory) and by the National Science Foundation (Grant CHE-9120454, Colorado State University).

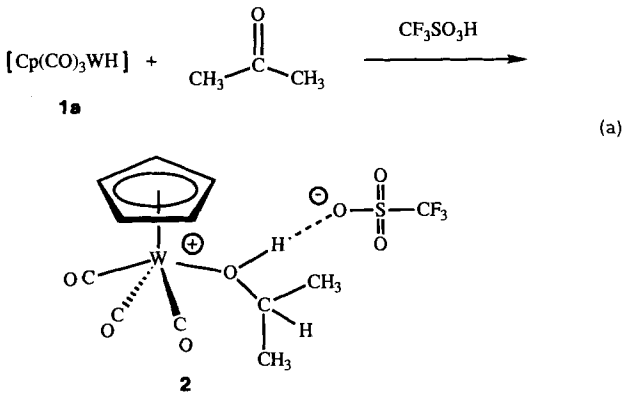

plexes with low-valent metal centers are known,[20, 23] and structural data for this unusual class of compounds are very scarce.

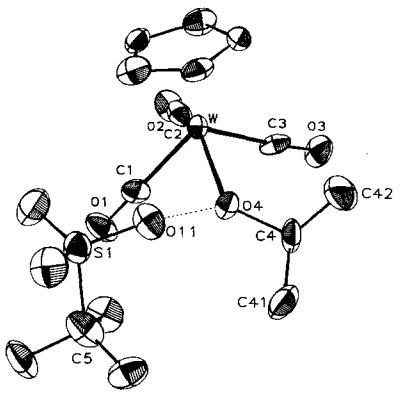

Fig. 1. ORTEP drawing of **2** showing 50% probability thermal ellipsoids. Selected bond lengths [Å] and angles [°]: O(4)···O(11) 2.63(1); W-C(1) 2.01(2); W-C(2) 1.99(2); W-C(3) 1.99(2); W-O(4) 2.186(9); O(4)-C(4) 1.47(2); C(1)-W-C(2) 76.1(5); C(2)-W-C(3) 77.2(6); C(1)-W-C(3) 110.6(6); C(2)-W-O(4) 139.8(5); C(1)-W-O(4) 78.2(5); C(3)-W-O(4) 83.7(4); W-O(4)-C(4) 131.2(7).

A variety of coordinatively saturated hydrido transition-metal complexes can serve as hydride donors in such reactions, examples being $[CpM(CO)_3H]$ (M = W, Mo), $[M(CO)_5H]$ (M = Mn, Re), and $[CpRe(NO)(PPh_3)H]$; in none of the cases examined does the hydride react with the ketone in the absence of acid. Ionic hydrogenation can also occur with acids of considerably different strengths (CF_3CO_2H, p-$CH_3C_6H_4SO_3H$, $C_6F_5CO_2H$, and CF_3SO_3H). With CF_3SO_3H/**1a** hydrogenation of propionaldehyde, 2-butanone, methyl benzyl ketone, 2,3-butanedione, adamantanone, or cyclohexanone gave high yields (>95% by NMR in CD_2Cl_2) of the $[Cp(CO)_3W(HOR)][OTf]$ complexes **3** with-in 5 minutes at room temperature, using 1.5–2 equivalents of both acid and hydride. For the synthesis of complexes **3**, typically about 1.5 equivalents of ketone (or aldehyde) and acid and 1 equivalent of **1a** were used; complexes **3** were obtained in 43–78% yield.

Despite the fact that these tungsten alcohol complexes can be isolated, they decompose slowly in solution, giving the free alcohol and the tungsten triflate complex $[CpW(CO)_3(OTf)]$ **4**. The decomposition half-life is about 14 hours at room temperature in CD_2Cl_2. The fact that an alcohol complex, rather than the more stable complex **4**, is the kinetic product suggests some W–O bond formation in the transition state of the hydride transfer.

When $(CH_3)_2CHCHO$ (0.049 M) was treated with excess $[CpMo(CO)_3H]$ **1b** (0.9 M) in the presence of CF_3CO_2H (0.23 M), at −30 °C in CD_2Cl_2, the apparent first-order rate constant k_{obs} for the disappearance of the aldehyde decreased as the reaction proceeded. However, with the acidity held constant by a quinuclidine-quinuclidinium buffer (total $[CF_3CO_2H] = 0.58$ M, total [quinuclidine] = 0.13 M), the rate of disappearance of the aldehyde was cleanly pseudo-first-order. The observed rate constant k_{obs} proved to be proportional to the concentration of **1b**, indicating that the reaction obeyed the rate law given in Equation (b). At −30 °C, $k = 3.5 \times 10^{-4}\ M^{-1}s^{-1}$.

$$\frac{-d[(CH_3)_2CHCHO]}{dt} = k[(CH_3)_2CHCHO][\mathbf{1b}] \qquad (b)$$

These results suggest that the reaction proceeds by rate-determining hydride transfer from the coordinatively saturated transition-metal hydride to the protonated form of the aldehyde or ketone [Eq. (c) and (d)]. This mechanism ac-

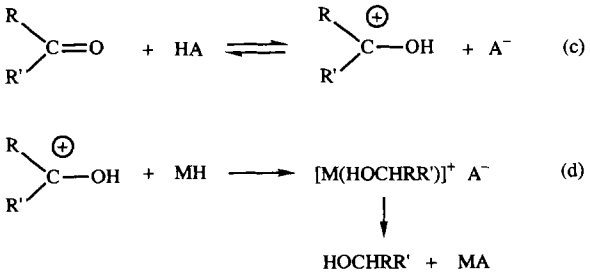

counts for the decrease of k_{obs} with time in the unbuffered reaction; since the reaction consumes protons as it proceeds, k_{obs} (which is a function of the acidity because it includes the equilibrium constant for Eq. (c)) will decrease. The acids effective in this hydrogenation range from those that protonate only a small amount of aldehyde at equilibrium (CF_3CO_2H) to strong acids (CF_3SO_3H) that protonate most of the aldehyde.

When p-$CH_3C_6H_4SO_3H$ is added to pivaldehyde and $[CpRe(NO)(PPh_3)H]$ in CH_2Cl_2, neopentyl alcohol is the only organic product formed. This implies that hydride transfer to the protonated pivaldehyde is occurring faster than the rearrangement of the protonated aldehyde to protonated isopropyl methyl ketone. The rate constant for this rearrangement has been estimated[24] as 0.6 s^{-1} at 25 °C in FSO_3H.

Selective incorporation of deuterium into the product alcohol can be effected under certain conditions, using deuterium labels on either the hydride or acid. For example, CH_3CHDOH results from ionic hydrogenation of acetaldehyde using $[CpMo(CO)_3D]$ and CF_3CO_2H. D^- transfer is thus faster than H/D exchange between the deuterido complex and trifluoroacetic acid under these conditions.[25]

Experimental Procedure

CF_3SO_3H (100 μL, 1.1 mmol) was added to a solution of **1a** (300 mg, 0.9 mmol) and acetone (80 μL, 1.1 mmol) in CH_2Cl_2 (10 mL) under Ar. The solution was stirred for 30 min at 22 °C, during which time the solution became burgundy-red. Et_2O (20 mL) and hexane (10 mL) were added by vacuum transfer, and the dark red microcrystalline product **2** (380 mg; 78%) was collected by filtration. ^1H NMR (CD_2Cl_2): $\delta = 7.49$ (d, $J = 7.3$ Hz, 1H, OH), 6.04 (s, 5H, Cp), 3.58 (d of septets, $J = 7.3$ Hz, 6.3 Hz, 1H, CH), 1.15 (d, $J = 6.3$ Hz, 6H, CH_3). ^{13}C NMR (CD_2Cl_2, 200 K): $\delta = 225.0$ (CO), 222.3 (2CO), 94.9 (Cp), 83.8 (CH), 22.2 (CH_3). IR (KBr): $\tilde{\nu}$ [cm^{-1}] = 3444 (w, br; OH), 2062 (vs; CO), 1983 (vs), 1953 (vs); 1022 (s; CO); correct C,H analysis.

Received: April 2, 1992 [Z 5273 IE]
German version: *Angew. Chem.* **1992**, *104*, 1280

CAS Registry numbers:
1a, 12128-26-6; **1b**, 12176-06-6; **2** (*i*Pr), 142866-81-7; **2** (Pr), 142866-83-9; **2** (*s*Bu), 142842-25-9; **2** [$CH(CH_3)CH_2Ph$], 142842-27-1; **2** [$CH(CH_3)COCH_3$], 142842-29-3; **2** (2-adamantyl), 142842-31-7; **2** (C_6H_{11}), 142842-33-9; CF_3SO_3H, 1493-13-6; CF_3CO_2H, 76-05-1; *p*-$CH_3C_6H_4SO_3H$, 104-15-4; $C_6F_5CO_2H$, 602-94-8; $HReCp(NO)(PPh_3)$, 79919-58-7; acetone, 67-64-1; propionaldehyde, 123-38-6; 2-butanone, 78-93-3; methyl benzyl ketone, 103-79-7; 2,3-butandione, 431-03-8; adamantanone, 700-58-3; cyclohexanone, 108-94-1; pivalinaldehyde, 630-19-3; neopentylalcohol, 75-84-3.

[1] For a recent comparison of H^- transfer reactions with H· and H^+ transfer reactions, see: R. M. Bullock, *Comments Inorg. Chem.* **1991**, *12*, 1–33.

[2] S. S. Kristjánsdóttir, J. R. Norton in *Transition Metal Hydrides* (Ed.: A. Dedieu), VCH, New York, **1991**, Chapter 9.

[3] a) R. T. Edidin, J. M. Sullivan, J. R. Norton, *J. Am. Chem. Soc.* **1987**, *109*, 3945–3953; b) S. S. Kristjánsdóttir, J. R. Norton, *ibid.* **1991**, *113*, 4366–4367.

[4] R. M. Bullock, *J. Am. Chem. Soc.* **1987**, *109*, 8087–8089.

[5] R. M. Bullock, E. G. Samsel, *J. Am. Chem. Soc.* **1990**, *112*, 6886–6898.

[6] D. C. Eisenberg, C. J. C. Lawrie, A. E. Moody, J. R. Norton, *J. Am. Chem. Soc.* **1991**, *113*, 4888–4895.

[7] J. A. Labinger in *Transition Metal Hydrides* (Ed.: A. Dedieu), VCH, New York, **1991**, Chapter 10. Recent examples of the insertion of ketones into the M–H bonds of coordinatively unsaturated metal hydrides include reactions of acetone with $[Re_3(H)(\mu OiPr)_3(OiPr)_5]$ [8] and $[Os(H)Cl(CO)(PiPr_3)_2]$ [9].

[8] D. M. Hoffman, D. Lappas, D. A. Wierda, *J. Am. Chem. Soc.* **1989**, *111*, 1531–1533.

[9] M. A. Esteruelas, C. Valero, L. A. Oro, U. Meyer, H. Werner, *Inorg. Chem.* **1991**, *30*, 1159–1160.

[10] R. M. Bullock, B. J. Rappoli, *J. Chem. Soc. Chem. Commun.* **1989**, 1447–1448.

[11] C. Walsh, *Enzymatic Reaction Mechanisms*, Freeman, San Francisco, **1979**, Chapter 10.

[12] D. H. Gibson, Y. S. El-Omrani, *Organometallics* **1985**, *4*, 1473–1475.

[13] P. L. Gaus, S. C. Kao, K. Youngdahl, M. Y. Darensbourg, *J. Am. Chem. Soc.* **1985**, *107*, 2428–2434.

[14] S. M. Geraty, P. Harkin, J. G. Vos, *Inorg. Chim. Acta* **1987**, *131*, 217–220.

[15] T. Ito, M. Koga, S. Kurishima, M. Natori, N. Sekizuka, K. Yoshioka, *J. Chem. Soc. Chem. Commun.* **1990**, 988–989.

[16] J.-F. Reynoud, J.-F. Leboeuf, J.-C. Leblanc, C. Moïse, *Organometallics* **1986**, *5*, 1863–1866.

[17] Although the kinetic barrier to protonating a monohydride complex H–M at M [2], or evolving H_2 gas from H^+ and H–M, is usually substantial, there is evidence that the formation of *dihydrogen complexes* from H^+ and H–M is kinetically facile [2]. The existence of facile equilibria between H–M/H^+ and the corresponding dihydrogen complexes suggests that the hydrogenations with dihydrogen complexes (of acetone with $[(H_3N)_5Os(\eta^2\text{-}H_2)]^{3+}$ [18], and of dimethyl maleate with $[(P(CH_2CH_2PPh_2)_3)Co(\eta^2\text{-}H_2)]^+$ [19]) may occur by ionic mechanisms.

[18] W. D. Harman, H. Taube, *J. Am. Chem. Soc.* **1990**, *112*, 2261–2263.

[19] C. Bianchini, C. Mealli, A. Meli, M. Peruzzini, F. Zanobini, *J. Am. Chem. Soc.* **1988**, *110*, 8725–8726.

[20] K. Sünkel, G. Urban, W. Beck, *J. Organomet. Chem.* **1985**, *290*, 231–240.

[21] Crystal data for $[(C_5H_5)(CO)_3W(HOCH(CH_3)_2)(OSO_2CF_3)]$, monoclinic space group $P2_1/n$ (a non-standard setting of $P2_1/c$, No. 14), $a = 8.139(1)$ Å, $b = 20.906(5)$ Å, $c = 10.516(2)$ Å, $\beta = 113.22(2)°$, $V = 1644(7)$ Å^3, $Z = 4$, $\rho_{calcd} = 2.190$ g cm^{-3}, Enraf-Nonius CAD-4 diffractometer, $\mu = 76.2$ cm^{-1} ($Mo_{K\alpha}$), analytical absorption correction, 200 K, $2\theta_{max} = 60°$, 5240 reflections measured, 2684 with $F_0 > 3\sigma(F_0)$, variables = 218. Heavy atom solution, full matrix least squares refinement (SHELX-76), all non-hydrogen atoms anisotropic thermal parameters, all hydrogens placed at calculated positions (except for the hydrogen on the oxygen of the isopropyl alcohol ligand, which could not be found). $R = 0.056$, $R_w = 0.072$. Further details of the crystal structure investigation are available on request from the Director of the Cambridge Crystallographic Data Centre, University Chemical Laboratory, Lensfield Road, Cambridge CB2 1EW, UK, on quoting the full journal citation.

[22] S. E. Kegley, C. J. Schaverien, J. H. Freudenberger, R. G. Bergman, S. P. Nolan, C. D. Hoff, *J. Am. Chem. Soc.* **1987**, *109*, 6563–6565 and references cited therein.

[23] S. K. Agbossou, W. W. Smith, J. A. Gladysz, *Chem. Ber.* **1990**, *123*, 1293–1299 and references cited therein.

[24] D. M. Brouwer, J. A. van Doorn, *Rec. Trav. Chim.* **1971**, *90*, 1010–1026.

[25] Note added in proof (August 11, 1992): J. Milke, C. Missling, K. Sünkel, W. Beck have characterized a similar alcohol complex, $[Cp(CO)(PPh_3)Ru(HOEt)]^+BF_4^-$, by X-ray crystallography (submitted to *J. Organomet. Chem.*). The results indicate that a hydrogen bond is formed between the hydrogen atom of the hydroxyl group and one of the F atoms of the BF_4^- ion. We thank Prof. W. Beck for a preprint of this paper.

$[Nb\{B(\eta^6\text{-}C_6H_5)_2(C_6H_5)_2\}(\eta^2\text{-}H_3CC_2CH_3)]$: the First Compound with Bent Tetraphenylborate as 12-Electron Donor Ligand**

By *Fausto Calderazzo, Ulli Englert, Guido Pampaloni,** and *Lucia Rocchi*

We recently reported a simple synthesis of the metallocene $[Nb(\eta^6\text{-mes})_2]$, (mes = 1,3,5-trimethylbenzene) and demonstrated that this compound opens up a convenient entry to niobium(I) systems.[1] Herein we report on the preparation of the niobium complexes **1** and on their thermal conversion into the complexes **2**.

$[Nb(\eta^6\text{-mes})_2(RC_2R)]BPh_4$ **1** $[Nb\{B(\eta^6\text{-}C_6H_5)_2(C_6H_5)_2\}(\eta^2\text{-}RC_2R)]$ **2**

a, R = CH_3; **b**, R = C_6H_5

Oxidation of $[Nb(\eta^6\text{-mes})_2]$ with $[FeCp_2]BPh_4$ in toluene, followed by treatment with a stoichiometric amount of alkyne, affords red to brown microcrystalline solids which are sparingly soluble in the reaction medium and were identified by IR spectroscopy as **1a,b** ($\tilde{\nu}_{CC} = 1818$ and 1767 cm^{-1} for **1a** and **1b**, respectively).

$$[Nb(\eta^6\text{-mes})_2] \xrightarrow{[FeCp_2]BPh_4} [Nb(\eta^6\text{-mes})_2]BPh_4 \xrightarrow{RC_2R} \mathbf{1} \qquad \text{(a)}$$

Upon heating **1** in toluene at ca. 100 °C, red to orange solutions were obtained, which, after filtration from black pyrophoric materials, concentration, and cooling at ca. −30 °C, deposited red to orange crystals of compounds **2**.

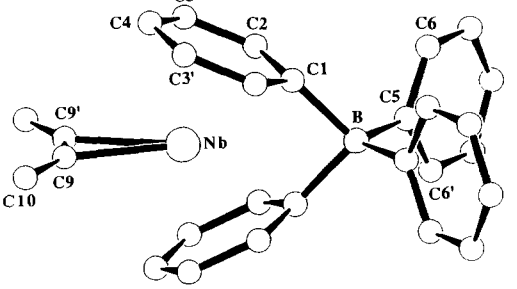

Fig. 1. SCHAKAL drawing of the crystal structure of **2a**. Selected bond lengths [Å] and angles [°]: Nb-C1, 2.369(3); Nb-C2, 2.373(2); Nb-C3, 2.420(2); Nb-C4, 2.420(1); C-C(η^6-C_6H_5, mean value), 1.419(3); C-C(other rings, mean value), 1.392(3); B-C1, 1.653(3); B-C5, 1.631(3); C5-B-C5', 112.8. For further data see text.

The structure of **2a** in the crystal[21] is shown in Figure 1. The niobium(I) atom is coordinated by two of the four phenyl rings of the tetraphenylborato ligand: the mean arene(centroid)–Nb distance is 1.931 Å, and the angle

[*] Dr. G. Pampaloni, Prof. F. Calderazzo, Dr. L. Rocchi
Dipartimento di Chimica e Chimica Industriale
Via Risorgimento 35, I-56126 Pisa (Italy)
Dr. U. Englert
Institut für Anorganische Chemie der Technischen Hochschule
Professor-Pirlet-Strasse 1, D-W-5100 Aachen (FRG)

[**] This work was supported by the Consiglio Nazionale delle Ricerche (CNR, Roma), and the Ministero dell'Università e della Ricerca Scientifica e Tecnologica (MURST).

formed between the arene centroids and the niobium atom is 131.6° (for comparison: 1.92 Å (mean value) and 147.7° in $[Nb(\eta^6\text{-mes})_2(CO)]BPh_4$[1b] and 1.91 Å (mean value) and 142.3° in $[Nb(\eta^6\text{-toluene})_2(PEt_3)]BF_4$[5]). The boron atom has a distorted tetrahedral geometry; the C1–B–C1′ angle is 92.3°.

The distances C9–C9′ [1.219(1) Å] and the Nb–C9 [2.269(3) Å] and the C10–C9–C9′ angle [150.8(3)°] are typical for niobium(I)–alkyne interaction with the alkyne behaving as a two-electron donor;[6] in contrast, longer C–C distances and shorter niobium(I)–carbon distances are generally observed in other disubstituted acetylene complexes,[7, 8] particularly when the ligand behaves as a four-electron donor.

Coordination of one[9] or more than one,[10] of the phenyl rings of the tetraphenylborate to transition metals in a 1:1 ratio has been reported in the literature; examples are $[Co\{B(\eta^6\text{-}C_6H_5)(C_6H_5)_3\}(py)_2]$[9b] and $[\{RuCp^*(\eta^6\text{-}C_6H_5)\}_4B]^{3+}$.[10] In the case of $Si(C_6H_5)_4$[11] two of the phenyl rings were found to be coordinated to the same metal atom in $[M\{Si(\eta^6\text{-}C_6H_5)_2(C_6H_5)_2\}]$, M = V, Cr.

To the best of our knowledge, compound **2** represents the first example of a metal complex containing two phenyl rings of the tetraphenylborate ligand coordinated to the same metal cation. The presence of the formal negative charge on the BPh_4^- ligand is important since its removal from the coordination sphere can be carried out only by ionization or by reduction in the presence of competitive ligands.

Experimental Procedure

2a: A suspension of **1a** (0.774 g, 1.09 mmol) in toluene (100 mL) was heated at 100 °C for 15 min and filtered. The volume of the orange-brown filtrate was reduced to ca. 25 mL, and the solution cooled at ca. −30 °C. Red crystals of **2a** (0.07 g) were isolated and dried in vacuo. Another crop of crystals (0.065 g) was isolated by further reduction of the volume of the solution to ca. 5 mL to give a total yield of 0.135 g (26%).—IR (nujol and poly(chlorotrifluoroethylene)): $\tilde{\nu}$ [cm^{-1}] = 3067w, 3047m, 2963m, 1919m, 1591s, 1481m, 1425s, 1347w, 1276w, 1261m, 1159m, 1089m, 1015m, 803m, 752s, 709s, 589m. Correct C, H and Nb elemental analyses.

Received: April 7, 1992 [Z 5286 IE]
German version: *Angew. Chem.* **1992**, *104*, 1230

[1] a) F. Calderazzo, G. Pampaloni, L. Rocchi, J. Strähle, K. Wurst, *Angew. Chem.* **1991**, *103*, 109–110; *Angew. Chem. Int. Ed. Engl.* **1991**, *30*, 102–103; b) *J. Organomet. Chem.* **1991**, *413*, 91–109; c) F. Calderazzo, F. Gingl, G. Pampaloni, L. Rocchi, J. Strähle, *Chem. Ber.*, **1992**, 125, 1005–1010.

[2] ENRAF-Nonius CAD4; $Mo_{K\alpha}$ radiation ($\lambda = 0.7093$ Å), graphite monochromator, empirical absorption correction (ψ-scans [3]); intensity data collected with the ω-scan method at room temperature. Crystal data for **2a**: crystal dimensions [mm]: 0.5 × 0.3 × 0.2, tetragonal, space group $P\bar{4}2_1m$ (No. 113); $a = 9.734(1)$, $c = 11.633(1)$ Å, $V = 1102.3(3)$ Å^3, $Z = 2$, $\rho_{calc} = 1.405$ g cm^{-3}, $\mu(Mo_{K\alpha}) = 5.331$ cm^{-1}; $F(000) = 480$; 6183 reflections in the scan range $3 < \theta < 29°$, 5570 with $I \geq 3\sigma(I)$, 1444 independent reflections with $I > 3\sigma(I)$ in structure solution and refinement [4] for 81 parameters. The point symmetry of the molecule is 2 *mm*; $R = 0.022$; $R_w = 0.031$; $w^{-1} = 1/\sigma^2(F_o)$, GOF = 1.115; anisotropic refinement for non-hydrogen atoms, hydrogen atoms from difference Fourier map in structure factor calculations. Highest residual electron density = 0.4 e Å^{-3}. Further details of the crystal structure determination are available on request from the Fachinformationszentrum Karlsruhe, Gesellschaft für wissenschaftlich-technische Information mbH, D-W-7514 Eggenstein-Leopoldshafen 2 (FRG), on quoting the depository number CSD-56367, the names of the authors, and the journal citation.

[3] A. C. T. North, D. Phillips, F. C. Mathews, *Acta Crystallogr. Sect. A* **1968**, *24*, 351–359.

[4] B. A. Frenz, *The Enraf-Nonius CAD4-SDP* (Hrsg.: H. Schenk, R. Olthof-Hazekamp, R. van Konigsveld, G. C. Bassi), Delft University Press, Delft, Netherlands, **1978**, p. 64; SDP-PLUS, Version 1.1, **1984**, und VAXSDP, Version 2.2, **1985**.

[5] J. A. Bandy, K. Prout, F. G. N. Cloke, H. C. de Lemos, J. M. Wallis, *J. Chem. Soc. Dalton Trans.* **1988**, 1475–1478.

[6] A. N. Nesmeyanov, A. I. Gusev, A. A. Pasynskii, K. N. Anisimov, N. E. Kolobova, Yu. T. Struchkov, *Chem. Commun.* **1969**, 739–740.

[7] A. N. Nesmeyanov, A. I. Gusev, A. A. Pasynskii, K. N. Anisimov, N. E. Kolobova, Yu. T. Struchkov, *Chem. Commun.* **1969**, 277–278; N. I. Kirillova, N. E. Kolobova, A. I. Gusev, A. B. Antonova, Yu. T. Struchkov, K. N. Anisimov, O. M. Khitrova, *Zh. Strukt. Khim.* **1974**, *15*, 651–658 [*Chem. Abstr.* **1974**, *81*, 142416 m].

[8] R. N. Vrtis, S. Liu, C. P. Rao, S. G. Bott, S. J. Lippard, *Organometallics* **1991**, *10*, 275–285; M. J. McGeary, A. S. Gamble, J. L. Templeton, *ibid.* **1988**, *7*, 271–279; P. A. Bianconi, R. N. Vrtis, K. P. Rao, I. D. Williams, M. P. Engeler, S. J. Lippard, *ibid.* **1987**, *6*, 1968–1977.

[9] See, for example: a) B. J. Thomas, S. K. Noh, G. K. Schulte, S. C. Sendlinger, K. H. Theopold, *J. Am. Chem. Soc.* **1991**, *113*, 893–902; b) G. Fachinetti, T. Funaioli, P. F. Zanazzi, *J. Chem. Soc. Chem. Commun.* **1988**, 1100–1101; c) R. D. Rogers, D. C. Hrncir, *Acta Crystallogr. Sect. C* **1984**, *40*, 1160–1161; d) P. Albano, M. Aresta, M. Manassero, *Inorg. Chem.* **1980**, *19*, 1069–1072; e) M. B. Hossain, D. van der Helm, *ibid.* **1978**, *17*, 2893–2900; f) G. J. Kruger, A. L. du Preez, R. J. Heines, *J. Chem. Soc. Dalton Trans.* **1974**, 1302–1305.

[10] P. J. Fagan, M. D. Ward, J. C. Calabrese, *J. Am. Chem. Soc.* **1989**, *111*, 1698–1719.

[11] C. Elschenbroich, J. Hurley, B. Metz, W. Massa, G. Baum, *Organometallics* **1990**, *9*, 889–897.

Alkyne(carbene) Complexes: Stabilization of an Intermediate of Carbene Annelation**

By *Karl Heinz Dötz,* Thomas Schäfer, Friedrich Kroll,* and *Klaus Harms*

Stable carbene complexes of the Fischer type are proving increasingly attractive reagents for organic synthesis.[1] Apart from established reaction patterns such as the cyclopropanation[2] and the Diels–Alder reaction,[3] they also undergo "nonclassical" cycloadditions, whose steps take place at the metal-template center.[4] A typical example for this is the chromium-induced coupling of an unsaturated carbene ligand with an alkyne and—in some cases—carbon monox-

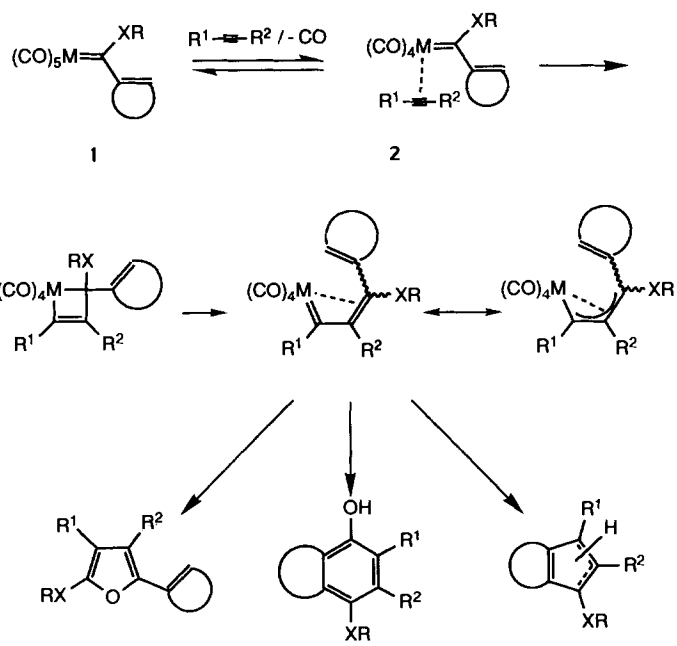

Scheme 1. M = Cr, Mo, W; X = O, NR, S.

[*] Prof. Dr. K. H. Dötz, Dr. T. Schäfer, F. Kroll, K. Harms
Fachbereich Chemie der Universität
Hans-Meerwein-Strasse, D-W-3550 Marburg (FRG)

[**] Reactions of complex ligands, part 53. This work was supported by the Deutsche Forschungsgemeinschaft (SFB 260), the Gradiertenkolleg "Metallorganische Chemie" and the Fonds der Chemischen Industrie.- Part 52: K. H. Dötz, A. Rau, K. Harms, *J. Organomet. Chem*, in press.

ide, which leads selectively to carbene annelation or to other cycloaddition products.[5]

According to a plausible proposal for the mechanism of the reaction based on the results of earlier kinetic investigations,[6] the reaction begins with the reversible decarbonylation of the pentacarbonyl(carbene) complex **1**, followed by the coordination of the alkyne.[7] Thereafter the alkyne(carbene) complex **2** undergoes a ligand coupling, as a result of which a σ,π allyl complex (alkyne insertion into the metal–carbene bond)[8] and a metallacyclobutene (alkyne addition to the metal–carbene bond)[9] are discussed. This step determines the regioselectivity with which the alkyne is incorporated into the final product (Scheme 1).

It has so far not been possible to isolate the alkyne(carbene) complex intermediate **2**, in which the alkyne behaves as a *two*-electron ligand, or to characterize it directly by spectroscopy;[10] a small metal–alkyne interaction was expected from calculations.[8, 9] We have now attempted to suppress the alkyne–carbene coupling by linking these two functions by a rigid C_2 arene bridge in the *ortho*-alkynyl carbene complex **3**. Here an insertion of the alkyne into the metal–carbene bond could occur only at the expense of the formation of an energy-rich benzocyclobutadiene intermediate (Scheme 2).

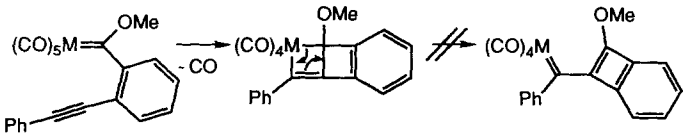

3

Scheme 2.

The *photochemically* induced low-temperature decarbonylation of the pentacarbonyl(*ortho*-alkynylarylcarbene) complexes of chromium and tungsten **3a,c** (accessible by the classical Fischer route[11]) affords the alkyne(carbene) complexes **4a,c**. In contrast, the molybdenum complex **3b** can be decarbonylated in a dark reaction under reduced pressure at 45 °C to give **4b** (Scheme 3). The X-ray structural analysis of the tungsten complex **4c**[12] (Fig. 1) shows unusually long

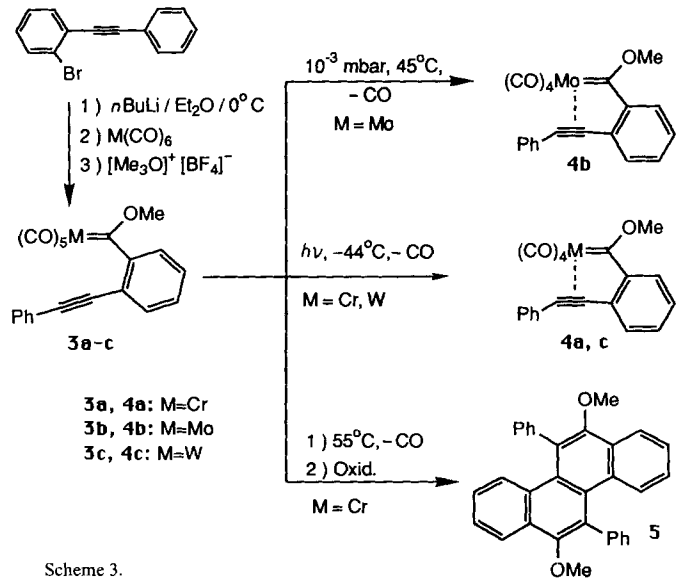

Scheme 3.

metal–C_{alkyne} distances (ca. 2.40 and 2.36 Å),[10] whereas the C_{alkyne}–C_{alkyne} bond (ca. 1.22 Å) is only lengthened slightly upon coordination. Together with the almost identical ^{13}C NMR chemical shifts for the alkyne carbon atoms in **3c** and **4c**,[13] these results prove a very weak coordination of the alkyne ligand.

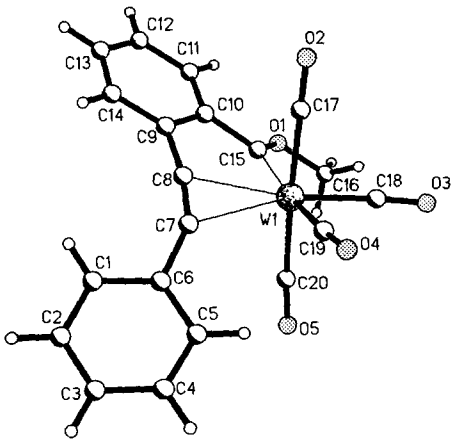

Fig. 1. Crystal structure of **4c**. Selected bond lengths [Å] and angles [°]: W1-C7 2.402(4), W1-C8 2.368(4), W1-C15 2.181(5), W1-C17 2.024(7), W1-C18 1.974(5), W1-C19 2.040(7), W1-C20 1.995(7), C7-C8 1.224(7), C15-O1 1.314(6); C7-W1-C8 29.7(2), C15-W1-C19 169.2(3), C17-W1-C20 176.1(2), C7-C8-C9 169.4(4), C6-C7-C8 151.9(4), C9-C10-C15 115.0(4), W1-C15-C10 118.2(0.4), W1-C15-O1 134.0(0.1), O1-C15-C10 107.6(0.4); torsion angle [°]: C15-W1-C8-C7 151.7(0.4), C9-C10-C15-O1 164.5(0.4), C8-C9-C10-C15 −2.6(0.7), C18-W1-C15-C10 −152.4(0.4).

The known special suitability of chromium carbene complexes for carbene annelation is also evident from compound **3a**. Its *thermal* decarbonylation leads—without in this case being able to isolate the alkyne(carbene) intermediate **4a**—by the formal dimerization of the carbene ligand directly to the chrysene derivative **5**, which according to NMR spectra recorded during the reaction is initially coordinated to $Cr(CO)_3$. After oxidative demetalation in air **5** is obtained in the form of colorless crystals.[12]

A plausible explanation for the formation of **5** is based on a weak coordination of the alkyne, which is also proven for the chromium complex **4a** by NMR spectroscopy.[13] A decoordination of the alkyne could lead to the formation of a doubly alkyne-bridged dinuclear complex, which undergoes an alkyne insertion into the neighboring metal–carbene bond. Thus, a central ten-membered ring with carbene functions lying opposite one another is formed, whose coupling

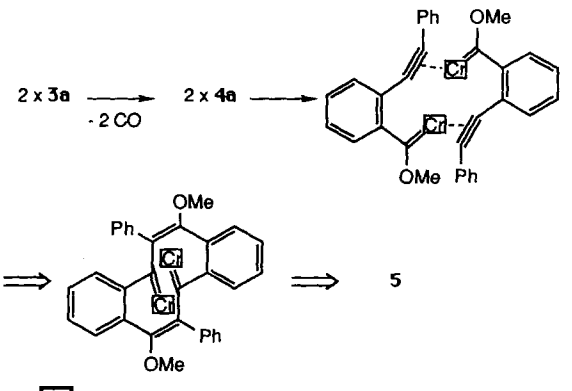

Scheme 4. Cr = $Cr(CO)_4$.

("carbene dimerization") leads to the chrysene framework (Scheme 4).

Experimental Procedure

4c: A solution of pentacarbonyl[methoxy(2-phenylethynyl)phenylcarbene]-tungsten (**3c**) (0.94 g, 1.73 mmol) [prepared according to the Fischer route [11] from hexacarbonyl tungsten, 2-bromodiphenylacetylene, *n*-butyllithium, and trimethyloxonium tetrafluoroborate in a yield of 73%] in diethyl ether (80 mL) was irradiated at −44 °C with a Hg high-pressure lamp (TQ 150, Heraeus) for 150 min. After removal of the solvent and chromatography on silica gel (PE/Et_2O 3/1, −40 °C) dark brown metallic shiny crystals of **4c** were obtained (0.45 g, 51%).– IR (PE): $\tilde{\nu}$[cm^{-1}] = 2039, 1959, 1933, 1905 [W(CO)$_4$]; ^{1}H NMR (300 MHz, CD_3COCD_3): δ = 7.30–8.00 (m, 9 H, H_{aryl}), 4.87 (s, 3 H, OCH_3); ^{13}C NMR (75 MHz, CD_3COCD_3): δ = 308.9 (t, $J_{W,C}$ = 90 Hz, W=C), 212.9 (CO_{trans}), 210.3 (CO_{trans}), 198.3 (t, $J_{W,C}$ = 120 Hz, 2 $CO_{all-cis}$), 164.0 (C-1), 139.2 (C-2), 134.1 (C_{tert}), 132.9 (C_{tert}), 131.2 (C_{tert}), 130.1 (C_{tert}), 129.9 (C_{tert}), 129.6 (C_{tert}), 128.8 (C_{quat}), 121.5 (C_{tert}), 92.5, 88.7 (C≡C), 71.5 (OCH_3).

5: A solution of pentacarbonyl[methoxy(2phenylethynyl)phenylcarbene]-chromium (**3a**) (1.30 g, 3.15 mmol) in *tert*-butylmethyl ether (20 mL) was warmed under reflux for 2 h. After the addition of acetone (50 mL) the mixture was stirred for another 12 h with exposure to the air. Filtration and chromatography on silica gel (PE/Et_2O 3/1) afforded colorless crystals of **5** (0.58 g, 55%). ^{1}H NMR (300 MHz, $CDCl_3$): δ = 8.20 (d, J = 7.8 Hz, 1 H, H_{aryl}), 7.20–7.60 (m, 7 H, H_{aryl}), 7.00 (d, J = 7.6 Hz, 1 H, H_{aryl}), 3.38 (s, 3 H, OCH_3); ^{13}C NMR (75 MHz, $CDCl_3$): δ = 151.8 (C-6, C-12), 140.1 (C_{quat}), 131.6 (C_{quat}), 131.4 (C_{tert}), 129.3 (C_{tert}), 128.6 (C_{tert}), 128.2 (C_{quat}), 128.0 (C_{quat}), 127.8 (C_{quat}), 127.0 (C_{tert}), 126.0 (C_{tert}), 124.6 (C_{tert}), 122.5 (C_{tert}), 60.3 (OCH_3); EI-MS (70 eV): *m/z* 440 (M^+, 100%).

Received: April 2, 1992 [Z 5275 IE]
German version: *Angew. Chem.* **1992**, *104*, 1257

CAS Registry numbers:
3a, 142581-49-5; **3b**, 142581-50-8; **3c**, 142581-51-9; **4a**, 142581-52-0; **4b**, 142581-53-1; **4c**, 142581-54-2; **5**, 142581-48-4; 2-bromodiphenylacetylene, 21375-88-2.

[1] Reviews: a) K. H. Dötz, *Angew. Chem.* **1984**, *96*, 573; *Angew. Chem. Int. Ed. Engl.* **1984**, *23*, 587; b) W. D. Wulff in *Comprehensive Organic Synthesis, Vol. 5* (Eds.: B. M. Trost, I. Fleming), Pergamon Press, New York, **1991**, p. 1065; c) L. S. Hegedus, *Pure Appl. Chem.* **1990**, *62*, 691; d) R. Aumann in *Advances in Metal Carbene Chemistry* (Ed.: U. Schubert), Kluwer Academic Press, Dordrecht, **1989**, p. 211.

[2] a) K. H. Dötz, E. O. Fischer, *Chem. Ber.* **1972**, *105*, 1356; b) H. U. Reißig *Organometallics in Organic Synthesis 2* (Eds.: H. Werner, G. Erker), Springer, Berlin, **1989**, p. 311; c) D. F. Harvey, K. P. Lund, *J. Am Chem. Soc.* **1991**, *113*, 8916.

[3] a) W. D. Wulff, W. E. Bauta, R. W. Kaesler, P. J. Lankford, R. A. Miller, C. K. Murray, D. C. Yang, *J. Am. Chem. Soc.* **1990**, *112*, 3642; b) K. H. Dötz, R. Noack, K. Harms, G. Müller, *Tetrahedron* **1990**, *46*, 1235.

[4] K. H. Dötz in *Organometallics in Organic Synthesis: Aspects of a Modern Interdisciplinary Field* (Eds.: H. tom Dieck, A. de Meijere), Springer, Berlin, **1988**, p. 85.

[5] Review: K. H. Dötz, *New J. Chem.* **1990**, *14*, 433.

[6] a) H. Fischer, J. Mühlemeier, R. Märkl, K. H. Dötz, *Chem. Ber.* **1982**, *115*, 1355; b) C. P. Casey, M. C. Cesa, *Organometallics* **1982**, *1*, 87.

[7] a) K. H. Dötz, B. Fügen-Köster, *Chem. Ber.* **1980**, *113*, 1449; b) C. P. Casey in *Reactive Intermediates, Vol. II* (Eds.: M. Jones, Jr., R. Moss), Wiley, New York, **1981**, p. 135.

[8] EH-MO calculations: a) P. Hofmann, M. Hämmerle, *Angew. Chem.* **1989**, *101*, 940; *Angew. Chem. Int. Ed. Engl.* **1989**, *28*, 908; b) P. Hofmann, M. Hämmerle, G. Unfried, *New J. Chem.* **1991**, *15*, 769.

[9] According to preliminary ab initio calculations a puckered chromacyclobutene intermediate has a flat energy minimum: J. Möllmann, G. Frenking, K. H. Dötz, unpublished.

[10] Alkyne(alkylidene) complexes of tungsten in *higher* oxidation states are known in which the alkyne acts as a four-electron donor: H. G. Alt, *J. Organomet. Chem.* **1983**, *256*, C12; A. Mayr, K. S. Lee, M. A. Kjelsberg, D. van Engen, *J. Am. Chem. Soc.* **1986**, *108*, 6079; A. Mayr, K. S. Lee, B. Kahr, *Angew. Chem.* **1988**, *100*, 1798; *Angew. Chem. Int. Ed. Engl.* **1988**, *27*, 1730.

[11] E. O. Fischer, *Angew. Chem.* **1974**, *86*, 651.

[12] a) Crystallographic data for **4c** ($C_{20}H_{12}CO_5W$, M = 516.16): Triclinic, space group $P\bar{1}$, a = 9.097(1), b = 9.616(1), c = 10.958(1) Å, α = 95.31(1), β = 93.44(1), γ = 108.19(1)°, Z = 2, ρ_{calcd} = 1.899 g cm^{-3}, $\mu(Mo_{K\alpha})$ = 65.6 cm^{-1}. Measurements on an Enraf-Nonius CAD4 diffractometer, ($Mo_{K\alpha}$ radiation, λ = 0.71073 Å, graphite monochromator, room temperature); 6248 measured reflections, of which 3124 were independent (R_{int} = 0.0228), 2610 with $F > 3.0\sigma$ (F_0) were considered as being observed. Solution by direct methods (Siemens SHELXTL Plus/VMS), refinement (Siemens SHELXTL Plus/VMS) to R = 0.0285, R_w = 0.020 ($w = 1/\sigma^2$), all non-hydrogen atoms anisotropic, H atoms with groupwise common isotropic temperature factors in calculated positions, 236 parameters. Empirical absorption correction. All calculations were carried out on a Micro-Vax II. b) Further details of the crystal structure investigations may be obtained from the Fachinformationszentrum Karlsruhe, Gesellschaft für wissenschaftlich-technische Information mbH, D-W-7514 Eggenstein-Leopoldshafen 2 (FRG) on quoting the depository number CSD-320423 (**4c**) and CSD-320422 (**5**), the names of the authors, and the journal citation.

[13] Selected ^{13}C NMR data: **3a** ($CDCl_3$, 100 MHz): δ = 354.0 ($C_{carbene}$), 94.7, 86.0 (C≡C); **4a** (CD_3COCD_3, 125 MHz, 223 K): δ = 336.8 ($C_{carbene}$), 80.8, 80.3 (C≡C); **3b** (CD_3COCD_3, 100 MHz, 253 K): δ = 346.7 ($C_{carbene}$), 94.4, 87.2 (C≡C); **4b** (CD_3COCD_3, 100 MHz, 253 K): δ = 326.9 ($C_{carbene}$), 87.5, 86.5 (C≡C); **3c** (CD_3COCD_3, 75 MHz): δ = 327.6 ($C_{carbene}$), 94.8, 87.1 (C≡C); **4c** (CD_3COCD_3, 75 MHz): δ = 308.9 ($C_{carbene}$), 92.5, 88.7 (C≡C).

Homodiboriranides: The Simplest Negatively Charged Homoaromatic Compounds**

By *Peter Willershausen, Claudia Kybart, Nicolaos Stamatis, Werner Massa, Michael Bühl, Paul von Ragué Schleyer,* and *Armin Berndt**

While many positively charged homoaromatic systems are known,[1] and a few such neutral species have been described,[2] the existence of negatively charged analogues is still controversial.[3] The homodiboriranides **3** we report here are the simplest negatively charged homoaromatics and supplement the known series of isoelectronic analogues **1**[1a] and **2**.[2a]

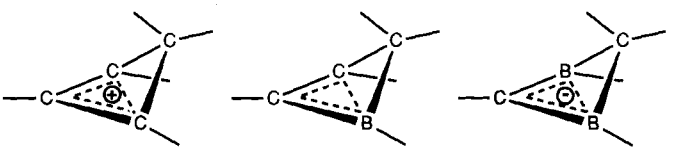

1 **2** **3**

Compound **3a** is formed together with the 2-borataallene **8** by heating (110 °C, 3 h) a toluene solution of the boriranide **5a**. Compound **5a** is accessible from the borandiylborirane **4**[4] and phenyllithium (Scheme 1). The reaction of **4** with duryllithium (2,3,5,6-tetramethylphenyllithium) at room temperature only gave **3b**; **5b** was not detected. The carbenes **6**[5] are likely intermediates in the formation of **8** and **3**, while the 1-bora-3-boratabutadienes **7** might also be involved on the pathway leading to **3**. The constitution of **5a**, **3a,b**, and **8** follow from the ^{13}C and ^{11}B NMR data (Table 1).

The central C atoms of the 1,3-diboraallylanion moieties of the (*Z*) and (*E*) isomers of **5a** have chemical shifts (δ = 106.0 and 110.6, respectively) similar to that of the central C atom in **9** (δ = 99.7).[6] In contrast, the corresponding C atoms in **3a** and **3b** (δ = 162.9 and 155.1, respectively) are

[*] Prof. Dr. A. Berndt, P. Willershausen, C. Kybart, N. Stamatis, Prof. Dr. W. Massa
Fachbereich Chemie der Universität
Hans-Meerwein-Strasse, D-W-3550 Marburg (FRG)

Dr. M. Bühl, Prof. Dr. P. von R. Schleyer
Institut für Organische Chemie der Universität Erlangen-Nürnberg
Henkestrasse 42, D-W-8520 Erlangen (FRG)

[**] This work was supported by the Deutsche Forschungsgemeinschaft and the Fonds der Chemischen Industrie.

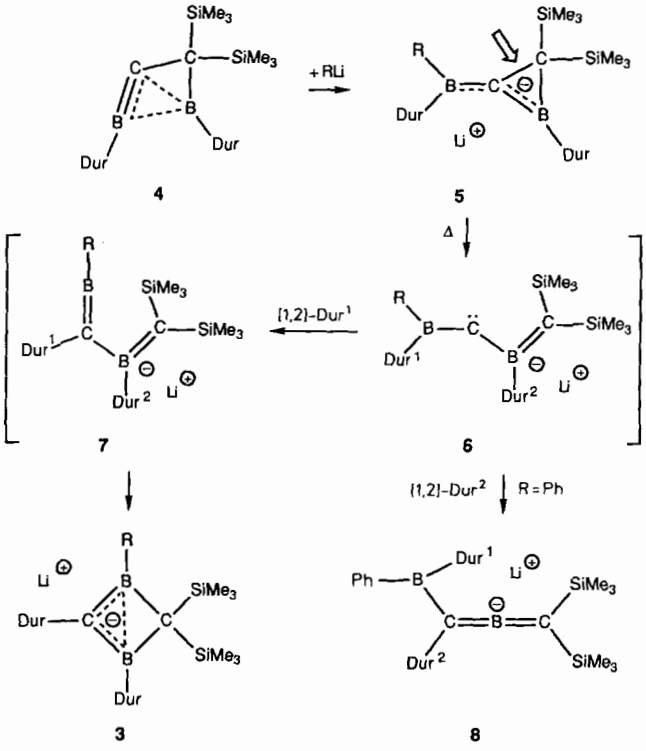

Scheme 1. Synthesis of the homodiboriranides **3**. **3**, **5**–**7**: **a**, R = phenyl; **b**, R = 2,3,5,6-tetramethylphenyl (Dur).

Table 1. Some physical data of the compounds **3a**, **3b**, **5a**, and **8**.

3a: colorless crystals, m.p. = 180 °C, yield 28%. – ^{1}H NMR (300 MHz, [D$_8$]THF, 25 °C): δ = – 0.21 (s, 18 H, Si(CH$_3$)$_3$), 1.88, 1.97, 2.01, 2.13, (each s, each 6 H, *o*- and *m*-CH$_3$), 6.25, 6.45 (each s, each 1 H, *p*-H(Dur)), 6.82–6.93 (m, 3 H, *m*- and *p*-H(phenyl)), 7.47 (d, 2H, *o*-H(phenyl)); ^{13}C NMR(125 MHz, [D$_8$]THF, –40 °C): δ = 4.5 (br. q, 6 C, Si(CH$_3$)$_3$), 20.4, 21.0, 21.4, 22.1, (each q, each 2 C, *o*- and *m*-CH$_3$), 33.4 (br. s, 1 C, CSi$_2$), 124.3, 125.0, 128.1, (each d, each 1 C, *p*-C), 126.2, (d, 2 C, *m*-C(phenyl)), 130.6, 130.8, 131.8, 136.2, (each s, each 2 C, *o*- and *m*-C(Dur)), 135.8 (d, 2 C, *o*-C(phenyl)), 143.1 (s, 1 C, *i*-C(C-Dur)), 151.1, 153.3 (each br. s, each 1 C, *i*-C(phenyl and B-Dur)), 162.9 (br. s, 1 C, CB$_2$); ^{11}B NMR(96 MHz, C$_6$D$_6$, 25 °C): δ = 37 ($\nu_{1/2}$ = 1440 Hz)

3b: colorless solid, m.p. = 190 °C (decomp.), yield 52% – ^{13}C NMR-(125 MHz, [D$_8$]THF, –40 °C): δ = 6.0 (q, 6 C, Si(CH$_3$)$_3$), 19.3, 21.0, 22.1 (each br. q, 12 C, *o*- and *m*-CH$_3$), 124.0 (br. d, 1 C, *p*-C(C-Dur)), 128.2 (d, 2 C, *p*-C(B-Dur)), 130.4, 130.6, 131.0, 136.2 (each s, in total 12 C, *o*- and *m*-C), 147.6 (s, 1 C, *i*-C(C-Dur)), 153.4 (br. s, 2 C, *i*-C(B-Dur)), 155.1 (br. s, 1 C, CB$_2$). The signal for CSi$_2$ is not observed in [D$_8$]THF, in C$_6$D$_6$ at 25 °C it is found at δ = 26; ^{11}B NMR(96 MHz, [D$_8$]THF, 25 °C): δ = 41 ($\nu_{1/2}$ = 1330 Hz)

5a: bright yellow solid m.p. = 235 °C (decomp.), yield 61% – In [D$_8$]THF the (*Z*)- and (*E*)-isomer are in the ratio of ca. 1:1. ^{1}H NMR (300 MHz, [D$_8$]THF, 25 °C): δ = – 0.16, 0.00 (each s, each 18 H, Si(CH$_3$)$_3$), 2.08, 2.14, 2.16, 2.17, 2.18, 2.22, 2.29, 2.41 (each *s*, each 6 H, *o*- and *m*-CH$_3$), 6.57, 6.61, 6.67, 6.75 (each s, each 1 H, *p*-H(Dur)), 6.82–7.02 (m, 6 H, *m*- and *p*-H(phenyl)), 7.52, 7.82 (each d, each 2 H, *o*-H(phenyl)); ^{13}C NMR (125 MHz, [D$_8$]THF, –40 °C): δ = 3.3, 3.4 (each q, each 6 C, Si(CH$_3$)$_3$), 12.3, 18.0 (each br. s, each 1 C, CSi$_2$), 15.9 (q, 2 C, CH$_3$(Et$_2$O)), 20.70, 20.87, 20.96, 20.99, 21.10, 21.30, 21.90 (each q, in total 16 C, *o*- and *m*-CH$_3$), 66.5 (t, 2 C, CH$_2$(Et$_2$O)), 106.0, 110.6 (each br. s, each 1 C, CB$_2$), 124.6, 125.4, 125.98, 126.04, 127.6, 127.8, 130.7, 130.8, 131.0, 131.5, 131.6, 131.9, 135.3, 135.4, 136.0, 136.1, 139.5, 141.3 (in total 30 C, *o*- *m*- and *p*-C), 140.4, 142.7, (each br. s, 1 C, *i*-C(phenyl)), 151.7, 153.3, 155.6, 157.2 (each br. s, each 1 C, *i*-C(Dur)); ^{11}B NMR (96 MHz, C$_6$D$_6$, 50 °C): δ = 43 ($\nu_{1/2}$ = 1950 Hz), 51 ($\nu_{1/2}$ = 1400 Hz).

8: yellow crystals, m.p. = 180 °C (decomp.), yield 26% – ^{1}H NMR(300 MHz, [D$_8$]THF, 25 °C): δ = – 0.24 (s, 18 H, Si(CH$_3$)$_3$), 2.07, 2.09, 2.23, 2.28 (each s, each 6 H, *o*- and *m*-CH$_3$), 6.42, 6.54 (each s, each 1 H, *p*-H(Dur)), 6.60 (m, 3 H, *m*- and *p*-H(phenyl)), 6.80 (d, 2H, *o*-H(phenyl)); ^{13}C NMR(125 MHz, [D$_8$]THF, –40 °C): δ = 5.1 (q, 6 C, Si(CH$_3$)$_3$), 19.6, 20.7, 21.3, 21.8 (each q, each 2 C, *o*- and *m*-CH$_3$), 39.6 (br. s, 1 C, CSi$_2$), 98.2 (br. s, 1 C, CB$_2$), 125.45, 125.51, 128.0 (each d, each 1 C, *p*-C), 126.3 (d, 2 C, *m*-C(phenyl)), 134.6 (d, 2 C, *o*-C(phenyl)), 130.8, 131.1, 132.8, 135.3 (each s, each 2 C, *o*- and *m*-C(Dur)), 150.0 (s, 1 C, *i*-C(C-Dur)), 150.7, 154.9 (each br. s, each 1 C, *i*-C(B-Dur, phenyl)); ^{11}B NMR (96 MHz, C$_6$D$_6$, 55 °C): δ = 54 ($\nu_{1/2}$ = 950 Hz), 65 ($\nu_{1/2}$ = 1400 Hz)

strongly deshielded. This deshielding indicates a cyclic homoaromatic delocalization of the π electrons as in the diboriranide **10** (δ_{BCB} = 147.8).[7]

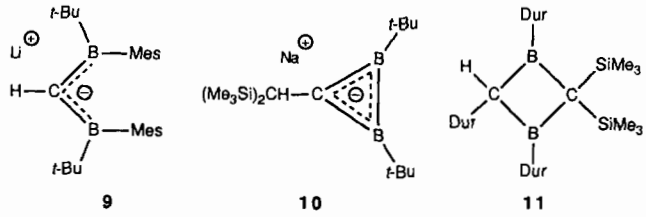

The partial bonding between the boron atoms in **3** is facilitated by the folding of the four-membered ring. Although the trimethylsilyl substituents are diastereotopic, the ^{13}C NMR spectrum of **3a** in [D$_8$]THF/[D$_{10}$]Et$_2$O (4/1) at room temperature shows only one sharp signal. Upon cooling, this signal broadens and splits into four peaks at –120 °C, one for a trimethylsilyl group (which can still rotate freely) and three for the second trimethylsilyl group whose rotation is frozen. From the chemical shift difference with slow exchange ($\Delta\delta$ = 250 Hz) and the coalescence temperature (176 K), a 7.9 kcal mol^{-1} barrier to ring inversion of **3a** (Scheme 2) can be estimated approximately. This value, a measure of the homoaromaticity of **3**, is similar to that determined for the isoelectronic cation **1** (8.4 kcal mol^{-1}).[1a]

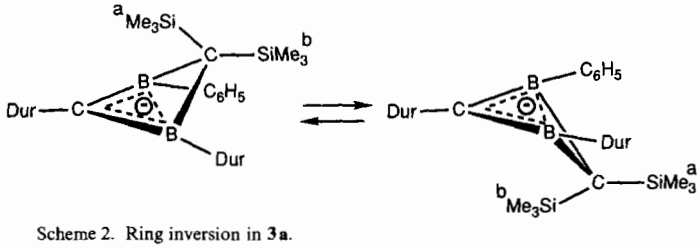

Scheme 2. Ring inversion in **3a**.

The crystal structure of **3a**[8] confirms the conclusions from the NMR data in solution (Fig. 1). The folding (147.1(9)°) at the B–B bond is similar to that found in derivatives of **1** (142.7, 143.6, 148.5°).[1c] The B–B distance (179.2(15) pm) is significantly shorter than the corresponding distance in **11** (203.1(7) pm), the product of the protona-

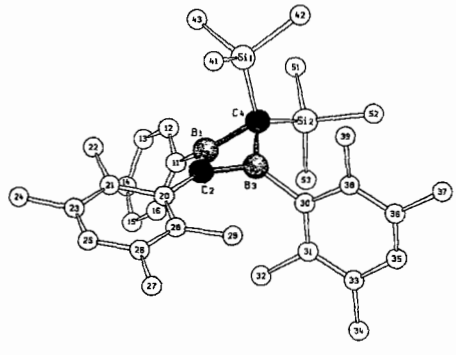

Fig. 1. Schakal drawing of the crystal structure of the anion in **3a**. Selected distances [pm] and angles [°]: B1-C2 148.4(13), C2-B3 148.2(13), B3-C4 160.4(14), C4-B1 158.7(13), B1-B3 179.2(15), B1-C11 161.4(12), C2-C20 145.0(13), B3-C30 161.9(14), C4-Si1 187.7(9), C4-Si2 185.1(9); B1-C2-B3 74.3(7), C2-B3-C4 102.0(8), B3-C4-B1 68.3(6), C4-B1-C2 102.8(7), Si1-C4-Si2 115.6(4).

tion of **3b**, for which the fold at the B–B bond is 153°. The Li^+ ion is far away from the charge-carrying centers B1, C2, and B3 (>700 pm) and is planar-coordinated with three partially disordered diethyl ether molecules.

The folding of **3a,b** is not due to steric interactions between the large substituents. This follows from ab initio calculations for the parent anion **3**, $C_2B_2H_5^-$ (C_s symmetry).[10] Fold angle (146°), B–B distance (185.9 pm), C–B distances (148.7 and 160.7 pm), energy difference to the planar conformation (7.4 kcal mol^{-1}), and the chemical shift for C2 (169) calculated with IGLO[11, 12] are in good agreement with the data for **3a** determined by experiment.

The 1,3 interaction in $C_2B_2H_5^-$ is evident from the calculated bond order of 0.23 (NPA, natural population analysis,[13] Wiberg's definition[14]). This value is somewhat smaller than that for the homocyclopropenium ion **1** (0.40). This can be explained as follows: In contrast to the usual descriptions with formal charges the boron atoms in $C_2B_2H_5^-$ are *positively* charged (NPA + 0.35). Fewer electrons are available for the transannular overlap than in **1** (NPA charge about 0). Analogously, in spite of the similar folding angle (145°) in **1**, a slightly higher inversion barrier is calculated (9.4 kcal mol^{-1}).[15]

The parent neutral compound **2**, C_3BH_5 (C_1 symmetry), shows the same evidence for a 1,3 interaction: the fold angle (147°) and the 1,3 bond order (0.24) are similar to the values for $C_2B_2H_5^-$, the inversion barrier (4.3 kcal mol^{-1}) is significantly smaller.

Received: April 6, 1992 [Z 5281 IE]
German version: *Angew. Chem.* **1992**, *104*, 1278

CAS Registry numbers:
3a, 142633-75-8; **3b**, 142633-72-5; **4**, 127628-93-7; **5a**, 142633-73-6; **8**, 142633-74-7; PhLi, 591-51-5; DurLi, 142633-71-4.

[1] a) G. A. Olah, J. S. Staval, R. J. Spear, G. Liang, *J. Am. Chem. Soc.* **1975**, *97*, 5489–5497, and references cited therein; b) L. A. Paquette. *Angew. Chem.* **1978**, *90*, 114–125; *Angew. Chem. Int. Ed. Engl.* **1978**, *17*, 106, and references cited therein; c) G. Maier, R. Emrich, K.-D. Malsch, K.-A. Schneider, M. Nixdorf, H. Irngartinger, *Chem. Ber.* **1985**, *118*, 2798–2810, and references cited therein; d) T. Laube, *J. Am. Chem. Soc.* **1989**, *111*, 9224–9232, and references cited therein.

[2] a) C. Pues, G. Baum, W. Massa, A. Berndt, *Z. Naturforsch. B* **1988**, *43*, 275–279, and references cited therein; b) P. J. Fagan, E. G. Burns, J. C. Calabrese, *J. Am. Chem. Soc.* **1988**, *110*, 2979–2981.

[3] P. von R. Schleyer, E. Kaufmann, A. J. Kos, H. Mayr, J. Chandrasekhar, *J. Chem. Soc. Chem. Commun.* **1986**, 1583–1585, zit. Lit.

[4] C. Wieczorek, J. Allwohn, G. Schmidt-Lukasch, R. Hunold, W. Massa, A. Berndt, *Angew. Chem.* **1990**, *102*, 435–436; *Angew. Chem. Int. Ed. Engl.* **1990**, *29*, 398–399.

[5] We have recently explained the 1,2 shift of a mesityl group from a three coordinated boron to the neighboring carbon atom by means of a diboryl carbene intermediate (there **8**). M. Pilz, J. Allwohn, W. Massa, A. Berndt, *Angew. Chem.* **1990**, *102*, 436–438; *Angew. Chem. Int. Ed. Engl.* **1990**, *29*, 399–401.

[6] M. Pilz, J. Allwohn, R. Hunold, W. Massa, A. Berndt, *Angew. Chem.* **1988**, *100*, 1421–1422; *Angew. Chem. Int. Ed. Engl.* **1988**, *27*, 1370–1372.

[7] R. Wehrmann, H. Meyer, A. Berndt, *Angew. Chem.* **1985**, *97*, 719–781; *Angew. Chem. Int. Ed. Engl.* **1985**, *25*, 788-790; H. Meyer, G. Schmidt-Lukasch, G. Baum, W. Massa, A. Berndt, *Z. Naturforsch. B* **1988**, *43*, 801–806.

[8] X-ray crystal structure analysis of **3a**: $C_{34}H_{49}B_2Si_2Li \cdot 3Et_2O$, space group $P2/c$, $Z = 4$, $a = 1971.2(4)$, $b = 1345.0(3)$, $c = 1891.6(4)$ pm, $\beta = 104.84(3)°$, 3836 independent reflections with $F_0 > 3\sigma(F_0)$ measured on a four-circle diffractometer CAD4 (Enraf–Nonius) with $Cu_{K\alpha}$ radiation at −80 °C; no absorption correction ($\mu = 9.2$ cm^{-1}). The structure was solved by direct methods and with full matrix refinement [9]. Anisotropic temperature factors were used for all C, O, and Si atoms, for the rest isotropic. For the anion all the H atoms were included in calculated positions with groupwise refined temperature factors. There are two symmetry independent $[Li(OEt_2)_2]^+$ ions present, both with C_2 symmetry, i.e. Li^+ and an O atom lie on a twofold axis, and Li^+ is planar surrounded. Both cations have a disordered ethyl group, which was described by a "split atom" model with 1:1 occupation. Because of the uncertain geometry no H atom positions were included in the calculations for these ethyl groups. Apart from the numerous peripheral methyl groups of the anion this positional disorder appears to be the reason for the relatively low accuracy of the structure determination, which for 448 parameters gave $R = 0.098$, $wR = 0.077$ (weights $w = 1/\sigma^2(F_0)$). Further details of the crystal structure investigation may be obtained from the Fachinformationszentrum Karlsruhe, Gesellschaft für wissenschaftlich-technische Information mbH, D-W-7514 Eggenstein-Leopoldshafen 2 (FRG) on quoting the depository number CSD-56362, the names of the authors, and the journal citation.

[9] G. M. Sheldrick, SHELXTL-Plus. Release 4.0 for Siemens R3 Crystallographic Research Systems, **1989**.

[10] Standard procedures and basis sets were used, see for example, W. Hehre, L. Radon, P. von R. Schleyer, J. A. Pople, *Ab Initio Molecular Orbital Theory*, Wiley, New York, **1986**. Geometric parameters refer to the MP2(Full)/6-31G* optimized structures, energies were determined on the QCISD(T)/6-31G*//MP2(Full)/6-31G* + ZPE(6-31G*) level.

[11] a) W. Kutzelnigg, *Isr. J. Chem.* **1980**, *19*, 193; b) M. Schindler, W. Kutzelnigg, *J. Chem. Phys.* **1982**, *76*, 1919; c) W. Kutzelnigg, M. Schindler, U. Fleischer in *NMR Basic Princ. Prog.* **1990**, *23*, 165.

[12] Huzinaga basis (S. Huzinaga, *Approximate Atomic Wave Functions*, University of Alberta, Edmonton, Canada, **1971**), contracted as follows: B, C, 7s3p (4111, 21), H 3s (21). The MP2/6-31G* optimized geometries were used (notation DZ/MP2//6-31G*).

[13] a) A. E. Reed, R. B. Weinstock, F. Weinhold, *J. Chem. Phys.* **1985**, *83*, 735; b) A. E. Reed, L. A. Curtis, F. Weinhold, *Chem. Rev.* **1988**, *88*, 899. The values given were obtained with the 6-31G* basis set for the MP2/6-31G* optimized geometries.

[14] K. Wiberg, *Tetrahedron* **1968**, *24*, 1083.

[15] R. C. Haddon, K. Raghavachari, *J. Am. Chem. Soc.* **1983**, *105*, 118–120; D. Cremer, E. Kraka, T. S. Shee, R. F. W. Bader, C. D. H. Lau, T. T. Nguyen-Dang, P. J. McDougall, *ibid.* **1983**, *105*, 5069–5075; J. W. de M. Carneiro, P. von R. Schleyer, unpublished.

Novel Cross-Conjugated Compounds Derived from Tetraethynylethene**

By *Armen M. Boldi, John Anthony, Carolyn B. Knobler,* and *François Diederich**

Recently, we reported the synthesis of tetraethynylethene (**1a**), the parent compound of an interesting class of highly unsaturated cross-conjugated hydrocarbons.[1] Besides **1a**, only the tetrasubstituted derivatives **1b–g** and compounds **1h,i** with two free ethynyl groups attached to the same ethene-carbon are known.[1–5] Tetraethynylethenes in which one or more alkyne units are functionalized became of interest to us for several reasons: 1) Compound **2a** ($R^1 = R^3$ = silyl protecting group, $R^2 = R^4 = H$) with a free *cis*-enediyne unit represents the precursor for oxidative coupling to hexaethynylhexadehydro[18]annulene derivatives and, ultimately, to a two-dimensional all-carbon network.[6] 2) Oxidative coupling of **2b** ($R^1 = R^4 \neq H$, $R^2 = R^3 = H$) with a free *trans*-enediyne unit should lead to linear chain polymers with pendant alkynyl groups along a poly(enebutadiyne) backbone. 3) Derivative **2c** ($R^1 = R^2 = R^3 \neq H$, $R^4 = H$) would be the first representative with a single terminal ethynyl group and provide access, via oxidative coupling, to extended cross-conjugated dimeric chromophores. In this communication, we present the first examples of compounds fitting the descriptions 2) and 3) and

[*] Prof. Dr. F. Diederich,[+] A. M. Boldi, J. Anthony, C. B. Knobler
Department of Chemistry and Biochemistry
University of California
Los Angeles, CA 90024-1569 (USA)

[+] Present address:
Laboratorium für Organische Chemie
ETH-Zentrum
Universitätstrasse 16, CH-8092 Zürich (Switzerland)

[**] We thank the U.S. National Science Foundation and the American Chemical Society (ACS graduate student fellowship to J. A.) for support of this work.

describe the synthesis and structural characterization of the tetraethynylethene derivatives **3a–d** and the dimerization products **4a,b**.

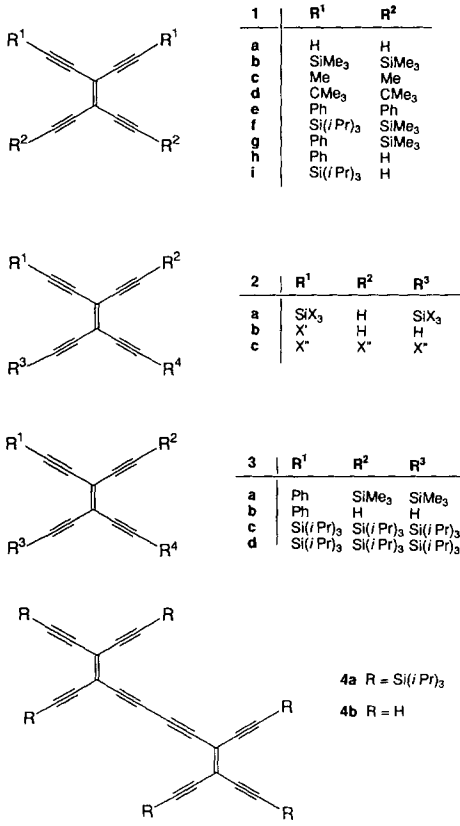

The seven-step synthesis of **3b** with a free *trans*-enediyne unit, which starts from dimethyl 2,3-dibromofumarate,[7] is shown in Scheme 1.[8] Upon slow evaporation of the solvent

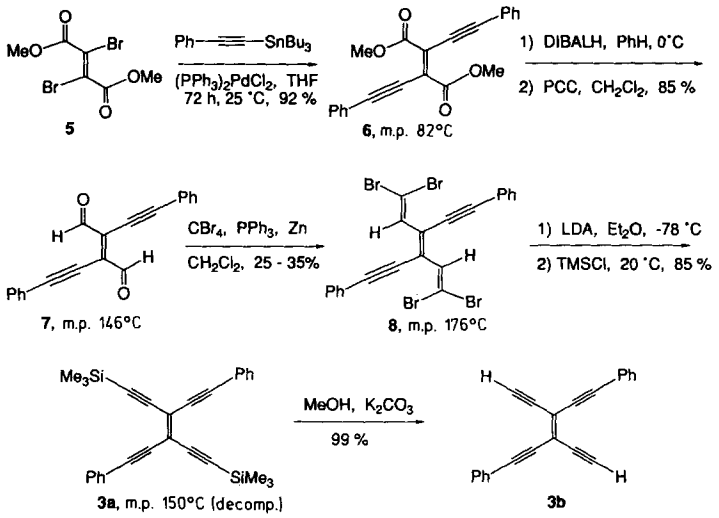

Scheme 1. DIBALH = Diisobutylaluminium hydride, PCC = pyridinium dichlorochromate, LDA = lithium diisopropylamide, TMS = trimethylsilyl.

dichloromethane, the stable pale-yellow TMS-protected derivative **3a** afforded crystals suitable for X-ray analysis (Fig. 1).[9] Except for the methyl groups on the two silicon atoms, the molecule is perfectly planar. Deprotection of **3a** with K_2CO_3 in MeOH proceeded smoothly and yielded **3b** in quantitative yield. In the 360 MHz ^1H NMR spectrum of **3b** in $CDCl_3$, the signal for the terminal ethynyl protons appears at $\delta = 3.66$ [IR (neat): $\tilde{\nu}$ [cm^{-1}] = 3307, ≡C–H]. Like the isomeric compound **1h**, derivative **3b** is only stable at room temperature in dilute solutions. Upon concentration, solutions in $CHCl_3$ or CCl_4 darken rapidly, even at −5 °C, and in the solid state decomposition is instantaneous.

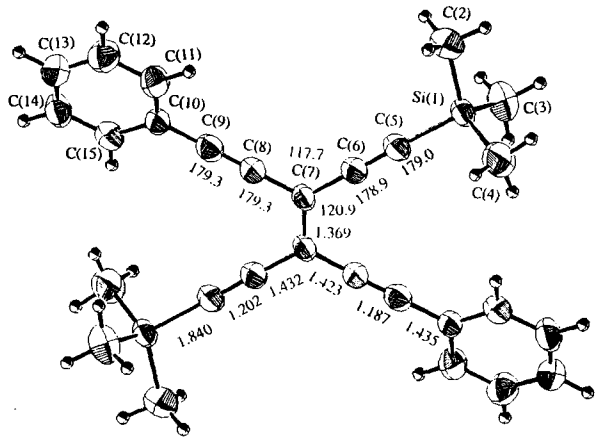

Fig. 1. X-ray crystal structure of **3a**.

For the preparation of **4b**, a carbon-rich compound with the molecular composition $C_{20}H_6$, the terminally mono-deprotected tetraethynylethene **3d** was synthesized (Scheme 2).

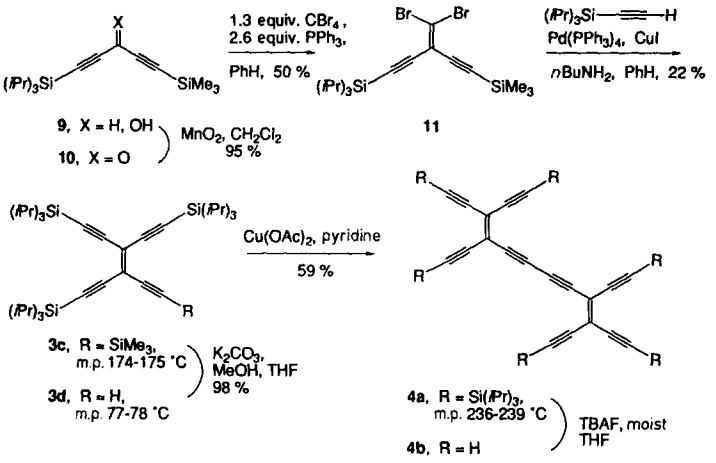

Scheme 2. Compounds for which no melting point is quoted are oils at 25 °C. TBAF = tetrabutylammonium fluoride.

The starting material in this route, the unsymmetrically protected 1,4-pentadiyne-3-ol **9**, was prepared in 48% yield by reaction of TMS-propargylaldehyde in THF with $(i\text{Pr})_3\text{Si–C}{\equiv}\text{CH}$ and *n*BuLi. The mono-deprotected tetraethynylethene **3d** was obtained as a stable solid [IR (neat): $\tilde{\nu}$ [cm^{-1}] = 3307, ≡C–H] which was transformed through oxidative coupling in 59% yield into the fully silyl-protected yellow compound **4a**. This remarkably extended cross-conjugated π-system is very stable with a high melting point of 236–239 °C (!) and, upon recrystallization from hexane/EtOH, afforded crystals suitable for X-ray analysis.[9] The molecule is nearly planar (Fig. 2) with a maximum deviation

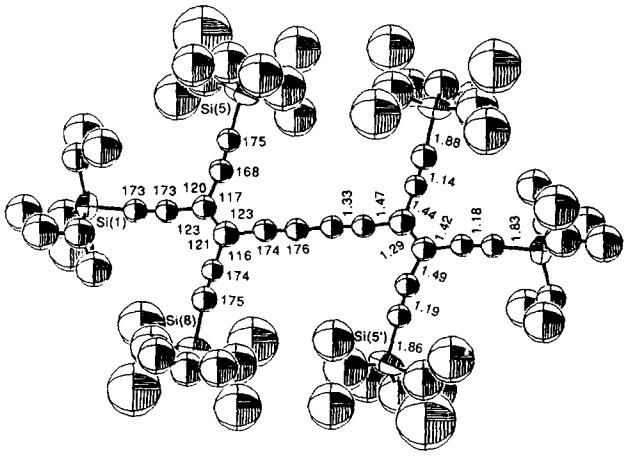

Fig. 2. X-ray crystal structure of **4a**.

from the least-squares plane through the dimeric framework including the six silicon atoms of 0.21(3) Å. Of two possible geometries, **4a** prefers the "transoid" alignment of the two ethenes with respect to the central butadiyne unit. The eighteen isopropyl groups are highly disordered, thus preventing a refinement of the structure beyond $R = 0.169$ ($R_w = 0.178$).

The extension of the π-electron conjugation in the new chromophore **4a** becomes clearly visible on comparison of its electronic absorption spectrum with that of the simple tetraethynylethene **1b** (Fig. 3). Both the location and the shape of the absorption bands of **4a** are very different from the bands in **1b**. In agreement with the planar molecular structure found by X-ray analysis, the UV/VIS spectrum of **4a** shows significant vibrational fine structure. Due to the extension of its chromophore, the end absorption of **4a** appears above 450 nm, and the longest wavelength band at $\lambda_{max} = 432$ nm is bathochromically shifted by 82 nm compared to the lowest energy absorption in **1b** ($\lambda_{max} = 350$ nm).

Deprotection of **4a** with tetra(*n*-butyl)ammonium fluoride in wet THF afforded the hexaethynyl derivative **4b** which is quite stable and soluble in pentane. The 360 MHz ^{1}H NMR spectrum of **4b** in [D$_6$]acetone showed three singlets of equal intensity for the terminal alkyne protons at $\delta = 4.51$, 4.57, and 4.60. Evaporation of the solvent yields a solid which, at room temperature even in the absence of oxygen and light, turns rapidly black yielding a polymer that is insoluble in organic solvents.

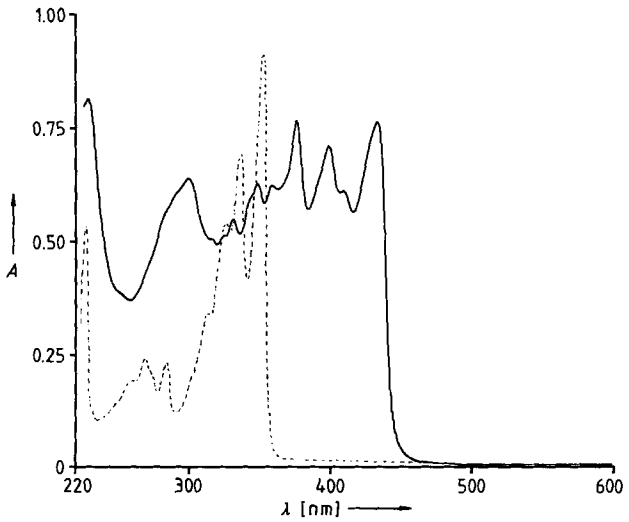

Fig. 3. Electronic absorption of **1b** (----) [1] and **4a** (——) in hexanes, $T = 25$ °C, $d = 1$ cm, $c = 2.74 \times 10^{-5}$ *M*. Spectrum of **4a**: $\lambda_{max} = 223$ sh ($\varepsilon = 36800$ cm^{-1}mol^{-1}L), 228 (37700), 253 sh (17500), 283 sh (25500), 291 sh (27800), 299 (29600), 316 (23200), 324 (23600), 331 (25300), 343 sh (27600), 347 sh (29000), 358 (28900), 374 (35600), 398 (33000), 408 (28300), 432 (35500).

The study of the polymerization chemistry of **3b** and **4b** as well as the preparation of tetraethynylethenes **2a** with free *cis*-enediynes are now under way.

Experimental

3a: To a solution of 3.2 g (5.4 mmol) of tetrabromide **8** in dry diethyl ether at −78 °C was added slowly 13.5 mL of a 2.0 M solution of LDA in THF (27 mmol). After 40 min, the stirred green solution was slowly warmed to 20 °C and 1.30 g (12 mmol) of TMSCl was added. After 3 h, the reaction was quenched with saturated NH_4Cl and extracted with water followed by saturated NaCl. The organic layer was dried and the solvent evaporated. The crude product was filtered through a short column of silica gel (CH_2Cl_2), and the solvent reduced to a volume of 5 mL. The residual solution was cooled to −5 °C, whereupon the product crystallized slowly to yield 1.9 g (85%) of **3a** as a pale yellow solid: m.p. 150 °C (decomp.). IR (KBr) $\tilde{\nu}$ [cm^{-1}] = 2205, 2141 (C≡C); ^{1}H NMR (360 MHz, $CDCl_3$): $\delta = 0.27$ (s, 18H, TMS), 7.36 (m, 6H, aryl), 7.54 (m, 4H, aryl); ^{13}C NMR (90.6 MHz, $CDCl_3$): $\delta = -0.23$, 87.24, 98.81, 101.14, 105.4, 118.1, 122.5, 128.3, 129.0, 131.9; UV/VIS (MeOH) λ_{max} [nm] = 232 (sh) ($\varepsilon = 17700$), 246 (18600), 256 (18900), 274 (24400), 380 (23500).

4a: To a solution of 266 mg (0.448 mmol) of **3d** in 45 mL of pyridine was added 1.6 g (8.96 mmol) of anhydrous $Cu(OAc)_2$. After stirring for 20 h at 20 °C, the solution was poured into 250 mL of pentane and 500 mL of 30% $CuSO_4$. The aqueous layer was extracted once with pentane, and the combined organic layers were washed twice with 500 mL of 30% $CuSO_4$, once with 250 mL of water, and once with 250 mL of saturated NaCl. After the organic layer was dried over $MgSO_4$, the solvent was removed to yield a brownish solid. The solid was re-suspended in pentane and filtered through flash silica gel. Removal of the solvent and recrystallization from MeOH/CH_2Cl_2 yielded 156 mg (59%) of **4a** as a yellow solid: m.p. 236–239 °C. IR (neat) $\tilde{\nu}$ [cm^{-1}] = 2156, 2125 (C≡C); ^{1}H NMR (360 MHz, $CDCl_3$): $\delta = 1.07$ (s, 126H, $CH(CH_3)_2$); ^{13}C NMR (90.6 MHz, $CDCl_3$): $\delta = 11.13$, 11.20, 11.24, 18.53, 18.61, 18.65, 82.34, 82.98, 101.55, 103.14, 103.34, 103.64, 103.70, 105.05, 115.91, 120.80.

Received: May 16, 1992 [Z 5356 IE]
German version: *Angew. Chem.* **1992**, *104*, 1270

CAS Registry numbers:
3a, 142761-75-9; **3b**, 142761-76-0; **3c**, 142761-77-1; **3d**, 142761-78-2; **4a**, 142761-79-3; **4b**, 142761-80-6; **5**, 116631-94-8; **6**, 142761-81-7; **7**, 142761-82-8; **8**, 142761-83-9; **9**, 142761-84-0; **10**, 142761-85-1; **11**, 142761-86-2; $Cu(OAc)_2$, 142-71-2; (phenylethynyl)tributylstannane, 3157-88-8; (triisopropylsilyl)-acetylene, 89343-06-6.

[1] Y. Rubin, C. B. Knobler, F. Diederich, *Angew. Chem.* **1991**, *103*, 708–710; *Angew. Chem. Int. Ed. Engl.* **1991**, *30*, 698–700.
[2] Y. Hori, N. Noda, S. Kobayashi, H. Taniguchi, *Tetrahedron Lett.* **1969**, 3563–3566.
[3] a) H. Hauptmann, *Angew. Chem.* **1975**, *87*, 490–491; *Angew. Chem. Int. Ed. Engl.* **1975**, *14*, 498–499; b) *Tetrahedron Lett.* **1975**, 1931–1934.
[4] a) H. Hopf, M. Kreutzer, *Angew. Chem.* **1990**, *102*, 425–426; *Angew. Chem. Int. Ed. Engl.* **1990**, *29*, 393–395; b) H. Hopf, M. Kreutzer, P. G. Jones, *Chem. Ber.* **1991**, *124*, 1471–1475.
[5] B. Ma, Y. Xie, H. F. Schaefer, III, *Chem. Phys. Lett.* **1992**, *191*, 521–526.
[6] F. Diederich, Y. Rubin, *Angew. Chem.* **1992**, *104*, 1123–1146; *Angew. Chem. Int. Ed. Engl.* **1992**, *31*, 1101.
[7] E. A. Shilov, I. V. Smirnov-Zamkov, *Izv. Akad. Nauk SSSR, Otd. Khim. Nauk.* **1951**, 32–41; *Chem. Abstr.* **1951**, *45*, 7952f.
[8] All new compounds have been fully characterized by ^{1}H and ^{13}C NMR, IR, and UV spectroscopy, as well as mass spectrometry. Correct elemental analyses were obtained for all stable derivatives; high-resolution mass spectra were measured for unstable compounds.
[9] X-ray crystal data for **3a** ($C_{28}H_{28}Si_2$); $M_r = 420.71$, monoclinic space group $P2_1/c$, $Z = 2$; $a = 9.0490(6)$, $b = 13.7296(8)$, $c = 10.4373(5)$ Å, $V = 1289$ Å^3, $Cu_{K\alpha}$ radiation, $2\theta \leq 115°$, 1761 unique reflections; the structure was solved by statistical methods (MULTAN80), yielding $R = 0.055$, $R_w = 0.080$ for 1589 independent reflections with $I > 3\sigma(I)$. X-ray crystal data for **4a** ($C_{74}H_{126}Si_6$); $M_r = 1184.32$, monoclinic space group $P2_1/a$, $Z = 2$ (centrosymmetric molecule); $a = 13.768(6)$, $b = 15.011(6)$, $c = 21.125(9)$ Å, $V = 1573$ Å^3, $Cu_{K\alpha}$ radiation, $2\theta \leq 95°$, 3788 unique reflections; the structure was solved by statistical methods (MULTAN80), yielding $R = 0.169$, $R_w = 0.178$ for 1573 independent reflections with $I > 2\sigma(I)$. Further details of the crystal structure investigations are available on request from the Director of the Cambridge Crystallographic Data Centre, University Chemical Laboratory, Lensfield Road, GB-Cambridge CB2 (UK), on quoting the full journal citation.

Photoswitchable Association of an Azobenzene–Bipyridinium Diad to Eosin: Photostimulated "On-Off" Guest Binding**

By *Itamar Willner**, *Sharon Marx*, and *Yoav Eichen*

Photoswitchable devices evoke continuous interest as information storage systems and signal amplification units of optical signals.[1, 2] Recent activities in photostimulation of macromolecules' functions[3] have demonstrated that physical properties of photochromic polymers such as permeability,[4] volume,[5] or viscosity[6] can be controlled by light. Similarly, catalytic[7] and binding properties of proteins containing photochromic components anchored to their backbones[8] can be activated by light (i.e., phototriggered).

Photostimulated "on–off" chemical reactivity at the molecular level has, however, been less explored. Photocontrolled binding of ions to photochromic ionophores such as azobenzene crown ethers[9] or "polyether spiropyran"[10] represent phototriggered chemical processes at the molecular level. Here we report on the photostimulated on–off binding of *N*-methyl-*N'*-[4-(phenylazo)benzyl]-4,4'-bipyridinium (Azo-V^{2+}, **1**) to eosin Y (Eo^{2-}, **2**).

The diad *trans*-**1** was synthesized by the reaction of *trans*-1-(bromomethyl)-4-phenylazobenzene, with *N*-methyl-4,4'-bipyridinium. The resulting diad exhibits photochromic properties: Illumination of *trans*-**1** ($\lambda = 366$ nm) results in isomerization to *cis*-**1**, and upon illumination of *cis*-**1** ($\lambda > 400$ nm) *trans*-**1** is restored. Recently, we reported

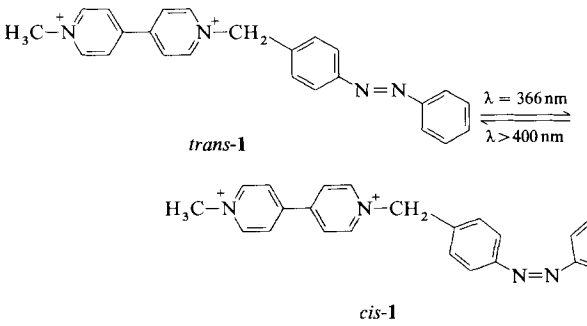

trans-**1**

cis-**1**

on the structural and chemical properties of donor–acceptor complexes formed between bipyridinium salts and xanthene dyes, such as eosin.[11] We found that electrostatic interactions as well as π–π donor–acceptor and charge-transfer interactions play important roles in stabilization of these complexes.

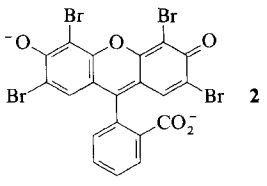

2

Trans-**1** as well as *cis*-**1** form 1:1 complexes with **2**, but the complexes differ substantially in their association constants. Figure 1 shows the spectral changes of **2** upon addition of *cis*-**1**. By applying the Benesi-Hildebrand relation,[12] the derived association constant $K_a(cis)$ is determined to be 38000 M^{-1}. The association constant $K_a(trans)$ of *trans*-**1** to **2** is 3000 M^{-1}. Thus, functionalization of the bipyridinium

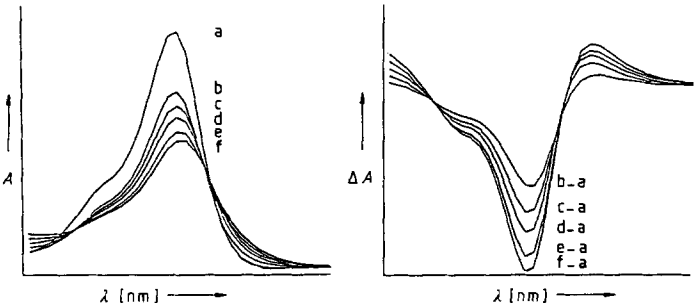

Fig. 1. Left: Spectral changes of Eo^{2-} (**2**, $c = 1.48 \times 10^{-5}$ M) at different *cis*-**1** concentrations. These concentrations for the different experiments are a) 0 M, b) 2.5×10^{-5} M, c) 5.02×10^{-5} M, d) 7.5×10^{-5} M, e) 1.0×10^{-4} M, f) 1.25×10^{-4} M. Right: difference spectra of **2** upon addition of *cis*-**1**. *A* = Absorption units.

component by an azobenzene unit results in a substantial difference in its association properties with **2**, and the association constant of **2** with *cis*-**1** is about twelve times greater than that with *trans*-**1**. A possible origin for this difference can be the changes in dipole moment associated with the isomerization of azobenzene. Isomerization of *trans*-azobenzene (0.5 D) is accompanied by an increase in the dipole moment (*cis*-azobenzene, 3.0 D). This larger dipole moment of the *cis*-azobenzene can participate synergetically in the stabilization of the charge-transfer complex between eosin and the bipyridinium unit. The association constant K_a of *N,N'*-dimethyl-4,4'-bipyridinium with eosin (in H_2O) is 4500 M^{-1}. This value implies that the enhanced binding of *cis*-**1** to eosin is associated with the increase in dipole moment of the azobenzene component.

The difference in the association constants of *trans*-**1** and *cis*-**1** to eosin allows us to design a molecular switch for association (Fig. 2). An aqueous solution of eosin ($c = 1.48 \times 10^{-5}$ M) and *trans*-**1** ($c = 6.2 \times 10^{-5}$ M) results in a system where the two components exhibit only weak mutual recognition and are essentially in a separated form. Upon illumination ($\lambda = 366$ nm), isomerization of *trans*-**1** to *cis*-**1** occurs. This results in the formation of a complex between *cis*-**1** and eosin, as evidenced by the decrease in the absorbance of the eosin dye [Eq. (a)]. Back isomerization of

$$\underset{\mathbf{2}}{Eo^{2-}} + \underset{trans\text{-}\mathbf{1}}{trans\text{-}Azo\text{-}V^{2+}} \underset{\lambda > 400\ nm}{\overset{\lambda = 366\ nm}{\rightleftharpoons}} [Eo^{2-} \cdots cis\text{-}Azo\text{-}V^{2+}] \qquad (a)$$

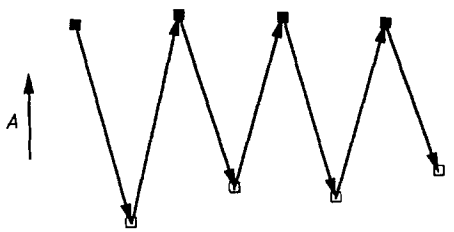

Fig. 2. Periodic complexation and decomplexation of diad **1** to and from eosin, followed by absorption differences of free and associated eosin. □: complexed Eo^{2-} in the presence of *cis*-**1**; ■: free Eo^{2-} in the presence of *trans*-**1**.

[*] Prof. Dr. I. Willner
Institute of Chemistry and the Farkas Center for Light-Induced Processes
The Hebrew University of Jerusalem
Jerusalem 91904 (Israel)

[**] This research was supported by the Basic Research Foundation administered by the Israel Academy of Sciences and Humanities. The Farkas Center is supported by the Bundesministerium für Forschung und Technologie and the Minerva Gesellschaft.

cis-**1** to *trans*-**1** ($\lambda > 400$ nm) results in separation of the complex, as evidenced by restoration of the absorption band of free eosin. Figure 2 shows the periodic complexation and separation [Eq. (a)] of the bipyridinium unit and eosin on remote photoinduced isomerization of the azobenzene component. In all photoinduced transformations of *trans*-**1** to *cis*-**1**, a photostationary state corresponding to 60% *cis* and 40% *trans* form is generated. Furthermore, the thermal reisomerization of *cis*-**1** is influenced by the complex formation, while transformation of *cis*-**1** to *trans*-**1** in dimethylsulfoxide (DMSO) proceeds at 323 K with a rate constant of $k = 4 \times 10^{-3}\ s^{-1}$. This is enhanced in the complex configuration, and the derived rate constant is $k = 3.9 \times 10^{-2}\ s^{-1}$.

We thus conclude that on–off photostimulated binding of the azobenzene-4,4′-bipyridinium diad to eosin proceeds by photoinduced isomerization of the photochromic component. The performance of this system resembles to some extent the functions of macroscopic machines. The separated form is analogous to the neutral position of a machine. Upon isomerization of *trans*-**1** to *cis*-**1** the system is geared into the complexed state. Further studies to modify the two complex components by including a catalytic site and a reactive site are now under way in our laboratory in an attempt to drive a catalytic transformation with the geared supramolecular assembly.

Received: April 22, 1992 [Z 5315 IE]
German version: *Angew. Chem.* **1992**, *104*, 1255

CAS Registry numbers:
cis-**1**, 142867-97-8; *cis*-**1**·**2**, 142867-99-0; *trans*-**1**, 142867-96-7; *trans*-**1**·**2**, 142867-98-9; **2**, 47604-22-8; **2**·*N,N′*-dimethyl-4,4′-bipyridinium, 137122-81-7.

[1] D. Hug, *Photochem. Photobiol. Rev.* **1978**, *3*, 1.
[2] K. Martinek, I. V. Berezin, *Photochem. Photobiol.* **1979**, *29*, 637.
[3] M. Irie, *Adv. Polym. Sci.* **1990**, *27*, 94.
[4] I. Willner, S. Rubin, T. Zor, *J. Am. Chem. Soc.* **1991**, *113*, 4014.
[5] M. Irie, D. Kungwatchakum, *Makromol. Chem. Rapid Commun.* **1984**, *5*, 829.
[6] a) M. Irie, K. Hayashi, *J. Macromol. Sci. Chem. A* **1979**, *13*, 511; b) M. Irie, K. Hirano, S. Hashimoto, K. Hayashi, *Macromolecules* **1981**, *14*, 262; c) M. Irie, M. Honda, *Makromol. Chem. Rapid Commun.* **1985**, *6*, 533.
[7] I. Willner, S. Rubin, A. Riklin, *J. Am. Chem. Soc.* **1991**, *113*, 3321.
[8] I. Willner, S. Rubin, unpublished.
[9] a) S. Shinkai, T. Nakaji, T. Ogawa, K. Shigematsu, O. Manabe, *J. Am. Chem. Soc.* **1981**, *103*, 111; b) S. Shinkai, K. Shigematsu, Y. Kusano, O. Manabe, *J. Chem. Soc. Perkin Trans. 1* **1981**, 3279; c) S. Shinkai, T. Ogawa, Y. Kusano, O. Manabe, K. Kikukawa, T. Goto, T. Matsuda, *J. Am. Chem. Soc.* **1982**, *104*, 1960; d) S. Shinkai, T. Minami, Y. Kusano, O. Manabe, *ibid.* **1982**, *104*, 1967.
[10] a) J. D. Winkler, K. Deshayes, B. Shao, *J. Am. Chem. Soc.* **1989**, *111*, 769; b) K. Kimura, T. Yamashita, M. Yokoyama, *Chem. Lett.* **1991**, 965.
[11] I. Willner, Y. Eichen, M. Rabinovitz, R. Hoffman, S. Cohen, *J. Am. Chem. Soc.* **1992**, *114*, 637.
[12] H. A. Benesi, J. H. Hildebrand, *J. Am. Chem. Soc.* **1949**, *71*, 2703.

Solid-State Columns Made from Twisted, Self-Complementary Terpyridine Units**

By *Chia-Yu Huang, Vince Lynch*, and *Eric V. Anslyn**

One goal in the design of self-assembling molecular arrays[1] is to confidently predict solid-state structures. The assembly of organic molecules into predictable motifs has potential in the preparation of organic materials with useful optical or electronic properties.[2] To accomplish self-organization, two compounds are typically used which serve as complementary recognition units that guide the crystallization into a desired pattern.[3] Hydrogen-bond donors and acceptors are convenient for this purpose, since the directionality of the hydrogen bonds can be predicted,[4] and such donors and acceptors can be synthetically incorporated into the monomeric units used to form a polymeric array. In order to construct crystalline materials whose physical properties can be systematically varied, one strategy would be to form a scaffold with repeating units that allow the attachment of electron donors or acceptors,[5] or possibly structures with good nonlinear optical properties.[6] The α-helical scaffold of a protein is a particularly attractive design to mimic, since the amino acid side chains protrude from the helix in predictable and repeatable spatial positions.[7] The hydrogen bonds that direct the assembly of the secondary structure are colinear or directed toward the helix axis, and thus are not perturbed by the side chains.[8] The α-helix structure forms a columnar scaffold in which functional groups (the side chains) project from the column, and whose basic structural components may be mimicked by assembly of self-complementary monomers. A schematic representation of such a scaffold is shown in Figure 1. We report here a crystalline material with a structure that conforms to this conceptual design.

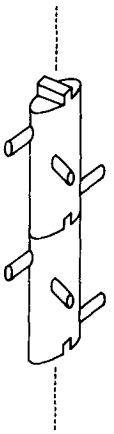

Fig. 1. A schematic representation of a columnar scaffold with sites for attachment of molecular units (the pegs). This scaffold is assembled by interactions of the recognition sites (the slots and teeth) along the column axis.

We reported recently on the complexation of nonplanar guests such as carbohydrates and their analogues with the polyaza cleft molecules **1** and **2**.[9] Since compounds **1** and **2** are twisted, we anticipated that in the solid state they might display the motif shown in Figure 1. The 2-aminopyridine groups could serve as the hydrogen-bond donors and acceptors to induce self-assembly, and the ethyl ester groups would point toward the outside of the scaffold. Herein, we show that compound **2** does indeed form such a structure, but compound **1** does not.

Both compounds **1** and **2** exist in solution as a mixture of *meso* as well as (+) and (−) isomers. According to molecu-

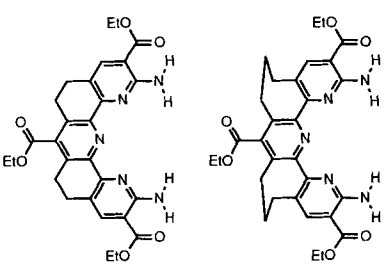

1 **2**

[*] Prof. Dr. E. V. Anslyn, C.-Y. Huang, V. Lynch
Department of Chemistry and Biochemistry
University of Texas at Austin
Austin, TX 78712 (USA)

[**] This work was supported by grants from the National Science Foundation (High Risk Research Program) and the Welch Foundation.

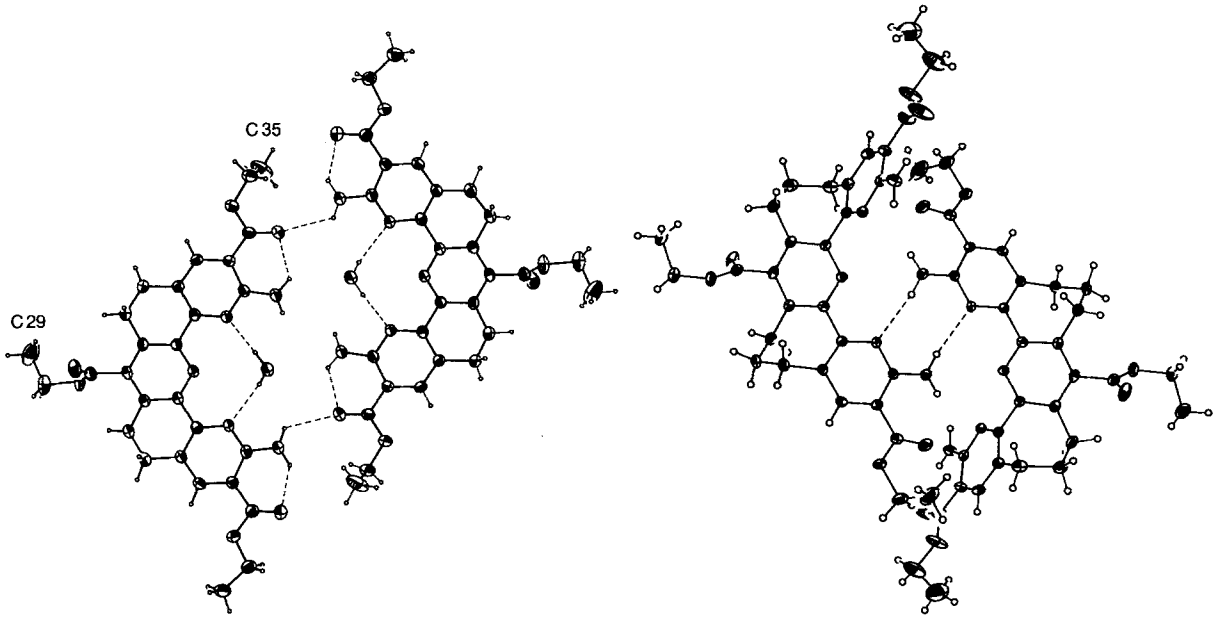

Fig. 2. Left: Dimeric structure of **1** in the solid state with two molecules of water. Right: Dimeric structure of **2** in the solid state showing the two intermolecular hydrogen bonds that ultimately lead to the columnar structure.

lar mechanics calculations,[10] the (+)/(−) isomers of **2** are typically 2 to 3 kcal mol^{-1} lower in energy than the *meso* isomer;[11] the energy difference for **1** is only about 1 kcal mol^{-1}. In the (+)/(−) isomers of **2** the angle formed by the two peripheral pyridine units is 80° in the calculated structure, and 79.8° in the crystal structure.[11] In contrast, the corresponding angle in **1** is calculated to be 24°, but is only 11° in the crystal structure. The discrepency between the calculated and the crystal structure is probably due to a water of crystallization found in **1** which would tend to make the host molecule less twisted so that it may form more linear hydrogen bonds with the water molecule (Fig. 2 left). Figure 2 shows the dimeric structures of compounds **1** and **2** in the solid state. In both cases the (+)/(−) isomers are found. In compound **2** (Fig. 2 right), the twist opens up the structure allowing each peripheral 2-aminopyridine moiety to associate with and form hydrogen bonds to an adjacent monomeric unit; this rigidifies the structure. Each hydrogen bond is close to linearity, and the N–N distance is nearly 3.0 Å. In contrast, compound **1** does not form a columnar scaffold but instead traps a water molecule between the peripheral 2-aminopyridine units. A molecular model of compound **1** suggests that a dihedral angle of only 24° between the peripheral 2-aminopyridines is not enough to allow dimerization of the monomers. "Polymerization" is thus prevented because of steric congestion.

Repetition of the hydrogen-bonding motif shown in Figure 2 leads to a columnar structure for compound **2** (Fig. 3). The ribbon (Fig. 3 middle) is drawn so as to depict the flow of the scaffold coplanar with the three pyridine rings of each

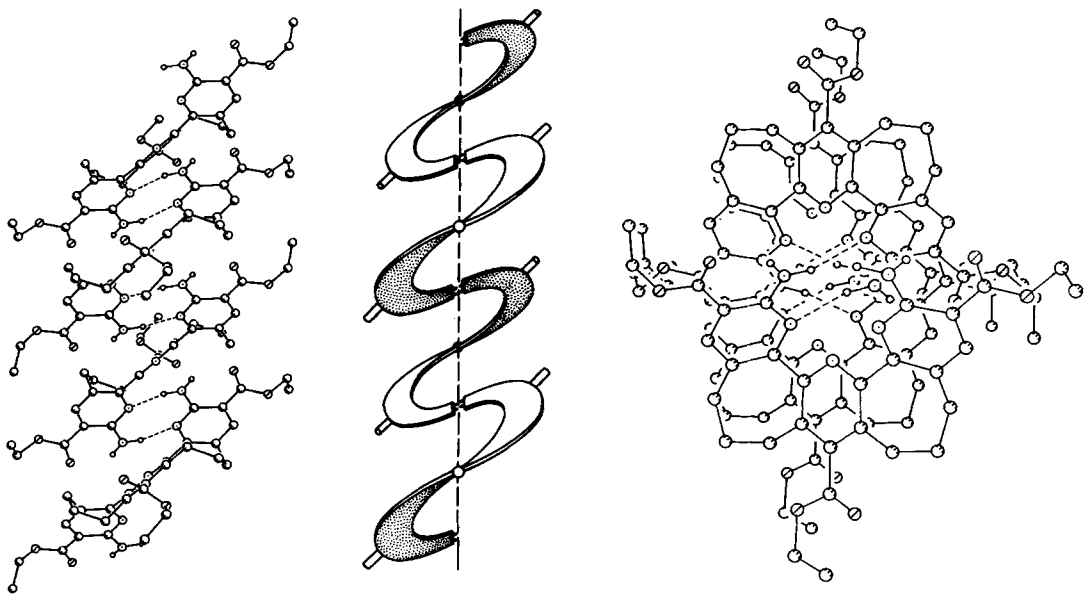

Fig. 3. Left: Four monomeric units of **2** of the self-assembled columnar scaffold. Middle: Schematic representation of the scaffold structure. Right: A view of the scaffold along the axis showing the interior hydrogen bonding that assembles the structure and the protruding ester groups.

monomer. The monomers are held together by two hydrogen bonds shown as two small dashed lines, and the ester groups are represented by pegs. The large dashed line drawn through the length of the ribbon is the column axis, and it passes through each pair of the hydrogen bonds. Two monomeric units are required to reach a translationally equivalent position along the column. The distance (the pitch of the helix) between equivalent positions is 10.8 Å. The perpendicular rise between the planes formed by the central pyridine rings is 3.74 Å, and the tilt angle of the central pyridines to the column axis is 48.2°. The tilt angle of the peripheral pyridines with respect to the column axis is 50°.

Figure 3 right shows a view of the scaffold down the column axis. Ethyl ester groups are oriented approximately 90° to each other when viewed down this axis. There are two types of ethyl ester groups: on two sides of the scaffold those of the peripheral pyridine units are stacked 5.4 Å apart and eclipse each other; on the other two sides the separation is also 5.4 Å but the ester groups of the central pyridine units are staggered. Thus on these sides of the scaffold, equivalent ester groups are 10.8 Å apart.

In summary, **2** forms a scaffold-type framework by self-complementarity, whereby the monomers are not covalently linked. Metal complexes of oligopyridine ligands have been extensively studied by Lehn et al. and Constable et al.[11,12] in an alternate approach to a similar helical columnar motif. We are currently testing if this structure is retained when the ethyl esters of **2** are derivatized. We are also preparing chiral monomers for the investigation of helix formation.

Experimental Procedure

Crystals of **1** [9] ($C_{28}H_{29}N_5O_6 \cdot H_2O$) were obtained as yellow plates from CH_2Cl_2/CH_3CO_2Et. One crystal was cut into a long needle $0.1 \times 0.2 \times 0.9$ mm. The X-ray data were collected at room temperature on a Nicolet P3 diffractometer with a graphite monochromator and $Mo_{K\alpha}$ radiation ($\lambda = 0.7107$ Å). Crystals of **2** [9] ($C_{30}H_{33}N_5O_6$) were obtained as pale yellow prisms and needles from $CHCl_3/CH_3CO_2Et$. The crystal selected for X-ray analysis was a prism of approximate dimensions $0.1 \times 0.2 \times 0.4$ mm. The data were collected at 173 K on a Nicolet R3 diffractometer, equipped with a Nicolet LT-2 low-temperature device and with a graphite monochromator and $Mo_{K\alpha}$ radiation ($\lambda = 0.7107$ Å). Four reflections were remeasured every 96 reflections to monitor the stability of the instrument and the crystal. A smoothed curve of the intensities of these control reflections was used to scale the data. The data were corrected for Lp effects but not for absorption. Data reduction and decay correction were performed with the SHELXTL-Plus software package. [13] Both structures were solved by direct methods and refined by full-matrix least-squares [13] with anisotropic thermal parameters for the non-H atoms. The hydrogen atoms were obtained from a ΔF map and refined with isotropic temperature factors. For **1**, the hydrogen atoms on C29 and C35 did not refine well and were idealized in the final refinement cycles (C–H 0.96 Å). The function, $\sum w(|F_o| - |F_c|)^2$ was minimized, where $w = 1/(\sigma(F_o))^2$ and $\sigma(F_o) = \{0.5\, kI^{-1/2}[(\sigma(I))^2 + (0.02\, I)^2]^{1/2}\}$. The intensity I is given by $(I_{peak} - I_{background}) \times$ scan rate, where 0.02 is a factor to downweight intense reflections and to account for instrument instability, and k is the correction due to Lp effects and decay. $\sigma(I)$ was estimated from counting statistics; $\sigma(I) = [(I_{peak} + I_{background})^{1/2} \times$ scan rate]. Neutral atom scattering factors for the non-H atoms were taken from Cromer and Mann, [14] with the corrections for anomalous dispersion taken from the work of Cromer and Liberman. [15] The scattering factors for the H atoms were obtained from Stewart, Davidson and Simpson. [16] Values used to calculate the linear absorption coefficient are from the International Tables for X-ray Crystallography (1974). [17] Other computer programs used in this work are listed elsewhere. [18] All figures were generated with SHELXTL-Plus. [13] Further details of the crystal structure investigation are availables on request from the Director of the Cambridge Crystallographic Data Centre, University Chemical Laboratory, Lensfield Road, GB-Cambridge CB2 1EW (UK), on quoting the full journal citation.

Received: March 23, 1992 [Z 5257 IE]
German version: *Angew. Chem.* **1992**, *104*, 1259

[1] F. J. DiSalvo, *Science (Washington D.C.)* **1990**, *247*, 608.
[2] F. L. Carter, *Molecular Electronic Devices II*, Marcel Dekker, New York, **1982**; R. W. Murray in *Chemical Sensors and Microinstrumentation* (Eds.: D. C. Melchior, R. L. Bassett), *ACS Symp. Ser. 403*, American Chemical Society, Washington DC, **1989**, pp. 1–19; J. D. Wright, *Molecular Crystals*, Cambridge Univ. Press, Cambridge, **1987**; G. R. Desiraju, *Crystal Engineering: The Design of Organic Solids*, Elsevier, New York, **1989**.
[3] S. J. Geib, S. C. Hirst, C. Vincent, A. D. Hamilton, *J. Chem. Soc. Chem. Commun.* **1991**, 1283; N. Shimuzu, N. Nishigaki, K. Osaki, *Acta Crystallogr. Sect. B* **1982**, *38*, 2309; M. C. Etter, D. A. Adsmond, *J. Chem. Soc. Chem. Commun.* **1990**, 479; J. A. Zerkowski, C. T. Seto, D. A. Wierda, G. M. Whitesides, *J. Am. Chem. Soc.* **1990**, *112*, 9025; M. Gallant, M. T. P. Viet, J. D. Wuest, *J. Org. Chem.* **1991**, *56*, 2284; J.-M. Lehn, *Angew. Chem.* **1988**, *100*, 91–116; *Angew. Chem. Int. Ed. Engl.* **1988**, *27*, 89–112; *ibid.* **1990**, *102*, 1347–1362 and **1990**, *29*, 1304–1319; H. C. Haddon, A. A. Lamola, *Proc. Natl. Acad. Sci. USA* **1985**, *82*, 1874–1878.
[4] M. C. Etter, *Acc. Chem. Res.* **1990**, *23*, 120–126, and references therein; L. Leiserowitz, M. Tuval, *Acta Crystallogr., Sect. B* **1978**, *34*, 1230; L. Leiserowitz, A. T. Hagler, *Proc. R. Soc. London A* **1983**, *288*, 133.
[5] F. Wudl, *Acc. Chem. Res.* **1984**, *17*, 227; J. M. Williams, M. A. Beno, H. H. Wang, P. C. Leung, T. J. Emge, U. Geiser, K. D. Carlson, *ibid.* **1985**, *18*, 261.
[6] D. J. Williams, *Angew. Chem.* **1984**, *96*, 637–651; *Angew. Chem. Int. Ed. Engl.* **1984**, *23*, 690–703; P. N. Prasad, B. A. Reinhardt, *Chem. Mater.* **1990**, *2*, 660.
[7] L. Pauling, R. B. Corey, *Proc. Int. Wool Text. Res. Conf. B* **1955**, 249. This predictability was recently used in the design and synthesis of an ion channel: N. Voyer, *J. Am. Chem. Soc.* **1991**, *113*, 1818.
[8] L. Pauling, *The Nature of the Chemical Bond*, Cornell University Press, Cornell, NY, USA, **1960**.
[9] C. Y. Huang, L. A. Cabell, E. V. Anslyn, *Tetrahedron Lett.* **1990**, *31*, 7411; C. Y. Huang, L. A. Cabell, V. Lynch, E. V. Anslyn, *J. Am. Chem. Soc.* **1992**, *114*, 1900.
[10] Macromodel Version 2.5, Clark Still, Columbia University.
[11] Calculations with the MM2, OPLSA, and AMBER force fields all found the (+)/(−) isomers to be lower in energy than the *meso* isomer.
[12] M. M. Harding, U. Koert, J.-M. Lehn, A. Marquis-Rigault, C. Piquet, J. Siegel, *Helv. Chim. Acta.* **1991**, *74*, 594; E. C. Constable, M. D. Ward, D. A. Tocher, *J. Chem. Soc. Dalton Trans.* **1991**, 1675; J.-M. Lehn, A. Rigault, J. Siegel, J. Harrowfield, B. Chevrier, D. Moras, *Proc. Nat. Acad. Sci. USA* **1987**, *84*, 2565–2569.
[13] G. M. Sheldrick, SHELXTL-PLUS (Version 4.1), Nicolet XRD, Madison, Wisconsin, USA, **1989**.
[14] D. T. Cromer, J. B. Mann, *Acta Crystallogr. Sect. A* **1968**, *24*, 321–324.
[15] D. T. Cromer, D. Liberman, *J. Chem. Phys.* **1970**, *53*, 1891–1898.
[16] R. F. Stewart, E. R. Davidson, W. T. Simpson, *J. Chem. Phys.* **1965**, *42*, 3175–3187.
[17] *International Tables for X-ray Crystallography, Vol. IV*, Kynoch Press, Birmingham, **1974**, p. 55.
[18] S. M. Gadol, R. E. Davis, *Organometallics* **1982**, *1*, 1607–1613.

Pheromones of Marine Brown Algae; A New Branch of the Eicosanoid Metabolism**

By *Klemens Stratmann, Wilhelm Boland,** and *Dieter G. Müller*

Most of the semiochemicals (pheromones) in the sexual cycle of marine brown algae (Phaeophyceae) known today are acyclic or cyclic hydrocarbons with the molecular formulas $C_{11}H_{14}$, $C_{11}H_{16}$, $C_{11}H_{18}$, or $C_{11}H_{14}O$.[1,2] Fertile female gametes of the brown alga *Ectocarpus siliculosus*, a species found worldwide, release a mixture of ectocarpene (**A**), dictyotene (**B**), hormosirene (**C**), and finavarrene (**D**) to attract male gametes[3] (Fig. 1). The two most important pheromones are (+)-(*S*)-ectocarpene (**A**) and (−)-(1*R*,2*R*)-hormosirene (**C**); their threshold concentrations are in the range of 0.1 to 1 nM.

(+)-(*S*)-Ectocarpene (**A**), dictyotene (**B**), and finavarrene (**D**) are also produced by terrestrial plants. According to

[*] Prof. W. Boland, Dr. K. Stratmann
Institut für Organische Chemie der Universität
Richard-Willstätter-Allee 2
D-W-7500 Karlsruhe (FRG)
Prof. D. G. Müller
Fakultät für Biologie der Universität
Postfach 5560, D-W-7750 Konstanz (FRG)

[**] We thank Michael Schöttler for his assistance.

modeling experiments with the South African *Senecio isatideus* (Asteraceae), these compounds arise in them from the multiply unsaturated C_{12} carboxylic acids **4** or **5** by oxidative decarboxylation[4, 5] (Scheme 1). We report here that in marine algae this class of compounds does not arise from the unsaturated C_{12} precursors **4** or **5** as previously thought, but is derived from the pool of polyunsaturated C_{20} fatty acids. Externally supplied [$^2H_8$]arachidonic acid **2** can be converted into labeled 6-butylcyclohepta-1,4-diene **1** (dictyotene **B**, Fig. 1) in high yield by female gametes of *E. siliculosus*. The relative amount of [$^2H_4$]-**1** obtained in the observed de novo synthesis from [$^2H_8$]-**2** under standard conditions[7] exceeds the amount of the natural accompanying component **1** by 800%, as is evident from the ratio of the signals of the respective molecular ions at *m/z* 150 and 154.

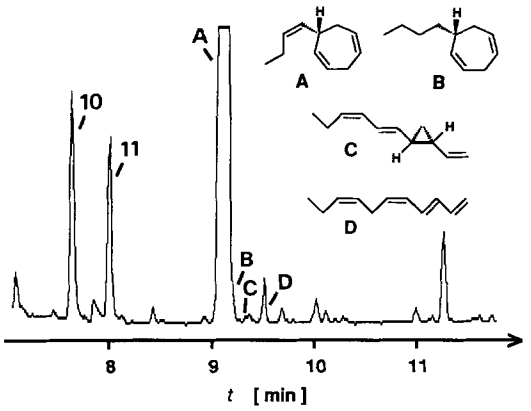

Fig. 1. Section of the gas chromatogram of the volatile compounds produced by the female gametes of the marine brown alga *Ectocarpus siliculosus*. **A**, **B**, **C**, and **D** are natural C_{11} compounds. **10** and **11** are the artificially derived C_{10} metabolites obtained after incubation with [$^2H_6$]-**7**. A similar product profile is observed after application of [$^2H_6$]-**7** to female gametes of *Sphacelaria rigidula*. GC conditions: RSL 300 (30 m × 0.32 mm; Alltech, Munich (FRG)) under programmed conditions (40 °C for 2 min, then heated at 10 °C min^{-1} to 250 °C); detector: Finnigan ion trap ITD 800.

The deuteration pattern[4] and the structure of [$^2H_4$]-**1** indicate that this $C_{11}H_{18}$ hydrocarbon is formed from the C(10) to C(20) segment of the arachidonic acid [$^2H_8$]-**2**. Logically, a $C_{11}H_{16}$ hydrocarbon, for example **A**, **C**, or **D** (cf. Fig. 1), should arise from the aliphatic terminus of the yet more unsaturated eicosapentaenoic acid (**6**). This was established for ectocarpene (**A**) and finavarrene (**D**) with the [$^2H_6$]-C_{19} carboxylic acid **7**, which was designed as a short-chain analogue of natural eicosapentaenoic acid (**6**)[6] (Scheme 1).

[$^2H_6$]-**7** was metabolized very efficiently by female gametes of the brown alga *E. siliculosus* into the two deuterated C_{10} hydrocarbons **10** and **11**. The terminus of the metabolic probe, [$^2H_6$]-**7**, is one carbon atom shorter than in **6**, thus guaranteeing that the artificial metabolites **10** and **11** can be analyzed without interference from the natural products **A** and **D**. Figure 1 shows a profile of the substances formed in a typical incubation[7] with [$^2H_6$]-**7**. Relative to the natural pheromone **A** the production of **10** and **11** amounts to 10%! The mass spectrum of [$^2H_6$]-**10** displays the expected signal of the molecular ion (*m/z* 140) and a fragmentation pattern characteristic for cycloheptadienes like **10**.[4, 5] Careful analysis of the mass spectrum indicates that the ring closure to **10** occurs between C(10) and C(16) in the precursor [$^2H_6$]-**7** with retention of the positions of the deuterium atoms. The fragmentation pattern of the second C_{10} metabolite, [$^2H_6$]-**11**, corresponds to that of an acyclic olefin related to finavarrene (**D**).[4] The overproportional amount of [$^2H_6$]-**11** formed (Fig. 1) may be related somehow to the shorter chain, since the short-chained substrates of the terrestrial plant *S. isatideus* (e.g. nona-3,6-dienoic acid) are converted exclusively to acyclic olefins (e.g. 1,3,5-octatriene).[4] A metabolite corresponding to the trace component **C** was not found.

In experiments in which the gametes of the marine brown algae *E. siliculosus* are incubated with the C_{12} trienecarboxylic acid **5** or with a [$^2H_6$]-C_{11} analogue with a shorter terminal chain, the corresponding ectocarpene or [$^2H_6$]-**10** and [$^2H_6$]-**11** are not produced. According to this, the *intact* framework of the eicosanoids **3** or **6** is essential to the formation of the $C_{11}H_{18}$ and $C_{11}H_{16}$ hydrocarbons; a preceding degradation to **4** or **5** (4 × β oxidation) does not take place in the female gametes of marine brown algae.

The description above also holds for other members of the class Phaeophyceae. In experiments with female gametes from *Sphacelaria rigidula*, which also release primarily ectocarpene (**A**),[8] a spectrum of products analogous to that from *E. siliculosus* is obtained (cf. Fig. 1). Especially impor-

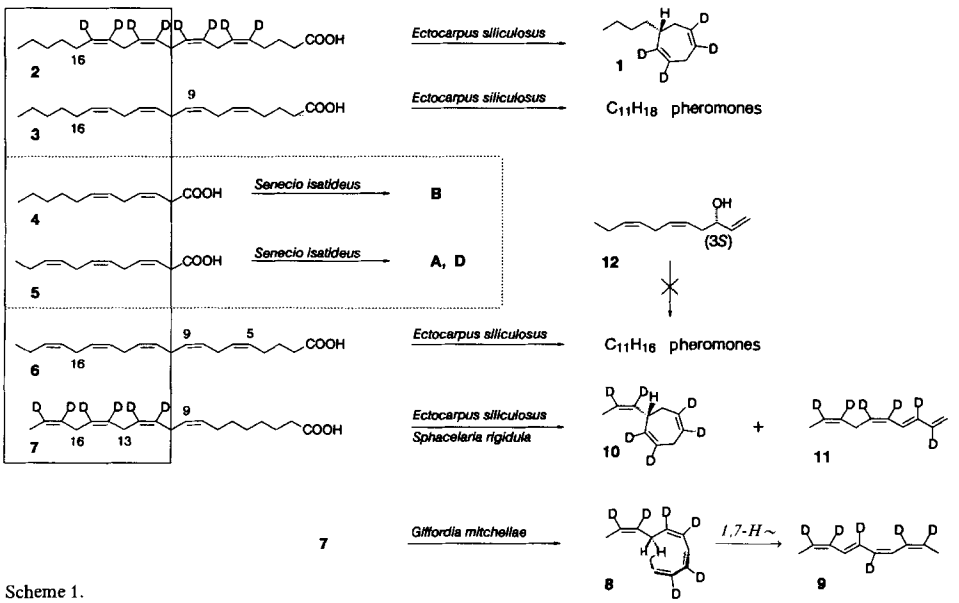

Scheme 1.

tant was the finding that [$^2H_6$]-**7** is transformed by the gametophytes of the brown alga *Giffordia mitchellae* into **9**, the C_{10} analogue of giffordene[9] (giffordene = (2*Z*,4*Z*,6*E*,8*Z*)-undeca-2,4,6,8-tetraene). In analogy to the biosynthesis of the acyclic tetraene **11**, which arises from **7** by loss of a hydrogen atom at C(13) and cleavage of the C(9)–C(10) bond, the formation of the intermediate (3*Z*,5*Z*,8*Z*)-decatetra-1,3,5,8-ene (**8**) must be postulated in order to account for the unusual geometry of **9**. Compound **8** is thermally labile and rearranges below room temperature into the isomeric tetraene **9** by an antarafacial [1,7] hydrogen shift.[9, 10] This electrocyclic reaction which otherwise occurs only in the biosynthesis of vitamin D[11] is now proven experimentally for the first time for the secondary metabolism of marine brown algae as well.

(3*S*,5*Z*,8*Z*)-Undeca-1,5,8-trien-3-ol (**12**),[12, 13] isolated from brown algae, was discussed by Moore and Jaenicke as an intermediate common to the fatty acid metabolism and the $C_{11}H_{16}$ pheromones.[14] A recently reported "biomimetic" synthesis of hormosirene (**B**) from **12** appears to support this hypothesis.[15] In analogy to the biosynthesis of the mushroom aroma oct-1-en-3-ol, **12** could be derived from a C_{20} polyene carboxylic acid.[16] Under standard conditions[7] all incubation experiments with a chain-shortened (5*Z*,8*Z*)-[5,6,8,9-$^2H_4$]-deca-1,5,8-trien-3-ol were negative. The expected [$^2H_4$]-propenylcycloheptadiene [$^2H_4$]-**10** was not found. Thus, we rule out the unsaturated alk-1-en-3-ols of type **12** as intermediates between the fatty acid metabolism and the C_{11} hydrocarbons. Because the eicosanoids are not catabolized into the multiply unsaturated C_{12} carboxylic acids **4** or **5**, we presume that 9-hydroxy- or 9-hydroperoxyeicosapentaenoic acid is the intermediate. In these compounds the functionalized C(9) of **3** and **6** corresponds to the carboxyl groups of **4** and **5** (Scheme 1), the precursors of the $C_{11}H_{18}$ and $C_{11}H_{16}$ hydrocarbons in higher plants. Thus, the group of C_{11} compounds in the brown algae could arise from the pool of eicosanoids according to the fragmentation $C_{20} \rightarrow C_{11} + C_9$, whereas in higher plants unsaturated fatty acids are converted to the olefins according to the scheme $C_{12} \rightarrow C_{11} + C_1$.

Received: April 10, 1992 [Z 5299 IE]
German version: *Angew. Chem.* **1992**, *104*, 1261

CAS Registry numbers:
7, 142781-27-9; **10**, 142864-29-7; **11**, 142781-26-8; dictyotene, 22735-58-6; arachidonic acid, 506-321-1.

[1] I. Maier, D. G. Müller, *Biol Bull.* **1986**, *170*, 145.
[2] W. Boland, *Biol. Unserer Zeit* **1987**, *17*, 176.
[3] D. G. Müller, C. E. Schmid, *Biol. Chem. Hoppe-Seyler* **1988**, *369*, 647.
[4] W. Boland, K. Mertes, *Eur. J. Biochem.* **1985**, *147*, 83.
[5] C. Neumann, W. Boland, *Eur. J. Biochem.* **1990**, *191*, 453.
[6] Eicosapentaenoic acid (**6**) and arachidonic acid (**3**) are the main components of the phospholipids found in the membranes of female gametes of *E. siliculosus*: C. E. Schmid, W. Eichenberger, D. G. Müller, *Biol. Chem. Hoppe-Seyler* **1991**, *372*, 540.
[7] *Experimental Procedure*: To a cell suspension of approximately 10^8 gynogametes of *E. siliculosus* in 15 mL of seawater was added 0.2 mg of [$^2H_6$]-**7** in 2 μL of DMSO. After 30 min at 18 °C the volatile components were collected over 24 h on a filter of active charcoal (1.5 mg; CLSA filter, CH-8405 Winterthur (Switzerland)) by means of a circulating stream of air (miniature circulation pump; Brey, D-W-8940 Memingen (FRG)) in a closed system. The dead volume of the circulating air was about 15 mL. The filter was eluted with CH_2Cl_2 (30 μL), and the metabolites were characterized by GC/MS. The method was modified from: W. Boland, P. Ney, L. Jaenicke, G. Gassmann in *Analysis of Volatiles* (Ed.: P. Schreier), de Gruyter, Berlin, **1984**, p. 371.
[8] D. G. Müller, W. Boland, L. Jaenicke, G. Gassmann, *Z. Naturforsch. C* **1985**, *40*, 457.
[9] W. Boland, N. Schroer, C. Sieler, M. Feigel *Helv. Chim. Acta* **1987**, *70*, 1025; W. Boland, L. Jaenicke, D. G. Müller, G. Gassmann, *Experientia* **1987**, *43*, 466.
[10] F. Näf, R. Decorzant, W. Thommen, B. Willhalm, G. Ohloff, *Helv. Chim. Acta* **1975**, *58*, 1016.
[11] M. Akhtar, C. J. Gibbons, *J. Chem. Soc. (London)* **1965**, 5964.
[12] K. Yamada, H. Tan, H. Tatematsu, M. Ojika, *Tetrahedron* **1986**, *42*, 3775.
[13] W. Boland, D. G. Müller, *Tetrahedron. Lett.* **1987**, 307.
[14] L. Jaenicke, D. G. Müller, R. E. Moore, *J. Am. Chem. Soc.* **1974**, *96*, 3324; R. E. Moore, *Acc. Chem. Res.* **1977**, *10*, 40.
[15] W. D. Abraham, T. Cohen, *J. Am. Chem. Soc.* **1991**, *113*, 2313.
[16] M. Wurzenberger, W. Grosch, *Biochem. Biophys. Acta* **1984**, *795*, 163.

Separation of Overlapping Multiplets in Two-Dimensional NMR Spectra by Selective "Injection" of Magnetization**

By *Catherine Zwahlen, Sébastien J. F. Vincent,* and *Geoffrey Bodenhausen**

Broadly speaking, multidimensional NMR spectra can be interpreted at two different levels of sophistication. In many cases, it is sufficient to focus on chemical shifts, but a more thorough analysis must also address the information contained in the fine-structure of cross-peak multiplets.[1] There are three major obstacles that may impair such a detailed analysis: excessive complexity, poor digital resolution, and accidental overlap. Very complicated structures can be simplified either by some means of decoupling during signal acquisition, or by partial deconvolution of the multiplets once they have been recorded.[2] The problem of digital resolution can be solved very effectively by "zooming in" on multiplets with the help of "soft" two-dimensional methods such as selective correlation spectroscopy (soft-COSY).[3] However, these methods are unsuitable when the experimentalist is confronted with overlapping multiplets. Serious cases of overlap call for some way of increasing the dimensionality of the spectra. While three-dimensional spectra recorded with non-selective pulses have the advantage that multiplets rarely suffer from overlap, their digital resolution is usually very poor. Thus, it is desirable to record three-dimensional spectra with *selective* pulses,[4] but three-dimensional experiments are relatively cumbersome and time-consuming, and it is difficult to present the outcome in a graphically pleasing way.

Fortunately, it is possible to achieve a similar separating effect by a "poor man's" form of three-dimensional spectroscopy, which amounts to recording signals in a plane $S(\omega_2,\omega_3)$ of a hypothetical $S(\omega_1,\omega_2,\omega_3)$ data cube, where one of the three frequency variables (i.e. ω_1) is fixed. This can be achieved by a variant of relayed magnetization transfer, where coherence is "injected" in a selective manner at the beginning of the evolution period of a soft-COSY sequence. Consider a soft-COSY experiment that is set up to correlate multiplets resonating in the vicinity of Ω_A in ω_1 and Ω_X in ω_2. If there are several spins that resonate at nearly or precisely degenerate frequencies Ω_A, $\Omega_{A'}$,... and Ω_X, $\Omega_{X'}$,..., the soft-COSY spectrum will consist of a superposition of cross-peaks due to coherence transfer processes $A \rightarrow X$, $A' \rightarrow X'$,... Now suppose that each of the nearly degenerate nuclei A, A',..., has a coupling partner M, M',..., and suppose that these are *not* degenerate amongst each other. In such a case,

[*] Prof. Dr. G. Bodenhausen, C. Zwahlen, S. J. F. Vincent
Section de Chimie, Université de Lausanne
Rue de la Barre 2, CH-1005 Lausanne (Switzerland)

[**] We thank Dr. W. Bermel, Karlsruhe, and Prof. H. Kessler, Garching, for a sample of *cyclo*-(L-Pro^1-L-Pro^2-D-Pro^3). This work was supported by the Swiss National Science Foundation and by the Commission pour l'Encouragement de la Recherche Scientifique (CERS).

one may carry out experiments where the soft-COSY sequence is preceded by a selective coherence transfer step $M \rightarrow A$, or $M' \rightarrow A'$, etc. In this manner, the soft-COSY multiplets of the processes $A \rightarrow X$, $A' \rightarrow X'$, etc., can be unraveled.[5]

We have recently shown[6, 7] how a doubly selective homonuclear Hartmann-Hahn (HOHAHA) transfer can be used in one-dimensional spectra. Figure 1a shows the pulse sequence for one-dimensional applications. In-phase magnetization I_x^M is first excited by a self-refocusing 270° Gaussian pulse truncated at 2.5% with a typical duration of 30 ms for a peak amplitude of 55 Hz.[8] More sophisticated pulses such as Gaussian cascades optimized by quaternions[9] or E-BURP pulses[10] may also be used. In Figure 1, the doubly selective irradiation of duration τ_{DSI} is implemented by modulating a rectangular radiofrequency (rf) pulse with a function $\cos(\omega_a t)$, where $\omega_a = \frac{1}{2}(\Omega_M - \Omega_A)$. This modulation

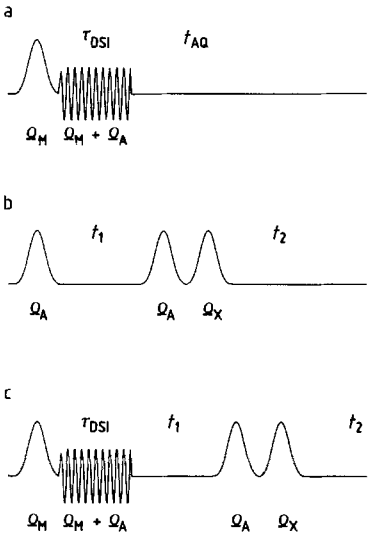

Fig. 1. a) Pulse sequence for selective in-phase coherence transfer in one-dimensional spectroscopy. The initial 270° Gaussian pulse, with a carrier frequency set at the chemical shift Ω_M, excites in-phase magnetization of spin M, which is transferred to spin A during the subsequent doubly selective irradiation period $\tau_{DSI} \approx 1/J_{AM}$, with two rf sidebands at Ω_M and Ω_A. The phase of the spin-locking field is orthogonal to the phase of the initial excitation pulse. b) Normal selective correlation experiment (soft-COSY) using three self-refocusing 270° Gaussian pulses, the first to excite A magnetization, the latter two for transferring magnetization from spin A to spin X. c) SPLIT-COSY sequence, consisting of a soft-COSY preceded by a doubly selective HOHAHA to inject in-phase coherence from spin M to spin A at the beginning of the evolution period. To suppress unwanted signals, the phases of the first pulse and of the receiver are alternated between 0 and 180° in all three sequences.

generates two sidebands at frequencies $\omega_{rf} \pm \omega_a$, which coincide with the chemical shifts Ω_M and Ω_A of the two chosen spins, provided the carrier frequency is placed at $\omega_{rf} = \frac{1}{2}(\Omega_M + \Omega_A)$. The optimum duration of the doubly selective irradiation is given by the inverse of the active coupling constant, $\tau_{DSI} = 1/J_{AM}$. The amplitude of the doubly selective irradiation must be optimized empirically to give the best in-phase transfer, as shown in Figure 2 for a transfer within the coupling network of L-proline[2] of *cyclo*(L-Pro[1]-L-Pro[2]-D-Pro[3]) **1**.[11]

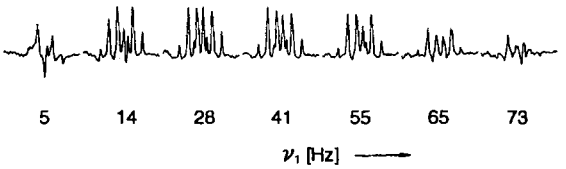

Fig. 2. Optimization of the rf amplitude ν_1 [Hz] for a HOHAHA transfer between the β^{cis} proton ($\delta = 2.10$) and the β^{trans} proton ($\delta = 1.62$) of L-proline[2] in **1** in $C_6D_6/CDCl_3$ (8/1) at 303 K. Since $J(\beta^{cis}\beta^{trans})$ is -12.8 Hz, τ_{DSI} is 78 ms. The experiments were performed on a Bruker MSL 300 spectrometer equipped with an Oxford Research Systems selective excitation unit.

Typically, the optimum radiofrequency amplitude ν_1 is 30 Hz for each sideband. If the amplitude is much weaker, it is impossible to lock all magnetization components within each multiplet simultaneously; if the rf amplitude is too large, various passive spins, some of which may have chemical shifts that lie accidentally in the vicinity of the rf sidebands, will also be perturbed.

Figure 1b shows the pulse sequence for normal selective correlation spectroscopy (soft-COSY). The in-phase magnetization I_x^A partly evolves into an anti-phase term $2I_x^A I_z^X$ during t_1.[12] The second and third pulses convert this term first into $2I_z^A I_z^X$, then into $2I_z^A I_x^X$, which evolves into observable magnetization I_x^X. The method can easily be adapted for soft-NOESY, by inserting a mixing period τ_m between the last two pulses.[8, 13] Figure 1c shows the sequence obtained by combining Figures 1a and 1b; in effect, the initial pulse of the soft-COSY experiment is applied at Ω_M rather than at Ω_A, and it is immediately followed by a doubly selective irradiation period τ_{DSI} for HOHAHA transfer from M to A. The only information needed prior to setting up the experi-

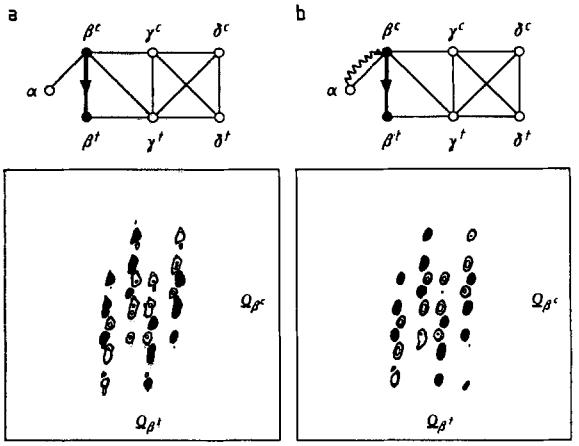

Fig. 3. a) Soft-COSY experiment correlating the β^{cis} proton (at $\delta = 1.23$ in the vertical ω_1 domain) and the β^{trans} proton ($\delta = 2.79$ in the horizontal ω_2 domain) of D-proline[3] in **1** obtained by exciting the magnetization of the β^{cis} proton by a simple 270° Gaussian pulse at the beginning of the evolution period. b) Same multiplet, but obtained by injection of magnetization from the α proton ($\delta = 4.49$) to the β^{cis} proton at the beginning of the evolution period, as indicated on the graph representing the coupling network. Since in D-proline[3] $J(\alpha\beta^{cis})$ is 6.5 Hz, τ_{DSI} is 154 ms. The spectral widths were 75 Hz in both ω_1 and ω_2. The matrices consisted of 128 × 1 K data points before and 256 × 1 K data points after zero filling. A Lorentz-Gauss transformation (LB = −0.3, GB = 0.05) was applied before Fourier transformation. With two scans for each t_1 increment and a relaxation delay of 10 s, the overall duration required for spectrum a was about 45 min; 16 scans were used for spectrum b.

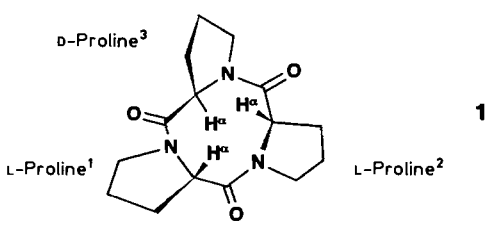

1

ment is the chemical shift Ω_M of a "passive" M spin which must be coupled to one of the A spins that we wish to distinguish. It is also desirable (though not essential) that we know the approximate value of the coupling constant J_{AM} to be able to estimate the optimum duration $\tau_{DSI} \approx 1/J_{AM}$ of the doubly selective irradiation period.

Before tackling difficult cases with overlapping multiplets, it appears advisable to check the efficiency of HOHAHA injection by an application to a harmless case within the coupling network of D-proline[3] of *cyclo*(L-Pro[1]-L-Pro[2]-D-Pro[3]) **1**.[11] The agreement of the patterns and pure absorption peak shapes in the multiplets shown in Figure 3 provides conclusive evidence that excitation by HOHAHA transfer, if done properly, is fully equivalent to excitation with a selective pulse. Figure 3 also shows graphs of coupling networks where the nodes represent the spins and the edges their mutual couplings.[14] To represent a soft-COSY experiment symbolically, a bold arrow runs from the spin that is active in t_1 to the one that carries the coherence in t_2, while HOHAHA transfer is represented by a wavy arrow.

Now consider a case where the multiplets appear to be hopelessly entangled. In earlier studies, the 1:3 mixture of the ethyl esters **2** of *cis*- and *trans*-2-phenylcyclopropanoic acid (R = $COOCH_2CH_3$, R' = C_6H_5) was used to test the limits of pattern recognition[14] and multiplet separation[15] procedures.

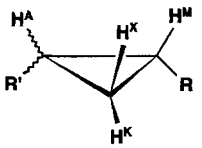

2

The protons A^{trans} and A^{cis} on the one hand, and X^{trans} and X^{cis} on the other, have pairwise nearly the same chemical shifts. This situation is very typical for a mixture of isomers. In a conventional soft-COSY experiment, one obtains two strongly overlapping multiplets due to the two transfer processes $X^{trans} \rightarrow A^{trans}$ and $X^{cis} \rightarrow A^{cis}$ (Fig. 4a). Fortunately, the existence of nondegenerate coupling partners M^{trans} and M^{cis} makes it possible to transfer magnetization selectively to either X^{trans} *or* X^{cis}. A soft-COSY sequence following selective transfer may provide pure cross-peaks of either $X^{trans} \rightarrow A^{trans}$ *or* $X^{cis} \rightarrow A^{cis}$, as illustrated in Figures 4c and 4b, respectively. We dubbed this novel experiment *S*eparation of *P*atterns by *L*ifting the *I*mbroglio of *T*ransfer in *Co*rrelation *S*pectroscop*y* (SPLIT-COSY).

Figure 5 illustrates an interesting case where our technique failed to split two overlapping cross-peaks due to an unforeseen case of degeneracy. In the normal soft-COSY spectrum corresponding to the region shown in Figure 5, one observes two severely overlapping multiplets due to $\gamma^{trans} \rightarrow \beta^{trans}$ and $\beta^{cis} \rightarrow \beta^{trans}$ in L-proline[1]. We hoped to split these by using a selective HOHAHA transfer to γ^{trans} from two other strongly coupled protons of the same amino acid, δ^{cis} and δ^{trans}. To our disappointment, the SPLIT-COSY spectrum obtained in this manner, which is shown in Figure 5, is virtually identical to the corresponding soft-COSY spectrum. This experiment shows that the magnetization received by γ^{trans} is in part transferred to β^{cis}, although the J coupling constants between β^{cis} and both δ^{cis} and δ^{trans} are vanishingly small. In general, when two coupled spins have nearly the same chemical shift, it is not possible to transfer magnetization to one of them selectively. Indeed, two such spins will always be irradiated at the same time by one of the rf sidebands, so that

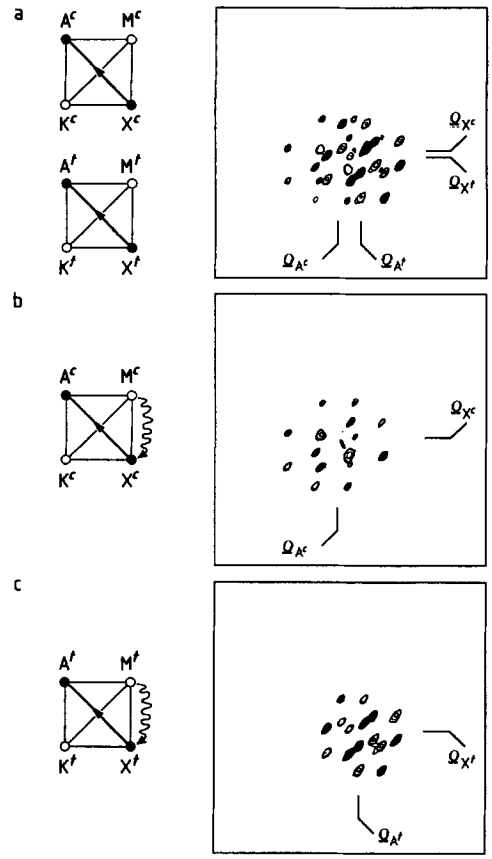

Fig. 4. a) Normal soft-COSY spectrum of **2** in $CDCl_3$ showing overlapping cross-peaks $X^{cis} \rightarrow A^{cis}$ and $X^{trans} \rightarrow A^{trans}$. The symbols A^c and A^t stand for the H^A protons of the *cis* and *trans* isomers of **2**. b) Clean $X^{cis} \rightarrow A^{cis}$ multiplet (centered at $\delta = 1.16$ and 2.42, respectively) obtained by SPLIT-COSY with injection from M^{cis} ($\delta = 1.95$) to X^{cis} with $\tau_{DSI} = 130$ ms. c) Clean $X^{trans} \rightarrow A^{trans}$ multiplet (centered at $\delta = 1.18$ and 2.40) obtained by an injection from M^{trans} ($\delta = 1.79$) to X^{trans}, with $\tau_{DSI} = 108$ ms. Experimental conditions were the same as for the spectra in Figure 3.

if any magnetization is transferred to one of them, it will automatically be transferred to the other, in the manner of total correlation spectroscopy (TOCSY).[16]

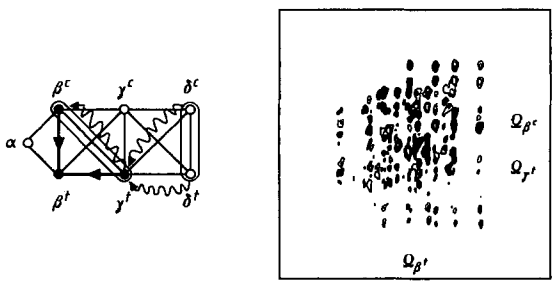

Fig. 5. SPLIT-COSY spectrum of **1** centered at $\delta = 1.59$ in ω_1 and 2.27 in ω_2, showing a superposition of two cross-peaks $\beta^{cis} \rightarrow \beta^{trans}$ and $\gamma^{trans} \rightarrow \beta^{trans}$ in L-proline[1]. In this case, a doubly selective HOHAHA period led to a transfer from δ^{cis} *and* δ^{trans} (which are nearly degenerate at $\delta = 3.55$) to γ^{trans} *and* β^{cis}, the latter being coupled and nearly degenerate in the vicinity of $\delta = 1.59$. Experimental conditions were the same as for the spectra in Figure 3.

Although the two-step transfer from $\delta^{cis} + \delta^{trans}$ to β^{cis} represents an obstacle to the separation of the two overlapping multiplets in Figure 5, the same phenomenon can be put to use in a constructive fashion to separate the multiplets in Figure 6a. These two multiplets originate from two different

proline residues. The L-proline[2] multiplet can be separated easily by a transfer from β^{cis} to β^{trans} as shown in Figure 6b. In order to excite only the β^{cis} proton of L-proline[1], magnetization was transferred from the strongly coupled pair $\delta^{cis} + \delta^{trans}$ to the strongly coupled pair $\beta^{cis} + \gamma^{trans}$. The resulting multiplet is represented in Figure 6c and corresponds perfectly to the pattern in Figure 6a obtained by soft-COSY.

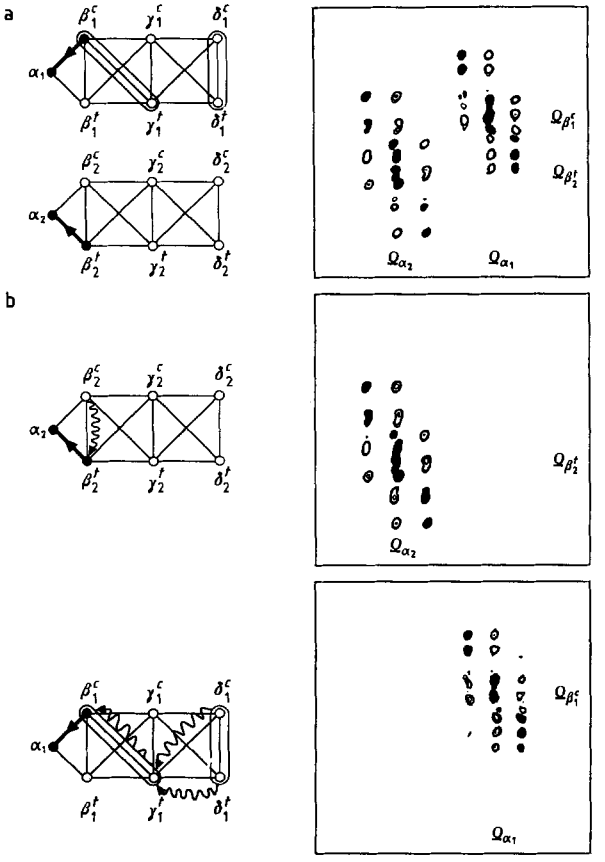

Fig. 6. a) Multiplets obtained with normal soft-COSY of **1**, centered at $\delta = 1.60$ in ω_1 and $\delta = 4.28$ in ω_2. To the left, cross-peak correlating the β^{trans} proton (at $\delta = 1.62$) and the α proton ($\delta = 4.32$) of L-proline[2]; to the right, cross-peak connecting the β^{cis} proton ($\delta = 1.58$) and the α proton ($\delta = 4.23$) of L-proline[1]. b) SPLIT-COSY multiplet of L-proline[2] alone obtained by injection of magnetization from β^{cis} ($\delta = 2.10$) to β^{trans} via $J(\beta^{cis}\beta^{trans}) = -12.8$ Hz with $\tau_{DSI} = 78$ ms. c) SPLIT-COSY multiplet of L-proline[1] alone obtained by injection of magnetization from the two nearly degenerate protons δ^{cis} ($\delta = 3.52$) and δ^{trans} ($\delta = 3.57$), with $J(\delta^{cis}\delta^{trans}) = -11.7$ Hz, to the two nearly degenerate and strongly coupled protons γ^{trans} and β^{cis} ($\delta = 1.61$ and 1.58, with $J(\gamma^{trans}\beta^{cis}) = 3.4$ Hz) via $J(\delta^{cis}\gamma^{trans}) = 3.1$ Hz and $J(\delta^{trans}\gamma^{trans}) = 6.7$ Hz. The cleanest in-phase magnetization was obtained for $\tau_{DSI} = 220$ ms. In this case, the double irradiation period was followed by a hard purging pulse in order to remove antiphase terms [6]. Experimental conditions were the same as those for the spectra in Figure 3.

Our new SPLIT-COSY technique allows one to separate overlapping multiplets in crowded parts of COSY spectra in order to extract hidden information. The structure of the resulting multiplets is the same as in soft-COSY, unlike the multiplets obtained in *S*electively *I*nverted *S*oft COSY (SIS-COSY).[15] In general, samples containing mixtures of isomers, which are likely to give overlapping cross-peaks, should become amenable to investigation, provided each isomer has at least one site with a distinct chemical shift. If necessary, several consecutive HOHAHA transfer steps may be used.

Received: April 7, 1992 [Z 5285 IE]
German version: *Angew. Chem.* **1992**, *104*, 1233

CAS Registry numbers:
1, 70493-40-2; *cis*-**2**, 946-39-4; *trans*-**2**, 946-38-3.

[1] R. R. Ernst, G. Bodenhausen, A. Wokaun, *Principles of Nuclear Magnetic Resonance in One and Two Dimensions*, Clarendon Press, Oxford, **1987**.
[2] J.-M. Le Parco, L. McIntyre, R. Freeman, *J. Magn. Reson.* **1992**, *97*, 553; P. Huber, G. Bodenhausen, *ibid.*, in press.
[3] R. Brüschweiler, J. C. Madsen, C. Griesinger, O. W. Sørensen, R. R. Ernst, *J. Magn. Reson.* **1987**, *73*, 380; J. Cavanagh, J. P. Waltho, J. Keeler, *ibid.* **1987**, *74*, 386.
[4] J. Friedrich, S. Davies, R. Freeman, *Mol. Phys.* **1988**, *64*, 691; C. Griesinger, O. W. Sørensen, R. R. Ernst, *J. Magn. Reson.* **1989**, *84*, 14.
[5] N. Müller, L. Di Bari, G. Bodenhausen, *J. Magn. Reson.* **1991**, *94*, 73.
[6] R. Konrat, I. Burghardt, G. Bodenhausen, *J. Am. Chem. Soc.* **1991**, *113*, 9135.
[7] B. Boulat, R. Konrat, I. Burghardt, G. Bodenhausen, *J. Am. Chem. Soc.*, **1992**, *114*, 5412.
[8] L. Emsley, G. Bodenhausen, *J. Magn. Reson.* **1989**, *82*, 211.
[9] L. Emsley, G. Bodenhausen, *J. Magn. Reson.*, **1992**, *97*, 135.
[10] H. Geen, S. Wimperis, R. Freeman, *J. Magn. Reson.* **1989**, *85*, 620; H. Geen, R. Freeman, *ibid.* **1991**, *93*, 93.
[11] H. Kessler, W. Bermel, A. Friedrich, G. Krack, W. E. Hull, *J. Am. Chem. Soc.* **1982**, *104*, 6297.
[12] O. W. Sørensen, G. W. Eich, M. H. Levitt, G. Bodenhausen, R. R. Ernst, *Prog. Nucl. Magn. Reson. Spectrosc.* **1983**, *16*, 163; U. Eggenberger, G. Bodenhausen, *Angew. Chem.* **1990**, *102*, 392; *Angew. Chem. Int. Ed. Engl.* **1990**, *29*, 374.
[13] H. Oschkinat, G. M. Clore, A. M. Gronenborn, *J. Magn. Reson.* **1988**, *78*, 371; H. Oschkinat, W. Bermel, *ibid.* **1989**, *81*, 220.
[14] M. Nović, G. Bodenhausen, *Anal. Chem.* **1988**, *60*, 582; P. Pfändler, G. Bodenhausen, *J. Magn. Reson.* **1988**, *79*, 99.
[15] L. Emsley, P. Huber, G. Bodenhausen, *Angew. Chem.* **1990**, *102*, 576; *Angew. Chem. Int. Ed. Engl.* **1990**, *29*, 517; L. Emsley, G. Bodenhausen, *J. Am. Chem. Soc.* **1991**, *113*, 3309.
[16] L. Braunschweiler, R. R. Ernst, *J. Magn. Reson.* **1983**, *53*, 521.

Se_2NCl_3 and $[Se_2NCl_2]^+[GaCl_4]^-$, Chloride Nitrides of Trivalent Selenium**

By *René Wollert, Antje Höllwarth, Gernot Frenking, Dieter Fenske, Helmut Goesmann,* and *Kurt Dehnicke**

The chemistry of selenium–nitrogen compounds has only livened up in the last few years, mainly because of the development of new synthetic processes.[1] Nevertheless, the research in this field is often limited by the properties of the starting materials: the explosive character of tetraselenium tetranitride or by the low solubility of the more stable tetraselenium dinitride.[2] We report herein about a readily accessible chloride nitride of trivalent selenium, which is soluble in organic solvents and stable, but at the same time is very reactive and suitable as a synthetic reagent.

Diseleniumtrichloride nitride (**1**) is formed by the action of tris(trimethylsilyl)amine on a suspension of selenium tetrachloride in boiling dichloromethane [Eq. (a)]. Upon cooling

$$2\,SeCl_4 + N(SiMe_3)_3 \longrightarrow \underset{\mathbf{1}}{Se_2NCl_3} + 3\,ClSiMe_3 + Cl_2 \qquad (a)$$

moisture-sensitive crystals can be isolated from the red solution. **1**, which when viewed against light appear red but viewed against a background appear a shiny, metallic green.

[*] Prof. Dr. K. Dehnicke, Dr. R. Wollert, Dipl.-Chem. A. Höllwarth, Prof. Dr. G. Frenking
Fachbereich Chemie der Universität
Hans-Meerwein-Strasse, D-W-3550 Marburg (FRG)
Prof. Dr. D. Fenske, Dr. H. Goesmann
Institut für Anorganische Chemie der Universität Karlsruhe

[**] This work was supported by the Deutsche Forschungsgemeinschaft and the Fonds der Chemischen Industrie.

According to the X-ray crystal structure analysis[3] **1** forms planar molecules shaped like dividers and with almost C_{2v} symmetry (Fig. 1). The two symmetry-independent molecules are only slightly different from each other. The Se–N bonds in **1** (174 pm) are significantly shorter than the values expected for a Se–N single bond (186 pm [4]); thus π bonding contributions can be assumed. Similar short distances are

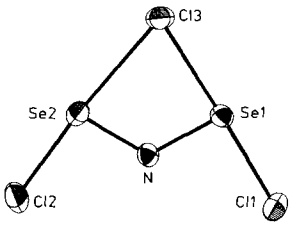

Fig. 1. Crystal structure of **1**.

also observed for other Se–N compounds with delocalized π bonding,[1] for example, in the cyclic anions $[SeN_2Se_2]_2^{2+}$ and $[SeN_2Se_2]^{2+}$ available from Se_4N_4 and arsenic pentafluoride.[5] The bond angle at the N atom in **1** (119.9°) is in accordance with sp^2 hybridization. The Se–Cl distances to the terminally bonded chlorine atoms in **1** are slightly longer (average value 223.4 pm) than the terminal Se–Cl bonds in the cubane structure of $[SeCl_4]_4$ (average value 216.4 pm);[6] in contrast the two bridging Se–Cl bonds in **1** are much shorter (average value 259.8 pm) than the Se–Cl bridging bonds in $[SeCl_4]_4$ (average value 279.4 pm). Nevertheless, the bridging chlorine atom in **1** is readily removed as chloride by the action of strong Lewis acids such as aluminum or gallium trichloride leading to the formation of **2** [Eq. (b)]. Com-

$$\mathbf{1} + GaCl_3 \longrightarrow \underset{\mathbf{2}}{[Se_2NCl_2]^+[GaCl_4]^-} \qquad (b)$$

pound **2** forms orange, moisture-sensitive crystals, which according to the X-ray crystal structure analysis[7] are ionic. The cation of **2** is formed by the rearrangement of the framework atoms of **1** (Fig. 2) and has a U-shaped structure. The

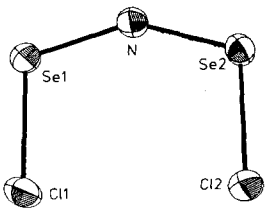

Fig. 2. Crystal structure of the cation of **2**.

cation is almost planar, and the Se–N and Se–Cl distances are the same within standard deviations, fulfilling the criteria for C_{2v} symmetry. As expected, all the bond lengths in **2** are slightly shorter than in **1**. The shortening of the Se–N bonds is accompanied by an opening of the Se-N-Se bond angle of 119.9° in **1** to 146.6° in **2**. This is also apparent in the IR spectra[8] from the shift of the υ_{as}Se-N-Se band from 830 cm^{-1} in **1** to 922 cm^{-1} in **2**.

Whereas the sulfur compound analogous to **1** is unknown, the $[N(SCl)_2]^+$ cation analogous to the cation of **2** is known with various counterions.[9–12]

Both **1** and **2** are diamagnetic; the ground state is thus a singlet state. In the ^{77}Se NMR spectra[13] in acetonitrile **1** shows a resonance signal at $\delta = 961$, the corresponding signal in the spectrum of **2** is shifted to $\delta = 1699$, which is explained by the deshielding of the selenium atoms in the cation of **2**. This signal lies in the range between that of **1** and those of the cations of $[Se_4^{2+}][AsF_6^-]_2$ ($\delta = 1936$ [14]) and $[SeN_2Se_2^{2+}][AsF_6^-]_2$ ($\delta = 2434$ [6]).

The results of quantum chemical ab initio calculations[15] of **1** and of the cation of **2** are in good agreement with the average values of the bond lengths and angles determined by experiment (Table 1). The deviations between the theoretical and the experimental values can partly be explained by crystal packing effects.

Table 1. Experimentally determined and theoretically calculated bond lengths [pm] and angles [°] of Se_2NCl_3 (**1**) and of $Se_2NCl_2^+$ the cation of **2**. Calculated partial charges q from the Mulliken population analysis.

	Se_2NCl_3		$Se_2NCl_2^+$	
	Experiment	Theory	Experiment	Theory
Se1-N1	174.2(5)	170.8	169.5(4)	167.9
Se2-N1	173.3(5)	170.8	169.4(4)	167.9
Se1-Cl1	226.9(2)	220.5	215.1(2)	212.2
Se2-Cl2	219.8(2)	220.5	214.3(2)	212.2
Se1-Cl3	251.9(2)	267.7		
Se2-Cl3	267.6(2)	267.7		
Se1-Cl3-Se2	70.7(1)	69.0		
Se1-N1-Se2	119.9(3)	126.7	146.6(3)	152.9
Cl1-Se1-N1	91.4(2)	101.0	108.3(1)	107.1
Cl2-Se2-N1	93.0(2)	101.0	108.3(1)	107.1
Cl3-Se1-N1	87.1(2)	82.2		
Cl3-Se2-N1	82.4(2)	82.2		
q(Cl3)		−0.61		
q(Cl1)		−0.21		−0.01
q(Se1)		+0.69		−0.70
q(N1)		−0.35		−0.38

The analysis of the occupied orbitals supports the assumption that the Se–N bonds in **1** and those in the cation of **2** have π bonding contributions. The orbital occupation shows five occupied valence orbitals with π symmetry for **1** and four occupied π orbitals for the cation of **2**. Of those, three and two, respectively, can be assigned to the π orbitals of the lone pairs at the chlorine atoms of **1** and in the cation of **2**, respectively. This means that the Se-N-Se unit in **1** and in the cation of **2** has two doubly occupied π orbitals and is therefore, with regard to the π bonds, valence isoelectronic with the allyl anion, which could be an explanation for the bond shortening. The bonding in **1** can be described with the mesomeric structures shown in Figure 3.

A topological analysis of the calculated wave function[16] of **1** indicates significant differences between the terminal

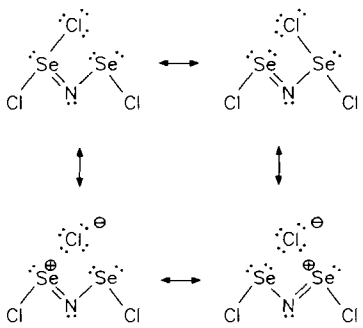

Fig. 3. Description of the bonding in **1** with mesomeric limiting structures.

Se–Cl bonds and the Se–Cl bridging bond. Figure 4 (left) shows the Laplacian distribution of the electron density of **1**. Whereas the electron density distribution of the bridging Cl atom is spherically symmetrical, the terminal Cl atoms show a significant distortion of the electron density distribution and an overlap with the electron density of the Se atoms. This indicates a covalent character for the terminal Se–Cl bonds, whereas the bridging Cl atom is rather ionically bound. The calculation of the charge distribution according to Mulliken[17] supports this interpretation (Table 1). The bridging Cl atom with a partial charge of -0.61 is clearly more negatively charged than the terminal Cl atoms (-0.21). The Se atoms in **1** have a positive partial charge ($+0.69$), which in the cation of **2** is almost identical ($+0.70$). The Laplacian distribution of the U-shaped cation (Fig. 4 right) shows that the only significant difference to the corresponding structural unit in **1** is the orientation of the Se-N-Se unit. Obviously the repulsion between the in-plane orbitals of the lone pairs at Cl and at N in the W-shaped structure of the cation of **2** is greater than that between Se and N in the U-shaped structure.

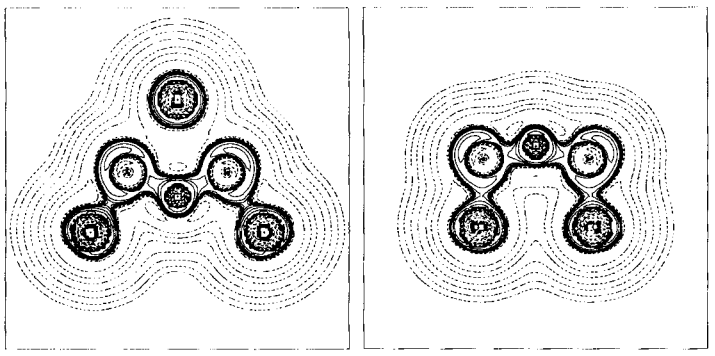

Fig. 4. Laplacian distribution of the electron density in **1** (left) and in the cation of **2** (right).

The calculated frequency spectra for **1** and for the cation of **2** show that the optimized structures are minima on the potential energy hypersurface (no negative eigenvalues of the Hessian matrix). In agreement with the experiment a frequency shift to higher wavenumbers is calculated for the highest positioned band (ν_{as}(Se-N-Se), b_2) from 862 cm^{-1} (**1**) to 909 cm^{-1} (cation of **2**) during the formation of **2** from **1**.

Experimental Procedure

1: A solution of tris(trimethylsilyl)amine (2.2 g, 9.4 mmol) in CH_2Cl_2 (20 mL) was added dropwise to a suspension of $SeCl_4$ (4.1 g, 18.7 mmol) in CH_2Cl_2 (30 mL) and stirred. This was refluxed for 12 h, filtered to remove small amounts of unreacted $SeCl_4$, and after concentration to 10 mL cooled to 5 °C. The red crystals were separated by filtration, washed with a little cold CH_2Cl_2, and dried in vacuum (yield 1.5 g, 57%, based on $SeCl_4$, m.p. 69 °C). The chlorine formed by this reaction reacted with a part of the tris(trimethysilyl)amine. An improvement in the yield strived for by the addition of larger quantities of amine is not advisable since explosive by-products are formed.

Received: March 27, 1992 [Z 5266 IE]
German version: *Angew. Chem.* **1992**, *104*, 1216

CAS Registry numbers:
1, 142581-22-4; **2**, 142581-23-5; $SeCl_4$, 10026-03-6; $N(SiMe_3)_3$, 1586-73-8; $GaCl_3$, 13450-90-3.

[1] M. Björgvinsson, H. W. Roesky, *Polyhedron* **1991**, *10*, 2353–2370.
[2] K. Dehnicke, F. Schmock, K. F. Köhler, G. Frenking, *Angew. Chem.* **1991**, *103*, 564–565; *Angew. Chem. Int. Ed. Engl.* **1991**, *30*, 577-578.
[3] Crystal data of **1** (−60): space group *Pbca*, $a = 1229.0(6)$, $b = 804.6(4)$, $c = 2433.6(12)$ pm, $Z = 16$, four-circle diffractometer STOE STADI IV, $Mo_{K\alpha}$ radiation, graphite monochromator, ω scan, $2\theta = 3$–$55°$, 2343 observed independent reflections ($I > 2\sigma(I)$) $R = 0.039$, $R_w = 0.035$ [7].
[4] A. F. Wells, *Structural Inorganic Chemistry*, Clarendon, Oxford, **1984**.
[5] E. G. Awere, J. Passmore, P. S. White, T. Klapötke, *J. Chem. Soc. Chem. Commun.* **1989**, 1415–1417.
[6] P. Born, R. Kniep. D. Mootz, M. Hein, B. Krebs, *Z. Naturforsch. B* **1981**, *36*, 1516–1519.
[7] Crystal data of **2** (−90): space group $P2_1/c$, $a = 948.3(4)$, $b = 1154.8(5)$, $c = 1042.9(5)$ pm, $\beta = 112.32(2)°$, $Z = 4$, four-circle diffractometer STOE STADI IV, $Mo_{K\alpha}$ radiation, graphite monochromator, ω scan, $2\theta = 3$–$54°$, 1867 observed independent reflections ($I > 2\sigma(I)$) $R = 0.031$, $R_w = 0.036$. Further details of the crystal structure investigation may be obtained from the Fachinformationszentrum Karlsruhe, Gesellschaft für wissenschaftlich-technische Information mbH, D-W-7514 Eggenstein-Leopoldshafen 2 (FRG) on quoting the depository number CSD-56328, the names of the authors, and the journal citation.
[8] IR spectra: Nujol mulls, CsI plates, Bruker IFS-88 (values in cm^{-1}). **1**: 830 st (ν_{as}SeNSe), 570 st, 545 m (δSeNSe), 340 vst ($\nu SeCl_{terminal}$), 220 vst (νSeClSe). **2**: 922 vst (ν_{as}SeNSe), 813 st (ν_sSeNSe), 595 m, 564 w, 546 w, (δSeNSe), 404 w, 352 st (νSeCl, $\nu GaCl_4$).
[9] O. Glemser, B. Krebs, J. Wegener, E. Kindler, *Angew. Chem.* **1969**, *81*, 568; *Angew. Chem. Int. Ed. Engl.* **1969**, *8*, 598.
[10] O. Glemser, E. Kindler, B. Krebs, R. Mews, F. M. Schnepel, *Z. Naturforsch. B.* **1980**, *35*, 657.
[11] H. G. Hauck, P. Klingelhöfer, U. Müller, K. Dehnicke, *Z. Anorg. Allg. Chem.* **1984**, *510*, 180.
[12] U. Müller, P. Klingelhöfer, U. Kynast, K. Dehnicke, *Z. Anorg. Allg. Chem.* **1985**, *520*, 18.
[13] ^{77}Se NMR spectra: acetonitrile solutions, external standard $SeMe_2$, measurement temperature 20 °C, Bruker AM 400, (76.312 MHz), 41046 scans for **1**, 2800 scans for **2**.
[14] M. J. Collins, R. J. Gillespie, J. F. Sawyer, G. J. Schrobilgen, *Inorg. Chem.* **1986**, *25*, 2053.
[15] The calculations were carried out with the program Gaussian 90 [18]. For Se the LANL1DZ pseudopotential [19] was used, which was expanded with a set of d functions (coefficient 0.038). For Cl a 3-21G(d) basis set [20a] and for N a 6-31G(d) basis set were applied [20b].
[17] R. S. Mulliken, *J. Chem. Phys.* **1955**, *23*, 1833.
[18] M. J. Frisch, M. Head-Gordon, G. W. Trucks, J. B. Foreman, H. B. Schlegel, K. Raghavachari, M. A. Robb, J. S. Binkley, C. Gonzalez, D. J. DeFrees, D. J. Fox, R. A. Whiteside, R. Seeger, C. F. Melius, J. Baker, R. Martin, L. R. Kahn, J. J. P. Stewart, S. Topiol, J. A. Pople, Gaussian 90, Gaussian Inc,. Pittsburgh, PA, **1990**.
[19] P. J. Hay, W. R. Wadt, *J. Chem. Phys.* **1985**, *82*, 284.
[20] a) P. C. Haraharan, J. A. Pople, *Chem. Phys. Lett.* **1972**, *66*, 217; b) W. J. Pietro, M. M. Francl, W. J. Hehre, D. J. DeFrees, J. A. Pople, J. S. Binkley, *J. Am. Chem. Soc.* **1982**, *104*, 5039.

Pyridine-2-thiolato Complexes of V^{II}, V^{III}, and V^{IV} with Unusual Structural Features**

By *John G. Reynolds,* Shawn C. Sendlinger, Ann M. Murray, John C. Huffman,* and *George Christou**

One of the stimuli for our continuing interest in vanadium–sulfur chemistry is the relevance of this area to industrial petroleum refining. Certain crude oils contain large amounts of vanadyl (VO^{2+}) impurities categorized into two types according to their ligands.[1] These are the vanadyl petroporphyrins, which have been well studied and characterized,[2] and the vanadyl nonporphyrins whose ligand environment is thought to contain S, N, and/or O donor atoms.[3] The presence of these vanadyl impurities leads to the formation of

[*] Prof. G. Christou, Dr. S. C. Sendlinger, Dr. J. C. Huffman
Department of Chemistry and Molecular Structure Center
Indiana University, Bloomington, IN 47405 (USA)
Dr. J. G. Reynolds, A. M. Murray,
Lawrence Livermore National Laboratory, Mail Stop L-524
P.O. Box 808
Livermore, CA 94550 (USA)

[**] This work was supported by the Office of Basic Energy Sciences, Division of Chemical Sciences, U.S. Department of Energy, Grant DE-FG02-87ER13702 (to G. C.) and Contract No. W-7405-ENG-48 (to J. G. R.)

vanadium sulfides (primarily V_2S_3 and V_3S_4) under the reducing and sulfur-rich hydrotreating conditions.[4] These sulfides have deleterious consequences on the activity and lifetime of the heterogeneous catalyst (e.g., Mo/Co/S on alumina) employed for upgrading crude oil. To model the progressive reduction, sulfide incorporation, and aggregation of VO^{2+} impurities in crude oil, we have studied a variety of vanadium–sulfur compounds which contain a number of thiolato ligands and range from mono- to tetranuclear in oxidation states from III to V.[5–11] More recently we have used the ligand pyridine-2-thiol (pytH) because it contains functional groups common in crude oils (thiolate S and arene N) and also has the ability to both chelate and bridge transition metals.[12] We herein report the syntheses of V^{II}, V^{III}, and V^{IV} complexes with pyt^- ligands which have unusual structural features; we also describe an extremely rare example of a thiolatovanadium(II) complex.

The addition of two equivalents of Na(pyt) to a solution of $[VOCl_2(thf)_2]$ in THF yields the vanadium(IV) compound **1**.[13] The structure of **1** (Fig. 1)[14, 23] displays an unusual

$[V_2O_2(pyt)_4]$ **1**

bridging arragement of two $\mu_2:\eta^1:\eta^2$-pyt^- ligands in which the N6 atom of pyridine makes up part of the base of the square-pyramidal coordination of V1 (vertices N6, N5, S2, S3′, O4) and the sulfur atom S3 of the same pyt^- unit occupies a basal position at V1′ [V1′–S3 = 2.457(4) Å]. In addition, the sixth position of the V1 coordination sphere *trans* to the oxo ligand is occupied by S3 [V1–S3 = 2.798(3) Å]. This complex is an extremely rare example of a compound with an unsymmetrical pyt^- bridge.[15] Two chelating pyt^- ligands complete the coordination sphere at each metal center. The V–O distance [1.583(6) Å] is normal for a triply bonded vanadyl unit, and the whole molecule has imposed C_i symmetry. The X-band EPR spectra of **1** dissolved in CH_2Cl_2 or THF recorded at room temperature show only the typical isotropic 8-line signals characteristic of mononuclear VO^{2+} species; this suggests that either the dinuclear arrangement is not retained in solution, or that the metal centers are noninteracting.

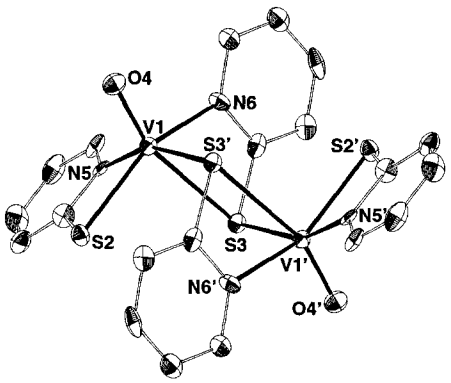

Fig. 1. ORTEP representation of complex **1** (ellipsoids at the 50% probability level). Primed and unprimed atoms are related by the inversion center. Selected interatomic distances [Å] and angles [°]: V1···V1′ 3.989(2), V1-S2 2.427(3), V1-S3 2.798(3), V1-S3′ 2.457(4), V1-O4 1.583(6), V1-N5 2.088(7), V1-N6 2.106(7); V1-S3-V1′ 98.65(9), O4-V1-S2 108.92(24), O4-V1-S3 158.99(24), O4-V1-S3′ 99.47(22), O4-V1-N5 101.13(28), O4-V1-N6 96.7(3), N5-V1-S3′ 158.11(19), S2-V1-N6 150.68(21), S2-V1-N5 68.51(19), S3-V1-N6 62.35(21).

Addition of four equivalents of Na(pyt) to a solution of $[VCl_3(thf)_3]$ in THF yields the vanadium(III) complex **2**.[16]

$[Na(thf)_2V(pyt)_4]$ **2**

The crystal structure of **2** (Fig. 2)[17, 23] shows a rare example of a vanadium(III) center with sevenfold coordination[18] which consists of three chelating pyt^- ligands and a fourth bound to the V atom by its sulfur atom (S23). The nitrogen

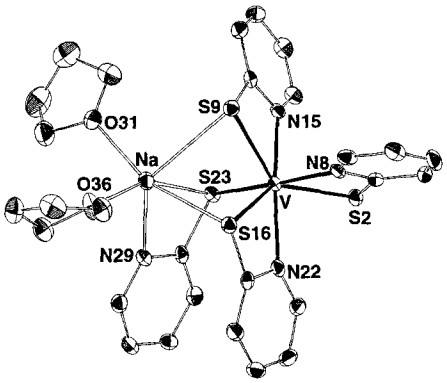

Fig. 2. ORTEP representation of complex **2** (ellipsoids at the 50% probability level). Selected distances [Å] and angles [°]: V-S2 2.526(1), V-S9 2.567(1), V-S16 2.543(1), V-S23 2.495(1), V-N8 2.121(3), V-N15 2.178(3), V-N22 2.187(3), Na-S9 3.042(2), Na-S16 2.887(2), Na-S23 2.951(2), Na-N29 2.400(3), Na-O31 2.286(3), Na-O36 2.325(3); S9-V-N15 64.39(9), S2-V-N8 66.59(9), S16-V-N22 64.57(9); Na-S9-V 77.15(7), Na-S16-V 80.44(7), Na-S23-V 79.96(7); N8-V-S23 168.14(9).

atom (N29) of this fourth pyt^- ligand is bound to a second metal center, the Na atom. There are also bonding interactions between the Na atom and S9, S16, and S23. Two THF molecules complete the coordination sphere of the Na atom. Complex **2** may best be described as a triply bridged heterobimetallic species because of the ligation mode of three of the four pyt^- ligands (particularly that containing S23 and N29). The formulation as an ion pair, $[Na(thf)_2]^+[V(pyt)_4]^-$, would be less accurate. In **2** the three pyt^- ligands are also in the rare μ_2: $\eta^1:\eta^2$ ligation mode.

Addition of two equivalents of Na(pyt) to a solution of $[VCl_2(tmeda)_2]$ (tmeda = tetramethylethylenediamine)[19] in CH_2Cl_2 or THF yields the vanadium(II) complex **3**,[20] an

$[V(pyt)_2(tmeda)]$ **3**

extremely rare example of a thiolatovanadium(II) complex.[22] Compound **3** (Fig. 3)[21, 23] is a mononuclear trischelate which has a distorted octahedral geometry because of the small bite angle of the pyt^- ligand. The molecule has imposed C_2 symmetry, and the S2-V-S2′ angle is 156.05(4)° rather than 180°. X-band EPR spectra of **3** dissolved in toluene recorded at room temperature show a broad signal near $g = 2$. At 115 K, an additional broad signal at $g = 4$ is observed, consistent with an $S = 3/2$ ground state.

The pyt^- complexes of V^{II}, V^{III}, and V^{IV} display unusual structural features and provide a useful family of related compounds for reactivity studies. Preliminary results show that both compounds **2** and **3** react with O_2 and S_8 to yield complex **1** and $[V_2S_2(pyt)_4]$, respectively. Also, dissolution of

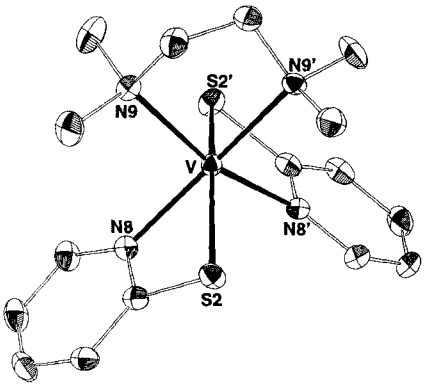

Fig. 3. ORTEP representation of complex **3** (ellipsoids at the 50% probability level). Selected distances [Å] and angles [°]: V-S2 2.547(1), V-N8 2.124(2), V-N9 2.252(2); S2-V-S2′ 156.05(4), S2-V-N8′ 97.24(6), S2-V-N8 66.85(8), S2-V-N9 97.63(6), S2-V-N9′ 100.45(6), N8-V-N8′ 99.89(13), N8-V-N9 90.65(9); N8-V-N9′ 164.27(8), N9-V-N9′ 81.64(12).

compound **2** in CH_2Cl_2 yields a white precipitate [Na(pyt) according to IR spectroscopy]. Efforts are currently underway to characterize this material, since mononuclear "$[V(pyt)_3]$" may be unstable with respect to aggregation.

Complexes **1** and **2** were studied by electron ionization mass spectrometry to determine gas-phase fragmentation pathways and probe possible C–S bond cleavage reactions. These transformations may serve as a models for some of the high-energy reactions occurring during hydrodemetallation/hydrodesulfurization of petroleum. Under normal ionization conditions, both compounds show one or more fragmentation pathways involving C–S bond cleavage, as previously detected in $[V(StBu)_4]$, in which the C–S bonds are more easily cleaved.[11] For example, $[VO(C_5H_4NS)_2]^+$ (*m/z* 287; 100% intensity) gives fragment ions assigned to $[VO(C_5H_4NS)(C_5H_4N)]^+$ (*m/z* 255; 4%), $[VO(C_5H_4N)_2]^+$ (*m/z* 223; 38%), and $[VO(C_5H_4NS)S]^+$ (*m/z* 208, 209; 10%) which appear to form through a one- or two-step process involving C–S bond cleavage. The ion $[V(C_5H_4NS)_3]^+$ responds similarly under the same conditions. Further details of both the mass spectrometric investigation and the reactivity studies will be reported in due course.

Received: April 8, 1992 [Z 5287 IE]
German version: *Angew. Chem.* **1992**, *104*, 1275

CAS Registry numbers:
1, 142839-69-8; **2**, 142865-80-3; **3**, 142865-18-9; $[VOCl_2(thf)_2]$, 29666-18-0; $[VCl_3(thf)_3]$, 19559-06-9; $[VCl_2(tmeda)_2]$, 122116-24-9.

[1] T. F. Yen in *The Role of Trace Metals in Petroleum*, Ann Arbor Science, Ann Arbor, Michigan, **1975**, Chapter 1.
[2] P. Psundararaman, *Anal. Chem.* **1986**, *57*, 2204.
[3] J. G. Reynolds, E. J. Gallegos, R. H. Fish, J. J. Komlenic, *Energy Fuels* **1987**, *1*, 36.
[4] a) B. G. Silbernagel, R. R. Mohan, G. H. Singhal, *ACS Symp. Ser.* **1984**, *248*, 91; b) B. G. Silbernagel, *J. Catal.* **1979**, *56*, 315; c) S. Asaoka, N. Nakata, C. Takeuchi, *ACS Symp. Ser.* **1987**, *344*, 275; d) M. Rose-Brussin, D. Moranta, *Appl. Catal.* **1984**, *11*, 85; e) P. C. H. Mitchell, C. E. Scott, J.-P. Bonnelle, J. G. Grimblot, *J. Chem. Soc., Faraday Trans. 1* **1985**, *81*, 1047.
[5] a) J. K. Money, J. C. Huffman, G. Christou, *Inorg. Chem.* **1985**, *24*, 3297; b) J. K. Money, K. Folting, J. C. Huffman, D. Collison, J. Temperly, F. E. Mabbs, G. Christou, *ibid.* **1986**, *25*, 4583.
[6] J. K. Money, J. R. Nicholson, J. C. Huffman, G. Christou, *Inorg. Chem.* **1986**, *25*, 4072.
[7] J. K. Money, J. C. Huffman, G. Christou, *J. Am. Chem. Soc.* **1987**, *109*, 2210.
[8] J. K. Money, K. Folting, J. C. Huffman, G. Christou, *Inorg. Chem.* **1987**, *26*, 944.
[9] J. K. Money, J. C. Huffman, G. Christou, *Inorg. Chem.* **1988**, *27*, 507.
[10] G. Christou, D. D. Heinrich, J. K. Money, J. R. Rambo, J. C. Huffman, K. Folting, *Polyhedron* **1989**, *8*, 1723.
[11] D. D. Heinrich, K. Folting, J. C. Huffman, J. G. Reynolds, G. Christou, *Inorg. Chem.* **1991**, *30*, 300.
[12] For recent examples, see: a) A. J. Deeming, M. Karim, P. A. Bates, M. B. Hursthouse, *Polyhedron* **1988**, *7*, 1401; b) K. Umakoshi, A. Ichimura, I. Kinoshita, S. Ooi, *Inorg. Chem.* **1990**, *29*, 4005; c) J. H. Yamamoto, W. Yoshida, C. M. Jensen, *Inorg. Chem.* **1991**, *30*, 1353 and references therein.
[13] A green-blue solution of $[VOCl_2(thf)_2]$ in THF turns dark brown on addition of Na(pyt). The solvent is removed under vacuum, the residue extracted with CH_2Cl_2, and the resulting solution filtered and placed in a freezer to allow the product to crystallize. Suitable crystals for the X-ray crystallographic study were obtained by filtering the initial reaction mixture through a fine frit and layering the solution with hexanes. Crystals so obtained lose solvent rapidly when removed from the mother liquor.
[14] Crystal data for $1 \cdot 2\ THF \cdot 1/3\ C_6H_{12}$: $C_{30}H_{36}N_{40}O_4S_4V_2$, 746.76 g mol^{-1}, hexagonal, $R\bar{3}$, $a = b = 30.888(21)$, $c = 8.960(6)$ Å, $V = 7402.84$ Å^3, $Z = 9$. A total of 1310 unique reflections with $I > 2.33\sigma(I)$ were refined to values of $R(R_w)$ of 0.0613 (0.0563).
[15] To our knowledge, only one complex with this ligation mode has been reported: M. V. Castano, A. Macias, A. Castineiras, A. S. Gonzalez, E. M. Martinez, J. S. Casas, S. Sordo, W. Hiller, E. E. Castellano, *J. Chem. Soc., Dalton Trans.* **1990**, 1001.
[16] Addition of Na(pyt) to a red solution of $[VCl_3(thf)_3]$ yields a black solution which slowly turns purple and finally turns blood-red. After overnight stirring, the solution was filtered and placed in a freezer to allow the product to crystallize.
[17] Crystal data for **2**: $C_{28}H_{32}N_4O_2S_4NaV$, 658.76 g mol^{-1}, triclinic, $P\bar{1}$, $a = 10.442(2)$, $b = 16.476(4)$, $c = 9.465(2)$ Å, $\alpha = 100.73(4)°$, $\beta = 109.20(4)°$, $\gamma = 87.86(3)°$, $V = 1510.33$ Å^3, $Z = 2$. A total of 3391 unique reflections with $I > 2.33\sigma(I)$ were refined to values of $R(R_w)$ of 0.0412 (0.0432).
[18] a) N. Vuletic, C. Djordjevic, *J. Chem. Soc., Dalton Trans.* **1973**, 1137; b) R. E. Drew, F. W. B. Einstein, *Inorg. Chem.* **1973**, *12*, 829; c) R. A. Levenson, R. J. G. Dominguez, M. A. Willis, F. R. Young III, *ibid.* **1974**, *13*, 2761; d) D. Begin, F. W. B. Einstein, J. Field, *ibid.* **1975**, *14*, 1785.
[19] J. J. H. Edema, W. Stauthamer, F. Bolhuis, S. Gambarotta, W. J. J. Smeets, A. L. Spek, *Inorg. Chem.* **1990**, *29*, 1302.
[20] A mixture of $[VCl_2(tmeda)_2]$ and two equivalents of Na(pyt) in CH_2Cl_2 or THF immediately turns a deep red-purple color. After several hours of stirring, the mixture is filtered and the solution is layered with hexanes to allow the product to crystallize.
[21] Crystal data for **3**: $C_{16}H_{24}N_4S_2V$, 387.45 g mol^{-1}, orthorhombic, $B22_12$, $a = 14.338(5)$, $b = 17.755(7)$, $c = 7.255(2)$ Å, $V = 1846.86$ Å^3, $Z = 4$. A total of 1192 unique reflections with $I > 2.33\sigma(I)$ were refined to values of $R(R_w)$ of 0.0220 (0.0261).
[22] W. Schmidt, G. Henkel, B. Krebs, *Proc. Int. Conf. Coord. Chem.* **1990**, *28*, 1–9. This conference abstract includes the structure of $(PPh_4)[V(pyt)_3]$.
[23] All structures were solved by direct methods and refined by full-matrix least-squares. Further details of the crystal structure investigations may be obtained from the Fachinformationszentrum Karlsruhe, Gesellschaft für wissenschaftlich-technische Information mbH, D-W-7514 Eggenstein-Leopoldshafen 2 (FRG), on quoting the depository number CSD-56417, the names of the authors, and the journal citation.

Aromatic Boron Heterocycles: The Generation of 1 H-Borepin and the Structure of Tricarbonyl(1-phenylborepin)molybdenum**

By *Arthur J. Ashe III,* Jeff W. Kampf, Yasuhiro Nakadaira,** and *Jennifer M. Pace*

Dedicated to Professor William von E. Doering on the occasion of his 75th Birthday

1*H*-Borepin (**1**) is of great interest because it is isoelectronic with tropylium (**2**).[1, 2] Prior work over thirty years has

[*] Prof. Dr. A. J. Ashe III, Dr. J. W. Kampf, J. M. Pace
Department of Chemistry
The University of Michigan
Ann Arbor, MI 48109-1055 (USA)
Prof. Dr. Y. Nakadaira
Department of Chemistry, The University of Electro-Communications
Chofu, Tokyo 182 (Japan)

[**] This work was supported by the Research Corporation and the donors of the Petroleum Research Fund, administered by the American Chemical Society.

produced a number of imaginative syntheses of highly substituted borepins,[3-9] while the minimally substituted 1-methylborepin (**3a**) has only recently been synthesized.[10] We report here on the first synthesis of the parent heterocycle **1** and on structural data which show that 1-substituted borepins can serve as η^7 aromatic ligands for transition metals.

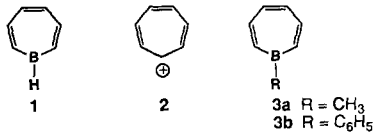

Borepins are most conveniently prepared by an exchange reaction of the appropriate stannepin with boron halides.[4,8-10] Thus, the reaction of 1,1-dibutylstannepin (**4**)[11] with phenylboron dibromide in benzene affords 1-phenylborepin (**3b**) in 30% yield. The reaction of **4** with excess BCl_3 in refluxing liquid butane affords 1-chloroborepin (**5**) as a volatile liquid (67% yield), which is easily purified by pot-to-pot distillation. Reaction of **5** with CH_3OH in CH_2Cl_2 gives 1-methoxyborepin (**6**) in 73% yield. These

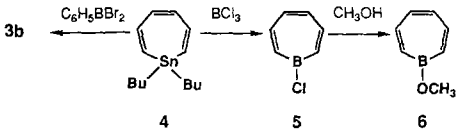

borepins are air sensitive and **5** is particularly sensitive, but they can be easily handled using Schlenk techniques. The NMR data for these compounds is summarized in Table 1.

When an excess of Bu_3SnH (50 mg) is added to a frozen solution of 10 mg of **5** in 500 μL of C_6D_6 in an NMR tube at −78 °C and then warmed to 25 °C, the ^1H NMR spectrum of the reaction mixture shows that the signals of **5** decrease over 15 min and new signals simultaneously appear. The spectrum after the reaction is complete is shown in Figure 1.[18] We assign this spectrum to 1*H*-borepin as discussed below. Since 1*H*-borepin is extremely moisture, oxygen, and heat sensitive, it has not been isolated. However, in a reaction characteristic of secondary boranes[13] **1** reacts with methanol to afford the methoxy derivative **6**.

The proof of the existence of 1*H*-borepin rests largely on the analysis of the ^1H, ^{11}B, and ^{13}C NMR spectra (Table 1). The ^1H NMR spectra of the four borepins **1**, **3b**, **5**, and **6** show virtually identical patterns of peaks, since the observed

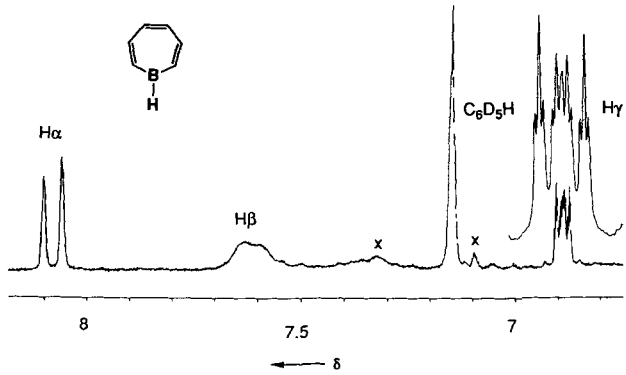

Fig. 1. The low-field region of the 300 MHz ^1H NMR spectrum of 1*H*-borepin in C_6D_6. The signals due to excess Bu_3SnH and Bu_3SnCl are not seen. The insert shows an expansion of the signal at $\delta = 6.89$ arising from the γ protons. Signals for unidentified oxidation products are marked with an x.

ring H–H coupling constants are all nearly equal.[14] The signals of the β protons are very broad doublets without fine structure because of strong quadrupolar coupling to ^{11}B, while the signals of the α protons are also somewhat broadened due to a weaker coupling. Only the signals for the remote γ protons are sharp. For **1** the signal of the proton bound to the boron atom was not observed presumably due to the signal width.[15] However, the ^{11}B NMR spectrum shows a broad doublet ($J = 99$ Hz), which collapses to a singlet on ^1H broad-band irradiation, indicating B–H coupling.

The ^{13}C NMR spectra of borepins **1**, **3b**, and **5** show that the α and β carbon atoms are almost identically deshielded while the signals of the γ carbon atoms are in the normal region for aromatic and olefinic carbon atoms. The STO-3G MO calculations on **1** give p–π orbital populations of 0.94, 0.94, and 0.98 electrons for the α, β, and γ carbon atoms, respectively.[2a] Since the ^{13}C NMR shifts are sensitive to changes in π electron density, the observed shifts are consistent with the calculations.

The low-field ^1H NMR shifts of the ring protons of substituted borepins have been taken as evidence of a diamagnetic ring current.[4,8-10] The low-field signals of **1**, particularly the signals of the α protons, also fit this pattern. Analysis of the ^1H NMR spectrum of **1** permits a discussion of its conformation. The Karplus relationship between the magnitude of the vicinal coupling constant $^3J_{H3,H4}$ and the torsion angle H3-C3-C4-H4 applies to cycloheptatriene and heterocycloheptatrienes.[16-18] The observed value of $^3J_{H3,H4}$ of 8.3 Hz is very close to that calculated from the torsion angle of 0° which is required for the planar conformation predicted by

Table 1. ^1H, ^{11}B, and ^{13}C NMR shifts of the new borepin derivatives and the borepin complex **7** (C_6D_6, 25 °C, coupling constants in Hz).

	1	**3b**	**5**	**6**	**7**
H2(7)	8.09 (d, $J(2,3) = 12.4$)	8.10 (d, $J(2,3) = 12.9$)	7.60 (d, $J(2,3) = 12.4$)	6.99 (d, $J(2,3) = 13.1$)	4.86 (d, $J(2,3) = 11.6$)
H3(6)	7.60 (br d)	7.62 (br d)	7.25 (br d)	7.30 (br d)	5.31 (br d)
H4(5)	6.89 (m, $J(3,4) = 8.3$)	6.85 (m, $J(3,4) = 8.0$)	6.57 (m, $J(3,4) = 8.3$)	6.56 (m, $J(3,4) = 8.4$)	4.64 (m, $J(3,4) = 7.8$)
B	48.0 (br d, $J = 99$)	48.8 (br)	47.9 (br)	40.0 (br)	28.1 (br)
C2(7)	152 (br)	149.5 (br)	150 (br)	140 (br)	98.1 (br)
C3(6)	149.2	148.2	148.3	146.2	112.1 [a]
C4(5)	136.4	135.4	135.4	132.7	96.8 [a]

[a] Assignment uncertain.

MO calculations.[18, 2a] Thus, the data suggest that borepin is a planar aromatic compound.

In order to explore further the aromaticity of borepins, we have prepared the $Mo(CO)_3$ complex **7** by the reaction of **3b** with tricarbonyltris(pyridine)molybdenum and $BF_3 \cdot OEt_2$. The NMR signals of the orange, air-stable complex **7** are shifted markedly upfield in comparison to those of the free ligand **3b**. Therefore the borepin ring is η^7-coordinated to Mo.[19] Since prior structural data are available only for complex **8** with the fused benzene ring,[4c] it was of interest to obtain a crystal structure for **7**.[20]

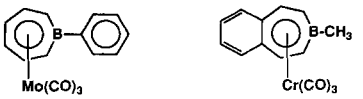

7 **8**

The structure of **7** (Fig. 2) shows a nearly planar borepin ring which is η^7-coordinated to the $Mo(CO)_3$ moiety. The B–Mo distance (2.523(3) Å) is somewhat larger than the C–Mo distances of 2.33–2.42 Å; the boron atom is slightly displaced (0.04 Å) from the plane of the ring. This is consistent with the larger size of the boron atom and conforms to a pattern shown by other heterocyclic boron ligands.[21] The uncoordinated phenyl ring is canted by 28° relative to the boron ring.

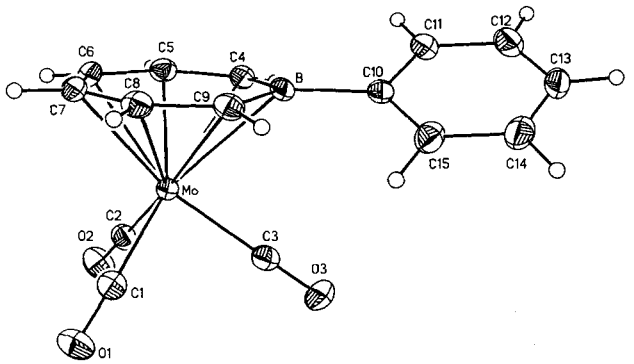

Fig. 2. Solid-state structure of 7 (ORTEP). Selected distances [Å]: MoB 2.523(3), MoC4 2.400(3), MoC5 2.346(3), MoC6 2.327(3), MoC7 2.348(3), MoC8 2.380(3), MoC9 2.416(3), BC4 1.525(4), BC9 1.532(4), BC10 1.578(4), C4C5 1.390, C5C6 1.421(4), C6C7 1.408(5), C7C8 1.423(4), C8C9 1.391(4).

The C–C bonding distances of the borepin ring (1.39–1.42 Å) are typical of those found for complexed monocyclic ligands containing boron. The small range of bond lengths (deviation 0.04 Å) indicates that the π bonds are not very localized. Interestingly, this range is identical to that shown by the C–C bond lengths of the phenyl ring (1.36–1.40 Å). The intraring B–C bond length (1.53 Å) is significantly shorter than the exocyclic B–C_6H_5 distance of 1.58 Å, indicating B–C π bonding in the borepin ring. These structural data clearly demonstrate that borepin can serve as an aromatic ligand.

Experimental

3b: Phenylboron dibromide (0.84 g, 3.4 mmol) in 5 mL of benzene was added dropwise with stirring to **4** (1.0 g, 2.4 mmol) in 5 mL of benzene at 25 °C. The reaction mixture turned green on addition. After 5 min the solvent was removed under reduced pressure, and the residue was subjected to pot-to-pot distillation (120 °C/0.05 Torr) giving 1.35 g of product. Analysis by ^{1}H NMR indicated that the product was approximately 10% 1-phenylborepin (30% yield), and the remainder was largely dibutyltin dibromide. This mixture can be used in subsequent reactions. Careful redistillation gave 70 mg (15%) of **3b** (b.p. 95 °C/0.05 Torr). – EI-MS: *m/z* (rel. intensity): 166 (45, M^+ for $C_{12}H_{11}{}^{11}B$), 165(100).

5: To a gently refluxing solution of BCl_3 (1.0 g, 8.5 mmol) in 10 mL of butane at 0 °C, **4** (1.0 g, 2.4 mmol) was added dropwise with stirring. On addition, the rate of reflux increased and the color of the reaction mixture turned green-brown as a brown precipitate formed. The mixture was allowed to stir as the butane and excess BCl_3 were removed by distillation. The reaction mixture was allowed to warm to 25 °C and finally heated to 50 °C. The brown residue was then subject to pot-to-pot distillation (50 °C/0.5 Torr) giving 200 mg (67%) of product which formed colorless crystals at −78 °C. EI-MS: *m/z* (rel. intensity): 126 (17, M^+, for $C_6H_6{}^{11}B\ {}^{37}Cl$) 123(100). High-resolution EI-MS: calcd for $C_6H_5{}^{11}B^{35}Cl$: 123.0173; found: 123.0171.

6: A solution of methanol (55 mg, 1.72 mmol) in 1.0 mL of CH_2Cl_2 was added to **5** (200 mg, 1.61 mmol) at −78 °C. The mixture was allowed to warm to 25 °C with stirring for 15 min. The solvent and excess methanol were removed under vacuum leaving an oil which was distilled pot-to-pot (50 °C, 1 Torr) to give 140 mg (73%) of **6**. EI-MS: *m/z* (rel. intensity): 120 (33, M^+ for $C_7H_9{}^{11}BO$), 119(100). High-resolution EI-MS: calcd. for $C_7H_8{}^{11}BO$: 119.0668; found: 119.0666.

7: A solution of 1.35 g of the mixture of **3b** and dibutyltin dibromide (0.8 mmol of **3b**) above in 5 mL of Et_2O was added to a suspension of $[(C_5H_5N)_3Mo(CO)_3]$ (0.38 g, 0.9 mmol) in 5 mL of Et_2O. The $BF_3 \cdot OEt_2$ (0.4 mL, 2.8 mmol) was added dropwise with stirring over 5 min. The reaction mixture gradually darkened to a golden brown. After 2 h the solvent was removed under vacuum, and the residue was extracted with hexane (2 × 25 mL). The yellow-brown extracts were washed with 10 mL H_2O and dried over anhydrous Na_2SO_4. Removal of solvent left a thick yellow oil (0.54 g) which solidified on cooling. ^{1}H NMR showed the material to be about 20% product. Recrystallation from pentane gave 10 mg bright orange crystals, m.p. 75–76 °C.

Received: April 8, 1992 [Z 5290 IE]
German version: *Angew. Chem.* **1992**, *104*, 1267

CAS Registry numbers:
1, 291-62-3; **3b**, 142868-01-7; **4**, 114245-35-1; **5**, 142868-02-8; **6**, 142868-03-9; **7**, 142868-00-6; $C_6H_5BBr_2$, 4151-77-3; BCl_3, 10294-34-5; Bu_2SnBr_2, 996-08-7; $[(C_5H_5N)_3Mo(CO)_3]$, 15279-79-5.

[1] M. E. Vol'pin, *Russ. Chem. Rev. (Engl. Transl.)* **1960**, *29*, 129.
[2] a) J. M. Schulman, R. L. Disch, M. L. Sabio, *J. Am. Chem. Soc.* **1982**, *104*, 3785; *ibid* **1984**, *106*, 7696; b) J. M. Schulman, R. L. Disch, M. L. Sabio, *Tetrahedron Lett.* **1983**, *24*, 1863; c) N. L. Allinger, J. H. Siefert, *J. Am. Chem. Soc.* **1975**, *97*, 752.
[3] E. E. van Tamelen, G. Brieger, K. G. Untch, *Tetrahedron Lett.* **1960**, No. 8, 14.
[4] a) A. J. Leusink, W. Drenth, J. G. Noltes, G. J. M. van der Kerk, *Tetrahedron Lett.* **1967**, 1263; b) G. Axelrad, D. Halpern, *Chem. Commun.* **1971**, 291; c) A. J. Ashe III, J. W. Kampf, C. M. Kausch, H. Konishi, M. O. Kristen, J. Kroker, *Organometallics* **1990**, *9*, 2944.
[5] A. T Jeffries III, S. Gronowitz, *Chem. Scr.* **1973**, *4*, 183.
[6] a) J. J. Eisch, J. E. Galle, *J. Am. Chem. Soc.* **1975**, *97*, 4436; b) However, see: A. Geisberger, Ph.D. Thesis, Universität Giessen, **1990**.
[7] W. Schacht, D. Kaufmann, *Angew. Chem.* **1987**, *99*, 682; *Angew. Chem. Int. Ed. Engl.* **1987**, *26*, 665.
[8] a) A. J. Ashe III, F. J. Drone, *J. Am. Chem. Soc.* **1987**, *109*, 1879; *ibid.* **1988**, *110*, 6599; b) A. J. Ashe III, F. J. Drone, C. M. Kausch, J. Kroker, S. M. Al-Taweel, *Pure Appl. Chem.* **1990**, 513.
[9] Y. Sugihara, T. Yagi, I. Murata, A. Imamura, *J. Am. Chem. Soc.* **1992**, *114*, 1479.
[10] Y. Nakadaira, R. Sato, H. Sakurai, *Chem. Lett.* **1987**, 1451.
[11] R. Sato, Ph.D. Thesis, Tohoku University, **1984**; Y. Nakadaira, R. Sato, H. Sakurai, 6th Int. Symp. Novel Arom. Comp. Osaka, **1989**, A-47.
[12] The same result is obtained with nBu$_2$SnH$_2$ or tBu$_2$SnH$_2$.
[13] H. C. Brown, E. Negishi, *J. Am. Chem. Soc.* **1971**, *93*, 6682.
[14] The observed spectra can be simulated with the PANIC program (Bruker). The following ^{1}H-^{1}H coupling constants were obtained for **1**: $J(2,3) = 12.4$, $J(2,4) = 1.0$, $J(2,5) = 0.7$, $J(2,6) = 0$, $J(2,7) = 3.2$, $J(3,4) = 8.3$, $J(3,5) = 1.0$, $J(3,6) = J(3,7) = 0$, $J(4,5) = 11.1$ Hz.
[15] The borale complex $[CpCoC_4Ph_4BH]$ displays similar behavior: F. E. Hong, C. W. Eigenbrot, T. P. Fehlner, *J. Am. Chem. Soc.* **1989**, *111*, 949.
[16] Y. Nakadaira, R. Sato, H. Sakurai, *Organometallics* **1991**, *10*, 435.
[17] M. Karplus, *J. Am. Chem. Soc.* **1963**, *85*, 2870.
[18] H. Günther, M. Gorlitz, H. Meizenheimer, *Org. Magn. Reson.* **1974**, *6*, 388.

[19] G. E. Herberich, E. Bauer, J. Hengesbach, U. Kölle, G. Huttner, H. Lorenz, *Chem. Ber.* **1977**, *110*, 760.

[20] **7**: Monoclinic, space group $P2_1/n$ (No. 14) with $a = 12.406(4)$, $b = 6.733(2)$, $c = 16.390(4)$ Å, $\beta = 95.11(2)°$, $V = 1363.6(5)$ Å^3, and $Z = 4$ ($\varrho_{calcd} = 1.685$ g cm^{-3}), $\mu(Mo_{K\alpha}) = 93.18$ cm^{-1}, 3997 unique reflections, 3777 with $F_0 \geq 0.6\sigma(F)$ were used in refinement; $R = 0.0466$, $R_w = 0.0452$; GOF = 1.22. Further details of the crystal structure investigation are available on request from the Director of the Cambridge Crystallographic Data Centre, University Chemical Laboratory, Lensfield Road, GB-Cambridge CB21EW (UK), on quoting the full journal citation.

[21] a) G. E. Herberich, W. Boveleth, B. Hessner, D. P. J. Köffer, M. Negele, R. Saive, *J. Organomet. Chem.* **1986**, *308*, 153; b) W. Siebert, M. Bochmann, J. Edwin, C. Krüger, Y.-H. H. Tsay, *Z. Naturforsch. B* **1978**, *33*, 1410; c) G. Huttner, W. Gartzke, *Chem. Ber.* **1974**, *107*, 3786; d) G. E. Herberich, B. Hessner, S. Beswetherick, J. A. K. Howard, P. Woodward, *J. Organomet. Chem.* **1980**, *192*, 421; e) G. E. Herberich, B. Hessner, M. Negele, J. A. K. Howard, *J. Organomet. Chem.* **1987**, *336*, 29.

Stepwise Stacking of Three Paramagnetic Metallocene Units: [CpNiCp(SiMe$_2$)$_2$CpCrCp(SiMe$_2$)$_2$CpNiCp]**

By *Pierre Bergerat, Janet Blümel, Monika Fritz, Johann Hiermeier, Peter Hudeczek, Olivier Kahn,* and *Frank H. Köhler**

Molecular materials which are ferro-, ferri, or antiferromagnetic as a result of interactions between spin-carrying metal centers are currently subjects of intensive research.[1] A particularly rich chemistry is derived from chelate compounds in which like and—more promisingly—unlike metals are assembled in close proximity.[1c] Other spin sources are organometallic compounds. Thus, the reactions of polyalkylmetallocenes with tetracyanoethylene and related electron acceptors yield the salts $[Cp^*_2M]^+$ [π anion]$^-$ which crystallize as stacks and exhibit spontaneous magnetization at low temperature when the metal is iron, manganese, or chromium.[2] In these materials the stacks are linear, that is, vertical with respect to the plane of the π ligands, and their stability is determined by ionic interactions. This organometallic/organic concept implies that different metal centers cannot be introduced in one stack by using simple sandwich molecules.

We wished to explore an alternative concept concerning pure organometallic compounds with stacking orientations other than vertical, with covalent bonding between the metallocenes, and with two different paramagnetic metal centers. We therefore synthesized biscyclopentadienyl ligands that may serve to link different metallocenes in a stereochemically well-defined manner.[3] After testing less reactive diamagnetic synthetic building blocks and their complexation behavior[4] we report here on the title compound **4**, the prototype of a heteronuclear compound containing three paramagnetic metallocene units.

The synthesis (Scheme 1) is based on the stepwise metalation of two doubly bridged cyclopentadienes.[4] Thus the cyclopentadienide **1**[3b] reacted with $C_5H_5^-$ and solvated nickel(II) bromide to give the nickelocene **2** (two pairs of enantiomers *syn*-**2a/b** and *anti*-**2a/b** in the ratio 5:1).[5] Deprotonation of **2** yielded the green anion **3**,[5] a key compound for further reaction with transition metal ions. The title compound **4**[5] was obtained after addition of solvated chromium(II) chloride to a solution of **3** in THF. **4** is an air-sensitive compound isolated as mossy green crystals of **4** · toluene from toluene and solvent-free olive-green glittering platelets from hexane (42% yield).

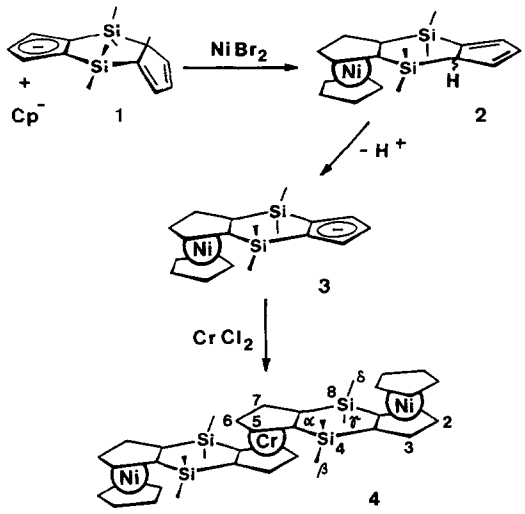

The cyclic voltammogram of **4** (Fig. 1) shows five electron transfers leading to a pentacation. An interaction between the two terminal nickelocenes is disclosed by splittings of 65 and 190 mV[6] associated with the potentials for the oxidation to the nickelocene monocations (near 1 V) and dications (near 2 V), respectively. Not surprisingly for highly charged

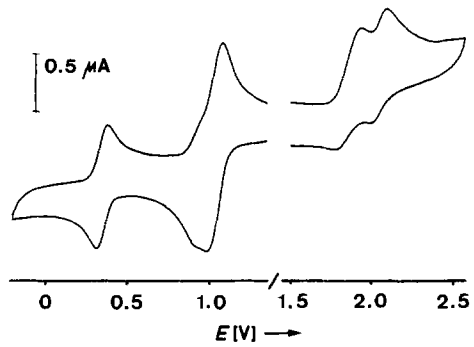

Fig. 1. Cyclic voltammogram of **4** in propionitrile, 8×10^{-4} mol L^{-1}, −20 °C, scan rate 200 mV s^{-1}, potential E vs internal Cp_2Co/Cp_2Co^+. Electron transfers from left to right: $E_{1/2}$ (ΔE_p) 340(65), 980(80), 1045(80), 1850(170), 2040(105) mV; assignment see text.

species, the electron transfers leading to the tetra- and pentacation are chemically not reversible. The central chromocene is oxidized more easily ($E_{1/2}$ = 340 mV) in accord with what is known from the parent metallocenes.[7] In addition, a broad, unresolved wave with $E_c = -1140$ mV indicates the irreversible reduction to 4^{3-}.

From the paramagnetic compound **4** we have obtained ^{13}C NMR signals in the range from $\delta = -400$ to $+1600$ (Fig. 2). Their number and their approximate areas are in

[*] Prof. Dr. F. H. Köhler, Dr. J. Blümel, Dr. M. Fritz, Dr. J. Hiermeier, Dipl.-Chem. P. Hudeczek
Anorganisch-chemisches Institut der Technischen Universität München
Lichtenbergstrasse 4, D-W-8046 Garching (FRG)
Prof. O. Kahn,[+] P. Bergerat
Université de Paris Sud
Laboratoire de Chimie Inorganique, CNRS URA 420
F-91405 Orsay (France)

[+] Wilhelm Manchot Research Professor of the Technische Universität München 1991.

[**] This work was supported by the Pinguin-Stiftung, the Deutsche Forschungsgemeinschaft, and the Fonds der Chemischen Industrie.

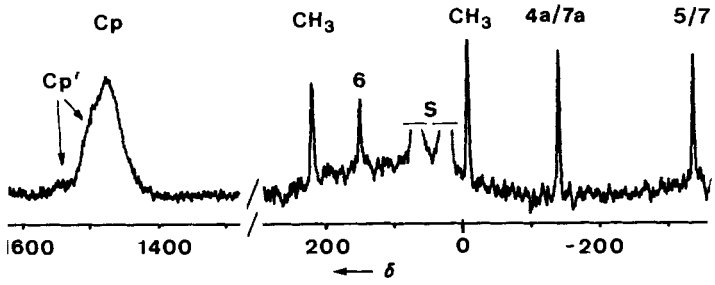

Fig. 2. ^{13}C NMR spectrum of **4** in [D$_8$]THF at 298 K; the two sections have different vertical scales. S = solvent, Cp' = C1-3, C3a, and C8a.

agreement with the structure shown in Scheme 1,[8] while their shifts are characteristic of substituted nickelocenes (weighted average $\delta \approx 1400$ to 1500[9]) and chromocenes (weighted average $\delta \approx -300$ to -400[9]). It follows that, at ambient temperature, **4** has six unpaired electrons with each metallocene unit accommodating two of them. This is confirmed by the ^1H NMR spectrum.[5] Surprisingly, however, the signals of H1-3 at $\delta = -221.6$ are shifted about 10% less than the Cp protons of mononuclear nickelocenes.[9] Since it was not clear whether this points to spin exchange between the metallocenes, we performed solid-state magnetic measurements.

The magnetic behavior is illustrated by the plot of $\chi_M T$ vs T (Fig. 3). At 250 K, $\chi_M T$ is equal to 2.94 cm^3 K mol^{-1}, which corresponds to what is expected for three uncoupled ions with $S_{Ni1} = S_{Ni2} = S_{Cr} = 1$[10] and is in agreement with the NMR results. When the temperature is lowered, $\chi_M T$ decreases more and more rapidly and reaches 0.83 cm^{3}Kmol^{-1} at 1.9 K. Such behavior may arise from the

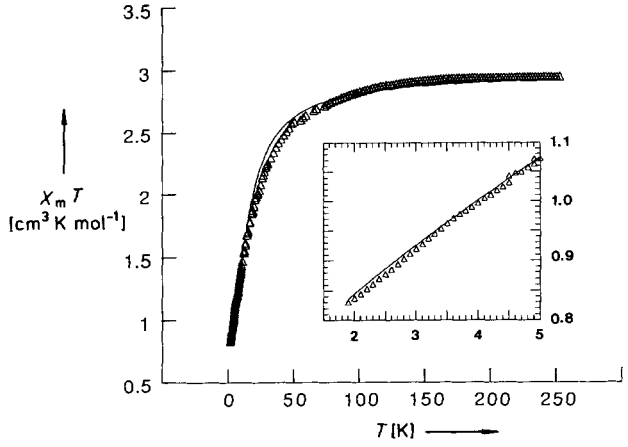

Fig. 3. Magnetic properties of **4** represented as a plot of $\chi_M T$ vs T with χ_M being the molar magnetic susceptibility and T the absolute temperature. Δ: Experimental values, solid line: calculated curve. Inset: expansion of the low-temperature range.

local anisotropies D_{Ni} and D_{Cr} of the metal(II) ions, and the isotropic intramolecular magnetic interaction J between the central Cr^{II} and the terminal Ni^{II} ions. Based on the pertinent spin Hamiltonian[11] the respective role of the two contributions becomes evident from the plot of $\chi_M T$ vs T when T approaches zero: neglecting J would result in $\chi_M T > 1.3$ cm^3 K mol^{-1}; neglecting D_{Ni} and D_{Cr} would result in a plateau with $\chi_M T \approx 1$ cm^3 K mol^{-1}. The latter corresponds to the temperature range in which only the triplet ground state is thermally populated. It turns out (Fig. 3) that both contributions are operative. These contributions are not correlated below 50 K, although they are correlated above 50 K, so that the fitting of the magnetic susceptibility χ_{Mu} along the direction u by Equation (a)[12] is expected to

$$\chi_{Mu} = \frac{N\beta \, \Sigma_i(-\partial E_{i,u}/\partial H_u) \exp(-E_{i,u}/kT)}{H_u \quad \Sigma_i \exp(-E_{i,u}/kT)} \qquad \text{(a)}$$

provide a reliable value of J. Since both D_{Ni} and D_{Cr} contribute to the zero-field splitting within the magnetic pair state they cannot be determined separately. We therefore assumed that D_{Cr} is negligible with respect to D_{Ni}. With somewhat idealized symmetry[13] the fitting yielded a Zeeman factor of $g = 1.98$, a zero-field splitting of $D_{Ni} = 28.7$ cm^{-1} (both are close to the values for nickelocene itself[14]), and the Ni^{II}–Cr^{II} interaction parameter $J = -1.95$ cm^{-1}; the agreement factor[12] was $R = 3.8 \times 10^{-4}$. The corresponding theoretical curve is given in Figure 3. Considering that D_{Cr} is not negligible leads to the same energy spectrum for the low-lying states with a different value for D_{Ni} but the same for J.

The magnetic properties are the crucial proof that the silyl bridges in **4** function as "valves" that allow a limited electron-exchange interaction. In this particular case it is antiferromagnetic. Other metal combinations and the manipulation of the silyl bridges are conceivable so that the magnetism of trinuclear metallocenes should be adjustable.

The properties of the title compound **4** illustrate that the approach discussed at the beginning, the stepwise stacking of metallocene units, actually works. Compound **4** is a good model for analogous polymers, since here structure, redox behavior, and interactions between the metallocene units, in particular magnetic exchange, may be investigated conveniently.

Received: January 23, 1992 [Z 5144IE]
German version: *Angew. Chem.* **1992**, *104*, 1285

CAS Registry numbers:
1, 142947-25-9; *syn*-**2**, 142947-26-0; *anti*-**2**, 142947-29-3; **3**, 142947-27-1; **4**, 142947-28-2; Cp$^-$, 12127-83-2; $NiBr_2$, 13462-88-9; $CuCl_2$, 10049-05-5.

[1] a) J. S. Miller, A. J. Epstein, W. M. Reiff, *Chem. Rev.* **1988**, *88*, 201–220; b) A. Caneschi, D. Gatteschi, R. Sessoli, *Acc. Chem. Res.* **1989**, *22*, 392–398; c) O. Kahn, *Phil. Trans. R. Soc. Lond. A* **1990**, *330*, 195–204; d) A. L. Buchachenko, *Russ. Chem. Rev. Engl. Transl.* **1990**, *59*, 307–319.

[2] a) J. S. Miller, J. C. Calabrese, A. J. Epstein, R. W. Bigelow, J. H. Zhang, W. M. Reiff, *J. Chem. Soc. Chem. Commun.* **1986**, 1026–1028; b) J. S. Miller, J. C. Calabrese, H. Rommelmann, S. R. Chittipeddi, J. H. Zhang, W. M. Reiff, A. J. Epstein, *J. Am. Chem. Soc.* **1987**, *109*, 769–781; c) W. E. Broderick, J. A. Thompson, E. P. Day, B. M. Hoffman, *Science* **1990**, *249*, 401–403; d) W. E. Broderick, B. M. Hoffman, *J. Am. Chem. Soc.* **1991**, *113*, 6334–6335; e) G. T. Yee, J. M. Manriquez, D. A. Dixon, R. S. McLean, D. M. Groski, R. B. Flippen, K. S. Narayan, A. J. Epstein, J. S. Miller, *Adv. Mater.* **1991**, *3*, 309–311.

[3] a) H. Atzkern, F. H. Köhler, R. Müller, *Z. Naturforsch. B.* **1990**, *45*, 329–343; b) J. Hiermeier, F. H. Köhler, G. Müller, *Organometallics* **1991**, *10*, 1787–1793; ligand **1** has been synthesized independently: U. Siemeling, R. Krallmann, P. Jutzi, *Abstr. IXth Int. Conf. Silicon Chem.* Edinburgh, 1990; U. Siemeling, P. Jutzi, *Chem. Ber.* **1992**, *125*, 31–35; U. Siemeling, P. Jutzi, B. Neumann, H.-G. Stammler, M. B. Hursthouse, *Organometallics* **1992**, *11*, 1328–1333.

[4] M. Fritz, J. Hiermeier, N. Hertkorn, F. H. Köhler, G. Müller, G. Reber, O. Steigelmann, *Chem. Ber.* **1991**, *124*, 1531–1539. In principle, the synthetic steps described for iron correspond to those used here for nickel.

[5] The isomer ratio of *syn*-**2a/b** to *anti*-**2a/b** was determined by ^1H NMR spectroscopy. *syn*-**2a/b**: ^{13}C NMR (THF, 310 K): $\delta = 655/597$ (Cα/δ), $-15.1/56.6$ (Cβ/γ), 114.6 (C2), 139.2/132.2 (C1/3); ^{29}Si NMR (THF, 319 K): $\delta = -845/-873$ (Si4/8). *anti*-**2a/b**: ^{13}C NMR (THF, 310 K): $\delta = 220/519$ (Cα/δ), 85.7/98.4 (Cβ/γ), 191.8 (C2), 140.6/127.9 (C1/3); ^{29}Si NMR (THF, 319 K): $\delta = -832/-852$ (Si4/8). The signal-to-noise ratio did not allow the localization of the broad Cp carbon signals expected at $\delta(^{13}C) > 1000$ similar as for **4** (Fig. 2). *syn*/*anti*-**2a/b** gave a satisfactory elemental analysis. EI-MS (70 eV): *m/z* (rel. intensity) *366* (M^+, 100), 351

($M^+ - CH_3$, 4), 300 ($M^+ - C_5H_6$, 2), 285 ($M^+ - CH_3 - C_5H_6$, 3), 183 (M^{2+}, 3); the M^+ signal shows the theoretically expected isotope pattern. – **3**: ^{13}C NMR (THF, 298 K): δ = 1600 (Cp, C5–7, C4a/7a), 511/34 (Cα-δ), 135.7 (C3a/8a), 125.6 (C2), 100.1 (C1/3); ^{29}Si NMR (THF, 298 K): δ = – 842. **4**: ^1H NMR ([D$_8$]toluene, 303 K) δ = – 239.6 (Cp), – 221.6 (H1–3), 224.0 (H5/7), 163.0 (H6), 0.6/0.3 (Hα-δ); ^{29}Si NMR (THF, 305 K): δ = 313; EI-MS (70 eV): *m/z* (rel. intensity) 784 (M^+, 100), 660 (M^+ -CPNi, 7) and small unassigned peaks; the M^+ signal shows the theoretically expected isotope pattern. A satisfactory elemental analysis was obtained for **4** · toluene.

[6] The poorly resolved splitting near 1 V was estimated as described in: H. Atzkern, J. Hiermeier, F. H. Köhler, A. Steck, *J. Organomet. Chem.* **1991**, *408*, 281–296.

[7] a) N. G. Connelly, W. E. Geiger, *Adv. Organomet. Chem.* **1984**, *23*, 1–93; b) V. V. Strelets, *Russ. Chem. Rev. Engl. Transl.* **1989**, *58*, 297–311.

[8] The study of the tris-iron analogues excludes the all-*cis* arrangement [6].

[9] F. H. Köhler, W. A. Geike, *J. Organomet.Chem.* **1987**, *328*, 35–37 and earlier contributions in the series. Note that we have changed the sign convention since.

[10] Calculated from $\chi_M T = (N\beta^2/3k)\ (4g_{Ni}^2 + 2g_{Cr}^2)$ where g_{Ni} and g_{Cr} are the local Zeeman factors and the other symbols have their usual meaning.

[11] $H = -J\ (S_{Ni1} + S_{Ni2})\ S_{Cr} + S_{Ni1}\ \boldsymbol{D}_{Ni}\ S_{Ni1} + S_{Ni2}\ \boldsymbol{D}_{Ni}\ S_{Ni2} + S_{Cr}\ \boldsymbol{D}_{Cr}\ S_{Cr} + \beta(S_{Ni1} + S_{Ni2})\ \boldsymbol{g}_{Ni} + S_{Cr} \cdot \boldsymbol{g}_{Cr} \cdot H$, where $\boldsymbol{D}_{Ni}$ and $\boldsymbol{D}_{Cr}$ are the local anisotropy tensors and $\boldsymbol{g}_{Ni}$ and $\boldsymbol{g}_{Cr}$ are the local Zeeman tensors.

[12] In Equation (a) the summation runs over the 27 levels $E_{i,u}$ in the presence of the magnetic field H_u. The powder magnetic susceptibility was calculated by averaging over 15 directions of the magnetic field. The energies $E_{i,u}$ were obtained by diagonalizing the spin Hamiltonian of ref. [11] using the $|M_s(Ni1), M_s(Cr), M_s(Ni2)>$ functions as a basis set. Then the parameters J, $\boldsymbol{D}_{Ni}$, and g were determined by minimizing the agreement factor $R = \sum[(\chi_M T)^{cal} - (\chi_M T)^{obs}]^2 / \sum[(\chi_M T)^{obs}]^2$.

[13] $\boldsymbol{D}_{Ni}$ and the zero-field splitting parameter D_{Ni} (= $3D_{Ni,zz}/2$) were assumed to be axial, and $\boldsymbol{g}_{Ni}$ and $\boldsymbol{g}_{Cr}$ to be isotropic with the same principal g value.

[14] P. Baltzer, A. Furrer, J. Hullinger, A. Stebler, *Inorg. Chem.* **1988**, *27*, 1543–1548 and references therein.

Chelate Stabilization of a Monomeric Lithium Tellurolate**

By *Heinz Gornitzka, Susanne Besser, Regine Herbst-Irmer, Ulrike Kilimann*, and *Frank T. Edelmann**

Metal complexes with alkoxide (RO^-) and thiolate ligands (RS^-) have been well studied.[1–3] However, only a few with selenolate and tellurolate ligands (RSe^- and RTe^-, respectively) are known.[4–6] They are of interest as precursors for metal chalcogenides,[7,8] and also play an ever increasing role as reagents in organic synthesis.[4–6,9–11] In both cases alkali metal chalcogenolates act as intermediates. Sodium tellurolates are for example accessible by the reduction of the corresponding ditellurides with sodium amalgam or sodium in liquid ammonia.[12] They can undergo reactions to give transition metal tellurolates[13] as well as compounds with Te–C bonds.[9–11] Very little is known about the structural chemistry of alkali metal tellurolates: only $[Li(thf)_3][2,4,6\text{-}tBu_3C_6H_2Te]$[14] as well as $[Na(tmeda)][2,4,6\text{-}Me_3C_6H_2Te]$ and $[K([18]crown\text{-}6)][2,4,6\text{-}iPr_3C_6H_2Te]$[15] have been structurally characterized. In all three cases bulky substituents led to a kinetic stabilization of the alkali metal tellurolate. We have now found that the stability of alkali metal chalcogenolates can also be increased dramatically by chelation. Crystalline lithium chalcogenolates are readily accessible also in the case of the higher homologues by incorporation of a Li–E unit (E = S, Se, Te) into a six-membered chelate system.

[*] Priv.-Doz. Dr. F. T. Edelmann, Dipl.-Chem. H. Gornitzka, Dipl.-Chem. S. Besser, Dr. R. Herbst-Irmer, Dipl.-Chem. U. Kilimann
Institut für Anorganische Chemie der Universität
Tammannstrasse 4, D-W-3400 Göttingen (FRG)

[**] This work was supported by the Deutsche Forschungsgemeinschaft.

2-(Dimethylaminomethyl)ferrocenyllithium (**1**) served as the starting material, which is readily accessible by metalation of (dimethylaminomethyl)ferrocene[16] with *n*-butyllithium.[17] In THF solution **1** rapidly reacts with elemental sulfur, selenium, or tellurium under insertion of a chalcogen atom into the lithium–carbon bond. The crystalline lithium chalcogenolates **2**–**4** can be isolated in high yield from the resulting solution. The yellow-brown solids are readily soluble in THF, but almost insoluble in diethyl ether and hydrocarbon solvents.

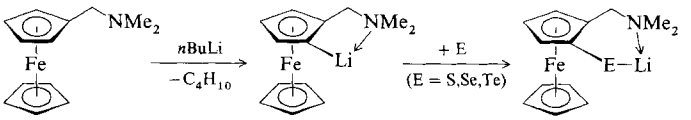

1

2, E = S (73%)
3, E = Se (84%)
4, E = Te (100%)

Red-brown single crystals of the composition [Li(dme)][CpFe{$C_5H_3(CH_2NMe_2)$Te}] were obtained by recrystallization of **4** from dimethoxyethane (DME). In contrast to other alkali metal tellurolates, which are very sensitive to oxidation, crystalline [Li(dme)][CpFe{$C_5H_3(CH_2NMe_2)$Te}] can be handled in air for a short period of time without noticeable decomposition. The X-ray structure analysis[18] reveals that the Li–Te unit is stabilized by intramolecular chelate formation (Fig. 1). The six-membered chelate ring

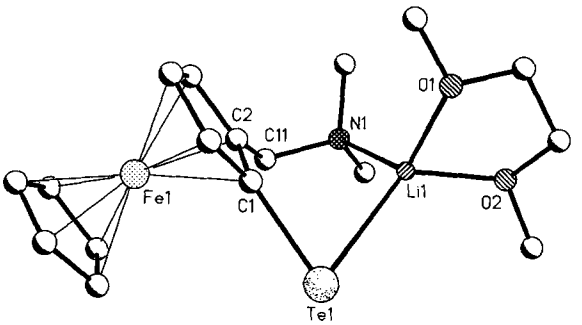

Fig. 1. Crystal structure of [Li(dme)][CpFe{$C_5H_3(CH_2NMe_2)$Te}]. Selected bond distances [pm] and angles [°]: Te1-Li1 273.4(4), Li1-N1 207.9(4), N1-C11 147.8(3), C11-C2 149.0(3), C2-C1 144.0(3), C1-Te1 212.2(2), Li1-O1 195.3(5), Li1-O2 201.0(4), C1-Fe1 206.3(2), C2-Fe1 203.9(2); C1-Te1-Li1 74.2(1), Te1-Li1-N1 103.7(2), Li1-N1-C11 111.0(2), N1-C11-C2 111.2(2), C11-C2-C1 124.5(2), C11-C2-C3 127.1(2), C2-C1-Te1 125.5(2), C5-C1-Te1 127.9(1), C2-C1-C5 106.6(2), Te1-C1-Fe1 128.1(1), C11-C2-Fe1 126.6(2).

adopts a slightly distorted boat conformation, in which Te1, C1, C2, and C11 are found almost in a plane. Noteworthy is the relatively small angle at the tellurium atom (74.2(1)°). The Te–C bond length (212.2(2) pm) lies in the normal range.

Their easy accessibility and unusual stability render the lithium chalcogenolates **2**–**4** of interest for subsequent reactions. Air oxidation of THF solutions leads to the corresponding dichalcogenides [{CpFe[$C_5H_3(CH_2NMe_2)$E]}$_2$] (E = S, Se, Te) as yellow crystalline solids.[19] Initial experiments show that the new ferrocenyl chalcogenolate ions are suitable ligands for transition metals and rare-earth elements. Thus, the ytterbium(III) thiolate [{CpFe[$C_5H_3(CH_2NMe_3)$S]}$_2$Yb] is accessible from **2** and $YbCl_3$.[20] As a typical example the reaction of **4** with $HgCl_2$ is outlined, which leads to the mercury(II) tellurolate **5**. The orange crys-

tals of **5** are stable in air and thermally stable up to about 170 °C.

$$HgCl_2 + 2\,\mathbf{4} \longrightarrow [\{CpFe[C_5H_3(CH_2NMe_2)Te]\}_2Hg] + 2\,LiCl$$
$$\mathbf{5}$$

Experimental Procedure

General Procedure: To a suspension of 2-(dimethylaminomethyl)ferrocenyllithium (**1**) (4.71 g, 18.9 mmol) in THF (100 mL) was added chalcogen (21.2 mmol) [S_8 was dissolved in THF (50 mL) and added dropwise at −20 °C]. The mixture was stirred at room temperature for 24 h (**2**: 1 h). After filtration and removal of the solvent in vacuo the residue was washed with ether (20 mL) and dried in vacuo.

2: Yellow solid, m.p. 190 °C (decomp.); yield 3.90 g (73%); IR (Nujol): ν[cm^{-1}]: 1268 m, 1166 m, 1105 s, 1036 m, 1006 m, 795 m; ^{1}H NMR (250 MHz, CD_3CN): δ = 4.10 (d, 1 H; J = 13 Hz, CH_2N), 4.05 (s, 1 H, C_5H_3), 3.92 (s, 1 H, C_5H_3), 3.81 (s, 5 H, C_5H_5), 3.70 (s, 1 H, C_5H_3), 2.51 (d, 1 H, J = 13 Hz, CH_2N), 2.07 (s, 6 H, NMe_2); ^{7}Li NMR (97 MHz, THF, C_6D_6): δ = 0.43 (s); FI-MS: m/z (rel. int. [%]) 562 (18, M_2^+), 288 (90, M^+ + Li), 281 (80, M^+), 230 (24, M^+ − Li − NMe_2), 186 (100, Cp_2Fe^+), 121 (74, $CpFe^+$), 66 (24, $C_5H_6^+$), 56 (48, Fe^+), 44 (34, NMe_2^+).

3: Yellow-brown solid, m.p. 117 °C (decomp.); yield 5.20 g (84%); IR (Nujol): ν[cm^{-1}]: 1262 m, 1175 m, 1104 m, 1045 s, 1000 m, 798 s, 722 m, 485 m; ^{1}H NMR (250 MHz, [D_8]THF): δ = 4.23 (d, 1 H, J = 13 Hz, CH_2N), 4.11 (s, br, 1 H, C_5H_3), 4.06 (d, 1 H, J = 6 Hz, C_5H_3), 3.90 (s, 1 H, C_5H_3), 3.82 (s, 5 H, C_5H_5), 2.58 (d, 1 H, J = 13 Hz, CH_2N), 2.16 (s, 6 H, NMe_2); ^{7}Li NMR (97 MHz, THF, C_6D_6): δ = 0.74 (s); FI-MS: m/z (rel. int. [%]) 322 (64, M^+ − Li), 279 (100, M^+ − Li − NMe_2), 242 (28, $[CpFe(C_5H_3CH_2NMe_2)]^+$), 199 (18, $FcCH_2^+$), 121 (48, $CpFe^+$).

4: Brown solid, m.p. 136 °C; Yield 7.20 g (100%); IR (Nujol): ν[cm^{-1}]: 1263 s, 1162 s, 1102 s, 1045 s, 1030 s, 1001 s, 964 m, 892 m, 812 s, 722 s; ^{1}H NMR (250 MHz, [D_8]THF): δ = 4.19 (s, 1 H, C_5H_3), 4.13 (d, 1 H, J = 12 Hz, CH_2N), 4.01 (s, 1 H, C_5H_3), 3.89 (s, 1 H, C_5H_3), 3.83 (s, 5 H, C_5H_5), 2.66 (d, 1 H, J = 12 Hz, CH_2N), 2.18 (s, 6 H, NMe_2); ^{7}Li NMR (97 MHz, THF, C_6D_6): δ = 1.21 (s); FI-MS: m/z (rel. int. [%]) 371 (54, M^+ − Li), 3.29 (26, M^+ − Li − NMe_2), 242 (99, $[CpFe(C_5H_3CH_2NMe_2)]^+$), 199 (100, $FcCH_2^+$), 66 (24, $C_5H_6^+$), 186 (16, Cp_2Fe^+), 121 (58, $CpFe^+$).

5: A freshly prepared solution of **4** (4.08 g, 10.8 mmol) in THF (100 mL) was added dropwise to $HgCl_2$ (1.47 g, 5.4 mmol) in THF (100 mL) and the mixture was stirred at room temperature for 12 h. After filtration, the dark brown filtrate was evaporated to dryness. The residue was washed with hexane (50 mL) and dried in vacuo. This afforded **5** (4.00 g, 79%) as an orange-brown solid. M.p. 173 °C (decomp.). IR (Nujol): ν[cm^{-1}]: 1261 s, 1171 m, 1105 s, 1061 m, 1026 m, 968 m, 804 s, 722 s; ^{1}H NMR (250 MHz, [D_8]THF): δ = 4.33 (m, 2 H, J = 12 Hz, CH_2N), 3.95 (s, 10 H, C_5H_5), 3.88 (m, 4 H, C_5H_3), 3.79 (m, 2 H, C_5H_3), 2.53 (d, 2 H, J = 12 Hz, CH_2N), 1.85 (s, 12 H, NMe_2); FI-MS: m/z (rel. int. [%]) 867 (3, $M^+ - CH_2NMe_2$), 327 (61, $[CpFe(C_5H_3CH_2Te)]^+$), 242 (100, $[CpFe(C_5H_3CH_2NMe_2)]^+$), 199 (67, $FcCH_2^+$), 121 (69, $CpFe^+$).

Received: February 11, 1992
Revised: May 12, 1992 [Z 5180 IE]
German version: *Angew. Chem.* **1992**, *104*, 1252

CAS Registry numbers:
2, 142761-70-4; **3**, 142761-71-5; **4**, 142761-72-6; **4** · DME, 142761-74-8; **5**, 142761-73-7; (dimethylaminomethyl)ferrocene, 1271-86-9.

[1] R. C. Mehrotra, *Adv. Inorg. Chem. Radiochem.* **1983**, *26*, 269.
[2] I. P. Rothwell, M. H. Chisholm in *Comprehensive Coordination Chemistry* (Eds.: G. Wilkinson, R. D. Gillard, J. A. McCleverty), Pergamon, New York, **1987**, Vol. 2, p. 335.
[3] A. Müller, E. Diemann in [2], p. 526.
[4] H. J. Gysling in *The Chemistry of Organic Selenium and Tellurium Compounds* (Eds.: S. Patai, Z. Rappoport), Wiley, New York, **1986**, Vol. 1, p. 679.
[5] F. J. Berry in [2], Chap. 17.
[6] H. J. Gysling, *Coord. Chem. Rev.* **1982**, *42*, 133.
[7] M. L. Steigerwald, C. R. Sprinkle, *J. Am. Chem. Soc.* **1987**, *109*, 7200.
[8] M. L. Steigerwald, *Chem. Mater.* **1989**, *1*, 52.
[9] K. J. Irgolic in *Methods of Org. Chem. (Houben-Weyl) Vol. E12b, 4th ed. 1952–, Vol. Organotellurium Compounds*, **1990**.
[10] Y. Aso, H. Yamashita, T. Otsubu, F. Ogura, *J. Org. Chem.* **1989**, *54*, 5627.
[11] T. Inokuchi, M. Kusumoto, S. Torii, *J. Org. Chem.* **1990**, *55*, 1548.
[12] J. Liesk, P. Schultz, G. Klar, *Z. Anorg. Allg. Chem.* **1977**, *435*, 98.
[13] I. Davies, W. R. McWhinnie, *J. Inorg. Nucl. Chem. Lett.* **1976**, *12*, 763.
[14] W.-W. Du Mont, R. Hensel, S. Kubiniok, L. Lange, T. Severengiz, *Phosphorus Sulfur Relat. Elem.* **1988**, *38*, 85.
[15] P. J. Bonasia, J. Arnold, *J. Chem. Soc. Chem. Commun.* **1990**, 1299.
[16] J. K. Lindsay, C. R. Hauser, *J. Org. Chem.* **1957**, *22*, 355.
[17] M. D. Rausch, G. A. Moser, C. F. Meade, *J. Organomet. Chem.* **1973**, *51*, 1.
[18] X-ray crystallographic data for [Li(dme)][CpFe{$C_5H_3(CH_2NMe_2)Te$}] (−120 °C): monoclinic, space group $P2_1/n$, a = 834.4(1), b = 2177.9(2), c = 1111.6(1) pm, β = 105.90(1)°, V = 1.9428 nm^3, Z = 4, ρ_{calcd} = 1.596 g cm^{-3}, 3512 observed reflections [$F_o > 4\sigma F_o$], 2θ = 8–55°, refined to R = 0.0230, Rw = 0.0256. Further details of the crystal structure investigation may be obtained from the Fachinformationszentrum Karlsruhe, Gesellschaft für wissenschaftlich-technische Information mbH, D-W-7514 Eggenstein-Leopoldshafen 2 (FRG) on quoting the depository number CSD-56440, the names of the authors, and the journal citation.
[19] H. Gornitzka, S. Besser, R. Herbst-Irmer, U. Kilimann, F. T. Edelmann, K. Jacob, *J. Organomet. Chem.*, in press.
[20] H. Gornitzka, F. T. Edelmann, K. Jacob, *J. Organomet. Chem.*, in press.

1,3-Dimetallabenzene Derivatives of Niobium or Tantalum**

By *Robert D. Profilet, Phillip E. Fanwick,* and *Ian P. Rothwell**

Interest in the structure, bonding, and reactivity of six-membered metallacyclic compounds that may be considered quasiaromatic has surged in the last few years.[1] We report here on the synthesis and structure of a series of novel six-membered dimetallacyclic derivatives of niobium and tantalum that appear to be a new class of 1,3-dimetallabenzenes.

We have recently shown that the alkylidyne-bridged dimer **1b** is a useful starting material for the synthesis of polyhydridoditantalum compounds.[2] We have also investigated the reaction of **1b** and its niobium analogue **1a** with various substituted alkynes in order to assess their potential as catalysts (or precursors) for alkyne metathesis.[3] Reaction of **1a** or **1b** with 3-hexyne does not occur over weeks at 25 °C. However, these sparingly soluble compounds will react with one equivalent of 3-hexyne at 110 °C over 3 days in toluene to produce new metallacyclic compounds **2** in 60% yield as dark red (**2a**) or red (**2b**) crystals from toluene/hexane.[4]

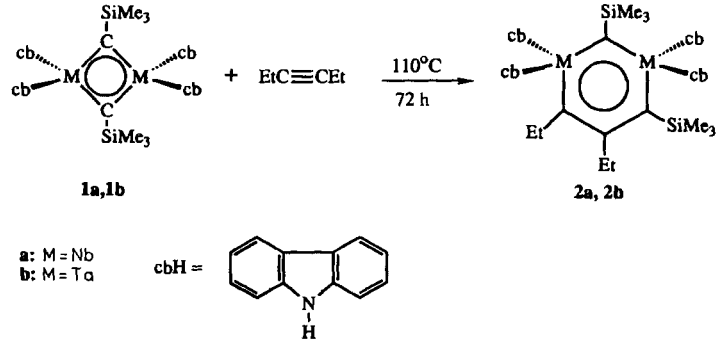

1a,1b **2a, 2b**

a: M = Nb
b: M = Ta

The solid-state structure of **2b** in Figure 1[5] shows a six-membered dimetallacycle formed by insertion of one hexyne molecule into one of the alkylidyne bridge groups in **1**. The coordination environment about each nonequivalent tantalum center is pseudotetrahedral involving two carbazole ni-

[*] Prof. I. P. Rothwell, R. D. Profilet, Dr. P. E. Fanwick
Department of Chemistry, Purdue University
West Lafayette, IN 47907 (USA)

[**] This work was supported by the National Science Foundation.

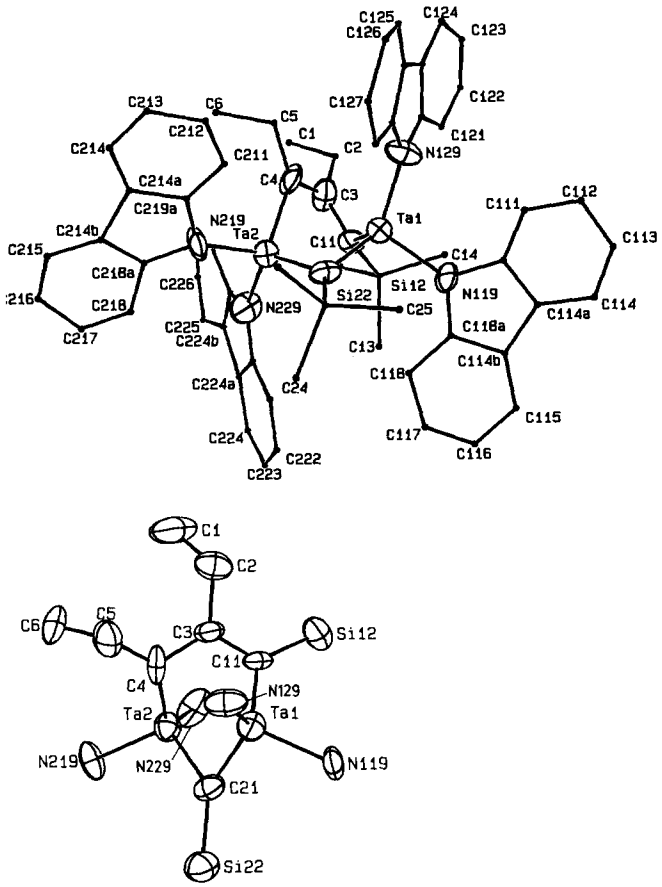

Fig. 1. Top: Solid-state structure of 1,3-dimetallabenzene **2b** (ORTEP). Bottom: Central section of the structure of **2b**. Distances [pm] and angles [°]: Ta1-N119 203(1), Ta1-N129 208(2), Ta2-N219 202(1), Ta2-N229 207(2), Ta2-C4 204(2), Ta2-C21 204(2), Ta1-C11 211(2), Ta1-C21 199(2), C3-C11 140(3), C3-C4 148(3); Ta1-C21-Ta2 90.5(7), C21-Ta2-C4 99.6(7), Ta2-C4-C3 98(1), C4-C3-C11 119(2), C3-C11-Ta1 93(1), C11-Ta1-C21 102.8(7), N119-Ta1-N129 105.8(7), N219-Ta2-N229 104.9(7).

trogen atoms and two carbon atoms within the ring. The six-membered dimetallacycle is distorted from planarity. The distortion can best be described as a twist (53°) of the $EtCC(Et)CSiMe_3$ and $(cb)_2TaC(SiMe_3)Ta(cb)_2$ units relative to each other. Inspection of the bond lengths within the dimetallacycle does indicate some localization of the (double) bonds, indicating more contribution from resonance form **A**.

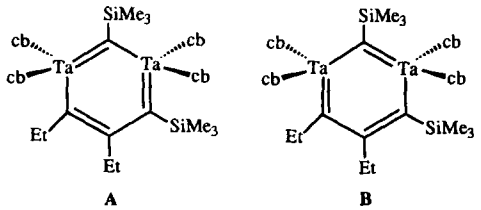

The observed solid-state structure of **2b** is maintained in solution as evidenced by ^1H and ^{13}C NMR spectra. The deviation from planarity is demonstrated in the ^1H NMR spectrum (25 °C) by the presence of diastereotopic methylene protons for the two ethyl substituent groups.[6] When the temperature of the solution is increased, the ABX_3 multiplets collapse into a simpler A_2X_3 pattern. From the coalescence temperature an estimate of the barrier for exchange of these protons of 16.1(5) kcal mol^{-1} at 328 K can be made. This barrier corresponds to the energy needed for the nonplanar ditantallacycle **2b** to achieve planarity before flipping into the other enantiomeric form. There is no evidence at 70 °C for exchange of nonequivalent Et, $SiMe_3$, or $Ta(cb)_2$ groups in **2b**, indicating that more extensive, reversible fragmentation or rearrangement of the dimetallacycle does not occur on the NMR timescale. The ^{13}C NMR spectrum of **2b** is also informative. The resonance of the carbon atom bound to both tantalum centers lies at $\delta = 393.0$, while those of the carbon atoms bound to only one tantalum center are found at $\delta = 253.9$ and 257.3. These latter two signals are in a region typical for α carbon atoms in tantalum alkylidene complexes.[7]

The alkylidyne-bridged compounds **1a** and **1b** both react over 24 hours at 80 °C with the terminal alkyne $Me_3SiC{\equiv}CH$ to produce a single regioisomer, **3a** and **3b**, respectively.[8] The presence of only the 2,4,6-trisubstituted regioisomer is indicated by both the ^1H and ^{13}C NMR spectra.[9] The most important feature of the spectroscopic data on **3a** and **3b** is the chemical shift of the proton directly attached to the six-membered ring. These protons resonate at $\delta = 8.43$ and 8.64 for **3a** and **3b**, respectively. The downfield position of these signals may be indicative of a ring current within compounds **3**, although the fact that this proton is in a position β to two high-valent metal centers complicates this assessment.

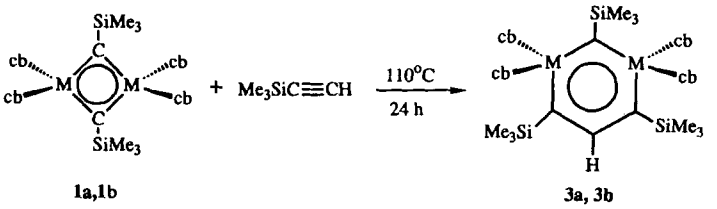

The isolation of these new dimetallacycles **2** and **3** allows the proposal of a possible new pathway for alkyne metathesis.[10, 11] Preliminary studies have shown that reaction of **1a** and **1b** with 2-pentyne at 100 °C leads to a mixture of regioisomeric dimetallacycles, but no evidence of alkyne metathesis has yet been found. Further work on these and related dimetallacycles continues.

Received: April 14, 1992 [Z 5302 IE]
German version: *Angew. Chem.* **1992**, *104*, 1277

CAS Registry numbers:
1a, 142842-18-0; **1b**, 142842-19-1; **2a**, 142842-20-4; **2b**, 142842-21-5; **3a**, 142842-22-6; **3b**, 142842-23-7; $EtC{\equiv}CEt$, 928-49-4; $Me_3SiC{\equiv}CH$, 1066-54-2.

[1] a) J. R. Bleeke, *Acc. Chem. Res.* **1991**, *24*, 271, and references therein; b) H. Chen, R. A. Bartlett H. V. Dias, M. M. Olmstead, P. P. Power, *Inorg. Chem.* **1991**, *30*, 3390, and references therein; c) J. R. Bleeke, Y. F. Xie, L. Bass, M. Y. Chiang, *J. Am. Chem. Soc.* **1991**, *113*, 4703; d) J. R. Bleeke, T. Haile, M. Y. Chiang, *Organometallics* **1991**, *10*, 19; e) J. R. Bleeke, Y. F. Xie, W. J. Peng, M. Y. Chiang, *J. Am. Chem. Soc.* **1989**, *111*, 4118; f) G. P. Elliott, W. R. Roper, J. M. Waters, *J. Chem. Soc. Chem. Commun.* **1982**, 811; g) M. S. Kralik, A. L. Rheingold, R. D. Ernst, *Organometallics* **1987**, *6*, 2612; h) D. L. Thorn, R. Hoffman, *Nouv. J. Chim.* **1979**, *3*, 39; i) for the chemistry of 1,3-diphosphabenzenes see H. Schmidbaur, S. Gamper, C. Paschalidis, O. Steigelmann, G. Müller, *Chem. Ber.* **1991**, *124*, 1525.
[2] R. D. Profilet, P. E. Fanwick, I. P. Rothwell, *Polyhedron*, **1992**, *11*, 1559.
[3] For the similar reactivity of 1,3-ditungstacyclobutadienes see a) M. H. Chisholm, J. A. Heppert, *Adv. Organomet. Chem.* **1986**, *26*, 97; b) M. H. Chisholm, R. M. Jansen, J. C. Huffman, *Organometallics* **1992**, *11*, 2305.
[4] **2b**: Analysis calcd for $Ta_2C_{62}H_{60}N_4Si_2$: C 58.21, H 4.73, N 4.38%; found C 57.91, H 4.77, N 4.22%.
[5] Crystal data (20 °C) for **2b**: space group $P2_1/c$, $a = 19.721(2)$,

$b = 11.7788(9)$, $c = 23.240(4)$ Å, $Z = 4$, $\beta = 98.571(9)°$, $\rho_{calcd} = 1.592\ g\,cm^{-3}$; 4548 unique reflections with $I > 3\sigma(I)$ yielded $R = 0.054$, $R_w = 0.076$. Further details of the crystal structure investigations may be obtained from the Fachinformationszentrum Karlsruhe, Gesellschaft für wissenschaftlich-technische Information mbH, D-W-7514 Eggenstein-Leopoldshafen 2 (FRG), on quoting the depository number CSD-56378, the names of the authors, and the journal citation.

[6] **2a**: ^{1}H NMR (C_6D_6, 30 °C): $\delta = 0.33$ (s, Nb_2CSiMe_3), −0.77 (s, $CCSiMe_3$), 0.13, 0.81 (t, CH_2CH_3), 1.56, 2.32 (br., CH_2CH_3); ^{13}C NMR (C_6D_6, 30 °C): $\delta = 5.6$ (Nb_2CSiMe_3), 1,3 ($CCSiMe_3$). – **2b**: ^{1}H NMR (C_6D_6, 30 °C): $\delta = 0.34$ (s, Ta_2CSiMe_3), −0.75 (s, $CCSiMe_3$), 0.21, 0.84 (t, CH_2CH_3), 1.85, 2.40, 2.68 (br., CH_2CH_3), 8.71 (d, *ortho* protons of cb, 6.59 (t, *meta* protons of cb ^{13}C NMR (C_6D_6, 30 °C): $\delta = 6.7$ (Ta_2CSiMe_3), 1.4 ($CCSiMe_3$), 16.0 (CH_2CH_3), 27.2, 27.7 (CH_2CH_3), 253.9 ($CCSiMe_3$), 257.3 (CCEt), 393.0 (Ta_2CSiMe_3).

[7] L. R. Chamberlain, I. P. Rothwell, J. C. Huffman, *J. Am. Chem. Soc.* **1982**, *104*, 7338.

[8] **3b**: Analysis calced for $Ta_2C_{61}H_{60}N_4Si_3 \cdot C_7H_8$: C 58.87, H 4.94, N 4.04%; found C 58.13, H 5.03, N 4.00%.

[9] A single-crystal X-ray diffraction analysis of **3a** has been carried out, it confirms the formulation of the compound as a dimetallabenzene derivative and clearly shows four equivalent Nb–C and two equivalent C–C distances within the ring **3a**: ^{1}H NMR (C_6D_6, 30 °C): $\delta = 0.07$ (s, Nb_2CSiMe_3), − 0.70 (s, $CCSiMe_3$), 8.43 (s, CH), 8.60 (d, *ortho* protons of cb); ^{13}C NMR (C_6D_6, 30 °C): $\delta = 5.8$ (Nb_2CSiMe_3), 0.1 ($CCSiMe_3$). – **3b**: ^{1}H NMR (C_6D_6, 30 °C): $\delta = 0.14$ (s, Ta_2CSiMe_3), − 0.63 (s, $CCSiMe_3$), 8.64 (s, CH), 8.73 (d, *ortho* protons of cb); ^{13}C NMR (C_6D_6, 30 °C): $\delta = 5.6$ (Ta_2CSiMe_3), − 0.3 ($CCSiMe_3$), 255.0 ($CCSiMe_3$), 386.5 (Ta_2CSiMe_3).

[10] a) R. R. Schrock, *J. Organomet. Chem.* **1986**, *300*, 249; b) *Acc. Chem. Res.* **1986**, *19*, 342.

[11] The possibility of tungstabenzene intermediates in alkyne metathesis has been discussed by J. H. Freudenberger, R. R. Schrock, M. R. Churchill, A. L. Rheingold, J. W. Ziller, *Organometallics* **1984**, *3*, 1563.

BOOK REVIEWS

Book Reviews are written by invitation from the editor. Suggestions for books to be reviewed and for book reviewers are welcome. Publishers should send brochures or (better) books to the following address: Redaktion Angewandte Chemie, Postfach 101161, D-W-6940 Weinheim, Federal Republic of Germany. The editor reserves the right of selecting which books will be reviewed. Uninvited books not chosen for review will not be returned.

Host-Guest Molecular Interactions. From Chemistry to Biology. (Series: Ciba Foundation Symposium No. 158.) Wiley, Chichester, 1991. IX, 278 pp., hardcover £ 39.50.—ISBN 0-471-92958-1

Under the auspices of the Ciba Foundation, a symposium on molecular recognition was held in London at the beginning of July 1990. The 15 papers presented at this small but illustrious gathering have provided the material for the book reviewed here. Following an introduction by I. Sutherland, the first paper is a contribution by J. F. Stoddart on the application of charge-transfer interactions to the synthesis of catenanes and rotaxanes. Next G. W. Gokel reports on experiments aimed at creating artificial ion channels based on crown ether derivatives. This is followed by an application-orientated contribution by D. N. Reinhoudt, on the problem of converting chemical information into electrical signals. The required selectivity can be obtained by using synthetic host molecules; for example, calixarene is the basis for a field-effect transistor responding to potassium ions. However, it is also possible to use enzymes for specifically converting substrates into products that can be detected electrochemically, and W. J. Albery describes how this method has been successfully used for in-vivo determination of blood sugar content. Next comes a report by J. P. Waltho and D. H. Williams on complexes between antibiotics of the vancomycin family and peptides, then an article on J. Rebek's well-known receptor molecules for adenine etc., which are derived from Kemp's tricarboxylic acid. The contribution by R. Breslow describes cooperative effects of bifunctional molecules in the binding of substrates, in the catalysis of supramolecular reactions, and in connection with the triggering of differentiation processes in tumor cells.

The second half of the book is mainly concerned with biopolymers, starting with nucleic acids and their complexes with antibiotics (M. Waring). N. T. Thuong and C. Hélène describe conjugates of oligonucleotides with acridine that make possible sequence-selective binding to DNA through the formation of triple helices. This topic is taken further in a report by M. H. Caruthers on the preparation and properties of dithioate-modified DNA. The next four articles are concerned with the structural self-organization of proteins and enzyme–substrate complexes. G. C. K. Roberts describes NMR studies on dihydrofolate reductase, R. I. Carey and M. Mutter report on synthetic proteins with template-controlled folding behavior, A. B. Edmundson contributes an article on the binding of peptides to immunoglobulins, and R. U. Lemieux describes studies on the stability of complexes between various modified tetrasaccharides and a lectin. The lectin results reported by Lemieux generated new speculations concerning the role of associated water molecules in the association of amphiphilic surfaces, and the discussion of this is reported here. The book concludes with an article by J. G. Vinter on molecular modeling approaches to the description of host–guest interactions.

Conference reports published in book form have certain unavoidable drawbacks, namely the lack of uniformity in the individual contributions, a relatively high price due to small print runs, and above all the fact that similar articles by the same authors can often be found in the regular journals, and sometimes already exist when the book appears. This volume is no exception in the latter respect, and, moreover, the articles are all very brief. However, this certainly does not mean that the book is superfluous, since by including an account of the discussions it achieves something that an individual paper cannot do, that is to convey something of the spirit of a conference in which the lively exchange of views reveals new aspects of the work reported. These discussions, which also include literature references and diagrams to make the main points clear, are given an appropriately large amount of space. In addition three "General Discussions" on important topics of interest are included. The volume is completed by a list of participants, an author index, and a brief subject index. The material has been carefully put together, and the standard of printing and production is good. This book is certainly of value for everyone interested in the subject.

Michael Göbel
Institut für Organische Chemie
der Universität Frankfurt (FRG)

Cyclobutarenes. The Chemistry of Benzocyclobutene, Biphenylene, and Related Compounds. (Series: Studies in Organic Chemistry, Vol. 44.) By *M. K. Shepherd.* Elsevier, Amsterdam, 1991, XIV, 322 pp., hardcover HFl 320.00.— ISBN 0-444-88171-9

Benzocyclobutene, biphenylene, and related compounds are of interest because of the rigidity of the four-membered ring linking the benzenoid parts of the structure, which confers planarity on molecules of this type and makes possible a mesomeric interaction between the individual π-systems. Furthermore, various higher analogues have recently been successfully synthesized, and heterocyclic compounds of this type can also be prepared. Against this background the publication of the book "Cyclobutarenes" by M. K. Shepherd, which gives a comprehensive survey of this class of compounds, is a welcome development.

The book contains eight chapters, two short appendices, and a subject index. In Chapter 1 the author describes the electronic configurations and physical properties of the cyclobutarenes. The chapter begins with an introduction discussing aromaticity, nonaromaticity, and antiaromaticity, starting with benzene and cyclobutadiene then moving on to the cyclobutarenes. A brief section on nomenclature is followed by sections on benzocyclobutene and annelated systems such as biphenylene, benzobiphenylenes, and lastly their heterocyclic and ionic analogues. Chapter 2 describes methods for preparing benzocyclobutene and related compounds, classified according to reaction types, with similar compounds grouped together in tables. The following chapter gives a thorough description of the chemistry of benzocyclobutene and related compounds. The main reactions discussed are dimerizations, cycloadditions with dienes and dienophiles, insertions, additions, metal complex formation, and redox reactions. Chapter 4 is concerned with methods for preparing biphenylene and related compounds, again subdivided according to reaction types; these include the dimerization of arynes, dehalogenation of 2,2′-biaryls, extrusion reactions from bridged biaryls, cyclotrimerization of alkynes, cycloaddition reactions with benzocyclobutene, the Wittig reaction, and condensations with benzocyclobutenedione. Chapter 5 then describes the chemistry of biphenylene and its derivatives, again arranged according to reaction types, namely electrophilic, nucleophilic, and homolytic substitutions, additions, insertions, cycloadditions, heat-induced reactions, photochemical reactions, and redox reactions. The following chapter deals with substituted biphenylenes, classified according to substituents: alkyl and aryl derivatives, carbonyl compounds, halides, nitrogen compounds, hydroxybiphenylenes, metalated derivatives, transition metal complexes, and lastly biphenylenequinones. Chapter 7 is devoted to annelated biphenylene derivatives, starting with the strained cyclopropane-anellated systems, then moving on to systems with four- and five-membered anellated rings, and continuing with a longer section on systems with six-membered rings, which also include the larger fully conjugated systems. The series then continues in the same way up to annelated systems with twelve-membered rings. The final chapter deals with heterocyclic biphenylenes and their derivatives, distinguishing between azabiphenylenes that are electron-deficient and those with an electron excess, and also covering furan and thiophene analogues. The book ends with two appendices listing ^1H and ^{13}C NMR data for many of the compounds mentioned, followed by a detailed subject index.

M. K. Shepherd has carried out a formidable task in writing this book, as is evident from the more than 1200 literature references. It is a mine of information for everyone working in this field, especially as it also includes many reactions that only give a specified compound in low yields. The subject matter is systematically arranged, although in some cases this reviewer felt that it would have been better to combine sections that are very short. In view of the wealth of information provided, the criticisms mentioned below are only of minor importance. For example, the author should have been aware that P. J. Garratt's book "Aromaticity" (Ref. 1a in Chapter 1), which first appeared in 1971, was succeeded in 1986 by a thoroughly revised new edition. In the appendix listing ^1H NMR data it is unfortunate that the solvent is not always given. It is especially regrettable that the publishers have not afforded the book a quality of production commensurate with the author's hard work and with the price. The text is directly reproduced (which no doubt accounts for the fact that it is noticeably free of errors), but the quality of the type and of the formula diagrams leaves something to be desired. Considering the facilities that are available with modern text processing, it would have been helpful if, instead of printing the formula numbers in normal type in parentheses, they were in bold type for easier readability. Substituents attached to arene rings should be shown joined on by lines. It would also have been helpful to include details of reagents, reaction conditions, and yields alongside the arrows in the reaction schemes, rather than mentioning them only in the text.

The book is of great value for chemists whose work is concerned with cyclobutarenes, but the high price will probably deter many potential private buyers. It has often been demonstrated by other publishers that books comparable in content to this one can be offered at a lower price and with a better standard of production.

Holger Butenschön
Max-Planck-Institut für Kohlenforschung
Wuppertal (FRG)

Registered names, trademarks, etc. used in this journal, even when not marked as such, are not to be considered unprotected by law.

© VCH Verlagsgesellschaft mbH, D-W-6940 Weinheim, 1992. – Printed in the Federal Republic of Germany by Konrad Triltsch Druck- und Verlagsanstalt Würzburg.

All rights reserved (including those of translation into foreign languages). No part of this issue may be reproduced in any form — by photoprint, microfilm, or any other means — nor transmitted or translated into a machine language without written permission from the publishers. Only single copies of contributions, or parts thereof, may be made for personal use. This journal was carefully produced in all its parts. Nevertheless, authors, editors, and publisher do not warrant the information contained therein to be free of errors. Readers are advised to keep in mind that statements, data, illustrations, procedural details, or other items may inadvertently be inaccurate.

Valid for users in the USA: The appearance of the code at the bottom of the first page of an article (serial) indicates the copyright owner's consent that copies of the article may be made for personal or internal use, or for the personal or internal use of specific clients. This consent is given on the condition, however, that the copier pay stated per-copy fee through the Copyright Clearance Center, Inc. (CCC), for copying beyond that permitted by Sections 107 or 108 of the U.S. Copyright Law. This consent does not extend to other kinds of copying, such as copying, for general distribution, for advertising or promotional purposes, for creating new collective works, or for resale. For copying from back volumes of this journal see 'Permissions to Photo-Copy: Publisher's Fee List' of the CCC.

Editorial office: Postfach 10 11 61, D-W-6490 Weinheim, Federal Republic of Germany, Telephone (06201) 602 315, Telex 465 516 vchwh d, Telefax (06201) 602 328, E-Mail Z16@DHDURZ2 in Earn Bitnet.

Editor: *Peter Gölitz*

Associate editors: *R. H. Schmidt-Radde, K. J. Schneider, A. Stimson.* **Editorial assistant:** *E. Schweikart*

Publishers: VCH Verlagsgesellschaft mbH. (Managing Directors: *Hans Dirk Köhler, Dr. Karlheinz Köpfer*), Pappelallee 3, D-W-6940 Weinheim, Federal Republic of Germany.

Advertising office (Advertising Manager: *R. J. Roth*): Postfach 10 11 61, D-W-6940 Weinheim, Federal Republic of Germany, Telephone (0 62 01) 104 556, Telefax (0 62 01) 104 550.

ANGEWANDTE CHEMIE
International Edition in English
Volume 31 · Number 10
October 1992
Pages 1265–1398

August Wilhelm Hofmann—"Reigning Chemist-in-Chief"**

By Christoph Meinel*

One hundred and twenty-five years ago, on November 11th, 1867, the German Chemical Society of Berlin held its inaugural meeting. The main purpose of the Society was to unite pure and applied chemistry and to foster cooperation between academic research and the chemical industry. And, indeed, it soon became the major forum of German and even European chemistry. Its program clearly bears the hallmark of a single individual: August Wilhelm Hofmann, the Society's first president, who died 100 years ago. For his contemporaries, Hofmann represented a new type of chemistry professor. At no time since have professional chemists felt as abundantly endowed with potential for the future and with public esteem. Hofmann's portrait was monumental even then, and still today it would belong in any gallery devoted to our distinguished forebears.

Anniversaries provide an opportunity to direct our attention toward the past—and thus to ourselves as well. We are, after all, heirs to that period from which the modern world derives its profile. Questions from our own time lead us to reacquaint ourselves with one of the founders of modern chemistry, but we may also benefit from a fresh look at an epoch which, beneath the surface of prosperity and progress, was as contradictory as our own, an epoch struggling to understand the role of science in the new industrial era.

In Liebig's Laboratory

We must envision the young Hofmann as a sensitive individual, rather inclined toward literature and the arts—and the direct opposite of someone with a clear plan for the future.[1] He was stamped with impressions gathered in educational travel, especially to Italy, where the boy was accompanied by his father, Johann Philipp Hofmann, privy councillor and provincial architect to the court of Darmstadt. "This awakened his early interest in the study of modern languages and a certain facility for expressing himself in tongues other than his native German, a factor not without its influence on his later career."[2] Hofmann registered as a student in his native city of Giessen at the age of eighteen. His father would have liked to have seen him study architecture, but the son found himself drawn rather to languages, "an idea contested vigorously by the father on the grounds that it could not lead to any satisfactory goal." The resolution of this dilemma was a decision in favor of law, a study "to which the next few years were dedicated, with occasional interruptions and little notable success." As far as the pursuit of a utilitarian education was concerned, Hofmann found it difficult to develop any enthusiasm, "always wavering between philology, law, and even architecture." In those days, preparing oneself to become an administrative official included learning the fundamentals of chemistry, so Hofmann became acquainted with the basic tenets of analytical chemistry in Liebig's laboratory. The name Liebig was already on

[*] Prof. C. Meinel
Lehrstuhl für Wissenschaftsgeschichte der Universität
Postfach, D-W-8400 Regensburg (FRG)

[**] This essay appears here as a preprint from *Die Allianz von Wissenschaft und Industrie: August Wilhelm Hofmann (1818–1892)–Zeit, Werk, Wirkung* (Eds.: C. Meinel, H. Scholz), VCH, Weinheim, November **1992**. In this volume, historians, historians of science, and chemists from industry and academia discuss Hofmann's life and work in the context of the society and economy of his time. They also trace those traditions that led to today's chemical research. The authors of this bilingual volume come from Germany, Great Britain, the USA, Czechoslovakia, the Netherlands, and Israel.

 © *VCH Verlagsgesellschaft mbH, W-6940 Weinheim, 1992* *0570-0833/92/1010-1265 $ 3.50+.25/0*

every tongue—his novel didactic methods had in fact attracted students to Giessen from all over Europe. It had already been necessary to expand the facilities of Liebig's institute on two occasions, and even to open a second branch, with construction activities carried out under the supervision of Hofmann's father. The resulting frequent—indeed, friendly—interchange between Herr Hofmann and Liebig was not without its effect on the son. According to one anecdote, Hofmann's father was moved to provide Liebig with an account of his son's indecisiveness and lack of academic success, to which Liebig is supposed to have responded: "give him to me, and I'll see what can be made out of him; he's a good lad, and he's certainly no fool; perhaps he just hasn't found the right path."[3]

Once within the sphere of attraction of the great master, he soon felt an irresistible pull toward the natural sciences, which confronted him with the lure of the novel in contrast to the singular course of his own previous studies. Thus began a new life, the study of law forgotten, philology relegated to the leisure hours, and the major part of his efforts dedicated to the study of chemistry, physics, and finally mathematics. Soon we see the young man working as a zealous pupil in the laboratory and ultimately taking part as an assistant in the research of the revered professor.[4]

Liebig's institute in Giessen is regarded as the prototype of the modern university laboratory. Here experimental research became incorporated directly into the educational function of the university, and laboratories were transformed into work stations dedicated to the production of new knowledge. It was also here that the idea of a division of labor was first applied to research activities, with distinctive roles assigned to the group leader, one or more assistants, and the research students. Moreover, contacts were established between university research and industry, and the organizational form of the university "institute" as a large-scale enterprise had its beginnings. It all began with a single piece of methodology: the elemental analysis of organic compounds, which was developed to the level of a routine procedure in 1832. This proved the key to organizing research along new lines: "turning out the most audacious discoveries in a factorylike fashion," as Liebig once described it.[5] These were also decisive years for the discipline of chemistry itself. Organic and physiological chemistry emerged from the context of "plant and animal chemistry" as distinct fields of research. Fundamental concepts, the notions of elements and molecules, nomenclature and formulas: all demanded clarification. The question of chemical "vitalism"—which was supposed to provide a distinction between the "organic" and the "inorganic"—was transported into the realm of experimental answers. Commercial applications promised to furnish the discipline with improvements in obsolete techniques in addition to attractive profits.

Liebig's recipe for success included introducing his gifted students to research at a very early stage.[6] There was no such thing as a fixed curriculum, and passing an oral examination was the sole requirement for a doctorate. Outstanding performance on the latter, as in Hofmann's case, constituted grounds for certification as a qualified university lecturer *(Habilitation)*. Within a very short time we find Hofmann working as an assistant, and entrusted with editing the *Annalen der Chemie und Pharmacie*. His own first research results appeared in this journal in 1843 under the title "Chemische Untersuchung der organischen Basen im Steinkohlen-Theeroel" ("Chemical Investigation of the Organic Bases in Coal-Tar Oil").[7]

How often does it happen that a young chemist takes on as his first research topic a substance that will become the basis for his later fame—and for an entire industry as well? And how often does he succeed at the same time in locating a substrate open to almost infinite variation? The owner of a tar distillery in Offenbach, himself a former student of Liebig, sent a sample of the material to Giessen for analysis, and Hofmann was assigned the task of its investigation. He found in this tar two previously described bases, known as "kyanol" and "leukol" [quinoline],[8] and after a great deal of effort extracted from it sufficient material to demonstrate that the "kyanol" was actually identical to substances also characterized in the literature as "krystallin," "benzidam," and "anilin." Moreover, he showed that it bore a relationship to phenol, one which could be expressed in terms of the common radical "phen" or $C_{12}H_{10}$ [C = 6]. Shortly thereafter it became apparent that the other base, "leukol," was identical to Gerhardt's quinoline. The latter was of considerable interest as a degradation product of quinine. Once Hofmann succeeded in obtaining larger quantities of aniline from the benzene in coal tar, he subjected it to nitration and subsequent reduction with zinc in acid, after which he began

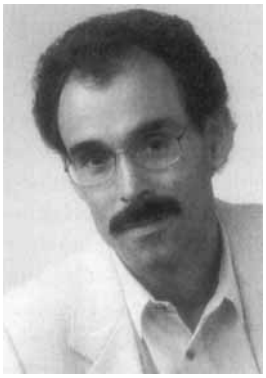

Christoph Meinel, born in Dresden in 1949, studied chemistry in Marburg. After receiving his Diplom, he turned toward the history of science and completed his Ph.D. in 1977 with a dissertation on the history of chemistry. Following a postdoctoral year at the University of Kent at Canterbury, he held positions at the Universities of Marburg and Hamburg and conducted research in the United States. In 1987 he completed his Habilitation in the field of history of science in Hamburg. He was Fellow at the Institute for Advanced Study, Berlin, in 1987/88, and later Heisenberg Fellow of the Deutsche Forschungsgemeinschaft and coordinator of the Verbund für Wissenschaftsgeschichte in Berlin. In 1990 he was appointed professor for history of science at Mainz but moved on to a chair for history of science at the University of Regensburg that same year. Since 1990 he has been chairman of the History of Chemistry Group in the Gesellschaft Deutscher Chemiker. His research interests include 18th- and 19th-century chemistry and early modern natural philosophy and theory of matter. He has published books on the history of chemistry at the University of Marburg, on the work of the 17th-century Hamburg naturalist and philosopher Joachim Jungius, and on the history of alchemy.

a systematic investigation of the various transformations. Indigo attracted his attention in this context, since it also led to aniline upon alkali fusion. A paper describing the properties of this dye[9] served as impetus for the preparation of its halogenated derivatives, in analogy to the chloro and bromo derivatives of isatin.

The matter proved to be of considerable interest. Accepted theory—in the Liebig school as elsewhere—held that a chemical compound should be regarded as a pairing of a stable, electropositive group of atoms, the "radical," with an electronegative element or group. It was recognized in the meantime, however, that an organic radical might incorporate electronegative elements like chlorine or bromine without altering its electropositive character. This observation was the starting point for a new "substitution theory," put forward and defended by Laurent and Dumas. The substitution theory made it possible for the first time to regard a molecule as a single entity, in which individual atoms might be replaced by other elements without fundamentally changing its chemical nature. This theory, championed by Liebig's bitterest opponents, had been the subject three years earlier of a malicious piece of satire formulated by Wöhler and Liebig and published in the *Annalen* under the pseudonym S. C. H. Windler ("swindler"). The alleged author reported that, thanks to the new French doctrine of "types and substitution," he had succeeded in replacing, one after another, all the atoms in cotton by chlorine, and that there was no significant change evident in the material's characteristics. Indeed, clothing manufactured from "spun chlorine" was said to be already on the market in London, where it was avidly sought by consumers! Was Liebig now expected to allow Hofmann's bromo- and chloroanilines to reignite this old controversy?

Facts

Hofmann must have known that he could never come to Liebig with a new theory. This was especially true since his mentor's research program had just recovered from a very serious crisis. Its origin can be traced to nearly insurmountable difficulties presented by the chemistry of nitrogen metabolism in animals. Liebig had struggled for a decade with the explanation for this phenomenon, using all the means available from a contemporary perspective. If chemistry were to satisfy the demands of the neo-humanist interpretation of science then it must demonstrate its powers in the context of a theoretical interpretation of natural phenomena.[10] And now his program was threatened with failure because of the complexity of the subject! The dilemma could only be resolved in one of two ways. Either the discipline must succeed in breaking new ground and convincingly translate its insights into practical results, thereby displaying to the world the utility it claimed to possess, or else the demand for a scientific interpretation of nature must be reduced to "hard" numbers and facts, with studious disregard for any speculative elements.

Hofmann chose the second path, adopting a compromising stance with respect to those aspects of his research that impinged upon bonding theory. Thus, while he acknowledged that hydrogen had been replaced by halogen, he emphasized at the same time the fact that the introduction of increasing amounts of bromine or chlorine caused the electrochemical character of the radical to be displaced in an electronegative direction. This left Liebig free to present this work in a footnote—not as evidence supporting the views of Dumas, but as a strike against Berzelius. Hofmann's own reserved attitude with respect to broad generalizations and theories is also apparent from the fact that he coupled his cautious compromise proposal with an express warning: "Nothing is more dangerous than attempting to draw general conclusions without the ability to stand on a mass of facts."[11] And when he submitted the work in a competition sponsored by the Société de Pharmacie in Paris, he took steps to ensure that he would not be accused of taking sides in the bonding theory controversy by adding the motto of the English author Edmund Burke: "Facts are to the mind what food is to the body."[12]

As it happens, this motto reveals to us one of the important characteristics of Hofmann's approach to research. To a much greater extent than most of his contemporaries, and comparable in this respect only to Wöhler, Hofmann avoided becoming involved in controversies surrounding the fundamental theories of chemistry. His papers speak instead the dispassionate language of "chemical facts." When confronted with the need to adopt a text for use in his classes in London, Hofmann chose to translate Wöhler's *Beispiele zur Übung in der analytischen Chemie* (Göttingen, 1853), a work that progresses through 122 chapters—very pragmatically, without any theory—proceeding from simple materials to complex situations involving applications. The translator's preface leaves no room for questioning the motive behind his choice: "General statements, general instructions, will always remain more or less unintelligible to the student, as long as he fails to have a sufficient number of facts at his disposal."[13] Thomas Gradgrind, director of the model school in *Hard Times*, would have taken a great deal of satisfaction from this textbook, which was published in precisely the same year as Charles Dickens' famous critique of the impending machine age, with its obsession for numbers and facts—a book that begins with the classic enjoinder: "Now, what I want is, Facts. Teach these boys and girls nothing but Facts. Facts alone are wanted in life. You can only form the minds of reasoning animals upon Facts: nothing else be of any service to them ... Stick to Facts, Sir!"[14]

Four years later, at the suggestion of Kekulé, chemists from all over the world assembled in Karlsruhe in an attempt to clarify the fundamental uncertainties surrounding the concept of atoms and molecules. Hofmann's was among the 45 signatures on the invitation, but he chose, in fact, not to make a personal appearance at this first congress of chemists. While others were publishing ambitious theoretical compendia, such as Kekulé's *Lehrbuch der organischen Chemie* (Erlangen, 1861–1887), Hofmann produced only a single small volume, almost conversational in style, entitled *Einleitung in die moderne Chemie*. This work does testify to his "conversion to 'Gerhardtism'"[15] and to the "types" notation, but otherwise maintains a very pragmatic tone, with commitment to clear, didactic presentation and to "extreme moderation, the most measured reserve"[16] with respect to theory. The most original part of the work—a computational method based strictly on gas volumes ("Krithen") rather than mass units, with the corresponding

formulas expressed graphically—was never copied by anyone else, and must have seemed, only six years after the Karlsruhe congress, oddly positivistic. When the sixth and last edition of the *Einleitung* appeared in 1877 it still contained no reference whatsoever to the periodic table, and the list of atomic weights of the elements is simply presented alphabetically! And yet, Hofmann was anything but "A man of realities, a man of facts and calculations" in the mold of Gradgrind. Precisely the tension arising between the bold geometrical speculations of a Kekulé or a van't Hoff and the massive production of tangible "chemical facts" by a Hofmann, the latter outrunning every theory—it is this dichotomy that explains the incredible dynamic of chemistry at that time.

What Marvelous Opportunities!

Giessen offered no place for Hofmann over the long term. Assistants with greater seniority had priority in terms of acquiring a professorship. Liebig played his cards close to the chest when it came to personnel matters. Consequently, Hofmann cleverly contrived during the master's absence to become engaged to his niece, at the same time transferring his activities to Bonn. Understandably enough, Liebig was "painfully moved" to discover that his protégé had seized the initiative "without consulting me and without telling me about it," in the process frustrating his own plan for establishing Friedrich Mohr in the Bonn position, which had already been proposed to him.[17] In the spring of 1845 Hofmann became a *Privatdozent* (instructor) in Bonn. What he had in mind was nothing less than establishing a copy of the successful Giessen model on Prussian soil. This should necessarily have appealed to Liebig, since it would have been equivalent to an intellectual-political triumph over the latter state, where Liebig had recently claimed there was not a single university offering practical training in chemistry.[18] Or did Liebig have an even more audacious plan in mind?

Exactly one month prior to Hofmann's introductory lecture in Bonn, Liebig set out on his fourth visit to England. Ever since the first wave of British students arrived in Giessen in 1836, Liebig had found himself irresistibly fascinated with this country.[19] Great Britain must have seemed a "land of unlimited opportunity" to a chemist. Liebig had even toyed with the idea of emigrating there in order to devote himself exclusively to his agrochemical experiments. The lightning visit in the spring of 1845 was intended as preparation for such a move. Under a seal of absolute secrecy, Liebig entrusted his friend Wöhler with the news that he wished this time to undertake "an enormous experiment" to verify his agrochemical ideas.[20] In fact, jointly with two British partners he had established a fertilizer factory in Liverpool.[21] Despite the fact that this firm was not blessed with great success, it is quite clear that an interest in practical applications was what Liebig was pursuing in England.

The date of the trip coincided with a decisive phase in British chemistry. After decades of stagnation the discipline had achieved a leading role in the modernization of science, in no small measure due to demands of the economy. Public recognition and professionalization in chemistry were much further advanced in England than on the continent; missing, however, was an appropriately modern educational facility. William Gregory, chemistry professor at Aberdeen and a former student of Liebig, had been stressing this point since 1842. Bullock and Gardner, also former Liebig students, made a public suggestion in 1844 that a private institution be founded, on the Giessen model, for education and research in chemistry.[22] The motives of these clever, business-oriented young men were an elevated status for the discipline and the promise of rich profits. They attracted support in a circle of wealthy landowners interested in improvements in agriculture and mining, as well as among physicians, druggists, and industrialists. The plan gained an important advocate in the person of the queen's physician, with whom Liebig also had close contacts. Before long a nucleus of subscribers had been assembled, and even the support of the crown had been won. Needless to say, only a student of Liebig could be considered for the role of director of such an institute. And so it was that Hofmann was offered the directorship of the Royal College of Chemistry in London. The proposal sounded not only speculative but even visionary.[23]

Fig. 1. A. W. Hofmann in his 28th year (1846), heliogravure from an (unknown) drawing, 116 × 91 mm, from Jacob Volhard and Emil Fischer, "August Wilhelm von Hofmann: Ein Lebensbild," *Ber. Dtsch. Chem. Ges.* **1902**, *35* (special issue), prior to p. 33.

The moment of decision came at a meeting in August 1845, when Queen Victoria and the Prince Consort were visiting Schloss Brühl as guests of the Prussian court. From there they made a trip to Bonn, where Prince Consort Albert was anxious to see once again the building in which he had lived as a student. In the meantime, who but Hofmann should have installed his laboratory in that very building! This favorable coincidence led to the confirmation of the appointment at the highest possible level, since both the Prussian ambassador and the Minister of Education were also in attendance. One formal obstacle—the fact that instructors were not employed members of the faculty, and thus not eligible for leaves of absence—was dealt with in an elegant fashion: the Minister of Education simply promoted Hofmann on the spot to the rank of assistant professor *(ausserordentlicher Professor)*, and then granted him a leave of absence. Hofmann was offered a laboratory with space for

40 students, assistants, and technicians, free lodging, and an annual income of £ 400 with a £ 2 supplement from the tuition of each student. After two years he was promised an annual raise of £ 100, up to a maximum stipend of £ 700—and in the interest of security, 600 talers [equivalent to £ 51] to permit him to return to Bonn. With ten times the income that a professor at Bonn could anticipate, Hofmann planned to return in two years as a successful man with 10000 talers in his pocket, suitably prepared for marriage. Full of self-confidence he wrote back to Giessen:

My dear professor, what will you say when you hear that in all probability I will be going to England. It may be that I overestimate my abilities, since recently all my investigations have been so crowned with splendid success, but I believe I am the man who can make something of the situation there. Once in a lifetime each of us is offered a very special chance, and the daring man seizes it. What marvelous opportunities to move forward in science and establish a reputation for oneself are not offered in England![24]

A Conspiracy

The outcome of this situation was hardly inopportune from Liebig's perspective. Or might it not be that he arranged the whole thing himself? At the very least it is noteworthy that Hofmann's contract became valid only after Liebig had approved the conditions. Having a reliable bridgehead in England was almost preferable to emigrating there himself. It would appear, however, that Liebig and Hofmann secretly pursued designs that none of their contemporaries could have imagined.[25] It may have been Hofmann's work on the bases in coal tar that gave Liebig the idea to investigate more closely the residues from cinchona bark and quinine production known as "quinoidine," which was discovered in 1822 to contain an amorphous mixture of alkaloids. Liebig discovered that this quinoidine could serve as a source for crystalline quinidine [a stereoisomer of quinine], with a composition identical to that of pure quinine itself and displaying equivalent therapeutical activity. This led to a scheme to buy up supplies of quinoidine from all over Europe, then patent the process, publish the analytical results, and finally sell the now valuable material at a good profit. Capital was of course required, but also important—from the standpoint of patent rights—were British comrades-in-arms. A consortium was therefore established in which Liebig, Hofmann, Bullock, and Gardner each held one-sixth shares. The chancellor of the University of Giessen, on the other hand, had two-sixths, since he represented the actual source of the funds. All but the latter belonged to the narrow circle around the founders of the Royal College of Chemistry. They must have felt rather like conspirators preparing to join in the new game of "capitalism." A sum of 50000 gulden had already been invested in the project when, through carelessness, the affair came out and the whole scheme collapsed.

The stereotype of Hofmann as one who ventured forth "from the spiritual heights of a German university ... inflamed" with "a pure passion for knowledge of the true and the beautiful, unsullied by the pursuit of material advantages,"[26] who arrived in a materialistic England and there capitulated against his will to the forces of industry—this stereotype is clearly due for revision. Indeed, it reveals all too openly the handwriting of its author, who was a master of stylization. In any event, Hofmann must have recognized in the quinidine affair a warning against future direct participation in business risks. He never succumbed to the "founders' fever" that later struck so many chemists. When his assistant William Perkin produced his first synthetic dye and—having just turned 18—wanted to try his luck in industry, Hofmann reacted "much annoyed, and spoke in a very discouraging manner ... Hofmann perhaps anticipated that the undertaking would be a failure, and was sorry to think that I should be so foolish as to leave my scientific work for such an object."[27] Nevertheless, to see Hofmann as the archetype of the pure scientist[28] would be a mistake. "Whatever you now do," he once advised Liebig (hardly an inexperienced bystander in such matters), "don't lift a finger unless there is financial compensation."[29]

Branching Off

Conceived originally as an educational institution, the Royal College of Chemistry was also a testing laboratory, which was supposed to provide its private financiers with certifications and analyses. Landowners and mine operators, apothecaries and druggists, industrialists and businessmen, all anticipated that their investments would be rewarded in productivity and the jingling of coins. But Hofmann was quite conscious of the dangers in an overly shortsighted, utilitarian operation. The fact that the Giessen model of research-oriented education had been transplanted into the more utilitarian climate of Britain meant that the character of the institution would necessarily change as well. London was not the place for the selfless pursuit of pure science. It was important instead to justify the research imperative as a pedagogic vehicle directed toward scientific results in the form of new laws and compounds that could in turn be applied in a beneficial way within industry and commerce. The gap between theory and practice, the tension between the demands of commerce and the ideals of scholarship—Hofmann dealt with these through a rhetoric that treated the utilitarian as a more or less inevitable spin-off from the scientific quest for knowledge.

Even though the curriculum of the College[30] offered a fixed three-year course of studies, what made it attractive was the fact that the extent and intensity of the required work could be tailored to the individual, who could enter the program at any stage. Fully half the students enrolled for only a single semester, often to conduct investigations important to their own particular professions. Others came to seek the qualifications necessary for carrying out research. Hofmann's ability to recognize talent and provide each applicant with an appropriate assignment from his rich storehouse of ideas was as famous as his knack for selecting outstanding associates. In this way the focus of the College shifted more and more in the direction of pure organic chemistry.

It is nearly impossible to describe all the projects undertaken by Hofmann and his students. As in any research

program, detours, special opportunities, and outside commissions played a role, and one substance or another inevitably resisted the will of the chemist. Nevertheless, Hofmann succeeded in developing a characteristic research style in London. One of his earliest projects, executed in Giessen but presented before the Chemical Society in April 1845, was introduced with the remarkable assertion that a new direction had become apparent in organic chemical research. Whereas in the past one had always operated in a purely analytical mode, and rarely "with the goal of preparing particular compounds postulated through prior speculation," now the groundwork had been laid to conduct targeted "synthetic experiments" for the artificial preparation of organic compounds. "If a chemist were to succeed in transforming naphthalene in a simple way into quinine, we would quite properly honor him as a benefactor of humanity. Such a transformation has not yet been accomplished, but that alone does not imply that it is impossible."[31]

The concept of synthesis is a key to Hofmann's way of thinking. If the analytical phase of organic chemistry began with Liebig, in Wöhler's synthesis of urea Hofmann saw the threshold to the next higher step: an "era of synthetic chemistry."[32] A decisive shift in emphasis for the discipline had thus been recognized. This change is associated in no small measure with the name of another man who also traveled to London in the fall of 1845: Hermann Kolbe. With acetic acid, Kolbe succeeded in completing the first targeted synthesis of an indisputably organic compound starting from its elements.[33] In fact, the synthetic program of modern chemistry evolved in very important ways from the work undertaken by Kolbe and Frankland at the Royal School of Mines in the 1840s. The idea of "synthesis," for which popular accounts had predicted so much, reached its programmatic summit in the work of Berthelot. But as early as 1858 Kolbe had prophesied:

> *In the present state of our still-youthful discipline one may make the bold claim that as soon as the chemical constitution of substances such as indigo, alizarin, quinine ... has been correctly diagnosed, we will be in a position to assemble these materials artificially from their more intimate components.*[34]

It was left to Hofmann to transform this agenda into practice, and this he did with spectacular success. At the same time, however, for Hofmann the concept of synthesis held more than a mere chemical connotation: consistent with his creative, esthetic, nonanalytical way of looking at things, synthesis appeared to offer a vision of creativity in the face of the emerging machine age, and the prospect of wholeness as opposed to a science increasingly dominated by division of labor and a narrow-minded concentration on detail.

It is certainly characteristic that Hofmann's research program was eminently product-oriented. His positivistic, theory-abstaining stance corresponded to the spirit of the new age itself, the spirit of goods and the marketplace. Hofmann thought strictly in terms of *classes* of substances, which were to be investigated systematically and thoroughly once a pilot study had revealed some synthetic access. Analogy was his leading heuristic principle; his method was to systematically chart possible derivatives, toward which targeted syntheses were then directed. Hofmann operated strategically, in accordance with the expansionism of his time. Extension and diversification were key words for him. He described chemistry as a "magical tree, reaching out in every direction with its branches and twigs and infinite ramifications."[35] His central and often repeated metaphor of the tree comprises three crucial aspects: the nineteenth-century notion of evolution, the image of motion and vitality, and the many ramifications of Hofmann's own research program, at the heart of which was the researcher, supplying both guidance and planning. That, at any rate, is how his students saw it, and they extolled "the fertility of mind which, while he himself was conducting simultaneously several investigations, continually branching off into new ramifications, enabled him to suggest a multitude of fresh subjects for work to his students ... and to hold the guiding strings of all firmly within his grasp."[36]

There is no need to explain to chemists that Hofmann could not have selected a better starting point for such an endeavor than aniline. This particular venture led to a series of ten "Contributions to an Understanding of the Volatile Organic Bases." The goal was to investigate the "remarkable analogy" between aniline and its derivatives, on the one hand, and ammonia, on the other.[37] Reactions with the halogens and alkyl halides were especially interesting. It became clear that the premise of the radical theory, according to which preformed ammonia must constitute one member of a "pair" in such compounds, was no longer tenable. In fact, the alkylated anilines could better be viewed as compounds in which the various hydrogen atoms of ammonia were successively replaced by organic residues. Application of the principle of homology permitted the number of possible combinations and their isomers to be increased almost without limit.

> *Here I find it impossible to avoid pointing out the wonderful versatility of isomeric compounds, to which a continuation of this investigation must necessarily lead. One sees at first glance that substances with the formula $C_{18}H_{13}N$ can be obtained by introduction of 1 equiv of methyl into xylidine, or 2 equiv of methyl into toluidine, or finally by attaching to aniline the radical (propyl) derived from the missing alcohol of propionic acid. We obtain in this way six alkaloids with the same formula, yet differing significantly in their constitution.*

$$\left.\begin{array}{ll}
\text{Cumidin} & \left\{\begin{array}{ll} & H \\ & H \\ C_{18} & H_{11} \end{array}\right\} N \\
\text{Methyloxylidin} & \left\{\begin{array}{ll} & H \\ C_2 & H_3 \\ C_{16} & H_9 \end{array}\right\} N \\
\text{Aethylotoluidin} & \left\{\begin{array}{ll} & H \\ C_4 & H_5 \\ C_{14} & H_7 \end{array}\right\} N \\
\text{Dimethylotoluidin} & \left\{\begin{array}{ll} C_2 & H_3 \\ C_2 & H_3 \\ C_{14} & H_7 \end{array}\right\} N \\
\text{Propylanilin} & \left\{\begin{array}{ll} & H \\ C_6 & H_7 \\ C_{12} & H_5 \end{array}\right\} N \\
\text{Methyläthylanilin} & \left\{\begin{array}{ll} C_2 & H_3 \\ C_4 & H_5 \\ C_{12} & H_5 \end{array}\right\} N
\end{array}\right\} = C_{18}\,H_{13}\,N.$$

> *This number, of course, increases the higher we climb up the ladder of organic compounds. Two members are added at each rung, so that when we reach diamylaniline $C_{32}H_{27}N$ we*

are confronted with no less than twenty bases, the calling into existence of which will not be overlooked in the progress of science. —A striking example of simplicity in variety, which characterizes the creations of organic chemistry.[38]

Types, Colors, Alliances

Substitution reactions had convinced Hofmann of the advantages of utilizing the notation of "types" for expressing

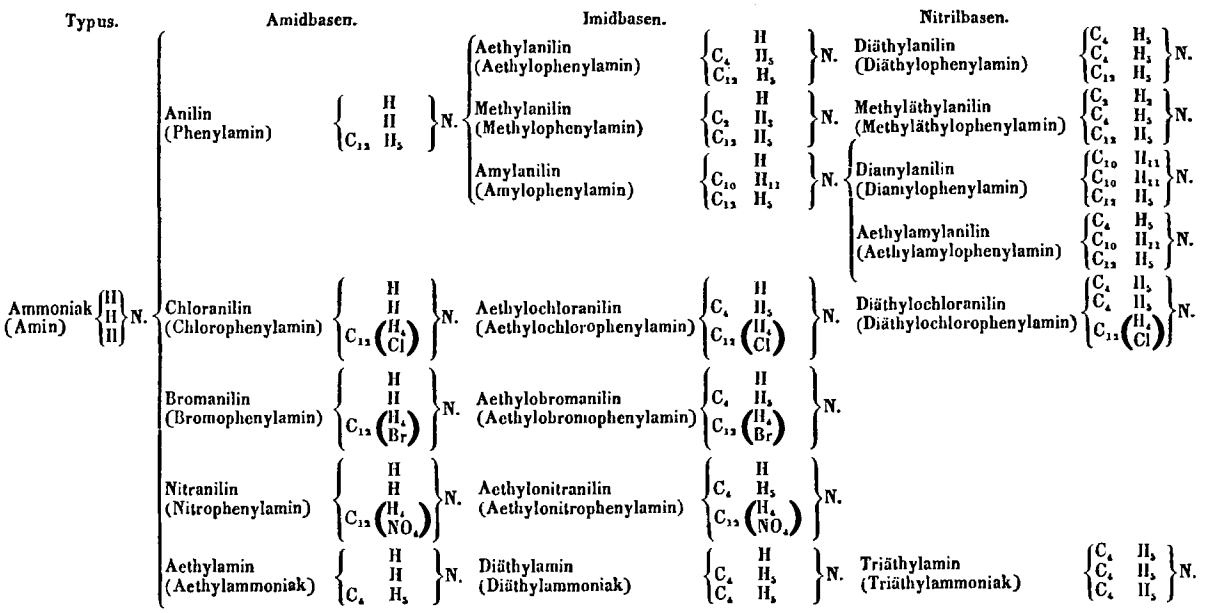

The basic structure of ammonia permits one to obtain in this way a complete range of homologous substitution products, which Hofmann later designated as primary, secondary, and tertiary amines. Even though individual twigs were still unknown on this tree of possibilities that had unfolded itself in Hofmann's mind's eye, he remained confident that their existence "should be supportable by facts without difficulty;"[39] indeed, the synthesis of complicated natural products appeared to have moved into the realm of the possible.

The natural bases [quinine, morphine, etc.], may possess a more entangled composition. But a series of well-conceived experiments will not fail to cast light on the constitution of these compounds, and in this way place us in the position of constructing them in the same way it has been possible with the alcohol bases.[40]

Before Hofmann no one had ever conducted chemistry in this way. His approach represents an anticipation of basic strategies of industrial research, with the development and variation of entire spectra of products.[41] The program was to prove its worth a hundred times over in the broad field of organic nitrogen compounds. It is thus no wonder that Hofmann once compared his role as director of the institute with "the position of an industrialist in command of a splendid machine."[42] Instead of following Liebig's ingenious principle of basing research on an instrumental method, elemental analysis, Hofmann transformed the laboratory into a gigantic piece of machinery for the systematic synthesis of "chemical facts" in the form of new compounds and derivatives.

chemical formulas. Substances with similar reactivities could thereby be assigned to a small number of basic types, in which atomic groupings were bound to one another in identical ways. Nevertheless, this was not meant to be an assertion regarding the true nature of either intramolecular groupings or bonding relationships; rather, the formulas were regarded simply as tools to aid in the classification of reactivity, and to assist in the search for analogies—a taxonomic model with no correlation with a reality that was assumed to be fundamentally unintelligible.[43] Compounds derived formally from a given inorganic primary substance all belonged to a single "chemical type." Hofmann seized upon this approach more firmly than his contemporaries as a guide to synthesis. He pictured it as a "type of construction" and a form of "template" in whose empty spaces atoms or atomic groups could be inserted like building blocks.[44] Hofmann's own model substance was of course ammonia.

Relative to all the other approaches to expressing chemical formulas, the type theory offered the tremendous advantage of permitting for the first time predictions regarding possible compounds of a given type. For this reason, type formulas were to provide the basis—along with the principles of analogy, homology, and variation—of the most important heuristic instrument and classification scheme in the new synthetic chemistry. Without his type theory, Hofmann's research program would have been impossible. He therefore remained true to the type notation even after it had been superseded by structural formulas. Entire series of publications on the volatile and nonvolatile organic bases [amines], the analogous phosphorus bases [phosphines] (17 papers, 1857–1860), and the "polyammonias" [polyamines] (24 pa-

pers, 1858–1863) testify to the effectiveness of the approach. Always pursuing several series of investigations simultaneously, and attacking across a broad front, Hofmann carried the art of serial publication to its first high point. He preferred to describe his method of operation as "analogic or template work."[45]

It was destined to prove its worth best in that field which to this day is still associated with Hofmann's name: coal-tar dyes. The corresponding history is too familiar to be repeated here in detail.[46] In 1856 Hofmann's assistant William Perkin oxidized aniline in the hope of obtaining quinine. The result was the first synthetic organic dye prepared in a research laboratory, aniline purple or mauve. This was followed two years later by Hofmann's discovery—and Verguin's independent discovery in Lyon—of fuchsin (magenta). The brilliance of these substances enchanted the ranks of high society, and they quickly acquired the status of "fashionable" colors. Industry and science instantly became conscious of the potential inherent in coal tar. Coal-tar dyes, together with their corresponding starting materials and intermediates, came to occupy the center of attention, leading in turn to a new relationship between chemical research and industry. The complexity of the substrate demanded the availability of professional chemists with both theoretical and analytical training, while translating results from the laboratory into industrial-scale ventures required the experience of industrialists. Virtually all the important subsequent innovations would come from the collaboration between these two worlds.

Hofmann himself first entered the new territory in 1860 in the context of his work on the polyamines.[47] The decisive factor was his contact with Edward Chambers Nicholson, whose company in London was one of the leading producers of chemical intermediates.[48] Studies related to aniline red (fuchsin), "chrysaniline," "rosaniline," and their derivatives, which we recognize today as triphenylmethane and acridine dyes, constituted thereafter the core of Hofmann's efforts. Systematically applying the principles of analogy and variation, he provided access to an enormous number of potential dyes and intermediates, at the same time clarifying their relationships to one another. Of outstanding significance was his discovery that the introduction of substituents into a dye molecule could lead to systematic changes in the dye's properties, facilitating the targeted development of specific nuances of color.

> *The facts elicited by the study of the action of iodide of ethyl upon rosaniline open a new field of research, which promises a harvest of results. The question very naturally suggests itself, whether the substitution for hydrogen in rosaniline of radicals other than methyl, ethyl, and amyl, may not possibly give rise to colours differing from blue; and whether chemistry may not ultimately teach us systematically to build up colouring molecules, the particular tint of which we may predict with the same certainty with which we at present anticipate the boiling-point and other physical properties of the compounds of our theoretical conceptions?*[49]

The chemical knowledge of the times, of course, set up certain barriers preventing the thorough classification and theoretical interpretation of the diversity of new dyes. This becomes especially apparent in Hofmann's case, since he remained firmly committed to thinking in terms of the ammonia type, which prevented him from ever understanding the true nature of the rosaniline dyes with respect to their triphenylmethane skeleton. Hofmann himself did not regard this as a particularly serious obstacle. Oriented in his thinking and in his work toward substances and away from theories, he saw it as precisely the point at which a purely scientific view must be supplemented by the pragmatic and problem-oriented approach of industry. "Though proud of her office as guide of industry, science acknowledges without blushing that there are territories on which she cannot advance without leaning on the strong arm of her powerful companion. Joint labours of this kind cannot fail to seal the pledge of alliance between industry and science."[50] Educated in a tradition that recognized a clear division of responsibilities and an even clearer intellectual priority of "pure" over "applied" chemistry,[51] Hofmann learned in England that the new era demanded new ways of thinking. In his report on the World's Fair of 1862, he concluded that industrial research constituted the highest and noblest activity, and should be accorded an equal status with pure science:

> *In the course of this review he [the reporter: Hofmann] has become more and more disposed to assign to the pursuit of industrial chemistry ... an equal rank with the very highest and noblest of the learned professions; and, in particular, to place it fully on a par with the pursuit of purely scientific investigations of any kind .... He desires to record it as his firm persuasion that pure and applied science will, hereafter, in an increasing degree, go hand in hand.*[52]

"To seal the pledge of alliance between industry and science"[53] was to become the equivalent of a magical formula for Hofmann.

In the Marketplace of Life

The London Great Exhibition[54] of 1851, a prestige project of the Prince Consort, marked a turning point in Hofmann's life. World's Fairs amounted to stages for the century itself, with commercial interests resplendent in a shimmer of glass and steel, light and national banners: masterpieces of consumption, shrines dedicated to the idolization of merchandise.[55] A vision of paradise on earth, offering glitter and luxury even to the masses—here it became truly palpable. Hofmann was active in the preparations for this first World's Fair, which was to set the pattern for those that followed. He was a member of both the German exhibition commission and the jury, and he edited the official report on "miscellaneous manufacture and small wares." The impetus to innovation emanating from the exhibition was of direct benefit to chemistry. A whole complex of new research establishments came into existence, and the Royal College of Chemistry was made a part of the School of Mines. As a result, Hofmann became director of a state institute of higher education as well as a British subject, and soon thereafter was named Assayer of the Royal Mint. Government agencies thought highly of him as a consultant, and he was an indispensable adviser to industry. In 1851 he was designated a Fellow of the Royal Society. The Chemical Society,

of which he had been a member since 1845, elected him in 1847 to the post of foreign secretary, and then in 1861 to the presidency.

Fig. 2. A. W. Hofmann as professor at the London Government School of Mines, engraving by [John William] Cook, 16 × 11 cm from James Sheridan Muspratt, *Chemistry, Theoretical, Practical and Analytical as Applied and Relating to the Arts and Manufactures*, Mackkenzie, Glasgow/Edinburgh/London/New York, **1853–1861**.

Aristocratic landowners introduced Hofmann into the ranks of high society. The climax appears to have been an invitation to the estate of Lord Ashburton in the company of Thomas Carlyle.[56] Hofmann sparkled as an orator, delivering popular scientific lectures in front of the laboring classes in London as well as to the Crown Prince and Princess of Prussia at Windsor Castle—and finally even before the Queen and her children. As Hofmann himself perceived it, the interests of science were no longer subjects reserved exclusively for scientists; they had passed out of the laboratories to take their stand "in the market-place of life."[57] And in their company Hofmann himself became a recognized figure in public life: courted, honored, and influential.

At the apex of Hofmann's fame an opportunity arose to return to Germany. Bismarck's Prussia was on the point of backing up its political and military pretensions to leadership by modernizing institutions at home. Professorial chairs in chemistry had come available at two of the important centers of the land: those of Bischof in Bonn and Mitscherlich in Berlin. Chemistry at both institutions had fallen behind the level of development characterizing even the smaller universities, to say nothing of Munich and Leipzig, but Prussia was determined to set a new tone by issuing calls to prominent professorial candidates. Even the names Wöhler and Liebig were discussed. In 1863 Hofmann received an offer from Bonn, shortly thereafter one from Berlin.

Hofmann did not hesitate about returning to Prussia, which was beginning to take the lead in the modernization of Germany. His move was carefully prepared in advance.[58] Nevertheless, few at the time would have been able to appreciate his true motives. Friends advised him not to relinquish his prominent position in England. Liebig, who would perhaps have gladly received the offer himself (if only to be able to reject it), warned him against "transporting himself into the misery of German university conditions."[59] Actually, Hofmann probably foresaw that the traditional structures of British society, business, and education were soon to become a hindrance to further progress in industry and science,[60] and he was one of the first to draw the obvious conclusion. Caro, Böttinger, König, Leonhardt, Martius, Meister, and other industrialists who had sought their fortunes as chemists in Britain during the 1840s and 1850s followed his example.[61]

The Germany to which Hofmann returned had little in common with the quiet land of his youth. The country was awakening. Within a few decades it would experience a modernization unparalleled in history. Provincialism and customs barriers were falling, and railroads and factory chimneys were reshaping the agrarian landscape of the "belated nation,"[62] which was preparing itself under Prussia's leadership to surpass its rivals. The era of factories and machines was dawning: the era of Borsig, Krupp, and Siemens. A wave of new incorporations reached its culmination in the chemical industry in the 1860s. Europe watched spellbound by the incredible tempo with which a new industrial sector arose, one that was destined in a short time to dominate the world market.[63]

Palaces and Temples

Universities also derived their share of spoils from the economic upturn. The Humboldt formula of "seclusion and freedom," once purchased dearly with a renunciation of political and economic power, was displaced by a new self-assurance in science that relied on the scientists' power to actually reshape the world. Chemistry assumed the leading role in the modernization of the universities. A new generation of magnificently equipped institutes came into being.[64] Bonn and Berlin represented a prelude. While still in London, Hofmann was assigned the task of preparing a report on the building plans. He accepted this commission with obvious pleasure, since he was very well aware of the symbolic significance of such "palaces and temples"[65] dedicated to progress and the religion of science. They gave clear expression to the new claims of scientists to validity and prestige: the "splendid suite of apartments for the director" at the institute in Bonn with its "imposing entrance hall, illuminated by a glass cupola above, and the splendid ball-room, extending through two stories, and amply satisfying the social requirements of a chemical professor of the second half of the nineteenth century!"[66] The proposed institute in the Dorotheen- and Georgenstrasse in Berlin was impressive on the basis of its size alone.[67] A total of 954000 marks had been allotted to the construction, two and one-half times as much as for the institute in Bonn. New standards were to be set here for modernity, albeit hidden again behind the type of Renaissance facade so dear to the industrialists and upper middle-class. Their economic power no longer bore any relationship to their political standing, and this led them to hide their historical perplexity behind historicizing pretense.[68] Hofmann was especially concerned to include terra-cotta medal-

lions of the great chemists between the window arches, as well as busts of Liebig, Wöhler, and Faraday in the foyer.[69]

On May 7th, 1865, Hofmann commenced his lectures in Berlin, establishing himself temporarily in Heinrich Rose's old laboratory. Three years later the new building was ready. It boasted three large work rooms for beginning and advanced students; spectroscopy and photometry rooms; clean-up, weighing, and titration areas; metallurgical and forensic laboratories; workshops; and a roomy, private laboratory for the director. Hofmann was now in a position to pursue a research program along the broadest possible front.[70] He supervised more than 150 doctoral dissertations in Berlin, and his co-workers must have handled an equal number. The unprecedented dimensions of the resulting intellectual productivity are attested to by 899 scientific publications "Aus dem Berliner Universitäts-Laboratorium," 150 of them from Hofmann himself. Applying the principles of analogy, homology, and variation to the targeted synthesis of derivatives and to the discovery of new classes of compounds, here he was able to develop his working style to perfection. At the center remained as always organic compounds containing nitrogen, together with dyes, especially the rosaniline and quinoline dyes, but also dyes derived from beechwood tar. Reactive starting materials and intermediates for synthetic purposes also became important. Aromatic diamines, benzidine, xylidine, and methylated aniline derivatives were among the key substrates. Using the analogy between alcohols and amines as a heuristic tool, Hofmann prepared the aliphatic amines from C_9 to C_1, for which purpose he devised a general technique of amide degradation involving bromine and base. Systematic studies were also conducted on the derivatives of guanidine, isonitriles, and aliphatic mustard oils. A synthesis of formaldehyde permitted Hofmann to prove the existence of this long-sought molecule.

Reigning Chemist-in-Chief[71]

The close connection between the university research program and practical application was apparent in constant efforts to supply the dye and fine-chemical industries with new classes of substances and derivatives. An intimate, virtually symbiotic relationship soon joined the laboratory in Berlin with the chemical industry through former students who had accepted industrial appointments. The central figure was Carl Alexander Martius, one of Hofmann's assistants in London. In Berlin Martius assumed leadership of the Aktiengesellschaft für Anilinfabrikation (AGFA), thereafter enjoying a virtual monopoly with respect to the discoveries in Hofmann's laboratory and the placement of his graduates.[72] Hofmann also maintained ties with the inorganic bulk-chemicals industry through Hugo Kunheim, and with the developing pharmaceutical industry through Ernst Schering. The "alliance between industry and science" of which Hofmann had once dreamed was now a reality, albeit in a form very much in keeping with the patriarchal structure of the Wilhelmian era. The result was a complex interplay of give and take, interests and powers, gains and concessions, which—due to problems with the relevant source materials—eludes even today the grasp of the historian. Only in limited areas, such as the role played by professors in the various World's Fairs,[73] has it so far been possible to analyze the relationships with greater clarity.

Hofmann remained a master of "synthesis" when it came to matters of influence and power, always willing to accept nominations for new offices. His work load was incredible.

> *When he was seized by a new challenge, bodily needs seemed for him no longer to exist. A long lunch break was a useless waste of time, and hours devoted to sleep were reduced to a minimum. Even younger associates found it difficult in those days to keep pace with Hofmann at work, and I venture to doubt whether the occasional invitations to his assistants at two or three in the morning to join him in a glass of punch in order then 'to finish the job just like that' were always received as an unmixed blessing.*[74]

Institute director and professor at the Friedrich-Wilhelms-Universität, as well as its rector (1880/1881), Royal Privy Councillor Hofmann was at the same time a professor in the Military Academy, full member of the Academy of Sciences, full member of the Scientific Delegations for Medical and Educational Affairs (from 1864) as well as the Delegation for Trade and Commerce (from 1864), member of the directorate of the Patent Rights Society (from 1873), member of the Imperial Patent Office (1877–1882), full member of the Imperial Office of Public Health (from 1880), chemical adviser to the Chancellor of the Reich, and an expert witness before the courts. When the Assembly of German Natural Scientists and Physicians *(Versammlung Deutscher Naturforscher und Ärzte)*, with all its rich tradition, survived a stormy controversy in 1890 that resulted in a new set of by-laws intended to enhance its professional standing, it was once again Hofmann who was entrusted with the delicate position of the presidency.

Nevertheless, it was the German Chemical Society *(Deutsche Chemische Gesellschaft)* that emerged as the true focal point for the diverse interests of chemical industry and chemical science.[75] The Society constituted an imaginary stage upon which Hofmann was to perform as the star in a production that seemed written just for him. Martius and Wichelhaus, his closest associates, took the initiative in founding the organization, but it is tempting to think that Hofmann himself was the source of the idea. He described its purpose as follows: "the new Society is actually designed to provide an opportunity for the mutual exchange of ideas between representatives of the speculative and applied branches of chemistry in order to seal anew the alliance between science and industry."[76] Founded on November 11th, 1867, in the Great Hall of the Institute of Trade, the Society elected August Wilhelm Hofmann to be its first president. He would occupy this chair fourteen times in the next twenty-five years. But even during the eleven years in which he was "only" vice-president, Hofmann held the reins of power in his own hands. "It is self-evident," he assured Wöhler when the latter was proposed for the presidency, "that your assumption of this office will not cause you the slightest worry, or trouble you in any way. We ask nothing more than the honor of seeing your name at the pinnacle of this Society."[77] Indeed, Wöhler's only obligation was that of adding his signature to documents presented to him by the secretary "in a cozy portfolio."[78] Hofmann appears to have directed the course of elections in other cases as well. Thus, when the

election of Hermann Kopp was under consideration, Hofmann turned to Bernhard Tollens with the request that he "add the weight of your voice, along with those of your friends, colleagues, and students, to the scales" in the interest of his friend.[79]

Hofmann maintained his leading role in the German Chemical Society for a quarter of a century by exercising incomparable diplomatic adroitness, and by using this instrument he helped to determine the overall development of chemistry in Germany. Walter Ruske acknowledged as "a phenomenon difficult to understand for a contemporary observer" the degree to which the style and image of the Society was stamped in the image of a single man: "It almost appears as though Hofmann was literally forced into the role of a hero of German chemistry by his admirers, and the descriptions they provided of their master bear all the marks of a patriarchal model."[80] Hofmann knew how to make full and ceremonial use of all the authority that flowed in his direction. With eloquence and politeness, coupled with an almost youthful charm, he was an expert at transforming tension into a communal sense of self-assurance, preventing conflicts from ever developing, and finding common ground where there appeared to be a direct conflict of interests—a master at synthesis in this context as well.

Dissonance and Jubilation

The chemists tried very hard to convey an impression of self-confidence, both progressive and imperial, but in reality they felt a certain insecurity. Ever since the declaration of the Reich, worries and skepticism with regard to "progress" had merged with the fervor of the "founders' years" *(Gründerzeit)*. The belated and correspondingly accelerated modernization threatened to redraw the established boundaries of class and status. Modernization and industrialization also made their appearance within the universities. In no other discipline was the new role played by the natural sciences in the industrial era so apparent as in chemistry. Conflict with the traditional self-image of the universities was unavoidable. It peaked with a demand that chemistry and the other applied natural sciences be excluded from the universities altogether and banished to polytechnics or appropriate specialist institutions.[81] "The 'spirit of New York' now making its way into Berlin," wrote Heinrich von Treitschke in 1873 in reference to the University of Berlin, "threatens to endanger the life of the nation; it would be impossible to take action too strong in establishing an optimum counterbalance against the forces of consumption and pleasure," especially since some of the faculty already perceived themselves as part of a "university *en décadence*."[82] Anyone hesitant to retreat into the "ivory tower of academics" could escape the trials of the time only in aesthetic ventures with the vision of a more perfect, nobler world. Idealization and tendencies toward harmonization left their distinctive mark on the picture of the imperial Reich. What followed was an era of pomp and posturing, festivals and parades.

Hofmann was a genius at staging, at careful and exacting preparation, and the grand gesture. Even his lectures were recognized as histrionic masterpieces, "very dramatic, indeed theatrically honed."[83] For example, in order to demonstrate the bleaching effect of chlorine he once ordered an entire basket of violets and robbed them of their color, after which "with friendly jests and charming grace Hofmann threw the bouquets to his pupils."[84] But his *pièces de résistance* were the celebrations of the German Chemical Society. The new building for the Chemical Institute at the University had barely been completed when Hofmann invited the members to a "club night with the President." His intent was to make up for the spirit of elegance and consecration that had been absent when work first commenced in the "halls of the new temple": "None of those distinguished and eminently distinguished gentlemen in whose radiance we might on this occasion have shone, no bemedalled dignitaries of the Reich with their followers, no blossoming wreath of white-clad maidens to greet us on the steps of the sanctuary!"[85]

In 1870 after two years in office as president of the German Chemical Society, Hofmann passed the position on to Rammelsberg. In doing so he invited all the members, together with colleagues from the academy and the university, ministers, state officials, and diplomats, to a banquet that was to become a model for all their future ceremonial gatherings: a veritable firework of speeches, witty toasts, and congratulatory telegrams from all over the world. The purpose of the event was obvious: the effusive ovations served no other end than to portray Hofmann's return to Germany and the renunciation of his magnificent position in London to become a "simple German professor" as a rejection of the banal utilitarianism of the English, a yearning for the "higher, more ideal interpretation of things" found only in the German universities—remarkable testimony to the posturing and pretense of the founders' years. Hofmann edited the ceremonial report himself, and distributed it at his own expense as a special issue of the *Berichte der deutschen Chemischen Gesellschaft*.[86] Its title page portrayed Hofmann posing as an Olympian; in place of the goddess Victory he held in his right hand a bottle of aniline as he reigned sovereign over a multitude of profitable dye-putti bearing sacks bursting with talers. We must not let ourselves be disappointed by the antiquated Germanic frame and the clumsy lines of the artist: had any German professor ever before appeared in such an undisguised imperial attitude, or assumed so shamelessly the attributes of political and economic power?

This was not to pass without protest, and one of the greatest scandals in the intellectual history of the imperial Reich followed in its wake.[87] From Leipzig, a stronghold of middle-class mistrust of the upstart capital Berlin, Kolbe raged against the "arrogance of that Society, which calls itself 'German.'"[88] His colleague, the astrophysicist Zöllner, launched an unbridled attack against Hofmann and the modern scientific establishment in general. Hermann Cochius, one of the founding members of the German Chemical Society, resigned in protest against the dominant tone soon after the Hofmann celebration, distancing himself explicitly from the "clique of Berlin *raisonneurs*."[89] Friedrich Mohr wrote quite openly: "There prevails in the German Chemical Society in Berlin an attitude of toadyism and subservience that would make anyone nauseous.... I myself have fought for some time ... against the patented science of the current leaders."[90] Friedrich Rüdorff, chemistry professor at the Berlin Archi-

tectural Academy, feared nothing could be altered by criticism: "at the least they are likely to proceed with undiminished strength about the business of the great European society founded for the purpose of mutual and self-adulation (of which I myself am one of the oldest members)."[91]

Rüdorff turned out to be right. The success of the experiment in "modernity" was increasingly called into question, contradictions began to intrude into business and society as a result of the ebbs and flows of economic cycles and the so-called founders' crises, societies and special-interest groups were organized, complaints were voiced over depersonalization and declining quality, and disputes arose concerning academic versus vocational education, universities versus technical colleges, culture versus civilization. Yet, the more differentiated and dissonant this Wilhelmian Germany became, the more brilliant and jubilant were the festivities of the German Chemical Society: expressions of a deep desire to rise above the conflicts of the day, to compensate for dissonance in society with the harmony of a community.

Harmony and Luster

No excuse for celebration was wasted. A drinking party was held for 1500 students in Berlin's largest ballroom in 1878 in honor of Hofmann's 60th birthday, followed by a magnificent dinner for 200 guests. Hofmann arranged for participation by delegates from the four corners of the earth.[92] A convention was held in 1886 by the Assembly of German Natural Scientists and Physicians, at which Virchow and Hofmann were named managing directors. The German Chemical Society was responsible for organizing the chemical sections. A ceremonial reception was included, and the Society distributed to all in attendance a witty publication called the *Berichte der durstigen* ("thirsty") *Chemischen Gesellschaft*,[93] from the same publisher and in the same format as its staid journal, the *Berichte der deutschen Chemischen Gesellschaft*. The light-hearted tone and coarse jokes of this "journal" were in stark contrast to the otherwise solemn demeanor of the distinguished assembly of professors, directors, and industrialists. For Hofmann's 70th birthday the Society contributed a marble bust, together with the initial funds for a Hofmann Foundation. A student fête followed in imperial Germany's great ceremonial style.

Finally, a stunning culmination was arranged in the form of an elaborately coordinated double event for the year 1890: a "benzene festival" in the chambers of the City Hall and an "aniline festival" in the Hotel Kaiserhof. The Kaiser himself was invited, together with the "highest dignitaries of the Reich"—of course to no avail.[94] The former celebration was a tribute to the 25th anniversary of the formula for benzene, as well as to Kekulé, its inventor. The latter saluted Hofmann's return to Germany 25 years previously, and the impact that had on industrial development. The centerpiece at the first festival was the brilliant architect of a courageous idea who, in the words of Hofmann in his laudation, "never had a dye in his hands, and yet ... by proposing his theory of benzene may have given the coal-tar dye industry a greater impetus than all of us together, who have devoted years of our lives to the investigation of dyes."[95] Meanwhile, at the other celebration, tribute was paid to the man of action, one whose syntheses had provided industry with building blocks for the future, "who carried the light of science into the workshops of technology, ... who raised Technology to a status equivalent to that of its sister: Science," in the words of Heinrich Caro, representing the dye manufacturers.[96] The question of academic standing versus practical application, which had sounded as a leitmotiv throughout chemistry's history as an academic discipline, was thus provided with a dual answer: "pure" science scatters applications in its wake, even if unintentionally, but only industry blessed with an equal share of rights is in a position to make science productive. The coal-tar dyes, products of the most complex of all industrial syntheses up to that point, would have been unthinkable in the absence of an alliance between science and industry. But even more was at issue with these magical substances.

The founders' years of the chemical industry were not a time for treating men and materials with velvet gloves. Sulfuric acid, chlorine bleach, and sulfite pulping operations produced hazardous emissions at a level scarcely imaginable today. Exploitation reached its height, and plumes belching from the smokestacks of the factories were the pride of every entrepreneur. Coal tar was recognized as a particularly repulsive by-product, and it was produced in vast quantities during the gasification of coal. And yet it was precisely this scourge that was to become the starting point for a blossoming industry. It is certainly no coincidence that whenever the occasion arose to illustrate the utility of chemistry, Hofmann chose as his example not the mass-produced chemicals or the metals, not the dramatic improvements achieved in soda and mineral-acid manufacture, not the crucial fertilizer sector, not the introduction of wood-based cellulose as the basis of a new mass culture, but always dyes—a field that in the 11th edition of Rudolf Wagner's *Handbuch der chemischen Technologie* (Leipzig, 1880) warranted a scant 72 out of 1100 pages. It was not actual utility that was here thrust into the debate: many of the early dyes were primarily used in the treatment of silk, purely a luxury item. Much more at issue was fascination with the transformation of a detestable raw material into shining offspring steeped in elegance and luxury: "the way from coal to colour,"[97] a scientific fulfillment of the alchemist's ancient dream of transmutation.[98] It was this theatrical display that had occupied the center of public attention at the Internation Exhibition of 1862. Some of the glow is reflected in Hofmann's report:

> *In these cases is displayed a series of most attractive and beautiful objects, set in sharp contract with a substance particularly ugly and offensive. This latter is a black, sticky, fetid semifluid, equally repulsive to sight, smell, and touch: one of the most noisome, as it is also one of the most abundant and (heretofore) embarrassing, of the gas manufacturer's waste products. It is, in a word, gas tar.*
> *The beautiful objects amidst wich [sic] the tar is placed are a series of silks, cashmeres, ostrich plumes, and the like, dyed in a diversity of novel colours allowed on all hands to be the most superb and brilliant that ever delighted the human eye. Language, indeed, fails adequately to describe the beauty of these splendid tints. Conspicuous among them are the crimsons of the most gorgeous intensity, purples of more than Tyrian magnificence, and blues ranging from light*

azure to the deepest cobalt. Constrasted with these are the most delicate roseate hues, shading by imperceptible gradations to the softest tints of violet and mauve.[99]

The aesthetic of shine and luster was as much a part of the image of Wilhelmian Germany as its inclination toward the decorative and colorful. The sober reality of power and material acquired a second and artificial skin, appearing to be ennobled to culture. It was a remarkable (but for the times typical) preference for the ceremonial over the commonplace that conferred such a high symbolic value on iridescence drawn from tar. Gottfried Semper had extolled the introduction of gas illumination for its enrichment of the festive,[100] and in a similar way the conspicuous rhetoric surrounding the coal-tar dyes constituted a part of the apparatus of idealization and ennoblement with which the aspiring profession of chemistry freighted its vision of the future: science could help transform the inhospitability of cities and their industries into a festival of bright colors. Critics have described the reign of Wilhelm II as an "age of festivals."[101] The monarch himself, with his peculiar inclination to the operatic, represented precisely what the public desired: pomp and glory. "Even the simplest of things was transformed in Bengalic illumination," observed Nicolaus Sombart.[102] The same words could almost have been used to characterize Hofmann's style in his later years.

Prestige and Effect

Through their unique mix of glorification of the free life of the student, of whimsical superabundance, of that drive to impress so characteristic of the founders' years, and of the general national pathos, the chemists' celebrations betrayed all too clearly how little this band of professionals had established its footing in the new role to which it had ascended on the strength of its academic and economic might. Status and acceptance were dominant social values of the time,[103] but in chemistry a wide gulf separated pretension from reality. Avoidance of things political after all constituted the core of that silent compromise into which intellect and capital had entered under the protective mantle of state authority. Neither party—scientists nor industrialists—had any serious part to play at the real center of power. The greatest height to which a scientist could hope to rise was to become a model for the educated middle class, the "Bildungsbürgertum," but chemistry rested on one of the lower rungs of the disciplinary ladder. Status in Prussia was measured on a prestige scale shaped by the aristocracy and the military. Professors were not even represented on the court's list of high-ranking individuals. This made all the more important the carefully crafted system of titles and honors with which the traditional elite attempted to ensnare members of the aspiring middle class. In the year 1888 Hofmann, too, was rewarded with a title of nobility by Kaiser Friedrich, whose brief reign was the subject of so many hopes.

The impression of a leading role for natural scientists in German society of the second half of the nineteenth century, conveyed so often by sources close to the scene, is simply a myth.[104] In Imperial Germany the truth lay elsewhere. Chemistry was never blessed with a du Bois-Reymond or a Helmholtz. Chemists rarely ventured beyond the bounds of their own discipline and its closely allied industry; even marriages were commonly arranged within this social group. The circle surrounding Hofmann was also curiously limited. Shortly after his arrival in Berlin he admittedly communicated to his brother what he perceived to be compensation for the shabbiness and pettiness with which he was otherwise confronted at every step: "In the circles in which I travel, an academic enjoys encounters with industry and high finance, with the highest officials of the state, officers of every rank, artists in every field;"[105] but in truth his association was essentially limited to industrialists, co-workers, and "special colleagues" from the natural-science branch of the philosophical faculty. Few prominent figures appeared even at the numerous celebrations held in Hofmann's honor, leaving aside those from closely related disciplines. It is therefore reasonable to suggest that the ostentatious celebrations were intended primarily to shape and enhance the self-image of a profession that was in fact still somewhat insecure with respect to its true significance in society.

Fig. 3. A. W. Hofmann, ca. 1871, photograph by Carl Günther, Berlin, 90 × 56 mm, Staatsbibliothek Preussischer Kulturbesitz, Berlin, Coll. Darmstaedter, G2 1858 (5), f. 162.

The impression made on the outside world was correspondingly weak. Hofmann seldom appeared as a public lecturer except among chemists. Only when his duties required it did he take a position in daily affairs. The speech he delivered upon assuming the position of Rector of the Friedrich-Wilhelms-Universität attracted wide attention, but what he actually had to say on that occasion regarding division of the Faculty of Philosophy into separate faculties of science and humanities came across as weak and conventional: a rearguard action in the attempt to maintain the advantages associated with university status. Hofmann never followed a true policy in science, let alone in politics. In 1880 when he opposed the recognition of an antisemitic student fraternity—but at the same time pressed for the dissolution of a student "Committee Opposed to Antisemitic Agitation"—he was acting merely in his role as rector, attempting to keep the university free of politics and party confrontation.[106] Hofmann had no head for politics. He accepted the notions of monarchy and dynasty as pivotal, and he dis-

played an almost childish veneration for Friedrich's empress, who as a princess in London had once eavesdropped on his chemistry lectures. One searches in vain among Hofmann's speeches and writings for the name of Bismarck. To characterize him as a liberal nationalist would be something of an overstatement. Indeed, the widely traveled Hofmann had been a British subject for twelve years, and he always refused to be a participant in the growing nationalism. As for the German Chemical Society, with its high percentage of foreign members, he governed it according to the age-old model of the transnational community of scholars, and in England this "denationalisation of chemical science" was praised as one of the Society's most lofty achievements.[107]

Monuments

The restless Reich attempted with the help of historical myths to obscure the impositions of modernity. An excessive cult of monuments was the result. The monument to Arminius (*Hermannsdenkmal*) in the Teutoberger Forest (1875) and the Niederwald monument near Rüdesheim (1883) set the national tone. In the following years monuments were erected everywhere. In a world of expanding markets, of proliferating cities and industrial landscapes, materials and materialism, greed and profits, in a world characterized by horizontal expansion, monuments offered an element of verticality and meaning, pointing upward toward the sublime and away from the crudely materialistic, toward a realm of culture in which all historical contradictions were resolved.[108] It was unthinkable that the chemists should be immune to this passion for monuments.[109] Hofmann's laboratory in Berlin was probably the first building of its type to incorporate in its facade a rich sculptural program honoring the traditions of European chemistry.[110] Hofmann attached great importance to the busts of Liebig, Wöhler, and Faraday displayed in the entrance hall. But it was important that the world outside take notice as well. April, 1873, marked the death of Liebig, and the German Chemical Society decided immediately that a monument should be dedicated to him. In that very year, though it was also to witness the first of the founders' crises and an economic depression, a collection for the purpose was initiated among the chemists, energetically pursued by Hofmann.[111] Meanwhile, the German population as a whole was engaged in a collection to build a great national monument. The two monuments were unveiled within a few weeks of each other in the summer of 1883: the Kaiser doing the honors for a victorious Germania atop the Niederwald, and Hofmann for the Liebig statue in Munich. A second monument was erected to Liebig in Giessen, in July of 1890, and two days later one to Wöhler in Göttingen. It goes without saying that Hofmann delivered both dedication addresses. The tradition he thereby initiated continued for many years: by 1911 the German Chemical Society had erected no less than 21 monuments throughout the Reich.

Perhaps no preceding era had ever felt a greater need for history. Historicized styles of every imaginable type literally blossomed. It is no coincidence that an independent historiography of the natural sciences developed at the same time. Hermann Kopp set the standards with his *Geschichte der Chemie* (*History of Chemistry*; 1843–1847), a work that Hofmann greatly respected. Other descriptions followed from the hands of Gerding (1867), Wurtz (1868), and Ladenburg (1869).[112] Whether motivated by fundamental principles of a historiographic concern for source criticism, or by those of a panegyric, all these works shared one common characteristic: they invested a young discipline devoid of a history of its own with a mantle of tradition and permanence. Spurred on by both expedience and inclination, Hofmann contrived to make history an integrating element within the German Chemical Society. His genre was necrology; his preferred source, correspondence. Beginning with a commemorative address for Thomas Graham in 1869, Hofmann created a colorful bouquet of life histories—no less than 51 in number—which now adorns the yellowing volumes of the *Berichte*. The finest were collected in 1888 as three sumptuous volumes of *Erinnerungen an vorausgegangene Freunde* (*Remembrances of Departed Friends*), where they were accompanied by selections from the correspondence between Liebig and Wöhler. Lively, and displaying a fine sense of cultural history, the portrayals by Hofmann are testaments to a culture of affirmation, projecting the contrasting world of a pre-industrial idyll in which at the end of the day's toil one might seek after-hours consolation. But they also preserve the vision of a science at the heart of which stood the individual researcher, with all his hopes and disappointments; a science in which the ideal was most important, and financial gain was irrelevant; the vision also of a community of scholars, far removed from nationalistic delusions and the arsenals of the present day.

Under the Protection of the Patriarchy

Hofmann's portrait gallery, indeed the world of the founders' years quite generally, must be envisioned as a male phenomenon. Women played at most a decorative role, as when a "blossoming wreath of white-clad maidens"[113] adorned the formal opening of an institute, or during a social evening "a rich garland of lovely ladies looked down into the colorfully animated room from the loges and balconies."[114] Even as the wives of professors, corporate directors, and privy councillors, women were absent from the chemists' circles. Prussia was a bastion of male chauvinism. Nowhere else was opposition to women students so powerful and so enduring. Initially tolerated only as auditors in 1895, women were first allowed to matriculate or acquire the doctorate in 1908.[115]

And yet there existed certain isolated niches under the protection of this patriarchy, although it required a patriarch with the stature of a Hofmann to employ a female private assistant for almost three years, subsequently going so far as to help her acquire a doctorate—all without the news ever leaking out in Berlin. This case is documented in confidential correspondence.[116] In the summer of 1874 Hofmann wrote a letter to Wöhler enjoining the latter to be of assistance to his "not only charming, but also thoroughly educated pupil, Fräulein Julie Lermontoff," whose knowledge far exceeded the norm and who had the singular ambition "to take home with her from Germany a doctorate." Fräulein Lermontoff wished to apply for this purpose to Göttingen. "With our severe regulations here we are unfortunately not in a position

to introduce to the scene something so unheard of as a doctoral degree for a woman." Shortly thereafter Hofmann once again requested that special considerations be accorded her due to the unusual circumstances: "despite her considerable knowledge Fräulein Lermontoff is naturally very shy, and would consider herself fortunate if the chalice of an examination might pass her by."[117] In October 1874, 28-year-old Julie Lermontoff from St. Petersburg received her doctorate in chemistry at Göttingen with physics as a minor, albeit not without standing for the usual examination.[118] This was certainly the first doctorate in chemistry for a woman in Germany, indeed the first by many years.[119]

The End of an Epoch

If we may accept the word of his brother-in-law and longtime co-worker Ferdinand Tiemann, Hofmann's image evolved in a contrapuntal way:[120] from that of a fiery combatant in the battle for science in a Germany only beginning to awaken from its Philistine repose; to one serious and strict in respecting his obligations, out of a regard for public welfare, as the new Reich contemplated assuming a strong-man posture on the way to becoming a modern state. He ultimately came to represent the one constant factor in the chemical world: cheerful, benevolent, of sparkling humor, and always mindful of conciliation as the epoch reeled in a *fin-de-siècle* fever toward its demise.

In 1890 the whole atmosphere of Wilhelmian Germany was transformed. Ever since Bismarck's withdrawal, the Reich had perceived itself facing an uncertain future. The supremacy of the past gave way to a labile equilibrium. Industrialization, fragmentation of the middle class, and a developing labor movement produced dangerous cracks in the apparent solidarity of a patriarchal order. Rampant materialism, specialization, and "professionalism": these were the bywords of the cultural crisis of the decade. The instruments of the founders' years, the program of conservative reform, no longer struck a resonant chord; even the vision of industrialism as conveyed by the literature of the times became inverted and assumed a distinctly negative character.[121] The contrasting image of the creative genius, as conjured up for example by Julius Langbehn's *Rembrandt als Erzieher* (*Rembrandt as Educator*, 1890) began to attract enthusiastic throngs. A diffuse and ambiguous critique of modernity established itself.[122] The Reich of Bismarck had gambled away the opportunity for modern industrialized society to guide a new elite toward new forms of scientific-economic-political cooperation.

Such circumstances called for one more grand celebration by the chemists in an attempt to promote unity: in honor of the 25th anniversary of the German Chemical Society. Preparations were well underway when, on May 5th, 1892, Hofmann died, in the fullness of life and with a completed manuscript lying on his desk: it was to be the 887th contribution "Aus dem Berliner Universitäts-Laboratorium."[123] His funeral was worthy of a prince.

Hofmann's death marked the end of an epoch. The generation of the founders had retired from the scene. Siemens, who had coined the phrase "scientific era," died six months later. A new generation of academic mandarins,[124] the privy councillors and grandiose professors, rejected exaggerated display and monumentality. Emil Fischer, Fritz Haber, and Walther Nernst, leading reformers and protagonists of a new style, distanced themselves through coolness, matter-of-factness, and precision from the exuberance of their predecessors. Their own plans for the future were based on complexity and competitiveness, not on hierarchies and a sense of community.[125] They no longer felt able to plaster over the rents and tensions plaguing the scientific establishment. In conflicts about state examinations, rights of the technical institutes, questions related to untenured faculty and instructors or the integration of research and teaching—everywhere the tones became harsher and more strident.

Is it any wonder that the times held fast to their image of Hofmann? That they in fact inflated it until it acquired monumental proportions, because modern scientists—and industrialists—were threatened with disappearance as individuals due to a new division of labor in the workplace? That they drew comfort from Hofmann's enormous vitality, because their era seemed powerless, hectic, and a primary cause of its own illness? That they rejoiced in the memory of Hofmann's unpretentious humor and winning charm, because times were now bad and the mood had become strident? That they swore by his ability to integrate and to synthesize, because industrial society had lost that unanimity and clarity that had characterized traditional society? "In times of almost feverish growth in activity in science and industry," began Tiemann in his obituary address before the German Chemical Society, "it is appropriate for us to look back more often than in the past in order not to lose sight of the broader perspective."[126] A biography that the Society commissioned Tiemann to prepare was not completed until 1902, and then by Volhard and Fischer. It finally appeared in the form of an impressive special issue of the *Berichte*: a testament of the preceding century, laid at the threshold of a new age.

Hofmann would be remembered once again. In April 1918, the German Chemical Society gathered to celebrate its own 50th anniversary and the 100th birthday of its founder.[127] Few were present because of the war, and indeed only a single foreigner. The atmosphere was one of dejection; achievements from the past were urgently recalled to counter the uncertainty of the future. Cabinet ministers and representatives of government agencies, the rectors of the university and the Technische Hochschule, presidents of the professional associations and of the Kaiser Wilhelm Society—all were duly in attendance, and tributes to the contributions of chemistry recorded "in the golden book of this war" were just as obligatory as telegrams praising Ludendorff and the "heroic" Kaiser. Only one of the seated dignitaries apparently maintained his silence through all the speeches and toasts: Fritz Haber, who came to represent the minister of war.

*

Speaking out of the feverish restlessness of the *fin de siècle*, from the deep strife characterizing the turn of the century, and from the trauma of war, the German Chemical Society and chemists individually swore their allegiance repeatedly to the image of Hofmann. And it is this image that tradition has handed down to us. The accomplishments of this remarkable man were phenomenal for the time. In the stormy

phase of economic rebirth and through the crises of the founder's years he was the central integrating figure, the figurehead. Hofmann's powers of synthesis were enviable. But must we therefore be envious of an era that stood in desperate need of such men?

Received: May 13, 1992 [A 879IE]
German version: *Angew. Chem.* **1992**, *104*, 1293
Translated by Dr. W. E. Russey, Huntington, PA (USA)

[1] Based on the classic portrayals by Jacob Volhard and Emil Fischer, "August Wilhelm von Hofmann: Ein Lebensbild", *Ber. Dtsch. Chem. Ges.* **1902,** *35* (special issue); L. Playfair, "Hofmann Memorial Lecture" in *Memorial Lectures delivered before the Chemical Society, 1893–1900*, Gurney & Jackson, London, **1901**, pp. 575–596; W. H. Perkin, "The origin of the coal-tar industry, and the contributions by Hofmann and his pupils," *ibid.*, pp. 596–637; Henry E. Armstrong, "Notes on Hofmann's scientific work," *ibid.*, pp. 637–732; F. Tiemann, "Gedächtnisrede auf A. W. Hofmann," *Ber. Dtsch. Chem. Ges.* **1892**, *25*, 3377–3398; B. Lepsius, "Festschrift zur Feier des 50jährigen Bestehens der Deutschen Chemischen Gesellschaft und des 100. Geburtstages ihres Begründers August Wilhelm von Hofmann",*Ber. Dtsch. Chem. Ges.* **1918**, *51* (special issue). More recent sources: Monika Müller, *Die Lehrtätigkeit des Chemikers A. W. von Hofmann in Zusammenhang mit seinen Leistungen als Forscher und Wissenschaftsorganisator*, Ph.D. Dissertation A, Humboldt Universität, Berlin, **1978**; "Aus dem Leben und Wirken des Chemikers und Hochschullehrers August Wilhelm von Hofmann (1818–1892)", *Beiträge zur Geschichte der Humboldt-Universität zu Berlin*, **1981**, *4*; Johann Mulzer, "Bedeutende Chemiker der Berliner Universität: August Wilhelm Hofmann und Emil Fischer" in *Berlinische Lebensbilder, Vol. 1: Naturwissenschaftler* (Eds.: Wilhelm Treue, Gerhard Hildebrandt), Einzelveröffentlichung der Historischen Komission zu Berlin, Vol. 60, Stapp, Berlin, **1987**, pp. 27–44; Michael Engel, Brita Engel, *Chemie und Chemiker in Berlin: Die Ära August Wilhelm von Hofmann, 1865–1892*, Studien und Quellen zur Geschichte der Chemie, Vol. 1, Verlag f. Wiss.- und Regionalgeschichte, Berlin, **1992**. A reliable personal bibliography does not exist. Sources are given in the present contribution only for literal quotations; additional information was derived from the literature assembled here.

[2] August Wilhelm Hofmann, fragment of an autobiography, no date, Staatsbibliothek Berlin, Sammlung Darmstädter, Sig. G2 1858 (5), folio 1; The two subsequent quotations are derived from the same source.

[3] W. Will, *Zum Gedächtnis an A. W. von Hofmann, Rede auf der Trauerfeier der Universität am 22. Juni 1892*, Friedländer, Berlin, **1892**, pp. 4–5; cf. *idem.*, "Festrede bei der Enthüllung des Denkmals für A. W. von Hofmann in Giessen am 8. Juli 1918," *Ber. Dtsch. Chem. Ges.* **1918**, *51*, 1693–1704, here p. 1695.

[4] Hofmann, autobiography (cf. note 2), folio 1v.

[5] Liebig to Wöhler (12 July 1840), Bayerische Staatsbibliothek München, Liebigiana II A 1 (Wöhler), No. 180.

[6] Frederic L. Holmes, "The complementarity of teaching and research in Liebig's laboratory," *Osiris* **1989**, *5*, 121–164.

[7] A. W. Hofmann, "Chemische Untersuchung der organischen Basen im Steinkohlen-Theeroel," *Ann. Chem. Pharm.* **1843**, *47*, 37–87.

[8] Compound names appear here in their original form. Where it would be useful for comprehension, modern designations have been appended in brackets.

[9] A. W. Hofmann, "Übersicht der in letzter Zeit unternommenen Forschung über den Indigo und seine Metamorphosen", *Ann. Chem. Pharm.* **1843**, *48*, 253–343.

[10] Justus Liebig, "Über das Studium der Naturwissenschaften und über den Zustand der Chemie in Preussen [1840]", in Justus von Liebig, *Reden und Abhandlungen*, Winter, Leipzig, **1874**, pp. 7–36, here p. 12.

[11] A. W. Hofmann, "Metamorphosen des Indigos: Erzeugung organischer Basen, welche Chlor und Brom enthalten", *Ann. Chem. Pharm.* **1845**, *53*, 1–57, here p. 56.

[12] Volhard/Fischer (**1902**), p. 22; "Facts are ... the body. The wisest in council, the ablest in debate, and the most agreeable companion in the commerce of human life, is that man who has assimilated to his understanding the greatest number of facts." George Seldes, *The Great Quotations*, Stuart, New York, **1967**, p. 336, no source provided.

[13] A. W. Hofmann, *Preface*, in Friedrich Wöhler, *Handbook of Inorganic Analysis* (Ed.: A. W. Hofmann), Walton & Maberly, London, **1854**, p. vii.

[14] Charles Dickens, *Hard Times* [1854], (Eds.: George Ford und Sylvère Monod), Norton Critical Editions, Norton, New York, **1966**, p. 1.

[15] Armstrong (**1901**), p. 725.

[16] A. W. Hofmann, *Einleitung in die moderne Chemie*, 5th ed., Vieweg, Braunschweig, **1871**, p. 222.

[17] Liebig to Mohr (9 November 1844), in *Justus Liebig und Friedrich Mohr in ihren Briefen von 1834–1870* (Ed.: G. W. A. Kahlbaum), *Monographien aus der Geschichte der Chemie*, Vol. 8, Barth, Leipzig, **1904**, pp. 82–83.

[18] Liebig (**1874**), p. 32.

[19] Eric Gray Forbes, "Liebig in Grossbritannien", *Nachrichtenblatt der Deutschen Gesellschaft für Geschichte der Medizin, Naturwissenschaft und Technik* **1983**, *33/3*, 115–133.

[20] Liebig to Wöhler (28 March 1845), in *Aus Justus Liebig's und Friedrich Wöhler's Briefwechsel in den Jahren 1829–1873, Vol. I*, (Ed.: A. W. Hofmann), Vieweg, Braunschweig, **1888**, p. 256.

[21] Liebig to Wöhler (26 April 1845), Bayerische Staatsbibliothek München, Liebigiana II A I (Wöhler), No. 279.

[22] Robert Bud and Gerrylynn K. Roberts, *Science versus Practice: Chemistry in Victorian Britain*, Manchester Univ. Press, Manchester, **1984**, pp. 52–53; G. K. Roberts, "The establishment of the Royal College of Chemistry: An investigation of the social context of early Victorian chemistry", *Historical Studies in the Physical Sciences* **1976**, *7*, 437–485; Jonathan Bentley, "The Chemical Department of the Royal School of Mines: Its origins and developments under A. W. Hofmann", *Ambix* **1970**, *17*, 153–181; A. W. Hofmann, "A page of scientific history: Reminiscences of the early days of the Royal College of Chemistry", *The Quarterly Journal of Science* **1871**, *8*, 145–153.

[23] Hofmann to Liebig (4 June 1845), in *Justus von Liebig und August Wilhelm Hofmann in ihren Briefen, 1841–1873* (Ed.: William Hodson Brock), Verlag Chemie, Weinheim, **1984**, p. 28.

[24] Hofmann to Liebig (24 June 1845), in Brock (**1984**), p. 31.

[25] Brock (**1984**), pp. 14–17.

[26] "Bericht über das Festmahl der Deutschen Chemischen Gesellschaft zu Ehren A. W. Hofmanns" (Eds.: C. A. Martius, H. Wichelhaus), *Ber. Dtsch. Chem. Ges.* **1870**, *3*, supplement; cited in Lepsius (**1918**), p. 6.

[27] Perkin (**1901**), p . 605.

[28] Anthony S. Travis, "Science's powerful companion: A. W. Hofmann's investigation of aniline red and its derivatives", *The British Journal for the History of Science* **1992**, *25*, 27–44; here p. 27; cf. also Peter Borscheid, *Naturwissenschaft, Staat und Industrie in Baden (1848–1914)*, Industrielle Welt, Vol. 17, Klett-Cotta, Stuttgart, **1976**, pp. 114–115.

[29] Hofmann to Liebig (26 June 1853), in Brock (**1984**), p. 159.

[30] Cf. the contribution by G. K. Roberts in *Die Allianz von Wissenschaft und Industrie: August Wilhelm Hofmann (1818–1892)—Zeit, Werk, Wirkung* (Eds.: C. Meinel, H. Scholz), VCH, Weinheim, **1992**.

[31] J. S. Muspratt and A. W. Hofmann, "Über das Toluidin, eine neue organische Basis", *Ann. Chem. Pharm.* **1845**, *54*, 1–29; here p. 3.

[32] A. W. v. Hofmann, "Die Ergebnisse der Naturforschung seit Begründung der Gesellschaft", *Verhandlungen der Gesellschaft Deutscher Naturforscher und Ärzte, 63. Versammlung zu Bremen 1890*, Leipzig, **1890**, pp. 1–55; here p. 50. Recent research no longer shares this appraisal of Wöhler's 1828 synthesis of urea, largely propagated by Hofmann himself; cf. John Hedley Brooke, "Organic synthesis and the unification of chemistry", *The British Journal for the History of Science* **1970/71**, *5*, 363–392.

[33] Hermann Kolbe, "Beiträge zur Kenntnis der gepaarten Verbindungen", *Ann. Chem. Pharm.* **1845**, *54*, 145–188.

[34] Hermann Kolbe, *Über die chemische Konstitution organischer Verbindungen*, Elwert, Marburg, **1858**, p. 6; cf. also Justus Liebig, *Chemische Briefe*, Winter, Heidelberg, **1844**, first letter.

[35] Hofmann (**1890**), p. 41. For the use of this metaphor cf. William H. Brock, O. Theodor Benfey, Susanne Stark, "Hofmann's benzene tree at the Kekulé festivities", *J. Chem. Ed.* **1991**, *68*, 887–888; and W. H. Brock in Meinel/Scholz (**1992**).

[36] Abel (**1901**), pp. 592–593.

[37] A. W. Hofmann, "Über einige neue Verbindungen und Zersetzungsprodukte des Anilins", *Ann. Chem. Pharm.* **1846**, *57*, 1846, 265–267, here p. 265.

[38] A. W. Hofmann, "Beiträge zur Kenntnis der flüchtigen organischen Basen, VIII", *Ann. Chem. Pharm.* **1850**, *74*, 117–177, here pp. 172–173, 177.

[39] *Ibid.*, p. 171.

[40] *Ibid.*, p. 175. In the terminology of the times, "alcohol bases" are *N*-alkylated compounds derived from ammonia by the introduction of "alcohol radicals".

[41] Georg Meyer-Thurow, "The industrialization of invention: A case study from the German chemical industry," *Isis* **1982**, *73*, 363–381.

[42] Hofmann to the Ministry (1873), Geheimes Staatsarchiv (Merseburg), Rep. 76, Va, Sec. 2, Tit. XV, No. 70, Vol. 2; cited after Fritz Welsch, *August Wilhelm von Hofmann, 1818–1892* (n.p, n.d. [printed in manuscript form, **1992**]), p. 67.

[43] John H. Brooke, "Laurent, Gerhardt, and the Philosophy of Chemistry", *Historical Studies in the Physical Sciences* **1976**, *6*, 405–429.

[44] A. W. Hofmann, "On Mauve and Magenta", *Proceedings of the Royal Institution of Great Britain* **1862**, *3*, 468–483, here pp. 472–473; Otto Krätz, "Historische Experimente (1849): A. W. Hofmann: Darstellung verschiedener organischer Basen (Zu den Anfängen der 'Typentheorie')", *Chemie, Experiment und Didaktik*, **1975**,*1*, 129–132.

[45] Müller (**1978**), pp. 93–95.

[46] John Joseph Beer, *The Emergence of the German Dye Industry*, Illinois Studies in the Social Sciences, Vol. 44, Univ. of Chicago Press, Urbana,

IL, USA, **1959**; "Organic Chemistry and High Technology, 1850–1950", *The British Journal for the History of Science*, **1992**, Special Issue 25, 1–167 (Eds.: Anthony S. Travis, Willem J. Hornix, Robert Bud); Anthony S. Travis, *The Rainbow Makers: The Origins of the Synthetic Dyestuff Industry in Western Europe*, Lehigh Univ. Press, Bethlehem, PA, USA, **1992**.

[47] A. W. Hofmann, "Notes of researches on the poly-ammonias: 20. On the colouring matters produced from aniline", *Proc. R. Soc.* **1862/63**, *12*, 2–13.

[48] Beer (**1959**); Travis (**1992**).

[49] A. W. Hofmann, "Researches on the colouring matters derived from coal-tar: II. On aniline-blue", *Proc. R. Soc.* **1863/64**, *13*, 9–14, here p. 14.

[50] A. W. Hofmann, "Researches on some artificial colouring matters: I. On the composition of the blue derivatives of the tertiary monamines derived from cinchonine", *Proc. R. Soc.* **1862/63**, *12*, 410–418, here p. 418.

[51] Christoph Meinel, "Reine und angewandte Chemie: Die Entstehung einer neuen Wissenschaftskonzeption in der Chemie der Aufklärung", *Berichte zur Wissenschaftsgeschichte* **1985**, *8*, 25–45; see also C. Meinel *Angew. Chem.* **1984**, *96*, 326–334; *Angew.Chem. Int. Ed. Engl.* **1984**, *23*, 339–347.

[52] A. W. Hofmann, "Chemical products and processes", in *International Exhibition 1862: Reports by the Juries*, Class II, Sect. A, Clowes, London, **1863**, p. 170.

[53] *Ibid.*, p. 418.

[54] Utz Haltern, *Die Londoner Weltausstellung von 1851: Ein Beitrag zur Geschichte der bürgerlich-industriellen Gesellschaft im 19. Jahrhundert*, Neue Münstersche Beiträge zur Geschichtsforschung, Vol. 13, Aschendorff, Münster, **1971**.

[55] Christian Beutler, *Weltausstellungen im 19. Jahrhundert*, Neue Sammlung, Munich, **1973**.

[56] Volhard/Fischer (**1902**), pp. 50–59.

[57] Hofmann, "On Mauve" (**1862**), p. 483.

[58] Jonathan Bentley, "Hofmann's return to Germany from the Royal College of Chemistry", *Ambix* **1972**, *19*, 196–203. Beginning as early as 1861 Hofmann was involved in the planning for the new chemical laboratories in Bonn.

[59] Liebig to Hofmann (14 November 1863), in Brock (**1984**), p. 197.

[60] Bud/Roberts (**1984**), pp. 97–166; Walter Wetzel, *Naturwissenschaften und Chemische Industrie in Deutschland: Voraussetzungen und Mechanismen ihres Aufstiegs im 19. Jahrhundert*, Frankfurter Historische Abhandlungen, Vol. 32, F. Steiner, Stuttgart, **1991**, pp. 79–83.

[61] *Ibid.*, pp. 135–140, 322–323.

[62] Helmuth Plessner, *Die verspätete Nation: Über die Verführbarkeit bürgerlichen Geistes* [1959], Collected Works, Vol. 6, Suhrkamp, Frankfurt am Main, **1982**.

[63] L. F. Haber, *The Chemical Industry during the Nineteenth Century: A Study of the Economic Aspect of Applied Chemistry in Europe and North America*, Clarendon, Oxford, **1958**; Wetzel (**1991**).

[64] Jeffrey A. Johnson, "Academic chemistry in Imperial Germany", *Isis* **1985**, *76*, 500–524; Gert Schubring, "The rise and decline of the Bonn Natural Sciences Seminar", *Osiris* **1989**, *5*, 57–93, here pp. 82–85.

[65] A. W. Hofmanm, *Die Frage der Theilung der philosophischen Facultät*, Akademie, Berlin, **1880**, p. 17.

[66] A. W. Hofmann, *The Chemical Laboratories in Course of Erection in the Universities of Bonn and Berlin*, Clowes & Sons, London, **1866**, pp. 29, 36.

[67] *Die naturwissenschaftlichen und medicinischen Staatsanstalten Berlins*, (Ed.: Albert Guttstadt), Hischwald, Berlin, **1884**, pp. 155–178; cf. Engel/Engel (**1992**), pp. 30–55.

[68] Plessner (**1982**), pp. 84–85.

[69] Hofmann to Wöhler (4 February 1867), Göttingen University Library, Manuscript Division, Sign. Wöhler 59, No. 4, and others.; cf. also Hofmann (**1866**), pp. 70–71.

[70] Engel/Engel (**1992**), pp. 55–86; cf. also Jeffrey A. Johnson, "Hierarchy and creativity in chemistry, 1871–1914", *Osiris* **1989**, *5*, 214–240.

[71] Wilhelm Ostwald, *Lebenslinien: Eine Selbstbiographie, Teil 1*, Klasing, Berlin, **1926**, p. 185.

[72] Beer (**1959**), p. 65.

[73] Otto Krätz, *Beilstein – Erlenmeyer: Briefe zur Geschichte der chemischen Dokumentation und des chemischen Zeitschriftenwesens*, Neue Münchner Beiträge zur Geschichte der Medizin und der Naturwissenschaften, Naturwissenschaftshistorische Reihe, Vol. 2, Fritsch, Munich, **1972**; cf. also the contribution by Elisabeth Vaupel in Meinel/Scholz (**1992**).

[74] Tiemann (**1892**), p. 3396.

[75] Walter Ruske, *100 Jahre Deutsche Chemische Gesellschaft*, Verlag Chemie, Weinheim, **1967**.

[76] A. W. Hofmann, *Ber. Dtsch. Chem. Ges.* **1868**, *1*, 3.

[77] Hofmann to Wöhler (6 November 1876), Göttingen University Library, Manuscript Division, Sign. Wöhler 59, No. 42.

[78] Hofmann to Wöhler (26 December 1876), *ibid.*, No. 44.

[79] Hofmann to Tollens (4 December 1879), *ibid.*, Sign. 4° Philos. 207, 10.

[80] Ruske (**1967**), p. 46.

[81] Rudolf Fittig, *Das Wesen und die Ziele der chemischen Forschung und des chemischen Studiums*, Quandt & Händel, Leipzig, **1870**, p. 3.

[82] Heinrich von Treitschke, *Die Lage der Universität Berlin* [1873] (Ed.: E. Riecke), Grosse, Göttingen, **1927**, pp. 5, 10; similarly in Rudolf Virchow, "Über die Aufgaben der Naturwissenschaften im neuen nationalen Leben Deutschlands [1871]" in Karl Sudhoff, *Rudolf Virchow und die Deutschen Naturforscherversammlungen*, Akadem. Verlagsges., Leipzig, **1922**, pp. 99–118.

[83] Ostwald (**1926**), p. 186.

[84] Based on a newspaper clipping of unknown origin (May 1892), Staatsbibliothek Berlin, Sammlung Darmstädter, Sig. 141/42.

[85] A. W. Hofmann, [Address at the "Club night with the President" on the occasion of the completion of the Chemical Institute on 15 May 1869], *Ber. Dtsch. Chem. Ges.* **1869**, *2*, 228–236, here p. 229.

[86] Martius/Wichelhaus (**1870**); illustration in Ruske (**1967**), p. 74.

[87] Christoph Meinel, *Karl Friedrich Zöllner und die Wissenschaftskultur der Gründerzeit: Eine Fallstudie zur Genese konservativer Zivilisationskritik*, Berliner Beiträge zur Geschichte der Naturwissenschaften und der Technik, Vol. 13, ERS-Verlag, Berlin, **1991**.

[88] Kolbe to Liebig (23 February 1873), Bayerische Staatsbibliothek, Liebigiana, No. 58; cf. Lepsius (**1918**), 21–22.

[89] Cochius to Zöllner (28 March 1872), cited after Johann Carl Friedrich Zöllner, *Über die Natur der Cometen: Beiträge zur Geschichte und Theorie der Erkenntniss*, 3. ed., Staackmann, Leipzig, **1883**, p. 411.

[90] Mohr to Zöllner (1871), cited after Felix Koerber, *Karl Friedrich Zöllner. Ein deutsches Gelehrtenleben*, Sammlung populärer Schriften (Ed.: Urania), Vol. 53, Paetel, Berlin, **1899**, pp. 56–57.

[91] Rüdorf to Zöllner (24 March 1872), cited after Zöllner (**1883**), p. 412.

[92] Lepsius (**1918**), pp. 30–32.

[93] *Berichte der durstigen Chemischen Gesellschaft*, Unerhörter Jahrgang, Nr. 20, Berlin, **1886**; Lepsius (**1918**), pp. 34–37; Ruske (**1967**), pp. 80–84.

[94] Gustav Schultz, "Bericht über die Feier der Deutschen Chemischen Gesellschaft zu Ehren August Kekulés", *Ber. Dtsch. Chem. Ges.* **1890**, *23*, 1265–1311, here pp. 1267–1268.

[95] Gustav Schultz, "August Wilhelm von Hofmanns Tischrede bei der Kekulé-Feier", *Ztsch. Farben.- u. Textilchemie* **1902**, *1*, 231–233.

[96] Heinrich Caro, "Das 25jährige Jubiläum der Wiederkehr August Wilhelm von Hofmanns nach Deutschland 1890," in H. Caro, *Gesammelte Reden und Vorträge*, Spamer, Leipzig, **1913**, pp. 59–63, here p. 59.

[97] Hofmann, "On Mauve" (**1862**), p. 468.

[98] A. W. Hofmann, *Berliner Alchemisten und Chemiker: Rückblick auf die Entwickelung der chemischen Wissenschaft in der Mark*, Schade, Berlin, **1882**, pp. 68–71.

[99] A. W. Hofmann, "Chemical products and processes," in *International Exhibition 1862: Reports by the Juries*, Class II, Sect. A, Clowes, London, **1863**, pp. 119–120.

[100] Dolf Sternberger, *Panorama oder Ansichten vom 19. Jahrhundert*, Govert, Hamburg, **1938**, p. 201; cf. also pp. 139–141.

[101] So described in a Social-Democratic handbill from 1913; cited in Klaus Sauer and German Werth, *Lorbeer und Palme: Patriotismus in deutschen Festspielen*, Deutscher Taschenbuch Verlag, Munich, **1971**, p. 138.

[102] Nicolaus Sombart, "Der letzte Kaiser war so, wie die Deutschen waren: Wilhelm II.", *Frankfurter Allgemeine Zeitung* (1 January 1979), cited after Hermann Glaser, *Die Kultur der Wilhelminischen Zeit: Topographie einer Epoche*, Fischer, Frankfurt, **1984**, p. 154, note 212.

[103] Richard Hamann and Jost Hermand, *Gründerzeit: Deutsche Kunst und Kultur von der Gründerzeit bis zum Expressionismus*, Vol. 1, Akademie-Verlag, Berlin, **1965**.

[104] Borscheid (**1976**), pp. 117–121.

[105] Hofmann to Fritz Hofmann (August 1865), in Volhard/Fischer (**1902**), pp. 100–104, here p. 103.

[106] *Die Vereine Deutscher Studenten: Zwölf Jahre akademischer Kämpfe*, (Ed.: Herman von Petersdorff), 3. ed., Breitkopf & Härtel, Leipzig, **1900**, pp. 25–62; *Der Berliner Antisemitismusstreit* (Ed.: Walther Boehlich), Sammlung Insel, Vol. 6, Insel, Frankfurt am Main, **1965**, does not mention Hofmann.

[107] Armstrong (**1901**), 729.

[108] Glaser (**1984**), p. 226.

[109] Ruske (**1967**), 54–60.

[110] These are larger-than-life terra-cotta medallions of Lavoisier, Scheele, Cavendish, Priestley, Dalton, Berthollet, Gay-Lussac, Davy, Berzelius, Mitscherlich, Klaproth, Rose, Gmelin, Gerhardt, and Laurent. Interestingly, there is none for G. E. Stahl, whose priority in the establishment of modern chemistry had been proclaimed polemically by German nationalists since 1870 (although his name was included among the finalists). Cf. Hofmann (**1866**), p. 71.

[111] Minutes of the Chemical Society, Staatsbibliothek Berlin, Sammlung Darmstädter, Sig. G2 1858 (5), Folios 15–26.

[112] Jost Weyer, *Chemiegeschichtsschreibung von Wiegleb (1790) bis Partington (1970): Eine Untersuchung über ihre Methoden, Prinzipien und Ziele*, Arbor scientiarum, Series A, Vol. 3, Gerstenberg, Hildesheim, **1974**.

[113] A. W. Hofmann, [Address at the "Club night with the President" on the occasion of the completion of the Chemical Institute on 15 May 1869], *Ber. Dtsch. Chem. Ges.* **1869**, *2*, 228–236, here p. 229.

[114] Lepsius (**1918**), p. 29, Students' party for Hofmann's 60th birthday.

[115] Regine Zott, "Zu den Anfängen des Frauenstudiums an der Berliner

Universität," in *Perspektiven interkultureller Wechselwirkung für den wissenschaftlichen Fortschritt*, ITW-Kolloquien, 48, Akademie, Berlin, **1985**, pp. 29–37.
[116] Hofmann to Wöhler (Berlin, 9 July 1874), Göttingen University Library, Manuscript Division, Sign. Wöhler 59, No. 23; cf. Margaret Alic, *Hypatias Töchter: Der verleugnete Anteil der Frauen an der Naturwissenschaft*, Unionsverlag, Zurich, **1987**, pp. 184–187.
[117] Hofmann to Wöhler (Berlin, 28 July 1874), *ibid.*, No. 24.
[118] Information gratefully received from Günther Beer and the Archive of the Universität Göttingen.
[119] It was a quarter of a century later before Clara Immerwahr, the first wife of Fritz Haber, earned her doctorate in chemistry at Breslau.
[120] Tiemann (**1892**), p. 3396.
[121] Hans Werner Niemann, "Der Industrielle in der deutschen Erzähllitteratur der Jahre 1890 bis 1945" in *Technik in der Literatur* (Ed.: Harro Segeberg), Suhrkamp, Frankfurt am Main, **1987**, pp. 174–232.
[122] Fritz Stern, *The Politics of Cultural Despair: A Study in the Rise of the Germanic Ideology*, Univ. of California Press, Berkeley, **CA (USA), 1961**; Rudolf Peter Sieferle, *Fortschrittsfeinde? Opposition gegen Technik und Industrie von der Romantik bis zur Gegenwart*, Sozialverträglichkeit von Energiesystemen, Vol. 5, Beck, Munich, **1984**.
[123] A. W. Hofmann and S. Gabriel, "Über das Product der Einwirkung des Jods auf Thiobenzamid", *Ber. Dtsch. Chem. Ges.* **1892**, *25*, 1578–1589.
[124] Fritz K. Ringer, *The Decline of the German Mandarins: The German Academic Community, 1890–1933*, Harvard Univ. Press, Cambridge, MA (USA), **1969**.
[125] Jeffrey Allan Johnson, *The Kaiser's Chemists: Science and Modernization in Imperial Germany*, Univ. of North Carolina Press, Chapel Hill/London, **1990**.
[126] Tiemann (**1892**), p. 3377.
[127] F. Mylius, "Festbericht über die Jubiläumsfeier," in Lepsius (**1918**), pp. 142–177.

A stop-gap solution?

If the latest library copy of Angewandte spends more time off the shelf than on, stop the gap with a personal subscription.

Just call or fax

VCH

USA: Tel. 1-(800) 422-8824; Fax (305) 428-8201
UK: Tel. (0223) 321111, Fax (0223) 313221

The Chemistry of GALLEX—Measurement of Solar Neutrinos with a Radiochemical Gallium Detector

By Edmund Henrich and Klaus H. Ebert*

In the GALLium EXperiment, GALLEX, low-energy solar neutrinos produced in the main hydrogen fusion reaction inside the Sun are being counted for the first time in a radiochemical gallium detector. In this way, the theories about stellar structure may be verified and the question of the existence of a neutrino rest mass be brought closer to a solution. The experiment is being carried out with international collaboration at the Gran Sasso underground laboratory (LNGS) in the Abruzzi mountains in Italy. In this paper we survey the planning, construction and initial experimental operation of the gallium detector, paying special attention to the chemical aspects of the experiment. The chemical problem to be solved is the separation of very few ^{71}Ge atoms from 100 metric tons of a highly concentrated $GaCl_3$ solution acidified with hydrochloric acid. In addition, these Ge atoms must be isolated and converted into germane, GeH_4, for low-level counting of ^{71}Ge in a gas proportional counter. After extensive preparatory work to meet the extreme requirements of the experiment, the first results have now become available.

1. Introduction

Direct information about the interior of the Sun, where fusion reactions take place in which energy is generated, can be obtained only by way of solar neutrinos. While it takes photons roughly a million years to diffuse to the surface of the Sun, undergoing profound changes in the process, neutrinos travel from the interior of the Sun to the Earth within 500 seconds. According to the Standard Solar Model (SSM),[1] there are essentially two types of solar neutrinos: 1) pp neutrinos, arising in the main reaction of the fusion cycle, with a maximum energy of 0.42 MeV; 2) higher energy neutrinos from side reactions, with maximum energies of up to 18.8 MeV.

So far, it has only been possible in sophisticated experiments to demonstrate the existence of the higher energy neutrinos, but the readings obtained are at least 50% below the calculated values from the SSM. This discrepency has fueled much discussion and speculation both about the correctness of the SSM and the problem of the rest mass of the neutrino.[2, 3] The solution to this riddle of the solar neutrinos is now expected to come from experiments in which pp neutrinos are counted in a radiochemical gallium detector.

Two such experiments have been under way for some time: SAGE,[4] a Russian–American collaboration in the Baksan underground laboratory[5] in the Caucasus mountains, and GALLEX,[6–8] an international collaboration carried out in the Gran Sasso underground laboratory in Italy.[9] All experiments conducted to prove the existence of solar neutrinos must be optimally shielded against cosmic radiation and, for this reason, are performed in laboratories below ground.

Neutrinos are difficult to detect because of their extremely weak interactions with matter. With low-energy neutrinos, these interactions are even less pronounced than with higher energy neutrinos. The higher energy neutrinos can be detected in real-time experiments, but this requires extremely large detectors. One such detector contains 680 tons of water as the scattering medium and detects the neutrinos, after collisions with electrons, by the Cerenkov radiation; it has been in operation in the Kamioka mine in Japan since 1987. In that experiment, Kamiokande, neutrinos with an energy >7.3 MeV have been detected.[10]

Neutrinos can also be detected by radiochemical detectors; the reaction is based on the capture of a neutrino by a nucleus corresponding to an inverse β-decay (as is well known, neutrinos are emitted in β-decays). This transmutation gives rise to the nucleus of a different element, which can be separated in a chemically selective way. At the present time, there are three radiochemical detectors which can be used for the detection of solar neutrinos: one chlorine detector and two gallium detectors.

The chlorine detector is based on the conversion of chlorine-37 into argon-37. This detector offers a number of excellent preconditions: 1) there are many cheap liquid compounds with high fractions of chlorine which may serve as targets; 2) argon-37 decays by electron capture with a half-life of 35 d; 3) the separation of argon from the liquid and its subsequent purification are relatively easy. Several hundred tons of chlorine are required to ensure that the number of argon-37 atoms is still large enough to be detected reliably by low-level counting techniques. The chlorine detector suffers from the disadvantage of responding only to neutrinos with an energy in excess of 0.81 MeV and, thus, is not sensitive to lower energy solar neutrinos. The chlorine detector was set up in the Homestake gold mine in South Dakota more than twenty years ago by pioneers in the field of radiochemical neutrino detectors, namely Raymond Davis and his colleagues from Brookhaven National Laboratory (BNL). It has been in operation since 1970.[11] The result of Davis's extensive measurements, shows that roughly only one third of the value expected from the SSM[12] is detected.

The gallium neutrino detector was proposed by Kuzmin as early as 1964.[13] It is based on the conversion of gallium-71 into germanium-71, and it is sensitive to neutrinos above an energy as low as 0.23 MeV. For many years, the gallium

[*] Prof. Dr. K. H. Ebert, Dr. E. Henrich
Kernforschungszentrum Karlsruhe, Institut für Heisse Chemie
P.O. Box 3640, W-7500 Karlsruhe (FRG)

 © *VCH Verlagsgesellschaft mbH, W-6940 Weinheim, 1992* *0570-0833/92/1010-1283 $ 3.50+.25/0*

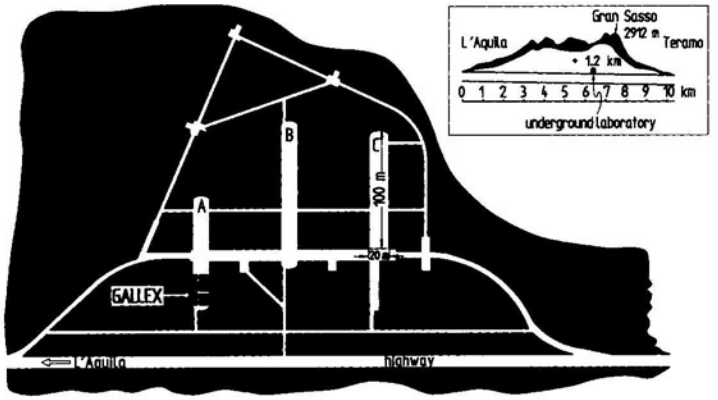

Fig. 1. Floor plan of LNGS underground laboratory with location of GALLEX in hall A.

detector was a utopian proposition because the worldwide annual production of gallium was far below the minimum of thirty tons required for the experiment. Only in the past decade, as the commercial demand picked up, has production increased.

The studies of the concept of a gallium neutrino detector were begun at BNL as long ago as the seventies; the chemical target selected was a concentrated $GaCl_3$ solution acidified with hydrochloric acid.[14, 15] The experiment was intended to be run in the underground laboratory of the Homestake mine, where access is limited by the main shaft. The approximately 100–150 tons of detector solution was to be contained in twenty or more tanks of approximately 3 m^3 each, and desorption was to be used to separate the $GeCl_4$ from this battery of tanks. The project[16] was abandoned in the USA in the mid-eighties due to lack of funding to purchase the large quantity of gallium required.

Upon the initiative of the Max-Planck-Institut für Kernphysik (MPIK), the GALLEX Collaboration was set up next. The decisive factors in favor of GALLEX were the ability to finance the amount of gallium needed, and the guarantee of space in the underground laboratory, being built in the Gran Sasso mountains by the Italian Istituto Nazionale di Fisica Nucleare (INFN). Figure 1 shows a floor plan of the LNGS underground laboratory[9] and the location of GALLEX.

The Standard Solar Model (SSM) and the Mass of Neutrinos

The most important fusion reactions in which hydrogen (protons p) is converted into helium can be subdivided into the main cycle (Scheme 1 A), secondary reactions (Scheme 1 B), and the CNO cycle with carbon-12 as "catalyst" (Scheme 1 C). The main cycle provides some 83% of the total energy of the Sun, while the secondary cycles produce 15% and the CNO cycle contributes only 1.6%. The various solar models[1, 17] differ in the contributions made by main and secondary reactions and, consequently, in the temperature assumed to exist in the Sun. At higher tempera-

Klaus Ebert, born in Berlin in 1928, studied chemistry in Vienna, where he gained his doctorate in 1953 for work on the properties of chemically altered silicate surfaces. In 1957, after carrying out postdoctoral work with Professor Paneth at the University of Durham (UK), and a spell as assistant at the Max-Planck-Institut für Chemie in Mainz (FRG), he took up an appointment as assistant to Professor F. Patat at the Institut für Technische Chemie der Technischen Hochschule München (FRG), where he habilitated in 1964 with work on the mechanism and kinetics of enzymatic dextran polymerization. In 1969, following a short period of employment in industry at BASF (1968–1969), he was appointed Professor for Applied Physical Chemistry at the University of Heidelberg, where he was also Dean of the Faculty for Chemistry and Natural Sciences (1969–1972) as well as vice-president. In 1980 he was appointed head of the Institut für Heisse Chemie des Kernforschungszentrum Karlsruhe (FRG) (on leave from the University of Heidelberg) and worked on the development of technology for the reprocessing of nuclear fuels. Since 1984 he has worked on the GALLEX project. Further research areas range from the influence of cosmic radiation on meteorites to the kinetics and modeling of complex chemical gas reactions (pyrolyses) and the degradation mechanisms of high-polymer materials to investigations of the chemistry of supercritical fluids. Klaus Ebert is a founder member of the Sonderforschungsbereich "Modeling of Complex Reactions", author of the VCH textbook "Computer Applications in Chemistry", and was a member of the "Studienreformkommission Chemie".

Edmund Henrich was born in 1941 in Kaiserslautern (FRG). From 1961 to 1967 he studied chemistry at the Universities of Mainz and Heidelberg and spent a period of time doing research at GERN in Geneva. After gaining his doctorate in 1971 for work on the preparation and properties of heptavalent transuranics under the supervision of Franz Baumgärtner he remained at Heidelberg until 1974 as research assistant. Since 1974 he has been employed as scientist at the Kernforschungszentrum Karlsruhe (FRG). His work focusses on the applicational development of new methods for the safer management of volatile radionuclides during reprocessing of spent nuclear fuel, especially in off-gas purification, the treatment of fission product iodine, the removal of fission product noble gases and refining by crystallization. Besides his contribution to the design, construction, and operation of the process engineering plant for GALLEX he has in recent years turned his interests to low waste technology.

tures, the contribution by secondary cycles increases. On the other hand, narrow limits are imposed by the total energy emitted, whose absolute level is known very precisely from the solar constant.

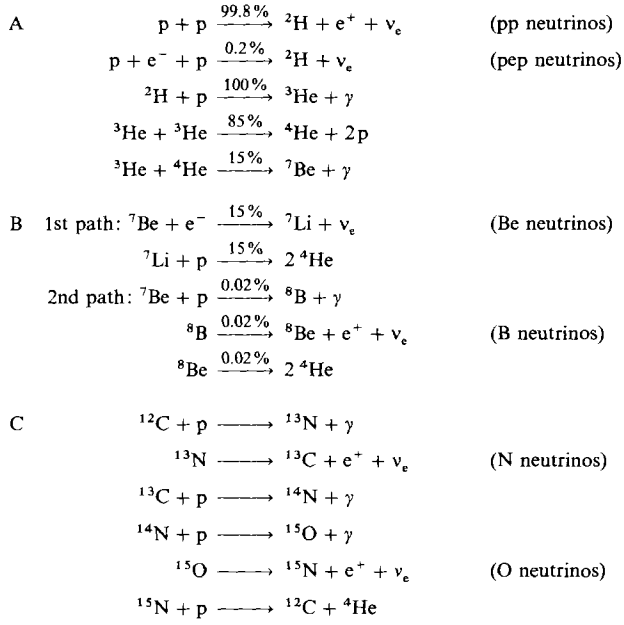

Scheme 1. Main reactions in the fusion of hydrogen. A) main cycle, B) secondary reactions, C) CNO cycle.

Six of the fusion reactions outlined above (Scheme 1) give rise to neutrinos (ν_e). These neutrinos are distinguished by prefixes indicating the elements from which they originate, e.g., pp neutrinos from the reaction of two protons, or Be neutrinos from the decay of the beryllium nucleus. The solar neutrino flux is made up of all neutrinos leaving the Sun. Their intensities are calculated by the SSM (Table 1). The neutrinos produced in the various fusion reactions have very different energies, partly discrete values, partly continuous energy spectra (Table 1, Fig. 2). For the total neutrino flux impinging on the Earth, the SSM produces a calculated value of 66 billion neutrinos per cm^2 per second.

Neutrinos are assumed to have no rest mass and no charge. As they are subject only to weak interaction, their interaction with matter is extremely rare, which makes measuring difficult. The cross-section decreases greatly as the energy decreases (Fig. 3), i.e., the low-energy neutrinos are even more difficult to detect than the high-energy variety. On

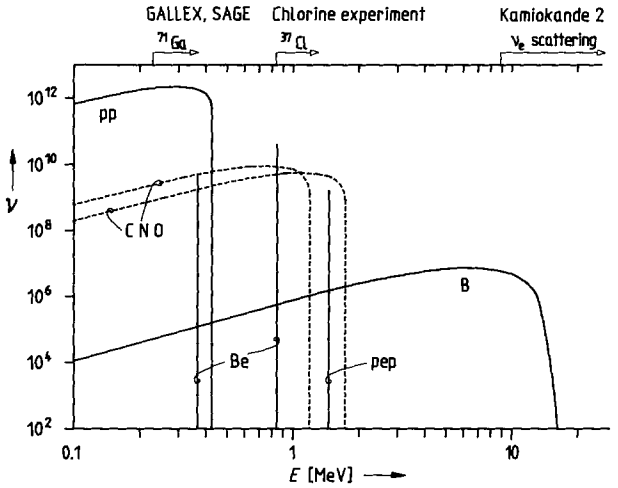

Fig. 2. Solar neutrino spectrum (for abbreviations see Scheme 1). E = neutrino energy; ν = solar neutrino flux to earth per cm^2, second and MeV; detection limits of the neutrino detectors are given above. Kamiokande 2 = neutrino detector in the Kamioka mine.

the other hand, the low-energy pp-neutrinos make up 91% of the neutrino flux according to the SSM. Only the gallium neutrino detector is sensitive to pp neutrinos, but, again, only above its 0.23 MeV threshold. The other detectors

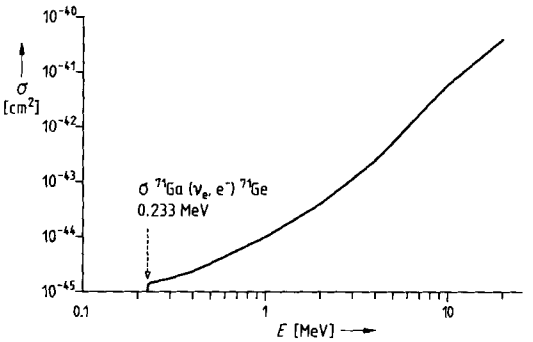

Fig. 3. Neutrino capture cross-section σ of gallium as a function of the neutrino energy E (after Ref. [1]). The dotted arrow indicates the threshold energy for neutrino detection.

(chlorine detector, Kamiokande) can count only the higher energy neutrinos from the secondary reactions, which contribute but slightly to the total fusion cycle. The limits of detection are indicated in Figure 2.

In recent years, the assumption that neutrinos have no mass has been doubted more and more seriously. The prob-

Table 1. Contributions of solar neutrinos to the production of ^{71}Ge and ^{27}Ar in the gallium and chlorine detectors.

Type [a]	Energy (absolute [MeV])		Neutrino flux [10^6 ν $cm^{-2}s^{-1}$]	[%]	% Contribution to neutrino capture $^{71}Ga(\nu_e, e^-)^{71}Ge$	$^{37}Cl(\nu_e, e^-)^{37}Ar$
pp	0–0.42		60000 ± 2%	91.0	53.6	0
pep	1.44	(100%)	140 ± 15%	0.21	2.3	2.5
Be	0.86	(90% abundance)	4700 ± 15%	7.1	26.0	14.0
	0.38	(10% abundance)				
B	0–15		5.8 ± 37%	0.009	10.6	77.5
CNO	0–1.20		1100 ± 58%	1.7	7.5	5.0
	0–1.73					
	0–1.74				100^{+15}_{-13} [b]	100 ± 33 [b]

[a] See Scheme 1. [b] Summed percentage contributions.

The GALLEX Collaboration

An experiment posing such extreme requirements in several areas of chemistry, physics, and process engineering can be carried out successfully only by collaboration among various working groups.

The GALLEX Collaboration was set up in 1984 following an initiative by the Max-Planck-Institute for Nuclear Physics in Heidelberg (MPIK),[*] soon after collaboration for the same research purpose between the Brookhaven National Laboratory (BNL) and MPIK had been wound up after BNL had reduced its solar neutrino program for financial reasons.

GALLEX was initiated with mainly West European collaboration in mind. It very soon became apparent that scientists from this region showed a very keen interest in the experiment, and that there was a real chance of raising the funds for the necessary investments. A decisive fact improving the prospects of GALLEX in the early stage was that the 30 tons of gallium, which amounted to almost one worldwide annual production, were purchased and financed thanks to grants from the Bundesministerium für Forschung und Technologie (BMFT), the Alfried-Krupp-von-Bohlen-und-Halbach-Stiftung, and the Max-Planck-Gesellschaft, and that sufficient space was offered by the Istituto Nazionale di Fisica Nucleare (INFN) in the Laboratorio Nazionale del Gran Sasso in the Abruzzi mountains (LNGS), the word's largest underground laboratory.

The GALLEX Collaboration was ready to start in 1986; it is made up of scientists from ten institutions. Its present members are:

P. Anselmann, W. Hampel, G. Heusser, J. Kiko, T. Kirsten, E. Pernicka, R. Plaga, U. Rönn, M. Sann, C. Schlosser, R. Wink, M. Wójcik (Max-Planck-Institut für Kernphysik (MPIK), Heidelberg (FRG)), R. von Ammon, K. H. Ebert, T. Fritsch, K. Hellriegel, E. Henrich, L. Stieglitz, F. Weirich (Institut für Heisse Chemie, Kernforschungszentrum Karlsruhe (IHCH-KFK), Karlsruhe (FRG)), M. Balata, E. Bellotti, N. Ferrari, H. Lalla, T. Stolarczyk (INFN—Laboratori Nazionali del Gran Sasso (LNGS), L'Aquila (Italy)), C. Cattadori, O. Cremonesi, E. Fiorini, S. Pezzoni, L. Zanotti (Dipartimento di Fisica, Università di Milano, and INFN—Sezione di Milano, Milan (Italy)), F. von Feilitzsch, R. Mössbauer, U. Schanda (Physikalisches Institut der Technischen Universität München (TUM), Garching (FRG)), G. Berthomieu, E. Schatzman (Observatoire de la Côte d'Azur, Nizza (France)), I. Carmi, I. Dostrovsky (Department of Environmental and Energy Research, Weizmann Institute of Science (WIS), Rehovot (Israel)), C. Bacci, P. Belli, R. Bernabei, S. d'Angelo, L. Paoluzi (Dipartimento di Fisica II Università di Roma, and INFN—Sezione di Roma 2, Rome (Italy)), S. Charbit, M. Cribier, G. Dupont, L. Gosset, J. Rich, M. Spiro, C. Tao, D. Vignaud (DAPNIA, CEN Saclay: Gif-sur-Yvette (France)), R. L. Hahn, F. X. Hartmann, J. K. Rowley, R. W. Stoenner, J. Weneser (Brookhaven National Laboratory (BNL), Upton, NY (USA)).—In addition, the following KfK staff members were instrumental in the construction and operation of the technical installation: J. Amend, O. Brenk, P. Fischer, W. Habicht, D. Heidt, M. Kluth, G. König, F. Koch, M. Persohn, J. Römer, W. Rösch, G. Schnabel, F. Schübel, P. Schwab, J. Unk, R. Will.

A collaborative venture of this size can succeed only if, on the one hand, responsibilities in planning, buildup, and execution are clearly delineated and, on the other hand, communication functions smoothly. Over the whole period of time, the GALLEX Collaboration has met every six months for GALLEX meetings from the beginning of the experiment, always at LNGS. At these meetings, the program has been discussed and defined in detail. Throughout the year, important information has been made accessible to each member of the Collaboration as "GALLEX News" by electronic mail, and the local GALLEX Coordinator appointed by each group on a basis of rotation ensured that GALLEX was always present at LNGS for ongoing business and for taking care of numerous visitors. In appointing Till Kirsten its Spokesman, the GALLEX Collaboration succeeded in finding a scientist who not only acted as a promoter of the project from the beginning, but also has been its Coordinator from the early days on. Special mention must be made of the excellent equipment available at the underground laboratory, which is in no way inferior to that of a modern experimental facility. In addition, the generous support offered by the staff of LNGS and its Director, Enrico Bellotti, must be emphasized. Cooperation within the Collaboration has been exemplary; all members have at all times given their full support to the experiment. Indeed, it was quite customary to see physicists participate in the operation of the chemical plant by running night shifts.

The main activities within the project are assigned to certain groups. Frequently, new problems and duties arose in the course of the experiment, which needed to be solved quickly; in most cases they were handled by interdisciplinary cooperation. In this way, collaboration has become closer and closer as the experiment went on. This should be taken into account when going through the list below of tasks assigned to the institutions:

- Scientific and technical infrastructure, and measurement of background radiation in the underground laboratory: INFN-LNGS; University and INFN Milan; University and INFN Rome
- Supply of the gallium chloride solution and specification control: MPIK.
- Planning, construction, and operation of the detector and technical process equipment; IHCH KfK
- Specification and chemistry of the detector solution: MPIK, KfK, BNL, TUM
- Side reactions in the detector: INFN, CEN Saclay, MPIK, KfK
- Conversion of $GeCl_4$ into GeH_4; purification and transfer into the counter: BNL, MPIK, and WIS
- Development and operation of the low-level counting systems; trace analysis (detector solution, in-plant analyses): MPIK
- Planning and construction of the 1.5 MCi ^{51}Cr neutrino source; neutron measurement in the process buillding: CEN Saclay.

All member groups of the Collaboration took part in the evaluation and assessment of measured results. It has been a particularly good idea of the initiators of GALLEX to include, from the outset, particle physicists and astrophysicists in the collaborative venture. At the GALLEX meetings and in many specialized discussions, they time and again have motivated the experimentalists, by their imaginative contributions, and it is largely due to their efforts that the publication of the first measured results [6] of GALLEX has been accompanied by an evaluation [7].

[*] T. Kirsten, *Jahresbericht des Max-Planck-Instituts für Kernphysik*, Heidelberg, **1984**, p. 139.

lem is of eminent importance to particle physics and astrophysics alike. Modern physics tells us that elementary particles can be grouped into three identical families, which differ only in their masses. The leptons (electrons and neutrinos) are classified in the electron, muon and tauon families. For the quarks it was proved that transformations—so-called oscillations—among the families are possible. However, such oscillations are confined to elementary particles with a rest mass. If proof can be obtained that also neutrinos oscillate, they are bound to have a mass, albeit a very small one.[2, 3, 18]

The fusion reactions in the Sun give rise only to electron neutrinos (ν_e). All radiochemical detectors of solar neutrinos are sensitive only to electron neutrinos. The rate at which neutrinos are converted into a different species, e.g. muon neutrinos, is very much a function of their energy. The experiments conducted so far to detect solar neutrinos, which are sensitive only to the higher energy neutrinos, have produced only one half to one third the signal expected. This has been interpreted as an indication of neutrino oscillations.[19] Consequently, it is of great interest to know whether such indications exist also for low-energy neutrinos. Only the gallium detector can tell us this, because it is the only instrument that is also sensitive to low-energy neutrinos.[20]

Should neutrinos be found in fact to have a finite rest mass, its value would give a strong boost to the grand unified theories (GUTs), especially by providing an indication of the scale of energy at which all electroweak and strong interactions can be described by a unified force.

In astrophysics it is also important to know whether neutrinos have a mass. Even if it were less than 10^{-4} the mass of an electron, it could contribute to the missing mass in the universe, as the number of neutrinos present in space is enormous. However, they do not disturb measurements of solar neutrinos on Earth, as their energy is much lower, and their interaction with matter is many orders of magnitude weaker than that of the pp neutrinos.

2. Basic Principles of GALLEX

2.1. ^{71}Ge Production from ^{71}Ga

In principle, gallium as a neutrino detector can be used in any chemical form. Germanium-71 is produced by the capture of an electron neutrino: $^{71}Ga(\nu_e, e^-)^{71}Ge$. The rate of production P of ^{71}Ge is given by the product of the number n of gallium-71 atoms, the neutrino capture cross-section σ, and the neutrino flux Φ [Eq. (a)]. The 30.3 t of natural gallium, the quantity available to GALLEX, contains 12 t, i.e. 1.037×10^{29} atoms, of ^{71}Ga.[21]

$$P = n \int_0^{E_{max}} \sigma(E_i)\Phi(E_i)dE \qquad \text{(a)}$$

As seen in Figure 2 the solar neutrino flux, Φ_i, is made up of fractions of various neutrinos with different energy spectra; the capture cross-sections also depend on energy.[1] The relatively complex calculation ends up in a production rate for GALLEX of 1.18 ^{71}Ge atoms a day. After four weeks, there are roughly 16 atoms of ^{71}Ge, as ^{71}Ge decays at a half-life of 11.4 d. These Ge atoms must be separated from the gallium target with a high yield and high selectivity, and must be counted by way of their radioactive decay. At a separation yield of 90% and a counting yield of 66%, the counting system would measure an average of 9.5 ^{71}Ge pulses. These procedures must be repeated again and again until the statistical error of measurement is so small that a reliable value is reached. This ultimately requires four years of measurements, in which a total of approximately 500 ^{71}Ge pulses will be registered. A first result based on ca. 70 ^{71}Ge pulses has been published recently by GALLEX.[6]

It must be ensured that all ^{71}Ge atoms have originated from the neutrino-capture reaction and not from other nuclear reactions. The most important side reaction of ^{71}Ga occurs with fast protons ($E_p \geq 1.02$ MeV), in which ^{71}Ge atoms are also produced[16, 22]: $^{71}Ga(p,n)^{71}Ge$.

Protons can be generated in three ways: 1) by fast muons from cosmic radiation; 2) by fast neutrons (>0.4 MeV) produced in the local environment of the gallium neutrino detector by α-radiation and spontaneous fission; 3) by α-radiation inside the detector. The side reactions must be kept so small as not to have a major impact on the value of the measured production rate of ^{71}Ge. This implies a number of requirements with respect to the purity of the detector solution, to the materials used for the equipment, and to the environment.

2.2. Separation of $GeCl_4$ from a $GaCl_3$ Solution

The sequence of experimental steps in GALLEX is shown in a simplified way in Figure 4. The process comprises three steps: 1) Separation of $GeCl_4$ from the detector tank and transfer into ca. 1 L of an aqueous solution. 2) Further concentration; conversion into germane (germanium tetrahy-

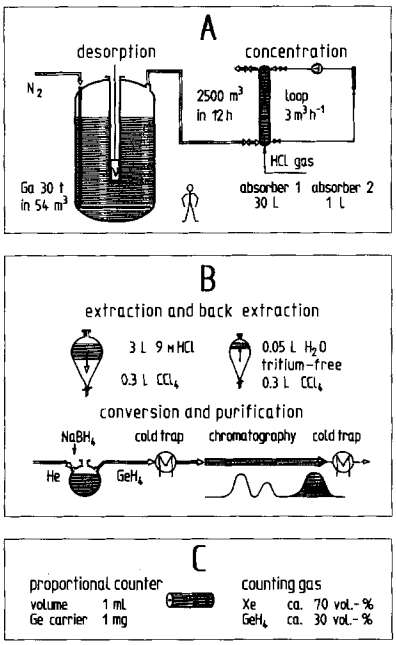

Fig. 4. Sequence of process steps of GALLEX. A: desorption, absorption and concentration in 1 L solution; B: extraction, conversion, and purification; C: counting of $^{71}GeH_4$.

dride, GeH_4); purification by gas chromatography; introduction into the 1 mL-volume counter. 3) Low-level counting and identification of the counting pulses.

Germanium tetrachloride, which is volatile in a solution acidified with hydrochloric acid, is desorbed from the detector solution by an inert gas (nitrogen) and reabsorbed in a small volume of liquid. The volatility of $GeCl_4$ depends very much on the HCl concentration (Fig. 5): at low acid concentrations, $GeCl_4$ hydrolyzes and dissolves, while it is volatile and can be expelled easily at high acid concentrations. In the target solution, however, a lower concentration of HCl is sufficient, as $GaCl_3$ contributes considerably to the volatility of $GeCl_4$.[16, 23] This is shown in Figure 6, which indicates the partition coefficients of Ge^{IV} as contours as a function of the $GaCl_3$ and HCl concentrations. The region of high volatility is shown by the grey area, reaching down to a nearly 1 M HCl concentration for an 8 M $GaCl_3$ solution. At this point, the volume of the solution, the concentration and the partial pressure of hydrochloric acid are all at a minimum. For this reason, only little inert gas is needed for desorption, and only a small amount of hydrochloric acid is discharged.

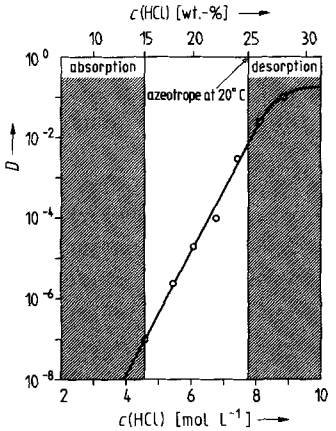

Fig. 5. Ge-partition coefficient D of Ge^{IV} in hydrochloric acid solution. D is defined as the ratio of the concentrations in the gas phase and in the liquid.

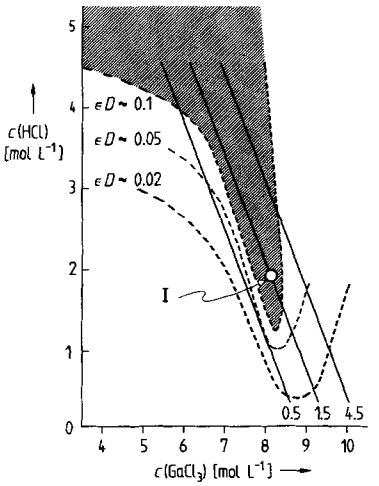

Fig. 6. Dynamic partition coefficients εD (broken curves) of Ge^{IV} as a function of the $GaCl_3$ concentration and HCl concentration; I = composition of the GALLEX detector solution; solid curves: partial concentration of the HCl over the solution. The values on the straight portions of the curves hold for 20 °C and are given in $g \cdot m^{-3}$.

When calculating desorption, it must be borne in mind that ^{71}Ge both decays and is growing-in during the desorption process. As a consequence, desorption time should be kept as short as possible. The amount of Ge is not important initially; if the desorption yield is to be determined, however, non-radioactive germanium carrier must be added; because of the small counters, this addition is limited to a quantity of 1 mg.

At a constant desorption rate, the concentration, c, of the germanium carrier in the detector solution decreases exponentially with time, t_d [Eq. (b)]; c_o is the initial concentration and τ_d is the mean residence time of Ge during desorption; it can be either measured or calculated from operating data [Eq. (c)], where $G(m3/h)$ = desorption gas flow, $L(m^3)$ = solution volume, D = Ge partition coefficient, and ε = gas phase saturation (normally between 0.5 and nearly 1).

$$R = c/c_o = e^{-t_d/\tau_d} \tag{b}$$

$$\tau_d = \frac{L}{G\varepsilon D} \tag{c}$$

When looking at processes involving only a small number of atoms, one must not forget that concentration data are mean values of a Poisson distribution.

The decrease of the ^{71}Ge concentration initially parallels that of the Ge carrier, but then flattens out at longer times.

The residual ^{71}Ge concentration ^{71}R is given by Equation (d) with R defined by Equation (b) and $A = \exp(-t_e/\tau)$, $B = \exp(-t_d/\tau)$; t_e is the exposure time, and τ is the mean lifetime of ^{71}Ge (16.5 d).

$$^{71}R = \frac{B-A}{1-A}R + \frac{\tau_d}{\tau_d+\tau} \cdot \frac{1-BR}{1-A} \tag{d}$$

The minimum concentration $^{71}R_{min}$ of ^{71}Ge in the target is found for $t_e = t_d$ to be approximately

$$^{71}R_{lim} \approx \frac{\tau_d}{(\tau_d+\tau)(1-A)} \tag{e}$$

The calculated desorption curves for the Ge carrier and ^{71}Ge from the detector tank are shown in Figure 7. They indicate that a desorption period of 12 hours is in the optimum range at a rate of 200 m^3/h; longer times will not add much more to the ^{71}Ge yield. At lower desorption rates, the desorption curve shows a correspondingly flatter shape, and the residual concentration of ^{71}Ge levels off at higher absolute concentrations. Thus, at an inert gas flow of 95 m^3/h and 20 h of desorption—the conditions prevailing in tank B in the first test series—a ^{71}Ge desorption yield of 97–98% is achieved.

The absorption of $GeCl_4$ from the inert gas in a scrubber is calculated by the model of transfer units.[24] As the $GeCl_4$ partial pressure is negligibly low over water and diluted hydrochloric acid, it decreases exponentially over the packing height. In a (1:9 scale) pilot plant the height of a transfer unit was determined and, in this way, the packing height of the absorbers in the plant was designed for a yield of 99.8%.

In the absorption process, $GeCl_4$ losses can arise also by desorption from the scrubbing acid, by entrainment of small droplets, and by condensation mist. Conditions were determined experimentally at which these losses remain below 1%; this is a very low level for a 10^5 ratio of gas throughput to scrubbing acid volume.

In the process, only the Ge-carrier can be measured to determine separation yields. While, in the detector solution, ^{71}Ge and the Ge carrier cannot be readily assumed to behave identically, after desorption, the carrier and ^{71}Ge are present in the same chemical form, $GeCl_4$, and at almost constant ratio (see Fig. 7).

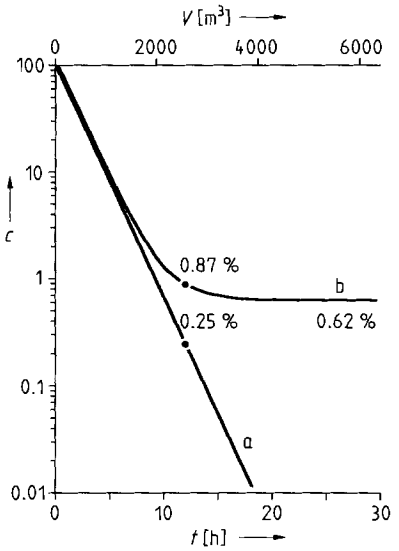

Fig. 7. Desorption of Ge carrier (a) and $^{71}GeCl_4$ (b) for a standard run in tank A (t_e = 27 d, τ_d = 2 h); c = Ge in solution in %, t = desorption time, V = initial gas volume. The percentages on the curves give the residual content of Ge carrier and ^{71}Ge relative to the initial concentration.

H_2GeO_3 solution is added as a carrier to the detector solution; however, ^{71}Ge is produced in a nuclear reaction. It is well known that recoil atoms from nuclear reactions are often present in another chemical form in an inert surrounding than the same species in a thermal equilibrium.[25] In the detector solution, which contains some 50 wt-% of chlorine, it is very probable for a ^{71}Ge atom initially to produce $GeCl_4$ after neutrino capture. As the carrier is present in the same form, also the chemical behavior ought to be the same. In addition, it was verified experimentally that ^{71}Ge atoms produced in the solution as a result of the β-decay of ^{71}As (EC, β^+, half-life 64 h), can be desorbed just as easily as a stable Ge carrier added at the same time.[16, 26]

2.3. Counting Gas and Low-level Counting Technique

The chemical procedure for quantitatively converting the separated germanium into GeH_4 was developed at BNL and, in contrast to the process steps up to this point, can be carried out on a laboratory scale. After acidifying the 1 L of concentrate, the Ge is transferred into 50 mL of low-tritium water by extraction with CCl_4 and back-extraction. Low-tritium $NaBH_4$ is added to convert it quantitatively into 0.3 mL of GeH_4 gas at a temperature of 90 °C and at a pH of 11. The GeH_4 is purified by gas chromatography and the gas volume is then measured for yield determination. Finally, the 0.3 mL of GeH_4 is mixed with 0.7 mL of xenon, and counted for six months in a gas proportional counter. Roughly 8 h pass from the beginning of extraction to the start of counting.

Counting these few ^{71}Ge atoms requires a special effort. The Heidelberg MPIK developed the miniaturized gas proportional counters of the Davis type to the ultimate level worldwide, especially in terms of low background count rates and high counting yields.[27] The high standard of the HD2 Fe/Si type GALLEX counters has contributed decisively to the possibility of running GALLEX on only 30 t of Ga.

^{71}Ge atoms decay by electron capture (K 87.7%, L 10.3%, M 2.0%), emitting Auger electrons and X-rays.[28] Because of their low energies of 10.4 (K capture) and 1.2 keV (L capture), these produce point-type ionization events in the counting gas which result in a rapid pulse rise. Pulse shape analysis allows these pulses to be differentiated from the slowly rising pulses of the high-energy Compton electrons or β-particles which produce extended ionization tracks. Figure 8 is a plot of counting pulses versus energy and rise time. The ^{71}Ge pulses are located in the K and L counting windows with a probability of 95%. The background count rate in the windows is approximately 2 pulses per month or even less in a few selected counters.

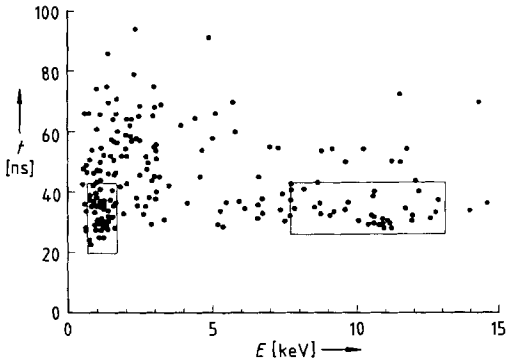

Fig. 8. Plot of pulses as a function of the energy E of the pulse and pulse rise time; as rise time t, the time for the pulse energy to increase from 10% to 70% of the maximum value was taken. The diagram shows all ^{71}Ge pulses of the first ^{71}Ge series of measurements during the first ^{71}Ge half-life (16.5 d) (after Ref. [6]).

Where counters are operated in the well of a large NaI pair spectrometer for simultaneous γ-counting, additional information about the types of decaying nuclides can be obtained by coincidence measurements from the γ-quanta emitted, albeit at the expense of a slightly higher background of ca. 1 pulse per week. Consequently, ^{68}Ge-decays can be distinguished from ^{71}Ge not only by their longer half-lives, but also by the delayed coincidence of the γ-radiation of the ^{68}Ga daughter. Decays of ^{69}Ge can be identified by direct γ-coincidence.

3. Process and Equipment

3.1. Process Concept

For the chemical form of the Ga target, either gallium metal (melting point, 29.8 °C) or a $GaCl_3$ solution can be used. Preparatory earlier work at BNL had decided in favor of the $GaCl_3$ solution, and a number of experiments were run, some of which were on a pilot scale, with 1.3 t of $GaCl_3$. The two types of target were evaluated primarily in terms of the simpler chemistry and process technology associated with the separation of ^{71}Ge from the $GaCl_3$ target. On the other hand, two advantages of the metal target are its ten times lower specific volume and lower sensitivity to trace impurities.

Modern technology in the making of containers of fiberglass-reinforced vinyl ester lined with PVDF (polyvinylidene fluoride) allowed the entire 100 t of $GaCl_3$ solution to be accommodated in one tank, which greatly facilitated the process engineering and operational aspects of desorption.[30] The properties of fiberglass-reinforced tanks with respect to corrosion resistance and weight exhibit clear advantages compared to enamel tanks. As hydrochloric acid has to be handled in an underground laboratory with a low rate of air exchange, and earthquakes had to be taken into account as well, a second tank, a large spill tray and emergency dump tanks (100 m^3) were necessary.

For desorption, a choice had to be made between a loop system and an open once-through system. The loop system seems to offer advantages because of its insensitivity to external impurities. The advantage is bought, however, at the expense of a more complicated process flowsheet. Consequently, that option was not pursued further, especially because of the impossibility of obtaining a suitable compressor (approx. 30 kW) resistant to hydrochloric acid. For this reason, a once-through flow system was designed in which liquid nitrogen is evaporated to provide the required desorption gas.[29, 30]

For the absorber system, three commercial glass columns with coolers in the circulating scrubbing acid were used. A three-column version is also easy to adapt to a loop mode of operation.[30] Concentration, i.e., the desorption of $GeCl_4$ from the scrubbing solution and reabsorption in a small column, was mainly carried out in laboratory-scale equipment; care had to be taken to minimize holdup and dead volumes.

All the materials used must be examined for corrosion, compatibility with germanium, and also for α-emitters; the latter can produce fast neutrons. Special attention had to be paid to the glass fibers used for the tank construction, and also to the substances to be put into the tank. For the glass fibers, so-called S2-type glass manufactured by Corning (USA) was used; it had by far the lowest contents of uranium and thorium among all glass fibers available.

3.2. Process Flowsheet

At the beginning of a run a carrier solution containing 1 mg of an enriched stable Ge isotope is added to the $GaCl_3$ solution. After three or four weeks of exposure time, desorption is carried out with 2500 m^3 of nitrogen over a period of 12 hours. Approximately 0.2% oxygen is added to keep the oxidation potential high enough to prevent the reduction of Ge^{IV} to non-volatile Ge^{II}. In each run, desorption is monitored by measuring the gas throughput and the amount of HCl in the scrubbers. $GeCl_4$ and HCl (roughly 4 kg) are absorbed from the gas flow by circulating water at 10–12 °C. In this step, the HCl content in the scrubbers must not exceed 15% if losses of Ge are to be avoided reliably. After the desorption process, all of the germanium is contained in the first scrubber in a volume of 25–30 L. The scrubber is then detached from the system and connected to the small concentration loop. After evacuation to 0.1 bar and acidification to 30% with electronic grade HCl gas, $GeCl_4$ is expelled from the scrubbing acid by means of a recirculating gas flow of 3 m^3/h and transferred to the small absorber of the concentration loop. After careful rinsing of the small absorber, all Ge is contained in ca. 1 L of diluted hydrochloric acid. The Ge yield is determined by atomic absorption spectrometry. Additional chemistry further concentrates the germanium, which is finally converted into germane.

To minimize ^{71}Ge losses due to radioactive decay, roughly 1% decays within four hours, all process steps must be performed as quickly as possible. Losses of ^{71}Ge can be tolerated if a faster operation ultimately results in the same amount of ^{71}Ge to be filled into the counters.

3.3. Yield Determination

The yield of the Ge carrier must be high and amenable to reliable predetermination. Since the chemical behavior of ^{71}Ge and Ge carrier is identical, the ^{71}Ge yield can be calculated from the carrier yield.

The yield is related to the amount of Ge carrier added at the beginning of each run. In a sequence of identical runs, losses caused by incomplete desorption are offset by the amounts left over from earlier runs, which affects the yield of an individual run as determined from the GeH_4 volume. Because carriers containing Ge isotopes enriched to different levels (^{72}Ge, ^{74}Ge, ^{76}Ge) are used, mass spectrometry can be used to determine whether Ge has been carried over from earlier experiments or from some outside source. This mass spectrometric examination of the counting gas is done at the end of the counting period. Consequently, the ultimate yield is not known until six months after completion of counting.

3.4. Technical Equipment

The entire facility is located in the process building in the southern wing of hall A (Fig. 9); only the supply of nitrogen gas is situated outside the building. The counters are installed in an adjacent low-level building. The process building is 14.6 m long, 9.2 m wide, and 9.6 m high. It includes the two detector tanks, the absorber system, the laboratory apparatus for the production and purification of germane, and a number of auxiliary systems (Fig. 10). The exhaust air of the building ventilation system and the building atmosphere

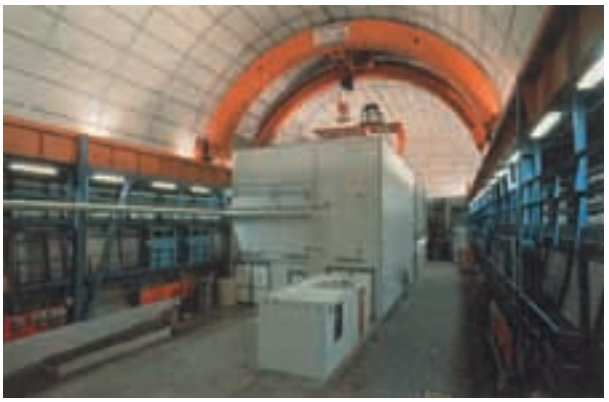

Fig. 9. GALLEX process building in hall A of the LNGS underground laboratory.

are passed through scrubbers and continuously monitored for HCl.

A general overview of the technical equipment is given in Figure 11. The detector tanks are two 70 m^3 vessels of vinyl ester resin reinforced with fiberglass, with an inner lining of 4 mm of PVDF; the outer dimensions are 3.9 m diameter and 7.8 m overall height. These dimensions just barely allow the tanks to be transported inside the tunnel (Fig. 12). The central tube to accommodate a calibration neutrino source exists only in tank A. The sparging system in tank A has been designed for a gas flow of 250 m^3/h and is made up of four concentric pipe rings perforated at the bottom. The sparging system in tank B consists of only one pipe ring and has been designed for ten times lower gas throughputs. The

Fig. 12. Transportation of a detector tank into the Gran Sasso tunnel.

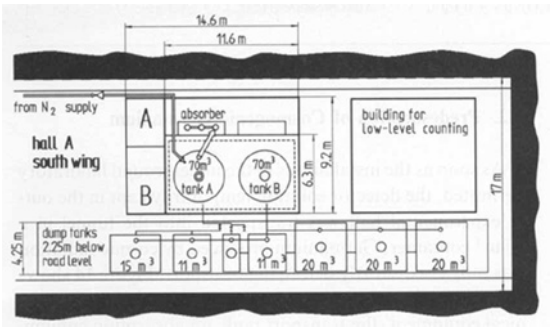

Fig. 10. Floor plan of the GALLEX facilities (without nitrogen supply). A: safety equipment, workshop, ^{37}Ar laboratory; B: building ventilation, storeroom, ^{71}Ge laboratory.

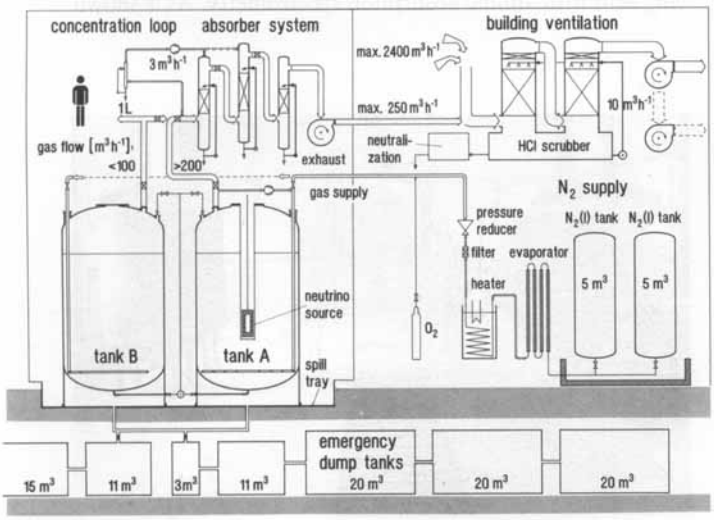

Fig. 11. Simplified flowsheet and survey of the technical equipment of the GALLEX facility.

solution contained in the tank can be thermostated at temperatures between 10 °C and 60 °C by means of tube bundle heaters; for thermal insulation, the tanks are enclosed in plastic film jackets. The inner surfaces of the tank, the supply ducts and pumps are all made of PVDF.

The absorber system consists of three commercial glass columns with diameters of 0.3 m and heights of 3.5 m, connected in series. The exchange regions are filled with 12 mm glass helices and have been designed for a maximum gas throughput of 250 m^3/h (gas flow rate, approx. 1 m/s). The scrubbing water can be thermostated to a temperature slightly above the dew point of the environment (8 °C) by means of heat exchangers made of tantalum.

4. The $GaCl_3$ Detector Solution

4.1. Supply and Specification

Purchasing the very large quantity of 30.3 t of gallium as a highly concentrated $GaCl_3$ solution that met special purity criteria was difficult to achieve in a relatively short period of time. The $GaCl_3$ solution was prepared at a Rhône-Poulenc facility in Salindres (France) and delivered to LNGS between December 1988 and May 1990; a total of 46 batches of roughly 2.2 t each arrived in specially designed shipping casks. All batches were carefully examined for weight, composition, and critical impurities before they were added to the contents of the interim storage tanks in the outer experimental hall. All of the batches met GALLEX acceptance criteria. The chemical analyses performed in three different laboratories yielded results which were in surprisingly good agreement. The specifications and the measured mean values

Table 2. Comparison of the measured and specified values of the GALLEX detector solution.

	Measured	Specified
Ga content [g L^{-1}]	567 ± 2	565 ± 10
Cl content [g L^{-1}]	937 ± 4	
Cl/Ga [mol/mol]	3.24 ± 0.01	>3.15
Density [g L^{-1}]	1887	
^{226}Ra content [pCi kg^{-1}]	≤0.04	<0.5 [a]
U content [ppb]	<0.04	<25 [a]
Th content [ppb]	<0.04	<2 [a]
Zn conent [ppb]	ca. 20	

[a] These values give a ^{71}Ge contribution of 1% according to the SSM.

are listed in Table 2, while the composition and the characteristics of the detector solution are shown in Table 3. The

^{68}Ge done at KfK and TU-Munich. The initial ^{68}Ge concentration roughly corresponded to the Ge-carrier concentration in a run. The desorption curve initially shows an exponential decrease but then flattens out below 0.1% (Fig. 13).[33] This less volatile fraction of germanium, which is also called the tail, is a sensitive indicator of trace impurities difficult to detect in any other way. Additional checks indicated the tails to have most likely been caused by traces of silicic acid.[31-33]

In an experiment conducted at such an extremely low level, the presence of a mere 60 atoms of ^{68}Ge, a figure eight orders of magnitude below the detection level of contamination monitors, can still double the counting background. This exemplifies the special care that must be exercised when working in the GALLEX facility.

Table 3. Composition and properties of the detector solution; 8.13 M $GaCl_3$, 2.0 M HCl.

	Spezies			Elements			
	$GaCl_3$	HCl	H_2O	Ga	Cl	H	O
m [t]	78.5	3.9	20.5	30.3	50.0	2.4	18.2
Wt.-%	75.9	3.9	20.2	30	49.6	2.4	18
10^3 Mol	435	107	1135	435	1411	2377	1135
Mol-%	25.9	6.4	67.7	8.1	26.3	44.4	21.2

Properties at 20 °C
Weight: 100.87 t Volume 53.46 m^3 Density 1.887 t m^{-3} Partial pressure (H_2O): 0.4 ± 0.1 gm^{-3} Partial pressure (HCl): 1.55 ± 0.1 gm^{-3} (+7% pro K)
Ge partition coefficent D: 0.14 (+ 2.4% pro K) Viscosity: 8 cPoise

composition of the solution, with approx. 76 wt-% $GaCl_3$, is rather like that of a "molten salt"; physicochemical data of diluted $GaCl_3$ solutions can be extrapolated only with great reservations. The solution carbonizes organic material, very much like concentrated sulfuric acid does, and is highly corrosive in the presence of air. This was taken into account in designing the process flowsheet by reducing all operations with the solution to the absolute minimum. Radioactive trace impurities due to the natural decay series in all of the delivered batches were measured by means of activation analyses for U-238 and Th-232, and Rn-222 desorption for Ra-226.[22, 32] In many instances, the radioactive impurity levels were far below specifications (see Table 2).

The existence of chemical impurities critical to $GeCl_4$ desorption was checked in samples of the detector solution by measurements of the desorption behavior of carrier-free

4.2. Predesorption of Cosmogenic Germanium

As soon as the installations in the underground laboratory permitted, the detector solution temporarily kept in the outer experimental hall was transported into the tunnel in a 10 m^3 container. Germanium produced by cosmic radiation was outgassed shortly before the transport. Figure 14 shows an interior view of the outer experimental hall with the technical equipment, the transport tank, an absorption column, and tanks for interim storage. Desorption of each of the eight transport batches was performed with 1000 m^3 of nitrogen during 24 hours. Desorption was monitored with a few mg of Ge carrier by concentration assays of the scrubbing acid with atomic absorption spectrometry. As is shown

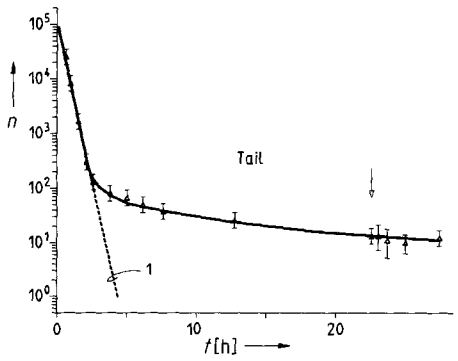

Fig. 13. Plot of ^{68}Ge-stripping from the detector solution; 1 = ideal stripping. n = number of ^{68}Ge pulses per mL. Values plotted after the arrow were recorded after 80 d.

Fig. 14. Interior view of the outer experimental hall with transport and storage tanks and weighbridge in foreground.

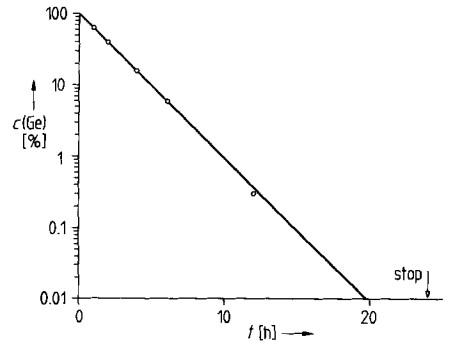

Fig. 15. Decrease in concentration of the Ge carrier during pre-desorption.

in Figure 15, an exponential desorption curve over two and a half orders of magnitude was obtained.

Only rough estimates can be made of the quantities of cosmogenic Ge radioactivity removed in the pre-desorption and of the fraction carried on into the tunnel. Existing measurements[16, 34] estimate the cosmogenic production of ^{71}Ge at sea level to be some 1000 atoms per day per ton of gallium. The production of ^{68}Ge and ^{69}Ge is roughly two and three times larger, respectively.[16, 35] In the outer experimental hall located roughly 1000 m above sea level the entire rate of Ge production is higher by a factor of two.[36]

When the gallium solution was manufactured, also the cosmogenic germanium was separated; but new cosmogenic germanium was produced in the solution during transport and storage. Averaging over the post-production periods of all 46 batches results in nearly saturation activity for the shorter lived ^{69}Ge and ^{71}Ge isotopes, and in a value of roughly 30% of the saturation level for the long-lived ^{68}Ge. The ^{68}Ge desorbed was measured in three pre-desorption steps. Extrapolation to the total quantity indicated about 18×10^6 ^{68}Ge atoms at the end of the storage period, or a saturation level of approx. 6×10^7 atoms, which is in good agreement with the estimate.

After pre-desorption, less than 0.1% of the volatile cosmogenic ^{68}Ge remains in solution. However some Ge activity grows in during desorption in the transport tank (six hours germanium mean residence time) and over the approximately four hours of transport into the tunnel; this corresponds approximately to 10 hours of exposure time. On the basis of these data, the number of cosmogenic ^{68}Ge atoms carried into the tunnel can be estimated at some 60000 (ca. 1 atom/L). Even this quantity upsets the measurement of ^{71}Ge; consequently, pre-desorption must be completed underground. If all ^{68}Ge atoms existed in a volatile form, three outgassing steps would be sufficient. If there are tails, the desorption is delayed and requires additional measures to be taken. For the short-lived ^{69}Ge, and for ^{71}Ge, this problem is solved automatically by the decay within a few months.

4.3. ^{68}Ge Desorption in the Detector Tank

The entire detector solution had been transferred to tank B by June 1990. The procedure employed to remove the residual ^{68}Ge activity was identical with that used in ^{71}Ge runs. After the first few runs, the release of ^{68}Ge was seen to be persistent at a level of 100–200 atoms/d, which was considerably higher than the tolerable amount of ≤ 3 atoms/d (Fig. 16). Blank tests were carried out to verify that the release was not simulated by memory effects in the absorbers or other parts of the equipment. The sparging system in tank B was run far into the overload range at a throughput of up to 95 m^3/h in order to attain the necessary desorption yields over a period not exceeding 20 hours. The resultant absorption losses due to solution entrainment and condensation mist amounted to a few percent. For the purpose of ^{68}Ge removal such losses were tolerable.

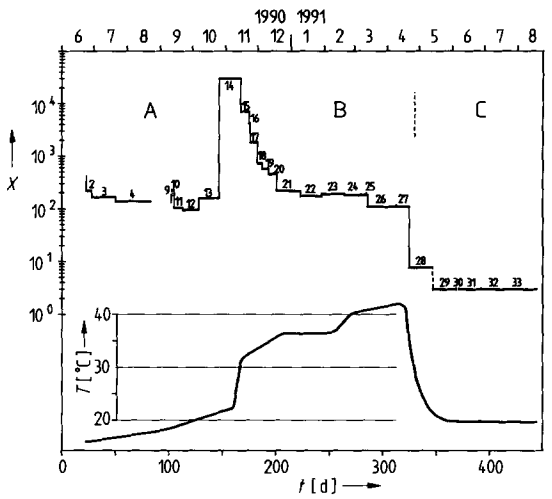

Fig. 16. Release x of ^{68}Ge in atoms per day in tank B (runs B2–B33) during the temperature treatment of the tank solution (lower curve). A: cold runs; B: warm runs; C: cold runs, ^{71}Ge measurement. The measurements relate to the period from June 1990 to July 1991 (upper scale).

The properties of the ^{68}Ge tails in the detector tank do not have to agree with those examined in the laboratory, as their concentrations differ by several orders of magnitude, and as they also have different histories. Consequently, an attempt was made to characterize the release rates by adding more carrier (four runs (B5–B8) with 10 mg each of Ge carrier), and by conducting runs with different exposure times (B9–B13). The persistent high release level (Fig. 16) documents the inertness to isotopic exchange of the tail species and is indicative of a uniform release from a deposit of ^{68}Ge which, at room temperature, does not decrease greatly beyond the lifetime of ^{68}Ge.

This was followed by thermal treatment; the solution was heated to 42 °C over a period of six months, left at that temperature for some time and then cooled again. Desorptions were carried out periodically during this period. When the solution was first heated to a temperature above 30 °C, some 600000 ^{68}Ge atoms were removed, which corresponds to some 5% of the original cosmogenic ^{68}Ge inventory. Despite further heating, the release rate then gradually dropped to the original level of approximately 100 ^{68}Ge atoms/d. Under the assumption that the release originated from the decomposition of a Ge tail species with an activation energy of approx. 100 kJ/mol, it was to be expected that the release of

^{68}Ge would drop back to the desired low level of ≤ 3 ^{68}Ge atoms/d after cooling (runs B27 and B28). After this was verified, it was possible to start the first measurement of ^{71}Ge produced by solar neutrinos. It was decided to continue these runs in tank B.

5. First Experimental Operation

5.1. Germanium Yields

When measuring the ^{71}Ge production rate in tank B, attention had to be devoted again to attaining high absorption yields. The absorption yields of $GeCl_4$ and HCl in the three columns are listed in Table 4 for various operating conditions. The numbers are averaged over runs conducted under the same operating conditions. In normal operation in tank A, $GeCl_4$ and HCl are absorbed at a rate in excess of 99% in the first column. Overload operation of the sparging system in tank B results in the formation of condensation mist and partly transfers these compounds to the second and third columns, where they are completely retained. The cause of mist formation is the sharp gas jet from the perforated sparging pipes in the overload regime; per 1 m^3 of gas, approx. 0.14 mL of solution is entrained in the form of droplets approximately 1 μm in size. In the wet gas phase of the scrubbers, supersaturated with HCl, they constitute good condensation nuclei which grow in the scrubber packing to roughly four times their original diameter, thus forming a condensation mist of 8 mL/m^3. If the pressure losses are low and the gas velocities ≤ 0.4 m/s, the mist droplets can pass the scrubber packing.[37] If the pressure losses are high the last scrubber is operated slightly below the flooding point, thus reliably retaining the mist.

Table 4. Percentage absorption yields of $GeCl_4$ and HCl.

Column	1	2	3
Tank A: Gas throughput ca. 200 $m^3 h^{-1}$			
$GeCl_4$	>99	<0.5	<0.5
HCl	>99.2	<0.7	<0.1
Tank B: Gas throughput ca. 95 $m^3 h^{-1}$			
$GeCl_4$	88.5	3.4	8.1
HCl	74.3	9.1	16.6
$GeCl_4$ [a]	88.6	9.3	2.1

[a] With acidification of the mist after column 1.

$GeCl_4$ and HCl are carried over from the first column exclusively by mist. For this reason, feeding HCl gas (4 kg in 7 h) downstream of the first column acidifies the mist so that $GeCl_4$ is released into the gas phase. It is then reabsorbed in the second column. After some 80% of $GeCl_4$ from the tank had been desorbed, the HCl feed was stopped to keep the HCl concentration in the scrubbing acid of the second column below 15 wt-%. The effectiveness of this simple measure can be seen from Table 4: instead of 8–9%, only some 2% of the $GeCl_4$ is carried over into the final column and, thus, is lost to the measurement.

The yield of germanium put into the counters, as determined from the GeH_4 volume, has an average value of 91.8 ± 2.2% for all runs after B35. These values still need to be corrected for the Ge residues from the previous run, which is obtained from the isotopic composition of the germanium in the counting gas. In most of the runs conducted so far, a fraction of 98.5–99% of the carrier used was removed during desorption, which is in good agreement with the value calculated on the basis of operating data (see also equations in Section 2.2).

Table 5 summaries the Ge mass balance for the Ge carrier and ^{71}Ge for the runs performed under standard conditions in tanks A and B. The decay losses of ^{71}Ge (difference between Ge carrier and ^{71}Ge yields) depend on the time required to perform the operations. The carrier residue (and the ^{71}Ge contained) must be taken into account when estimating desorption losses. Table 6 is a summary of the yields of all runs in the ^{71}Ge series.

Table 5. Mass balance for the Ge carrier and ^{71}Ge in tanks A and B.

	Tank B	Tank A
GeH_4 yield [%]		
Ge carrier	91 ± 2	$95 + \pm 2$
(^{71}Ge	86 ± 2	$91 + \pm 2$)
Losses [%] *upon:*		
Desorption	1.5	0.3 [a]
Absorption	3	1
Concentration	1	1
Sampling	1	0.5
Preparation of counting gas	2.5	2

[a] Determined from operational data.

5.2. ^{71}Ge Production in Side Reactions

Contributions to ^{71}Ge production by side reactions were estimated from a number of additional investigations. The fluxes of cosmic muons and fast neutrons were measured directly in the underground laboratory.[38, 39] The integral ^{71}Ge production cross-sections in the detector solution were determined from irradiations with muon beams[35] and Pu-Be neutron sources of known intensity.[16] On the basis of the reaction cross-section and the particle flux, the ^{71}Ge production rate is calculated for the muons in the underground laboratory, which increases the expected SSM value by 2.9 ± 0.9%. For fast neutrons, the correction was found to be less than 0.2%.

The integral ^{71}Ge production rate of α-particles was measured directly in an 8 M $GaCl_3$ solution.[14, 16] On this basis, the number, Z, of α-particles required for the production of one ^{71}Ge atom was calculated by means of the approximation Equation (f).

$$\log_{10} Z = 15.36 - 0.67\, E_\alpha, \quad E_\alpha\ 4\text{–}9\ \text{MeV} \qquad \text{(f)}$$

The calculation indicates that, e.g., 1% of the value expected in the SSM is produced by 0.2 g of ^{232}Th in equilibri-

Table 6. Carrier yields in the first ^{71}Ge runs.

Run	Exposure completed	duration [d]	Ge carrier isotope/amount [μmol]	Ge carrier yields after absorption [%]	after concentration [%]	in counting gas [%]
B29	4.6.91	20.96	74/15.68	100.3	90.2	83.7
B30	5.6.91	1.27	72/13.87	102.9	87.4	88.0
B31	26.6.91	20.77	76/15.42	103.5	89.0	84.4
B32	17.7.91	21.00	74/14.29	n.b. [a]	89.1	85.0
B33	7.8.91	21.00	72/13.80	n.b. [a]	85.4	87.0
B34	28.8.91	21.00	76/16.27	97.8	87.4	85.2
B35 [b]	19.9.91	22.25	74/15.88	97.0	94.2	92.6
B36	9.10.91	19.70	72/13.35	94.4	96.0	93.5
B37	10.10.91	1.17	76/15.14	95.2	97.3	92.8
B38	30.10.91	19.88	74/15.03	100.7	89.1	88.8
B39	20.11.91	20.96	72/11.94	104.5	92.5	92.4
B40	21.11.91	1.17	76/14.64	104.9	96.4	92.8
B41	11.12.91	19.88	74/14.86	107.0	89.5	90.9
B42	8.1.92	27.96	72/14.83	96.7	90.0	90.6
B43	9.1.92	1.17	76/15.25	99.7	100.3	94.2
B44 [c]	29.1.92	19.88	74/13.82	101.6	–	[d]
B45	19.2.92	20.96	72/13.35	105.0	95.2	92.8
B46	20.2.92	1.21	76/13.12	98.3	96.2	93.8
B47	11.3.92	19.81	74/15.02	n.b. [a]	92.9	86.1
B48	12.3.92	1.19	72/13.56	n.b. [a]	99.2	92.8
B49	31.3.92	18.83	76/14.83	98.3	97.5	93.2
B50	29.4.92	29.00	74/15.23	99.0	95.5	89.1
[e, f]				100.5 ± 3.8	94.7 ± 3.5	91.8 ± 2.2
[f, g]				101.1 ± 2.6	88.1 ± 1.7	85.6 ± 1.6

[a] Not determined. [b] Acidification of mist and standard conditions after B35. [c] Reduction of the static holdup in the concentrating absorber from 0.07 to 0.05 after B44. [d] Loss on preparation, B44 is not included in the averaging. [e] Average values under standard conditions (B35–B50). [f] The error of the average values contain both the error of analytical determination as well as the reproducibility of the experiment. The most accurate analytically determinable counting tube yields are reproducible to +2%. [g] Average values without acidification of the mist (B29–B34).

um with its daughters. The more effective short-lived higher energy α-emitters are generated as daughters of long-lived nuclides, which is why the long-lived radioelements of the natural decay series must be monitored very accurately. In our present environment, transuranium elements should also be included in these checks. Consequently, α-spectrometric assays for transuranium elements and for ^{210}Pb, ^{210}Po, and ^{228}Ra were carried out.[40] Investigations conducted so far have shown the sum total of all known contributions by side reactions caused by α-emitters to be below 0.2% of the expected standard solar signal.

The gallium detector solution is much more sensitive to fast neutrons ($\geq$0.4 MeV) than to α-particles. In the case of heavy nuclei, such as ^{244}Pu and ^{252}Cf, the emission of neutrons in spontaneous fission contributes more to the production of ^{71}Ge than do the α-particles emitted at the same time. As α-spectrometric analysis is too insensitive, global detection of spontaneous fission events in the tank by separating and measuring the ^{133}Xe fission product (half-life, 525 d) is currently being organized. In addition, more information about spurious side reactions is to be obtained by way of measuring the production of ^{69}Ge.

5.3. Results of the Series of ^{71}Ge Measurements[6]

Between May 1991 and April 1992, 16 runs with either 3 or 4 weeks of exposure time and five runs with short exposure times (ca. 1.2 d) were performed (runs 29 to 50). The short runs serve as blank tests in which Ge activity carried over is detected; they were spread over the entire measurement period and provided very low levels of 6(+12, −6)% of the SSM signal, consistent with a null result.

The counting gas yields (Table 6) comprise all operations, including filling of the counting gas into the counters. The counting periods of 13 runs had not been completed by June 1992, which means that precise determination of the counting background has not yet been accomplished. The results obtained in the first counting period comprise a total of 295 days of exposure.

The counting pulses due to ^{71}Ge were selected on the basis of pulse energy and rise time. Figure 8 shows all the pulses registered during the first lifetime of ^{71}Ge. The two "counting windows" for the K and L peaks were determined by calibration for each counter. A maximum-likelihood-analysis was applied in calculating the rate of ^{71}Ge production from the pulses within the two windows.[41] The original number of ^{71}Ge atoms was obtained by assuming a half-life of 11.43 d for ^{71}Ge and a constant background. The results are summarized in Figure 17; the diagram contains the count rates (in pulses/d) of all L and K pulses of 14 runs plotted as a function of counting time. The solid line represents the best fit with the measured value of the counting background. Figure 18 shows the results of the individual ^{71}Ge counting runs. Monte Carlo simulations showed deviations to be within the statistical error range which, because of the small total number of pulses (an approximate aggregate of 70), is still relatively high.

Analysis of the counting pulses indicated a mean rate of ^{71}Ge production in the detector tank of 0.80 ± 0.17 ^{71}Ge atoms per day. As, in astrophysics, one neutrino capture per second per 10^{36} target atoms is called 1 SNU

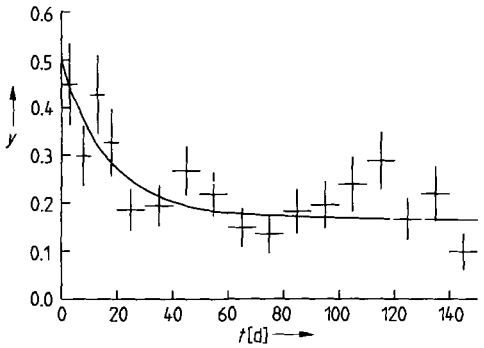

Fig. 17. Decrease in ^{71}Ge count rate (number of pulses per day y) averaged over 14 runs (after Ref. [6]).

(Solar Neutrino Unit), the resultant value is 90 ± 19 SNU. The corrections to be subtracted from this value are: 1) induced by muons, 3.7 ± 1.1 SNU; 2) due to α-emitters in the detector solution, 0.2 SNU; 3) due to fast neutrons, 0.15 ± 0.1 SNU; 4) due to radon, 2 ± 1 SNU; 5) because of ^{69}Ge from muons and ^{8}B neutrinos, 1 ± 1 SNU.

In addition, contributions to the systematic error by the counting yield ($\pm 3.6\%$), the definition of the limits to pulse rises ($\pm 1.6\%$), and the chemical yield ($\pm 1.5\%$) must also be taken into account. The result then obtained for the flux of solar neutrinos is given by (g) or (h).

$(83 \pm 19$ [statistical] ± 8 [systematic]/SNU (for 1σ error) (g)

$(63 \pm 14$ [statistical] ± 6 [systematic])% of the expected value of 132 SNU in the SSM (h)

This average SNU value is shown on the far right in Figure 18. A fit to the measured values in Figure 17 produced a value of the lifetime of ^{71}Ge of 13.5 ($+5.2 - 3.5$) d, which is in statistical agreement with the known value of 16.5 d.

Evaluation of this result[7] in the light of the theories about stellar structure and the fusion reactions inside stars as well as the properties of neutrinos allows the conclusion to be drawn that GALLEX, for the first time, has proved the existence of low-energy pp neutrinos originating in the main reaction of the Sun. The result of GALLEX may be in agreement with the SSM if the error, which is still relatively large, is taken into account. As far as the question of whether neutrinos have a rest mass is concerned, the findings are not that unequivocal. However, it is possible to indicate limits to the neutrino mass together with the results of the chlorine experiment[11,2] and the measurements conducted in the Kamioka detector[10] and, perhaps even more important, to exclude certain ranges of mass. Consequently, the most probable region of the difference between the squared masses of electron neutrino the muon neutrino seems to be around 10^{-5} eV, which would lead to a mass of a few 10^{-3} eV for the heavier muon neutrino. For astrophysical purposes, this value is too small to explain the "missing" mass in the universe.

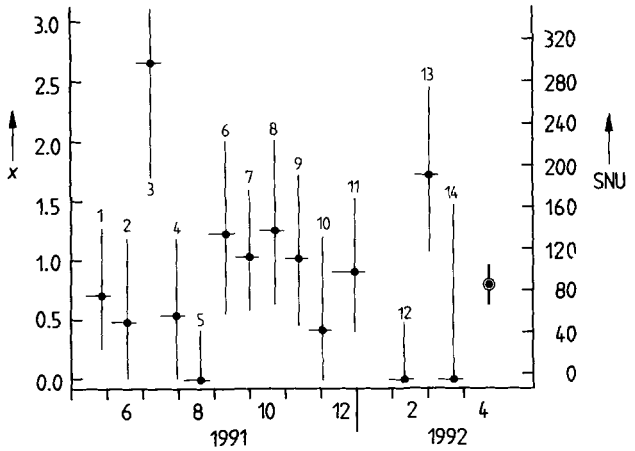

Fig. 18. Results of the first series of measurements (May 1991 – April 1992, 14 runs). The mean value is given on the extreme right (after Ref. [6]). x = ^{71}Ge production in atoms per day (after Ref. [6]).

6. Outlook

The GALLEX experiment is scheduled to run for a period of four years. The accuracy of the final result depends critically on high yields of ^{71}Ge and on tight checks being kept on all credible side reactions. The latter aspect will continue to be worked on intensively. However, even checks on further side reactions are not expected to lead to any fundamental change in the results obtained so far. As far as yields are concerned, we have reached a satisfactory point beyond which no significant improvements are possible, especially now (since June 1992) that desorption is being performed in tank A, specifically designed for that purpose.

Measurements of the ^{71}Ge production by solar neutrinos were continued after August 1992 (2nd period of operation) and are planned to continue for another year. At intervals of four weeks, runs with 27 d and runs with 1 d of exposure are to be performed alternately. A large number of short runs allows, by extrapolation to zero exposure time, a background level for the production of ^{71}Ge to be measured and spurious effects due to extraneous Ge activity to be excluded.

An important confirmation of the measured results is the calibration of the GALLEX detector with a chromium-51 neutrino source (half-life 28 d), which is produced by the irradiation of enriched chromium-50 metal in the Grenoble high-flux reactor. It will have an intensity in excess of 1.5 MCi and produce a ^{71}Ge signal in the detector solution which, initially, will be ten times stronger than that produced by the solar neutrinos. Preparations for the two calibration experiments planned after the second period of operation, for late 1993 and 1994, are on schedule. These calibration experiments are to check once more the correct conceptual design of the experiment, its setup, and the execution of all operations. Afterwards, there will be another two years of solar exposures in order to reduce further the statistical error in the result.

When, after four years, a final result about the fusion reactions in the Sun will be in hand, this certainly will not be the end of the GALLEX mission. The question of a relationship between longer-term fluctuations of the neutrino flux and the eleven-year sunspot cycles may be another worthwhile activity for GALLEX.

Received: July 24, 1992 [A 882 IE]
German version: *Angew. Chem.* **1992**, *104*, 1310
Translated by Ralph Friese, Karlsruhe

[1] J. N. Bahcall, *Neutrino Astrophysics,* Cambridge University Press, **1989**; J. N. Bahcall, R. K. Ulrich, *Rev. Mod. Phys.* **1988**, *60*, 297.

[2] S. P. Mikheev, A. Y. Smirnov, *Nuovo Cimento Soc. Ital. Fis. C* **1986**, *9*, 17; L. Wolfenstein, *Phys. Rev. D* **1978**, *17*, 2369.

[3] T. K. Kuo, J. Pantaleone, *Rev. Mod. Phys.* **1989**, *61*, 937.

[4] SAGE-collaboration, *Phys. Rev. Lett.* **1991**, *67*, 3332; SAGE-collaboration, *16th Int. Symp. Neutrino Mass Rel. Top.* (Japan, (**1988**), CONF-880369-3-LA-UR 1461.

[5] A. A. Pomansky, *Nucl. Instrum. Methods Phys. Res. Sect. B* **1986**, *17*, 406–410.

[6] GALLEX-collaboration, *Phys. Lett. B* **1992**, *285*, 376–389.

[7] GALLEX-collaboration, *Phys. Lett. B* **1992**, *285*, 390–397.

[8] T. Kirsten, *Neutrino 90 (Nucl. Phys. B. (Proc. Suppl.)* **1991**, *19*, 77); T. Kirsten in *Particles and Fields 91, Vol. 2* (Eds.: D. Axen et al.), World Scientific, Singapore 2, **1992**, p. 942.

[9] E. Belotti, *Nucl. Instrum. Methods Phys. Res. Sect. A* **1988**, *264*, 1; L. Paoluzi, *ibid.* **1989**, *279*, 133.

[10] K. S. Hirata, K. Inoue, T. Kajita, T. Kifune, K. Kihara, M. Nakahata, K. Nakamura, S. Ohara, N. Sato, Y. Suzuki, Y. Totsuka, Y. Yaginuma, M. Mori, Y. Oyama. A. Suzuki, K. Takahashi, M. Yamada, M. Koshiba, T. Suda, T. Tajima, K. Miyano, H. Miyata, H. Takei, Y. Fukuda, E. Kodera, Y. Nagashima, M. Takita, K. Kaneyuki, T. Tanimori, E. W. Beier, L. R. Feldscher, E. D. Frank, W. Frati, S. B. Kim, A. K. Mann, F. M. Newcomer, R. Van Berg, W. Zhang, *Phys. Rev. Lett.* **1990**, *65*, 1297; K. S. Hirata, K. Inoue, T. Ishida, T. Kajita, K. Kihara, M. Nakahata, K. Nakamura, S. Ohara, N. Sato, Y. Suzuki, Y. Totsuka, Y. Yaginuma, M. Mori, Y. Oyama, A. Suzuki, K. Takahashi, M. Yamada, M. Koshiba, K. Nishijima, T. Suda, T. Tajima, K. Miyano, H. Miyata, H. Takei, Y. Fukuda, E. Kodera, Y. Nagashima, M. Takita, K. Kaneyuki, T. Tanimori, E. W. Beier, L. R. Feldscher, E. D. Frank, W. Frati, S. B. Kim, A. K. Mann, F. M. Newcomer, R. Van Berg, W. Zhang, *Phys. Rev. D* **1991**, *44*, 2241..

[11] R. Davis, D. S. Harmer, K. C. Hoffmann, *Phys. Rev. Lett.* **1968**, *20*, 1205.

[12] R. Davis in *Proc. of the 21st Int. Cosmic Ray Conf., Vol. 12* (Ed.: R. J. Protheroe), University of Adelaide Press, **1990**, p. 143.

[13] V. A. Kuzmin, *Sov. Phys. JETP (Engl. Transl.)* **1966**, *22*, 1051.

[14] J. N. Bahcall, B. T. Cleveland, R. Davis, I. Dostrovsky, J. C. Evans, W. Frati, G. Friedlander, K. Lande, J. K. Rowley, R. W. Stoenner, J. Weneser, *Phys. Rev. Lett.* **1978**, *40*, 1351.

[15] I. Dostrovsky in *Proc. of Informal Conf. on Status and Future of Solar Neutrino Research, Vol. 1 (Brookhaven Natl. Lab. ReP. BNL* **1978**, *50879*, 231).

[16] R. Davis, B. T. Cleveland, J. K. Rowley, S. Katcoff, L. Remsberg, G. Friedlander, J. Weneser: Proposal for a Fundamental Test of the Theory of Nuclear Fusion in the Sun with a Gallium Solar Neutrino Detector, Brookhaven Natl. Lab., Dept. of Chemistry, April 15, 1981; J. N. Bahcall, L. P. Remsberg, J. Weneser, B. T. Cleveland, G. Friedlander, J. K. Rowley, T. Kirsten, W. Hampel, J. Kiko, G. Heuser, E. Pernicka, R. Schlotz, M. Heubner, R. Wunderlich, G. Eymann, I. Dostrovsky: Proposal for Gallium Solar Neutrino Experiment, submitted to National Science Foundation, April 21, 1983, Brookhaven Natl. Lab.: Proposal of DOE for a Gallium Solar Neutrino Experiment, BNL-37801, 1985.

[17] S. Turck-Chièze, S. Cahen, M. Casse, C. Dom, *Astrophys. J.* **1988**, *335*, 415.

[18] B. Pontercorvo, *Sov. Phys. JETP (Engl. Transl.)* **1968**, *26*, 984.

[19] A. J. Baltz, J. Weneser, *Phys. Rev. D* **1987**, *35*, 528; *ibid.* **1988**, *37*, 3364; J. Bouchez, M. Cribier, W. Hampel, J. Rich, M. Spiro, D. Vignaud, *Z. Phys. C.* **1986**, *32*, 499; L. Wolfenstein, *Nature* **1986**, *323*, 579; M. Cribier, W. Hampel, J. Rich, D. Vignaud, *Phys. Lett. B* **1986**, *182*, 89.

[20] W. Hampel, *Habilitationsschrift*, Universität Heidelberg, **1987**.

[21] J. W. Gramlich, L. A. Machlan, *Anal. Chem.* **1985**, *57*, 1788.

[22] A. Lenzing, Dissertation, Universität Heidelberg, **1989**.

[23] K. Rowley, R. W. Stoenner, *Brookhaven Natl. Lab. Rep. BNL* **1984**, *40818*.

[24] T. K. Sherwood, R. L. Pigford, *Absorption and Extraction*, New York, **1952**.

[25] G. Stöcklin, *Chemie heisser Atome,* Verlag Chemie, Weinheim, **1969**.

[26] R. Hahn, Lecture at the *14th Gallex Meeting* (Italy, October 1991).

[27] R. Wink, Dissertation, Universität Heidelberg **1988**; R. Plaga, T. Kirsten, *Nucl. Instrum. Methods Phys. Res. Sect. A* **1991**, *309*, 560; W. Hampel et al., *Proc. 19th Int. Cosmic Ray Conf. Vol. 5* (USA **1985**), 422; G. Heusser, *Proc. 2nd Conf. Trends Astroparticle Phys.* (Aachen, **1992**), in press.

[28] C. M. Lederer, V. S. Shirley, *Table of Isotopes,* 7th Edit., Wiley, New York, **1978**.

[29] R. von Ammon, K. Ebert, E. Henrich, G. Knittel, J. Unk, *KFK-Nachr.* **1987**, *19*(2), 67.

[30] E. Henrich, R. von Ammon, K. Ebert, T. Frisch, K. Hellriegel, M. Balata, *KFK-Nachr.* **1990**, *22*(3), 125.

[31] E. Henrich, R. von Ammon, K. Ebert, T. Frisch, W. Habicht, K. Hellriegel, W. Rösch, L. Stieglitz, F. Weirich, R. Will, M. Balata, *KFK-Nachr.* **1992**, *25*(3).

[32] E. Pernicka, Lecture at the *13th GALLEX Meeting* (Italy, March 1991).

[33] U. Schanda, Diplomarbeit, Technische Universität München, **1989**, and lectures at Gallex Meetings **1990–1991**.

[34] V. N. Gavrin, Yu. I. Zakharov, *Institute for Nuclear Research, USSR Academy of Sciences,* Moscow, Preprint-0560, **1987**.

[35] T. Storarczyk, Dissertation, Université de Paris-sud, CEA-N-2660, **1991**.

[36] D. Lal, B. Peters in *Handbuch der Physik, Band XLVI/2* (Ed.: S. Flügge), Springer, Heidelberg, **1967**, p. 551.

[37] G. L. Fairs, in *Gas Purification for Air Pollution Control* (Ed.: G. Nonhebel), Newnes-Butterworths, London, **1972**, p. 520.

[38] S. P. Ahlen et al., *Phys. Lett. B* **1990**, *249*, 149; P. Belli et al., *Nuovo Cimento Soc. Ital. Fis. A* **1989**, *101*, 959.

[39] R. Aleksan et al., *Nucl. Instrum. Methods Phys. Res. Sect. A* **1989**, *274*, 203.

[40] The α-spectrometric measurements (Universität Regensburg) are not yet completed.

[41] B. Cleveland, *Nucl. Instrum. Methods Phys. Res.* **1983**, *216*, 451.

[42] M. Cribier, B. Pichard, J. Rich, M. Spiro, D. Vignaud, A. Besson, A. Bevilacqua, F. Caperan, G. Dupont, P. Sire, J. Gorry, W. Hampel, T. Kirsten, *Nucl. Instrum. Methods Phys. Res.* **1983**, *214*, 451; F. X. Hartmann, R. L. Hahn, Brookhaven Natl. Lab. *Rep. BNL* **1991**, *51281*.

Scanning Tunneling Microscopy and Atomic Force Microscopy in Organic Chemistry

By Jane Frommer*

When Kekulé awoke from dreams of snakes biting their own tails, he didn't have the benefit of a scanning tunneling microscope (STM) image to confirm that his vision of benzene as a cyclic molecule was accurate. References to STM in the chemical literature increase steadily, although the technique was perhaps oversold in its early days of the 1980s, with such promises as DNA sequencing and tailored bi-molecular chemical reactions (literally, two molecules). Publications alternate between attempting to explain the process by which images of traditional insulators are obtained and simply presenting the end images themselves as stunning views of atoms and molecules. While imaging mechanisms are still being debated, these instruments' ability to "see" single molecules has been established, albeit at the fringes of our expectations. For example, whereas STM studies at present might not be able to answer the question of why adsorption of CO doubles the density of platinum atoms on the surface of a single crystal of the metal, the images go far in illustrating that this *is* a process which platinum undergoes. As with any emerging analytical tool, these scanning, very localized microscopic methods are undergoing the growing pains of irreproducible results and mis-marketed artifacts. Nonetheless, we assemble here, primarily for the uninitiated, a collection of careful and credible studies to mark the progress of scanning tunneling microscopy and atomic force microscopy into chemistry, and to encourage a healthy blend of idealism and skepticism toward future work.

1. Introduction to the Scanning Tunneling Microscope

In 1986 a Nobel prize was awarded for scientific progress made five years earlier: a microscope based on electron tunneling.[1] What about this instrument endowed it with such recognition? This new imaging technique enabled *direct atomic-scale* measurements to be made. This high-resolution measuring and imaging technique afforded an enormous magnification, allowing atomic information not from an average over many atoms, but rather recorded locally, atom by atom. The development of this method continues in new directions; it is a dynamically evolving method rather than a mature one.[2]

The operating principle of the scanning tunneling microscope (STM; this abbreviation is used for the instrument and the technique) takes advantage of an electrical current that flows between two conductors that are separated by very small distances, typically angstroms. This current, known as the tunneling current, is an electrical current through an extremely thin, insulating layer such as vacuum, air, or liquid. The electrons "tunnel" through this electrically insulating layer, giving rise to a measurable current which displays an exponential dependence on the distance between the two conductors, that is, the thickness of the insulating layer [Eq. (a)] where I is the tunneling current, V is the voltage applied across the two conductors, φ is the effective tunneling barrier (eV), c is a constant, and s is the spacing between the two conductors (Å).[3]

$$I \propto V \exp(-c\sqrt{\varphi}s) \qquad \text{(a)}$$

It is the *exponential* dependence of the tunneling current on the distance between the two conductors (STM tip and the analyzed surface) that provides the sensitivity of the measured current that can be interpreted as the surface structure. As the equation shows, other factors influence the current as well, such as the electron band structure of the two conductors (φ).

At the time of the STM's conception,[4] the theories of tunneling were not new. Indeed, experimental setups were already in operation, mostly in the form of planar tunnel junctions.[5] The novelty of the STM arose when the mechanics of piezoelements became refined enough to allow control over motion on the subangstrom scale.[6] This control enables positioning a probe over an individual atom and scanning it over an array of atoms, thereby providing a surface analysis with atomic resolution (Fig. 1). In the STM, the probe is one of the two conductors, configured as a tip. A very localized stream of electrons tunnels from it to the second conductor, the surface being analyzed. As the tip is scanned over the surface, the tunneling current is collected

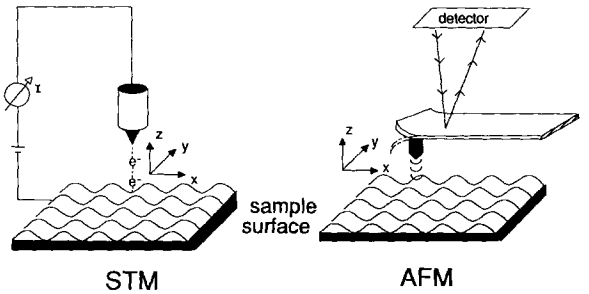

Fig. 1. Schematic illustration of the scanning tunneling microscope and the atomic force microscope, highlighting their common feature of a localized probe that scans a surface composed of atomic or molecular features and collects data directly over very localized sites of angstrom or nanometer dimensions.

[*] Dr. J. Frommer
IBM Almaden Research Center
San Jose, CA 95120 (USA)
and
Institut für Physik der Universität
Klingelbergstrasse 82, CH-4056 Basel (Switzerland)

from a series of points, angstrom by angstrom, that is, on the level where atoms are joined together. When this atomic information is pieced together laterally, like the pieces of a puzzle, an image of the whole is obtained, be it the face of a crystal lattice or the backbone of a hydrocarbon chain.

By monitoring the tunneling current over each point (x, y) on a surface, the electronic topography of a surface is recorded experimentally. In cases of homogeneous materials, such as a metal single crystal, this current map reflects the surface topography; atoms appear as "hills" of higher current and the bonds between them as "valleys" of lower current. Figure 2 is a map of the tunneling current that flows between the tip and surface as the tip is scanned piezoelectrically over a (7×7) reconstructed[*] silicon (111) surface.[7] It reflects the atomic surface structure of the sample displayed as an array of single atoms that make up the sample. The STM's atomic resolution arises from the extremely narrow stream of tunneling electrons which is spatially confined between a few atoms on the tip and a few atoms in the sample.

Lattice parameters are available from other techniques, such as X-ray and neutron scattering. Where, then, does the STM offer an advantage, or an improvement in our previous knowledge? A fundamental difference is the scale on which the STM collects its data: an STM image is not the result of averaging over large areas containing many atoms; rather it is a composite picture of data points collected separately and directly over each individual atom. By avoiding both the averaging of data from many sites and the Fourier transform from reciprocal space, information can be obtained for very localized features such as an irregular atomic defect, a grain boundary, or small, irregularly shaped domains. Figure 2b contains two examples of defects in a silicon lattice: a shifted atom and a vacancy or reacted atom These details would be lost in analytical techniques that provide atomic information from averaging data from many sites.

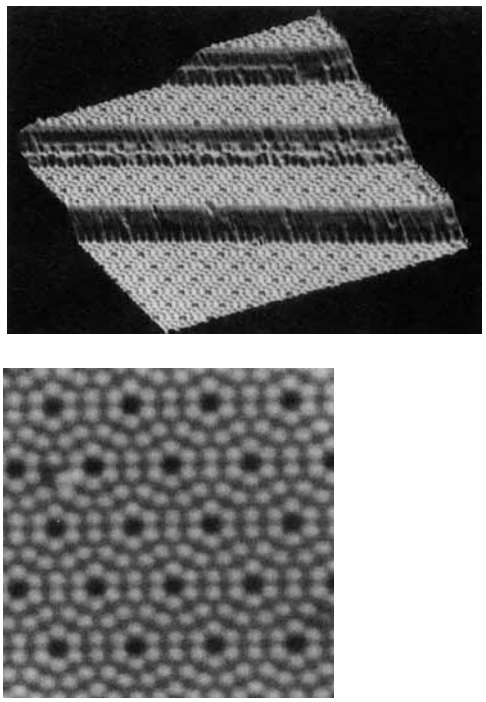

Fig. 2. STM images of a silicon (111) crystal (7×7) reconstructed surface resolving atomic spacing[7]: a) a 3-D rendition of a scan (size 320×360 Å^2) showing three steps of varying heights up to about 12 Å high. The step heights are multiples of the silicon (111) double-layer height of 3.13 Å. b) Top view of a $(100 \times 100$ Å^2) scan. Two defects can be seen in this image: a shifted adatom (top left) and a reacted adatom or surface impurity (bottom right).

1.1. Units

In this article, measurements will be discussed that have been performed with the STM on organic molecules, rendering information from the angstrom scale to the submicron scale, that is, from intramolecular features such as bond lengths and angles to intermolecular spacings and long-range packing. Data from the atomic force microscope (AFM) are collected over nanometers to microns (Section 9). Resolution with the AFM is currently limited, principally by tip geometries, to molecular resolution on organic molecules; however, interatomic spacing is often obtained for inorganic salts.

Results are reported in units of angstroms (10^{-10} m) or nanometers (nm, 10^{-9} m). For reference, examples of bond lengths are 1.4 Å between lithium and fluorine atoms in a LiF crystal, 2.2 Å between silicon atoms in a Si single crystal, 1.5 Å between adjacent carbon atoms in an alkane, and 1.4 Å between carbon atoms in benzene. Within the context of organic solids, intermolecular spacings (e.g., noncovalent bonding interactions due to van der Waals forces) are on the order of 3 to 10 Å.

[*] On reconstructed surfaces the surface atoms are arranged differently from the bulk crystal to minimize energy. In the case of Si(111), (7×7) reconstruction means a rhombohedral unit cell, the sides of which are seven atoms long (see also ref. [1]).

Jane Frommer was born in 1952 in New England (USA). She obtained her Bachelor of Science degree in chemistry in 1975 from Tufts University (Massachusetts) after carrying out an undergraduate research project at MIT in mechanistic organic chemistry. Following a year of research in Vitamin D photobiochemistry at Massachusetts General Hospital Endocrine unit, she entered California Institute of Technology (Pasadena) where she obtained a Ph.D. in organometallic chemistry in 1980 under R. G. Bergmann. Since 1980 she has been active in industrial research laboratories, first at the Allied Corporation (New Jersey) and then at IBM (Almaden Research Laboratory, San Jose, CA, USA). Her research areas have included electronically conducting polymers and STM and AFM investigations of molecular interfaces. Since 1990 she has been on sabbatical from IBM at the Physics Institute of the University of Basel, Switzerland.

1.2. The Scanning Tunneling Microscope

An STM workstation consists of several components (Fig. 1). The actual measuring device is mounted on a stable surface (for example, a vibration isolation table). At the heart of the device, a delicate metal tip scans over the sample surface. The scanning is controlled electronically with piezoelectric transducers, over spans of hundreds of microns to several angstroms. During the scan the tunneling current is recorded over each point on the sample, the signals are digitized, and an image is assembled from the collection of these points with a computer. The contrast in STM images is based on an arbitrarily chosen scale of shades of grey to indicate the magnitude of the measured currents, where high currents are typically assigned light shades and low currents dark shades. Artificial coloring is occasionally used to render data from different atoms or molecular moieties separable to the eye. The STM workstation is completed with associated hardware and software to drive the data acquisition, to convert the electronic signals into images that can be displayed in various formats, such as line scans or 3-D renderings, and finally to store the scanned information.

The electrode fashioned into a tip rarely terminates in a single-atom point; instead the effective operating area is provided by several atoms at the end of a fortuitous protrusion on the macroscopic tip. STM tips are commonly prepared by electrochemically etching a tungsten wire (about 0.25 mm in diameter) partially immersed in an NaOH solution until the end of the wire has a conical shape.[8] Platinum/iridium (80/20) wire, cut with pliers, can also serve as a tip. Ultimately it is the dependence of the tunneling process on s, the separation between the two electrodes [Eq. (a)], that defines the *functional* tip as the point on the macroscopic tip that is closest to the scanned surface. Regardless of the tip preparation method, its geometry can influence the collected image and introduce artifacts (see Section 1.5 and Fig. 3).

In recording an STM image, the tip is scanned in an x, y plane over the sample surface while the tunneling current flows between the sample and the tip along the orthogonal z direction. In practice, greater control over a broader dynamic range is afforded when the instrument is operated in the constant current mode: under the control of a feedback loop, a fixed current is maintained between tip and sample by allowing the tip to adjust its distance from the sample automatically as it scans over surface features. This motion of the tip in the z direction is then plotted as surface contours. Typical values for scanning parameters range from millivolts to a few volts for the bias voltage between tip and sample, and picoamperes to nanoamperes for the tunneling current. These are adjustable parameters, used to maximize resolution for each individual sample.

In imaging organic materials, the STM samples only the layer or layers closest to the interface with the conducting substrate. Under feedback loop control, the tunnel tip advances through macroscopic quantities of organic material until it reaches a distance from the substrate that sustains a tunneling current, typically 5–10 Å. At this distance the tunneling and scanning parameters are optimized and the images are recorded. Physical contact between the tip and substrate is avoided to prevent damage to either. Confirmation of the proximity of the tip from the substrate during scanning is provided by studies which show that both substrate and adsorbate images can be recorded (nearly) simultaneously.[9–12] This is done by rapidly switching between the two sets of parameters that optimize the recording of each. It is still being debated whether this process disrupts the assembled film reversibly or irreversibly.[12] Some perturbations in the adsorbate layer have been documented.[13] Typical values for voltage and currents in experiments are 0.3–1 V and 0.05–1 nA to resolve the adsorbates and 0.1–0.3 V and 0.3–10 nA to resolve the substrate.[9, 12, 13]

It can take from several seconds to several minutes to record an image, depending on the scan size, the surface roughness, and the level of resolution. Fast scan rates (kHz) can produce series of images that are then stored on video tape. In reviewing the data, the successive frames are played back as a "movie".[14] This mode of data storage and presentation is advantageous in monitoring dynamic processes, on the timescale of the STM measurements—seconds to hours (see Section 1.3).

Most scanning tunneling microscopes are operated at room temperature; however, instruments have been customized to operate at variable temperatures. Examples are STMs operated at low temperatures of 1–4 K in ultrahigh vacuum (UHV).[15–17] Mildly elevated temperatures (30–85 °C) have been achieved in instruments operated in air by simply incorporating a heated stage under the sample.[9, 18] For recording STM images during higher temperature experiments (up to 725 K), the STM has been incorporated into a controlled environment and coupled with other surface science tools.[19, 20] For example, variable temperature STM imaging (150–450 K) of chemical processes in UHV can be performed in a surface analysis chamber that also permits monitoring chemical reactions that occur at temperatures too high for stable operation of an STM (up to 1200 K). This was achieved in a design where the sample and STM were not in thermal contact, but remained in close proximity within the chamber, affording rapid cooling (a few degrees per second) of the sample to stable imaging temperatures.[19, 21] In the following section, studies are presented in which these instruments are used.

1.3. Dynamics

The STM is able both to monitor the dynamics of processes in real time and to induce atomic and molecular rearrangements. Events of atomic and molecular manipulation can be performed.[16, 17, 22] For example, xenon atoms[16] and carbon monoxide molecules[17] were deposited with an STM tip in preselected patterns on metal surfaces in an instrument held at liquid helium temperature ($\sim$ 4 K). At room temperature, silicon atoms were individually removed from their crystal lattice and redeposited elsewhere.[22]

Phase transitions were monitored in semiconductor surfaces and in organic adsorbates. In the field of semiconductors, thermally activated phase transformations on silicon[20, 23] and germanium[24] were studied, documenting phenomena of diffusion of atoms, reactivity of step edges, and defect stability. A stable, high-termperature STM enabled in situ "watching" of the dynamic behavior of single

silicon atoms at temperatures up to 850 K.[20] In the field of organics, a smectic-to-isotropic phase transition was induced in a liquid crystal by the scanning action of the STM tip at elevated temperatures (see Section 6).[18]

The dynamics of certain phenomena have also been recorded in the form of "before-and-after" STM images. Examples include the process of graphitization of ethene on a platinum surface[19] (see Section 7.3), layer-by-layer etching of metal chalcogenide surfaces,[25] and domain-boundary shifts of hydrocarbons adsorbed on graphite.[26]

The extension of STM into electrochemistry is resulting in new STM configurations with electrochemically active electrodes as the tunneling tip or planar sample[27–29] In most of these studies, the STM was operated in situ in the electrochemical cell, submerged in electrolyte; for example, in this configuration, the potential-induced reconstruction of a Au (111) surface was observed[29] and assessed as comparable to the reconstructed gold surfaces observed by STM in UHV.[30] In another electrochemical approach, the STM tip was configured as an ultramicroelectrode and thus was called the Scanning Electrochemical Microscope.[28] With this instrument, dynamic processes such as redox reactions of bound enzymes and adsorption isotherms are now undergoing scrutiny on the 100 nm scale by electrochemical reactions between the tip and its surroundings.

1.4. Field Effects

Of tantamount importance is the influence of the applied voltage across the tunnel junction on the material being studied. If one normalizes the applied voltage to laboratory dimensions by simply linearly scaling from the tunneling distance of several angstroms, one arrives at electric field strengths on the order of about $10^8\ Vm^{-1}$ (from potential/distance $\approx 10^{-1}\ V/10^{-9}\ m$). This field strength is of a similar magnitude as those measured in experiments on the Stark effect in spectral hole burning, where a single molecule can experience an effective internal field of $10^8\ Vm^{-1}$ arising from the environment of surrounding molecules.[31] Future work will focus on coupling the approaches of STM and photochemical hole burning.

Other questions which will catalyze future work in this field arise in constructing a model for the environment of the molecule under the STM tip. They involve the issues of conductance and polarizability of the surrounding medium[32, 33] and creation of surface charges and charge trapping on the substrate.[34]

There is no doubt that electric field strengths can be large enough to induce further reactions. Evidence is accumulating for field-induced and field-enhanced effects in the tunnel junction.[35–37] Among these reports is the deposition of gold particles from a gold tip by field evaporation of tip atoms enhanced by the proximity of the substrate;[35] selective ionization and desorption of silicon atoms from a silicon crystal by field evaporation, mediated by the STM tip;[23] and CVD (chemical vapor deposition) lithography in the tunnel junction onto silicon wafers from gold- and tungsten-containing volatile organometallic precursors.[37]

1.5. Difficulties and Artifacts

The apparent success of the STM in obtaining atomically and molecularly resolved images of materials has been accompanied by a fair share of "failures". These failures can be divided into those experiments that give no recognizable results, and those results that mislead. The first category speaks to the practical difficulties in preparing organic samples for scanning; the hurdle is to arrive at a conformation of the molecule on the substrate that is both immobilized and oriented to give identifiable and reproducible images (see Sections 3.2 and 4.1). The present state-of-the-art of interpreting STM images requires that the molecule present a readily recognizable shape to differentiate its outline from random features in the STM image. A goal, of course, is to increase the STM image database with reproducible images of known molecules to the point of bestowing confidence on the identification of "unknowns" or amorphous samples.

The STM's capacity for high resolution is not restricted to the materials intentionally under study. It is also sensitive to

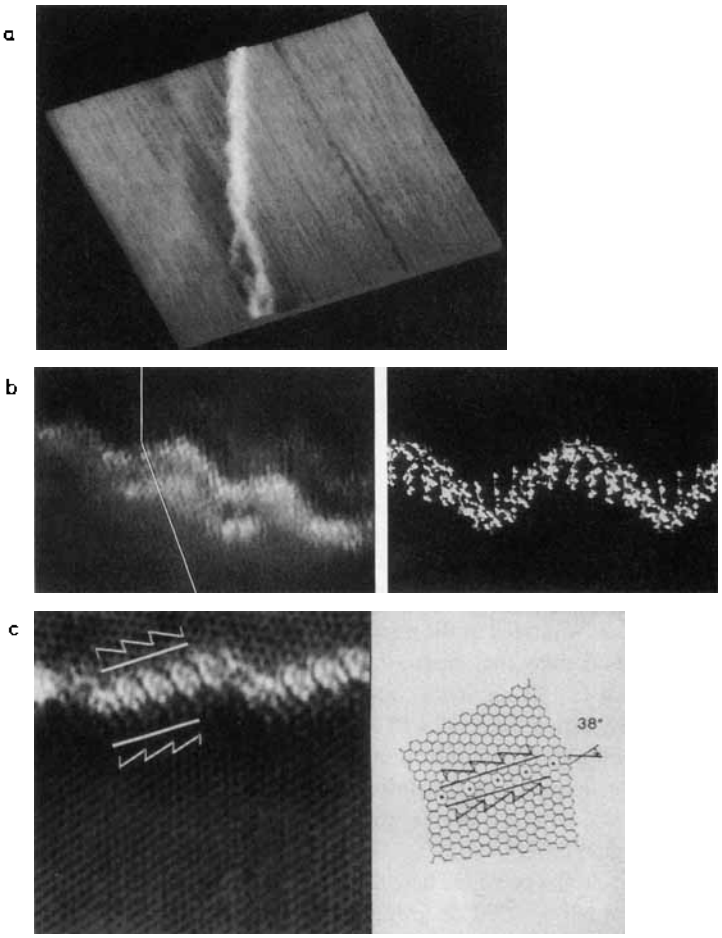

Fig. 3. STM images of features in or on graphite itself that mimic features of macromolecules [39]: a) Scanned area: $190 \times 190\ Å^2$. A grain boundary in graphite, collected with a "faulty" STM tip composed of two minitips that record simultaneously and produce an image which mimics the winding conformation of two DNA strands. b) Scanned area: $110 \times 78\ Å^2$. Left: A grain boundary in graphite. This image resembles a single strand of DNA (scanned with a double tip), which is modeled with a computer molecular graphics program on the right. c) Scanned area: $76 \times 76\ Å^2$. A graphite surface, showing the intersection of two domains with different orientations. The bright polymerlike feature arises from a 38° misorientation between the two domains. Adjacent sketch shows the origin of the defect relative to the graphite lattice vectors.

impurities. The field has been subjected to self-criticism with certain reported results, particularly in the fields of molecular biology[38, 39] and polymer research.[40] This reevaluation resulted from the discovery in several laboratories that substrates *alone* can produce images with features akin to those of molecules.[38–41] These features can be traced to defects or step edges in the substrate lattice, to tip shape, or to spurious impurities (Fig. 3). Additional artifacts can be introduced by the STM tip.[42, 43] A commonly observed one is a convolution of the tip shape into the sample's image. For example, in the case of a "double tip", images of apparent dimer-like features can be traced back to simultaneous imaging of a single surface feature by two points on the STM tip.[44] The healthy effect of these alarms is to compel researchers to be more vigilant in analyzing images and to tighten standards in reporting results.

1.6. Studies of Long-Range Electronic Structure

The STM's sensitivity to electron energy levels is not limited to the atomic scale. It is also capable of detecting electron density distribution over larger regions. A good example is provided by STM images of semiconductors. Unlike metals, in which the electronic state density on the surface correlates closely with the atoms' positions, semiconductors can show preferential localization of states over specific sites in the surface. For example, charge density waves resulting from a Peierls phase transition (a periodic lattice distortion accompanied by a change in band structure) have been recorded on $TaSe_2$ and TaS_2 as a $(\sqrt{13} \times \sqrt{13})$ superlattice of ~ 12.4 Å periodicity superimposed on the atomic lattice periodicity of ~ 3.4 Å.[45]

1.6.1. Graphite

Another example of an electronic superstructure is given by one of the most studied, yet still enigmatic materials, graphite. In Figure 4b of Rb-intercalated graphite (C_8Rb), a (2×2) superlattice of electron distribution is evident, presumably pinned to the underlying dopant ions.[46] Figure 4c demonstrates that the Rb-doped graphite is a dynamic system. Over 15–30 minutes at room temperature, the boundaries have shifted from a (2×2) to a $(\sqrt{3} \times 4)$ pattern, mirroring an equilibration and diffusion of electrons (and possibly ions) with time. All of this information is superimposed on the STM's atom-by-atom map of the carbon lattice of graphite (Figure 4a).

It should be added here that large-scale patterns have been recorded by STM on graphite even in the absence of (intentional) doping agents.[41] Various explanations for these superlattices have been proffered, among which is the rotation of the topmost layer of graphite relative to the stack of layers below.[41]

In scanning the basal plane of graphite, a puzzle of localized electronic structure presents itself: typical STM images of graphite display only every other carbon atom of the hexagonal lattice. In producing these "50 percent" images, the STM is exhibiting its sensitivity to the difference in electronic environments of two carbon sites. It has been proposed that the STM is distinguishing between those carbon atoms (α sites) which are situated directly over a carbon atom in the underlying graphite layer, and those carbon atoms (β sites) which are not (see sketch accompanying Figure 4a). Calculations predict a higher electronic density of states at the Fermi level for β sites than α sites.[47]

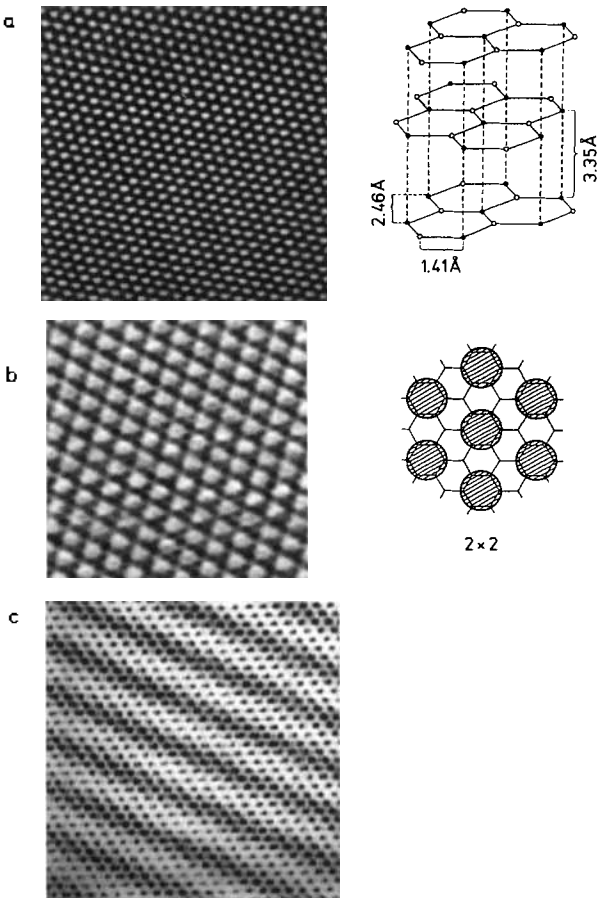

Fig. 4. STM images of the intercalation process in graphite[46]. a) Scanned area 60×60 Å^2. Undoped, pristine graphite, showing the position of every second carbon atom (see text) in a hexagonal pattern with a lattice constant of 2.46 Å. Accompanying sketch shows inter- and intraplanar distances. Dark circles are carbons that lie directly above/below a carbon atom in the adjacent layer; open circles are those carbons that lie above/below the centers of a hexagon in the adjacent layer. b) Scanned area 50×60 Å^2. Rubidium-doped graphite, C_8Rb, immediately after doping. Adjacent sketch shows the placement of the Rb^+ dopant ions relative to the hexagonal graphite lattice. c) Scanned area 50×60 Å^2. The same rubidium-doped graphite, C_8Rb, ~15–30 minutes after doping. The new contrast pattern in the STM image, arising from the intercalated graphite's electronic structure, indicates that a redistribution of electron density has occurred in the interim.

An intriguing recent observation is that from a single sheet of graphite on a platinum crystal (see Section 7.3), *still* only 50% of the graphitic carbon atoms appear in the STM images.[19] This calls into question previous explanations for graphite images that invoked underlying layers of graphite in the electronic interactions that produced the 50% images of the graphite surface.[47]

1.7. The Scanning Tunneling Microscope as a Local Spectroscopic Tool

An extension of scanning tunneling microscopy that still holds much potential is spectroscopy. Several approaches to garnering information about the band structure of samples have already been taken. Some examples are briefly listed here: the density of states of occupied and unoccupied π surface states on a silicon(111) surface was recorded, along with doping-induced shifts in the density of states arising from a shift in the surface Fermi level;[48] also on silicon, entire I–V curves were obtained with spatial resolution in a study of a chemical reaction of the surface with ammonia;[49] STM studies on the compound semiconductors GaAs and $ReSe_2$ illustrated the method of voltage dependent imaging as a way of understanding spatially resolved electronic structure;[50] and the superconducting gap was measured in the type-II superconductor $NbSe_2$ by using a low-temperature STM operating at 1–2 K.[15]

Finally, on a related topic, an STM and a variation, the scanning capacitance microscope, have been used to probe the relaxation of photoexcited carriers on a silicon surface on a picosecond timescale.[51] Using the instrument's tip as a local detector, the investigators have monitored the system's return to equilibrium by measuring surface photovoltage.

2. Scanning Tunneling Microscopy of Inorganic Materials

The image of silicon in Figure 2 is one example of STM studies on inorganic materials. In fact, most STM studies have been performed on surfaces that chemical nomenclature would classify as inorganic[52] (to set them apart from the carbon-containing organic surfaces). They are derived from diverse classes of materials and include single crystal metals, semiconductors, superconductors, and even thin insulating layers. Since the emphasis of this paper is on organic materials, the "inorganic" studies will not be described further, except to provide some examples and references. Examples of metal surface processes that have been investigated by STM include CO-induced structural transformation of platinum,[53] oxidation of copper, [54] electrochemical potential-induced surface reconstruction of gold,[29] and atomic-scale electroplating with copper.[55] Among semiconductors, silicon has been most widely studied,[2, 7, 20, 22, 23, 48, 51, 56] in addition to GaAs,[50, 57] InSb,[58] and $ReSe_2$.[50] Papers on STM studies of oxides and oxide formation deal with SiO_n,[59] ZnO_n,[60] RuO_n,[61] and NiO_n.[62] A review[45] covers the transition metal dichalcogenides $TaSe_2$, TaS_2, $NbSe_2$, VSe_2, $TiSe_2$ and TiS_2. Finally, STM studies on superconductors have detected flux lines and morphological screw dislocations in addition to atomic lattices: $Bi_2Sr_2Ca_1Cu_2O_{8+x}$,[63] $Tl_2Ba_2Ca_1Cu_2O_{8+x}$,[64] $Y_1Ba_2Cu_3O_{7-x}$,[65] and $NbSe_2$.[15]

3. Scanning Tunneling Microscopy of Organic Materials

In STM studies of organic materials, the layer of molecules deposited onto the conducting substrate must be sufficiently thin (≤ 10 Å) to allow electrons to tunnel between the tip and the conducting substrate. Although numerous pathways have been proposed, the actual mechanism for electron transport through these insulating organic materials is still under debate (see Section 3.1). Nonetheless, a rapidly growing list of organic materials is being inspected with the STM, including ordered monolayers,[66, 68] polypeptides,[69] polysaccharides (denatured),[70] conducting polymers,[71] fullerenes,[72] nucleic acid bases,[10, 73] and biological materials[66, 74, 75]. The topic has been covered in several review articles as well.[76]

3.1. Tunneling Mechanism through Organic Materials

Organic materials have been studied by STM predominantly in the form of thin films. Since the bulk organic material itself is (usually) not intrinsically conductive, it is deposited as a thin layer of adsorbate on a conducting substrate, thin enough still to allow electrons to tunnel between the tip and substrate. Thus, the combination of adsorbate and underlying substrate acts as the planar electrode that is raster scanned by the tip. Despite the insulating nature that most organic materials display in bulk, within the tunnel junction they do not impose an impenetrable insulating barrier. The applied voltages in these STM experiments (0.5 to 1.9 eV) are well below the band gaps that characterize most of these organic materials in spectroscopic and electrochemical measurements (5 to 10 eV). Nonetheless, images reflecting the adsorbate's molecular structure are obtained from these samples with the STM.

The mechanism by which images of adsorbates on conducting substrates are obtained is not straightforward. The tunnel junction is made up of three components: two electrodes and the space between them, the latter being occupied by organic molecules in the case of organic adsorbates. Instead of considering these components individually in a theoretical treatment of the tunnel junction, one can consider tunneling into states of a "hybrid" material at this interface. This hybrid is composed of the material in the area of contact between the substrate and the adsorbate, the two being in intimate contact with each other. Furthermore, the hybrid is likely not a single species, but rather a gradient of species as a function of distance from the electrode surface, as in the description of classical boundary conditions. (The difference from the classical situation is that in the case of the tunnel junction's angstrom-scale dimensions, the boundary is the entire reaction site.) This description is not exclusive to the adsorbate–substrate interaction; it also characterizes states on the tip arising from adsorption of organics on the metallic atoms of the tip. The material at these interfaces can be described in analogy to organometallic complexes in which ligands are bonded to metals through bonds such as π bonds, where no formal charge transfer has occurred but both ligand and metal orbitals have been perturbed by each other's presence. In this scenario, tunneling occurs into or out of a hybrid material that has accessible energy levels and an electron distribution that mirrors the adsorbate's molecular structure. A somewhat related mechanism of localized modulation of the substrate's work function by a polarizable

adsorbate has been postulated.[77] Other models or techniques to describe some aspect of electron transport through adsorbates or solvents have been proposed, including atomic and molecular orbital calculations,[9,43,78-80] resonant tunneling,[81,11] deconvolution of tunneling data to recover densities of states,[82] ionic conduction,[83] and favorable molecular configurations that lower the effective barrier height and promote charge exchange.[84]

3.2. Sample Preparation

There is no single set method for preparing organic materials for scanning. The chief requirement is immobilization, that is, the organic adsorbate must remain (or appear to remain) stationary under the scanning probe. Physisorption has been the most common means of attaching molecules to the conductive substrate.[85] Chemisorption has been operative in UHV STM studies on clean metal crystals exposed to submonolayers of organic reactants[19,80,86,87] and on covalently bound thin films, such as thioalkyls on gold.[66]

In most of these STM studies, the organic materials have assembled into ordered planes of molecules, typically thousands of angstroms in dimension, by processes of self-assembly or registration with the substrate. Registration can be viewed in analogy to surface science processes for growth of one material on another.[67] In the example of epitaxial growth, the internal order of an overlayer is dictated by the registry (lateral positions of atoms in a surface) of the underlayer. The growing number of STM results indicate that many organic adsorbates assume an ordered orientation analogous to epitaxial growth when they are absorbed on an ordered substrate. Individual molecules are locked into position by their interaction with the underlying surface and their closely packed lateral neighbors. The images of the planes are then recorded as ordered arrays, consisting of individual molecules as subunits. In some studies of particularly high resolution, molecular subunits of moieties or atoms are observed individually.

Alkylation might enable images of certain organic molecules to be acquired, because alkyl chains energetically favor 2-D crystallization (see Section 7.1). Of course, the steric nature of the parent molecule will have to be taken into account so that the contact area between molecule and surface is not overly compromised.

A major requirement for a good STM substrate, besides conductivity, is flatness. If data are to be recorded on the molecular scale, then the rms (root mean square) roughness of the substrate must be on or below this scale. Layered materials that are easily cleaved afford good surfaces, particularly for sample preparation in air. These include graphite,[88] MoS_2,[89,90], WSe_2,[68e] and mica (metal-coated for conductivity).[91] Other flat, conductive surfaces used for adsorption of organics have included melted gold spheres,[92] PtC-coated glass,[75] metal single crystals and semiconductors.[72c,93] The last two are usually employed under inert (typically vacuum) conditions.

Sample preparation involves primarily introduction of the organic adsorbate to the conductive substrate. Samples have been prepared for scanning by a variety of deposition techniques: sublimation, adsorption from solution, melting, and application of a neat liquid. Regardless of the preparation technique, the STM samples only the layer or layers closest to the interface with the conducting substrate.

Several alternative sample configurations have been found. For example, if the organic layer itself is conductive, it can act as the planar electrode, as in the case of charge-transfer salts[94] and conducting polymers.[71] Additional, puzzling cases have been found in which tunneling has occurred through relatively thick layers (e.g., tens to hundreds of angstroms) of organic material that is traditionally considered electronically insulating, for example, paraffins,[95] Langmuir–Blodgett (LB) films,[68] and lipids.[32] Alternate electron pathways from tip to conductive support have been proposed, such as surface and defect conductivity, to rationalize the tunneling currents detected through these particularly thick organic samples,[96] but to date their mechanism of conductivity and image contrast remains an enigma.

As shown in the above examples, successful imaging can be performed on sample surfaces in a variety of environments, for instance, in vacuum, under solutions, or in air. However, all of these cases share the requirement that the sample consist of or be deposited onto a conducting plane which acts as the second electrode in the tunneling process.

4. Specific Studies: Imaging Liquid Crystals

As mentioned above, the largest number of STM results are emerging from organic adsorbates that are highly ordered on surfaces. Although this might appear to be a restrictive requirement, many molecules in fact take on a degree of intermolecular order when placed on an ordered substrate.[67] For example, acetone and DMSO have provided images with long range order when deposited on graphite.[97] The class of organic molecules that has been most extensively imaged to date is liquid crystals, which are molecules displaying more highly ordered phases than a normal liquid. They are favorable molecules for STM study since they self-organize to form a stable molecular lattice. This lattice is then anchored to the graphite basal plane through surface–adsorbate interactions. STM images depict the highly ordered two-dimensional molecular "crystals" that form on surfaces such as graphite and MoS_2. Following an early success in imaging these materials,[98] many research groups[100] have contributed additional pieces to the puzzle of adsorbate packing on surfaces. The distinct patterns and high degree of order that these molecules display on assembly facilitate identification with the STM. Particularly important for interpreting the images is the differentiation of adsorbate structure from the underlying substrate structure. Their readily identifiable molecular shapes make this discrimination particularly easy for liquid crystals. Furthermore, the diversity of molecular compositions among liquid crystals allows for systematic studies on large numbers of analogues with common core structures. However, as discussed elsewhere in this article (Section 4.4), the role of the underlying substrate in determining adsorbate images can not be underestimated.

4.1. Liquid Crystal Sample Preparation

STM studies of liquid crystals have been performed under ambient conditions on instruments located in standard laboratory environments.

The choice of preparation technique depends, in part, on the phase of the liquid crystal at the experiment's operating temperature (usually room temperature). For example, a material in the smectic or nematic phase at room temperature can be introduced as a neat, macroscopic drop onto the substrate, or a material that is crystalline at room temperature might be melted onto a warmed substrate, followed by slow cooling to the operating temperature.[9, 11] Alternatively, the instrument can be operated at elevated temperatures.[9, 18]

Since present scanning and imaging methods require immobilizing the molecules so that they are not continually displaced by the action of the scanning tip, the characteristic behavior of liquid crystals to form extended ordered phases makes them ideal objects for STM investigations. The ability of the STM to focus on the monolayer(s) closest to the substrate provides new information on the role of the substrate in affecting long- and short-range intermolecular order. The driving force for assembly comes from both intermolecular and adsorbate–substrate interactions; evidence for both is described below.

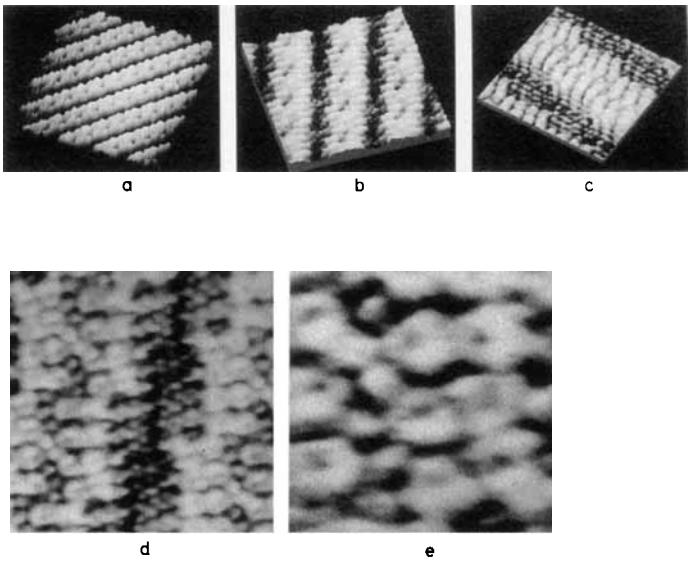

Fig. 5. STM images of 8CB (**1a**) on a graphite substrate [9,98,101]. a) Scanned area 250 × 250 Å^2. Long-range order of smectic planes, side-on. b) Scanned area 114 × 114 Å^2. Smectic layers resolved as rows of molecules. c) Scanned area 57 × 57 Å^2. Cyanobiphenyl headgroup differentiable from alkyl tails. d) Scanned area 57 × 57 Å^2. Individual phenyl groups resolved as rings. e) Scanned area 25 × 25 Å^2. Dipolar alignment seen in interdigitation of CN groups.

4.2. Alkylcyanobiphenyls[*]

The first use of the STM to study the ordering of liquid crystals on graphite was published in 1988.[98] The initial material studied, 4-*n*-octyl-4′-cyanobiphenyl, (8CB, **1a**) has since proven to be especially popular in STM studies of organic adsorbates.[9, 11, 89, 90, 101, 103].

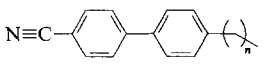

1a, $n = 7$
1b, $n = 9$
1c, $n = 11$
1d, $n = 5$
1e, $n = 6$

STM images of 8CB on the graphite basal plane have been collected on various scales, from large areas (250 × 250 Å^2) to smaller areas (20 × 20 Å^2) (Figs. 5 and 6).[9] In large scans, (Fig. 5a) the long-range ordering of molecules is evidenced as rows, 38 Å wide and extending for hundreds of angstroms. Occasionally these rows terminate at domain boundaries (Fig. 6a, b) that originate either within the organic layer or in the underlying substrate (discussed further in Section 5).[98, 105–107]

On narrowing the scan range to 112 × 112 Å^2 and then to 57 × 57 Å^2, the increased resolution distinguishes rows of parallel molecules (Fig. 5b, c). The cyanobiphenyl head group appears as a brighter oval, while the alkane tail appears as a fainter chain (areas of higher and lower current, respectively. See Section 1.2). Each row interacts in amphiphilic fashion with neighboring rows: head-to-head and tail-to-tail.

From these images it can be seen that the molecules are lying on the graphite surface, as opposed to extending their long axes out normal to the substrate plane, as in LB films (Fig. 7). The rows are subdivided into discrete packets of molecules, each packet, or unit cell, containing eight molecules. Each consecutive unit cell is laterally offset ~7 Å from its neighboring cell within the row. This periodic offset, every eight molecules, is possibly a mechanism by which strain from incommensurate packing is relieved. Close examination of the angle formed between the biphenyl group and the alkyl group reveals a progressive increase in angle, from 12° to 35° on going from the first to the fourth molecule on one side of the unit cell (better discerned in Figure 9). This bond angle could be reflecting, or accommodating, an increasingly unfavorable lattice match between the adsorbate and substrate structures which is relieved every eighth molecule by an offset of the entire unit cell by 7 Å. This is a description of a "molecular solution" to incommensurate packing: the unit cell assembly of eight molecules accommodates the mismatch until a point where the lattice mismatch becomes predominantly unfavorable; then the row is broken, and a new repeat unit of eight molecules is assembled.

In another perspective of a scan area of 57 × 57 Å^2, the individual rings of the biphenyl unit are visible (Fig. 5d). The biphenyl groups appear as pairs of bright rings and the aliphatic tails as darker zig-zag chains of spots, each spot associated with an alternating methylene group (Fig. 5c, d; see also Fig. 9). The position of the cyano group can also be seen as a bright spot off the phenyl ring, *para* to the biphenyl linkage. In images like these of phenyl groups which resolve as actual ringlike structures, the rings are considered to be lying flat on the substrate. This conclusion is supported by comparing intermolecular distances from various images in order to correlate the larger intermolecular distances measured (e.g., 6.5 Å) with flat-lying rings and the smaller inter-

[*] Names like cyanobiphenyls in this section and Sections 4.5.1 and 4.5.2 are treated as trivial names. The IUPAC nomenclature for cyanobiphenyl is biphenylylcyanide or biphenylcarbonitrile.

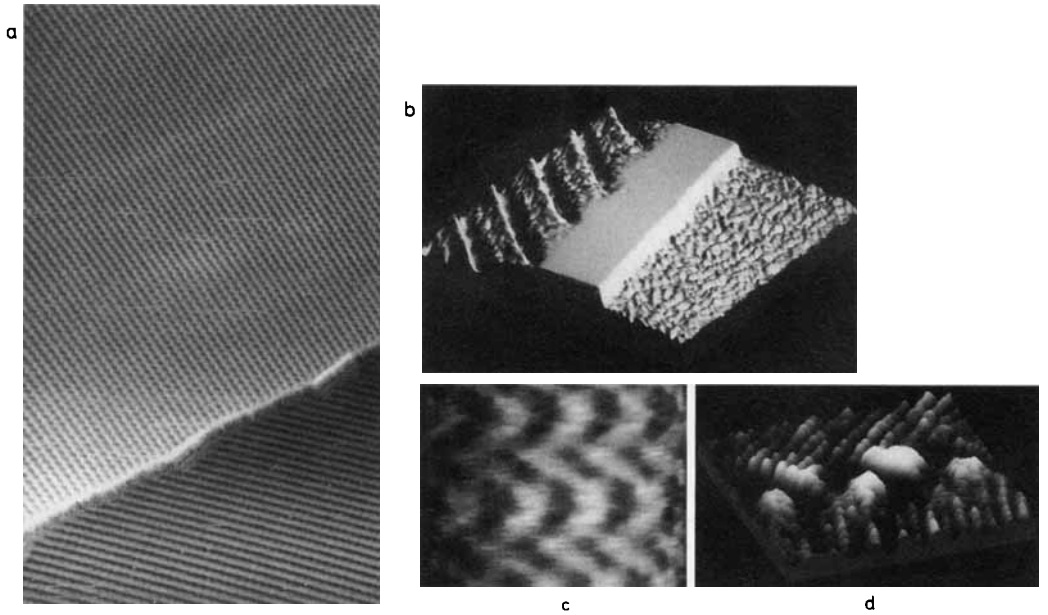

Fig. 6. STM images of boundaries: a) Scanned area 1350×2600 Å^2. 10CB (**1b**) on graphite with a step height of 3.5 Å (one layer of graphite)[106]. b) Scanned area 150×150 Å^2. 8CB (**1a**) on graphite. A smectic plane terminates at a step edge of ~ 10 Å. The contrast in this image is adjusted to optimize resolution of the molecular rows on the upper plane, so the higher central section of the image is out of the range of the STM electronics (see text). The lower plane is shown in Figure 6c, with optimized scanning parameters. c) Scanned area 105×105 Å^2. The lower plane of Figure 6b, brought into better resolution, revealing a moiré pattern for the packing of 8CB on graphite[105]. d) Scanned area 72×72 Å^2. 5CBN (**6**) on graphite. A boundary between two domains oriented 30° to each other[98].

molecular spacings (e.g., 5.5 Å) with tilted rings (the approximate diameter of a phenyl ring is ~ 5.4 Å[108]. This point will be discussed further in the next section with the example of 6CB (**1d**).

One of the most outstanding features of these STM images of 8CB is illustrated in Figure 5e, a scan area focused on the interaction between vicinal headgroups (25×25 Å^2). Figure 5e provides a direct view of interdigitation, where cyano groups are aligned side-by-side yet in opposing directions. This alignment reduces electrostatic repulsions between the dipoles of the cyano groups (Fig. 8) by striving to "cancel" the dipole moment of the nitrile (C≡N) group. Dipolar alignment has been considered a major driving force in the assembly of CN-containing liquid crystals.[109] Now, with the STM, it can actually be visualized, molecule by molecule. In images like that of Figure 5e, the power of the STM as a tool in characterizing intra- and intermolecular order is clearly demonstrated.

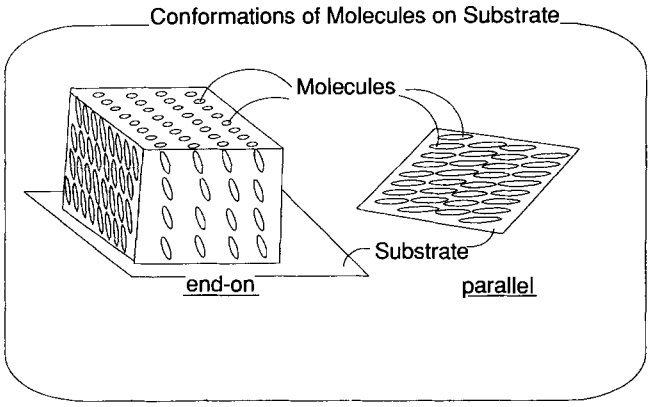

Fig. 7. Schematic representation of molecular orientation on a substrate for the classes of molecules discussed in the text. The end-on conformation is observed in the AFM studies of LB films (see Section 12) and the parallel conformation is recorded in the STM studies of liquid crystals (see Section 4).

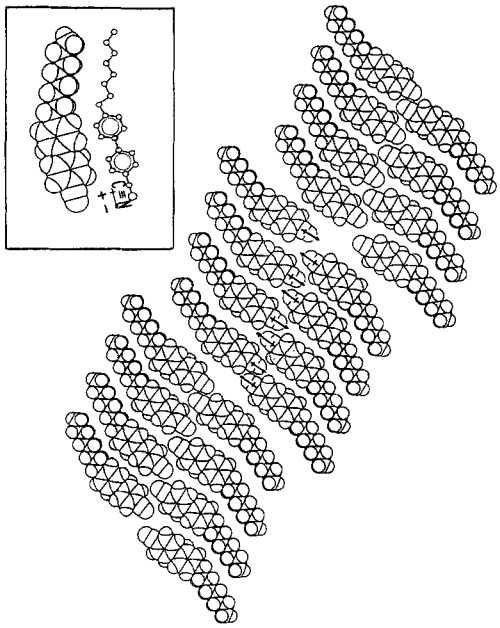

Fig. 8. Cartoon depicting the cyanobiphenyl molecules **1** in the alignment observed in the STM images of Figures 5 and 9. The alignment of nitrile dipoles is highlighted.

4.3. Systematic Studies of Alkylcyanobiphenyl Homologues

The current lack of a definitive theory for STM imaging of organic molecules that was discussed earlier is compensated,

in part, by the ability of organic chemists to make systematic modifications in the molecules and to monitor the changes in the STM images.

Table 1 is a list of organic systems for which images with "submolecular" recognition have been recorded. Prominent among these are liquid crystals, particularly the alkylcyanobiphenyls. Therefore, the following discussion of systematic studies on organic compounds will focus on the alkylcyanobiphenyls by assembling and integrating data from various laboratories worldwide.

Table 1. Representative STM studies on organic materials.

Class	Structure	Reference
liquid crystals	$N\equiv C-C_6H_4-C_6H_4-(CH_2)_xCH_3$, $x = 5 \rightarrow 11$ **1**	[11, 89, 98, 101, 116] [9, 90, 104, 107]
	$N\equiv C-C_6H_4-C_6H_4-OC_4H_9$ **2**	[18, 77]
	$N\equiv C-C_6H_4-(c\text{-}C_6H_{10})-C_5H_{11}$ **6**	[98, 116]
	$N\equiv C-(c\text{-}C_6H_{10})-(c\text{-}C_6H_{10})-C_3H_7$ **3**	[18, 77]
	$C_9H_{19}-C_4N_2H_2-C_6H_4-OR$; $R = C_6H_{13}$, C_9H_{19} **4**, **5**	[18, 77, 116]
	$C_8H_{17}O-C_6H_4-CO_2-C_6H_4-C_6H_4-C(O)C^*H(CH_3)C_6H_{13}$	[99]
n-alkanes	$CH_3(CH_2)_nCH_3$	[12, 118–121]
n-alcohols	$CH_3(CH_2)_nOH$	[12, 120, 121]
carboxylic acids	$CH_3(CH_2)_nCOOH$	[121, 126]
DNA bases	guanine	[10]
	adenine	[73]
	thymine	[73]
arenes	benzene	[86]
	naphthalene	[87]
	phthalocyanine	[80]
	perylene dianhydride	[13]
	p-di(dodecyl)benzene	[121]
	graphite clusters	[18]

4-*n*-Alkyl-4′-cyanobiphenyls **1** (*n*CB, n = number of carbon atoms in the alkyl chain) are well-known and well-used in both academic and industrial studies of liquid crystals. Many of the *n*CB molecules studied to date by STM order similarly on graphite. For example, both decyl and dodecyl derivatives pack in extended rows, approximately two molecules wide (Fig. 9), with the same head-to-head orientation seen for 8CB (Fig. 5).[101] These rows are derived from smectic planes, viewed side-on. Actually, their degree of order is more crystalline than smectic, with very regular correspondence between rows as well as within the rows. Although it is more accurate to refer to the patterns viewed in these pictures as two-dimensional crystals, the tendency has been to borrow nomenclature from the traditional field of liquid crystals in describing molecular orientation in the STM images.

A linear relationship is recorded between increasing alkyl chain length and increasing (smectic) row spacing for cyanobiphenyl derivatives of different alkyl chain lengths (Fig. 9 and 10).[101] For example, the width of the "unit cell" of eight

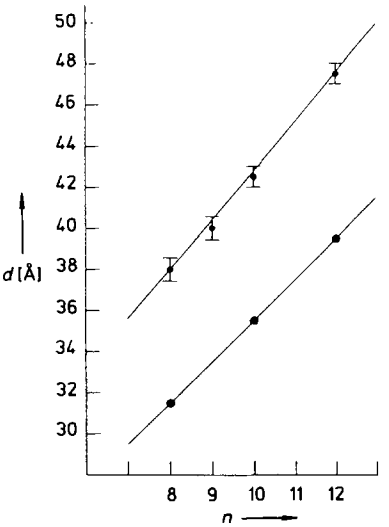

Fig. 10. Dependence of smectic spacing d on number of carbons n in the tail of cyanobiphenyl derivatives **1** from STM measurements (◆, data from [101] and X-ray diffraction (●, data from [109]).

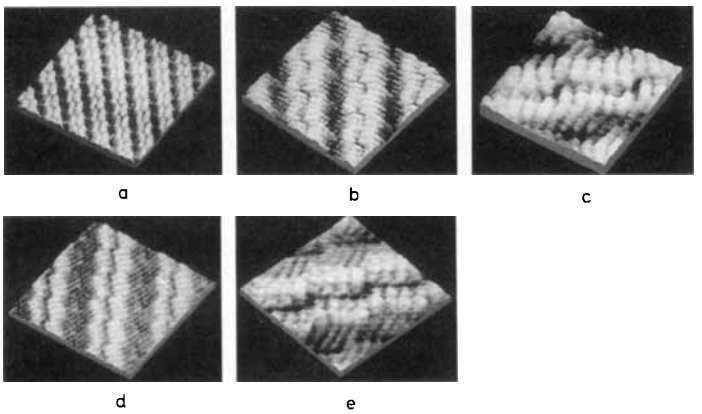

Fig. 9. STM images of 10CB (**1b**) and 12CB (**1c**) on a graphite substrate [9,101]: a) Scanned area 285 × 285 Å². Long-range order of 10CB showing side-on arrangement of smectic planes. b) Scanned area 114 × 114 Å². Smectic layers of 10CB resolved as rows of molecules, with "unit cells" of 10 molecules. c) Scanned area 57 × 57 Å². The changing bond angle between tail and head groups of 10CB is evident on going from the first to the fifth molecule on one side of the unit cell. d) Scanned area 114 × 114 Å². Smectic layers of 12CB resolved as rows of molecules, with "unit cells" of eight molecules. e) Scanned area 57 × 57 Å² 12CB.

molecules in 8CB (**1a**), measured from the terminal methyl group across the interdigitated heads to the terminal methyl group of the molecule opposite, is 38 Å. This width is 43 Å in 10CB (**1b**), the decyl derivative with two more methylene units per molecule, and 47 Å in 12CB (**1c**). The stepwise increases of 4–5 Å on going from octyl to decyl to dodecyl derivatives corresponds to a predictable increase in chain length of 1.25 Å per methylene unit (note: there are two molecular lengths per row width).

Extension of the series in the opposite direction, to shorter chain lengths, results in more changes than just narrowing of the widths of the rows. The hexyl derivative 6CB (**1d**) forms a pattern which resembles that of the higher weight analogues (long rows of parallel molecular axes and head-to-head contact);[104, 110] however, it differs in the orientation of phenyl rings relative to the underlying substrate (Fig. 11). With 6CB, every second biphenyl unit appears to be canted, wedged between its two adjacent biphenyl neighbors, which are lying flat. The hexyl tails in these images are less obvious than their higher molecular weight homologues, perhaps due to thermal motion.

Since 6CB, 8CB, 10CB, and 12CB all share a common head group structure, the cyanobiphenyl unit, one looks to

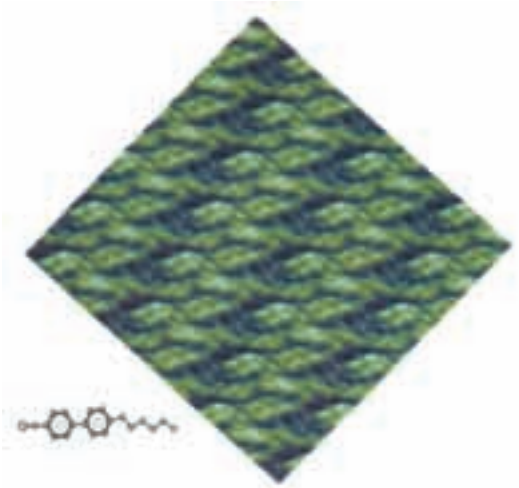

Fig. 11. STM image of 6CB (**1d**) on graphite (scanned area 70×70 Å^2). The ring structure is resolved in every second molecule within a row, which is interpreted as biphenyl groups alternately lying flat or canted relative to the flat, underlying graphite substrate [110].

the influence of the tail in explaining the differences in their images. The principle change on proceeding from the dodecyl (C12) through the decyl (C10) to the octyl (C8), and finally to the hexyl (C6) derivative in the cyanobiphenyl series is the successive shortening of the alkyl component by two methylene units (~ 2.5 Å). Thus, the rather major difference in the position of C6 molecules on the surface indicates that n = hexyl is below a threshold for the alkyl group to influence (to a certain extent) the ordering to the nCB molecules. Apparently, at shorter chain lengths the alkyl component is below the "critical mass" required for strongly directing the intermolecular ordering that is common to 8CB, 10CB, and 12CB on graphite. The lack of well-ordered tails in 6CB perhaps releases the constraint on the phenyl head groups to accommodate alkyl tail intermolecular spacing. (The width of an alkyl chain is ~ 4 Å and that of a flat-lying phenyl ring ~ 5.4 Å.)[108] The interactions of the head groups having little "tail mass" to constrain them could be the dominating driving force in the alternate 6CB packing pattern. In any case, the lower observed order in the hexyl chain is consistent with the fact that 6CB is in the nematic phase at room temperature, the temperature of the STM experiments, whereas the others are in the more highly ordered smectic phases.

An STM study of 7CB, the heptyl derivative **1e**, produces images that reveal an alternative packing for the nCBs on graphite.[111] In fact, this alternative packing pattern has also been observed on rare occasions with 8CB on graphite (Fig. 13) and with some nCBs on other substrates (discussed in full in Section 4.4). The difference in 7CB's behavior could arise from its odd number of carbons in the alkyl moiety, which subjects it to odd/even alternation effects often observed for alkanes.[111] Like 6CB, 7CB is a room-temperature nematic in the bulk.

Finally, meaurements of interlayer spacings in the smectic phase by STM and by X-ray and neutron scattering[109] give different results. On average, this spacing for 8CB, 10CB, and 12CB is 1.2 times greater when measured by STM (see Fig. 10[101, 109]). This discrepancy is not surprising when the molecules' environment is considered: X-rays and neutrons interact with molecules in the bulk, that is, molecules that are surrounded by like molecules.[67] The STM, however, measures molecular spacings in a layer of molecules located at the "edge" of the bulk, at the interface with a substrate. The factor of 1.2 is due to the influence of the interface such as a lattice mismatch with the substrate on the ordering of the proximal organic adsorbate (see Section 4.4). The shorter spacing in the smectic phase detected by X-rays on the bulk crystal could be due to a number of molecular origins, for example, less extended alkyl tails. This example of a notable difference between results obtained from the bulk and from the interface emphasizes that caution must accompany interpretations of STM images. Direct extensions of phenomena and principles from the bulk to the angstrom scale at interfaces could be misleading.

4.4. Substrate Effects

4.4.1. Graphite as a Substrate

Evidence for substrate effects has been provided by the dependence of unit cell size on alkyl chain length in the series 8CB/10CB/12CB. Close inspection of Figure 9, the STM image of the decyl derivative 10CB, reveals a unit cell of ten molecules—two more than in the case of 8CB (Fig. 5). 12CB again conforms to the 8-molecule unit cell of 8CB. This change in unit-cell size on minor modification of the molecular length implies that energies for bonding to the substrate and bonding to nearest neighbor molecules are comparable. Apparently, the favorable energy of intermolecular interaction is offset by an increasing strain between the substrate and adsorbate every eight or ten molecules, depending on the length of the alkyl chains. The difference in adsorption energies between two consecutive members of the series C12-C10-C8-C6 (where the molecular structure of the head group stays fixed and only the length of the alkyl tail changes) can be estimated at 1.6 eV (≈ 160 J and ≈ 38 kcal) per unit cell (for a unit cell of eight molecules) by applying an approximate value for adsorption energy of 0.1 eV (that is, 10 kJ, ≈ 2.4 kcal) per methylene unit.[112, 113]

Among the proposed mechanisms for registration with the substrate are hydrogen atom positioning over graphite rings.[113, 114] Molecular models can be used to illustrate adsorbate registration with the underlying lattice[90], though one must be wary of carrying bulk parameters of bond lengths and angles over to the interface between the metallic surface and hydrocarbon. Relaxation of these parameters to geometries which are distorted from ground state geometries (as known from the bulk or the gas phase) is worth considering, as are interactions with the image dipole in the underlying substrate.

4.4.2. MoS_2 as a Substrate

Dramatic evidence for the influence of the substrate on adsorbate order is provided in the comparison of STM images from two different substrates. The well-studied liquid crystals of type **1** have also been imaged on MoS_2[89, 90], and the resulting molecular patterns have been compared to those on graphite (Fig. 12). Most striking is the deviation in

the case of 8CB. Instead of the long rows of parallel molecules all aligned head-to-head within a row, on MoS_2 a row is made up of a pattern of alternating head-to-head and tail-to-tail parallel dimers. The attractive contacts between rows come from interactions with neighboring rows; this interface also contains alternating head-to-head and tail-to-tail interactions. In Figure 12 details of the molecular structure of 8CB are noticeably less well-resolved than on graphite; although the alkyl and cyanobiphenyl moieties can be distinguished from each other, both lack internal structure.

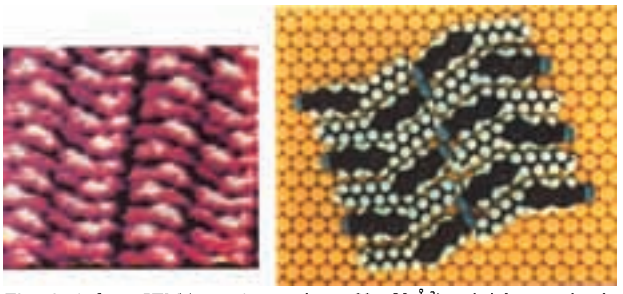

Fig. 12. Left, an STM image (scanned area 80×80 Å^2) and right, a molecular model of 8CB (**1a**) on a MoS_2 substrate [89,90].

10CB and 12CB maintain a similar packing pattern on MoS_2 and graphite.[89,90] For 10CB, where the pattern of molecular packing is the same on these two substrates, the intermolecular spacing within rows of 10CB molecules is greater on MoS_2 than on graphite (5.47 Å vs. 4.25 Å). This is consistent with the larger lattice constant of MoS_2 (3.16 Å compared to graphite's 2.46 Å. See Fig. 4).

It is tempting to conclude from the difference between adsorbate packing patterns on the two substrates that adsorbate–substrate interactions dominate intermolecular ones. In the majority of scans this appears to be so. However, there are a minor number of counter examples which don't allow such a generalization. Figure 12 presents one such exception: 8CB on graphite in the molecular packing pattern more commonly observed on MoS_2.[116] An image of 7CB has also been recorded on graphite with this molecular packing pattern,[111] as noted in the previous section. These exceptions imply that this adsorbate system is in a delicate balance between intermolecular and substrate–adsorbate forces. This balance can be disturbed by obvious influences, such as changing the substrate or the sample's thermal history, as well as by less obvious ones. In some cases the STM image of a "deviant" packing pattern is providing us with a snapshot of a metastable state.

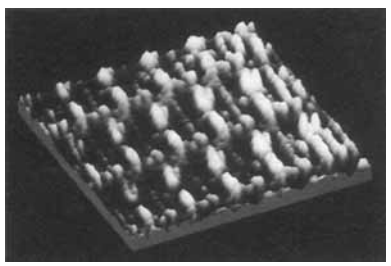

Fig. 13. An STM image [116] of 8CB (**1a**) on graphite (scanned area 105×105 Å^2) with a similar (rare) molecular packing pattern as observed for 8CB on MoS_2 (Fig. 12) [89, 90].

4.5. A Collection of Diverse, Yet Related, Compounds

A few of the other liquid crystals listed in Table 1 are briefly discussed below to point out the effect of modifying chemical functionalities on their STM images.

4.5.1. An Alkoxycyanobiphenyl

In two more examples of liquid crystals containing cyano groups, one (**2**) provides another look at interdigitation of dipoles while the second (**3**) leaves open the provocative question of tunneling mechanisms.[18, 77]

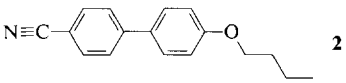

2

In the first, 4-cyano-4′-butoxybiphenyl (4OCB, **2**), the cyanobiphenyl head group is appended to an alkoxy tail four carbons long. The STM images portray parallel molecules arrayed in long rows of head-to-head pairs (Fig. 14a). The cyanobiphenyl head group resolves distinctly as two moieties; its position relative to its opposite neighbor is dictated by the interdigitation of the cyano groups, as discussed earlier for 8CB (see Fig. 5e and 8).

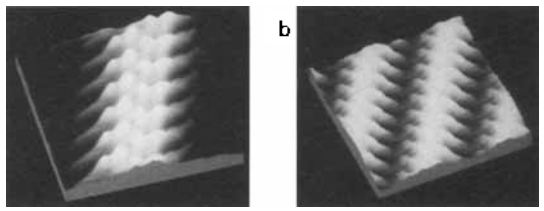

Fig. 14. STM images of two additional CN-containing liquid crystals, 4OCB (**2**) and CCH3 (**3**) on graphite substrates [18,77]. a) 4OCB, scanned area 30×30 Å^2. The biphenyl unit resolves distinctly as two separate features; positioned to reflect the interdigitation of the nitrile groups. b) CCH3, scanned area 52×52 Å^2. The bicyclohexyl and alkyl groups resolve as one continuous feature, again interdigited with the neighboring row. Note that this compound does not contain aromatic structures, so the contrast can not be attributed to transitions in energetically low-lying orbitals of the phenyl unit.

4.5.2. A Cyanobicyclohexyl

The last CN-containing liquid crystal discussed here is 4-(4-*n*-propylcyclohexyl)cyanocyclohexane (CCH3, **3**), a compound containing no aromatic moiety. Instead, it is composed of a core of two cyclohexyl groups with a cyano group at one

3

end and a short propyl tail at the other. The image of a single molecule is diffuse, with no distinction between the straight chain hydrocarbon tail and the hydrocarbon core of two cyclohexane units.[18, 77] Perhaps the conformation of the cyclohexyl groups does not allow continuous and close contact between the atoms of the adsorbate and the substrate, a proposed requisite for atomic resolution of adsorbates. The row width (26 Å) resolves as an interdigitated bilayer, directed by the cyano groups. This particular compound was chosen for study by STM in the series of liquid crystals because it contains no aromatic structures. One hypothesis of tunneling through organic adsorbates invokes accessible energy levels in the HOMO and/or LUMO of the phenyl units;[9, 80] this would be consistent with conduction mechanisms proposed for electronically conducting organic molecules.[115] However, Figure 14b demonstrates that no single, particular moiety is "most" responsible for the conductivity, and therefore the contrast that produced these images.

4.5.3. Phenylpyrimidines

"A long aliphatic chain interrupted by an aromatic core" is one description of the members of the 2-(4-alkoxyphenyl)-5-alkylpyrimidines (PYP). Of the two examples from this family of molecules given here, one yields STM images with a repeat unit of a single row of parallel molecules (PYP909); the other shows a repeat unit of two rows, each of a different molecular orientation (PYP906).[18, 77, 116]

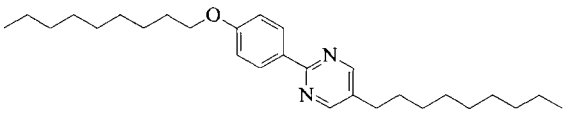

4

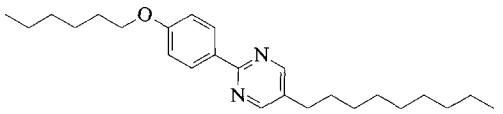

5

2-(4′-Nonyloxyphenyl)-5-nonylpyrimidine (PYP909, **4**) on graphite produces an image of long rows of parallel molecules, in which the bright oval areas correspond to the phenylpyrimidine cores from which the dimmer, aliphatic side chains extend (Fig. 15a). The molecules are spaced about 6 Å apart. The two substituents on the phenylpyrimidine core come off at two different angles from the core (ca. 15° and 0°); the level of resolution in this image does not allow assignment of the alkyl and alkoxy substituents. Interaction between neighboring rows comes from overlap of the alkyl chains, depicted as small areas of increased current; it is not surprising then that the row width is 25 Å, approximately 7 Å shorter than the molecule's extended length, when this overlap is taken into account.

The second member of the phenylpyrimidine series examined, PYP906 (**5**), is three methylene units shorter than PYP909 in the alkoxy sidechain. The STM image ofPYP906 on graphite also shows long rows of parallel molecular axes, adjacent molecules spaced 6 Å apart, and alkyl substituents forming bond angles of 15° and 0° with the core (Fig. 15b). However, the similarities end here. The long-range repeat pattern of the central ring systems of the molecules reveals that the rows are not all identical; rather, they alternate between two distinctive packing patterns, providing a bilayer repeat unit. The long axes of the aromatic cores of one row form an angle of approximately 180° with the axes of the adjacent row. The reason for the different packing mode is not yet known – it could arise from the odd-even chain length effect cited earlier.

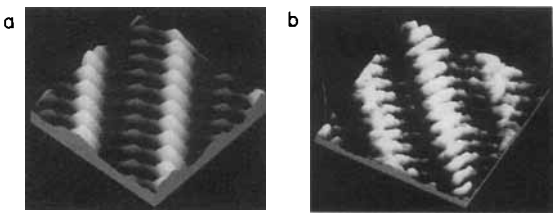

Fig. 15. STM images of PYP 909 (**4**) and PYP 906 (**5**) on graphite substrates [18,77]: a) Scanned area 43 × 52 Å². In PYP 909, the *para*-disubstituted phenylpyrimidine cores resolve as bright ellipses in straight rows. The alkyl and alkoxy substituents resolve as fainter chains that overlap between rows. The overlap appears as a short, brighter stretch in the chain. b) Scanned area 52 × 52 Å². PYP 906 differentiates itself from PYP 909 in the alternating row pattern, constituting a repeat unit of bilayers. The phenylpyrimidine cores of adjacent rows are roughly perpendicular to each other.

The resolution of STM images of liquid crystals **2**–**5** is on the molecular, or submolecular scale, and not on the atomic scale. However, they still serve well in comparative studies to demonstrate the powerful effect that chemical modification can have on the STM images of similar molecules.

5. Domain Boundaries

Domain boundaries are occasionally observed in the STM images of adsorbates,[11, 26, 98, 107] as seen already in the image of 8CB (**1a**) on graphite which shows the termination of smectic rows (Fig. 6b). In this image, the contrast is adjusted to optimize resolution of the molecular rows; consequently, the higher central section of the image is saturated (that is, out of the dynamic range of the electronics) and appears artificially as a flat, white plane. When the contrast is adjusted for the lower plane of Figure 6b, it resolves into a completely different pattern for 8CB (Fig. 6c), best described as a moiré pattern.[116] This moiré pattern is one of several examples of deviations[107, 116] from the more commonly observed 8CB structure of Figure 5. In the examples of Figures 6a and b, the boundary is probably caused by a step edge in the underlying graphite. Figure 6a illustrates this phenomenon in a particularly good, large-scale image of 10CB recorded over thousands of angstroms and interrupted by a step of 3.5 Å, corresponding to a step of graphite one atom high.[106]

The origin of the boundary in Figure 6d is probably not a defect in the underlying substrate, but an impurity in the overlying adsorbate, even though the boundary separates two domains oriented 30° to each other, an angle consistent with (and perhaps directed by) the sixfold symmetry of the under-

lying graphite.[98] The material in this image, 4-(4-*n*-pentylcyclohexyl)benzonitrile (5CBN, **6**) is nematic in the bulk at room temperature.

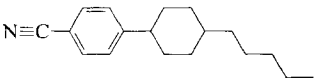

6

Individual molecular moieties are not differentiable in this image, other than a regular 2.5 Å spacing between features, a typical distance recorded by STM from alternating methylene groups in alkanes on graphite. The large islandlike features have not been identified. However, it is clear that they are associated with a boundary from which the molecules align.

In these examples of observed discontinuities, the term "domain boundary" has been borrowed from traditional disciplines, for example surface science. The strict definitions might not carry over to the topographical phenomena observed with the STM; nonetheless, the terms are applied, in part to avoid inventing new terms. In fact, the different domains could be different phases, impurities, or degrees of order in either the substrate or adsorbate.

6. A Phase Transition Viewed on the Angstrom Scale

Liquid crystals are ideally suited to the study of phase transitions since they display distinct phase transitions as a function of temperature. To this end, tunneling microscopes have been modified with variable temperature stages.[9, 11, 18] An example[18] is provided in a study of the aforementioned PYP906 (**5**), a room temperature smectic with an isotropic transition at 72 °C in the bulk. On heating the adsorbed PYP906 to 72 °C, no change in order is observed. Surprisingly on continued heating to temperatures 10–15 °C above this temperature the order is still maintained. At 85 °C the order of the mesophase can be intentionally perturbed by lowering the scanning STM tip. In the absence of the perturbing tip, the molecular order persists, even at these elevated temperatures.

These observations reflect a significant physisorption energy of the molecules to the graphite substrate. They could also be reflecting a more highly ordered phase at this temperature on the ordered substrate than in the corresponding bulk phase, requiring more thermal energy for disruption. Such highly ordered surface phases have been postulated to explain unexpected features in the X-ray reflection data of similar liquid crystal molecules.[117]

The roles of variable temperature and variable pressure are currently creating interest and activity in the field of STM and AFM. Most of the published reports are on metal or semiconductor surfaces in UHV (see Section 1.3). More reports on organic systems are sure to appear in the near future.

7. Studies on Alkanes and Arenes

Since the first liquid crystal images were obtained, several other STM studies have been performed on the smaller molecular moieties that constitute part of the liquid crystals' molecular structure: alkanes and arenes. The alkane samples studied to date have been applied to the substrate either neat or by selective adsorption from a solution with sterically bulky solvent, such as iso-octane. Imaging is performed on a substrate surface immersed in this solution. The studies of arenes have been primarily performed in UHV on monolayer or submonolayer coverages deposited on metal single crystals. These contrasting operating conditions have supplied information consistent with each other and with our previous knowledge or intuition about organic molecules such as straight-chain or cyclic configurations and intramolecular carbon–carbon spacing, discussed below.

7.1. Alkanes

One of the most striking examples of STM imaging of organic monolayers has been with long-chain *n*-alkanes.[12, 118–121] The simple chemical structure of these molecules yields clear-cut STM images of hydrocarbon order and registry on a graphite surface (Fig. 16). The STM images of *n*-alkanes also nicely corroborate the images of the hydrocarbon components in the earlier liquid crystal studies (Fig. 5, 9).[9, 101] Images with atomic resolution show the spacing between parallel molecules of dotriacontane (**7**, $C_{32}H_{66}$) to be 4.5 ± 0.5 Å (Fig. 16)[119].

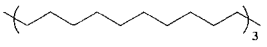

7

Interchain distances measured by X-ray on solid paraffins are in this range; for example, in the triclinic unit cell of *n*-$C_{18}H_{38}$, $a = 4.28$ Å and $b = 4.82$ Å.[125]

In the STM images, within an individual hydrocarbon molecule, interatomic spacings of 2.5 Å are recorded. This value corresponds to the distance between every second carbon in the extended conformation of an *n*-alkane (see diagram in Fig. 16). Which entity gives rise to these 2.5 Å-

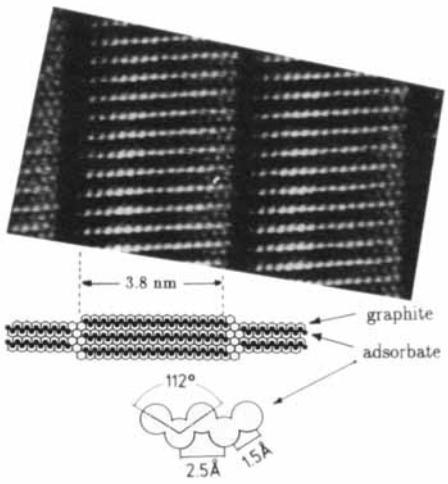

Fig. 16. STM image (scanned area 100 × 60 Å²) and graphic rendition of the paraffin dotriacontane (**7**, $C_{32}H_{66}$) on graphite. The molecules form close-packed rows. The width of the row corresponds to the length of a molecule (38 Å). The bright spots that make up each molecule correspond to every second methylene group, spaced 2.5 Å apart [119].

spaced features is still under debate: their source has been attributed both to tunneling directly into states on the methylene group and to enhanced tunneling into sites in the substrate lattice. (The lattice spacing a_0 of graphite is 2.46 Å; Fig. 4.) In the latter explanation, the hydrocarbon adlayer commensurate with the graphite spacings is assigned the role of enhancing the tunneling current into the substrate.[119] As mentioned in Section 4.4, one should not a priori expect ground state geometry, but rather consider the possibility of distortion of gas-phase or crystalline ground-state geometries on adsorption to the underlying substrate lattice.

In the STM studies on *n*-alkanes, samples are prepared by applying a drop of the alkane either neat or in dilute isooctane and decane solution to the graphite substrate surface. In the latter case, the longer alkanes were preferentially adsorbed out of solution onto the graphite. It has been shown that adsorbed layers of liquids can take on solidlike properties.[127–129] It is likely that the adsorbed hydrocarbon layers imaged with the STM have this solidlike property.

The alkanes of these STM studies are of the higher molecular weight of paraffins. From calorimetric,[114, 122, 123] low energy electron diffraction (LEED),[124] and neutron diffraction studies,[124] they are known to adsorb preferentially from dilute solutions in nonpolar organic solvents to form a close-packed monolayer of molecules oriented with their long axes parallel to the graphite basal plane. The measured heat of adsorption increases uniformly with the chain length and reaches values of 209 kJ mol^{-1} ($\approx$2 eV mol^{-1}, $\approx$50 kcal mol^{-1}) for dotriacontane ($C_{32}H_{66}$, **7**).[114] The calorimetric studies that preceded the STM imaging assigned the overriding driving force for the preferential absorption of long-chain alkanes either to lateral intermolecular interaction or to adsorbate–substrate interaction. In the argument for lateral interaction within the adsorbed layer,[122] the interpretation of the solution isotherms was based on a temperature dependence characteristic of a highly cooperative effect, such as molecular ordering. In the argument for adsorbate–substrate interactions,[114] the driving force for assembly was assigned to the registry of methylene groups in the alkane with underlying hexagons in the graphite. This approach required a compression of the molecular chains by 8–12% relative to their arrangement in the solid paraffin.

Support for the first argument is building from a range of functionalized alkanes whose adsorption behaviors have been studied by both calorimetry and STM. The methods used in the original STM study of alkanes have been applied to imaging functionalized hydrocarbons, such as alcohols,[12, 120, 121] carboxylic acids,[121, 126] and alkylated carbohydrates.[70] Because of the variety of packing modes observed for these assembled adsorbates, the ordering appears to be more a function of the derivatized hydrocarbon's atomic composition than of the unchanging lattice parameter of the underlying graphite.

These STM images of straight-chain hydrocarbons constitute one of the most straight-forward examples of imaging of electric insulators with a current of tunneling electrons.

7.2. Arenes

In the context of modeling catalytically active surfaces, the (111) surface of a crystal of rhodium has been dosed with stoichiometric quantities of benzene and carbon monoxide gases.[130] The surface was then observed in an ultrahigh vacuum instrument.[86] A high-resolution STM image of this system depicts benzene as a three-cornered ring (Fig. 17).

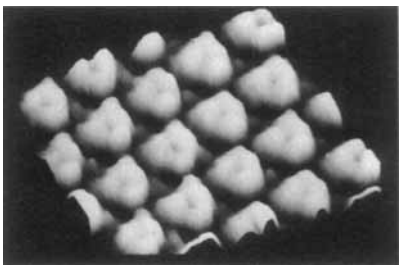

Fig. 17. STM image of benzene and carbon monoxide (molar ratio 1:2) coadsorbed on the (111) surface of a rhodium crystal. The benzene appears as three-cornered rings; the CO, bound end-on through the carbon to the metal surface, is only weakly detected [86].

The triangular shape is ascribed to the registry of the rhodium lattice with three of the benzene's carbons. The barely resolved small bumps in the dark areas at the corners of the benzene rings are assigned to CO; from LEED and high-resolution electron energy loss spectroscopy (HREELS) studies CO is known to bind to the metal end-on through a metal–carbon bond.[130] The current level of understanding of the tunneling mechanism through organic adsorbates cannot yet explain the pronounced difference in tunnel current between the benzene and carbon monoxide molecules. A similar effect has been observed in a combined LEED, X-ray, and STM investigation of perylene dianhydride on graphite.[13] In this study, the tunnel current above the arene rings is distinctly greater than that over the anhydride units; only the perylene moiety is depicted, appearing as a double-ringed structure. The oxygen-containing anhydride eludes detection by STM.

Additional UHV-STM studies of aromatic adsorbates on metals include copper phthalocyanine on copper (100)[80] and naphthalene on platinum (111).[87] In the former, the STM images reveal a submonolayer distribution over the metal surface of isolated phthalocyanine rings with four distinct lobes. In the naphthalene study, three distinct rotational orientations, 120° apart, are observed for the bi-lobed naphthalene molecules on the metal surface.[87] These three orientations correspond to the (3×3) lattice spacing of the platinum substrate.

7.3. The Transformation of Alkenes into Arenes

An outstanding example of the use of the STM to monitor chemical reactions is provided by a study of the reaction pathway from ethene to graphite on a platinum surface.[19] In this study, performed in a variable-temperature UHV apparatus, the individual steps along the thermally activated reaction pathway from adsorption of C_2H_4 on Pt(111) to formation of graphite are documented, including ethylidyne intermediates, 5–10 Å carbon particles, and the penultimate morphology of small islands of graphite (Fig. 18). This particular instrument is capable of high-temperature (to 1070 K) genera-

tion of intermediates and low-temperature (to 180 K) STM documentation of them. The low temperature is necessary to observe the ethene since it converts to ethylidyne at temperatures above 230 K. The low temperature also presumably freezes out low-frequency motions of the ethylidyne surface species that would limit resolution at higher temperatures.

Because of the controlled amounts of ethene used in forming the monolayer on platinum, the final grapite product is one monolayer thick. Several superstructures with periodicities up to 22 Å are evident in the STM images of the final product; they are attributed to the higher order commensurability of the graphite and platinum lattices at different relative rotations (Fig. 18).

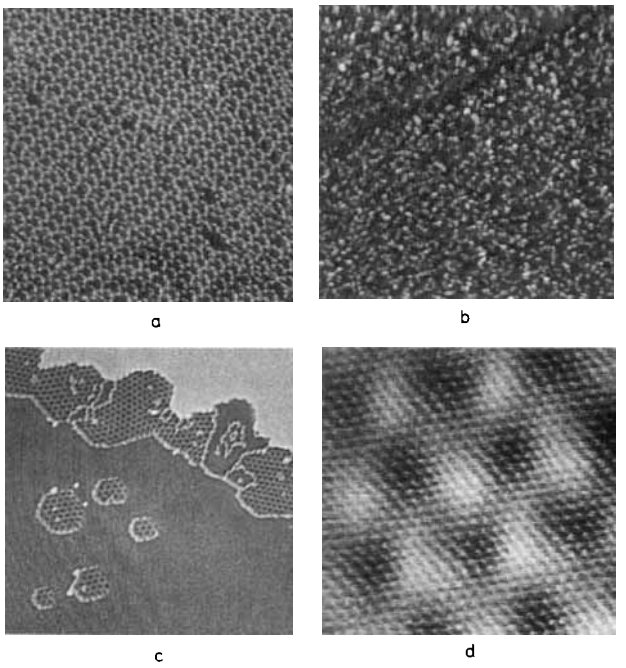

Fig. 18. STM images of stages in the process of graphitization of ethene on a platinum surface[119]. a) Scanned area 200×200 Å^2. A monolayer of ethene adsorbed in a regular pattern on Pt(111), recorded at 150 K. b) Scanned area 1000×1000 Å^2. On heating to 700 K, carbon species have agglomerated into particles, approximately 10–15 Å in diameter, containing no more hydrogen (determined by thermal desorption measurements). A step in the platinum surface runs across the upper left quadrant of the image. Image recorded at room temperature. c) Scanned area 1000×1000 Å^2. Annealing at 900 K creates islands of graphite, 20–30 Å in diameter, on the platinum terraces. Further annealing up to 1230 K results in larger structures of graphite, principally at lower step edges in the platinum, with some large, regularly shaped islands remaining on terraces (this image). Image recorded at room temperature. d) Scanned area 65×65 Å^2. A close-up of a graphite area on the platinum surface. The hexagonal arrangement of dots represent every other carbon in the graphite lattice (see text), spaced with the ~2.5 Å lattice constant of graphite (see Fig. 4). A 22 Å period superstructure is superimposed on the image as a hexagonal array of larger maxima and minima. It arises from the mismatch between the Pt(111) substrate lattice and that of the graphite adlayer.

In the STM images of the single layer of graphite on Pt(111) surfaces, only three of the six carbons in the graphite rings are visible. As mentioned in Section 1.6, this sheds new light onto explanations for the contrast in STM images of bulk graphite; it had been reasoned that only 50% of the carbon in the surface of bulk graphite is imaged due to interactions with the underlying graphite planes.[47] The C_2H_4/Pt(111) STM results now challenge this explanation.

8. Concluding Remarks on the Impact of STM in Chemistry

The physics of tunneling microscopy is contributing to chemistry in diverse ways. The limited width of the probing stream of tunneling electrons (on the order of angstroms) focuses directly on single atoms and the bonds between them. In this way, images are produced of atoms and molecules ranging from phthalocyanines and alkanes to alkylidynes. The method's means of deriving local and direct data from material renders information not only about regular, ordered arrays of atoms and molecules, but also about defects and anomalies in the bonds that hold them together, for instance, missing atoms in a crystal structure and a strained bond angle between a phenyl ring and its alkyl substituent.

For chemistry on the trace level, the STM allows focusing on a single layer of a species or on a submonolayer coverage of adsorbate. These are realms that are often untouchable for they fall below the detection threshold of most techniques.

The STM's role is not limited to passive analysis of chemical species. Instances of STM-induced change, intentional and unintentional, are appearing with increased frequency. The instrument has been used to rearrange matter, atomic unit by atomic unit, to create oligomers from single atoms or molecules, and to induce phase transitions.

Finally, there are many more chemical systems waiting to challenge the technique further into innovative and nonconventional uses. They await the collaboration of imaginative chemists and competent STM instrumentalists.

9. Introduction to the Atomic Force Microscope

Five years after the initial STM experiments, an STM was mounted in a novel configuration above a cantilever.[131] To the underside of the cantilever was mounted a fragment of diamond to act as a stylus. A sample, mounted on a piezo-driven stage, was then placed underneath the stylus and scanned in an x,y plane. Repulsive and attractive interactions between the stylus and the sample surface were registered as deflections in the cantilever and detected quantitatively by the STM positioned above. In this experiment the recording of surface structure directly, with the fine, subnanometer control of piezo devices, was expanded to include nonconducting samples, certainly a larger class of materials than those which conduct. In contrast to the STM, which detects a current of tunneling electrons between a scanning tip and a sample, the atomic force microscope (AFM) does not require electrically conductive surfaces. Instead, the AFM measures interactions between the scanned tip and the surface such as electrostatic, van der Waals, frictional, capillary, and magnetic forces. Like the STM, the measurements are localized, typically over areas nanometers in dimension. For studies of larger scale topographies, the same operating principles are applied with wider range scanners.

The range of samples investigated by AFM to date includes inorganic, organic, and biological materials, as well as technological samples. Since the instrument can be adjusted to sense specific forces, almost no class of materials is unsuitable for this technique, particularly as it is sensitive even to ubiquitous van der Waals forces. The force microscopes have

been adapted for a wide variety of environments as well. For example, since the instrument can operate reliably when the tip–sample interface is submersed in liquid, measurements have been made on operating electrodes,[132] hydrated proteins,[133, 134] and lubricated disks.[135] A number of reviews[2, 136–138, 142] address the rapidly growing presence of AFM in physics and chemistry; some have focused on biology.[74, 139] The emphasis in the following sections is on organic molecules and their assemblies.

To avoid confusion, it should be pointed out that this instrument was originally known as the AFM (*A*tomic *F*orce *M*icroscope). As its use expanded to include detection of forces on various scales and from various different sources, the nomenclature diversified. The term scanning force microscope (SFM) refers to the class of instruments which scan and collect data locally, and includes magnetic force microscopes (MFM), electrostatic force microscopes (EFM), friction force microscopes (FFM), etc. An attempt has been made to simplify the rapidly expanding number of acronyms by creating a generic term for both scanning force and scanning tunneling microscopes: SXM or SPM, for scanning probe microscopes.

9.1. Units

As with the discussion of length units presented earlier in the STM section, it is worthwhile briefly to review units of force and pressure, and their associated energy, before entering into a discussion of techniques that meddle with these parameters.

The force exerted by the measuring AFM probe is in the range of 10^{-9} to 10^{-6} newtons. A newton (N) is the force which imparts to a body of 1 kg an acceleration of 1 $m s^{-2}$. To put this in perspective, an apple on a tree experiences a force due to gravity of about one newton.[140] Typical stylus profilometers exert a force of $\sim 10^{-4}$ N on the samples surface.

An object that is configured as a spring or a cantilever has a characteristic spring constant (or force constant) from which the force exerted by the spring (cantilever) can be calculated. For example, a piece of aluminum foil, cut to a size of 4 mm × 1 mm, has a spring constant of 1 $N m^{-1}$.[142] A Slinky toy displays approximately the same spring constant. A bond between two atoms can be viewed as a spring, with a typical spring constant of 10 $N m^{-1}$ (determined from vibrational frequencies). Typical AFM cantilevers have spring constants of 0.1–100 $N m^{-1}$.

Pressure is defined as a force applied over a certain area: for example, 1 $N m^{-2}$. The units of pressure have the area term already incorporated: 1 $N m^{-2}$ = 1 pascal (Pa) ($\approx 10^{-5}$ atm; $\approx 7.5 \times 10^{-3}$ mmHg). In the AFM experiment, applied pressures are estimated from an approximated contact area between probe and sample: $\sim 10^{-9}$–10^{-8} N applied over 10–100 nm^2 gives pressures of ~10 MPa–1 GPa (10^7–10^9 Pa).

Finally, to put into perspective the magnitude of forces introduced to chemical systems during the AFM measurement, it is worthwhile to include units of energy and their relation to force and pressure. A joule (J) is the amount of energy expended to push with a force of 1 N over one meter (1 J = 1 Nm). (1 cal = 4.18 J and 1 eV corresponds to 100 $kJ mol^{-1}$.) The energy imparted by the AFM probe is estimated to be in the range of ~0.1–50 $kJ mol^{-1}$. This is calculated from a typical force of 10^{-9}–10^{-8} N applied over a vertical distance of 1–5 Å above a surface area of 25–100 nm^2 (which is 100–400 molecules in an end-on orientation with intermolecular spacing of 5 Å, as in Fig. 7 and 22). For comparison, examples of chemical bonding energies include van der Waals (~2 $kJ mol^{-1}$), hydrogen bonding (~20 $kJ mol^{-1}$), and covalent carbon–carbon bonds (~350 $kJ mol^{-1}$).[141]

Evidence that the AFM indeed operates within the energy range of 0.1–50 $kJ mol^{-1}$ is provided in examples of intentional modification of LB films with an AFM: assemblies of molecules held together by van der Waals forces can be disrupted and displaced by careful adjustment of applied forces in this energy range (see Section 12.5).

9.2. The Atomic Force Microscope

The AFM image is a map of information obtained from each point on a surface. A deflection in the cantilever is recorded over each *x,y* coordinate of the sample as it is scanned under the probe, a process which takes from several seconds to several minutes per image, depending on the scan size, the surface roughness, and the resolution. The *x,y*-registered data are then assembled into a 2-D surface map, much as described above for the operation of an STM. However, unlike the STM's map of locally recorded currents, the resulting image from the AFM is a map of forces detected over each point on the sample. This force map is interpreted as a reflection of the surface structure, be it magnetic, electrostatic, or geometric topography.

The contrast in an AFM topography image is based on an arbitrarily chosen gray scale to indicate the relative heights of features on a surface. High features are assigned light shades and low features dark shades. Analogously, in modified AFMs the gray scale is applied to whatever force is being measured; for example, with the friction force microscope, areas of high friction are assigned lighter shades and areas of low friction darker shades.

Forces of 10^{-13} N to 10^{-6} N are measured with the AFM. Typical forces in conventional profilometers are 10^{-4} N over submicron areas. Experimentally, the probing tip is attached to a cantilever-type spring (Fig. 1). During scanning, the tip/cantilever assembly deflects in response to forces sensed in the sample. A displacement sensor then measures those deflections (from the backside of the cantilever) which can be detected down to 10^{-2} Å. The first displacement sensor was based on electron tunneling.[131] Later, sensors based on optical interferometry,[143] optical beam deflection,[144] or capacitance[145] were introduced. Currently the most commonly used force microscope configuration incorporates optical detection methods, which facilitate alignment with the cantilever. Most of the cantilevers and tips in use today are produced by microlithography on silicon or silicon nitride. Cantilevers are designed with dimensions of ~100–200 μm in length, ~10–20 μm in width, and ~0.5 μm in thickness. Tips are typically a few microns high and come to a macroscopic point of ~108°, depending on the manufacturing methods and materials. Different shapes have been made for

special applications, for example, sharp tips are available with angles as steep as $\sim 20°$. The force constant and resonance frequency associated with this configuration are in the range of $\sim 0.1-100$ Newton m^{-1} and $\sim 1-100$ kHz, respectively. To avoid disturbances from ambient vibrations, mechanical designs strive to maximize the resonance frequency of the whole instrument, by keeping the assembled apparatus as compact as possible and incorporating a cantilever with as high a resonance frequency as feasible.

9.3. Coupled Atomic Force and Scanning Tunneling Microsope Measurements

Instruments that are able to measure tunneling current and forces simultaneously are being custom-built.[32, 146] One goal with these instruments is to distinguish between a sample's physical topography and its electronic structure. Another aim is to determine the role of pressure in the tunnel junction in obtaining STM images. Theoretical work is simultaneously evolving on the interrelation between tunneling and force in the several angstrom wide tunnel gap; for example, tip and sample deformation has been proposed in a model of tip–sample forces to explain the (anomolously low) barrier heights recorded in STM measurements.[147] Meanwhile, parallel studies to compare AFM and STM images of the same molecular system are proceeding;[25, 148, 149] for example, similar periodicities have been obtained by the two methods on liquid crystals, although the mechanisms by which the contrasts are generated remain unclear.[149] In a study on metal chalcogenides, AFM measurements have determined that hole formation during STM measurements is caused by abrasion with the scanning probe.[25]

9.4. Variations on the Atomic Force Microscope's Operating Mode

Most scanning force microscopes operate under ambient conditions. More elaborate, customized systems incorporate UHV, controllable atmospheres, variable temperature capabilities, sophisticated software and electronics, and/or interfaces with other analytical instruments. Within the generic description of the operating principles of the scanning force microscope lie many variations. For example, the magnetic force microscope (MFM) incorporates a tip with a magnetic moment so that it can respond to the field of a magnetized sample.[150] In doing so, it can depict magnetic features such as bit patterns. An electrostatic force microscope (EFM) senses isolated charges on surfaces by monitoring the electrostatic interaction between a tip and charged sample.[151] This has proven fruitful, for example, in mapping charge on a polymer surface. In these latter two cases, the detection scheme of the AFM is modified to detect the longer range magnetic and electrostatic forces. Instead of measuring single deflections of a cantilever, a vibrating cantilever is used and the change in the resonance frequency of the cantilever is measured as it interacts with the field imposed by the sample. In this mode, the probe is not in physical contact with the sample, and resolution is possibly more limited, for example, to tens of nanometers.[152] For higher resolution studies, short range forces are detected by operating the AFM in the contact mode. In this mode, repulsive contact forces between tip and sample are monitored. Although the dimensions of the tip are nearly macroscopic (terminating tip radius of ~ 300 Å, height of ~ 3 μm), an attempt is made to limit the point of contact with the sample by applying very small forces to the tip ($\sim 10^{-10}$–10^{-8} N).

9.5. Topography Measurements: Principles

As with scanning tunneling microscopy on organic molecules, theoretical explanations for the rapidly expanding body of AFM experimental results are evolving simultaneously.[153, 154] Models of the interface between the AFM probe and the sample surface include interrelated surface and intermolecular forces.[138, 155] The former are classified under the phenomena of capillary action, adhesion, friction, etc. The latter are derived from attractive van der Waals and repulsive interactions. Ultimately, at the scale that most contact AFM measurements are made, these two regimes merge.

The AFM can be operated in the noncontact, attractive mode or in the contact, repulsive mode. Most of the topographic images of organic systems collected with the AFM have been recorded in the contact mode. Under these conditions, the repulsive part of the Lennard–Jones potential describes the interaction of two bodies as they are brought within several angstroms contact, the model gap for the interface between the AFM probe and the sample surface. The $1/r^{12}$ distance dependence of this repulsion forms the basis for the AFM's ability to detect force gradients over small intermolecular distances. Several calculations have been performed, based on idealized tip and surface interfaces of several atoms,[153] and extending to larger areas over which an exchange of tip and substrate atoms is proposed during plastic deformation.[154] Much work remains to be done in the field.

As with the STM, the possibility that the measuring instrument itself induces the observed results must also be considered, since the estimated, locally applied pressures can be as high as a gigapascal (see Section 9.1). This value is comparable to hydrogen bonding of ~ 20 kJ mol^{-1} and attractive van der Waals forces (dispersion forces, ~ 2 kJ mol^{-1}) that hold molecules together in non-covalent assemblies.[141] Indeed, examples of surface modification with the AFM are increasing, particularly in studies aimed at microlithography (see Section 12.5).

9.6. A Related Technique: Surface Force Apparatus

Finally, it is important to relate the results from the atomic force microscope to those of the surface force apparatus (SFA) since they arise from the same or similar phenomena.[108, 128, 129] The SFA is an arrangement of two cylindrical surfaces placed at right angles to each other to provide a molecularly smooth, small contact area (10^{-4}–10^{-1} mm^2). Samples are placed within this juncture and the force between the two surfaces is measured interferometrically as a function of the thickness of material between them. These

measurements enable the tracking of many properties down to the molecular scale where interesting nonlinearities can occur. For example, when the viscosity of a liquid is studied from the bulk down to the monolayer, a transition to solid-like behavior can be detected for the last layers.[129] Results like these serve to reinforce the caveat about linear scaling of properties from the bulk to the monolayer.

10. Atomic Force Microscopy of Inorganic Materials

As in the case of STM, the preponderance of AFM studies has been performed on materials which would be classified as inorganic, although this is apt to change since AFM is compatible with an aqueous (biological) environment. Crystal lattice parametrs have been measured directly on free-standing, macroscopic crystals of salts and minerals. In the examples of NaCl,[156] LiF,[157] and AgBr,[158] the images are composed of regularly spaced features (4.0, 2.8, and 4.1 Å respectively) corresponding to every second atom in the lattice (Figure 19); that is, the observed periodicity indicates that the instrument is sensitive to only one of the two atomic species. In the AFM images of these ionic crystals, the features have been assigned to the larger of the two ions in the salt (Cl^- in NaCl, F^- in LiF, and Br^- in AgBr) based on a contact hard-sphere model of the crystal surfaces.[157] In contrast, both the anion and cation were observed in an AFM image of KBr performed in a UHV instrument run at liquid helium temperatures.[159]

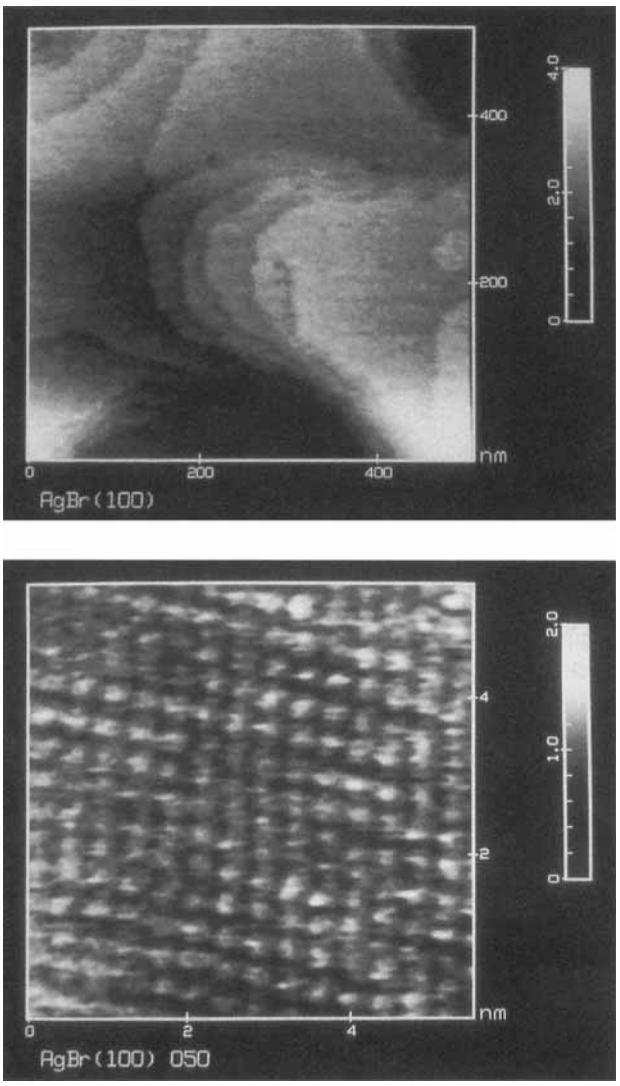

Fig. 19. AFM images of AgBr(100)[158]: a) Scanned area 500×500 nm^2. Crystal surface containing monoatomic steps (2.9 Å) and a screw dislocation (center). b) Scanned area 6×6 nm^2. Crystal lattice with spacing between repeated features of 4.1 Å, corresponding to every second ion in the crystal (presumably the bromine ions, see text).

AFM images of minerals such as the layered compounds mica[160] and molybdenite (MoS_2)[161, 162] contain interatomic spacings corresponding to the elements in the topmost layer of the cleaved samples. The upper layer imaged in MoS_2 was of sulfur atoms, while in mica it was of SiO_4 tetrahedra.

Atomic corrugation has also been observed in the AFM images of graphite,[162, 163] a layered material which has found great popularity as a substrate for STM imaging of organics.[76] AFM studies on the etching process in metal chalcogenides (e.g., $SnSe_2$, $NbSe_2$, TaS_2, SnS_2) correlate etch rates with applied forces and humidity.[25] The same study attributes surface modification to physical tip–sample contact in prior STM studies on the same materials.

Other AFM studies on inorganic materials include boron nitride,[162] $TaSe_2$,[164] copper on gold,[132] and $ReSe_2$.[51]

11. Atomic Force Microscopy of Organic Materials

The first AFM studies of organic maerials were mainly on macromolecules, for example, fibrin[139] and polydiacetylenes.[165] In some cases, periodicities consistent with the intermolecular distances between smaller molecules (around 5 Å) have been observed, for example in crystals of the amino acid leucine.[166] Only recently have AFM results achieved the resolution needed to distinguish between different molecular orientations[133, 167] or to provide lattice information not already available by other methods.[168]

In the first example, a phospholipid membrane has produced images composed of repeat units with aspect ratios that correspond to the dimensions of individual headgroups (2 Å × 5 Å).[133] This reconstituted lipid is deposited on alkylated mica for scanning and maintained in an aqueous environment during the scanning.

The next examples have been generated in the context of addressing surface reconstructions in organic molecular crystals. Surface photonic processes, excitons, and nonlinear behavior have been implicated in investigations into the physics of organic solids; however, physical sources for these phenomena elude detection, in part due to difficulties in limiting sampling depths to the top layer(s) of molecules in crystals. A comparative study on several molecular crystals has demonstrated the AFM's ability to distinguish a reconstructed arrangement of atoms in a crystal surface from the crystal's internal atomic structure.[167, 168] In the course of a study of fused arenes, the surface of freshly cleaved crystals of tetracene (**8**) was shown to have lattice spacings that cor-

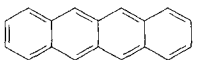

8

Table 2. Crystal lattice parameters of tetracene (**8**) and pyrene (**9**) from X-ray diffraction and AFM measurements [a].

Cmpd	Length of sides [Å]			Angles [°]		
	a	*b*	*c*	α	β	γ
8	7.90	6.03	13.53	100.3	113.2	86.3
	(8.0)	(6.3)				(85.5)
9	13.65	9.26	8.47	90.0	100.28	90
	(6.2)	(6.0)				(58)

[a] X-ray diffraction data from ref. [169, 170]. AFM data in parentheses; from [167, 168].

respond to their bulk crystal parameters.[167] Table 2 contains the X-ray and AFM data for tetracene. In addition to confirming that the intermolecular spacing on the surface is the same as in the bulk,[169] the AFM image of the surface of tetracene also distinguishes between the two translationally nonequivalent molecules that make up the tetracene unit cell (Fig. 20). This ability arises from the interaction of the

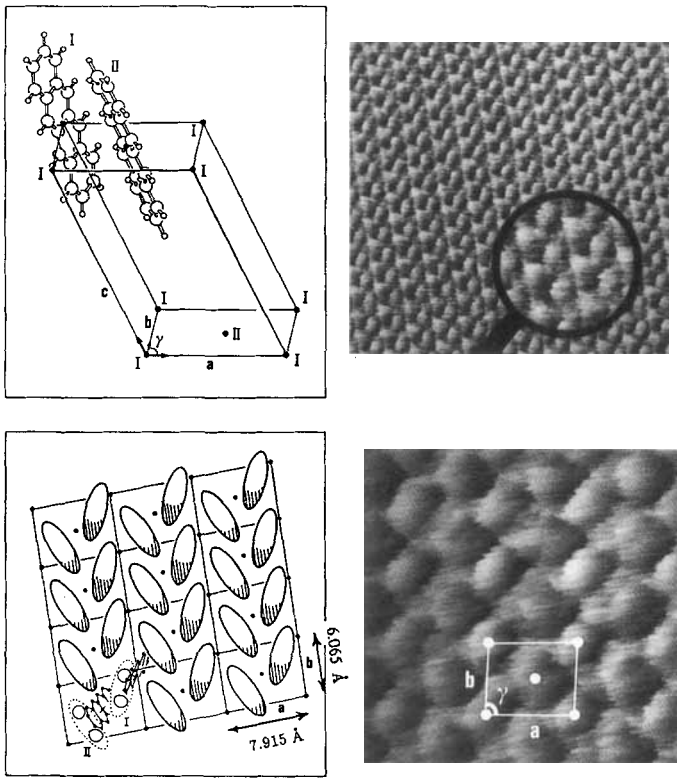

Fig. 20. AFM images and crystal packing of tetracene (**8**)[167]. Top: Scanned area 100×100 Å^2. The scanned crystal surface is the *a,b* cleavage plane. Rows are 8 Å wide, corresponding to the width of the unit cell. The magnified circle is an area of ~ 20 Å in diameter. Bottom: Scanned area 30×30 Å^2. The unit cell parameters measured on the surface of the crystal, marked on the image, correspond to those of the bulk (see Table 2).

AFM probe with the two different orientations of the molecules in the surface of the unit cell: within the unit cell, they are not parallel to each other (the planes of their σ electron systems are roughly perpendicular) and their short axes intersect with the imaged *a,b* cleavage plane at two different angles. The AFM probe therefore "sees" different surface orientations for the two tetracene molecules: not only are their broad, flat σ systems not parallel to one another, but the molecules are tilted in such a way that their short axes present different angles to the scanned cleavage plane.

However, pyrene (**9**), a different tetracyclic arene, shows no such correspondence between the surface and bulk structure.[168] In the bulk, pyrene molecules exist in pairs with

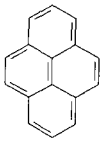

9

lattice spacing of 8.47 Å and 9.26 Å in the *a,b* plane (Table 2). The two molecules of a dimer are separated by 3.5 Å.[170] AFM images of the surface of a pyrene crystal indicate no evidence of dimers; instead, the surface consists of monomers regularly spaced 6.0 ± 0.3 Å apart (Fig. 21, Table 2). Confirmation that the features are monomers is provided by the density of molecules on the surface: it corresponds fairly well to the surface density of molecules in the dimeric packing pattern. This change in molecular spacing on the surface is perhaps not surprising when the dielectric environment of the surface layer is compared to that of an internal, bulk site. Nonetheless, at present it is difficult to predict when and how a surface will reconstruct.[67] The bulk crystal data, together with the final surface configuration of molecules provided by the AFM, present us with the initial and final points of a physical process. Efforts are currently under way to model the pathway inbetween.

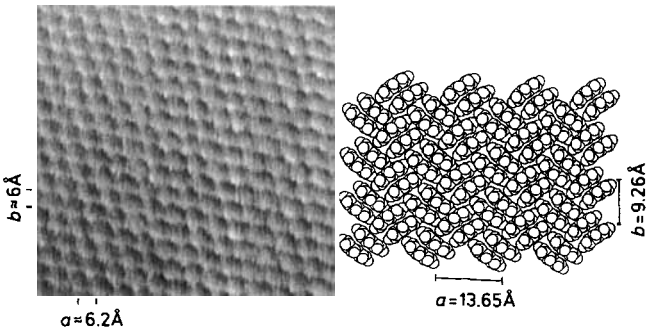

Fig. 21. AFM image (scanned area 100×100 Å^2) and bulk crystal structure of pyrene (**9**) [168,170]. Left: The scanned crystal surface is the *a,b* cleavage plane; however, the unit cell parameters measured on the surface of the crystal (marked on the image) do not correspond to those of the bulk. The surface density of the regularly spaced features in the image support an assignment of monomers to the surface species. Surface area per molecule ≈ 37 Å^2. The bulk crystal packing of dimers oriented perpendicular to one another, and lattice parameters are shown on the right for comparison [168,170]. Surface area per molecule ≈ 32 Å^2.

12. Specific Study: Atomic Force Microscopy on Organic Thin Films

Reports of tailored organic films are appearing with increasing frequency in the technical literature.[171] Often the films serve as models for more complex systems such as idealized membranes for protein adsorption and selective permeation. They are also used increasingly as molecularly

engineered systems for 2-D interfacial processes, for example, nonlinear optics and microlithography.

Films composed of amphiphilic molecules assembled into a high degree of order occur naturally in biological systems in the forms of membranes and micelles. Laboratory-made films are currently synthesized by a variety of techniques, including self-assembly and externally directed, ordered adsorption. Prominent among tailored films are Langmuir–Blodgett (LB) films: they are 3-D assemblies of 2-D ordered layers of amphiphilic molecules that can be made with high precision and reliability (Fig. 23).[171] Briefly, the LB technique involves orientation of amphiphilic molecules at a hydrophobic/hydrophilic interface on a fluid medium, followed by an orderly transfer of the molecules, in the form of a monolayer, from the fluid surface onto a dipped, solid substrate. Repeated dipping yields films of controlled numbers of monolayers. LEED, HREELS, RHEED (reflection high energy electron diffraction) and ATR-FTIR (attenuated total reflectance fourier transform infrared spectroscopy) are among the many analytical techniques that have provided structural information on the lattice structure of the films, such as orientations of molecular axes relative to the substrate plane and interplanar spacings.[171]

However, gaps exist in our knowledge of molecular systems on scales inaccessible to conventional analytical techniques. For example, some features go undetected because the samples are not crystalline or are too fragile to withstand sample preparation or incident radiation.[172] Furthermore, and perhaps most importantly, features that are randomly distributed throughout a sample elude detection by methods which average over different locations on a sample. With X-rays and related techniques, data is provided primarily from the ordered structures of crystalline domains.

The AFM shares with the STM the ability to access information on a very local and direct scale, over very small dimensions, from microns to angstroms. In doing so, AFM studies have provided thin film information on dimensions not available before, for example, degrees of coverage as manifested by boundaries, holes, and islands; step-heights in samples of mixed monolayers, bilayers, and multilayers; and well-defined interfaces, not only between films and air or substrates, but also between domains within multicomponent films (Section 12.8).

The development of the force microscope has benefited from the organic thin-film samples as well. These have not only provided the AFM a topography to study on both the atomic and macromolecular scale, but have also served as compliant objects for localized manipulation and friction studies. Such studies will also be discussed below.

12.1. Thin Langmuir–Blodgett films: a Bilayer or Two of Cadmium Arachidate

One of the more commonly studied Langmuir–Blodgett films is composed of the cadmium salt of arachidic acid (icosanoic acid, **10a**). For these particular AFM studies, the LB films were prepared as follows:[173] Silicon(111) wafer substrates are pretreated[173] to render their surfaces hydrophobic.[174] The fatty acid salt is deposited onto the silicon

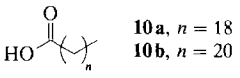

10a, $n = 18$
10b, $n = 20$

substrate during the downstroke into the LB bath with the alkyl "tails" directed toward the hydrophobized surface and the carboxylate head groups away from the surface. On the upstroke of the dipping process, a second monolayer is deposited onto the first to give a bilayer film whose carboxylate headgroups are oriented toward the center of the film, and alkyl tails are oriented toward the two interfaces, with air and with the substrate (Fig. 22). The thickness of this film corresponds to approximately twice the length of the arachidate molecule (~54 Å). Double bilayers of ~108 Å thickness are obtained by performing the above process twice.

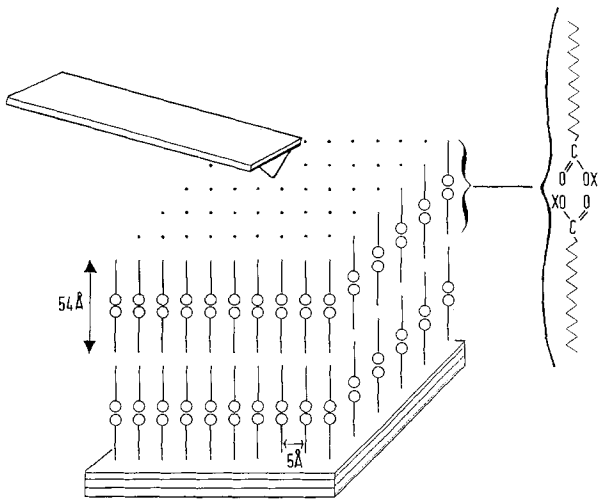

Fig. 22. Schematic representation of a Langmuir–Blodgett film being scanned by an AFM probe. The pictured film is a double bilayer of cadmium arachidate (**10a**) deposited onto a hydrophobized silicon wafer [175,189]. X = Cd, second anion omitted.

AFM images of the LB films of cadmium arachidate produced in this manner contain large expanses of smooth film over 95% of the sample surface (Fig. 23. See also

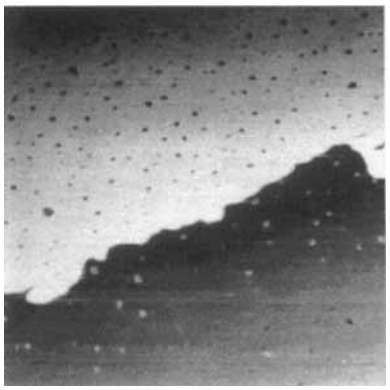

Fig. 23. AFM image (scanned area $3.5 \times 3.5\ \mu m^2$) of the edge of a double bilayer cadmium arachidate film. The flat terraces extend over microns, and cover ~90% of the substrate. A step height is 54 Å which corresponds to a bilayer. The steps are curved and have no preferential orientation. On the flat terraces pores are visible, and on the silicon substrate round islands are visible [175,177,186].

Fig. 26a).[175–177] These planes extend over hundreds of microns. The contours of the organic film on the inorganic substrate can be likened to a coastline. Film edges take on the appearance of geologists' topographical maps, with islands, inlets, peninsulas, and bays reflecting a fluid origin (Fig. 24). The similarity between geography over thousands of kilometers and over thousands of angstroms illustrates the fractal character of nature.

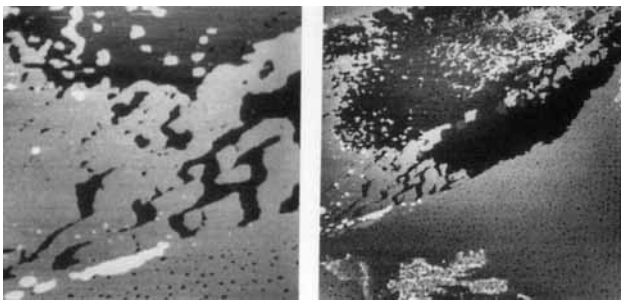

Fig. 24. Additional AFM images of the double bilayer cadmium arachidate films of Figure 23, showing long-range morphology and film boundaries. Islands of material scattered on the film's flat terraces have heights that are also of bilayer dimensions (54 Å). The contours of the film edges resemble coastlines viewed from an airplane [175, 177]. The scanned area in a) is $3.5 \times 3.5\ \mu m^2$ and in b) $10 \times 10\ \mu m^2$.

Step heights of both 54 Å and 108 Å can be observed, corresponding to single and double bilayers. This is particularly visible in larger scale images obtained on films with regions of incomplete bilayer coverage. Single monolayer steps of 27 Å are measured at single bilayer edges and in experiments where a bilayer has been intentionally "peeled apart" with the AFM probe (see Section 12.5).

Interspersed in the large, flat planes of cadmium arachidate are pores of one bilayer depth and 20–100 nm diameter (Fig. 23 and 24). On double bilayer films, pores are a bilayer deep, although occasionally a double bilayer depth is observed. These pores are difficult to detect with other analytical methods because they are randomly distributed; methods which sample over large dimensions in general average signals from regular film features, thereby producing data dominated by signals from the preponderance of ordered molecules. In the particular cadmium arachidate system studied, the total combined area of holes constitutes $\leq 10\%$ of the film's surface. Holes have been found in the surfaces of other Langmuir–Blodgett films, although hole-free films have also been observed (see Sections 12.4 and 12.8). The origin of these localized voids is currently not known. They could reflect bath composition, transferred to the films on deposition. Or they could form subsequent to deposition, for example, as a mechanism to lower surface energy at the interface between the ordered film structure and air or substrate. To resolve these issues, systematic studies on film formation and stability must be pursued. There is also plenty of opportunity here for studying the fundamental properties of 2-D crystals, and for performing molecular dynamics calculations.

12.1.1. Molecular Resolution

On increasing magnification of one of the broad, flat planes of cadmium arachidate, resolution on the scale of individual molecules becomes possible (Fig. 25).[175] Regularly spaced features, ~5 Å apart, are assigned to the methyl termini of the close-packed alkyl tails. The degree of accuracy of these measurements ($\pm 5\%$) does not allow a more rigorous assignment of space group to the observed pseudo-hexagonal packing of molecules. In fact, since the radius of the effective probing stylus tip probably does not lie in the subnanometer range, the ~5 Å molecular spacing is likely a local averaging over many angstroms, that is, over several molecules. However, observation of this 5 Å periodicity does indicate a degree of order in the films on the molecular scale. The packing density (area per molecule) of $24 \pm 2\ Å^2$ is in reasonable agreement with literature values for ordered cadmium arachidate films on metal single crystals (measured by LEED).[178] It is also in qualitative agreement with STM images recorded on LB films on ordered substrates of graphite and WS_2.[68] Apparently, the lack of local order in the surface of the silicon substrate does not prevent ordering of the molecules into regular arrays close to the absorbate–substrate interface; dense and regular packing is recorded on the surface of a single bilayer, at a distance of ~54 Å from the silicon substrate. This observation of long-range order in extremely thin LB films on an amorphous surface demonstrates that the driving force for ordering from intermolecular interactions is great enough to overcome the influence of disorder from the underlying substrate surface.

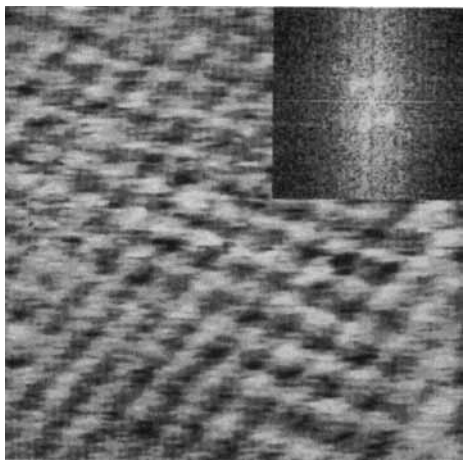

Fig. 25. Higher resolution AFM image, (scanned area $53 \times 51\ Å^2$), of the double bilayer cadmium arachidate film of Figure 23, together with its 2-D fast Fourier transform. The spacing between the protrusions is ~5 Å, which corresponds well to the intermolecular spacing of the alkyl tails (see Fig. 22). Another example of atomic resolution on an LB film is given in Figure 28 [175, 177].

12.2. A Thicker Langmuir–Blodgett film: Cadmium Behenate

LB films prepared from another fatty acid, the cadmium salt of behenic acid (**10b**) have also been examined by

AFM.[179] The cadmium behenate films are thicker than those of cadmium arachidate discussed above: seven bilayers deposited on a hydrophobized silicon substrate.[180] Again, widespread, flat, close-packed films are recorded over a hundred microns (Fig. 26a). In a scan of $100 \times 100\,\mu m$, most evident in the overall flat film are large-scale, irregular "cracks", 10–40 μm long, and all oriented in the same direction. At higher magnification ($5 \times 5\,\mu m$) these cracks turn out to be shallow, only a bilayer deep and 0.5–1 μm wide (Fig. 26b). The bottom surface of a crack shows a similar

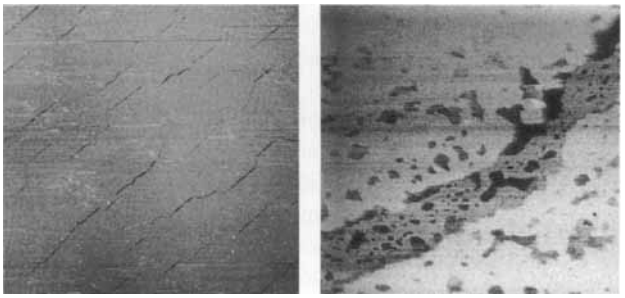

Fig. 26. AFM images of a Langmuir–Blodgett film composed of seven bilayers of cadmium behenate (**10b**) on hydrophobized silicon [180]. a) Scanned area $100 \times 100\,\mu m^2$. A long-range, very flat morphology is observed, interrupted regularly with nearly unidirectional cracks. b) Scanned area $5 \times 5\,\mu m^2$. Increased resolution of the cracks show them to be only one bilayer deep. The scattering of bilayer-deep holes recorded in this film is often observed by AFM in LB films [177, 182].

morphology of distributed, irregular holes as the upper surface of the film. The origin of these cracks is not yet known. They could arise during deposition, or later on aging or sample handling.

12.3. A Comparative Film Quality Study on Langmuir–Blodgett films of Liquid Crystals

In a preliminary study comparing the surface structure of two films composed of the same molecules but of different thicknesses, the use of the AFM in tracking qualitative film differences has been demonstrated. The LB technique used in preparing the previous two examples of fatty acid films has been applied to another class of molecules, liquid crystalline alkoxybiphenylesters.[181] Crystalline films of the heptoxy derivative, 4′-*n*-heptoxybiphenyl carboxylic acid methyl ester (**11**), on hydrophobized silicon have been made for AFM studies in two thicknesses: 12 and 20 bilayers (~480 Å and ~800 Å, respectively).[179, 182]

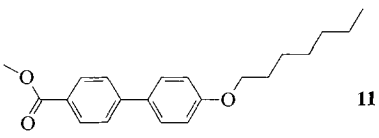

11

Differences in the AFM images from these two samples allow comparison of relative film quality (Fig. 27). For example, a $5 \times 5\,\mu m$ image of the surface of the 12-bilayer film shows the now-familiar, continuous, flat film, interrupted occasionally by holes of one bilayer (40 Å) depth.[182] Images of the 20-bilayer film also exhibit the "hole" morphology. But the thicker film also displays scattered "islands" on the film surface, one bilayer high and 100 nm to 500 nm in diameter. These islands might arise from impurities in the film peparation. Although these two thicknesses of 12 and 20 bilayers represent only two points along a continuum of film-forming steps, a comparison of their images illustrates the utility of the force microscope in tracking film quality during the film-forming process.

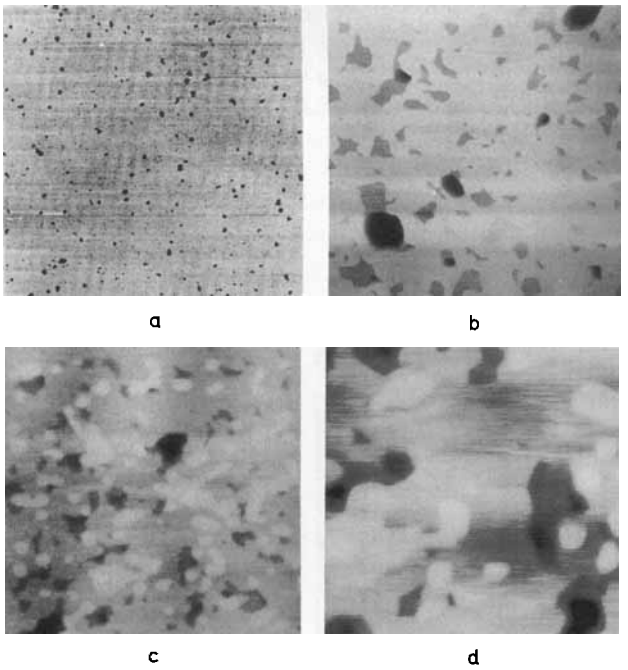

Fig. 27. AFM images of Langmuir–Blodgett films of the liquid crystalline alkoxybiphenylester **11** of different thicknesses and histories [181]. a) Scanned area $50 \times 50\,\mu m^2$. A 12-bilayer film showing overall flat morphology, punctured regularly with holes that are mostly of one bilayer depth (40 Å). b) Scanned area $5 \times 5\,\mu m^2$. Smaller scan area of a). c) Scanned area $5 \times 5\,\mu m^2$. A 20-bilayer film showing, in addition to the flatness and the bilayer-deep holes of the 12-bilayer film, islands of extra material, also one-bilayer high. d) Scanned area $2 \times 2\,\mu m^2$. Smaller scan area of c) [182].

12.4. Transferred, Freely Suspended Films

A similar alkoxybiphenylester molecule to that of the two LB films of the previous section has been handled in another manner to produce a different type of film.[183] A thin film of a two-dimensional fluid of the octoxy derivative, 4′-*n*-octoxybiphenyl carboxylic acid ethyl ester (**12**), is drawn across

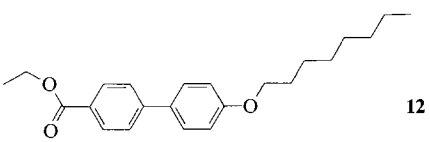

12

an aperture at 100 °C to create a freely suspended film,[184] which is then transferred to a hydrophobized substrate,

Fig. 28. AFM images of freely suspended liquid crystalline films, transferred to a hydrophobized silicon substrate [182]. The molecule **12**, an alkoxybiphenylester, is similar to **11** of the LB film of Figure 27, but with minor modification of the substituents [183, 184]. a) Scanned area $5 \times 5\ \mu m^2$. Flat, hole-free, irregularly shaped planes of films are observed. The overall film thickness is ~18–22 nm, corresponding to 8 layers. Layer steps (24 Å) are also measured. b) Scanned area $50 \times 50\ \mu m^2$. In a large-scale image, part of the film resembles a peninsula. The scan also shows the surrounding exposed silicon substrate. Note scattered small islands on the substrate (see text). Darker, square features superimposed on the shore of the peninsula are the result of local manipulation experiments, such as those performed in Figure 30 and described in Section 12.5 [182]. c) Scanned area $12 \times 12\ nm^2$. Molecular resolution, from which lattice constants of 7.3 Å × 5.8 Å with an angle of 71° between them are measured. (Measurement bars superimposed on image.)

cooled, and examined under the AFM in its crystalline phase.[182, 183] Unlike the previously discussed films, these are hole-free. Large, flat planes, microns across and ~18–22 nm (8 layers) thick are observed (Fig. 28). These planes are irregularly shaped and overlayed, resembling ice floes. A measured step height of 24 Å is consistent with layer spacing from X-ray measurements,[182] which corresponds to the length of the molecule. The adjacent surface of the fused quartz (hydrophobized) is widely and randomly dotted with islands. These might arise from the substrate itself, the silanizing agent (octadecyltrichlorosilane), or the film.[186] Molecular resolution on one of the flat film planes yields unit cell dimensions of 7.3 Å × 5.8 Å with an angle of 71° between them. These values are not totally consistent with electron diffraction measurements obtained from this film, which indicates substrate effects or surface rearrangements.[182]

12.5. Local Manipulation

The AFM cantilever is chosen to be "soft" enough to detectibly respond to interactions with the scanned surface, yet "stiff" enough to reversibly maintain its integrity – that is, to be able to return to an equilibrium position between interactions. By modifying the cantilever specifications and/or the scanning conditions, the AFM can be transformed from a relatively passive imaging tool into an active modifying tool. For example, incorporation of stiff cantilevers and tip modulation techniques have led to a system for "plowing through" a polycarbonate film (Fig. 29) in order to write lines, dots, and features on the submicron scale of the cantilever tip.[187, 188] Other examples of localized plastic deformation have been demonstrated on actin filaments and AgBr.[134, 177] Sometimes the features created by the AFM probe are unstable and rearrange to more stable surface configurations. When this occurs on the time scale of the AFM measurement (1 frame of ~250 scans min^{-1} over nanometer dimensions), the AFM can be used to monitor the kinetics of diffusion.[177] Metal-coating an AFM tip has allowed lithography to be performed with linewidths of 70 nm on a photoresist. This was done by applying a bias across the polymer, between an underlying gold film and the metalized tip while scanning.[187c]

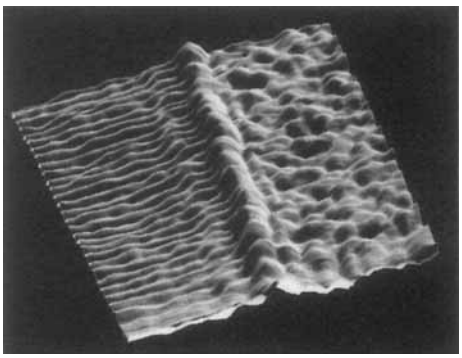

Fig. 29. AFM image (scanned area $1.35 \times 1.35\ \mu m^2$) of a pattern created in a polycarbonate film with an AFM probe. The traces are created by the lateral movement of a lever tip under an applied force (10^{-7} N) higher than that required for imaging. After the pattern is created, its image was recorded under a lower applied force of 5×10^{-9} N. An individual trace is typically 10 nm deep and 70 nm wide [188].

When scanning conditions are changed to increase both the applied force (from 10^{-8} to 10^{-7} N) and scan rate (from 0.5 to 5 $\mu m\, s^{-1}$), holes one or two layers deep can be intentionally introduced into the cadmium arachidate LB films of Section 12.1.[189] Figure 30 shows areas of 0.5–1 μm dimension which have been plowed aside in the top bilayer of the double bilayer of cadmium arachidate discussed above, exposing the bilayer below. Further application of this abrasive technique to the lower bilayer produces holes two bilayers deep and exposes the silicon substrate below. Thus a two-tiered hole with tier heights corresponding to a bilayer thickness has been produced (Fig. 30c).

The film has been observed to respond to this deformation in two ways: either by amassing piled-up debris (typically one bilayer thick) at the hole's edges (Fig. 30b) or by decreasing the density of naturally occurring holes in the vicin-

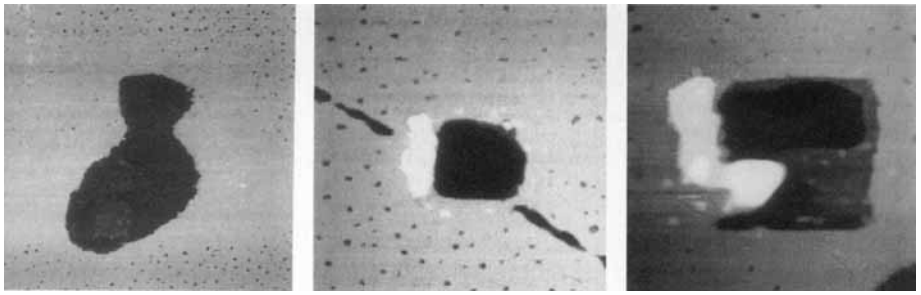

Fig. 30. AFM images of manipulations performed in the double bilayer cadmium arachidate films of Figures 22–25 [175, 177]. a) Scanned area $3.5 \times 3.5\ \mu m^2$. An intentionally scribed hole that has changed its contour over the period of several hours. Note the decrease in pore density surrounding the hole. This decrease could be a result of the pores' role as shock-absorbers during the process of creating the holes with the AFM probe. b) Scanned area $3 \times 3\ \mu m^2$. An intentionally scribed hole superimposed on a naturally occurring linear defect in the film that originates in the substrate. Note that the displaced material from the hole-forming process is amassed at the hole's edge. It is typically one bilayer high. c) Scanned area $1.35 \times 1.35\ \mu m^2$. A hole-within-a-hole. The first hole is created by removing one bilayer over $\sim 0.5 \times 0.5\ \mu m^2$, exposing the underlying bilayer. A second hole, $\sim 0.25 \times 0.25\ \mu m^2$ is then scribed in this underlying layer, exposing the underlying substrate. Displaced film is piled up at the left edge of the hole.

ity of the intentionally scribed hole (Fig. 30a). In this latter mode, the holes appear to behave as "buffers" or "shock absorbers", taking up the extra displaced material within the plane of the film. Some holes made in the cadmium arachidate films have been observed to diffuse and even coalesce over several hours.

Holes one monolayer deep have also been made, when the starting surface is covered by only one bilayer. In this case, the adhesion between substrate and the first monolayer is strong enough to allow removal of the top half of a bilayer without disrupting the bottom half. In all, layers have been "sheared" with an AFM at various levels: between bilayers, within bilayers, and between the substrate and the first bilayer.[177] Relative adhesive strengths can be ordered from these comparative studies, which demonstrate a relative increase in adhesion on going from interplanar, to interlayer, and finally to interfacial interactions. Additional shearing experiments have been performed on multilayer films composed of different classes of molecules, for example, comparing fatty acids,[190] alkoxybiphenyl acid esters,[182] and fluorinated alkanes.[191] These studies show that film composition affects the ease with which intentional modifications in the film are made with the AFM stylus.[189]

12.6. Very Local Friction

The ability of the AFM probe to locally displace adsorbate from the substrate produced a new sample surface – a heterogeneous surface of inorganic silicon and organic bilayer. This surface then became the object of a study using a slightly modified AFM,[190] a friction force microscope (also called the lateral force microscope, LFM) which measures simultanously the lateral and normal deflections of a cantilever-type probe.[192] In this configuration, the microscope's cantilever and detection scheme are constructed to allow measurement of forces acting against the lever that are parallel to the scanned plane,[193] in addition to the more common normal force detection mode in which only lever deflections perpendicular to the sample surface are recorded. Normal deflections provide information on the topography of the surface. Lateral torsions and bending of the cantilever provide information on elastic and inelastic (or, perhaps more accurately, adiabatic and dissipative) interactions with the sample surface. These measurements of lateral forces are of great interest in studies of lubrication and friction, often classified under the term tribology.[194]

The mixed surface of exposed substrate and organic adsorbate has been scanned, to measure both normal and lateral forces (Fig. 31).[177, 190] From the normal forces (Fig. 31a), an image of topography is produced in which two levels of film on an underlying substrate are evident; the contrast scales are assigned such that the upper film is light gray, the lower film is dark gray, and the underlying substrate is black.

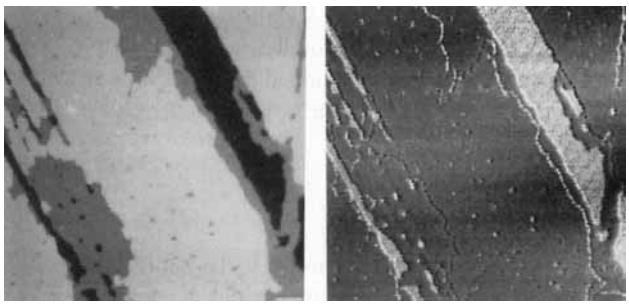

Fig. 31. AFM images recorded on the double bilayer cadmium arachidate films of Figure 23, simultaneously in the normal force mode for topography and lateral force mode for friction [190]. a) Scanned area $3 \times 3\ \mu m^2$. Topography image. Principally three levels are observed: the substrate (darkest), one bilayer (gray) and two bilayers (lightest). Most of the film is a double bilayer. The height difference between these levels corresponds to the thickness of a bilayer, ~ 54 Å. Occasional islands of extraneous bilayer are seen on top of the double bilayer. b) Scanned area $3 \times 3\ \mu m^2$. Friction image. The difference in the lateral force signals from the bilayer and double bilayer surfaces is small. In fact, often only at the interface (step) between these two is any contrast observed (and this contrast is due to torsion, not friction). However, the difference between the lateral force signal from the organic layers and that from the silicon substrate is significant (intensity ratio 1:10). Comparison of the normal and lateral force images demonstrates that the lateral force measurement is sensitive to material properties derived from chemical composition (see text).

The difference in height between adjacent levels is 54 Å, consistent with the thickness of a bilayer cadmium arachidate LB film. Occasional, small islands of extraneous material are encountered on the top surface of the film. From this image, however, no compositional information is provided; that is, only the absolute height differentiates the lower substrate from the upper organic film. In contrast, the frictional force measurement (Figure 31 b) affords additional information about material properties of the surface from the interaction between the two components in dynamic contact with each other during the measurement: the probe and the particular area on the surface. In this measuring mode, the tip responds remarkably differently to interactions with the organic film and interactions with the silicon, shown as darker and light areas, respectively, in Figure 31 b. The lateral response to the organic film remains rather constant, whether on the single or double bilayer level. In fact, were it not for a lateral, torsional response to the edge of the upper bilayer during scanning (seen as thin contour lines at borders and spots at holes), the LFM image would be devoid of indication that a second bilayer exists. The frictional forces between the probe and silicon are approximately ten times those between the probe and the organic film, reflecting the difference in material properties of the inorganic and organic layers quite consistently. This order of magnitude reduction in friction on coating a surface with an organic layer is consistent with measurements made on boundary lubrication in the traditional materials science field of tribology.[194, 195]

Interpretation of these early images indicating local variations in the friction coefficient on both the micron and molecular scale is still preliminary. It will undoubtedly require previous knowledge of macroscopic phenomena such as "stick–slip" behavior in lubrication, and then modification for the unprecedented local scale of these measurements.

12.7. A Comparative Study: Fluorocarbon vs. Hydrocarbon Surface

Langmuir–Blodgett films assembled from fluorinated carboxylic acids have provided fluorinated surfaces with which to study the response of the AFM probe to a chemically modified surface.[191, 197] The representative films presented here have been synthesized according to established LB techniques from a partially fluorinated carboxylic acid **13**.[198] The subphase is *N*-methylated polyvinylpyridine (14).[199]

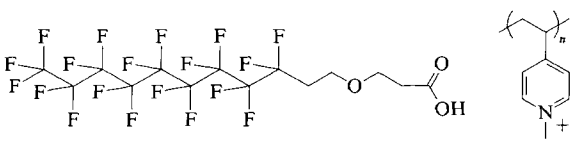

13 **14**

LB films of arachidic acid (**10a**) on the same polyvinylpyridine subphase have also been measured as a control experiment. Comparison of the behaviors of the two films—from the perhydroarachidate and the fluorocarbon terminated carboxylate—indicate a higher degree of cohesive in-plane binding within the fluorocarbon film (Fig. 32 b) than in the hydrocarbon film (Fig. 32 a). Distinctively different surfaces are recorded from the two films during the AFM measurements. The fluorinated film is characterized as resistant to deformation, robust, and fairly homogeneous. The hydrocarbon film is randomly defaced with cracks and holes, and is more deformable. Earlier studies on the mechanical properties of fluorinated Langmuir–Blodgett films also reported a better resistance to rupture during sliding than their hydrogen-containing counterparts.[196]

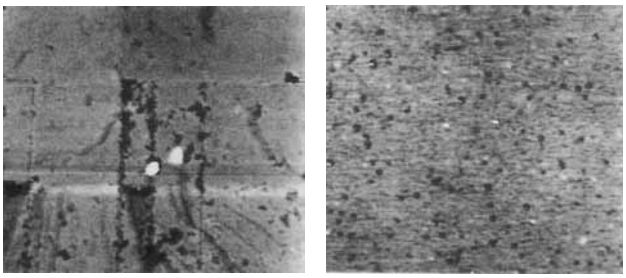

a b

Fig. 32. AFM images comparing Langmuir–Blodgett films composed of a normal, hydrogenated carboxylate **10a** to that of a partially fluorinated carboxylate **13**. Both films are prepared in the same manner with an *N*-methylated polyvinylpyridine **14** as subphase on hydrophobized silicon (100) [198, 199]. (See schematic drawing in Figure 33.) a) Scanned area $5 \times 5\ \mu m^2$. A film of perhydro arachidate (ions of **10a**) shows long-range, flat morphology, irregularly decorated with defects and holes. b) Scanned area $5 \times 5\ \mu m^2$. A film of partially fluorinated anions of carboxylic acid **13** shows long-range, homogeneous morphology.

12.8. Mixed Monolayers: Distinguishing Domain Boundaries

The ability of the AFM to document surface features on thin, somewhat fluid organic films has, by now, been well demonstrated in this article. One challenge lies in differentiating subtle features, such as compositional changes *within* a film. An ideal system to test the LFM for sensitivity to differences between materials is a mixed monolayer of two chemical species. Many issues are raised on constructing such films, including molecular miscibility and segregation into domains. How is the origin of bulk properties related to domain size: do localized properties of individual molecules or domains scale up to the macroscopic whole?

The localized properties of adhesion, elasticity, and friction have now been probed with a force microscope within single domains in LB films composed of mixtures of molecules with hydrocarbon and fluorocarbon moieties.[191, 197] A representative film is presented here, which is synthesized according to establish LB techniques from a 1:1 molar mixture of arachidic acid (**10a**) and partially fluorinated carboxylic acid **13**.[198] The subphase is *N*-methylated polyvinylpyridine **14**.[199] The mixed film is therefore composed of the two molecular species from the previous comparative study of fluorocarbon and hydrocarbon films. The mixed film images show distinct, phase-separated domains that have distinct properties (Fig. 33). From the topography image, boundaries within the film define circular, flat-topped

domains of 500 nm to 1000 nm in diameter that are ~16 Å higher than the surrounding flat film. Because of the difference in molecular lengths between the two component molecules (arachidic acid is ~25 Å long and the partially fluorinated carboxylic acid **14** is ~20 Å long), the higher, circular domains are assigned to the hydrocarbon. Further experiments with more closely controlled monolayers of the two components are under way.[191]

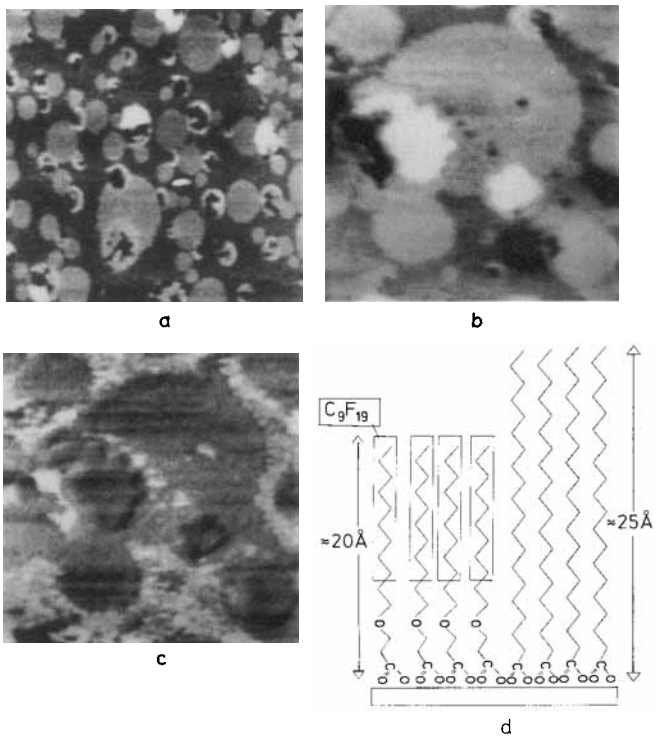

Fig. 33. AFM images recorded on a LB film comprising a mixed layer of the two components of the films of Figure 32: anions of perhydroarachidic acid (**10a**) and the fluorinated carboxylic acid **13**. The normal and lateral force modes are compared, each yielding different information [191, 197]. The accompanying schematic drawing is intended as a qualitative description of the LB film components, and neglects such features as tilt angles and intermolecular spacing. a) Scanned area $5 \times 5\ \mu m^2$. Topography image. Flat, circular domains are ~16 Å higher than surrounding flat film. They are attributed to the longer perhydrocarboxylate. Note that holes occur only in these hydrocarbon domains, consistent with the hydrocarbon film of Figure 31, and extend down to the substrate (darkest features). The surrounding flat film is hole-free, which supports its assignment as fluorocarbon (see Figure 31). Occasional islands are scattered across the films (highest, brightest features), the origin of which can not be identified from this topography image. b) Scanned area $2 \times 2\ \mu m^2$. Topography image on the same film as in a). c) Scanned area $2 \times 2\ \mu m^2$. Friction image recorded simultaneously over the same area as in b). Lateral force signal differentiates between the material compositions of the domains. The fluorinated regions respond with higher friction than the hydrocarbon domains (see text). In this recording mode, it is possible to ascertain the origin of the scattered islands since they give the same friction response as the circular hydrocarbon domains. The highest friction (brightest areas) is recorded over the silicon substrate, exposed at the bottom of the holes. The relative friction (hydrocarbon:fluorocarbon:silicon) in this sample is 1:4:10. d) Schematic representation of the composition of the mixed layer of anions of **10a** and **13** on a polymer with cationic centers.

Holes in the film are confined to the large, circular domains assigned as hydrocarbon domains; this is not surprising since in the control study above, only the hydrocarbon film shows evidence of holes while the fluorinated film remains fairly uniform. The holes in the mixed films are irregularly shaped, and extend down to the substrate (~50 Å deep). Using the AFM tip as an indenter reveals that the hydrocarbon regions are more deformable than the fluorocarbon regions, again consistent with the control films and an apparent higher in-plane binding among the fluorinated chains.

Lateral force measurements (Fig. 33c) indicate a fourfold higher friction over the fluorinated regions than over hydrocarbon regions. This perhaps goes against our social familiarity with teflon cookware (and labware); however, further studies on wettability will have to be carried out to bridge this gap between the macro- and the micro-world. On the scale of the AFM measurement, this higher friction on the fluorocarbon is accompanied by (and perhaps explained by) a higher local elasticity measurement. Higher elasticity could be explained by the greater stiffness of fluorocarbon chains. This result is supported by earlier investigations of sliding friction between monolayers in which fluorinated Langmuir–Blodgett films were found to have higher shear strengths than their hydrogen-containing counterparts.[196] These studies also reported that despite the high shear strengths, the fluorinated films showed good resistance to rupture during sliding – a result consistent with the observation that it is very difficult to puncture the fluorinated surfaces with the AFM probe.

Finally, scattered islands of 'extraneous' material appear in the topography image as higher (brighter) spots sitting atop the hydrocarbon domains (Fig. 33b). The lateral force image assigns these a hydrocarbon identity, based on their low friction signal identical with that observed from the hydrocarbon domains (Fig. 33c). This is an assignment of composition that is not possible in the topography mode, which tracks absolute physical features, nearly independent of the material make-up. Lateral force measurements reflect a more intimate interaction between the probe and the scanned surface, which reflects some material properties.

This final example of the mixed hydrocarbon–fluorocarbon films serves as an apt concluding study for the use of the AFM and its derivatives in the investigation of film surfaces. Surface topography of extensive planes, holes, and distinct domains are documented. These features are then embellished with compositional information from lateral force measurements that assign higher friction to fluorinated regions, and track impurities to hydrocarbon origin.[191, 197]

13. Concluding Remarks on the Atomic Force Microscope in Chemistry

In focusing on the last layer of molecules between two media, the effect of one material on the other can be assessed. This statement is of fundamental importance for friction and lubrication, adhesion and diffusion, or miscibility and phase separation. The AFM is entering into these and other disciplines, although it is reasonable to question just what properties and phenomena are being sampled on the molecular scale.

When scanning, the forces exerted by the probe itself must be questioned. Such a localized perturbation is difficult to corroborate with a second technique since most other techniques operate on a larger scale. Despite this lack of quantifi-

cation, researchers are taking advantage of the intentional physical displacement of material by the AFM probe to create tiny designer structures. This kind of localized manipulation of material has been performed on polymers, membranes, and salts.

The AFM's sensitivity to only the topmost nanometers of a material is at once a strength and a drawback. This superficial regime often eludes other analytical techniques which average over greater depths and lateral distances and require deconvolution of signals from reciprocal space. The AFM provides direct information about surface structure, down to the molecular scale. On an optimistic note, the downside of being confined to the surface layer(s) provides the challenge to the next generation of experiments to apply the fine, local resolution of AFM to the interior interstices of 3-D samples.

14. Concluding Remarks on the Impact of the Scanning Tunneling Microscope and the Atomic Force Microscope on Chemistry: The Emperor's New Clothes

The STM and AFM are able to provide information about molecular environments not directly observed before. The two methods are not redundant. They probe different properties on different scales. The STM probes electronic levels of atoms and molecules over a sampling area defined by the confined stream of tunneling electrons, on the order of 1 Å. From the STM one obtains atomic topography when electronic structure coincides with atomic structure. The AFM senses forces originating in surfaces: van der Waals, magnetic, electrostatic, etc. The effective sampling area of an AFM is determined by the interactive area of the tip, typically hundreds of angstroms. From the AFM one obtains maps of molecular topography when local material properties, such as elasticity, coincide with molecular structure. The AFM can be customized to sense specific forces, thereby producing maps of, for example, charge distribution or friction over a surface. The STM has the potential of performing localized spectroscopy. In recording electronic structure over an atom or two, chemical analysis is added to the topographical information. The fact that the STM sample must be conducting, or in very close proximity to a conductor, places a limitation on what samples can be studied. With the AFM, this restriction is lifted, rendering the AFM more suitable for most organic materials, and biological systems. In particular, biological systems will benefit from the AFM's ability to operate in native environments, such as the physiological conditions under which in vivo processes take place.

Samples have been taken from the formal disciplines of catalysis, optics, surface science, and tribology. What the STM and AFM work from these seemingly diverse areas has shown is that on the molecular scale, the departmentalization becomes artificial, and the molecules are returned to their unclassified, bare selves. In this analogy to the fairy tale, "The Emperor's New Clothes", we have the opportunity to transcend the artificial boundaries between chemistry, physics, and biology and look instead for the commonality of properties on the molecular scale. This is not to over-simplify the beautiful diversity of materials, but rather to foster a wider perspective when thinking about the results that these instruments produce and about future systems for study.

Finally, both the STM and AFM are still in a stage of continuous development and change. Both have caught molecules in the act of dynamic processes, rearrangements and reconstructions of surfaces. The database of credible images is growing and will soon allow the identification of unknowns. This will be supported by the concomitant development of other localized probes coupled into the scan head that will provide elemental and spectroscopic information. The use of such combined and compatible techniques will enable us proudly to reclothe the Emperor.

I take great pleasure in acknowledging colleagues John Foster, Jackie Spong, Ed Barrall, Bob Twieg, Doug Smith, Wolfgang Heckl, Ernst Meyer, Rene Overney, Dario Anselmetti, Gero Decher, Doug Thomson, Masamichi Fujihira, Terry Lang, John Hemminger, and George Comsa for their fine technical abilities in operating the instruments and recording credible images, and/or for their enthusiasm and encouragement in making inroads for these new instruments into chemistry. I would also like to acknowledge the helpful input of my colleagues and my family's perseverance during the writing of this article. The support of IBM Research and The University of Basel (H.-J. Güntherodt) is gratefully acknowledged.

Received: January 7, 1992 [A 880 E]
German version: *Angew. Chem.* **1992**, *104*, 1325

[1] G. Binnig, H. Rohrer, *Angew. Chem.* **1987**, *99*, 622; *Angew. Chem. Int. Ed. Engl.* **1987**, *26*, 606.
[2] For a background to STM and AFM, and an overview of the recent directions, see the proceedings of two international meetings on STM and AFM: a) *Proc. Int. Conf. Scanning Tunneling Microscopy (STM'91) Interlaken, Switzerland, August* **1991** (Ultramiscroscopy **1992**, Vol. 42–44; b) *J. Vac. Sci. Technol B* **1991**, *9*, 401–1211; c) see also Scanning Tunneling Microscopy, I and II (Eds.: R. Wiesendanger, H. Güntherodt), Springer, Berlin, 1992.
[3] G. Binnig, H. Rohrer, *Surf. Sci.* **1983**, *126*, 236.
[4] G. Binnig, H. Rohrer, C. Gerber, E. Weibel, *Phys. Rev. Lett.* **1982**, *49*, 57.
[5] D. Walmsley, *Surf. Sci.* **1987**, *181*, 1.
[6] Electronically controlled piezo tubes operate on the basis of the (inverse) piezoelectric effect: a controlled change in the geometry of a material on application of a controlled voltage: G. Binnig, D. Smith, *Rev. Sci. Instrum.* **1986**, *57*, 1688; C. Chen, *Appl. Phys. Lett.* **1992**, *60*, 132; C. Chen in [2a], 1653.
[7] R. Wiesendanger, G. Tarrach, D. Bürgler, H. Güntherodt, *Europhys. Lett.* **1990**, *12*, 57.
[8] H. Lemke, T. Göddenhenrich, H. Bochem, U. Hartmann, C. Heiden, *Rev. Sci. Instrum.* **1990**, *61*, 1538; R. Penner, M. Heben, T. Longin, N. Lewis, *Science* **1990**, *250*, 1118; A. Bryant, D. Smith, C. Quate, *Appl. Phys. Lett.* **1986**, *48*, 832.
[9] D. Smith, J. Hörber, G. Binnig, H. Nejoh, *Nature* **1990**, *344*, 641.
[10] W. Heckl, D. Smith, G. Binnig, H. Klagges, T. Hänsch, J. Maddocks, *Proc. Natl. Acad. Sci. USA* **1991**, *88*, 8003.
[11] W. Mizutani, M. Shigeno, Y. Sakakibara, K. Kajimura, M. Ono, S. Tanishima, K. Ohno, N. Toshima, *J. Vac. Sci. Technol. A* **1990**, *8*, 675.
[12] K. Yackoboski, Y. Yeo, G. McGonigal, D. Thomson, in [2a] 963.
[13] C. Ludwig, B. Gompf, W. Glatz, J. Petersen, W. Eisenmenger, *Z. Phys. B.* **1992**, *86*, 397.
[14] A. Bryant, D. Smith, G. Binnig, W. Harrison, C. Quate, *Appl. Phys. Lett.* **1986**, *49*, 936.
[15] H. Hess, R. Robinson, R. Dynes, J. Valles, J. Waszak, *Phys. Rev. Lett.* **1989**, *62*, 214.
[16] D. Eigler, E. Schweizer, *Nature* **1990**, *344*, 524; D. Eigler, C. Lutz, W. Rudge, *ibid.* **1991**, *352*, 600.
[17] J. Stroscio, D. Eigler, *Science* **1991**, *254*, 1319.
[18] J. Spong, L. LaComb, M. Dovek, J. Frommer, J. Foster, *J. de Phys.* **1989**, *50*, 2139.
[19] T. Land, T. Michely, R. Behm, J. Hemminger, T. Comsa, *Appl. Phys. A* **1991**, *A53*, 414; *Surf. Sci.* **1992**, *264*, 261.
[20] J. Zandvliet, H. Elswijk, E. van Loenen, *Surf. Sci.* **1992**, in press; S. Kitamura, T. Sato, M. Iwatsuki, *Nature* **1991**, *351*, 215.

[21] K. Besocke, *Surf. Sci.* **1987**, *181*, 145.
[22] I. Lyo, P. Avouris, *Science* **1991**, *253*, 173.
[23] R. Feenstra, M. Lutz, *Surf. Sci.* **1991**, *243*, 151.
[24] R. Feenstra, A. Slavin, G. Held, M. Lutz, *Phys. Rev. Lett.* **1991**, *66*, 3257.
[25] E. Delawski, B. Parkinson, *J. Am. Chem. Soc.* **1992**, *114*, 1661; B. Parkinson, *ibid.* **1990**, *112*, 7498.
[26] J. Rabe, S. Buchholz, *Phys. Rev. Lett.* **1991**, *66*, 2096.
[27] H. Siegenthaler, R. Christoph, in *Scanning Tunneling Microscopy and Related Methods* (Eds.: R. Behm, N. Garcia, H. Rohrer), Kluwer, Dordrecht, **1990**, p. 315; R. Christoph, H. Siegenthaler, H. Rohrer, H. Wiese, *Electrochim. Acta* **1989**, *34*, 1011; H. Siegenthaler in [2c] II, Chapter 2.
[28] A. Bard, F. Fan, D. Pierce, P. Unwin, D. Wipf, F. Zhou, *Science* **1991**, *254*, 68.
[29] X. Gao, A. Hamelin, M. Weaver, *J. Chem. Phys.* **1991**, *95*, 6993; X. Gao, A. Hamelin, M. Weaver, *Phys. Rev. Lett.* **1991**, *67*, 618.
[30] J. Barth, H. Brune, G. Ertl, R. Behm, *Phys. Rev. B Condens. Matter* **1990**, *42*, 9307.
[31] L. Kador, S. Jahn, D. Haarer, R. Silbey, *Phys. Rev. B Condens. Matter* **1990**, *41*, 12215; A. Meixner, A. Renn, S. Bucher, U. Wild, *J. Phys. Chem.* **1986**, *30*, 6777; A. Meixner, A. Renn, U. Wild, *Chem. Phys. Lett.* **1992**, *190*, 75.
[32] M. Specht, F. Ohnesorge, W. Heckl, *Surf. Sci. Lett.* **1991**, *257*, L653.
[33] H. Nejoh, *Nature* **1991**, *353*, 640.
[34] M. Fox, *Nature* **1992**, *355*, 500, and references cited therein.
[35] H. Mamin, P. Guethner, D. Rugar, *Phys. Rev. Lett.* **1990**, *65*, 2418.
[36] I. Lyo, P. Avouris, *J. Chem. Phys.* **1990**, *93*, 4479; C. Whitman, J. Stroscio, R. Dragoset, R. Celotta, *Science* **1991**, *251*, 1206.
[37] M. McCord, D. Kern, T. Chang, *J. Vac. Sci. Technol. B* **1988**, *6*, 1877.
[38] C. Clemmer, T. Beebe, *Science* **1991**, *251*, 640.
[39] W. Heckl, G. Binnig, in [2a] p. 1073.
[40] H. Chang, A. Bard, *Langmuir* **1991**, *7*, 1143.
[41] C. Liu, H. Chang, A. Bard, *Langmuir* **1991**, *7*, 1138, and references cited therein.
[42] H. Mamin, E. Ganz, D. Abraham, R. Thomson, J. Clarke, *Phys. Rev. B. Condens. Matter* **1986**, *34*, 9015.
[43] M. Ramos, A. Sutton, A. Stoneham, *J. Phys. Condens. Matter* **1991**, *3*, S. 127.
[44] T. Albrecht, H. Mizes, J. Nogami, S. Park, C. Quate, *Appl. Phys. Lett.* **1988**, *52*, 362.
[45] R. Coleman, R. Giambattista, P. Hansma, A. Johnson, W. McNairy, C. Slough, *Adv. Phys.* **1988**, *37*, 559.
[46] D. Anselmetti, V. Geiser, G. Overney, R. Wiesendanger, H. Güntherodt, *Phys. Rev. B Condens. Matter* **1990**, *42*, 1848; D. Anselmetti, V. Geiser, D. Brodbeck, G. Overney, R. Wiesendanger, H.-J. Güntherodt, *Synth. Met.* **1990**, *38*, 157; S. Kelty, C. Lieber, *J. Phys. Chem.* **1989**, *93*, 5983.
[47] P. Batra, N. Garcia, H. Rohrer, H. Salemink, E. Stoll, S. Ciraci, *Surf. Sci.* **1987**, *181*, 126; D. Lawunmi, M. Payne, *J. Phys. Condens. Matt.* **1990**, *2*, 3811; D. Tomanek, S. Louie, H. Mamin, D. Abraham, R. Thomson, E. Ganz, J. Clarke, *Phys. Rev. B Condens. Matter* **1987**, *35*, 7790; D. Tomanek, S. Louie, *ibid.* **1988**, *37*, 8327; J. LaFemina, J. Lowe, *Int. J. Quantum Chem.* **1986**, *30*, 769; M. Soto, *J. Mircrosc. (Oxford)* **1988**, *152*, 779.
[48] R. Feenstra, J. Stroscio, A. Fein, *Surf. Sci.* **1987**, *181*, 295.
[49] R. Hamers, P. Avouris, F. Bozso, *J. Vac. Sci. Technol. A.* **1988**, *6*, 508.
[50] R. Feenstra, J. Stroscio, J. Tersoff, A. Fein, *Phys. Rev. Lett.* **1987**, *58*, 1192; B. Parkinson, J. Ren, M. Whangbo, *J. Amer. Chem. Soc.* **1991**, *113*, 7832.
[51] R. Hamers, D. Cahill, in [2b], p. 514.
[52] A recent review of STM in inorganic chemistry: X. Wu, C. Lieber, *Prog. Inorg. Chem.* **1991**, *39*, 432.
[53] T. Gritsch, D. Coulman, R. Behm, G. Ertl, *Phys. Rev. Lett.* **1989**, *63*, 1086.
[54] F. Chua, Y. Kuk, P. Silverman, *Phys. Rev. Lett.* **1989**, *63*, 386; D. Coulman, J. Wintterlin, R. Behm, G. Ertl, *Phys. Rev. Lett.* **1990**, *64*, 1761.
[55] O. Magnussen, J. Hotlos, R. Nichols, D. Kolb, R. Behm, *Phys. Rev. Lett.* **1990**, *64*, 2929. For STM images of clean gold surfaces, see [30].
[56] X. Wang, J. Goldberg, N. Bartlet, T. Einstein, E. Williams, *Phys. Rev. Lett.* **1990**, *65*, 2430.
[57] L. Whitman, J. Stroscio, R. Dragoset, R. Celotta, *Phys. Rev. Lett.* **1991**, *66*, 1338, and references cited therein.
[58] L. Whitman, J. Stroscio, R. Drogoset, R. Celotta, *J. Vac. Sci. Technol. B* **1991**, *9*, 770.
[59] J. Pelz, R. Koch, *J. Vac. Sci. Technol. B.* **1991**, *9*, 775; W. Kobayashi, K. Sugii, *ibid.* **1991**, *9*, 748.
[60] G. Rohrer, D. Bonnell, *J. Vac. Sci. Technol. B* **1991**, *9*, 783.
[61] R. Behm, *J. Phys. Condens. Matter* **1991**, *3*, S117.
[62] E. Kopatzki, R. Behm, *Surf. Sci.* **1991**, *245*, 255.
[63] M. Kirk, J. Nogami, A. Baski, D. Mitzi, A. Kapitulnik, T. Geballe, C. Quate, *Science* **1988**, *242*, 1673.
[64] X. Wu, C. Lieber, D. Ginley, R. Boughmann, *Appl. Phys. Lett.* **1989**, *55*, 2129.
[65] C. Gerber, D. Anselmetti, J. Bednorz, J. Mannhart, D. Schlom, *Nature* **1991**, *360*, 279; M. Hawley, I. Raistrick, J. Beery, R. Houlton, *Science* **1991**, *251*, 1587; H. Lang, T. Frey, H. Güntherodt, *Europhys. Lett.* **1991**, *15*, 667.
[66] C. Widrig, C. Alves, M. Porter, *J. Am. Chem. Soc.* **1991**, *113*, 2805; L. Häussling, B. Michel, H. Ringsdorf, H. Rohrer, *Angew. Chem.* **1990**, *103*, 568; *Angew. Chem. Int. Ed. Engl.* **1991**, *30*, 569; Y. Kim, A. Bard, *Langmuir* **1992**, 8, 1096.
[67] M. van Hove, G. Ertl in *The Nature of the Surface Chemical Bond* (Eds.: T. Rhodin, G. Ertl), North Holland Publishing Company, Amsterdam, **1979**, pp. 276–380; G. Somorjai, *Chemistry in Two Dimensions: Surfaces*, Cornell University Press, Ithaca, **1981**, especially Chapter 5.
[68] Reports of STM images on Langmuir Blodgett films include: a) D. Smith, A. Bryant, C. Quate, J. Rabe, C. Gerber, J. Swalen, *Proc. Natl. Acad. Sci. USA* **1987**, *84*, 969; b) W. Mizutani, M. Shigeno, K. Saito, K. Watanabe, M. Sugi, M. Ono, K. Kajimura, *Jpn. J. Appl. Phys.* **1988**, *27*, 1803; c) C. Lang, J. Hörber, T. Hänsch, W. Heckl, H. Möwald, *J. Vac. Sci. Technol. A.* **1988**, *6*, 368; d) H. Fuchs, *Phys. Scr.* **1988**, *38*, 264; e) H. Fuchs, S. Akari, K. Dransfeld, *Z. Phys. B. Condens. Matter* **1990**, *80*, 389.
[69] T. McMaster, H. Carr, M. Miles, P. Cairns, V. Morris, *Macromolecules* **1991**, *24*, 1428.
[70] I. Lee, E. Atkins, M. Miles in [2a] p. 1107.
[71] R. Yang, K. Naoi, D. Evans, W. Smyrl, W. Hendrickson, *Langmuir* **1991**, *7*, 556.
[72] STM studies on fullerenes: a) R. Wilson, G. Meijer, D. Bethune, R. Johnson, D. Chambliss, M. de Vries, H. Hunziker, H. Wendt, *Nature* **1990**, *348*, 621; b) J. Wragg, J. Chamberlain, H. White, W. Krätschmer, D. Huffman, *Nature* **1990**, *348*, 623; c) Y. Li, M. Chander, J. Patrin, J. Weaver, L. Chibante, R. Smalley, *Science* **1991**, *253*, 429; d) T. Chen, S. Howells, M. Gallagher, L. Yi, D. Sarid, D. Lichtenberger, K. Nebesny, C. Ray in [2b], p. 2461; e) H. Lang, V. Thommen-Geiser, J. Frommer, A. Zahab, P. Bernier, H. Güntherodt, *Europhys. Lett.* **1992**, *18*, 29.
[73] M. Allen, M. Ballooch, S. Subbiah, R. Tench, W. Siekhaus, R. Balhorn, *Scanning Microsc.* **1991**, *5*, 625; W. Heckl, *Mol. Cryst. Lig. Sci. Technol. Sect B: Nonlinear Optics* **1992**, *2*, 231.
[74] Recent reviews on the use of the STM and AFM on biological materials: a) A. Engel, *Ann. Rev. Biophys. Chem.* **1991**, *20*, 79–108; b) A. Engel in *STM and SFM in Biology* (Ed.: O. Marti), Academic Press, London, **1992**, in press; c) W. Heckl, *Thin Solid Films* **1992**, *210–211*, 640; d) H. Arakawa, K. Umemura, A. Ikai, *Nature* **1992**, 171, 358; e) R. Guckenberger, T. Hartmann, W. Wiegräbe, W. Baumeister in [2c] II, Chapter 3.
[75] R. Guckenberger, W. Wiegräbe, A. Hillebrand, T. Hartmann, Z. Wang, W. Baumeister, *Ultramicroscopy* **1989**, *31*, 327.
[76] Recent reviews on the use of the STM and AFM on organic materials include: S. Chiang in [2c], Chapter 7; J. Rabe, *Ultramicroscopy*, **May 1992**; D. Smith, J. Frommer in *STM and SFM in Biology* (Ed.: O. Marti), Academic Press, London, **1992**, in press.
[77] J. Spong, H. Mizes, L. La Comb, M. Dovek, J. Frommer, J. Foster, *Nature* **1989**, *338*, 137.
[78] M. Youngquist, R. Driscoll, T. Coley, W. Goddard, J. Baldeschwieler, *J. Vac. Sci. Technol. B* **1991**, *9*, 1304; T. Coley, W. Goddard, J. Baldeschwieler, *ibid.* **1991**, *9*, 470.
[79] D. Eigler, P. Weiss, E. Schweizer, N. Lang, *Phys. Rev. Lett.* **1991**, *66*, 1189.
[80] P. Lippel, R. Wilson, M. Miller, C. Wöll, S. Chiang, *Phys. Rev. Lett.* **1989**, *62*, 171.
[81] S. Lindsay, O. Sankey, L. Li, C. Herbst, A. Rupprecht, *J. Phys. Chem.* **1990**, *94*, 4655.
[82] C. Chen. in [2a], p. 147.
[83] J. Yuan, Z. Shao, C. Gao, *Phys. Rev. Lett.* **1991**, *67*, 863.
[84] J. Sass, J. Gimzewski, *J. Phys. Condens. Matter* **1991**, *3*, 121.
[85] For examples of physisorption, see, for example, [9] and [119], in addition to the review articles of [76].
[86] H. Ohtani, R. Wilson, S. Chiang, C. Mate, *Phys. Rev. Lett.*, **1988**, *60*, 2398; S. Chiang, R. Wilson, C. Mate, H. Ohtani, *Vacuum* **1990**, *41*, 118.
[87] V. Hallmark, S. Chiang, J. Brown, C. Wöll, *Phys. Rev. Lett.* **1991**, *66*, 48.
[88] Since most of the examples of STM imaging of physisorbed molecules to date have been performed on graphite, they are too numerous to list explicitly. See other references throughout the text, particularly those articles about artifacts on graphite [38–41], in addition to the review articles of organic [76] and biological [74] imaging.
[89] Y. Iwakabe, M. Hara, K. Kondo, K. Tochigi, A. Mukoh, A. Yamada, A. Garito, H. Sasabe, *Jpn. J. Appl. Phys.* **1991**, *30*, 2542; *ibid.* **1990**, *29*, L2243; M. Hara, Y. Iwakabe, K. Tochigi, H. Sasabe, A. Garito, A. Yamada, *Nature* **1990**, *344*, 228.
[90] D. Smith, W. Heckl, *Nature* **1990**, *346*, 616.
[91] R. Emch, J. Nogami, M. Dovek, C. Lang, C. Quate, *J. Appl. Phys.* **1989**, *65*, 79.
[92] J. Wiechers, T. Twomey, D. Kolb, R. Behm, *J. Electroanal. Chem.* **1988**, *248*, 451; J. Clavilier, R. Faure, G. Guinet, R. Durand, *ibid.* **1989**, *107*, 205; A. Hamelin in *Modern Aspects of Electrochemistry* (Eds.: B. Conway, R. White, J. Bockris), Plenum, New York, **1986**, Chapter 1.
[93] R. Möller, R. Coenen, A. Esslinger, B. Koslowski, *J. Vac. Sci. Technol. A* **1990**, *8*, 659.
[94] T. Sleator, R. Tycko, *Phys. Rev. Lett.* **1988**, *60*, 1418.

[95] B. Michel, G. Travaglini, H. Rohrer, C. Joachim, M. Amrein, *Z. Phys. B Condens. Matter* **1989**, *76*, 99.
[96] R. Garcia, N. Garcia, *Chem. Phys. Lett.* **1990**, *173*, 44.
[97] J. Hubacek, R. Brockenbrough, R. Gammie, S. Skala, J. Lyding, *J. Microsc.* (Oxford) **1989**, *152*, 221.
[98] J. Foster, J. Frommer, *Nature* **1988**, *333*, 542.
[99] M. Hara, T. Umemoto, H. Takezoe, A. Garito, H. Sasabe, *Jpn. J. Appl. Phys.* **1991**, *30*, 2052.
[100] For examples of STM images of liquid crystals, see, e.g., references [9,11,18,77,89,90,99,101–104,116], in addition to the review articles of [76].
[101] D. Smith, H. Hörber, C. Gerber, G. Binnig, *Science* 989, *245*, 43.
[102] W. Mizutani, M. Shigeno, M. Ono, K. Kajimura, *Appl. Phys. Lett.* **1990**, *56*, 1974.
[103] T. McMaster, H. Carr, M. Miles, P. Cairns, V. Morris, *J. Vac. Sci. Technol. A* **1990**, *8*, 672.
[104] S. Brand, D. DiLella, R. Colton, in [2b], p. 1115.
[105] J. Foster, J. Frommer, unpublished.
[106] D. Anselmetti, C. Gerber (IBM Zurich) unpublished.
[107] D. Smith, *J. Vac. Sci. Technol. B.* **1991**, *9*, 1119.
[108] For molecular dimensions: J. Israelachvili, *Intermolecular and Surface Forces*, Academic Press, **1985**.
[109] G. Brownsey, A. Leadbetter, *Phys. Rev. Lett.* **1980**, *44*, 1608; A. Leadbetter, J. Frost, J. Gaughan, G. Gray, A. Mosley, *J. Phys. (Paris)* **1979**, *40*, 375.
[110] D. Smith, H. Klagges, W. Heckl (IBM Munich) unpublished.
[111] A. Kitaigorodsky, *Molecular Crystals and Molecules*, Academic Press, New York, **1973**, p. 48–62.
[112] N. Avgul, A. Kiselev in *Chemistry and Physics of Carbon, Vol. 6* (Ed.: P. Walker) Dekker, New York, **1970**, p. 1–124.
[113] F. Hansen, H. Taub, *Phys. Rev. B S. Condens. Matter* **1979**, *19*, 6542.
[114] A. Groszek, *Nature* **1962**, *196*, 531; *Nature* **1964**, *204*, 680; *Proc. R. Soc. London A* **1970**, *314*, 473.
[115] J. Frommer, R. Chance in *Encyclopedia of Polymer Science and Engineering, Vol. 5*, 2nd ed., Wiley, New York **1986**, p. 462–507; J. Frommer, *Acc. Chem. Res.* **1986**, *19*, 2.
[116] J. Foster, J. Frommer, J. Spong, *Proc. SPIE Int. Soc. Opt. Eng.* **1989**, *1080*, 200.
[117] P. Pershan, A. Breslau, A. Weiss, *Phys. Rev. A Gen. Phys.* **1987**, *35*, 4800.
[118] R. Bernhardt, G. McGonigal, R. Schneider, D. Thomson, *J. Vac. Sci. Technol. A* **1990**, *8*, 667.
[119] G. McGonigal, R. Bernhardt, D. Thomson, *Appl. Phys. Lett.* **1990**, *57*, 28.
[120] G. McGonigal, R. Bernhardt, Y. Yeo, D. Thomson, in [2b], p. 1107.
[121] J. Rabe, S. Buchholz, *Science* **1991**, *253*, 424.
[122] G. Findenegg, M. Liphard, *Carbon* **1987**, *25*, 119, and references cited therein.
[123] C. Brown, D. Everett, A. Powell, P. Thorne, *Faraday Discuss. Chem. Soc.* **1975**, 97.
[124] J. Krim, J. Suzanne, H. Shechter, R. Wang, H. Taub, *Surf. Sci.* **1985**, *162*, 446.
[125] A. Müller, K. Lonsdale, *Acta Crystallogr.* **1948**, *1*, 129; see also on excellent presentation of crystallographic work on paraffin in ref. [111], Chapter 1.
[126] R. Kuroda, E. Kishi, A. Yamano, K. Hatanaka, H. Matsuda, K. Eguchi, T. Nakagiri, in [2b], p. 1180.
[127] D. Everett, G. Findenegg, *Nature* **1969**, *223*, 52.
[128] J. Israelachvili, P. McGuiggan, M. Gee, A. Homola, M. Robbins, P. Thompson, *J. Phys. Condens. Matter* **1990**, *2*, SA89.
[129] M. Gee, P. McGuiggan, J. Israelachvili, A. Homola, *J. Chem. Phys.* **1990**, *93*, 1895; H. Hu, G. Carson, S. Granick, *Phys. Rev. Lett.* **1991**, *66*, 2758.
[130] C. Mate, G. Somorjai, *Surf. Sci.* **1985**, *160*, 542; R. Lin, G. Blackmann, M. VanHove, G. Somorjai, *Acta Crystallogr. Sect. B* **1988**, *43*, 368.
[131] G. Binnig, C. Quate, C. Gerber, *Phys. Rev. Lett.* **1986**, *56*, 930.
[132] S. Manne, P. Hansma, J. Massie, V. Elings, A. Gewirth, *Science* **1991**, *251*, 183.
[133] M. Egger, F. Ohnesorge, A. Weisenhorn, S. Heyn, B. Drake, C. Prater, S. Gould, P. Hansma, H. Gaub, *J. Struct. Biol.* **1990**, *103*, 89.
[134] A. Weisenhorn, B. Drake, C. Prater, S. Gould, P. Hansma, F. Ohnesorge, M. Egger, S. Heyn, H. Gaub, *Biophys. J.* **1990**, *58*, 1251.
[135] H. Heinzelmann, E. Meyer, L. Scandella, P. Grütter, T. Jung, H. Hug, H. Hidber, H. Güntherodt, *Wear* **1989**, *135*, 107.
[136] J. Frommer, E. Meyer, *J. Phys. Condens. Matter* **1991**, *3*, S1.
[137] H. Heinzelmann, E. Meyer, H. Rudin, H. Güntherodt in *Scanning Tunneling Microscopy and Related Methods* (Ed.: R. Behm), Kluwer, Dordrecht, **1990**, p. 443–467; E. Meyer, H. Heinzelmann in [2c] II, Chapter 4.
[138] N. Burnham, R. Colton in *Scanning Tunneling Microscopy: Theory and Application* (Ed.: D. Bonnell), VCH Publishers, New York, **1992**, in press.
[139] S. Gould, B. Drake, C. Prater, A. Weisenhorn, S. Manne, H. Hansma, P. Hansma, J. Massie, M. Longmire, V. Elings, B. Dixon, B. Mukergee, C. Peterson, W. Stoeckenius, T. Albrecht, C. Quate, *J. Vac. Sci. Technol. A* **1990**, *8*, 369; B. Drake, C. Prater, A. Weisenhorn, S. Gould, T. Albrecht, C. Quate, D. Cannell, H. Hansma, P. Hansma, *Science* **1989**, *243*, 1586; M. Miles, *Phys. World* **1990**, *3*, No. 10. 28; see also [74c].
[140] P. W. Atkins, *Physical Chemistry*, 2nd ed., Oxford University Press, Oxford, **1984**, p. 23–24.
[141] P. W. Atkins, *General Chemistry*, Scientific American Books, New York, **1989**, p. 354 and 850.
[142] D. Rugar, P. Hansma, *Phys. Today* **1990**, *43*, 23.
[143] D. Rugar, H. Mamin, R. Erlandsson, J. Stern, B. Terris, *Rev. Sci. Instrum.* **1988**, *59*, 2337.
[144] G. Meyer, N. Amer, *Appl. Phys. Lett.* **1988**, *53*, 1045.
[145] T. Göddenhenrich, H. Lemke, U. Hartmann, C. Heiden, *J. Vac. Sci. Technol. A* **1990**, *8*, 383; G. Neubauer, S. Cohen, G. McClelland, D. Horne, C. Mate, *Rev. Sci. Instrum.* **1990**, *61*, 2296.
[146] D. Anselmetti, Ch. Gerber, B. Michel, H. Güntherodt, H. Rohrer, *Rev. Sci. Instrum.*, **1992**, *63*, 3003, and references cited therein.
[147] C. Chen, R. Hamers, *J. Vac. Sci. Technol. B* **1991**, *9*, 503.
[148] L. Eng, H. Fuchs, K. Jandt, J. Petermann, in [2a], p. 989.
[149] H. Yamada, S. Akamine, C. Quate, in [2a], p. 1044.
[150] Y. Martin, H. Wickramasinghe, *Appl. Phys. Lett.* **1987**, *50*, 1455; P. Grütter, T. Jung, H. Heinzelmann, A. Wadas, E. Meyer, H. Hidber, H. Güntherodt, *J. Appl. Phys.* **1990**, *67*, 1437; D. Rugar, J. Mamin, P. Güthner, S. Lambert, J. Stern, I. McFadyen, T. Yogi, *Appl. Phys. Lett.* **1990**, *68*, 1169; P. Grütter, H. Mamin, D. Rugar in [2c] II, Chapter 5.
[151] B. Terris, J. Stern, D. Rugar, H. Mamin, *Phys. Rev. Lett.* **1989**, *63*, 2669; J. Stern, B. Terris, H. Mamin, D. Rugar, *Appl. Phys. Lett.* **1988**, *53*, 2717.
[152] Y. Martin, C. Williams, H. Wickramasinghe, *J. Appl. Phys.* **1987**, *61*, 4729; M. Nonnenmacher, J. Greschner, O. Wolter in [2b], 1358.
[153] S. Ciraci in *Scanning Tunneling Microscopy and Related Methods* (Ed.: R. Behm), Kluwer, Dordrecht, **1990**; G. Overney, W. Zhong, D. Tomanek, in [2b], p. 479.
[154] U. Landman, W. Luedthke, N. Burnham, R. Colton, *Science* **1990**, *248*, 454.
[155] R. Rand, V. Parsegian, *Biochim. Biophys. Acta* **1989**, *988*, 351.
[156] G. Meyer, N. Amer, *Appl. Phys. Lett.* **1990**, *56*, 2100.
[157] E. Meyer, H. Heinzelmann, D. Brodbeck, G. Overney, R. Overney, L. Howald, H. Hug, T. Jung, H. Hidber, H. Güntherodt, in [2b], p. 1329.
[158] E. Meyer, H. Güntherodt, H. Haefke, G. Gerth, M. Krohn, *Europhys. Lett.* **1991**, *15*, 319.
[159] F. Giessibl, G. Binnig, in [2a], p. 281.
[160] R. Erlandsson, G. Hadziioannou, C. Mate, G. McClelland, S. Chiang, *J. Chem. Phys.* **1988**, *89*, 5190.
[161] W. Heckl, F. Ohnesorge, G. Binnig, M. Specht, M. Hashmi, in [2b], p. 1072.
[162] T. Albrecht, C. Quate, *J. Vac. Sci. Technol. A* **1988**, *6*, 271.
[163] G. Binnig, C. Gerber, E. Stoll, T. Albrecht, C. Quate, *Europhys. Lett.* **1987**, *3*, 1281.
[164] E. Meyer, D. Anselmetti, R. Wiesendanger, H. Güntherodt, F. Levy, H. Berger, *Europhys. Lett.* **1989**, *9*, 695.
[165] O. Marti, H. Ribi, B. Drake, T. Albrecht, C. Quate, P. Hansma, *Science* **1988**, *239*, 51.
[166] S. Gould, O. Marti, B. Drake, L. Hellemans, C. Bracker, P. Hansma, N. Keder, M. Eddy, G. Stucky, *Nature* **1988**, *332*, 332.
[167] R. Overney, L. Howald, J. Frommer, E. Meyer, J. Güntherodt, *J. Chem. Phys.* **1991**, *94*, 8441.
[168] R. Overney, L. Howald, J. Frommer, E. Meyer, D. Brodbeck, H. Güntherodt, in [2a], p. 983.
[169] R. Campbell, J. Robertson, *Acta Crystallogr.* **1962**, *15*, 289; C. Truscott, B. Ault, *J. Phys. Chem.* **1984**, *89*, 1741.
[170] A. Camerman, J. Trotter, *Acta Crystallogr.* **1965**, *18*, 636.
[171] For articles in the field of ordered, thin organic films and its analytical methods see A. Ulman, *An Introduction to Ultrathin Organic Films from Langmuir Blodgett to Self-Assembly*, Academic Press, San Diego, **1991**; J. Swalen, *Annu. Rev. Mater. Sci.* **1991**, *21*, 373.
[172] P. Laibinis, R. Graham, H. Biebuzck, G. Whitesides, *Science* **1991**, *254*, 981.
[173] M. Schreck, D. Schmeisser, W. Goepel, H. Schier, H. Habermeier, S. Roth, L. Dulog, *Thin Solid Films* **1989**, *175*, 95.
[174] W. Kern, *RCA Engineer* **1983**, *28*, 99; G. Trucks, K. Raghavachari, G. Higashi, Y. Chabal, *Phys. Rev. Lett.* **1990**, *65*, 504.
[175] E. Meyer, L. Howald, R. Overney, H. Heinzelmann, J. Frommer, H. Güntherodt, T. Wagner, H. Schier, S. Roth, *Nature* **1991**, *349*, 398.
[176] L. Bourdieu, P. Silberzan, D. Chatenay, *Phys. Rev. Lett.* **1991**, *67*, 2029; H. Fuchs, L. Chi, L. Eng, K. Graf, *Thin Solid Films* **1992**, *210–211*, 655.
[177] E. Meyer, L. Howald, R. Overney, D. Brodbeck, R. Lüthi, H. Haefke, J. Frommer, H. Güntherodt, in [2a], p. 274.
[178] V. Vogel, C. Wöll, *J. Chem. Phys.* **1986**, *84*, 5200.
[179] These films were kinldy provided by G. Decher and coworkers H. Merle, J. Maclennan, J. Reibel, P. Quint and U. Sohling, University of Mainz (FRG).
[180] Cadmium behenate LB films were prepared with standard Langmuir Blodgett techniques [171].
[181] G. Decher, U. Sohling, *Ber. Bunsenges. Phys. Chem.* **1991**, *95*, 1538.

[182] R. Overney, E. Meyer, J. Frommer, H. Güntherodt, G. Decher, J. Reibel, U. Sohling *Langmuir*, in press.
[183] J. Maclennan, G. Decher, U. Sohling, *Appl. Phys. Lett.* **1991**, *59*, 917; G. Decher, J. Maclennan, J. Reibel, U. Sohling, *Adv. Mater.* **1991**, *3*, 617.
[184] G. Decher, J. Maclennan, U. Sohling, J. Reibel, *Thin Solid Films* **1992**, *210–211*, 504.
[185] AFM experiments are currently underway to produce images of freely suspended films directly. E. Meyer, R. Lüthi, R. Overney, University of Basel (Switzerland).
[186] Similar features to these islands are seen by AFM on glass surfaces alone.
[187] a) E. Hamada, R. Kaneko, *J. Phys. D. Appl. Phys.* **1992**, *25*, A53; b) in [2a], p. 184; c) L. Nagahara, P. Oden, A. Majumbar, J. Carrejo, J. Graham, J. Alexander, *Scanning Probe Microscopies (SPIE Vol. 1639)* **1992**, 171.
[188] T. Jung, A. Moser, H. Hug, D. Brodbeck, R. Hofer, H. Hidber, U. Schwarz, in [2a], p 1446.
[189] We find that the instrumental operating conditions necessary to deform a film vary widely with the type of molecules that comprise the film. For example, some films require a lower scanning speed, and others a higher one. We postulat capillary and adhesive forces as a source of this effect.
[190] E. Meyer, R. Overney, D. Brodbeck, L. Howald, R. Lüthi, J. Frommer, H. Güntherodt, *Phys. Rev. Lett.* **1992**, *69*, 1777.
[191] E. Meyer, R. Overney, R. Lüthi, D. Brodbeck, J. Frommer, H. Güntherodt, O. Wolter, M. Fujihira, H. Takano, Y. Gotoh, *Thin Solid Films* **1992**, *220*, 132.
[192] Recent reviews on measuring friction on the atomic scale include: G. McClelland, S. Cohen, *Tribology at the Atomic Scale* in *Chemistry and Physics of Solid Surfaces VIII*, (Eds.: R. Vanselow, R. Rowe) Springer, Berlin, **1990**, S. 419; G. McClelland, J. Glosli, Friction at the Atomic Scale, in *Of Friction*, (Eds.: H. Pollok, I. Singer), Kluwer, Dordrecht, **1992**, in press; G. McClelland, Friction at Weakly Interacting Interfaces in *Springer Series in Surface Sciences Vol. 17 (Adhesion and Friction)* (Eds.: M. Grunze, H. Kreuzer), Springer Berlin, **1988**, p. 1.
[193] C. Mate, G. McClelland, R. Erlandsson, S. Chiang, *Phys. Rev. Lett.* **1987**, *59*, 1942; G. Meyer, N. Amer, *Appl. Phys. Lett.* **1990**, *56*, 2100; O. Marti, J. Colchero, J. Mlynek, *Nanotechnology* **1990**, *1*, 141; T. Miyamoto, R. Kaneko, S. Miyake, in [2b], p. 1336.
[194] For a recent overview of the field of tribology, see the issue of the *MRS* (Materials Research Society) *Bulletin* dedicated to this topic: **October 1991**, *Volume XVI*, pages 30–58 und 69.
[195] A. Bailey, J. Courtney-Pratt, *Proc. R. Soc. London A* **1954**, *227*, 501; J. Israelachvili, D. Tabor, *Wear* **1973**, *24*, 386.
[196] B. Briscoe, D. Evans, *Proc. R. Soc. London A* **1982**, *380*, 389.
[197] R. Overney, E. Meyer, J. Frommer, D. Brodbeck, L. Howald, H. Güntherodt, M. Fujihira, H. Takano, Y. Gotoh, *Nature* **1992**, *359*, 133.
[198] M. Fujihira, Y. Gotoh in *Nanostructures Based on Molecular Materials* (Eds.: W. Göpel, C. Ziegler), VCH, Weinheim, **1992**.
[199] Selected papers on LB films or monolayers complexed to polyions include: J. Umemura, Y. Hishiro, T. Kawai, T. Takenaka, Y. Gotoh, M. Fujihira, *Thin Solid Films* **1989**, *178*, 281; K. Nishiyama, M. Fujihira, *Chem. Lett.* **1988**, 1257; K. Nishiyama, M. Kurihara, M. Fujihira, *Thin Solid Films* **1989**, *179*, 477.

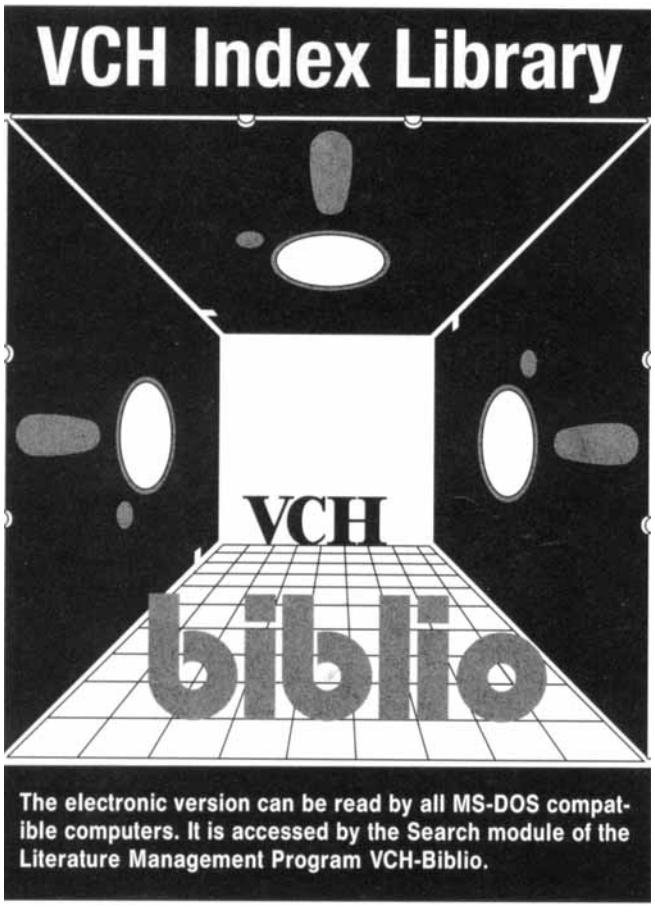

The electronic version can be read by all MS-DOS compatible computers. It is accessed by the Search module of the Literature Management Program VCH-Biblio.

ANGEWANDTE CHEMIE
A Journal of the Gesellschaft Deutscher Chemiker
International Edition in English

30 Year Index of Reviews
– in print or on diskette –

The reviews in Angewandte Chemie are amongst the most often cited chemical publications. Many have become classics of the chemical literature. The 30 year review index was compiled to provide easy access to these important documents of the rapid development of our discipline. The index—both a chemical dictionary and a history book—offers you:

1. A list of all authors, indicating the main author and the title of the review.
2. A subject index giving the main author.
3. Both indexes provide complete information on date of issue and first and last pages of the German and English editions.

The electronic version of the index is available on 5¼" and 3½" diskettes and costs DM 98.00 or sFr 96.00 (plus shipping costs). This is your last chance to order a copy of the **printed version.** In order to clear out our warehouse we are selling the remaining lot for the reduced price of DM 48.00, £ 19.00, or sFr 41.00 (plus shipping costs). Please order by telephone or in writing to **VCH, Software und Datenbanken, Postfach 10 11 61, D-W-6940 Weinheim, Tel. 0 62 01/6 02-2 71, Telefax 0 62 01/6 02-3 28. U.S. customers please contact VCH Publishers, Inc., 303 N.W. 12th Avenue, Deerfield Beach, FL 33442-1788; Telephone 1-(800) 422-8824; Telefax (305) 428-8201.**

Compounds with Three-Membered Rings Containing Boron

By *Hansjörg Grützmacher**

Apart from the well-established cyclopropanes, a series of homologous cyclopropanes of the general formula X_3 ($X = CR_2$, SiR_2, GeR_2, SnR_2) has also been prepared in the last few years. Several derivatives of these compounds, obtained by replacing a ring building block X by a different one (Y, e.g., CR_2, SiR_2, NR, O, S, Se, Te), have also been structurally characterized.[1-6]

Common features of the molecular structures determined can be summarized as follows: if a ring building block X in an X_3 three-membered ring is replaced by a heteroatom or a group Y of greater electronegativity, the basal X–X bond is shortened. Within a series X_2Y this reduction in the bond length increases with increasing electronegativity of the ring building block Y. At the same time the angle α, a measure of the planarization at the basal atoms, increases (Scheme 1).

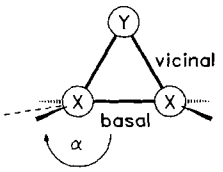

Scheme 1.

The unusual molecular properties of three-membered rings have stimulated numerous quantum chemical studies. In accordance with the Dewar–Chatt–Duncanson model developed for transition metal–olefin complexes, the bonding in heterocyclopropanes can be described in a simplified way as a π complex of the X=X unit and the ring building block Y (Scheme 2).[7] The observed shortening of the basal X–X

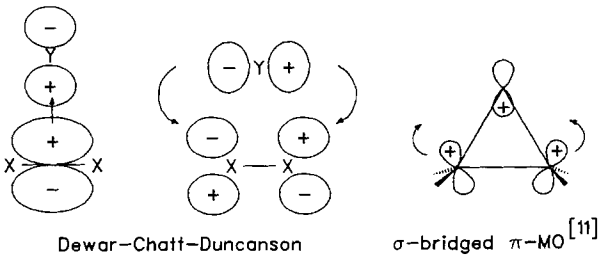

Scheme 2.

bond with increasing electronegativity of Y is therefore considered to result from reduced backbonding from an occupied p(Y) orbital into the π^* orbital of the X=X unit. Alternatively, the molecular structures of three-membered rings can be explained by a high contribution of the "σ-bridged π orbital" in the bonding molecular orbitals.[11] Cremer and Kraka have translated this "molecular orbital model" into an "electron density model" for three-membered rings.[8] In qualitative agreement with the π complex model a deformation of the σ electron density is found, which is reminiscent of that of a π bond and which is delocalized in the plane of the three-membered ring (surface delocalization). The path of the maximum (valence) electron density (MED), however, does not agree with the nucleus–nucleus axes Y–X and X–X, but takes a bent course.

It is possible to distinguish between cases with outwardly (convex) and inwardly (concave) bent bonds. Cyclopropane **1** is an example for the first case and protonated oxirane **2** an example for the second.[8a] Therefore, a short distance between the nuclei in the X–X unit is not necessarily a result of particularly high π character in this bond, but of a strong bend. In actual fact, the calculated length of the bent C–C and Si–Si bond in the series of heterocyclopropanes agrees well with those of the corresponding single bonds.[1] In both models it is possible to establish simple rules, which allow the prediction of the geometries of heterocyclopropanes as well as substituent effects.[8b, 10]

According to calculations by Allen et al. the parent compound of the oxadiboriranes $(HB)_2O$ (**3**) has a remarkable geometry.[11] The calculated B–B bond length in **3** is only

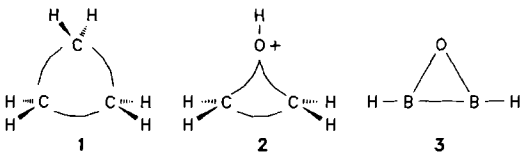

1.594 Å and the H-B-B-H grouping is almost linear ($\alpha = 173.9°$). Paetzold et al. have now been able to synthesize the first alkyl-substituted oxadiborane **5** in a rather a simple way [Eq. (a)].[12] They started from a chlorine-substituted diboryloxide **4**, which was coupled reductively with sodium/potassium alloy to give **5**. Previously, Nöth et al. and also Paetzold et al. sucessfully prepared azadiboranes **6**;[13] however, these either had amino groups (isopropylamino;

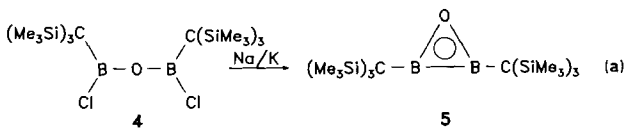

2,2,6,6-tetramethylpiperidino) at the boron atoms which interact strongly with the electronically unsaturated boron atoms, or the crystals were not suitable for an accurate structural investigation. Also in **5** the oxygen atom is disordered with respect to the crystallographic C_2 axis; nevertheless, the ring geometry can be determined accurately enough. In good agreement with the calculations a very short B–B bond

[*] Priv.-Doz. Dr. H. Grützmacher
Anorganisch-chemisches Institut der Universität
Im Neuenheimer Feld 270, D-W-6900 Heidelberg (FRG)

(1.60 Å) and an almost linear C-B-B skeleton (177.7°) are found. The B–O distances are not that well reproduced (obsd B–O 1.55, 1.52 Å; calcd B–O 1.409 Å). The packing of the B-O-B three-membered ring in the sheath of the very bulky, lipophilic $(Me_3Si)_3C$ ("trisyl") substituents, however, transforms it into a chemical "rock": in contrast to the remarkably reactive azadiborirane **6**, R = R^1 = *t*Bu, **5** does not react with O_2, H_2O, CO, azides, BH_3, phosphanes, or alkynes. The reaction of **6**, R = R^1 = *t*Bu, with CO leads to the tricyclic product **7**, whose structure with two B-N-C

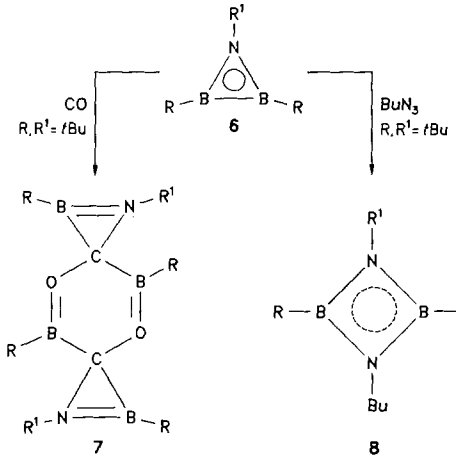

three-membered rings is confirmed by an X-ray structural analysis.[14] With azides the azadiborirane ring can be expanded to give diazadiboretidine **8**. Only reactions of **5** with formic or acetic acid to give **9** (R^2 = H and Me, respectively) were observed.

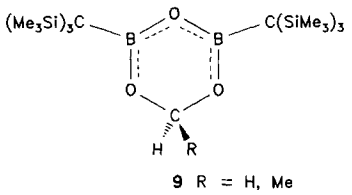

On the basis of the isolobal analogy B $\leftrightarrow$ C^+, boriranes are related to cyclopropyl cations. The latter generally isomerize exothermically ($\Delta G = -38$ kcal mol^{-1}) to give allyl cations. An exception is the most recently prepared cyclo-

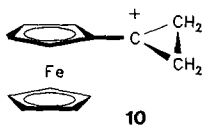

propyl cation **10**, which, because it is stabilized by a ferrocenyl group, can be studied by NMR spectroscopy in solution at −60 °C.[15] Methylborirane (**11**) is in contrast 27.5 kcal mol^{-1} more stable than its isomer **12**.[16] Denmark et al. recently reported indications for 1,2,3-triphenylborirane (**13**) with a thermal stability (>150 °C).[17]

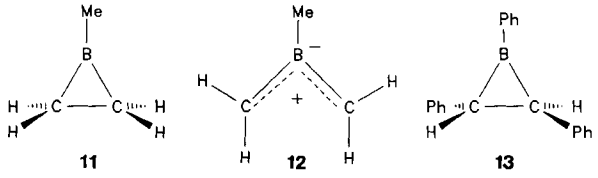

Following the synthesis and complete characterization of the three-membered ring compounds containing boron, **14**, **15**, and **16** (Scheme 3),[18, 19] Berndt et al. have now success-

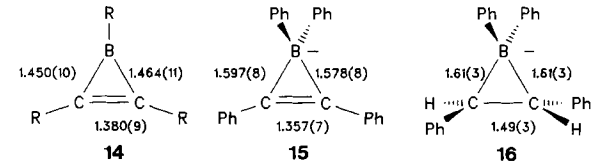

Scheme 3. The C_2B ring compounds **14**–**16** with the relevant experimentally determined B–C bond lengths [Å] given. R = 2,4,6-trimethylphenyl.

fully prepared the first boriranes **18a–c** from the borandiylboriranes **17a,b** (Scheme 4). The molecular structures of **18a** and **18c** have been confirmed by X-ray crystal structure analysis.[20]

The new three-membered rings **18a–c** supplement the family of the heterocyclopropanes with an example in which a significantly more electropositive ring building block Y = BR replaces a more electronegative X = CR_2. Furthermore, an R_2B group as strong π acceptor is connected to a ring carbon atom. The structure determined experimentally with a highly extended basal C–C bond (1.636 Å) is in agreement with the theoretical results. Thermally (60 °C, 46 h),

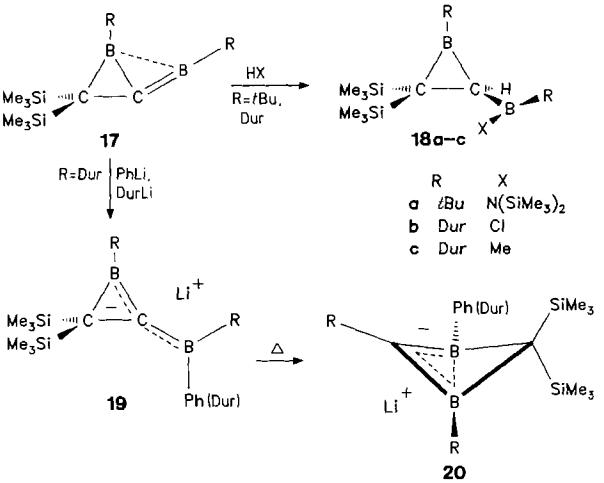

Scheme 4. Dur = 2,3,5,6-tetramethylphenyl.

18a rearranges into a *C*-borylaminomethyleneborane, and at higher temperature (120 °C, 4 h) the borirane **18c** rearranges into a 1,2,3,4-tetrahydro-1,3-diboranaphthaline. The authors explain these results by the cleavage of a ring bond (basal C–C bond, or C–B bond) opposing the R_2B substituents, but in both cases the proposed rearrangements leave enough room for speculation.

Finally, Berndt et al. have reported the first unequivocal proof of a negatively charged homoaromatic system **20**, which they obtained from the thermolysis of **19**, the addition product of aryllithium compounds to the borandiylborirane **17b** (Scheme 4).[21] The fact that this compound actually possesses the cyclic delocalized π bonding system of a homoaromatic compound with 2π electrons is revealed by NMR spectroscopy. In comparison with **19** the signal due to the tricoordinate carbon atom in **20** is shifted to lower field by about $\Delta\delta = 60$ (**20**: $\delta = 162.9$; **19**: $\delta = 106.0/110.6$). The crystal structure was determined by X-ray structural analysis. The C_2B_2 ring is folded about the B–B axis by roughly 33°; the transanular B–B distance (1.792 Å) is in the range of bonding B–B interactions. The energy barrier $\Delta G^{\neq}$ (176 K) for ring inversion was estimated by dynamic NMR spectroscopy at approximately 7.9 kcal mol^{-1}. The experimental results were supported by ab initio calculations [fold angle 34°, B–B distance 1.859 Å; ΔE (ring, folded)$-\Delta E$ (ring, planar) $= -7.4$ kcal mol^{-1}, $\delta(^{13}C) = 169$ (IGLO)]. The somewhat lower calculated bond order of the 1,3 interaction relative to that in the homocyclopropenium ion (0.23 vs 0.40) can be attributed to the lower electronegativity of the boron atom in comparison with the carbon atom.

Molecular chemistry is alive! Together with the authors of the papers discussed we look forward to and eagerly await new boron-containing three-membered rings. The synthesis of a diborirane **21**, in particular, now seems to be almost

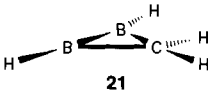

21

within reach. For this compound the calculations predict a carbon atom with a planar coordination geometry.[22]

German version: *Angew. Chem.* **1992**, *104*, 1358

[1] J. A. Boatz, M. S. Gordon, *J. Phys. Chem.* **1989**, *93*, 3025, and references cited therein.

[2] T. Tsumuraya, S. A. Batcheller, S. Masamune, *Angew. Chem.* **1991**, *103*, 916; *Angew. Chem. Int. Ed. Engl.* **1991**, *30*, 902, and references cited therein.

[3] R. Peng-Koon Tan, G. R. Gillette, D. R. Powell, R. West, *Organometallics* **1991**, *10*, 546.

[4] a) T. Tsumuraya, S. Sato, W. Ando, *Organometallics* **1990**, *9*, 2061; b) T. Tsumuraya, Y. Kabe, W. Ando, *J. Chem. Soc. Chem. Commun.* **1990**, 1159.

[5] A. Schäfer, M. Weidenbruch, W. Saak, S. Pohl, H. Marsmann, *Angew. Chem.* **1991**, *103*, 873; *Angew. Chem. Int. Ed. Engl.* **1991**, *30*, 834.

[6] H. Grützmacher, H. Pritzkow, *Angew. Chem.* **1991**, *103*, 976; *Angew. Chem. Int. Ed. Engl.* **1991**, *30*, 1017.

[7] A. Greenberg, J. F. Liebman, *Strained Organic Molecules*, Academic Press, New York, **1978**, S. 280–282, and references cited therein.

[8] a) D. Cremer, E. Kraka, *J. Am. Chem. Soc.* **1985**, *107*, 3800; *ibid.* **1985**, *107*, 3811. The advantage of this concept attributed to Bader et al. [9] is that a random assignment of the electron density onto the bonding and nonbonding electron pairs is avoided. The π character of a bond is described by the anisotropy ε of the charge concentration $p(r_b)$ at special points r_b of the bond (bond critical points).

[9] R. F. W. Bader, P. J. MacDougall, C. D. H. Lau, *J. Am. Chem. Soc.* **1984**, *106*, 1594, and references cited therein.

[10] T. Clark, G. W. Spitznagel, R. Klose, P. von R. Schleyer, *J. Am. Chem. Soc.* **1984**, *106*, 4412.

[11] C. Liang, L. C. Allen, *J. Am. Chem. Soc.* **1991**, *113*, 1878.

[12] P. Paetzold, L. Géret-Baumgarten, R. Boese, *Angew. Chem.* **1992**, *104*, 1071; *Angew. Chem. Int. Ed. Engl.* **1992**, *31*, 1040.

[13] a) F. Dirschl, E. Hanecker, H. Nöth, W. Rattay, W. Wagner, *Z. Naturforsch. B* **1986**, *41*, 32; b) R. Boese, B. Kröckert, P. Paetzold, *Chem. Ber.* **1987**, *120*, 1913; c) K.-H. van Bonn, P. Schreyer, P. Paetzold, R. Boese, *ibid.* **1988**, *121*, 1045.

[14] P. Paetzold, B. Redenz-Stormanns, R. Boese, *Angew. Chem.* **1990**, *102*, 910; *Angew. Chem. Int. Ed. Engl.* **1990**, *29*, 900.

[15] G. K. Surya Prakash, H. Buchholz, V. Prakash Reddy, A. de Meijere, G. A. Olah, *J. Am. Chem. Soc.* **1992**, *114*, 1097.

[16] M. Bühl, P. von R. Schleyer, M. A. Ibrahim, T. Clark, *J. Am. Chem. Soc.* **1991**, *13*, 2466, and references cited therein.

[17] S. E. Denmark, K. Nishide, A.-M. Faucher, *J. Am. Chem. Soc.* **1991**, *113*, 6675.

[18] J. J. Eisch, B. Shafii, J. D. Ordon, A. L. Rheingold, *J. Am. Chem. Soc.* **1990**, *112*, 1847.

[19] M. A. Kropp, M. Baillargeon, K. M. Park, K. Bhamidapaty, G. B. Schuster, *J. Am. Chem. Soc.* **1991**, *113*, 2155.

[20] P. Willershausen, G. Schmidt-Lukasch, C. Kybart, J. Allwohn, W. Massa, M. L. McKee, P. von R. Schleyer, A. Berndt, *Angew. Chem.* **1992**, *104*, 1417; *Angew. Chem. Int. Ed. Engl.* **1992**, *31*, 1384

[21] P. Willershausen, C. Kybart, N. Stamatis, W. Massa, M. Bühl, P. von R. Schleyer, A. Berndt, *Angew. Chem.*, **1992**, *104*, 1278; *Angew. Chem. Int. Ed. Engl.* **1992**, *31*, 1238.

[22] K. Krogh-Jespersen, D. Cremer, D. Poppinger, J. A. Pople, P. von R. Schleyer, J. Chandrasekhar, *J. Am. Chem. Soc.* **1979**, *101*, 4843.

 © *VCH Verlagsgesellschaft mbH, W-6940 Weinheim, 1992* *0570-0833/92/1010-1331 $ 3.50+.25/0*

Cascade Cyclizations

By *H. Martin R. Hoffmann**

Cascade cyclizations, also called tandem, zip, or domino reactions, are multiple consecutive cyclizations which have fascinated organic chemists for more than 35 years. Several reasons account for this interest. Rings are not built up tediously step by step, but convergently in one fell swoop. Proper induction and termination of the cyclization cascade provide a major challenge, as does stereocontrol over the generation of several new chiral centers. To this end, a suitable tether must be constructed, the conformation and stereoelectronics of which facilitate coupling and ring closure.

Multiple consecutive cyclizations can be triggered by stoichiometric and catalytic amounts of reagents. Biomimetic cascades of cations which follow the biogenetic isoprene rule,[1] were among the first reactions of this type to be studied. Thus, many functionalized polyenes containing 1,5-diene units have been cyclized to give higher terpenes.[2]

Recently, these reactions have been terminated in a novel way with internal oxygen nucleophiles such as carbonyl, hydroxyl, and β-ketoester groups. For example, *trans,trans*-farnesylacetone (**1**), readily available from farnesol, was submitted to the Nishizawa cyclization protocol[3] with mercuric triflate/*N,N*-dimethylaniline to give sensitive endocyclic enol ether **2**, capable of surviving in the presence of the electrophilic trigger. Demercuration of **2** furnished sclareol oxide **3**,[4] a well known constituent of clary (*Salvea sclarea*) which fulfills Ohloff's syntriaxial rule[5] and is used as a precursor of ambergris odorants.

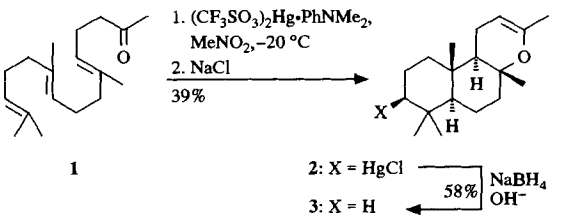

More conventionally, tandem cyclizations of polyenes have been initiated with a variety of other electrophiles including protons, bromine cations, Lewis acids,[2] sulfenium ions (from methyl benzenesulfenate $PhSOCH_3$ and BF_3[6]) and benzeneselenenyl triflate PhSeOTf.[7]

In the 1980s radical reactions emerged as efficient processes for carbon–carbon bond formation in the synthesis of natural products. An oxidative cyclization is the central step in Snider's synthesis of podocarpic acid.[8] The reaction is induced by electrophilic radical **5**, which is generated from the enol precursor by a one-electron oxidation. Termination of the cascade is feasible by the oxidation of **6** to cation **7** and straightforward deprotonation.

Perhaps the best known tandem radical cyclizations terminating in radical rather than ionic fashion were developed by

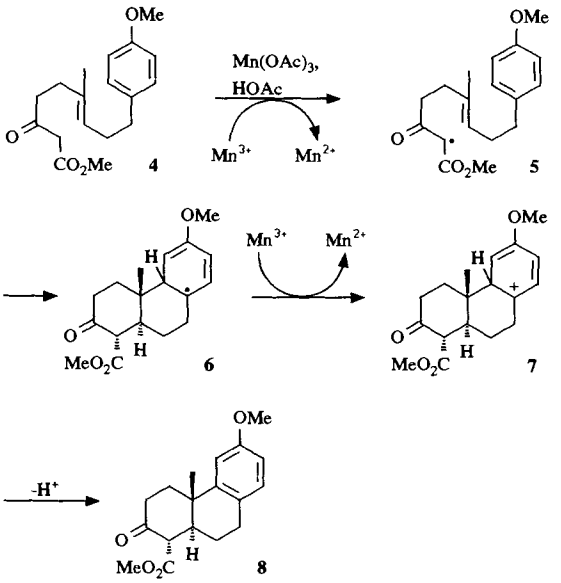

Curran et al. and relate to the synthesis of both linear (**9** → **12**) (AIBN = azobis(isobutyronitrile) and angular triquinanes (**13** → **14**).[9] The formation of the less stable vinyl radical **11** from the more stable tertiary radical **10**

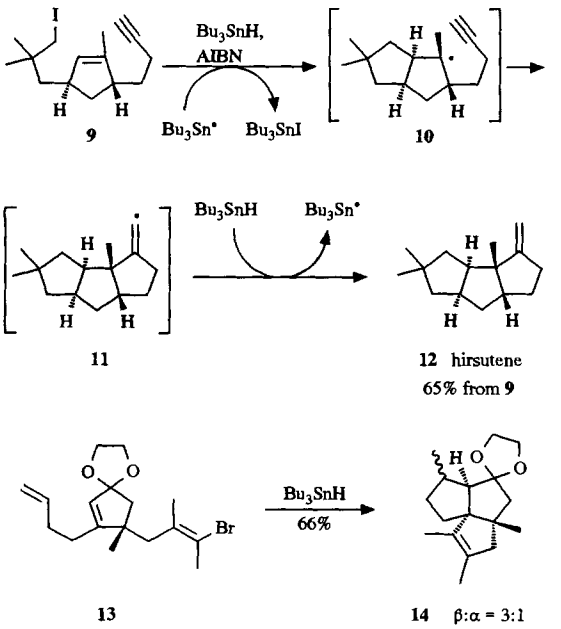

might seem surprising at first glance. However, the reaction is accompanied by loss of a weak acetylenic π bond and formation of a strong vinylic carbon–carbon bond. Furthermore, termination by hydrogen atom transfer affords a strong vinylic carbon–hydrogen bond (CH_2 = CH–H, ΔH^0 = 108 kcal mol^{-1}) which compares with ΔH^0 = 91 kcal mol^{-1} for the bond between hydrogen and a tertiary carbon atom. Thus, the success of the cyclization may depend on factors other than those in cationic cyclizations in which the stability of the cation generated on termination is often critical. It is also obvious that the stereochemistry of the vinylic bromide **13** (*E* or *Z*) is irrelevant to the success of the cascade, since the resulting vinylic radical is linear.

[*] Prof. H. M. R. Hoffmann
Institut für Organische Chemie der Universität
D-W-3000 Hannover (FRG)

Recently, the cedrane skeleton **19** was constructed in two steps from nitroolefin **15** and the γ,δ-unsaturated aldehyde **16**.[10] As in the synthesis of **14** from **13**, the key step is the tandem cyclization **18** → **19**, consisting of consecutive 5-*exo*-trigonal ring closure reactions. Delivery of the hydrogen atom in the terminating step occurs antiperiplanar to the face of the double bond, resulting in an equatorial methyl group. As in the examples above, the two five-membered rings in **19** must be *cis*-fused, since a *trans*-bicyclo[3.3.0]-octane substructure would be too strained.

The synthesis of **19** also testifies to the synthetic versatility of the nitro group in reactions of three fundamental mechanistic types, namely, pericyclic, ionic, and free radical. Nitroolefin **15** is the Diels–Alder adduct of isoprene and nitroethylene. The nitro group not only activates the dienophile, but also controls regioselectivity ("*para*"). Nitroalcohol **17** is formed in an ionic nitroaldol reaction (Henry reaction). Finally, since the nitro group is attached to a tertiary carbon in **17**, it serves as a convenient leaving group in the generation of the tertiary radical **18**,[10] thus demonstrating excellent overall efficiency in the use of this one functional group.

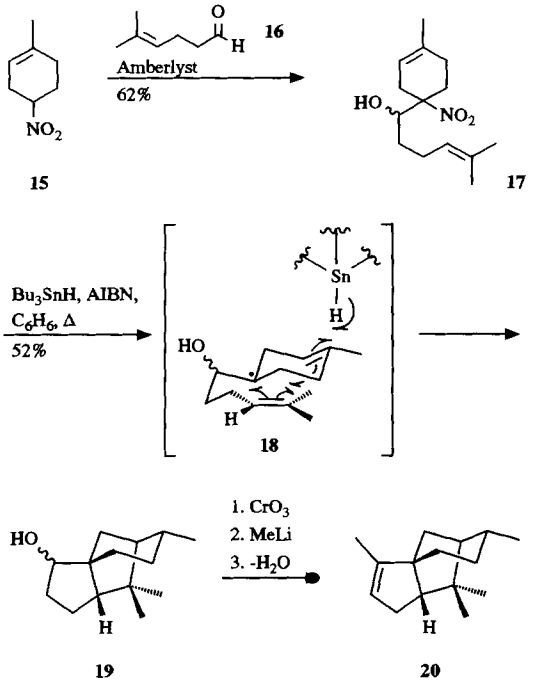

Hanessian and Léger[11] have recently cyclized a series of dienes and trienes with trimethyltin hydride Me_3SnH rather than Bu_3SnH. Me_3SnH is sterically less encumbered and therefore probably more reactive than Bu_3SnH. It has been generated conveniently in situ, from Me_3SnCl and $NaBH_3CN$, which is superior to the more reactive $LiAlH_4$ as a hydride donor. The (trimethylstannyl)methyl group in the cyclization product **22** does not lead the synthesis into a cul-de-sac, since this group can be converted into a masked aldehyde by a novel oxidative destannylation. The oxidation probably involves single-electron transfer (SET) from stannane to $(NH_4)_2Ce(NO_3)_6$ (CAN) to produce a (trimethylstannyl)methyl radical cation which disproportionates reversibly to the most stable radical, namely, the primary

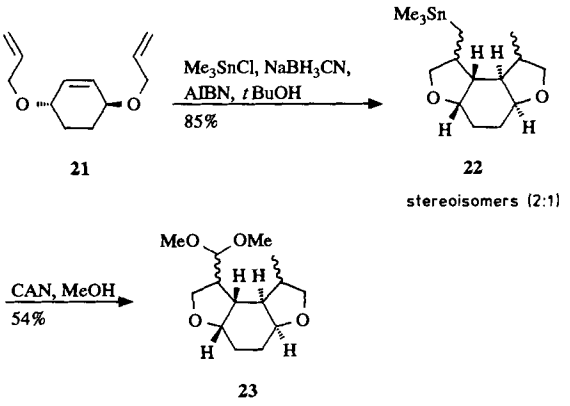

radical **24** (rather than Me$^\bullet$) and trimethylstannylium ion **25**. Even if the double cyclization had been successful with Bu_3SnH instead of Me_3SnH, any differentiation of alkyl groups during the oxidation step would have been lost!

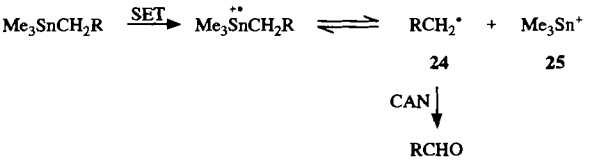

A monocyclization reaction was applied in the synthesis of the lignan antibiotic burseran (**31**).[12] Starting from 1,6-diene **26**, Hanessian and Léger prepared tetrahydrofuran **27**,

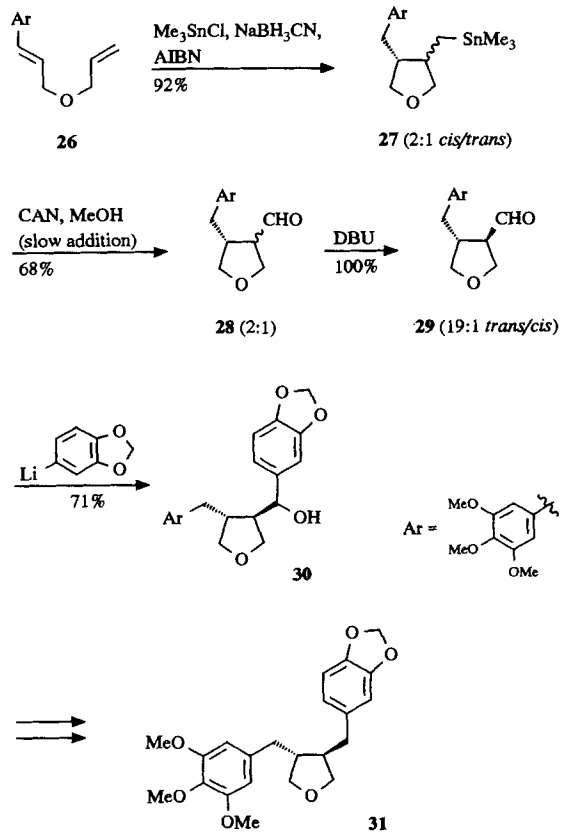

substituted in the 3 and 4 positions with typically the *cis* isomer predominating. Since tetrahydrofurans such as **27** and related five-membered heterocycles are usually difficult to obtain with substituents in the 3 and 4 positions, the radical route is very useful. Oxidation of **27** with CAN gave the aldehyde **28**, without attack of the electron-rich aromatic moiety or alteration of the ratio of isomers (2:1) of **27**. Further steps furnished (±)-burseran (**31**), which was also obtained enantiomerically pure when the racemic mixture was resolved at an earlier stage in the synthesis (DBU = 1,8-diazabicyclo[5.4.0]undec-7-ene).

The stereochemical outcome of cyclization cascades such as **9** → **12**, **13** → **14** is dictated by the stereochemistry of the central five-membered ring which serves as a platform for the construction of two new rings. For example, for steric reasons radical **10** has little option but form *cis-anti-cis*-fused hirsutene **12** (cf. also **21** → **22**). In contrast, not only the conformation must be decided but also the choice between a C-C double bond and a C-C triple bond must be made in the reactions of the radicals generated from functionalized 1,5-enyne **32**, which has recently been shown to enter into radical-mediated, sequential 5-*exo*-trigonal, 6-*endo*-digonal cyclizations. The 6-*endo*-digonal closure is unusual in itself and requires heating to 100 °C. The overall reaction **32** → **33** + **34** is a cycloisomerization, that is, the radical chain is driven by iodine atom transfer. Interestingly, the cascade has

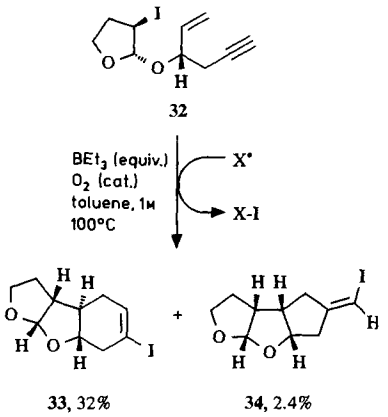

also been terminated by hydrogen atom transfer (with catalytic amounts of cobaloxime and $NaBH_4$) under milder conditions, that is at 50 °C. The tricyclic compound **33** arises from an "abnormal" boat transition state with transoid pseudo-axial substituents, whereas formation of compact dioxatriquinane **34** requires a cisoid chair transition state. According to a CAS online search, both the tricyclic 5 · 5 · 6 ring system in **33** and the corresponding 6 · 5 · 6 ring system are new.[13]

Synthetic methods based on reactions of radicals have come of age and are now almost standard procedures for carbon–carbon bond formation.[14, 15] High chemoselectivity, stereoselectivity, and the possibility of working without protecting groups as well as taking advantage of umpolung provide new opportunities for using old compounds. In this fashion, the "reaction windows" of organic reactions are defined more clearly. Apart from many obvious and important practical applications and advantages, the intellectual base of organic chemistry has been broadened and strengthened decisively.

German version: *Angew. Chem.* **1992**, *104*, 1361

[1] A. Eschenmoser, L. Ruzicka, O. Jeger, D. Arigoni, *Helv. Chim. Acta* **1955**, *38*, 1890; G. Stork, A. W. Burgstahler, *J. Am. Chem. Soc.* **1955**, *77*, 5068. Cf. R. Bohlmann, *Angew. Chem.* **1992**, *104*, 596; *Angew. Chem. Int. Ed. Engl.* **1992**, *31*; 582; C. H. Heathcock, *ibid.* **1992**, *104*, 675 and **1992**, *31*, 665.

[2] W. S. Johnson, S. D. Lindell, J. Steele, *J. Am. Chem. Soc.* **1987**, *109*, 5852. Cf. *Chemtracts: Org. Chem.* **1988**, *1*, 32. For a transannular π-cyclization terminated by simultaneous formation of a bridgehead cation–bridgehead olefin see U. Vogt, U. Eggert, A. M. Z. Slawin, D. J. Williams, H. M. R. Hoffmann, *Angew. Chem.* **1990**, *102*, 1530; *Angew. Chem. Int. Ed. Engl.* **1990**, *29*, 1456; H. M. R. Hoffmann, U. Eggert, *Synlett* **1991**, 337.

[3] H. Takenaka, T. Sato, M. Nishizawa, *Tetrahedron Lett.* **1989**, *30*, 2267; M. Nishizawa, H. Takenaka, H. Nishide, Y. Hayashi, *ibid.* **1983**, *24*, 2581, and references therein.

[4] A. S. Gopalan, R. Prieto, B. Mueller, D. Peters, *Tetrahedron Lett.* **1992**, *33*, 1679.

[5] G. Ohloff: *Riechstoffe und Geruchssinn. Die molekulare Welt der Düfte*, Springer, Heidelberg, **1990**.

[6] S. R. Harring, T. Livinghouse, *Tetrahedron Lett.* **1989**, *30*, 1499; S. R. Harring, T. Livinghouse, *J. Chem. Soc. Chem. Commun.* **1992**, 502, 503.

[7] S. Murata, T. Suzuki, *Tetrahedron Lett.* **1990**, *31*, 6535, and references therein.

[8] B. B. Snider, R. Mohan, S. A. Kates, *J. Org. Chem.* **1985**, *50*, 3659.

[9] Reviews: C. P. Jasperse, D. P. Curran, T. L. Fevig, *Chem. Rev.* **1991**, *91*, 1237; W. B. Motherwell, D. Crich, *Best Synthetic Methods. Free Radical Chain Reactions in Organic Synthesis*, Academic Press, London, **1991**; D. H. R. Barton, *The Invention of Chemical Reactions: The Last Five Years* (*Tetrahedron* **1992**, *48*, 2529).

[10] Y.-J. Chen, W.-Y. Lin, *Tetrahedron Lett.* **1992**, *33*, 1749. For a review of aliphatic nitro compounds in organic synthesis, see R. Tamura, A. Kamimura, N. Ono, *Synthesis* **1991**, 423.

[11] S. Hanessian, R. Léger, *J. Am. Chem. Soc.* **1992**, *114*, 3115.

[12] S. Hanessian, R. Léger, *Synlett* **1992**, 402.

[13] U. Albrecht, R. Wartchow, H. M. R. Hoffmann, *Angew. Chem.* **1992**, *104*, 903; *Angew. Chem. Int. Ed. Engl.* **1992**, *31*, 910.

[14] The converse also applies: chemoselective C-C bond cleavage in complex, polyfunctionalized molecules is feasible. For example, the fragmentation of anomeric carbohydrate alkoxy radicals affords acyclic chiral building blocks: P. de Armas, C. G. Francisco, E. Suárez, *Angew. Chem.* **1992**, *104*, 746; *Angew. Chem. Int. Ed. Engl.* **1992**, *31*, 772.

[15] Transition metal (Pd, Zr) mediated zip cyclizations provide a range of further synthetic possibilities; see for example B. M. Trost, Y. Shi, *J. Am. Chem. Soc.* **1991**, *113*, 701; B. M. Trost, *Science* **1991**, *254*, 1471; E. Negishi, *Pure Appl. Chem.* **1992**, *64*, 323.

[16] *Note added in proof* (Sept. 9, 1992): The tricyclo[9.3.1.0]pentadecane system of the taxanes has been synthesized by a spectacular 12-*endo*-trig,6-*exo*-trig cyclization: S. A. Hitchcock, G. Pattenden, *Tetrahedron Lett.* **1992**, *33*, 4843.

Communications may be submitted in English *or* in German. Further details regarding the submission of communications can be found in the "Notice to Authors" reproduced in the January issue of the journal. Copies thereof may be obtained from the editorial office upon request.

Intermolecular Additions and Cycloisomerizations by a Pd-Catalyzed Sequence of an Intramolecular Redox Reaction and an Addition**

By *Barry M. Trost,* Walter Brieden,* and *Karl H. Baringhaus*

Adjusting oxidation states by intramolecular hydrogen shifts[1, 2] is more efficient and "atom economical" than conventional reduction/oxidation sequences in organic synthesis. Such hydrogen shifts may generate trappable reactive intermediates, ultimately leading to simple additions.[3] This fits in with our program to enhance atom economy[4]—that is, to minimize the number of atoms required in the building blocks of a reaction sequence and to maximize the use of processes that require only catalytic amounts of any additional reactants—and to generate macrocycles by cycloisomerization.[4, 5] Our previous work suggested that a hydridopalladium complex isomerizes acetylenes to allenes.[2a] We postulated that the latter may undergo a second hydropalladation to form a π-allylpalladium complex, which could undergo a subsequent addition [Eq. (1)]. This overall

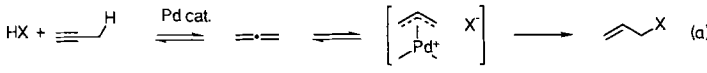

(a)

process would constitute an internal redox reaction and an addition. We wish to report the development of such a process whereby propargylic acetates are converted into novel allylic *gem*-diacetates.[7]

In initial experiments the propargylic acetate **1a** was treated with 2.5 mol% tris(dibenzylidenacetone) complex **3** and 35 mol% triphenylphosphine in toluene with 5 equivalents of acetic acid. The resulting geminal diacetate **2a** was isolated in 77% yield exclusively as the (*E*) isomer (proven by NMR spectroscopy) [Eq.(b)]. Only slightly lower yields (72%) were obtained with as little as 1 equivalent of acetic acid. A precipitous drop in yield (to 28%) resulted when a palladium complex with an acceptor ligand like trifurylphosphine was used. When complexes with bidentate ligands like bis(diphenylphosphino)butane (dppb) were employed, the reaction was shut down completely. Replacement of the methoxy group OR′ in **1a** with a siloxy substituent (**1b**) led again exclusively to the geminal diacetate product, in this case **2b**. In all the cases examined all the products were obtained as (*E*) isomers.

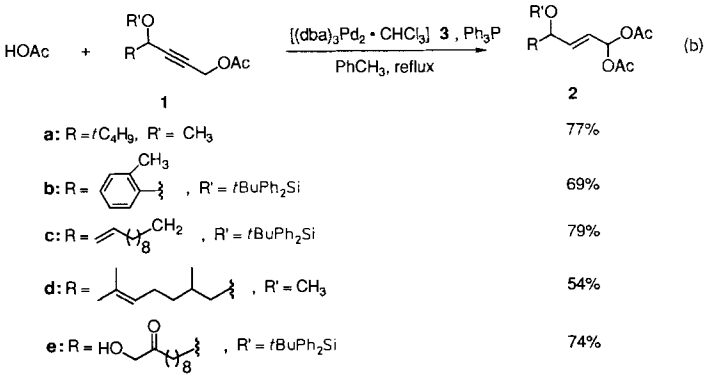

(b)

Reaction (b) exhibits excellent chemoselectivity. Neither double bonds (**1c** and **1d**), nor carbonyl and hydroxyl functions on the R group (**1e**) are affected. Compounds **4** and **6**, both derived from ketones, react as smoothly as compounds **1a–e** to give the corresponding geminal diacetates **5** and **7** [Eqs.(c) and (d)]. Remarkably, even compounds with carboxyl groups react analogously when 13 equivalents of acetic acid are used to suppress the intramolecular reaction with the acid function. Mixed geminal carboxylates such as **8** are also available [Eq.(e)].

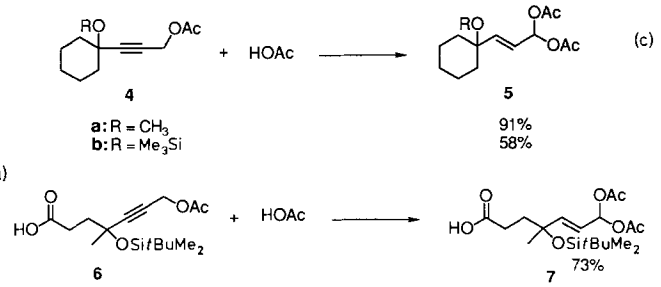

(c)
(d)

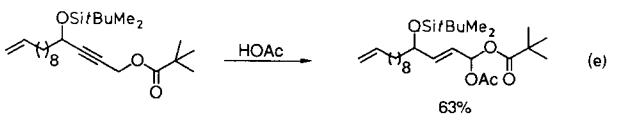

(e)

Gratifyingly, this new sequence consisting of an intramolecular redox reaction and an addition may be performed intramolecularly in relatively concentrated solutions to gener-

[*] Prof. Dr. B. M. Trost, W. Brieden, K. H. Baringhaus
Department of Chemistry, Stanford University
Stanford, CA 94305-5080 (USA)

[**] This research was supported by the National Science Foundation, the General Medical Sciences Institute of the National Institutes of Health (NIH) and the Deutsche Forschungsgemeinschaft (stipends for W. B. and K. H. B.) The mass spectra were recorded at the Mass Spectrometry Facility of the University of California at San Francisco, which is sponsored by the Division of Resources of the NIH.

ate macrocycles [Eq.(f)]. For example, a 0.01 M solution of carboxylic acid **9** in benzene was heated at reflux with 3–5 mol% **3** and 30 mol% triphenylphosphine for 16 h to furnish the macrolide **10** in 52% yield as a 1.5:1 mixture of isomers. The 15.5–15.7 Hz coupling constants for the

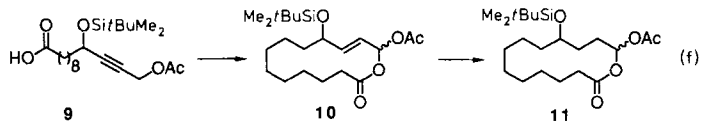

9 10 11 (f)

olefinic hydrogens suggested that the product was a mixture of diastereomeric acetates, both with (*E*) geometry, rather than (*E*) and (*Z*) olefins. This conclusion was confirmed by the catalytic hydrogenation of the product mixture to a similar mixture of saturated isomeric macrolides **11**. The chemoselectivity of the cyclization is established by the reaction of diyne **14** [Eq. (g)], readily available from our Pd-catalyzed coaddition of the terminal acetylene **12** with ynoate **13**

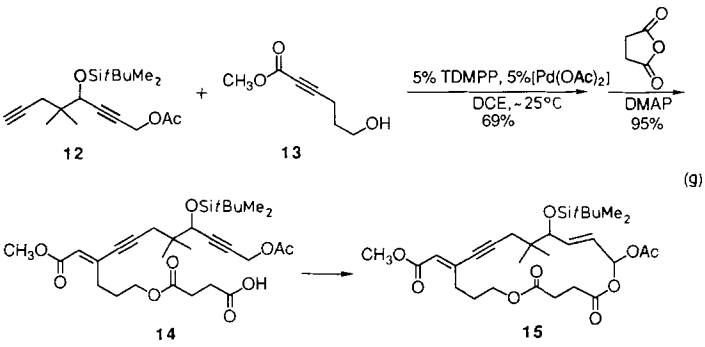

12 13 14 15 (g)

(TDMPP = tris(2,6-dimethoxyphenyl)phosphine, DCE = 1,2-dichloroethene, DMAP = 4-dimethylaminopyridine).[8] The excellent yield of macrodiolide **15** (87–90%) illustrates the innocuousness of the normally reactive yneoate units in substrate **14** under these reaction conditions. The diastereoselectivity here (4:1) is higher than that observed in the cyclization leading to **10** and suggests that the diastereoselectivity depends upon substituents on the tether.

To our knowledge the Pd-catalyzed sequence of intramolecular redox reaction and addition described here leading to synthetically interesting geminal dicarboxylates is unprecedented. It stands in contrast to the Pd^0 catalyzed substitution reactions of propargyl carboxylates[9] and the Pd^{2+} catalyzed additions of carboxylic acids to triple bonds.[10] The isomerization of an alkyne to an alkene was reported recently, however, as the first step in the isomerization of alk-2-ynedi-1,4-ols to 1,4-dicarbonyl compounds.[2b] Rhodium and ruthenium complexes also have been reported to catalyze direct addition to triple bonds.[11] The new reaction described here also exhibits excellent atom economy and should allow access to highly functionalized macrolides.

Experimental Procedure

Acetic acid (0.150 mL, 2.62 mmol) was added to a solution of **3** (33.8 mg, 0.0327 mmol) and triphenylphosphine (89.1 mg, 0.340 mmol) in toluene (20 mL) at 20–30 °C. After 5 min **4a** (325 mg, 1.54 mmol) was added and the resultant mixture heated at reflux for 20 h. The reaction mixture was concentrated under vacuum and the residue chromatographed directly (silica gel, hexane/ethyl acetate, 10:1) to give **5a** (379.5 mg, 91% yield).

Received: May 2, 1991 [Z 5328 IE]
German version: *Angew. Chem.* **1992**, *104*, 1392

[1] Cf. Cr: M. Sodeoka, H. Yamada, M. Shibasaki, *J. Am. Chem. Soc.* **1990**, *112*, 4906; Fe: N. Iranpoor, E. Mottaghinejad, *J. Organomet. Chem.* **1992**, *423*, 399; J. C. Barborak, J. W. Herndon, J.-W. Wong, *J. Am. Chem. Soc.* **1979**, *101*, 7430; J. U. Strauss, P. W. Ford, *Tetrahedron Lett.* **1975**, 2917; F. G. Cowerd, J. L. von Rosenberg, *J. Am. Chem. Soc.* **1969**, *91*, 2157; R. Damico, T. J. Logan, *J. Org. Chem.* **1967**, *32*, 2356; G. F. Emerson, R. Pettit, *J. Am. Chem. Soc.* **1962**, *84*, 4591; Co: F. Piacenti, S. Pucci, M. Bianchi, P. Pino, *ibid.* **1968**, *90*, 6847; R. W. Goetz, M. Orchin, *ibid.* **1963**, *85*, 1549; M. Brock, A. Heesing, *Chem. Ber.* **1989**, *122*, 1925; Rh and Ru: B. M. Trost, R. J. Kulawiec, *Tetrahedron Lett.* **1991**, *32*, 3039; S. H. Bergens, B. Bosnich, *J. Am. Chem. Soc.* **1991**, *113*, 958; W. Smadja, G. Ville, C. Georgoulis, *J. Chem. Soc. Chem. Commun.* **1980**, 594; M. Dedieu, Y.-L. Pascal, *C.R. Acad. Sci. Ser. C* **1976**, *282*, 65; W. Strohmeier, L. Weigelt, *J. Organomet. Chem.* **1975**, *86*, C17; Y. Sasson, G. L. Rempel, *Tetrahedron Lett.* **1974**, 4133; J. K. Nicholson, B. L. Shaw, *Proc. Chem. Soc. London* **1963**, 282; Os: A. J. Deeming, S. Hasso, *J. Organomet. Chem.* **1976**, *114*, 313; Ir: D. Baudry, M. Ephritikine, H. Felkin, *Nouv. J. Chim.* **1978**, *2*, 355; D. Ma, X. Lu, *Tetrahedron* **1990**, *46*, 3189, 6319; Pt: H. C. Clark, H. Kurosawa, *Chem. Commun.* **1972**, 150.

[2] Pd: a) B. M. Trost, T. Schmidt, *J. Am. Chem. Soc.* **1988**, *110*, 2301; b) X. Lu, J. Ji, D. Ma, W. Shen, *J. Org. Chem.* **1991**, *56*, 5774; c) C. Guo, X. Lu, *Tetrahedron Lett.* **1991**, *32*, 7549; d) H. Sheng, S. Lin, Y. Huang, *ibid.* **1986**, *27*, 4893.

[3] H. Nemoto, H. N. Jimenez, Y. Yamamoto, *J. Chem. Soc. Chem. Commun.* **1990**, 1304.

[4] B. M. Trost, *Science* **1991**, *254*, 1471.

[5] For some of our recent work see, B. M. Trost, B. A. Vos, C. M. Brzezowski, D. P. Martina, *Tetrahedron Lett.* **1992**, *33*, 717; B. M. Trost, Y. Shi, *J. Am. Chem. Soc.* **1992**, *114*, 791; B. M. Trost, M. K. Trost, *Tetrahedron Lett.* **1991**, *32*, 3647; B. M. Trost, Y. Kondo, *ibid.* **1991**, *32*, 1613; B. M. Trost, M. K. Trost, *J. Am. Chem. Soc.* **1991**, *113*, 1850; B. M. Trost, Y. Shi, *ibid.* **1991**, *113*, 701; B. M. Trost, M. Lautens, C. Chan, D. J. Jebaratnam, T. Müller, *ibid.* **1991**, *113*, 636; B. M. Trost, *Acc. Chem. Res.* **1990**, *23*, 34; B. M. Trost, S. Matsubara, J. Caringi, *J. Am. Chem. Soc.* **1989**, *111*, 8745.

[6] Cf. R. C. Larock, N. G. Berrios-Pena, C. A. Fried, *J. Org. Chem.* **1991**, *56*, 2615; K. Koerber, J. Gore, J.-M. Vatele, *Tetrahedron Lett.* **1991**, *32*, 1187; J. S. Prasad, L. S. Liebeskind, *ibid.* **1988**, *29*, 4253, 4257; M. Ahmar, J. J. Barrieux, B. Cazes, J. Gore, *Tetrahedron* **1987**, *43*, 513; N. Chatani, T. Takeyasu, T. Hanafusa, *Tetrahedron Lett.* **1986**, *27*, 1841.

[7] B. M. Trost, J. Vercauteren, *Tetrahedron Lett.* **1985**, *26*, 131.

[8] B. M. Trost, C. Chan, G. Rühter, *J. Am. Chem. Soc.* **1987**, *109*, 3486.

[9] J. Tsuji, H. Watanabe, I. Minami, I. Shimizu, *J. Am. Chem. Soc.* **1985**, *107*, 2196.

[10] N. Yanagihara, C. Lambert, K. Iritani, K. Utimoto, H. Nozaki, *J. Am. Chem. Soc.* **1986**, *108*, 2753.

[11] K. Sakai, K. Kondo, *Chem. Lett.* **1990**, 1665; D. M. T. Chan, B. Marda, D. Milstein, N. J. Taylor, *J. Am. Chem. Soc.* **1987**, *109*, 6385.

Chemoenzymatic Syntheses of the Optically Active Hydroperoxides of Phosphatidylglycerol and Phosphatidylethanolamine with Lipase, Lipoxygenase, and Phospholipase D**

By *Kenji Yoneda, Keiji Sasakura, Shoichi Tahara, Junkichi Iwasa, Naomichi Baba*, Takao Kaneko,* and *Mitsuyoshi Matsuo*

Recent studies have demonstrated that in vivo formation of lipid peroxides is responsible for aging and for some serious diseases and dysfunctions such as arteriosclerosis or cancer.[1]

For studies in this field, different types of pure, optically active lipid hydroperoxides are urgently needed. We previ-

[*] Prof. Dr. N. Baba, K. Yoneda, K. Sasakura, S. Tahara, Prof. Dr. J. Iwasa
Bioresources Chemistry, Faculty of Agriculture
Okayama University
1-1-1 Tsushimanaka, Okayama 700 (Japan)
Dr. T. Kaneko, Dr. M. Matsuo
Tokyo Metropolitan Institute of Gerontology
35-2 Sakaecho, Itabashiku, Tokyo 173 (Japan)

[**] This work was supported by the Ministry of Education of Japan (grant 0455 6015).

ously reported the synthesis of a phospholipid hydroperoxide, 1-stearoyl-2-[13-(*S*)-hydroperoxy-(9*Z*, 11*E*)-octadecadienoyl]-*sn*-glycero-3-phosphocholine.[2] Here we wish to describe the syntheses of optically active hydroperoxides of phosphatidylethanolamine and phosphatidylglycerol containing a hydroperoxidized linoleic acid moiety.

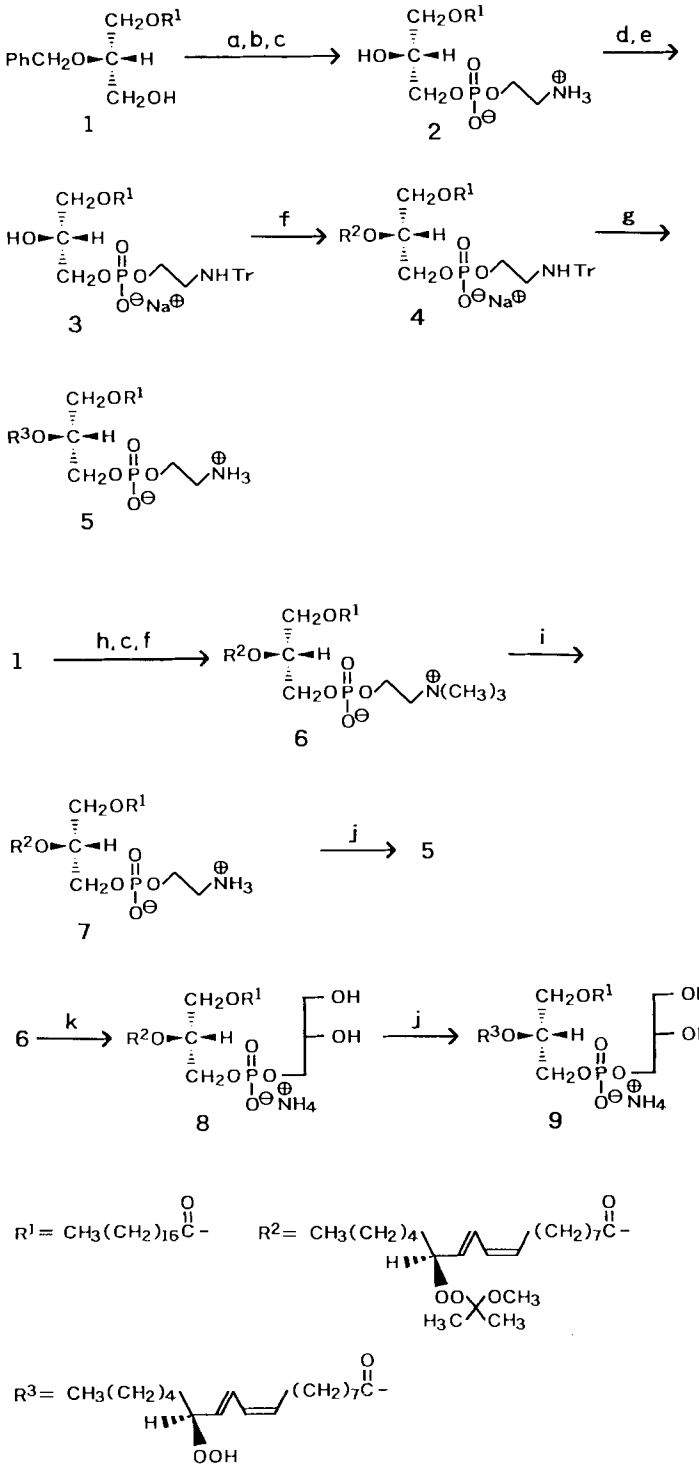

Scheme 1. Reagents for the syntheses of phospholipid hydroperoxides **5** and **9**. a) $POCl_3$, $H_2NCH_2CH_2OH$; b) H_3O^+; c) $H_2/Pd(OH)_2$; d) TrCl, NEt_3; e) Na_2CO_3; f) DCC, DMAP, R^2OH; g) $AcOH/H_2O/THF$ (4:1:5); h) $POCl_3$, choline tosylate; i) $H_2NCH_2CH_2OH$, phospholipase D; j) $THF/AcOH/H_2O$ (4:2:1); k) glycerol, phospholipase D. Tr = trityl, DCC = Dicyclohexylcarbodiimide, DMAP = 4-dimethylaminopyridine.

The synthetic routes to these compounds are shown in Scheme 1. Optically active 1-stearoyl-*sn*-glycerol **1** (100% optical purity) was prepared by enantioselective, lipase-catalyzed stearoylation of 2-*O*-benzylglycerol with vinyl stearate.[2] The optically active 1-stearoyl-*sn*-glycerol obtained was converted to 1-stearoyl-*sn*-lysophosphatidylethanolamine **2** according to the method of Eible.[3] The nucleophilicity of its amino group was decreased by tritylation, which afforded **3**. A hydroxy group of the phosphatidyl glyceride **3** was then esterified by the DCC method (DCC = dicyclohexylcarbodiimide) with 13-(*S*)-α-methoxyisopropylperoxy-(9*Z*, 11*E*)-octadecadienoic acid (96% optical purity), which was prepared from linoleic acid by the action of soybean lipoxygenase followed by the acetalization of a hydroperoxy group with 2-methoxypropene.[2] This esterification gave rise to **4** (24% yield from **2**). On treatment of **4** with a mixture of THF, AcOH, and H_2O (5:4:1) at 45 °C for 24 h, the acetal and trityl residues were simultaneously removed. The desired hydroperoxide **5** was obtained without any side reactions (83% yield). The hydroperoxide was purified by preparative thin-layer chromatography (TLC) on silica gel with a mixture of methanol, chloroform, and 28% ammonium hydroxide (15:30:2; $R_f = 0.6$) as eluent. The presence of a hydroperoxy group in **5** was confirmed by potassium iodide coloration, and its structure was deduced from the ^1H NMR and FAB mass spectra.[4]

The second route to **5** involved transphosphatidylation catalyzed by phospholipase D. The glycerol **1** was converted to the choline peroxide **6** as described previously.[2] In the presence of excess (58 mol equiv) of ethanolamine in acetate buffer (0.1 M, pH 5.6), **6** was treated with phospholipase D (153 units) from *Streptomyces sp.*[5] at ambient temperature for 3 h. Usual workup and isolation by preparative TLC on silica gel afforded **7**, from which the final product **5** was obtained by hydrolysis of the peracetal with a mixture of $THF/AcOH/H_2O$ (4:2:1). All the analytical and spectroscopic data of **5** prepared by the two synthetic routes were consistent.

Phosphatidylglycerol hydroperoxide **9** was also synthesized by a similar approach. The hydroperoxide **9** was purified by TLC with a mixture of methanol, chloroform, and 28% ammonium hydroxide [(70:130:1); $R_f = 0.48$] as an eluent. Its structural integrity was confirmed by ^1H NMR spectroscopy and FAB mass spectrometry.[4]

In conclusion, two kinds of pure, optically active phospholipid hydroperoxides **5** and **9** were synthesized for the first time through protection of the hydroperoxy group by acetalization and the amino group by tritylation, and subsequent simultaneous deprotection followed by transphosphatidylation catalyzed by phospholipase.

The toxicities towards human endthelial cells of both hydroperoxides are now being investigated. The present chemical and enzymatic approaches can be applied to the other biologically important phospholipid hydroperoxides with well-defined chemical structures.

Received: April 14, 1992 [Z 5304]
German Version: *Angew. Chem.* **1992** *104*, 1386

CAS Registry numbers:
1, 85647-89-8; **2**, 69747-55-3; **3**, 143447-32-9; **4**, 143447-33-0; **5**, 143447-34-1; **6**, 132194-62-8; **7**, 143447-35-2; **8**, 143447-36-3; **9**, 143447-37-4; 13-(*S*)-α-methoxyisopropylperoxy-(9*Z*,11*E*)-octadecadienoic acid, 132194-61-7; ethanolamine, 141-43-5; glycerin, 56-81-5.

[1] *Lipid Peroxides in Biology and Medicinie* (Ed.: K. Yagi), Academic Press, New York, **1982**.
[2] N. Baba, K. Yoneda, S. Tahara, J. Iwasa, T. Kaneko, M. Matsuo, *J. Chem. Soc. Chem. Commun.* **1990**, 1281–1282.

[3] H. Eible, *Proc. Natl. Acad. Sci. USA* **1978**, *75*, 4074–4077.

[4] Spectroscopic data: **5**, $[\alpha]_D^{25} = +2.01$ ($c = 1.19$ in $MeOH/CHCl_3$, 1:1 v/v); ^1H NMR (500 MHz, $CDCl_3$): $\delta = 0.88$ (m, 6H; 2 ω-Me), 1.24 (m, 44H; 22 CH_2), 1.58 (m, 4H; $OCOCH_2CH_2$ in each chain), 2.18 (m, 2H; C_8'-H), 2.28 (m, 4H; $OCOCH_2$ in each chain), 3.13 (m, 2H; CH_2NH_3), 3.94 (m, 2H; -OCH_2-CH-CH_2O-), 4.07 (m, 2H; $OCH_2CH_2NH_3$), 4.14 (m, 1H; 1H of -OCH_2-CH-CH_2O-), 4.36 (m, 2H; 1H of -OCH_2-CH-CH_2O-, C_{13}'-H), 5.21 (m, 1H; CHOCO), 5.46 (m, 1H; C_9'-H), 5.72 (m, 1H; C_{12}'-H), 6.00 (dd, ^3J (H,H) = 10.7 Hz, 1H; C_{10}'-H), 6.53 (m, ^3J (H,H) = 10.7 Hz, 1H; C_{11}'-H), FAB-MS: m/z 775 (MH^+).
9, $[\alpha]_D^{25} = +3.76$ ($c = 1.07$ in $MeOH/CHCl_3$, 1:1 v/v); ^1H NMR (500 MHz, $CDCl_3$): $\delta = 0.88$ (m, 6H; 2 ω-Me), 1.28 (m, 44H; 22 CH_2), 1.57 (m, 4H; $OCOCH_2CH_2$ in each chain), 2.17 (m, 2H; C_8'-H), 2.28 (m, 4H; $OCOCH_2$ in each chain), 3.62 (m, 2H; PO-CH_2-CHOH-CH_2), 3.90 (m, 5H; 2 CH_2OP, CHOH), 4.15 (m, 1H; 1H of OCH_2-CH-CH_2O-), 4.35 (m, 2H; 1H of -OCH_2-CH-CH_2O-, C_{13}'-H), 5.22 (br, 1H; CHOCO), 5.46 (m, 1H; C_9'-H), 5.58 (m, 1H; C_{12}'-H), 6.00 (m, 1H; C_{10}'-H), 6.54 (m, 1H; C_{11}'-H), FAB-MS: m/z 805 $(M-H)^+$.

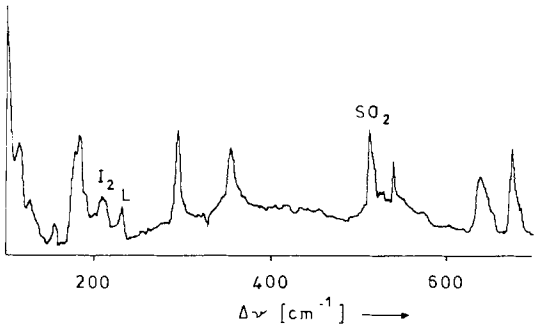

Fig. 1. Raman spectrum of **1** in SO_2 solution in the range 100–700 cm^{-1} (647.09 nm, 20 mW, −50 °C, 3 scans, 1 s/p, 1 s integration time) L: laser peak.

Azidoiodoiodine(1+) Hexafluoroantimonate: The First Binary Nitrogen–Iodine Cation**

By *Inis C. Tornieporth-Oetting, Peter Buzek, Paul von Ragué Schleyer,* and Thomas M. Klapötke**

So far only two neutral binary iodine–nitrogen compounds have been described, which as a result of the very labile I–N bond[1] and the associated thermodynamic instability are both explosive: NI_3[2] (or $NI_3 \cdot NH_3$[3]) and IN_3[4]. Our attempts at the synthesis of the $[NI_4]^+$ ion analogous to $[NCl_4]^+$[5] have so far been unsuccessful.[2] We report here, the preparation and characterization starting from iodoazide, of the first binary iodine–nitrogen cation.

The reaction of iodoazide freshly prepared from silver azide and iodine in $CFCl_3$ (R-11) with I_2/SbF_5 (intermediate formation of "[I][SbF_6]", see ref. [6]) leads to the formation of a $[I_2N_3]^+$ salt [Eq. (a)].

$$IN_3 + 1/2\ I_2 + 3/2\ SbF_5 \xrightarrow{-90\,°C/-40\,°C} \underset{\mathbf{1}}{[I_2N_3]\,[SbF_6]} + 1/2\ SbF_3 \quad (a)$$

After removing the $CFCl_3$ at −50 °C and dissolving the product mixture in SO_2 (−50 °C) **1** can be separated from SbF_3 which is insoluble in SO_2 (evidence from MS, IR spectroscopy). The compound **1**, which is deep carmine red both in the solid state as well as in solution, is more easily accessible from the reaction of fresh AgN_3 with $[I_3][SbF_6]$ in liquid SO_2 [Eq. (b)], since here the step of pumping to dryness (**caution**: high danger of explosion) is no longer necessary.

$$AgN_3 + [I_3]\,[SbF_6] \xrightarrow{-50\,°C} AgI + \mathbf{1} \quad (b)$$

If **1** is prepared according to Equation (b), only the precipitated AgI (analytically proven) needs to be separated by a low-temperature filtration, and the residual SO_2 solution can be used directly for the characterization by Raman spectroscopy.[7] The Raman spectrum of **1** (Fig. 1) shows, apart from the bands of the solvent SO_2 and those of the $[SbF_6]^-$ ion, only bands which can be assigned unequivocally to the $[I_2N_3]^+$ ion.[7] It is noteworthy that the I–I stretch in **1** (182 cm^{-1}) in comparison to that in iodine I_2 (215 cm^{-1}) is shifted to lower wavenumber, whereas the N–I stretch in **1** (355 cm^{-1}) in contrast to that in IN_3 (338 cm^{-1}) is observed at higher wavenumber (Table 1). The position of the N–I vibrational bands of **1** corresponds to a calculated bond distance of 2.72 Å and thus also agrees with the empirical correlation between the I–I bond length and the wavenumber of the I–I vibration (Table 1). Similarly, the calculated N–I bond length in **1** (2.07 Å) which is shorter than that in IN_3 (2.13 Å) is in good agreement with the spectroscopic data.

Table 1. I–I and N–I bond lengths d and vibrational frequencies ν [17].

	ν(I-I) [cm^{-1}] calcd. [a]	exp.	d(I-I) [Å] exp.	calcd. [c]	ν(N-I) [cm^{-1}] exp.	d(N-I) [Å]
$[I_2]^+$	237	235 [6]	2.56 [6]	2.65		
I_2	208	215 [6]	2.66 [6]	2.73		
$[I_3]^-$	113	114 [9]	2.90 [10]	2.99		
IN_3					338 [4]	2.13 [b]
$[I_2N_3]^+$	188	182		2.72 [b]	355	2.07 [b]

[a] Estimated from: $\nu[cm^{-1}] = -1170.8 + 1356.0d[Å] - 314.9d^2[Å^2]$ [8]. [b] MP2 optimized [c] MP2/Basis.

We have estimated the enthalpy for the reaction carried out according to Equation (c) for the thermodynamically

$$IN_3(g) + 1/2\ I_2(s) + 3/2\ AsF_5(g) \longrightarrow [I_2N_3][AsF_6](s) + 1/2\ AsF_3(l) \quad (c)$$

comparatively stable $[I_2N_3][AsF_6]$[6]—as a result of better accessibility of the data—based on a simple Born–Haber cycle (see ref. [2, 6]) to be $\Delta H°(c) = -20 \pm 4$ kcal mol^{-1}.[17] With $\Delta H_f°(IN_3) = +90.2$[11] and $\Delta H_f°(AsF_5) = -295.6$ kcal mol^{-1}[6] a standard heat of formation for $[I_2N_3][AsF_6]$ of $\Delta H_f°([I_2N_3][AsF_6]) = -275$ kcal mol^{-1} is obtained. The decomposition given in Equation (d) is, however, strongly favored with $\Delta H°(d) = -97$ kcal mol^{-1} [6] (furthermore $[I_2]^+$ dimerizes exothermally to $[I_4]^{2+}$ [6]), and both N_2 (gas discharge) and $[I_2]^+$ ($[I_4]^{2+}$) were observed as decomposition products of **1** in solution above −10 °C ($[I_2]^+$ also occurs as the decomposition product at −50 °C, if the laser power for the Raman spectroscopy exceeds 25 mW). The desired slow decomposition of a sample of **1** prepared according to Equation (b) afforded (after separation of AgI,

$$[I_2N_3][AsF_6](s) \longrightarrow [I_2][AsF_6](s) + 3/2\ N_2(g) \quad (d)$$

[*] Priv.-Doz. Dr. T. M. Klapötke, Dr. I. C. Tornieporth-Oetting
Institut für Anorganische und Analytische Chemie
der Technischen Universität
Strasse des 17. Juni 135, D-W-1000 Berlin 12 (FRG)
Prof. Dr. P. von R. Schleyer, Dipl.-Chem. P. Buzek
Institut für Organische Chemie der Universität
Henkestrasse 42, D-W-8520 Erlangen (FRG)

[**] This work was supported by the Deutsche Forschungsgemeinschaft (KL/636/2-1), the Fonds der Chemischen Industrie, and the Bundesminister für Bildung und Wissenschaft (Graduiertenkolleg "Synthese und Strukturaufklärung niedermolekularer Verbindungen").

yield > 90%) $[I_4][SbF_6]_2$ in approximately 90% yield (residual nitrogen content ca. 0.4–0.5%; cf. **1**, calcd. 7.9%) [Eq.(e)].

$$2\,\mathbf{1} \longrightarrow [I_4][SbF6]_2 + 3\,N_2 \qquad (e)$$

It would have been also conceivable that the reaction of IN_3 with "I^+" [Eq.(a)] could have resulted in a particle isomeric to the cation in **1**. Since the strong asymmetric N_3 vibration (ν_{as} = 2067 cm^{-1})[7] in the Raman spectrum made the linear arrangement of the two iodine atoms at the N_3 unit seem unlikely,[14] we calculated a structure with a bent I_2 unit and another with C_{2v} symmetry for the cation in **1** based on ab initio MO calculations (Fig. 2). The calculations were

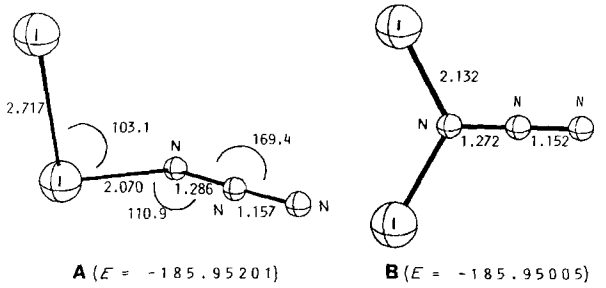

Fig. 2. MP2 optimized structures for the $[I_2N_3]^+$ ion, basis sets see text; (bond angles [°], distances [Å], energies [Hartree])[17]: **A**: nonplanar, chainlike structure of the cation in **1**, **B**: energetically next most favorable C_{2v} structure.

carried out with the Gaussian 90 program using the 6-31 + G* standard basis set for nitrogen.[15a, b] For iodine a quasi-relativistic pseudopotential[16a] and a [5s5p1d]/(3s3p1d)(DZ + P) basis set were used.[16b] The geometries were fully optimized in accord with the electron correlation according to Møller–Plesset 2nd order (MP(FU)). In agreement with the experimental spectroscopic results, the ab initio calculation also shows that the nonplanar chainlike structure of the $[I_2N_3]^+$ ion proposed by us is favored by about 1 kcal mol^{-1} to the (not observed) C_{2v} structure.

In a detailed work we will report the ab initio calculations of IN_3 and other energetically more unfavorable, terminal coordinated and cyclic $[I_2N_3]^+$ ions as well as about an improved preparative method for the preparation of IN_3 in gram quantities.

Experimental Procedure

A solution of $[I_3][SbF_6]$ (0.50 g, 0.81 mmol) in SO_2 (5 mL) at −70 °C was added to a suspension of AgN_3 (0.12 g, 0.80 mmol) [freshly prepared, washed with ethanol and ether, and dried in vacuo] in SO_2 (2 mL). After the mixture was swirled for 3 h at −50 °C it was filtered by decantation the precipated AgI under constant cooling [7,18]. **Caution**: The explosive nature increases greatly from AgN_3 to IN_3 to **1**! Compound **1** often shows also below −20 °C explosive decomposition.

Received: May 9, 1992 [Z 5332IE]
German version: *Angew. Chem.* **1992**, *104*, 1391

CAS Registry numbers:
A_9N_3, 13863-88-2; $[I_3][SbF_6]$, 117818-72-1; $[I_2N_3][SbF_6]$, 143007-78-7; $[I_4][SbF_6]_2$, 117041-30-2.

[1] R. H. Davies, A. Finch, P. N. Gates, *J. Chem. Soc. Chem. Commun.* **1989**, 1461.
[2] I. Tornieporth-Oetting, T. Klapötke, *Angew. Chem.* **1990**, *102*, 726; *Angew. Chem. Int. Ed. Engl.* **1990**., *29*, 677.
[3] H. Hartl., H. Bärnighausen, J. Jander, *Z. Anorg. Allg. Chem.* **1968**, *375*, 225.
[4] K. Dehnicke, *Angew. Chem.* **1976**, *88*, 612; *Angew. Chem. Int. Ed. Engl.* **1976**, *15*, 553.
[5] R. Minkwitz, *Angew. Chem.* **1990**, *102*, 185; *Angew. Chem. Int. Ed. Engl.* **1990**, *29*, 181.
[6] N. Burford, J. Passmore, J. C. P. Sanders in *From Atoms to Polymers* (Eds.: J. F. Liebman, A. Greenberg), VCH, Weinheim, **1989**, p. 53.
[7] Raman (**1** in SO_2 solution; 647.09 nm, 20 mW, − 50 °C); $\Delta\nu$[cm^{-1}] (intensity) assignment cf. ref. [4]: 182 (10), ν(I-I): 295 (8), $\nu_5(SbF_6^-)$; 355 (6), ν(N-I); 540(3), $\nu(N_3)$; 638(5), $\delta(N_3)$; 675 (8), $\nu_1(SbF_6^-)$; 1286(7), $\nu_s(N_3)$; 2067 (8), $\nu_{as}(N_3)$. A band (238 cm^{-1} [6]) assignable to the starting material $[I_3][SbF_6]$ could not be observed.
[8] I. C. Tornieporth-Oetting, T. M. Klapötke, unpublished.
[9] K. Nakamoto, *Infrared and Raman Spectra of Inorganic and Coordination Compounds*, 4. ed., Wiley, New York, **1986**.
[10] N. N. Greenwood, A. Earnshaw, *Chemistry of the Elements*, Pergamon, **1984**.
[11] Estimated from ΔH_f° (N_3^-,g) = +105 kcal mol^{-1} [12] and $\Delta H_f^\circ(I^-, g)$ = +25.56 kcal mol^{-1} [13].
[12] K. Jones in *Comprehensive Inorganic Chemistry, Vol. 2*, (Eds.: J. C. Bailar, J. J. Emeléus, R. Nyholm, A. F. Trotman-Dickenson), Pergamon, Oxford, **1973**, p. 276.
[13] D. A. Johnson, *Some Thermodynamic Aspects of Inorganic Chemistry*, Cambridge University Press, Cambridge, **1982**, appendix.
[14] D. W. H. Rankin, *J. Chem. Soc. Dalton Trans.* **1972**, 869.
[15] a) M. J. Frisch, M. Head-Gordon, G. W. Trucks, J. B. Forseman, H. B. Schlegel, K. Raghavachari, M. Robb, J. S. Binkley, C. Gonzalez, D. J. Defrees, D. J. Fox, R. A. Whiteside, R. Seeger, C. F. Melius, J. Baker, R. L. Martin, L. R. Kahn, J. J. P. Stewart, S. Topiol. . A. Pople: *Gaussian 90, Revision F*, Gaussian Inc., Pittsburgh, PA, **1990**; b) W. J. Hehre, L. Radom, P. von R. Schleyer, J. A. Piople, *Ab Initio Molecular Orbital Theory*. Wiley, New York, **1986**.
[16] a) P. Schwertfeger, M. Dolg, W. H. E. Schwarz, G. A. Bowmaker, P. D. W. Boyd, *J. Chem. Phys.* **1989**, *91*, 1762; b) M. Kaupp, P. von R. Schleyer, H. Stoll, H. Preuss, *J. Am. Chem. Soc.* **1991**, *113*, 607.
[17] Since it is internationally acceptable the following non-SI units were used: 1 Å = 10^{-10} m; 1 cal = 4.18 J; 1 Hartree = 27.2 eV = 627.4 kcal mol^{-1}.
[18] Attempts at recording of a ^{14}N NMR spectrum of a SO_2 solution of $[I_2N_3][SbF_6]$ were unsuccessful (cf. ref.[2]). Furthermore, we were also not in the position to carry out a favorable synthesis for AgN_3, starting from commercial $^{15}NH_4Cl$.

Control of the Reaction of *n*-Butyllithium with Benzo[*b*]tellurophene by the Solvent—Either Metalation or Tellurium–Lithium Exchange To Give an Interesting Lithiostyryllithium**

By *Adalbert Maercker,* Heinrich Bodenstedt,* and *Lambert Brandsma*

Dedicated to Professor Ulrich Schöllkopf on the occasion of his 65th birthday

The reductive cleavage of diphenylmethylene cyclobutane with elemental lithium leads to 2,5-dilithio-1,1-diphenyl-1-pentene (**1**), which is rearranged by a 1,7 proton shift into the stable dilithio compound **2a**.[1] According to 2D NMR investigations[2] **2a** has a lithium double bridge, similar to the metalated addition product of *n*-butyllithium with diphenylacetylene (tolane) **2b**.[3]

It was now of interest to prepare the parent compound of both compounds **2** with $R^1 = R^2 = H$, that is, (*Z*)-2-lithiostyryllithium (**8**). The readily accessible benzo[*b*]tellurophene (**4**)[4] was clearly a potential starting material that should be

[*] Prof. Dr. A. Maercker, Ing.-grad. H. Bodenstedt
Institut für Organische Chemie der Universität
Adolf-Reichwein-Strasse, D-W-5900 Siegen (FRG)
Prof. Dr. L. Brandsma
Department of Preparative Organic Chemistry
University of Utrecht, Padualaan 8
NL-3584 CH Utrecht (The Netherlands)

[**] Polylithiumorganic Compounds, Part 18. This work was supported by the Fonds der Chemischen Industrie. Part 17: A. Maercker, K.-D. Klein, *J. Organomet. Chem.* **1991**, *410*, C35–C38.

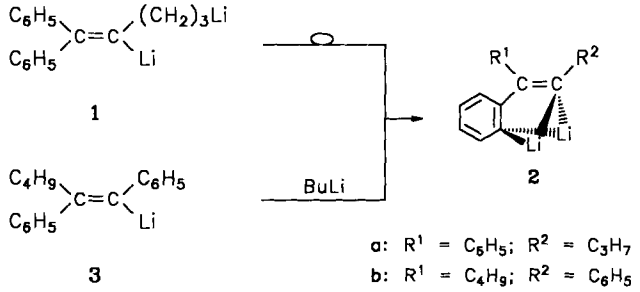

converted stereospecifically into **8** by tellurium–lithium exchange.

However, if benzo[*b*]tellurophene (**4**) is treated under the usual conditions for tellurium–lithium exchange[5] with *n*-BuLi in THF, then at −78 °C no reaction occurs, whereas at 0 °C—as also previously in diethyl ether at room temperature[6]—exclusively α-metalation was observed leading to 2-lithiobenzo[*b*]tellurophene (**5**). The reaction of **5** with methyl iodide afforded **6**[6] in 88% yield, and from deuterolysis **7** is obtained with a degree of deuteration of > 98% in the α position.

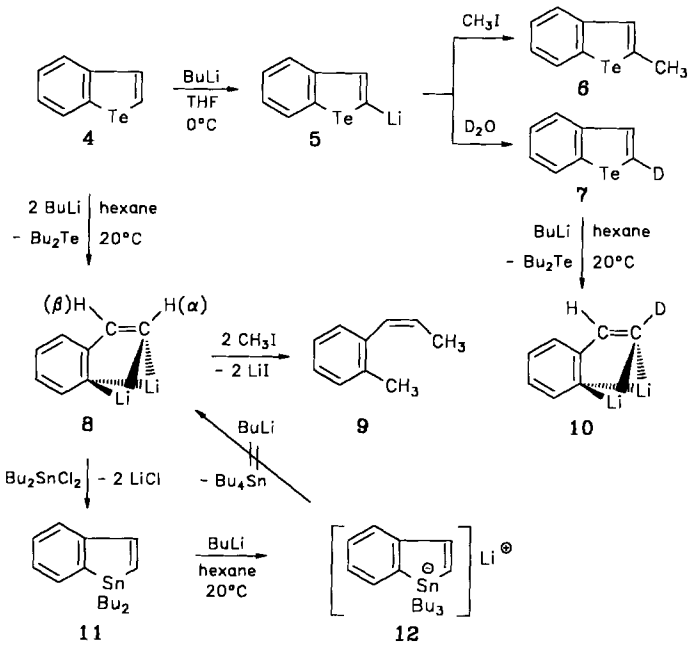

Surprisingly, the reaction of *n*-BuLi with **4** in hexane as solvent occurred very differently. If the components are stirred under an inert atmosphere at room temperature, within 5–10 min a fine, light-brown precipitate is formed, which proved to be the pure dilithium compound **8** (94% yield). The powder, which is beige when dry, is highly pyrophoric and dissolves in diethyl ether to give a red-brown solution. Following hydrolysis the mother liquor, apart from the theoretically expected quantities of dibutyltellurium, contains only traces of styrene.

The reaction of a suspension of **8** in hexane with methyl iodide or—better—dimethylsulfate affords pure **9**,[7] which is identical with the *cis* part of a *cis–trans* mixture prepared as a reference. Interestingly, 1,1-di-*n*-butylbenzo[*b*]stannophene (**11**) (82% yield, Table 1) formed from **8** and di-*n*-butyldichlorostannane could not be converted back into **8** by tin–lithium exchange. On the contrary the reaction in hexane stopped at the deep violet ate-complex **12** (Table 1). Stannates of the type **12** are discussed[8] as intermediates of the tin–lithium exchange and have been detected already for other special cases.[9]

In contrast, the conversion of **11** into **8** is achieved via the diiodo compound **13** (Table 1), which undergoes a double iodine–lithium exchange. The Wittig reaction of bromo-

Table 1. Important physical data for the compounds **8** and **11**–**13**.

8: ^{1}H NMR: see text; ^{13}C NMR (100.6 MHz, [D$_{10}$]Et$_2$O): δ = 177.65 (m, $^1J(^{13}C^6Li)$ = 8.8, 4.4 Hz, =CHLi), 173.1 (m, $^1J(^{13}C^6Li)$ = 8.2, 4.1 Hz, Ar-Li), 156.6, 156.2, 144.7, 128.8, 126.5, 124.0; ^{6}Li NMR (58.9 MHz, [D$_{10}$]Et$_2$O, standard 0.1 M LiBr in THF, external): δ = 1.4, 0.9 (1:1)

11: ^{1}H NMR (200 MHz, CDCl$_3$): δ = 7.57 (d, ^3J = 10.5 Hz), 7.53 (d, ^3J = 7.9 Hz), 7.29–7.14 (m), 6.73 (d, ^3J = 10.5 Hz), 1.67–0.82 (m); ^{13}C NMR (50.3 MHz; CDCl$_3$): δ = 150.0, 149.6, 139.7, 135.7, 133.1, 128.5, 127.1, 126.3, 29.2, 27.0, 13.6, 11.8; ^{117}Sn NMR (142 MHz, [D$_{10}$]Et$_2$O, Standard 0.2 M (CH$_3$)$_4$Sn in Et$_2$O, external): δ = −6.4; MS (70 eV): *m*/*z* 335 (*M*$^{\oplus}$, 0.2%), 279 (73), 223 (73), 221 (63), 120 (66), 41 (65), 29 (100); B.p. = 84–88 °C/0.002 Torr; correct element analysis

12: ^{1}H NMR (400 MHz, [D$_{10}$]Et$_2$O): δ = 6.75 (d, ^3J = 6.9 Hz), 6.65 (t, ^3J = 7.7 Hz), 6.39 (d, ^3J = 7.7 Hz), 5.87 (t, ^3J = 6.9 Hz, 5.20 (d, ^3J = 10.6 Hz), 3.45 (d, ^3J = 10.6 Hz), 1.54 (m), 1.36 (m), 1.12 (t, ^3J = 8.4 Hz), 0.87 (t, ^3J = 7.3 Hz); ^{13}C NMR (100.6 MHz, [D$_{10}$]Et$_2$O): δ = 152.6, 138.1, 129.5, 127.7, 113.9, 112.0, 97.5, 30.6, 28.5, 14.4, 10.3; ^{117}Sn NMR (142 MHz, [D$_{10}$]Et$_2$O, standard 0.2 M (CH$_3$)$_4$Sn in Et$_2$O, external): δ = −44.0

13: ^{1}H NMR (200 MHz, CDCl$_3$): δ = 7.86 (d, ^3J = 7.9 Hz), 7.53 (d, ^3J = 7.6 Hz), 7.37 (t, ^3J = 7.6 Hz), 7.21 (d, ^3J = 8.4 Hz), 7.02 (t, ^3J = 7.9 Hz), 6.70 (d, ^3J = 8.4 Hz); ^{13}C NMR (50.3 MHz, CDCl$_3$): δ = 143.1, 141.3, 139.1, 129.8, 129.7, 127.9, 99.0, 84.2; MS (70 eV): *m*/*z* 356 (*M*$^{\oplus}$, 4%), 229 (96), 102 (100), 76 (20), 75 (24), 74 (16), 50 (20); b.p. = 65–75 °C/0.001 Torr (decomp.); correct elemental analysis

methylenetriphenylphosphorane[10] with *o*-bromobenzaldehyde in contrast affords a *cis–trans* mixture of the corresponding dibromo compound, which in contrast to **13** does not lead to a sterically uniform product after halogen–metal exchange.

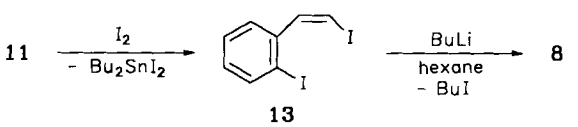

For the preparation of **8** there are therefore no suitable alternatives to the tellurium–lithium exchange **4** → **8**. It is noteworthy that this reaction was successful in a hydrocarbon solvent; furthermore, **8** is the first dilithium organic compound with two different anionic centers, which was made accessible by a tellurium–lithium exchange.

The structure and stereochemistry of the lithiostyryllithium (**8**) are also derived from the NMR spectra.[11] Particularly characteristic in the ^{1}H NMR spectrum (80 MHz, [D$_{10}$]diethyl ether) is the doublet of the vinyl proton in the β position to the lithium atom at δ = 8.50 (^3J = 17.0 Hz), which, as expected, yields a singlet[12] in the α-deuterated compound **10**, and the doublet of the aryl proton in the *ortho* position to the lithium atom at δ = 7.96 (^3J = 6.7 Hz). The doublet of the vinyl proton in the α position (δ = 7.17) relative to the lithium atom lies partially beneath the signals of the remaining arene protons (δ = 6.8–7.1), so only the peak at lower field (δ = 7.25) can be seen. Obviously no signal is detected for **10** in this region. The ^{13}C and ^{6}Li NMR spectra (Table 1) are in agreement with a dimeric structure for **8**, as this has already been observed for compounds **2**[2, 3] under certain conditions. The result[11] is however novel and unex-

pected in that this information can already be taken from the spectra recorded at room temperature, whereas cooling to $-70\,^{\circ}C$ was necessary for the resolution of the $^{13}C,^{6}Li$ coupling in **2**.

Experimental Procedure

A solution of 1.6 M *n*BuLi (50 mL, 80 mmol) in hexane (Metallgesellschaft, Frankfurt am Main) was added under argon at room temperature to **4** (6.9 g, 30 mmol)[4]. This formed a pale yellow, clear solution which after 5–10 min clouded and became light brown as a result of precipitated **8**. After the mixture was stirred for 3 h (magnetic stirrer), the precipitate was separated by decantation, washed three times with dry pentane (50 mL), and dried in vacuo. Yield: 3.3 g (94%) **8** as a fine, beige powder which ignites immediately on contact with air.

Received: May 21, 1992 [Z 5341 IE]
German version: *Angew. Chem.* **1992**, *104*, 1387

CAS Registry numbers:
4, 272-35-5; **6**, 50519-02-3; **7**, 143077-01-4; **8**, 143077-02-5; **10**, 143077-03-6; **11**, 143077-04-7; **12**, 143077-06-9; **13**, 143077-05-8; BuLi, 109-72-8.

[1] A. Maercker, K.-D. Klein, *J. Organomet. Chem.* **1991**, *401*, C1–C4.
[2] a) O. Eppers, H. Günther, K.-D. Klein, A. Maercker, *Magn. Res. Chem.* **1991**, *29*, 1065–1067; b) H. Günther, O. Eppers, K.-D. Klein, A. Maercker, unpublished.
[3] W. Bauer, M. Feigel, G. Müller, P. von R. Schleyer, *J. Am. Chem. Soc.* **1988**, *110*, 6033–6046.
[4] L. Brandsma, H. Hommes, H. D. Verkruijsse, R. L. P. de Jong, *Recl. Trav. Chim. Pays-Bas* **1985**, *104*, 226–230.
[5] a) D. Hellwinkel, G. Fahrbach, *Chem. Ber.* **1968**, *101*, 574–584; b) D. Seebach, A. K. Beck, *ibid.* **1975**, *108*, 314–321; c) E. Luppold, E. Müller, W. Winter, *Z. Naturforsch. B.* **1976**, *31*, 1654–1657; d) M. J. M. Schoufs, Dissertation, Universität Utrecht, **1978**; e) T. Kauffmann, H. Ahlers, *Chem. Ber.* **1983**, *116*, 1001–1008; Review: T. Kauffmann, *Angew. Chem.* **1982**, *94*, 401–420; *Angew. Chem. Int. Ed. Engl.* **1982**, *21*, 410–429; f) T. Hiiro, N. Kambe, A. Ogawa, N. Miyoshi, S. Murai, N. Sonoda, *ibid.* **1987**, *99*, 1221–1222 and **1987**, *26*, 1187–1188; g) S. M. Barros, J. V. Comasseto, J. Berriel, *Tetrahedron Lett.* **1989**, *30*, 7353–7356; h) Review: N. Petragnani, J. V. Comasseto, *Synthesis* **1991**, 793–817, 897–919.
[6] J.-L. Piette, J.-M. Talbot, J.-C. Genard, M. Renson, *Bull. Soc. Chim. Fr.* **1973**, 2468–2471.
[7] R. Wehrli, H. Heimgartner, H. Schmid, H.-J. Hansen, *Helv. Chim. Acta* **1977**, *60*, 2053.
[8] H. J. Reich, N. H. Phillips, *J. Am. Chem. Soc.* **1986**, *108*, 2102–2103; *Pure Appl. Chem.* **1987**, *59*, 1021–1026.
[9] A. J. Ashe III, L. L. Lohr, S. M. Al-Tawee, *Organometallics* **1991**, *10*, 2424–2431.
[10] G. Köbrich, H. Trapp, K. Flory, W. Drischel, *Chem. Ber.* **1966**, *99*, 689–697.
[11] Thorough 2D NMR investigations are in progress: H. Günther, H.-E. Mons, H. Bodenstedt, A. Maercker, L. Brandsma, unpublished.
[12] Theoretically this is a 1:1:1 triplet with $^{3}J(^{1}H,^{2}H) = 2.6$ Hz, however it is not resolved.

"[Cp*Co=CoCp*]" is a Hydride**

By *Jörg L. Kersten, Arnold L. Rheingold, Klaus H. Theopold,* Charles P. Casey, Ross A. Widenhoefer,* and *Cornelis E. C. A. Hop*

Recently, bis(η^5-pentamethylcyclopentadienyl)dicobalt ([Cp*Co=CoCp*], **1**) was reported to have been prepared by a metal-atom vapor synthesis employing cobalt and pentamethylcyclopentadiene.[1] This unusual compound features a formal Co–Co double bond without any bridging ligands.[1] Some of the physical properties and the reactivity of **1** were surprising to us in light of the proposed structure. Despite its even valence electron count (28 valence electrons per dimer, Co^{I}, d^{8}), **1** was reported to be paramagnetic. It apparently did not react with ethylene or carbon monoxide. Finally, the X-ray crystal structure featured considerable residual electron density ($2.5\,e\,Å^{-3}$) in a position bridging the two metal atoms. Sensitized to the difficulty of characterizing paramagnetic hydrides by our recent work on $[\{Cp^{*}Cr(\mu_3\text{-}H)\}_4]$,[2] we wondered whether **1** might not contain bridging hydride ligands,[3] and if this compound could be prepared by straightforward solution chemistry. Herein we report the combined results of independent experiments in this regard by two laboratories (in Delaware and Wisconsin), which led us to conclude that **1** is really the mixed-valent cobalt hydride $[Cp^{*}_{2}Co_2(\mu_2\text{-}H)_3]$.[4]

In work carried out at the University of Delaware, reaction of $[\{Cp^{*}Co(\mu\text{-}Cl)\}_2]$[5] with 0.5 equivalents of $LiAlH_4$ at ambient temperature in THF gave a dark red solution. Subsequent removal of THF, extraction with pentane, filtration, and evaporation of the solvent yielded the crude reaction product as a black solid. ^{1}H NMR analysis of this solid in [D_6]benzene revealed two major broad resonances at $\delta = 62.0$ and 29.6 of roughly equal intensity, besides minor diamagnetic contaminants. Vacuum sublimation at 50 °C afforded a purple solid, which could be further purified by recrystallization from pentane. The resulting material (**2**) exhibited one resonance in the ^{1}H NMR spectrum ([D_6]benzene) at $\delta = 29.6$. The sublimation residue was recrystallized from pentane to yield black crystals; the ^{1}H NMR spectrum ([D_6]benzene) of the latter consisted of a single broad resonance at $\delta = 62.0$, very close to the value reported for **1**. As the original report gave NMR shifts in [D_8]toluene ($\delta = 61.3$ at 30 °C),[1] we recorded spectra in the same solvent ($\delta = 63.0$ at 20 °C and 60.3 at 30 °C). Given the apparent temperature dependence of the chemical shift, we considered all of these values to be identical within experimental uncertainty.

Presuming to have prepared **1** by an alternate route, we determined the crystal structure of our black compound ex-

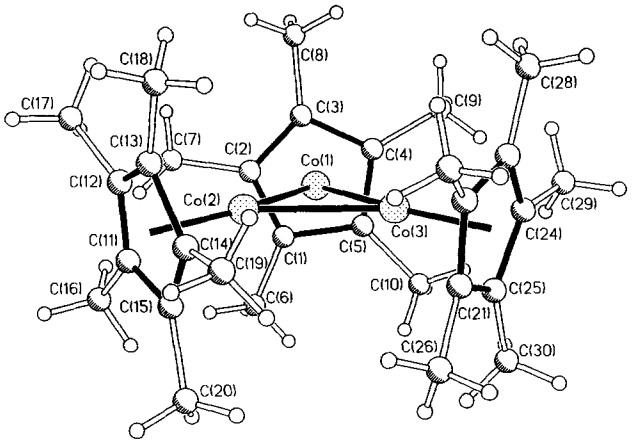

Fig. 1. The molecular structure of $[Cp^{*}_{3}Co_3(\mu_2\text{-}H)_3(\mu_3\text{-}H)]$ (**3**). The hydride ligands were not located and thus are not shown. Selected bond distances [Å] and angles [°]: Co(1)-Co(2) 2.479(4); Co(1)-Co(3) 2.472(4); Co(2)-Co(3) 2.477(4); Co-C 2.109 (average); Co(2)-Co(1)-Co(3) 60.0(1); Co(1)-Co(2)-Co(3) 59.8(1); Co(1)-Co(3)-Co(2) 60.1(1). The Cp* centroids are displaced below the Co_3 plane by an average distance of 0.193 Å.

[*] Prof. K. H. Theopold, J. L. Kersten, Prof. A. L. Rheingold
Department of Chemistry and Biochemistry
University of Delaware
Newark, DE 19716 (USA)
Prof. C. P. Casey, R. A. Widenhoefer, Dr. C. E. C. A. Hop
Department of Chemistry
University of Wisconsin
Madison WI 53706 (USA)

[**] This work was supported by grants from the Petroleum Research Fund of the American Chemical Society and the U.S. National Science Foundation (KHT) and by the U.S. Department of Energy, Division of Basic Energy Sciences (CPC). Cp* = C_5Me_5.

hibiting the $\delta = 62.0$ resonance. To our consternation it turned out to be a trinuclear cobalt complex (**3**, see Fig. 1).[6] Whereas its cobalt atoms form an almost perfect equilateral triangle, the Cp* centroids are all displaced by approximately 0.2 Å to one side of the plane defined by the metal atoms. This distortion presumably results from the presence of stereochemically active hydride ligands. No hydrides could be located during the structure solution and refinement; however, based on mass spectral measurements (see below) we suggest that **3** has four such ligands. Three of the latter probably bridge the edges of the Co_3 triangle on the side opposite to the Cp* ligands, while the fourth hydride ligand presumably caps the other trigonal face, thus giving **3** the formula $[Cp^*_3Co_3(\mu_2\text{-}H)_3(\mu_3\text{-}H)]$.

We have also determined the crystal structure of the other reaction product, **2**.[7] Much to our surprise its structure (see Fig. 2) was that previously reported for **1**! The unit cell parameters, as well as the bond distances, were close enough to the published values to virtually ensure that this compound is identical to **1**, whatever its true chemical nature. Compari-

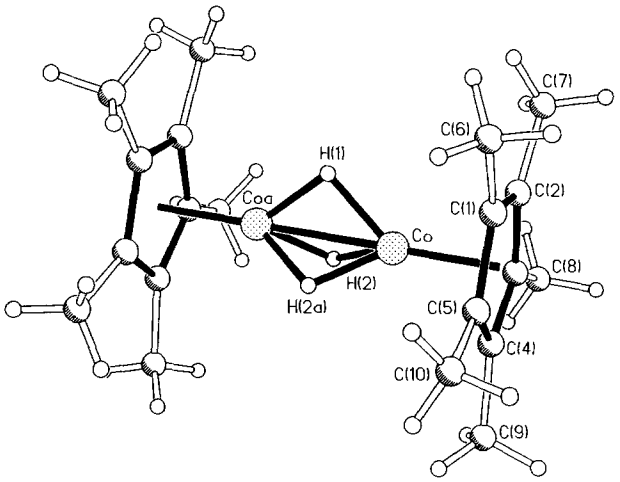

Fig. 2. The molecular structure of $[Cp^*_2Co_2(\mu_2\text{-}H)_3]$ (**2**). Selected bond distances [Å] and angles [°]: Co-Co_a 2.249(1) [**1**: 2.253(1) [1]]; Co-C 2.074 (average); Co-Cp*-centroid 1.681 [**1**: 1.689]; Co-H(1) 1.50(4); Co-H(2) 1.50.(6); Co-H(2a) 1.42(5); Co-H(1)-Co_a 97(3); Co-H(2)-Co_a 101(3).

son of the final R factors (this work: $R = 0.030$, $R_w = 0.040$; previously reported: $R = 0.040$, $R_w = 0.062$) indicated our structure determination to be the more reliable. After anisotropic refinement of all non-hydrogen atoms, the difference map revealed the presence of several peaks of residual electron density (ca. 0.5 eÅ^3), consistent with hydride ligands bridging the Co–Co bond. The best structural model featured three bridging hydride ligands; however, their positions as determined by X-ray diffraction must of course be viewed with some caution. Given the apparent contradiction between our observations and the reported NMR spectrum of **1**, it was important to confirm that the crystal used in our structure determination consisted of material exhibiting an ^{1}H NMR resonance at $\delta = 29.6$. Dissolution of said crystal in a minimal amount of [D_6]benzene yielded a faintly purple solution, and extended accumulation of scans confirmed the presence of a broad resonance at approximately $\delta = 31$ and the complete absence of any signal near $\delta = 60$.

To confirm the presence of hydride ligands in **2** and **3**, their synthesis was repeated using $LiAlD_4$. A sample of **2** prepared with $LiAlH_4$ exhibited a weak IR band at 1231 cm^{-1} (KBr), which was replaced by a very weak band at 806 cm^{-1} in material isolated from a reaction with $LiAlD_4$. These observations also suggest the presence of bridging hydride ligands in **2**.[8] The IR spectra of labeled and unlabeled **3** were indistinguishable. The mass spectrum of **2**, recorded under very mild ionization conditions (sample temperature 50 °C, electron energy 10 eV), showed its base peak at m/z 391, consistent with the formula $[Cp^*_2Co_2H_3]$. Under similar conditions the mass spectrum of **3** contained a strong peak at m/z 586, consistent with the molecular ion of $[Cp^*_3Co_3H_4]$.[9] At room temperature, solid **2** exhibited an effective magnetic moment (μ_{eff}) of 2.2(2) μ_B; this value is only slightly higher than the spin-only moment for one unpaired electron. Whereas pseudo-octahedral Co^{III} should be diamagnetic, the Co^{II} ion in the ligand field of a Cp* ligand and three hydrides (forming a trigonal piano stool) is expected to give rise to one unpaired electron, in accord with the measurement. Reaction of **2** with 4.0 equivalents of gaseous HCl (THF, 60 °C) liberated only 2.00(6) equivalents of H_2 (measured with a Töpler pump). We suggest that initial protonation may induce reductive elimination of H_2, thereby reducing the pool of hydrides available for protonation.

Parallel work carried out at the University of Wisconsin began with the reaction of cobalt(III) complex $[\{Cp^*CoCl_2\}_2]$[10] with excess $LiAlH_4$ in ether for 10 hours, followed by quenching of the reaction mixture with EtOH at −80 °C. The ^{1}H NMR spectrum in [D_6]benzene showed a 1:3 ratio of the resonances at $\delta = 62.1$ (**3**) and 29.6 (**2**) for the two major paramagnetic products. When the reaction was carried out at −45 °C for 30 minutes before quenching with EtOH at −80 °C, a 63% isolated yield of a 4.5:1 mixture of **3** and **2** was obtained. Recrystallization of the mixture from hexane gave the pure black paramagnetic complex **3** with a ^{1}H NMR resonance at $\delta = 62.4$ in [D_8]toluene at 22 °C, very close to the value reported by Schneider for **1**.[1] The high-resolution mass spectrum of **3** had a signal for the molecular ion at m/z 586.1819 (M^+; calcd 586.1825) and 587.1886 (^{13}C isotopomer; 32.8% of M^+; calcd 587.1858, 34.6% of M^+), consistent with the formulation $[Cp^*_3Co_3H_4]$.

The reported failure of **1** to react with CO appeared highly unusual. Casey et al. recently prepared $[Cp^*(CO)_2Re{=}Re(CO)_2Cp^*]$,[11] which has a Re=Re bond[12] supported by semibridging carbonyl groups; this complex reacted instantaneously with CO at −80 °C to produce $[\{Cp^*(CO)_2Re\}_2(\mu\text{-}CO)]$. The reaction of a black solution of **3** with CO (1 atm) produced a yellow-orange solution within 10 minutes at ambient temperature. ^{1}H NMR analysis with C_6Me_6 as an internal standard showed quantitative formation of $[Cp^*Co(CO)_2]$.[13] Gas chromatography of the gases over the solution showed the presence of H_2, and comparison with standard mixtures indicated a Co:H ratio of 1.02 ± 0.04, corresponding to 82% yield of H_2 from $[Cp^*_3Co_3H_4]$. Reaction of **3** with $CH_2{=}CH_2$ and with CCl_4 also released H_2. The effective magnetic moment of **3** determined by the Evans NMR method[14] was 3.9 ± 0.2 μ_B, consistent with the presence of multiple unpaired electrons.

Reaction of **2** (isolated by vacuum sublimation, see above) with CO rapidly produced $[Cp^*Co(CO)_2]$ (80% yield) and H_2 (66% yield; Co:H 2:2.46). The determination by the Evans method indicated an effective magnetic moment of 1.8 ± 0.2 μ_B in solution, consistent with the one unpaired electron predicted by MO calculations.[3]

In consideration of the results detailed above, we conclude that [Cp*Co=CoCp*] (**1**) remains unknown. The complex whose crystal structure was previously interpreted as that of **1** has the formula $[Cp^*_2Co_2(\mu_2\text{-}H)_3]$ (**2**). Furthermore, the

complex whose ^{1}H NMR spectrum was assigned to **1** is probably identical to $[Cp^*_3Co_3(\mu_2\text{-}H)_3(\mu_3\text{-}H)]$ (**3**). While both **2** and **3** can apparently be prepared by reaction of cobalt atoms with Cp*H, they are also accessible by simple solution procedures. We are now exploring the reactivity of these paramagnetic hydrides.

Received: May 27, 1992
Revised: July 13, 1992 [Z 5375/5405 IE]
German version: *Angew. Chem.* **1992**, *104*, 1364

CAS Registry numbers:
1, 135075-06-8; **2**, 143345-91-9; **3**, 143345-92-0.

[1] J. J. Schneider, R. Goddard, S. Werner, C. Krüger, *Angew. Chem.* **1991**, *103*, 1145; *Angew. Chem. Int. Ed. Engl.* **1991**, *30*, 1124. Editorial note: see also the Corrigendum in this issue: J. J. Schneider, Angew. Chem. **1992**, *104*, 1422; *Angew. Chem. Int. Ed. Engl.* **1992**, *31*, 1392.

[2] R. A. Heintz, B. S. Haggerty, H. Wan, A. L. Rheingold, K. H. Theopold, *Angew. Chem.* **1992**, *104*, 1100; *Angew. Chem. Int. Ed. Engl.* **1992**, *31*, 1077.

[3] H. B. Abrahamson, G. P. Niccolai, D. M. Heinekey, C. P. Casey, B. E. Bursten, *Angew. Chem.* **1992**, *104*, 464; *Angew. Chem. Int. Ed. Engl.* **1992**, *31*, 471.

[4] There exists ample precedent for this kind of structure in the cobalt group: a) P. Dapporto, S. Midollini, L. Sacconi, *Inorg. Chem.* **1975**, *14*, 1643; b) R. H. Crabtree, H. Felkin, G. E. Morris, T. J. King, J. A. Richards, *J. Organomet. Chem.* **1976**, *113*, C7; c) R. Bau, W. E. Carroll, D. W. Hart, R. G. Teller, T. F. Koetzle, *Adv. Chem. Ser.* **1978**, *167*, 73; d) I. R. Butler, W. R. Cullen, T.-J. Kim, F. W. B. Einstein, T. Jones, *J. Chem. Soc. Chem. Commun.* **1984**, 719; e) C. Bianchini, F. Laschi, D. Masi, C. Mealli, A. Meli, F. M. Ottaviani, D. M. Proserpio, M. Sabat, P. Zanello, *Inorg. Chem.* **1989**, *28*, 2552.

[5] U. Koelle, B. Fuss, M. Belting, E. Raabe, *Organometallics* **1986**, *5*, 980.

[6] Crystal data for **3**: $C_{30}H_{48}Co_3$, $M_r = 586.5$, monoclinic, $P2_1/n$, $a = 14.941(3)$, $b = 10.728(4)$, $c = 18.078(4)$ Å, $\beta = 90.43(3)°$, $V = 2897.6(10)$ Å^3, $Z = 4$, $\rho_{calc} = 1.338$ g cm^{-3}, $T = 243$ K. Of 4683 reflections collected ($4° < 2\theta < 48°$, Siemens P4, $Mo_{K\alpha}$) 4387 were independent, and 1748 were observed ($5\sigma F_o$). All examined specimens of the trimer diffracted weakly and somewhat asymmetrically. Criteria for the rejection of asymmetric reflections were lowered slightly to increase the available data. During attempted anisotropic refinement of all non-hydrogen atoms, several carbon atoms (3–5, 21, and 22) refined to "non-positive definite" values and were returned to isotropic status. All methyl-group hydrogen atoms were placed in idealized locations. The hydride ligands were not located. The highest and lowest peaks on the final difference map were 1.12 and -0.91 eÅ^{-3}. $R(F) = 9.79\%$ and $R(wF) = 12.70\%$.

[7] Crystal data for **2** (values in square brackets are those reported for **1** [1], note temperature difference!): $C_{20}H_{33}Co_2$, $Fw = 391.3$, monoclinic, $P2/c$, $a = 9.540(2)$ [9.533(1)], $b = 8.572(2)$ [8.514(2)], $c = 12.588(3)$ [12.376(2)] Å, $\beta = 105.62(2)°$ [105.95(1)°], $V = 991.4(4)$ [965.8] Å^3, $Z = 2$, $\rho_{calc} = 1.314$ g cm^{-3}, $T = 235$ K [100 K]. Of 2044 absorption-corrected reflections collected ($4° < 2\theta < 52°$, Siemens P4, $Mo_{K\alpha}$), 1951 were independent and 1410 were considered observed ($6\sigma F_o$). The centrosymmetric space group alternative was initially preferred from the statistical distribution of the normalized structure factors; the successful refinement validated this choice. All nonhydrogen atoms were refined anisotropically. Methyl-group hydrogen atoms were placed in calculated positions based on at least one found location per methyl group. The bridging hydrogen atoms were located from a difference map and isotropically refined. The highest and lowest difference peaks were, respectively, 0.35 and -0.25 eÅ^{-3}. $R(F) = 3.03\%$ (4.70% for all data) and $R(wF) = 3.98\%$ (4.51% for all data) for 108 refined parameters. Further details of the crystal structure investigations are available on request from the Director of the Cambridge Crystallographic Data Centre, University Chemical Laboratory, Lensfield Road, GB-Cambridge CB2 1EW (UK), on quoting the full journal citation.

[8] H. D. Kaesz, R. B. Saillant, *Chem. Rev.* **1972**, *72*, 231.

[9] Mass spectra; **2** (10 eV): m/z 390 (31.0%), 391 (100.0%, M^+), 392 (23.1%, ^{13}C isotopomer, expected intensity 22.5%); **3** (16 eV): m/z 329 (100%, $Cp^*_2Co^+$), 586 (80.6%, M^+; HRMS: 586.1878), 587 (25.7%, ^{13}C isotopomer, expected intensity 27.1%).

[10] M. L. H. Green, R. B. A. Pardy, *J. Chem. Soc. Dalton Trans.* **1979**, 355.

[11] C. P. Casey, H. Sakaba, P. N. Hazin, D. R. Powell, *J. Am. Chem. Soc.* **1991**, *113*, 8165.

[12] A rhenium compound with an unbridged M=M bond has been reported recently; see R. Toreki, R. R. Schrock, M. G. Vale, *J. Am. Chem. Soc.* **1991**, *113*, 3610.

[13] ^{1}H NMR ([D$_6$]benzene, $\delta = 1.59$) and IR spectrum (hexane, $\tilde{\nu} = 2008$(s), 1948(s) cm^{-1}) were identical with the spectra of an authentic sample; see U. Kölle, B. Fuss, *Chem. Ber.* **1984**, *117*, 743.

[14] a) D. F. Evans, *J. Chem. Soc.* **1959**, 2005. b) R. S. Drago, *Physical Methods for Chemists*, 2nd ed., Saunders College Publ., Orlando, FL, USA, **1992**.

Tetrakis(η^1-phosphabenzene)nickel**

By *Christoph Elschenbroich,* Mathias Nowotny, Andreas Behrendt, Werner Massa,* and *Sigrid Wocadlo*

Complexes of Ni in the oxidation state zero must be stabilized by strong σ donor/π acceptor ligands such as CO, RNC, PF_3 or $P(OR)_3$.[2] The function of weaker coordinating moieties such as alkenes, organophosphanes, and pyridines critically depends on the chelate effect. Thus, for example, homoleptic neutral nickel complexes with pyridine as a ligand are unknown[3a]—as are neutral complexes $[M(py)_m]$ of other metals[3b–i]—in contrast to the chelate bipyridine complex $[Ni(bpy)_2]$.[4] During our research into the coordination chemistry of heteroarenes of Group 15 we have now studied the modes of bonding of phosphabenzene to Ni^0[3j]. Since from the experience so far gained for heteroarenes C_5H_5E (E = N, P, As) with increasing atomic number of E, η^6 coordination predominates over η^1 coordination,[5–7] the formation of the homoleptic complex $[(\eta^6\text{-}C_5H_5P)(\eta^1\text{-}C_5H_5P)Ni]$ with 18 valence electrons could not be a priori excluded. We have now found, however, that the reaction of bis(1,5-cyclooctadiene)nickel (**1**) with phosphabenzene **2** forms tetrakis(η^1-phosphabenzene)nickel (**3**) in the form of orange, air-stable crystals, which are thermally stable up to 180 °C [Eq.(a)]. In solution **3** is air sensitive.

$$\underset{\mathbf{1}}{[(cod)_2Ni]} + 4\,\underset{\mathbf{2}}{C_5H_5P} \xrightarrow[25\,^\circ C]{CH_3\ C_6H_{11}} \underset{\mathbf{3}}{[(\eta^1\text{-}C_5H_5P)_4Ni]} + 2\,cod \qquad (a)$$

Analogous reactions with pyridine or arsabenzene lead to decomposition with deposition of a nickel slurry.[21] Compound **3** is the first homoleptic $\sigma(\eta^1)$ neutral complex of a heteroarene; it complements the $\pi(\eta^6)$ complexes **4**,[5] **5**,[1] and **6**[7] prepared by us previously.

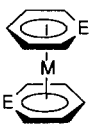

	M	E
4	Cr	N
5	V	P
6	Cr	As

The X-ray structural analysis[8] reveals the tetrahedral framework of **3** with point symmetry $\bar{4}$ (S_4) and almost ideal tetrahedral angles P-Ni-P of 108.6 and 109.9°; the most important bond parameter is the distance Ni–P = 212.7 pm (Fig. 1). To our knowledge shorter Ni–P distances are only found in $[Ni(PF_3)_4]$ (210–211 pm)[10a] and in $[Ni\{PF_2(2\text{-thienyl})\}_4]$ (209.3 pm),[10b] whereas typical values for Ni–P distances in tetrahedral organophosphane nickel complexes lie in the range 214–220 pm.[11] The short Ni–P distance indicates considerable double bond character between these elements, $Ni \xrightarrow{\pi} P$ back bonding being favored by the relatively low energy of the $b_1(\pi^*)$ ligand orbital,[12] the large MO coefficients at the P atom in this orbital,[13] and the low promotional energy of the configuration $Ni^0(d^{10})$.[14] The P–C and C–C distances in the phos-

[*] Prof. Dr. C. Elschenbroich, Dipl.-Chem. M. Nowotny, Dipl.-Chem. A. Behrendt, Prof. Dr. W. Massa, S. Wocadlo
Fachbereich Chemie der Universität
Hans-Meerwein-Strasse, D-W-3550 Marburg (FRG)

[**] Metal Complexes of Heteroarenes, Part 4. This work was supported by the Deutsche Forschungsgemeinschaft, the Fonds der Chemischen Industrie, and the NATO Scientific Affairs Division.-Part 3: [1].

phabenzene ligands in **3** are the same within the limits of error and in comparison to those of the free ligands,[15] slightly shortened. The six-membered rings are planar (maximum deviation from a best-fit plane 0.4(4) pm), and the Ni–P bond (1.7°) is slightly bent "upward" (Fig. 1). The inclination of the rings towards the P-Ni-P′ plane, which contains the $\bar{4}$ axis, is $\pm 58.5°$; thus the two "upper" and "lower" rings, which can be mutually transformed by the twofold axis lie almost perpendicular to each other (84.9°). The upper rings form an interplanar angle of 62.9° with the lower ones.

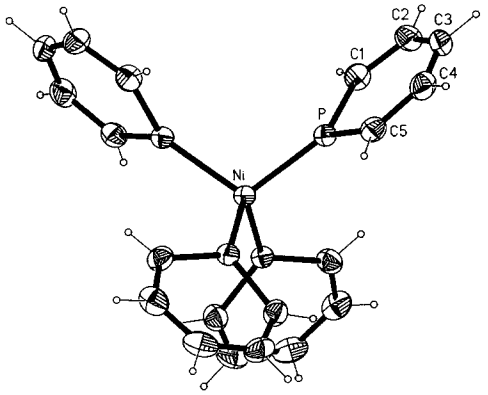

Fig. 1. XP drawing [9] of a molecule of **3**. Vibrational ellipsoids with 50% probability of occupation, selected bond lengths [pm] and angles [°]: Ni-P 212.74(5), P-C1 171.4(2), P-C5 171.8(2), C1-C2 138.0(3), C2-C3 138.7(3), C3-C4 137.2(3), C4-C5 138.6(3); C-H 87(2)–94(2); P-Ni-P′ 108.57(2), P-Ni-P″ 109.93(1), Ni-P-C1 129.45(6), Ni-P-C5 129.17(7), C1-P-C5 101.34(9), P-C1-C2 124.8(2), C1-C2-C3 123.1(2), C2-C3-C4 122.8(2), C3-C4-C5 123.7(2), P-C5-C4 124.2(2).

In addition to the bond length criterion a high Ni–P bond order in **3** is also suggested by the ν(Ni–P) stretching frequency. Thus, in the Raman spectrum the totally symmetric stretch a_1 is observed at 168 cm^{-1} which lies in the range of the absorptions of related complexes such as [Ni{P(OMe)$_3$}$_4$] (178 cm^{-1}), [Ni{P(OEt)$_3$}$_4$] (169 cm^{-1}), and [Ni(PF$_3$)$_4$] (195 cm^{-1}). Since experimental findings (drastic reduction of the proton affinity according to $C_5H_5N > C_5H_5P$; P in C_5H_5P is not quaternized by R_3O^+[16]) as well as the results of quantum chemical calculations[17] indicate a decrease in the σ electron density at the heteroatom, the surprisingly high stability of **3** must be traced to the π bonding contribution to the Ni–P bond. To a lesser extent this also seems to apply to the η^1 coordination of phosphaferrocene to the [Fe(CO)$_4$] complex fragment in **7**[18a] as well as of mesityl(diphenylmethylene)phosphane in **8**[18b] and in **9**, R = mesityl.[18c] Since such a Ni(3d$_\pi$)–P(3p$_\pi$) interaction decreases with increasing orbital contraction at the central atom it is not surprising that the cation $3^{+\cdot}$ proves to be unstable in solution: cyclic voltammetry attests to irreversibility for the pair $3^+/3^0$ even at −40 °C [anodic peak potential E_{pa} = 0.41 V in DME/nBu$_4$NClO$_4$ at glassy carbon versus a saturated calomel electrode (SCE)]. The reduction $3^0/3^-$ ($E_{pc(1)} = -2.11$ V) is also irreversible. This cathodic wave is followed by a second step ($E_{pc(2)} = -2.28$ V) assigned to the reduction of the free ligand by comparison with authentic phosphabenzene.

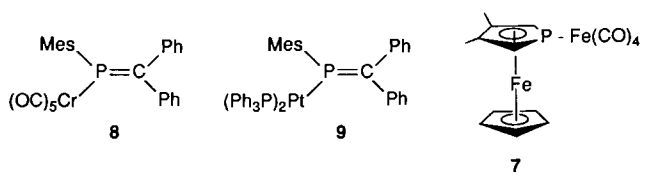

Solutions of **3** appear orange in benzene or methylcyclohexane and dark brown in THF. The same change in color also results for solutions of **3** in hydrocarbons with increasing temperature. Since in both cases the change in color can be reversed by the addition of small quantities of phosphabenzene this observation points to the existence of a dissociation equilibrium $[(\eta^1\text{-}C_5H_5P)_4Ni] \rightleftharpoons [(\eta^1\text{-}C_5H_5P)_3Ni] + C_5H_5P$. This assumption is supported by the presence of an isosbestic point (λ = 471 nm), which lies between the absorption maximum of **3** (λ_{max} = 389 nm) and a weak maximum ($\lambda \approx 530$ nm), which can possibly be assigned to the compound $[(\eta^1\text{-}C_5H_5P)_3Ni]$ or its solvate (Fig. 2). Yet, in the ^{1}H and ^{31}P NMR spectra of **3** in solution signals for the free ligand and the threefold coordinated complex are not observed. If free ligand is added, the spectra show an additional signal to that of the complex **3** and the $J(^1H,^{31}P)$ couplings can be resolved. Evidently, a situation prevails which Tolman[19a] referred to as type I (low complex dissociation, slow ligand exchange). The dissociation of **3** is surprising since for [Ni(PMe$_3$)$_4$], which possesses ligands of almost identical Tolman cone angle[19b] (θ(PMe$_3$) = 118°, θ (C_5H_5P) = 116°), such a partial cleavage is not observed.[20]

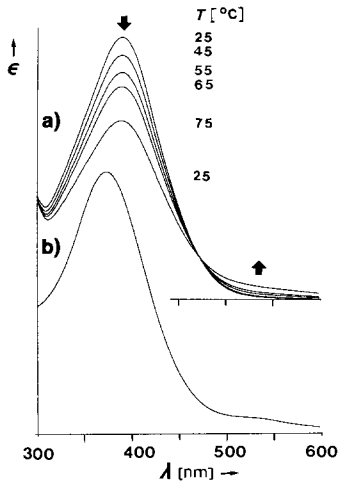

Fig. 2. UV/VIS spectra of $[(\eta^1\text{-}C_5H_5P)_4Ni]$ (**3**) a) in benzene at different temperatures and b) in THF at 25 °C.

Experimental Procedure

3: Phosphabenzene (0.45 g, 4.68 mmol) was added dropwise to [Ni(cod)$_2$] (212 mg, 0.77 mmol), dissolved in methylcyclohexane (50 mL) and stirred, whereupon a fine crystalline orange solid precipitated immediately, which was separated and taken up with the addition of phosphabenzene (0.1 mL) in THF (20 mL). After filtration the filtrate was layered with hexane (20 mL) at 4 °C. Within a day **3** (180 mg, 0.41 mmol, 53%) separated in the form of orange needles, m.p. 199 °C (decomp.), correct C,H, analysis. FD/MS: m/z 442 ($M^{\oplus}$, 100%); UV/VIS (benzene): λ_{max} [nm] (ε) = 389 (21 500); ^{31}P NMR (121.5 MHz, [D]$_8$THF + C_5H_5P, 25 °C): δ = 213.3, $\Delta\delta$ (relative to free C_5H_5P) = 6.3; ^{1}H NMR (300 MHz, [D]$_8$THF, 25 °C, TMS): δ = 8.20 (^2J(P,H) = 24.6 Hz; H-2,6), 7.65 (H-3,5), 7.17 (H-4), $\Delta\delta$(C_5H_5P) = −0.57 (H-2,6), −0.22 (H-3,5), −0.38 (H-4); ^{13}C NMR (125.77 MHz, [D]$_8$THF, 25 °C):

$\delta = 146.9$ ($^1J(C,H) = 157.2$ Hz; C-2,6), 136.4 ($^1J(C,H) = 155.9$ Hz; C-3,5), 124.0 ($^1J(C,H) = 158.5$ Hz; C-4), $\Delta\delta(C_5H_5P) = -8.2$ (C-2,6), -1.7 (C-3,5), -5.8 (C-4).

Received: May 9, 1992 [Z 5333 IE]
German version: *Angew. Chem.* **1992**, *104*, 1388

CAS Registry numbers:
1, 1295-35-8; **2**, 289-68-9; **3**, 143331-78-6.

[1] C. Elschenbroich, M. Nowotny, B. Metz, W. Massa, J. Graulich, K. Biehler, W. Sauer, *Angew. Chem.* **1991**, *103*, 601; *Angew. Chem. Int. Ed. Engl.* **1991**, *30*, 547.

[2] *Comprehensive Coordination Chemistry* (Eds.: G. Wilkinson, R. D. Gillard, J. A. McCleverty), Pergamon, Oxford, **1987**, Chap. 50.

[3] The formation of $[(C_5H_5N)_4Ni]$ from $[Ni(acac)_2]$ and C_5H_5N in toluene was postulated, the pyridine complex was however neither isolated nor characterized in solution: a) L. Conoira, J. G. Rodriguez, *J. Chem. Res. Synop.* **1988**, 68. Better documented are however several homoleptic complex cations $[(\eta^1\text{-}C_5H_5N)_nM]^{n+}$; b) $[(C_5H_5N)_6Cr]^{2+}$, presumed as the building block of $CrX_2 \cdot 6$ py (X = Br, I): D. G. Holah, J. P. Fackler, Jr., *Inorg. Chem.* **1965**, *4*, 1112; c) $[(C_5H_5N)_4Cr(PF_6)_2]$, axial coordination by two F atoms of the counterions: G. Fochi, J. Strähle, F. Gingl, *ibid.* **1991**, *30*, 4669; d) $[(C_5H_5N)_6Fe][Fe_4(CO)_{13}]$, isolated $[Fe(py)_6]^{2+}$ octahedra: R. J. Doedens, L. F. Dahl, *J. Am. Chem. Soc.* **1966**, *88*, 4847; e) $[(C_5H_5N)_6Co]^{2+}$, proposed to be present in solutions of $[(C_5H_5N)_4Co(PF_6)_2]$ in pyridine: D. W. Herlocker, M. R. Rosenthal, *Inorg. Chim. Acta* **1970**, *4*, 501; f) $[(C_5H_5N)_6Ni]^{2+}$, spectroscopically identified in solutions of $[(C_5H_5N)_4Ni(BF_4)_2]$ in pyridine: M. R. Rosenthal, R. S. Drago, *Inorg. Chem.* **1965**, *4*, 840; g) $[(C_5H_5N)_4Pd]^{2+}$, X-ray structural analysis, B. Freckmann, K. F. Tebbe, *Acta Crystallogr. Sect. A* **1981**, *37*, C 228; h) $[(C_5H_5N)_4Pt]^{2+}$, X-ray structural analysis, C. H. Wei, B. E. Hingerty, W. R. Busing, *Acta Crystallogr. Sect. C*, **1989**, *45*, 26; i) $[(C_5H_5N)_4Cu,Ag]^+$, X-ray structural analysis, K. Nilsson, A. Oskarsson, *Acta Chem. Scand. Ser. A* **1982**, *36*, 605; j) see also: H. Lehmkuhl, R. Paul, R. Mynott, *Liebigs Ann. Chem.* **1981**, 1139.

[4] H. Behrens, A. Müller, *Z. Anorg. Allg. Chem.* **1965**, *341*, 124.

[5] C. Elschenbroich, J. Koch, J. Kroker, M. Wünsch, W. Massa, G. Baum, G. Stork, *Chem. Ber.* **1988**, *121*, 1983.

[6] A. J. Ashe III, J. C. Colburn, *J. Am. Chem. Soc.* **1977**, *99*, 8099.

[7] C. Elschenbroich, J. Kroker, W. Massa, M. Wünsch, A. J. Ashe III, *Angew. Chem.* **1986**, *98*, 562; *Angew. Chem. Int. Ed. Engl.* **1986**, *25*, 571.

[8] Crystal structure determination of **3**: An orange single crystal of dimensions ca. $0.27 \times 0.13 \times 0.10$ mm^3 was measured on a four-circle diffractometer (CAD4, Enraf-Nonius, $Mo_{K\alpha}$ radiation, graphite monochromator) at 193 K. It proved to be tetragonal, space group $P42_1c$, $Z = 2$, with the lattice constants refined from 25 reflections with $\theta > 15°$ $a = 1219.7(2)$, $c = 686.6(1)$ pm and a density $\rho_{calcd} = 1.440$ Mg m^{-3}. In total 4623 reflections (complete sphere in the reciprocal space up to $\theta = 23°$) were collected. After a numerical absorption correction ($\mu = 12.6$ cm^{-1}, min./max. transmission 0.85/0.89) there were ($R_{int} = 0.017$) 701 independent reflections, all $F > 4\sigma(F)$. The structure was solved by direct methods and refined with anisotropicic temperature factors for all heavy atoms [9]. The high quality of the data set allowed all the H atoms to be localized and be freely refined with isotropic temperature factors. Furthermore, the correct orientation of the structure to the polar axis could be clearly determined by refinement of Rogers η parameter [9] (to 1.00(3)). By the use of an extinction correction and a weighting according to $1/\sigma^2(F_0)$ reliability factors of $R = 0.013$, $wR = 0.014$ were achieved, whereas for the inverted structure only $R = 0.031$ and $wR = 0.037$ were obtained. Further details of the crystal structure investigation may be obtained from the Fachinformationszentrum Karlsruhe, Gesellschaft for wissenschaftlich-technische Information mbH, D-W-7514 Eggenstein-Leopoldshafen 2 (FRG) on quoting the depository number CSD-56415, the names of the authors, and the journal citation.

[9] G. M. Sheldrick, SHELXTL-Plus. Release 4.0 for Siemens R3 Crystallographic Research systems, Siemens Analytical X-Ray Instruments, Inc., Madison, Wisconsin, USA, **1989**.

[10] a) A. Almenningen, B. Andersen, E. E. Astrup, *Acta Chem. Scand.* **1970**, *24*, 1579; J. C. Marriott, J. A. Salthouse, M. J. Ware, J. M. Freeman, *Chem. Commun.* **1970**, 595; b) G. M. Sheldrick, *Acta Crystallogr. Sect. B* **1975**, *31*, 305.

[11] X-ray structural analyses of homoleptic organophosphane–Ni complexes are, apart from ref. [10b], only known for chelate complexes of the type $[(P\text{-}P)_2Ni]$: a) P–P = $CH_2[P(cyhex)_2]_2$, Ni–P average 221 pm, C. Krüger, Y.-H. Tsay, *Acta Crystallogr. Sect. B* **1972**, *28*, 1941; b) P–P = *trans*-2,3.bis(diphenylphosphino)bicyclo[2.2.1]heptane, renorphos, Ni–P 219.5, H. Brunner, G. Vitulli, W. Porzio, M. Zocchi, *Inorg. Chim. Acta* **1985**, *96*, 67; c) P-P = $[Cp_2Zr(CH_2PMe_2)_2]$, Ni-P 216.7, H. H. Karsch, G. Müller, C. Krüger, *J. Organomet. Chem.* **1984**, *273*, 195; d) P-P = $Ph_2P\text{-}(CH_2)_2PPh_2$, Ni-P 216.5, H. Hartung, U. Baumeister, B. Walther, M. Maschmeier, *Z. Anorg. Allg. Chem.* **1989**, *578*, 177; e) P-P = $[(Me_2P\text{-}\eta^6\text{-}C_6H_5)_2Cr]$, Ni-P 214.9, C. Elschenbroich, G. Heikenfeld, M. Wünsch, W. Massa, G. Baum, *Angew. Chem.* **1988**, *100*, 397; *Angew. Chem. Int. Ed. Engl.* **1988**, *27*, 414; f) P-P = $MeP(CH_2PMe_2)_2$, Ni-P 213.8, G. Müller, H. H. Karsch, *Acta Crystallogr. Sect. C* **1987**, *43*, 663.

[12] Compare [1] Figure 2 and literature cited therein. According to electron transmission spectroscopy the anionic state $^2B_1(\pi^*)$ of C_5H_5P is binding: P. D. Burrow, A. J. Ashe III, D. J. Belleville, K. D. Jordan, *J. Am. Chem. Soc.* **1982**, *104*, 425.

[13] From the EPR spectrum of the radical anion $C_5H_5P^{-\bullet}$ the high π spin population $\rho_p = 0.47$ (c_p^2, b_1) can be deduced: F. Gerson, G. Plattner, A. J. Ashe III, G. Märkl, *Mol. Phys.* **1974**, *28*, 601.

[14] R. S. Nyholm, *Proc. Chem. Soc.* **1961**, 273.

[15] A. J. Ashe III, *Acc. Chem. Res.* **1978**, *11*, 153.

[16] a) R. V. Hodges, J. L. Beauchamp, A. J. Ashe III, W.-T. Chan, *Organometallics* **1985**, *4*, 457; b) G. Märkl, *Lect. Heterocycl. Chem.* **1972**, *1*, 69.

[17] D. T. Clark, I. W. Scanlan, *J. Chem. Soc. Faraday Trans. II* **1974**, *70*, 1222.

[18] a) J. Fischer, A. Mitschler, L. Ricard, F. Mathey, *J. Chem. Soc. Dalton Trans.* **1980**, 2522; B. Deschamps, F. Mathey, J. Fischer, J. Nelson, *Inorg. Chem.* **1984**, *23*, 3455; b) T. C. Klebach, R. Lourens, F. Bickelhaupt, C. H. Stam, A. van Herk, *J. Organomet. Chem.* **1981**, *210*, 211; c) T. A. van der Knaap, F. Bickelhaupt, H. van der Poel, G. van Koten, C. H. Stam, *J. Am. Chem. Soc.* **1982**, *104*, 1756.

[19] a) C. A. Tolman, W. C. Seidel, L. W. Gosser, *J. Am. Chem. Soc.* **1974**, *96*, 53; b) C. A. Tolman, *Chem. Rev.* **1977**, *77*, 313.

[20] Compare with $[Ni(PPh_3)_4] \rightleftharpoons [Ni(PPh_3)_3] + PPh_3$, R. Mynott, A. Mollbach, G. Wilke, *J. Organomet. Chem.* **1980**, *199*, 107.

[21] Note added in proof (August 10, 1992): Very recently from bis(2,4-dimethylpentadienyl)iron and phosphabenzene we have obtained pentakis(η^1-phosphabenzene)iron, space group $P2/n$, $Z = 4$, $a = 1600.1(2)$, $b = 972.2(1)$, $c = 1618.8$ pm, $\beta = 102.126(5)°$, mean Fe–P distance = 216 pm.

Catalytic Oxidation of Partially and Fully Fluorinated Olefins with Osmium Tetroxide**

By *Wolfgang A. Herrmann,* Stefan J. Eder,* and *Wolfgang Scherer*

The oxidation of olefins catalyzed by osmium tetroxide is a reliable method for the synthesis of vicinal *cis* diols.[1] The catalytic and stereochemical efficiency of this reaction can be explained by the formation of an intermediate cyclic osmate(VI) ester from the olefin and OsO_4 in the presence of pyridine bases, which undergoes hydrolytic cleavage. Current literature is still based on the assumption that very electron-poor olefins do not react with the metal oxide, and thus are also not oxidizable.[1, 2] We report here the contrary, namely, the formation of cycloadducts of partially and fully fluorinated olefins and their conversion into fluorinated diols and products of subsequent reactions.

Fluoroalkenes **1a–i** including those in which fluorine is directly bound to the carbon atoms of the double bond (**1e–i**), react with osmium tetroxide in hexane in the presence of pyridine and other nitrogen-containing bases at room temperature without irradiation.[3] In all cases, the isolable, thermally stable, cyclic osmate(VI) esters **2a–i** were obtained quantitatively within minutes or hours according to Scheme 1. Tetracyanoethylene **1j** is converted into the analogous cycloadduct **2j**. In comparison to the known complexes of this type, the fluorinated derivatives **2e–i** are extremely sensitive to hydrolysis.

The structure of the new osmate esters was determined by a single-crystal X-ray diffraction study of **2h**.[4] Complex **2h**

[*] Prof. W. A. Herrmann, Dr. S. J. Eder, W. Scherer
Anorganisch-chemisches Institut der Technischen Universität München
Lichtenbergstrasse 4, D-W-8046 Garching (FRG)

[**] Multiple Bonds between Main-Group Elements and Transition Metals, Part 107. This research was supported by the Fonds der Chemischen Industrie and the Hauptlaboratorium of Hoechst AG (Frankfurt). – Part 106: R. Buffon, A. Anroux, F. Lefebvre, M. Leconte, A. Choplin, J. M. Basset, W. A. Herrmann, *J. Mol. Catal.*, in press.

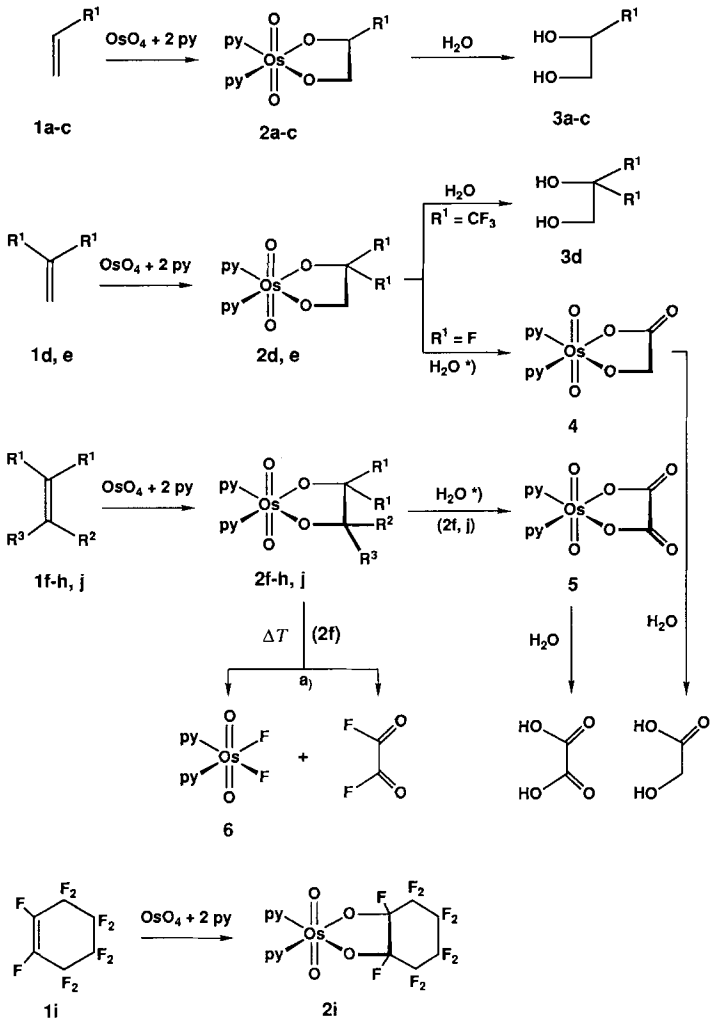

	a	b	c	d	e	f	g	h	i	j
R^1	CF_3	C_6F_{13}	C_6F_5	CF_3	F	F	F	CF_3	[a]	CN
R^2	H	H	H	H	H	F	F	F		CN
R^3	H	H	H	H	H	F	CF_3	C_2F_5		CN

[a] For the structures of compounds **1i** and **2i** see above.

Scheme 1. py = Pyridine. *) Liberation of HX. a) Vacuum.

has a *trans*-configurated linear osmyl group $(OsO_2)^{2+}$ with octahedral geometry about the osmium center (Fig. 1). A comparison with the structures of non-fluorinated osmate esters shows that the numerous electron-withdrawing groups do not affect the structural parameters of **2h**.[5]

The thermolysis and hydrolysis of the new osmate esters are dependent upon their constitution: hydrolysis of the fluoro- and cyano-substituted osmate esters occurs primarily on the ring systems. Hydrolysis of **2e** and **2f, j**, for example, provides the respective isolable hydroxyacetato and oxalato complexes **4** and **5**. Continued hydrolysis yields the corresponding osmium-free hydroxycarboxylic acid and dicarboxylic acids (Scheme 1). Of the series of osmate esters examined, **2f**, derived from tetrafluoroethylene **1f**, is most thermally labile:[6, 7] when **2f** is heated under vacuum at 150 °C, the previously unknown difluoride **6** is obtained as a stable pyridine complex in 80% yield by elimination of oxalyl fluoride. Esters **2a–e** and **2g–i** are thermally stable to at least 110 °C, **2h** to approximately 190 °C.

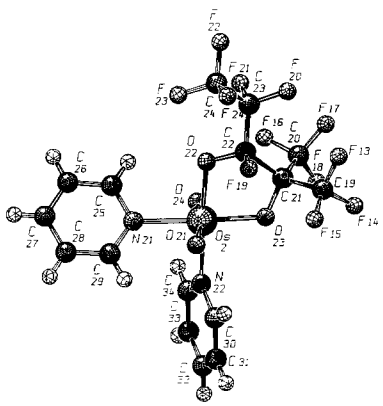

Fig. 1. SCHAKAL representation of one of the two crystallographically independent molecules of the perfluorinated osmate ester **2h**. Selected distances [pm] and angles [°]: Os2-O21 173.2(5), Os2-O24 172.3(5), Os2-O22 199.6(5), Os2-O23 196.9(5), Os2-N21 212.8(7), C21-O23 138.6(9), C22-O22 132.0(9), C21-C22 159(1), C22-F19 143.9(9); O22-Os2-O23 81.9(2), Os2-O23-C21 116.2(5), O22-C22-C21 112.4(7).

Aside from these exceptional cases, the hydrolysis of osmate esters **2a–d** with electron-withdrawing groups such as CF_3 and C_6F_5 is synthetically useful. For synthetic application the catalytic variant of this reaction appears to be especially advantageous. Thus the typical fluoroolefins **1a–d** can be converted under standard conditions into the 1,2-diols **3a–d** by treatment with potassium hexacyanoferrate(III), with hydrogen peroxide as the primary oxidant on free or supported[8] osmium tetroxide, or with the salt $K_2[OsO_2(OH)_4]$. A representative selection of data on these reactions is listed in Table 1. When α-fluoroalcohols are formed (e.g. from **1e–i**), ketones or 1,2-diketones arise after spontaneous elimination of HF (Table 1). Although this loss of fluorine appears to be a drawback, this method holds promise for the preparation of fluorinated mono- and diketones in special cases, since fully fluorinated olefins are often more easily accessible than their partially fluorinated congeners.

Table 1. Catalytic oxidation of selected fluoroolefins with H_2O_2 or $K_3[Fe(CN)_6]$.

Fluoroolefin	Oxidation product	Oxidant H_2O_2 cat.	Oxidant $Fe^{(III)}$ cat.	stoichiometric
1a	**3a**	67%	95%	>99%
1b	**3b**	68%	>99%	>99%
1c	**3c**	85%	98%	>99%
1d	**3d**	48%	>99%	>99%
1g	$HOOC-CO-CF_3$	80%	63%	80%
1h	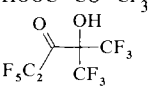	87%	70%	80%
1i	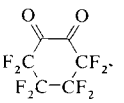	88%	83%	>90%
	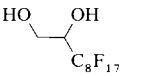	70%	> 99%	>99%
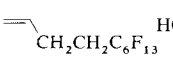	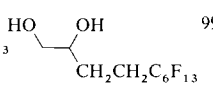	99%	> 99%	

We demonstrate here that even the most electron-poor olefins undergo OsO_4-catalyzed oxidations. The reduced reactivity of chloroolefins relative to their fluorine counterparts is explained by a size effect; in all other respects the chloroolefins behave analogously.[7] The procedure is also applicable to strained fluoroolefins, for example norbornene derivatives.

Our results cannot be rationalized with the frequently held conception of the mechanism of the osmylation as the electrophilic attack of osmium tetroxide on the olefin. The pyridine base effect discussed by Corey et al. and Hoffmann et al.[9] is more applicable. According to this mechanistic description, the polarized *cis*-OsO_2 group reacts by a [2 + 3] cycloaddition (*trans* influence of the pyridine base). The remarkable reactivity of polar fluoroolefins such as vinylidene fluoride $F_2C{=}CH_2$ (**1f**), $(CF_3)_2C{=}CF_2$, and $F(CF_3)C{=}C(OC_6H_5)_2$ supports this interpretation.

Although α-hydroxyfluorides react further by elimination of HF, the catalytic variant of the reaction sequence described here provides a new, convenient route to oxygenated organofluorine compounds. Osmium tetroxide can now be considered a universal oxidizing agent for olefins. The optimization of the less toxic, immobilized variants[8] is thus of even greater importance.

Experimental Procedure

2f: C_2F_4 was separated from the stabilizing agent α-pinene by cooling to −35 °C, and was then passed through a solution of OsO_4 (2.00 g, 7.9 mmol) in toluene (80 mL) and pyridine (1.3 mL) at 25 °C. After a few minutes **2f** separated as an ochre precipitate. The reaction mixture was concentrated and the residue dried under vacuum to give analytically pure **2f**. Yield 4.0 g (99%). M.p. 143 °C (decomp)[10a]. After compound **2f** was heated for 6 h at 135 °C/10^{-3} Torr, the residue was recrystallized from CH_2Cl_2 (−30 °C) to give analytically pure $[(py)_2OsO_2F_2]$ in 80% yield[10b].

Catalytic oxidation with hexacyanoferrate(III): $K_2[OsO_2(OH)_4]$ (100 mg, 0.27 mmol), pyridine (0.36 mL), $K_6[Fe(CN)_6]$ (14.7 g, 45 mmol), and K_2CO_3 (6.2 g) were dissolved in a mixture of H_2O (100 mL) and *t*-C_4H_9OH (100 mL)[11]. This solution was vigorously stirred while 15–20 mmol of the olefin was added. The reaction mixture was stirred for 24 h, $Na_2SO_3 \cdot 7H_2O$ (11.4 g) was added, and the mixture stirred an additional 1 h. The organic phase was separated, the aqueous phase washed with CH_2Cl_2 (2 × 50 mL), the collected organic layers dried over $MgSO_4$, and concentrated. For yields see Table 1.

Catalytic oxidation with hydrogen peroxide: OsO_4 (80 mg, 0.315 mmol) was dissolved in THF (30 mL) and immobilized on cross-linked poly(4-vinylpyridine) (Reillex 402, 1 g)[8]. An "oxidation solution" made from *tert*-butanol (100 mL) and 30% H_2O_2 (25 mL) and dried over aqueous $MgSO_4$ was used along with the heterogeneous catalyst to oxidize the olefins listed in Table 1 (25–100 mmol). Standard workup, for yields see Table 1.

Received: May 13, 1992 [Z 53451E]
German version: *Angew. Chem.* **1992**, *104*, 1371

[1] Reviews: a) M. Schröder, *Chem. Rev.* **1980**, 80, 187–213; b) W. P. Griffith in *Gmelins Handbuch der Anorganischen Chemie, Band Osmium, Suppl. Vol. 1* (Eds.: K. Swars), Springer, Berlin, **1980**, p. 184ff; c) J. L. Courtney in *Organic Syntheses by Oxidation with Metal Compounds* (Eds.: W. J. Mijs, C. R. H. I. de Jonge), Plenum, New York, **1986**, Chapter 8, p. 449; d) H. Waldmann, *Nachr. Chem. Techn. Lab.* **1992**, *40*, 702–708; e) A. H. Haines, *Methods for the Oxidation of Organic Compounds*, Academic Press, New York, **1985**, pp. 280–285.

[2] a) H. B. Henbest, W. R. Jackson, B. C. G. Robb, *J. Chem. Soc (B)* **1966**, 803–807; b) D. G. Lee in *Techniques and Applications in Organic Synthesis, Vol. 1* (Ed.: R. L. Augustine), Dekker, New York, **1969**, p. 11ff; c) M. Hudlicky, *Chemistry of Organic Fluorine Compounds*, 2nd ed., E. Horwood, London **1976**.

[3] Cf. J. M. Wallis, J. K. Kochi, *J. Am. Chem. Soc.* **1988**, *110*, 8207–8223.

[4] Complex **2h** crystallized from toluene/CH_2Cl_2 at −20 °C in the monoclinic space group $P2_1/c$ with $a = 1548.1(9)$, $b = 1769.7(4)$, $c = 1519.2(9)$ pm, $\beta = 94.85(3)°$, $Z = 8$, $V = 4147 \times 10^6$ pm^3, $\delta = 2.282$ g cm^{-3}, $F(000) = 2688$; $Mo_{K\alpha}$ radiation, CAD-4 Enraf-Nonius diffractometer, ω scan, maximum 90 s, 7846 measured reflections $1° < \theta < 25°$ (0/18), (0/21), (−18/18), 6477 independent reflections, of these 5516 with $I > 3.0\sigma(I)$ were used for refinement, structure solution by the Patterson method, no intensity correction, empirical absorption correction ($\mu = 62.9$ cm^{-1}), $R = \Sigma(||F_o| - |F_c||)/\Sigma|F_o| = 0.035$; $R_w = [\Sigma w(|F_o| - |F_c|)^2/\Sigma w|F_o|^2]^{1/2} = 0.035$, residual electron density $+1.18/-0.93$ e$_o \cdot$Å^3. Figure 1 shows one of the two crystallographically independent molecules. Further details of the crystal structure investigation may be obtained from the Fachinformationszentrum Karlsruhe, Gesellschaft für wissenschaftlich-technische Information mbH, D-W-7514 Eggenstein-Leopoldshafen 2 (FRG), on quoting the depository number CSD-56416, the names of the authors, and the journal citation.

[5] B. A. Cartwright, W. P. Griffith, M. Schröder, A. C. Skapski, *Inorg. Chim. Acta* **1981**, 53, L129–L130.

[6] The osmate ester $[(py)_2OsO_2(OCCl_2CCl_2O)]$ obtained from $Cl_2C{=}CCl_2$ is thermally also not very stable; nevertheless, it could be characterized.

[7] S. J. Eder, Dissertation, Technische Universität München, **1992**.

[8] W. A. Herrmann, G. Weichselbaumer (Hoechst AG), WO 91/00143 from January 10, 1991.

[9] K. A. Jørgensen, R. Hoffmann, *J. Am. Chem. Soc.* **1986**, 108, 1867–1876; b) E. J. Corey, P. D. Jardine, S. Virgil, P.-W. Yuen, R. D. Connell, *ibid.* **1989**, *111*, 9243–9244; c) E. J. Corey, G. I. Lotto, *Tetrahedron Lett.* **1990**, *31*, 2665–2668.

[10] a) ^{19}F NMR (235.3 MHz, CD_3CN, vs. CF_3CO_2H): $\delta = -17.34$ (s); ^{13}C NMR (100.5 MHz, CD_3CN): $\delta = 128.8$ (tt, $^1J(C,F) = 263$, $^2J(C,F) = 47$ Hz, CF_2), 151.46 (*o*, $^1J(C,H) = 186$, C_5H_5N), 144.03 (*p*, $^1J(C,H)$ 168), 127.99 (*m*, $^1J(C,H) = 172$ Hz); IR (KBr): $\nu(OsO) = 857$ cm^{-1} (st). Correct C, H, N, F analyses. – b) ^{19}F NMR (see above, CH_2Cl_2): $\delta = -31.06$ (s, OsF); IR (KBr): $\nu(OsO) = 855$ cm^{-1}. Correct C, H, N, F analyses.

[11] K. B. Sharpless, W. Amberg, M. Beller, H. Chen, J. Hartung, Y. Kawanami, D. Lübben, E. Manoury, Y. Ogino, T. Shibata, T. Ukita, *J. Org. Chem.* **1991**, *56*, 4585–4588.

High Molecular Weight Polypropylene through Specifically Designed Zirconocene Catalysts

By *Walter Spaleck,* Martin Antberg, Jürgen Rohrmann, Andreas Winter, Bernd Bachmann, Paul Kiprof, Joachim Behm,* and *Wolfgang A. Herrmann**

Only a few years after the discovery of the isotactic polymerization of propylene with zirconocene catalysts,[1,2] more than 250 patents and numerous original publications document a fascinating, rapid development. Nevertheless, all variants of these "stereorigid" zirconocene/methylalumoxane catalysts remained merely of academic interest. Practical application failed because of the insufficient molecular mass of the polymeric products. For instance, the catalyst **1** described first gave only polymeric waxes with $M_w < 30000$ g mol^{-1} under technically reasonable conditions (> 40 °C) in the presence of methylalumoxane (MAO) as cocatalyst.[1,3] Modification of the zirconocene complexes brought only gradual improvements.[4–6] The structurally analogous hafnium derivatives[7] could also not solve the technical problems,

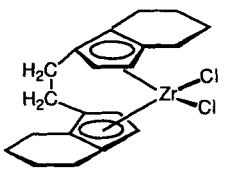

1

[*] Prof. Dr. W. A. Herrmann, Dr. P. Kiprof, Dr. J. Behm
Anorganisch-chemisches Institut der Technischen Universität München
Lichtenbergstrasse 4, D-W-8046 Garching (FRG)
Dr. W. Spaleck, Dr. M. Antberg, Dr. J. Rohrmann, Dr. A. Winter, Dr. B. Bachmann
Hoechst AG
Brüningstrasse 50, D-W-6230 Frankfurt am Main 80 (FRG)

 © VCH Verlagsgesellschaft mbH, W-6940 Weinheim, 1992

because their activities were less than 5% of those of the reference zirconocene catalysts.[8] Under these peripheral conditions, the required demand for pure hafnium would make catalyst production particularly uneconomical. This report on the synthesis of polypropylene of molecular mass far above $M_w = 100000\ g\,mol^{-1}$ announces the technical breakthrough for polymerization with zirconocene catalysts.

A glance at Table 1 shows that for the polymerization of propylene with the catalysts **2b** and **3b** the molecular weight of the polymers formed at technically acceptable reaction temperatures are drastically higher than those formed with the complexes known to date (**2a** and **3a**), in spite of the only slight variation in the catalyst system. In the simplest case the

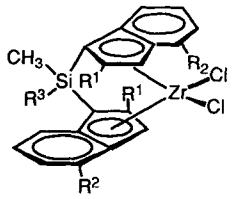

2a-e

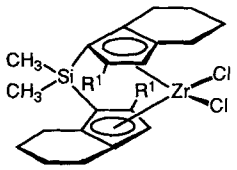

3a,b

introduction of a methyl group at the indenyl ligand ($R^1 = CH_3$; **2b**) in the immediate proximity of the silylene bridge suffices. This change alone increases the molecular weight of the polymer fivefold and provides distinctly improved tacticity (> 96%; m.p. 145–148 °C). Although the same effect can be achieved with the hafnium derivative **2a'**, it shows only a fraction of the activity of the zirconium reference catalyst **2a** (Table 1; see also [8]). Larger 2-substituents adjacent to the bridge ($R^1 = C_2H_5$, **2c**), do not result in improved polymer properties. However, another substituent in 4-position, that is, at the annelated benzene ring, effects a further increase in molecular weight ($R^2 = iC_3H_7$, **2d**), and this complex is much more active than the reference catalyst **2a**. Furthermore, the isotacticity also increases (98%, m.p. 152 °C). The catalyst **2d** is therefore a realistic candidate for technical applications. Modification of R^3 on the silyl group can also be advantageous for high molecular weight polymers, as indicated by the exchange of methyl (**2b**) by phenyl (**2e**).

The underlying ligand system of those catalysts **2**, in which $R^1 = CH_3$, was synthesized from the ketoaldehyde (a) according to the new, generalizable sequence outlined in Scheme 1.[9, 10]

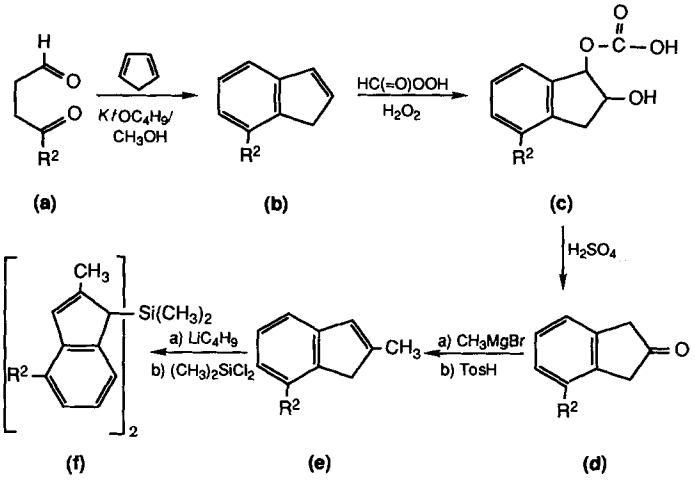

Scheme 1. Synthesis of the ligand systems of catalysts **2**. Yields of the individual steps: (b) 52%, (c) + (d) 79%, (e) 50%, (f) 91%. $R^2 = CH(CH_3)_2$.

The R^1 effect seems to be of a general nature, since it is also observed in the tetrahydroindenyl derivatives **3** (Table 1). Replacing H (**3a**) with CH_3 (**3b**) doubles the polypropylene mass and increases the isotacticity. Nevertheless, the achievable molecular weights are much lower than those of the analogous systems of **2** with aromatic six-membered rings. This demonstrates that for technical catalysts for propylene polymerization not only the 2-alkyl substitution but also the benzoannelation of the five-membered ring is crucial.

Although our results appeared to be able to be explained by a distortion of the catalyst framework, this conclusion proved false, because the molecular structures of the reference catalyst **2a** and its methyl derivative **2b** are identical in all parameters (Table 2, Fig. 1 and 2).[11] As may be seen in Figure 2, right, the methyl groups present in **2b** in 2-position are turned away from the spatial segment relevant for catalysis. A direct steric influence of this group on the chain termination reaction and thus on the polymer mass is therefore not expected.[12, 13] In our opinion an electronic effect is dominant. It is reasonable to assume[14] that a decrease in the local Lewis acidity at the (cationic) zirconium atom of the active species[2, 15] lowers its tendency to abstract a β-H atom. The number of chain terminations thereby decreases and the molecular mass thus increases (**2a** → **2b**). Additional alkyl substitution enhances this effect (**2d**), while loss of aromaticity of the six-membered ring weakens it drastically (**3b**). The alkyl substituents in 2- and 4-position provide in

Table 1. Bulk polymerization of propylene at 50 °C in the presence of zirconocene catalysts of type **2** and **3**. PP = polypropylene.

Catalyst (+ MAO)	R^1	R^2	R^3	Activity $\left[\frac{kg\ PP}{mmol\ cat.\ h}\right]$	M_w [10^3 g mol^{-1}]	M.p. [°C]	Isotacticity [%]	Proportion of isotact. pentads *mmmm* [%]
Indenyl type								
2a	H	H	CH_3	60	60	141	94.2	82.2
2a' [a]	H	H	H	2	350	138	94.6	82.7
2b	CH_3	H	CH_3	40	340	148	96.8	90.2
2c	C_2H_5	H	CH_3	30	370	145	96.4	90.1
2d	CH_3	i-C_3H_7	CH_3	105	460	152	98.0	91.6
2e	CH_3	H	C_6H_5	35	450	148	[b]	[b]
Tetrahydroindenyl type								
3a	H			35	32	147	94.0	85.8
3b	CH_3			10	65	153	96.0	90.2

[a] For comparison with **2a**, the hafnocene derivative with the same structural formula, **2a'**, has been listed. [b] Not determined.

 © VCH Verlagsgesellschaft mbH, W-6940 Weinheim, 1992 0570-0833/92/1010-1348 $ 3.50+.25/0 Angew. Chem. Int. Ed. Engl. 1992, 31, No. 10

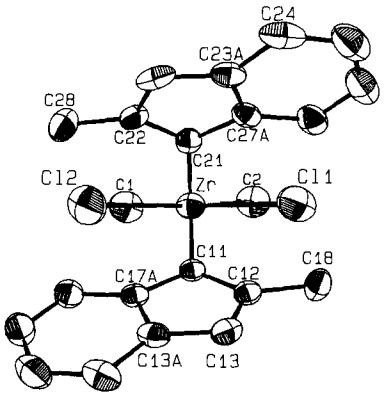

Fig. 1. Crystal structure and molecular structure of the *ansa*-zirconocene catalyst **2b** ($R^1 = R^3 = CH_3$; $R^2 = H$). The ellipsoids represent 50% probability; hydrogen atoms are omitted.

2d the currently optimal catalyst by increasing the basicity of the aromatic ligand without placing a steric obstacle in the path of the growing polymer chain.

In accord with this interpretation, electron-withdrawing substituents lower the molecular mass. A 5-chloro substituent in the catalyst yields molecular weight of $M_w = 9900\ g\,mol^{-1}$ for polypropylene;[16a] similar effects are known for bridged and nonbridged indenyl complexes of the same type.[16b, c]

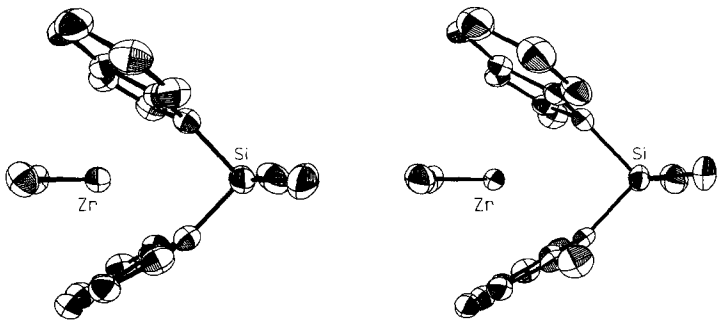

Fig. 2. Comparison of the structure of the catalysts **2a** (left) and **2b** (right); view onto the edge of the Zr plane (ORTEP drawing).

The higher stereospecificity (higher proportion of isotactic pentads, polymer's higher melting point) observed with all these new complexes **2b–d** compared with the parent catalyst **2a** is striking. A subordinate spatial effect of the substituents on the exact position of the reactant at the active site must therefore be assumed.

Table 2. Comparison of the structure of the unsubstituted and methyl-substituted zirconocene catalysts **2a** and **2b**.

	2a	**2b**	Δ
Zr-Cl [pm]	243.14(2)	241.9 [a]	1.2
Cl-Zr-Cl [°]	98.76(1)	99.06	0.3
C-Si-C [°]	94.57(6)	94.3(1)	0.3
Cp-Zr [b] [pm]	224.13(1)	224.4 [a]	0.3
Cp-Zr-Cp [b] [°]	127.81(1)	128.11(1)	0.3
E1-E2 [c] [°]	61.94	61.39	0.6
Zr-C [pm]	247.0(1)-265.9(1)	246.2(3)-266.3(5)	–
α [d] [°]	110	110	0
β [c] [°]	0	0	0

[a] Average value. [b] Centers of the five-membered rings of the indenyl ligands. [c] Interplanar angle between the two indenyl ligands. [d] Aperture gap according to [12b]. [e] Obliquity angle according to [12b].

Our interpretation of these results suggests that another optimization of the catalysts derived from the indenyl complex **2a** would be possible if the effects of the 2- and 4-substituents can be combined in a way to avoid steric hindrance at the active site. Modified CVFF force field calculations have shown that all these derivatives should have the same framework structures as **2a** and **2b** within experimental error.[17]

Experimental Procedure

All manipulations were conducted in an inert argon atmosphere.

Ligand systems: A solution of the relevant indene [9,18a] (30 mmol) in THF (30 mL) was slowly treated with a solution of butyllithium (12 mL, 30 mmol, 2.5 M) in *n*-hexane at 25 °C and heated for 1 h under reflux. The solution was then added dropwise to a solution of dimethyl- or methylphenyldichlorosilane (15 mmol) in THF (10 mL) at 25 °C and stirred for 15 h. The mixture was poured onto ice water and extracted with diethyl ether. The residue remaining after removal of the solvent was chromatographed on silica gel 60. The unchanged starting material for the ligand was eluted with solvent mixtures of *n*-hexane/CH_2Cl_2 (between 20:1 and 10:1); yield 35–60%.

2a–2e: A solution of the appropriate indene (10 mmol) in THF (30 mL) was treated with a solution of butyllithium (8 mL, 22 mmol, 2.5 M) in *n*-hexane at 25 °C and stirred for 15 h. The solvent was removed, and the solid residue washed with *n*-hexane and dried in vacuum (oil pump) for 5 h. The powdered dilithium salt was added to a suspension of $ZrCl_4$ (2.33 g, 10 mmol) in CH_2Cl_2 at −78 °C. The mixture was allowed to warm to 25 °C (15 h) and was then evaporated to dryness under vacuum. The process yielded a 1:1 mixture of the *rac* and *meso* isomer. The residue was dried at 10^{-3} Torr and extracted with toluene. The pure racemate (an orange-yellow crystalline powder) was recovered from the extract by crystallization (− 35 °C); further recrystallization is possible from CH_2Cl_2 or THF; yield of pure compound 10–25% (*rac*).

3a,b: The aromatic analogues **2a,b** were hydrogenated according to [18b]. Yield 50%.

Propylene polymerization: A dry 16-L, thermostatable steel reactor was charged with nitrogen and 10 L of liquid propylene at 30 °C. Then a solution of methylalumoxane in toluene (30 mL, 40 mmol Al; average molar mass 950 $g\,mol^{-1}$) was added. Simultaneously, 0.02 mmol of metallocene was dissolved in an identical solution of methylalumoxane in toluene (20 mL) and left to stand for 15 min to be "activated". The orange-red solution was then added to the reactor. The reactor was heated to 50 °C and kept at this temperature for 1 h. The reaction was stopped by the addition of isopropanol (10 mL), cooled, the pressure released, and the product dried in vacuum. The yield was determined by weighing.

Polymer analysis: Molecular masses were determined by gel permeation chromatography (as solution in 1,2-dichlorobenzene at 135 °C; molar mass distribution M_w/M_n in total < 3), melting points by DSC, triad isotaxies and proportion of isotactic pentades by ^{13}C NMR spectroscopy [18c] (Bruker WP 300, 110 °C, hexachlorobutadiene/$CDCl_2CDCl_2$).

Received: May 16, 1992 [Z 5355 1E]
German version: *Angew. Chem.* **1992**, *104*, 1373

CAS Registry numbers:
2a, 119821-97-5; **2a'**, 124684-46-4; **2b**, 143278-86-8; **2c**, 143278-92-6; **2d**, 143346-94-5; **2e**, 143346-95-6; **3a**, 115701-70-7; **3b**, 143346-96-7; polypropylene (isotactic homopolymer), 25085-53-4.

[1] a) W. Kaminsky, K. Külper, H. H. Brintzinger, F. R. W. P. Wild, *Angew. Chem.* **1985**, *97*, 507; *Angew. Chem. Int. Ed. Engl.* **1985**, *24*, 507; b) W. Kaminsky, *Angew. Makromol. Chem.* **1986**, *145/146*, 149.
[2] P. Pino, P. Ciani, M. Galimberti, J. Wei, N. Piccolrovazzi in *Transition Metals and Organo-Metallics as Catalysts for Olefin Polymerization* (Eds.: W. Kaminsky, H. Sinn), Springer, Berlin, **1988**.
[3] W. Kaminsky, K. Külper, S. Niedoba, *Makromol. Chem. Macromol. Symp.* **1986**, *3*, 377.
[4] W. A. Herrmann, J. Rohrmann, E. Herdtweck, W. Spaleck, A. Winter, *Angew. Chem.* **1989**, *101*, 1536; *Angew. Chem. Int. Ed. Engl.* **1989**, *28*, 1511.
[5] T. Mise, S. Miya, H. Yamazaki, *Chem. Lett.* **1989**, 1853.
[6] J. W. Röll, H.-H. Brintzinger, B. Rieger, R. Zolk, *Angew. Chem.* **1990**, *102*, 339; *Angew. Chem. Int. Ed. Engl.* **1990**, *29*, 279.
[7] J. A. Ewen, L. H. Haspeslagh, J. L. Atwood, H. Zhang, *J. Am. Chem. Soc.* **1987**, *109*, 6544.
[8] W. Spaleck, M. Antberg, V. Dolle, R. Klein, J. Rohrmann, A. Winter, *New J. Chem.* **1990**, *14*, 499.
[9] a) G. Erker, D. Reuschling, J. Rohrmann, R. Nolte, M. Aulbach, A. Weiß (Hoechst AG), DE-OS 4104931 of February 18, 1991; b) J. Rohrmann, M. Antberg, W. Spaleck (Hoechst AG), DE-OS 4128238 of August 26, 1991.
[10] ^1H NMR (100 MHz, $CDCl_3$, 25 °C) **2a**: δ = 6.9–7.7 (m, 5H, arom. H), 6.85 (s, 2H, 3-H), 2.2–2.8 (m, 4H, CH_2), 1.30 (s, 6H, $SiCH_3$), 1.10 (t, 6H, CH_3). – **2b**: δ = 6.92–7.75 (m, 8H, arom. H), 6.80 (s, 2H, β-H), 2.18 (s, 6H, CH_3), 1.25 (s, 6H, $SiCH_3$). – **2c**: δ = 7.0–8.2 (m, 13H, arom. H), 6.90

(s, 2H, β-H), 2,67 (s, 3H, CH_3), 2.45 (s, 3H, CH_3), 1.50 (s, 3H, $SiCH_3$). – **2d**: δ = 6.7–7.5 (m, 6H, arom. H), 6.85 (s, 2H, β-H), 3.0 (m, 2H, CH), 2.23 (s, 6H, CH_3), 1.17–1.37 (m, 12H, CH_3), 1.27 (s, 6H, $SiCH_3$). – **3b**: δ = 6.05 (s, 2H, β-H), 2.44–3.37 (m, 8H, CH_2), 2.10 (s, 6H, CH_3), 1.43–1.93 (m, 8H, CH_2), 0.90 (s, 6H, $SiCH_3$).

[11] **2b**: monoclinic (space group $P2_1/c$, no. 14), $a = 878.2(2)$, $b = 2668.8(2)$, $c = 921.9(2)$ pm, $\beta = 112.24(1)°$, $V = 1999 \times 10^6$ pm^3, $Z = 4$, $\rho_{calcd} = 1.583$ g cm^{-1}, $M = 476.6$. Lattice parameters from 25 reflections at high diffraction angles ($33.2° < 2\theta < 44.8°$). Data collection on a CAD4 single crystal diffractometer (Enraf-Nonius), $Mo_{K\alpha}$ radiation ($\lambda = 71.07$ pm, graphite monochromator) at room temperature in ω scan to $\theta_{max} = 25°$ ($t_{max} = 90$ s, scan width: $1.2 + 0.3 \tan\theta$). Intensity data from 3837 observed reflections $h(-10/0)$, $k(0/31)$, $l(-10/10)$, of 2969 independent reflections 576 reflections with $I/\sigma(I) < 0.01$ suppressed, 2704 with $I > 1\sigma(I)$ used, structure solution through direct methods with subsequent difference Fourier syntheses; no absorption correction ($\mu = 8.7$ cm^{-1}), observed decomposition (5.7% in 107 h) not corrected; H atoms calculated in ideal positions, included in the calculation of the structure factors, but not refined. Refinement according to the least-squares method, $R = \sum||F_o| - |F_c||/\sum|F_o| = 0.046$; $R_w = [\sum w(|F_o| - |F_c|)^2/\sum w|F_o^2|]^{1/2} = 0.029$; GOF $= [\sum w(|F_o| - |F_c|)^2/(NO-NV)]^{1/2} = 1.993$. Residual electron density + 0.51 e Å^{-3} 121 pm beside Zr1 and −0.45 e Å^{-3} 88 pm beside Zr1. Further details of the crystal structure investigation may be obtained from the Fachinformationszentrum Karlsruhe, Gesellschaft for wissenschaftlich-technische Information mbH, D-W-7514 Eggenstein-Leopoldshafen 2 (FRG) on quoting the depository numbers CSD-53960 (**2a**) and 56457 (**2b**), the names of the authors, and the journal citation.

[12] a) L. Cavallo, P. Corradini, G. Guerra, M. Vacatello, *Polymer* **1991**, *32*, 1329; b) K. Hortmann, H.-H. Brintzinger, *New J. Chem.* **1992**, *16*, 51.

[13] A theoretical consideration of the problem leads to the conclusion that methyl substitution at the 2-position does not influence the transition state of the polymerization reaction [12a]. This statement seems to be substantiated since the quoted loss of stereospecificity is actually observed on 3-methyl substitution. The + I effect of the methyl substituents, which improves the molecular mass of polypropylene, is also seen in the series of $(CH_3)_2$Si-bridged cyclopentadienyl complexes; cf. [5].

[14] J. A. Ewen, M. J. Elder, R. L. Jones, S. Curtis, H. N. Cheng in *Catalytic Olefin Polymerization* (Eds.: T. Keii, K. Soga), Tokio, **1990**.

[15] R. F. Jordan, R. E. La Pointe, C. S. Bajgur, R. Willet, B. Scott, *J. Am. Chem. Soc.* **1986**, *108*, 7410.

[16] a) H. M. Riepl, Dissertation, Technische Universität München 1992; b) W. Spaleck, J. Rohrmann, M. Antberg, unpublished; c) N. Piccolrovazzi, P. Pino, G. Consiglio, A. Sironi, M. Moret, *Organometallics* **1990**, *9*, 3098.

[17] W. A. Herrmann, J. Behm, unpublished, 1992.

[18] a) M. Adamczyk, D. S. Watt, D. A. Netzel, *J. Org. Chem.* **1984**, *49*, 4226; b) F. R. W. P. Wild, L. Zsolnai, G. Huttner, H. H. Brintzinger, *J. Organomet. Chem.* **1982**, *232*, 233; c) A. Zambelli, P. Locatelli, A. Provasoli, D. F. Ferro, *Macromolecules*, **1980**, *13*, 267.

Phosphorus(v) Selenides with Phosphorus in a Trigonal-Planar Environment**

By *Alfred Schmidpeter,* Georg Jochem, Konstantin Karaghiosoff,* and *Christian Robl*

In phosphorus(v) chalcogenides the phosphorus atom is generally tetracoordinated: dichalcogeno(organo)-λ^5-phosphanes **1**, Y = S, Se, form dimers **2**,[1,2] and phosphinoyl halides **4** show no tendency to dissociate with the formation of a chalcogeno(diorgano)phosphonium ion **3**.

The tricoordinate phosphorus atom in **1** and **3** should be highly electrophilic. Compounds **1** and **3** are therefore postulated as the reactive species for the O/S exchange with Lawesson reagent[1] or for the $AlCl_3$ catalyzed electrophilic substitution with thiophosphinoyl chlorides.[3]

1 **2** **3** **4**

For Y = S the monomers **1** with R = Me, Et could be detected as the products of the gas-phase thermolysis of **2**.[4] In the condensed phase so far only one representative of **1**, namely with the large 2,4,6-tri-*tert*-butylphenyl substituent, has been described and structurally confirmed;[5] the corresponding compound with Y = Se is also known.[6] To our knowledge there is so far not sufficient evidence for **3**.

Both of the above equilibria are shifted to the left with ylide substituents R. Monomeric dithioxo- and diselenoxo-λ^5-phosphanes **1** and ionic selenophosphonium halides **3** can be isolated because of the stabilizing effects of these R groups.

Dichloro[organo(triphenylphosphonio)methanidyl]phosphanes **5**[7] react smoothly with sodium diselenide in THF to give the corresponding ylide-substituted diselenoxo-λ^5-phosphanes **7**, which can be isolated as orange-yellow crystals.

The reaction comprises a reduction of the diselenide and an oxidation of the phosphorus. The ylide-substituted diselenaphosphirane **6** assumed as intermediate, however, cannot be observed. Compound **7** is formed by cleavage of the Se–Se bond and flattening of the coordination environment of the phosphorus. In the case of S instead of Se, and H instead of the ylide substituent, a value of −9 kcal mol^{-1} is calculated for the corresponding ring opening.[8] In view of the comparable electronegativities of S and Se, a similar value is to be expected for the selenium compound; however, because of the ylide substituent the formation of **7** should be considerably more favorable energetically.

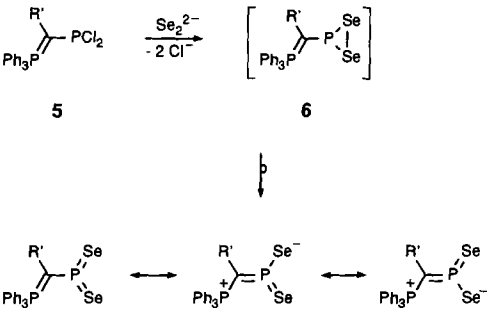

5 **6**

7, R' = Me, Et, Ph, *m*-MeC_6H_4

The structure of compounds **7** follows from their NMR spectra. The most important information is the nonequivalence of the two selenium atoms. This shows that the two parts of the molecule (ylide and PSe_2 moiety) are planar and lie in a common plane and cannot easily be twisted against each other, and that thus the 1,4-dipolar resonance formulas are of great importance. In contrast to this, the planes of the aryl group and of the PS_2 moiety in the aforementioned compound **1** with R = 2,4,6-tri-*tert*-butylphenyl and Y = S lie almost perpendicular to each other (dihedral angle = 80°).[5] Thus, the phosphorus atom is sterically protected and remains trigonal planar coordinated. In contrast, tricoordination is electronically stabilized by the ylide substituent in **7**.

The ^{31}P NMR spectra of **7** (at 25 °C) show doublets at $\delta \approx 21$ and 214 for the PPh_3 and PSe_2 group, respectively, with ^2J(P,P) about 40 Hz. Thus, the PSe_2 signal of **7** lies in

[*] Prof. Dr. A. Schmidpeter, Dipl.-Chem. G. Jochem, Dr. K. Karaghiosoff, Priv.-Doz. Dr. C. Robl
Institut für Anorganische Chemie der Universität
Meiserstrasse 1, D-W-8000 München 2 (FRG)

[**] This work was supported by the Deutsche Forschungsgemeinschaft and the Fonds der Chemischen Industrie.

the same region as that of tBu$_3$C$_6$H$_2$PSe$_2$ (δ = 273),[6] however, at somewhat higher field. It is accompanied by two pairs of satellites. In keeping with this, the ^{77}Se NMR spectrum shows a doublet each for the isotopomer with ^{77}Se *trans* and *cis* to R′ at $\delta \approx$ 600, ^1J(Se,P) average 816 Hz, and at $\delta \approx$ 495 (R′ = Me, Et) and 575 (R′ = Ph, *m*-tolyl), ^1J(Se,P) average 844 Hz. The isotopomer with two ^{77}Se atoms (R′ = Et) contributes satellites with ^2J(Se,Se) = 133 Hz. The assignment of the ^{77}Se signals is based on the fact that the second shift mentioned is strongly dependent on whether R′ is an alkyl or an aryl group, since the *cis*-positioned aryl group has an anisotropic effect. This assignment, however, is only provisional.

The X-ray structural analysis[9] of a single crystal of **7**, R′ = Ph, reveals that here also discrete molecules occur without detectable interactions (shortest intermolecular Se–Se distance 6.04 Å, shortest intermolecular P1–Se distance 6.04 Å, Fig. 1). The intramolecular Se–Se distance (3.68 Å)

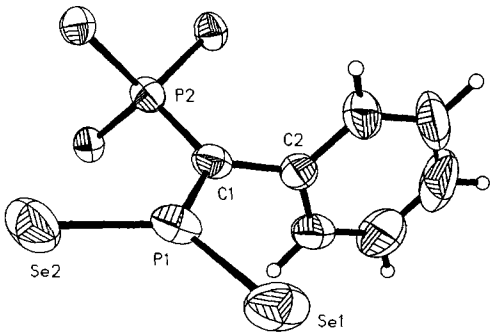

Fig. 1. Crystal structure of **7**, R′ = Ph, (of the P-positioned phenyl groups only the *ipso* carbon atom is given, thermal ellipsoids with 50% probability). Bond lengths [Å] and angles [°] (with standard deviations): P2-C1 1.751(5), P1-C1 1.696(5), P1-Se1 2.081(2), P1-Se2 2.079(2); P2-C1-C2 116.3(3), C2-C1-P1 120.7(4), P1-C1-P2 122.9(4), C1-P1-Se1 117.0(2), Se1-P1-Se2 124.5(1), Se2-P1-C1 118.4(2).

is also too great for a Se–Se bond to be considered. Both the ylide carbon atom and also the phosphorus atom have planar coordination environments; the two planes are only tilted towards each other by about 9.7°. The central P–C distance is almost as short as in the P=C unit of a bismethylene-λ^5-phosphorane[10] and, thus, confirms the participation of the polar resonance formulas. The two P–Se distances are not significantly different.

In the same way, dichlorophosphanes **5** react with sodium sulfide affording the ylide-substituted dithioxo-λ^5-phosphanes **8**. Their structure is revealed by the ^{31}P NMR data, which are very similar to those of **7**: $\delta \approx$ 22 (PPh_3), 243 (PS_2); ^2J(P,P) about 50 Hz.

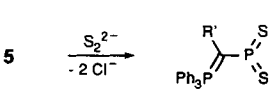

8

The bisylide-substituted monochlorophosphanes (Ph_3P-R′C)$_n$PCl$_{3-n}$ with n = 2, which follow the compounds **5** (n = 1) in the series of the ylide-substituted chlorophosphanes, are ionic "phosphenium" chlorides (IUPAC nomenclature phosphanylium chlorides) **9**, X = Cl.[7] In comparison to other phosphenium ions[11] the central phosphorus atom of these cations is not only a weaker acceptor but also more nucleophilic. Thus, it reacts with gray selenium in a base-catalyzed reaction with the formation of bisylide-substituted selenoxophosphonium chloride **10**, X = Cl, which is isolated as yellow crystals.

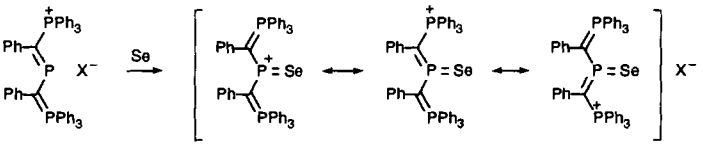

9 **10**

From the NMR data it follows that the product is ionic like the starting compound, despite the oxidation of the phosphorus, and monomeric: $\delta(^{31}P)$ = 24.1 (d, PPh_3), 196.6 (t, PSe), ^2J(P,P) = 68.7 Hz; $\delta(^{77}Se)$ = 276.7 (d), ^1J(Se,P) = 846.8 Hz. The addition of $AlCl_3$ to a solution of **10**, X = Cl, in dichloromethane does not change the NMR shifts of the phosphorus atoms. In order to further support the ionic structure and to supplement these findings, the preparation was repeated starting from **9**, X = Br. The NMR data of the product were the same, thus confirming the presence of a cation not influenced by the anion.

Compounds **10** are not only the first chalcogeno(diorgano)phosphonium halides but also the first isolated salts of chalcogenophosphonium ions in general. Diaminothioxophosphonium salts with PF_6^-,[12] $AlCl_4^-$,[13,14] and $GaCl_4^-$ [14] counterions are proposed in solution. In the solid state, however, the assumed tetrachloroaluminates are found to be either the $AlCl_3$ adduct of the covalent chlorothioxo-λ^5-phosphane, or the cation dimerizes just like the corresponding selenoxo cation,[14] or their cation is stabilized by transferring a methyl group from a N(SiMe$_3$)$_2$ substituent to the phosphorus.[14] In all cases the phosphorus atom thus attains tetracoordination.

Experimental Procedure

7, R′ = Ph: **5** (3.64 g, 8.0 mmol), R′ = Ph, was stirred with Na_2Se_2 (0.88 g, 8.0 mmol)[15] in THF (25 mL) at 20 °C. After 5 h the NaCl formed was filtered off with a frit, the orange filtrate was concentrated under vacuum to 15 mL and mixed with benzene (5 mL). Orange prisms of **7**·0.5 C_6H_6 crystallized over a period of several days; yield 3.20 g (69%), m.p. 143–145 °C.

10, X = Cl: To a solution of **9** (2.43 g, 3.2 mmol), X = Cl, in dichloromethane (4 mL) was added gray selenium (0.50 g, 6.4 mmol) and diethylamine (0.12 g, 1.6 mmol). After the mixture was stirred for 3 h at 20 °C the unreacted selenium was filtered off with a frit, the orange-red filtrate was concentrated to about half of its original volume and mixed with benzene (8 mL). Yellow needlelike crystals of **10**·C_6H_6 (1.57 g, 53%) were obtained, which when dried under vacuum crumbled to a yellow powder, m.p. 144–148 °C (decomp).

Received: May 27, 1992 [Z 5378 IE]
German version: *Angew. Chem.* **1992**, *104*, 1420

CAS Registry numbers:
5 (R′ = Ph), 140199-75-3; **7** (R′ = Ph), 143265-88-7; **7**·0.5 C_6H_6 (R′ = Ph), 143265-89-8; **8** (R′ = Ph), 143265-91-2; **9** (X = Cl), 140199-81-1; **10** (X = Cl), 143265-90-1.

[1] M. Meisel in *Multiple Bonds and Low Coordination in Phosphorus Chemistry* (Eds.: M. Regitz, O. J. Scherer), Thieme, Stuttgart, **1990**, p. 415, and references therein.
[2] J. C. Fitzmaurice, D. J. Williams, P. T. Wood, J. D. Woollins, *J. Chem. Soc. Chem. Commun.* **1988**, 741–743; K. Karaghiosoff, G. Jochem, *Phosphorus Sulfur Silicon Relat. Elem.* **1989**, *41*, 460.
[3] L. Maier, *Z. Anorg. Allg. Chem.* **1966**, *345*, 29–34.
[4] M. Meisel, H. Bock, B. Solouki, M. Kremer, *Angew. Chem.* **1989**, *101*, 1378–1381; *Angew. Chem. Int. Ed. Engl.* **1989**, *28*, 1373–1376; M. Binnewies, H. Bock, B. Solouki, M. Kremer, *Chem. Ber.* **1992**, *125*, 315–320.

[5] R. Appel, F. Knoch, H. Kunze, *Angew. Chem.* **1983**, *95*, 1008–1009; *Angew. Chem. Int. Ed. Engl.* **1983**, *22*, 1004–1005.
[6] M. Yoshifuji, K. Shibayama, N. Inamoto, *Chem. Lett.* **1984**, 603–606.
[7] A. Schmidpeter, G. Jochem, *Tetrahedron Lett.* **1992**, *33*, 471–474.
[8] W. W. Schoeller in *Multiple Bonds and Low Coordination in Phosphorus Chemistry* (Eds.: M. Regitz, O. J. Scherer), Thieme, Stuttgart, **1990**, p. 5.
[9] X-ray structural analysis of $7 \cdot 0.5 C_6H_6$ (R' = Ph). Orange prisms, $C_{28}H_{23}P_2Se_2$, $M_r = 579.3$, triclinic, space group $P\bar{1}$, $a = 9.288(2)$, $b = 10.476(2)$, $c = 14.801(3)$ Å, $\alpha = 75.40(1)$, $\beta = 74.61(2)$, $\gamma = 70.10(1)°$, $V = 1284.7(4)$ Å^3, $Z = 2$, $\rho_{calcd} = 1.498$ g cm^{-3}, $F(000) = 756$; $\mu = 2.73$ cm^{-1}. Data collection at 295 K, Siemens R3m/V diffractometer, $Mo_{K\alpha}$ radiation ($\lambda = 0.71073$ Å), graphite monochromator, ω scans $5.0° \leq 2\theta \leq 50°$, 4962 measured reflections of which 4522 were independent ($R_{int} = 0.0140$), 3214 with $|F_o| > 3\sigma_{|Fo|}$, empirical absorption correction. The structure was solved by direct methods with Siemens SHELXTL PLUS (MikroVAX II). The full matrix least squares refinement (290 parameters) gave $R = 0.0571$, $R_g = 0.0295$, and $R_w = 0.0381$. Further details of the crystal structure investigation may be obtained from the Fachinformationszentrum Karlsruhe, Gesellschaft für wissenschaftlich-technische Information mbH, D-W-7514 Eggenstein-Leopoldshafen 2 (FRG) on quoting the depository number CSD-56 554, the names of the authors, and the journal citation.
[10] R. Appel, E. Gaitzsch, K.-H. Dunker, F. Knoch, *Chem. Ber.* **1986**, *119*, 535–542.
[11] M. Sanchez, M. R. Mazières, L. Lamandé, R. Wolf in *Multiple Bonds and Low Coordination in Phosphorus Chemistry* (Eds.: M. Regitz, O. J. Scherer), Thieme, Stuttgart, **1990**, p. 129.
[12] R. W. Light, R. T. Paine, *Phosphorus Sulfur Relat. Elem.* **1980**, *8*, 255–258.
[13] M. Sanchez, M. R. Marre, J. F. Brazier, J. Bellan, R. Wolf, *Phosphorus Sulfur Relat. Elem.* **1983**, *14*, 331–334.
[14] N. Burford, R. E. von H. Spence, *J. Am. Chem. Soc.* **1989**, *111*, 5006-5008; N. Burford, R. E. von H. Spence, R. D. Rogers, J. Chem. Soc. Dalton Trans 1990, 3611-3619; N. Burford, S. Mason, R. E. von H. Spence, J. M. Whalen, J. F. Richardson, R. D. Rogers, *Organometallics* **1992**, *11*, 2241-2250.
[15] D. P. Thompson, P. Boudjouk, *J. Org. Chem.* **1988**, *53*, 2109–2112.

The Structure of the [1.1]Ruthenocenophane Dication: Metal–Metal Bond Formation and the Consequences of Proximity

By *Ulrich T. Mueller-Westerhoff,* Arnold L. Rheingold,* and *Gerhard F. Swiegers*

When the [1.1]ruthenocenophane **1** was first synthesized[1] and studied,[2] one of the most surprising results was its unusually low oxidation potential. Whereas, relative to the reversible oxidation of ferrocene near 400 mV, the mononuclear ruthenocene is oxidized at a much higher potential (irreversible two-electron oxidation at 920 mV),[2, 3] the [1.1]ruthenocenophane showed a reversible two-electron oxidation at 380 mV to a stable diamagnetic dication $\mathbf{1}^{2+}$. The ^{1}H NMR

$[Ru_2(\eta^5\text{-}C_5H_4CH_2\text{-}\eta^5\text{-}C_5H_4)_2]$ **1**

data (four Cp-H multiplets and a sharp singlet for the CH_2 bridges) seemed difficult to interpret,[2] because the sharpness of the bridge proton signal appeared to indicate a rapid rotational exchange, as was familiar from the neutral metallocenophanes of iron and ruthenium.[4] However, this did not allow a satisfactory assignment of the four ruthenocene multiplets; the structural details had to be left unresolved.

[*] Prof. Dr. U. T. Mueller-Westerhoff, Dr. G. F. Swiegers
Department of Chemistry
University of Connecticut
Storrs, CT 06269-3060 (USA)
Prof. Dr. A. L. Rheingold
Department of Chemistry
University of Delaware
Newark, DE 19716 (USA)

A plausible structural proposal was advanced by Taube et al.[5] when the oxidation product of osmocene was isolated and structurally characterized: the dication $[Cp_2Os]^{2+}$ reacts with a neutral osmocene to form the dimer $[Cp_4Os_2]^{2+}$, containing an Os–Os bond. A related structure could exist in our ruthenocenophane dication.

The recent improvement in the synthesis of ruthenocene[6] enticed us to apply this method to the synthesis of **1** and enabled its isolation in reasonable yields. The oxidation of **1** to $\mathbf{1}^{2+}$ was accomplished by reaction with benzoquinone and $BF_3 \cdot Et_2O$ in CH_3CN. Single crystals of the **1**-$(BF_4)_2$ were grown by slow diffusion of Et_2O into a CH_3CN solution of this salt.

The results of X-ray diffraction studies[7] on these crystals fully confirm Taube's proposal.[5] A Ru–Ru bond holds the molecule rigidly in an unusually twisted conformation (Fig. 1). Viewed down the Ru–Ru axis, the two ruthenocene

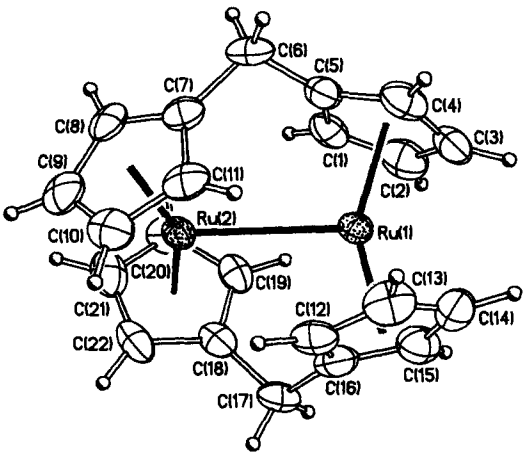

Fig. 1. View of $\mathbf{1}^{2+}$ (ORTEP), drawn with 35% thermal ellipsoids. Hydrogen atoms have arbitrary radii.

units in $\mathbf{1}^{2+}$ form an angle of approximately 75°, as measured by the angle between the two centroid-Ru-centroid planes (Fig. 2). To allow the two ruthenium atoms to approach each other, the Cp rings deviate from coplanarity and form a dihedral angle between the Cp planes of 28° (average

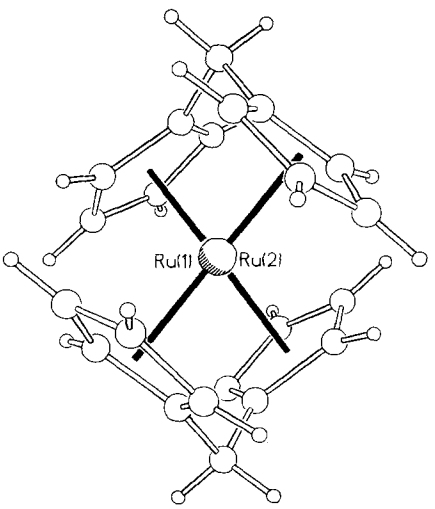

Fig. 2. View of $\mathbf{1}^{2+}$ along the Ru–Ru bond, showing the strong twist and the equivalence of the bridge protons.

centroid-Ru-centroid angle 152°). The resulting Ru–Ru bond of 2.953(1) Å must be considered to be a single bond (the Os–Os distance in $[Cp_4Os_2]^{2+}$ is 3.04 Å, in agreement with the very similar atomic radii of Ru and Os). The Cp ligands are approximately staggered and the two α protons and the two β protons of each ring are nonequivalent. The two protons of each CH_2 bridge appear different in the projection of Figure 1, but a view along the Ru–Ru axis (Fig. 2) clearly shows their equivalence. This structural detail explains the observed ^1H NMR data.

Comparison of the structure of the neutral precursor **1** (Fig. 3) with those of the Fe–Fe and the Fe–Ru [1.1]metallocenophanes[8] shows that all three are twisted to relieve the steric crowding of the inner α hydrogens but that **1** is more twisted (twist angle 33.4°) than the other two. Consequently, the metal atoms in **1** approach more closely than in the other two cases (4.70 vs. 4.82 and 4.80 Å, respectively). This still is far beyond metal–metal bonding distances, and the two ruthenocenes in **1** are fully independent and symmetrical, with exactly coplanar Cp ligands in each subunit.

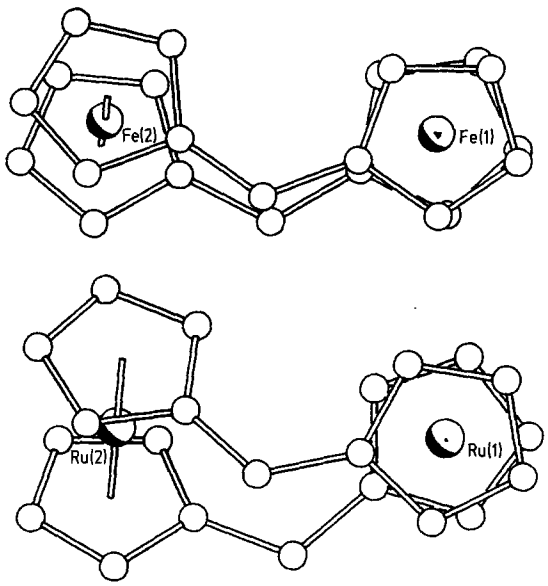

Fig. 3. Schematic top views of [1.1]ferrocenophane and [1.1]ruthenocenophane (**1**), as revealed in single-crystal X-ray diffraction studies. The Fe–Fe distance is 4.82 Å, but the more twisted **1** has a shorter Ru–Ru distance of 4.70 Å. There is no indication of any distortion of the metallocenes (the M–C distances all are equal within standard deviations).

It is of interest to analyze and compare the oxidations of ruthenocene and [1.1]ruthenocenophane. Under the usual conditions, the oxidation of Cp_2Ru is an electrochemically irreversible two-electron process at relatively high (>900 mV) potential.[9] The initially formed dication can be stabilized by adding a second, neutral metallocene (Fig. 4, Path A), which of course, first has to be located in the surrounding solution.[10,11] In [1.1]ruthenocenophane **1**, however, a second metallocene is in the immediate vicinity, and the "dimer" state is reached directly. This corresponds to a pathway (Fig. 4, Path B) in which the expected high-energy intermediate (consisting of one ruthenocene dication linked to a neutral ruthenocene) and the separate reactions $[Cp_2Ru \rightarrow Cp_2Ru^{2+} \rightarrow Cp_4Ru_2^{2+}]$ are avoided.

An obvious interpretation is that the closeness of the two ruthenium atoms leads to a metal–metal interaction in the neutral molecule and that Ru–Ru bond formation lowers the

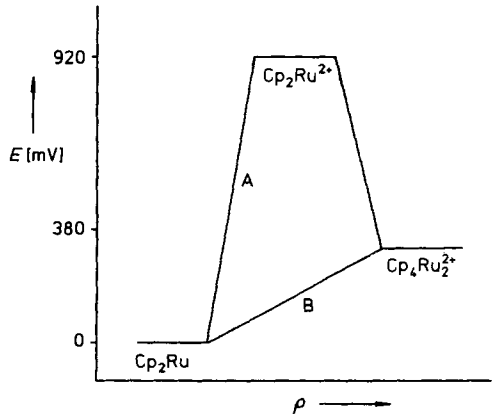

Fig. 4. Energies (in mV relative to $[Cp_2Ru]$) of the oxidation products of ruthenocene. ρ = reaction coordinate

activation energy of the oxidation process. However, the structure of the neutral species **1** shows[8] no obvious sign of metal–metal interaction. In its absence, the removal of two electrons would have to occur from only one $[Cp_2Ru]$ unit. Since this would require an oxidation potential above 900 mV, which experimentally is not the case, another explanation must be sought, to account for the fact that two electrons are lost from an orbital of much higher energy than in ruthenocene itself.

It is a unique structural feature of **1** that the two ruthenocenes can approach closer than in any solution experiment with independent ruthenocenes.[11] We suggest that the low oxidation potential and the electrochemical reversibility in **1** must be a consequence of this spatial proximity. In fact, a nonbonding interaction between the two Ru atoms produces the unusual redox properties. As shown in Figure 5, the crucial interaction is between two filled d AOs which face each other, leading to a splitting of these two levels into a bonding and an antibonding orbital. This interaction does not consti-

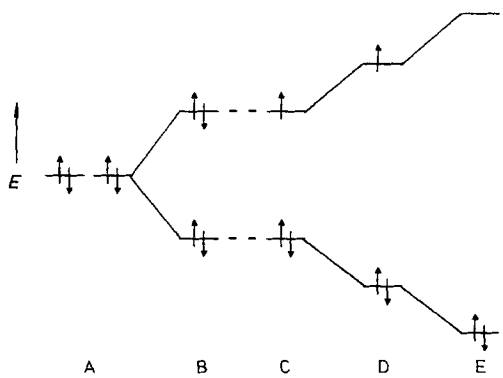

Fig. 5. Qualitative molecular orbital diagram of the relevant 4d AOs and Ru–Ru bond formation in the oxidation of [1.1]ruthenocenophane. A: degenerate, noninteracting 4d orbitals in the absence of Ru–Ru interactions; B: splitting of the 4d levels due to interaction leads to no net bonding (bond order $p = 0$); C: removal of one electron results in $p = 0.5$ and increased splitting; D: the second electron is lost more easily than the first and a Ru–Ru single bond (E, $p = 1.0$) is formed.

tute a metal–metal bond because the net bond order is zero.[13,14] Upon oxidation, an electron is removed from the antibonding orbital, which accounts for the lowering of the oxidation potential. Loss of an electron from this orbital results in an increase in the bond order to 0.5 and therefore

increased splitting. A second electron can then be removed at an even lower potential, which explains why the oxidation process involves two electrons. Loss of the second antibonding electron leads to a bond order of 1.0 for the Ru–Ru single bond. In solution, **1** undergoes a rapid *syn-syn* exchange[4] with a strongly twisted transition state containing nearly orthogonal ruthenocenes. This brings the two Ru atoms very close (Ru–Ru distance estimated from models, 3.6 Å). This further increases the splitting and leads to the very low oxidation potential.

None of the above considerations would be relevant if the reaction product were not stabilized by some form of intramolecular interaction.[15] In another case in [1.1]metallocenophane chemistry[16] we have seen independent evidence that the proximity of a reaction partner and the stabilization of the product (in an unusual way by the formation of a C-H-C bond) are the deciding factors which allow the reaction to occur. The reaction $\mathbf{1} \rightarrow \mathbf{1}^{2+}$ is driven by the proximity of the metals and stabilization of the product through a Ru–Ru bond. The ease with which this bond can form in the oxidation of **1**, especially when compared to the conditions in the oxidation of $[Cp_2Ru]$ itself, is a consequence of the interaction of the two proximate metals. The existence of a metal–metal bonding interaction or of ligand-mediated interactions in **1** is not a prerequisite.

Received: February 17, 1992
Revised: July 6, 1992 [Z 5193 IE]
German version: *Angew. Chem.* **1992**, *104*, 1398

CAS Registry numbers:
1, 83601-21-2; **2**, 143331-77-5.

[1] U. T. Mueller-Westerhoff, A. Nazzal, M. Tanner, *J. Organomet. Chem.* **1982**, *236*, C41.

[2] A. Diaz, U. T. Mueller-Westerhoff, A. Nazzal, M. Tanner, *J. Organomet. Chem.* **1982**, *236*, C45.

[3] The initial confusion about the nature of the Cp_2Ru oxidation has been resolved: a) G. Wilkinson, *J. Am. Chem. Soc.* **1952**, *74*, 6146; b) D. E. Bublitz, G. Hoh, T. Kuwana, *Chem. Ind. (London)* **1959**, *653*; c) T. Kuwana, D. E. Bublitz, G. Hoh, *J. Am. Chem. Soc.* **1960**, *62*, 5811; d) A. V. Savitskii, Y. K. Syrkin, *Tr. Khim. Khim. Tekhnol.* **1961**, *4*, 165; e) A. N. Nesmeyanov, A. A. Lubovich, L. P. Yur'eva, S. P. Gubin, E. G. Perevalova, *Izv. Akad. Nauk SSSR, Ser. Khim.* **1967**, 935; f) S. P. Gubin, S. A. Smirnova, L. I. Denisovich, A. A. Lubovich, *J. Organomet. Chem.* **1971**, *30*, 243; g) S. A. Smirnova, S. P. Gubin, A. A. Lubovich, L. I. Denisovich, *Dokl. Akad. Nauk SSSR* **1971**, *200*, 605; h) D. N. Henrickson, Y. S. Soh, W. H. Morrison, Jr., H. B. Gray, *Inorg. Chem.* **1972**, *11*, 808; i) Y. S. Sohn, A. W. Schlueter, D. N. Hendrickson, H. B. Gray, *ibid.* **1974**, *13*, 301; j) P. Borrell, E. Henderson, *J. Chem. Soc. Dalton Trans.* **1975**, 432; k) S. V. Kukharenko, A. A. Bezrukova, A. Z. Rubezhov, V. Strelets, *Metalloorg. Khim.* **1990**, *3*, 634.

[4] U. T. Mueller-Westerhoff, *Angew. Chem.* **1986**, *98*, 700; *Angew. Chem. Int. Ed. Engl.* **1986**, *25*, 702.

[5] M. W. Droege, W. D. Harman, H. Taube, *Inorg. Chem.* **1987**, *26*, 1309.

[6] U. T. Mueller-Westerhoff, G. F. Swiegers, *Synth. React. Inorg. Met. Org. Chem.*, submitted.

[7] Crystallographic data for **1**-$(BF_4)_2$: $C_{22}H_{20}B_2F_8Ru_2$, dark red, nearly black crystals, $M_r = 636.13$, monoclinic, *Ia*, $a = 15.726(6)$, $b = 20.012(6)$, $c = 14.721(6)$ Å, $\beta = 106.06(3)°$, $V = 4452(3)$ Å^3, $Z = 8$, $\rho_{calcd} = 1.898$ g cm^{-3}, $T = 294$ K, $R(F) = 0.0399$ for reflections with $F_o \geq 3\sigma(F_o)$ ($R(F) = 0.0415$ for all data). The crystallographic asymmetric unit contains two dications and four anions; the cations are chemically identical. The centrosymmetric space group, *I2/a*, was initially preferred because $Z = 8$, and **1**-$(BF_4)_2$ had two potential crystallographic twofold axes. However, structure development beyond the metal atoms was not possible; in the final structure, none of the molecular twofold axes are aligned with the crystallographic *b* axis. The Rogers test was used to determine the correct enantiomorph ($\eta = 0.92(5)$ for the reported enantiomer). Further details of the crystal structure investigation are available on request from the Director of the Crystallographic Data Centre, University Chemical Laboratory, Lensfield Road, GB-Cambridge CB2 1EW (UK) on quoting the full journal citation.

[8] Full details of the X-ray diffraction study of **1**-$(BF_4)_2$ will be reported separately, together with the structures of the [1.1]metallocenophanes of iron and ruthenium: A. Rheingold, U. T. Mueller-Westerhoff, G. F. Swiegers, T. J. Haas, *Organometallics*, in press.

[9] A recent communication (M. G. Hill, W. M. Lamanna, K. R. Mann, *Inorg. Chem.* **1991**, *30*, 4690) has shown that all three metallocenes can undergo quasi-reversible one-electron oxidations in noncoordinating media. The oxidation of $[Cp_2Ru]$ under these conditions occurs at an even higher potential (1.03 V) than we observed. For the present case, a mechanism based on two reversible one-electron oxidations is not applicable, because it would, as in the parallel case of [1.1]ferrocenophane, lead to two well-separated waves.

[10] In chemical oxidations, such as by halogens, the dication can also be stabilized by addition of a halide ion to form the monocation $[Cp_2RuX]^+$. Oxidation at a Hg electrode leads to the dication $[Cp_2Ru(\mu\text{-Hg})RuCp_2]^{2+}$ [3i].

[11] This consideration might suggest that the oxidation potentials of $[Cp_2Ru]$ and $[Cp_2Os]$ are concentration-dependent, and should show a lowering of the potential at high concentrations. This has not been tested experimentally. In cyclic voltammetry, the peak potential of an oxidation also may shift to more negative voltage (and that of a reduction to more positive ones) if a subsequent and rapid reaction follows the initial electron transfer (EC mechanism), and such potential shifts are concentration-dependent [12]. Thus, the rate of Ru_2 cation formation will certainly be much higher on oxidation of **1** than of ruthenocene itself. The observed decrease in oxidation potential clearly reflects this trend, although the magnitude of the difference (540 mV) cannot be explained this way.

[12] A. L. Bard, L. R. Faulkner, *Electrochemical Methods*, J. Wiley & Sons, New York, **1980**, Chapter 11.

[13] This is strictly true only in the "complete neglect of overlap" approximation. If nonzero overlap integrals are considered, the antibonding orbital is destabilized more than the bonding one is stabilized, which leads to a net repulsive interaction (e.g. in He_2). Given the 4.7 Å Ru–Ru distance, in **1** the Ru–Ru overlap integrals will be vanishingly small and their complete neglect is the best choice.

[14] Similar interpretations have been invoked to explain the chemistry of binuclear Pt, Rh, and Ir complexes. For a related interpretation, see: D. C. Smith, V. M. Miskowski, W. R. Mason, H. B. Gray, *J. Am. Chem. Soc.* **1990**, *112*, 3759. UM-W wishes to thank H. B. Gray (California Institute of Technology) for helpful discussions on this point.

[15] A low-potential two-electron oxidation involving metal–metal bond formation has, however, also been seen in a case where the metals are assumed to be not close to each other in the neutral species: N. G. Connelly, A. R. Lucy, J. D. Payne, A. M. R. Galas, W. E. Geiger, *J. Chem. Soc. Dalton Trans.* **1983**, 1879. See also: W. E. Geiger, *Prog. Inorg. Chem.* **1985**, *33*, 276. Our results suggest that a nonbonding metal–metal interaction exists in this case as well.

[16] For instance, the deprotonation of [1.1]ferrocenophane by BuLi in THF leads to a carbanion that is stabilized by a C-H-C bond. However, it is not possible to deprotonate diferrocenyl methane under the same conditions, because it does not have any means to stabilize the resulting carbanion: U. T. Mueller-Westerhoff, A. Nazzal, W. Prössdorf, *J. Am. Chem. Soc.* **1981**, *103*, 7678.

Octakis(1,1,2-trimethylpropyl)octasilacubane: Synthesis, Molecular Structure, and Unusual Properties**

By *Hideyuki Matsumoto,* Koichi Higuchi, Soichiro Kyushin, and Midori Goto**

Polycyclic compounds of Group 4 elements Si, Ge, and Sn continue to attract considerable attention.[1–4] In recent years, we have studied the synthesis and properties of polycyclopolysilanes consisting of fused four-membered rings;[5, 6]

[*] Prof. Dr. H. Matsumoto, K. Higuchi, Dr. S. Kyushin
Department of Applied Chemistry,
Faculty of Engineering Gunma University
Kiryu, Gunma 376 (Japan)
Dr. M. Goto
National Chemical Laboratory for Industry
Tsukuba, Ibaraki 305 (Japan)

[**] This work was supported by a Grant-in-Aid for Scientific Research of Priority Area of Organic Unusual Valency (03233105 to H. M.) and of Molecular Design (02230101 to H. M.), from the Ministry of Education, Science and Culture, Japan. We also thank Shin-etsu Chemical Co. Ltd., Toshiba Silicone Co. Ltd., and Yuki Gousei Kogyo Co. Ltd. for financial support.

the primary goal of our study is to assess the electronic properties arising from their strained Si–Si σ-bonded frameworks. Earlier we reported on the synthesis of $Si_8(SiMe_2tBu)_8$ (**2**), the first octasilacubane.[6, 7] Ab initio molecular orbital calculations, however, predict that a silyl-substituted octasilacubane, $Si_8(SiH_3)_8$, is 10 kcal mol^{-1} less strained than an alkyl-substituted derivative, Si_8Me_8, at HF/6-31G* level, due to the electronic perturbation of the Si_8 ring by the silyl substitution.[8] This prompted us to synthesize octakis(1,1,2-trimethylpropyl)octasilacubane (**1**), which provides the first opportunity for assessing the electronic properties of the peralkyl Si_8 framework.[9]

The reductive coupling of (1,1,2-trimethylpropyl)trichlorosilane (**3**)[10] with sodium in toluene yielded peralkyloctasilacubane **1** (2.6% yield) (Scheme 1).[11] Compound **1** was characterized by IR and NMR spectroscopy, mass spectrometry, and X-ray crystallography.[12]

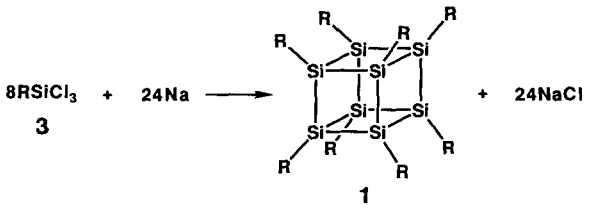

Scheme 1. R = CMe_2CHMe_2.

Compound **1** forms red-orange crystalline prisms (m.p. 220.0–221.5 °C, decomp, sealed tube), which are moderately soluble in organic solvents [benzene, toluene, hexane, 3-methylpentane (3-MP), THF, CH_2Cl_2, and $CHCl_3$]. It is surprisingly stable in air: **1** in crystalline form exhibits no change in color upon exposure to atmosphere for two weeks and can be handled without the protection of an inert atmosphere.[13] Therefore, the 1,1,2-trimethylpropyl group is a promising protective moiety for conferring a kinetic stability upon the octasilacubane framework. Also important to note is the thermodynamic stability of the framework. In a thermogravimetric analysis **1** remained stable under argon to 200 °C, after which gradual weight loss occurred. In the mass spectrometer, the dominant mode of fragmentation for **1** is the initial loss of a 1,1,2-trimethylpropyl group followed by successive loss of an olefin, 2,3-dimethyl-2- or 2,3-dimethyl-1-butene; the eight-membered charged ions remain intact under electron impact conditions.

The molecular structure of **1** (Fig. 1) is slightly distorted from an ideal octasilacubane geometry: the molecule possesses only one C_2 axis passing through the midpoint of Si1–Si1′ and Si3–Si3′ bonds; the Si–Si bond lengths range from 2.398(2) to 2.447(2) Å, and the Si-Si-Si bond angles vary from 87.2(1) to 92.6(1)°; the Si–C bond lengths lie between 1.963(5) and 1.978(6) Å, longer than the normal value; the Si-Si-C [116.2(2)–133.4(2)°] and the Si-C-C [104.5(4)–114.5(4)°] bond angles show scatter within a wide range. This distortion from an ideal cube may be due to the strained structure, caused by the need to minimize steric repulsion from eight bulky 1,1,2-trimethylpropyl groups. The packing of molecules in the unit cell is shown in Figure 2. The closest intermolecular C···C contact [C(3)···C(3) 3.72 Å] is less than the contact distance of 4 Å between the van der Waals radii of terminal methyl groups. Therefore, crystal packing forces may also have some influence on the molecular structure of **1**.

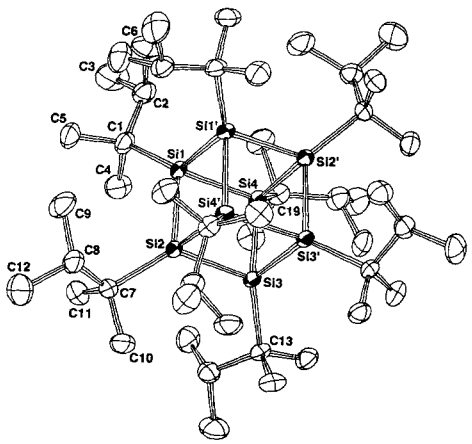

Fig. 1. Molecular structure of R_8Si_8 **1**, (R = CMe_2CHMe_2). Primed atoms are related to nonprimed atoms by the crystallographic C_2 axis at 0, *y*, 1/4 in the unit cell. Selected bond lengths [Å] and bond angles [°]: Si1-Si2 2.425(2), Si1-Si4 2.420(2), Si-Si1′ 2.447(2), Si2-Si3 2.416(2), Si2-Si4′ 2.398(2), Si3-Si4 2.424(2), Si3-Si3′ 2.440(2), Si1-C1 1.963(5), Si2-C7 1.963(5), Si3-C13 1.964(5), Si4-C19 1.978(6); Si2-Si1-Si4 90.5(1), Si2-Si1-Si1′ 87.2(1), Si4-Si1-Si1′ 91.5(1), Si1-Si2-Si3 89.5(1), Si1-Si2-Si4′ 92.6(1), Si3-Si2-Si4′ 89.6(1), Si2-Si3-Si4 90.6(1), Si2-Si3-Si3′ 90.5(1), Si4-Si3-Si3′ 88.4(1), Si1-Si4-Si3 89.4(1), Si1-Si4-Si2′ 88.5(1), Si3-Si4-Si2′ 91.3(1), Si2-Si1-C1 126.2(2), Si4-Si1-C1 116.2(2), Si1′-Si1-C1 133.4(2), Si1-Si2-C7 124.2(2), Si3-Si2-C7 127.9(2), Si4′-Si2-C7 122.6(2), Si2-Si3-C13 121.1(2), Si4-Si3-C13 131.1(2), Si3′-Si3-C13 123.7(2), Si1-Si4-C19 128.5(2), Si3-Si4-C19 125.0(2), Si2′-Si4-C19 122.8(2), Si1-C1-C2 110.0(4), Si1-C1-C4 104.5(4), Si1-C1-C5 114.5(4), Si2-C7-C8 110.6(3).

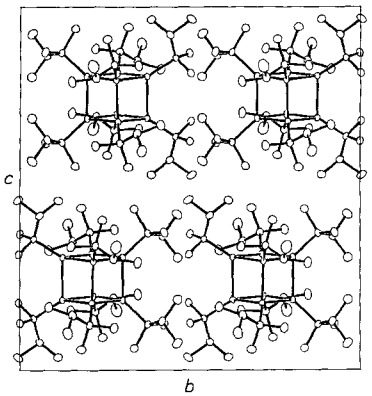

Fig. 2. Arrangement of molecules of **1** in the unit cell (*a* projection).

The highly strained silicon framework in **1** gives rise to unusual electronic properties. The UV/VIS spectrum of **1** exhibits absorption maxima at 252 (ε = 30800), 350 (ε = 850), and around 500 nm (ε = 70) (Fig. 3)[14–16]. By comparison, the corresponding spectrum of the persilyl deriva-

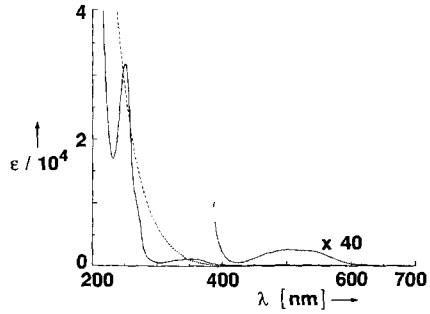

Fig. 3. UV/VIS spectra of octasilacubanes **1** (—) and **2** (– – –).

tive **2** showed only tailing absorption commencing at 470 nm. The absorption maximum of 500 nm, which is responsible for the red-orange color of **1**, is the longest wavelength electronic transition in any cyclopolysilanes with an all-silicon σ framework [e.g., 304–412 nm for $(R^1R^2Si)_3$][1, 17] suggesting a small HOMO–LUMO energy difference. A cyclic voltammogram of **1** (CH_2Cl_2, Bu_4NClO_4, standard calomel electrode (SCE), room temperature) showed an irreversible wave with anodic peak potential at 0.43 V. This value reflects the high strain energy of the Si_8 framework and is less positive than that observed for other cyclic polysilanes (e.g., 0.72 V (CH_2Cl_2, SCE) for $[Si(CH_2tBu)]_3$].[18]

Experimental Procedure

1: All manipulations were carried out under argon atmosphere. To a suspension of sodium sand (3.4 g, 150 mmol) and toluene (170 mL) was added dropwise a solution of **3** (10.4 g, 47.3 mmol) in toluene (40 mL) at 120 °C over 40 min. The resulting mixture was stirred for 5 hours. The reaction mixture was filtered to remove sodium chloride and excess sodium. After removal of toluene, the residue was taken up in hexane (10 mL). Column chromatography on silica gel 60 with hexane as eluent, and crystallization from butan-2-one afforded **1** (0.140 g, 2.6% yield), as a red-orange powder. Recrystallization from pentane gave an analytically pure sample of **1** (0.110 g), as red-orange prisms. ^{1}H NMR (200 MHz, C_6D_6): δ = 2.45 (sept, J = 6.8 Hz, 8H; CH), 1.54 (s, 48H; $C(CH_3)_2$), 1.19 (d, J = 6.8 Hz, 48H; $CH(CH_3)_2$); $^{13}C\{^1H\}$ NMR (50 MHz, C_6D_6): δ = 38.07 (CCH), 36.18 (SiC), 26.15 (CCH_3), 20.82 ($CHCH_3$); $^{29}Si\{^1H\}$ NMR (17.9 MHz, $C_6D_5CD_3$): δ = 22.24; IR (KBr): $\tilde{\nu}$ [cm^{-1}] = 2948, 2864, 1453, 1371, 1360, 1148, 1125, 1084, 742; EI-MS (25 eV): rel. intensities *m/z* (R = CMe_2CHMe_2): 908 (12, M + 4), 907 (65, M + 3), 906 (74, M + 2), 905 (94, M + 1), 904 (100, M^+), 819 (48, Si_8R_7), 735 (24, $Si_8R_6(H)$), 651 (48, $Si_8R_5(H_2)$), 567 (13, $Si_8R_4(H_3)$), 483 (10, $Si_8R_3(H_4)$), 399 (9, $Si_8R_2(H_5)$).

Received: May 14, 1992 [Z 5347IE]
German version: *Angew. Chem.* **1992**, *104*, 1410

CAS Registry numbers:
1, 143447-31-8; **2**, 18151-53-6.

[1] Review: T. Tsumuraya, S. A. Batcheller, S. Masamune, *Angew. Chem.* **1991**, *103*, 916; *Angew. Chem. Int. Ed. Engl.* **1991**, *30*, 902.

[2] For accounts on silicon clusters see a) T. Lange, T. P. Martin, *Angew. Chem.* **1992**, *104*, 179; *Angew. Chem. Int. Ed. Engl.* **1992**, *31*, 172; b) C. Zybill, *ibid.* **1992**, *104*, 180 and **1992**, *31*, 173.

[3] Experimental studies: a) S. Masamune, Y. Kabe, S. Collins, D. J. Williams, R. Jones, *J. Am. Chem. Soc.* **1985**, *107*, 5552; b) R. Jones, D. J. Williams, Y. Kabe, S. Masamune, *Angew. Chem.* **1986**, *98*, 173; *Angew. Chem. Int. Ed. Engl.* **1986**, *25*, 176; c) Y. Kabe, M. Kuroda, Y. Honda, O. Yamashita, T. Kawase, S. Masamune, *ibid.* **1988**, *100*, 1793 and **1988**, *27*, 1725; d) M. Weidenbruch, F. T. Grimm, S. Pohl, W. Saak, *ibid.* **1989**, *101*, 201 and **1989**, *28*, 198; e) A. Sekiguchi, C. Kabuto, H. Sakurai, *ibid.* **1989**, *101*, 97 and **1989**, *28*, 55; f) A. Sekiguchi, H. Naito, H. Nameki, K. Ebata, C. Kabuto, H. Sakurai, *J. Organomet. Chem.* **1989**, *368*, C1; g) L. R. Sita, R. D. Bickerstaff, *J. Am. Chem. Soc.* **1989**, *111*, 3769; h) L. R. Sita, I. Kinoshita, *Organometallics* **1990**, *9*, 2865; i) Y. Kabe, T. Kawase, J. Okada, O. Yamashita, M. Goto, S. Masamune, *Angew. Chem.* **1990**, *102*, 823; *Angew. Chem. Int. Ed. Engl.* **1990**, *29*, 794; j) R. Sita, I. Kinoshita, *J. Am. Chem. Soc.* **1991**, *113*, 1856.

[4] Theoretical studies: a) S. Nagase, T. Kudo, M. Aoki, *J. Chem. Soc. Chem. Commun.* **1985**, 1121; b) D. A. Clabo, Jr., H. F. Schaefer III, *J. Am. Chem. Soc.* **1986**, *108*, 4344; c) A. F. Sax, J. Kalcher, *J. Chem. Soc. Chem. Commun.* **1987**, 809; d) S. Nagase, M. Nakano, T. Kudo, *ibid.* **1987**, 60; e) A. F. Sax, J. Kalcher, R. Janoschek, *J. Comput. Chem.* **1988**, *9*, 564; f) S. Nagase, M. Nakano, *Angew. Chem.* **1988**, *100*, 1098; *Angew. Chem. Int. Ed. Engl.* **1988**, *27*, 1081; g) S. Nagase, *ibid.* **1989**, *101*, 9 and **1989**, *28*, 329; h) S. Nagase, *Polyhedron* **1991**, *10*, 1299.

[5] a) H. Matsumoto, H. Miyamoto, N. Kojima, Y. Nagai, *J. Chem. Soc. Chem. Commun.* **1987**, 1316; b) H. Matsumoto, H. Miyamoto, N. Kojima, Y. Nagai, M. Goto, *Chem. Lett.* **1988**, 629.

[6] H. Matsumoto, K. Higuchi, Y. Hoshino, H. Koike, Y. Naoi, Y. Nagai, *J. Chem. Soc. Chem. Commun.* **1988**, 1083.

[7] X-ray structural analysis of Si_8R_8 **2** (R = $tBuMe_2Si$): triclinic, space group $P\bar{1}$, Si-Si bond lengths, 2.39(1)–2.45(1) Å; Si-Si-Si bond angles, 86.8(5)–92.6(5)° in the Si_8 ring: M. Goto, *Kagaku Gijutsu Kenkyusho Hokoku* **1991**, *86*, 127. Details of the X-ray structural analysis will be published elsewhere.

[8] The HF/6-31G* values of the strain energies of octasilacubanes: Si_8Me_8: 88.9; $Si_8(H_3Si)_8$: 77.9 kcal mol^{-1}, S. Nagase, Yokohama National University (Japan), private communication.

[9] **Note added in proof** (Sept. 11, 1992): After this paper was accepted for publication, the syntheses of octasilacubanes Si_8R_8 were published. R = 2,6-$Et_2C_6H_3$, A. Sekiguchi, T. Yatabe, H. Kamatani, C. Kabuto, H. Sakurai, *J. Am. Chem. Soc.* **1992**, *114*, 6291; R = *t*Bu: K. Furukawa, M. Fujino, N. Matsumoto, *Appl. Phys. Lett.* **1992**, *60*, 2744.

[10] a) H. Tobita, Y. Kawano, M. Shimoi, H. Ogino, *Chem. Lett.* **1987**, 2247; b) Y. Kawano, H. Tobita, H. Ogino, *J. Organomet. Chem.* **1992**, *428*, 125.

[11] The low yield of **1** is presumably due to the large steric demands imposed upon the cyclization process. In fact, the major products from the reductive coupling reaction showed strong Si-H absorption bands in the IR spectra, but the structures of the products were not further examined. In relevant work, Masamune et al. have reported that reductive oligomerization of $Cl_2tBuSiSitBuCl_2$ with lithium naphthalenide in dimethoxyethane proceeded in a unique and somewhat unexpected manner to provide tricyclo[2.2.0.0^{2,5}]hexasilanes and tetracyclo[3.3.0.0^{2,7}.0^{3,6}]octasilane.[3b,c] Also, Weidenbruch et al.[3d] and Sakurai et al.[3f] have described the synthesis of a tetracyclo[3.3.0.0^{2,7}.0^{3,6}]octagermane derivative by the oligomerization of $X_2tBuGeGetBuX_2$ (X = Br, Cl) or $tBuGeCl_3$.

[12] Crystal structure data: Enraf-Nonius CAD4, graphite-filtered $Cu_{K\alpha}$ radiation, $C_{48}H_{104}Si_8$, monoclinic, space group $C2/c$, a = 13.802(1), b = 19.246(1), c = 20.916(1) Å, β = 99.476(3)°, V = 5480.2(5) Å^3, Z = 4, ϱ_{calcd} = 1.098 g cm^{-3}, $\mu(Cu_{K\alpha})$ = 19.76 cm^{-1}. 4592 independent reflections up to 2θ = 130° by the 2θ-ω scan technique, 3706 with $F > 3\sigma(|F_o|)$, empirical absorption correction based on ψ scans for a relative transmission of 0.8785–0.9998, solution by direct methods [Multan 78 (P. Main, S. E. Hull, K. Lassinger, G. Germain, J.-P. Declercq, M. M. Woolfson, *A System of Computor Programs for the Automatic Solution of Crystal Structures for the X-ray Diffraction Data*, Multan 78, **1978**)]. Refinement by full-matrix least-squares using UNICS III programm (T. Sakurai, K. Kobayashi, *Rikagaku-Kenkyujo Hokoku*, **1978**, *55*, 69). 102 hydrogen atoms (all but 2 atoms) found in the difference Fourier map and fixed, all non-hydrogen atoms anisotropic, overall isotropic temperature factor for hydrogen atoms, R = 0.0396, R_w = 0.0416. Further details of the crystal structure investigation are available on request from the Director of the Cambridge Crystallographic Data Centre, University Chemical Laboratory, Lensfield Road, GB-Cambridge CB21EW (UK), on quoting the full journal citation.

[13] Compound **1** is more stable to air-oxidation than the persilyl compound **2**, which decolorizes upon exposure to the atmosphere for several days at room temperature [6].

[14] The longest wavelength absorption was fitted by three Gaussian peaks with relative intensities of 1/5.5/1. These peaks have their maxima at 464, 508, and 561 nm, respectively.

[15] Recently, it has been reported that blue colloidal sodium-metal particles formed during the reaction of dichloromethylphenylsilane with sodium in diethyl ether and that they showed a single broad absorption band centered around 560 nm (R. E. Benfield, R. H. Cragg, R. G. Jones, A. C. Swain, *Nature* **1991**, *353*, 340). However, crystals of **1** were found by atomic absorption spectrometry to contain only 0.039% sodium. Therefore, the possibility that the absorption around 500 nm is due to the colloidal sodium can be virtually excluded.

[16] Compound **1** is photoactive under UV irradiation. In a preliminary experiment, upon irradiation (> 300 nm) at 77 K, a 3-MP glass of **1** in a sealed evacuated UV cell showed a new absorption band at 708 nm, the intensity of which attained the highest value after 0.5 h. This band, however, disappeared after the glass was warmed to the room temperature. Work including a trapping experiment is under way.

[17] M. Weidenbruch, K.-L. Thom, S. Phol and W. Saak, *J. Organomet. Chem.* **1987**, *329*, 151.

[18] H. Watanabe, K. Yoshizumi, T. Muraoka, M. Kato, Y. Nagai, T. Sato, *Chem. Lett.* **1985**, 1683.

Structure of a Product of Double Addition to C_{70}: $[C_{70}\{Ir(CO)Cl(PPhMe_2)_2\}_2] \cdot 3C_6H_6$**

By *Alan L. Balch,* Joong W. Lee*, and *Marilyn M. Olmstead*

Studies of the chemical behavior of the fullerenes have shown that they can undergo multiple addition reactions.[1] However, isolation and structural characterization of isomerically pure products of these addition reactions have

[*] Prof. A. L. Balch, J. W. Lee, Dr. M. M. Olmstead
Department of Chemistry, University of California
Davis, California 95616 (USA)

[**] This work was supported by the National Science Foundation (Grant CHE 9022909). We thank Johnson Matthey, Inc. for a gift of iridium chloride.

proven difficult. For the multiple addition products of C_{60}, published structural information is limited to $[C_{60}\{Pt(PEt_3)_2\}_6]$,[2] its palladium analogue,[2] and $C_{60}Br_{24}$.[3] Multiple additions to C_{70} have been mentioned,[4] but until now no structural information on these was available.

In previous work we have shown that Vaska's complex, $[Ir(CO)Cl(PPh_3)_2]$, reacts readily and reversibly with C_{60}[5] and C_{70}[6] to yield adducts in which the fullerene binds in an η^2 fashion through a double bond common to two six-membered rings (6-6 ring junction) to the iridium atom. By utilizing $[Ir(CO)Cl(PPhMe_2)_2]$, which is known to be more reactive than $[Ir(CO)Cl(PPh_3)_2]$ in oxidative-addition reactions,[7] we have succeeded in placing two metal complexes on the exterior surface of C_{70}.

Treatment of C_{70} with a six- to twelvefold molar amount of $[Ir(CO)Cl(PPhMe_2)_2]$ in benzene produces black, feather-shaped crystals of **1**[8] [IR (fluorolube): $\tilde{\nu}[cm^{-1}] = 2001$ (C≡O), $^{31}P\{^1H\}$ NMR (121.7 MHz, CD_2Cl_2, 25 °C): $\delta = -38.7$]. The broad single in the ^{31}P NMR spectrum appears as eleven individual lines at −70 °C. This suggests that several isomers are in dynamic equilibrium in solution. However, both the observation of a uniform, characteristic morphology and identical cell constants for crystals from several different preparations suggest that crystalline samples contain exclusively the isomer reported here.

$[C_{70}\{Ir(CO)Cl(PPhMe_2)_2\}_2] \cdot 3C_6H_6$ **1**

The molecular structure, as revealed by an X-ray diffraction study, is shown in Figure 1, left.[9] The molecule possesses a crystallographically imposed twofold axis which bisects the C35–C35′ bond. Each iridium atom is bound to a 6-6 ring junction at opposite poles of the C_{70} molecule. The attachment of the iridium atoms to the a-b bonds of C_{70} is similar to that seen earlier in $[(\eta^2\text{-}C_{70})Ir(CO)Cl(PPh_3)_2]$.[6] The positioning of the two substituents can be explained by combination of structural and electronic factors. The a-b bonds of C_{70} are the 6-6 ring junctions that have the highest degree of pyramidalization within the molecule. Since η^2-coordination of olefins causes pyramidalization of the two carbon atoms involved, it is not surprising that the iridium fragment preferentially binds at the a-b sites. Once one iridium complex has added to C_{70}, it is likely that the local steric and electronic effects will direct further reactivity away from that pole of the molecule. At the opposite pole, there is a choice of three distinct a-b bonds (A, B, and C in Fig. 1, right) to which the second iridium atom can add. In **1**, the second addition has occurred at site B. At site C, the two substituents would be furthest apart, while at site A they would be closest together. Careful examination of computer-generated representations of these three possible structures reveals no untoward contacts that would disfavor the formation of any form, even for addition at A where the two iridium complexes would be closest.

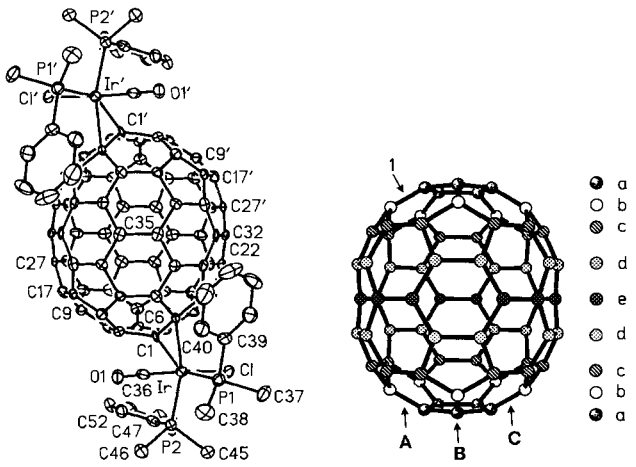

Fig. 1. Left: A perspective view of **1** with 50% thermal contours for all atoms. Selected distances [Å]: Ir-C1, 2.194(7); Ir-C6, 2.156(7); C1-C6, 1.523(11); the e-e bonds C31-C32, 1.456(11); C33-C34, 1.464(12); C35-C35′, 1.448(18). Right: Idealized structure of C_{70}. 1 indicates the bond at which the first addition occurs **A**, **B**, and **C** mark possible sites for the second addition.

The form of the C_{70} molecule in **1** conforms to the structural features noted earlier for $[(\eta^2\text{-}C_{70})Ir(CO)Cl(PPh_3)_2]$[6] and for those predicted theoretically for the unsubstituted molecule.[10, 11] Average bond lengths in Å (excluding those modified by iridium coordination) are: a-a, 1.44(1) Å; a-b, 1.39(1); b-c, 1.46(1); c-c, 1.37(1); c-d, 1.44(1); d-d, 1.43(1); d-e, 1.42(1); and e-e, 1.46(1). The report of an unusually short e-e distance that came from an electron diffraction study of a C_{70} film is not confirmed by this structure.[12]

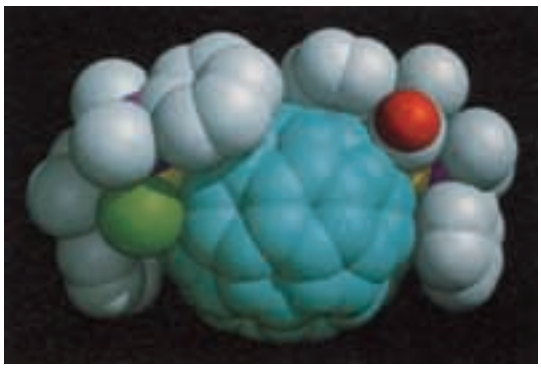

Fig. 2. A view of **1** showing van der Waals surfaces. Notice how the phenyl substituents hug the surface of C_{70}. C_{70} is light blue; other carbons, white; oxygen, red; chlorine, green; iridium, yellow; and phosphorus, purple.

We have previously noted that arene/fullerene π–π contacts are important factors in the solid-state structure of fullerene derivatives.[13] In the case of **1**, the phenyl substituents of the phosphane ligands lie over the surface of the C_{70} portion although these could have assumed positions further from the C_{70} portion by simple rotation of the PMe_2Ph unit about the Ir-P bonds (see Fig. 2). Moreover

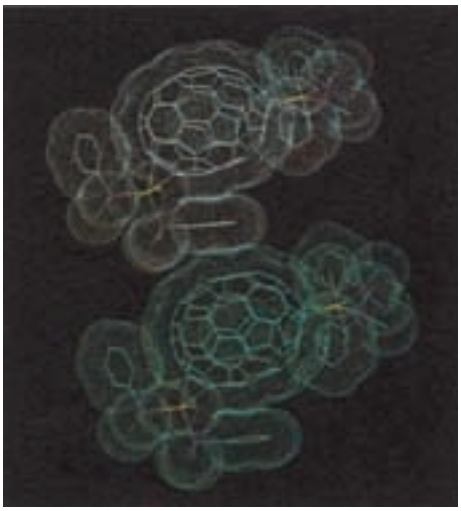

Fig. 3. A view of the contact of two molecules of **1** in the solid state. Van der Waals surfaces are represented by dots, and the two molecules appear in different colors.

adjacent molecule of **1**. This close approach of two molecules of **1** is shown in Figure 3. The three benzene solvent molecules in **1**, however, do not adopt positions that place their flat surfaces in contact with the C_{70} unit. These benzene molecules are merely occupying what would otherwise be voids within the solid.

In summary, a double addition product of C_{70} has been structurally characterized. Because of potential differences in the chemical reactivity of the eight discrete bond types in C_{70}, it may be easier to characterize multiple addition products for C_{70} than for C_{60}.

Experimental Procedure

A yellow solution of 84 mg (0.16 mmol) of $[Ir(CO)Cl(PMe_2Ph)_2]$ in 0.5 mL of benzene was added to a reddish brown solution of 20 mg (0.024 mmol) of C_{70} in 12 mL of benzene. The resulting solution was thoroughly mixed and then allowed to stand undisturbed for four days. The black, crystalline product was collected by filtration and washed with benzene and ethyl ether. Yield: 30 mg, 60% based on C_{70}.

Received: June 12, 1990 [Z 5403 IE]
German version: *Angew. Chem.* **1992**, *104*, 1400

CAS Registry numbers:
1, 143667-85-0; $[Ir(CO)Cl(PMe_2Ph)_2]$, 22685-99-0; C_{70}, 115383-22-7.

[1] J. H. Holloway, E. G. Hope, R. Taylor, G. J. Langley, A. G. Avent, T. J. Dennis, J. P. Hare, H. W. Kroto, D. R. M. Walton, *J. Chem. Soc. Chem. Commun.* **1991**, 966; A. Hirsch, Q. Li, F. Wudl, *Angew. Chem.* **1991**, *103*, 1339; *Angew. Chem. Int. Ed. Engl.* **1991**, *30*, 1309; W. A. Kalsbeck, H. H. Thorp, *J. Electroanal. Chem.* **1991**, *314*, 363; P. J. Krusic, E. Wasserman, P. N. Keizer, J. R. Morton, K. F. Preston, *Science* **1991**, *254*, 1183; T. Suzuki, Q. Li, K. C. Khemani, F. Wudl, O. Almarsson, *ibid.* **1991**, *254*, 1186; G. A. Olah, I. Bucsi, C. Lambert, R. Aniszfeld, N. J. Trivedi, D. K. Sensharma, G. K. S. Prakash, *J. Am. Chem. Soc.* **1991**, *113*, 9387; *ibid.* **1991**, *113*, 9385; F. N. Tebbe, J. Y. Becker, D. B. Chase, L. E. Firment, E. R. Holler, B. S. Malone, P. J. Krusic, E. Wasserman, *ibid.* **1991**, *113*, 9900; F. Wudl, *Acc. Chem. Res.* **1992**, *25*, 157; J. M. Hawkins, *ibid.* **1992**, *25*, 150.

[2] P. J. Fagan, J. C. Calabrese, B. Malone, *J. Am. Chem. Soc.* **1991**, *113*, 9408; *Acc. Chem. Res.* **1992**, *25*, 134.

[3] F. N. Tebbe, R. L. Harlow, D. B. Chase, D. L. Thorn, G. C. Campbell, Jr., J. C. Calabrese, N. Herron, R. J. Young, Jr., E. Wasserman, *Science* **1992**, *256*, 822.

[4] J. M. Wood, B. Kahr, S. H. Hoke, II, L. Dejarme, R. G. Cooks, D. Ben-Amotz, *J. Am. Chem. Soc.* **1991**, *113*, 5907; S. H. Hoke, II, J. Molstad, G. L. Payne, B. Kahr, D. Ben-Amotz, R. G. Cooks, *Rapid Commun. Mass Spectrom.* **1991**, *5*, 472.

[5] A. L. Balch, V. J. Catalano, J. W. Lee, *Inorg. Chem.* **1991**, *30*, 3980.

[6] A. L. Balch, V. J. Catalano, J. W. Lee, M. M. Olmstead, S. R. Parkin, *J. Am. Chem. Soc.* **1991**, *113*, 8953.

[7] A. J. Deeming, B. L. Shaw, *J. Chem. Soc. A* **1969**, 1802.

[8] When the ratio of C_{70} and $[Ir(CO)Cl(PPhMe_2)_2]$ in benzene is 1:1, $[(\eta^2\text{-}C_{70})Ir(CO)Cl(PPhMe_2)_2]\cdot 2C_6H_6$ crystallizes as black, rectangular needles that are visually distinctly different from **1**. They form in the triclinic space group $P\bar{1}$. A completed X-ray diffraction study to be published separately shows that this product closely resembles $[(\eta^2\text{-}C_{70})Ir(CO)Cl(PPh_3)_2]$ [6] where the iridium is bound to an a-b bond of C_{70}.

[9] Crystal structure analysis of **1** at 130 K: $C_{122}H_{62}Cl_2Ir_2O_2P_4$, monoclinic space group $C2/c$, $a = 17.893(4)$ Å, $b = 20.988(5)$ Å, $c = 22.127(5)$ Å, $\beta = 103.51(2)°$, $Z = 4$, $\rho_{calcd} = 1.758$ mg m^{-3}, $Mo_{K\alpha}$ radiation ($\lambda = 0.71073$ Å), Siemens R3m/V; 9262 independent reflections, 6360 observed reflections with $F > 4.0\,\sigma F$, $R = 0.054$, $R_w = 0.051$. As is typical for this class of compounds, the Cl and CO groups are disordered [6]. The figure shows the predominant form (0.64 fractional occupancy). Solution by direct methods (SHELXTL PLUS (VMS)). Further details of the crystal structure investigation may be obtained from the Director of the Cambridge Crystallographic Data Centre, University Chemical Laboratory, Lensfield Road, Cambridge, CB2 1EW (U.K.) on quoting the full journal citation.

[10] F. Negri, G. Orlandi, F. Zerbetto, *J. Am. Chem. Soc.* **1991**, *113*, 6037.

[11] G. E. Scuseria, *Chem. Phys. Lett.* **1991**, *180*, 451.

[12] D. R. McKenzie, C. A. Davis, D. J. H. Cockayne, D. A. Muller, A. M. Vassallo, *Nature* **1992**, *355*, 622.

[13] A. L. Balch, V. J. Catalano, J. W. Lee, M. M. Olmstead, *J. Am. Chem. Soc.* **1992**, *114*, 5455.

avium Trisaccharide (Serovar 21) for the Preparation of a Neoglycoprotein for Immunological Studies**

By *Thomas Ziegler**

Dedicated to Cornelis P. J. Glaudemans on the occasion of his 60th birthday

Disseminated infections by microorganisms of the MAI complex (*Mycobacterium avium intracellulare*), which normally do not cause diseases, are often observed in AIDS patients as serious complications.[1-3] The early recognition of the infection and the clear diagnostic discrimination between these "atypical" mycobacteria and tuberculosis (*Mycobacterium tuberculosis, bovis*) is essential for the specific treatment of the infection. However, this is only possible after laborious and time-consuming cultivation of the isolated bacteria.[4] A quicker and more selective detection of atypical mycobacteria (e.g., serologically, by ELISA techniques or skin tests) would therefore be desirable for routine clinical examinations. However, access to MAI-specific antigens that enable the preparation of suitable antisera or the determination of antibody titers is necessary for such tests. A recent attempt to use MAI-specific protein antigens showed that interfering cross-reactions with antigens of *M. tuberculosis* can occur, which thus prevents an unambiguous diagnosis.[5]

Far more promising is the use of species-specific oligosaccharide haptenes, which are found in the characteristic glycopeptidolipids of the cell membrane of MAI.[6-8] These are tri- to pentasaccharides that form an *O*-glycosidic linkage with the threonine unit of a tetrapeptide (Scheme 1). The

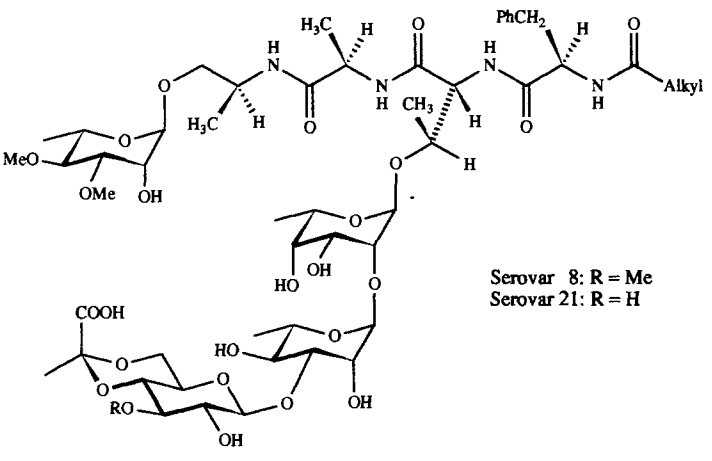

Scheme 1. Structure of the MAI glycopeptide lipids (serovars 8 and 21).

protein-bound disaccharide residue α-L-Rha*p*-(1 → 2)-6-deoxy-α-L-Tal*p* is conserved for all MAI serovars, whereas the serologically differentiable species are determined by the saccharide residue at the nonreducing end.[9] The serovars 8 and 21, which both bear an immunodominant 4,6-pyruvylated

[*] Dr. T. Ziegler
Institut für Organische Chemie und Isotopenforschung
Pfaffenwaldring 55, D-W-7000 Stuttgart 80 (FRG)

[**] This work was supported by the Deutsche Forschungsgemeinschaft. Abbreviations used: *p* = pyranose, Rha = rhamnose, Tal = talose, Bn = benzyl, Bz = benzoyl, Ac = acetyl, Z = benzyloxycarbonyl, Tos = tosyl, TMSOTf = trimethylsilyltriflate, BSA = bovine serum albumin, PBS = phosphate buffered saline, EE = ethyl acetate, RT = room temperature.

β-D-Glc*p* residue are particularly interesting.[9, 10] We now describe an efficient chemical synthesis of a trisaccharide neoantigen of MAI (serovar 21), which can be employed directly for diagnostic purposes or for the preparation of specific antibodies. For the first time the complete synthesis of a complex oligosaccharide containing a pyruvate acetal was possible.

A blockwise construction of the trisaccharide was chosen for the synthesis so that a minimum of manipulation of protecting groups was required. The monosaccharide building blocks **3** and **12** were synthesized from the readily accessible[11–14] L-rhamnopyranoside derivative **1** (Scheme 2).

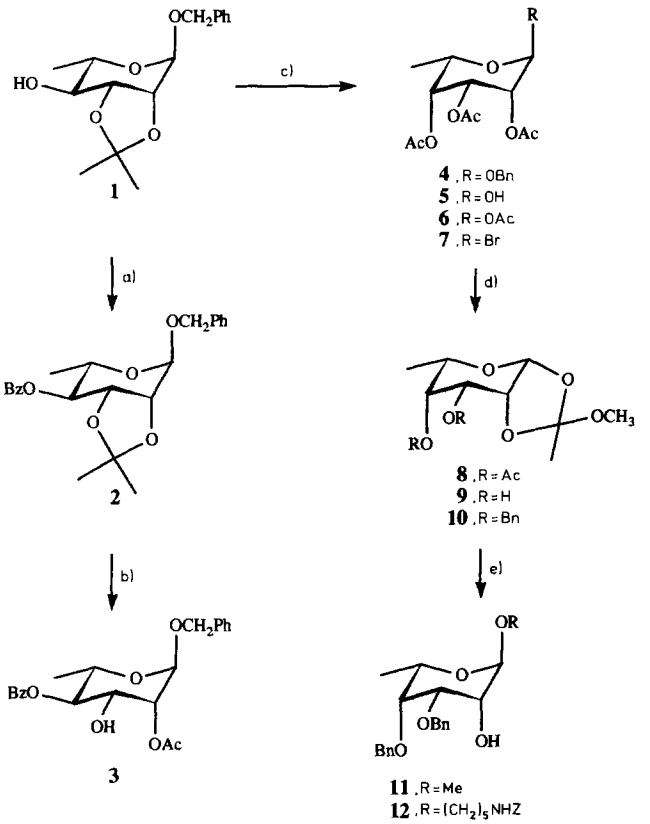

Scheme 2. Synthesis of the monosaccharide building blocks **3** and **12**. a) BzCl in pyridine. b) 1) AcOH (90%); 2) $MeC(OMe)_3$, TosOH (cat.) in DMF; 3) AcOH (80%). c) 1) Ref. [8]; 2) H_2, Pd (10% on activated charcoal) in EE; 3) Ac_2O in pyridine; 4) HBr in AcOH, → 94% **7**. d) 1) 2,6-lutidine in MeOH; 2) NaOMe (cat.) in MeOH; 3) BnBr, NaH in THF. e) 1) $HO(CH_2)_5NHZ$, $HgBr_2$ (cat.) in MeCN; 2) NaOMe (cat.) in MeOH, →18% **11**, → 55% **12**.

Benzoylation of **1** yielded the crystalline derivative **2** (72%), which was converted into the L-rhamnosyl acceptor **3** (65%). The 6-deoxy-L-talosyl acceptor **12** should bear a 5-aminopentyl aglycon so that the saccharide can be subsequently linked to a protein. For the synthesis of **12**, compound **1** was transformed into the known L-taloside **4**.[12, 13] After hydrogenation of the benzyl group (**4** → **5**) and acetylation, the resulting tetraacetate **6** was treated without further purification with HBr to afford 2,3,4-tri-*O*-acetyl-6-deoxy-α-L-talopyranosyl bromide (**7**, 94%). The latter was subsequently converted into the orthoester **8** with methanol. After cleavage of the acetate groups at O3 and O4 (Zemplén and benzylation of the intermediate **9**, the yield of the L-talopyranose derivative **10** was 79%. All synthetic steps for the conversion **4** →**10** proceeded without the formation of by-products, which made the time-consuming isolation and characterization of the intermediates **5**–**9** unnecessary. This contributed to the efficiency of our chosen synthesis of **10**. Reaction of **10** with 5-benzyloxycarbamidopentanol catalyzed by $HgBr_2$[15] and deblocking of the 2-position afforded the desired acceptor **12** (55%). Also produced as a side product was L-talopyranoside **11** (18%), which was recently prepared differently and used in the synthesis of the MAI tetrasaccharide (serovar 4).[8] The overall yield of the building blocks **3** and **12** was thus 47% (based on **1**) and 40% (based on **4**), respectively.

The construction of the MAI trisaccharide was now begun from the nonreducing end (Scheme 3), which required a suitable pyruvylated glucosyl donor. The trichloroacetimidate **13** proved particularly valuable for this purpose. It can be synthesized easily from glucose.[16] The trimethylsilyltriflate-

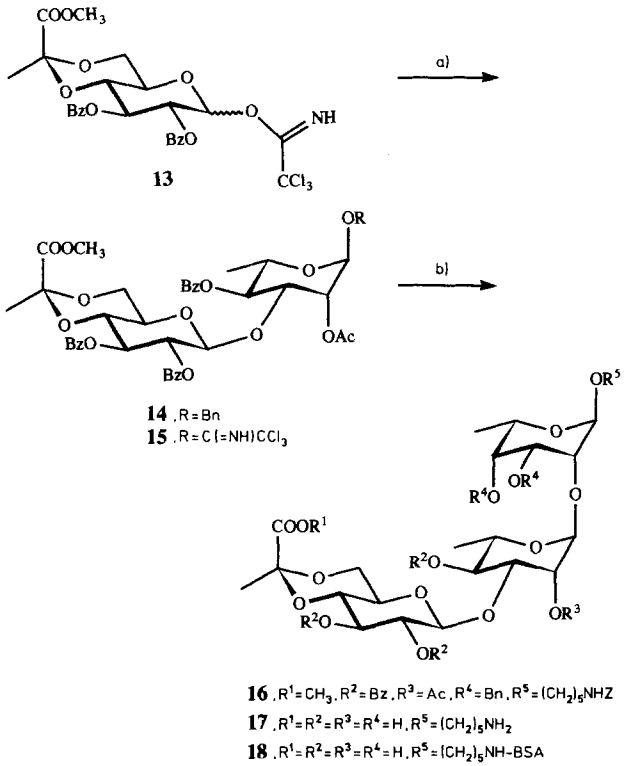

Scheme 3. Synthesis of the MAI neoglycoprotein **18** from the precursors **3**, **12**, **13**. a) 1) **3**, 10 mol% TMSOTf in CH_2Cl_2, 1 h, −20 °C, →72% **14**,; 2) H_2, Pd (10% on activated charcoal) in EE, 3 h, RT; 3) Cl_3CN, K_2CO_3 in CH_2Cl_2, 4 h, RT, →77% **15**. b) 1) **12**, 10 mol% TMSOTf in CH_2Cl_2, 1 h, −20 °C, →70% **16**; 2) NaOMe (cat.) in MeOH, 24 h, RT; 3) NaOH in H_2O, 48 h, RT; 4) H_2, Pd (10% on activated charcoal) in H_2O, 12 h, RT, → 76% **17**; 5) **17** (10 μmol), BSA (0.3 μmol), glutardialdehyde solution (28%, 15 mL) in PBS buffer (pH 7.2), 1 h, 0–4 °C, then $NaBH_4$ (0.3 g), 1 h, 0–4 °C; 6) dialysis against PBS, then lyophilization →**18**.

catalyzed coupling of **3** and **13** by the inverse addition procedure[17] furnished the crystalline β-(1 → 3)-linked disaccharide **14**. Hydrogenation of the latter and subsequent reaction with trichloroacetonitrile afforded the diglycosyl donor **15** (77%). The protected trisaccharide was finally prepared in 70% yield by coupling of **12** and **15**. Both glycosylation steps proceeded diastereoselectively; in neither case could the undesired anomer be detected. For the deblocking of **16**, first the acyl residues were cleaved (Zemplén), and then the methyl ester of the pyruvate acetal was saponified, followed by a hydrogenolytic cleavage of the benzyl groups. The deprotected trisaccharide **17** was obtained in 76% yield.

Table 1. Selected physical data of compounds **2**, **3**, **10**, **12**, and **14**–**17**.

2: M.p. 143 °C; $[\alpha]_D = -25.1$ ($c = 0.6$, $CHCl_3$); ^1H NMR ($CDCl_3$, TMS): $\delta = 5.13$ (s, $J_{1,2} = 0$, 1H; H1); ^{13}C NMR ($CDCl_3$, TMS): $\delta = 96.2$ (C1), 76.1, 75.8, 75.0 (C2,3,4), 69.3 (Bn), 64.3 (C5), 17.1 (C6).

3: M.p. 117–118 °C; $[\alpha]_D = -58.0$ ($c = 0.6$, $CHCl_3$); ^1H NMR ($CDCl_3$, TMS): $\delta = 4.95$ (d, $J_{1,2} = 1.6$, 1H; H1); ^{13}C NMR ($CDCl_3$, TMS): $\delta = 96.8$ (C1), 75.3 (C3), 72.7 (C4), 68.7 (C2), 66.3 (C5), 69.7 (Bn), 17.5 (C6).

10: $[\alpha]_D = +6.7$ ($c = 0.3$, $CHCl_3$); ^1H NMR ($CDCl_3$, TMS): $\delta = 5.33$ (d, $J_{1,2} = 2.3$, 1H; H1); ^{13}C NMR ($CDCl_3$, TMS): $\delta = 125.0$ ($C_{quart.}$), 97.6 (C1), 76.5, 75.4, 74.1 (1C, 1C, 2C; C2,3,4,5), 70.6, 69.5 (2 Bn), 49.1 (OMe), 25.4 (Me), 17.4 (C6).

12: $[\alpha]_D = -37.6$ ($c = 0.4$, $CHCl_3$); ^1H NMR ($CDCl_3$, TMS): $\delta = 4.86$ (d, $J_{1,2} = 2.1$, 1H; H1); ^{13}C NMR ($CDCl_3$, TMS): $\delta = 101.5$ (C1), 78.8 (C3), 75.5 (Bn), 74.5 (C4), 69.8 (Bn), 68.0 (C2), 67.5 (Bn), 66.7 (Bn), 66.4 (C5), 40.9 (CH_2N), 29.8, 29.1, 23.4 (CH_2), 16.9 (C6).

14: M.p. 211 °C; $[\alpha]_D = +43.2$ ($c = 0.2$, $CHCl_3$); ^1H NMR ($CDCl_3$, TMS): $\delta = 4.86$ (d, $J_{1,2} = 1.7$, 1H; H1), 1.13 (d, $J_{5,6} = 6.2$, 3H; H6), 4.83 (d, $J_{1',2'} = 7.7$, 1H; H1'), 3.80 (s, 3H; COOMe), 1.46 (s, 3H; Me); ^{13}C NMR ($CDCl_3$, TMS): $\delta = 101.6$ (C1'), 99.3 ($C_{quart.}$), 96.9 (C1), 75.0 (C4'), 74.5 (C3), 72.6 (C3'), 72.2 (C2'), 72.0 (C4), 71.5 (C2), 69.8 (Bn), 66.7 (C5), 65.1 (C6'), 66.0 (C5'), 52.8 (COO*Me*), 25.2 (Me), 17.4 (C6).

15: $[\alpha]_D = +31.3$ ($c = 0.2$, $CHCl_3$); ^1H NMR ($CDCl_3$, TMS): $\delta = 6.23$ (d, $J_{1,2} = 1.9$, 1H; H1), 1.17 (d, $J_{5,6} = 6.3$, 3H, H6), 4.86 (d, $J_{1',2'} = 7.7$, 1H; H1'), 3.81 (s, 3H; COOMe), 1.46 (s, 3H; Me); ^{13}C NMR ($CDCl_3$, TMS): $\delta = 101.8$ (C1'), 99.4 ($C_{quart.}$), 94.7 (C1), 90.9 (CCl_3), 74.5 (C4'), 74.4 (C3), 72.2 (C3'), 71.9 (2C, C4,2'), 70.1 (C2), 69.6 (C5), 66.1 (C5'), 65.0 (C6'), 52.8 (COO*Me*), 25.2 (Me), 17.5 (C6).

16: $[\alpha]_D = +26.4$ ($c = 0.1$, $CHCl_3$); ^1H NMR ($CDCl_3$, TMS): $\delta = 4.92$ (brs, $J_{1,2} < 0.5$, 1H; H1), 1.34 (d, $J_{5,6} = 6.5$, 1H; H6), 4.66 (d, $J_{1'',2''} = 1.9$, 1H; H1''), 1.12 (d, $J_{5'',6''} = 6.3$, 1H; H6''), 4.29 (d, $J_{1'',2''} = 7.5$, 1H; H1''), 3.76 (s, 3H; COOMe), 1.45 (s, 3H; Me); ^{13}C NMR ($CDCl_3$, TMS): $\delta = 101.0$ (C1''), 99.5 (C1), 99.2 (C1'), 99.1 ($C_{quart.}$), 77.2 (C3), 75.4 (C4''), 74.4 (2C, C4,3'), 73.1 (Bn), 72.5 (C3''), 72.0 (2C, C2',2''), 71.2 (C4'), 71.0 (Bn), 67.5 (3C, C2, Bn, CH_2O), 67.3 (C5'), 66.7 (2C, C5,5''), 65.2 (C6''), 52.6 (COO*Me*), 41.0 (CH_2N), 29.1 (CH_2), 25.7 (Me), 23.4, 23.2 (CH_2), 17.5 (C6'), 17.1 (C6).

17: $[\alpha]_D = -161.3$ ($c = 0.1$, H_2O); ^{13}C NMR (D_2O): $\delta = 178.2$ (COO), 107.1 (C1''), 105.4 (C1'), 104.4 ($C_{quart.}$), 101.7 (C1), 82.4 (C2), 80.1 (C3'), 78.8 (C4''), 77.1 (C2''), 75.7 (C3''), 74.4 (C3), 73.9 (CH_2O), 72.5 (C4), 72.1 (2C, C4',5), 70.7 (C2'), 70.0 (C5'), 68.8 (C5''), 67.2 (C6''), 42.3 (CH_2N), 30.8 (CH_2), 29.4 (CH_2), 27.5 (Me), 25.3 (CH_2), 19.6 (C6), 18.3 (C6').

Attachment of saccharide **17** to a carrier protein can be achieved by different methods.[18–20] However, the use of the heterobifunctional coupling reagent 3-maleimidopropionyl-*N*-hydroxysuccinimide ester[21] yielded, after lyophilization, an insoluble conjugate with bovine serum albumin (BSA) that was therefore unsuitable as neoantigen. Advantageous, on the other hand, was the particularly simple and quick attachment of **17** to BSA with glutardialdehyde. The concentrations chosen here for the coupling step (Scheme 3) by this method provided a highly soluble neoglycoprotein **18** that contained 12 mol **17** per mol BSA according to the determination of bound sugar by the phenol–sulfuric acid method.[22] The conjugate **18** should therefore be ideally suited tor further immunological studies.

Received: June 2, 1992 [Z 5384 IE]
German version: *Angew. Chem.* **1992**, *104*, 1369

CAS Registry numbers:
1, 53270-14-7; **2**, 105285-86-7; **3**, 143332-41-6; **4**, 88818-93-3; **5**, 143332-42-7; **6**, 143394-72-3; **7**, 41881-45-2; **8**, 143394-73-4; **9**, 143394-74-5; **10**, 143394-75-6; **11**, 138552-37-1; **12**, 143332-43-8; **13**, 143394-76-7; **14**, 143332-44-9; **15**, 143332-45-0; **16**, 143332-46-1; **17**, 143332-47-2; 5-benzyloxycarbamidopentanol, 87905-98-4.

[1] P. Zakowski, S. Fligiel, G. W. Berlin, B. L. Johnson, *J. Am. Med. Assoc.* **1982**, *248*, 2920–2982.
[2] J. M. Wallace, J. B. Hannah, *Chest* **1988**, *93*, 926–932.
[3] L. S. Young, *J. Infect. Dis.* **1988**, *157*, 863–867.
[4] H. M. Sommers, J. K. McClatchy in *Cumitech 16: Laboratory Diagnosis of the Mycobacteriosis* (Ed.: J. A. Morello), American Society for Microbiology, Washington, D.C., USA, **1983**.
[5] D. A. Rouse, S. L. Morris, A. B. Karpas, J. C. Mackall, P. G. Probst, S. D. Chaparas, *Infect. Immun.* **1991**, *59*, 2595–2600.
[6] B. Rivoire, B. J. Ranchoff, D. Chatterjee, H. Gaylord, A. Y. Tsang, A. H. J. Kolk, G. O. Aspinall, P. J. Brennan, *Infect. Immun.* **1989**, *57*, 3147–3158.
[7] W. R. Thayer, C. M. Bozic, R. T. Camphausen, M. McNeil, *J. Clin. Microbiol.* **1990**, *28*, 714–718.
[8] M. K. Gurjar, G. Viswanadham, *Tetrahedron Lett.* **1991**, *32*, 6191–6194.
[9] P. J. Brennan, S. W. Hunter, M. McNeil, D. Chatterjee, M. Daffe in *Microbial Determinants of Virulence and Host Response* (Eds.: E. M. Ayoub, G. H. Cassell, W. C. Branche, T. J. Henry), American Society for Microbiology, Washington, DC, USA, **1990**, pp. 55–75.
[10] P. J. Brennan, G. O. Aspinall, J. E. Nam Shin, *J. Biol. Chem.* **1981**, *256*, 6817–6822.
[11] J. S. Brimacombe, L. C. N. Tucker, *Carbohydr. Res.* **1967**, *5*, 36–44.
[12] J. S. Brimacombe, F. Hunedy, A. K. Al-Radhi, *Carbohydr. Res.* **1969**, *11*, 331–340.
[13] G. O. Aspinall, K. Takeo, *Carbohydr. Res.* **1983**, *121*, 61–77.
[14] A. Eßwein, R. R. Schmidt, *Liebigs Ann. Chem.* **1988**, 675–678.
[15] D. Chatterjee, S.-N. Cho, P. J. Brennan, *Carbohydr. Res.* **1986**, *156*, 39–56.
[16] T. Ziegler, E. Eckhardt, G. Herold, *Liebigs Ann. Chem.* **1992**, 441–451.
[17] R. Bommer, W. Kinzy, R. R. Schmidt, *Liebigs Ann. Chem.* **1991**, 425–433.
[18] C. P. Stowell, Y. C. Lee, *Adv. Carbohydr. Chem. Biochem.* **1980**, *37*, 225–281.
[19] S. Muller, *Lab. Tech. Biochem. Mol. Biol.* **1988**, *19*, 95–130.
[20] B. F. Erlanger, *Methods Enzymol.* **1980**, *70*, 85–104.
[21] T. Kitagawa, T. Shimozono, T. Aikawa, T. Yoshida, H. Nishimura, *Chem. Pharm. Bull.* **1981**, *29*, 1130–1135.
[22] M. Dubois, K. A. Gilles, J. K. Hamilton, P. A. Rebers, F. Smith, *Anal. Chem.* **1956**, *28*, 350–356.

Novel Strategies for the Synthesis and Crystallization of Electrophilic Dinuclear Cations: Solution and Solid-State Properties of $[Re_2(NCCH_3)_{10}][Mo_6O_{19}]_2$ **

By *Stacey N. Bernstein* and *Kim R. Dunbar**

Dedicated to Professors F. Albert Cotton and Richard A. Walton

Beginning with the earliest reports in 1858, mononuclear transition metal acetonitrile complexes have been a topic of considerable interest to inorganic chemists,[1] but surprisingly little is known about analogous metal–metal bonded species; in fact only two examples have been reported to date, namely, $[M_2(NCCH_3)_{10}]^{4+}$ (M = Mo, Rh),[2] these being derived from acidification or alkylation reactions of $M_2(O_2CCH_3)_4$. Recent years have seen a marked increase of interest in acetonitrile cation complexes, particularly with respect to their use as precursors for metal–containing polymers and molecular materials,[3] catalysts,[4] and biologically relevant coordination compounds.[5] We now report two entirely new strategies for the synthesis of novel solvated dinuclear cations beginning from halide and phosphine complexes.

Reactions of $[(n\text{Bu})_4N]_2[Re_2Cl_8]$ with $HBF_4 \cdot Et_2O$ in CH_3CN/CH_2Cl_2 solvent mixtures produced, in approximately 15% yield, a bright blue solid characterized as **1**.[6]

$[Re_2(NCCH_3)_8][BF_4]_4$ **1**

[*] Prof. K. R. Dunbar, S. N. Bernstein
Department of Chemistry, Michigan State University
East Lansing, MI 48824 (USA)

[**] This work was supported by the National Science Foundation (Grants CHE-89149, CHE-8403823, CHE-8908088, and CHE-88-00770), the Camille and Henry Dreyfus Foundation, and the National Institutes of Health (Grant No. 1-S10-RR04750-01). We thank Dr. J. Amarasekera and Professor T. J. Pinnavaia for help with the TGA analyses and Dr. J. Ledford for the XPS studies. We also thank Dr. A. Quillevéré for helpful discussions and Dr. D. Ward for help with the ORTEP.

Analogous protonation reactions of $[Re_2Cl_4(PnPr_3)_4]$ also led to **1**, and in much higher yields (ca. 80%). Single crystals of the $[BF_4]^-$ salt were obtained by slow diffusion of CH_2Cl_2 into a CH_3CN solution of **1** over a period of 3 days.[7] Preliminary X-ray results of **1** revealed a body-centered cubic lattice that shows a threefold disorder of the dirhenium units. Poor diffraction coupled with considerable refinement difficulties for three independent cubic crystals prompted us to resort to an unusual strategy to reduce the crystal symmetry and improve packing: we replaced the small tetrahedral $[BF_4]^-$ counterions with large octahedral $[Mo_6O_{19}]^{2-}$ polyoxometalate anions. This not only led to a perfectly ordered array of dinuclear cations within the interstices provided by the anions, but opened up the possibility of studying solid-state reactivity of the trapped solvated cations as well.

$[Re_2(NCCH_3)_{10}][Mo_6O_{19}]_2$ **2**

The molybdate salt **2** was prepared by an anion exchange reaction of **1** and $[(nBu)_4N]_2[Mo_6O_{19}]$ in CH_3CN; crystals suitable for X-ray studies were grown by slow diffusion of separate CH_3CN solutions of the two salts that were layered in a sealed tube.[8] Single-crystal X-ray data revealed its identity as $[Re_2(NCCH_3)_{10}][Mo_6O_{19}]_2 \cdot 4CH_3CN \cdot 2H_2O$. The ORTEP plot of the three constituent ions in **2** is depicted in Figure 1, and a selection of important distances and angles are listed in the caption. The molecule crystallizes in the

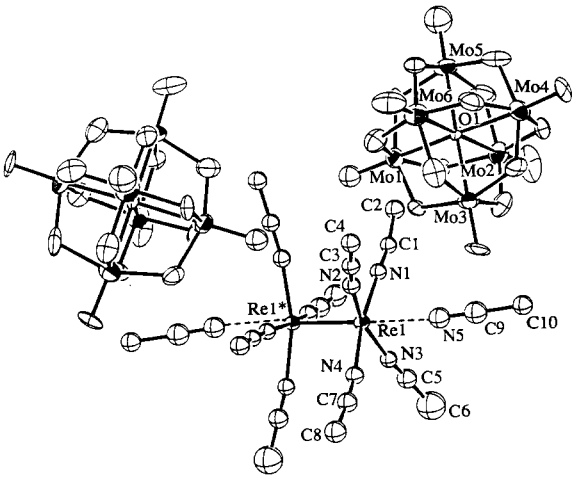

Fig. 1. Selected distances [Å] and angles [°] for **2**: Re1-Re1* 2.259(4); Re1-N1 2.07(3); Re1-N2 2.02(3); Re1-N3 2.06(2); Re1-N4 2.16(3); Re1-N5 2.51(3); N1-C1 1.06(3); N2-C3 1.12(3); N3-C5 1.18(3); N4-C7 1.13(4); N5-C9 1.09(3); C1-C2 1.33(5); C3-C4 1.47(4); C5-C6 1.37(4); C9-C10 1.39(4); Re1-Re1*-N1 97.8(6); Re1-Re1*-N2 92.6(7); Re1-Re*-N5 174.6(6); Re1-N1-C1 170(3); N1-C1-C2 179(4); Re1-N2-C3 176(2); N2-C3-C4 172(3); Re1-N5-C9 168(3); N5-C9-C10 178(4).

monoclinic space group $C2/c$, and the midpoint of the Re-Re bond resides on a twofold symmetry axis. Each Re^{II} center is pseudooctahedral, consisting of four nearly planar CH_3CN ligands and two additional vertices defined by a weakly interacting axial CH_3CN group (Re–N = 2.51 (3) Å) and the other Re atom. The new molecule adopts a staggered conformation in which the two $Re(NCCH_3)_4$ units are rotated by $\chi_{av} = 44.5\ (1)^\circ$, as expected for a triply bonded species. The Re–Re distance of 2.259 (4) Å in **2** falls in the range observed for dirhenium compounds containing metal–metal triple bonds of the electron-rich $\sigma^2\pi^4\delta^2\delta^{*2}$ configuration, although the metal centers are highly charged in **2** and are not coordinated to strong σ or π donors such as phosphine or halide ligands.[9] In the $[Mo_6O_{19}]^{2-}$ anion, the average Mo–O distances correlate well with those previously observed.[10] The three-dimensional packing arrangement within a 10 Å radius from the center of the Re–Re bond revealed that the $[Re_2]^{4+}$ cations occupy pseudooctahedral sites in the lattice defined by the spherical $[Mo_6O_{19}]^{2-}$ anions.

An IR spectrum of crystals of **2** reveal absorptions arising from coordinated CH_3CN and the $[Mo_6O_{19}]^{2-}$ counterion.[11] The IR spectrum of **1** exhibits similar absorptions for coordinated CH_3CN and $[BF_4]^-$.[11] A ^1H NMR spectrum of **1** in CD_3CN exhibits a resonance at $\delta = +3.37$ attributed to the equatorially bound CH_3CN groups and a minor feature at +1.95 due to free CH_3CN.[12] The electronic spectrum of **1** in the visible region consists of a very broad low-energy transition at λ_{max} (ε) = 663 nm (630 $M^{-1}cm^{-1}$) in addition to a strong feature of nearly equal intensity at 593 nm (590 $M^{-1}cm^{-1}$) with two shoulders, located at 458 and 866 nm. Bands in the UV region fall at 244 (2.7×10^4 $M^{-1}cm^{-1}$) and 203 nm (5.1×10^4 $M^{-1}cm^{-1}$). Electrochemical measurements performed in 0.05 M $[(nBu)_4N][BF_4]/CH_3CN$ solutions revealed, surprisingly, an extremely accessible quasi-reversible reduction at $E_{1/2} = +0.24$ V along with two irreversible reductions at $E_p^c = -0.20$ V and -0.76 V vs. Ag/AgCl.[13] These results are in sharp contrast to the redox properties of other complexes containing triple bonds of the type $\sigma^2\pi^4\delta^2\delta^{*2}$, which exhibit one or two accessible oxidations but not reductions. The high charge of the cation coupled with the fact that the supporting ligand set comprises only moderate-strength σ-donors undoubtedly contributes to the electrophilic character of **2**.

A test of the thermal stability of **2** by thermogravimetric analysis under N_2 (Fig. 2) reveals that loss of coordinated CH_3CN is essentially quantitative upon gradual heating to 350 °C.[14] The resulting black amorphous mixed-metal oxide constitutes the first example of a ternary ReMo oxide of any type. Preliminary studies by X-ray photoelectron spectroscopy (XPS) confirmed the absence of carbon or nitrogen components and revealed that Mo^{VI} and two different oxidation states of Re are at the surface of the material. Further characterization by transmission electron spectroscopy, neutron scattering, and EXAFS are in progress. Similar materials have been synthesized from the salts $[M_2(NCCH_3)_{10}][M'_6O_{19}]_2$ (M = Mo, Rh; M' = Mo, W).

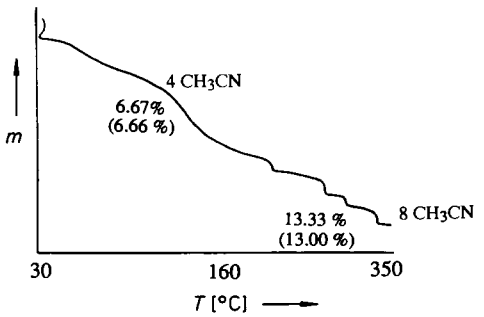

Fig. 2. Thermogravimetric analysis curve for a sample of $[Re_2(NCCH_3)_8][Mo_6O_{19}]_2$ heated under N_2 to 350 °C. The salt undergoes sequential loss of all 8 CH_3CN groups to yield a ternary oxide. m = weight of the sample. The percentages refer to the theoretical (experimental) weight loss.

This paper reports two findings of importance to molecular and solid-state chemistry of transition metals. The fact that a hitherto unknown dinuclear solvated cation may be easily synthesized from $[Re_2Cl_8]^{2-}$ and $Re_2Cl_4(PnPr_3)_4$

complexes is remarkable, considering the demonstrated stability of such species.[9] This method is currently being extended to related complexes of W and Os.[15] Furthermore, the low-temperature desolvation approach to mixed-metal oxides from salts comprising acetonitrile cations and various polyoxometalate anions is a potentially very useful route to new oxides of previously unknown stoichiometries and structures. In principle, one may carefully select the identity of the metals to optimize properties such as catalytic activity and magnetism, especially if 3d metals are included.

Experimental Procedure

1: $[(n\mathrm{Bu})_4\mathrm{N}]_2[\mathrm{Re}_2\mathrm{Cl}_8]$ (1.00 g, 0.865 mmol) was dissolved in 50 mL of CH_3CN and treated with 5 mL of $HBF_4 \cdot Et_2O$ (85% HBF_4 solution). After complete addition of the acid, the pressure in the reaction vessel was reduced to remove gaseous HCl, and 200 mL of CH_2Cl_2 was slowly added. The solution was heated under reflux for five hours, after which time the intensely blue solid was collected, washed with CH_2Cl_2 and Et_2O, and dried in vacuo. Yield 150 mg, 15%.

Alternative procedure: $[\mathrm{Re}_2\mathrm{Cl}_4(P\mathrm{Pr}_3)_4]$ (350 mg, 0.303 mmol) was suspended in a mixture of CH_3CN (10 mL) and CH_2Cl_2 (3 mL) and treated with 1 mL of $HBF_4 \cdot Et_2O$ under reduced pressure. The reaction mixture turned green within 5 min and gradually became blue after heating at reflux for 12 h. The solution was then treated with 20 mL of CH_2Cl_2 to yield a bright blue solid which was collected, washed with CH_2Cl_2 and Et_2O, and dried in vacuo. Yield 253 mg, 80%.

Received: April 23, 1990 [Z 5318IE]
German version: *Angew. Chem.* **1992**, *104*, 1412

[1] W. Henke, *Justus Liebigs Ann. Chem.* **1858**, *106*, 280; R. A. Walton, *Q. Rev. Chem. Soc.* **1965**, *19*, 126; B. N. Storhoff, H. C. Lewis, *Coord. Chem. Rev.* **1977**, *23*, 1; J. A. Davies, F. R. Hartley, *Chem. Rev.* **1981**, *81*, 79; A. P. Zuur, W. L. Groeneveld, *Recl. Trav. Chim. Pays-Bas* **1967**, *86*, 1103; J. Reedijk, A. P. Zuur, W. L. Groeneveld, *ibid.* **1967**, *86*, 1127; J. Reedijk, W. L. Groeneveld *ibid.* **1968**, *87*, 513, 553, 1079; J. Reedijk, *ibid.* **1969**, *88*, 86; B. J. Hathaway, A. E. Underhill, *J. Chem. Soc.* **1960**, 3705; B. J. Hathaway, D. G. Holah, A. E. Underhill, *ibid.* **1962**, 2444; B. J. Hathaway, D. G. Holah, *ibid.* **1964**, 2400; I. Rapaport, L. Helm, A. E. Merbach, P. Bernhard, A. Ludi, *Inorg. Chem.* **1988**, *27*, 873; M. Bown, X. L. R. Fontaine, N. N. Greenwood, J. D. Kennedy, M. J: Thornton-Pett, *J. Chem. Soc. Dalton Trans.* **1987**, 1169; A. Sen, T.-W. Lai, *J. Am. Chem. Soc.* **1981**, *103*, 4627; R. R. Thomas, A. Sen, *Inorg. Synth.* **1989**, *26*, 128; C. K. Alesbury, M. C. R. Symons, *J. Chem. Soc. Faraday Trans. 1* **1980**, *76*, 244; K. Nilsson, A. Oskarsson, *Acta. Chem. Scand. A* **1984**, *38*, 79; A. Bruckner, H. Vogt, L. Riesel, *Z. Chem.* **1987**, *27*, 415; A. De Renzi, A. Panunzi, A. Vitagliano, G. Paiaro, *J. Chem. Soc. Chem. Commun.* **1976**, 47; P. R. Johnson, J. M. Pratt, R. I. Tilley, *ibid.* **1978**, 606; R. R. Thomas, V. Chebolu, A. Sen, *J. Am. Chem. Soc.* **1986**, *108*, 4096.

[2] F. A. Cotton, K. J. Wiesinger, *Inorg. Chem.* **1991**, *30*, 871; J. M. Mayer, E. H. Abbott, *ibid.* **1983**, *22*, 2774; K. R. Dunbar, *J. Am. Chem. Soc.* **1988**, *110*, 8247; L. M. Dikareva, V. I. Andrianov, A. N. Zhilyaev, I. B. Baranovskii, *Russ. J. Inorg. Chem.* (Engl. Transl.) **1989**, *34*, 240.

[3] See, for example, J. Michl, *Science* **1991**, *252*, 511; S. C. Huckett, S. Batten, R. Gable, B. F. Hoskins, R. Robson, Paper INORG 345 (201st ACS National Meeting, Atlanta, Georgia), **1991**; B. F. Hoskins, R. Robson, *J. Am. Chem. Soc.* **1990**, *112*, 1546; B. F. Abrahams, B. F. Hoskins, R. Robson, *J. Am. Chem. Soc. Chem. Commun.* **1990**, 60.

[4] Z. Jiang, A. Sen, *J. Am. Chem. Soc.* **1990**, *112*, 9655; A. Sen, *Acc. Chem. Res.* **1988**, *21*, 421, and references cited therein.

[5] See, for example, M. Shibata, *Top. Curr. Chem.* **1983**, *110*, 13–16; D. M. Eichhorn, W. H. Armstrong, *Inorg. Chem.* **1990**, *29*, 3607.

[6] Reactions of $[\mathrm{Re}_2(O_2C_4H_7)_4Cl_2]$ with $AgBF_4$ followed by Et_3OBF_4 also produce low yields of **1**. K. R. Dunbar and A. Quillevéré, unpublished results.

[7] Compound **1** crystallizes in a body-centered cubic space group with lattice parameters 29.22(1) Å and $V = 24947(22)$ Å^3.

[8] Calculated for $[\mathrm{Re}_2(\mathrm{NCCH}_3)_8][\mathrm{Mo}_6O_{19}]_2$: C 8.09, H 1.02, N 4.72. Found: C 8.39, H 1.20, N 4.78. Allowances for small amounts of residual CH_3CN in the lattice improves the analysis. Crystal data for $\mathbf{2} \cdot 4CH_3CN \cdot 2H_2O$ at $-90\,^\circ$C: $C_{24}H_{40}N_{12}O_{40}Mo_{12}Re_2$, $M = 2742.44$, monoclinic space group $C2/c$ with unit cell parameters $a = 18.36(2)$, $b = 22.67(2)$, $c = 17.45(2)$ Å, $\beta = 90.31(9)^\circ$, $V = 7263(22)$ Å^3, $Z = 4$, $\varrho_{calcd} = 2.508$ g cm^{-1}, and $\mu(\mathrm{Mo}_{K\alpha}) = 54.03$ cm^{-1}. The intensity data were collected on a Rigaku AFC6-S diffractometer by an ω-2θ scan technique. 6508 unique data were collected in the range $6 \le 2\theta \le 50^\circ$ and corrected for Lorentz and polarization effects. The intensities of three check reflections decreased by ~60%; a linear correction factor was applied to account for this considerable decay. An empirical absorption correction based on azimuthal scans of several reflections with χ near 90° was also applied. A total of 2805 data with $F_o^2 > 3\sigma(F_o^2)$ were used to refine 298 variables to residuals of R (R_w) = 0.066 (0.083) and quality-of-fit of 2.56. The largest shift/esd in the final cycle was 0.13; the largest peak in the final difference Fourier map was 1.95 e$^-$/Å^3 and is the ghost of a Re atom. Further details of the crystal structure investigation are available on request from the Director of the Cambridge Crystallographic Data Centre, University Chemical Laboratory, Lensfield Road, GB-Cambridge CB21EW (UK), on quoting the full journal citation.

[9] F. A. Cotton, R. A. Walton, *Multiple Bonds Between Metal Atoms*, Wiley-Interscience, New York, **1982** and references therein; R. A. Walton, *Isr. J. Chem.* **1985**, *25*, 196; F. A. Cotton, R. A. Walton in *Structure and Bonding, (Berlin)*, **1985**, *62*, 7.

[10] P. Dahlstrom, J. Zubieta, B. Neaves, J. R. Dilworth, *Cryst. Struct. Commun.* **1982**, *11*, 463; H. R. Allcock, E. C. Bissell, E. T. Shawl, *Inorg. Chem.* **1973**, *12*, 2963.

[11] Selected IR absorptions (KBr pellet, $\tilde{\nu}$ [cm^{-1}]): **2**: 2350m, 2285w, 2250w, (ν(C≡N)); 956vs, 793vs, 598ms, 492m, (ν(Mo–O)); **1**: 2328m, 2295w, (ν(C≡N)); 1025vs, 520s, (ν(B–F)).

[12] The formulation of the cation as $[\mathrm{Re}_2(\mathrm{NCCH}_3)_{10}]^{4+}$ is based on the low-temperature crystal structure of **2**. Crystals of **1** and **2** lose solvent rapidly, however, when removed from the mother liquor, and appear to stabilize after axial solvent loss, that is, at $[\mathrm{Re}_2(\mathrm{NCCH}_3)_8]^{4+}$.

[13] Electrochemistry was performed at a Pt electrode and referenced to Ag/AgCl. The E_p^c and E_p^a values for the reduction at $E_{1/2} = +0.24$ V are +0.185 and +0.295, respectively. A cathodic current was observed at potentials more negative than $E_p^c = +0.295$ V; therefore the couple represents a reduction.

[14] At 350 °C, a 13.00% weight loss was observed (heating rate 1 °C min^{-1}; the calculated value for loss of 8 CH_3CN groups is 13.33% for **2** (Fig.2). Similar low-temperature loss of coordinated CH_3CN was observed for organometallic cations cocrystallized with Keggin ions, A. R. Siedle, W. B. Gleason, R. A. Newmark, R. P. Skarjune, P. A. Lyon, C. G. Markell, K. O. Hodgson, A. L. Roe, *Inorg. Chem.* **1990**, *29*, 1667; A. R. Siedle, U.S.-A 4 673 753.

[15] S. N. Bernstein, K. R. Dunbar, L. E. Pence, unpublished.

$[Ga(C_5H_5)]$: Synthesis, Identification, and Ab Initio Investigations**

By *Dagmar Loos, Hansgeorg Schnöckel,* Jürgen Gauss,** and *Uwe Schneider*

Monovalent compounds of the third main group are interesting synthetic targets in inorganic chemistry.[1] Whereas for the heavier elements gallium, indium, and thallium[2] as well as for boron[3] a series of formally monovalent compounds are well known and have been characterized in detail, the corresponding aluminum compounds have only been obtained recently in solution[4–7] and as solids.[5] Of particular interest in this context is the synthesis and crystal structural analysis of $[Al_4Cp^*_4]$, $Cp^* = C_5Me_5$,[5] which shows an Al_4 tetrahedron with each Cp* bonded η^5 to one of the aluminum atoms. Besides the tetramer, the monomer was recently obtained by warming a solution of $[Al_4Cp^*_4]$ in toluene up to 100 °C and was then identified by NMR spectroscopy.[7] The unambiguous assignment of the NMR signal was possible due to the theoretical calculation of the ^{27}Al NMR shifts. Following the successful preparation of [AlCp*], [GaCp] (**4**) was the only missing member in the series of the cyclopentadienyl compounds of the monovalent third main group elements. [InCp] and [TlCp], $Cp = C_5H_5$, were described more than 35 years ago by E. O. Fischer et al.[8] and H. Meister[9], respectively.

[*] Prof. Dr. H. Schnöckel, Dipl.-Chem. D. Loos
Institut für Anorganische Chemie der Universität
Meiserstrasse 1, D-W-8000 München 2 (FRG)
Dr. J. Gauss, Dipl.-Chem. U. Schneider
Institut für Physikalische Chemie der Universität
Kaiserstrasse 12, D-W-7500 Karlsruhe (FRG)

[**] This work was supported by the Deutsche Forschungsgemeinschaft and the Fonds der Chemischen Industrie. We thank Prof. Dr. R. Ahlrichs for his generous support and for many helpful discussions.

We report in this communication the preparation of [GaCp] (**4**), the first molecular, organometallic compound of monovalent gallium. The synthesis is achieved in an analogous way to that of the cyclopentadienylaluminum(I) compounds[5] by the reaction of a metastable solution of GaCl (**1**) in toluene/diethyl ether[10, 11] with $[MgCp_2]$ (**2**) [Eq. (a)]. Compound **3**, which precipitates in a crystalline

$$\underset{\mathbf{1}}{GaCl_{solv.}} + \underset{\mathbf{2}}{[MgCp_2]} \xrightarrow{PhCH_3/Et_2O} \underset{\mathbf{3}}{\tfrac{1}{2}[CpMgCl \cdot Et_2O]_2} + \underset{\mathbf{4}}{[GaCp]} \quad (a)$$

form at $-30\,^{\circ}C$, was characterized by an X-ray structural analysis.[12] Compound **4** is also formed if [LiCp] is used instead of magnesocene [Eq. (b)].

$$\underset{\mathbf{1}}{GaCl_{solv.}} + [LiCp] \xrightarrow{PhCH_3/Et_2O} LiCl + \underset{\mathbf{4}}{[GaCp]} \quad (b)$$

In both cases the formation of metallic gallium occurs as a side reaction. This finding corresponds to the formation of metallic indium in the synthesis of [InCp].[13]

The ^{71}Ga NMR spectra[14] of the solutions obtained from reactions (a) and (b) reveal a single signal at $\delta = -714$ with a full width at half-maximum of 250 Hz.[15] This resonance at very high field suggests by comparison with the shifts reported by H. Schmidbaur for arene complexes of monovalent gallium[2] that [Ga^{I}Cp] has been formed. The assignment is also supported by ab initio calculations, which we will discuss in the second part of this communication, and is also in agreement with NMR spectroscopic investigations of other low-valent main group cyclopentadienyl compounds. Thus, the resonances of the metal atoms of $[SnCp_2]$,[16] $[SiCp^*_2]$,[17] [AlCp*],[5, 7] and [TlCp][18] are observed at very high field compared with those of normal-valent species. As a result of the shielding effect of the Cp group, however, the ^{6}Li NMR signals of [LiCp] and its derivatives are also shifted to higher field.[19]

The isolation of pure **4** by removal of the solvent in vacuo has not been successful. At $-50\,^{\circ}C$ **4** condenses together with the solvent in the receiving flask cooled to $-196\,^{\circ}C$ and can be detected by NMR spectroscopy.[14, 20] The δ values are -714 (^{71}Ga), 106.8 (^{13}C), and 5.71 (^{1}H). Furthermore, **4** can also be detected by mass spectrometry[21] in the gas phase above the receiving flask cooled to $-70\,^{\circ}C$: at 20 eV excitation energy the signals of the highest mass are those due to monomeric **4** at m/z 134 and 136.[22] Their intensity ratio corresponds to that of the natural $^{69}Ga/^{71}Ga$ isotope distribution. By comparison of the intensities of the solvent and of the [GaCp] peak the vapor pressure of [GaCp] (**4**) at $-70\,^{\circ}C$ can be estimated to about 0.1 to 1 mbar. Thus, it is of the same order of magnitude as the partial pressures of the solvents toluene and ether used in the synthesis.

Solid, colorless **4** can be obtained if pentane is added to the condensate at room temperature. However, because of its high volatility **4** could not be isolated in a pure form free of solvent. These attempts were furthermore hampered by the photolability and the extreme air-sensitivity of **4**.

Since according to electron diffraction studies[23, 24] the monovalent metals form η^5 bonds to the cyclopentadienyl ring in the homologous monomeric compounds [TlCp] and [InCp], and since ab initio calculations predict the same bonding for [AlCp],[25] an analogous structure should be expected for [GaCp] (**4**). To confirm this expectation and to support the interpretation of the experimental results, we carried out ab initio calculations[26] for the structure of **4** as well as for its spectroscopic properties.

The structure calculated with the MP2 method[27] which explicitly considers electron correlation effects is shown in Figure 1.[28] Like the corresponding aluminum compound[29] the equilibrium structure of [GaCp] has C_{5v} symmetry. The distance of the metal atom to the center of the ring is 209.6 pm, thus only slightly greater than in [AlCp] (203.7 pm). A Mulliken population analysis[30] shows that strong π(Cp)–π(Ga) interactions are responsible for the stability as in the case of [AlCp]. Figure 2 shows a contour line diagram of the MO $7e_1$, which contains the main contributions of the π(Cp)–π(Ga) bonding.

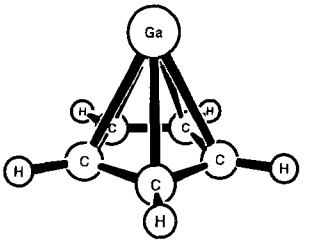

Fig. 1. Calculated structure of **4**. The geometrical parameters obtained with the MP2 method are: $r(GaC) = 242.0$, $r(CC) = 142.0$, $r(CH) = 108.7$ pm, and $\sphericalangle(HCX) = 179.7°$. X denotes the center of the Cp ring; the hydrogen atoms point away from the gallium atom.

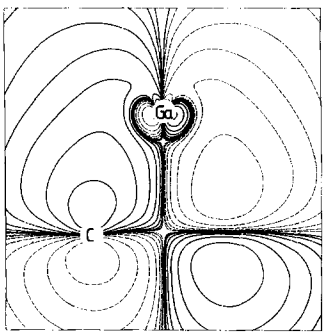

Fig. 2. Contour line diagram of the molecular orbital $7e_1$ (HOMO in e_1 symmetry), which makes the main contribution to the π(Cp)–π(Ga) bonding.

A force field calculation (analytical second derivatives of the SCF energy with respect to the nuclear coordinates) for the geometry obtained with the SCF method reveals that the calculated C_{5v} structure corresponds to a minimum on the potential hypersurface: as the calculated vibrational frequencies collected in Table 1 show, only real frequencies result for the C_{5v} structure of [GaCp] (**4**). For an IR spectroscopic characterization of **4** the frequency of the Ga–Cp stretching mode (a_1) is most significant. The calculated values of 272 cm^{-1} (SCF) and 285 cm^{-1} (MP2)[31] can serve as a reference for the IR spectroscopic identification of **4**, in particular since the calculated intensities (57.5 km mol^{-1} (SCF) and 42.1 km mol^{-1}(MP2)) indicate that the corresponding band should be relatively intense. Further confirmation of the assignment might be obtained by the detection of the $^{69}Ga/^{71}Ga$ isotopic pattern with a calculated splitting of 2 cm^{-1}.

Of particular importance for the confirmation of the experimental results given here is the calculation of the ^{71}Ga NMR shift of **4**.[32] The SCF method yields $\delta = -635$, a value which deviates by about 80 ppm from the experimental shift of $\delta = -714$, whereas the chemical shift calculated with the MP2 approach, $\delta = -696$, is in good agreement with the experiment.

Thus, the ab initio calculations support the conclusion drawn from the experiments that monomeric **4** is formed by

Table 1. Calculated IR spectra of **4** [harmonic vibrational frequencies $\tilde{\nu}$ in cm^{-1}, IR intensities I in km mol^{-1}].

Vibration	Symmetry	Characterization [a]	SCF $\tilde{\nu}$	SCF I	MP2 $\tilde{\nu}$	MP2 I
1	e_1	Ga-Cp-valence (asym.)	210	6.9		
2	a_1	Ga-Cp-valence (sym.)	272	57.5	285	42.1
3	e_2	CC-def. (out-of-plane)	649	0.0		
4	a_1	CH-def. (out-of-plane)	894	236	818	182.7
5	e_1	CH-def. (out-of-plane)	895	2.6		
6	e_2	CC-def. (in-plane)	921	0.0		
7	e_2	CH-def. (out-of-plane)	1007	0.0		
8	e_1	CC-valence (asym.)	1090	11.1		
9	e_2	CH-def. (in-plane), CC-valence (asym.)	1140	0.0		
10	a_1	CC-valence (sym.)	1203	16.8	1150	9.3
11	a_2	CH-def. (in-plane)	1390	0.0		
12	e_2	CC-valence (asym.)	1465	0.0		
13	e_1	CH-def. (in-plane), CC-valence (asym.)	1573	17.0		
14	e_2	CH-valence (asym.)	3350	0.0		
15	e_1	CH-valence (asym.)	3368	2.4		
16	a_1	CH-valence (sym.)	3381	10.8	3291	2.9

[a] valence = valence stretch, def. = deformation

the reaction of GaCl (**1**) with $[MgCp_2]$ (**2**) or [LiCp]. Furthermore, the calculations confirmed the expected C_{5v} structure with η^5 bonding between gallium and the cyclopentadienyl ring.

Experimental Procedure

A solution of **2** (1.7 mmol) in toluene (9.5 mL) was added dropwise to a dark red solution of **1** (3.0 mmol) in toluene/diethyl ether (11 mL) at −78 °C. After the solution was kept at −30 °C for 7 days, colorless, cubic crystals **3** (318 g, 95%) were separated from the yellow solution. By recondensation at ca. 10^{-2} mbar a colorless, air-sensitive solution of **4** (ca. 50%) in toluene and diethyl ether was obtained in the receiving flask at −196 °C.

Received: May 26 and 27, 1992
Revised version: 1 July, 1992 [Z 5374/5376 IE]
German version: *Angew. Chem.* **1992**, *104*, 1376

CAS Registry numbers:
1, 17108-85-9; **2**, 63757-86-8; **3**, 143345-90-8; **4**, 143332-35-8; [LiCp], 16733-97-4.

[1] P. Paetzold, *Angew. Chem.* **1991**, *103*, 559; *Angew. Chem. Int. Ed. Engl.* **1991**, *30*, 544.
[2] H. Schmidbaur, *Angew. Chem.* **1985**, *97*, 893; *Angew. Chem. Int. Ed. Engl.* **1985**, *24*, 893.
[3] See for example J. A. Morrison in *Advances in Boron and the Boranes* (*Mol. Struct. Energ.* **1988**, *5*), p. 151.
[4] M. Tacke, H. Schnöckel, *Inorg. Chem.* **1989**, *28*, 2895.
[5] C. Dohmeier, C. Robl, M. Tacke, H. Schnöckel, *Angew. Chem.* **1991**, *103*, 594; *Angew. Chem. Int. Ed. Engl.* **1991**, *30*, 564.
[6] N. Wiberg in *Frontiers of Organosilicon Chemistry* (Eds.: A. R. Bassindale, P. P. Gaspar), The Royal Society of Chemistry, Cambridge, **1991**, p. 263.
[7] J. Gauss, U. Schneider, R. Ahlrichs, C. Dohmeier, H. Schnöckel, *J. Am. Chem. Soc.*, submitted.
[8] E. O. Fischer, H. P. Hofmann, *Angew. Chem.* **1957**, *69*, 639.
[9] H. Meister, *Angew. Chem.* **1957**, *69*, 533.
[10] M. Tacke, H. Kreienkamp, L. Plaggenborg, H. Schnöckel, *Z. Anorg. Allg. Chem.* **1991**, *604*, 35.
[11] A ^{71}Ga NMR signal at $\delta = -653$ of the solution from the reaction between GaCl and $[MgCp_2^*]$ indicates the formation of [GaCp*] (D. Loos, H. Schnöckel, unpublished).
[12] C. Dohmeier, D. Fenske, D. Loos, C. Robl, H. Schnöckel, *J. Organomet. Chem.*, submitted.
[13] J. S. Poland, D. G. Tuck, *J. Organomet. Chem.* **1972**, *42*, 307.
[14] 61.0 MHz, external standard $[Ga(H_2O)_6]^{3+}$, 25 °C, Bruker AC 200.
[15] The metastable solution of GaCl in toluene/diethyl ether shows no detectable ^{71}Ga NMR signal.
[16] J. D. Kennedy, W. McFarlane in *NMR and the Periodic Table* (Eds.: R. K. Harris, B. E. Mann), Academic Press, London, **1978**, p. 342.
[17] P. Jutzi, U. Holtmann, D. Kanne, C. Krüger, R. Blom, R. Gleiter, I. Hyla-Kryspin, *Chem. Ber.* **1989**, *122*, 1629.
[18] H. Köppel, J. Dallorso, B. Walther, *Z. Anorg. Allg. Chem.* **1976**, *427*, 24.
[19] L. A. Paquette, W. Bauer, M. R. Sivik, M. Bühl, M. Feigel, P. von R. Schleyer, *J. Am. Chem. Soc.* **1990**, *112*, 8776.
[20] ^{13}C NMR: 50.3 MHz, internal standard [D_8]toluene ($\delta(C_1) = 137.5$), 25 °C, Bruker AC 200; ^1H NMR: internal standard [D_8]toluene ($\delta(CH_3) = 2.09$), Jeol GSX-270.
[21] Varian CH7 (Finnigan).
[22] Apart from the solvent peaks the fragment ions $^{69}Ga^+$, $^{71}Ga^+$, $(C_5H_5)^+$, and $(C_5H_6)^+$ were detected.
[23] S. Shibata, L. S. Bartell, R. M. Gavin, Jr., *J. Chem. Phys.* **1964**, *41*, 717.
[24] R. Blom, H. Werner, J. Wolf, *J. Organomet. Chem.* **1988**, *354*, 293.
[25] R. Ahlrichs, M. Ehrig, H. Horn, *Chem. Phys. Lett.* **1991**, *183*, 227.
[26] The ab initio calculations were carried out with the program package TURBOMOLE (R. Ahlrichs, M. Bär, M. Häser, H. Horn, C. Kölmel, *Chem. Phys. Lett.* **1989**, *162*, 165) and ACES II (J. F. Stanton, J. Gauss, J. D. Watts, W. J. Lauderdale, R.J. Bartlett, *Int. J. Quantum Chem. Symp.*, in press).
[27] C. Møller, M. S. Plesset, *Phys. Rev.* **1934**, *46*, 618. MP2 denotes the treatment of electron correlation in the second order of perturbation theory, starting from the Hartree–Fock wave function.
[28] For the geometry optimization and the calculation of the vibrational frequencies the following basis sets were used: Ga [14s10p6d/5s4p3d] with $\eta(4d) = 0.207$, Cl [10s7p1d/4s3p1d] with $\eta(d) = 0.65$, C [7s3p1d/3s2p1d] with $\eta(d) = 0.8$ and H [4s1p/2s1p] with $\eta(p) = 0.8$ (A. Schäfer, H. Horn, R. Ahlrichs, *J. Chem. Phys.*, in press).
[29] For ab initio investigations of aluminum(I) compounds see D. J. Swanton, R. Ahlrichs, *Theor. Chim. Acta* **1989**, *75*, 163; D. J. Swanton, R. Ahlrichs, M. Häser, *Chem. Phys. Lett.* **1989**, *155*, 325; U. Schneider, R. Ahlrichs, H. Horn, A. Schäfer, *Angew. Chem.* **1992**, *104*, 327; *Angew. Chem. Int. Ed. Engl.* **1992**, *31*, 353.
[30] R. Mulliken, *J. Chem. Phys.* **1955**, *23*, 1833, 2343. For the population of the 4pπ orbitals a value of 0.23 is obtained.
[31] Only the frequencies and intensities of the vibrations with a_1 symmetry were calculated with the MP2 method. The force constant matrix was determined by numerical differentiation of the analytically calculated forces.
[32] The chemical shifts were calculated with the GIAO (gauge-including atomic orbitals) method (R. Ditchfield, *Mol. Phys.* **1974**, *27*, 789), which guarantees gauge invariance by the use of explicitly field-dependent atomic orbitals. For a description of the GIAO method within the framework of the SCF approximation see K. Wolinski, J. F. Hinton, P. Pulay, *J. Am. Chem. Soc.* **1990**, *112*, 8291; M. Häser, R. Ahlrichs, H. P. Baron, P. Weiss, H. Horn, Theor. *Chim. Acta*, in press. For GIAO calculations within the framework of the MP2 approach see J. Gauss, Chem. *Phys. Lett.* **1992**, *191*, 614. In the SCF calculations the following basis sets were used: Ga [14s10p6d/8s6p4d] with $\eta(4d) = 0.2$, Cl [12s9p2d/7s6p2d] with $\delta(d) = 1.1258$ and 0.375, C [10s5p2d/6s3p2d] with $\eta(d) = 1.386$ and 0.462 as well as H [5s1p/3s1p] with $\eta(p) = 0.8$ (see ref.[28]). The basis sets in the MP2 calculations were the same as those for the geometry optimizations. In the MP2 calculations polarization functions were only used for heavy atoms. Conversion of the calculated shielding constants σ into the usual experimentally obtained relative shifts δ is possible with the experimental known value for $[GaCl_4]^-$ of $\delta = +247$.[2] As a comparison of the SCF and MP2 results shows, electron correlation effects are of no great significance for the calculation of the shielding constants of Ga in [GaCp] (**4**) $\Delta\delta = \delta(MP2) - \delta(SCF) = -18$, whereas for $[GaCl_4]^-$ the correlation correction with a value of $\Delta\delta = -78$ is no longer negligible. Calculations with different basis sets indicate that the remaining error can be estimated to approximately 20 to 30 ppm.

$[Ga_4\{C(SiMe_3)_3\}_4]$ with a Tetrahedral Ga_4 Skeleton**

By *Werner Uhl,* Wolfgang Hiller, Marcus Layh,* and *Wolfgang Schwarz*

Recently, we synthesized and determined the crystal structure of an organoelement compound with a gallium–gallium bond (**1**), which is formed in good yields by the reaction of

[*] Dr. W. Uhl, Dr. M. Layh, Dr. W. Schwarz
Institut für Anorganische Chemie der Universität
Pfaffenwaldring 55, D-W-7000 Stuttgart 80 (FRG)
Prof. Dr. W. Hiller
Anorganisch-chemisches Institut der Technischen Universität München

[**] This work was supported by the Deutsche Forschungsgemeinschaft and the Fonds der Chemischen Industrie.

readily accessible $Ga_2Br_4 \cdot 2$ dioxane[1] with four equivalents of bis(trimethylsilyl)methyllithium.[2] Because of the high stability and the planar and thus unusual molecular structure of **1**, we are trying to synthesize further derivatives, in

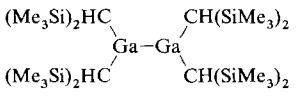

1

order to thoroughly characterize this new class of compounds. However, with sterically less demanding substituents and analogous reaction conditions disproportionation occurs exclusively with the formation of elemental gallium and gallium(III) derivatives.[3]

Tris(trimethylsilyl)methyllithium suitable for the introduction of a sterically more demanding group has so far only been described as an adduct with ethers or amines;[4] the reactions of these derivatives with the gallium(II) bromide dioxane adduct gave tris(trimethylsilyl)methane $HC(SiMe_3)_3$ as the only isolable product, which is probably formed by the reaction of the alkyllithium compound with the complex-bound solvent molecules. In contrast, when a suspension of the gallium compound in *n*-pentane was combined at $-60\,^{\circ}C$ with a solution of the ether-free Li compound recently prepared for the first time by us[5] in the same solvent, the initially colorless reaction mixture changed from yellow to pale red upon warming. After the usual workup procedures we isolated a dark red, crystalline compound, tris(trimethylsilyl)methylgallium(I) (**2**) with the gallium atom in the unusual[6] oxidation state + I which is formed by disproportionation.

The molar ratio of the starting materials of 1:3 given in Equation (a) corresponds to the setup for optimized yields; **2** is also formed as the major product by changing this ratio

$$4\ Ga_2Br_4 \cdot 2\ \text{dioxane} + 12\ LiC(SiMe_3)_3 \longrightarrow$$

$$\underset{\mathbf{2}}{[\{GaC(SiMe_3)_3\}_4]} + 12\ LiBr + 4\ \text{"}GaBr[C(SiMe_3)_3]_2\text{"}$$

in the range from 1:2 to 1:4 and is obtained as a pure substance after repeated recrystallization from *n*-pentane or toluene. As by-products we isolated a little tris(trimethylsilyl)methane as well as small quantities of the colorless 1,3-disiletane $[Me_2Si{-}C(SiMe_3)_2]_2$,[7] which is probably formed by the elimination of MeLi from $LiC(SiMe_3)_3$ or of a GaMe fragment from a corresponding gallium compound via a silaethene intermediate. Because of this side reaction the dialkylgallium bromide formulated in Equation (a) and to be expected from an ideal course of the disproportionation is not isolated; however, after the separation of the crystalline products from the mother liquor a highly viscous residue remains, which shows a large number of signals of unidentifiable compounds in the ^1H NMR spectrum.

Compound **2** is remarkably thermally stable and decomposes only above 255 °C; in the air it can be stored for several months without change. Depending on the method of characterization one of several degrees of oligomerization is determined: in the mass spectrum only the monomer with a relative intensity of 100% is detected, and the isotope pattern agrees very well with the calculated distribution of masses. Heavier fragments, such as those expected for oligomeric units, are not observed. The cryoscopic molar mass determination in benzene in the usual concentration range ($0.023\ mol\,L^{-1}$) indicates approximately a trimer, whereas with increasing dilution the dissociation increases and at $0.0014\ mol\,L^{-1}$ finally only the monomer is present. The UV/VIS spectrum shows absorptions at 252, 294, and 435 nm. On the basis of a comparison with the spectra of the bis(trimethylsilyl)methyl-substituted digallium(4) (**1**) (360 nm[2]) and diindium(4) compounds (380 nm[8]) we attribute the long-wavelength absorption to the presence of metal–metal bonds. It is exceptionally intense and, in contrast to the two other bands, only falls completely in the measurable intensity range at very high dilution, then, however, it surprisingly has the lowest extinction. Optically, this is noticeable from a change in the solution from red to pale yellow. We attribute these observations to the monomerization of **2** increasing with the dilution of the sample.

The crystal structure determination of **2** reveals an almost undistorted tetrahedral Ga_4 skeleton (Fig. 1). The molecules are disordered via a pseudo mirror plane in $x = 0.25$, which approximately coincides with a triangular face of the tetrahedron (Ga 1, Ga 2, Ga 3); nevertheless with occupation factors of 0.77 and 0.23 for the two positions a satisfactory refinement of the structural parameters[9] of the Ga_4 skeleton was possible. The Ga–Ga distances in the cluster are

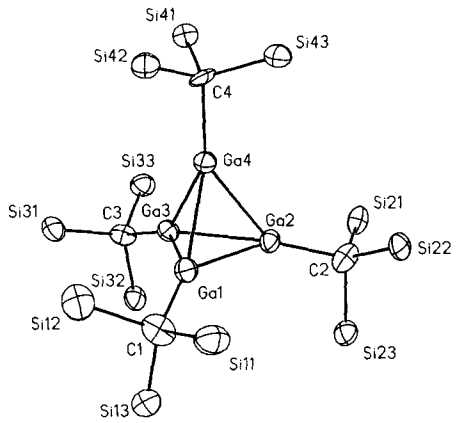

Fig. 1. Crystal structure of **2** (ellipsoids with 40% probability). For the sake of clarity the methyl groups of the $SiMe_3$ moieties were omitted from the drawing. Selected bond lengths [pm] and angles [°]: Ga1-Ga2 269.2(4), Ga1-Ga3 268.5(4), Ga1-Ga4 268.0(4), Ga2-Ga3 270.2(3), Ga2-Ga4 268.9(4), Ga3-Ga4 267.8(4), Ga1-C1 206(2), Ga2-C2 206(2), Ga3-C3 207(2), Ga4-C4 211(2); Ga-Ga-Ga 59.6(1)–60.5(1), Ga-Ga-C 143.4(6)–146.3(7).

267.8(4) to 270.2(4) pm (average: 268.8 pm); thus as expected they are approximately 15 pm longer than in the tetraalkyldigallium(4) derivative **1** with an isolated Ga–Ga bond (254.1(1) pm[2]). Analogous differences in distances (11 pm) are observed between $[Al_4Cp^*_4]$, $Cp^* = C_5Me_5$, also with a tetrahedral cluster structure (Al–Al 276.9(5) pm)[10] and the dialuminum(4) derivative isotypical to **1** with an isolated Al–Al bond (266.0(1) pm).[11] In addition the Ga–C bond lengths (average 208 pm) are significantly longer than standard values[2] and lie in the range obtained recently by our research group for bonds to bridging carbon atoms.[3] Compound **2** supplements the series of recently published tetrahedral molecules from elements of the third main group: tetra(*tert*-butyl)tetraborane(4)[12] and tetrakis(pentamethylcyclopentadienyl)tetraaluminum(4).[10] Meanwhile, we have obtained the indium compound analogous to **2** by the same method from $In_2Br_4 \cdot 2$ TMEDA and $LiC(SiMe_3)_3$.

Experimental Procedure

All operations were carried out in an atmosphere of purified argon with dried solvents.

To a suspension of $Ga_2Br_4 \cdot 2$dioxane [1] (0.79 g, 1.24 mmol) in *n*-pentane (20 mL) was added dropwise a solution of tris(trimethylsilyl)methyllithium [5] (0.89 g, 3.7 mmol) at $-60\,^{\circ}C$ in 30 mL of the same solvent. After the mixture was warmed to room temperature it was stirred for a further hour, filtered, and the red filtrate was concentrated to ca. 10 mL and cooled to $-30\,^{\circ}C$. The precipitating impurities were discarded. The mother liquor was concentrated to a few mL; at $-60\,^{\circ}C$ **2** crystallized in the form of dark red columns, mixed together with the disiletane described in the text,[7] which can be enriched by sublimation in vacuo. Following repeated recrystallizations of the crude product from *n*-pentane, cyclopentane, or toluene, pure **2** was finally obtained in a yield of 0.21 g (56%).

Decomp. (under argon): 255 °C. Molar mass (by cryoscopy in benzene) [g mol^{-1}]: obsd 848 (0.023 mol L^{-1}), 322 (0.0014 mol L^{-1}): calcd 903.9 (trimer) and 301.3 (monomer); MS (425 K, 20 eV): *m/z* 300 (M^+(monomer), 100%), 285 ($M^+ - CH_3$, 90%); ^{1}H NMR (C_6D_6, 200 MHz): $\delta = 0.51$; $^{13}C\{^1H\}$ NMR (C_6D_6, 50.32 MHz): $\delta = 7.7$ ($SiMe_3$), no signal for α-C; IR (Nujol, CsBr plates): $\tilde{\nu}$ [cm^{-1}] = 1270 m (sh), 1260 s, 1255 m (sh) δCH_3; 1030 w (br); 865 vs, 845 vs, 805 w (sh), 775 w, 730 w ρCH_3(Si); 695 vw (sh), 680 m, 660 m (sh), 655 m νSiC_3; 585 s νGaC; 460 w; UV/VIS (*n*-pentan): λ_{max} [nm] (ε) = 252 (5000), 294 (6000), 435 (2000).

Received: May 27, 1992 [Z 5377 IE]
German version: *Angew. Chem.* **1992**, *104*, 1378

CAS Registry numbers:
2, 143237-39-2; $LiC(SiMe_3)_3$, 28830-22-0; $Ga_2Br_4 \cdot 2$ dioxane, 68317-89-5.

[1] J. C. Beamish, R. W. H. Small, I. J. Worrall, *Inorg. Chem.* **1979**, *18*, 220.
[2] W. Uhl, M. Layh, T. Hildenbrand, *J. Organomet. Chem.* **1989**, *364*, 289.
[3] W. Uhl, K.-W. Klinkhammer, M. Layh, W. Massa, *Chem. Ber.* **1991**, *124*, 279.
[4] Z. H. Aiube, C. Eaborn, *J. Organomet. Chem.* **1984**, *269*, 217; C. Eaborn, P. B. Hitchcock, J. D. Smith, A. C. Sullivan, *J. Chem. Soc. Chem. Commun.* **1983**, 827; N. H. Buttrus, C. Eaborn, P. B. Hitchcock, J. D. Smith, J. G. Stamper, A. C. Sullivan, *ibid.* **1986**, 969.
[5] W. Hiller, M. Layh, W. Uhl, *Angew. Chem.* **1991**, *103*, 339; *Angew. Chem. Int. Ed. Engl.* **1991**, *30*, 324.
[6] Inorganic Ga^I derivatives: see inorganic text books; survey in [2] and [11]; W. Frank, W. Hönle, A. Simon, *Z. Naturforsch. B* **1990**, *45*, 1; M. Tacke, H. Kreienkamp, L. Plaggenborg, H. Schnöckel, *Z. Anorg. Allg. Chem.* **1991**, *604*, 35. – Complexes of arenes and Ga^I: H. Schmidbaur, *Angew. Chem.* **1985**, *97*, 893; *Angew. Chem. Int. Ed. Engl.* **1985**, *24*, 893; P. Paetzold, *ibid.* **1991**, *103*, 559 and **1991**, *30*, 544.
[7] N. Wiberg, G. Preiner, O. Schieda, *Chem. Ber.* **1981**, *114*, 2087.
[8] W. Uhl, M. Layh, W. Hiller, *J. Organomet. Chem.* **1989**, *368*, 139.
[9] Five diffraction data sets of **2** were collected for different crystals and under different conditions. They all gave the tetrahedral Ga_4 structure with approximately the Ga–Ga distances given in Figure 1; they showed, however, significantly different disorders, especially in the region of the $SiMe_3$ groups, which were in part not completely localized. The best structural model up to now is shown in Figure 1 and described in the following: $[Ga_4\{C(SiMe_3)_3\}_4]$·cyclopentane; diffractometer CAD 4; $Cu_{K\alpha}$ radiation; −60 °C; programs VAXSDP and SHELXTL; orthorhombic, $P2_12_12_1$; $a = 1361.6(3)$, $b = 1694.2(4)$, $c = 3061.5(6)$ pm; $V = 7062.3$ Å^3; $Z = 4$; crystal dimensions $0.2 \times 0.2 \times 0.3$ mm; θ–2θ scan; 4021 measured values with $F > 6\sigma(F)$; 553 parameters; $R = 0.087$. The molecule is disordered via a pseudo mirror plane in $x = 0.25$; whereas the C, Si, and Ga atoms were fully refined anisotropically for the more occupied position, for the second position this was only successful for the free apex of the tetrahedron. This was used for the optimization of the occupation factor (0.77 to 0.23). The positions of the atoms in the region of the almost common base face were each calculated anew for the less occupied position via the pseudo mirror plane; most of them could not be sensibly refined and were therefore included rigid in the calculation of the structure factors. By the use of substituents of lower symmetry it should be possible to eliminate the disorder of the almost spherical molecules **2** in the solid state. We are currently trying therefore to synthesize appropriate derivatives for a more exact structural determination. Further details of the crystal structure investigation may be obtained from the Fachinformationszentrum Karlsruhe, Gesellschaft für wissenschaftlich-technische Information mbH, D-W-7514 Eggenstein-Leopoldshafen 2 (FRG) on quoting the depository number CSD-56418, the names of the authors, and the journal citation.
[10] C. Dohmeier, C. Robl, M. Tacke, H. Schnöckel, *Angew. Chem.* **1991**, *103*, 594; *Angew. Chem. Int. Ed. Engl.* **1991**, *30*, 564; see also E. P. Schram, N. Sudha, *Inorg. Chim. Acta* **1991**, *183*, 213.
[11] W. Uhl, *Z. Naturforsch. B* **1988**, *43*, 1113.
[12] T. Mennekes, P. Paetzold, R. Boese, D. Bläser, *Angew. Chem.* **1991**, *103*, 199; *Angew. Chem. Int. Ed. Engl.* **1991**, *30*, 173.

$[V(SNC_9H_6)_3]$ and $[V(SNH_2C_6H_4)_2(SNHC_6H_4)]^-$, Homoleptic Vanadium(III) Complexes with Sulfur–Nitrogen Donor Ligands, and $[V(SNC_5H_4)_3]^-$, the First Thiolatovanadium(II) Complex**

By *Gerald Henkel,** *Bernt Krebs,* and *Wilfried Schmidt*

In the vanadium-based nitrogenases discovered only a few years ago,[1] the metal atom is bound to sulfur and probably also to nitrogen and/or oxygen atoms simultaneously.[2] In our search of useful model complexes for biologically active vanadium centers we have investigated various reactions of di- and trivalent vanadium with bifunctional chelating ligands. We[3] and others[4] have already reported the results from the reaction of VCl_3 with ethane-1,2-dithiolate. Interestingly, the dinuclear species $[V_2(SCH_2CH_2S)_4]^{2-}$ with four thiolato bridges formed in this reaction cannot be cleaved with additional thiolate to mononuclear trischelate complexes. Such a disassembly is probably unfavorable because of coulombic repulsions. Similar arguments can also be used to explain why pure homoleptic thiolato complexes of divalent vanadium have not been observed so far.

The problem of charge can be circumvented effectively when the bifunctional ligands possess a (charged) thiolate function as well as a formally uncharged donor atom.[5] We report here the synthesis and characterization of mononuclear homoleptic thiolatovanadium complexes that are stabilized by bidentate ligands with sulfur and nitrogen donor functions.

The reaction of $VCl_2 \cdot 4MeOH$[6] with sodium pyridine-2-thiolate in acetonitrile gave rise to the complex anion **1**, which could be isolated as the tetraphenylphosphonium salt **2**. In contrast, when $VCl_2 \cdot 4MeOH$ was treated with sodium aniline-2-thiolate under the same conditions, the vanadium atom was oxidized and the complex anion **3** was obtained,

$[V(SNC_5H_4)_3]^-$	**1**	$[Ph_4P][V(SNC_5H_4)_3]$	**2**
$[V(SNH_2C_6H_4)_2(SNHC_6H_4)]^-$	**3**	$[Ph_3MeP][V(SNH_2C_6H_4)_2(SNHC_6H_4)]$	**4**
$[V(SNC_9H_6)_3]$	**5**	$[V(SNC_9H_6)_3] \cdot MeCN$	**6**

the ligands of which are not protonated to the same extent. Anion **3** was crystallized as the triphenylmethylphosphonium salt **4**. The neutral complex **5** was formed in the reaction of VCl_3 with quinoline-8-thiolate and precipitated as solvate **6** from acetonitrile in the form of red-green needles.

To our knowledge, compound **2** is the first structurally characterized thiolatovanadium(II) complex (Fig. 1). The coordination environment of each of the vanadium atoms is distorted octahedral and composed of three sulfur and three nitrogen atoms of the pyridine-2-thiolato ligands. Opposite to each nitrogen is a sulfur atom from the neighboring ligand which gives rise to a *facial* arrangement of the donor atoms of the same type. The mean metal–ligand distances are 2.545 (V–S) and 2.113 Å (V–N). The three four-membered chelate rings are completely planar within the experimental error.

[*] Prof. G. Henkel
Fachgebiet Anorganische Chemie/Festkörperchemie der Universität
Lotharstrasse 1, D-W-4100 Duisburg 1 (FRG)
Prof. B. Krebs, Dr. W. Schmidt
Anorganisch-chemisches Institut der Universität
Wilhelm-Klemm-Strasse 8, D-W-4400 Münster (FRG)

[**] This research was supported by the Deutsche Forschungsgemeinschaft, the Bundesminister für Forschung und Technologie, and the Fonds der Chemischen Industrie.

The complex salt **2** forms chiral crystals (space group $P1$) from acetonitrile. The unit cell contains two symmetry-independent complex anions **1** which can be superimposed.[7] Minor differences in geometry are attributed to packing effects. The sample under investigation contained complex anions in the Λ configuration.

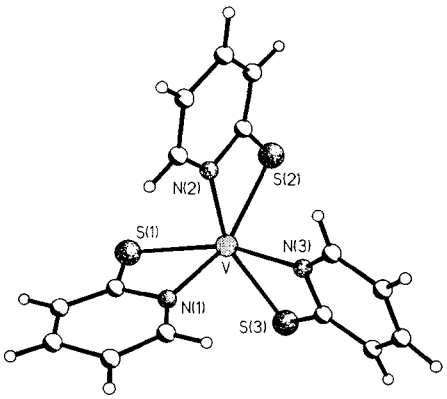

Fig. 1. The complex anion $[V(SNC_5H_4)_3]^-$ (**1**) in crystals of **2**.

In the complex anion **3** (Fig. 2), the three ligands are present in two different protonation states. Whereas two ligands have one thiolate group and a neutral amine function each, in the third ligand both the mercapto group and the amine function are deprotonated. Salt **4** is thus the first known compound in which both an electronically neutral amine function and a charged amide function are bound to the same metal center. The coordination is distorted octahedral with a *facial* arrangement of the donor atoms of particular type. As in **1**, this causes the thiolate groups of the ligands to adopt a *trans* orientation to the amine or amide groups of the neighboring ligands. The coordinated amide group is distinguished by its comparably short bond to vanadium (1.94 Å). This group also exerts a significant *trans* effect; the sulfur atom opposite to the amide group (V–S 2.508 Å) is on the average 0.090 Å further away from the vanadium center than the other two sulfur atoms (V–S 2.418 Å). The mean $V-N_{amine}$ bond is 2.18 Å in length. The complex salt **4** crystallizes in the space group $P2_1$[7] and, as in the case of **2**, with two symmetry-independent complex anions **3**. These are found as mirror images of each other so that in the crystal investigated **4** is racemic (Λ and Δ isomers).

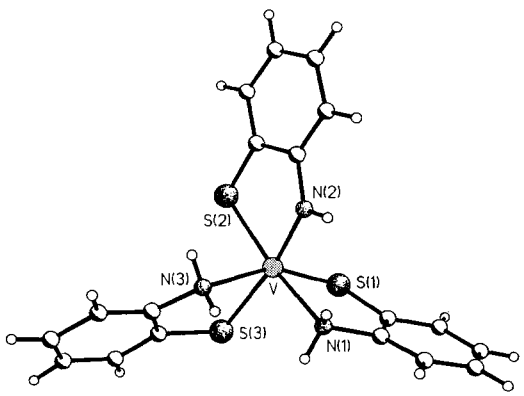

Fig. 2. The complex anion $[V(SNH_2C_6H_4)_2(SNHC_6H_4)]^-$ (**3**) in crystals of **4**.

Crystals of **6** have inversion centers and are composed of mononuclear neutral trischelate complexes **5**, which differ fundamentally from the related complex anions **1** and **3** with respect to the orientation of the donor atoms.[7] The quinoline-8-thiolato ligands are positioned so that a distorted octahedral coordination of the vanadium atom with *meridional* arrangement of the donor atoms of a particular type results (Fig. 3). Two statistically equivalent orientations of the molecule are found in the crystal; they can be superimposed exactly by a 180° rotation about the axis that passes through the middle of a S···S edge of the octahedron and through the central atom. The mean V–S and V–N bond lengths, 2.364 and 2.18 Å, respectively, fall within the range expected for single bonds.

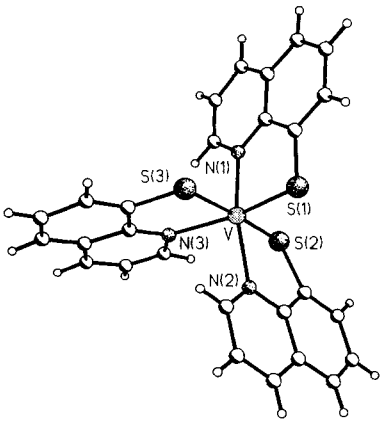

Fig. 3. The neutral trischelate complex $[V(SNC_9H_6)_3]$ (**5**) in crystals of **6**.

We have also determined the oxidation states of the vanadium atoms in the trischelate complexes **1**, **3**, and **5** directly by magnetic measurements. The susceptibilities determined fit the Curie law from 90 to 296 K. The experimental magnetic moment for complex salt **2** is $\mu_{exp} = 3.73\ \mu_B$; this value deviates only slightly from the spin-only value of divalent vanadium (d^3, $\mu_{eff} = 3.87\ \mu_B$. As anticipated, the observed magnetic moments for compounds **4** and **6**, $\mu_{exp} = 2.85$ and $2.78\ \mu_B$, respectively, are somewhat smaller. This convincingly confirms the assignment (V^{3+}, d^2, $\mu_{eff} = 2.83\ \mu_B$) made on the basis of the X-ray structure analyses.

Experimental Procedure

2: A solution of sodium (0.35 g, 15 mmol) in EtOH (25 mL) was treated with pyridine-2-thiol (1.66 g, 15 mmol) and concentrated to dryness. The residue was taken up in MeCN (10 mL), the suspension again concentrated to dryness, and finally treated again with MeCN (70 mL). To this was added $VCl_2 \cdot 4MeOH$ (1.25 g, 5 mmol); the solution turned deep violet immediately upon addition. After the reaction mixture was stirred for ca. 1 h, the small amount of a black precipitate that had formed was filtered off. The filtrate was treated with Ph_4PBr (2.10 g, 5 mmol) and kept at room temperature. After 2 d, compact, deep dark-red crystals had formed which appear black in direct light.

4: Sodium (0.4 g, 17 mmol) and aniline-2-thiol (1.57 g, 15 mmol) were dissolved in EtOH (20 mL). The solution was then concentrated to dryness, the yellow residue treated with MeCN (20 mL), the resulting suspension again concentrated to dryness, and subsequently taken up again in MeCN (70 mL). After addition of $VCl_2 \cdot 4MeOH$ (1.25 g, 5 mmol), the reaction mixture immediately became a clear, red solution. This was stirred for ca. 1 h and then filtered to remove a black precipitate. The filtrate was treated with Ph_3MePBr (1.79 g, 5 mmol) and kept at + 5 °C. Compact, dark red crystals formed in the course of a week.

6: Sodium (0.35 g, 15 mmol) and quinoline-8-thiol (2.97 g, 15 mmol) were dissolved in EtOH (25 mL). After this solution was concentrated to dryness, the resulting yellow residue was taken up in MeCN (50 mL). To this solution was added VCl_3 (0.79 g, 5 mmol), and the color of the reaction mixture changed

from yellow to red and finally to green. After the reaction mixture had been stirred for about 1 h, a black precipitate was filtered off. The filtrate was kept at −20 °C, and after a few days small, red-green needles separated from the solution.

Received: June 2, 1992 [Z 5381 IE]
German version: *Angew. Chem.* **1992**, *104*, 1380

CAS Registry numbers:
2, 143306-07-4; **4**, 143293-26-9; **6**, 143293-28-1.

[1] a) R. L. Robson, R. R. Eady, T. H. Richardson, R. W. Miller, M. Hawkins, J. R. Postgate, *Nature* **1986**, *322*, 388; b) B. J. Hales, E. E. Case, J. E. Morningstar, M. F. Dzeda, L. A. Mauterer, *Biochemistry* **1986**, *25*, 7251.

[2] a) C. D. Garner, J. M. Arber, I. Harvey, S. S. Hasnain, R. R. Eady, B. E. Smith, E. de Boer, R. Wever, *Polyhedron* **1989**, *8*, 1649; b) J. M. Arber, B. R. Dobson, R. R. Eady, S. S. Hasnain, C. D. Garner, T. Matsushita, M. Nomuras, B. E. Smith, *Biochem. J.* **1989**, *258*, 733; c) G. N. George, C. L. Coyle, B. J. Hales, S. P. Cramer, *J. Am. Chem. Soc.* **1988**, *110*, 4057.

[3] D. Szeymies, B. Krebs, G. Henkel, *Angew. Chem.* **1983**, *95*, 903; *Angew. Chem. Int. Ed. Engl.* **1983**, *22*, 885; *Angew. Chem. Suppl.* **1983**, 1176.

[4] a) J. R. Dorfman, R. H. Holm, *Inorg. Chem.* **1983**, *22*, 3179; b) R. W. Wiggins, J. C. Huffman, G. Christou, *J. Chem. Soc. Chem. Commun.* **1983**, 1313.

[5] W. Schmidt, G. Henkel, B. Krebs, *Proc. Int. Conf. Coord. Chem.* **1990**, *28*, 1–9.

[6] H. J. Seifert, T. Auel, *Z. Anorg. Allg. Chem.* **1968**, *360*, 50.

[7] Crystal structure analyses: Syntex $P2_1$ four-circle diffractometer, $Mo_{K\alpha}$ radiation ($\lambda = 0.71073$ Å), graphite monochromator, scintillation counter, 140 K, empirical absorption corrections, SHELXTL-PLUS programs, direct methods, least-squares refinement. **2**: $C_{39}H_{32}N_3PS_3V$, $M = 720.77$, triclinic, space group $P\bar{1}$, $a = 9.678(3)$, $b = 13.304(5)$, $c = 13.836(5)$ Å, $\alpha = 88.84(3)$, $\beta = 89.06(3)$, $\gamma = 85.19(3)°$, $V = 1775$ Å^3, $Z = 2$, $\rho_{calc} = 1.349$ g cm^{-3}, $\mu(Mo_{K\alpha}) = 0.53$ mm^{-1}, crystal dimensions $0.25 \times 0.18 \times 0.12$ mm, ω-2θ scan, $2\theta_{max} = 48°$, 5593 independent reflections, $R(R_w) = 0.0503$ (0.0376) for 3663 observed reflections ($I > 3\sigma(I)$), 859 variables (2 blocks), all non-hydrogen atoms anisotropic, H atoms calculated at idealized positions and fixed, isotropic temperature factors of the H atoms refined in groups, one scaling factor. **4**: $C_{37}H_{35}N_3PS_3V$, $M = 699.77$, monoclinic, space group $P2_1$, $a = 11.252(4)$, $b = 21.345(6)$, $c = 14.308(15)$ Å, $\beta = 94.91(2)°$, $V = 3424$ Å^3, $Z = 4$, $\rho_{calc} = 1.358$ g cm^{-3}, $\mu(Mo_{K\alpha}) = 0.55$ mm^{-1}, crystal dimensions $0.20 \times 0.20 \times 0.10$ mm, ω-2θ scan, $2\theta_{max} = 52°$, 4280 independent reflections, R (R_w) = 0.0540 (0.0448) for 1932 observed reflections ($I > 3\sigma(I)$), 412 variables (2 blocks), V, S, and P atoms anisotropic, N and C atoms isotropic, H atoms calculated at idealized positions and fixed, one common isotropic temperature factor was refined, one scaling factor. **6**: $C_{29}H_{31}N_4S_3V$, $M = 572.62$, monoclinic, space group $P2_1/c$, $a = 10.407(4)$, $b = 15.663(5)$, $c = 16.115(7)$ Å, $\beta = 99.91(3)°$, $V = 2588$ Å^3, $Z = 4$, $\rho_{calc} = 1.470$ g cm^{-3}, $\mu(Mo_{K\alpha}) = 0.65$ mm^{-1}, crystal dimensions $0.30 \times 0.25 \times 0.20$ mm, ω-2θ scan, $2\theta_{max} = 54°$, 5690 independent reflections, R (R_w) = 0.0775 (0.0711) for 2265 observed reflections ($I > 3\sigma(I)$), 363 variables, all non-hydrogen atoms anisotropic, H atoms calculated at idealized positions and fixed ($U_H = 0.04$ Å^{-2}), one scaling factor. Further details of the crystal structure investigation may be obtained from the Fachinformationszentrum Karlsruhe, Gesellschaft für wissenschaftlich-technische Information mbH, D-W-7514 Eggenstein-Leopoldshafen 2 (FRG) on quoting the depository number CSD-56467, the names of the authors, and the journal citation.

Novel Metal Thiolates: $[Co_2(SC_3H_7)_5]^-$, the First Complex with Face-Sharing MS_4 Tetrahedra**

By *Gerald Henkel*,* and *Stefan Weissgräber*

Transition metal complexes with thiolato ligands are a well-studied class of compounds. Not only are they important model complexes for the study of biological metal–sulfur centers,[1] but they are also suitable starting materials for the synthesis of mixed sulfido–thiolato clusters.[2]

A common feature of thiolato complexes with divalent metal atoms and sterically unemcumbered ligands is the coordination number 4; the central atom often has tetrahedral or, less frequently, square-planar coordination geometry. The latter type of coordination is generally limited to complexes with d^8 metal centers.[3] The mononuclear square-planar anions $[Cr(SCH_2CH_2S)_2]^{2-}$[4] and $[Fe(SC_6H_4S)_2]^{2-}$[5] are exceptions; both have bifunctional 1,2-dithiolato ligands.

Besides the mononuclear complexes with the general formula $[M(SR)_4]^{2-}$, metal thiolates with tetrahedral coordination also include the respective di- and tetranuclear complexes $[M_2(SR)_6]^{2-}$ and $[M_4(SR)_{10}]^{2-}$. In the dinuclear complexes the MS_4 tetrahedra are linked by common edges, in the tetranuclear ones by common vertices. Compounds with other connectivities were previously not known; even the only reported trinuclear thiolates with tetrahedral coordination, $[Hg_3(SCH_2CH_2S)_4]^{2-}$[6] and $[Hg_3(SCH_2C_6H_4CH_2S)_4]^{2-}$,[7] are constructed of either only edge-, or vertex- and edge-sharing MS_4 tetrahedra. We report here on a homoleptic thiolatocobalt(II) complex, the first compound to contain two MS_4 tetrahedra which share a face.

Cobalt(II) nitrate was treated with sodium propane-2-thiolate in methanol/DMF. After subsequent addition of tetramethylammonium chloride, a black product could be isolated, the analytical data of which was completely consistent with a complex salt of composition $[Me_4N]_2[Co_4(SC_3H_7)_{10}]$ and thus with a complex anion which adopts the adamantane-like structure. However, this initial assumption was soon questioned because of the color which is unusual for complexes of this type.

According to the results of an X-ray structure analysis,[8] the novel dinuclear compound **1** (Fig. 1 left) was formed instead under the reaction conditions described above. This complex anion differs fundamentally from other metal thiolates in the binding arrangement of its ligands.

$[Co_2(SC_3H_7)_5]^-$ **1** $[Me_4N][Co_2(SC_3H_7)_5]$ **2**

Crystals of **2** are composed of discrete complex anions **1** (idealized C_s symmetry) and Me_4N^+ cations (idealized T_d

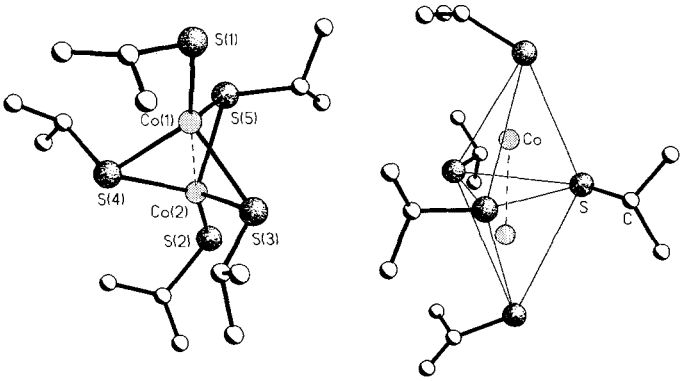

Fig. 1. Left: Structure of the complex anion **1** in the tetramethylammonium salt **2** (H atoms omitted). Important distances [Å] and angles [°]: Co(1)-Co(2) 2.491(1), Co(1)-S(1) 2.210(2), Co(1)-S(3) 2.343(2), Co(1)-S(4) 2.268(2), Co(1)-S(5) 2.293(2), Co(2)-S(2) 2.209(2), Co(2)-S(3) 2.346(2), Co(2)-S(4) 2.289(2), Co(2)-S(5) 2.303(2); S(1)-Co(1)-S(3) 123.4(1), S(1)-Co(1)-S(4) 128.5(1), S(1)-Co(1)-S(5) 115.1(1), S(3)-Co(1)-S(4) 92.9(1), S(3)-Co(1)-S(5) 93.1(1), S(4)-Co(1)-S(5) 95.7(1), S(2)-Co(2)-S(3) 123.1(1), S(2)-Co(2)-S(4) 129.6(1), S(2)-Co(2)-S(5) 115.5(1), S(3)-Co(2)-S(4) 92.3(1), S(3)-Co(2)-S(5) 92.7(1), S(4)-Co(2)-S(5) 94.8(1). Right: The metal-centered bitetrahedral Co_2S_5 framework in **1**.

[*] Prof. G. Henkel, Dipl.-Chem. S. Weissgräber
Fachgebiet Anorganische Chemie/Festkörperchemie der Universität Lotharstrasse 1, D-W-4100 Duisburg 1 (FRG)

[**] This research was supported by the Deutsche Forschungsgemeinschaft, the Bundesminister für Forschung und Technologie, and the Fonds der Chemischen Industrie.

symmetry). The separation of the cobalt atoms in the dinuclear complex is remarkably short (2.491(1) Å) and results from the unusual arrangement of the five thiolate S atoms which occupy the vertices of a trigonal bipyramid and simultaneously also surround the two metal atoms in a tetrahedral fashion (Fig. 1 right). The cobalt atoms thus occupy the centers of two sulfur tetrahedra, which have a common face (S3-S4-S5). The three bridging ligands are positioned so that the isopropyl groups have a paddlewheel-like arrangement, that is, they are symmetric with respect to a local threefold axis. Two different orientations of the complex anion are found in the crystal which are superimposable by a simple rotation. One of the orientations appears to be energetically favored with an occupancy of approximately 64%.

The two CoS_4 tetrahedra are distorted in a very characteristic manner. The ideal geometry would not only lead to very small bond angles of about 39° at the bridging sulfur atoms, but also to an unrealistically short metal–metal distance of about 1.52 Å. The observed structure results from an ideal tetrahedral arrangement when the bipyramid is stretched along the apices until the bonding angles at the bridging atoms approach the mean value of 65.4°. At the same time the Co–Co distance increases to 2.491 Å while the mean distance between the three sulfur atoms of the bridging ligands decreases to 3.362 Å. Consequently, the mean (μ-S)-Co-(μ-S) angle is also quite small (93.58°).

The Co–S bonds of the terminal thiolato ligands are not completely parallel to the Co–Co axis. The slight tilt (8.1°) gives rise to three different S-Co-(μ-S) angles (mean values 115.3, 123.2, and 129.1°). The mean lengths of the Co–(μ-S) and Co–S bonds, 2.307 and 2.210 Å, respectively (average 2.283 Å), are somewhat shorter than those in other thiolatocobalt(II) complexes; this is especially evident in the comparison with the dinuclear complex anion $[Co_2(SC_2H_5)_6]^{2-}$, in which each Co atom is bound to two terminal and two bridging thiolato ligands. The corresponding values here are 2.355 and 2.270 Å for the *syn*, and 2.363 and 2.273 Å for the *anti* conformation.[2]

The example of *syn*- and *anti*-$[Co_2(SC_2H_5)_6]^{2-}$[2] clearly illustrates that in complexes with tetrahedral CoS_4 units and monofunctional ligands, the change from edge- to face-sharing has a drastic influence on the Co–Co distance. For the *anti* isomer, this change results in an increase of 0.554 to 3.045(2) Å (+ 22.2%) relative to **1**, and for the *syn* isomer of 0.529 to 3.020(3) Å (+ 21.2%).

The situation is somewhat different for complexes that are strained as a result of specific ligand influences, for example $[Co_2(SCH_2C_6H_4CH_2S)_3]^{2-}$ with edge-sharing CoS_4 tetrahedra.[9] Here the bifunctional ligands are bound so that the central $Co_2(\mu\text{-}S)_2$ four-membered ring is significantly folded. Although the Co–Co distance is thereby reduced to 2.786(1) Å, this value is still 0.3 Å longer than in the title compound **1**.

These results show that the chemistry of complexes with thiolato ligands is much more diverse than originally assumed. We suggest that the surprising formation of units with tetrahedral coordination which have common faces is controlled by specific electronic properties of the ligands. We already have the first experimental evidence of the existence of novel iron thiolates with bitetrahedral Fe_2S_5 centers.

Experimental Procedure

All reactions were conducted in a glovebox under nitrogen.

A solution of $Co(NO_3)_2 \cdot 6H_2O$ (1.46 g, 5 mmol) in methanol (20 mL) was added dropwise to a stirred solution of sodium isopropanethiolate (1.23 g, 12.5 mmol) in methanol/DMF (20 mL, 1:1) whereby the reaction mixture turned black. After the addition of the cobalt solution was complete, the reaction mixture was treated with Me_4NCl (0.55 g, 5 mmol) and filtered. Diethyl ether (25 mL) was added to the filtrate, and the mixture was stored at −26 °C. In the course of a few days black rectangular prisms formed. Yield: 1.51 g (2.66 mmol, 53.2%). Correct C,H,N analysis. UV/VIS (MeCN): λ_{max} [nm] (ε) = 294 (4500), 332 (4900), 351 (5300), 388 (5600), 538 (500), 598 (500), 778 (300).

Received: June 6, 1992 [Z 5392 IE]
German version: *Angew. Chem.* **1992**, *104*, 1382

CAS Registry numbers:
2, 143293-41-8; Co, 7440-48-4.

[1] B. Krebs, G. Henkel, *Angew. Chem.* **1991**, *103*, 785; *Angew. Chem. Int. Ed. Engl.* **1991**, *30*, 769, and references therein.
[2] K. S. Hagen, R. H. Holm, *Inorg. Chem.* **1984**, *23*, 418, and references therein.
[3] W. Tremel, M. Kriege, B. Krebs, G. Henkel, *Inorg. Chem.* **1988**, *27*, 3886, and references therein.
[4] C. Pulla Rao, J. R. Dorfman, R. H. Holm, *Inorg. Chem.* **1986**, *25*, 428.
[5] D. Sellmann, U. Kleine-Kleffmann, L. Zapf, G. Huttner, L. Zsolnai, *J. Organomet. Chem.* **1984**, *263*, 321.
[6] G. Henkel, P. Betz, B. Krebs, *J. Chem. Soc. Chem. Commun.* **1985**, 1498.
[7] G. Henkel, P. Betz, B. Krebs, *Inorg. Chim. Acta* **1987**, *134*, 195.
[8] Crystal structure analysis: Siemens P4RA four-circle diffractometer, $Mo_{K\alpha}$ radiation (λ = 0.71073 Å), graphite monochromator, rotating anode generator, scintillation counter, 150 K, empirical absorption correction, SHELXTL-PLUS programs, direct methods, least squares refinement; $C_{19}H_{47}NS_5Co_2$, M = 567.75, monoclinic, space group $P2_1/c$, a = 10.755(3), b = 10.733(3), c = 25.957(5) Å, β = 101.60(2)°, V = 2935 Å^3, Z = 4, ρ_{calc} = 1.282 g cm^{-3}, $\mu(Mo_{K\alpha})$ = 1.47 mm^{-1}, transmission range 0.585–0.528, crystal dimensions 0.32 × 0.27 × 0.24 mm, ω scan, $2\theta_{max}$ = 54°, 6392 independent reflections, R (R_w) = 0.0533 (0.0583) for 4254 observed reflections ($I > 2\sigma(I)$), 273 variables, all non-hydrogen atoms anisotropic, H atoms fixed at idealized positions (U_H = 1.2 U_C), one scaling factor, one isotropic extinction parameter. Further details of the crystal structure investigation may be obtained from the Fachinformationszentrum Karlsruhe, Gesellschaft für wissenschaftlich-technische Information mbH, D-W-7514 Eggenstein-Leopoldshafen 2 (FRG) on quoting the depository number CSD-56492, the names of the authors, and the journal citation.
[9] W. Tremel, B. Krebs, G. Henkel, *Angew. Chem.* **1984**, *96*, 604; *Angew. Chem. Int. Ed. Engl.* **1984**, *23*, 634.

On the Mechanism of Coherent Dihydrogen Tunneling in Transition Metal Trihydrides**

By *Hans-Heinrich Limbach,* Gerd Scherer, Marcus Maurer,* and *Bruno Chaudret*

The solution ^{1}H NMR spectra of transition metal trihydrides (T) exhibit very large temperature-dependent scalar coupling constants J between the metal-bonded hydrogen atoms H_a and H_b (Fig. 1).[1–7] Zilm et al.[5] and Weitekamp et al.[6] have clearly identified this phenomenon as a mutual quantum exchange process between the two identical forms T and T*, characterized by a coherent hydrogen tunneling frequency that is directly related to the observed exchange coupling J. At high temperatures the hydrogen atoms are subject to a classical, that is, stochastic exchange process which can be characterized by a rate constant k.[3] The quantum process was treated in terms of a one-dimensional tunneling model. Since the reaction coordinate had not yet been

[*] Prof. Dr. H.-H. Limbach, Dr. G. Scherer, M. Maurer
Institut für Organische Chemie der Freien Universität Berlin
Takustrasse 3, D-W-1000 Berlin 33 (FRG)
Dr. B. Chaudret
Laboratoire de Chimie de Coordination du CNRS (UP 8241)
205, route de Narbonne, F-31077 Toulouse-Cedex (France)

[**] This work was supported by the Fonds der Chemischen Industrie. We also thank Prof. K. Zilm, Yale University, New Haven (USA) for helpful discussions of the manuscript.

discussed in detail,[6, 7] we explored different possible reaction pathways for the hydrogen motion and checked their compatibility with the experimental results.

In the one-dimensional approximation one can imagine two different reaction pathways (Fig. 1). In I the reaction

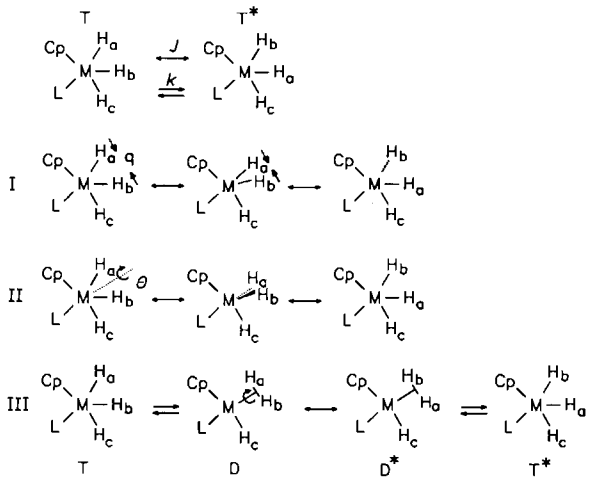

Fig. 1. Mutual hydrogen exchange in a metal trihydride complex (M = Ru, Ir, Nb; L = ligand) between the degenerate forms T and T*. J is the coherent tunnel frequency, k the classical exchange rate constant. H_b and H_c are also subject to a similar exchange process. I: The reaction coordinate corresponds to the motion of the two hydrogen atoms along their internuclear distance vector $\boldsymbol{q}$. II: The reaction coordinate corresponds to a rotation of angle θ of the internuclear distance vector around an axis in the MH_aH_b plane. III: The reaction takes place in two steps: firstly, a metastable dihydrogen complex D is formed by an activated rate process; subsequently, rotational tunneling takes place in D.

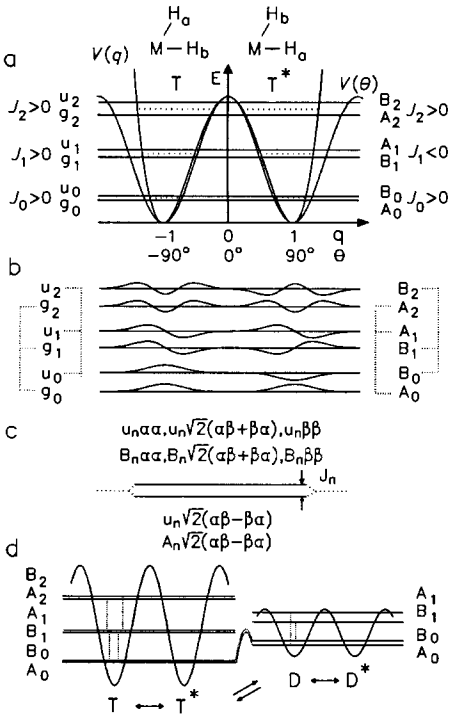

Fig. 2. a) One-dimensional potential curves $V(q)$ and $V(\theta)$ and corresponding energy eigenvalues (schematically) for the coherent hydrogen exchange according to pathways I and II. J_n is the splitting of the nth pair of states, also called exchange coupling constant. b) Eigenfunctions (schematically) of the states in Figure 2a. c) Energy level diagram and combined antisymmetric spatial and nuclear spin functions for the nth pair of states (schematically); α and β are the usual single nuclear spin functions. d) One-dimensional potential curves for pathway III.

coordinate corresponds to the internuclear H_a–H_b distance vector $\boldsymbol{q}$, and in II to the angle θ of a rotation around an axis located in the MH_aH_b plane perpendicular to $\boldsymbol{q}$. In pathway III first an intermediate dihydrogen complex D is formed by an activated rate process in which the rotation to D* takes place. The formation of D can be characterized by an equilibrium constant $K = \exp(-\Delta S/R)\exp(-\Delta H/RT)$, where ΔH is the reaction energy and ΔS the reaction entropy. Theoretical evidence for a metastable D state has been obtained recently by ab initio calculations.[8]

The eigenvalues and eigenfunctions for the double minimum potential $V(\boldsymbol{q})$ of pathway I[9] and for the periodic potential $V(\theta)$ of pathway II[10] can be calculated and are shown schematically in Figure 2. The wave functions are given in good approximation as the sum or the difference of the isoenergetic harmonic oscillator functions of the left and the right potential well. In pathway I the states are either symmetric (g) or antisymmetric (u) with respect to inversion at the center of the H_a–H_b distance vector, while in pathway II they are symmetric (A) or antisymmetric (B) with respect to the C_2 symmetry operation. It follows from Figure 2 that the energy splittings $J_n = E_{u_n} - E_{g_n}$ are always positive but that the sign of $J_n = E_{B_n} - E_{A_n}$ alternates. According to the Pauli exclusion principle the total wave function must be antisymmetric for a pair of protons. Therefore, it is necessary to combine the spatial antisymmetric with the symmetric nuclear spin states and vice versa as shown in Figure 2c[5, 6]. The diagram of Figure 2c cannot be distinguished from the energy level diagram of an ordinary scalar, coupled two-spin system in the absence of an external magnetic field,[5, 6] where the energy splitting corresponds to the magnetic scalar coupling constant J^{mag}. Therefore, the energy splitting J_n has been called exchange coupling constant.[5, 6]

Thus, the MH_aH_b group in the vibrational state n will contribute the spectral features of an ordinary AX, AB, or A_2 spin system to the ^1H NMR spectra, characterized by the effective scalar coupling constant $J_n + J^{mag}$ and the chemical shift difference $\Delta\nu_n$ between the exchanging protons.

In real proton-transfer systems the reaction barriers can change when vibrational modes that couple to the reaction coordinate are excited,[11, 12] or when the reactive system interconverts between different molecular conformations or environments.[13] In the trihydride exchange problem one can expect that the rotational barrier is greatly reduced in the dihydrogen state D as indicated schematically for pathway III in Figure 2c.

The question now arises as to how the observed exchange couplings are related to the individual exchange couplings in the different states. Generally, in polyatomic molecules, fast stochastic vibrational relaxation takes place within picoseconds,[14] which destroys coherent tunneling together with solvent relaxation on a timescale typical for NMR spectroscopy.[15] However, in the case of trihydride complexes, vibrational relaxation takes place only within the manifold of states of the same spatial symmetry[6] as indicated in Figure 2 by broken lines. Relaxation between states of different symmetry would require a conversion of nuclear spins states, which is a slow process. In addition, stochastic exchange between the trihydride form T and the dihydrogen form D in pathway III will also be faster than nuclear spin conversion. The averaging between vibrational and conformational states indicated in Figure 2b and c can be described in terms of usual dynamic NMR theory.[16] If this process is very fast, the usual signal pattern of an averaged AX, AB, or A_2 spin system will be obtained that is characterized by an averaged exchange coupling constant J. Since the different states are populated

according to the Boltzmann distribution, the average tunnel splitting J becomes a function of temperature T.

To elucidate the behavior of $J(T)$ for the different pathways we have performed numerical calculations. Some representative results are shown in Figure 3.[17] A variation of

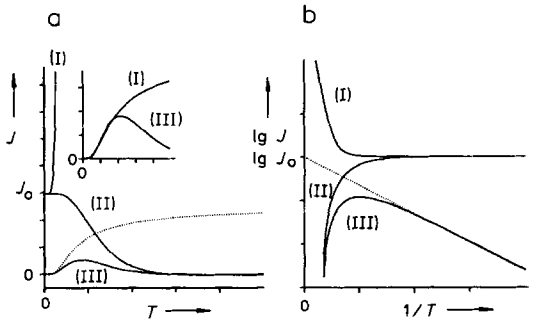

Fig. 3. Average exchange coupling constants J vs. temperature T (Fig. 3a) and lg J vs. $1/T$ (Fig. 3b) calculated [17] for pathways I to III with particular parameter sets. The broken line represents the equilibrium constant of formation of the metastable dihydrogen intermediate D from the trihydride form T. J_0 for pathways I and II were set equal to $J_{0D}\exp(-\Delta S/R)$ of pathway III.

the parameters used, namely, energy barriers, hydrogen atom distances, ΔH and ΔS values, did not seem to change the general shapes of the curves significantly. For pathway I we observe a behavior described previously:[5, 6] J is equal to J_0 at low temperatures and increases exponentially when T increases. By contrast, for the rotation pathway II J decreases as temperature is increased and eventually becomes zero. This behavior has not yet been discussed before in the trihydride case; it is, however, well known in the case of methyl group tunneling.[19] Finally, for pathway III where tunneling in the trihydride form has been neglected, first an increase of J with T is expected as the lowest lying tunneling states of D are populated and then a decrease as the higher tunneling states in D are occupied. At low temperature an Arrhenius-type equation holds for all pathways [Eq. (1)]. E_1 is the average energy of the first excited pair of vibrational states. If the

$$|J - J_0| \approx |A|\exp(-E_a/RT) \qquad (1)$$

$|A| \approx J_1$, $E_a \approx E_1$ (pathways I and II)

$|A| \approx J_{0D}\exp(-\Delta S/R)$, $E_a \approx \Delta H$, $J_0 = 0$ (pathway III)

low-temperature approximation is not valid E_1 and J_1 will be overestimated when experimental data are interpreted in terms of Equation (1). By contrast, in the case of pathway III, ΔH and $J_{0D}\exp(-\Delta S/R)$ will be underestimated. It follows from Equation (1) that pathways I and III can practically only be distinguished if either a temperature independent value of $J = J_0 \neq 0$ can be observed at low temperature or a decrease of J with increasing T at the high temperature. In order to illustrate this difficulty we have scaled the two functions in the inset of Figure 3a to each other by multiplication with an arbitrary factor.

We have plotted in Figure 4 the experimental values of lg J vs. $1/T$ for the examples that have been reported. We obtain fairly straight lines within the error limits. Since all J values increase with increasing temperature, pathway II can be rejected, but the experiments cannot distinguish unambiguously between pathway I and III, since no evidence is found either for the temperature-independent low-temperature value $J = J_0$ expected for I, or for the decrease in J at high temperature predicted for III. At high temperature J is obscured by the onset of classical stochastic exchange. The

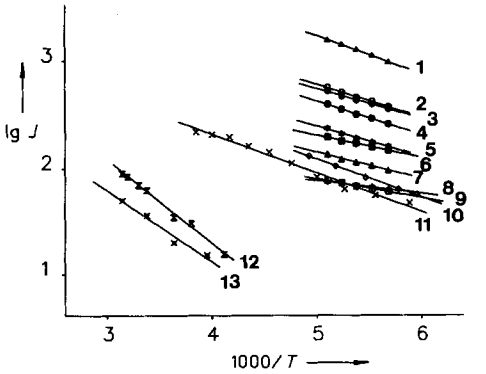

Fig. 4. Plot of the observed exchange couplings J as a function of $1/T$. The lines were calculated from the low-temperature approximation [Eq. (1)]. **1**: $[CpIrH_3(mtpb)]^+$ [5c], **2**: $[CpIrH_3AsPh_3]^+$ [5c], **3**: $[CpIrH_3P(OPh)_3]^+$ [5c], **4**: $[CpIrH_3PPh_3]^+$ [5c], **5**: $[CpIrH_3PMe_2Ph]^+$ [5c], **6**: $[CpIrH_3SbPh_3]^+$ [5c], **7**: $[CpIrH_3PMe_3]^+$ [5c], **8**: $[CpIrH_3PiPr_3]^+$ [5c], **9**: $[CpIrH_3PCy_3]^+$ [5c], **10**: $[Cp^*RuH_3(PiPr_3)]$ [2], **11**: $[\{Cp^*RuHPCy_3(\mu-H_2)\}_2Cu]PF_6$ [2] and this work; preliminary values obtained by lineshape analysis, **12**: $[Cp'_2NbH_3]$ [2], **13**: $[Cp'_2NbH_3]$ [2], $Cp' = C_5H_4SiMe_3$, $Cp'' = C_5H_3(SiMe_3)_2$, $Cp^* = C_5Me_5$, mtpb = 1-methyl-4-phospha-3,5,8-trioxabicyclo[2.2.2]octane, Cy = *cyclo*-C_6H_{11}. Parameters of the calculations for compounds **1** to **13** assuming a magnetic scalar coupling constant of $J^{mag} = -10/0/10$ Hz: E_a/kJ mol^{-1}: 6.8/6.9/6.9, 5.8/5.9/6.1, 5.2/5.4/5.5, 5.8/6.0/6.3, 5.2/5.5/5.8, 3.8/4.0/4.3, 4.3/4.7/5.2, 2.0/2.3/2.7, 3.0/3.4/4.0, 6.1/6.8/7.7, 6.3/6.9/22.1, 11.8/15.1/22, 9.4/12.9/22; $|A|$/Hz: 104000/107000/110000, 20100/21300/22800, 13200/13900/14800, 14300/15500/17100, 5900/6630/7650, 2100/2330/2600, 2050/2410/3000, 300/310/340, 540/630/780, 5050/7220/11600, 4500/5860/8400, 8800/28900/180000, 2060/6560/400000.

values of $|A|$ and E_a depend somewhat on the estimated values of the magnetic scalar coupling constant J^{mag}. We note in Figure 4 a large variation of the slopes of the curves, that is, of the E_a values, a circumstance which can easily be explained in terms of pathway III with a structural dependence of reaction enthalpies ΔH between the trihydride and the dihydrogen form. It is a little bit more difficult to explain this variation in terms of the model of pathway I, although not impossible.[5d] The latter will involve a very high barrier since the nuclei occupy the same position at $q = 0$. Therefore, in fact a combined one-dimensional inversion/rotation pathway was discussed previously[5, 6] in which the two nuclei only approach a certain minimal distance, that is, they slide along each other. This pathway would, however, need a two-dimensional description from which it could be discerned whether the tunnel splittings will alternate in sign or not as vibrational excitation occurs, that is, whether J should really increase or decrease with temperature.

In conclusion, we have proposed a novel mechanism (pathway III in Fig. 1) as an alternative origin of exchange couplings in transition metal trihydride complexes. This pathway represents the simplest model that is in agreement with the experimental observations. We hope to obtain more information on this problem by measuring the exchange couplings over a wider temperature range as well as the rate constants k of the classical exchange processes including the multiple kinetic HH/HD/DD isotope effects.[20]

Received: February 18, 1992 [Z 5196 IE]
German version: *Angew. Chem.* **1992**, *104*, 1414

[1] T. Arliguie, B. Chaudred, J. Devillers, R. Poilblanc, C. R. Acad. Sci. Ser. 2 **1987**, *305*, 1523.
[2] A. Antinolo, B. Chaudret, G. Commenges, M. Fajardo, F. Jalon, R. H. Morris, A. Otero, C. T. Schweitzer, *J. Chem. Soc. Chem. Comm.* **1988**, 1210.
[3] T. Arliguie, C. Border, B. Chaudret, J. Devillers, R. Poilblanc, *Organometallics* **1989**, *8*, 1308.
[4] R. R. Paciello, J. M. Manriquez, J. E. Bercaw, *Organometallics* **1990**, *9*, 260.

 © VCH Verlagsgesellschaft mbH, W-6940 Weinheim, 1992 0570-0833/92/1010-1371 $ 3.50+.25/0

[5] a) D. M. Heinekey, N. G. Payne, G. K. Schulte, *J. Am. Chem. Soc.* **1988**, *110*, 2303; b) D. M. Heinekey, J. M. Millar, T. F. Koetzle, N. G. Payne, K. W. Zilm, *ibid.* **1990**, *112*, 909; c) K. W. Zilm, D. M. Heinekey, J. M. Millar, N. G. Payne, P. Demou, *ibid.* **1989**, *111*, 3088; d) K. W. Zilm, D. M. Heinekey, J. M. Millar, N. G. Payne, S. P. Neshyba, J. C. Duchamp, J. Szczyrba, *ibid.* **1990**, *112*, 920; e) K. W. Zilm, J. M. Millar, *Adv. Magn. Reson.* **1990**, *15*, 163.

[6] a) D. Jones, J. A. Labinger, J. Weitekamp, *J. Am. Chem. Soc.* **1989**, *111*, 3087; b) C. R. Bowers, D. H. Jones, N. D. Kurur, J. A. Labinger, M. G. Pravica, D. P. Weitekamp, *Adv. Magn. Reson.* **1990**, *15*, 269.

[7] T. Arliguie, B. Chaudret, F. A. Jalon, A. Otero, J. A. Lopez, F. J. Lahoz, *Organometallics* **1991**, *10*, 1888.

[8] J. C. Barthelat, B. Chaudret, J. P. Dauday, Ph. De Loth, R. Poilblanc, *J. Am. Chem. Soc.* **1991**, *113*, 9896.

[9] a) P. M. Morse, E. C. G. Stückelberg, *Helv. Phys. Acta* **1931**, *4*, 337; b) R. L. Somorjai, D. F. Hornig, *J. Phys. Chem.* **1962**, *36*, 1980; c) J. Brickmann, H. Zimmermann, *Ber. Bunsenges. Phys. Chem.* **1966**, *70*, 157; d) *ibid.* **1966**, *70*, 521; e) *ibid.* **1967**, *71*, 160; *J. Chem. Phys.* **1969**, *50*, 1608; f) J. Brickmann, H. Zimmermann, *Z. Naturforsch* **1968**, *23A*, 11; g) J. Laane, *Appl Spectrosc.* **1970**, *24*, 73.

[10] a) D. Wallach, W. A. Steele, *J. Chem. Phys.* **1976**, *52*, 2534; b) National Bureau of Standards, Tables relating to Mathieu functions, Columbia University Press, New York, **1951**.

[11] J. Brickmann, *Z. Naturforsch.* **1973**, *28A*, 1759.

[12] L. Meschede, H. H. Limbach, *J. Phys. Chem.* **1991**, *95*, 10267.

[13] a) B. Wehrle, H. Zimmermann, H. H. Limbach, *J. Am. Chem. Soc.* **1988**, *110*, 7014; b) B. Wehrle, H. H. Limbach, *Chem. Phys.* **1988**, *136*, 223.

[14] J. D. McDonald, *Annu. Rev. Phys. Chem.* **1979**, *30*, 29.

[15] R. A. Harris, R. Silbey, *J. Phys. Chem.* **1983**, *78*, 7330.

[16] G. Binsch, *J. Am. Chem. Soc.* **1969**, *91*, 1304.

[17] The average value for J was calculated according to the following equation [18]:

$$J = \nu_{12} - \nu_{34},\ \nu_{ij} = \sum_n (E_n^i - E_n^j)\{\exp[-E_n^i/RT] - \exp[-E_n^j/RT]\}/\sum_n \{\exp[-E_n^i/RT] - \exp[-E_n^j/RT]\}$$

where E_n^i, $i = 1,4$ refers to the well known energy levels of the AX, AB, or A_2 two-spin system in the nth environment, here the nth pair of split states as indicated in Figure 2. As long as J is much smaller than the Zeeman energy one can show that this equation reduces to the simpler form [6]

$$J = \sum_n J_n \exp[-E_n/RT]/\sum_n \exp[-E_n/RT]$$

where E_n is the average energy of the nth pair of states. The energies were calculated according to references [9, 10] assuming three pairs of split states below the barrier.

[18] D. H. Jones, N. D. Kurur, D. P. Weitekamp, 33rd Experimental NMR Conference Asilomar, Pacific Grove, USA, **1992**, Book of Abstracts, p. 79

[19] We thank Dr. H. P. Trommsdorf (Grenoble) for pointing out the similarity with the methyl group rotational tunneling problem. See for example E. O. Stejskal, H. S. Gutowsky, *J. Chem. Phys.* **1958**, *28*, 388; S. Clough, A. Heidemann, *J. Phys. C: Solid State Phys.* **1979**, *12*, 761; J. Haupt, *Z. Naturforsch.* **1971**, *26A*, 1578; W. Müller-Warmuth, R. Schüler, M. Prager, A. Kollmar, *J. Magn. Reson.* **1979**, *34*, 83; H. Langen, A. S. Montjoie, W. Müller-Warmuth, H. Stiller, *Z. Naturforsch.* **1987**, *42A*, 1266.

[20] H. H. Limbach, *Dynamic NMR Spectroscopy in the Presence of Kinetic Hydrogen Deuterium Isotope Effects*, Chapter 2 in *NMR Basic Principles and Progress, Vol. 26*, Springer, Berlin, **1990**.

Diastereoselective Addition of Allylsilanes to Aldehydes: Synthesis of Enantiomerically Pure Homoallylic Alcohols**

By *Lutz F. Tietze,* Angelika Dölle,* and *Kai Schiemann*

Dedicated to Professor Theophil Eicher on the occasion of his 60th birthday

Homoallylic alcohols are interesting synthetic building blocks which can be prepared quite simply by the Lewis acid induced addition of allylsilanes to aldehydes.[1] Numerous procedures have been developed to allow access to these compounds in enantiomerically pure form.[2] Usually the aldehydes are converted with chiral diols into cyclic acetals, typically dioxolanes, dioxanes, dioxolanones, or dioxanones.[3, 4] Acyclic acetals have also been employed; however, poor selectivity was achieved. One negative aspect of these methods is that the acetals are frequently formed as mixtures of diastereomers which must then be purified. Chiral homoallylic alcohols may also be prepared by the reaction of aldehydes with chiral, nonracemic, allyl–metal compounds often with very good selectivities.[6]

We describe here a method for the direct and simple preparation of homoallylic ethers with excellent *de* values (> 99%) from aliphatic aldehydes and trimethylsilyl ether derivatives of chiral 1,2-aminoalcohols.

The best results were obtained with the trimethylsilyl ether of (1*R*,2*R*)-*N*-trifluoroacetylnorpseudoephedrine (**2**) (Scheme 1).[7] Two equivalents of the aldehydes **1a–g** were stirred at

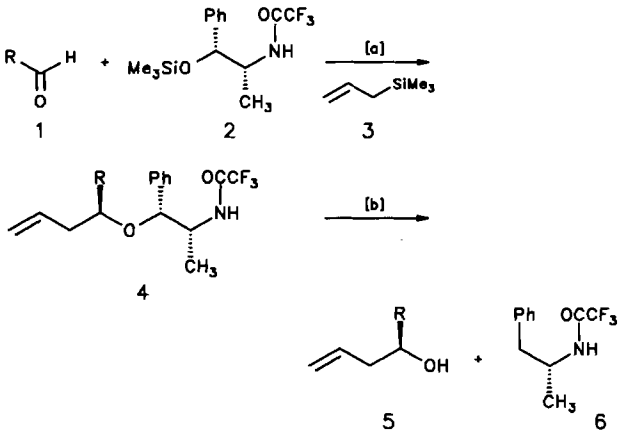

Scheme 1. Synthesis of the homoallylic alcohols **5** (R groups see Table 1). [a] CH_2Cl_2, −78 °C, 0.1 equiv TMS-OTf. After 1 h, addition of allyltrimethylsilane **3** and another 0.1 equiv TMS-OTf. [b] THF, liquid NH_3, −78 °C, 2.5 equiv sodium. After 15 min, addition of methanol.

−78 °C with one equivalent of **2** in dichloromethane in the presence of 0.1 equivalents of the trimethylsilyl trifluoromethanesulfonate (TMS-OTf) for one hour. The reaction mixture was then treated with two equivalents of allyltrimethylsilane **3** and 0.1 equivalents of TMS-OTf at −78 °C, and allowed to stir for 48 hours at this temperature. After aqueous workup and chromatography (silica gel, *tert*-butyl methyl ether/petroleum ether) the homoallylic ethers **4a–g** were obtained in total yields of 49–81% (Table 1). Side products in these reactions are the desilylated **2** (< 5%), the oxazolidine derivatives **7** (10–25%), and the acetals **8** (< 5%). If aromatic aldehydes **1h–k** are employed, the stereoselectivity is reduced (Table 1).

Application of other aminoalcohols as chiral inductors resulted in considerably lower yields and stereoselectivities. Reactions of aliphatic aldehydes with the trimethylsilyl ethers of (1*S*,2*R*)-*N*-trifluoroacetylnorephedrine and (1*S*,2*R*)-*N*-trifluoroacetylephedrine provided products with respective *de* values of 52–78, and 56–62% and respective yields of 25–

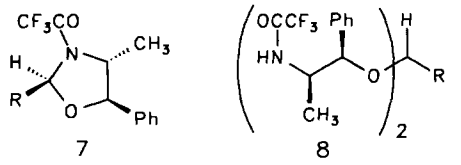

[*] Prof. L. F. Tietze, Dr. A. Dölle, Dipl.-Chem. K. Schiemann
Institut für Organische Chemie der Universität
Tammannstrasse 2, D-W-3400 Göttingen (FRG)

[**] This research was supported by the Fonds der Chemischen Industrie.

Table 1. Conversions of **1a–k**, **2**, and **3** to **4a–k** and **5a–g**.

1, 4, 5	R	4: Yield [%] [a]	*de* [%] [b]	$[\alpha]_D^{20}$ [c]	M.p. [°C] [d]	5: Yield [%]
a	CH_3	52(21)	>99 [e]	+1.5	60.2	[g]
b	CH_2CH_3	73	>99 [e]	+9.6	70.6	[g]
c	$(CH_2)_5CH_3$	81	>99 [e]	−4.2	34.3	[g]
d	$(CH_2)_7CH_3$	65	>99 [e]	−6.6	30.8	87
e	$CH(C_2H_5)_2$	71	>99 [f]	−9.7	75.8	88
f	$C(CH_3)_3$	55(31)	>99 [f]	+38.5	57.0	82
g	C_6H_{11}	49(38)	90 [f]	−5.3	73.2	90
h	$CH{=}CH{-}C_6H_5$	61	66 [f]	−133.5	94.0	0
i	C_6H_5	73	56 [f]	−108.0	84.8	0
j	C_6H_4-*m*-Br	89	82 [f]	−101.2	114.7	0
k	C_6H_4-*p*-OMe	80	96 [f]	−125.4	103.5	75

[a] Amount of recovered **2** in parentheses. [b] Determination by GC (Chromopack WOCT CP Sil 19CB, 0.22 mm × 50 m, H_2). [c] Optical rotation of **4** ($c = 1$ in chloroform). [d] Melting point of **4**, recrystallized from *tert*-butyl methyl ether/petroleum ether. [e] The major product has (*R*) configuration. [f] The major product has (*S*) configuration. [g] The alcohol in the crude reaction mixture was derivatized and then detected.

63 and 32–34%. Even worse results were obtained with aromatic aldehydes.

The homoallylic ethers **4a–g** could be converted by reductive cleavage with sodium in liquid ammonia[8] into the homoallylic alcohols **5a–g** in good yields without racemization (Table 1; THF, 2.5 equiv sodium, −78 °C, 15 min). As an additional product the enantiomerically pure amphetamine **6** was obtained which can easily be removed by distillation or chromatography (silica gel, *tert*-butyl methyl ether/petroleum ether). The homoallylic ether **4k** prepared from *p*-methoxybenzaldehyde may also be cleaved selectively to **5k** and **6**; the reductive cleavage of the homoallylic ethers **4h–j** obtained from aromatic aldehydes **1i,j** and cinnamaldehyde did not proceed as desired.

For the determination of the absolute configuration of **5**, an 87:13 mixture of the enantiomers of *ent*-**5b** and **5b** was esterified with (*R*)-(+)-α-methoxy-α-trifluoromethyl-phenylacetyl chloride, and examined by spectroscopy. The absolute configuration of the homoallylic alcohols could be deduced following Mosher's rules[9] from the positions of the signals for 2-H_2 and 4-H_2 of the ester of **5b** ($\delta = 1.61, 2.41$), and for 2-H_2 and 4-H_2 of the ester of *ent*-**5b** ($\delta = 1.69, 2.35$). The assignment was confirmed by comparison of the optical rotation of (*R*)-dodec-1-en-4-ol (**5d**) ($[\alpha]_D^{20} = +10.5$, $c = 0.65$ in CCl_4) with the literature value ($[\alpha]_D^{20} = +10.2$, $c = 3.5$ in CCl_4).[4]

The high stereoselectivity of the reaction is probably due to the selective formation of the oxazolidinium ion **9**, which is subsequently opened in an S_N2-type reaction. This hypothesis is also supported by the appearance of side product **7**; interestingly, treatment of **7** with **3** in the presence of Brönsted or Lewis acids does not lead to **4**. The low selectivity achieved

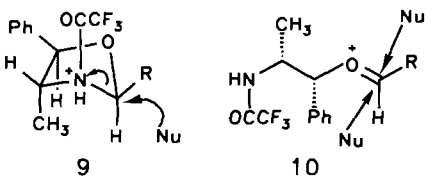

when aromatic aldehydes are employed may be explained by the existence of the acyclic oxonium ion **10**. The possible mesomerism when R is a phenyl group should make this intermediate lower in energy than when R is a alkyl group.

Received: April 11, 1992 [Z 5301 IE]
German version: *Angew. Chem.* **1992**, *104*, 1366

CAS Registry numbers:
1a, 75-07-0; **1b**, 123-38-6; **1c**, 111-71-7; **1d**, 124-19-6; **1e**, 96-17-3; **1f**, 630-19-3; **1g**, 2043-61-0; **1h**, 104-55-2; **1i**, 100-52-7; **1j**, 3132-99-8; **1k**, 123-11-5; **2**, 143143-10-6; **3**, 762-72-1; **4a**, 143143-11-7; **4b**, 143143-12-8; **4c**, 143143-13-9; **4d**, 143143-14-0; **4e**, 143143-15-1; **4f**, 143143-16-2; **4g**, 143143-17-3; **4h** (isomer 1), 143143-18-4; **4h** (isomer 2), 143234-59-7; **4i**, (isomer 1) 143143-19-5; **4i** (isomer 2), 143234-60-0; **4j** (isomer 1), 143143-20-8; **4j** (isomer 2), 143234-61-1; **4k**, 143143-21-9; **5a**, 64584-92-5; **5b**, 51795-28-9; **5c**, 143143-22-0; **5d**, 85029-09-0; **5e**, 143143-23-1; **5f**, 67760-86-5; **5g**, 94340-22-4; **5k**, 115413-90-6; (1*R*,2*R*)-norpseudoephedrine hydrochloride, 53643-20-2; methyl trifluoroacetate, 431-47-0.

[1] Reviews: J. S. Panek in *Comprehensive Organic Synthesis, Vol. 1* (Eds.: B. M. Trost, I. Fleming), Pergamon, Oxford, **1991**, pp. 579–627; I. Fleming, *Org. React. N.Y.* **1989**, *37*, 57; G. Majetich, *Org. Synth. Theory Appl.* **1989**, *1*, 173, *Organosilicon and Bioorganosilicon Chemistry: Structure, Bonding, Reactivity and Synthetic Application* (Ed.: H. Sakurai), Halsted, New York, **1985**.

[2] Reviews: D. Seebach, R. Imwinkelried, T. Weber, *Mod. Synth. Methods* **1986**, *4*, 125–259; D. Schinzer, *Janssen Chim. Acta* **1988**, *6*, 11; H. J. Altenbach, *Nachr. Chem. Tech. Lab.* **1988**, *36*, 1212–1217.

[3] D. Seebach, R. Imwinkelried, G. Stucky, *Helv. Chim. Acta* **1987**, *70*, 448–464; S. E. Denmark, N. G. Almstead, *J. Am. Chem. Soc.* **1991**, *113*, 8089–8110; W. S. Johnson, J. D. Elliot, *ibid.* **1983**, *105*, 2088–2089; J. M. McNamara, Y. Kishi, *ibid.* **1982**, *104*, 7371–7374; H. G. Howell, P. R. Brodfuehrer, C. Sapino, *J. Org. Chem.* **1985**, *50*, 2598–2600; S. F. Martin, C. Gluchowsky, C. L. Campbell, R. C. Chapman, *ibid.* **1984**, *49*, 2513–2516.

[4] D. Seebach, R. Imwinkelried, G. Stucky, *Angew. Chem.* **1986**, *98*, 182–183; *Angew. Chem. Int. Ed. Engl.* **1986**, *25*, 178.

[5] I. E. Markò, A. Mekhalfia, *Tetrahedron Lett.* **1991**, *32*, 4779–4782; S. E. Denmark, T. M. Wilson, *J. Am. Chem. Soc.* **1989**, *111*, 3475–3476; D. Seebach, R. Imwinkelried, *Angew. Chem.* **1985**, *97*, 781–782; *Angew. Chem. Int. Ed. Engl.* **1985**, *24*, 765.

[6] R. W. Hoffmann, G. Niel, A. Schlapbach, *Pure Appl. Chem.* **1990**, *62*, 1993–1998; H. C. Brown, R. S. Randad, K. S. Bhat, M. Zaidlewicz, U. S. Racherla, *J. Am. Chem. Soc.* **1990**, *112*, 2389–2392; R. O. Duthaler, M. Riediker, *Angew. Chem.* **1989**, *101*, 488–490; *Angew. Chem. Int. Ed. Engl.* **1989**, *28*, 494; E. J. Corey, C. M. Yu, S. S. Kim, *J. Am. Chem. Soc.* **1989**, *111*, 5495–5496; M. M. Midland, S. C. Preston, *ibid.* **1982**, *104*, 2330–2331.

[7] The hydrochloride of (1*R*,2*R*)-norpseudoephedrine was dissolved in methanol and treated with 1.1 equiv triethylamine. After the addition of 1.2 equiv methyl trifluoroacetate (0 °C), the reaction mixture was stirred for 15 h at room temperature. The solvent was removed completely under vacuum and the residue dissolved in dichloromethane. This solution was cooled to 0 °C, treated with 2.5 equiv triethylamine and 1.2 equiv chlorotrimethylsilane, and stirred for 15 h at room temperature. After aqueous workup the trifluoroacetylated silyl ether was purified by distillation [B.p. 78 °C (0.01 mbar); $[\alpha]_D^{20} = +16.0$ ($c = 1$ in methanol)].

[8] M. Hudlicky, *Reduction in Organic Chemistry*, Wiley, New York, **1984**, p. 82.

[9] H. A. Mosher, J. A. Dale, *J. Am. Chem. Soc.* **1973**, *95*, 512–519; H. A. Mosher, J. A. Dale, D. L. Dull, *J. Org. Chem.* **1969**, *31*, 2543–2549.

5′-*P*-Borane-Substituted Thymidine Monophosphate and Triphosphate**

By *Jeno Tomasz,* Barbara Ramsay Shaw,* Ken Porter, Bernard F. Spielvogel,** and *Anup Sood**

We describe here the synthesis and some properties of 5′-*P*-borane-substituted thymidine phosphate **5** and triphosphate **6** (boranophosphates, -triphosphates), the first nucleoside 5′-boranophosphates and -triphosphates, respec-

[*] Dr. J. Tomasz, Dr. B. R. Shaw, Dr. K. Porter
Chemistry Department, Duke University
Durham, NC 27706 (USA)
Dr. B. F. Spielvogel, Dr. A. Sood
Boron Biologicals, 533 Pylon Drive
Raleigh, NC 27606 (USA)

[**] Boron-Containing Nucleic Acids, Part 3. This research was supported by the U.S. National Institute of Health (1 R43 AI 30887-01) and the American Cancer Society (NP 741). The HPLC study by F. Huang is gratefully acknowledged. – Part 2: [2].

tively,[1] in which a negatively charged BH_3 group replaces one nonbridging O^- of a phosphate group. Boranophosphates of types **5** and **6** have charge distributions and a prochiral (**5**) or chiral (**6**) phosphorus atom analogous to those of the nucleoside 5′-thiophosphates or nucleoside 5′-*O*-(1-thiotriphosphates), respectively. Because of these similarities it has been anticipated that the boranophosphates may be useful like the thiophosphates in biochemical and molecular biological investigations. The latter have found widespread applications in the study of the stereochemistry of enzyme-catalyzed nucleotidyl- and phosphoryltransfer reactions[3] and have been successfully employed in sequencing,[4] oligonucleotide-directed mutagenesis[5] and the labeling of hybridization probes.[6] An additional pharmacological application for boranophosphates may be as carriers of ^{10}B in boron neutron capture therapy for the treatment of cancer.[7]

The crucial step in the synthesis of compounds **5** and **6** (Scheme 1) is the attachment of the BH_3 group to the phosphorus atom. This was performed at the stage of the nucleoside 5′-phosphite by using the exchange reaction[8] with an amine–borane. 3′-*O*-Acetylthymidine **1** was phosphitylated with (CEO)P(N*i*Pr$_2$)Cl[9] to give **2**. Phosphite **2** was treated in situ with excess *i*Pr$_2$EtN · BH_3. The postulated product of this reaction, phosphite · borane **3**, was not isolated but converted directly to **4** with NH_4OH. Acid hydrolysis of **4**[10] gave **5**,[11]

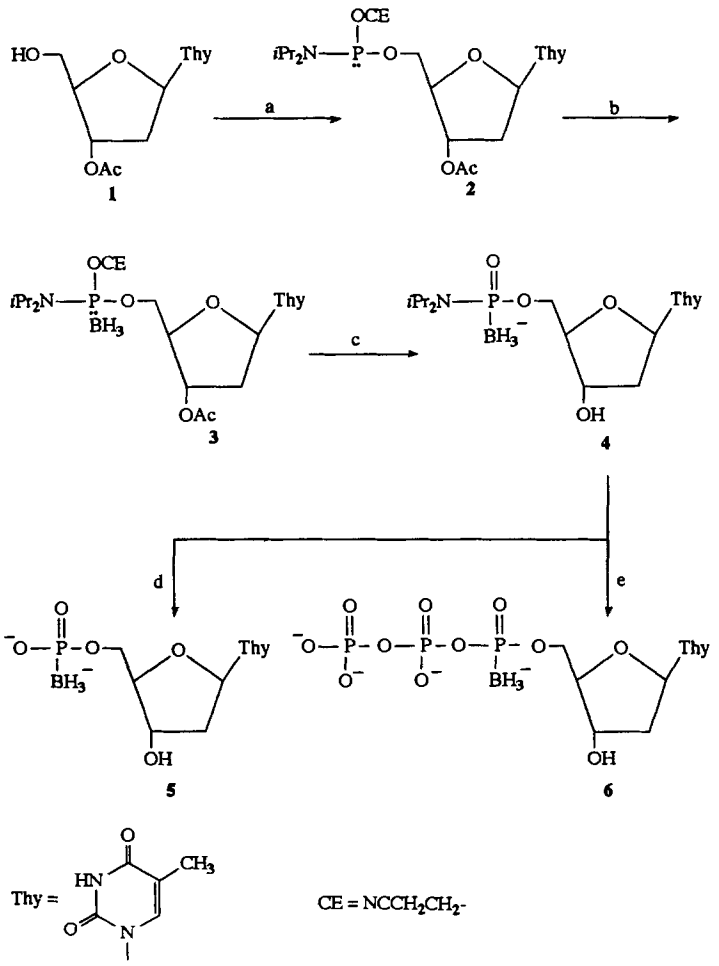

Scheme 1. Synthesis of boranophosphates **5** and **6**: a) (CEO)P(N*i*Pr$_2$)Cl, *i*Pr$_2$NEt, 4-dimethylaminopyridine, CH_3CN, 20 °C, 1 h; b) *i*Pr$_2$NEt · BH_3, 20 °C, 12 h; c) MeOH/conc. NH_4OH (1.5:1), 20 °C, 5 h; d) 0.1 M aqueous trifluoroacetic acid, 20 °C, 0.5 h; e) $(Bu_3NH)_2H_2P_2O_7$, *N*,*N*-dimethylformamide, 55 °C, 4 h.

Table 1. Selected physical data of **5** and **6** [a,b].

5: ^1H NMR: $\delta = 0.149$ (dq, $^1J(B,H) = 84.0$ Hz, $^2J(P,H) = 21.6$ Hz, 3H; BH_3), 1.787 (s, 3H; CH_3), 2.147–2.291 (m, 2H; 2′-H), 3.715–3.811 (m, 2H; 5′-H), 3.978 (unresolved, 1H; 4′-H), 4.424 (unresolved, 1H; 3′-H), 6.182 (t, $^3J(H,H) = 6.9$ Hz, 1H; 1′-H), 7.690 (s, 1H; 6-H); $^{31}P\{^1H\}$ NMR: $\delta = 79.3$ (q, $^1J(P,B) = 168$ Hz); ^{11}B NMR: $\delta = -37.9$(m); UV(H_2O): λ_{max}[nm] (ε)$_{max}$ λ_{min}-[nm] = 268 (9100) 236 (pH 2.0 and 7.0), 268 (7500) 244 [pH 11.0]; MS (electrospray ionization, 3000 V): *m/z* 321 (**5** + 3H)$^+$; DC: $R_{dTMP} = 1.25$; RP-HPLC (C_{18}, A: 0.02 M KH_2PO_4, B:CH_3CN, 0 → 25% B/5 min, 3.0 mL min^{-1}, t_R = 4.98 min).

6: ^1H NMR: $\delta = -0.249$–0.804 (2 br.m, 3H; BH_3), 1.780, 1.788 (2s, 3H; CH_3), 2.194–2.216 (m, 2H; 2′-H), 3.961–4.168 (2*m*, 3H; 4′-H, 5′-H), 4.449–4.497, 4.536–4.584 (2m, 1H; 3′-H), 6.190 (t, $^3J(H,H) = 6.7$ Hz, 1H; 1′-H), 7.571, 7.557 (2s, 1H; H-6); $^{31}P\{^1H\}$ NMR: $\delta = -21.4$ (t, $^2J(P,P) = 21.4$ Hz, 1P; P^2), −5.50 (unresolved, 1P; P^5), 82–84 (br.m, 1P; P^1); ^{11}B NMR: $\delta = -38.6$ (m, $^1J(B,P) = 137$ Hz, $^1J(B,H) = 92$ Hz); MS: *m/z* 498 (**6** + 4H + NH_4)$^+$; DC: $R_{dTTP} = 1.40$; RP-HPLC (C_{18}, A: 0.2 M triethylammonium acetate, pH = 7.5, B:methanol, 0 → 10% B/20 min, then 10% B/10 min, 4.0 mL min^{-1}, t_R = 20.91 (60%) and 24.57 (40%) min.

[a] All NMR measurements were conducted in D_2O + 0.1 M NaOD at 20 °C and 300 (^1H), 121.4 ($^{31}P\{^1H\}$, 85% H_3PO_4), or 28.7 (^{11}B, BF_3 · Et_2O) MHz. [b] Thin-layer chromatography (TLC) was performed on silica gel 60 F_{254} plates with a solvent mixture of 1-propanol/NH_4OH/H_2O (11:7:2). R_{dTMP} and R_{dTTP}: R_f values relative to dTMP and dTTP, respectively.

whereas the reaction of **4** with excess $(Bu_3NH)_2H_2P_2O_7$[12] yielded **6**.[13] Compounds **5** (52%) and **6** (30%, 3:2 mixture of phosphorus diastereoisomers according to HPLC) were isolated after ion-exchange chromatography on a QA-cellulose[HCO_3^-] column as HPLC-pure ammonium salts (Table 1).

Preliminary studies on **5** show that thymidine (dT) is the sole UV-absorbing hydrolysis product between pH 1–13. The fact that **5** does not hydrolyze to give thymidine 5′-phosphate (dTMP) reflects the stability of the P–BH_3 bond to water. Like monoalkyl phosphates that have a maximum rate of hydrolysis around pH 4,[14] **5** is least stable in the slightly acidic pH range. This suggests that the mechanism of the hydrolysis of **5** is analogous to that of the monoalkyl phosphates and proceeds via $H_3BPO_2^-$, the borane derivative of monomeric metaphosphate in the transition state.[15] At the same time, **5** is significantly more labile than monoalkyl phosphates.[16]

Acid phosphatase [EC 3.1.3.2] from sweet potato or 5′-nucleotidase [EC 3.1.3.5] from *Crotalus adamanteus* venom completely hydrolyzes **5** to dT. On the other hand, **5** is a very poor substrate or, like thymidine 5′-thiophosphate,[17] may even be an inhibitor of alkaline phosphatase [EC 3.1.3.1] from *Escherichia coli*. In accordance with the above findings, hydrolysis of triphosphate **6** by acid phosphatase or 5′-nucleotidase also gives dT, while that by alkaline phosphatase yields **5**.

Compound **6**—possibly only one of two diastereoisomers analogous to the thiotriphosphates[18]—can substitute for thymidine 5′-triphosphate (dTTP) in the extension of a deoxyribo 17-mer primer by Sequenase (modified T7 DNA polymerase) using a 25-mer template containing one 2′-deoxyadenosine residue. Extension was performed at 37 °C for 15 min with 0.1 μM primer/template and 6.5 units of the enzyme in the presence of 100 μM 2′-deoxyadenosine 5′-triphosphate, 2′-deoxycytidine 5′-triphosphate, 2′-deoxyguanosine 5′-triphosphate, and either 100 μM **6** or 100 μM dTTP. The extension products were separated by denaturing polyacrylamide gel electrophoresis. Autoradiography showed that in both cases the primer was extended to completion without any detectable pause.

These preliminary results indicate that boranophosphates may open a new chapter in nucleotide chemistry.

Received: April 22, 1992 [Z 5314 IE]
German version: *Angew. Chem.* **1992**, *104*, 1404

CAS Registry numbers:
1, 21090-30-2; **2**, 143446-82-6; **3**, 143446-86-0; **4**, 143446-83-7; **5**, 143446-84-8; **6** (*R*) isomer, 143446-85-9; **6** (*S*) isomer, 143491-59-2; iPr$_2$NEt · BH$_3$, 88996-23-0.

[1] Two short oligonucleotide derivatives of similar structure were prepared recently [2].

[2] A. Sood, B. R. Shaw, B. F. Spielvogel, *J. Am. Chem. Soc.* **1990**, *112*, 9000–9001.

[3] F. Eckstein, *Angew. Chem.* **1983**, *95*, 431–447; *Angew. Chem. Int. Ed. Engl.* **1983**, *22*, 423–439; *Annu. Rev. Biochem.* **1985**, *54*, 362–402.

[4] G. Gish, F. Eckstein, *Science* **1988**, *240*, 1520–1522; K. L. Nakamaye, G. Gish, F. Eckstein, H.-P. Vosberg, *Nucleic Acids Res.* **1988**, *16*, 9947–9959; D. B. Olsen, F. Eckstein, *ibid.* **1989**, *17*, 9613–9620.

[5] K. L. Nakamaye, F. Eckstein, *Nucleic Acids Res.* **1986**, *14*, 9679–9698; J. R. Sayers, W. Schmidt, F. Eckstein, *ibid.* **1988**, *16*, 791–802.

[6] A. T. Haase, D. Walker, L. Stowring, P. Ventura, A. Geballe, H. Blum, M. Brahic, R. Goldberg, K. O'Brien, *Science* **1985**, *227*, 189–192; S. Bahmanyar, G. A. Higgins, D. Goldgaber, D. A. Lewis, J. H. Morrison, M. C. Wilson, S. K. Shankar, D. C. Gajdusek, *ibid.* **1987**, *237*, 77–80.

[7] A. H. Soloway in *Progress in Boron Chemistry* (Eds.: H. Steinberg, A. L. McCloskey), Macmillan, New York, **1964**, p. 203.

[8] T. Reetz, *J. Am. Chem. Soc.* **1960**, *82*, 5039–5042; C. W. Heitsch, J. G. Verkade, *Inorg. Chem.* **1962**, *1*, 392–398; J. G. Verkade, C. W. Heitsch, *Inorg. Chem.* **1963**, *2*, 512–515.

[9] S. L. Beaucage, M. H. Caruthers, *Tetrahedron Lett.* **1981**, *22*, 1859–1862; T. Dorper, E.-L. Winnacker, *Nucleic Acids Res.* **1983**, *11*, 2575–2584; N. D. Sinha, J. Biernat, J. McManus, H. Koster, *ibid.* **1984**, *12*, 4539–4557; N. Usman, K. K. Ogilvie, M.-Y. Jiang, R. J. Cedergren, *J. Am. Chem. Soc.* **1987**, *109*, 7845–7854.

[10] Selected physical data of **4**. ^{1}H NMR: $\delta = -0.079$–0.739 (2 br.m, 3H; BH$_3$), 0.973, 0.981, 0.997, 1.021, 1.105, 1.127 (6s, 12H; C(CH$_3$)$_2$), 1.764, 1.772 (2s, 3H; CH$_3$), 2.142–2.244 (m, 2H; 2′-H), 3.269–3.402 (m, 2H; 5′-H), 3.720–3.795 (m, 2H; N-CH), 3.973–4.027, 4.375–4.455 (2m, 1H; 3′-H), 6.154, 6.230 (2t, ^3J(H,H) = 7.1 Hz, 1H; 1′-H), 7.481, 7.519 (2d, ^4J(H,H) = 1.0 Hz, 1H; 6-H); ^{31}P{^{1}H} NMR: δ = 92.2, 93.2 (2q, ^1J(P,B) = 147 Hz). ^{11}B NMR: $\delta = -36.8$; DC: $R_{dTMP} = 1.42$. See [a], [b] in Table 1.

[11] For the sensitivity of P–N bond toward acids, see for example: R. F. Hudson, *Structure and Mechanism in Organo-Phosphorus Chemistry*, Academic Press, New York, **1965**, p. 274; A. J. Kirby, S. G. Warren, *The Organic Chemistry of Phosphorus*, Elsevier, Amsterdam, **1967**, p. 294.

[12] J. Tomasz, *Nucleosides Nucleotides* **1983**, *2*, 63–79.

[13] Selected papers for the synthesis of nucleoside 5′-triphosphates from nucleoside 5′-phosphoramidates: J. G. Moffatt, H. G. Khorana, *J. Am. Chem. Soc.* **1961**, *83*, 649–658; J. G. Moffatt, *Can. J. Chem.* **1964**, *42*, 559–604; J. H. van Boom, R. Crea, W. C. Luyten, A. B. Vink, *Tetrahedron Lett.* **1975**, 2779–2782; J. Tomasz, A. Simoncsits, M. Kajtár, R. M. Krug, A. J. Shatkin, *Nucleic Acids Res.* **1978**, *5*, 2945–2957.

[14] J. Emsley, D. Hall, *The Chemistry of Phosphorus*, Harper & Row, London, **1976**, p. 311, and references cited therein.

[15] W. W. Butcher, F. H. Westheimer, *J. Am. Chem. Soc.* **1955**, *77*, 2420–2424; P. W. C. Barnard, C. A. Bunton, D. R. Llewellyn, K. G. Oldham, B. L. Silver, C. A. Vernon, *Chem. Ind. (London)* **1955**, 760–763; S. L. Buchwald, J. M. Friedman, J. R. Knowles, *J. Am. Chem. Soc.* **1984**, *106*, 4911–4916; J. M. Friedman, S. Freeman, J. R. Knowles, *ibid.* **1988**, *110*, 1268–1275.

[16] For example at pH 4.8 and 37 °C, **5** is completely converted to dT within 22 h, while dTMP is unchanged.

[17] F. Eckstein, H. Sternbach, *Biochim. Biophys. Acta* **1967**, *146*, 618–619.

[18] P. M. J. Burgers, F. Eckstein, *J. Biol. Chem.* **1979**, *254*, 6889–6893; P. J. Romaniuk, F. Eckstein, *ibid.* **1982**, *257*, 7684–7688.

Cationic Metallocene Polymerization Catalysts. Synthesis and Properities of the First Base-Free Zirconocene Hydride**

By *Xinmim Yang, Charlotte L. Stern,* and *Tobin J. Marks**

Growing evidence from spectroscopic studies of reactions and investigations of model compounds[1] indicates that the active components of potent[2] and highly stereoselective[3] homogenous and heterogenous olefin polymerization catalysts based on Group 4 metallocenes and Lewis acids (e.g., Al_2O_3,[4] alumoxane,[2, 5] and organoboranes[6]) are electrophilic, base-free, cation-like alkyl complexes of type **A** (M = Ti, Zr, Hf; R = alkyl).[7, 8] Since hydrogenolysis and β-hydride eliminination are essential for the molecular

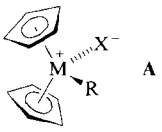

A

weight control and chain-transfer processes in metallocene-centered olefin polymerization, elucidating the presently unknown chemical and structural properties of the corresponding cationic metallocene hydrides (bis(cyclopentadienyl)-hydridometal(IV) cations) would be of great interest. We report here on the synthesis, reactivity, and structural characterization of the first base-free cationic zirconocene hydride.[9] This compound displays high electrophilicity and polymerization activity and also offers further insight into the structure and dynamics of ion-pairing in such species.

The metallocene cation **1** (Cp′ = η^5-(CH$_3$)$_5$C$_5$)[6] undergoes rapid, stepwise hydrogenolysis to yield mono- and dihydrido complexes **2** and **3**, respectively (Scheme 1). Alternatively, **3** can be prepared by hydride abstraction from **4**.[10]

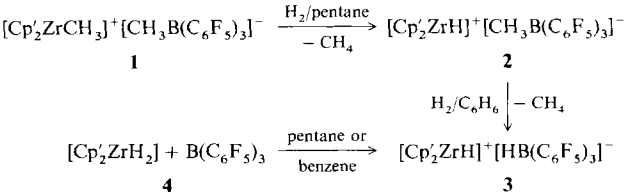

Scheme 1. Hydrogenolysis (**1** → **2** → **3**) and hydride abstraction (**4** → **3**) as routes to the cationic hydrido complexes **2** and **3**.

Complexes **2** and **3** were characterized by standard spectroscopic and analytical techniques (see Experimental Procedure). In the ^{1}H NMR spectra, the downfield shifts of the Zr–H resonances (δ = 7.70 (**2**), 8.18 (**3**) vs. δ = 7.46 (**4**)) are particularly instructive. The signal of the B-bound H atom in **2** exhibits the expected broadening due to the ^{11}B quadrupole,[11] and any Zr–H/B–H exchange processes at 0 °C are slow on the NMR timescale. Very high electrophilicity is evidenced by the facile Zr–H/C–D exchange reactions exhibited by **2** and **3** in deuterated aromatic solvents ($t_{1/2}$ for the disappearance of the Zr–H signal is ca. 12 h and 6 min, respectively, in C$_6$D$_6$). In the IR spectra (Nujol mulls), the $\tilde{\nu}_{Zr-H}$ modes of the cationic hydrides are shifted to higher frequencies: **2**, $\tilde{\nu}_{Zr-H}$ = 1642 ($\tilde{\nu}_{Zr-D}$ = 1174) and **3**, $\tilde{\nu}_{Zr-H}$ = 1663, 1604 cm^{-1}.[12] The analogous values for **4** and [Cp′$_2$Zr(H)(O*t*Bu)][10] are 1555 and 1582 cm^{-1}, respectively.

The crystal structure of **3** (Fig. 1)[13] consists of a [Cp′$_2$ZrH]$^+$ ion with a "bent-sandwich" structure (unexceptional metrical parameters)[6, 10a, 14] weakly coordinated to a [HB(C$_6$F$_5$)$_3$]$^-$ ion. The most interesting aspect of the ion-pairing is the non-involvement of the B–H functionality (a priori, structure **B** might be anticipated based upon several known examples of **C**[6, 14]). The reason appears to be a combination of steric and electronic factors, with the latter involving weak, but nonnegligible Zr···F–C interactions.[15] Thus, the Zr–F separations here (Zr–F1 = 2.416(3)

[*] Prof. T. J. Marks, Dr. X. Yang, C. L. Stern
Department of Chemistry, Northwestern University
Evanston, IL 60208-3113 (USA)

[**] This work was supported by the Division of Chemical Sciences, Office of the Basic Energy Sciences, Office of Energy Research, U.S. Department of Energy (Grant DE-FG02-86ER13511) and by Akzo Chemicals.

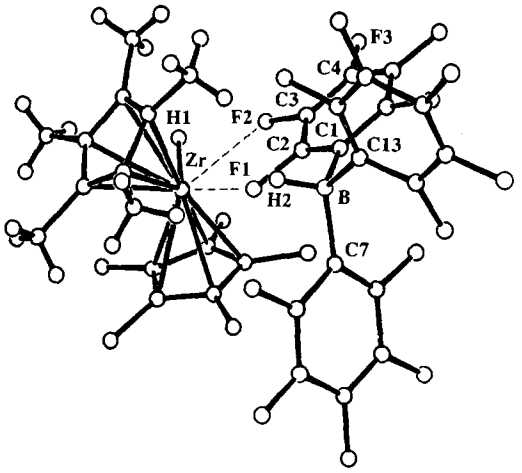

Fig. 1. Molecular structure of **3**. Important distances [Å] and angles [°]: Zr-H1 2.00(5), Zr-H2 4.87(5), Zr-F1 2.416(3), Zr-F2 2.534(3), B-H2 1.06(6); H2-B-C1 104(3), H2-B-C7 109(3), H2-B-C13 105(3), C1-B-C7 112.9(4), C1-B-C13 111.9(4), H1-Zr-F1 128(1), H1-Zr-F2 65(1). Only one of the two possible orientations of the disordered Cp′ ring is shown.

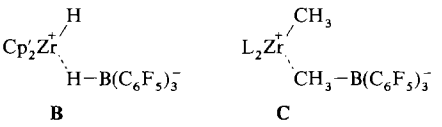

B **C**

L = Cp′, 1,2-$(CH_3)_2C_5H_3$

and Zr–F2 = 2.534(3) Å) can be compared to those in Cp_2ZrF_2 (1.98(1) Å)[16] and in the cation in **5** (2.108(2) and 2.118(2) Å).[14] A small but significant elongation in the C2–F1 separation (1.396(5) Å) versus C–F_{av} (1.354(4) Å) is also evident. The boron valence angles are approximately tetra-

$[Cp'_2Zr(CH_3)(\mu\text{-}F)Zr(CH_3)Cp'_2]^+[CH_3B(C_6F_5)_3]^-$ **5**

hedral. Interestingly, the ^{19}F NMR spectrum of **3** at −75 °C is consistent with the symmetry found in the solid state (Fig. 1); however, as the temperature is increased to −20 °C rapid exchange of the fluorine sites within the rings and between the rings is observed.

Compounds **2** and **3** are active homogenous catalysts for olefin polymerization. Ethylene polymerization proceeds rapidly at 25 °C/1 atm to yield linear (by NMR)[17] polyethylene ($M_w = 4.34 \times 10^5$; $M_n = 1.54 \times 10^5$ by gel permeation chromatography (GPC)). The turnover rate N_t is approximately 32 s^{-1} (3.2×10^6 g polyethylene (mol Zr)$^{-1}$ h^{-1} atm^{-1}). Propylene polymerization proceeds at 0 °C in toluene to yield atactic (by ^{13}C NMR)[17] polypropylene ($M_w = 3900$; $M_n = 2500$ by GPC) with $N_t \approx 2.1$ s^{-1} (3.2×10^5 g polypropylene (mol Zr)$^{-1}$ h^{-1}); analysis of the end groups of the polypropylene by ^1H and ^{13}C NMR spectroscopy indicates 90% vinyl/isopropyl and 10% vinylidene/*n*-propyl structures. Both the kinetic data and product microstructures are therefore comparable to those associated with $[Cp'_2Zr(CH_3)_2]$/methylalumoxane catalysts.[2, 6, 18]

These results afford the first picture of the properties of base-free zirconocene hydrides. Noteworthy are the electrophilicity, polymerization activity, and the presence of ion-pairing effects not based on bridging hydrogen atoms.

Experimental Procedure

All operations involving air- and moisture-sensitive complexes were carried out under rigorously anhydrous and anaerobic conditions.

2: $Cp'_2Zr(CH_3)_2$ (82 mg, 0.21 mmol) and $B(C_6F_5)_3$ (123 mg, 0.24 mmol) were transferred into a 25 mL reaction flask. Pentane (15 mL) was condensed in at −78 °C. The flask was then backfilled with 1 atm of H_2. The suspension was stirred at −78 °C for 2 h, then at 25 °C for 15 h. It was filtered, and the product, a light yellow solid, was collected, washed with pentane, and dried under vacuum. Yield, 80%. ^1H NMR (300 MHz, C_6D_6, 25 °C): δ = 7.70 (s, 1H; ZrH), 1.48 (s, 30H; Cp′), 0.10 (br. s, 3H; BCH_3); ^{19}F NMR (282 MHz, C_6D_6, 25 °C); δ = −132.94 (d, ^3J = 22.6 Hz, 6F; *o*-F), −159.80 (t, ^3J = 20.6 Hz, 3F; *p*-F), −176.02 (m, 6F; *m*-F); IR (Nujol): $\tilde{\nu}$ [cm^{-1}] = 1642 (Zr-H), 1174 (Zr-D). Correct C,H analysis.

3: Procedure A: A procedure similar to that for **2** was employed except the reaction was carried out in benzene (in which **2** is soluble). Procedure B: $[Cp'_2ZrH_2]$ (150 mg, 0.41 mmol) and $B(C_6F_5)_3$ (230 mg, 0.45 mmol) were allowed to react in 15 mL of toluene in a 25 mL flask at −78 °C for 0.5 h, then at 25 °C for 1 h. The resulting solution was filtered. Pentane (25 mL) was condensed onto the toluene filtrate resulting in the formation of yellow powdery product which was then isolated by filtration, washed with pentane, and dried under vacuum. Yield, 75%. ^1H NMR (300 MHz, [D_8]toluene, 0 °C): δ = 8.18 (s, ZrH), 3.98 (br, d, BH), 1.50 (s, Cp′); ^{19}F NMR (282 MHz C_6D_6, 25 °C): δ = −137.08 (br. s, 6F; *o*-F), −160.75 (t, $^3J \approx 20.6$ Hz, 3F; *p*-F), −168.36 (br. s, 6F; *m*-F); IR (Nujol): $\tilde{\nu}$ [cm^{-1}] = 1663, 1604 (Zr-H), 2364 (B-H). Correct C, H analysis.

Ethylene and propylene polymerizations were carried out using procedures described previously[6,19]. In a typical ethylene polymerization experiment, a solution of **3** (7.5 mg in 5 mL of toluene) was quickly injected with a gas-tight syringe equipped with a spraying needle into a 250 mL flask containing 50 mL of toluene which was rapidly stirring (and pre-saturated) under 1 atm of rigorously purified ethylene. The reaction was quenched with CH_3OH after a short time period (78 s) at which point copious amounts of polymer precipitated. Polymer was collected using standard procedures yield 0.61 g. In a typical propylene polymerization experiment, a flame-dried quartz pressure tube was charged with 7.5 mg of **3** together with 4 mL of toluene and 10–15 mL of rigorously purified liquid propylene. After 2 h of vigorous stirring at 0 °C, unreacted monomer was vented. Polymeric product was collected using standard procedures; yield 5.5 g. Polymerization experiments conducted on a larger scale (1 L reactor) and for longer durations gave similar polymerization activities[20].

Received: April 22, 1992 [Z 5317 IE]
German version: *Angew. Chem.* **1992**, *104*, 1406

CAS Registry numbers:
1, 133445-52-0; **2**, 143565-17-7; **3**, 143565-18-8; **4**, 61396-34-7; $[Cp'_2Zr(CH_3)_2]$, 67108-80-9; $B(C_6F_5)_3$, 1109-15-5; ethylene, 74-85-1; propylene, 115-07-1.

[1] T. J. Marks, *Acc. Chem. Res.* **1992**, *25*, 57–65, and references therein.
[2] a) H. Sinn, W. Kaminisky, *Adv. Organomet. Chem.* **1980**, *18*, 99–149; b) W. Kaminisky, M. Miri, H. Sinn, R. Woldt, *Makromol. Chem. Rapid Commun.* **1983**, *4*, 417–421; c) L. Resconi, S. Bossi, L. Abis, *Macromolecules* **1990**, *23*, 4489–4491, and references therein.
[3] a) W. Kaminisky, K. Külper, H. H. Brintzinger, F. R. W. P. Wild, *Angew. Chem.* **1985**, *97*, 507–508; *Angew. Chem. Int. Ed. Engl.* **1985**, *24*, 507–508, and references therein; b) L. Resconi, R. M. Waymouth, *J. Am. Chem. Soc.* **1990**, *112*, 4953–4954. c) J. A. Ewen, M. J. Elder, R. L. Jones, L. Haspeolagh, J. L. Atwood, S. G. Bott, K. Robinson, *Makromol Chem. Macromol. Symp.* **1991**, *48/49*, 253–295, and references therein.
[4] K.-H. Dahmen, D. Hedden, R. L. Burwell, Jr., T. J. Marks, *Langmuir* **1988**, *4*, 1212–1214.
[5] a) C. Sishta, R. Hathorn, T. J. Marks, *J. Am. Chem. Soc.* **1992**, *114*, 1112–1114; b) E. Giannetti, G. M. Nicoletti, R. Mazzocchi, *J. Polym. Sci. Chem. Ed.* **1985**, *23*, 2117–2133.
[6] a) X. Yang, C. Stern, T. J. Marks, *J. Am. Chem. Soc.* **1991**, *113*, 3623–3625; b) J. A. Ewen, M. J. Elder, CA-A 2027145, **1991**; *Chem. Abstr.* **1991**, *115*, 136998g.
[7] a) R. F. Jordan, *Adv. Organomet. Chem.* **1991**, *32*, 325–387, and references therein; b) M. Bochmann, A. J. Jaggar, *J. Organomet. Chem.* **1992**, *424*, C5-C7, and references therein; c) J. J. Eshuis, Y. Y. Tan, J. H. Teuben, J. Renkema, *J. Mol. Catal.* **1990**, *62*, 277; d) G. G. Hlatky, H. W. Tuner, R. R. Eickman, *J. Am. Chem. Soc.* **1989**, *111*, 2728–2729; e) H. W. Turner, G. G. Hlatky, EP-B 277004, **1988**; *Chem. Abstr.* **1989**, *110*, 58290a; f) R. Taube, L. Krukowa, *J. Organomet. Chem.* **1988**, *347*, C9; g) Z. Lin, J.-F. L. Marechal, M. Sabat, T. J. Marks, *J. Am. Chem. Soc.* **1987**, *109*, 4127–4129.
[8] a) J. J. Eisch, K. R. Caldwell, S. Werner, C. Krüger, *Organometallics* **1991**, *10*, 3417–3419; b) P. G. Gassmann, M. R. Callstrom, *J. Am. Chem. Soc.* **1987**, *109*, 7875–7876; c) J. J. Eisch, A. M. Piotrowski, S. K. Brownstein, E. J. Gabe, F. L. Lee, *ibid.* **1985**, *107*, 7219–7200; d) F. S. D'yachkovskii, A. K. Shilova, A. Y. Shilov, *J. Polym. Sci. Part C Polym. Symp.* **1967**, 2333-2339; e) D. S. Breslow, N. R. Newburg, *J. Am. Chem. Soc.* **1957**, *79*, 5072.
[9] For the synthesis of hydrido complexes stabilized by coordination to Lewis bases see a) R. F. Jordan, C. S. Bajgur, W. E. Dasher, A. L. Rheingold *Organometallics* **1987**, *109*, 1041–1051; b) R. J. Jordan, R. E. LaPointe, P. K. Bradley, N. Baenziger, *ibid.* **1989**, *8*, 2892–2903; c) R. B. Grossman, R. A. Doyle, S. L. Buchwald, *ibid.* **1991**, *10*, 1501–1506.

[10] a) L. E. Schock, T. J. Marks, *J. Am. Chem. Soc.* **1988**, *110*, 7701–7715 b) J. M. Manriquez, D. R. McAlister, R. D. Sanner, J. E. Bercaw, *ibid.* **1978**, *100*, 2716.
[11] a) H. Nöth, B. Wrackmeyer, *Nuclear Resonance Spectroscopy of Boron Compounds* in *NMR, Principles and Progress Vol. 14*, (Eds.: P. Diehl, E. Fluck, R. Kosfeld), Springer, Berlin, **1978**, Chapters 4 and 7; b) T. J. Marks, J. R. Kolb, *Chem. Rev.* **1977**, *77*, 263–293.
[12] Two equally intense $\tilde{\nu}_{Zr-H}$ modes are observed, presumably a consequence of the Cp′ rotamers [13] and/or correlation field effects.
[13] Crystal structure analysis of **3**: $ZrF_{15}C_{38}BH_{32}$; monoclinic, space group $P\bar{1}$ (No. 2), $a = 11.899$ (4), $b = 12.643$ (4), $c = 13.681$ (4) Å, $\alpha = 84.47$ (2), $\beta = 76.12$ (3), $\gamma = 65.34$ (3)° at −120 °C; $V = 1816$ (2) Å^3; $\varrho_{calcd} = 1.601$ g/cm^3; $Z = 2$. Data were collected on an Enraf-Nonius CAD-4 diffractometer ($Mo_{K\alpha}$ radiation, $\lambda = 0.71069$ Å, $2\theta = 48.9°$). The structure was solved by a combination of Patterson and direct methods (SHELXS 86) using 5136 reflections with $I > 3.00\sigma(I)$. Hydrogen atoms on Zr and on B atoms were located on the electron density map and refined. One of the Cp′ rings was disordered with site occupancy refining to 59% and the other to 41%. The non-hydrogen atoms were refined anisotropically (Texsan) except for the carbon atoms of the disordered Cp′ ring which were refined isotropically; $R = 0.060$, $R_w = 0.082$. Further details of the crystal structure investigation are available on request from the Director of the Cambridge Crystallographic Data Centre, University Chemical Laboratory, Lensfield Road, GB-Cambridge CB2 1EW (UK), on quoting the full journal citation.
[14] $[Cp'_2ZrCH_3]^+[CH_3B(C_6F_5)_3]^-$, $[Cp'_2Zr(CH_3)(\mu\text{-}F)Zr(CH_3)Cp'_2]^+$ $[CH_3B(C_6F_5)_3]^-$ (**5**): X. Yang, Ph.D. Thesis, Northwestern University, 1991.
[15] For another example where weak coordination of a fluoroarylborate counterion was detected by NMR, see: A. D. Horton, A. G. Orpen, *Organometallics* **1991**, *10*, 3910–3918.
[16] M. A. Bush, G. A. Sim, *J. Chem. Soc. A* **1971**, 2225.
[17] a) F. A. Bovey, *Chain Structure and Confirmation of Macromolecules*, Academic Press, New York, **1982**, pp. 78–91; b) A. E. Tonelli, *NMR Spectroscopy and Polymer Microstructure*, VCH Publishers, New York, **1989**.
[18] L. Resconi, F. Piemontesi, G. Franciscono, L. Abis, T. Fiorani, *J. Am. Chem. Soc.* **1992**, *114*, 1025–1032.
[19] G. Jeske, H. Lauke, H. Mauermann, P. N. Sweptson, H. Schumann, T. J. Marks, *J. Am. Chem. Soc.* **1985**, *107*, 8091–8103.
[20] G. M. Smith (Akzo Chemicals), private communication.

The Formation of *cyclo*-P_4 Ligands with Maximum Electron Donor Ability**

By *Manfred Scheer,** *Christa Troitzsch*, and *Peter G. Jones*

The transformation of the P_4 tetrahedron **A** to the *cyclo*-P_4 **B** is observed for the reaction of white phosphorus with carbonyl chromium and carbonyl tungsten complexes.[1] The *cyclo*-P_4 ligand in the $[(CO)_4M\{\eta^4\text{-}P_4[M(CO)_5]_4\}]$ (M = Cr or W) formed has twelve valence electrons (VE) available for the overall complex. The question of the mechanism of the transformation of **A** into **B** is answered by the results of the three-component reaction (a) of P_4 and $[RhCp'(CO)_2]$ ($Cp' = \eta^5\text{-}C_5H_4t\text{Bu}$) in the presence of $[Cr(CO)_5(thf)]$[2] at 60–70 °C.

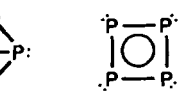

A B

The tetraphosphane complexes **1** and **2** are formed by the reaction (a); with a large excess of $[Cr(CO)_5(thf)]$ **2** is formed exclusively. Compound **2** can also be obtained by the thermolysis of **1**.

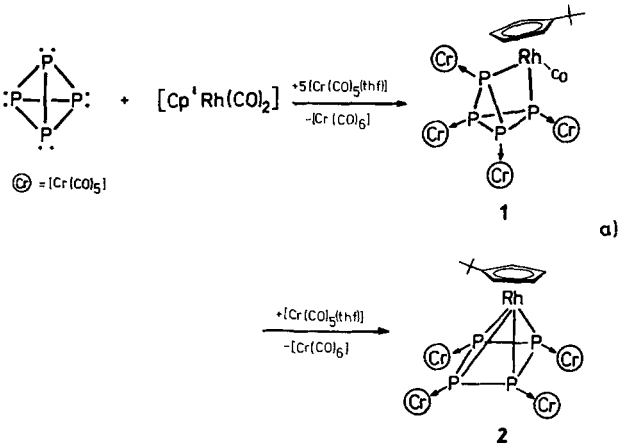

Compound **1** forms black platelets and **2** red needles which are readily soluble in CH_2Cl_2, moderately soluble in benzene, and slightly soluble in *n*-pentane. Both compounds can be handled in the air for a short period of time. Their solutions also only decompose in the air after quite a long time (ca. 30 min).

Compounds **1** and **2** were characterized by NMR and IR spectroscopy as well as by mass spectrometry.[6]

The crystal structural analysis of **1**[7] (Fig. 1) reveals two independent molecules with very similar structural parameters. Compound **1** contains a tetraphosphabicyclobutane ligand, an open-edged P_4 tetrahedron, which is bound along its open P–P edge to a [RhCp′(CO)] complex fragment. All the P atoms are also coordinated via their lone pairs to $[Cr(CO)_5]$ complex fragments. The P···P distance of the

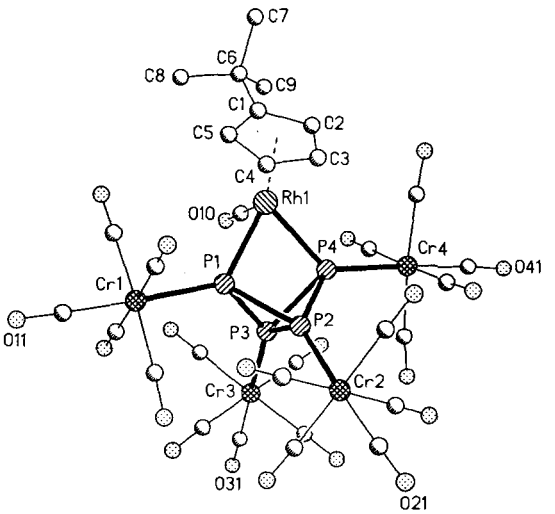

Fig. 1. Crystal structure of **1** (only one of the two independent molecules is shown).

[*] Dr. M. Scheer,[+] C. Troitzsch
Institut für Allgemeine und Anorganische Chemie der Universität
Weinbergweg 16, D-O-4050 Halle (Saale) (FRG)
Prof. Dr. P. G. Jones
Institut für Anorganische
und Analytische Chemie der Technischen Universität
Hagenring 30, D-W-3300 Braunschweig (FRG)
[+] Present address:
Department of Chemistry
Chemistry Building, Indiana University
POB 242, Bloomington, IN 47405 (USA)

[**] P_4 Ligands with Maximum Electron-Donating Ability, Part 4. This work was supported by the Fonds der Chemischen Industrie. Degussa AG is thanked for the donation of $RhCl_3 \cdot nH_2O$. The authors also thank Dr. M. Dargatz and L. Hilfert for recording and the simulation of the NMR spectra, and Dr. K. Schenzel for carrying out the IR measurements. Part 3 : M. Scheer, M. Dargatz, A. Rufinska, *J. Organomet. Chem.*, in press.

open edge 2.815(4) Å (2.808(4) Å) is greater than in the Co complex **3** (2.606(1) Å),[8] whose P_4M skeleton is isostructural with that of **1**. Also the P–P bond lengths (P1P2, P1P3, P2P4, P3P4) are on average (2.222(4) Å) slightly longer than those in **3** (2.210(2) Å) (d_{PP} = 2.21 Å for the single bond). They correspond more closely to those in the tetraphosphabicyclobutanes **4**[9] and **5**,[10] which contain sterically demanding organic substituents. In contrast to **3**–**5**, the P–P bond between the bridgehead atoms P2 and P3 in **1** (2.201(3) Å for both independent molecules) is lengthened (**3**: 2.158(2), **4**: 2.129, **5**: 2.166(2) Å). Obviously the lengthening of the P–P bonds of the tetraphosphabicyclobutane skeleton is caused by the coordination of the lone pairs of all P atoms to sterically demanding $[Cr(CO)_5]$ complex fragments.

$[CoCp^*(CO)(\eta^2\text{-}P_4)]$ **3**

$Cp^* = \eta^5\text{-}C_5Me_5$

$P_2(PR_2)$ **4**, R = $N(SiMe_3)_2$
5, R = 2,4,6-$tBu_3C_6H_2$

The bonds P1–Cr1 and P4–Cr4 (2.335(2)–2.350(3) Å, average 2.344 Å) are slightly longer than P2–Cr2 and P3–Cr3 (2.308(2)–2.329(2) Å, average 2.321 Å). The P–Cr bonds in **1** are longer than those in complexes such as **6** (2.301(4) Å)[11] and **7** (2.307(5) Å)[11] with P_1 and P_2 ligands, respectively.

$[Fe_3(CO)_6\{\mu_3\text{-}PCr(CO)_5\}\{\mu_3\text{-}PFe(CO)_4\}]$ **6**

$[Fe_2(CO)_6(\mu\text{-}CO)\{\mu,\eta^2\text{-}\{PCr(CO)_5\}_2\}]$ **7**

$[Co(triphos)\{\eta^3\text{-}P_3[Cr(CO)_5]_2\}]$ **8**

triphos = $MeC(CH_2PPh_2)_3$

In the sterically bulky complex **8** with a P_3 ligand[12] the P–Cr bonds (2.426(4) Å) are somewhat longer than in **1**. The fold angle of the tetraphosphabicyclobutane skeleton in **1** (94° (93°)) is only slightly less than in **3** (95°), **4** (95.2°), and **5** (95.5°).

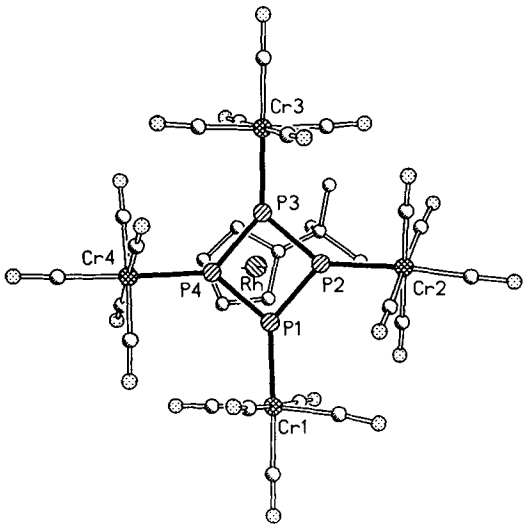

Fig. 2. Crystal structure of **2** (view of the *cyclo*-P_4 moiety).

The crystal structure of **2**[7] reveals a planar *cyclo*-P_4 ligand, which is capped centrosymmetrically by a Cp'Rh cap, and the lone pairs of all P atoms coordinate to the $[Cr(CO)_5]$ complex fragments (Fig. 2). The P–P bond lengths are very similar (2.143(2)–2.160(2) Å, average 2.149 Å) and shorter than single bond lengths. Only the distance between the atoms P3 and P4 (2.160(2) Å) is slightly lengthened in contrast to the others (2.146(3) Å). The reason could be that one C–C edge of the Cp' ligand is arranged above this P–P bond, whereas only corners of the Cp' ligand lie above the other P–P edges (Fig. 2). A kite-shaped distortion of a *cyclo*-P_4 ligand is observed in **9**,[13] where the CO groups of the capping $[NbCp^*(CO)_2]$ complex fragment are parallel to the elongated bonds of the P_4 ligand.

$[NbCp^*(CO)_2(\eta^4\text{-}P_4)]$ **9**

The four P atoms in **2** form a plane at a distance of 1.88 Å from the capping Rh atom (Fig. 3). The Cp' plane and the *cyclo*-P_4 ligand are inclined to each other by about 7°, which is traced back to the repulsion of the *t*Bu group of the Cp' ligand with the $[Cr(CO)_5]$ group at the P2 atom. Thus, the Cr2 atom is deflected away from the plane of the remaining three Cr atoms by about 0.38 Å, which is found about 0.22 Å below the P_4 plane. The P2–Cr2 distance (2.327(2) Å) is insignificantly greater than the average P–Cr bond length of 2.321(2) Å.

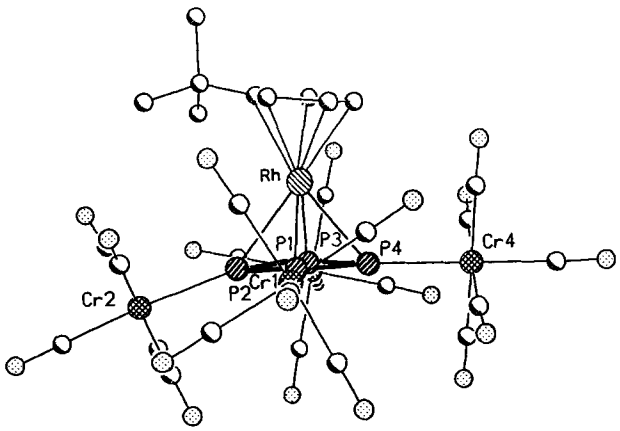

Fig. 3 Crystal structure of **2** (side view).

The structure of the products **1** and **2** provides an explanation of the method of formation of **B** starting from the tetrahedron **A**. Firstly, a P–P edge of the P_4 tetrahedron is opened by the Rh complex. Only in this step are the lone pairs of all phosphorus atoms of the now formed tetraphosphabicyclobutane chemically active for coordination [14] and coordinate to pentacarbonylchromium(0) complex fragments with the formation of **1**. The attack of a second [RhCp'(CO)] complex at the P–P edge is prevented by the $[Cr(CO)_5]$ groups. Therefore the CO abstraction at the coordinating Rh complex triggers the opening of a further P–P bond in the molecule **1** and complex **2** is formed with a planar *cyclo*-P_4 moiety. The P_4 ligand in **1** provides ten and in **2** twelve VE to the overall complex.

Experimental Procedure

To a solution of P_4 (140 mg, 1.13 mmol) and $[Cr(CO)_5(thf)]$ (6.78 mmol) in THF (25 mL), prepared by the UV irradiation of a THF solution of $[Cr(CO)_6]$ (1.6 g), was added $[RhCp'(CO)_2]$ (316 mg, 1.13 mmol). The solution was stirred at room temperature for 10 min and subsequently for 10 min at a bath temperature of 60–70 °C and evaporated to dryness under vacuum. The solid was suspended in *n*-pentane (40 mL) and filtered off over a frit. It was extracted hot with the filtrate. The volume of the pentane extract was reduced to a fifth in vacuo, and a mixture (0.45 g) of **1**, **2**, and $[Cr(CO)_6]$ crystallized at 5 °C. The latter was sublimed under high vacuum at 60 °C. The fractional crystallization of the residue from CH_2Cl_2 at 0 °C afforded **1** (110 mg, 8.5%) and **2** (150 mg, 12%). The residue from the filtration of the pentane extraction was taken up in CH_2Cl_2, whereby a further 0.3 g of solid was obtained, from which an additional 200 mg (16%) of **2** could be obtained at 0 °C.

Received: May 22, 1992 [Z 5369 IE]
German version: *Angew. Chem.* **1992**, *104*, 1395

CAS Registry numbers:
1, 143492-90-4; **2**, 143492-91-5; $[Cr(CO)_5thf]$, 15038-41-2; $[RhCp'(CO)_2]$, 143492-92-6.

[1] M. Scheer, E. Herrmann, J. Sieler, M. Oehme, *Angew. Chem.* **1991**, *103*, 1023–1025; *Angew. Chem. Int. Ed. Engl.* **1991**, *30*, 969–971; cf. the photochemical synthesis of $[\{W(CO)_4\{\eta^4\text{-}P_4[W(CO)_5]_4\}\}(CH_2Cl_2)]$: M. E. Barr, S. K. Smith, B. Spencer, L. F. Dahl, *Organometallics* **1991**, *10*, 3983–3991. review article about the reaction of P_4 with metal complex fragments: M. Scheer, E. Herrmann, *Z. Chem.* **1990**, *30*, 41–55; O. J. Scherer, *Angew. Chem.* **1990**, *29*, 1137–1155; *Angew. Chem. Int. Ed. Engl.* **1990**, *29*, 1104–1122.

[2] The reaction (a) without $[Cr(CO)_5(thf)]$ takes a different reaction pathway. According to our investigations no reaction occurs between $[RhCp'(CO)_2]$ and P_4 up to 110 °C. The reaction of P_4 with $[RhCp^x(CO)_2]$ ($Cp^x = \eta^5\text{-}C_5Me_4Et$) at 110° in toluene leads to the tetraphosphabutadiene derivative $[RhCp^x(P_4)\{RhCp^x(CO)\}]$[3] and at even higher temperatures to $[(RhCp^x)_2(\mu,\eta^2\text{-}P_2)_2]$, which has two separate P_2 moieties [4]. The reaction to give $[RhCp^x(CO)(\eta^2\text{-}P_4)]$ is only observed if the dimeric compound $[\{RhCp^x(CO)\}_2]$ is used as the starting material [5].

[3] O. J. Scherer, M. Swarowsky, H. Swarowsky, G. Wolmershäuser, *Angew. Chem.* **1988**, *100*, 738–739; *Angew. Chem. Int. Ed. Engl.* **1988**, *27*, 694–

[4] O. J. Scherer, M. Swarowsky, G. Wolmershäuser, *Angew. Chem.* **1988**, *100*, 423–424; *Angew. Chem. Int. Ed. Engl.* **1988**, *27*, 405–406.

[5] O. J. Scherer (Universität Kaiserslautern), private communication.

[6] $^{31}P\{^1H\}$ NMR (32.438 MHz, CD_2Cl_2, 85proz. H_3PO_4 ext.) **1** (301 K): AE_2MX Spin system (A = P2, E = P1, P4, M = P3, X = Rh), $\delta = -74.1$ (P_A), -95.0 (P_E), -114.8 (P_M); $J(AE) = 138.7$, $J(AM) = 117.7$, $J(EM) = 139$, $J(AX) = 3.8$, $J(EX) = 63.5$, $J(MX) = -1$ Hz; **2** (301 K): $\delta = 151.5$ (d, $J(RhP) = 34.5$ Hz); ^1H NMR (200.17 MHz, $CDCl_3$, 298 K, TMS) **1**: $\delta = 1.23$ (s, 9H), 5.58 (m, 1H), 5.63 (m, 1H), 5.99 (m, 1H), 6.08 (m, 1H); **2**: $\delta = 1.23$ (s, 9H), 6.58 (m, 2H), 6.20 (m, 2H). IR (Nujol): $\tilde{\nu}$(CO) [cm^{-1}] **1**: 2086 (m), 2062 (s), 1938 (vs, br); **2**: 2076 (m), 2055 (s), 2043 (m), 2001 (w), 1987 (m), 1950 (s, br), 1922 (s, br). EI-MS of **2** (70 eV, 160 °C): *m/z* 1116 (M^+, 2), 924 ($M^+ - [Cr(CO)_5]$, 5), 732 ($M^+ - 2[Cr(CO)_5]$, 4), 220 ($[Cr(CO)_6]$, 12), 124 (P_4, 3), 28 (CO, 100%) as well as additional signals of fragments which are due to losses of CO from the molecular ion and the fragment ions.

[7] X-ray structural determination: **1**, $P2_1/n$, $a = 11.364(2)$, $b = 35.047(8)$, $c = 21.945(5)$ Å, $\beta = 104.68(2)°$ (at -95 °C), $Z = 8$ (two independent molecules), $wR = 0.048$ for 8770 reflections. **2**: $P\bar{1}$, $a = 10.035(2)$, $b = 14.112(3)$, $c = 14.253(3)$ Å, $\alpha = 87.66(2)$, $\beta = 89.04(2)$, $\gamma = 83.60(2)°$ (at -95 °C), $Z = 2$, $wR = 0.038$ for 4865 reflections. Further details of the crystal structure investigations may be obtained from the Fachinformationszentrum Karlsruhe, Gesellschaft for wissenschaftlich-technische Information mbH, D-W-7514 Eggenstein-Leopoldshafen 2 (FRG) on quoting the depository number CSD-56468, the names of the authors, and the journal citation.

[8] O. J. Scherer, M. Swarowsky, G. Wolmershäuser, *Organometallics* **1989**, *8*, 841–842.

[9] E. Niecke, R. Rüger, B. Krebs, *Angew. Chem.* **1982**, *94*, 553; *Angew. Chem. Int. Ed. Engl.* **1982**, *21*, 544.

[10] R. Riedel, H.-D. Hausen, E. Fluck, *Angew. Chem.* **1985**, *97*, 1050; *Angew. Chem. Int. Ed. Engl.* **1985**, *24*, 1056; E. Fluck, R. Riedel, H.-D. Hausen, G. Heckmann, *Z. Anorg. Allg. Chem.* **1987**, *551*, 85–94. Cf. also with $P_2(PCp^*)_2$: P. Jutzi, T. Wippermann, *J. Organomet. Chem.* **1985**, *287*, C5–C7; P. Jutzi, U. Meyer *ibid.* **1987**, *333*, C18–C20.

[11] H. Lang, G. Huttner, L. Zsolnai, G. Mohr, B. Sigwarth, U. Weber, O. Orama, I. Jibril, *J. Organomet. Chem.* **1986**, *304*, 157–179.

[12] C. A. Ghilardi, S. Midollini, A. Orlandini, L. Sacconi, *Inorg. Chem.* **1980**, *19*, 301–306; S. Midollini, A. Orlandini, L. Sacconi, *Angew. Chem.* **1979**, *91*, 93; *Angew. Chem. Int. Ed. Engl.* **1979**, *18*, 81.

[13] O. J. Scherer, J. Vondung, G. Wolmershäuser, *Angew. Chem.* **1989**, *101*, 1395–1397; *Angew. Chem. Int. Ed. Engl.* **1989**, *28*, 1355.

[14] ^{31}P NMR investigations of reaction mixtures from P_4 and $[M(CO)_5(thf)]$ (M = Cr or W) indicate no noticeable interaction between the two reaction partners at room temperature (cf. also [1]).

Synthesis and Biological Activity of D-3-Deoxy-3-Fluorophosphatidylinositol—A New Direction in the Design of non-DNA Targeted Anticancer Agents**

By *Alan P. Kozikowski,* Werner Tückmantel,* and *Garth Powis*

Ligand-activated growth factor and mitogen receptors activate phosphatidylinositol (PtdIns) phospholipase C, which hydrolyzes phosphatidylinositol 4,5-biphosphate to form inositol 1,4,5-trisphosphate [Ins(1,4,5)P_3] and diacylglycerol.[1] Ins(1,4,5)P_3 releases Ca^{2+} from nonmitochondrial stores to increase the cytoplasmic free Ca^{2+} concentration, whereas diacylglycerol is an activator of protein kinase C (PKC).[2] The increase in cytoplasmic free Ca^{2+} concentration and the increased activity of PKC leads to a sequence of events that culminate in DNA synthesis and cell proliferation.[3] Recently, another pathway through which PtdIns can function as a signal molecule has been identified and linked to the action of some growth factors and oncogenes. Phosphatidylinositol-3′-kinase (PtdIns-3′-kinase) is found associated with a number of protein tyrosine kinases, including the ligand-activated receptors for insulin, platelet-derived growth factor (PDGF), epidermal growth factor (EGF), and colony stimulating factor (CSF), as well as oncogene protein tyrosine kinases.[4] The PtdIns-3′-kinase phosphorylates the D-3 position of the *myo*-inositol ring of PtdIns to yield a class of PtdIns-3′-phosphates that cannot be hydrolyzed by PtdIns phospholipase C,[5] and therefore appear to exert their signaling action independently of the inositol phosphate pathway. The relative contributions of the inositol phosphate and PtdIns-3′-kinase signaling pathways in mediating the effects of growth factors and oncogenes on cell proliferation remain to be determined.[6]

We have recently reported on the synthesis and biological activity of a variety of 3-substituted 3-deoxy-*myo*-inositol derivatives.[7] Some of these compounds exhibit antiproliferative effects toward both normal and transformed cell lines, while a subset of these compounds has been found to selectively block the growth of oncogene transformed cells. Based upon results obtained from the study of a tritiated derivative of D-3-azido-3-deoxy-*myo*-inositol,[8] we believe that these analogues may owe their action to the blockade of mitogenic signals issuing from the action of PtdIns-3′-kinase. However, because the antiproliferative action of all of the analogues synthesized to date decreases significantly in the presence of normal serum concentrations of *myo*-inositol (40 μM), it is unlikely that these compounds will be active in vivo.[7] Therefore, we have considered the possibility of preparing a phosphatidylinositol derivative substituted at the 3-position of the *myo*-inositol ring in order to examine its inhibitory effects on cell growth. Since the ability of an inositol isostere to block the action of PtdIns-3′-phosphate depends upon its incorporation into a membrane-associated phosphatidylinositol—a transformation that would require competition of the isostere with endogeneous inositol for uptake as well as reaction with PtdIns synthetase—the direct administration

[*] Prof. Dr. A. P. Kozikowski, Dr. W. Tückmantel
Neurochemistry Research, Mayo Clinic Jacksonville
4500 San Pablo Road, Jacksonville, FL 32224 (USA)
Dr. G. Powis
Arizona Cancer Center

[**] This work was supported by the National Institutes of Health (grants CA 42286 for G. P. and CA 50175 for A. P. K.). We also thank Dr. A. H. Fauq for helpful discussions.

of a PtdIns isostere would circumvent these earlier steps in order to arrive at the presumed active structure (see Fig. 1).

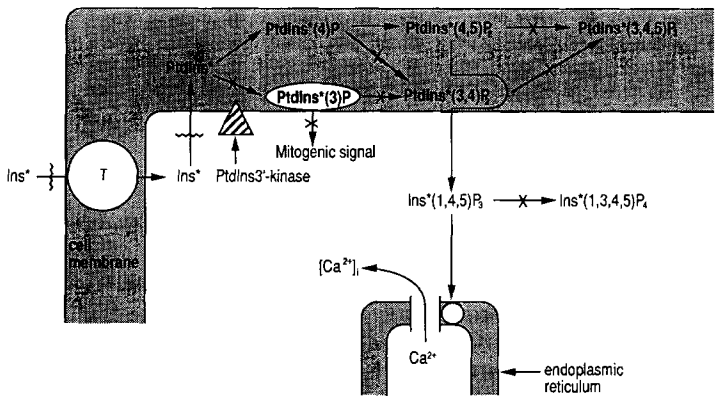

Fig. 1. Possible pathways for D-3-substituted *myo*-inositol analogues in the cell. Ins* is the analogue that is taken up by the *myo*-inositol transport process. It is then incorporated into inositol phospholipids and may give rise to D-3-substituted inositol phosphates or D-3'-substituted phosphatidylinositols. The formation of some of the phosphatidylinositol phosphates and inositol 1,3,4,5-tetrakisphosphate is blocked (indicated by crossed out arrows) because of the substitution at the D-3-position. T = transport protein. The wavy line indicates where Ins* and Ins compete.

To test this hypothesis, a D-3-deoxy-3-fluorophosphatidylinositol (**7**, 3-FPI) was synthesized starting from D-3-deoxy-3-fluoro-*myo*-inositol (**1**). As illustrated in Scheme 1, **1** (prepared by methods described previously[9]) was transformed into the fully protected intermediate **4** by a sequence of conventional steps. The MOM protecting group was removed, and the 1-position phosphitylated with benzyloxybis(diisopropylamido)phosphorus to afford **5**. Next, **5** was coupled with 1,2-dipalmitoyl-*sn*-glycerol (Sigma), and the phosphite oxidized to phosphate (**6**). Finally, all benzyl groups were removed by hydrogenolysis over $Pd(OH)_2/C$ in *t*BuOH. *t*BuOH was chosen as the solvent to minimize the possibility of transesterification of the palmitoyl groups of the diacylglycerol moiety. Of all of the steps executed to procure **7**, the hydrogenolysis reaction proved to be the most capricious, and the conditions detailed in step k were established only after considerable experimentation. Satisfactory ^1H, ^{13}C, ^{19}F, and ^{31}P NMR spectra were obtained for this PtdIns analogue,[10] which notably appears to represent the first analogue of this genre to have been synthesized.[11]

Table 1. Inhibition of cell growth by 3-FPI (**7**) and D-3-deoxy-3-fluoro-*myo*-inositol (**1**). IC_{50} values in μM with standard deviations [a].

Compound	Mouse Cell Type NIH 3T3	v-*sis* NIH 3T3
7	110 ± 20	107 ± 15
7 + *myo*-inositol	99 ± 13	81 ± 11
1	7,000 ± 130	1,100 ± 600
1 + *myo*-inositol	NT [b]	NT [b]

[a] The NIH 3T3 and v-*sis* NIH 3T3 cells were plated at 5×10^3 cells in 1.6 cm diameter culture wells for 24 h in Dulbecco's Modified Eagle Medium (DMEM) with 10% heat-inactivated calf serum, and then grown in *myo*-inositol free DMEM or DMEM with 10% dialyzed heat-inactivated calf serum for 3 days in the presence of the analogues. The number of attached cells was measured with an automated cell counter. All incubations were conducted in quadruplicate. Values listed are the concentration of analogue which produces 50% inhibition of cell growth (IC_{50}). [b] NT = nontoxic, that is, $IC_{50} > 33$ mM.

The cell growth inhibitory properties of 3-FPI toward wild-type mouse NIH 3T3 and v-*sis* NIH 3T3 cells were studied (Table 1).[7] The IC_{50} was found to be approximately

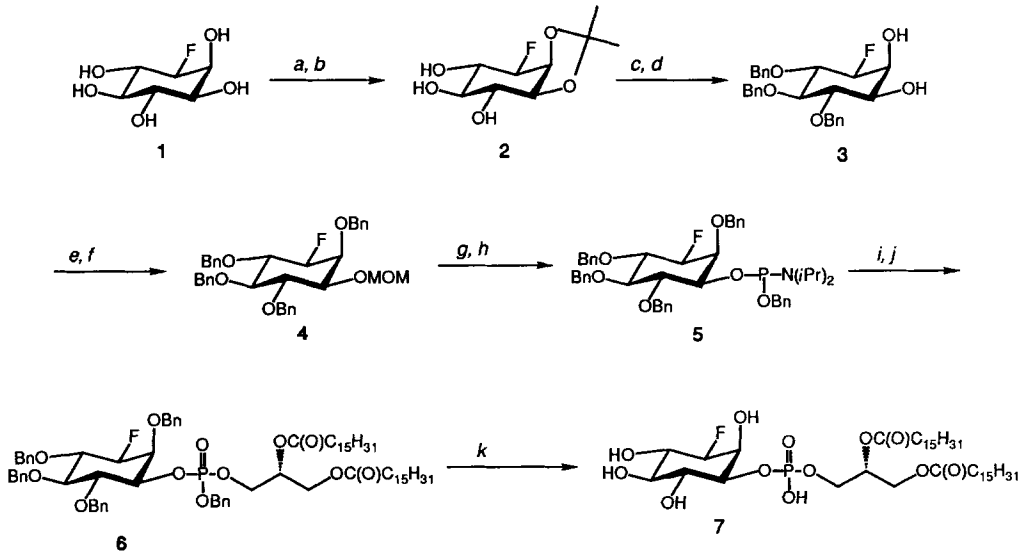

Scheme 1. Synthesis of D-3-deoxy-3-fluorophosphatidylinositol **7**; MOM = methoxymethyl, Bn = benzyl. Reagents and conditions: a) 2-methoxypropene (4 equiv), camphorsulfonic acid (cat.), dimethylformamide (DMF), 80 °C, 4 h (84%); b) AcCl (cat.), $MeOH/CH_2Cl_2$ (1/2), room temperature (RT), 20 min (80%); c) NaH (10 equiv), $PhCH_2Br$ (10 equiv), DMF, 9.5 h, 0 °C → RT (96%); d) 37% HCl (cat.), MeOH, RT, 20 h (100%); e) Bu_2SnO (1 equiv), MeOH, reflux, 70 min; $MeOCH_2Cl$ (1.1 equiv), DMF, 0 °C, 1 h (66%); f) NaH (2 equiv), $PhCH_2Br$ (3 equiv), DMF, RT, 5 h (98%); g) $MeOH/H_2O$/37% HCl (100/10/1), reflux, 8 h (93%); h) $BnOP(NiPr_2)_2$ (1.2 equiv), diisopropylammonium tetrazolide (0.5 equiv), CH_2Cl_2, RT (97%); i) 1,2-dipalmitoyl-*sn*-glycerol (1.08 equiv), tetrazole (2 equiv), CH_2Cl_2/CH_3CN (1/1), RT, 5 h, 35–40 °C, 64 h (79%); j) *t*BuOOH (1.5 equiv), 0 °C, 1.5 h, RT, 3 h (92%); k) 5 atm H_2, 20% $Pd(OH)_2/C$, *t*BuOH, RT, 1 d (71–83%).

100 μM in both cell types. For comparison, Table 1 also shows the effects of D-3-deoxy-3-fluoro-*myo*-inositol which was 10 to 70 times less active as an inhibitor of cell growth.[7] Of considerable significance, however, is the finding that while the growth inhibitory effects of the inositol isostere (**1**) were completely inhibited by the presence of *myo*-inositol at physiological levels (40 μM) in the medium, the presence or absence of *myo*-inositol had no effect on the activity of 3-FPI (**7**). 3-FPI also inhibited colony formation by HT-29 human colon tumor cells in soft agarose (IC_{50} 37 ± 3 μM).

The measured IC_{50} values are within a range that should make studies with 3-FPI in blocking tumor cell growth in vivo possible. While the synthesis of other substituted PtdIns analogues that may show cell selectivity as well as an improved potency is under way, it is clear that disruption of the PtdIns-based signaling events may provide an exciting new direction in the discovery of non-DNA targeted anti-cancer agents.

Received: April 29, 1992 [Z 5325 IE]
German version: *Angew. Chem.* **1992**, *104*, 1408

CAS Registry numbers:
1, 120444-24-8; **2**, 143446-76-8; **3**, 143446-77-9; **4**, 143446-78-0; **5**, 143446-79-1; **6**, 143446-80-4; **7**, 143446-81-5; 1,2-dipalmitoyl-*sn*-glycerine, 30334-71-5.

[1] a) B. Margolis, S. G. Rhee, S. Felder, M. Mervic, R. Lyall, A. Levitzki, A. Ullrich, A. Zilberstein, J. Schlessinger, *Cell* **1989**, *57*, 1101; b) P. Secrist, I. Sehgal, G. Powis, R. Abraham, *J. Biol. Chem.* **1990**, *265*, 20394; c) T. K. Harden, *Am. Rev. Respir. Dis.* **1990**, *141*, S119.

[2] M. J. Berridge, R. F. Irvine, *Nature* **1989**, *341*, 197.

[3] M. Whitman, L. Cantley, *Biochem. Biophys. Acta* **1988**, *948*, 327.

[4] a) K. R. Auger, L. A. Serunian, S. P. Soltoff, P. Libby, L. C. Cantley, *Cell* **1989**, *57*, 167; b) J. D. Bjorge, T.-O. Chan, M. Antczak, H.-J. Kung, D. J. Fujita, *Proc. Natl. Acad. Sci. USA* **1990**, *87*, 3816; c) S. R. Coughlin, J. A. Escobedo, L. T. Williams, *Science* **1989**, *243*, 1191; d) S. A. Courtneidge, A. Heber, *Cell* **1987**, *50*, 1031; e) J. A. Escobedo, L. T. Williams, *Nature* **1988**, *335*, 85; f) Y. Fukui, S. Kornbluth, S.-M. Jong, L.-H. Wang, H. Hanafusa, *Oncogene Res.* **1989**, *4*, 283.

[5] a) D. L. Lips, P. W. Majerus, *J. Biol. Chem.* **1989**, *264*, 19911; b) L. A. Serunian, M. T. Haber, T. Fukui, J. W. Kim, S. G. Rhee, J. M. Lowenstein, L. C. Cantley, *ibid.* **1989**, *264*, 17809.

[6] a) T. D. Hill, N. M. Dean, L. J. Mordan, A. F. Lau, M. Y. Kanemitsu, A. L. Boynton, *Science* **1990**, *248*, 1660; b) R. W. Tucker, D. T. Chang, K. Meade-Cobun, *J. Cell Biochem.* **1989**, *61*, 203.

[7] a) G. Powis, I. A. Aksoy, D. C. Melder, S. Aksoy, H. Eichinger, A. H. Fauq, A. P. Kozikowski, *Cancer Chemother. Pharmacol.* **1991**, *29*, 95; b) A. P. Kozikowski, A. H. Fauq, G. Powis, D. C. Melder, *Med. Chem. Res.* **1991**, *1*, 277.

[8] G. Brunn, A. H. Fauq, S. Chow, A. P. Kozikowski, G. Powis, unpublished.

[9] A. P. Kozikowski, A. H. Fauq, J. M. Rusnak, *Tetrahedron Lett.* **1989**, *30*, 3365.

[10] Physical and spectral properties for **7**: colorless amorphous solid; m.p. 132–133 °C (after sintering); ^{1}H NMR ($CDCl_3/CD_3OD$ 2/1, TMS): δ = 5.27 (m, 1H, 2-H of glycerol), 4.45–4.35 (m, 2.5H), 4.27–4.15 (m, 3.5H), 4.02 (br, 1H), 3.97 (dt, 1H, J = 9.5 Hz (t), 12 Hz (d)), 3.86 (br.t, 1H, J = 8.5 Hz), 3.24 (t, 1H, J = 9.5 Hz), 2.36 (t, 2H, J = 7.5 Hz), 2.33 (t, 2H, J = 7.5 Hz), 1.62 (m, 4H), 1.27 (m, 48H), 0.89 (t, 6H, J = 7 Hz); ^{13}C NMR ($CDCl_3/CD_3OD$ 2/1): δ = 173.67, 173.30, 91.30 (d, J = 182.5 Hz), 73.46 (d, J = 12.5 Hz), 70.82 (d, J = 4 Hz), 70.42 (d, J = 18 Hz), 69.52 (d, J = 6 Hz), 69.08 (d, J = 17.5 Hz), 64.85, 64.79, 61.86, 33.84, 33.73, 31.60, 29.34, 29.18, 29.00, 28.79, 24.53, 22.32, 13.57; ^{19}F NMR ($CDCl_3/CD_3OD$ 2/1, $CFCl_3$ ext.): δ = −204.51 (ddd, J = 47, 11, 10 Hz); ^{31}P NMR ($CDCl_3/CD_3OD$ 2/1, 85proz. H_3PO_4 ext.): δ = −0.94 (br.); IR (KBr): $\tilde{\nu}$[cm^{-1}] = 3416, 2920, 2851, 1740, 1630, 1468, 1383, 1038; $[\alpha]_0^{25}$ = −1.3, $[\alpha]_{578}^{23}$ = −1.3, $[\alpha]_{365}^{23}$ = −4.2 (c = 5.6 g L^{-1}, $CHCl_3$/MeOH 2/1).

[11] a) For the synthesis of PtdIns analogues in which the phosphorus atom is linked to the diacylglycerol moiety through a carbon atom rather than an oxygen atom (i.e. phosphinyl analogue), see: S. S. Yang, T. R. Beattie, P. L. Durette, T. F. Gallagher, T.-Y. Shen, Merck & Co., Inc., Rahway NJ (USA), US-A 4515722, **1985**; b) for the synthesis of a PtdIns analogue with *scyllo* configuration, see: S. S. Yang, T. R. Beattie, T.-Y. Shen, *Tetrahedron Letters* **1982**, *23*, 5517.

Synthesis and Complexation Properties of a Cyclodextrin-Derived Siderophore Analogue

By *Anthony W. Coleman,* Chang-Chun Ling,* and *Marcel Miocque*

The natural siderophores, exemplified by enterobactin,[1,2] parabactin,[3–5] and agrobactin,[3–5] are a class of molecules excreted by microorganisms to sequester and solubilize iron under iron-deficient conditions. Structurally, they are composed of three bidentate ligands allowing the octahedral geometry necessary for Fe^{III}. In many cases the required three bidentate ligands, often spermidine units, are incorporated into the same skeleton.

Recently, considerable efforts have been dedicated to the synthesis of analogues of the natural siderophores. Raymond et al.[6–8] and Vögtle et al.[9–11] have synthesized macrocycles containing three catechol units in a favorably geometric arrangement using 1,3,5-trisubstituted benzene derivatives, and these systems have a proven efficiency in ferric ion coordination. Most recently Raymond et al.[12] have used tris(ω-aminoalkyl)amines as building blocks in the synthesis of 2,3-dihydroxyterephthalamide derivatives. We are interested in preparing siderophore analogues with a cyclodextrin framework. Cyclodextrins are cyclic oligosaccharides possessing an axial symmetry arising from the presence of six, seven, or eight α-1,4-glucopyranose units (giving α, β, and γ cyclodextrins, respectively). Their structure, a truncated cone with two hydrophilic faces surrounding a less polar cavity, allows the inclusion of a wide variety of guest molecules.[13] The advantage of these cyclodextrin siderophores should be their potential to coordinate biologically and pharmaceutically interesting ions while retaining a "free" cavity in which a second series of molecules can be included and transported. To this end we have synthesized the ligand $6^A,6^C,6^E$-triamino-*N*,*N*′,*N*″-tris(2,3-dihydroxybenzoyl)-pentadeca-*O*-methyl-α-cyclodextrin (**1**, H_6L), which possesses a threefold axial symmetry (Scheme 1).

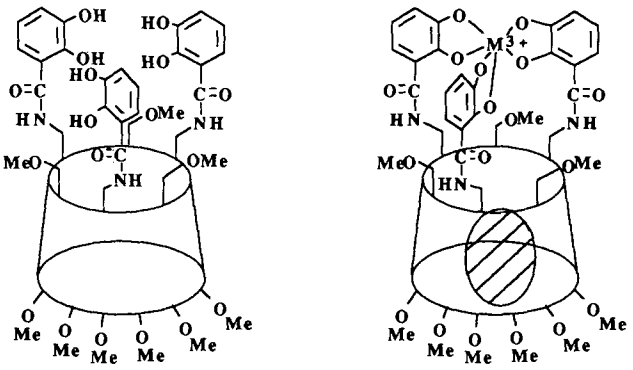

1

Scheme 1. Schematic representation of the structures of ligand **1** (left) and its complexes (right). The hatched oval symbolizes an included active molecule.

Our experience with the multiple tritylation of α-cyclodextrin[14] led us to synthesize **1** (Scheme 2) via the previously described $6^A,6^C,6^E$-triamino-pentadeca-*O*-methyl-α-cyclodextrin trihydrochloride (**6**),[15] prepared now by an im-

[*] Dr. A. W. Coleman, Dr. C.-C. Ling, Prof. M. Miocque
CNRS, Laboratoire de Chimie Organique
Centre Pharmaceutique, Université de Paris Sud
F-92290 Châtenay-Malabry (France)

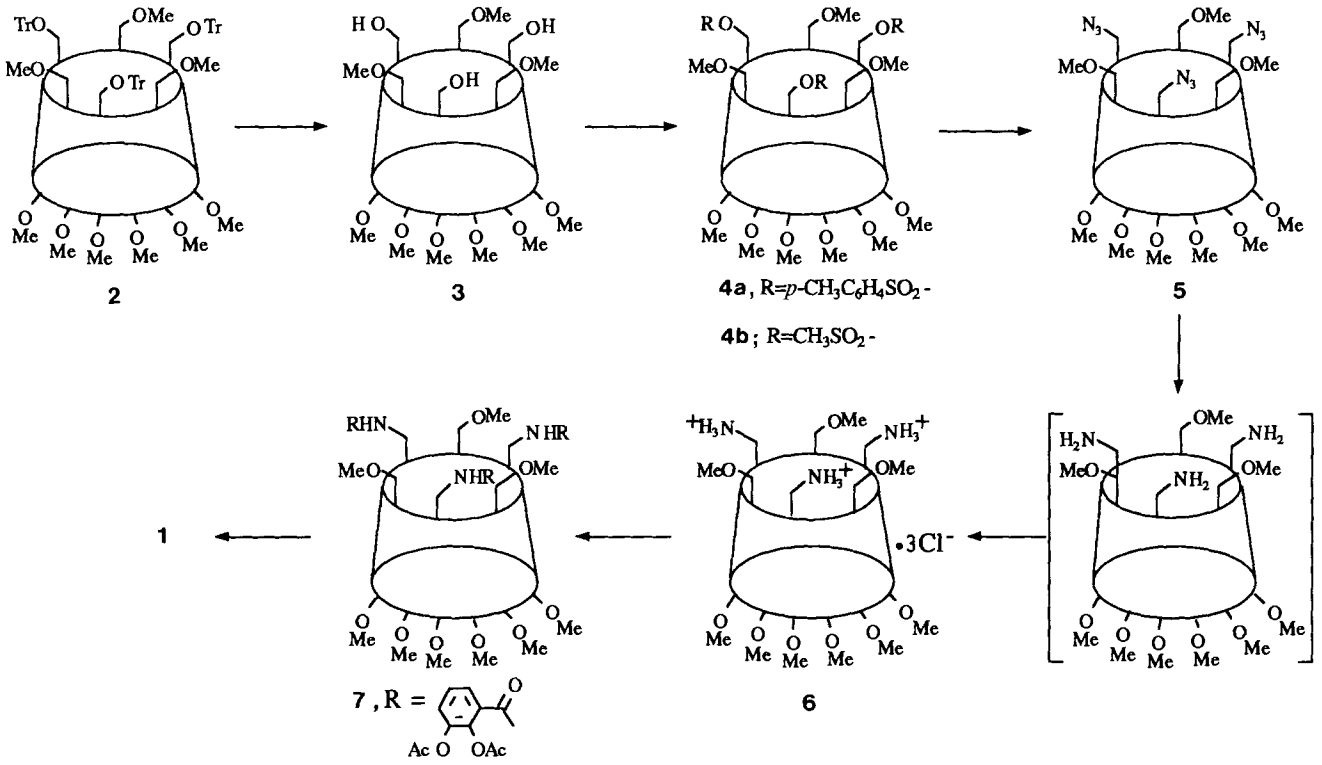

Scheme 2. Synthesis of ligand **1**. Tr = trityl.

proved method. Derivative **2** was smoothly detritylated with HBF_4 (34%)/CH_3CN[16] in good yield (87%), whereas the method of Boger et al.[15] (concentrated HCl/$CHCl_3$) led generally to incomplete detritylation at 0 °C and partial hydrolysis of cyclodextrin at room temperature. The trihydroxyl derivative **3** was converted into both the trimesylate **4a** and tritosylate **4b** in 63% and 96% yields, respectively. These compounds were converted to triazide, which was reduced with triphenylphosphine–ammonia to give the triamine as the hydrochloride salt. Treatment of **6** with 2,3-diacetoxybenzoyl chloride[17] in anhydrous tetrahydrofuran with triethylamine as base gave the protected ligand **7** in 82% yield. The acetate groups were removed with $NaOCH_3/CH_3OH$ to provide the desired ligand **1** in 97% yield.

The ^1H NMR spectra of the two catechol-containing derivatives **7** and **1** clearly show retention of the threefold molecular symmetry and the rotational liberty of the catechol groups. Spectra of **1** in [D_6]DMSO display two doublets (δ = 5.04 and 4.84) and a triplet (5.95) corresponding to the two types of anomeric protons and one type of amide protons, respectively. The two signals due to the protons of the phenol groups are observed at δ = 13.6 (*ortho*) and 8.95 (*meta*). The ^{13}C NMR spectrum of **1** in $CDCl_3$ confirms the expected symmetry: a single CONH signal is observed at δ = 170.3, two C-1 signals at δ = 100.4 and 99.4, and one CH_2NH signal at δ = 40.7.

Complexation of $FeCl_3$ by **1** in water [**1**/$FeCl_3$ = 1/1, 2.59×10^{-4} M; μ = 0.10 M (NaCl)] was studied spectrophotometrically in the pH range 3–11. At pH values greater than **4** the dark red color of the complex is observed, and an absorption maximum is recorded at 545 nm. Between pH 6.88 and 8.20, a sharp isosbestic point at 563 nm is found; between pH 8.25 and 9.40 a second (at 535 nm) is observed. A potentiometric titration experiment of the aqueous solution of **1**/$FeCl_3$ (1/1) proves that the two isosbestic points are due to two protonation equilibria ($FeLH^{2-} + H^+ \rightleftharpoons FeLH_2^-$; $FeL^{3-} + H^+ \rightleftharpoons FeLH^{2-}$). Using the Schwarzenbach plot,[18] we were able to calculate the first protonation constant $\lg K_{FeLH^{2-}} = 8.4$, and the second protonation constant $\lg K_{FeLH_2^-} = 7.4$, as both plots follow linearity.

The extremely strong binding of Fe^{3+} by the ligand **1** precludes a direct measurement of the formation constant $K_{FeL^{3-}}$ which is defined in Equation (a). Thus a competition

$$K_{FeL^{3-}} = \frac{[FeL^{3-}]}{[Fe^{3+}][L^{6-}]} \quad \text{(a)}$$

experiment[19] was carried out at pH 7.85 with solutions containing a tenfold excess of EDTA at 25 °C. Equilibrium was attained after 24 h according to the spectrophotometric results. The ligand protonation constants of **1** are still unknown, but if one reasonably assumes that the logarithms of the first three protonation constants of ligand **1** correspond to those of dihydroxybenzamide (7.6, 8.4, 9.2) and the remaining three protonation constants are 12.1,[19] then the stability constant K^* dependent on proton concentration [Eq. (b)] can be determined as $10^{2.82}$. The formation con-

$$K^* = \frac{[FeL^{3-}][H^+]^3}{[Fe^{3+}][H_3L^{3-}]} \quad \text{(b)}$$

stant $K_{FeL^{3-}}$ can then be calculated as 10^{39}, a value comparable with those of other cyclic ligands (10^{40} for CYCAM,[7] 10^{38} for CYCAMS[20]), but still several orders of magnitude lower than that of enterobactin (10^{52}).[19]

In order to test the capacity of **1** to both complex metal ions and transport organic molecules, we have studied its interaction with diamagnetic Al^{3+} in D_2O at pD 11 [**1**/Al-$(NO_3)_3$ = 1/1]. The complexation is reflected by the dramatic shifts of the aromatic protons (Fig. 1a,b) and also the methyl protons of the B, D, and F glucopyranose units (3.35 to 2.85 ppm). The retention of the threefold symmetry before and after complexation is evident from the simplicity of the spectra and the observation of only two doublets for the anomeric protons.

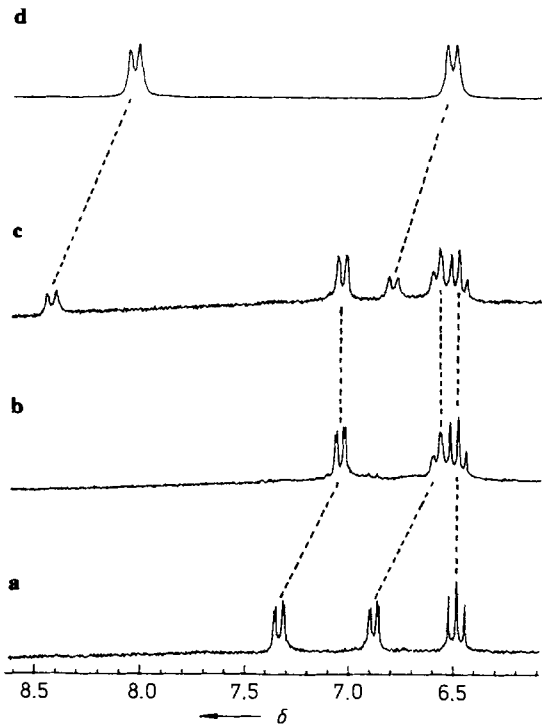

Fig. 1. ^{1}H NMR spectrum of the aromatic protons of a) ligand **1**, b) ligand **1** + $Al(NO_3)_3$ (1:1), c) ligand **1** + $Al(NO_3)_3$ (1:1) in the presence of 1 equiv sodium *p*-nitrophenolate, d) sodium *p*-nitrophenolate in D_2O at pD 11.

Inclusion experiments with AlL^{3-} were carried out with *p*-nitrophenolate. The inclusion is clearly demonstrated by the induced chemical shifts for the *ortho* protons which are displaced from 8.0 to 8.4 ppm and *meta* protons, from 6.5 to 6.7 ppm (Fig. 1d,c). The shifts of the aromatic protons of AlL^{3-} are not affected by the inclusion (Fig. 1b,c), whilst some changes are observed for cyclodextrin protons in the region $\delta = 3.8-4.0$. These observations are in agreement with the simultaneous complexation of a metal ion and inclusion of an organic molecule within the cyclodextrin cavity.

We have synthesized an α-cyclodextrin-derived siderophore and demonstrated its ability to complex Fe^{III} and Al^{III}. With Al^{III} simultaneous formation of an inclusion complex was also evident.

Experimental Procedure

3: To a stirred solution of **2** (2.42 g) in acetonitrile (40 mL), was added tetrafluoroboric acid (34%, 2.0 mL). This mixture was stirred at room temperature for 30 min, then Et_3N (1.4 mL) was added. The solvent was evaporated and the residue was subjected to column chromatography to give **3** [15] (1.30 g, 87%).

4a: A solution of **3** (200 mg), *p*-toluenesulfonyl chloride, and *N,N*-dimethylaminopyridine (50 mg) in anhydrous pyridine (3 mL) was stirred for 48 h. H_2O (0.5 mL) was added and the solution was diluted with ethyl acetate (15 mL). This solution was washed with H_2O (15 mL), HCl (2 M, 15 mL), NaOH (2 M, 15 mL), and H_2O (20 mL), dried over Na_2SO_4, and concentrated. Column chromatography (EtOH/$CHCl_3$ = 4/96 v/v) gave **4a** (174 mg, 63%). ^{1}H NMR ($CDCl_3$, signal assignments from the spectra of COSY DQF at 500 MHz): δ = 7.71 (6H, d, tosyl), 7.29 (6H, d, tosyl), 4.89 (3H, d, H-1_{ACE}), 4.85 (3H, d, H-1_{BDF}), 4.58 (3H, m, H-6_{ACE}), 4.34 (3H, dd, H-$6'_{ACE}$), 4.02 (3H, m, H-5_{BDF}), 3.91 (3H, H-6_{BDF}), 3.83 (3H, H-5_{BDF}), 3.70 (3H, H-4_{BDF}), 3.55 (3H, H-3_{BDF}), 3.42 (3H, H-$6'_{ACE}$), 3.38 (3H, H-4), 3.14 (3H, dd, H-2_{BDF}), 3.04 (3H, dd, H-2_{ACE}).

4b, **5** and **6** are prepared according to the published procedure [15].

7: Compound **6** (100 mg) and 2,3-diacetoxybenzoyl chloride (119 mg) were dissolved in anhydrous THF (5 mL) at 0 °C, then Et_3N (0.33 mL) was added. After 1 h the temperature was allowed to rise to room temperature, and the reaction was continued for 15 h. H_2O was added and the solvent was evaporated. The residue was redissolved in ethyl acetate (60 mL), and this solution was washed with H_2O (15 mL), saturated $NaHCO_3$ solution (2 × 15 mL), and H_2O (15 mL), dried over Na_2SO_4, and concentrated to dryness. Column chromatography (MeOH/CH_2Cl_2 = 5/95 v/v) gave **7** as a white solid (117 mg, 82%). IR (KBr), $\tilde{\nu}_{max}$[cm^{-1}] = 3463, 1779, 1665; ^{1}H NMR (200 MHz, $CDCl_3$): δ = 6.62 (3H, t, CONH), 5.14 (3H, d, H-1), 5.02 (3H, d, H-1), 3.15 (9H, s, MeO-6_{BDF}), 2.18 (9H, s, Ac), 2.22 (9H, s, Ac). ^{13}C NMR (J. Mod., 50 MHz, $CDCl_3$): δ = 167.8, 167.9 (COO), 165.1 (CONH), 142.7 (C-2'), 139.9 (C-3'), 129.9 (C-1', 126.6, 125.9 (C-4',5',6'), 99.2 (C-1), 83.6, 81.9, 81.8, 81.5, 81.1, 81.0 (C-2,3,4), 71.3, 70.1 (C-5_{ACE}, C-5_{BDF}), 70.6 (C-6_{BDF}), 61.5 (MeO-2_{ACE}, MeO-2_{BDF}), 59.1 (MeO-6_{BDF}), 58.0, 57.9 (MeO-3_{ACE}, MeO-3_{BDF}), 41.0 (C-6_{ACE}), 20.4 (CH_3). Correct C,H,N analyses.

1: Compound **7** (100 mg) was dissolved in absolute methanol (degassed, 5 mL), and $NaOCH_3$ (20 mg) was added. The solution was stirred under argon for 1 h, and the solvent was evaporated. The residue was redissolved in degassed water (5 mL) and the pH of the solution adjusted to 7. This solution was extracted with ethyl acetate (20 mL), then the organic phase was separated and washed with H_2O (2 × 10 mL), dried over Na_2SO_4, and concentrated to dryness. The residue was recrystallized from ethyl acetate/hexane to give analytically pure **1** (84 mg, 97%). IR (KBr): $\tilde{\nu}_{max}$[cm^{-1}] = 3302, 1640. ^{1}H NMR (200 MHz, [D_6]DMSO): δ = 13.60 (3H, s, OH-2'), 8.95 (3H, s, OH-3'), 5.95 (3H, t, CONH), 5.04 (3H, d, H-1), 4.84 (3H, d, H-1). ^{13}C NMR (J. Mod., 50 MHz, $CDCl_3$): δ = 170.3 (CONH), 149.1 (C-2'), 145.8 (C-3'), 118.6, 116.0 (C-4',5',6'), 113.8 (C-1'), 100.4, 99.4 (C-1), 84.5, 82.2, 82.1, 81.9, 81.1 (C-2,3,4), 71.7, 70.4 (C-5), 70.8 (C-6_{BDF}), 61.9, 61.6 (MeO-2), 59.5 (MeO-6), 58.2, 57.8 (MeO-3), 40.7 (CH_2NH-6_{ACE}). Correct C,H,N analyses.

Received: February 26, 1992
Revised: July 18, 1992 [Z 5212 IE]
German version: *Angew. Chem.* **1992**, *104*, 1402

CAS Registry numbers:
1, 143345-94-2; **1**/Fe, 143345-97-5; **1**/Al, 143345-98-6; **1**/Al·*p*-nitrophenolate, 143346-00-3; **2**, 72665-48-6; **3**, 72360-03-3; **4a**, 143345-95-3; **4b**, 139622-75-6; **5**, 72665-49-7; **6**, 72665-51-1; **7**, 143345-96-4; 2,3-diacetoxybenzoyl chloride, 65055-19-8.

[1] J. R. Pollack, J. B. Neilands, *Biochim. Biophys. Res. Commun.* **1970**, *38*, 989.
[2] I. G. O'Brien, F. Gibson, *Biochim. Biophys. Acta* **1970**, *215*, 393.
[3] G. H. Tait, *Biochem. J.* **1975**, *146*, 191.
[4] T. Peterson, J. B. Neilands, *Tetrahedron Lett.* **1979**, 4805.
[5] T. Peterson, K. E. Falk, S. A. Leong, M. P. Klein, J. B. Neilands, *J. Am. Chem. Soc.* **1980**, *102*, 7715.
[6] F. L. Weitl, K. N. Raymond, *J. Am. Chem. Soc.* **1979**, *101*, 2728.
[7] W. R. Harris, K. N. Raymond, *J. Am. Chem. Soc.* **1979**, *101*, 6534.
[8] D. J. Ecker, L. D. Loomis, M. E. Cass, K. N. Raymond, *J. Am. Chem. Soc.* **1988**, *110*, 2457.
[9] W. Kiggen, F. Vögtle, *Angew. Chem.* **1984**, *96*, 712; *Angew. Chem. Int. Ed. Engl.* **1984**, *23*, 714.
[10] W. Kiggen, F. Vögtle, S. Franken, H. Puff, *Tetrahedron* **1986**, *42*, 1859.
[11] P. Stutte, W. Kiggen, F. Vögtle, *Tetrahedron* **1987**, *43*, 2065.
[12] T. M. Garrett, T. J. McMurry, M. W. Hosseini, Z. E. Reyes, F. E. Hahn, K. N. Raymond, *J. Am. Chem. Soc.* **1991**, *113*, 2965.
[13] J. Szejtli, *Cyclodextrin Technology*, Kluwer, Dordrecht, **1988**.
[14] C.-C. Ling, A. W. Coleman, M. Miocque, *Carbohydr. Res.* **1992**, *223*, 287.
[15] J. Boger, J. R. Knowles, *J. Am. Chem. Soc.* **1979**, *101*, 7631.
[16] S. Cottaz, H. Driguez, *Synthesis* **1989**, 755.
[17] R. J. Bergeron, K. A. McGovern, M. A. Channing, P. S. Burton, *J. Org. Chem.* **1980**, *45*, 1589.
[18] G. Anderegg, F. L'Eplattenier, G. Schwarzenbach, *Helv. Chim. Acta* **1963**, *46*, 1409.
[19] W. R. Harris, C. J. Carrano, S. R. Cooper, S. R. Sofen, A. E. Avdeef, J. V. McArdle, K. N. Raymond, *J. Am. Chem. Soc.* **1979**, *101*, 6079.
[20] W. R. Harris, K. N. Raymond, F. L. Weitl, *J. Am. Chem. Soc.* **1981**, *103*, 2667.

Boriranes: Structures and Thermal Ring Openings**

By *Peter Willerhausen, Günter Schmidt-Lukasch, Claudia Kybart, Jürgen Allwohn, Werner Massa, Michael L. McKee, Paul von Ragué Schleyer,* and *Armin Berndt**

Although borirenes **1**,[1] boratirenes **2**,[2] and boratiranes **3**[2] have been completely characterized in spectroscopic and structural investigations, simple[3] boriranes **4** have only been studied theoretically.

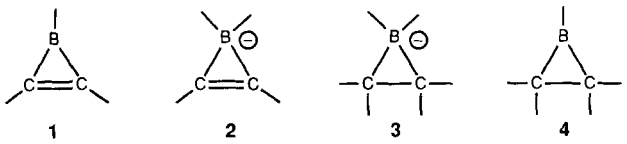

1 **2** **3** **4**

Boriranes are isoelectronic with the cyclopropyl cations (**5**), whose disrotatory ring opening to allyl cations (**6**) has been extensively investigated.[6, 7] The analogous ring opening **4** → **7**, endothermic according to calculations,[6] has not been observed experimentally.[8] We describe here the first crystal structures of boriranes and the thermal cleavages of their C–C and C–B bonds.

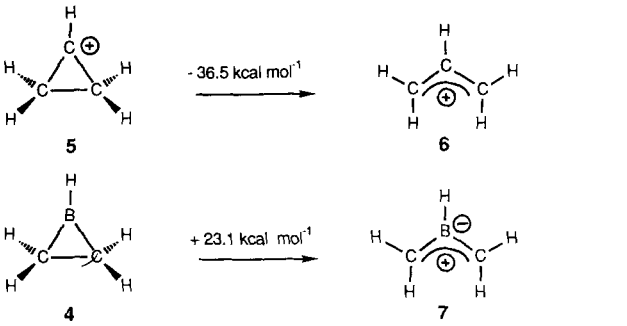

5 **6** **4** **7**

Scheme 1. The relative energies are calculated at the MP2 (FULL)/6.31G*// MP2(FULL)/6-31G* level.

Boriranes **4a** and **4b** were obtained from the additions of $HN(SiMe_3)_2$ and of HCl to the B–C double bonds of boranediylboriranes **8a**[9] and **8b**, respectively.[5] Compound **4b** reacted with methyllithium to give **4c**.

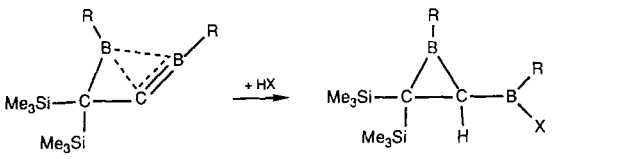

8a : R = *t*Bu
8b : R = duryl

4a : R = *t*Bu, X = $N(SiMe_3)_2$
4b : R = duryl, X = Cl
4c : R = duryl, X = CH_3

[*] Prof. A. Berndt, Dr. P. Willershausen, Dr. G. Schmidt-Lukasch, C. Kybart, Dr. J. Allwohn, Prof. Dr. W. Massa
Fachbereich Chemie der Universität
Hans-Meerwein-Strasse, D-W-3550 Marburg (FRG)
Prof. P. von Ragué Schleyer
Institut für Organische Chemie der Universität Erlangen-Nürnberg
Henkestrasse 42, D-W-8520 Erlangen (FRG)
Prof. M. L. McKee
Department of Chemistry, Auburn University
Auburn, AL 36849 (USA)

[**] This research was supported by the Deutsche Forschungsgemeinschaft and the Fonds der Chemischen Industrie.

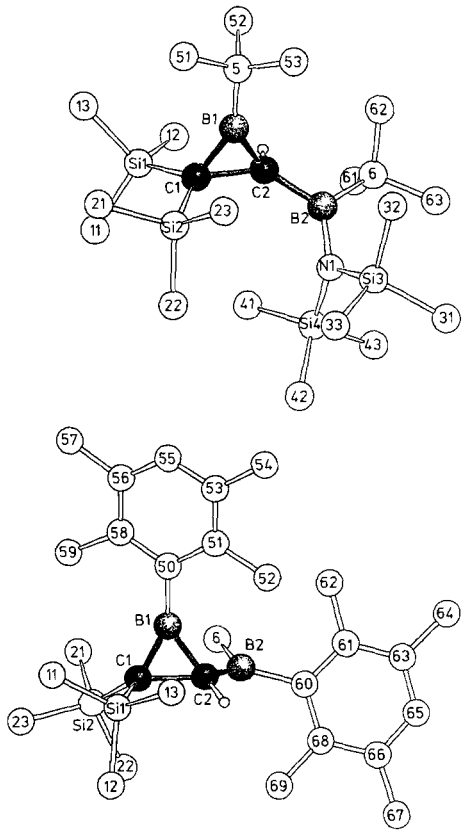

Fig. 1. Top: Crystal structure of **4a** (Schakal). Projection approximately 30° from the B1-C1-C2 plane. Bottom: Crystal structure of **4c** (Schakal). Projection roughly on the B1-C1-C2 plane.

The crystal structures of **4a** and **4c** are shown in Figure 1.[10] Table 1 compares important distances and angles of **4a** and **4c** to those calculated for *B*-methylborirane **4d**[6c] (MP2/6-31G*) and **4e** (6-31G*).

Table 1. Important distances [pm] and angles [°] in **4a**, **4c**, and **4d**.

	4a	**4c**	**4d**	**4e** (6-31G*)
C1-C2	163.6(5)	162.0(5)	155.1	156.4
C1-B1	150.0(5)	149.5(5)	153.4	151.9
C2-B1	153.9(5)	158.0(5)	153.4	155.6
C2-B2	156.8(5)	152.9(5)	–	155.1
C5-B1 [a]	155.6(5)	154.8(5)	154.9	156.2
B2-C2-B1	139.2(3)	115.0(3)	–	117.7
B2-C2-C1	139.4(3)	129.3(3)	–	123.3
C6-B2-C2-B1 [b]	−98.8(5)	−44.8(5)	–	−49.6
X-B2-C2-C1 [c]	−5.2(6)	−163.4(3)	–	−162.2
C6-B2-C2-C1 [b]	168.5(4)	20.3(6)	–	18.9
X-B2-C2-B1 [c]	87.5(5)	131.6(3)	–	129.3

[a] **4c**: C50 instead of C5, **4d**, **4e**: C3 instead of C5. [b] **4e**: C5 instead of C6. [c] **4a**: X = N1, **4c**: X = C60, **4e**: X = C4.

Relative to the B2-C2-B1 and B2-C2-C1 angles in **4c** (115.0 and 129.3°, respectively), the larger angles in **4a** (139.2 and 139.4°, respectively) as well as the long C2–B2 bond (156.8(5) versus 152.9 pm in **4c**) can be attributed to strong steric interactions. These data argue against significant electronic interaction of the boryl substituent with the borirane ring in **4a**. The bond between the carbon atom with the two trimethylsilyl substituents and the B1 atom is 3.4 pm shorter than the related bond in **4d**. This difference results from hyperconjugation of the C–Si bond with the empty p orbital

of the boron atom in the three-membered ring. The markedly longer C1–C2 bond (Δ = 8.5 pm, **4a** versus **4d**) is rationalized by the steric interactions between the large, *cis* substituents on C1 and C2.

The C2–B1 bond (158.0 pm) in **4c** is considerably longer than that in **4d** (153.4 pm); the C1–B1 bond in **4c** is even shorter than that in **4a**. This relationship is reminiscent of those found in cyclopropylcarbinyl cations[11] and in cyclopropylboranes:[6c] the distal bonds in the three-membered ring are shortened, while the vicinal bonds are lengthened. In contrast, the vicinal bonds are *not* equivalent in borylboriranes **4**. The bond with the electropositive boron substituent has stronger σ–π interactions with the exocyclic electron-poor center than the bond with the electronegative C atom. In **4c** the C2–B1 bond describes a torsion angle of 40° with the axis of the p oribital of the exocyclic boron atom; the torsional angle involving the C2–C1 bond, on the other hand, is 72°.

The electronic influence of the diorganylboryl substituents on the structure of the borirane ring in the absence of the steric and additional electronic effects of the trimethylsilyl and aryl groups was investigated by ab initio calculations on dimethylboryl-*B*-methylborirane (**4e**). When electron correlation is included (MP2/6-31G*), a bridged structure **4e*** results. Note the similar features of the bridged methyleneborane **8** which has a C2–B2 single bond and an additional methyl bridge.

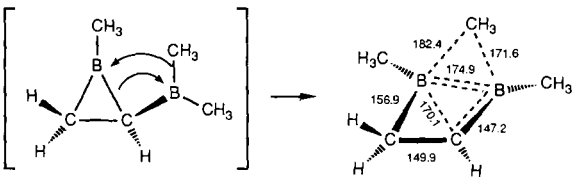

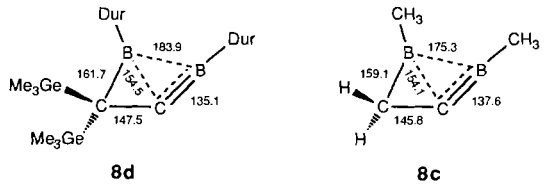

Thus the geometry of **4e** (MP2-6-31G*) cannot serve as a model for **4c**. The electron deficiency of the boron atom of the three-membered ring in **4c** is apparently reduced relative to that in **4e** by C–Si hyperconjugation and π–π delocalization through the duryl ring (see NMR data). The larger substituents may also help prevent the formation of a bridge.

The ^{13}C NMR signals of the C atoms in the borirane ring are relatively sharp for such boron-bound species. This may be attributed to the high p character of the bonds in the three-membered ring. The correspondingly increased s character of the exocyclic C–H bonds is evident in the large ^{13}C–H coupling constants for the C–H groups adjacent to two boron atoms: 115 (**4a**), 142 (**4b**), and 140 Hz (**4c**) (cf. 96 Hz for **11**). The relatively small coupling constant for **4a** and the large B1-C2-B2 and C1-C2-B2 angles (139.2 and 139.4°, respectively) reflect the increased s character of the C2–B2 bond, and thus the reduced s character in the C2–H bond. The shielding of the boron atom in the ring in **4a** (δ = 77) compared to that in **4d** (calculated with IGLO: δ = 93.4[6c]) can be considered further evidence of the C–Si hyperconjugation. The B ring atoms of boriranes with aryl substituents are shifted another $\Delta\delta$ = 5–8 ppm relative to those with *tert*-butyl substituents. The effects of π–π interactions between the boron atom in the three-membered ring and the aryl ring are also evident in the deshielding of the *ortho* C atoms (144.3), the shielding of the *ipso* C atom (131.1), and the small angle (26.1°) between the planes of the borirane and the aryl rings.

When compound **4a** was heated in chloroform for 46 hours at reflux, *C*-borylaminomethyleneborane **9** was the only reaction product detected by ^{13}C NMR spectroscopy. The structural data for **9**[12] are in good agreement with those of known aminomethyleneboranes.[13]

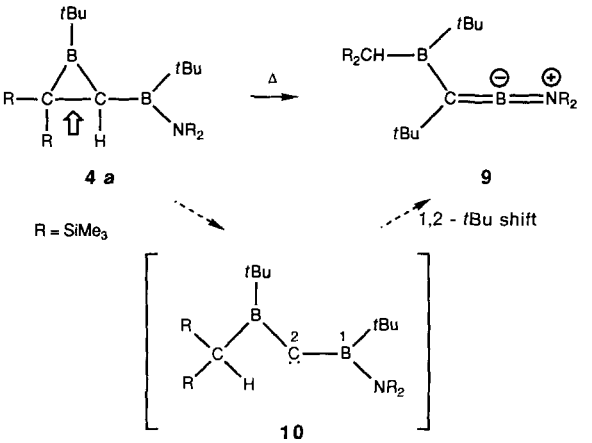

The C–C bond of the borirane ring is cleaved during the conversion of **4a** into **9**. We assume that diborylcarbene[14] **10** may be formed initially by the migration of the proton from the C atom between the two boron atoms to the C atom with the two trimethylsilyl groups. 1,2-Migration of the *tert*-butyl group from the boron atom bearing the amino substituent to the neighboring carbene C atom would then lead to **9**.

When heated in toluene at reflux for four hours, **4c** rearranges into tetrahydrodiboranaphthalene **11** (roughly 80%) and an unknown product. As for similar boriranes,[16] the preferred reaction is cleavage of the Si_2C–*B* bond of the borirane ring by the addition of a C–H bond of an *ortho* methyl group at the duryl group at the exocyclic boron atom.

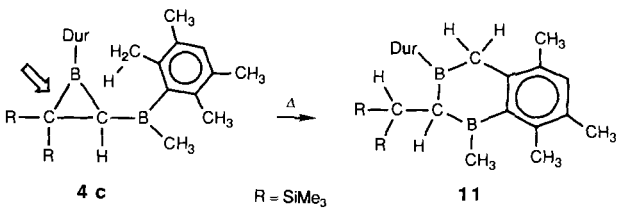

The structure assigned to **11** is supported by the ^{13}C NMR spectrum: broad signals for the C atoms of the CH_2 group bound to boron at δ = 32.9 (triplet, $J(^{13}C\text{-}H)$ = 116 Hz) and for the CH group at δ = 66.7 (doublet, $J(^{13}C\text{-}H)$ = 96 Hz), as well as the sharp signal at δ = 15.3 (doublet, $J(^{13}C\text{-}H)$ = 105 Hz) for the methine C atom of the $(Me_3Si)_2CH$ group *not* bound to boron (Table 2).

Cleavage of the borirane C–B bond adjacent to the exocyclic boron atom occurs during the reaction of **8a,b** with ethyl vinyl ether. The 2,5-dihydroboroles **13a,b**[17] are formed even at room temperature. The vinylboriranes **12a,b** are probable intermediates; these react under considerably

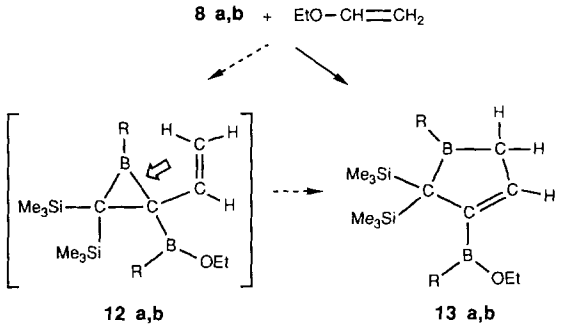

Table 2. Selected data for compounds **4a**, **4c**, **9**, **11**, and **13**.

4a: Colorless crystals, m.p. 180 °C (decomp.), yield: 65%. – ^{1}H NMR (300 MHz, $CDCl_3$, 25 °C): δ = 0.20 (s, 18H, $SiMe_3$), 0.08, 0.29 (each s, each 9H, $SiMe_3$), 1.05, 1.18 (each s, each 9H, *t*bu), 1.54 (s, 1H, BCH); ^{13}C NMR (100 MHz, $CDCl_3$, −40 °C): δ = 2.2, 3.5, 4.7, 4.9 (each q, each 3C, $SiMe_3$), 16.3 (s, 1C, CSi_2), 23.6, 29.7 (each br. s, each 1C, CMe_3), 27.5, 30.7, (each q, each 3C, $C(CH_3)_3$), 33.4 (br. d, 1C, BCH, $^1J(^{13}C,H)$ = 115 Hz); ^{11}B NMR (96 MHz, $CDCl_3$, 25 °C): δ = 69, 77.

4c: Colorless crystals, m.p. 128 °C (decomp.), yield: 55%. – ^{1}H NMR (300 MHz, $CDCl_3$, 25 °C): δ = 0.20, 0.44 (each s, each 9H, $SiMe_3$), 1.04 (s, 3H, B-CH_3), 2.14, 2.35, 2.39, 2.65 (each s, 24H, *o*- and *m*-CH_3), 7.02, 7.33 (each s, each 1H, *p*-H), the signal for B_2CH could not be localized; ^{13}C NMR (125 MHz, $CDCl_3$, −40 °C): δ = 1.4, 5.2 (each q, each 3C, $SiMe_3$), 15.1 (br. q, 1C, B-CH_3), 19.4, 20.2, 20.3, 20.5, 20.9, 21.3 (each q, 8C, *o*- and *m*-CH_3), 22.3 (s, 1C, CSi_2), 38.6 (br. d. 1C, B_2CH, $^1J(^{13}C,H)$ = 140 Hz), 130.6 (d, 1C, *p*-C), 131.1 (br. s, 1C, *i*-C), 132.7, 133.2, 133.7, 133.8 (each s, each 1C, *o*- or m-C), 134.2 (s, 2C, *m*-C), 137.5 (d, 1C, *p*-C), 144.3 (s, 2C, *o*-C), 151.3 (br. s, 1C, *i*-C); ^{11}B NMR (96 MHz, toluene, 90 °C): δ = 72, 78.

9: Colorless crystals, m.p. 184 °C (decomp.), yield: 68%. – ^{1}H NMR (300 MHz, $CDCl_3$, 25 °C): δ = 0.10, 0.32 (each s, each 18 H, $SiMe_3$), 1.00, 1.20 (each s, each 9 H, *t*bu), 1.47 (, 1H, Si_2CH); ^{13}C NMR (100 MHz, $CDCl_3$, 25 °C): δ = 2.6, 4.4 (each q, each 6C, $SiMe_3$), 20.5 (br. d, 1C, BCH, $^1J(^{13}C,H)$ = 91 Hz), 25.8 (br. s, 1C, $BCMe_3$), 32.2 (s, 1C, $CCMe_3$), 33.5, 35.9 (each q, each 3C, $C(CH_3)_3$), 86.8 (br.s, 1C, CB_2); ^{11}b NMR (96 MHz, $CDCl_3$, 25 °C): δ = 70, 58; IR (KBr): $\tilde{\nu}$ [cm^{-1}] = 1614, 1662 (4:1, ^{11}B = C, ^{10}B = C).

11: Colorless crystals, m.p. 162 °C (decomp.), yield: 45%. – ^{1}H NMR (300 MHz, $CDCl_3$, 25 °C): δ = 0.00, 0.12 (each s, each 9 H, $SiMe_3$), 0.97 (s, 1H, Si_2CH), 1.38 (s, 3H, B-CH_3), 1.94, 2.10, 2.25, 2.28, 2.32, 2.37, 2.47 (each s, each 3H, *o*- and *m*-CH_3), 2.78, 3.08 (each 1H, AB, ^2J(H,H) = 22.3 Hz), 4.04 (s, 1H, B_2CH), 7.01, 7.15 (each s, each 1H, *p*-H); ^{13}C NMR (125 MHz, $CDCl_3$, −30 °C): δ = 0.0, 2.8 (each q, each 3C, $SiMe_3$), 14.8 (d, 1C, Si_2CH, $^1J(^{13}C$-H) = 105 Hz), 16.4 (br. q, 1C, B-CH_3), 19.3, 19.5, 19.8, 20.2, 0.26, 20.29, 21.3 (each q, each 1C, *o*- and *m*-CH_3), 32.8 (br. t, 1C, CH_2, $^1J(^{13}C,H)$ = 116 Hz), 66.3 (br. d, 1C, B2CH, $^1J(^{13}C,H)$ = 96 Hz), 130.7 (d and s, 2C, *p*-C and *o*- or *m*-C), 133.2 (d, 1C, *p*-C), 131.9, 133.3, 133,9. 134.3, 134.4, 135.5, 138.3 (each s, each 1C, *o*- and *m*-C), 144.7, 146.3 (each br. s, each 1C, *i*-C); ^{11}B NMR (96 MHz, $CDCl_3$, 25 °C): δ = 83.

13b: Colorless crystals, m.p. 167 °C (decomp.), yield: 67%. – ^{13}C NMR (75 MHz, $CDCl_3$, 25 °C): δ = 3.7 (q, 6C, $SiMe_3$), 17.0 (q, 1C, CH_2-CH_3), 19.4, 19.57, 19.61, 22.1 (each q, each 4C, *o*- and *m*-CH_3), 40.3 (t, 1C, B-CH_2, $^1J(^{13}C,H)$ = 119 Hz), 52.6 (s, 1C, Si_2C), 63.1 (t, 1C, OCH_2), 130.1, 130.8 (each d, each 2C, *p*-C), 131.0, 132.8, 133.4, 134.4 (each s, each 2C, *o*- and *m*-C), 141.4, 147.3, 153.3 (each br. s, each 1C, *i*-C and BC = CH), 158.5 8d, 1C, BC = *CH*, $^1J(^{13}C,H)$ = 161 Hz); ^{11}B NMR (96 MHz, $CDCl_3$, 25 °C): δ = 47, 92.

milder conditions than those required by vinylcyclopropanes[18] to give the corresponding five-membered compounds. We conclude that all types of bonds in the three-membered rings of suitably substituted boriranes can open thermally.

Received: April 6, 1992 [Z 5278 IE]
German version: *Angew. Chem.* **1992**, *104*, 1417

[1] J. J. Eisch, B. Shafii, J. D. Odom, A. L. Rheingold, *J. Am. Chem. Soc.* **1990**, *112*, 1847–1853, and references therein; A. Höfner, B. Ziegler, W. Massa, A. Berndt, *Angew. Chem.* **1989**, *101*, 188–190; *Angew. Chem. Int. Ed. Engl.* **1989**, *28*, 186–187, and references therein.

[2] M. A. Kropp, M. Baillargeon, K. M. Park, K. Bhamidapaty, G. B. Schuster, *J. Am. Chem. Soc.* **1991**, *113*, 2155–2163, and references therein.

[3] Bicyclic boriranes [4] could not be obtained as single crystals because of their instability. Boranediylboriranes [5] are quite distorted as a result of very strong σ–π interactions.

[4] H. Klusik, A. Berndt, *Angew. Chem.* **1983**, *95*, 895–896; *Angew. Chem. Int. Ed. Engl.* **1983**, *22*, 877–878.

[5] C. Wieczorek, J. Allwohn, G. Schmidt-Lukasch, R. Hunold, W. Massa, A. Berndt, *Angew. Chem.* **1990**, *102*, 435–436; *Angew. Chem. Int. Ed. Engl.* **1990**, *29*, 389–399, and references therein; P. H. M. Budzelaar, K. Krogh-Jespersen, T. Clark, P. von R. Schleyer, *J. Am. Chem. Soc.* **1985**, *107*, 2773–2779, and references therein.

[6] a) P. H. M. Budzelaar, A. J. Kos, T. Clark, P. von R. Schleyer, *Organometallics* **1985**, *4*, 429–437, and references therein; b) C. A. Taylor, M. C. Zerner, B. Ramsey, *J. Organomet. Chem.* **1986**, *317*, 1–10; c) M. Bühl, P. von R. Schleyer, M. A. Ibrahim, T. Clark, *J. Am. Chem. Soc.* **1991**, *113*, 2466–2471, and references therein.

[7] L. Radom, J. A. Pople, P. von R. Schleyer, *J. Am. Chem. Soc.* **1973**, *95*, 8193–8195, P. von R. Schleyer, M. Bremer, *J. Org. Chem.* **1988**, *53*, 2362–2369, and references therein.

[8] S. E. Denmark, K. Nishide, A.-M. Faucher, *J. Am. Chem. Soc.* **1991**, *113*, 6675–6676.

[9] H. Meyer, G. Schmidt-Lukasch, G. Baum, W. Massa, A. Berndt, *Z. Naturforsch. B* **1988**, *43*, 801–806.

[10] X-ray structure analysis with a four-circle diffractomer (CAD4, Enraf-Nonius) with $Cu_{K\alpha}$ radiation: **4a**: $C_{22}H_{55}B_2Si_4N$, space group *Pccn*; Z = 8; a = 977.6(2), b = 3090.5(13), c = 2038.4(7) pm, ϱ = 1.009 g cm^{-3}; 3289 independent reflections with $F_0 > 3\sigma(F)$ measured at −100 °C; no absorption correction (μ = 17.4 cm^{-1}). Hydrogen atoms at calculated positions, collective isotropic temperature factors refined for groups, the H atom on C2 was refined separately. Anisotropic temperature factors were used for all other atoms except boron. Refinement with full matrix. 272 parameters, R = 0.044, wR = 0.043 (weighted $w = 1/\sigma^2(F_0)$). **4c**: $C_{29}H_{48}B_2Si_2$, space group $P4_1$; Z = 4; a = 876.85(4), c = 3901.8(2) pm; ϱ = 1.051 g cm^{-3}; 1842 independent reflections with $F_0 > 4\sigma(F)$ measured at −80 °C, no absorption correction (μ = 11.5 cm^{-1}). Except for those of the methyl group C12, all hydrogen atoms were all localized, but were calculated with the riding model. Collective isotropic temperature factors were refined for them. Anisotropic temperature factors were used for all other atoms except boron. Refinement with the block-diagonal matrix technique. 309 Parameters, R = 0.033, wR = 0.035, (weighted $w = 1/\sigma^2(F_0)$). The existence of the enantiomeric structure (space group $P4_3$) was not likely since Rogers η parameter could be refined to 1.23(9). Further details of the crystal structure investigation may be obtained from the Fachinformationszentrum Karlsruhe, Gesellschaft für wissenschaftlich-technische Information mbH, D-W-7514 Eggenstein-Leopoldshafen 2 (FRG) on quoting the depository number CSD-56363, the names of the authors, and the journal citation.

[11] R. F. Childs, M. D. Kostyk, C. J. L. Lock, M. Mahendran, *J. Am. Chem. Soc.* **1990**, *112*, 8912–8920, and references therein.

[12] The X-ray structure analysis provided the following distances and angles for **9**: C=B 140.8(5) pm, B-N 136.7(5) pm, C=B-N 175.8(4)°, B-C-B 121.3(3)°. J. Allwohn, Diplomarbeit, Marburg, **1988**.

[13] B. Glaser, E. Hanacker, H. Nöth, H. Wagner, *Chem. Ber.* **1987**, *120*, 659–667; R. Boese, P. Paetzold, A. Tapper, *ibid.* **1987**, *120*, 1069–1071.

[14] Similar carbenes disubstituted by boron have been postulated to explain products resulting from the cleavage of the C–C bond of boriranides [15].

[15] P. Willershausen, C. Kybart, W. Massa, M. Bühl, P. von R. Schleyer, A. Berndt, *Angew. Chem.* **1992**, *104*, 1278; *Angew. Chem. Int. Ed. Engl.* **1992**, *31*, 1238.

[16] P. Willershausen, Dissertation, Marburg, **1992**.

[17] The structure of **13b** is secured by X-ray structure analysis. J. Allwohn, Dissertation, Marburg, **1991**.

[18] J. Salaun in *The Chemistry of the Cyclopropyl Group* (Ed.: Z. Rapport), Wiley, New York, **1987**, p. 809.

Stereoselective Synthesis of Phosphate-Modified Building Blocks of DNA**

By *Wendelin Samstag* and *Joachim W. Engels**

Dedicated to Professor Fritz Eckstein on the occasion of his 60th birthday

As a result of little electrostatic repulsion, nonionic DNA analogues form very stable complexes with complementary

[*] Prof. Dr. J. Engels, Dipl.-Chem. W. Samstag
Institut für Organische Chemie der Universität
Niederurseler Hang, D-W-6000 Frankfurt am Main 50 (FRG)

oligonucleotides[1] and are resistant towards cellular nucleases.[2] They have long half-lives in living systems and diffuse more easily through cell membranes.[3] Nonionic DNA analogues are thus excellent candidates for the study of DNA–DNA and DNA–protein interactions, as well as for application as antisense oligonucleotides. Among the nonionic oligonucleotides analogous to phosphate oligomers are the phosphotriesters, phosphoramidates, and alkylphosphonates. The alkylphosphonates are characterized by particularly high stability towards nucleases and therefore the oligonucleoside methylphosphonates belong to the most extensively studied compounds for the antisense approach.[4] Difluoromethyl- and phenylphosphonates have also been synthesized and are currently under investigation.[5, 6] The influence of the methyl group of the methylphosphonate on helix formation has not yet been elucidated in detail. We therefore reasoned that it would be interesting to incorporate sterically bulkier organic groups as modification at the phosphorus atom to study their effect on stereoselection and thus to influence the configuration and the molecular geometry by design. We report here a simple experimental access to predominantly *Sp*-configurated alkyl- and benzylphosphonates, based on the reaction of organozinc halides with PCl_3.

The reaction of the Grignard reagent **1** with $ZnCl_2$ gives the organozinc halides **2**, which react further with PCl_3 to yield the desired alkyl- or benzyldichlorophosphanes **3** (Scheme 1).

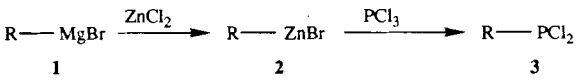

Scheme 1. Synthesis of the phosphonylation reagents. R = *i*Pr, benzyl, (*S*)-(+)-2-methylbutyl.

In a one-pot reaction, the phosphonylation reagent **3** is treated successively with two protected nucleosides. The resulting phosphonous acid diester is oxidized without prior isolation to its alkyl- or benzylphosphonate (**4**–**12**) by addition of *tert*-butylhydroperoxide (Scheme 2).

The symmetric reference compounds, 3′-3′- and 5′-5′-linked phosphonates **7**–**9** and **10**–**12**, respectively, are accessible by treating two equivalents of each of 5′-*O*-tritylthymidine and 3′-*O*-(*tert*-butyldimethylsilyl)thymidine with the phosphonylation reagent. Reaction of 5′-*O*-tritylthymidine and 3′-*O*-(*tert*-butyldimethylsilyl)thymidine with $RPCl_2$ yields **4**–**6**, which contain the 3′,5′-linkage. The 3′,3′-phosphonates **7**–**9** are always formed as side products, but the formation of **10**–**12** (on reaction of 3′-*O*-(*tert*-butyldimethylsilyl)thymidine with unchanged $RPCl_2$) can easily be suppressed by a small excess (0.06 equiv) of 5′-*O*-tritylthymidine.

The introduction of this modification generates a chiral center at the phosphorus atom. The compounds **4**–**6** form two diastereomers (**a**, **b**) that can be separated by preparative reverse-phase HPLC. As also observed for the methylphosphonates, the *Rp*-configurated isomer has the shorter retention time. According to the latest findings an unambiguous assignment by ^{31}P NMR spectroscopy is not possible.[10] The configuration of the diastereomers **4** was determined with the ROESY NMR technique.[7] To do so, the ROEs between the benzylic methylene protons and the sugar protons in the immediate vicinity must be measured. Interestingly, according to our current assignment a selection in favor of the *Sp* isomer is observed, whereas in the synthesis of the

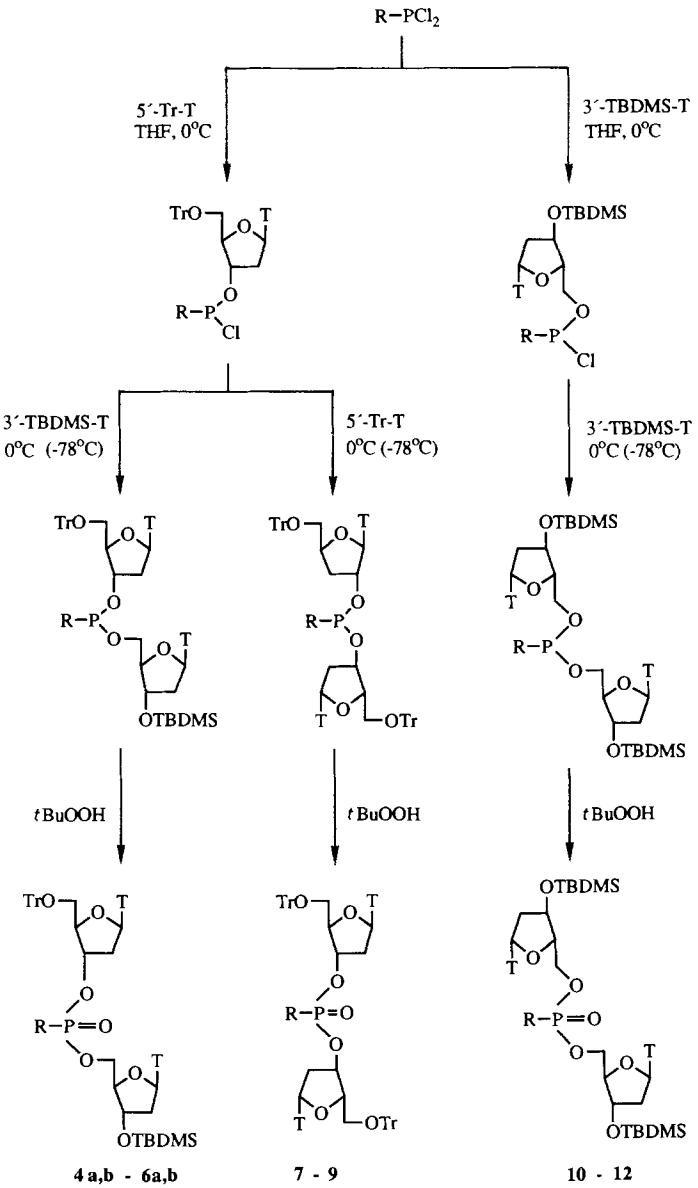

Scheme 2. Synthesis of the 3′,5′- (**4**–**6**), 3′,3′- (**7**–**9**), and 5′,5′-linked (**10**–**12**) alkyl- and benzyl phosphonates. **4**, **7**, **10**: R = *i*Pr; **5**, **8**, **11**: R = benzyl; **6**, **9**, **12**: R = (*S*)-(+)-methylbutyl. The compounds **4**–**6** occur as diastereomers. These *Rp*/*Sp* isomers are labeled **a** or **b**.

methylphosphonates the *Rp* isomer is always formed preferentially (Table 1).

The configuration at the phosphorus atom has a drastic influence on the stability of duplexes of modified oligonucleotides and complementary sequences. Oligonucleoside–methylphosphonates with predominantly *Rp*-configurated diastereomers afford more stable hybrids with complementary DNA than the naturally occurring analogues, while duplexes with predominantly *Sp*-configurated isomers are less

Table 1. Dependence of the diastereoselectivities on the substituents at the phosphorus atom at different temperatures.

P substituent	*T* [°C]	*Rp*/*Sp*	P substituent	*T* [°C]	*Rp*/*Sp*
methyl	+4	2.0:1.0	isopropyl	+4	1.0:2.8
methyl	−78	5.0:1.0	isopropyl	−78	1.0:3.9
benzyl	+4	1.0:1.6	(*S*)-(+)-2-methylbutyl	+4	1.0:2.2
benzyl	−78	1.0:2.7	(*S*)-(+)-2-methylbutyl	−78	1.0:2.8

stable.[9] The reason for this behavior is not clear. We hope to throw more light on the subject by building the new nucleosidephosphonates into oligonucleotides and studying their behavior toward duplex formation. As UV and CD measurements on many diastereomerically pure methylphosphonate dimers show, the bases of the *Rp* dimer occur in the stacked form, whereas the extended form prevails for the *Sp* isomer.[10] In the *Sp* configuration of the phosphodiester linkage, the substituent at the P atom is in a pseudoaxial position and thus in the vicinity of the nucleoside bases. Since this is the clearly preferred isomer in the synthesis presented here, the possibility exists that the structure of the molecule can be intentionally changed by a suitable choice of substituents. Now, further influence of either a steric, electronic, or covalent nature opens a new field for molecular modeling at DNA molecules.

The preferential formation of one isomer is in accord with our concept of the reaction mechanism. The diastereomeric selection takes place at the reaction of the monoester with the second nucleoside; we assume that it is a $S_N2(P)$ mechanism. The two approaches from which the attack can be initiated are blocked to different extents by the trityl protecting group on one side and the substituent at the phosphorus on the other. One approach is thereby energetically favored.[11] If the substituent at the phosphorus atom is small, the attack is predominantly from this side and affords the *Rp* configurated product. However, if the substituent at the P atom is bulky, the attack from the side of the trityl group is more favorable, and the *Sp* isomer forms preferentially. In this case the yield decreases, since the space around the phosphorus atom in the monoester is already severely congested. Even the use of a chiral substituent, here (*S*)-(+)-2-methylbutyl, does not lead to a further increase in the diastereomeric ratio. Phosphorusamidites are also easily accessible as building blocks for solid-state synthesis via the monoester step; however, no statement about stereoselectivities and yields is yet possible.

Experimental Procedure

3: A solution of $ZnCl_2$ (0.1 mol) in ether was added dropwise under argon at 0 °C to the Grignard compound **1** (0.1 mol) dissolved in ether (300 mL). A gray precipitate formed. The suspension was stirred for 15 min before it was transferred to an addition funnel and added dropwise to a boiling solution of PCl_3 (0.3 mol) and ether (50 mL). The mixture was stirred for a further 1 h under reflux, cooled to room temperature, and filtered by suction, and the residue washed with ether. The filtrate was evaporated to dryness, and the recovered solid fractionated in a stream of argon. ^{31}P NMR (121.5 MHz, $CDCl_3$, 295 K, 85% H_3PO_4 external): benzyldichlorophosphane: $\delta = 179.3$; dichloroisopropylphosphane: $\delta = 199.8$; dichloro-(*S*)-(+)-2-methylbutylphosphane: $\delta = 198.1$.

4–**6**: 5′-Tritylthymidine (0.76 mmol) and 3′-(*tert*-butyldimethylsilyl)thymidine (0.725 mmol) were coevaporated with THF into separate tapered flasks. THF (2 mL), collidine (1.5 mmol), and phosphonylation reagent **3** (0.745 mmol) were placed in a flask that had previously been degassed by heating, flushed with argon, and sealed with a septum. The solution was cooled to 4 °C before the nucleoside, protected at the 5′-position and dissolved in 3 mL of THF, was added within 5 min with stirring from a Hamilton syringe. A white precipitate formed. After 10 min the 3′-protected nucleoside dissolved in THF was added at 4 °C or −78 °C within 5 min, and the mixture was stirred for a further 30 min. Either at 4 °C or after thawing to −20 °C, the product was oxidized with *tert*-butylhydroperoxide within 10 min. The suspension was evaporated to dryness, and the residue taken up in $CHCl_3$ (150 mL). The mixture was washed with 5% $NaHCO_3$ solution, 5% Na_2SO_4 solution, and H_2O, then dried over Na_2SO_4, and filtered. The solvent removed in a rotary evaporator, and the residue was dissolved in a little $CHCl_3$. The product was precipitated with *n*-hexane, filtered by suction, washed, and dried on a vacuum line (oil pump). Yield based on unchanged TrT: **4a,b**: 47% (4 °C), 38% (−78 °C); **5,b**: 56% (4 °C), 28% (−78 °C); **6a,b**: 31% (4 °C), 11% (−78 °C). Preparative HPLC separation of the diastereomers: **4a,b**: Lichrospher RP-C18 Semiprep. 5 μm; 3 mL min^{-1} triethylammonium acetate (TEAA) 0.1 M/CH_3CN 28/72 isochratic. **5a,b**: Bondapack C18 prep. 10 μm; 15 mL min^{-1} TEAA 0.1 M/CH_3CN 51/49 isochratic. **6a,b**: Bondapack C18 prep. 10 μm; 15 mL min^{-1} TEAA 0.1 M CH_3CN 47/53 isochratic. ^{31}P NMR (121.5 MHz, $CDCl_3$, 295 K, 85% H_3PO_4 external): **4**: $\delta = 29.1$ (*Rp*), 28.1 (*Sp*); **5**: $\delta = 37.9$ (*Rp*), 37.1 (*Sp*); **6**: $\delta = 34.9$ (*Rp*), 34.0 (*Sp*).

Received: May 23, 1992 [Z 5370 IE]
German version: *Angew. Chem.* **1992**, *104*, 1367

CAS Registry numbers:
1, R = Pr, 920-39-8; **1**, R = CH_2Ph, 1589-82-8; **1** R = (*s*)-$CH_3CHMeEt$, 35026-81-4; **3** R = *i*Pr, 25235-15-8; **3** R = CH_2Ph, 4545-85-1; **3** R = (*s*)-$CH_2CHMeEt$, 113738-71-9; **4** (*R*) phosphorus isomer, 143331-43-5; **4** (*S*) phosphorus isomer, 143394-41-6; **5** (*R*) phosphorus isomer, 143331-44-6; **5** (*S*) phosphorus isomer, 143394-42-7; **6** (*R*) phosphorus isomer, 143331-45-7; **6**, (*S*) phosphorus isomer, 143394-43-8; **7**, 143331-46-8; **8**, 143331-47-9; **9**, 143331-48-0; **10**, 143331-49-1; **11**, 143331-50-4; **12**, 143331-51-5; 5′-tritylthymidine, 7791-71-1; 3′-(*tert*-butyldimethylsilyl)thymidine, 40733-27-5.

[1] L. S. Kan, D. S. Cheng, P. S. Miller, J. Yano, P. O. Ts'O, *Biochemistry* **1980**, *19*, 2122.
[2] J. C. Barrett, P. S. Miller, P. O. Ts'O, *Biochemistry* **1974**, *13*, 4897.
[3] J. C. Marcus-Sekura, A. Woerner, K. Shinozuka, G. Zon, G. Quinnan, *Nucleic Acids Res.* **1987**, *15*, 5749.
[4] P. S. Miller, *Bio/Technology* **1991**, *9*, 358.
[5] D. E. Bergstrom, P. W. Shum, *J. Org. Chem.* **1988**, *53*, 3953.
[6] K. L. Agarwal, F. Riftina, *Nucleic Acids Res.* **1979**, *6*, 3009.
[7] T. Löschner, J. W. Engels, *Nucleic Acids Res.* **1990**, *18*, 5083.
[8] T. Löschner, J. W. Engels, *Tetrahedron Lett.* **1989**, *30*, 5587.
[9] J. Lesnikowski, M. Jaworska, W. J. Stec, *Nucleic Acids Res.* **1990**, *18*, 2109.
[10] A. V. Lebedev, E. V. Vyazovkina, A. Frauendorf, J. W. Engels, *Tetrahedron*, submitted.
[11] J. W. Engels, T. Löschner, A. Frauendorf, *Nucleosides & Nucleotides* **1991**, *10*, 347.

Fullerene Sugars: Preparation of Enantiomerically Pure, Spiro-Linked *C*-Glycosides of C_{60}**

By *Andrea Vasella,* Peter Uhlmann, Christian A. A. Waldraff, François Diederich,** and *Carlo Thilgen*

Whereas the initial fullerene research primarily focused on the physical properties of the pure carbon spheres, synthetic chemists lately have become interested in their functionalization, especially that of C_{60}. Examples for reactions with fullerenes are the hydrogenation,[1] halogenation,[2] epoxidation,[3] the formation of exohedral transition metal complexes,[4] cycloadditions and carbene additions,[5] as well as alkylations and arylations.[6] In agreement with the expectations for molecules with multiple reactive sites, many of these derivatizations yielded nonseparable mixtures of constitutional isomers and polyfunctionalized compounds. In some cases, selective conversions were achieved,[2–5] leading to well defined and pure compounds.

In this paper we describe the preparation and complete characterization of the fullerene sugars **4** and **5**, which were obtained in good yields from the reaction of C_{60} with nucleophilic glycosylidene carbenes. These spiro-linked C-glycoside-like compounds are of interest because they are the first chiral *and* enantiomerically pure derivatives of fuller-

[*] Prof. A. Vasella, P. Uhlmann, C. A. A. Waldraff
Organisch-chemisches Institut der Universität
Winterthurerstrasse 190, CH-8057 Zürich (Switzerland)
Prof. F. Diederich, Dr. C. Thilgen
Laboratorium für Organische Chemie
ETH-Zentrum
Universitätstrasse 16, CH-8092 Zürich (Switzerland)

[**] Glycosylidene Carbenes, Part 9. We thank D. Nanz, T. Plüss, and O. Zerbe for recording the NMR spectra and V. Purghart, Spectronex AG, for recording the mass spectra. Part 8: A. Linden, A. Vasella, C. Witzig, *Helv. Chim. Acta*, in press.

enes. In addition, deprotection of the sugar residues should generate ambiphilic buckyballs and therefore provide an entry into investigations of the biochemical and pharmacological potential of this fascinating class of compounds.

As precursors of nucleophilic or ambiphilic carbenes, alkyl- and acyl-protected 1-azi derivatives of monosaccharides react with acceptor- and donor-substituted alkenes to yield spiro-linked glycosylidene cyclopropanes.[7-9] In a similar way, the *O*-benzyl protected diazirine **2**[10] reacted with C_{60} (**1**) to afford the monoglycosylated adduct **4** in 55% yield (74% based on reacted **1**) (Scheme 1). Evidence for double or even multiple carbene additions as the main side-reactions was obtained by ^{1}H NMR spectroscopy. The significant difference in the R_f values of **1** and **4** (ΔR_f (toluene): 0.38, SiO_2) facilitated the chromatographic purification of **4** and the almost complete recovery of unreacted **1**. In analogy, the *O*-pivaloylated diazirine **3**[9] afforded the addition product **5** (ΔR_f (toluene): 0.67) in 54% yield (76% based on reacted **1**).

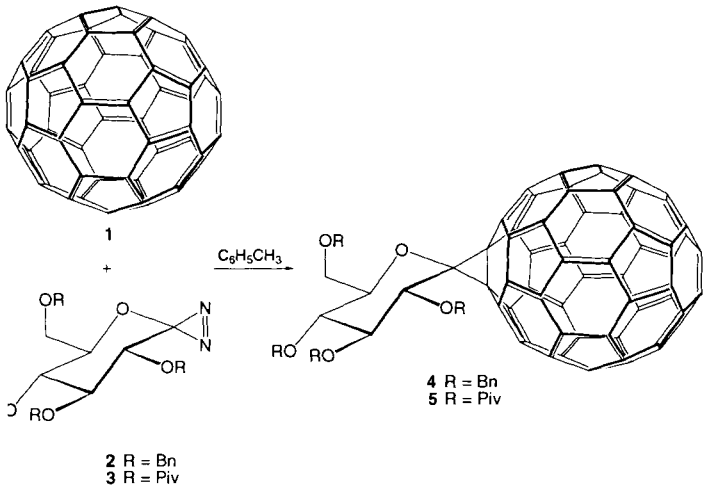

Scheme 1. Synthesis of the fullerene sugars **4** and **5**. Bn = benzyl, Piv = pivaloyl.

The formation of **4** and **5** through monoaddition is confirmed by elemental analyses and NMR data. The ^{1}H NMR spectrum of **4** shows chemical shifts and coupling patterns typical of *O*-benzyl protected derivatives of glucose in the $^4C_1$ conformation. Compared to known *O*-benzyl protected glycosylidene cyclopropane derivatives,[7] the ^{1}H NMR resonances of the new compound (**4**) are shifted downfield; the signal for the proton on C2 is shifted the most ($\Delta\delta = 1$). The signals of the glycosylidene moiety of **5** are also shifted significantly downfield in comparison to the related known cyclopropanes;[9] the signal for the proton on C2 is particularly affected ($\delta = 6.77$). The coupling constant $^{2,3}J$ (3.9 Hz) in **5** indicates a remarkable deformation of the chair conformation, probably as a result of steric interactions between the C_{60} moiety and the pivaloyloxy group at C2.

In the ^{13}C NMR spectra of **4** and **5** (Fig. 1), the resonances of the carbon atoms C2 to C6 appear in the typical chemical shift region $\delta = 68-86$ and $\delta = 62-75$, respectively. Evidence for a cyclopropane structure is obtained by comparison of the NMR data with that of known glycosylidene cyclopropane derivatives.[7,9] In particular, the peaks at $\delta = 74.04$ and 72.81, respectively, (probably C1) as well as the two peaks of identical, but lower intensity at 78.24 and

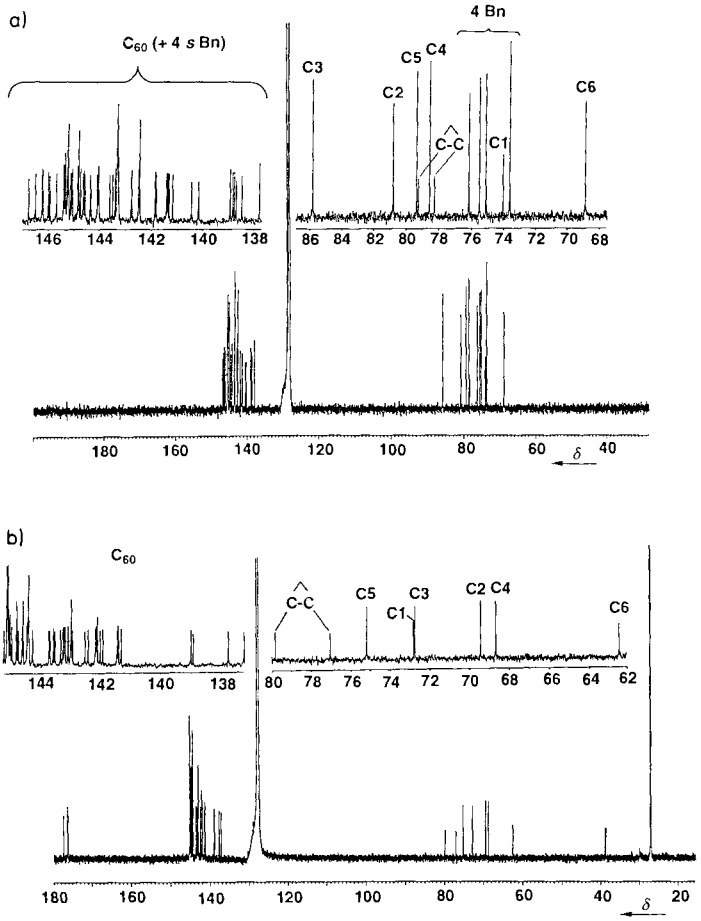

Fig. 1. ^{13}C NMR spectra (150.7 MHz, C_6D_6) of **4** (a) and **5** (b).

79.29 (**4**) and 77.05 and 79.84 (**5**) are characteristic of a three-membered ring structure. In the region $\delta = 137-147$, 48 and 44 singlets (partially overlapping) for **4** and **5**, respectively, are observed, arising from the C_{60} moieties.

Besides the characteristic bands of the glycosylidene residue, the IR spectra of **4** and **5** exhibit four (1426, 1186,

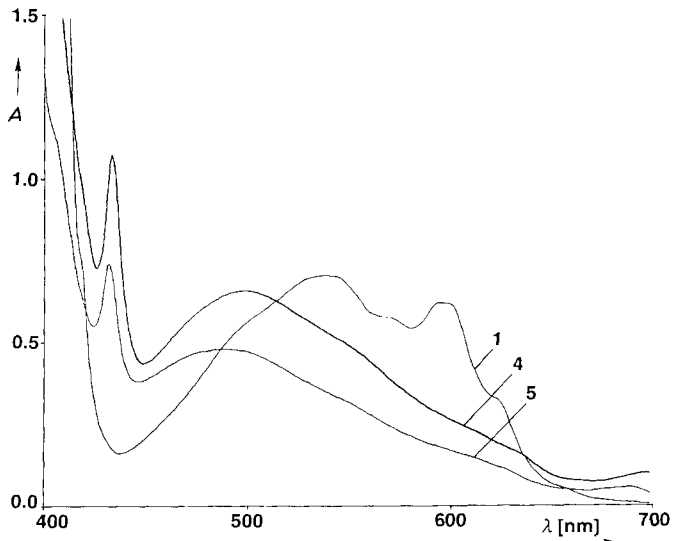

Fig. 2. UV/VIS spectra (toluene) of **1**, **4**, and **5**.

574, 526 cm^{-1}) and three (1428, 574, 527 cm^{-1}) bands, respectively, of the fullerene moiety. The UV/VIS spectra of **4** and **5** (Fig. 2) are nearly identical, and absorption maxima are located at 499 ($\varepsilon = 2660$) and 489 nm ($\varepsilon = 1802$), respectively, and at 433 ($\varepsilon = 1629$) and 432 nm ($\varepsilon = 1163$). Both spectra show the same loss of the C_{60} absorption fine structure between 500 and 650 nm, and the absorption maxima resemble those of the buckminsterfullerene oxide, $C_{60}O$.[3b]

Interestingly, the CD spectra of **4** and **5** (Fig. 3) exhibit several maxima and differ significantly from each other. It is not clear yet whether the differences originate directly from the protecting groups or indirectly from a conformational change of the fullerene framework. The interpretation of the

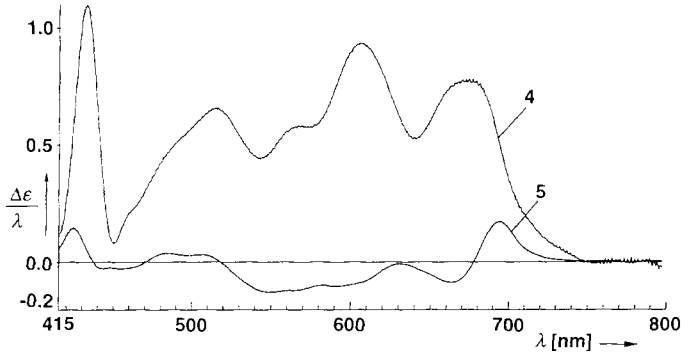

Fig. 3. CD spectra [$\Delta\varepsilon/\lambda$] of **4** (toluene, $c = 0.402$ mM) and **5** (toluene, $c = 1.19$ mM).

CD spectra, the proof for the regioselectivity of the addition, the nature of the cyclopropane unit, and the deprotection of the sugar moieties are currently subjects of further investigations.

Experimental Procedure:

4: A solution of 35 mg (0.049 mmol) of **1** in 35 mL of toluene was treated with 26.7 mg (0.049 mmol) of **2** under argon at 23 °C. The solution was stirred for 3 h, and a color change from violet to wine red was observed. The solvent was removed under vacuum, and the brownish residue was purified by flash chromatography (SiO_2, toluene) to yield 33 mg (55%) of **4** in addition to 9 mg (26%) of unreacted **1**. The product can be precipitated as a brown powder from a toluene solution by addition of methanol. R_f (SiO_2, toluene): 0.43; UV/VIS (toluene): λ_{max} [nm] (ε) = 433 (2660), 499 (1629); IR (KBr): $\tilde{\nu}$ [cm^{-1}] = 3060w, 3027w, 2920w, 2855w, 1604w, 1536w, 1495m, 1452m, 1426m (C_{60}), 1402w, 1359m, 1319w, 1249w, 1208m, 1186w (C_{60}), 1155m, 1089s, 1073s, 1028m, 1002m, 907w, 840w, 799w, 732s, 695s, 645w, 594w, 574w (C_{60}), 562w, 550w, 526s (C_{60}), 479w, 462w; ^{1}H NMR (300 MHz, $CDCl_3$): $\delta \approx 7.35-7.06$ (m; 20 arom. H), 5.11 (d, ^3J(H,H) = 11.2 Hz, 1H; $PhCH_2$), 5.01 (d, ^3J(H,H) = 10.8 Hz, 1H; $PhCH_2$), 4.95 (d, ^3J(H,H) = 10.8 Hz, 1H, $PhCH_2$), 4.94 (d, ^3J(H,H) = 8.3 Hz; H-C2), 4.92 (d, ^3J(H,H) ≈ 10.8 Hz, 2H; $PhCH_2$), 4.68 (d, ^3J(H,H) = 12.2 Hz, 1H; $PhCH_2$), 4.64 (d, ^3J(H,H) = 10.7 Hz, 1H; $PhCH_2$), 4.53 (d, ^3J(H,H) = 12.2 Hz, 1H; $PhCH_2$), 4.42 (pseudo t, ^3J(H,H) ≈ 8.0 Hz, H-C3), 4.25 (dd, ^3J(H,H) = 7.8, 9.8 Hz; H-C4), 4.18 (ddd, ^3J(H,H) = 2.0, 3.0, 9.9 Hz; H-C5), 3.89 (dd, ^3J(H,H) = 3.3, 11.0 Hz; H_A-C6), 3.82 (dd, ^3J(H,H) = 2.0, 11.0 Hz; H_B-C6); ^{1}H NMR (600 MHz, C_6D_6): $\delta = 7.47-7.14$ (m; 20 arom. H), 5.13 (d, ^3J(H,H) = 11.1 Hz, 1H; $PhCH_2$), 5.09 (d, ^3J(H,H) = 11.2 Hz, 1H; $PhCH_2$), 5.04 (d, ^3J(H,H) = 11.2 Hz, 1H; $PhCH_2$), 5.00 (d, ^3J(H,H) = 11.1 Hz, 1H; $PhCH_2$), 4.91 (d, ^3J(H,H) = 7.9 Hz; H-C2), 4.90 (d, ^3J(H,H) = 11.0 Hz, 1H; $PhCH_2$), 4.81 (d, ^3J(H,H) = 11.3 Hz, 1H; $PhCH_2$), 4.64 (pseudo t, ^3J(H,H) ≈ 7.9 Hz; H-C3), 4.60 (d, ^3J(H,H) = 12.1 Hz, 1H; $PhCH_2$), 4.56 (dd, ^3J(H,H) = 7.9, 9.8 Hz; H-C4), 4.51 (pseudo dt', ^3J(H,H) ≈ 9.8, 2.6 Hz; H-C5), 4.50 (d, ^3J(H,H) = 12.1 Hz; $PhCH_2$), 3.94 (d, ^3J(H,H) = 2.7 Hz, 2H; H-C6); ^{13}C NMR (150.7 MHz, C_6D_6): $\delta = 146.76$(s), 146.49(s), 146.24(s), 146.20(s), 145.99(s), 145.93(s), 145.67(s), 145.40(s), 145.38(s), 145.34(s), 145.27(s), 145.25(2s), 145.22(2s), 145.13(s), 145.09(s), 145.06(s), 144.85(s), 144.81(2s), 144.75(s), 144.64(s), 144.61(s), 144.57(s), 144.37(s), 144.34(s), 144.10(s), 144.06(s), 144.04(s), 144.02(s), 143.59(s), 143.48(s), 143.38(s), 143.30 (≈7s), 143.25(s), 142.76(s), 142.73(s), 142.49(s), 142.47(s), 142.45(2s), 141.85(s), 141.81(s), 141.41(s), 141.36(s), 141.32(s), 141.18(s), 140.44(s), 140.15(s), 138.92(s), 138.81(s), 138.75(s), 138.68(s), 138.45(s), 137.77(s), 129.80-127.5(m), 85.82 (d; C3), 80.80 (d; C2), 79.34 (d; C5), 79.23(s), 78.55 (d; C4), 78.25(s), 76.17(t), 75.50(t), 75.10(t), 74.04 (s;C1), 73.62(t), 68.87 (d; C6); Low Density Time of Flight Mass Spectrum (LD-TOF-MS): *m/z* 799 (5%), 721(100), 698(8), 267(5), 225(16), 212(5), 181(31), 163(14), 149(5), 123(9), 91 (90, $[C_7H_7]^+$), 60(10); correct elemental analysis.

5: To a solution of 35 mg (0.049 mmol) of **1** in 18 mL of absolute toluene stirred under argon at 45 °C was added an ice-cold solution of 26 mg (0.049 mmol) of **3** in 17 mL of toluene. After the mixture had been stirred at 45 °C for an additional 2 h, a color change similar to the one observed during the preparation of **4** occurred. The same workup and isolation procedure provided 32 mg (54%) of **5** as well as 10 mg (28%) of unreacted **1**. R_f (hexanes/AcOEt 4:1) 0.59 (**5**), 0.73 (**1**); R_f (toluene) 0.14 (**5**), 0.81 (**1**); UV/VIS (toluene): λ_{max} [nm] (ε) = 432 (1802), 489 (1163); FT-IR (KBr): $\tilde{\nu}$ [cm^{-1}] = 2971s, 2932m, 2871m, 1743s, 1479s, 1459m, 1428m (C_{60}), 1397m, 1366m, 1277s, 1228w, 1207w, 1122s (br.), 1036m, 940w, 885w, 796w, 761w, 743w, 574w (C_{60}), 563w, 527s (C_{60}), 480w; ^{1}H NMR (600 MHz, C_6D_6): $\delta = 6.77$ (d, ^3J(H,H) = 3.9 Hz; H-C2), 5.98 (t, ^3J(H,H) = 4.2 Hz; H-C3), 5.90 (dd, ^3J(H,H) = 4.3, 9.9 Hz; H-C4), 4.88 (ddd, ^3J(H,H) = 2.1, 5.6, 9.7 Hz; H-C5), 4.62 (dd, ^3J(H,H) = 1.8, 12.6 Hz; H_A-C6), 4.43 (dd, ^3J(H,H) = 5.7, 12.7 Hz; H_B-C6), 1.27, 1.24, 1.21 (3s, 4$C(CH_3)_3$); ^{13}C NMR (150.7 MHz, C_6D_6): $\delta = 177.32$ (s, C=O), 176.37 (s, C=O), 176.25 (s, C=O), 176.12 (s, C=O), 145.26(s), 145.17(s), 145.16(s), 145.13(s), 145.07(s), 145.06(s), 145.00(s), 144.84(s), 144.78(s), 144.65(s), 144.62(s), 144.49(s), 144.47(s), 144.44(s), 144.42(s), 144.30(s), 143.75(s), 143.72(s), 143.60(s), 143.55(s), 143.36(s), 143.29(s), 143.24(s), 143.21(s), 143.12(s), 143.11(s), 143.03(s), 143.01(s), 142.96(s), 142.54(s), 142.43(s), 142.19(s), 142.16(s), 142.13(s), 142.03(s), 141.94(s), 141.46(s), 141.43(s), 141.41(s), 141.31(s), 139.01(s), 138.94(s), 137.78(s), 137.25(s), 79.84(s), 77.05(s), 75.20 (d, C5), 72.81 (s, C1), 72.75 (d, C3), 69.43 (d, C2), 68.67 (d, C4), 62.48 (t, C6), 38.98, 38.76, 38.74, 38.62 (4s, 4$C(CH_3)_3$), 27.19, 27.06, 27.03, 26.87 (4q, 12 CH_3); LD-TOF-MS: *m/z* 720 (36%, C_{60}^+), 224(4), 188(4), 110(3), 98(3), 85 (6, $[C_5H_9O]^+$), 57 (100, $[C_4H_9]^+$); correct elemental analysis.

Received: June 23, 1992 [Z 5425 IE]
German version: *Angew. Chem.* **1992**, *104*, 1383

CAS Registry numbers:
1, 99685-96-8; **2**, 126709-14-6; **3**, 143494-97-7; **4**, 143705-57-1; **5**, 143705-58-2.

[1] R. E. Haufler, J. Conceicao, L. P. F. Chibante, Y. Chai, N. E. Byrne, S. Flanagan, M. M. Haley, S. C. O'Brien, C. Pan, Z. Xiao, W. E. Billups, M. A. Ciufolini, R. H. Haugem, J. L. Margrave, L. J. Wilson, R. F. Curl, R. E. Smalley, *J. Phys. Chem.* **1990**, *94*, 8634.

[2] a) F. N. Tebbe, R. L. Harlow, D. B. Chase, D. L. Thorn, G. C. Campbell, Jr., J. C. Calabrese, N. Herron, R. J. Young, Jr., E. Wassermann, *Science* **1992**, *256*, 822; b) G. A. Olah, I. Bucsi, C. Lambert, R. Aniszfeld, N. J. Trivedi, D. K. Sensharma, G. K. S. Prakash, *J. Am. Chem. Soc.* **1991**, *113*, 9385; c) J. H. Holloway, E. G. Hope, R. Taylor, G. J. Langley, A. G. Avent, T. J. Dennis, J. P. Hare, H. W. Kroto, D. R. M. Walton, *J. Chem. Soc. Chem. Commun.* **1991**, 966; d) H. Selig, C. Lifshitz, T. Peres, J. E. Fischer, A. R. McGie, W. J. Romanow, J. P. McCanley, Jr., A. B. Smith III, *J. Am. Chem. Soc.* **1991**, *113*, 5475; e) P. R. Birkett, P. B. Hithcock, H. W. Kroto, R. Taylor, D. R. M. Walton, *Nature* **1992**, *357*, 479.

[3] a) Y. Elemes, S. K. Silverman, C. Sheu, M. Kao, C. S. Foote, M. M. Alvarez, R. L. Whetten, *Angew. Chem.* **1992**, *104*, 364; *Angew. Chem. Int. Ed. Engl.* **1992**, *31*, 351; b) K. M. Creegan, J. L. Robbins, W. K. Robbins, J. M. Millar, R. D. Sherwood, P. J. Tindall, D. M. Cox, A. B. Smith III, J. P. McCauley, Jr., D. R. Jones, R. T. Gallagher, *J. Am. Chem. Soc.* **1992**, *114*, 1103; c) F. Diederich, R. Ettl, Y. Rubin, R. L. Whetten, R. Beck, M. M. Alvarez, S. J. Anz, D. Sensharma, F. Wudl, K. C. Khemani, A. Koch, *Science* **1991**, *252*, 548.

[4] a) J. M. Hawkins, *Acc. Chem. Res.* **1992**, *25*, 150; b) P. J. Fagan, J. C. Calabrese, B. Malone, *ibid.* **1992**, *25*, 134; c) R. S. Koefod, M. F. Hudgens, J. R. Shapley, *J. Am. Chem. Soc.* **1991**, *113*, 8957; d) A. L. Balch, V. J. Catalano, J. W. Lee, M. M. Olmstead, S. R. Parkin, *ibid.* **1991**, *113*, 8953; e) A. L. Balch, V. J. Catalano, J. W. Lee, *Inorg. Chem.* **1991**, *30*, 3980.

[5] F. Wudl, *Acc. Chem. Res.* **1992**, *25*, 157.

[6] a) J. W. Bausch, G. K. S. Prakash, G. A. Olah, D. S. Tse, D. C. Lorents, Y. K. Bae, R. Malhotra, *J. Am. Chem. Soc.* **1991**, *113*, 3205; b) G. A. Olah, I. Bucsi, C. Lambert, R. Aniszfeld, N. J. Trivedi, D. K. Sensharma, G. K. S. Prakash, *ibid.* **1991**, *113*, 9387; c) P. J. Krusic, E. Wasserman, K. F. Preston, J. R. Morton, P. N. Keizer, *Science* **1991**, *254*, 1183.

[7] A. Vasella, C. A. A. Waldraff, *Helv. Chim. Acta* **1991**, *74*, 585.

[8] A. Vasella, C. Witzig, R. Husi, *Helv. Chim. Acta* **1991**, *74*, 1362.

[9] L. Panza, A. Vasella, C. A. A. Waldraff, submitted to *Helv. Chim. Acta.*

[10] a) K. Briner, A. Vasella, *Helv. Chim. Acta* **1989**, *72*, 1371; b) K. Briner, A. Vasella, *ibid.* **1990**, *73*, 1764.

Configuratively Stable Dipeptide Aldehydes from D-Glucosamine Hydrochloride**

By *Thomas Kolter, Annegret Klein,* and *Athanassios Giannis**

Chiral N-protected α-amino aldehydes play an increasingly important role in preparative organic chemistry;[1] however, they are not completely attractive synthetic building blocks because of their chemical and configurative instability.[1] To solve this problem, suitable protecting groups for the amino function have been developed to prevent the racemization of the amino aldehydes during their synthesis, storage, and in subsequent reactions. Rapoport et al.[2] adopted the phenylfluorenyl group, while Reetz et al.[3] studied the *N,N*-dibenzyl function, which in addition leads to notable diastereoselectivity in the addition of organometallic reagents to the protected aminoaldehydes.[3]

With D-glucosamine hydrochloride (**1**)[4] as a chirality-transfer agent, we found an efficient route to *N*-Boc-L-serinal (Boc = *tert*-butoxycarbonyl), a chemically and configuratively stable α-amino aldehyde which can be treated with stabilized phosphorus ylides to provide the corresponding allyl amino alcohols without racemization.[5] This induced us to replace the Boc protecting group with *N*-benzyloxycarbonyl-protected chiral amino acids[6] and thus considerably broaden the synthetic potential of the N-protected serinaldehydes.

Amino aldehydes **4**, with an *N*-benzyloxycarbonylamino acid residue, are available in two steps from D-glucosamine hydrochloride in gram amounts (Scheme 1). These are crystalline substances that can be stored at room temperature and are chemically and configuratively stable. We attribute the unusual stability of these compounds to their oligomeric structure;[7] because of the formation of an intramolecular hemiaminal and an intermolecular hemiacetal, the α H atom has considerably reduced acidity. Thus, in the complex ^{1}H NMR spectra of compounds **4** only a weak (<0.1 H) signal is seen in the range of aldehyde protons. The configuration of the chiral center, the α C atom, was retained under the conditions of the Wittig reaction with stabilized phosphorus ylides. The amino aldehydes **4** were treated with a twofold excess of the phosphorus ylide in refluxing acetonitrile. The resulting Wittig products **5** with *E*-configured double bonds were isolated in 75–80% yield and provided simple ^{1}H NMR spectra.

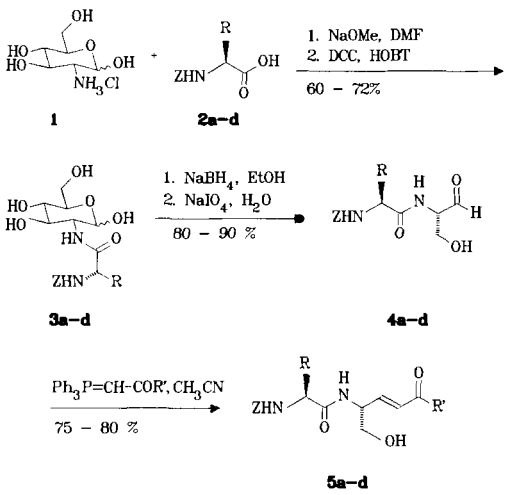

Scheme 1. Synthesis of the configuratively stable dipeptide aldehydes **4a–d** and peptide Michael acceptors **5** from D-glucosamine hydrochloride **1** and protected amino acids **2a–d**. Z = CO_2CH_2Ph, DCC = dicyclohexylcarbodiimide, HOBT = *N*-hydroxybenzotriazole, DMF = *N,N*-dimethylformamide. **a**: R = *i*Pr, **b**: R = CH_2*i*Pr, **c**: R = CH_2Ph, **d**: R = Me, **5a**: R = *i*Pr, R' = O*t*Bu, **b**: R = CH_2*i*Pr, R' = O*t*Bu, **c**: R = CH_2Ph, R' = O*t*Bu, **d**: R = *i*Pr, R' = Me.

Because these α-amino aldehydes with the *N*-benzyloxycarbonyl-protected amino acid residue can also be considered as dipeptide aldehydes with defined stereochemistry, the method described here provides a new route to peptide aldehydes. The first isolation of naturally occurring peptide aldehydes was conducted by Umezawa, and they are of great pharmacological interest as protease inhibitors.[8]

Compounds related to the peptide Michael acceptor **5** have been described as novel irreversible inhibitors of thiol-proteases.[9]

Experimental Procedure

All new compound were characterized by ^{1}H NMR spectroscopy, (high-resolution) mass spectrometry, and elemental analysis. Representative procedures are given.

3a: A solution of **1** (4.32 g, 20 mmol) in DMF (80–100 mL) cooled to 0 °C was treated with sodium methoxide (1.08 g, 20 mmol). The mixture was stirred for 10 min at 0 °C, then **2a** (5.02 g, 20 mmol), hydroxybenzotriazole (5.40 g, 40 mmol), and finally dicyclohexylcarbodiimide (4.54 g, 22 mmoL) were added. After the reaction mixture had been stirred for 1 h, the cooling bath was removed and the mixture stirred another 24 h at room temperature. The precipitate was then removed by filtration, the filtrate treated with diethyl ether (800 mL), and the resulting mixture stored in a refrigerator. The crystalline product that formed was filtered off, and a further crop could be obtained when the filtrate was diluted with diethyl ether. The crude product was recrystallized from ethanol. Yield: 5.90 g (71.5%) **3a**.

M.p. 215 °C (decomp). R_f (dichloromethane: methanol = 4:1) = 0.74. Anomeric ratio $\alpha:\beta = 1:4$. ^{1}H NMR (200 MHz, [D$_6$]DMSO): δ = 0.82 (d, J = 6.5 Hz, 3H), 0.87 (d, J = 6.5 Hz, 3H), 1.93 (m, 1H), 3.00–3.70 (m, 7H), 3.85–4.02 (m, 1H), 4.38–5.10 (m, 6H), 6.48 (d, J = 4.7 Hz, 0.2H), 6.55 (d, J = 6.0 Hz, 0.8H), 7.08 (d, J = 9 Hz, 0.2H), 7.17 (d, J = 9 Hz, 0.8H), 7.24–7.40 (m, 5H), 7.65 (d, J = 7.8 Hz, 0.8H), 7.83 (d, J = 7.8 Hz, 0.2H). Correct C,H,N analysis for **3a**. 0.5 H_2O.

4a: Glucosamine derivative **3a** (4.12 g, 10 mmol) was dissolved in ethanol (250 mL) and treated with sodium borohydride (0.57 g, 15 mmol). After the reaction was complete (monitored by TLC), the reaction mixture was filtered through celite and the volatiles were removed by distillation. The residue was taken up in water (250 mL), neutralized with 2N sulfuric acid, and the resulting solution of the polyol with treated with a solution of sodium periodate (6.42 g in 100 mL water, 30 mmol). When starting material could no longer be detected by TLC (dichloromethane: methanol = 4:1), the reaction mixture was extracted with dichloromethane (4 × 100 mL). The collected organic layers were dried over magnesium sulfate and the solvent removed under reduced pressure. The aldehyde was obtained as a white solid. Yield: 2.7 g (8.37 mmol, 83.7%) **4a**.

M.p. 150 °C. $[\alpha]_D$ +16.8(c = 1.1, DMSO). R_F (CH_2Cl_2/MeOH = 10:1) = 0.44, 0.53. ^{1}H NMR (200 MHz, $CDCl_3$): δ = 0.82–1.08 (m, 6H), 1.95–2.20 (m, 1H), 3.35–4.40 (m, 4H), 4.55–5.95 (m, 4H), 6.90–8.00 (m, 6.9H), 9.55–9.65 (m, 0.1H). Correct C,H,N analysis for **4a** · H_2O. MS (70 eV): $C_{16}H_{22}N_2O_5$ (M^+) calcd.: m/z 322.1529, found: m/z 322.1528: IR: $\tilde{\nu}$ [cm^{-1}] = 3400 (s, shoulder), 3300(s), 3.080(w), 3060(w), 3020(w), 2950(s), 2920(m), 2860(w), 1700(s), 1650(s), 1520(s), 1250(s), 1090(s), 1030(s), 750(m), 700(s).

5a: Aldehyde **4a** (1 equiv) was dissolved in acetonitrile (3 mmol in 50 mL), and after the addition of *tert*-butoxycarbonylmethylenetriphenylphosphorane (2 equiv) the mixture was heated at reflux for 4 h. The reaction mixture was then neutralized with the calculated amount of acetic acid, the solvent removed by distillation, and the remaining oily residue chromatographed on silica gel eluting with hexane:acetone (2:1). Compound **5a** was obtained as a white solid. Preparation: 1.0 g (3.1 mmol) **4a**, yield: 1.0 g (2.38 mmol, 76.8%) **5a**.

M.p. 120–122 °C. $[\alpha]_D$ −16.4 (c = 0.5, $CHCl_3$), R_F (hexane:acetone = 2:1) = 0.32.

^{1}H NMR (400 MHz, $CDCl_3$): δ = 0.93 (d, 6.8 Hz, 3H; CH_3), 0.97 (d, 6.8 Hz, 3H; CH_3), 1.45 (s, 9H; $(CH_3)_3$), 2.09 (m, 1H; 3'-CH), 2.99 (t, 6.0 Hz, 1H; OH), 3.63 (m, 1H; 5-H_A), 3.71 (m, 1H; 5-H_B), 4.01 (dd, 8.4 Hz, 6.6 Hz, 1H; 2'-H),

[*] Priv.-Doz. Dr. A. Giannis, Dipl.-Chem. T. Kolter, A. Klein
Institut für Organische Chemie und Biochemie der Universität
Gerhard-Domagk-Strasse 1, D-W-5300 Bonn 1 (FRG)

[**] This research was supported by the state of North Rhine-Westphalia (stipend for T.K.) We thank Prof. Dr. K. Sandhoff for his support of this work.

4.71 (m, 1H; 4-H), 5.01 (d, 12.0 Hz, 1H; benzyl-H_A), 5.10 (d, 12.0 Hz, 1H; benzyl-H_B), 5.57 (d, 8.4 Hz, 1H; NH), 5.90 (d, 16.0 Hz, 1H; 2-H), 6.77 (dd, 16.0 Hz, 5.2 Hz, 1H; 3-H), 6.83 (d, 8.0 Hz, 1H; NH), 7.28–7.38 (m, 5H; aryl-H). Correct C,H,N analysis. MS (70 eV): $C_{22}H_{32}N_2O_6$ (M^+) calcd.: *m/z* 420.2260, found: *m/z* 420.2258. IR (KBr): $\tilde{\nu}$ [cm^{-1}] = 3410(m), 3280(s), 3060(w), 3010(w), 2960(m), 2920(m), 2860(w), 1710(s), 1650(s), 1530(s), 1240(s), 1150(s), 1035(s), 750(w), 700(m).

Received: May 8, 1992 [Z 5331 IE]
German version: *Angew. Chem.* **1992**, *104*, 1394

CAS Registry numbers:
1, 66-84-2; **2a**, 1149-26-4; **2b**, 2018-66-8; **2c**, 1161-13-3; **2d**, 1142-20-7; **3a** (α), 142981-16-6; **3a** (β, 16684-38-1; **4a**, 142981-11-1; **5a**, 142981-12-2; **5b**, 142981-13-3; **5c**, 142981-14-4; **5d**, 142981-15-5.

[1] J. Jurczak, A. Golebiowski, *Chem. Rev.* **1989**, *89*, 149.
[2] W. D. Lubell, H. J. Rapoport, *J. Am. Chem. Soc.* **1987**, *109*, 236.
[3] M. T. Reetz, M. W. Drewes, A. Schmitz, *Angew. Chem.* **1987**, *99*, 1186; *Angew. Chem. Int. Ed. Engl.* **1987**, *26*, 1141.
[4] A. Giannis, T. Henk, *Liebigs Ann. Chem.* **1991**, 789.
[5] A. Giannis, T. Henk, *Tetrahedron Lett.* **1990**, *31*, 1253.
[6] Conjugates of D-glucosamine and amino acids have already been synthesized as components of immunomodulators: O. Lockhoff, *Angew. Chem.* **1991**, *103*, 1639; *Angew. Chem. Int. Ed. Engl.* **1991**, *30*, 1611. As components of glycolipids with antiviral activity: S. Horvat, L. Varga, J. Horvat, A. Pfützner, S. Suhartono, H. Rübsamen-Waigmann, *Helv. Chim. Acta* **1991**, *74*, 951. The procedure we used for the synthesis of such a conjugate (**3**) follows that in W. König, R. Geiger, *Chem. Ber.* **1979**, *103*, 788.
[7] A related example: V. Jäger, V. Wehner, *Angew. Chem.* **1989**, *101*, 512; *Angew. Chem. Int. Ed. Engl.* **1989**, 28, 469. The authors describe (*R*)- and (*S*)-2-*O*-benzyl-glycerinaldehydes, which are chemically and configuratively stable as a result of their oligomeric structure.
[8] H. Umezawa in *Conformationally Directed Drug Design*, (Eds.: J. A. Vida, M. Gordon) American Chemical Society, Washington D.C., **1984**, p. 73; R. M. McConnell, G. E. Barnes, C. F. Hoyng, J. Martin Gunn, *J. Med. Chem.* **1990**, *33*, 86; S. Bajusz, E. Szell, D. Bagdy, E. Barabas, G. Horvath, M. Dioszegi, Z. Fittler, G. Szabo, A. Juhasz, E. Tomori, G. Szilagyi, *ibid.* **1990**, *33*, 1729. An automated synthesis of peptides with a *C*-terminal aldehyde function: A. M. Murphy, R. Dagnino, P. L. Vallar, A. J. Trippe, S. L. Sherman, R. H. Lumpkin, S. Y. Tamura, T. R. Webb, *J. Am. Chem. Soc.* **1992**, *114*, 3156.
[9] S. A. Thompson, P. R. Andrews, R. P. Hanzlik, *J. Med. Chem.* **1986**, *29*, 104; S. Liu, R. P. Hanzlik, *ibid.* **1992**, *35*, 1067, and references therein; D. Brillon, G. Sauvé, *J. Org. Chem.* **1992**, *57*, 1838.

CORRIGENDUM

On the Reaction of Pentamethylcyclopentadiene with Cobalt Atoms: A Reexamination**

By *Jörg J. Schneider**

Over a year ago we reported in this journal the reaction of pentamethylcyclopentadiene Cp*H (**1**) with cobalt atoms.[1] We described the formation of the mononuclear η^4-η^5-sandwich complex **2**, as well as the two Co_2 compounds **3** and "[Cp*Co=CoCp*]" (**4**).[1] Theoretical studies by Abrahamson et al.[2] and preparative work by Theopold et al.[3] prompted us to investigate the title reaction anew. Our former interpretation of the identity of **4** is corrected here.

We succeeded in separating **2** from the multinuclear reaction products **3** and **4** by chromatography and could isolate them as crystals from the eluate by repeated crystallization.[1] A reexamination by mass spectrometry (15 eV, high resolution) of single crystals of **4** yielded a base peak at *m/z* 391.12427 (calculated for $[Cp^*_2Co_2H_3]$ **5**: 391.12461). The ^{1}H NMR study of solutions of these single crystals shows a signal at $\delta_{para} = 29$ (CH_3 on Cp*). More recent MS and ^{1}H NMR investigations of crystals from the mother liquor of **3** and **4** gave a base signal of *m/z* 586 (10 eV, calculated for $[Cp^*_3Co_3H_4]$ **6**: 586.52) and a ^{1}H NMR signal at $\delta_{para} = 61$ (CH_3 on Cp*). This signal had been incorrectly assigned to **6** previously.[1] Because of the almost identical composition, the elemental analyses in general could not distinguish between **4** (now **5**) and **6**. Our initial MS studies of the crude

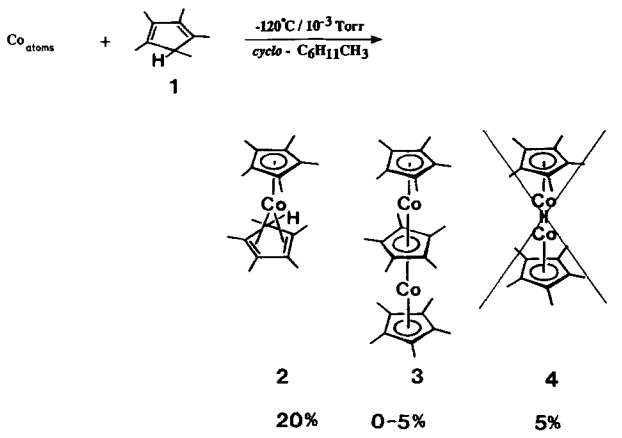

materials (standard conditions, 70 eV) also gave no evidence of the presence of different compounds with *m/z* 391 and 586.[1]

In conclusion, $[Cp^*_2Co_2]$ (**4**) remains unknown. The compound we described as $[Cp^*_2Co_2]$ is, in fact, $[Cp^*_2Co_2H_3]$ (**5**). $[Cp^*_3Co_3H_4]$ (**6**) is the major component in the eluate of the chromatography after separation of **2** (yield of **6**: 10%), but we formerly did not recognize this.[4]

[*] Dr. J. J. Schneider
Max-Planck-Institut für Kohlenforschung
Kaiser-Wilhelm-Platz 1, D-W-4330 Mülheim a.d. Ruhr (FRG)

[**] I thank Prof. Dr. K. H. Theopold, University of Delaware, Newark, USA, and Prof. Dr. C. P. Casey, University of Wisconsin, Madison, USA, for communicating their results before publication.

[1] J. J. Schneider, R. Goddard, S. Werner, C. Krüger, *Angew. Chem.* **1991**, *103*, 1145–1147; *Angew. Chem. Int. Ed. Engl.* **1991**, *30*, 1124–1126.
[2] H. B. Abrahamson, G. P. Niccolai, D. M. Heinekey, C. P. Casey, B. E. Bursten, *Angew. Chem.* **1992**, *104*, 464–466; *Angew. Chem. Int. Ed. Engl.* **1992**, *31*, 471–473.
[3] K. H. Theopold, J. L. Kersten, A. L. Rheingold, C. P. Casey, R. A. Wiedenhoefer, C. E. C. A. Hop, *Angew. Chem.* **1992**, *104*, 1364–1366; *Angew. Chem. Int. Ed. Engl.* **1992**, *31*, Nr. 10.
[4] We shall soon report on our studies of reactions of cobalt atoms with substituted cyclopentadienes.

Book Reviews are written by invitation from the editor. Suggestions for books to be reviewed and for book reviewers are welcome. Publishers should send brochures or (better) books to the following address: Redaktion Angewandte Chemie, Postfach 101161, W-6940 Weinheim, Federal Republic of Germany. The editor reserves the right of selecting which books will be reviewed. Uninvited books not chosen for review will not be returned.

Modern Synthetic Methods 1992. Vol. 6. Edited by *R. Scheffold*. Verlag Helvetica Chimica Acta, Basel/VCH Verlagsgesellschaft, Weinheim/VCH Publishers, New York, 1992. 489 pp., hardcover DM 108.00.—ISBN 3-906390-00-4/3-527-28489-3/1-56081-255-9

The 6th International Symposium on Modern Synthetic Methods was held on the 4th and 5th of May 1992 in Interlaken. The proceedings volume of this latest in a well-established series of symposia contains reviews on the following topics: "Regio- and Stereoselective Formation of Enolates and the Consequences of Enolate Configuration and Subsequent Reactions", by C. H. Heathcock; "Acetylenes in Synthesis", by E. Winterfeldt; "Superbases as Powerful Tools in Organic Synthesis", by M. Schlosser; "Enantiopure Building Blocks from Sugars and their Utilization in Natural Product Synthesis", by F. W. Lichtenthaler; "Carbohydrate Synthesis via Thiazoles", by A. Dondoni; and "Protective Group Strategies in the Synthesis of Functionalized Carbohydrates", by C. A. A. van Boeckel.

All the contributions reflect the latest state of knowledge, with detailed literature references extending up to 1991. The convenient arrangement of subject matter and the clear schemes make for easy reading. It is pleasing to note that, as a general rule, a reaction arrow represents only a single transformation. All the articles except the one on alkynes contain many examples of laboratory recipes, which enable one to work through the syntheses. Unlike previous volumes there is, for the first time, a subject index, which is a valuable aid when using the book.

C. H. Heathcock gives a lucid overview of the chemistry of enolates, from its beginnings up to the present state of knowledge. Reactions leading to regio- and stereoselective formation of enolates are discussed in detail. The author then describes the influence of the configuration of enolates on the stereochemistry of subsequent reactions, especially aldol additions.

E. Winterfeldt reports on the latest developments in the use of alkynes in synthesis. These include thermal and organometallic reactions of alkynes, such as $[2\pi + 2\pi]$-cycloadditions, 1,3-dipolar additions, Diels–Alder, en, and pericyclic reactions, free radical and carbene reactions, and reactions of organometallic compounds. Some applications of ionic reactions of alkynes are also described.

M. Schlosser deals with the preparation and synthetic applications of superbases. Methods for forming metal–carbon bonds and for activating metal compounds by forming superbases are described, as well as the use of superbases in achieving metalation at aliphatic, olefinic, and heterocyclic positions. The review is completed by examples of arene metalations influenced by neighboring groups, and of regio- and stereocontrolled reactions of allylic carbanions prepared from superbases.

The use of cheap carbohydrates as precursors for the preparation of enantiomerically pure synthetic building blocks, and their applications in natural products syntheses, are discussed by F. W. Lichtenthaler. The emphasis is on syntheses using simple, easily obtainable reagents and protecting groups, and on avoiding the need for laborious work-up procedures.

A. Dondoni devotes his contribution to the synthesis of carbohydrates by the addition of aldehydes to thiazole derivatives. By means of this versatile synthetic strategy one can, in a stepwise procedure, stereoselectively build up the carbon skeleton of a sugar around one, two, or three carbon atoms by combining a suitable 2-substituted thiazole derivative with an aldehyde.

C. A. A. van Boekel describes syntheses of biologically active oligosaccharides, in particular of heparin fragments. The regio- and stereoselective synthesis of these highly functionalized molecules is achieved by the clever use of appropriate protecting group techniques and glycosidation methods.

Each of these articles provides an excellent overview of the topic covered, and offers a rapid way into it for the newcomer. The book can therefore be recommended unreservedly for all synthetic chemists and also for advanced students, and it should be in every chemical library. The sturdy binding (an improvement on the previous paperback volumes) and the careful preparation of the volume, including the index, complete the favorable overall impression.

Fritz Theil
Zentrum für Selektive Organische Synthese
Berlin-Adlershof (FRG)

Design and Optimization in Organic Synthesis. (Series: Data Handling in Science and Technology, Vol. 8.) By *R. Carlson*. Elsevier, Amsterdam, 1991. XVI, 536 pp., hardcover HFl 330.00.—ISBN 0-444-89201-X

During the last few years many books on the design of experiments have been virtually thrown onto the market. It is all the more pleasing, therefore, that Rolf Carlson has allowed time for his contribution to the subject to mature, and has produced a book that is excellent from both the pedagogic and scientific standpoints. It is by no means merely "... yet another introductory text on statistics written by a non-statistician", as Carlson, who is himself an organic chemist at the University of Umea, the stronghold of chemometrics in Sweden, fears in his preface that it might be judged.

This book of around 500 pages includes a brief but comprehensive index, a detailed bibliography, references to suitable software, about 30 pages of tables, a few graphics, and a number of detailed examples. There are 19 chapters, six of which might be described as the essential core of the book: "Models as tools" (Ch. 3), "Two-level factorial designs" and "Two-level fractional factorial designs" (Chs. 5 and 6), "Response surface methods" (Ch. 12), "Principal properties" (Ch. 15), and "Quantitative relations between observed responses and experimental variations" (Ch. 17).

 © *VCH Verlagsgesellschaft mbH, W-6940 Weinheim, 1992* *0570-0833/92/1010-1393 $ 3.50+.25/0*

In "Models as tools" the concept of a model is developed, and the types of models generally used for the design of experiments are described. The reader first encounters statistics towards the end of this chapter, in connection with the validation of models. The two chapters on factorial designs (together with Chs. 4, 7, and 8) contain a detailed treatment of factorial screening, and in particular they explain the connection between calculated primary effects and interaction effects and the response surface models that are treated in more detail in Chapter 12. This chapter also introduces quadratic models and uses this concept to describe the yields of various reactions. Chapter 15 is concerned with principal component analysis, and its application to selecting a few test systems from a very large number of possibilities (different catalysts, solvents, etc.). Chapter 17 then considers how one investigates the effects of the reaction conditions on the most important product characteristics (descriptors), and explains the PLS (partial least squares or projections to latent structures) method.

The rest of the chapters serve to put the statistical methods described into the context of organic chemistry. Thus, there are three chapters on strategies (Chs. 1, 13, and 16); these are concerned with general strategies for organic synthesis, strategies for optimizing reaction conditions, and strategies for selecting test systems. Unfortunately, however, there are also three short chapters on optimization methods, which interrupt the flow of the book to some extent, and do not have any direct applications (p. 242: "... applications in organic chemistry are, however, remarkably few"). Possibly these methods have been included in the book so that in later chapters they can serve as a sort of heuristic basis for the selection of suitable test systems, in connection with applications of principal component analysis.

To summarize, this book makes worthwhile reading for the organic chemist who would like to plan his or her work a little more systematically, or who simply wishes to find out what statistical methods applied to the design, interpretation, and optimization of experiments are all about.

Andreas Orth
Hoechst AG
Frankfurt am Main (FRG)

Principles of Nuclear Magnetic Resonance Microscopy. By *P. T. Callaghan.* Clarendon Press, Oxford, 1991. XVII, 492 pp., hardcover £ 60.00.—ISBN 0-19-853944-4

This monograph is the first handbook devoted to NMR imaging at microscopic resolution. It covers recent technical developments as well as a broad range of applications to biological, mineral, and synthetic materials in a rapidly growing area of research. Examples range from small laboratory animals to eggs, from pathological tissue specimens to plants, and from sandstones to polymers.

NMR microscopy is defined as the acquisition of proton NMR images with volume elements smaller than $(0.1\ \mathrm{mm})^3$. While two-dimensional images often exhibit an in-plane linear resolution that is about one order of magnitude better than the chosen slice thickness, three-dimensional imaging aims at isotropic spatial resolution. Although the achievable resolution is much coarser than for optical and electron microscopy, significant advantages of the NMR approach are due to (i) the examination of the full three-dimensional structure of a sample without restriction to its surface, (ii) the non-destructive investigation of biological materials or even living systems, and (iii) the potential for dynamic studies of functional properties.

Although not specifically indicated, the book is structured into three main parts, complemented by a small section on hardware considerations. The first part of the monograph comprising Chapters 1–3 (170 pages) deals with imaging principles, basic NMR, and magnetic field gradients in NMR imaging, respectively, and thus covers the whole range of essentials for microscopic imaging by NMR. More difficult theoretical parts may be skipped by the neophyte, but will turn out to be useful for a rigorous treatment at later stages. In addition, principles such as the Fourier transformation and the convolution theorem are discussed with many illustrative examples and figures. The introduction to NMR is confined to some basic quantum mechanics emphasizing the classical treatment (Bloch equations) of magnetizations subject to simple radiofrequency (r.f.) pulse sequences (excluding two-dimensional NMR spectroscopy). The use of magnetic field gradients for NMR imaging is discussed in great detail. Starting from spin density projections of a sample obtained by acquiring its NMR signal in the presence of a magnetic field gradient, the chapter describes slice-selective excitation, NMR image reconstruction, and actual r.f. pulse and gradient sequences popular in medical NMR imaging.

The second part formed by Chapters 4 and 5 (150 pages) focusses on the principles and applications of NMR microscopy. Limitations of the spatial and temporal resolution are addressed that are due to the achievable signal-to-noise ratio (SNR), short NMR relaxation times, molecular self-diffusion and other motions (macroscopic movements, flow, intracellular streaming, fluid penetration of solid materials, swelling of polymers, etc.), and the presence of magnetic field inhomogeneities caused by susceptibility differences in the sample. An almost complete summary of applications is given that creates a realistic picture of the state of the art (1990), by presenting numerous examples from both the "liquid" phase and the solid state. Where appropriate, the applications are accompanied by further detailed descriptions of more complex NMR techniques. For example, microscopy studies of nuclei other than protons may require heteronuclear polarization transfer to improve the SNR, while NMR imaging of solid specimens may be performed in conjunction with spectral line-narrowing by multi-pulse techniques and/or magic angle spinning synchronized to rotating magnetic field gradients.

The third part, Chapters 6–8 (120 pages), expands in considerable detail on the relevance of translational motions for NMR microscopy. Following largely theoretical discussions of various types of mobility and their effects on the NMR signal, more practical aspects are concerned with NMR imaging methods to visualize or even quantitatively determine properties such as anisotropic and/or restricted diffusion, or spatial distributions of flow velocities. The final chapter (20 pages) discusses the design of optimized gradient coils for generating strong, uniform, and time-varying magnetic field gradients as required in high-resolution NMR imaging.

A strength of this book is a detailed and comprehensive coverage of NMR imaging, including fundamental NMR techniques and mathematical treatments. This provides the necessary background information, particularly for those readers who are primarily concerned with microscopy as a problem-solving tool, but have little or no experience in NMR. However, my feeling is that many parts will be best appreciated by physicists, but not so easily followed by specialists from other areas of this multidisciplinary field. Microscopy studies are extensively discussed in a major part of the book and include many up-to-date examples. The tabu-

lated summaries provide an excellent overview and facilitate access to the original literature. While some of the examples may soon become outdated due to continuous and rapid progress, the adequate outline of the principles and problems will make this book a useful investment for those interested in the future potential of NMR microscopy.

Jens Frahm
Max-Planck-Institut für biophysikalische Chemie
Göttingen (FRG)

The Chemistry of Amidines and Imidates. Vol. 2. (Series: The Chemistry of Functional Groups; series editor: *S. Patai*). Edited by *S. Patai* and *Z. Rappoport*. Wiley, Chichester, 1991. XIV, 918 pp., hardcover £ 225.00.—ISBN 0-471-92457-1

This bulky second volume on amidines and imide esters, in Patai's well-known and comprehensive series, fulfills two functions. Firstly, nine of the sixteen chapters expand on topics treated in Volume 1 (1975) by including work published up to 1989, mostly with new authors. Secondly, the remaining seven chapters deal with new aspects of the title compounds that were not covered in Volume 1. Many of the chapters also report on the guanidines, which are closely related chemically, and also in some cases on (hetero)cyclic amidines and imidates. Eight of the chapters are concerned with physicochemical and spectroscopic properties, while the other eight deal with syntheses and mechanisms.

The first three chapters are concerned with the structures and dynamics of the title compounds. Chapter 1 (G. Häfelinger and F. K. H. Kuske) contains a clear and comprehensive presentation of general aspects and of theoretical results, mainly from ab initio calculations, which are then compared with the available experimental data. Chapter 2 seems somewhat anomalous. In it the authors (T. M. Krygowski and K. Woźniak) present results, in a condensed form, obtained by applying statistical methods to analyze more than 600 crystal structures. Only 22 literature references are given, mainly to the authors' own publications, and thus one is not given proper access to the original literature. Although Chapter 3, by C. L. Perrin, overlaps in places with Chapter 1, it is interesting since the emphasis is mainly on dynamic and stereoelectronic aspects.

Chapter 4 (I. Buśko-Oszczapowicz and J. Oszczapowicz) deals with chromatography and spectroscopy, and Chapter 5 (S. Fornarini) with mass spectrometry. Other chapters are devoted to thermochemistry (Ch. 6, K. Pihlaja), the acid-base and complexation chemistry of the title compounds (Ch. 12, J. Oszczapowicz), and to electronic effects (Ch. 13, J. Shorter).

The synthesis of amides, imidates, and guanidines, and their reactions are treated in Chapters 7 and 8 (G. V. Boyd), 9 (D. G. Nelson), 10 (Y. Yamamoto and S. Kojima), and 11 (I. Min-kin and I. E. Mikhailov). Here the great importance of these classes of compounds for the synthesis of a wide variety of heterocyclic ring systems of pharmaceutical significance becomes clearly evident. The book concludes with some more specialized chapters on radiation chemistry (Ch. 14, Z. B. Alfassi), catalytic properties (Ch. 15, P. Ahlberg and L. Swahn), and electrochemistry (Ch. 16, J. S. Jaworski and M. K. Kalinowski).

Comparing the coverage with my own collection of literature references shows that in general the authors have been thorough in their searches and careful in their selection. The fact that a number of East European authors have contributed shows that science too is deriving benefits from political changes, as also is the thorough coverage of publications from the East. This volume in the Patai series therefore succeeds well in the aim of providing a key to the original literature, although some of the chapters (e.g. Chs. 1, 3, 6, 12, 13) have more of a monograph character, and thus invite more careful study. This excellent work is indispensable for scientific libraries.

Ernst-Ulrich Würthwein
Institut für Organische Chemie
der Universität Münster (FRG)

My 132 Semesters of Chemistry Studies. By *V. Prelog*. American Chemical Society, Washington, DC, 1991. XXIV, 120 pp., hardcover $ 24.95.—ISBN 0-8412-1772-6

In an article on the Czech chemist Emil Votoček (G. B. Kauffman and F. Jursík, *Chem. Br.* **1989**, *25*, 495), I mistakenly referred to Vlado Prelog as deceased. Our library provided me with the supposed date of his death, and in view of the lengthy duration of his career and the near-classic status of his contributions to chemistry (he is truly a legend in his own time), I neglected to verify the date. I am now delighted to report that this prolific and still active octagenarian has written his scientific memoirs as the shortest volume published to date (Prelog is succinct and modest about his achievements) in Jeffrey I. Seeman's projected series of 22 autobiographies of prominent organic chemists, *Profiles, Pathways, and Dreams*.[*] With characteristic, self-deprecating humor, he chose the title of his book to reflect his post-1976 "retirement" position of "postdoctoral student" at Zürich's Eidgenössische Technische Hochschule (ETH). The Latin subtitle, "Studium chymiae nec nisi cum morte finitur" (The study of chemistry is concluded only with death) underscores his lifelong commitment to chemistry. As a perfectionist, he was unwilling to draft his manuscript in English despite his superb fluency in this language. His German text was felicitously translated by his friend David Ginsburg, who died before completing the translation, which was finished by Otto Theodor Benfey.

Born on July 23, 1906 in Sarajevo, Yugoslavia, Prelog served as a "flower boy" on the occasion of the ill-fated visit (June 28, 1914) of Austrian Archduke Franz Ferdinand, whose assassination provided the spark that ignited World War I. Following his parents' separation in 1915, he lived with his aunt in Zagreb, Croatia, where he spent his first three years of high school (*Realgymnasium*) and at the age of 12 began his first experiments in his home chemistry laboratory. A 1918 portrait of this juvenile chemist (without goggles!) is one of the book's 34 formal and informal illustrations. His first article (*Chem.-Ztg.* **1921**, *45*, 736) was written when he was 15. After completing high school in Zagreb in 1924, he entered the Chemical Engineering School of Prague's Institute of Technology, from which he received his Ing.-Chem. (1928) and doctorate (1929). He remained in Prague carrying out research until 1935, when he became a poorly paid lecturer (docent) (1935–40), and subsequently Associate Professor (1940–41) at the University of Zagreb. With the help of Nobel laureates Richard Kuhn and Leopold Ružička, in 1941 he emigrated from German-occupied Zagreb to Zürich, where he has remained ever since at the ETH (*Privat-Dozent* 1942; Associate Professor 1947; Professor 1950–76).

[*] See also: H. Hopf, *Angew. Chem. Int. Ed. Engl.* **1991**, *30*, 1190.

These personal details notwithstanding, Prelog concentrates primarily on the chemical contributions of himself and his collaborators (some 400 papers with about 100 *Doktoranden*)—work on alkaloids and other natural products, heterocyclic compounds, dyes, medicinal products, adamantane, organ extracts, steroids, medium-sized rings, microbial metabolites, antibiotics, transannular reactions, asymmetric syntheses, stereoselectivity of microbial and enzymatic reactions, and the seminal Cahn–Ingold–Prelog (CIP) nomenclature system for stereoisomers. Nevertheless, in a book replete with numerous structural formulas, equations, and reaction schemes as well as almost 200 references, this charming and witty Nobel (1975) laureate does not neglect his travels, lectures, meetings, and interactions with dozens of internationally known scientists (the volume reads like a *Who's Who* of organic chemists). Despite his well-deserved reputation as a raconteur, it was only on Seeman's urging that Prelog related in an epilogue just seven of his innumerable anecdotes "because stories are mostly apocryphal, or at least, they tend to deviate from the truth, and I wished to avoid that." I highly recommend this inexpensive, fascinating, and informative book to practicing chemists and anyone interested in the history of chemistry and the conduct of research.

George B. Kauffman
California State University, Fresno
Fresno, CA (USA)

Dictionary of Plants Containing Secondary Metabolites. By *J. S. Glasby*. Taylor and Francis, London, 1991. 488 pp., hardcover £ 95.00.—ISBN 0-85066-423-3

Research into the immense potential of biologically active compounds found in the plant kingdom, where the number of species is estimated as between 250000 and 500000, is currently undergoing a remarkable renaissance. The practical aim underlying these efforts is to find new structural themes for developing biologically active compounds. During the course of evolution plants have developed many secondary metabolites with regulatory or protective functions, which are now becoming increasingly recognized, and these offer good opportunities for such developments. At the very beginning of the interdisciplinary chain of research that may lead to a biologically active structure, one needs to find out what, if any, phytochemical studies have already been carried out on the chosen plant species; getting this information demands a thorough search of the widely scattered literature.

This book by J. S. Glasby is intended as an aid to carrying out that task. In this comprehensive work nearly 8500 species of higher plants, as well as lichens and mosses, are listed alphabetically according to genus and species, together with the substances that they contain, arranged under compound classes. The accompanying literature citations extend up to the end of 1987. Linked to this main part of the dictionary is an index of compounds, containing an impressive total of nearly 18300 secondary metabolites. Altogether this is the fruit of a painstaking compilation; the amount of information is so great that this must surely be approaching the limit of what a single author can achieve, as one soon finds on starting to examine the book in more detail. Nevertheless, the book's weakness undoubtedly lies in its lack of completeness, a fact that is also referred to by the author himself in his short preface. Whereas some classes of compounds are very fully represented, one searches in vain for the steroid alkaloids havanin, aculeamin, or epikibatalin, the tropane alkaloids schizanthin A and B, and the lichen constituents rangiformic acid and ovoic acid with their botanical origins, to name just a few examples. Only three of the nine triterpenes found in two Araliaceae are listed, and of the 23 brassinosteroids discovered in plants up to 1987, one again finds only three. Also one cannot fail to notice that a good many printing errors have crept in, both in the plant names and the compound names.

Despite these reservations, this sturdily bound work of reference should prove useful, at least as a first source of information on the subject of secondary metabolites in plants. If the plant species or compound that one is looking for cannot be found in this book, there is no alternative but to carry out one's own literature search with the help of a data bank.

Günter Adam
Institut für Pflanzenbiochemie
Halle (FRG)

Solid State Chemistry—Compounds. Edited by *A. K. Cheetham* and *P. Day*. Oxford University Press, Oxford, 1992. XII, 304 pp., hardcover £ 40.00.—ISBN 0-19-855166-5

As a sequel to the book "Solid State Chemistry—Techniques" from the same editors in 1988, this second volume contains contributions by various authors dealing with classes of compounds that are important in modern solid state chemistry. The largest emphasis is on compounds with especially interesting electronic properties, such as superconductors (J. Etourneau, Bordeaux), low-dimensional solids (P. Day, London), and metal cluster compounds (A. Simon, Stuttgart). The second focus of interest is on materials that are important in relation to heterogeneous catalysis. This includes chapters on zeolites (J. M. Newsam, San Diego), layer structures (A. J. Jacobson, Houston), and an introduction to heterogeneous catalysis (A. W. Sleight, Oregon), although this chapter is very brief compared with the rest of the contributions. The book is completed by a short article on ferroic materials (C. N. R. Rao and K. J. Rao, Bangalore).

The introductory chapter (P. A. Cox, Oxford) is concerned with the electronic structures of solids. Unfortunately, this topic is only treated very superficially, the information given being hardly more than one finds in a general textbook. At this point an easily understandable introduction to the band theory (*k*-space, band structures, density of states, etc.) would certainly have been more appropriate, as a knowledge of that would be extremely useful in the chapters that follow (on compounds with one-dimensional physical behavior, and metal-rich compounds). The literature references for this first chapter, which in any case seem very incomplete, should at least have directed the reader to relevant review articles such as those by R. Hoffmann or J. K. Burdett.

The material in the subsequent chapters is arranged according to the chemical composition and structural characteristics of the various classes of compounds. The chapters on superconductors, metal clusters, layer-forming compounds, and zeolites succeed particularly well in elucidating the relationships between chemical composition, the structure of the solid, and the resulting physical and chemical properties. Furthermore, indications are often given of opportunities for interesting studies in the future. Thus, the book can certainly be recommended for the user groups en-

 © VCH Verlagsgesellschaft mbH, W-6940 Weinheim, 1992 0570-0833/92/1010-1396 $ 3.50+.25/0

visaged by the editors, namely students about to take their final examinations and scientists engaged in solid state research.

An important foundation for any kind of experimental investigation on chemical compounds is the preparative chemistry involved. Unfortunately this important topic is given only a small amount of space in this book. A notable exception to this is the comprehensive and clearly written chapter on zeolites, which gives in about 50 pages a well-balanced overview of the compositions, structures, methods of preparation, properties, characterization, and applications of this important group of materials. In contrast most of the other chapters give no information on methods for synthesizing the compounds discussed. On the other hand, theoretical aspects occupy a considerable proportion of the book. For example, nearly a half of the chapter on superconductors is devoted to theoretical considerations that are normally covered in textbooks (BCS theory, thermodynamic aspects, etc.). However, the second part of this chapter contains details of known superconducting materials, arranged under compound classes. This clearly shows the great variety of chemical compositions and structures with superconducting properties. This is followed by a concise discussion of the structural and atomic characteristics that seem to be important in relation to superconductivity.

The very informative and concise chapter on metal clusters also succeeds well in explaining the structural and chemical conditions that lead to the occurrence of metal-rich compounds. Here too the book does not merely list compounds, but explains interrelationships and analogies. Considered as a whole this book offers the reader an interesting insight into the latest developments and knowledge in modern solid state chemistry. Although the selection of topics cannot be regarded as covering the whole of solid state chemistry, the particular aspects treated are of broad interest and considerable importance. The interested reader will therefore look forward eagerly to the follow-up volume mentioned by the editors in the preface, which will contain further articles on topics such as solid electrolytes, and materials with properties relevant to magnetic and optoelectronic applications.

Wolfgang Schnick
Institut für Anorganische Chemie
der Universität Bonn (FRG)

Biotechnology. A Multi-Volume Comprehensive Treatise. Vol. 4. Measuring, Modelling and Control. 2nd edition. Edited by *K. Schügerl*. VCH Verlagsgesellschaft, Weinheim/VCH Publishers, New York, 1991. XIII, 658 pp., hardcover DM 490.00.—ISBN 3-527-28314-5/1-56081-154-4

This volume in the "Biotechnology" series is the first one to appear in the second edition of the series. The book is intended to be equally useful to university academics, scientists in research institutes, and practical users of biotechnology. It offers a valuable resource for the reader who wishes to become familiar with particular aspects of measurement and control in the field of biotechnology.

The volume is divided into four main areas: measuring instruments, measurement techniques, modeling, and control/automation, which are treated in 19 chapters altogether. Its attractive features include the clear division of the subject matter, with a list of contents and symbols for each chapter which makes the book especially easy to use, the uniformity of the typography, and the quality of the figures. Despite the fact that the introduction at the beginning is rather short, the book offers the reader far more than just a narrow view of each specialized area. For example, Chapter 13 on models for aerobic waste-water treatment processes begins with a brief discussion of the purpose and usefulness of models, which goes far beyond merely generating and manipulating large amounts of numerical data. Chapter 14, on anaerobic water treatment, is complementary to the previous chapter, and contains a good introduction to the thermodynamics and kinetics of the relevant processes. Altogether one is given a good coherent overview of the field. Exceptions such as the very brief and rather isolated Chapter 8, on sampling techniques, merely serve to emphasize the consistency of the rest.

The book's coverage is not limited to describing the current state of the art in the various topics: some of the chapters treat topics which, although not at present familiar to everyone, are certain to become more important in the future, such as assessing the conditions in bioreactors (Chapter 7). On the other hand, whether the use of expert systems (Chapter 19) will become established in practice remains to be seen.

Despite the fact that some chapters are of an advanced theoretical nature, examples of practical applications are also often mentioned; thus, an entire chapter (Chapter 12) is devoted to a case study on the optimization of yeast production. Chapter 2 links the theory and practice of gas analysis in fermentation processes in a highly instructive way. I agree with the comment, made by the volume editor in the preface, that the discussion of the control of downstream processing remains too brief in the present edition, due to the lack of information on this topic.

Although individuals may be somewhat deterred by the price of DM 490.00 for this single volume, no specialist library should be without the book, and everyone interested in the field is strongly recommended to make use of it.

Karlheinz Drauz
Forschung und Entwicklung
Organische und Biologische Chemie
Degussa AG, Hanau (FRG)

Reaction Mechanisms of Inorganic and Organometallic Systems. By *R. B. Jordan*. Oxford University Press, Oxford, 1991. 292 pp., hardcover £ 30.00.—ISBN 0-19-506945-5

This book is the result of a one-semester course given to senior undergraduate and graduate students by the author over the past 20 years. It is a well-balanced presentation, which not only goes into the basic principles involved, but also gives a detailed account of mechanistic studies, dealing with inorganic, organometallic, and bioinorganic systems.

The first two chapters are devoted to the tools of the trade, rate law and mechanism, in which an appropriate account of the experimental and theoretical background for the study of reaction mechanisms is given. Chapter 3 is devoted to ligand substitution reactions in which typical tests for particular mechanisms are treated in much detail. The account includes a well-balanced presentation of the present understanding of such processes. Stereochemical changes in inorganic and organometallic compounds are treated in Chapter 4. Ligand substitution, insertion, and oxidative addition reactions of organometallic systems are treated in Chapter 5, along with a discussion on catalytic hydrogenation of alkanes and homogeneous catalysis by organometallic compounds. Chapter 6 is devoted to a treatment of oxidation–reduction reactions, in which inner-sphere and outer-sphere electron

transfer reactions, as well as intervalence and electron transfer in metallo-proteins, receive adequate attention. The topic of inorganic photochemistry is presented in Chapter 7. Most of the selected examples originate from classical coordination compounds (Co^{III}, Rh^{III}, Cr^{III}), but some information is also included on organometallic systems. Details on the intimate reaction mechanisms of excited state species are not given. In the final chapter the author discusses mechanistic studies on bioinorganic systems, and treats reactions of vitamin B_{12}, carbonic anhydrase, and enzymatic reactions of dioxygen. Following this chapter a series of problems taken from the literature are given, which enables the student to check his understanding of the material presented.

Throughout the book ample references to the most recent work (up to 1990) are included. The book is easy to read, it is technically well finished, and should be very popular among students interested in this area. It is highly suitable for the level it is aimed at, and it is obvious from the clear treatment that the author is an active researcher in this area.

Rudi van Eldik
Institute for Inorganic Chemistry
University of Witten/Herdecke (FRG)

Oligonucleotides and Analogues. A Practical Approach. (The Practical Approach Series.) Edited by *F. Eckstein*. Oxford University Press, Oxford, 1991. XIV, 313 pp., paperback £ 22.50.—ISBN 0-19-963279-0

Since the publication of the last book on this topic [*Oligonucleotide Synthesis. A Practical Approach*. (Ed.: M. Gait), **1984**], there have been further rapid developments in the synthesis of oligonucleotides and their analogues, and until now these have not been summarized in monograph form. Oligonucleotides are now attracting increased interest in the scientific world, owing to their potential as therapeutically active compounds (antisense oligonucleotides, ribozymes, aptamers) and their applications in DNA diagnostics, and methods for synthesizing them have therefore assumed a special importance. In this book the editor has very successfully remedied the gap that existed in the literature, and one can confidently predict that it will become a frequently cited standard work.

The book's twelve chapters provide the reader with a good knowledge of the theory and practice of methods for synthesizing the compounds named in the title, in the form of detailed laboratory recipes. Unmodified oligodesoxynucleotides can nowadays be synthesized without difficulty using commercially available DNA synthesizers, as described in the first chapter, but if even minor variations in the molecule are required one needs to adopt completely different strategies. These are dealt with in the subsequent chapters. The compounds whose syntheses are described include oligoribonucleotides, 2′-*O*-methylribooligonucleotides, and oligonucleotides with modified bases. As examples of analogues with modified phosphate backbones, the chapters deal with methylphosphonates, phosphorothioates, and phosphorodithioates. Another part of the book is concerned with the synthesis of oligonucleotide-conjugate molecules, e.g., conjugates with chemical nucleases and with non-radioactive labeling groups. Such groups may be introduced via the 5′ or 3′ terminal positions, via bases, or via the phosphate backbone. As well as recipes for synthesis and purification, methods are also given in some cases for applications, e.g., in the isolation of proteins by affinity-selection, in DNA sequencing, in DNA hybridization, and in antisense cell culture experiments.

It is, of course, inevitable that with such a many-faceted subject it has not been possible to cover every aspect. Nor, indeed, has the editor sought to achieve completeness in that sense. Nevertheless, this reviewer would have liked to see further chapters included, e.g., on phosphoramidates and on the scale-up of oligonucleotide syntheses. Also methods for purification and analysis, the importance of which is often underestimated, deserved to be given a separate chapter. They are included, but are scattered throughout the book under the individual compound classes.

The individual contributions are written by recognized experts, who in many cases have themselves had an important role in the development of the areas covered. Nevertheless, where it seemed appropriate they have avoided describing their own work in detail, giving instead an account of the current state of the art, with a beneficial effect on the book's quality. Furthermore, there is no overlapping between the chapters, thanks to the editor's good organization.

In keeping with the good reputation of the "Practical Approach" series in this respect, there is a degree of consistency in the presentation that is unusual in a multi-author book. The list of contents and the key-word index are entirely satisfactory, and attention has even been given to such little matters as providing a list of suppliers of chemicals. The book will soon find its way onto the shelves of all students and scientists with an active interest in the applications of oligonucleotides.

A. Peyman
Allgemeine Pharmaforschung
Hoechst AG, Frankfurt/Main (FRG)

Registered names, trademarks, etc. used in this journal, even when not marked as such, are not to be considered unprotected by law.

© VCH Verlagsgesellschaft mbH, D-W-6940 Weinheim, 1992. – Printed in the Federal Republic of Germany by Konrad Triltsch Druck- und Verlagsanstalt Würzburg.

All rights reserved (including those of translation into foreign languages). No part of this issue may be reproduced in any form — by photoprint, microfilm, or any other means — nor transmitted or translated into a machine language without written permission from the publishers. Only single copies of contributions, or parts thereof, may be made for personal use. This journal was carefully produced in all its parts. Nevertheless, authors, editors, and publisher do not warrant the information contained therein to be free of errors. Readers are advised to keep in mind that statements, data, illustrations, procedural details, or other items may inadvertently be inaccurate.

Valid for users in the USA: The appearance of the code at the bottom of the first page of an article (serial) indicates the copyright owner's consent that copies of the article may be made for personal or internal use, or for the personal or internal use of specific clients. This consent is given on the condition, however, that the copier pay stated per-copy fee through the Copyright Clearance Center, Inc. (CCC), for copying beyond that permitted by Sections 107 or 108 of the U.S. Copyright Law. This consent does not extend to other kinds of copying, such as copying, for general distribution, for advertising or promotional purposes, for creating new collective works, or for resale. For copying from back volumes of this journal see 'Permissions to Photo-Copy: Publisher's Fee List' of the CCC.

Editorial office: Postfach 10 11 61, D-W-6490 Weinheim, Federal Republic of Germany, Telephone (06201) 602 315, Telex 465 516 vchwh d, Telefax (06201) 602 328, E-Mail Z16@DHDURZ2 in Earn Bitnet.

Editor: *Peter Gölitz*

Associate editors: *R. H. Schmidt-Radde, K. J. Schneider, A. Stimson.* **Editorial assistant:** *E. Schweikart*

Publishers: VCH Verlagsgesellschaft mbH. (Managing Directors: *Hans Dirk Köhler, Dr. Karlheinz Köpfer*), Pappelallee 3, D-W-6940 Weinheim, Federal Republic of Germany.

Advertising office (Advertising Manager: *R. J. Roth*): Postfach 10 11 61, D-W-6940 Weinheim, Federal Republic of Germany, Telephone (0 62 01) 104 556, Telefax (0 62 01) 104 550.

ANGEWANDTE CHEMIE
International Edition in English
Volume 31 · Number 11
November 1992
Pages 1399–1540

The Photochemistry of Stilbenoid Compounds and Their Role in Materials Technology

By Herbert Meier*

Stilbenes and compounds containing stilbene units in their structures form the material basis for numerous research projects in photophysics and photochemistry. Moreover, because these compounds are easy to synthesize and are thermally and chemically stable, they are taking on an increasingly prominent role in the area of materials science investigations into optical, electrical, and optoelectronic properties. In accordance with the interdisciplinary nature of such studies, this article aims to provide a bridge extending from molecular theory and photophysical measurements, through preparative applications, to material effects and their potential technical applications.

1. Introduction

Stilbenes (**1**) are certainly one of the most thoroughly studied classes of compounds from the standpoint of mechanistic and preparative photochemistry. Considerable attention is devoted to stilbenes in modern textbooks on photochemistry,[1] and they have been covered in numerous reviews.[2] Theoretical calculations and the application of modern physical methods such as time-resolved laser spectroscopy in the picosecond and femtosecond range, jet studies, and photoacoustic measurements are yielding an increasingly detailed knowledge of the fundamental photophysics and photochemistry of these systems. However, they are now revealing that even such apparently simple processes as the *cis–trans* (or *Z–E*) isomerization of stilbenes are actually complex and still inadequately understood in detail. Recently materials science investigations have increasingly provided a stimulus for further fundamental research. The connection between stilbenoid compounds and light is a theme that has implications for optical brighteners, laser dyes, optical data storage, photoconductors, photoresists, photochemically crosslinked polymers, nonlinear optics, and many more areas of application. Thus the photochemistry of stilbenoid compounds has taken on an interdisciplinary character, and the number of publications appearing each year has grown at a remarkable rate.

By stilbenoid compounds we mean systems that are made up of stilbene units, ranging from (*E*)- and (*Z*)-stilbene (1,2-diphenylethene, **1**) through oligostyrylarenes (e.g., **2** and **3**) up to poly(phenylenevinylene)s (PPVs, **4**).

In all these four types of compounds, benzene rings are linked by 1,2-ethenediyl groups. This feature is associated with a strong absorption in the UV/VIS spectrum corre-

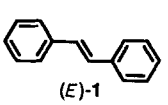
(*E*)-1

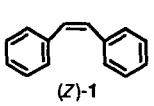
(*Z*)-1

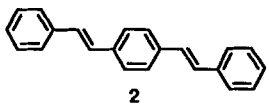
2

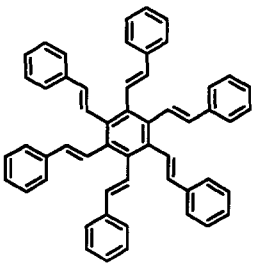
3

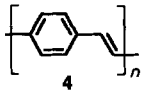
4

[*] Prof. Dr. H. Meier
Institut für Organische Chemie der Universität
J.-J.-Becher-Weg 18–22, D-W-6500 Mainz (FRG)

 © *VCH Verlagsgesellschaft mbH, W-6940 Weinheim, 1992* *0570-0833/92/1111-1399 $ 3.50+.25/0*

sponding to the excitation of π electrons of the conjugated ethenediyl group into π* orbitals. Substituted chromophores still fall within the definition of stilbenoid compounds if they do not impose their own characteristic photochemistry on the compounds. Heteroatoms such as nitrogen may also be introduced into the ring skeleton, provided that their lone pairs of electrons do not result in a completely different photophysical and photochemical character. Thus, the almost colorless compound 3,6-distyrylpyridazine (**5**) is essentially similar to the hydrocarbon **2** in its photochemical behavior, whereas the deep red compound 3,6-distyryl-1,2,4,5-tetrazine (**6**) shows typical tetrazine properties.[3]

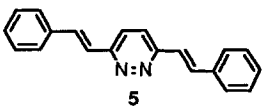

5

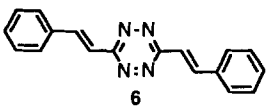

6

The introduction of heteroatoms or substituents, or even the presence of certain types of basic stilbenoid units, can result in additional weaker adsorption bands close to the strong $\pi \rightarrow \pi^*$ transition, which often completely or partially obscures them. When they occur in the spectrum at shorter wavelength than the main band, their effect can be neglected. Even in cases where an S_2 state becomes populated, a fast radiationless transition to such an S_1 state ($S_2 \rightsquigarrow S_1$) usually occurs. On the other hand, if the weak band is situated on the longer wavelength side of the main band, it can have a much greater effect. Either direct excitation of the S_1 state or internal conversion $S_2 \rightsquigarrow S_1$ then gives an electronically excited singlet state with different photophysical, and possibly also photochemical, properties. Nevertheless, if the energy difference is small and mixing of the S_1 and S_2 states occurs, this can actually favor the photochemical behavior of the stilbenes (see Section 4.1).

The photochemistry of stilbenoid compounds in their pure state or in inert media can be divided into four types of reactions: a) *Z*–*E* isomerizations, b) cyclizations, c) cyclodimerizations, and d) oligomerizations. If additional components are present, other reactions may be added to this list. This is not the case for a simple energy transfer, is sometimes the case when a charge transfer occurs, and always the case for photoadditions or photocycloadditions with other reaction partners. The last reaction type will not be considered in this article.[4] A brief discussion of synthetic routes to stilbenoid systems will be followed by an account of the fundamental molecular theory and the photophysics, and of the individual types of photoreactions. Lastly the article will discuss the applications of the photophysical and photochemical properties of stilbenoid compounds in materials technology.

2. The Synthesis of Stilbenoid Compounds

The methods for the synthesis of stilbenoid compounds can be classified into two groups. On one hand are those in which the stilbene units arise directly during the construction of the carbon skeleton by formation of single or double carbon–carbon bonds. On the other hand are methods in which the carbon skeleton is first constructed and the olefinic double bonds are subsequently introduced.

Altogether there are many synthetic routes, and consequently only the advantages and disadvantages of the most important methods will be considered here. Structural and configurational purity of the products are of extreme importance for applications in materials technology.

Scheme 1 summarizes three methods for forming C=C bonds: the Wittig–Horner reaction,[5] the Siegrist method,[6] and the McMurry reaction.[7] Starting from methylarenes

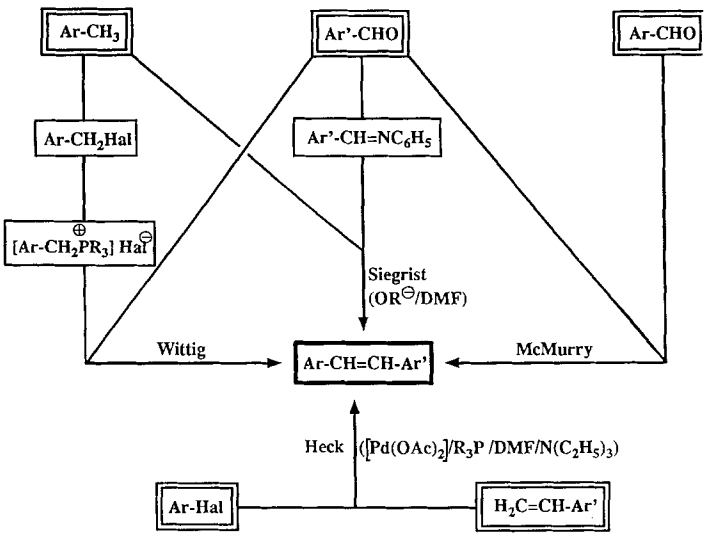

Scheme 1. The most important synthetic routes to stilbenoid compounds. Hal = halogen, DMF = dimethylformamide.

Herbert Meier, born in 1939 in Prague, studied Chemistry and Mathematics at the University of Tübingen and the Freie Universität Berlin, obtaining his doctorate under Eugen Müller in Tübingen in 1968 on the Mills-Nixon effect. After habilitating there in Organic Chemistry and Photochemistry in 1972, he continued as dozent and in 1975 as extraordinary professor. In 1982 he accepted a professorship as successor to L. Horner at the Johannes Gutenberg University in Mainz. His research interests include the synthesis and application of strained carbo- and heterocycles with emphasis on photolytic and pyrolytic methods and the study of photosensitive materials. He is co-author of a widely known textbook on spectroscopic methods in organic chemistry.

and/or aromatic aldehydes one obtains 1,2-diarylethenes in good yields. The total yields of the Siegrist method is often inferior to those of the other two methods—its main advantage is its remarkably high stereoselectivity. For example, our syntheses of **10** (Ar = *p*-$CH_3C_6H_4$ and Ar′ = C_6H_5) showed that the selectivity is more than 1000:1 in favor of the *E* configuration.[8] The decisive factor here is the anti-elimination (E2 or E1cB) from the least energetic conformation **9**.

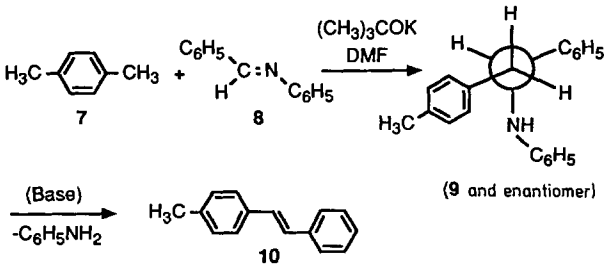

Of the two other methods of forming a C=C bond, neither the stereoselective variants[9] nor a subsequent catalytic *Z*/*E* isomerization yields a higher fraction of the *E* conformer than the thermodynamic equilibrium value.[10] All three methods can be used to build compounds with a chain structure of the poly(phenylenevinylene) type **4**. The Siegrist method is especially suitable for this purpose, not only because of its stereoselectivity but also because it gives nearly quantitative yields when the acidic character of the CH_3 group is increased by the presence of the methyl group and the imine function in the same molecule as in **11**.[11]

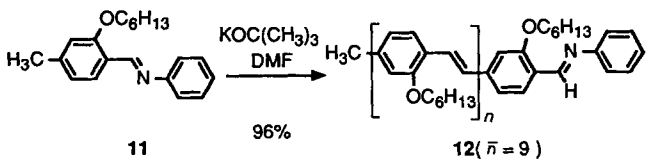

Besides linear polycondensations it is also possible to achieve cyclocondensations. This affords an easy preparative route to the arene-condensed [18]annulenes (e.g. **14**), which are nonplanar and thus, in principle, stilbenoid systems.[12]

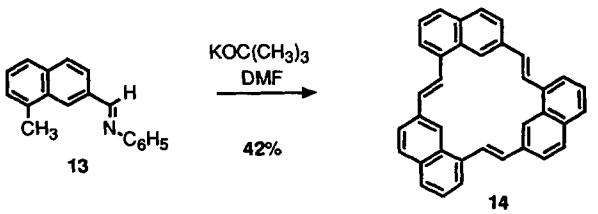

With none of the above three methods of forming C=C bonds can four or more styryl groups be linked into one central arene ring. However, this objective can be achieved by using the Heck reaction[13] to form four or more C–C bonds in the last stage of the reaction (see Scheme 1). Thus, for example, hexastyrylbenzene (**3**) can be prepared either from hexabromobenzene (**15**) and styrene[14] or from **16** by a triple Wittig–Horner reaction and a triple Heck reaction.[15]

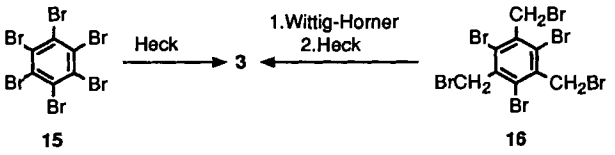

The Heck reaction is also useful for synthesizing linear polymers with stilbene units.[16] A particular problem with all multiple condensation reactions that afford relatively rigid molecules is the products' poor solubility, because precipitation causes a premature termination of the reaction. This can be avoided by introducing groups such a alkyl, alkoxy, or alkoxycarbonyl, which increase the solubility. Another possibility is to form the carbon skeleton in a first stage and then to introduce the double bonds. This method is often used to synthesize poly(phenylenevinylene)s (PPV, **4**) via so-called precursor polymers.[17, 18]

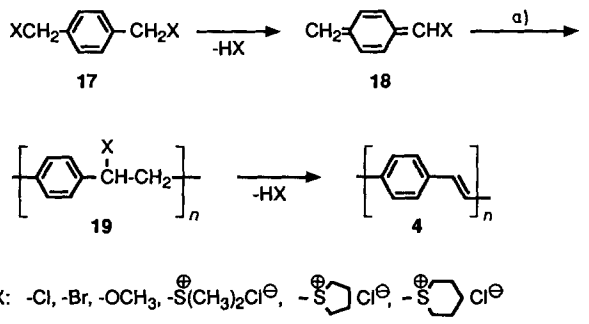

Scheme 2. Synthesis of **4** via precursor polymers. a) Polymerization.

The use of sulfonium moieties as leaving groups has been found to have particular advantages.[19, 20] With increasing size of the groups X and increasing rigidity of the prepolymers such as **19**, the structural consistency of the PPV chains increases, but the degree of ordering between the chains is reduced.[20]

3. Stilbenoid Compounds in the Ground State

3.1. Molecular Parameters of (*E*)- and (*Z*)-Stilbene

X-ray structural analysis of crystalline (*E*)-stilbene shows that the molecule is nearly planar.[21] Electron diffraction measurements in the gas phase indicate a structure with C_2 symmetry and a twist angle θ of about 32° for the phenyl groups.[22] Molecular mechanics calculations[23, 24] yield appreciably smaller θ values, but show that the anharmonic potential curve for rotation of the benzene rings out of the plane of the double bond is very flat. If one ensures that there is no surplus vibrational energy, as in ultra-cold jet conditions, one can assume a quasi-planar structure for (*E*)-**1** with

C_{2h} symmetry.[21] Electron diffraction studies indicate that (*Z*)-**1** has a propeller-type structure with C_2 symmetry and a twist angle $\theta = 43°$,[25] in good agreement with theoretical calculations, notably by the MM2'[24] and AM1[23] methods. There is some uncertainty regarding the torsion at the olefinic double bond, which in contrast to the situation for the *E* isomer cannot automatically be assumed to be negligible. Relative to other structural parameters, a noticeable feature is the opening of the bond angles α at the olefinic carbon atoms, which are somewhat larger in the *Z* isomer (129°) than in the *E* isomer (126° or 127°).[21,22,25] From the geometric data a greater degree of electron delocalization can be predicted for (*E*)-**1** than for (*Z*)-**1**. However, in both cases the benzene rings are linked together through an olefinic bridge with no additional resonance stabilization;[26-28] thus the average resonance energy per π electron is even smaller than in benzene.[26,29]

3.2. Thermal *Z*/*E* Isomerization

In the ground state S_0 there is a high activation barrier separating (*E*)- and (*Z*)-**1** (Fig. 1). Differential thermal analysis shows that the $Z \rightarrow E$ isomerization in the pure phase does not become efficient until the temperature reaches about 300 °C. The thermogram has a maximum at 385 °C, and the activation energy is calculated[30] to be $192 \pm 9\ kJ\,mol^{-1}$. Measurements in the gas phase[31-33] give similar results. For isomerization reactions in solution the activation energies are probably slightly lower. In solution, however, it is difficult to exclude the possibility of catalysis by trace impurities, since there is a great variety of catalysts that can influence the *Z*/*E* isomerization of stilbenoid compounds; these range from metals such as palladium to nonmetals such as iodine. The latter is often used in preparative work to establish the *Z*/*E* equilibrium. The iodine molecules can be induced to dissociate either thermally or photochemically. Figure 1 shows the energy profile for the *Z*/*E* equilibration of stilbene, drawn with values found by Saltiel et al.[34] from measurements in *tert*-butylbenzene; the value for the Arrhenius activation energy E_a is in agreement with a measurement by Kistiakowsky et al.[35]

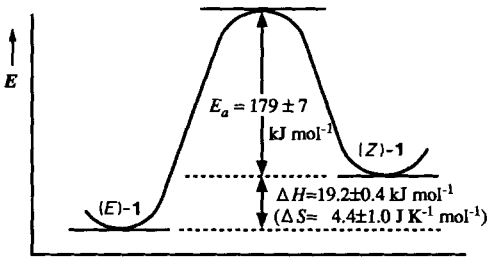

Fig. 1. Energy profile for the thermal equilibration of (*Z*)- and (*E*)-stilbene (**1**) in *tert*-butylbenzene. Rk = reaction coordinate.

The published values for $\Delta G°$ range from 10.7 to $23.8\ kJ\,mol^{-1}$; the data determined from the equilibrium constants (15.5[36] and $17.6\ kJ\,mol^{-1}$[34]) are more reliable than those obtained from corrected heats of combustion[37] or heats of hydrogenation.[38] According to this the proportion of the *Z* isomer under thermal equilibrium conditions is small; for example, at 30 °C in benzene it is less than 0.1%, and it increases to slightly more than 1% in *tert*-butylbenzene at 188 °C.[34] For the great majority of stilbenoid compounds, the proportion of the *Z* isomer in the thermal equilibrium remains small ($\leq 5\%$). However, for PPV compounds **4**, even a small fraction of the double bonds in the *Z* configuration can result in serious defects in the material.

4. Stilbenoid Compounds in Electronically Excited Singlet States

4.1. Electronic Excitation and Physical Deactivation Processes

Both (*E*)- and (*Z*)-stilbene (**1**) have strong UV adsorption bands. As can be seen from Figure 2, the band at longer wavelength is weaker in the *Z* than in the *E* isomer, and shifted slightly to shorter wavelengths. At low temperatures

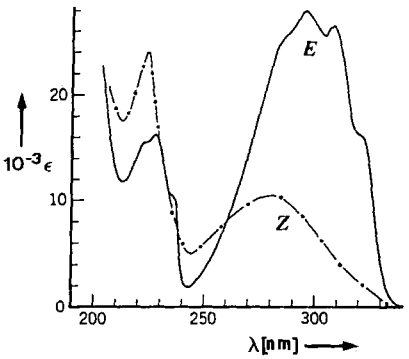

Fig. 2. UV spectra of (*E*)- and (*Z*)-stilbene (**1**) in hexane at room temperature.

the spectrum of (*E*)-**1** shows a well-defined vibrational structure, whereas the band of the more severely twisted (*Z*)-**1** continues to show no fine structure.

Figure 3 depicts the HOMO–LUMO electronic transition $\pi_7 \rightarrow \pi_8^*$. The highest occupied orbital π_7 is localized to a large extent in the region of the olefinic double bond. Consequently, the electronic excitation process reduces the bond order of the C=C bond, with a corresponding effect on the relevant stretching vibration. This effect is greatest in the gas phase, where the $S_0 \rightarrow S_1$ transition in (*E*)-**1** reduces the C=C vibrational frequency from 1654 cm^{-1} to about 1550 cm^{-1}; the olefinic double bond lengthens (136 to 144 pm), whereas the adjacent bonds to the phenyl groups contract from 148 to 142 pm.[39,40]

The dipole moment of asymmetrically substituted (*E*)-stilbenes is greater for the S_1 state than for the ground state. This effect can be described by the empirical relationship $\mu(S_1) = 3.11\ \mu(S_0) - 1.46$.[44] A more extreme effect can occur for donor–acceptor disubstituted stilbenes. For example, (*E*)-4-dimethylamino-4'-cyanostilbene (**20**) forms a TICT (*t*wisted *i*ntramolecular *c*harge *t*ransfer) state, which gives rise to an additional fluorescence band. In the S_1 state of this

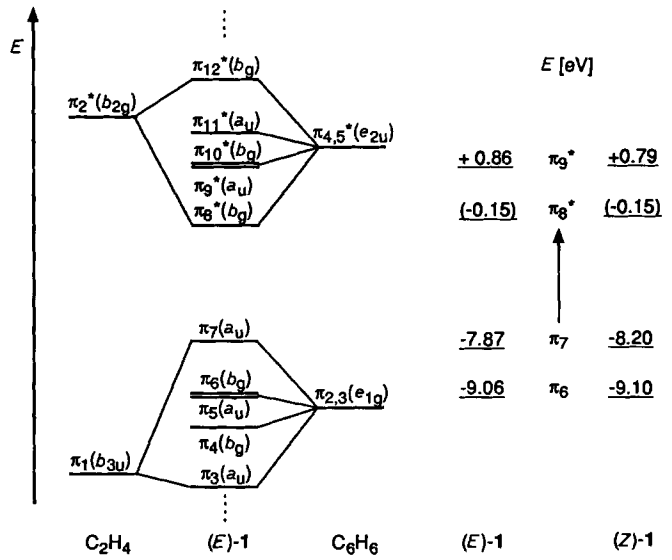

Fig. 3. Correlation diagram for the highest occupied π-orbitals and lowest unoccupied π^*-orbitals of (*E*)-stilbene, derived from ethene and benzene, showing the HOMO–LUMO electronic transitions: (*E*)-**1**: $A_{1g} \rightarrow B_{1u}$ (idealized point group C_{2h}) and (*Z*)-**1**: $A \rightarrow B$ (point group C_2). The orbital energies *E* correspond to ionization energies *I* measured by photoelectron spectroscopy [41, 42] and to electron affinities *EA* measured by electron transmission spectroscopy (ETS) [43]; the LUMO energies given in parentheses have been calculated by the Pariser-Parr-Pople (PPP) method [43], since the stable anions cannot be measured by ETS because $EA > 0$.

molecule, the twisting of the 4-dimethylaminophenyl moiety competes with rotation about the double bond (isomerization).[45]

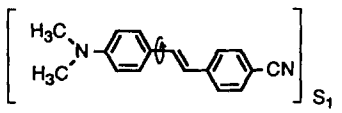

20

Physical deactivation of the S_1 state can occur by fluorescence ($S_1 \rightarrow S_0$), by internal conversion (IC, $S_1 \rightsquigarrow {}^1S_0$), and by intersystem crossing (ISC, $S_1 \rightsquigarrow T_1$). For (*E*)-**1** the fluorescence quantum yield ϕ_F has been measured as 0.07–0.08 at room temperature,[46] and 0.90 at 77 K;[47] at still lower temperatures it may approach the limiting value of 1.0. For a long time it was assumed that (*Z*)-**1** does not fluoresce in solution at room temperature, but only does so in glasses at low temperatures or in the vibrationally relaxed state in jet experiments. Recently, however, the emission spectrum has been successfully measured in hexane at room temperature.[48] The spin inversion or ISC process, leading to the least energetic triplet state T_1, plays only a very minor role for (*E*)-stilbene. The fluorescence intensity of pure (*E*)-**1** in solution at room temperature shows a monoexponential decay,[46, 49, 50] from which average fluorescence lifetimes τ of between 80 and 140 ps have been measured for this exited state. At 77 K the value of τ increases to 1.2–1.4 ns.[49] For (*Z*)-stilbene the mean lifetime of the S_1 state is considerably shorter (0.7–1.4 ps).[51] Evidently for both (*E*)- and (*Z*)-**1**, "chemical" deactivation of the S_1 state into product channels (see Sections 4.2 and 4.3) is of great importance. The relative contributions of physical and chemical deactivation processes depend not only on the temperature and the medium, but also on the excess thermal energy relative to the origin of the $S_0 \rightarrow S_1$ transition, as is shown by results from supersonic jet experiments.[52] A crucial factor in this context is the existence of activation thresholds along the reaction coordinates (see Section 4.2). Higher excited singlet states S_n with energies close to that of S_1 exist. On the basis of results from two-photon spectroscopy and also from theoretical calculations, it has been postulated[53] that (*E*)-**1** has at least six additional excited singlet states below 50000 cm^{-1}. When these states become populated they decay only partly to S_1 by internal conversion, since they can also lead directly to the product channels.[54]

An investigation of arenes with two or more styryl groups reveals that these can be divided into two categories. Figure 4 shows spectra for two typical examples. (*E,E*)-1,4-Distyrylbenzene (**2**) belongs to category I.[55, 56] These compounds are spectroscopically rather similar to the parent compound (*E*)-stilbene (**1**). For **2** a strong absorption band (λ_{max} = 353 nm) overlaps with the fluorescence band in the region of the $0 \rightarrow 0$ transition. The excitation (Exc) and absorption (A) spectra are identical. The fluorescence quantum yield ϕ_F at room temperature is 62%.[55, 57] (*E,E*)-1,2-Distyrylbenzene (**21**) represents category II.[55] Its absorption is less intense than that of **2** and shows a hypsochromic shift. The excitation spectrum differs from the absorption spectrum, ϕ_F is considerably smaller (11%), and a large Stokes shift is observed between the absorption and fluorescence bands. The latter effect provides a very simple criterion for distinguishing between the two categories. The *meta*-substituted compound **22** behaves similarly to the *ortho*-substituted compound **21**.[56]

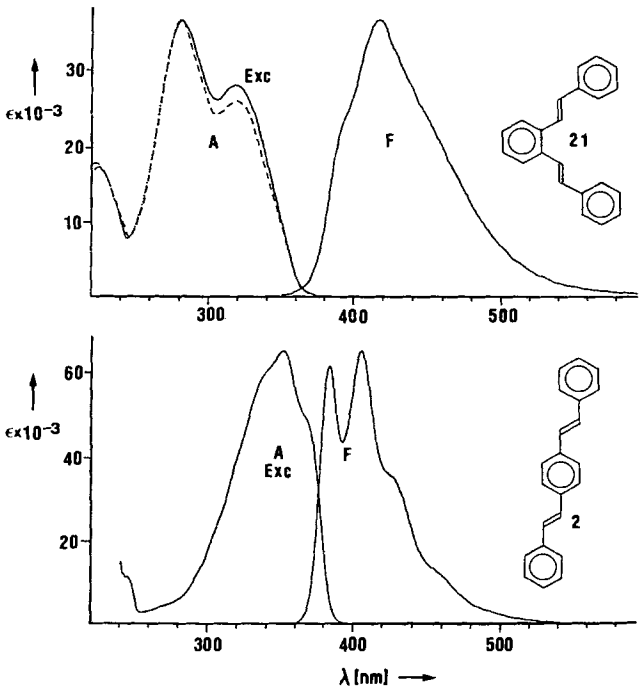

Fig. 4. Absorption, excitation, and fluorescence spectra (A, Exc, F) for (*E,E*)-1,2- and (*E,E*)-1,4-distyrylbenzene (**21** and **2**, respectively) in ethanol at room temperature.

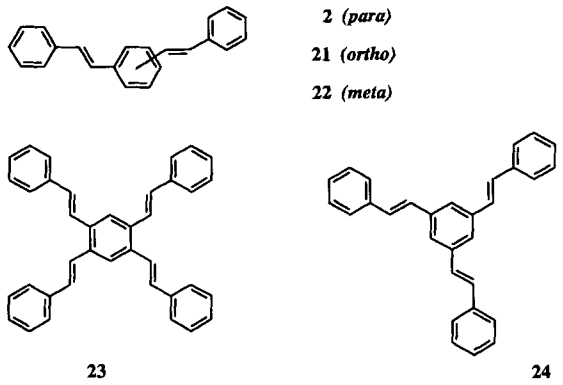

Stilbenoid systems often exist as several rotamers, which can differ in their photophysical and photochemical properties.[2k, 55] Thus, the fluorescence decay curves are not always monoexponential. For example, seven rotamers are theoretically possible for (*E,E,E,E*)-1,2,4,5-tetrastyrylbenzene (**23**); the statistical distribution is 4:4:2:2:2:1:1. So far as the actual populations are concerned, at least three conformers are excluded from the outset on steric grounds because their energies are too high; the remainder show identical fluorescence behavior in toluene at room temperature, with a mean fluorescence lifetime of $\tau = 7.8$ ns.[56] A contrasting example is (*E,E,E*)-1,3,5-tristyrylbenzene, **24**, for which both theory and experiment indicate the existence of two rotamers. Under the same conditions as above the τ values are 9.4 and 13.6 ns, while at 50 K in hexane they are 16.4 and 43.0 ns (Fig. 5). When one compares the τ values for the two categories of stilbenoid compounds, a further important difference becomes apparent; this is especially obvious from the intrinsic lifetimes $\tau_o = \tau\phi_F^{-1}$. Whereas τ_0 is of the order of 1 ns for (*E*)-**1** and other compounds of category I, the intrinsic lifetimes in category II are up to 300 times greater. Corresponding differences are found in the behavior of the two categories of compounds in bimolecular photoreactions (see Section 4.4). In category I the absorption band at longer wavelength ($S_0 \rightarrow S_1$) corresponds to an allowed electronic transition A → B, whereas in category II the intensity of the $S_0 \rightarrow S_1$ transition is weak (A → A). In the example of **24** in Figure 5, the latter transition can be seen on the long-wavelength side of the strong band.[56]

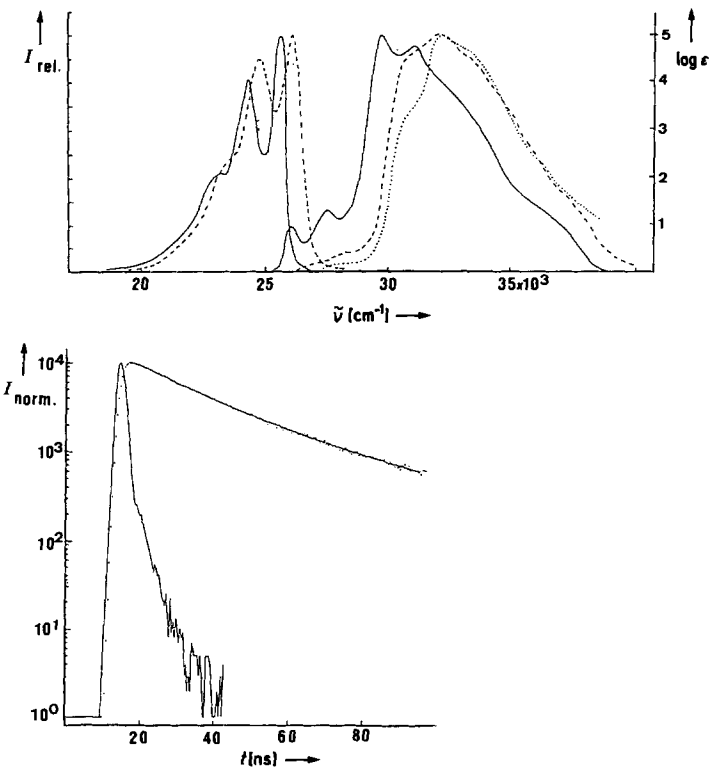

Fig. 5. Top: Absorption, excitation, and fluorescence spectra [56] for **24** in hexane [···· absorption (293 K), ---- excitation and fluorescence (293 K), —— excitation and fluorescence (50 K)]; bottom: fluorescence decay curve for **24** in hexane at 50 K ($\tau_1 = 16.4$ ns, $\tau_2 = 43.0$ ns, with pre-exponential factors $A_1 = 0.121$, $A_2 = 0.045$) [56].

The difference in the nature of the $S_0 \rightarrow S_1$ excitation process already becomes apparent from a simple MMX calculation for 1,3- and 1,4-distyrylbenzene (**22** and **2**, respectively), as shown in Figure 6. The $b_g \rightarrow a_u$ electronic excitation process in **2** corresponds to the transition $S_0(A_g) \rightarrow S_1(B_u)$, whereas the $a_2 \rightarrow a_2$ excitation in **22** corresponds to the transition $S_0(A_1) \rightarrow S_1(A_1)$. The configurational interaction does not alter the fact that in each case the HOMO–LUMO transition leads to the band of lowest energy. Unlike the $A_g \rightarrow B_u$ transition, the $A_1 \rightarrow A_1$ transition is polarized only in the direction of the C_2 symmetry axis, that is, perpendicular to the longitudinal extension of the molecule **22**. Measurements of the polarization P again provide a distinction between categories I and II. The high values of P for the bands of substances in category I are in contrast to the low values for those in category II, since the absorbing and emitting states are not identical, and a difference in direction between the transition moments leads to depolarization. If the bands are partly separated (as in Fig. 5, top), P changes at the crossover point.[58]

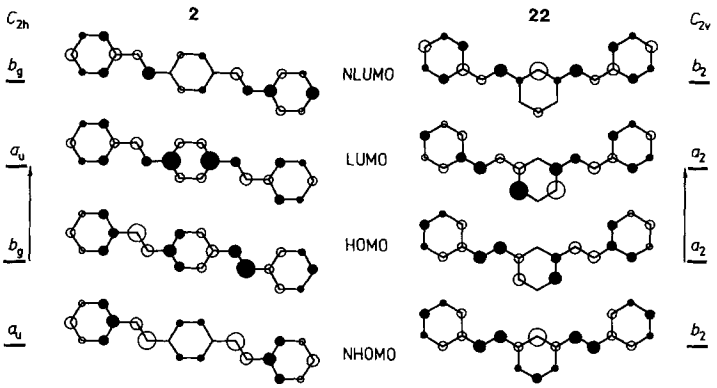

Fig. 6. Frontier orbitals for **2** and **22**, and HOMO–LUMO electronic transitions (selected conformers).

Figure 7 shows for a number of styrylbenzenes a comparison of the energies of the 0 → 0 transitions of the weak absorption A, the strong absorption B, and the fluorescence F, measured at 77 K in hexane or ethanol. For compounds in category I the energies are typically in the sequence F, B, A, whereas for category II the sequence is F, A, B. This observation also sheds a new light on the simplest of the criteria for distinguishing between categories I and II, namely the large Stokes shift between the strong absorption band and the fluorescence band. The fluorescence transition $S_1 \rightarrow S_0$

should always be related to the absorption transition $S_0 \rightarrow S_1$, even when this absorption can only be recognized as a weak shoulder on the strong absorption band, or is actually completely hidden by the latter. Adopting this procedure ensures that overlapping of the bands occurs in the region of the $0 \rightarrow 0$ transition (see also Fig. 5). In general it can be stated that stilbenoid systems in which (linear) conjugation is blocked, either on a priori grounds or due to steric hindrance, will belong to category II.

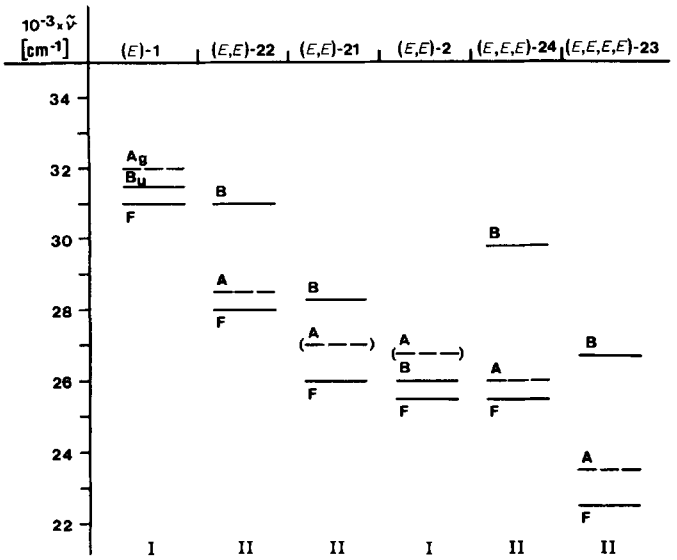

Fig. 7. Schematic diagram showing the energies of the $0 \rightarrow 0$ transitions for the allowed absorption (B), the forbidden or weak absorption (A), and the fluorescence (F) for selected styrylbenzenes in categories I and II.

After the discussion of sterically hindered or blocked conjugation, we now examine the situation in greatly extended conjugated systems. In this context we consider the series of compounds **1**, **2**, and **4**, with the all-(*E*) configuration. The poor solubility of compounds **4** with $n \geq 2$ present difficulties; it is therefore better to make comparisons with compounds **25** containing *tert*-butyl substituents, which have been studied by K. Müllen et al.[59] Whereas for **4** the limit of convergence appears to be reached at $n = 4$, for **25** a more reliable limit in the region $n = 7$ to 10 can be assumed.[59] For

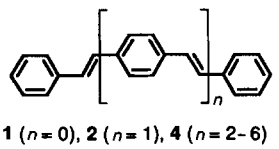

1 ($n = 0$), **2** ($n = 1$), **4** ($n = 2$–6)

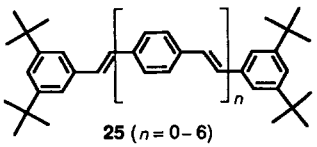

25 ($n = 0$–6)

	λ_{max} [nm] (solvent)[60]	λ_{max} [nm]/chloroform[58]
$n = 0$	295 (hexane)	≈ 309
$n = 1$	350 (hexane)	360
$n = 2$	385 (chloroform)	387
$n = 3$	385 (dioxan, 80°C)	403
$n = 4$	388 (dioxan, 80°C)	412
$n = 5$	388 (dioxan, 80°C)	418
$n = 6$	388 (1-methylnaphthalene, 90°C)	415

Scheme 3. Dependence of the absorption on the chain length for compounds **1**, **2**, **4**, and **25**.

the corresponding monoanions an effectively conjugated chain segment is not reached until nine or ten stilbene units are present.[59] The effective conjugation length is essentially limited by the torsion of the benzene rings; this effect is expected to be even more pronounced in solution than in the solid. The oligo- and poly(phenylenevinylene)s with all-(*E*) configuration show strong fluorescence bands which, like the adsorption bands, are shifted to longer wavelengths as *n* is increased. Our measurements, which are not yet completed, indicate that on increasing *n*, ϕ_F passes through a maximum (see Section 6.3).

4.2. *Z*/*E* Isomerization

The *cis–trans* or *Z–E* isomerization of stilbenes has been known for more than 80 years;[61] in recent years it has received much attention as a model reaction for the study of ultra-fast reaction kinetics.[2j] The first detailed mechanism was proposed in 1967/68 by Saltiel.[62] The more recent models based on that of Saltiel have mainly continued to assume one-dimensional reaction coordinates. Reducing the reaction coordinate to a single molecular parameter, the torsion angle θ about the olefinic double bond, is a crude simplification; nevertheless, the sections $E(\theta)$ through the potential energy surfaces then correctly describe the basic features of this photoisomerization. Figure 8 shows the Orlandi–Siebrand model,[63] in which the direct *E–Z* isomerization reaction follows a nonadiabatic mechanism, characterized by the avoided crossing of the lowest electronically excited singlet state $S_1(B_u^*$ or $B^*)$ with a doubly excited state $S_2(A_g^*$ or $A^*)$. Experimental evidence has also been obtained[64] for

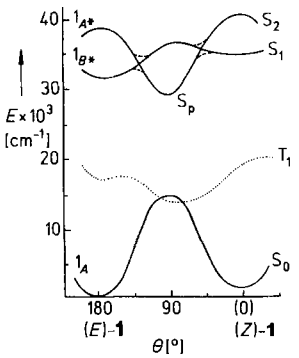

Fig. 8. Schematic reaction profile for the *E*/*Z* isomerization of stilbene (**1**). The reaction coordinate θ is the torsion angle about the olefinic double bond.

an S_n state, corresponding to a two-photon transition. According to an ab initio calculation,[63] the energy of B_u^* increases in the range from $\theta = 180° - 90°$, whereas that of A_g^* decreases. The vibrationally induced internal conversion leads over an activation barrier to the energy minimum S_p, which was previously called a phantom singlet state.[62] A similar reaction sequence leads from the (*Z*) configuration ($\theta \cong 0°$) to S_p. However, whereas the barrier between S_1 and S_p can have a value up to 15 kJ mol^{-1} for (*E*)-**1**, that on the *Z* side is less than 4 kJ mol^{-1}.[51, 65, 66] Thus, temperature has an appreciable influence on the competition between fluorescence and $E \rightarrow Z$ isomerization.[2e] On the *Z* side the competition from fluorescence is much less important than the alternative reaction path of photocyclization (see Sec-

tion 4.3). The lifetime of S_p is less than 150 fs.[51] The system in the representative area for the twisted state rapidly jumps through a funnel to an area near the saddle point on the ground state surface S_0, and from there with similar probability moves along the surface to the ground state configurations (*Z*)- and (*E*)-**1**. Results from laser studies with femtosecond resolution are consistent with an isomerization model with a spatially fixed C_2 symmetry axis.[51, 67]

Many details of the Orlandi–Siebrand model are still unclear. For example, it is uncertain whether the energy profile for the S_1 (*B*) state has a maximum at $\theta = 90°$, or whether there is a monotonic increase up to $\theta \simeq 0°$.[63] A monotonic increase could explain why a small fraction (0.16–0.20%) of the (*Z*)-stilbene molecules in the S_1 state does not follow the isomerization path described, but undergoes an adiabatic process forming (*E*)-**1** in the S_1 state, which is detected by the fluorescence from (*E*)-**1**.[48] An important modification to the Orlandi–Siebrand model was introduced by Hohlneicher and Dick,[53] who showed that (*E*)-**1** has a whole series of electronically excited singlet states with higher energy than S_1 and *A*- and *B*-type symmetry. Twisting of the molecule by the angle θ increases the energy of these states, except for an A^* state with the $\pi\pi^*$ configuration of the ethenediyl group, whose energy is reduced. Thus, depending on the symmetry there is either crossing of surfaces, or interactions in which crossing is strongly or weakly avoided. A minimum at S_p on the potential energy curve, flanked by an activation threshold corresponds to a weakly avoided crossing of the falling A^* state S_5 with a rising A^* state S_3.[53] To investigate the involvement of a higher excited singlet state, Sumitani and Yoshihara[54] devised an interesting experiment. They used a laser pulse at 266 nm wavelength to excite (*E*)-**1** to the S_1 (B_u) state, and 90 ps later a second pulse at 532 nm to raise the energy into an S_n (A_g) state. The second pulse has the effect of weakening the fluorescence $S_1 \rightarrow S_0$, with a corresponding increase in the isomerization tendency. This applies even at 90 K, a temperature at which single excitation no longer leads to isomerization. Thus, the activation barrier can be circumvented by directly populating the $S_n(A_g{}^*)$ state.

An alternative model for *Z*/*E* isomerization is the proposal by Troe.[68] MNDO-CI calculations provide no evidence for the nonadiabatic involvement of higher excited singlet states. The apparent cause of the experimentally observed barrier is the change in the configurational interaction in S_1, which is greater in the *E* configuration ($\theta = 180°$) than for $\theta = 90°$. The photostationary equilibrium for direct *Z*/*E* isomerization can be calculated for monochromatic irradiation from the quantum yields and the extinction coefficients, according to Equation (a). Since the ratio of the quantum

$$\frac{[Z]}{[E]} = \frac{\phi_{E\rightarrow Z}\,\varepsilon_E}{\phi_{Z\rightarrow E}\,\varepsilon_Z} \qquad \text{(a)}$$

yields is usually close to 1, it is possible by a suitable choice of the wavelengths to obtain a high degree of enrichment in one configuration. For example, with $\lambda = 313$ nm 91.5% conversion of (*E*)-**1** into the *Z* configuration can be attained.[69] This method is of particular interest from a preparative standpoint in cases where one of the two configurational isomers is difficult or impossible to obtain in other ways.[70]

The rate of the isomerization of the *E* isomer to the *Z* isomer depends to a large extent on the medium. The reverse ($Z \rightarrow E$) isomerization for (*Z*)-**1** in the first electronically excited singlet state is complete in 1–2 ps, even in highly viscous media.[71, 72] As the lifetime of the S_p state is also very short, the (*E*)-stilbene molecules formed are "hot", that is, not in thermal equilibrium with their environment.[65] Medium effects such as solvation, temperature, pressure, and especially viscosity, have been studied in detail.[51, 73–82] A typical result is the observed lowering of the activation barrier in alcohols (polar, protic media) relative to that of hydrocarbons.[75, 78, 82] The application of the Kramer's theory[83] to account for the viscosity effects observed in this isomerization is somewhat controversial, but it gives useful results in most cases.[2i] An important point to bear in mind here is that the macroscopic viscosity is not a good measure of the microscopic friction. To account for this discrepancy, Saltiel et al.[74] have defined a specific microviscosity based on diffusion coefficients. Substituents can drastically alter the dynamics of the isomerization. In Figure 9 the initial phases of the isomerizations (*E*)-**1** → (*Z*)-**1** and (*E*)-**26** → (*Z*)-**26** when irradiated in cyclohexane and in hexadecane are compared. The more viscous medium has a considerably greater retarding effect on the isomerization of the long-chain substituted system **26**.[94]

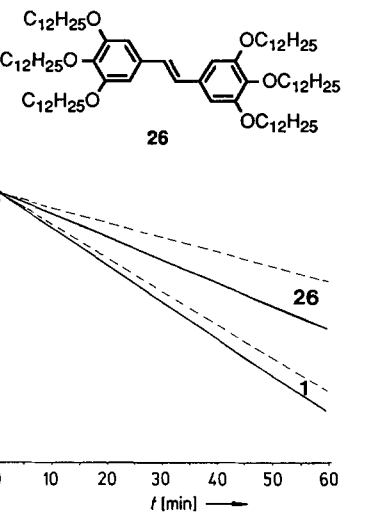

Fig. 9. Initial disappearance of the *E* configuration of **1** and **26** during irradiation at $\lambda = 313$ nm [84]; – – – in hexadecane, — in cyclohexane. This nearly linear early phase is followed by an asymptotic approach to the photostationary equilibrium, which is not shown.

Even more pronounced effects on the photochemical and photophysical properties of stilbenes than those caused by solvent cages occur as a result of adsorption at surfaces,[85, 86] or inclusion in the cavities of zeolites[87] or cyclodextrins.[88] The restricted molecular mobility not only slows down the isomerization, but can also alter the product ratio. Adsorption of substrates accompanied by partial ionization[85] already leads to an intended charge transfer. In fact, the photoisomerization of stilbenes can also proceed by an electron-transfer mechanism.[89–92] For example, if the acceptor (A) 9,10-dicyanoanthracene ($E_s = 2.90$ eV) is irradiated in acetonitrile in the presence of (*E*)- or (*Z*)-**1** as a

donor (D), then the excited single state, $A(S_1)$, and $D(S_0)$ generate, via the exciplex, a radial ion pair consisting of a 9,10-dicyanoanthracene radical anion and a stilbene radical cation.[89] The oxidation potentials are 1.95 eV for (*E*)-stilbene and 2.06 eV for (*Z*)-stilbene. The (*E*)-**1** radical cations have a higher probability of leaving the ion pair solvent cage than the (*Z*)-**1** radical cations. However, although the $E \rightarrow Z$ isomerization has a low efficiency ($\phi \approx 0.002$), only the photoisomerization in the $Z \rightarrow E$ direction is concentration-dependent. The quantum yield ϕ increases linearly with the concentration of (*Z*)-**1** and exceeds the value 1 at about 0.2 M.[89] The reaction chain probably involves dimeric structures (Scheme 4), though the details still need to be clarified.

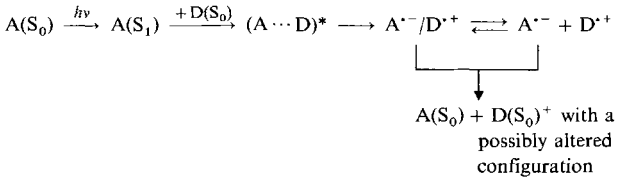

Scheme 4. Photoisomerization of stilbenes (donor D) in the presence of an acceptor (A) by an electron-transfer mechanism.

Most stilbenoid compounds behave like the parent compound **1** with regard to direct *Z*/*E* isomerization. In oligostyrylarenes all the double bonds can take part in a stepwise process, and in asymmetric cases it is even possible for the isomerization to take place preferentially on the less sterically favored side. For example, in **27** the quantum yield for the isomerization of double bond ① is significantly greater, despite the fact that in the photostationary state the *Z* configuration of double bond ② predominates (Scheme 5).[93]

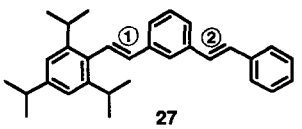

27

	①	②	
$\Phi_{E \rightarrow Z}$	0.34	0.026	
photostationary equilibrium:	*E*	*E*	8 %
	Z	*E*	20 %
	E	*Z*	31 %
	Z	*Z*	41 %

Scheme 5. Quantum yield for the $E \rightarrow Z$ isomerization of **27** and the position of the photostationary equilibrium with respect to the double bonds ① and ②.

A special case is that of stilbenoid compounds with extended conjugation. Even for 1,4-distyrylbenzene (**2**) the quantum yield for the photoisomerization (*Z*,*E*)-**2** → (*E*,*E*)-**2** is one to two orders of magnitude greater than for the reverse reaction.[94, 95] AM1 calculations indicate that for an adiabatic reaction sequence the forward and reverse reactions would have to overcome activation thresholds on the S_1 potential energy surface of 25 and 51 kJ mol^{-1}, respectively.[96] Experimental results for the tetra-*tert*-butyl derivative **25** ($n = 1$) support the assumption of a one-way photoisomerization (*Z*,*Z*) → (*Z*,*E*) → (*E*,*E*). It is not yet clear whether the reverse reaction (*E*,*E*)-**2** → (*Z*,*E*)-**2**, which occurs somewhat more readily with derivatives of **2** containing methyl or isopropyl substituents,[95] is a singlet or a triplet process. (The quantum yields are around 1 %, a range in which there is a significant probability of intersystem crossing.) One-way photoisomerization was first observed by Tokumaru et al.[97] for anthryl olefins in the triplet state; H.-D. Becker et al.[98] subsequently found that such adiabatic processes can occur on singlet and triplet potential energy surfaces. Each absorbed photon can produce a rotation about more than one double bond. For still greater conjugation lengths, as in the PPV systems (**4**), isomerization processes have not been observed in all-(*E*) compounds of high configurational purity prepared by the Siegrist method (Section 2).

4.3. Cyclization

The photocyclization of stilbene (**1**) was first observed by Smakula[99] in the 1930s, although the products were identified much later;[100] nowadays the oxidative cyclization of stilbenoid compounds is the method of choice for the synthesis of a wide variety of polycondensed arenes.[2f, g, i] If (*Z*)-**1** is irradiated at $\lambda = 313$ nm, it affords, in addition to the (*E*) isomer ($\phi = 0.35$), *trans*-4a,4b-dihydrophenanthrene (**28**) in a competing reaction with a quantum yield of about 10 % (Scheme 6).[101] In accordance with the orbital symmetry

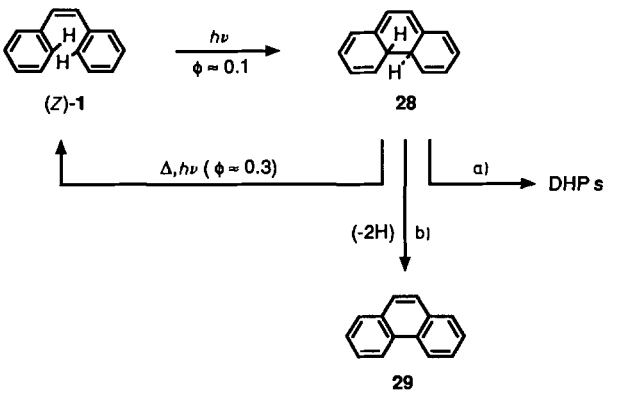

29

Scheme 6. Cyclization of (*Z*)-**1**. a) isomerization, b) oxidation; DHP = dihydrophenanthrene.

rules, the reaction is a photochemically allowed, conrotatory, electrocyclic ring closure involving six π electrons. (The signs of the orbital coefficients of the LUMO of (*Z*)-**1** at the carbon centers involved correspond to those of the coefficients for 1,3,5-hexatriene.) Dihydrophenanthrene **28** ($\lambda_{max} = 450$ nm) dissolved in isopropanol at room temperature has a mean lifetime of about 9 s.[102] It reverts thermally and photochemically to (*Z*)-**1**. Although the thermal interconversion (*Z*)-**1** ⇄ **28** is forbidden, being a conrotatory process, this only applies strictly for the direction (*Z*)-**1** → **28**, which would have to overcome a high activation barrier of about 220 kJ mol^{-1}.[103] The energy of **28** lies considerably higher on the S_0 energy surface for molecules with the consti-

tutional formula $C_{14}H_{12}$ than that of (*Z*)-**1**; consequently the activation energy E_a for the back reaction is only about 73 kJ mol^{-1}. For substituted compounds, steric effects result in a rather wide spread of E_a values from 30 to 125 kJ mol^{-1}.[2f] Steric effects can also greatly reduce the quantum yield in the photochemical back reaction. According to the theory of the photostationary equilibrium, the enrichment in **28** is markedly dependent on the irradiation wavelength. The optimal conditions are given by $\lambda = 290$ nm (the absorption maximum of **1**), low temperature, and exclusion of ambient light. Dihydrophenanthrene **28** can be removed from the equilibrium mixture by oxidizing with iodine, atmospheric oxygen, or other oxidizing agents. The recently discovered iodine/propene oxide system is especially effective.[104] Oxidation occurs irreversibly to give phenanthrene, (**29**). If there is a suitable leaving group (halogen, alkoxy, CN, CH_3, etc.) at the 4a position, the reaction can also proceed under nonoxidative conditions.[2c] An alternative to complete aromatization is, in principle, a partial aromatization by isomerization of 4a,4b-dihydrophenanthrene to 1,2-, 1,4-, 3,4-, or 9,10-dihydrophenanthrene.[105] The first double 1,3-H shift proceeding with a high yield was the formation of *trans*-9,10-dihydrophenanthrene-9,10-dinitrile on irradiation of 2,3-diphenylmaleic dinitrile.[106] Pericyclic H shifts, and even suprafacial thermal [1,5]shifts, can rarely compete with dihydrophenanthrene ring-opening, and consequently these isomerizations are usually carried out as base- or acid-catalyzed reactions.[105]

In principle this method of synthesis can be used to prepare a very wide variety of condensed arenes and heteroarenes. Instead of the olefinic double bond, C=N, N=NH, C=NH, NH-CO, or N=CO groups, or even O, N and S bridging groups can be used.[2g] The reaction mechanisms then proceeds through tripled states; however, in the standard example of the stilbenoid systems (*Z*)-**1** → **28**(→ **29**), only pure singlet states are involved. Following the electronic excitation $S_0 \rightarrow S_1$, the adiabatic process takes place over an activation barrier of 5–6 kJ mol^{-1}, in competition with the process $S_1 \rightarrow S_p$.[101, 107] The branching ratio between these two routes is about 30:70. Subsequently a return to the ground state of either (*Z*)-**1** or **28** occurs, again in the ratio 70:30, resulting in a final quantum yield of about 10% for the formation of dihydrophenanthrene.[107, 108] Since (*Z*)-**1** is continuously formed during the irradiation from the equilibrium (*E*)-**1** ⇄ (*Z*)-**1**, despite the only moderate quantum yields, product yields for the arenes vary from good to very good. With cyclohexane/iodine/atmospheric oxygen as medium, phenanthrene itself is obtained with a yield of 73%.[109] In cases where several different cyclization reactions are possible, considerable effort has already been devoted to seeking criteria for predicting the preferred reaction path. If the free valencies in the S_1 state for the C centers that are to be linked are represented by F_r^* and F_s^* then $F_{rs}^* = R_r^* + F_s^*$ should be preferably greater than 1. If several combinations can be formulated, the pair with the greatest value of F_{rs}^* is expected to be realized.[110–113] This simple rule works well in practice, apart from a few exceptions. As an example we consider here 1,3-distyrylbenzene (**22**).[111, 113, 114]

As expected, the main product (70%) from **22** is benzo[*c*]chrysene (**33**) but an 8% yield of dibenz(*a*,*j*)anthracene (**32**) is also obtained.[114, 115] Substituents can greatly influence the course of the photocyclization.[115] In the cyclization of 1,2-distyrylbenzene (**21**) to picene, and of 1,4-distyrylbenzene (**2**) to dibenzo[*c*,*g*]phenanthrene and benzo[*g*,*h*,*i*]perylene, a direct reaction path is ruled out on the basis of the F_{rs}^* values; Laarhoven et al.[113] assume an indirect route via dimeric intermediates (see Section 4.4). In consi-

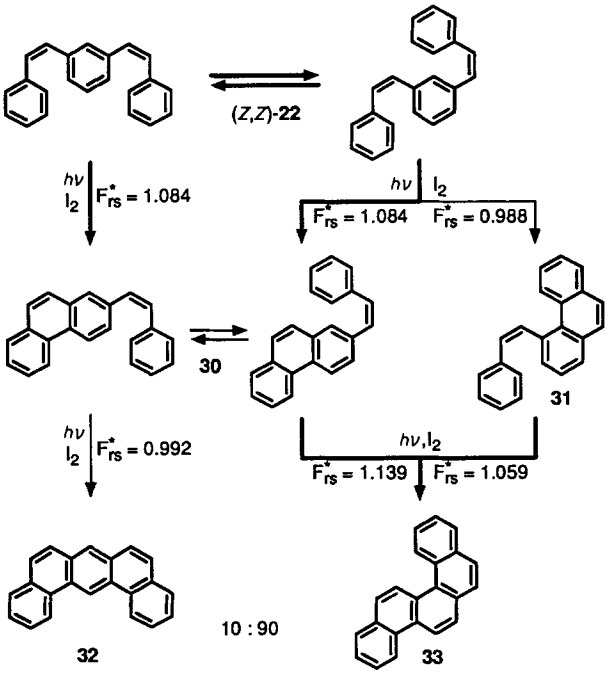

dering alternative reaction paths one must take into account that the selectivity can be achieved at the thermal oxidation stage as well, since the cyclizations are always reversible.[116] Finally, this method has been used to prepare a wide variety of helicenes,[117] and even asymmetry syntheses are possible by using polarized light,[118] chiral substituents,[119] chiral solvents,[120] or cholesteric liquid crystalline phases.[121]

4.4. Cyclodimerization

The photocyclodimerization of (*E*)-stilbene (**1**) was discovered as early as the beginning of the twentieth century by Ciamician and Silver,[122] who rank among the pioneers of photochemistry. The structure of the main product **35** was determined 45 years later by Fulton and Dunitz.[123] The side product **36** was identified in the 1960s by Shechter

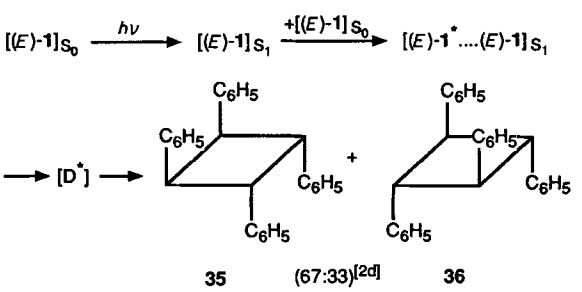

et al.[124] The first excited singlet state S_1 undergoes a stereospecific $[\pi^2s + \pi^2s]$ cycloaddition by diffusion-controlled formation of nonfluorescent singlet excimers **34**. These excimers, which correspond to flat energy minima,[125] transfer to the minima D* of doubly excited singlet state for a pericyclic geometry of the intermediate ("pericyclic minimum") and are rapidly deactivated to the ground state of the products.[126]

The geometry at the pericyclic minimum causes the energy of the D* state to dip below that of the degenerate S_1 state of these excimers within a narrowly defined local region. The avoided crossing of the energy surfaces probably results in a small energy barrier in the reaction profile. Excimers and pericyclic minima determine the stereochemistry and, in the asymmetrical case, also the regiochemistry. Predicting the regiochemistry is difficult, since according to perturbation theory the head-to-head adducts should give the most stable excimers and the head-to-tail adducts the most stable pericyclic minima.[126] The stereoselectivity of the cycloaddition is also linked to the formation of excimers. (*Z*)-**1** has an S_1 state that is much too short-lived, but also it does not, as a molecule in the ground state, take part in the formation of an exciplex $[(E)\text{-}\mathbf{1}^* \cdots (Z)\text{-}\mathbf{1}]S_1$.[127] Thus (*E*)-**1** dimerizes in concentrated solutions under irradiation to form **35** and **36**, (*Z*)-**1** does not dimerize, even in the pure liquid state, and a mixture of (*Z*)-**1** and (*E*)-**1** does not give a mixed cycloadduct. Irradiation at shorter wavelengths leads to stereoselective cycloreversion of the four-membered rings:[128, 129] irradiating with $\lambda = 254$ nm at 300 K causes scission of **35** and **36** to form (*E*)-**1** with quantum yields of 84% and 62%, respectively. Typically, the C–C bond that bears groups in a *cis* configuration is preferentially cleaved (the "*cis effect*").[128] The limiting quantum yield for the dimerization in concentrated solution is 77%.[2h] In principle, the forward and reverse reactions can involve different mechanisms. Whereas a 1,4-diradical is not an intermediate in the dimerization of stilbene,[130] it may take part in the back reaction;[128, 129] the observed stereoselectivity does not rule out the possibility of a short-lived 1,2,3,4-tetraphenylbutane-1,4-diyl species in the singlet state. A diradical of this kind has also been postulated to account for the formation of 1,2,3-triphenyl-1,2,3,3a-tetrahydroazulene with a 10% yield during the irradiation of 1,2,3,4-tetraphenylcyclobutane.[131]

According to a strikingly simple theory developed by Caldwell,[132] one can predict the cyclodimerization behavior from Equation (b), which gives the resonance integral γ in the transition state of the C–C bonds to be linked. The

$$\gamma = (2E_T - E_S)/c^2 \qquad \text{(b)}$$

smaller the value of γ, the more efficient the cyclodimerization process. When the triplet energy E_T is 205 kJ mol^{-1}, the singlet energy E_S is 357 kJ mol^{-1}, and c^2 the sum of the products of the HOMO and LUMO orbital coefficients at the reactive centers is 1.55, an extremely favorable value of γ (34 kJ mol^{-1}) is obtained for (*E*)-**1**. For styrene this value is 51 and for a simple alkene about 67 kJ mol^{-1}.[132]

Here one should not forget that efficient monomolecular processes exist for the deactivation of the S_1 state in (*E*)-**1** (see Sections 4.1 and 4.2). Thus the quantum yield for the photocyclodimerization increases with the concentration c of (*E*)-**1**, at the expense of fluorescence and $E \rightarrow Z$ isomerization. For preparative work it is desirable to have $c \geq 0.1$ mol L^{-1}. At small concentrations the dimerization comes to a standstill, as the molecules in the first excited singlet state can no longer meet a dimerization partner by diffusion within their lifetime. Aqueous or alcoholic solutions are exceptions that form stilbene aggregates down to 10^{-6} M and therefore give favorable conditions for dimerization.[133, 134] For example, the distribution of products on irradiating 5.5×10^{-4} M solutions of (*E*)-**1** in benzene and water for 24 hours is summarized in Table 1.[133]

Table 1. The dependence of the product ratio for the irradiation of (*E*)-**1** (24 h, 5.5×10^{-4} M) on solvent.

Solvent	(*E*)-**1**	(*Z*)-**1**	Cyclization	Dimerization
benzene	12	84	4	0
water	33	11	33	22
water /LiCl	27	7	25	42

Addition of lithium chloride affects the water structure in a way that favors dimerization of (*E*)-**1**. On the other hand, β-cyclodextrin or the micelle-forming salt, sodium dodecylsulfate, form hydrophobic cavities which favor a deaggregation of stilbene in water, thereby reducing the dimerization tendency.[133] (*E*)-**1** cannot be dimerized in the crystalline form, since the average distance between two adjacent double bonds is greater than 420 pm.[135] For some substituted stilbenes, however, topochemically controlled cyclodimerizations in the crystalline state are known. For ex-

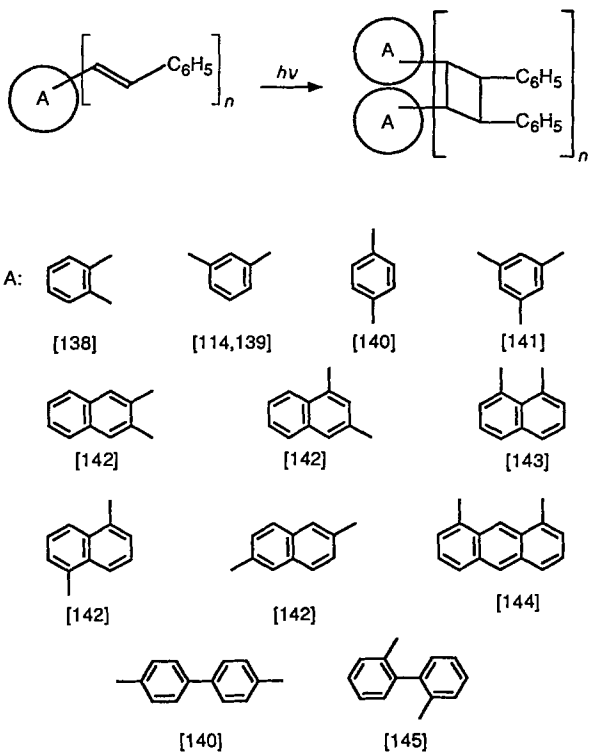

Scheme 7. Formation of cyclophanes through photocyclodimerization. The lines on the arenes mark the positions of the styryl substituents, and the numbers in square brackets the relevant reference.

ample, whereas the photolysis of (*E*)-2,4-dichlorostilbene in solution gives both a head-to-head and a head-to-tail cycloadduct of type **35**, in the solid state one finds an excimer emission band and selective formation of only the head-to-head product.[136]

An extension of the principle of photocyclodimerization to oligostyrylarenes yields special cyclophane systems in which the central arene rings (decks) are linked through four-membered rings (Scheme 7).[137] In concentrated solutions competition from intramolecular cycloaddition reactions is usually negligible. An exception is 2,2'-distyryldiphenyl,[145] in which cyclophane formation is largely suppressed. Moreover, adsorption on silica gel completely alters the photochemistry of for example, 1,2-distyrylbenzene (**21**) in favor of monomolecular processes.[146]

Regiospecific head-to-head cycloadditions are an essential precondition for all dimerizations to cyclophanes of the type shown in Scheme 7. In addition, there is a high degree of stereoselectivity in some cases.[142]

Here again the formation of excimers is a key factor. This is illustrated by the example of the double photocyclodimerization of 1,3-distyrylbenzene (**22**; Scheme 8, R = C_6H_5).[114, 139] This compound can exist as three rotamers; the form shown in Scheme 8, bottom left is the least abundant, owing to its slightly higher steric energy. The three

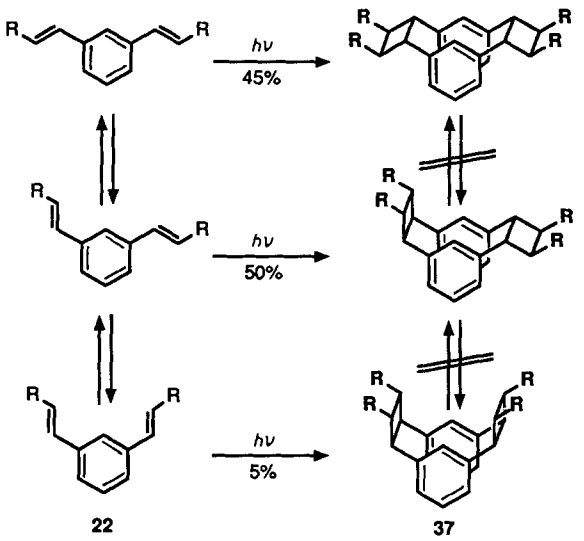

Scheme 8. Formation of three cyclophanes from three rotamers of compound **22**.

rotamers lead to different *syn*-[2.2](1,3)cyclophanes. According to the "NEER" principle (*n*on*e*quilibrium of *e*xcited *r*otamers), the original distribution between the rotamers is preserved in the S_1 state.[147] After the first four-membered ring has been formed, the distribution in the S_0 state might change, but since the steric conditions are similar to those in **22**, the rotamer populations remain essentially unaltered. The thermodynamically unfavorable *syn* stereochemistry becomes fixed by the formation of excimers. The stabilization energies *E* for these complexes, which exist only in the S_1 state, can be estimated from first-order, and/or second-order perturbation theory.[142] The HOMO–HOMO and LUMO–LUMO interactions play a crucial role. The expressions for E_1 and E_2 involve a summation over all the pairs *i,j* of overlapping π centers for molecules 1 and 2 (Scheme 9).

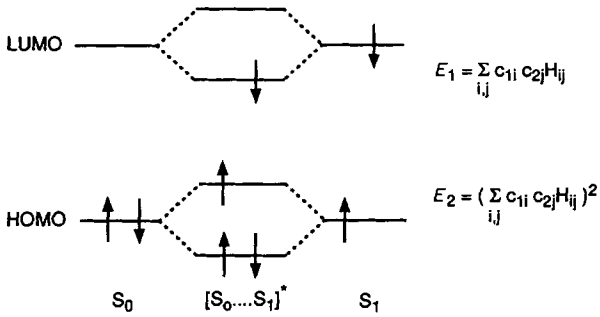

Scheme 9. Frontier orbital interactions for the formation of excimers.

By far the largest stabilization is achieved by the maximal overlap that occurs when the molecules are in a parallel arrangement. *Anti*-[2.2] (1.3)cyclophanes are therefore ruled out. This also serves to explain the head-to-head selectivity. From (*E,E,E*)-1,3,5-tristyrylbenzene (**24**) one obtains exclusively [2.2.2](1,3,5)cyclophane **38**, despite the fact that a triple head-to-tail dimerization would yield the much less strained [3.3.3](1,3,5)cyclophane **38'**.[141] However, for the latter interaction E_1 and E_2 both are zero.

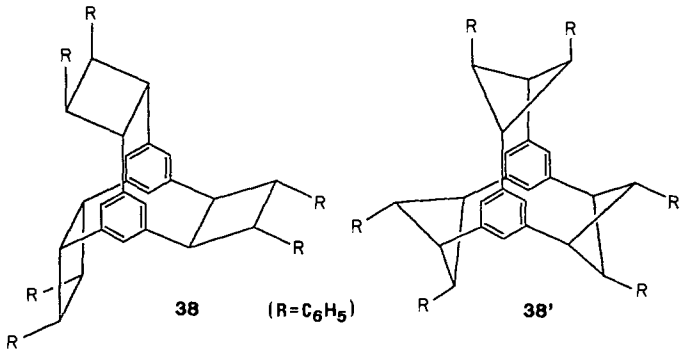

Thus, neither the photocyclization (Section 4.3) nor the photocyclodimerization reactions are controlled by the energy content of the products. Compounds **22** and **24** are category II stilbenoid chromophores; because of the relatively long lifetime of the S_1 state, dimerization can still occur even in dilute solutions ($c \approx 0.5 \times 10^{-3}$ M).

The principle of repeated photocyclodimerizations (oligomerizations) of stilbenoid compounds offers interesting possibilities for building up polymers[148, 149] (see Section 6.2).

5. Stilbenoid Systems in the Triplet State

5.1. Excitation and Physical Deactivation

For stilbene itself and for most stilbenoid compounds the quantum yield for intersystem crossing $S_1 \rightsquigarrow T_1$ is extremely small ($\phi_{ISC} \approx 0.002$).[2e] To populate the T_1 state the energy

transfer requires a triplet sensitizer. However, substituents such as nitro groups, halogens, or aroyl groups can increase ϕ_{ISC}.[150, 151] For example, 4-nitrostilbene in benzene yields 86% of the triplet state for the *E* configuration and 59% for the *Z* configuration.[151, 152] If chlorine or bromine are substituents, ϕ_{ISC} has values between 0.1 and 0.5, and singlet and triplet processes are observed simultaneously.[2c, 2j]

The physical deactivation of the T_1 state in stilbenoid compounds by phosphorescence is so limited that it is difficult to detect; for example, for (*E*)-**1** in ethanol at 77 K, ϕ_P is not greater than 10^{-5}.[153] The heavy atom effect[154] or the restriction of molecular mobility increases the phosphorescence.[153, 155] Nevertheless, even for (*E*)-4-nitrostilbene in ethanol at 77 K, a large majority of the molecules undergoes the transition into the T_1 state, but only about 0.03% subsequently emit phosphorescence radiation (λ_{max} = 614 and 673 nm); the fluorescence quantum yield, $\phi_F = 3 \times 10^{-3}$, is still ten times greater than that for phosphorescence.[153] By far the most efficient process is radiationless deactivation[151, 156] (see Section 5.2). The lifetime of the triplet state under these conditions is around 10 ms; deuterium substitution increases the lifetime,[156] whereas bromine and other heavy atoms reduce it.[153]

5.2. Sensitized *Z*/*E* Isomerization

The pioneering studies on triplet-sensitized *Z*/*E* isomerization in stilbenes were carried out in the 1960s by Hammond et al.[157] The sensitizers (donors) D_1 with triplet energies E_T of at least 255 kJ mol^{-1} transfer their energy to (*E*)-**1** and (*Z*)-**1** in a diffusion-controlled process. The model in Scheme 10 proceeds from an initial donor–acceptor collision complex, which generates T_1 states without change of spin (corresponding to vertical transitions, which retain the ground state geometry). From the triplet state $[(E)\text{-}\mathbf{1}]_T$, a relaxation process takes place on the T_1 potential energy surface, leading to a state T_P, which represents a molecule twisted through 90° (formerly called a "phantom triplet").[157] The ground state energy surface S_0 should intersect or touch the T_1 hypersurface in the immediate vicinity of T_P, so that a transition to $[(Z)\text{-}\mathbf{1}]S_0$ or $[(E)\text{-}\mathbf{1}]S_0$ can occur (see Fig. 8).[34, 158] The exact form of the potential surface is not known with certainty. The $[(E)\text{-}\mathbf{1}]_T$ and T_P states are relatively close together in energy, and consequently the order of these can alter, and different equilibria can become established depending on the solvent.[158] When the *E* configuration approaches the geometry of T_P, one can assume a small activation threshold; this is less likely to occur on the *Z* side of the reaction profile. Unlike $[(Z)\text{-}\mathbf{1}]_T$, T_P can transfer its triplet energy to an acceptor.[24, 159] The mean lifetime of T_P at room temperature is about 60 ns.[159, 160]

The photostationary equilibrium of the triplet-sensitized reaction can be described by Equation (c). For a high sen-

$$\frac{[(Z)\text{-}\mathbf{1}]}{[(E)\text{-}\mathbf{1}]} = \frac{k_1}{k_2} \cdot \frac{k_4}{k_3} \qquad (c)$$

sitizer energy, one has $k_1 \approx k_2$, and the value of $k_4/k_3 = \phi_{E\to Z}/\phi_{Z\to E}$ is also approximately 1, resulting in equilibria with 50–60% of the *Z* isomer. For the benzophenone-sensi-

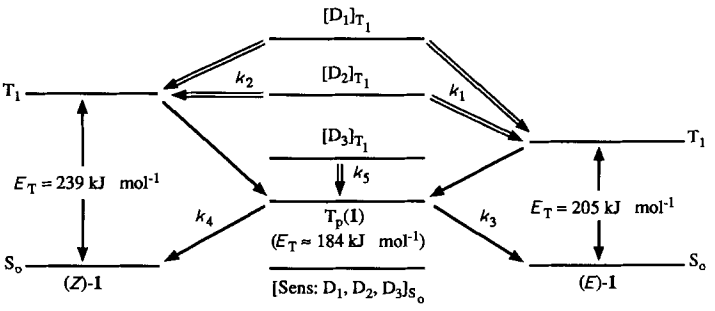

Scheme 10. Model for the energy transfer from donors D_1, D_2, and D_3 to stilbene 1 in the sensitized *Z*/*E* isomerization. Sens = sensitizer.

tized reaction (E_T = 289 kJ mol^{-1}) the quantum yields are $\phi_{Z\to E} = 0.41$ and $\phi_{E\to Z} = 0.55$, resulting in a ratio $[(Z)\text{-}\mathbf{1}]/[(E)\text{-}\mathbf{1}] = 58:42$. The sum of the quantum yields is 0.96, which is very close to 1, suggesting that a common intermediate (T_P) is involved. If the triplet energy of the donor is reduced to 239 kJ mol^{-1}, the same as the triplet energy of (*Z*)-**1** the transfer to the **Z** configuration is considerably slowed down by a small activation barrier. However, in this case (sensitizer D_2) an efficient energy transfer to $[(E)\text{-}\mathbf{1}]_T$ still takes place. In the formula for the photostationary equilibrium state the important term is the ratio k_1/k_2, and the *Z* fraction is increased. If one has a sensitizer D_3 with a triplet energy E_T (equal to that of (*E*)-**1**) of 205 kJ mol^{-1} or less, the energy transfer to $[(E)\text{-}\mathbf{1}]_T$ should also cease. In fact, however, an energy transfer is still observed even in this situation, although it is less efficient.[157, 158] As Figure 10 shows, the *E* fraction in the photostationary equilibrium then increases again. A likely explanation is that there is a nonvertical ener-

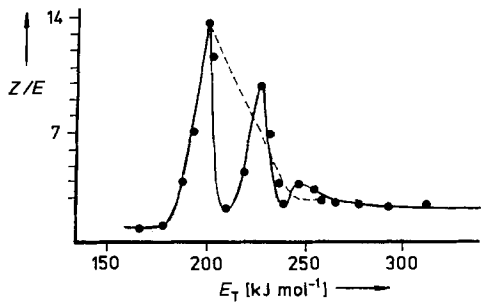

Fig. 10. Photostationary *Z*/*E* equilibrium for the isomerization of stilbene (**1**) with triplet sensitizers of different energies *E*, [157]. The dashed line shows the theoretical curve expected for a diffusion-controlled energy transfer involving spectroscopic states.

gy transfer process with the formation of T_P ($E \simeq$ 184 kJ mol^{-1});[160] such a process has smaller activation enthalpy on the (*Z*) side (and a slightly more negative activation entropy).[158] The question then arises whether, in principle, an energy transfer with formation of T_P can also occur for D_1 and D_2.[158] Other models involving vibrationally excited molecules[161] or triplet exciplexes[1a] have also been proposed as alternatives to the nonvertical energy transfer. Balzani, Orlandi, et al. have discussed this problem from both the classical and quantum-mechanical standpoints.[162] Derivations from the theoretical curve shown in Figure 10 indicate that, leaving aside differences in the methods used to

determine the data, steric effects too can have an important influence on the energy transfer process. An interesting example of this is again provided by **27**. In contrast to the direct photolysis situation, in the benzophenone-sensitized reaction the quantum yields for the isomerization (*E,E*)-**27** → (*Z,E*)-**27** are small on the sterically hindered side ($\phi = 0.026$) and large on the other side ($\phi = 0.49$). The quasi-stationary equilibrium state has the ratios[93] (*E,E*):(*Z,E*):(*E,Z*):(*Z,Z*) = 39:8:44:9. In 1,4-distyrylbenzene (**2**), the extended conjugation leads to a very low efficiency for the $E \rightarrow Z$ isomerization in the S_1 state (see Section 4.2), whereas the benzophenone-sensitized reaction has a quantum yield of 53%.[95] Triplet-sensitized *E–Z* isomerization is of particular synthetic interest in cases where direct photolysis fails. For preparative purposes one can also use polymer-bound sensitizers[163] or sensitizers which favor the *E* isomer.[164] To end this section it should be mentioned that sensitized *Z/E* isomerization can also be achieved by means of an electron transfer process [Equation (d)]. Here, of

$$[D]_{S_1} \xrightarrow{+A} [D^{\bullet+}A^{\bullet-}]_{S_1} \xrightarrow{ISC} [D^{\bullet+}A^{\bullet-}]_{T_1} \xrightarrow[-D]{} [A]_{T_1} \longrightarrow \cdots \qquad \text{(d)}$$

course, *Z/E* isomerization can, in principle, also occur at the stages where one has radical pairs or charge-transfer stabilized exciplexes. This leads into the topic of photocatalysis. Thirty years ago such mechanisms were discussed by Schenck et al.[165] If a donor D (or an acceptor) forms a σ bond to the stilbene system, rotation about the formerly olefinic bond is possible (Scheme 11). In the singlet case this process is similar to catalysis by iodine.

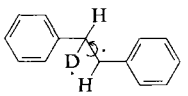

Scheme 11. A *Z/E* isomerization at the radical ion pair stage can lead to rotation about the former double bond.

6. Applications in Materials Science

Stilbenoid systems and light is a many-faceted topic in materials science, and has grown rapidly in importance in the last few years. Some of the most important applications, which are either already technological realities or show potential are optical brighteners, laser dyes, scintillators, light-emitting diodes, optical switching, optical data storage, photopolymerization, photochemical crosslinking, photoinitiators, photoresists, photoconductors, and nonlinear optics.

In this review the emphasis will be on recent developments, and an attempt will be made to illustrate the link between the photophysics and photochemistry of stilbenoid compounds and the technology.

6.1. Utilization of Light Emission

The high quantum yield of fluorescence of many stilbenoid compounds led to their early introduction as optical brighteners. The first successful products of this kind appeared on the market during the 1940s under the trade name Blankophor®; these products (**39**) were derivatives of 4,4′-diaminostilbene-2,2′-disulfonic acid.[166] Incorporating heterocyclic rings such as 1,3,5-triazines, 1,2,3-triazoles, or benzoxazoles improves their fluorescence properties; nevertheless, the resulting products are different from fluorescent dyes in which the chromophores themselves are entirely heterocyclic. Optical brighteners based on **39** continue to play a major role in industrial processes, but there are also other technologically interesting products such as **40** and **41**, based on the stilbenoid structures (*E,E*)-1,4-distyrylbenzene and (*E,E*)-4,4′-distyrylbiphenyl.[167] The common physical characteristics of compounds **39**–**41** are a strong UUV/VIS absorption with a maximum between 350 and 375 nm and an intense fluorescence band (ϕ_F of nearly 1) in the range from 415 to 445 nm. Thus the absorbed UV radiation is converted to light in the violet to blue-green region, compensating for the yellow cast of many textiles, papers, plastics, etc. To overcome the blue deficiency of these materials it is also important that both the absorption band and the fluorescence band fall off steeply on the longer wavelength side.

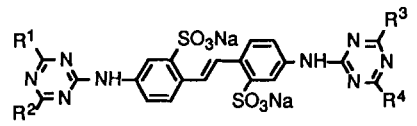

39(R^i = NHR′, NR_2', OR′ ...)

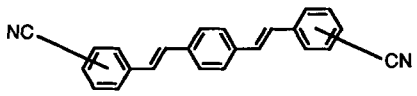

40

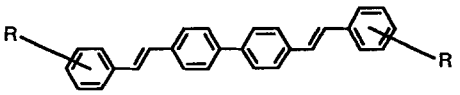

41(R = SO_3Na, OCH_3, Cl)

The closer ϕ_F is to 1, the less likely is it that the S_1 or T_1 states will lead to unwanted photoreactions. Of these, the one that must be considered most seriously is the isomerization of the *E* isomer to the nonfluorescent *Z* isomer. In the compounds **39**–**41**, however, the quantum yield for the $E \rightarrow Z$ isomerization is small, especially in the absorbed state (see Section 4.2). In this case the nature of the interaction with the support, which can extend from simple contact to covalent bonding, is very important.[168, 169] Another unwanted reaction could occur when singlet oxygen, which is extremely reactive, is generated; depending on the nature of the substituents, stilbene-based optical brighteners can sometimes function as sensitizers or quenchers for singlet oxygen.[168]

The good fluorescence properties of stilbenoid compounds also make them interesting as scintillators[170, 171] and laser dyes.[172] Continuous dye lasers were developed in 1970 by Peterson, Tuccio, and Snavely.[173] Because of their tunability, dye lasers are now found in a very wide variety of

applications. They can also be used to generate extremely short pulses—less than 30 fs.[174] The electronic excitation of the dissolved fluorescent dye, known as optical pumping, is achieved by means of a flash tube or gas laser; very often an excimer laser (based on xenon chloride or krypton fluoride) is employed. A typical fluorescent dye of the stilbenoid type is **42**, generally known as stilbene-1.

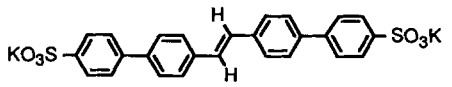

42

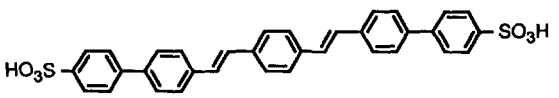

43

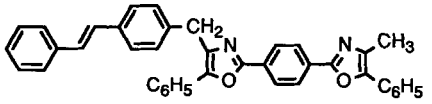

44

When an argon ion laser is used as the excitation source, the tunable wavelength range extends from 395 to 435 nm in the violet.[175] The typical dye laser is a four-level laser. The excitation of the fluorescent dye from the ground state to a vibrational level of the S_1 state ($S_0 \rightarrow S_1^v$) is followed by relaxation into the lowest vibrational level of S_1, from which spontaneous and stimulated emission of the fluorescence radiation occurs ($S_1 \rightarrow S_0^v$). The relaxation to the lowest vibrational level of S_0 occurs very rapidly; thus, only a low population in the S_1 state is necessary for the population inversion on which the laser action depends. An important criterion for suitability as a laser dye is a high fluorescence quantum yield; it is therefore appropriate to carry out tests on the stilbenoid compounds developed as optical brighteners, to assess their suitability as laser dyes.[176-178] Such experiments are usually confined to the violet to blue spectral emission region. A serious disadvantage is the tendency of the dyes to fade,[175] caused by the conversion of stilbenes from the *E* configuration to the nonfluorescent *Z* configuration, which then undergoes secondary photoreactions.[179, 180] the partial quantum yields in the range $313 \leq \lambda \leq 365$ for **42** in oxygen containing ethylene glycol are given in Equation (e).

$$(E)\text{-}\mathbf{42} \underset{\phi = 0.5}{\overset{\phi = 0.016}{\underset{h\nu}{\rightleftharpoons}}} (Z)\text{-}\mathbf{42} \xrightarrow[\phi = 0.0001]{h\nu} \text{secondary products} \quad \text{(e)}$$

Using a laser dye based on 1,4-distyrylbenzene as the chromophore suppresses the $(E) \rightarrow (Z)$ isomerization. For **43** the value of $\phi_{E \rightarrow Z}$ is only 1×10^{-5}, and the proportion of the *Z* isomer in the photostationary equilibrium is reduced to 4%.[179] Stilbenes are also employed for a quite different purpose in laser dye technology, as triplet quenchers, since significant competition from the intersystem crossing process $S_1 \rightsquigarrow T_1$ would reduce the fluorescence yield. A better alternative to mixing a triplet quencher with the dye is to attach it to the dye by covalent, nonconjugative bonding. The first successful application of this principle was realized in the bisoxazole laser dye **44**.[181]

Another way of achieving light emission with stilbenoid compounds of high molecular mass is electroluminescence. Poly(arylenevinylene)s with opposite charge carriers can form excitons, which dissipate their energy by light emission, as shown in Scheme 12.[182-184] The interaction of positive

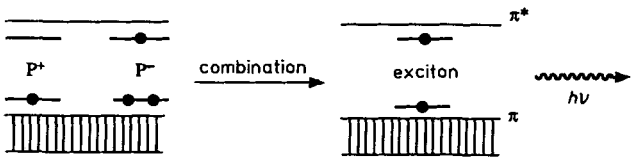

Scheme 12. The formation of excitons, which lose energy by emission of light. P^+,P^- are polarons.

and negative polarons P causes a splitting of the energy levels in the band gap, with the result that the doubly occupied level falls back into the π band, whereas the empty level is raised to π*. A material for use in a light-emitting diode should have ionization potential and electron affinity values that ensure balanced flows of positive and negative charge carriers from the attached electrodes. Also both types of charge carriers must be able to travel far enough in the material to allow the formation of excitons. The fluorescence process responsible for the electroluminescence competes with multiphonon emission (internal conversion), the formation of triplet states (intersystem crossing), exciton–exciton annihilation, and lastly exciton–polaron and exciton–bipolaron interactions. Bipolarons are very efficient "catalysts" for the radiationless decay of excitons.[183] The yield of emitted photons per transferred electron is usually small. However, in a remarkable experiment[183] the photon yield for a PPV copolymer was increased from 0.01% to 0.3% by incorporating about 10% of 2,5-dimethoxy-*p*-phenylenevinylene units into the chain. The homopolymer of the dimethoxy compound has a band gap of about 2.1 eV, which is 0.3–0.4 eV smaller than that of PPV, but its photoluminescence is much lower. Its incorporation into the copolymer in the optimal proportion of 10% produces local energy sinks in the chain, which act as "exciton traps", resulting in an enhanced radiation emission.[183] Using calcium instead of aluminum as the electrode material can even increase the efficiency to more than 1%.[184]

6.2. Utilization of Photochemical Transformations

Whereas reactions stimulated by light are a nuisance in the materials applications discussed in Section 6.1, photochemical processes in stilbenoid compounds provide the basis for the materials and effects described in this section. A new field of study concerns the effects of light on liquid crystalline (LC) systems containing stilbene chromophores, which are calamitic or discotic mesogens.[185-187] One can easily envisage that highly ordered smectic or nematic phases may be modified by $E \rightarrow Z$ isomerization, cyclodimerization, or polymerization to such an extent that the mesophases under-

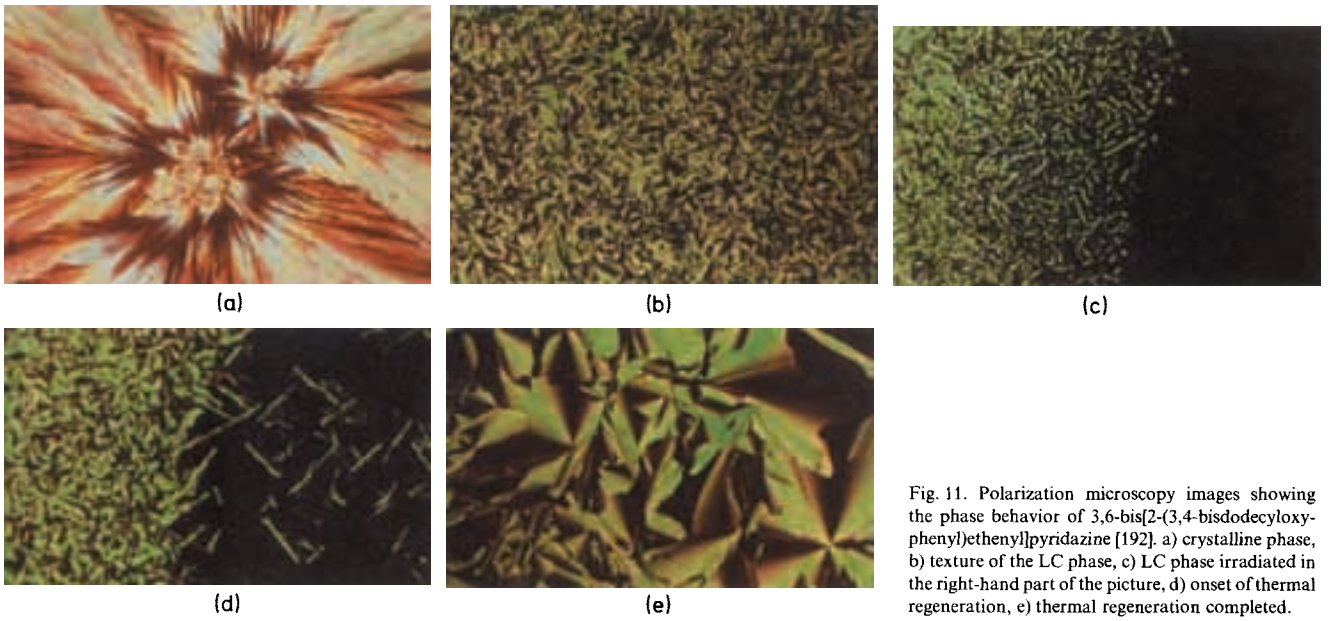

Fig. 11. Polarization microscopy images showing the phase behavior of 3,6-bis[2-(3,4-bisdodecyloxyphenyl)ethenyl]pyridazine [192]. a) crystalline phase, b) texture of the LC phase, c) LC phase irradiated in the right-hand part of the picture, d) onset of thermal regeneration, e) thermal regeneration completed.

go a transition to the isotropic melt phase well below the original clearing point. Here a distinction must be made between reversible and irreversible processes. Based on the change in the optical properties which accompanies the phase transformations, these effects find application on the one hand in optical switches, and on the other hand in permanent optical data storage. As the following examples show, liquid crystalline phases are observed in a wide variety of stilbenoid compounds.

(*E*)-stilbenes such as **45** with *p*-alkoxy substituents were among the earliest LC systems described in the literature;[188] to these have since been added many other stilbene derivatives containing alkyl, alkylamino, and ester groups,

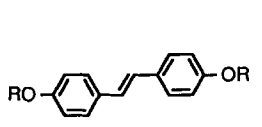

45

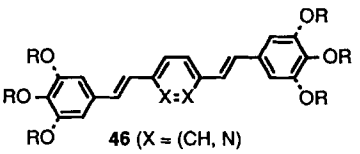

46 (X = (CH, N)

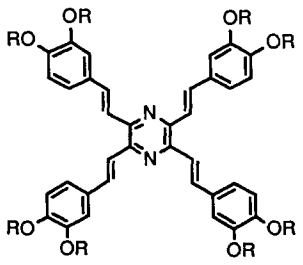

47

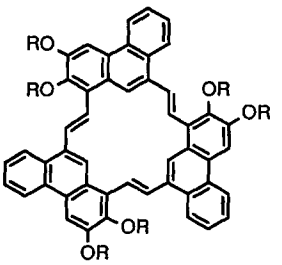

48

and also push–pull compounds containing nitro groups.[189] If one increases the length of the rod-shaped mesogen, as in the compounds **46**, then in addition to *p*-substitution one can have long-chain alkoxy substituents at one or even both of the *meta* positions.[185, 191] The calamitic systems are then transformed into phasmidic systems.[190] The compounds **47** and **48** are new types of discotic mesogens.[12, 191] Figure 11 illustrates a reversible breakdown of a liquid crystalline phase under UV illumination.[192]

Only a very small degree of conversion is sufficient to break down the LC phases; the photocyclodimerizations and photopolymerizations are irreversible processes, the $E \rightarrow Z$ transformation is reversible. In highly viscous LC phases, isomerizations of the stilbenoid compounds can only take place with difficulty compared with experiments in solution; on the other hand, the high degree of ordering in these phases favors dimerizations. However, these are limited to the formation of only one four-membered ring. We have not so far found any examples of cyclophanes in LC phases of stilbenoid compounds (see Section 4.4). Since the S_1 state is expected always to result in a higher proportion of irreversible reactions, research activity is tending to concentrate more on triplet sensitization. The aim is to develop a multicomponent system consisting of a stilbenoid mesogen/chromophore, a triplet sensitizer absorbing at long wavelengths, and a catalyst for the thermal back reaction ($Z \rightarrow E$ isomerization). The cyclization of stilbene units (Section 4.3) should also be of interest in this area of materials science, if liquid crystals based on helicene structures can be prepared. Finally, stilbene units can be incorporated into the backbone or side chains of polymers,[193] which creates materials with light-sensitive LC phases.

This topic leads into the general principle of photo-crosslinking of polymers through stilbene units (Scheme 13).[194] The basis of a negative photoresist is a soluble polymer that becomes insoluble as a result of crosslinking. Although it has often been postulated that photopolymerization of stilbenoid systems in solution involves the formation of four-membered rings, our experience indicates that the dominant mechanism is usually a free radical chain reaction, leading to polymers with little structural uniformity. Hasegawa et al.[148] recognized a considerable time ago that a repeated photocyclodimerization in the solid state could be an interesting principle for building polymers.[149] Here again the topochemically controlled reaction is associated with a fa-

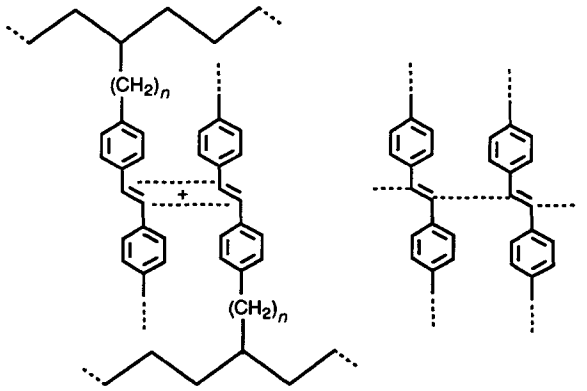

Scheme 13. Photo-crosslinking of polymers through stilbene units.

vorable arrangement of the C=C bonds in the crystal lattice (see Section 4.4); however, lattice defects can play an important role in the progress of the reaction. For example, whereas (*E,E*)-1,4-distyrylbenzene (**2**) is photostable in the crystalline phase, the aza analogues (*E,E*)-1,4-bis[2-(2-pyridyl)-ethyl]benzene[195] and (*E,E*)-2,5-distyrylpyrazine (**49**) form photopolymers such as **50**.[148]

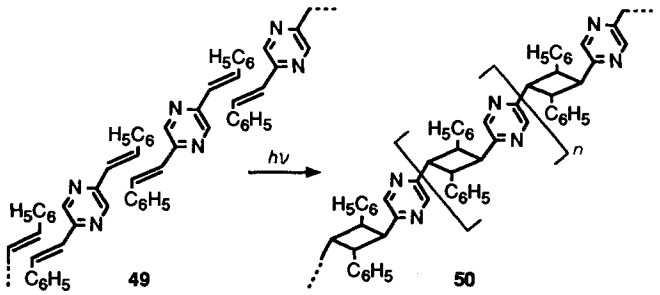

6.3. Other Electrical, Optical, and Optoelectronic Applications

This last section will review some applications of stilbenoid compounds in materials technology in situations where neither photochemical transformations nor light emission are desired. It was originally thought that polymers of high structural purity with fully conjugated chains would be electrical conductors.[196] Using poly(1,4-phenylenevinylene) (**4**) as example Hörhold and Opfermann[197] were able to show that, in fact, these polymers were semiconductors of high resistivity, with a relatively large band gap of about 2.4 eV. Oxidative or reductive doping was found to increase the conductivity σ from less than 10^{-15} S cm^{-1} by many orders of magnitude—in extreme cases even up to 3×10^3 S cm^{-1}.[17] In the context of this article the photoconductivity of undoped poly(arylenevinylenes) is of particular importance. With direct illumination or triplet-sensitization, remarkably high values of the photocurrent I have been measured. The dependence $I(\lambda)$ of intensity on wavelength observed on irradiating unsensitized PPV films is very similar to the absorption curve. The maxima of the two curves are close together in the visible region, at wavelengths between 400 and 600 nm depending on substitution. Figure 12 shows typical capacitor discharge curves measured in the dark and with illumination, together with results on the sensitivity as a function of wavelength.

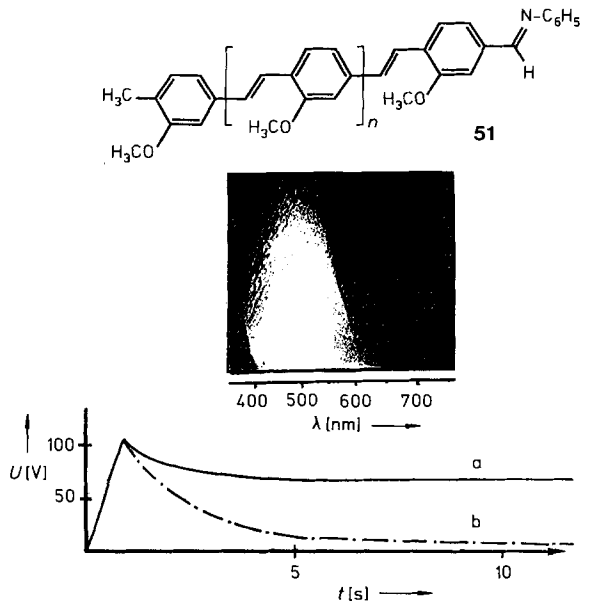

Fig. 12. Measurement of the photoconductivity of the PPV system **51** in a dispersed film, showing the decay of the voltage $U(t)$ and the sensitivity as a function of wavelength. a) In the dark; b) on irradiation.

The photoconductivity in PPV can be explained by assuming a light-induced disproportionation into radical ion pairs.[17] The short-lived charge carriers that are generated in this way according to the effectively conjugated chain segments (ECS) theory[17] are undoubtedly augmented at the electrodes by radical ions produced by transfer of charge onto electronically excited particles. The details of the mechanism of conduction are not fully understood; the fast transfer of the charge can be explained by an almost activationless transport in the chain and electron-hopping processes between chains. Mechanistic studies[198a] and synthetic efforts in which the polymer structure **52** is subjected to wide variation[198] should contribute to a better understanding of these effects. Alkoxy groups R in **52** not only reduce the band gap,

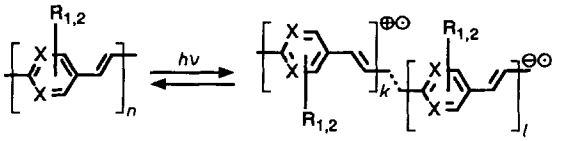

52 (X = CH,N; R = OCH_3,...,$OC_{16}H_{33}$)

but also influence the arrangement of the chains in such a way that when the convergence limit for n (see Section 4.1) is exceeded, the photoconductivity passes through a maximum as the length of the side chains is increased. The efficiency of the light-induced ion formation is reduced by the fluorescence of **52**, but is even more drastically affected by photochemical processes. When monochromatic light (λ = 436 nm) in the region of the longer wavelength absorption maximum

($\lambda_{max} \approx 450$ nm) is used for irradiation, ion formation competes with fluorescence ($\phi_F \approx 0.2$), but even when the irradiation is continued for several months no photochemical change in the material is detected. The mean lifetime of the excited state is too short for cyclodimerization to occur (see Section 4.4), and $E \rightarrow Z$ isomerization does not take place, since for $n \leq 3$ the isomerizations proceed in only one direction, $Z \rightarrow E$ (see Section 4.2). If instead the irradiating light is in the short-wave UV region ($\lambda = 254$ nm), **52** is converted relatively quickly into nonconjugated oligomers with $\lambda_{max} \approx 270$ nm; at the same time the photoconductivity disappears.[198] The application of such materials in electrophotographic recording depends essentially on the photostability, and also on the resistance to atmospheric oxygen and bonding agents.

Another highly topical investigation of stilbenoid compounds in materials technology is in connection with nonlinear optical properties. Due to the electric field component of light waves, molecules become polarized. In the case of linear optical behavior the induced dipoles emit radiation of the same frequency. The polarization P is then proportional to the field strength E, which corresponds to the model of a harmonic oscillator. In the anharmonic oscillator model, which is a closer approximation to reality at very high light intensities, P still increases monotonically with E, but no longer linearly [Eq. (f)]. Here, in addition to the linear polar-

$$P = \alpha E + \beta EE + \gamma EEE + \ldots \qquad \text{(f)}$$

izability α, we have the tensors β and γ representing the second- and third-order polarizabilities, the so-called hyperpolarizabilities. In this case, whereas the function describing the E vector of the incoming light waves is sinusoidal, the polarization is nonsinusoidal. The Fourier analysis of the periodic function of the polarization yields a series of sinusoidal components $P(n\omega)$ with $n = 0,1,2,3\ldots$. In addition to the static component $P(0)$, which describes the optical rectification effect, and the fundamental wave $P(\omega)$, we obtain $P(2\omega)$ (second harmonic generation, SHG) and $P(3\omega)$ (third

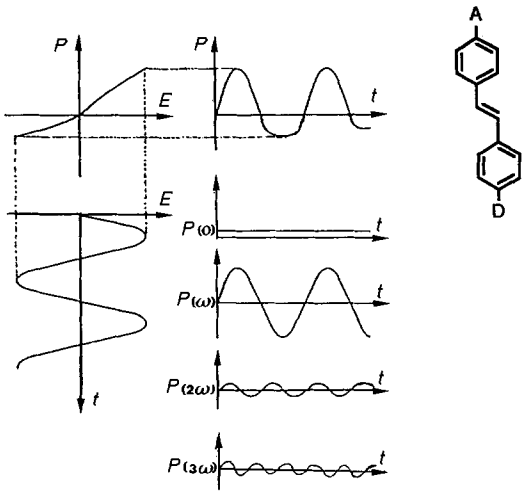

Fig. 13. Polarization $P(t)$ of a stilbene system by the oscillating electric field component $E(t)$ of a light wave, and its resolution into the Fourier components $P(0)$, $P(\omega)$, $P(2\omega)$, and $P(3\omega)$.

harmonic generation, THG).[199] Translating this to the macroscopic level gives Eq. (g). Thus, in addition to the

$$P = \chi^{(1)}E + \chi^{(2)}EE + \chi^{(3)}EEE \qquad \text{(g)}$$

linear susceptibility $\chi^{(1)}$, the materials considered here have the nonlinear susceptibilities $\chi^{(2)}$ and $\chi^{(3)}$.[200] These relationships are illustrated in Figure 13 for a stilbene derivative that is assumed to be oriented so that the light wave produces the greatest polarization in the direction of the substituents; the substituents themselves constitute a donor-acceptor pair, as in the canonical structures **53**. The charge transfer band for

53

such a molecule is polarized in the direction of the longest axis. Although in the ground state the dipolar canonical structure is only of minor significance, in the electronically excited singlet state the dipole moment is considerably greater (see Section 4.1). If the stilbene had identical substituents in the 4 and 4′ positions, the molecule would have C_{2h} symmetry with a center of inversion as a symmetry element. For centrosymmetric molecules, $P(E)$ and $P(-E)$ must be equal, which means that in the power series for P the terms with even-numbered exponents are zero. From the condition $\beta E^2 = 0$ it follows that $\beta = 0$. In the monocrystalline form the arrangement of the molecules can still be centrosymmetric even though the individual molecule is not itself centrosymmetric; this means that we can have $\chi^{(2)} = 0$ with $\beta \neq 0$. Push-pull compounds have a tendency to form crystalline arrangements of this kind, and therefore a common procedure is to embed such a chromophore in a polymer matrix and polarize by applying an electric field. For materials technology applications a system with a high quadratic hyperpolarizability is needed, and one therefore aims for noncentrosymmetric structures in which charge transfer transitions can take place at low energies. (*E*)-stilbene derivatives are especially suitable in this respect.[201] As λ_{max} for the electronic transition at longer wavelength increases, β also increases. Plotting log β against log λ_{max} gives a line whose gradient is greater than that for analogous benzene derivatives.[202] Although (*E*)-4-methoxy-3-methyl-4′-nitrostilbene only has a moderately high β-value of $18-26 \times 10^{-30}$ esu (at $\lambda = 1064$ nm), the SHG value for this compound in powder form is very high; it is 1250 times greater than the value for urea [$\chi^{(2)} = (3.4 \pm 1) \times 10^{-9}$ esu], which is often used as a standard.[202, 203] The relevant range of $\chi^{(2)}$ values for organic compounds extends from 10^{-9} to about 10^{-5} esu. Stilbazolium systems are at the upper end of this scale. Instead of using the host–guest relationship of polymers with chromophores having nonlinear optical (NLO) properties, as described earlier, the NLO-active compounds may be directly incorporated into systems that can be photochemically polymerized and crosslinked. In this way one can achieve a high concentration of the NLO-active component.[204] Another interesting development is the production of NLO-active compounds that form thermotropic liquid crystals.[205]

In contrast to compounds with second-order optical nonlinearity, third-order NLO-active systems demand fewer structural preconditions, because the symmetry criterion no longer applies. Unsubstituted (*E*)-stilbene has γ values (THG coefficients) of 27 and 18×10^{-36} esu at $\lambda = 1064$ and 1907 nm respectively.[206] The most promising of the stilbenoid systems are the poly(phenylenevinylene)s in which the largest component of the γ tensor lies in the direction of the extended conjugation. Stretched polymers of this type with chains aligned parallel to each other should give particularly large $\chi^{(3)}$ values. This has been confirmed in studies of the anisotropic behavior.[207] For a uniaxially stretched PPV film the $\chi^{(3)}$ value measured in the stretching direction was 1.2×10^{-9} esu (at $\lambda = 602$ nm).[208] For the 2,5-dimethoxy derivative, which has a smaller band gap, a four-wave mixing experiment in the subpicosecond region yielded, at the same wavelength, $\chi^{(3)} = 4 \times 10^{-9}$ esu.[209] For unorientated PPV films a $\chi^{(3)}$ value of $(1.5 \pm 0.6) \times 10^{-10}$ esu was observed at $\lambda = 1064$ nm.[210] The high light intensities generated by the lasers that are used make high demands on the photostability of the NLO materials. Where possible the direct resonance condition is avoided, and resonance with two-photon transitions should also be excluded.

7. Outlook

Stilbenoid compounds will undoubtedly continue to be a central topic in photochemistry in the future. From the theoretical physicochemical standpoint, flash spectroscopy extending into the femtosecond region is expected to yield further knowledge about the nature of the reactive species along the reaction coordinates followed on light absorption or energy transfer. This will provide new impetus and ideas for synthesis and matrials technology, making it possible to refine ways of either eliminating unwanted radiation effects or increasing the efficiency of the desired photoreactions, depending on the type of application. The road from new substances with interesting properties to fully developed technological materials is often long and arduous. Stilbenes, which are already being used very successfully in a number of industrial sectors, are now making progress on a still wider front.

Received: March 30, 192 [A 883 IE]
German version: *Angew. Chem.* **1992**, *104*, 1425
Translated by Dr. J. K. Becconsall, Gwynedd, Wales.

[1] a) N. J. Turro, *Modern Molecular Photochemistry*, Benjamin/Cummings, Menlo Park, USA, **1978**; b) M. Klessinger, J. Michl, *Lichtabsorption und Photochemie organischer Moleküle*, VCH, Weinheim, **1989**; c) J. Michl, V. Bonačič-Koutecký, *Electronic Aspects of Organic Photochemistry*, Wiley, New York, **1990**; d) H. G. O. Becker, *Einführung in die Photochemie*, Deutscher Verlag der Wissenschaften, Berlin, **1991**; e) G. von Bünau, T. Wolff, *Photochemie, Grundlagen, Methoden, Anwendungen*, VCH, Weinheim, **1987**; f) J. Kopecký, *Organic Photochemistry:* A Visual Approach, VCH, Weinheim, **1992**; g) A. M. Brown, M.-T. Maurette, E. Oliveros, *Technologie Photochimique*, Presses Polytechniques Romandes, Lausanne, **1986**.

[2] More recent review articles on individual topics: a) J. Saltiel, J. D'Agostino, E. D. Megarity, L. Metts, K. R. Neuberger, M. Wrighton, O. C. Zafirou, *Organic Photochemistry* **1983**, *3*, 1–113; b) J. Saltiel, D. W. L. Chang, E. D. Megarity, A. D. Rousseau, P. T. Shannon, B. Thomas, A. K. Uriarte, *Pure Appl. Chem.* **1975**, *41*, 559–579; c) H. Meier, *Methoden Org. Chem. (Houben-Weyl)* **1975**, Vol. IV, 5a, 1, pp. 511–538; d) G. Kaupp, *ibid.* **1975**, Vol. IV, 5a, 1, pp. 326–347, 360–369; e) J. Saltiel, J. L. Charlton in *Rearrangements in Ground and Excited States*, Vol. 3 (Ed: P. DeMayo), Academic Press, New York, **1980**, p. 25ff; f) K. A. Muszkat, *Top. Curr. Chem.* **1980**, *88*, 89–143; g) F. B. Mallory, C. W. Mallory, *Org. React.* **1983**, *30*, 1–456; h) F. D. Lewis, *Adv. Photochem.* **1986**, *13*, 165–235; i) W. H. Laarhoven, *Org. Photochem.* **1987**, 9, pp. 129–224; j) D. H. Waldeck, *Chem. Rev.* **1991**, *91*, 415–436; k) U. Mazzucato, F. Momicchioli, *ibid.* **1991**, *91*, 1679–1719.

[3] H. Meier, T. Lifka, unpublished; see also U. Mazzucato, *Gazz. Chim. Ital.* **1987**, *117*, 661–665.

[4] For a summary see Ref. [2h].

[5] H. J. Bestmann, O. Vostrowsky, *Top. Curr. Chem.* **1983**, *109*, 85–164; H. Pommer, P. C. Thieme, *ibid.* **1983**, *109*, 165–188.

[6] A. E. Siegrist, *Helv. Chim. Acta* **1967**, *50*, 906–957; see also H. Meier, F. Kosteyn, N. Hanold, H. Rau, G. Gauglitz, *Chem. Ber.* **1992**, *125*, 889–892, and references cited therein.

[7] J. E. McMurry, *Acc. Chem. Res.* **1983**, *16*, 405–411.

[8] H. Meier, unpublished.

[9] E. G. McKenna, B.-J. Walker, *Tetrahedron Lett.* **1988**, *29*, 485–488, and references cited therein.

[10] Although the *Z* fraction is usually below 5%, this can cause problems in the preparation of materials of high structural purity, especially when the number of C–C linkages per molecule is large.

[11] H. Kretzschmann, H. Meier, *Tetrahedron Lett.* **1991**, *32*, 5059–5062.

[12] H. Meier, H. Kretzschmann, H. Kolshorn, *J. Org. Chem.*, in print.

[13] R. F. Heck, *Org. React.* **1981**, *27*, 345–390.

[14] A. deMeijere, University of Göttingen, private communication.

[15] N. Hanold, H. Kalbitz, H. Meier, unpublished.

[16] A. Greiner, W. Heitz, *Makromol. Chem. Rapid Commun.* **1988**, *9*, 581–588.

[17] H.-H. Hörhold, M. Helbig, D. Raabe, J. Opfermann, U. Scherf, R. Stockmann, D. Weiß, *Z. Chem.* **1987**, *27*, 126–137, and references cited therein.

[18] H.-H. Hörhold, *Z. Chem.* **1972**, *12*, 41–52.

[19] R. A. Wessling, R.-G. Zimmermann (Dow Chemical Co.), USA 3401152, **1968**; *Chem. Abstr.* **1968**, *69*, P 87735q.

[20] P. L. Burn, A. B. Holmes, A. Kraft, D. D. C. Bradley, A. R. Brown, R. H. Friend, R. W. Gymer, *Nature* **1992**, *356*, 47–49, and references cited therein.

[21] A. Hoekstra, P. Meertens, A. Vos, *Acta Crystallogr. Sect. B* **1975**, *31*, 2813–2817.

[22] M. Traetteberg, E. B. Frantsen, F. C. Mijlhoff, A. Hoekstra, *J. Mol. Struct.* **1975**, *26*, 57–68.

[23] M. Müller, G. Hohlneicher, *J. Am. Chem. Soc.* **1990**, *112*, 1273–1274.

[24] S. Tsuzuki, K. Tanabe, Y. Nagawa, H. Nakanishi, *J. Mol. Struct.* **1989**, *212*, 45–52.

[25] M. Traetteberg, E. B. Frantsen, *J. Mol. Struct.* **1975**, *26*, 69–76.

[26] A. Moyano, J. C. Paniagua, *J. Org. Chem.* **1986**, *51*, 2250–2257.

[27] W. C. Herndon, H. Hosoya, *Tetrahedron* **1984**, *40*, 3987–3995.

[28] Cf. W. R. Roth, O. Adamczak, R. Breuckmann, H.-W. Lennartz, R. Boese, *Chem. Ber.* **1991**, *124*, 2499–2521.

[29] B. A. Hess, Jr., L. A. Schaad, *J. Am. Chem. Soc.* **1971**, *93*, 305–310.

[30] A. V. Santoro, E. J. Barrett, W. H. Hoyer, *J. Am. Chem. Soc.* **1967**, *89*, 4545–4546.

[31] W. W. Schmiegel, F. A. Litt, D. O. Cowan, *J. Org. Chem.* **1968**, *33*, 3334–3335.

[32] See also C. L. Hickson, H. McNab, *J. Chem. Res. Synop.* **1989**, 176–177.

[33] We have measured a free energy of activation $\Delta G^{\neq}$ of 210 ± 12 kJ mol^{-1} for (*Z,E*)-1,3-distyrylbenzene relative to the (*E,E*) configuration.

[34] J. Saltiel, S. Ganapathy, C. Werking, *J. Phys. Chem.* **1987**, *91*, 2755–58.

[35] G. B. Kistiakowsky, W. R. Smith, *J. Am. Chem. Soc.* **1934**, *56*, 638–642.

[36] G. Fischer, K. A. Muszkat, E. Fischer, *J. Chem. Soc. B*, **1968**, 1156–1158.

[37] E. L. Eliel, E. Brunet, *J. Org. Chem.* **1986**, *51*, 1902–1904.

[38] R. B. Williams, *J. Am. Chem. Soc.* **1942**, *64*, 1395–1404.

[39] T. Urano, H. Hamaguchi, M. Tasumi, K. Yamanouchi, S. Tsuchiya, *Chem. Phys. Lett.* **1987**, *137*, 559–563; *J. Chem. Phys.* **1989**, *91*, 3884–3894; T. Urano, M. Maegawa, K. Yamanouchi, S. Tsuchiya, *J. Phys. Chem.* **1989**, *89*, 3459–3465.

[40] B. B. Champagne, J. F. Pfanstiel, D. F. Plusquellic, D. W. Pratt, W. M. van Herpen, W. L. Meerts, *J. Phys. Chem.* **1990**, *94*, 6–8.

[41] G. Hohlneicher, M. Müller, M. Demmer, J. Lex, J. H. Penn, L. X. Gann, P. D. Lösel, *J. Am. Chem. Soc.* **1988**, *110*, 4483–4494.

[42] H. Güsten, L. Klasinc, I. Novak, M. Šanjek, *Z. Naturforsch. A* **1984**, *39*, 1230–1234.

[43] P. D. Burrow, J. A. Michejda, K. D. Jordan, *J. Chem. Phys.* **1987**, *86*, 9–24.

[44] L. A. Shmulevich, A. N. Shchapov, R. M. Basaev, F. P. Cheruyakovskii, *Zh. Fiz. Khim.* **1983**, *57*, 225–226; *Chem. Abstr.* **1983**, *98*, 125326r.

[45] W. Rettig, *Nachr. Chem. Techn. Lab.* **1991**, *39*, 398–406; *Angew. Chem.* **1986**, *98*, 969–986; *Angew. Chem. Int. Ed. Engl.* **1986**, *25*, 971–990; E. Gilabert, R. Lapouyade, C. Rulliere, *Chem. Phys. Lett.* **1988**, *145*, 262–268; see also W. Rettig, J. Majenz, *ibid.* **1989**, *154*, 335–341; H. Gruen, H. Görner, *J. Phys. Chem.* **1989**, *93*, 7144–7152.

[46] C. H. Pyun, T. A. Lyle, H. G. Daub, S. M. Park, *Chem. Phys. Lett.* **1986**, *124*, 48–52, and references cited therein.

[47] H. Görner, *J. Phys. Chem.* **1989**, *93*, 1826–1832.

[48] J. Saltiel, A. Waller, Y. P. Sun, D. F. Sears, Jr., *J. Am. Chem. Soc.* **1990**, *112*, 4580–4581, and references cited therein.
[49] H. P. Good, U. P. Wild, E. Haas, E. Fischer, E. P. Resewitz, E. Lippert, *Ber. Bunsen-Ges. Phys. Chem.* **1982**, *86*, 126–129.
[50] See also P. E. Brown, D. G. Whitten, *J. Phys. Chem.* **1985**, *89*, 1217–1220.
[51] S. Abrash, S. Repinec, R. M. Hochstrasser, *J. Chem. Phys.* **1990**, *93*, 1041–1053.
[52] A. Amirav, J. Jortner, *Chem. Phys. Lett.* **1983**, *95*, 295–300.
[53] G. Hohlneicher, B. Dick, *J. Photochem.* **1984**, *27*, 215–231.
[54] M. Sumitani, K. Yoshihara, *J. Chem. Phys.* **1982**, *76*, 738–740.
[55] D. Oelkrug, K. Rempfer, E. Prass, H. Meier, *Z. Naturforsch. A* **1988**, *43*, 583–590.
[56] H. Meier, R. Zertani, K. Noller, D. Oelkrug, G. Krabichler, *Chem. Ber.* **1986**, *119*, 1716–1724.
[57] See also T. E. Bush, G. W. Scott, *J. Phys. Chem.* **1981**, *85*, 144–146 and R. Erckel, H. Frühbeis, *Z. Naturforsch. B* **1982**, *37*, 1472–1480.
[58] T. Damerau, unpublished.
[59] R. Schenk, H. Gregorius, K. Müllen, *Adv. Mater.* **1991**, *3*, 492–493; R. Schenk, H. Gregorius, K. Meerholz, J. Heinze, K. Müllen, *J. Am. Chem. Soc.* **1991**, *113*, 2634–2647; B. Tian, G. Zerbi, R. Schenk, K. Müllen, *J. Chem. Phys.* **1991**, *95*, 3191–3197; B. Tian, G. Zerbi, K. Müllen, *ibid.* **1991**, *95*, 3198–3207.
[60] H.-H. Hörhold, *Z. Chem.* **1972**, *12*, 41–52.
[61] R. Störmer, *Ber. Dtsch. Chem. Ges.* **1909**, *42*, 4865–4871.
[62] J. Saltiel, *J. Am. Chem. Soc.* **1967**, *89*, 1036–1037, *ibid.* **1968**, *90*, 6394–6400.
[63] G. Orlandi, W. Siebrand, *Chem. Phys. Lett.* **1975**, *30*, 352–354; G. Orlandi, P. Palmieri, G. Poggi, *J. Am. Chem. Soc.* **1979**, *101*, 3492–3497; G. Orlandi, F. Zerbetto, *J. Mol. Struct.* **1986**, *138*, 185–191; F. Negri, G. Orlandi, F. Zerbetto, *J. Phys. Chem.* **1989**, *93*, 5124–5128; F. Negri, G. Orlandi, *ibid.* **1991**, *95*, 748–757.
[64] T. M. Stachalek, T. A. Pazoha, W. M. McClain, R. P. Drucker, *J. Chem. Phys.* **1977**, *66*, 4540–4543.
[65] R. J. Sension, S. T. Repinec, R. M. Hochstrasser, *J. Chem. Phys.* **1990**, *93*, 9185–9188.
[66] V. Sundström, T. Gillbro, *Chem. Phys. Lett.* **1984**, *109*, 538–543.
[67] R. J. Sension, S. T. Repinec, R. M. Hochstrasser, *J. Phys. Chem.* **1991**, *95*, 2946–2948.
[68] J. Troe, K. M. Weitzel, *J. Chem. Phys.* **1988**, *88*, 7030–7039.
[69] H. Meier, *Methoden Org. Chem.* (Houben-Weyl) **1975**, Vol. IV, 5a, 1, p. 191.
[70] 2,3-Diaryl-2-hydroxyacrylic acid derivatives are usually only obtainable in the chelated *Z* configuration; recently, however, we succeeded in isolating the *E* isomers by a photochemical isomerization of the *Z* isomer (M. Buß, H. Meier, unpublished).
[71] S. A. Abrash, S. T. Repinec, R. M. Hochstrasser, *J. Chem. Phys.* **1990**, *93*, 1041–1053.
[72] D. C. Todd, J. M. Jean, S. J. Rosenthal, A. J. Ruggerio, D. Yang, G. R. Fleming, *J. Chem. Phys.* **1990**, *93*, 8658–8668.
[73] J. Schröder, D. Schwarzer, J. Troe, F. Voss, *J. Chem. Phys.* **1990**, *93*, 2393–2404.
[74] Y. P. Sun, J. Saltiel, *J. Phys. Chem.* **1989**, *93*, 8310–8316; J. Saltiel, Y. P. Sun, *ibid.* **1989**, *93*, 6246–6250.
[75] N. Sivakumar, E. A. Hoburg, D. H. Waldeck, *J. Phys. Chem.* **1989**, *90*, 2305–2316.
[76] M. Lee, J. N. Haseltine, A. B. Smith III, R. M. Hochstrasser, *J. Am. Chem. Soc.* **1989**, *111*, 5044–5051.
[77] N. S. Park, D. H. Waldeck, *J. Chem. Phys.* **1989**, *91*, 943–952.
[78] S. K. Kim, S. H. Courtney, G. R. Fleming, *Chem. Phys. Lett.* **1989**, *159*, 543–548.
[79] J. M. Hicks, M. T. Vandersall, E. V. Sitzmann, K. B. Eisenthal, *Chem. Phys. Lett.* **1987**, *135*, 413–420.
[80] J. Lee, S. B. Zhu, G. W. Robinson, *J. Phys. Chem.* **1987**, *91*, 4273–4277.
[81] J. Schröder, J. Troe, *J. Phys. Chem.* **1986**, *90*, 4215–4216.
[82] V. Sundström, T. Gillbro, *Ber. Bunsen-Ges. Phys. Chem.* **1985**, *89*, 222–226; *Chem. Phys. Lett.* **1984**, *109*, 538–543.
[83] H. A. Kramers, *Physica* **1940**, *7*, 284.
[84] H. Meier, K. Müller, unpublished.
[85] D. Oelkrug, G. Krabichler, W. Honnen, F. Wilkinson, C. J. Willsher, *J. Phys. Chem.* **1988**, *92*, 3589–3594.
[86] T. W. Scott, J. Liu, C. Doubleday, Jr., *J. Chem. Phys.* **1990**, *146*, 327–342.
[87] V. Ramamurthy, J. V. Caspar, D. R. Corbin, D. F. Eaton, J. S. Kauffman, C. Dybowski, *J. Photochem. Photobiol. A* **1990**, *51*, 259–263; F. Gessner, A. Olea, J. H. Lobough, L. J. Johnston, J. C. Scaiano, *J. Org. Chem.* **1989**, *54*, 259–261.
[88] M. S. Symala, S. Devanathan, V. Ramamurthy, *J. Photochem.* **1986**, *34*, 219–229; G. L. Duveneck, E. V. Sitzmann, K. B. Eisenthal, N. J. Turro, *J. Phys. Chem.* **1989**, *93*, 7166–7170.
[89] F. D. Lewis, A. M. Bedell, R. E. Dykstra, J. E. Elbert, J. R. Gould, S. Farid, *J. Am. Chem. Soc.* **1990**, *112*, 8055–8064; F. D. Lewis, R. E. Dykstra, *J. Photochem. Photobiol. A* **1989**, *49*, 109–119; Y. Kuriyama, T. Arai, H. Sakuragi, K. Tokumaru, *Chem. Phys. Lett.* **1990**, *173*, 253–256; I. K. Lednev, M. V. Alfimov, Y. Kuriyama, T. Arai, H. Sakuragi, K. Tokumaru, *J. Photochem. Photobiol. A* **1992**, *63*, 201–209, and references cited therein.
[90] J. L. Courtneidge, A. G. Davies, P. S. Gregory, *J. Chem. Soc. Perkin Trans.* **1987**, *2*, 1527–1532.
[91] A. I. Kruppa, O. I. Mikhailovskaya, T. V. Leshina, *Chem. Phys. Lett.* **1988**, *147*, 65–71.
[92] Vgl. S. Angel, K. S. Peters, *J. Phys. Chem.* **1989**, *93*, 713–717.
[93] Y. Ito, T. Dote, Y. Uozo, T. Matsuura, *J. Am. Chem. Soc.* **1986**, *108*, 141–142; Y. Ito, Y. Uozu, T. Dote, M. Ueda, T. Matsuura, *ibid.* **1988**, *110*, 189–198.
[94] G. Gauglitz, D. Oelkrug, University of Tübingen, private communication.
[95] See Y. Ito, Y. Uozu, T. Matsuura, *Tetrahedron Lett.* **1987**, *28*, 3493–3496.
[96] K. Sandros, M. Sundahl, O. Wennerström, U. Norinder, *J. Am. Chem. Soc.* **1990**, *112*, 3082–3086; see also M. Sundahl, O. Wennerström, K. Sandros, T. Arai, K. Tokumaru, *J. Phys. Chem.* **1990**, *94*, 6731–6734.
[97] T. Arai, T. Karatsu, H. Sakuragi, K. Tokumaru, *Tetrahedron Lett.* **1983**, *24*, 2873–2876; T. Arai, T. Karatsu, H. Misowa, Y. Kuriyama, H. Okamoto, T. Hiresaki, H. Furuuchi, H. Zeng, H. Sakuragi, K. Tokumaru, *Pure Appl. Chem.* **1988**, *60*, 989–998, and references cited therein; K. Tokumaru, T. Arai, *J. Photochem. Photobiol. A* **1992**, *65*, 1–13, and references cited therein.
[98] K. Sandros, H.-D. Becker, *J. Photochem.* **1987**, *39*, 301–315.
[99] A. Smakula, *Z. Phys. Chem. Abt. B* **1934**, *25*, 90–98.
[100] C. O. Parker, P. E. Spoerri, *Nature* **1950**, *166*, 603; R. E. Buckles, *J. Am. Chem. Soc.* **1955**, *77*, 1040–1041.
[101] T. Wismonski-Knittel, G. Fischer, E. Fischer, *J. Chem. Soc. Perkin Trans.* **1974**, *2*, 1930–1940.
[102] P. Takach, A. C. Testa, *J. Photochem.* **1987**, *37*, 347–354.
[103] K. A. Muszkat, W. Schmidt, *Helv. Chim. Acta* **1971**, *54*, 1195–1207.
[104] L. Liu, B. Yang, T. J. Katz, M. K. Poindexter, *J. Org. Chem.* **1991**, *56*, 3769–3775.
[105] J. B. Somers, A. Couture, A. Lablache-Combier, W. H. Laarhoven, *J. Am. Chem. Soc.* **1985**, *107*, 1387–1394.
[106] M. V. Sargent, C. J. Timmons, *J. Chem. Soc.* **1964**, 5544–5552.
[107] K. A. Muszkat, E. Fischer, *J. Chem. Soc. B* **1967**, 662–678; H. Petek, K. Yoshihara, Y. Fujiwara, Z. Lin, J. H. Penn, J. H. Frederick, *J. Phys. Chem.* **1990**, *94*, 7539–7543.
[108] J. H. Frederick, Y. Fujiwara, J. H. Penn, K. Yoshihara, H. Petek, *J. Phys. Chem.* **1991**, *95*, 2845–2858.
[109] F. B. Mallory, C. S. Wood, J. T. Gordon, *J. Am. Chem. Soc.* **1964**, *86*, 3094–3102; C. S. Wood, F. B. Mallory, *J. Org. Chem.* **1964**, *29*, 3373–3377.
[110] M. Scholz, F. Dietz, M. Mühlstädt, *Z. Chem.* **1967**, *7*, 329–338; *Tetrahedron Lett.* **1967**, 665–668.
[111] F. Dietz, M. Scholz, *Tetrahedron* **1968**, *24*, 6845–6849.
[112] W. H. Laarhoven, *Recl. Trav. Chim. Pays-Bas* **1983**, *102*, 185–204, 241–254; W. H. Laarhoven, T. H. J. M. Cuppen, R. J. F. Nivard, *ibid.* **1968**, *87*, 687–698.
[113] W. H. Laarhoven, T. H. J. M. Cuppen, R. J. F. Nivard, *Tetrahedron* **1970**, *26*, 1069–1083.
[114] R. Zertani, H. Meier, *Chem. Ber.* **1986**, *119*, 1704–1715, and references cited therein.
[115] K. Noller, F. Kosteyn, H. Meier, *Chem. Ber.* **1988**, *121*, 1609–1615.
[116] W. H. Laarhoven, University of Nijmegen, private communication.
[117] Reviews: G. Oremek, U. Seiffert, A. Janecka, Chem. Ztg. **1987**, *111*, 69–75; R. H. Martin, *Angew. Chem.* **1974**, *86*, 727–738; *Angew. Chem. Int. Ed. Engl.* **1974**, *13*, 649–669.
[118] A. Moradpour, J. F. Nicoud, G. Balavoine, H. Kagan, G. Tsoucaris, *J. Am. Chem. Soc.* **1971**, *93*, 2353–2354.
[119] Y. Cochez, J. Jespers, V. Libert, K. Mislow, R. H. Martin, *Bull. Soc. Chim. Belg.* **1975**, *84*, 1033–1036.
[120] W. H. Laarhoven, T. Cuppen, *J. Chem. Soc. Chem. Commun.* **1977**, 47; *Perkin Trans. 2* **1978**, 315–318.
[121] M. Nakazaki, K. Yamamoto, K. Fujiwara, *Chem. Lett.* **1978**, 863–864.
[122] G. Ciamician, P. Silber, *Chem. Ber.* **1902**, *35*, 4128–4131.
[123] J. D. Fulton, J. D. Dunitz, *Nature* **1947**, *160*, 161–162; J. D. Dunitz, *Acta Crystallogr.* **1949**, *2*, 1–13.
[124] H. Shechter, W. J. Link, G. V. D. Tiers, *J. Am. Chem. Soc.* **1963**, *85*, 1601–1605.
[125] Stilbene excimers are difficult to detect experimentally; for details of an experiment using γ-radiation see: B. Brocklehurst, D. C. Bull, M. Evans, P. M. Scott, G. Stanney, *J. Am. Chem. Soc.* **1975**, *97*, 2977–2978; see also F. D. Lewis, D. E. Johnson, *J. Photochem.* **1977**, *7*, 421–423, F. D. Lewis *Acc. Chem. Res.* **1979**, 152–158.
[126] V. Bonačić-Koutecký, J. Koutecký, J. Michl, *Angew. Chem.* **1987**, *99*, 216–236; *Angew. Chem. Int. Ed. Engl.* **1987**, *26*, 170–189.
[127] H. Stegemeyer, *Chimia* **1965**, *19*, 535–536.
[128] G. Kaupp, *Angew. Chem.* **1974**, *86*, 741–742; *Angew. Chem. Int. Ed. Engl.* **1974**, *13*, 817–818; G. Kaupp, M. Stark, *Chem. Ber.* **1977**, *110*, 3084–3110.
[129] H. Shizuka, I. Seki, T. Morita, T. Iizuka, *Bull. Chem. Soc. Jpn* **1979**, *52*, 2074–2078.

[130] F. D. Lewis, T. L. Field, M. Sabat, *Photochem. Photobiol.* **1990**, *52*, 277–281.
[131] M. Sauerbier, *Tetrahedron Lett.* **1972**, *13*, 551–552.
[132] R. A. Caldwell, *J. Am. Chem. Soc.* **1980**, *102*, 4004–4007.
[133] M. S. Symala, V. Ramamurthy, *J. Org. Chem.* **1986**, *51*, 3712–3715.
[134] See also Y. Ito, T. Kajita, K. Kunimoto, T. Matsuura, *J. Org. Chem.* **1989**, *54*, 587–591.
[135] G. M. J. Schmidt, *Pure Appl. Chem.* **1971**, *27*, 647–678; M. D. Cohen, *Angew. Chem.* **1975**, *87*, 439–447; *Angew. Chem. Int. Ed. Engl.* **1975**, *14*, 386–394.
[136] M. D. Cohen, B. S. Green, Z. Ludmer, G. M. J. Schmidt, *Chem. Phys. Lett.* **1970**, *7*, 486–490; B. S. Green, L. Heller, *J. Org. Chem.* **1974**, *39*, 196–201.
[137] H. Meier, J. Juriew, W. Winter, *J. Photochem.* **1981**, *17*, 92.
[138] E. Müller, H. Meier, M. Sauerbier, *Chem. Ber.* **1970**, *103*, 1356–1363; T. E. M. Van den Hark, P. T. Beurskens, W. H. Laarhoven, *J. Cryst. Mol. Struct.* **1974**, *4*, 227–242.
[139] H. Meier, E. Praß, K. Noller, *Chem. Ber.* **1988**, *121*, 1637–1641.
[140] The dominant photoreaction is polymerization; the cyclopane and dimeric head-to-tail adducts are formed only in trace amounts.
[141] J. Juriew, T. Skorochodova, J. Merkushew, W. Winter, H. Meier, *Angew. Chem.* **1981**, *93*, 285–286; *Angew. Chem. Int. Ed. Engl.* **1981**, *20*, 269–270; W. Winter, U. Langjahr, H. Meier, J. Merkushew, J. Juriew, *Chem. Ber.* **1984**, *117*, 2452–2463.
[142] H. Meier, E. Praß, R. Zertani, H.-L. Eckes, *Chem. Ber.* **1989**, *122*, 2139–2146.
[143] J. Meinwald, J. W. Young, *J. Am. Chem. Soc.* **1971**, *93*, 725–731.
[144] K. Müllen, H. Meier, unpublished results.
[145] W. H. Laarhoven, T. J. H. M. Cuppen, *J. Chem. Soc. Perkin Trans. 1* **1972**, 2074–2079.
[146] A. J. W. Tol, W. H. Laarhoven, *J. Org. Chem.* **1986**, *51*, 1663–1668.
[147] H. J. C. Jacobs, E. Havinga, *Adv. Photochem.* **1979**, *11*, 305–373.
[148] M. Hasegawa, Y. Suzuki, *Polymer Lett.* **1967**, *5*, 813–815; H. Iguchi, H. Nakanishi, M. Hasegawa, *J. Polym. Sci. Part A* **1968**, *6*, 1055–1057; H. Nakanishi, K. Ueno, M. Hasegawa, Y. Sasada, *Chem. Lett.* **1972**, 301–304; M. Hasegawa, M. Harashina, S. Kato, K. Saigo, *Macromolecules* **1986**, *19*, 1276–1278; M. Hasegawa, T. Katsumata, Y. Ito, K. Saigo, *ibid.* **1988**, *21*, 3134–3138.
[149] Reviews: G. Wegner, *Pure Appl. Chem.* **1977**, *49*, 443–454; W. L. Dilling, *Chem. Rev.* **1983**, *83*, 1–47; M. Hasegawa, *ibid.* **1983**, *83*, 507–518; *Pure Appl. Chem.* **1986**, *58*, 1179–1188.
[150] D. Gegiou, K. A. Muszkat, E. Fischer, *J. Am. Chem. Soc.* **1968**, *90*, 12–18, 3907–3918.
[151] D. Schulte-Frohlinde, H. Görner, *Pure Appl. Chem.* **1979**, *51*, 279–297, and references cited therein.
[152] H. Görner, *Ber. Bunsen-Ges. Phys. Chem.* **1984**, *88*, 1199–1208; H. Görner, D. Schulte-Frohlinde, *ibid.* **1978**, *82*, 1102–1107; *ibid.* **1984**, *88*, 1208–1216.
[153] H. Görner, *J. Phys. Chem.* **1989**, *93*, 1826–1832.
[154] J. Saltiel, G.-E. Khalil, K. Schanze, *Chem. Phys. Lett.* **1980**, *70*, 233–235, *ibid.* **1980**, *73*, 199.
[155] T. Ikeyama, T. Azumi, *J. Phys. Chem.* **1985**, *89*, 5332–5333; *ibid.* **1988**, *92*, 1383–1384; V. Ramamurthy, J. V. Caspar, D. R. Corbin, *Tetrahedron Lett.* **1990**, *31*, 1097–1100.
[156] G. Heinrich, G. Holzer, H. Blume, D. Schulte-Frohlinde, *Z. Naturforsch. B* **1970**, *25*, 496; G. Heinrich, H. Güsten, F. Mark, G. Olbrich, D. Schulte-Frohlinde, *Ber. Bunsen-Ges. Phys. Chem.* **1973**, *77*, 103–108.
[157] G. S. Hammond, J. Saltiel, *J. Am. Chem. Soc.* **1962**, *84*, 4983–4984; G. S. Hammond, J. Saltiel, A. A. Lamola, N. J. Turro, J. S. Bradshaw, D. O. Cowan, R. C. Counsell, V. Vogt, C. Dalton, *ibid.* **1964**, *86*, 3197–3217; D. Valentine, Jr., G. S. Hammond, *ibid.* **1972**, *94*, 3449–3464; L. M. Stephenson, G. S. Hammond, *Angew. Chem.* **1969**, *81*, 279–289; *Angew. Chem. Int. Ed. Engl.* **1969**, *8*, 261–270.
[158] J. Saltiel, A. D. Rousseau, B. Thomas, *J. Am. Chem. Soc.* **1983**, *105*, 7631–7637; J. Saltiel, G. R. Marchand, E. Kirkor-Kaminska, W. K. Smothers, W. B. Müller, J. L. Charlton, *ibid.* **1984**, *106*, 3144–3151, and references cited therein.
[159] C. V. Kumar, S. K. Chattopadhyay, P. K. Das, *Chem. Phys. Lett.* **1984**, *106*, 431–436.
[160] J. A. Lavilla, J. L. Goodman, *Chem. Phys. Lett.* **1987**, *141*, 149–153.
[161] V. Ramamurthy, R. S. H. Liu, *J. Am. Chem. Soc.* **1976**, *98*, 2935–2942; P. J. Wagner, B. J. Schewe, *ibid.* **1977**, *99*, 2888–2892; K. Sandros, *Acta Chem. Scand.* **1973**, *27*, 3021–3032; A. Farmilo, F. Wilkinson, *Chem. Phys. Lett.* **1975**, *34*, 575–580.
[162] V. Balzani, F. Boletta, F. Scandola, *J. Am. Chem. Soc.* **1980**, *102*, 2152–2163; G. Orlandi, S. Monti, F. Barigelletti, V. Balzani, *J. Chem. Phys.* **1980**, *52*, 313–319.
[163] R. Martinez-Utrilla, F. Catalina, R. Sastre, *Makromol. Chem.* **1987**, *188*, 1703–1711.
[164] R. Searle, J. L. R. Williams, D. E. DeMeyer, J. C. Doty, *J. Chem. Soc. Chem. Commun.* **1967**, 1165; J. A. Mercer-Smith, D. G. Whitten, *J. Am. Chem. Soc.* **1978**, *100*, 2620–2625.
[165] G. O. Schenck, P. Steinmetz, *Bull. Soc. Chim. Belg.* **1962**, *71*, 781–800.
[166] B. Wendt, IG Farbenindustrie, DE-A 752677, **1940**.
[167] Reviews: A. E. Siegrist, C. Eckhardt, J. Kaschig, E. Schmidt, *Ullmanns Encycl. Ind. Chem.* **1991**, *A18*, 153–176; H. Gold, *Environ. Qual. Saf. Suppl.* **1975**, *4*, 25–46; *Chem. Abst.* **1975**, *85*, 110066p; A. Dorlars, C.-W. Schellhammer, J. Schröder, *Angew. Chem.* **1975**, *87*, 693–707; *Angew. Chem. Int. Ed. Engl.* **1975**, *14*, 665–679.
[168] R. S. Davidson, G. M. Ismail, D. M. Lewis, *J. Soc. Dyers Colour.* **1988**, *104*, 86–93 (*Chem. Abstr.* **1988**, *109*, 24167); *ibid.* **1987**, *103*, 261–264 (*Chem. Abstr.* **1987**, *108*, 39502p).
[169] For the influence of functional groups on the stilbene skeleton, see: R. P. Hurd, B. M. Reagan, *J. Soc. Dyers. Colour.* **1990** *106*, 49–54; W. R. Findley, *J. Am. Oil Chem. Soc.* **1988**, *65*, 679–683; *Chem. Abstr.* **1988**, *108*, 223499 u.
[170] L. Pichat, P. Pesteil, J. Clément, *J. Chim. Phys.* **1953**, *50*, 26–41; C. H. Pyun, S. M. Park, *Anal. Instrum.* **1984**, *13*, 159–171; *Chem. Abstr.* **1985**, *102*, 38818v.
[171] See also R. Hofstadter, *Naturwiss. Rundsch.* **1984**, *37*, 45–52.
[172] More recent review: R. Raue in *Ullmanns Encycl. Ind. Chem.* **1990**, *A15*, 151–164.
[173] O. G. Peterson, S. A. Tuccio, B. B. Snavely, *Appl. Phys. Lett.* **1970**, *17*, 245–247.
[174] P. W. Smith, A. M. Weiner, IEEE Circuits and Devices **1988**, *4*, 3.
[175] W. Hüffer, R. Schieder, H. Telle, R. Raue, W. Brinkwerth, *Opt. Commun.* **1979**, *28*, 353–354.
[176] W. Majewski, J. Krasinski, *Opt. Commun.* **1976**, *18*, 255–259.
[177] H. Telle, U. Brinkmann, R. Raue, *Opt. Commun.* **1978**, *24*, 33–37.
[178] J. Kuhl, H. Telle, R. Schieder, U. Brinkmann, *Opt. Commun.* **1978**, *24*, 251–254.
[179] G. Gauglitz, R. Goes, W. Stooß, R. Raue, *Z. Naturforsch. A* **1985**, *40*, 317–323.
[180] G. Gauglitz, R. Goes, W. Schmid, *J. Photochem.* **1986**, *34*, 339–348.
[181] B. Liphardt, B. Liphardt, W. Lüttke, *Chem. Ber.* **1982**, *115*, 2997–3010; *Opt. Commun.* **1981**, *38*, 207–210.
[182] J. H. Burroughes, D. D. C. Bradley, A. R. Brown, R. N. Marks, K. D. Mackay, R. H. Friend, P. L. Burn, A. B. Holmes, *Nature* **1990**, *347*, 539–541.
[183] D. D. C. Bradley, A. R. Brown, P. L. Burn, R. H. Friend, A. B. Holmes, A. Kraft, *Proceedings IWEPP* **1991**, Kirchberg
[184] D. Braun, A. J. Heeger, *Appl. Phys. Lett.* **1991**, *58*, 1982–1984.
[185] H. Meier, E. Praß, G. Zerban, F. Kosteyn, *Z. Naturforsch. B* **1988**, *43*, 889–896; W. E. Haas, F. F. Nelson, J. A. Adams, G. A. Dir, *J. Electrochem. Soc.* **1974**, *121*, 1667–1669.
[186] See also F. Kosteyn, G. Zerban, H. Meier, *Chem. Ber.* **1992**, *125*, 893–897.
[187] H. Menzel, *Nachr. Chem. Tech. Lab.* **1991**, *39*, 636–647.
[188] D. Vorländer, *Ber. Dtsch. Chem. Ges.* **1970**, *40*, 4527–4540.
[189] W. R. Young, A. Aviram, R. J. Cox, *J. Am. Chem. Soc.* **1972**, *94*, 3976–3981; W. R. Young, I. Haller, A. Aviram, *Mol. Cryst. Liquid. Cryst.* **1972**, *15*, 311–327; C. Fouquey, J.-M. Lehn, J. Malthête, *J. Chem. Soc. Chem. Commun.* **1987**, 1424–1426.
[190] Cf. J. Malthête, A. M. Levelut, N. H. Tinh, *J. Phys. Lett.* **1985**, *46*, L 875.
[191] G. Zerban, Dissertation, University of Mainz, **1991**.
[192] H. Meier, *Chem. Ind. Frankfurt*, **1992**, 44–46.
[193] M. Suzuki, J.-C. Lim, T. Taegusa, *Makromolecules* **1990**, *23*, 1574–1579; W. Memeger, Jr. *ibid.* **1989**, *22*, 1577–1588; V. Percec, T. Dimitris, *Polymer* **1990**, *31*, 1658–1662; W. Heitz, U. Kampschulte, W. Brügging, H. W. Schmidt (Bayer AG), DE-A 3719578 A_1, **1988**.
[194] Cf. F. A. Stuber, H. Ulrich, D. V. Rao, A. A. R. Sayigh, *J. Appl. Polym. Sci.* **1969**, *13*, 2247–2255 and the extensive recent patent literature.
[195] If the 2-pyridyl group is replaced by a 3- or 4-pyridyl group, the method fails.
[196] Cf. M. Becher, H. F. Mark, *Angew. Chem.* **1961**, *73*, 641–646.
[197] H.-H. Hörhold, J. Opfermann, *Makromol. Chem.* **1970**, *131*, 105–132.
[198] a) P. Strohriegl, D. Haarer, *Makromol. Chem. Macromol. Symp.* **1991**, *44*, 85–95; M. Gailberger, A. Greiner, H. Bässler *Synth. Met.* **1991**, *41–43*, 1269–1272; S. Rentsch, J. P. Yang, M. Lenzner, H. Bergner, *ibid.* **1991**, 41–43. 1369–1372, and references cited therein. H. Meier, H. Kretschmann, M. Lang, W. Fraß, C. Albrecht, K. März, unpublished.
[199] D. J. Williams, *Angew. Chem.* **1984**, *96*, 637–651; *Angew. Chem. Int. Ed. Engl.* **1984**, *23*, 690–703.
[200] β and $\chi^{(2)}$ are third-order tensors whose functional relationship is not trival, as it involves a transformation from molecular coordinates to the coordinates of the macroscopic sample. Some simpler special cases are uniaxial symmetries ($C_{\infty v}$) and Langmuir–Blodgett (mono)layers. Analogous considerations apply to the relationship between γ and $\chi^{(3)}$.
[201] J. L. Qudar, *J. Chem. Phys.* **1977**, *67*, 446–457; A. Dulcic, C. Flytzanis, C. L. Tang, D. Pépin, M. Fétizon, Y. Hoppilliard, *ibid.* **1981**, *74*, 1559–1563.
[202] W. Tam, L.-T. Cheng, J. D. Bierlein, L. K. Cheng, Y. Wang, A. E. Feiring, G. R. Meredith, D. F. Eaton, J. C. Calabrese, G. L. J. A. Rikken in *Materials for Nonlinear Optics, Chemical Perspectives* (Eds.: S. R. Marder, J. E. Sohn, G. D. Stucky), ACS, Washington, **1991**, p. 158.

[203] W. Tam, B. Guerin, J. C. Calabrese, S. H. Stevenson, *Chem. Phys. Lett.* **1989**, *154*, 93–96.
[204] D. R. Robello, C. S. Willand, M. Scozzafava, A. Ulman, D. J. Williams, in *Materials for Nonlinear Optics, Chemical Perspectives* (Eds.: S. R. Marder, J. E. Sohn, G. D. Stucky), ACS, Washington, **1991**, and references cited therein.
[205] C. Fouquey, J.-M. Lehn, J. Malthête, *J. Chem. Soc. Chem. Commun.* **1987**, 1424–1426.
[206] J. W. Perry in *Materials for Nonlinear Optics* (Ed.: S. R. Marder, J. E. Sohn, G. D. Stucky), ACS, Washington, **1991**, p. 67.
[207] B. P. Singh, P. N. Prasad, F. E. Karasz, *Polymer* **1988**, *29*, 1940–1942; D. McBranch, M. Sinclair, A. J. Heeger, A. O. Patil, S. Shi, S. Askari, F. Wudl, *Synth. Met.* **1989**, *29*, E85–E90.
[208] F. E. Karasz, P. N. Prasad, unpublished.
[209] J. Swiatkiewicz, P. N. Prasad, F. E. Karasz, M. Druy, P. Glatoski, *Appl. Phys. Lett.* **1990**, *56*, 892; J. Swiatkiewicz, P. N. Prasad, C. Lee, unpublished.
[210] G. Bubeck, A. Kaltbeitzel, R. W. Lenz, D. Neber, J. D. Stenger-Smith, G. Wegner in *Nonlinear Optical Effects in Organic Polymers* (Eds.: J. Messier, F. Kajzar, P. Prasad, D. Ulrich), (NATO ASI Series), Kluwer, Dordrecht **1989**, p. 143; see also T. Kaino, K. Kubodera, S. Tomaru, T. Kurihara, S. Saito, T. Tsutsui, S. Tokito, *Electron. Lett.* **1987**, *23*, 1095.

A stop-gap solution?

If the latest library copy of Angewandte spends more time off the shelf than on, stop the gap with a personal subscription.

Just call or fax

VCH

USA: Tel. 1-(800) 422-8824; Fax (305) 428-8201
UK: Tel. (0223) 321111, Fax (0223) 313221

Cubanes: Starting Materials for the Chemistry of the 1990s and the New Century

By Philip E. Eaton*

Dedicated to Professor Horst Prinzbach on the occasion of his 60th birthday

The study of non-natural products has led to a broad understanding of bonding and reactivity in organic chemistry. Many times, compounds thought impossible have been realized in the course of such studies. Cubane, a landmark in the world of "impossible" compounds, has been found to have a rich chemistry, full of the unexpected. The recent renaissance of cubane chemistry, triggered by potential applications of the system to the production of high-energy fuels and the like, has led to many discoveries including the first methods for systematic substitution on strained, saturated systems and a new process for the metalation of arenes, *ortho* magnesiation. Reactive intermediates with exceptional bonding parameters have been uncovered and characterized including 1(9)-homocubene, the most twisted olefin; cubene, the most pyramidalized olefin; cubyl cation, once the "least likely" cation; cubylmethyl radical, a saturated radical that rearranges on the picosecond timescale; and many other extraordinary species. There is certainly good reason to believe that future work in the cubane arena will be at least as productive (probably more so), and that it will help develop a deeper understanding of chemistry.

1. Introduction

Cubane **1** is immensely strained; the geometry at each carbon atom is far from tetrahedral. Originally there was doubt that the skeleton could even hold together.[1] Only later was it appreciated that no kinetically viable paths exist for the thermal rearrangement of cubane. On one hand, orbital symmetry considerations show that the energy of concerted two-bond ring-opening reactions is very high.[2a, b] On the other, there is little to be gained by breaking just one bond, as the concomitant change in geometry is small, and the resulting biradical is still very strained.[2c]

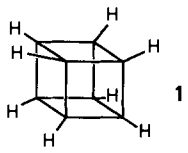

1

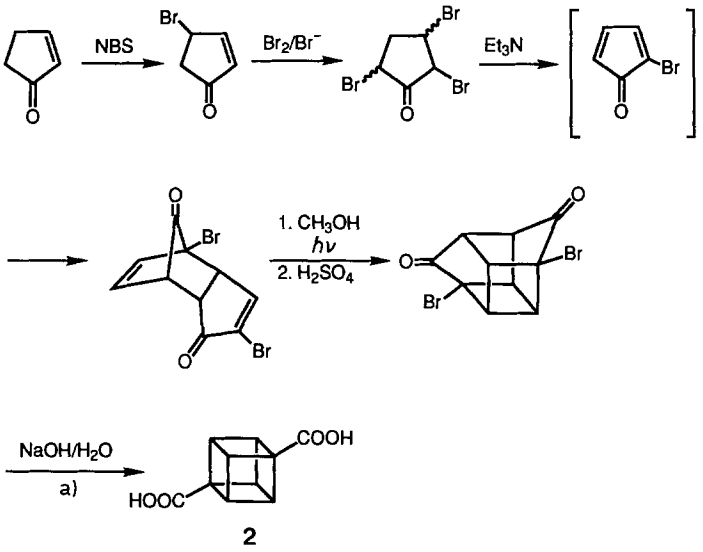

2

Scheme 1. The first entry into the cubane system. a) Reflux. NBS = *N*-bromosuccinimide.

2. Entry into the Cubane System

In 1964, at The University of Chicago, Tom Cole and I achieved the first synthesis of the cubane system (Scheme 1).[3] The Favorskii rearrangements (semibenzilic mechanism) by which the bishomocubane system is contracted were the critically important steps. This is true to this day for most cubane syntheses; all but two depend on this reaction.[4]

Even in retrospect, the whole sequence is really rather good, although the early part of the procedure requires the preparation of 4-bromocyclopentenone, a tricky matter. A few years after the original synthesis was published, N. B. Chapman et al. in England,[4c, 5] following up on my work with Hudson on bromocyclopentadienone ketals,[6] found that the ethylene ketal of 2-bromocyclopentadienone could be made easily and undergoes spontaneous dimerization. From this discovery the cubane synthesis ultimately evolved into a simple five-step process providing cubane-1,4-dicarboxylic acid **2** in about 25% overall yield (Scheme 2).

2.1. Availability of Cubanes

The synthesis of **2** has been scaled up and is conducted in small pilot plants by Fluorochem in California and EniChem Synthesis in Milan. Cubane-1,4-dicarboxylic acid is being

[*] Prof. P. E. Eaton
Department of Chemistry
The University of Chicago
5735 South Ellis Avenue, Chicago, IL 60637 (USA)

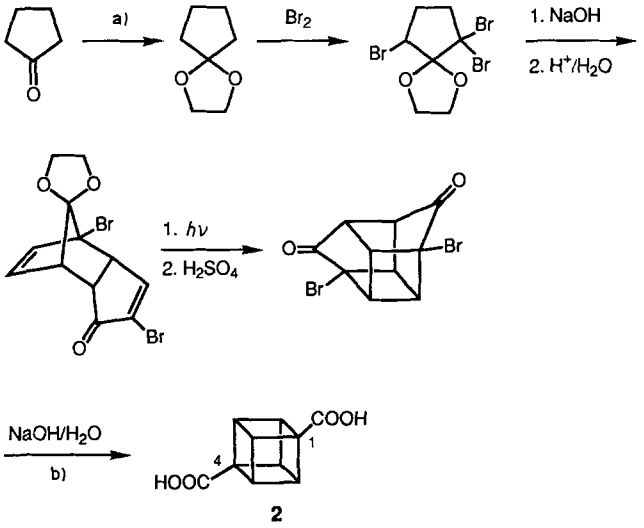

Scheme 2. The best synthetic route known for the cubane system. a) Glycol, H^+; b) reflux.

made in multi-kilogram batches! Nonetheless, as is often the case with experimental compounds, cubane **1** and its derivatives are still expensive to purchase. Fortunately, any good student, having gone through the procedure once to become familiar with its details, can easily make 10 grams of **2** in a month or so. It is a very satisfying procedure and an excellent way to introduce students to the delights of distillation and the thrill of crystallization. It is unfortunate that in today's academic synthesis laboratories these joys are often missed.

2.2. The Hydrocarbon

The original method for the decarboxylation of cubanedicarboxylic acid **2** to provide the pure hydrocarbon itself proceeded via the *tert*-butyl perester.[3] The present method is much superior. Following from the lovely work of Derek Barton et al.,[7] we now use the radical-induced decomposition of diester **3**, which is prepared simply from **2**. Cubane, the hydrocarbon, is thus obtained easily on a 10-gram scale

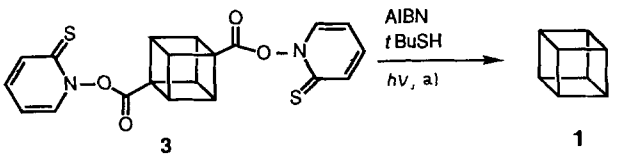

Scheme 3. The decomposition of **3** provides **1** in good yields. a) Reaction in THF at reflux; irradiation (tungsten filament).

in very nearly quantitative yield. It is beautifully crystalline; alas, the crystals are rhombohedral, not cubic.

3. Physical Properties

Because of its exceptional structure, strain, and symmetry, cubane is a benchmark in organic chemistry. Cubane has been studied extensively, and much concerning its properties has been published.[8] A few physical parameters are given in Table 1.

Table 1. Selected data for cubane.

C–C distance	1.5727 ± 0.0019 Å [a]	Boiling point	≈133 °C
C–H distance	1.118 ± 0.008 Å	Melting point	130–131 °C
Color	transparent [b]	Solubility	≈18 wt% (hexane)
Toxicity	nontoxic	Heat of formation [d]	+144 kcal mol^{-1}
Stability	inert to light, water, air		(+159 kcal mol^{-1})
Decomposition	>220 °C [c]	Strain energy [d]	166 kcal mol^{-1}
Density	1.29 g cm^{-3}		(181 kcal mol^{-1})
Vapor pressure	1.1 mm (25 °C)		

[a] Old value 1.551 Å. [b] To below 200 nm. [c] Very slow. [d] Values not in parentheses from Margrave et al. [12]; values in parentheses from Domalski et al. [13].

The bond lengths given in Table 1 are from a recent electron diffraction study by L. and K. Hedberg et al.[9] and agree reasonably well with the earlier data of Almenningen et al.[10] The C–C bond length is a bit longer than that obtained in the original (and crucial) X-ray structure determination by Fleischer in 1964.[11a] It is interesting that this distance is not much different than the C–C bond length in a simple cyclobutane.[11b] The values for the heat of formation and strain energy given in parentheses below the results of Margrave et al.[12] were derived by Domalski et al. at the U.S. National Institute of Standards from the heat of combustion of 1,4-di(methoxycarbonyl)cubane.[13] We hope soon to have new data directly from combustion of cubane.

Molecular mechanics calculations, and semiempirical and ab initio quantum mechanical treatments of cubane abound. Robiette et al. have provided an excellent overview.[9] The agreement between methods is fair, but to my mind certainly less than completely reassuring. Whatever one's opinions about the calculated properties of cubane, the bottom line experimentally is that cubane is remarkably stable. Cubane melts just above 130 °C; measurable decomposition occurs only above 200 °C. Martin et al. have shown that the energy of activation for the thermolysis of cubane at 230–260 °C

Philip E. Eaton was born in New York in 1936. He received his undergraduate degree from Princeton University in 1957, then did his Ph. D. work with Peter Yates at Harvard University, graduating in 1961. From 1960 to 1962 he was an assistent professor of chemistry at the University of California at Berkeley. He then accepted a position at The University of Chicago, where he is a full professor. Eaton has received the Rohm and Haas Award for Research, an Alfred P. Sloan Foundation Fellowship, and a Senior Scientist Award from the Alexander von Humboldt Foundation. His research interests include the synthesis of important non-natural products and their applications in materials science.

is 43.1 ±1.0 kcal mol^{-1}, an extraordinarily high value.[2b] Cubane is entirely stable to light, air, water, and most common reagents.

4. The Cubane Renaissance

Although many physical properties of cubane have been measured, until a few years ago cubane was considered just a laboratory curiosity of interest only to academics. That changed in the early 1980s when Gilbert of the U.S. Army Armament and Development Command (now ARDEC) pointed out that cubane's very high heat of formation[12] and its exceptionally high density (1.29 g cm^{-3})[11a]—higher than almost all other hydrocarbons[14]—could make certain cubane derivatives important explosives. His colleagues Sandus and Alster at ARDEC provided theoretical support and estimated that octanitrocubane **4** might be 20–25% more effective than HMX (octogen), the present-day standard.[15] It is sufficient to comment here that detonation of

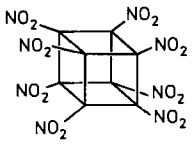

4

octanitrocubane would lead to an awesome amount of very hot gas [Eq. (a)].

$$C_8(NO_2)_8 \longrightarrow 8\,CO_2 + 4\,N_2 \qquad (a)$$

Miller at the U.S. Office of Naval Research realized quickly that some substituted cubanes could be very useful propellants for the space and "Star Wars" programs. The synthesis of **4** and related compounds are formidable tasks. The challenge made us aware that we did not know how to prepare substituted cubanes beyond a very few simple examples.[4] At the time we returned to cubane chemistry in 1983 there was little methodology for taking the most readily available cubane compound, the 1,4-dicarboxylic acid **2**, and doing anything besides manipulating the carboxyl groups.

5. Functional Group Transformations

As it turned out, the carboxylic acid groups of **2**, like most other functional groups on cubane, are exceedingly well-behaved. Most typical functional group transformations can be applied successfully. This can be appreciated in the preparations of 1,4-dinitrocubane worked out at Chicago by Shankar et al. and Wicks et al. (Scheme 4).[16] Here, modern versions of classical methodology are used. These conversions are as easy to do on the cubane system as on any standard carboxylic acid. Note, just as one example of the "convenient" behavior of most cubane derivatives, that the intermediate cubyl-1,4-diisocyanate in Scheme 4 is a stable, crystalline material (m.p. 112–114 °C) and an obvious precursor for polyurethanes. Such materials may find application as high-energy binders for propellants. Cubylamines (and more particularly cubylmethyl amines) are of interest as antiviral agents given the relation of their size and shape to the important drugs Symmetrel® and Rimantadine® (DuPont). 1,4-Dinitrocubane, the final product in Scheme 4, is perfectly easy to handle. It is less shock-sensitive than TNT

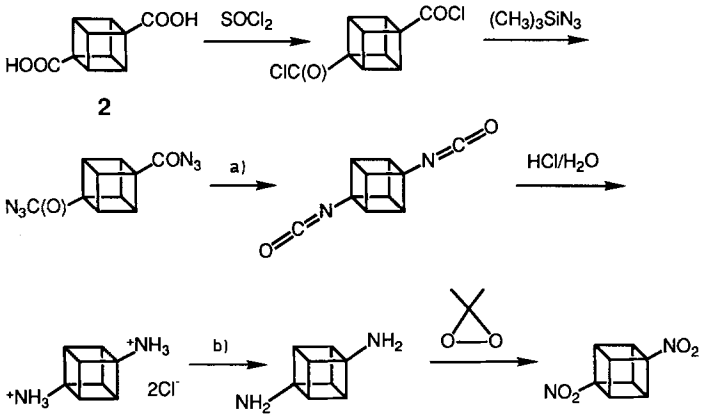

Scheme 4. Functional group transformations on the cubane framework. a) Warming; b) neutralization.

and remarkably stable thermally (decomp. 260 °C). [This is not true of some other cubanes; cubyl azides, diazoketones, and diazomethanes are shock sensitive and dangerous. **Caution** is advised in handling any cubane, since all are high-energy compounds. Safety shields should always be used, and particular care should be taken in the workup of crude mixtures that might contain acidic or heavy-metal contaminants.]

6. Substitution on the Cubane Framework

Functional group transformations are useful for preparing many mono- and disubstituted cubanes, as the corresponding carboxylic acids are readily available.[3] But this does not suffice for the preparation of more highly substituted cubanes. As Reddy et al. have shown, substitution of the cubane framework by way of the cubyl radical is fairly easy. However, as is usually the case with radical reactions, mixtures of products are obtained. Light-induced iodination of cubane with *tert*-butyl hypoiodite gives mono-, di-, triiodocubanes, etc.[17] The challenge is to achieve systematic and controlled substitution onto the cubane frame. This requires a real understanding of the structure of cubane.

6.1. The Nature of the C–H Bond in Cubane

The geometry of the cubane system dictates substantial rehybridization of the component tetravalent carbon atoms away from sp^3 hybridization. The carbon–carbon bonds become p-rich, and the exocyclic carbon orbital used for the C–H bond becomes s-rich. There is about 31% s character in this orbital as calculated from the observed ^{13}C–^1H coupling constant of 155 Hz.[3, 18] Thus, the hydrogen atoms of

cubane are expected to be more acidic than those of strain-free, saturated hydrocarbons. This has been demonstrated decisively.[19] The kinetic acidity of cubane is about 63000 times that of cyclohexane. Nonetheless, this is far too low to be useful for direct synthetic applications.

6.2. Amide Activation for *ortho* Metalation

Our idea was to use neighboring group activation to assist metalation of cubane. It was already well known from the work of Meyers, Beak, Snieckus, and others that an amide substituent on an arene aids lithiation in the *ortho* position by activation of the arene hydrogen atom.[20] There are certain similarities between cubanes and arenes: both have C–H bonds with enhanced s character, and in both the adjacent (*ortho*) substituents are forced to be coplanar (Scheme 5). Thus, we speculated that it might be possible to lithiate cubanamides.

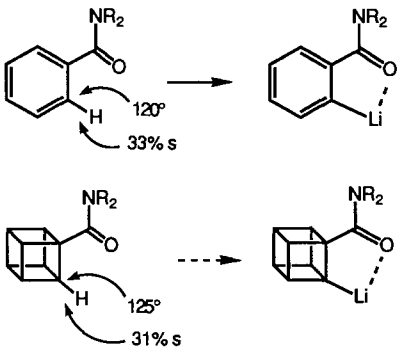

Scheme 5. A comparison of important features of benzamide, cubanamide, and their *ortho*-lithiated derivatives. The similarity between arenes and cubanes is reflected in the similar CCH angle and amount of s character in the C–H bond.

The seminal work was done in my laboratory by Graziano Castaldi.[21] He showed that a small equilibrium concentration of the *ortho*-lithiated derivative **6** is indeed formed when the diisopropylamide **5** of cubanecarboxylic acid is treated with a large excess of a strong, non-nucleophilic base like lithium tetramethylpiperidide (LiTMP). (Alkyllithium reagents are not suitable because they attack the amide group.) When the reaction mixture was quenched with CH_3OD the recovered cubanamide contained approximately 3% deuterium in the 2 position (*ortho*); dideuterated material could not be detected.

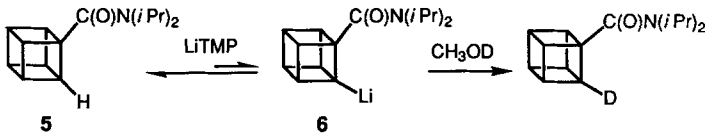

This result was very satisfying to us as physical organic chemists since it was logically derived and demonstrated that activated saturated systems can be metalated.[22, 23] Nonetheless, this observation alone was not particularly useful in synthesis. A small concentration of a carbanion in the presence of a huge excess of base is not an easy thing to work with.

6.3. Transmetalation

In a key step forward, Castaldi showed transmetalation to be the golden link in the synthesis of substituted cubanes.[21] When lithiation of a cubanamide is performed in the presence of mercury salts, the lithium compound first formed is quickly mercuriated, and the very polar C–Li bond is replaced by the more nearly covalent (and relatively inert) C–Hg bond. In this way, the starting material **5** can be completely converted into a metalated cubane (Scheme 6). The

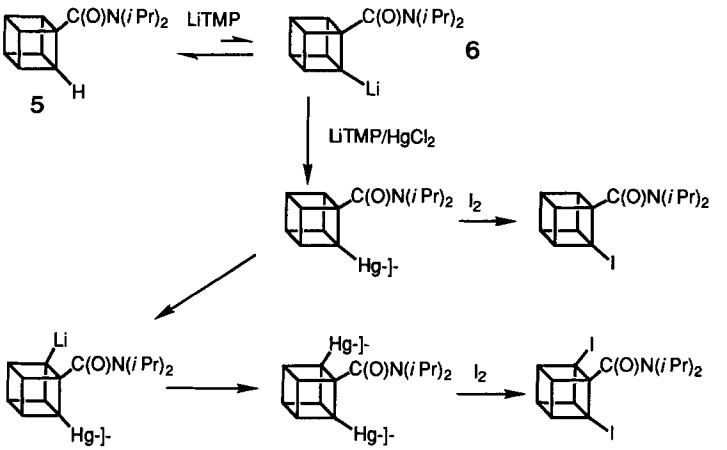

Scheme 6. Metalation/transmetalation: a method for the complete metalation of the activated cubane framework.

amide group is important in stabilizing the intermediate lithiated cubane, but not the mercuriated compound. Once lithium is replaced by mercury, the amide group is again able to assist removal of another *ortho*-hydrogen atom, and the process can continue.

Metalation/transmetalation is the basis of a complete synthetic methodology for the preparation of a great variety of substituted cubanes. Mercuriated cubanes are useful for the formation of halocubanes, as the C–Hg bond is readily cleaved by halogens such as iodine. Other metalated cubanes are more reactive and thus more useful. Higuchi et al. showed that zinc, silicon, and tin derivatives of cubane could be made in a similar way (Scheme 7) and are of great synthetic utility.[24]

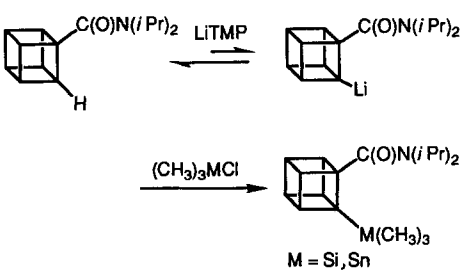

Scheme 7. Preparation of silyl- and stannylcubanes by metalation/transmetalation.

6.4. Reverse Transmetalation

Cunkle, a postdoc in my group, worked out a reverse transmetalation methodology for converting mercuriated cubane compounds into more reactive metallocubanes.[25a] This extraordinary (if roundabout) process allows the quantitative preparation of dilithiated cubanes (Scheme 8), materials not available by direct lithiation of cubanamides. The method has also found use in the synthesis of dimetalated arenes.[25b]

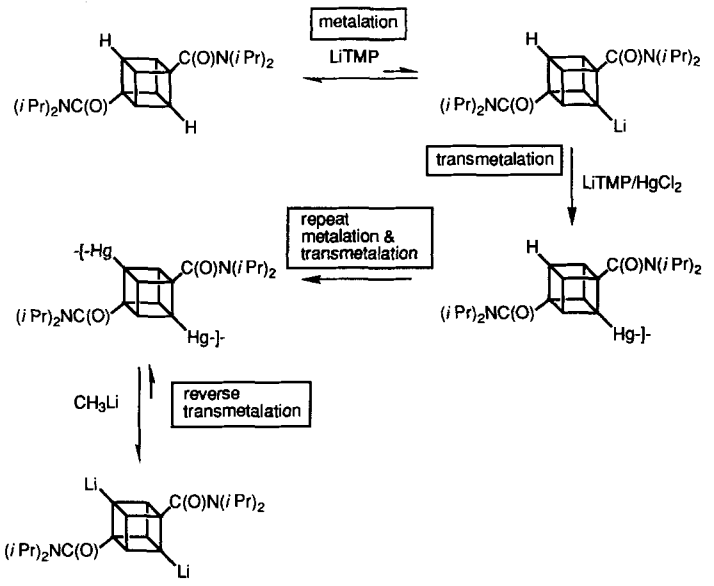

Scheme 8. Metalation/transmetalation/reverse transmetalation: a roundabout route to not easily accessible compounds.

6.5. Cubyl Grignard Reagents

Bashir-Hashemi at Geo-Centers introduced transmetalation with magnesium salts and thereby provided easy access to cubyl mono- and bis-Grignard reagents.[26] This works exceedingly well. The conversion proceeds by stepwise lithiation/bromomagnesiation. The second metalation of the

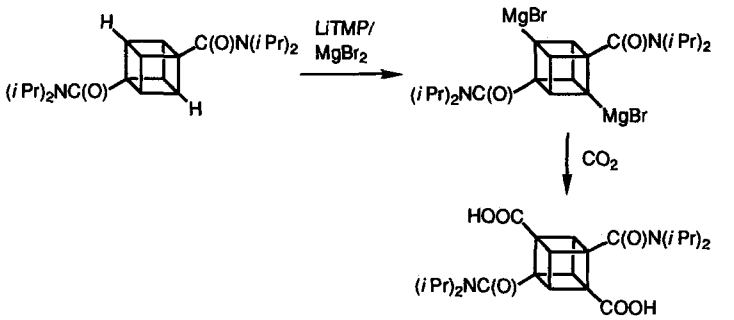

Scheme 9. *ortho*-Magnesiation by metalation/transmetalation: a useful method.

cubane framework occurs at a position remote from the first—quite understandable considering the polarities of the intermediates. Further metalation does not take place. In most cases, the overall conversion of these reactions is extraordinarily good; in the example shown in Scheme 9 yields of 90–95% are easy to achieve in both small- and large-scale runs.[27]

6.6. The Amide Activating Group

The diisopropyl amide activating group used in these various reactions was chosen because it is quite inert to the amide bases employed for *ortho* metalation. As always, there is a price to be paid for the luxury of judicious choice: such amides cannot be hydrolyzed to the corresponding carboxylic acid, the functional group most amenable to further transformations. For a time this problem was the "Achilles heel" of the reaction sequence. We did find finally that borane reduction of the amide followed by oxidation of the amine so produced with dimethyldioxirane (Scheme 10)[27a] or (on larger scale) with potassium permanganate provided a successful solution.[27b]

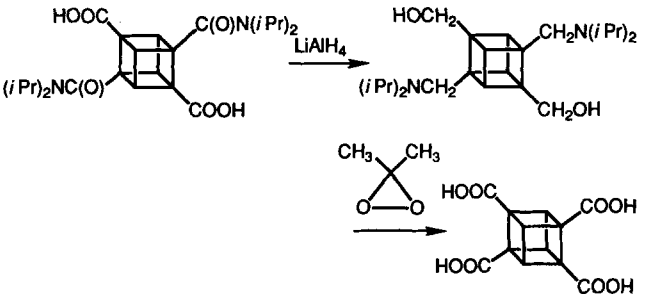

Scheme 10. A novel way to "hydrolyze" a recalcitrant amide group.

Bottaro, Schmitt, et al. introduced later the use of the *tert*-butyl ethyl amide as an activating group for *ortho* metalation that could be completely hydrolyzed in strong acid.[28] Subsequently, we found that just the *tert*-butyl group alone can be removed in mild acid, and then the resulting amide (in our case a methyl amide) can be taken to the free carboxylic acid with either acid- or, better, base-catalyzed hydrolysis.

6.7. *ortho* Magnesiation

In the course of extending our work to the synthesis of cubanes with different substitution patterns, we found that treatment of the 2,4-dicyanocubanamide **7** with LiTMP gives two isomeric tetrasubstituted cubane carboxylic acids (**8** and **9**) after carboxylation.[29] The electron-withdrawing

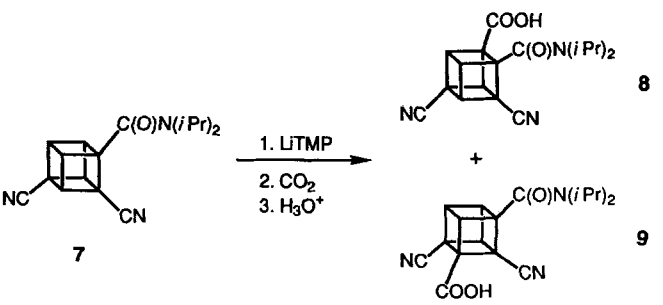

effects of the cyano groups along with the amide stabilizes both intermediate lithiated cubanes so well that only a small excess of LiTMP is needed to achieve fairly complete deprotonation even at −78 °C. In the initial lithiation step, the activation of a cubane C–H bond by two flanking cyano groups rivals the *ortho* activation by the one amide group. This results in competitive lithiations and a mixture of products. In attempts to achieve greater selectivity in this reaction, we examined the effect of added $MgBr_2$. When the ratio of LiTMP to $MgBr_2$ was 1.5:1, the product ratio was improved to 9:1 favoring carboxylation *ortho* to the amide function. This suggests an important, previously unknown reaction: direct magnesiation by TMPMgBr (a Hauser base)[30] and/or by $(TMP)_2Mg$. Lee and Xiong in my laboratory have expanded this idea into a powerful new process dubbed *ortho* magnesiation, and we have found that magnesium amide bases are exceedingly useful in synthesis.[31, 32]

These bases can be made very simply. The reaction of 2,2,6,6-tetramethylpiperidine (TMPH) in refluxing THF with one equivalent of ethylmagnesium bromide or with 0.5 equivalents of dibutylmagnesium gives, respectively, clear solutions of TMPMgBr and $(TMP)_2Mg$. The reactions are complete within a few hours. Solutions of the corresponding diisopropylamine derivatives can be obtained similarly.[31] These magnesium amide bases are stable in refluxing THF for hours. In this way they differ markedly from the corresponding lithium amides, which rapidly decompose at this temperature; indeed, LiTMP is unstable above 0 °C in THF. Since the magnesium amide bases can be used in refluxing THF, reactions with materials of otherwise low solubility or low reactivity are possible.

When dicyanocubanamide **7** is treated with TMPMgBr or $(TMP)_2Mg$ the only product after carboxylation (90% yield!) is **8** in which the carboxyl group is next to the amide activating group.[29] This reaction proceeds well even at −78 °C. The inductive effect of the cyano group clearly enhances the reaction, but the cyano group itself is not an *ortho* director for magnesiation.

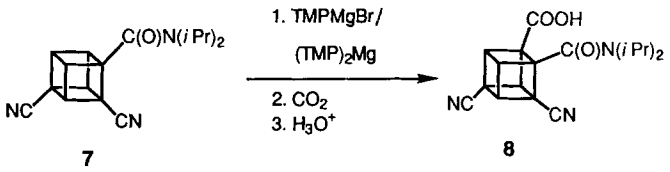

7 8

The uses of *ortho* magnesiation extend far beyond the cubane system; for example, the method can be applied productively to aromatic systems. "By-products" such as this have arisen often from our work on the cubane system and as in this case have brought new, important insights. Since the original work by Gilman on *ortho* lithiation of substituted arenes, it has always been assumed that the metalation depends crucially, if not exactly explicably, on the properties of lithium. Now we know that direct *ortho* magnesiation can be accomplished as well. Such processes complement *ortho* lithiation and sometimes also offer distinct advantages, as shown in the new synthesis of pyromellitic acid (**10**). This,

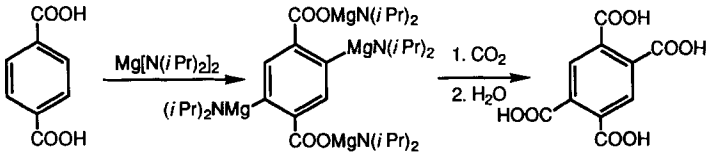

10

and further extensions of the *ortho* magnesiation process are discussed in more detail elsewhere.[31, 33–35]

7. Synthesis of Cubanes with Different Substitution Patterns

Although activation by a single amide group suffices for the metalation of cubanes, the presence of additional electron-withdrawing groups enhances reactivity enormously. 4-Cyanocubanamide is much more reactive than the unsubstituted amide. Magnesiation occurs quickly and exclusively *ortho* to the amide. As Puranik, a postdoc in my group, has shown for certain cases, namely when the electrophile can coexist with the base, it is possible to substitute all three positions *ortho* to the amide in a wonderfully simple, one-pot reaction proceeding by sequential metalations. Thus, for example, 4-cyanocubanamide can be converted directly into the tri(*tert*-butylcarbonyl) derivative **11**.[36]

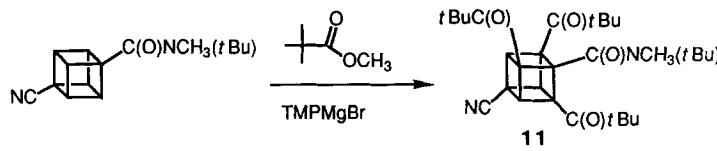

11

As the Baeyer–Villiger oxidation of *tert*-butyl cubyl ketones is completely specific—only the *tert*-butyl group migrates—triketone **11** can be converted easily to the polycarboxylated cubane **12**.[36]

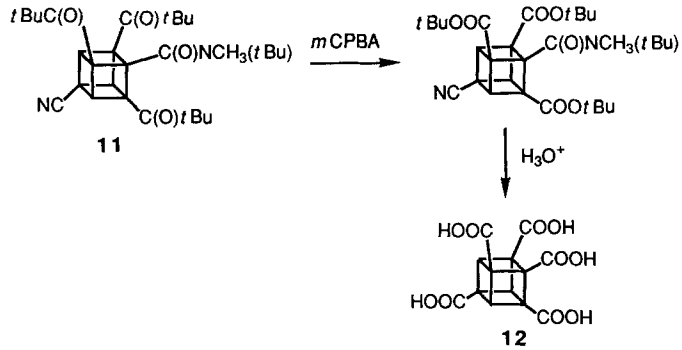

We have used processes like these to produce many different cubanes. It is fair to say that almost any combination or permutation of functional groups and positions on the cubane nucleus can be achieved now by fairly simple chemistry.[37] In Scheme 11, for example, are six tetrasubstituted

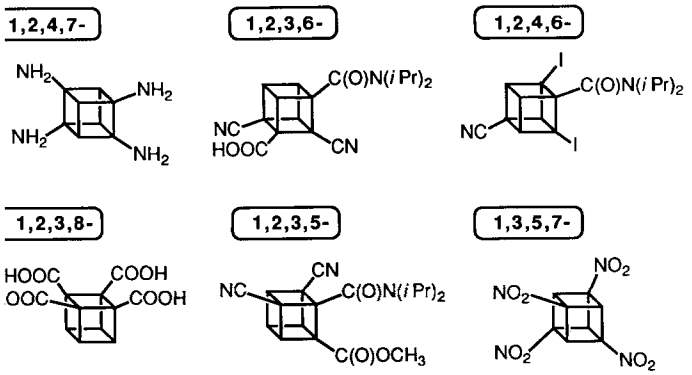

Scheme 11. Tetrasubstituted cubanes with different substitution patterns.

cubanes we have made, each with a different substitution pattern.

We have even synthesized cubanes like **13** with fused heterocyclic rings.[38] Quite different from expectation these "heteropropellano cubanes" are remarkably stable. The nitrogen atoms can be alkylated or nitrated without interference from ring-opening reactions. Interestingly, the C–C bond shared by the urea ring and the cubane system is substantially shorter than the equivalent bond in cubanes or cyclic ureas. The origin of this effect is not known.[38]

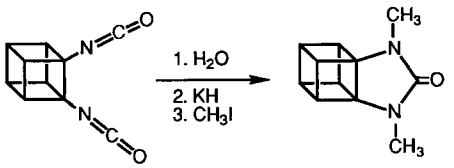

13

8. Cubane as a Building Block for Pharmaceuticals

Because the cubane frame is rigid, substituents have precise spatial relationships to one another. The distance across the cube (the body diagonal) is almost the same as that between the *para* positions of the benzene ring. On cubane, one can add substituents in "the benzene plane", as well as above and below it, so to speak. This offers fascinating possibilities for the synthesis of new pharmaceuticals. A number of cubane derivatives have already been obtained which show interesting activity in anti-AIDS and anti-tumor screens. Admittedly, the activity/toxicity balance is not yet satisfactory. We do know, however, that the cubane system is not inherently toxic; most cubanes are biologically innocuous. The search for pharmaceutically significant cubanes has just begun. At this point, cubane should be viewed as a biologically stable, lipophilic platform on which the chemist can install a wide choice of substitutents in a variety of well-defined spacial relationships. Developments in drug design programs should allow the judicious choice of substituents.

9. Cubanes as Precursors to Reactive Intermediates

Having solved the problems associated with the synthesis of substituted cubanes, we can now start with the cubane system, itself an extraordinary structure, and move outward in our continuing exploration of the limits of bonding in organic compounds.

9.1. Cubyl Cation

One of the biggest surprises we have had in our work was the discovery that cubyl cation is much more accessible than expected.[39] Everything about cubyl cation seems unfavorable: 1) The geometry about the positively charged carbon atom is very far from flat; 2) the exocyclic orbitals in cubane are s-rich; 3) hyperconjugative stabilization would require high-energy, cubene-type structures. Ab initio calulations (6-31G*, without electron correlation) place cubyl cation about 20 kcal mol^{-1} higher in energy than *tert*-butyl cation and about 5 kcal mol^{-1} higher in energy than 1-norbornyl cation.[40] Nevertheless, we came across numerous reactions (Scheme 12) that might involve the intermediacy of the cubyl cation.[41]

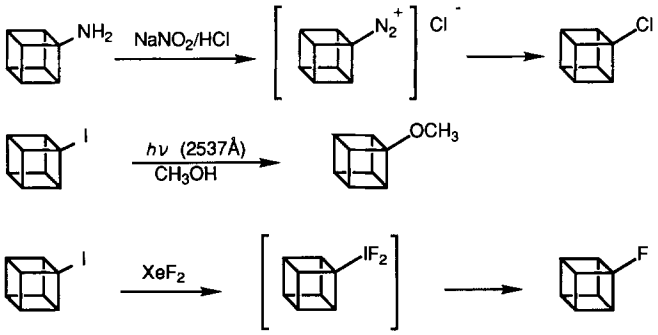

Scheme 12. Substitution reactions of cubane derivatives that probably proceed via the cubyl cation.

9.1.1. Solvolysis of Cubyl Triflate

Since some of the substitution reactions in Scheme 12 do not have clearly defined mechanisms, and there are possibilities for front-side attack, "hot intermediates", etc., we turned to an examination of simple solvolysis reactions.[39a] As it turned out, the solvolysis of cubyl triflate **14** in pure dry methanol is remarkably facile. Its half-life at 70 °C is only

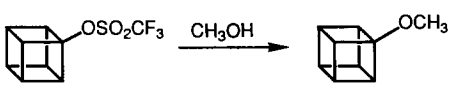

14 **15**

15 minutes. The reaction is very clean. No rearrangement is observed, and the only product is cubyl methyl ether **15**. Labeling studies have established that the methoxy group is

attached to the same carbon as the original triflate group. There is no hydrogen scrambling nor skeletal rearrangement.

9.1.2. A Comparison of Experimental and Calculated Solvolysis Rates

Cubyl triflate is very much more reactive than 1-norbornyl triflate which is not solvolyzed noticeably by methanol at 70 °C even after 250 hours. In hexafluoroisopropanol at 60 °C norbornyl triflate is only 90% solvolyzed in 85 hours, whereas cubyl triflate is converted completely in this solvent to cubyl hexafluoroisopropyl ether within 5 minutes at room temperature.

The logarithm of the S_N1 solvolysis rate is, in a first approximation, inversely related to the difference in the strain energy of the non-ionized starting material and the intermediate cation. Schleyer et al.[42] have shown that this energy difference can be estimated successfully by careful application of molecular mechanics calculations. In Table 2 published rate data for solvolysis have been adjusted (in so far as possible)[43] to a common set of conditions, and are compared to the values predicted by molecular mechanics. The

Table 2. Comparison of the experimentally determined and the calculated relative rates of solvolysis of some tertiary tosylates in acetic acid at 70 °C.

Tosylate	Exp.	Calc.	Tosylate	Exp.	Calc.
tert-butyl	1	1	1-norbornyl	10^{-13}	10^{-14}
1-adamantyl	10^{-3}	10^{-4}	cubyl	10^{-10}	$<10^{-25}$
1-bicyclo[2.2.2]octyl	10^{-7}	10^{-8}			

agreement is within one or two orders of magnitude—astonishing considering the substantial corrections. Cubyl tosylate is the exception; here the theoretical and experimental rates of hydrolysis differ by more than 15 orders of magnitude!

9.1.3. The Bonding in Cubyl Cation

Why is cubyl cation so much more easily formed than expected?[44] Put another way, what differentiates the cubane derivative from the other compounds in Table 2? As discussed earlier in Section 6, the geometric constraints inherent in the cubane skeleton force significant rehybridization in the bonding orbitals of carbon away from sp^3. The C–C bonds in cubane are p-rich in comparison to those in the other systems listed in Table 2. The electronic structure of the bonding system in cubane is quite different from that of the others; molecular mechanics does not take this into account.[45] The matter has been treated quantitatively by Borden and Hrovat with ab initio 6-31G* calculations including electron correlation.[40] This has led to the conclusion that the positive charge is delocalized by interaction with the strained C–C bonds in cubane; namely, there is positive bond order between the p orbital at the positively charged carbon atom and the p orbital aligned with it at each of the β carbon atoms (C3). Population analysis reveals that the γ-CH (C4) and α-CH (C2) groups bear considerable positive charge (0.16), more than the β-CH groups.

9.1.4. Substituent Effects on the Rate of Solvolysis of Cubyl Triflate

Considering the calculated charge distribution in cubyl cation, it is not surprising that electron-withdrawing substituents at position 4 (body diagonal, *para*) suppress solvolysis effectively (Table 3). We were unable to detect any signif-

Table 3. Comparison of the half-lives $t_{1/2}$ for the hydrolysis of a number of 4-substituted cubyl triflates.

4-X-1-Triflate	T [°C]	$t_{1/2}$	4-X-1-Triflate	T [°C]	$t_{1/2}$
X = H	20	< 5 min [a]	H	25	67 h [c]
CH_3O	60	> 133 h [a]	CH_3	25	200 h [c]
Cl	60	> 20 d [a]	$(CH_3)_3Si$	25	37 min [c]
CF_3SO_3	100	[b]	$(CH_3)_3Sn$	25	[d]

[a] In $(CF_3)_2CHOH$. [b] Reaction time in $(CF_3)_2CHOH$ was too long to measure. [c] In CH_3OH. [d] Reaction time in CH_3OH was too short to measure.

icant solvolysis of the bistriflate of cubane-1,4-diol after it was heated in methanol at 85 °C for 5 days, in aqueous 80% ethanol at 100 °C for 5 days, or in hexafluoroisopropanol at 100 °C for 6 days.[46] On the other hand, as Borden et al. insightfully pointed out,[40] π-donor substituents cannot stabilize cubyl cation effectively, since the C-to-substituent bond at C4 is along the axis of the cylindrically symmetric LUMO of the cation.[47] Thus, substituents such as methyl and methoxy normally associated with the hyperconjugative and resonance stabilization of cations fail to do so in cubyl cation. Indeed, as can be seen in Table 3, only their destabilizing inductive effects are mirrored in the observed rates. The symmetry restriction limiting the stabilizing effects of π-donor substituents of course does not apply to σ donors. Jian Ping Zhou in my laboratory has found that silyl and tin substituents at C4 markedly enhance the rate of solvolysis of cubyl triflates.[48] Indeed, solvolysis of 4-trimethylstannylcubyl triflate in methanol is so fast (about 3000 times faster than cubyl triflate) that its rate could only be obtained by extrapolation from the reaction of the corresponding mesylate.

9.2. Dehydrocubanes

Cubane is a saturated hydrocarbon of extraordinary geometry and strain. Although it was once dismissed as impossible, it has been shown to be stable. Similarly, cubyl cation has been found to be far more readily accessible than once imagined. With these lessons in mind, it is prudent not to dismiss other uncommon notions out of hand.

9.2.1. 1,2-Dehydrocubane (Cubene)

1,2-Dehydrocubane, cubene **16**, is the most extreme example of a pyramidalized olefin.[49, 50] Obviously, the ge-

ometry about the vinyl carbon atom can be nowhere near planar. Hrovat and Borden have calculated a pyramidalization angle of 84° for **16**.[50b]

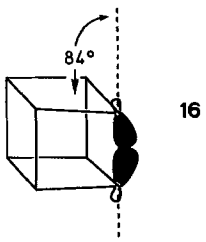

16

Using the newly developed methods for the synthesis of substituted cubanes discussed earlier, Maggini, a postdoc in my group, prepared 1,2-diiodocubane.[51] He found that the chemistry of this vicinal dihalide could be rationalized most efficiently by invoking the intermediacy of cubene (Scheme 13).[51] Critical to the reasoning behind this hypothesis is the fact that reaction of monoiodocubane with *tert*-butyllithium gives essentially only cubyllithium; no significant amount of *tert*-butylcubane is formed. The formation of *tert*-butylcubane and cubylcubanes in the reactions of 1,2-diiodocubane presumably reflects the susceptibility of cubene to nucleophilic attack. Certainly, nucleophilic addition to highly strained olefins is well precedented in the lovely work of Szeimies et al. on bridged bicyclobutenes.[49]

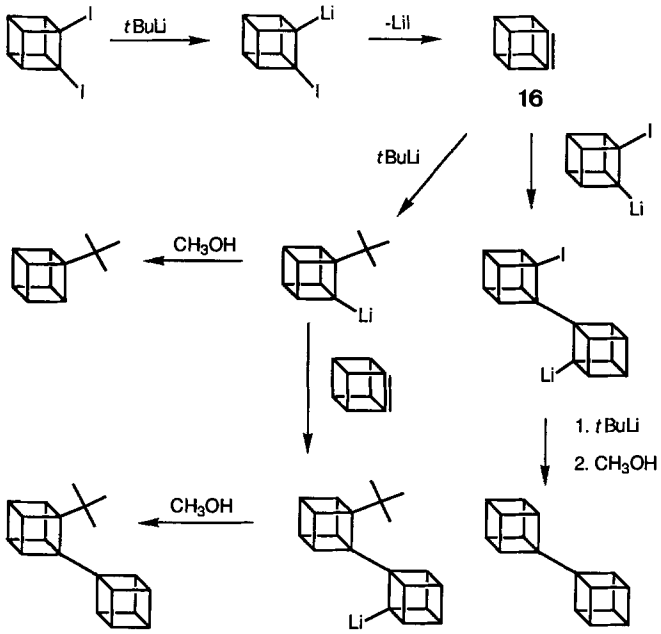

Scheme 13. The reaction of 1,2-diiodocubane with *t*BuLi.

Cubene is an immensely strained, relatively "open", and sterically unhindered olefin. As such, it can be expected to be very reactive in Diels–Alder additions. Indeed, when the deiodination of 1,2-diiodocubane was conducted at room temperature with *tert*-butyllithium in benzene in the presence of 11,12-dimethylene-9,10-dihydro-9,10-ethanoanthracene, the 1:1 Diels–Alder adduct **17** was formed in 64% isolated yield. Cubane-on-a-pedestal!

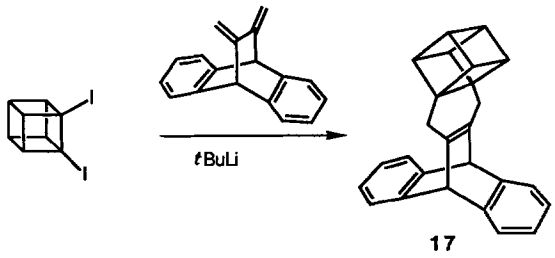

17

9.2.2. 1,4-Dehydrocubane (1,4-Cubanediyl)

The extraordinary chemistry of 1,2-diiodocubane induced us to examine the 1,4-diiodo compound,[52] a material readily available from cubane-1,4-dicarboxylic acid.[53] In my laboratory, Tsanaktsidis showed that the reactions of 1,4-diiodocubane with alkyllithium reagents (Scheme 14) give rise to products related to those obtained from the reactions of 1,2-diiodocubane, that is, materials resulting from the nucleophilic additions of lithium compounds to some very reactive intermediate.[54]

Our labeling experiments provide good evidence that the products arise from a symmetrical intermediate. There are a number of possible structures, for example **18**–**21**, but some of these can be eliminated from serious consideration. 1,4-Dilithiocubane (**18**) can be prepared if the exchange reaction between 1,4-diiodocubane and *tert*-butyllithium is conducted at −100 °C; **18** behaves as would be expected, quite differently from the intermediate generated in the reaction performed at −70 °C. It is not likely that Grob fragmentation of the diiodide gives **19**, surely a reactive olefin, since the addition of suitable trapping dienes like furan and 9,10-diphenylisobenzofuran does not change the observed course of the reaction. Borden et al.[55] and Michl et al.[56] have calculated independently that structure **20** with a body-diagonal bond is unlikely given its exceedingly high strain and

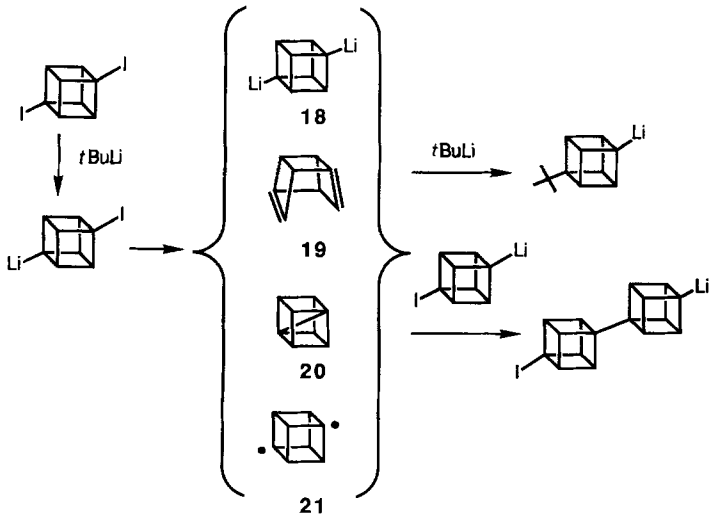

Scheme 14. Possible intermediates **18**–**21** in the reaction of 1,4-diiodocubane with *t*BuLi.

orbital phase mismatch.[57] Ab initio calculations by both groups indicate that the actual intermediate is probably 1,4-cubanediyl (**21**).

The singlet state **22** of 1,4-cubanediyl is calculated to be > 10 kcal mol^{-1} more stable than the triplet state, a result of substantial through-bond interaction. Indeed, 1,4-cubanediyl does not behave like a diradical. It does not react with cyclohexene; neither hydrogen abstraction from, nor addition to the olefin is observed. Michl et al. have obtained spectroscopic evidence for cubanediyl by matrix isolation (argon, 12 K) of the products from the gas-phase metal-induced dehalogenation of 1,4-dihalocubanes.[56]

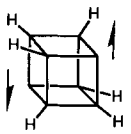

22

10. Cubylcubanes and Oligocubanes

Cubene (1,2-dehydrocubane) and 1,4-cubanediyl (1,4-dehydrocubane) are enormously strained compounds which cannot be isolated under standard conditions. They both undergo nucleophilic additions very readily, and this has provided us access to the cubylcubane series (see Schemes 13 and 14). Gilardi[58] has shown by X-ray structure analysis that the central cubylcubane bond is exceedingly short (1.458 Å, Scheme 15) as might be expected, since the exocyclic orbitals of cubane are s-rich and close to the nucleus.[59] The central bond in cubylcubane has about the same length as the C–C single bond made from sp^2 orbitals in 1,3-butadiene. Note that the central bond in adamantyladamantane, constructed from sp^3 orbitals, is 1.578 Å long.[60]

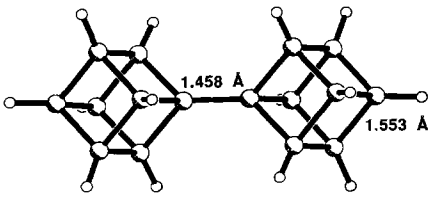

Scheme 15. The molecular structure of cubylcubane. The C–C bond lengths were determined by X-ray structure analysis [58].

10.1. Arylated Cubylcubanes

Tsanaktsidis[54] found that 4-haloiodocubane reacts with phenyllithium to give, ultimately, 1-iodo-4-phenylcubane. He demonstrated that the reactions proceed by way of the 1,4-diyl (Scheme 16).[49]

K. Pramod extended and modified the sequence in a way that permits the preparation of a host of [*n*]cubylcubanes (Scheme 17).[61, 62]

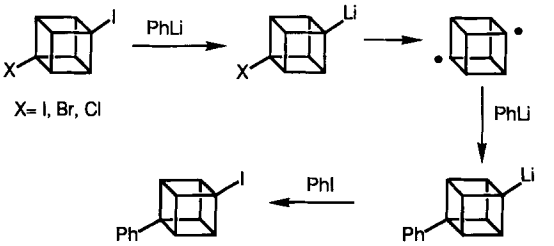

Scheme 16. The reactions of 4-halo-1-iodocubanes with phenyllithium.

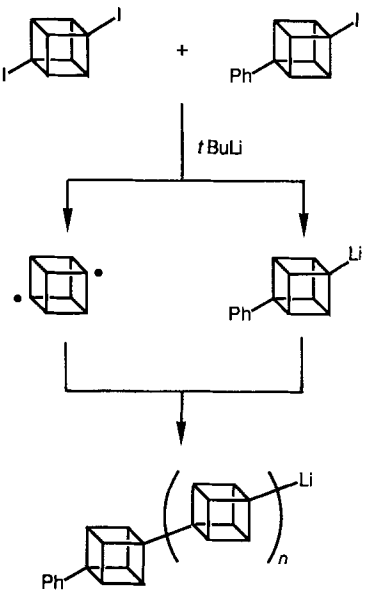

Scheme 17. The key steps in the synthesis of arylated [*n*]cubylcubanes.

The [*n*]cubylcubanes have rigid, rod-shaped skeletons and allow the preparation of sets of compounds with interacting groups separated in space by precise distances. Each cubane unit adds 4.15 Å to the length of the molecule. Pramod developed smooth methods to place different arene substituents at opposite ends of cubylcubanes. Thus, for example, he could trap the product from Scheme 17, the lithiocubane with $n = 2$, with phenanthrene-9,10-epoxide and then dehydrate the resulting intermediate to give **23**.[62]

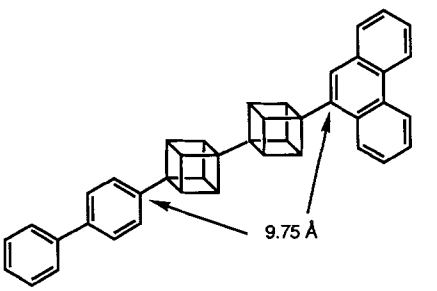

23

The group of Gerhard Closs (deceased May 24, 1992), my late colleague at The University of Chicago, is now measuring the rates of electron transfer between such substituents as a function of the distance separating them.

10.2. Alkylated Cubylcubanes

The preparation of alkyl-substituted cubylcubanes in good yield by the addition of alkyllithium reagents to cubanediyls is more difficult than the synthesis of the aryl analogues. Nucleophilic addition reactions most probably proceed by way of single-electron transfers, and a good match of the orbital energies is required for this to be effective. Aryl- and cubyllithium add easily to 1,4-cubanediyl, but alkyllithium reagents do not. Yusheng Xiong in my laboratory found a way around this limitation by making intelligent use of Grignard intermediates as shown in Scheme 18.[63]

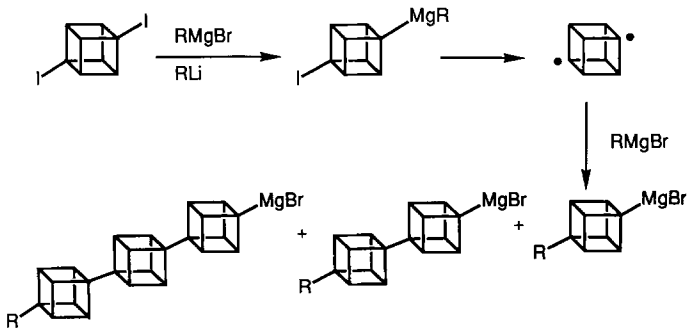

Scheme 18. The key steps in the synthesis of alkylated [*n*]cubylcubanes. In the first step, RLi is added slowly. R = methyl, butyl, or a long-chain substituent.

The Grignard products can be taken on in a variety of ways. One of particular interest to us at this time is the possibility of making liquid crystals with exceptional properties (e.g. UV transparency) from oligocubanes.[64] To this end Xiong has prepared materials like **24** as shown in Scheme 19.

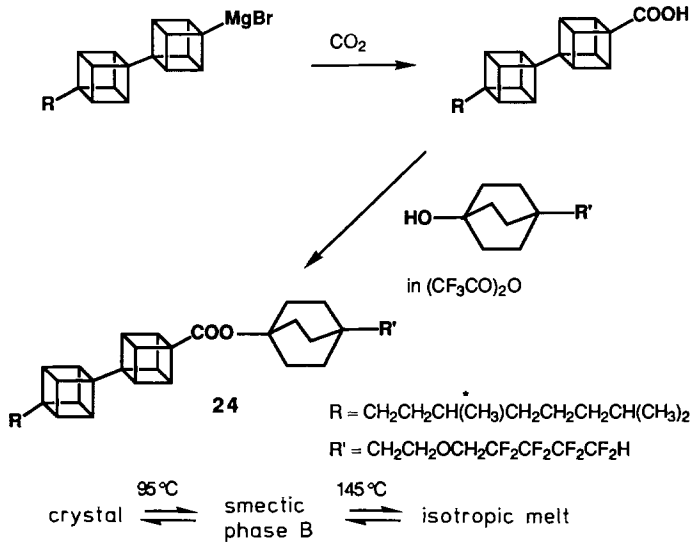

Scheme 19. Synthesis of trial liquid-crystalline compounds derived from cubylcubane.

It is worth noting here that esterification of the cubylcubanecarboxylic acid in Scheme 19 with the highly hindered bicyclo[2.2.2]octan-1-ol cannot be achieved in standard ways. The successful esterification conducted in trifluoroacetic anhydride depends on the formation of cubylacyl cation, an intermediate whose existence was demonstrated by Xiong using NMR spectroscopy.

10.3. Higher Cubylcubanes

As the number of linked cubane units increases, that is, as n increases, the solubility of [*n*]cubylcubanes plunges; at $n = 3$ most are essentially insoluble in ordinary solvents. This problem can be relieved by having moderately long alkyl substituents on the "monomer". Virtuani has converted 2,7-di-*n*-hexyl-1,4-diiodocubane (**25**) into the corresponding diyl, whose polymerization, presumably initiated by addition of 4-iodo-1-lithio- or 2,7-di-*n*-hexyl-1,4-dilithiocubane, gives an oligomeric cubylcubane with a molecular weight of approximately 10000. This corresponds to a polycubyl rod about 150 Å long containing on average 40 cubane units![65]

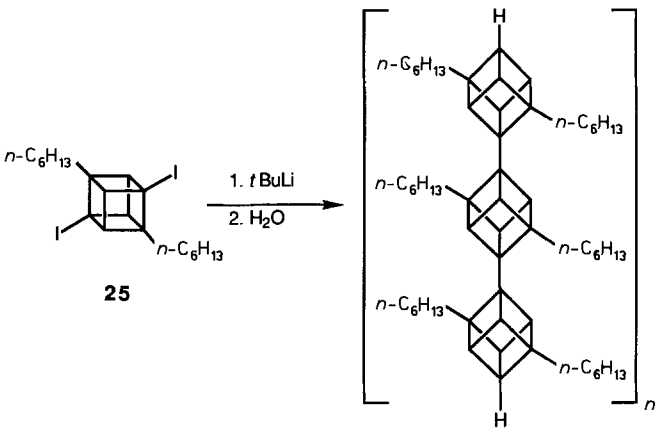

11. Ring-Opening Reactions of Cubanes

Cubane and many substituted cubanes are very stable compounds, indeed remarkably so considering the extreme strain energy of the skeleton (> 166 kcal mol^{-1}). There is no symmetry-allowed, concerted pathway for ring opening. When reagents or substituents open other paths, the molecule rearranges.

11.1. Electron-Rich Cubanes

Although cubanols can be isolated with care, they are fragile. 4-Methylcubanol **26**, like the others, opens by way of homoketonization to a tricyclooctenone, which in turn rearranges further to a vinylcyclobutenylketene.[66] Cubyl-

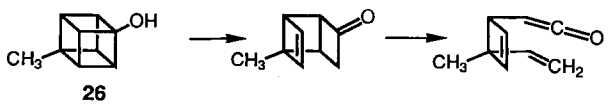

amines show similar ring-opening proclivities, but their ammonium salts are quite stable. Clearly, the ring-opening process is initiated by the shift of electrons into the ring. The tendency toward ring opening is greater when there is an electron acceptor at C2. No cubylamine or cubanol with a carbonyl substituent *ortho* to the electron donor has ever been obtained. Similarly, 2-nitrocubylamine has never been isolated. A simple push–pull mechanism can easily rationalize the rapid bond cleavages which account for the instability of such compounds.

11.2. Cubane–Homocubane Rearrangements

The framework of homocubane is at least 20 kcal mol^{-1} less strained than that of cubane. When a path is opened, cubanes rearrange to homocubanes.

11.2.1. Cubylcarbenium Ions

Great care is necessary in the isolation of cubylmethyl alcohols such as **27** with a nucleofuge on the methyl carbon atom. These compounds are exceedingly fragile and rearrange into the homocubyl system with exceptional ease.[67]

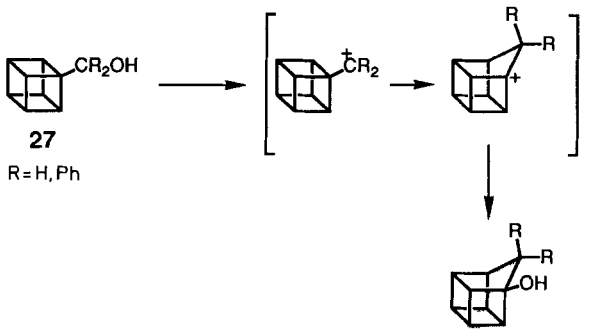

This probably occurs by way of a tight ion pair, as the usual product is primarily that of internal return. The Wagner–Meerwein 1,2 shift occurs even when the positively charged carbon atom is stabilized by two phenyl groups.

11.2.2. 1(9)-Homocubenes

K.-L. Hoffmann in my group showed that cubyl phenyl diazomethane **28** on thermolysis or photolysis is converted

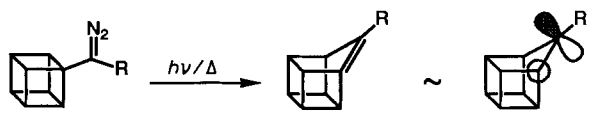

28a: R=Ph
28b: R=H

29

to 9-phenyl-1(9)-homocubene **29a**.[68] Later, Jones showed that the same reaction occurs when R = H.[69]

The 1(9)-homocubene system contains the most twisted C–C double bond known. If rehybridization and pyramidalization did not occur the angle between the p orbitals of the unsaturated carbons would be 90°. This is the anti-Bredt olefin nonpareil! Its chemistry is extraordinary. 1(9)-Homocubenes rearrange to 9-homocubylidenes. These conversions are amongst the rare examples of the rearrangement of an olefin to a carbene.[70] For the cases at hand, using ^{13}C-labeling, Appell et al. have shown that the rearrangement occurs reversibly,[71] and White et al. have proven that it proceeds by the shift of a C–C bond in the homocubane framework.[72] The rearrangement can best be rationalized by invoking a zwitterionic contributor to the olefin structure (Scheme 20). Platz, Jones, et al. have determined the equilibrium constant for the olefin–carbene rearrangement.[73]

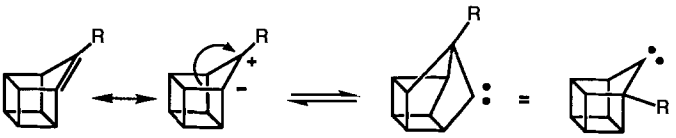

Scheme 20. Rearrangement of 1(9)-homocubenes to the corresponding homocubylidenes.

The investigation of such 1(9)-homocubene species is a very active area.[73] Most recently we have obtained optical spectra of *para*-substituted 9-phenylhomocubenes frozen out in 77 K glasses.[74] We shall discuss these in detail elsewhere.

11.2.3. 9-Azahomocubene

The solvolysis of cubyl azide **30** may also proceed by way of a homocubene, in this case 9-azahomocubene.[75] As yet

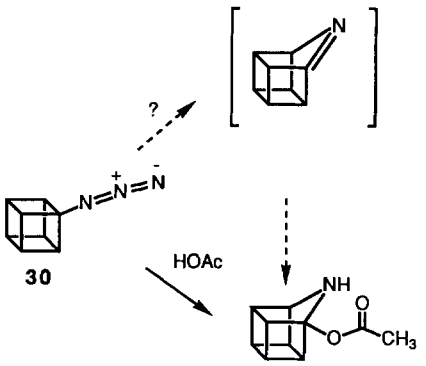

30

there is no proof for the intermediacy of such an anti-Bredt imine;[76] the observed acetolysis product could also be accounted for by a mechanism in which solvolysis, C–C bond migration, and nitrogen loss are linked together.

12. Cubylmethyl Radicals

The cubylmethyl radical has been generated from cubylmethyl bromide and from the *N*-hydroxy-2-pyridinethione

ester **31** of cubylacetic acid under various conditions favoring hydrogen-atom transfer to the radical. The behavior of the radical has been studied in detail by Yip Yu Chi in my laboratory[77a] and with Newcomb[77b] at Wayne State University. Methylcubane is formed only in the presence of high concentrations of the hydrogen donor PhSeH. Otherwise the cubylmethyl radical rearranges. There is no evidence of a 1,2 shift to give the homocubyl system, even though this would be extremely favorable energetically. Instead, one, two, or three bonds of the cubane framework cleave, leading to olefinic products. These can be accounted for by a mechanism in which σ bonds break sequentially and regioselectively; processes in which there is good overlap between the radical orbital and that of the breaking bond are favored (Scheme 21).[78] The distribution of products depends qualitatively on the survival time of the radical intermediates, in other words, on the concentration and effectiveness of the hydrogen-atom-transfer agent. From product distributions, the rate constant for ring opening of the cubylmethyl radical is calculated to be at least $2.7 \times 10^{10}\ s^{-1}$; this value is substantially greater than that of any radical derived to date from a saturated hydrocarbon system. The lifetime of cubylmethyl radical at 25 °C is about 35 ps.[77b]

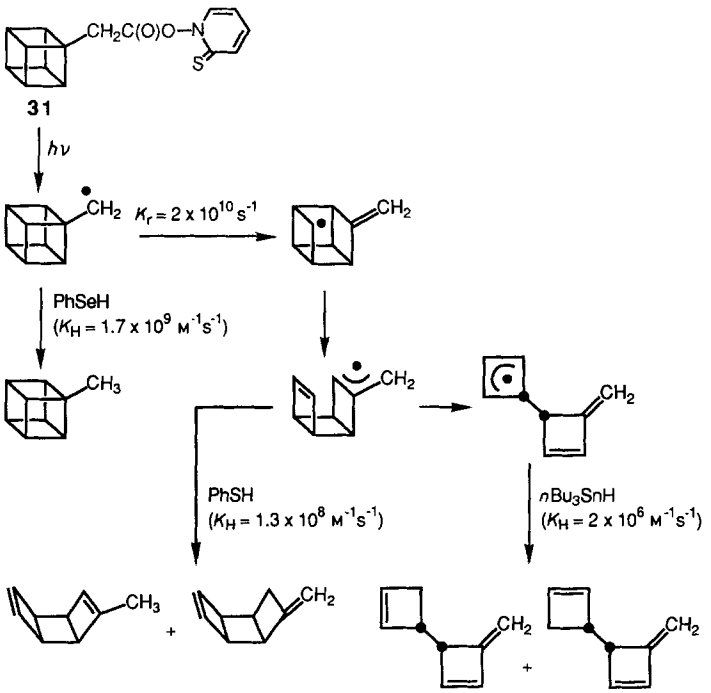

Scheme 21. Generation of the cubylmethyl radical and its reactions with various trapping reagents. The rate constants K for these reactions and the ring-opening reactions are given.

13. Metal-Induced Reactions of Cubanes

More than 20 years ago Halpern, Cassar, and I showed that various metal catalysts lead to the facile rearrangement or ring opening of cubane at room temperature. Thus, for example, oxidative addition to Rh^I triggers opening of the cubane frame to the *syn*-tricyclooctadiene system **32**.[79] Treatment with Ag^+ or H^+ induces rearrangement to cuneane (**33**).[80]

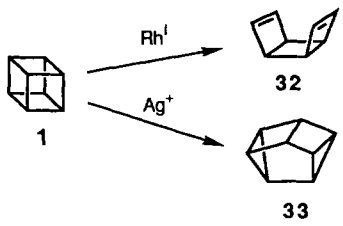

The details of such reactions were used at the time to help unscramble the very nature of metal-induced olefin rearrangements and olefin metathesis. Now, these early studies are starting to pay off in a different way. The Rh^I-catalyzed ring-opening to *syn*-tricyclooctadiene is particularly useful, because this intermediate is in turn readily converted at 50–60 °C into cyclooctatetraene. In my group, Chou and Pramod have shown that this also works well with substituted cubanes, allowing much easier access to substituted cyclooctatetraenes (e.g. **34**) and oligomeric cyclooctatetraenes (e.g. **35**) than previously possible (Scheme 22).[81] Indeed, the chemistry of cubane opens the way to new and exciting cyclooctatetraene derivatives, for example **36**.

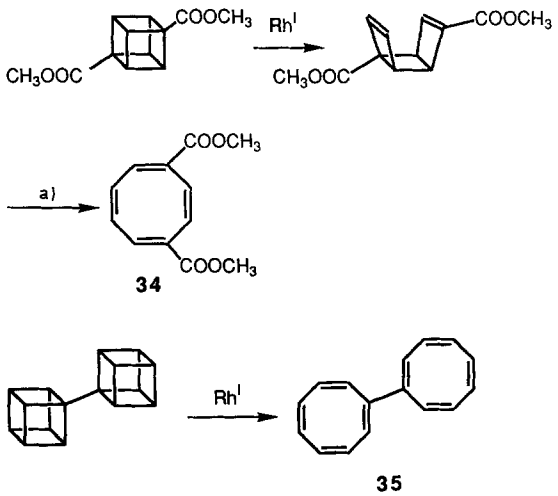

Scheme 22. Metal-induced ring-opening of cubane to give cyclooctatetraene. a) Warming.

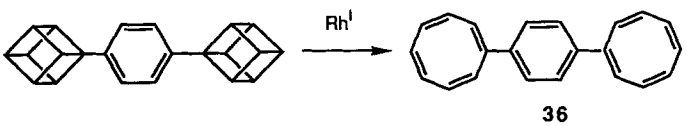

14. The Future

Much (but certainly nowhere near all) of the fundamental chemistry of the cubane system is now understood. Many new cubane derivatives and important, new high-energy sys-

tems can be made from cubane. But what about the more pragmatic aspects? Do cubanes have a role to play in practical chemistry? Will they prove to be important outside the university?

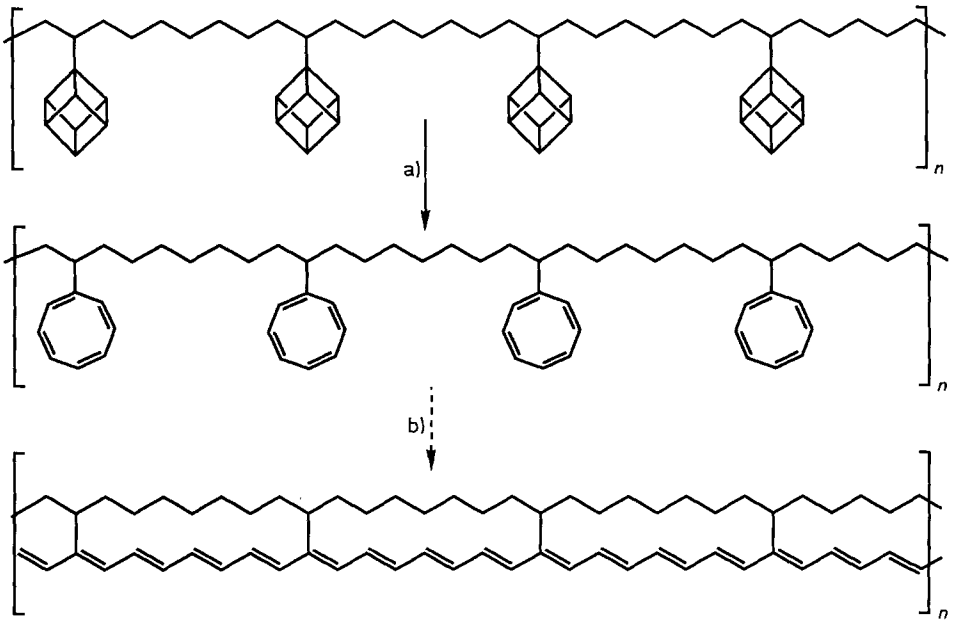

Scheme 23. Hypothetical route to polymer-bound polyacetylene. a) [{Rh(norbornadiene)Cl}$_2$]; b) metathesis catalyst.

I think the answer is a clear "yes". Not only are cubanes ideally suited for drug design, high-energy cubanes are also under consideration as explosives and propellants. Racing-car and missile manufacturers are looking to cubanes as the fuels of the future. In other lines of applications, optically transparent cubanes and cubylcubanes have been proposed as building blocks for rigid liquid-crystal compounds. UV-active cubanes, for example cubyl ketones, are readily transformed photochemically into colored cyclooctatetraenes; this conversion could be used for permanent information storage. We are currently focusing our efforts on polymers with cubane in the backbone or as a pendant group along a polymer chain.[82] The cubane subunits in these polymers can be rearranged easily to cyclooctatetraenes. We expect to convert these polycyclooctatetraenes to polyacetylenes by way of ring-opening metathesis polymerization.[83] In this way (Scheme 23), we hope to make polyacetylenes whose properties (e.g. stability, extrudability) are enhanced by the chain being intrinsically part of another polymer (e.g. a polyester or polyethylene). Of course, Scheme 23 is paper chemistry at its most optimistic. Such propositions have innumerable problems, not the least being conformational and configurational irregularities, cross-linking, and back-biting. But it is time that chemists address the possibility of controlled intramolecular polymerization of "polymeric monomers". The early history of cubane lends credence to the old adage that "the impossible just takes a little longer".

Although cubane and cubane derivatives are available on pilot-plant scale, they are still too expensive for industrial applications. Conceptually, cubane can be regarded as a stable oligomer of acetylene, a cheap starting material available in immense quantities. If it were possible to convert acetylene to cubane catalytically, cubane and its derivatives might be made cheaply. Under these circumstances cubanes could become the fuels of choice, not only for military applications but for ordinary transportation as well. One can speculate with some pleasure on the enormous impact this conversion would have on the way we live.

The energy balance of the conversion is good; the tetramerization is energetically favourable even when entropy is considered. One goal we have is to discover how to achieve this conversion and thus complete the transformation of cubane from a laboratory curiosity to an industrial material. I invite your participation.

The U. S. Office of Naval Research, the U. S. Army Research, Development and Engineering Center, the National Institutes of Health, and the National Science Foundation have all helped support my work. Richard Miller at the U. S. Office of Naval Research and Jack Alster at ARDEC have been particularly encouraging. It is a truly a pleasure to acknowledge the work of my students and postdocs. They made our achievements possible, and they made the work itself exciting and fun.

Received: November 4, 1991 [A881 IE]
German version: *Angew. Chem.* **1992**, *104*, 1447

[1] W. Weltner, Jr., *J. Am. Chem. Soc.* **1953**, *75*, 4224–4231.
[2] a) H.-D. Martin, P. Pföhler, T. Urbanek, R. Walsh, *Chem. Ber.* **1983**, *116*, 1415–1421; b) H.-D. Martin, T. Urbanek, P. Pföhler, R. Walsh, *J. Chem. Soc. Chem. Commun.* **1985**, 964–965; c) W. von E. Doering, W. R. Roth, R. Breuckmann, L. Figge, H.-W. Lennartz, W.-D. Fessner, H. Prinzbach, *Chem. Ber.* **1988**, *121*, 1–9.
[3] P. E. Eaton, T. W. Cole, Jr., *J. Am. Chem. Soc.* **1964**, *86*, 962–964, 3157–3158.
[4] a) J. C. Barborak, L. Watts, R. Pettit, *J. Am. Chem. Soc.* **1966**, *88*, 1328–1329; b) P. E. Eaton, T. W. Cole, Jr., *J. Chem. Soc. Chem. Commun.* **1970**, 1493–1494; c) N. B. Chapman, J. M. Key, K. J Toyne, *J. Org. Chem.* **1970**, *35*, 3860–3867; d) C. G. Chin, H. W. Cuts, S. Masamune, *J. Chem. Soc. Chem. Commun.* **1966**, 880–881; e) G. W. Griffin, A. Chaudhuri, L. W. Reichel, R. A. Breyer, M. M. Condon, T. Elhajj, D. C. Lankin, E. D.

Stevens, Y. J. Li, *Abstracts of Papers*, 149th National Meeting of the American Chemical Society, New Orleans, LA, Aug. 30-Sept. 4, 1987; American Chemical Society: Washington, D.C., 1987; ORGN 11. Only the synthesis of octakis(trifluoromethyl)cubane (L. F. Pelosi and W. T. Miller, *J. Am. Chem.Soc.* **1976**, *98*, 4311–4312) and the tetrabridged cubane, propella[3$_4$]prismane (J. Spanget-Larsen, R. Gleiter, L. A. Paquette, M. J. Carmody, C. R. Degenhardt, *Theor. Chim. Acta* **1978**, *50*, 145–158) are different in concept, employing intramolecular photochemical [2 + 2]-cycloaddition to produce cubanes directly. Unfortunately, such cycloadditions are not applicable to the synthesis of simple cubanes; see, for example, R. Criegee, *Angew. Chem.* **1962**, *74*, 703–712; *Angew. Chem. Int. Ed. Engl.* **1962**, *1*, 519–527.

[5] Cf. T.-Y. Luh, L. M. Stock, *J. Org. Chem.* **1972**, *37*, 338–339.

[6] P. E. Eaton, R. A. Hudson, *J. Am. Chem. Soc.* **1965**, *87*, 2769–2770.

[7] D. H. R. Barton, D. Crich, W. B. Motherwell, *J. Chem. Soc. Chem. Commun.* **1983**, 939–941.

[8] References through late 1988 can be found in G. W. Griffin, A. P. Marchand, *Chem. Rev.* **1989**, *89*, 997–1010.

[9] L. Hedberg, K. Hedberg, P. E. Eaton, N. Nodari, A. G. Robiette, *J. Am. Chem. Soc.* **1991**, *113*, 1514–1517.

[10] A. Almenningen, T. Jonvik, H.-D. Martin, T. Urbanek, *J. Mol. Struct.* **1985**, *128*, 239–247.

[11] a) E. B. Fleischer, *J. Am. Chem. Soc.* **1964**, *86*, 3889–3890; b) N. L. Allinger, P. E. Eaton, *Tetrahedron Lett.* **1983**, *24*, 3697–3700.

[12] K. D. Kybett, S. Carroll, P. Natalis, D. W. Bonnell, J. L. Margrave, J. L. Franklin, *J. Am. Chem. Soc.* **1966**, *88*, 626.

[13] D. R. Kirklin, K. L. Churney, E. S. Domalski, *J. Chem. Thermodyn.* **1989**, *21*, 1105–1113.

[14] For comparison: the density of adamantane is approximately 1.09 $g cm^{-1}$.

[15] J. Alster, O. Sandus, ARDEC, personal communication.

[16] a) P. E. Eaton, B. K. Ravi Shankar, G. D. Price, J. J. Pluth, E. Gilbert, J. Alster, O. Sandus, *J. Org. Chem.* **1984**, *49*, 185–186; b) P. E. Eaton, E. Wicks, *ibid.* **1988**, *53*, 5353–5355.

[17] D. S. Reddy, M. Maggini, J. Tsanaktsidis, P. E. Eaton, *Tetrahedron Lett.* **1990**, *31*, 805–806.

[18] E. W. Della, P. T. Hine, H. K. Patney, *J. Org. Chem.* **1977**, *42*, 2940–2941.

[19] a) T.-Y. Luh, L. M. Stock, *J. Am. Chem. Soc.* **1974**, *96*, 3712–3713; b) R. E. Dixon, A. Streitwieser, P. G. Williams, P. E. Eaton, *ibid.* **1991**, *113*, 357–358.

[20] For reviews see: a) H. W. Geschwend, H. R. Rodriguez, *Org. React. N.Y.* **1979**, *26*, 1–360; b) P. Beak, V. Snieckus, *Acc. Chem. Res.* **1982**, *15*, 306–312. I am particularly grateful to Prof. Snieckus for introducing me to the power of this method.

[21] P. E. Eaton, G. Castaldi, *J. Am. Chem. Soc.* **1985**, *107*, 724–726.

[22] For somewhat related examples see: G. W. Klumpp, M. Kool, A. H. Veefkind, M. Shakel, R. F. Schmitz, *Recl. Trav. Chim. Pays-Bas* **1983**, *102*, 542–543, and references therein.

[23] a) C-H activation by an amide substituent also works for cyclopropane: P. E. Eaton, R. G. Daniels, D. Casucci, G. T. Cunkle, P. Engel, *J. Org. Chem.* **1987**, *52*, 2100–2102. b) Less strained analogues (less s character in the C-H bonds) like adamantane or cyclobutane do not show this phenomenon: R. Daniels, P. E. Eaton, unpublished results.

[24] P. E. Eaton, H. Higuchi, R. Millikan, *Tetrahedron Lett.* **1987**, *28*, 1055–1058.

[25] a) P. E. Eaton, G. Cunkle, G. Marchioro, R. M. Martin, *J. Am. Chem. Soc.* **1987**, *109*, 948–949; b) P. E. Eaton, R. M. Martin, *J. Org. Chem.* **1988**, *53*, 2728–2732.

[26] A. Bashir-Hashemi, *J. Am. Chem. Soc.* **1988**, *110*, 7234–7235.

[27] a) A. Bashir-Hashemi, P. E. Eaton, unpublished results; b) C.-X. Yang, P. E. Eaton, unpublished results.

[28] J. C. Bottaro, P. E. Penwell, R. J. Schmitt, *J. Org. Chem.* **1991**, *56*, 1305–1307; see also: D. B. Reitz, S. M. Massey, *ibid.* **1990**, *55*, 1375–1379.

[29] P. E. Eaton, C.-H. Lee, Y. Xiong, *J. Chin. Chem. Soc. (Taipei)* **1991**, *38*, 303–306.

[30] a) C. R. Hauser, H. G. Walker, *J. Am. Chem. Soc.* **1947**, *69*, 295–297; b) C. R. Hauser, F. C. Frostlick, *ibid.* **1949**, *71*, 1350–1352.

[31] P. E. Eaton, C.-H. Lee, Y. Xiong, *J. Am. Chem. Soc.* **1989**, *111*, 8016–8018.

[32] Cf. R. Sanchez, W. Scott, *Tetrahedron Lett.* **1988**, *29*, 139–142.

[33] C.-H. Lee, Ph.D. Thesis, University of Chicago, **1990**.

[34] The intermediates in many of these reactions are $R'MgNR_2$ compounds. We have dubbed them "amido Grignard reagents" and are now studying this class of Grignard reagents and their applications in synthesis. A note is made in passing: when these amido Grignard reagents are made from chiral amines, chirality transfer can be (and has been) achieved in C-C bond-forming reactions.

[35] P. E. Eaton, R. G. Daniels, D. Casucci, G. T. Cunkle, P. Engel, *J. Org. Chem.* **1987**, *52*, 2100–2102.

[36] P. E. Eaton, J. Puranik, unpublished results.

[37] For related work in other research groups see, for example: A. Bashir-Hashemi, H. L. Ammon, C. S. Choi, *J. Org. Chem.* **1990**, *55*, 416–420.

[38] P. E. Eaton, K. Pramod, R. Gilardi, *J. Org. Chem.* **1990**, *55*, 5746–5750.

[39] a) P. E. Eaton, Y. Xiong, C.-X. Yang, *J. Am. Chem. Soc.* **1990**, *112*, 3225–3226; b) R. M. Moriarty, S. M. Tuladhar, R. Penmasta, A. L. Awasthi, *ibid.* **1990**, *112*, 3228–3230.

[40] D. A. Hrovat, W. T. Borden, *J. Am. Chem. Soc.* **1990**, *112*, 3227–3228.

[41] a) A. J. H. Klunder, B. Zwanenburg, *Tetrahedron* **1972**, *28*, 4131–4138; b) P. E. Eaton, S. Reddy, G. P. Sollott, *J. Org. Chem.* **1989**, *54*, 722–723; P. E. Eaton, J. Tsanaktsidis, unpublished results.

[42] R. C. Bingham, P. von R. Schleyer, *J. Am. Chem. Soc.* **1971**, *93*, 3189–3199. See also P. Müller, J. Mareda, *Helv. Chim. Acta* **1987**, *70*, 1017–1024.

[43] a) E. Grunwald, S. Winstein, *J. Am. Chem. Soc.* **1948**, *70*, 846–854; b) T. W. Bentley, K. Roberts, *J. Org. Chem.* **1985**, *50*, 4821–4828.

[44] There are other systems which also give cations with unexpected ease. See for example: a) K. B. Wiberg, V. Z. Williams, *J. Am. Chem. Soc.* **1967**, *89*, 3373–3374; b) E. W. Della, P. M. W. Gill, C. H. Schiesser, *J. Org. Chem.* **1988**, *53*, 4354–4357.

[45] For more recent treatments of cubyl cation with molecular mechanics see: a) P. Müller, D. Milin, *Helv. Chim. Acta* **1991**, *74*, 1808–1816; b) P. Müller, D. Milin, W. Q. Feng, R. Houriet, E. W. Della, *J. Am. Chem. Soc.* **1992**, *114*, 6169–6172.

[46] The effects of electron-withdrawing groups have also been noted by others; see [39b] and D. Kevill, M. J. D'Souza, R. M. Moriarty, S. M. Tuladhar, R. Penmasta, A. K. Awasthi, *J. Chem. Soc. Chem. Commun.* **1990**, 623–624.

[47] The point has not been accepted (nor appreciated) by some authors, [39b] and [46].

[48] P. E. Eaton, J. Zhou, *J. Am. Chem. Soc.*, **1992**, *114*, 3118–3120.

[49] For a review, see: G. Szeimies, *React. Intermed. (Plenum)* **1983**, *3*, 299.

[50] For a few relevant examples, see: a) G. Szeimies, J. Harnisch, O. Baumgärtel, O. D. A. Hrovat, W. T. Borden, *J. Am. Chem. Soc.* **1977**, *99*, 5183–5184; b) D. A. Hrovat, W. T. Borden, *ibid.* **1988**, *110*, 7229–7230; c) D. A. Hrovat, W. T. Borden, *ibid.* **1988**, *110*, 4710–4718; d) J. Schäfer, G. Szeimies, *Tetrahedron Lett.* **1988**, *29*, 5253–5254.

[51] P. E. Eaton, M. Maggini, *J. Am. Chem. Soc.* **1988**, *110*, 7230–7232.

[52] 1,3-Diiodocubane is presently under investigation in my laboratory.

[53] J. Tsanaktsidis, P. E. Eaton, *Tetrahedron Lett.* **1989**, *30*, 6967–6968, and references therein.

[54] P. E. Eaton, J. Tsanaktsidis, *J. Am. Chem. Soc.* **1990**, *112*, 876–878.

[55] D. A. Hrovat, W. T. Borden, *J. Am. Chem. Soc.* **1990**, *112*, 875–876.

[56] K. Hassenrück, J. G. Radziszewski, V. Balaji, G. S. Murthy, A. J. McKinley, D. E. David, V. M. Lynch, H.-D. Martin, J. Michl, *J. Am. Chem. Soc.* **1990**, *112*, 873–874.

[57] Nevertheless, it is amusing to point out that **20** (= **20'**) is related to [2.2.2]propellane **A**, a compound synthesized many years ago in my laboratory The formation of single bonds in highly strained molecules by through-space dehalogenation has a checkered history; see footnote 2 in ref. [54] for a brief discussion. P. E. Eaton, G. H. Temme, *J. Am. Chem. Soc.* **1973**, *95*, 7508–7510.

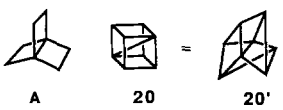

[58] R. Gilardi, M. Maggini, P. E. Eaton, *J. Am. Chem. Soc.* **1988**, *110*, 7232–7234; see also [56].

[59] O. Ermer, J. Lex, *Angew. Chem.* **1987**, *99*, 455–456; *Angew. Chem. Int. Ed. Engl.* **1987**, *25*, 447–449.

[60] R. A. Alden, J. Kraut, T. G. H. Taylor, *J. Am. Chem. Soc.* **1968**, *90*, 74–82.

[61] I am grateful to D. S. Reddy and A. Basir-Hashemi for informing me of the results of their initial exploration of this reaction.

[62] P. E. Eaton, K. Pramod, unpublished results.

[63] P. E. Eaton, Y. Xiong, unpublished results.

[64] This work is being done in collaboration with D. Walba, University of Colorado, and M. Wand, Displaytech, Inc.

[65] P. E. Eaton, M. Virtuani, K. Pramod, unpublished results. The molecular weight assigned assumes the applicability of the universal calibration parameter, see Z. Grubisic, P. Rempp, H. Benoit, *Polymer Lett.* **1967**, *5*, 753.

[66] R. E. Hormann, Ph.D. Dissertation, University of Chicago, **1987**.

[67] a) T. W. Cole, Jr., Ph.D. Dissertation, University of Chicago, **1966**; b) T.-Y. Luh, Ph.D. Dissertation, University of Chicago, **1974**.

[68] P. E. Eaton, K.-L. Hoffmann, *J. Am. Chem. Soc.* **1987**, *109*, 5285–5286.

[69] M. Jones, Jr., N. Chen, *J. Phys. Org. Chem.* **1988**, *1*, 305; *Tetrahedron Lett.* **1989**, *30*, 6969–6972.

[70] See footnotes 13, 14, 15 in ref. [68] and also a) T. J. Barton, M.-H. Yeh, *Tetrahedron Lett.* **1987**, *28*, 6421–6424; b) B. Halton, J. H. Bridle, E. G. Lovett, *ibid.* **1990**, *31*, 1313–1314.

[71] P. E. Eaton, R. B. Appell, *J. Am. Chem. Soc.* **1990**, *112*, 4055–4057.

[72] P. E. Eaton, A. J. White, *J. Org. Chem.* **1990**, *55*, 1321–1323.
[73] See, for example: N. Chen. M. Jones, Jr., W. W. White, M. S. Platz, *J. Am. Chem. Soc.* **1991**, *113*, 4981–4992; P. E. Eaton, R. Appell, W. R. White, M. S. Platz, unpublished results.
[74] R. B. Appell, Ph.D. Dissertation, University of Chicago, **1990**.
[75] P. E. Eaton, A. M. Fisher, R. E. Hormann, *Synlett* **1990**, 737–738.
[76] Photolysis of cubyl azide leads to the formation of homopentaprismanecarbonitrile. Matrix isolation studies proved insufficient to demonstrate the intermediacy of azahomocubene: P. E. Eaton, R. E. Hormann, *J. Am. Chem. Soc.* **1987**, *109*, 1268–1269.
[77] a) P. E. Eaton, Y. C. Yip, *J. Am. Chem. Soc.* **1991**, *113*, 7692–7697; b) S.-Y. Choi, P. E. Eaton, M. Newcomb, Y. C. Yip, *ibid.* **1992**, *114*, 6326–6329.
[78] For earlier examples, see: a) M. Castaing, M. Pereyre, M. Ratier, P. M. Blum, A. G. Davies, *J. Chem. Soc.* **1979**, 287; b) A. L. J. Beckwith, G. Moad, *J. Am. Chem. Soc.* **1980**, *92*, 1083, and references therein; c) K. U. Ingold. B. Maillard, J. C. Walton, *ibid.* **1981**, *93*, 970, and references therein.
[79] L. Cassar, P. E. Eaton, J. Halpern, *J. Am. Chem. Soc.* **1970**, *92*, 3515–3518.
[80] a) L. Cassar, P. E. Eaton, J. Halpern, *J. Am. Chem. Soc.* **1970**, *92*, 6366–6368; b) J. E. Byrd, L. Cassar, P. E. Eaton, J. Halpern, *J. Chem. Soc. Chem. Commun.* **1971**, 40–41.
[81] P. E. Eaton, C.-T. Chou, K. Pramod, unpublished results.
[82] a) P. E. Eaton, S. Giacobbe, S. Cohen, Poster Presentation, Amoco Oil Company, October, **1991**; b) P. E. Eaton, C. T. Chou, S. Giacobbe, L. Zhu, unpublished results.
[83] See, for example: F. L.Klavetter, R. H. Grubbs, *J. Am. Chem. Soc.* **1988**, *110*, 7807–7813.

Oxoniobates Containing Metal Clusters

By Jürgen Köhler,* Gunnar Svensson,* and Arndt Simon*

Dedicated to Professor Rudolf Hoppe on the occasion of his 70th birthday

Metal clusters, discrete or condensed, are characteristic of the structures of many compounds which contain transition metals in low oxidation states. The highly reduced oxoniobates support the concept of condensed clusters. They contain Nb_6O_{12} clusters which are either isolated or linked at the apices of the Nb_6 octahedra to form oligomeric chains or networks. The analysis of the bonding relationships allows the identification of different types of Nb atoms and thus the quantitative prediction of valence electron concentrations for finite or infinite structures composed of these condensed M_6X_{12} clusters.

1. Introduction

Metal–metal bonding and metal clusters have changed our understanding of the chemistry of metals in low oxidation states. It is not that long ago that elements in a large section of the periodic table were assigned only integer oxidation states. Only structural insight shows that the oxidation state II for molybdenum in $MoCl_2$—just to take one example—is more or less accidental, as the $[Mo_6Cl_8]^{n+}$ cluster in this compound could well take other values than $n = 4$. The rich chemistry of reduced niobium halides avoids integer oxidation states in spite of strictly stoichiometric compositions. The most metal-rich chlorides and iodides of niobium are $NbCl_{1\,4/6} = NbCl_{2.\bar{3}}$[1] and $NbI_{1\,1/6} = NbI_{1.8\bar{3}}$,[2] and not the dihalides. The allowance for such unusual compositions is due to the fact that any excess of valence electrons on the metal atoms can be used for covalent M–M bonding with the formation of $[Nb_6Cl_{12}]^{2+}$ and $[Nb_6I_8]^{3+}$ clusters in the compounds mentioned above. Such clusters had to be recognized for the understanding of the remarkably strict stoichiometry of NbO,[3] a compound with "divalent" niobium which formally has a defect rocksalt structure but is actually a "condensate" of Nb_6O_{12} clusters linked through all the apices of the Nb_6 octahedra.[4]

Numerous compounds turned out to contain such condensed clusters.[5] In particular, condensation along edges or faces of M_6 octahedra is quite common and leads to a wealth of oligomeric and infinite cluster structures as in, for example, the oxomolybdates[6–8] and molybdenum chalcogenides.[9, 10] Compared to this mode of condensation the linkage through apices of the M_6 octahedra, as found in NbO, was rare and the number of examples negligible. However, after the discrete Nb_6O_{12} cluster had been found in an oxoniobate,[11] one hoped for a rich chemistry for compounds with condensed clusters, intermediates between a compound containing isolated clusters and the final member, NbO, with clusters joined through all the apices. This approach created sufficient interest for the investigation of reduced oxoniobates with a wide variety in the countercations and the Nb/O ratio. The suspicion that reduced oxoniobates might exhibit superconductivity at room temperature[12] led to an increased interest in reduced oxoniobates and resulted in an number of investigations. So far, the hope of finding new high-temperature superconductors has not been fulfilled. Nevertheless, superconductivity below 12 K has been found in various reduced oxoniobates.[13–16]

The field of reduced oxoniobates has grown to such an extent, that at this stage a review seems desirable, in which the known compounds are listed, the structural and bonding principles are outlined, and some physical properties are summarized.

2. Preparation and Characterization

At first glance the syntheses of reduced oxoniobates seem to be rather straightforward. They can be carried out as solid-state reactions from appropriate mixtures of binary or ternary starting compounds with Nb and NbO as reducing agents. In spite of this rather basic approach, special care is necessary for a number of reasons. Most of the starting materials and products are solids up to very high temperatures leading to low reaction rates even at temperatures above 1300 K. At these temperatures volatile components like alkali metal oxides may react with the container material. In order to prevent evaporation of the reaction components inert gas atmosphere is thus always preferred over vacuum. Reduced oxoniobates, in particular those in which the Nb atoms have an average oxidation state well below IV, have very low oxygen partial pressures[18] and call for special container materials. Most often sealed Au, Pt, or Nb ampules or corundum crucibles are used; in the latter two cases, the ampule or the reaction mixture is protected by an Ar-filled quartz ampule.[19–21] Ampules made solely of quartz can be used at temperatures up to 1500 K; however, the walls of the reaction vessel are attacked to some extent.[11, 20, 22, 23] Alkaline or alkaline earth compounds react partially with formation of silicates. When traces of moisture are present, chemical transport reactions lead to noticeable changes in the compositions of the products, for example the formation of Nb_5Si_3 via $SiO_{(g)}$.[24] Closed Pt tubes allow temperatures up to 1800 K. Nb ampules seem best for the syntheses as they do not introduce any components not already in the starting materials. They can be used above

[*] Dr. J. Köhler, Dr. G. Svensson,[+] Prof. A. Simon
Max-Planck-Institut für Festkörperforschung
Heisenbergstrasse 1, D-W-7000 Stuttgart 80 (FRG)

[+] Permanent address: Arrhenius Laboratory
Department of Inorganic Chemistry, University of Stockholm
S-10691 Stockholm (Sweden)

 © *VCH Verlagsgesellschaft mbH, W-6940 Weinheim, 1992* *0570-0833/92/1111-1437 $ 3.50+.25/0*

2300 K in an inert gas atmosphere. However, Nb ampules can be used only for the preparation of the most reduced compounds which are stable in equilibrium with elemental Nb.

Of course, what has been said about container materials holds true for the system components. Only oxides of very electropositive metals can be used to provide the countercations in the reduced oxoniobates, because all others will be reduced to their elemental state during the synthesis.

Besides Nb and NbO, carbon has also been used to reduce mixtures of $BaCO_3$ and Nb_2O_5 under vacuum at temperatures between 1500 and 1900 K.[25, 26] It is even possible to reduce $BaNb_2O_6$ in a hydrogen flow at 1600 K with the formation of $Ba_2Nb_5O_9$.[27]

Mineralizers or fluxes such as alkaline or alkaline earth fluorides, chlorides, or borates have been used successfully to reduce the necessary reaction temperatures, in particular, to obtain single-crystal specimens.[20, 22, 28–32] However, fluxes can lead to unintended changes of the compositions of the reaction products. Phosphates cannot be used as flux materials since they are reduced with the formation of NbP.[33] In several cases a compound did not form when a flux was employed, as was seen for $NaNb_3O_6$. When using fluorides as mineralizers one always has to bear in mind that fluorine can be incorporated into the crystal lattice and is indistinguishable from oxygen in X-ray investigations.

In many cases the crystal structures of reduced oxoniobates proved to be extremely complicated, and single crystals were essential for solving their structures and determining their compositions. Others, fortunately, were simple enough to be solved by X-ray powder methods. Particularly for the more reduced oxoniobates the early investigations were limited to microcrystalline products; here high-resolution electron microscopy gave valuable insight into structures and structural relationships.

3. On the Way Toward Clusters

Besides many examples of fully oxidized oxoniobates a large number of reduced phases with Nb atoms in oxidation states between IV and V are known. With a few exceptions

Jürgen Köhler was born April 11, 1953, in Bobenheim am Rhein (FRG). He studied chemistry at the Justus-Liebig-Universität in Giessen and completed his doctorate in 1984 under the direction of R. Hoppe in the area of alkali metal oxogallates and oxothallates. Since 1984 he has been in the research group of A. Simon at the Max-Planck-Institut für Festkörperforschung in Stuttgart. His research interests focus on the preparation and characterization of metal-rich oxides and reduced fluorides of the rare-earth metals, as well as the oxidation of metals at low temperatures. He is also interested in the development of new methods for recognizing relationships between crystal structures.

Gunnar Svensson was born in 1960 in Sweden. He received his Ph.D. in 1989 at the Institute for Inorganic Chemistry at the University of Stockholm under the direction of L. Kihlborg. He received an Alexander von Humboldt stipend in 1991 and joined the research group of A. Simon for a year, during which he prepared and characterized reduced oxoniobates. He has been on the staff of the Institute for Inorganic Chemistry at the University of Stockholm since 1992. His research interests lie in the preparation of transition metal oxides and oxonitrides and their characterization with high-resolution electron microscopy as well as with powder and single-crystal X-ray diffraction.

Arndt Simon was born in January 1940 in Dresden. He started his chemistry studies in 1960 at the University of Münster and received his Ph.D. in 1966 for his research with H. Schäfer. After his habilitation in 1972 he became a professor of inorganic chemistry in Münster. He was made a member of the Max-Planck-Gesellschaft and director at the Max-Planck-Institut für Festkörperforschung in Stuttgart in 1974. In 1975 the University of Stuttgart made him an honorary professor. He turned down offers from the University of Münster (successor of H. Schäfer, 1979) and Cornell University (successor of M. J. Sienko, 1985). His research interests range from the studies of metal-rich compounds such as alkali metal suboxides, cluster compounds of heavy d metals, and metal-rich binary and ternary halides of the lanthanoids to the development of new apparatus (Guinier–Simon camera), and the structure and phase transformations in molecular crystals. Further interests include the structure relationships of intermetallic compounds and the investigation of superconductors with the goal of understanding the chemical basis for the phenomenon.

these compounds crystallize in several basic structure types, namely perovskite,[34, 35] tetragonal tungsten bronze (TTB),[36, 37] and $Ba_3Nb_8O_{21}$ types.[38, 39] As in the block-type structures,[40–43] these compounds are built mainly from NbO_6 octahedra. They do not have direct M–M bonds even when they are metallic. These compounds contrast the more reduced nonmetallic oxides $ANbO_2$ (A = Li, Na),[44, 45] which adopt a filled MoS_2 structure in which the A atoms occupy octahedral voids between trigonal-prismatic NbO_2 layers. It is not unusual that atoms with d^2 configuration prefer trigonal-prismatic coordination. The short Nb–Nb distances ($LiNbO_2$ 290, $NaNbO_2$ 295 pm) give evidence for M–M bonding, and Extended Hückel (EH) calculations provide further support.[46]

Although $LiVO_2$ undergoes a phase transition with formation of trigonal V_3 clusters having short V–V distances,[47] this could not be found for the corresponding niobates. Deintercalation of $LiNbO_2$, by the way, leads to Li_xNbO_2 ($x \approx 0.45$) which becomes superconducting at temperatures below 11 K.[13] This property seems closely related to a tendency towards structural instability caused by charge density waves, that is, a tendency to distortion accompanied by cluster formation. Such transitions from a delocalized to a localized electronic system are well known, for example for NbO_2.[48–50] In the high-temperature (HT) form of NbO_2 the chains of *trans*-edge-sharing NbO_6 octahedra are undistorted, the electrons are delocalized, and the compound is metallic. In the low-temperature (LT) form every second joined edge is lengthened, and the Nb atoms form pairs with short Nb–Nb distances (274 pm) corresponding to Nb–Nb single bonds (Fig. 1).[*]

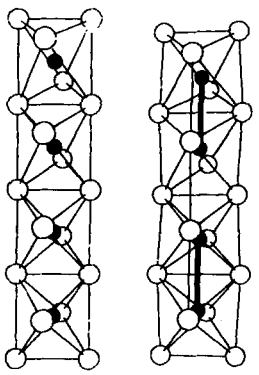

Fig. 1. Chains of *trans*-edge-sharing NbO_6 octahedra in HT-NbO_2 (left) and LT-NbO_2 (right).

A discrete Nb_2O_8 cluster (Fig. 2) was first discovered in the isotypic compounds $NaNb_3O_{6-x}F_x$ ($0 \leq x \leq 0.5$),[20, 51] $Ca_{0.75}Nb_3O_6$,[52] and $Ca_{0.95}Nb_3O_6$.[53] Similar units are also found as molecular species, for example $[Re_2Cl_8]^{n-}$,[54] as well as in the crystal structures of reduced rare earth rhenium oxides such as $La_4Re_6O_{19}$.[55] In the above-mentioned compounds with Nb_2O_8 clusters each Nb–Nb dumbbell is surrounded by four additional Nb atoms with octahedral coordination (indicated by dashed lines in Fig. 2). In $NaNb_3O_6$ the Nb–Nb distances within the dumbbells of Nb(1) atoms are 262 pm and between atoms Nb(1) and Nb(2) 308 pm.

[*] In this and subsequent figures the Nb and O atoms are represented by small black and large white circles, respectively. Large cations (Fig. 4 and following) are denoted by hatched circles.

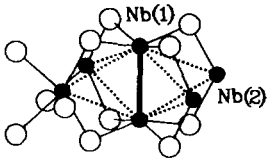

Fig. 2. Nb_2O_8 cluster in $NaNb_3O_6$ and related compounds together with surrounding Nb atoms and a coordination octahedron for one of these. Heavy lines indicate Nb–Nb multiple bonding, dotted lines weak Nb–Nb bonding.

The corresponding distances in the isotypic Ca compounds are a little shorter. The long Nb–Nb distances can still be interpreted in terms of weak M–M bonding. An extensive discussion of the bonding on the basis of EH calculations[56] for $NaNb_3O_6$ supports the hypothesis that the Nb–Nb bond within the dumbbell is a double bond and that some additional Nb–Nb bonding to the four surrounding Nb atoms is present.

4. Principles of Structures Based on the Nb_6O_{12} Cluster

The compounds to be discussed in this section contain the most complicated as well as very simple structures. The common principle in these structures is the common close-packing of structural units which have comparable sizes. These units are O atoms, Nb_6 octahedra, and large A atoms which serve as countercations. The description of the compounds will start with those containing discrete Nb_6O_{12} clusters and end with those with condensed cluster phases.

4.1. Discrete Nb_6 Octahedra

Since the early discovery of a compound containing discrete Nb_6O_{12} clusters[11] a whole series of reduced oxoniobates with such clusters has been found (Table 1). A $Nb_6O^i_{12}O^a_6$ cluster is shown in Figure 3. The twelve O atoms above the edges of a Nb_6 octahedron belong to the inner sphere and form a cuboctahedron. They are designated O^i if they belong to one cluster, or O^{i-i} if they connect adjacent clusters.[4] As many as six O atoms above the apices of the octahedron constitute the outer ligand sphere and may belong to one cluster only (O^a), or link clusters with identical (O^{a-a}), as well as different functionality (O^{a-i}, O^{i-a}).

In each compound given in Table 1 the Nb–Nb distances in the Nb_6O_{12} cluster fall within the narrow range of 279–289 pm. The distances between the Nb and O^a atoms are usually between 215 and 235 pm, while Nb–O^i distances range from 202 to 213 pm, which is about $1/2 \times \sqrt{2} \times d_{Nb-Nb}$ (285 pm). Therefore, each Nb atom lies no further than 5 pm from the plane formed by four surrounding O^i atoms (inside the cuboctahedron). This situation is different with Nb_6X_{12} clusters with X = Cl or Br in which the distances d_{Nb-Nb} are much smaller than $\sqrt{2} \times d_{Nb-X}$ resulting in a contraction of the M_6 octahedron relative to the X_{12} cuboctahedron. For topological reasons the Nb_6O_{12} clusters are therefore much more suited for a condensation through the apical atoms then the corresponding halide clusters; in addition, ligand deficiency is easier to attain with (divalent) oxygen than with (monovalent) halogen atoms.

As mentioned above, O atoms, Nb_6 octahedra, and, if present, large atoms of the electropositive metal A (A = Na,

Table 1. Unit cell parameters [pm] and properties of compounds containing discrete Nb_6O_{12} clusters.

Compound	Space group	a	b	c	Z	Color	Electrical property [a]	Ref.
$Mg_3Nb_6O_{11}$	$P\bar{3}m1$	604.2	–	746.6	1	dark green	s	[19, 21]
$Mn_3Nb_6O_{11}$	$P\bar{3}m1$	608.0	–	762.7	1	dark green	s	[21]
$Na(V_{3-x}, Nb_x)Nb_6O_{14}$ ($x \approx 1.0$)	$p6_3/m$	1603.4	–	1807.9	3	golden [b]	s	[62]
$Na_3Al_2Nb_{34}O_{64}$	$R\bar{3}$	784.4	–	7065.0	3	golden [b]	s	[22]
$Na(SiNb)Nb_{10}O_{19}$	$R\bar{3}$	784.1	–	4221.8	6	red	s	[22]
$K(SiNb)Nb_{10}O_{19}$	$R\bar{3}$	783.7	–	4236.0	6	golden [b]	–	[33]
$K_3Al_2Nb_{34}O_{64}$	$R\bar{3}$	783.0	–	7051.0	3	golden [b]	–	[33]
$K_4Al_2Nb_{35}O_{70}$	$P\bar{3}$	782.2	–	2632.0	1	brown	–	[33]
$KSiNb_{10}O_{19}$	$P6_3$	779.2	–	1443.0	2	golden [b]	–	[33]
$Rb_4(SiNb)_2Nb_{35}O_{70}$	$P\bar{3}$	782.1	–	2651.3	1	golden [b]	–	[71]
$Ba_3Si_2Nb_{20.8}O_{44}$	$P\bar{3}$	777.4	–	1676.5	1	black	–	[11]
$BaSiNb_{10}O_{19}$	$P6_3$	777.7	–	1451.0	2	black	s	[63]
$Ba_2Nb_{15}O_{32}$	$R\bar{3}$	777.7	–	3551.8	3	golden [b]	s	[32]
KNb_8O_{14}	*Pbam*	935.2	1026.8	592.9	2	golden [b]	s	[72]
$KNb_8O_{14-x}F_x$ ($x \approx 1.0$)	*Pbam*	932.7	1028.0	593.7	2	golden [b]	s	[72]
$SrNb_8O_{14}$	*Pbam*	925.7	1030.1	595.4	2	golden [b]	s	[28]
$BaNb_8O_{14}$ (I)	*Pbam*	931.1	1033.1	595.4	2	golden [b]	s	[30]
$BaNb_8O_{14}$ (II)	*Pcab*	2371.0	1036.0	942.2	8	golden [b]	s	[30, 32]
$LaNb_8O_{14}$	*Pbam*	919.4	1033.7	596.2	2	golden [b]	s	[72]
$EuNb_8O_{14}$	*Pbam*	927.7	1031.1	596.4	2	golden [b]	s	[73]
$NaNb_{10}O_{18}$	$P2_1/c$ ($\beta = 110.48°$)	784.9	931.6	1028.1	2	golden [b]	m	[29]

[a] s = Semiconducting, m = metallic. [b] Extrinsic property.

K, Rb, Sr, Ba, La, Eu) form a conventional close-packing. Smaller M atoms fill tetrahedral (M = Al, Si, Mg, Mn), octahedral (M = Nb, V, Mg, Mn), and trigonal-bipyramidal voids (M = V, Nb) within the O sublattices. These additional atoms stabilize the structures and formally act as electron donors for the Nb_6O_{12} clusters.

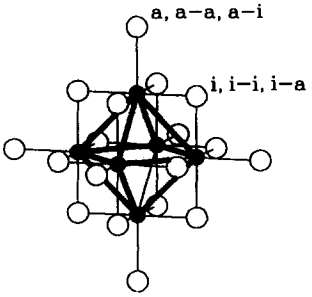

Fig. 3. $Nb_6O^i_{12}O^a_6$ cluster with notations according to ref. [4].

In the following discussion the structural principle of a common close-packing is outlined in more detail. The structures known at present can be described and compared on the basis of only a few features. As usually done with close-packed arrangements of spheres, the packings are decomposed into 3^6 layers[57] which are of four types in the structures discussed here. The first is made up solely of O atoms, the second consists of A and O atoms, the third contains O atoms and Nb_6 octahedra, and the fourth is composed of O and A atoms together with Nb_6 octahedra. The latter two allow an infinite number of different arrangements (and compositions). Only the layer types with Nb_6 octahedra shown in Figure 4 a–e have been found so far. The layers shown in Figure 4a and b have Nb_6:O ratios of 1:3 and 1:6, respectively. They represent the limiting cases with all O atoms bonded as O^{i-i} (layer a) and O^i atoms (layer b). A particularly simple case in between with both O^i and O^{i-i} atoms is one which contains linear chains with O^{i-i} bridges

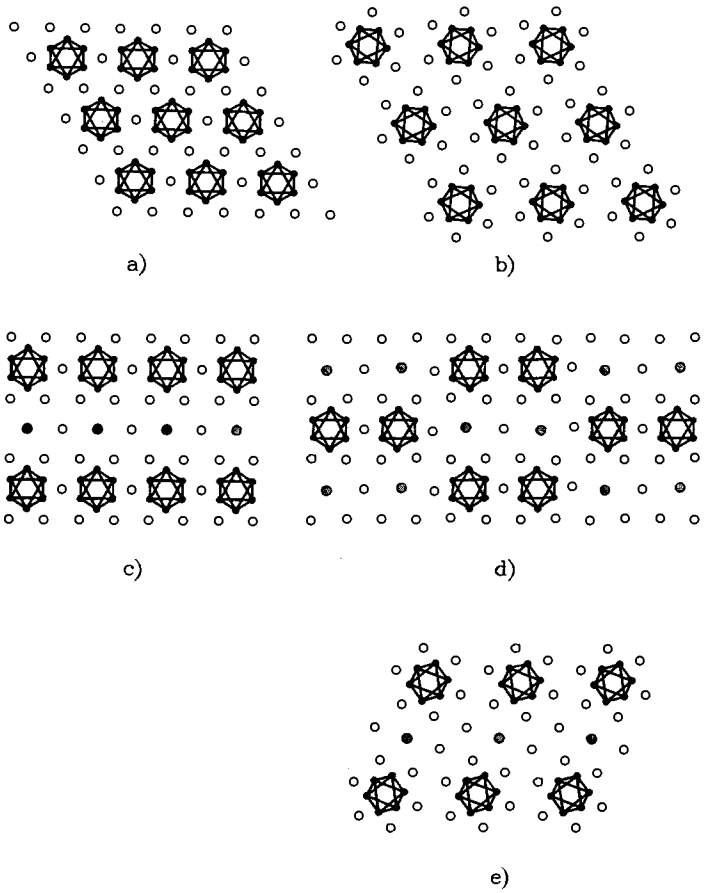

Fig. 4. Common close-packed layers of large cations, O atoms, and Nb_6 octahedra as found in reduced oxoniobates with discrete Nb_6O_{12} clusters.

as in $Nb_6O^i_4O^{i-i}_{2/2}$. Such chains separated by AO chains occur in the layers c and have the composition ANb_6O_6. Variations are possible when the chains are terminated by "chemical shear".[86] Layer d is an example of a layer with only one O^{i-i} bridge. It has the composition $Nb_6O_{11} + A_2O =$

$A_2Nb_6O_{12}$. Last but not least, layer e is related to type b in so far as all O atoms around the Nb_6 octahedron are of O^i type. Such nonconnected cluster sections are combined with a zigzag AO_2 chain to yield a layer with the composition ANb_6O_8.

There are certain (trivial) rules to be obeyed when stacking such individual layers. Three O atoms are added above and below the Nb_6 unit in order to complete the Nb_6O_6 fragment and form a Nb_6O_{12} cluster. A stacking of only type a layers leads to the structure of NbO. In metal-rich oxoniobates with discrete Nb_6O_{12} clusters discussed in subsequent sections, layers of types a–e are always surrounded by pure O or AO_x layers.

For a simplified description of the existing compounds it is helpful to limit the discussion to characteristic slabs formed from several layers. Figure 5 summarizes the different kinds which have been found. Type I slabs contain the Nb_6O_{12} clusters and are of primary interest. The index a–e is included in the notation to indicate the kind of central

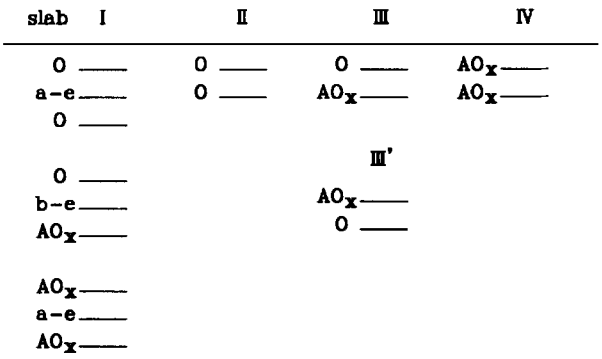

Fig. 5. Schematic representation of characteristic slabs formed from close-packed layers in compounds with discrete Nb_6O_{12} clusters (see text).

layer according to Figure 4. No differences are made, however, with respect to whether the envelope consists of pure O or AO_x layers. These differences enter the notation (II–IV) for the types or contacts between the cluster slabs.

Layers a: The structures of $M_3Nb_6O_{11}$ (M = Mn, Mg),[19, 21] and $Na(V_{3-x}Nb_x)Nb_6O_{14}$[62] (idealized $NaV_2Nb_7O_{14}$) contain type I_a slabs (Figs. 6 and 7). The particularly simple atomic arrangement in $Mg_3Nb_6O_{11}$ is well suited to illustrate the system of notation. The sequence I_a,

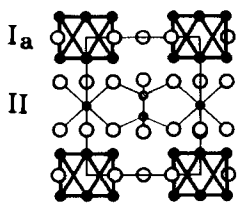

Fig. 6. Projection of the structure of $Mg_3Nb_6O_{11}$ on (100) in the range $-0.5 \leq x \leq +0.5$. Small gray circles represent Mg atoms. MgO_4 tetrahedra and MgO_6 octahedra are highlighted.

II... indicates that layer a is surrounded by layers of O atoms and that the resulting type I_a slabs are simply stacked. Mg atoms occupy one-fourth of the tetrahedral and one-fourth of the octahedral holes between the layers of O atoms in such a way that the MO_6 octahedra and MO_4 tetrahedra are

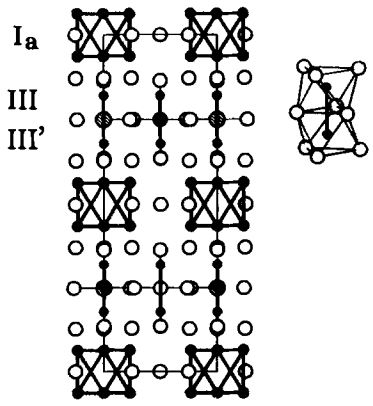

Fig. 7. Projection of the structure of $NaV_2Nb_7O_{14}$ on (100) in the range $-0.5 \leq x \leq +0.5$ and the separate drawing of a V_2O_9 cluster.

linked only by shared corners. The structure of $Na(V_{3-x}Nb_x)Nb_6O_{14}$ can be described by the sequence I_a, III, III' .... The combination of III and III', in this case, results in a hexagonal stacking of the O, AO_x, and O layers leading to trigonal-bipyramidal voids occupied by Nb atoms. Moreover, pairs of face-sharing O_6 octahedra are present, both of which are filled by V atoms forming V_2O_9 clusters. Such M_2X_9 clusters are known, for example, from the halides $Cs_3M_2Cl_9$ (M = Cr, Mo, W).[60, 61] The M atoms are shifted towards one another in the case of M = Mo and W to form short M–M bonds of 261 and 251 pm, respectively. The lack of M–M bonding when M = Cr is indicated by shifts in opposite directions (d_{Cr-Cr} = 313 pm). The V_2O_9 cluster has the same topology as the Cr complex; however, the V–V distance is short enough (256 pm) that M–M bonding must be assumed. The distances between the V atoms and O atoms of the common face are 207 pm and longer than the other V–O distances of 199 pm.

Layers b: Six structure types containing type I_b slabs have been found so far. They all crystallize in trigonal space groups with *a* axes of nearly equal length (777–784 pm). The number of layers per unit cell in a structure can be calculated by dividing the length of the *c* axis by the average repeat distance of neighboring layers ($\approx$235 pm).

The simple sequence I_b, III'... is found in the structure of $BaSiNb_{10}O_{19}$;[63] the isotypic compound $KSiNb_{10}O_{19}$[33] is also known (Fig. 8). Single Nb and Si atoms occupy octahe-

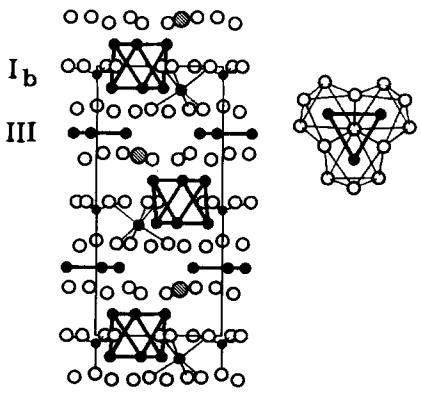

Fig. 8. Projection of the structure of $BaSiNb_{10}O_{19}$ on (210) together with a drawing of a Nb_3O_{13} cluster (d_{Nb-Nb} = 282 pm).

dral and tetrahedral sites, respectively, within slab I_b. Additional Nb atoms fill three adjacent octahedral voids in III'. The common edges of the coordination octahedra are rather long (314 pm), and the Nb atoms form a Nb_3 triangle with short Nb–Nb distances (282 pm). Thus, $MSiNb_{10}O_{19}$ contains a second metal cluster, Nb_3O_{13}, as well as Nb_6O_{12}. The M_3O_{13} cluster is well known from the oxomolybdates, $M_2Mo_3O_{13}$ (M = Li, Zn, Sc, Ni...),[64, 65] which have a variable number of valence electrons (6–8) in M–M bonding states.[66, 67] A comparable variability of the electron count is found with halide clusters Nb_3X_8 (X = Cl, Br).[68, 69] As will be shown later, the Nb_3O_{13} cluster can act as an electron buffer in reduced oxoniobates.

A sufficient amount of Si is necessary for the formation of $KSiNb_{10}O_{19}$, otherwise a compound with nearly the same composition, $K(Si_xNb_{1-x})Nb_{10}O_{19}$,[33] but a completely different structure is formed which is isotypic to $Na(Si_xNb_{1-x})Nb_{10}O_{19}$ ($x \approx 0.75$)[22, 70] (Fig. 9). In this structure type I_b slabs are directly joined, and these twin slabs alternate with intermediate slabs III and III' to form the sequence I_b, I_b, III, III' .... As in $BaSiNb_{10}O_{19}$, octahedral and tetrahedral holes within I_b are occupied by Nb and Si atoms, respectively. Yet, there is a crucial difference. Since the coordination tetrahedron about Si has a common face with one of the coordination octahedra about Nb, they can be occupied only alternately (Fig. 9). The $Si^{IV}:Nb^{V}$ ratio is approximately 0.75, and the variation of this ratio is another type of electron buffer. The occupation of octahedral voids within III and III' by Nb atoms follows the same pattern as in $BaSiNb_{10}O_{19}$; however, another mode of cluster formation arises from these neighboring slabs. Nb atoms pair up across the slabs (d_{Nb-Nb} = 274 pm), that is, the NbO_6 octahedra are joined along common edges as in LT-NbO_2 (Fig. 1). This bonding situation is typical for Nb^{IV} with a d^1 configuration.

The compound $A_3Al_2Nb_{34}O_{64}$(A = Na, K) provides one more example of a structure type[22, 23] that contains all the features discussed so far, and in spite of its complexity, illustrates the underlying simple building block system. The structure is described by the sequence I_b, III', I_b, III, I_b, III, III'... (Fig. 10). Single Nb atoms fill octahedral voids within slabs I_b, and Al atoms occupy tetrahedral voids. M–M-

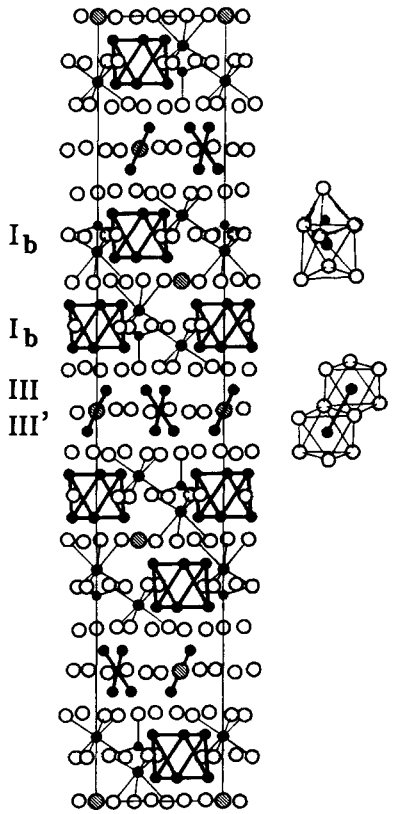

Fig. 9. Projection of the structure of $Na(Si_xNb_{1-x})Nb_{10}O_{19}$ on (210) with separate drawings of the Nb_2O_{10} cluster and the adjacent octahedral and tetrahedral voids which are occupied alternately with Nb and Si, respectively.

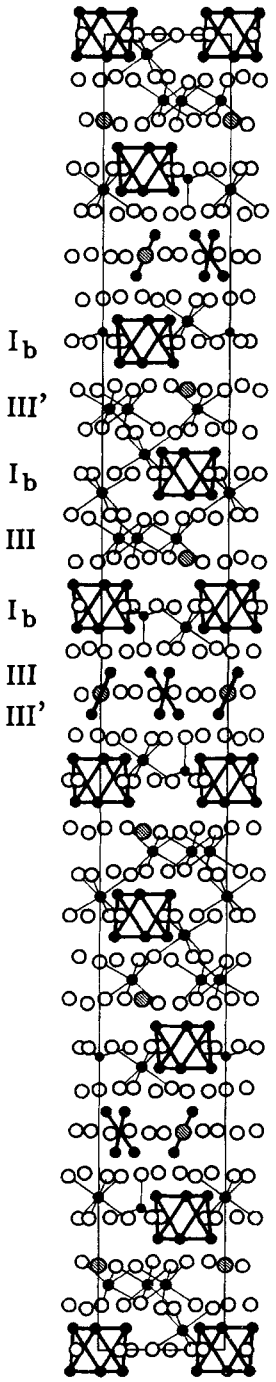

Fig. 10. Projection of the structure of $Na_3Al_2Nb_{34}O_{64}$ on (210).

bonded Nb_2 units are formed across neighboring slabs III, III' as in $Na(Si_xb_{1-x})Nb_{10}O_{19}$. The octahedral voids in the single slabs of types III and III' are occupied as in $BaSiNb_{10}O_{19}$, but in contrast, the Nb–Nb distances within the Nb_3O_{13} unit are considerably longer (317 pm).

In the structures of $Ba_3Si_2Nb_{20.8}O_{44}$,[11] $M_4(SiNb)_2Nb_{35}O_{70}$ (M = K, Rb),[33, 71] and $Ba_2Nb_{15}O_{32}$[32] one more feature is added (Figs. 11–13). Neighboring AO_6 layers lead to the formation of type IV slabs. Only one-seventh

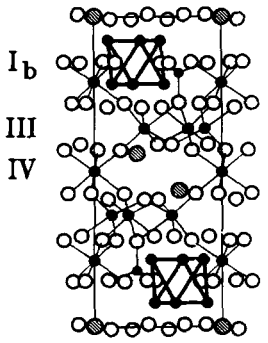

Fig. 11. Projection of the structure of $Ba_3Si_2Nb_{20.8}O_{44}$ on (210).

of the octahedral voids between the layers can be occupied, resulting in more highly oxidized compounds with an O:Nb ratio ≥ 2.0 in contrast to the compounds discussed previously in which the O:Nb ratio is < 2.0. The existence of only a few links between the layers of type IV slabs always leads to platelike crystals and easy cleavage parallel to IV. Besides these mechanical consequences of the weak bonding between the layers, there are chemical consequences. The distances between AO_6 layers and thus the size of the octahedral void can vary and allow an occupation by Nb atoms in different oxidation states (IV, V, or of intermediate valency). Thus, we meet yet another kind of electron buffer in the reduced oxoniobates.

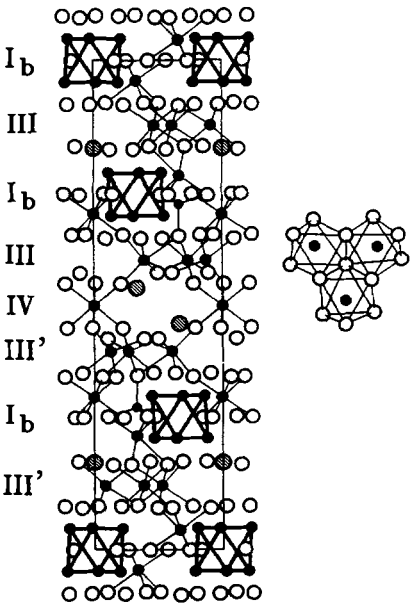

Fig. 12. Projection of the structure of $Rb_4(SiNb)_2Nb_{35}O_{70}$ on (210) together with a drawing of a Nb_3O_{13} unit ($d_{Nb \cdot Nb} = 335$ pm).

More about the electronic buffer mentioned previously, the Nb_3O_{13} unit, can be learned from $Rb_4(SiNb)_2Nb_{35}O_{70}$.[71] As seen in Figure 12 there are two different kinds of such units. Those which are sandwiched by two I_b slabs exhibit Nb–Nb distances of 306 pm indicating weak Nb–Nb bonding; in contrast those between slabs I and IV have Nb–Nb distances of 335 pm. In all compounds known so far, shortened Nb–Nb distances within Nb_3O_{13} units are only observed if these units are embedded between type I_b slabs, cf. $BaSiNb_{10}O_{19}$, $Ba_3Si_2Nb_{20.8}O_{44}$, and $Ba_2Nb_{15}O_{32}$.

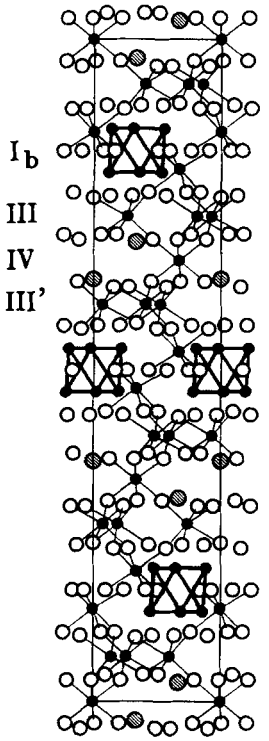

Fig. 13. Projection of the structure of $Ba_2Nb_{15}O_{32}$ on (210).

$Rb_4(SiNb)_2Nb_{35}O_{70}$ allows for a most intricate adjustment of electronic balance. Besides the buffer systems previously discussed, the $Si^{IV}:Nb^{V}$ ratio in adjacent tetrahedral and octahedral voids (cf. $Na(Si_xNb_{1-x})Nb_{10}O_{19}$) and the partial occupation of the cuboctahedral voids with Rb atoms come into play. As will be discussed later, this introduces considerable ambiguity into the determination of a "magic" concentration of valence electrons for the Nb_6O_{12} cluster.

Layers c: The structure of the compounds ANb_8O_{14} (A = K, Sr, Eu)[72, 28, 73] is shown in Figure 14. Type I_c slabs are stacked simply with a repeat length of 930 pm for two I_c

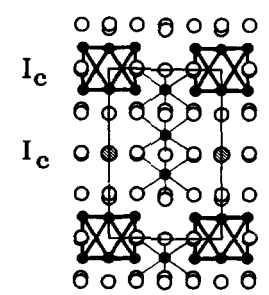

Fig. 14. Projection of the structure of $SrNb_8O_{14}$ on (010) in the range $-0.25 \leq x \leq +0.25$. The NbO_6 octahedra are highlighted; I_c slabs appear different because of a relative shift by 0.5 in the viewing direction.

slabs. Adjacent voids are filled by Nb atoms such that two NbO_6 octahedra have a common corner. Together with the surrounding A atoms, the part of the structure between the clusters represents a fraction of the perovskite structure. Many more examples of such intergrowth will be described in connection with condensed clusters.

Layers d: Larger countercations in ANb_8O_{14} (A = Ba, La) lead to structures significantly different from that of $SrNb_8O_{14}$. Although an isotypic phase of $BaNb_8O_{14}$[30] was observed, the broad lines of the X-ray diagram indicate severe disorder. Careful annealing leads to a new structure which still contains some disorder (C-centered lattice type[30]) or is entirely ordered (primitive lattice[32]). The ordered structure of $BaNb_8O_{14}$ with a simple stacking of I_d slabs is shown in Figure 15. The infinite chains of O^{i-i} linked Nb_6O_{12} clusters as they occur in $SrNb_8O_{14}$ are interrupted after two clusters. This chemical shear also disrupts the linear arrangement of Ba atoms. As a result the surrounding O_{12} cuboctahedron is larger than between I_c slabs. $LaNb_8O_{14}$[72] has been found with only an even more pronounced disorder.

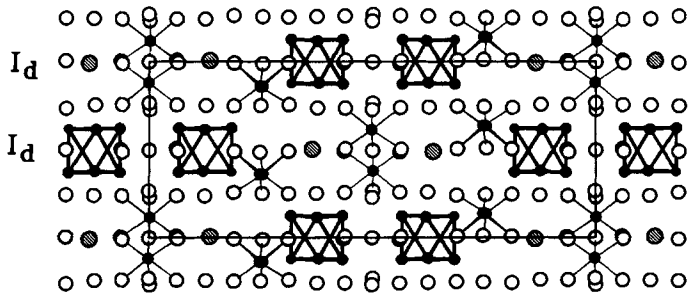

Fig. 15. Projection of the ordered structure of $BaNb_8O_{14}$ on (100) in the range $-0.25 \leq x \leq +0.25$. I_d slabs appear different because of a relative shift by 0.5 in the viewing direction.

Layers e: Finally, I_e slabs connected to one another are found in the structure of $NaNb_{10}O_{18}$[29] (Fig. 16). Compared to the structure of $SrNb_8O_{14}$, the Nb_6 octahedra here are even more separated as no O^{i-i} bridges occur. Four additional Nb atoms occupy octahedral sites, which are linked along shared edges to form a chain fragment. The central Nb–Nb distance is 294 pm, two outer Nb–Nb distances are 313 pm. The outer Nb atoms of such chain fragments exhibit short distances to Nb atoms of the cluster (309 pm), in contrast to the corresponding distances in $SrNb_8O_{14}$, which are considerably longer (330 pm).

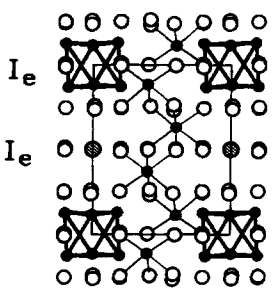

Fig. 16. Projection of the structure of $NaNb_{10}O_{18}$ on (001) in the range $-0.25 \leq x \leq +0.25$. I_e slabs appear different because of a relative shift by 0.5 in the viewing direction.

The structures discussed so far are built from discrete Nb_6O_{12} clusters linked by O atom bridges. In the following section structures will be shown in which such units share Nb atoms, resulting in condensed clusters.

4.2. Condensed Nb_6 Octahedra

Nb_6O_{12} clusters can be condensed in one, two, or three dimensions. Although a number of such compounds has been found during the last four years, at present $K_4Al_2Nb_{11}O_{21}$ is the only representative with oligomeric clusters.[74, 75] This compound contains two Nb_6 units condensed at a common vertex to form the cluster $[Nb_{11}O^i_{20}]O^a_{10}$ (Fig. 17). The Nb–Nb distance from the central Nb atom to the eight neighboring Nb atoms (289 pm) is significantly longer than the others in the cluster (280 or 284 pm).

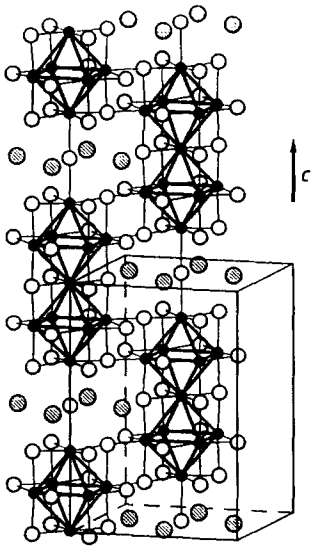

Fig. 17. Unit cell and a characteristic section of the structure of $K_4Al_2Nb_{11}O_{21}$.

Each cluster is connected to eight neighboring clusters by O^{i-a} bridges forming a three-dimensional network. This linkage yields rather short Nb–Nb distances of 308 pm between clusters, which will be discussed later in more detail. In the z direction the clusters are rather weakly connected by two linear O^{a-a} bridges.[76] Within the three-dimensional cluster framework the voids are occupied by K and Al atoms.

As in compounds containing discrete Nb_6O_{12} clusters, the atomic arrangement in $K_4Al_2Nb_{11}O_{21}$ can be rationalized in terms of a common close-packing of K and O atoms together with Nb_6 units. The close-packed arrangement itself can be decomposed into columns which present an alternation of the $Nb_{11}O_{30}$ cluster and a fragment of the perovskite-type structure.

One can imagine an alternative kind of intergrowth between perovskite-type fragments and infinitely condensed Nb_6O_{12} clusters as fractions of the NbO structure by extending the structural principles discussed for compounds with discrete Nb_6O_{12} clusters. As mentioned earlier, simple stacking of only Nb_6O_3 layers leads to the NbO structure

(Fig. 4a). Three such layers are outlined in Figure 18. If a limited number of NbO layers is sandwiched by pure O atoms, slabs cut parallel {111} from the NbO structure with the general formula $Nb_{3n+6}O_{3n+11}$ (n = number of layers) result. The limiting cases are the NbO structure itself ($n = \infty$) and the Nb–O framework of $Mg_3Nb_6O_{11}$ ($n = 0$). Any structures with $1 \leq n < \infty$ are possible but unknown at present. A similar stacking of only layers c leads to a general formula $A_nNb_{4n+2}O_{6n}$. The limiting cases here are ANb_4O_6 ($n = \infty$), a compound which exists with A = Ba[31] (see Fig. 18b), and the Nb–O framework of $SrNb_8O_{14}$ ($n = 1$). Again none of the possible intermediate structures with $1 < n < \infty$ has been observed so far. In contrast to the limited number of structures based on the NbO-type layers cut parallel {111}, intergrowth phases based on layers cut parallel {100} have been frequently observed in the K–, Sr–, Ba–, and Eu–Nb–O systems, and have turned out to be veritable treasure troves of condensed cluster compounds.

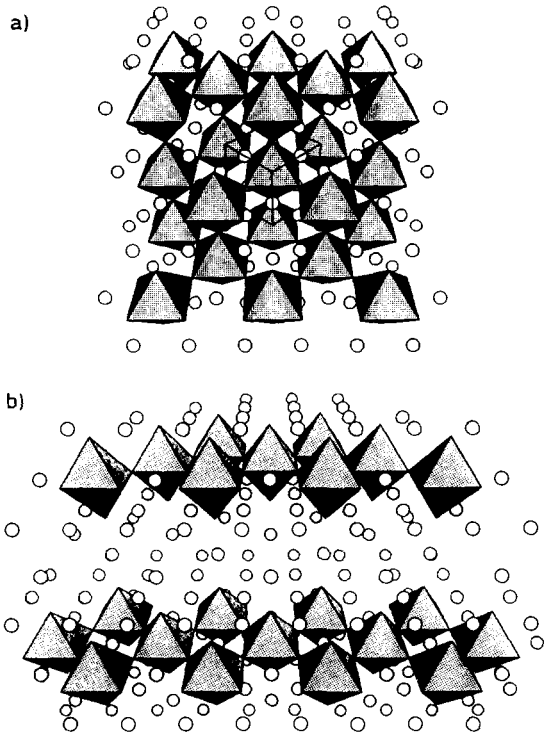

Fig. 18. The structures of a) NbO projected along [111] showing the 3D-condensed Nb_6 octahedra and b) $BaNb_4O_6$ projected along [112] revealing layers of 2D-condensed Nb_6 octahedra.

The arrangements of atoms in NbO[3, 77] and $BaNbO_3$[34, 78, 79] fit together well (Fig. 19). It is therefore possible to mutually dilute them. Either the three-dimensional condensate of Nb_6O_{12} clusters in NbO can be fragmented by a systematic insertion of perovskite-type sections or the perovskite-type section can be intersected by fragments of the NbO structure. Thus, a remarkably complex chemistry results. Intergrowth of the perovskite and NbO structure along [100] results in at least one short axis (410–419 pm). This short repeat unit corresponds approximately to the heights of the Nb_6 as well as the NbO_6 octahedra and therefore makes the compounds excellent candidates for investigation by High-Resolution Electron Microscopy (HREM).

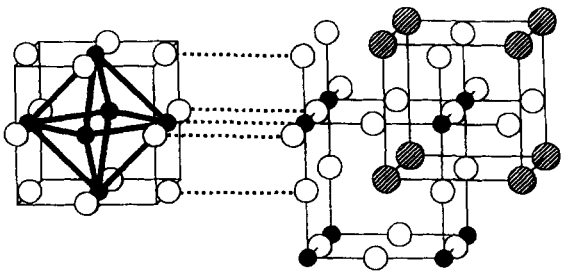

Fig. 19. Topological similarity of the structure of NbO (left, a = 421 pm) and $BaNbO_3$ (right, a = 408.5 pm for $Ba_{0.95}NbO_3$).

4.2.1. α-Phasoid

The high melting points of niobium oxides and BaO are the cause of considerable disorder in the oxoniobates prepared without flux at "moderate" temperatures (1300–1500 K). The phase diagram for BaO–NbO–NbO_2 is shown in Figure 20. HREM images of the samples with compositions close to the line NbO/$BaNbO_3$ are shown in Figure 21.

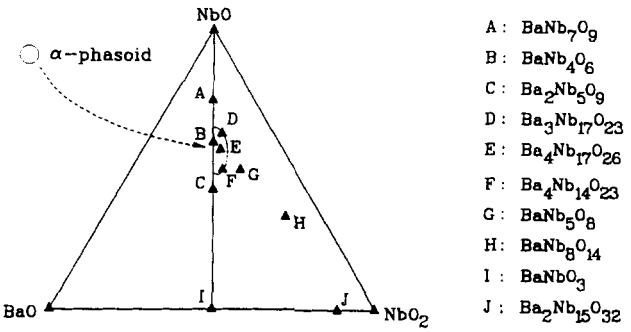

Fig. 20. The BaO–NbO–NbO_2 system. The region with the approximate composition of the α-phasoid is circled.

Crystals can be found in an area near NbO in which perfect regions of the NbO-type structure are intersected by single perovskite-type layers (Fig. 21a). The metal atoms in the Nb_6 octahedra forming the NbO slabs appear as large black spots, or rather crosses, and the perovskite slabs are clearly recognized as light stripes. In crystals with an excess of the perovskite component the situation may be inverted (Fig. 21b). Large domains of the perovskite are intersected by single layers of the NbO-type structure. The square net of metal atoms in the perovskite domains is clearly seen.

A change in the composition toward NbO leads to the compound $Ba_2Nb_5O_9$ which has regular layered intergrowth (Fig. 21c); this structure will be discussed later in detail. Moving still further toward NbO, a remarkable compound with a Ba:Nb ratio of approximately 1:4 exists as a homogeneous "phase" in the shaded region to the right of the $BaNbO_3$/NbO line.[80]

In crystals of this compound the two-dimensionally extended blocks of both structure types are shown before decomposition into one-dimensional fragments (Fig. 22a). The dark crosses again correspond to columns of Nb_6 octahedra and the smaller spots in between to the Ba and Nb atoms in the perovskite-type regions. Despite the amount of disorder in the crystals, one can assume that the columns along the

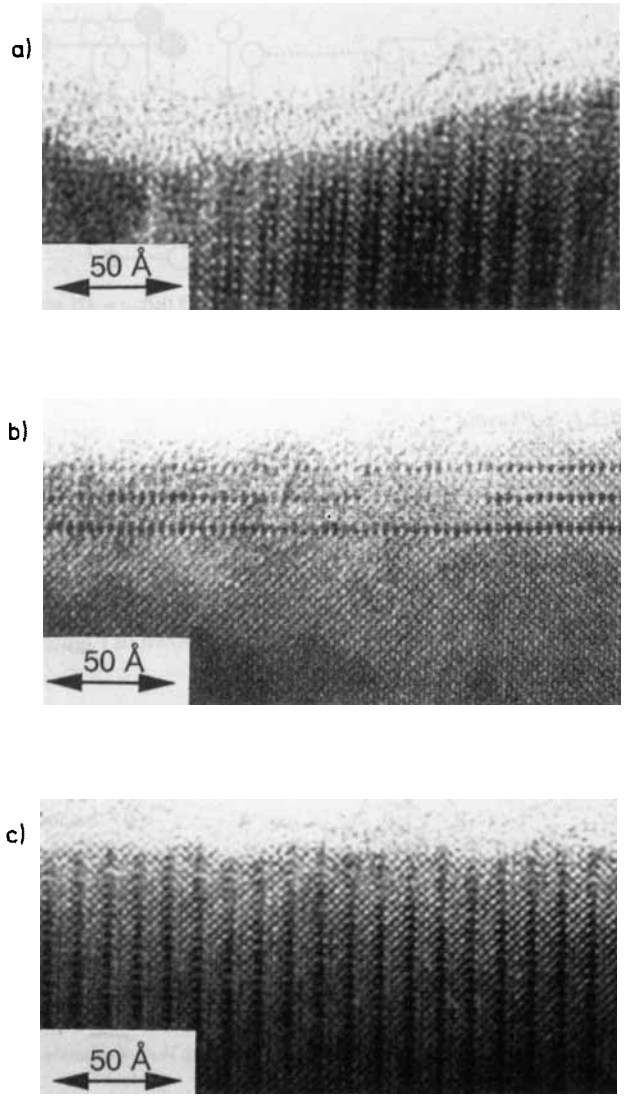

Fig. 21. a) HREM image of a crystallite exhibiting 1D intergrowth of perovskite (light) in NbO (dark). b) HREM image of a crystallite exhibiting 1D intergrowth of NbO in $BaNbO_3$. c) HREM image of $Ba_2Nb_5O_9$ viewed along [001]. Dark lamella of NbO are interleaved with a square lattice of dark spots corresponding to Ba and Nb atoms.

viewing direction are not interrupted and that the number of defects is very limited along these columns.[81-83]

The exact meaning of the term "phase" may be questioned here. The less rigidly defined term "phasoid" introduced by Magnéli[84, 85] can be used very appropriately as a common description of these intergrowth structures. Of course, such a phasoid, called α-phasoid in the Ba–Nb–O system,[82] is thermodynamically instable, but it forms because the difference in its energy of formation compared to possible discrete phases is rather small. Apparently, shortly after the reaction has started, this disordered intergrowth forms rather quickly, and once the phasoid has formed the reaction stops at moderate temperatures.[87]

The one-dimensional structural features of the α-phasoid which contrast the layered intergrowth near NbO or $BaNbO_3$ deserve some comment. If one considers the different types of intergrowth that are probably due to a slight but significant difference in the metrics of NbO and $BaNbO_3$, single slabs of the minority component can adjust to the crystal structure of the majority component. If the ratio $BaNbO_3:Nb_3O_3$ is close to one, large and in particular two-dimensionally extended blocks are avoided, because small fragments of both structures can mutually adjust more easily.

The HREM images of the α-phasoid are rather easy to interpret in spite of the complexity of its intergrowth. A magnification of the region marked in the image and two possible interpretations are shown in Figure 22. The smaller spots in the perovskite blocks correspond to strings of Nb and O atoms (41 and 8 electrons, respectively) and Ba atoms (56 electrons) which are aligned parallel to the viewing direc-

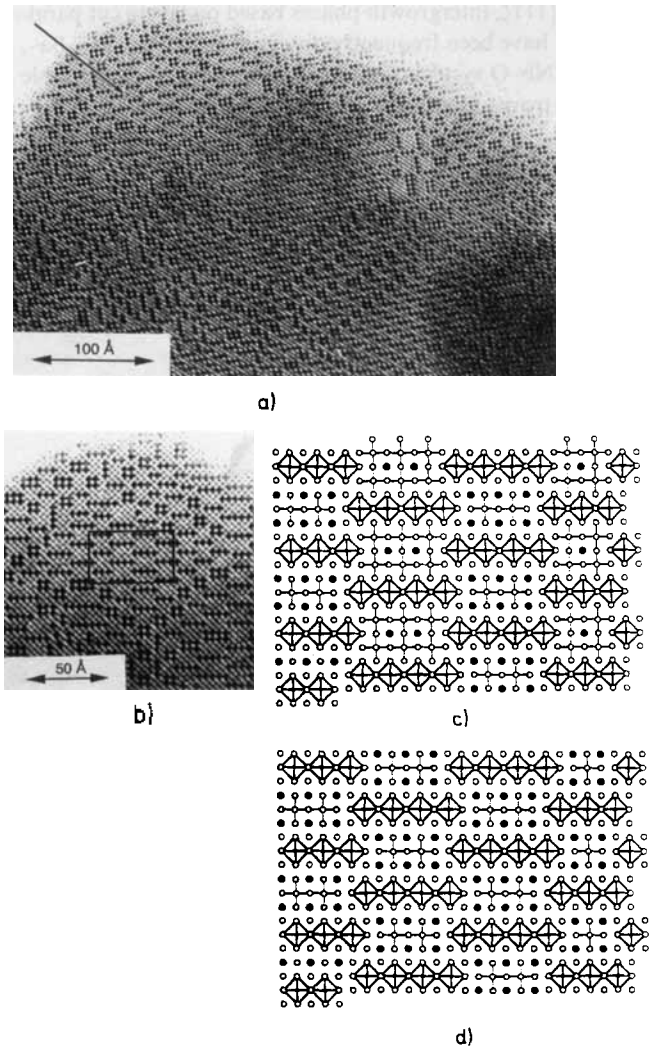

Fig. 22. a) HREM image of the α-phasoid in the Ba–Nb–O system. NbO blocks are seen as large spots or crosses, and the Ba and Nb atoms in the perovskite blocks as smaller spots in between. b) Enlargement of the area marked in a). Two different interpretations of the enclosed area are indicated in c) and d). In c) the perovskite matrix between the NbO blocks is assumed to be coherent; in d) perovskite blocks between the NbO blocks are independently oriented. The models yield a Nb:Ba ratio of 5.2 for c) and 3.4 for d).

tion approximately 290 pm apart. The average number of electrons in the two types of strings are rather similar. As a result, structure models differing only in the distribution of the metal atoms among the projected positions can give rise to more or less identical simulated HREM images. This

makes it difficult to distinguish between models as shown in Figure 22c and d without further information from X-ray structure analyses of ordered phases.

In Figure 22a one can see many regions of the image with rather ordered distributions of uniformly sized blocks, which are interpreted in terms of "microphases".[82] Although these regions are quite small, their identification has helped to systematize and to give a better understanding of the structural and compositional variations within the α-phasoid. These microphases can then be considered members of many different homologous series.

To simplify the discussion the following notation will be used as a description of the cluster substructures. The NbO-type substructures are described in terms of the matrix $[p \times q \times r]$, where p, q, and r refer to the number of condensed Nb_6 octahedra in the three directions of space. A discrete Nb_6O_{12} cluster and NbO are represented by $[1 \times 1 \times 1]$ and $[\infty \times \infty \times \infty]$, respectively. A similar description, $\{s \times t \times u\}$, is used for the perovskite units, where s, t, and u correspond to the number of perovskite-type units as well as the number of A atoms. In general, each NbO-type block is linked to four neighboring blocks by O^{i-a} bridges, resulting in rather short Nb–Nb intercluster distances (ca. 300 pm). The O^{i-a} linkage also separates the perovskite blocks from one another thus enabling them to orient out of phase with respect to each other.

An infinite number of homologous series can be derived from combinations of $[p \times q \times r]$ and $\{s \times t \times u\}$. However, for practical reasons only four basic series are considered[82] (Fig. 23). According to the notation given above they are described as $[p \times q \times \infty]$ with $1 \leq q \leq \infty$ and p = constant. Increasing values of q correspond to an increase of the sizes of the NbO- and simultaneously the perovskite-type blocks. The end members of all series are of the type $[p \times \infty \times \infty]$ and

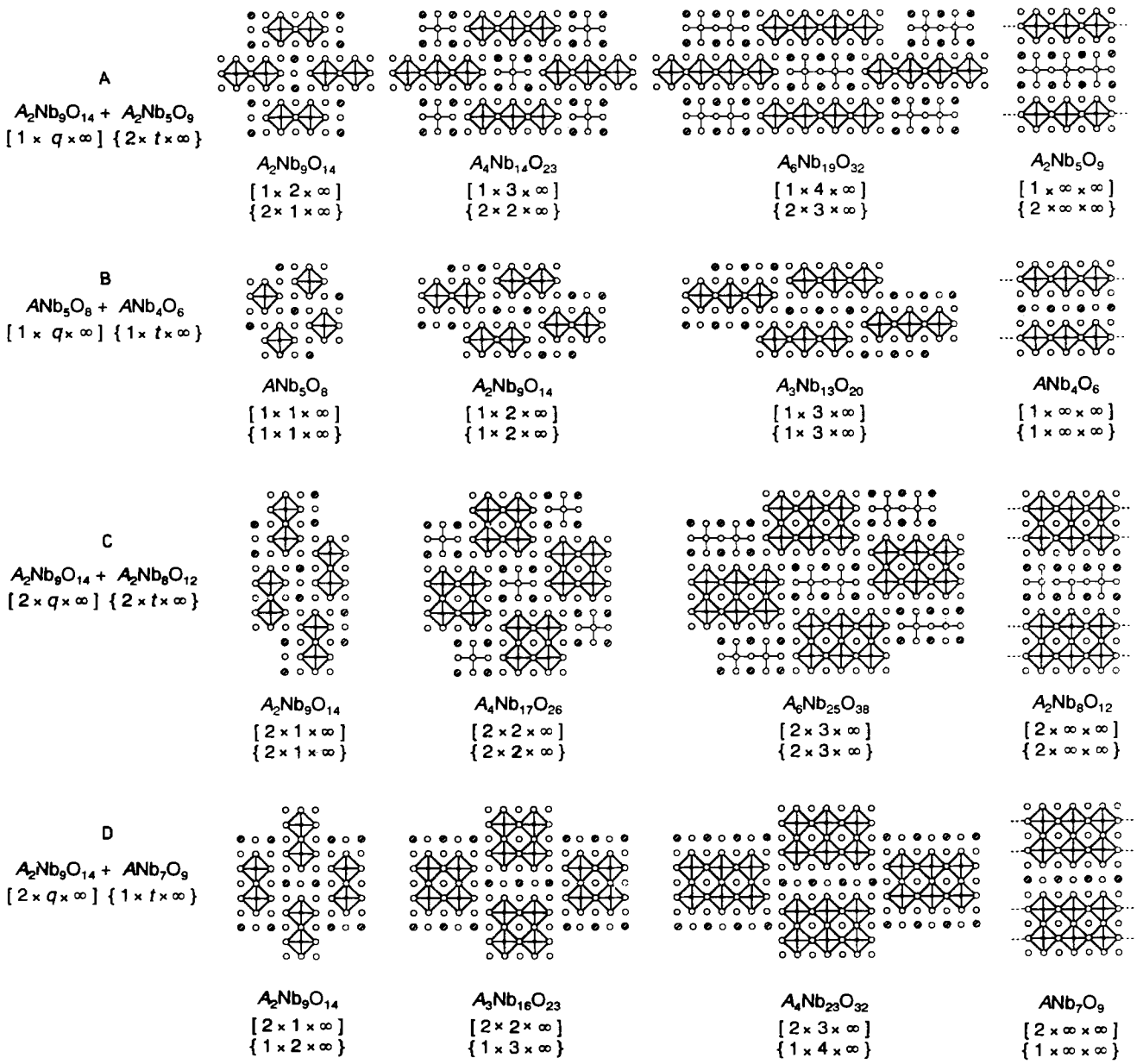

Fig. 23. Four homologous series A–D describing intergrowth compounds between perovskite and NbO structures. Each homologous series corresponds to $\{s \times t \times \infty\}$ with s = const, $t = 1, 2, \ldots \infty$ and $[p \times q \times \infty]$ with p = const, $q = 1, 2, \ldots \infty$. The end members with $t = q = \infty$ form a homologous series of their own, $A_sNb_{s+3p}O_{3s+3p}$.

Table 2. Unit cell parameters [pm] and properties of compounds containing condensed Nb_6O_{12} clusters.

Compound	Space group	a	b	c	Z	Color	Electrical property [a]	Ref.
$K_4Al_2Nb_{11}O_{21}$	$I4/mmm$	879.9	–	1252.7	2	black	s	[33, 74, 75]
$K_4Al_2Nb_{11}O_{21-x}F_x$ ($x \approx 0.2$)	$I4/mmm$	878.6	–	1263.7	2	black	s	[33, 74, 75]
$Ba_{1-x}Nb_5O_8$ ($x \approx 0.2$)	$P4/m$	660.8		410.7	1	black	m	[25]
$Ba_4Nb_{14}O_{23}$	$Cmmm$	2080.7	1245.2	415.1	2	black	–	[94]
$Ba_{4-x}Nb_{17}O_{26}$ ($x \approx 1.0$)	$P4/m$	1210.0	–	414.8	1	black	–	[96]
KNb_4O_6	$P4/mmm$	413.9	–	825.4	1	black	m	[100, 101]
$BaNb_4O_6$	$P4/mmm$	418.2	–	821.3	1	black	m	[26, 31, 127]
$K_2Nb_5O_9$	$P4/mmm$	413.8	–	1210.1	1	black	m	[101]
$Sr_2Nb_5O_9$	$P4/mmm$	414.1	–	1204.4	1	black	m	[101–103]
$Ba_2Nb_5O_9$	$P4/mmm$	417.2	–	1224.0	1	black	m	[26, 31, 101]
$Eu_2Nb_5O_9$	$P4/mmm$	413.8	–	1203.7	1	black	m	[73, 95]
$BaNb_7O_9$	$P4/mmm$	419.5	–	1242.6	1	black	m	[98]
NbO	$Pm3m$	421.1	–	–	1	golden	m	[3, 77]

[a] s = Semiconducting, m = metallic.

thus represent structures containing two-dimensionally condensed Nb_6O_{12} clusters. These structures belong to a series of $A_sNb_{s+3p}O_{3s+3p}$ where s is the number of perovskite-type slabs $\{s \times \infty \times \infty\}$ and p the number of NbO-type slabs $[p \times \infty \times \infty]$.

4.2.2. Ordered Structures

There are many examples in the literature in which ranges of homogeneity could be split into discrete ordered line phases by careful choice of the preparative conditions.[88–92] Several of the phases predicted in the homologous series of reduced oxoniobates (Fig. 23) have been synthesized (Table 2). We concentrate here on the discussion of the Ba compounds which present the largest diversity.

Three compounds have been found with one-dimensionally condensed clusters. $Ba_{1-x}Nb_5O_8$ ($x = 0.2$)[25] contains single chains of the type $[1 \times 1 \times \infty]$ which alternate with single columns of perovskite units $\{1 \times 1 \times \infty\}$ containing barium atoms cuboctahedrally coordinated by O atoms (Fig. 23). This phase is the starting member of the series B depicted in Figure 23. The structure is based on Rietfeld refinement on neutron powder data leading to a significant Ba atom deficiency.

Trimers $[1 \times 3 \times \infty]$ of cluster chains are found in $Ba_4Nb_{14}O_{23}$,[94] again one of the phases in Figure 23. The compound occurred together with the α-phasoid. Its structure was characterized from HREM images, and the unit cell parameters were obtained from X-ray powder patterns. Within each perovskite block of the size $\{2 \times 2 \times \infty\}$ one Nb atom occupies an octahedral void. Quadruple chains $[2 \times 2 \times \infty]$ together with perovskite blocks $\{2 \times 2 \times \infty\}$ are found in $Ba_4Nb_{17}O_{26}$.[95, 96] The calculated X-ray powder pattern fits the observed powder pattern; however, the given atomic positions are not very accurate.[97]

More accurate structural data are available for the phases with two-dimensionally condensed Nb_6O_{12} clusters. These are $BaNb_4O_6$,[26, 31] $Ba_2Nb_5O_9$,[26, 31] and $BaNb_7O_9$ (Fig. 24).[98] All belong to the series $A_sNb_{s+3p}O_{3s+3p}$. The first member is $BaNb_4O_6$ with $s = 1$ and $p = 1$. Its structure therefore exhibits a regular alternation of single NbO-type slabs $[1 \times \infty \times \infty]$ and single perovskite-type slabs $\{1 \times \infty \times \infty\}$. The apical Nb atoms in the NbO layers are also constituents of the perovskite layers in between. A step toward an extended perovskite-type $BaNbO_3$ is realized in $Ba_2Nb_5O_9$. Single slabs of NbO alternate with double slabs of perovskite according to $[1 \times \infty \times \infty]$ and $\{2 \times \infty \times \infty\}$, respectively. Figure 24b shows that the perovskite slabs contain additional Nb atoms in octahedral environments. Thus the Ba atoms have the complete first and second coordination spheres of the extended perovskite structure. The corresponding step toward an extended NbO structure, on the other hand, is realized in $BaNb_7O_9$. Here, double slabs of NbO-type are stacked with single perovskite-type slabs according to $[2 \times \infty \times \infty]$ and $\{1 \times \infty \times \infty\}$, respectively (Fig. 24c).

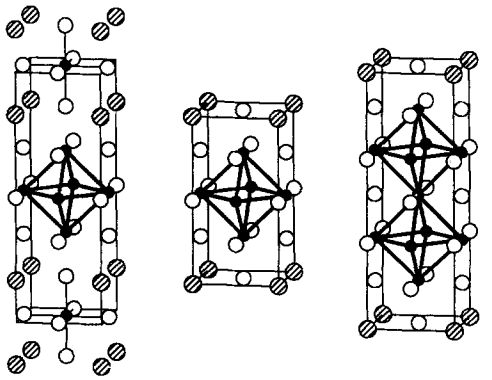

Fig. 24. Crystal structures of a) $Ba_2Nb_5O_9$, b) $BaNb_4O_6$, and c) $BaNb_7O_9$ on (100).

Several compounds with the previously described structures could be synthesized with A = K, Sr, Eu because of the compatibility in atomic structure and unit cell metrics.[99] These are "KNb_4O_6"[100, 101] and $A_2Nb_5O_9$ (A = K,[101] Sr,[101–103] Eu[73, 95]). The last two compounds were also prepared with mixed cations A: $SrBaNb_5O_9$[101] and $Eu_{1-x}Ba_xNb_5O_9$ ($0 \leq x \leq 2$).[95]

Single-crystal structure analyses have been performed on $BaNb_4O_6$,[31] $Ba_2Nb_5O_9$,[31] $BaNb_7O_9$,[98] and $Sr_2Nb_5O_9$.[102] The structural parameters for "KNb_4O_6"[100] have been determined by profile refinement of X-ray powder patterns. Only unit cell parameters and very approximate atomic coordinates have been reported for $K_2Nb_5O_9$[101] and $Eu_2Nb_5O_9$.[73]

The severe structural disorder indicated in some of the refinements is not surprising considering the easy formation of the α-phasoid discussed previously. The compositions of compounds may therefore deviate significantly from the compositions of the idealized structures. The methods of HREM and X-ray diffraction complement each other and together allow for a detailed understanding of such deviations. To give an example, both powder diffraction and energy dispersive microanalysis of individual crystallite fragments of "KNb_4O_6" unequivocally indicate Nb deficiency with a Nb:K ratio of about 3.4. A possible explanation for this result was found in the HREM images.[100] In Figure 25a a number of structural defects can be seen. The NbO-type slab, in particular, is terminated and continues as a perovskite-type slab. The suggested model for this defect is

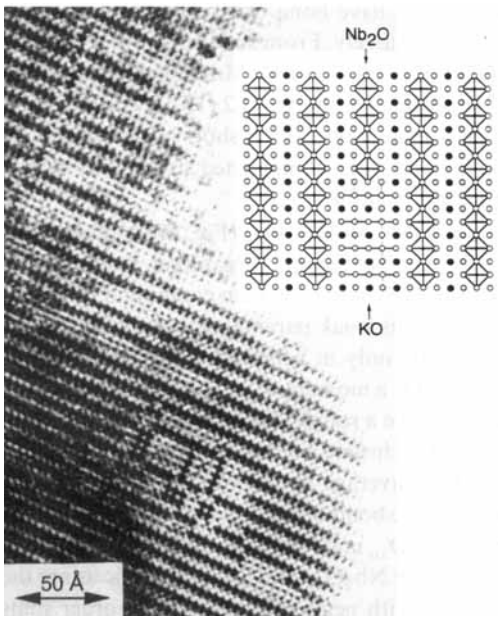

Fig. 25. a) HREM image of "KNb_4O_6" with both ordered and disordered areas. Inset: Graphic interpretation of the transition between a NbO- and a perovskite-type slab.

shown in Figure 25b. As a result of this defect the composition of the phase is $K_{1+x/2}Nb_{4-x}O_6$ with the experimentally determined value $x \approx 0.24$.[100] Another kind of (expected) disorder is shown for crystals of $BaNb_7O_9$ in Figure 26, where some of the NbO double slabs are replaced by single slabs.

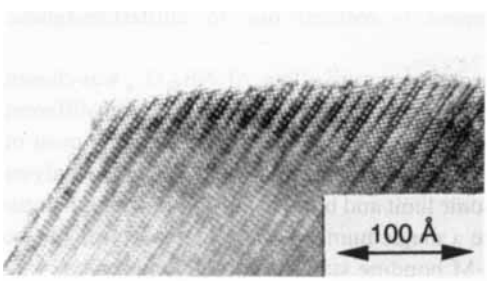

Fig. 26. HREM image showing defects in $BaNb_7O_9$ wherein the $[2 \times \infty \times \infty]$ NbO slabs have been replaced by $[1 \times \infty \times \infty]$ slabs.

Whereas HREM clearly explains the disorder phenomena observed in X-ray structure analyses of reduced oxoniobates, the latter provide sufficiently accurate structural parameters for an analysis, for example, of the mutual adjustment of the different structure types in the intergrowth phases. A comparison of the known Ba oxoniobate structures with two-dimensionally condensed clusters reveals a gradual increase of the lengths of the comparable axes with the relative amount of NbO-type slabs, or to put it in other terms, with the degree of condensation of the Nb_6O_{12} clusters (Fig. 27). The relief of strain by mutual adjustment is apparent from distortions of the coordination polyhedra. In $BaNb_4O_6$, $Ba_2Nb_5O_9$,[31] and $BaNb_7O_9$[98] the BaO_{12}

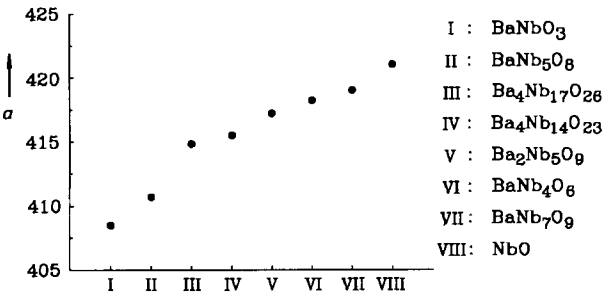

Fig. 27. Plot of the shortest unit cell axes of the reduced compounds in the Ba–Nb–O system versus the relative amount of NbO in the structures.

cuboctahedra are stretched in the *ab* plane (2%) and contracted (2%) along the *c* axis compared to bulk $Ba_{0.95}NbO_3$. The same kind of distortion, but larger due to the greater strain relief needed, is found in $Sr_2Nb_5O_9$ (3.0 and 3.7%)[102] and in KNb_4O_6 (3.1 and 3.5%).[100] The average A–O bond lengths that result are close to the values found for the corresponding bulk perovskites (Table 3). The adjustment of the NbO_6 octahedra to the NbO slab in the *ab* plane results in Nb–O bond lengths of 207.0 pm in $Sr_2Nb_5O_9$ and 208.6 pm in $Ba_2Nb_5O_9$.

Although the interatomic distances within the perovskite-type parts of the structures can be understood in terms of mutual adjustments, such reasoning does not explain

Table 3. A–O and Nb–Nb bond lengths [pm] in the structures containing Nb_6O_{12} clusters together with A–O bond lengths [pm] in oxoniobates with perovskite structure.

Compound	Average d_{A-O}	Range d_{A-O}	Average d_{Nb-Nb}	Range d_{Nb-Nb}
Oxoniobates with discrete Nb_6O_{12} clusters	–	–	281	277–288
$K_4Al_2Nb_{11}O_{21}$	–	–	285	280–289
$Ba_{0.95}NbO_3$	289	289	–	–
$Ba_{1-x}Nb_5O_8$	293	292–293	287	286–288
$BaNb_4O_6$	291	289–296	293	291–296
$Ba_2Nb_5O_9$	291	285–295	291	289–295
$BaNb_7O_9$	292	290–296	295	290–298
$Sr_{0.95}NbO_3$	285	285	–	–
$Sr_2Nb_5O_9$	287	277–293	289	287–293
$KNbO_3$	284	280–288	–	–
$K_{1-x/2}Nb_{4-x}O_6$	289	287–293	296	293–297
NbO	–	–	298	298

changes of the Nb–Nb distances within the NbO-type parts. One must also take into account the electron balance in the structures. In the perovskite phases $ANbO_3$ (A = Sr, Ba) the Nb atoms have the oxidation state IV. Because of similar distances within the NbO_6 octahedra in $A_2Nb_5O_9$, the oxidation state IV could also be assigned for the Nb atoms, implying that ten valence electrons per unit cell are available for M–M bonding in the NbO-type section as in $BaNb_4O_6$. However, all Nb–Nb bonds in $Ba_2Nb_5O_9$ are significantly shorter than in $BaNb_4O_6$ (Table 3). This difference is evidence of an electron transfer δ from the single Nb atoms to the cluster atoms resulting in $10 + \delta$ valence electrons involved in M–M bonding. The shorter Nb–O and Nb–Nb bonds in the respective NbO_6 and the Nb_6 units of $Sr_2Nb_5O_9$ then should be associated with an even larger charge transfer. This discussion leads to the more general topic of chemical bonding in reduced oxoniobates with discrete and condensed Nb_6O_{12} clusters which will be discussed in the next section.

5. Structures, Properties, and Bonding

Most of the reduced oxoniobates are mixed-valent compounds, that is, they contain niobium in different oxidation states. In descriptions of the phases with discrete clusters it has been mentioned that certain structural components, for example Nb_3O_{13} units, may act as electron buffers. In the discussion of the intergrowth phases, structural details indicate a charge transfer between perovskite- and NbO-type subunits. A more detailed analysis is necessary in order to reach a quantitative understanding of the electron balances in these phases. The final aim of such analysis is to find "magic" numbers for the electron concentrations in specific discrete clusters and condensed cluster structures. Arguments based on bond length/bond strength, and band structure calculations will be used in conjunction with observed properties of the compounds to reach this goal.

5.1. Bond Order Sums

A simple approach for relating bond lengths and bond orders was first introduced by Pauling.[104] This idea was further developed by many others and successfully applied to determine oxidation states[105] and electron concentrations in M–M bonded systems such as reduced oxomolybdates.[106] To derive the bond order or bond strength s corresponding to an experimental distance r, Equation (a) intro-

$$s = \exp[(r_o - r)/B] \qquad \text{(a)}$$

duced by Brown[107] is widely used, where B is normally set to 37 pm, and r_o is an empirically determined parameter for a single bond between two elements. The reference distance r_o for Nb–O bonds has been determined to be 191.1 pm from 228 different oxoniobates with an estimated standard deviation of 3.1 pm. Bond order summations have been performed for most of the reduced oxoniobates. The results of such calculations will be presented for selected examples of increasing complexity and discussed with respect to possible conclusions as well as to limitations of the procedure.

The compounds $Mg_3Nb_6O_{11}$ and $Mn_3Nb_6O_{11}$ are greenish black semiconductors. $Mg_3Nb_6O_{11}$ is nonmagnetic, that is, the diamagnetism is nearly compensated by a temperature-independent paramagnetism as often found for cluster compounds containing only paired electrons. $Mn_3Nb_6O_{11}$ has a magnetic moment $\mu_{eff} = 5.83\ \mu_B$ close to that expected for Mn^{2+} ions. The ionic limit $(Mg^{2+})_3(Nb^{16/6+})_6(O^{2-})_{11}$ leads to 14 electrons in M–M bonding states for the Nb_6O_{12} cluster.

Bond order summations for $Mg_3Nb_6O_{11}$ ($Mn_3Nb_6O_{11}$) clearly indicate a hierarchy in bond strengths. The average bond order sums for the O^i and O^a atoms are 2.11 and 1.84, respectively, indicating that the inner sphere of O atoms is strongly bonded to the Nb_6 core to form a rigid $Nb_6O^i_{12}$ cluster. The rigidity of the cluster framework hardly allows for full adjustments of the sizes of individual voids filled by the M^{2+} ions. The Mg(Mn) atoms in both the octahedral and tetrahedral voids have bond order sums of 2.07 (2.20) and 1.80 (1.98), respectively. From such bond order summations the number of electrons in M–M bonding states of the Nb_6O_{12} cluster is calculated to be 13.2 (13.4). The deviation from 14, which is mainly due to the short Nb–O^i distances, must be born in mind when complicated structures are analyzed as in the next example.

The structure of $Na_3Al_2Nb_{34}O_{64}$ (Fig. 10) contains four chemically different Nb atoms organized according to $(Nb_6)_3(Nb_3)_2(Nb_2)_3(Nb)_4$. The golden compound is a semiconductor and exhibits weak paramagnetism which follows the Curie–Weiss law only in a limited temperature range. Between 20 and 200 K a moment $\mu_{eff} \approx 2.2\ \mu_B$ is found. Bond order summations give a rough idea of the electron distribution. In the Nb_6O_{12} cluster, similar to $Mg_3Nb_6O_{11}$, the O^i and O^a atoms have average bond order sums of 2.12 and 1.90, respectively. The bond order sums for the Al (3.05) and Nb atoms in the Nb_2O_{10} units (4.00) are in perfect agreement with expectation. The Nb_2O_{10} unit is diamagnetic as are the four NbO_6 entities with pentavalent Nb (bond order sums 4.72 and 4.75). The Curie–Weiss behavior of the compound must therefore originate from either the Nb_6O_{12} clusters, the Nb_3O_{13} entities, or both. There might be some indication for an occupied M–M bonding state in the Nb_3O_{13} unit. The bond order sum is slightly reduced (4.5 instead of 5.0), and in spite of a more expanded matrix of O atoms in $Na_3Al_2Nb_{34}O_{64}$ the Nb–Nb distances are shorter (317 pm) than in $Ba_2Si_4Nb_{20.8}O_{44}$ (330 pm). Weak M–M bonding in the Nb_3O_{13} units in $Na_3Al_2Nb_{34}O_{64}$ seems to be present and is further corroborated by the sum of Nb–O bond orders for the Nb_6O_{12} cluster which indicates one electron less in M–M bonding states than in $Mg_3Nb_6O_{11}$. It is possible that the observed magnetic moment is reduced due to antiferromagnetic coupling.

The complicated structure of $Na_3Al_2Nb_{34}O_{64}$ was chosen to illustrate the intricate electronic balance between different parts of the structure. Such balance is also found in most of the other phases with discrete Nb_6O_{12} clusters. Analyses based on the ionic limit and bond length/bond strength arguments indicate a magic number of about 14 electrons to be present in M–M bonding states in Nb_6O_{12} clusters.

With only one exception, $NaNb_{10}O_{18}$, all compounds containing discrete clusters are insulators or semiconductors

and hence exhibit electronic delocalization only in certain components like the Nb_6O_{12} cluster. Remarkably, the expected paramagnetism for clusters analyzed as odd-electron species from the ionic limit (13 or 15 electrons) is not observed. If one does not believe in strong antiferromagnetism in all phases, an explanation for the nonoccurence of paramagnetism has to be sought in deviations from the stoichiometry derived by X-ray structure analysis and possibly also in a breakdown of general bond length/bond strength relations in rigid framework structures like the reduced oxoniobates. The following example might serve to spotlight both aspects. The golden $Na(Si_xNb_{1-x})Nb_{10}O_{19}$ ($x \approx 0.75$) contains two crystallographically different kinds of Na atoms (Fig. 12). In particular, those atoms between type I_b slabs are characterized by very low Na–O bond order sums of 0.53. These ions are housed in cages of O atoms that are far too voluminous for Na^+. With ions that are able to change their oxidation state, such a deviation from the expected bond order sum could be entirely misleading. With Na, however, any incomplete electron transfer to the Nb–O framework can be ruled out by ^{23}Na NMR spectroscopic results. These Na atoms are characterized by unusually large temperature factors indicative of a rattling motion. Any Na atom deficiency would therefore be well hidden. In fact, there is evidence that the golden color of the crystals is an extrinsic property; $Na(Si_xNb_{1-x})Nb_{10}O_{19}$ has also been prepared as red transparent crystals.[108]

A partial occupation of cuboctahedral voids by cations, well known from the perovskite-type compounds A_xNbO_3 (A = Sr, Ba), could also occur with the more reduced oxoniobates. This makes the exact determination of the ionic limit and the number of electrons in M–M bonding states of Nb_6O_{12} more difficult. Problems also arise when bond length/bond strength relationships are used for the analyses of structures. These limitations become particularly obvious for the structures with infinitely condensed Nb_6O_{12} clusters.

In the structures containing slabs of NbO alternating with perovskite-type slabs all O atoms which belong to the latter have bond order sums similar to those found in structures with discrete Nb_6O_{12} clusters, whereas the corresponding values for the O^{i-i} atoms coordinated by four Nb atoms inside the NbO-type slabs are usually high (2.34 in $BaNb_7O_9$ to 2.6 in $Sr_2Nb_5O_9$). The increased value is not too surprising since the corresponding O atom in NbO itself has the same kind of coordination and a bond order sum of 2.41. The very high value of 2.6 found for $Sr_2Nb_5O_9$ results from the pronounced structural misfit between the perovskite $Sr_{0.95}NbO_3$ ($a = 402$ pm) and NbO ($a = 421$ pm) which calls for an extreme compromise when the intergrowth structure is formed. Obviously, strong polarization and covalency effects can increase the bond order sum for an O atom to a value which is also found in the CO molecule (2.6). Under such extreme conditions any assignment of oxidation states for the Nb atoms with octahedral coordination must be ambiguous. However, Nb–O bond order sums of 4.6 and 4.3 in the respective structures of $Sr_2Nb_5O_9$ and $Ba_2Nb_5O_9$ indicate some electron transfer from these atoms to the NbO-type slabs, possibly suggesting that these atoms are in an intermediate oxidation state and contribute to the metallic conductivity observed.[127]

5.2. Band Structure Calculations

Band structure calculations by the EH method[110] have been used successfully for the interpretation of bonding in metal-rich oxides such as reduced oxomolybdates,[111, 112] NbO,[113] $LiNbO_2$,[46] and $NaNb_3O_6$.[56] For simple enough structures like NbO self-consistent band structure calculations can be performed[114] which quantitatively support the EH results.[115] To obtain more detailed insight into the complex bonding situation and especially the distribution of valence electrons in reduced oxoniobates, EH calculations were conducted for a number of compounds containing discrete and condensed clusters.[116, 117]

The nature of orbitals in discrete M_6Cl_{12} clusters has been previously examined in detail.[118, 119] Figure 28a shows the corresponding M–M bonding levels a_{1g}, t_{1u}, t_{2g}, and a_{2u} for the $Nb_6O^i_{12}O^a_6$ cluster. Nb–O antibonding character is present in all states. In the case of the a_{2u} level this antibonding contribution dominates and leads to an overall antibonding character. In this respect the oxo cluster differs from the chloro cluster for which the a_{2u} level is overall nonbonding and, hence, easily occupied, for example in species such as $Nb_6Cl_{12}^{2+}$.[120] Interestingly, the closed-shell configuration, which in a valence bond description corresponds to eight three-center two-electron bonds at the faces of the M_6 octahedron,[114, 119] is disadvantageous in the case of the oxo cluster because of a stronger metal–ligand interaction. The occupancy of all M–M bonding states by 16 electrons has not been observed experimentally for the Nb_6O_{12} cluster. In fact, the 14-electron species seems much preferred in agreement with the calculation.

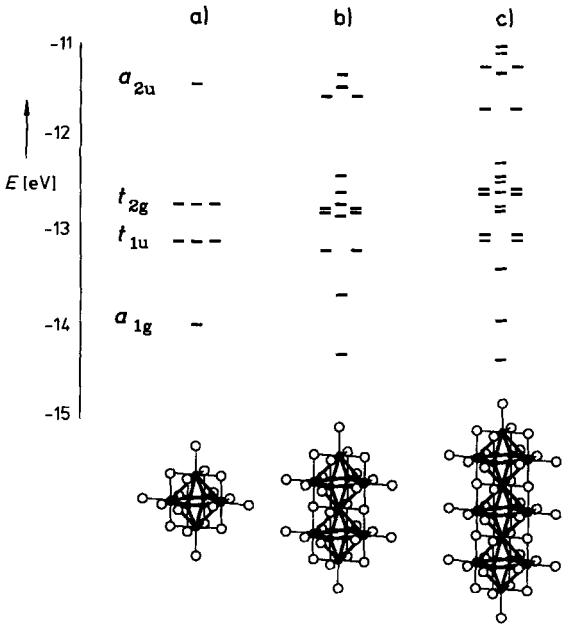

Fig. 28. Energy level diagrams for the metal-centered orbitals of the a) $Nb_6O^i_{12}O^a_6$, b) $Nb_{11}O^i_{20}O^a_{10}$, and c) the (hypothetical) $Nb_{16}O^i_{28}O^a_{14}$ clusters. The diagrams were obtained from full band structure calculations at the Γ point ($k = 0$). In the calculations atomic parameters were used from a) $Mg_3Nb_6O_{11}$, b) $K_4Al_2Nb_{11}O_{21}$, and c) an extended model derived from $K_4Al_2Nb_{11}O_{21}$ with corresponding interatomic distances.

The distortions of the Nb_6O_{12} clusters in all reduced oxoniobates are minor, and therefore the energy level diagram of the discrete cluster can be recognized in the corresponding Density Of States (DOS) for oxoniobates containing such discrete clusters. The band structure of $SrNb_8O_{14}$ depicted in Figure 29 serves as an example. Rather narrow bands appear in the projection of the DOS for the Nb atoms of the cluster below the Fermi level at approximately -14, -13, and -12.5 and -12.2 eV which correspond to the seven low-ly-

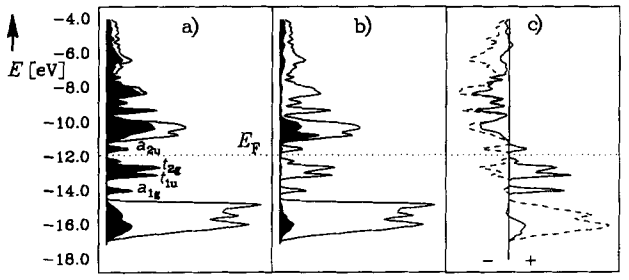

Fig. 29. a) Total DOS for $SrNb_8O_{14}$ with the projection of the Nb cluster atoms (black). The energy levels corresponding to the discrete Nb_6O_{12} cluster are labeled. b) Projection of the DOS for the Nb atoms in octahedral environments, and c) COOP curves for the Nb–Nb (solid) and Nb–O (dashed) interactions in the Nb_6O_{12} cluster.

ing states of the discrete cluster. The band near -11.5 eV corresponds to the a_{2u} orbital. As previously pointed out, the character of this band is overall antibonding because of the dominance of the Nb–O interactions within the cluster which is clearly reflected in the corresponding Crystal Orbital Overlap Population (COOP[111]) curves (Fig. 29b). The optimal stability of the compound is reached with 14 valence electrons in Nb–Nb bonding bands which are entirely filled, in agreement with the DOS and the semiconducting properties of the compound. The Nb_6O_{12} cluster in $SrNb_8O_{14}$ contains indeed all 14 electrons without any significant transfer of negative change to the Nb atoms in octahedral environments, which becomes apparent by inspection of the Atomic Orbital Projection (AOP) for these atoms. The bands near the Fermi level contain essentially no contribution from these Nb atoms.

The situation changes when more than 14 electrons are available for M–M bonding in the Nb_6O_{12} cluster. Other bands originating from interactions between clusters, clusters and adjacent Nb atoms, or between noncluster Nb atoms may then be filled. In $NaNb_{10}O_{18}$, for example, the band corresponding to the a_{2u} level is partly occupied as well as the d band, which originates from the Nb atoms in octahedral environments (Fig. 30). The metallic conductivity of this compound is thus easily explained. The corresponding COOP curves indicate that there are strong bonding interactions between the d orbitals of the octahedrally coordinated Nb atoms in a chain, but not with the Nb atoms of the Nb_6O_{12} cluster (Fig. 30c).

Band structure calculations for metallic $BaSiNb_{10}O_{19}$ (Fig. 31) indicate that Nb–Nb bonding bands of both the Nb_6O_{12} and Nb_3O_{13} clusters are occupied. The d states of the remaining Nb atoms in octahedral environments lie high

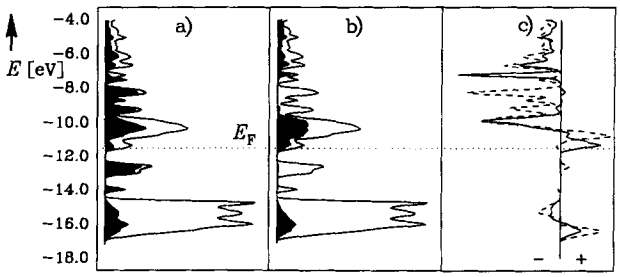

Fig. 30. Total DOS for $NaNb_{10}O_{18}$ with projections for a) the Nb cluster atoms (black) and b) Nb atoms in octahedral environments (black). c) COOP curves for the Nb–Nb interactions between octahedrally coordinated atoms only (solid) and Nb cluster atoms (dashed).

above the Fermi level indicating an oxidation state of v for these atoms.

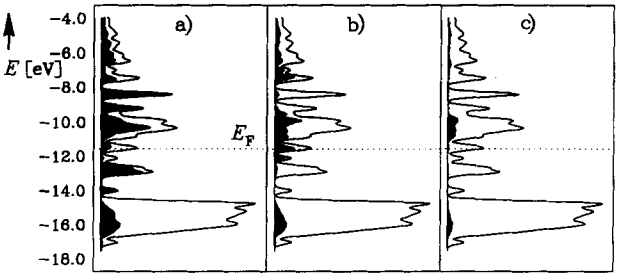

Fig. 31. Total DOS for $BaSiNb_{10}O_{19}$ with projections for a) the Nb cluster atoms (black), b) the Nb atoms of the Nb_3O_{13} unit (black), and c) the remaining Nb atoms in octahedral environments (black).

In order to discuss bonding in the Nb_3O_{13} units with different Nb–Nb distances as they occur in $BaSiNb_{10}O_{19}$, $Rb_4(Si,Nb)_2Nb_{35}O_{70}$, and $Na_3Al_2Nb_{34}O_{64}$, the respective COOP curves are compared (Fig. 32). The familiar energy level scheme (a_2'', e', a_1') for such molecular units[118] is only reflected in the COOP curve for the Nb_3 units in $BaSiNb_{10}O_{19}$, the Nb–Nb distances of which are rather

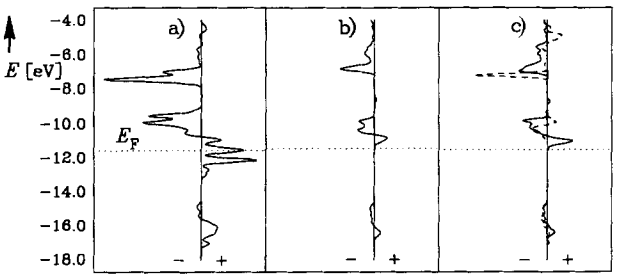

Fig. 32. COOP curves for the Nb–Nb interactions in the different Nb_3O_{13} units of a) $BaSiNb_{10}O_{19}$ (d_{Nb-Nb} = 282 pm), b) $Na_3Al_2Nb_{34}O_{64}$ (d_{Nb-Nb} = 315 pm), and c) $Rb_4Si_2Nb_{35}O_{70}$ (d_{Nb-Nb} = 306 pm (solid) and d_{Nb-Nb} = 335 pm (dashed)).

short (282 pm). Here, the Nb–Nb bonding states are filled to approximately 60% corresponding to four valence electrons in M–M bonding states of the Nb_3 unit instead of six to eight usually found in oxomolybdates such as $M_2Mo_3O_8$.[131] The corresponding COOP curve for $Na_3Al_2Nb_{34}O_{64}$ (d_{Nb-Nb} = 317 pm) shows only a weak unstructured Nb–Nb

bonding band slightly above the Fermi level (Fig. 32b). The situation is similar for $Rb_4(SiNb)_2Nb_{35}O_{70}$ where one kind of Nb_3 unit is located between I_b slabs and exhibits Nb–Nb distances of 306 pm. In the COOP curve for the other type of Nb_3 unit in this structure (d_{Nb-Nb} = 335 pm) the Nb–Nb antibonding state, curiously enough, lies below the Nb–Nb bonding state (Fig. 32c). In this case the Nb–O–Nb interaction is stronger than the direct Nb–Nb interaction; this is comparable to the situation found in CdI_2-type structures which do not exhibit direct M–M bonding.[121]

Before extending the discussion to structures with condensed clusters a word of caution seems appropriate here. All EH calculations were performed with the same parameters for different types of Nb atoms.[117] Since Nb atoms in octahedral environments have a much higher charge than the Nb cluster atoms, the energies of their d states are raised in the calculation with respect to the energy levels of the cluster atoms. If such a relative shift is on the scale of a few tenths of an electronvolt, then the partial occupation of the bands which correspond to the a_{2u} state in $BaSiNb_{10}O_{19}$, $Rb_4(SiNb)_2Nb_{35}O_{70}$, and $Na_3Al_2Nb_{34}O_{64}$ could be an artifact, and the d states close to the Fermi level of Nb atoms in octahedral environments are more or less filled.[132] This also holds true for the electron distribution between Nb atoms of the cluster and the Nb atoms in $NaNb_{10}O_{18}$ with octahedral environments.

The first step of the condensation of Nb_6O_{12} clusters is realized in the $Nb_{11}O_{21}$ cluster in $K_4Al_2Nb_{11}O_{21}$. The M–M bonding levels for the discrete cluster $Nb_{11}O^i_{20}O^a_{10}$ are drawn in Figure 28b. This energy level diagram can also be recognized in the DOS obtained from a full band structure calculation for $K_4Al_2Nb_{11}O_{21}$ (Fig. 33a) indicating the rather localized and therefore dispersionless cluster states. For this cluster an e' orbital results from the combination of t_{2g} orbitals of two monomers which has almost the same energy as the levels derived from a_{2u} orbitals.[74] The COOP curves (Fig. 33b) indicate that this group of orbitals has Nb–Nb bonding and strong Nb–O antibonding character like the a_{2u} orbitals in the monomeric cluster. Therefore, 12 low-lying levels result which can be filled by 24 electrons for the optimal electronic stabilization of this cluster.

The structure of $K_4Al_2Nb_{11}O_{21}$ is well suited for the analysis of the Nb–Nb interaction between clusters with Nb–Nb distances as short as 305 pm across the common O^i–O^a edges. The COOP curves (Fig. 33c), which have been calculated for all Nb–Nb distances between clusters, indicate that the intercluster bonding is negligible compared to the intracluster bonding. The same holds for the short interchain Nb–Nb distance (305 pm) in $BaNb_5O_8$, and it is reasonable to conclude that M–M bonding is also absent between the one-dimensional fragments of the NbO structure in the α-phasoid. The bonding is different than in TiO whose structure is derived from Ti_6O_{12} clusters which are condensed into chains by corner-sharing of the Ti_6 octahedra[5, 133] like in $BaNb_5O_8$. However, there is significant Ti–Ti bonding here between Ti atoms belonging to neighboring chains. In the chain compound Ti_5Te_4 based on corner-condensed Ti_6Se_8clusters,[134] interchain Ti–Ti bonding becomes even dominant and replaces some of the intrachain bonding.

The analysis of a hypothetical linear trimeric cluster is an appropriate transition to the discussion of the infinite chain compound. The energy level diagram for this cluster, $Nb_{16}O^i_{28}O^a_{14}$, with Nb–Nb and Nb–O distances taken from the dimeric cluster is presented in Figure 28c. The Nb–Nb bonding states appear as groups around the energies of the levels for the $Nb_6O^i_{12}O^a_6$ cluster. Seventeen states with Nb–Nb bonding character lie below the energy of the d orbitals for the free Nb atom (−12.1 eV) and eight states above due to strong Nb–O antibonding interactions. Such a trimeric cluster should therefore have its optimal stability with 34 valence electrons in M–M bonding states.

In the discussion of $BaNb_5O_8$ the first step was made toward structures containing infinitely condensed Nb_6O_{12} clusters. All compounds belonging to this class are metallic. The band structure of the infinite chain compound $BaNb_5O_8$ (Fig. 34) is reminescent of the "fingerprint" of levels characterizing the discrete clusters. The energy gap around −12 eV

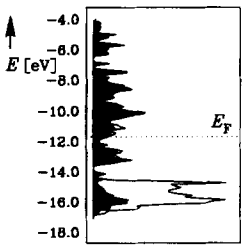

Fig. 34. Total DOS for $BaNb_5O_8$ with the projection of the Nb cluster atoms (black).

which exists for the mono-, di-, and trimeric clusters (Fig. 28) is closed in agreement with metallic property of $BaNb_5O_8$. The band filling corresponds to an optimization with respect to Nb–Nb bonding and Nb–O antibonding interactions (Fig. 34b). An optimized band filling comparable to that of $BaNb_5O_8$ with infinite chains is found for $BaNb_4O_6$ which contains layers of condensed Nb_6O_{12} clusters (Fig. 35). Fewer electrons would not take full advantage of M–M bonding;

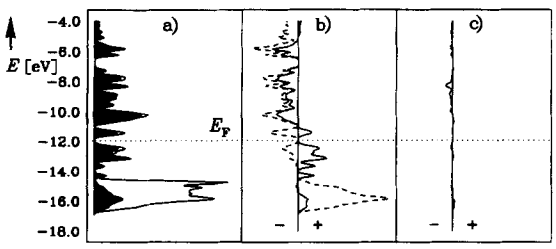

Fig. 33. a) Total DOS for $K_4Al_2Nb_{11}O_{21}$ with the projection of the Nb cluster atoms (black). b) COOP curves for the Nb–Nb intracluster and Nb–O (dashed) interactions, and c) for the Nb–Nb intercluster interactions.

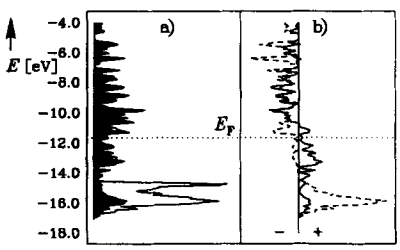

Fig. 35. a) Total DOS for $BaNb_4O_6$ with the projection of the Nb cluster atoms (black). b) COOP curves for the Nb–Nb and Nb–O (dashed) interactions.

more electrons would occupy strong Nb–O antibonding levels. One of the basic questions in the discussion of the related structure of $Ba_2Nb_5O_9$ is the electron distribution between the cluster sheet and the Nb atoms in octahedral environments. Band structure calculations suggest that all d bands arising from the latter atoms lie above the Fermi level and are therefore empty (Fig. 36). As a consequence, the M–M bonding bands of the Nb_4O_6 cluster sheet seem to contain one more electron in $Ba_2Nb_5O_9$ (11) than in $BaNb_4O_6$ (10).

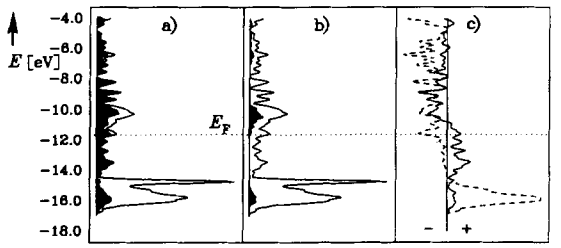

Fig. 36. Total DOS for $Ba_2Nb_5O_9$ with a) the projection of the Nb cluster atoms (black) and b) the Nb atoms with octahedral environments (black). c) COOP curve for the Nb–Nb and Nb–O (dashed) interactions of the Nb cluster atoms.

The observed average Nb–O distances for the Nb atoms in octahedral environments, however, indicate tetra- rather than pentavalency for these atoms. As discussed earlier, the calculated energies for the d bands related to highly charged ions are obviously too high and should be used with caution. However, a partial electron transfer from the cluster layers to these ions obviously occurs and results in an oxidation state $v - \delta$ for the octahedrally coordinated Nb atoms as in bronzes.

Finally, the most metal-rich ordered compound discovered so far, $BaNb_7O_9$, is of particular interest. Close similarities between the DOS for $BaNb_7O_9$ and NbO become obvious upon comparison of Figures 37 and 38. Two layers of the NbO-type structure are sufficient to model the essentials of

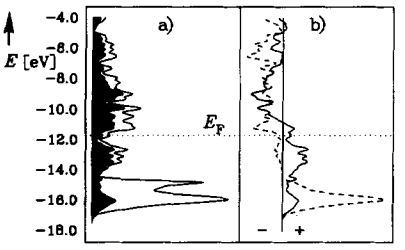

Fig. 37. a) Total DOS for $BaNb_7O_9$ with the projection of the Nb atoms (black). b) COOP curves for the Nb–Nb and Nb–O (dashed) interactions.

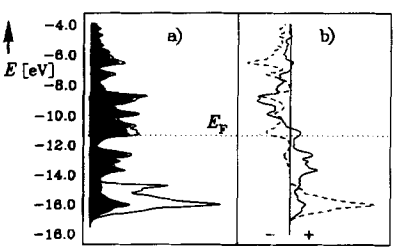

Fig. 38. a) Total DOS for NbO with the Nb projection (black). b) COOP curve for the Nb–Nb and Nb–O (dashed) interactions.

the electronic structure of bulk NbO. The COOP curves for both structures indicate optimal electron concentrations. The bands are filled up to a level at which the Nb–Nb bonding character is just overcompensated by the Nb–O antibonding character. For $BaNb_7O_9$ and NbO this situation is met with nineteen and three electrons, respectively, in M–M bonding bands. The possibility of any further occupation of M–M bonding bands, for example in $BaNb_7O_9$ by a partial substitution of Ba by La, seems highly improbable as bands with strongly antibonding character must then be occupied. On the other hand, a slightly reduced electron concentration could be tolerated, particularly in NbO since the band states down to 0.5 eV below the Fermi level are rather nonbonding due to the compensation of the Nb–Nb bonding and Nb–O antibonding contributions. The partial substitution of Nb by Ti in the structure of NbO found experimentally is in agreement with this result.[135]

To summarize, band structure calculations indicate optimal valence electron concentrations for both discrete and condensed Nb_6O_{12} clusters, governed by an exact balance between Nb–Nb bonding and Nb–O antibonding contributions. These optimal (magic) electron numbers are in close agreement with those derived from the ionic limit.

5.3. Magic Electron Numbers

The structures of oxoniobates based on Nb_6O_{12} clusters cover the whole spectrum from discrete clusters ("zero-dimensional", 0D) to 1D, 2D, and 3D corner-condensed cluster frameworks. The situation therefore seems to be more complicated than with edge-sharing Mo_6 octahedra as observed in oxomolybdates[122–126] or face-sharing as in molybdenum chalcogenides,[9] where in both cases only 1D condensation occurs. On the other hand, both edge and face condensation lead to a loss of the nonmetal atoms above the edges and faces involved in condensation. As a consequence the bonding orbitals of the discrete cluster reorient considerably in systems with edge- and face-condensed clusters. In contrast, condensation at the corners of the M_6 octahedron keeps the M_6X_{12} entity complete and uses only the outer lobes of the M–M bonding orbitals of the discrete cluster.[114] This makes the derivation of optimized electron concentrations (after some thinking) straightforward in the case of corner condensation.

Rules for optimized electron numbers in oligomeric clusters formed from edge-condensed Mo_6O_{12} as well as face-condensed Mo_6Se_8 clusters have been worked out before.[137] They covered the compounds known and were used successfully as guidelines in the search for new compounds.[136] These rules were derived from cutting the infinite chains into Mo_4O_6 and Mo_3Se_3 fragments (face and corner condensation) and combining the electron concentrations for the fragments with those for the single Mo_6O_{12} and Mo_6Se_8 clusters.

The procedure in the case of corner-condensed Nb_6O_{12} clusters is somewhat different. Key systems are the Nb_6O_{12} cluster with 14 electrons in M–M bonding states and hence $14/6 = 2.\bar{3}$ electrons for each of the equivalent Nb atoms, the compound NbO with 3D-condensed clusters and 3.0 electrons per equivalent Nb atom, and finally the dimeric cluster

$Nb_{11}O_{20}$ with 24 electrons in M–M bonding states and three kinds of nonequivalent Nb atoms. The central Nb atom in the $Nb_{11}O_{20}$ cluster has the same environment as the Nb atom in NbO and therefore donates three electrons to three-center bonds in altogether eight faces. The two peripheral Nb atoms are bonded as in the Nb_6O_{12} cluster and therefore contribute $2.\bar{3}$ electrons to M–M bonding in four faces. The remaining eight equivalent basal Nb atoms then need to contribute $16.\bar{6}$ electrons ($\approx 2.0\,e^-$ per Nb atom) to M–M bonding in order to reach the optimal electron count of 24. The same counting scheme leads to $2\times 2.\bar{3} + 2\times 3.0 + 3\times 4\times 2.0 = 34.\bar{6}$ as an optimal number of electrons in M–M bonding states for the trimeric cluster, in close agreement with 17 bonding states in the energy level diagram presented in Figure 28c.

With the electron numbers depicted for the different types of Nb atoms in Figure 39a simple prediction of electron concentrations for all kinds of terminated (oligomers) or infinite (polymers) condensates of M_6O_{12} clusters linked

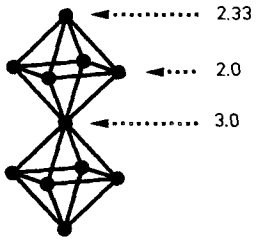

Fig. 39. Assignment of number of electrons for the different kinds of Nb atoms in condensed Nb_6O_{12} clusters.

Table 4. Magic electron numbers for condensed Nb_6O_{12} clusters.

Compound	Cluster unit	Predicted NVE [a]/cluster	Observed NVE [a]/cluster
Nb_6O_{12} discrete cluster	$[1\times 1\times 1]$	14	13–15
$K_4Al_2Nb_{11}O_{21}$	$[1\times 1\times 2]$	23.67	23–24
$BaNb_2O_6$	$[1\times 1\times \infty]$	11	11
$Ba_4Nb_{14}O_{23}$	$[1\times 3\times \infty]$	31	31–32
$Ba_4Nb_{17}O_{26}$	$[2\times 2\times \infty]$	40	40–41
KNb_4O_6	$[1\times \infty\times \infty]$	10	9
$BaNb_4O_6$	$[1\times \infty\times \infty]$	10	10
$K_2Nb_5O_9$	$[1\times \infty\times \infty]$	10	9
$Sr_2Nb_5O_9$	$[1\times \infty\times \infty]$	10	10–11
$Ba_2Nb_5O_9$	$[1\times \infty\times \infty]$	10	10–11
$Eu_2Nb_5O_9$	$[1\times \infty\times \infty]$	10	10–11
$BaNb_7O_9$	$[2\times \infty\times \infty]$	19	19
NbO	$[\infty\times \infty\times \infty]$	9	9

[a] NVE = Number of valence electrons in Nb–Nb bonding states.

through the apices of the M_6 octahedron can be made. As Table 4 indicates, the predicted values are in perfect agreement with those observed experimentally.

Received: March 6, 1992 [A 884 IE]
German version: *Angew. Chem.* **1992**, *104*, 1463

[1] A. Simon, H. G. Schnering, H. Wöhrle, H. Schäfer, *Z. Anorg. Allg. Chem.* **1965**, *339*, 155.
[2] A. Simon, *Z. Anorg. Allg. Chem.* **1967**, *355*, 311.
[3] G. Brauer, *Z. Anorg. Allg. Chem.* **1941**, *248*, 1.
[4] H. Schäfer, H. G. Schnering, *Angew. Chem.* **1964**, *76*, 833.
[5] A. Simon, *Angew. Chem.* **1981**, *93*, 23; *Angew. Chem. Int. Ed. Engl.* **1981**, *20*, 1.
[6] R. E. McCarley, K.-H. Lii, P. A. Edwards, L. F. Brough, *J. Solid State Chem.* **1985**, *57*, 17.
[7] J. D. Corbett, R. E. McCarley in *Crystal Chemistry and Properties of Materials with Quasi-One-Dimensional Structures* (Ed.: J. Rouxel), Reidel, Dordrecht, **1986**, p. 179.
[8] H. Mattausch, A. Simon, E.-M. Peters, *Inorg. Chem.* **1986**, *25*, 3428.
[9] R. Chevrel, P. Gougeon, M. Potel, M. Sergent, *J. Solid State Chem.* **1985**, *57*, 25.
[10] R. Chevrel, M. Sergent in *Crystal Chemistry and Properties of Materials with Quasi-One-Dimensional Structures* (Ed.: J. Rouxel), Reidel, Dordreht, **1986**, p. 315.
[11] D. M. Evans, L. Katz, *J. Solid State Chem.* **1973**, *6*, 459.
[12] T. Ogushi, G. N. Suresha, Y. Honjo, I. Kawano, T. Numata and Y. Hakuraku, *J. Low. Temp. Phys.* **1987**, *69*, 451.
[13] M. J. Geselbracht, T. J. Richardson, A. M. Stacy, *Nature* **1990**, *345*, 324.
[14] J. Akimitsu, J. Amano, H. Sawa, O. Nagase, K. Gyoda, M. Kogai, *Jpn. J. Appl. Phys. Part 1* **1991**, *30*, 1155.
[15] Transitions to superconductivity below 8 and 6 K have been found in phases with the composition $Ba_{2-x}La_xNb_3O_9$ ($0.2 \le x \le 0.5$) [16]. The transition at 8 K probably originates from NbO_x ($0.0 < x < \le 0.125$) [17].
[16] J. Long, J. Köhler, G. Svensson, R. K. Kremer, A. Simon, unpublished results.
[17] C. D. Wiseman, *J. Appl. Phys.* **1966**, *37*, 3599.
[18] S. Berglund, *Chem. Scr.* **1981**, *18*, 73.
[19] B. O. Marinder, *Chem. Scripta* **1977**, *11*, 97.
[20] J. Köhler, A. Simon, *Angew. Chem.* **1986**, *98*, 1011; *Angew. Chem. Int. Ed. Engl.* **1986**, *25*, 996.
[21] R. Burnus, J. Köhler, A. Simon, *Z. Naturforsch. B* **1987**, *42*, 536.
[22] J. Köhler, A. Simon, *Z. Anorg. Allg. Chem.* **1987**, *553*, 106.
[23] G. Svensson, *Mater. Res. Bull.* **1988**, *23*, 437.
[24] H. Schäfer, K.-D. Dohmann *Z. Anorg. Allg. Chem.* **1959**, *299*, 197.
[25] V. G. Zubkow, V. A. Perelyayev, I. F. Berger, I. A. Kontzevaya, O. B. Makarova, S. A. Turshevskii, V. A. Gubanov, V. I. Voronin, A. V. Mirmelstein, A. E. Karkin, *Sverkhprovodimost. Fiz. Khim. Tekh.* **1990**, *3*, 2121.
[26] V. G. Zubkov, V. A. Perelyayev, I. F. Berger, V. I. Voronin, I. A. Kontzevaya, G. P. Shveikin, *Dokl. Akad. Nauk. SSSR*, **1990**, *312*, 615.
[27] G. Svensson, unpublished results.
[28] J. Köhler, A. Simon, S. J. Hibble, A. K. Cheetham, *J. Less-Common Met.* **1988**, *142*, 123.
[29] J. Köhler, A. Simon, *Z. Anorg. Allg. Chem.* **1989**, *572*, 7.
[30] S. J. Hibble, A. K. Cheetham, J. Köhler, A. Simon, *J. Less-Common Met.* **1989**, *154*, 271.
[31] G. Svensson, J. Köhler, A. Simon, *J. Alloys Comp.* **1991**, *176*, 123.
[32] B. Hessen, S. A. Sunshine, T. Siegrist, A. T. Fiory, *Chem. Mater.* **1991**, *3*, 528.
[33] R. Tischtau, Dissertation, Universität Stuttgart, **1991**.
[34] R. Kreiser, A. Ward, *J. Solid State Chem.* **1970**, *1*, 368.
[35] D. Ridgeley, A. Ward, *J. Am. Chem. Soc.* **1955**, *77*, 6132.
[36] F. Galasso, L. Katz, A. Ward, *J. Am. Chem. Soc.* **1959**, *81*, 5898.
[37] A. Feltz, H. Langbein, *Z. Anorg. Allg. Chem.* **1976**, *425*, 47.
[38] D. Groult, J. M. Chailleux, J. Choisnet, B. Raveau, *J. Solid State Chem.* **1976**, *19*, 235.
[39] J. M. Chailleux, D. Groult, C. Mercy, F. Studer, B. Raveau, *J. Solid State Chem.* **1981**, *37*, 122.
[40] H. Schäfer, R. Gruehn, *Angew. Chem.* **1966**, *78*, 28.
[41] A. Hibst, R. Gruehn, *Angew. Chem.* **1981**, *93*, 23; *Angew. Chem. Int. Ed. Engl.* **1981**, *20*, 1.
[42] K. Naito, N. Kamageshira, N. Sasaki, *J. Solid State Chem.* **1980**, *35*, 305.
[43] H. Hibst, R. Gruehn, *Z. Anorg. Allg. Chem.* **1978**, *442*, 49.
[44] G. Meyer, R. Hoppe, *J. Less-Common Met.* **1976**, *46*, 55.
[45] G. Meyer, R. Hoppe, *Z. Anorg. Allg. Chem.* **1976**, *424*, 128.
[46] J. K. Burdett, T. Hughbanks, *Inorg. Chem.* **1985**, *24*, 1741.
[47] J. B. Goodenough, *Phys. Rev.* **1955**, *100*, 564.
[48] B. O. Marinder, *Ark. Kem.* **1962**, *19*, 435.
[49] A. K. Cheetham, C. N. R. Rao, *Acta Crystallogr. Sect B* **1976**, *32*, 1579.
[50] H.-J. Schweizer, R. Gruehn, *Z. Naturforsch. B* **1982**, *37*, 1361.
[51] It is difficult to determine the fluorine content in $NaNb_3O_{6-x}F_x$, however, the maximum value is $x = 1.0$. Data for the pure oxide $NaNb_3O_6$ ($x = 0$) are: space group *Immm* (no. 71), $Z = 4$, $a = 647.1(1)$, $b = 1026.9(2)$, $c = 708.7(1)$ pm (Guinier-data). Diffractometer CAD4; $Mo_{K\alpha}$; 330 reflections, 207 with $F_0 \ge 2.0\sigma(F_0)$, $R = 0.025$, $R_w = 0.019$ $\rho_{calc.} = 6.07\,g\,cm^{-3}$. Positional parameters: Na 4*e* with $x = 0.2682(1)$, Nb(1) 4*f* with $x = 0.2990(1)$, Nb(2) 8*l* with $y = 0.7781(1)$, $z = 0.7298(1)$, O(1) 4*g* with $y = 0.1665(1)$, O(2) 4*h* with $z = 0.6750(2)$, O(3) 16*o* $x = 0.7731(2)$, $y = 0.3654(2)$, $z = 0.1949(1)$. Further details of the crystal structure investigation may be obtained from the Fachinformationszentrum Karlsruhe, Gesellschaft für wissenschaftlich-technische Information, mbH, D-W-7514 Eggenstein-Leopoldshafen (FRG), on quoting the depository number CSD-51994, the names of the authors, and the journal citation.

[52] S. J. Hibble, A. K. Cheetham, D. E. Cox, *Inorg. Chem.* **1987**, *26*, 2389.
[53] P. Alemany, V. G. Zubkov, S. Alvarez, V. P. Zhubkov, V. A. Perelyayev, I. Kontsevaya, A. Tyutyunnik, unpublished.
[54] F. A. Cotton, *Chem. Soc. Rev.* **1975**, *4*, 27.
[55] K. Walterson, *Acta Crystallogr. Sect. B* **1976**, *32*, 1485.
[56] M. J. Calhorda, R. Hoffmann, *J. Am. Chem. Soc.* **1988**, *110*, 8376.
[57] Each point in the net belongs to six triangles, see notation according to Schläfli [58], see also ref. [59].
[58] W. B. Pearson, M. O'Keefe, B. G. Hyde, *Philos. Trans. R. Soc. London A* **1980**, *295*, 553.
[59] W. B. Pearson, *The Crystal Chemistry and Physics of Metals and Alloys*, Wiley, New York, **1972**, p. 3.
[60] W. H. J. Watson, J. Waser, *Acta Crystallogr.* **1958**, *11*, 689.
[61] G. J. Wessel, W. J. D. Ijdo, *Acta Crystallogr.* **1957**, *10*, 466.
[62] J. Köhler, G. Miller, A. Simon, *Z. Anorg. Allg. Chem.* **1989**, *568*, 8.
[63] K. B. Kersting, W. Jeitschko, *J. Solid State Chem.* **1991**, *93*, 350.
[64] W. H. McCaroll, L. Katz, G. B. Ansell, *J. Am. Chem. Soc.* **1957**, *79*, 5410.
[65] G. B. Ansell, L. Katz, *Acta Crystallogr.* **1966**, *21*, 482.
[66] F. A. Cotton, *Inorg. Chem.* **1964**, *3*, 1217.
[67] F. A. Cotton, X. Feng, *Inorg. Chem.* **1991**, *30*, 3666.
[68] A. Simon, H. G. von Schnering, *J. Less-Common Met.* **1966**, *11*, 31.
[69] J. R. Kennedy, A. Simon, *Inorg. Chem.* **1991**, *30*, 2564.
[70] With A = Na only the latter compound has been found in many experiments illustrating that besides a delicate electron balance, critical size relationships are of importance.
[71] J. Köhler, R. Tischtau, A. Simon, *J. Alloys Comp.* **1992**, *182*, 343.
[72] J. Köhler, R. Tischtau, A. Simon, *J. Chem. Soc. Dalton Trans.* **1991**, 829.
[73] J. Köhler, R. K. Kremer, A. Simon, unpublished results.
[74] J. Köhler, A. Simon, R. Tischtau, G. Miller, *Angew. Chem.* **1989**, *101*, 1695; *Angew. Chem. Int. Ed. Engl.* **1989**, *28*, 1662.
[75] $K_4Al_2Nb_{11}O_{21}F$: Space group *I4/mmm* (no. 139), $Z = 2$, $a = 878.57(6)$, $c = 1263.7(1)$ pm (Guinier data). CAD4 diffractometer; $Mo_{K\alpha}$; 315 with $F_0 \geq 2.0\sigma(F_0)$, $R = 0.097$, $R_w = 0.074$ $\rho_{calc} = 5.35\ g\,cm^{-3}$. Positional parameters: Nb(1) 2*a*, Nb(2) 16*m* with $x = 0.1620(2)$ and $z = 0.1643(2)$, Nb(3) 4*e* with $z = 0.3186$, Al 4*d*, K 8*j* with $x = 0.313(1)$, O(1) 8*h* with $x = 0.830(3)$, O(2) 16*n* with $x = 0.335(3)$, O(3) 16*m* with $x = 0.832(2)$ and $z = 0.328(1)$, F 2*b*. Further details of the crystal structure investigation may be obtained from the Fachinformationszentrum Karlsruhe, Gesellschaft für wissenschaftlich-technische Information mbH, D-W-7514 Eggenstein-Leopoldshafen (FRG), on quoting the depository number CSD-53992, the names of the authors, and the journal citation.
[76] The O^{a-a} atoms can be replaced by F atoms to give $K_4Al_2Nb_{11}O_{21-x}F_x$ ($0 \leq x \leq 1.0$). It is not possible to determine this replacement by means of structural analysis; however, it clearly shows up in the magnetic behavior and particularly in the lengths of the *c* axes, see Table 2.
[77] A. L. Bowman, T. C. Wallace, J. L. Yarnell, R. G. Wenzel, *Acta Crystallogr.* **1966**, *21*, 843.
[78] B. Hessen, S. A. Sunshine, T. Siegrist, R. Jimenez, *Mater. Res. Bull.* **1991**, *26*, 85.
[79] G. Svensson, P.-E. Werner, *Mater. Res. Bull.* **1990**, *25*, 9.
[80] Left of the line $Ba_2Nb_5O_9$, NbO, and Nb coexist.
[81] G. Svensson, *Solid State Ionics* **1989**, *32/33*, 126.
[82] G. Svensson, *Microsc. Microanal. Microstruct.* **1990**, *1*, 343.
[83] L. Kihlborg, *Prog. Solid State Chem.* **1990**, *20*, 101.
[84] A. Magnéli, *Chem. Scr.* **1986**, *26*, 535.
[85] A. Magnéli, *Microsc. Microanal. Microstruc.* **1990**, *1*, 1.
[86] B. G. Hrde, S. Andersson, *Inorganic Crystal Structures*, Wiley, New York, **1989**, p. 19.
[87] A similar phasoid exists in the Sr–Nb–O system.
[88] Vernier phases [89] or other "solid solutions" with fluorite structure such as the CeO_2–Y_2O_3 system and the block structures found among the slightly reduced niobium oxides serve as examples [90–92]. On the other hand, ordered compounds may contain extended structural defects which are the only structural features of a new compound when the appropriate preparative conditions are chosen. For example, before $YBa_2Cu_4O_9$ was actually synthesized it was identified as a defect in $YBa_2Cu_3O_{7-\delta}$ [93].
[89] E. Makovicky, B. G. Hyde, *Struct. Bonding (Berlin)* **1981**, *46*, 101.
[90] R. Wallenberg, R. Withers, D. J. M. Bevan, J. G. Thompson, P. Barlow, B. G. Hyde, *J. Less-Common Met.* **1989**, *156*, 1.
[91] K. M. Nimmo, J. S. Anderson, *J. Chem. Soc. Dalton Trans.* **1972**, 2328.
[92] H. Hibst, R. Gruehn, *Z. Anorg. Allg. Chem.* **1978**, *442*, 49.
[93] B. Domengès, M. Hervieu, C. Michel, B. Raveau, *Europhys. Lett.* **1987**, *4*, 211.
[94] G. Svensson, J. Köhler, A. Simon, *Z. Anorg. Allg. Chem.*, in press.
[95] V. G. Zubkov, V. A. Perelyayev, D. G. Kellermann, V. E. Stapsev, V. P. Dyakina, I. A. Kontzevaya, O. B. Makarova, G. P. Sveikin, *Dokl. Akad. Nauk SSSR* **1990**, *313*, 367.
[96] V. G. Zubkov, V. A. Perelyayev, G. P. Sveikin, *Dokl. Akad. Nauk SSSR*, in press.
[97] HREM studies indicate the existence of a greatly disordered compound $Ba_3Nb_{16}O_{23}$ containing $[2 \times 2 \times \infty]$ and $\{1 \times 3 \times \infty\}$ blocks.
[98] G. Svensson, J. Köhler, A. Simon *Angew. Chem.* **1992**, *104*, 192; *Angew. Chem. Int. Ed. Engl.* **1992**, *31*, 212.
[99] Cubic A_xNbO_3 (A = Sr, Ba, and Eu) is A-deficient with $0.7 \leq x \leq 0.95$ for Sr [34] and $x \approx 0.95$ for Ba and $0.7 \leq x \leq 0.9$ for Eu. $KNbO_3$ crystallizes in a distorted perovskite structure.
[100] G. Svensson, *J. Solid State Chem.* **1991**, *90*, 249.
[101] C. F. Michelson, P. E. Rauch, F. J. DiSalvo, *Mater. Res. Bull* **1990**, *25*, 971.
[102] G. Svensson, J. Köhler, A. Simon, *Acta Chem. Scand.*, **1992**, *46*, 244.
[103] G. Svensson, *Acta Chem. Scand.* **1990**, *44*, 222.
[104] L. Pauling, *The Nature of the Chemical Bond*, 3rd ed., Cornell University Press, New York, **1960**, Chapter 5, pp. 145–182.
[105] I. D. Brown, *Chem. Soc. Rev.* **1978**, *7*, 359.
[106] R. E. McCarley, *Polyhedron* **1986**, *5*, 51.
[107] I. D. Brown, D. Altermatt, *Acta Crystallogr. B* **1985**, *41*, 244.
[108] In some experiments with added NaF as a flux a few red transparent crystals were formed [33]. They exhibit nearly identical structural parameters as the golden crystals except for a slightly different $x \approx 0.8$ and, more importantly, a ring-shaped distribution of the scattering density for Na around the center of the too-large cuboctahedral cavity. Of course, the Na–O bond order sum is slightly increased by such (statistical) off-center positions of Na^+. The result is reminiscent of Na_4Si_4 which was described as having dark metallic luster before it was prepared in pure form as red transparent crystals [109].
[109] H. G. von Schnering, M. Schwarz, R. Nesper, *Angew. Chem.*, **1986**, *98*, 558; *Angew. Chem. Int. Ed. Engl.* **1986**, *25*, 566.
[110] R. Hoffmann, *J. Chem. Phys.* **1963**, *39*, 1397.
[111] T. Hughbanks, R. Hoffmann, *J. Am. Chem. Soc.* **1983**, *105*, 3528.
[112] R. A. Wheeler, R. Hoffmann, *J. Am. Chem. Soc.* **1988**, *110*, 7315.
[113] J. K. Burdett, T. Hughbanks, *J. Am. Chem. Soc.* **1984**, *106*, 3101.
[114] O. K. Andersen, S. Sathpathy in *Basic Properties of Binary Oxides* (Eds.: A. Dominguez, J. Castaing, R. Marquez), Publ. Univ. Sevilla, **1983**, p. 21.
[115] T. Hughbanks, *Prog. Solid State Chem.* **1989**, *19*, 329.
[116] EH approximation [110]. H_{ij} matrix elements: J. H. Ammeter, H.-B. Bürgi, J. C. Thibeault, R. Hoffmann, *J. Amer. Chem. Soc.* **1978**, *100*, 3686; Tight-binding modification: M.-H. Whangbo, R. Hoffmann, *J. Amer. Chem. Soc.* **1978**, *100*, 6093; special *k* points: R. Ramirez, M. C. Böhm, *Int. J. Quantum Chem.* **1986**, *30*, 391. R. H. Summerville, R. Hoffmann, *J. Amer. Chem. Soc.* **1976**, *98*, 7240.
[117] Parameters used in the EH calculations: Atomic orbital energies H_{ij} [eV] (coefficients ζ_1): O: 2s −32.3 (2.275), 2p −14.8 (2.275), Ba: 6s −6.62 (1.214), 6p −3.92 (1.214), Si: 3s −17.3 (1.383), 3p −9.2 (1.383), Al: 3s −12.3 (1.167), 3p −6.50 (1.167), Mg: 3s −9.0 (1.100), 3p −4.50 (1.100), Nb: 5s −10.1 (1.89) 5p −6.86 (1.85), 4d −12.10 (4.08) Double ζ functions have been used for Nb with C_1 0.6401, ζ_2 1.64, and C_2 0.5516.
[118] F. A. Cotton, T. E. Haas, *Inorg. Chem.* **1964**, *3*, 10.
[119] S. F. A. Kettle, *Theoret. Chim. Acta* **1965**, *3*, 211.
[120] B. Spreckelmeyer, H. G. von Schnering, *Z. Anorg. Allg. Chem.* **1971**, *386*, 27.
[121] G. Miller, Iowa State University, private communication.
[122] C. C. Torardi, R. E. McCarley, *J. Am. Chem. Soc.* **1979**, *101*, 3963
[123] R. Hoffmann, R. Hoppe, K. Bauer, K. J. Range, *J. Less-Common Met.* **1990**, *161*, 279.
[124] A. Simon, W. Mertin, H. Mattausch, R. Gruehn, *Angew. Chem.* **1986**, *98*, 831; *Angew. Chem. Int. Ed. Engl.* **1986**, *22*, 845.
[125] S. J. Hibble, A. K. Cheetham, A. R. L. Bogle, H. R. Wakerly, D. E. Cox, *J. Am. Chem. Soc.* **1988**, *110*, 3295.
[126] P. Gougeon, P. Gall, R. E. McCarley, *Acta Crystallogr. Sect. C* **1991**, *47*, 1585.
[127] S. A. Davydov, B. N. Goschchitskii, E. A. Karkin, A. V. Mirmelstein, V. I. Voronin, V. D. Parkhomenko, V. G. Zubkov, V. A. Perelyayev, I. F. Berger, I. A. Kontzevaya, *Int. J. Mod. Phys. B* **1990**, *4*, 1531.
[128] J.-P. Fayolle, F. Studer, G. Desgardin, B. Raveau, *J. Solid State Chem.* **1975**, *13*, 57.
[129] G. V. Bazuev, G. P. Shveikin, *Russ. J. Inorg. Chem. (Engl. Transl.)* **1985**, *30*, 1497.
[130] L. Katz, H. D. Megaw, *Acta Crystallogr.* **1967**, *22*, 639.
[131] C. C. Torardi, R. E. McCarley, *Inorg. Chem.* **1985**, *24*, 476.
[132] G. Miller, Iowa State University, private communication.
[133] D. Watanabe, J. R. Castles, A. Jostons, A. S. Malin, *Acta Crystallogr.* **1967**, *23*, 307.
[134] F. Gronvold, A. Kjekshus, F. Raaum, *Acta Crystallogr.* **1961**, *14*, 930.
[135] G. Brauer, H. Morawietz, *Z. Anorg. Allg. Chem.* **1962**, *317*, 13.
[136] R. Dronskowski, A. Simon, *Angew. Chem.* **1989**, *101*, 775; *Angew. Chem. Int. Ed. Engl.* **1989**, *28*, 758.
[137] A. Simon, *Angew. Chem.* **1988**, *100*, 163, *Angew. Chem. Int. Ed. Engl.* **1988**, *27*, 159.

Proteins from the D-Chiral World

By *Günther Jung**

Chirality and symmetry in general have always intrigued mankind. This fascination can be traced over the course of thousands of years by reference to many buildings and works of art created by humans with their mirror-image hands. Ever since the work of Louis Pasteur, Emil Fischer, and van't Hoff, stereochemistry has constantly provided chemical research with new impetus. Recently Kent et al.[1] have achieved a much discussed aim by synthesizing the first enzymatically active D-protein. Kent's experience with the optimized total chemical synthesis of many highly pure analogues of the HIV-1 protease,[2, 3] which also yielded single crystals suitable for X-ray analysis, encouraged him to attempt the total chemical synthesis of the 99 amino acid long D-enantiomeric protein chain.

The Merrifield synthesis based on the *t*Boc (*tert*-butyloxycarbonyl) strategy which still dominates in the USA was carried out using a modified Applied Biosystems 430 A synthesizer for fast synthesis cycles. Two syntheses were carried out according to the identical procedure, one using commercially available N^{α}-*t*Boc-L-amino acid derivatives, the other using commercially available N^{α}-*t*Boc-D-amino acid derivatives with the appropriate side-chain protecting groups. As in previous syntheses of crystalline L-HIV-1 protease, α-amino-*n*-butyric acid (Aba) was used as an isosteric replacement for cysteine residues at positions 67 and 95; this modification does not affect folding or enzyme activity. According to the manufacturers of the D-amino acid derivatives, these contained only 0.01–0.08% of L-enantiomers. The coupling was carried out with preactivation by benzotriazolyltetramethyluronium hexafluorophosphate (HBTU) and simultaneous in situ neutralization; this has been shown by Henklein et al.[4] to result in negligible levels of racemization. As a check during the course of the synthesis, samples of peptides cleaved from the resin with hydrogen fluoride were sequenced by matrix-assisted laser desorption time-of-flight mass spectrometry. Up until the present time the properties of the two enantiomeric proteins have been compared using amino acid analysis, ion spray mass spectrometry (L-enzyme: 10748 ± 4 Da, D-enzyme: 10751 ± 3 Da, calculated monoisotopic mass: 10748 Da) and high-pressure liquid chromatography (HPLC). The circular dichroism (CD) spectra revealed, as was to be expected, equal and opposite Cotton effects.

The synthetic D- and L-proteins have identical sequences of amino acids. Therefore, if it is true that the amino acid sequence alone determines the final folded 3-D structure, they should fold in exactly the same way to give identical three-dimensional (tertiary structure) structures. A comparison of the enzyme activities powerfully demonstrates the mirror-image folding (Fig. 1) from the denatured state to the homodimer with correct quaternary structure. Thus the L-enzyme cleaved only the fluorogenic L-hexapeptide substrate, whereas the D-enzyme cleaved only the corresponding D-substrate, 2-aminobenzoyl-all-D-Thr-Ile-Nle-Phe(p-NO_2)-Gln-Arg-NH_2 (Nle = norleucine). Reciprocal chiral specificity was also demonstrated with acetylated D- and L-pseudohexapeptidamide chiral inhibitors with the structure Ac-Thr-Ile-Nle-Ψ[CH_2-NH]-Nle-Gln-Arg-NH_2 (Ac = acetyl). The achiral protease inhibitor Evans Blue was a potent inhibitor of both enantiomers of the enzyme.

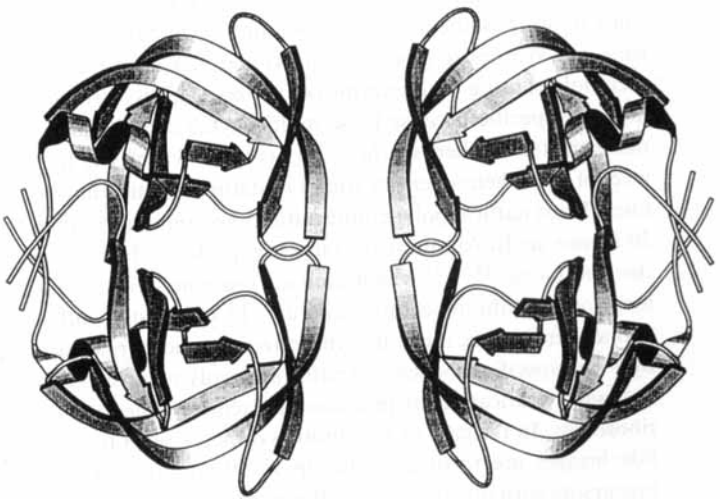

Fig. 1. Three-dimensional structure of the L- (left) and D-HIV proteases (right) (from ref. [1]).

Up to this point everything as was to be expected, most people might say. But do D-proteins offer us any advantages apart from the chiral properties and substrate specificities experimentally demonstrated for the first time? One of the most important advantages is the resistance to proteases as exhibited by many polypeptide antibiotics containing D-amino acids.

It is well established that polypeptides built of L-amino acids form right-handed α-helices and that polypeptides with D-amino acids form left-handed α-helices. Merrifield et al.[5, 6] demonstrated that three helical polypeptides, cecropin A, magainin-2-amide, and melittin, which form potential-dependent ion channels in lipid bilayers, are also antibacterial as D-enantiomers. Another recent paper[10] describes enantiomeric gramicidin A channels. Gramicidin A is a polypeptide antibiotic built up from alternating D- and L-amino acids. In this case, however, the biological activity does not depend on a chiral receptor molecule, that is to say that left- and right-handed channels built from peptide aggregates should allow the passage of ions to the same extent.

There should, however, be a small but noticeable difference in experiments with lipid bilayers, because helices with opposite handedness should interact differently with chiral lipid membranes. Apparently the difference is so small that

[*] Prof. Dr. G. Jung
Institut für Organische Chemie der Universität
Auf der Morgenstelle 18, D-W-7400 Tübingen (FRG)

 © VCH Verlagsgesellschaft mbH, W-6940 Weinheim, 1992 0570-0833/92/1111-1457 $ 3.50+.25/0

it is not measurable even with very sensitive electrical measuring devices (see also ref. [7]). We were able to demonstrate some time ago that homopolypeptides built up from the achiral α-aminobutyric acid (Aib), for example Z-$(Aib)_{10}$-O*t*Bu, interconverted from a left-handed to right-handed 3_{10}-helix and vice versa 1200 times per second. These enantiomeric helices also form ion-conducting channels in lipid bilayers, in spite of the interconversion between the two forms (isotoperization) at room temperature. The three synthetic D-enantiomeric peptide antibiotics with full antibiotic activity are especially interesting because of their resistance to proteases, which means that they may retain their activity when taken orally. Tam[11] also recently synthesized D-peptide antibiotics containing cysteine bridges with antibacterial activity, defensins with a β-pleated sheet structure.

In the majority of the hundreds of known peptide antibiotics, nature has already built in D-amino acids. Microorganisms can synthesize mixed L- and D-peptides as secondary metabolites using multienzyme complexes. This is, however, not very specific because these multienzyme complexes can make mistakes when synthesizing, as is shown by the high level of microheterogeneity found in natural peptide antibiotics. Most natural polypeptide antibiotics contain less than 20 amino acids. Amongst the largest peptide antibiotics are the lantibiotics,[12, 13] which contain D-amino acids in the form of a lanthionine ring structure. In contrast to other peptide antibiotics, these are synthesized by microorganisms by a very specific biochemical pathway involving post-translational modification of precursor proteins synthesized on ribosomes. In the case of lantibiotic synthesis, several disulfide bridges are formed in the up to 60 amino acid long precursors with inversion of configuration at the C_α atom of the original serine and threonine residues.[14]

This recent work shows that peptide chemists are able to synthesize active all-D-peptide compounds and even a pure D-enzyme. In addition, newly elucidated biosynthetic pathways using microorganisms allow, for example, *meso*-lanthionine and α,β-didehydroamino acids to be built into protein structures. Equal chirality of each building block is a prerequisite for a three-dimensional biopolymer with a high percentage of ordered structural elements like the α-helix and β-pleated sheet. A functional enzyme built from D-amino acids and L-amino acids, is conceivable, however, if enough D-amino acids in sequence could form a left-handed α-helix which could then, for example, form a "D-domain" α-helix-turn-β-pleated sheet with a β-pleated sheet of D-amino acids. Other domains could consist of L-amino acids and contain enzymatic cleavage sites. Such a chimera could be constructed by combining segments produced by peptide chemistry and by biotechnology. Recently, there have been promising attempts at the total chemical synthesis of artificial enzymes with the help of templates.[15, 16] In the future, D-domains should be considered in the de novo design of such molecules. The human imagination is held in check only by the size of peptides that can be chemically synthesized, currently around 150 amino acids. This figure may increase to around 250 amino acids by the year 2000 (for details of new developments in solid-phase synthesis see refs. [17, 18]).

The resistance of synthetic D-enzymes to proteases has led to speculation about possible therapeutic applications.[1, 11] D-Enzymes could react with achiral substrates with a long-lived in-vivo activity, because they are resistant to attack by the L-proteases found in mammals. An additional advantage would be that D-proteins are presumably very slightly immunogenic or nonimmunogenic. A boostable and long-lasting immune response requires the processing and presentation of the peptide antigen to the MHC (major histocompatibility complex) molecules to enable recognition by helper T cells (by MHC class II) or by cytotoxic lymphocytes (CTL, by MHC class I). This requires that a peptide fragment with an MHC-specific recognition sequence[19] be cut from the D-proteins, and this is not possible. Nevertheless, the synthesis and purification of a totally nonimmunogenic D-protein is not possible with the present state of technology and methodology. This is not because of the presence of failure sequences in them which are certainly present due to incomplete coupling reactions. Rather, the reason is to be found in the extremely sensitive and highly specific recognition reaction between peptide antigen, MHC molecule, T cell receptor, and associated proteins such as β-microglobin. In fact, this multimeric complex could be used for in-vitro assays for CTL epitopes in the attomole range. None of the current amino acid activation reactions operate without some degree of racemization. So even if very sensitive racemization tests fail to indicate the presence of L-amino acids in D-proteins, recognition is possible due to antibodies already present, and a T cell mediated immunological response is to be expected after repeated application. This means that any traces of material that can be cleaved by L-proteases must be removed, in order to produce D-protein drugs which do not evoke an immune response.

Other nontherapeutic applications, above and beyond purely academic interest, make D-proteins interesting as well. The unfortunately extremely expensive D-enzymes could enable the production of hard-to-produce chiral products. Especially attractive is the enzymatic synthesis or modification of L-carbohydrates. Would it be possible to create an L-sugar world with D-proteins and even an L-RNA/DNA world with L-ribose/L-deoxyribose linked bases?

Let us return to the practical and realizable possibilities which synthetic D-proteins offer. Zawadake and Berg[20] synthesized a D-protein for completely different reasons. They synthesized the iron–sulfur protein D-rubredoxin, which is part of the electron transport chain in microorganisms. The synthetic D-rubredoxin was mixed with synthetic L-rubredoxin to give a racemate, exactly that mixture which one usually tries to painstakingly separate with sophisticated methods. However, the authors obtained through this procedure single crystals of the highest quality with a centrosymmetric space group. This space group led to a simplification of the phase problem and a quicker solution of the structure by X-ray crystallography. In addition, the resolution of the X-ray structural analysis should be greatly improved, and it seems easier to obtain good crystals from the racemate compared to the pure enantiomers. If only the last application proves to be practicable, then at least as far as the protein crystallographers are concerned, the enormous effort put into the synthesis is well worthwhile, as Petsko[11] has already pointed out.

German version: *Angew. Chem.* **1992**, *104*, 1484

[1] R. C. del Milton, S. C. F. Milton, S. B. H. Kent, *Science* **1992**, *256*, 1445–1448.
[2] A. Wlodawer, M. Miller, M. Jaskólski, B. K. Sathyanarayana, E. Baldwin, J. T. Weber, L. M. Selk, L. Clawson, J. Schneider, S. B. H. Kent, *Science* **1989**, *245*, 616–621.
[3] M. Miller, J. Schneider, B. K. Sathyanarayana, M. V. Toth, G. R. Marshall, L. Clawson, L. M. Selk, S. B. H. Kent, A. Wlodawer, *Science* **1989**, *246*, 1149–1152.
[4] P. Henklein, M. Beyermann, B. Costisella, R. Sohr, M. Haußner in *Innovation and Perspectives in Solid Phase Synthesis* (Ed.: R. Epton), Intercept, Andover, **1992**, pp. 401–403.
[5] R. B. Merrifield, H. G. Boman, D. Andreu, Z. Li, J. Fink, D. Wade in *Peptides 1990, Proc. 21st Eur. Pept. Symp.* (Eds.: E. Giralt, D. Andreu), Escom, Leiden, **1991**, pp. 3–16.
[6] D. Wade, A. Boman, B. Wahlin, C. M., Drain, D. Andreu, H. G. Boman, R. B. Merrifield, *Proc. Natl. Acad. Sci. USA* **1990**, *87*, 4761–4765.
[7] a) E. Neher, *Angew. Chem.* **1992**, *104*, 837–843; *Angew. Chem. Int. Ed. Engl.* **1992**, *31*, 824–829; b) B. Sakmann, *ibid.* **1992**, *104*, 844–856 and **1992**, *31*, 830–841.
[8] R.-P. Hummel, C. Toniolo, G. Jung, *Angew. Chem.* **1987**, *97*, 1180–1182; *Angew. Chem. Int. Ed. Engl.* **1987**, *26*, 1150–1152.
[9] G. Boheim, C. Toniolo, G. Jung, unpublished results.
[10] R. E. Koeppe II, L. L. Providence, D. V. Greathouse, F. Heitz, Y. Trudelle, N. Purdie, O. S. Andersen, *Proteins: Struct. Funct. Genet.* **1992**, *12*, 49–62.
[11] Cf. note by G. A. Petsko, *Science* **1992**, *256*, 1403–1404.
[12] G. Jung, *Angew. Chem.* **1991**, *103*, 1067–1084; *Angew. Chem. Int. Ed. Engl.* **1991**, *30*, 1051–1068.
[13] *Nisin and Novel Lantibiotics* (Eds.: G. Jung, H. G. Sahl), Escom, Leiden, **1991**.
[14] N. Schnell, K.-D. Entian, U. Schneider, F. Götz, H. Zähner, R. Kellner, G. Jung, *Nature* **1988**, *333*, 276–278.
[15] M. Mutter, S. Vuilleumier, *Angew. Chem.* **1989**, *101*, 551–571; *Angew. Chem. Int. Ed. Engl.* **1989**, *28*, 535–555.
[16] J. M. Stewart, J. R. Cann, K. W. Hahn, W. A. Klis in *Peptides, Chemistry and Biology, Proc. 12th Am. Pept. Symp.* (Eds.: J. A. Smith, J. Rivier), Escom, Leiden, **1992**, S. 335–336.
[17] E. Bayer, *Angew. Chem.* **1991**, *103*, 117–133; *Angew. Chem. Int. Ed. Engl.* **1991**, *30*, 96–112.
[18] G. Jung, A. G. Beck-Sickinger, *Angew. Chem.* **1992**, *104*, 375–391; *Angew. Chem. Int. Ed. Engl.* **1992**, *31*, 367–383.
[19] K. Falk, O. Rötzschke, S. Stevanović, G. Jung, H. G. Rammensee, *Nature* **1991**, *351*, 290–296.
[20] L. Zawadske, J. Berg, *J. Am. Chem. Soc.* **1992**, in press, cf. ref. [11].

Asymmetric Deprotonation as an Efficient Enantioselective Preparation of Functionalized Secondary Alcohols

By *Paul Knochel**

The enantioselective preparation of chiral secondary alcohols has been achieved through a number of methods with great success. One pathway that is widely used is the asymmetric addition of organometallic compounds R^1M to aldehydes[1] (retrosynthetic pathway **A** of Scheme 1). A disconnection involving inversion of polarity[2] is also possible [retrosynthetic pathway **B** of Scheme 1]. In this case, the sec-

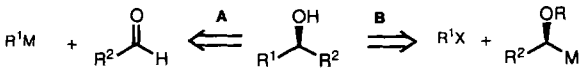

Scheme 1.

ondary alcohol is formed by a substitution reaction of an α-oxygen-substituted carbenoid **1**.[3] Although this alternative route has been frequently used for synthetic applications, the multistep procedures[4] required for the enantioselective preparation of the carbenoids have limited the utility of this approach. Furthermore, to be synthetically attractive, the chiral carbenoid has to be configurationally stable under the reaction conditions, and its reaction with electrophiles has to proceed with a well-defined stereochemistry (retention or inversion).

Enantioselective deprotonation reactions have been known for several years and have led to several elegant synthetic applications.[5] Hoppe et al. found that this method allows an expedient access to a wide range of chiral α-oxygen carbenoids **1** [M = Li, Eq. (a), Scheme 1][6–12] starting from readily available achiral carbamates **2** and the complex of an alkyllithium compound and (−)-sparteine **3**.[13]

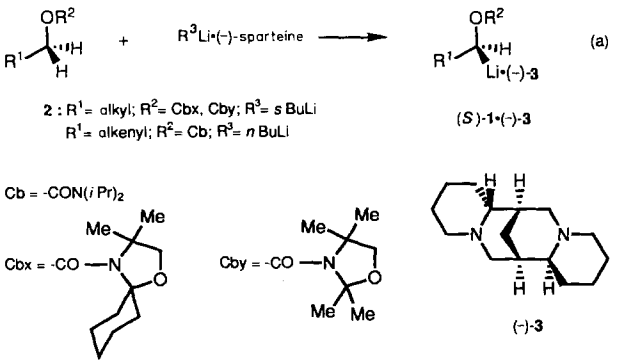

The deprotonations are complete within a few hours at −78 °C and afford the lithium carbenoid · sparteine complexes (*S*)-**1** · (−)-**3** with excellent enantioselectivities.[6–12] Whereas sparteine complexes of lithiated secondary allyl and primary alkyl carbamates are configurationally stable below −30 °C, those of primary allyl carbamates such as **4** · (−)-**3** are not configurationally stable even at −70 °C. It is, however, possible to use these reagents in synthesis, since the preferential crystallization of the *S* diastereoisomer in pentane/cyclohexane drives the equilibrium completely to one side. After a low-temperature transmetalation of (*S*)-**4** · (−)-**3** with an excess of tetraisopropoxytitanium, the allylic titanium reagent (*R*)-**5** is obtained with inversion of configuration. The addition of various aldehydes to (*R*)-**5**

[*] Prof. Dr. Paul Knochel
Fachbereich Chemie der Philipps-Universität
Hans-Meerwein-Strasse, D-W-3550 Marburg (FRG)

furnishes homoaldol adducts of type **6** with high *anti* diastereoselectivity and very good enantioselectivity (82–90% *ee*) (Scheme 2). They can be further converted into lactones as shown in the synthesis of the insect pheromone (+)-eldanolide (92% *ee*).[6d]

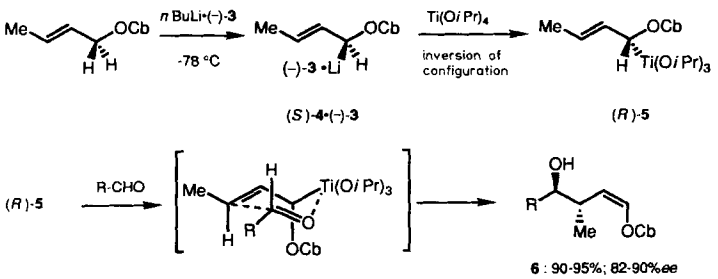

Scheme 2. Enantioselective synthesis of homoallyl alcohols by asymmetric deprotonation.

A crystal structure analysis of a complex between a lithiated primary carbamate and (−)-sparteine **3** unambiguously established the *S* configuration.[14]

Of considerable interest for synthetic applications are the deprotonations of alkyl carbamates RCH_2OCbx or RCH_2OCby with *sec*-butyllithium · (−)-sparteine, followed by the alkylation with an electrophile.[7] Most electrophiles such as CO_2, Me_3SnCl, Me_3SiCl, MeI, Me_2CHCHO react with retention of configuration to afford protected alcohols of the type **7** [Eq. (b)]. This provides a very general enantioselective synthesis of secondary alcohols. The enantioselectivities of the deprotonations are better than 95% *ee* in most cases. These high enantiodifferentiations are kinetic in nature, and MNDO calculations show that the stabilities of the two diastereomeric ion-pairs (+)-**1** · (−)-**3** and (−)-**1** · (−)-**3** are comparable.[15] Efforts have also been made to determine the structure of the chiral base RLi · (−)-**3**, but only the structure of the complex $(iPrLi)_2$ · (−)-**3** in ether has been determined, by NMR techniques.[16]

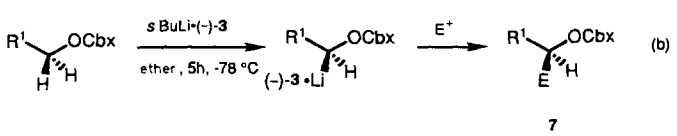

The Cbx-protecting group of **7** can be removed under mild conditions. An acid treatment ($MeSO_3H$, MeOH, reflux, 16 h) affording the intermediate carbamate **8** followed by a basic treatment ($Ba(OH)_2 \cdot 8H_2O$, MeOH, reflux, 4 h) leads to the chiral alcohol **9** [Eq. (c)][7] in excellent yield.

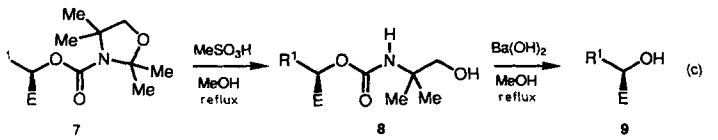

Remarkably, this method can be applied to carbamates bearing a functional group in close proximity to the OCbx or OCby group. High enantiomeric excesses are obtained, although chelating groups such as $N(CH_2Ph)_2$[8, 11] or an OR[9, 10] group are present. Thus the β-dibenzylaminocarbamate **10** can be deprotonated with high enantioselectivity with *s*BuLi · (−)-**3** (3 equiv; −78 °C, 3 h) and treated with various electrophiles to give almost enantiomerically pure 1,2-aminoalcohols **11** [Eq. (d)].[8] Interestingly, the presence of a substituent at the α position to the nitrogen functionality strongly influences the rate and controls the enantioselectivity of the deprotonation. This can be clearly seen in the case of the carbamate **12**, derived from (*S*)-*N*,*N*-dibenzylleucinol. After the reaction with an electrophile, substrate-controlled deprotonation yields the aminoalcohol derivative **13**

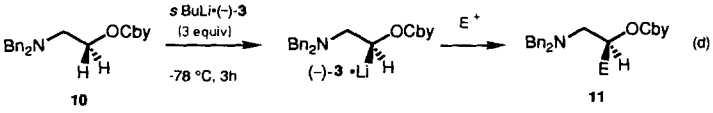

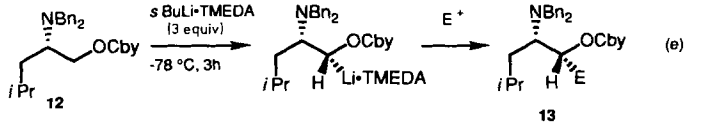

[Eq. (e)].[8] Finally, the utility of the method has been demonstrated by Hoppe et al. with a short enantioselective synthesis of (*R*)-pentolactone **14** [Eq. (f)].[9]

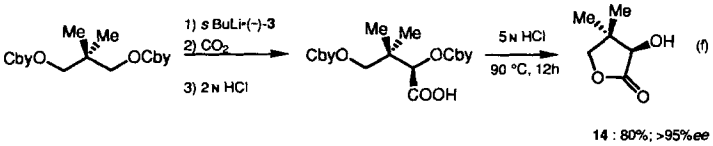

An asymmetric deprotonation of (*tert*-butoxycarbonyl)-pyrrolidines **15** has been recently developed by Beak et al. allowing a highly enantioselective synthesis of a variety of 2-substituted pyrrolidines [Eq. (g)].[17]

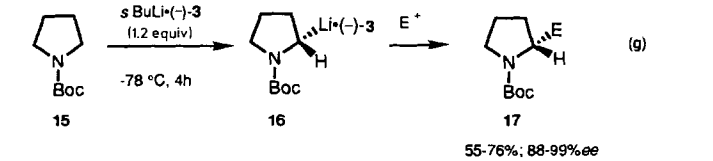

The enantioselective deprotonation at the α position to oxygen- or nitrogen-substituted carbamates with RLi · sparteine complexes allows the most practical and efficient synthesis of the corresponding chiral organolithium compounds. The high enantioselectivity of the deprotonation, the high stereoselectivity observed in the course of the reaction of these species with electrophiles, as well as the compatibility with some donating functional groups in the lithium organometallic compound make this methodology a very powerful tool for the construction of nonracemic chiral molecules.

German version: *Angew. Chem.* **1992**, *104*, 1486

[1] For recent advances in this field see: a) G. Solladié in *Asymmetric Synthesis, Vol. 2* (Ed.: J. D. Morrison), Academic Press, New York, **1983**, pp. 157–200; b) D. A. Evans, *Science* **1988**, *240*, 420–426; c) R. Noyori, M. Kitamura, *Angew. Chem.* **1991**, *103*, 34–55; *Angew. Chem. Int. Ed. Engl.* **1991**, *30*, 49–69; d) B. Schmidt, D. Seebach, *ibid.* **1991**, *103*, 1383–1385 and **1991**, *30*, 1321.

[2] D. Seebach, *Angew. Chem.* **1979**, *91*, 259–278; *Angew. Chem. Int. Ed. Engl.* **1979**, *18*, 239.

[3] a) H. Ahlbrecht, G. Boche, K. Harms, M. Marsch, H. Sommer, *Chem. Ber.* **1990**, *123*, 1853–1858; b) G. Boche, A. Opel, M. Marsch, K. Harms, F. Haller, J. C. W. Lohrenz, C. Thümmel, W. Koch, *ibid.* **1992**, *143*, in press.

[4] a) W. C. Still, C. Sreekumar, *J. Am. Chem. Soc.* **1980**, *102*, 1201–1202; b) V. J. Jephcote, A. J. Pratt, E. J. Thomas, *J. Chem. Soc. Chem. Commun.* **1984**, 800–802; *J. Chem. Soc. Perkin Trans. 1* **1989**, 1529–1535; c) J. M. Chong, E. K. Mar, *Tetrahedron* **1989**, *45*, 7709–7716; d) D. S. Matteson, P. B. Tripathy, A. Sarkar, K. N. Sadhu, *J. Am. Chem. Soc.* **1989**, *111*, 4399–4402; e) R. J. Linderman, A. Ghannam, *ibid.* **1990**, *112*, 2392–2398; f) J. A. Marshall, W. Y. Gung, *Tetrahedron* **1989**, *45*, 1043–1052.

[5] For an excellent review see: H. Waldmann, *Nachr. Chem. Tech. Lab.* **1991**, *39*, 413–418.

[6] a) D. Hoppe, O. Zschage, *Angew. Chem.* **1989**, *101*, 67–69; *Angew. Chem. Int. Ed. Engl.* **1989**, *28*, 65–67; b) O. Zschage, J.-R. Schwark. D. Hoppe, *ibid.* **1990**, *102*, 336–337 and **1990**, *29*, 296; c) O. Zschage, D. Hoppe, *Tetrahedron* **1992**, *48*, 5657–5666; d) H. Paulsen, D. Hoppe, *ibid.* **1992**, *48*, 5667–5670; e) O. Zschage, J.-R. Schwark, D. Hoppe, *ibid.* **1992**, *48*, in press.

[7] D. Hoppe, F. Hintze, P. Tebben, *Angew. Chem.* **1990**, *102*, 1457–1459; *Angew. Chem. Int. Ed. Engl.* **1990**, *29*, 1422.

[8] J. Schwerdtfeger, D. Hoppe, *Angew. Chem.* **1992**, *104*, 1547; *Angew. Chem. Int. Ed. Engl.* **1992**, *31*, 1505.

[9] M. Peatow, H. Ahrens, D. Hoppe, *Tetrahedron Lett.* **1992**, *33*, 5323–5326.

[10] H. Ahrens, M. Paetow, D. Hoppe, *Tetrahedron Lett.* **1992**, *33*, 5327–5330.

[11] P. Sommerfeld, D. Hoppe, *Synlett* **1992**, 764–766.

[12] F. Hintze, D. Hoppe, *Synthesis* **1992**, in press.

[13] (−)-Sparteine has been used as additive in several types of asymmetric reactions with moderate success; see, for example, H. Nozaki, T. Aratani, T. Toraya, R. Noyori, *Tetrahedron* **1971**, *27*, 905–913.

[14] M. Marsch, K. Harms, O. Zschage, D. Hoppe, G. Boche, *Angew. Chem.* **1991**, *103*, 338–339; *Angew. Chem. Int. Ed. Engl.* **1991**, *30*, 321–323.

[15] H.-U. Würthwein, unpublished results.

[16] D. J. Gallagher, S. T. Kerrick, P. Beak, *J. Am. Chem. Soc.* **1991**, *114*, 5872–5873.

[17] S. T. Kerrick, P. Beak, *J. Am. Chem. Soc.* **1991**, *113*, 9708–9710.

Communications may be submitted in English *or* in German. Further details regarding the submission of communications can be found in the "Notice to Authors" reproduced in the January issue of the journal. Copies thereof may be obtained from the editorial office upon request.

The Structure of Pentamethyltantalum**

By *Thomas A. Albright** and *Huang Tang*

For a d^0 or d^{10} ML_5 transition metal complex there is a spherical field around the transition metal. As a result, the Valence Shell Electron Pair Repulsion (VSEPR) model[1] clearly predicts that a trigonal-bipyramidal (TBP) structure will be preferred over other alternatives, including the square-pyramidal (SP). Force field calculations[2] have also demonstrated that the TBP structure is favored over the SP on purely steric grounds. A number of theoretical studies have been carried out on the structural preferences of d electron counts between zero and ten.[3] In this work, we would like to communicate our theoretical work on two d^0 complexes, $[TaH_5]$ and $[Ta(CH_3)_5]$, in which the influence of strong π-donors and steric bulk of the ligands does not play a role in determining the structure. Our contention is that there is a persistent electronic factor that, contrary to the VSEPR model, favors the SP structure.

An idealized orbital correlation diagram for the TBP and SP structures is given in Figure 1. The electron count is appropriate for a d^0 complex, and for simplicity hydrido ligands are assumed. The construction of these valence orbitals is quite straightforward and has been presented elsewhere[3f] for the structure with D_{3h} symmetry. The orbital lowest in energy, $1a_1'$, does not change much in form or energy on going from TBP to SP geometry. The xy[4] component of the e' set is destabilized (coordinate system on the upper left of Figure 1); overlap between metal d orbitals and hydrogen s orbitals decreases as the H_{eq}-M-H_{eq} angle increases. The $x^2 - y^2$ component of e' stays basically at constant energy. There is some orbital mixing with $2a_1'$ so that it becomes a y^2 orbital at the metal. Likewise, the $2a_1'$ level evolves into an $x^2 - z^2$ function at the metal. The relative energy of $2a_1'$ at the SP geometry depends critically on the H_{ap}-M-H_{ba}[4] angles. With typical angles of approximately 115° (see below),

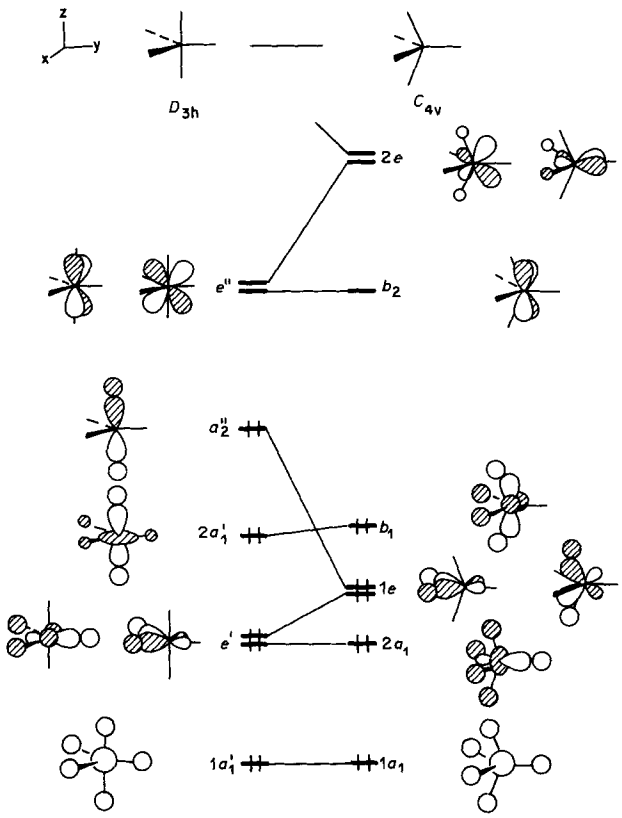

Fig. 1. An orbital correlation diagram connecting the structures of $[TaH_5]$ with D_{3h} (TBP) and C_{4v} (SP) symmetry.

there is a small net loss of overlap between metal d orbitals and the appropriate orbitals of the ligands so that there is a small increase in energy on going from the TBP to SP for this molecular orbital. The a_2'' and e'' levels are absolutely critical to this analysis. At the TBP geometry, the a_2'' orbital has exclusively metal z character and overlaps with the hydrogen s atomic orbitals, whereas the e'' set has rigorously metal xz and yz character with no hydrogen contribution. Upon distortion, the a_2'' level and the yz component of the e'' level strongly intermix so that the former is stabilized considerably, becoming one component of the $1e$ set on the SP side, and metal yz is correspondingly destabilized. Now, a_2'' is filled while the e'' set is empty; consequently, the total stabilization afforded to a_2'' influences greatly which geometry will be the more stable one. In the absence of strong π-donor groups on the ligand, the e''/a_2'' energy gap primarily determines the magnitude of this second-order perturbation.[4] As the electronegativity of the ligands decreases (and the ligand σ-donor strength increases), the energy gap will decrease and a_2'' will be stabilized to a greater extent. Hence, an SP structure for a d^0 complex can be a viable possibility. This argument is simply based on a second-order Jahn–Teller effect; a small energy gap implies a potential distortion of $e'' \times a_2'' = e'$ symmetry which converts a trigonal bipyramid into a square pyramid. A related view draws on the fact that valence p atomic orbitals of the metal lie at a much higher energy than the d set. In a localized sense, the hybridization at the metal will have increased d and less p character at the SP geometry. This will afford greater stabilization when the M–L bond is reasonably covalent.

[*] Prof. T. A. Albright, H. Tang
Department of Chemistry, University of Houston
Houston, TX 77204-5641 (USA)

[**] This research was supported by the Robert A. Welch Foundation and the Petroleum Research Fund as administered by the American Chemical Society. We appreciate a generous allocation of supercomputer time from the National Science Foundation at the Pittsburgh Supercomputing Center. We are very grateful to Professor A.Haaland (University of Oslo) for communicating unpublished results (see also the following communication).

To test these ideas, we have carried out ab initio calculations[5] on $[TaH_5]$ and $[Ta(CH_3)_5]$. $[TaH_5]$ is unknown, although the d^8 complexes $[CoH_5]^{4-}$ and $[IrD_5]^{4-}$ in $Mg_2[CoH_5]$ and $Sr_2[IrD_5]$ are known.[8] At the Hartree–Fock (HF) level, the optimized D_{3h} (TBP) structure was found to have Ta–H_{ax} and Ta–H_{eq} bond lengths of 186 and 174 pm, respectively. Inclusion of electron correlation was carried out at the MP2 level. The Ta–H_{ax} and Ta–H_{eq} distances were found to be 188 and 176 pm, respectively. Likewise, we found little difference between the HF and MP2 optimized structures for the C_{4v} (SP) isomer. The Ta–H_{ap}, Ta–H_{ba} bond lengths and H_{ap}-Ta-H_{ba} bond angles were 180 pm (182), 175 pm (177), and 117.2° (117.6°), respectively, where the numbers in parentheses refer to the MP2 optimized values. Most importantly, at the HF level the C_{4v} structure was found to be 16.4 kcal mol^{-1} more stable than the D_{3h} one. This value increases to 19.9 kcal mol^{-1} at the MP2 level! The vibrational frequencies (MP2 level) for the C_{4v} isomer were computed to be all real, thus categorizing this structure as a minimum on the potential energy surface. However, the D_{3h} structure was found to possess imaginary frequencies of e' and a_2'' symmetry. Therefore, it is a higher order saddle point. Clearly, the contribution of the d orbitals to Ta–H bonding is very large here. One interesting manifestation of this thesis is that the Ta–H_{ba} bonds are shorter than the Ta–H_{ap} bonds. Rossi and Hoffmann[3a] have indicated that the basal M–L bonds should be shorter than the apical ones for a d^0 electron count at the metal only when the L_{ap}-M-L_{ba} angle is less than approximately 98°. However, if the involvement of metal in the b_1 orbital (see Fig. 1) is very large, then this pattern should be retained for even larger angles. The pattern of longer Ta–H_{ax} distances compared to the Ta–H_{eq} ones that we find for the D_{3h} structure is consistent with Rossi and Hoffmann's analysis.[3a]

The orientation of the methyl groups is a complicating feature for $[Ta(CH_3)_5]$. For the TBP isomer, the C_{3h} structure shown by **1** in Scheme 1 would certainly appear to be the most viable on steric grounds. In a preliminary HF calculation on a structure in which the axial methyl groups were rotated by 60° about the Ta–C bond the energy was 2.0 kcal mol^{-1} higher. Optimization of **1** (within C_{3h} symmetry) at the HF level yielded Ta–C_{ax} and Ta–C_{eq} distances of 224 and 216 pm, respectively. The C–H distances and Ta-C-H angles are unexceptional; average values are 110 pm and 111.2°, respectively. Three rotamers, structures **2**–**4** in Scheme 1, were considered for the SP isomer. In each case, only C_s symmetry was imposed on the optimization (HF level). MP2 calculations were then performed on each resulting stationary point. The relative energies (in kcal mol^{-1}) are listed alongside each structure in Scheme 1; the values at the HF level are given in parentheses. The square-pyramidal structure **2** was found to be the most stable. At the MP2 level, the trigonal-bipyramidal structure **1** lies 7.7 kcal mol^{-1} higher in energy. This result is consistent with the electron diffraction structure reported by Haaland and co-workers.[9] The structural details of optimized **2** are compared to the experimental data[9] in Table 1. The agreement between theory and experiment is outstanding! The theoretical values in Table 1 were averaged from those obtained in the full optimization with C_s symmetry. However, the individual bond lengths do not differ by more than 0.5 pm and the bond angles by more than 0.8° (0.1° for the C-Ta-C angles) from those reported.

Table 1. Interatomic distances [pm] and valence angles [°] for $[Ta(CH_3)_5]$ from the HF optimized structure **2** and the corresponding experimental values [9].

Parameter	Theory [a]	Experiment [b]
Ta–C_{ap}	215.4	211(2)
Ta–C_{ba}	218.7	218.0(5)
C–H	109.9	110.6(6)
Ta-C-H	111.2	110.3(16)
C_{ap}-Ta-C_{ba}	111.6	111.7(13)
C_{ba}-Ta-C_{ba}	82.2	82.2(9)

[a] The theoretical values are averaged ones from the optimization in C_s symmetry. [b] Estimated standard deviations are given in parentheses, in units of the last digit.

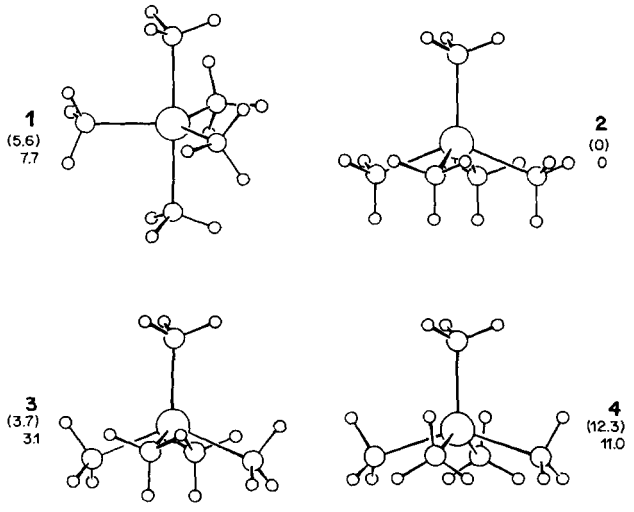

Scheme 1.

Notice that structure **4** has a very high relative energy (Scheme 1). We feel that the reason for this is primarily steric in origin. In **4** there are four more eclipsing H-C-Ta-C interactions than in **2**. Furthermore, the closest nonbonded H···H distances between adjacent basal methyl groups in **2** are 240 pm, whereas in **4** they are reduced to 217 pm. The latter value lies well within the van der Waals contact, given a van der Waals radius for hydrogen of approximately 130 pm. In the SP rotamer **3**, there are two more eclipsing H-C-Ta-C interactions compared to **1**; however, the orientation of the methyl groups is such that the nonbonded H···H contacts lie far outside of the van der Waals contact. Thus, the energy of **3** lies only 3.1 kcal mol^{-1} higher than **2**. There is evidence from both the ab initio and extended-Hückel wavefunctions for hyperconjugation between the filled methyl group orbitals and the empty d orbitals at the metal. However, no compelling evidence was found that the orientation of the methyl groups is dependent on the magnitude of these hyperconjugative interactions. Furthermore, there is no structural evidence from our optimizations which indicates that the magnitude of hyperconjugation is strong enough to distort the methyl groups toward agostic bonding as seen in other electron-deficient transition metal complexes.[10] We can make no assurances that **2** represents the global minimum. There may be one or more rotamers whose energy lies close to that of **2**. Because of resource limitations

we have also not computed the vibrational frequencies associated with **1–4**. The photoelectron spectrum of $[Ta(CH_3)_5]$ was assigned on the basis of a TBP structure.[11] We hesitate to make an assignment here on the basis of our molecular orbital calculations because the eigenvalues for the valence region around the metal are very sensitive to the orientation of the methyl groups. The finding here that $[TaH_5]$ and $[Ta(CH_3)_5]$ have SP rather than TBP structures nicely confirms the validity of the model outlined above based on second-order Jahn–Teller effects. It is well known[12] that 3d orbitals for vanadium are much more contracted and, hence, overlap more weakly with the orbitals of ligand σ-donor functions than the 4d orbitals of niobium or 5d orbitals of tantalum. Thus, we expect that the structure of the unknown $[Nb(CH_3)_5]$ should be very similar to that found for $[Ta(CH_3)_5]$; however, we expect that the TBP–SP energy difference for hypothetical $[V(CH_3)_5]$ will be considerably smaller than that found here for $[Ta(CH_3)_5]$. The application of the model also fits into the broader context of structural preferences for other d^0 ML_n complexes.[13] We have deliberately avoided examining what will occur when the auxiliary ligands possess strong π-donor functions. The preference of one distinct geometry (TBP or SP) is greatly affected by the number of π-donor functions, as well as whether they are single or double-faced π-donors.

Received: May 15, 1992 [Z 5350 IE]
German version: *Angew. Chem.* **1992**, *104*, 1532

[1] a) R. J. Gillespie, R. S. Nyholm, *Q. Rev. Chem. Soc.* **1957**, *11*, 339; R. J. Gillespie, *Molecular Geometry*, Van-Nostrand-Reinhold, London, **1972**; b) R. J. Gillespie, I. Hargittai, *The VSEPR Model of Molecular Geometry*. Allyan and Bacon, Boston, **1991**.

[2] H. K. McDowell, H.-L. Chiu, J. F. Geldard, *Inorg. Chem.* **1988**, *27*, 1674.

[3] a) A. R. Rossi, R. Hoffmann, *Inorg. Chem.* **1975**, *14*, 365; b) M. Elian, R. Hoffmann, *ibid.* **1975**, *14*, 1058; c) J. K. Burdett, *ibid.* **1975**, *14*, 375; *J. Chem. Soc. Faraday Trans. 2*, **1974**, *70*, 1599; d) P. J. Hay, *J. Am. Chem. Soc.* **1978**, *100*, 2411; e) Y. Jean, O. Eisenstein, *Polyhedron* **1988**, *7*, 405; El-I. I. Rachidi, O. Eisenstein, Y. Jean, *New J. Chem.* **1990**, *14*, 671; J.-F. Riehl, Y. Jean, O. Eisenstein, M. Pelissier, *Organometallics* **1992**, *11*, 729; f) T. A. Albright, J. K. Burdett, M.-H. Whangbo, *Orbital Interactions in Chemistry*, Wiley, New York, **1985**.

[4] The notations xy, $x^2 - y^2$, z, etc. stand for the d_{xy}, $d_{x^2-y^2}$, P_z, etc. orbitals. The subscripts ax, eq, ap, and ba refer to the axial, equatorial, apical, and basal positions, respectively.

[5] The calculations were conducted with the GAUSSIAN 82 program [6]. The Ta basis set employed a relativistic effective core potential for the 1s through 4d electrons and an associated double zeta basis set for the 5s, 5p, 5d, 6s, and 6p electrons [7a]. For $[TaH_5]$ the hydrogen basis set was 3-21G [7b]; for $[Ta(CH_3)_5]$ a 3-21G basis set was used for C [7b] and a STO-3G basis set for hydrogen [7c].

[6] J. S. Binkley, M. Frisch, K. Raghavachari, E. Fluder, R. Seeger, J. A. Pople, *Gaussian* 82, Carnegie-Mellon Publishing Unit, Pittsburgh, **1982**.

[7] a) P. J. Hay, W. R. Wadt, *J. Chem. Phys.* **1985**, *82*, 299; b) J. S. Binkley, J. A. Pople, W. J. Hehre, *J. Am. Chem. Soc.* **1980**, *102*, 939; c) W. J. Hehre, R. F. Stewart, J. A. Pople, *J. Chem.Phys.* **1969**, *51*, 2657.

[8] a) P. Zolliker, K. Yvon, P. Fischer, J. Schefer, *Inorg. Chem.* **1985**, *24*, 4177; b) J. Zhuang, J. M. Hastings, L. M. Corliss, R. Bau, C.-Y. Wei, R. O. Moyer, *J. Solid State Chem.* **1981**, *40*, 352.

[9] A. Haaland, A. Hammel, K. Rypdal, H. P. Verne, H. V. Volden, C. Pulham, J. Brunvoll, J. Weidlein, M. Greune, *Angew. Chem.* **1992**, *104*, 1534; *Angew. Chem. Int. Ed. Engl.* **1992**, *31*, 1464 (the following communication).

[10] For leading theoretical efforts on this issue see: R. Goddard, R. Hoffmann, E. D. Jemmis, *J. Am. Chem. Soc.* **1980**, *102*, 7667; A. Demolliens, Y. Jean, O. Eisenstein, *Organometallics* **1986**, *5*, 1457, and references therein.

[11] a) J. C. Green, D. R. Lloyd, L. Galyer, K. Mertis, G. Wilkinson, *J. Chem. Soc. Dalton Trans.* **1978**, 1403; b) L. Galyer, G. Wilkinson, D. R. Lloyd, *J. Chem. Soc. Chem. Commun.* **1975**, 497.

[12] See, for example, G. Ohanessian, W. A. Goddard III, *Acc. Chem. Res.* **1990**, *23*, 386.

[13] For a preliminary communication on the d^0 ML_6 problem, see S. K. Kang, T. A. Albright, O. Eisenstein, *Inorg. Chem.* **1989**, *28*, 1611. Experimental verification has been found for $[W(CH_3)_6]$: A. Haaland, A. Hammel, K. Rypdal, H. V. Volden, *J. Am. Chem. Soc.* **1990**, *112*, 4547.

The Structures of Pentamethyltantalum and -Antimony: One Square Pyramid and One Trigonal Bipyramid**

By *Colin Pulham, Arne Haaland,* Andreas Hammel, Kristin Rypdal, Hans Peter Verne,* and *Hans Vidar Volden*

The synthesis of pentamethylantimony $[Sb(CH_3)_5]$ was reported by Wittig and Torsell in 1953.[1] Infrared and Raman spectra of the neat liquid provide strong evidence for an SbC_5 frame of D_{3h} symmetry.[2] ^1H NMR spectra in CS_2 solution consist of one narrow line down to −100 °C, which shows that equatorial and axial methyl groups undergo rapid exchange on the NMR timescale,[3] presumably through Berry pseudorotation.[4] The synthesis of pentamethyltantalum $[Ta(CH_3)_5]$ was reported by Schrock and Meakin in 1974.[5] ^1H NMR spectra in $[D_8]$toluene at −10 °C show that all protons are magnetically equivalent.[5] The photoelectron spectra are consistent with D_{3h} molecular symmetry.[6]

In this communication we report the molecular structures of $[Ta(CH_3)_5]$ and $[Sb(CH_3)_5]$ determined by gas-phase electron diffraction (GED). This study is not only the first investigation of these molecules by diffraction techniques, but the first structure determinations of any pentaalkyl complex.

$[Sb(CH_3)_5]$ was synthesized from $[(CH_3)_3SbCl_2]$ and $LiCH_3$ in diethyl ether;[1, 7] $[Ta(CH_3)_5]$ was synthesized from $[(CH_3)_3TaCl_2]$ and $LiCH_3$ in the same solvent.[5] Both compounds were purified by distillation at reduced pressure.

The GED data were recorded at room temperature with a Balzers Eldigraph KDG-2 with an all-glass inlet system.[8] Since $[Ta(CH_3)_5]$ may detonate spontaneously at room temperature, it was treated according to procedures described in our study of hexamethyltungsten.[9] The data were processed by standard procedures.[10] Atomic scattering factors were taken from ref. [11]. Further information on the intensity data is given in Table 1. The molecular structures were refined by least-squares calculations on the modified molecular intensity curves with diagonal weight matrices.[10]

Molecular models of $[M(CH_3)_5]$ with trigonal-bipyramidal and square-pyramidal coordination of the metal atom are shown in Figure 1. A model with trigonal-bipyramidal coordination, that is, an MC_5 frame with D_{3h} symmetry, may be described by four independent structural parame-

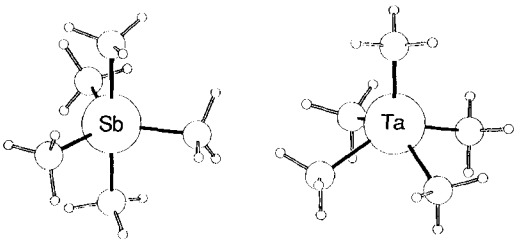

Fig. 1. Molecular models (PLUTON-91 [12]) of $[Sb(CH_3)_5]$ with trigonal-bipyramidal coordination, molecular symmetry (equatorial H atoms excluded) D_{3h}, and of $[Ta(CH_3)_5]$ with square-pyramidal coordination, molecular symmetry (apical H atoms excluded) C_{4v}.

[*] Prof. A. Haaland, Dr. A. Hammel, Dr. K. Rypdal, H. P. Verne, Ing. H. V. Volden
Department of Chemistry, University of Oslo
Box 1033 Blindern, N-0315 Oslo (Norway)
Dr. C. Pulham
Inorganic Chemistry Laboratory, South Parks Road
GB-Oxford OX1 3QR (UK)

[**] This work was supported by the Norwegian Research Council for Science and the Humanities, the VISTA program of STATOIL, and the Norwegian Academy of Science and Letters.

Table 1. Experimental conditions, background polynominals, s ranges and increments of modified molecular intensity curves, weight factors in least squares calculations, and R factors.

	$[Sb(CH_3)_5]$		$[Ta(CH_3)_5]$	
Nozzle to plate distance [cm]	50	25	50	25
Number of plates	6	6	6	6
s range [nm^{-1}]	13.75–145.00	35.00–200.00	22.50–125.00	30.00–260.00
Increment, Δs [nm^{-1}]	1.25	2.50	1.25	2.50
Background; degree of polynominal	4	6	6	8
Least squares calculations; weight	1.00	0.30	1.00	0.20
$R = [\sum W(I_{obs} - I_{calc})^2/\sum I_{obs}^2]^{1/2}$	0.031	0.115	0.038	0.187

ters: the axial and equatorial bond lengths M–C_{ax} and M–C_{eq}, a mean C–H bond length, and a mean M-C-H valence angle. Least squares refinements of a D_{3h}-symmetric model for $[Sb(CH_3)_5]$ proceeded without difficulty. Ten vibrational amplitudes could be refined in addition to the four structural parameters.[13] The final overall R factor was 0.057. The best estimates for the most important parameters are listed in Table 2,[14] and calculated and experimental radial distribution curves are compared in Figure 2.

Table 2. Interatomic distances, valence angles [°], and root mean square vibrational amplitudes l for $[Sb(CH_3)_5]$ and $[Ta(CH_3)_5]$. Estimated standard deviations in parentheses in units of the last digit. Parameters in square brackets have not been refined.

	$[Sb(CH_3)_5]$ D_{3h} symmetry			$[Ta(CH_3)_5]$ C_{4v} symmetry	
Bond lengths	r_a [pm]	l [pm]		r_a [pm]	l [pm]
Sb–C_{eq}	214.0(5)	[5.4]	Ta–C_{ap}	211(2)	[5.4]
Sb–C_{ax}	226.4(11)	[6.1]	Ta–C_{ba}	218.0(5)	[5.8]
C–H (mean)	110.4(6)	10.3(7)	C–H (mean)	110.6(7)	8.4(15)
Nonbonded distances					
Sb···H_{eq}	271(3)	13.4(15) [a]	Ta···H_{ap}	270(3)	17(2) [a]
Sb···H_{ax}	282(4)	13.7(15) [a]	Ta···H_{ba}	276(3)	17(2) [a]
C_{ax}···C_{eq}	310.9(7)	11.3(18)	C_{ba}···C_{ba}	286(2)	14(4)
C_{eq}···C_{eq}	370.0(9)	23(10)	C_{ap}···C_{ba}	355(3)	12(3)
C_{ax}···C_{ax}	451.3(22)	12(9)	C_{ba}···C_{ba}	405(4)	19(7)
Valence angles					
Sb-C-H (mean)	110.5(22)		Ta-C-H (mean)	110.3(16)	
C_{ax}-Sb-C_{eq}	[90]		C_{ap}-Ta-C_{ba}	111.7(13)	
C_{eq}-Sb-C_{eq}	[120]		C_{ba}-Ta-C_{ba}	82.2(9)	

[a] Pairs of amplitudes refined with constant difference.

A molecular model of $[M(CH_3)_5]$ with square-pyramidal coordination, in which the MC_5 frame has C_{4v} symmetry, may be described by five independent structure parameters: the apical and basal bond lengths M–C_{ap} and M–C_{ba}, a mean C–H bond length, a mean M-C-H valence angle, and the angle C_{ap}-M-C_{ba}. Least squares refinements of a C_{4v} model for $[Sb(CH_3)_5]$ yielded R factors above 0.12 and failed to converge. When refinements were carried out on a model with C_{2v} symmetry, calculations with starting parameters corresponding to nearly C_{4v} symmetry converged to models with close to D_{3h} symmetry. We conclude that C_{4v}-symmetric models are incompatible with the GED data. Our investigation thus confirms the conclusion reached in the earlier investigation by vibrational spectroscopy.[2]

Although refinements of a D_{3h}-symmetric molecular model of $[Ta(CH_3)_5]$ yielded overall R factors above 0.17, only a limited number of parameters could be refined without divergence. Comparison of experimental and calculated radial distribution curves revealed considerable disagreement in the region around $r = 305$ pm, the value calculated for the nonbonded C_{ax}···C_{eq} distance. Refinements of a C_{4v}-symmetric model proceeded without difficulties to yield a final overall R factor of 0.070. Six vibrational amplitudes were refined along with the five structural parameters.[15] The best estimates for the most important parameters are listed in Table 2, and calculated and experimental radial distribution curves are compared in Figure 2. We conclude that the structure of $[Ta(CH_3)_5]$ is square pyramidal.[16]

We recorded the ^{13}C NMR spectra of $[Sb(CH_3)_5]$ down to $-90\,^{\circ}C$ in CD_2Cl_2 and of $[Ta(CH_3)_5]$ down to $-120\,^{\circ}C$ in a 1:1 mixture of $CFCl_3$ and $[D_8]$toluene. Both spectra consist of one line which remains sharp down to the lowest temperatures. If axial and equatorial methyl groups in $[Sb(CH_3)_5]$ are exchanged by Berry pseudorotation, the transition state presumably has C_{4v} or nearly C_{4v} symmetry.[4] Similarly apical and basal methyl groups in $[Ta(CH_3)_5]$ may exchange over a transition state of D_{3h} or nearly D_{3h} symmetry.

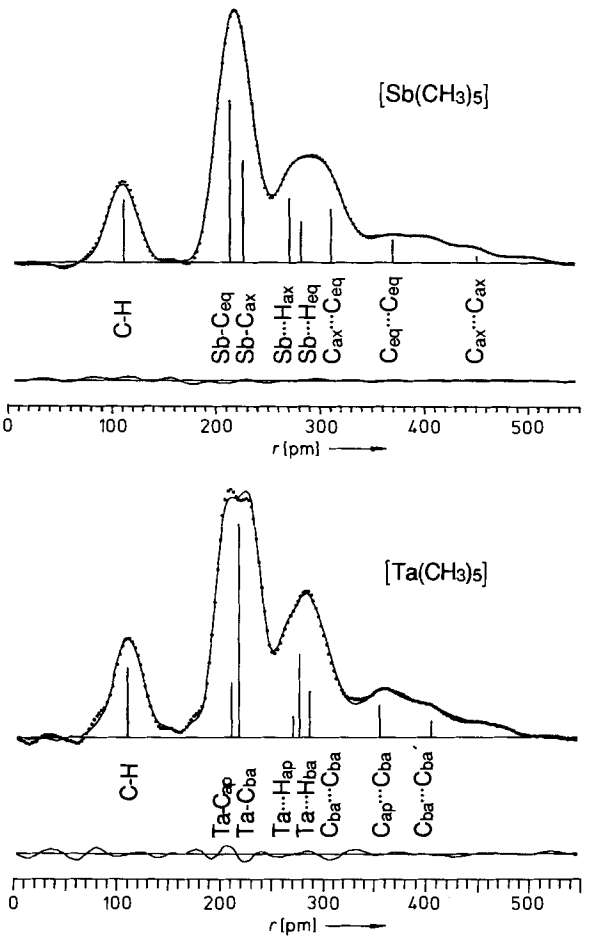

Fig. 2. Calculated (solid line) and experimental (·) radial distribution curves of $[Sb(CH_3)_5]$ (top) and $[Ta(CH_3)_5]$ (bottom). Artificial damping constants $k = 30\ pm^2$.

Thus, even though the two pentamethyl complexes have different equilibrium structures, the ^{13}C NMR spectra indicate that the energy difference between the two coordination geometries is small for both molecules. We have carried out ab initio MO calculations on $[Sb(CH_3)_5]$ with a split valence shell basis set and find that the energy of an optimized C_{4v} model is only 12.1 kJ mol^{-1} higher than that of an optimized D_{3h} model.[17]

The axial bond length in $[Sb(CH_3)_5]$ is about 12 pm longer than the equatorial, and the apical bond in $[Ta(CH_3)_5]$ is probably a few pm shorter than the basal. The average M–C bond lengths in the two compounds are, however, very similar: Sb–C (mean) = 219 pm; Ta–C (mean) = 217 pm.

The small C_{ba}-Ta-C_{ba} angle (82.2(9)°) is remarkable. The square base in $[Ta(CH_3)_5]$ is, however, similar to the rectangular faces in the trigonal-prismatic complex $[W(CH_3)_6]$: in the latter compound the angles defined by the metal atom and neighboring C atoms in the rectangular faces are 76.1(6)° and 86.0(2)°.[9] These angles are difficult to rationalize on the basis of electron-pair or interligand repulsion, and so we suggest that they are caused by an electronic factor.

Because of the small energy differences between the two coordination geometries, any attempt to rationalize the different equilibrium structures of $[Sb(CH_3)_5]$ and $[Ta(CH_3)_5]$ may be likened to performing surgery with a blunt axe. Nevertheless we suggest that the different structures adopted may reflect the different properties of the d orbitals available for bonding. The 5d orbitals of Sb are outside the valence shell, higher in energy, and more diffuse than the valence shell 5s or 5p orbitals. The 5d orbitals of Ta are part of the valence shell and may be more effective in bond formation than the valence shell 6p orbitals.

The three equatorial Sb–C bonds in $[Sb(CH_3)_5]$ may be described as two-center two-electron bonds formed from sp^2 hybrid orbitals on Sb. Bonding between Sb and the two axial C atoms may be described in terms of two-center two-electron bonds formed from two $p_z d_{z^2}$ hybrids on Sb, or in terms of a three-center four-electron system involving the $5p_z$ orbital only.[18] The first description implies that the population of the $5d_{z^2}$ orbital is about one electron, the second that the $5d_{z^2}$ orbital remains unoccupied. Mulliken population analysis of the SCF MO wave functions of $[Sb(CH_3)_5]$ in the D_{3h} configuration yields a total population of the d orbitals of 20.62 and a total population of the d_{z^2} orbitals of 4.32 electrons, corresponding to a $5d_{z^2}$ population of 0.32 compared to a total population of the 5d orbitals of 0.62 electrons. For what they are worth, the Mulliken populations suggest that though a description in terms of three-center four-electron bonding may be more appropriate, the role of the $5d_{z^2}$ orbital is not negligible.[19]

In his classical paper published in 1932, Hultgren set out to form hybrid orbitals from one s, three p, and five d functions, which at the outset were assumed to be equally effective for formation of two-center two-electron bonds.[20] Hultgren required the hybrid orbitals formed to have identical shapes and to have cylindrical symmetry. He found that there were four ways of forming six identical orbitals. Two of the sets contained hybrid orbitals with very small angles between them, but two sets seemed to be well suited for formation of bonds to six (identical) ligands. One set was formed by the well-known octahedral sp^3d^2 hybrids, the other was formed by sp^2d^3 hybrids pointing towards the corners of a trigonal prism with square faces.

Five hybrid orbitals with identical shape may obviously be obtained by removing one hybrid orbital from the set of octahedral or trigonal prismatic hybrids, but there is an additional possibility: five hybrids orbitals pointing towards the corners of a square pyramid. The angle between the hybrid orbital pointing towards the apex and one pointing toward a corner of the base is 120°, and the angle between hybrid orbitals pointing towards neighboring corners of the base is 75.5°. The composition of these orbitals is $sp^{1.2}d^{3.2}$.

In conclusion, we suggest that the 5d orbitals of Ta or W are more effective for bond formation than the 6p orbitals, and that in the absence of significant repulsion between ligands, greater participation of the d orbitals in bond formation favors square-pyramidal over trigonal-bipyramidal, and trigonal-prismatic over octahedral configurations.

Received: May 15, 1992 [Z 5351 IE]
German version: *Angew. Chem.* **1992**, *104*, 1534

[1] G. Wittig, K. Torsell, *Acta Chem. Scand.* **1953**, *7*, 1293.
[2] A. J. Downs, R. Schmutzler, I. A. Steer, *Chem. Commun.* **1966**, 221.
[3] E. L. Muetterties, W. Mahler, K. J. Packer, R. Schmutzler, *Inorg. Chem.* **1964**, *3*, 1298.
[4] R. S. Berry, *J. Chem. Phys.* **1969**, *32*, 933.
[5] R. R. Schrock, P. Meakin, *J. Am. Chem. Soc.* **1974**, *96*, 5288; R. R. Schrock, *J. Organomet. Chem.* **1967**, *122*, 209.
[6] J. C. Green, D. R. Loyd, L. Galyer, K. Merties, G. Wilkinson, *J. Chem. Soc. Dalton Trans.*, **1978**, 1403.
[7] We are grateful to Professor Johann Weidlein and Dr. Michael Greune, Institute of Inorganic Chemistry, University of Stuttgart, for the sample of $[Sb(CH_3)_5]$.
[8] O. Bastiansen, R. Graber, L. Wegmann, *Balzers High Vacuum Report*, **1969**, *25*, 1.
[9] A. Haaland, A. Hammel, K. Rypdal, H. V. Volden, *J. Am. Chem. Soc.* **1990**, *112*, 4547.
[10] B. Andersen, H. M. Seip, T. G. Strand, R. Stølevik, *Acta Chem. Scand.* **1969**, *23*, 3224.
[11] L. Schäfer, A. C. Yates, R. A. Bonham, *J. Chem. Phys.* **1971**, *55*, 3055; *International Tables for X-ray Crystallography, Vol. 4*; Kynoch Press, Birmingham, **1974**.
[12] PLUTON-91, A. L. Spek, University of Utrecht, the Netherlands.
[13] The refinements were carried out under the constraints of a geometrically consistent r_a structure (K. Kuchitsu, S. J. Cyrin in *Molecular Structures and Vibrations* (Ed.: S. J. Cyvin), Elsevier, Amsterdam, **1972**, Chapter 12, p. 183. Correction coefficients for thermal motion $D = r_a - r_a$ and root mean square vibrational amplitudes were calculated from a molecular force field by combining the valence force field of the SbC_5 frame (B. A. Nevett, A. Perry, *J. Mol. Spectr.* **1977**, *66*, 331) with the methyl group force field (A. Müller, W. Nolte, S. J. Cyvin, B. N. Cyvin, A. J. P. Alix, *Spectrochim. Acta* **1978**, *34A*, 383). Nonrefined vibrational amplitudes were fixed at the calculated values.
[14] Since the refinements were carried out with a diagonal weight matrix, the estimated standard devitions listed in Table 2 have been multiplied by a factor of 3.0 to include the uncertainty introduced by data correlation and nonrefined vibrational amplitudes, and then expanded to include an estimated scale uncertainty of 0.1%.
[15] We recorded the IR spectra of $[Ta(CH_3)_5]$ in N_2 and Ar matrices at 20K and the IR and Raman spectra of the solid at 77K, and made tentative assignments for the nine normal modes of the TaC_5 frame of C_{4v} symmetry. A diagonal force field has been obtained and used to calculate Ta–C and C–C vibrational amplitudes. The least squares refinements were made under the constraints of a geometrically consistent r_a structure. The vibrational amplitudes of the Ta–C bonds were fixed at the calculated values. $[Ta(CH_3)_5]$ is thermally unstable. The volatile decomposition products are 98% methane and contain no Ta-containing species [5]. The mole fraction of methane with known molecular structure, L. S. Bartell, K. Kuchitsu, R. J. de Neui, *J. Chem. Phys.* **1971**, *35*, 1211, was included as an additional parameter in the least squares calculations. The resulting value was $x = 0.10(30)$. The scattering power of CH_4 is, of course, much smaller than that of $[Ta(CH_3)_5]$.
[16] Crystalline $[Nb(N(CH_3)_2)_5]$ (C. Heath, M. B. Hursthouse, *Chem. Commun.* **1971**, 145) and gaseous $[Ta(N(CH_3)_2)_5]$ (K. Hagen, C. J. Holwill, D. A. Rice, V. D. Runacles, private communication) adopt distorted square-pyramidal structures. We believe, however, that $[Ta(CH_3)_5]$ is the first five-coordinate d^0 metal complex found to a adopt a square-pyramidal configuration in the gas phase with a pure σ bond to the apical substituent.
[17] SCF MO calculations were performed with the MOLECULE SWEDEN program package: MOLECULE is a vectorized Gaussian integral program written by J. Almlöf, and SWEDEN is a vectorized SCF-program written by P. Siegbahn, B. Roos, P. Taylor, A. Heiberg, J. Almlöf, S. R. Langhoff, and D. P. Chong. For Sb we used a basis set of (15,11,8) primitive Gaussian functions (A. Strömberg, O. Gropen; U. Wahlgren, *J. Comp. Chem.* **1983**, *4*, 181), supplemented by two diffuse d functions with

exponents 0.20 and 0.05 and contracted to ⟨6,5,4⟩. For C we used a (7,4) basis set (F. B. van Duijnevelt, *IBM Technical Research Report No. RJ-945*, **1971**), and for H a (3) basis set (S. Huzinaga, *J. Chem. Phys.* **1965**, *42*, 1293) contracted to ⟨3,2⟩ and ⟨2⟩ respectively. The methyl groups were fixed at the experimental geometry. The optimal Sb–C_{eq} and Sb–C_{ax} bond lengths for the D_{3h} model were 219 and 224 pm, respectively.

[18] J. I. Musher, *Angew. Chem.* **1969**, *81*, 68; *Angew. Chem. Int. Ed. Engl.* **1969**, *8*, 54.

[19] For three recent articles on the participation of outer d orbitals for bonding in hypervalent compounds of main group elements see A. E. Reed, F. Weinhold, *J. Am. Chem. Soc.* **1986**, *108*, 3586; A. E. Reed, P. von R. Schleyer, *ibid.* **1990**, *112*, 1434; A. Magnusson, *ibid.* **1990**, *112*, 7940.

[20] R. Hultgren, *Phys. Rev.* **1932**, *40*, 891.

Perfluorotriethylamine: An Amine with Unusual Structure and Reactivity

By *Markus Gaensslen, Udo Gross, Heinz Oberhammer,** and *Stephan Rüdiger**

Simple amines NX_3, for example with X = H, F, or Cl, and trialkylamines NR_3 with R = methyl or ethyl have a pyramidal structure with tetrahedral or smaller bond angles at nitrogen. A marked widening of the C-N-C bond angle has recently been observed for triisopropylamine, in which the repulsion between the sterically demanding isopropyl groups forces a flattening of the NC_3 unit with a C-N-C angle of 119.2(3)°.[1] Similarly, fluorination of trimethylamine to $N(CF_3)_3$ also leads to a widening of the pyramidal structure (∢C-N-C) from 110.9(6)° to 117.9(4)°.[2] This pronounced influence of fluorination on the bond angles is remarkable because the C-C-C angle in alkanes is hardly affected by fluorination (e.g., ∢C-C-C is 112.0(10)° in $CH_3CH_2CH_3$ and 113.9(6)° in $CF_3CH_2CF_3$[3]). The structure of perfluorotriethylamine (PTEA) is of particular interest, therefore, to study the influence of fluorination on the nitrogen–carbon skeleton. During the last decade mainly medical research showed an interest in perfluorinated organic compounds. These compounds are less attractive for synthetic chemists because of their extremely low reactivity. The lack of physiological activity of these compounds and their high capacity for dissolving gases render them very promising as components in blood substitutes. The synthesis and isolation of PTEA was achieved by standard methods, as described, for example, in ref. [4]: triethylamine was fluorinated electrochemically in liquid hydrofluoric acid, the crude product was treated with a strong nucleophile, and the PTEA isolated by repeated distillation. The purity of the PTEA, determined by gas chromatography, was 99.2%.

PTEA, like many other perfluorinated compounds, is not crystalline, but solidifies as a glass. Solid-state structure investigations are not, therefore, possible. As a consequence, the structure was determined by electron diffraction (ED) in the gas phase.[5] Many model structures with various symmetries were tested: 1) All three ethyl groups are rotated around the N–C bonds with the same torsion angle τ(N–C) (C_3 symmetry). 2) One methyl group is aligned synperiplanar ($\tau_1 = 0°$) or antiperiplanar ($\tau_1 = 180°$) to the lone pair on nitrogen while the two other methyl groups are rotated with the same angle either in the opposite direction ($\tau_2 = -\tau_3$, C_s symmetry), or 3) in the same direction ($\tau_2 = \tau_3$, C_1 symmetry). The various models were judged under two aspects: the agreement between calculated and experimental radial distribution functions (Fig. 1) and no F···F contacts (except geminal contacts) should be less than 220 pm. If reasonable

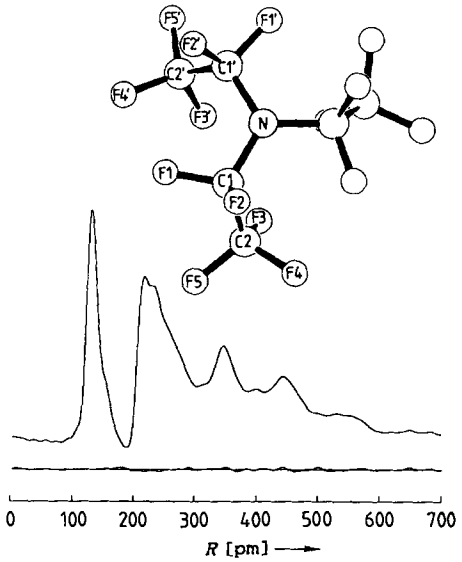

Figure 1. Radial distribution function for PTEA with difference curve and molecular model with atomic numbering.

bond lengths and C-C-C and F-C-F bond angles are assumed, these conditions are only fulfilled by those models with C_3 symmetry, a value for τ(N–C) of approximately 150°, and an almost planar configuration at the nitrogen atom. In addition, a twisting of the trifluoromethyl group about by C–C bond by τ(C–C) from the staggered position must be assumed to obtain complete agreement with the experimental radial distribution.

The preliminary model was then refined with the method of least squares.[6] The agreement between the final model and the experimental data is indicated by the difference curve in Figure 1. The optimized structure parameters are presented in Table 1. The NC_3 unit is almost planar (∢C-N-C = 119.3(4)°). A negligible bending of the N–C bond out of the plane (α = 4.8(27)°) in the direction of the CF_3 groups can be seen. In addition to a widening of the C-N-C angle the steric strain also leads to an increase in the N-C-C angle to

Table 1. Structural parameters for perfluorotriethylamine.

Parameter	Value [a]	Parameter	Value [a]
C–F	133.0(2)	N-C-C	118.2(26)
N–C	148.2(7)	F-C1-F	105.0(16)
C–C	159.2(8)	F-C2-F	108.8(5)
α [b]	4.9(25)	τ(N–C) [c]	147.0(5)
C-N-C	119.3(4)	τ(C–C) [d]	25.6(11)

[a] Distances in pm and angles in degrees. Uncertainties correspond to 3σ values. [b] Angle between an N–C bond and the plane through nitrogen perpendicular to the C_3 axis. [c] Torsion angle about an N–C bond. For τ(N–C) = 0° the C–C bond is synperiplanar to the lone electron pair on nitrogen. [d] Torsion angle about a C–C bond. For τ(C–C) = 0° the CF_3 groups are staggered to the CF_2 groups.

[*] Prof. Dr. H. Oberhammer, Dipl.-Chem. M. Gaensslen,
Institut fur Physikalische und Theoretische Chemie der Universitat
Auf der Morgenstelle 8, D-W-7400 Tübingen (FRG)
Dr. S. Rüdiger, Dr. U. Gross,
Projektgruppe Fluorchemie
Rudower Chaussee 5, D-O-1199 Berlin (FRG)

[**] This work was supported by the Deutsche Forschungsgemeinschaft.

118.2(26)° and a marked increase (about 5 pm) in the N–C and the C–C bond lengths. The N–C bonds are stretched from 142.6(6) in $N(CF_3)_3$ to 148.2(7) in PTEA and the C–C bonds from 154.5(8) in CF_3–CF_3[7] to 159.2(8) in PTEA. In spite of this distortion of the molecular geometry, F···F contacts are present between non-geminal atoms that are considerably shorter than the corresponding van der Waals distance of 270 pm: F1···F'4 = 234, F1···F5 = 256, F3···F'3 = 259, F2···F4 = 260 pm.

The most prominent chemical difference between tertiary amines and their perfluorinated analogues is the strongly reduced basicity of the latter, apparently as a result of the strong electron withdrawing effect of the perfluorinated groups attached to nitrogen, the lone pair of which is partially delocalized over the neighboring CF_2 or perfluoroalkyl groups. The increased electron density on the α carbon atoms leads to a certain reactivity of the CF_2 groups. Thus, under extreme conditions (e.g. oleum at 170 °C or SbF_5 at 100–170 °C) electrophilic attack on an α-C atom is possible, which can lead to perfluorolactams[8] or perfluoroazomethines.[9]

The structure of PTEA also directly reflects its chemical behavior. A partial delocalization of the electron lone pair on nitrogen allows the transition from a pyramidal to an almost planar structure of the NC_3 unit. The arrangement of the CF_3 groups all on the same side of the molecule shows that the residual electron density on nitrogen still has a profound effect on the structure. A model of PTEA with van der Waals radii (Fig. 2) shows that the central nitrogen atom

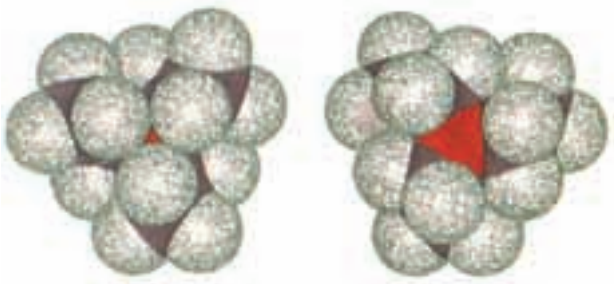

Figure 2. Structure model with van der Waals radii. Color key: N = red, C = black, F = green. View towards the CF_3 groups (left) and towards the CF_2 groups (right).

(in red) is almost completely covered by the fluorine atoms of the CF_3 groups (left) and that more space is available for the lone electron pair in the direction of the CF_2 groups (right).

Received: June 11th, 1992 [Z 5401 IE]
German version: *Angew. Chem.* **1992**, *104*, 1525

CAS Registry number:
Perfluorotriethylamine, 359-70-6.

[1] H. Bock, I. Göbel, Z. Havlas, S. Liedle, H. Oberhammer, *Angew. Chem.* **1991**, *103*, 193; *Angew. Chem. Int. Ed. Engl.* **1991**, *30*, 187.
[2] H. Bürger, H. Niepel, G. Pawelke, H. Oberhammer, *J. Mol. Struct.* **1979**, *54*, 159.
[3] H. G. Mack, H. Oberhammer, M. Grosser, M. Dakkouri, *J. Mol. Struct.* **1992**, *268*, 135.
[4] A. Dimitrov, W. Radeck, S. Rüdiger, V. E. Platonov, *J. Fluorine Chem.* **1991**, *52*, 317.
[5] The ED intensities were recorded with a gas diffractograph KD-G2 for two camera distances (25 and 50 cm) and an accelerating voltage of about 60 kV. The temperature of the sample was −28 °C, that of the nozzle 10 °C, and the pressure of the apparatus was approximately 10^{-5} mbar. For each camera distance two photographic plates (Kodak Electron Image, 13 × 8 cm) were evaluated according to standard methods (H. Oberhammer, W. Gombler, H. Willner, *J. Mol. Struct.* **1981**, *70*, 273). The molecular scattering intensity in the *s*-ranges 20–180 and 80–350 nm^{-1} ($s = (4\pi/\lambda)\sin\theta/2$, λ = electron wavelength, θ = scattering angle) were used for the structure determination. The radial distribution function was calculated by Fourier transformation.
[6] In the least-squares structure refinement, the scattering intensities were modified with a diagonal weighting matrix and known scattering amplitudes and phases (J. Haase, *Z. Naturforsch. A*, **1970**, *25*, 936). For the CF_2 and the CF_3 groups C_{2v} or C_{3v} symmetry was assumed. Vibrational amplitudes were collected in groups according to the type and length of the interatomic distances. Two correlations between geometric parameters are larger than |0.7|: α/N-C-C = 0.97, ∢F-C1-F/∢F-C2-F = 0.85. The *R* factors are 0.086 and 0.037 for the intensities of the 25 cm or 50 cm camera distances.
[7] K. L. Gallaher, A. Yokozeki, S. H. Bauer, *J. Phys. Chem.* **1974**, *78*, 2389.
[8] E. Hayashi, T. Abe, S. Nagase, *J. Fluorine Chem.* **1988**, *41*, 213.
[9] V. A. Petrov, G. G. Belen'kii, L. S. German, *Izv. Akad. Nauk SSSR Ser. Khim.* **1985**, 1934.

Product Predictions for Nucleophilic Additions to C_{70}

By *Heinrich R. Karfunkel** and *Andreas Hirsch*

If fullerenes are provided with functional groups, three-dimensional arrangements that are not possible for planar arenes or heteroarenes are generated. To utilize these new opportunities, it is essential that the course of the addition of these groups can be controlled. Besides the addition of radicals,[1] dienes, and 1,3-dipoles,[2, 3] the nucleophilic addition with alkyllithium or Grignard reagents presents further possibilities for derivatizing fullerenes.[3, 4]

Recently we developed a new method of directed nucleophilic addition to a single 6-6 "double bond" (the bond common to the annelated six-membered rings) in C_{60}.[5] Semiempirical quantum mechanical calculations (MOPAC/AM1[6, 7] agreed with the experimental findings: the addition to the 6-6 bond of C_{60} is energetically favored over all other potential additions, irrespective of nucleophile used. This synthetic method can be applied to C_{70} and other fullerenes. However, already for C_{70} the situation is considerably more complex than for C_{60}. The number of conceivable reaction products is too large for chemical intuition alone to predict the result; we employed MO calculations for this purpose.

The nucleophilic addition to C_{70} proceeds in two steps (Scheme 1). Three questions arise: a) Which are the most

1. $C_{70} + Nu^- \longrightarrow C_{70}Nu^-$ (nucleophilic attack)

2. $C_{70}Nu^- + H^+ \longrightarrow C_{70}NuH$ (proton addition)

Scheme 1.

probable isomers of $C_{70}NuH$? b) Is the result in a) dependent on the nature of the nucleophile? c) How reliable are predictions based on calculations?

[*] Priv.-Doz. Dr. H. R. Karfunkel
Ciba-Geigy AG
R-1008.823, CH-4002 Basel (Switzerland)
Dr. A. Hirsch
Institut für Organische Chemie der Universität
Auf der Morgenstelle 18, D-W-7400 Tübingen (FRG)

If a reasonable error tolerance is chosen and it is assumed that no rearrangement takes place on proton addition, the answer is that only two (in the case of $C_{70}t$BuH three) isomers are possible as addition products. These isomers are largely independent of the nature of the nucleophile. Rearrangement on proton addition increases the number of possible isomers slightly.

A nomenclature system for the isomers of $C_{70}XY$ (X,Y are two added groups) does not yet exist. For this reason we introduce a new system here. C_{70} in D_{5h} symmetry has five sets of equivalent atoms arranged radially about the symmetry axis. In Figure 1 these sets are labeled e (for equatorial), 1, 2, 3, and N (for North Pole). For the second hemisphere the corresponding sets of equivalent atoms are given a minus sign.

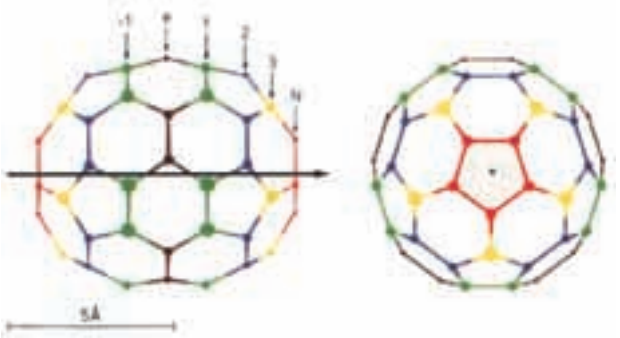

Fig. 1. C_{70} in D_{5h} symmetry, viewed looking at the equator (left) and at the pole (right). The fivefold rotation axis is indicated by the long arrow (left) and the dot (right). The sets of equivalent atoms are indicated in color (pole in red, etc.) and their labeling by arrows (e,1,2,3,N for one hemisphere and -1 etc. for the other).

The first nucleophilic attack can take place at any of these sets and yields five possible isomers of $C_{70}Nu^-$. The next proton addition can proceed at each of the 69 free positions of the anion. Hundreds of products are thus possible in principle. An isomer of C_{70}NuH is characterized by the position of the nucleophilic attack, followed by a slash (/) and the shortest path to the position of the added proton: for example (see also Fig. 2), 2/2 means a nucleophilic attack at set 2 and proton addition at the adjacent atom of the same set; 2/2,3,N corresponds to a 1,4 addition in which the nucleophilic attack is at set 2 and the proton is added to the final atom of the path from 2 via 2 (only one possibility) and 3 (only one possibility), to N (only one possibility); finally 1/e,-1,-1 corresponds to a 1,4 addition across the equator. In some cases the suffixes *t* and *c* (for *trans* and *cis*) are also needed to specify a particular path unambiguously.

Initial geometries were generated with the program MACROMODEL.[8] These were then optimized with MOPAC 6.0[6] through the use of AM1 parametrization (options: EF, PRECISE, and XYZ). All AM1 calculations were performed on a RS-6000 workstation. AM1 calculations were carried out on each of the five isomers of $C_{70}Nu^-$ for each of the three nucleophiles H^-, Me^-, and tBu$^-$. The resulting energies for the geometry-optimized structures (AM1 standard heats of formation or HOF) are presented in Table 1.

Three conclusions about the first step of the nucleophilic addition to C_{70} may be drawn from these results: 1) A nucleophilic attack at the equator does not take place (although the greatest positive charge is localized there). 2) The most probable sites for nucleophilic attack are the positions (or sets) 1 and 2, followed by the pole N. 3) There is excellent agreement for the three nucleophiles. This good correlation of the $C_{70}Nu^-$ energies and our experience with C_{60}[5] (which is experimentally substantiated) allows an efficient global search for the most stable isomers of C_{70}NuH.

Table 1. AM1 standard enthalpies of formation (AM1-HOF) [kcal mol^{-1}] for the five isomers of $C_{70}H^-$, $C_{70}Me^-$, and $C_{70}t$Bu$^-$. The numbers in parentheses ranks the relative energy of the isomers in increasing order.

C_{70} site	Mulliken charge	H^-	Me^-	tBu$^-$
N	+0.0045	961.33(3)	959.03(3)	950.44(3)
3	−0.0098	965.23(4)	962.94(4)	954.33(4)
2	+0.0051	958.07(2)	955.94(1)	947.46(1)
1	−0.0146	957.61(1)	955.94(1)	948.25(2)
e	+0.0243	979.07(5)	977.31(5)	969.64(5)

The time required for the computation makes the calculation of all the isomers of $C_{70}H_2$, C_{70}MeH, and $C_{70}t$BuH impossible. Nevertheless, the results in Table 1 permit a reliable search with little effort. All the $C_{70}H_2$ isomers (a total of 130) that can be generated from the four most stable isomers of $C_{70}H^-$ of Table 1 were found, and their energies calculated (to be sure that none were missed, the products from the unlikely 3/ isomer were also considered). Then only from the most stable isomers of $C_{70}H_2$ (see Table 2) were a small number of C_{70}MeH and $C_{70}t$BuH isomers generated by substitution of a H atom by a methyl or *tert*-butyl group, and their energies calculated. This search methodology can also be applied to higher fullerenes.

Table 2. The relative stability (AM1-HOF in kcal mol^{-1}) of the seven most stable $C_{70}H_2$ isomers. The relative AM1-HOF of the anionic intermediate $C_{70}H^-$ is given in the last column for completeness.

No. (rank)	Isomer	Mulliken charge [a]	Relative AM1 HOF (isomer)	Relative AM1 HOF (intermediate)
1	2/2	−0.25	0.00	0.46
2	N/3	−0.28	1.05	3.72
	(3/N)	(−0.31)		(7.62)
3	1/e,−1,−1	−0.18	1.74	0.00
4	2/2,3,N	−0.06	3.17	0.46
	(N/3,2,2)	(−0.14)		(7.62)
5	1/1	−0.19	6.80	0.00
6	3/2,2,3	−0.13	6.85	7.62
7	1/1,2,2	−0.12	9.81	0.00
	(2/2,1,1)	(−0.16)		(0.46)

[a] Position of the added proton.

The results for the final products as well as for the anionic intermediates are collated in Tables 2–4. Relative energies are quoted as only the differences in energy are relevant for comparison.

Two aspects of the reliability of the calculations must be taken into account: the reliability of the AM1 calculations and the reliability of the search process for the most stable isomers of C_{70}MeH and $C_{70}t$BuH.

Statistical studies[9] have shown that the error (RMS error) of the AM1 standard enthalpies of formation is approximately 10 kcal mol^{-1}. However, if comparisons of energy

Table 3. The relative stability (AM1-HOF in kcal mol^{-1}) of the eight most stable C_{70}MeH isomers.

No. (rank)	Isomer	Mulliken charge [a]	Relative AM1 HOF (isomer)	Relative AM1 HOF (intermediate)
1	2/2	−0.25	0.00	0.00
2	N/3	−0.28	0.84	3.09
3	3/N	−0.30	0.91	7.00
4	1/e,−1,−1	−0.18	1.66	0.00
5	N/3,2,2	−0.14	2.56	3.09
6	2/2,3,N	−0.06	2.70	0.00
7	3/2,2,3	−0.13	6.27	7.00
8	1/1	−0.19	6.84	0.00

[a] Position of the added proton.

are made within a generic family of substances (e.g., the comparison of structurally similar isomers), the error in these $\Delta\Delta H$ values are almost an order of magnitude smaller.[10] If one considers that the calculations assume idealized relationships, that is, the molecules are in the gas phase and no entropy effects are considered, an error limit of 2.5 kcal mol^{-1} seems reasonable. The conclusions drawn below are based on the assumption that isomers differing in AM1 energy by more than 2.5 kcal mol^{-1} from the most stable isomer may be neglected.

Table 4. The relative stability (AM1 energies in kcal mol^{-1}) of the eight most stable $C_{70}t$BuH isomers.

No. (rank)	Isomer	Mulliken charge [a]	Relative AM1 HOF (isomer)	Relative AM1 HOF (intermediate)
1	2/2	−0.24	0.00	0.00
2	1/e,−1,−1	−0.19	0.61	0.79
3	N/3	−0.27	0.66	2.98
4	N/3,2,2	−0.14	0.66	2.98
5	3/N	−0.30	0.78	6.87
6	2/2,3,N	−0.06	1.01	0.00
7	3/2,2,3	−0.13	4.4	6.87
8	1/1	−0.19	6.89	0.79

[a] Position of the added proton.

Since the correlation between the energies of the analogous isomers for the three nucleophiles is good, it is hardly conceivable that other isomers of C_{70}MeH or $C_{70}t$BuH exist, whose calculated AM1 energy differ from that of the 2/2 isomer by less than 2.5 kcal mol^{-1}. Conclusions from the AM1 calculations: irrespective of whether reaction 1 of nucleophilic addition (nucleophilic attack) or reaction 2 (proton addition) is rate-determining, the most probable product for all nucleophiles is the 2/2 isomer. It should be noted that the sets 1 and 2 have twice as many sites as sets 3 and N, which also affects the probabilities. The six most stable isomers (Fig. 2) are at any rate identical, and although there are slight changes in order of stability for different nucleophiles, the correlation between the energies is excellent. In other words, the nucleophilic addition is largely independent of the nature of the nucleophile. As for C_{60}, a 1,2 addition to C_{70} also takes place exclusively at a 6-6 "double bond". A surprising result of the calculations is that in contrast to C_{60}, for C_{70} 1,4 addition products are also anticipated, and predominantly the 1/e,−1,−1 transequatorial isomer. Consideration of the tolerances mentioned above lead to the following predictions: 1) Unless there are

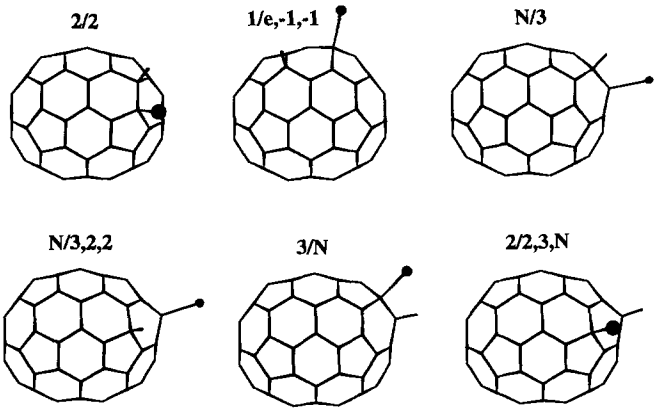

Fig. 2. The six energetically most favorable isomers of C_{70}NuH (viewed from the side). The nucleophile (H, Me, or *t*Bu) is indicated (in perspective) by a solid ball and the added proton by a dash. The labeling of the isomers is derived by giving the position of the nucleophile (character before the slash) followed by the path to the position of the added proton (see text).

rearrangements on proton addition, the 2/2 and 1/e,−1,−1 isomers are possible for $C_{70}H_2$ and C_{70}MeH and the 2/2, 1/e,−1,−1, and 2/2,3,N isomers for $C_{70}t$Bu. 2) If rearrangements take place on proton addition, the 2/2, N/3, and 1/e,−1,−1 isomers are likely for $C_{70}H_2$, the isomers 2/2, N/3, 3/N, and 1/e,−1,−1 for C_{70}MeH, and the 2/2,1/e,−1,−1, N/3, N/3,2,2, 3/N, and 2/2,3,N for $C_{70}t$Bu (Fig. 2). Finally the paper of Balch et al. should be mentioned, which deals with the additions of $[(Ph_3P)_2Pt]$ and $[Ir(CO)Cl(PPh_3)_2]$ to C_{70}.

An unambiguous identification of the isomers by methods other than X-ray diffraction will probably be extremely difficult. For structure elucidation with 2D NMR methods (2D-NOE studies), the interproton distances are of crucial importance. Geometry-optimized AM1 structures reveal that for C_{70}MeH (in which H_{Nu} is the closest proton to the added H^+), the H–H_{Nu} distance is identical for the possible 1,2-addition products (the 2/2, N/3, and 3/N isomers) and amounts to 2.4 Å. The H–H_{Nu} distance for the 1/e,−1,−1 isomer is 2.93 Å. For $C_{70}t$Bu the H–H_{Nu} distances for the 1,2-addition products are identical and are 2.01 Å, while for the 1,4-addition products the H–H_{Nu} distance of the transequatorial 1/e,−1,−1 isomers is 0.5–0.6 Å smaller than in the N/3,2,2 or 2/2,3,N isomers.

Received: July 20, 1992 [Z 5473 IE]
German version: *Angew. Chem.* **1992**, *104*, 1529

[1] P. J. Krusic, E. Wassermann, P. N. Keizer, J. R. Morton, K. F. Preston, *Science* **1991**, *254*, 1183.
[2] T. Suzuki, Q. Li, K. Khemani, F. Wudl, Ö. Almarson, *Science* **1991**, *254*, 1186.
[3] F. Wudl, A. Hirsch, K. Khemani, T. Susuki, P.-M. Allemand, A. Koch, H. Eckert, G. Srdanov, H. Webb in *Fullerenes* (Eds.: G. S. Hammond, V. J. Kuck) (*ACS Symp. Ser.* **1992**, *481*, 161).
[4] A. Hirsch, Q. Li, F. Wudl, *Angew. Chem.* **1991**, *103*, 1339; *Angew. Chem. Int. Ed. Engl.* **1991**, *30*, 1309.
[5] A. Hirsch, A. Soi, H. R. Karfunkel, *Angew. Chem.* **1992**, *104*, 808; *Angew. Chem. Int. Ed. Engl.* **1992**, *31*, 766.
[6] J. J. P. Stewart, QCPE 455, MOPAC Version 6.0, **1990**.
[7] M. J. S. Dewar, E. G. Zoebisch, E. F. Healy, J. J. P. Stewart, *J. Am. Chem. Soc.* **1985**, *107*, 3902.
[8] F. Mohamadi, N. G. J. Richards, W. C. Guida, R. Liskamp, M. Lipton, C. Caufield, G. Chang, T. Hendrickson, W. C. Still, *J. Comput. Chem.* **1990**, *11*, 440.
[9] J. J. P. Stewart, *J. Comput. Chem.* **1989**, *10*, 221.
[10] D. Bakowies, W. Thiel, *J. Am. Chem. Soc.* **1991**, *113*, 3704.
[11] A. L. Balch, V. J. Catalano, J. W. Lee, *J. Am. Chem. Soc.* **1991**, *113*, 8953.

Paramagnetic Chiral Smectic C Materials: A New Class of Ferroelectric Liquid Crystals**

By *Mercedes Marcos,* José Luis Serrano, Teresa Sierra,* and *María José Giménez*

Chiral liquid-crystalline phases, in particular smectic C* phases, have attracted great interest over recent years because of their ferroelectric and nonlinear optical (NLO) properties.[1] Furthermore, interest in the synthesis of liquid-crystalline compounds incorporating transition metal ions is currently increasing, since potential applications originate from the presence of a metal ion in ordered fluid phases.[2] The high electron density of the metallic center may lead to an increase in polarizability and high birefringence, and under the right conditions complexes may exhibit a NLO response.[3]

Up until now, the typical ferroelectric liquid crystals have been chiral rodlike organic molecules. However, recently we described a ferroelectric liquid-crystalline material consisting of a dimer of an *ortho*-palladated azine complex, in which chirality is introduced through chiral carboxylate bridges.[4] Our group has also published several papers on copper(II) and vanadium(IV) Schiff base complexes that exhibit a smectic C phase among other mesphases.[5] This led us to envisage a new class of ferroelectric liquid crystals that incorporate a metallic center in their mesogenic core and have the general structure ML_2 (Scheme 1). These complexes are of special interest, because they are the first paramagnetic, ferroelectric metallomesogens.

The synthesis of ligand L and complexes ML_2 is shown in Scheme 1. Schiff base L, synthesized by condensation of 4-(decyloxy)-2-hydroxybenzaldehyde **3** with chiral amine **7** (see Experimental Procedure), reacts with copper acetate or vanadyl sulfate in a 2:1 molar ratio affording a brown copper complex or a green oxovanadium complex, whose elemental analyses and IR spectra are in full agreement with the proposed structures.

The phase sequence and transition temperature of L and the copper(II) and vanadium(IV) complexes studied by differential scanning calorimetry (rate of heating 10 °C min^{-1}) and optical microscopy are listed in Table 1. The ligand and both the complexes exhibit a chiral smectic C mesophase and a smectic A phase. A photomicrograph of the S_{C^*} phase of the copper(II) complex is shown in Figure 1.

Their physical properties, spontaneous polarization Ps, switching time τ, and rotational viscosity γ, were determined simultaneously by the triangular wave method[6, 7] in 10 μm cells with indium tin oxide (ITO) electrodes coated with polyimide in an electrical field of 30 V peak to peak and 50 Hz for the ligand. For the complexes, the electric field was 40 V peak to peak and it was necessary to decrease the frequency to 40 Hz for CuL_2 and 5 Hz for VOL_2 in order to obtain the Ps saturation values. The dependence of Ps on temperature is shown in Figure 2. A maximum spontaneous polarization Ps_{max} of 44 nC cm^{-2} was measured for the ligand and of 23 and 20 nC · cm^{-2} for the copper and oxovanadium complexes respectively (Table 1). The rotational viscosity of the oxovanadium complex is much larger than that of the copper complex, which is even lower than that for the

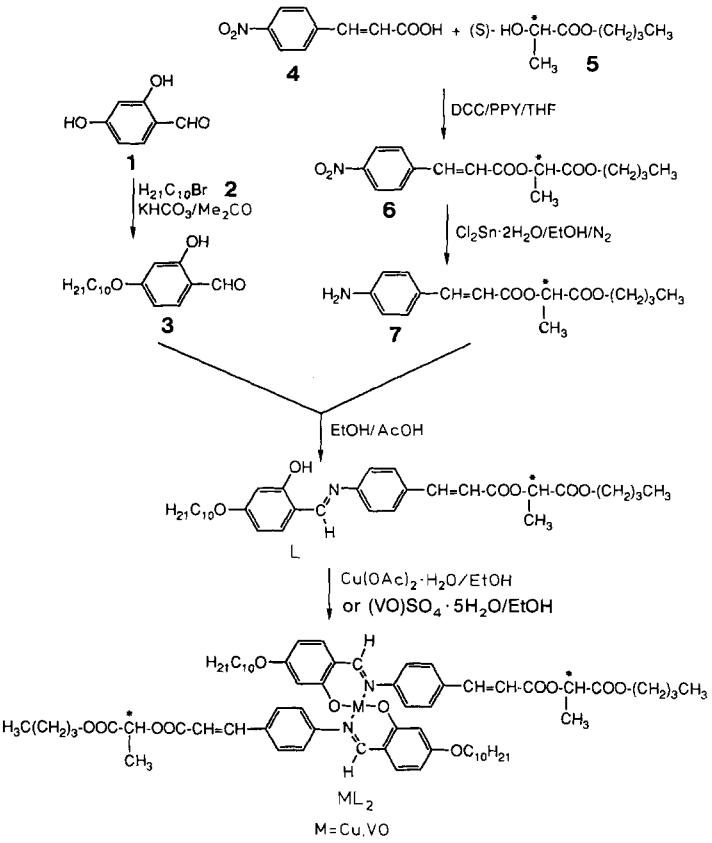

Scheme 1. Synthesis of L and ML_2. DCC = dicyclohexylcarbodiimide, PPY = 4-pyrrolidinopyridine.

Table 1. Phase transitions, spontaneous polarization Ps_{max}, rotational viscosity γ_{max}, and switching time τ_{max} for the ligand and their complexes.

Compd	Phase [a] and Phase transition Temperatures [°C]	Ps_{max} [nC cm^{-2}]	γ_{max} [Pa s]	τ_{max} [μs V μm^{-1}]
L	C 51.7 S_{C^*} 92 [b] S_A 113.3 I	44	0.23	1104
CuL_2	C 109.2 S_{C^*} 120 [b] S_A 160.1 I	23	0.14	1247
VOL_2	C 125.0 S_{C^*} 137 [b] S_A 177.7 I	20	0.87	8217

[a] C = crystal, S_{C^*} = chiral smectic C; S_A = smectic A; I = isotropic. [b] From optical data.

Fig. 1. Photomicrograph of the CuL_2 complex in its chiral smectic C phase at 115 °C, viewed between crossed polars; 1 cm ≙ 200 μm.

[*] Dr. M. Marcos, Dr. J. L. Serrano, Dr. T. Sierra, M. J. Giménez
Química Orgánica, Facultad de Ciencias-I.C.M.A.
Universidad de Zaragoza-C.S.I.C.
E-50009-Zaragoza (Spain)

[**] This work was supported by Comisión Internacional de Ciencia y Tecnología (C.I.C.Y.T.) (Spain) under projects MAT90-0813 and MAT91-0962-CO2-01.

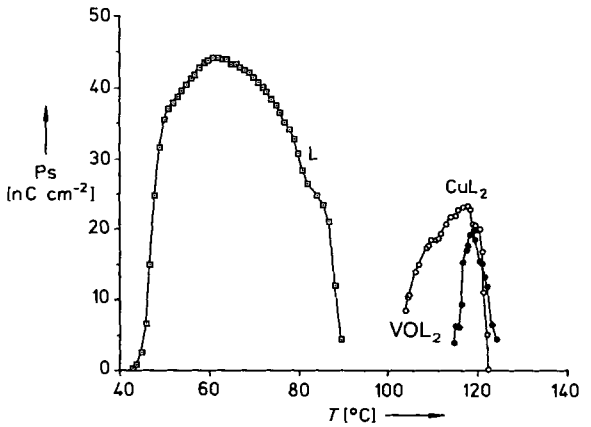

Fig. 2. Temperature dependence of the spontaneous polarization of ligand L and complexes CuL_2 and VOL_2.

ligand. Consequently, as both complexes exhibit similar Ps_{max} values, the switching time is longer in VOL_2 than in CuL_2 (Table 1). These complexes exhibit switching times in the millisecond range, comparable to the switching time exhibited by polymeric ferroelectric liquid crystals,[8] but slightly longer than that of most of ferroelectric organic liquid crystals (FOLCs), which are normally in the range of microseconds.[9] However, it is noteworthy that in this case the switching time for the organic ligand L is also in the range of milliseconds.

The Ps of FLCs is determined by the magnitude of the molecular dipole moment, the relative intramolecular motions of the dipole moment of the chiral part, and the rotation of the molecule around its long axis. As can be seen in Figure 2, the Ps_{max} of the ligand decreases from 44 nC cm^{-2} to 23 or 20 nC cm^{-2} on complexation, probably because the dipole moments of a chain cancel each other out when their orientations differ.

In conclusion, these ferroelectric metallomesogens are interesting not for the usual applications in which classical FOLCs are employed, but rather for applications in which a combination of the ferroelectric properties of the chiral smectic C phase with the magnetic orientability of paramagnetic complexes in a magnetic field is important, as these complexes can be aligned parallel or perpendicular to the magnetic field, depending on the anisotropy of the magnetic susceptibility of the complex.[10]

Experimental Procedure

All compounds were characterized by C,H,N analyses and IR and ^{1}H NMR spectroscopy.

6: (−)-Butyl-L-lactate (**5**) available in 97% enantiomeric purity from Fluka, served as chiral starting material. It was coupled to *p*-nitrocinnamic acid **4** (each 71.8 mmol) with DCC (79 mmol) as esterification agent and PPY (7.18 mmol) as catalyst in dry THF (20 mL) according to the method described by Hassner and Alexanian [11]. The product **6** was purified by flash chromatography (dichloromethane).

7: The nitro group of **6** (25 mmol) was reduced with $SnCl_2 \cdot 2H_2O$ (125 mmol) in ethanol (100 mL) under an inert atmosphere (N_2) according to the Bellamy method [12]. The amine obtained was used without further purification in the condensation step.

L: Schiff base L was synthesized along standard procedures [13] by mixing an ethanolic solution of **3** (5.7 mmol) with chiral amine **7** (5.7 mmol) and a few drops of acetic acid as catalyst, and purified by two recrystallizations from ethanol and hexane. Selected spectroscopic data for L: ^{1}H NMR ($CDCl_3$) δ = 13.52 (s, 1H), 8.52 (s, 1H), 7.73 (d, J = 16.1 Hz, 1H), 7.55 (d, J = 8.4 Hz, 2H), 7.2–7.3 (m, 3H), 6.41–6.54 (m, 3H), 5.20 (J = 6.9 Hz, 1H), 4.16 (t, 2H), 3.98 (t, 2H), 1.84–1.20 (m, 20H), 1.53 (d, 3H), 0.92 (t, 3H), 0.86 (t, 3H); IR (nujol) $\tilde{\nu}$ [cm^{-1}]: 1752, 1719 (CO=O), 1630 (CH=CH), 1630 (C=N) overlapping signals.

ML_2: An ethanolic solution containing copper acetate or vanadyl sulfate (1 mmol) was added to a hot ethanolic solution of L (2 mmol). The color of the reaction solution changed from yellow to green. The solution was refluxed for 1 h and then cooled. The precipitate was collected by filtration and recrystallized from chloroform/ethanol (1/3). The brown copper complex and green oxovanadium compound were characterized by IR spectroscopy and elemental analysis. The ^{1}H NMR spectra of the complexes exhibit large shifts relative to the free ligand, and all signals are broadened as a result of the paramagnetic metallic ion. CuL_2: IR (nujol) $\tilde{\nu}$ [cm^{-1}]: 1755, 1719 (CO=O), 1633 (CH=CH), 1609 (C=N); VOL_2: IR (nujol) $\tilde{\nu}$ [cm^{-1}]: 1761, 1717 (CO=O), 1634 (CH=CH), 1608 (C=N), 976 (V=O).

Received: June 9, 1992 [Z 5398 IE]
German version: *Angew. Chem.* **1992**, *104*, 1523

CAS Registry numbers:
1, 95-01-2; **2**, 112-29-8; **3**, 68075-69-4; **4**, 619-89-6; **5**, 34451-19-9; **6**, 143958-68-3; **7**, 143958-67-2; L, 143958-66-1; CuL_2, 143968-95-0; VOL_2, 143968-96-1; $Cu(OAc)_2$, 142-71-2; $VOSO_4$, 27774-13-6.

[1] D. M. Walba, M. B. Ros, N. A. Clark, R. Shao, M. G. Robinson, J. Y. Lin, K. M. Johnson, D. Doroski, *J. Am. Chem. Soc.* **1991**, *113*, 5471; A. Taguchi, K. Kajikawa, Y. Ouchi, H. Takezoe, A. Fukuda in *Materials for Nonlinear Optics of Organics and Semiconductors* (Ed.: T. Kobayashi), Springer, Berlin, **1989**, p. 250; H. Kapitza, R. Zentel, R. J. Twieg, C. Neguyen, S. U. Vallerien, F. Kremer, C. G. Willson, Adv. Mater. **1990**, *2*, 539.
[2] P. M. Maitlis, A. M. Giroud-Godquin, *Angew. Chem.* **1991**, *103*, 370; *Angew. Chem. Int. Ed. Engl.* **1991**, *30*, 375.
[3] J. A. Bandy, H. E. Bunting, M. H. García, M. L. H. Green, S. R. Marder, M. E. Thompson, D. Bloor, P. V. Kolinsky, R. J. Jones in *Organic Materials for Non-Linear Optics* (Eds.: R. A. Hann, D. Bloor), Royal Society of Chemistry, London, **1989**, p. 225.
[4] P. Espinet, J. Etxebarria, M. Marcos, J. Pérez, A. Remón, J. L. Serrano, *Angew. Chem.* **1989**, *1*, *Angew. Chem. Int. Ed. Engl.* **1989**, *28*, 1065.
[5] M. Marcos, P. Romero, J. L. Serrano, C. Bueno, J. A. Cabeza, L. A. Oro, *Mol. Cryst. Liq. Cryst.* **1989**, *167*, 123; M. Marcos, P. Romero, J. L. Serrano, J. Barberá, A. M. Levelut, *Liq. Cryst.* **1990**, *7*, 251; M. Marcos, P. Romero, J. L. Serrano, *Chem. Mater.* **1990**, *2*, 495.
[6] M. R. de la Fuente, A. Ezcurra, M. A. Pérez-Jubindo, J. Zubia, *Liq. Cryst.* **1990**, *7*, 51.
[7] C. Escher, T. Geelhaar, E. Böhm, *Liq. Cryst.* **1988**, *3*, 469.
[8] H. Poths, A. Schönfeld, R. Zentel, F. Kremer, K. Siemensmeyer, *Adv. Mater.* **1992**, *4*, 351.
[9] S. Arakawa, K. Nito, J. Seto, *Mol. Cryst. Liq. Cryst.* **1991**, *204*, 15; M. Marcos, A. Omenat, J. L. Serrano, T. Sierra, A. Ezcurra, *Adv. Mater.* **1992**, *4*, 285.
[10] M. Marcos, J. L. Serrano, *Adv. Mater.* **1991**, *3*, 285.
[11] A. Hassner, V. Alexanian, *Tetrahedron Lett.* **1978**, 4475.
[12] F. D. Bellamy, K. Ou, *Tetrahedron Lett.* **1984**, *25*, 839.
[13] P. Keller, L. Liebert, *Solid State Phys. Suppl.* **1986**, *14*, 19.

Solving the Structure of a Metal-Substituted Aluminum Phosphate Catalyst by Electron Microscopy, Computer Simulation, and X-ray Powder Diffraction**

By *Paul A. Wright, Srinivasan Natarajan, John Meurig Thomas,* Robert G. Bell, Pratibha L. Gai-Boyes, Richard H. Jones,* and *Jiesheng Chen*

Of the large number of new molecular sieves based on microporous aluminum phosphates (ALPOs) reported since their discovery ten years ago,[1–3] many have not yet had

[*] Prof. Sir J. M. Thomas, Dr. P. A. Wright, Dr. S. Natarajan, Dr. R. G. Bell, Dr. R. H. Jones, Dr. J. Chen
Davy Faraday Research Laboratory,
The Royal Institution of Great Britain
21 Albemarle Street, GB-London W1X 4BS (UK)
Dr. P. L. Gai-Boyes
Central Research and Development, E. I. du Pont de Nemours (USA)

[**] This work was supported by the Science and Engineering Research Council (UK).

their crystal structures determined, mainly because they do not form crystals of a quality good enough for single-crystal X-ray analysis. Particularly interesting members of the MeALPO family, in which a divalent metal (Me) substitutes for Al^{3+} in the framework, are MeALPO-36 (Me = Mg, Mn, Co, Ni, Zn) and MeALPO-34 (Me = Mg, Mn, Be, Co). In some MeALPO structures silicon may also replace a fraction of both the phosphorus and aluminum; such products are designated MeALPSOs or MeAPSOs. Most of these are active, uniform heterogeneous catalysts[3, 4] for the conversion of hydrocarbons and methanol. The active sites (readily detachable protons loosely bound to a framework oxygen atom close to the divalent metal) are distributed in a uniform manner throughout the bulk of the microporous solid and are accessible to small reactant molecules.[5, 6] MeALPO-34 has a framework structure exactly analogous to that of the zeolitic mineral chabazite ($Ca_6[Al_{12}Si_{24}O_{72}] \cdot 40H_2O$), but that of MeALPO-36 has hitherto not been known. We describe herein how the three-dimensional structure of this catalyst was solved on the basis of evidence garnered from high-resolution electron microscopy,[7, 8] electron diffraction, and other methods including energy minimization.[9]

Monophasic samples of MgALPO-36, MgALPSO-36, and ZnALPO-36 were synthesized according to published procedures.[10] The similarity of their X-ray powder diffraction patterns indicates that they have the same framework structure. Thin sections of the needlelike crystals (both parallel and perpendicular to the needle axis) of specimens of the ZnALPO-36 (taken as representative) were examined under the electron microscope. The diffraction patterns and high-resolution images suggested an orthorhombic cell, approximately $13.1 \times 21.6 \times 5.0$ Å, with two one-dimensional, wide-pored channels (known from previous adsorption measurements[10] to be bounded by twelve tetrahedrally surrounded atoms) parallel to the c axis and situated at 0,0 and $a/2$, $b/2$ in the unit cell.

The determination of the short 5 Å c axis was particularly helpful, because it restricts the possible structures to those built up of zigzag chains of tetrahedra parallel to the short axis. Examples of such structures include the zeolites bikitaite,[11] cancrinite,[12] Theta-1,[13] and ZSM-23[14] as well as the aluminum phosphate ALPO-31.[15] A consideration of possible frameworks of appropriate dimensions and with the observed size and spatial distribution of unidimensional, large-pore channels suggests a trial structure with idealized symmetry *Cmcm*, illustrated in Figure 1a. (Initial coordinates were refined by using distance least-squares (DLS)[16] constraints on the bond lengths and angles applicable for high silica zeolites.)

We next took advantage of computational methods designed to achieve energy minimization of the solid with respect to its structural parameters, using the procedures that have proved to be a powerful tool for modeling the structure of high silica zeolites.[17] We have applied the METAPOCS[9, 18] method for the minimization of the lattice energy at constant pressure, which allows cell dimensions and symmetry elements to relax in addition to the atomic coordinates. We first replaced each tetrahedrally surrounded atom by a silicon atom; which approximates to keeping Al and P disordered in terms of the long-range structural order. The resulting structure remained orthorhombic (*Cmcm*), and the atoms shifted little from their values refined by DLS. However, we know that in ALPOs, and also probably in MeALPOs and MeALPSOs where the degree of substitution of Al for Me, and Si for P and Al is small, the Al (and Me) and P atoms will be strictly ordered on alternate tetrahedra. Therefore, by putting Al and P (ordered) into the high-symmetry *Cmcm* structure (thereby breaking the mirror and glide symmetry), and by using Al and P potentials derived by van Beest et al.[19] the lattice energy was again minimized. Because of the presence of mirror planes perpendicular to a in the high-symmetry form, only one distinct Al/P ordering scheme is possible. The resulting triclinic cell ($a = 13.46$, $b = 22.17$, $c = 5.29$ Å; $\alpha = 90.16$, $\beta = 92.01$, $\gamma = 89.95°$) retained $C\bar{1}$ symmetry and was close to pseudomonoclinic. The atomic coordinates are given in Table 1.

The X-ray powder diffraction profiles simulated from the atomic coordinates and cell parameters derived from the energy-minimized "SiO_2" and "AlPO" structural models are given in Figure 2a. They can be compared with experimental X-ray diffraction patterns of the representative aluminophosphate MgALPSO-36 recorded in dry helium with a special in situ cell[20] at temperatures of 150 and 375 °C (Fig. 2b). The close agreement of the diffraction pattern of the high-symmetry "SiO_2" structure with that of the pattern obtained experimentally at high temperature is clear. However, at the lower temperature, the (131) peak is split ($\Delta 2\theta = 0.375°$), and the entire profile approximates much more closely to that predicted from the "ALPO" energy-minimized structure, although the predicted lattice parameters are larger (by about 2.5 %) than those actually observed.

The diffraction pattern collected at the lower temperature was then matched by applying the Rietveld profile method.[21, 22] The atomic coordinates obtained from the

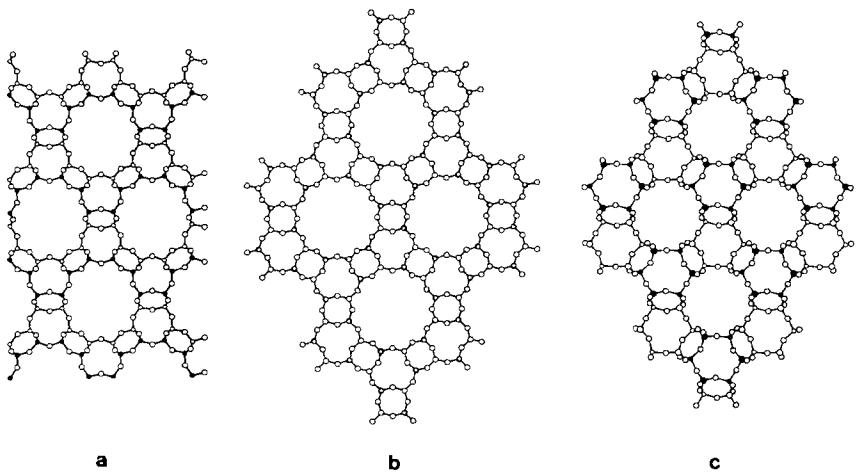

Fig. 1. a) and b) Projections down [001] of the high-symmetry (Al and P disordered) models for MeALPO-36 (*Cmcm*) as a generalized structure and calcined ALPO-5 [24], respectively; c) projection of the structure of aluminosilicate cancrinite. For a) and c) the open circles representing tetrahedrally coordinated atoms are separated in the direction of the z axis by a distance of $c/2$ from those tetrahedrally coordinated atoms represented by closed circles. In c) the smaller tetrahedrally surrounded atoms represent Al, the larger Si.

Table 1. Atomic coordinates for MeALPO-36 (energy minimized) using a hypothetical end-member $AlPO_4$ composition.

Atom	x	y	z
Al(1)	0.1200	0.9608	0.2681
Al(2)	0.8085	0.8235	0.2714
Al(3)	0.3838	0.7438	0.2749
P(1)	0.8800	0.9587	0.2313
P(2)	0.1905	0.8251	0.2349
P(3)	0.6141	0.7441	0.2240
O(1)	0.1821	0.8924	0.2548
O(2)	0.8235	0.9006	0.2409
O(3)	0.9911	0.9447	0.2466
O(4)	0.1409	0.0008	0.5477
O(5)	0.8592	0.9920	0.9875
O(6)	0.2960	0.8027	0.2602
O(7)	0.6862	0.7962	0.2440
O(8)	0.1486	0.8040	0.9809
O(9)	0.8655	0.2044	0.5554
O(10)	0.8584	0.7990	0.5630
O(11)	0.1290	0.2128	0.9732
O(12)	0.5077	0.7629	0.2457

"ALPO" energy minimization were used, and the lattice and thermal parameters refined. No attempt was made to refine the 54 independent atomic coordinates because of the limited amount of reflection intensity data available from the powder diffraction data. The final fit is illustrated in Figure 3. The average bond lengths for Al–O 1.71(1) and P–O 1.48(1) Å are identical (within experimental error) with the values obtained from a single-crystal study of ALPO-5.[23]

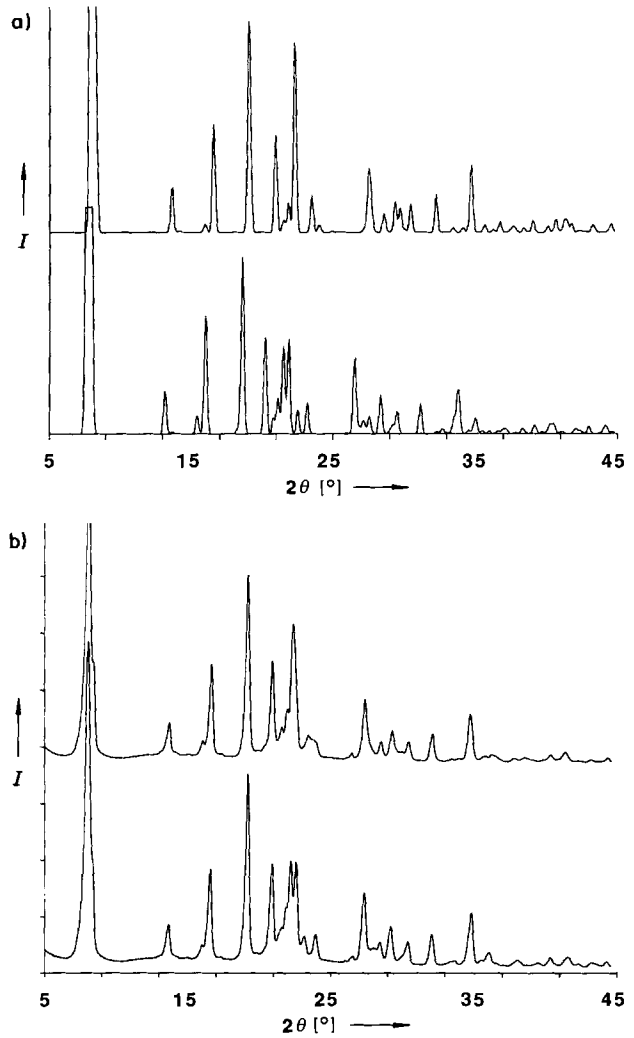

Fig. 2. a) Simulated X-ray diffraction patterns for SiO_2 (top) and ALPO (bottom) energy-minimized structures. b) Experimental X-ray diffraction patterns for MgALPSO-36 recorded at 375 (top) and 150 °C (bottom). I = intensity in arbitary units.

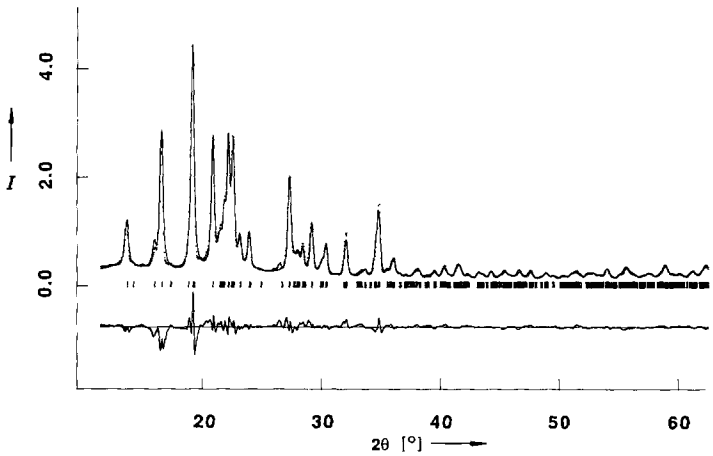

Fig. 3. Experimental (dots) and fitted (solid line) diffraction profiles (top) with difference plot (bottom) and peak markers (middle) for the X-ray diffraction data collected at 150 °C and for the atomic coordinates from the ALPO energy minimization (I = counts $\times 10^{-4}$). The refined cell parameters for MgALPSO-36 are $a = 13.161(2)$, $b = 21.649(3)$, $c = 5.189(1)$ Å, $\alpha = 89.96(2)$, $\beta = 92.17(2)$, and $\gamma = 90.02(3)°$. The isotropic temperature factors (U_i) of the tetrahedrally surrounded atoms (constrained to be a single value) and of the oxygen atoms (a single, independent value) refined to 0.015 and 0.030 $Å^2$, respectively. The final weighted profile R-factor (R_{wp}) was 0.098.

For comparison, DLS refinement was performed in the same unit cell and space group, with Al/P ordering, and with experimental bond lengths from the single-crystal study of ALPO-5.[23] The DLS-derived atomic coordinates were within 0.06(2) Å for the tetrahedrally surrounded atoms and 0.10(7) Å for the oxygens of the energy-minimized structure and fitted the observed X-ray diffraction data well ($R_{wp} = 0.112$ as against 0.098 for the energy-minimized structure).

The framework of MeALPO-36 is built of four- and six-membered rings and contains wide-pore channels bounded by twelve-membered rings half at $z = 0$ and half at $z = 1/2$ (Fig. 4). In projection, MeALPO-36 (Fig. 1a) is similar to ALPO-5 (Fig. 1b[24]) and possesses nearly identical adsorption properties. (However, in ALPO-5, the largest apertures are effectively circular, and the smallest are squares, whereas in MeALPO-36 both the largest and smallest apertures are oval.) MeALPO-36 is also very similar to the zeolite cancrinite in projection (Fig. 1c), and an aluminophosphate with the cancrinite structure could easily intergrow on the (010) plane of MeALPO-36. We are currently investigating whether such intergrowths can explain faults determined by high-resolution electron microscopy (HREM) on the (010) plane of ZnALPO-36.

Two significant general conclusions may be drawn from this work. First, the use of energy minimization procedures in elucidating structural detail is likely to be widely applicable to other solids (irrespective of whether or not they are uniform catalysts), particularly those that are available only as powders. Details of distortions away from idealized symmetry—expected in ALPOs as a consequence of strict Al/P ordering—may be predicted with a physical model rather than relying on diffraction data. Whereas for MeALPO-36 it is possible to approach the energy-minimized structure by

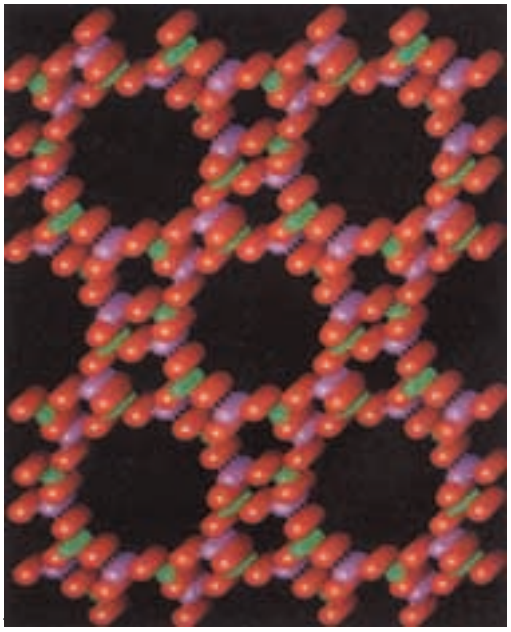

Fig. 4. The energy minimized "ALPO" structure for MeALPO-36, Me = Mg, Zn, etc. Note that Al and P alternate in the tetrahedra. Red = oxygen, green = phosphorus, violet = aluminum (+Me in synthesized samples).

DLS-modeling, this requires prior knowledge of the unit cell and space group, which cannot generally be determined unambiguously. Second, a knowledge of the three-dimensional structure of uniform heterogeneous catalysts (such as that of MeALPO-36) provides far greater insight into the properties of the catalyst than is the case for nonuniform, multicomponent ones (such as a typical Fischer–Tropsch, supported catalyst).

After completing this study we became aware of an as yet unpublished report of the structure of MeALPO-36, Me = Mg.[25] This report gives details of the average disordered structure in space group $C2/c$ with $a = 13.1$, $b = 21.6$, $c = 5.2$, $\beta = 92.0°$.

Experimental Procedure

Samples of MgALPO-36, MgALPSO-36, and ZnALPO-36 (seeded with MgALPO-36) were prepared from gels with tripropylamine as a base [10] by heating the gels under autogenous pressure in a Teflon-lined autoclave at 110 °C for 24 h and 150 °C for 22 h. The bulk Mg:Al:P, Mg:Al:P:Si, and Zn:Mg:Al:P contents were 0.14:0.86:1.00, 0.04:0.91:0.90:0.15, and 0.04:0.03:0.91:1.01, respectively, as determined by inductively coupled plasma (ICP) atomic emission spectrometry. The organic template was removed by calcination in oxygen at 550 °C for 12 h. Electron microscopy was performed on a Philips CM30 microscope operating at 300 keV. DLS calculations, X-ray powder profile simulations, and plotting were performed with Biosym Technologies Catalysis software on a Silicon Graphics Personal Iris workstation. Energy refinements were performed with the METAPOCS code on a CONVEX C210 computer. X-ray diffraction patterns were collected with flat-plate geometry on dehydrated samples in an environmental GTP cell under flowing helium with a Siemens D500 diffractometer with a STOE rotating anode Cu X-ray source operating at 6 kW with a Ni filter. The profile refinement was performed over the range $2\theta = 11$–$63°$ with the GSAS program of Larson and Von Dreele [26].

Received: June 17, 1992 [Z 5409 IE]
German version: *Angew. Chem.* **1992**, *104*, 1526

[1] S. T. Wilson, B. M. Lok, C. A. Messina, T. R. Cannon, E. M. Flanigen, *J. Am. Chem. Soc.* **1982**, *104*, 1146.
[2] B. M. Lok, C. A. Messina, R. L. Patton, T. R. Gajeh, T. R. Cannon, E. M. Flanigen, *J. Am. Chem. Soc.* **1984**, *106*, 6092.
[3] E. M. Flanigen, B. M. Lok, R. L. Patton, S. T. Wilson in *New Developments in Zeolite Science and Technology* (Ed.: P. A. Jacobs), Elsevier, Amsterdam, **1986**, p. 103.
[4] J. M. Thomas, Y. Xu, C. R. A. Catlow, J. W. Couves, *Chem. Mater.* **1991**, *3*, 667.
[5] J. M. Thomas, *Angew. Chem.* 1988, *100*, 1735; *Angew. Chem. Int. Ed. Engl.* **1988**, *27*, 1673.
[6] J. M. Thomas, *Philos. Trans. R. Soc. London A* **1990**, *333*, 173.
[7] J. M. Thomas, *Ultramicroscopy* **1982**, *8*, 13.
[8] J. M. Thomas in *Zeolites: facts, figures, future* (Ed.: P. A. Jacobs, R. A. van Santen), Elsevier, Amsterdam, **1989**, p. 3.
[9] C. R. A. Catlow, A. N. Cormack, F. Theobald, *Acta Crystallogr. Sect. B* **1984**, *40*, 195.
[10] S. T. Wilson, E. M. Flanigen in *Zeolite Synthesis* (*ACS Symp. Ser.* **1989**, *398*), p. 329.
[11] K. Stahl, A. Kvick, S. Ghose, *Zeolites* **1989**, *9*, 303.
[12] Yu. I. Smolin, Yu. F. Shepelev, I. K. Butikova, I. B. Kobyakov, *Kristallografia* **1981**, *26*, 63.
[13] S. A. I. Barri, G. W. Smith, D. White, D. Young, *Nature* **1985**, *312*, 533.
[14] P. A. Wright, G. R. Millward, J. M. Thomas, S. A. I. Barri, *J. Chem. Soc. Chem. Commun.* **1985**, 1117.
[15] J. M. Bennett, R. M. Kirchner, *Zeolites* **1992**, *12*, 338.
[16] C. Baerlocher, A. Heppe, W. M. Meier, DLS-76, Manual, Institut of Crystallography and Petrology, ETH, Zürich, Switzerland, **1977**.
[17] R. G. Bell, R. A. Jackson, C. R. A. Catlow, *J. Chem. Soc. Chem. Commun.* **1990**, 782.
[18] R. A. Jackson, C. R. A. Catlow, *Mol. Simul.* **1989**, *1*, 207.
[19] B. W. H. van Beest, G. J. Kramer, R. A. van Santen, *Phys. Rev. Lett.* **1990**, *64*, 1955.
[20] P. J. Maddox, J. Stachurski, J. M. Thomas, *Catal. Lett.* **1988**, *1*, 191.
[21] H. M. Rietveld, *J. Appl. Crystallogr.* **1969**, *2*, 65.
[22] J. W. Couves, R. H. Jones, J. M. Thomas, B. J. Smith, *Adv. Mater.* **1990**, *2*, 181.
[23] J. M. Bennett, J. P. Cohen, E. M. Flanigen, J. J. Pluth, J. V. Smith, in *Intrazeolite Chemistry* (*ACS Symp. Ser.* **1983**, *218*), p. 109.
[24] J. W. Richardson, Jr., J. J. Pluth, J. V. Smith, *Acta. Crystallogr. Sect. C* **1987**, *43*, 1469.
[25] J. V. Smith, J. J. Pluth, K. J. Andries, *Zeolites*, submitted; cited in *Atlas of Zeolite Structure Types* (Ed. W. M. Meier, D. H. Olson), Butterworth-Heinemann, London, **1992**, p. 50.
[26] A. C. Larson, R. B. von Dreele, *Generalized Crystal Structure Analysis System*, Los Alamos National Laboratory, USA, **1988**.

Decamethylcucurbit[5]uril**

By *Anthony Flinn, Gordon C. Hough, J. Fraser Stoddart,** and *David J. Williams*

Rigid toroidal receptor molecules, which resemble collars,[1] belts,[1] and doughnuts,[2] have appealing molecular architectures. On the one hand, they may be regarded as progenators of molecular cages:[3] on the other hand, they can serve as components in the construction of molecular abacuses.[4] The synthesis of cucurbituril[5] during the last decade demonstrated the use of self-assembly[6] in synthesis to construct a rigid, hollow structure of D_{6h} symmetry consisting of six glycoluril units mutually linked by pairs of methylene groups to form a macropolycyclic array. Molecular modeling suggests that both the immediately lower and higher order homologues of this cyclic hexamer have almost strain-free structures. Here, we describe the synthesis of a cyclic pentamer **2** by self-assembly of dimethylglycoluril (**1**) (Scheme 1) and the full structural characterization of **2** (Fig. 1).

[*] Prof. J. F. Stoddart, G. C. Hough
School of Chemistry, University of Birmingham
Edgbaston, GB-Birmingham B15 2TT (UK)
Dr. A. Flinn
Hexcel Chemical Products Limited
Seal Sands Road, Seal Sands
GB-Middlesbrough TS2 1UB (UK)
Dr. D. J. Williams
Chemical Crystallography Laboratory
Department of Chemistry, Imperial College
GB-London SW7 2AY (UK)

[**] This work was supported by the Science and Engineering Research Council and Hexcel Chemical Products Limited.

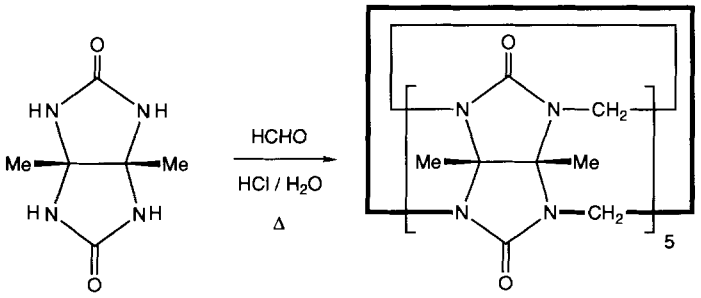

1 2

Scheme 1.

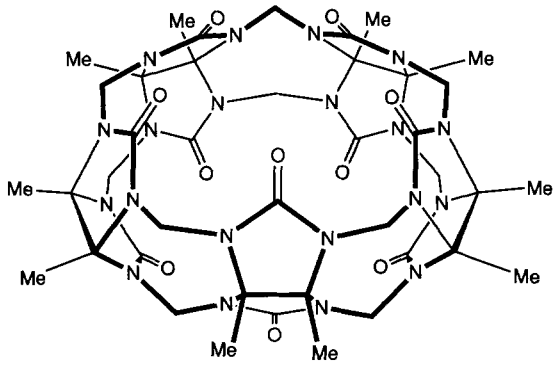

Fig. 1. The structure of decamethylcucurbit[5]uril (**2**).

The X-ray structural analysis[8, 9] of the crystalline material obtained from dilute HNO_3 shows (Fig. 2) that, in the solid state,[9] the decamethylcucurbit[5]uril[10] molecule (**2**) deviates only slightly from D_{5h} symmetry. The crystallographic symmetry is C_2. Despite the steric crowding associated with the adjacent Me substituents around the periphery of the molecule, all the atoms that comprise its equatorial plane are coplanar to within 0.06 Å. The formation of the cyclic pentamer involves a small amount of molecular strain, which is reflected in an enlargement of the NCN angles at the bridging methylene groups from 109° to between 114 and 116°. There is, however, no out-of-plane distortion at any of the nitrogen atoms. The inclusion of a "molecule of nitric acid"[11] within the molecular cavity of **2** results (Fig. 3) in a distortion of the pentagonal arrays of carbonyl oxygen atoms that form the portals of the receptor. The angles between adjacent atoms of these arrays are in the range 103–114°, and the associated O···O distances are between 3.14 and 3.22 Å. The exterior surface of the molecular receptor is discus-shaped with a diameter of about 15 Å and a thickness of about 9 Å. The diameter of the interior along the σ_h plane is approximately 6 Å. The diameters of the oxygen-bounded portals are about 2.5 Å. The inclusion of HNO_3, or the NO_3^- ion, within the molecular cavity demonstrates that these portals can expand to permit the passage of this guest through the orifice. The nature of the binding of HNO_3, or the NO_3^- ion, within the receptor cannot be defined precisely. There are, however, short contacts of 2.82 and 2.85 Å between two of the three $(H)NO_3$ oxygen atoms and the oxygen and carbon atoms of two different carbonyl groups. The former could represent a hydrogen bonding interaction and the latter an electrostatic one.

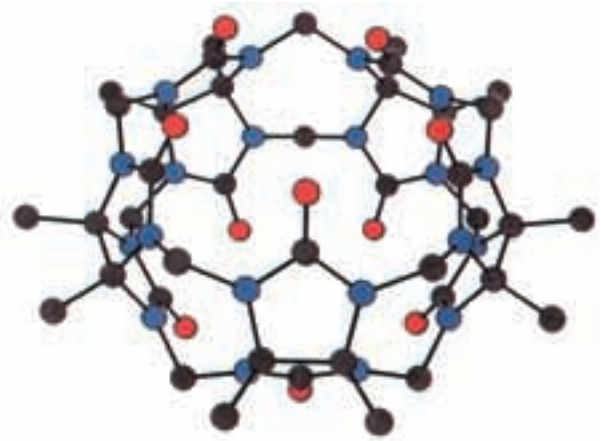

Fig. 2. The ball-and-stick representation of the structure of **2**. Gray C, blue N, pink O.

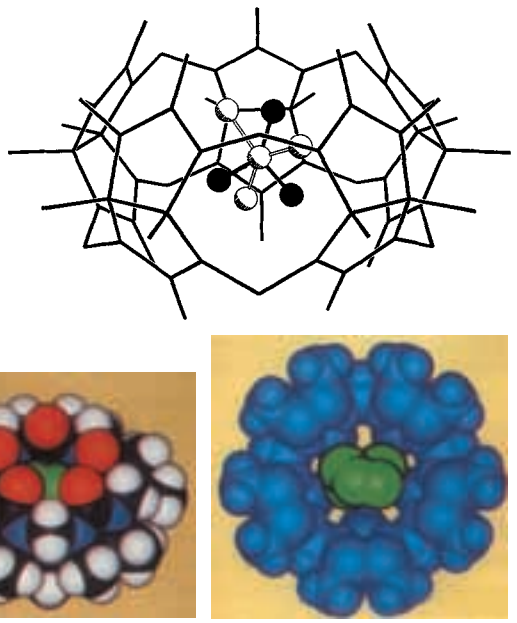

Fig. 3. Top: The positioning of the disordered nitric acid "molecule" within the molecular cage of **2**. The O atoms of the differently oriented nitric acids are depicted, one shaded, and the other unshaded. Bottom left: The space-filling representation of this inclusion complex. Black C, blue N, red O, green nitric acid "molecule". Bottom right: A space-filling representation of **2** · nitric acid viewed along the principal axis of **2** showing the interior of the molecular cavity produced by removing the upper rim of atoms and groups in **2**. Host molecule, blue: guest molecule, green.

The self-assembly,[6] isolation, and unambiguous characterization of decamethylcucurbit[5]uril[10] (**2**) raises the prospect of synthesizing a family of cucurbituril receptors in addition to the previously characterized cyclic hexamer formed between glycoluril and formaldehyde.

Experimental Procedure

2: Dimethylglycoluril (**1**) (4 g, 23 mmol), 37% aqueous HCHO solution (8 mL), concentrated HCl (16 mL), and H_2O (5 mL) were heated under reflux for 2 h. H_2O (70 mL) was added, and the dark red solution was heated under reflux for a further 1 h, before being allowed to cool gradually. The precipitate was collected by filtration, washed (H_2O), and dried in vacuo to give **2** as a white solid. Yield: 750 mg, 16%; m.p. > 280 °C; positive-ion FAB-MS: *m/z* = 971, 989, and 1009 for $[M + H]^+$, $[M + H_3O]^+$, and $[M + K]^+$, respective-

ly; ^{1}H NMR (300 MH]$_z$, CF_3CO_2D): $\delta = 1.99$ (s, 30H), 4.61 (d, $^2J = 16$ Hz, 10H), 6.04 (d, $^2J = 16$ Hz, 10H); ^{13}C NMR (75 MHz, CF_3CO_2D): $\delta = 16.9$, 44.1, 78.3, 156.3. Single crystals suitable for X-ray crystallography were obtained from a solution of **2** in dilute HNO_3 by slow evaporation over a period of 12 months.

Received: July 11, 1992 [Z 5461 IE]
German version: *Angew. Chem.* **1992**, *104*, 1550

[1] F. H. Kohnke, A. M. Z. Slawin, J. F. Stoddart, D. J. Williams, *Angew. Chem.* **1987**, *99*, 941; *Angew. Chem. Int. Ed. Engl.* **1987**, *26*, 892; P. R. Ashton, N. S. Isaacs, F. H. Kohnke, A. M. Z. Slawin, C. Spencer, J. F. Stoddart, D. J. Williams, *ibid.* **1988**, *100*, 981 and **1988**, *27*, 966; P. R. Ashton, G. R. Brown, N. S. Isaacs, D. Giuffrida, F. H. Kohnke, J. P. Mathias, A. M. Z. Slawin, D. R. Smith, J. F. Stoddart, D. J. Williams, *J. Am. Chem. Soc.*, **1992**, *114*, 6330.

[2] W. Saenger, *Angew. Chem.* **1980**, *92*, 343; *Angew. Chem. Int. Ed. Engl.* **1980**, *19*, 344; J. F. Stoddart, *Carbohydr. Res.* **1989**, *192*, xii; *Angew. Chem.* **1992**, *104*, 860; *Angew. Chem. Int. Ed. Engl.* **1992**, *31*, 846.

[3] D. J. Cram, *Nature* **1992**, *356*, 29.

[4] M. V. Reddington, A. M. Z. Slawin, N. Spencer, J. F. Stoddart, C. Vicent, D. J. Williams, *J. Chem. Soc. Chem. Commun.* **1991**, 630; A. Harada, J. Li, M. Kamachi, *Nature* **1992**, *356*, 325.

[5] W. A. Freeman, W. L. Mock, N.-Y. Shih, *J. Am. Chem. Soc.* **1981**, *103*, 7367; W. A. Freeman, *Acta Crystallogr. Sect. B* **1984**, *40*, 382; W. L. Mock, N.-Y. Shih, *J. Org. Chem.* **1986**, *51*, 4440; *J. Am. Chem. Soc.* **1988**, *110*, 4706; *ibid.* **1989**, *111*, 2697; W. L. Mock, J. Pierpont, *J. Chem. Soc. Chem. Commun.* **1990**, 1509.

[6] J. S. Lindsey, *New J. Chem.* **1991**, *15*, 153; D. Philp, J. F. Stoddart, *Synlett* **1991**, 445; G. M. Whitesides, J. P. Mathias, C. T. Seto, *Science* **1991**, *254*, 1312.

[7] V. L. Himes, C. R. Hubbard, A. Mighell, A. J. Fatiadi, *Acta Crystallogr. Sect. B* **1978**, 34, 3102. A compound has been obtained (N.-Y. Shih, PhD Thesis, University of Chicago at Illinois, **1981**; *Diss. Abstr. Int. B* **1982**, *42*, 4071) from the condensation of dimethylglycoluril with formaldehyde under acidic conditions. This compound was assumed to be a cyclic pentamer or tetramer on the basis of an elemental analysis and the failure to form inclusion complexes with alkylamines in aqueous formic acid solutions.

[8] Siemens P4/PC diffractometer, ω-scans, $Mo_{K\alpha}$ radiation (graphite monochromator). The structure was solved by direct methods and the major occupancy atoms refined anisotropically, the minor occupancy atoms isotropically. Further details of the crystal structure investigation can be obtained from the Director of the Cambridge Crystallographic Data Centre, University Chemical Laboratory, Lensfield Road, GB-Cambridge CB2 1EW (UK), on quoting the full journal citation.

[9] Crystal data for $2 \cdot 3HNO_3 \cdot 6H_2O$: monoclinic, $a = 24.693(5)$, $b = 17.744(4)$, $c = 13.293(3)$ Å, $\beta = 116.39(3)°$, $V = 5217$ Å^3, space group $C2/c$, $Z = 4$ (the molecule has crystallographic C_2 symmetry) $\varrho_{calcd} = 1.614$ g cm^{-3}, $\mu(Mo_{K\alpha}) = 1.4$ cm^{-1}, 2603 independent observed reflections with $|F_o| > 3\sigma(|F_o|)$, $2\theta \leq 45°$, refined to $R = 0.067$, $R_w = 0.070$. The HNO_3 units occupy one full and two partial occupancy sites in the asymmetric unit, and the water molecules eight partial occupancy sites.

[10] We propose a simple nomenclature system for cucurbituril derivatives which is reminiscent of that proposed for the calixarenes (C. D. Gutsche, *Calixarenes*, Royal Society of Chemistry, Cambridge, **1989**, p. 26). The number of glycoluril or substituted glycoluril units is indicated by the number inside the square brackets. Substituents at the ring junction between the five-membered rings in the glycoluril units are indicated by a prefix.

[11] It should be noted that, in dilute aqueous solution, nitric acid is approximately 93% dissociated at 0.1 M concentration (F. A. Cotton and G. Wilkinson, *Advanced Inorganic Chemistry*, 5th ed, Wiley, New York, **1988**, p. 113).

The $[(\mu_3\text{-}WSe_4)_3(\mu_3\text{-}Se)_2(Cu_3)_2]^{4-}$ Anion, an Inorganic Cluster with a Pinwheel Shape**

By *Christopher C. Christuk, Mohammad A. Ansari,* and *James A. Ibers**

The rich chemistry of soluble sulfidometalates has been developed over the past two decades. There are now numerous examples of both homometallic[1] and mixed-metallic[2] compounds. Although the chemistry of selenido- and telluridometallates is very new,[3] most species that have been prepared have no sulfido analogues. Examples include $[Ni_4Se_4(Se_3)_5(Se_4)]^{4-}$,[4] $[Ni_4Te_4(Te_3)_4(Te_2)_2]^{4-}$,[5] $[In_2(Se_4)_4(Se)_5]^{4-}$,[6] $[NbTe_{10}]^{3-}$,[7] and $[W(AsSe_5)_2]^{2-}$.[8] In the search for new selenidometalates we investigated the chemistry of cubane-like clusters based on the MSe_4^{2-} core (M = Mo, W). Using the cubane **1**[9] we have synthesized the striking anion **2**.

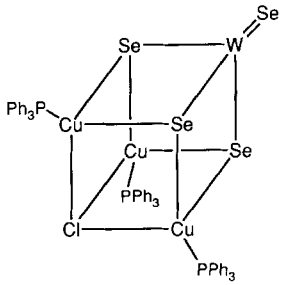

1

$[(\mu_3\text{-}WSe_4)_3(\mu_3\text{-}Se)_2(Cu_3)_2]^{4-}$ **2**

The precursor **1** is prepared from the stoichiometric reaction of $(NPr_4)_2[WSe_4]$, $[Cu(PPh_3)]^+$, and NH_4Cl in dimethylformamide (DMF). It has the same basic structure as other known cubanes,[2, 10] although their reaction chemistry has not been probed. A slurry of Li_2Se (15 mg, 0.16 mmol) in DMF (10 mL) was added with stirring to **1** (239 mg, 0.16 mmol) and NEt_4Cl (26 mg, 0.16 mmol) in 15 mL DMF under anaerobic conditions in oven-dried glassware. Red microcrystals filled the solution. Heating for 45 min produced a clear red solution that was filtered and stored at −15 °C. Deep red, block-shaped crystals of $(NEt_4)_4$-**2** · 2DMF were obtained after two weeks (34 mg, 32% yield).[11] The supernatant was pale, suggesting that most metal-containing species were no longer in solution. Precipitation of LiCl, heat, and insolubility of the NEt_4^+ salt of the anion provide the driving forces for the reaction. We speculate that the cubane is opened upon reaction with Se_2^{2-} and these remnants are linked by Se atoms. There is no spectroscopic evidence for the formation of $SePPh_3$.

The structure[12] of **2** (Fig. 1) can be described as two Cu_3 triangles (Cu1,Cu3,Cu5 and Cu2,Cu4,Cu6) bridged by tridentate WSe_4^{2-} ligands and capped by Se atoms (Se14 and Se13, respectively). Charge balance suggests that this anion contains the formal oxidation states Cu^I and W^{VI}. The Cu–Cu distances within the equilateral Cu_3 triangles (Cu-Cu-Cu angles between 58.1(1)° and 62.5(1)°), each capped by a Se atom, average 2.880(3) Å, while distances between these eclipsed Cu_3 triangles range from 3.519(3) to 3.580(3) Å. These distances between the triangles are too large for Cu–Cu interactions, and hence the structure cannot be described in terms of a Cu_6 trigonal prism. Numerous Cu_3 triangles[13] and chalcogen-capped M_3 triangles[2, 14] have been observed, but none in which these two features are present in the same molecule. While MQ_4^{2-} units (M = Mo, W, Q = S or more rarely Se) frequently act as monodentate[2] and bidentate[2, 15] ligands, there are far fewer examples in which they act as tridentate[2, 9, 10] or tetradentate[16] ligands. In anion **2** the WSe_4^{2-} ligands are tridentate.

The coordination at the W centers remains nearly tetrahedral: the angles range from 106.8(1)° to 110.9(1)°, slightly smaller than the related angles in the starting material **1**

[*] Prof. Dr. J. A. Ibers, C. C. Christuk, Dr. M. A. Ansari
Department of Chemistry, Northwestern University,
Evanston, IL 60208-3113 (USA)

[**] This work was supported by the U. S. National Science Foundation (Grant CHE89-22754).

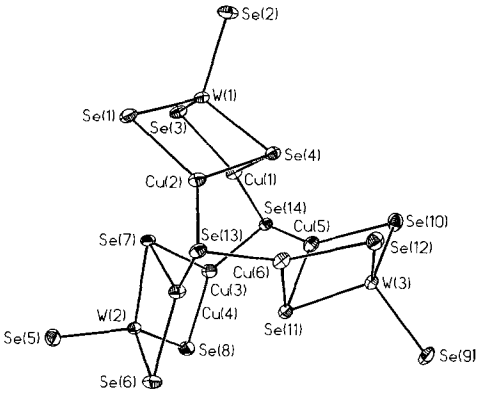

Fig. 1. Sketch of the structure of **2**. The thermal ellipsoids are shown at the 50% level. Selected bond lengths [Å] and angles [°]: W(1)-Se(1) 2.339(2), W(1)-Se(2) 2.289(2), W(1)-Se(3) 2.338(2), W(1)-Se(4) 2.400(2), W(1)-Cu(1) 2.741(2), W(1)-Cu(2) 2.734(3), Cu(1)-Se(3) 2.369(3), Cu(1)-Se(4) 2.386(3), Cu(1)-Se(14) 2.339(3), Cu(1)-Cu(3) 2.842(3), Se(1)-W(1)-Se(2) 110.2(1), Se(1)-W(1)-Se(3) 109.2(1), Se(1)-W(1)-Se(4) 109.3(1), W(1)-Se(3)-Cu(1) 71.2(1), W(1)-Se(4)-Cu(1) 69.9(1), Se(3)-Cu(1)-Se(4) 108.5(1), Se(3)-Cu(1)-Se(14) 125.0(1), Se(4)-Cu(1)-Se(14) 124.1(1), Cu(1)-Se(14)-Cu(3) 75.0(1), Cu(1)-Se(14)-Cu(5) 76.2(1), Cu(3)-Se(14)-Cu(5) 74.1(1).

(108.13(8)°–111.4(1)°). Variations in Se_{bridge}-W-$Se_{terminal}$ compared with Se_{bridge}-W-Se_{bridge} angles closely mirror those observed in related compounds.[2, 17] Angles about the capping Se atoms are acute (between 74.1(1)° and 79.3(1)°) similar to analogous angles for other capping chalcogens.[16, 18] The steric limitations imposed by the WSe_4^{2-} ligand result in the placement of the capping Se atoms away from the center of the cluster. A slight opening of the Se-Cu-Se angles (108.2(1)°–109.8(1)°) from those in the starting cubane **1** (104.2(1)°–108.6(1)°) probably also arises from steric effects.

Four types of Se atoms are present in **2**: capping Se atoms bonded to three Cu atoms and three-, two-, and one-coordinate Se atoms in the WSe_4 moieties. Consequently, three different ranges of Cu–Se bond lengths are observed: 2.327(3)–2.347(3) Å (capping Se), 2.355(3)–2.369(3) Å (two-coordinate Se), and 2.385(3)–2.388(3) Å (three-coordinate Se) as opposed to the average Cu–Se distance of 2.408(3) Å in the parent cubane.[9]

The W–Se bond lengths similarly fall into three categories. Terminal Se atoms are found at an average distance of 2.290(2) Å from the W atoms, an elongation from the 2.201(4) Å distance observed in **1**. The W–Se_{bridge} distances, which average 2.376(3) Å in the cubane, lengthen to 2.397(3) Å for three-coordinate Se atoms or shorten to 2.344(2) Å for two-coordinate Se atoms. An average W–Cu distance of 2.738(3) Å in the WSe_4Cu_2 moiety may imply a slightly stronger W^{VI}–Cu^{I} interaction than in the cubane where the average distance is 2.753(3) Å and where the orbitals of three Cu atoms, rather than two, compete for overlap with those of the W atom.

Received: June 24, 1992
Revised version: August 31, 1992 [Z 5428 IE]
German version: *Angew. Chem.* **1992**, *104*, 1519

CAS Registry numbers:
1, 143618-53-5; **2**, 143901-53-5; $(NPr_4)_2[WSe_4]$, 143594-19-8; $[Cu(PPh_3)]^+$, 81218-61-3

[1] A. Müller, E. Diemann, *Adv. Inorg. Chem.* **1987**, *31*, 89–122.
[2] A. Müller, H. Bögge, U. Schimanski, M. Penk, K. Nieradzik, M. Dartmann, E. Krickemeyer, J. Schimanski, C. Römer, M. Römer, H. Dornfeld, U. Wienböker, W. Hellmann, M. Zimmermann, *Monatsh. Chem.* **1989**, *120*, 367–391.
[3] M. A Ansari, J. A. Ibers, *Coord. Chem. Rev.* **1990**, *100*, 223–266.
[4] J. M. McConnachie, M. A. Ansari, J. A. Ibers, *J. Am. Chem. Soc.* **1991**, *113*, 7078–7079.
[5] J. M. McConnachie, M. A. Ansari, J. A. Ibers, *Inorg. Chim. Acta* **1992**, *198–200*, 85–93.
[6] M. G. Kanatzidis, S. Dhingra, *Inorg. Chem.* **1989**, *28*, 2024–2026.
[7] W. A. Flomer, J. W. Kolis, *J. Am. Chem. Soc.* **1988**, *110*, 3682–3683.
[8] S. C. O'Neal, W. T. Pennington, J. W. Kolis, *Inorg. Chem.* **1992**, *31*, 888–894.
[9] C. C. Christuk, M. A. Ansari, J. A. Ibers, unpublished results.
[10] A. Müller, H. Bögge, U. Schimanski, *Inorg. Chim. Acta* **1983**, *69*, 5–16.
[11] Satisfactory elemental analyses for C,H,N.
[12] Crystallographic data for $(NEt_4)_4$-**2** · 2DMF: $M_r = 2705.5$, monoclinic, $a = 13.932(1)$, $b = 17.240(2)$, $c = 14.475(2)$ Å, $\beta = 92.31(1)°$, $V = 3473.9$ Å^3, $T = 106$ K, $\lambda(Mo_{K\alpha_1}) = 0.70926$ Å, space group C_2^2-$P2_1$, $Z = 2$, $\mu = 141$ cm^{-1}, 9654 observations, 7802 unique reflections having $F_o^2 \geq 3\sigma(F_o^2)$, 428 variables, $R = 0.049$, $R_w = 0.044$. Data were collected on an Enraf-Nonius CAD4 diffractometer with the use of ω-2θ scans for $\theta \leq 28°$. The structure was solved and refined with the Siemens SHELXTL.PC package (G. M. Sheldrick, SHELXTL.PC, Version 4.1). The positions of all non-hydrogen atoms were determined from successive difference electron-density maps. The final refinement involved absorption-corrected data and anisotropic refinement of the W, Se, Cu, O, and N atoms. Further results of the crystal structure investigation may be obtained from the Fachinformationszentrum Karlsruhe, Gesellschaft für wissenschaftlich-technische Informationen mbH, D-W-7514 Eggenstein-Leopoldshafen 2, FRG on quoting the depository number CSD-56659, the names of the authors, and the journal citation.
[13] A. Camus, N. Marsich, G. Nardin, L. Randaccio, *J. Organomet. Chem.* **1973**, *60*, C39-C42; N. Bresciani, N. Marsich, G. Nardin, L. Randaccio, *Inorg. Chim. Acta* **1974**, *10*, L5-L6; G. Nardin, L. Randaccio, E. Zangrando, *J. Chem. Soc. Dalton Trans.* **1975**, 2566–2569; J. A. Tiethof, J. K. Stalick, P. W. R. Corfield, D. W. Meek, *J. Chem. Soc. Chem. Commun.* **1972**, 1141–1142; T. H. Lemmen, J. C. Huffman, K. G. Caulton, *Angew. Chem.* **1986**, *98*, 267–268; *Angew. Chem. Int. Ed. Engl.* **1986**, *25*, 262–264; G. Doyle, K. A. Eriksen, D. Van Engen, *J. Am. Chem. Soc.* **1986**, *108*, 445–451; *ibid.* **1985**, *107*, 7914–7920; C. P. Rao, J. R. Dorfman, R. H. Holm, *Inorg. Chem.* **1986**, *25*, 428–439; D. M. Ho, R. Bau, *ibid.* **1983**, *22*, 4079–4083; H. C. Kang, Y. Do, C. B. Knobler, M. F. Hawthorne, *ibid.* **1988**, *27*, 1716–1725.
[14] C. Lensch, P. G. Jones, G. M. Sheldrick, *Z. Naturforsch.* **1982**, *37*, 944–949; R. C. Haushalter, *Angew. Chem.* **1985**, *97*, 412–414; *Angew. Chem. Int. Ed. Engl.* **1985**, *24*, 432–433.
[15] A. Müller, E. Diemann, R. Jostes, H. Bögge, *Angew. Chem.* **1981**, *93*, 957–977; *Angew. Chem. Int. Ed. Engl.* **1981**, *20*, 934–955.
[16] G. Zhou, Y. Guo, S. Zhang, Y. Tang, *Huaxue Xuebao* **1985**, *43*, 107–112; *Chem. Abstr.* **1985**, *102*, 196819r; G. Jin, X. Xin, A. Dai, J. Wu, B. Wang, P. Zheng, *Ziran Zazhi* **1987**, *10*, 873; *Chem. Abstr.* **1987**, *109*, 84947 u.
[17] A. Müller, I. Paulat-Böschen, B. Krebs, H. Dornfeld, *Angew. Chem.* **1976**, *88*, 691–692; *Angew. Chem. Int. Ed. Engl.* **1976**, *15*, 633; Y.-J. Lu, J. A. Ibers, *Acta Crystallogr. Sect. C* **1991**, *47*, 1600–1602.
[18] D. Fenske, H. Krautscheid, M. Müller, *Angew. Chem.* **1992**, *104*, 309–312; *Angew. Chem. Int. Ed. Engl.* **1992**, *31*, 321–323.

Synthesis of Esterase-resistant 9-*O*-Acetylated Polysialoside as Inhibitor of Influenza C Virus Hemagglutinin

By *René Roy**, *Fredrik O. Andersson*, *Günter Harms*, *Sørge Kelm*, and *Roland Schauer*

Human infections by influenza viruses are mediated by the adherence of the viral membrane protein hemagglutinin to the host-cell glycoproteins and glycolipids.[1] Recent X-ray data,[2] proton NMR spectroscopic studies,[3] and inhibition experiments with synthetic sialosides[4] have clearly defined the minimum and effective structural ligand requirements of the viral hemagglutinin. These receptor determinants have

[*] Prof. Dr. R. Roy, Dr. F. O. Andersson
Department of Chemistry, University of Ottawa
Ottawa, Ontario K1N 6N5 (Canada)
Prof. Dr. R. Schauer, G. Harms, Dr. S. Kelm
Biochemisches Institut, Christian-Albrechts-Universität
Kiel (FRG)

been identified as the sialic acid *N*-acetylneuraminic acid (Neu5Ac, **1**) for influenza A and B viruses[1–5] and its corresponding 9-*O*-acetylated derivatives (Neu5,9Ac$_2$) for influenza C virus isolates.[6] The influenza C viruses also possess a receptor-destroying enzyme, which was characterized as a sialate 9-*O*-acetyl esterase.[6] The binding site for Neu5,9Ac$_2$ (hemagglutinin) and the acetyl esterase activity are located together with a fusion activity on a single viral glycoprotein.[7]

Moreover, influenza A and B viruses contain a sialidase besides hemagglutin. Thus, a general strategy for the prevention of viral adherence to the host cell may reside in the design of sialidase-resistant sialic acid conjugates. To be of general use, these synthetic inhibitors must be "universal" and stable target receptors. At the same time, they should have several binding sites ("be multivalent") in order to account for the low binding affinities of α-sialosides to the hemagglutinin, since a dissociation constant K_d of only 2.8×10^{-3} M has been determined.[3] Previous work on the synthesis of sialic acid containing neoglycoproteins[8] and glycopolymers[8, 9] allowed the design of suitable influenza A virus inhibitors.[10] This approach was recently confirmed by other groups.[11] Furthermore, divalent sialosides have also been used to study the influence of spatial structure on their binding to the hemagglutinin.[12]

Recent findings have also established that hemagglutinin inhibition is not the sole factor that can prevent infections.[10] It could be postulated that the sialidase activity, common to all influenza A and B viruses, also participates in a complementary fashion to the infection and the spreading

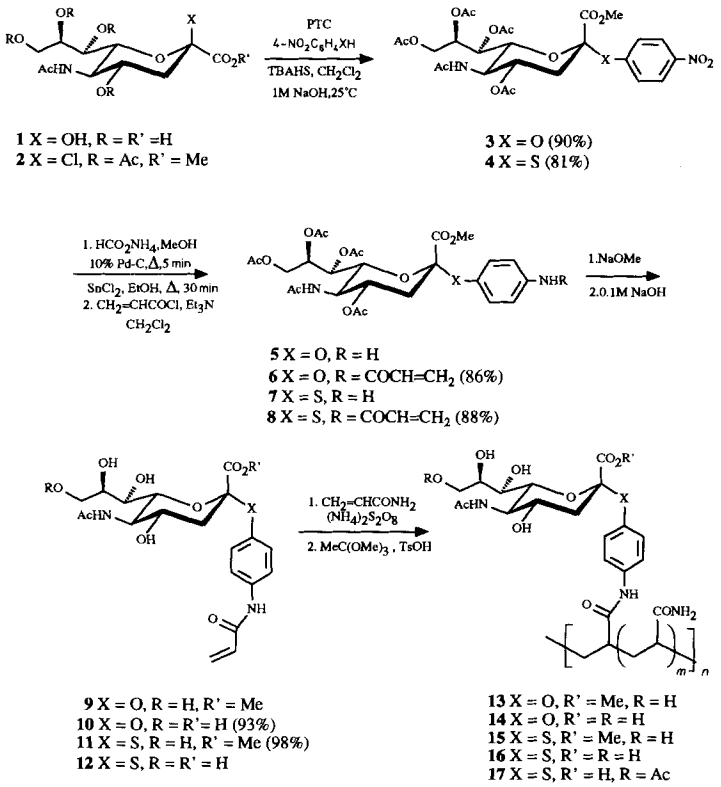

Scheme 1. Ts = $CH_3C_6H_4SO_2$.

of the virus particles. To answer these questions we have synthesized glycopolymers containing multivalent sialic acid, which should act as both hemagglutinin and sialidase inhibitors.

The general strategy for the stereospecific synthesis of the aryl α-sialoside precursors is based on phase transfer catalysis (PTC). The synthesis of the new glycopolymers is depicted in Scheme 1 and involves acrylamide copolymerization of suitable *N*-acryloylated carbohydrate derivatives.[13] Thus, transformation of Neu5Ac (**1**) into the known acetochloroneuraminic acid[14] glycosyl donor **2** was effected in two steps following previously modified procedures (1: MeOH, H^+; 2: AcCl, AcOH).[8] Stereospecific introduction of the *para*-nitrophenyl- and *para*-nitrophenylthio-α-sialosides (**3** and **4**, respectively)[15] was effected using PTC conditions in dichloromethane and tetrabutylammonium hydrogen sulfate (TBAHS) as catalyst (90% and 81% yield, respectively; for physical properties, see Table 1). No β-glycoside was detected in the crude reaction mixtures. However, some dehydrochlorination and hydrolysis by-products were formed

Table 1. Physical data of **3** and **4**.

3: M.p. 87–88 °C; $[\alpha]_D^{23}$ + 26.6 (*c* 1.28, $CHCl_3$). ^{1}H NMR (300 MHz, $CDCl_3$, 25 °C, TMS): δ = 1.90 (s, 3H, NAc), 2.02–2.17 (4s, 12H, OAc), 2.28 (dd, $^3J(H_{3a,4})$ = 12.5, $^2J(H_{3a,3e})$ = 12.8 Hz, 1H, H3a), 2.72 (dd, $^3J(H_{3e,4})$ = 4.7 Hz, 1H, H3e), 3.67 (s, 3H, CO_2Me), 4.05–5.38 (m, 8H), 7.12 (d, $^3J(H_{o,m})$ = 9.3 Hz, aryl H-*ortho*), 8.16 (d, aryl H-*meta*); ^{13}C NMR: 20.5–23.0 (5×, Ac), 38.5 (C3), 49.0 (C5), 59.2 (OMe), 62.0 (C9), 66.8–68.2 (3×, C4, C7, C8), 73.6 (C6), 99.4 (C2), 118.5 (2×, C-*ortho*), 125.7 (2×, C-*meta*), 143.4 (C-*para* (NO_2)), 159.1 (C-*ipso*), 168.2–170.9 (6×, C=O).

4: M.p. 170–171 °C; $[\alpha]_D^{23}$ +18.2° (*c* 1.01, $CHCl_3$). ^{1}H NMR, δ = 1.85 (s, 3H, NAc), 2.00–2.11 (4s, 12H, OAc), 2.05 (dd, coupling constants as for **3**, H3a), 2.85 (dd, H3e), 3.60 (s, 3H, CO_2Me), 3.90–4.10 (m, 2H, H5, H6), 4.07–5.30 (m, 6H), 7.62 (d, aryl H-*ortho*), 8.17 (d, aryl H-*meta*); ^{13}C NMR: 20.5–22.8 (5×, Ac), 38.1 (C3), 48.8 (C5), 52.9 (OMe), 62.0 (C9), 67.1–69.2 (3×, C4, C7, C8), 74.4 (C6), 86.8 (C2), 123.8 (2×, C-*ortho*), 135.0 (2×, C-*meta*), 137.9 (C-*para*), 148.1 (C-*ipso*), 167.5–170.9 (6×, C=O). Correct C,H,N,S analysis for $C_{26}H_{32}N_2O_{14}S$.

in small quantities. Catalytic transfer hydrogenation with ammonium formate and 10% Pd–C provided the unstable *para*-aminophenyl derivative of the glycoside **5**, which was *N*-acryloylated directly (CH_2=CH–COCl, Et_3N, CH_2Cl_2) to provide **6** in 86% yield from **3**. The above reducing conditions were unsuccessful when applied to the *S*-glycoside **4**. However, **4** could be successfully reduced with tin(II) chloride in refluxing ethanol. *N*-acryloylation of crude **7**, as described above, provided the *para*-*N*-acryloylaminophenylthio-α-sialoside (**8**) in 88% overall yield from **4**. Zemplén de-*O*-acetylation (NaOMe, MeOH) of the *O*- and *S*-glycosides **6** and **8** afforded the *N*-acryloylaminophenyl glycosides **9** and **11** as methyl ester in almost quantitative yields. Hydrolysis of the methyl ester with an aqueous solution of 0.1 M NaOH gave the free acid **10** in 93% yield. When these conditions were applied to the *S*-glycoside **11**, the methyl ester was partly hydrolyzed to give **12** only in low yield. This hydrolysis was accompanied by extensive Michael addition of the hydroxide ions to the *N*-acryloylamino function (detected by ^{1}H and ^{13}C NMR analyses). After several attempts at hydrolysis with different conditions, the methyl ester of the thiosialoside (**11**) was used in the polymerization reaction.

The monomeric precursors **10** and **11** were copolymerized with acrylamide in various molar ratios in a deoxygenated mixture of dimethyl sulfoxide and water (1:2) with ammonium persulfate as initiator in a boiling water bath, or with *N,N,N',N'*-tetramethylethylenediamine (TMEDA) at room temperature. After 10 min further quantities of the initiator were added when required (monitored by TLC). The reac-

tions were stopped after 15–20 min (heat) or 12 h (TMEDA, room temperature). The reaction mixtures were exhaustively dialyzed against distilled water and freeze-dried to provide the water-soluble polymers **13** and **15** in yields ranging from 60 to 77%. The ratio of acryloylamine units to sialosides within the glycopolymer was controlled by the ratio in the reaction mixture. This feature is typical for *N*-acryloyl carbohydrate monomers[13] and differs from those of the slow reacting alkenyl glycosides.[8] Polymers with sialic acid to acrylamide ratios of 1:5 and 1:10 were thus prepared. Methyl ester hydrolysis of the polymer **15** containing *S*-glycoside (0.1 M NaOH) afforded a quantitative yield of the free polymer **16**. The sialic acid content of the polymers were determined with ^{1}H NMR spectroscopy. Their reactivity with wheat germ agglutinin was demonstrated by using standard serological methods. The molecular weights of the polymers were estimated at between 75–150 kDa by gel permeation chromatography on a TSK G-4000 SWXL column.[13]

The *S*-sialosyl glycopolymer **16** features characteristics that possibly allow interaction with both hemagglutinin and sialidase of influenza A or B viruses. However, in hemagglutination inhibition assays with human erythrocytes,[4] polymer **16** did not inhibit the hemagglutinin of X31 and X31HS influenza A virus (H3N2) at concentrations up to 0.8×10^{-3} M in sialic acid residues. In previous studies with a different polyacrylamide glycopolymer containing Neu5Ac,[10] hemagglutination inhibition was reported at much lower concentrations. However, the density of Neu5Ac in these polymers was higher (1:7 instead of 1:10). The hemagglutination inhibition of such polymers varies over orders of magnitude depending on the density of the sialic acid residues.[11] In addition, the spacer used may influence the inhibitory potency as has been shown for X31 with the aglycon of monomeric sialic acid analogues.[16]

In contrast to influenza A and B viruses, influenza C virus requires 9-*O*-acetyl sialosides as receptors.[6] To study the interaction of influenza C virus with this kind of polymer as well, selective 9-*O*-acetylation was attempted. This modification was directed at the synthesis of an inhibitor of influenza C virus. A selective orthoester/hydrolysis sequence was performed under known conditions[17] (1: $MeC(OMe)_3$, TsOH; 2: H_3O^+) to provide 9-*O*-acetyl *S*-α-sialoside polymer **17** in quantitative yield (recovery). The ^{1}H NMR spectrum of the polymer showed that about 70% of the sialic acid residues contained *O*-acetyl groups, and these were located exclusively at the C9 position (Table 1, *Experimental Procedure*). Attempts to push the reaction further provided polymers with more than one acetyl group per sialic acid residue. Binding of influenza C virus (Johannesburg/1/66) to glycopolymer **17** was demonstrated in a microtitre plate assay[18] (Fig. 1). Furthermore, in a hemagglutination inhibition assay[4] with murine erythrocytes, glycopolymer **17** inhibited influenza C virus at concentrations as low as 3.3×10^{-6} M. The specificity towards 9-*O*-acetylated sialic acid residues was shown by the lack of binding of influenza C virus to the glycopolymer **16** and its methyl ester **15**.

Interestingly, the 9-*O*-acetylated glycopolymer **17** was a poor substrate for the virus esterase (Fig. 2). This suggests that the structural requirements for the biological activity of

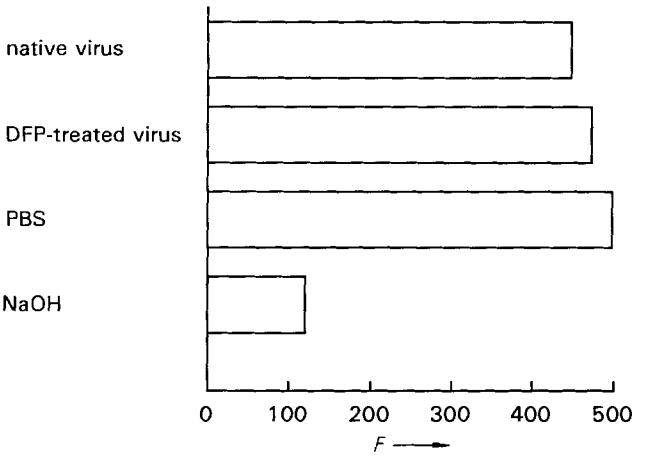

Fig. 2. Resistance of glycopolymer **17** to influenza C esterase. F = relative fluorescence as a measure of the esterase activity. 250 μg of glycopolymer **17** was incubated at 37 °C in 35 μL PBS with native influenza C virus (1.9 mU esterase) or DFP-treated (DFP = diisopropylfluorophosphate) virus in 35 μL for 1 h. Reactions were stopped by adding 315 μL ice-cold PBS, and virus was removed by centrifugation at $10^5 \times g$ for 90 min. As control, 250 μg of glycopolymer **17** was saponified with 0.1 M NaOH or PBS at 0 °C for 1 h. The reaction was stopped by adding an equal volume of 0.1 M HCl or NaCl, respectively, and diluted to 350 μL with PBS. To determine the amount of 9-*O*-acetyl groups remaining on glycopolymer **17** after these treatments, 100 μL were coated onto microtitre plate wells in triplicate and assayed as described for Figure 1.

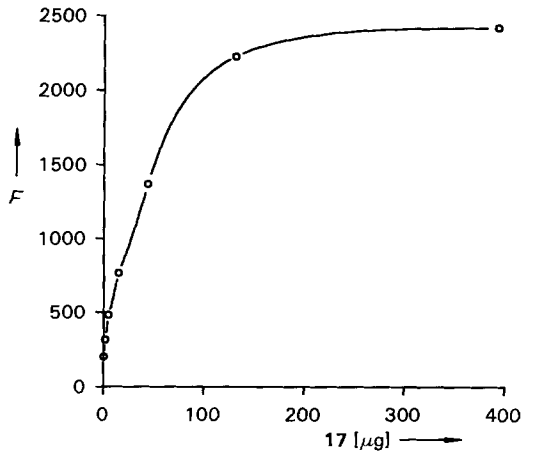

Fig. 1. Binding of influenza C virus to glycopolymer **17**. *F* = relative fluorescence as a measure of the esterase activity. The amount of substance **17** indicated was coated to microtitre plate wells in 100 μL phosphate buffer solution (PBS), pH = 7.2, approximately 12 h. Influenza C virus was allowed to bind to these wells. The amount of bound virus was then determined by assaying the esterase activity with the fluorogenic substrate 4-methylumbelliferyl acetate as described [18].

the hemagglutinin and the esterase are different. Similar observations were made with natural compounds. For example, whereas influenza C virus binds well to 9-*O*-acetylated gangliosides,[18] the *O*-acetyl groups of these compounds are hydrolyzed only very slowly by the esterase.[19] These findings show that compound **17** may serve as a basis for the development of esterase-resistant drugs designed to combat influenza C infections.

Experimental Procedure

Polymerization: A solution of **11** (10.3 mg, 22 μmol) and acrylamide (7.7 mg, 109 μmol, 5 equiv) in a deaerated water–dimethyl sulfoxide mixture (2:1, 300 μL) was treated with ammonium persulfate (15 μL of a 100 mg mL^{-1} solution) and stirred at 100 °C for 15 min. After a further 15 min and 25 min, more ammonium persulfate solution was added (15 μL). This process ensured that all the monomer **11** had reacted. After 30 min, the reaction mixture was cooled and dialyzed against distilled water. Lyophilization afforded **15** as a white fluffy powder (10.8 mg, 60%). ^{1}H NMR showed a ratio of sialic acid residues to acrylamide of 1:5. Transformation of **15** into **16** was conducted in 0.1 M NaOH at room temperature (approximately 12 h). Dialysis and freeze-drying as above

provided pure **16** devoid of the CO_2Me signal at $\delta = 3.70$. Transformation of **16** into **17** as described in ref. [17] afforded **17** which showed the characteristic *O*-acetyl signal in the ^1H NMR spectra (D_2O, $\delta = 2.0$, signal intensity corresponds to 0.7 acetyl units). Moreover, the signals of H9a and H9b in **17** appeared downfield at $\delta = 4.00$ and 4.20, respectively, in accord with the structure. Molecular weight determination of **15**–**17** were effected on a Waters 991/625 LC HPLC system equipped with a diode array detector and a TSK G-4000 SWXL column (7.5 × 300 mm) as described in ref. [13c].

Received: April 21, 1992 [Z 5312 IE]
German version: *Angew. Chem.* **1992**, *104*, 1551

CAS Registry numbers:
1, 131-48-6; **2**, 67670-69-3; **3**, 59694-37-0; **4**, 124974-13-6; **5**, 130087-26-2; **6**, 143857-99-2; **7**, 124925-06-0; **8**, 143858-00-8; **9**, 143858-84-2; **10**, 143858-01-9; **11**, 143858-02-0; **12**, 143858-03-1; **13**, 143858-05-3; **14**, 143886-97-9; **15**, 143858-06-4; **16**, 143858-07-5; **17**, 143858-09-7; CH_2=CHCOCl, 814-68-6; 4-$NO_2C_6H_4OH$, 100-02-7; 4-$NO_2C_6H_4SH$, 1849-36-1; esterase, 9013-79-0; acrylamide, 79-06-1.

[1] D. C. Wiley, J. J. Skehel, *Annu. Rev. Biochem.* **1987**, *56*, 365; J. C. Paulson, G. N. Rogers, S. M. Carroll, H. H. Higa, T. J. Pritchett, G. Milks, S. Sabesan, *Pure Appl. Chem.* **1984**, *56*, 797; Y. Suzuki, Y. Nagao, H. Kato, M. Matsumoto, K. Nerome, K. Nakajima, E. Nobusawa, *J. Biol. Chem.* **1986**, *261*, 17057.
[2] I. A. Wilson, J. J. Skehel, D. C. Wiley, *Nature (London)* **1981**, *289*, 366; W. Weiss, J. H. Brown, S. Cusak, J. C. Paulson, J. J. Skehel, C. D. Wiley, *ibid.* **1988**, *333*, 426.
[3] N. K. Sauter, M. D. Bednarski, B. A. Wurzburg, J. E. Hanson, G. M. Whitesides, J. J. Skehel, D. C. Wiley, *Biochemistry* **1989**, *28*, 8388.
[4] T. J. Pritchett, R. Brossmer, U. Rose, J. C. Paulson, *Virology* **1987**, *160*, 502; T. J. Pritchett, J. C. Paulson, *J. Biol. Chem.* **1989**, *264*, 9850.
[5] Y. Suzuki, Y. Nagao, H. Kato, T. Suzuki, M. Matsumoto, J. Murayama, *Biochim. Biophys. Acta* **1987**, *903*, 417.
[6] G. Herrler, R. Rott, H.-D. Klenk, H.-P. Müller, A. K. Shukla, R. Schauer, *EMBO J.* **1985**, *4*, 1503.
[7] G. Herrler, I. Dürkop, H. Brecht, H.-D. Klenk, *J. Gen. Virol.* **1988**, *69*, 839.
[8] R. Roy, C. A. Laferrière, A. Gamian, H. J. Jennings, *J. Carbohydr. Chem.* **1987**, *6*, 161; R. Roy, C. A. Laferrière, *Can. J. Chem.* **1990**, *68*, 2045.
[9] R. Roy, C. A. Laferrière, *Carbohydr. Res.* **1988**, *177*, C1; R. Roy, C. A. Laferrière, *J. Chem. Soc. Chem. Commun.* **1990**, 1709.
[10] A. Gamian, M. Chomik, C. A. Laferrière, R. Roy, *Can. J. Microbiol.* **1991**, *37*, 233.
[11] M. N. Matrosovich, L. V. Mochalova, V. P. Marinina, N. E. Byramova, N. V. Bovin, *FEBS Lett.* **1990**, *272*, 209; A. Spaltenstein, G. M. Whitesides, *J. Am. Chem. Soc.* **1991**, *113*, 686; N. E. Byramova, L. V. Mochalova, J. M. Belyanchikov, M. N. Matrosovich, N. V. Bovin, *J. Carbohydr. Chem.* **1991**, *10*, 691.
[12] G. D. Glick, J. R. Knowles, *J. Am. Chem. Soc.* **1991**, *113*, 4701; S. Sabesan, J. O. Duus, P. Domaille, S. Kelm, J. C. Paulson, *ibid.* **1991**, *113*, 5865.
[13] a) R. Roy, F. D. Tropper, T. Morrison, J. Boratynski, *J. Chem. Soc. Chem. Commun.* **1991**, 536; b) R. Roy, C. A. Laferrière, *ibid.* **1990**, 1709; c) R. Roy, F. D. Tropper, A. Romanowska, *Bioconjugate Chem.* **1992**, *3*, 256.
[14] R. Kuhn, P. Lutz, D. L. McDonald, *Chem. Ber.* **1966**, *99*, 611.
[15] All new compounds were characterized by elemental analysis (C, H, N, S), NMR spectroscopy, and mass spectrometry. See also Table 1.
[16] S. Kelm, J. C. Paulson, U. Rose, R. Brossmer, W. Schmid, B.-P. Bandgar, E. Schreiner, M. Hartmann, E. Zbiral, *Eur. J. Biochem.* **1992**, *205*, 147.
[17] H. Ogura, K. Furukata, S. Sato, K. Anazawa, M. Itoh, Y. Shitori, *Carbohydr. Res.* **1987**, *167*, 77.
[18] G. Zimmer, G. Reuter, R. Schauer, *Eur. J. Biochem.* **1992**, *204*, 209.
[19] R. Schauer, G. Reuter, S. Stoll, F. Posadas del Rio, G. Herrler, H.-D. Klenk, *Biol. Chem. Hoppe-Seyler* **1988**, *369*, 1121.

N-Perbenzylation of Oligopeptides with P4-Phosphazene Base; A New Protecting-Group Technique for Modification and Solubilization of Peptides in Apolar Organic Solvents**

By *Thomas Pietzonka* and *Dieter Seebach**

Peptides are normally constructed from the appropriate amino acids. The modification of a peptide, not at the side chains but directly at the carbon atoms of the peptide skeleton itself, seemed impossible a short time ago. We have already been able to form lithium enolates of sarcosine units in oligopeptides containing up to eleven amino acids, and to treat them with electrophiles, to achieve C,C-bond formation if the amino acid following the sarcosine was *N*-methylated[1] (see **1**). Problems arise because of the low solubility in aprotic media of many peptides required for enolate formation,[2] the necessity to remove all NH and OH hydrogen atoms from the peptide (polylithiation!), and the impossibility of demethylation of *N*-methyl groups, the presence of which is objectionable in most cases.

We have recently discovered that the P4-phosphazene base **2** developed by Schwesinger and Schlemper[3] is able to mediate alkylation of BOC- or Z-protected linear and cyclic peptides. At low temperature in THF, in the presence of benzyl or allyl bromide, alkylation occurs at all NH groups of the peptide backbone and, if available, at the terminal COOH group too [see the conversions of BOC-valyl-glycyl-leucine (**3a**) to the products **3b** and **3c** in Scheme 1, and further examples (**4**–**12**) in Table 1]. For these reactions the peptide need not initially be in solution: even the extremely sparingly soluble tetrapeptide derivative **8a** (≤ 0.8 mg mL^{-1} THF at $-75\,^{\circ}C$)[2a] reacts under these conditions, and dissolves completely. In general, the perbenzylated peptides are readily soluble in apolar solvents, as is reflected by their R_F values on thin-layer silica plates (see Table 1). For example, perbenzylated BOC-Val-Gly-Leu **3b** is very soluble in pentane (!).

The new benzyl and allyl derivatives may be viewed as protected peptides. Debenzylation of the amine nitrogens is not possible by hydrogenolysis, but occurs easily through the procedure developed by Weygand and Steglich[5] (liquid am-

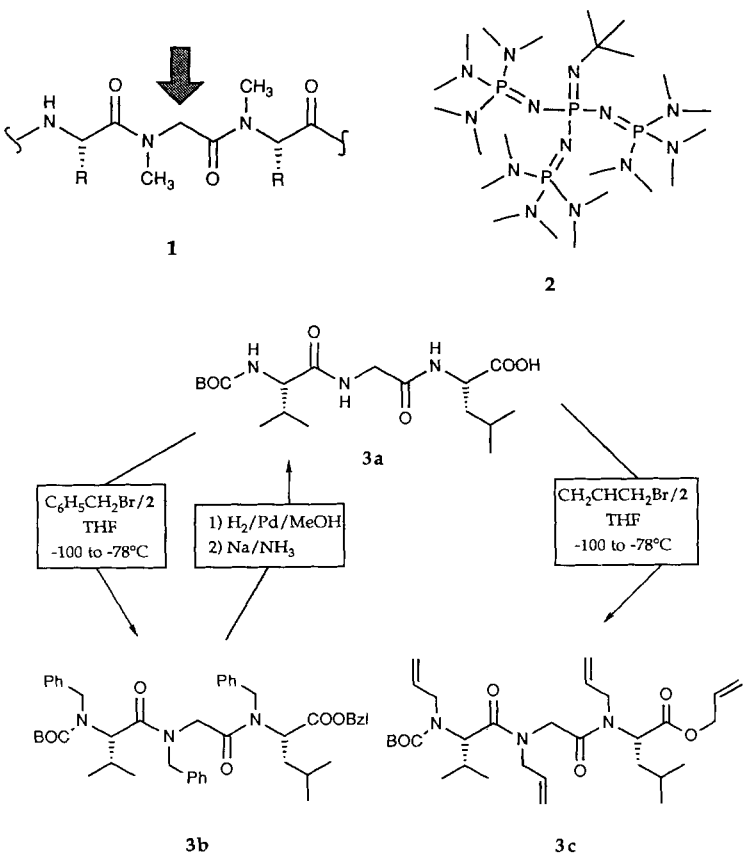

Scheme 1. Perbenzylation/debenzylation and perallylation of BOC-Val-Gly-Leu with P4-base. BOC = *tert*-butyloxycarbonyl.

[*] Prof. Dr. D. Seebach, Dipl.-Chem. T. Pietzonka
Laboratorium für organische Chemie der Eidgenössischen Technischen Hochschule
ETH-Zentrum, Universitätstrasse 16, CH-8092 Zürich (Switzerland)

[**] Part of the planned Ph.D. thesis of T. Pietzonka. We thank E. Devaquet for performing some of the experimental work during her advanced OC-lab course.

Table 1. Yields and some properties of benzylated peptide derivatives prepared with P4-base (**2**).

Peptide [a]	Number of OH + NH in Peptide	Number of Benzyl in Product	Product No.	Yield [%]	R_F (Et_2O/C_5H_{12} 1:1) before benzylation	R_F (Et_2O/C_5H_{12} 1:1) after benzylation	$[\alpha]_D$ (solvent) [b] before benzylation	$[\alpha]_D$ (solvent) [b] after benzylation
BOC-Val-Gly-Leu-OH **3a**	4	4	**3b**	51	0	0.47	−13 (M)	−75
BOC-Ala-Gly-Leu-OH **4a**	4	4	**4b**	63	0	0.35	−10 (E)	−54
BOC-Leu-Gly-Val-OH **5a**	4	4	**5b**	57	0	0.55	−11 (E)	−30
Z-Leu-Gly-Val-OBn **6a**	3	3	**6b**	14	0	0.30	−19 (E)	−38
BOC-Val-Ala-Gly-Leu-OH **7a**	5	5	**7b**	58	0	0.35	−21 (E)	−95
BOC-Ala-Gly-Gly-Gly-OH [8] **8a**	5	7	**8b**	35	0	0.16	−3 (E)	
BOC-Val-Leu-Gly-Abu-Ile-OH **9a**	5	5	**9b**	51	0	0.45	−31 (E)	−51
cyclo-(D-Ala-Sar-MeLeu-Gly) **10a**	2	2	**10b**	46	0	0.20	−15 (W)	−40 (C)
cyclo-(Gly-Val-Sar-Sar) **11a**	2	2	**11b**	30	0	0.11 [c]	+37 (E)	+59 (C)
	2	3	**11c**	80	0	0.37 [c]	+37 (E)	+47 (C)
cyclo-(Leu-Sar-Sar-Gly) **12a**	2	2	**12c**	46	0	0.11 [c]	−13 (C)	+18 (M)
	2	3	**12d**	20	0	0.36 [c]	−13 (C)	+41 (M)

[a] Z = benzyloxycarbonyl. [b] E = ethanol, M = methanol, C = chloroform, W = water. [c] 5% MeOH in Et_2O.

monia/sodium). Thus, the BOC peptides **3a** and **5a** were regenerated from the corresponding benzyl derivatives **3b** and **5b**. The BOC peptides can be cleaved into their components on treatment with concentrated HCl at 110 °C. The amino acids obtained were derivatized to the (*N*-pentafluoropropionyl)isopropyl esters and analyzed by gas chromatography on a Chirasil-Val GC column.[6] It was observed that no epimerization occurred at either of the stereogenic centers on the way to the tetrabenzylated peptide and back. Analysis by NMR spectroscopy of the chromatographically uniform, linear, perbenzylated peptide products is complicated by the presence of many rotamers, even at 180 °C. Nevertheless, an examination of the products by FAB mass spectrometry not only showed the correct molecular weight, but also the expected *N*-benzyl amino acid fragment peaks. In addition, the increase in specific optical rotation $[\alpha]_D$ after the introduction of benzyl groups is noteworthy (up to fivefold, see Table 1). In contrast to those of the open-chain peptides (**3a**–**9a**), the NMR spectra of the cyclic tetrapeptides (**10a**–**12a**)[1c] are very well resolved, containing sharp signals. The positions of the benzyl groups can be clearly determined, mainly by NOE measurements. Thus, we discovered that for *cyclo*-(Leu-Sar-Sar-Gly) (**12a**) the first *N*-benzylation occurs at the glycine unit (→**12b**), and the second at the leucine-*N* atom (→**12c**).[7]

Preliminary investigations have shown that benzyl-protected peptides (after hydrogenolytical removal of the *C*-terminal benzyl group) can be methylated by treatment with 2 equivalents of lithium diisopropylamide (LDA)/CH_3I in THF, via the corresponding lithium enolate of the glycine unit. However, the P4-base is also able to deprotonate the sarcosine CH_2 group of benzyl-protected peptides. Thus, the dibenzylated product **12c** was *C*-alkylated with a further equivalent benzyl bromide (→**12d**). Using optimal reaction conditions, we were able to isolate the tribenzylated compound **11c** as the main product in 80% yield, starting from *cyclo*-tetrapeptide **11a**.[8] As in the case of **12c**, hydrogen H_{Si} of the sarcosine adjacent to the valine was replaced by a benzyl group (precursor **11b** contains a total of seven α-carbonyl hydrogen atoms!).

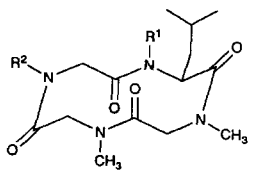

12b (R^1 = H, R^2 = CH_2Ph)
12c (R^1 = CH_2Ph, R^2 = CH_2Ph)

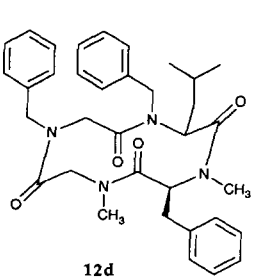

12d

Experimental Procedure

To a solution of 138 mg (0.45 mmol) of *cyclo*-(Leucyl-sarcosyl-sarcosyl-glycine) **12a** in THF (5 mL) was added 0.25 mL (1.6 mmol) of benzylbromide. The mixture was cooled to −100 °C and 0.70 g (1.1 mmol) of P4-base in THF (2 mL) introduced carefully, dropwise, in order to control the resulting exothermic reaction. After the reaction mixture had been stirred for 3 h at −78 °C, it was allowed to warm to room temperature. The solvent was then evaporated, and the crude product purified by flash chromatography (SiO_2/5% MeOH in diethyl ether). Yield: 100 mg (46%) **12b** colorless powder. M.p. 206.5–207.5 °C; $[\alpha]_D$ +18.1 (*c* = 0.98 in MeOH); ^1H NMR (300 MHz, $CDCl_3$, 25 °C, TMS): δ = 0.91 (d, $^3J(H,H)$ = 7 Hz, 3H; CH_3), 1.00 (d, $^3J(H,H)$ = 7 Hz, 3H; CH_3), 1.40–1.75 (m, 2H; CH_2-Leu), 1.78–1.90 (m, 1H; CH-Leu), 3.00 (s, 3H; CH_3-N), 3.11 (s, 3H; CH_3-N), 3.15 (d, $^3J(H,H)$ = 18 Hz, 1H; H-Gly), 3.30 (d, $^3J(H,H)$ = 14 Hz, 1H; H-Sar_2), 3.65 (d, $^3J(H,H)$ = 14 Hz, 1H; H-Ph(Gly)), 3.72 (d, $^3J(H,H)$ = 18 Hz, 1H; H-Sar_1), 4.06 (d, $^3J(H,H)$ = 18 Hz, 1H; H'-Gly), 4.32 (dxd, $^3J(H,H)$ = 25 Hz, 2H; CH_2-Ph(Leu)), 4.57 (d, $^3J(H,H)$ = 18 Hz, 1H; H'-Sar_1), 5.27 (d, $^3J(H,H)$ = 14 Hz, 1H; H'-Sar_2), 5.52 (t, $^3J(H,H)$ = 6 Hz, 1H; CH-Leu), 7.2–7.6 (m, 10H; aromatic H).

Received: July 18, 1992 [Z 5472 IE]
German version: *Angew. Chem.* **1992**, *104*, 1543

CAS Registry numbers:
2, 111324-04-0; **3a**, 82537-91-5; **3b**, 144002-63-1; **3c**, 144002-75-5; **4a**, 144002-55-1; **4b**, 144002-64-2; **5a**, 144002-56-2; **5b**, 144002-65-3; **6a**, 144002-57-3; **6b**, 144002-66-4; **7a**, 144002-58-4; **7b**, 144002-67-5; **8a**, 64263-99-6; **8b**, 144002-68-4; **9a**, 144002-59-5; **9b**, 144002-69-7; **10a**, 144002-60-8; **10b**, 144002-70-0; **11a**, 144002-61-9; **11b**, 144002-71-1; **11c**, 144002-73-3; **12a**, 144002-62-0; **12b**, 144002-76-6; **12c**, 144002-72-2; **12d**, 144002-74-4; benzylbromide, 100-39-0; allylbromide, 106-95-6.

[1] a) D. Seebach, *Angew. Chem.* **1988**, *100*, 1685–1715; *Angew. Chem. Int. Ed. Engl.* **1988**, *27*, 1624–1654; b) D. Seebach, H. Bossler, H. Gründler, S.-i. Shoda, R. Wenger, *Helv. Chim. Acta* **1991**, *74*, 197–224; c) S. A. Miller, S. L. Griffiths, D. Seebach, *ibid.* **1992**, in press.
[2] a) D. Seebach, A. Thaler, A. K. Beck, *Helv. Chim. Acta* **1989**, *72*, 857–867; b) A. Thaler, D. Seebach, F. Cardinaux, *ibid.* **1991**, *74*, 617–627 and 628–643.
[3] R. Schwesinger, H. Schlemper, *Angew. Chem.* **1987**, *99*, 1212–1214; *Angew. Chem. Int. Ed. Engl.* **1987**, *26*, 1167–1169; *Nachr. Chem. Tech. Lab.* **1990**, *38*, 1214–1226.
[4] For cleavage of an allyl amide see: T. Fukuyama, A. Laird, C. Schmidt, *Tetrahedron Lett.* **1984**, *25*, 4709–4712.
[5] F. Weygand, W. Steglich, J. Bjarnason, R. Akhtar, N. Khan, *Tetrahedron Lett.* **1966**, 3483–3487.
[6] S. Abdalla, E. Beyer, *Chromatographia* **1987**, *23*, 83–85.
[7] The crystal structure of compound **12c** has been solved. It confirms the conformation of the 12-membered ring represented in the structural formula. Detailed data will be published in the future.
[8] Minor quantities of *C*-benzylated products also form with linear peptides, but they can be separated by flash chromatography because of their higher R_F values. Starting from tetrapeptide **8a** a heptabenzyl derivative was obtained as the main product. The structure has not been determined as yet, but from the GC analysis mentioned in the text above, the alanine unit in product **8b** has not epimerized.

Crosslinking of Adjacent Guanine Residues in an Oligonucleotide by *cis*-$[Pt(NH_3)_2(H_2O)_2]^{2+}$: Kinetic Analysis of the Two-Step Reaction**

By *Florence Gonnet, Jiři Kozelka,** and *Jean-Claude Chottard*

The antitumor drug *cis*-diamminedichloroplatinum(II) ("cisplatin") binds to DNA to form preferentially the d(GpG) intrastrand crosslink.[1] This macrochelate is formed in a two-step process (Scheme 1), and the reactive platinum species is one of the hydrolyzed cisplatin forms, that is, *cis*-$[PtCl(NH_3)_2(H_2O)]^+$ (X = Cl^-; Y = H_2O) or *cis*-$[Pt(NH_3)_2(H_2O)_2]^{2+}$ (X = Y = H_2O). Between 60 and 65% of the DNA-bound platinum appears as the GG crosslink, as shown both by in vitro and by in vivo experiments.[2-7] This percentage significantly exceeds the probability of finding a guanine residue adjacent to another, and since the reactions in Scheme 1 are irreversible under the experimental conditions, the guanine residues in GG sequences must be more reactive than in other positions. The origin of this differential guanine reactivity is unknown. One possible factor is the enhancement of the negative potential at the guanine N7 atom caused by a neighboring guanine, which is predicted by ab initio calculations.[8] However, as we have recently shown using molecular modeling,[1] nonbonding interactions in the transition state,[9] that is, those between the platinum ligands and the DNA residues adjacent to the guanine being platinated, could also play a role. Such a mechanism would be ligand-dependent, which opens the interesting possibility of influencing the binding selectivity of the platinum complex by an appropriate choice of ligands.

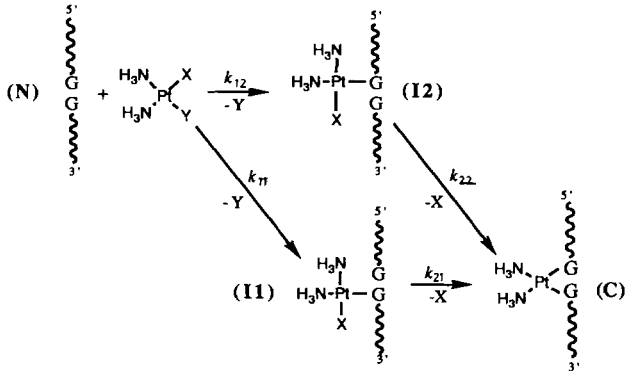

Scheme 1. Binding of a *cis*-$[Pt(X)(Y)(NH_3)_2]$ complex (X, Y = leaving groups) to a GpG sequence of an oligonucleotide.

One question that arises is whether the 5'-guanine of a d(GpG) sequence enhances the reactivity of the 3'-guanine, or vice versa. No answer to this question could be given so far, since it was not possible to measure the rate constants for the platination of the two guanines (k_{11} and k_{12} in Scheme 1) separately.

In this paper, we describe a technique that enables the measurement not only of the two primary platination rate constants k_{11} and k_{12} but also of the two chelation constants k_{21} and k_{22} and apply it to the reaction between the single-stranded oligonucleotide d(TpGpG) and the diaqua form of cisplatin, *cis*-$[Pt(NH_3)_2(H_2O)_2]^{2+}$. The method consists of treating known amounts of oligonucleotide with approximately stoichiometric platinum complex in aqueous solution and, at intervals, taking aliquots which are quenched by addition of a saturated KCl solution and cooled to liquid nitrogen temperature. The conserved aliquots are subsequently analyzed by HPLC. Figure 1 displays a typical chromatogram showing peaks for all four species **N**, **I1**, **I2**, and **C** defined in Scheme 1 for d(TGG). The high resolution of our system allows a precise integration of peaks, and thus an accurate determination of the concentrations. A computer program written in our laboratory calculates for each time t_i the four concentrations $[\mathbf{N}]_i$, $[\mathbf{I1}]_i$, $[\mathbf{I2}]_i$, and $[\mathbf{C}]_i$, based on assumed rate constants k_{11}, k_{12}, k_{21}, and k_{22}, and optimizes the fit by iteration on the constants as described in the appendix.

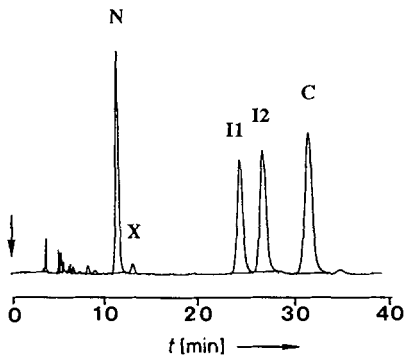

Fig. 1. A typical HPL chromatogram for a stoichiometric reaction of d(TGG) (10^{-3} M) with *cis*-$[Pt(NH_3)_2(H_2O)_2](NO_3)_2$ in 0.1 M $NaClO_4$, after quenching by addition of an excess of KCl. T = 293 K; pH = 4.4; t = 12 min (X = impurity; for the other identifiers, see Scheme 1).

Since, in general, only the concentration of the platinum complex can be determined precisely (that of the oligonucleotide is measured by means of UV absorbance), the excess (or shortfall) of oligonucleotide with respect to the platinum complex is used as a fifth variable. The correct functioning of the program has been tested in two control experiments in which a defined large excess of oligonucleotide was employed. The excess determined by the program deviated by up to 10% from the value determined by UV spectroscopy, which corresponds to the error of the concentration measurement. The four rate constants determined in these two control experiments were similar to those found in the other runs.

Figure 2 shows a typical fit of the four concentration curves, after optimization of the five variables, for the reaction of d(TGG) with *cis*-$[Pt(NH_3)_2(H_2O)_2]^{2+}$. The following rate constants were obtained for this system at 293 K (mean values of five experiments):

$k_{11} = 0.90 \pm 0.07\ M^{-1}s^{-1}$ $\quad k_{12} = 0.89 \pm 0.08\ M^{-1}s^{-1}$
$k_{21} = (1.76 \pm 0.09)\ 10^{-3}s^{-1}$ $\quad k_{22} = (1.27 \pm 0.09)\ 10^{-3}s^{-1}$

Apparently, in this trinucleotide the two guanine residues are equally reactive. The chelation of the 3'-intermediate **I1** is slightly faster than that of the 5'-intermediate **I2**.

Our ultimate goal in this research is to compare the rate constants for reactions of oligonucleotides of different lengths and sequences (including duplexes) with different

[*] Dr. J. Kozelka, F. Gonnet, Dr. J.-C. Chottard
URA 400, Laboratoire de Chimie et Biochimie Pharmacologiques et Toxicologiques
45 rue des Saints Pères, F-75270 Paris Cedex 06 (France)

[**] We thank Dr. J. Igolen for supplying the d(TGG) trinucleotide. The authors acknowledge EEC support (grant no. ST2J-0462-C) allowing regular scientific exchange with the group of Prof. J. Reedijk, Leiden (The Netherlands).

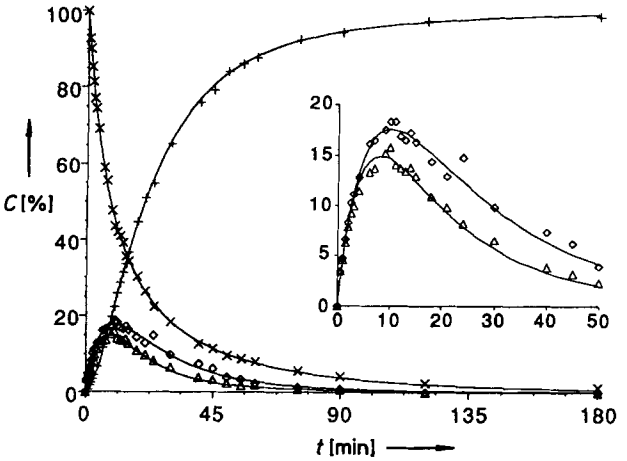

Fig. 2. Calculated curves and observed values for the four relative concentrations [N] (x), [I1] (Δ), [I2] (○), and [C] (+).

platinum complexes. An understanding of the high affinity of cisplatin towards GG sequences, and specifically, of the role that the ligands play in this affinity, will possibly provide a means to modify this affinity by appropriate changes in the ligands. In this way, it should be possible to test whether there is a relationship between sequence-specific DNA binding and antitumor activity of platinum complexes.

The kinetic analysis of a reaction between TGG and *cis*-$[PtCl(NH_3)_2(H_2O)]^+$ is currently being investigated in our laboratory. The experimental procedure is exactly the same as with the diaqua complex *cis*-$[Pt(NH_3)_2(H_2O)_2]^{2+}$, since the quenched products are the same. However, the evaluation of the rate constants is more complicated because of the equilibrium (a).

$$cis\text{-}[PtCl(NH_3)_2(H_2O)]^+ + H_2O \rightleftharpoons cis\text{-}[Pt(NH_3)_2(H_2O)_2]^{2+} + Cl^- \quad (a)$$

The determination of the rate constants for the reaction system with *cis*-$[Pt(NH_3)_2(H_2O)_2]^{2+}$ is prerequisite for the more complex system involving *cis*-$[PtCl(NH_3)_2(H_2O)]^+$. As far as other platinum complexes are concerned, their reactions with oligonucleotides can be analyzed by our method, provided that the starting, intermediate, and final products can be quenched in a simple way and separated by HPLC.

Experimental Procedure

The reactions were typically initiated by mixing a solution of about 2 μmol of d(TGG) (measured by UV spectrophotometry, $\varepsilon_{254} = 22170\ M^{-1}cm^{-1}$) [10] in 0.1 M $NaClO_4$ with a solution containing 2 μmol of *cis*-$[Pt(NO_3)_2(NH_3)_2]$ (prepared according to Ref. [11]) in 2 mL H_2O. The pH of the mixture was adjusted to pH = 4.4 by addition of $HClO_4$. After an initial increase to pH = 4.5 resulting from liberation of coordinated water, the pH decreased slowly to a value of 4.3, presumably due to dissolution of CO_2 from the atmosphere. The reaction temperature was kept at 293 ± 0.2 K. In initial intervals of 30 s (beginning) to 15 min (end), aliquots of 30 μL were withdrawn and quenched with 30 μL of a saturated KCl solution in an Eppendorf tube, and after 1.75 min incubation at 293 K (conversion of monoaqua to monochloro adducts) [12], dipped into liquid nitrogen and stored at 77 K until they were analyzed by HPLC. The cooling to 77 K is important, since at 193 K (dry ice temperature), the monocoordinated species **I1** and **I2** (Scheme 1) still slowly convert to the chelate **C**, despite KCl excess. As the subsequent HPLC analyses are quite time-consuming, and thus some of the samples have to be conserved for several days, this slow conversion significantly modifies the relative concentrations.

The HPLC analyses were performed on a Spectra Physics SP 8800 Chromatograph with a Nucleosil C18 column (250 × 4.6 mm ID, 5 μm, 100 Å; Macherey Nagel). Standard operating conditions were: mobile phase, ammonium acetate buffer (Merck, 0.01 M, pH = 4.70) and acetonitrile (Merck, 95:5 v/v); flow rate 0.8 mL min^{-1}; $T = 298$ K. At the detection wavelength of 255 nm, the absorbance of the reaction mixture decreased by 4% during the reaction; this decrease correlated roughly with the formation of the chelate **C**. The concentration of **C** based on peak integration was therefore corrected by a factor of 1.04.

Identification of the monoadducts was achieved by using enzymatic digestion of the corresponding fractions by the exonuclease Venum phosphodiesterase (VPD, Sigma). VPD digests the 5'-monoadduct (**I2**) to *cis*-$[PtCl(NH_3)_2d(TpG\text{-}N7)]$ and dpG, whereas the 3'-monoadduct (**I1**) remains undigested [13].

Appendix

The integration of the differential equations describing the kinetics of the reaction system shown in Scheme 1 yields the following expressions for the four concentrations [N], [I1], [I2], and [C], at the time t (W = excess of *cis*-$[Pt(NH_3)_2(H_2O)_2](NO_3)_2$ over the oligonucleotide **N**):

$$[N] = \frac{W}{e^{(k_1 t + A)W} - 1}$$

$$A = \frac{\ln(W/[N]_0 + 1)}{W};\ k_1 = k_{11} + k_{12};\ W = [Pt] - [N]$$

$$[I1] = k_{11} e^{-k_{21}t} \int [N]([N] + W) e^{k_{21}t} dt$$

$$[I2] = k_{12} e^{-k_{22}t} \int [N]([N] + W) e^{k_{22}t} dt$$

$$[C] = [N]_0 - [N] - [I1] - [I2]$$

The integrals in the expressions for [I1] and [I2] were calculated numerically with time steps of 1 s. The optimization procedure was based on perpendicular distances of the experimental points from the calculated curves (**p** in Fig. 3), rather than on vertical distances corresponding to the difference between calculated and experimental concentrations (**v** in Fig. 3). This approach, which takes into account the experimental errors for both time and concentration, is, of course, meaningful only if both variables are scaled in units corresponding to the uncertainty in their measurement.

In the minimized function (1), $\mathbf{p}_i^{\mathbf{X}}$ are the perpendicular deviations of the experimental points i from the calculated curve, determined as from Equation (2).

$$F = [\sum_i (\mathbf{p}_i^{\mathbf{N}})^2]^2 + [\sum_i (\mathbf{p}_i^{\mathbf{I1}})^2]^2 + [\sum_i (\mathbf{p}_i^{\mathbf{I2}})^2]^2 + [\sum_i (\mathbf{p}_i^{\mathbf{C}})^2]^2 \quad (1)$$

$$\mathbf{p}_i^{\mathbf{X}} = \{[\mathbf{X}]_i^{obs} - [\mathbf{X}]_i^{calc}\} \cos\alpha = \{[\mathbf{X}]_i^{obs} - [\mathbf{X}]_i^{calc}\}(1 + \tan^2\alpha)^{-1/2} \quad (2)$$

with $\tan\alpha = \{d[\mathbf{X}]^{calc}/dt\}_i \{s(t)/s([\mathbf{X}])\}$

$[\mathbf{X}]_i^{obs}$ and $[\mathbf{X}]_i^{calc}$ are the observed and calculated concentrations of the product **X** at the time t_i, and $s(t)$ and $s([\mathbf{X}])$ are the errors in the determination of time and concentration, estimated to be 4 s and 2% of the initial oligonucleotide concentration, respectively. The individual sums in Equation (1) were taken as the second power to prevent the program from fitting one curve considerably worse than the others. Our optimization procedure used a grid search algorithm [14].

Received: May 14, 1992 [Z 5348 IE]
German version: *Angew. Chem.* **1992**, *104*, 1494

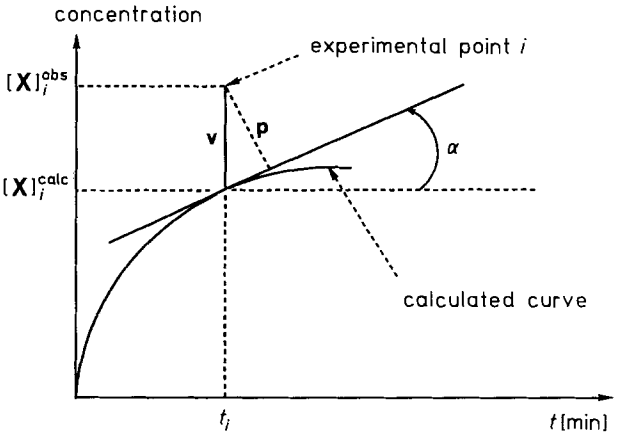

Fig. 3. Two distances relating an experimental point with the calculated curve: **v**, the vertical distance; **p**, the normal to the curve through the experimental point. In the linear approximation, $\mathbf{p} = \mathbf{v} \cos\alpha$. The variables are scaled in units of their inherent experimental errors. Whereas **v** reflects only the uncertainty in the concentration measurement, **p** takes into account the imprecision of both variables.

CAS Registry numbers:
N, 34727-11-2; **C**, 144017-98-1; **I1**, 144041-54-3; **II2**, 144017-99-2; *cis*-$[Pt(NH_3)_2(H_2O)_2]^{2+} \cdot 2NO_3^-$, 52241-26-6; *cis*-$[PtCl(NH_3)_2 \cdot (H_2O)]^+$, 53861-42-0.

[1] A. Laoui, J. Kozelka, J. C. Chottard, *Inorg. Chem.* **1988**, *27*, 2751–2753.
[2] A. Eastman, *Biochemistry* **1983**, *22*, 3927–3933.
[3] A. Eastman, *Biochemistry* **1985**, *24*, 5027–5032.
[4] A. Eastman, M. A. Barry, *Biochemistry* **1987**, *26*, 3303–3307.
[5] A. Eastman, N. Schulte, *Biochemistry* **1988**, *27*, 4730–4734.
[6] A. M. J. Fichtinger-Schepman, P. H. M. Lohman, J. Reedijk, *Nucleic Acids Res.* **1982**, *10*, 5345–5356.
[7] A. M. J. Fichtinger-Schepman, J. L. Van der Veer, J. H. J. Den Hartog, P. H. M. Lohman, J. Reedijk, *Biochemistry* **1985**, *24*, 707–713.
[8] A. Pullman, C. Zakrzewska, D. Perahia, *Int. J. Quantum Chem.* **1979**, *16*, 395–403.
[9] The modeled species was, in fact, the pentacoordinated intermediate, since the assumption was made that the structure of the transition state would not be very different.
[10] This value was approximated as $\varepsilon_{254}\{d(TGG)\} \approx \varepsilon_{254}(dT) + 2\varepsilon_{254}\{d(pG)\}$; $\varepsilon_{254}(dT)$ and $\varepsilon_{254}\{d(pG)\}$ were measured on Sigma products, and their analytically determined water content taken into account as 5850 $M^{-1}cm^{-1}$ and 8160 $M^{-1}cm^{-1}$, respectively.
[11] Y. N. Kukushkin, S. C. Dhara, *Indian J. Chem.* **1970**, *8*, 184–185.
[12] It is essential to allow the monoaqua products (**I**, X = H_2O) to convert to monochloro species (**I**, X = Cl^-), otherwise the chelation reactions proceed during HPLC analysis, leading to smearing of the peaks. The minimum time necessary at 293 K is 1.75 min. Longer incubations should be avoided, since the chelation reactions are not sufficiently inhibited at this temperature.
[13] K. Inagaki, Y. Kidani, *Inorg. Chim. Acta* **1985**, *106*, 187–191.
[14] J. A. McCammon, S. C. Harvey, *Dynamics of proteins and nucleic acids*, Cambridge University Press, Cambridge, **1987**, p. 48.

Stable Cyclic Germanediyls ("Cyclogermylenes"): Synthesis, Structure, Metal Complexes, and Thermolyses**

By *Wolfgang A. Herrmann,* Michael Denk, Joachim Behm, Wolfgang Scherer, Franz-Robert Klingan, Hans Bock, Bahman Solouki,* and *Matthias Wagner*

Substituted ethylenediamine **2a** and its derivatives form volatile, spirocyclic titanium amides, which precipitate from the gas phase (produced thermally or plasma-induced) as titanium carbonitrides.[1] We discovered that this type of ligand is generally suited for the stabilization of main group and subgroup elements with unusual valencies and report here on new applications in the chemistry of germanium.

The cyclic germanium(IV) diamide **3a**[2] was formed in almost quantitative yields from $GeCl_4$ (**1a**) and diamine **2a** in the presence of triethylamine. Reductive dehalogenation of **3a** then provided the new germanediyl ("germylene") **3b** (Scheme 1).[3] In another approach to **3b** the dilithium salt **2b** was allowed to react with germanium dichloride·1,4-dioxane (**1b**). Surprisingly, the CC-unsaturated germanediyl **3c** obtained by a formal dehydrogenation was isolated as a side product (Scheme 1). Compound **3c** can be prepared

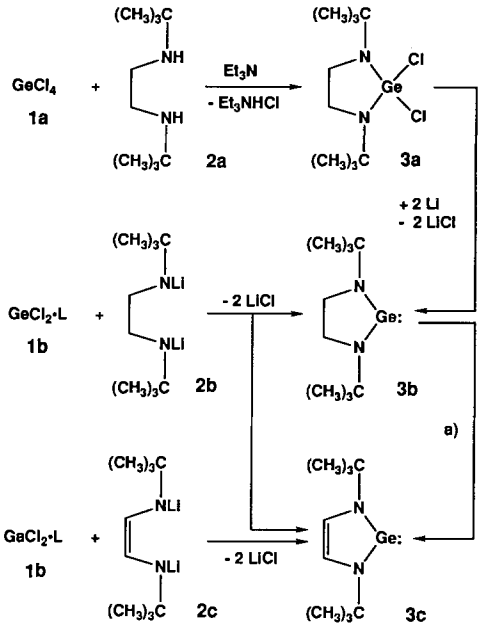

Scheme 1. a) $+[(CH_3)_3Si]_2NLi$; $-[(CH_3)_3Si]_2NH$, $-LiH$; THF, 2 h, 60 °C. L = 1,4-dioxane.

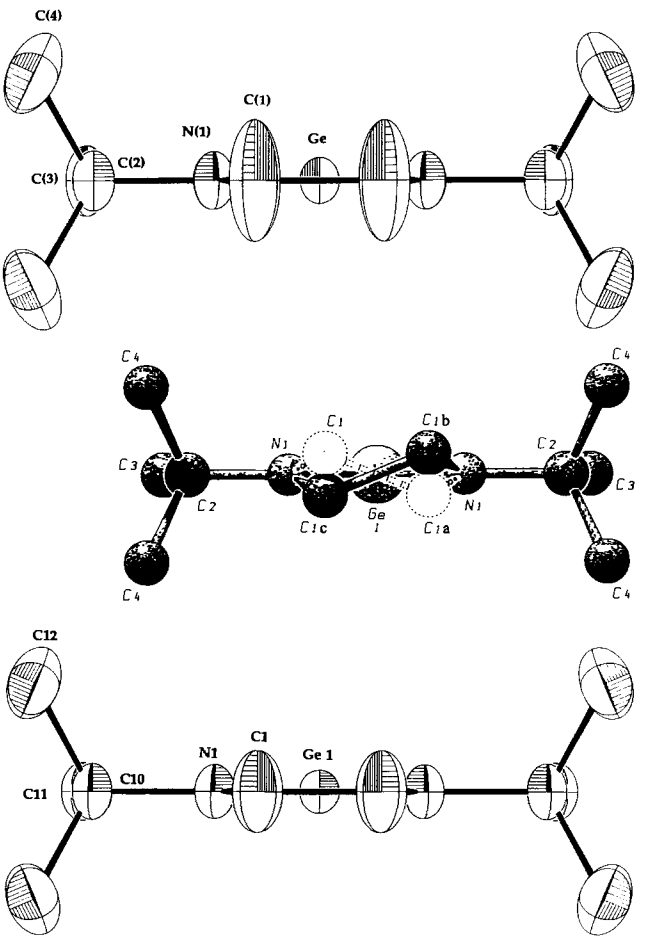

Fig. 1. Top: Crystal structure of **3b** at −70 °C (ORTEP, without hydrogen atoms, thermal ellipsoids at the 50% probability level). Middle: Model of the disorder in **3b** (SCHAKAL, see text). Selected distances [pm] and angles [°]: Ge-N1 183.3(2), N1-C1 145.9(4), C1-C1a 157.1(7), N1-C2 146.7(4); N1,Ge,N1′ 88.0(1), N1,C1,C1a 105.7(2), Ge,N1,C1 113.1(2), C2,N1,Ge 128.2(2); shortest Ge–Ge distance: 643 pm. Bottom: Crystal structure of **3c** at −50 °C. Selected distances [pm] and angles [°]: Ge-N1 185.6(1), N1-C1 138.4(1), C1-C1′ 136.4(1), N1-C10 149.3(1); N1,Ge,N1′ 84.8(1), N1,C1,C1′ 144.3(1), Ge,N1,C1 113.3(1); shortest Ge–Ge distance: 641 pm.

[*] Prof. Dr. W. A. Herrmann, Dr. M. Denk, Dr. J. Behm, W. Scherer, F.-R. Klingan
Anorganisch-chemisches Institut der Technischen Universität München
Lichtenbergstrasse 4, D-W-8046 Garching (FRG)
Prof. Dr. H. Bock, Dr. B. Solouki
Anorganisch-chemisches Institut der Universität Frankfurt
Dr. M. Wagner
Anorganisch-chemisches Institut der Universität München

[**] Cyclic Metal Amides, Part 2. This research was supported by the Bundesministerium für Forschung und Technologie. Part 1: ref. [1b].

cleanly from treatment of the dilithium salt **2c** with **1b** (85%).[4]

Both germanediyls are infinitely stable at 25 °C under inert gas. The extraordinarily volatile compounds (both sublime at 45 °C and 1 Torr; **3b**: m.p. 45 °C, **3c**: m.p. 51 °C) are highly prone to hydrolysis. Compared to **3b**, compound **3c** is less reactive, thermally more stable, and can even be handled briefly in air in the crystalline state. Germanediyls **3b** and **3c** are monomeric not only in solution (osmometry) and in the gas phase (CI-MS, electron diffraction[5a]), but also in the solid state (Fig. 1), and thus belong to a rare class of compounds.[6] Merely replacing the *t*-butyl groups on the N atom with methyl groups leads to dimerization or trimerization.[6] The tin derivative analogous to **3b** is dimeric.[5b]

According to the X-ray structure analysis of **3b**,[7a] the atoms of the C_2N_2Ge five-membered ring appear to lie in a mirror plane, which could imply a planar framework. However, the large vibration ellipsoids of C1 and C1′ (view parallel to the mirror plane, Fig. 1 top) cannot be rationalized completely in terms of thermal vibrations. In addition, the C1–C1′ bond is too short (142.8(7) pm) for a CC single bond. These features can be explained by a model in which the disorder is caused by two superimposed twist conformations (Fig. 1 middle).[7a] The refinement of this model provides the same *R* values,[7] but leads to a CC bond length (157.1(7) pm) reasonable for a single bond. Calculations also predict that **3b** should have a twist conformation in the ground state.[10a] In contrast, **3c** is planar (Fig. 1 bottom);[7b] the bond lengths and bond angles at germanium differ only marginally from those of **3b** and give no evidence of electronic differences between the two molecules.

$[Ni(CO)_4]$ reacts with **3b** to furnish the monogermanediyl complex **4a**, and with excess **3b** to give the bis(germanediyl) complex **5a** (Scheme 2). The structure of **5a**[8] was determined by X-ray diffraction (Fig. 2). The zero-valent metal atom has an almost ideal tetrahedral coordination geometry, the respective carbonyl and germanediyl ligands are nonequivalent, and the GeN_2C_2 five-membered rings are nonplanar, as in the free ligand **3b**. Their CC bonds thus appear to be shortened, but this effect is caused once again by a twist disorder of the ethylene bridge. The angles at N, Ge, and N′ are almost identical to those in **3b**. Germanium has trigonal-planar coordination (sum of the angles is ca. 360°). Each N_2GeNi plane is coplanar with a carbonyl group. The resulting nonequivalence of the two *tert*-butyl groups of each germanediyl ligand is also evident in solution [$^1H/^{13}C$ NMR; coalescence temperature + 65 °C (^{13}C NMR)]. The Ni–Ge distances (ca. 230 pm) are not shorter than the single bonds in the few known germylnickel complexes.[9] As the ^{15}N NMR and IR data (νCO) show, the nickel atom (d orbitals) cannot compete effectively with N–Ge backbonding: $[Ni(CO)_4]$ 2057 (T_2), $[Ni(CO)_2\{P(C_6H_5)_3\}_2]$ 2000 (A_1)/1941 (B_1), **5a** 2003 (A_1)/1945 (B_1) cm^{-1}; the corresponding force constants for CO stretching have the following respective values $\kappa = 17.9$, 14.1, and 14.2 $N\,cm^{-1}$. Thus, germanediyl **3b** is a ligand with relatively good σ-donor and poor π-acceptor qualities, and in this respect is similar to triphenylphosphine.

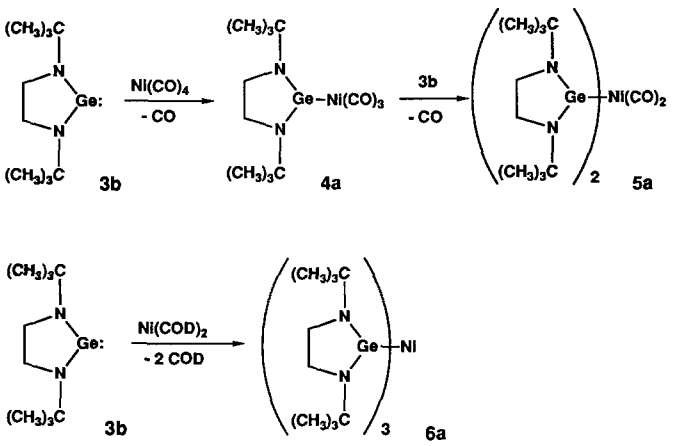

Scheme 2.

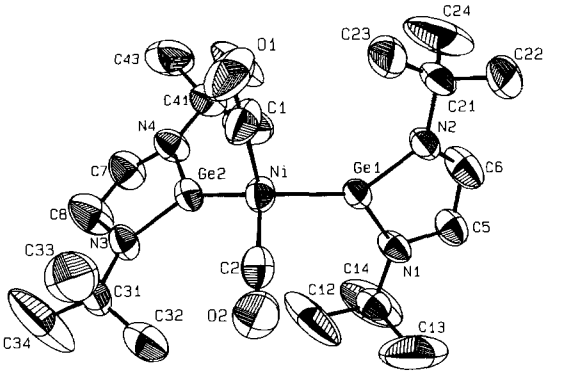

Fig. 2. Crystal structure of **5a** (ORTEP, without hydrogen atoms, thermal ellipsoids at the 50% probability level). Selected distances [pm] and angles [°]: Ge1-Ni 229.69(4), Ge2-Ni 229.13(3), C1-Ni 177.2(3), C2-Ni 176.9(2), C1-O1 113.1(2), C2-O2 113.3(2), Ge-N1 182.6(2), Ge1-N2 181.9(1), Ge2-N3 183.0(1), Ge2-N4 181.3(2); Ge1,Ni,Ge2 106.67(1), C1,Ni,C2 111.6(1), Ge1,Ni,C1 113.71(8), Ge1,Ni,C2 106.3(1), Ni,C1,O1 176.4(3), Ni,C2,O2 176.3(2), N1,Ge1,N2 88.62(7), N3,Ge2,N4 89.22(7), Ge1,N1,C5 112.2(1), Ge1,N1,C11 129.3(1), C5,N1,C11 118.3(2), Ge1,N2,C6 111.8(1), Ge1,N2,C21 129.8(1), C6,N2,C21 118.1(2).

Ab initio calculations of the model compound $(NH_2)_2Ge$: (planar ground state, symmetry point group C_{2v}) showed unexpectedly strong Ge–N backbonding. The barrier to rotation about the first Ge–N bond with pyramidalization is 12.8 kcal mol^{-1}, about the second 21.8 kcal mol^{-1}. The second NH_2 group apparently provides some of the charge density which the Ge atom loses when the first NH_2 group is orthogonal.[10]

The reaction of **3b** with $[Ni(1,5\text{-cod})_2]$ (cod = cyclooctadiene), furnished the extremely air- and moisture-sensitive tris(germanediyl) complex **6a** (Scheme 2), which crystallized as brick-red crystals from *n*-hexane. The NMR spectra (^1H, ^{13}C, ^{15}N) indicate that the compound has D_{3h} symmetry.

Investigations of the chemical vapor deposition (CVD) to $[Ge]_\infty$ or $[Ge/GeH]_\infty$ were conducted in a flow tube under controlled conditions;[11a, b] the gas was analyzed by photoelectron (PE) spectroscopy. Surprisingly, the thermolysis of **3b,c** gave rise to isobutene and HCN; H_2 could not be detected. Besides the ionization pattern of isobutene,[11c] the region of contourless bands between 11–16 eV presumably also contains the one of isobutane. The thermolyses analyzed by PE spectroscopy suggest the following reaction sequence for the extrusion of $[Ge]_\infty$ or $[Ge/GeH]_\infty$ (Scheme 3). At 470 K **3b** decomposes to **3c** and **2a**. At 900 K **3b** and **3c** give identical PE spectra in which isobutene and HCN can be identified by their characteristic ionization peaks besides residual **3c**. These results indicate that the CVD decomposition of **3b,c** may be optimized for the preparation of (hydrogen-containing) germanium layers.

The different thermal stabilities of the saturated and unsaturated cyclogermanediyls were approximated by ab initio

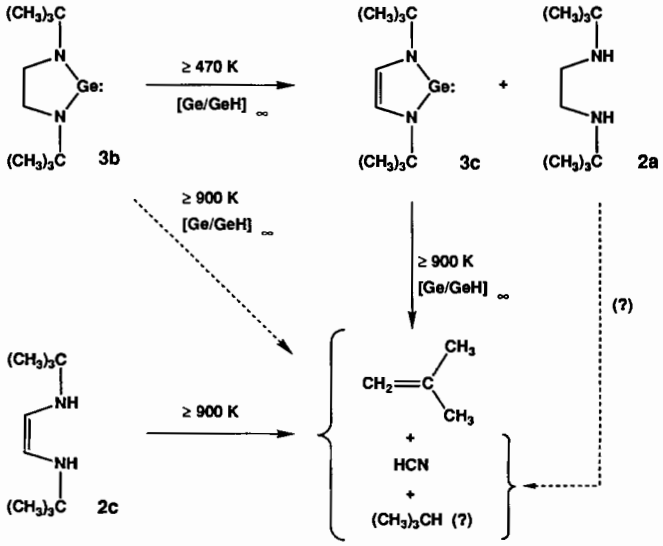

Scheme 3.

calculations[10a] of the hydrogenation enthalpies of the model compounds **3b'** and **3c'** [isodesmic Eqs. (a) and (b)]. The unsaturated cyclogermanediyl **3c'** is 41 kJ mol^{-1} lower in energy than the saturated compound **3b'** (RHF/LANL1DZ//RHF/LANL1DZ); when electron correlation is included (MP2/LANL1DZ//RHF/LANL1DZ), **3c'** is 54 kJ mol^{-1} more stable than **3b'**.[10a] The optimized geometry is in excellent agreement with the structural data (Fig. 1). In the triplet state, in which seven electrons occupy the π molecular orbitals of **3c'**, there is *no* significant difference between the hydrogenation enthalpies of the model compounds and those of the hypothetical germane derivatives [Eqs. (a) and (b)].

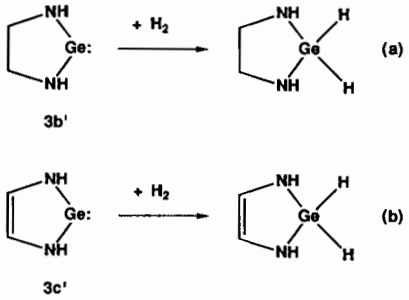

The theoretical and experimental results (planarity, ^{1}H/^{15}N NMR data,[2, 3, 5a] reduced reactivity) can best be explained by assuming a cyclic delocalization of the π electrons in **3c** in the ground state. In light of the results reported here, as well as the work of Arduengo et al.[12] on the structurally analogous carbenes (C instead of Ge), the corresponding silanediyls should also be stable.

Experimental Procedure

3b: A solution of **3a** (1.29 g, 4.12 mmol) in THF (5 mL) was treated with Li granules (57 mg) (the reaction mixture turned brown). After 5–6 h the solvent was removed under vacuum and replaced with *n*-pentane (10 mL). Filtration (G3 Schlenk frit) and evaporation of the solvent gave a thick, light yellow oil, which upon sublimation (1 Torr, 40 °C) provided analytically pure **3b** in the form of colorless needles (750 mg, 75%). Occasionally a small amount of a yellow, volatile impurity was observed which could be removed by sublimation.

3c: A solution of *N*,*N'*-bis(*tert*-butyl)-1,4-diazabutadiene (59.4 mmol, 1 molequiv) in THF (200 mL) was treated with Li granules (830 mg, 0.12 g-atom, 2 molequiv) and stirred overnight (reaction mixture turned red). A solution of **1b** (13.8 g) in THF (50 mL) was added dropwise at 25 °C over 10 min (reaction mixture turned brown and warmed to 30–40 °C). The solvent was removed under vacuum after 1 h, the residue stirred with *n*-pentane (100 mL), and the mixture filtered (G3 or G4 Schlenk frit). The solvent was evaporated, and sublimation provided **3c** as dull colorless needles (11.5 g, 80%). Correct complete analysis.

4a: [Ni(CO)$_4$] (5 mL, excess) was added dropwise to a stirred solution of **3b** (900 mg, 3.705 mmol) in THF (5 mL) at 25 °C. After a short induction period, a vigorous evolution of gas began and lasted ca. 3 min (reaction mixture turned pale yellow). After 1 h at 25 °C, the solvent was removed under vacuum, the orange-yellow, clear, glasslike residue taken up in *n*-pentane (10 mL), and the solution stored at −25 °C (1 d) and −78 °C (1 d). **4a** was obtained as colorless crystals with a slightly gray tinge (1.17 g, 82%). ^{1}H NMR (270 MHz, C_6D_6, 25 °C): δ = 1.23 (s, CH_3); 3.08 (s, CH_2); ^{13}C NMR (100.54 MHz, C_6D_6, 25 °C): δ = 32.2 (q, ^1J(C,H) = 125 Hz; CH_3), 48.7 (t, ^1J(C,H) = 136 Hz; CH_2), 55.5 (s; $C(CH_3)_3$), 195.9 (s; CO); ^{17}O NMR (36.64 MHz, [D_8]toluene, 25 °C, D_2O standard): δ = −197.1 (s; CO); ^{15}N NMR (40.51 MHz, C_6D_6, 25 °C, CH_3NO_2 standard): δ = −226.1 (s).

5a: To a solution of **3b** (900 mg, 3.705 mmol) in *n*-hexane (5 mL) was added [Ni(CO)$_4$] (161 μL, 0.212 g, 1.235 mmol). After a short induction period, a vigorous evolution of gas began and lasted ca. 3 min. The solvent was removed by distillation under vacuum and the residue heated at 90 °C (oil bath temperature) in a sublimation apparatus under high vacuum for 1 d. The clear, glassy remaining material was taken up in *n*-pentane (10 mL) and crystals formed at −25 °C. Yellow, transparent prisms were obtained (830 mg, 75%). IR (Nujol, CsI): ν(CO) = 2003 (s), 1945 (s) cm^{-1}; ^{1}H NMR (400 MHz, C_6D_6, 25 °C): δ = 1.41, 1.48 (s; CH_3), 3.09 (s; CH_2); ^{13}C NMR (100.54 MHz, [D_8]toluene, 25 °C): δ = 31.9, 32.2 (q, ^1J(C,H) = 125 Hz; CH_3), 48.6, 48.7 (t, ^1J(C,H) = 136 Hz; CH_2), 55.4 (s, $C(CH_3)_3$), 195.7 (s; CO); ^{17}O NMR (36.64 MHz, C_6D_6, 25 °C, D_2O standard): δ = 207.7 (s); ^{15}N NMR (40.51 MHz, C_6D_6, 25 °C, CH_3NO_2 standard): δ = −222.2 (s). Correct complete analysis.

6a: A solution of **3b** (840 mg, 3.46 mmol) in THF (5 mL) at −78 °C was treated with [Ni(1,5-cod)$_2$] (317 mg, 1.15 mmol) (reaction mixture turned red immediately). The reaction mixture was allowed to warm to 25 °C, and the volatiles were removed by distillation. The remaining material was heated at 60 °C (oil bath temperature) for 2 h under argon and then 8 h under vacuum. The red-brown crystalline residue was dissolved in *n*-hexane (10 mL) and cooled to −30 °C for ca. 15 d to provide deep red needles (810 mg, 89%). ^{1}H NMR (400 MHz, C_6D_6, 25 °C): δ = 1.45 (s; CH_3), 3.24 (s; CH_2); ^{13}C NMR (100.54 MHz, [D_8]toluene, 25 °C): δ = 32.4 (q, ^1J(C,H) = 125 Hz; CH_3), 48.6 (t, ^1J(C,H) = 135 Hz; CH_2), 54.5 (s; $C(CH_3)_3$); ^{15}N NMR (40.51 MHz, [D_8]toluene, 25 °C, CH_3NO_2 standard): δ = −234.7 (s); CI-MS (isobutene, positive ions): *m*/*z* 242 (LGe^+, 100%); CI-MS (isobutene, negative ions): *m*/*z* 749 (**6a**$^{\cdot -}$ − 3CH_3, 42%), 394(30), 315(23), 279(10), 208(9), 149(100). Correct complete analysis.

Received: June 22, 1992
Revised: August 25, 1992 [Z 5432 IE]
German version: *Angew. Chem.* **1992**, *104*, 1489

CAS Registry numbers:
1b, 28595-67-7; **2a**, 4062-60-6; **3a**, 143970-59-6; **3b**, 143970-60-9; **3c**, 143970-61-0; **4a**, 143970-63-2; **5a**, 144000-21-5; **6a**, 143970-64-3; [Ni(cod)$_2$], 1295-35-8; [Ni(CO)$_4$], 13463-39-3; *N*,*N'*-Bis(*tert*-butyl)-1,4-diazabutadiene, 143970-62-1.

[1] a) W. A. Herrmann, M. Denk, S. Vepřek, unpublished results, 1991/1992; b) W. A. Herrmann, M. Denk, R. W. Albach, J. Behm, E. Herdtweck, *Chem. Ber.* **1990**, *124*, 683–689.

[2] **3a**: ^{1}H NMR (270 MHz, C_6D_6, 25 °C): δ = 1.21 (s, 18H; CH_3), 2.75 (s; CH_2); ^{13}C NMR (67.94 MHz, C_6D_6, 25 °C): δ = 29.3 (q, ^1J(C,H) = 126 Hz; CH_3), 43.6 (t, ^1J(C,H) = 139 Hz; CH_2), 54.0 (s; $C(CH_3)_3$); ^{15}N NMR (40.51 MHz, C_6D_6, 25 °C, Standard CH_3NO_2): δ = −302.5 (s; $C(CH_3)_3$); EI-MS (70 eV, positive ions): *m*/*z* 318 ($M^{\cdot +}$, 1%), 299 ($M^{\cdot +}$ − CH_3, 100). Correct complete analysis.

[3] **3b**: ^{1}H NMR (C_6D_6, 270 MHz, 25 °C): δ = 1.28 (s, 9H; CH_3), 3.27 (s, 2H; CH_2); ^{13}C NMR (C_6D_6, 67.9 MHz, 25 °C): δ = 32.1 (q, ^1J(C,H) = 125 Hz; CH_3), 54.3 (s, $C(CH_3)_3$), 49.7 (t, ^1J(C,H) = 135 Hz, ^2J(C,H) = 3 Hz; CH_2); ^{15}N NMR (C_6D_6, 40.51 MHz, 20 °C, CH_3NO_2 standard): δ = −207.3 (s); CI-MS (isobutene, positive ions): *m*/*z* 242 (65%), 229(28), 173(100). Correct complete analysis.

[4] **3c**: ^{1}H NMR (270 MHz, C_6D_6, 25 °C): δ = 1.43 (s, 18H; CH_3), 7.05 (s, 2H; CH); ^{13}C NMR (67.94 MHz, C_6D_6, 25 °C): δ = 33·2 (q, ^1J(C,H) = 125.1 Hz; CH_3), 55.7 (s, $C(CH_3)_3$), 121.4 (dd, ^1J(C,H) = 173.0 Hz,

^2J(C,H) = 11.0 Hz; CH); ^{15}N NMR (C_6D_6, 40.51 MHz, 25 °C, CH_3NO_2 standard): $\delta = -136.3$ (s); CI-MS (isobutene, positive ions): m/z 242 (60%), 194(47), 169(100). Correct complete analysis.

[5] a) A. Haaland, P. Kiprof, W. A. Herrmann, M. Denk, unpublished; b) M. Denk, Dissertation, Technische Universität München, **1992**.

[6] a) M. F. Lappert, M. J. Slade, J. L. Atwood, *J. Chem. Soc. Chem. Commun.* **1980**, 621–622; b) J. Pfeiffer, W. Maringgele, M. Noltemeyer, A. Meller, *Chem. Ber.* **1989**, *122*, 245–252; c) R. A. Bartlett, P. P. Power, *J. Am. Chem. Soc.* **1990**, *112*, 3660–3662; d) M. Veith, L. Stahl, V. Huch, *J. Chem. Soc. Chem. Commun.* **1990**, 359–361.

[7] a) X-ray structure analysis of **3b** ($C_{10}H_{22}GeN_2$): Irregular fragment of a crystal obtained by sublimation. Systematic extinctions $h00$ ($h = 2n+1$) and $0k0$ ($k = 2n+1$), space group $P\bar{4}2_1m$ (no. 113), $a = 998.09(4)$, $c = 643.12(5)$ pm, $V = 640 \cdot 10^6$ pm^3, $Z = 2$, $\rho_{calc} = 1.259$ g cm^{-3}, Enraf-Nonius CAD4, $\lambda = 71.07$ pm ($Mo_{K\alpha}$, graphite monochromator), $T = -70$ (±3) °C, range of measurement $1.0° < \theta < 25.0°$, ω-scan, scan width $(1.2 + 0.25\tan\theta)°$ (±25%) before and after each reflection to determine the background, $t_{max} = 60$ s, empirical absorption correction based on Ψ-scan data, $\mu = 23.2$ cm^{-1}, no decomposition, direct structure determination, difference Fourier technique, 620 independent reflections, of which 620 had $I > 0.01\sigma(I)$, 67 parameters refined by full-matrix least-squares, reflection/parameter relationship 9.25, all six heavy atoms except C1 with anisotropic thermal motion parameters, all hydrogen atoms found and independently refined, anomalous dispersions accounted for, shift/error < 0.001, residual electron density 0.20 Δe_o Å^{-3} (105 pm off the Ge atom) and $-0.31\ \Delta e_o$ Å^{-3}, $R = \Sigma(\|F_o| - |F_c\|)/\Sigma|F_o| = 0.017$, $R_w = [\Sigma w(|F_o| - |F_c|)^2/\Sigma w|F_o|^2]^{1/2} = 0.019$. The refinement of the other enantiomer gave a larger R value (0.0263). Three additional sets of data were collected from another crystal between −35 and −110 °C for further support the model of disorder. All four measurements confirm the model of disorder and thus the nonplanarity of the C_2N_2Ge ring, since the large vibration ellipsoids were shown to be temperature invariant and best rationalized by disorder. The structure refinement provided almost identical behavior for the main axes of the thermal parameters. b) X-ray structure analysis of **3c** ($C_{10}H_{20}GeN_2$): $a = 1378.40(4)$, $b = 1403.12(3)$, $c = 641.45(1)$ pm, $V = 1240 \cdot 10^6$ pm^3, measurement at −50 °C, $\rho_{calc} = 1.289$ g cm^{-3}, $\mu = 30.2$ cm^{-1}, $Z = 4$, orthorhombic crystal system, space group $Pmmn$, Enraf-Nonius CAD4, $\lambda = 154.184$ pm, $Cu_{K\alpha}$, graphite monochromator), $\omega/2\theta$-scan, 4635 measured reflections, $(-h, \pm k, \pm l)$ of which 1143 were independent, structure determination with Patterson methods and difference Fourier syntheses, empirical absorption correction, transmission coefficients 0.8592–0.999, 118 refined parameters, $R = \Sigma(\|F_o| - |F_c\|)/\Sigma|F_o| = 0.035$, $R_w = [\Sigma w(|F_o| - |F_c|)^2/\Sigma w|F_o|^2]^{1/2} = 0.029$, residual electron density + 0.68, −0.76 Δe_o Å^{-3}. c) Further details of the crystal structure investigation may be obtained from the Fachinformationszentrum Karlsruhe, Gesellschaft für wissenschaftlich-technische Information mbH, D-W-7514 Eggenstein-Leopoldshafen 2 (FRG), on quoting the depository number CSD-56578, the names of the authors, and the journal citation.

[8] X-ray structure analysis of **5a** ($C_{22}H_{44}Ge_2N_4NiO_2$): $a = 965.1(1)$, $b = 1671.8(2)$, $c = 1811.5(2)$ pm, $\beta = 101.51°$, $V = 2864 \cdot 10^6$ pm^3, measurement at 25 °C, $\rho_{calc} = 1.39$ g cm^{-3}, $\mu = 33.8$ cm^{-1}, $F_{000} = 1248$, $Z = 4$, monoclinic crystal system, space group $P2_1/c$, Enraf-Nonius CAD4, $\lambda = 154.184$ pm ($Cu_{K\alpha}$, graphite monochromator), $\omega/2\theta$-scan, 5288 measured reflections $(\pm h, -k, +l)$, 4651 of which were independent, 4645 used for refinement, structure solution with Patterson methods and difference Fourier syntheses, empirical absorption correction, transmission coefficients 0.939–0.999, 280 refined parameters, $R = \Sigma(\|F_o| - |F_c\|)/\Sigma|F_o| = 0.052$, $R_w = [\Sigma w(|F_o| - |F_c|)^2/\Sigma w|F_o|^2]^{1/2} = 0.049$, residual electron density + 0.98, −0.74 Δe Å^{-3}. See also ref. [7c].

[9] Cf. for example F. Glocking, A. McGregor, M. L. Schneider, H. M. M. Shearer, *J. Inorg. Nucl. Chem.* **1970**, *32*, 3101. Few metal complexes of stable germane- and stannanediyls have been reported previously; see for example W. P. Neumann, *Chem. Rev.* **1991**, *91*, 311, and references therein; M. S. Holt, W. L. Wilson, J. H. Nelson, *ibid.* **1989**, *89*, 11.

[10] a) The calculations were conducted on a Cray vector computer with the GAUSSIAN-90 program package; cf. W. J. Hehre, C. Radom, P. von R. Schleyer, J. A. Pople, *Ab Initio Molecular Orbital Theory*, Wiley, New York, **1986**; T. Clark, *A Handbook of Computational Chemistry*, Wiley, New York, **1985**. Geometries were optimized at the RHF (singlet states) or the UHF level (triplet states) within the given symmetry restrictions with the LANL1DZ basis set. The frequencies were calculated in the same way for the determination of local minima. The energies listed were obtained from single-point calculations on the RHF/LANL1DZ geometries with up to second-order perturbation theory (MP2); cf. P. J. Hay, W. R. Wadt, *J. Chem. Phys.* **1985**, *82*, 270–283, 284–298, 299–310. b) For π-electron delocalization cf. S. S. Shaik, P. C. Hiberty, J.-M. Lefour, G. Ohanessian, *J. Am. Chem. Soc.* **1987**, *109*, 363.

[11] a) H. Bock, B. Solouki, H. S. Aygen, M. Bankmann, O. Breuer, R. Dammel, J. Dörr, M. Hann, D. Jaculi, J. Mintzer, S. Mohumand, H. Müller, P. Rosmus, B. Roth, J. Wittmann, H.-P. Wolf, *J. Mol. Struct.* **1988**, *173*, 31; H. Bock, M. Kremer, H. Schmidbaur, *J. Organomet. Chem.* **1992**, *429*, 1. b) Quartz tube (40 × 1.5 cm) with three plugs of quartz wool each 1.5 cm long in a 30-cm tubular oven connected to a Leybold Heraeus UPG 200 PE spectrometer (resolution ca. 20 meV, 2000 counts s^{-1}). The spectra were recorded at a pressure of 10^{-4} mbar and calibrated with Ar ($^2P_{3/2}$) = 15.76 eV. c) Cf. for example K. Kimura, S. Katsumata, Y. Achiba, T. Yamazaki, S. Iwata, *Handbook of He-I Photoelectron Spectra of Fundamental Organic Molecules*, Halstead Press, New York, **1981**. d) The assignment of the PE spectra of **3b** and **3c** following Koopman's correlation $IE_n^v = -\varepsilon_j^{MNDO}$, with MNDO eigenvalues was not reliable, since in the optimization of the parameters for Ge (M. J. S. Dewar, G. L Grady, E. F. Healy, *Organometallics* **1987**, *6*, 186–189) $MeGeNMe_2$ was the only nitrogen compound considered. Under C_{2v} symmetry, the order of the first three bands should be $n_N - (a_2) < N_{Ge}(a_1) \approx n_N + (b_1)$ is expected qualitatively; the bands of the last $M^{\cdot+}$ states overlap.

[12] a) A. J. Arduengo III, R. L. Harlow, M. Kline, *J. Am. Chem. Soc.* **1991**, *113*, 361; b) A. J. Arduengo III, H. V. Rasika Dias, R. L. Harlow, M. Kline, *ibid.* **1992**, *114*, 5530; c) D. A. Dixon, A. J. Arduengo III, *J. Phys. Chem.* **1991**, *95*, 4180.

Quest for Higher Ladderanes: Oligomerization of a Cyclobutadiene Derivative**

By *Goverdhan Mehta,* M. Balaji Viswanath, G. Narahari Sastry, Eluvathingal D. Jemmis,* D. Sivakumar K. Reddy,* and *Ajit C. Kunwar**

The name [*n*]-ladderane has been given to novel molecular arrays composed entirely of linearly concatenated cyclobutanes for example, **1**.[1] Thus, cyclobutane, bicyclo[2.2.0]-hexane, and tricyclo[4.2.0.0^{2,5}]octane are [1]-, [2]-, and [3]-ladderane, respectively. These multifused, cyclobutanoid systems hold great promise as spacers in view of the latitude they offer in terms of rigidity, distal variation, steric disposition, and an accommodating σ framework. However, only [2]-ladderanes have been exploited as spacers thus far.[2] Ladderanes with $n \geq 11$, which possess functional groups at the terminal rings [e.g., **2** ($x \geq 9$)], have been considered as precursors of configurational isomers of higher [*n*]-prismanes for example, israelane **3** and helvetane **4**.[3, 4] However, to our knowledge, the ladderane route to the fascinating hydrocarbons **3** and **4** has never progressed beyond the realm of fanciful ideas.[4, 5] The major impediment in the exploitation of the potentially rich chemistry of ladderanes has been their inaccessibility. It has not yet been possible to assemble a linear array of more than four cyclobutane rings, and only a handful of [4]-ladderanes are known.[6] Herein, we report a new approach for the rapid assembly of higher ladderanes, and describe the characteristics of [5]- and [7]-ladderane derivatives.

The simplest and shortest approach to the higher ladderanes **1**/**2** ($x \geq 3$) would be by the controlled oligomerization of a cyclobutadiene. However, cyclobutadiene and its derivatives are known to dimerize only.[7] If we can understand why the oligomerization of cyclobutadiene does not proceed beyond the dimer stage, it should be possible to design cyclobutadiene derivatives that may exhibit enhanced

[*] Prof. G. Mehta, M. B. Viswanath, G. N. Sastry, Prof. E. D. Jemmis
School of Chemistry
University of Hyderabad
Hyderabad 500134 (India)
Dr. D. S. K. Reddy
ARDEC, Picatinny Arsenal, NJ (USA)
Dr. A. C. Kunwar
Indian Institute of Chemical Technology
Hyderabad 500007 (India)

[**] This work was supported, in part, by the Council of Scientific and Industrial Research, New Delhi (Research Fellowships for MBV and GNS).

propensity towards further [4 + 2] cycloaddition and thus promote a cycloaddition cascade process leading to higher ladderanes **2**. To this end, we examined the frontier orbitals

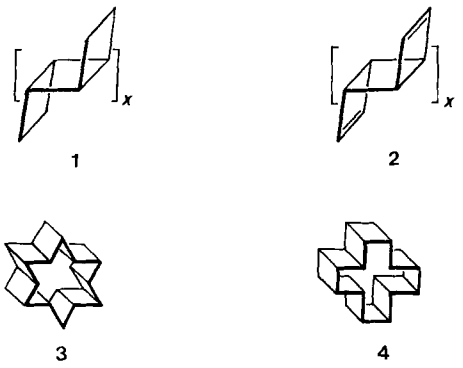

involved in the oligomerization and performed molecular orbital calculations at the AM1 level.[8] The HOMO–LUMO and LUMO–HOMO gaps calculated for oligomerization of **5a**, **b** are given in Scheme 1. The HOMO–LUMO gap of 8.46 eV for the dimerization of **5a** is within the range of successful [4 + 2] reactions.[9] The reaction of the dimer **6a** with **5a** has a considerably larger HOMO–LUMO or LUMO–HOMO gap (9.64 and 9.70 eV, respectively). Reactions with a HOMO–LUMO gap larger than 9.0 eV tend not to be very facile.[9] Formation of the tetramer **8a** from **5a** and **7a** has an equally unfavorable HOMO–LUMO (LUMO–HOMO) gap of 9.68 (9.64) eV. Electron withdrawing groups in the 1,2 position as in **5b** should reduce the HOMO and LUMO of the system. While this may not affect the dimerization substantially, it could facilitate further oligomerization because the HOMO and LUMO in this case have to be from different molecules.

Accordingly, the dicarboxylic acids **5b**–**8b** were optimized at the AM1 level. Scheme 1 shows that for the dimerization of **5b**, the HOMO–LUMO gap is somewhat lower

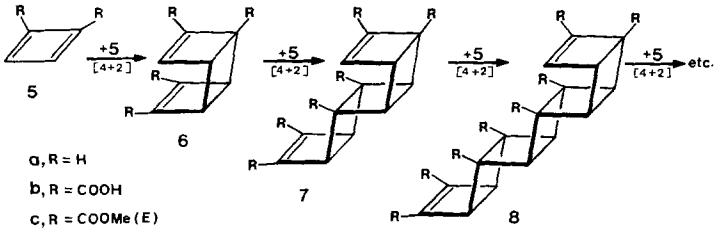

Reaction	HOMO–LUMO (LUMO–HOMO) [eV]	
	R = H	R = CO_2H
5 + **5** → **6**	8.46	8.12
5 + **6** → **7**	9.64 (9.70)	8.37 (9.29)
5 + **7** → **8**	9.68 (9.64)	8.35 (9.29)

Scheme 1.

than that for **5a**. The HOMO–LUMO gaps calculated for the trimerization and the tetramerization (8.37 and 8.35 eV, respectively) are even more encouraging. These are more than 1 eV lower than those calculated for the parent system, and therefore **5b** can be considered a good candidate for oligomerization.

Based on these predictions, the tricarbonyl iron complex of dimethyl 1,2-cyclobutadienedicarboxylate (**9**) (1.2 mmol)[10] was treated with cerium(IV) ammonium nitrate (CAN, 5 equiv) in dry acetone (10 mL, 0–5 °C), which liberated the methyl ester **5c** (Scheme 2). Usual workup and chromatography led to the isolation of three crystalline products, dimer **6c**, trimer **7c**, and tetramer **8c** in an approximate 3:2:1 ratio and 55% yield along with minor quantities of uncharacterized products. The structures of **6c**–**8c** were revealed by their high-field ^1H and ^{13}C NMR parameters, which indicated the presence of four, six, and eight methylester moieties, respectively (Table 1). All the protons were duly assigned on

Table 1. ^1H and ^{13}C NMR chemical shifts and melting points of **6c**–**8c**.

Compound (M.p.)	^1H NMR (400 MHz, $CDCl_3$) chemical shifts	^{13}C NMR (100 MHz, $CDCl_3$) chemical shifts
6c (114–115 °C)	6.76 (1H, d, J_{ab} = 0.6 Hz; H_a), 3.94 (1H, d, J_{cd} = 3.4 Hz; H_c), 3.77 (3H, s; COOMe), 3.73 (3H, s; COOMe), 3.71 (3H, s; COOMe), 3.67 (3H, s; COOMe), 3.52 (1H, dd, J_{bd} = 8.3 Hz, J_{ab} = 0.6 Hz; H_b), 3.47 (1H, dd, J_{bd} = 8.3 Hz, J_{cd} = 3.4 Hz; H_d)	170.59, 161.15, 160.68, 160.53, 144.68, 142.44, 141.65, 136.66, 52.50, 52.19, 51.94, 51.62, 49.92, 41.67, 35.75, 35.57
7c (120–121 °C)	6.88 (1H, d, J_{ab} = 0.9 Hz; H_a), 3.77 (3H, s; COOMe), 3.76 (3H, s; COOMe), 3.74 (3H, s; COOMe), 3.73 (1H, dd, J_{bd} = 8.2 Hz, J_{ab} = 0.9 Hz; H_b), 3.72 (1H, d, J_{cd} = 5.6 Hz; H_c), 3.70 (3H, s; COOMe), 3.64 (3H, s; COOMe), 3.61 (1H, d; J_{ef} = 2.4 Hz; H_e), 3.51 (3H, s; COOMe), 3.48 (1H, d, J_{fe} = 2.4 Hz; H_f), 3.14 (1H, dd, J_{bd} = 8.2 Hz, J_{cd} = 5.6 Hz; H_d)	170.66, 169.68, 168.78, 160.60, 160.45, 160.43, 148.93, 143.19, 142.51, 140.14, 60.32, 57.49, 53.28, 52.38, 52.11, 52.08, 51.82, 51.69, 51.58, 46.92, 45.86, 45.07, 41.74, 39.82
8c (132–133 °C)	6.88 (1H, d, J_{ab} = 1 Hz; H_a), 3.79 (3H, s; COOMe) 3.77 (1H, d, J_{cd} = 5.6 Hz; H_c), 3.76 (3H, s; COOMe), 3.72 (3H, s; COOMe), 3.71 (3H, s; COOMe), 3.70–3.68 (1H, ddd, J_{bd} = 8.4 Hz, J_{ab} = 1 Hz, J_{bc} = 0.5 Hz; H_b), 3.65 (3H, s; COOMe), 3.58 (1H, d, J_{gh} = 2.4 Hz; H_g), 3.56 (3H, s; COOMe), 3.55 (3H, s; COOMe), 3.51 (1H, d, J_{hg} = 2.4 Hz; H_h), 3.48 (3H, s; COOMe), 3.25 (1H, d, J_{ef} = 3.6 Hz; H_e), 3.18 (1H, dd, J_{bd} = 8.4 Hz, J_{cd} = 5.6 Hz; H_d), 3.15 (1H, d, J_{fe} = 3.6 Hz, H_f)	170.68, 169.09, 168.38, 168.17, 167.90, 160,62, 160.57, 160.24, 147.81, 143.53, 142.35, 139.97, 58.10, 56.58, 55.74, 54.92, 54.21, 52.40, 52.19, 52.13, 51.74, 51.36, 51.26, 51.13, 50.73, 50.28, 47.47, 47.05, 45.91, 43.38, 42.11

the basis of expected chemical shifts and decoupling data. The stereochemistry of the oligomers **6c**–**8c** was determined by detailed and complimentary NOE experiments (Scheme 2). These assignments were further confirmed by the analysis of NOESY spectra.

The regio- and stereochemistry of the ladderanes **6c**–**8c** are in agreement with the results of the calculations carried out for **5b**–**8b**. For example, the regio- and stereochemistry of **6c** follows from the coefficients and the energies of the HOMO and LUMO of **5c** and potential secondary orbital interactions during the dimerization. Similarly, the regiochemistry of **7c** is dictated by the LUMO of **6c**, which is

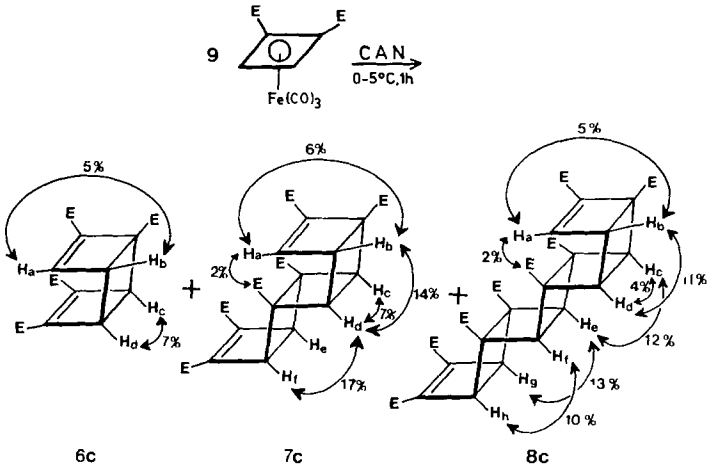

Scheme 2. E = COOMe.

localized on the more substituted double bond. The stereochemistry of **7c**, in the absence of any secondary orbital interaction, is determined by steric interactions. The formation of **8c** follows the same pattern.

Structures **7c** and **8c** have five and seven linearly fused cyclobutane rings, respectively, as well as many ester groups positioned on one face. This "polarofacial" disposition should confer special properties on these compounds and make them interesting as spacers and new materials. We are actively pursuing these aims, particularly the synthesis of even higher ladderanes.

Received: June 29, 1992 [Z 5437 IE]
German version: *Angew. Chem.* **1992**, *104*, 1557.

CAS Registry numbers:
5c, 1120-53-2; **6c**, 143859-21-6; **7c**, 143859-22-7; **8c**, 143859-23-8.

[1] M. A. Miller, J. M. Schulman, *J. Mol. Struct.* **1988**, *163*, 133.
[2] Related literature for systems with the bicyclo[2.2.0]hexane ([2]-ladderane) as spacers: M. N. Paddon-Row, *Acc. Chem. Res.* **1982**, *15*, 245; H. Overing, M. N. Paddon-Row, M. Heppener, A. M. Oliver, E. Cotsaris, J. W. Verhoeven, N. S. Hush, *J. Am. Chem. Soc.* **1987**, *109*, 3258; D. C. Craig, J. M. Lawson, A. M. Oliver, M. N. Paddon-Row, *J. Chem. Soc. Perkin Trans. 1* **1990**, 3305; R. N. Warrener, P. Groundwater, I. G. Pitt, D. N. Butler, R. A. Russell, *Tetrahedron Lett.* **1991**, *32*, 1885.
[3] E. Osawa, J. M. Rudzinski, D. A. Barbiric, E. D. Jemmis in *Strain and its Implications in Organic Chemistry*, (Eds.: A. de Meijere, S. Blechert), NATO-ASI Series, Kluwer, London, **1989**, p. 259.
[4] G. Dinsburg, *Nouv. J. Chim.* **1982**, *6*, 175.
[5] A. Nickon, E. F. Silversmith, *Organic Chemistry: The Name Game*, Pergamon Press, New York, **1987**, p. 87. A stepwise approach to an [11]-ladderane en route to **3** and **4**, conceptualized by A. Eschenmoser, is mentioned in this book.
[6] H. D. Martin, M. Hekman, *Angew. Chem.* **1973**, *85*, 615. *Angew. Chem. Int. Ed. Engl.* **1973**, *12*, 572; J. Meinwald, J. Mioduski, *Tetrahedron Lett.* **1974**, 3839; H. D. Martin, M. Hekman, *ibid.* **1978**, 1183; H. D. Martin, B. Mayer, M. Putter, H. Hochstetter, *Angew. Chem.* **1981**, *90*, 695; *Angew. Chem. Int. Ed. Engl.* **1981**, *20*, 677. For an annulated derivative, see G. Mehta, M. B. Viswanath, M. Nethaji, K. Venkatesan, *J. Chem. Soc. Chem. Commun.* **1992**, 82.
[7] T. Bally, S. Masamune, *Tetrahedron* **1980**, *36*, 343; G. Maier, K. Euler, H. Irngartinger, M. Nixdorf, *Chem. Ber.* **1985**, *118*, 409; I. G. Pitt, R. A. Russell, R. N. Warrener, *Syn. Commun.* **1986**, *16*, 1627; G. Maier, *Angew. Chem.* **1988**, *100*, 317; *Angew. Chem. Int. Ed. Engl.* **1988**, *27*, 309.
[8] M. J. S. Dewar, E. G. Zoebisch, E. F. Healy, J. J. P. Stewart, *J. Am. Chem. Soc.* **1985**, *107*, 3902.
[9] I. Fleming, *Frontier Orbitals and Organic Chemical Reactions*, Wiley, New York, **1976**.
[10] G. Berens, F. Kaplan, R. Rimerman, B. W. Roberts, A. Wissner, *J. Am. Chem. Soc.* **1975**, *97*, 7076.

Ether-Soluble Ti^0 and Bis(η^6-arene)titanium(0) Complexes from the Reduction of $TiCl_4$ with Triethylhydroborate**

By *Helmut Bönnemann** and *Barbara Korall*

The reduction of transition metal salts with alkali metal triethylhydroborates in THF yields finely divided, noncrystalline metal powders.[1] We have found that the analogous reaction of titanium or zirconium halides leads surprisingly to ether-soluble metal species.

Within 2 hours $TiCl_4 \cdot 2\,THF$ and $TiCl_3 \cdot 3\,THF$ reacted in THF with $K[BEt_3H]$ with evolution of H_2 to give brown-black solutions from which roughly 90% of the precipitated KCl could be removed by filtration. Solvent and BEt_3 (identified by ^{11}B NMR spectroscopy) were removed under vacuum (10 Pa) leaving a black residue which was extracted with THF. This THF solution was treated with pentane to give a brown-black precipitate, which according to elemental analysis was composed of 23.7% C, 4.4% H, 7.9% O, 0.3% B, 8.5% Cl, 8.8% K, and 46.7% Ti; after thorough drying under vacuum this solid was pyrophoric. The K and Cl components were identified as KCl by X-ray diffraction measurements. The material contained almost no boron. It dissolved in THF and ether but was insoluble in pentane and in arene solvents. Complete dissolution in THF provided a 0.5 M solution which could be concentrated without formation of a precipitate to approximately 2.5 M by distilling off THF.

During the reduction only about one mol of H_2 was released per mol of titanium. The hydrogen which is not accounted for, approximately one mol, should be found bound to titanium. To test this hypothesis we conducted the reduction with $K[BEt_3D]$. During the reaction, 48% of the amount of D_2 theoretically anticipated was released. In the protonolysis of the reaction mixture with 2 N HCl a mixture of HD and H_2 formed [Eq.(a)]. Following Equation (a) the D/Ti ratio in "TiD_m" was determined to be $m = 2$ from the amount of HD produced from material with a known titanium content.

$$\text{"}TiD_m\text{"} + nH^+ \longrightarrow m\,HD\uparrow + (n-m)/2\,H_2\uparrow + Ti^{3+} \qquad \text{(a)}$$

After workup and drying, the product had a D/Ti ratio of only $m = 0.3$. Thus, compound **1** is found in solution, but it loses hydrogen under vacuum. Our results are best summarized in Scheme 1.

$$TiCl_4 \cdot 2\,THF + 4\,K[BEt_3H] \xrightarrow[2\,h,\,40\,^\circ C]{THF} \underset{\mathbf{1}}{(TiH_m \cdot x\,THF)_{soluble}} + 4\,BEt_3 + 4\,KCl\downarrow + (2-m/2)\,H_2\uparrow$$

$$\text{vacuum} \;\Big|\; \begin{array}{l} -\,BEt_3 \\ -\,THF \\ -\,H_2 \end{array} \Big\downarrow$$

$$\underset{\mathbf{2}}{Ti \cdot 0.5\,THF}$$

Scheme 1. The course of the reduction of $TiCl_4$ with $K[BEt_3H]$ in THF.

[*] Prof. Dr. H. Bönnemann, Dr. B. Korall
Max-Planck-Institut für Kohlenforschung
Postfach 101353, D-W-4330 Mülheim an der Ruhr (FRG)

[**] We thank Dr. K. Seevogel for recording the IR spectra on a Nicolet FT-IR spectrometer 7199 and interpreting them, Dr. G. Block (Krupp Industrietechnik GmbH, Essen) for X-ray diffractograms, Prof. Dr. R. Courths (Universität-Gesamthochschule Duisburg) for XPS spectra with ESCALAB Mark II, and Prof. Dr. P. Kleinschmit (Degussa AG, ZN Wolfgang) for the gift of the metal sponges.

The protonolysis of **2** with 2N HCl provided 1.5–2 mol of H_2 per mol of titanium. Theoretically, 1.5 mol H_2 are expected for Ti^0. This shows that in **2** Ti^0 has various amounts of residual hydrogen.

According to the IR spectrum of **2** intact THF is coordinated to the metal center. Neither the IR nor ^1H NMR spectra give evidence of Ti-bound hydrogen. Likewise, there is no spectroscopic proof of a cleavage of THF by Ti^0. In the X-ray diffractogram of **2** besides the reflections of the KCl impurity only a diffuse, small peak at $2\theta = 30°$ is seen, the position of which matches that of the peak of amorphous titanium. The accompanying lattice distance, approximately 0.3 nm, corresponds to that in metal. In the XPS spectrum of **2** (Fig. 1d) the Ti 2p peak is found 2.3 eV higher in energy than in the spectrum of TiO_2 (Fig. 1a). Although metallic titanium as finely divided as **2** was not available for control experiments, it can be deduced from the XPS spectra (Fig. 1) that titanium in **2** is almost as reduced as titanium metal. The

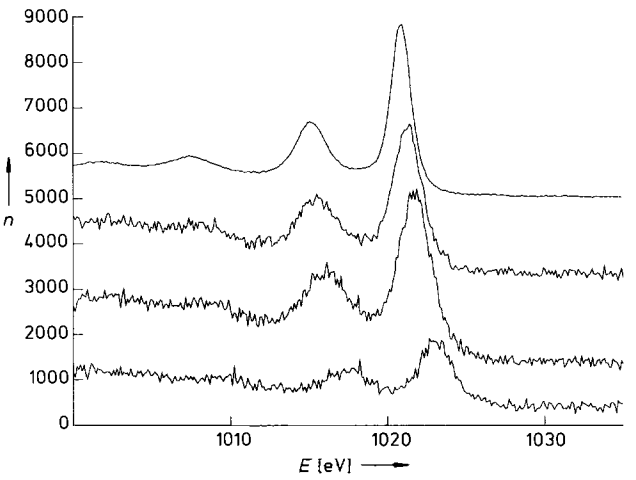

Fig. 1. XPS spectra (double peak $Ti\,2p_{1/2}$ and $Ti\,2p_{3/2}$) of a) TiO_2,b) TiO_2 from **2**, c) a sample of **2** with an oxidized surface, d) Ti·0.5THF **2**. n = Number of recorded pulses.

lack of the typical broad peak between 990 and 1010 eV for **2** indicates the absence of TiO_2 (no oxidation of the sample during the measurement). As a comparison for the measured values, the curves from TiO_2 produced from **2** (Fig. 1b) and from an oxidized sample (Fig. 1c) are also displayed.

Two titanium–hydrogen compounds are known. α-TiH_x ($x < 0.46$) can be described as elemental titanium with incorporated hydrogen, whereas β-TiH_y (ca. $1 < y < 2$)[2] has a CaF_2-type structure. The radial distribution function of an initial EXAFS analysis fitted with the experimentally determined titanium phase function (of titanium metal) shows three shells of titanium for **2** with the Ti–Ti distances listed in Table 1. A hexagonal structure type similar to that of α-titanium can be deduced from these values. The lattice is somewhat expanded,[4] possibly by the included hydrogen.

The characterization of **2** up to this point supports its description as colloidal titanium stabilized by complexed THF and containing included residual hydrogen. The determination of the particle size by transmission electron microscopy has not been conducted.

The analogous reduction of $ZrCl_4$ with $K[BEt_3H]$ in THF also provided a product soluble in THF; its composition was determined to be 34.1% C, 8.0% H, 11.4% O, 3.7% B,

Table 1. Comparison of the Ti–Ti distances in **2**, α-Ti and β-$TiH_{1.971}$.

Shell	**2**	α-Ti (a = 2.952, c = 4.689 Å [3])	β-$TiH_{1.971}$ (a = 4.440 Å [3])
1	2.96 Å	2.90 Å, 2.95 Å } 2.925 Å 2.95 Å	3.14 Å
2	4.21 Å	4.14 Å	4.44 Å
3	5.68 Å	5.85 Å	5.44 Å

5.2% Cl, 17.9% K, and 19.4% Zr. The purification and closer characterization are not yet complete.

When the reduction of $TiCl_4$ with $K[BEt_3H]$ was conducted in arene solvents (benzene, toluene, *p*-xylene, and mesitylene) instead of THF, the corresponding bis(η^6-arene)titanium complexes were obtained under standard conditions in up to 20% yield.[5] Previously these compounds could be prepared only by the metal-atom vapor technique.[6] The two-step synthesis of the bis(η^6-arene)titanium complexes by reaction of **2** with the appropriate arene did not succeed.

Complex **2** and the bis(η^6-arene)titanium complexes may find application as dopants for noble metal hydrogenation catalysts; this should increase the catalytic activity and the lifetime considerably.[5, 7] Complex **2** and the analogous zirconium compound catalyze the hydrogenation of titanium and zirconium sponges as well as of a hydride battery alloy.

Experimental Procedure

Synthesis of **2**: To a stirred solution of $TiCl_4 \cdot 2THF$ (6.68 g, 20 mmol) in THF (250 mL) at 40 °C was added 70 mL of a 1.15 M solution of $K[BEt_3H]$ (80 mmol) in THF over 2 h. Approximately 20 mmol of H_2 were released during the reaction. After the addition was complete, the reaction mixture was stirred another 30 min at 40 °C. The precipitated KCl was removed by filtration with a D4 frit. BEt_3 (^{11}B NMR (THF, 300 K): $\delta = 76.73$) and THF were removed from the brown filtrate under vacuum (10 Pa), and the residue extracted with THF (100 mL). Insoluble material was removed by filtration, and the filtrate was concentrated under vacuum to a volume of roughly 20 mL. The brown-black precipitate formed by addition of pentane to this solution was filtered and dried under vacuum for 16 h. Yield: 1.68 g (82%) **2**, 5.24 g (88%) KCl. – IR: $\tilde{\nu}[cm^{-1}]$ = 867 s, 915 vw, 1035 s, 1340 br, 1455 w; ^1H NMR ([D_8]THF, 300 K, TMS): $\delta = 1.77$ (m, 2H), 3.61 (m, 2H); MS: m/z 72 ($C_4H_8O^+$); X-ray diffraction: KCl, titanium portion is amorphous (small diffuse peak at $2\theta \approx 30°$); DSC: exothermic reaction at 73 and 147 °C; protonolysis of **2** with 2N HCl provides a H/Ti ratio of 1.7:1.

Reduction of $ZrCl_4$: Procedure analogous to that described for **2**; yield of Zr-containing product: 31.93 g (81%),

Synthesis of the bis(η^6-arene)titanium complexes:

a)Bis(η^6-benzene)titanium: To a solution of $TiCl_4$ (2.2 mL, 20 mL) in benzene (50 mL) in an ultrasonic bath at room temperature was added 160 mL of a 0.5 M solution of $K[BEt_3H]$ (80 mmol) in benzene over 1 h. After the addition was complete the reaction mixture was left in the ultrasonic bath another 1 h. A black precipitate was filtered away from the clear, red solution with a D4 frit and then washed with benzene (3 × 50 mL). The filtrate and the washes were combined and concentrated to dryness. The residue was taken up in pentane, and insoluble material was removed from the red solution by filtering through a D4 frit. The pentane was removed under vacuum, and the residue was recrystallized from pentane. Bis(η^6-benzene)titanium was obtained as deep red, shiny plates. Yield: 0.449 g (11%). ^1H NMR ([D_6]benzene, 300 K, TMS): $\delta = 4.92$ (s, 6H, CH) (according to ref.[8]: δ (in [D_6]benzene) = 5.04); IR (KBr): $\tilde{\nu}[cm^{-1}]$ = 673 vs, 694 vs, 943 s, 973 s, 1406 w, 1478 w (according to ref.[8]: $\tilde{\nu}[cm^{-1}]$ = 946 s, 979 s).

b) Bis(η^6-toluene)titanium: Procedure analogous to that described in a); toluene was used as the solvent. Yield: 1.014 g (22%), satisfactory C,H,Ti analysis. ^1H NMR ([D_6]benzene, 300 K, TMS): $\delta = 2.13$ (s, 3H, CH_3), 5.01 (m, 5H, CH) (according to ref.[8]: δ (in [D_{12}]$SiMe_4$) = 2.15, 4.89); MS m/z 232 [$(H_{16}C_{14})^{48}Ti^+$, 52%], 140 [$(H_8C_7{}^{48}Ti^+$, 100], 138 [$(H_6C_7{}^{48}Ti^+$, 35], 116 [$(H_{16}C_{14})^{48}Ti^{2+}$, 6], 70 [$(H_8C_7)^{48}Ti^{2+}$, 4], 48 [$^{48}Ti^+$, 13).

c) Bis(η^6-*p*-xylene)titanium: Procedure analogous to that described in a); *p*-xylene was used as the solvent, reaction mixture treated for 4 h in the ultrasonic bath. Yield: 0.462 g, (9%). ^1H NMR ([D_6]benzene, 300 K, TMS): $\delta = 1.96$ (s, 6H, CH_3), 4.84 (s, 4H, CH); MS: m/z 260 [$(H_{20}C_{16})^{48}Ti^+$, 100%], 154

$[(H_{10}C_8)^{48}Ti^+$, 85], 152 $[(H_8C_8)^{48}Ti^+$, 41], 130 $[(H_{20}C_{16})^{48}Ti^{2+}$, 14], 77 $[(H_{10}C_8)^{48}Ti^{2+}$, 9], 48 $[^{48}Ti^{2+}$, 5].

d) Bis(η^6-mesitylene)titanium: Procedure analogous to that described in a); mesitylene was used as the solvent, reaction mixture treated for 16 h in the ultrasonic bath. Yield: < 5%. ^{1}H NMR ([D$_6$]benzene, 300 K, TMS): δ = 1.99 (s, 9H, CH_3), 4.74 (s, 3H, CH); (according to ref.[8]; δ (in [D_{12}]$SiMe_4$) = 1.96, 4.69); MS: *m/z* 288 $[(H_{24}C_{18})^{48}Ti^+$, 100%], 168 $[(H_{12}C_9)^{48}Ti^+$, 42], 166 $[(H_{10}C_9)^{48}Ti^+$, 38], 144$[(H_{24}C_{18})^{48}Ti^{2+}$, 21], 48$[^{48}Ti^+$, 4].

Received: June 27, 1992
Revised: July 28, 1992 [Z 5436 IE]
German version: *Angew. Chem.* **1992**, *104*, 1506

CAS Registry numbers:
2, 143746-11-6; TiH*m*, 11140-68-4; TiD*m*, 53095-13-9; ZrH*m*, 11105-16-1; $[(C_6H_6)_2Ti]$, 52462-43-8; $[(C_6H_5Me)_2Ti]$, 55527-82-7; $[(C_6H_4Me_2)_2Ti]$, 143746-12-7; $[(C_6H_3Me_3)_2Ti]$, 57347-27-0; $TiCl_4 \cdot 2THF$, 31011-57-1; $ZrCl_4$, 10026-11-6; C_6H_6, 71-43-2; C_6H_5Me, 108-88-3; $C_6H_4Me_2$, 106-42-3; $C_6H_3Me_3$, 108-67-8; $K[BEt_3H]$, 22560-21-0; $K[BEt_3D]$, 143773-88-0.

[1] H. Bönnemann, W. Brijoux, T. Joußen, *Angew. Chem.* **1990**, *102*, 324–326; *Angew. Chem. Int. Ed. Engl.* **1990**, *29*, 273–275.
[2] A. Chrétien, W. Freundlich, M. Bichara, *C. R. Hebd. Seances Acad. Sci.* **1954**, *238*, 1423.
[3] S. S. Sidhu, L. Heaton, D. D. Zauberis, *Acta Crystallogr.* **1956**, *9*, 607.
[4] Dr. L. Aleandri, Max-Planck-Institut für Kohlenforschung, Mülheim an der Ruhr, **1991**. The X-ray absorption spectrum was recorded on the Ti K-edge (77 K) with an EXAFS 3 spectrometer in DCI (French Synchrotron Facility in Lure) with monochromatic X-ray radiation.
[5] H. Bönnemann, W. Brijoux, R. Brinkmann, E. Dinjus, R. Fretzen, T. Joußen, B. Korall, *J. Mol. Catal.*, **1992**, *74*, 323–333.
[6] F. Benfield, M. L. H. Green, J. S. Ogden, D. Young, *J. Chem. Soc. Chem. Commun.* **1973**, 866–867; P. N. Hawker, E. P. Kündig, P. L. Timms, *ibid.* **1978**, 730–731. See also D. W. Blackburn, D. Britton, J. E. Ellis, *Angew. Chem.* **1992**, *104*, 1520; *Angew. Chem. Int. Ed. Engl.* **1992**, *31*, 1495.
[7] H. Bönnemann, W. Brijoux, R. Brinkmann, E. Dinjus, T. Joußen, B. Korall, *Angew. Chem.* **1991**, *103*, 1344–1346; *Angew. Chem. Int. Ed. Engl.* **1991**, *30*, 1312–1314.
[8] M. T. Anthony, M. L. H. Green, D. Young, *J. Chem. Soc. Dalton Trans.* **1975**, 1419–1422.

High-Yield Synthesis of Lipid Systems with Giant Rings**

By *Fredric M. Menger,* Stephen Brocchini,* and *Xiangyang Chen*

Phospholipids, a major constituent of biological membranes, possess two alkyl chains each made up of 14–18 carbon atoms (see e.g. **I**). Since the chains are connected only at the ester ends, they have a certain amount of freedom within the membrane bilayer to bend, reorient, and interdigitate.[1] We wondered how membrane behavior (e.g. thermotropic properties,[2] permeability,[3] etc.) would be affected when the two distal ends are joined as in **II**, thereby restricting independent motion. Answering this simple but intriguing question required the synthesis of "giant rings" up to 72 atoms in size.[4] Any synthesis chosen to construct the macrocyclic lipids[5] had to proceed in high yields if we were to secure sufficient amounts for subsequent physical/chemical studies.[2, 3] And the route had to be flexible enough to give, in addition to the looped diesters, the diether analogues (interesting molecules because of their similarity to lipids of archaebacterial thermophiles).[6] Our answer to the synthetic challenge is described in the ensuing text.

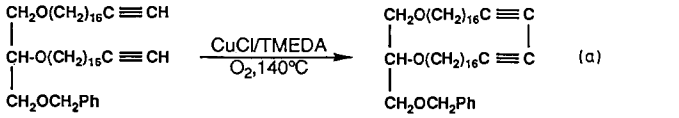

(a)

Our method is based on Glaser oxidation of dialkynyl compounds [Eq. (a)]. When the reaction was carried out by slow addition of the dialkynyl compound (syringe pump, 4–5 h), and at higher than usual temperatures (140 °C), yields were consistently and reproducibly high (Table 1). The procedure seems preferable to those used in the only two previously reported syntheses of cyclic lipids.[5]

Table 1. Yields for high-temperature Glaser cyclization of seven giant-ring lipids [a].

Lipid type	Ring size	Yield [%]
Diester	32	52
Diester	36	64
Diester	40	60, 68
Diether	32	78, 79
Diether	36	83
Diether	40	77, 78, 85
Diether	44	71

[a] Reactions were conducted with 0.9 to 2.8 g diyne as described in the text. Yields refer to the amounts of material after purification by column chromatography.

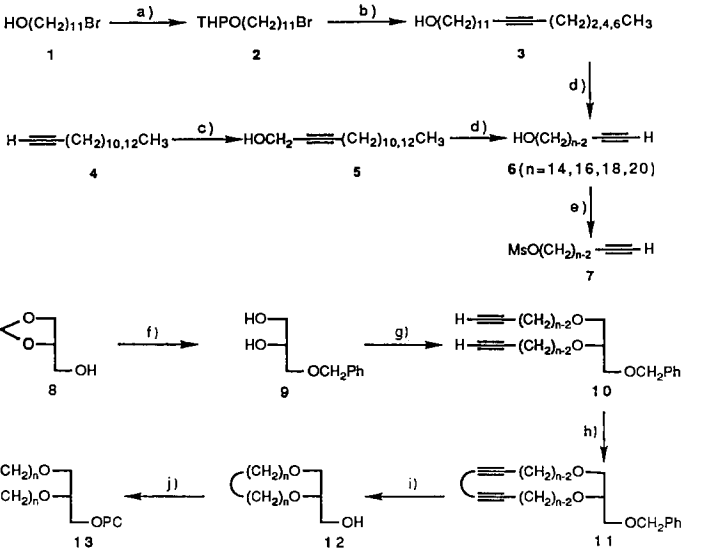

Scheme 1. a) Dihydropyran (DHP), *p*-TsOH, 90%; b) 1. 1-alkyne, *n*BuLi, hexamethylphosphoric triamide (HMPA); 2. MeOH, *p*-TsOH, pH = 3–4, 75%; c) 1. *n*BuLi, HMPA; 2. $(CH_2O)_n$, 84%; d) 1. Li, $H_2N(CH_2)_3NH_2$; *t*BuOK, (from **3**), 44% (from **5**), 70%; e) MesCl, Et_3N, 90%; f) 1. $PhCH_2Cl$, dimethylsulfoxide (DMSO), powdered KOH; 2. 10% HOAc, 90 °C, 66%; g) powdered KOH, DMSO, **7**, 76%; h) O_2, CuCl, TMEDA, 140 °C, 71–85%; i) H_2, 10% Pd/C, 60–74%; j) 1. 2-chloro-2-oxo-1,3,2-dioxaphospholane, Et_3N, benzene, 2 h; 2. Me_3N, MeCN, 60–65 °C, 48 h, 35–66%.

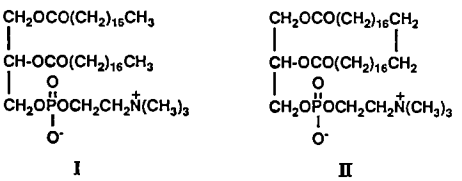

[*] Prof. Dr. F. M. Menger, S. Brocchini, X. Chen
Department of Chemistry, Emory University
Atlanta, GA 30322 (USA)

[**] The authors gratefully acknowledge the support of the Dow Chemical Co. and the National Institutes of Health.

A total synthesis of the cyclic ether lipids, incorporating our high-temperature Glaser cyclization as its key step, is given in Scheme 1. The corresponding cyclic diester phospholipids were prepared by first esterifying (*R*)-3-benzyloxy-1,2-propanediol with two equivalents of an ω-alkynyl fatty acid and then proceeding as outlined for **10** → **13** in Scheme 1.

Reaction (b) exemplifies the surprising ease with which giant rings are constructed under the modified Glaser condi-

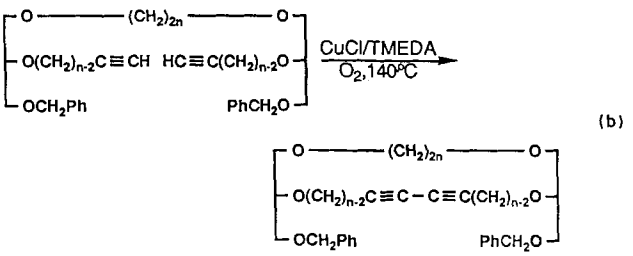

tions described here. Thus, chromatographically pure macrocycles of 64 atoms ($n = 14$) and 72 atoms ($n = 16$) were formed in 66 and 54% yield, respectively. Reaction (b) provides an entry into new "double" phospholipids.

It is unclear why giant-ring formation is so efficient, especially since the chains are devoid of substituents that often aid ring closures leading to macrocycles. Perhaps van der Waals attractions promote side-by-side alignment of the chains, although this would favor both intramolecular closures and the competing intermolecular reactions.

Differential scanning calorimetry studies[7] show that the cyclic ester lipids have higher transition temperatures than their acyclic counterparts. For example, transition temperatures of 41.7, 55.6, and 66.5 °C have been recorded for the acyclic series with 16, 18, and 20 carbon atoms per chain, respectively. Linking the chain ends raises these values to 50.4, 70.1, and 82.6 °C, respectively. Clearly, cyclization produces a substantial barrier to chain-melting.

Experimental Procedure

In a typical cyclization reaction 0.37 g of copper(I) chloride and 0.60 mL of tetramethylethylenediamine were added to 200 mL of reagent-grade xylenes in a 500 mL, three-necked flask fitted with a reflux condenser. Oxygen was bubbled through the mixture with a glass pipet while heating at 140 °C with an oil bath. A solution of 1.02 g of the diyne in 40 mL of xylenes was added over 4 h with a syringe pump. The reaction mixture was cooled and concentrated to dryness. The residue was dissolved in 300 mL of ethyl acetate and washed with 100 mL of water and 5% HCl. The organic layer was dried over Na_2SO_4 and the solvent removed to give the crude product. The material was purified by chromatography (60 Å silica gel, 200–425 mesh) eluting with ethyl acetate/hexane (1:6) to obtain 0.78 g (77%) of product (pure by NMR spectroscopy). Hydrogenation of the giant ring and cleavage of the benzyl group gave an alcohol with the correct elemental analysis and ^1H NMR, ^{13}C NMR, and FAB mass spectra.

Received: July 10, 1992
Revised: August 17, 1992 [Z 5457 IE]
German version: *Angew. Chem.* **1992**, *104*, 1542

CAS Registry numbers:
1, 1611-56-9; **2**, 52056-69-6; **3**, (n = 2), 144002-31-3; **3**, (n = 4), 21721-01-7; **3**, (n = 6), 144002-32-4; **4**, (n = 10), 26186-02-7; **4**, (n = 12), 765-13-9; **5**, (n = 10), 51309-22-9; **5**, (n = 12), 2833-99-0; **6**, (n = 14), 18202-12-5; **6**, (n = 16), 62914-53-8; **6**, (n = 18), 87640-08-2; **6**, (n = 20), 144017-86-7; **7**, (n = 14), 144002-33-5; **7**, (n = 16), 144002-34-6; **7**, (n = 18), 144002-35-7; **7**, (n = 20), 144002-36-8; **8**, 22323-82-6; **9**, 56522-80-8; **10**, (n = 14), 144002-37-9; **10**, (n = 16), 144002-38-0; **10**, (n = 18), 144002-39-1; **10**, (n = 20), 144002-40-4; **11**, (n = 14), 144002-41-5; **11**, (n = 16), 144002-42-6; **11**, (n = 18), 144002-43-7; **11**, (n = 20), 144002-44-8; **12**, (n = 14), 144002-45-9; **12**, (n = 16), 144002-46-0; **12**, (n = 18), 144002-47-1; **12**, (n = 20), 144002-48-2; **13**, (n = 14), 144002-49-3; **13**, (n = 16), 144002-50-6; **13**, (n = 18), 144002-51-7; **13**, (n = 20), 144002-52-8; 1-pentyne, 627-19-0; 1-heptyne, 628-71-7; 1-nonyne, 3452-09-3; 13-butadecynoic acid, 82909-47-5; 15-hexadecynoic acid, 99208-90-9; 17-octadecynoic acid, 34450-18-5; diester lipid (n = 13), 144002-53-9; diester lipid (n = 15), 113960-54-6; diester lipid (n = 17), 144002-54-0.

[1] M. Edidin, *Annu. Rev. Biophys. Bioeng.* **1974**, *3*, 179; N. O. Petersen, S. I. Chan, *Biochemistry* **1977**, 16, 2657.
[2] F. M. Menger, M. G. Wood, Jr., Q. Z. Zhou, H. P. Hopkins, J. Fumero, *J. Am. Chem. Soc.* **1988**, *110*, 6804.
[3] F. M. Menger, D. S. Davis, R. A. Persichetti, J-J. Lee, *J. Am. Chem. Soc.* **1990**, *112*, 2451.
[4] *Macrocycles* are commonly regarded as molecules with rings containing twelve or more atoms. Since most synthetic work on macrocycles has focused on rings with less than twenty atoms, we refer to **II** as a "giant ring". For useful methods of synthesizing macrocycles, see ref. [9] in S. F. Martin, M. Yamashita, *J. Am. Chem. Soc.* **1991**, *113*, 5478; M. Hesse, *Ring Enlargement in Organic Chemistry*, VCH, Weinheim, **1991** and ref. [1–3] in D. L. Boger, R. J. Mathvink, *J. Am. Chem. Soc.* **1990**, *112*, 4008; *Macrocycles* (Eds.: E. Weber, F. Vögtle), Springer, Berlin, **1992**.
[5] An analogue of **II** with a 36-membered ring was synthesized in only 8% yield by a macrolactonization. See K. Yamauchi, I. Yamamoto, M. Kinoshita, *J. Chem Soc. Chem. Commun.* **1988**, 445. An analogue of **II** with a 32-membered ring was synthesized in 50–60% yield by a Glaser coupling with 10 equivalents of $Cu(OAc)_2 \cdot H_2O$ in refluxing pyridine. N. Hébert, A. Beck, R. B. Lennox, G. Just, *J. Org. Chem.* **1992**, *57*, 1777. In our hands, this procedure gave substantial amounts of starting material and hydrolysis product.
[6] K. Yamauchi, Y. Sakamoto, A. Moriya, K. Yamada, T. Hosokawa, T. Higuchi, M. Kinoshita, *J. Am. Chem. Soc.* **1990**, *112*, 3188.
[7] The calorimetry work was carried out by Prof. Harry Hopkins, Georgia State University. A joint report on the data is planned.

Arborols Based on Luminescent and Redox-Active Transition Metal Complexes**

By *Scolastica Serroni, Gianfranco Denti,* Sebastiano Campagna,* Alberto Juris, Mauro Ciano,* and *Vincenzo Balzani**

The development of strategies for synthesizing supramolecular species ("nanostructures") with specific functions is one of the most important challenges now facing chemistry.[1] "Cascade molecules"[2–4] (also called arborols or dendrimers) are of great interest in this regard. We have designed a strategy to obtain arborols, based on transition metal complexes, which exhibit interesting photophysical and electrochemical properties. In this paper we illustrate our synthetic strategy and report the properties of a luminescent and redox-active arborol which contains 22 metal centers.

[*] Prof. Dr. G. Denti, Dr. S. Serroni
Laboratorio di Chimica Inorganica
Istituto di Chimica Agraria dell'Università
I-56124 Pisa (Italy)
Dr. S. Campagna
Dipartimento di Chimica Inorganica e Struttura Molecolare
dell'Università
I-98166 Messina (Italy)
Prof. Dr. V. Balzani, Prof. Dr. A. Juris, Dr. M. Ciano
Dipartimento di Chimica dell'Università
and Istituto FRAE-CNR
I-40126 Bologna (Italy)

[**] This work was supported by the Ministero della Università e della Ricerca Scientifica e Tecnologica and by the Consiglio Nazionale delle Ricerche (Progetto Finalizzato Chimica Fine II and Research Grant 91.03355-CT03). We wish to thank V. Cacciari for technical assistance.

The arborols described here are polynuclear metal complexes with Ru^{II} as the metal ion, 2,3-bis(2-pyridyl)pyrazine (2,3-dpp) as the bridging ligand, and 2,2'-bipyridine (bpy) as the terminal ligand (Fig. 1). Extension to other metal ions (e.g., Os^{II}), bridging ligands (e.g., 2,5-dpp), and terminal ligands (e.g., 2,2'-biquinoline) is straightforward.[5]

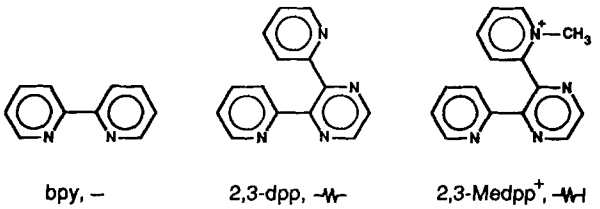

Fig. 1. Formulas, abbreviations, and graphic symbols for the ligands.

The synthetic method, illustrated in Scheme 1 (for the symbols see Fig. 1), is based on a protection/deprotection procedure in which a complex is used as a ligand and another is used as a metal ("complexes-as-ligands/complexes-as-metals" synthetic strategy).[5, 6] The first step is the construction of a core, $[Ru(2,3\text{-}dpp)_3]^{2+}$ (**1**), which contains three open sites for chelation (complex as ligand). At each of these sites, a bifurcate branch can be grafted (Scheme 1, top) by using the novel $[Ru(2,3\text{-}Medpp)_2Cl_2]^{2+}$ (**2**) building block (for 2,3-$Medpp^+$ see Fig. 1). The dication **2** contains two easily replaceable Cl^- ligands (and therefore the complex can play the role of a metal) and two bridging ligands in which the chelating sites not used for metal coordination have been protected by methylation. The reaction of **1** with **2** leads to the novel tetranuclear metal complex **3** (first generation of our arborols). Deprotection of the six peripheral chelating sites of **3** (Scheme 1, middle) yields compound **4**, to which six units of the building block **2** can again be grafted, to yield a second-generation compound (**5**, Scheme 1, bottom). In principle, the above procedure can be iterated to obtain larger species by a divergent synthetic approach. If the bridging ligands of the building block **2** are replaced by simple chelating ligands like bpy, the species obtained are "sterile" since they can no longer be used as "cores" for larger structures.

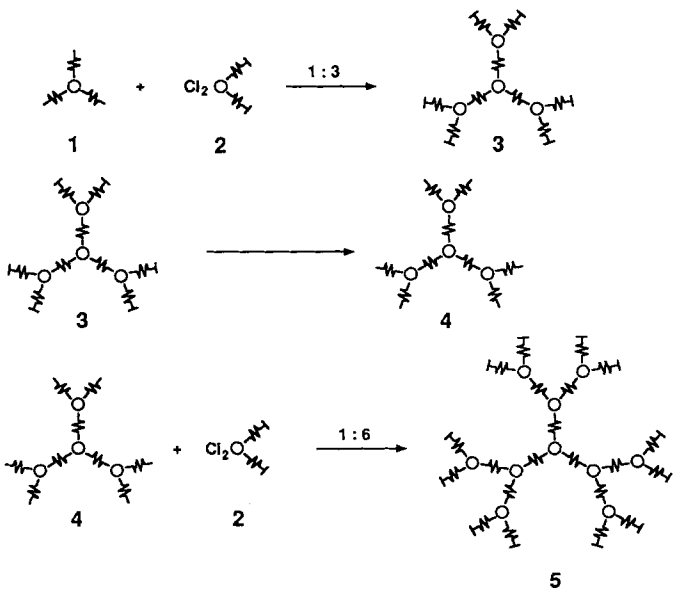

Scheme 1. The circles represent ruthenium atoms. The other symbols are explained in Figure 1.

To explore the feasibility of the synthetic strategy illustrated in Scheme 1, we prepared the docosanuclear[7] metal complex **6** (Scheme 2) which, to our knowledge, is the largest Werner-type transition metal complex obtained so far.

The dication **1** was prepared as previously described.[5a, 8] The treatment of 2,3-$Medpp^+$[9] with $RuCl_3 \cdot 3H_2O$ in water/ethanol 1:2 (v/v) containing a sevenfold excess of LiCl afforded **2** (yield 90% after purification by size exclusion chromatography (SEC)). Reaction of **2** with **1** (3:1 molar ratio; water/ethanol 1:2; pretreatment with $AgNO_3$) gave **3** in 70% yield after purification. Demethylation of the chelating sites of **3** (dry CH_3CN, large excess of diazabicyclo[2.2.2]octane (DABCO), reflux) gave rise to **4** (yield 60% after purification). The novel compounds **2**–**4** were characterized by elemental analysis (as PF_6^- salts), by NMR, IR, UV/VIS, and luminescence spectra, and by their conductivities and electrochemical behavior.[10] Reaction of **4** with the trinuclear building block $[Ru\{(\mu\text{-}2,3\text{-}dpp)Ru(bpy)_2\}_2Cl_2]^{4+}$ (**7**)[9] gave **6** in 73% yield after purification (Scheme 2).[13, 14]

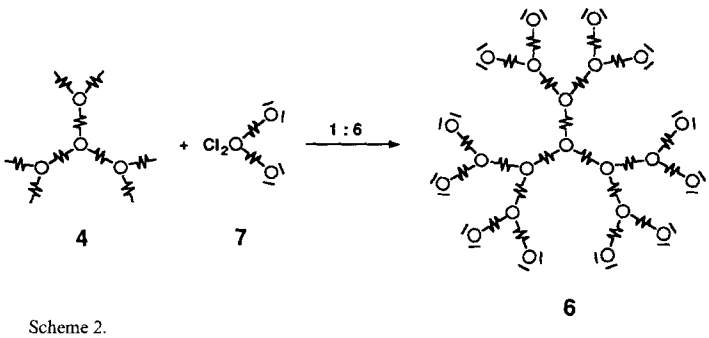

Scheme 2.

If the PF_6^- counterions are neglected, **6** is made of 1090 atoms, has a relative molecular mass of 10890, and an estimated size of about 5 nm. Its absorption spectrum extends across the UV/VIS spectral region (ε = 681500 $M^{-1}cm^{-1}$ at 284 nm and ε = 202400 $M^{-1}cm^{-1}$ at 542 nm). It exhibits a luminescence band with a maximum at 784 nm in acetonitrile solution at room temperature and at 730 nm in methanol/ethanol 4:1 (v/v) at 77 K (rigid matrix), as expected for peripheral $[Ru(bpy)_2(\mu\text{-}2,3\text{-}dpp)]^{2+}$ units.[5, 11e, f] Upon electrochemical oxidation, a peak corresponding to twelve electrons is observed at 1.52 V vs. saturated calomel electrode (SCE) (ΔE_p = 220 mV), as expected for oxidation of twelve equivalent and weakly interacting peripheral units.[5b, 17]

In conclusion, we have designed a general synthetic strategy to obtain luminescent and redox-active arborols from building blocks made of transition metal complexes. By choosing building blocks of different composition (e.g., $[Cl_2Os(2,3\text{-}Medpp)_2]^{2+}$ or $[Cl_2Ru(2,5\text{-}Medpp)_2]^{2+}$ in the place of **2**), it will be possible to obtain arborols made of concentric shells each chemically different,[5b] that is, to create species with a high information content which could be used for the design of photochemical molecular devices[18] (e.g., for light harvesting in solar energy conversion systems[19]).

Received: July 1, 1992 [Z 5443 IE]
German version: *Angew. Chem.* **1992**, *104*, 1540

[1] a) J.-M. Lehn, *Angew. Chem.* **1988**, *100*, 91; *Angew. Chem. Int. Ed. Engl.* **1988**, *27*, 89; b) *Molecular Electronic Devices* (Eds.: F. L. Carter, R. E. Siatkowski, H. Woltjen), North Holland, Amsterdam, **1988**; c) J.-M. Lehn, *Angew. Chem.* **1990**, *102*, 1347; *Angew. Chem. Int. Ed. Engl.* **1990**, *29*, 1304; d) G. M. Whitesides, J. P. Mathias, C. T. Seto, *Sience* **1991**, *254*, 1312.

[2] E. Buchlein, W. Wehner, F. Vögtle, *Synthesis* **1978**, 155; see also H.-B. Mekelburger, W. Jaworek, F. Vögtle, *Angew. Chem.* **1992**, *104*, No. 12; *Angew. Chem. Int. Ed. Engl.* **1992**, *31*, No. 12 (Highlight).

[3] For recent papers see, a) T. Nagasaki, M. Ukon, S. Arimori, S. Shinkai, *J. Chem. Soc. Chem. Commun.* **1992**, 608; b) G. R. Newkome, C. N. Moorefield, G. R. Baker, M. J. Saunders, S. H. Grossman, *Angew. Chem.* **1991**, *103*, 1207; *Angew. Chem. Int. Ed. Engl.* **1991**, *30*, 1178; c) C. J. Hawker, R. Lee, J. M. J. Fréchet *J. Am. Chem. Soc.* **1991**, *113*, 4583; d) K. R. Gopidas, A. R. Leheny, G. Caminati, N. J. Turro, D. A. Tomalia, *ibid.* **1991**, *113*, 7335; e) K. Shahlai, H. Hart, *ibid.* **1990**, *112*, 3687.

[4] For a comprehensive review, see D. A. Tomalia, A. M. Naylor, W. G. Goddard III; *Angew. Chem.* **1990**, *102*, 119; *Angew. Chem. Int. Ed. Engl.* **1990**, *29*, 138.

[5] a) S. Campagna, G. Denti, L. Sabatino, S. Serroni, M. Ciano, V. Balzani, *J. Chem. Soc. Chem. Commun.* **1989**, 1500; b) G. Denti, S. Campagna, S. Serroni, M. Ciano, V. Balzani, *J. Am. Chem. Soc.* **1992**, *114*, 2944; c) G. Denti, S. Serroni, S. Campagna, V. Ricevuto, A. Juris, M. Ciano, V. Balzani, *Inorg. Chim. Acta* **1992**, *198–200*, 507.

[6] G. Denti, S. Serroni, S. Campagna, A. Juris, M. Ciano, V. Balzani in *Perspectives in Coordination Chemistry* (Eds.: A. F. Williams, C. Floriani, A. E. Merbach), Helvetica Chimica Acta Verlag and VCH, Basel and Weinheim, p. 153.

[7] That is, a species containing 22 metal ions; see P. B. Block, W. H. Powell, W. C. Fernelius, *Inorganic Chemical Nomenclature*, American Chemical Society, Washington, DC, **1990**.

[8] K. J. Brewer, W. R. Murphy, Jr., S. R. Spurlin, J. D. Petersen, *Inorg. Chem.* **1986**, *25*, 882.

[9] S. Serroni, G. Denti, *Inorg. Chem.*, in press.

[10] NMR: ^{1}H NMR spectrum of **2** and **3** in [D$_3$]acetonitrile solution showed several signals between $\delta = 4.20$ and 4.47 that can be attributed to *N*-methyl groups of different stereoisomers. These signals completely disappear on demethylation and are, in fact, absent in **4**. Conductivity values (Ω^{-1}cm^{-1}mol^{-1}; 1.0×10^{-3} M solutions in acetonitrile, 20 °C): **2**, 364.0; **3**, 874.7; **4**, 472.3. IR [5, 9, 11]: the most characteristic bands are those of bridged (system of four bands between 1470 and 1390 cm^{-1}), unbridged (990 cm^{-1}), and *N*-methylated (1626 cm^{-1}) 2,3-dpp ligands. UV/VIS spectra (acetonitrile solutions) [5, 11]: ligand-centered 2,3-dpp bands: λ_{max} [nm] (ε, [M^{-1}cm^{-1}]): **2**, 304 (25100); **3**, 296 (137000); **4**, 264 (108000); metal-to-ligand charge transfer bands: λ_{max} [nm] (ε, [M^{-1}cm^{-1}]): **2**, 575 (8490); **3**, 456 (42600); **4**, 461 (38200). Luminescence at 298 K (in acetonitrile solution) [5]: λ_{max} [nm]: **3**, 714; **4**, 722; at 77 K (methanol/ethanol 4:1 (v/v) rigid matrix) [5]: λ_{max} [nm]: **3**, 700; **4**, 698. Compound **2** is not emissive. Electrochemical oxidation (potentials [V] vs. SCE; number of electrons involved; ΔE_p [mV] [12]: **2**: +0.63, 1, 70, **3**: +1.70, 3, 110; electrochemical analysis of **4** was prevented by adsorption of the compound at the electrodes.

[11] a) Y. Fuchs, S. Lofters, T. Dieter, W. Shi, R. Morgan, T. C. Strekas, H. D. Gafney, A. D. Baker, *J. Am. Chem. Soc.* **1987**, *109*, 269; b) W. R. Murphy, Jr., K. J. Brewer, G. Gettliffe, J. D. Petersen, *Inorg. Chem.* **1989**, *28*, 81; c) K. Kalyanasundaram, M. K. Nazeeruddin, *ibid.* **1990**, *29*, 1888; d) T. S. Akasheh, I. Jibril, A. M. Shraim, *Inorg. Chim. Acta.* **1990**, *175*, 171; e) G. Denti, S. Campagna, L. Sabatino, S. Serroni, M. Ciano, V. Balzani, *Inorg. Chem.* **1990**, *29*, 4750; f) S. Campagna, G. Denti, S. Serroni, M. Ciano, V. Balzani, *ibid.* **1991**, *30*, 3728.

[12] Acetonitrile was used as solvent and tetrabutylammonium tetrafluoroborate as supporting electrolyte. Cyclic voltammograms were usually obtained at a scan rate of 20 mV s^{-1}. Differential-pulse voltammetry was performed with a scan rate of 20 mV s^{-1}, a pulse height of 50 mV, and a duration of 50 ms. Ferrocene (5×10^{-4} M) was employed as a reference. The multielectron nature of some peaks was elucidated as in ref. [5b].

[13] [Ru{(μ-2,3-dpp)Ru(bpy)$_2$}$_2$Cl$_2$](PF$_6$)$_4$ (**7**) (0.084 g, 0.042 mmol) in water/ethanol 1:1 (v/v) (5 mL) was treated with silver nitrate (0.014 g, 0.084 mmol). After the mixture had been stirred at room temperature for 2 h, a solution of [Ru{(μ-2,3-dpp)Ru(2,3-dpp)$_2$}$_3$](PF$_6$)$_8$ (**4**) (0.025 g, 0.007 mmol) in ethylene glycol (3 mL) was added. The reaction mixture was refluxed for seven days, then cooled to room temperature. AgCl was separated by repeated centrifugations, the mother liquor concentrated by evaporation in vacuum, and an excess of solid NH_4PF_6, methanol (2 mL), and diethyl ether (10 mL) were added. The crude product was filtered off and then purified by SEC on Sephadex G-75 (acetonitrile eluant). The eluate was concentrated in a rotary evaporator to 2 mL, and the product **6** was recovered as a cyclamen (very dark reddish purple) powder by addition of diethyl ether (about 15 mL). Yield: 0.086 g (73%) after purification. Anal.: Calcd. including 25 H_2O: C 36.2, H 2.6, N 10.0. Found: C 35.9, H 2.3, N 10.4. Conductivity [Ω^{-1}cm^{-1}mol^{-1}] (1.0×10^{-3} M solution in acetonitrile, 20 °C): 2297.4. IR: system of four bands between 1470 and 1390 cm^{-1}, typical of bridged 2,3-dpp. No typical band for unbridged 2,3-dpp at 990 cm^{-1} is present.

[14] In principle, the complexes **1**–**7** can exist as different isomers, depending on the arrangement of the ligands around the metal ions. A careful analysis of the 2D-COSY 400 MHz ^{1}H NMR spectrum of the [Ru(2,3-dpp)$_3$]$^{2+}$ precursor that permitted a complete assignment of the signals [15], has shown that the purified material was obtained as a mixture of the *mer* and *fac* isomers in which the *mer* isomer was predominant (92%). The oligometallic complexes can also be a mixture of several diastereoisomeric species, since each metal center is also a stereogenic center. For these reasons structural investigations on these systems are difficult [11e]. Differences arising from the presence of isomeric species are not expected to be large in the electrochemical and spectroscopic results described in this paper [16].

[15] G. Predieri, C. Vignali, G. Denti, S. Serroni, unpublished.

[16] R. Hage, A. H. J. Dijkhnis, J. G. Haasnoot, R. Prins, J. Reedijk, B. E. Buchanan, J. G. Vos, *Inorg. Chem.* **1988**, *27*, 2185.

[17] J. B. Flanagan, S. Margel, A. J. Bard, F. C. Anson, *J. Am. Chem. Soc.* **1978**, *100*, 4248.

[18] V. Balzani, F. Scandola, *Supramolecular Photochemistry*, Ellis Horwood, Chichester, England, **1991**, Chapter 12.

[19] a) R. Amadelli, R. Argazzi, C. A. Bignozzi, F. Scandola, *J. Am. Chem. Soc.* **1990**, *112*, 7099; b) B. O'Regan, M. Grätzel, *Nature* **1991**, *353*, 737.

A New Approach to Bis(arene)titanium(0) and -titanium(−1) Complexes; Structure of Bis(arene)titanates(1−)

By *David W. Blackburn, Doyle Britton,* and *John E. Ellis**

Dedicated to Professor Wolfgang Beck on the occasion of his 60th birthday

Until very recently[1] bis(arene)titanium complexes were prepared only by metal atom–ligand cocondensations that employed either titanium[2–7] or potassium[8,9] atoms as key reagents. These procedures required the use of specialized equipment[10] unavailable to most chemists. We now report the syntheses of compounds of this class that do not utilize metal atoms or metal-atom reactors and also describe the first structural characterizations of bis(arene)titanate monoanions, of which only two examples were previously known.[11] Our method involves the reduction of $TiCl_4 \cdot 2\,THF$ by arene anions and requires only conventional laboratory apparatus and procedures.

Although there is a rich tradition in employing arene anions, especially the naphthalene radical anion, in inorganic and organometallic syntheses,[12] surprisingly few reports on their designed use as reagents for the syntheses of bis(arene)metal complexes exist.[13,14] Indeed, to our knowledge, [Cr(biphenyl)$_2$]$^+$[15] and [Cr(tetralin)$_2$][16] are the only examples of such compounds to be isolated from the interaction of arene anions and transition metal reagents in syntheses not involving the use of metal atoms.[17]

Equations (a) and (b) summarize the syntheses of new Ti compounds, (see Experimental Procedure for further details).

[*] Prof. Dr. J. E. Ellis, D. W. Blackburn, Prof. Dr. D. Britton
Department of Chemistry, University of Minnesota
Minneapolis, Minnesota 55455 (USA)

[**] Highly Reduced Organometallics, Part 30. This work was supported by the U.S. National Science Foundation (NSF) and the Petroleum Research Fund administered by the American Chemical Society. D. W. B. thanks the NSF for a predoctoral fellowship. Part 29: J. E. Ellis, K.-M. Chi, A. J. DiMaio, S. R. Frerichs, J. R. Stenzel, A. L. Rheingold, B. S. Haggerty, *Angew. Chem.* **1991**, *103*, 196; *Angew. Chem. Int. Ed. Engl.* **1991**, *30*, 194.

$$TiCl_4 \cdot 2THF + 5K(arene) \xrightarrow[THF]{-78\,^\circ C} \underset{\mathbf{K[1]},\ \mathbf{K[2]}}{K[Ti(arene)_2]} + 3arene + 4KCl \quad (a)$$

$$K[Ti(arene)_2] + 1/2\,I_2 \xrightarrow[THF]{-78\,^\circ C} \underset{\mathbf{3,\ 4}}{[Ti(arene)_2]} + KI \quad (b)$$

1, **3**: arene = biphenyl **2**, **4**: arene = 4,4′-di-*tert*-butylbiphenyl

The deep purple, paramagnetic anions **1** and **2** were isolated as satisfactorily pure $[K([15]crown\text{-}5)_2]^+$ or [K([2.2.2]-cryptand)]$^+$ salts ([2.2.2]cryptand = 4,7,13,16,21,24,-hexaoxa-1,10-dazobicyclo[8.8.8]hexacosane) in 70–80% yields, while the deep green, diamagnetic metallocenes **3** and **4** were best obtained by an in situ oxidation of freshly prepared **1** and **2**, respectively, with I_2 in [Eq. (b)]. Potassium ion complexants were unnecessary in the latter syntheses, which provided 20–30% yields of satisfactorily pure **3** and **4**. These complexes are both thermally robust species as pure solids (decomp ca. 170 °C) and have NMR and mass spectra which are consistent with the assigned formulations (cf. Experimental Procedure). The purified complexes **3** and **4** do not appear to be contaminated by products of the type $[Ti_2(arene)_2]$ or $[Ti_2(arene)_3]$, analogous to known chromium complexes where arene is biphenyl.[18]

Anion **1** has been shown to undergo facile carbonylation at low temperature to provide, after workup, a 56% isolated yield [Eq. (c)] of the known [K([2.2.2]cryptand)]$_2$

$$2[K([2.2.2]cryptand)][\mathbf{1}] + CO(1\ atm) \xrightarrow[-70\,^\circ C,\ 12\,h]{THF} [K([2.2.2]cryptand)]_2[Ti(CO)_6] + \ldots \quad (c)$$

$[Ti(CO)_6]$.[19] This is the first reaction to be reported for a bis(arene)titanate(1−) and suggests that similar complexes are involved in the original, "phosphane-free" alkali metal naphthalenide route to $[Ti(CO)_6]^{2-}$.[19] It is anticipated that these and related labile bis(arene)titanium species will have a rich chemistry.

Single-crystal X-ray studies on **1** and **2** as [K([2.2.2]-cryptand)]$^+$ salts were carried out to confirm their existence in the solid state and thereby provide the first structural characterization of bis(arene)metalates(1−) of the Group 4 elements.[20] Figure 1 depicts the unit cell of [K([2.2.2]cryptand)][**1**] showing two independent bis(biphenyl)-titanate(1−) ions, **1A** and **1B**, which are essentially *anti* and *syn* rotamers, respectively. Both **1A** and **1B** are situated at a center of symmetry in the unit cell. In **1A** the Ti atom lies on the inversion center as the ion is completely ordered. The center in **1B** is between two half-occupied Ti positions.[21] The disorder of the Ti atoms is paralleled by a real but not obvious disorder in the phenyl rings since each phenyl ring depicted is the superposition of equal numbers of bound and free rings. Since the positions of the carbon atoms in the latter are averaged, large uncertainties are present in the interatomic distances for **1B**: average Ti–C distance is 2.2(2) and the average C–C distance in the ring 1.40(2) Å. However, the corresponding values for **1A** are more precise and informative: the average distances are Ti–C 2.27(2), C–C in the bound ring 1.42(1), C–C in the free ring 1.39(1), Ti–ring plane 1.78(2) Å. The dihedral angle between the bound and free ring is 31°. The bound rings in **1A** are eclipsed, parallel

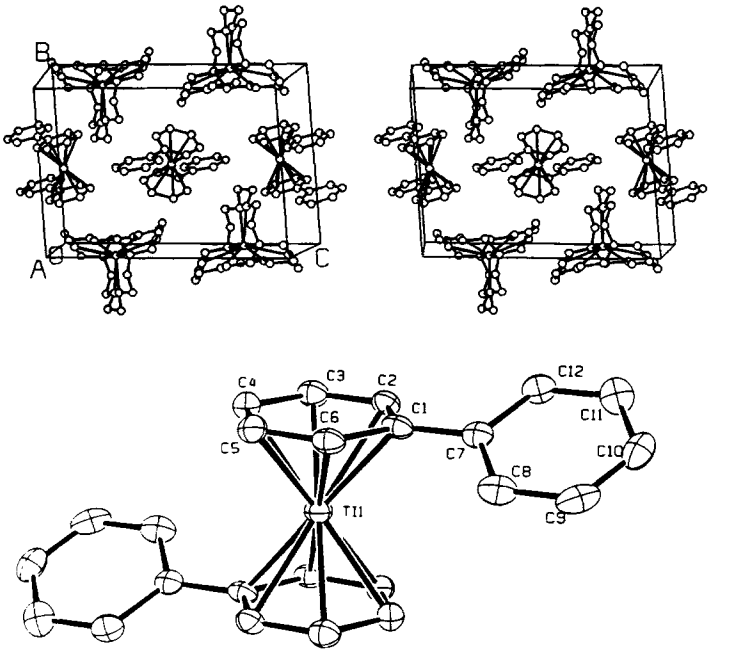

Fig. 1. Top: Stereoview of the unit cell of [K([2.2.2]cryptand)][**1**] showing independent anions **1A** and **1B** and cations. Note that the *syn* rotamer, **1B**, lies on a center of symmetry, and the titanium has half occupancy at each site. For clarity one of the two titanium positions in **1B** has been omitted. Each ring in **1B** is an average of one bound and free phenyl group, and therefore the carbon positions are averaged. Bottom: View of **1A**. Important bond lengths [Å]: Ti-C1 2.290(4), Ti-C2 2.284(4), Ti-C3 2.277(5), Ti-C4 2.271(5), Ti-C5 2.265(4), Ti-C6 2.256(5), C1-C2 1.416(6), C1-C6 1.442(6), C2-C3 1.418(6), C3-C4 1.414(6), C4-C5 1.412(7), C5-C6, 1.421(7), C1-C7 1.472(6), C7-C8 1.394(7), C7-C12 1.402(6), C8-C9 1.386(7), C9-C10 1.386(7), C10-C11 1.371(7), C11-C12 1.387(7).

to each other, and planar. Corresponding data for **2** (Fig. 2) are quite similar to those for **1A**, that is, the average distances are Ti–C 2.29(4), C–C in the bound ring 1.42(2), C–C in the free ring 1.38(2), Ti–ring plane 1.79(1) Å; the bound rings are planar. However, unlike **1**, the bound rings are tilted (dihedral angle 7.6°), and their distance from each other is greatest (3.7 Å) near the *tert*-butyl groups. Also, as shown in a view of **2** approximately down the centroid–centroid vector of the bound rings (Fig. 2 bottom), the latter are substantially staggered, apparently to minimize interactions of the 4-*tert*-butylphenyl and 4′-*tert*-butylphenyl substituents on neighboring rings. In both salts the cations are well separated from the anions in the crystalline lattices, and the geometry of the [K([2.2.2]cryptand)]$^+$ units is essentially identical and in good agreement with the structure of the corresponding iodide salt.[22] Bis(benzene)titanium(0) and bis(toluene)titanium(0) are the only other bis(arene)titanium species for which structural data have been reported.[23] They both contain shorter Ti–ring plane (average 1.74 Å) and Ti–C distances (average 2.24 Å) than those in **1** and **2**. Bis(mesitylene)vanadate(1−) is apparently the only other anionic bis(arene)metal complex to have been structurally characterized.[24]

We are currently investigating whether arene anions are generally useful for the syntheses of bis(arene) complexes of other metals.

Experimental Procedure

All operations except the carbonylation step were conducted under an atmosphere of argon.

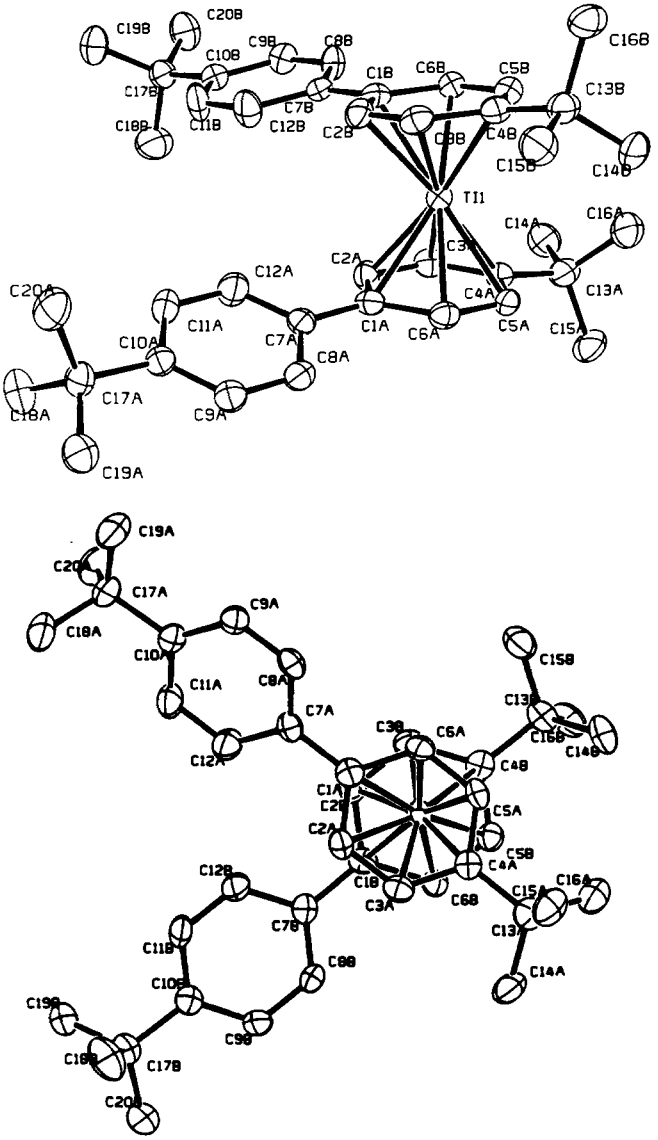

Fig. 2. Top: Molecular structure of **2**. Important bond lengths [Å]: Ti-C1A 2.299(6), Ti-C2A 2.254(5), Ti-C3A 2.267(6), Ti-C4A 2.318(5), Ti-C6A 2.283(6), Ti-C1B 2.286(6), Ti-C2B 2.250(6), Ti-C3B 2.284(6), Ti-C4B 2.334(6), Ti-C5B 2.298(6), Ti-C6B 2.273(6), C1A-C2A 1.426(8), C1A-C6A 1.434(8), C2A-C3A 1.416(8), C3A-C4A 1.419(8), C4A-C5A 1.423(8), C4A-C13A 1.539(8), C1A-C7A, 1.471(8), C7A-C8A 1.388(8), C7A-C12A 1.393(8), C8A-C9A 1.397(8), C9A-C10A 1.394(8), C10A-C11A 1.372(9), C11A-C12A 1.384(8), C10A-C17A 1.537(8). Bottom: View of **2** approximately down the centroid–centroid vector of the bound rings.

[K([15]crown-5)$_2$][**1**]: A cold (−78 °C) solution of $TiCl_4 \cdot 2THF$ (1.67 g, 5.00 mmol) in THF (175 mL) was added to a deep blue solution (−78 °C) of $K[C_{12}H_{10}]$ (25.2 mmol) in THF (200 mL). The reaction mixture changed to the deep purple color, characteristic of **1**, while the solution slowly warmed from −78 °C to room temperature over 15 h. It was then filtered into a solution of [15]crown-5 (2.2 g, 10 mmol) in THF (25 mL). After the mixture had been stirred for 2 h, the solvent was removed in vacuo. The resulting crude product was purified by crystallization from THF/heptane and washed thoroughly to remove unchanged biphenyl. In this manner 3.13 g (75% yield based on Ti) of purple-black microcrystalline solid was obtained (correct analysis for C, H, K, Ti). The corresponding $[K([2.2.2]cryptand)]^+$ salt was prepared and isolated by the same procedure in 81% yield. A saturated THF solution of the latter product was layered with excess diethyl ether/heptane (2:1 by volume). Long swordlike iridescent green crystals were slowly deposited from this solution over ten days at room temperature. One of these was selected for the X-ray study.

Reaction of [K([2.2.2]cryptand)][**1**] with CO: A cold solution (−70 °C) of [K([2.2.2]cryptand)] [**1**] (1.00 g, 1.30 mmol) in THF (250 mL) was stirred under CO at atmospheric pressure for 12 h while slowly warming to room temperature. A soluble carbonyl complex of unknown composition and an insoluble component were present. The latter was isolated and recrystallized from pyridine/THF; yield: 0.38 g (56%) of the previously described $[K([2.2.2]cryptand)]_2[Ti(CO)_6]$ [19].

[K([2.2.2]cryptand)][**2**] · THF: By analogous methods the reaction of $TiCl_4 \cdot 2THF$ (0.541 g, 1.62 mmol) with $K[4,4'\text{-}tBu_2C_{12}H_8]$ (9.80 mmol) in THF (300 mL) provided a deep purple solution which was filtered, the filtrate stirred with [2.2.2]cryptand (1.22 g, 3.24 mmol) for 3 h at room temperature, and the solvent removed in vacuo. The resulting crude black solid was crystallized from THF/pentane to provide 1.72 g (93% yield based on Ti) of purple-black microcrystalline product, which provided satisfactory elemental analyses (C,H). A cold saturated THF solution of this material was layered with excess heptane. After seven days at −30 °C square platelike crystals had formed, which were used in the X-ray study.

3: A solution of K[**1**] was prepared as described above from the reduction of $TiCl_4 \cdot 2THF$ (3.34 g, 10.0 mmol) by $K[C_{12}H_{10}]$ (51.4 mmol), and a solution of I_2 (1.27 g, 5.00 mmol) in THF (100 mL) was then added dropwise at −40 °C. Removal of solvent from the resultant green solution gave a crude product. This was crystallized from THF/pentane to provide 0.82 g (23% based on $TiCl_4 \cdot 2THF$) of deep green microcrystalline **3**, which gave satisfactory elemental analyses (C, H, Ti; m.p. 170 °C (decomp)). ^1H NMR (300 MHz, C_6D_6, 20 °C): $\delta = 4.9$ (m, 6H; bound ring CH); 5.38 (m, 4H; bound ring CH); 6.9–7.2 (br m, 10H; free ring). $^{13}C\{^1H\}$NMR (75 MHz, C_6D_6, 20 °C) $\delta = 83.0$, 83.6, 84.1 (bound ring C); 124.8, 125.5, 129.0 (free ring C), quaternary carbons not observed; high-resolution mass spectrum: calcd for $^{12}C_{24}\ ^1H_{20}\ ^{48}Ti$: 356.1044; found, 356.1060.

4: A solution of K[**2**] was prepared as described above from the reduction of $TiCl_4 \cdot 2THF$ (1.67 g, 5.00 mmol) by $K[4,4'\text{-}tBu_2C_{12}H_8]$ (25.2 mmol) in THF (400 mL) at −70 °C, and a solution of I_2 (0.63 g, 2.50 mmol) in THF (50 mL) added dropwise at room temperature. After 39 mL of the latter had been added, the purple color of K[**2**] was replaced by the dark green color of **4**, and the addition of I_2 was stopped. Removal of solvent from the reaction mixture gave a crude product, from which free 4,4'-di-*tert*-butylbiphenyl was removed by sublimation (75 °C, 10^{-5} Torr). Recrystallization of the residue from pentane provided 0.81 g (28% based on $TiCl_4 \cdot 2THF$) of greenish-black **4**; satisfactory elemental analyses (C, H, Ti; m.p. 175 °C (decomp)). ^1H NMR (300 MHz, C_6D_6, 20 °C) $\delta = 1.18$ (s, 18H; *t*Bu of free ring), 1.26 (s, 18H, *t*Bu of bound ring), 5.08, 5.44 (AA'BB', $J = 8$ Hz, 8H; protons on bound ring), 7.29, 7.52 (AA'BB', $J = 9$ Hz, 8H; protons on free ring) $^{13}C\{^1H\}$ NMR (75 MHz, C_6D_6, 20 °C) $\delta = 31.5$ ($C(CH_3)_3$ on free ring), 32.3 ($C(CH_3)_3$ on bound ring), 34.4 ($C(CH_3)_3$ on free ring), 34.9 ($C(CH_3)_3$ on bound ring), 83.5, 85.3 (*C*H groups of bound ring), 95.6 ($CC(CH_3)_3$ of bound ring), 117.0 (CC_5H_4tBu of bound ring), 124.2, 125.6 (*C*H groups of free ring), 139.1 ($CC(CH_3)_3$ of free ring), 148.1 (CC_5H_4tBu of free ring). Assignments of the ^1H and ^{13}C NMR signals of the uncoordinated ring in the complex were made on the basis that they closely matched those of the free arene ligand (same solvent, temperature, concentration). The remaining signals were then assigned to those of the coordinated ring. High-resolution mass spectrum: calcd for $^{12}C_{40}\ ^1H_{52}\ ^{48}Ti$: 580.3548; found, 580.3514.

Received: June 15, 1992 [Z 5404 IE]
German version: *Angew. Chem.* **1992**, *104*, 1520

[1] Recently several bis(arene)titanium(0) complexes have been prepared by the interaction of $TiCl_4$, $K[BEt_3H]$, and the appropriate arene with ultrasound: B. Korall, Doctoral Dissertation, Technische Hochschule Aachen, March **1992**. We thank a referee for bringing this work to our attention. See also the related communication in this issue: H. Bönnemann, B. Korall, *Angew. Chem.* **1992**, *104*, 1506; *Angew. Chem. Int. Ed. Engl.* **1992**, *31*, 1490.

[2] F. W. S. Benfield, M. L. H. Green, J. S. Ogden, D. Young, *J. Chem. Soc. Chem. Commun.* **1973**, 866.

[3] M. T. Anthony, M. L. H. Green, D. Young, *J. Chem. Soc. Dalton Trans.* **1975**, 1419.

[4] E. P. Kündig, P. L. Timms, *J. C. S. Chem. Commun.* **1977**, 912.

[5] P. D. Morand, C. G. Francis, *Inorg. Chem.* **1985**, *24*, 56.

[6] F. G. N. Cloke, M. F. Lappert, G. A. Lawless, A. C. Swain, *J. Chem. Soc. Chem. Commun.* **1987**, 1667.

[7] F. G. N. Cloke, K. A. E. Courtney, A. A. Sameh, A. C. Swain, *Polyhedron* **1989**, *8*, 1641.

[8] P. N. Hawker, E. P. Kündig, P. L. Timms, *J. Chem. Soc. Chem. Commun.* **1978**, 730.

[9] P. N. Hawker, P. L. Timms, *J. Chem. Soc. Dalton Trans.* **1983**, 1123.

[10] See M. P. Andrews *Using Metal Atoms and Molecular High-Temperature Species in New Materials Synthesis, Apparatus and Techniques*, in *Experimental Organometallic Chemistry: A Practicum in Synthesis and Characterization* (Eds. A. L. Wayda, M. Y. Darensbourg), (*ACS Symp. Ser.* **1987**, 357, Chapter 7.).

[11] J. A. Bandy, A. Berry, M. L. H. Green, R. N. Perutz, J.-N. Verpeaux, *J. Chem. Soc. Chem. Commun.* **1984**, 729.

[12] a) J. E. Ellis, *Polyhedron* **1989**, *8*, 1611, and references cited therein; see also: b) H. Shapiro, H. E. Podall *J. Inorg. Nucl. Chem.* **1962**, *24*, 925; c) R. Gompper, E. Bartmann, *Liebigs Ann. Chem.* **1979**, 229; d) V. S Leong, N. J. Cooper, *Organometallics* **1987**, *6*, 2000; e) M. N. Bochkarev, A. A.

Trifonov, E. A. Fedorova, N. S. Emelyanova, T. A. Basalgina, G. S. Kalinina, G. A. Razuvaev, *J. Organomet. Chem.* **1989**, *372*, 217; f) K. Jonas, G. Burkart, C. Häselhoff, P. Betz, C. Krüger, *Angew. Chem.* **1990**, *102*, 291; *Angew. Chem. Int. Ed. Engl.* **1990**, *29*, 322; g) J. A. Corella, R. L. Thompson, N. J. Cooper, *ibid.* **1992**, *104*, 55 and **1992**, *31*, 83.

[13] a) G. Henrici-Olivé, S. Olivé, *J. Am. Chem. Soc.* **1970**, *92*, 4831; b) C. G. Dewey, J. E. Ellis, K. L. Fjare, K. M. Pfahl, G. F. Warnock, *Organometallics* **1983**, *2*, 388.

[14] Cyclooctatetraene dianion and related $(4n+2)\pi$ electron systems are excluded from this discussion.

[15] K. Lühder, *Z. Chem.* **1969**, *9*, 31.

[16] C. Elschenbroich, R. Möckel, *Angew. Chem.* **1977**, *89*, 908; *Angew. Chem. Int. Ed. Engl.* **1977**, *16*, 870. See footnote [4] in this citation.

[17] Timms et al. [8, 9] suggested but did not confirm that arene radical anions were involved in their potassium atom vapor route to bis(arene)metal complexes.

[18] C. Elschenbroich, J. Heck, *J. Am. Chem. Soc.* **1979**, *101*, 6773.

[19] K. M. Chi, S. R. Frerichs, S. B. Philson, J. E. Ellis, *J. Am. Chem. Soc.* **1988**, *110*, 303.

[20] Crystal data for [K([2.2.2]cryptand)][**1**]: $C_{84}H_{112}N_4O_{12}K_2Ti_2$: triclinic, $P\bar{1}$ (no. 2), $a = 11.250(7)$, $b = 11.338(6)$, $c = 15.90(1)$ Å, $\alpha = 94.50(5)$, $\beta = 105.34(6)$, $\gamma = 95.02(5)°$, $V = 1937(5)$ Å^3, $Z = 1$, $\varrho_{calcd} = 1.323$ g cm^{-3}, $\mu(Mo_{K\alpha}) = 3.72$ cm^{-1}, Crystal dimensions: $0.60 \times 0.50 \times 0.15$ mm^3. The intensities of 7581 reflections were measured at -105 °C ($0 < \theta < 26°$) on an Enraf-Nonius CAD 4 diffractometer using $Mo_{K\alpha}$ radiation. The structure was solved by direct methods and all non-hydrogen atoms were refined anisotropically (full-matrix least squares). For 4806 unique observed reflections [$(I) \geq 2.0\,\sigma(I)$], $R = 0.061$ and $R_w = 0.082$. Crystal data for [K([2.2.2]cryptand)][**2**] · THF: $C_{62}H_{96}N_2O_7KTi$: monoclinic $P2_1/n$ (no. 14), $a = 11.829(9)$, $b = 21.40(1)$, $c = 23.77(1)$ Å, $\beta = 91.95(5)°$, $V = 6013(1)$ Å^3, $Z = 4$, $\varrho_{calcd.} = 1.180$ g cm^{-3}, $\mu(Mo_{K\alpha}) = 2.58$ cm^{-1}, crystal dimensions: $0.55 \times 0.55 \times 0.35$ mm^3. 9574 reflections were measured at -101 °C ($0 < \theta < 24°$) on an Enraf-Nonius CAD4 diffractometer using $Mo_{K\alpha}$ radiation. The structure was solved by direct methods and all non hydrogen atoms were refined anisotropically (full matrix least squares). For 5142 unique observed relections [$(I) \geq 2.20\,\sigma(I)$], $R = 0.057$ and $R_w = 0.067$. Further details of the crystal structure investigations are available on request from the Director of Cambridge Crystallographic Data Centre, University Chemical Laboratory, Lensfield Road, GB-Cambridge CB21EW (UK) on quoting the full journal citation.

[21] When first solved, the structure appeared to contain both $[Ti(biphenyl)_2]^-$ and the "dimeric" $[Ti_2(biphenyl)_2]^-$. However, the R value was poor (0.099) and the temperature factor for the titanium in the dimeric anion was about twice the size of the atoms to which it was connected. This, and the chemical evidence, suggested that the "dimer" was really another form of $[Ti(biphenyl)_2]^-$ in a disordered centric location. Refinement with Ti2 having half occupancy converged with $R = 0.061$ and with a reasonable temperature factor.

[22] B. Metz, D. Moras, R. Weiss, *Chem. Commun.* **1971**, 444.

[23] a) G. G. Tairova, E. F. Krashina, O. N. Krasochka, G. A. Kichigina, Y. A. Shvetsov, E. M. Lisetsky, L. O. Atovmyan, Y. G. Borodko, *Nouv. J. Chim.* **1981**, *5*, 603; b) G. G. Tairova, O. N. Krasochka, V. I. Ponomaryov, E. F. Krashina, Y. A. Shvetsov, E. M. Lisetsky, D. P. Kiryukhin, L. O. Atovmyan, Y. G. Borodko, *Transition Met. Chem. (Weinheim, Ger.)* **1982**, *7*, 189; c) X-ray characterization of bis(1,3,5-tri-*tert*-butylbenzene)titanium(0) has been noted, but no structural details have been reported to date [7].

[24] G. Fochi, D. Braga, P. Sabatino, *Organometallics*, **1988**, *7*, 565.

Molecular Switching by Electron Transfer—the Spiroperimidine/Quinonimine System**

By *Josef Salbeck, Vitaly N. Komissarov, Vladimir I. Minkin,* and *Jörg Daub**

Building blocks for molecular memory devices, sensors, and switches contain components with two or more metastable states. Dyes containing functional groups occupy a prominent position amongst them.[1, 2] According to previous studies, spiroperimidine (**1**) shows photochromic behavior; the forward reaction forming quinonimine (**2**) was photochemical ($\lambda_{max} = 615$ nm, in hexane) and the reverse reaction **2** → **1** thermal (Scheme 1).[3] We now report a reversible rearrangement **1**/**2** with electrochemical activation.

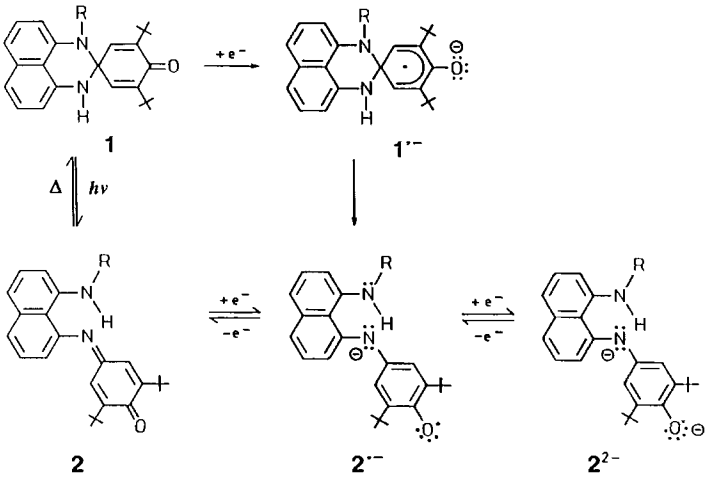

Scheme 1. R = CH_3.

The cyclic voltammogram of **1** (Fig. 1a) shows an irreversible reduction signal [$E_p^r = -2150$ mV vs. ferrocene (Fc)], two back-oxidation signals shifted to distinctly more positive potentials (E_p^{o1} and E_p^{o2}), and a pronounced crossing effect (arrow) of reduction and oxidation traces (trace crossing). Such a curve form is evidence for the stability and reactivity of the radical anions and can be attributed to a homogeneous disproportionation of the radical anion $\mathbf{1}^{\bullet-}$.[4]

We deduce from the thin-layer voltammogram (Fig. 1b) that two electrons are transferred on reduction, whereas the two oxidation steps are one-electron transfers. Furthermore, a multisweep experiment shows that from the second cycle a corresponding reduction signal is present for both oxidation steps, while the original reduction signal of the starting compound no longer appears: **1** is thus reduced to a dianion in a multistep process consisting of electrochemical and chemical substeps (ECE step sequence). Through the valence isomerization occurring at the radical anion stage, $\mathbf{1}^{\bullet-} \rightarrow \mathbf{2}^{\bullet-}$, the acceptor capability of the compound is raised so much that the redox potential for dianion formation of the quinoid form becomes more positive than E_p^r. For this reason only a single, but more intense wave is observed for the first reduction in the cyclic voltammetric experiment. After reversing the potential scan, two distinctly separated voltammetric signals appear, which correspond to the oxidation of $\mathbf{2}^{2-}$ via $\mathbf{2}^{\bullet-}$ to **2**. Since in the thin-layer voltammogram the compound **2** formed in the first cycle cannot diffuse away from the electrode into the solution and the thermal rearrangement of **2** to **1** is slow at room temperature, the subsequent cycles show only the reduction of **2** via $\mathbf{2}^{\bullet-}$ to $\mathbf{2}^{2-}$ and the corresponding back oxidation. The original signal for **1** is no longer observed. The overall process is summarized in Scheme 1.[5] The cycle **1** → $\mathbf{2}^{2-}$ → $\mathbf{2}^{\bullet-}$ → **2** induced by reduction/oxidation is also confirmed by UV/VIS/near IR spectroelectrochemistry. With this experimental technique the

[*] Prof. Dr. J. Daub, Dr. J. Salbeck
Institut für Organische Chemie der Universität
Universitätsstrasse 31, D-W-8400 Regensburg (FRG)
Prof. Dr. V. I. Minkin, Dr. V. N. Komissarov
Institute for Physical and Organic Chemistry of the University
Rostov on Don (Russia)

[**] This work was supported by the Bundesministerium für Forschung und Technologie and the Fonds der Chemischen Industrie.

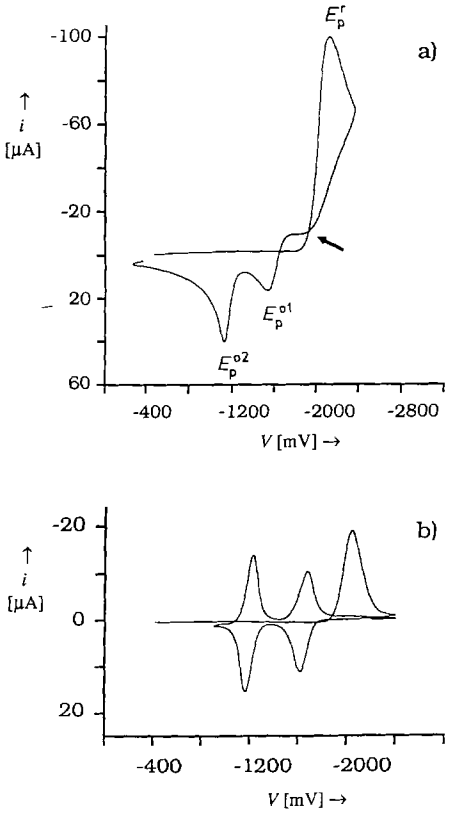

Fig. 1. Cyclic voltammetry (CV): a) semi-infinite conditions, reduction of **1** and back oxidation (in acetonitrile/nBu$_4$NPF$_6$ 0.1 M, $c = 2.5$ mM, $v = 250$ mVs^{-1}), b) thin-layer CV (double cycle), layer thickness $d = 15$ μm, $v = 25$ mVs^{-1}.

thermal back reaction of the electrochemically formed quinoid form to the spiro form (**2** → **1**) could also be detected, which proves the complete reversibility of the overall cycle. The absence of side reactions during the transformations is characterized by isosbestic points. Electrochemical and spectroscopic data of the individual species and intermediates are listed in Table 1.

Table 1. Reduction potentials $E_{1/2}$ and the position of the absorption bands λ [medium: acetonitrile/nBu$_4$NPF$_6$ (0.1 M)].

Compound	$E_{1/2}$ [mV] [a]	λ [nm]
1	−2150 [b]	229, 330, 340, 400
2	−1230	218, 304, 595
2$^{\bullet-}$	−1705	347, 525, 800
2^{2-}		209, 260 (s), 336, 415

[a] $E_{1/2}$ (vs. Fc). [b] Peak potential, irreversible.

The spectroelectrochemistry yields even more evidence for the mechanism (Scheme 2) of the electrochemically induced valence isomerization: derivative voltabsorptometry, in which the first derivative of the absorption signal is recorded at a particular wavelength during a potential sweep,[6] reveals that the reduction of **1** to **2**$^{2-}$ passes through the quinonimine radical anion **2**$^{\bullet-}$.

In Figure 2 the signal at 525 nm, the position of the most intense absorption of **2**$^{\bullet-}$, and the thin-layer voltammogram registered at the same time are depicted. In derivative

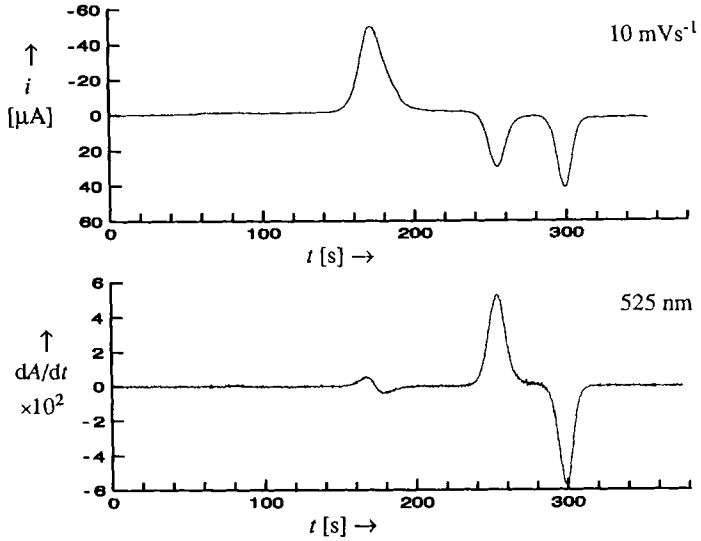

Fig. 2. Derivative voltabsorptometry during the reduction of **1** and the back oxidation of **2**$^{2-}$ to **2**. Top: Thin-layer CV in current/time (i/t) mode (in acetonitrile/nBu$_4$NPF$_6$ 0.1 M, $c = 2.5$ mM, $v = 10$ mVs^{-1}). Bottom: Simultaneously registered derivative voltabsorptogram at 525 nm.

voltammetry a positive peak corresponds to the formation, and a negative peak to the disappearance of the species absorbing at the particular wavelength. Thus a positive peak in the derivative voltabsorptogram occurs at 525 nm simultaneously with the reoxidation signal of **2**$^{2-}$ to **2**$^{\bullet-}$ in the cyclic voltammogram, whereas the further oxidation of **2**$^{\bullet-}$ to **2** is accompanied by a negative peak at this wavelength. During the reduction of the spiroperimidine compound **1** to quinonimine dianion **2**$^{2-}$ the interesting effect of a sinusoidal wave can be seen in the derivative voltabsorptogram; that is, in the course of this reduction a species that absorbs at 525 nm is formed as intermediate. The interpretation that this intermediate is the quinonimine radical anion **2**$^{\bullet-}$ is supported by the observation that at 800 nm, the position of the second absorption band of **2**$^{\bullet-}$, the same effect occurs.

The radical anion **1**$^{\bullet-}$ formed from **1** rapidly converts into **2**$^{\bullet-}$, which is immediately reduced further to **2**$^{2-}$ at the existing electrode potential. Moreover, **2**$^{2-}$ reacts further with **1** in a homogeneous redox reaction to form two molecules of **2**$^{\bullet-}$ that are in turn reduced at the electrode to **2**$^{2-}$ (Scheme 2). The redox cycle in the frame explains both the absorption of **2**$^{\bullet-}$ that appears as an intermediate and the

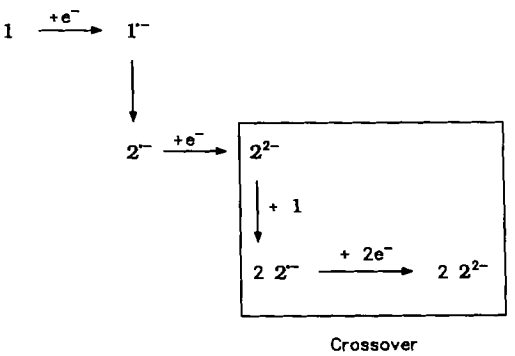

Scheme 2. Schematic representation of the intermediate steps in the formation of the quinonimine dianion **2**$^{2-}$.

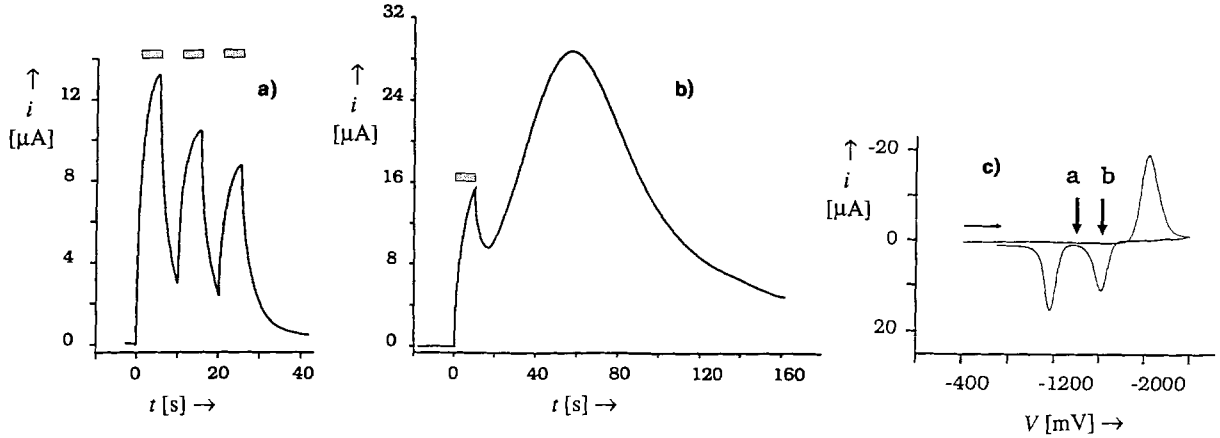

Fig. 3. Photomodulation amperometry: variation in the current signals on illumination with visible light (filter (Schott BG 14) indicated by a gray rectangle; medium acetonitrile/nBu$_4$NPF$_6$ 0.1 M, c = 2.5 mM). a) Working potential −1400 mV vs. Fc; b) working potential −1600 mV vs. Fc; c) record of the working potentials a and b.

trace crossing effect that is seen in the cyclic voltammogram under bulk conditions.

The amperometry "modulated by photochemistry" depicted in Figure 3 presents additional evidence for the proposed mechanism. By this method **2** is generated by irradiation from **1** (photochromism) in a spectroelectrochemical thin-layer cell under potentiostatic conditions. On applying a potential at which **2** is reduced to $\mathbf{2}^{\bullet-}$ (see Scheme 3 and Fig. 3c), a cathodic current is observed as signal, which decays again after extinguishing the light (Fig. 3a). The slow decrease in amplitude for the subsequent light pulses is explained by the decrease in concentration of **1** in the thin-layer cell.

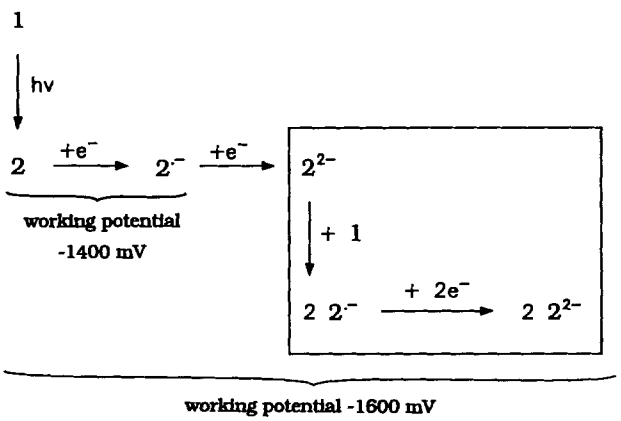

Scheme 3. Schematic representation of the course of the reaction in the photomodulation amperometry experiment.

If the working potential of the photomodulation amperometry is set at a value at which **2** is reduced to the dianion, the curve depicted in Figure 3b is obtained. A light pulse of 10 s, as in the previous experiment, causes a steep increase in the current, which, however, does not drop to zero on closing the shutter, but after an initial decrease, rises to a new maximum before again decreasing slowly. The photomodulation thus provides further support for the mechanism of Scheme 2, in which the cathodically generated dianion $\mathbf{2}^{2-}$ accelerates the reduction of **1**.

Whereas in the experiment in Figure 3a, only the first direct electrochemical reduction of the photochemically generated **2** to $\mathbf{2}^{\bullet-}$ is responsible for the current, in the second the reduction of the photochemically generated **2** proceeds to the dianion $\mathbf{2}^{2-}$ as well (Scheme 3). This is also observed in the greater height of the signal. In the dark the homogeneous cycle continues further: the $\mathbf{2}^{2-}$ formed reduces neutral **1** with the formation of two molecules of $\mathbf{2}^{\bullet-}$. The $\mathbf{2}^{\bullet-}$ formed in this step is reduced further to $\mathbf{2}^{2-}$ at the electrode until the entire content of **1** in the thin-layer cell has been transformed. This also confirms that the electrochemically induced valence isomerization of **1** takes place *at the radical anion stage*.

These studies show a) the properties of a multiswitchable spiroperimidine/quinonimine system, b) the application of combination methods of spectroscopy and electrochemistry for the mechanistic elucidation of this electron-transfer reaction, c) the detection of an electron-transfer catalysis by photomodulation amperometry, and d) the close relationship between the photoreaction driven by "inner electron excitation" and a reaction induced by intermolecular electron transfer.

Received: May 8, 1992 [Z 5330 IE]
German version: *Angew. Chem.* **1992**, *104*, 1498

CAS Registry numbers:
1, 120608-41-5; **2**, 12057-52-7.

[1] F. L. Carter, *Molecular Electronic Devices, Vol. 1* und *Vol. 2*, Dekker, New York, **1982** and **1987**.

[2] a) J. Daub, C. Fischer, S. Gierisch, J. Sixt, *Mol. Cryst. Liq. Cryst.* **1992**, *217*, 177; b) J. Daub, J. Salbeck, T. Knöchel, C. Fischer, H. Kunkely, K. M. Rapp, *Angew. Chem.* **1989**, *101*, 1541; *Angew. Chem. Int. Ed. Engl.* **1989**, *28*, 1494; c) J. Daub, C. Fischer, J. Salbeck, K. Ulrich, *Adv. Mater.* **1990**, *2*, 366; d) J. Daub, S. Gierisch, J. Salbeck, *Tetrahedron Lett.* **1990**, *31*, 3113; e) J. Achatz, C. Fischer, J. Salbeck, J. Daub, *J. Chem. Soc. Chem. Commun.* **1991**, 504.

[3] V. N. Komissarov, V. A. Kharlanow, L. Yu. Ukhin, V. I. Minkin, *Dokl. Acad. Nauk USSR* **1988**, *301*, 902 [*Chem. Abstr.* **1989**, *110*, 211855k].

[4] a) C. Amatore, J. Pinson, J. M. Savéant, *J. Electroanal. Chem.* **1980**, *107*, 59; b) K. Hinkelmann, J. Heinze, *Ber. Bunsenges. Phys. Chem.* **1987**, *91*, 243–249.

[5] For electrochemically induced valence isomerization, see: a) M. A. Fox, J. R. Hurst, *J. Am. Chem. Soc.* **1984**, *106*, 7626; b) L. L. Miller, R. F. Boyer, *ibid.* **1971**, *93*, 646; c) H. Kiesele, *Angew. Chem.* **1983**, *95*, 253; *Angew. Chem. Int. Ed. Engl.* **1983**, *21*, 254; d) J. R. Dodd, R. F. Winton, R. M. Pagni, C. R. Watson, J. Bloor, *J. Am. Chem. Soc.* **1974**, *96*, 7846; e) S. F. Nelsen, J. P. Gillespie, *J. Org. Chem.* **1973**, *38*, 3592; f) A. Böhm, K. Meerholz, J. Heinze, K. Müllen, *J. Am. Chem. Soc.* **1992**, *114*, 688.

[6] E. E. Bancroft, J. S. Sidwell, H. N. Blount, *Anal. Chem.* **1981**, *53*, 1390.

Trigonal-Monopyramidal M^{III} Complexes of the Type $[M(N_3N)]$ ($M = Ti, V, Cr, Mn, Fe$; $N_3N = [(t\mathrm{BuMe_2Si)\ddot{N}CH_2CH_2]_3N}$)**

By *Christopher C. Cummins, Jenny Lee, Richard R. Schrock,* and William D. Davis*

We wish to report the syntheses of a series of unusual monopyramidal complexes, $[M(N_3N)]$ (M = Ti, V, Cr, Mn, and Fe; $N_3N = [(t\mathrm{BuMe_2Si)\ddot{N}CH_2CH_2]_3N}$), in which the trigonal-monopyramidal (TMP) coordination geometry is enforced by the triamido ligand[1-4] and the empty axial coordination position is encircled by sterically demanding trialkylsilyl substituents. In this work the TMP geometry[5-7] is represented for the first time among early transition metal complexes. The object of this work is to synthesize inorganic or organometallic complexes with metals in relatively high oxidation states that contain unusual substrates, including complexes that contain dinitrogen or partially reduced dinitrogen ligands (N_2H_x).[8,9] A potentially important feature of the TMP geometry is the availability of three d orbitals (d_{xz}, d_{yz}, and d_{z^2}) for substrate binding, a circumstance that is analogous to that found in complexes that contain the $W(\eta^5\text{-}C_5Me_5)Me_3$ core.[10].

The M^{III} target molecules were prepared by one of three methods (Scheme 1), each of which employs white, crystalline, pentane-soluble $Li_3[N_3N]\cdot Et_2O$.[1] The Cr (green) and Fe (brown) derivatives were prepared by the "direct" route a. In the "reduction" route b yellow Ti^{IV} and blue-black V^{IV} monochloro complexes[1] were prepared first and then reduced by sodium amalgam in pentane[11] to the blue (Ti) and aquamarine (V) $[M(N_3N)]$ complexes. The "oxidation" route c was employed to provide dark green $[Mn(N_3N)]$; a pink, pentane-soluble compound formulated as $[Li(thf)][Mn(N_3N)]$ (by analogy with the known $[Li(thf)][Mn\{N(SiMe_3)_2\}_3]$[12]) was generated first from manganocene[13] and then oxidized in cold ether with $[FeCp_2]OTf$.[14] All M^{III} complexes can be prepared in gram quantities, and can be purified readily by recrystallization from pentane.[15]

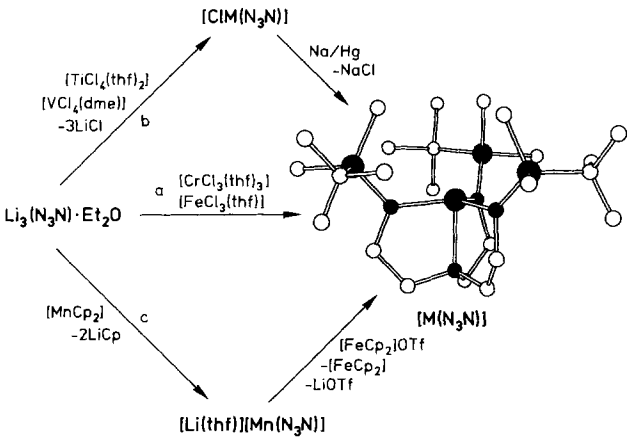

Scheme 1. Methods for the synthesis of $[M(N_3N)]$ complexes for a) M = Cr, Fe; b) M = Ti, V; c) M = Mn.

The TMP geometry was verified by an X-ray diffraction study of $[V(N_3N)]$[24] (see Fig. 1 and Scheme 1). The symmetry of the complex is close to C_3, with V and the apical amine donor lying on the pseudo-threefold axis. The vanadium atom is displaced slightly from the equatorial N_3 plane (by 0.16 Å) in the direction of the vacant coordination site, which leads to an average $N_{eq}\text{-}V\text{-}N_{ax}$ angle of 85.3°. The planes of the planar amido groups and the threefold axis are nearly coincident (average $Si\text{-}N_{eq}\text{-}V\text{-}N_{ax}$ dihedral angle 12°), and therefore the $t\mathrm{BuMe_2Si}$ groups point almost straight up and encircle the vacant coordination site. Comparison of this structure with that obtained recently for

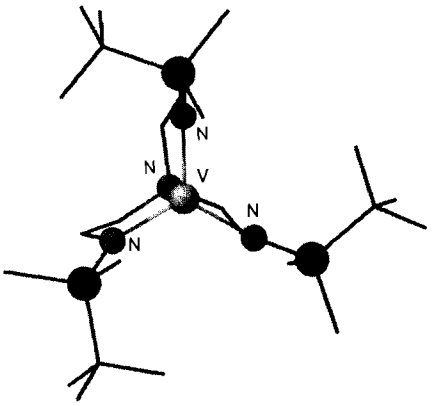

Fig. 1. Crystal structure of $[V(N_3N)]\cdot 0.5$ toluene.

$[ClV\{(Me_3SiNCH_2CH_2)_3N\}]$[1] reveals lengthened $V\text{–}N_{amide}$ bonds (average 1.930 vs. 1.883 Å), consistent with an increase in ionic radius on going from V^{IV} to V^{III} (0.67 and 0.78 Å respectively), while the bond between V and the axial nitrogen atom is shortened (2.083 vs. 2.238 Å), as should be expected in the absence of any ligand in the *trans* position. A preliminary X-ray study (as yet incompletely refined) of the analogous Cr^{III} complex reveals a similar coordination geometry.

The $[M(N_3N)]$ complexes are all high spin, as indicated by comparison of the observed magnetic moments (Evans method[16,17]) with the theoretical spin-only values (Table 1). Extended Hückel calculations (in which the threefold axis serves as the z axis) suggest that the d_{z^2} orbital (a, σ^*) is close in energy to the $d_{x^2-y^2}$, d_{xy} set (e, σ^*), while the d_{xz}, d_{yz} set (e, nonbonding) is relatively low lying. Despite

Table 1. Magnetic and selected ^{1}H NMR data for $[M(N_3N)]$ complexes.

M	μ_{eff} [a]	μ_s [b]	$\delta SiMe_2(\Delta\nu_{1/2})$ [c]
Ti	2.26(1)	1.73	5.25(40)
V	3.08(2)	2.83	6.63(750)
Cr	4.03(10)	3.87	43.36(1400)
Mn	5.01(1)	4.90	38.40(960)
Fe	5.95(5)	5.92	36.50(1360)

[a] In units of μ_B. The number in parentheses is σ for three independent measurements (multiplied by 10^{-2}). [b] Spin-only values of the magnetic moment expected for an M^{III} ion; in units of μ_B. [c] Relative to internal C_6D_5H ($\delta = 7.15$); peak width at half-maximum in Hz.

[*] Prof. Dr. R. R. Schrock, C. C. Cummins, J. Lee, Dr. W. M. Davis[+]
Department of Chemistry
Massachusetts Institute of Technology
Cambridge, MA 02139 (USA)

[+] X-ray structure analysis

[**] This work was supported by the National Science Foundation (CHE 91 22827) and the National Institutes of Health (GM 31978). C. C. C. thanks the National Science Foundation for a Predoctoral Fellowship.

their paramagnetic nature, all the complexes give rise to assignable proton NMR spectra (see Table 1 and *Experimental Procedure*) in which the isotropic shift and signal width increase substantially as a function of the number of unpaired spins. Solution IR spectra of the five $[M(N_3N)]$ complexes are very similar, and all were found to be monomeric in pentane (Signer method[18]). These data suggest that all five species are structurally analogous, monomeric species in the solid state and in solution.

That trigonal-monopyramidal complexes may lead to unusual binding of substrates is presaged by the observation of reversible binding of carbon monoxide to $[Ti(N_3N)]$ ($\tilde{\nu}_{CO} = 2003\ cm^{-1}$), a reaction that is accompanied by a color change from blue to green and a shifting and broadening of the ^1H NMR signals attributed to the triamide ligand. We could find no other example of a reversible binding of carbon monoxide to a d^1 metal center.[19] We are continuing to explore the reaction chemistry of complexes with first row transition metals that contain the N_3N ligand, but are also interested in designing related $(RNCH_2CH_2)_3N$ ligands that may be stable to protic environments and in synthesizing complexes with heavier metals, especially Ta, Mo, or W.

Experimental Procedure

$[Ti(N_3N)]$: To a flask containing 40 mL pentane at −40 °C was added $[TiCl_4(thf)_2]$ [20] (1.990 g, 5.959 mmol) with stirring, followed by $Li_3(N_3N) \cdot Et_2O$ (3.020 g, 5.198 mmol). The reaction mixture was allowed to warm to 25 °C and stirred 12 h, at which point the precipitated LiCl was filtered. The ^1H NMR spectrum of an aliquot of the crude orange filtrate revealed the presence of only $[ClTi(N_3N)]$, indicating essentially quantitative reaction. The orange filtrate was concentrated to dryness, and the solid yellow-orange residue was dissolved in a minimum amount of pentane; the product crystallized at −40 °C as yellow needles (1.220 g in two crops, 2.143 mmol, 41%). ^1H NMR (C_6D_6): $\delta = 3.447$ (t, CH_2), 2.288 (t, CH_2), 1.112 (s, *t*Bu), 0.360 (s, $SiMe_2$). $^{13}C\{^1H\}$ NMR (C_6D_6): 63.88 (CH_2), 51.93 (CH_2), 27.71 ($SiC(CH_3)_3$), 22.08 ($SiCMe_3$), −2.21 ($Si(CH_3)_2$). Satisfactory C,H,N-analysis. To a stirred solution of $[ClTi(N_3N)]$ (760 mg, 1.335 mmol) in 15 mL pentane was added Na/Hg (0.5%, 17.369 g, 3.776 mmol Na), and the reaction mixture was allowed to stir 72 h. After the gray Na/Hg/NaCl mixture was allowed to settle, the blue solution was decanted and filtered, and concentrated to dryness. The crystalline residue was dissolved in a minimum amount of pentane and chilled to −40 °C, whereupon blue crystals were obtained (374 mg, 701 μmol, 52%). ^1H NMR (C_6D_6): $\delta = 5.25$ ($\Delta\nu_{1/2} \approx 40$ Hz, 18H, $SiMe_2$), 1.15 ($\Delta\nu_{1/2} = 11$ Hz, *t*Bu), −0.93 ($\Delta\nu_{1/2} = 49$ Hz, CH_2), −18.77 ($\Delta\nu_{1/2} = 54$ Hz, CH_2). Mol wt (pentane): calcd. 533.88, found 504. Satisfactory C,H,N analysis.

$[V(N_3N)]$: To a flask containing 250 mL pentane at −40 °C was added $[VCl_4(dme)]$ [21] (2.791 g, 9.867 mmol) with stirring, followed by $Li_3(N_3N) \cdot Et_2O$ (5.000 g, 8.607 mmol). The reaction mixture was allowed to warm to 25 °C and stirred for 14 h, at which point the precipitated LiCl was filtered off, and the solvent was removed from the blue-black filtrate in vacuo. The gummy residue was dissolved in a minimum amount of pentane, and the solution was cooled to −40 °C to give green-black crystals (1.609 g). A ^1H NMR spectrum of the crystalline product showed it to be a mixture of 28% $[ClV(N_3N)]$ (^1H NMR (C_6D_6): $\delta = 1.77$ ($\Delta\nu_{1/2} = 45$ Hz, $SiMe_2$), 0.85 ($\Delta\nu_{1/2} = 23$ Hz, *t*Bu), −16.21 ($\Delta\nu_{1/2} = 186$ Hz, CH_2), −40.84 ($\Delta\nu_{1/2} = 308$ Hz, CH_2)) and 72% $[V(N_3N)]$. The mixture was dissolved in pentane (40 mL) and treated with Na/Hg (13.55 g, 0.5%, 2.945 mmol Na). The reaction mixture was stirred for 12 h, at which point the NaCl/Na/Hg mixture was allowed to settle. The aquamarine pentane solution was decanted and filtered, and the filtrate was concentrated in vacuo to give a crystalline residue that was dissolved in a minimum amount of toluene. The toluene solution was cooled to −40 °C to give 1.148 g (2.138 mmol, 73%) of crystalline $[V(N_3N)]$. ^1H NMR (C_6D_6): $\delta = 6.63$ ($\Delta\nu_{1/2} = 750$ Hz, $SiMe_2$), 1.93 ($\Delta\nu_{1/2} = 190$ Hz, *t*Bu), −19.83 ($\Delta\nu_{1/2} = 1440$ Hz, CH_2), −84.18 ($\Delta\nu_{1/2} \approx 2600$ Hz, CH_2). Mol wt (pentane): calcd. 536.94, found 456. Satisfactory, C,H,N analysis.

$[Cr(N_3N)]$: To a stirred slurry of $[CrCl_3(thf)_3]$ [22] (2.957 g, 7.892 mmol) in 80 mL pentane at −40 °C was added $Li_3(N_3N) \cdot Et_2O$ (4.000 g, 6.885 mmol). The reaction mixture was allowed to warm to 25 °C and stirred for 48 h, at which point the precipitated LiCl was removed by filtration. The filtrate was concentrated to dryness, and the residue was dissolved in a minimum of pentane. The pentane solution was chilled to −40 °C to give 1.639 g of green crystals (3.047 mmol, 44%). ^1H NMR (C_6D_6): $\delta = 43.36$ ($\Delta\nu_{1/2} = 1430$ Hz, $SiMe_2$), 0.02 ($\Delta\nu_{1/2} = 370$ Hz, *t*Bu). Mol wt (pentane): calcd. 538.00, found 531.

$[Mn(N_3N)]$: To a stirred solution of $[MnCp_2]$ [13] (1.593 g, 8.606 mmol) in 30 mL THF was added solid $Li_3(N_3N) \cdot Et_2O$ (5.000 g, 8.607 mmol) in portions over a period of 1 min. After 3 h the solvents were removed in vacuo, and the residue was extracted with 125 mL of pentane. The pentane solution was filtered through a bed of Celite to remove LiCp (89% isolated yield of LiCp, ^1H NMR (C_5D_5N): $\delta = 6.430$ (s, Cp)), and the filtrate was concentrated to dryness. The residue was recrystallized from a minimum of ether/pentane to afford 3.235 g of light pink crystals of $[Li(thf)][Mn(N_3N)]$ (5.218 mmol, 61%) in two crops. To a stirred solution of $[Li(thf)][Mn(N_3N)]$ (750 mg, 1.210 mmol) in ether at −40 °C was added solid $[FeCp_2]OTf$ [14] (405 mg, 1.210 mmol); the color rapidly changed to dark green. The reaction mixture was allowed to warm to 25 °C and stirred for 2 h, at which point the solvents were removed in vacuo. The residue was extracted with 30 mL pentane, LiOTf was removed by filtration, and the filtrate was concentrated in vacuo. Ferrocene was removed by sublimation at room temperature over a period of 5 h (0.05 Torr) onto a probe cooled to −78 °C. The remaining green-black solid was taken up in a minimum amount of pentane, and the solution was chilled to −40 °C to give 336 mg of green-black crystals (621 μmol, 51%). ^1H NMR (C_6D_6): $\delta = 38.40$ ($\Delta\nu_{1/2} = 960$ Hz, $SiMe_2$), 0.02 ($\Delta\nu_{1/2} = 316$ Hz, *t*Bu). Mol wt (pentane): calcd. 540.94, found 552. Satisfactory C,H,N analysis.

$[Fe(N_3N)]$: To a stirred solution of $Li_3(N_3N) \cdot Et_2O$ (3.04 g, 5.233 mmol) in 70 mL THF at −40 °C was added $[FeCl_3(thf)]$ [23] (1.226 g, 5.233 mmol) all at once. The reaction mixture was allowed to warm to 25 °C and stirred for 3 h, at which point the solvents were removed in vacuo, and the residue was extracted with 100 mL pentane. The extract was filtered and the filtrate was concentrated to dryness in vacuo. The residue was dissolved in a minimum of pentane, and the solution was chilled to −40 °C to give 1.347 g of brown microcrystals (2.486 mmol, 48%) in two crops. ^1H NMR (C_6D_6): $\delta = 36.50$ ($\Delta\nu_{1/2} = 1360$ Hz, $SiMe_2$), 13.90 ($\Delta\nu_{1/2} = 646$ Hz, *t*Bu). Mol wt (pentane): calcd. 541.85, found 556.

Received: June 19, 1992 [Z 5415 IE]
German version: *Angew. Chem.* **1992**, *104*, 1510

CAS Registry numbers:
$[Ti(N_3N)]$, 143924-27-0; $[TiCl_4(thf)_2]$, 31011-57-1; $[ClTi(N_3N)]$, 143924-28-1; $[V(N_3N)]$, 143924-29-2; $[VCl_4(dme)]$, 17035-16-4; $[ClV(N_3N)]$, 143924-30-5; $[Cr(N_3N)]$, 143924-31-6; $[CrCl_3(thf)_3]$, 10170-68-0; $[Mn(N_3N)]$, 143924-32-7; $[Cp_2Mn]$, 73138-26-8; $[Li(thf)][Mn(N_3N)]$, 143924-34-9; $[Fe(N_3N)]$, 143924-35-0; $[FeCl_3(thf)]$, 36470-52-7; $[V(N_3N)] \cdot 0.5$ toluene, 143924-36-1.

[1] C. C. Cummins, R. R. Schrock, W. M. Davis, *Organometallics* **1992**, *11*, 1452.
[2] D. Gudat, J. G. Verkade, *Organometallics* **1989**, *8*, 2772.
[3] W. Plass, J. G. Verkade, *J. Am. Chem. Soc.* **1992**, *114*, 2275.
[4] A. A. Naiini, W. M. P. B. Menge, J. G. Verkade, *Inorg. Chem.* **1991**, *30*, 5009.
[5] C. Mealli, L. Sacconi, *J. Chem. Soc. Chem. Commun.* **1973**, 886.
[6] K. D. Karlin, P. L. Dahlstrom, J. R. Hyde, J. Zubieta, *J. Chem. Soc. Chem. Commun.* **1980**, 906.
[7] J. de Mendoza, E. Mesa, J.-C. Rodríguez-Ubis, P. Vásquez, F. Vögtle, P. M. Windscheif, K. Rissaneu, J.-M. Lehn, D. Lilienbaum, R. Ziessel, *Angew. Chem.* **1991**, *103*, 1365; *Angew. Chem. Int. Ed. Engl.* **1991**, *30*, 1331.
[8] R. R. Schrock, T. E. Glassman, M. G. Vale, *J. Am. Chem. Soc.* **1991**, *113*, 725.
[9] S. Cai, R. R. Schrock, *Inorg. Chem.* **1991**, *30*, 4105.
[10] T. E. Glassman, M. G. Vale, R. R. Schrock, *Inorg. Chem.* **1991**, *30*, 1985.
[11] K. J. Covert, P. T. Wolczanski, *Inorg. Chem.* **1989**, *28*, 4565.
[12] B. D. Murray, P. P. Power, *Inorg. Chem.* **1984**, *23*, 4584.
[13] G. Wilkinson, F. A. Cotton, J. M. Birmingham, *J. Inorg. Nucl. Chem.* **1956**, *2*, 95.
[14] R. R. Schrock, L. G. Sturgeoff, P. R. Sharp, *Inorg. Chem.* **1983**, *22*, 2801.
[15] Due to the extreme sensitivity of the $[M(N_3N)]$ complexes to air, elemental analyses have not yet given satisfactory results for $[Cr(N_3N)]$ and $[Fe(N_3N)]$.
[16] D. F. Evans, *J. Chem. Soc.* **1959**, 2003.
[17] S. K. Sur, *J. Magn. Reson.* **1989**, *82*, 169.
[18] E. P. Clark, *Ind. Eng. Chem. Anal. Ed.* **1941**, *13*, 820.
[19] J. G. Brennan, R. A. Andersen, J. L. Robbins, *J. Am. Chem. Soc.* **1986**, *108*, 335.
[20] L. E. Manzer, *Inorg. Synth.* **1982**, *21*, 135.
[21] B. E. Bridgland, G. W. A. Fowles, R. A. Walton, *J. Inorg. Nucl. Chem.* **1965**, *27*, 383.
[22] J.-H. So, P. Boudjouk, *Inorg. Chem.* **1990**, *29*, 1592.
[23] L. S. Brenner, C. A. Root, *Inorg. Chem.* **1972**, *11*, 652.
[24] Data were collected at −72 °C on an Enraf-Nonius CAD-4 diffractometer with graphite-monochromated $Mo_{K\alpha}$ radiation. A total of 8416 reflections were collected to a 2θ value of 54.9°, of which 8057 were unique

($R_{int} = 0.032$); equivalent reflections were merged. The structure was solved by a combination of Patterson and difference Fourier techniques. The final cycle of full-matrix least-squares refinement was based on 5784 observed reflections ($I > 3.00\sigma(I)$) and 326 variable parameters and converged (largest parameter shift was less than 0.009 times its esd) with $R = 0.060$ and $R_w = 0.063$. A final difference Fourier map showed no chemically significant features. Crystal data are $a = 13.084(2)$, $b = 13.089(2)$, $c = 13.194(2)$ Å, $\alpha = 60.08(1)$, $\beta = 64.78(1)$, $\gamma = 72.88(1)°$, $V = 1762(1)$ Å^3, space group $P\bar{1}$, $Z = 2$. Further details of the crystal structure investigation may be obtained from the Fachinformationszentrum Karlsruhe, Gesellschaft für wissenschaftlich-technische Information mbH, D-W-7514 Eggenstein-Leopoldshafen 2 (FRG), on quoting the depository number CSD-56535, the names of the authors, and the journal citation.

Catecholates as σ- and π-Donating Ligands: The Synthesis and Structure of $(Et_4N)_2[W(CO)_4(O_2C_6H_4)]$ and the "Sixteen Electron" Analogue Resulting from CO Dissociation**

By *Donald J. Darensbourg,* Kevin K. Klausmeyer, Brian L. Mueller,* and *Joseph H. Reibenspies*

Carbon dioxide insertion into the metal–oxygen bond of metal hydroxides, alkoxides, and aryloxides is a fundamental step in several chemical and biochemical catalytic processes. Notable among these processes are the coupling of CO_2 and epoxides to provide cyclic carbonates[1] or polymeric materials,[2] and the hydration of CO_2 to afford carbonic acid.[3] Attendant with reactions involving low-valent anionic Group 6 metal alkoxy- or aryloxycarbonyl complexes is the lability of the carbonyl ligands which can subsequently lead to β-hydrogen elimination or metal aggregation reactions.[4] In this communication, we report the synthesis and structural characterization of carbonyl catecholatotungsten complexes and the effect of the π-donating property of these dihydroxo ligands on the reactivity patterns of the metal complexes.

A solution of $[W(CO)_5thf]$ (prepared photochemically from 1.9 mmol of $[W(CO)_6]$ in tetrahydrofuran) was transferred to a Schlenk flask containing 3.8 mmol of $(Et_4N)(OC_6H_4OH)$ and stirred. An orange powder precipitated within one hour and orange crystals of **1** were isolated by filtration (1.3 g or 90% yield) and recrystallization from CH_3CN/ether. The infrared spectrum of **1** in CH_3CN exhibited ν_{CO} vibrations at 1975(w), 1829(vs), 1807(m, sh) and 1773(m) cm^{-1}. Two sharp doublets of equal intensity were observed for the CO ligands in the ^{13}C NMR spectrum at $\delta = 217.6$ ($J_{W,C} = 165$ Hz) and 207.5 ($J_{W,C} = 131$ Hz).

$(Et_4N)_2[W(CO)_4(O_2C_6H_4)] \cdot HOC_6H_4OH$ **1**

Definitive assignment of the structure of **1** was obtained by X-ray crystallography; the result is shown in Figure 1.[5] The solid-state structure of **1** is characterized by continuous hydrogen bonding between the bridging catechol moiety and two adjacent dianions. The structure shows typical hydrogen-bond lengths (O···O 2.535(10) Å[6]) and tungsten to oxygen-bond lengths of 2.175(11) Å. One notable feature in the structure is the deviation from linearity of the axial carbonyl groups (C-W-C angle of 167.3(8)°).

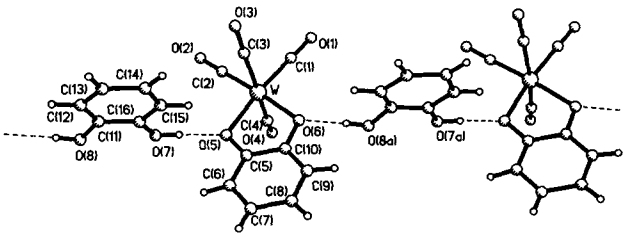

Fig. 1. Ball-and-stick representation of the non-hydrogen atoms of the anion of **1**.

The complex **2** containing only coordinated catechol was obtained by reacting 1.6 mmol of **1** with three equivalents of

$(Et_4N)_2[W(CO)_4(O_2C_6H_4)]$ **2**

NaOMe in acetonitrile. $Na_2O_2C_6H_4$ and excess NaOMe were removed by filtration through Celite, and dark orange crystals (yield 0.91 g, 82%) were obtained upon addition of THF/Et_2O to the filtrate. As anticipated, the ν_{CO} vibrations of **2** in CH_3CN (1965(w), 1817(vs), 1800(m,sh) and 1763(m) cm^{-1}) are shifted to lower frequencies than those of **1**, indicative of some hydrogen bonding of **1** in solution as well. Similarly the two ^{13}C NMR resonances in CH_3CN shift downfield to $\delta = 219.6$ ($J_{W,C} = 159$ Hz) and 208.8 ($J_{W,C} = 133$ Hz). More importantly, in contrast to species **1**, the carbonyl ligands in the non-hydrogen-bonded form of the complex are fluxional. Coalescence of the two carbonyl carbon signals into one symmetrical peak at $\delta = 214.2$ occurred at temperatures greater than 23 °C.[7] The activation parameters for the CO exchange were determined to be $\Delta H^{\ddagger} = 12.0 \pm 0.7$ kcal mol^{-1} and $\Delta S^{\ddagger} = -4.5 \pm 2.5$ cal K^{-1} mol^{-1}.[8] The facile nature of this process is attributed to the π-donor property of the catecholato ligand. This conclusion is supported by the fact that upon addition of excess catechol, which forms hydrogen bonds to the ligated catechol and hence diminishes its π-donor character, the fluxional process is slowed down.[9] Furthermore, in the instance where the catecholate ligand contains electron-releasing *tert*-butyl substituents in the 3,5-positions (→ **4**), the coalescence temperature is much lower than ambient temperature.

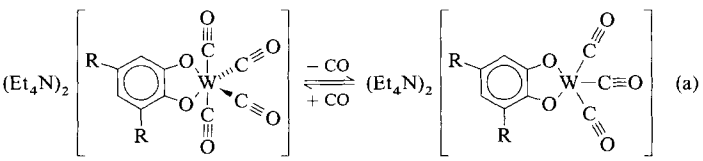

(a)

2, R = H
4, R = *t*Bu

3, R = H
5, R = *t*Bu

In a slower process, **2** readily expels CO to provide the tricarbonyl derivative **3** [Eq. (a)].[10] Formation of **3** was indicated by the two bands for the ν_{CO} vibrations in CH_3CN

[*] Prof. Dr. D. J. Darensbourg, Dipl.-Chem. K. K. Klausmeyer, Dr. B. L. Mueller, Dr. J. H. Reibenspies
Department of Chemistry, Texas A & M University
College Station, TX 77843 (USA)

[**] This work was supported by the National Science Foundation (Grant 91-19737) and the Robert A. Welch Foundation.

(1863(s) and 1726(vs) cm^{-1}), and a single broad ^{13}C NMR signal at $\delta = 234.2$ at $-35\,^{\circ}C$. Upon exposing an acetonitrile solution of **3** to a carbon monoxide atmosphere, **2** is regenerated rapidly and quantitatively. Hence, an equilibrium between the 18-electron complex **2** and its formally "16-electron" unsaturated species **3** exists in solution. Because the reaction is carried out in a strongly coordinating solvent, CH_3CN, it is possible that CH_3CN is in the coordination sphere of **3**.

Synthesis of the 3,5-di-*tert*-butyl derivative of **2** was accomplished in a completely analogous manner. The ν_{CO} region of the solution infrared spectrum indicated the presence of both the tetra- and tricarbonyl species (**4** and **5**) even in the absence of a CO atmosphere, that is, a four band pattern (1962(w), 1815(s), 1796(m,sh), and 1755(m) cm^{-1}) and a two band pattern (1859(s) and 1721(vs) cm^{-1}), respectively. Consistent with the presence of the electron-donating *t*-butyl groups, this equilibrium lies farther to the right than that formulated in Equation (a). The ^{13}C NMR spectrum of the tetracarbonyl derivative, stabilized by a CO atmosphere, exhibited three resonances at $\delta = 220.2, 219.8$, ($J_{W,C} = 161$ Hz) and 209.0 ($J_{W,C} = 136$ Hz) of intensity ratio 1:1:2 at $-40\,^{\circ}C$. That is, the two equatorial CO ligands are not equivalent because of the unsymmetrically substituted catecholate ligand. The coalescence of the three carbon signals occurred at temperatures above $5\,^{\circ}C$.

Proof of the structure of the tricarbonyl derivative **5** was obtained by X-ray crystallography (Fig. 2).[11] The structure is quite similar to that previously reported for its manganese analogue,[12] in which the coordination geometry is intermediate between trigonal bipyramidal and square pyramidal, and there is no CH_3CN in the metal's coordination sphere. The tungsten atom lies out of the plane defined by the two carbonyl carbon atoms, C1 and C2, and one of the catecholate's oxygen atoms O5 by 0.048 Å (towards the axial O4 atom). The O4-W-C3 angle is 166.7°. The W–O5 bond, which is *ortho* to the electron-releasing *t*-butyl substituent, is significantly shorter than the W–O4 bond (2.059 vs. 2.154 Å). Indeed, both W–O bond lengths are shorter than those in the tetracarbonyl species **1**. Concomitantly, the W–C1 bond, which is closest to *trans* to O5 ($\sphericalangle$O5-W-C1 = 143.3°), is the shortest W–C bond. The bond lengths within the catecholato ligands in complexes **1** and **5** are extremely similar.

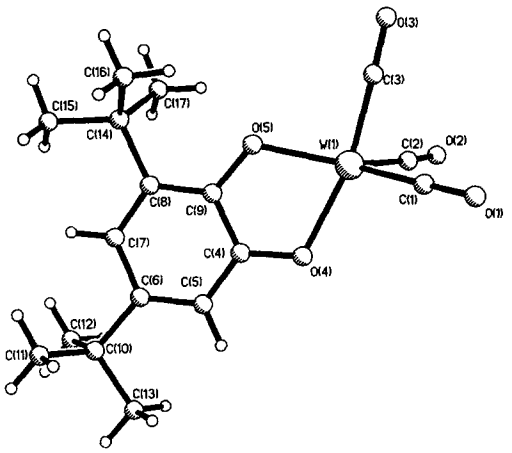

Fig. 2. Ball-and-stick representation of the non-hydrogen atoms of the anion of **5**.

These results emphasize the emerging opinion that strongly π-donating hydroxo ligands stabilize unsaturated organometallic derivatives.[13] The reactivity of the coordinatively unsaturated derivatives **3** and **5** with dihydrogen or carbon dioxide are currently under investigation. Preliminary observations indicate that these catecholato complexes readily react with one equivalent of CO_2 at low temperature to afford cyclic carbonato metal complexes.

Received: June 19, 1992 [Z 5418 IE]
German version: *Angew. Chem.* **1992**, *104*, 1501

CAS Registry numbers:
1, 143958-31-0; **2**, 143958-30-9; **3**, 143958-33-2; **3**·CH_3CN, 143958-35-4; **4**, 143958-37-6; **5**, 143958-39-8.

[1] a) R. J. De Pasquale, *J. Chem. Soc. Chem. Commun.* **1973**, 157; b) J. E. Bäckvall, O. Karlsson, S. O. Ljunggren, *Tetrahedron Lett.* **1980**, 4985; c) M. Ratzenhofer, H. Kisch, *Angew. Chem.* **1980**, *92*, 303; *Angew. Chem. Int. Ed. Engl.* **1980**, *19*, 317; d) D. P. Klein, J. C. Hayes, R. G. Bergman, *J. Am. Chem. Soc.* **1988**, *110*, 3704; e) K.-T. Aye, L. Gelmini, N. C. Payne, J. J. Vittal, R. J. Puddephatt, *ibid.* **1990**, *112*, 2464.

[2] a) S. Inoue, *CHEMTECH* **1976**, 588; b) A. Rokicki, W. J. Kuran, *Macromol. Sci-Rev. Macromol. Chem.* **1981**, *C21(1)*, 135; c) T. Aida, M. Ishakawa, S. Inoue, *Macromolecules* **1986**, *19*, 8.

[3] a) R. S. Brown in *Enzymatic and Model Carboxylation and Reduction Reactions for Carbon Dioxide Utilization* (*NATO ASI Ser. C* **1990**, *314*, 145–180); b) R. Alsfasser, S. Trofimenko, A. Looney, G. Parkin, H. Vahrenkamp, *Inorg. Chem.* **1991**, *30*, 4098; c) R. Han, G. Parkin, *J. Am. Chem. Soc.* **1991**, *113*, 9707.

[4] a) P. A. Tooley, C. Ovalles, S. C. Kao, D. J. Darensbourg, M. Y. Darensbourg, *J. Am. Chem. Soc.* **1986**, *108*, 5465; b) T. J. McNeese, T. E. Mueller, D. A. Wierda, D. J. Darensbourg, T. J. Delord, *Inorg. Chem.* **1985**, *24*, 3465; c) T. J. McNeese, M. B. Cohen, B. M. Foxman, *Organometallics* **1984**, *3*, 552; d) D. J. Darensbourg, K. M. Sanchez, J. H. Reibenspies, A. L. Rheingold, *J. Am. Chem. Soc.* **1989**, *111*, 7094; e) D. J. Darensbourg, B. L. Mueller, J. H. Reibenspies, C. J. Bischoff, *Inorg. Chem.* **1990**, *29*, 1789; f) D. J. Darensbourg, B. L. Mueller, C. J. Bischoff, C. C. Johnson, K. M. Sanchez, J. H. Reibenspies, *Isr. J. Chem.* **1990**, *30*, 369.

[5] **1**: Crystallographic data ($-80\,^{\circ}C$): $a = 17.742(5)$, $b = 19.452(5)$, $c = 10.345(2)$ Å, $Z = 4$, space group $Pna2_1$; 2306 reflections with $I > 2\sigma(I)$ used, $R = 0.050$, $R_w = 0.049$ [14].

[6] a) K. Osakada, Y. Kim, M. Tanaka, S. Ishiguro, A. Yamamoto, *Inorg. Chem.* **1991**, *30*, 197; b) Y. Kim, K. Osakada, A. Takenaka, A. Yamamoto, *J. Am. Chem. Soc.* **1990**, *112*, 1096; c) S. E. Kegley, C. J. Schaverien, J. H. Fruedenberger, R. G. Bergman, S. P. Nolan, C. D. Hoff, *J. Am. Chem. Soc.* **1987**, *109*, 6563; d) D. Braga, P. Sabatino, C. Di Bugno, P. Leoni, M. Pasquali, *J. Organomet. Chem.* **1987**, *334*, C46.

[7] a) NMR spectra were simulated by a density matrix procedure (software by Dr. John Horner at Wayne State University) for an exchange between two sites of equal population to determine rate constants; b) J. I. Kaplan, *J. Chem. Phys.* **1958**, *28*, 278; *ibid.* **1958**, *29*, 462.

[8] Activation parameters were calculated by the method of Christian and Tucker. S. K. Christian, E. E. Tucker, *Am. Lab. (Fairfield, CT)* **1982**, *14* (8), 36; S. D. Christian; E. E. Tucker *Am. Lab. (Fairfield, CT)* **1982**, *14* (9), 31.

[9] A slight excess of catechol was added to the NMR tube containing the sample used in the variable temperature experiment. After addition of the alcohol the ^{13}C NMR spectrum showed no broadening of the axial and equatorial carbonyl resonance signals at ambient temperature.

[10] Preliminary rate measurements for CO dissociation in these derivatives indicate rate constants in the range of 10^{-2} sec^{-1} at $5\,^{\circ}C$, whereas the rate constant for intramolecular CO exchange at $0\,^{\circ}C$ was determined to be 153 sec^{-1}.

[11] **5**: Crystallographic data ($-80\,^{\circ}C$): $a = 18.089(4)$, $b = 8.618(2)$, $c = 22.194(5)$ Å, $\beta = 91.25(2)^{\circ}$, $V = 3459.0(14)$ Å^3, $Z = 4$, space group $C2$; 3266 reflections with $I > 2\sigma(I)$ used, $R = 0.047$ and $R_w = 0.048$ [14].

[12] F. Hartl, A. Vlček, Jr., L. A. deLearie, C. G. Pierpont, *Inorg. Chem.* **1990**, *29*, 1073.

[13] D. M. Lunder, E. B. Lobkovsky, W. E. Streib, K. G. Caulton, *J. Am. Chem. Soc.* **1991**, *113*, 1837.

[14] Further details of the crystal structure investigations are available on request from the Fachinformationszentrum Karlsruhe, Gesellschaft für wissenschaftlich-technische Information mbH, D-W-7514 Eggenstein-Leopoldshafen 2 (FRG), on quoting the depository number CSD-56480, the names of the authors, and the journal citation.

Stereoselective Generation of 1-Acyloxy-2-amino Carbanions by Deprotonation; Synthesis of Enantiomerically and Diastereomerically Pure β-Amino Alcohols**

By *Jörg Schwerdtfeger* and *Dieter Hoppe**

Dedicated to Professor Ulrich Schöllkopf on the occasion of his 65th birthday

Synthetic equivalents of 2-amino-1-hydroxy carbanions **A** that allow the preparation of more highly substituted 2-amino alcohols **B** by stereoselective electrophilic substitutions are hitherto unknown.[1] In the one related example, Beak et al.[2] generated the racemic, dipole-stabilized 2,4,6-triisopropylbenzoate **1** and isolated its deuterium analogue. We report here a simple and highly stereoselective approach to this problem.

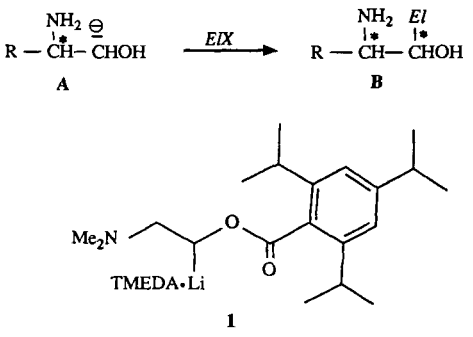

Lithiocarbanions of type **2** unsubstituted in the alkyl portion can be prepared by the enantioselective deprotonation of the related *O*-alkylcarbamates with *sec*-butyllithium/(−)-sparteine[3] with high stereoselectivity. The trick is protecting the hydroxyl group while simultaneously activating the neighboring methylene protons by means of the sterically demanding, and yet acid-labile, 1,3-oxazolidine-3-carbonyl group and stabilizing the ion pair by chelation. The enantiomers are differentiated in the deprotonation because of the complex ligand (−)-sparteine (**3**); the *Si* proton is abstracted with selectivities > 95% *ee* to give configurationally stable lithium (1*S*)-(acyloxy)alkanides of type **2**. These compounds can be substituted with most electrophiles with retention of stereochemistry.[3, 6] The alkyl group R may have alkoxy substituents[7] in the γ and δ positions without deleterious effects on the yield and stereoselectivity.

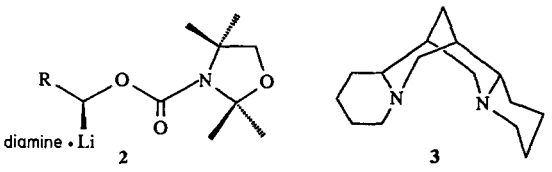

[*] Prof. D. Hoppe,[+] Dipl.-Chem. J. Schwerdtfeger
Institut für Organische Chemie der Universität
Olshausenstrasse 40–60, D-W-2300 Kiel (FRG)
[+] New address: Organisch-chemisches Institut der Universität
Corrensstrasse 40, D-W-4400 Münster (FRG)

[**] This research was supported by the Deutsche Forschungsgemeinschaft, the Fonds der Chemischen Industrie, and the Pharmaforschungszentrum of Bayer AG, Wuppertal.

We had anticipated that the *N*,*N*-dialkylamino group in the substrate would compete with (−)-sparteine in complexation and that the stereoselectivity would suffer.[8] To our surprise carbamate **4**,[9, 10] obtained from 2-(*N*,*N*-dibenzylamino)ethanol, was deprotonated smoothly with 3 equiv *sec*-butyllithium/(−)-sparteine in diethyl ether at −78 °C. The intermediate ion pair **5**·(−)-**3** was trapped with electrophiles to provide the expected substitution products **6**[10] in good yields and with enantiomeric enrichments of > 95%[11] (Scheme 1, Table 1). The (*R*) configuration of **6d** was confirmed by conversion into diol (*R*)-**7**;[12] its enantiomer (*S*)-**7** was synthesized from the commercially available glycerin derivative (*R*)-**8** for comparison.[12] The racemates *rac*-**6** were obtained in similar yields when *N*,*N*,*N*′,*N*′-tetramethylenediamine (TMEDA) was used instead of (−)-**3**.

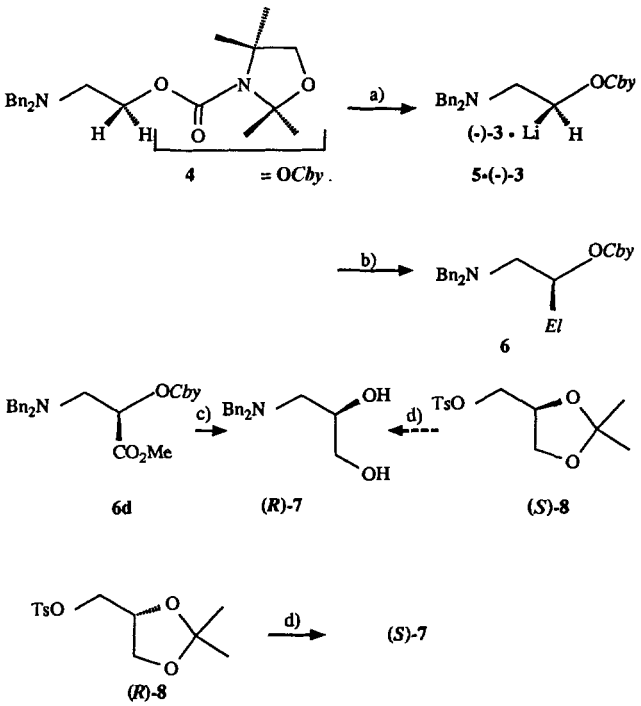

Scheme 1. a) 3 equiv *s*BuLi/(−)-**3**, Et_2O, −78 °C, 3 h; b) EIX; c) $LiAlH_4$; d) 1. Bn_2NH, $C_6H_5CH_3$, 65%; 2. $MeSO_3H$, MeOH, 65%. Bn = benzyl.

Carbamate **9**[9, 10], derived from (*S*)-*N*,*N*-dibenzylleucinol,[13] could not be deprotonated at −78° with *sec*-butyllithium/(−)-sparteine. When TMEDA was used as a complexing agent, however, the lithium complex **10** was formed and subsequently methylated to give the diastereomerically pure substitution product **11a**[10] (Scheme 2, Table 1). The liberation of the hydroxyl group led to amino alcohol (2*R*,3*S*)-**12a**,[14] which is also the major product from the substrate-controlled Grignard addition of methylmagnesium iodide to (*S*)-*N*,*N*-dibenzylleucinal **13**.[13] Thus the *Re* proton in **9** was replaced exclusively. The internal and external chiral inductions oppose because of the pronounced *Si* preference of the *sec*-butyllithium/(−)-sparteine complex. This is reflected in the markedly reduced reactivity of the "mismatched pair".[15]

Similar results were obtained with the (*S*)-prolinol derivative **14**.[9, 10] Here too, deprotonation in the presence of TMEDA provided lithium compound **15**, and the *Re* proton

Table 1. Enantio- or diastereoselective deprotonation and substitution of carbamates **4**, **9**, and **14**.

Starting material	Diamine	EIX	Product [a]	El	Yield [%] [b]	*ee* or *ds* [%]	Config. [c]	$[\alpha]_D^{20}$ [d]
4	(−)-**3**	CH_3I	**6a**	CH_3	72	>95	*S*	−34.7
4	(−)-**3**	Me_3SiCl	**6b**	Me_3Si	70	>95	*S*	+6.2
4	(−)-**3**	Bu_3SnCl	**6c**	Bu_3Sn	70	>95	*S*	+28.4
4	(−)-**3**	CO_2 [e]	**6d**	CO_2Me	56	>95	*R*	−7.8
9	TMEDA	CH_3I	**11a**	CH_3	84	>95:5 [f]	1*R*,2*S*	−35.2
9	TMEDA	CO_2	**11e**	CO_2H	84	>95:5 [f]	1*S*,2*S*	+2.2
9	TMEDA	$(CH_3)_2CHCH{=}O$	**11f**	$(CH_3)_2CHCHOH$	49	>95:5 [g]	1*S*,2*S*,1′*RS* [i]	–
14	TMEDA	CH_3I	**16a**	CH_3	72	>95:5 [f]	2′*R*,2*S*	−51.0
14	(−)-**3**	CH_3I	**16a**	CH_3	56	>95:5 [f]	2′*R*,2*S*	−51.4
14	TMEDA	Bu_3SnCl	**16c**	Bu_3Sn	71	>95:5 [f]	2′*R*,2*S*	−69.6
14	TMEDA	CO_2 [e]	**16d**	CO_2Me	40	>95:5 [f]	2′*S*,2*S*	−19.2
14	TMEDA	$(CH_3)_2CHCH{=}O$	**16f**	$(CH_3)_2CHCHOH$	85	>95:5 [h]	2′*S*,2*S*,2″*RS* [i]	–
14	TMEDA	$(CH_3)_2C{=}O$	**16g**	$(CH_3)_2COH$	33	>95:5 [f]	2′*S*,2*S*	−7.4

[a] See ref[10]. [b] Yield after chromatography. [c] The numbering does not correspond to the IUPAC names; see Schemes 1–3. [d] In $CHCl_3$, $c = 1.0–1.5$. [e] After esterification of the crude product with diazomethane. [f] A second diastereomer was not found after careful chromatographic separation and analysis by ^1H NMR spectroscopy. [g] Two diastereomers, 55:45. [h] Two diastereomers, 73:27. [i] The relative configuration of the additional stereocenter was not determined.

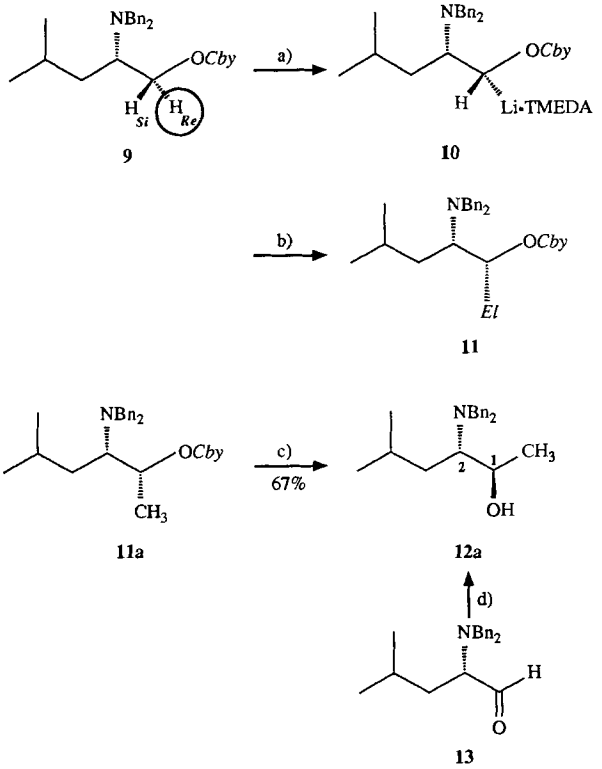

Scheme 2. a) 3 equiv *s*BuLi/TMEDA, Et_2O, −78 °C, 3 h; b) EIX; c) 5 N HCl; d) CH_3MgI, Et_2O, 0 °C, 1 h, 85%, **12a**: *epi*-**12a** = 90: 10.

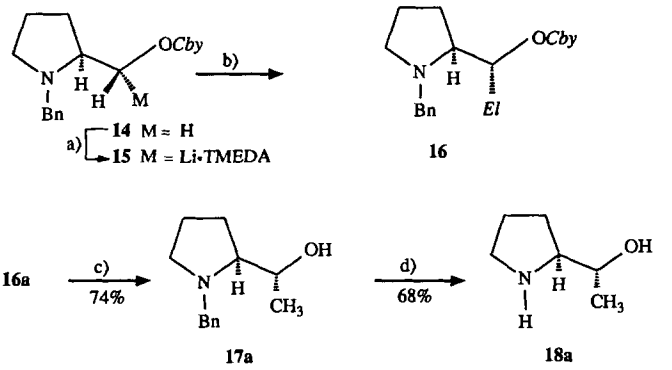

Scheme 3. a) 3 equiv *s*BuLi/TMEDA, Et_2O, −78 °C, 3 h; b) EIX; c) 1. $MeSO_3H$, MeOH, 16 h; 2. $Ba(OH)_2$, 4 h; d) Pd black, MeOH, HCOOH.

was replaced exclusively (Scheme 3, Table 1). The configuration of the acetone adduct **16g** was confirmed by an X-ray structure analysis.[16] We also observed a deprotonation when (−)-sparteine was employed, but the subsequent methylation led to the uniform *u* diastereomer **16a** in lower yield. This implies that the diastereoselectivity is controlled by the stereogenic center in the substrate. In the addition of prostereogenic aldehydes to the carbanionic intermediates **10** and **15**, only minimal stereodifferentiation was observed at the carbonyl group (see Table 1, **11f** and **16f**).

The conversion of the methylation product **16a** via **17a**[3, 10, 17] into the free amino alcohol **18a**[3, 10, 17, 18] demonstrates that the amino[19] and hydroxyl[3] groups can be removed by standard procedures.

We have found a novel, broadly applicable method for the highly stereoselective synthesis of β-amino alkanols and 2-amino-1-hydroxycarboxylic acids. Moreover, we have proven that *N*-benzylamino groups are capable of effecting differentiation not only between diastereotopic faces[13] but also between diastereotopic groups like protons.

Experimental Procedure

A solution of 1.0 mmol of the carbamate and 3.0 mmol of the diamine in 8 mL of anhydrous diethyl ether at −78 °C was treated with 3.0 mmol[20] of *sec*-butyllithium (ca. 1.4 M in cyclohexane/hexane). The reaction mixture was stirred at −78 °C for 3 h, 3.0 mmol of the electrophile was added, and the reaction mixture was then allowed to warm to room temperature. After workup with diethyl ether and water (2 mL), the crude product was purified by flash chromatography on silica gel or alumina (activity 2–3) eluting with diethyl ether/pentane. An excess of carbon dioxide was used as the electrophile in the preparation of the methyl esters **7a** and **16d**. The reaction mixture was acidified to pH 5 with 2 N HCl and the crude carboxylic acids treated with diazomethane.

Received: June 22, 1992 [Z 5422 IE]
German version: *Angew. Chem.* **1992**, *104*, 1547

CAS Registry numbers:
(−)-**3**, 90-39-1; **4**, 143746-13-8; **6a**, 143746-16-1; **6b**, 143746-17-2; **6c**, 143746-18-3; **6d**, 143746-19-4; (*R*)-**7**, 143837-93-8; (*S*)-**7**, 143837-94-9; **8** (isomer 1), 23788-74-1; **9**, 143746-14-9; **11a**, 143746-20-7; **11e**, 143746-21-8; **11f** (isomer 1), 143746-22-9; **11f** (isomer 2), 143837-95-0; **12a**, 111085-50-8; *epi*-**12a**, 111060-90-3; **13**, 111060-65-2; **14**, 143746-15-0; **16a**, 143746-23-0; **16c**, 143746-24-1; **16d**, 143790-27-6; **16f** (isomer 1), 143746-25-2; **16f** (isomer 2), 143837-96-1; **16g**, 143746-26-3; **17a**, 143746-27-4; **18a**, 113865-57-9; *ent*-**18a**, 113865-55-7; TMEDA, 110-88-9; CH_3I, 74-88-4; Me_3SiCl, 75-77-4; Bu_3SnCl, 1461-22-9; CO_2, 9224-50-1; $(CH_3)_2CHCH{=}O$, 78-84-2; $(CH_3)_2C{=}O$, 67-64-1; dibenzylamine, 103-49-1.

[1] Reviews: a) J. E. Saavedra in *Umpoled Synthons* (Ed.: T. Hase), Wiley, New York, **1981**, p. 101; b) D. Seebach, *Angew. Chem.* **1990**, *102*, 1363; *Angew. Chem. Int. Ed. Engl.* **1990**, *29*, 1320.
[2] P. Beak, L. G. Carter, *J. Org. Chem.* **1981**, *46*, 2363.
[3] a) D. Hoppe, F. Hintze, P. Tebben, *Angew. Chem.* **1990**, *102*, 1457; *Angew. Chem. Int. Ed. Engl.* **1990**, *29*, 1422; b) F. Hintze, D. Hoppe, *Synthesis* **1992**, in press; c) Patent application D. Hoppe, P. Tebben, F. Hintze, T. Raffel, EP 464439 (January 8, 1992).
[4] For the X-ray structure analysis of a (1-lithioallyl)carbamate–sparteine complex see: M. Marsch, K. Harms, O. Zschage, D. Hoppe, G. Boche, *Angew. Chem.* **1991**, *103*, 338; *Angew. Chem. Int. Ed. Engl.* **1991**, *30*, 321.
[5] Review of earlier attempts at chiral modification of lithiocarbanions with sparteine: R. Noyori, M. Kitamura, *Angew. Chem.* **1991**, *103*, 34; *Angew. Chem. Int. Ed. Engl.* **1991**, *30*, 49.
[6] Enantioselective deprotonation and substitution of *N*-Boc-pyrrolidine by *s*BuLi/(−)-sparteine: S. T. Kerrick, P. Beak, *J. Am. Chem. Soc.* **1991**, *113*, 9708; D. J. Gallagher, S. T. Kerrick, P. Beak, *ibid.* **1992**, *114*, 5872.
[7] M. Paetow, H. Ahrens, D. Hoppe, *Tetrahedron Lett.* **1992**, *33*, 5323, 5327.
[8] P. Sommerfeld, D. Hoppe, *Synlett* **1992**, 764.
[9] Preparation following the alkoxide method, ref [3].
[10] All new compounds were obtained analytically pure (C,H ±0.3%).
[11] Determined by ^{1}H NMR spectroscopy in ca. 0.05 M solution ($CDCl_3$) with 1–2 mol% tris[3-(heptafluoropropylhydroxymethylene)-(+)-camphorato]praseodym [Pr(hfc)$_3$] for **6b** and the free alcohol obtained from **6a**.
[12] (*R*)-**7**: M.p. 55 °C (ether/pentane): $[\alpha]_D^{20}$ + 45.6 (c = 1.0, $CHCl_3$); (*S*)-**7**: $[\alpha]_D^{20}$ −48.8 (c = 1.0, $CHCl_3$).
[13] Review: a) M. T. Reetz, *Angew. Chem.* **1991**, *103*, 1559; *Angew. Chem. Int. Ed. Engl.* **1991**, *30*, 1531; b) M. T. Reetz, M. W. Drewes, A. Schmitz, *ibid.* **1987**, *99*, 1186 and **1987**, *26*, 1141.
[14] **12a**: Oil; $[\alpha]_D^{20}$ +28.0 (c = 1.0, $CHCl_3$).
[15] Review on double stereodifferentiation: S. Masamune, W. Choy, J. S. Petersen, L. R. Sita, *Angew. Chem.* **1985**, *97*, 1; *Angew. Chem. Int. Ed. Engl.* **1985**, *24*, 1.
[16] We thank Dr. M. Göhrt, Bayer AG, Leverkusen (FRG) for the structure analysis. These results will be reported elsewhere.
[17] **17a**: Oil; $[\alpha]_D^{20}$ −85.0 (c = 0.7, $CHCl_3$). **18a**: M.p. 86 °C (ether/pentane); $[\alpha]_D^{20}$ −36.4 (c = 1.0, MeOH). The data reported for *ent*-**18a** [18] differ significantly.
[18] A. K. Ganguly, S. Szmulewicz, O. Z. Sarre, D. Greeves, J. Morton, J. McGlotten, *J. Chem. Soc. Chem. Commun.* **1974**, 395.
[19] B. El Amin, G. M. Anantharamaiah, G. P. Royer, G. E. Means, *J. Org. Chem.* **1979**, *44*, 3442.
[20] When only 1.5 equiv of *sec*-butyllithium/(−)-sparteine was used in the reaction with **4**, the yields were markedly lower.

^{99m}Tc Labeled Biotin Conjugate in a Tumor "Pretargeting" Approach with Monoclonal Antibodies**

By *Peter Koch* and *Helmut Robert Mäcke**

An important link between chemistry, biology, and medicine is the synthesis and use of bifunctional chelators specific for radioactive metal ions and designed for covalent coupling to biomolecules.[1] Among the biomolecules used clinically as radiopharmaceuticals are monoclonal antibodies (MAbs).[2] In particular, tumor-associated MAbs are potential diagnostic and therapeutic agents when labeled with γ-ray emitting (i.e. image producing) or particulate radiation emitting (i.e. cytotoxic) radioisotopes. Although somewhat successful in diagnosic applications, MAbs have drawbacks such as slow blood clearance and unspecific binding to normal tissues. This results in an unfavorable tumor/nontumor ratio and, more importantly, in a high and unnecessary radiation exposure for the patient.

One promising way to circumvent the problem of long-circulating, radioactive antibodies is the so-called pretargeting strategy. We report on the successful development of the chemical and physicochemical science of such a strategy with the avidin/biotin system.[3] The approach is schematically depicted in Figure 1. It has been used in a variety of biochemical studies, for example a strategy for selective protein cleavage,[4] and in many analytical in vitro applications.[5]

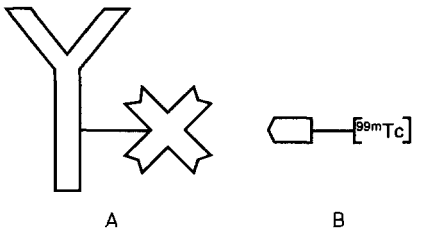

Fig. 1. Schematic representation of the antibody/avidin/biotin pretargeting approach. Avidin is a glycoprotein (M = 68000) with four binding sites for biotin ($K_D = 10^{-15}$ M^{-1}) which is a naturally occurring vitamin. A = Conjugate of MAb (left) and avidin (right), B = conjugate of PnAO–biotin and ^{99m}Tc.

In the pretargeting strategy, avidin is covalently attached to a tumor-specific antibody at a site that does not interfere with the biological activity of the antibody. The nonradioactive conjugate is injected and allowed to localize in the tumor for several days. Finally, a radiolabeled biotin derivative is injected. Because of its fast blood clearance it binds quickly and irreversibly to avidin at the tumor site and can be localized by imaging with an external gamma camera. The radionuclide of choice is ^{99m}Tc, a transition metal which has a short half-life and optimal nuclear physical characteristics for use in vivo. As the metal-coordinating properties of biotin are very weak,[6] the molecule must be modified by conjugation to a bifunctional ligand. Such a conjugate must then fulfill the following requisites: 1) fast formation of the ^{99m}Tc chelate under mild conditions at a $^{99m}TcO_4^-$ concentration of roughly 10^{-7} M; 2) high kinetic stability of the ^{99m}Tc-labeled conjugate under physiological conditions, that is, no transfer of the radionuclide to competing ligands in serum and tissue; 3) retained biological activity of modified biotin, in other words, its binding to avidin must be complete.

We synthesized a PnAO–biotin derivative **1**[7] (Fig. 2, Table 1) by treatment of (+)-biotin *N*-hydroxysuccinimide ester with copper(II) 6-*p*-aminobenzyl-3,3,9,9-tetramethyl-4,8-diazaundecane-2,10-dionedioxate in anhydrous dimethyl sulfoxide, followed by removal of the protecting Cu^{2+} ion with NaCN, and purification of the conjugate by medium-pressure chromatography (MPLC) on silica gel

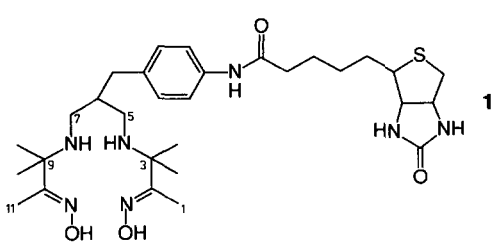

1

Fig. 2. Biotinylated 6-*p*-aminobenzyl-3,3,9,9-tetramethyl-4,8-diazaundecane-2,10-dionedioxime = PnAO–biotin = **1**.

[*] Prof. Dr. H. R. Mäcke, Dipl.-Chem. P. Koch
Institut für Nuklearmedizin
Universitätsspital Basel
Petersgraben 4, CH-4031 Basel (Switzerland)

[**] This research was supported by the Schweizerische Nationalfonds zur Förderung der wissenschaftlichen Forschung (no. 31-27739.89) and the Regionale Krebsliga beider Basel. We are grateful to Dr. G. Paganelli, University of Milan, for pictures from his clinical studies.

Table 1. ^{13}C NMR, ^{1}H NMR, and MS data of PnAO-biotin **1** [a].

^{13}C NMR (90 MHz, [D$_6$]DMSO, 25 °C, TMS): $\delta = 9.06$ ($(CH_3)C{=}NOH$), 25.03 ($CH_2CH_2(CO)NH$), 25.56 ($(CH_3)_2CNH$), 27.97 (CH_2CHS), 28.13 (CH_2CH_2CHS), 36.00 ($PhCH_2CH$), 36.05 ($CH_2(CO)NH$), 39.85 (SCH_2CH), 40.91 ($PhCH_2CH$), 44.45 (CH_2NH), 55.25 (CH_2CHS), 56.68 ($(CH_3)_2CNH$), 59.06 (SCH_2CHNH), 60.90 ($CH_2CHCHNH$), 118.68 (Ph), 128.79 (Ph), 135.24 (C(Ph)NH(CO)), 136.78 (C(Ph)CH_2), 159.69 (C=NOH), 162.50 (NH(CO)NH), 170.69 (C(Ph)NH(CO))

^{1}H NMR (360 MHz, [D$_6$]DMSO, 25 °C, TMS): $\delta = 1.10$ (d, 12H, $(CH_3)_2CNH$), 1.38 (m, 2H, CH_2CHS), 1.50 (m, 2H, $CH_2CH_2(CO)$), 1.62 (m, 2H, CH_2CH_2CH), 1.68 (s, 6H, $CH_3C{=}NOH$), 2.08 (m, 1H, Ph-CH_2CH), 2.20 (d, 4H, CH_2NH), 2.28 (t, 2H, $CH_2(CO)NH$), 2.47 (m, 2H, $PhCH_2CH$), 2.58 (d, 1H, SCH_2CHNH), 2.82 (q, 1H, SCH_2CHNH), 3.12 (m, 1H, CH_2CHS), 4.12 (m, 1H, $CHCHNH$), 4.31 (m, 1H, SCH_2CHNH), 6.39 (d, 2H, NH(CO)NH), 7.08 (d, 2H, Ph), 7.46 (d, 2H, Ph), 9.77 (s, 1H, $PhNH(CO)$), 10.37 (s, 2H, C=NOH)

FAB-MS (8 keV): m/z 604 (M^+)

[a] The NMR signals could be assigned with HCCORR and COLOC experiments.

with acetonitrile/25% NH_3 10/1.[8] The synthesis of the ^{99m}Tc complex depends on two important, fairly restrictive requisites. The preparation must start with an approximately 10^{-7} M solution of TcO_4^- in physiological saline, that is, the starting material, generator-eluted TcO_4^-, is present in low concentrations and must be reduced to an oxidation state suitable for coordinative binding. This is usually done with Sn^{2+} as a two-electron reducing agent in the presence of tartrate or citrate. These weak ligands are used to avoid formation of Tc/Sn colloids and serve to transfer technetium(v) to the biomolecule-conjugated ligand. We developed a labeling protocol on this basis which gives 99% labeling yield within 15 min at room temperature and physiological pH (see *Experimental Procedure*).

Quality control of ^{99m}Tc–PnAO–biotin was performed with high-pressure liquid chromatography (HPLC). The labeled conjugate (> 99%) eluted after 2 min 18 s, TcO_4^- after 1 min 30 s, and the ^{99m}Tc–tartrate complex after 1 min 5 s.

The biological activity of ^{99m}Tc–PnAO–biotin was tested in two related experiments. In the first, the labeled conjugate was mixed with avidin at 37 °C in phosphate buffer (pH 7.4) and incubated for 10 min with shaking. The mixture was then subjected to gel filtration (Sephadex G50). Approximately 99% of ^{99m}Tc was bound to the high-molecular-weight protein avidin, which indicated that the modified biotin retained its biological activity. In the second experiment, which more closely resembled the situation in a solid tumor, the binding capacity was checked with avidin immobilized on beaded agarose. ^{99m}Tc–PnAO–biotin was slowly passed through the column (1 mL per min) and the column washed with phosphate buffer (pH 7.3). 98 ± 2% (average of five experiments) of the radioactivity was strongly bound to the immobilized avidin, again showing that the modified biotin retained its high affinity for avidin.

The kinetic stability of ^{99m}Tc–PnAO–biotin in terms of loss of the metal ion, disproportionation, or transfer of ^{99m}Tc to serum proteins was determined by its incubation with phosphate-buffered saline solution (pH 7.3, 37 °C) over 24 h. Aliquots were taken (after 1, 2, 3, 4, 5, 6, 12, 18, and 24 h) and analyzed by HPLC and TLC (silica gel, isopropanol/25% NH_3 9/1). No significant loss of bound ^{99m}Tc was found within the first 6 h, and after 24 h only 2.5% TcO_4^- was detected. In a second experiment freshly prepared human serum was incubated with ^{99m}Tc–PnAO–biotin and analyzed by gel filtration (Biogel P2). The conjugate proved to be stable under these conditions as well.

Physicochemical data show that the Tc–PnAO complex is neutral and lipophilic: it can be readily extracted into diethyl ether and does not move on paper electrophoresis. PnAO derivatives have been tested as chelators for technetium, and an X-ray crystal structure revealed five-coordinate ^{99m}Tc in one such complex with a Tc=O unit at the apex of a square pyramid and the tetradentate ligand in a pseudo-macrocyclic arrangement with an intramolecular hydrogen bond between the oxime oxygen atoms. On coordination of TcO^{3+} the two amine nitrogens lose their protons resulting in the neutral complex.[9]

After its sterility and pyrogenicity (pyrogen = fever-producing substance) had been tested, ^{99m}Tc–PnAO–biotin was successfully applied in a three-step approach in the diagnosis of patients with different types of tumors, and a clinical trial on 15 patients with brain tumors was completed. The stability found in the in vitro experiments was confirmed in vivo. Moreover, the high affinity of ^{99m}Tc–PnAO–biotin for tumor-associated avidin was shown by imaging with an external gamma camera. A typical example of a positive scan of a brain tumor is shown in Figure 3.[10] This is the first use of a ^{99m}Tc complex in a pretargeting approach in patients. Similar complexes for use in therapy are being developed.

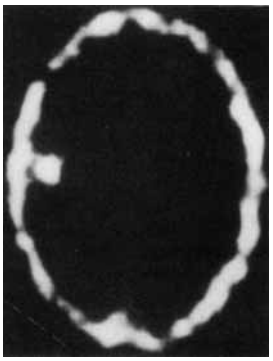

Fig. 3. Single-photon emission computed tomography (SPECT) scan of a patient with a brain tumor 30 min after injection of ^{99m}Tc–PnAO–biotin. Tumor-specific avidinated MAb was injected 3 days before. The tumor can be seen on the left side.

Experimental Procedure

The nine-step synthesis of **1** will be published elsewhere.

Labeling of **1** with ^{99m}Tc: 1.7 mL of a N_2-purged solution containing 900 μg (1.49 μmol) **1**, 4.5 μg (0.02 μmol) $SnCl_2 \cdot 2H_2O$ and 8.05 mg (28.5 μmol) potassium sodium tartrate tetrahydrate was adjusted to pH 7.5 with NaOH. To this solution was added 740–1100 MBq $^{99m}TcO_4^-$, freshly eluted from a generator. The mixture was left at room temperature for 15 min and after sterility filtration was ready for quality control and injection. For highly specific activity labeling, the excess of unlabeled PnAO–biotin was easily removed with a C_{18} Sepak cartridge. The more hydrophilic PnAO–biotin was washed from the cartridge with water, whereas ^{99m}Tc–PnAO–biotin was removed with methanol, and the solvent was evaporated at 40 °C with a stream of N_2. The residue was dissolved in phosphate buffer for injection.

Received: April 8, 1992
Revised: June 4, 1992 [Z 5292 IE]
German version: *Angew. Chem.* **1992**, *104*, 1492

[1] M. K. Moi, C. F. Meares, S. J. DeNardo, *J. Am. Chem. Soc.* **1988**, *110*, 6266–6267; D. J. Hnatowich, U. U. Layne, R. J. Childs, D. Lateigne, M. A. Davis, T. W. Griffin, P. W. Doherty, *Science* **1983**, *220*, 613–617; M. W. Brechbiel, O. A. Gansow, R. W. Atcher, J. Schlom, J. Esteban, D. E. Simpson, D. Colcher, *Inorg. Chem.* **1986**, *25*, 2772–2781; G. Ruser, W. Ritter, H. R. Maecke, *Bioconjugate Chem.* **1990**, *2*, 345–349.
[2] J. P. Mach, S. Correl, M. Forni, J. Ritschard, A. Donath, P. Alberto, *N. Engl. J. Med.* **1980**, *303*, 5–10; T. A. Waldmann, *Science* **1991**, *252*, 1657–1662.
[3] M. Wilchek, E. A. Bayer, *Immunol. Today* **1984**, *5*, 39–42.
[4] D. Hoyer, H. Cho, P. G. Schultz, *J. Am. Chem. Soc.* **1990**, *112*, 3249–3250.

[5] M. Wilchek, E. A. Bayer, *Trends Biochem. Sci.* **1989**, *14*, 408–412.
[6] H. Sigel, *Experientia* **1981**, *37*, 789–798.
[7] PnAO is an acronym used for this type of ligand. PnAO is the abbreviation for the bifunctional derivative of propylenediamine dioxime.
[8] The product was pure by TLC (silica gel, CH_3CN/25% NH_3 10/1, $R_f = 0.18$) and HPLC (C18, Bondapak 10 μm, 0.01 M ammonium acetate (pH 7)/CH_3CN 2/3). The ^{13}C and ^1H NMR spectra as well as FAB mass spectra were consistent with the proposed structure.
[9] S. Jurisson, E. O. Schlemper, D. E. Troutner, L. R. Canning, D. P. Nowotnik, R. D. Neirinckx, *Inorg. Chem.* **1986**, *25*, 543–549.
[10] In a few patients the pretargeting approach was compared with the usual direct application of a ^{99m}Tc labeled antibody. The pretargeting approach showed the tumor very clearly with very little unspecific uptake and a good tumor/nontumor ratio, whereas the direct labeling showed high unspecific uptake. The comparative study will be published elsewhere, but supplementary material is available on request.

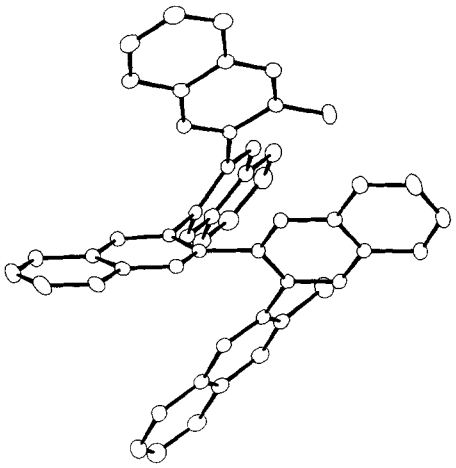

Fig. 1. Structure of **4**. CH_2SiMe_3 groups and hydrogen atoms are omitted for clarity.

Enantioselective Polymerization of 1,2-Diisocyanoarenes—Synthesis of Optically Active, Helical Poly(quinoxaline-2,3-diyl)s

By *Yoshihiko Ito*,* *Eiji Ihara*, and *Masahiro Murakami*

The synthesis of an optically active polymer from an achiral monomer using a chiral catalyst is a significant challenge.[1] We now report an enantioselective polymerization of 1,2-diisocyanoarenes induced by new chiral palladium catalysts having helical conformations.

We reported recently that a new living polymerization of 1,2-diisocyanoarenes **1** was catalyzed by *trans*-bromo(methyl)bis(phosphine)palladium(II) to give poly(quinoxaline-2,3-diyl)s **3** with narrow molecular weight distributions.[2] Noteworthy was that several of the propagating palladium(II) complexes **2**, which were still reactive in the polymerization, were isolated and fully characterized.

The X-ray crystallographic study of pentamer **4**, revealed a helical structure (Fig. 1).[3] This finding prompted us to undertake a synthesis of optically active poly(quinoxaline-2,3-diyl) **3**, whose chirality emanates from the helical

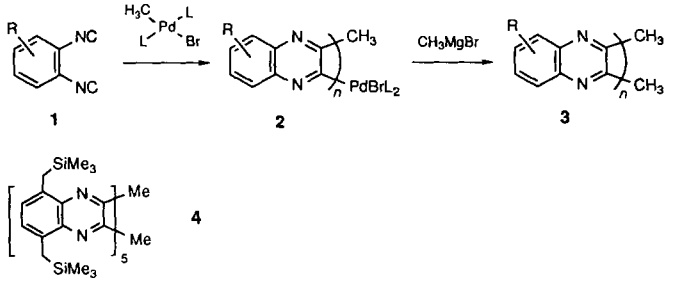

structure. Oligomerization of 1,2-diisocyano-3,6-di-*p*-tolylbenzene (4 equiv) catalyzed by *trans*-bromobis[bis{(*S*)-2-methylbutyl}phenylphosphine]methylpalladium(II) (1 equiv) gave a mixture of oligo(5,8-di-*p*-tolylquinoxaline-2,3-diyl)palladium(II) complexes in quantitative yield. Gel permeation chromatography (GPC) on polystyrene allowed the isolation of pentamer **5**. Of note was that subsequent highly resolved, preparative high-pressure liquid chromatography (HPLC) permitted the separation of two isomers **5a** and **5b** (3:4), which were conformationally stable in solution. Circular dichroism (CD) spectra of **5a** and **5b** showing large Cotton effects are nearly mirror images of each other and indicative of enantiomers with opposite helicities (Fig. 2). After removal of the chiral bis(phosphine)palladium(II) moiety by the reaction with methylmagnesium bromide, **5** gave quinque(quinoxaline-2,3-diyl)s **6**, which have identical spectroscopic properties[4] and optical rotations in opposite directions; **6a** $[\alpha]_D = +25$ ($c = 0.1$, $CHCl_3$), **6b**:$[\alpha]_D = -25$ ($c = 0.1$, $CHCl_3$). The CD spectra of **6a** and **6b** exhibit weak Cotton effects. Based on these results, the two isomers **5a** and **5b** were assigned to the diastereomers which arise from

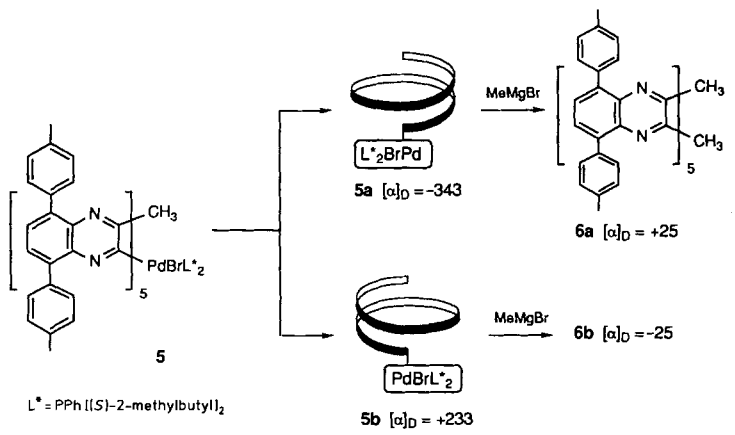

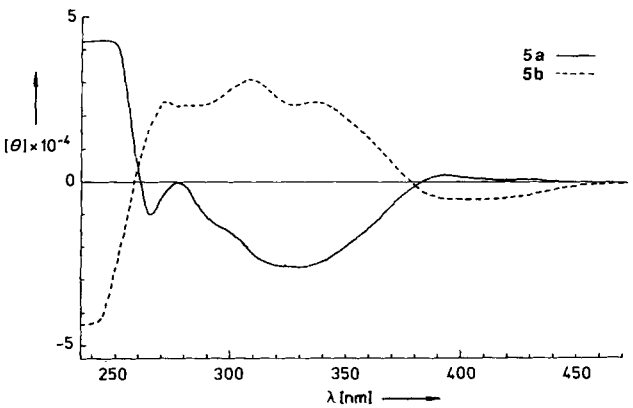

Fig. 2. CD spectra of **5a** and **5b** in CH_2Cl_2.

[*] Prof. Dr. Y. Ito, E. Ihara, Dr. M. Murakami
Department of Synthetic Chemistry
Faculty of Engineering, Kyoto University
Yoshida, Kyoto 606 (Japan)

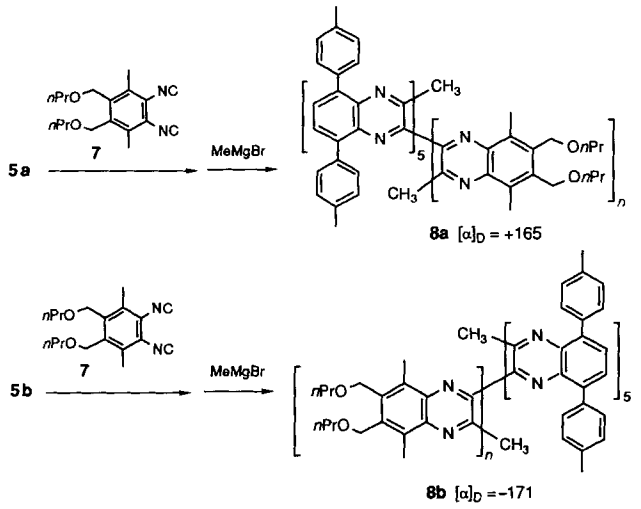

the combination of the helical secondary structure and the chirality of the phosphine ligand.

We thought that the rigid and stable conformations of **5a** and **5b** might induce further polymerization of 1,2-diisocyanoarenes with stereocontrol, resulting in the extension of the helical chain. Indeed, enantioselective polymerization of 1,2-diisocyano-3,6-dimethyl-4,5-bis(propoxymethyl)benzene (**7**)[5] was accomplished with the diastereomerically pure palladium(II) complex **5a** as a chiral initiator. After removal of the chiral palladium(II) moiety, optically active poly(quinoxaline-2,3-diyl) **8a** ($[\alpha]_D = +165$ ($c = 0.54$, $CHCl_3$), $M_n = 11\,200$ (vapor-pressure osmometry in $CHCl_3$)) was obtained which showed a larger optical rotation and much more distinct Cotton effects than **6a** (Fig. 3).[6] Similarly, the other diastereomer **5b** gave poly(quinoxaline-2,3-diyl) **8b**,

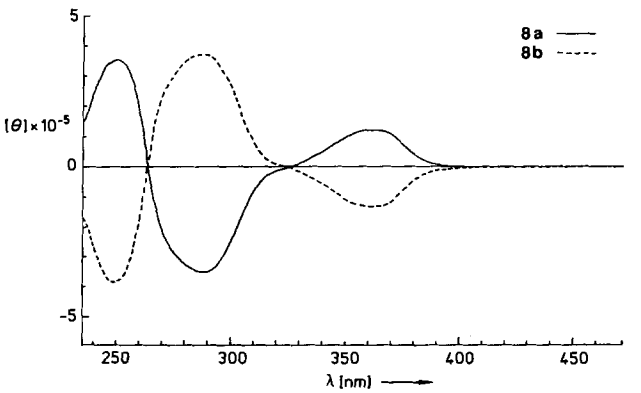

Fig. 3. CD spectra of **8a** and **8b** in CH_2Cl_2.

whose optical rotation is almost identical, but with the opposite sign ($[\alpha]_D = -171$ ($c = 0.56$, $CHCl_3$), $M_n = 10\,000$ (vapor-pressure osmometry in $CHCl_3$)). The CD spectrum of **8b** is the complete mirror image of that of **8a** (Fig. 3). These observations indicate that poly(quinoxaline-2,3-diyl)s **8a** and **8b** have helical structures which are the mirror images of each other.

Experimental Procedure

1,2-Diisocyanoarenes: 1,2-Diisocyano-3,6-di-*p*-tolylbenzene and **7** were prepared from the corresponding 1,2-diformamidoarenes by the procedure previously reported [7].

5: MeMgBr (2 mmol, 2M solution in ether) was added to a solution of *trans*-bis[bis{(*S*)-2-methylbutyl}phenylphosphine]dibromopalladium(II) (66 mg, 86 μmol) in benzene (5 mL) cooled in an ice-water bath and then stirred for 20 min. The mixture was quenched with water and extracted with benzene. The collected organic phases were dried, and the solvent was removed under vacuum to give *trans*-bis[bis{(*S*)-2-methylbutyl}phenylphosphine]bromo(methyl)-palladium(II) (57 mg, 81 μmol) in almost pure form. To this were added 1,2-diisocyano-3,6-di-*p*-tolylbenzene (99 mg, 0.32 mmol) and THF (5 mL). The mixture was stirred at room temperature for 12 h and then concentrated to afford a mixture of oligo(5,8-di-*p*-tolylquinoxaline-2,3-diyl)palladium(II) complexes quantitatively. Pentamer **5** (48 mg) was isolated by preparative GPC (polystyrene, $CHCl_3$). Two isomers **5a** and **5b** were separated by preparative HPLC on silica gel (hexane: EtOAc:EtOH = 200:20:1). **5a**: UV (CH_2Cl_2): λ_{max} [nm] (ε) = 263 (139000); $[\alpha]_D = -343$ ($c = 0.7$, $CHCl_3$). **5b**: UV (CH_2Cl_2): λ_{max} [nm] (ε) = 263 (175000); $[\alpha]_D = +233$ ($c = 0.8$, $CHCl_3$).

8a: A solution of **7** (31 mg, 0.10 mmol) and **5a** (4.9 mg, 2.2 μmol) in THF (6 mL) was stirred at room temperature for 36 h before MeMgBr (0.6 mmol, 2 M solution in ether) was added. After the reaction mixture had been stirred for 1 h, water was added, and the mixture was extracted with $CHCl_3$. The collected organic phases were dried, and the solvent was removed under vacuum. Preparative GPC (polystyrene, $CHCl_3$) afforded **8a**. Yield: 27 mg (78%). UV (CH_2Cl_2): λ_{max} [nm] (ε) = 287 (905000), 349 (345000).

8b: Following the procedure for **8a**, **7** (30.5 mg, 0.10 mmol) and **5b** (4.9 mg, 2.2 μmol) provided **8b**. Yield: 28 mg (83%). UV (CH_2Cl_2): λ_{max} [nm] (ε) = 288 (912000), 349 (339000).

Received: May 2, 1992 [Z 5327 IE]
German version: *Angew. Chem.* **1992**, *104*, 1508

CAS Registry numbers:
4, 144043-06-1; **5a**, 144071-96-5; **6a**, 144043-08-3; **7** (homopolymer), 144043-01-6; *trans*-$BrPd(CH_3)[P(Ph)\{(S)\text{-}CH_2CH(CH_3)CH_2CH_3\}_2]_2$, 144043-09-4; 1,2-diisocyano-3,6-di-*p*-tolylbenzene, 144043-07-21.

[1] Examples of optically active helical polymers: polyisocyanide: P. C. J. Kamer, R. J. M. Nolte, W. Drenth, *J. Am. Chem. Soc.* **1988**, *110*, 6818; poly(triarylmethylmethacrylate): Y. Okamoto, H. Mohri, T. Nakano, K. Hatada, *ibid.* **1989**, *111*, 5952; polychloral: K. Ute, K. Hirose, H. Kashimoto, K. Hatada, O. Vogl, *ibid.* **1991**, *113*, 6305; poly(β-pyrrole): P. Magnus, W. Danikiewicz, T. Katoh, J. C. Huffman, K. Folting, *ibid.* **1990**, *112*, 2465.
[2] Y. Ito, E. Ihara, M. Murakami, M. Shiro, *J. Am. Chem. Soc.* **1990**, *112*, 6446.
[3] **4**: Monoclinic, $P2_1/a$, $a = 25.287(8)$, $b = 24.423(8)$, $c = 15.842(7)$ Å, $\beta = 93.52(3)°$, $V = 9766(3)$ Å^3, $Z = 4$, $\lambda(Cu_{K\alpha}) = 1.54178$ Å, Mac Science MXC3 diffractometer. The structure was solved by direct methods and Fourier synthesis (CRYSTAN program package). $R = 0.068$, $R_w = 0.080$ for 8462 reflections [$F_0 > 4\sigma(F_0)$]. Further details of the crystal structure investigation are available on request from the Director of the Cambridge Crystallographic Data Centre, University Chemical Laboratory, Lensfield Road, GB-Cambridge CB2 1EW (UK), on quoting the full journal citation.
[4] **6**: UV (CH_2Cl_2): λ_{max} [nm] (ε) = 263 (73500) 321 (35500); MS: *m/z* 1572.7 (MH^+).
[5] Compound **7** was used as a monomer to ensure higher solubility of the resulting polymer in THF.
[6] The CD bands (250 and 290 nm) were assigned to the helical chromophore of **8** by quantum mechanical calculations [8] of the helical poly(quinoxaline-2,3-diyl).
[7] Y. Ito, A. Ohnishi, H. Ohsaki, M. Murakami, *Synthesis* **1988**, 714.
[8] Theoretical CD curves for helical poly(quinoxaline-2,3-diyl) were computed on the basis of the exciton theory (R. W. Woody, *J. Polym. Sci. Macromol. Rev.* **1977**, *12*, 181), on the model compound 2-butyl-5,6,7,8-tetramethylquinoxaline taking into account a π–π^* transition at 252 nm polarized along the long axis of the molecule. Details of the CD spectral analysis will be published in due course.

Triphosphatrisilacyclohexanes as Tridentate Coronands in Cr and Mo Complexes: Activation of Si–H in an Early Stage versus Phosphane Coordination

By *Matthias Driess,* Michael Reisgys,* and *Hans Pritzkow*

Dedicated to Professor Hermann Schildknecht on the occasion of his 70th birthday

Only isolated examples of cyclic multidentate phosphane ligands such as phospha crown ethers are known, and these

[*] Dr. M. Driess, Dipl.-Chem. M. Reisgys, Dr. H. Pritzkow
Anorganisch-chemisches Institut der Universität
Im Neuenheimer Feld 270, D-W-6900 Heidelberg (FRG)

[**] This work was supported by the Deutsche Forschungsgemeinschaft. We thank the referees for valuable tips.

are difficult to prepare.[1] Nevertheless, an increasing demand exists for such phosphane ligands containing a large potential for varying the substituents, so that the design of metal complexes (e.g. as catalytic active substances) may be achieved more efficiently than is possible with acyclic systems. The difficult access to cyclic multidentate organophosphanes contrasts with the simple synthesis of cyclophosphasilanes,[2] whose suitability as chelate ligands in organometallic chemistry has hardly been studied.[3] The only cyclophosphasilane with a P_3Si_3 ring framework that has been described is $(PhP–SiPh_2)_3$, which can coordinate through three phosphorus atoms to $[Mo(CO)_3]$, but not to $[Cr(CO)_3]$.[4] Till now, neither the free ligand nor the complex with $[Mo(CO)_3]$ has been structurally characterized.

We report here on the first hexaorgano-substituted, crystalline triphosphatrisilacyclohexanes **1a,b** (Scheme 1) containing one Si–H bond per Si atom and their unusual coordination to $[M(CO)_3]$ fragments (M = Cr, Mo). Ligand **1a** and the $[Cr(CO)_3]$ fragment surprisingly form the Si,H,Cr

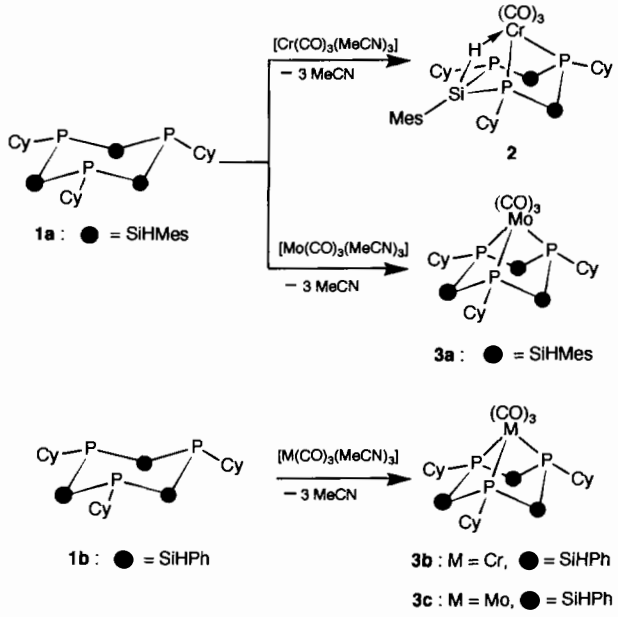

Scheme 1. Synthesis of complexes **2** and **3**. Cy = cyclohexyl, Mes = 2,4,6-trimethylphenyl (mesityl). The Si-bound H atoms are located in axial positions in all compounds.

three-center two-electron complex **2**, and only with $[Mo(CO)_3]$ is the anticipated coordination by three phosphorus atoms observed (**3a**). In contrast, **1b** functions exclusively as a tridentate phosphane ligand towards $[M(CO)_3]$ (M = Cr, Mo; **3b,c**). The P_3Si_3 heterocycles **1a,b** (Table 1) are formed by cyclocondensation of $RSiHCl_2$ (R = Mes, Ph) with LiPH(Cy). The P_3Si_3 ring inverts rapidly in solution on the NMR timescale. Similar ring flexibility and low inversion barriers at phosphorus atoms occur in $(PhP–SiPh_2)_3$ and $(HP–SiMe_2)_3$.[4] The substituents at Si and P are expected to occupy equatorial positions because of their bulk; a single-crystal X-ray analysis confirms this for **1a** (Fig. 1). The P_3Si_3 ring is in a chair conformation and is considerably distorted on account of the different endocyclic bond angles at phosphorus and silicon.

If ligand **1a** is stirred with $[Cr(CO)_3(MeCN)_3]$ in benzene at 25 °C, **2** forms instead of the chromium complex

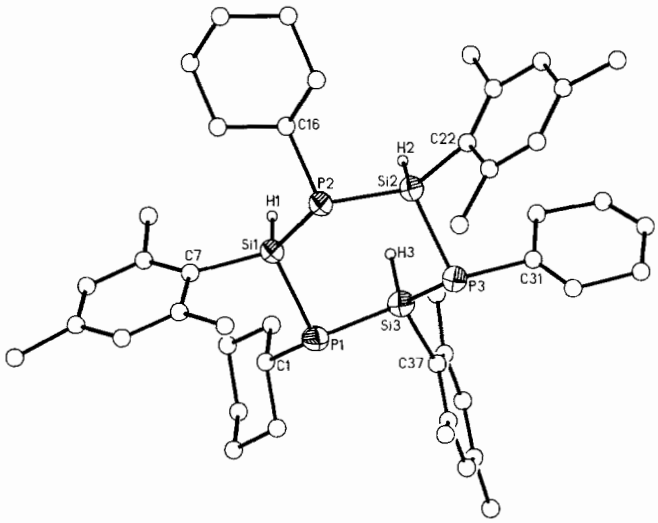

Fig. 1. Molecular structure of **1a** in the crystal. Selected distances [Å] and angles [°]: P1–Si1 2.258(4), P1–Si3 2.252(4), Si1–H1 1.26(6), Si1–P2 2.272(3), Si2–P2 2.267(3), Si2–H2 1.44(6), Si2–P3 2.266(4), Si3–P3 2.252(3), Si3–H3 1.38(7); Si3-P1-Si1 99.5(1), P2-Si1-P1 113.3(1), Si2-P2-Si1 98.4(1), P3-Si2-P2 108.6(1), Si3-P3-Si2 97.8(1), P3-Si3-P1 100.2(1).

analogous to **3a**. A notable feature of **2** is an agostic Si–H function at the chromium center (see Scheme 1). The constitution of **2** is deduced from the ^1H, ^{31}P, and ^{29}Si NMR spectra (Table 1). The presence of a Si,H,Cr three-center

Table 1. Selected physical data of **1–3**.

1a: ^1H NMR (C_6D_6, 25 °C, 200 MHz): δ = 0.8–1.7 (m, 33H, C_6H_{11}), 2.01 (s, 9H, *p*-Me), 2.76 (br., 9H, *o*-Me), 3.31 (br., 9H, *o*-Me), 6.28 (s, 3H, SiH), 6.75–6.80 (br., 6H, arom. H); ^{31}P NMR (81 MHz): δ = –162.1 (s); $^{29}Si\{^1H\}$ NMR (39.7 MHz): δ = –24.3 (m); IR (vSiH, CH_2Cl_2): $\tilde{\nu}$[cm^{-1}] = 2142; MS (EI, 70 eV): *m/z* (%) 785 ($(M-H)^+$, 2), 702 ($(M-H-C_6H_{11})^+$, 100), 267 (Mes_2SiH^+, 39). M.p. 211–213 °C

1b: ^1H NMR (C_6D_6, 25 °C, 200 MHz): δ = 0.90–1.70 (m, 33H, C_6H_{11}), 5.47 (m, 3H, SiH), 7.37–7.76 (m, 15H, arom. H); ^{31}P NMR (36 MHz): δ = –158.0 (s); IR (vSiH, CH_2Cl_2): $\tilde{\nu}$[cm^{-1}] = 2144; MS (EI, 70 eV): *m/z* (%) 660 (M^+, 2), 577 ($(M-C_6H_{11})^+$, 100), 183 (Ph_2SiH^+, 31). M.p. 232–234 °C

2: ^1H NMR (C_6D_6, 25 °C, 200 MHz): δ = –7.69 (d, 1H, SiHCr, *J*(P,H) = 33.6 Hz), 0.8–1.76 (m, 33H, C_6H_{11}), 1.87 (s, 3H, *p*-Me), 2.00 (s, 3H, *p*-Me), 2.11 (s, 3H, *p*-Me), 2.36–3.17 (m, 18H, *o*-Me), 5.64 (d, 1H, SiH, *J*(P,H) = 26.1 Hz), 6.50 (m, 1H, SiH), 6.73 (s, 2H, arom. H), 6.6–6.78 (m, 4H, arom. H); ^{31}P NMR (81 MHz): δ = –204.9 (d, *J*(P,P) = 28.3 Hz), –118.0 (dd, *J*(P,P) = 28.3, 90.7 Hz), –41.1 (d, *J*(P,P) = 90.7 Hz); ^{29}Si NMR (39.7 MHz): δ = –45.2 (dm, ^1J(Si,H) = 135.7, ^1J(Si,P) = 69 Hz, SiHCr), –20.5 (br.d, ^1J(Si,H) = 228.6, ^1J(Si,P) = 9 Hz, –16.9 (dd, ^1J(Si,H) = 210.9, ^1J(Si,P) = 56 Hz); IR (vSiH, CH_2Cl_2): $\tilde{\nu}$[cm^{-1}] = 2142 (SiH), 1994 (SiHCr); MS (EI, 70 eV): *m/z* (%) 922 (M^+, 1), 838 ($(M-3CO)^+$, 60), 703 ($(M-Cr(CO)_3-C_6H_{11})^+$, 100), 267 (Mes_2SiH^+, 65). M.p. 209–212 °C (decomp)

3a: ^1H NMR (C_6D_6, 25 °C, 200 MHz): δ = 0.8–1.8 (m, 33H, C_6H_{11}), 2.31 (s, 9H, *p*-Me), 2.57 (s, 9H, *o*-Me, 3.12 (s, 9H, *o*-Me), 6.92 (s, 3H, arom. H), 6.97 (s, 3H, arom. H), 7.88 (m, 3H, SiH); ^{31}P NMR (81 MHz): δ = –129.8 (s); ^{29}Si NMR (39.7 MHz): δ = 33.3 (d, ^1J(Si,H) = 205 Hz); IR (vSiH, CH_2Cl_2): $\tilde{\nu}$[cm^{-1}] = 2165; MS (EI, 70 eV): *m/z* (%) 968 (M^+, 0.3), 703 ($(M-Mo(CO)_3-C_6H_{11})^+$, 100), 267 (Mes_2SiH^+, 22). M.p. 205 °C (decomp)

3b: ^1H NMR (C_6D_6, 25 °C, 200 MHz): δ = 0.89–2.25 (br.m, 33H, C_6H_{11}), 6.12 (br., 3H, SiH), 7.07–7.79 (m, 15H, arom. H); ^{31}P NMR (81 MHz): δ = –66.3 (s); ^{29}Si NMR (39.7 MHz): δ = 8.3 (d, ^1J(Si,H) = 210 Hz, SiH); IR (vSiH, CH_2Cl_2): $\tilde{\nu}$[cm^{-1}] = 2120; MS (EI, 70 eV): *m/z* (%) 796 (M^+, 1.3), 712 ($(M-3CO)^+$, 63), 577 ($(M-Cr(CO)_3-C_6H_{11})^+$, 100), 183 (Ph_2SiH^+, 90). M.p. 215–217 °C (decomp)

3c: ^1H NMR (C_6D_6, 25 °C, 200 MHz): δ = 0.7–1.9 (m, 33H, C_6H_{11}), 7.68 (br., 15H, arom. H), 8.27 (s, 3H, SiH); ^{31}P NMR (81 MHz): δ = –137.5 (s); ^{29}Si NMR (39.7 MHz): δ = 33.5 (d, ^1J(Si,H) = 209 Hz, SiH), IR (vSiH, CH_2Cl_2): $\tilde{\nu}$[cm^{-1}] = 2124; MS (EI, 70 eV): *m/z* (%) 842 (M^+, 0.4), 786 ($(M-2CO)^+$, 0.5), 758 ($(M-3CO)^+$, 0.3), 575 ($(M-Mo(CO)_3-C_6H_{11}-2H)^+$, 19), 56 ($C_4H_8^+$, 100). M.p. 215–220 °C (decomp)

two-electron bond is shown beyond doubt by the ^{29}Si and ^{1}H NMR spectra: **2** yields three ^{29}Si NMR signals split into multiplets by ^{31}P and ^{1}H coupling. Experiments with selective ^{1}H decoupling confirm the assignment of the multiplet at $\delta = -45.2$ to the ^{29}Si nucleus participating in the Si,H,Cr bond. The $J_{Si,H}$ coupling constant of 135.7 Hz is the largest value reported for a complex with agostic Si–H bonding.[6] In contrast, the ^{29}Si nuclei in **2** whose Si–H bonds are not affected show typical $^{1}J_{Si,H}$ coupling constants of 210.9 and 228.6 Hz. In related three-center complexes with manganese and chromium as coordination centers, $[(\eta^5\text{-}C_5R_5)(CO)LMn(H)SiR_3]$ and $[(\eta^6\text{-}C_6Me_6)(CO)_2Cr(H)(SiHPh_2)]$, the values of the coupling constants lie between 65 and 80 Hz, which is considered a sure sign of a Si–H bond.[6] The value drops to 10–20 Hz if no Si–H bonding interaction is present. Probably the relatively weak Si–H activation in **2** is mainly attributable to the special geometric features of the molecule. Apparently in this case the coordination through the Si–H bond instead of through the third phosphorus atom lessens the unfavorable steric interactions of the substituents in the Cr complex. At any rate the exchange of the chromium atom for the larger molybdenum atom is enough to result in **3a** in which all three phosphorus atoms of **1a** are coordinated to the metal center.

In the ^{1}H NMR spectrum the agostic proton of **2** is easily distinguished from the nonagostic protons: the H atom coordinated to Cr gives rise to a doublet at characteristically high field ($\delta = -7.69$, $J_{P,H} = 33.6$ Hz), whereas the signals for the other two H atoms occur at $\delta = 5.64$ ($J_{P,H} = 26.1$ Hz) and $\delta = 6.50$ (overlapping signal group).

The constitution of **2** derived from the NMR spectra was confirmed by an X-ray crystal structure analysis (Fig. 2).[7] The H atoms bound to Si could be localized with the difference Fourier map, and the Si–H, Cr–H, and Cr–Si distances are all in accord with the finding that the Si,H,Cr three-center bond represents an unusually early stage of Si–H activation. The Si–H distance in the Si,H,Cr bridge is 1.52(4) Å, while the nonagostic Si–H bonds are on average 1.36(4) Å long. The Cr–Si distance (agostic Si) of 2.616(1) Å is distinctly longer than that in Cr complexes with terminally bound silyl ligands. The Cr–H distance (agostic H) is 1.75(5) Å long. In contrast, the related complex also containing a Si,H,Cr three-center bond, $[(\eta^6\text{-}C_6Me_6)(CO)_2Cr(H)(SiHPh_2)]$,[6] has clearly shorter Cr–H (1.61(4) Å) and Cr–Si distances (2.456(1) Å) and at the same time a longer Si–H bridgehead bond (1.61(4) Å) and normal terminal Si–H bond lengths (1.39(3) Å). Moreover, the Cr atom in **2** is coordinated to the atoms P1 and P2 that are in 3- and 1-position relative to the agostic Si atom.

The ligand **1a** reacts with $[Mo(CO)_3(CH_3CN)_3]$ to form **3a**, which is convincingly shown by the NMR spectra (Table 1). The crystal structure analysis[8] (Fig. 3) shows that the P_3Si_3 ligand is forced into a pronounced crownlike chair conformation by its tridentate coordination to the Mo atom.

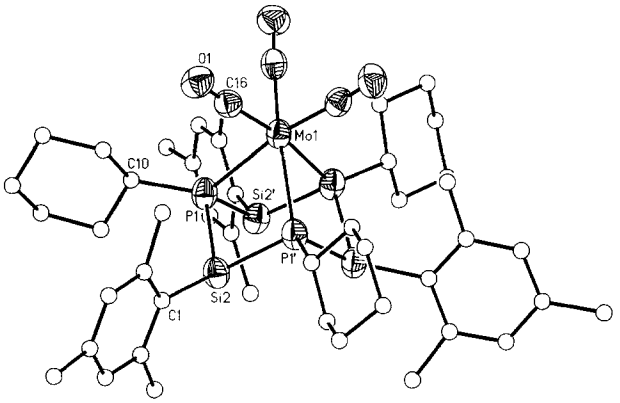

Fig. 3. Molecular structure of **3a** in the crystal. Selected distances [Å] and angles [°]: Mo1–P1 2.616(2), Mo1–C16 1.936(6), P1–Si2 2.290(2), P1–Si2' 2.284(2); P1-Mo1-P1' 74.8(1), P1-Si2-P1' 88.0(1), Si2-P1-Si2' 97.2(1).

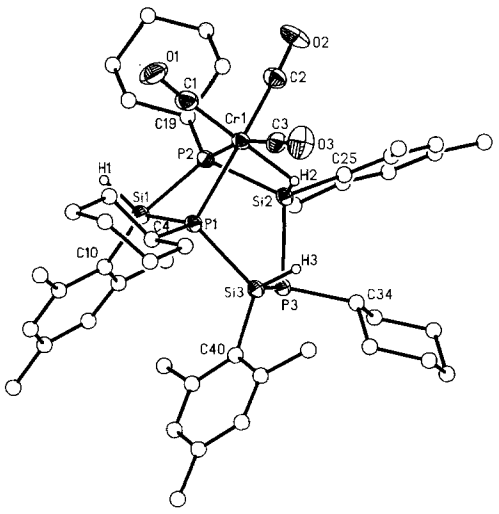

Fig. 2. Molecular structure of **2** in the crystal. Selected distances [Å]: Cr1–P1 2.407(1), Cr1–P2 2.372(1), Cr1–P3 4.24, Cr1–Si2 2.616(1), Cr1–H2 1.75(5), P1–Si1 2.279(2), P1–Si3 2.271(2), P2–Si2 2.208(2), P2–Si1 2.229(2), P3–Si2 2.272(2), P3–Si3 2.250(1), Si1–H1 1.34(5), Si2–H2 1.52(4), Si3–H3 1.38(4).

In contrast to **1a**, **1b** (phenyl instead of mesityl groups at Si) surprisingly reacts not only with $[Mo(CO)_3]$ but also with $[Cr(CO)_3]$ to afford analogous compounds **3b** and **3c**. This finding was confirmed by NMR spectroscopy (Table 1) and the crystal structure analyses of **3b,c**.[9] The crystallographic investigations of the complexes **3** reveal no significant structural variations. That the bulky mesityl group determines the different behavior of **1a** toward $[Cr(CO)_3]$ is clear from molecular models. If the phenyl groups are exchanged for mesityl groups in the crystallographically determined structure of the Cr complex **3b**, the structure obtained is less favorable than that of **2** because of the *ortho* methyl groups on the phenyl groups. We assume that **2** does not form by rearranging from this less stable isomer, but by the stepwise ligation of $[Cr(CO)_3(MeCN)_3]$ to **1a**. The *syn* position of the Si-bound H atoms and chromium in **2** arises without difficulty from the inversion of the configuration of the phosphorus atoms P1 and P2. Further investigations into whether the competition between Si–H activation and phosphane coordination in cyclophosphasilanes is also influenced by *electronic* effects such as the nature of the metal and its oxidation state are under way.

Experimental Procedure

1a: $C_6H_{11}PH_2$ (4.5 g, 39 mmol) was dissolved in THF (50 mL) and lithiated with *n*BuLi in hexane (2.5 M, Aldrich, 39 mmol) at about −70 °C. The resulting lithium phosphide solution was added within 30 min to a solution of MesSiH-

Cl_2 (4.27 g, 19.5 mmol) in THF (100 mL) at −60 °C. After removal of the volatile components under vacuum (10^{-2} Torr), the residue was taken up in benzene (30 mL) and filtered to remove LiCl. The filtrate was evaporated to dryness in vacuum, and the residue taken up in hexane. At −5 °C **1a** crystallizes as a colorless solid (2.32 g, 2.9 mmol, 45%).

1b: From $C_6H_{11}PH_2$ (5.4 g, 46.5 mmol) in Et_2O (80 mL), a solution of LiHPC$_6H_{11}$ was prepared analogously to the procedure for **1a**. To this lithium phosphide solution at −70 °C, a solution of $PhSiHCl_2$ (8.23 g, 46.5 mmol) in Et_2O (30 mL) was added slowly. The mixture was allowed to warm to 25 °C, then stirred for 2 h, and again cooled to −90°C. A solution of *t*BuLi (27.3 mL, 46.5 mmol; 1.7 M in pentane, Aldrich) was added. The suspension was warmed to 25 °C within 8 h and evaporated to dryness under vacuum (10^{-2} Torr). The residue was extracted with hot toluene. Cooling to −30 °C yielded **1b** as a colorless solid (4.13 g, 6.26 mmol, 40%).

2: **1a** (750 mg, 0.95 mmol) and $[Cr(CO)_3(MeCN)_3]$ (250 mg, 0.96 mmol) were stirred with benzene (40 mL) at 25 °C in a Schlenk tube for about 16 h. The solvent was removed under vacuum, and the residue taken up in CH_2Cl_2 (10 mL) and filtered. The filtrate was added dropwise with stirring to pentane (50 mL), upon which **2** precipitated as an ochre solid. Yield: 340 mg, 0.37 mmol, 38.9%.

3a: **1a** (440 mg, 0.56 mmol) and $[Mo(CO)_3(MeCN)_3]$ (180 mg, 0.59 mmol) were suspended in hexane (80 mL) and heated in a closed Schlenk tube (Teflon tap) for 6 h at 60 °C. The solvent and volatile components were removed under vacuum, and the bright red residue dissolved in CH_2Cl_2 (40 mL). After filtration, crystallization at −10 °C yielded orange-red crystals (510 mg, 0.53 mmol, 94.6%).

3b: **1b** (1.68 g, 2.56 mmol) and $[Cr(CO)_3(MeCN)_3]$ (660 mg, 2.55 mmol) were treated with pentane (50 mL) in a Schlenk tube and heated for 20 h at 40 °C. A yellow precipitate formed, which was filtered off, dissolved in CH_2Cl_2 (10 mL), and again filtered. **3b** precipitated on addition of pentane as a yellow solid (yield: 910 mg, 1.14 mmol, 44.5%).

3c: In an analogous synthesis to that of **3b**, **1b** (480 mg, 0.73 mmol) was allowed to react with $[Mo(CO)_3(MeCN)_3]$ (220 mg, 0.72 mmol) in hexane (10 mL) at 60 °C. Red crystals were obtained by crystallization from CH_2Cl_2 (480 mg, 0.57 mmol, 78%).

Received: June 16, 1992 [Z 5408 IE]
German version: *Angew. Chem.* **1992**, *104*, 1514

CAS Registry numbers:
1a, 143970-53-0; **1b**, 143970-54-1; **2**, 143970-55-2; **3a**, 143970-56-3; **3b**, 143970-57-4; **3c**, 143970-58-5; $[Cr(CO)_3(MeCN)_3]$, 16800-46-7; $[Mo(CO)_3(MeCN)_3]$, 15038-48-9; $C_6H_{11}PH_2$, 822-68-4; $MesSiHCl_2$, 117560-00-6; $PhSiHCl_2$, 1631-84-1.

[1] Review: F. Vögtle, *Supramolekulare Chemie*, Teubner, Stuttgart, **1991**, p. 45.
[2] Review: D. A. Armitage in *The Silicon-Heteroatom Bond* (Eds.: S. Patai, Z. Rappoport), Wiley, New York, **1991**, p. 167, and references cited therein.
[3] R. T. Oakley, D. A. Stanislawski, R. West, *J. Organomet. Chem.* **1978**, *157*, 389; J. C. Calabrese, R. T. Oakley, R. West, *Can. J. Chem.* **1979**, *57*, 1909; G. Fritz, R. Uhlmann, *Z. Anorg. Allg. Chem.* **1980**, *463*, 143.
[4] $(PhPSiPh_2)_3$: H. Schumann, H. Benda, *Angew. Chem.* **1970**, *82*, 46; *Angew. Chem. Int. Ed. Engl.* **1970**, *9*, 76; $(HPSiMe_2)_3$: G. Fritz, R. Biastoch, *Z. Anorg. Allg. Chem.* **1986**, *535*, 63.
[5] X-ray structure analysis of **1a**: space group $P\bar{1}$, $a = 9.275(6)$, $b = 13.408(9)$, $c = 21.822(15)$ Å, $\alpha = 93.10(5)$, $\beta = 97.62(5)$, $\gamma = 108.58(5)°$, $V = 2536$ Å^3, $Z = 2$; 3606 observed reflections, $R = 0.077$, $R_w = 0.087$ [10].
[6] Review: U. Schubert, *Adv. Organomet. Chem.* **1990**, *30*, 151, references cited therein.
[7] X-ray structure analysis of **2**: space group $P2_1/c$, $a = 11.462(3)$, $b = 21.616(9)$, $c = 23.793(16)$ Å, $\beta = 103.46(5)°$, $V = 5733$ Å^3, $Z = 4$; 6008 observed reflections ($T = -60$ °C), $R = 0.059$, $R_w = 0.070$ [10].
[8] X-ray structure analysis of **3a**: space group $P\bar{3}$, $a = 14.843(9)$, $b = 14.843(9)$, $c = 14.533(9)$ Å, $V = 2773$ Å^3, $Z = 2$; 2251 observed reflections, $R = 0.058$, $R_w = 0.065$ [10].
[9] X-ray structure analysis of **3b**: space group $P\bar{1}$, $a = 11.664(6)$, $b = 13.848(9)$, $c = 16.644(8)$ Å, $\alpha = 84.99(4)$, $\beta = 86.98(3)$, $\gamma = 66.43(3)°$, $V = 2454$ Å^3, $Z = 2$; 5240 observed reflections, $R = 0.087$, $R_w = 0.112$; of **3c**: space group $P2_1/n$, $a = 13.369(8)$, $b = 21.661(12)$, $c = 14.833(9)$ Å, $\beta = 97.47(5)°$, $V = 4259$ Å^3, $Z = 4$; 6573 observed reflections, $R = 0.043$, $R_w = 0.052$ [10].
[10] All analyses were performed with a four-circle diffractometer, $Mo_{K\alpha}$ radiation, ω scan, $I > 2\sigma(I)$. Further details of the crystal structure investigations may be obtained from the Fachinformationszentrum Karlsruhe, Gesellschaft für wissenschaftlich-technische Information mbH, D-W-7514 Eggenstein-Leopoldshafen 2 (FRG) on quoting the depository number CSD-56539, the names of the authors, and the journal citation.

Multifield Saturation Magnetization Measurements of Oxidized and Reduced Ribonucleotide Reductase from *Escherichia coli*

By *Mohammed Atta, Corinne Scheer, Pascal H. Fries, Marc Fontecave,* and *Jean-Marc Latour**

Ribonucleotide reductases are found in all living organisms where they catalyze the conversion of ribonucleotides to deoxyribonucleotides, an essential step in DNA biosynthesis. The enzyme from *Escherichia coli* has been shown to consist of two homodimeric subunits R1 and R2.[1] The X-ray crystal structure determination[2] of the oxidized form of protein R2 has shown that its active site contains a binuclear iron center similar to the one found in hemerythrin. However, its resolution was insufficient to identify clearly the nature of the group bridging the two iron atoms; the presence of an oxo bridge was demonstrated from spectroscopic measurements.[1, 3] In accord with this, a magnetic susceptibility study[4] has shown that the two high-spin iron(III) ions are strongly antiferromagnetically coupled; however, due to experimental limitations a precise determination of the exchange interaction was not achieved ($-J = 106 \pm 22$ cm^{-1}; $H = -2J\,S_1 \cdot S_2$). A tyrosyl residue, essential for the enzyme function, is present about 5 Å from the closest iron atom.

Much less is known, however, on the binuclear iron center of the reduced enzyme. Reduction of the iron center is an essential step during the formation of the tyrosyl radical and the resulting activation of the enzyme.[5] Mössbauer experiments[6] have concluded that the two iron sites are essentially equivalent and that the spin coupling between the two iron(II) ions, if present, is smaller than the zero-field splittings. On the other hand Ehrenberg et al. have determined the coupling from NMR studies ($-J = 5 \pm 5$ cm^{-1}) and concluded that the interaction in the iron center is weak, if it exists at all.[7] Accordingly, a weak exchange interaction is anticipated for reduced ribonucleotide reductase. In hemerythrin, protonation of the oxo bridge occurs simultaneously with reduction of the diiron(III) center,[8] and an analogous process might be operative in ribonucleotide reductase. The magnetic interaction between two iron ions depends critically on the nature of their bridging ligands. It is well known that carboxylate bridges are poor mediators of exchange interactions in these systems. Magnetic susceptibility measurements performed both on proteins and on synthetic analogues clearly identify the range of values of the magnetic exchange interaction associated with every bridging ligand.[9] Starting from a high value ($-J = 80$–140 cm^{-1}) for oxo derivatives, this interaction decreases with protonation to $-J = 10$–50 cm^{-1} for a hydroxo bridge.[10] A weak but definitely positive value of J is supposedly associated with further protonation in several natural systems.[8, 11] It follows that magnetization studies constitute a valuable tool for investigating the transformations involved in the reduction of the diiron center.

In this paper, we report multifield saturation magnetization studies of both the oxidized and the reduced forms of ribonucleotide reductase. The high exchange interaction cal-

[*] Dr. J.-M. Latour, C. Scheer, Dr. P. H. Fries
Laboratoire DRFMC/SESAM/CC
Centre d'Etudes Nucléaires de Grenoble
F-85X 38041 Grenoble Cedex (France)
M. Atta, Prof. M. Fontecave
L.E.D.S.S./Université Joseph Fourier
F-BP 53X F 38041 Grenoble Cedex (France)

 © VCH Verlagsgesellschaft mbH, W-6940 Weinheim, 1992 0570-0833/92/1111-1513 $ 3.50+.25/0

culated here provides additional support for the presence of an oxo bridge in the oxidized enzyme; moreover, magneto-structural correlations suggest that the diiron center is structurally similar to the one found in methemerythrin derivatives. In the case of reduced ribonucleotide reductase, this study points to an extremely weak exchange interaction, if it exists at all; this strongly suggests that the oxo bridge has been protonated and then eliminated during reduction. A structural hypothesis is proposed accordingly.

Multifield saturation magnetization data were collected on two different protein samples,[12] R2 and reduced R2, with a SHE 900 SQUID susceptometer according to the procedure outlined by Day et al.[13] The sample was contained in a quartz bucket etched overnight with a 10% HF solution. Measurements were performed in the 5–200 K temperature range at six field strengths (0.5, 1, 2, 3, 4, and 5 T). The data was treated according to the method of Day et al.[13]

Figure 1 illustrates the magnetic properties of oxidized ribonucleotide reductase as the temperature dependence of the product of the magnetic susceptibility and the

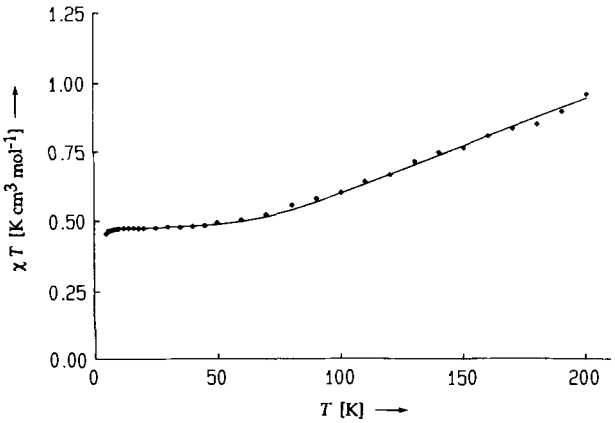

Fig. 1. Oxidized R2: Temperature dependence of the product of the magnetic susceptibility and the temperature. The experimental data (•) are the mean values of the data collected at the six field strengths. The solid line corresponds to the theoretical values (see text).

temperature. This curve clearly shows a plateau at $\chi T \approx 0.45\ \mathrm{K\,cm^3\,mol^{-1}}$ at temperatures lower than 50 K and an increase of χT at higher temperatures. Such behavior is fully consistent with an isolated spin $S = 1/2$ contributing to the plateau ($\chi T \approx 0.4\ \mathrm{K\,cm^3 mol^{-1}}$) and an antiferromagnetically coupled pair of high-spin Fe^{III} ions, whose contribution is negligible at low temperature. Simulation of the experimental data with an equation derived from the corresponding Heisenberg Hamiltonian, taking into account the presence of a small amount (p) of adventitious high-spin Fe^{III}, leads to the best fit parameters $g = 2.00$, $J = -84(5)\ \mathrm{cm^{-1}}$, and $p = 0.022(2)$. This value of J is at the upper end of the range estimated by Ehrenberg et al.[4] ($-128 < J < -83\ \mathrm{cm^{-1}}$). Undoubtedly, such a strong antiferromagnetic coupling is indicative[9] that the iron atoms are bridged by an oxide ion, in agreement with the conclusions drawn from spectroscopic measurements.[3]

Analyzing the structural and magnetic properties of three dozen (μ-oxo)diiron(III) complexes, Gorun and Lippard[14] have recently proposed a correlation between the exchange interaction (J) and the Fe–O distance (P), the shortest exchange pathway between the two iron(III) ions. Introducing the above J value into this relation leads to a value of 1.82 Å for the Fe–O distance P and 130° for the Fe-O-Fe angle on using the Fe–Fe distance of 3.3 Å obtained from the X-ray analysis. The same value of the Fe-O-Fe angle was deduced from resonance Raman data.[15] These values are quite reasonable for a (μ-oxo)(μ-carboxylato)diiron(III) entity[9] and in very good agreement with the ones measured on methemerythrin derivatives.[16]

Figure 2 presents the magnetization data of reduced ribonucleotide reductase over the 5–200 K temperature range at six field strengths. In Figure 2a the susceptibilities for the six fields are plotted versus the inverse temperature; Figure 2b displays the variation of the product χT with the temperature for the two extreme fields (0.5 and 5 T).

The spin Hamiltonian for the two exchange-coupled iron spins $S = 2$ is given in Equation (a), where the anisotropic Zeeman interaction $\mathscr{H}_{iz}$ is represented by Equation (b). J is

$$\mathscr{H} = -2J\vec{S}_1 \cdot \vec{S}_2 + \sum_{i=1,2} [D(S_{iz}^2 - 2) + E(S_{ix}^2 - S_{iy}^2) + \mathscr{H}_{iz}] \quad \text{(a)}$$

$$\mathscr{H}_{iz} = \mu_B(g_x H_x S_{ix} + g_y H_y S_{iy} + g_z H_z S_{iz}) \quad \text{(b)}$$

the isotropic coupling constant. D and E are the axial and rhombic parameters of the zero-field splitting (ZFS) tensors which are assumed to be equal for both ions. The usual hypothesis is made that for each ion the ZFS tensor and the Zeeman g factor can be simultaneously diagonalized.[17a] The calculations have been performed while fixing or floating the various parameters to assess their relative importance. It follows from this procedure that inclusion of the rhombicity in the calculation (either as $E \neq 0$ or as $g_x \neq g_y$)

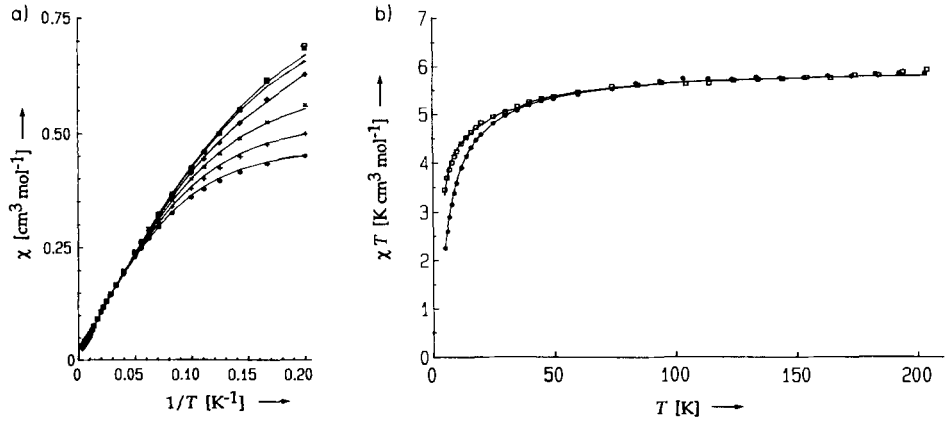

Fig. 2. Reduced R2: a) Dependence of the magnetic susceptibility on the inverse temperature at the six experimental fields: 0.5 (□), 1 (△), 2 (○), 3 (×), 4 (+), and 5 T (*). The solid lines are the calculated values (see text). b) Temperature dependence of the product of the magnetic susceptibility and the temperature at the two extreme field strengths: 0.5 (□) and 5 T (*). The solid lines are the calculated values (see text).

leads to a slight but hardly significant improvement of the statistical index. In any case, the E value never exceeded 1 cm^{-1} and g_x never differed from g_y by more than 0.1. On the other hand, a small J value was found and fixing J to 0 induced a significantly poorer fit. Accordingly, the final calculations were done with five parameters: J, D, $g_x = g_y$, g_z.

The solid lines in Figure 2 were calculated with the following set of parameters:[18] $g_x = 1.63(5)$, $g_y = 1.63(5)$, $g_z = 2.56(5)$, $J = 0.3(2)\ cm^{-1}$, and $D = 9.8(5)\ cm^{-1}$. The value estimated for the axial zero-field splitting is comparable to the one observed for deoxyhemerythrin derivatives,[8, 11] but the most remarkable feature is the extreme weakness of the exchange interaction J. In the case of reduced hemerythrin $-J$ is $12-38\ cm^{-1}$, in agreement with the presence of a hydroxo bridge.[8] A further protonation to an aqua bridge is presumed to occur with the binding of some exogeneous anions and results in the decrease of the exchange interaction. When the counterion is azide, the coupling even changes sign ($J = 1.7\ cm^{-1}$)[11] and the interaction becomes ferromagnetic, which leads to an EPR-active $S = 4$ ground state of the deoxyHrN_3 protein. In its reduced form methane monooxygenase (MMO), another diiron protein, presents the same kind of EPR signal characterized by a high g value ($g \approx 16$).[19] It is worth mentioning that reduced ribonucleotide reductase from *E. coli* is EPR silent[20] for conditions under which deoxyHrN_3 and reduced MMO exhibit the high g value spectrum. This observation might suggest that a water molecule is not the ligand bridging the iron atoms in reduced ribonucleotide reductase, but which bridging ligands could then be present in reduced ribonucleotide reductase? During reduction of the oxidized enzyme, a weakly binding aqua bridge could conceivably be formed upon protonation of the oxo bridge and subsequently be replaced by the carboxylate group from glutamate 238. This residue is terminal and monodentate in oxidized R2 and would become bridging and bidentate in the reduced protein. From the structural analysis of a wealth of carboxylato metal complexes, Lippard et al.[21] have shown that such a change in the coordination mode of a carboxylate residue from terminal to bridging is a viable possibility. Moreover, the carboxylate group from aspartate 84 would probably become monodentate resulting in the hypothetical situation illustrated in Figure 3. Interestingly, a similar structure has been

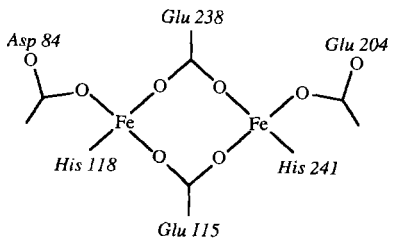

Fig. 3. Structural hypothesis for the diiron center of reduced protein R2. It is highly likely that the coordination of the iron(II) ions is completed by water molecules as found for oxidized R2

found recently by X-ray crystallography for a new form of protein R2 in which the iron centers have been replaced by divalent manganese ions.[22] This observation gives additional support to the above hypothesis.

Received: May 12, 1992 [Z 5342 IE]
German version: *Angew. Chem.* **1992**, *104*, 1558

[1] M. Fontecave, P. Nordlund, H. Eklund, P. Reichard, *Adv. Enzymol.* **1992**, *65*, 147.
[2] P. Nordlund, H. Eklund, B.-M. Sjöberg, *Nature* **1990**, *345*, 593.
[3] a) J. Sanders-Loehr in *Iron Carriers and Iron Proteins*, (Ed.: T. Loehr), VCH, New York, **1989**, p. 373; b) L. Que, Jr., A. E. True, *Prog. Inorg. Chem.* **1990**, *38*, 97.
[4] L. Petersson, A. Gräslund, A. Ehrenberg, B.-M. Sjöberg, P. Reichard, *J. Biol. Chem.* **1980**, *255*, 6706.
[5] a) M. Fontecave, R. Eliasson, P. Reichard, *J. Biol. Chem.* **1989**, *264*, 9164; b) M. Fontecave, C. Gerez, D. Mansuy, P. Reichard, *ibid.* **1990**, *265*, 10919.
[6] J. B. Lynch, C. Juarez-Garcia, E. Münck, L. Que, Jr., *J. Biol. Chem.* **1989**, *264*, 8091.
[7] M. Sahlin, A. Gräslund, L. Petersson, A. Ehrenberg, B.-M. Sjöberg, *Biochemistry* **1989**, *28*, 2618.
[8] R. C. Reem, E. I. Solomon, *J. Am. Chem. Soc.* **1987**, *109*, 1216.
[9] D. M. Kurtz, *Chem. Rev.* **1990**, *90*, 585.
[10] W. A. Armstrong, S. J. Lippard, *J. Am. Chem. Soc.* **1984**, *106*, 4632.
[11] M. P. Hendrich, L. L. Pearce, L. Que, Jr., N. D. Chasteen, E. P. Day, *J. Am. Chem. Soc.* **1991**, *113*, 3039.
[12] Proteins R2 and apoR2 were prepared in Tris buffer (0.1 M, pH 7.5, 20% glycerol). The solvent of both solutions was then exchanged for D_2O by successive concentration followed by dilution with D_2O in an Amicon YM-30 centricon. Finally the protein solution was concentrated (1×10^{-3} M, 125 µL) and deaerated on a manifold argon/vacuum line. Reduced R2 was prepared in an anaerobic glove box by adding four equivalents of ammonium iron(II) sulfate to an apoR2 solution in D_2O. That iron was correctly incorporated was shown from the appearance of the tyrosyl radical upon exposure to air. This is observed both by EPR and UV/VIS spectroscopy. Moreover, no free iron(III) could be detected in the reoxidized sample by EPR spectroscopy (signal with $g = 4.3$).
[13] E. P. Day, T. A. Kent, P. A. Lindahl, E. Münck, W. H. Orme-Johnson, H. Roder, A. Roy, *Biophys. J.* **1987**, *52*, 837.
[14] S. M. Gorun, S. J. Lippard, *Inorg. Chem.* **1991**, *30*, 1625.
[15] B. M. Sjöberg, T. M.Loehr, J. Sanders-Loehr, *Biochemistry* **1982**, *21*, 96.
[16] R. E. Stenkamp, L. C. Sieker, L. H. Jensen, *J. Am. Chem. Soc.* **1984**, *106*, 618.
[17] a) Also note that the single-ion ZFS tensors are assumed to be colinear. This simplification places very little restriction on a frozen solution when the J value is small, as found. The average molar magnetization $m_{av}(H)$ along the direction of the magnetic field H is calculated numerically from the partial derivative of the free energy [17 b]. The six parameters J, D, E, g_x, g_y, and g_z of the Hamiltonian are obtained through a least-squares fit to the experimental values of the product $m_{av}(H)\ T$ for all the magnetic fields and temperatures; b) N. W. Ashcroft, N. D. Mermin, *Solid State Physics*, Saunders, Philadelphia, **1976**, p. 643.
[18] The average value for g is 1.992, too low for an iron(II) derivative. We believe that the uncertainty in protein quantitation is responsible for this result, as outlined by Day et al. [11]. The other parameters (J, D, E) are unaffected.
[19] M. P. Hendrich, E. Münck, B. G. Fox, J. D. Lipscomb, *J. Am. Chem. Soc.* **1990**, *112*, 5861.
[20] Que, Jr. [6] reported that reduced ribonucleotide reductase exhibits a broad EPR signal at low field, but does not rule out that it is associated to adventitious Fe(II) ions. We have never detected such a signal in our preparations of the reduced enzyme.
[21] R. L. Rardin, W. B. Tolman, S. J. Lippard, *New J. Chem.* **1991**, *15*, 417.
[22] M. Atta, P. Nordlund, A. Åberg, H. Eklund, M. Fontecave, *J. Biol. Chem.* in press.

Mono- and Binuclear Molybdenum Complexes Incorporating 4-(4-Hydroxyphenyl)pyridine: Metal–Metal Interactions Across an Asymmetric Bridging Ligand**

By *Amitava Das, John C. Jeffery, John P. Maher, Jon A. McCleverty,* Erik Schatz, Michael D. Ward,** and *Gerd Wollermann*

The study of binuclear complexes whose metal centers are linked by an unsaturated bridging ligand is of relevance to

[*] Prof. J. A. McCleverty, Dr. M. D. Ward, Dr. A. Das, Dr. J. C. Jeffery, Dr. J. P. Maher, E. Schatz, G. Wollermann
School of Chemistry
Cantock's Close, GB-Bristol BS8 1TS (United Kingdom)

[**] We thank the Science and Engineering Research Council (SERC) for a postdoctoral fellowship (A.D.) and for a grant for the purchase of an EPR spectrometer.

intramolecular electron transfer in mixed-valence systems[1] and the study of magnetic interactions between paramagnetic centers. The most extensively studied such complex is the Creutz–Taube ion;[2] more recently 4,4′-bipyridine-bridged binuclear complexes have received much attention.[3, 4] The synthesis of the symmetrical binuclear complex $[\{Mo(NO)L^*Cl\}_2(\mu\text{-bpy})]$ [L* = tris(3,5-dimethylpyrazolyl)-hydridoborate, bpy = 4,4′-bipyridine] was recently reported,[4] in which a strong electronic coupling between the [Mo(NO)L*Cl] centers caused a difference of 765 mV between the reductions of the first and the second metal centers; EPR spectroscopy showed rapid site exchange of the two unpaired electrons at room temperature. We now report the syntheses, and electrochemical and EPR spectroscopic properties of asymmetric, mixed-valent (17e–16e) and homovalent (17e–17e) (e = valence electrons) binuclear molybdenum complexes containing a 4-(4-hydroxyphenyl)pyridine bridge, and present evidence that metal–metal interactions are assisted by a nearly planar conformation of the bridging ligand.

The precursor L^2 was prepared by extensions of known procedures,[5–7] and demethylated with pyridinium chloride[8] to give HL^1 (Scheme 1). Syntheses of the complexes

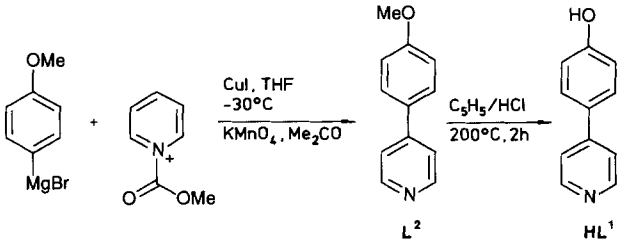

Scheme 1. Syntheses of the ligands L^2 [6] and HL^1.

are outlined in Scheme 2.[7] Reaction of $[MoL^*(NO)Cl_2]$ with HL^1 afforded **1**, in which the phenoxide terminus of L^1 is attached to the 16-electron Mo center and the pyridyl group is pendant. This reaction is apparently controlled by the difference in reaction rate between the anionic phenolate and the neutral pyridine with the electron-deficient

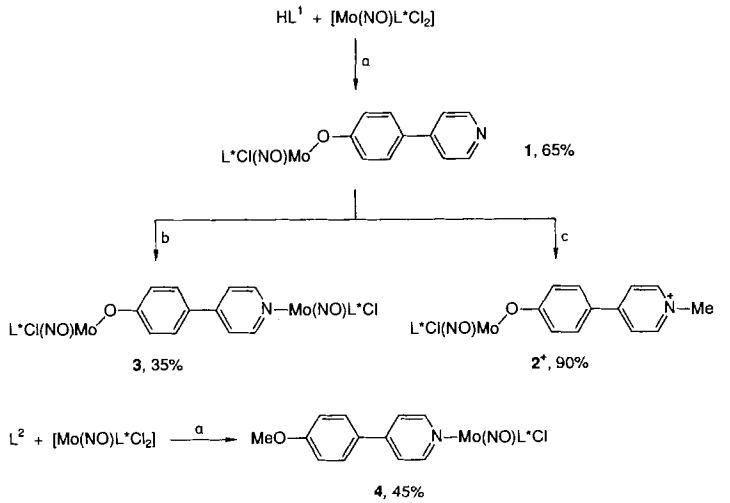

Scheme 2. Syntheses of the complexes **1**–**4** under an N_2 atmosphere. a) Toluene, Et_3N, 4 h under reflux; b) $[Mo(NO)L^*Cl_2]$, toluene, Et_3N, 6 h under reflux; c) MeI, CH_2Cl_2, 18 h under reflux.

$[Mo(NO)L^*Cl_2]$. Attachment of the pyridyl terminus to molybdenum could only be achieved if the phenol group was protected, as in L^2; thus, reaction of $[Mo(NO)L^*Cl_2]$ with L^2 produced **4** which has a pendant methoxyphenyl group. This complex has 17 valence electrons; attachment of the pyridyl ligand is accompanied by a one-electron reduction of the molybdenum center, probably by the Et_3N, which is known to act as a hydridic reducing agent.[9]

Methylation of the pendant pyridyl group in **1** gave $\mathbf{2}^+$, isolated as its PF_6^- salt. The electrochemical data (Table 1) show that the metal-centered reduction is anodically shifted

Table 1. Electrochemical and EPR data for the new complexes.

	Electrochemical processes [a]		EPR parameters	
	$E_{1/2}$	$E_{1/2}$	g [b]	Hyperfine splitting [mT]
1	−0.70 (75) [c]	–	–	–
$\mathbf{1}^-$ [d]	–	–	1.969	5.1
$\mathbf{2}^+$	−0.58 (80) [c] −1.85 (100) [e]	–	–	–
2 [d]	–		−1.971	5.1
3	−0.65 (90) [c]	+0.12 (80) [f] −2.00 (180) [g]	1.979	4.9
$\mathbf{3}^-$ [d]	–	–	1.973	2.6
4	–	+0.11 (70) [f] −1.87 (100) [g]	1.978	5.0

[a] Potentials quoted in V vs. the ferrocene/ferrocenium couple, with peak–peak separations [mV] in parentheses. Electrochemical measurements were made with Pt-bead working and auxiliary electrodes and a saturated calomel electrode as reference electrode in a 0.1 M solution of $(Bu_4N)PF_6$ in CH_2Cl_2. In all cases ferrocene was used as an internal reference. [b] Average value of the g factor. [c] Potentials for the 16e–17e reduction of the [Mo(NO)L*Cl-(phenolate)] moiety. [d] 17e complex produced by in situ reduction of the parent 16e complex with cobaltocene. [e] Potentials for the reduction of the methylpyridinium moiety. [f] Potentials for the 17e–16e oxidation of the [Mo(NO)L*Cl(pyridyl)] moiety. [g] Potentials for the 17e–18e reduction of the [Mo(NO)L*Cl(pyridyl)] moiety.

by 120 mV on *N*-methylation of the pendant pyridyl group. This is in marked contrast to the behavior of polypyridine–ruthenium(II) complexes containing 4,4′-bipyridyl groups, where *N*-methylation of the pendant pyridyl groups results in an anodic shift of the Ru^{II}/Ru^{III} redox couples by just 20 mV per methylpyridinium group.[10] The large interaction in $\mathbf{2}^+$ is due to charge recombination in the deprotonated, methylated ligand resulting in a quinonoidal structure (Fig. 1). This constrains the ligand to be planar, prevents free rotation about the central C–C bond normally associated with biphenyls, and causes a decrease of electron density at the metal center by removal of the phenolate negative charge, thereby facilitating the 16e–17e reduction.

Reaction of **1** with further $[Mo(NO)L^*Cl_2]$ produced the mixed-valence complex **3**,[11] in which the N-coordinated

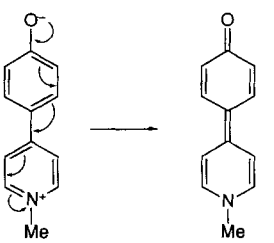

Fig. 1. Resonance structures of the deprotonated, *N*-methylated ligand HL^1.

molybdenum atom has 17 valence electrons, whereas the O-coordinated molybdenum atom has only 16. Thus, here also the addition of the pyridyl ligand is accompanied by a reduction of the molybdenum center. Electrochemical measurements (Table 1) confirm the presence of an electronic interaction between the two metal centers; whereas the difference between the reductions at the metal centers in **1** and **4** is 1.17 V, the presence of a direct link between them in **3** results in a $\Delta(E_{1/2})$ value of 1.35 V, that is, an increase of 180 mV. Again, this may be accounted for by a quinonoidal contribution to the structure of the bridging ligand which results in decreased electron density at the O-terminus and increased electron density at the N-terminus. This contribution will be more significant in **3** than in **1**, due to stabilization of the electron-rich pyridyl N atom by attachment to a 17-electron Mo center; the pyridyl group thus functions as a π donor rather than as a π acceptor, which is its more common role.

The EPR spectra of **4** and the reduced complexes $\mathbf{1}^-$ and **2** (produced by in situ reduction of the 16-electron species **1** and $\mathbf{2}^+$ with cobaltocene) all show hyperfine coupling constants of about 5.0 mT due to coupling to a single molybdenum center (Table 1). The coupling constant is similar for **3**; this indicates that the unpaired electron is trapped at the pyridyl-coordinated molybdenum center, which is to be expected considering the difference in the 16e–17e redox potentials for the two molybdenum sites. The localization of the unpaired electron in **3** is confirmed by virtually identical values of g for **3** (1.979) and **4** (1.978).

One-electron reduction of **3** with cobaltocene affords the 17e–17e species $\mathbf{3}^-$, a biradical where the two electrons are in redox levels 0.77 V apart. Despite this energy gap, the EPR spectrum (Fig. 2) indicates a change from localized to delocalized electrons on the EPR timescale. A single signal is observed at $g = 1.973$, midway between the values for the mononuclear components $\mathbf{1}^-$ and **4** ($g = 1.969$ and 1.978, respectively); this places a lower limit of 4×10^7 Hz on the electron-exchange frequency,[12] a reasonable value since studies of electron transfer across saturated hydrocarbon bridges have shown transfer rates in the region 10^6 to $10^9\ s^{-1}$.[13] Also the hyperfine splitting is halved to 2.6 mT. This confirms that, as with $[\{Mo(NO)L^*Cl\}_2(\mu\text{-bpy})]$,[4] there is fast electron exchange between the two metal centers with $|J| \gg A_0$ ($|J|$ is the exchange integral, A_0 is the hyperfine interaction);[14] in such cases the hyperfine splitting is predicted to be 0.5 ($A_0/g\beta$), that is, half the value found in the spectra of the mononuclear components. No half-field resonance was observed either at room temperature or 77 K, which may be ascribed to the intermetallic separation.[4] Although the complex is asymmetric, there is no barrier to electron exchange arising from reorganization of the metals' coordination spheres, since both metal centers possess 17 valence electrons before and after any exchange. To our knowledge this is the first example of fast exchange in an asymmetric biradical, bimetallic system.

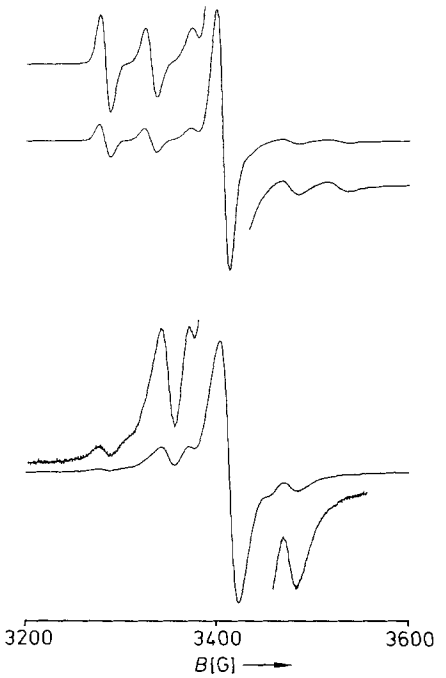

Fig. 2. Room-temperature EPR spectra of **3** and $\mathbf{3}^-$.

The crystal structure of **4** is shown in Figure 3.[15] The coordination geometry is approximately octahedral. The most interesting feature is the nearly coplanar aromatic rings of L^2 (dihedral angle of 5°). By contrast, in the isoelectronic complex $[Mo(NO)L^*(ppy)_2]^+$ (ppy = 4-phenylpyridine, an analogue of L^2 without the electron-donating methoxy group), the torsion angles between the rings are 30 and 41°.[18] This is consistent with our view that planarity of L^2 in **4**, and of L^1 in the other complexes, is due to partial quinonoidal character, although the central C–C bond length in **4** [1.476(9) Å] is close to the average value for biphenyl-type structures[19] and not significantly different from the corresponding distances in $[Mo(NO)L^*(ppy)_2]^+$ [1.430(15) and 1.497(13) Å]. Although near-planarity in the crystal structures of biphenyl-type species may often be ascribed to favorable stacking interactions between the aromatic rings,[19] this does not appear to apply in **4**; the aromatic rings are not especially close to any other groups, so it is less likely that the ligand is being forced into planarity by crystal packing effects.

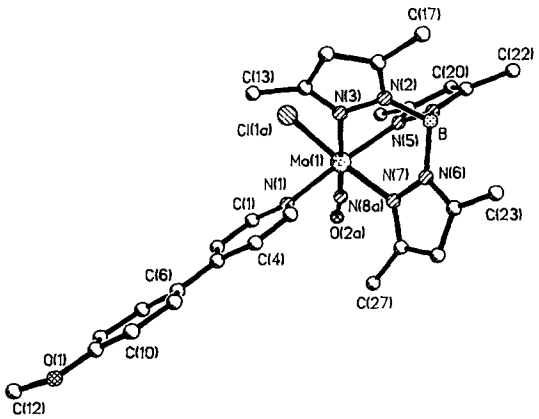

Fig. 3. Molecular structure of **4**. Selected bond lengths [Å] and angles [°]: Mo(1)-Cl(1a) 2.432(6), Mo(1)-N(8a) 1.85(2), Mo(1)-N(1) 2.204(5), Mo(1)-N(3) 2.246(5), Mo(1)-N(5) 2.163(5), Mo(1)-N(7) 2.196(5); N(1)-Mo(1)-N(7) 87.4(2), N(1)-Mo(1)-N(3) 86.9(2), N(8a)-Mo(1)-N(1) 92.0(6), Cl(1a)-Mo(1)-N(1) 93.6(2), Cl(1a)-Mo(1)-N(8a) 91.2(6), Cl(1a)-Mo(1)-N(3) 89.7(2), Cl(1a)-Mo(1)-N(5) 95.4(2), N(8a)-Mo(1)-N(5) 96.5(6), N(8a)-Mo(1)-N(7) 94.4(6).

Received: June 30, 1992 [Z 5440 IE]
German version: *Angew. Chem.* **1992**, *104*, 1554

CAS Registry numbers:
1, 144018-72-4; $\mathbf{1}^-$, 144018-79-1; **2**, 144018-77-9; $\mathbf{2}^+PF_6^-$, 144018-74-6; **3**, 144018-75-7; $\mathbf{3}^-$, 144018-78-0; **4**, 144018-76-8; $\mathbf{4}\cdot CH_2Cl_2$, 144018-80-4; HL^1, 77409-99-5; L^2, 5938-16-9; $[MoL^*(NO)Cl_2]$, 24981-81-5; 4-bromoanisole, 104-92-7; methyl chloroformate, 79-22-1; pyridine, 110-86-1.

[1] N. S. Hush, *Prog. Inorg. Chem.* **1967**, *8*, 391.
[2] C. Creutz, *Prog. Inorg. Chem.* **1983**, *30*, 1.
[3] D. J. Salmon, M. J. Powers, R. W. Callahan, T. J. Meyer, *Inorg. Chem.* **1976**, *15*, 894; J. E. Sutton, H. Taube, *ibid.* **1981**, *20*, 3125; M. M. Zulu, A. J. Lees, *ibid.* **1989**, *28*, 85; A. J. Downard, G. E. Honey, L. F. Phillips, P. J. Steel, *ibid.* **1991**, *30*, 2259; R. L. Blackburn, J. T. Hupp, *J. Phys. Chem.* **1988**, *92*, 2817; B. L. Loeb, G. A. Neyhart, L. A. Worl, E. Danielson, B. P. Sullivan, T. J. Meyer, *ibid.* **1989**, *93*, 717; E. C. Constable, M. D. Ward, *J. Chem. Soc. Dalton Trans.* **1990**, 1405.
[4] S. L. W. McWhinnie, C. J. Jones, J. A. McCleverty, D. Collison, F. E. Mabbs, *J. Chem. Soc. Chem. Commun.* **1990**, 940.
[5] D. L. Comins, A. H. Abdullah, *J. Org. Chem.* **1982**, *47*, 4375.
[6] Preparation of L^2: To an ice-cold, stirred suspension of anhydrous CuI (0.1 g, 0.53 mmol) and dry pyridine (1.19 g, 15 mmol) in dry THF (25 cm^3) under N_2 was added methyl chloroformate (0.95 g, 10 mmol); a white precipitate appeared. The mixture was cooled to $-30\,^\circ C$, and a solution of the Grignard reagent prepared from 4-bromoanisole (2.06 g, 11 mmol) and Mg turnings (0.34 g, 14 mmol) in THF (20 cm^3) was added dropwise over 15 min. The mixture was stirred for 15 min at $-30\,^\circ C$ and then at room temperature for 1 h. After hydrolysis with aqueous NH_4Cl, the intermediate dihydropyridine was extracted with ether, concentrated, and rearomatized with $KMnO_4$ in acetone at $0\,^\circ C$. The product L^2 was obtained as a white solid in 65% yield after chromatography on alumina with CH_2Cl_2.
[7] All new compounds gave satisfactory elemental analyses. Data for HL^1: M.p. 250–252 °C. ^1H NMR (270 MHz, CD_3OD, TMS): $\delta = 6.91$ (d, $J = 8.6$ Hz, 2H; phenyl-H^2, -H^6), 7.63 (d, $J = 8.6$ Hz, 2H; phenyl-H^3, -H^5), 7.65 (d, $J = 5.6$ Hz, 2H; pyridyl-H^3, -H^5), 8.49 (d, $J = 5.6$ Hz, 2H; pyridyl-H^2, -H^6); MS: m/z 185 (M^+, 100%). Data for L^2: M.p. 95–96 °C. ^1H NMR (270 MHz, CD_3OD, TMS): $\delta = 3.84$ (s, 3H; OMe); 7.06 (d, $J = 8.6$ Hz, 2H; phenyl-H^2, -H^6), 7.69 (d, $J = 8.6$ Hz, 2H; phenyl-H^3, -H^5), 7.71 (d, $J = 5.6$ Hz, 2H; pyridyl-H^3, -H^5), 8.50 (d, $J = 5.6$ Hz, 2H; pyridyl-H^2, -H^6); MS: m/z 171 (M^+, 100%). FAB mass spectra of complexes **1**–**4** show molecular ion peaks at m/z 630, 644, 1088, and 644, respectively (based on the masses of the most abundant isotopes).
[8] C. Dietrich-Buchecker, J.-P. Sauvage, *Tetrahedron* **1990**, *46*, 503.
[9] G. S. Daitmazova, N. P. Gambaryan, E. M. Rokhlin, *Russian Chem. Rev.* **1989**, *58*, 1145.
[10] M. A. Hayes, C. Meckel, E. Schatz, M. D. Ward, *J. Chem. Soc. Dalton Trans.* **1992**, 703; B. P. Sullivan, H. Abruna, H. O. Finklea, D. J. Salmon, J. K. Nagle, T. J. Meyer, H. Sprintschnik, *Chem. Phys. Lett.* **1978**, *58*, 389.
[11] In addition to mass spectrometry and elemental analysis, the molybdenum complexes have characteristic $\tilde{\nu}$(NO) stretching frequencies. **1**: $\tilde{\nu}(NO) = 1686\ cm^{-1}$; **4**: $\tilde{\nu}(NO) = 1607\ cm^{-1}$; **3**, which contains one Mo center of each type, $\tilde{\nu}(NO) = 1611$ and $1687\ cm^{-1}$.
[12] The difference between the signals at $g = 1.978$ and $g = 1.969$ is 15 G. At an average magnetic field of approximately 3400 G and a microwave frequency of approximately 9 GHz, the rate of electron exchange necessary to give an averaged signal is simply given by $\upsilon_{min} = (15/3400) \times (9 \times 10^9) \approx 4 \times 10^7$ Hz.
[13] J. R. Miller, L. T. Calcaterra, G. L. Closs, *J. Am. Chem. Soc.* **1984**, *106*, 3047; G. L. Closs, P. Piotrowiak, J. M. MacInnis, S. R. Fleming, *ibid.* **1988**, *110*, 2652.
[14] D. C. Reitz, S. I. Weissmann, *J. Chem. Phys.* **1960**, *33*, 700.
[15] **4**: $C_{27}H_{33}BClMoN_8O_2 \cdot CH_2Cl_2$, $M = 728.7$, triclinic, space group $P\bar{1}$, $a = 10.641(4)$, $b = 10.893(4)$, $c = 14.865(7)$ Å, $\alpha = 96.43(3)$, $\beta = 98.00(3)$, $\gamma = 98.56(3)^\circ$, $V = 1672(1)$ Å^3, $Z = 2$, $\varrho_{calcd} = 1.45\ g\,cm^{-3}$, $F(000) = 746$, $\mu(Mo_{K\alpha}) = 6.7\ cm^{-1}$, $R = 0.066$ ($R_w = 0.067$) for 4403 unique data [293 K, Wyckoff-ω-scans, $2\theta \leq 50^\circ$, $F \geq 5\sigma(F)$]; Data were collected with a Siemens R3m/V diffractometer ($Mo_{K\alpha}$ radiation, graphite monochromator, $\lambda = 0.71069$ Å). The data were corrected for Lorentz, polarization, and X-ray absorption effects. The structure was solved by conventional heavy-atom methods and successive difference Fourier syntheses were used to locate all non-hydrogen atoms. The Cl and NO ligands are mutually disordered (relative site occupancies 76:24), and only the major sites for these ligands are shown in Figure 3. There was no evidence of disorder in the remainder of the complex. Final refinements by full matrix least-squares procedures were performed on a Micro Vax computer with the SHELXTL system of programs [16]. Scattering factors with corrections for anomalous dispersion were taken from ref. [17]. Further details of the crystal structure investigation are available on request from the Director of the Cambridge Crystallographic Data Centre, University Chemical Laboratory, Lensfield Road, Cambridge CB2 1EW (UK), on quoting the full journal citation.
[16] G. M. Sheldrick, *SHELXTL programs for use with a Nicolet X-ray System*, Cambridge, **1976**, updated Göttingen, **1981**.
[17] *International Tables for X-Ray Crystallography, Vol. 4*, Kynoch Press, Birmingham, **1974**.
[18] F. McQuillan, C. J. Jones, J. A. McCleverty, T. A. Hamor, unpublished results.
[19] C. P. Brock, R. P. Minton, *J. Am. Chem. Soc.* **1988**, *111*, 4586.

$Se_3N_2Cl_2$, a Novel Selenium–Nitrogen Chloride: Reinvestigation of "Se_4N_2"**

By *Jari Siivari*, *Tristram Chivers*,* and *Risto Laitinen*

The development of selenium–nitrogen (Se–N) chemistry has been impeded by the lack of readily available Se–N reagents.[1] For example, the selenium analogue of the useful synthon $S_3N_2Cl_2$[2] (**1a**) is unknown, although the mixed sulfur–selenium halides $S_2SeN_2Cl_2$ (**1b**)[3] and $SSe_2N_2Cl_2$ (**1c**)[4] have been structurally characterized recently.

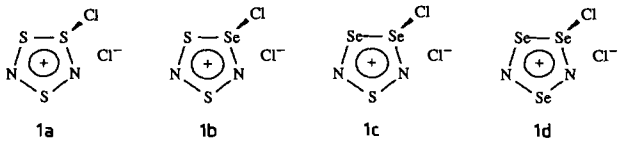

In 1991 Dehnicke reported the preparation of tetraselenium dinitride obtained as a black powder [Eq. (a)].[5, 6] The

$$2\,Se_2Cl_2 + 4\,Me_3SiN_3 \xrightarrow{CH_2Cl_2} Se_4N_2 + 5\,N_2 + 4\,Me_3SiCl \qquad (a)$$

identification of Se_4N_2 relied solely on a comparison of the IR spectrum with that of the structurally characterized sulfur analogue *cyclo*-1,3-S_4N_2, which is a six-membered ring in the half-chair conformation,[7, 8] and with the calculated (3-21G*) vibrational frequencies.[5] The formation of 2:1 and 1:1 adducts of Se_4N_2 with $SnCl_4$ and $TiCl_4$, respectively, has also been reported.[9] These adducts were characterized by IR spectroscopy and by chemical analyses.

The reported stability of Se_4N_2 up to 80 °C[5] appeared to us to be incompatible with the facile thermal decomposition of diiminoselanes RN=Se=NR (R = *t*Bu,[10] $SiMe_3$[11]) above 0 °C. These observations, and our interest in heterocycles of the type $Se_xS_{4-x}N_2$ ($x = 1-4$),[12] prompted us to reinvestigate reaction (a). We report here that the compound formulated by Dehnicke et al. as Se_4N_2 is, in fact, $Se_3N_2Cl_2$ (**1d**) and describe an alternative route to this novel selenium–nitrogen halide.

The reaction of trimethylsilyl azide with diselenium dichloride was carried out according to the literature proce-

[*] Prof. T. Chivers, J. Siivari
Department of Chemistry
The University of Calgary
Calgary, Alberta T2N 1N4 (Canada)
Prof. R. Laitinen
Department of Chemistry
University of Oulu (Finland)

[**] This work was funded by the Natural Sciences and Engineering Research Council (NSERC) (Canada) and the Academy of Finland. J. Siivari is an exchange Ph.D. student at the University of Calgary supported by Neste Oy Foundation, Espoo, Finland.

dure to give an insoluble black powder with an IR spectrum in good agreement with that reported by Dehnicke et al.[5] The insolubility of this black powder in organic solvents and in liquid SO_2 and the possibility of explosions[13] combine to make its characterization by spectroscopic methods (e.g. NMR) difficult. However, complete elemental analyses are consistent with the formula $Se_3N_2Cl_2$ rather than Se_4N_2.[14, 15] Furthermore, when the reaction is carried out with the stoichiometry indicated in Equation (a), the ^{1}H NMR spectrum of the filtrate reveals the presence of unchanged Me_3SiN_3 ($\delta = 0.26$). When the stoichiometry is adjusted to that shown in Equation (b), Me_3SiN_3 is com-

$$3\,Se_2Cl_2 + 2\,Me_3SiN_3 \longrightarrow \underset{\mathbf{1d}}{2\,Se_3N_2Cl_2} + 2\,Me_3SiCl + N_2 \qquad (b)$$

pletely consumed, and the ^{1}H NMR spectrum shows only Me_3SiCl ($\delta = 0.41$). The yield of $Se_3N_2Cl_2$ (found: Cl, 19.75; Se, 70.00) is approximately 70% after 16 h.

Compound **1d** may also be prepared in high yield by the reaction of bis[bis(trimethylsilyl)amino]selane[17] with a mixture of selenium halides designed to mimic "$SeCl_3$" in dichloromethane [Eq. (c)]. The ^{1}H NMR spectrum of the

$$3\,[(Me_3Si)_2N]_2Se + 4\,SeCl_4 + Se_2Cl_2 \longrightarrow \underset{\mathbf{1d}}{3\,Se_3N_2Cl_2} + 12\,Me_3SiCl \qquad (c)$$

filtrate revealed that Me_3SiCl ($\delta = 0.39$) is the exclusive proton-containing product of this reaction, which proceeds according to Equation (c) to give analytically pure samples of $Se_3N_2Cl_2$ (**1d**). The infrared spectra of the products obtained from the reactions (a), (b), and (c) are identical.

The synthesis of $Se_3N_2Cl_2$ completes the series **1a**–**1d** in which one of the sulfur atoms of **1a** is successively replaced by selenium. Although **1b** and **1c** are represented as ionic, we note that covalent forms of both derivatives have been structurally characterized.[3, 4] Thus **1d** may also exist in both covalent and ionic forms. The thermal instability of **1d** relative to the other members of the series is probably due to the presence of the labile NSeN group in **1d** and, as mentioned earlier,[15] samples should be stored at low temperatures to avoid loss of chlorine.

Finally, we note that attempts to convert $Se_3N_2Cl_2$ to the known compound $[Se_3N_2](AsF_6)_2$[18] by reaction with $AgAsF_6$ in liquid SO_2, or to prepare $Se_3N_2Cl^+$ salts by the treatment of $Se_3N_2Cl_2$ with chloride ion acceptors in dichloromethane or liquid SO_2, were unsuccessful, probably due to the insolubility of $Se_3N_2Cl_2$ in these solvents.

Experimental Procedure

A solution of $[(Me_3Si)_2N_2]Se$ [17] (0.200 g, 0.5 mmol) in CH_2Cl_2 (5 mL) was added to a mixture of Se_2Cl_2 (0.0345 g, 0.15 mmol) and $SeCl_4$ (0.143 g, 0.65 mmol) in CH_2Cl_2 (20 mL) at $-78\,^\circ C$ under a dry nitrogen atmosphere. The dark red solution was allowed to warm to room temperature (20 h) and gave a black precipitate, which was washed with CH_2Cl_2 (3 × 5 mL), to give $Se_3N_2Cl_2$ (0.16 g, 0.48 mmol, 95% yield). Analyses: calcd. Cl, 21.12; N, 8.34; Se, 70.54%; found: Cl, 20.73; N, 9.02; Se, 70.44%. IR (Nujol) $\tilde{\nu}$ [cm^{-1}] = 829(s), 584(s), 571(sh), 555(vs), 424(w).

Received: June 12, 1992 [Z 5402 IE]
German version: *Angew. Chem.* **1992**, *104*, 1539

CAS Registry numbers:
1d, 143958-69-4; $[(Me_3Si)_2N]_2Se$, 107886-86-2; Se_2Cl_2, 10025-68-0; $SeCl_4$, 10026-03-6; $[Se_3N_2](AsF_6)_2$, 127435-54-5; $Se_3N_2Cl^+$, 125454-90-2; *cyclo*-1,3-Se_4N_2, 132724-39-1; Me_3SiN_3, 4648-54-8.

[1] T. Klapötke in *The Chemistry of Inorganic Ring Systems*, (Ed.: R. Steudel). Elsevier, Amsterdam, **1992**, pp. 409–427.
[2] a) W. L. Jolly, K. D. Maguire, *Inorg. Synth.* **1967**, *9*, 102; b) A. Zalkin, T. E. Hopkins, D. H. Templeton, *Inorg. Chem.* **1966**, *6*, 1767; T. Chivers in *The Chemistry of Inorganic Homo- and Heterocycles*, (Eds.: I. Haiduc, D. B. Sowerby), Academic Press, London, **1987**, pp. 793–870.
[3] R. J. Gillespie, J. P. Kent, J. F. Sawyer, *Inorg. Chem.* **1990**, *29*, 1251.
[4] A. Haas, J. Kasprowski, K. Angermund, P. Betz, C. Krüger, Y.-H. Tsay, S. Werner, *Chem. Ber.* **1991**, *124*, 1895.
[5] K. Dehnicke, F. Schmock, K. F. Köhler, G. Frenking, *Angew. Chem.* **1991**, *103*, 564; *Angew. Chem. Int. Ed. Engl.* **1991**, *30*, 577.
[6] In fact, the reaction of selenium monochloride and trimethylsilyl azide in dichloromethane had previously been reported to produce an explosive, blue-black Se–N compound. F. A. Kennett, G. K. MacLean, J. Passmore, M. N. S. Rao, *J. Chem. Soc. Dalton Trans.* **1982**, 851.
[7] R. W. H. Small, A. J. Banister, Z. V. Hauptman, *J. Chem. Soc. Dalton Trans.* **1981**, 2188.
[8] T. Chivers, P. W. Codding, W. G. Laidlaw, S. W. Liblong, R. T. Oakley, M. Trsic, *J. Am. Chem. Soc.* **1983**, *105*, 1186.
[9] S. Vogler, M. Schäfer, K. Dehnicke, *Z. Anorg. Allg. Chem.* **1991**, *606*, 73.
[10] a) K. B. Sharpless, T. Mori, L. K. Truesdale, C. O. Dietrich, *J. Am. Chem. Soc.* **1976**, *98*, 269; b) M. Herberhold, W. Jellen, *Z. Naturforsch. B* **1986**, *41*, 144.
[11] F. Fockenberg, A. Haas, *Z. Naturforsch. B* **1986**, *41*, 413.
[12] J. Siivari, R. S. Laitinen, Y. Hiltunen, *Phosphorus, Sulfur Silicon Relat. Elem.* **1991**, *65*, 177. and unpublished results.
[13] **Caution**: It is reported that this product "can be handled with ease at room temperature" [5]. We find, however, that the *dry* powder is extremely hazardous. For example, it explodes violently on contact with a metal spatula. We recommend, therefore, that it is stored under a hydrocarbon solvent.
[14] No analytical data were reported in ref. [5].
[15] To minimize the risk of explosions in handling the black powder, a weighed sample was mixed with Nujol prior to each analysis. Chloride was determined gravimetrically on sample sizes in the range 100–280 mg, and selenium was determined as red selenium on 100–300 mg samples by using a published procedure. [16] Anal. calcd. for $Cl_2N_2Se_3$: Cl, 21.12; N, 8.34; Se, 70.54. Found: Cl, 20.09; N, 7.45; Se, 72.68. These are average values for two (Se and Cl) and three (N) analyses. It is essential to use freshly prepared samples in order to obtain satisfactory analyses. Samples which have aged for a week give low values for Cl, for example, 13.4 and 15.8%, for two different week-old samples.
[16] C. W. Cooper in *Selenium* (Ed.: R. A. Zingaro, C. W. Cooper), Van Nostrand Reinhold, New York, **1974**, p. 615.
[17] M. Björgvinsson, H. W. Roesky, F. Pauer, D. Stalke, G. M. Sheldrick, *Inorg. Chem.* **1990**, *29*, 5140.
[18] E. G. Awere, J. Passmore, P. S. White, T. Klapötke, *J. Chem. Soc. Chem. Commun.* **1989**, 1415.

The New Subnitride $NaBa_3N$; an Extension of Alkali Metal Suboxide Chemistry**

By *Paul E. Rauch* and *Arndt Simon**

The heavy alkali metals rubidium and cesium form a series of suboxides with unusual structures which display a special separation of metallic and ionic bonds.[1] We were interested in extending this chemistry of alkali metal suboxides to alkaline earth metal subnitrides. Addison et al.[2] showed that barium dissolved in liquid sodium is quite reactive with nitrogen gas, and Ba_2N eventually precipitates. Before the precipitation of Ba_2N begins, however, there appears to be for-

[*] Prof. Dr. A. Simon
Max-Planck-Institut für Festkörperforschung
Heisenbergstrasse 1, D-W-7000 Stuttgart 80 (FRG)
Dr. P. E. Rauch
Harvard University, Department of Chemistry
12 Oxford Street, Cambridge, MA 02138 (USA)

[**] P. E. R. thanks the Alexander von Humboldt Foundation for financial support. We thank Dr. H. Borrmann for aid in the structure determination, Dr. N. Perchenek for helpful discussions, and Dr. J. Köhler for the band-structure calculation.

mation of metal-rich clusters that remain in solution. Here we report the synthesis and structure of the new compound $NaBa_3N$.

$NaBa_3N$ was synthesized by slowly cooling a solution of barium and nitrogen in liquid sodium. Hard black needles were obtained.[3] The hexagonal structure consists of a close packing of Na and Ba atoms, that is, a packing of $NaBa_3$ layers, with the trigonal-antiprismatic voids formed by the Ba atoms filled with N atoms. The Ba and N atoms form rods composed of face-sharing Ba_6N octahedra, with single Na atoms arranged between these close-packed rods (Fig. 1). This structure corresponds to the hexagonal perovskite structure known for compounds such as $CsNiCl_3$.[4]

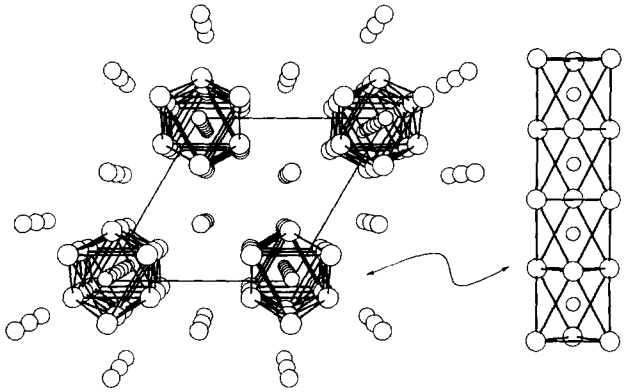

Fig. 1. Central projection of the structure of $NaBa_3N$ along [001] and a Ba_3N column along [210]. The Ba_3N columns are designated by interconnections between the Ba atoms. Distances [Å]: Ba-N 2.734(1), Ba-Ba 3.645(2) (within triangles), 4.076(1) (between triangles), and 4.796(2) (between chains), Ba-Na 4.234(1) and 4.456(1).

The Ba–N and Ba–Ba distances in $NaBa_3N$ (see legend to Fig. 1) compare favorably with the corresponding distances in the structure of the other known barium subnitride Ba_2N (2.760(5) and 3.788(5), 4.016(1), and 4.476(5) Å, respectively).[5] The Ba–Ba distance in Ba metal is 4.341 Å.[6] The shorter of the observed Ba–Na distances (4.234(1) Å) corresponds closely to the sum of the radii (4.154 Å)[7] for Ba and Na in the metals.

A simple model of the chemical bonding in $NaBa_3N$ is based on the much greater electronegativity of nitrogen versus barium and sodium. Tubes of Ba atoms with central N atoms, $\{[Ba^{2+}]_3N^{3-}\}$ $3e^-$, exhibit ionic bonding on the inside and metallic bonding on the "skin" of the tubes and between the tubes and Na atoms, leading to an overall metallic character. This model is verified by the results of a band-structure calculation, which show a low-lying, narrow, filled N2p band; the Fermi level is in a wide band of barium and sodium character.

As we hoped, the metallic and heteropolar bonding are segregated into separate regions in a way that has been seen previously in alkali metal suboxides.[1] Indeed, there is a close structural and bonding relationship between $NaBa_3N$ and the alkali metal suboxides. For example, in Rb_9O_2[8] and Rb_6O,[9] Rb_9O_2 units occur, which represent the first step towards the condensation of M_6X units by face sharing. This finally results in infinite chains as found in $NaBa_3N$.[10] Also in Rb_6O, alkali metal atoms are inserted between the clusters, as reflected in the formula $Rb_3Rb_9O_2$. In another alkali metal suboxide, $Rb_7Cs_{11}O_3$,[14] we see the same preference of different metal atoms for one or the other kind of bond type, as in $NaBa_3N$; the Cs atoms form clusters with oxygen, and the Rb atoms insert between the clusters. The structure of $NaBa_3N$ extends the chemistry of the alkali metal suboxides from discrete clusters to low-dimensional frameworks and on to the layered structure of Ba_2N.[5, 15]

The structure of $NaBa_3N$ helps complete a unified picture of metal cluster compounds.[16] Metal clusters can be grouped into electron-rich species, electron-poor species, and species with an intermediate number of electrons for metal–metal bonding. Within each of these groups we find discrete clusters, quasi-two-dimensional structures (sheets), and quasi-one-dimensional structures (chains).

In the electron-rich case there are enough electrons to form bonds with electronegative elements (Cl, S, etc.) outside the cluster and enough electrons to hold the clusters together by M–M bonding. Examples from this group include Mo_6Cl_{12},[17] Nb_6Cl_{14}[18] (discrete clusters), $ZrCl$[19] (sheets), and $TlMo_3Se_3$[20] (chains). In the intermediate case there are again enough electrons to form bonds with electronegative elements outside the cluster, but interstitial atoms in the cluster are now necessary to stabilize the assembly. Examples from this group include $Nb_6I_{11}H$[21] and $Zr_6Cl_{14}C$[22] (discrete clusters), $GdClH_x$[23] (sheets), and Gd_4I_5C[24] and Ta_4SiTe_4[25] (chains). Finally, in the electron-poor case there are not enough electrons to form bonds with electronegative elements outside the cluster, and an interstitial atom is required. Previously in this category, only discrete clusters such as Rb_9O_2 and $Cs_{11}O_3$, and sheets such as Ba_2N,[5, 14] were known. Now $NaBa_3N$ completes this set with a quasi-one-dimensional chain compound.

Experimental Procedure

The barium metal was purified by distillation, and the sodium metal by filtration of the liquid, prior to use.

$NaBa_3N$: Barium (0.4731 g, 3.445 mmol) and sodium (0.0696 g, 3.02 mmol) were heated to 410 °C in a tantalum crucible under argon (0.0347 MPa), and 27.52 mL of nitrogen (99.99%, 0.0253 MPa at 26.5 °C; ca. 0.28 mmol N_2) was added to this system. The total pressure (argon and nitrogen) was initially 0.0080 MPa. After 1 h this value stopped decreasing to give a final pressure of 0.0047 MPa. Next, enough argon was added to bring the pressure up to 0.0399 MPa, and the reaction mixture was heated at 400 °C for 3.5 h, and then cooled to 100 °C over the next 15 h. Many large (> 1 mm), hard, needle-shaped, black crystals formed, which could be easily separated from the soft solidified "flux" of Ba and Na. Quantitative removal of the crystals from the flux was not possible, hence a yield could not be determined, although $NaBa_3N$ appeared to be the main product.

Received: June 19, 1992 [Z 5417 IE]
German version: *Angew. Chem.* **1992**, *104*, 1505

CAS Registry numbers:
$NaBa_3N$, 143968-89-2; Ba, 7440-39-3; N_2, 7727-37-9; Na, 7440-23-5.

[1] A. Simon, *Struct. Bonding (Berlin)* **1979**, *36*, 81.
[2] C. C. Addison, R. J. Pulham, E. A. Trevillion, *J. Chem. Soc. Dalton Trans.* **1975**, 2080.
[3] a) Crystal data of $NaBa_3N$: space group $P6_3/mmc$; $a = 8.4414(6)$, $c = 6.9817(8)$ Å; $Z = 2$; $\varrho_{calcd} = 3.461\ g\,cm^{-3}$; Ba in 6h ($x = 0.1439(1)$), Na in 2c, N in 2a; $R = 0.0328$, $wR = 0.0219$; 195 observed reflections. $F(000) = 372$; Syntex $P2_1$ diffractometer, 2θ-scan, 2θ-range of 4.0–55.0°, $Mo_{K\alpha}$ radiation. b) Further details of the crystal structure investigation may be obtained from the Fachinformationszentrum Karlsruhe, Gesellschaft für wissenschaftlich-technische Information mbH, D-W-7514 Eggenstein-Leopoldshafen 2 (FRG) on quoting the depository number CSD-56436, the names of the authors, and the journal citation.
[4] G. N. Tishchenko, *Trans. Inst. Kristallogr. Akad. Nauk. USSR* **1955**, *11*, 93.
[5] H.-T. Künzel, *Metallreiche Bariumnitride*, Dissertation, Universität Stuttgart, **1980**.
[6] W. B. Pearson, *A Handbook of Lattice Spacings and Structures of Metals and Alloys, Vol. 2*, Pergamon, London, **1967**, p. 80.
[7] W. B. Pearson, *The Crystal Chemistry and Physics of Metals and Alloys*, Wiley-Interscience, New York, **1972**, p. 151.
[8] A. Simon, *Z. Anorg. Allg. Chem.* **1977**, *43*, 5.

[9] A. Simon, H. J. Deiseroth, *Rev. Chim. Minér.* **1976**, *13*, 98.
[10] The Ba_3N chains correspond to those reported in Cs_3O [11], but there is some doubt about the correctness of the reported structure [12]. Crystals of Cs_3O exhibit strong diffuse superstructure reflections not taken into account in the reported structure [13]. The diffraction pattern of $NaBa_3N$ is free of any such diffuse reflections.
[11] K.-H. Tsai, P. M. Harris, E. N. Lassettre, *J. Phys. Chem.* **1956**, *60*, 338.
[12] A. Simon, *Z. Anorg. Allg. Chem.* **1973**, *395*, 301.
[13] F. Okino, A. Simon, unpublished results, **1985**.
[14] A. Simon, W. Brämer, H. J. Deiseroth, *Inorg. Chem.* **1978**, *17*, 875.
[15] S. M. Ariya, E. A. Prokofyeva, I. I. Matveeva, *J. Gen. Chem. USSR* **1955**, *26*, 609.
[16] A. Simon, *Angew. Chem.* **1988**, *100*, 163; *Angew. Chem. Int. Ed. Engl.* **1988**, *27*, 159.
[17] H. Schäfer, H. G. von Schnering, J. Tillack, F. Kuhnen, H. Wöhrle, H. Baumann, *Z. Anorg. Allg. Chem.* **1967**, *353*, 281.
[18] A. Simon, H. G. von Schnering, H. Wöhrle, H. Schäfer, *Z. Anorg. Allg. Chem.* **1965**, *339*, 155.
[19] D. Adolphson, J. D. Corbett, *Inorg. Chem.* **1976**, *15*, 1820.
[20] M. Potel, R. Chevrel, M. Sergent, *Acta Crystallogr. Sect. B* **1980**, *36*, 1545.
[21] A. Simon, *Z. Anorg. Allg. Chem.* **1967**, *355*, 311.
[22] R. P. Ziebarth, J. D. Corbett, *J. Solid State Chem.* **1989**, *80*, 56.
[23] H. Mattausch, W. Schramm, R. Eger, A. Simon, *Z. Anorg. Allg. Chem.* **1985**, *530*, 43.
[24] A. Simon, *J. Solid State Chem.* **1985**, *57*, 2; S. M. Kauzlarich, T. Hughbanks, J. D. Corbett, P. Klavins, R. N. Shelton, *Inorg. Chem.* **1988**, *27*, 1791.
[25] M. E. Badding, F. J. DiSalvo, *Inorg. Chem.* **1990**, *29*, 3952.

Enantioselective Complexation of Chiral Dicarboxylic Acids in Clefts of Functionalized 9,9′-Spirobifluorenes**

By *Victoria Alcazar* and *François Diederich**

The results of several studies on the enantioselective recognition of chiral substrates by optically active receptors have led to the conclusion that large differences in stability between diastereomeric complexes are preferentially obtained when the receptors are *conformationally homogenous*[1, 2] and when differential *oriented bonding interactions*, for example hydrogen bonding, are effective in the complexes.[3–6] Following these guidelines, we recently prepared the receptors **1** and **2** which incorporate a cleft formed by a rigid 9,9′-spirobifluorene unit functionalized with hydrogen-bonding residues. The 9,9′-spirobifluorene unit had previously been introduced by Prelog et al.[7] as spacer in chiral crown ethers. Binding studies with the racemic hosts showed that **1**, but not **2**, was capable of forming 1:1 complexes with aliphatic and aromatic dicarboxylic acids in chloroform (association constants $K_a \approx 10^3$ to 10^5 L mol^{-1} at 293 K). These complexes are mainly stabilized by hydrogen bonds between the two COOH groups of the guests and the two aminopyridine residues in **1** (Scheme 1a).[8, 9] On the other hand, monocarboxylic acids form much weaker complexes ($K_a \approx 100$ to 400 L mol^{-1}). In this report, we describe first investigations of the *enantioselective* complexation of chiral dicarboxylic acids by the enantiopure receptors (*R*)- and (*S*)-**1** and compare their chiral recognition potential to that of similarly functionalized but more flexible 1,1′-binaphthyl hosts.

[*] Prof. Dr. F. Diederich, Dr. V. Alcazar
Laboratorium für Organische Chemie, ETH-Zentrum
Universitätstrasse 16, CH-8092 Zürich (Switzerland)
and
Department of Chemistry and Biochemistry
University of California
Los Angeles, CA 90024-1569 (USA)

[**] This work was supported in part by the U.S. National Institutes of Health and by the Fulbright Foundation (fellowship for V.A.).

For the preparation of (*R*)- and (*S*)-**1**, the racemic dicarboxylic acid **3** was prepared according to Prelog et al. and optically resolved via the diastereomeric amides obtained by reaction of the corresponding acyl halide with (−)-dehydroabietylamine.[7b] The conversion of the acyl halides, prepared from (*R*)-(+)- and (*S*)-(−)-**3**,[10] with 2-amino-6-methylpyridine afforded the enantiopure receptors (*R*)-**1** ($[\alpha]_D^{22}$ +177.5 (c = 0.435 in $CHCl_3$) and (*S*)-**1** ($[\alpha]_D^{22}$ −180.0 (c = 0.570 in $CHCl_3$)). The optically active amino acid derivatives needed as substrates for the binding studies were either commercially available or were prepared according to routine procedures.[10] The optically active 2,2′,7,7′-tetrasubstituted spirobifluorene (*S*)-**4** ($[\alpha]_{589}^{22}$ +3.1 (c = 0.450 in acetone)) was obtained by acylation of (*S*)-**3** ($C_7H_{15}COCl$, $AlCl_3$, CS_2, 67% yield).

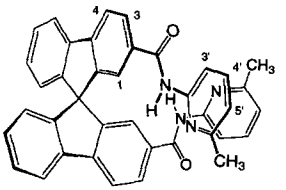

1

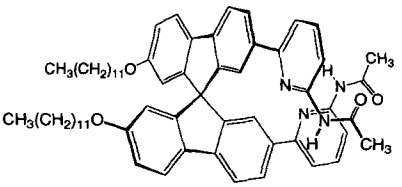

2

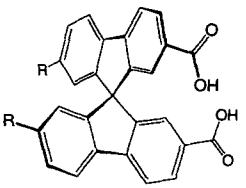

3 R = H
4 R = $CH_3(CH_2)_6CO$

Table 1 shows the results of ^{1}H NMR binding titrations executed under fast-exchange conditions and in significant concentration ranges.[11] The following findings are of particular interest:

1) The *N*-protected derivatives **5**–**8** of the acidic amino acids L-aspartic acid (L-Asp) and L-glutamic acid (L-Glu) are selectively recognized by the enantiomeric receptors. Differences in stability as high as $\Delta(\Delta G^\circ) = 0.9$ kcal mol^{-1} are measured for the diastereomeric complexes of the *N*-carbobenzyloxy (Cbz) protected substrates. Interestingly, L-Asp and L-Glu prefer binding to different host enantiomers. The Asp derivatives **5** and **6** form the most stable complexes with (*S*)-**1**, whereas the Glu derivatives **7** and **8** bind strongest to (*R*)-**1**. As a consequence of the different chain length, which is even-numbered in **5**/**6** and odd-numbered in **7**/**8**, the terminal carboxyl residues adopt very different orientations in the complexes, which ultimately leads to an inversion of the favored host configuration. This explanation is currently being tested in computer modeling studies.[12]

Binding constants of similar magnitude are measured for the complexes of the Cbz derivatives and the *n*-butylcarba-

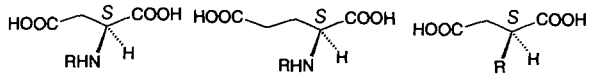

5 R = $C_6H_5CH_2OCO$ **7** R = $C_6H_5CH_2OCO$ **9** R = C_6H_5S
6 R = *n*BuOCO **8** R = *n*BuOCO **10** R = C_6H_5Se

Table 1. Association constants K_a and binding free energies $-\Delta G°$ (uncertainty 0.1 kcal mol^{-1}) of the diastereomeric complexes formed by the enantiopure receptors **1** and **12** in $CDCl_3$ at 293 K. The value of $\Delta(\Delta G°)$ indicates the difference in stability between diastereomeric complexes.

Host	Guest	K_a [L mol^{-1}]	$-\Delta G°$ [kcal mol^{-1}]	$\Delta(\Delta G°)$ [kcal mol^{-1}]
(*R*)-**1**	**5**	820	3.9	
(*S*)-**1**	**5**	4200	4.8	0.9
(*R*)-**1**	**6**	1400	4.2	
(*S*)-**1**	**6**	4800	4.9	0.7
(*R*)-**1**	**7**	14000	5.6	0.8
(*S*)-**1**	**7**	3900	4.8	
(*R*)-**1**	**8**	23000	5.8	0.4
(*S*)-**1**	**8**	10000	5.4	
(*R*)-**1**	**9**	680	3.8	
(*S*)-**1**	**9**	3400	4.7	0.9
(*R*)-**1**	**10**	800	3.9	
(*S*)-**1**	**10**	2200	4.5	0.6
(*R*)-**1**	**11b**	420	3.5	
(*S*)-**1**	**11b**	680	3.8	0.3
(*R*)-**1**	(*S*)-**4**	490	3.6	
(*S*)-**1**	(*S*)-**4**	11300	5.4	1.8
(*R*)-**12**	**7**	20800	5.8	0.1
(*S*)-**12**	**7**	19400	5.7	
(*R*)-**12**	(*R*)-**13**	8500	5.3	0.1
(*S*)-**12**	(*R*)-**13**	7200	5.2	

mates. This indicates that the phenyl residues of the Cbz groups do not have specific stabilizing aromatic interactions with the spirobifluorene unit. This assumption is further supported by the absence of specific, complexation-induced changes in the ^{1}H NMR chemical shifts as well as by the absence of significant intermolecular Nuclear Overhauser effects in the complexes. For stable complexation *and* efficient chiral recognition, the presence of two carboxyl residues in the guest is essential. This is clearly shown in a series of control experiments: Compounds **11a–e** formed weaker complexes ($K_a \approx 10-700$ L mol^{-1}) with binding strengths similar to those exhibited by complexes with monocarboxylic acids, and chiral recognition was less effective (Table 1). On the other hand, considerable enantioselectivity was observed in the complexation of the two chiral succinic acid derivatives **9** and **10**.

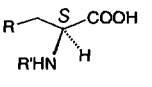

11	R	R'
a	HO	Cbz
b	C_6H_5	Cbz
c	C_6H_5	C_6H_5NHCO
d	H_2NCOCH_2	Cbz
e	C_6H_5NHCOO	Cbz

2) Whereas complexation has a pronounced effect on the equilibrium between the *cis* and *trans* conformations of the NH–CO carbamate bond of **5**, no such effect is seen with **7**.[13] The integration of the NH and C(α)H proton NMR resonances, which appear at higher field in the *trans* and at lower field in the *cis* conformation,[14] shows that the *cis*/*trans* ratio of 3:1 in the free substrate **5** changes to 8:1 in the two diastereomeric complexes formed with (*R*)- and (*S*)-**1**. In contrast, the same *cis*/*trans* ratio of 8:1 is measured for both free and complexed carbamate **7**.

3) A very high enantioselectivity, $\Delta(\Delta G°) = 1.8 \pm 0.1$ kcal mol^{-1}, was measured for the complexation of the (*S*)-spirobifluorene-2,2′-dicarboxylic acid **4** by (*R*)- and (*S*)-**1**. The origin of this large difference in stability becomes apparent in examinations of CPK molecular models (Scheme 1b). Only in the complex of similarly configurated host and guest are the two spirobifluorene units capable of assembling in a way to lead to the formation of four hydrogen bonds. In the other diastereomeric complex, the interactions of two COOH groups with the H-bonding functionality of the host are impossible for geometrical reasons. Therefore, the association constant of the latter complex is small and of a magnitude characteristic for 1:1 complexes of monocarboxylic acids and amidopyridines. This result suggests that enantiopure host **1** could be prepared by resolving its direct precursor, the racemic spirobifluorenedicarboxylic acid **3**, through complexation with previously formed optically pure (*R*)- and (*S*)-**1** followed by crystallization, extraction, or chromatography.

4) The findings with the spirobifluorene receptors (*R*)- and (*S*)-**1** are in sharp contrast to the results obtained with the analogous 1,1′-binaphthyl cleft molecules (*R*)-**12** ($[\alpha]_D^{22}$ −19.40 (c = 1.01 in $CHCl_3$)) and (*S*)-**12** ($[\alpha]_D^{22}$ +19.28 (c = 1.12 in $CHCl_3$)).[2b, 8b] Although substrates **5–8** and the dicarboxylic acid (*R*)-**13** ($[\alpha]_D^{22}$ +14.74 (c = 0.231 in $CHCl_3$)) form stable complexes with the binaphthyl receptors, no significant degree of chiral recognition was observed (Table 1).[15] In contrast to the rigid spirobifluorene frame, the binaphthyl unit is conformationally flexible and capable of adopting geometries which fit both substrate enantiomers. As a consequence, diastereomeric complexes of similar ener-

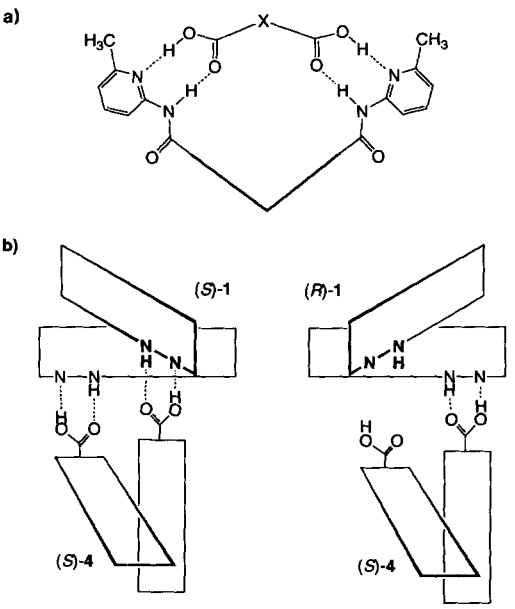

Scheme 1. a) Optimal hydrogen-bonding array in the complexes formed by (*R*)- and (*S*)-**1** with dicarboxylic acids, as supported by computer modeling studies [8a]. b) Hydrogen bonds in the diastereomeric complexes of (*R*)- and (*S*)-**1** with (*S*)-**4**.

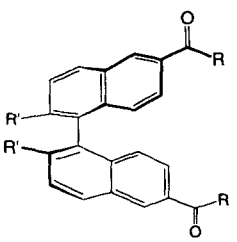

	R	R'
12	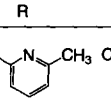	$C_6H_5CH_2O$
13	OH	$C_{12}H_{25}O$

gy are formed. However, through careful control of the 1,1'-binaphthyl geometry, for example by an additional binding site in the 2,2'-positions,[16] it should be possible to rigidify the cleft molecule and enhance its efficiency in chiral recognition. Experiments in this direction are now under way.

Received: June 19, 1992 [Z 5433 IE]
German version: *Angew. Chem.* **1992**, *104*, 1503

CAS Registry numbers:
(*R*)-**1**·(*S*)-**4**, 144017-09-4; (*R*)-**1**·**5**, 144017-06-1; (*R*)-**1**·**6**, 144068-54-2; (*R*)-**1**·7, 144068-55-3; (*R*)-**1**·**8**, 144068-56-4; (*R*)-**1**·**9**, 144017-07-2; (*R*)-**1**·**10**, 144017-08-3; (*R*)-**1**·**11b**, 144068-57-5; (*S*)-**1**·(*S*)-**4**, 143957-65-7; (*S*)-**1**·**5**, 143957-58-8; (*S*)-**1**·**6**, 143968-92-7; (*S*)-**1**·7, 143957-59-9; (*S*)-**1**·**8**, 143968-94-9; (*S*)-**1**·**9**, 143957-61-3; (*S*)-**1**·**10**, 143957-63-5; (*S*)-**1**·**11b**, 144000-09-9; (*R*)-**12**·7, 143957-67-9; (*R*)-**12**·(*R*)-**13**, 143957-71-5; (*S*)-**12**·7, 143957-69-1; (*S*)-**12**·(*R*)-**13**, 143957-72-6.

[1] a) R. Liu, P. E. J. Sanderson, W. C. Still, *J. Org. Chem.* **1990**, *55*, 5184–5186; b) J.-I. Hong, S. K. Namgoong, A. Bernardi, W. C. Still, *J. Am. Chem. Soc.* **1991**, *113*, 5111–5112.
[2] a) T. M. Georgiadis, M. M. Georgiadis, F. Diederich, *J. Org. Chem.* **1991**, *56*, 3362–3369; b) P. P. Castro, F. Diederich, *Tetrahedron Lett.* **1991**, *32*, 6277–6280.
[3] W. H. Pirkle, T. C. Pochapsky, *Chem. Rev.* **1989**, *89*, 347–362.
[4] a) K. S. Jeong, A. V. Muehldorf, J. Rebek Jr., *J. Am. Chem. Soc.* **1990**, *112*, 6144–6145; b) M. Famulok, K.-S. Jeong, G. Deslongchamps, J. Rebek, Jr., *Angew. Chem.* **1991**, *103*, 880–882; *Angew. Chem. Int. Ed. Engl.* **1991**, *30*, 858–860.
[5] A. Galán, D. Andreu, A. M. Echavarren, P. Prados, J. de Mendoza, *J. Am. Chem. Soc.* **1992**, *114*, 1511–1512.
[6] P. P. Castro, T. M. Georgiadis, F. Diederich, *J. Org. Chem.* **1989**, *54*, 5835–5838.
[7] a) V. Prelog, *Pure Appl. Chem.* **1978**, *50*, 893–904; b) G. Haas, V. Prelog, *Helv. Chim. Acta* **1969**, *52*, 1202–1218; c) V. Prelog, D. Bedekovic, *ibid.* **1979**, *62*, 2285–2302; d) V. Prelog, S. Mutak, *ibid.* **1983**, *66*, 2274–2278; e) M. Dobler, M. Dumić, M. Egli, V. Prelog, *Angew. Chem.* **1985**, *97*, 793–794; *Angew. Chem. Int. Ed. Engl.* **1985**, *24*, 792–794.
[8] a) V. Alcazar Montero, L. Tomlinson, K. N. Houk, F. Diederich, *Tetrahedron Lett.* **1991**, *32*, 5309–5312; b) V. Alcazar, J. R. Moran, F. Diederich, *Isr. J. Chem.*, in press.
[9] F. Garcia-Tellado, S. Goswami, S.-K. Chang, S. J. Geib, A. D. Hamilton, *J. Am. Chem. Soc.* **1990**, *112*, 7393–7394.
[10] The assignment of the absolute configuration was made according to Prelog et al., see ref. [7c]. All new compounds were completely characterized by IR and ^{1}H NMR spectroscopy, mass spectrometry, melting point, and elemental analysis.
[11] Examples for complexation-induced downfield shifts of the ^{1}H NMR signals of the host in the (*R*)-**1**·7 complex at saturation binding: $\Delta\delta_{sat}$ = +0.245 (1-H); +0.057 (3-H); +0.048 (3'-H); +0.116 (4'-H); +0.044 (5'-H); +2.628 (NH). Both the shifts of the aromatic resonances and the amide protons were evaluated to determine the association constants given as average values in Table 1.
[12] L. Tomlinson, K. N. Houk, V. Alcazar, F. Diederich, unpublished results.
[13] C. Vicent, S. C. Hirst, F. Garcia-Tellado, A. D. Hamilton, *J. Am. Chem. Soc.* **1991**, *113*, 5466–5467.
[14] J. L. Dimicoli, M. Ptak, *Tetrahedron Lett.* **1970**, 2013–2016.
[15] For similar independent findings see: F. Garcia-Tellado, J. Albert, A. D. Hamilton, *J. Chem. Soc. Chem. Commun.* **1991**, 1761–1763.
[16] F. Diederich, M. R. Hester, M. A. Uyeki, *Angew. Chem.* **1988**, *100*, 1775–1777; *Angew. Chem. Int. Ed. Engl.* **1988**, *27*, 1705–1706.

The Uncatalyzed Transfer Hydrogenation of α-Methylstyrene by Dihydroanthracene or Xanthene—a Radical Reaction**

By *Christoph Rüchardt,** *Matthias Gerst,* and *Margot Nölke*

During an investigation of the thermolysis of 3-(1-methyl-1-phenylethyl)pentane-2,4-dione at 290 °C with dihydroanthracene DHA **2a** as a radical trap, we observed that α-methylstyrene (**1**) formed initially was hydrogenated to cumene and that anthracene was an additional product. In independent experiments it was demonstrated that α-methylstyrene (**1**) is hydrogenated by DHA **2a** almost quantitatively at 280–310 °C in an uncatalyzed H-transfer reaction.

Hydrogen-transfer reactions between H donors and H acceptors catalyzed by transition metals are well known,[1] and examples catalyzed by Lewis acids have also been described.[2] Yet the literature contains few examples of uncatalyzed H-transfer reactions between organic or organometallic H donors and unsaturated hydrocarbons. The mechanisms of these reactions were either not examined more closely,[3] or they were described as pericyclic synchronous transfers.[4] For DHA **2a** and xanthene (**2b**) a pericyclic reaction is not possible, since it either cannot be formulated or it is symmetry forbidden as a thermal reaction (e.g. the reaction of **1** with **2a** of the type $[_\sigma 2_s + _\pi 2_s + _\sigma 2_s + _\pi 4_s]$[4c]). Recently, multistep mechanisms have been formulated in which bimolecular radical formation proceeds by H transfer;[5-7] most of the examples concern the assumed initiation steps of radical chains as in the uncatalyzed polymerization of styrene,[5a] the thermal chain addition of alkanes to alkenes,[5b] and the thermal decomposition of dihydronaphthalenes[6] and isotoluene.[7] These reactions are not suitable for an exact mechanistic study. The stoichiometric disproportionantion of DHA **2a** and 2-ethylanthracene[8a] which proceeds by H transfer, and the gas-phase reaction of ethylene and cyclopentene which occurs at 400–500 °C[8b] are exceptions.

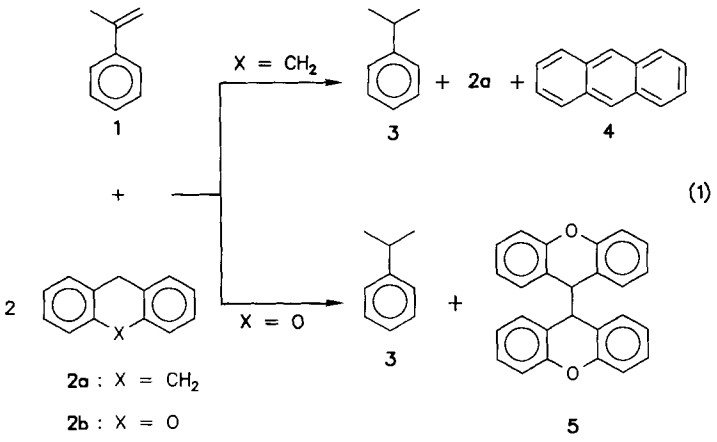

(1)

We report here on experiments that prove that the hydrogenation of α-methylstyrene (**1**) by DHA **2a** is one of the few examples of a *stoichiometric*, solution-phase, uncatalyzed transfer hydrogenation of an alkene initiated by the bimolecular formation of a radical by H transfer from a C–H bond. Thus this reaction is a suitable subject for a mechanistic study of the type of "molecule-induced"[9] radical formation discussed as the initiation step in the uncatalyzed polymerization of styrene.

Kinetic measurements (Table 1) show that the rate of the H-transfer reaction [Eq. (1)] is first order in DHA **2a** and in α-methylstyrene (**1**) up to high conversions. Both the decrease in the concentration of **1** (k_2) and the increase of the concentration of **3** (k'_2) were followed by gas chromatography and provided the same results.

The rate constant of the bimolecular reaction is almost independent of the concentration of the H donor, invariant to oxygen, and also unchanged upon addition of the initiator

[*] Prof. C. Rüchardt, Dipl.-Chem. M. Gerst, Dipl.-Chem. M. Nölke
Institut für Organische Chemie und Biochemie der Universität
Albertstrasse 21, D-W-7800 Freiburg (FRG)

[**] Bimolecular Formation of Radicals by Hydrogen Transfer, Part 1. This research was supported by the Fonds der Chemischen Industrie.

Table 1. Kinetic data for the transfer hydrogenation of α-methylstyrene (**1**) by dihydroanthracene **2a** or xanthene (**2b**) in diphenyl ether at 250–310 °C.

Cmpd.	T [°C]	[**2**] [mol L^{-1}]	[**1**] [mol L^{-1}]	**2**:**1**	$10^5 k_2 \pm \sigma$ [a]		$10^5 k_2' \pm \sigma$ [a]	
2a	250.0	1.570	0.082	19:1	0.56	1.2	0.56	3.3
	270.0	1.570	0.082	19:1	1.42	1.3	1.45	3.4
	280.0	0.848	0.082	10:1	4.15	1.3	4.14	2.4
	290.0	1.570	0.074	21:1	7.36	2.0	7.35	4.9
	290.0	0.888	0.089	10:1	6.36	4.2	6.34	1.3
	290.0	0.888	0.044	20:1	6.06	6.5	6.06	3.0
	300.0	0.849	0.075	11:1	12.54	1.2	12.35	2.8
	300.0 [b]	0.851	0.071	11:1	6.09	1.8	6.05	1.6
	310.0	0.405	0.042	10:1	20.89	4.5	20.88	3.5
	310.0	0.848	0.077	11:1	19.66	0.8	19.65	2.6
	310.0 [c]	0.848	0.077	11:1	17.86	2.1	17.82	2.9
	310.0 [d]	0.848	0.077	11:1	17.34	2.8	17.41	2.1
	310.0	1.635	0.155	10:1	16.26	1.9	16.24	4.5
		$\Delta G^{\neq}$(300 °C) $\pm \sigma$		$\Delta H^{\neq} \pm \sigma$			$\Delta S^{\neq} \pm \sigma$	
		44.7 ± 1.4 [e,g]		35.9 ± 1.4 [e,g]			−15.3 ± 2.5 [f, g]	
2b	280.0	0.836	0.075	11:1	5.84	2.1	5.84	1.8
	290.0	0.836	0.075	11:1	11.27	3.1	11.34	3.8
	300.0	0.836	0.075	11:1	17.38	1.9	17.38	4.4
	310.0	0.836	0.075	11:1	26.34	1.5	26.39	1.5
		$\Delta G^{\neq}$(300 °C) $\pm \sigma$		$\Delta H^{\neq} \pm \sigma$			$\Delta S^{\neq} \pm \sigma$	
		44.2 ± 2.4 [e,g]		31.4 ± 2.4 [e,g]			− 22.3 ± 4.3 [f, g]	

[a] k_2 in s^{-1}M^{-1}, σ in %. k: decrease in **1** was followed, k': increase in **3** was followed. [b] Deuterated **2a** (95% deuterium incorporation in the methylene position). [c] Addition of 5 mol% of 9,9′-bifluorene [10] relative to **1**, $\tau_{1/2} = 1$ h at 270 °C. [d] Addition of 10 mol% of 9,9′-bifluorene relative to **1**. [e] In kcal mol^{-1}. [f] In e.u. (cal K^{-1}mol^{-1}). [g] The activation data were calculated from the Eyring plot of all values of k_2 from **2a** and **2b** (exception: k_2 at 300 °C with deuterated **2a**).

9,9′-bifluorene[10] ($\tau_{1/2} = 1$ h at 270 °C). Radical chain reactions can thus be ruled out.

We assume a bimolecular radical formation[5, 6] [Eq.(2)] followed by H transfer from DHA **2a** to the cumyl radical **6** [Eq.(3)] and subsequent disproportionation of **7a** [Eq.(6)].

Isotopic labeling of **2a** (95% deuterium incorporation at the methylene position) showed that an H atom is transferred from **2a** to **1** in the rate-determining step. The kinetic isotope effect $k_2(H)/k_2(D)$ at 300 °C was 2.1;[11] it has the same order of magnitude as known values.[5b, 8a]

According to isotope analyses by mass spectrometry, the back reaction with $v_{-2} = k_{-2}$[**6**][**7a**] does not take place, since deuterium is not incorporated into α-methylstyrene (**1**) and only dideuteriocumene is formed. Thus the rate of disappearance of **1** is governed solely by $v_2 = k_2$[**1**][**2a**]. Apparently, the reaction with $v_3 = k_3$[**2**][**6**] proceeds much faster than the back reaction with v_{-2} under the reaction conditions and thus certainly faster than the alternative disproportionation according to Equation (4). The reaction enthalpy of the H-transfer reaction [Eq.(2)] calculated from thermodynamic data,[12] ΔH°(25 °C,g) = 31.5 ± 2.0 − 34.2 ± 2.3 kcal mol^{-1}, is only somewhat less than the activation enthalpy $\Delta H^{\neq} = 35.9 \pm 1.4$ kcal mol^{-1} (Table 1); this supports the proposed mechanism. The back reaction should be a disproportionation without activation enthalpy. A metathesis reaction of **7a** and **1**[5b] combined with Equation (3) leads formally to a radical chain reaction. According to the kinetic results of the reaction of **1** with **2a** upon addition of bifluorene, this chain reaction does not seem to occur (Table 1); the radicals **7a** react faster following Equation (6).

The uniform reaction sequence is remarkable when one considers the possible competing side reactions of the radicals involved. The rate constants of the potential reactions of

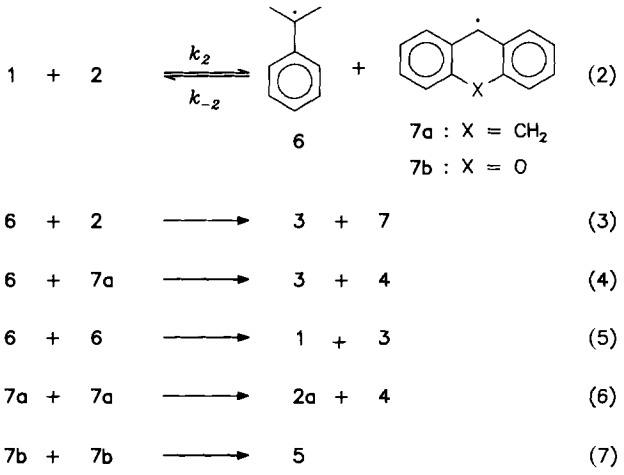

radicals **6** and **7a** discussed were estimated, and the change in the experimental concentrations of **1** and **3** over time were calculated with the simulation program KISS.[13] The rate of the H transfer from the H donor **2a** to **6** [Eq.(3)] was found to be 10^3 times faster than formation of **3** by the disproportionation reactions in Equations (4) or (5). The fact that $v_3 = k_3$[**2a**][**6**] is favored over $v_4 = k_4$[**6**][**7a**] and $v_5 = k_5$[**6**][**6**] is explained by the low concentration of the radicals. According to work of Fischer et al.,[14] Equation (5) should be neglible relative to Equation (4), since when short-lived radicals **6** and long-lived radicals **7** are formed in equimolar amounts the cross termination reaction [Eq.(4)] dominates.

Moreover, it should be considered that mobile dimerization equilibria exist for the radical recombination of **6** and **7a**; nevertheless, the radicals are converted irreversibly into the reaction products.[15–17] In addition, the polymerization of **1** is outweighed by the corresponding depolymerization.[18]

Because of the fast disproportionation reaction [Eq.(6)], the steady-state concentration of radicals **7a** was too low for proof of their existence by ESR spectroscopy. Thus, we employed xanthene (**2b**) as the H-transfer agent, as xanthyl radicals **7b** cannot disproportionate following Equation (6). The reaction of **2b** proceeded analogously to that of **2a** (Table 1). The difference in the activation enthalpy $\Delta\Delta H^{\neq} = 4.5$ kcal mol^{-1} is related to the difference in the bond dissociation energy in **2a** and **2b** (Δ(C–H bond dissociation energy) = 0.8–3.8 kcal mol^{-1}).[12d, e]

Intense, well-resolved ESR spectra typical of **7b**[16] could be observed during the reaction (280 °C). 9,9′-Bixanthene[16] (**5**) was formed according to Equation (7) in yields of > 90%, thereby reconfirming the two-stage H-transfer hydrogenation with initial bimolecular radical formation. The activation parameters of both reactions (Table 1) are in line with the expectations for bimolecular processes and are similar to the values reported by Stein et al.[8] for the related disproportionation of 2-ethylanthracene and DHA **2a** ($\Delta G^{\neq}_{300\,°C} = 45.7 \pm 1.3$ kcal mol^{-1}, $\Delta H^{\neq} = 36.3 \pm 1.3$ kcal mol^{-1}, $\Delta S^{\neq} = -16.5 \pm 2.2$ e.u.). The effect of the polarity of the solvent on the transfer hydrogenation from **2b** to **1** between 280 and 310 °C in *tert*-butylbenzene (E_T value = 33.7),[19] diphenyl ether (E_T value = 35.3), *ortho*-dichlorobenzene (E_T value = 38.1), and benzonitrile (E_T value = 42) was minimal for k_2 (factor < 5). It is therefore very unlikely that ions or zwitterions are involved.

Initial studies showed that *para*-methylstyrene is also hydrogenated under the same conditions ($k_2^{309\,°C} = 21.6 \times 10^{-5}$ kcal mol^{-1} ± 1.4%), but cyclohexene, acrylonitrile,

and methyl methacrylate are not. Further experiments will show if these substrates will react under more forcing conditions or with more effective H-transfer reagents. Phenalene, known to be an especially reactive H donor, was used successfully.[20]

This uncatalyzed H-transfer reaction with its unequivocal, undisturbed reaction sequence is a good subject for further investigation of additional mechanistic details of the bimolecular radical formation by hydrogen transfer. The structure–reactivity relationships may then be better understood.

Received: July 23, 1992 [Z 5476 IE]
German version: *Angew. Chem.* **1992**, *104*, 1516

CAS Registry numbers:
1, 98-83-9; **2a**, 613-31-0; **2b**, 92-83-1; D_2, 7782-39-0.

[1] R. A. W. Johnstone, A. H. Wilby, I. D. Entwistle, *Chem. Rev.* **1985**, *85*, 129.
[2] J. J. Eisch, S. R. Sexsmith, M. Singh, *Energy Fuels* **1989**, *3*, 761.
[3] B. A. Arbuzov, L. A. Shapshinskaya, G. A. Prytkova, *Izv. Akad. Nauk. SSSR, Otd. Khim. Nauk* **1962**, 2084 [*Chem. Abstr.* **1963**, *58*, 8995].
[4] a) J. W. Rosenthal, W. von E. Doering, *J. Am. Chem. Soc.* **1967**, *89*, 4534; b) K. Mackenzie, G. Proctor, D. J. Woodnutt, *Tetrahedron* **1987**, *43*, 5981; J. A. K. Hobard, K. Mackenzie, R. E. Johnson, *Tetrahedron Lett.* **1989**, *30*, 5005; J. P. Melder, H. Prinzbach, *Chem. Ber.* **1991**, *124*, 1271; L. A. Paquette, G. A. O'Doherty, *J. Am. Chem. Soc.* **1991**, *113*, 7761; T. Gerres, A. Heesing, *Chem. Ber.* **1992**, *125*, 1439; M. L. McKee, D. M. Stanbury, *J. Am. Chem. Soc.* **1992**, *114*, 3214; c) K. N. Houk, Y. Li, J. D. Evanseck, *Angew. Chem.* **1992**, *104*, 711; *Angew. Chem. Int. Ed. Engl.* **1992**, *31*, 682.
[5] a) W. A. Pryor, W. D. Graham, J. G. Green, *J. Org. Chem.* **1978**, *43*, 526; Y. K. Chong, E. Rizzardo, D. H. Solomon, *J. Am. Chem. Soc.* **1983**, *105*, 7761; H. K. Hall, *Angew. Chem.* **1983**, *95*, 448; *Angew. Chem. Int. Ed. Engl.* **1983**, *22*, 440; b) J. O. Metzger, *ibid.* **1983**, *95*, 914 and **1983**, *22*, 889; *ibid.* **1986**, *98*, 79 and **1986**, *25*, 80; J. Hartmanns, K. Klenke, J. O. Metzger, *Chem. Ber.* **1986**, *119*, 488; J. Hartmanns, J. O. Metzger, *ibid.* **1986**, *119*, 500; c) J. W. Grissom, T. L. Calkins, *Tetrahedron Lett.* **1992**, *33*, 2315; d) J. Halpern, *Pure Appl. Chem.* **1979**, *51*, 2171.
[6] J. A. Franz, D. M. Camaioni, R. R. Beishline, D. K. Dulling, *J. Org. Chem.* **1984**, *49*, 3563; K. R. Kopecky, M.-P. Lau, *ibid.* **1978**, *43*, 525; A. Heesing, W. Müllers, *Chem. Ber.* **1980**, *113*, 9, 19, 24.
[7] J. J. Gajewski, A. M. Gotva, *J. Am. Chem. Soc.* **1982**, *104*, 334.
[8] a) R. Billmers, L. L. Griffith, S. E. Stein, *J. Phys. Chem.* **1986**, *90*, 517; b) S. W. Benson, *Int. J. Chem. Kin.* **1980**, *12*, 755.
[9] W. A. Pryor, L. D. Lasswell, *Advances in Free Radical Chemistry, Vol. 5* (Ed.: G. H. Williams), Academic Press, New York, **1975**, p. 27; J. A. K. Harmony, *Methods in Free Radical Chemistry, Vol. 5* (Ed.: E. S. Huyser), Dekker, New York, **1974**, p. 101.
[10] J. Schaetzer, Dissertation, Universität Freiburg, **1986**.
[11] This value was not corrected for incomplete deuterium incorporation. This small isotope effect supports the assumption that the hydrogen transfer is almost complete in the transition state. The same holds for Reaction (2), the back reaction of which (disproportionation) should proceed without activation enthalpy. Halpern et al. reported similar results in transfer hydrogenations with pentacarbonylhydridomangenese [5d].
[12] ΔH_f°(25 °C,g) **2a** = 38.2 ± 1.1 kcal mol^{-1}, J. B. Pedley, R. D. Naylor, S. P. Kirby, *Thermochemical Data of Organic Compounds*, 2nd ed., Chapman and Hall, London, **1986**; b) ΔH_f°(25 °C,g) **1** = 24.9 kcal mol^{-1}, Dr. H.-D. Beckhaus (Universität Freiburg), private communication (MM2 force field); c) ΔH_f°(25 °C,g) **6** = 33.2 kcal mol^{-1}, ΔH_f°(25 °C,g) **7a** = 61.4 ± 1.5 kcal mol^{-1}, D. F. McMillen, D. M. Golden *Ann. Rev. Phys. Chem.* **1982**, *33*, 493; if the C–H bond dissociation energy of the methylene protons in **2a** (76.3 [12d] or 78 kcal mol^{-1} [12e]) is used for the calculation of ΔH°_f(25 °C,g) **7a**, values of 62.4 ± 1.5 and 64.1 ± 2 kcal mol^{-1} result; d) S. E. Stein, *J. Am. Chem. Soc.* **1991**, *113*, 787; M. J. Rossi, D. F. McMillen, D. M. Golden, *H. Phys. Chem.* **1984**, *88*, 5031; e) F. G. Bordwell, J. P. Cheng, G. Zhen, A. V. Satish, X. Zhang, *J. Am. Chem.* **1991**, *113*, 9790.
[13] B. A. Gottwald, *Simulation* **1981**, *37*, 169.
[14] H. Fischer, *J. Am. Chem. Soc.* **1986**, *108*, 3925; H. Fischer, H. Paul, *Acc. Chem. Res.* **1987**, *20*, 200.
[15] R. E. Miller, S. E. Stein, *J. Phys. Chem.* **1981**, *85*, 580.
[16] C. Herberg, Dissertation, Universität Freiburg, **1992**.
[17] C. Rüchardt, H.-D. Beckhaus, *Top. Curr. Chem.* **1985**, *130*, 1.
[18] a) J. Brandrup, E. H. Immergut, *Polymer Handbook*, Interscience Publishers, New York, **1965**, Chapter 2, p. 390; b) C. H. Bamford, C. F. H. Tipper, *Comprehensive Chemical Kinetics, Vol. 14, Degradation of Polymers*, Elsevier, Amsterdam, **1975**, p. 50.
[19] E_T values are empirical parameters of solvent polarity: C. Reichart, K. Dimroth, *Fortschr. Chem. Forsch.* **1968**, *11*, 1.
[20] M. Gerst, C. Rüchardt, unpublished results.

Novel Binuclear Phosphinidene Compounds by Dimerization of the P–H-Functional Phosphenium Complexes $[C_5R_5(CO)_2W{=}PH(Mes)]$ (R = H, Me)**

By *Wolfgang Malisch,* Ulrich-Andreas Hirth, Theresa A. Bright, Harald Käb, Teja Sebastian Ertel, Sabine Hückmann,* and *Helmut Bertagnolli*

Diverse terminal coordination possibilities (η^1, linear, or bent),[1] but above all the bridging μ^2 – μ^4 forms,[2] substantiate the coordination capability of phosphinidenes PR. Most of the known μ^2-phosphinidene complexes have the open structure **A**, in which the sp^2-hybridized phosphorus atom symmetrically bridges two 16-electron metal complex fragments ($ML_n = M(CO)_5$ for M = Cr, Mo, W; $Mn(CO)_2Cp$).[2a] More exceptional are the compounds of type **B** containing 15-electron metal complex fragments (ML_n = $Co(CO)_3$; $M(CO)_2Cp$ for M = Mo, W), in which a metal–metal bond is an additional structural feature.[2b]

In attempts to synthesize PH-functional phosphenium complexes $[L_nM{=}PH(R)]$, we have now obtained the novel structural type **C**. It shows the coordination of a phosphinidene to electronically nonequivalent metal units—a 15-

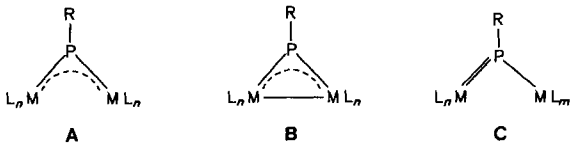

and a 17-electron fragment—which implies the formation of one M–P single and one M–P double bond. Form **C** may thus be described as a metalliophosphenium complex.[3]

As starting materials for the synthesis of the H(R)P=M systems we used the phosphane complexes *cis*-**1a,b**, accessible by thermal reactions from $[C_5R_5(CO)_3WCl]$ (R = H, Me) and $MesPH_2$ (Mes = mesityl (2,4,6-trimethylphenyl)). Treatment with 1,8-diazabicyclo[5.4.0]undec-7-ene (DBU) in dichloromethane yielded spontaneously and almost quantitatively the phosphinidene complexes **3a,b**. The mesitylphosphenium complexes **2a,b** initially expected on dehydrochlorination of **1a,b** cannot be detected even at −78 °C by NMR spectroscopy, but their presence is proven by trapping reactions with Me_3P that furnish the metallophosphanes **4a,b** (Scheme 1). Phosphinidene complexes **3a,b** are thus the product of the dimerization of the mesitylphosphenium complexes **2a,b**. The addition of a P–H function to the W–P double bond in this dimerization involves a hitherto unknown type of M–P bond formation occurring under unusually mild conditions.

[*] Prof. Dr. W. Malisch, Dr. U.-A. Hirth, Dr. T. A. Bright, Dr. H. Käb
Institut für Anorganische Chemie der Universität
Am Hubland, D-W-8700 Würzburg (FRG)
Dr. T. S. Ertel, Dipl.-Chem. S. Hückmann, Prof. Dr. H. Bertagnolli[+]
Institut für Physikalische Chemie der Universität Würzburg

[+] Present address: Institut für Physikalische Chemie
Pfaffenwaldring 55, D-W-7000 Stuttgart 80 (FRG)

[**] Phosphenium Complexes, Part 18. This work was supported by the Deutsche Forschungsgemeinschaft within project SFB 347 ("Selektive Reaktionen Metall-aktivierter Moleküle") and the Fonds der Chemischen Industrie. T. S. E. thanks the Fonds der Chemischen Industrie for a study grant. Part 17: A. Fried, W. Malisch, M. Schmeusser, U. Weis, *Phosphorus, Sulfur, Silicon Relat. Elem.* **1992**, *64*, 441. The internationally accepted terms phosphinidene and phosphenium complexes have been used instead of the little used IUPAC expressions λ^3- and λ^4-phosphandiyl complexes.

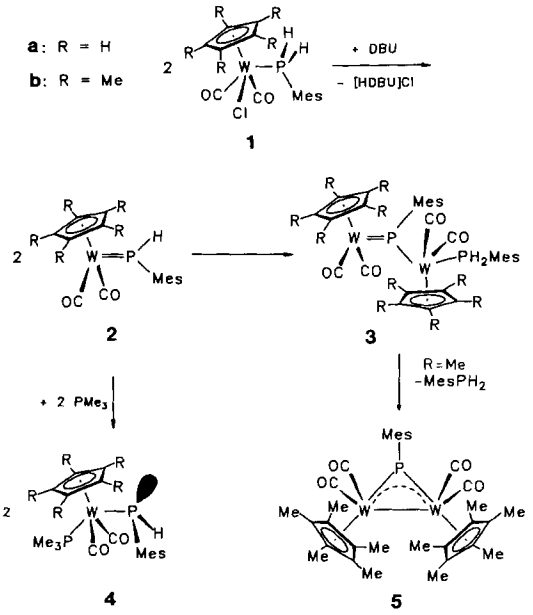

Scheme 1.

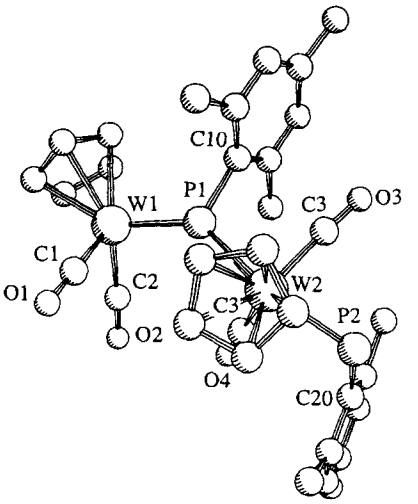

Fig. 1. Molecular structure of **3a** in the solid state. The hydrogen atoms are omitted for clarity. Selected bond lengths [Å] and angles [°]: W1–P1 2.281(3), W2–P1 2.550(3), W2–P2 2.440(3), P1–C10 1.845(4), W1-P1-C10 113.2(3), W2-P1-C10 110.1(3), W1-P1-W2 136.65(8).

Although **3a** is thermally extremely stable and remains unchanged even on heating to 100 °C in toluene, the C_5Me_5 analogue **3b** is only stable at low temperatures. Above −40 °C it reacts to form a "closed" phosphinidene complex **5** (type **B**) by elimination of $MesPH_2$. Therefore, form **C** has to be attributed a role as intermediate in the formation of **B**.

The constitution of **3a,b** is deduced from spectroscopic data as well as X-ray structural analysis and an EXAFS study (EXAFS = *E*xtended *X*-ray *A*bsorption *F*ine *S*tructure). In the ^{31}P NMR spectrum the signal for the bridging phosphorus atom is in the low-field region typical for phosphenium complexes (**3a**: δ = 313.9, **3b**: 397.4), and the widely differing $J(^{183}W^{31}P)$ coupling constants (**3a**: 485.3, 113.1; **3b**: 436.2, 135.6 Hz) are characteristic for a double and a single W–P bond (Table 1).

Table 1. Spectroscopic data of complexes **1a,b**, **3a,b**, **4a,b**, and **5**.

1a/1b: ^{31}P NMR (36 MHz, C_6D_6, 25 °C): δ = −78.9/−67.9 (s, ^1J(P,W) = 269.4/271.1 Hz). IR (benzene): ν(CO) = 1964 (vs), 1877 (s)/1945 (vs), 1863 (vs); ν(PH) = 2350 (w)/2318 (w) cm^{-1}.

3a/3b: ^{31}P NMR (36 MHz, C_6D_6, 25 °C): δ = 313.9/397.4 (d, ^1J(P,W) = 485.3/436.2, ^1J(P,W) = 113.1/135.6, ^2J(P,W,P) = 11.9/36.7 Hz; W=P), −82.8/−60.8 (d, ^1J(P,W) = 225.0 Hz/273.1 Hz; H_2PMes). IR (benzene)/(dichloromethane): ν(CO) = 1954 (m), 1931 (m), 1898 (vs), 1882 (s), 1805 (m)/1943 (s), 1928 (s), 1864 (vs), 1845 (vs), 1807 (m); ν(PH) = 2319 (w)/2320 (w) cm^{-1}.

4a/4b: ^{31}P NMR (36 MHz, C_6D_6/$CDCl_3$, 25 °C): δ = −157.6/−42.9 (d, ^1J(P,W) = 68.4/75.5, ^2J(P,W,P) = 39.1/42.1 Hz; PH(Mes)), −13.5/−21.7 (d, ^1J(P,W) = 249.0/262.3, ^2J(P,W,P) = 39.1/42.1 Hz; PMe_3). IR (benzene): ν(CO) = 1913 (m), 1837 (vs)/1902 (m), 1824 cm^{-1}.

5: ^{31}P NMR (36 MHz, CD_2Cl_2, 25 °C): δ = 589.4 (s, ^1J(P,W) = 335.7 Hz). IR (pentane): ν(CO) = 1927 (m), 1867 (vs) cm^{-1}.

The X-ray structural analysis of **3a** (Fig. 1) shows a trigonal-planar coordination at the P1 atom (angle sum 360°). The largest angle is that between the two metal fragments (W1-P1-W2 = 137°),[4] and the short W1–P1 bond length of 2.28 Å corresponds to that of $[Cp(CO)_2W{=}P(tBu)_2]$.[3] The W2–P1 distance of 2.55 Å represents the first example of a P(sp^2)–W single bond. The interatomic distance between W2 and the phosphorus atom of the $MesPH_2$ ligand (2.44 Å) lies in the anticipated range. For steric reasons the plane defined by W2-P1-C10 is twisted from the orthogonal orientation to the Cp ligand on W1 that would be optimal for metal-d-π–phosphorus-p-π interaction (Cp_z-W1-P1-C10 = −7.77°, Cp_z-W1-P1-W2 = −170.08°). The mesityl group is almost perpendicular to this plane (W1-P1-C10-C11 = 87.7°).

The EXAFS study in solution (Fig. 2) is in excellent agreement with the single-crystal structural data.[5] In benzene three types of W–P distances are detected, and their values of 2.33, 2.48, and 2.67 Å correspond to those for the W1–P1, W2–P2, and W2–P1 bonds, respectively, in the crystal. In addition, the distances between the ligands and the tungsten center could be identified (carbonyl unit: W–C 1.91 and W–(carbonyl)O 3.17 Å (1.90–1.97 and 3.08–3.11 Å, respectively, in the crystal); Cp unit: 2.37 Å (2.28–2.34 Å, in the crystal)). This study shows that the ability of EXAFS spectroscopy to distinguish between different interatomic distances of the same absorber–scatterer pairs[6] can be used for the structural characterization of complexes with different M–P distances that exist only in solution.

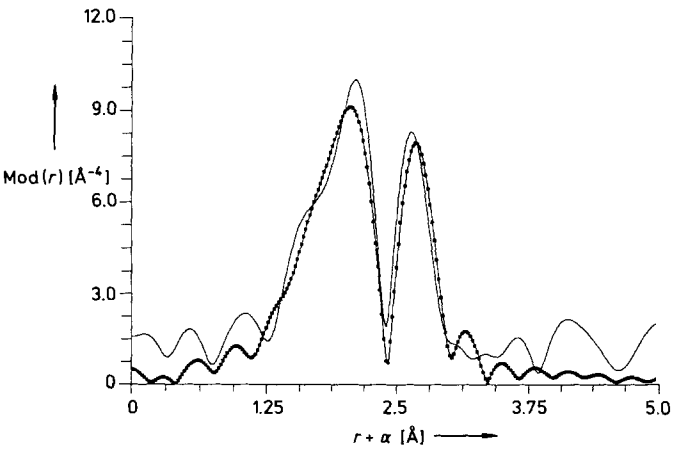

Fig. 2. Fourier transformed $k^3X(k)$ function of **3a** (solid line) and the Fourier transformed result of curve fitting (•).

The M=P unit of the phosphinidene complexes described here represents a reactive center, which we are now investigating with respect to its suitability for the construction of metallacycles and cluster compounds by cycloaddition.

Experimental Procedure

All manipulations were performed in the absence of air and moisture.

1a/b: A suspension of $[Cp(CO)_3WCl]$ (857 mg, 2.33 mmol)/$[C_5Me_5(CO)_3WCl]$ (1.735 g, 3.96 mmol) in methylcyclohexane (20 mL) was treated with $MesPH_2$ (355 mg, 2.33 mmol)/(603 mg, 3.96 mmol) and stirred for 3 h/5 h at 110 °C. After the mixture was cooled to room temperature, the desired product was separated off, washed with pentane, and dried in vacuum. Yield: 964 mg (84%)/1.905 g (85%), orange crystalline powder, m.p. 111 °C (decomp)/127 °C (decomp).

3a: A solution of **1a** (222 mg, 0.45 mmol) in dichloromethane (20 mL) was treated with DBU (69 mg, 0.45 mmol) at room temperature. After removal of the solvent in vacuum, the residue was taken up in toluene (5 mL), insoluble material separated, and the filtrate worked up by column chromatography (15 × 2 cm column; Al_2O_3, activity grade III, neutral; toluene). The first dark green fraction yielded **3a** after the solvent had been removed in vacuum. Yield: 177 mg (86%), green crystalline powder, m.p. 145 °C.

3b: A solution of **1b** (135 mg, 0.24 mmol) in dichloromethane (20 mL) was treated with DBU (36 mg, 0.24 mmol) at −78 °C. Above −40 °C the transformation to $MesPH_2$ and **5** starts, and is quantitative within 30 min at room temperature.

4a/b: A solution of **1a** (254 mg, 0.52 mmol)/**1b** (254 mg, 0.45 mmol) and trimethylphosphane (40 mg, 0.52 mmol/35 mg, 0.45 mmol) in toluene (10 mL) was treated with DBU (79 mg, 0.52 mmol/68 mg, 0.45 mmol) at room temperature. After insoluble material had been removed, the filtrate was concentrated to 2 mL and worked up by column chromatography (10 × 2 cm column; Al_2O_3, activity grade III, neutral; **4a**: toluene; **4b**: toluene/ether). The bright yellow fraction yielded the desired product after removal of the solvent in vacuum. Yield: 235 mg (85%)/196 mg (72%), bright yellow/lemon-yellow crystalline powder, m.p. 128 °C/126 °C).

Received: May 9, 1992 [Z5335IE]
German version: *Angew. Chem.* **1992**, *104*, 1537

CAS Registry numbers:
1a, 143733-37-3; **1b**, 143733-38-4; **3a**, 143733-39-5; **3b**, 143733-40-8; **4a**, 143744-99-4; **4b**, 143733-42-0; **5b**, 143733-41-9; $[Cp(CO)_3WCl]$, 12128-24-4; $[C_5Me_5(CO)_3WCl]$, 89916-32-5; $MesPH_2$, 68357-98-2.

[1] a) P. B. Hitchcock, M. F. Lappert, W. P. Leung, *J. Chem. Soc. Chem. Commun.* **1987**, 1287; b) F. Mathey, *Angew. Chem.* **1987**, *99*, 285; *Angew. Chem. Int. Ed. Engl.* **1987**, *26*, 275; c) A. H. Cowley, B. Pellerin, J. L. Atwood, S. G. Bott, *J. Am. Chem. Soc.* **1990**, *112*, 6734.

[2] a) G. Huttner, K. Evertz, *Acc. Chem. Res.* **1986**, *19*, 406; b) A. M. Arif, A. H. Cowley, N. C. Norman, A. G. Orpen, M. Pakulski, *Organometallics* **1988**, *7*, 309; c) G. Huttner, K. Knoll, *Angew. Chem.* **1987**, *99*, 765; *Angew. Chem. Int. Ed. Engl.* **1987**, *26*, 743; d) H. Vahrenkamp, *Adv. Organomet. Chem.* **1983**, *22*, 169.

[3] a) K. Jörg, W. Malisch, W. Reich, A. Meyer, U. Schubert, *Angew. Chem.* **1986**, *98*, 103; *Angew. Chem. Int. Ed. Engl.* **1986**, *25*, 92; b) A. H. Cowley, R. A. Kemp, *Chem. Rev.* **1985**, *85*, 367.

[4] X-ray structural analysis of **3a** ($C_{32}H_{34}O_4P_2W_2$): $M_r = 912.27$; green crystals (0.2 × 0.10 × 0.15 mm); triclinic; space group $P\bar{1}$ (no. 2); $a = 9.24(1)$, $b = 10.63(1)$, $c = 18.88(2)$ Å, $\alpha = 74.842(1)$, $\beta = 78.453(1)$, $\gamma = 71.288(2)°$, $V = 1.682(4)$ nm^3, $Z = 2$; $\rho_{calcd} = 1.801$ g cm^{-3}, $\mu(Mo_{K\alpha}) = 71.08$ cm^{-1}; four-circle diffractometer CAD4 Enraf–Nonius (graphite monochromator, scintillation counter, $Mo_{K\alpha}$), 4923 independent reflections ($1.8° < \theta < 23°$) of which 4325 with $I > 3\sigma(I)$ used for structure solution (direct methods) and refinement (389 parameters); all non-hydrogen atoms were refined anisotropically, H atoms were taken into account in calculated positions in the calculation of the structure factor; $R = 0.031$ ($R_w = 0.036$, $w^{-1} = \sigma^2(F) + 0.0003\,F^2$). Further details of the crystal structure investigation may be obtained from the Fachinformationszentrum Karlsruhe, Gesellschaft für wissenschaftlich-technische Information mbH, D-W-7514 Eggenstein-Leopoldshafen 2 (FRG) on quoting the depository number CSD-56414, the names of the authors, and the journal citation.

[5] The EXAFS experiment was performed at a RÖMO II work station (HASYLAB at DESY Hamburg) in transmission at the W-LIII-edge on a 0.08 M solution of **3a** in an inert atmosphere with a liquid path length of 115 μm; Si-311 crystal monochromator, energy calibration with 4 μm thick tungsten foil. The experimental data of the reference material were folded with Gauss functions of different half-widths and determined from the intersection of the curves obtained thus. On the front edge a Victoreen function was fitted in the range 10000.0 to 10175.0 eV. The background $\mu_0(E)$ was determined with a Smoothing Spline routine that was applied to a spectrum folded with a Gauss function of half-width 24.0 eV and the Fourier transform performed on the k^3-weighted structure function $k^3X(k)$ obtained thus, in the range 2.8–12.8 Å^{-1}. B. K. Teo, *EXAFS: Basic Principles and Data Analysis*, Springer, Berlin, **1986**; D. C. Konigsberger, R. Prins, *X-ray Absorption: Principles, Applications, Techniques of EXAFS, SEXAFS, and XANES*, Wiley, New York, **1988**; T. S. Ertel, S. Hückmann, U. Kolb, D. Peter, H. Bertagnolli, *Appl. Spectrosc.*, in press.

[6] Back transformation of the ranges 1.26–2.40 Å, 2.40–3.20 Å, and 1.26–3.20 Å in the impulse space and fitting of the theoretical EXAFS equation to the experiment with theoretical amplitude and phase functions yields the contributions of the individual back scatterers; these are the distance r[Å], the coordination number N, and the Debye–Waller factor σ[Å] (A. G. McKale, *J. Am. Chem. Soc.* **1988**, *110*, 3763): W1-P1: $r = 2.33$, $N = 0.49$, $\sigma = 0.508$; W2-P2: $r = 2.48$, $N = 1.56$, $\sigma = 0.0551$; W2-P1: $r = 2.67$, $N = 0.39$, $\sigma = 0.0708$; W1-C1,2 and W2-C3,4: $r = 1.91$, $N = 1.06$, $\sigma = 0.0545$; W1-C5-9 and W2-C30-34: $r = 2.37$, $N = 2.27$, $\sigma = 0.1497$; W1-O1,2 and W2-O3,4: $r = 3.17$, $N = 2.78$, $\sigma = 0.0390$; W1-C18: $r = 3.44$, $N = 1.87$, $\sigma = 0.1099$.

A Paramagnetic, Mononuclear Organometallic Iridium(II) Complex: $[Ir(C_6Cl_5)_2(cod)]$**

By *María P. García,* M. Victoria Jiménez, Luis A. Oro, Fernando J. Lahoz*, and *Pablo J. Alonso*

Iridium and rhodium complexes with a d^7 electronic configuration are very uncommon, especially as monomeric species.[1] Very recently some paramagnetic, mononuclear rhodium(II) complexes have been described,[2] but in the chemistry of iridium(II) there are only a limited number of reports concerning either species generated by electrolysis that were not isolated[3] or isolated complexes that were examined only with regards to their magnetic properties.[4] To the best of our knowledge, only two paramagnetic, mononuclear Ir^{II} coordination compounds have been structurally characterized, the square-planar complexes *trans*-$[Ir(t\mathrm{Bu}_2PC_6H_3XO)_2]$, X = H, CH_3.[5]

One of our current research interests is the chemistry of pentafluorophenyl derivatives of rhodium, and we reported[6] the preparation of the anion $[Rh(C_6F_5)_5]^{2-}$. Using this complex anion as a starting material, we prepared neutral[7] and anionic[8] mono- and dinuclear rhodium(III) complexes. This research is now extended to complexes with the pentachlorophenyl ligand; we expected that in the same way that this ligand stabilizes the unusual +III oxidation state of platinum,[9] it could allow the preparation of rhodium(II) and iridium(II) complexes. We now report the first fully characterized organometallic Ir^{II} complex, an Ir^{II} compound whose ligands are bound exclusively at C atoms.

The remarkably stable iridium(I) complex **1** (cod = 1,5-cyclooctadiene), prepared according to Equation (a), reacted

$$[\{Ir(\mu\text{-}Cl)(cod)\}_2] + 4\,LiC_6Cl_5 \xrightarrow{-2\,LiCl} 2\,Li[Ir(C_6Cl_5)_2(cod)] \xrightarrow[-2\,LiBr]{+2\,NBu_4Br} 2\,[NBu_4][Ir(C_6Cl_5)_2(cod)] \quad \mathbf{1} \qquad \text{(a)}$$

[*] Dr. M. P. García, Dipl.-Chem. M. V. Jiménez, Prof. Dr. L. A. Oro, Dr. F. J. Lahoz
Departamento de Química Inorgánica
Instituto de Ciencia de Materiales de Aragón
Universidad de Zaragoza-C.S.I.C.
E-50009 Zaragoza (Spain)
Prof. Dr. P. J. Alonso
Departamento de Física de la Materia Condensada
Universidad de Zaragoza-C.S.I.C
E-50009 Zaragoza (Spain)

[**] This work was supported by the D.G.I.C.Y.T. (Dirección General de Investigación Científica y Técnica), projects PB 88 0386 and PB 87 0289.

with iodine in dichloromethane (ratio 1:1) at room temperature, or with silver perchlorate (1:1) at $-10\,^{\circ}C$ to yield a brown solid (almost insoluble in CH_2Cl_2 and acetone) identified as the mononuclear iridium(II) complex **2**. The reaction of **1** with $[Ph_3PAgOClO_3]$ (1:1) in tetrahydrofuran gave rise to the pentacoordinated complex **3**. This complex is very unstable: in solution it decomposes to give the iridium(I) compound **4** identified by its spectroscopic data (IR, NMR), mass spectrometry, and elemental analysis.

$[Ir(C_6Cl_5)_2(cod)]$ **2**

$[Ir(C_6Cl_5)_2(cod)(PPh_3)]$ **3**

$[Ir(C_6Cl_5)(cod)(PPh_3)]$ **4**

The oxidation of complex **1** to yield **2** can also be achieved electrochemically. When an increasing voltage (-1 to $+1$ V with sweep rate of 0.1 Vs^{-1}) is applied to an orange solution of **1** in CH_2Cl_2 (0.5 mM), an oxidation wave is observed at 0.054 V (Fig. 1). The reduction peak is at -0.021 V. The value of $E_p^{ox}-E_p^{red}$ (0.07 V) and the ratio i_c/i_a (1/1) show the process to be reversible and diffusion controlled. We also used cyclic voltammetry to study the reduction of complex **2** and the subsequent reoxidation. Unfortunately the low solubility of this compound prevents the preparation of 0.50 mM solutions; however, with the same scanning conditions, the reduction and oxidation peaks were localized at values identical to those observed for complex **1**, although the peak intensities were smaller.

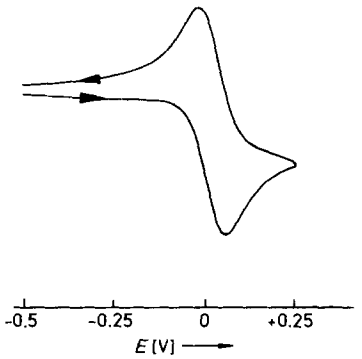

Fig. 1. Cyclic voltammogram of a solution of 0.50 mM of **2** in CH_2Cl_2/0.1 M $[NBu_4][PF_6]$ at room temperature; sweep rate = 0.1 Vs^{-1}, Pt electrode.

The molecular structure of **2** was determined by a single-crystal X-ray diffraction study.[10] Figure 2 shows the structure of the complex. The iridium atom, situated on a site of C_2 symmetry, exhibits a roughly square-planar coordination geometry (maximum deviation from the least-squares plane 0.217(5) Å for C(1)), and is bonded to two carbon atoms of the two symmetry-related pentachlorophenyl groups and to the olefinic bonds of a cyclooctadiene molecule. The perhalogenated aryl ligand is disposed almost perpendicular to the metal coordination plane (dihedral angle 93.0(1)°), and slightly twisted [Ir-C(1)-C(4) 8.9(2)°] so that the *ortho* chlorine atoms (Cl(6) and Cl(6′)) above and below the coordination plane can interact with the iridium center (Ir···Cl(6) 3.077(1) Å). This weak interaction could be partially responsible for the stability of this compound, as it could make oxidation sterically more difficult.

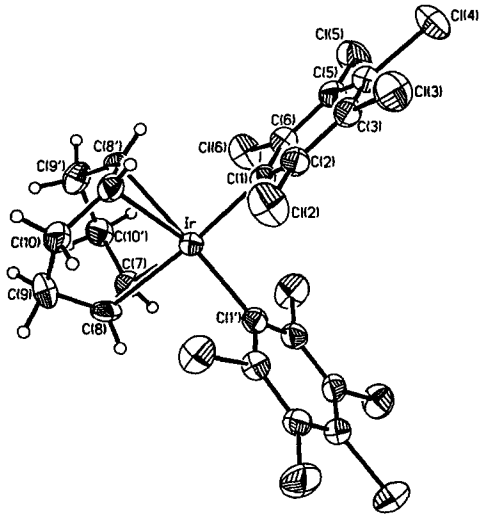

Fig. 2. Crystal structure of **2**. Selected distances [Å] and angles [°]: Ir-C(1) 2.073(5), Ir-C(7) 2.210(5), Ir-C(8) 2.274(5), C(7)-C(8) 1.372(8); C(1)-Ir-C(1′) 93.9(2), C(1)-Ir-M(1) 169.2(2), M(1)-Ir-M(1′) 84.4(1). (M(1) represents the midpoint of C(7)-C(8) olefinic bond; C(1′) and M(1′) are related to C(1) and M(1) by the symmetry relation $1-x, y, 1+(1/2-z)$).

The EPR spectra[11] of polycrystalline samples of **2** and **3** are shown in Figure 3 (solid lines). The spectra are very similar with only minor differences. In spite of iridium having two isotopes with $I = 3/2$ and very close nuclear g-factors, no hyperfine structure was observed. These spectra can be interpreted with an standard electronic Zeeman term with $S = 1/2$ and principal g-factors: $g_x = 3.00 \pm 0.02$, $g_y = 2.79 \pm 0.02$ and $g_z = 1.85 \pm 0.02$. The dotted lines in Figure 3 represent the spectra calculated using a Lorentzian lineshape with peak-to-peak distances in the first derivative of the signal of 25 and 20 mT for **2** and **3**, respectively. This interpretation of the EPR data is in agreement with an iridium(II) ion with an unpaired electron.

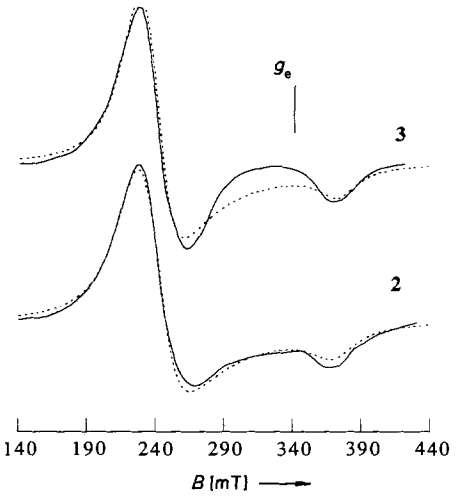

Fig. 3. EPR spectra of powdered samples of complexes **2** and **3** measured at room temperature. The solid lines represent the experimental spectra and the dotted lines the calculated spectra.

Experimental Procedure

1: To a solution of LiC_6Cl_5 (1.5 mmol) in diethyl ether (40 mL) (prepared by slow addition of a solution of *n*BuLi (1.5 mmol) in diethyl ether (10 mL) to a suspension of C_6Cl_6 (0.427 g, 1.5 mmol) in the same solvent (30 mL)) at $-50\,^{\circ}C$ was added solid $[\{Ir(\mu\text{-}Cl)(cod)\}_2]$ (0.200 g, 0.30 mmol). The solid was dissolved in approximately 30 min, and the solution turned orange-brown. As the reaction mixture was allowed to warm to room temperature (over ca. 4 h), an orange oily solid was formed together with a brown solution. The solution was removed and the solid washed twice with 10 mL of aqueous diethyl ether. The residue was treated with a solution of NBu_4Br (0.192 g, 0.60 mmol) in methanol (10 mL) yielding complex **1** (orange crystalline solid; 0.450 g, 70% yield). Correct C,H,N analysis. ^1H NMR ($CDCl_3$): $\delta = 2.1$ (br. m, 8H, CH_2(cod)), 3.4 (br. m, 4H, =CH(cod)), 2.7, 1.4, 1.1, 0.9 (m, 8:8:8:12, NBu_4^+).

2: This complex was prepared by two methods: a) To a solution of **1** (0.100 g, 0.096 mmol) in dichloromethane (4 mL) was added a solution of iodine (0.024 g, 0.096 mmol) in the same solvent (2 mL). The yellow solution changed to red, and a brown solid formed. The reaction mixture was stirred for 30 min, the volume of the solution reduced to 2 mL, and a brown, crystalline solid precipitated upon addition of 4 mL of acetone (0.053 g, 69% yield). Correct elemental analysis. b) Brown crystals of **2** were obtained by slow diffusion at $-10\,^{\circ}C$ of a solution of $AgClO_4$ (0.02 g, 0.096 mmol) in acetone (5 mL) into a solution of $[NBu_4][Ir(C_6Cl_5)_2(cod)]$ (0.100 g, 0.096 mmol) in dichloromethane (3 mL) under a nitrogen atmosphere and with exclusion of light. Crystals could be separated from the metallic silver formed because of the density difference between the crystals and the silver powder. The crystals were washed with acetone and dried under vacuum (0.040 g, 52% yield).

3: To a solution of **1** (0.100 g, 0.096 mmol) in tetrahydrofuran (10 mL) was added solid $[Ph_3PAgOClO_3]$ (0.045 g, 0.096 mmol). The solution was stirred for 1 h under a nitrogen atmosphere and with exclusion of light to yield a black solid (metallic silver) which was removed by filtration through Kieselguhr. Concentration of the resulting solution under reduced pressure to a volume of 1 mL and addition of methanol (5 mL) afforded **3** as a reddish solid which was filtered off, washed with methanol, dried under vacuum (0.053 g, 52% yield). Correct elemental analysis.

4: Concentrated solutions of **3** in dichloromethane or chloroform yielded pink crystals of **4** which were filtered off, washed with diethyl ether, and dried under vacuum. Correct elemental analysis. ^1H NMR ($CDCl_3$): $\delta = 4.57$, 3.19, 2.28, 2.15, 1.89, 1.76 (m, 2H each, cod); 7.23–7.56 (m, 15H, PPh_3). $^{31}P\{^1H\}$: $\delta = 17.45$ (s). IR (Nujol suspension between polyethylene sheets): $\tilde{\nu}(C_6Cl_5)$ [cm^{-1}]: 1335 s, 1320 s, 1285 s, 865 m, 615 s. MS(FAB): *m/z* 812 (M^+, 90%).

Received: June 20, 1992 [Z 5414 IE]
German version: *Angew. Chem.* **1992**, *104*, 1512

CAS Registry numbers:
1, 143887-03-0; **2**, 143859-27-2; **3**, 143859-28-3; **4**, 143859-29-4; $[\{Ir(\mu\text{-}Cl)(cod)\}_2]$, 12112-67-3; LiC_6Cl_5, 6782-80-5; $Ph_3PAgOClO_3$, 73165-02-3.

[1] N. Serpone, M. A. Jamieson in *Comprehensive Coordination Chemistry, Vol. 4* (Eds.: G. Wilkinson, R. D. Gillard, J. A. McCleverty), Pergamon, Oxford, **1987**, p. 1120.

[2] K. R. Dunbar, S. C. Haefner, *Organometallics* **1992**, *11*, 1431, and references therein; R. S. Hay-Motherwell, S. U. Koschmieder, G. Wilkinson, B. Hussain-Bates, M. B. Hursthouse, *J. Chem. Soc. Dalton Trans.* **1991**, 2821.

[3] G. Pilloni, G. Schiavon, G. Zotti, S. Zecchin, *J. Organomet. Chem.* **1977**, *134*, 305; S. Zecchin, G. Zotti, G. Pilloni, *ibid.* **1985**, *294*, 379.

[4] A. Aràneo, F. Morazzoni, T. Napoletano, *J. Chem. Soc. Dalton Trans.* **1975**, 2039; G. Mercati, F. Morazzoni, *ibid.* **1979**, 569; M. Angoletta, T. Beringhelli, F. Morazzoni, *Spectrochim. Acta Part A* **1982**, *38*, 1177.

[5] R. Mason, K. M. Thomas, H. D. Empsall, S. R. Fletcher, P. N. Heys, E. M. Hyde, C. E. Jones, B. L. Shaw, *J. Chem. Soc. Chem. Commun.* **1974**, *612*.

[6] M. P. García, L. A. Oro, F. J. Lahoz, *Angew. Chem.* **1988**, *100*, 1766; *Angew. Chem. Int. Ed. Engl.* **1988**, *27*, 12.

[7] M. P. García, M. V. Jiménez, F. J. Lahoz, L. A. Oro, A. Tiripicchio, J. A. López, *J. Chem. Soc. Dalton Trans.* **1990**, 1503.

[8] M. P. García, M. V. Jiménez, L. A. Oro, *J. Organomet. Chem.*, in press.

[9] R. Usón, J. Forniés, M. Tomás, B. Menjón, K. Sünkel, R. Bau, *J. Chem. Soc. Chem. Commun.* **1984**, 751; R. Usón, J. Forniés, M. Tomás, B. Menjón, R. Bau, K. Sünkel, E. Kuwabara, *Organometallics* **1986**, *5*, 1576.

[10] Four-circle Siemens AED diffractometer, graphite-monochromated $Mo_{K\alpha}$ radiation. Complex **2** crystallizes in the monoclinic space group *C*2/*c* with $a = 15.4214(7)$, $b = 8.0742(5)$, $c = 18.977(2)$ Å, $\beta = 91.42(1)^{\circ}$, $V = 2362.2(3)$ Å^3, $\rho_{calcd.} = 2.247$, $\mu = 67.8$ cm^{-1} and $Z = 4$. Data collection range $3 \le 2\theta \le 45^{\circ}$, ω-2θ scan mode ($T = 295$ K), 4365 measured reflections, 1350 observed with $F \ge 5.0\sigma(F)$. Absorption correction based on Ψ-scan measurements. Full anisotropic model (isotropic hydrogens), 161 parameters; $R = 0.023$ and $R_w = 0.0301$. Further details of the crystal structure investigation are available on request from the Director of the Cambridge Crystallographic Data Centre, University Chemical Laboratory, Lensfield Road, GB-Cambridge, CB2 1EW (UK), on quoting the full journal citation.

[11] Electron paramagnetic resonance spectra were recorded at room temperature with a Varian E-112 spectrometer working in the X-band. The magnetic field was measured with a NMR gaussmeter Bruker ER035M and the diphenylpicrylhydrazyl (DPPH) resonance signal ($g = 2.0037 \pm 0.0002$) was used for determining the microwave frequencies.

Formate-Driven, Non-Enzymatic NAD(P)H Regeneration for the Alcohol Dehydrogenase Catalyzed Stereoselective Reduction of 4-Phenyl-2-butanone**

Von *Dorothée Westerhausen, Sabine Herrmann, Werner Hummel*, and *Eberhard Steckhan**

Biotransformations of organic substrates with enzymes or microorganisms have found widespread application because of their capability to perform stereoselective reactions. The use of redox enzymes for synthetic purposes, however, has been limited because of the necessary cofactor regeneration. For reductions with NAD(P)H-dependent enzymes, enzyme-coupled regeneration systems have been developed. These systems employ either a regeneration enzyme such as formate dehydrogenase (FDH)[1] for NADH-dependent production enzymes, or the production enzyme itself, as in the case of NADPH-dependent alcohol dehydrogenase (ADH) of *Thermoanaerobium brockii* (TBADH).[2]

We developed a non-enzymatic regeneration system for NADH and NADPH with $[(C_5Me_5)Rh^{III}(bpy)(H_2O)]Cl_2$ and similar complexes as the homogeneous redox catalysts and either the electrode[3, 5, 6] or formate[4, 5] as the donor. The reaction mechanism for the formate-driven NAD(P)H regeneration is described by Equations (a)–(c). The important step is the hydride transfer from the intermediate hydridorhodium complex to $NAD(P)^+$ [Eq. (c)] which has been

$$[(C_5Me_5)Rh^{III}(bpy)L]^{2+} + HCOO^- \xrightarrow{K} [(C_5Me_5)Rh^{III}(bpy)(HCO_2)]^+ + L \quad (a)$$

$$[(C_5Me_5)Rh^{III}(bpy)(HCO_2)]^+ \xrightarrow{rds} [(C_5Me_5)Rh^{III}H(bpy)]^+ + CO_2 \quad (b)$$

$$[(C_5Me_5)Rh^{III}H(bpy)]^+ + L + NAD(P)^+ \xrightarrow{fast} [(C_5Me_5)Rh^{III}(bpy)L]^{2+} + NAD(P)H \quad (c)$$

found to take place at a very high rate leading selectively to enzymatically active NAD(P)H.[3–6] Here we describe the formate-driven, non-enzymatic NAD(P)H regeneration for the ADH-catalyzed stereoselective reduction of carbonyl compounds.

[*] Prof. Dr. E. Steckhan, Dipl.-Chem. D. Westerhausen, Dr. S. Herrmann
Institut für Organische Chemie und Biochemie der Universität
Gerhard-Domagk-Strasse 1, D-W-5300 Bonn 1 (FRG)
Priv.-Doz. Dr. W. Hummel
Institut für Enzymtechnologie der Universität Düsseldorf
in der KFA Jülich GmbH
Postfach 2050, Wilhelm-Johnen-Strasse, D-W-5170 Jülich (FRG)

[**] This work was supported by the Bundesministerium für Forschung und Technologie (0319410A), the BASF Aktiengesellschaft, and the Fonds der Chemischen Industrie. We are grateful to the BASF AG and the DEGUSSA AG for chemicals. We thank Prof. Dr. M.-R. Kula, Düsseldorf, and Prof. Dr. C. Wandrey, Jülich, for their support.

In a first model system, the horse liver ADH (HLADH) catalyzed reduction of hexanal with formate-driven, in-situ NADH regeneration catalyzed by $[(C_5Me_5)Rh(bpy\text{-}5\text{-}OAc)(H_2O)]Cl_2$ was examined (Table 1). With a 1:1 ratio of substrate (0.1 M) to formate (0.1 M), 21 U HLADH (acetaldehyde/ethanol), 1 mol% of NAD^+, and 0.5 mol% of redox catalyst, 50% turnover was achieved after about 6 hours. After 30 hours, all of the substrate had been reduced. A comparable result was obtained with butanal as the substrate.

Table 1. Results of the enzymatic reduction of hexanal with formate-driven, in-situ regeneration of NADH [a].

c (Hexanal) [mM]	t [h]	c (Hexanol) [mM]	Turnover number redox cat.	NAD
100.0	0	0	0	0
92.8	1	7.2	14	7
84.6	3	15.4	31	15
57.2	5	42.8	86	43
1.0	24	99.0	198	99
0	30	100.0	200	100

[a] Concentrations: HCOONa = 0.1 M; aldehyde = 0.1 M; NAD^+ = 1 mM; $[(C_5Me_5)Rh(bpy\text{-}5\text{-}OAc)(H_2O)]Cl_2$ = 0.5 mM; HLADH = 21 units (acetaldehyde/ethanol); in 50 mL 0.1 M sodium phosphate buffer, pH 7.5; T = 25 °C; argon atmosphere; GLC analysis.

We then applied this method to the reduction of the interesting prochiral ketone 4-phenyl-2-butanone (Fig. 1). Four different enzymes were compared with respect to the turnover and stereoselectivity in this reaction. Two commercially available alcohol dehydrogenases, HLADH and TBADH, together with two recently isolated secondary alcohol dehydrogenases from *Lactobacillus kefir*[7] (PhEDH = phenylethanol-DH) and from *Rhodococcus* sp.[8] (S-ADH) were investigated. Yeast ADH was not included in the study, as it proved to be very slow in the reduction of 4-phenyl-2-butanone. HLADH and S-ADH are NADH-dependent enzymes while the others are NADPH-dependent.

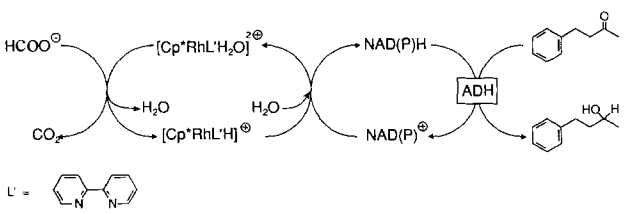

Fig. 1. Enzymatic reduction of 4-phenyl-2-butanone with in-situ cofactor regeneration using $[(C_5Me_5)Rh(bpy)(H_2O)]Cl_2$ as a redox catalyst and formate as a donor.

As standard conditions, 10 mL of KP_i buffer (0.1 M, pH 7) containing the oxidized cofactor (1 mM), $[(C_5Me_5)Rh(bpy)(H_2O)]Cl_2$ (0.5 mM), sodium formate (0.066 M), and 4-phenyl-2-butanone (0.033 M) were used. Because of the low solubility of the ketone in the aqueous buffer system an emulsion was formed. The progress of the reaction was followed by GLC with an HP-1 glass capillary column; the enantiomeric excess was also determined by GLC with a β-cyclodextrin modified capillary column (50 m, FS-Cyclodex beta-I/P, CS-Chromatographie Service GmbH) after esterification of the alcohol with acetic anhydride.

From the study of the reaction progress (Fig. 2), it is obvious that PhEDH, S-ADH, and especially HLADH all lead to a turnover of between 76 and 90% at 30 °C under batch conditions. Although TBADH reaches a turnover of only 24% at 30 °C after 24 h, it reacts much faster and more efficiently at 60 °C giving a turnover of 75% already after 5 h. Initial studies showed that the TBADH preparation used here contains a side-activity leading to NADPH inactivation. This seems to be more an important factor at lower temperatures and leads to the low turnover at 30 °C.

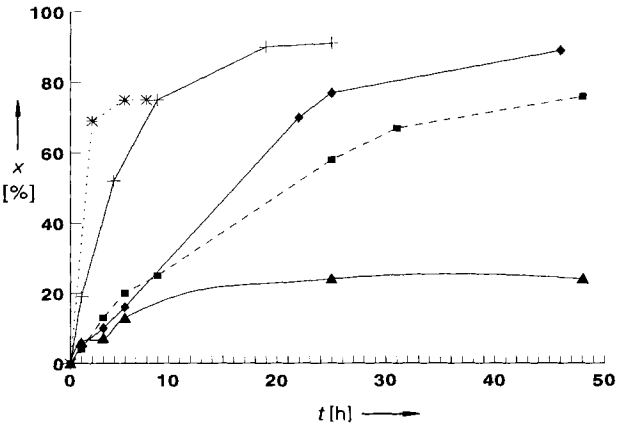

Fig. 2. Dependence of the turnover x on time t for the enzymatic reduction of 4-phenyl-2-butanone with in-situ, formate-driven cofactor regeneration with HLADH at 30 °C (+), TBADH at 30 °C (▲), TBADH at 60 °C (*), PhEDH at 30 °C (■), and S-ADH at 30 °C (◆). [Conditions: 4-phenyl-2-butanone: 33 mM; HCOONa: 66 mM; $NAD(P)^+$: 1 mM; $[(C_5Me_5)Rh(bpy)(H_2O)]Cl_2$: 0.5 mM; in 10 mL 0.1 M KP_i buffer of pH 7; at 30 °C and 60 °C (TBADH only); HLADH: 9 U (4-phenyl-2-butanone); TBADH: 5 U (4-phenyl-2-butanone); PhEDH: 20 U (4-phenyl-2-butanone); S-ADH: 20 U (4-phenyl-2-butanone)].

Comparison of the values for the enantiomeric excess *ee* and the turnover x for the four different enzymes at 30, 38, and 60 °C (Table 2) show that the *ee* values are the same as with other cofactor regeneration systems. TBADH and S-ADH reach values of more than 99% *ee* for the (*S*)-alcohol, while HLADH gives values of about 96% *ee* for the same enantiomer. Interestingly, PhEDH favors the formation of the (*R*)-alcohol (96% *ee*). The high values for the enantiomeric excess prove convincingly that the reaction proceeds selectively by means of the enzyme and not by a direct hydride transfer from the intermediate rhodium hydride to the substrate. This is not only true for a 2:1 formate to substrate ratio, but also even for a ratio of 15:1. A slightly lower enantiomeric excess was observed only in the case of

Table 2. Turnover x and enantiomeric excess *ee* in the enzymatic reduction of 4-phenyl-2-butanone with in-situ, formate-driven redox-catalytic cofactor regeneration [a].

Enzyme activity [U] [b]	Cofactor conc. [mM]	T [°C]	t [h] [c]	x [%]	ee [%]
HLADH [9]	NAD^+ [1]	30	24	90	96 (*S*)
HLADH [9]	NAD^+ [1]	38	24	75	96 (*S*)
TBADH [5]	$NADP^+$ [1]	30	24	24	>99 (*S*)
TBADH [5]	$NADP^+$ [1]	38	24	45	>99 (*S*)
TBADH [5]	$NADP^+$ [1]	60	5	75	>99 (*S*)
PhEDH [20]	$NADP^+$ [1]	30	45	76	96 (*R*)
PhEDH [20]	$NADP^+$ [1]	38	24	81	96 (*R*)
S-ADH [20]	NAD^+ [1]	30	43	89	>99 (*S*)

[a] Conditions identical to those in Fig. 2. [b] Units always with respect to 4-phenyl-2-butanone. [c] Time at which the change in turnover became insignificant.

HLADH for a 15:1 ratio of formate to substrate. The direct hydride transfer from the hydrido complex to the ketone in the absence of cofactor and enzyme leads only to a very low turnover of 7% after 52 hours at 25 °C and 13% after 45 hours at 30 °C. Even at 60 °C, the direct hydride transfer cannot compete with the enzymatic reaction leading to 99% *ee* (see TBADH at 60 °C). For all enzymes studied, the maximum turnover rate of the substrate was already reached with a formate to substrate ratio of 2:1, while with equimolar concentrations the turnover was about 30% lower after the identical reaction time. Possible enzymatic inhibition by the rhodium complex was excluded after intensive studies: After preincubation of the four enzymes with the rhodium complex (0.5 mM) at 30 °C for 5 min, 1 h, 8 h, and 24 h the initial reaction rate was determined and compared with the values obtained in the absence of the rhodium complex. No influence was observed. The turnover rates for the applied enzymes with our new non-enzymatic cofactor regeneration system were usually higher than with the coupled substrate approach (under otherwise identical conditions) using ethanol (HLADH) or isopropanol (TBADH, PhEDH) as cosubstrates. For example, with HLADH in the presence of ethanol as cosubstrate a turnover of 33% was obtained at 25 °C after 24 hours.

The temperature dependence of the reactions with the four enzymes is different. While for HLADH and S-ADH the optimum turnover is reached at 30 °C, the temperature optimum for PhEDH is observed at 35 °C, and for TBADH the turnover increases considerably up to a temperature of 60 °C.

In the case of HLADH, we studied the influence of dioxane as a cosolvent. While with the addition of dioxane to up to 5% by volume the turnover was diminished only to a very small extent and the enantiomeric excess was unchanged, at higher dioxane concentrations the turnover decreased considerably.

We will now apply this system in an enzyme membrane reactor with our water-soluble high-molecular weight rhodium complexes as redox catalysts.[5, 6, 9] Thus, a continuous enzymatic reduction should be possible.

Received: June 22, 1992 [Z 5420 IE]
German version: *Angew. Chem.* **1992**, *104*, 1496

[1] C. Wandrey, R. Wichmann, A. F. Bückmann, M.-R. Kula, *Umschau* **1984**, *84*, 88–91; C. Wandrey, R. Wichmann, W. Berke, M. Morr, M.-R. Kula, *Prepr. 3rd. Eur. Congr. Biotechnol.* **1984**, 239–244; C. Wandrey, R. Wichmann in *Enzymes and Immobilized Cells in Biotechnology* (Ed. A. I. Laskin), Benjamin/Cummings, Menlo Park, CA, USA, **1985**, pp. 177–208; M.-R. Kula, C. Wandrey, *Methods Enzymol.* **1986**, *136*, 9–21; D. Vasic-Racki, M. Jonas, C. Wandrey, W. Hummel, M.-R. Kula, *Appl. Microbiol. Biotechnol.* **1989**, *31*, 215–222; H. Schütte, J. Floßdorf, H. Sahm, M.-R. Kula, *Eur. J. Biochem.* **1976**, *62*, 151–160; Z. Shaked, G. M. Whitesides, *J. Am. Chem.Soc.* **1980**, *102*, 7104–7108.

[2] T. R. Röthig, K. D. Kulbe, F. Bückmann, G. Carrea, *Biotechnol. Lett.* **1990**, *12*, 353–356; E. Keinan, E. K. Hafeli, K. K. Seth, R. Lamed, *J. Am. Chem. Soc.* **1986**, *108*, 162–169.

[3] R. Ruppert, S. Herrmann, E. Steckhan, *Tetrahedron Lett.* **1987**, *28*, 6583–6586.

[4] R. Ruppert, S. Herrmann, E. Steckhan, *J. Chem. Soc. Chem. Commun.* **1988**, 1150–1151.

[5] E. Steckhan, S. Herrmann, R. Ruppert, E. Dietz, M. Frede, E. Spika, *Organometallics* **1991**, *10*, 1568–1577.

[6] E. Steckhan, M. Frede, S. Herrmann, R. Ruppert, E. Spika, E. Dietz, *DEHEMA-Monographien* **1992**, *125*, 723–752.

[7] W. Hummel, *Biotechnol. Lett.* **1990**, *12*, 403–408; W. Hummel, *Appl. Microbiol. Biotechnol.* **1990**, *34*, 15–19; C. W. Bradshaw, W. Hummel, C.-H. Womg, *J. Org. Chem.* **1992**, *57*, 1532–1536.

[8] W. Hummel, unpublished results.

[9] E. Steckhan, S. Herrmann, R. Ruppert, J. Thömmes, C. Wandrey, *Angew. Chem.* **1990**, *102*, 445–447; *Angew. Chem. Int. Ed. Engl.* **1990**, *29*, 388–390.

Induction of Ferroelectricity in Polymeric Systems through Hydrogen Bonding**

By *Uday Kumar, Jean M. J. Fréchet,* Takashi Kato, Seiji Ujiie,* and *Kazuyoshi Timura*

Ferroelectric liquid crystals have attracted much attention since the discovery of surface-stabilized ferroelectric liquid crystal devices capable of switching on the nanosecond timescale.[1] Recently, ferroelectricity was induced in polymeric liquid crystals by covalently attaching a chiral mesogen of low molar mass onto a polymer backbone by means of a flexible polymethylene spacer.[2a–e] We report here a novel approach to the preparation of ferroelectric liquid crystals through the thermodynamically favorable self-assembly[3] of a suitable hydrogen-bond donor with a hydrogen-bond acceptor.

The concept of inducing ferroelectricity through hydrogen bonding was realized with assemblies such as **1**, which consists of polysiloxanes **2a–2d** with pendant *p*-alkoxybenzoic acid groups complexed with an optically active (*S*)-(−)-*trans*-4-(2-methoxypropyloxy)-4′-stilbazole (**3**).

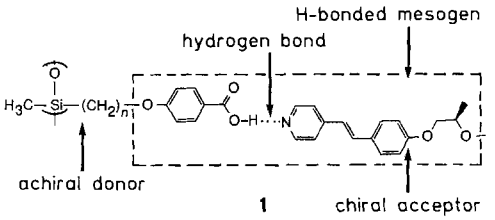

1

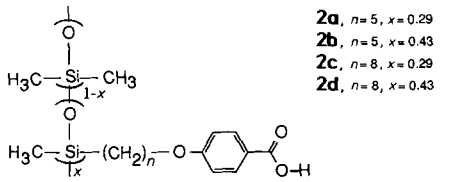

The complexes are designed to form chiral smectic (S_{C^*}) phases over an extended temperature range as a result of the formation of linear structures such as **1** with a large length to breadth ratio. As in liquid crystals of low molar mass, the presence of a strong terminal lateral dipole (methoxy group) and a polarizable core in **1** should aid in the formation of tilted smectic phases.[4] Furthermore the proximity of the chiral center to the linear stilbazole frame restricts its independent motion and should facilitate the spontaneous polarization of the H-bonded structures such as **1**.[5]

Mesogenic polysiloxanes **2a–2d** containing *p*-alkoxybenzoic acid groups in their side chains were prepared as described previously.[6] The weight average molecular weights

[*] Prof. Dr. J. M. J. Fréchet, Dr. U. Kumar
Department of Chemistry, Baker Laboratory
Cornell University
Ithaca, NY 14853 (USA)
Dr. T. Kato
Institute of Industrial Science, University of Tokyo
Minato-ku, Tokyo 106 (Japan)
S. Ujiie, Prof. K. Iimura
Department of Chemistry, Science University of Tokyo
Shinjuku-ku, Tokyo 162 (Japan)

[**] This work was supported by the IBM Corporation (Materials and Processing Science Program), the Cornell University Material Science Center (NSF DMR-8818558), and S. C. Johnson and Sons.

of polymers **2a**–**2d** determined by gel permeation chromatography with a viscometric detector with universal calibration were in the range $\bar{M}_r = 7000-12000$. Stilbazole **3** was made from (*S*)-(−)-ethyl lactate (Scheme 1).[7]

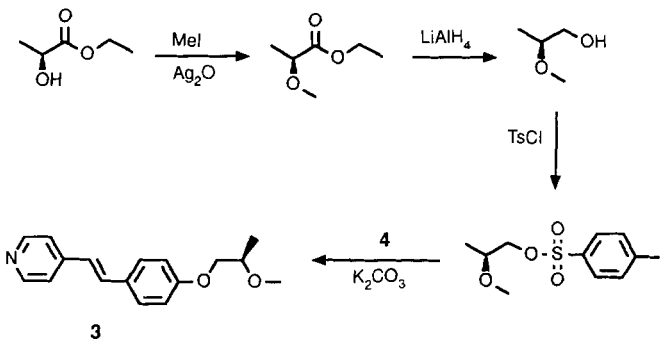

Scheme 1. Synthesis of *trans*-4-(2-methoxypropyloxy)-4′-stilbazole **3** from (*S*)-(−)-ethyl lactate. TsCl: *p*-toluenesulfonyl chloride; **4**: *trans*-4-hydroxy-4′-stilbazole.

The thermal properties of equimolar blends of polymer **2a**–**2d** and stilbazole **3** are given in Table 1. Unless otherwise stated all transition temperatures were measured by differential scanning calorimetry (DSC) on annealed samples, while assignment of the various liquid crystalline phases was done on the basis of DSC, hot stage microscopy, and X-ray experiments. The transition temperatures are dependent on the thermal history. In the following discussion equimolar complexes are represented by [**a**/**b**] where **a** and **b** represent polysiloxane and stilbazole, respectively. The temperatures at which the liquid crystalline complexes [**2a**/**3**], [**2b**/**3**], [**2c**/**3**], and [**2d**/**3**] become isotropic (isotropization temperatures) are higher than either the clearing temperature of the corresponding uncomplexed polymers **2a**–**2d** or the melting point of **3**. This is a consequence of the formation of extended H-bonded assemblies such as **1**, which stabilize the smectic phase. The clearing temperature of [**2c**/**3**] is lower than that of [**2d**/**3**] because of the lower concentration of H-bonded mesogenic structures in the former complex. None of the complexes show a glass transition temperature. The relatively high enthalpy of isotropization is in keeping with the requirement that strong H-bonds be broken during the conversion from the smectic to the isotropic state. The DSC thermogram of an annealed sample of [**2b**/**3**] is shown in Figure 1. Two overlapping endothermic processes at 80 and 90 °C corresponding to solid → solid and crystalline → smectic (K → S) transitions followed by a smectic → isotropic (S → I) transition at 162 °C are observed during heating (Fig. 1a). An isotropic to smectic (I → S) transition at 145 °C followed by two overlapping peaks at 75 and 63 °C are observed during the cooling run (Fig. 1b).

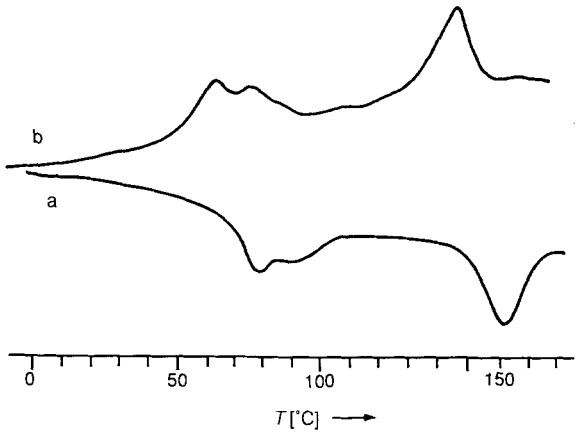

Fig. 1. DSC thermogram of the annealed equimolar complex [**2b**/**3**]. Rate 15 K min^{-1}. [a] Heating run. [b] Cooling run. Endothermic processes are reflected by negative slopes.

The IR spectrum of polymer **2b** shows a strong broad band and two medium-intensity absorptions due to the OH group at 2960, 2675, and 2560 cm^{-1}. In the case of complexes such as [**2b**/**3**], the presence of two intense absorptions at 1930 and 2500 cm^{-1} confirm the existence of a strong hydrogen bond between the COOH group of polysiloxane **2b** and the pyridyl N atom of stilbazole **3**.[3, 8] The non-ionic character of the complexes is further supported by NMR measurements.[6]

The spontaneous polarization was measured by the Sawyer–Tower method[9] from the hysteresis loops (Fig. 2). Ferroelectricity measurements were possible, as the complexes are non-ionic. Plots of the spontaneous polarization P_s of [**2d**/**3**] and [**2b**/**3**] as a function of temperature are given in Figures 3a and 3b, respectively. The decrease of P_s with increasing temperature as is seen for [**2d**/**3**] is normally found in most chiral smectics.[2b, d, 10] This is a result of the decrease

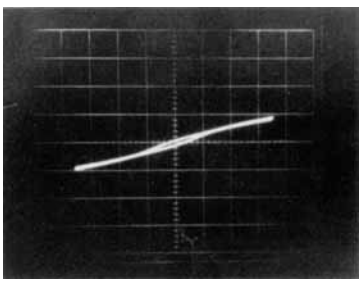

Fig. 2. Hysteresis loop of [**2d**/**3**] at 110.2 °C and 20 Hz. $P_s = 3.2$ nC cm^{-2}. Divisions on the vertical axis: 21.2 nC cm^{-2}; divisions on the horizontal axis: 2.2 kV m^{-1}.

Table 1. Transition temperatures [a] of equimolar blends of polysiloxanes **2a**–**2d** and optically active stilbazole **3**.

Cmpd. or Complex	T_g [°C]	$T_{K\rightarrow S}$ [°C]	T_{soft} [°C]	$T_{S\rightarrow I}$ [°C]	$\Delta H_{S\rightarrow I}$ [J g^{-1}]
2a	31	–	95	108	12
2b	58	–	125	134	16
2c	−7	–	81	111	8
2d	10	–	79	133	24
[**2a**/**3**]	–	85	–	154	14
[**2c**/**3**] [b]	–	88	–	151	8
[**2b**/**3**] [c]	–	90	–	162	15
[**2d**/**3**]	–	91	–	170	11

[a] T_g: glass transition temperature; $T_{K\rightarrow S}$: temperature of the crystalline → smectic transition; T_{soft}: softening temperature, temperature at which sample shows fluidity and birefringence; $T_{S\rightarrow I}$: temperature of the smectic → isotropic transition; $\Delta H_{S\rightarrow I}$: enthalpy of smectic → isotropic transition; m.p. of stilbazole **3** is 111 °C. [b] A solid → solid transition at 79 °C overlaps with the K → S transition. [c] Solid → solid peak at 80 °C overlaps with the K → S transition.

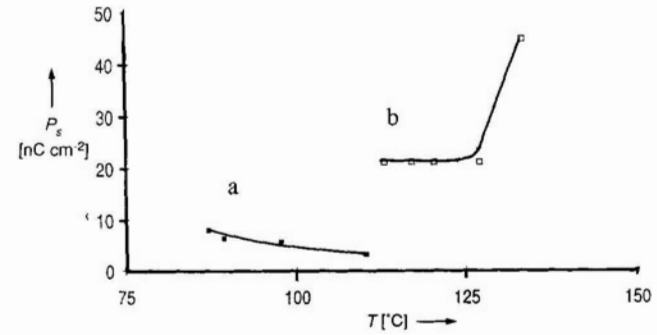

Fig. 3. Temperature dependence of the spontaneous polarization for some equimolar complexes of polysiloxane **2** and optically active stilbazole **3**. [a]: [**2d**/**3**]; [b]: [**2b**/**3**].

in dipolar ordering that occurs with increasing temperature as a consequence of increased rotations about the molecular axis. The increase of P_s with increasing temperature observed for complex [**2b**/**3**] is rather unusual, though a similar phenomenon has recently been reported for a polyacrylate.[12e]

Table 2. X-ray diffraction studies [a] of equimolar blends of polysiloxanes **2a**–**2d** and optically active stilbazole **3**.

Complex	T [°C]	Layer spacing d [Å]
[**2a**/**3**]	110	45.5 (s) 7.2 (d)
	140	44.1 (s) 7.6 (d)
	145	42.8 (s) 8.0 (d)
[**2b**/**3**]	110	40.1 (s) 7.5 (d)
	140	38.4 (s) 7.6 (d)
[**2c**/**3**]	120	45.0 (s) 21.9 (w) 7.6 (d)
	130	46.4 (s) 7.6 (d)
	140	49.6 (s) 7.6 (d)
[**2d**/**3**]	110	43.7 (s) 21.8 (w) 7.7 (d)
	115	44.1 (s) 22.1 (w) 7.9 (d)
	135	43.2 (s) 21.7 (w) 7.9 (d)
	140	42.8 (s) 21.3 (w) 7.7 (d)
	150	42.1 (s) 21.4 (w) 8.0 (d)
	155	41.6 (s) 21.2 (w) 8.0 (d)

[a] Complexes are crystalline below their crystalline → smectic transition temperatures; the diffuse ring at around 4.5 Å is present in all samples; (s) sharp; (w) weak; (d) diffuse.

The large difference in the magnitude of P_s between [**2d**/**3**] and [**2b**/**3**] is probably related to the more hindered rotation of the H-bonded mesogen about its molecular axis in the latter complex because of the proximity to the polymer backbone.

X-ray diffraction data of the annealed unoriented samples are given in Table 2. An intense ring (sometimes accompanied by its second-order reflection) together with the spontaneous polarization, point to a smectic C phase comprising two overlapping H-bonded moieties such as **1**. Although DSC traces do not indicate a $S_C \rightarrow S_A$ transition, investigations with optical microscopy suggest the possibility of a higher temperature S_A phase.

Our approach, the self-assembly of a complex from two complementary compounds, provides excellent opportunities for the preparation of materials with defined mesophase stability, polarization, dielectric anisotropy, viscosity, and refractive index. New developments may thus be anticipated in the study of liquid crystals.

Received: May 18, 1992 [Z 5358 IE]
German version: *Angew. Chem.* **1992**, *104*, 1545

[1] N. A. Clark, S. T. Lagerwall, *Appl. Phys. Lett.* **1980**, *36*, 899.
[2] a) V. P. Shibaev, M. V. Koslovsky, L. A. Beresnev, L. M. Blinov, N. A. Plate, *Polym. Bull.* **1984**, *12*, 299; b) M. Dumon, H. T. Nguyen, M. Mauzac, C. Destrade, M. F. Achard, H. Gasparoux, *Macromolecules* **1990**, *23*, 355; c) S. Uchida, K. Morita, K. Miyoshi, K. Hashimoto, K. Kawasaki, *Mol. Cryst. Liq. Cryst.* **1988**, *155*, 93; d) T. Suzuki, T. Okawa, T. Ohnuma, S. Yohata, *Makromol. Chem. Rapid Commun.* **1988**, *9*, 755; e) H. J. Coles, H. F. Gleeson, C. Scherowsky, A. Schliwa, *Mol. Cryst. Liq. Cryst. Lett.* **1990**, *7*, 117.
[3] a) T. Kato, J. M. J. Fréchet, *J. Am.Chem. Soc.* **1989**, *111*, 8533; b) T. Kato, J. M. J. Fréchet, *Macromolecules* **1989**, *22*, 3818. T. Kato, H. Adachi, A. Fujishima, J. M. J. Fréchet, *Chem. Lett.* **1992**, 265.
[4] G. W. Gray, *Molecular Structure and Properties of Liquid Crystals*, Academic Press, New York, **1962**.
[5] J. W. Goodby, T. M. Leslie, *Mol. Cryst. Liq. Cryst.* **1984**, *110*, 175.
[6] U. Kumar, T. Kato, J. M. J. Fréchet, *J. Am. Chem. Soc.* **1992**, *114*, in press.
[7] **3**: M.p. 111 °C; $[\alpha]^{25}$ −28.8°; ^{1}H NMR (300 MHz, $CDCl_3$, 25 °C): δ = 8.52, 7.32 (C_5H_5N), 7.48, 7.22, 6.91, 6.85 (C_6H_4, CH = CH), 3.98 (OCH_2), 3.75 (CH), 3.47 (OCH_3), 1.29 (H_3CH).
[8] S. E. Odinikov, A. A. Mashkovsky, V. P. Glazunov, A. V. Iogansen, B.-V. Rassadin, *Spectrochim. Acta A* **1976**, *32*, 1355.
[9] a) C. B. Sawyer, C. H. Tower, *Phys. Rev.* **1930**, *35*, 269; b) K. Yoshino, T. Uemoto, Y. Inuishi, *Jpn. J. Appl. Phys.* **1977**, *16*, 571.
[10] S. T. Lagerwall, B. Otterholm, K. Skarp, *Mol. Cryst. Liq. Cryst.* **1987**, *152*, 503.

BOOK REVIEWS

Book Reviews are written by invitation from the editor. Suggestions for books to be reviewed and for book reviewers are welcome. Publishers should send brochures or (better) books to the following address: Redaktion Angewandte Chemie, Postfach 101161, D-W-6940 Weinheim, Federal Republic of Germany. The editor reserves the right of selecting which books will be reviewed. Uninvited books not chosen for review will not be returned.

Chemical Evolution. Origin of the Elements, Molecules and Living Systems. By *S. F. Mason*. Clarendon Press, Oxford, 1991. IX, 317 pp., hardcover £ 19.50.—ISBN 0-19-855272-6

Stephen F. Mason, the author of this book, has made contributions towards answering many unsolved problems of chemical evolution, in particular by studies of stereochemistry, optical activity, and chirality. He has also become well known for his historical studies, and for his book on the history of science. It is becoming increasingly recognized that not only biology, but also chemistry, has an important historical aspect. It is from this standpoint that the book

reviewed here has been written by a chemist who is well versed in the history of the subject, and who thinks of it historically, reflecting all the many different aspects of chemistry. The particular strength of this account is that it unites chemistry, the history of chemistry, and the history of the chemical elements. The early stages of these are described best and in greatest detail, whereas the treatment of prebiotic chemistry and related research is rather brief. Thus one finds an excellent analysis of the early stages of chemical evolution and the contributions of chemists such as Bunsen, Kirchhoff, Fisher, and van't Hoff, whereas the origins of the chemical basis of life and the corresponding work of Oparin, Haldane, Bernal, Urey, Miller, Calvin, etc. are not discussed so thoroughly. To that extent the book does not entirely fulfill the claim of accurately reflecting the state of knowledge at the end of the 1980s, but despite this it can be strongly recommended.

The author gives an excellent description of the formation of the lighter chemical elements in the "big bang", then leads the reader on through the formation of the heavier elements in the stars, and describes the origin of the solar system and of geological minerals. He treats with equal thoroughness the interstellar medium, interstellar dust, meteorites, and comets. The account of the chemical basis of life is divided into the separate aspects of bioenergetics, replication, and polymerization. The last chapter deals with the question of chirality, where the author bases the discussion on his previous work, starting from the concept of the amplification of weak electrical asymmetry.

Subject to the reservations mentioned above, the book can be recommended for study by chemists, physicists, biologists, geologists, and astrophysicists who are interested in chemical evolution. It should also be of considerable interest to scientific historians.

Werner Ebeling
Institut für Theoretische Physik
der Humboldt-Universität Berlin (FRG)

Microscopy. 2nd edition. (Series: Physical Methods of Chemistry, Vol. 4.) Edited by *B. W. Rossiter* and *J. F. Hamilton*. Wiley, Chichester, 1991. XI, 539 pp., hardcover £ 109.00.—ISBN 0-471-08026-8

This book describes methods of microscopy by which images can be obtained through different "illumination methods". The volume encompasses ten contributions, each fitting well with the others, from internationally recognized specialists. The contents are best indicated by the chapter titles, given here in order of the contributing authors: 1. Introduction: Principles and Practice of Electron Microscopy, 3. Electron Microscopy of Defects in Crystals (Medium Resolution), and 7. Special Electron Microscopy Techniques, by John M. Cowley; 2. Electron Microscopy of Biological (and Organic) Materials, and 4. High-Resolution Imaging of Crystalline and Amorphous Materials, by David J. Smith; 5. Electron Diffraction and Microdiffraction, by John C. H. Spence; 6. Microanalysis by Electron Energy Loss Spectroscopy and Energy Dispersive X-Ray Analysis, by Peter Rez; 8. Scanning Electron Microscopy, by Ludwig Reimer; 9. Light Microscopy, by Walter C. McCrone; 10. Determination of Particle Size, by George L. Beyer.

Two-thirds of the book is devoted to electron microscopy, which indicates the importance of and the increasing interest in this method. Modern developments are also to be found in light microscopy, and the contribution about light microscopy makes it clear that this field should in no way be forgotten. The contribution on particle size determination provides a practical example of, among other things, the application of light and electron microscopy (also for automated measurement methods).

With the development of electron microscopy to higher resolution it is increasingly the differences and not the analogies between light and electron microscopy that emerge. Electron microscopy has therefore been considered in this book as consistently as possible from the standpoint of the theory of coherent images, whereas light microscopy was usually described using the concept of incoherent images. The wave properties of electrons and the corresponding diffraction effects are set in the foreground. This volume does not attempt to describe the field completely with results, but sufficient reference is made to the literature for examples of applications and further methods. The emphasis on methods contributes to clarity because the fundamental principles are not concealed by detail. This book shows both where the value and the limits of each method lie and gives an impression of the necessary expenditure of time and effort. All important ideas are explained in an easily comprehensible form. The good general index makes the keywords, otherwise to be found scattered in specialized publications, easily accessible. The individual contributions are so fluently written that one will not only consult them but read further with interest.

The fact that transmission electron microscopy constitutes the book's main theme shows that, in this area alone, unusually *fast* and significant advances have been made in the last few years. All types of equipment and imaging techniques now available are introduced, for example, diffraction in a convergent beam, possibilities for imaging and analysis with scanning transmission microscopy, image processing, and simulation procedures. Even the very promising method of holography with electrons is mentioned. Some of these working methods have only become available for normal use by outfitting apparatus with digital technology and by employing computers. All the modern methods of contrast generation, scanning microscopy, and image processing are described in the section on light microscopy. Every chapter is well provided with diagrams, schemes, and illustrations.

This volume, which presents a sound, up-to-date survey, can be highly recommended to all scientists who want to be informed about these methods, their theoretical basis, and the necessary equipment.

Wilhelm Merten
Institut für Anorganische und Analytische Chemie
der Universität Gießen (FRG)

Reductions by the Alumino- and Borohydrides in Organic Synthesis. By *J. Seyden-Penne*. VCH Publishers, New York/VCH Verlagsgesellschaft, Weinheim/Lavoisier TEC & DOC, Paris, 1991. XIII, 193 pp., hardcover DM 108.00.—ISBN 1-56081-099-8/3-527-28247-5.

Alumino- and borohydrides can be used to achieve selective reductions in high yields, requiring only a simple protocol, and they have therefore rapidly become an indispensable aid to organic synthesis. Because of the wide variety of special reagents now available, and the large number of efficient reductions that have been described in the primary literature, there was a pressing need for an up-to-date review. This report on the latest situation by J. Seyden-Penne does not claim to be complete, but by reviewing 605 publications,

most of which have appeared during the last decade (35 during 1990), it offers an extensive reference source with particular emphasis on the chemo-, regio-, and stereoselectivity of the reactions.

The book is divided into three parts. The first part, consisting of 13 pages, briefly describes the relevant properties (solubility, stability, reactivity) of the most commonly used alumino- and borohydrides, and of a few boranes. The second part (126 pp.) deals with reductions of the most important functional groups. This main part of the book covers the reductive scission of CX, CO, CN, and CP single bonds, and the reactions of the title reagents with CC, CO, and CN double bonds, and with CC and CN triple bonds, and ends with a chapter on the reduction of other substrates (N-, Hg-, Pd-, S-, P-, Si-, and B-containing compounds). The third part (12 pp.) gives a tabular survey of reductive preparations for the most important functional groups, listing the products, educts, reagents, and relevant sections in the book. These synoptic tables arranged according to the structure of the product, together with the list of contents subdivided according to the structure of the substrate and an additional 11-page index organized according to reaction types, enable the reader to readily locate particular transformations of interest.

The examples chosen to illustrate the selectivities include numerous synthetically relevant polyfunctional substrates, making up a very useful compilation. The main strength of the book undoubtedly lies in the detailed discussion of the differential reactivities of various functional groups towards alumino- and borohydrides, and the clear information that is given regarding suitable chemoselective reagents for each case. An appropriate amount of space is also devoted to substrate- and reagent-induced stereoselective transformations, but the pleasure in reading these sections is marred for the reasons explained below. Nowhere is there any mention of yields; however, a few random checks in the original papers that are cited indicate that the reactions described give high yields.

Unfortunately, the book contains many errors that could easily have been avoided by conscientious proofreading. These include simple slips (for example, p. 39: "most hindered double bond" instead of "least substituted ...", p. 99: "trapping of the aluminum enolates obtained from alkyl halides" instead of "... with alkyl halides", p. 143: "to treat the sulfones" instead of "... the sulfoxides"), wrongly or incompletely drawn structures (for example, p. 26: sultone instead of sulfate, p. 32: free alcohol instead of TMS-ether, pp. 36 and 148: primary ozonide instead of secondary ozonide and, accordingly, wrong products shown, p. 94: missing imide nitrogen atom and missing CH_2 group in the chiral auxiliary, p. 52: stereochemistry of the ring junction in the decalones omitted, p. 97: relative configurations of the 3,5-dimethylcyclohexanones not shown), inappropriate descriptions (e.g. p. 29: "the reaction proceeds with configuration inversion" and p. 37: "the reaction can be regioselective", as comments on reactions that do not show the selectivities referred to, or p. 71: "the reduction follows the Felin–Anh rule", as an explanation of the stereoselective reduction of ketones that do not have a stereogenic center at the α carbon atom), and misleading representations, which are frequent (of all places) in the important chapters on the stereoselective reduction of ketones (for example, pp. 49, 50, 54: confusion between the major and minor products in the reduction of C-22 ketones of the steroids series—here also the methyl group on C-20 is sometimes missing, pp. 62–63: interchanging of the major and minor products in the reduction of 2-acyl-1,3-oxathiones and the wrong enantiomers shown, p. 68: the irrelevant statement that "the two conformations C_1 and C_2 are equally populated", where one is dealing with different reactivities). Readers interested in the stereoselective synthesis of steroid side chains or in applying Eliel's method for the enantioselective preparation of α-hydroxyaldehydes must definitely consult the original publications.

To summarize, therefore, this book leaves one with a mixed impression; a thorough revision would be necessary before this reviewer could agree unreservedly with the recommendation by H. C. Brown in the preface that "this book should be in the personal library of every chemist engaged in organic synthesis".

Peter Metz
Organisch-chemisches Institut
der Universität Münster (FRG)

The World of Peptides. A Brief History of Peptide Chemistry. By *T. Wieland* and *M. Bodanszky*. Springer, Berlin, 1991. XII, 298 pp., hardcover DM 198.00.—ISBN 3-540-52830-X

When, in 1901 in Berlin, Emil Fischer prepared glycylglycine, the first free "peptide", no one guessed that this compound marked the beginning of the history of a fascinating class of substances. Peptides constitute the link between amino-acids and proteins. The great variety of peptide structures includes compounds with remarkable biological activities. Many important hormones, antibiotics, toxins, sleep regulators, pain regulators, immunostimulants, immunosuppressants, antitumor and anti-AIDS agents, and a variety of other active substances, are peptides.

This "world of peptides" is described in the book by Theodor Wieland and Miklos Bodanszky. The ten chapters (298 pp.) are as follows: 1. Introduction. Aminoacids and a Few Early Paradigmatic Peptides; 2. Synthesis of Peptides. The First Epoch; 3. The Era After Emil Fischer. The Carbobenzoxy Group, Max Bergmann and his Scientific Circle; 4. A Second Breakthrough: New Methods for the Formation of the Peptide Bond; 5. A New Technology: Solid Phase Peptide Synthesis; 6. Structure Elucidation; 7. Peptide Hormones; 8. Biologically Active Fragments of Proteins; 9. Biologically Active Peptides from Microorganisms and Fungi; 10. Peptide Research Around the World.

Reading this highly interesting account one is aware on every page that the authors are thoroughly at home in this world. Indeed, in their scientific careers they have had a part in shaping the history of these developments, through their fundamental contributions to experimentation and to the literature. The first few chapters describe in detail the work of the founders of peptide chemistry (Fischer, Curtius, Abderhalden, Leuchs, Bergmann, and others) and of the pioneers of the post-war period (Du Vigneaud, Rudinger, Merrifield, etc.). One learns more about the difficult relationship between Fischer and Curtius, and about the temporary shift of the center of gravity of peptide research from Germany to the USA. Pioneering advances are related to the subsequent developments in an admirable fashion; for example, the discovery of the Leuchs anhydrides is linked to an excellent review of later work on the chemistry of NCA and polyamino-acids, and that of the benzyloxycarbonyl residue by Bergmann and Zervas is linked to an account of work on protecting groups during the years that followed. The rapid development of peptide chemistry after the Second World War led to numerous innovations in methods of synthesis

 © VCH Verlagsgesellschaft mbH, W-6940 Weinheim, 1992 0570-0833/92/1111-1535 $ 3.50+.25/0

and analysis, to the discovery of many new naturally occurring peptide structures, and to the elucidation of a variety of structure–activity relationships. The careful choice of subject matter covers all the important facts and highlights. However, it seems to this reviewer that the application of genetic engineering methods to peptide synthesis has not been treated in adequate detail. One can hardly accept that a few more pages here would have exceeded the planned length of the book.

In Chapter 10 one learns that research in peptide chemistry is now being carried out in 27 countries throughout the world (the names of about 800 peptide chemists are listed, and the appendix contains photographs and short biographical notes on about 60 of the field's "élite").

A comprehensive bibliography at the end of each chapter facilitates quick access to the original publications. Other useful information (not only for the expert) is given in a chronological list of international symposia on peptides (Ch. 3, Ref. 42), and in references to the standard works on the subject.

The "Brief History of Peptide Chemistry" announced in the book's subtitle turns out in practice to be a valuable monograph on the topic. This considerably broadens the potential readership. Scientists with an interest in the history of the subject, especially chemists, biochemists, medical scientists, pharmaceutical chemists, and students of all these disciplines, will find here a wealth of information that could otherwise only be gathered with a great deal of effort. Altogether this is a book that belongs in every specialist library, and that everyone concerned will need to have read.

Hans Jeschkeit
Institut für Organische Chemie
der Universität Halle (FRG)

Molecular Electronics. Edited by *G. J. Ashwell.* Research Studies Press, Taunton (UK)/Wiley, Chichester, 1992. X, 362 pp., hardcover £44.50.—ISBN 0-86380-125-0/0-471-93386-4

Molecular electronics is an intriguing term, which can be understood to include several quite different fields of research. Essentially, however, two major areas can be distinguished. Firstly there is the search for molecular materials that can be used in electronics or microelectronics to make components with improved functions. Secondly one can understand it to cover various investigations, some of which involve highly speculative ideas, with the aim of developing a form of electronics based on individual molecules. The hope here is that an element performing an electronic function can be incorporated within a single molecule or a small number of molecules. It is this latter possibility in particular that has seized the imagination of researchers. The book reviewed here deals only with the first of these problem areas, and even here it does not claim to cover the whole topic. A more appropriate title would therefore have been something like "Molecular Materials for Electronics—Selected Topics".

The six chapters are essentially independent of each other, and cover several aspects that are important in relation to potential applications of molecular materials in electronics. The first chapter, "Molecular Electronic Materials", by G. J. Ashwell, I. Sage, and C. Trundle, begins with a 27-page survey of such interesting topics as photochromism, electrochromism, organic conductors, superconductors, and nonlinear materials. The most important areas of application are in optical data storage, molecular rectifiers, and frequency doubling. A review as short as this is inevitably far from complete, and many important publications do not appear in the bibliography. This is followed by a 30-page review of the physical and chemical properties of liquid crystals, which has no obvious relevance to the theme of the book. The second chapter, on "Conjugated Polymers", by M. F. Rubner, explains conductivity in polymers by introducing the concept of solitons and polarons, then discusses aspects such as stability and processing behavior, and describes applications of conducting polymers as active layers in electronic components, in Schottky junctions, and in field-effect transistors. In Chapter 3 on "Langmuir–Blodgett Films", I. R. Peterson first gives a detailed description (60 pp.) of the preparation and characterization of these films, which allow the development of a "molecular architecture" and make it possible to arrange molecules in well-defined structures. This is followed by 15 pages devoted to potential applications (thin insulating films, dielectrics in capacitors, in lithography, and in nonlinear photonics), the general impression being rather pessimistic. In Chapter 4 on "Nonlinear Optics", S. Allen gives a good overview of the prospects for measuring nonlinear optical properties of organic materials and influencing these chemically, and also of incorporating such molecules into a suitable matrix. However, no practical applications in electronics are cited, which probably reflects the true situation. In Chapter 5, "Piezoelectricity, Pyroelectricity and Ferroelectricity", J. Sworakowski gives an introduction to this group of topics, with particular emphasis on molecular solids. Although there are potential applications in molecular electronics, for sensors, storage devices, and similar purposes, the author's view is that, with the exception of polar monomers, these are unlikely to be realized in the near future. The final chapter by K. Firth on "Holography" gives a short and superficial account of the main features of holography, without really relating this to molecular electronics. Recent developments such as holography based on bacteriorhodopsin are not mentioned.

It is not clear for whom this book is intended. The six chapters contain little that will be new to specialists, although they do provide something of an overview of this broadly interdisciplinary field of research. The interested non-specialist, although not finding as much in the book as its title appears to offer, can nevertheless learn something about several interesting aspects of materials research.

Hans Christoph Wolf
Physikalisches Institut
der Universität Stuttgart (FRG)

The Science of Crystallization. Microscopic Interfacial Phenomena. By *W. A. Tiller.* Cambridge University Press, Cambridge (UK), 1991. XXX, 391 pp., hardcover £40.00.—ISBN 0-521-38138-9/paperback £15.00.—ISBN 0-521-38827-9

The two monographs "The Science of Crystallization. Macroscopic Phenomena and Defect Generation" and "The Science of Crystallization. Microscopic Interfacial Phenomena" together form a complete set from this publisher. As the author indicates in his preface, they are suitable as textbooks for students at postgraduate or advanced undergraduate levels in materials science, chemistry, or related subjects. These compact and straightforwardly presented volumes are themselves a *crystallization* of Tiller's long experience in teaching and research, during a period of far-reaching developments

that laid the basis of modern knowledge of crystal growth phenomena and techniques. Here the chemist, in the narrower sense of the word, may learn how complex spatial, temporal, and energetic factors influence the formation or breakdown of crystalline morphological forms, and how these effects can be understood in terms of the chemical thermodynamics and kinetics of multiphase systems. The volume reviewed here consists of three parts. The first treats general and specific aspects of interfacial phenomena, with examples drawn from the semiconductors field; the second presents "background science" relevant to both volumes (introductory discussions of phase systems, nucleation phenomena, etc.); and the third contains example problems (although solutions are not given).

The general discussion begins by considering research on crystallization phenomena from the standpoint of a "response" theory, from which one arrives at a realistic estimate of the necessary research effort (in man-years) using different approaches. This shows that if one adopts a "black-box" approach (with the emphasis on crystal growth and experimental procedures), then the $(j + k)$-dimensional space of variables (where j is the number of different materials and k the number of experimental parameters) leads in practice to an "art-based technology" (in which crystal-growing becomes an art and a collection of recipes). On the other hand, a "system" approach based on a "clustering" that imposes a predetermined structure leads to a "science-based technology" (with a strategically planned procedure and a minimum of experimentation). The consequences of this viewpoint are then systematically developed. Lastly, Tiller considers an *intelligent* approach in which one chooses "scientific trajectory segments" (p. 34) and aims to minimize the experimental work required. The theoretical procedure is illustrated by examples of experiences with semiconductor materials especially (Si, GaAs); these mainly involve crystallization from the melt, and the wealth of available experimental data allows a quantitative study of the crystallization process. Although Tiller discusses the theory using examples drawn mainly from the semiconductors field, many of the results remain valid for the crystallization of other substances, and under different conditions (solutions or the gas phase).

Although the chemist who frequently encounters difficult crystallization problems is likely to find this knowledge interesting in principle, it will probably not be of great help from a practical standpoint. For those working in the area of crystallization, these two volumes will make interesting, and perhaps essential, reading. On the other hand, the chemist seeking help in this area can certainly learn from this book about modern ideas on interfacial phenomena of crystal growth, but should also refer to other works such as that by K.-T. Wilke and J. Bohm (*Kristallzüchtung*, H. Deutsch, **1988**). For newly synthesized materials that need to be crystallized in order to determine their solid state properties, thermodynamic formulas are only of limited use in general, since one does not usually have sufficient data on the thermodynamic parameters. Thus, success is likely to come more quickly from an approach based on the intuition of the crystal-grower, or on computer-aided empirical strategies (P. van der Sluis et al., *J. Cryst. Growth* **1991**, *112*, 719; G. L. Gilliland, *ibid.* **1988**, *90*, 51).

If there is something to be said against this excellent book, it is that a discussion of the energetic and kinetic aspects of interfacial phenomena should have included recent studies, by methods such as light scattering measurements and in-situ synchrotron radiation experiments, that have shown the existence of a labile transitional region between the growing (or dissolving) crystal and the mobile phase, and have led to a better understanding of its structure (e.g., R. Steiniger et al., *J. Cryst. Growth* **1991**, *112*, 203; D. Cunningham et al., *ibid.* **1990**, *99*, 1065). Also, it would be worthwhile to publish a supplementary volume giving solutions to the exercise problems, which are generally of a very high standard; these examples drawn from practical calculations would serve to elucidate the theoretical methods even better.

Jürg Hulliger
Institut für Quantenelektronic
der Eidgenössischen Technischen Hochschule Zürich
(Switzerland)

Transition Metal Hydrides. Edited by *A. Dedieu*. VCH Publishers, New York/VCH Verlagsgesellschaft, Weinheim, 1992. X, 399 pp., hardcover DM 182.00—ISBN 0-89573-781-7/3-527-27985-7

Since Hieber's synthesis of tetracarbonyldihydrido-iron $Fe(CO)_4H_2$, in 1931, hydrido-transition metal complexes have occupied a central position in coordination chemistry. Complexes containing a metal–hydrogen bond are usually regarded as belonging to organometallic chemistry, due mainly to the enormous importance of such compounds in homogeneous catalysis. For example, the role of $Co(CO)_4H$ as the catalytically active species in the Roelen oxo-synthesis was recognized at a very early stage, and the insertion of small molecules into the metal–hydrogen bond has long been one of the key reactions of homogeneous catalysis. More recently, transition metal complexes with molecular hydrogen as a ligand came onto the scene, following the discovery by Kubas in 1984 of the prototype compound $[W(P\{iPr\}_3)_2(CO)_3(\eta^2\text{-}H_2)]$.

This superbly produced book "Transition Metal Hydrides" consists of ten review articles devoted *exclusively* to theoretical and physicochemical aspects of hydrido-transition metal complexes. All the articles have been written by internationally recognized experts, who present the current state of knowledge on hydrido-transition metal complexes in a thoroughly competent way from their own particular viewpoints.

In the first chapter Armentrout and Sunderlin describe the results of studies on hydride species in the gas phase, and report experimental data on the bond energies of apparently simple binary species of the type MH. The experimental techniques used are also described by way of introduction. In the following chapter Sweany reviews matrix isolation studies on hydrido complexes. Particular attention is devoted to the elementary reaction of molecular hydrogen with "naked" metal atoms, and spectroscopic methods for investigating metal–hydrogen interactions are critically reviewed.

The middle five chapters of the book discuss, from the standpoint of theoretical chemistry, practically all the areas of the chemistry of hydrido-transition metal complexes that are currently of interest. Bauschlicher and Langhoff summarize the results of theoretical calculations on bonding in binary species of the type MH, and compare these with spectroscopic data. In Chapter 4 Hay reports on ab-initio and semiempirical calculations on oxidative addition and reductive elimination reactions of molecular hydrogen and of saturated hydrocarbons, while Burdett, Eisenstein, and Jackson discuss the nature of the bonding in complexes having molecular hydrogen as a ligand ("non-classical" hydrido complexes). They also discuss polyhydrido complexes, which are still a subject of much structural and spectroscopic investigation. Koga and Morokuma, in a very comprehensive chapter, deal with hydrogen transfer reactions, including both intramolec-

ular (insertion) and intermolecular reactions. These Japanese authors describe how, thanks to the enormous computing capacities that have become available in the last few years, ab-initio methods can now be applied not only to calculations of molecular geometry, but also in many cases to reaction profiles of catalytic cycles. To complete this group of topics, in Chapter 7 Daniel and Veillard discuss theoretical aspects of the photochemistry of hydrido complexes.

The last three chapters are devoted to some properties of hydrido complexes in solution. Bullock gives a detailed account of results on isotope effects in hydrido complexes, and an excellent review of isotope exchange methods as an important tool for mechanistic studies. In the following chapter Kristjánsdóttir and Norton describe results from the extensive studies carried out in Norton's group on the determination of the acidity of hydrido-transition metal complexes. The tables of pK_a values given here will certainly be very useful for comparison purposes. Lastly, Labinger discusses the very interesting question of exactly what is meant by hydride character, and considers which factors influence the nucleophilic properties of hydrido-metal complexes.

The editor Dedieu then rounds off the book with some general comments on the topics treated. The differences in layout and presentation that are often unavoidable in multi-author works, but are nevertheless a continual source of irritation, have been successfully minimized here, and the book is virtually free of printing errors. With its over 1000 literature references and detailed subject index, it offers readers with an interest in this field an up-to-date overview of theoretical and physicochemical aspects of hydrido-transition metal complexes.

Jun Okuda
Department of Chemistry
State University of New York, Albany (USA)

Metal–Surface Reaction Energetics. Theory and Applications to Heterogeneous Catalysis, Chemisorption, and Surface Diffusion. Edited by *E. Shustorovich*. VCH Publishers, New York/VCH Verlagsgesellschaft, Weinheim, 1991. XII, 232 pp., hardcover DM 144.00.—ISBN 0-89573-776-0/3-527-27938-5

The interaction of gases with surfaces is an area of chemistry that has been studied intensively for many years. This book offers, in five chapters, a review of theoretical methods for describing the energetics of interactions between gases and metal surfaces, including surface diffusion, dissociative and non-dissociative chemisorption, and catalytic processes. The individual chapters are rounded off by comparing theoretical results with experimental data.

The first chapter (approx. 50 pp.) is concerned with the study of adsorption energies and dissociative reaction pathways using quantum-chemical cluster calculations. After introducing the theoretical concept of cluster calculations, P. E. Siegbahn and U. Wahlgren discuss its capabilities and practical limitations with the help of a number of examples. This chapter impresses by its straightforward presentation of the basic features of this complex topic, and it should be understandable even by non-specialists.

In the following chapter, also of about 50 pages, J. B. Benzinger describes thermodynamic methods for treating the energetics of adsorption and reactions at surfaces. The main emphasis is on applications of the bond order conservation (BOC) method to the estimation of adsorption and reaction energies, which can then be used to determine kinetic parameters. Owing to the complexity of this field and the scarcity of relevant thermodynamic data, the methods described here are, of course, heavily reliant on approximations and empirical procedures.

The next chapter (R. C. Baetzold, approx. 30 pp.) deals with the diffusion of atomic and molecular adsorbates on surfaces. This area of study, which is important in relation to the dynamics of surface processes such as nucleation, crystal growth, and surface reactions, again involves the application of the BOC model.

In the fourth chapter (approx. 40 pp.) D. Halstead and S. Holloway describe simulation calculations on dissociative and non-dissociative adsorption using the split operator method (example: H_2 on metal surfaces). In this method the development with time of the wave function of a molecule is treated by taking into account the translational, rotational, and vibrational degrees of freedom when scattering occurs at a surface potential. After introducing the method of calculation, the authors present results obtained by applying it to model potentials with different reaction barriers.

In the final chapter (approx. 30 pp.) A. T. Bell discusses approaches based on the BOC method for treating mechanisms and kinetics of heterogeneously catalyzed reactions. The chapter begins with an explanation of the underlying concept, then discusses several examples and simulation calculations aimed at determining reaction energetics and pathways.

The book is intended for scientists working in the fields of surface chemistry or heterogeneous catalysis. Although the individual chapters are essentially of a theoretical nature, the material is presented in such a way that it can also be understood by non-theoretical readers. The book can therefore be recommended also for final year students. As it contains many tables listing experimental and calculated energy data for different adsorbates and a wide variety of metallic substrates, it also has some value as a work of reference. Aspects that may be criticized are the overlapping in subject matter between some of the chapters, and the fact that some of them concentrate too heavily on the BOC formalism. In the preface the editor expresses the view that a mutual understanding between theoreticians and experimentalists will be of crucial importance for future progress. This book is a very welcome contribution towards that aim.

Helmut Kuhlenbeck
Institut für Physikalische Chemie
der Universität Bochum (FRG)

Intermolecular Forces. An Introduction to Modern Methods and Results. Edited by *P. L. Huyskens, W. A. P. Luck*, and *T. Zeegers-Huyskens*. Springer, Berlin, 1991. X, 490 pp., hardcover DM 198.00.—ISBN 3-540-53410-5

The properties of chemical substances are greatly dependent on intermolecular interactions. In particular, the occurrence of hydrogen bonding in a substance fundamentally affects its physical and chemical properties. Despite this, according to the editors of this book the subject receives too little attention in undergraduate teaching. Their book, which is based on the contributions presented at a 1989 "Erasmus" course, is thus seen by the editors as, not least, a stimulus for university teachers to give the subject a greater emphasis.

A glance at the contents list of this book of 21 chapters quickly reveals that the main emphasis is on describing recent results on hydrogen bonding. Although this is not in keeping with the book's title, which suggests a more general

concern with intermolecular forces, it undoubtedly takes into account the extreme importance of hydrogen bonding in chemistry and biochemistry. Consequently, the two articles concerned with studies on clusters and with experiments on molecular collisions in the gas phase seem almost out of place in the otherwise uniformly orientated subject matter.

The book consists of three parts. The first part contains a general introduction to intermolecular interactions. T. Zeegers-Huyskens and P. L. Huyskens report on cohesion forces and on specific intermolecular forces. The first of these two sections deals briefly with van der Waals forces, but regrettably does not relate this topic to recent research in the field of cluster physics. The second section discusses hydrogen bonding and related interactions and describes examples. For this introduction it would perhaps have been better to start with van der Waals interactions, and then to proceed via charge-transfer interactions to hydrogen bonding. However, this is put right in the second chapter by L. G. Vanquickenborne, who is concerned solely with the quantum chemical aspects of hydrogen bonding, and gives a detailed description of the Morokuma model for explaining the nature of hydrogen bonding. The first part of the book concludes with chapters on "How to Understand Liquids", by W. A. P. Luck, and "Dynamic Aspects of Intermolecular Interactions", by L. C. M. De Maeyer.

The second part consists of eight chapters describing spectroscopic studies of intermolecular interactions. Six of these are concerned with hydrogen bonding, mainly in the liquid phase. A. Ceulemans gives an introduction to the theoretical treatment of vibrational spectra of hydrogen-bonded systems. T. Zeegers-Huyskens then links this to IR spectroscopic investigations of intermolecular stretching vibrations. W. A. P. Luck discusses the application of IR overtone vibrational spectroscopy to studies of hydrogen-bonded liquids. The same author, in a further chapter entitled "Water—The Most Anomalous Liquid", describes the unique macroscopic properties of water and attempts to explain their causes. K. Rademann gives a short introduction to the various forms of spectroscopy for studying clusters in molecular beams, and shows how these new techniques can be used to investigate intermolecular forces. This part on spectroscopic methods concludes with chapters by H. Kleeberg on "Cooperative Effects Involved in H-Bond Formation", by H. H. Limbach on "NMR Studies of Elementary Steps of Multiple Proton and Deuteron Transfers in Liquids, Crystals and Organic Glasses", and by G. Maes on "Matrix Spectroscopy of Hydrogen-Bonded Complexes".

The third part consists of nine chapters describing non-spectroscopic methods of investigation. For example, U. Buck deals with the determination of intermolecular potentials by scattering experiments with crossed molecular beams. P. Bopp shows what can be achieved by applying "Molecular Dynamics (MD) Computer Simulations of Hydrogen-Bonded Liquids" to the interpretation of experimental results. P. L. Huyskens and G. G. Siegel, in their article on "Hydrogen Bonding and Entropy", attempt a quantitative description of hydrophobic effects.

The appearance of the book gives a good impression, and the quality of the figures and formulas is excellent. A detailed keyword index makes it easy to find one's way around the many chapters. Further help in quickly locating information is provided by the short summary given at the beginning of each chapter, and by the contents lists for the individual chapters. A brief examination of the ample lists of references appended to the chapters shows that the most recent results have been cited.

The book can be recommended for everyone seeking a review of the current state of research in the area of molecular interactions, especially hydrogen bonding. Unfortunately however, recent studies using molecular beams receive only marginal coverage. Also, the wealth of methods and results in the rapidly growing field of research on clusters cannot be adequately covered in only a single chapter. Nevertheless, this is more a criticism of the choice of title for the book, which is too general, than of the otherwise comprehensive and well-balanced contents.

Harald Krause
Institut für Physikalische und Theoretische Chemie
der Technischen Universität München
Garching (FRG)

Stereochemistry of Organic Compounds. Principles and Applications. By *D. Nasipuri.* Wiley, Chichester, 1991. XX, 527 pp., hardcover £33.95.—ISBN 0-470-21639-5

A new 500-page book on stereochemistry? One's reaction might be: well, at last!—this raises high expectations—but to write such a book must be a very difficult task, in view of the continuing rapid development of modern methods.

Nasipuri has divided his book into three main subject areas. Following an introductory chapter on the different types of chemical bonding and molecular geometry, he goes on to consider increasingly complex questions of stereochemistry. The basic principles, methods of classification, and definitions are explained with the help of good illustrations and examples of reactions. This first part, consisting of eight chapters, is followed by a second part giving a detailed description of molecular conformations of cyclic and acyclic systems. The discussion includes physicochemical methods of conformational analysis, and conformational behavior of polycyclic and heterocyclic compounds, considering both individual examples and general characteristics. The third part is concerned with dynamic stereochemistry, and consists of three chapters dealing in turn with relationships between conformation and reactivity, stereoselective transformations, and pericyclic reactions. Each chapter of the book begins with a brief introduction outlining the main aspects of the topics to be discussed. Occasional excursions into the historical background serve to stimulate the reader's interest. Each of the fifteen chapters is subdivided into numerous sections, and ends with a brief summary and a bibliography.

The book is intended mainly for advanced undergraduate and post-graduate students. Its greatest strength lies in the first part, which deals with the basic concepts of organic stereochemistry. In many places the text strikes one as material designed to accompany a course of lectures, and often the reader will wish that the author could act as a "course tutor" to explain difficult points. The preface indicates that the literature references cover publications up to 1990; in fact, most of the citations refer to older monographs, review articles, and original papers, which describe results of fundamental importance. It is annoying to find that a lengthy search is often needed to locate a citation in the bibliography. The citations are identified in the text by the author's name and the year, but instead of being listed at the end of the chapter in alphabetical order as one would expect, they are just given in the order of appearance in the text. The frequency of errors is noticeably high, especially in names (e.g., "J. N. Lehn", p. 42; "Nögradi", p. 404; "Gröb fragmentation, Gröb 1969", p. 365; "Yamamotoa", p. 444; "Stereochemie der Kohlenstoffverdunger", p. 105; and

many more). There are also some very unusual abbreviations for journal names, and different ones appear at different places. In a student textbook it would surely have been appropriate to use the standard citation methods of the *Chemical Abstracts Source Index*. Also it is very annoying when a citation given in the text does not appear in the bibliography (e.g., Phillips 1954, p. 236).

The very detailed description of the conformations of organic compounds in the middle part of the book is followed by a compilation of stereoselective transformations and asymmetric synthesis methods. In contrast to the careful and patient explanations of complex matters in the earlier chapters, the style of this part seems hurried and very condensed. The author describes individual examples, but neglects important theoretical explanations, giving repeated references (rather old ones in many cases) for further reading; this is justified by the statement that "...space does not permit any further discussion on this topic" (p. 475). Here it was evidently felt that there was a need to update the book by including in the bibliography some additional citations that are not mentioned in the text (Chapter 13). However, the choice of these seems very haphazard. Some newer areas of research, such as stereoselective free radical reactions and the application of force field calculations to conformational analysis, are completely absent, or are only mentioned incidentally in the text.

Nasipuri's textbook can be thoroughly recommended for its good and detailed introduction to the basic concepts of organic stereochemistry. However, in its treatment of dynamic stereochemistry, and especially of asymmetric synthesis, it still leaves one with the need for a comprehensive textbook dealing effectively with these topics. The relatively low price makes this an attractive new textbook, but does not excuse the poor quality of the typography and binding.

Carsten Bolm
Institut für Organische Chemie
der Universität Basel (Switzerland)

Corrigenda

In the correspondence "The Epidemic Spread of Fullerene Research" by T. Braun (*Angew. Chem. Int. Ed. Engl.* **1992**, *31*, 558), an entry in Table 3 is missing. The University of Pennsylvania with 21 papers should follow the University of California, Los Angeles.

In the review "Flexible Molecules with Defined Shape—Conformational Design" by R. W. Hoffmann (*Angew. Chem. Int. Ed. Engl.* **1992**, *31*, 1124), the structure of lardolure **9** on p. 1125 is incorrect and should be replaced with the following structural formula:

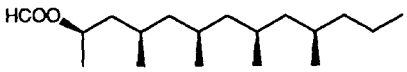

9

The author thanks Dr. M. Morr, Gesellschaft für Biotechnologische Forschung, Braunschweig (FRG), for pointing out this error.

Registered names, trademarks, etc. used in this journal, even when not marked as such, are not to be considered unprotected by law.

© VCH Verlagsgesellschaft mbH, D-W-6940 Weinheim, 1992. – Printed in the Federal Republic of Germany by Konrad Triltsch Druck- und Verlagsanstalt Würzburg.

All rights reserved (including those of translation into foreign languages). No part of this issue may be reproduced in any form — by photoprint, microfilm, or any other means — nor transmitted or translated into a machine language without written permission from the publishers. Only single copies of contributions, or parts thereof, may be made for personal use. This journal was carefully produced in all its parts. Nevertheless, authors, editors, and publisher do not warrant the information contained therein to be free of errors. Readers are advised to keep in mind that statements, data, illustrations, procedural details, or other items may inadvertently be inaccurate.

Valid for users in the USA: The appearance of the code at the bottom of the first page of an article (serial) indicates the copyright owner's consent that copies of the article may be made for personal or internal use, or for the personal or internal use of specific clients. This consent is given on the condition, however, that the copier pay stated per-copy fee through the Copyright Clearance Center, Inc. (CCC), for copying beyond that permitted by Sections 107 or 108 of the U.S. Copyright Law. This consent does not extend to other kinds of copying, such as copying, for general distribution, for advertising or promotional purposes, for creating new collective works, or for resale. For copying from back volumes of this journal see 'Permissions to Photo-Copy: Publisher's Fee List' of the CCC.

Editorial office: Postfach 10 11 61, D-W-6490 Weinheim, Federal Republic of Germany, Telephone (06201) 606 315, Telex 465 516 vchwh d, Telefax (06201) 606 328, E-Mail Z16@DHDURZ2 in Earn Bitnet.

Editor: *Peter Gölitz*

Associate editors: *R. H. Schmidt-Radde, K. J. Schneider, N. A. Compton.* **Editorial assistant:** *E. Schweikart*

Publishers: VCH Verlagsgesellschaft mbH. (Managing Directors: *Hans Dirk Köhler, Dr. Karlheinz Köpfer*), Pappelallee 3, D-W-6940 Weinheim, Federal Republic of Germany.

Advertising office (Advertising Manager: *N. Schippel*): Postfach 10 11 61, D-W-6940 Weinheim, Federal Republic of Germany, Telephone (0 62 01) 606 312, Telefax (0 62 01) 606 328.

ANGEWANDTE CHEMIE
International Edition in English
Volume 31 · Number 12
December 1992
Pages 1541–1696

Emil Fischer's Proof of the Configuration of Sugars: A Centennial Tribute**

By Frieder W. Lichtenthaler*

Today's textbooks convey the deceptive impression that chemistry developed in a rational and orderly process with discoveries following one upon another in a vertical progression—an impression that tends to classify Fischer's achievement as a matter-of-fact historical development. This misconception does not consider the instances of serendipity invariably involved, and entirely fails to appreciate the human endeavor, the intellectual struggle of the dedicated researcher, and the forging force of his personality that eventually led to this key insight. The hundredth anniversary of Fischer's classical piece of work provides a welcome opportunity not only to highlight its paramount importance for the development of carbohydrate chemistry, and of organic chemistry in general, but to trace the creative processes underlying this fundamental discovery, the thought patterns at a conceptual level, and the constructive reasoning that eventually led to it. Their understanding and appreciation is essential for emulating Fischer's achievement in a modern context.

Die Geschichte einer Wissenschaft
ist diese Wissenschaft selbst
J. W. von Goethe[***]

The rapid pace and volume of scientific discoveries tend to eclipse not only those of past decades, but those of the past century in particular. This leads to a gross underestimation of the basic contributions of the pioneers of our science who laid the very foundations of current research. Pertinent examples of this are the foundation of organic structural chemistry and the proposal of the benzene formula by Kekulé in 1865[1] and, ten years later, the postulation of tetrahedral geometry for carbon by Le Bel and van't Hoff,[2, 3] which provided an explanation for the occurrence of numerous isomers inexplicable on the basis of the then current structural formulas. Another case in point, substantially undervalued in its impact on the development on organic chemistry, is the establishment of the relative configurations of the sugars by Emil Fischer in 1891,[4, 5] a most remarkable piece of research which not only put carbohydrate chemistry on a rational basis but—more importantly for that time—provided unequivocal proof for the validity of the Le Bel–van't Hoff theory of stereoisomerism.

The essence of what was to become the sugar family tree, and what inaugurated a new mode of writing stereoformulas is contained in two publications by Fischer (Fig. 1) in the *Berichte der Deutschen Chemischen Gesellschaft*, the first appearing in the September issue of 1891[4] (Fig. 2) and the second only two months later.[5] Both papers carried the

[*] Prof. Dr. F. W. Lichtenthaler
Institut für Organische Chemie der Technischen Hochschule
Petersenstrasse 22, D-W-6100 Darmstadt (FRG)

[**] Based on a Commemorative Lecture presented at the 203rd American Chemical Society Meeting, San Francisco, April 8, 1992, on the occasion of the Symposium "Emil Fischer—100 Years of Carbohydrate Chemistry".
This account is dedicated to Professor Klaus Hafner on the occasion of his 65th birthday; his exemplary tribute to Kekulé on his 150th birthday gave the essential impulses to this centennial.

[***] "The history of a science is the science itself."

 © *VCH Verlagsgesellschaft mbH, W-6940 Weinheim, 1992* *0570-0833/92/1212-1541 $ 3.50+.25/0*

Fig. 1. Emil Fischer (1852–1919) in 1889 [6].

modes title "Über die Configuration des Traubenzuckers und seiner Isomeren" (On the Configuration of Grape Sugar and its Isomers), yet the introductory sentence of the first of these (see Fig. 2) gives a clear indication of the fundamental question to be addressed, and the solution that was achieved:

> "All previous observations in the sugar group are in such complete agreement with the theory of the asymmetric carbon atom, that, by now, one may dare to use this theory as a basis for the classification of those substances."

This not only announced the advent of a rational sugar chemistry but, de facto, that of applied organic stereochemistry as well; the discovery was to shape the development of organic chemistry to an extent that can be compared only with the impact that Kekulé's benzene formula[6] had made 25 years earlier.

Modern textbooks give the deceptive impression that chemistry developed in a rational and orderly way in which discoveries follow one after another in a vertical progression—an impression that tends to classify Fischer's achievement as purely an historical development, accomplished by some remote, legendary historical figure. This misconception does not consider the instances of serendipity invariably involved, and entirely fails to appreciate the human endeavor, the intellectual struggle of the dedicated researcher, and the forging force of his personality that eventually led to this key insight. The hundredth anniversary of this classical piece of work provides a unique opportunity not only to highlight and appraise its paramount importance for the development

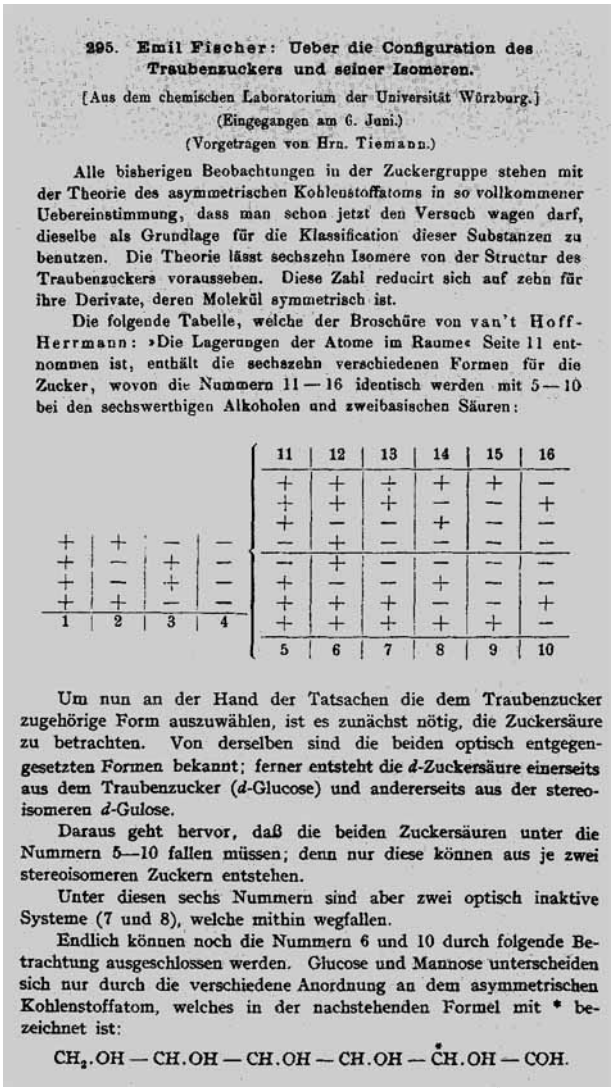

295. **Emil Fischer: Ueber die Configuration des Traubenzuckers und seiner Isomeren.**

[Aus dem chemischen Laboratorium der Universität Würzburg.]

(Eingegangen am 6. Juni.)

(Vorgetragen von Hrn. Tiemann.)

Alle bisherigen Beobachtungen in der Zuckergruppe stehen mit der Theorie des asymmetrischen Kohlenstoffatoms in so vollkommener Uebereinstimmung, dass man schon jetzt den Versuch wagen darf, dieselbe als Grundlage für die Klassification dieser Substanzen zu benutzen. Die Theorie lässt sechszehn Isomere von der Structur des Traubenzuckers voraussehen. Diese Zahl reducirt sich auf zehn für ihre Derivate, deren Molekül symmetrisch ist.

Die folgende Tabelle, welche der Broschüre von van't Hoff-Herrmann: »Die Lagerungen der Atome im Raume« Seite 11 entnommen ist, enthält die sechszehn verschiedenen Formen für die Zucker, wovon die Nummern 11—16 identisch werden mit 5—10 bei den sechswerthigen Alkoholen und zweibasischen Säuren:

1	2	3	4	11	12	13	14	15	16
+	+	−	−	+	+	+	+	+	−
+	−	+	−	+	+	+	−	−	+
+	−	+	−	+	−	−	+	−	−
+	+	−	−	−	+	−	−	−	−
+	−	+	−	−	+	−	−	−	−
+	−	+	−	+	−	−	+	−	−
+	+	−	−	+	+	+	−	−	+
+	+	−	−	+	+	+	+	+	−
1	2	3	4	5	6	7	8	9	10

Um nun an der Hand der Tatsachen die dem Traubenzucker zugehörige Form auszuwählen, ist es zunächst nötig, die Zuckersäure zu betrachten. Von derselben sind die beiden optisch entgegengesetzten Formen bekannt; ferner entsteht die *d*-Zuckersäure einerseits aus dem Traubenzucker (*d*-Glucose) und andererseits aus der stereoisomeren *d*-Gulose.

Daraus geht hervor, daß die beiden Zuckersäuren unter die Nummern 5—10 fallen müssen; denn nur diese können aus je zwei stereoisomeren Zuckern entstehen.

Unter diesen sechs Nummern sind aber zwei optisch inaktive Systeme (7 und 8), welche mithin wegfallen.

Endlich können noch die Nummern 6 und 10 durch folgende Betrachtung ausgeschlossen werden. Glucose und Mannose unterscheiden sich nur durch die verschiedene Anordnung an dem asymmetrischen Kohlenstoffatom, welches in der nachstehenden Formel mit * bezeichnet ist:

$$CH_2.OH - CH.OH - CH.OH - CH.OH - \overset{*}{C}H.OH - COH.$$

Fig. 2. Title page of the first [4] of Fischer's two landmark papers in 1891 on the configuration of sugars.

of organic stereochemistry in general, and carbohydrate chemistry in particular—this has been done, over the years, in many specialized accounts[7–14]—or for keeping pivotal facts from oblivion. During the past hundred years there has been almost unbelievable material and conceptual progress; what has not changed, however, are the creative processes underlying a fundamental discovery and the constructive reasoning that eventually led to it. Their understanding and

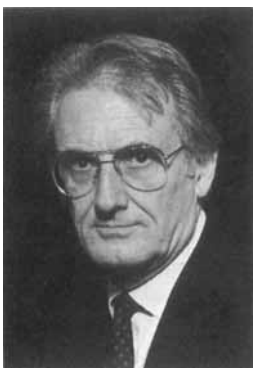

Frieder W. Lichtenthaler, born 1932 in Heidelberg, studied chemistry at the University of Heidelberg from 1952–1956 and received his doctorate there in 1959 under F. Cramer for research on enol phosphates. The following three years he spent as a postdoctoral fellow at the University of California, Berkeley, with Hermann O. L. Fischer—the only of Emil Fischer's three sons who survived the first World War.[10d] He subsequently worked as an assistant at the Technische Hochschule Darmstadt, where he acquired his "Habilitation" in 1963, was appointed associate professor in 1968, and was promoted to full professor in 1972. His research activities center on the generation of enantiopure building blocks from sugars, their utilization in the synthesis of oligosaccharides and complex non-carbohydrate natural products, the computer simulation of chemical and biological properties of sugars, and studies towards the utilization of carbohydrates as organic raw materials.

appreciation is required to emulate Fischer's achievement in a modern context.

The attempt to trace these processes starts with the analytical reagent which Fischer was the first to use in carbohydrate chemistry in 1884, and with which he established the relative configurations of the sugars only seven years later: *phenylhydrazine*, a base, which he accidentally discovered in 1875 at the age of 23, while working as an assistant in Baeyer's Strassburg laboratory. The resulting publication[15] (Fig. 3) is unusual in several respects. First, Baeyer, in whose institute the work was done, allowed him to publish it on his own; that there isn't even an acknowledgement to his teacher attests to the seemingly high esteem and encouraging attitude Baeyer had for his gifted pupil; second, the paper is formulated in a concise, clear style undoubtedly adopted from his teacher, and written in the first person. For example, in the paper reproduced in Figure 3, he writes,

> "I have again taken up experiments on the reduction of diazo compounds. ... I arrived at a class of well-characterized bases, for which I propose the name hydrazine compounds".

A rather self-confident statement for a young chemist who had just received his doctorate, and the more so as the parent compound, hydrazine, was discovered only twelve years later, in 1887, by Curtius.[16] Reading Fischer's paper of 1875 today engenders the sensation of contemplating the modest source of what was to become a mighty river within the next 15 years.

The research school of Adolf Baeyer (1835–1917[17]), from which Fischer emerged—first in Strassburg, and then for 40 years after 1875 at the University of Munich—was a major "forge" of talent. A group photograph[18] of 1878 attests to that almost literally: the unusually wide hood in the background is certainly more reminiscent of a forge than of a laboratory. In the center Adolf Baeyer, wearing a prominent hat; since several others also wear headgear, we may deduce that in the winter of 1878 the heating was deficient in that laboratory. To the right of Baeyer the 25-year-old Emil Fischer, in a peaked cap and strikingly self-confident three years after his Ph.D.; to the left Jacob Volhard (1834–1910), who was in charge of the analytical division in Baeyer's institute, and whose successor Fischer was to become in Munich a year later (1879), and at the University of Erlangen in 1882. Far to the left Fischer's cousin Otto Fischer, with whom he did extensive work on rosaniline dyes.[20] Between Baeyer and Volhard stands Wilhelm Koenigs (1851–1906[21]) who in 1900, together with his co-worker Eduard Knorr, discovered the Ag_2CO_3-induced glycosidation of acetobromoglucose,[22] known today as the Koenigs–Knorr reaction.

A survey of the early papers of Emil Fischer indicates the curious fact that although the ability of phenylhydrazine to react with aldehydes was quickly observed by him—the phenylhydrazones of acetaldehyde, benzaldehyde, and furfural were unequivocally characterized and structurally secured[23]—Fischer does not appear to have recognized the tremendous values of the compound for the characterization and identification of carbonyl compounds until nearly 10 years later, in 1884,[24] when he finally applied it to the sugars. This 'induction period' had several reasons:

Over a number of years (1876–1880) he did extensive investigations on rosaniline dyes with his cousin Otto Fischer.[20]

He pursued his habilitation and completed it in the spring of 1878.

In the fall of 1878, he took charge of the analytical division of Baeyer's institute, as the successor to J. Volhard.

In 1881 he started work on purines, investigating the structure caffeine. Although he initially devised an erroneous formula,[25] the research eventually led to his classification of purines.

In 1882 at the age of 30, he moved from Munich to Erlangen, accepting the chair of chemistry at that university, and there he was intensely occupied with the conversion of phenylhydrazine into N-heterocycles,[26] which led to the Fischer indole synthesis.[27]

Another reason for not applying phenylhydrazine to sugars earlier, although their "aldehyde nature" was known, may have been the desolate state in which the chemistry of sugars was at that time. Because of the nature of these substances, their study was fraught with great difficulty, especially since impure sugars tend to form syrups, which in the second half of last century could not be analyzed reliably. A compound had to be crystalline, and be recrystallizable to a constant melting point and optical rotation to be considered pure. Thus, it is not surprising that early progress in the field of carbohydrates could not be achieved, whereas, for example, the chemistry of the aromatic compounds was well-developed.

Around 1870, chemists recognized two aldohexoses, glucose and galactose, and one ketose (levulose, later named

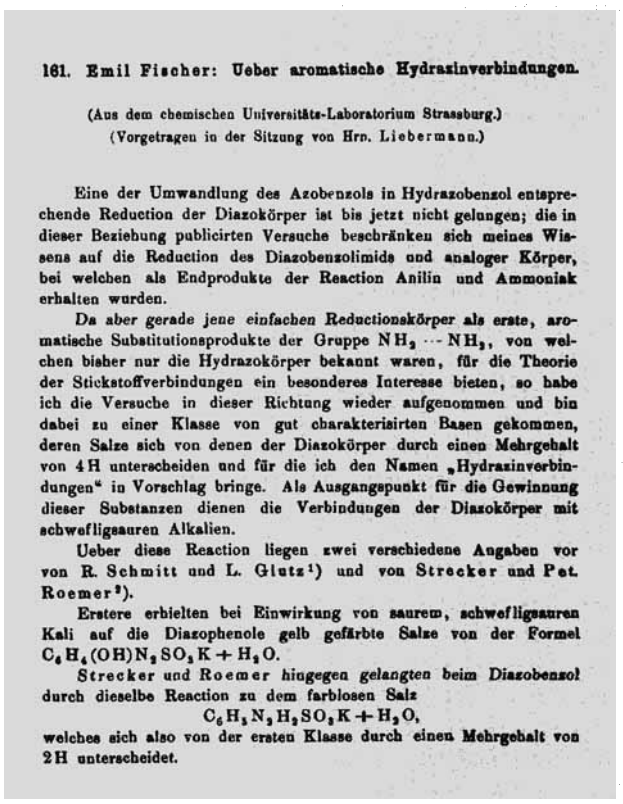

161. Emil Fischer: Ueber aromatische Hydrazinverbindungen.

(Aus dem chemischen Universitäts-Laboratorium Strassburg.)
(Vorgetragen in der Sitzung von Hrn. Liebermann.)

Eine der Umwandlung des Azobenzols in Hydrazobenzol entsprechende Reduction der Diazokörper ist bis jetzt nicht gelungen; die in dieser Beziehung publicirten Versuche beschränken sich meines Wissens auf die Reduction des Diazobenzolimids und analoger Körper, bei welchen als Endprodukte der Reaction Anilin und Ammoniak erhalten wurden.

Da aber gerade jene einfachen Reductionskörper als erste, aromatische Substitutionsprodukte der Gruppe $NH_2 \cdots NH_2$, von welchen bisher nur die Hydrazokörper bekannt waren, für die Theorie der Stickstoffverbindungen ein besonderes Interesse bieten, so habe ich die Versuche in dieser Richtung wieder aufgenommen und bin dabei zu einer Klasse von gut charakterisirten Basen gekommen, deren Salze sich von denen der Diazokörper durch einen Mehrgehalt von 4H unterscheiden und für die ich den Namen „Hydrazinverbindungen" in Vorschlag bringe. Als Ausgangspunkt für die Gewinnung dieser Substanzen dienen die Verbindungen der Diazokörper mit schwefligsauren Alkalien.

Ueber diese Reaction liegen zwei verschiedene Angaben vor von R. Schmitt und L. Glutz[1]) und von Strecker und Pet. Roemer[2]).

Erstere erhielten bei Einwirkung von saurem, schwefligsauren Kali auf die Diazophenole gelb gefärbte Salze von der Formel $C_6H_4(OH)N_2SO_3K + H_2O$.

Strecker und Roemer hingegen gelangten beim Diazobenzol durch dieselbe Reaction zu dem farblosen Salz

$$C_6H_5N_2H_2SO_3K + H_2O,$$

welches sich also von der ersten Klasse durch einen Mehrgehalt von 2H unterscheidet.

Fig. 3. Title page of Fischer's 1875 paper on the discovery of phenylhydrazine [15].

Fig. 4. Photograph of the Baeyer group in 1878 at the laboratory of the University of Munich (room for combustion analysis), with inscriptions from Fischer's hand [18].

fructose by Fischer). Three disaccarides, sucrose, lactose, and maltose were also characterized as distinct compounds. The experimental evidence for their structures was very scarce, yet it had gradually led to the assumption that they may be straight-chain pentahydroxyaldehydes. Thus, A. Baeyer in an 1870 Berichte paper[28] expressed the opinion:

> "On the basis of all known experience the constitution of grape sugar must correspond to one of the two formulas [shown in Fig. 5 (top left)], or at least be very closely related thereto."

Hugo Schiff, in the same year, formulated "grape sugar as the first aldehyde of mannitol" (Fig. 5 top right).[29] The most elaborate formulations (Fig. 5 bottom) stem from Rudolph Fittig (1835–1910) in 1871:[30]

> "Grape sugar is the aldehyde of mannitol, and mannitol is the saturated sixfold acidic alcohol of hexane. On gentle oxidation of grape sugar, like with all other aldehydes, the CHO group is converted into carboxyl COOH, and a unibasic acid of six atoms $C^6H^{12}O^7$, gluconic acid, is formed. Since gluconic acid contains a second oxidizable CH^2OH group, further oxidation must result in a dibasic acid. This acid is sugar acid, which contains four hydroxyl atoms apart from the two carboxyl groups."

Fittig's formulas (Fig. 5 bottom) did not show any stereochemical relationships of the various hydroxyl groups, and thus many reactions of the sugars were far from being understood.

This explains why, in the course of the 15 years following, very little progress was made either experimentally or conceptually. The interrelationships of the sugars remained something of a black box, except maybe for the fact that in 1883 Tollens (Fig. 6)[31] intuitively anticipated the cyclic hemiacetal forms of sugars, without, of course, fully realizing their significance (see Fig. 7): glucose ("Dextrose") forms a seven or five-membered ring, fructose ("Laevulose") was thought to adopt the furanoid form, which happens to be the one realized in sucrose ("Rohrzucker").

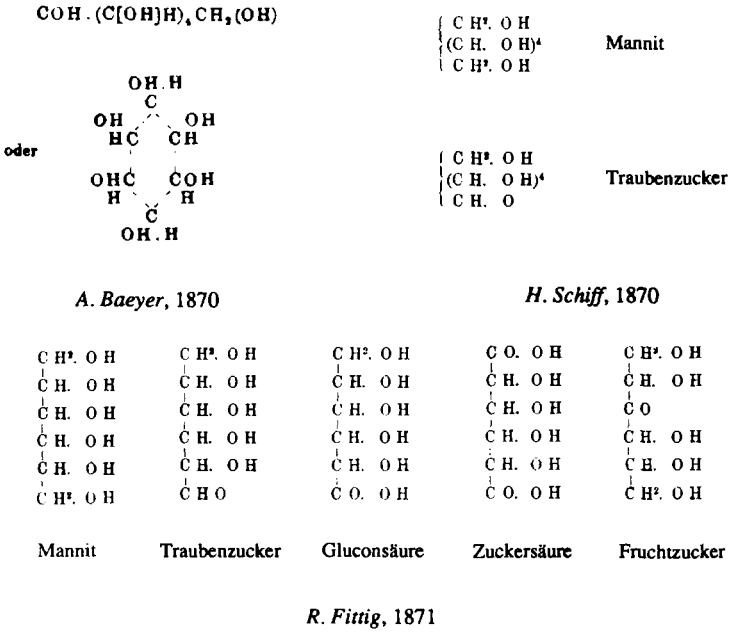

Fig. 5. Structural concepts on sugars around 1870 by Adolf Baeyer [28], Hugo Schiff [29], and Rudolph Fittig [30].

A year after Tollens's intuitive foresight, that is, in 1884, Emil Fischer began his studies with sugars and phenylhydrazine. He found that when heated with this base, glucose and fructose yielded the same, beautifully crystalline compound, which, unlike the free sugars, was readily characterizable; it was designated "phenylglucosazone". Fischer noted that the course of the reaction with these sugars was decisively different from that of standard aldehydes, but understandably, the individual steps of the osazone formation were not clear initially.[24] He formulated only the stoichiometric equation (Fig. 8 top) with the commentary "I cannot say anything definite yet on the fate of the two hydrogen atoms".

In an ensuing paper from 1887,[32] Fischer discovered the intermediate phenylhydrazone by performing the reaction in the cold. Thus, he was able to supply the necessary information for deducing the correct constitutional formula (Fig. 8 bottom).[32]

These hydrazones and osazones have not only rendered invaluable service for the identification and isolation of the

Fig. 6. Bernhard Tollens (1841–1918) in 1890 [6].

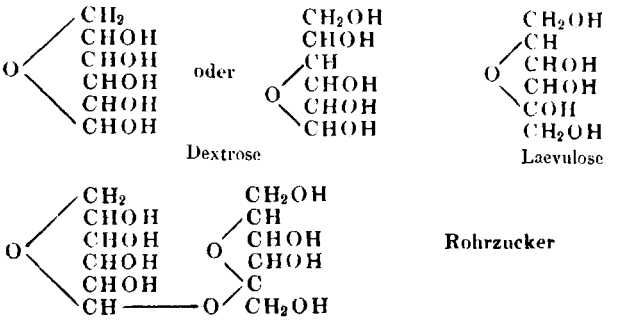

Fig. 7. Tollens' 1883 conception of cyclic hemiacetal formulas for glucose ("Dextrose"), fructose ("Laevulose"), and sucrose ("Rohrzucker") [31].

then existing sugars, but also have been instrumental in the preparation of new ones. At this early stage of his studies, in 1887, Fischer discovered a new hexose in this way: gentle oxidation of mannitol with nitric acid and exposure of the resulting mixture to phenylhydrazine led to a phenylhydrazone, isomeric with the one generated from glucose. By the acid hydrolysis of this product he obtained an as yet unknown hexose, which he named mannose.[33] This study soon led to an important conceptual result: glucose and

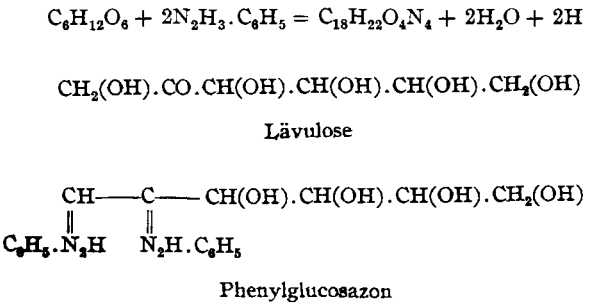

Fig. 8. Formation of osazones from glucose and fructose ("Lävulose") [24, 32].

mannose yield different hydrazones but the same osazone (Fig. 9), hence they must be 2-epimeric aldoses. For the rationalization of these data Fischer, in a 1889 paper with Hirschberger,[34] made use of the Le Bel–van't Hoff theory for the first time:

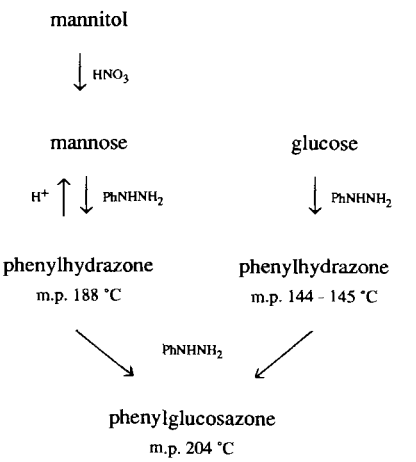

Fig. 9. Glucose and mannose yield the same osazone.

"In the sugar group, dextrose and mannose are the first examples of two isomers, which have the same structure and can be converted into each other. For the explanation of this form of isomerism, we draw entirely on the principles of the Le Bel–van't Hoff theory.
The formula contains four asymmetric carbon atoms, which we find appropriate to differentiate by the designations as_1, as_2, as_3, and as_4:

$$\underset{as_1}{CHO.CHOH}.\underset{as_2}{CHOH}.\underset{as_3}{CHOH}.\underset{as_4}{CHOH}.CH_2OH$$

Each of these carbon atoms causes the existence of two geometric isomers, yielding no less than 16 isomers predicted by theory. From the experimental material at hand it can now be easily proved that the isomerism of dextrose and mannose is determined by carbon atom as_1. The phenylhydrazones of the two sugars are distinctly different, yet with particular ease they give the same osazone with the structural formula

$$HC(N_2HC_6H_5).C(N_2HC_6H_5).\underset{as_2}{CHOH}.\underset{as_3}{CHOH}.\underset{as_4}{CHOH}.CH_2OH$$

in which carbon as_1 has lost its asymmetry. Since it is highly improbable that the carbon atoms as_2, as_3, and as_4 change their steric arrangements during the smooth and particularly easy osazone formation, one must assume that the difference between mannose and dextrose rests on the asymmetry of carbon atom as_1."[34]

The accessibility of mannose was soon greatly improved by its discovery in nature, first in salep mucilage[35] and then in the seeds of the tagua palm,[36] also known as ivory nut, at the time a commercial product used to make buttons. Ivory nut turned out to be a mannose polysaccharide, which yielded a sugar on acid hydrolysis that was identical with the product obtained by gentle oxidation of mannitol (Fig. 10). By further oxidation with bromine water the corresponding aldonic acid was prepared, whilst more rigorous oxidative conditions (HNO_3) led to the aldaric acid, which on the basis of their derivation were named mannonic and mannaric acid, respectively:[37]

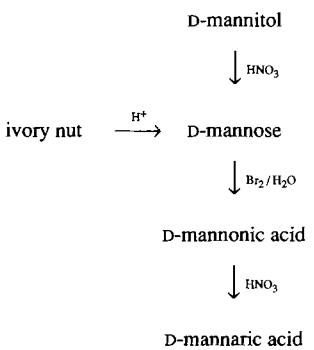

Fig. 10. Elaboration of the ensuing chemistry of mannose after it became available on a large scale by the acid hydrolysis of ivory nut shavings [37, 38].

The experimental difficulties encountered in this type of work because of the techniques available around 1890 were formidable, which made great demands on the experimental skill and patience of Fischer's Ph.D. students who carried out the work. The following excerpt from a letter of Fischer's to his mentor and friend A. Baeyer, dated January 12, 1889, gives ample proof thereof:[39]

"The investigations on sugars are proceeding very gradually. It will perhaps interest you that mannose is the geometrical isomer of grape sugar. Unfortunately, the experimental difficulties in this group are so great, that a single experiment takes more time in weeks than other classes of compounds take in hours, so only very rarely a student is found who can be used for this work. Thus, nowadays, I often face difficulties in trying to find themes for the doctoral theses."

The research of Heinrich Kiliani (1855–1945[40]) proceeded parallel to these studies. His application of the cyanohydrin reaction for the reduction of sugars in 1885[41] was to have a major bearing on unraveling the sugar configurations. The polyhydroxy acids resulting from the hydrolysis of the hydrocyanic acid adducts contained one more carbon atom than the parent sugar, and on reduction with hydrogen iodide/red phosphorus afforded the corresponding "dehydroxylated" carboxylic acids. In this way, Kiliani established that the natural arabinose is a straight-chain aldopentose (1887)[42] and convincingly proved that glucose and galactose are aldohexoses,[43, 44] and that fructose must be a 2-ketohexose since it forms a 2-methyl-branched hexanoic acid (Fig. 11).[41]

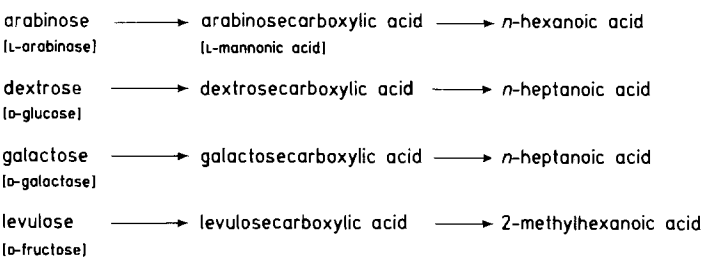

Fig. 11. Kiliani's results, 1885–1889, on the cyanohydrin extension of the sugars, and his proof of their straight-chain nature by reductive "dehydroxylation" with hydrogen iodide/red phosphorus to the corresponding alkanoic acids [41–44].

At this stage of the gradually unfolding interrelationships between the sugars in that still very "black box", an observation was made by Fischer that was to lead to a key insight: the mannonic acid obtained from mannose derived from ivory nut on gentle oxidation proved to be identical—in the form of its nicely crystalline lactone—with that obtained by Kiliani from natural arabinose by cyanohydrin extension, except for the sign of rotation[45] (Fig. 12). Consequently, the two products had to be mirror images, that is, enantiomers—a conclusion Fischer corroborated by comparing the corresponding 1,6-dicarboxylic acids, the sugars themselves, and the sugar alcohols,[44] thus providing an entire set of enantiomeric products. In an 1890 lecture Fischer attests to the conceptual importance of these results:[46]

"The observation that the mannonic acid obtained by oxidation of natural mannose is the optical isomer of ara-

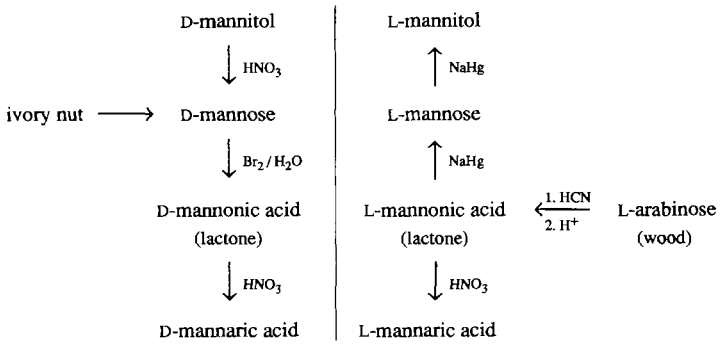

Fig. 12. Elaboration of the first complete set of enantiomers in the sugar group by Fischer [45].

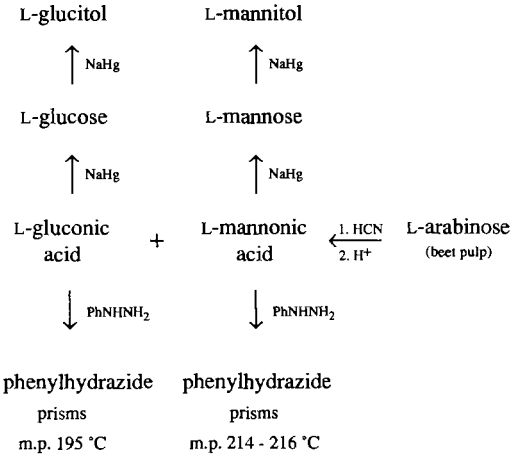

Fig. 13. The first example of an asymmetric synthesis recorded in the literature: not only L-mannonic acid is formed by cyanohydrin synthesis from L-arabinose, but also the 2-epimeric L-gluconic acid, as evidenced by its crystalline phenylhydrazide [51]

binosecarboxylic acid provided the key to determining the interrelationships in the mannitol group."

Fischer had discovered in 1889 that the lactones of sugar acids could be reduced by sodium amalgam to yield the corresponding aldoses.[47] The combination of this reduction with Kiliani's cyanohydrin procedure, which entered the literature as the Kiliani–Fischer synthesis, did not only become a standard method for the chain extension of sugars, (Fischer applied it extensively for the preparation of heptoses,[48] octoses, and nonoses[48, 49]), but more important for the time around 1890, it enabled the intercorrelation of the relative configurations of the individual sugars.

A 100 years ago the purification and unequivocal identification of a compound was a formidable task, requiring crystallinity of the compound as well as a preferably sharp melting point and a constant optical rotation. Hexonic acids certainly formed crystalline lactones, but only under special conditions, and since these lactones exhibited mutarotation, their rotational values were not very useful for comparisons. Here for a second time, phenylhydrazine—and as serendipitously as for the formation of the osazones—proved to be a most useful reagent: when heated with an aldonic acid in aqueous acetic acid, the phenylhydrazides of these acids are formed, which crystallize exceedingly well, exhibit sharp melting points and constant rotational values, and thus, were ideal derivatives for the purification and identification of such sugar acids.[50]

Accordingly, when Fischer repeated Kiliani's work on the C_1 extension of the arabinose derived from sugar beet, and—for identification purposes—heated the reaction mixture (allegedly containing only L-mannonic acid) with phenylhydrazine, he obtained not one, but two phenylhydrazides. Both crystallized in the form of prisms, but their melting points were 20 °C apart.[50] After a lengthy purification procedure he succeeded in isolating the one with the lower melting point in pure form (Fig. 13), which, upon hydrolysis, proved to be the enantiomer of the acid derived from natural glucose by gentle oxidation. In this way a second complete set of enantiomers, namely D- and L-glucose, became available.[51]

As it turned out, this is the first example of an asymmetric synthesis recorded in the literature, on which Fischer commented in the following way:[52]

"The simultaneous formation of the two stereoisomeric products on the addition of hydrogen cyanide to aldehydes, which was observed here for the first time, is quite remarkable in theory as well as in practice."

This first example of an asymmetric synthesis was soon to be followed by a second case, since sodium amalgam reduction of fructose gave rise to two stereoisomeric products, namely, mannitol and sorbitol.[53] Fischer clearly realized the basic importance of this result:

"The reduction of fructose is the second reaction in the sugar group, which generates two stereoisomeric products due to the formation of an asymmetric carbon atom. The same phenomenon will undoubtedly be observed much more frequently in the future, and most probably will be generally found with all compounds that are asymmetric a priori."[53]

Another milestone in the quest for the configurations of sugars proved to be the ensuing chemistry of xylose.[54] The discovery of this sugar in cherry gum in 1886[55] and the establishment of its pentose structure by Tollens et al. two years later[56] came at a most opportune time for Fischer's work. In 1890 he undertook a study of xylose by applying the cyanohydrin synthesis, which led to a hexonic acid different from any yet encountered.[57, 58] It could be reduced to a new sugar and oxidized to a 1,6-dicarboxylic acid, which proved to be the enantiomer of the one obtained from natural glucose. This new sugar was named gulose by Fischer "by exchanging the letter l and u in glucose and eliminating the c".[58] Figure 14 summarizes these interrelationships, refraining from the use of chemical formulas—as Fischer did at the time—yet providing the D- and L-assignments later adopted[38a, b] for clarity.

The correlation between D-glucose and D-gulose revealed by this set of reactions, and particularly the fact that they become identical—as mirror images—at the stage of their dicarboxylic acids, must have given Fischer the strong indication that the two sugars are head-to-tail enantiomers, that is, that gulose has its aldehyde group where glucose has the hydroxymethyl function, and vice versa. This rationalization was soon confirmed by another set of reactions starting from D-glucose-derived 1,6-dicarboxylic acid (D-glucaric acid), in

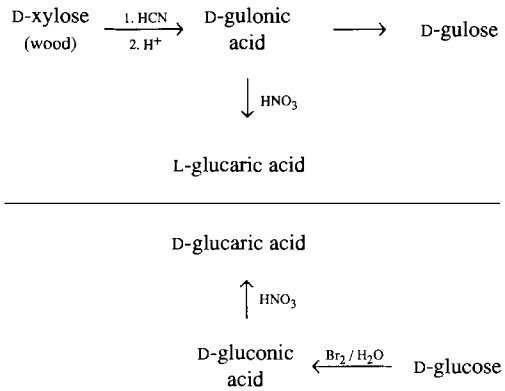

Fig. 14. Experiments which show that D-glucose and D-gulose—on the basis of their 1,6-dicarboxylic acids—are head-to-tail enantiomers. [58, 59].

the form of its 1,4-lactone:[59] sodium amalgam reduction first led to D-glucuronic acid, which was identical with the compound isolated from urine 12 years before by Schmiedeberg and Meyer.[60] Further reduction generated L-gulonic acid,[59, 61] the optical antipode to the hexonic acid obtained from D-xylose by cyanohydrin synthesis.[62] In turn, the 1,4-lactone of L-gulonic acid gave L-gulose on treatment with sodium amalgam.[59]

The level of comprehension reached by these sets of intercorrelating reactions is clearly evident from a passage of the relevant paper published with Piloty:[59]

"A simple consideration shows that gluconic and gulonic acid have the same structure and a very similar configuration. They differ only in the position of the carboxyl group as illustrated by the two formulas,

$$COOH.CHOH.CHOH.CHOH.CHOH.CH_2OH$$

$$CH_2OH.CHOH.CHOH.CHOH.CHOH.COOH$$

which are to be viewed stereometrically. Thus, gluconic and gulonic acid are the first examples of stereoisomeric substances which give identical products if the molecule is symmetrical after the conversion of the terminal alcohol groups into carboxyl functions. This observation appears to be an important confirmation of the theory of the asymmetric carbon atom, which predicts 16 isomers for a compound having the structure of gluconic acid; in the case of dibasic acids, their number is reduced to 10. This indicates that one will soon be in a position to determine the configurations of the sugars in terms of the Le Bel–van't Hoff theory from the factual observations made."

Although the structural formulas given in the citation were to be viewed "stereometrically", half a year prior to his two 1891 landmark papers[4, 5] Fischer still avoided the use of configurational representations—an attitude that dramatically changed after unraveling them.

Now, before discussing the actual proof contained in these two publications, a final piece of evidence has to be mentioned which was to have major bearing on uncovering the configurational relationships, namely, the rotational values of the pentose-derived sugar alcohols and 1,5-dicarboxylic acids. The two pentoses known at the time, xylose and arabinose, gave the respective pentitols on reduction, neither of which showed any rotation.[58, 63] This meant that both are *meso* compounds (Fig. 15). For Fischer, however, this conclusion was too important to be based on the optical inactivity of one compound only, especially since it was known that the alditols encountered so far had comparatively small rotational values.

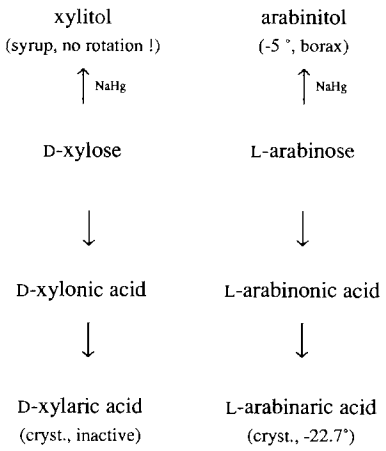

Fig. 15. Correlation between configuration and optical activity of the pentitols and their trihydroxyglutaric acids.

To substantiate this conclusion, Fischer prepared the respective 1,5-dicarboxylic acids by nitric acid oxidation, which each gave crystalline products (Fig. 15). The trihydroxyglutaric acid derived from xylose was indeed optically inactive,[64] yet the arabinaric acid showed a distinct negative rotation. Therefore, Fischer again inspected the rotation of the arabinitol; only on addition of borax, that is, with arabinitol in the form of its boric acid complex, was a small negative rotation finally observed,[58] thus completing the scheme (Fig. 15).

In this context, we are in the fortunate position to add some personal details to these sober experimental facts. In Fischer's autobiography "Aus meinem Leben"[19] there is a delightful passage, which refers to the trihydroxyglutaric acids, and I would like to quote the relevant section:[65]

"The Easter Holidays of 1891 I spent at Bordighera on the Italian Riviera in the company of Baeyer. Needless to say, on our extensive walks, and during the meals we took together, we had intense discussions; there was no important problem of chemistry which we would not have covered. I particularly remember one stereochemical question. In the preceeding winter of 1890/91 I was occupied with the task of clarifying the configuration of the sugars without completely achieving my goal. In Bordighera the idea occurred to me to make the decision concerning the configuration of the pentoses from their relationships to the trioxyglutaric acids. Unfortunately, due to the lack of models I could not determine how many of such acids were theoretically possible, and thus, I put this question to Baeyer. He took up such questions with great warmth and immediately started to construct carbon atom models from toothpicks and little balls of bread. However, after many attempts he finally gave up, allegedly because it

Fig. 16. Jacobus Henrikus van't Hoff (1852–1911) around 1889 [6].

became too difficult for him. Later only back in Würzburg, I succeeded in finding the final solution by extensive study of good models."

The solution Fischer succeeded in finding was based on the theory of Le Bel and van't Hoff.[2, 3] On the basis of purely theoretical considerations, van't Hoff (Fig. 16) had predicted in 1874 that for the case with four chiral carbon centers 16 isomers can be expected. These 16 isomers of the general formula

$$C(R^1R^2R^3)\,C(R^4R^5)\,C(R^4R^5)\,C(R^1R^2R^3)$$

were formulated by van't Hoff as depicted in Figure 17, in which the + and − signs allude to the sign of rotation of the individual chiral centers.

1	2	3	4
+	+	−	−
+	−	+	−
+	−	+	−
+	+	−	−

11	12	13	14	15	16
+	+	+	+	+	−
+	+	+	−	−	+
+	−	−	+	−	−
−	+	−	−	−	−
−	+	−	−	−	−
+	−	−	+	−	−
+	+	+	−	−	+
+	+	+	+	+	−
5	6	7	8	9	10

Fig. 17. Van't Hoff's prediction of configurational isomers for compounds with four chiral carbon centers, in his + and − notation [3].

Accordingly, the isomers 1 and 4 are enantiomers, as are the isomers 2 and 3; the other twelve possibilities are listed in such a way as to illustrate the head-to-tail mirror-image symmetry: isomer 5 is the enantiomer of 11, this relationship is also valid for 6 and 12, 7 and 13 etc. In the case where both ends have identical substitutents, as in the hexitols and 1,6-dicarboxylic acids, the isomers 5–10 become identical with 11–16, so the total number of isomers then would be reduced to 10.

The task with which Fischer had been occupied in the years preceeding 1891 was a formidable one: to select the configuration from the sixteen possibilities that represent grape sugar, on the basis of the experimental evidence that had been accumulated. This required models. Those van't Hoff used for his theoretical deductions are shown in Figure 18. Fischer must have used these too, since van't Hoff[3] gave detailed instructions on how to prepare them from cardboard in an appendix to his brochure.

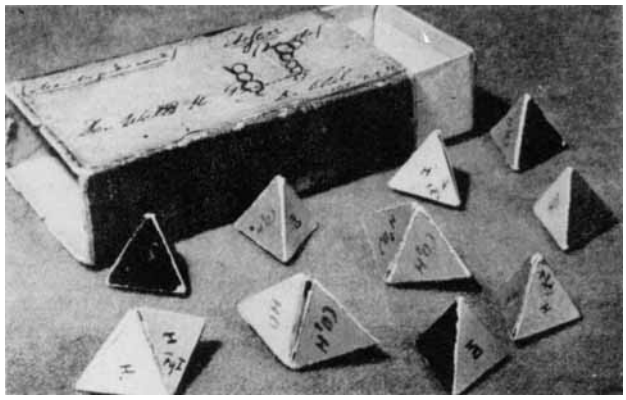

Fig. 18. "Match box" models of van't Hoff (preserved in the chemistry museum of the Maison de la Chimie of the French Chemical Society, Paris).

In his second landmark paper of 1891,[5] however, Fischer also referred to the use of "Friedländer rubber models", the essentials of which were described by V. Meyer:[66]

"They consist of four short pieces of rubber tubing, whose inner diameter is approximately the thickness of a match, and which are soldered together in the middle, so that they extend into space in a tetrahedral arrangement."

These models appear to be very close to the ball and stick models, or those of the Fieser or Dreiding type in use today. Evidently as a result of his extensive use of models, and his intense intellectual involvement in correlating the experimental data available with the 16 sugar configurations available, Fischer arrived at the solution laid down in his first 1891 paper: grape sugar, the natural glucose, has the −+++ configuration (Fig. 19), D-mannose has the ++++ configuration, and D-fructose with only three asymmetric centers, correspondingly, +++.[4]

Now, rather than presenting the Fischer proof of the sugar configuration in the terms of the van't Hoff notation, it is more appropriate and expedient to proceed here as Fischer did: within two months of proposing the sugar configurations in the +/− terminology, he discarded this system altogether, and replaced it by his own. There was ample reason for that. The + and − signs used by van't Hoff for designating the configurations at asymmetric carbon atoms are very confusing, because they are derived by observing the individual tetrahedra—as arrayed in a model (Fig. 20)—from a point within the model, namely, its center. This refers to the center of the whole molecule and not that of an individual tetrahedron. For tartaric acid, the center of the molecule is clear: its the apex where the two tetrahedra are joined (marked by an asterisk in Figure 20); on looking up from that point of reference, the sequence of OH → H is perceived to be counterclockwise, so the asymmetric carbon atom receives a − sign, whereas looking down from the apex results

Aldosen: $COH.CH(OH).CH(OH).CH(OH).CH(OH).CH_2OH$

d. Glucose	−	+	+	+
l. Glucose	+	−	−	−
d. Mannose	+	+	+	+
l. Mannose	−	−	−	−

Ketosen: $CH_2OH.CO.CH(OH).CH(OH).CH(OH).CH_2OH$

d. Fructose	+	+	+
l. Fructose	−	−	−

Alkohole: $CH_2OH.CH(OH).CH(OH).CH(OH).CH(OH).CH_2OH$

d. Sorbit	−	+	+	+
l. Sorbit	+	−	−	−
d. Mannit	+	+	+	+
l. Mannit	−	−	−	−

Zweibasische Säuren:
$COOH.CH(OH).CH(OH).CH(OH).CH(OH).COOH.$

d. Zuckersäure	−	+	+	+
l. Zuckersäure	+	−	−	−
d. Mannozuckersäure	+	+	+	+
l. Mannozuckersäure	−	−	−	−

Fig. 19. Fischer's configurational assignments to glucose, mannose, and fructose in the van't Hoff notation [4].

in a clockwise order of OH towards H, and it is given a + sign. The signs compensate each other, as would do the individual rotational contributions of the two carbon atoms, hence they denote the *meso* form of tartaric acid.

The situation becomes more difficult in cases with three chiral centers, since the "center" of the molecule has to be defined. For pentoses this was placed at the apex between the first and second asymmetric carbon (see position of the asterisk in Fig. 20, center), which results in a + + + sequence of signs for D-arabinose. In hexoses, the point of reference is again the center of the molecule, (Fig. 20 right) which results in the − + + + sequence for D-glucose.

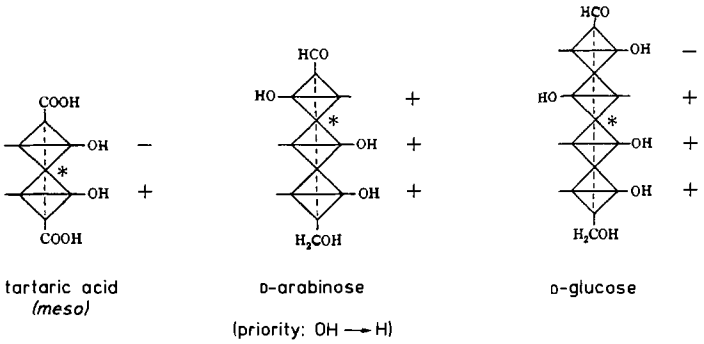

Fig. 20. Derivation of van't Hoff's + and − signs from the "center" (marked by *) of the respective molecules.

Fischer soon realized[5] that "the designation of spacial relationships by + and −, which were introduced by van't Hoff and which were retained by me in unchanged form, can easily lead to an erroneous view in the case of such complicated molecules. To prevent this, I consider a more detailed interpretation of the formula an urgent necessity."

Thus, within two months after the submission of the first 1891 paper (received at Berichte on June 6[4]) Fischer dispatched a second one (received: August 8[5] (Fig. 21) in which he replaced the + and − system of van't Hoff by his

48. Emil Fischer: Über die Konfiguration des Traubenzuckers und seiner Isomeren. II.

[Aus dem chemischen Laboratorium der Universität Würzburg.]

(Eingegangen am 8. August.)

In der ersten Abhandlung[1]) habe ich für den Traubenzucker die Formel

$CH_2(OH).CH(OH).CH(OH).CH(OH).CH(OH).COH$
$\quad + \quad + \quad + \quad -$

entwickelt. Die Bezeichnung der räumlichen Anordnung durch + und −, welche von van't Hoff eingeführt und von mir in unveränderter Form beibehalten wurde, kann aber bei solchen komplizierten Molekülen leicht eine irrtümliche Auffassung zur Folge haben. Um dies zu verhüten, halte ich eine ausführlichere Interpretation der Formeln für nötig.

COOH	COOH
H — C — OH	HO — C — H
HO — C — H	H — C — OH
H — C — OH	HO — C — H
H — *C — OH	HO — C — H
COOH	COOH

Ich wähle wieder willkürlich für die *d*-Zuckersäure die Form I, wobei es natürlich unentschieden bleibt, ob bei dem mit * bezeichneten Kohlenstoffatom die Reihenfolge von Hydroxyl und Wasserstoff im Sinne des Uhrzeigers oder umgekehrt statthat. Dann ergeben sich für Traubenzucker und seine Isomeren folgende Formen:

COH	COH	COH	COH
H — C — OH	HO — C — H	HO — C — H	H — C — OH
HO — C — H	H — C — OH	HO — C — H	H — C — OH
H — C — OH	HO — C — H	H — C — OH	HO — C — H
H — C — OH	HO — C — H	H — C — OH	HO — C — H
CH_2OH	CH_2OH	CH_2OH	CH_2OH
Traubenzucker	*l*-Glucose	*d*-Mannose	*l*-Mannose

Fig. 21. The second of Fischer's 1891 landmark papers on the configurations of the sugars, with which he introduced the Fischer mode of writing stereoformulas [5].

own: representation of tetrahedral space relationships by their projection into a plane. The resulting formulas were simple to write and easy to visualize, yet required the setting up of conventions; the ones he chose seem as few in number and as simple in character as possible: The carbon chain of a sugar is oriented vertically and to the rear with the aldehyde group at the top; the hydrogen atoms and hydroxyl groups at the asymmetric carbon atoms stand out in front. The resulting three-dimensional model is then imagined to be flattened and the groups are laid on the plane of the paper. If the lowermost asymmetric center (i.e., C-5 in glucose) has the OH group to the right, it is considered to have the D-configuration. Fischer's decision to place the OH group of natural glucose to the right, hence D-glucose, was purely arbitrary, yet proved to be a fortunate one, since much later in 1951, it was proved by special X-ray structural techniques[6,7] that he had made the right choice.

The change of the + and − notation to the projection mode of writing stereoformulas is strikingly evident in the second 1891 paper,[5] (Fig. 21) and this was soon universally adopted. In this presentational mode, by using Fischer's convention that the asymmetric carbon atoms (tetrahedra) have the lower edge in the plane of the paper whilst the corners carrying the H and OH groups lie above this plane can now be delineated.[6,8]

1. Since glucose was selected by definition as having the OH group at the lowermost asymmetric carbon atom at the

right, all chemically interrelated compounds are of D-configuration:

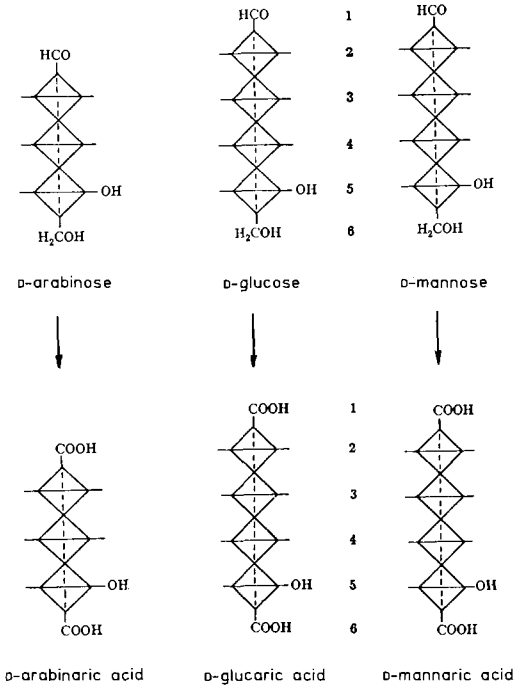

2. The D-arabonic acid showed a distinct optical rotation, thus cannot be a *meso* compound. This means that the OH group at C-2 of D-arabinaric acid must be to the left and thus determines the relative configuration at C-3 of the two hexoses. Therefore, in the entire set of compounds depicted here the OH group is to be placed to the left:

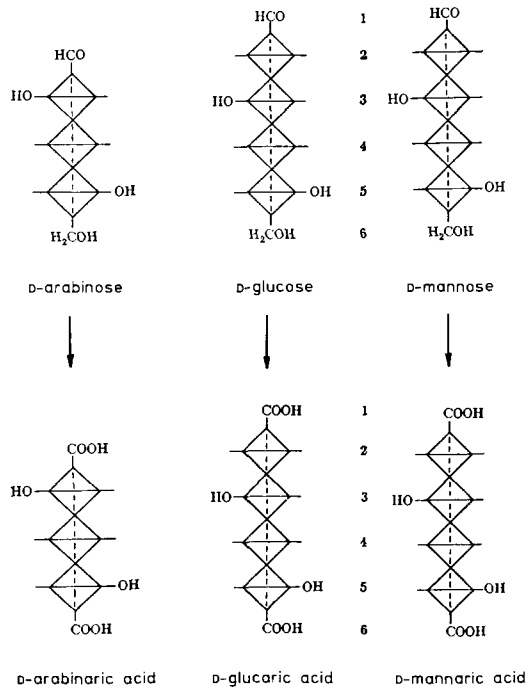

3. D-Glucose and D-mannose are C-2 epimers; hence their 2-hydroxyl groups are oriented in opposite directions. Either one may be selected as having the OH on the right; in the following Figure D-glucose is—for now—arbitrarily considered to have the C-2 OH group to the right, and consequently this group is oriented to the left in D-mannose:

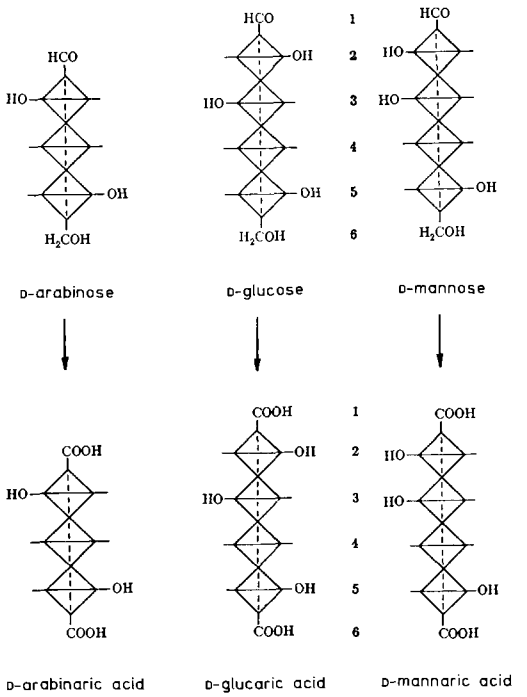

4. Since both D-glucaric and D-mannaric acids are optically active, the configuration of neither of them can possess end-to-end symmetry; hence the OH group on C-4 must be on the right (if it were on the left, the glucaric acid would have end-to-end symmetry and, hence be optically inactive). At this stage the configuration of D-arabinose and its dicarboxylic acid have been established:

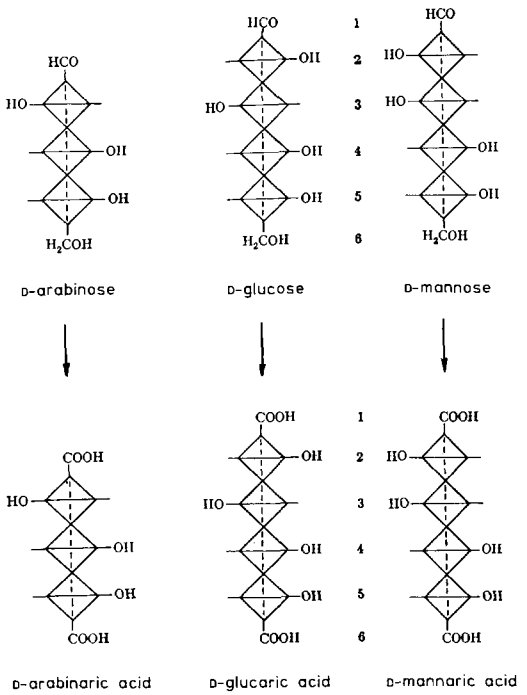

5. D-Glucose and D-mannose have been limited to two configurations but final specification remains to be established. This was done on the basis of the following reason-

ing: D-glucaric acid is obtained from the oxidation of D-glucose, the enantiomeric L-glucaric acid analogously from L-glucose, but also from D-gulose. This is only possible, if D-gulose is the head-to-tail configurational isomer to L-glucose:

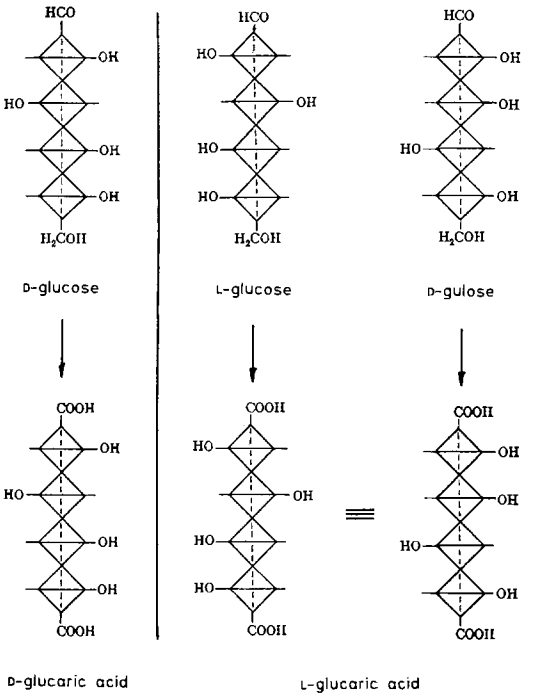

D-Gulose, upon exchange of its aldehyde group with CH_2OH and vice versa, yields a different aldose, namely, L-glucose. Applying the same operation to D-mannose, the product is again D-mannose, thus providing a further substantiation of conclusions 1–5:

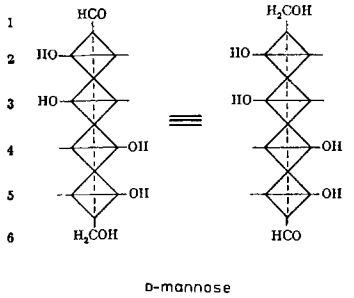

Thus, the deduction is now in itself conclusive. This proof not only became the basis for the sugar family tree (Fig. 22) as it is—100 years later—in our textbooks today; it also provided a major impulse for the development of organic stereochemistry, which thereafter made rapid and sweeping progress. Up to 1891 relative configurational assignments are not found in the literature. As it turned out, the sugars became the point of reference on which all other configurations—those of hydroxy acids and amino acids in particular—were based by chemical correlation. So, we are con-

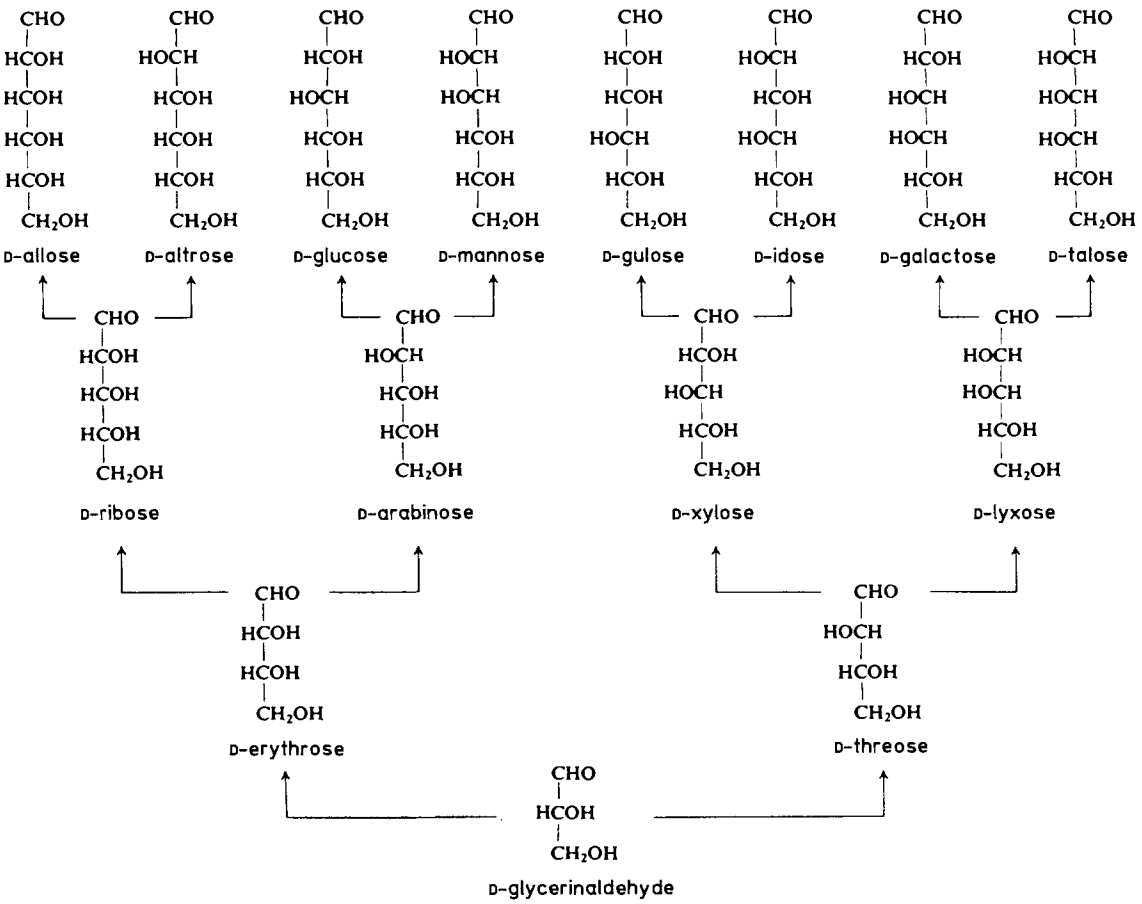

Fig. 22. The sugar family tree of D-aldoses.

fronted with the paradox that at this stage the development of chemistry did not proceed from the understanding of simple cases to the gradual comprehension of more complex ones, but vice versa.

In this context, a number of contemporaries had all the knowledge at hand to unravel the sugar configurations—Kiliani,[69] for example, and Tollens, who later was to write the first comprehensive treatise on carbohydrate chemistry[70]—but it was Emil Fischer who, endowed with a brilliant mind and the necessary self-confidence and perseverance, attacked the problem systematically and after only seven years of involvement with the chemistry of the sugars found the solution.

This classical piece of work was not to remain the only great service Fischer rendered to chemistry, since later he returned to the work he had started in 1882 in Munich on purines. This led to the classification of this class of substances[71] and subsequently to the synthesis of the first nucleosides.[72] Around the turn of the century Fischer began his third great series of investigations on amino acids, polypeptides, and proteins and laid the chemical and biochemical foundations for this field.[13] Finally in 1908 he began work on a further class of natural products, the tannins.[74] The brilliant synthetic work in the sugar series, however, and the manner in which he applied and developed the van't Hoff–Le Bel theory for elucidating their stereochemistry stands out—in my opinion—as the pinnacle of his scientific career.

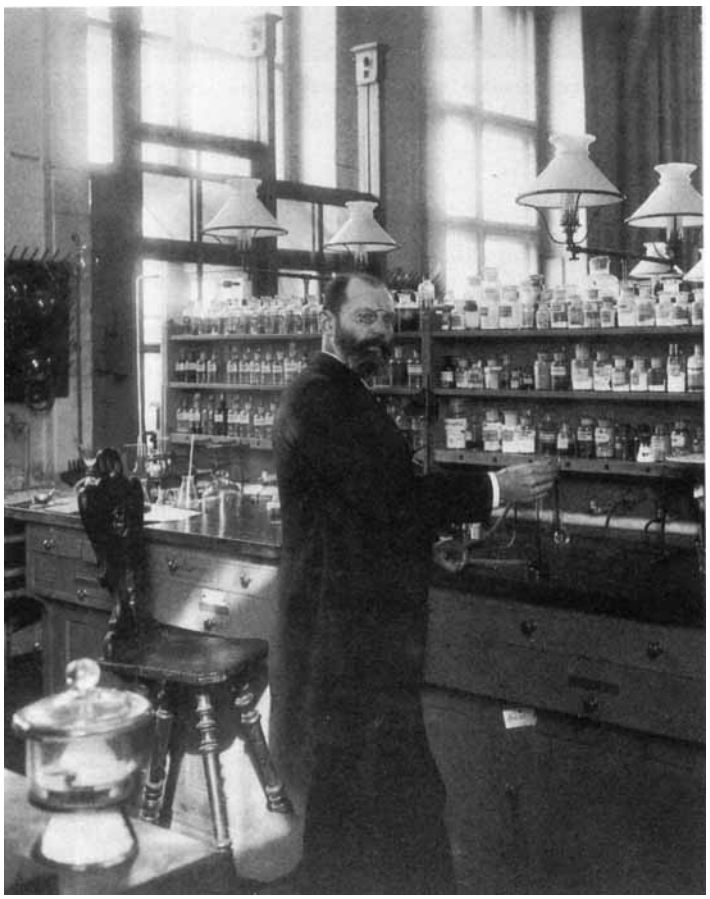

Fig. 23. Emil Fischer around the turn of the century in his laboratory at the University of Berlin [18].

Not only we today, a century later, marvel at this classic example of exact mathematical reasoning in an experimental science, and at the man who accomplished it; his contemporaries also recognized his genius by bestowing many honors on Fischer of which two are mentioned here: in 1892 at the age of 40, mostly on the basis of his work on the sugars, Fischer was offered the most coveted chair of chemistry at the time, at the University of Berlin (Fig. 23), to become successor to A. W. von Hofmann (1818–1892), and in 1902 he was awarded the Nobel Prize in chemistry, the second one ever to be awarded; notably, the recipient of the first in 1901 was van't Hoff. The president of the Royal Swedish Academy of Sciences put his appreciation into the following words:[75]

> "The specific type of research which has characterized organic chemistry during the final decades of the nineteenth century, attained its zenith of development and its finest form in Fischer's studies of sugars and purines. From the experimental point of view they are unsurpassed."

In concluding this centennial tribute to one of the really great figures of our science, a passage from his 1890 lecture at the Universiy of Berlin, in which he outlined the strategy he followed in the pursuit of the sugar configurations, may give a final glimpse of the spirit of the man in his quest for knowledge:[76]

> "I would like to compare chemical investigations of this sort which become more difficult with every step, with the construction of a tunnel. If a mountain ridge is not too wide, one succeeds in driving the tunnel through in one direction. Otherwise, the engineer is forced to start work from the opposite site. However, he is in the fortunate position of being able to predetermine the site of the attack by exact measurements and, thus, is assured of joining the tracks inside.
>
> Our science, unfortunately, is as yet not deductive enough to allow such calculations. The chemist may consider himself fortunate if he drives his tunnels through matter from opposite sites and finds the connection inside, albeit after several zigzag moves. Such a piece of good luck led me to the target."

This should remind us that hard experimental work, clear evaluation of results, mathematical reasoning, and a superb strategy is not all. A piece of serendipity is also involved in the solution of the fundamental problems of science.

Received: April 30, 1992 [A 885 IE]
German version: *Angew. Chem.* **1992**, *104*, 1577

[1] A. Kekulé, *Bull Soc. Chim. Fr.* **1865**, *3*, 98; *Justus Liebigs Ann. Chem.* **1866**, *137*, 129; K. Hafner, *Angew. Chem.* **1979**, *81*, 685; *Angew. Chem. Int. Ed. Engl.* **1979**, *18*, 641.

[2] J. A. Le Bel, *Bull. Soc. Chim. Fr.* **1874**, *22*, 337.

[3] J. H. van't Hoff, *Die Lagerung der Atome im Raume*, Vieweg, Braunschweig, **1877**. This, at the time widely distributed, 53-page booklet is the thoroughly revised German version of van't Hoff's brochure *La chimie dans l'espace* (Bazendijk, Rotterdam, **1875**), which, in turn, is a French translation (by van't Hoff himself) of the original Dutch text *Voorstel tot uitbreiding der tegenwoordig in de scheikunde gebruikte structurformules in*

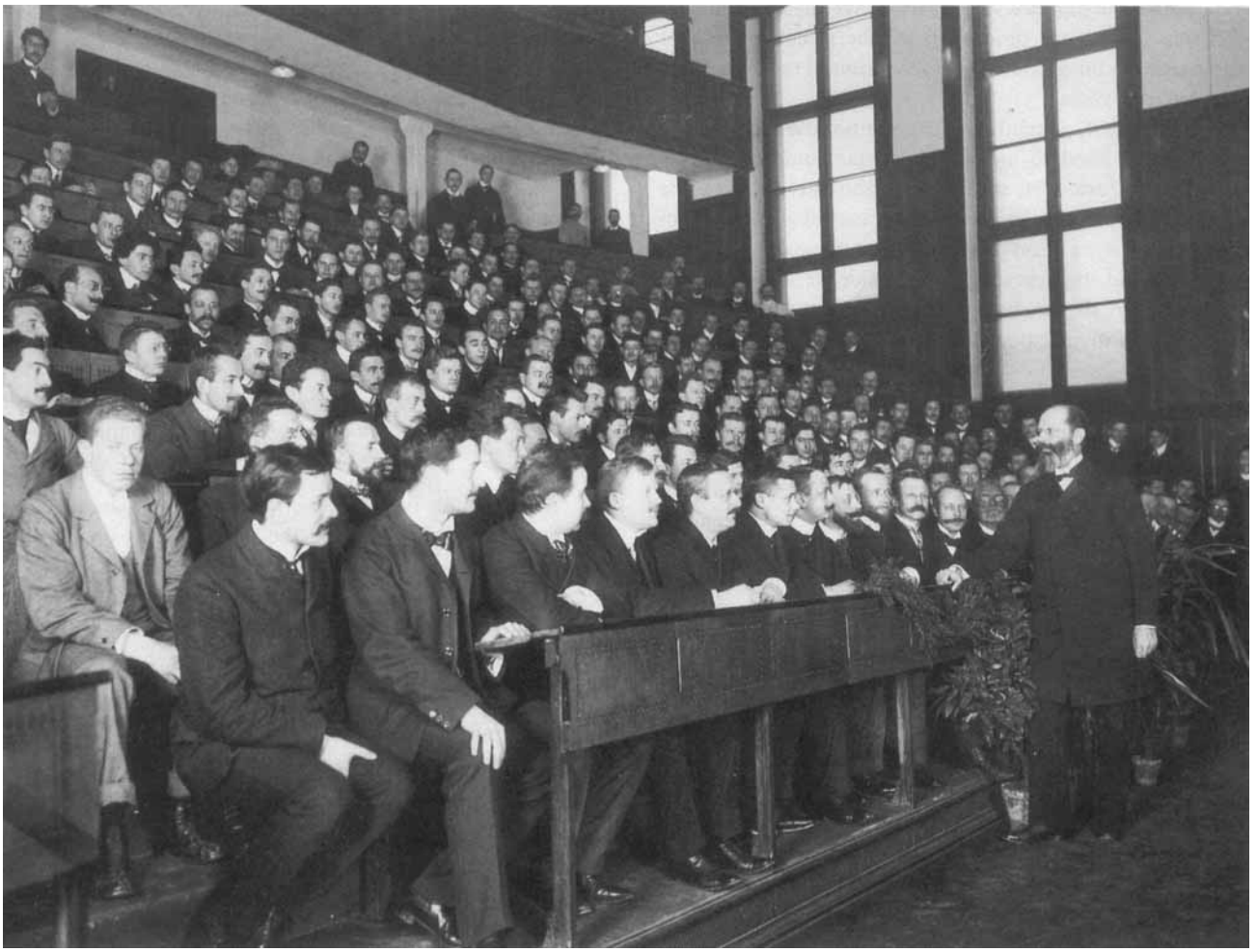

Fig. 24. Festive Colloquium on December 16, 1902 in the Fischer Lecture Hall of the Chemical Institute of the University of Berlin, in honor of Emil Fischer having received the Nobel Prize in Chemistry the week before [18].

de reimte (Greven, Utrecht, **1874**). The translation into German was done by F. Herrmann instigated by J. Wislicenus, who contributed a most favorable preface, in which he stood up against "the multifold, obstinate misunderstanding of the ideas" (of van't Hoff), by appraising them as "a real and important step forward". E. Fischer used this 1877 German version for his stereochemical deductions referring to it as "Broschüre von van't Hoff-Herrmann".

[4] E. Fischer, *Ber. Dtsch. Chem. Ges.* **1891**, *24*, 1836.

[5] E. Fischer, *Ber. Dtsch. Chem. Ges.* **1891**, *24*, 2683.

[6] Picture from the congratulatory album of photographs presented to August von Kekulé on the occasion of his 60th birthday (September 6, 1889). The original document is in the collection of Kekulé papers, in the Institut für Organische Chemie, Technische Hochschule Darmstadt.

[7] L. Knorr, "Über die wissenschaftlichen Arbeiten und die Persönlichkeit Emil Fischers", *Ber. Dtsch. Chem. Ges.* **1919**, *52*, 132–149.

[8] C. Harries, "Emil Fischer's wissenschaftliche Arbeiten", *Naturwissenschaften* **1919**, *7*, 843–860.

[9] M. O. Forster, "Emil Fischer Memorial Lecture", *Trans. Chem. Soc. (London)* **1920**, *117*, 1157–1201.

[10] K. Hoesch, "Emil Fischer, sein Leben und sein Werk", *Ber. Dtsch. Chem. Ges.* (special issue) **1921**, *54*; also issued as a book with the same title, Verlag Chemie, Berlin/Leipzig (**1922**). This biography, written in an overly pathetic, pompous style appears to been well perceived by many of Fischer's contemporaries, as evidenced by enthusiastic letters of approval from C. Duisberg, A. Gabriel, C. Neuberg and H. Pringsheim [10a]. However, it also met strong criticism; C. Harries who over years had been the assistant in the experimental lecture courses given by A. W. von Hofmann and from 1892 on by E. Fischer, happened to be president of the Deutsche Chemische Gesellschaft, which had commissioned the biography. He strongly disapproved of the fact that he was deprived of seeing the manuscript before publication, and added [10b]: "It is a poetic achievement, a well-accomplished dithyramb on the adored teacher. Unfortunately, however, the author has got carried away by his temperament and made statements that transgress the poetically allowed, which for historical reasons cannot remain uncontradicted. What primarily has to be objected is the comparison of A. W. von Hofmann, Adolf von Baeyer, and Viktor Meyer with Emil Fischer. It is certainly permitted to make comparative evaluations of illustrious personalities, however, a protest must be made about the form, in which this was done here. Quite bluntly the intended portrayal of Emil Fischer unconditionally as the greatest is obvious. A. W. von Hofmann and Viktor Meyer come off quite badly. Instead, we should be delighted that we had such a series of great men, and hence should not attempt to exalt one to be the most important, since each of them more or less stood on th shoulders of the others." R. Willstätter [10c] also criticizes Hoeschs's presentation for lack of depth, insufficient inside knowledge, and its "pathetic style", in sharp contrast with Fischer's refreshing informality. H. O. L. Fischer (1888–1960 [10d]), Emil Fischer's son, initially (1922) approved of the biography: "I am delighted that you have solved your task in a literarily splendid, comprehensive, and sympathetic, warmhearted form" [10a]; in later years (1959), however, he had arrived at a distinctly different opinion: "The Hoesch biography of my father is essentially unreadable, even by an educated German" [10e]. a) The relevant letters to K. Hoesch, dating from 1922 and 1923, are in the Emil Fischer Collection in the Bancroft Library, University of California, Berkeley, the citations given with their kind permission. b) Presentation at a meeting of the Deutsche Chemische Gesellschaft in Berlin on July 3, 1923; the manuscript is in possession of the Bancroft Library. c) R. Willstätter, *Aus meinem Leben*, 3rd edition, VCH, Weinheim, **1979**, p. 212. An English translation was prepared by L. S. Hornig, Benjamin, New York, **1965**. d) H. O. L. Fischer, "Fifty Years in the Service of Biochemistry", *Annu. Rev. Biochem.* **1960**, *29*, 1–14; F. W. Lichtenthaler, *Carbohydr. Res.* **1987**, *156*, 1–22. e) Personal communication to C. E. Ballou and the author.

[11] C. S. Hudson, "Emil Fischer's Discovery of the Configuration of Glucose", *J. Chem. Educ.* **1941**, *18*, 353–357.

[12] C. S. Hudson, "Historical Aspects of Emil Fischer's Fundamental Conventions for Writing Stereoformulas in a Plane", *Adv. Carbohydr. Chem.* **1948**, *3*, 1–22.
[13] K. Freudenberg, "Emil Fischer and His Contribution to Carbohydrate Chemistry", *Adv. Carbohydr. Chem.* **1966**, *21*, 1–38.
[14] J. S. Fruton, *Contrasts in Scientific Style. Research Groups in the Chemical and Biochemical Sciences*, Am. Phil. Soc., Philadelphia, **1990**, pp. 163–229 and 375–403.
[15] E. Fischer, *Ber. Dtsch. Chem. Ges.* **1875**, *8*, 589; G. B. Kauffmann, R. P. Ciula, *J. Chem. Educ.* **1977**, *54*, 295.
[16] T. Curtius, *Ber. Dtsch. Chem. Ges.* **1887**, *20*, 1632.
[17] R. Huisgen, *Angew. Chem.* **1986**, *98*, 297; *Angew. Chem. Int. Ed. Engl.* **1986**, *25*, 303.
[18] The original and numerous other photographs are contained in the Collection of Emil Fischer Papers, housed in the Bancroft Library at the University of California, Berkeley. This scientific bequest consists of 34 boxes of material: lab notes, manuscripts, drafts of his autobiography "Aus meinem Leben", which differ from the published version [19], and about 5000 letters, mostly handwritten that reached Fischer during his 40-year scientific career; for example, 157 letters during 1889–1915 from his teacher A. von Baeyer, others from F. Beilstein (11), A. Hantsch (56), F. Haber (35), J. H. van't Hoff (31), A. W. Hofmann (5), A. von Kekulé (6), H. Kiliani (16), V. Meyer (46), W. Nernst (67), B. Tollens (20), P. Walden (13), O. Wallach (46), and R. Willstätter (33); Fischers intense interaction with industry is documented by 181 letters from C. Duisberg (from 1895–1919), from Bayer (271), BASF (54), Boehringer Mannheim (116), Hoechst (50) and Merck (33). Surprisingly, the collection contains also two letters from Konrad Adenauer, written in 1918 as Lord Mayor of Cologne, concerning the establishment of a Kaiser-Wilhelm Institute for Physiology. The papers eventually reached Berkeley through Fischer's son, Hermann Otto Laurens Fischer, [10d] who carried this collection along with him through all the stations of his unusually cosmopolitan career: Privatdozent in Berlin, Professor of Pharmaceutical Chemistry in Basel, Director of the Banting Institute, Toronto, and Professor of Biochemistry at the University of California, Berkeley. The papers were donated to the Bancroft Library by Mrs. H. O. L. Fischer in November 1970.
[19] E. Fischer, *Aus meinem Leben*, Springer, Berlin, **1987**, (reprint of the original 1922 version with an english commentary by B. Witkop).
[20] E. Fischer, O. Fischer, *Ber. Dtsch. Chem. Ges.* **1876**, *9*, 891; *Justus Liebigs Ann. Chem.* **1878**, *194*, 242; *Ber. Dtsch. Chem. Ges.* **1880**, *13*, 2204.
[21] T. Curtius, J. Bredt, "Wilhelm Koenigs", *Ber. Dtsch. Chem. Ges.* **1912**, *45*, 3787–3830.
[22] W. Koenigs, E. Knorr, *Sitzungsber. Bayr. Akad. Wiss.* **1900**, *30*, 108; *Ber. Dtsch. Chem. Ges.* **1901**, *34*, 957.
[23] E. Fischer, *Ber. Dtsch. Chem. Ges.* **1876**, *9*, 880; *Justus Liebigs Ann. Chem.* **1878**, *190*, 134.
[24] E. Fischer, *Ber. Dtsch. Chem. Ges.* **1884**, *17*, 579.
[25] E. Fischer, *Ber. Dtsch. Chem. Ges.* **1881**, *14*, 637, 1905; *ibid.* **1882**, *15*, 29, 453; *Justus Liebigs Ann. Chem.* **1882**, *215*, 253.
[26] E. Fischer, F. Jourdan, *Ber. Dtsch. Chem. Ges.* **1883**, *16*, 2241; E. Fischer, O. Hess, *ibid.* **1884**, *17*, 559; E. Fischer, *Justus Liebigs Ann. Chem.* **1886**, *236*, 116.
[27] P. A. Roussel, *J. Chem. Educ.* **1953**, *30*, 122; B. Robinson, *Chem. Rev.* **1963**, *63*, 373.
[28] A. Baeyer, *Ber. Dtsch. Chem. Ges.* **1870**, *3*, 67.
[29] H. Schiff, *Ann. Chem. Pharm.* **1870**, *154*, 344.
[30] R. Fittig, *Über die Constitution der sogenannten Kohlenhydrate*, L. F. Fues, Tübingen, **1871**. This 35-page treatise was attached to the invitation for the academic celebration of the birthday of his Majesty, King Karl of Württemberg, on March 6, 1871 and, due to its low circulation, responsible for the oversight of Fittig's contribution by most of his contemporaries. A copy is in the possession of the Hessische Landesbibliothek, Darmstadt, evidently due to the fact that the Grandduke of Hesse, who resided in Darmstadt, received such an invitation.
[31] B. Tollens, *Ber. Dtsch. Chem. Ges.* **1883**, *16*, 923.
[32] E. Fischer, *Ber. Dtsch. Chem. Ges.* **1887**, *20*, 821.
[33] E. Fischer, J. Hirschberger, *Ber. Dtsch. Chem. Ges.* **1888**, *21*, 1805.
[34] E. Fischer, J. Hirschberger, *Ber. Dtsch. Chem. Ges.* **1889**, *22*, 365.
[35] R. Gans, W. E. Stone, B. Tollens, *Ber. Dtsch. Chem. Ges.* **1888**, *21*, 2148; R. Gans, B. Tollens, *Justus Liebigs Ann. Chem.* **1888**, *249*, 256.
[36] R. Reiss, *Ber. Dtsch. Chem. Ges.* **1889**, *22*, 609.
[37] E. Fischer, J. Hirschberger, *Ber. Dtsch. Chem. Ges.* **1889**, *22*, 3218.
[38] In Figures 10–15 the gradually evolving affiliation of the individual sugars and their derivatives to the D- or L-series has already been made. It should be noted though, that Fischer only introduced the symbols *d* and *l* as late as 1890 [38a], deriving their meaning from the sign of rotation: "Since sugar derivations change their sign of rotation from right to left and vice versa, I propose to designate all compounds of a series according to the sign of rotation of the aldehyde with the letters *d* (dextro) or *l* (levo), just like the letters *o*, *m* and *p* are used in the case of benzene derivatives". [38] Only later did Fischer take this a step further, so that the signs *d* and *l* were not uniformly derived from the sign of rotation of the parent sugar, but they were also used to express similar or identical steric arrangements between related compounds. "Thus, I desginated natural fructose, which features the same configuration as *d*-glucose, the *d*-designation despite its levorotation [38b]." Rosanoff in 1906 [38c], and Wohl and Freudenberg in 1923 [38d] brought the use of the *d* and *l* symbols on a logical, genetic basis by selecting the enantiomeric glyceraldehydes as points of reference, such that any sugar belongs to the *d*-series, if it can be derived from *d*-glyceraldehyde by successive Kiliani–Fischer syntheses. For sugars defined in this way Rosanoff originally proposed to use δ- and λ-symbols, which did not gain general acceptance. The present use of the D- and L-notation [38e] started around 1940 [38f]. a) E. Fischer, *Ber. Dtsch. Chem. Ges.* **1890**, *23*, 370; b) *ibid.* **1907**, *40*, 102; c) M. A. Rosanoff, *J. Am. Chem. Soc.* **1906**, *28*, 114; d) A. Wohl, K. Freudenberg, *Ber. Dtsch. Chem. Ges.* **1923**, *56*, 309; e) Rules of Carbohydrate Nomenclature, No. 4 and 5, in *The Carbohydrates, Vol. IIB* (Eds.: W. Pigman, D. Horton), Acad. Press, New York, **1970**, p. 809ff; f) In the monographs of F. Micheel (*Chemie der Zucker und Polysaccharide*, 1st Edition, Akad. Verlagsges., Leipzig, **1939**) and H. Elsner (*Grundriß der Kohlenhydratchemie*, Verlag Parey, Berlin, **1941**) the *d* and *l* symbols are still used exclusively.
[39] The Emil Fischer Collection in the Bancroft Library [18] not only contains the original letters (157) written by Baeyer to Fischer, but also carbon copies of those written by Fischer to his mentor.
[40] W. Hückel, "Heinrich Kiliani", *Chem. Ber.* **1949**, *82*, I-IX.
[41] H. Kiliani, *Ber. Dtsch. Chem. Ges.* **1885**, *18*, 3066; *ibid.* **1886**, *19*, 221.
[42] H. Kiliani, *Ber. Dtsch. Chem. Ges.* **1886**, *19*, 3029; *ibid.* **1887**, *20*, 282, 339.
[43] H. Kiliani, *Ber. Dtsch. Chem. Ges.* **1886**, *19*, 767, 1128.
[44] H. Kiliani, *Ber. Dtsch. Chem. Ges.* **1888**, *21*, 915; *ibid.* **1889**, *22*, 521.
[45] E. Fischer, *Ber. Dtsch. Chem. Ges.* **1890**, *23*, 370.
[46] E. Fischer, *Ber. Dtsch. Chem. Ges.* **1890**, *23*, 2114; quotation from p. 2123.
[47] E. Fischer, *Ber. Dtsch. Chem. Ges.* **1889**, *22*, 2204; *ibid.* **1890**, *23*, 930.
[48] E. Fischer, F. Passmore, *Ber. Dtsch. Chem. Ges.* **1890**, *23*, 2226.
[49] E. Fischer, *Justus Liebigs Ann. Chem.* **1892**, *270*, 64; *ibid.* **1895**, *288*, 139.
[50] E. Fischer, F. Passmore, *Ber. Dtsch. Chem. Ges.* **1889**, *22*, 2728.
[51] E. Fischer, *Ber. Dtsch. Chem. Ges.* **1890**, *23*, 2611.
[52] See [46], p. 2134.
[53] E. Fischer, *Ber. Dtsch. Chem. Ges.* **1890**, *23*, 3684.
[54] a) The naturally occurring levorotatory xylose, that is, D-xylose in todays nomenclature, was originally designated as *l*-xylose by Fischer [58]. Correspondingly, the products resulting from cyanohydrin synthesis, hydrolysis, and reduction were denoted *l*-gulonic acid and *l*-gulose [58]; in the scheme of Figure 14, the D-notation has been applied to these alleged *l*-compounds, as they are all derived from D-glyceraldehyde. This has to be taken into consideration when studying the older literature [54b, 58]. b) E. Fischer, I. W. Fay, *Ber. Dtsch. Chem. Ges.* **1895**, *28*, 1975; E. Fischer, O. Ruff, *ibid.* **1990**, *33*, 2142.
[55] F. Koch, *Pharm. Z. Russl.* **1886**, *25*, 619, 635, 651, 747, 763; *Ber. Dtsch. Chem. Ges.* **1887**, *20*, 145.
[56] H. J. Wheeler, B. Tollens, *Justus Liebigs Ann. Chem.* **1889**, *254*, 304.
[57] E. Fischer, *Ber. Dtsch. Chem. Ges.* **1890**, *23*, 2625.
[58] E. Fischer, R. Stahel, *Ber. Dtsch. Chem. Ges.* **1891**, *24*, 528.
[59] E. Fischer, O. Piloty, *Ber. Dtsch. Chem. Ges.* **1891**, *24*, 521.
[60] O. Schmiedeberg, H. Meyer, *Z. Physiol. Chem.* **1879**, *3*, 422.
[61] H. Thierfelder, *Z. Physiol. Chem.* **1891**, *15*, 71.
[62] "Encumbered" with the present-day knowledge on the reactions outlined in Figure 14, one can't refrain from marveling at the series of fortuitous circumstances which led Fischer to these rather sparse experimental results. For example, the fact that cyanohydrin synthesis of D-xylose, on subsequent hydrolysis, yields a mixture of D-gulonic acid and its C-2 epimer D-idonic acid (E. Fischer, I. W. Fay, *Ber. Dtsch. Chem. Ges.* **1895**, *28*, 1975), from which the former could only be isolated because its 1,4-lactone crystallizes outstandingly well: "The gulonic acid lactone belongs to the most beautiful compounds of the sugar group. By slow evaporation of its aqueous solution one easily obtains magnificently formed crystals of 1 cm in diameter" [58].

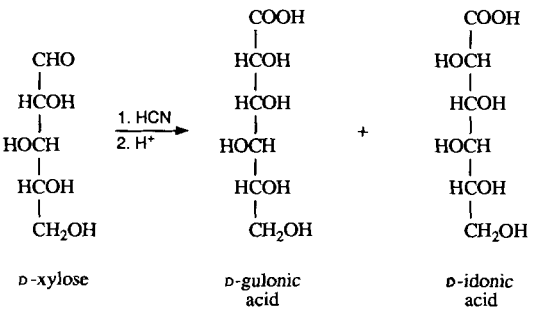

On the other hand, D-glucaric acid forms two monolactones, and only the lactonized carboxyl function is reduced by sodium amalgam to the aldehyde and subsequently to the primary alcohol. Undoubtedly a case of

serendipity, that "the sugar acid liberated from its cadmium salt by hydrogen sulfide, on concentration to a syrup and subsequent heating on a water bath for 5–6 hours" [59], mainly contained the 1,4-lactone of D-glucaric acid, which gave L-gluconic acid on reduction, isolated as its superbly crystalline 1,4-lactone in 10% yield [59]. If Fischer and Piloty had made efforts to purify the sirupy "Zuckerlactonsäure" as obtained above, they would have acquired the crystalline 3,6-lactone, (H. Kiliani, *Ber. Dtsch. Chem. Ges.* **1925**, *58*, 2344). On reduction this would have yielded D-gluonic acid; of no value in unraveling the interrelationships of the sugars. The formulas are presented as Fischer projections, since present day graphic presentations are not necessarily more appropriate for such configurational comparisons.

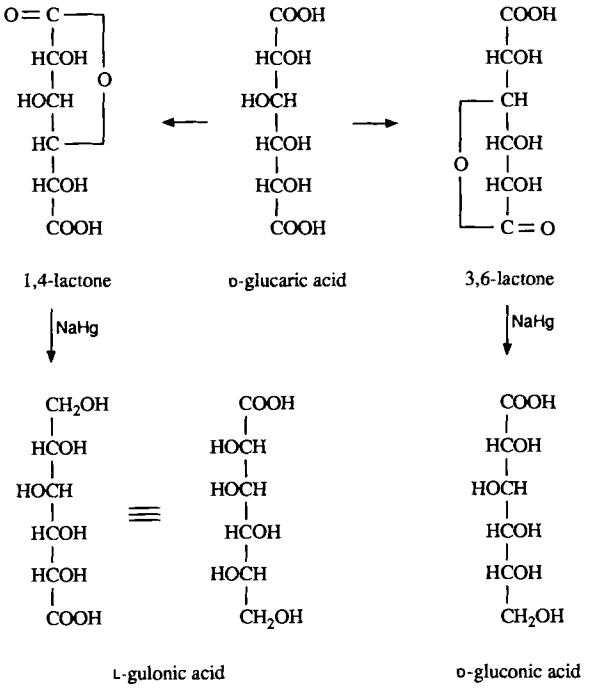

[63] H. Kiliani, *Ber. Dtsch. Chem. Ges.* **1887**, *20*, 1234.
[64] See [58], p. 538.
[65] See [19], p. 133 and 134.
[66] V. Meyer, *Ber. Dtsch. Chem. Ges.* **1890**, *23*, 572.
[67] A. F. Peerdemann, A. J. van Bommel, J. M. Bijvoet, *Nature* **1951**, *168*, 271; J. Trommel, J. M. Bijvoet, *Acta Crystallogr.* **1954**, *7*, 703; J. M. Bijovet, *Endeavour* **1955**, *14*, 71.
[68] The individual progressive steps of the proof given here try to trace and follow Fischer's chain of reasoning that undoubtedly developed from the van't Hoff thought patterns. For that reason the projection formulas used are provided with the corresponding tetrahedra, from which they are thought to emerge. A similar presentational mode was used by C. S. Hudson in 1941 [11]. It is rare that one finds a textbook of today, which follows the steps of the original proof. A notable exception is *Organic Chemistry* by R. T. Morrison and R. N. Boyd (2nd ed, Allyn and Bacon, Boston, **1970**, p. 993–997) which gives a detailed, impressively clear derivation of the sugar configurations in slightly modernized form.
[69] In his obituary for H. Kiliani, W. Hückel comments on this as follows: [40] "Here Kiliani passed the gate, through which, only little later, Emil Fischer arrived at the stereochemistry of the sugars. Kiliani, with his experiments, turned the key twice and, thereby closed it again; he would have had to turn only once to open it."
[70] B. Tollens, *Kurzes Handbuch der Kohlenhydrate*, J. A. Barth, Leipzig, **1895**; further editions in 1898, 1914 and 1935 (revised by H. Elsner).
[71] E. Fischer, *Untersuchungen in der Puringruppe* (1882–1906), Springer, Berlin, **1907**.
[72] E. Fischer, B. Helferich, *Ber. Dtsch. Chem. Ges.* **1914**, *47*, 210.
[73] E. Fischer, *Untersuchungen über Aminosäuren, Polypeptide und Proteine* (1899–1906), Springer, Berlin, **1906**.
[74] E. Fischer, *Untersuchungen über Depside und Gerbstoffe* (1908–1919), Springer, Berlin, **1921**.
[75] *Nobel Lectures Including Presentation Speeches and Laureates Biographies, Chemistry, 1901–1921* (Ed.: Nobel Foundation), Elsevier, Amsterdam, **1966**, pp. 15–39.
[76] See [46], quotation from p. 2130.

Synchrotron X-ray and Neutron Diffraction Studies in Solid-State Chemistry

By Anthony Kevin Cheetham* and Angus Paul Wilkinson

Neutron diffraction studies, especially with powders, play an important role in structural solid-state chemistry, making possible the precise determination of the location of light atoms, particularly hydrogen, and enabling a distinction to be made between certain neighboring elements in the periodic table that are difficult to distinguish in experiments with X-rays. Neutron diffraction investigations also make a unique contribution in the area of magnetic structure determination. The availability of intense synchrotron X-rays sources, however, is opening up new opportunities to the structural chemist, many of them complementary to the "traditional" strengths of neutron methods. The key features of synchrotron radiation in relation to structural studies are the wavelength tunability, which facilitates the use of resonant diffraction methods, and the high brightness and excellent vertical collimation of the source, which make possible the construction of diffractometers with unparalleled angular and spatial resolution. The following types of experiments are now possible with synchrotron X-ray diffraction: 1) The ab initio determination of structures from powder diffraction data. 2) The differentiation between different oxidation states of an element (valence contrast experiments) based upon the sensitivity of an absorption edge to the valence of the element in question. 3) The differentiation of elements adjacent to each other in the periodic table, which is now feasible with synchrotron X-rays for all elements beyond chromium. 4) Site-selective X-ray absorption spectroscopy. 5) The study of cation occupancies in materials where more than one element occupies a site that is, or may be, partially occupied. (Such problems are important in zeolite chemistry and high-temperature superconductors.) 6) The determination of crystal structures from microcrystals. 7) In situ and rapid, time-resolved diffraction studies. This review examines the roles played by X-ray and neutron diffraction studies in modern solid-state chemistry, and describes some recent examples in which the use of neutron radiation or synchrotron X-rays has been advantageous.

1. Introduction

Our current knowledge of the chemistry of inorganic materials relies heavily upon information obtained from X-ray diffraction studies. For example, the X-ray powder pattern of a compound provides a convenient and characteristic fingerprint which can be used in qualitative analysis; precise values of the d spacings (which are properties of the material itself, independent of the X-ray wavelength) and of estimated line intensities can be compared with those listed in the JCPDS Powder Diffraction File,[1] which contains entries for approximately 40000 inorganic compounds. Powder diffraction studies are also used for the precise determination of lattice parameters and in the elucidation of phase diagrams as a function of composition and temperature. As in other areas of chemistry, single-crystal studies also play a central role, providing the detailed structures of crystalline compounds that form the pillar of our understanding of the solid state. The Inorganic Crystal Structure Database (ICSD),[2] for example, details the structures of approximately 32000 materials. The vast majority of crystal structure determinations are performed using laboratory X-ray sources, but there are circumstances in which the use of the intense beams available from a synchrotron X-ray source may be advantageous. For other experiments, an alternative radiation, commonly neutron radiation, may be appropriate. The essential features of diffraction methods with neutrons and synchrotron X-rays are discussed below.

[*] Prof. A. K. Cheetham, Dr. A. P. Wilkinson
Materials Department, University of California
Santa Barbara, CA 93106 (USA)

1.1. Neutron Diffraction

The wave nature of neutrons leads in principle to the possibility of doing diffraction experiments, and this was first demonstrated in 1936 with a radium–beryllium source.[3] At the present time the most common source of neutrons for diffraction experiments is the nuclear reactor, but in recent years there has been a growth in the number of facilities producing neutrons by spallation from metal targets bombarded with high-energy (approximately 500 MeV) protons.[4]

Unlike X-rays, which are scattered by the electrons of atoms, neutrons are scattered by the nucleus. Consequently, the interference effects that cause X-ray scattering to diminish with $(\sin\theta)/\lambda$ are absent with neutrons, and the scattering intensity shows no angular dependence. Because scattering power is a nuclear property, it shows only a weak dependence upon atomic number and, unlike X-ray scattering amplitude, it may vary dramatically from one element to the next (Fig. 1).[5] The neutron also has a magnetic moment, and magnetic scattering is observed from paramagnetic ions, in addition to nuclear scattering. These properties lead to the principal applications of neutron diffraction to solid-state chemistry, namely the location of light atoms, especially hydrogen atoms, in the presence of heavy elements, the differ-

 © VCH Verlagsgesellschaft mbH, W-6940 Weinheim, 1992 0570-0833/92/1212-1557 $ 3.50+.25/0

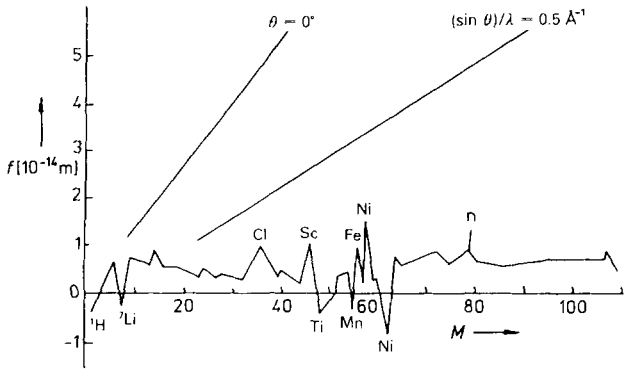

Fig. 1. The variation of neutron scattering power f with atomic weight M. The X-ray scattering amplitudes of the elements shown for comparison increase linearly with atomic number and diminish with increasing scattering angle (or more correctly with increasing $(\sin\theta)/\lambda$).

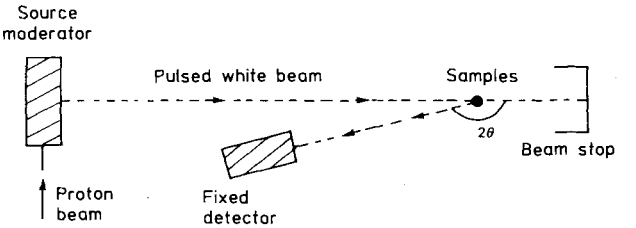

Fig. 2. A schematic diagram of a time-of-flight (TOF) powder neutron diffractometer. A high-energy, pulsed proton beam (energy ca. 500 MeV) is directed onto a metal target, producing pulses of "white" neutrons by spallation. In the simplest diffractometer arrangement, the diffraction pattern of a powder can be collected at a single, fixed detector by measuring the transmitted intensity within each pulse as a function of the time-of-flight (see text). Long-wavelength (low-energy) neutrons within each pulse will arrive after the short-wavelength (high-energy) neutrons. Data from successive pulses (typically 10^6) are summed to give adequate statistics.

entiation between adjacent elements in the periodic table, and the determination of the spin arrangements in magnetically ordered materials (e.g. antiferromagnets).

We noted earlier that the latest generation of intense neutron sources is based upon accelerators rather than nuclear reactors. The pulsed neutron beams that are emitted by such a source can conveniently be used to collect diffraction patterns by time-of-flight (TOF) methods. In a simple case, the neutron detector is placed at a fixed scattering angle, and the different scattering planes, which give rise to the peaks in the diffraction patterns, can be sampled by measuring the times that neutrons with different wavelengths (and therefore different speeds) take to reach the counter (Fig. 2); the neutron velocity is sufficiently slow to permit this. This experiment can be described by the Bragg equation [Eq. (a)]. In a conventional experiment, λ is fixed and θ is varied.

$$\lambda = 2d_{hkl}\sin\theta \qquad \text{(a)}$$

One of the features of the TOF method is that it can readily provide powder diffraction patterns with exceptionally high resolution. As a consequence, data collected on the high-resolution powder diffractometer at ISIS (Rutherford Appleton Laboratory) were used in the first demonstration of solving an unknown crystal structure by powder neutron diffraction.[6] Data collected on the same instrument at low temperature have been used to refine the structure of buckminsterfullerene with good precision.[7]

1.2. Synchrotron X-ray Diffraction

Synchrotron X-rays are produced when electrons (or positrons) with relativistic velocities are held in a circular orbit by magnetic fields.[8] The principal features that distinguish synchrotron X-rays from conventional X-rays, insofar as their applications to inorganic materials are concerned, are the high intensity, the excellent vertical collimation, and the white (continuous) spectral distribution.[9] The excellent instrumental resolution that can be achieved as a consequence of the first two factors is comparable to that obtainable with the best TOF neutron diffractometer (see Section 1.1). Several types of study are greatly facilitated by

Anthony Cheetham is the Director of the Materials Research Laboratory at the University of California, Santa Barbara, and Professor in both the Materials and Chemistry Departments. He has also held the Chair in Solid State Chemistry at the Royal Institution of Great Britain since 1986. His research interests lie in the area of inorganic materials, and embrace the synthesis, characterization, and properties of such materials. Prior to moving to UCSB in 1991, he was the Reader in Inorganic Materials at the University of Oxford. He was awarded the Corday Morgan Medal and Prize by the Royal Society of Chemistry in 1982, and the Medal for Solid State Chemistry in 1988.

Angus Wilkinson (not pictured) gained his doctorate at the University of Oxford in 1991 and is currently a postdoctoral researcher in the Materials Department at the University of California, Santa Barbara. He also holds a Junior Research Fellowship at Christ Church, Oxford. His research interests are in the use of synchrotron X-ray and neutron diffraction methods for the structural characterization of inorganic solids.

such high resolution. An important example is the routine determination of crystal structures from powder data, which will be illustrated later with some recent work on inorganic solids. In another application, high-resolution measurements are uniquely sensitive to the subtle phase transitions that are found in various types of materials, including ferroelectrics.

The continuous spectral distribution of the radiation offers the possibility of performing energy dispersive diffraction (EDXD) experiments (Section 3.4) and allows the radiation to be tuned for monochromatic experiments. The latter point leads to the possibility of 1) determining oxidation-state distributions in mixed-valent compounds, 2) differentiating between neighboring elements in the periodic table, and 3) locating exchangeable cations in ion-exchanged zeolites and other complex materials. These experiments rely on the use of anomalous scattering (Section 3.2) and have been conducted primarily on powders to date. In studies of single-crystals two developments are of great interest: the study of micron-size crystals and the use of imaging plates as detectors for the rapid collection of high-quality diffraction data.

Some of the characteristic features of synchrotron X-ray and neutron diffraction methods are apparent in Figure 3, in which the patterns of rutile (TiO_2) collected by the two techniques are compared. The angular dependence of the X-ray

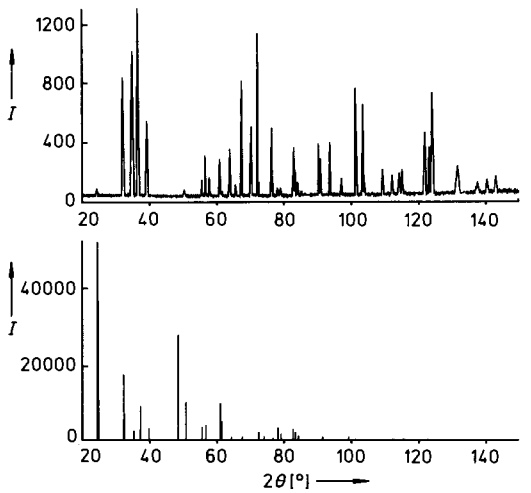

Fig. 3. A comparison of powder diffraction patterns for rutile (TiO_2) from neutron (top) and synchrotron X-ray radiation (bottom). The X-ray data were collected at Daresbury Laboratory (UK) with a mean wavelength of 1.37725 Å; the neutron data were collected at Lucas Heights (Australia) with a mean wavelength of 1.377 Å. The angular dependence of the X-ray scattering amplitudes, described in Figure 1, is clearly seen in the bottom pattern.

scattering intensity leads to poorer signal-to-noise ratios at large angles, and the different scattering factors for neutrons and X-rays are seen in the different relative intensities in the two patterns. The resolution comparison, on the other hand, is somewhat exaggerated, since the neutron data were collected on a medium-resolution instrument.

To a considerable extent, information that can be obtained by synchrotron X-ray diffraction and neutron diffraction is complementary. This point will be illustrated in Sections 2 and 3 by selected examples. On the other hand, there are several areas in which synchrotron X-ray diffraction studies can provide information traditionally extracted from neutron diffraction; this aspect will be examined in the context of locating light atoms and differentiating between neighboring elements in the periodic table. We shall also describe some of the ways in which the combined strengths of the two methods can be harnessed together to provide answers to problems in the solid state.

2. Applications of Neutron Diffraction

2.1. Location of Light Atoms

Many important applications of neutron diffraction are based on the dependence of neutron scattering powers (or scattering lengths, as they are known) upon atomic number (see Fig. 1). The average scattering power shows a rather slow increase with atomic number, with the consequence that light elements, which scatter X-rays weakly, make a more substantial contribution to a neutron diffraction pattern. This leads to better precision in the location of light atoms by neutron diffraction, an advantage that is especially useful in the study of hydrogen-containing materials. As a result, a number of studies of metal hydrides, systems with hydrogen bonds, and biological macromolecules have been conducted. Figure 4[10] shows the neutron diffraction pattern obtained from a powder sample of cerium hydride, or rather cerium deuteride. (Deuterium has superior scattering

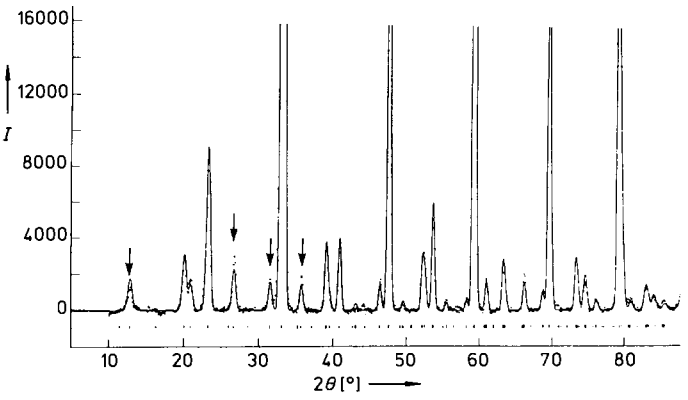

Fig. 4. The powder neutron diffraction pattern of $CeD_{2.5}$. Arrows indicate some of the reflections that arise from the long-range ordering of interstitial deuterium atoms. The corresponding X-ray pattern shows only the strong substructure reflections from the face-centered cubic arrangement of cerium atoms; it contains no information about the distribution of the deuterium atoms.

properties for diffraction experiments.) The key point here is that the diffraction pattern contains specific information about the disposition of the hydrogen (deuterium) atoms. The corresponding X-ray diffraction pattern would contain virtually no such information. In a subtle variation on this experiment Somenkov et al. used the difference in the scattering power of hydrogen and deuterium to show that in CeD_2H hydrogen preferentially occupies the octahedral sites and deuterium the tetrahedral sites.[11] Only with neutron diffraction can such isotopic ordering be detected.

In another example that illustrates the location of light atoms by neutron diffraction, a pyridine molecule was de-

tected inside a zeolite catalyst (Fig. 5).[12] The sorbate forms a Lewis acid–base complex with the K^+ ion, whilst enjoying a short-range, nonbonding interaction with the aluminosilicate framework of the zeolite. This study and other more

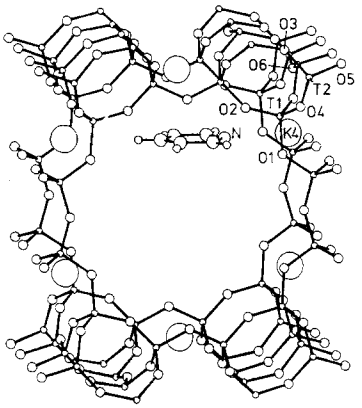

Fig. 5. The location of pyridine in the catalyst potassium zeolite-L determined by neutron diffraction. The nitrogen atom of the pyridine molecule forms a Lewis acid–base complex with the potassium ion, whilst the aromatic ring enjoys short-range interactions with the aluminosilicate framework.

recent examples[13–15] demonstrate unequivocally that adsorbed molecules are preferentially situated in positions close to the inner surfaces of the zeolite; this is a valuable insight into the behavior of organic species in these important catalysts.

2.2. Differentiation between Elements

A second important type of neutron diffraction experiment relies upon the variations in scattering that are sometimes found between elements adjacent to each other in the periodic table. Figure 1 reveals that the elements of the first transition series, for example manganese, iron, and cobalt, have quite different scattering powers; neutron diffraction is therefore able to differentiate between these elements. Their X-ray scattering powers, on the other hand, are almost identical because they have similar numbers of electrons; it is therefore difficult to distinguish them by X-ray methods. The significance of this advantage of using neutron diffraction can be seen in the extensive work that has been done on ferrite magnets. These compounds crystallize in the same structure as the mineral spinel ($MgAl_2O_4$), and their magnetic properties depend crucially upon the distribution of the different transition metal ions in the available cation sites. Until very recently, this information could be obtained only by neutron diffraction. A typical example is provided by a study of the spinel $NiCo_2O_4$[16] which, rather surprisingly, revealed 92% occupancy of the tetrahedral site by cobalt, corresponding to a spinel structure with almost complete inversion.

2.3. Magnetic Structure Determination

A third important class of experiments also relates to magnetic materials, but relies upon the magnetic scattering of neutrons. When the magnetic moments or spins in a material become aligned in a regular manner, for example in what a layman would call a magnet, the neutron diffraction pattern will exhibit additional peaks that contain information about the spin arrangement. Figure 6 shows the patterns of nonstoichiometric ferrous oxide $Fe_{1-x}O$[17] both above and below the temperature at which the spins become antiferromagnetically ordered (200 K). Note the appearance of peaks

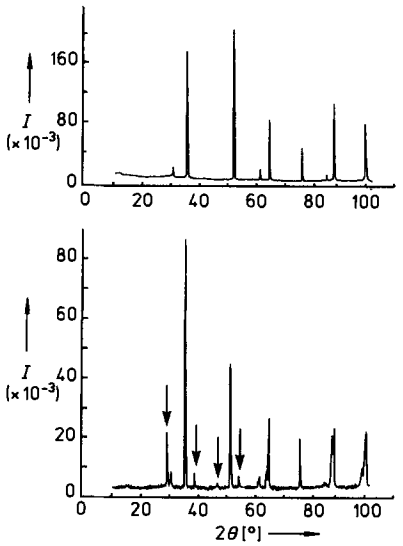

Fig. 6. Powder neutron diffraction patterns of $Fe_{0.943}O$; top: above (293 K) and bottom: below (4.2 K) the magnetic ordering transition at 200 K. Note the appearance of reflections in the low-temperature pattern resulting from magnetic ordering (marked with arrows), and the peak splittings at high scattering angles due to a lowering of symmetry from cubic to rhombohedral at the magnetic ordering temperature.

due to magnetic scattering in the low-temperature pattern. In this and many other magnetic compounds, neutron diffraction provides an unrivaled insight into their behavior at the atomic level.

The sensitivity of magnetic scattering experiments can be dramatically enhanced by utilizing a neutron beam containing neutrons of only one spin and measuring the polarization of the diffracted neutrons.[5] In the case of $Fe_{1-x}O$, such measurements have revealed that the magnetic spins of the iron atoms lie in the (111) plane in the bulk of the crystal, but are perpendicular to that plane in the vicinity of defects comprising octahedral iron vacancies and tetrahedral interstitial Fe^{3+} ions.[18]

Magnetic scattering studies can also be used to form the basis for establishing the charge distribution in mixed-valent compounds. In $Fe^{II}Fe^{III}PO_5$, for example, in which there are two crystallographically distinct iron sites in the crystal structure, magnetic neutron diffraction measurements yielded magnetic moments of $M1 = 3.89(3)\,\mu_B$ and $M2 = 4.22(3)\,\mu_B$, consistent with Fe^{2+} and Fe^{3+} at the positions Fe1 and Fe2, respectively[19] (see Section 3.2.1).

2.4. Rietveld Profile Analysis

Since the flux of a neutron beam is relatively low compared with that of an X-ray source, rather large samples (at

least 1 mm^3) are required for single-crystal neutron diffraction experiments. Such crystals are certainly difficult to prepare; thus powder neutron diffraction techniques have been developed to a point where they can now be used to refine complex, low-symmetry structures. A conventional refinement with structure factors from single, integrated powder intensities is quite feasible for high-symmetry structures, but is clearly impracticable for low-symmetry materials because of overlap between adjacent Bragg reflections (Fig. 7).

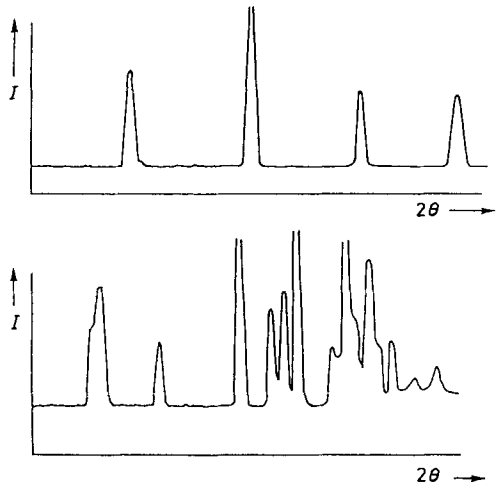

Fig. 7. Schematic representations of powder diffraction patterns of samples with high symmetry (top) and low symmetry (bottom). In the latter case, the intensities of individual Bragg reflections may be difficult or impossible to determine due to peak overlap.

Rietveld[20] has devised a method for analyzing the more complex patterns by means of a curve-fitting procedure in which the least-squares refinement minimizes the difference between the observed and calculated profiles, rather than individual reflections. In order to do this with neutron diffraction patterns, it can normally be assumed that the reflections have a Gaussian distribution, and the calculated intensity at each point (say, 0.05° in 2θ steps) on the profile is obtained by summing the contributions from the Gaussian functions that overlap at that point. Besides the conventional parameters in the least-squares refinement (atomic coordinates and temperature factors of the individual atoms), additional parameters are required: the lattice parameters which determine the positions of the reflections, a correction factor for setting the zero point of the detector, and three parameters that describe the variation of the half-width of the Gaussian distribution (full width at half-maximum intensity) with scattering angle. The Rietveld method was initially developed for the analysis of neutron diffraction data because of the relative simplicity of the peak-shape function, and it has been used in the examination of a wide range of problems in solid-state chemistry.[21–23] A typical example is shown in Figure 8.[24]

Profile analysis procedures have also been developed for the analysis of TOF powder data. The procedure is essentially the same as that used in constant-wavelength experiments except that the peak-shape function is more complex and wavelength-dependent terms must be taken into account.[25] One advantage of TOF powder methods is that the whole

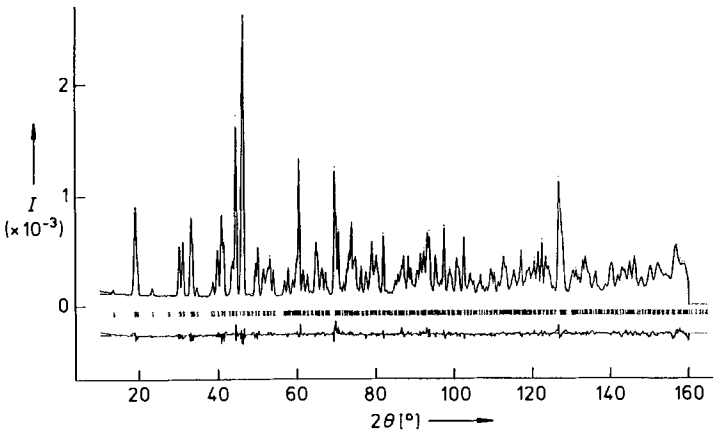

Fig. 8. The observed, calculated, and difference (lower curve) profiles resulting from the Rietveld analysis of powder neutron diffraction data collected on Sr_3CuPtO_6. The ticks mark the calculated positions of the possible reflections. $\lambda = 1.5940$ Å.

diffraction pattern is collected simultaneously (since the detector remains stationary). Thus, it is an attractive way of following structural changes with time, temperature, or pressure. In addition, since the incident and scattered beams can pass through small apertures, such measurements can easily be conducted on materials in special environments, for example in a high-pressure cell[26] (see Section 2.5).

Profile analysis is limited by the same drawback that applies to powder methods in general: the loss of information arising from the compression of the three-dimensional diffraction pattern into a single dimension. The inability to assign intensities to individual reflections, except in the simplest cases, normally leads to difficulties in solving crystal structures from powder data. For example, Patterson techniques may not yield the information necessary to locate heavy atoms and solve the phase problem, and direct methods are also difficult to apply. This serves to underline the fact that profile analysis, though an excellent technique for *refining* structures, requires a good starting model and is *not* a suitable method for *structure determination*. However, this problem should be overcome gradually as instrumental resolution and computational methods improve, giving larger numbers of individual reflections (see Section 3.1).

2.5. In Situ Powder Diffraction Studies

Currently, the majority of powder neutron diffractometers that are used for collecting data for structure refinements require data collection over several hours for a single diffraction pattern. However, it is possible to collect complete diffraction patterns in just a few minutes if a high incident neutron flux is available, efficient detection systems are employed, and a high degree of pattern resolution is not required. This opens up the possibilities of examining the progress of chemical reactions as they occur, or collecting data as a function of some external variable such as temperature or pressure. Neutron diffraction is in many ways well suited to these types of experiments: 1) Most materials do not significantly absorb neutrons; this markedly simplifies the construction of the sample environment (reaction vessel,

electrochemical cell, furnace, pressure cell, etc.). 2) Processes involving light atoms, such as dehydration, can be followed. 3) A fixed-angle detector can be used with TOF techniques (Fig. 2), again considerably simplifying the construction of certain types of sample environment, for example high-pressure cells. However, even the most advanced neutron sources offer considerably lower fluxes than those available with modern X-ray sources, particularly synchrotron storage rings. Consequently, synchrotron X-ray diffractometers are potentially able to follow dynamic processes on a much shorter timescale (see Section 3.4).

2.5.1. *Real-Time Neutron Diffraction*

Some of the applications of real-time neutron powder diffraction have been reviewed.[27-29] Dehydration/hydration reactions such as the industrially important dehydration of gypsum ($CaSO_4 \cdot 2H_2O$) in the manufacture of plaster of Paris have been studied.[30] In this case, the background incoherent scattering in the diffraction pattern provides a sensitive probe of the residual water (proton) content of the material, while the diffraction pattern itself identifies the crystalline phases that are present.

The reaction of gases and solids, for example the absorption of deuterium by the alloys $LaNi_{2.18}$ and $CeNi_{2.16}$, have also been examined.[31] The observed shifts in peak positions and changes in relative peak intensities were interpreted as suggesting that deuterium atoms are initially incorporated into a crystalline phase. As the reaction proceeded, a smooth increase in pattern background intensity combined with a decrease in intensity of the Bragg peaks was observed; this was ascribed to the formation of an amorphous hydride phase.

The processes occurring in electrochemical cells, for instance the study of the reversibility of hydrogen-absorbing TiNi electrodes, have been investigated.[32] The recorded powder patterns demonstrated that when the test cell was charged, the initial TiNi alloy electrode was converted to a new crystalline phase, $TiNiD_x$, but when the cell was discharged the crystalline alloy did not reform and only a small amount of the electrochemically inserted deuterium could be removed from the deuteride.

Intercalation processes, such as the absorption of THF by CsC_{24} have also been studied with real-time neutron diffraction.[33] The time-resolved diffraction patterns clearly showed the formation of $Cs(THF)_{1.74}C_{24}$ via an intermediate compound. The presence of "liquid rings" (diffuse scattering) in the diffraction pattern of the product, but not the intermediate, were interpreted as suggesting that the intercalated solvent is highly disordered (liquidlike) in the former material and ordered in the latter compound.

2.5.2. *High-Pressure Neutron Diffraction*

Neutron diffraction has been used for many years to study the influence of pressure on crystal structure,[34, 35] for example the occurrence of phase transitions and for the measurement of compressibility. The penetrating power and constant scattering power with respect to $(\sin\theta)/\lambda$ make the technique suitable for the acquisition of diffraction data of sufficient quality for quantitative analysis by Rietveld refinement or other methods. This has found application in several areas, including the examination of the influence of pressure on crystal structure in high-temperature superconductors and the correlation of these data with those obtained from T_c measurements.[36] In high-pressure X-ray studies of powder samples, it is often not possible to use the data in crystal structure analysis due to powder averaging problems (i.e. insufficient number of crystallites).

Unfortunately, the low flux of neutrons available from current sources requires that large sample volumes be employed; this is a severe limitation on the design of high-pressure neutron diffraction experiments as there is generally an inverse correlation between the maximum pressure achievable and the sample volume. As a consequence of this restriction, the majority of neutron experiments have been performed at less than 50 kbar in piston/cylinder cells. By contrast, the much higher flux available from synchrotron X-ray sources allows the performance of experiments at very high pressures (in excess of 1 Mbar) on small samples in diamond anvil cells (DACs).

3. Applications of Synchrotron X-ray Diffraction

3.1. Determination of Crystal Structures from Powder Data

A great deal of the development work in the field of structure determination from powder data has relied on conventional, laboratory X-ray sources, and there have been a number of important successes in the area.[37, 38] However, synchrotron X-rays have profound advantages over conventional X-rays for structure determination. In particular, the combination of the high brightness and excellent vertical collimation can be harnessed for the construction of diffractometers with unparalleled resolution. Cox's instrument at the National Synchrotron Light Source (NSLS), Brookhaven National Laboratory,[39] for example, has a resolution at the focusing position of $<0.02°$ in 2θ. This is achieved in part by constructing the instrument in the vertical plane, since the vertical divergence θ_v is only about $0.01°$ at 2.5 GeV. With high-resolution data, the solution of structures from powder data is greatly facilitated, and several successful structure solutions and refinements have recently been performed (Table 1).[40] On the other hand, very few structures have been solved from powder neutron diffraction data. This is partly a consequence of the lower resolution of most neutron diffractometers, but it is mainly due to the near equivalence of the neutron scattering powers for most elements (as a result of which, the phase problem cannot be solved on the basis of locating a small subset of dominant scatterers).

With single-crystal X-ray data that has been collected on an automatic diffractometer, the determination of a crystal structure is normally routine. The unit cell can be identified from an automatic peak search, the space group determined from systematic absences, and the phase problem solved by Patterson or direct methods. Patterson methods are normally used if there are one or more dominant scatterers present, as in many organometallic and coordination compounds,

Table 1. Some examples of ab initio structure determinations from synchrotron X-ray powder data.

Compound	Space group	Number of atoms [a]	Ref.
α-$CrPO_4$	*Imma*	8	[41]
I_2O_4	$P2_1/c$	6	[42]
$Al_2Y_4O_9$	$P2_1/c$	15	[42]
$MnPO_4 \cdot H_2O$	$C2/c$	6	[43]
PbC_2O_4	$P1$	7	[44]
Clathrasil, Sigma-2	$I4_1/amd$	17	[45]
$LaMo_5O_8$	$P2_1/a$	14	[46]
BeH_2	*Ibam*	4	[47, 48]
UPd_2Sn	*Pnma*	4	[49]
$C_5H_{11}NO_2$	$Pna2_1$	19	[50]
$NaCD_3$	*I*222	10	[51, 52]
$C_{10}N_6SH_{16}$	$P2_1/n$	33	[53]
$BaBiO_{2.5}$	$P2_1/c$	5	[54]
$(VO)_3(PO_4)_2 \cdot 9H_2O$	$P2_1/n$	13 (non-H)	[55]
$CuPt_3O_6$	$Pn2_1m$	10	[56]
$Ga_2(HPO_3)_3 \cdot 4H_2O$	$P2_1$	29	[57]

[a] Number of atoms in the asymmetric unit.

and direct methods are particularly suitable for organic compounds, minerals, and other regular solids. The structure can then be refined with a combination of least-squares and difference Fourier techniques. With powders, however, there are serious difficulties, most of which arise because the three-dimensional intensity data is compressed into a single dimension in the powder experiment. This results in peak overlap, which introduces complications at each stage of the structure determination.

The first hurdle to be overcome, that is, indexing of the reflections and determination of the unit cell, is nontrivial, although in our recent experience few determinations now falter at this stage. Several excellent autoindexing programs are available.[58–61] They require very accurate *d*-spacing data, but these can normally be obtained by peak-fitting of individual reflections provided that all systematic errors can be eliminated. Clearly, the autoindexing procedure is greatly facilitated if high-resolution data are available.

Following the determination of the unit cell it may be possible to identify the structure by comparison with a related material, for example, by searching in an appropriate database. In the many cases in which this is not possible, however, the solution of the crystal structure may present formidable obstacles. In particular, the solution of the phase problem is likely to be difficult, largely because the overlapping of adjacent reflections introduces ambiguity into the assignment of intensities to particular *hkl* values. This problem arises with both low-symmetry structures, where the density of reflections may become very high, and high-symmetry structures, where there may be unavoidable overlap of nonequivalent reflections. Ideally, unambiguous intensity data are needed for both Patterson and direct methods calculations.

The extraction of the maximum amount of integrated intensity data I_{hkl} from the powder diffraction pattern is perhaps the most difficult stage in the determination. Both Pawley[62] and Le Bail[63] have developed profile fitting methods by which the observed powder pattern can be decomposed into integrated intensities. It should be stressed that no structural model is required for any of these methods and that this crucial step can be performed more effectively with high-resolution data, underlining again the advantages of using synchrotron X-rays.

From this stage onwards, the analysis mirrors that of a single-crystal study. The possible space groups can be assigned from the systematic absences, although in cases of uncertainty it may be useful to carry out pattern decomposition in a number of possible space groups, or to obtain a series of electron diffraction patterns. The phase problem can be solved by conventional crystallographic methods. The principal difficulties are that the data set will be considerably smaller than that obtained from a single crystal and that some of the data will be unreliable for the reasons discussed above. It is a tribute to the robustness of modern structure-solving techniques that it is still possible to determine structures under these circumstances.

In the first structure solved from synchrotron X-ray powder data carried out in 1986 by Attfield et al.,[41] the orthorhombic structure of α-$CrPO_4$ with eight atoms in the asymmetric unit was solved by Patterson methods using a vector search procedure; 68 well-resolved peaks were utilized. A relatively poor R_{pr} factor (19.3%) was obtained for the final Rietveld refinement with the synchrotron data, no doubt due to problems with preferred orientation and *hkl*-dependent line-broadening effects. But a subsequent medium-resolution neutron study (on the D1a instrument at ILL Grenoble) gave an excellent fit ($R_{pr} = 8.3\%$), confirming the correctness of the model obtained with synchrotron X-ray diffraction. A comparison[64] of the atomic coordinates obtained from these investigations and a subsequent single-crystal study[65] nicely illustrate the relative strengths of the different methods (Table 2). We note that with neutron diffraction the parameters for almost all atoms are more precise in spite of the modest resolution of the data. The level of

Table 2. Structural parameters for α-$CrPO_4$ refined with synchrotron X-ray (X) and neutron (N) diffraction data; space group *Imma* (No. 74), estimated standard deviations in parentheses [64]. Parameters from the reported single-crystal study [65] (S) are given for comparison.

Atom	*x*	*y*	*z*	B_{iso} [a]
Cr1	1/2	1/2	0	0.3(2) N
				0.283(6) S
Cr2	1/4	0.3660(3) X	1/4	
		0.3650(4) N		0.0(1) N
		0.36611(3) S		0.316(4) S
P1	1/2	1/4	0.0819(12) X	
			0.0790(8) N	0.0(1) N
			0.0825(2) S	0.30(1) S
P2	1/4	0.5738(4) X	1/4	
		0.5739(2) N		0.47(8) N
		0.57358(5) S		0.345(7) S
O1	0.3790(10) X	1/4	0.2269(17) X	
	0.3766(3) N		0.2280(5) N	0.53(8) N
	0.3773(2) S		0.2268(3) S	0.42(2) S
O2	0.3603(6) X	0.4914(5) X	0.2145(11) X	
	0.3610(2) N	0.4907(1) N	0.2142(3) N	0.62(6) N
	0.3611(1) S	0.4902(1) S	0.2146(2) S	0.42(1) S
O3	0.2263(6) X	0.6352(5) X	0.0576(10) X	
	0.2240(1) N	0.6368(2) N	0.0546(3) N	0.68(5) N
	0.2238(1) S	0.6363(1) S	0.0552(2) S	0.56(1) S
O4	1/2	0.3509(8) X	−0.0457(15) X	
		0.3486(2) N	−0.0422(4) N	0.31(7) N
		0.3496(2) S	−0.0432(3) S	0.50(2) S

[a] For the refinement of the powder X-ray data the overall isotropic temperature factor was $B_{iso} = 0.24(7)$ Å^2.

agreement between the results of powder and single-crystal measurements suggests an underestimate of the estimated standard deviations with the Rietveld method, a feature that is apparent in other comparisons of this type.[66]

3.2. Resonant Diffraction

The tunability of synchrotron radiation allows us to modify the scattering factor f for a particular element by selecting an X-ray wavelength that is in close proximity to an absorption edge. This leads to resonance effects that require modifications to the scattering factor according to Equation (b), where f' is the real part of the correction and f'' is the imaginary part; these corrections have essentially no dependence on $\sin(\theta/\lambda)$. Both f' and f'' can have quite large values. For example, at the iron K-edge f' and f'' reach minima and maxima of -8 and $+4$ electrons, respectively,[67] compared to $f^0 = 26$ at $(\sin\theta)/\lambda = 0$. Such resonant (anomalous) scattering effects can have a marked influence on X-ray patterns and are opening up some exciting opportunities in the study of condensed matter, as will be discussed below. Unfortunately, powder diffraction patterns show poor sensitivity to changes in f''.[68] As a consequence, most experiments involving such materials rely upon the influence of f'.

$$f = f^0 + f' + if'' \qquad \text{(b)}$$

The two components of the anomalous scattering correction, f' and f'', are related to each other by the so-called Kramers–Kronig integral; where ω_i is the angular frequency of the radiation [Eq. (c)]. The term f'' is related to the X-ray

$$f'(\omega_i) = (2/\pi)\int_0^\infty \omega f''(\omega)/(\omega^2 - \omega_i^2)\,\mathrm{d}\omega \qquad \text{(c)}$$

absorption cross section $\sigma(\omega)$ by the optical theorem [Eq. (d)], where r_e is the classical radius of an electron. This close relationship between anomalous scattering and X-ray

$$f''(\omega) = (\omega/4\pi r_e c)\sigma(\omega) \qquad \text{(d)}$$

absorption has implications for several types of experiment. Since the energy of the absorption edge increases by a few eV for each unit increase in oxidation state, it is possible to differentiate between the oxidation states of an element by selectively tuning the wavelength (valence contrast experiments). Additionally, the local coordination environment of an atom affects the anomalous scattering corrections in the vicinity of the absorption edge as a consequence of its influence on the absorption spectrum of the atom (application in XANES and EXAFS experiments).

3.2.1. Valence and Neighboring Element Contrast Experiments

There have already been several illustrations of the opportunities that synchrotron radiation presents for the study of oxidation states and neighboring element contrast (Table 3).

Table 3. Some examples of valence (V) and neighboring element (NE) contrast experiments from synchrotron X-ray studies.

Compound	Exp.	Ref.	Compound	Exp.	Ref.
Y-doped ZrO_2	NE	[69]	Eu_3O_4	V	[76]
$YBa_2Cu_3O_7$	V	[70, 71]	$FeNi_2BO_5$	NE	[77]
$La_{0.9Gd}0.9Sr_{0.2}CuO_4$	NE	[72]	$GaCl_2$	V	[78]
$Fe_{0.5}Co_{0.48}V_{0.02}$	NE	[73]	$FeCo_2(PO_4)_2$	NE	[79]
$Cr_{0.48}Fe_{0.52}$	NE	[74]	α-Fe_2PO_5	V	[19]
$Fe_{0.52}Cr_{0.31}Ni_{0.08}Mo_{0.07}Mn_{0.02}$	NE	[75]	$PbBi_2S_4$	NE	[80]
$EuSm_2O_4$	NE, V	[76]			

The recent study[19] of α-Fe_2PO_5 affords an interesting example, since the same system was also investigated by magnetic neutron diffraction (see Section 2.3). The essence of such a valence contrast experiment is illustrated schematically in Figure 9 for a gallium compound. In the case of the

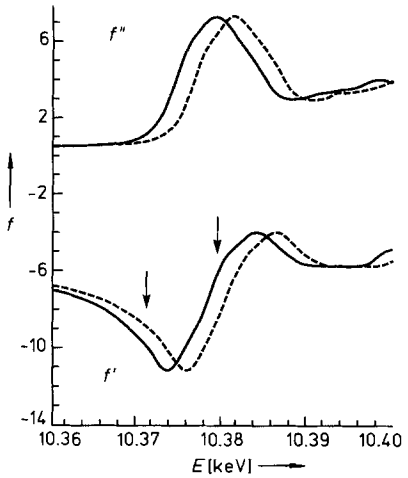

Fig. 9. A schematic diagram illustrating the principles involved in valence contrast experiments. The variations in f' and f'' [electrons] are shown for lower (solid line) and higher (broken line) oxidation states in the vicinity of an absorption edge. In experiments of the type described in the text, datasets are collected well below the edge and at two energies close to the absorption edge (the latter are indicated by arrows).

α-Fe_2PO_5, X-ray data were collected at three wavelengths: one well below the Fe K absorption edge, the second close to the Fe^{2+} edge (as determined by X-ray absorption measurements), and the third close to the Fe^{3+} edge. Since the absorption edge shifts to higher energies with increasing oxidation state, the real part of the anomalous scattering correction should be more negative for the Fe^{2+} site in the second experiment, and for the Fe^{3+} site in the third (see Fig. 9); for the first data set (well below the K absorption edge), the corrections for both iron positions M1 and M2 are expected to be approximately the same. The results, which are presented in Table 4, show that f' is more negative at site M1 in the second experiment and more negative at M2 in the third, consistent with the presence of Fe^{2+} at M1 and Fe^{3+} at M2, and in agreement with the findings from neutron diffraction studies given in Section 2.3. Paradoxically, these sophisticated studies do not afford such a clear-cut answer as simple valence bond calculations,[81] which yield $\sum\sigma_{M1} = 2.077(3)$ and $\sum\sigma_{M2} = 2.997(7)$ based upon the room-temperature crystal structure.

Table 4. Refined values of f' obtained for the M1 and M2 sites in α-Fe_2PO_5 (data collected on diffractometers at SRS, Daresbury Laboratory) [19].

Beamline	8.3	8.3	9.1
Wavelength [Å]	1.78316(4)	1.74179(1)	1.74018(6)
Energy [eV]	6953.1(1)	7118.3(1)	7124.8(3)
ΔE from Fe^{2+} K edge [eV]	−165.2(5)	−2.6(5)	3.9(5)
Estimated bandpass [eV]	3.0(2)	3.0(2)	1.6(2)
f' (M1) [electrons]	−3.57(4)	−9.74(5)	−6.75(11)
f' (M2) [electrons]	−3.56(5)	−8.04(7)	−10.01(17)
f'' (M1) [electrons]	0.472	1.8	4.0
f'' (M2) [electrons]	0.472	1.7	3.2

The ability to distinguish between neighboring elements in the periodic table, which has previously been possible only with neutrons, and even then only when the neutron scattering strengths are reasonably disparate, is now possible for many elements by resonant powder diffraction. For example, Warner et al.[79] have recently shown that the distribution of Fe and Co in $[Fe_2Co(PO_4)_2]$ can be determined with a precision that is comparable to that obtained by neutron diffraction (Table 5). Both experiments confirm that

Table 5. Occupancy of sites M1 and M2 by Fe atoms in $[FeCo_2(PO_4)_2]$ as determined by neutron diffraction and resonant X-ray diffraction experiments [79].

Site	M1	M2
Multiplicity	4	2
Coordination number	5	6
Random distribution	1/3	1/3
Occupancy from neutron data	0.246(5)	0.508(9)
Occupancy from X-ray data	0.243(5)	0.514(10)

iron preferentially occupies the site with octahedral coordination, M2. The differentiation between iron and cobalt is one of the classical applications of neutron diffraction (see Section 2.2), since the relative neutron scattering lengths are $+0.95 \times 10^{-14}$ and $+0.25 \times 10^{-14}$ m for Fe and Co atoms, respectively.[5] However, the X-ray contrast between Fe and Co atoms can be increased from approximately 1 to over 6 electrons by matching the wavelength to the Fe K absorption edge. Since the anomalous scattering corrections are approximately independent of scattering angle, a change of −6 electrons can have a profound influence on the intensities of reflections at large angles. It is already clear that this technique will enable us to tackle many structural problems that have previously been impenetrable with either conventional X-ray or neutron diffraction; the anomalous X-ray scattering approach is feasible for all elements that have an absorption edge in an energy range that is suitable for diffraction studies (i.e. the wavelength required is not too short or too long). With the next generation of synchrotron sources giving high fluxes of short-wavelength X-rays, such experiments will be practicable for all adjacent elements in the periodic table starting at approximately titanium.

3.2.2. *The Effect of Coordination Geometry on Anomalous Scattering*

As a consequence of the close relationship between the anomalous scattering corrections and X-ray absorption, anything that affects the absorption spectrum will also influence the anomalous scattering corrections f' and f''. This implies that anomalous scattering corrections are sensitive to coordination geometry, since the latter influences both the EXAFS (Extended X-ray Absorption Fine Structure) and the XANES (X-ray Absorption Near-Edge Structure) observed in absorption spectra. In practice, the impact of EXAFS on the anomalous scattering corrections is small and can probably be neglected, but in many cases the XANES does have a significant effect. This was recently demonstrated by a series of resonant diffraction experiments on the garnet $Y_3Ga_3^1Ga_2^2O_{12}$ (Ga^1 = tetrahedral, Ga^2 = octahedral coordination geometry).[82] The Ga^{3+} ions in this material with tetrahedral and octahedral coordination environments show distinct X-ray scattering behavior at energies in the near-edge region; the difference between f' for the two sites varies over a range of about four electrons.

This effect is large enough to be of importance in experiments for which a knowledge of the anomalous scattering correction is necessary for the accurate analysis of diffraction data, for example in neighboring element contrast and valence contrast experiments, and for structure solutions. Additionally, it could also provide the basis for a new type of experiment: the examination of the coordination geometry of a given atom through crystallographic determinations of f' or f'' (site-selective XANES). The latter approach could provide information on an atom's coordination environment in an elemental and site-specific fashion. This is something that is not possible with either conventional crystallography or X-ray absorption. Unfortunately, a large amount of resonant diffraction data must be obtained and analyzed in order to obtain any useful information, and this is likely to severely restrict the application of this method.

3.2.3. *Problems Due to Multiple Occupancy in Disordered Materials*

In many crystalline materials of interest to solid-state chemists more than two distinct species are located on a single crystallographic site. The superconductor $La_{0.9}Gd_{0.9}Sr_{0.2}CuO_{0.4}$ which has potentially three types of cations located on the same site is one such compound; it is not possible to determine uniquely the distribution of the cations on the site from a single diffraction data set.[72] In order to solve a problem of this type unambiguously, one diffraction pattern is required for every unknown occupancy, and each of these diffraction patterns has to be measured in such a way that the form factors for the disordered elements vary between them. This can be achieved by collecting both X-ray and neutron diffraction data, using isotope substitution in combination with neutron diffraction, or by using anomalous scattering to alter the X-ray scattering power of an element.

In the case of the superconductor just mentioned, a minimum of two diffraction data sets are required, as there are three cations and each crystallographic site is fully occupied. However, in partially zinc-exchanged sodium zeolite-Y ($Na_{0.07}Zn_{0.11}Al_{0.28}Si_{0.72}O_2$), in which there are potentially only two cations (Zn and Na) on each of the extra-framework sites, two diffraction data sets are still required as these

sites are not necessarily fully occupied. It was possible to resolve the latter problem by collecting two X-ray data sets, one near the Zn K absorption edge (1.284 Å) and the other at much shorter wavelength (0.8 Å).[82] The difference in scattering powers for Zn at these wavelengths is sufficient to allow the determination of the distribution of cations in the extra-framework sites.

3.2.4. Structure Solution Using Anomalous Scattering

Anomalous scattering plays a very important role in the solution of the phase problem for macromolecules,[83] but it has found little use in the solution of inorganic crystal structures from single-crystal or powder diffraction data. In the case of single-crystal data, it is nearly always possible to solve the crystal structure without recourse to such an expensive technique if the crystal is of reasonable quality, and the few examples of its use tend to be illustrating points of technique rather than solving new structures.[84, 85] While there have been no examples of the application of anomalous scattering data in solving structures from powder diffraction, there has been some discussion as to how this may be achieved.[40, 86] There may be some advantage here in using multiwavelength anomalous scattering data for structure solution rather than a single powder pattern. The extra information provided by the anomalous scattering may be able to partially compensate for that lost due to the overlap of reflections in the pattern.

3.3. Rietveld Analysis with Synchrotron X-ray Data

The extension of Rietveld profile analysis to laboratory X-ray diffraction data is now widely practiced, although, in general, the method does not appear to be as precise as its neutron counterpart. One disadvantage of using X-rays is that the falloff in intensity with increasing $(\sin\theta)/\lambda$ reduces the amount of useful data that can be measured, a serious drawback for a method that is intrinsically short of data compared with single-crystal experiments. In extending the technique to synchrotron data, the higher quality of the data leads to improved precision in the final structure, although Rietveld analysis can be more difficult at high resolution if sample effects such as anisotropic strain or particle-size broadening give rise to complex peak shapes. Nevertheless, Cox et al.[87] and other authors have shown that profile analysis can be applied routinely to synchrotron data; an example is shown in Figure 10.[88]

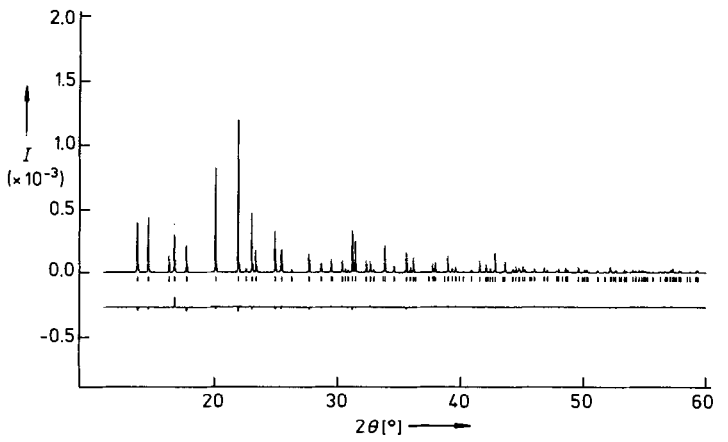

Fig. 10. The observed, calculated, and difference patterns (lower curve) resulting from the Rietveld analysis of the synchrotron X-ray powder pattern of $LiNbO_3$. The ticks mark the calculated positions of the possible reflections. The data were collected on beamline X7A at the NSLS, Broookhaven National Laboratory. $\lambda = 0.6543$ Å.

3.4. Synchrotron X-ray Diffraction In Situ

The use of synchrotron X-ray diffraction for time-resolved studies offers one major advantage over neutron diffraction: the radiation from synchrotron X-ray sources is typically many orders of magnitude more intense than that from neutron sources. This suggests that faster processes can be studied and that samples with smaller volumes can be examined. The latter point is of great importance when the design of the sample cell places severe restrictions on the amount of material that can be used, as for example in high-pressure experiments with diamond anvil cells (DACs).

There are several possible approaches to time-resolved X-ray experiments. 1) A conventional angle-scanning diffractometer can be used to perform short scans. However, while this approach has been used for some laboratory studies such as the formation of synthesis gas from methane over $Eu_2Ir_2O_7$,[89] it is only suitable for the examination of processes over extended times due to the time difference between the recording of the beginning and end of the diffraction pattern.

2) A position-sensitive detector can be used to simultaneously record either the entire monochromatic diffraction pattern or a substantial section of it. This method often, but not necessarily, gives diffraction patterns which are of lower angular resolution than those recorded in the angle-scanning mode. The timescale on which processes can be studied, usually a few seconds, is to some extent limited by the counting electronics typically employed with such detectors, although it could be improved considerably. The technique has found use in the study of electrode surfaces in situ[90] and has been employed in combination with time-resolved X-ray absorption spectroscopy to study the decomposition of carbonate precursors to oxide catalysts and the reduction of oxide mixtures.[91]

3) In energy-dispersive X-ray diffraction (EDXD) techniques, data are collected using "white" synchrotron radiation in an experiment similar to the TOF neutron diffraction experiment. The detector is again placed at a fixed 2θ value, but the different wavelengths are resolved, not by time-of-flight, but with an energy-dispersive X-ray detector (for example a Li-drifted silicon detector). As in the neutron diffraction experiment, this has the advantage that the whole diffraction pattern is accumulated simultaneously. The technique generally gives low pattern resolution due to the poor energy resolution of the detector, but it does offer some advantages over angle-dispersive techniques. EDXD enables the experimenter to employ a large fraction of the hard X-ray photons produced by the source and consequently allows the rapid collection of data. Once again, the timescale on which data can be collected is sometimes limited by the counting

electronics, but this problem can be overcome partly by examining selected areas of the diffraction pattern.[92] It has been demonstrated that data can be acquired on a 20 ms timescale.[93] Since EDXD is a fixed-angle experiment, it is an attractive technique for the study of samples in highly restricted environments, as in DACs. This, in combination with the high intensity of synchrotron radiation, has led to the extensive use of the technique for the investigation of phase relationships at very high pressures and the kinetics of phase transitions.[93,94] Examples include the transformation of CsI from an orthorhombic to an hexagonal structure type at approximately 2 Mbar[95] and the conversion of the olivine form of Mg_2GeO_4 to a spinel.[96] In addition, the technique has been applied in the study of the crystallization of metallic glasses,[97,98] the hydration of cements,[97] and the formation of crystalline zirconium(IV) oxide from hydroxide gels.[98] A recent application to the formation of a catalyst from a pyrochlore precursor as shown in Figure 11.[99]

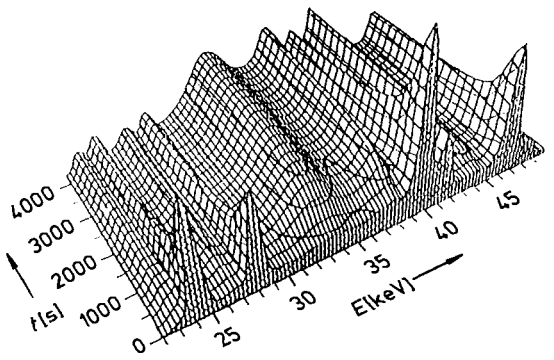

Fig. 11. The time-dependent evolution of the EDXD pattern of $Eu_2Ir_2O_7$ as the compound decomposes to Ir and Eu_2O_3 under a stream of CH_4/CO_2 at 888 K. The formation of small particles of iridium metal (diameter ca. 40 Å) is evident by the appearance of the broad peak at 35 KeV. Data were collected at Daresbury Laboratory.

3.5. Single-Crystal Studies

3.5.1. Microcrystal Experiments

The use of intense synchrotron X-ray sources to collect diffraction data on very small crystals promises to bring advances in three main areas: 1) the structural study of compounds which cannot be obtained as single crystals large enough for conventional diffractometry, 2) the collection of extinction-free data (at short wavelengths) for use in high-accuracy crystal structure analysis, and 3) the examination of materials in special environments, particularly under high pressures where the samples should be small in volume in order to simplify the construction of the cell and minimize any pressure gradients across the sample.

There have been several articles in which microcrystal diffraction experiments are discussed.[100-103] The published studies focused on test specimens such as CaF_2 (minimum size 2.2 μm^3),[104-106] the zeolite cancrinite (800 μm^3),[107] molybdenum (0.3 μm^3),[108] and bismuth (0.4 μm^3),[109] as well as a small number of materials whose crystal structures were not well determined previously, for instance piperazine silicate (25 200 μm^3)[110] and zeolite theta-1 (4000 μm^3).[111]

The majority of the early studies in this area were performed with conventional detectors and angle-scanning diffractometers.[104-107] Although this approach is capable of providing high-quality data, it suffers from the disadvantage that the time required for data acquisition may be long, since the crystal must be oriented for each Bragg reflection and then scanned. Two other techniques have been employed in an attempt to reduce the time required for data collection. Area detectors such as the CCD (Charged Coupled Device) camera[110,111] or imaging plates have been used with monochromatic radiation, and Laue diffraction studies have been conducted with either film,[112] imaging plates,[109] or in one case a solid-state detector.[108] The Laue technique is undoubtedly the quickest way of obtaining data, but unfortunately it is perhaps the most demanding in terms of crystal quality; crystals with large mosaic spreads produce data that are hard to analyze.

While the number of crystal structures that have been solved and refined from data collected on microcrystals is small, it appears likely that this technique will rapidly find widespread application. Many compounds that are currently regarded as only being available in powder form are potentially characterizable as microcrystals; this approach would considerably simplify the solution of their crystal structures.

3.5.2. Data Collection with Imaging Plates

Imaging plates (IPs) were originally developed for medical radiography as an alternative to film.[113] They offer the advantages of reduced radiation exposure to the patient and less expenditure on consumable materials. Each plate consists of a plastic sheet coated with a thin layer of an organic binder containing a phosphor (e.g. Eu-doped BaFBr). X-ray exposure produces color centers in the phosphor which can subsequently be "read out" by irradiation with laser light and monitoring of the resultant photostimulated luminescence (PSL). In addition, imaging plates have also found use as area detectors in the recording of X-ray diffraction patterns, both in the laboratory and at synchrotron X-ray sources.[114-117]

The use of IPs for the recording of X-ray diffraction patterns has largely been motivated by the need to reduce the radiation exposure required to obtain a given signal-to-noise ratio in the resulting diffraction pattern. However, there are several other advantages associated with their use as area detectors: 1) IPs have a large dynamic range, which permits the recording of the strong and weak data together on a single plate; X-ray film often requires multisheet packs of film. 2) There is effectively no limitation on count rate with imaging plate detectors, unlike pulse-counting devices such as multiwire proportional chambers. 3) The image recorded on an IP is essentially free of distortion, which is a significant improvement over video detectors. 4) IPs offer good spatial resolution. Together, these characteristics lead to a detection system that allows the rapid collection of high-quality diffraction data over a large area of reciprocal space. While this is particularly important in the case of protein samples that are often easily damaged by radiation exposure,[118-121] it is

also of use in time-resolved[122, 123] and diffuse-scattering studies, and the examination of small sample volumes. Furthermore, results obtained by using an imaging plate with short-wavelength radiation have demonstrated a dramatic enhancement in the sensitivity to hydrogen atoms, for example in organic clathrates.[124]

For inorganic compounds, which are not usually sensitive to radiation exposure, the reduction in the time required for the acquisition of a dataset is clearly advantageous, particularly in the case of time-resolved studies such as the examination of the diffuse scattering during a phase transformation in a single crystal of AgZn.[125] It appears likely, however, that the main application will be to high-pressure studies. To date there have been several studies of materials in diamond anvil cells, for example Ag, Mn, Cs, BN, Br, I,[126] InSb, and La_2CuO_4.[127] In such cases the two-dimensional nature of the imaging plate detector combined with suitable integration around the Debye–Scherrer rings recorded on the plate facilitate the collection of data with a reasonable signal-to-noise ratio and a significant improvement in powder averaging. The latter point is important if quantitative analysis of the intensity data is envisaged.

4. Conclusions and Future Prospects

The preceding sections underline the substantial and wide-ranging contributions that the use of neutron and synchrotron X-ray diffraction have already made to our understanding of solid-state chemistry, and the future is certain to bring new and exciting applications of these powerful tools. Furthermore, as a result of recent advances in software, there will be a growing awareness of the scope for combined X-ray and neutron refinements. For example, the simultaneous Rietveld analysis of X-ray and neutron powder data is now possible with the GSAS[128] suite of programs. In a recent study, the structure of $K_{0.5}Na_{0.5}TiOPO_4$ (a material with nonlinear optical properties) was analyzed by this method.[129] The neutron diffraction data gave better precision for the oxygen atoms than was possible with X-ray diffraction data, but the distribution of K^+ and Na^+ ions over the two available cation sites could not be determined, since the neutron scattering powers of potassium and sodium are almost identical.[5] When the X-ray data were included in the refinement, it became clear that sodium occupies one cation site and potassium occupies the other.

Another area in which X-ray and neutron diffraction data have traditionally been combined is in the determination of deformation densities; X–N maps, for example, show how the electron density is redistributed when atoms come together to form molecules.[130] In such experiments the neutron diffraction data is used to determine the nuclear positions and the X-ray diffraction data reveals the electron density distribution. In some cases this may lead to small differences in atomic coordinates between the two types of crystal structure analysis, especially for light elements. While we are unaware of any cases in which X–N maps have been calculated using synchrotron X-ray data, such data has been employed in the calculation of so-called X–X maps.[131] Here the X-ray diffraction data collected at high scattering angles is used to define the nuclear positions and that at low scattering angles provides information on the redistribution of charge density due to bonding. Synchrotron X-ray diffraction potentially offers significant advantages over conventional X-ray diffraction for such studies, in particular a reduction in the effects of extinction and absorption as a consequence of using small crystals at short wavelengths. However, there are several technical difficulties in performing such experiments[131] and further effort is needed in the area.

The examples described in Sections 2 and 3 illustrate many of the strengths and weaknesses of neutron and synchrotron X-ray diffraction for structural studies in the solid state. Whilst neutron diffraction is a mature area that has benefitted from the evolution of high-flux beam reactors and pulsed sources during the last three decades, it continues to play a vital role in key areas such as high-temperature superconductivity and zeolite catalysis. By contrast, synchrotron X-ray methods are less well developed because most facilities have only become available during the 1980s. The construction of advanced synchrotron sources, which operate at higher ring energies and give access to shorter X-ray wavelengths, is well under way in both Europe (the European Synchrotron Radiation Facility, ESRF) and the USA (the Advanced Photon Source, APS). These will certainly open up new possibilities, beyond the ideas discussed in this review. In some areas, particularly light-atom detection and neighboring element contrast, the unique role of neutron diffraction is already under some pressure from experiments with synchrotron radiation, and future developments will certainly lead to further inroads. Nevertheless, there are many experimental applications for which the use of neutron diffraction will continue to be mandatory. These include the study of magnetic materials (notwithstanding the recent advances in the magnetic scattering of X-rays, in particular, resonant enhancement[132, 133]), neighboring element contrast for light elements, and the use of neutron diffraction to give superior precision for most atoms in Rietveld analysis.[68] X-rays and neutron diffraction will always have their protagonists in the crystallographic community, but there will clearly continue to be a role for both methods in solid-state chemistry.

APW would like to acknowledge Christ Church, Oxford (UK) for giving him leave from a Junior Research Fellowship. We are also grateful to Shell for financial support and Dr. R. J. Cernik and Dr. C. J. Howard for providing the data in Figure 3.

Received: March 23, 1992 [A 886 IE]
German version: *Angew. Chem.* **1992**, *104*, 1594

[1] JCPDS, Powder diffraction file, International Center for Diffraction Data, 1601 Park Lane, Swarthmore, PA 19081-2389, USA.
[2] ICSD, Inorganic Crystal Structure Database, Institute for Inorganic Chemistry, University of Bonn.
[3] D. P. Mitchell, P. N. Powers, *Phys. Rev.* **1936**, *50*, 486–487.
[4] C. G. Windsor, *Pulsed Neutron Scattering*, Taylor and Francis, London, **1981**.
[5] G. E. Bacon, *Neutron Diffraction*, 3rd ed., Oxford, **1975**.
[6] A. K. Cheetham, W. I. F. David, M. M. Eddy, R. J. B. Jakeman, M. W. Johnson, C. C. Torardi, *Nature (London)* **1986**, *320*, 46–48.
[7] W. I. F. David, R. M. Ibberson, J. C. Matthewman, K. Prassides, T. J. S. Dennis, J. P. Hare, H. W. Kroto, R. Taylor, D. R. M. Walton, *Nature (London)* **1991**, *353*, 147–149.
[8] *Synchrotron Radiation Research* (Eds.: H. Winich, S. Doniach), Plenum, New York, **1980**.

[9] Å. Kvick, *Chemical Crystallography with Pulsed Neutrons and Synchrotron X-Rays*, (Eds.: M. A. Carrondo, G. A. Jeffrey) *(NATO Ad. Study Inst. Ser. Ser. C* **1988**, *221*, 187–203).
[10] C. G. Titcome, A. K. Cheetham, B. E. F. Fender, *J. Phys. C: Solid State Phys.* **1974**, *7*, 2409–2416.
[11] V. A. Somenkov, I. R. Entin, M. E. Kost, S. Sh. Shil'shtein, *Fiz. Tverd. Tela (Leningrad)* **1975**, *17(8)*, 2368–2373.
[12] P. A. Wright, J. M. Thomas, A. K. Cheetham, A. K. Nowak, *Nature (London)* **1985**, *318*, 611–613.
[13] A. N. Fitch, H. Jobic, A. Renouprez, *J. Phys. Chem.* **1986**, *90*, 1311–1318.
[14] R. Goyal, A. N. Fitch, H. Jobic, *J. Chem. Soc. Chem. Commun.* **1990**, 1152–1153.
[15] M. Czjzek, H. Fuess, T. Vogt, *J. Phys. Chem.* **1991**, *95*, 5255–5261.
[16] P. D. Battle, A. K. Cheetham, J. B. Goodenough, *Mater. Res. Bull.* **1979**, *14*, 1013–1024.
[17] P. D. Battle, A. K. Cheetham, *J. Phys. C: Solid State Phys.* **1979**, *12*, 337–345.
[18] C. Wilkinson, A. K. Cheetham, G. J. Long, P. D. Battle, D. A. O. Hope, *Inorg. Chem.* **1984**, *23*, 3136–3141.
[19] J. K. Warner, A. K. Cheetham, D. E. Cox, R. B. Von Dreele, *J. Am. Chem. Soc.*, **1992**, *114*, 6074–6080.
[20] H. M. Rietveld, *J. Appl. Crystallogr.* **1969**, *2*, 65–71.
[21] A. K. Cheetham, J. C. Taylor, *J. Solid State Chem.* **1977**, *21*, 253–275.
[22] A. Albinatti, B. T. M. Willis, *J. Appl. Crystallogr.* **1982**, *15*, 361–374.
[23] A. W. Hewat, *Chem. Scr.* **1986**, *26 A*, 119–130.
[24] A. P. Wilkinson, A. K. Cheetham, W. Kunnman, Å. Kvick, *Eur. J. Solid State Inorg. Chem.* **1991**, *28*, 453–459.
[25] R. B. Von Dreele, J. D. Jorgensen, C. G. Windsor, *J. Appl. Crystallogr.* **1982**, *15*, 581–589.
[26] J. D. Jorgensen in *Chemical Crystallography with Pulsed Neutrons and Synchrotron X-Rays* (Eds.: M. A. Carrondo, G. A. Jeffrey), (*NATO Ad. Study Inst. Ser. Ser. C* **1988**, *221*, 159–185).
[27] C. Riekel, *Prog. Solid State Chem.* **1980**, *13*, 89–117.
[28] J. Pannetier, *Chem. Scr.* **1986**, *26 A*, 131–139.
[29] J. Pannetier, *Real-Time Neutron Powder Diffraction: New opportunities for Solid State Chemistry*, **1980**, distributed at the Galerne meeting.
[30] W. Abriel, K. Reisdorf, J. Pannetier, *J. Solid State Chem.* **1990**, *85*, 23–30.
[31] V. Paul-Boncour, C. Lartigue, A. Percheron-Guégan, J. C. Achard, J. Pannetier, *J. Less-Common Met.* **1988**, *143*, 301–313.
[32] C. Poinsignon, M. Forestier, M. Anne, D. Fruchart, S. Miraglia, A. Rouault, J. Pannetier, *Z. Phys. Chem. (München)* **1989**, *164*, 1515–1520.
[33] M. Goldmann, J. Pannetier, F. Beguin, B. Gonzalez, *Synth. Met.* **1988**, *23*, 133–138.
[34] C. J. Carlile, D. C. Salter, *High Temp.-High Pressures* **1978**, *10*, 1-27.
[35] D. B. McWhan, *Rev. Phys. Appl.* **1984**, *19*, 715–718.
[36] A. W. Hewat, *Phys. Scr.* **1991**, *44*, 38–50.
[37] J. Plévert, M. Louër, D. Louër, *J. Appl. Crystallogr.* **1989**, *22*, 470–475, and references therein.
[38] A. Le Bail, G. Ferey, P. Amoros, D. Beltran-Porter, *Eur. J. Solid. State Inorg. Chem.* **1989**, *26*, 419–434, and references therein.
[39] D. E. Cox, J. B. Hastings, L. P. Cardoso, L. W. Finger, *Mater. Sci. Forum* **1986**, *9*, 1–20.
[40] A. K. Cheetham, A. P. Wilkinson, *J. Phys. Chem. Solids* **1991**, *52*, 1199–1208.
[41] J. P. Attfield, A. W. Sleight, A. K. Cheetham, *Nature (London)* **1986**, *322*, 620–622.
[42] M. S. Lehmann, A. N. Christensen, H. Fjellvag, R. Feidenhans'l, M. Nielsen, *J. Appl. Crystallogr.* **1987**, *20*, 123–129.
[43] P. Lightfoot, A. K. Cheetham, A. W. Sleight, *Inorg. Chem.* **1987**, *26*, 3544–3547.
[44] A. N. Christensen, D. E. Cox, M. S. Lehmann, *Acta Chem. Scand.* **1989**, *43*, 19–25.
[45] L. B. McCusker, *J. Appl. Crystallogr.* **1988**, *21*, 305–310.
[46] S. J. Hibble, A. K. Cheetham, A. R. L. Bogle, H. R. Wakerley, D. E. Cox, *J. Am. Chem. Soc.* **1988**, *110*, 3295–3296.
[47] G. S. Smith, Q. C. Johnson, D. E. Cox, R. L. Snyder, D. K. Smith, A. Zalkin, *Adv. X-ray Anal.* **1987**, *30*, 383–388.
[48] G. S. Smith, Q. C. Johnson, D. K. Smith, D. E. Cox, R. L. Snyder, R.-S. Zhou, A. Zalkin, *Solid State Commun.* **1988**, *67*, 491–494.
[49] M. Marezio, D. E. Cox, C. Rossel, M. B. Maple, *Solid State Commun.* **1988**, *67*, 831–835.
[50] M. Kurahashi, K. Honda, M. Goto, *Photon factory activity report* **1989**, 7, 170.
[51] E. Weiss, S. Corbelin, J. K. Cockcroft, A. N. Fitch, *Angew. Chem.* **1990**, *102*, 728; *Angew. Chem. Int. Ed. Engl.* **1990**, *29*, 650–652.
[52] E. Weiss, S. Corbelin, J. K. Cockcroft, A. N. Fitch, *Chem. Ber.* **1990**, *123*, 1629–1634.
[53] R. J. Cernik, A. K. Cheetham, C. K. Prout, D. J. Watkin, A. P. Wilkinson, B. T. M. Willis, *J. Appl. Crystallogr.* **1991**, *24*, 222–226.
[54] P. Lightfoot, J. A. Hriljac, S. Pei, Y. Zheng, A. W. Mitchell, D. R. Richards, B. Dabrowski, J. D. Jorgenson, D. G. Hinks, *J. Solid State Chem.* **1991**, *92*, 473–479.
[55] R. G. Teller, P. Blum, E. Kostiner, J. A. Hriljac, *J. Solid State Chem.* **1992**, *97*, 10–18.
[56] J. A. Hriljac, J. B. Parise, G. H. Kwei, K. B. Schwartz, *J. Phys. Chem. Solids* **1991**, *52*, 1273–1279.
[57] R. E. Morris, W. T. A. Harrison, J. M. Nicol, A. P. Wilkinson, A. K. Cheetham, *Nature* **1992**, *359*, 519–522.
[58] J. W. Visser, *J. Appl. Crystallogr.* **1969**, *2*, 89–95.
[59] P.-E. Werner, L. Eriksson, M. J. Westdahl, *J. Appl. Crystallogr.* **1985**, *18*, 367–370.
[60] D. Louër, M. Louër, *J. Appl. Crystallogr.* **1972**, *5*, 271–275.
[61] D. Louër, R. Vargas, *J. Appl. Crystallogr.* **1982**, *15*, 542–545.
[62] G. S. Pawley, *J. Appl. Crystallogr.* **1981**, *14*, 357–361.
[63] A. Le Bail, H. Duroy, J. L. Fourquet, *Mater. Res. Bull.* **1988**, *23*, 447–452.
[64] J. P. Attfield, A. K. Cheetham, D. E. Cox, A. W. Sleight, *J. Appl. Crystallogr.* **1988**, *21*, 452–457.
[65] R. Glaum, R. Gruehn, M. Möller, *Z. Anorg. Allg. Chem.* **1986**, *543*, 111–116.
[66] J. Köhler, A. Simon, S. J. Hibble, A. K. Cheetham, *J. Less-Common Met.* **1988**, *142*, 123–133.
[67] R. Begum, M. Hart, K. R. Lea, D. P. Siddons, *Acta Crystallogr. Sect. A* **1986**, *42*, 456–464.
[68] A. P. Wilkinson, D. E. Cox, A. K. Cheetham, *J. Phys. Chem. Solids* **1991**, *52*, 1257–1266.
[69] L. M. Moroney, P. Thompson, D. E. Cox, *J. Appl. Crystallogr.* **1988**, *21*, 206–208.
[70] R. S. Howland, T. H. Geballe, S. S. Laderman, A. Fischer-Colbrie, M. Scott, J. M. Tarascon, P. Barboux, *Phys. Rev. Sect. B* **1989**, *39*, 9017–9027.
[71] J. P. Attfield, *J. Phys. Chem. Solids* **1991**, *52*, 1243–1249.
[72] G. H. Kwei, R. B. Von Dreele, S.-W. Cheong, Z. Fisk, J. D. Thompson, *Phys. Rev. Sect. B* **1990**, *41*, 1889–1893.
[73] A. Williams, G. H. Kwei, A. T. Ortiz, M. Karnowski, W. K. Warburton, *J. Mater. Res.* **1990**, *5*, 1197–1200.
[74] H. L. Yakel, *Acta Crystallogr. Sect. B* **1983**, *39*, 20–28.
[75] H. L. Yakel, *Acta Crystallogr. Sect. B* **1983**, *39*, 28–33.
[76] J. P. Attfield, *Nature (London)* **1990**, *343*, 46–49.
[77] D. A. Perkins, J. P. Attfield, *J. Chem. Soc. Chem. Commun.* **1991**, 229–230.
[78] A. P. Wilkinson, D. E. Cox, A. K. Cheetham, *Acta Crystallogr. Sect. B* **1991**, *47*, 155–161.
[79] J. K. Warner, A. P. Wilkinson, A. K. Cheetham, D. E. Cox, *J. Phys. Chem. Solids* **1991**, *52*, 1251–1256.
[80] R. Wulf, *Acta Crystallogr. Sect. A* **1990**, *46*, 681–688.
[81] I. D. Brown, D. Altermatt et al., STRUMO – A modelling program for inorganic structures, Version 1991.3.12, Institute for Materials Research, McMaster University, Hamilton, Ontario L8S 4MI, Canada.
[82] a) A. P. Wilkinson, Dissertation, University of Oxford, **1991**; b) A. P. Wilkinson, A. K. Cheetham, S. C. Tang, W. J. Reppart, *J. Chem. Soc. Chem. Commun.* **1992**, 1485–1487.
[83] I. D. Glover, J. R. Helliwell, M. Z. Papiz, *Top. Curr. Chem.* **1988**, *147*, 32–55.
[84] G. Chapius, D. H. Templeton, L. K. Templeton, *Acta Crystallogr. Sect. A* **1985**, *41*, 274–278.
[85] K. F. Fischer, *Z. Kristallogr.* **1987**, *179*, 77–95.
[86] W. Prandl, *Acta Crystallogr. Sect. A* **1990**, *46*, 988–992.
[87] D. E. Cox, J. B. Hastings, W. Thomlinson, C. T. Prewitt, *Nucl. Instrum. Methods* **1983**, *208*, 573–578.
[88] A. P. Wilkinson, A. K. Cheetham, D. E. Cox, R. H. Jarman, unpublished results.
[89] R. H. Jones, A. T. Ashcroft, D. Waller, A. K. Cheetham, J. M. Thomas, *Catal. Lett.* **1991**, *8*, 159–174.
[90] M. E. Heron, S. E. Doyle, K. J. Roberts, J. Robinson, F. C. Walsh, *Daresbury Laboratory preprint*, September **1991**, DL/SCI/P780E.
[91] A. J. Dent, G. E. Derbyshire, G. N. Greaves, C. A. Ramsdale, J. W. Couves, R. Jones, C. R. A. Catlow, J. M. Thomas, *Daresbury Laboratory preprint*, August **1991**, DL/SCI/P774E.
[92] S. M. Clark, M. C. Miller, *Rev. Sci. Instrum.* **1990**, *61(8)*, 2253–2255.
[93] E. F. Skelton, S. B. Qadri, W. T. Elam, A. W. Webb in *Solid State Physics Under Pressure* (Ed.: S. Minomura), KTK scientific publishers, Tokyo, **1985**, 329–334.
[94] W. A. Basset, G. E. Brown, Jr., *Annu. Rev. Earth Planet. Sci.* **1990**, *18*, 387–447.
[95] H. K.Mao, Y. Wu, R. J. Hemley, L. C. Chen, J. F. Shu, L. W. Finger, *Science* **1989**, *246*, 649–651.
[96] J. Lauterjung, G. Will, *Physica B* **1986**, *139/140*, 343–346.
[97] W. Minor, B. Schönfeld, B. Lebech, B. Buras, W. Dmowski, *J. Mater. Sci.* **1987**, *22*, 4144–4152.
[98] P. Barnes, *J. Phys. Chem. Solids* **1991**, *52*, 1299–1306.
[99] A.T. Ashcroft, A. K. Cheetham, S. M. Clark, R. H. Jones, S. Natarajan, J. M. Thomas, D. Waller, unpublished results.
[100] J. M. Newsam, K. S. Liang, *Int. Rev. Phys. Chem.* **1989**, *8*, 289–338.

[101] J. M. Newsam, C. Z. Yang, H. E. King, Jr., R. H. Jones, D. Xie, *J. Phys. Chem. Solids* **1991**, *52*, 1281–1288.
[102] M. M. Harding, *Chem. Br.* **1990**, 956–958.
[103] M. M. Harding, *J. Phys. Chem. Solids.* **1991**, *52*, 1293–1298.
[104] R. Bachmann, H.Köhler, H. Schulz, H.-P. Weber, *Acta Crystallogr. Sect. A* **1985**, *41*, 35–40.
[105] W. Rieck, H. Euler, H.Schulz, W. Schildkamp, *Acta Crystallogr. Sect. A* **1988**, *44*, 1099–1101.
[106] W. Rieck, H. Schulz, M. Siedel, *J. Phys. Chem. Solids* **1991**, *52*, 1289–1291.
[107] P. Eisenberger, J. M. Newsam, M. E. Leonowicz, D. E. W. Vaughan, *Nature (London)* **1984**, *309*, 45–47.
[108] E. F. Skelton, J. D. Ayers, S. B. Qadri, N. E. Moulton, K. P. Cooper, L. W. Finger, H. K. Mao, Z. Hou, *Science* **1991**, *253*, 1123–1125.
[109] K. Ohsumi, K. Hagiya, M. Ohmasa, *J. Appl. Crystallogr.* **1991**, *24*, 340–348.
[110] S. J. Andrews, M. Z. Papiz, R. McMeeking, A. J. Blake, B. M. Lowe, K. R. Franklin, J. R. Helliwell, M. M. Harding, *Acta Crystallogr. Sect. B* **1988**, *44*, 73–77.
[111] M. Z. Papiz, S. J. Andrews, A. M. Damas, M. M. Harding, R. Highcock, *Acta Crystallogr. Sect. C* **1990**, *46*, 172–173.
[112] M. M. Harding, S. J. Maginn, J. W. Campbell, I. Clifton, P. Machin, *Acta Crystallogr. Sect. B* **1988**, *44*, 142–146.
[113] M. Sonoda, M. Takano, J. Miyahara, H. Kato, *Radiology* **1983**, *148*, 833–838.
[114] J. Miyahara, K. Takahashi, Y. Amemiya, N. Kamiya, Y. Satow, *Nucl. Inst. Methods. Phys. Res. Sect. A* **1986**, *246*, 572–653.
[115] Y. Amemiya, Y. Satow, T. Matsushita, J. Chikawa, K. Wakabayashi, J. Miyahara, *Top. Curr. Chem.* **1988**, *147*, 121–144.
[116] Y. Amemiya, T. Matsushita, A. Nakagawa, Y. Satow, J. Miyahara, J. Chikawa, *Nucl. Inst. Methods Phys. Res. Sect. A* **1988**, *266*, 645–653.
[117] I. Tanaka, M. Yao, M. Suzuki, K. Hikichi, T. Matsumoto, M. Kozasa, C. Katayama, *J. Appl. Crystallogr.* **1990**, *23*, 334–339.
[118] N. Watanabe, K. Sakabe, N. Sakabe, T. Higashi, K. Sasaki, S. Aibara, Y. Morita, K. Yonaha, S. Toyama, H. Fukutani, *J. Biochem.* **1989**, *105*, 1–3.
[119] Z. Dauter, H. Terry, H. Witzel, K. S. Wilson, *Acta Crystallogr. Sect. B* **1990**, *46*, 833–841.
[120] I. Fujii, Y. Morimoto, Y. Higuchi, N. Yasuoka, C. Katayama, K. Miki, *Acta Crystallogr. Sect. B* **1991**, *47*, 137–144.
[121] N. Sakabe, *Nucl. Inst. Methods Phys. Res. Sect. A* **1991**, *303*, 448–463.
[122] K. Wakabayashi, Y. Amemiya, H. Tanaka, H. Sugi, T. Mitsui, *J. Muscle Res. Cell Motil.* **1986**, *7*, 277–278.
[123] Y. Amemiya, S. Kishimoto, T. Matsushita, Y. Satow, M. Ando, *Rev. Sci. Instrum.* **1989**, *60*, 1552–1556.
[124] Z. Dauter, K. S. Wilson, European Molecular Biology Laboratory, Heidelberg (FRG), private communication.
[125] H. Iwasaki, Y. Matsuo, K. Ohshima, S. Hashimoto, *J. Appl. Crystallogr.* **1990**, *23*, 509–514.
[126] O. Shimomura, K. Takemura, H. Fujihisa, Y. Fujii, Y. Ohishi, T. Kikegawa, Y. Amemiya, T. Matsushita, *Rev. Sci. Instrum.* **1992**, *63*, 967–973, and references therein
[127] R. J. Nelmes, P. D. Hatton, M. I. McMahon, R. O. Piltz, J. Crain, R. J. Cernik, G. Bushnell-Wye, *Rev. Sci. Instrum.* **1992**, *63*, 1039–1042.
[128] A. C. Larson, R. B. Von Dreele, *GSAS – General Structure Analysis System. Tech. Report LA-UR-86-748, Los Alamos Laboratory*, **1987**.
[129] S. J. Crennell, J. J. Owen, C. P. Grey, A. K. Cheetham, J. A. Kaduk, R. H. Jarman, *J. Mater. Chemistry* **1991**, *1*, 113–119.
[130] *Electron Distributions and the Chemical Bond* (Eds.: P. Coppens, M. B. Hall), Plenum, New York, **1982**.
[131] F. S. Nielsen, P. Lee, P. Coppens, *Acta Crystallogr. Sect. B* **1986**, *42*, 359–364.
[132] D. E. Moncton, D. Gibbs, J. Bohr, *Nucl. Inst. Methods Phys. Res.Sect. A* **1986**, *246*, 839–844.
[133] J. Bohr, *J. Magn. Magn. Mater.* **1990**, *83*, 530–534.

Dendrimers, Arborols, and Cascade Molecules: Breakthrough into Generations of New Materials

By *Hans-Bernhard Mekelburger, Wilfried Jaworek,* and *Fritz Vögtle**

Over a decade ago dendritic (Greek: branched) molecules began to attract ever increasing attention in organic, supramolecular, and polymer chemistry, and recently also in coordination chemistry. The initial impetus can be traced to our cascadelike synthesis of noncyclic, branched polyamines in 1978 (Scheme 1).[1] Thereafter the research groups of

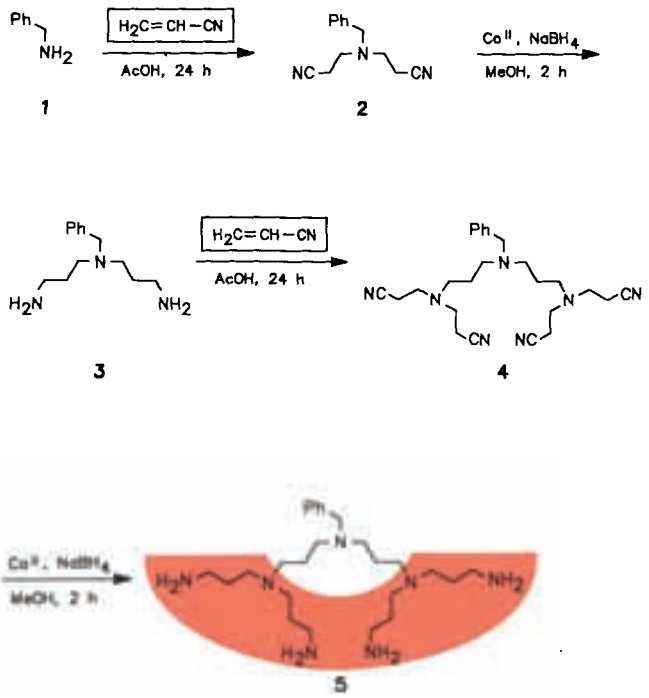

Denkewalter, Newkome, Tomalia, and others expanded this theme considerably (Scheme 2).[2] The extremely branched molecules are mainly synthesized from identical building blocks that contain branching sites, and often have a variety of functional groups on the periphery. These dendrimers[3] are constructed in stages in repeatable synthesis steps (repetitive synthesis strategy[1]). Each reaction cycle creates a new "generation". In the schemes we have highlighted the first, third, and fifth generation in red; the "core" (K) that is usually in the center of the molecule and the even generations are not highlighted (see in particular **27** in Scheme 6). The divergent synthesis method (construction, as it were, from the center outwards) is distinguished from the convergent method in which larger fragments are built up first and then coupled to the core; both methods have their strengths and their weaknesses.[4]

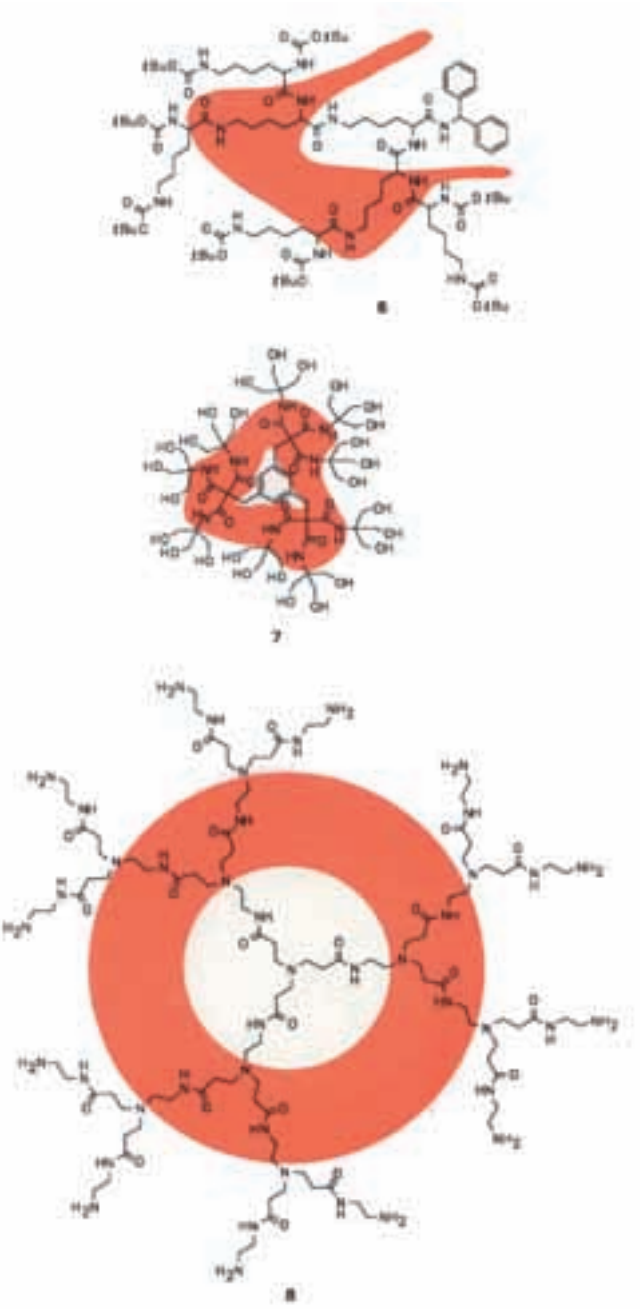

Scheme 2. Three examples of dendrimers [2]: polylysine **6** (Denkewalter et al.), arborol **7** (Newkome et al.), and polyamidoamine **8** (Tomalia et al.).

[*] Prof. Dr. F. Vögtle, H.-B. Mekelburger
Institut für Organische Chemie und Biochemie der Universität
Gerhard-Domagk-Strasse 1, D-W-5300 Bonn 1 (FRG)
Dr. W. Jaworek
Textar GmbH Grundsatzentwicklung/EPN

 © VCH Verlagsgesellschaft mbH, W-6940 Weinheim, 1992 0570-0833/92/1212-1571 $ 3.50+.25/0

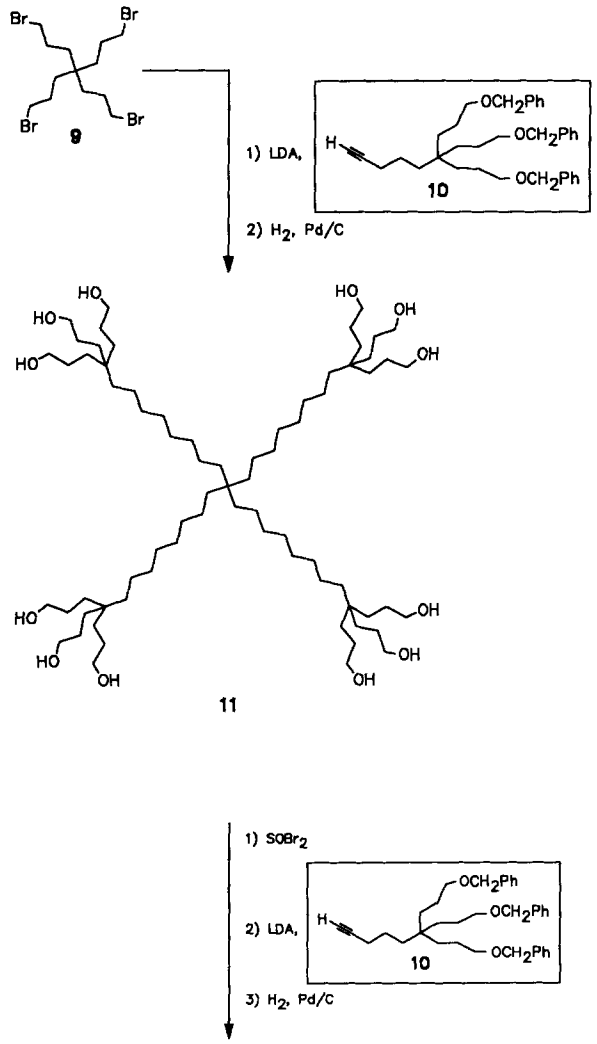

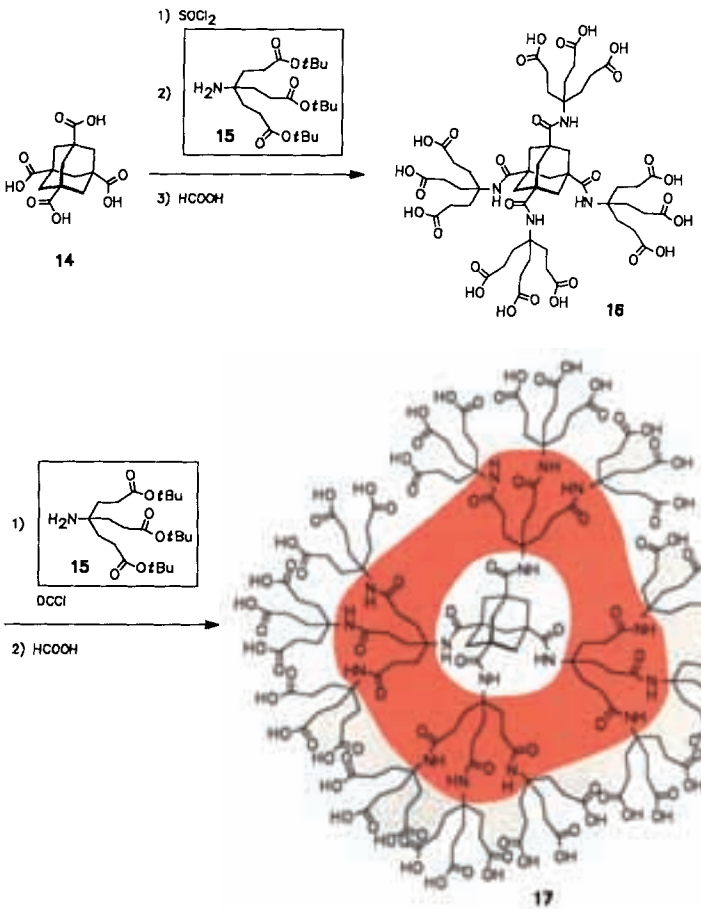

Scheme 4. Preparation of the dendrimer **17** containing 36 carboxy groups.

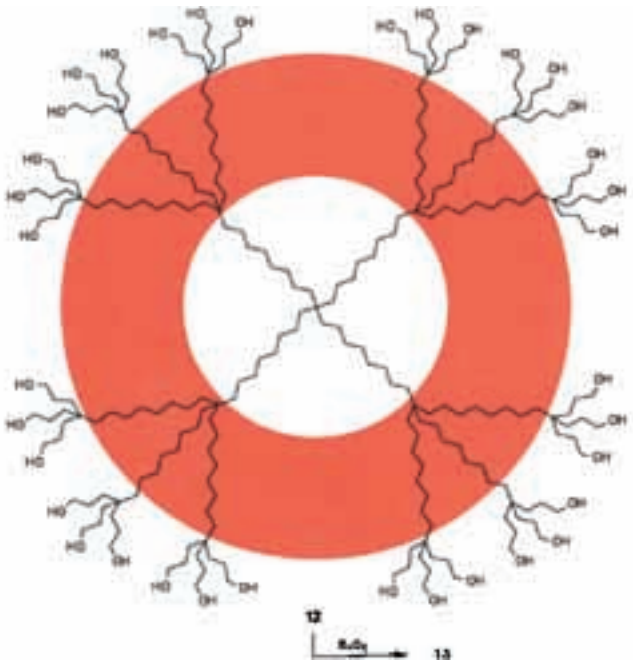

Scheme 3. Divergent synthesis of arborols with an exclusively hydrocarbon skeleton [7].

The pronounced branching provides the higher generations with an increasingly three-dimensional structure that is characterized by a growing number of cavities within the molecule. One aim in the design of new dendrimers is therefore the formation of niches tailormade for specific guests in order to generate host/guest relationships and aggregates. The dendrimers became even more attractive after it was shown that their surfaces displayed fractal (self-imaging) features. This contribution explores the most important developments in this field.

Newkome et al. reported the synthesis of arborols[6] with saturated hydrocarbon skeletons. They have the characteristics of globular micelles (Scheme 3).[7] Treatment of the core unit **9** with the anion of the alkyne **10** yielded the dodecahydroxy compound **11** after cleavage of the protecting groups and hydrogenation of the triple bond. After bromination with thionyl bromide the reaction sequence was repeated. Like its lower analogue **11**, the 36-fold alcohol **12** is very soluble in alcohol, but only slightly soluble in chloroform or water. Finally this second generation polyalcohol was oxidized with ruthenium tetroxide to form hexatriacontacarboxylic acid **13**, from which the water-soluble ammonium and tetramethylammonium derivatives were made. Both these dendrimers accept nonpolar molecules (for example, diphenylhexatriene, chlorotetracycline, or pinacyanol chloride) as guests in the niches within their lipophilic framework. They do not aggregate and can therefore be considered "unimolecular micelles".[8]

Newkome also approached the preparation of micellar dendrimers with a hydrophilic surface and a compact lipophilic interior from the core building block adamantanetetracarboxylic acid (**14**, Scheme 4), lengthening the chains through the amide bonds.[9] Each amine molecule **15** has three *tert*-butyl ester groups. Their hydrolysis yielded the dodecacarboxylic acid **16**, which was again treated with the amine **15**. Another hydrolysis afforded the water-soluble second generation dendrimer **17** containing 36 carboxyl groups at its periphery.

Recently the same author reported on poly(amidoalcohol)s with two spherical head groups joined to a central C–C triple bond through alkyl chains.[10] These dumbbell-shaped arborols form rodlike structures constructed by helical or scissorlike stacking, which can in turn cluster together to form aggregates of higher order. This property is reflected in the macroscopic tendency to form thermally reversible aqueous gels.

Fréchet et al.[4] employed the convergent method to synthesize dendritic polyethers up to the sixth generation. Bromide **18**, which is at the periphery of the dendrimer and contains two benzyl ether units, was treated with 3,5-dihydroxybenzyl alcohol **19**, a monomeric building block (Scheme 5). On reaction with tetrabromomethane and triphenylphosphane in excess, another bromide (**20**) was formed that could be extended with the monomeric building block **19** to give the second generation. At the end of the synthesis the reaction of the wedge-shaped bromides (e.g. **20**, **21**, **22**) with the trifunctional core unit afforded spherical polyethers such as **24**. In a variation of this synthesis, even unsymmetrically substituted polyethers could be obtained.[11] The attraction of the convergent method is the small number of molecules that are involved in the reaction steps to give each successive generation. The large excesses of reagents can be avoided, which results in good yields. However, for higher generations the yields decrease because of increasing steric hindrance at the reacting functional groups. The use of more flexible monomers (e.g. **25**) should therefore provide better yields. After convergent synthesis and cleavage of the benzylic protecting groups, Fréchet et al. obtained the sixfold phenol **26** (Scheme 6) that was used as extended core for a divergent procedure in a reaction with the bromide of the third generation (**22**) to give the spherical dendrimer (**27**).[12]

Miller, Neenan et al.[13] also used the convergent method to prepare aromatic hydrocarbon dendrimers. Aryl boronic

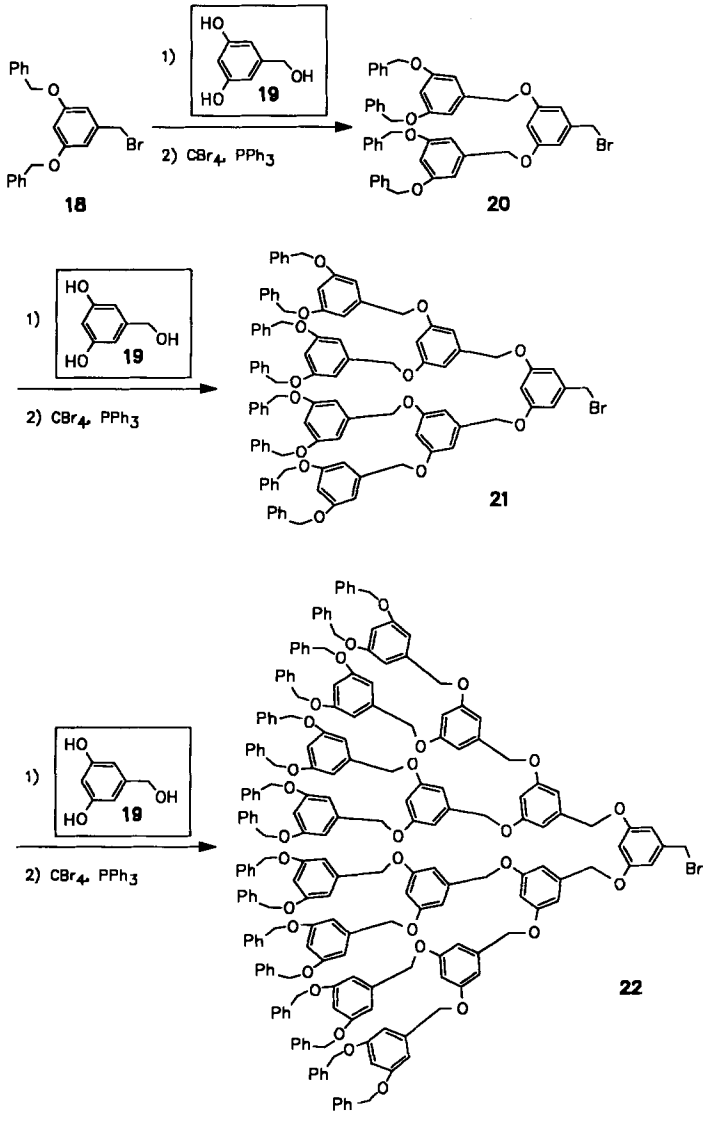

Scheme 5. Convergent synthesis of polyether dendrimers [4].

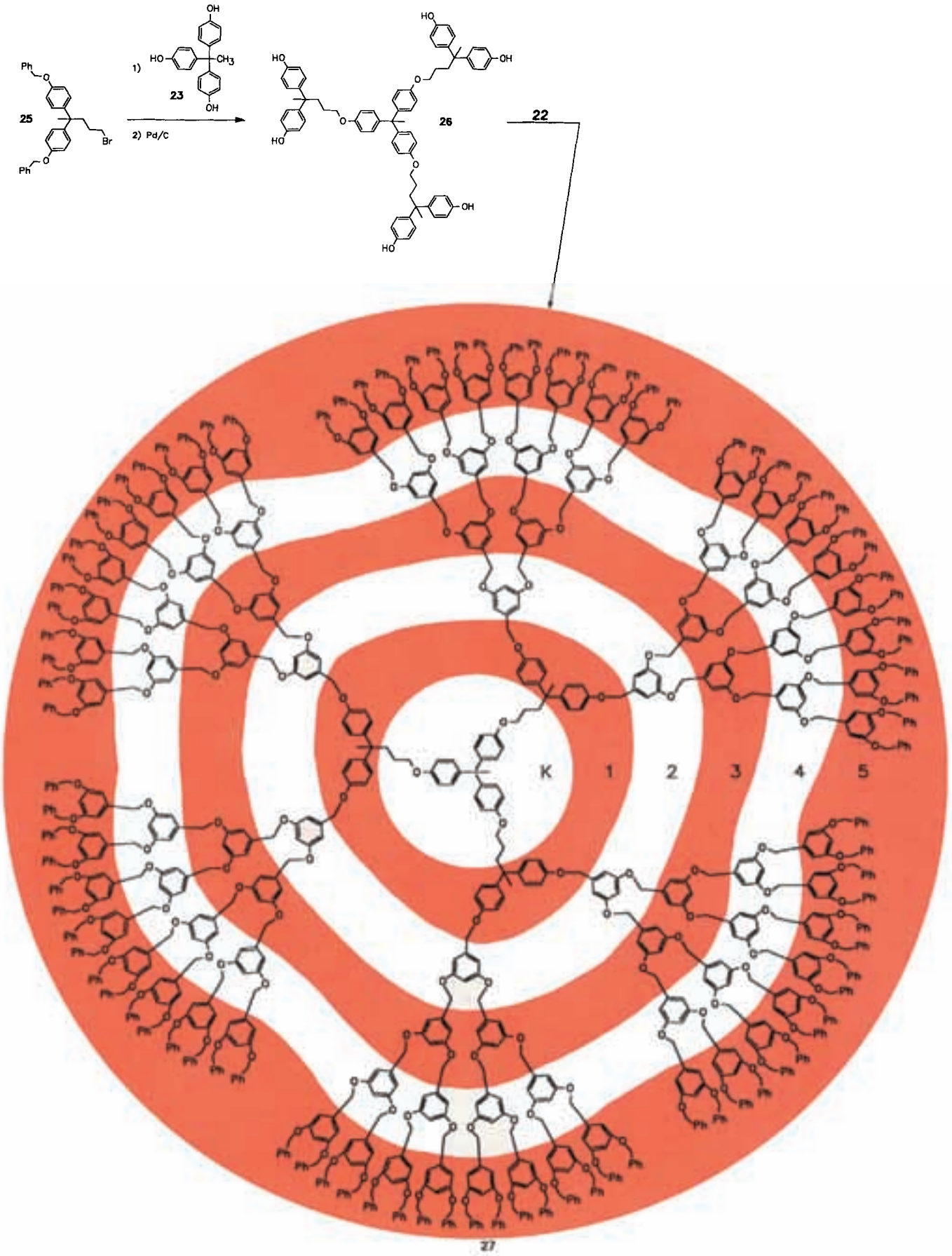

Scheme 6. Convergent–divergent synthesis of larger polyethers through incorporation of more flexible building blocks [12].

acids were coupled to the building block 3,5-dibromo-1-trimethylsilylbenzene in a Suzuki reaction, and the aryltrimethylsilane was subsequently transformed into an aryl boronic acid again. This procedure yielded poly(1,3,5-phenylene)s after the final coupling with the core molecule 1,3,5-tribromobenzene. The hydrocarbon of the third generation, containing 46 benzene rings, was obtained in a combined convergent–divergent synthesis. These dendrimers, with the exception of the sparingly soluble first generation, dissolve in THF, toluene, and chloroform and are thermally stable.

Only a short while ago Moore et al. [14] succeeded in preparing particularly stiff dendrimers constructed from phenylacetylene building blocks. Using the palladium-catalyzed Heck reaction in a convergent synthesis, they obtained the largest pure hydrocarbon yet isolated (molecular mass over 14 kDa). The incorporation of numerous *tert*-butyl groups on the periphery of the molecule ensured an excellent solubility in organic solvents.

Masumune et al.[15] reported the synthesis of silicon dendrimers[16] up to the third generation. The repetitive sequence consists of two steps: the terminal Si–H groups are first transformed catalytically into Si–OH groups, and then the new generation is produced in a reaction with chlorosilane building blocks. The surface of these dendrimers is therefore covered with many Si–H groups. Their facile transformations make other functional groups readily accessible, which enables the modulation of the physical properties of these dendrimers.

Dendrimers having charges within the cascade structure were described by Engel et al. These polyphosphonium[17] and polyammonium salts[18] contain tris(*p*-methoxymethylphenyl)phosphane and triethanolamine as monomeric building blocks, respectively. Whereas the ammonium dendrimers are soluble in alcohols and particularly in water, the phosphonium dendrimers display somewhat different behaviour. To the second generation they are soluble in organic solvents and slightly soluble in water; however, from the third generation the solubility is very limited.

Recently Shinkai et al.[19] reported the first arborols incorporating crown ethers. After the divergent method failed to achieve the desired goal, a dendrimer of the second generation was synthesized stepwise in a convergent process through amide bonds. Apart from aromatic building blocks it contains nine diaza[18]crown-6 units. The oily substance should be able to bind alkali metal ions selectively, but this has not yet been demonstrated.

Polynuclear transition metal complexes of a dendritic nature were first described by Balzani et al.;[20] their building blocks are not linked exclusively by covalent bonds but also by metal–ligand bonds (Scheme 7). In a divergent synthesis strategy ruthenium(II) ions form complexes with ligands of the 2,3-bis(2-pyridyl)pyrazine type and are therefore deliberately placed a definite distance apart. The complex **28** containing 22 metal centers can be oxidized and shows luminescence effects.

We prepared dendrimers with large monomeric units in a divergent synthesis (Scheme 8).[21] Readily soluble dendrimers were formed up to the third generation (**29**). This general synthesis can be extended to other core units and to higher generations. Further synthetic goals are "functional dendrimers" with properties characteristic, for example, of dyes, complexing agents for metals, or liquid crystals. For instance, a dendrimer containing six azobenzene groups undergoes reversible switching processes on irradiation with light of a suitable wavelength.[22]

Scheme 7. Dendritic metal complex **28** containing 22 ruthenium ions [20].

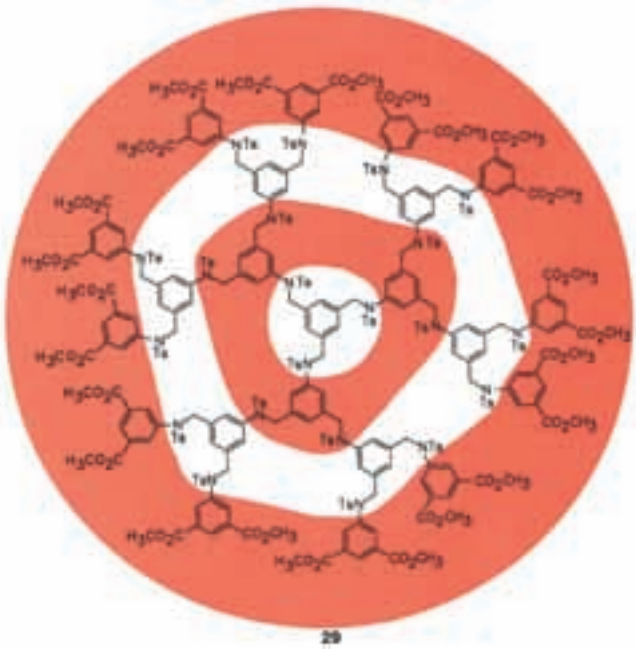

Scheme 8. Aromatic–aliphatic dendrimer **29** containing 24 carboxy groups [21].

All these examples from the past two years show that dendrimers (or cascade molecules) are a topical field of research[23] because their hierarchical architecture promises interesting properties and applications (the micelles are only one example). Nevertheless, the properties of strongly branched molecules are largely unknown and await discovery. In this connection the chemical reactions between multifunctional dendrimers, for example, may be mentioned, as well as dendrimers with many chiral elements, which might display chiroselective recognition.

Above all, the synthesis of large, branched molecules bordering on polymers challenges synthetic and analytical chemists alike. A large number of reaction centers or considerable steric congestion hinders the synthesis of monodisperse molecules. The classical methods of analysis in organic chemistry are sometimes pushed to their limits. NMR spectra and elemental analyses are becoming increasingly less informative, and mass spectrometry of very heavy molecules also is not without problems. Likewise the nomenclature of cascade molecules according to the common rules has its difficulties. The names become extremely long and the fundamental structure of the molecule is not immediately clear from them. And then the effort of naming a dendrimer of the second generation is out of all proportion. Newkome et al.[24] therefore recently proposed a new system that reflects the structure in the sense that it names the molecule from the core towards the periphery.[25] Furthermore, the class of compound becomes clear, since the names begin with "Z-Cascade", where Z is the number of functional groups on the periphery.

In conclusion, these dendritic compounds cross the boundaries of classical organic chemistry and as new materials will penetrate deeper into the topical fields of "nanostructures", supermolecules, and polymers in the future. Even now the dendrimers form a bridge to "soft materials", as de Gennes called polymers, tensides, liquid crystals, and colloids in his Nobel lecture.[26]

German version: *Angew. Chem.* **1992**, *104*, 1609

[1] E. Buhleier, W. Wehner, F. Vögtle, *Synthesis* **1978**, 155–158; F. Vögtle, E. Weber, *Angew. Chem.* **1979**, *91*, 813–837; *Angew. Chem. Int. Ed. Engl.* **1979**, *18*, 753; since then the reduction method has been improved: R. Moors, F. Vögtle, unpublished.

[2] Review with many related references: D. A. Tomalia, A. M. Naylor, W. A. Goddard III, *Angew. Chem.* **1990**, *102*, 119–157; *Angew. Chem. Int. Ed. Engl.* **1990**, *29*, 138–175.

[3] The term "starburst *dendrimers*" was favored by D. A. Tomalia. The first word refers to the explosive propagation of the "arms" of the molecule, and the second emphasizes the *dendr*itic (branched), oligo*mer*ic nature of this species.

[4] C. J. Hawker, J. M. J. Fréchet, *J. Am. Chem. Soc.* **1990**, *112*, 7638–7647; see also I. Gitsov, K. L. Wooley, J. M. J. Fréchet, *Angew. Chem.* **1992**, *104*, 1282–1285; *Angew. Chem. Int. Ed. Engl.* **1992**, *31*, 1200–1202.

[5] D. Farin, D. Avnir, *Angew. Chem.* **1991**, *103*, 1409–1410; *Angew. Chem. Int. Ed. Engl.* **1991**, *30*, 1379.

[6] The name *arborol*, coined by G. R. Newkome, is a composite term derived from "*arbor*" (tree) and "alcoh*ol*".

[7] G. R. Newkome, C. N. Moorefield, G. R. Baker, A. L. Johnson, R. K. Behera, *Angew. Chem.* **1991**, *103*, 1205–1207; *Angew. Chem. Int. Ed. Engl.* **1991**, *30*, 1176–1178.

[8] G. R. Newkome, C. N. Moorefield, G. R. Baker, M. J. Saunders, S. H. Grossman, *Angew. Chem.* **1991**, *103*, 1207–1209; *Angew. Chem. Int. Ed. Engl.* **1991**, *30*, 1178–1180.

[9] G. R. Newkome, A. Nayak, R. K. Behera, C. N. Moorefield, G. R. Baker, *J. Org. Chem.* **1992**, *57*, 358–362.

[10] G. R. Newkome, C. N. Moorefield, G. R. Baker, R. K. Behera, G. H. Escamillia, M. J. Saunders, *Angew. Chem.* **1992**, *104*, 901–903; *Angew. Chem. Int. Ed. Engl.* **1992**, *31*, 917.

[11] K. L. Wooley, C. J. Hawker, J. M. J. Fréchet, *J. Chem. Soc. Perkin Trans. 1* **1991**, 1059–1076.

[12] K. L. Wooley, C. J. Hawker, J. M. J. Fréchet, *J. Am. Chem. Soc.* **1991**, *113*, 4252–4261.

[13] T. M. Miller, T. X. Neenan, R. Zayas, H. E. Blair, *J. Am. Chem. Soc.* **1992**, *114*, 1018–1025.

[14] Z. Xu, J. S. Moore, *Angew. Chem.* **1993**, *105*, in press; *Angew. Chem. Int. Ed. Engl.* **1993**, *32*, in press.

[15] H. Uchida, Y. Kabe, K. Yoshino, A. Kawamata, T. Tsumuraya, S. Masamune, *J. Am. Chem. Soc.* **1990**, *112*, 7077–7079.

[16] Another synthesis of silicon dendrimers by polymerization: L. J. Mathias, T. W. Carothers, *J. Am. Chem. Soc.* **1991**, *113*, 4043–4044.

[17] K. Rengan, R. Engel, *J. Chem. Soc. Perkin Trans. 1* **1991**, 987–990.

[18] K. Rengan, R. Engel, *J. Chem. Soc. Chem. Commun.* **1992**, 757–758.

[19] T. Nagasaki, M. Ukon, S. Arimori, S. Shinkai, *J. Chem. Soc. Chem. Commun.* **1992**, 608–610.

[20] S. Serroni, G. Denti, S. Campagna, A. Juris, M. Ciano, V. Balzani, *Angew. Chem.* **1992**, *104*, 1540–1542; *Angew. Chem. Int. Ed. Engl.* **1992**, *31*, 1493–1495.

[21] H.-B. Mekelburger, F. Vögtle, *Supramolecular Chemistry*, in press.

[22] H.-B. Mekelburger, F. Vögtle, unpublished.

[23] Other syntheses of dendrimers: a) A. Higuchi, H. Inada, T. Kobata, Y. Shirota, *Adv. Mater.* **1991**, *3*, 549–550; E. C. Constable, A. M. W. C. Thompson, *J. Chem. Soc. Chem. Commun.* **1992**, 617–619; F. Moulines, B. Gloaguen, D. Astruc, *Angew. Chem.* **1992**, *104*, 452–454; *Angew. Chem. Int. Ed. Engl.* **1992**, *31*, 458; Y. H. Kim, *J. Am. Chem. Soc.* **1992**, *114*, 4947–4948; A. W. van der Made, P. W. N. M. van Leeuwen, *J. Chem. Soc. Chem. Commun.* **1992**, 1400–1401.

[24] G. R. Newkome, G. R. Baker, J. K. Young, personal communication.

[25] Cf. the related nomenclature of open-chain oligoethers (podands): E. Weber, F. Vögtle, *Inorg. Chim. Acta* **1980**, *45*, L65–L67.

[26] P.-G. de Gennes, *Angew. Chem.* **1992**, *104*, 856–859; *Angew. Chem. Int. Ed. Engl.* **1992**, *31*, 842.

The Structure of Water—A Mixture of Cubes and Planar Four-Membered Rings?

By *Helmut Bertagnolli**

The structure of water—a theme without end? One may have been under the impression that the structure had been explained. Many X-ray, neutron, and electron diffraction measurements have been carried out and modern spectroscopic techniques utilized to determine the microscopic structure of water.[1] Statistical-mechanical calculations and computer simulations have used these results and concluded the correctness of the applied model. However, all this has been put into question, since Benson and Siebert[2] proposed a completely different model for the structure of liquid water.

The starting point of all previous calculations had been the intermolecular interaction potential, which was determined with the help of extensive quantum-mechanical procedures. From this potential, statistical-mechanical methods[3] were used to calculate thermodynamic quantities and provide information about the microscopic structure from the calculation of pair distribution functions $g_{\alpha\beta}(r)$, which give the probability of finding an atom of type β at a distance r from an atom of type α. These functions contain, however, one-dimensional information only, and the inference of a three-dimensional structure cannot be clearly drawn.

The computer simulations[4] also start with the intermolecular potential. If the positions and velocities of all particles are known at a certain time, the forces acting on the particles can be calculated from the potential, and the positions of the particles can be determined at a later time. In this way the microscopic structure and its development with time can be simulated. This procedure is known as molecular dynamic simulation. The Monte–Carlo method dispenses with the strictly deterministic solution of the motion equations; here the particles are shifted at random, and the change of the total energy is used as the criterion for whether this shift can be accepted or not. Thus, both methods generate a set of configurations, which should be representative for the microscopic structure. By averaging all the configurations, both microscopic and also macroscopic physical-chemical quantites can be calculated.

In order to test the results of the computer simulations, preferably those quantites are used that provide information about the short-range order, for example, the pair distribution functions $g_{\alpha\beta}(r)$, which can be determined from diffraction experiments. In contrast, the energy of the system and its derivation with respect to the volume or temperature, which by definition leads to the pressure and the heat capacity, respectively, at constant volume is seldom used. The latter two quantities in particular are not entirely suitable for a comparison, since they are defined as ensemble average values, and the size of the systems, despite powerful computers is limited to edge lengths of approximately 100 Å. According to these calculations, the structure of liquid water resembles a disordered network with partly formed hydrogen bonds. Thus, the structure of water appeared to have been explained, and research consequently turned to the simulation of more complex systems, for example, the treatment of phase boundary surfaces.

However, is this picture correct? S. W. Benson and E. D. Siebert[2] do not think so. They dispense with extensive computer simulations and attempt to derive the structure of water based on thermodynamic quantities. The starting point is the energy of sublimation of ice. The authors assume that this energy is used mainly for breaking of hydrogen bonds and from this estimate the energy of one hydrogen bond. With this value and the assumption that for the melting of ice only hydrogen bonds are broken, the number of the hydrogen bonds still intact in liquid water per H_2O molecule is determined to be approximately 1.75 from the enthalpy of melting. In the opinion of the authors—and this is a decisive assumption—discrete units must occur in liquid water, which can move independently of each other. However, which structures might these units have that contain 1.75 hydrogen bonds per H_2O molecule, but possess no ring strain? The simplest ring structure is a cyclic tetramer consisting of four H_2O molecules. If two tetramers dimerize, a cube is formed with eight H_2O molecules and 1.5 hydrogen bonds per water molecule, thus a number, which is already closer to the value of 1.75. Furthermore, if the octamers are linked through hydrogen bonds, the missing 0.25 hydrogen bonds per H_2O can be easily explained. Thus, the structure of water is a mixture of tetramers and octamers! Scheme 1 shows (left) the classical perception of the microscopic structure of water and (right) the structure of the octamer.

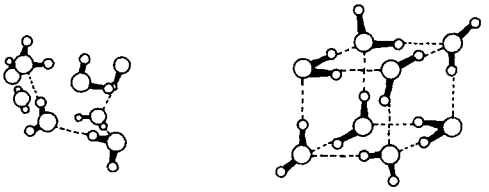

Scheme 1.

This formulation could be easily dismissed as unproven if Benson and Siebert had not used it to explain the heat capacity of water. They assume an ideal mixture of n_o mol H_2O, bound in the octamers, and n_t mol H_2O, bound in the tetramers, with $n_o + n_t = 1$, whose mixture enthalpy is given by (a).

$$H_{mix} = n_o H_o + n_t H_t = H_o + n_t(H_t - H_o) \quad (a)$$

The heat capacity C_p of the mixture is defined as the derivative of H_{mix} with respect to the temperature [Eq. (b)],

$$\left(\frac{dH_{mix}}{dT}\right)_p = C_p = C_{p,0} + n_t \Delta C_p \quad (b)$$

with $\Delta C_p = d(H_t - H_o)/dT$. This formulation would be correct if an equilibrium between tetramers and octamers did

[*] Prof. Dr. H. Bertagnolli
Institut für Physikalische Chemie der Universität
Pfaffenwaldring 55 D-W-7000 Stuttgart (FRG)

not occur and thus n_t is temperature dependent. Formula (b) is thus to be replaced by Equation (c).

$$C_p = C_{p,o} + n_t \Delta C_p + (H_t - H_o)\left(\frac{dn_t}{dT}\right) \quad (c)$$

This term is new. It completely changes the calculation of C_p. The isomerization equilibrium contributes to the heat capacity. To calculate the heat capacity Benson and Siebert estimate the reaction entropy $\Delta S°$, the reaction enthalpy $\Delta H°$, and from this, the free reaction enthalpy $\Delta G° = \Delta H° - T\Delta S°$ on the basis of known data. The equilibrium constant K can then be calculated from $\Delta G°$ according to $-\Delta G° = RT \ln K$ and once the equilibrium constant is known, from that n_t can be calculated. The calculation of the change of n_t with temperature is then also no longer difficult. Since $\Delta H°$ is known, the temperature dependence of the equilibrium constant can be calculated according to van't Hoff's equation $d(\ln K)/dT = \Delta H°/(RT^2)$, and from this also that of n_t, that is, dn_t/dT can be determined. There still remains the estimation of the quanities $C_{p,o}$ and ΔCp. This is achieved by the calculation of the librational and torsional degrees of freedom of the octamer and the tetramer according to the classical formula: per vibrational degree of freedom the contribution is given by the value of the gas constant R. The remaining internal motions of one molecule relative to another within the cluster have been assumed to be icelike.

Thus, all that is needed is the application of classic physical-chemical formulas! And what is the result? The temperature dependence of the heat capacity between 0 and 100°C is reproduced with an accuracy of ±2%. An astounding result! The introduction of an equilibrium between two forms of water clusters which additionally contributes to the heat capacity is the decisive factor. This is certainly an aspect, which so far has not received enough attention and which will lead to a re-examination of the calculation of heat capacities, particularly for systems with hydrogen bonds such as formic or benzoic acid. In comparison, the kind of isomers is of minor significance. The numerical values suggest an equilibrium between tetramers and octamers, however, as the authors admit, it could also be one between pentamers and decamers. Perhaps completely different forms of water clusters are also possible. The postulated structures of tetramers and octamers are contrary to the results of the diffraction experiments, which one might say deliver the spatial average from a snapshot of the liquid structure. For an assumed O–O distance of 2.89 Å, distances of 4.09 Å and 5.01 Å should be found preferably for the existence of square tetramers and cubic octamers, respectively. However, the second maximum in the pair distribution function lies at 4.5 Å,[1] which is more indicative of a tetrahedral structure. This indication, however, does not detract from the fundamental significance of this work.

German version: *Angew. Chem.* **1992**, *104*, 1615

[1] *Water – a Comprehensive Treatise, Vol. 1–6* (Ed.: F. Franks), Plenum, New York, **1975**.
[2] S. W. Benson, E. D. Siebert, *J. Am. Chem. Soc.* **1992**, *114*, 4269.
[3] J. P. Hansen, I. R. McDonald, *Theory of Simple Liquids*, Academic Press, New York, **1976**.
[4] M. P. Allen, D. J. Tildesley, *Computer Simulation of Liquids*, Clarendon Press, Oxford, **1987**.

A Milestone in Genome Sequencing: The Complete DNA Sequence of the Yeast Chromosome III**

By *Ernst-L. Winnacker**

Baker's or brewer's yeast is one of the most useful organisms in the immediate environment of our own species *Homo sapiens*. Though we make great use of it for our nourishment and for our pleasure with equal enthusiasm, there is more to yeast than just these aspects. For decades, it has been one of the favorite and most important tools of biochemistry and molecular biology. It is cheap and easy to manipulate, but it is nonetheless not simply a bacterium. Yeast is a eucaryotic microorganism with (almost) all the attributes of higher cells, including a cell nucleus, cellular organelles such as mitochondria and lysosomes, and even such a typical characteristic of higher organisms as sexuality. The great biochemists of this century, from Eduard Buchner to Hans Krebs and Feodor Lynen, to name but a few, made just as much use of yeast in their experiments as do today's geneticists and molecular biologists. Without these studies on baker's yeast, what would we know today about the structure of the cell membrane, about the cell cycle, mechanisms of signal transfer, and intracellular protein transport?

In spite of this background it may come as a surprise that it is only eight years ago that the exact number of chromosomes in yeast, namely 16, was first determined. This result, which at a first glance is anything but exciting, nonetheless created a furor in the field when it first appeared. It was not simply the result of a glance through a microscope—yeast chromosomes are far too small for that—but the outcome of applying a novel electrophoresis technique, pulsed field gel electrophoresis. In this method, developed by Cantor and Schwartz,[1] a sophisticated arrangement of electrodes is used and pulses of current are applied in alternating patterns, making possible the separation of very large biological macromolecules, even as large as entire chromosomes. These

[*] Prof. Dr. E.-L. Winnacker
Laboratorium für molekulare Biologie
Genzentrum und Institut für Biochemie
Am Klopferspitz, D-W-8033 Martinsried (FRG)

[**] I thank Dr. H. W. Mewes, Dr. H. Ibelgaufts, and Dr. H. Domdey for their help in preparing this manuscript.

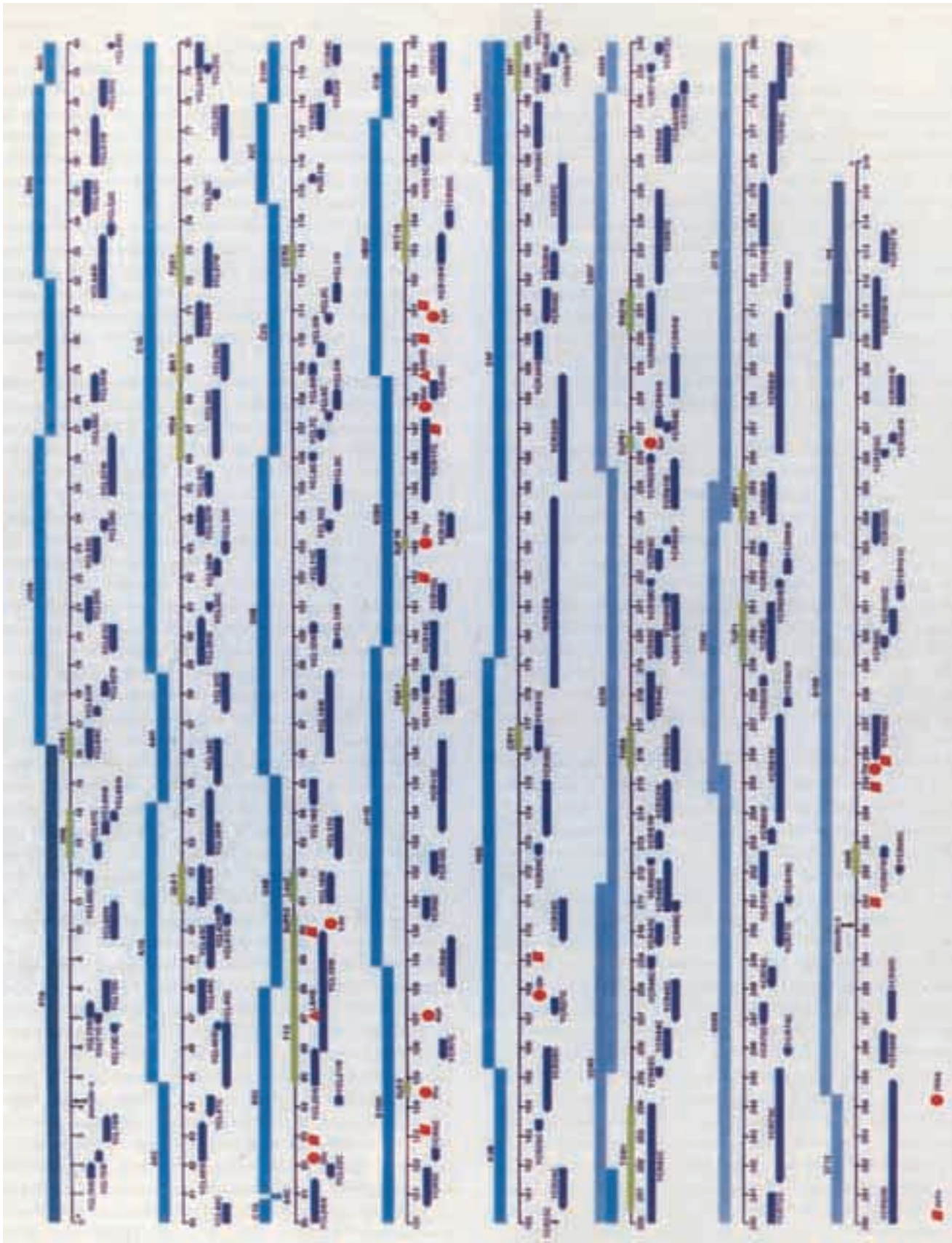

Fig. 1. Positions of the open reading frames and the known genetic markers on chromosome III of yeast.

can hence not only be counted, but can actually be isolated. This method has therefore become one of the decisive prerequisites for the elucidation of the structure of individual chromosomes of living organisms, including those of baker's yeast.

A few weeks ago the first result of these endeavors was revealed with the publication, by a consortium of 35 European laboratories, of the total DNA sequence of chromosome III from the yeast *Saccharomyces cerevisiae*, with its 315357 base pairs (Fig. 1).[2] The project, which began three years ago and for which the European Commission paid the 147 participating scientists 5 ECU per base pair (1 ECU = ca. 2 DM or $ 1.35), was initiated and coordinated by the Belgian biochemist André Goffeau. He was assisted by Stephen G. Oliver of the Manchester Biotechnology Centre UMIST in England, who as co-coordinator was responsible for the distribution of the DNA samples, and by a group at the Martinsried Institute for Protein Sequences (MIPS) at the Max Planck Institute for Biochemistry, who carried out the evaluation of the sequence data.

Whether this news is worth a "Highlight" in *Angewandte Chemie* is indeed a good question. The technique used for DNA sequencing is in fact by no means new; the authors themselves point out that only 25000 base pairs, that is, approximately 7%, were sequenced by new, automated sequencing procedures, while the rest were assigned conventionally and by hand, based on the work of Sanger in 1977. In addition, chromosome III of yeast is the third smallest of the yeast chromosomes and represents only about 2% of the entire yeast genome. It is therefore only a drop in the ocean on the way to sequencing the whole genome, with its 14 million base pairs (14 megabasepairs (MBp)); this "drop" would nonetheless fill some fifty pages of *Angewandte Chemie*.

And yet the importance of this result cannot be overestimated. It represents the largest continuous DNA sequence that has ever been determined, a record held until now by the genome of the cytomegalovirus with its 230000 base pairs. It is the first sequence of a complete, intact chromosome, and is therefore a milestone on the way to the characterization of human chromosomes, the eventual goal of these endeavors. The logistics required for the project should not be underestimated either. Thirty-five European laboratories were successfully harnessed together over a period of two and a half years to one scientific target. It is such an achievement which makes this project a model and example for the even larger, global arrangements which will be required to sequence the human genome. Finally, however, this result is fascinating mainly because of its wealth of scientific data and surprises. The sequence contains 182 open reading frames coding for proteins longer than 100 amino acids. On the classical genetic map, only 34 genes were marked on chromosome III of yeast. Thus, even in such a well-studied organism as baker's yeast, classical genetic and biochemical methods had only been able to localize 20% of the actual number of genes. If one extrapolates this result to the human genome, which is genetically much less studied than that of yeast, then the estimate of the number of our genes must be revised dramatically upwards, to 500000 or more. This is also a result arising from this study.

However, the most interesting aspect of a DNA sequence is not so much the mere sequence of its base pairs, but how it is converted into biological function. DNA is essentially nothing more than a carrier of information, though this information exists at multiple levels, and includes many kinds of signals for a multitude of functions, not least those for its own replication. The best known of these functions is, however, translation into proteins, which is why first priority in analyzing a DNA sequence is always given to the search for open reading frames. This was the case here, too. Since yeast genes only rarely come in pieces, the problem was not too difficult to solve. The decisive question which remained, however, was that of assigning biological functions to the open reading frames that had been found. To answer this question, at least two options are open to the biochemist or molecular biologist: sequence comparisons with known sequences, and the so-called Knock-Out (KO) technology.

Computer-assisted sequence comparisons are a routine procedure today, and because of their great usefulness, they are even carried out in our beginners' practical courses.[3] The programs used must always be able to fulfill two requirements: they must be able to find similarities between two sequences, and measure the significance of these similarities. In other words, they must be able to determine whether the similarity found is a purely chance one, or whether it represents real relatedness. The extreme case, complete identity, is, of course, simple to analyze. If two protein or DNA sequences are identical over long stretches, this cannot be due to chance. The situation becomes more difficult, however, if the two sequences contain gaps, if conservative amino acid exchanges occur, or if proteins are pieced together from sections or domains of various other proteins. These are of course the situations which are most interesting to the biochemist, since biological function may be conserved despite considerable amino acid exchanges. It requires great experience to carry out such "low-stringency" searches in a manner which allows identification of functionally related proteins on the basis of only slight similarities. The number of sequences known is growing rapidly—at the end of June 1992 there were approximately 90 million base pairs in almost 60000 reading frames—and with today's programs the assignment of unknown reading frames to particular protein families is becoming more and more reliable.

In the specific case of chromosome III of yeast such assignments were possible for 54 of the 145 unknown reading frames. They showed homologies to, for example, protein kinases, ion channels, methyltransferases, peptidyl-prolyl-*cis*,*trans*-isomerases, and G-proteins. Remarkably, homologies were found not only to the corresponding proteins from yeast, but also to organisms as diverse as the fruit fly *Drosophila*, the frog *Xenopus*, tobacco, and even *Homo sapiens*. This result leads to a new definition of the gene. If it is really true that genes from organisms representing the whole spectrum of life on earth are not only closely related to those of yeast, but can even replace them functionally, then the gene can no longer be defined in an organismic sense. Instead of speaking of a yeast gene, a fly gene, or a human gene, we must regard the gene as a continuum of biological information: Nature has conserved its function for as long as it has proved serviceable over millions of years.

In the present case, the most unusual of the relationships found was a high homology to the gene *nif*S from the nitrogenase operon of nitrogen-fixing bacteria (Fig. 2). Yeast can-

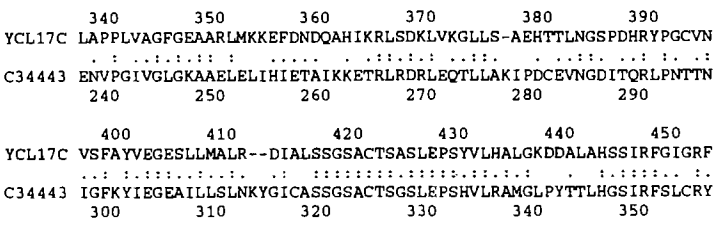

Fig. 2. Sequence comparison between a segment of reading frame YCL17C of yeast chromosome III and the *nif*S gene product from *Anabaena*. Identical bases are marked by two dots, exchanges between functionally related amino acids (e.g. between valine and isoleucine) by one dot. Gaps in the sequence are bridged with hyphens. The homology in this segment is 43.6% over a total length of 383 amino acids.

not fix nitrogen, but this gene is nonetheless essential for its existence. It must therefore code for a gene product which in the relevant bacteria is concerned with the formation of the nitrogenase operon proteins, but can, and must, also carry out its role in the biosynthesis of other proteins. It is assumed to fulfill a "modulating" function, that is, a function of general nature which may perhaps play a part in the formation of tRNA from its precursors, or in protein folding.

Once the search for protein families has been exhausted, it can be extended to a search for protein domains. One of the most important advances of recent years has been the recognition that proteins with different function may carry domains with related sequences, each with a particular partial functionality. Membrane proteins of any category are characterized by trans-membrane domains which anchor them in the membrane; DNA-binding proteins reveal so-called zinc-finger or helix-loop-helix motifs, which help them to recognize specific DNA sequences; short sequences of basic amino acids predestine the protein for the cell nucleus, while nucleotide-binding domains, at which ATP is bound and hydrolyzed, are found in specific types of transport proteins. The search for these and other domains was also successful here, so that in the end it was possible to assign particular functions to about 42% of the unknown reading frames using the sequence comparison procedure. Biochemistry will have to check each of these predictions individually, but this "computer biochemistry" makes the task significantly easier.

The second way in which the function of the unknown reading frames may be investigated is by so-called gene inactivation. This process, also called "knock-out", is based on the principle of general genetic recombination.[4] It involves the exchange of DNA between two identical (homologous) DNA double strands, and is normally responsible for the genetic diversity in the offspring of sexual reproduction. If the maternal and paternal chromosomes come to be aligned with each other after fertilization, an actual, physical exchange of DNA takes place between the two strands, between identical sequences on the chromosomes, leading to chromosomal chimeras. In general this process takes place statistically, that is, at random along the chromosomes. It is therefore impossible to predict which sequences derive from the paternal and which from the maternal chromosome. An effect on the phenotype is of course only seen if the two differ at a particular position. Even within one and the same species such differences are not rare, which explains the variations in phenotypes observed between parents and their offspring.

Under certain circumstances, the process of recombination can also take place in a directed manner. If a plasmid bearing only a short DNA sequence is introduced into a living cell, such as a yeast cell, then recombination events between this sequence and its partner on the yeast chromosome will lead, at a certain frequency, to the substitution of the endogenous gene by the exogenous one. If the reading frame in the exogenous gene has previously been destroyed by mutation, then this mutation is transferred into the chromosome by the recombination process, and the endogenous gene is thereby inactivated. This process is not particularly efficient, so an additional gene is usually added to the inactivated reading frame, often an antibiotic resistance gene. In this way inactivation of a particular gene is coupled to a selection marker so that in the presence of the antibiotic only the inactivated cells can grow, and they can thus be separated easily from those in which the exchange has not occurred. The selected cells can then be studied to determine what effect inactivation of the gene in question has on each cell.

For 55 of the unknown reading frames on chromosome III, this has already been carried out. For three of the genes, their deletion was lethal for the cell; for 24 of the others, a series of phenotypic changes were observed, ranging from heat- or cold-sensitivity, to sterility or to morphological changes. Although the deletions were compatible with life, they nonetheless led to recognizable changes. The biochemical defects responsible for these changes can now be analyzed in detail. For about half of the reading frames, however, their loss had no perceivable effects on the phenotype. This was extremely surprising, because it cannot seriously be suggested that half of the genes in yeast are dispensable for its existence. Even if these genes simply represented redundant systems, which Nature has built in to ensure survival of the species, they must, in the end, have provided a selective advantage of some sort. In the course of the millennia, yeast would surely have lost any gene sequences for which it had no use.

The knock-out experiments therefore show that molecular biology is far ahead of biochemistry in this field. They also prove how little we really know, even about an organism such as baker's yeast, which seemed to have been exhaustively studied. In many ways, then, the sequence determination of yeast chromosome III opens up undreamed of perspectives for a new biology and biochemistry of yeast. Not only is the number of genes vastly greater than previously thought, but the analysis of the function of their products afforded associations with known biochemical functions for only half of the genes. What is concealed behind the other half will now have to be shown by future studies.

Presumably, similar veins of gold can be expected to be unearthed by the genome projects of many other organisms which have been initiated, ranging from the nematode *C. elegans*, to the mouse-ear cress (Arabidopsis) *A. thaliana*, to *Homo sapiens*. Even the most enthusiastic supporters of these projects could not have expected such interesting scien-

tific perspectives to emerge. The discussion of the sense and nonsense of the projected mapping and sequencing of the human genome has thus died down to a large extent. Its direction has been set worldwide for some time now. A detailed description of the human genome project is beyond the scope of such a highlight, but it is clear that its dimensions are orders of magnitude greater than those of the yeast project. The human genome is approximately 300 times larger than that of yeast. In the past year, on average, one human gene was identified and sequenced every day around the world. For 500000 genes, then, our present technology would require several hundred years to complete this project. To predict with optimism that it will be finished in 15 to 20 years therefore requires not simply an improvement of current technologies, but the development of fundamentally new methods for mapping and sequencing. These may be in sight. Given the results that can be expected, it is to be hoped that Germany, including the pharmaceutical industry, will also take an intensive part in this project. Industry as well as biomedical research will be able to make rapid use of the possibilities described.

German version: *Angew. Chem.* **1992**, *104*, 1618

[1] D. C. Schwarz, C. R. Cantor, *Cell* **1984**, *37*, 67.
[2] S. G. Oliver et al., *Nature* **1992**, *357*, 38; J. Hodgson, *Biotechnology* **1992**, *10*, 760.
[3] W. R. Pearson, D. J. Lipman, *Proc. Natl. Acad. Sci. USA* **1988**, *85*, 2444; for an introduction to this area see: R. F. Doolittle, *Of URFs and ORFs*, University Science Books, Mill Valley, CA (USA), **1986**; *MIPS NEWS*, a newsletter form the Martinsried Institute for Protein Sequences, Am Klopferspitz 18, D-W-8033 Martinsried near Munich (Fax: within Germany 089-85782655, international 49 89 85782655).
[4] R. J. Rothstein, *Meth. Enzymol.* **1983**, *101*, 202; M. E. Goebl, T. D. Petes, *Cell* **1986**, *46*, 983.

A stop-gap solution?

If the latest library copy of Angewandte spends more time off the shelf than on, stop the gap with a personal subscription.

Just call or fax

VCH

USA: Tel. 1-(800) 422-8824; Fax (305) 428-8201
UK: Tel. (0223) 321111, Fax (0223) 313221

Communications may be submitted in English *or* in German. Further details regarding the submission of communications can be found in the "Notice to Authors" reproduced in the January issue of the journal. Copies thereof may be obtained from the editorial office upon request.

The First Metal–Metal Silyl Migration in a Heterobimetallic Complex, and the Structure of the Rearrangement Product $[(OC)_4Fe(\mu\text{-}PPh_2)Pt\{Si(OMe)_3\}(PPh_3)]$ (*Fe–Pt*)**

By *Pierre Braunstein,* Michael Knorr, Brigitte Hirle, Georg Reinhard,* and *Ulrich Schubert*

Dedicated to the memory of Ernest Colomer

Metal–silicon single or multiple bonds are key functionalities in a number of important catalytic transformations, such as the hydrosilylation of alkenes and alkynes and the coupling of organosilanes by dehydrogenation.[1] This largely accounts for the considerable research endeavor devoted to the organometallic chemistry of silicon. Whereas migration of a metal-bound silyl group to a ligand has been observed in mononuclear[2] and cluster compounds,[3] we report here on the first examples in molecular chemistry of the migration of a silyl group from one metal center to another. In this process, which requires very mild reaction conditions, the silyl group is transferred from the iron to the platinum center in Fe–Pt bimetallic complexes.

Oxidative addition of $[Fe(H)\{Si(OMe)_3\}(CO)_3(PPh_2H)]$ (**1a**)[4b] to $[Pt(C_2H_4)(PPh_3)_2]$ across the P–H and Fe–H bonds (Scheme 1) afforded the Fe–Pt complex **2a** with a phosphido bridge.[4a, 6] Despite the lability of the PPh_3 ligand (see reaction to give **3a**), the ^1H NMR spectrum of **2a** shows a singlet at $\delta=3.68$ for the nine equivalent methoxy protons, which rules out a dative MeO → Pt interaction and thus the occurrence of the unusual η^2-μ_2-SiO coordination recently discovered in some Fe–Pd, Fe–Pt, and Fe–Rh complexes.[4] When CO was bubbled through a CH_2Cl_2 solution of **2a**, substitution of PPh_3 occurred, which led to the rapid and quantitative formation of **3a** ($^{31}P\{^1H\}$ NMR monitoring $\delta PPh_2=159\cdot5$, $^1J(Pt,P) = 2657$ Hz). The *cis* arrangement of the P atoms [$^2J(P,P) = 13$ Hz] is consistent with previous observations on $[M(\mu\text{-}PR_2)Pt(CO)(PR_3)]$(*M–Pt*) systems, which revealed the preference of the Pt-bound CO ligand to occupy the position *trans* to the phosphido bridge.[7] The IR spectrum of **3a** contains CO bands for the Fe-bound ligands at 1989 (m) and 1928 (s, br) cm^{-1} and for the Pt-bound CO ligand at 2061 (m) cm^{-1}.

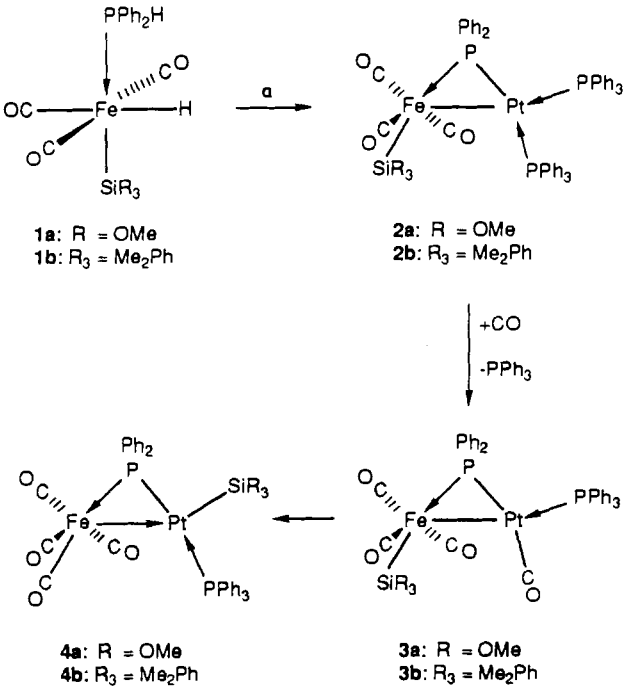

Scheme 1. Synthesis of the complexes **2**–**4**. a) $[Pt(H_2C{=}CH_2)(PPh_3)_2]$, in toluene, 298 K; loss of $H_2C{=}CH_2$ and H_2.

Unexpectedly, complex **3a** quantitatively rearranges in solution within approximately 1 h to its isomer **4a**, in which the Si atom is now bound to Pt, whereas the Pt-bound CO ligand has migrated to the Fe center, as established by an X-ray structure analysis (Fig. 1).[8]

The $^{31}P\{^1H\}$ NMR signal of the phosphido bridge of **4a** now appears at $\delta = 116.9$ and shows a strong *trans* coupling to the PPh_3 ligand [$^2J(P,P) = 308$ Hz]. Interestingly, the po-

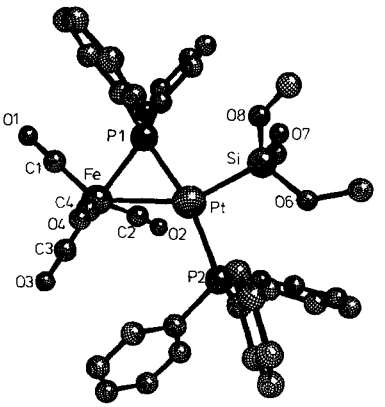

Fig. 1. Selected bond lengths [Å] and angles [°] in **4a**: Fe-Pt 2.7669(7), Pt-P1 2.250(1), Pt-P2 2.293(1), Pt-Si 2.288(1), Fe-P1 2.274(1), Fe-C1 1.776(6), Fe-C2 1.799(4), Fe-C3 1.794(5), Fe-C4 1.804(5), Si-O6 1.630(5), Si-O7 1.640(4), Si-O8 1.633(4); Fe-Pt-P1 52.69(3), Fe-Pt-P2 112.94(3), Fe-Pt-Si 150.51(4), P1-Pt-P2 165.60(4), P1-Pt-Si 98.00(5), P2-Pt-Si 96.28(5), Pt-Fe-P1 51.91(3), Pt-Fe-C1 141.4(2), Pt-Fe-C2 69.5(2), Pt-Fe-C3 122.9(2), Pt-Fe-C4 74.0(2), P1-Fe-C1 89.6(2), P1-Fe-C2 89.4(1), P1-Fe-C3 174.7(2), P1-Fe-C4 87.6(2), Pt-P1-Fe 75.41(4).

[*] Dr. P. Braunstein, Dr. M. Knorr
Laboratoire de Chimie de Coordination, URA 416 du CNRS
Université Louis Pasteur
4 rue Blaise Pascal, F-67070 Strasbourg Cédex (France)
Dipl.-Chem. B. Hirle, Dipl.-Chem. G. Reinhard, Prof. Dr. U. Schubert
Institut für Anorganische Chemie der Universität
Am Hubland, D-W-8700 Würzburg (FRG)

[**] This work was supported by the Commission of the European Communities (Contract no. ST 2J-0347-C), the Centre National de la Recherche Scientifique, the Deutsche Forschungsgemeinschaft, and the Alexander von Humboldt-Stiftung (award to P. B.).

sition of the CO bands in the IR spectrum of **4a** is almost identical with that in the spectrum of $[Fe(CO)_4(PPh_3)]$ in CH_2Cl_2 [2049 (vs), 1974 (m), and 1938 (vs) cm^{-1}].[9] Only a splitting of the *E* vibration mode is observed, presumably due to steric factors, which induce a slight distorsion of the Fe moiety of **4a** away from the C_{3v} symmetry found for $[Fe(CO)_4(PPh_3)]$. This also supports the assumption that **4a** is a $Fe(d^8) \rightarrow Pt(d^8)$ system with a dative bond between a Fe^0 and a Pt^{II} center.

Without the introduction of CO, pure **2a** in CH_2Cl_2 or toluene is transformed only slowly (4–5 days at room temperature) into **4a** (the slow decomposition of **2a** liberates CO), that is, the introduction of CO significantly accelerates the reaction **2a** → **4a**.[10]

In order to evaluate the influence of the ligands R attached to Si on this SiR_3 transfer reaction, **3b** was prepared quantitatively from **2b**. In contrast to **3a**, which rearranges too rapidly, **3b** can be isolated in a pure form as a yellow, air-stable solid. In CH_2Cl_2, however, it rearranges quantitatively at room temperature within approximately 5 h to the isomer **4b** (IR and $^{31}P\{^1H\}$ NMR monitoring). The IR spectrum of **4b** is similar to that of **4a** in the CO stretching frequency region; the bands are slightly shifted to lower wavenumbers owing to the stronger electron-donating properties of the $SiMe_2Ph$ group.

Migration of the silyl group from Fe to Pt is prevented by stronger σ-donor/ π-acceptor ligands on Pt, for example, *t*BuNC in **5**, or $Ph_2PCH_2PPh_2$ (dppm) in **6**. That the silyl-

$[(OC)_3(Ph_3Si)Fe(\mu\text{-}PPh_2)Pt(PPh_3)(CO)]$ **3c**

$[(OC)_3\{(MeO)_3Si\}Fe(\mu\text{-}PPh_2)Pt(PPh_3)(CN\,tBu)]$ **5**

$[(OC)_3\{(MeO)_3Si\}Fe(\mu\text{-}PPh_2)Pt(dppm)]$ **6**

group transfer reported here is strongly influenced by subtle changes in the molecule is further illustrated by the fact that neither the $SiPh_3$ derivative **3c**, nor the complexes analogous to **2a** and **3a**, which contain a μ-PHPh or a μ-PHCy (Cy = *cyclo*-C_6H_{11}) bridge, isomerize under similar conditions. A possible explanation invokes the Thorpe–Ingold effect,[11] whereby bulky geminal substituents on the μ-P atom would promote the formation of transition-state or intermediate structures containing additional bridging ligands and thus facilitate their transfer from one metal to another. This effect has also been put forward to account for the suppression of intramolecular, intermetal transfer of CO in heteronuclear complexes $[M(\mu\text{-}PR_2)Pt]$ on going from $\mu\text{-}PR_2$ to μ-PRH systems.[12] Whereas silatropic shifts are well known in organic chemistry,[13] and intramolecular metal to ligand migrations of silyl substituents have been reported,[2, 3] this CO-promoted transfer of a silyl-group from *one metal to another* is unprecedented. It may open up the possibility of "switching on" a catalyst system by converting a M–Si into a M′–Si bond under very mild conditions. It is particularly notable that a Pt–Si bond results from this migration, since platinum is known to be an important metal for catalysts in the chemistry of silicon compounds.[1]

Experimental Procedure

2a: **1a** (0.448 g, 1 mmol) [4b] was treated with $[Pt(C_2H_4)(PPh_3)_2]$ (0.749 g, 1 mmol) in toluene (15 mL). The solution was stirred for 1 h at 25 °C and concentrated. The product was precipitated by addition of hexane and obtained in 78% yield as an air-stable, yellow powder. IR (CH_2Cl_2): $\tilde{\nu}$ [cm^{-1}] = 2006s, 1942sh, 1932vs (ν(CO)); ^1H NMR (200 MHz, C_6D_6, 303 K, TMS): δ = 3.68 (s, 9H, OCH_3), 6.95–7.51 (m, 40H, C_6H_5). $^{31}P\{^1H\}$ NMR (81.02 MHz, [D_6]benzene/CH_2Cl_2, external reference H_3PO_4, for all compounds): δ = 27.8 (d, PPh_3(Pt), ^2J(P,P) = 9, ^1J(Pt,P) = 3482 Hz), 35.8 (d, PPh_3(Pt), ^2J(P,P) = 232, ^1J(Pt,P) = 3209 Hz), 181.9 (dd, μ-PPh_2, $^2J(P,P_{trans})$ = 232, $^2J(P,P_{cis})$ = 9, ^1J(Pt,P) = 2636 Hz).

2b was prepared in a manner similar to **2a** starting from **1b**. [5] $^{31}P\{^1H\}$ NMR: δ = 27.5 (d, PPh_3(Pt), ^2J(P,P) = 12, ^1J(Pt,P) = 3469 Hz), 36.2 (d, PPh_3(Pt), ^2J(P,P) = 228, ^1J(Pt,P) = 3239 Hz), 183.7 (dd, μ-PPh_2, $^2J(P,P_{trans})$ = 228, $^2J(P,P_{cis})$ = 12, ^1J(Pt,P) = 2643 Hz).

3b was prepared by purging a solution of **2b** (0.945 g, 1 mmol) in CH_2Cl_2 (30 mL) at 25 °C with a stream of CO. The reaction is quantitative (ca. 10 min, IR monitoring of the CO bands). The solution was concentrated to approximately 6 mL and slow addition of hexane (20 mL) induced precipitation of yellow **3b**. IR (CH_2Cl_2): $\tilde{\nu}$ [cm^{-1}] = 2055m, 1974m, 1910sh, 1902vs (ν(CO)); $^{31}P\{^1H\}$ NMR: δ = 26.9 (d, PPh_3(Pt), ^2J(P,P) = 16, ^1J(Pt,P) = 3436 Hz), 163.6 (d, μ-PPh_2, ^2J(P,P) = 16, ^1J(Pt,P) = 2589 Hz).

4a: A solution of **2a** (0.583 g, 0.5 mmol) in CH_2Cl_2 (15 mL) was purged at 25 °C with a stream of CO. After rearrangement was complete (ca. 1 h, IR-monitoring of the disappearence of the CO bands due to **3a**), the yellow-brown solution was concentrated to approximately 5 mL and hexane (20 mL) was slowly added, inducing precipitation of 0.429 g (92%) yellow **4a**. IR (CH_2Cl_2): $\tilde{\nu}$ [cm^{-1}] = 2040vs, 1975m, 1949s, 1927s (ν(CO)); ^1H NMR (200 MHz, C_6D_6, 303 K): δ = 3.12 (s, 9H, OCH_3), 7.06–8.12 (m, 25H, C_6H_5); $^{31}P\{^1H\}$ NMR: δ = 36.0 (d, PPh_3(Pt), ^2J(P,P) = 308, ^1J(Pt,P) = 3027 Hz), 116.9 (d, μ-PPh_2, ^2J(P,P) = 308, ^1J(Pt,P) = 2152 Hz).

4b: IR (CH_2Cl_2): $\tilde{\nu}$ [cm^{-1}] = 2034vs, 1972s, 1945s, 1920s (ν(CO)); $^{31}P\{^1H\}$ NMR: δ = 31.4 (d, PPh_3(Pt), ^2J(P,P) = 315, ^1J(Pt,P) = 3168 Hz), 118.5 (d, μ-PPh_2, ^2J(P,P) = 315, ^1J(Pt,P) = 2324 Hz).

5: IR (CH_2Cl_2): $\tilde{\nu}$ [cm^{-1}] = 2180s (ν(CN)), 1969s, 1900vs, br. (ν(CO)); ^1H NMR ($CDCl_3$, 303 K): δ = 1.26 (s, 9H, *t*Bu), 3.72 (s, 9H, OCH_3), 7.07–7.35 (m, 25H, C_6H_5); $^{31}P\{^1H\}$ NMR: δ = 27.4 (d, PPh_3(Pt), ^2J(P,P) = 7, ^1J(Pt,P) = 3618 Hz), 153.0 (d, μ-PPh_2, ^2J(P,P) = 7, ^1J(Pt,P) = 2709 Hz).

6: IR (CH_2Cl_2): $\tilde{\nu}$ [cm^{-1}] = 1964s, 1892vs, br. (ν(CO)); ^1H NMR ($CDCl_3$, 303 K): δ = 3.53 (s, 9H, OCH_3), 4.76 (t, 2H, CH_2, ^2J(P,H) = 9.5, ^3J(Pt,H) = 40.4 Hz), 7.24–7.83 (m, 30H, C_6H_5).

All new compounds gave satisfactory elemental analyses.

Received: May 29, 1992 [Z 5380 IE]
German version: *Angew. Chem.* **1992**, *104*, 1641

[1] a) J. F. Harrod, A. J. Chalk in *Organic Synthesis Via Metal Carbonyls* (Eds.: I. Wender, P. Pino), Wiley, New York, **1977**, p. 673; b) J. L. Speier, *Adv. Organomet. Chem.* **1979**, *17*, 407; c) I. Ojima in *The Chemistry of Organic Silicon Compounds* (Eds.: S. Patai, Z. Rappoport), Wiley, New York, **1989**, Chapter 25, p. 1479; d) E. Colomer, R. J. P. Corriu, *Top. Curr. Chem.* **1981**, *96*, 79; e) K. M. Mackay, B. K. Nicholson in *Comprehensive Organometallic Chemistry* (Eds.: G. Wilkinson, F. G. A. Stone, E. W. Abel), Pergamon, Oxford, **1982**, Chapter 43; f) B. J. Aylett, *Adv. Inorg. Chem. Radiochem.* **1982**, *25*, 1; g) U. Schubert, *J. Organomet. Chem.* **1988**, *358*, 215; h) T. D. Tilley, *Comments Inorg. Chem.* **1990**, *10*, 37; i) M. J. Hostetler, R. G. Bergman, *J. Am. Chem. Soc.* **1990**, *112*, 8621; j) T. Takahashi, M. Hasegawa, N. Suzuki, M. Saburi, C. J. Rousset, P. E. Fanwick, E. Negishi, *ibid.* **1991**, *113*, 8564; k) Y. Ito, M. Suginome, T. Matsuura, M. Murakami, *ibid.* **1991**, *113*, 8899; l) Y. Tsuji, Y. Obora, *ibid.* **1991**, *113*, 9368; m) C. Zybill, *Top. Curr. Chem.* **1991**, *160*, 1; n) X. Coqueret, G. Wegner, *Organometallics* **1991**, *10*, 3139; o) L. N. Lewis, K. G. Sy, G. L. Bryant, Jr., P. E. Donahue, *ibid.* **1991**, *10*, 3750; p) S. B. Duckett, R. N. Perutz, *ibid.* **1992**, *11*, 90; q) M. R. Kesti, R. M. Waymouth, *ibid.* **1992**, *11*, 1095; r) R. H. Heyn, T. D. Tilley, *J. Am. Chem. Soc.* **1992**, *114*, 1917; s) H. Brunner, M. Rötzer, *J. Organomet. Chem.* **1992**, *425*, 119.

[2] See for example a) P. J. Harris, J. A. K. Howard, S. A. R. Knox, R. J. McKinney, R. P. Phillips, F. G. A. Stone, P. Woodward, *J. Chem. Soc. Dalton Trans.* **1978**, 403; b) G. Thum, W. Ries, D. Greissinger, W. Malisch, *J. Organomet. Chem.* **1983**, *252*, C67; c) K. C. Brinkman, A. J. Blakeney, W. Krone-Schmidt, J. A. Gladysz, *Organometallics* **1984**, *3*, 1325; d) U. Schubert, A. Schenkel, J. Müller, *J. Organomet. Chem.* **1985**, *292*, C11; e) P. Pasman, J. J. M. Snel, *ibid.* **1986**, *301*, 329; f) U. Schubert, A. Schenkel, *Chem. Ber.* **1988**, *121*, 939; g) G. L. Crocco, C. S. Young, K. E. Lee, J. A. Gladysz, *Organometallics* **1988**, *7*, 2158; h) For an example of a $SiMe_3$-migration from Si to Pt see: L. S. Chang, M. P. Johnson, M. J. Fink, *ibid.* **1989**, *8*, 1369.

[3] a) I. Ojima, N. Clos, R. J. Donovan, P. Ingallina, *Organometallics* **1990**, *9*, 3127; b) I. Ojima, P. Ingallina, R. J. Donovan, N. Clos, *ibid.* **1991**, *10*, 38; c) I. Ojima, R. J. Donovan, N. Clos, *ibid.* **1991**, *10*, 2606; d) R. D. Adams, J. E. Cortopassi, M. P. Pompeo, *ibid.* **1992**, *11*, 1.

[4] a) P. Braunstein, M. Knorr, A. Tiripicchio, M. Tiripicchio Camellini, *Angew. Chem.* **1989**, *101*, 1414; *Angew. Chem. Int. Ed. Engl.* **1989**, *28*, 1361; b) P. Braunstein, M. Knorr, U. Schubert, M. Lanfranchi, A. Tiripicchio, *J. Chem. Soc. Dalton Trans.* **1991**, 1507; c) P. Braunstein, M. Knorr,

H. Piana, U. Schubert, *Organometallics* **1991**, *10*, 828; d) P. Braunstein, M. Knorr, E. Villarroya, A. DeCian, J. Fischer, *ibid.* **1991**, *10*, 3714.
[5] G. Reinhard, B. Hirle, U. Schubert, *J. Organomet. Chem.* **1992**, *427*, 173.
[6] See for example: J. Powell, M. R. Gregg, J. F. Sawyer, *J. Chem. Soc. Chem. Commun.* **1987**, 1029; *Inorg. Chem.* **1988**, *27*, 4526.
[7] a) J. Powell, J. F. Sawyer, S. J. Smith, *J. Chem. Soc. Chem. Commun.* **1985**, 1312; b) T. Blum, P. Braunstein, A. Tiripicchio, M. Tiripicchio Camellini, *New J. Chem.* **1988**, *12*, 539; c) P. Braunstein, E. de Jesùs, A. Dedieu, M. Lanfranchi, A. Tiripicchio, *Inorg. Chem.* **1992**, *31*, 399.
[8] X-ray structure analysis of **4a** (25 °C): $M_r = 931.63$; yellow crystal (dimensions $0.2 \times 0.2 \times 0.3$ mm); triclinic; space group $P\bar{1}$; $a = 1044.1(2)$, $b = 1151.8(3)$, $c = 1747.6(4)$ pm, $\alpha = 81.55(2)$, $\beta = 85.14(2)$, $\gamma = 64.41(2)°$, $V = 1874 \times 10^6$ pm^3, $Z = 2$, $\rho_{calcd} = 1.65$ g cm^{-3}, $\lambda(Mo_{K\alpha}) = 71.93$ pm; $\mu = 43.1$ cm^{-1}; $F(000) = 920$. A total of 5862 unique reflections (up to $2\theta = 48°$), of which 5370 with $F > 2\sigma(F)$ were used for structure solution (direct methods) and refinement (full-matrix least squares); $R = 0.023$, $R_w = 0.025$. All non-hydrogen atoms were refined anisotropically. The hydrogen atoms were calculated and fixed in idealized positions (d(C–H) = 0.96 Å, $U = 1.2\ U_{iso}$ for the carbon to which it was attached). Further details of the crystal structure investigation may be obtained from the Fachinformationszentrum Karlsruhe, Gesellschaft für wissenschaftlich-technische Information mbH, D-W-7514 Eggenstein-Leopoldshafen 2 (FRG), on quoting the depository number CSD-56493, the names of the authors, and the journal citation.
[9] H. Inoue, T. Nakagome, T. Kuroiwa, T. Shirai, E. Fluck, *Z. Naturforsch. B* **1987**, *42*, 573, and references therein.
[10] A base-assisted hydrogen transfer from Pt to Re has been observed in a Re(μ-PCy$_2$)Pt system: J. Powell, J. F. Sawyer, M. V. R. Stainer, *J. Chem. Soc. Chem. Commun.* **1985**, 1314.
[11] E. L. Eliel, N. L. Allinger, S. J. Angyal, G. A. Morrisson, *Conformational Analysis*, Interscience, New York, **1965**, p. 191.
[12] J. Powell, E. Fuchs, M. R. Gregg, J. Phillips, M. V. R. Stainer, *Organometallics* **1990**, *9*, 387, and references therein.
[13] J. Slutsky, H. Kwart, *J. Am. Chem. Soc.* **1973**, *95*, 8678.

Detection of the Tungsten–Carbene–Olefin Intermediates in Catalytic Metathesis Systems Containing High-Valent Metal Centers

By *Jacky Kress** and *John A. Osborn*

Metal–carbene–olefin complexes have been postulated as key intermediates in catalytic olefin metathesis reactions and in cycloolefin ring-opening metathesis polymerization (ROMP) reactions.[1] Although several such complexes have been reported,[2] these do not lead to metathesis,[3] probably because the transition metal is in low or medium oxidation states. Adducts between olefins and high-valent, d^0[4] metal–alkylidene complexes, which would be intermediates or at least models for the most active catalyst systems,[1] are still unknown, although their formation has been predicted by several theoretical studies[6] and on the basis of indirect experimental arguments.[7] We now report the first characterization of such alkylidene–olefin complexes with a d^0 metal center which are also intermediates in catalytic ROMP reactions of cycloalkenes.

Cycloheptene (**2**) was shown by low-temperature ^{13}C NMR (Fig. 1) to interact with the tungsten–cyclopentylidene complex **1**[8] following Scheme 1. The equilibrium is displaced toward the π olefin adduct **3** at low temperature, and toward the two reactants at high temperature. No polycycloheptene[9] is detected after 30 min at (or below) 245 K. The carbene–olefin nature of **3** is clearly established by the presence at 200 K of a signal at $\delta = 355.3$ (^1J(W,C) = 142 Hz), which is assigned to the α C atom of the cyclopentylidene

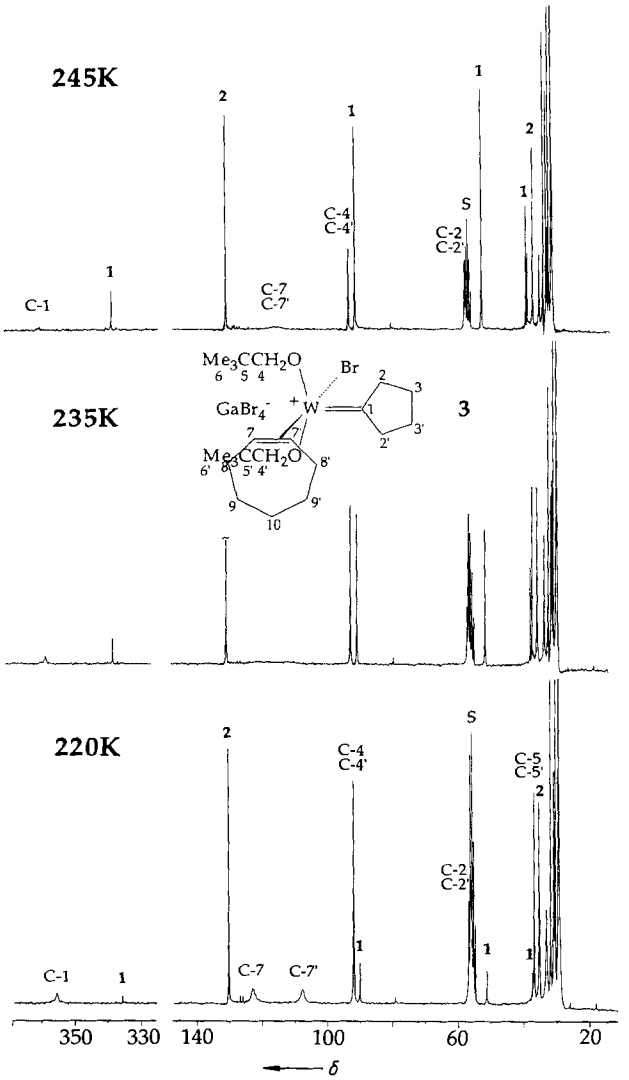

Fig. 1. ^{13}C NMR spectra (50 MHz) of the reaction mixture obtained after addition of 1.8 equiv of cycloheptene (**2**) to **1** (0.28 M in CD_2Cl_2 (S)) at 177 K.

unit, and of two signals at $\delta = 124.4$ and 107.8 (^1J(C,H) = 165 Hz) corresponding to two nonequivalent olefinic carbon atoms.[10] The assumption that $GaBr_4^-$ has left the coordination sphere of tungsten to yield a cationic complex is based on the large low-field shift of the alkylidene carbon atom and on the substantial decrease of the coupling constant ^1J(W,C),

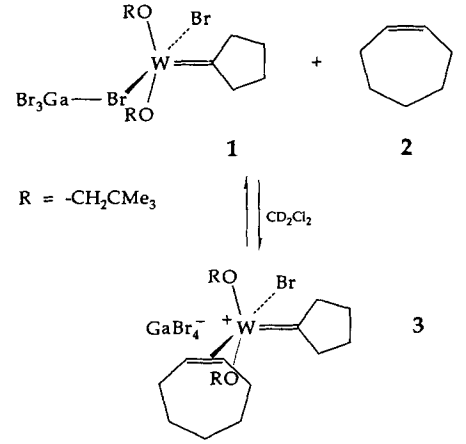

Scheme 1. Formation of the tungsten–carbene–olefin adduct **3**.

[*] Dr. J. Kress, Prof. Dr. J. A. Osborn
Laboratoire de Chimie des Métaux de Transition et de Catalyse
URA au CNRS n° 424
Université Louis Pasteur, Institut Le Bel
4 rue Blaise Pascal, F-67000 Strasbourg (France)

which suggest that the tungsten center is significantly more electron deficient in **3** than in **1** ($\delta = 335.6$ and $^1J(W,C) = 169$ Hz[8c]).[11] The limiting spectrum observed at 200 K[10] is fully consistent with a trigonal-bipyramidal coordination geometry (Fig. 1) with an equatorial "parallel" position for the cyclopentylidene ligand.[12] The arrangement of the two neopentoxo ligands with respect to the cyclopentylidene group is similar to that found for **1**.[8c] The olefin occupies an apical site with its C=C axis aligned with the W=C axis and with its "plane" parallel to that of the cyclopentylidene ligand.[14] Notably, this particular conformation is the only one suitable for subsequent conversion into a metallacyclobutane,[15] one of the fundamental steps of the metathesis mechanism.[1]

The ^{1}H NMR spectra[16] confirm these observations, showing moreover that the two hydrogen atoms of each β-methylene group of the cyclopentylidene ligand, as well as those of the neopentoxo methylene groups, are also nonequivalent, in agreement with the structure proposed for **3**. The two signals for the olefinic hydrogen atoms, on the other hand, are not distinguishable, giving rise to a single multiplet at $\delta = 5.64$. The position of this signal is shifted remarkably little from the corresponding signal of free cycloheptene ($\delta = 5.76$). The corresponding ^{13}C resonance signal ($\delta = 132.4$, $^1J(C,H) = 154$ Hz for free **2**), on the other hand, is shifted to an average position of $\delta = 116.1$.[10] Such small changes, compared to classical non-alkylidene d^2 olefin complexes,[17] tend to show that the alkylidene complex **3** should be viewed as a d^0 metal complex in which the olefin is bound mainly through donation of its π electrons into an empty d orbital of tungsten. A weak additional interaction of the π^* orbital with the π electrons of the W=C bond may, however, be at the origin of the parallel configuration and of the substantial barrier to rotation (see below).

Measuring the equilibrium constants at various temperatures, from the integrals of ^{1}H and ^{13}C NMR signals ($K = [\mathbf{3}]\,[\mathbf{1}]^{-1}\,[\mathbf{2}]^{-1} = 4.5 \pm 1\ \text{M}^{-1}$ at 235 K, for instance) allowed us to draw a linear Van't Hoff plot from which the thermodynamic values, $\Delta H^0 = -13.6 \pm 0.5$ kcal mol^{-1} and $\Delta S^0 = -55 \pm 3$ cal K^{-1}mol^{-1}, could be obtained for the formation of **3**.

Raising the temperature leads to the reversible coalescence of several of the ^{13}C and ^{1}H NMR signals of **3**. Most notable is the coalescence at 240 K of the two ^{13}C NMR signals of the olefinic C atoms C-7/C-7′ (Fig. 1). Other pairs such as C-3/C-3′, C-5/C-5′,[10] and $H_c/H_{c'}$[16] also coalesce to singlets at 215, 210, and 220 K respectively, whereas the two AB (2H) patterns due to CH_aH_b and $CH_{a'}H_{b'}$[16] simplify into a single AB (4H) pattern above 225 K; the same applies for the two AB patterns due to the two -OCH_2- groups. Using the Eyring equation,[18] equal and concentration-independent values for the free energy of activation are obtained for all these coalescences ($\Delta G^{\neq} = 10.6 \pm 0.1$ kcal mol^{-1}), showing that they result from a single intramolecular dynamic process. In this process, equilibration of the two neopentoxo ligands and of the two sides of both cycloheptene and cyclopentylidene ligands occurs, leaving their CH_2 protons nonequivalent. This can only be reconciled with the occurrence in **3** of olefin ligand rotation about the tungsten–olefin bond axis (Scheme 2). Such rotational barriers are relevant to the stereoselectivity in olefin metathesis and ROMP reactions.[1]

If the temperature is raised above 255 K, the catalytic ROMP reaction of cycloheptene[9, 19] begins in the reaction mixture, indicating that **3** can be considered as a true initiating intermediate in this catalytic system. No further intermediate, initiating or propagating, can however be detected,

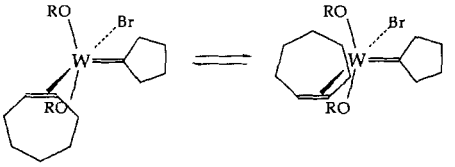

Scheme 2. Olefin ligand rotation about the tungsten–olefin bond axis.

and **1** is almost not consumed in this reaction, showing that the conversion of **3** into the metallacyclobutane derivative (Scheme 3) is slower than the following steps of this process.

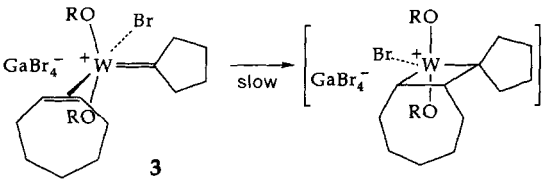

Scheme 3. Conversion of **3** into the corresponding metallacyclobutane derivative.

Furthermore, we found that: 1. Replacing bromides by chlorides[20a] cyclopentylidene by cyclohexylidene,[20b] or cycloheptene by cyclooctene[20c] leads to similar observations. In particular, the small low-field shift of the $^1H_{ol}$ NMR signal of cyclooctene on complexation to **1**[20c] confirms our description of the metal–olefin bonding in **3**. 2. When one bromo ligand is replaced by a neopentoxo group, or cyclopentylidene by neopentylidene, no intermediate can be detected, and polymerization of cycloheptene occurs at temperatures as low as 240 K. This suggests that the difference in energy between the initial carbene–olefin intermediate and the metallacyclobutane derivative as well as the reactants is smaller in these systems, and shows that the stability of **3** actually limits the rate of polymerization of **2** in the presence of **1**. 3. No interaction can be found between **1** and cyclohexene, indicating that ring-strain relief is involved in the formation of the cycloolefin adducts.[21] This may significantly contribute to the negative values found for ΔH^0. As expected, cyclohexene does not undergo polymerization by ring opening in the presence of **1**. 4. Replacing the cyclopentylidene ligand by *n*-pentylidene leads instead to a metallacyclobutane species as the main observable intermediate,[22] and the ROMP reaction of **2** starts at even lower temperatures (220 K). This behavior is similar to that found for the more strained norbornenes[23] and arises probably from further ring-strain relief on conversion of the carbene–olefin complexes into the metallacyclobutanes. The cycloalkylidene–monocycloolefin complexes described here are thus more stable than their metallacyclobutane derivatives (Scheme 3), probably because the tricyclic structure of the latter is more strained.

These results show that subtle changes in the nature of the metal–alkylidene catalyst or of the olefin substrate can lead to important modifications in the relative stability of the three types of intermediates involved in catalytic olefin metathesis reactions.

Received: July 6, 1992 [Z 5450 IE]
German version: *Angew. Chem.* **1992**, *104*, 1660

CAS Registry numbers:
1, 112069-32-6; **2**, 628-92-2; **3**, 144587-68-8.

[1] K. J. Ivin, *Olefin Metathesis*, Academic Press, London, **1983**.

[2] a) K. Angermund, F. W. Grevels, C. Krüger, V. Skibbe, *Angew. Chem.* **1984**, *96*, 911; *Angew. Chem. Int. Ed. Engl.* **1984**, *23*, 904; b) C. Alvarez, A. Pacreau, A. Parlier, H. Rudler, *Organometallics* **1987**, *6*, 1057; c) M. J. McGeary, T. L. Tonker, J. L. Templeton, *ibid.* **1985**, *4*, 2102; d) C. P. Casey, N. L. Hornung, W. P. Kosar, *J. Am. Chem. Soc.* **1987**, *109*, 4908; e) J. H. Wengrovius, R. R. Schrock, M. R. Churchill, H. J. Wasserman, *ibid.* **1982**, *104*, 1739.

[3] In one case only were olefin metathesis products observed on decomposition [2d].

[4] Here, the carbene/alkylidene group is considered as a dianionic 4e donor ligand [5].

[5] E. V. Anslyn, W. A. Goddard III, *Organometallics* **1989**, *8*, 1550.

[6] a) A. Dedieu, O. Eisenstein, *New J. Chem.* **1982**, *6*, 337; b) M. Sodupe, J. M. Lluch, A. Oliva, J. Bertran, *ibid.* **1991**, *15*, 321; c) T. H. Upton, A. K. Rappé, *J. Am. Chem. Soc.* **1985**, *107*, 1206.

[7] E. V. Anslyn, R. H. Grubbs, *J. Am. Chem. Soc.* **1987**, *109*, 4880.

[8] a) J. Kress, J. A. Osborn, *J. Am. Chem. Soc.* **1983**, *105*, 6346; b) J. Kress, A. Aguero, J. A. Osborn, *J. Mol. Catal.* **1986**, *36*, 1; c) M. T. Youinou, J. Kress, J. Fischer, A. Aguero, J. A. Osborn, *J. Am. Chem. Soc.* **1988**, *110*, 1488.

[9] T. J. Katz, S. J. Lee, N. Acton, *Tetrahedron Lett.* **1976**, *47*, 4247.

[10] ^{13}C NMR of **3** (50 MHz, CD_2Cl_2, 200 K): δ = 355.3 (C-1), 124.4, 107.8 (C-7, C-7'), 91.7 (C-4, C-4'), ≈54.4 (C-2, C-2'), 33.8, 33.5 (C-5, C-5'); 31.9 (C-10), 30.0, 29.4 (C-3, C-3'), 27.3 (C-9, C-9'), 25.8 (C-6, C-6'), ≈25.2, 24.8 (C-8, C-8'). The assignments are based on chemical shifts, signal intensities, gate-decoupled and DEPT NMR experiments; numbering of the nuclei is given in Figure 1.

[11] Similar variations in the NMR spectra were found for related complexes after conversion of $GaBr_3$ adducts into cationic species [8a], coordination of Lewis acids to a bromo ligand [8a,b], or replacement of neopentoxo ligands by less π electron donating bromo ligands [8b]. The neutral pentacoordinate alkylidene complexes were moreover shown to be only weak Lewis acids [8b], and their interaction with olefins to produce hexacoordinate π olefin adducts is unlikely. However, addition of excess $GaBr_4^-$ (1 equiv/**1**) in the form of its tetrabutylammonium salt has only little effect on the equilibrium position, according to the ^1H MR spectra [16], indicating that **3** is better viewed as non-separate ion pairs.

[12] This was shown to be the most favorable configuration for such complexes, both theoretically [6b, 13] and experimentally [8c].

[13] M. Sodupe, J. M. Lluch, A. Oliva, J. Bertran, *Organometallics* **1989**, *8*, 1837.

[14] This results in the dissymmetry observed for both cycloheptene and cyclopentylidene ligands, and in the non-equivalency of the two neopentoxo ligands [10].

[15] O. Eisenstein, R. Hoffmann, A. R. Rossi, *J. Am. Chem. Soc.* **1981**, *103*, 5582.

[16] ^1H NMR (200 MHz, CD_2Cl_2, $[1]_0$ = 0.05 M, $[2]_0/[1]_0$ = 4.3, 210 K, **3** = $[W(=C\overset{\alpha}{C}H_a\overset{\beta}{H_b}CH_2\overset{\gamma}{C}H_2\overset{\delta}{C}H_2\overset{\varepsilon}{C}H_{a'}H_{b'})(OCD_2tBu)_2Br(\overset{\alpha'}{C}H_{\alpha'}=\overset{\beta'}{C}H_{\alpha'}\overset{\gamma'}{C}H_{c'}\overset{\delta'}{H_{d'}}CH_2\overset{\varepsilon'}{C}H_2\overset{\zeta'}{C}H_2\overset{\eta'}{C}H_{d}H_{d'})(GaBr_4)]$: δ = 5.64 (2H; $H_{\alpha,\alpha'}$), 4.89 (3H; $H_{a',b'}$ + H_b), 4.42 (d, $^2J(H_a,H_b)$ = 20 Hz, 1H; H_a), 2.73 (1H; H_c), 2.37 (1H; $H_{c'}$), 1.88, 0.87 (s, 18H; *t*Bu). All signals (except the latter) are ill-resolved multiplets; the other expected lines were not distinguishable; the assignments were ensured by decoupling experiments. In the presence of OCH_2tBu instead of OCD_2tBu ligands, two additional AB patterns were observed for the $-OCH_2-$ protons at δ = 4.54 and 4.12 (d, $^2J(H,H)$ = 12 Hz, 1H + 1H), and 4.43 and 4.32 (d, $^2J(H,H)$ = 12 Hz, 1H + 1H).

[17] a) S. A. Cohen, P. R. Auburn, J. E. Bercaw, *J. Am. Chem. Soc.* **1983**, *105*, 1136; b) F. M. Su, C. Cooper, S. J. Geib, A. L. Rheingold, J. M. Mayer, *ibid.* **1986**, *108*, 3545; c) L. J. Guggenberger, P. Meakin, F. N. Tebbe, *ibid.* **1974**, *96*, 5420; d) J. D. Fellmann, R. R. Schrock, D. D. Traficante, *Organometallics* **1982**, *1*, 481.

[18] H. Günther, *NMR-Spektroskopie*, Thieme, Stuttgart, **1973**.

[19] The C=C double bonds in the initial polycycloheptene chains are 50% *cis* (by ^{13}C NMR). Secondary metathesis and formation of a saturated polymer occur simultaneously, especially above 270 K.

[20] a) $\Delta H^0 = -12.9$ kcal mol^{-1}, $\Delta S^0 = -48$ cal K^{-1}mol^{-1}, $\Delta G^* = 10.8$ kcal mol^{-1}, δ $^1H_{ol,ol'}$ (210 K) = 5.49; b) $\Delta H^0 = -12.9$ kcal mol^{-1}, $\Delta S^0 = -51$ cal K^{-1}mol^{-1}, $\Delta G^* = 10.6$ kcal mol^{-1}, δ $^1H_{ol,ol'}$ (225 K) = 5.66; c) $\Delta H^0 = -16$ kcal mol^{-1}, $\Delta S^0 = -62$ cal K^{-1}mol^{-1}, $\Delta G^* = 10.1$ kcal mol^{-1}, δ $^1H_{ol,ol'}$ (225 K) = 5.66 (5.58 in free cyclooctene); ^{13}C NMR (200 K): δ = 356.9 ($^1J(W,C)$ = 148 Hz; C-1), 127.7, 109.7 ($^1J(C,H)$ = 161 Hz; C-7, C-7'). Polymerization of cyclooctene occurs above 240 K (65% *cis*).

[21] N. S. Zefirov, V. I. Sokolov, *Russ. Chem. Rev. (Engl. Transl.)* **1967**, *36*, 87.

[22] ^{13}C NMR: δ = 192 ($^1J(C,H)$ = 166 Hz; C_α), 119.2 ($^1J(C,H)$ = 157 Hz, $^1J(W,C)$ = 55 Hz; $C_{\alpha'}$); ^1H NMR (210 K): δ = 7.67, 4.24 (H_α,$H_{\alpha'}$).

[23] a) J. Kress, J. A. Osborn, R. M. E. Greene, K. J. Ivin, J. J. Rooney, *J. Am. Chem. Soc.* **1987**, *109*, 899; b) J. Kress, J. A. Osborn, V. Amir-Ebrahimi, K. J. Ivin, J. J. Rooney, *J. Chem. Soc. Chem. Commun.* **1988**, 1164; c) J. Kress, J. A. Osborn, K. J. Ivin, *ibid.* **1989**, 1234.

C–C Coupling with NO_2/Alkyl Substitution at the Vinylic Carbon by Reaction of 2-Aryl-1-nitro-1-alkenes with Dialkylzinc Compounds—A Novel Reaction**

By *Dieter Seebach,* Harald Schäfer, Beat Schmidt,* and *Martin Schreiber*

In the course of our work on enantioselective Michael additions of diethylzinc to ω-nitrostyrene in the presence of chiral titanates[1] we were surprised to find not only the expected 1-nitro-2-phenylbutane but also 1-phenyl-1-butene,[2a] the product of the substitution of the vinylic nitro group by an ethyl group.[2b]

We soon found that substitution is preferred in the absence of a Lewis acid[2c] and in ethereal solvents. Under the optimized conditions shown in Scheme 1, 2-aryl- and 2-heteroarylnitroethenes reacted with both primary and secondary dialkylzinc compounds, affording the substitution products **1**–**6** in 30 to 40% yield[2d] (Scheme 1, Table 1). Due to their low polarity, these products[3] are readily purified by filtration through silica gel. According to their IR and NMR spectra all products **1**–**6** have (*E*) configuration, even if the starting material has (*Z*) configuration.[4] The nitroolefins used are readily available,[5] Et_2Zn (Schering) and $(octyl)_2Zn$[6] were used in pure form and dissolved in the required ethereal solvent, while $(iPr)_2Zn$ and $(tBu)_2Zn$ were prepared in situ and salt free, according to a recently published experimental procedure.[1b]

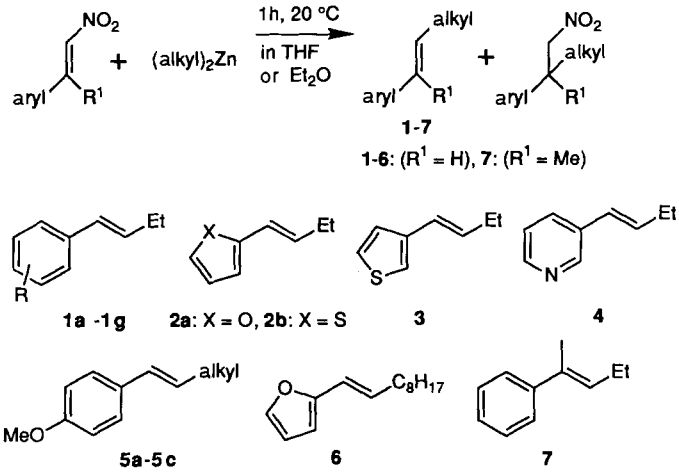

Scheme 1. Olefins **1**–**6** and **7** prepared by substitution of the NO_2 group of 1-aryl-2-nitroethenes and 1-nitro-2-phenylpropene, respectively, upon reaction with dialkylzinc compounds (for the specification of R and alkyl see Table 1).

The reaction is sensitive to steric hindrance in the starting materials (see for example **1c**, **5c**, **7**);[7] the substitution reaction was not successful with diallyl-, dibenzyl-, and diphenylzinc, nor with 3,3-dimethyl-1-nitrobutene (led to Michael adducts).

[*] Prof. Dr. D. Seebach, Dipl.-Chem. H. Schäfer, Dr. B. Schmidt, M. Schreiber
Laboratorium für Organische Chemie der Eidgenössischen Technischen Hochschule, ETH-Zentrum
Universitätstrasse 16, CH-8092 Zürich (Switzerland)

[**] The results described herein form part of the dissertation of B. Schmidt, ETH Nr. 9698 (1992) and part of the projected dissertation of H. Schäfer. The scholarship awarded to H. Schäfer by the Studienstiftung des deutschen Volkes is gratefully acknowledged.

Table 1. Products **1**–**7**, synthesized as shown in Scheme 1. The quoted yields refer to chromatographically purified products (pure according to ^{1}H NMR spectroscopy). For the typical synthetic procedure refer to the text.

Cmpd.	Product		Yield
	aryl	alkyl	[%]
1a	C_6H_5	Et	32
1b	4-Me-C_6H_4	Et	37
1c	2,4,6-$Me_3C_6H_2$	Et	18
1d	3-MeO-C_6H_4	Et	32
1e	4-MeO-C_6H_4	Et	38
1f	3,4-$(OCH_2O)C_6H_3$	Et	39
1g	4-NC-C_6H_4	Et	37 [a]
2a	2-furyl	Et	30 [b]
2b	2-thienyl	Et	37 [b]
3	3-thienyl	Et	31 [b]
4	3-pyridyl	Et	36 [a]
5a	4-MeO-C_6H_4	C_8H_{17}	40 [c,d]
5b	4-MeO-C_6H_4	*i*Pr	30 [d]
5c	4-MeO-C_6H_4	*t*Bu	15
6	2-furyl	C_8H_{17}	48 [b,d]
7	see Scheme 1		22

[a] Flash chromatography performed with additional 15% EtOAc in the eluent. [b] Sample ca. 90%, pure could not be further purified by distillation or chromatography. [c] Flash chromatography, eluent C_5H_{12}/CH_2Cl_2 (8:1), column 20 × 3 cm. [d] The reaction time was longer (ca. 20 h) than that given in Scheme 1.

The substitution reaction described herein is remarkable for the following two reasons: a) Normally, the nitro group acts as a leaving group only in special cases[8] and probably is the best "activator" for Michael additions.[9] b) Vinylic C–C coupling is usually carried out with halides and organometallic coumpounds, and normally requires a Pd or Ni catalyst (e.g. the Heck reaction).[2e, 10]

Since the starting materials leading to the products **1**–**7** are more accessible (aldehyde or ketone + CH_3NO_2)[5] than the corresponding vinyl halides or metal derivatives, the reaction described here could be applied preparatively[11] in some cases, despite the low yields achieved to date.[12]

Experimental Procedure

Typical synthetic procedure: A solution of 1.00 g (5.58 mmol) of 1-(4-methoxyphenyl)-2-nitroethene in 25 mL THF, under argon at room temperature was treated with 1.4 equiv of a 2 M Et_2Zn solution in THF. After 1 h, the reaction was quenched at 0 °C with 20 mL of saturated NH_4Cl solution and stirred for half an hour at room temperature. The mixture was filtered through celite and the solids washed with Et_2O (alternatively the precipitated zinc salts can be dissolved by addition of 2 M HCl). The organic layer was washed with 50 mL brine, dried over $MgSO_4$, and the solvent evaporated in vacuo. The oil obtained was filtered through silica gel (14 × 3 cm, ca. 70 mL dry material, ca. 400 mL C_5H_{12}/CH_2Cl_2 (5:1)), and 1-(4-methoxyphenyl)-1-butene **1e** was eluted as the least polar product. After removal of most of the solvent, the residue was further dried at ca. 0.1 Torr for 10 min[13] to give pure **1e** in 38% yield. Spectroscopic data [14] for **1e**: ^{1}H NMR (200 MHz, $CDCl_3$): $\delta = 6.30$ (d, $J = 16$ Hz, 1 H; C1-H), 6.08 (dt, $J = 15.8$ Hz, $J = 6.3$ Hz, 1 H; C2-H); IR ($CHCl_3$): $\tilde{\nu}$[cm^{-1}] = 966.

Received: August 13, 1992 [Z 5516 IE]
German version: *Angew. Chem.* **1992**, *104*, 1680

[1] a) B. Schmidt, D. Seebach, *Angew. Chem.* **1991**, *103*, 1383–1385; *Angew. Chem. Int. Ed. Engl.* **1991**, *30*, 1321–1323; b) J. L. von dem Bussche-Hünnefeld, D. Seebach, *Tetrahedron* **1992**, *48*, 5719–5730.

[2] a) The Michael adduct was essentially racemic; b) The "wrong" nucleophilic addition of $(alkyl)_2Zn$ to the nitroolefin is disfavored by many powers of ten [$pK_a(ArCH_2alkyl) > 35$, $pK_a(alkylCH_2NO_2)$ ca. 10]; c) Other Lewis acids, i.e. 2.8 equiv of $MgBr_2/MgCl_2$ in Et_2O (suspension), led selectively to the Michael adduct [e.g. 94% yield of 2-(4-methoxyphenyl)-1-nitrobutane starting from 1-(4-methoxyphenyl)-2-nitroethene and Et_2Zn in Et_2O at 20 °C]; d) Addition of 6 equiv of 1,3-dimethyl-2-oxo-hexahydropyrimidine (DMPU) (T. Mukhopadhyay, D. Seebach, *Helv. Chim. Acta* **1982**, *65*, 385–391) caused the yield of **1e** to increase to 44%; e) In the presence of $[Pd\{P(C_6H_5)_3\}_4]$, **1e** was obtained in 22% yield. We believe that the observed substitution is not caused by some metal impurity in the dialkylzinc compounds, because not only were they generated from different sources but were also purified by different methods.

[3] In addition to the Michael adduct (ca. 40%), a product aryl-CH(alkyl)-CH(alkyl)-NO_2 (ca. 5%) arising from a second addition was isolated.

[4] Tested with (*Z*)-1-nitro-2-phenylethene (D. B. Miller, P. W. Flanagan, H. Shechter, *J. Org. Chem.* **1976**, *41*, 2112–2120; D. Seebach, A. K. Beck, J. Golinsky, J. N. Hay, T. Laube, *Helv. Chim. Acta* **1985**, *68*, 162–172).

[5] a) H. G. Padeken, O. von Schickh, A. Segnitz in *Methoden Org. Chem. (Houben Weyl), 4th Ed.* **1971**, Vol. X1, pp. 342–360; b) H. Ohta, N. Kobayashi, K. Ozaki, *J. Org. Chem.* **1989**, *54*, 1802–1804.

[6] K. Nützel in *Methoden Org. Chem. (Houben Weyl) 4th Ed.* **1973**, Vol. 13/2a, 595.

[7] With 2-nitro-1-phenyl-1-propene [5a] we did not observe any substitution.

[8] R. Tamura, A. Kamimura, N. Ono, *Synthesis* **1991**, 423–434; N. Kornblum, *Aldrichimica Acta* **1990**, *23*, 71–78; D. Seebach, E. W. Colvin, F. Lehr, T. Weller, *Chimia* **1979**, *33*, 1–18, and references therein.

[9] *Nitroalkanes and Nitroalkenes in Synthesis (Tetrahedron* **1990**, *46*, 7313–7598; A. G. M. Barrett, *Chem. Soc. Rev.* **1991**, *20*, 95–127.

[10] a) J. P. Collman, L. S. Hegedus, J. R. Norton, R. G. Finke in *Principles and Applications of Organotransition Metal Chemistry*, University Science Books, Mill Valley, CA, **1987**, Chapter 14.4–14.5, pp. 710–727; b) R. F. Heck in *Palladium in Organic Synthesis*, Academic Press, New York, **1985**.

[11] It is difficult to compete successfully with the Wittig–Horner reaction, McMurry coupling, and other olefination reactions, as well as with the partial hydrogenation of acetylenes.

[12] Experiments investigating the mechanism of the reaction are in progress (see also ref. [2]), and may lead to an improvement of the yield.

[13] Particular care was taken with the furyl and phenyl derivatives, which were kept in vacuo for a shorter time because of their higher volatility.

[14] In the ^{1}H NMR spectra of the compounds **1**, **2b**, **3**, and **5a** the vinylic protons have chemical shifts $\delta = 6.3$ to 6.5 (C1-H) and 6.0 to 6.2 (C2-H) and coupling constants $J = 15$–16 Hz. For protons C2-H and C3-H_2 the coupling constant is ca. 6.2 Hz. The IR spectra of the compounds **1** to **6** contain strong bands between 953 and 972 cm^{-1}, typical of 1,2-disubstituted (*E*) olefins.

A Homologous Series of Stable Polyenes: Synthesis, Structure, and Redox Behavior**

By *Alfried Kiehl, Anke Eberhardt, Martin Adam, Volker Enkelmann,* and *Klaus Müllen**

Dedicated to Professor Klaus Hafner on the occasion of his 65 th birthday

Linear polyenes serve on one hand as textbook examples for the description of "the electron in a one-dimensional box" in molecular orbital theory[1] and on the other as defect-free model compounds for electrically conducting materials such as polyacetylene.[2] We describe here a facile way to a homologous series of monodisperse polyenes, based on the palladium-catalyzed coupling of organotin compounds with electrophiles, developed by Stille. Furthermore, we followed the electron-transfer behavior of the polyenes by cyclic voltammetry and proved the unusual layered structure of dodecahexaene (all-(*E*)-**10**) by X-ray crystallography.

Recently Schrock and Knoll[4] described a synthesis of polyenes that was based on the metathetical ring opening of cyclobutene derivatives and yielded polydisperse mixtures; chromatographic separation is required to provide defined homologues. We have developed a "warehouse" of olefin precursors that allow stable and soluble polyenes of defined

[*] Prof. Dr. K. Müllen, Dipl.-Chem. A. Kiehl, A. Eberhardt, Dipl.-Chem. M. Adam, Dr. habil. V. Enkelmann
Max-Planck-Institut für Polymerforschung
Ackermannweg 10, D-W-6500 Mainz (FRG)

[**] This work was supported by the Volkswagen Stiftung. We thank BASF AG for cyclooctatetraene.

chain length to be obtained in good yields. A further advantage of our procedure is the significantly smaller amount of catalyst required (2–5%), which simplifies the recovery of very pure samples.[5] The *tert*-butyl terminal groups in the title compounds provide the steric protection for the chain ends and ensure good solubility. In contrast to the carotenoids, the main chain of the polyenes should remain unsubstitued to prevent a twisting of the π-electron system.[6]

By hydroalumination of *tert*-butylacetylene with diisobutylaluminum hydride (DIBA) and subsequent cleavage by iodine, one obtains the iodide **2** as pure (*E*) isomer in 67% yield.[7] The butadiene **4** can be prepared from (*E*,*E*)-dichlorobutadiene **3**[8] and two equivalents of trimethylstannyllithium.[9] This procedure yields a distillable mixture of 65% (*E*,*E*), 31% (*E*,*Z*), and 4% (*Z*,*Z*) isomers.[10]

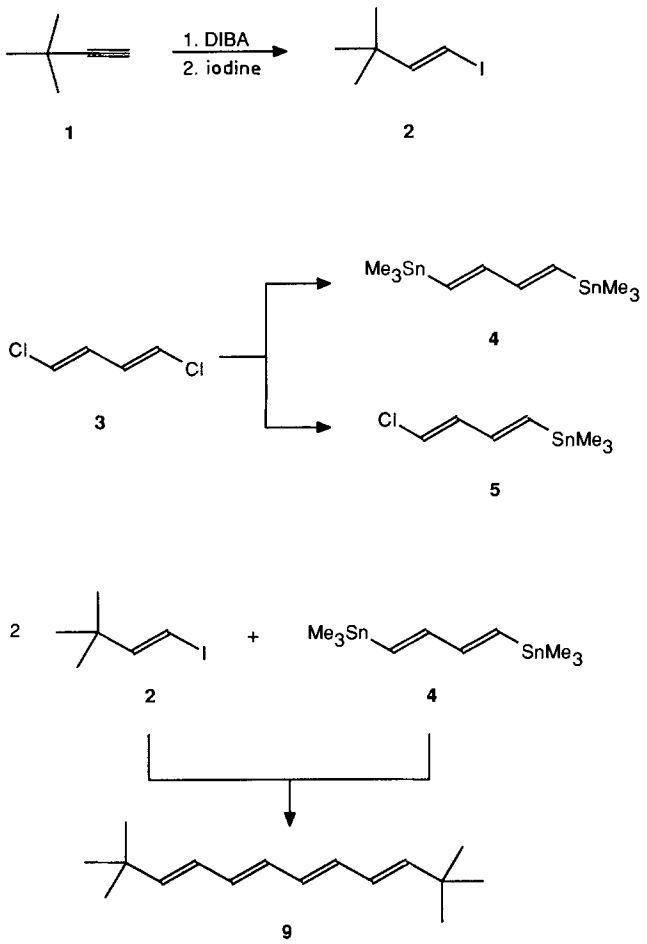

The best catalyst systems for the coupling of the vinyl iodide **2** with the bifunctional organyltin compound **4** proved to be $[PdCl_2(CH_3CN)_2]$/DMF and $[Pd(tfp)_2]$/DMF (tfp = trifurylphosphane, DMF = dimethyl formamide).[11] With these the tetraene **9** could be isolated after about 1 h in gram quantities and satisfactory yields (42%). The coupling of **9** also affords about 20% of **10** and small amounts of still higher oligomers with even numbers of double bonds in the chain. This finding can be explained by an exchange of iodine and trimethyltin in the catalyst, which leads, for example, to the formation of **8**.

All coupling reactions proceed with complete retention of the olefin configuration; that is, there is no isomerization of the starting materials **2** and **4** in the product **9**. Pure all-(*E*)-tetraene **9** is obtained by a simple recrystallization from ethyl acetate.

The dichloride **3** can be transformed into 1-chloro-4-trimethylstannyl-1,3-butadiene **5**, a bifunctional building block, with less than the stoichiometric amount of trimethylstannyllithium. The chlorohexatriene **6** is formed in 64% yield through a coupling reaction between **5** and the iodide **2** in which the chloro substituent, which is significantly more inert than iodine, remains unchanged. A further stannylation of **6** affords the hexatriene **7**. This product can also be obtained through a direct coupling of the iodide **2** with the stannane **4**, but small amounts of **4** are always present as impurity (5–10%). The iodine hexatriene **8** arises on cleavage of the stannyl group from **7** by iodine. Thus the way to the higher polyenes is open: the coupling reaction of the hexatrienes **7** and **8** furnishes di-*tert*-butyldodecahexaene **10** in 82% yield. This higher yield relative to tetraene **9** results from the already described exchange reaction. Since the transformation of **7** and **8** always yields **10** as final coupling product, higher oligomers are not formed. Finally reaction of the iodide **8** with the distannylbutadiene **4** gives rise to the hexadecaoctaene **11** in 39% yield. As in the coupling to form tetraene **9**, UV spectroscopy and mass spectrometry detect higher enes as side products, in particular di-*tert*-butylicosadecaene **12**. The physical properties of the compounds **5**–**8** are summarized in Table 1.

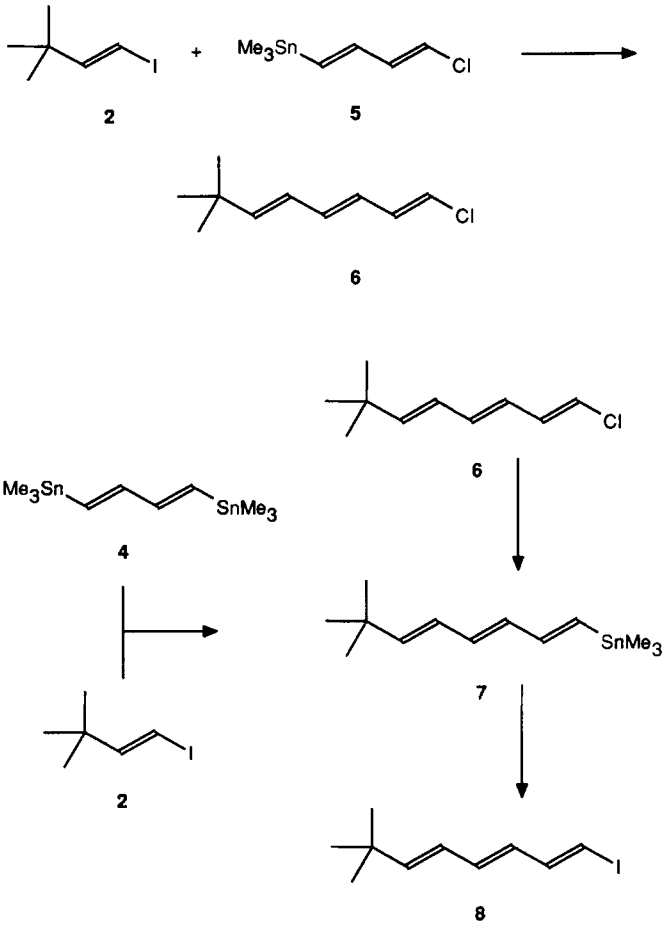

Compared with other polyenes, the di-*tert*-butyl polyenes thus accessible under mild reaction conditions (see ref. [5] and *Experimental Procedure*) display a remarkable thermal

Table 1. Selected physical data of the compounds **5**–**8** [a].

5: ^{1}H NMR: $\delta = 0.16$, 0.23 (2s, 9H, CH_3), 6.10–7.00 (m, 4H, olefin CH); ^{13}C NMR: $\delta = -9.29$, -8.06 (CH_3), 121.30, 123.41 (C4), 135.97, 136.77, 136.86, 137.22, 142.12, 142.26 (C1-C3); MS (70 eV): *m/z* 161 (17.0%), 163 (26.3%), 165 (36.0%, $(H_3C)_3Sn$), 233 (35.7%), 235 (73.6%), 237 (100%), 239 (35.9%; $M^+ - CH_3$), 248 (1.6%), 250 (3.9%), 252 (5.0%), 254 (1.6%, M^+).

6: ^{1}H NMR: $\delta = 1.04$, 1.06 (2s, 9H, CH_3), 5.75–7.00 (m, 6H, olefin CH); ^{13}C NMR: $\delta = 29.90$ (CH_3), 33.95, 34.00 (quat. C), 119.84, 120.39, 121.18, 123.23, 125.21, 126.59, 129.93, 131.59, 134.35, 134.89, 148.25, 149.08 (olefin C1-C6); MS (70 eV): *m/z* 170, 172 (M^+ with ^{35}Cl, ^{37}Cl).

7: ^{1}H NMR: $\delta = 0.14$, 0.22 (2s, 9H, $(H_3C)_3Sn$), 1.04, 1.05 (2s, 9H, $(H_3C)_3C$), 5.7–7.1 (m, 6H, olefin CH); ^{13}C NMR: $\delta = -9.23$, -8.00 ($(H_3C)_3Sn$), 30.01 (*tert*-butyl-CH_3), 33.79 (quat. C), 125.95, 125.63, 132.98, 133.45, 133.80, 133.89, 134.29, 135.97, 146.94, 147.12, 147.43, 147.68 (C1-C6); MS (70 eV): *m/z* 57 (18.7%, *tert*-butyl), 135 (100%, $M^+ - (H_3C)_3Sn$), 281 (7.8%), 283 (13.72%), 285 (17.0%, $M^+ - CH_3$), 296 (2.1%), 298 (3.1%), 300 (3.9%, M^+).

8: ^{1}H NMR: $\delta = 1.04$, 1.06 (2s, 9H, CH_3), 5.8–7.1 (m, 6H, olefin. CH); ^{13}C NMR: $\delta = 29.84$ (CH_3), 33.99 (quat. C), 77.68, 81.35 (C1), 125.01, 125.65, 130.44, 130.80, 134.81, 138.36, 138.93, 145.92, 149.02, 149.49 (C2-C6); MS (70 eV): *m/z* 57 (66.9%, *tert*-butyl), 105 (100%, C_8H_9), 135 (20.6%, $M^+ - I$), 262 (53.0%, M^+).

[a] ^{1}H NMR (200 MHz, $CDCl_3$), ^{13}C NMR (50 MHz, $CDCl_3$); 30 °C; all values relative to tetramethylsilane.

stability and inertness.[12] Low temperature crystallization from *n*-pentane yields square crystals of the dodecahexaene **10**. The crystal structure of **10**[13] is depicted in Figure 1 in two projections. In the layered structure the molecules are tilted both relative to the plane of the layer and to the plane of projection shown to provide an angle of about 90° between the oligoene chains in adjacent layers. Remarkably, this packing accommodates the bulky *tert*-butyl groups in the spaces between the layers in such a way that each polyene chain is surrounded by six neighbors, and an arrangement with a subcell structure very similar to that of *trans*-polyacetylene[14] results. Therefore, analogously to other polyenes, **10** can be regarded as a model for the packing in *trans*-polyacetylene. The subcell is indicated at the top of Figure 1, and as projection in the direction of the chain at the bottom.

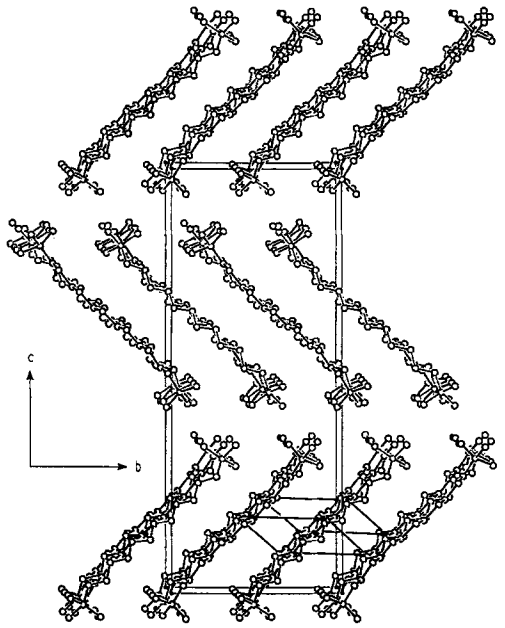

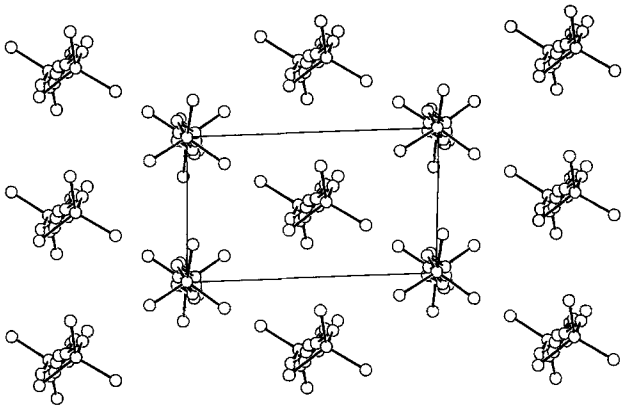

Fig. 1. Top: Unit cell of **10** (hydrogen atoms omitted). In addition the subcell of *trans*-polyacetylene is indicated. Bottom: view in the direction of the molecular axis of **10**.

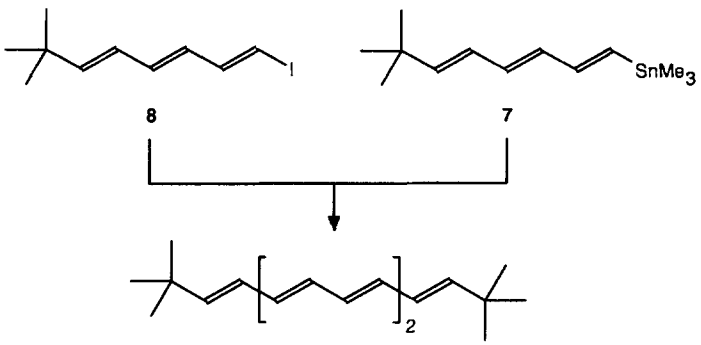

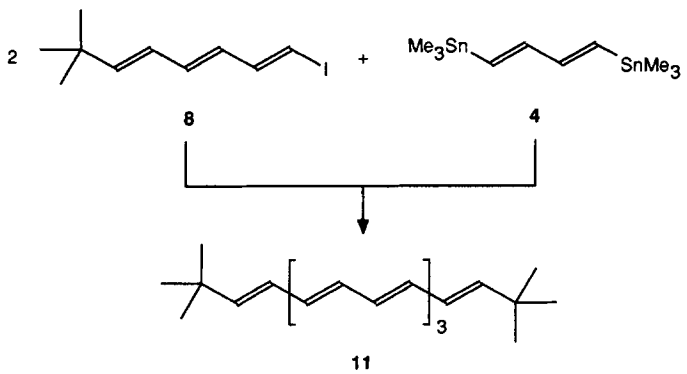

As in *trans*-polyacetylene,[16] the lengths of the double and single bonds in **10** are not completely equivalent. Instead it shows an alternating structure. The average length of the double bonds is 1.34 Å and that of the single bonds, 1.44 Å. A contraction of the bond lengths toward the center of the molecule[15] is not observed; the lengths of both double and single bonds are subject only to statistical variations.

The dodecahexaene **10** and its higher homologues can also serve as models for doped polyacetylene, because polyenes containing six to ten double bonds are comparable with those regions of the polyacetylene chain that become charged on oxidation or reduction.[17] If the layered structure can be maintained on reduction, intercalation com-

Table 2. Cyclovoltammetric data of **9**, **10**, and **11** [a]. $E_{1/2}$ in volt; reference electrode: saturated calomel electrode.

Compd.	Reduction (in THF)				Oxidation (in CH_2Cl_2)			
	$E^4_{1/2}$	$E^3_{1/2}$	$E^2_{1/2}$	$E^1_{1/2}$	$E^1_{1/2}$	$E^2_{1/2}$	$E^3_{1/2}$	ΔE [eV]
9			− 2.88 [b]	− 2.52	0.99	2.0 [b]		3.5
10			− 2.46 [b]	− 2.20	0.79	1.11 [b]		2.9
11	− 2.98 [b]	− 2.79 [b]	− 2.14 [b]	− 1.96	0.63	0.83 [b]	1.45 [b]	2.6
11 [c]	− 2.75 [b]	− 2.60 [b]	− 2.08 [b]	− 1.80				

[a] $T = -20\,^{\circ}C$, $v = 100\ mVs^{-1}$, electrolyte: $n Bu_4NPF_6$, electrode material: gold. [b] Irreversible charge transfer as a result of the deposition of films on the electrode surface. [c] In DMF/$n Bu_4NPF_6$ at $-30\,^{\circ}C$.

pounds should arise in which the charged oligoene layers are separated by layers of counterions.

As in polyacetylene,[18, 19] the oligomers described here have a high redox activity. The cyclic voltammogram of even the tetramer **9** (see Table 2) reveals two oxidation and two reduction peaks. The HOMO-LUMO energy difference ΔE can be estimated at 3.5 eV from the first reduction and oxidation potentials. The hexamer **10** does not show a more extended redox sequence, but the energy gap ΔE decreases to about 2.9 eV. Finally, in hexadecaoctaene **11** seven successive charge-transfer steps from tetraanion to trication can be detected, and ΔE is decreased even further to 2.6 eV. The band gap of polyacetylene can be calculated by plotting ΔE against $1/n$ (n = the number of double bonds) and extrapolating.[20] The resulting value of 1.7 eV agrees well with the band gap (1.4–1.8 eV) determined experimentally and theoretically for polyacetylene itself.[18]

Our investigations have shown that the structurally well-defined polyenes **9**–**11** make a valuable contribution to the understanding of the properties and the structure of polyacetylene. In addition the syntheses presented here open a versatile alternative to conventional methods of preparation for polyenes such as the Wittig reaction.[7, 21] In a later publication we shall describe how homologues with an uneven number of double bonds and, in particular, homologues with even longer chains are accessible.

Experimental Procedure

Palladium-catalyzed coupling reactions (general procedure): Into a "deactivated" Schlenk tube under an argon atomsphere was placed 2–5 mol% of catalyst. About 10 mL of DMF per mmol of stannyl equivalent was distilled into the tube. When $[Pd^0_2(dba)_3]$ (dba = dibenzylidene acetone) was used, two equivalents of trifurylphosphane were also added. Then the iodide and the stannane were injected into the solution. The course of the reaction could be followed clearly by thin-layer chromatography. At room temperature the reaction time varied between 30 and 90 minutes, depending on the subtrate. As workup the solution was taken up in ether, the organic phase washed three times with degassed water and subsequently dried over $MgSO_4$. The ether was then distilled off, and the final workup of the products was either by chromatography on degassed silica gel or by distillation.

Further workup of the polyenes **9**, **10**, and **11**: Low temperature chromatography ($-30\,^{\circ}C$) with n-pentane/$CHCl_3$ mixtures. The isolation of isomerically pure all-(*E*)-polyenes is achieved by irradiation with light of suitable wavelength [$\lambda > 300$ nm for **9** (in the presence of iodine) and **10**, $\lambda > 345$ nm for **11**] and subsequent recrystallization.

All analytical data agree with those of Schrock et. al (see ref. [4]).

Received: July 9, 1992 [Z 5456 IE]
German version: *Angew. Chem.* **1992**, *104*, 1623

CAS Registry numbers:
1, 917-92-0; **2**, 61382-45-4; **3**, 3588-12-3; **4**, 112008-10-3; **4**(*E*,*Z*), 112008-09-0; **4**(*Z*,*Z*), 112008-08-9; **5**, 144193-66-8; **6**, 144193-67-9; **7**, 144193-68-0; **8**, 144193-69-1; **9**, 121987-85-7; **10**, 121987-87-9; **11**, 121987-89-1.

[1] I. N. Levine, *Quantum Chemistry*, 3. Aufl., Allyn and Bacon, Boston, **1983**.
[2] T. A. Skotheim, *Handbook of Conducting Polymers*, Marcel Dekker, New York, **1986**; H. Kuzmany, M. Mehring, S. Roth, *Electronic Properties of Conjugated Polymers*, Springer Series in Solid State Sciences, *Vol. 76*, Springer, New York, **1988**.
[3] J. K. Stille, *Angew. Chem.* **1986**, *98*, 504–519; *Angew. Chem. Int. Ed. Engl.* **1986**, *25*, 508–524.
[4] K. Knoll, R. R. Schrock, *J. Am. Chem. Soc.* **1989**, *111*, 7989–8004.
[5] J. K. Stille, J. H. Simpson, *J. Am. Chem. Soc.* **1987**, *109*, 2138–2152.
[6] F. Effenberger, H. Schlosser, *Synthesis* **1990**, *11*, 1085; W. Göhring, S. Roth, M. Hanack, *Synth. Met.* **1987**, *17*, 259–262.
[7] G. Zweifel, C. C. Whitney, *J. Am. Chem. Soc.* **1967**, *89*, 2753.
[8] R. Criegee, W. Hörauf, W. D. Schellenberg, *Chem. Ber.* **1953**, *86*, 126–132.
[9] C. Tamborski, F. E. Ford, E. J. Soloski, *J. Org. Chem.* **1963**, *28*, 237–239.
[10] T. N. Mitchell, C. Nettelbeck, *Org. Magn. Reson.* **1987**, *25*, 879. On stannylation of **3** it is essential that no more than two equivalents of the organyllithium compound is used, because the butadiene **4** would otherwise be partially destannylated again. This finding contradicts the report of Ashe et al. (A. J. Ashe, S. Mahmoud. *Organometallics* **1988**, *7*, 1878–1880).
[11] First coupling experiments of **2** and **4** with tetrakis(triphenylphosphino)palladium(0) gave no reaction even after a week at room temperature. With $[PdCl(bz)(PPh_3)_2]$ (bz = benzyl) in THF, the tetraene **9** was isolated after three days in 21% yield and with $[PdCl_2(PPh_3)_2]$ in the same period, in 42% yield.
[12] F. Sondheimer, D. A. Efraim, R. Wolovsky, *J. Am. Chem. Soc.* **1961**, *83*, 1675–1681; R. Snyder, E. Arvidson, C. Foote, L. Harrigan, L. Christensen, *ibid.* **1985**, *107*, 4117–4122.
[13] Enraf-Nonius CAD4 diffractometer ($Cu_{K\alpha}$ radiation, graphite monochromator, $\lambda = 1.5404$ Å), $C_{20}H_{30}$, monoclinic crystals of the space group *Cc*. $a = 11.470(4)$, $b = 11.448(3)$, $c = 27.992(3)$ Å, $\beta = 92.01(2)^{\circ}$, $V = 3673$ Å^3, $Z = 8$, $\rho_{calcd} = 0.978\ g cm^{-3}$, $\mu = 3.707\ cm^{-1}$, 2451 measured relections of which 2202 observed ($I > 3\sigma(I)$). The structure was solved by direct methods (SIR). Two crystallographically independent molecules are found in the unit cell, whose binding geometries cannot be distinguished within experimental error. An empirical absorption correction was applied. In the last full-matrix refinement cycle the calculated hydrogen atoms in "riding" mode were provided with isotropic temperature coefficients and the C atoms with anisotropic temperature coefficients. ($R = 0.056$, $R_w = 0.058$ for $w = 1$ and 181 parameters.) The subcell of **10** (see Fig. 1) is slightly larger than that of polyacetylene: $a = 8.10$, $b = 4.56$, $c = 2.47$ Å, $V = 91.23$ Å^3. Further details of the crystal structure investigation may be obtained from the Fachinformationszentrum Karlsruhe, Gesellschaft für wissenschaftlich-technische Information mbH, D-W-7514 Eggenstein-Leopoldshafen 2 (FRG) on quoting the depository number CSD-56661, the names of the authors, and the journal citation.
[14] R. H. Baughman, S. L. Hsu, L. R. Anderson, G. P. Pez, A. J. Signorelli, *NATO Conf. Ser.* **1979**, *6*, 187.
[15] R. H. Baughman, B. E. Kohler, I. J. Levy, C. Spangler, *Synth. Met.* **1985**, *11*, 37–52.
[16] J. C. Chien, F. E. Karasz, K. Shimamura, *Makromol. Chem. Rapid Commun.* **1982**, *3*, 655.
[17] H. Kuzmany, M. Mehring, S. Roth, *Electronic Properties of Polymers and Related Compounds (Springer Ser. Solid State Sci. 63)*, Springer, Berlin, **1985**.
[18] P. M. Lathi, J. Obrzut, F. E. Karasz, *Macromolecules 1987*, *20*, 2023–2026.
[19] P. J. Nigrey, A. G. McDiarmid, A. J. Heeger, *Mol. Cryst. Liq. Cryst.* **1982**, *83*, 309–317.
[20] J. L. Bredas, R. Silbey, D. S. Boudreaux, R. R. Chance, *J. Am. Chem. Soc.* **1983**, *105*, 6555–6559.
[21] C. W. Spangler, P.-K. Liu, A. A. Dembek, K. O. Havelka, *J. Chem. Soc. Perkin Trans. 1* **1991**, 799, and references therein.

Chlorins Designed for Photodynamic Tumor Therapy and as Model Systems for Photosynthesis**

By *Franz-Peter Montforts,* Axel Meier, Gerhard Scheurich, Gerold Haake,* and *Jan. W. Bats*

Dedicated to Professor Emanuel Vogel on the occasion of his 65th birthday

Chlorophyll a (**1**), the green photosynthesis pigment, is the prototype of the chlorin class of natural products,[1] which has recently been expanded to include a number of compounds[2] with differing structures, biological sources, and functions. The common structural unit in this class is the chlorin framework **2** with a partially saturated pyrrole ring, which is derived from the completely unsaturated porphyrin. The photophysical properties of the chlorins resulting from this structural modification predestine them as pigments for photosynthesis[3] and for medical applications, for example in photodynamic tumor therapy (PDT).[4]

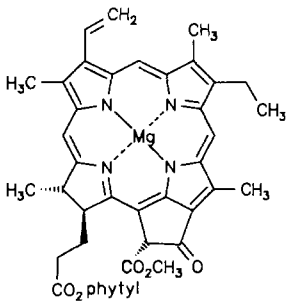

1

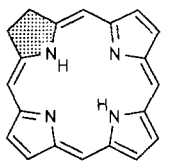

2

The chlorin *rac*-**3**[5] with geminal dialkyl substitution in the saturated pyrrole ring was easily obtained from the red blood pigment heme and functionalized in the 3 position by degradation of the double bond. Artifical photosynthesis systems may thus be prepared containing "natural" chlorins as the structural units in contrast to the previously synthesized model systems based on porphyrins. The functionalized chlorin *rac*-**8** may be modified to provide sensitizer structures and fluorescence markers[6] for photodynamic tumor therapy and other diagnostic/therapeutic applications.

Chlorin *rac*-**3** was first complexed with zinc(II) ions to protect the chromophore (Scheme 1). The oxidative cleavage of the exocyclic double bond and subsequent decomplexation under acidic conditions led to oxochlorin *rac*-**7**. The amide function in *rac*-**6** was hydrolyzed readily due to the anchimeric participation of the 3-oxo group to give *rac*-**14**. The preparation of the corresponding nickeloxochlorin *rac*-**11** required the hydrolysis of the amide function and cleavage of the double bond by iodolactonization, followed by a retro-aldol-type fragmentation and oxidation with MnO_2.[7] The X-ray structure analysis[8] of the nickeloxochlorin *rac*-**11**, which was conducted in light of the coenzyme function of metal-containing chlorins,[2g, k] proved to be difficult: all of

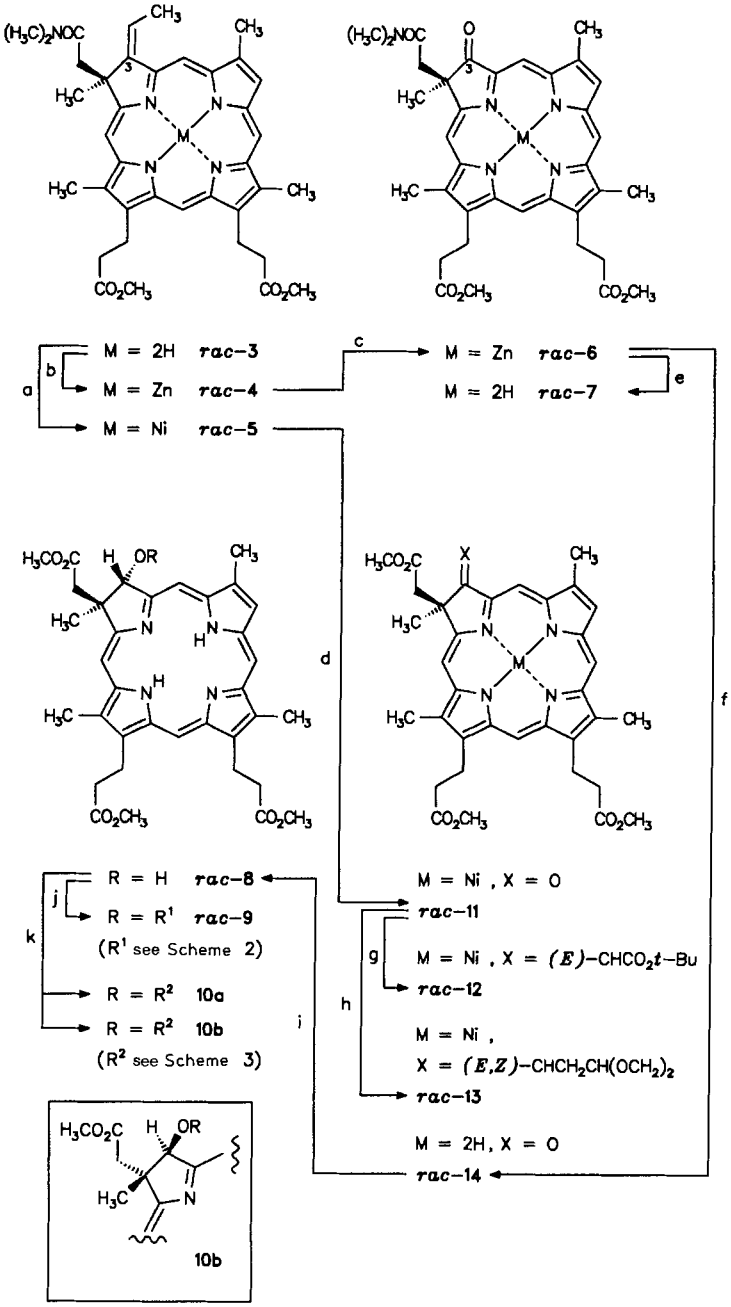

Scheme 1. a) 5 Equiv Ni^{II} acetylacetonate, $CHCl_3$, reflux, 10 h; flash chromatography, silica gel, CH_2Cl_2/ethyl acetate (6/1); recrystallization ($CHCl_3$/petroleum ether); *rac*-**5** (*Z* isomer) 67% and *E* isomer 14%. b) 10 Equiv Zn^{II} acetylacetonate, $CHCl_3$, reflux, 10 h; flash chromatography, silica gel, CH_2Cl_2/methyl acetate (6/1); recrystallization ($CHCl_3$/*n*-hexane); *rac*-**4** (*Z* isomer) 61% and *E* isomer 12%. c) K_2CO_3, $NaIO_4$, 0.1 equiv $KMnO_4$, *tert*-butanol + water, room temperature, 30 min; flash chromatography, silica gel, CH_2Cl_2/methyl acetate (6/1); recrystallization ($CHCl_3$/*n*-hexane); *rac*-**6** 56%. d) 1. 1.4 Equiv I_2, THF + water, room temperature, 5 h (87% stereoisomeric iodolactones); 2. 5M KOH, MeOH, 100 °C, 60 h; 3. 5 equiv MnO_2, MeOH, room temperature, 1 h; 4. CH_2N_2, MeOH + ether, room temperature, 1 h; flash chromatography, silica gel, CH_2Cl_2/ethyl acetate (20/1); recrystallization ($CHCl_3$/petroleum ether); *rac*-**11** 63%. e) 1N HCl, methanol, room temperature, 30 min; flash chromatography, silica gel, CH_2Cl_2/methyl acetate (6/1); recrystallization ($CHCl_3$/*n*-hexane); *rac*-**7** 98%. f) 1. KOH in methanol (saturated), reflux, 40 h; 2. pH 4 buffer (formation of the tricarboxylic acid and removal of zinc); 3. CH_2N_2, methanol + ether, room temperature, 1 h; flash chromatography, silica gel, CH_2Cl_2/methyl acetate (20/1); recrystallization ($CHCl_3$/*n*-hexane); *rac*-**14** 82%. g) 1. $(H_3CO)_2P(O)CH_2CO_2C(CH_3)_3$, *n*BuLi, THF, −78 °C, 1.5 h; 2. addition of the lithium phosphonate to *rac*-**11**, reflux, 20 h; flash chromatography, silica gel, CH_2Cl_2/methyl acetate (20/1); recrystallization ($CHCl_3$/*n*-hexane); *rac*-**12** 47%. h) 1. $[(H_5C_6)_3PCH_2CH_2CH(OCH_2)_2]^+Br^-$, NaN[$Si(CH_3)_3$]$_2$, THF, reflux, 1 h; 2. addition of the ylide to *rac*-**11**, reflux, 20 h; flash chromatography, silica gel, CH_2Cl_2/methyl acetate (20/1); recrystallization ($CHCl_3$/*n*-hexane); *rac*-**13** 33% (66% based on reacted *rac*-**11**). i) 1.

[*] Prof. Dr. F.-P. Montforts, Dr. A. Meier, Dr. G. Scheurich, Dipl.-Chem. G. Haake
Institut für Organische Chemie, FB 2 der Universität
Leobener Strasse/NW 2, D-W-2800 Bremen 33 (FRG)
Dr. J. W. Bats
Institut für Organische Chemie der Universität Frankfurt

[**] This research was supported by the Deutsche Forschungsgemeinschaft and the Fonds der Chemischen Industrie.

34 Equiv $LiAlH(OtBu)_3$, THF, room temperature, 30 min; 2. $NaHCO_3$; flash chromatography, silica gel, CH_2Cl_2/methyl acetate (6/1); recrystallization ($CHCl_3$/*n*-hexane); *rac*-**8** 81%. j) 1. 10 Equiv **16**, 0.9 equiv $N(nBu)_4Br$, 50% aq NaOH, CH_2Cl_2 room temperature, evacuated sealed tube, 90 h; 2. pH 4 buffer; 3. 5 M KOH, THF, 50 °C, vacuum, 90 h; 4. pH 4 buffer; flash chromatography, silica gel CH_2Cl_2/methanol (9/1), then methanol/water (1/1); 5. methanol, 10 vol% conc H_2SO_4, room temperature, 18 h; flash chromatography, silica gel, CH_2Cl_2/methyl acetate (6/1), recrystallization ($CHCl_3$/*n*-hexane); *rac*-**9** 42%. k) 1. 9.5 Equiv **19**, 0.9 equiv $N(nBu)_4Br$, 50% aq NaOH, CH_2Cl_2, room temperature, evacuated sealed tube, 90 h; 2. pH 4 buffer; 3. 5 M KOH, THF, 50 °C, vacuum, 90 h; 4. pH 4 buffer; flash chromatography, silica gel, CH_2Cl_2/methanol (9/1), then methanol/water (1/1); 5. methanol, 10 vol% conc H_2SO_4, room temperature, 18 h; flash chromatography, silica gel, CH_2Cl_2/methyl acetate (6/1), recrystallization ($CHCl_3$/*n*-hexane); binary mixture of diastereomers **10a** + **10b**, each 24%; analytical HPLC, Polygosil 60-10, CH_2Cl_2/methyl acetate (95/5), 2 mL min^{-1}, t_{R1} = 7.7 min, t_{R2} = 9.2 min, separation of the diastereomers.

the crystals were twinned, two crystallographically independent molecules are found in the unit cell, and these molecules have a certain degree of disorder. Both molecules, which differ primarily in the conformations of the side chains, are saddle-shaped and deviate from planarity (Fig. 1).[9] Some

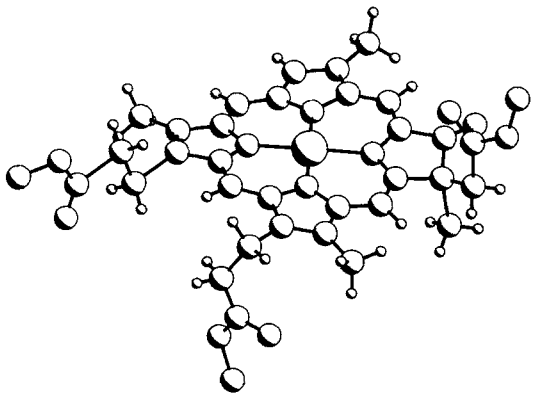

Fig. 1. Crystal structure of one of the two independent molecules of *rac*-**11** with the d_m parameter[9] 0.21 Å. The side view shows the marginal deviation of the ligand system from planarity ("ruffling"). The second molecule differs only in the relative orientation of its side chains.

of the atoms in the molecules have large values for the anisotropic temperature parameter in the direction perpendicular to the ring system. This indicates that each of the two molecules actually has at least two conformations that are less planar than the structures obtained in the X-ray analysis. The Ni–N distances range from 191(1) to 199(1) pm; as expected the Ni–N bond to the saturated pyrrole ring is the longest. We are currently investigating the effect the saddle-shaped deformation has on the redox behavior of chlorin, as this could be of importance in the biological function of metallochlorins.

The Wittig and Wittig–Horner reactions were used to attach functionalized residues to the keto group of the nickelchlorin *rac*-**11** to yield *rac*-**12** and *rac*-**13**; the metal-free oxochlorin *rac*-**14** did not react. The keto function of *rac*-**14** was reduced stereoselectively with excess $LiAl(OtBu)_3H$ under the directing influence of the acetic acid side chain to give the α-hydroxychorin *rac*-**8**. The trace amounts of the β-alcohol reacted with the acetic acid side chain also positioned β to form a lactone which could be removed easily by chromatography.

The hydroxyl group in *rac*-**8** was etherified with various alkyl groups under phase-transfer catalysis. With a view to photosynthesis models we treated the hydroquinone bromide **16**, available from **15** in five steps (Scheme 2), with *rac*-**8** to provide the chlorinhydroquinone ether *rac*-**9**.

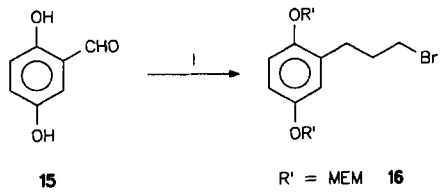

R^1 = **16** without Br, R'=H

Scheme 2. l) 1. 3 Equiv methoxyethoxymethyl chloride (MEMCl), 3 equiv *N*,*N*-diisopropylethylamine, 0.01 equiv 4-dimethylaminopyridine (DMAP), CH_2Cl_2, 0 °C to room temperature, 20 h; flash chromatography, silica gel, CH_2Cl_2/methyl acetate (9/1), ether/petroleum ether (2/1); 73%; 2. $(H_3CO)_2P(O)CH_2CO_2CH_3$, *n*BuLi, THF, −10 °C, 15 min; addition of the lithium phosphonate, 0 °C to room temperature, 6 h; flash chromatography, silica gel, ether/petroleum ether (2/1); 93%; 3. H_2 (1 atm), Pd/C (10%), methyl acetate, room temperature, 20 h; flash chromatography, silica gel, ether/petroleum ether (2/1); 85%; 4. 2.9 equiv $LiBH_4$, diglyme, 110 °C, 5.5 h; flash chromatography, silica gel, ether/petroleum ether (2/1); 70%; 5. 1.4 equiv methanesulfonyl chloride, 1.5 equiv triethylamine, CH_2Cl_2, −10 °C, 2 h; 3.2 equiv KBr, 2.7 equiv [18]crown-6, acetone, room temperature, 18 h, flash chromatography, silica gel, ether/petroleum ether (2/1); **16** 91% (37% based on **15**).

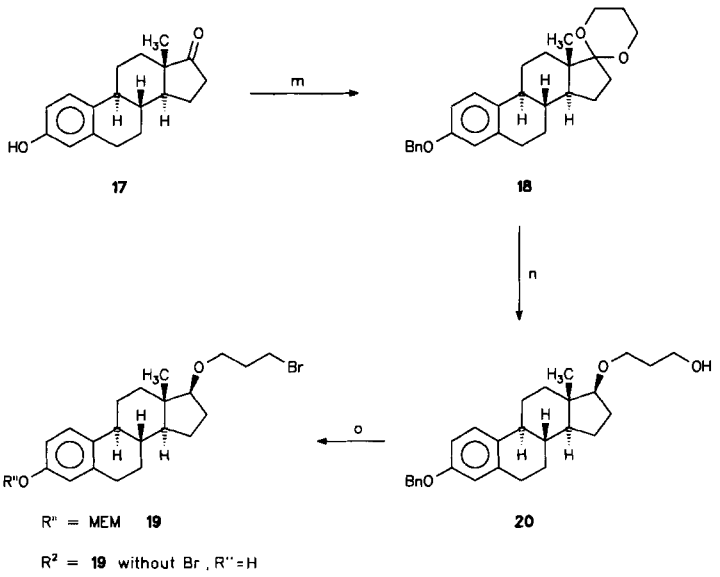

R^2 = **19** without Br, R"=H

Scheme 3. m) 1. 1.1 Equiv benzyl chloride, 1.1 equiv K_2CO_3, ethanol, reflux, 6 h; 0.5 M NaOH; 94%; 2. 2.2 equiv propane-1,3-diol, 0.03 equiv *p*-toluenesulfonic acid monohydrate, Na_2SO_4, 3 Å molecular sieves, toluene, reflux, 22 h; flash chromatography, silica gel, CH_2Cl_2/petroleum ether (5/1); **18** 67% (63% based on **17**). n) 1. 1.25 Equiv $H_3B{\cdot}S(CH_3)_2$, 1.26 $F_3CSO_3Si(CH_3)_3$, CH_2Cl_2, −78 °C, 1.5 h [10]; 2. saturated aq $NaHCO_3$ solution; flash chromatography, silica gel, CH_2Cl_2/methyl acetate (19/1), recrystallization (methanol); **20** 92%. o) 1. 1.6 Equiv benzoyl chloride, 0.09 equiv DMAP, pyridine, 0 °C to rooom temperature, 3.5 h; kugelrohr distillation; flash chromatography, silica gel, CH_2Cl_2/petroleum ether (4/1), recrystallization (acetone); 91%; 2. H_2 (1 atm), Pd/C (10%), ethyl acetate, room temperature, 16 h; flash chromatography, silica gel, CH_2Cl_2/methyl acetate (19/1); 94%; 3. 1.2 equiv *n*BuLi, THF, −10 °C, 30 min; addition of 1.3 equiv MEMCl, −10 °C, 2 h; flash chromatography, silica gel, CH_2Cl_2/methyl acetate (19/1); 92%; 4. NaOMe/NaOH, methanol/water (3/1), room temperature, 20 h; flash chromatography, silica gel, CH_2Cl_2/methyl acetate (9/1); 96%; 5. 1.3 equiv methanesulfonyl chloride, 1.5 equiv triethylamine, CH_2Cl_2 −15 °C, 2 h; 7 equiv KBr, 5 equiv [18]crown-6, acetone, room temperature, 18 h; flash chromatography, silica gel, CH_2Cl_2/petroleum ether (9/1); **19** 75% (57% based on **20**).

Chorin *rac*-**8** was attached to estradiol derivative **19**, which was prepared in a few steps (Scheme 3), in order to optimize the biological properties of photodynamically active sensitizers and to bind chlorins to the estrogen receptors as fluorescence markers.[6a] In estrogens the structural region with the phenolic hydroxyl group is crucial for receptor binding;[6b] thus the chlorin was attached with a diether spacer of appropriate length to the 17-hydroxyl function of the estradiol.

The homochiral diastereomeric estrogen chlorin ethers **10a** and **10b** obtained by the introduction of the enantiomerically pure estrogen unit were separated by analytical HPLC; this should also be possible for the preparative-scale resolution of chlorin *rac*-**8**. Spectroscopic data for selected compounds are provided in Table 1.

Table 1. Selected spectroscopic data for *rac*-**8**, *rac*-**9**, *rac*-**10a,b**, *rac*-**11**, and *rac*-**14**.

rac-**8**: M.p. 207–208 °C; UV/VIS ($CHCl_3$): λ_{max} [nm] (ε) = 391 (144800), 489 (8700), 495 (8800), 523 (200), 591 (1600), 616 (1400), 643 (37400); ^{1}H NMR (360 MHz, $CDCl_3$): $\delta = -2.65$ (m, br, 2 H, NH), 1.80 (s, 3 H, CH_3 an C-2), 3.65, 4.04 (AB system, $J_{AB} = 17.9$ Hz, 2 H, CH_2 on C-2), 4.60 (m, br, 1 H, OH), 6.81 (d, $J_{HCOH} = 3$ Hz, 1 H, 3-H), 8.73, 8.95, 9.30, 9.75, 9.78 (5 s, 5 H, 5-, 8-, 10-, 15-, 20-H); MS (70 eV): *m/z* 628 (M^+, 100%), 555 ($M^+ - CH_2CO_2CH_3$, 50).
rac-**9**: M.p. 80-85 °C; UV/VIS ($CHCl_3$): λ_{max} [nm] (ε) = 390 (154600), 639 (39300); MS (70 eV): *m/z* 778 (M^+, 1.4%), 626 ($M^+ - C_9H_{12}O_2$, 19), 612 ($M^+ - C_9H_{10}O_3$, 71), 539 (612 − $CH_2CO_2CH_3$, 57), 538 (612 − $CH_3CO_2CH_3$, 43), 150 ($(C_6H_3(OH)_2CH_2CH{=}CH_2^+$, 35); High-resolution MS: *m/z* for $C_{44}H_{50}N_4O_9$ calc. 778.3578, found 778.3568.
rac-**10a, b**: Binary mixture of diastereomers; m.p. 82–86 °C; UV/VIS ($CHCl_3$): λ_{max} [nm] (ε) = 391 (162300), 640 (40900); MS (70 eV): *m/z* 940 (M^+, 3%), 684 ($M^+ - C_{18}H_{22}O$, −2H, 3), 626 ($M^+ - C_{21}H_{28}O_2$, −2H, 19), 612 ($M^+ - C_{21}H_{28}O_3$, 48), 538 (612-$CH_3CO_2CH_3$, 89), 330 ($C_{21}H_{30}O_3^+$, 48); High-resolution MS: *m/z* for $C_{56}H_{68}N_4O_9$ calc. 940.4986, found 940.4949.
rac-**11**: M.p. 178 °C; UV/VIS ($CHCl_3$): λ_{max} [nm] (ε) = 289 (18400), 372 (34100), 409 (98500), 544 (5400), 570 (7900), 614 (47400); ^{1}H NMR (360 MHz, $CDCl_3$): $\delta = 1.77$ (s, 3 H, CH_3 on C-2), 3.79, 3.82 (AB system, $J_{AB} = 16.9$ Hz, 2 H, CH_2 on C-2), 8.56, 8.68, 9.39, 9.40, 9.42 (5 s, 5 H, 5-, 8-, 10-, 15-, 20-H); MS (70 eV): *m/z* 682 (M^+ with ^{58}Ni, 100%), 609 ($M^+ - CH_2CO_2CH_2CH_3$, 72).
rac-**14**: M.p. 195 °C; UV/VIS ($CHCl_3$): λ_{max} [nm] (ε) = 404 (154800), 484 sh (5800), 504 (10100), 540 (8900), 585 (5100), 642 (35800); ^{1}H NMR (360 MHz, $CDCl_3$): $\delta = -3.02$, −2.84 (2 s, 2 H, NH), 1.95 (s, 3 H, CH_3 on C-2), 3.93, 4.01 (AB system, $J_{AB} = 17$ Hz, 2 H, CH_2 on C-2), 9.05, 9.10, 9.88, 9.90, 9.93 (5 s, 5 H, 5-, 8-, 10-, 15-, 20-H); MS (70 eV): *m/z* 626 (M^+, 100%), 553 ($M^+ - CH_2CO_2CH_3$, 29).

Received: July 14, 1992 [Z 5464 IE]
German version: *Angew. Chem.* **1992**, *104*, 1650

CAS Registry numbers:
rac-**3**, 101544-04-1; *rac*-**4** (*Z* isomer), 144320-56-9; *rac*-**4** (*E* isomer), 144407-37-4; *rac*-**5** (*Z* isomer), 138749-68-5; *rac*-**5** (*E* isomer), 138608-12-5; *rac*-**6**, 144320-57-0; *rac*-**7**, 144320-47-8; *rac*-**8**, 144320-49-0; *rac*-**9**, 144320-51-4; **10a**, 144320-53-6; **10b**, 144407-36-3; *rac*-**11**, 144320-58-1; *rac*-**12**, 144320-59-2; *rac*-**13** (*Z* isomer), 144320-60-5; *rac*-**13** (*E* isomer), 144407-38-5; *rac*-**14**, 144320-48-9; **15**, 1194-98-5; **16**, 144320-50-3; **17**, 53-16-7; **18**, 144320-54-7; **19**, 144320-52-5; **20**, 144320-55-8; $(H_3CO)_2P(O)CH_2CO_2C(CH_3)_3$, 62327-21-3; $[(H_5C_6)_3PCH_2CH_2CH(OCH_2)_2]^+Br^-$, 86608-70-0; $(H_3CO)_2P(O)CH_2CO_2CH_3$, 5927-18-4.

[1] H. Brockmann Jr. in *The Porphyrins, Vol. 2* (Ed.: D. Dolphin), Academic Press, New York, **1978**, pp. 287–326.
[2] a) E. Lederer, *C. R. Acad. Sci.* **1939**, *209*, 528–529; b) J. A. Ballantine, A. F. Psaila, A. Pelter, D. Murray-Rust, V. Ferrito, P. Schembri, V. Jaccarini, *J. Chem. Soc. Perkin Trans.* **1980**, 1080–1089; c) F.-P. Montforts, C. M. Müller, A. Lincke, *Liebigs Ann. Chem.* **1990**, 415–418; d) R. Deeg, H.-P. Kriemler, K.-H. Bergmann, G. Müller, *Hoppe-Seyler's Z. Physiol. Chem.* **1977**, *358*, 339–352; e) K.-H. Bergmann, R. Deeg, K. D. Gneuss, H.-P. Kriemler, G. Müller, *ibid.* **1977**, *358*, 1315–1332; f) M. Imfeld, D. Arigoni, R. Deeg, G. Müller in *Vitamin B_{12}* (Eds.: B. Zagalak, W. Friedrich), de Gruyter, Berlin, **1979**, pp. 315–316; g) C. Sotiriou, C. K. Chang, *J. Am. Chem. Soc.* **1988**, *110*, 2264–2270; h) R. Timkovich, M. S. Cork, R. B. Gennis, P. Y. Johnson, *ibid.* **1985**, *107*, 6069–6075; i) P. Karuso, P. R. Bergquist, J. S. Buckleton, R. C. Cambie, G. R. Clark, C. F. Rickard, *Tetrahedron Lett.* **1986**, *27*, 2177–2178; j) K. Sakata, K. Yamamoto, H. Ishikawa, A. Yagi, H. Etoh, K. Ina, *ibid.* **1990**, *31*, 1165–1168; k) K. C. Bible, M. Buytendorp, P. D. Zierath, K. L. Rinehart, *Proc. Natl. Acad. Sci. USA* **1988**, *85*, 4582–4586.
[3] a) J. Deisenhofer, O. Epp, K. Miki, R. Huber, H. Michel, *J. Mol. Biol.* **1984**, *180*, 385–398; b) R. Huber, *Angew. Chem.* **1989**, *101*, 849–871; *Angew. Chem. Int. Ed. Engl.* **1989**, *28*, 848–869; c) J. Deisenhofer, H. Michel, *ibid.* **1989**, *101*, 872–892 and **1989**, *28*, 829–847.
[4] a) H. van den Bergh, P. Cornaz, *Nachr. Chem. Tech. Lab.* **1985**, *33*, 582–589; b) T. J. Dougherty, J. H. Kaufmann, A. Goldfarb, K. R. Weishaupt, D. Boyle, A. Mittleman, *Cancer Res.* **1976**, *38*, 3628; c) T. J. Dougherty in *Methods in Porphyrin Photosensitization* (Ed.: D. Kessel), Plenum, New York, **1985**, pp. 313–328; d) S. Beckmann, T. Wessel, B. Franck, W. Hönle, H. Borrmann, H. G. von Schnering, *Angew. Chem.* **1990**, *102*, 1439–1441; *Angew. Chem. Int. Ed. Engl.* **1990**, *29*, 1395; e) F.-P. Montforts, A. Meier, G. Haake, F. Höper, *Tetrahedron Lett.* **1991**, *32*, 3481–3482.
[5] a) F.-P. Montforts, G. Zimmermann, *Angew. Chem.* **1986**, *98*, 451–452; *Angew. Chem. Int. Ed. Engl.* **1986**, *25*, 458–459; b) G. Haake, A. Meier, F.-P. Montforts, G. Scheurich, G. Zimmermann, *Liebigs Ann. Chem.* **1992**, 325–336.
[6] a) G. M. Anstead, J. L. Ensign, C. S. Peterson, J. A. Katzenellenbogen, *J. Org. Chem.* **1989**, *54*, 1485–1491; b) R. Hahnel, E. Twaddle, T. Ratajczak, *J. Steroid Biochem.* **1973**, *4*, 21; c) A. Vessières, S. Top, C. Vaillant, D. Osella, J.-P. Mornon, G. Jaouen, *Angew. Chem.* **1992**, *104*, 790–792; *Angew. Chem. Int. Ed. Engl.* **1992**, *31*, 753–755.
[7] a) F.-P. Montforts, F. Romanowski, J. W. Bats, *Angew. Chem.* **1989**, *101*, 471–473; *Angew. Chem. Int. Ed. Engl.* **1989**, *28*, 480–483; b) F.-P. Montforts, G. Mai, F. Romanowski, J. W. Bats, *Tetrahedron Lett.* **1992**, *33*, 765–768.
[8] *rac*-**11**: Triclinic, space group P_1, $a = 13.250(2)$, $b = 16.315(2)$, $c = 17.757(6)$ Å, $\alpha = 100.28(2)$, $\beta = 108.96(2)$, $\gamma = 107.44(1)^\circ$, $V = 3298(3)$ Å^3, $Z = 4$ (two independent molecules), $\rho_{calc} = 1.377$ g cm^{-3}, $\mu(Cu_{K\alpha}) = 12.7$ cm^{-1}. The structure was determined by direct methods (Multan 80 program). $R(F) = 0.120$ for the 3864 reflections employed. Enraf-Nonius CAD-4 diffractometer; SDP program system. Further details of the crystal structure investigation may be obtained from the Fachinformationszentrum Karlsruhe, Gesellschaft für wissenschaftlich-technische Information mbH, D-W-7514 Eggenstein-Leopoldshafen 2 (FRG) on quoting the depository number CSD-55235, the names of the authors, and the journal citation.
[9] The ruffling in the structures of the two independent molecules is described by d_m parameters of 0.21 and 0.17 Å. For a definition of d_m cf. a) C. Kratky, R. Waditschatka, C. Angst, J. E. Johansen, J. C. Plaquevent, J. Schreiber, A. Eschenmoser, *Helv. Chim. Acta* **1985**, *68*, 1312–1337; b) A. Eschenmoser, *Angew. Chem.* **1988**, *100*, 5–40; *Angew. Chem. Int. Ed. Engl.* **1988**, *27*, 5.
[10] R. Hunter, B. Bartels, J. P. Michael, *Tetrahedron Lett.* **1991**, *32*, 1095–1098.

$KCeSe_4$: A New Solid-State Lanthanide Polychalcogenide**

By *Anthony C. Sutorik* and *Mercouri G. Kanatzidis**

Although interest in both solid-state and soluble metal polychalcogenide compounds has increased over the last few years, the extension of this work to the lanthanides and actinides has yet to be fully realized. At present only a handful of these compounds have been confirmed to possess polychalcogenido ligands, although several others are suspected to by analogy.[1] Rare earth metals are highly oxophilic, which precludes the use of oxygen-containing solvents commonly employed for solution reactions. A preparative

[*] Prof. Dr. M. G. Kanatzidis, A. C. Sutorik
Department of Chemistry and
Center for Fundamental Materials Research
Michigan State University
East Lansing, MI 48824 (USA)

[**] This work was supported by the National Science Foundation and the NASA Graduate Student Researchers Program. The authors wish to thank Isaac S. Sutorik and Gregori Kanatzidis for many stimulating and productive discussions.

method which satisfies the requirements of being both oxygen-free and enables the use of large quantities of polychalcogenides is the molten salt technique. The use of molten alkali metal polychalcogide fluxes as both reactant and media has been shown to give a wide variety of new alkali metal/transition metal polychalcogenide compounds, especially when the reaction temperature is maintained within the range of 250–400 °C, which favors polychalcogenide formation.[2, 3] We have studied the reactivity of lanthanides and actinides in various alkali metal polychalcogenide fluxes, and we now report on the synthesis of $KCeSe_4$, a new solid-state lanthanide polychalcogenide compound with a novel, but remarkably simple, structure, containing exclusively Se_2^{2-} units.

In the $KCeSe_4$ structure,[4] Ce and Se form anionic layers with K^+ ions in the cavity between the layers. The anionic layers themselves are further partitioned into two layers of Se_2^{2-} units, which sandwich a layer of Ce^{3+} ions. The Ce^{3+} ions are in a square antiprismatic environment, coordinated to the ends of eight diselenide ions, four above the Ce plane and four below (see Fig. 1). The Se_2^{2-} units point in one direction within one layer and this direction is reversed in the layer below. The net effect is such that when projected onto the (001) plane, a pattern of two crosses with a common center as inversion center is seen. Each Se_2^{2-} unit bridges four Ce^{3+} ions, whereby each Se atom acts as a μ_2 bridge; the expanded anionic layer is shown in Figure 2. The K^+ ions are not shown but are, in fact, colinear with the Ce^{3+} ions and are displaced from these by only half the length of the c axis. Hence, except for their distances from the Se_2^{2-} layers, Ce^{3+} and K^+ have the same coordination environment. A further feature of this structure is the formation of channels parallel to (110), which are bound on both sides by Ce^{3+} and above and below by Se_2^{2-} (Fig. 3). Their dimensions are 4.16 Å (Ce–Ce) by 3.61 Å (Se–Se), and hence, they are too small for intercalation of most species, although Li intercalation may be possibile by the reduction of Se_2^{2-} to $2Se^{2-}$.

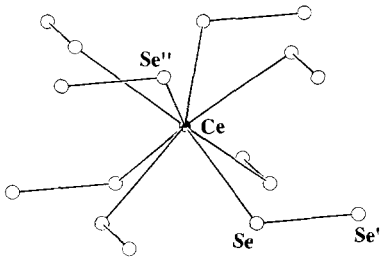

Fig. 1. Immediate coordination environment of Ce^{3+} in $KCeSe_4$. The Ce^{3+} ion is coordinated to one end of eight separate Se_2^{2-} units in a square-antiprismatic arrangement. The Ce^{3+} ion has the point symmetry of 422 and the Se atom resides on a mirror plane; hence, all Se atoms are crystallographically equivalent. Selected bond lengths [Å] and angles [°]: Ce-Se 3.075(1); Se-Se' 2.385(3); Se-Ce-Se'' 69.92(3); Ce-Se-Se' 110.20(3).

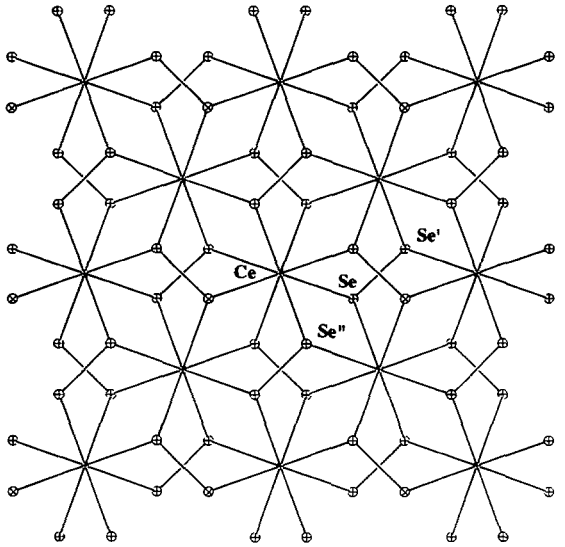

Fig. 2. View along the c axis of the anionic layers in $KCeSe_4$. The Ce^{3+} ions are represented by the eight-coordinate, shaded ellipses, and the Se atoms by the nonshaded ellipses.

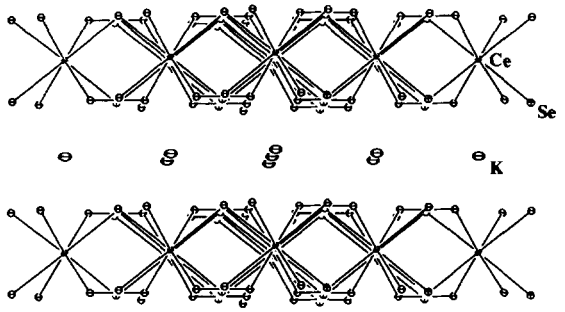

Fig. 3. View of $KCeSe_4$ showing intralayer channels parallel to the (110) planes. K^+ ions are included between the layers. The dimensions of the intralayer channels are 4.16 Å (Ce–Ce) by 3.61 Å (Se–Se).

The repeating unit shown in Figure 1 is the same unit which is found in two closely related three-dimensional structure types: $CuAl_2$ and $NbTe_4$. The former is found in several compounds of the formula TX_2 (T = transition metal, X = Sb, Ge, Sn, or Pb).[5] It is simply the result of fusing the anionic layers of $KCeSe_4$, through face-sharing at the square antiprisms, into a three-dimensional structure. Indeed, since K and Ce share coordination spheres, $KCeSe_4$ can be considered as a derivative of $CuAl_2$, in which the two cations alternate in the Cu positions along the c axis. The $NbTe_4$ structure[6] is also closely related to $CuAl_2$; the Nb cations reside in half of the Cu positions and are ordered such that every second plane of metal positions is vacant, forming a porous structure. $NbTe_4$ has Te_2^{2-} units, analogous to the Se_2^{2-} units in $KCeSe_4$.

Previously, only two structure types had been known for alkali metal(A) lanthanide(Ln) chalcogenide(Q) systems. Both have the stoichiometry $ALnQ_2$.[7] The first type is simply a NaCl structure with the A^+ and Ln^{3+} ions randomly distributed in the lattice. The second is the α-$NaFeO_2$ structure type, itself derived from the NaCl structure, in which the two cations are partitioned into alternating layers throughout the lattice. Thus, $KCeSe_4$ represents a new structural motif for a potential new family of alkali metal lanthanide polychalcogenides.[8]

A solid-state far-IR spectrum of $KCeSe_4$ shows only a broad absorption band beginning at 250 cm^{-1}. A conductivity measurement on a pressed pellet using four probes was performed at 300 K. A value of 5.1×10^{-6} $S cm^{-1}$ was found, indicating a semiconducting material. The diffuse reflectance spectrum of a microcrystalline sample of $KCeSe_4$ measured in the range of 2500 to 190 nm shows an abrupt absorption edge at approximately 780 nm, which suggests a band gap in the neighborhood of 1.59 eV.

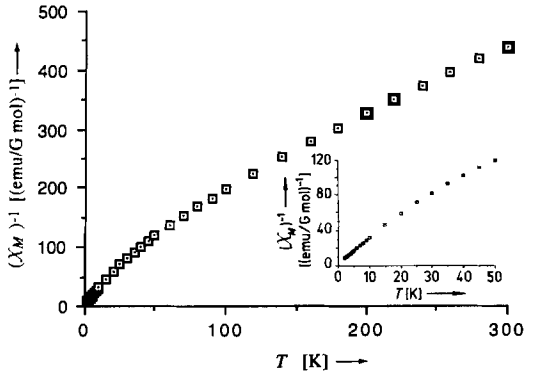

Fig. 4. Plot of $1/\chi_m$ vs. T; data taken at 500 G for $KCeSe_4$. The inset graph shows an expanded plot of the region between 2–50 K.

The magnetic susceptibility of $KCeSe_4$ was measured from 2 to 300 K at 500 G; a plot of $1/\chi$ vs. T is shown in Figure 4. $KCeSe_4$ appears to be paramagnetic, although several anomalies in the data are present. At temperatures below 100 K, the curve deviates negatively from a straight line extrapolated from the higher temperature data. Similar deviations have been reported for several Ce^{3+} compounds and have been attributed to crystal-field splitting of the cation's $^2F_{5/2}$ ground state.[9] At temperatures above 100 K, the Curie–Weiss law is not strictly adhered to, and a slight curvature remains in the data. In this temperature range an average μ_{eff} value of 2.29 μ_B has been calculated. This value is in accordance with the usual range for Ce^{III} compounds (2.3–2.5 μ_B) and is close to that of the free ion (2.54 μ_B) due to the shielding effect the outer electron cloud has on the embedded f orbitals.[10] We found that the measurements must be done on freshly prepared samples of $KCeSe_4$; older samples tend to give artificially high values for μ_{eff}, implying a phase change. This phase change probably occurs to a small extent on the sample surface because the bulk of the sample remains intact as shown by X-ray powder diffraction.

With the synthesis of $KCeSe_4$, we have demonstrated that alkali metal polychalcogenide fluxes can be employed to synthesize new lanthanide polychalcogenide materials. This, along with the recently discovered molecular complex $[U(Se_2)_4]^{4-}$,[11] also synthesized from a molten salt flux, opens the entire f block to further investigation. Given the potential these metals have for eightfold coordination and the known structural diversity of polychalcogenido ligands, the possibilities for synthesizing new and novel structure types become intriguingly vast.[8]

Experimental Procedure

$KCeSe_4$ was synthesized from a reaction of K_2Se (0.078 g, 0.5 mmol), Ce (0.035 g, 0.25 mmol), and Se (0.158 g, 2 mmol). These starting materials were thoroughly mixed in a glove box under a nitrogen atmosphere and loaded into pyrex tubes, which were subsequently evacuated to approximately 2×10^{-3} mbar and flame-sealed. The mixture was heated at 300 °C for 6 days and cooled at a rate of 2 °C h^{-1} to 100 °C then cooled to 50 °C in 1 h. The product was isolated by dissolving away the residual polyselenide flux with several portions of degassed dimethylformamide (DMF) under a nitrogen atmosphere until the solvent remained clear, indicating complete removal of the polyselenide. The remaining material consisted of deep blue to black chunks of $KCeSe_4$. The product was insoluble in DMF and was inert in both air and water for extended periods, although some surface degradation was evidence in the magnetic susceptibility studies. Homogeneity was confirmed by a comparison of the product's powder X-ray diffraction against one calculated with X-ray single-crystal data. A yield of 61%, based on Ce, was typical.

Received: June 9, 1992 [Z 5396 IE]
German version: *Angew. Chem.* **1992**, *104*, 1674

CAS Registry numbers:
$KCeSe_4$, 144586-78-7; K_2Se, 1312-74-9; Se, 7440-45-1; Ce, 7782-49-2.

[1] J. Flahaut in *Handbook on the Physics and Chemistry of Rare Earths: Vol. 4: Non-Metallic Compounds* (Eds.: K. A. Gschneidner, Jr., L Eyring), North-Holland, Amsterdam, **1979**, p. 1, and references therein.

[2] a) M. G. Kanatzidis, *Chem. Mater.* **1990**, *2*, 353–363; b) M. G. Kanatzidis, Y. Park, *J. Am. Chem. Soc.* **1989**, *111*, 3767–3769; c) M. G. Kanatzidis, Y. Park, *Chem. Mater.* **1990**, *2*, 99–101; d) Y. Park, M. G. Kanatzidis, *Angew. Chem.* **1990**, *102*, 945–947; *Angew. Chem. Int. Ed. Engl.* **1990**, *29*, 914–915.

[3] a) S. A. Sunshine, D. Kang, J. A. Ibers, *J. Am. Chem. Soc.* **1987**, *109*, 6202–6204; b) D. Kang, J. A. Ibers, *Inorg. Chem.* **1988**, *27*, 549–551.

[4] Crystals of $KCeSe_4$ are tetragonal, space group $P4/nbm$ (no. 125) with $a = 6.376(2)$, $c = 8.329(1)$ Å, $V = 338.6(2)$ Å^3, $Z = 2$, $\varrho_{calc} = 4.855$ g cm^{-3}; Measured reflections: 949; independent reflections: 916; reflections with $F_o^2 > 3\sigma(F_o^2)$: 302. Complete anisotropic refinement (11 variables), resulted in a final $R = 0.039$, $R_w = 0.049$. Measurement temperature 23 °C, Rigaku AFC6 diffractometer ($Mo_{K\alpha}$ radiation, $\mu = 572.140$ cm^{-1}, $2\theta_{max} = 60.00°$); structure was solved with TEXSAN, empirical absorbtion correction (DIFABS). Further details of the crystal structure investigation may be obtained from the Fachinformationszentrum Karlsruhe, Gesellschaft für wissenschaftlich-technische Information mbH, D-W-7514 Eggenstein-Leopoldshafen 2 (FRG), on quoting the depository number CSD-56489, the names of the authors, and the journal citation.

[5] F. Hulliger, *Struct. Bonding (Berlin)* **1968**, *4*, 83–229.

[6] K. Selte, A. Kjekshus, *Acta Chem. Scanda.* **1964**, *18*, 690–696.

[7] a) Compounds of the type $ALnQ_2$ (A = Na; Ln = La, Ce, Pr, Nd; Q = S) were first synthesized by Ballestracci and Bertaut (R. Ballestracci, E. F. Bertaut, *Bull. Soc. Fr. Mineral. Crystallogr.* **1964**, *87*, 512). They and others expanded the range of compounds to include A = Li, K, Rb, Cs; Q = Se; and several other lanthanides L_n [7b–h]. In general the compounds with large values for the radius ratio, r_{Ln3+}/r_{A+} favor the disordered NaCl structure, whereas smaller values (0.6–1.2) tend toward the α-$NaFeO_2$ structure type [7i,j]; b) R. Ballestracci, E. F. Bertaut, *ibid.* **1965**, *88*, 136; c) R. Ballestracci, *ibid.* **1965**, *88*, 207; d) M. Tromme, *C. R. Seances Acad.Sci. Ser. C.* **1971**, *273*, 849; e) W. Bronger, R. Elter, E. Mans, T. Schmidt, *Rev. Chim. Miner.* **1974**, *10*, 147; f) S. Kabre, M. Julien-Pouzol, M. Guittard, *Bull. Soc. Chim. Fr.* **1974**, *10*, 1881; g) C. M. Plug, G. C. Verschoor, *Acta Crystallogr. Sect. B* **1976**, *32*, 1856; h) T. Ohtani, H. Honjo, H. Wada, *Mater. Res. Bull.* **1987**, *22*, 829–840; i) W. Bronger, *Crystallography and Crystal Chemistry of Materials with Layered Structures* (Ed.: F. Levy), Reidel Dordrecht, **1976**, p. 93; j) M. Brunel, F. DeBergevin, M. Gondrand, *J. Phys. Chem. Solids* **1972**, *33*, 1927.

[8] Recently we have succeeded in synthesizing and structurally characterizing by X-ray diffraction a new phase isostructural to $KCeSe_4$: $RbCeTe_4$. The space group of $RbCeTe_4$ is $P4/nbm$ with $a = 6.952(3)$ and $c = 9.084(4)$ Å. The Ce–Te, Te–Te, and Rb–Te bonds are 3.285(1), 2.776(2) and 3.765(1) Å, respectively. $R = 0.031$, $R_w = 0.024$.

[9] a) H. Lueken, W. Bruggemann, W. Bronger, J. Fleischhauer, *J. Less-Common Met.* **1979**, *65*, 79–88; b) M. Duczmal, L. Pawlak, *J. Magn. Magn. Mater.* **1988**, *76–77*, 195–196.

[10] N. N. Greenwood, A. Earnshaw, *Chemistry of the Elements*, Pergamon Press, **1984**, p. 1443.

[11] A. C. Sutorik, M. G. Kanatzidis, *J. Am. Chem. Soc.* **1991**, *113*, 7754–7755.

Mutual Catalysis of Neutral and Anionic Cobalt Carbonyls in Their CO Scrambling Reactions**

By *Giuseppe Fachinetti** and *Tiziana Funaioli*

Carbonyl substitution is thought to be an important step in many syntheses and catalytic processes involving metal carbonyls, and there is a considerable interest in methods of assisting thermal substitution of CO ligands.[1] It was thought that $[Co(CO)_4]^-$, like a number of mononuclear 18-electron carbonylmetalates, for example $[V(CO)_6]^-$, $[Mn(CO)_5]^-$, $[Re(CO)_5]^-$, does not react with either labeled CO or phosphanes.[2] However, it was recently shown that alkali metal counterions accelerate the substitution reactions

[*] Prof. Dr. G. Fachinetti, Dr. T. Funaioli
Dipartimento di Chimica e Chimica Industriale Università di Pisa
Via Risorgimento, 35, I-56106 Pisa (Italy)

[**] This work was supported by Ministero dell' Università e della Ricerca Scientifica e Tecnologica (MURST). We thank Dr. G. Fochi for helpful discussions.

of CO groups in $[Co(CO)_4]^-$ in tetrahydrofuran (THF) solution:[3] the important role of ion-pairing phenomena was recognized, and the involvement of the 16-electron species $[Co(CO)_3]^-$ suggested.

Fig. 1. IR spectrum of a solution of $[NaCo(CO)_4]$ (0.02 M) in THF equilibrated under a ^{13}CO atmosphere (ratio $CO/^{13}CO = 1/1$).

Our own investigations of the factors affecting lability of CO ligands in $[Co(CO)_4]^-$, however, show that ion pairing with alkali metal counterions does not promote thermal CO dissociation from the carbonylmetalate at room temperature. Such a dissociation would require ^{13}CO exchange with $Na[Co(CO)_4]$ to occur in THF, in which ion pairs are evident.[4] However, this is not the case if the solution is pretreated with a reducing agent in order to destroy adventitious oxidants. The addition of the homogeneous reducing agent $[CoCp_2]$ (Cp = η^5-cyclopentadienyl) to a 0.02 M solution of $Na[Co(CO)_4]$ (1:10 molar ratio) completely inhibits the scrambling reaction between $[Co(CO)_4]^-$ and gaseous ^{13}CO. On the other hand, CO exchange is initiated by oxidizing the solution with sufficient oxygen to destroy the added $[CoCp_2]$: the IR spectrum shown in Figure 1 is obtained within 30 to 90 min at room temperature, when the CO ligands of $Na[Co(CO)_4]$ are equilibrated with an equimolar amount of ^{13}CO in THF. It seems possible, therefore, that the previously reported facile substitution reactions of $[Co(CO)_4]^-$ with acidic counterions in THF[3a] had arisen from a mechanism induced by traces of oxygen. Thus, the ion-pairing phenomena may merely increase the air sensitivity of $[Co(CO)_4]^-$ due to perturbation by the polarizing cation.[4b] Accordingly, the symmetrical $[Co(CO)_4]^-$ with a PPN^+ (PPN^+ = bis(triphenylphosphoranylidene)ammonium) counterion reacts only slowly with air, and was found to be inert towards substitution reactions.

These findings indicate that CO scrambling reactions of $[Co(CO)_4]^-$ follow a chemical oxidation and are therefore an example of electron-transfer catalysis (ETC).[5] A radical-chain mechanism would account for this ETC: trace amounts of oxygen react with $[Co(CO)_4]^-$, when the latter is activated by ion pairing; the intermediate $[Co(CO)_4]^\bullet$ could thus be generated. Like other 17-electron metal carbonyl radicals $[Co(CO)_4]^\bullet$ is expected to be prone to substitution:[6] electronic stabilization of the 19-electron hypervalent transition state, resulting from the association between the 17-electron radical and the incoming ligand, supplies the low-energy pathway for the substitution process.

An alternative mechanism for the CO scrambling of $[Co(CO)_4]^-$ catalyzed by electron transfer suggested itself when we found the anionic cluster $[Co_3(CO)_{10}]^-$ as a product of the reaction between the ion-pair activated $[Co(CO)_4]^-$ and traces of oxygen. After the short exposure of a 0.015 M diethyl ether solution of $Na[Co(CO)_4]$ to air, the formation of $[Co_3(CO)_{10}]^-$ was revealed by the appearance of an intense red color (λ_{max} = 530 nm); moreover analysis of the solution by IR spectroscopy revealed an absorption at 2006 cm^{-1}, characteristic for $[Co_3(CO)_{10}]^-$.[7] On the other hand, it has been stated that $[Co_3(CO)_{10}]^-$ participates in the fast equilibrium reaction (a),[7, 8] and it has also been observed that CO groups of this anionic cluster interchange rapidly with each other through a fast equilibrium between terminal and edge-bridging CO groups [see Eq. (a)].[9]

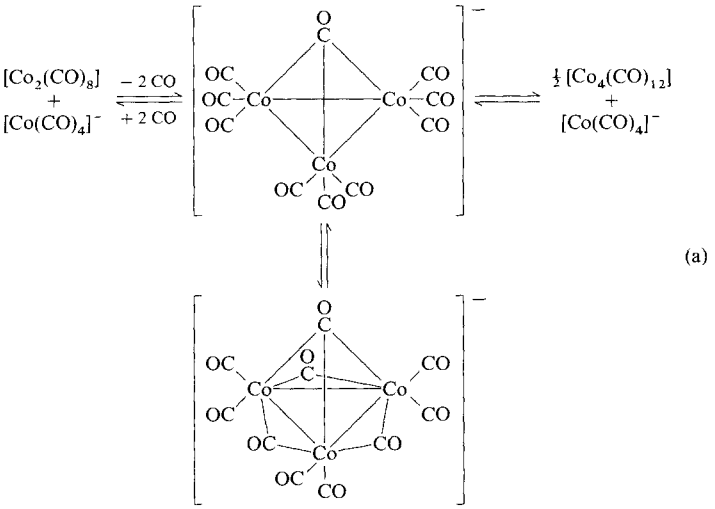

(a)

Therefore, we propose that $[Co_3(Co)_{10}]^-$ is the intermediate which causes the observed lability of the CO ligands of both neutral and anionic cobalt carbonyls in a solution where $[Co(CO)_4]^-$ and $[Co_2(CO)_8]$ or $[Co_4(CO)_{12}]$ exist simultaneously. This hypothesis requires that even the CO ligands of the reportedly inert $PPN[Co(CO)_4]$[3a] are activated by catalytic amounts of either $[Co_2(CO)_8]$ or $[Co_4(CO)_{12}]$ and that, reciprocally, catalytic amounts of $[Co(CO)_4]^-$ salts make the CO ligands of neutral cobalt carbonyls labile. We found that under a CO atmosphere, catalytic amounts of $[Co_2(CO)_8]$ promote CO scrambling in $PPN[Co(CO)_4]$ (case a), under an inert atmosphere, catalytic amounts of $[Co_4(CO)_{12}]$ promote the CO scrambling between $PPN[Co(CO)_4]$ and $PPN[Co(^{13}CO)_4]$ (case b), and that reciprocally, catalytic amounts of $Na[Co(CO)_4]$ accelerate the CO scrambling between $[Co_2(CO)_8]$ and gaseous ^{13}CO (case c) and promote the scrambling between $[Co_4(CO)_{12}]$ and $[Co_4(^{13}CO)_{12}]$ under an inert atmosphere (case d).

Case a: While $PPN[Co(CO)_4]$ is known not to incorporate ^{13}CO at room temperature,[3a] upon addition of $[Co_2(CO)_8]$ to a 0.016 M THF solution of the PPN^+ salt ($[Co_2(CO)_8]/PPN[Co(CO)_4]$, 0.05 molar ratio), a fast CO scrambling occurs. The IR spectrum shown in Figure 2 is obtained within 15 min when CO ligands bonded to cobalt are allowed to equilibrate with equimolar amounts of gaseous ^{13}CO.

Case b: Under an argon atmosphere, no CO scrambling is observed in a solution of $PPN[Co(CO)_4]$ and $PPN[Co(^{13}CO)_4]$ (each 0.08 M) in THF: the CO stretching region of the IR spectrum (Fig. 2 dashed line) remains unchanged for hours and shows two strong bands at 1887 and 1842 cm^{-1} due to unperturbed $[Co(CO)_4]^-$ and $[Co(^{13}CO)_4]^-$, respectively. A weak absorption at 1808 cm^{-1} accompanies the

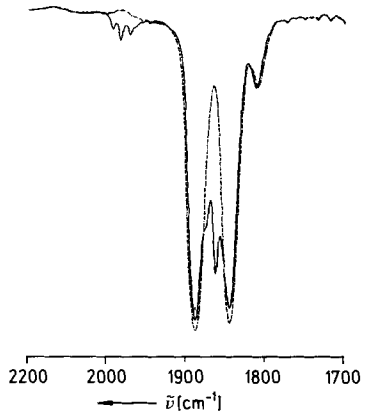

Fig. 2. IR spectrum of a solution of PPN[Co(CO)$_4$] and PPN[Co(^{13}CO)$_4$] in THF (both 0.08 M) (dashed line) and after the addition of a catalytic amount of [Co$_4$(CO)$_{12}$] (solid line).

band at 1842 cm^{-1} and is probably due to traces of ^{13}C^{18}O. However, if [Co$_4$(CO)$_{12}$] is added to the solution of PPN[Co(CO)$_4$] and PPN[Co(^{13}CO)$_4$] ([Co$_4$(CO)$_{12}$]/tetracarbonylcobaltates, 0-01 molar ratio), the IR spectrum in Figure 2 (solid line) shows that complete CO scrambling occurs immediately after mixing.

Case c: In agreement with Brown et al.,[10] we found that the [Co$_2$(CO)$_8$]/^{13}CO scrambling reaction proceeds even in the absence of [Co(CO)$_4$]$^-$; however, the addition of Na[Co(CO)$_4$] accelerates this reaction in Et$_2$O at 0 °C. As monitored by IR spectroscopy (Fig. 3), equilibration of a 0.013 M solution of [Co$_2$(CO)$_8$] in Et$_2$O with ^{13}CO at atmospheric pressure requires 50 min, whereas following the addition of Na[Co(CO)$_4$] to this solution (0.1 molar ratio) complete scrambling is attained within 10 min.

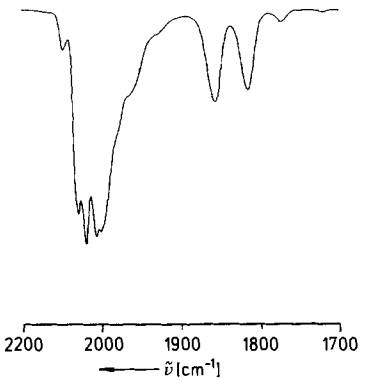

Fig. 3. IR spectrum of solution of [Co$_2$(CO)$_8$] (0.013 M) in Et$_2$O equilibrated under a ^{13}CO atmosphere (ratio CO/^{13}CO = 1/1).

Case d: Under an argon atmosphere, no CO scrambling is observed in a solution of [Co$_4$(CO)$_{12}$] and [Co$_4$(^{13}CO)$_{12}$] (each 0.008 M) in Et$_2$O on the timescale of the subsequent experiment for the catalysis with Na[Co(CO)$_4$]. After one hour at room temperature, the CO stretching region of the IR spectrum of this solution is still the sum of the spectra of isotopically pure [Co$_4$(CO)$_{12}$] and [Co$_4$(^{13}CO)$_{12}$] (Fig. 4a). However, the IR spectrum recorded immediately after the addition of Na[Co(CO)$_4$] (molar ratio 1:20) (Fig. 4b) shows that the [Co(CO)$_4$]$^-$ catalyzed CO scrambling occurs extremely rapidly.

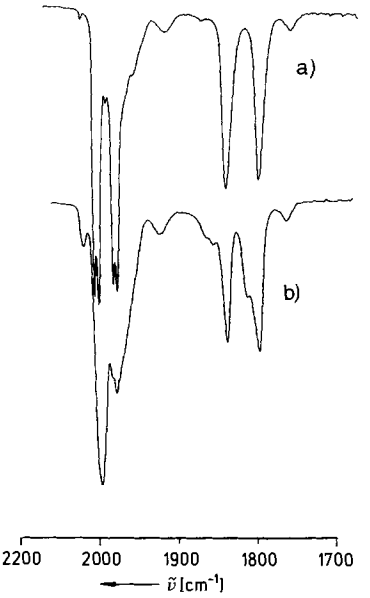

Fig. 4. IR spectra of a solution of [Co$_4$(CO)$_{12}$] and [Co$_4$(^{13}CO)$_{12}$] in Et$_2$O (both 0.008 M) a) before, and b) after the addition of a catalytic amount of Na[Co(CO)$_4$].

Our findings indicate that CO scrambling reactions of [Co(CO)$_4$]$^-$ are electron transfer catalyzed processes that can be initiated by traces of oxygen. While a radical-chain mechanism was documented for other oxidatively induced CO substitutions in metal carbonyls,[5] in the present case a redox condensation mechanism is proposed. In fact a redox condensation between [Co(CO)$_4$]$^-$ and the neutral cobalt carbonyls formed by the oxidation of [Co(CO)$_4$]$^-$ has been observed[7] [Eq. (a)]; this accounts for the mutual catalysis of their respective CO scrambling. Furthermore, a radical-chain mechanism based on [Co(CO)$_4$]$^\bullet$ cannot justify the extremely rapid CO scrambling observed under an inert atmosphere (cases b and d), when compared to the relatively moderate catalytic effect under a CO atmosphere (cases a and c). On the contrary, the fact that the free, incoming CO ligand slows the mutually catalyzed CO scrambling of both neutral and anionic cobalt carbonyls can be rationalized by assuming [Co$_3$(CO)$_{10}$]$^-$ as an intermediate. Its steady-state concentration in a [Co$_2$(CO)$_8$]/[Co(CO)$_4$]$^-$ solution is indeed controlled by CO partial pressure.[7] Apart from the mechanism which needs further support, this work demonstrates that the fundamental property of both neutral and anionic cobalt carbonyls, that is, CO ligand lability, is influenced dramatically by the presence of complexes belonging to the other class.

These observations are of general interest, first because the [Co(CO)$_4$]$^-$ ions formed in disproportionation reactions always accompany neutral cobalt carbonyls, unless in hydrocarbon solvents and under strictly controlled conditions, and second neutral cobalt carbonyls can be formed by oxidation of [Co(CO)$_4$]$^-$.

Experimental Procedure

Solid Na[Co(CO)$_4$] (78 mg, 0.40 mmol) was added under argon to a pale red solution of [CoCp$_2$] (0.002 M) in THF (20 mL) in a 150 mL closed vessel. Through a rubber septum, ^{13}CO (99% isotopical purity, MSD Isotopes) (38 mL, 1.6 mmol) was added to the atmosphere above the solution with a syringe. After the solution had been stirred for 24 h, a sample was withdrawn for IR analysis. 3 mL of air were then added, and additional samples were withdrawn after 15, 30, 60, and 90 min. The CO scrambling in PPN[Co(CO)$_4$],

$[Co_2(CO)_8]$, and $[Co_4(CO)_{12}]$ was studied by similar techniques. $Na[Co(^{13}CO)_4]$ was synthesized by Hieber's cyanide method [11]. The product was isolated as an analytically pure solid on saturation of the water solution with NaCl followed by continuous extraction with Et_2O. The extract was dried with Na_2SO_4 and finally evaporated to dryness. Typical yields were 60% based on the ^{13}CO introduced. $PPN[Co(^{13}CO)_4]$ was prepared by a metathesis reaction between PPNCl and $Na[Co(^{13}CO)_4]$ in CH_3OH/H_2O.

$[Co_4(^{13}CO)_{12}]$: To a suspension of $Na[Co(^{13}CO)_4]$ (480 mg, 2.42 mmol) in *n*-hexane (100 mL) was added HCl (60 mL, 2.50 mmol) through a rubber septum. The suspension was stirred for 24 h at 50 °C and then refluxed for 3 h. Solid impurities were removed by filtration, and black crystals of $[Co_4(^{13}CO)_{12}]$ were obtained (210 mg; 60% yield) by cooling the mother liquor to −20 °C.

Received: June 19, 1992 [Z 5419 IE]
German version: *Angew. Chem.* **1992**, *104*, 1692

CAS Registry numbers:
$[Co(CO)_4]^-$, 14971-27-8; $[Co_2(CO)_8]$, 10210-68-1.

[1] J. P. Collmann, L. S. Hegedus, J. R. Norton, R. G. Finke, *Principles and Applications of Organotransition Metal Chemistry*, University Science Book, Mill Valley, CA, USA, **1987**, Chapter 4, and references therein.
[2] a) R. D. W. Kemmitt, D. R. Russel in *Comprehensive Organometallic Chemistry, Vol. 5* (Eds.: G. Wilkinson, F. G. A. Stone, E. W. Abels), Pergamon Press, Oxford, **1982**; b) A. Davison, J. R. Ellis, *J. Organomet. Chem.* **1971**, *31*, 239; c) W. Hieber, K. Wollmann, *Chem. Ber.* **1962**, *95*, 1552; d) P. A. Bellus, T. L. Brown, *J. Am. Chem. Soc.* **1980**, *102*, 6020.
[3] a) F. Ungvary, A. Wojcicki, *J. Am. Chem. Soc.* **1987**, *109*, 6848; b) F. Ungvary, J. Gallucci, A. Wojcicki, *Organometallics* **1991**, *10*, 3053.
[4] a) D. P. Schussler, W. R. Robinson, W. F. Edgell, *Inorg. Chem.* **1974**, *13*, 153; b) M. Y. Darensbourg, *Prog. Inorg. Chem.* **1985**, *33*, 221.
[5] T. Graaf, R. M. J. Hofstra, P. G. M. Schilder, M. Rijkhoff, D. J. Stufkens, J. G. M. Linden, *Organometallics* **1991**, *10*, 3668, and references therein.
[6] M. J. Therien, W. C. Trogler, *J. Am. Chem. Soc.* **1988**, *110*, 4942.
[7] G. Fachinetti, *J. Chem. Soc. Chem. Commun.* **1979**, 396.
[8] G. Fachinetti, T. Funaioli, M. Marcucci, *J. Organomet. Chem.* **1988**, *353*, 393.
[9] H.-N. Adams, G. Fachinetti, J. Strähle, *Angew. Chem.* **1980**, *92*, 411; *Angew. Chem. Int. Ed. Engl.* **1980**, *19*, 404.
[10] M. Absi-Halabi, J. D. Atwood, N. P. Forbus, T. L. Brown, *J. Am. Chem. Soc.* **1980**, *102*, 6248.
[11] W. Hieber, C. Bartenstein, *Z. Anorg. Allg. Chem.* **1954**, *276*, 1.

C_{60} and C_{70} in a Basket? – Investigations of Mono- and Multilayers from Azacrown Compounds and Fullerenes

By *Francois Diederich, Jochem Effing, Ulrich Jonas, Ludovic Jullien, Thomas Plesnivy, Helmut Ringsdorf,* Carlo Thilgen,* and *David Weinstein*

The spreading behavior of fullerenes at the air–water interface and the formation of Langmuir–Blodgett (LB) films on solid substrates has already been described in several publications. [1–4] The results are in part contradictory. The behavior of pure fullerenes C_{60} and C_{70} at the air–water interface indicates a collapsed film rather than a homogeneous monolayer. Even mixed films of C_{60} and fatty acids or long-chain alcohols in a 1:1 ratio[2–4] do not give the expected areas, but also point to C_{60}-aggregates; we have confirmed these results.[5] We report here on mono- and multilayers of 1:1 mixtures of the C_{60} and C_{70} fullerenes (represented by **1**) and amphiphilic molecules **2** containing a lipophilic cavity (the "basket") (Scheme 1).

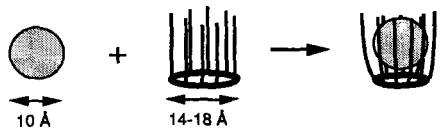

1 **2**

Scheme 1.

Although hydrophobic cyclodextrins,[6, 7] calixarenes,[7] and alkylated and acylated azacrown derivatives of different ring sizes were used as component **2** of Scheme 1, only the results with the alkylated hexaazacrown compound **3** and the acylated octaazacrown compound **4** will be reported here.

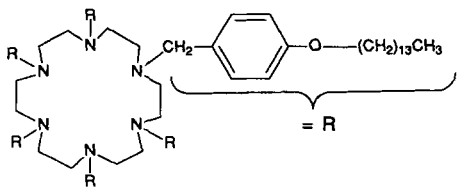

3

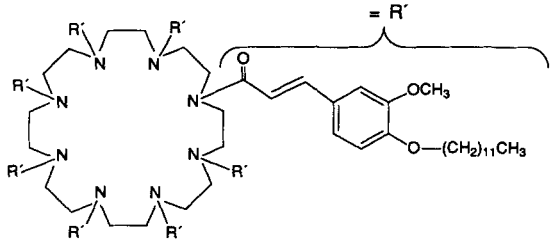

Figure 1 shows the surface pressure–area behavior of pure hexaazacrown **3** and that of 1:1 mixtures of **3** with C_{60} or C_{70}. The surface density, that is, the number of spread molecules **3** per air–water surface area, was the same in all experiments.[8] All curves are reproducible, and repeated compression–expansion experiments (hysteresis curves) give identical plots.

The fact that for all three systems similar collapse areas were found is a first indication that the fullerenes may at least partially be situated inside the cavities of the crown molecules. This is supported by the comparison of the width of the "transition regions" of the different mixing ratios (C_{60}/**3**). The less C_{60} is incorporated into the crowns, the narrower is the width of the plateau. Further indications pointing to such a complexation are the slight shifts in the UV/VIS spectra of the multilayers (see below).

The incorporation of the fullerenes into the monolayers of the azacrown compounds has a stabilizing effect on the film as clearly shown in Figure 2 for the octaazacrown **4** with C_{60} and C_{70}.

Although **4** has a larger diameter than **3**, the collapse area of **4** increases slightly in the presence of the fullerenes (average of three experiments); this is not the case for **3**. The

[*] Prof. Dr. H. Ringsdorf, Dipl.-Chem. J. Effing, U. Jonas, Dr. L. Jullien, Dipl.-Chem. T. Plesnivy
Institut für Organische Chemie der Universität
J. J. Becher-Weg 18–20, D-W-6500 Mainz (FRG)
Prof. Dr. F. Diederich, Dr. C. Thilgen
Laboratorium für Organische Chemie, ETH-Zentrum
CH-8092 Zürich (Switzerland)
D. Weinstein
Department of Chemistry and Biochemistry
University of California
Los Angeles, CA 90024-1596 (USA)

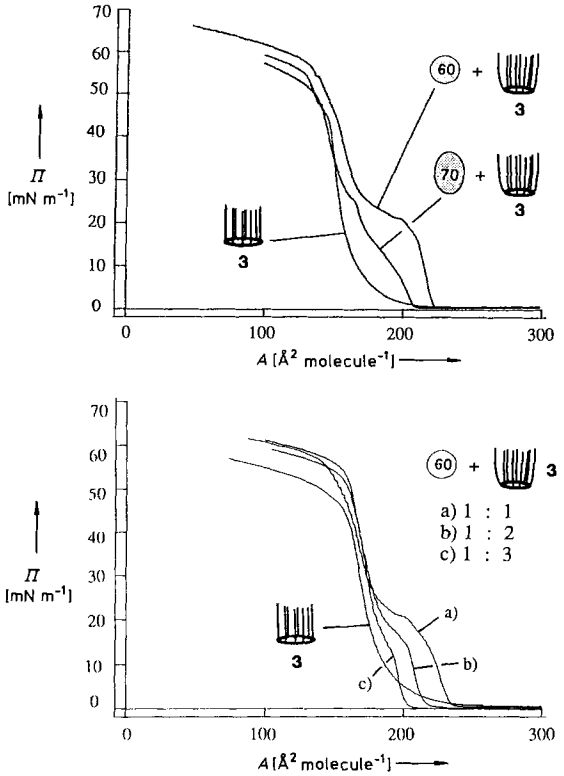

Fig. 1. Top: Surface pressure–area diagram (Π/A isotherms) of pure hexaazacrown **3** and the 1:1 mixtures of **3** with C_{60} and C_{70} [8]. Bottom: Π/A isotherms of pure hexaazacrown **3** and the 1:1, 2:1, and 3:1 mixtures of **3** with C_{60}.

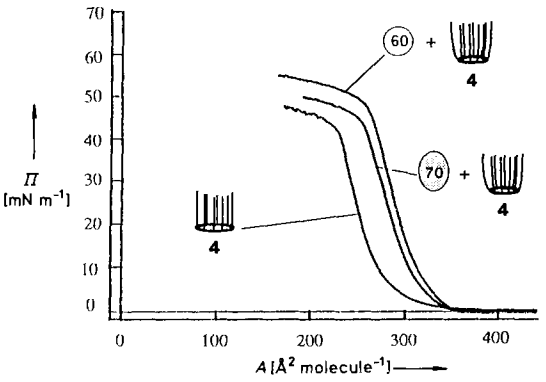

Fig. 2. Π/A isotherm of pure oxtaazacrown **4** and the 1:1 mixtures of **4** with C_{60} and C_{70} [8].

collapse area, the collapse pressure, and the area at pressure 0 mN m^{-1} of the azacrown/fullerene monolayers are given in Table 1.

Table 1. Data for monolayers of the hexa- and octaazacrown compounds **3** and **4**, respectively, with and without C_{60} or C_{70} [a].

Film	A_c [Å^2 mol^{-1}]	p_c [mN m^{-1}]	A_0 [Å^2 mol^{-1}]
3	148 ± 3	47 ± 3	170 ± 6
3/C_{60}	141 ± 6	52 ± 3	225 ± 5
3/C_{70}	137 ± 6	54 ± 3	205 ± 15
4	229 ± 3	40 ± 1	275 ± 2
4/C_{60}	263 ± 12	48 ± 1	325 ± 15
4/C_{70}	269 ± 8	46 ± 3	325 ± 9

[a] A_c: collapse area, p: collapse pressure, A_0: area at 0 mN m^{-1} pressure. A [Å^2 mol^{-1}] = area per crown molecule or fullerene/crown molecule pair. The numbers are average values of three or four experiments.

In addition, apparently well-defined multilayers can be built from all monolayers of azacrown/fullerene mixtures by the LB technique. However, all attempts to transfer pure hexaazacrown **3** to a hydrophilic substrate (quartz, glass, mica) or to hydrophobic supports (teflon, hydrophobized quartz) were unsuccessful. Likewise, it was not possible to transfer a defined monolayer of pure C_{60}, as already shown by other researchers.[2–4] Multilayers from mixtures of C_{60} with classical amphiphiles like icosanoic acid[3] or octadecanol,[4] which themselves can form stable multilayers, were described. Both **3** and the fullerene are unable to form LB films alone. In contrast, the 1:1 mixtures of **3** with C_{60} and C_{70} form homogeneous LB multilayers (Y-type, both on hydrophilic and on hydrophobic substrate) with an average bilayer thickness of approximately 47 Å (SAXS[9]). The incorporation of **3** and of the fullerenes into the multilayers was confirmed by UV/VIS spectroscopy. Figure 3 shows the absorption spectrum of the C_{60}/**3** LB film and a calculated spectrum (addition of the spectra of the components). Similar results were obtained for the multilayers of C_{70}/**3**. The microscopic environment of the fullerene molecules in the azacrown films (layer composition) seems to remain unchanged if more layers are added, as shown by the linear relationship between the number of layers and the absorption maxima of the peaks in the UV/VIS spectra.

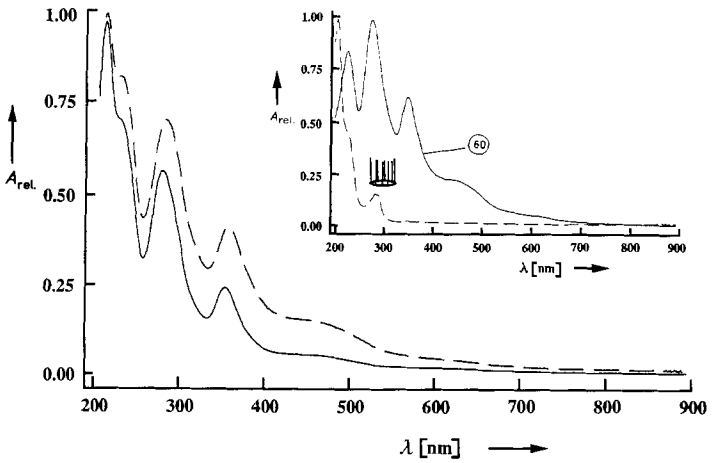

Fig. 3. Experimental and theoretical UV/VIS spectra of an LB multilayer consisting of LB films of a 1:1 mixture of C_{60} and **3** (2 × 17.5 bilayers). Solid line: recorded spectrum. Broken line: the spectrum obtained by addition of the spectra of films of pure **3** and C_{60}. The absorption values are relative ($A_{rel.}$); the highest peak is arbitrarily set to 1. The inset shows the UV/VIS spectra of the films of pure **3** and C_{60}.

The UV/VIS spectrum of the C_{60}/**4** film (Fig. 4) shows, in addition to the typical absorptions of the two pure compounds, a new peak at 256 nm, possibly arising from interactions between the C_{60} π-electron system and the cinnamic amide π electrons. Another interesting feature of the multilayer spectra is the fact that the broad band of the absorption of pure C_{60} (at 400–480 nm), arising from the interaction between different fullerene molecules (microcrystallites),[10] is diminished. This could indicate that the C_{60}-aggregation existing in the solid is in this case somewhat reduced.

As observed with the films of **3**, the regularity of the formation of the multilayers of **4** with and without the fullerenes was also confirmed by SAXS measurements (see Fig. 5). For all three multilayers Kiesig fringes were found. The bilayer thickness of the pure azacrown derivative **4** is about 40 Å, and thus only slightly greater than that for the 1:1 mixtures:

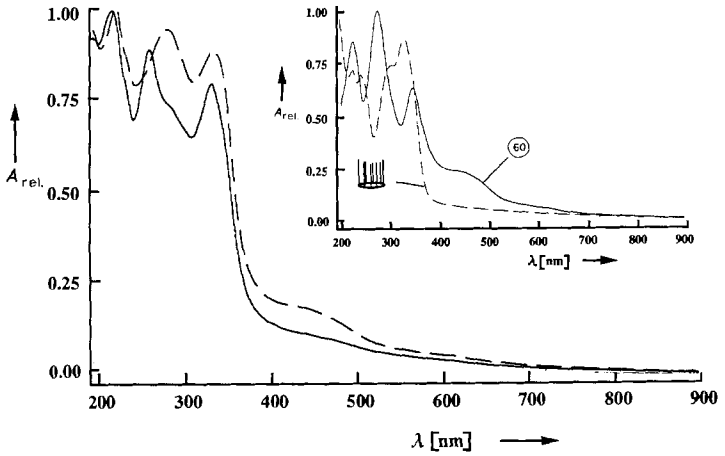

Fig. 4. Experimental and theoretical UV/VIS spectra of a LB multilayer consisting of LB films of a 1:1 mixture of C_{60} and **4** (2 × 12.5 bilayers). Solid line: recorded spectrum. Broken line: the spectrum obtained by addition of the spectra of films of pure **4** and C_{60}. The absorption values are relative ($A_{rel.}$), the highest peak is arbitrarily set to 1. The absorption at 256 nm is not present in the spectra of the pure compounds shown in the inset.

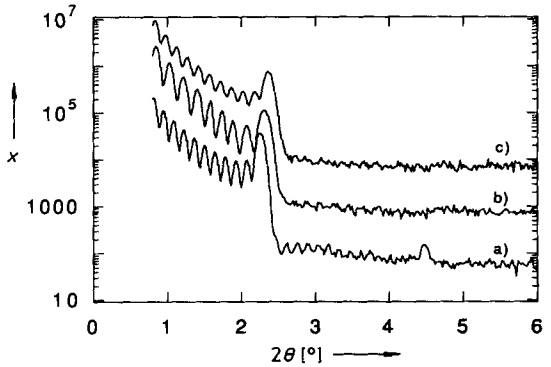

Fig. 5. Small-angle X-ray scattering plots of a) the LB film of pure **4** (15.5 bilayers), b) the C_{60}/**4** film (12.5 bilayers), and c) the C_{70}/**4** film (15.5 bilayers), all on quartz. The upper two curves are shifted in intensity by a factor of 12 for b) and by a factor of 120 for c). x = counts per 5s.

approximately 37 Å for the C_{60}/**4** LB film and approximately 38 Å for the C_{70}/**4** film.

On the basis of the present data one can only speculate on the real packing of the multilayers. Since the measured bilayer thicknesses of the pure **4** film and the 1:1 mixture films differ by just 2–3 Å, the possibility of finding the fullerenes in ordered layers on top of the films of **4** (**C** in Scheme 2) seems unlikely. Two hypothetical structures for regular films are depicted in Scheme 2 as **A** and **B**. In **B** the fullerenes would sit between the deformed crown compounds. However, this structure cannot explain the slight increase in area of the fullerene/crown complexes at the air–water interface (see Table 1). We prefer the hypothetical structure **A**, in which each fullerene molecule is located inside a crown molecule: C_{60} in the basket.

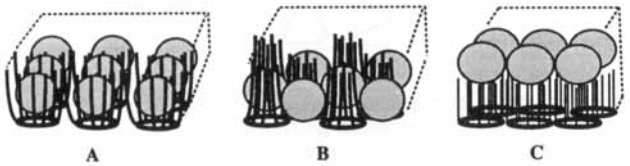

Scheme 2.

We obtained some support for the structure **A** from atomic force microscopy (AFM) measurements. Monolayers of pure **4** have homogeneous, flat surfaces. However, when the **4**/C_{60} mixture is transferred at 25 mN m^{-1}, irregular aggregates (ca. 1000 × 200 Å) appear, indicating C_{60} microcrystallites. These aggregates are also observed in the system **3**/C_{60} (Fig. 6b); here they are transferred at the same pressure (above the "transition region" in Fig. 1). If the mixed monolayer is transferred below the "transition region" at 5 mN m^{-1}, the surface is flat, and no aggregates are visible in the AFM image (Fig. 6a). This can indicate a well-mixed monolayer at low pressure in which C_{60} molecules are possibly situated inside the crown molecules. At pressures of 15–20 mN m^{-1} a demixing might occur, resulting in crystallization of the fullerenes.[11, 12]

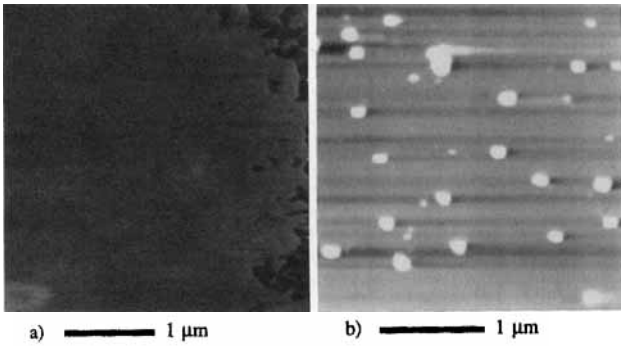

Fig. 6. Atomic force micrographs of monolayers of C_{60}/**3** (1:1 mixture) a) transferred at 5 mN m^{-1} and showing a flat film on mica (film edge visible on the right); b) transferred at 25 mN m^{-1} and revealing crystallites on the film.

In addition, AFM measurements on monolayers of calixarenes and hydrophobized cyclodextrins acting as "baskets" are under way [7]. Their mono- and multilayer behavior agree very well with the results described here for the aza-crown/fullerene mixtures.

Received: June 5, 1992
Revised: September 5, 1992 [Z 5391IE]
German version: *Angew. Chem.* **1992**, *104*, 1683

[1] Fullerene fever (T. Braun, *Angew. Chem.* **1992**, *104*, 602–603 (see also p. 1697); *Angew. Chem. Int. Ed. Engl.* **1992**, *31*, 588–589 (see also p. 1350)) could not be cooled by water—as shown by this and other publications [2–4] about C_{60} at the air–water interface!
[2] Y. S. Obeng, A. J. Bard, *J. Am. Chem. Soc.* **1991**, *113*, 6279–6280.
[3] T. Nakamura, H. Tachibana, M. Yumura, M. Matsumoto, R. Azumi, M. Tanaka, Y. Kawabata, *Langmuir* **1992**, *8*, 4–6.
[4] J. Milliken, D. D. Dominguez, H. H. Nelson, W. R. Barger, *Chem. Mater.* **1992**, *4*, 252–254.
[5] Area–pressure measurements were performed on a self-built, computer-controlled teflon trough with a surface of approximately 180 cm^2 and a Langmuir pressure pickup system. The measured area for the fullerenes is dependent on the spreaded amount and varied from ca. 70 Å^2 molecule^{-1} (spreading volume: 0.14 μL cm^{-2} of a 0.1 mM concentrated solution) to ca. 25 Å^2 molecule^{-1} (1.7 μL cm^{-2}; 0.1 mM) in the case of C_{60}. Areas from ca. 50 Å^2 molecule^{-1} (0.14 μL cm^{-2}; 0.1 mM) to ca. 25 Å^2 molecule^{-1} (1.7 μL cm^{-2}; 0.1 mM) were obtained for C_{70}. This behavior varies with the trough dimensions, and is most probably due to crystallization and collapse of the film at the water–teflon rim.
[6] A γ-cyclodextrin/C_{60} complex was previously described by T. Anderson, K. Nilsson, M. Sundahl, G. Westman, O. Wennerström (*J. Chem. Soc. Chem. Commun.* **1992**, 604–606).
[7] V. Böhmer, F. Diederich, J. Effing, U. Jonas, L. Jullien, T. Plesnivy, H. Ringsdorf, W. Vogt, unpublished.

[8] The alkylated hexaazacrown **3** and the acylated octaazacrown **4** were spread from a 0.1 mM solution of the pure crown compound in benzene at 20 °C on a water subphase (distilled, millipore filtered, 18 MΩcm). The same trough as in [5] was used, on which 50 or 100 μL were spread in different runs. The 1:1 mixtures were prepared by combining equal volumes of the fullerene and the crown solution (both 0.1 mM in benzene). To obtain the same surface density of the crown compounds, 100 and 200 μL of these 1:1 mixtures were spread. As a result of the hypothesis that fullerenes are accommodated inside the crown molecule, all area calculations are based on the concentration of the crown molecules.

[9] Small-angle X-ray scattering (SAXS) measurements were performed on LB films consisting of about 17 bilayers on quartz slices with a θ-2θ goniometer from Siemens.

[10] The long wavelength absorption between 400 and 480 nm due to C_{60} aggregation is relatively intense and must not be mistaken for the very weak bands between 500 and 650 nm for homogeneous solutions of C_{60} (violet!). Arguments that this relatively strong absorption at 400–480 nm is caused by C_{60} aggregation result from the comparison of the spectrum of a hexane solution (H. Ajie, M. M. Alvarez, S. J. Anz, R. D. Beck, F. Diederich, K. Fostiropoulos, D. R. Huffman, W. Krätschmer, Y. Rubin, K. E. Schriver, D. Sensharma, R. L. Whetten, *J. Phys. Chem.* **1990**, *94*, 8630) with a solid C_{60} film (W. Krätschmer, L. D. Lamb, K. Fostiropoulos, D. R. Huffman, *Nature* **1990**, *347*, 354–358). Furthermore, the spectrum of a $C_{60}/CHCl_3$ solution with C_{60} precipitate, which shows the normal absorptions of the dissolved fullerene, changes upon sonication to the spectrum of solid C_{60} (suspension of C_{60} aggregates, brown color).

[11] In cooperation with Dr. Lifeng Chi and Dr. Harald Fuchs (BASF Aktiengesellschaft); measured in air with commercially available force microscope (Park Scientific Instruments).

[12] In cooperation with Dr. Christoph Gerber and Dr. Bruno Michel (IBM Research Laboratories Rüschlikon, Switzerland), measured in air with a commercially available force microscope (Nanoscope III, Scientific Instruments).

The Isomers of the Acetylene Derivatives C_2Li_4: Transferable Structural Units in Hyperlithiated Compounds**

By *Andrea E. Dorigo, Nicolaas J. R. van Eikema Hommes, Karsten Krogh-Jespersen*, and *Paul von Ragué Schleyer**

Hyperlithiated molecules[1a] such as CLi_6,[1,2] OLi_4,[3] PLi_5,[4] and OLi_6,[1a,4] which formally violate the octet rule, cannot be defined in terms of classical Lewis structures. Instead they involve bonding between the metal ligands[5] and between the metal ligands and the central atom. We now describe C_2Li_4 isomers which are not ethylene-like but which also exhibit hypermetallic bonding. Several stable Li_n structural units common to hyperlithiated molecules are discernable in the optimized structures.

The experimental evidence for C_2Li_4 is modest: Lagow et al. observed C_2D_4 among the deuterolysis products of lithiated substrates.[6] Although we have computed various structures of C_2Li_4 for over more than a decade, no thorough comprehensive study has been undertaken before. Only a few calculations of several possible C_2Li_4 structural candidates, performed at the SINDO1, HF/STO-3G, and HF/3-21G levels, have been mentioned in the literature.[7,8] However, the highly symmetrical structures **1**–**5** (Scheme 1)

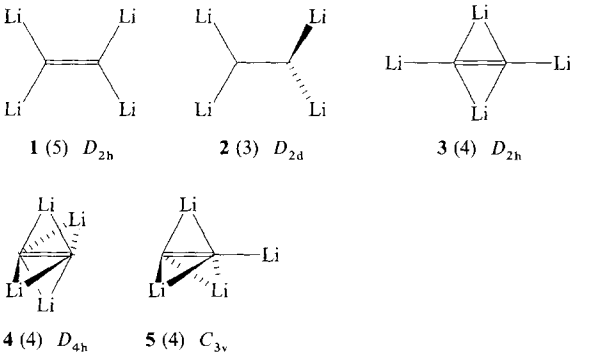

Scheme 1. Schematic structures of isomers **1**–**5**. The numbers in parentheses indicate the number of imaginary frequencies at the HF/3-21G level. None of these isomers corresponds to a minimum on the potential energy surface and all are much higher in energy than **6**–**13**.

have now proven to be high in energy and to have several imaginary frequencies; we will not refine them further at higher levels here. Note in particular that at the HF/3-21G level the ethylene-like D_{2h} structure **1** has five imaginary frequencies and is 41.0 kcal mol^{-1} higher in energy than structure **6**. Structures **6**–**13** (Scheme 2) are energetically much more favorable. All geometries were optimized[9] at the electron-correlated MP2/6-31G* level, and single-point calculations were carried out at the MP4(SDTQ)(FC)/6-31+G* level [MP4(SDTQ)(FC)/6-31+G*//MP2(FU)/6-31G*].[10] Structures **6**–**13** all have short carbon–carbon bonds (1.265–1.281 Å), and while the average length ex-

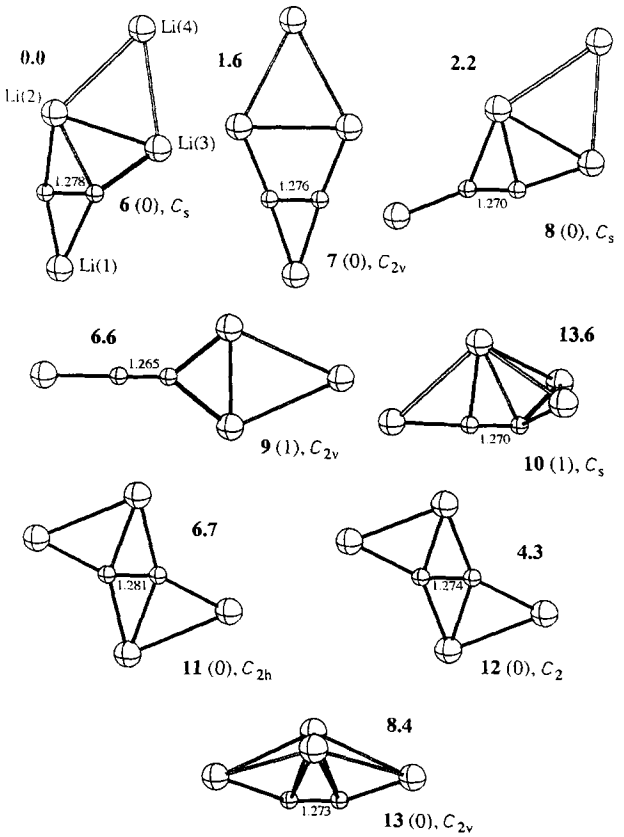

Scheme 2. MP2/6-31G* optimized structures and relative energies of the C_2Li_4 isomers **6**–**13**. The number of imaginary frequencies (0 = minimum, 1 = transition state) at the MP2/6-31G* level is given in parenthesis after the compound number. Relative energies (bold, in kcal mol^{-1}) were calculated at the MP4(SDTQ)/6-31+G*//MP2/6-31G* level.

[*] Prof. Dr. P. von R. Schleyer, Dr. A. E. Dorigo,
Dr. N. J. R. van Eikema Hommes
Institut für Organische Chemie der Universität Erlangen-Nürnberg
D-W-8520 Erlangen (FRG)
Prof. Dr. K. Krogh-Jespersen
Department of Chemistry, Rutgers
The State University of New Jersey
New Brunswick, NJ 08903 (USA)

[**] This work was supported in Erlangen by the Fonds der Chemischen Industrie, the Deutsche Forschungsgemeinschaft, and the Convex Computer Corporation. A. E. D. was supported through a postdoctoral fellowship from the Alexander von Humboldt Stiftung. We thank J. A. Pople, E. D. Jemmis, and A. J. Kos for early computations on this project.

ceeds that in acetylene (1.21 Å), both linear and doubly bridged C_2Li_2 forms have similar C–C bond lengths.[11] Hence, all C_2Li_4 isomers we have studied are acetylene rather than ethylene derivatives! The C_2^{2-} ion is bound to different Li_n structural units in **6**–**13**. Thus, the global minimum at the MP4(SDTQ)/6-31+G* level (**6**) can be characterized as $Li^+C_2^{2-}Li_3^+$: an acetylide triple ion "salt" with Li^+ and Li_3^+ counterions. In the cyclic Li_3^+ moiety,[12] the two lithium atoms closest to the C_2^{2-} unit (Li(2) and Li(3) in Scheme 2) have large fractional positive charges, while the third, more remote Li(4) is calculated to have a negative charge.[13, 14] The $Li^+C_2^{2-}Li_3^+$ description is also valid for **7** (C_{2v}) and **8** (C_s), which also are energy minima, as well as for **9** (C_{2v}), which is a transition structure for the interconversion of two equivalent forms of **8**. Since no interaction between the lithium atoms and the π_{C-C} bond takes place, the energy of **9** is 6.6 kcal mol^{-1} higher than that of **6**.

Lithium atoms in bridging positions are known to be favorable, for example in LiCN.[15] In C_2Li_2[11] the isomer with two bridging lithium atoms is the global minimum. A bridging lithium atom is also present in **10**. However, even though all three atoms of the Li_3^+ unit interact with the C_2 fragment, **10** is a transition structure lying 13.6 kcal mol^{-1} higher in energy than **6**, in which only two Li–C_2 interactions are present. The preference for the edge interaction in **6** over the face interaction in **10** is due to the polarization of the Li_3^+ unit in **6**. This leads to an alternating quadrupole-like distribution of charges.[13] In polylithium compounds with cyclic Li_3^+ moieties, edge coordination is generally preferred to face coordination, for example, in OLi_4 with C_{2v} symmetry ($Li^+O^{2-}Li_3^+$).[3]

Structures **11** and **12** both contain another such lithium cluster "fragment", namely the $Li_2^{\bullet+}$ radical cation, which has been identified in OLi_5 (i.e. $Li_2^{\bullet+}O^{2-}Li_3^+$).[1a] Two such $Li_2^{\bullet+}$ units in a molecule may give rise either to singlet or triplet electronic states. The singlet species **11** (+6.7 kcal mol^{-1} above **6**) can be viewed as a complex of C_2^{2-} and two $Li_2^{\bullet+}$ radical cations. Structure **12** is a triplet molecule which lies 4.3 kcal mol^{-1} above **6**. Still higher levels of theory may be necessary to refine the singlet–triplet energy difference, but the structural features we describe are not expected to change.

Finally, **13** (C_{2v}) contains another intriguing Li_n structural unit—a four-center, two-electron Li_4^{2+} ion.[16] This description is supported both by the natural charges and the roughly tetrahedral arrangement of the lithium atoms; the distortion of the Li_4 unit is due to the C_2^{2-} unit which opens up one edge of the tetrahedron. For the free Li_4^{2+} ion the T_d structure is the global minimum on the potential energy surface,[16] and it is also preferred by OLi_4,[3] in which the O^{2-} ion fits into the center of the Li_4^{2+} tetrahedron. The alternative $Li_3^+O^{2-}Li^+$ isomer, analogous to **6**, is a higher energy minimum.[1a, 3] In C_2Li_4 the C_2^{2-} unit is too bulky to fit into the tetrahedral cage without considerable distortion, and therefore **13** is less stable than **6**.

C_2Li_4 illustrates the richness of structural possibilities available even to small polylithium compounds. The identification of similar discernable Li_n structural fragments recurring in other molecules will be the subject of future reports.

Received: June 2, 1992
Revised: September 3, 1992 [Z 5382 IE]
German version: *Angew. Chem.* **1992**, *104*, 1678

CAS Registry number:
9, 144372-76-9.

[1] a) P. von R. Schleyer in *New Horizons of Quantum Chemistry* (Eds.: P.-O. Löwdin, A. Pullman), Reidel, Dordrecht, **1982**, pp. 95–105; b) P. von R. Schleyer, E.-U. Würthwein, E. Kaufmann, T. Clark, J. A. Pople, *J. Am. Chem. Soc.* **1983**, *105*, 5930; c) A. E. Reed, F. Weinhold, *ibid.* **1985**, *107*, 1919; d) see also the highlight by A. Maercker, *Angew. Chem.* **1992**, *104*, 598; *Angew. Chem. Int. Ed. Engl.* **1992**, *31*, 584.
[2] C. S. Ewig, J. R. van Wazer, *J. Am. Chem. Soc.* **1990**, *112*, 109; J. P. Ritchie, S. M. Bachrach, *ibid.* **1987**, *109*, 5909.
[3] P. von R. Schleyer, E.-U. Würthwein, J. A. Pople, *J. Am. Chem. Soc.* **1982**, *104*, 5839.
[4] C. J. Marsden, *J. Chem. Soc. Chem. Commun.* **1989**, 1356; K. Jug, *J. Comput. Chem.* **1984**, *5*, 555.
[5] CLi_4 and $SiLi_4$ can likewise be described in terms of metallic cluster bonding models: A. E. Reed, P. von R. Schleyer, R. Janoschek, *J. Am. Chem. Soc.* **1991**, *113*, 1885. For a review on the bonding in multilithiated compounds, see: P. von R. Schleyer, *Pure Appl. Chem.* **1984**, *56*, 151; A. Maercker, M. Theis, *Top. Carb. Chem.* **1987**, *138*, 1. For a review of the bonding in clusters of alkali metal elements, see V. Bonačić-Koutecký, P. Fantucci, J. Koutecký, *Chem. Rev.* **1991**, *91*, 1035.
[6] L. A. Shimp, J. A. Morrison, J. A. Gurak, J. W. Chinn, Jr., R. J. Lagow, *J. Am. Chem. Soc.* **1981**, *103*, 5951.
[7] SINDO1 calculations on some C_2Li_4 structures have previously been reported by: K. Jug, N. D. Epiotis, S. Buss, *J. Am. Chem. Soc.* **1986**, *108*, 1640.
[8] Data for the structures **1**, **3** and **5** are reported in *The Carnegie-Mellon Quantum Chemistry Archive* (Eds.: R. A. Whiteside, M. J. Frisch, J. A. Pople), Department of Chemistry, Carnegie-Mellon University, Pittsburgh, PA, USA, **1983**.
[9] The Gaussian 90- and Cadpac programm packages were used. *Gaussian 90*: M. J. Frisch, M. Head-Gordon, G. W. Trucks, J. B. Foresman, H. B. Schlegel, K. Raghavachari, M. A. Robb, J. S. Binkley, C. Gonzalez, D. J. Defrees, D. J. Fox, R. A. Whiteside, R. Seeger, C. F. Melius, J. Baker, R. L. Martin, L. R. Kahn, J. J. P. Stewart, S. Topiol, J. A. Pople, Gaussian, Inc., Pittsburgh, PA, USA, **1990**; *Cadpac*: R. D. Amos, J. E. Rice, issue 4.0, Cambridge, UK, **1987**.
[10] The total energy of **6** at the MP4(SDTQ)(FC)/6-31+G*//MP2(FU)/6-31G* level is −105.84222 Hartree (where FC = frozen core and FU = full correlation).
[11] P. von R. Schleyer, *J. Phys. Chem.* **1990**, *94*, 5560, and references therein.
[12] The first reference to the cyclic Li_3^+ ion an be found in: P. A. Kollman, J. F. Liebman, L. C. Allen, *J. Am. Chem. Soc.* **1970**, *92*, 1142. This cation is also a discernable fragment in C_2Li_6: W. Thiel, P. von R. Schleyer, *Tetrahedron Lett.* **1980**, *21*, 2151. The analogous Na_3^+ unit has been described in: E.-U. Würthwein, P. von R. Schleyer, J. A. Pople, *J. Am. Chem. Soc.* **1984**, *106*, 6973.
[13] The calculated natural[14] charges (HF/6-31G*) for Li(2), Li(3), and Li(4) (see **6** in Scheme 1) are 0.63, 0.59, and −0.38, respectively.
[14] A. E. Reed, F. Weinhold, *J. Am. Chem. Soc.* **1985**, *107*, 1919.
[15] P. von R. Schleyer, A. Sawaryn, A. E. Reed, P. Hobza, *J. Comput. Chem.* **1986**, *7*, 666.
[16] M. Glukhovtsev, A. Stein, P. von R. Schleyer, unpublished.

1-Borabutadiene(cyclopentadienyl)cobalt Complexes**

By *Gernot Gabbert, Wolfgang Weinmann, Hans Pritzkow,* and *Walter Siebert**

Dedicated to Professor Klaus Hafner on the occasion of his 65th birthday

2,3-Dihydro-1,2-diboroles **1** should react with fragments of organometallic compounds or metal complexes analogously to the isomeric 2,3-dihydro-1,3-diboroles,[1] as a 3e ligand, to give oligodecker[2] and polydecker compounds with elimination of a H atom. In contrast, from the reactions of **1** with 14 valence electron (VE) complex fragments the for-

[*] Prof. Dr. W. Siebert, Dipl.-Chem. G. Gabbert, Dipl.-Chem. W. Weinmann, Dr. H. Pritzkow
Anorganisch-chemisches Institut der Universität
Im Neuenheimer Feld 270, D-W-6900 Heidelberg (FRG)

[**] This work was supported by the Deutsche Forschungsgemeinschaft (SFB 247), the Fonds der Chemischen Industrie, and BASF AG.

mation of a B-H-B bridge is to be expected by the migration of one H atom,[3] so that the heterocycle can now act as a 4e donor as in **2**. The preparation of a derivative of **1** (R^1 = H, R^2 = N*i*Pr$_2$, R^3 = Me) was achieved starting from 4-methylene-1,2-diborolane **3a**.[4] We report herein about the synthesis and structure of the 3-methylene-1,2-diborolane **3b** as well as the reactions of **3a,b** with $[(C_5H_5)Co(C_2H_4)_2]$ to give mononuclear complexes.

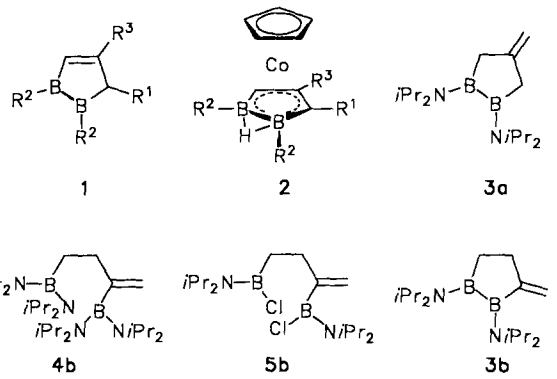

Analogous to the formation of 1,2-diborolane **3a**[4] the diboryl compound **4b** is formed by the reaction of 2,4-dilithio-1-butene[5] with ClB(N*i*Pr$_2$)$_2$; the subsequent substitution of one diisopropylamino group at each boron by chlorine leads to **5b**, and its reductive ring closure with Na/K alloy affords **3b**.[6] The constitution of **3b** was deduced from the spectroscopic data and confirmed by a crystal structure analysis.[7] The heterocycle is strongly folded along the line C3–B1 (angle between the planes C3-B2-B1/C3-C4-C5-B1 = 46.4°), and the bond lengths lie within the expected range (Fig. 1).

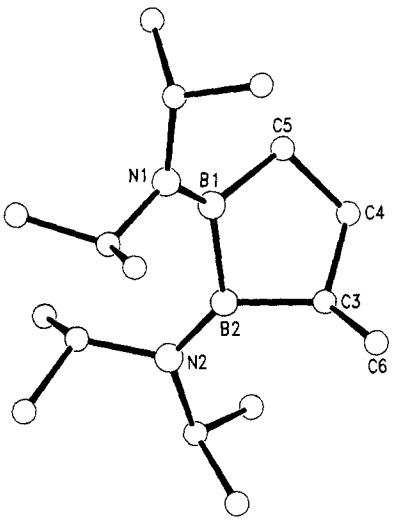

Fig. 1. Molecular structure of **3b**. Selected bond lengths [Å] and angles [°]: B1-B2 1.709(4), B1-C5 1.601(4), B2-C3 1.583(4), C3-C4 1.532(4), C4-C5 1.540(5), C3-C6 1.319(5), B1-N1 1.400(3), B2-N2 1.398(3); C5-B1-B2 101.1(2), C3-B2-B1 96.4(2), C4-C3-B2 104.1(2), C6-C3-B2 128.1(3), C6-C3-C4 120.5(3), C3-C4-C5 107.3(3), C4-C5-B1 106.5(3).

The two 1,2-diborolanes **3a** and **b** react with $[(C_5H_5)Co(C_2H_4)_2]$ in hexane, with the liberation of ethene, to give red solutions, from which red crystals (**A**) and a red oil (**B**), respectively, can be isolated by chromatographic workup in 73% and 42% yields, respectively. Both complexes show the required signals for the molecular ions of **2a,b** in the mass spectrum. Surprisingly, however, they show differing ^{11}B NMR signals: Substance **A** shows a broad singlet at δ = 35, and **B** two signals in a ratio of 1:1 at δ = 46 and 24, which are not in agreement with **2b** but with **6b**. We assign the low-field signal to the noncomplexed boron atom in the opened heterocycle. Both the ^{11}B NMR and the ^{1}H NMR spectrum of **A** are in accordance with **2a** and with a fluctuating molecule **6a**: the two CH groups of the ligand result in one signal, but that a doublet, as a result of the coupling with the BHB hydrogen. Temperature-dependent ^{1}H NMR spectra (to 180 K) show only a freezing of the free rotation (at 293 K) of the diisopropylamino groups about the B–N bond at 195 K. The protons of the CH groups are still magnetically equivalent at this temperature; that is, in the molecule the mirror plane through the Co atom and the substituent R^3 = Me is retained within the NMR time scale.

The crystal structure analysis[8] of **A** shows that by the metal-induced migration of a hydrogen atom to each of the atoms B5 and C6, the heterocycle **3a** is opened to give the complexed 4-boryl-1-borabutadiene in **6a** (Fig. 2). The ligand is only coordinated to the Co atom by the atoms B1, C2, C3, and C4. Since the B1–C2 bond length (1.493 Å), like the one in (B=C)π complexes,[9] corresponds to a very short BC single bond, and because C2–C3 as well as C3–C4 have identical interatomic distances (1.404 Å) this ligand can be described as a heterobutadiene. However, the likewise short

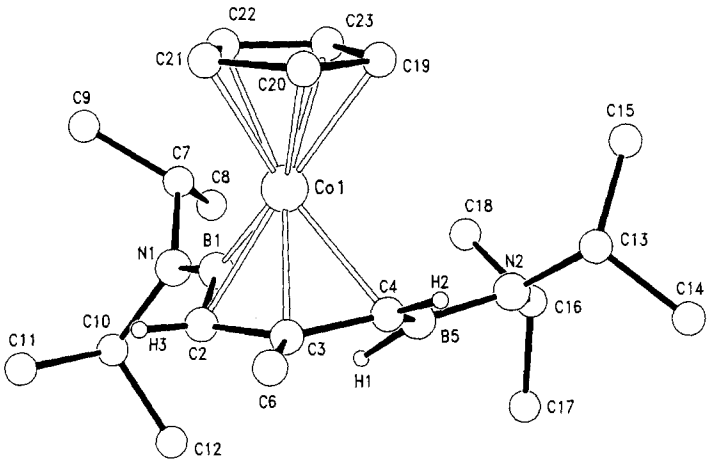

Fig. 2. Molecular structure of **6a**. Selected bond lengths [Å] and angles [°]: Co1-C2 2.022(3), Co1-C3 1.992(3), Co1-C4 2.072(2), Co1-B1 1.987(3), Co1-B5 2.714(3), B1-C2 1.493(4), B1-B5 2.758(5), B5-C4 1.522(4), C2-C3 1.404(4); C3-C4 1.404(4), B1-H1 2.31(4), B5-H1 1.15(3), B1-N1 1.390(3), B5-N2 1.409(3); N1-B1-C2 139.3(4), B1-C2-C3 119.9(2), C2-C3-C4 119.3(2), C3-C4-B5 125.9(2), C4-B5-N2 124.9(2), H1-B5-N2 118(1), H1-B5-C4 117(1), N1-B1-Co1 146.6(2).

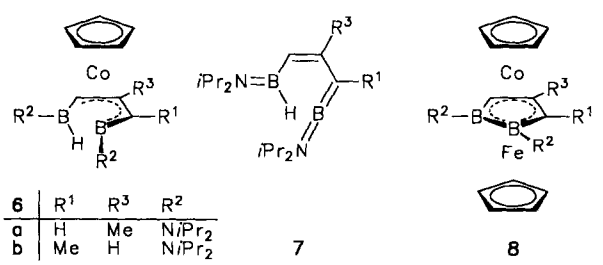

B5–C4 bond (1.524 Å) indicates a partial extension of the π electrons of the heterobutadiene onto B5, which obviously makes the above-mentioned fluctuation of the molecule **6a** easier.

The Co1–B1 distance (1.957 Å) is, in contrast to many metal complexes with B–C=C bonding, shorter than the Co1–C2 bond (2.022 Å). This can be explained by a strong back bond from the cobalt to the boron (population of the (B=C)π* MOs).[9] Furthermore, the geometry of the N1-B1-C2 group is very similar with that of the first (B=C)π ligand 9-fluorenylidene(2,2,6,6-tetramethylpiperidino)borane in the $(C_5H_5)Co(CO)$ and in the $Fe(CO)_4$ complex,[9a] whose electronic structure of has been described in detail.[9c] Therefore, for the previously unknown free diisopropylamino-substituted 4-boryl-1-borabutadiene **7** we also expect a N=B=C structure analogous to the 9-fluorenylidene(2,2,6,6-tetramethylpiperidino)borane.[9] In the solid state no interaction between Co1 and B5 (2.714 Å) occurs, the hydrogen H1 is only bound to B5 (B5–H1 1.15, B1–H1 2.31 Å). By a small rotation of the boryl groups about C3–C4 and C2–C3, respectively, a rapid exchange of the positions of H1 and B1 occurs, which can be observed in solution. This is not observed in **6b** because of the different position of the methyl group at the ring. We assume that the opening of the heterocycle in **2** is caused by the electronic saturation of the amino-substituted boron atoms. When R^2 is an alkyl group, the thus stabilized **2** should also enable the formation of the triple-decker sandwich complex **8**.[2]

The (*Z*)-4-boryl-1-borabutadiene **7** in the complexes **6a,b** is, with regard to its bonding situation, comparable with the H-bridged 1,3-diboraallyl R^1-C(R^2-B)$_2$(μ-H),[10] from which it is formally derived by the inclusion of a H-C=C unit.

Experimental Procedure

4b: Crystallization from hexane, yield: 48%; m.p. 68 °C; ^{1}H NMR (300 MHz, C_6D_6): Signals of the CH_2-C protons overlapped by the methyl of *i*Pr; $\delta = 6.68$ (s, 1H), 5.30 (s, 1H), 3.64 (sept, 4H), 3.56 (sept, 4H), 2.45 (m, 2H), 1.27 (d, 24H), 1.22 (d, 24H); ^{13}C NMR (75 MHz, C_6D_6): $\delta = 160$ (br.), 116.5, 48.0, 46.9, 33.1, 25.4, 24.8, 18 (br.); ^{11}B NMR (29 MHz, C_6D_6): $\delta = 38$; EI MS: *m/z* 476 (M^+, 28%), 461 ($M^+ - Me$, 26), 433 ($M^+ - i$Pr, 100).

5b: Filtration, distillation 92 °C/5×10^{-3} Torr; yield: 82%; ^{1}H NMR (200 MHz, $CDCl_3$): Signals of the CH_2-C protons overlapped by the methyl of *i*Pr; $\delta = 5.18$ (s, 1H), 4.94 (s, 1H), 4.08 (sept, 1H), 4.01 (sept, 1H), 3.62 (sept, 1H), 3.42 (sept, 1H), 2.30 (m, 2H), 1.38 (d, 6H), 1.19 (d, 12H), 1.11 (d, 6H); ^{13}C NMR (75 MHz, $CDCl_3$): $\delta = 154$ (br.), 116.2, 51.5, 47.9, 47.5, 45.7, 32.4, 23.3, 23.1, 22.2, 19.3, 19 (br.); ^{11}B NMR (29 MHz, $CDCl_3$): $\delta = 37.5$; EI-MS: *m/z* 346 (M^+, 7%), 331 ($M^+ - Me$, 28), 303 ($M^+ - i$Pr, 2).

3b: **5b** (7.5 g, 21.4 mmol) was added dropwise to a suspension of $NaK_{2.8}$ (2.03 g, 42.6 mmol) in pentane at 20 °C. Filtration and distillation (35 °C/5×10^{-3} Torr) afforded **3b** in 38% yield. ^{1}H NMR (300 MHz, $CDCl_3$): Signals of the C4 protons overlapped; $\delta = 4.97$ (m, 1H), 4.82 (m, 1H), 3.71 (sept, 1H), 3.62 (sept, 1H), 3.46 (sept, 1H), 3.28 (sept, 1H), 2.59 (m, 2H), 1.25 (d, 6H), 1.18 (d, 6H), 1.12 (d, 6H), 1.09 (d, 6H); ^{13}C NMR (75 MHz, $CDCl_3$): a C atom attached to a boron was not observed; $\delta = 163$ (br.), 110.6, 57.0, 55.7, 46.6, 45.1, 35.0, 25.6, 24.7, 22.6, 22.5; ^{11}B NMR (29 MHz, $CDCl_3$): $\delta = 53$; EI MS: *m/z* 276 (M^+, 56%), 261 ($M^+ - Me$, 100), 232 ($M^+ - i$Pr, 7).

6a: **3a** (1.10 g, 3.99 mmol) was added to a solution of $[(C_5H_5)Co(C_2H_4)_2]$ (0.69 g, 3.69 mmol) in hexane at −10 °C. After chromatography (at −40 °C, Al_2O_3, deactivated with 5% H_2O) **6a** remained in 72% yield, m.p. 97 °C; ^{1}H NMR (200 MHz, C_7D_8, 293 K): $\delta = 4.63$ (s, 5H), 3.62 (sept, 4H), 3.12 (C2-H and C4-H, d, 2H; $^3J_{CH-BH} = 2.8$ Hz), 2.32 (s, 3H), 1.2 (BH, t, br., 1H), 1.18 (d, 12H), 1.12 (d, 12H); ^{1}H NMR (200 MHz, C_7D_8, 180 K): $\delta = 4.51$ (s, br., 5H), 4.10 (sept, br., 2H), 3.05 (s, br., 2H), 2.72 (sept, br., 2H), 2.35 (s, 3H), 1.10 (br., 24H); ^{13}C NMR (50 MHz, C_7D_8, 293 K): $\delta = 115.2$, 81.0, 51.0, 47.6, 27.3, 24.8, 23.6; ^{13}C NMR (50 MHz, C_7D_8, 180 K): $\delta = 115.3$, 80.0, 49.7, 44.0, 27.1, 25.1, 23.0; ^{11}B NMR (29 MHz, C_7D_8): $\delta = 35$; EI MS: *m/z* 400 (M^+, 35%), 357 ($M^+ - i$Pr, 100).

6b: **3b** (290 mg, 1.10 mmol) was added to a solution of $[(C_5H_5)Co(C_2H_4)_2]$ (189 mg, 1.11 mmol) in hexane at −10 °C. After chromatography at −78 °C (Al_2O_3, deactivated with 5% H_2O) **6b** remained as an air-sensitive oil in 42% yield. ^{1}H NMR (200 MHz, C_6D_6): BH not found; $\delta = 5.86$ (d, 1H), 4.68 (s, 5H), 3.93 (sept, 2H), 3.32 (sept, 2H), 2.98 (dd, 1H), 1.51 (s, 3H), 1.23 (d, 6H), 1.18 (d, 6H), 1.06 (d, 12H); ^{13}C NMR (50 MHz, C_6D_6): $\delta = 102.1$, 80.3, 50.4, 46.7, 25.2, 24.2, 23.9, 23.2, 22.9; ^{11}B NMR (64 MHz, C_6D_6): $\delta = 46$, 24; EI MS: *m/z* 400 (M^+, 38%), 357 ($M^+ - i$Pr, 100).

Received: April 10, 1992
Revised version: September 18, 1992 [Z 5296 IE]
German version: *Angew. Chem.* **1992**, *104*, 1670

CAS Registry numbers:
3a, 128270-31-5; **3b**, 144156-92-3; **4b**, 144156-90-1; **5b**, 144156-91-2; **6a**, 144156-93-4; **6b**, 144191-76-4; $ClB(NiPr_2)_2$, 28049-80-1; $(C_5H_5)Co(C_2H_4)_2$, 69393-67-5; 2,4-dilithio-1-butene, 118112-74-6.

[1] W. Siebert, *Angew. Chem.* **1985**, *97*, 924; *Angew. Chem. Int. Ed. Engl.* **1985**, *24*, 943.
[2] W. Siebert, *Nachr. Chem. Tech. Lab.* **1977**, *25*, 59.
[3] Comparable with both BHB bridges in $[(\eta^5\text{-}C_5H_5)Co\{\eta^5\text{-}1,2\text{-}(CR)_2(BH)_3H_2\}]$: R. N. Grimes, *Pure Appl. Chem.* **1987**, *59*, 847.
[4] G. E. Herberich, C. Ganter, L. Wesemann, R. Boese, *Angew. Chem.* **1990**, *102*, 914; *Angew. Chem. Int. Ed. Engl.* **1990**, *29*, 912; G. E. Herberich, U. Englert, C. Ganter, L. Wesemann, *Chem. Ber.* **1992**, *125*, 23. Complex formation with **3a**-H_2 as bridging ligand in the "slipped" triple-decker complex $[\{(cod)Rh\}_2\text{-}\mu,\eta^4,\eta^5\text{-}(\mathbf{3a}\text{-}H_2)]$: G. E. Herberich, C. Ganter, L. Wesemann, *J. Organomet. Chem.* **1990**, *394*, C1.
[5] A. Maercker, K.-D. Klein, *Angew. Chem.* **1989**, *101*, 63; *Angew. Chem. Int. Ed. Engl.* **1989**, *28*, 83.
[6] G. Gabbert, Diplomarbeit, Universität Heidelberg, **1991**. Earlier attempted syntheses for **1** and **3**: H. Seyffer, Dissertation, Universität Heidelberg, **1986**; G. Knörzer, Dissertation, Universität Heidelberg, **1990**.
[7] $C_{16}H_{34}B_2N_2$: $M_r = 276.09$, $a = 6.391(2)$, $b = 17.856(6)$, $c = 17.021(6)$ Å, $\beta = 93.57(3)°$, $V = 1939$ Å^3, space group $P2_1/n$, $Z = 4$, 1893 observed reflections ($I > 2\sigma_I$). Refinement: non-hydrogen atoms anisotropic, the methylene protons in observed positions, all other hydrogen atoms in calculated positions or as part of a rigid group, $R = 0.063$, $R_w = 0.059$ (232 parameters) [11].
[8] $C_{21}H_{39}B_2CoN_2$: $M_r = 400.17$, $a = 10.142(4)$, $b = 13.132(4)$, $c = 18.038(4)$ Å, $\beta = 99.15(4)°$, $V = 2372$ Å^3, space group $P2_1/n$, $Z = 4$, 3231 observed reflections ($I > 2\sigma_I$). Refinement: non-hydrogen atoms anisotropic, hydrogen atoms isotropic, the methyl protons as part of a rigid group, $R = 0.043$, $R_w = 0.048$ (313 parameters) [11].
[9] a) S. Helm, H. Nöth, *Angew. Chem.* **1988**, *100*, 1378; *Angew. Chem. Int. Ed. Engl.* **1988**, *27*, 1331; b) S. Channareddy, G. Linti, H. Nöth, *ibid.* **1990**, *102*, 222 and **1990**, *29*, 199; c) S. W. Helm, G. Linti, H. Nöth, S. Channareddy, P. Hofmann, *Chem. Ber.* **1992**, *125*, 73.
[10] R. Wehrmann, H. Meyer, A. Berndt, *Angew. Chem.* **1985**, *97*, 779; *Angew. Chem. Int. Ed. Engl.* **1985**, *24*, 788.
[11] Further details of the crystal structure investigation may be obtained from the Fachinformationszentrum Karlsruhe, Gesellschaft für wissenschaftlich-technische Information mbH, D-W-7514 Eggenstein-Leopoldshafen 2 (FRG) on quoting the depository number CSD-56441, the names of the authors, and the journal citation.

$[(\pi\text{-}Me_5C_5)_2SiH]^+$—A Novel Silyl Cation

By *Peter Jutzi** and *Ernst-August Bunte*

Dedicated to Professor Ulrich Wannagat on the occasion of his 70th birthday

Despite intensive investigations, the possible existence of triorganosilyl cations R_3Si^+ in solution or in the solid state is still debated. In contrast, the existence of related alkyl cations in which carbon is the cationic center has been proven unequivocally.[1] According to the extensive studies of Lambert et al., triorganosilyl cations can be detected in very dilute solution in the presence of perchlorate anions.[2] Olah et al. maintained that the effects Lambert observed arose from impurities and contested the dissociation of triorganosilylium perchlorates.[3] Eaborn also questioned the

[*] Prof. Dr. P. Jutzi, Dr. E.-A. Bunte
Fakultät für Chemie der Universität
Universitätsstrasse, D-W-4800 Bielefeld (FRG)

existence of R_3Si^+ ions.[4] The current state of the controversy was recently summarized by Lickiss.[5] Here we report on the first example of a new type of R_3Si^+ cation in which π ligands contribute to the stabilization of the cationic center.

The reaction of the π complex decamethylsilicocene Cp^*_2Si (**1**) ($Cp^* = Me_5C_5$) and catechol in toluene first gave rise to aryloxysilane **2** by means of an oxidative addition to the divalent silicon atom (Scheme 1). Compound **2** is not stable

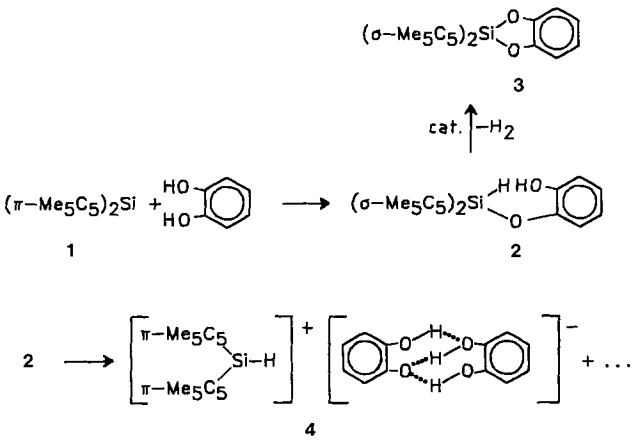

Scheme 1.

for very long, but its structure is supported by conclusive NMR data. The structure of the analogous addition product from the reaction of **1** with 4-methylcatechol was proven by an X-ray structure analysis conducted at $-100\,^\circ C$.[7, 8] The transition from **1** to **2** is associated with an η^5–η^1 slippage of the Cp* ligand.

Compound **2** can react further by two paths: With catalysis[8] and loss of H_2 **2** was converted to heterocycle **3**, whose structure was determined by X-ray structure analysis.[8, 10] Compound **2** decomposes in toluene solution after a few hours to give **4** as the unexpected main product containing the cation $[(\pi\text{-}Me_5C_5)_2SiH]^+$. When the reaction of **1** with catechol in toluene was conducted at 60 °C, **4** was obtained directly (see Experimental Procedure).

Compound **4** was obtained as a colorless, extremely air- and moisture-sensitive, amorphous[11] solid. It is soluble in toluene, tetrahydrofuran, and nitrobenzene; in acetonitrile and nitromethane the compound decomposes instantaneously.[12] Even in toluene, tetrahydrofuran, and nitrobenzene **4** decomposes slowly. Compound **4** is stable for longer periods at $-40\,^\circ C$ dissolved in toluene as well as in the solid state. Freshly prepared solutions of **4** were used in the investigations described here.[13]

The molecular mass, determined with a 0.025 M solution of **4** in nitrobenzene, is 300; this is roughly half of the expected value (518) and supports a dissociation of **4**. The results of conductance measurements in nitrobenzene can be explained by the presence of a 1:1 electrolyte. The products of the hydrolysis or decomposition of **4** can be ruled out as sources of the measured conductance.[14]

In the ^1H and ^{13}C NMR spectra of **4**,[15] the cation has signals for only one type of methyl group and one type of ring C atom, which are independent of concentration and temperature.[16] This finding is in agreement with the existence of π-bound Cp* ligands;[17] σ-bound Cp* ligands in related compounds (e.g. **2** or $Cp^*_2SiH_2$[18]) give rise to broad signals at room temperature and resolved signals at lower temperatures as a result of sigmatropic rearrangements that are slow on the NMR timescale. The signal for the Si–H proton in **4** at $\delta = 3.23$ is in the expected range.[20]

In the coupled ^{29}Si NMR spectrum of **4** a doublet is observed at $\delta = -12.1$ (J(Si,H) = 302 Hz). The δ value corresponds to a downfield shift of $\Delta\delta = 386$ upon conversion of **1** to $[(\pi\text{-}Me_5C_5)_2SiH]^+$. According to calculations, a ^{29}Si resonance at $\delta = 350$ would be expected for bonding situations with σ-bound ligands, as in Me_3Si^+.[21] The effectiveness of the π-bound Cp* ligands in reducing the electron deficiency at the silicon atom relative to that in Me_3Si^+ is reflected in the position of the ^{29}Si NMR signal.

The comparison of the J(Si,H) coupling constants in **4** (302 Hz), **2** (217 Hz), and $Cp^*_2SiH_2$ (194 Hz) is also diagnostic.[19] The tremendous increase of the coupling constants upon going from $Cp^*_2SiH_2$ and **2** to $[(\pi\text{-}Me_5C_5)_2SiH]^+$ is in agreement with the increased amount of s character in the Si–H bond of $[(\pi\text{-}Me_5C_5)_2SiH]^+$, as expected for sp^2-hybridized silicon.[22, 23]

The IR spectrum of a 0.2 M solution of **4** in THF shows a Si–H stretch at $\tilde{\nu} = 2200\ cm^{-1}$; this value is best explained by a positively polarized hydrogen atom[24] and correlates well with the value for the J(Si,H) coupling constant according to a known relationship.[25]

The anion in **4**, $H_4C_6O_2H_3O_2C_6H_4^-$, has been described as the Bu_4N^+ salt.[26] The ^1H and ^{13}C NMR spectra of the anions in **4** and in the ammonium salt are identical; the two types of aromatic H atoms and three types of C atoms support the symmetric structure with exchanging OH protons.[27] One of the possible static bonding situations for the anion in **4** is represented in Scheme 1.

According to Austin Model 1 (AM1) calculations,[28] the phenyl groups in the anion in **4** are oriented perpendicular to each other. The resulting tetrahedral arrangement of the oxygen atoms in the O_4H_3 unit allows an effective shielding of the negative charge. To our knowledge anions of this type have not been used previously to stabilize especially electrophilic cations, but apparently they are not very nucleophilic.

The deuterated cation $[(\pi\text{-}Me_5C_5)_2SiD]^+$ was prepared by the reaction of **1** with deuterated catechol $C_6H_4(OD)_2$; the ^2D NMR signal at $\delta = 3.18$, the ^{29}Si NMR signal at $\delta = -12.3$ (triplet), and the J(Si,D) coupling constant of 46.0 Hz have the expected values.[29]

Exactly how **4** arises from **2** is not yet understood. The addition of one equivalent of catechol to **2** surprisingly did not lead to **4**, but to complete decomposition and ill-defined products. Compound **2** was not even formed at a 1:2 stoichiometry of **1** and catechol. Compounds analogous to **4** were prepared with the catechol derivatives 4-methyl, 4-*tert*-butyl- and 4,6-di-*tert*-butylcatechol. The cation in **4** may most likely also be generated by the reaction of **1** with two equivalents of trifluoromethanesulfonic acid.[30] Up to this point it has not been possible to generate this cation by halide abstraction from precursors of the type $(\sigma\text{-}Me_5C_5)_2SiHHal$.

Cations that are significantly stabilized by π-bound cyclopentadienyl ligands are not unknown in the chemistry of the p-block elements as shown by the following examples: $[(\pi\text{-}Me_5C_5)BX]^+$, X = Cl, Br, I,[31] $[(\pi\text{-}Me_5C_5)Ge]^+$,[32] $[(\pi\text{-}Me_5C_5)Sn]^+$,[32, 33] $[(\pi\text{-}Me_5C_5)PNHtC_4H_9]^+$,[34] $[(\pi\text{-}Me_5C_5)_2As]^+$,[35] and $[(\pi\text{-}Me_5C_5)_2Sb]^+$.[35] We propose that the cation $[(\pi\text{-}Me_5C_5)_2SiH]^+$ has a structure with η^2/η^3-bound Cp* ligands, whereby the π ligands undergo rapid haptotropic rearrangements. A similar situation is found for the iso(valence)electronic cation $[(\pi\text{-}Me_5C_5)_2As]^+$. In $[(\pi\text{-}Me_5C_5)_2SiH]^+$, however, one finds a covalent bond to a hydrogen atom instead of a lone pair on the central atom.

Experimental Procedure

4: A solution of **1** (960 mg, 3.22 mmol) and catechol (354 mg, 3.22 mmol) in toluene (20 mL) was stirred at 60 °C for 16 h. The volatile components were removed under vacuum, and the residue was washed repeatedly with pentane. Compound **4** was isolated as a colorless solid; yield 560 mg (34% based on **1**). ^{1}H NMR (C_6D_6): $\delta = 1.77$ (s, 30 H, C_5Me_5), 3.22 (s, 1 H, Si-H), 6.68–6.71 (m, 4 H) and 7.00–7.03 (m, 4 H, AA'BB' spectrum for phenyl-H); ^{13}C NMR (C_6D_6): $\delta = 10.8$ (s, C_5Me_5), 113.5 (s, phenyl-C), 120.4 (s, C_5Me_5), 121.0 (s, phenyl-C), 149.3 (s, phenyl-C-O). MS (70eV): m/z 299 ($[\pi\text{-}C_5Me_5)_2SiH]^+$, 32%), 137 ($Cp^*H_2^+$, 100), 135 ($Cp^{*+}$, 74). Correct C,H analysis.

Received: February 6, 1992 [Z 5171 IE]
German version: *Angew. Chem.* **1992**, *104*, 1636

CAS Registry numbers:
1, 100189-23-9; **2**, 144181-18-0; **3**, 144181-19-1; **4**, 144181-22-6; $(Me_5C_5)_2Si(H)OC_6(Me)H_3(OH)$, 144181-23-7; $[(Me_5C_5)_2SiH][(F_3CSO_3)_2H]$, 144181-25-9; catechol, 120-80-9; 4-methylcatechol, 452-86-8.

[1] G. A. Olah, *Top. Curr. Chem.* **1979**, *80*, 19.
[2] a) J. B. Lambert, L. Kania, W. Schilf, J. A. A. McConnell, *Organometallics* **1991**, *10*, 2578; b) J. B. Lambert, W. J. Schulz, Jr., J. A. A. McConnell, W. Schilf, *J. Am. Chem. Soc.* **1988**, *110*, 2201; c) J. B. Lambert, W. Schilf, *ibid.* **1988**, *119*, 6364; d) J. B. Lambert, J. A. A. McConnell, *ibid.* **1986**, *108*, 2482.
[3] G. A. Olah, L. Heiliger, X.-Y. Li, G. K. S. Prakash, *J. Am. Chem. Soc.* **1990**, *112*, 5991; G. K. S. Prakash, S. Keyaniyan, R. Aniszfeld, L. Heiliger, G. A., Olah, R. C. Stevens, H. K. Choi, R. Bau, *ibid.* **1987**, *109*, 5123.
[4] C. Eaborn, *J. Organomet. Chem.* **1991**, *405*, 173.
[5] P. D. Lickiss, *J. Chem. Soc. Dalton Trans.* **1992**, 1333.
[6] P. Jutzi, U. Holtmann, D. Kanne, C. Krüger, R. Blom, R. Gleiter, I. Hyla-Kryspin, *Chem. Ber.* **1989**, *122*, 1629.
[7] Crystal structure data for $[(Me_5C_5)_2Si(H)OC_6(Me)H_3(OH)]$: space group $P\bar{1}$; Cp*-Si 1.903, Si-O 1.663 Å; Cp*SiCp* 121.5, Cp*SiO 109.3, SiOC 126.0°.
[8] P. Jutzi, E. A. Bunte, U. Holtmann, B. Neumann, H. G. Stammler, *J. Organomet. Chem.*, in press.
[9] This reaction is catalyzed by H_2O, pyridine, or Cp_2^*Si.
[10] Crystal structure data for **3**: space group *Pnn*2; Cp*-Si 1.883, Si-O 1.677, O-C 1.381 Å; Cp*SiCp* 122.2°, Cp*SiO: 106.9, OSiO 95.7, SiOC 108.8°.
[11] Crystallizations have failed so far.
[12] Immediate decomposition of **4** in solution is evident from the violet color.
[13] After the measurements on **4** the identity of the sample was double-checked by NMR spectroscopy.
[14] Equivalent conductances [$m^2\Omega val^{-1}$] in nitrobenzene: **4**: 10^{-3}; $nBu_4N^+H_4C_6O_2H_3O_2C_6H_4^-$: 10^{-2}; catechol: $< 5\times10^{-6}$; decomposition products of **4**: 10^{-6}; for comparison, $Ph_3C^+ClO_4^-$: 2×10^{-2} (in CH_3CN)[2c].
[15] Measurements in C_6D_6; measurements in [D_5]nitrobenzene provide almost the same values.
[16] Measurements in the concentration range 0.25 to 0.005 mol L^{-1} and temperature range + 26 to −80 °C.
[17] For information on molecular dynamics in cyclopentadiene systems: P. Jutzi, *Chem. Rev.* **1986**, *86*, 983.
[18] NMR data for the Me_5C_5 groups a) in **2**: ^{1}H NMR (C_6D_6): $\delta = 1.40$–1.80 (br.); ^{13}C NMR(C_6D_6): $\delta = 12.4$ (br.), 137.4 (br.); b) in $Cp_2^*SiH_2$[19]: ^{1}H NMR ($CDCl_3$): $\delta = 1.62$ (br., $\tau_{1/2} = 53$ Hz); ^{13}C NMR ($CDCl_3$): $\delta = 11.8$ (br.), 135.4 (br.); at 243 K: $\delta = 11.2$, 11.4, 15.9, 51.8, 134.4, 137.0.
[19] P. Jutzi, D. Kanne, M. Hursthouse, A. J. Howes, *Chem. Ber.* **1988**, *121*, 1299.
[20] The ^{29}Si–H signal (d, J(Si,H) = 302 Hz) can also be seen when the intensity is increased.
[21] Calculated value for Me_3Si^+: $\delta = 355.7$ [5] and $\delta = 351$: W. Kutzelnigg, U. Fleischer, M. Schindler in *NMR Basic Princ. Prog.* **1991**, *23*, 231.
[22] For a comparison showing the increase of the J(C,H) coupling constant on going from Ph_2CH_2(J(C,H) = 127 Hz) to Ph_2CH^+ (J(C,H) = 169 Hz) see J. B. Stothers, *Carbon-13-NMR-Spectroscopy*, Academic Press, New York, **1972**, p. 331.
[23] The increase of the J(Si,H) coupling constant on going from $Cp_2^*Si_2$/**2** to **4** eliminates the possibility of a molecule with a σ-Cp* ligand and a higher coordinated silicon atom: B. Becker, R. Corriu, G. Guerin, B. Henner, Q. Wang, *J. Organomet. Chem.* **1989**, *368*, C25.
[24] For comparison: $\tilde{\nu}$(Si-H) in $HSiBr_3$: 2239 cm^{-1} [25].
[25] H. Bürger, W. Kilian, *J. Organomet. Chem.* **1964**, *18*, 299.
[26] A. W. Hansen, A. W. McCulloch, A. G. McInnes, *Tetrahedron Lett.* **1982**, *23*, 607.
[27] The signals of the O–H protons are not seen in the ^{1}H NMR spectrum of **4**.
[28] For the method: M. J. S. Dewar, E. G. Zoebesch, E. F. Healy, J. J. P. Stewart, *J. Am. Chem. Soc.* **1985**, *107*, 3902.
[29] H. Friebolin, *Ein- und zweidimensionale NMR-Spektroskopie*, VCH, Weinheim, **1988**, p. 88.
[30] The compound $[Cp_2^*SiH][(F_3CSO_3)_2H]$ was obtained as an extremely sensitive oil; a more thorough characterization (conductance measurements, molecular weight determination) was thus not possible. ^{1}H NMR (C_6D_6): $\delta = 1.50$ (Cp*), 3.30 (SiH); ^{29}Si NMR (C_6D_6): $\delta = 51.6$ (^1J(Si,H) = 338 Hz). IR: $\tilde{\nu}$(Si–H) = 2245 cm^{-1}. See U. Holtmann, Dissertation, Universität Bielefeld, **1988**. The fact that the ^{29}Si NMR data are not identical to those of **4** suggests different π-bonding situations in the two systems (possibly caused by different cation–anion interactions). Different chemical shift values and coupling constants are not unusual for ionic species, see: R. N. Young, *Prog. Nucl. Magn. Reson. Spectrosc.* **1979**, *12*, 261.
[31] P. Jutzi, A. Seufert, *Angew. Chem.* **1977**, *89*, 339; *Angew. Chem. Int. Ed. Engl.* **1977**, *16*, 330; P. Jutzi, A. Seufert, W. Büchner, *Chem. Ber.* **1979**, *112*, 2488.
[32] P. Jutzi, F.-X. Kohl, P. Hofmann, C. Krüger, Y. H. Tsay, *Chem. Ber.* **1980**, *113*, 757.
[33] P. Jutzi, F.-X. Kohl, C. Krüger, *Angew. Chem.* **1979**, *91*, 81; *Angew. Chem. Int. Ed. Engl.* **1979**, *18*, 59.
[34] D. Gudat, M. Nieger, E. Niecke, *J. Chem. Soc., Dalton Trans.* **1989**, 643.
[35] P. Jutzi, Th. Wippermann, *Angew. Chem.* **1983**, *95*, 244; *Angew. Chem. Int. Ed. Engl.* **1983**, *22*, 250.

Distortional Isomerism in Oxomolybdenum Systems; the Evidence Re-evaluated**

By *Alan P. Bashall, S. W. Annie Bligh, Andrew J. Edwards, Vernon C. Gibson,* Mary McPartlin,** and *Oliver B. Robinson*

In recent years, there has been an upsurge of widespread interest in the phenomenon of distortional or bond stretch isomerism.[1–4] The term distortional isomerism was proposed in 1971 by Chatt, Manojlovic-Muir, and Muir[5] to describe two forms of $[Mo(O)Cl_2(PMe_2Ph)_3]$, one blue with $\tilde{\nu}$(Mo=O) at 954 cm^{-1} and the other green with $\tilde{\nu}$(Mo=O) at 943 cm^{-1}. These are members of a range of analogous blue and green oxomolybdenum compounds with high or low (Mo=O) vibrational frequencies, respectively, reported earlier by Butcher and Chatt and thought at first to be *cis* and *trans* isomers.[6] X-ray structure determinations showed that blue $[Mo(O)Cl_2(PMe_2Ph)_3]$ and the green diethylphenylphosphane derivative [$\tilde{\nu}$(Mo=O) = 940 cm^{-1}] in fact possessed similar *cis–mer* configurations, but with strikingly different organophosphane orientations and markedly different Mo=O bond lengths.

Based on these observations Chatt and co-workers proposed a new form of isomerism involving "two equilibrium arrangements of ligands which differ in the distortions of the highly strained coordination polyhedron of the metal". They suggested that the blue and green forms of *cis–mer*-$[Mo(O)Cl_2(PMe_2Ph)_3]$, which they concluded had different organophosphane orientations (resulting in C_s symmetry in the blue complex and C_1 in the green), exhibited this type of "distortional isomerism".

[*] Prof. M. McPartlin, Dr. S. W. A. Bligh, Dr. A. J. Edwards, A. P. Bashall
School of Chemistry, University of North London
London N7 8DB (UK)
Dr. V. C. Gibson, O. B. Robinson
Department of Chemistry, University Science Laboratories
South Road, Durham DH1 3LE (UK)

[**] We thank the Scientific and Engineering Research Council (UK) for a studentship (O. B. R.), financial support (A. J. E. and M. McP.), and for access to the CSSR Data Base at Daresbury, and Courtaulds PLC (O. B. R.) and B. P. Chemicals (V. C. G.) for financial support. The award of the Frankland Fellowship by the Royal Society of Chemistry is gratefully acknowledged (V.C.G.).

The marked differences in Mo=O bond length between these two isomers[7, 8] led Hoffmann to include them within the description of bond stretch isomerism,[9] a term that had originally been coined to describe hypothetical isomers "whose *only* structural difference is a relatively small increment in the length of one or several bonds" but not in any rotation or topological change.[10] Thus, recently the terms distortional isomerism and bond stretch isomerism have both been used somewhat arbitrarily to describe either phenomenon. Here we present results arising from a reinvestigation of the oxomolybdenum system which show that two blue forms of $[Mo(O)Cl_2(PMe_2Ph)_3]$ exist; they may reasonably be described as distortional isomers, but not bond stretch isomers.

The groups of Parkin and Enemark have recently subjected the Chatt system to detailed scrutiny. Extensive X-ray[11] studies by Parkin and coworkers, and independent spectroscopic[12] work by the Enemark group show that green $[Mo(O)Cl_2(PMe_2Ph)_3]$ [$\tilde{\nu}$(Mo=O) = 943 cm^{-1}] arises from cocrystallization of blue $[Mo(O)Cl_2(PMe_2Ph)_3]$ [$\tilde{\nu}$(Mo=O) = 943 cm^{-1}] with a yellow contaminant, $[MoCl_3(PMe_2Ph)_3]$, and they therefore concluded there was no need to invoke the existence of a second oxomolybdenum species in this system. Central to this argument is the absence of a second Mo=O stretch in the infrared spectra, although Butcher and Chatt had clearly recorded two Mo=O stretches, at 943 and 954 cm^{-1}, for the green and blue forms respectively. Following a thorough spectroscopic reinvestigation of the system, Enemark and coworkers concluded that the 954 cm^{-1} assignment was incorrect, since they had never been able to observe this band in any of their samples. Thus, the simple and persuasive contaminant theory gained widespread acceptance as providing an explanation for all the spectroscopic and crystallographic observations surrounding this distortional isomer system.[1, 3]

We, however, remained puzzled by the discrepancies between the infrared data recorded by Chatt on blue $[Mo(O)Cl_2(PMe_2Ph)_3]$ and subsequently by Enemark, not only in the Mo=O region but also in the Mo–Cl stretching region of the spectrum. One clue to a possible explanation for these was the fact that the Mo–Cl bond lengths reported by Parkin[11] for blue $[Mo(O)Cl_2(PMe_2Ph)_3]$ are significantly different from those reported in the original determination by Manojlovic-Muir.[7] It thus seemed possible that two blue oxo forms with differing bond lengths exist, thus providing an explanation for the discrepancies in the spectroscopic data.[2] In the hope of isolating the elusive Chatt blue isomer with $\tilde{\nu}$(Mo=O) at 954 cm^{-1}, we have explored methods as close as possible to those used in the earlier work and have been successful in isolating two blue forms of $[Mo(O)Cl_2(PMe_2Ph)_3]$ (**1a** and **1b**) and their bromo analogues (**2a** and **2b**) (see Scheme 1).

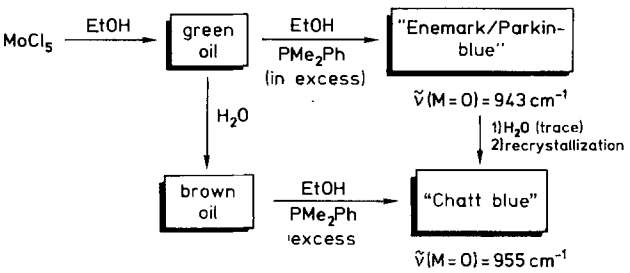

Scheme 1. The synthesis of the high (**1a**) and low (**1b**) frequency isomers of $[MoOCl_2(PMe_2Ph)_3]$.

In the original report Butcher and Chatt[6] described the reaction of molybdenum pentachloride with ethanol (added dropwise) to give a "brown" oil. This was subsequently treated with excess PMe_2Ph and refluxed for 5 min in ethanol to give a good yield of the blue isomer displaying $\tilde{\nu}$(Mo=O) at 954 cm^{-1}. During our attempts to reproduce this synthesis, we invariably obtained a green oil (reported earlier by Wardlaw and Webb to be molybdenyl chloride $[Mo(O)Cl_3]$[13]); upon subsequent treatment with PMe_2Ph followed by recrystallization from ethanol, this green oil afforded blue crystals that correspond to the compound described by Parkin and Enemark and displaying $\tilde{\nu}$(Mo=O) at 943 cm^{-1} (Scheme 1). However, when water was added dropwise to the green oil it turned brown. This led, on identical workup, to the Chatt blue isomer with $\tilde{\nu}$(Mo=O) at 955 cm^{-1}.

Solution IR spectra of the two blue forms at room temperature are identical and show an intermediate $\tilde{\nu}$(Mo=O) of 947 cm^{-1}. It therefore seems likely that the form that crystallizes depends upon the nature of the nucleation sites, possibly influenced by trace amounts of water. Indeed a solution of the "Enemark/Parkin blue", upon reflux in ethanol in the presence of a small amount of added water, gives the "Chatt blue" isomer on crystallization.

The bromide analogues $[Mo(O)Br_2(PMe_2Ph)_3]$, namely **2a** [$\tilde{\nu}$(Mo=O) 956 cm^{-1}] reported by Butcher and Chatt and the previously unknown form **2b** [$\tilde{\nu}$(Mo=O) 943 cm^{-1}], have been synthesized by treatment of the chloro isomers with LiBr, followed by recrystallization from ethanol.

X-ray structure analyses[14] show highly symmetrical dimethylphenylphosphane orientations in molecules of almost exact C_s symmetry for **1a** and **2a** (Fig. 1a) similar to that established[7] for the original Chatt blue $[Mo(O)Cl_2(PMe_2Ph)_3]$, while the molecules of the two low frequency compounds, **1a** and **2b**, have virtually identical asymmetric conformations of the dimethylphenylphosphanes resulting in only C_1 symmetry (Fig. 1b). The low frequency form (**1b**) of C_1 symmetry proves to be identical to the blue component of "green $[Mo(O)Cl_2(PMe_2Ph)_3]$" for which full structural details are now available[15] and is clearly a different blue form to that of C_s symmetry reported by Chatt.

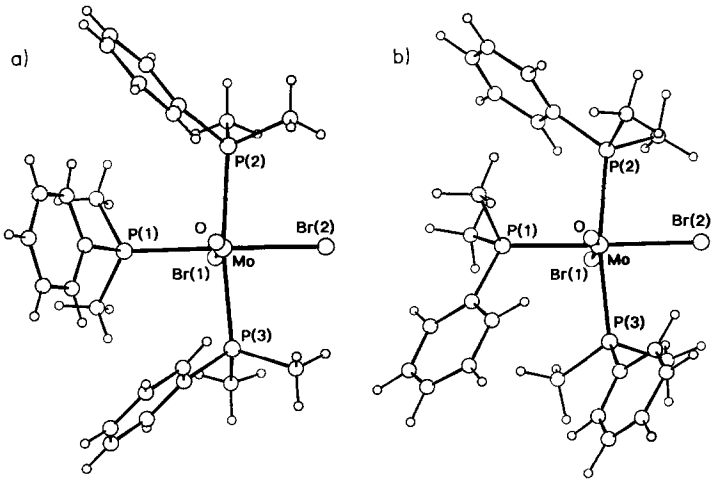

Fig. 1. The structures of the two forms of $[Mo(O)X_2(PMe_2Ph)_3]$ (X = Cl or Br), illustrated for X = Br. a) The structure of C_s symmetry for the high frequency form **1a**, **2a**. For selected bond lengths and angles see Table 1. b) The structure of C_1 symmetry for the low frequency form **1b**, **2b**. For selected bond lengths and angles, see Table 1.

The parameters of the two isomers differ most dramatically in large variations between equivalent angles at the metal atom (for example the angle Cl2-Mo-P1 has the nearly linear value of 177.8(1)° in **1b** but is reduced to 162.4(1)° in **1a**), and these distortions are reflected in significant differences in many of the metal–ligand bond lengths. The Mo=O length of 1.663(2) Å observed in the high frequency from **1a** is significantly shorter than 1.675(3) Å, the length in **1b**,[15] in line with the 12 cm^{-1} difference in their (Mo=O) stretching frequency. This difference in Mo=O length together with the differences in other bonds to the metal are undoubtedly related to the distortions of the coordination polyhedron and Chatt's original description of distortional isomers would still seem quite appropriate.[16] The phenomenon is not simple polymorphism because it has been clearly established that the differences are not merely a result of two different crystal packings; the two blue forms contain different molecules readily distinguished by their characteristic (Mo=O) stretching frequencies and symmetry.[17] Confirmation that the (Mo=O) stretching frequencies are molecular properties of the two isomers, not the result of a particular crystalline arrangement, is provided by the stretching frequency $\tilde{\nu}$(Mo=O) at 943 cm^{-1} exhibited by the low symmetry isomer in both the pure orthorhombic crystalline modification and in the contaminated monoclinic polymorph studied by Enemark[12] and Parkin.[15]

Table 1. Selected bond lengths [Å] and angles [°] of **1** (X = Cl) and **2** (X = Br).

	1a [a]	**1b** [b]	**2a**	**2b**
Mo-O	1.663(2) [1.676(7)]	1.682(7) [1.675(3)]	1.693(13)	1.672(10)
Mo-X(1)	2.538(1) [2.551(3)]	2.523(1) [2.528(1)]	2.654(4)	2.669(3)
Mo-X(2)	2.454(1) [2.464(3)]	2.478(3) [2.482(1)]	2.601(3)	2.618(2)
Mo-P(1)	2.491(1) [2.500(3)]	2.484(3) [2.489(1)]	2.506(6)	2.500(5)
Mo-P(2)	2.542(1) [2.541(3)]	2.519(3) [2.529(1)]	2.557(6)	2.527(5)
Mo-P(3)	2.539(1) [2.558(3)]	2.530(3) [2.533(1)]	2.559(6)	2.545(5)
O-Mo-X(1)	169.3(1) [168.8(3)]	170.0(3) [169.8(1)]	170.6(5)	168.5(3)
P(1)-Mo-X(2)	162.4(1) [162.4(1)]	177.8(1) [177.6(1)]	162.2(2)	178.5(1)
P(2)-Mo-P(3)	171.2(1) [171.2(1)]	160.4(1) [160.5(1)]	171.2(2)	160.4(2)

[a] Values for "Chatt blue" in parentheses [7]. [b] Values for "Enemark/Parkin blue" in parentheses [15].

This study demonstrates the importance of distinguishing between the phenomena of distortional isomerism and bond stretch isomerism. It should be noted that different ligand conformations cannot explain the differences in IR spectra reported for systems where the two "bond stretch isomers" are isostructural and give isomorphous crystals.[18]

Received: April 15, 1992
Revised version: September 8, 1992 [Z 5309 IE]
German version: *Angew. Chem.* **1992**, *104*, 1664

CAS Registry numbers:
1, 30134-06-6; **2**, 30134-05-5.

[1] J. M. Mayer, *Angew. Chem.* **1992**, *104*, 293; *Angew. Chem. Int. Ed. Engl.* **1992**, *31*, 286; G. Parkin, *Acc. Chem. Res.* **1992**, *25*, 455.
[2] V. C. Gibson, M. McPartlin, *J. Chem. Soc. Dalton Trans.* **1992**, 947.
[3] R. Baum, *Chem. Eng. News* **1991**, *69*, (9) 20; I. Amato, *Science* **1991**, *254*, 1452.
[4] L. Milgrom, *New Sci.* **1991**, *131* (1788) 22.
[5] J. Chatt, Lj. Manojlovic-Muir, K. W. Muir, *Chem. Commun.* **1971**, 655; Lj. Manojlovic-Muir, K. W. Muir, *J. Chem. Soc. Dalton Trans.* **1972**, 686.
[6] A. V. Butcher, J. Chatt, *J. Chem. Soc. A* **1970**, 2652.
[7] Lj. Manojlovic-Muir, *Chem. Commun.* **1971**, 147; *J. Chem. Soc. A* **1971**, 686.
[8] B. L. Haymore, W. A. Goddard III, J. N. Allison, *Proc. Int. Conf. Coord. Chem. 23rd* **1984**, 535.
[9] Y. Jean, A. Liedos, J. K. Burdett, R. Hoffmann, *J. Am. Chem. Soc.* **1988**, *110*, 4506.
[10] W.-D. Stohrer, R. Hoffmann, *J. Am. Chem. Soc.* **1972**, *94*, 1661.
[11] K. Yoon, G. Parkin, A. L. Rheingold, *J. Am. Chem. Soc.* **1991**, *113*, 1437.
[12] P. J. Desrochers, K. W. Nebesny, M. J. LaBarre, S. E. Lincoln, T. M. Loehr, J. H. Enemark, *J. Am. Chem. Soc.* **1991**, *113*, 9193.
[13] W. Wardlaw, H. W. Webb, *J. Chem. Soc.* **1930**, 2100.
[14] Crystal data: All crystals were orthorhombic, space group *Pbca*, $Z = 8$. **1a**: $[C_{24}H_{33}Cl_2MoOP_3]$, $a = 16.922(3)$, $b = 16.446(3)$, $c = 19.262(4)$ Å, $M = 597.3$, $V = 5360.6$ Å^3, $\varrho_{calcd} = 1.480$ g cm^{-3}, $F(000) = 2448$, $R = 0.038$ for 4265 reflections, $\mu(Mo_{K\alpha}) = 8.4$ cm^{-1}, blue crystal, $0.21 \times 0.18 \times 0.16$ mm^3. **1b**: $[C_{24}H_{33}Cl_2MoOP_3]$, $a = 11.300(2)$, $b = 17.636(3)$, $c = 28.277(6)$ Å, $M = 597.3$, $V = 5635.2$ Å^3, $\varrho_{calcd} = 1.408$ g cm^{-3}, $F(000) = 2448$, $R = 0.0539$ for 1914 reflections, $\mu(Mo_{K\alpha}) = 7.6$ cm^{-1}, blue crystal, $0.33 \times 0.32 \times 0.15$ mm^3. **2a**: $[C_{24}H_{33}Br_2MoOP_3]$, $a = 17.020(4)$, $b = 16.797(4)$, $c = 19.348(5)$ Å, $M = 686.2$, $V = 5531.3$ Å^3, $\varrho_{calcd} = 1.648$ g cm^{-3}, $F(000) = 2736$, $R = 0.0768$ for 1869 reflections, $\mu(Mo_{K\alpha}) = 34.9$ cm^{-1}, blue crystal, $0.31 \times 0.24 \times 0.18$ mm^3. **2b**: $[C_{24}H_{33}Br_2MoOP_3]$, $a = 11.439(2)$, $b = 17.660(3)$, $c = 28.283(6)$ Å, $M = 686.2$, $V = 5713.5$ Å^3, $\varrho_{calcd} = 1.595$ g cm^{-3}, $F(000) = 2736$, $R = 0.0632$ für 1953 reflections, $\mu(Mo_{K\alpha}) = 33.2$ cm^{-1}, blue crystal, $0.41 \times 0.38 \times 0.22$ mm^3. Diffractometer data with $I/\sigma(I) \geq 3.0$ were used in all determinations, collected in the θ-ranges 3–30° (**1a**) and 3–25° (**1b**, **2a**, and **2b**).
[15] K. Yoon, G. Parkin, A. L. Rheingold, *J. Am. Chem. Soc.* **1992**, *114*, 2210.
[16] Different orientations of bulky organophosphane ligands in metal complexes were shown previously to cause significant differences in bond lengths and angles but such a distinct and marked effect on the IR spectrum has not been noted before. For example *cis*-$[PtCl_2(PMePh_2)_2]$ crystallizes in two forms, differing markedly in phosphane orientation [Ho K.-C., G. M. McLaughlin, M. McPartlin, G. B. Robertson, *Acta Cryst. B38*, **1982**, 421–425]. Very accurate X-ray structure analyses showed small but significant differences in the Pt–Cl lengths related to marked differences in the angles at the Pt atom.
[17] The concepts involved in this type of isomerism in some ways parallel those invoked for isomerism in the tetrahedral cluster systems $[(Ph_3P)_2N][H_3M_4(CO)_{12}]$ (M = Ru and Os). Tautomeric anions of C_{3v} or C_2 symmetry equilibrate rapidly in solution and can only be separated in the solid state [J. W. Koepke, J. R. Johnson, S. A. R. Knox, H. D. Kaesz, *J. Am. Soc.* **1975**, *97*, 3947; B. F. G. Johnson, J. Lewis, P. R. Raithby, G. M. Sheldrick, K. Wong, M. McPartlin, *J. Chem. Soc. Dalton Trans.* **1978**, 673]. The two ruthenium isomers have been structurally characterized in the solid state, but in the case of osmium, the two different crystalline forms proved to be polymorphs each containing the same monoanion isomer of C_2 symmetry [M. McPartlin, W. H. Nelson, *J. Chem. Soc. Dalton Trans.* **1986**, 1557].
[18] A. Bashall, V. C. Gibson, T. P. Kee, M. McPartlin, O. B. Robinson, *Angew. Chem.* **1991**, *103*, 1021; *Angew. Chem. Int. Ed. Engl.* **1991**, *30*, 980; K. Wieghardt, G. Backes-Dahmann, B. Nuber, J. Weiss, *ibid.* **1985**, *97*, 773 bzw. **1985**, *24*, 777.

Determination of the H^N–H^α Coupling Constant in Large Isotopically Enriched Proteins**

By *Stephan Seip, Jochen Balbach*, and *Horst Kessler**

New multidimensional pulse techniques in NMR spectroscopy in combination with isotopic enrichment of the important heteronuclei ^{15}N and ^{13}C allow the structure determination of larger proteins up to a molecular weight of >30 kDa.[1–3] The information obtained from the coupling constants becomes more and more important in conformational analysis and molecular dynamics calculations.[4, 5] The H^N–H^α coupling constant plays an important role in the

[*] Prof. Dr. H. Kessler, Dr. S. Seip, Dipl.-Chem. J. Balbach
Organisch Chemisches Institut der Technischen Universität München
Lichtenbergstrasse 4, W-8046 Garching (FRG)

[**] This work was supported by the Deutsche Forschungsgemeinschaft and the Fonds der Chemischen Industrie. The authors thank Prof. Dr. B. Erni and K. Flükiger for the preparation of the sample of the uniformly labelled P13 domain. Stephan Seip thanks the Fonds der Chemischen Industrie for a grant.

determination of the backbone conformation, because it restricts the range of values of the angle Φ[6] (Fig. 1). It can be obtained from the splitting of the H^N or H^α signal in the one-dimensional spectra of small peptides. For larger peptides (up to medium-sized proteins), methods are available that allow the determination of the desired coupling from antiphase crosspeaks in COSY spectra.[7, 8] This requires sufficient magnetization transfer by homonuclear J-coupling. No homonuclear transfer is possible, however, for larger proteins (>30 kDa). Therefore, a method must be chosen that combines high sensitivity and large spectral dispersion of the heteronuclear couplings to reduce overlap of resonances. In addition, it is desirable to determine the coupling constant independent of the width of the signal.

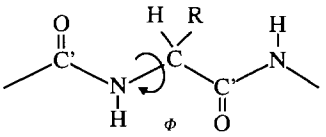

Fig. 1. Part of the polypeptide chain with definition of the angle Φ. The range of Φ can be restricted with the aid of the H^N-H^α coupling constant.

A number of pulse sequences were previously described that allow for the measurement of the H^N–H^α coupling constant in $^{15}N/^{13}C$ enriched proteins.[9–11] They all exploit the "E. COSY" pattern in the $F1/F3$ planes of a 3D spectrum for extraction of the coupling constant: The large coupling of the directly bound proton ($^1J_{C,H}$) is used to separate the two multiplet components of the C^α signal (H^α in α and in β state) in $F1$, where C^α is allowed to evolve (that means no proton decoupling is used in that dimension). This separation prevents mutual interference between the two components, which may lead to a wrong coupling constant. The $^3J_{H^N,H^\alpha}$ coupling leads to a displacement of the two multiplet components in the directly detected dimension and is therefore extracted in $F3$ (the dimension with the best digital resolution).

We propose two pulse sequences that utilize the same principle, but are optimized for sensitivity. The determination of the $^3J_{H^N,H^\alpha}$ coupling constant with high sensitivity, even for proteins that are larger than 30 kDa, can be achieved with these sequences. The pulse sequences correlate C^α, N, and H^N through large one-bond couplings ($^1J_{N,H}$ (ca. 90 Hz) and $^1J_{C,N}$ (ca. 11 Hz)).

The pulse sequences shown in Figure 2 excite the C^α nucleus (via the NH proton and nitrogen), which evolves in $F1$ as antiphase magnetization with respect to ^{15}N during t_1 without proton decoupling. After the constant-time evolution of ^{15}N in t_2, the magnetization is then transferred back to protons and detected during t_3. The "E.COSY" pattern of the $C^\alpha(F1)$–$H^N(F3)$ crosspeaks is achieved by selective excitation of the protons bound to nitrogen, thereby avoiding the mixing of the H^α spin states.[12] In practice, this is achieved by a "jump–return" sequence at the end of the pulse train, which acts as a selective 90° pulse for H^N.[13]

The application to larger proteins requires careful optimization of all pulsewidths and delays. In particular, the delays must be optimized under consideration of the relaxation behavior of the different nuclei. Equation (a) is found for 2τ, Equation (b) for $\tau_1 + \tau_2 + \delta$; the latter should be

$$A(\tau') = \sin(\pi\,{}^1J_{N,C}2\tau')\cos(\pi\,{}^2J_{N,C}2\tau')\exp(2\tau'/T_{2,N(SQ)}) \quad (a)$$

$$A(\tau_1,\tau_2,\delta) = \sin(\pi\,{}^1J_{N,C}(\tau_1+\tau_2+\delta)) \cdot\cos(\pi\,{}^2J_{N,C}(\tau_1+\tau_2+\delta))\exp((\tau_1+\tau_2+\delta)/T_{2,NH}) \quad (b)$$

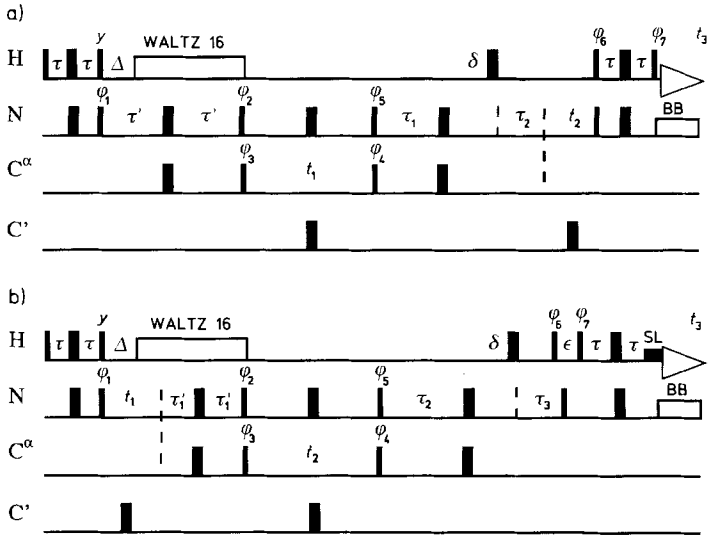

Fig. 2. Pulse sequences for the determination of the H^N–H^α coupling constants in large proteins. Both sequences correlate ^{15}N with $^{13}C^\alpha$ and H^N. The rf field strength from the X channel is reduced to 4 kHz for the selective excitation of the C^α carbon nuclei without affecting the C′ nuclei, by using the first zero crossing of the excitation function. Phase-modulated pulses [2,3] are used for selective inversion of the C′ spins, without switching of the transmitter frequency. a) Coupled HNCA (correlates H, N, and α-C) with "constant-time" evolution of nitrogen chemical shifts and jump–return pulse for selective excitation of the H^N resonances. $\tau = 2.25$, $\Delta = 4.5$, $\tau' = 13$, $\tau_1 = 10$, $\delta = 7.75$, $\tau_2 = 2.25$ ms. τ_1 is decremented with increasing t_2. The WALTZ decoupling is performed with an 8 kHz field. The water resonance is irradiated during the relaxation delay. b) Coupled HNCA with "constant-time" evolution of the nitrogen chemical shifts. The proton frequency is set on the water resonance. The jump–return pulse leads to a sinusoidal offset-dependent excitation. In this way excitation of the H^α protons is avoided (prerequisite for the "E. COSY" pattern) and the water resonance is suppressed. Sequence b) is superior to sequence a) when presaturation of the water resonance may lead to saturation transfer of H^N protons. Parameters are the same as in a) except for: $\tau_2 = 10$, $\tau_3 = 2.25$ ms, $\varepsilon = 60$ µsec (at 600 MHz). τ_1' is decremented with increasing t_1. Phase cycling for both experiments is $\phi_1 = x, x, -x, -x$, $\phi_2 = x, x, -x, -x$, $\phi_3 = x, \phi_4 = 8(x), 8(-x)$, $\phi_5 = 16(x), 16(-x)$, $\phi_6 = x, -x, \phi_7 = -x, x$, receiver $= x, -x, -x, x, -x, x, x, -x, 2(-x, x, x, -x, x, -x, -x, x), x, -x, -x, x, -x, x, x, -x$. All other pulses are applied from the x axis.

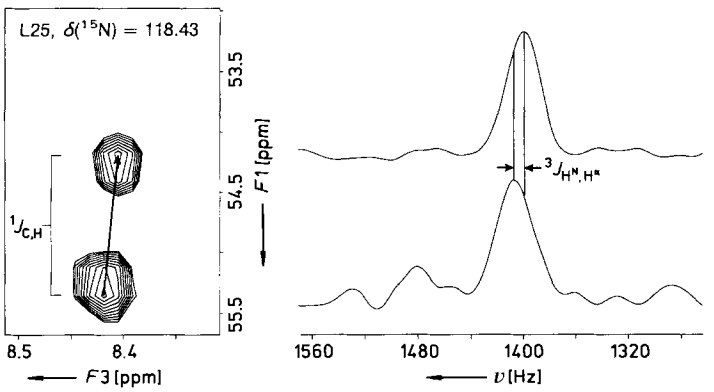

Fig. 3. Application of the pulse sequence shown in Figure 2a on a 1 mM solution of uniformly ^{15}N, ^{13}C labeled P13 domain of mannose permease of *E. coli*. The experiment was performed on a Bruker AMX 600 spectrometer equipped with a multichannel interface and a triple-resonance probe. 128 × 54 × 512 real points were taken with 32 scans each. Total measuring time was 74 hours. Multiplication with a 70° shifted $\sin^2$ function was applied in all dimensions to avoid truncation artifacts. The final spectrum consisted of 128 × 64 × 512 real points. Left: Section of the 2D plane with the crosspeak of Leu^{25} at a ^{15}N resonance frequency of $\delta = 118.43$. The "E.COSY" pattern is evident. For the determination of the coupling constants two rows which crossed the maxima of the two peaks along the $F3$ dimension were extracted from the spectrum. The displacement of the two maxima was measured after inverse Fourier transformation, zero-filling to 8192 points, and retransformation. The coupling constant is 8.0 Hz (the error is estimated at ±1 Hz).

shorter than $2t'$, because of the strong dipolar relaxation of the proton, $N_{x,y}H_z$ antiphase magnetization decays faster than ^{15}N in-phase magnetization which is present during $2\tau'$.[14] The T_2 times can be extracted from Heteronuclear Single Quantum Correlation (HSQC) and refocused HSQC spectra.[15]

The evaluation of the 3D spectrum is shown for the C^{α}–H^{N} crosspeak of Leu^{25} in the fully $^{15}N/^{13}C$ labeled P13 domain of mannose permease (31 kDa)[16] (Fig. 3). Because of the low digitization in the 3D spectrum, the coupling constant is best determined from selected rows, in analogy to the DISCO procedure.[17] The pulse sequence from Figure 2b yields an identical spectrum. Evaluation is performed in the $F2/F3$ planes.

The experiments described here allow for the determination of the homonuclear $^{3}J_{H^{N},H^{\alpha}}$ coupling constant even in very large (by NMR standards) proteins, which do not show any correlations in COSY or TOCSY spectra. Coupling constants provide structural information, which, together with distances determined from NOESY spectra, significantly enhance the quality of protein structures obtained by NMR spectroscopy.

Received: August 12, 1992 [Z 5514 IE]
German version: *Angew. Chem.* **1992**, *104*, 1656

CAS Registry number:
Mannose permease, 99442-22-5.

[1] M. Ikura, L. E. Kay, A. Bax, *Biochemistry* **1990**, *29*, 4659–4667.
[2] G. M. Clore, A. M. Gronenborn, *Prog. Nucl. Magn. Reson. Spectrosc.* **1991**, *23*, 43–92.
[3] L. E. Kay, M. Ikura, R. Tschudin, A. Bax, *J. Magn. Reson.* **1991**, *91*, 422–428.
[4] Y. Kim, J. H. Prestegard, *Proteins Struct. Funct. Genet.* **1990**, *8*, 377–382.
[5] D. M. Mierke, H. Kessler, *Biopolymers*, **1992**, *32*, 1277–1282.
[6] M. Kurz, P. Schmieder, H. Kessler, *Angew. Chem.* **1991**, *103*, 1341–1342; *Angew. Chem. Int. Ed. Engl.* **1991**, *30*, 1329–1331.
[7] H. Kessler, M. Gehrke, C. Griesinger, *Angew. Chem.* **1988**, *100*, 507–554; *Angew. Chem. Int. Ed. Engl.* **1988**, *27*, 490–536.
[8] Y. Kim, J. H. Prestegard, *J. Magn. Reson.* **1989**, *84*, 9–13.
[9] G. T. Montelione, G. Wagner, *J. Am. Chem. Soc.* **1989**, *111*, 5474–5475.
[10] G. T. Montelione, G. Wagner, *J. Magn. Reson.* **1990**, *87*, 183–188; G. Wagner, P. Schmieder, V. Thanabal, *ibid.* **1991**, *93*, 436–440.
[11] O. W. Sørensen, *J. Magn. Reson.* **1990**, *90*, 433–438.
[12] C. Griesinger, O. W. Sørensen, R. R. Ernst, *J. Magn. Reson.* **1987**, *75*, 474–492.
[13] L. Mueller, *J. Am. Chem. Soc.* **1979**, *101*, 4481–4484.
[14] S. Campbell-Burk, P. Domaille, L. Mueller, *J. Magn. Reson.* **1991**, *93*, 171–176.
[15] A. Bax, M. Ikura, L. E. Kay, D. A. Torchia, R. Tschudin, *J. Magn. Reson.* **1990**, *86*, 304–318.
[16] B. Erni, B. Zanolari, H. P. Kocher, *J. Biol. Chem.* **1987**, *262*, 5238–5247.
[17] H. Kessler, A. Müller, H. Oschkinat, *Magn. Reson. Chem.* **1985**, *23*, 844–852.

Butatrienes by Desulfurization of Cyclic Trithiocarbonates**

By *Rainer Herges** and *Christoph Hoock*

Most of the numerous butatriene syntheses[1, 2] are based on dehalogenation of 1,4-dichloro-2-butynes.[3, 4] Recently we reported a novel method for the synthesis of the parent butatriene **3** (R = H) starting from 1,4-dihalo- or 1,4-bistosyl-2-butyne **1** via 4-vinylidene-1,3-dithiolane-2-thione **2**.[5] The subsequent Corey–Winter desulfurization to butatriene **3** (R = H) was accomplished with the phosphorous base 1,3-dimethyl-2-phenyl-1,3,2-diazaphospholidine at 0 °C with yields exceeding 90%.

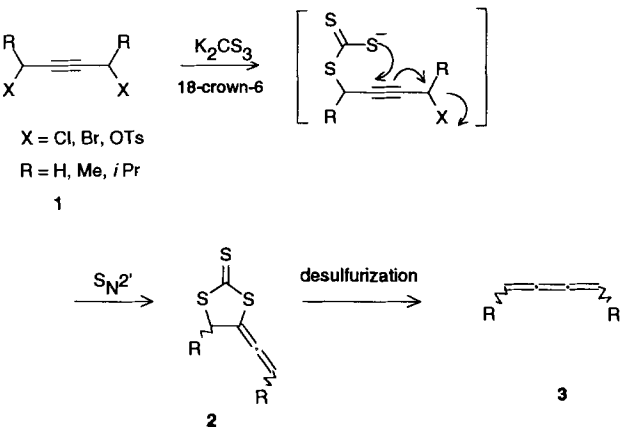

The net reaction is homologous to a fragmentation reaction that we discovered recently using computer-aided reaction design,[6] namely the reaction of 1,4-dichloro-2-butene with potassium trithiocarbonate and subsequent desulfurization to 1,3-butatriene. Compared with the conventional method of Schubert et al.[3] and Brandsma et al.[4] for the synthesis of butatriene, our method gives higher yields and a very pure product. For the extension to alkyl-substituted butatrienes, one could use the easily accessible bistosylates **1** (X = OTs) instead of the 1,4-dihalogen-2-butynes **1** (X = Br, Cl, R = alkyl), which are difficult to prepare. Unfortunately, the reaction is restricted to the parent butatriene when the conventional phosphorous bases for Corey–Winter reactions are used. All attempts to desulfurize alkyl-substituted dithiolanes **2** with the phosphorous bases trimethyl phosphite, triphenyl phosphite, tris(dimethylamino)phosphane, and diazaphospholidine to the corresponding cumulenes failed. After testing a number of transition metals and transition metal complexes[7] we found Raney nickel[8] (deactivated with ketones) to be an excellent desulfurization agent.

Alkylated 1,4-butynediols **1** (X = OH) were easily prepared from acetylene and aldehydes or ketones.[9] The corresponding bistosylates **1** (X = OTs) were then synthesized in almost quantitative yields according to a slightly modified method of Brandsma[10] with tosyl chloride. Reaction with anhydrous potassium trithiocarbonate was accomplished in dichloromethane with 10 mol% crown ether and using ultrasound to give excellent yields of the dithiolanes **2** (Table 1).[5] Dithiolanes **2** are yellow, light- and air-sensitive oils that can be stored in solution under nitrogen at −30 °C for several weeks. Characteristic spectroscopic features of **2** are the low-field NMR shift of the trithiocarbonate carbon atom (δ = 223–224),[11] the large C–H coupling constant of the terminal allene carbon atom (165–171 Hz), the strong IR stretching vibration of the C=S bond at 1070–1060 cm^{-1},[12] and the strong UV absorption at 330–338 nm (ε_{max} = 4000–15000 $L\,mol^{-1}\,cm^{-1}$).[13] According to the ^{13}C and ^{1}H NMR spectra, the two stereoisomeres *syn*- and *anti*-**2** (R = Me, *i*Pr) are formed in a 1:1 ratio (Fig. 1).

For subsequent desulfurization the crude product can be used without purification. A proper choice of the solvent was crucial for the desulfurization. Dimethylformamide and other higher boiling formamides are most suitable. The sensitive

[*] Dr. R. Herges, Dipl.-Chem. C. Hoock
Institut für Organische Chemie der Universität Erlangen-Nürnberg
Henkestrasse 42, D-W-8520 Erlangen (FRG)

[**] This research was supported by the Deutsche Forschungsgemeinschaft.

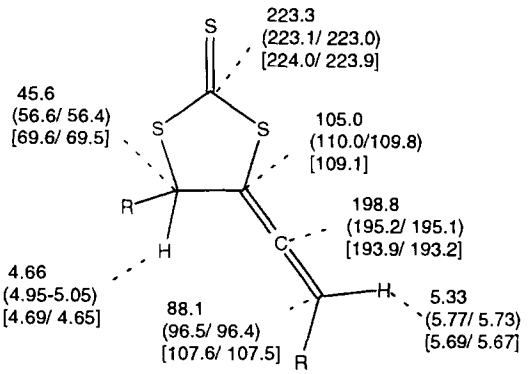

Fig. 1. The most important ^1H and ^{13}C NMR data (δ, $CDCl_3$) of dithiolanes **2** (data for R = H, R = Me (in parentheses), and R = *i*Pr (in brackets)). The spectra of the *syn* and *anti* isomers of the substituted dithiolanes formed in a 1:1 ratio are distinguishable and the chemical shifts are given separately.

butatrienes were removed from the reaction mixture under reduced pressure as they formed and were condensed in cold traps. Deactivation of the Raney nickel with ketones (acetone, acetophenone, or benzophenone) is recommended in order to avoid formation of alkanes (which are formed under not rigorously anhydrous conditions). The yields of butatrienes **3** range from 20 (R = H) to 95% (R = *i*Pr) (Table 1). The products are unequivocally characterized as butatrienes not only by comparison to the reported ^1H and ^{13}C NMR, and IR spectra, but also by the extraordinary large C–H coupling constants of the terminal cumulene carbon atoms (166.6–171.1 Hz).[14]

Table 1. Yields [%] for the preparation of dithiolanes **2** from bistosylates **1** and for the desulfurization of **2** to provide **3**.

R	**2** [a]	**3** [b]	Ref. [c]
H	71	20	[3, 4, 14]
Me	72	70	[17]
*i*Pr	82	95	[18]

[a] Yields after chromatographic purification. [b] Yields determined by ^1H NMR spectroscopy in $CDCl_3$ at −40 °C, after condensation and addition of a standard. [c] References giving the spectroscopic data of the butatrienes.

In order to investigate the stereochemistry of the S_N2' addition and the desulfurization to the butatrienes **3**, we synthesized the *meso* isomer of 2,7-dimethyl-3,6-ditosyl-4-octyne **1** (X = OTs, R = *i*Pr)[15] and treated it with potassium trithiocarbonate. Two stereoisomeric dithiolanes **2** were formed in a 2:1 ratio (Scheme 1).

NOE experiments suggest that the main product is the *syn* compound which arises by an internal *anti* S_N2' reaction.[16]

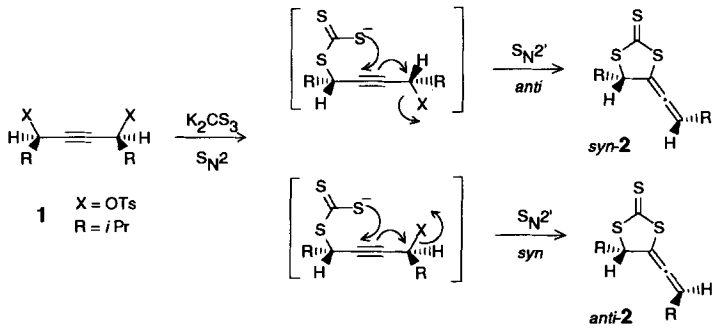

Scheme 1. Stereochemistry of the S_N2' reaction.

Since the two isomers could not be separated in preparative scale, the mixture was used for desulfurization with Raney nickel and a 1:1 mixture of *E*- and *Z*-substituted butatriene **3** (R = *i*Pr) was obtained. In contrast to the Corey–Winter reaction, the fragmentation is apparently not stereoselective or the cumulenes isomerize immediately after formation by coordination to nickel.

Experimental Procedure

1 (X = OTs, R = H, Me, *i*Pr): To a 10% solution of 19.1 g (0.1 mol) tosyl chloride in diethyl ether was added a concentrated solution of 0.04 mol diol **1** (X = OH) in ether or THF, and the reaction mixture was cooled to −15 °C. Thereafter 20 g (0.36 mol) finely powdered potassium hydroxide was added in small portions (1 g per min) to the vigorously stirred solution; the temperature was kept below −5 °C. To complete the reaction, the solution was stirred for another 1–2 h at 0–5 °C and then poured into ice water. The aqueous phase was extracted several times with ether or dichloromethane. After the collected organic extracts were dried over magnesium sulfate, the solvent was removed in vacuo and the crude product recrystallized. Yields were 80–90% after crystallization. The colorless crystals can be stored at −30 °C for several months without decomposition.

2: (R = H, Me, *i*Pr): To a suspension of 2.0 g (11 mmol) anhydrous potassium trithiocarbonate in 100 mL anhydrous dichloromethane were added 10 mmol bistosylate **1** (X = OTs) and 10 mg (0.04 mmol) 18-crown-6 under a nitrogen atmosphere. After treatment of the suspension with ultrasound at 20 °C for 12 h most of the red suspended potassium trithiocarbonate had reacted. The light-yellow precipitate was removed by filtration, the filtrate reduced in vacuo to 20 mL, and the yellow solution chromatographed over silica gel eluting with tetrachloromethane (to remove small amounts of polymers and crown ether). The yellow oily products were pure according to thin-layer chromatography (TLC), and ^1H and ^{13}C NMR spectroscopy; however, they polymerized rapidly when exposed to oxygen, moisture, or light. Solutions of 10% in dichloromethane are stable at −30 °C for several weeks. For desulfurization the crude product can be used without chromatographic purification.

3: (R = H, Me, *i*Pr): 10 g Raney nickel (Fluka, suspended in water) was dried in vacuo at 10^{-2} Torr and deactivated by stirring for 20 min with 30 mL acetophenone (in the case of R = *i*Pr deactivation with a solution of the higher boiling benzophenone in ether is recommended). After filtration from acetophenone under nitrogen, the Raney nickel was suspended in 40 mL anhydrous dimethylformamide (*N*-formylmorpholine, in the case of R = *i*Pr). The solution was heated to 60–70 °C, and a solution of 5 mmol dithiolane **2** in 10 mL dimethylformamide (or *N*-formyl-morpholine) was added dropwise. The product formed was continuously removed from the reaction mixture at 20 Torr (10^{-2} Torr for R = *i*Pr) and condensed in two cold traps at −198 °C. Small amounts of carbon disulfide were removed by condensation in vacuo. The stability of the butatrienes to oxygen and polymerization decreases in the series R = *i*Pr, Me, H. Whereas butatriene polymerizes vigorously even at 0 °C, the diisopropyl substituted triene can be destilled at 10 Torr under nitrogen.

Received: August 5, 1992 [Z 5503 IE]
German version: *Angew. Chem.* **1992**, *104*, 1652

[1] H. Hopf in *The Chemistry of Ketenes, Allenes and Related Compounds, Part 2* (Ed.: S. Patai), Wiley, New York, **1980**, p. 863–901.
[2] M. Murray, *Methoden Org. Chem. (Houben Weyl) 4th Ed.* **1952**–, Vol. 5/2a (*Alkine, Di- und Polyine, Allene, Kumulene*), Thieme, Stuttgart, **1977**, p. 913–1076.
[3] W. M. Schubert, T. H. Liddicoet, W. A. Lanka, *J. Am. Chem. Soc.* **1954**, *76*, 1929.
[4] P. P. Montijn, L. Brandsma, J. F. Arens, *Recl. Trav. Chim. Pays-Bas* **1967**, *86*, 129.
[5] R. Herges, C. Hoock, *Synthesis* **1991**, 1151.
[6] R. Herges, C. Hoock, *Science* **1992**, *255*, 711.
[7] See, for example a) J. Daub, V. Trautz, U. Ehrhardt, *Tetrahedron Lett.* **1972**, 4435; b) J. Daub, G. Endress, U. Erhardt, K. H. Jogun, J. Kappler, A. Laumer, R. Pfiz, J. J. Stezowski, *Chem. Ber.* **1982**, *115*, 1787; c) M. F. Semmelhack, R. D. Stauffer, *Tetrahedron Lett.* **1973**, 2667; d) S. Sakai, N. Wada, Y. Todo, T. Shibata, T. Fujinami, *Nippon Kagaku Kaishi*, **1985**, 282.
[8] W. V. Ruyle, T. Y. Shen, A. A. Patchett, *J. Org. Chem.* **1965**, *30*, 4353.
[9] W. Ziegenbein in *The Chemistry of Acetylenes* (Ed.: H. G. Viehe), Marcel Dekker, **1969**, p. 169.
[10] L. Brandsma, *Preparative Acetylenic Chemistry*, 2nd ed. Elsevier, Amsterdam, **1988**, p. 256.

[11] C. Copeland, R. J. Conway, J. J. Patroni, R. V. Stick, *Aust. J. Chem.* **1981**, *34*, 555.
[12] A. Lüttringhaus, J. Grohmann, *Z. Naturforsch. B.* **1955**, *10*, 365.
[13] D. Braun, M. Kiessel, *Monatsh. d. Chemie* **1965**, *96*, 631.
[14] N. J. Koole, M. J. A. de Bie, P. E. Hansen, *Org. Magn. Reson.* **1984**, *22*, 146.
[15] a) W. Krestinski, W. Marjin, *Chem. Ber.* **1927**, *60*, 867; b) J. Huang, V. Goedken, H. M. Walborsky, *J. Org. Chem.* **1988**, *53*, 4128.
[16] This is in accord with theoretical investigations of Epiotis et al. and experimental observations of Stork et al., according to which the *anti* elimination is preferred if the nucleophile and the leaving group are negatively charged, probably due to the coulombic repulsion. a) R. L. Yates, N. D. Epiotis, F. Bernardi, *J. Am. Chem. Soc.* **1975**, *97*, 6615; b) G. Stork, A. F. Kreft, *J. Am. Chem. Soc.* **1977**, *99*, 3850; *ibid.* 3852.
[17] W. R. Roth, H.-D. Exner, *Chem. Ber.* **1976**, *109*, 1158.
[18] H. Kleijn, M. Tigchellaar, R. J. Bullee, C. J. Elsevier, J. Meijer, P. Vermeer, *J. Organomet. Chem.* **1982**, *240*, 329.

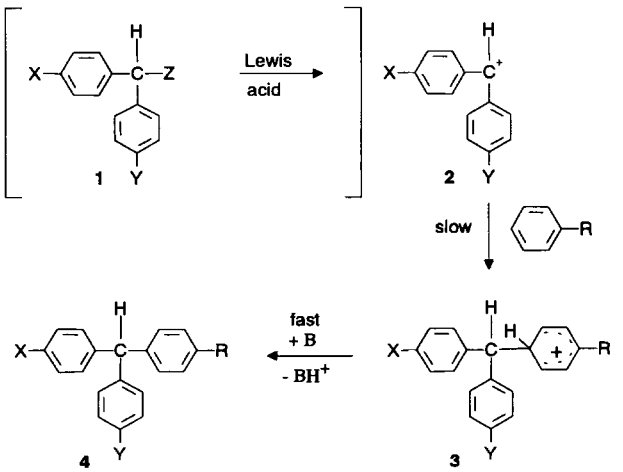

Scheme 1. For X, Y, Z see Table 1.

Rate Constants for the Attack of Carbenium Ions at Arenes—A Link between the Chemistry of Aliphatic and Aromatic π Systems**

By *Herbert Mayr,* Jörg Bartl,* and *Gisela Hagen*

Dedicated to Professor Klaus Hafner on the occasion of his 65th birthday

The mechanism of the Friedel–Crafts alkylation is one of the most thoroughly investigated in organic chemistry,[1] and countless investigations have been concerned with the determinations of relative reactivities of differently substituted arenes.[2] Amazingly, absolute rate constants for the attack of carbenium ions at arenes, the key step of these reactions, have hardly been available. Some investigations on the attack of metal-coordinated carbenium ions at highly activated arenes[3] and studies of fluorenyl cations generated by laser flash photolysis published[4a] recently in this journal are, to our knowledge, the only sources of such data.[4b]

We now report that the method, which we used for the determination of the nucleophilicity of aliphatic π systems,[5] can also be applied to arenes. As described previously, diarylhalomethanes **1** are quantitatively ionized by Lewis acids to give colored solutions of diarylcarbenium ions **2**; addition of nucleophiles causes bleaching, which can be monitored photometrically (Scheme 1). The methoxy-substituted arenes are so reactive that the kinetics of their reactions with donor-substituted benzhydryl cations **2** (X = OCH_3, Y = H, OCH_3) can be studied without difficulty. Since alkoxy-substituted arenes form complexes with those Lewis acids (BCl_3, $TiCl_4$, or $GaCl_3$) usually employed for the ionization **1** → **2**, we used trimethylsilyl triflate (Me_3SiOTf) for the ionization of the diarylchloro- and diarylfluoromethanes in these cases. The reactions of the arenes with the benzhydryl cations thus generated follow a second-order rate law (first order with respect to Ar_2CH^+, first order with respect to arene). The reaction rate is independent of the concentration of Me_3SiOTf (excess), and the coordination of Me_3SiOTf with the oxygen of the aryl ether can thus be excluded.

The strong Lewis acid $GaCl_3$ was used for the generation of the highly electrophilic bis(*p*-chlorophenyl)carbenium ion, which was then allowed to react with benzene and its methyl derivatives. Complex rate laws were observed for ion concentrations $\leq 10^{-4}$ mol L^{-1}, which may indicate that the alkylation step is partially reversible. In accord with this hypothesis, we found that addition of benzyltriethylammonium tetrachlorogallate (10^{-3}–10^{-2} mol L^{-1}) accelerates the reaction and gives rise to second-order kinetics, since at high concentrations of $GaCl_4^-$[6] (which acts as a base) the intermediate benzenium ion is rapidly deprotonated. The irreversibility of the C–C bond-forming step under these conditions is supported by the absence of a primary kinetic isotope effect for the reaction of $(p\text{-}ClC_6H_4)_2CH^+GaCl_4^-$ with *p*-deuteriotoluene ($k_H/k_D = 1.01$). As shown in several previous investigations,[5, 7] the nature of the counterion does not affect the electrophilicity of the diarylcarbenium ions, and the rate constants given in Table 1 can directly be compared with each other.

From the partial rate constants of the reactions with benzene and toluene, the large value of $\rho = -13$ is derived for the reaction constant, which indicates a transition state with pronounced benzenium character. In accord, the slopes of the correlations between nucleophilic reactivity and basicity of the arenes[8] are 0.94–1.05 (Fig. 1), which are reduced to 0.63–0.80 when one accounts for the different temperatures to which equilibrium and rate constants refer. As the correlation lines are almost parallel, one can now estimate rate

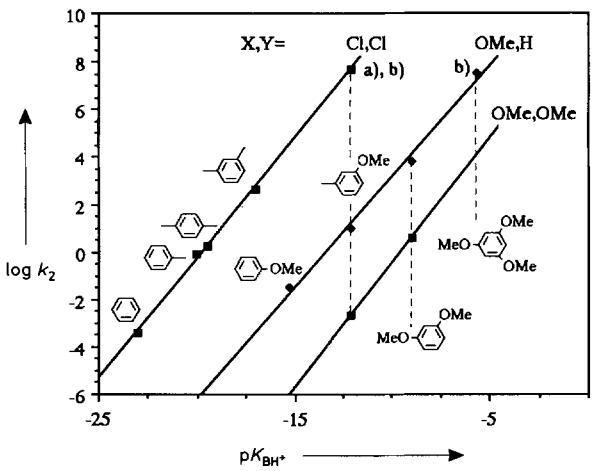

Fig. 1. Relationship between the basicity of arenes and their reactivity to diarylcarbenium ions (CH_2Cl_2, −70 °C). a) Since the value of pK_{BH^+} is not available for this compound the value of the abscissa was set. b) Ref. [14].

[*] Prof. Dr. H. Mayr, Dr. J. Bartl, Dr. G. Hagen
Institut für Organische Chemie der Technischen Hochschule Darmstadt
Petersenstrasse 22, D-W-6100 Darmstadt (FRG)

[**] This work was supported by the Deutsche Forschungsgemeinschaft and the Fonds der Chemischen Industrie.

Table 1. Rate constants (CH_2Cl_2, $-70\,^{\circ}C$) and activation parameters for the reactions of *para*-substituted benzhydryl salts $[(XC_6H_4)(YC_6H_4)CH^+Z^-]$ with arenes.

Arene	X, Y	Z^-	k_2 ($-70\,^{\circ}C$) [$L\,mol^{-1}s^{-1}$]	$\Delta H^{\neq}$ [$kJ\,mol^{-1}$]	$\Delta S^{\neq}$ [$J\,mol^{-1}K^{-1}$]
	Cl, Cl	$GaCl_4^-$	$\approx 4\times10^{-4}$	≈ 34.7	≈ -136
	Cl, Cl	$GaCl_4^-$	7.8×10^{-1}	24.9	-121
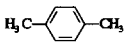	Cl, Cl	$GaCl_4^-$	1.8		
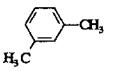	Cl, Cl	$GaCl_4^-$	4.2×10^{2}	15.5	-115
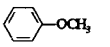	OMe, H	OTf^-	3.1×10^{-2}	31.2	-117
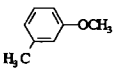	Cl, Cl	Cl^-	$\approx 5\times10^{7}$ [a]		
	OMe, H	OTf^-	1.0×10^{1}	24.8	-100
	OMe, OMe	OTf^-	2.2×10^{-3}	31.3	-138
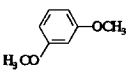	OMe, H	OTf^-	6.4×10^{3}		
	OMe, OMe	OTf^-	3.9	21.9	-123
	OMe, OMe	OTf^-	18 (CH_3CN) [b]	20.5	-117
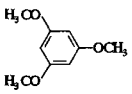	OMe, H	Cl^-	3.3×10^{7} [a]		

[a] These values were determined with carbenium ions generated by laser flash photolysis in acetonitrile at 20 °C [14]. In view of the reactivity range that covers many orders of magnitude these rate constants can be compared directly with the others in this column, since the solvent effect in these reactions is generally small (cf. penultimate entry in Table 1 and ref. [5a]). A temperature correction is not necessary because $\Delta H^{\neq} = 0$. [b] Extrapolated from the activation data.

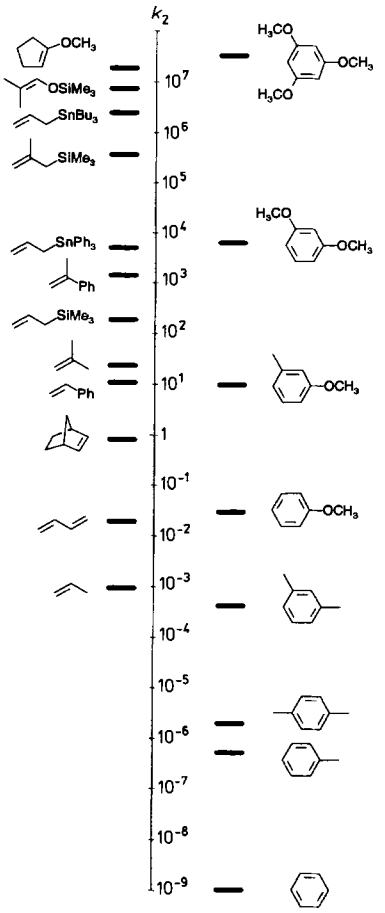

Fig. 2. Comparison of the nucleophilicity of alkenes [7c,d], allyl main group element compounds [7b], and arenes toward the *p*-methoxy substituted diphenylcarbenium ion ($-70\,^{\circ}C$).

constants for the reactions of the *p*-methoxy substituted benzhydryl cation with benzene, toluene, and the two xylenes. Since this carbenium ion has also been employed to characterize the nucleophilicity of numerous aliphatic π systems,[7] one can now directly compare the nucleophilic reactivities of aliphatic and aromatic π systems. Figure 2 shows, for example, that *m*-xylene and propene, *m*-methylanisole and styrene, and 1,3,5-trimethoxybenzene and various enol ethers show similar reactivities toward carbon electrophiles. A competition experiment corroborates the relationship between aliphatic and aromatic reactivity derived from the absolute rate constants: according to the product analysis 1,3-dimethoxybenzene is 16 times more reactive than allyltrimethylsilane towards $(p\text{-}MeOC_6H_4)_2CHCl/Me_3SiOTf$; absolute rate constants yield a rate ratio of 14.

In summary, it is now possible to recognize relation ships between aliphatic and aromatic reactivity and plan new reactions in one of these areas on the basis of known reactions in the other. The experience of the preparative chemist that methylene iminium ions react with α-methylstyrene but not with styrene or dialkylethylenes, and with 1,3,5-trimethoxybenzene and 1,3-dimethoxybenzene but not with anisole,[9] is in accordance with the nucleophilicity order given in Figure 2. Interestingly, Figure 2 can also be used to rationalize reactions with other types of electrophiles. From the chemistry of arenes it is known, for example, that anisole reacts with the 2,4-dinitrobenzenediazonium ion but not with the 4-nitrobenzenediazonium ion.[10] Accordingly, reactions of the 2,4-dinitrobenzenediazonium ion with various 1,1-dialkylethylenes,[11] styrene,[11] and allylsilanes[12] have been described, while we have not been able to achieve reactions with monoalkylated ethylenes.

For the reactions of carbenium ions with aliphatic π systems we had observed that in several cases the relative nucleophilicities of the π systems depend somewhat on the nature of the reference electrophile.[7a, 13] We intend to account for this fact by introducing an additional parameter in order to increase the predictive power of the nucleophilicity scale of Figure 2.

Received: July 10, 1992 [Z 5458 IE]
German version: *Angew. Chem.* **1992**, *104*, 1689

CAS Registry numbers:
bis(4-chlorophenyl)methylium tetrachlorogallate, 142581-67-7; (4-methoxyphenyl)(phenyl)methylium triflate, 135375-89-2; bis(4-chlorophenyl)methylium chloride, 128083-81-8; bis(4-methoxyphenyl)methylium triflate, 134310-96-6; (4-methoxyphenyl)(phenyl)methylium chloride, 128083-72-7; benzene, 71-43-2; toluene, 108-88-3; 1,4-dimethylbenzene, 106-42-3; 1,3-dimethylbenzene, 9225-20-1; anisole, 100-66-3; 1-methoxy-3-methylbenzene, 100-84-5; 1,3-dimethoxybenzene, 151-10-0; 1,3,5-trimethoxybenzene, 621-23-8.

[1] a) *Friedel-Crafts and Related Reactions, Vol. 1–4* (Ed.: G. A. Olah), Interscience, New York, **1963–1965**; b) G. A. Olah, *Friedel-Crafts Chemistry*, Wiley, New York, **1973**; c) R. M. Roberts, A. A. Khalaf, *Friedel-Crafts Alkylation Chemistry*, Dekker, New York, **1984**; d) M. Zander, C. Grundmann in *Methoden: Org. Chem. (Houben-Weyl) 4th Ed.*, **1981**, Vol. V/2b, p. 154; e) G. A. Olah, *Acc. Chem. Res.* **1971**, *4*, 240; f) R. Taylor, *Electrophilic Aromatic Substitution*, Wiley, New York, **1990**; g) T. H. Lowry, K. S. Richardson, *Mechanismen und Theorie in der Organischen Chemie*, VCH, Weinheim, **1980**, p. 387; h) L. M. Stock, H. C. Brown, *Adv. Phys. Org. Chem.* **1963**, *1*, 35; i) G. A. Olah, R. Malhotra, S. C. Narang, *Nitration: Methods and Mechanism*, VCH, Weinheim, **1989**; j) E. Berliner, *Prog. Phys. Org. Chem.* **1964**, *2*, 253; k) J. March, *Advanced Organic Chemistry*, 3rd ed., Wiley, New York, **1985**.

[2] a) In [1b], Chapter 5, 6; b) in [1f], Chapter 6.

[3] a) G. R. John, L. A. P. Kane-Maguire, *J. Chem. Soc. Dalton Trans.* **1979**, 1196; b) T. I. Odiaka, L. A. P. Kane-Maguire, *Inorg. Chem. Acta* **1979**, *37*, 85; c) J. C. Calabrese, S. D. Ittel, H. S. Choi, S. G. Davis, D. A. Sweigart, *Organometallics* **1983**, *2*, 226; d) G. R. John, L. A. P. Kane-Maguire, T. I. Odiaka, C. Eaborn, *J. Chem. Soc. Dalton Trans.* **1983**, 1721; e) L. A. P. Kane-Maguire, E. D. Honig, D. A. Sweigart, *Chem. Rev.* **1984**, *84*, 525; f) T. G. Bonner, K. A. Holder, P. Powell, *J. Organomet. Chem.* **1974**, *77*, C37; g) T. G. Bonner, K. A. Holder, P. Powell, E. Styles, *ibid.* **1977**, *131*, 105.

[4] a) F. Cozens, J. Li, R. A. McClelland, S. Steenken, *Angew. Chem.* **1992**, *104*, 753; *Angew. Chem. Int. Ed. Engl.* **1992**, *31*, 743; b) see also F. P. DeHaan, W. H. Chan, J. Chang, T. B. Cheng, D. A. Chiriboga, M. M. Irving, C. R. Kaufmann, G. Y. Kim, A. Kumar, J. Na, T. T. Nguyen, D. T. Nguyen, B. R. Patel, N. P. Sarin, J. H. Tidwell, *J. Am. Chem. Soc.* **1990**, *112*, 356, and references therein.

[5] a) H. Mayr, R. Schneider, C. Schade, J. Bartl, R. Bederke, *J. Am. Chem. Soc.* **1990**, *112*, 4446; b) R. Schneider, U. Grabis, H. Mayr, *Angew. Chem.* **1986**, *98*, 94; *Angew. Chem. Int. Ed. Engl.* **1986**, *25*, 89.

[6] The formula $GaCl_4^-$ is chosen for simplicity and is not meant to indicate that only mononuclear counterions are formed.

[7] a) Review: H. Mayr, *Angew. Chem.* **1990**, *102*, 1415; *Angew. Chem. Int. Ed. Engl.* **1990**, *29*, 1371; b) G. Hagen, H. Mayr, *J. Am. Chem. Soc.* **1991**, *113*, 4954; c) J. Bartl, S. Steenken, H. Mayr, *ibid.* **1991**, *113*, 7710; d) H. Mayr, R. Schneider, B. Irrgang, C. Schade, *ibid.* **1990**, *112*, 4454.

[8] a) R. Stewart, *The Proton: Applications to Organic Chemistry*, Academic Press, Orlando, **1985**; b) O. A. Reutov, I. P. Beletskaya, K. P. Butin, *CH-Acids*, Pergamon, Oxford, **1978**; c) D. M. Brouwer, E. L. Mackor, C. MacLean in *Carbonium-Ions, Vol. 2* (Eds.: G. A. Olah, P. von R. Schleyer), Wiley, New York, **1970**, p. 837.

[9] H. Böhme, H. G. Viehe, *Iminium Salts in Organic Chemistry, Vol. 9/1*, Wiley, New York, **1979**, p. 190, 202.

[10] H. K. Schündehütte, *Methoden Org. Chem. (Houben-Weyl) 4th Ed.*, **1965**, Vol. X/3, p. 232.

[11] a) H. Marxmeier, E. Pfeil, *Chem. Ber.* **1964**, *97*, 815; b) H. Marxmeier, E. Pfeil, *Liebigs Ann. Chem.* **1964**, *678*, 28.

[12] H. Mayr, K. Grimm, *J. Org. Chem.* **1992**, *57*, 1057.

[13] H. Mayr, R. Schneider, U. Grabis, *J. Am. Chem. Soc.* **1990**, *112*, 4460.

[14] J. Bartl, S. Steenken, H. Mayr, unpublished results.

Spectroscopic Characterization of Two Types of Tetraarylporphyrin Cation Radicals**

By *Zeev Gross** and *Claudia Barzilay*

Characterization of metalloporphyrins with metal ions in high oxidation states remains an intriguing challenge in the context of understanding and mimicking the chemistry of heme-dependent enzymes.[1, 2] These include catalases (CAT), peroxidases [especially horseradish (HRP) and cytochrome c (CCP) peroxidase], chloroperoxidases, and cytochrome P-450 enzymes, for which the intermediates obtained from two- and one-electron oxidations (starting from Fe^{III}) are referred to as compounds I and II, respectively. A considerable number of spectroscopic methods, including UV/VIS, ESR, NMR, and resonance Raman (RR) spectroscopy,[3] was utilized in the characterization of the intermediate isolated from the two-electron oxidation of (TMP)FeCl (**2**, M = Fe instead of Zn; TMP = tetramesitylporphyrin).[4] As a result of these and related studies it is presently accepted that upon oxidation of (TMP)FeCl only one electron is removed from the metal ion, forming an oxoiron(IV) center, while the second electron is removed from the porphyrin ligand, which is thus oxidized to the cation radical. The diverse types of interactions between the porphyrin radical and the metallic center are emphasized by close inspection of supposedly similar compounds. Whereas in the oxidation product of (TMP)FeCl the two paramagnetic centers strongly interact ferromagnetically,[4, 5] in the corresponding products of (TDCPP)FeCl (**3**, M = Fe instead of Zn; TDCPP = tetrakis(2,6-dichlorophenyl)porphyrin) and HRP the interaction is very weak and antiferromagnetic;[5, 6] for CCP an amino acid and not the porphyrin is oxidized;[7] in chloroperoxidase the interaction is antiferromagnetic and moderately strong,[8] and finally in cytochrome P-450, compound I remains elusive. Another point of concern is that in porphyrin cation radicals the unpaired electron can reside in one of two neighboring orbitals, A_{2u} and A_{1u} (in D_{4h} symmetry). As the spin distributions in these orbitals differ considerably, the interaction of the porphyrin radical with the metal center will vary according to symmetry considerations.[9] An early example emphasizing the importance of these possibilities and the relationship between oxidized enzymes and their synthetic analogues is the similarity of the electronic spectra of the cation radicals of zinc and magnesium complexes of tetraphenylporphyrin (TPP) and octaethylporphyrin (OEP) to those of compounds I of HRP and CAT, respectively, and their relation to the two different possible magnetic orbitals, A_{2u} and A_{1u}, respectively.[10]

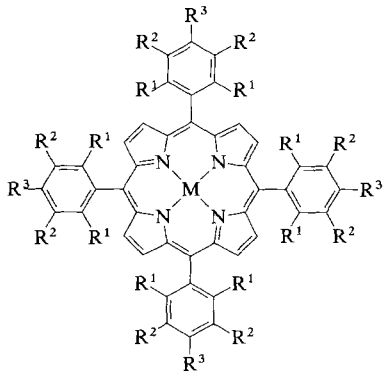

1, M = Zn, $R^1 = R^2 = R^3 = H$
2, M = Zn, $R^1 = R^3 = CH_3$, $R^2 = H$
3, M = Zn, $R^1 = Cl$, $R^2 = R^3 = H$
4, M = Mg, $R^1 = R^2 = R^3 = F$
5, $[1]^{\cdot+}$ $SbCl_6^-$
6, $[2]^{\cdot+}$ $SbCl_6^-$
7, $[3]^{\cdot+}$ $SbCl_6^-$
8, $[4]^{\cdot+}$ $SbCl_6^-$

Since OEP and TPP have very different structures, great efforts were expended in trying to obtain the two types of radicals from each of the porphyrin classes. For OEP this was accomplished by several groups,[10, 11] but to our knowledge in all tetraarylporphyrin radicals studied to date the unpaired electron was considered to be located in an A_{2u} orbital. We present here evidence, which indicates that in oxidized phenyl-substituted tetraphenylporphyrins, the magnetic orbital can be an A_{2u} as well as an A_{1u} orbital, depending on the properties of the substituents.

The cation radicals **5**–**8** were quantitatively prepared by oxidation of ZnTPP **1**, ZnTMP **2**, ZnTDCPP **3**, and MgTpFPP **4** with [PH(SbCl$_6$)] (PH = phenoxathiin radical cation) and isolated as black solids.[12] In the solid state the compounds were found to be stable for days, and no fast decomposition was observed in degassed $CHCl_3$ or CH_2Cl_2

[*] Dr. Z. Gross, C. Barzilay
Department of Chemistry
Technion, Israel Institute of Technology
Technion City, Haifa 32000 (Israel)

[**] This research was supported by the Koebner-Klein Edowment Fund, the New York Metropolitan Research Fund, the Pollard Biochemical Engineering Research Fund, and the Fund for Promotion of Research at the Technion.

solutions; where they appeared green as expected for porphyrin cation radicals. Addition of nBu$_4$NI regenerated the unoxidized precursors, thus eliminating the possibility of irreversible oxidation to isoporphyrins. All spectroscopic data of our ZnTPP oxidation product **5** was identical to that of ZnTPP$^{\cdot+}$ClO$_4^-$ reported previously.[13]

The four complexes **5**–**8** were characterized by ESR, UV/VIS, and IR spectroscopy.[10, 14, 15, 16] The ESR spectra (Fig. 1) clearly separate the four compounds into two groups; the spectra of ZnTPP$^{\cdot+}$ **5** and ZnTMP$^{\cdot+}$ **6** are almost identical, but very different from those of ZnTDCPP$^{\cdot+}$ **7** and MgTpFPP$^{\cdot+}$ **8**, whose spectra also resemble each other. In particular, for A_{2u} cation radicals an ESR spectrum with nine lines is expected due to high unpaired spin densities at the four equivalent nitrogen atoms and at the *meso* carbon atoms. These lines may be broad because of the interactions of the

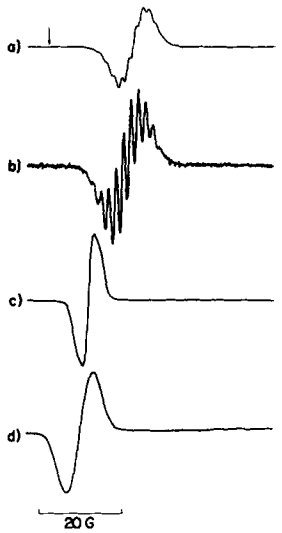

Fig. 1. ESR spectra at room temperature for a) **5**, b) **6**, c) **7**, d) **8**. Arrow indicates the position of $g = 2.0015$ (Mn^{2+} in MgO). The g values of **5**, **6**, **7**, and **8** are 2.0050, 2.0068, 2.0117, and 2.0126, respectively.

C spin centers with the phenyl protons. As shown in traces a and b of Figure 1, compounds **5** and **6** satisfy this expectation and thus provide definite evidence for the identity of the magnetic orbital as A_{2u} (the spectral narrowing of **6** relative to **5** is qualitatively similar to that observed in the spectra recorded for *ortho*- and *para*-deuterated ZnTPP$^{\cdot+}$ClO$_4^-$).[17] The broad and quite characterless VIS spectrum of **6** (solid line in Fig. 2) is also in accord with previous reports of A_{2u} cation radicals.[10]

On the other hand, the intense red shifts in the VIS spectra of **7** (broken line in Fig. 2) and **8** (not shown but very similar to that of **7**) were previously observed only for OEP$^{\cdot+}$ and similar compounds with an A_{1u} magnetic orbital.[15] Since for such radicals, theory and experiment suggest unpaired spin densities only at the α (mostly) and β carbon atoms of the pyrrole units[18] and not at the nitrogen atoms or at the *meso* carbon atoms, the ESR spectra of **7** and **8** (c and d in Fig. 1) should be very different from those of **5** and **6**. The spectra of **7** and **8** do not necessarily have to resemble that of OEP$^{\cdot+}$ because of the absence of *meso* protons in the former and the absence of pyrrole protons in the latter. Rather, the broad singlets observed in the ESR spectra of **7** and **8** indicate that most of the spin density is located at the α carbon atoms of the pyrrole units with some unresolved splitting from the β hydrogen atoms of the pyrrole units contributing to the linewidths. Furthermore, the remarkable similarity

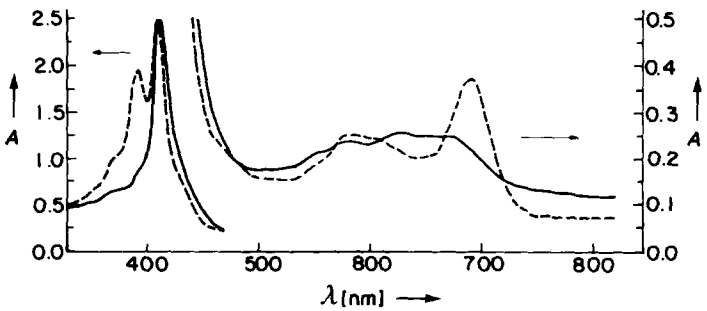

Fig. 2. Electronic absorption spectra of **6** (solid line) and **7** (broken line). The spectra of **5** and **8** are very similar to that of **6** and **7**, respectively. A = absorbance.

between the spectra of **7** and **8** is very strong evidence for essentially zero, unpaired spin density at the *meso* positions, since otherwise the fluorine substituents in **8** would be expected to cause very large splitting and thus affect the spectrum dramatically.

The examination of the IR spectra of porphyrin cation radicals showed that new bands at 1270–1290 cm^{-1} are diagnostic for TPP A_{2u} cation radicals, whereas for OEP A_{1u} cation radicals these bands appear at 1520–1570 cm^{-1}.[15] Attempts to identify these absorptions for compounds **6** and **8** were hampered by the strong bands of their unoxidized precursors **2** and **4** in that spectral region, thus only the spectra of **7** and its precursor **3** are shown in Figure 3. As can be judged by comparison of the spectra of **3** and **7**, the main new band appears at 1283 cm^{-1} together with two very weak bands at 1467 and 1580 cm^{-1}. These features are thus remarkably similar to those in the spectrum of **5** and not to those of OEP$^{\cdot+}$ despite the assignment of **7** as a A_{1u} cation radical. Thus, we might conclude that the position of the IR bands of porphyrin cation radicals is not sensitive to electronic configuration but rather to structural parameters. A similar conclusion was reached previously based on the IR spectra of the two types of cobalt OEP cation radicals.[15]

In summary, we have shown that cation radicals of tetraarylporphyrins with an A_{1u} magnetic orbital can be produced, which is understandable if the high spin density at *meso* carbons for A_{2u} radicals is considered. This should be disfavored by the electron-withdrawing substituents in **7** and **8**.[19] These results provide further insight into the factors affecting the inherent structural and electronic variations in the "compound I" of heme-dependent enzymes and their synthetic analogues; for any given axial ligand or geometry (e.g., displacement of the metal center from the porphyrin plane or deviation of the porphyrin from planarity, *the interaction of a paramagnetic metal center with a porphyrin cation*

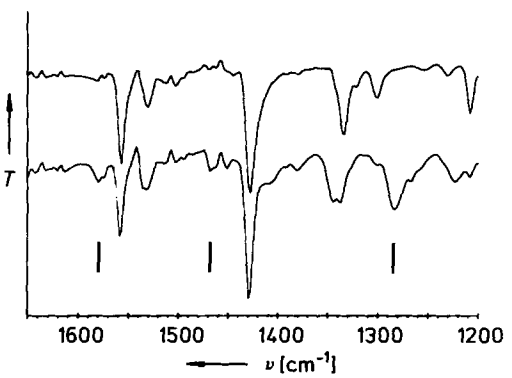

Fig. 3. FTIR spectra of **7** (bottom) and its neutral precursor **3** (top). The vertical lines indicate new bands which appear in **7**. T = transmittance.

radical is much smaller for an A_{1u} than for an A_{2u} orbital, because of the negligible spin density at the nitrogen atoms in the former. In order to test the generality of this phenomena, we are currently investigating the oxidized iron and manganese complexes of the porphyrins described here.

Received: July 30, 1992 [Z 5490 IE]
German version: *Angew. Chem.* **1992**, *104*, 1672

CAS Registry numbers:
1, 14074-80-7; **2**, 104025-54-9; **3**, 100506-72-7; **4**, 144588-07-8; **5**, 144588-08-9; **6**, 144608-58-2; **7**, 144588-09-0; **8**, 144588-11-4; phenoxathiin radical cation-$SbCl_6^-$, 84071-05-6; catalase, 9001-05-2; peroxidase, 9003-99-0; cytochrome p450, 9035-51-2; cytochrome c peroxidase, 9029-53-2; chloroperoxidase, 9055-20-3.

[1] B. Morgan, D. Dolphin, *Struct. Bonding (Berlin)* **1987**, *64*, 115.
[2] H. Fujii, K. Ichikawa, *Inorg. Chem.* **1992**, *31*, 1110; W. R. Scheidt, H. Song, K. J. Haller, M. K. Safo, R. D. Orosz, C. A. Reed, P. G. Debrunner, C. E. Schulz, *ibid.* **1992**, *31*, 941; J. W. Buchler, A. De Cian, S. Elschner, J. Fischer, P. Hammerschmitt, R. Weiss, *Chem. Ber.* **1992**, *125*, 107; A. Nanthakumar, H. M. Goff, *Inorg. Chem.* **1991**, *30*, 4460.
[3] a) RR spectroscopy: S. Hashimoto, Y. Tatsuno, T. Kitagawa, *J. Am. Chem. Soc.* **1987**, *109*, 8096; J. R. Kincaid, A. J. Schneider, K.-J. Paeng, *ibid.* **1989**, *111*, 735; b) Mössbauer and ESR spectroscopy: E. Bill, X.-Q. Ding, E. L. Bominaar, A. X. Trautwein, H. Winkler, D. Mandon, R. Weiss, A. Gold, K. Jayaraj, W. E. Hatfield, M. L. Kirk, *Eur. J. Biochem.* **1990**, *188*, 665; c) NMR spectroscopy: A. L. Balch, L. Latos-Grazynski, M. W. Renner, *J. Am. Chem. Soc.* **1985**, *107*, 2983; d) UV/VIS spectroscopy: ref. [4]; e) electrochemistry: T. S. Calderwood, W. A. Lee, T. C. Bruice, *J. Am. Chem. Soc.* **1985**, *107*, 8272.
[4] J. T. Groves, R. C. Haushalter, M. Nakamura, T. E. Nemo, B. J. Evans, *J. Am. Chem. Soc.* **1981**, *103*, 2884; J. T. Groves, Y. Watanabe, *ibid.* **1986**, *108*, 507.
[5] A. Gold, K. Jayaraj, P. Doppelt, R. Weiss, E. Bill, X.-Q. Ding, E. L. Bominaar, A. X. Trautwein, H. Winkler, *New J. Chem.* **1989**, *13*, 169.
[6] J. E. Roberts, B. M. Hoffman, R. Rutter, L. P. Hager, *J. Biol. Chem.* **1981**, *256*, 2118.
[7] B. M. Hoffman, J. E. Roberts, C. H.Kang, E. Margoliash, *J. Biol. Chem.* **1981**, *256*, 6556.
[8] R. Rutter, L. P. Hager, H. Dhonau, M. Hendrick, M. Valentine, P. Debrunner, *Biochemistry* **1984**, *23*, 6809.
[9] For schematic presentation of the spin distribution in the relevant orbitals, see M. Gouterman in *The Porphyrins, Vol. III* (Ed.: D. Dolphin), Academic Press, New York, **1978**, p. 93. More recent calculations and presentation as well as comprehensive discussion of that subject can be found in references [18] and [19b].
[10] D. Dolphin, R. H. Felton, *Acc. Chem. Res.* **1974**, *7*, 26.
[11] M. Satoh, Y. Ohba, S. Yamauchi, M. Iwaizumi, *Inorg. Chem.* **1992**, *31*, 298, and references therein.
[12] Compounds **1**–**4** were prepared by the Lindsey method for porphyrin synthesis (J. S. Lindsey, R. W. Wagner, *J. Org. Chem.* **1989**, *54*, 828) followed by metal insertion in dimethyl formamide (DMF) (A. D. Adler, F. R. Longo, F. Kampas, J. Kim, *J. Inorg. Nucl. Chem.* **1970**, *32*, 2443). Complexes **5**–**8** were prepared by adding freshly prepared solid phenoxathiin hexachloroantimonate (P. Gans, J.-C. Marchon, C. A. Reed, J.-R. Regnard, *Nouv. J. Chim.* **1981**, *5*, 203) to dried and argon-saturated CH_2Cl_2 solutions of their corresponding neutral zinc or magnesium porphyrins under a stream of argon. The products which precipitated within a few minutes were filtered, washed with hexane and dried in air.
[13] J. Fajer, D. C. Borg, A. Forman, D. Dolphin, R. H. Felton, *J. Am. Chem. Soc.* **1970**, *92*, 3451.
[14] J. Fajer, M. S. Davis in *The Porphyrins, Vol. IV* (Ed.: D. Dolphin), Academic Press, New York, **1979**, Chapter 4.
[15] E. T. Shimomura, M. A. Phillippi, H. M. Goff, W. F. Scholz, C. A. Reed, *J. Am. Chem. Soc.* **1981**, *103*, 6778.
[16] Complexes **5**–**8** were examined by ESR spectroscopy on an E4 Varian spectrometer at microwave power of 5 mW (sealed quartz cuvettes) as dried and oxygen-free CH_2Cl_2 solutions and by UV/VIS spectroscopy on a HP 8452A spectrophotometer. FTIR spectra of the complexes as KBr and NaCl pellets were measured on Nicolet 520 and Bruker IFS 48 instruments.
[17] J. Fajer, D. C. Borg, A. Forman, R. H. Felton, L. Vegh, D. Dolphin, *Ann. N. Y. Acad. Sci.* **1973**, *206*, 349.
[18] S. Nakashima, H. Ohya-Nishiguchi, N. Hirota, H. Fujii, I. Morishima, *Inorg. Chem.* **1990**, *29*, 5207.
[19] a) Magnetic circular dichroism (MCD) studies on nonoxidized zinc porphyrins have revealed that the ordering of the relevant orbitals is sensitive to similar substituent effects: J. D. Keegan, E. Bunnenberg, C. Djerassi, *Spectrochim. Acta A* **1984**, *40*, 287; b) Substitution of the β hydrogen atoms of pyrrole units of CoTPP by a variety of substituents was also recently found to affect the relative order of the orbitals: R. A. Binstead, M. J. Crossley, N. S. Hush, *Inorg. Chem.* **1991**, *30*, 1259.

DNA Recognition by Hybrid Oligoether–Oligodeoxynucleotide Macrocycles**

By *Squire Rumney IV* and *Eric T. Kool**

The sequence-specific binding of RNA and DNA by synthetic oligonucleotides and analogues is important as a diagnostic tool in the study of naturally ocurring polynucleotides and is the subject of intense research as a potential therapeutic strategy as well.[1–3] Two limitations of natural DNA oligomers in these applications are their low binding affinity[2] and also their limited stability, due to cleavage by exo- and endonucleases which occur in natural systems.[4, 5] We report here the construction of circular hybrid molecules which contain two oligonucleotide domains bridged by two oligoethylene glycol chains. These molecules bind with high affinity to complementary strands of RNA and DNA and display exceptional resistance to degradation by nucleases.

Oligoethylene glycol chains have been successfully used as simple linking groups which replace nucleotide units in linear oligonucleotide chains[6] and in hairpin-shaped oligonucleotides in duplexes and triplexes as well.[7] We wished to determine whether such spacers could be incorporated into circular structures and what the effect on their recognition properties and stability would be. We have previously shown that circular oligonucleotides can display very strong binding affinity[8] and high sequence selectivity[9] for single-stranded DNA and RNA by forming bimolecular triple helices. These macrocycles bind by forming bonds on two sides of a linear target strand, and their unusual recognition characteristics arise from the preorganized circular structure.[10]

Examination of models[11] and published data on DNA triple helices[12] revealed that a group 19–21 Å long would be ideal for bridging the outer pyrimidine strands, and that five-base nucleotide loops might be replaced with penta- or hexaethylene glycol chains. In addition to confirming our model for the binding, such a replacement might lead to favorable properties, such as lower cost and higher synthesis yield (by decreasing the number of nucleotide units), longer lifetimes in biological media, and possibly, improved membrane permeability (by decreasing total negative charge).

The linear precursors to the compounds investigated in this study **1**–**3** were constructed by automated DNA syn-

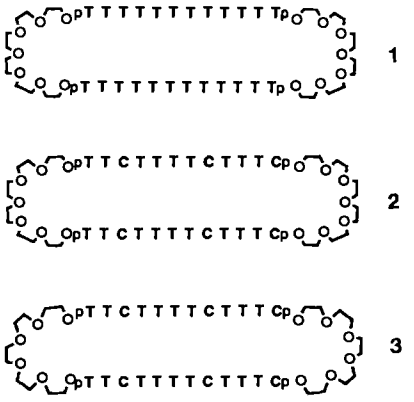

[*] Prof. Dr. E. T. Kool, S. Rumney IV
Department of Chemistry, University of Rochester
Rochester, 14627 (USA)

[**] This work was supported in part by a grant from the National Institutes of Health (RO1-GM46625). E.T.K. acknowledges awards from the Young Investigator Programs of the Office of Naval Research (1992–1995) and the Arnold and Mabel Beckman Foundation (1992–1994).

thesis methods[13] (*Experimental Procedure*) with the introduction of the synthetic dimethoxytrityl hexa- or pentaethylene glycol (HEG or PEG) phosphoramidites[7] at two positions. The oligomers $d(A)_{12}$ (for **1**) and dAAGAAAAGAAAG (for **2** and **3**) were used as templates in cyclization to align the reactive phosphate and hydroxyl ends in an intramolecular esterification reaction in the presence of BrCN, imidazole, and $NiCl_2$, as reported previously.[10]

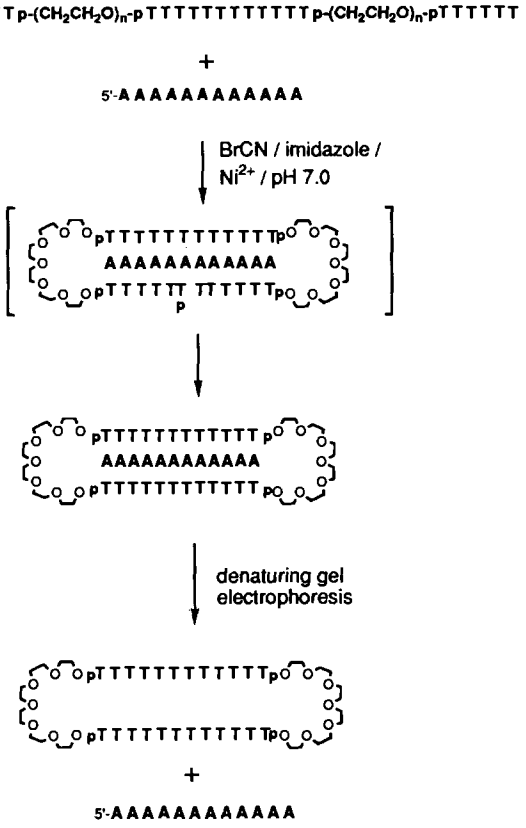

Thermal denaturation studies were carried out to investigate the binding properties of the macrocycles with their complementary 12-base oligonucleotides (Table 1) at a concentration of 3 μM in a buffer approximating physiological conditions (pH 7.0, 100 mM NaCl, 10 mM $MgCl_2$). The dissociation curves reveal sharp, two-state transitions, and similar hyperchromicities for both complexes, with an average value of 28% at 260 nm. Mixing curves of absorbance (at 260 nm) vs. mole ratio for both complexes confirm a 1 : 1 stoichiometry of binding, consistent with a bimolecular triple-helical structure. The complex of compound **1** and $d(A)_{12}$ has a melting transition (T_m) of 51 °C, which is 14 °C higher than the corresponding Watson–Crick duplex, $d(A)_{12} \cdot d(T)_{12}$[8] (Table 1). Curve-fitting analysis[14] gives an estimated free energy (37 °C) of -15 kcal mol^{-1} for the complex of **1** and $d(A)_{12}$, which is 7 kcal mol^{-1} more favorable than the duplex. Similarly, compound **2** binds its complementary oligonucleotide to give a complex with a T_m of 58 °C ($\Delta G^\circ_{37} = -17$ kcal mol^{-1}), compared to 42 °C (-10 kcal mol^{-1}) for the analogous duplex.

Thus, in both cases the binding by the macrocycles is much stronger than that achieved by simple Watson–Crick binding of the same sequences, giving equilibrium binding constants (K_{assoc}) which are approximately five orders of magnitude greater than those of the duplexes at 37 °C. Comparison with

Table 1. Melting temperatures (T_m) and free energies of complexation ($-\Delta G^\circ_{37}$) for linear duplexes and complexes of oligonucleotides and circular ether–DNA hybrids.

Complex [a]	T_m [°C] [b,c]	$-\Delta G^\circ_{37}$ [kcal mol^{-1}]
TTTTTTTTTTTT AAAAAAAAAAAA	37	8
HEG pTTTTTTTTTTTTp HEG pTTTTTTTTTTTTp	51	15
TTCTTTTCTTTC AAGAAAAGAAAG	42	10
PEG pTTCTTTTCTTTCp PEG pTTCTTTTCTTTCp	53	15
HEG pTTCTTTTCTTTCp HEG pTTCTTTTCTTTCp	58	17

[a] Hexa- and pentaethylene glycol are abbreviated as HEG and PEG, respectively. [b] The data are for pH 7.0, 100 mM NaCl, 10 mM $MgCl_2$, and oligomer concentrations of 3 μM in each strand. [c] Precision in T_m values is ± 1 °C, and in free energies, ± 10%.

the all-DNA analogues containing nucleotide loops reveals that these synthetic hybrid macrocycles bind only slightly less strongly. For example, the analogue of **1** containing five-base loops (sequence -CACAC-) forms a complex with a T_m of 57 °C ($\Delta G^\circ_{37} = -16$ kcal mol^{-1}) under identical conditions.[8] The small decrease of this value upon introduction of the HEG chain may be due to the increased flexibility relative to a more rotationally restricted nucleotide chain. The fact that the effect is small also helps to confirm the model for "circle binding",[10] which requires loops mainly for bridging and not for other more specific interactions.

Model studies[11] and fiber diffraction data[12] indicate that a bridge between the outer pyrimidine strands at a given base triad in a DNA triple helix must span a distance of approximately 20 Å. Molecular modeling studies indicate that in its extended conformation, HEG-monophosphate has a length of 23 Å, while penta- (PEG) and tetraethylene glycol (TEG) monophosphates have lengths of 19 and 16 Å, respectively. To test this length requirement, we also attempted construction of versions of **2** with these shorter spacers. Melting studies of the complex of the PEG-bridged macrocycle **3** with its template complement show that this complex is somewhat less stable than the analogous HEG complex (T_m = 53 °C, 5 °C less than the T_m of the adduct of **2**). Attempts at constructing the TEG circle failed; apparently, this bridge is too short to span the distance required for full complexation of the 12-base template in the cyclization reaction. Thus, it appears that of these three cases the hexaethylene glycol spacer is the best suited for optimum complexation, and the spacer length of 23 Å is consistent with published models for triple-helix structure.[11]

The primary cause of degradation of standard DNA oligomers in biological applications is a 3′-exonuclease activity found in cells.[4, 5] Although present in lower activity, endonucleases are also found, which degrade DNA oligomers at internal phosphodiester bonds.[2] Attempts at cleavage of **1** and **2** by exonucleases confirm that they are completely resistant, due to their circular structures. Interestingly, we find that exonucleases cleave the linear precursors of **1** and **2** only through the first six bases from the end, leaving

the oligoether units, which are apparently not recognized by the enzymes.

In order to test susceptibility of such macrocyclic DNA compounds to degradation in a biological medium, we incubated compound **2** and its all-DNA analogue (see Table 2) in fresh human serum at 37 °C and removed aliquots periodically, analyzing the structural integrity by gel electrophoresis (data not shown here). A linear version of this sequence was found to have a half-life for cleavage of 20–30 min, while both circular compounds showed no sign of cleavage after two days. Thus, circular oligomers are highly resistant in this medium, and exonucleases appear to be the dominant cleaving enzymes in serum, consistent with published findings.

To examine specifically the sensitivity to an endonuclease, we studied the cleavage of compound **2** by Nuclease S1, a single-strand-specific DNA-cleaving enzyme. We compared the results to those for the 34-base all-DNA analogue (Table 2). The sensitivity to degradation was tested with oligomers both alone and in the presence of a complementary oligonucleotide, since the resulting secondary structures (such as triple helices) may not be recognized by enzymes and thus confer added resistance.

Table 2. Susceptibility of synthetic circular DNA and DNA–ether compounds to degradation by staphylococcal endonuclease (S1) in the absence and presence of the complementary oligonucleotide sequence.

Oligomer(s) [a]	Nuclease cleavage $t_{1/2}$ [min]
	1
	20
	1
	>24 h

[a] Hexaethylene glycol loops are abbreviated as HEG.

The experiments show that both types of macrocycles are susceptible to single-strand endonuclease cleavage (Table 2). Both linear and circular sequences showed the same rates of cleavage (data not shown here). Interestingly, we find that both circular oligomers are considerably more resistant to cleavage when bound to their complement. This is evidently due to the fact that they are held in a tight triple-helical secondary structure in the complex. More significant is the finding that whereas the all-DNA compound is still cleaved, albeit at a slower rate, when bound, we find no evidence for any cleavage of the DNA–oligoether macrocycle **2** after 24 hours of incubation. This difference is likely due to the variance in loop structure for the two complexes: the all-DNA compound still presents single-stranded cleavable nucleotides in the complex, while in **2** there is no single-stranded region of DNA exposed to solvent. In the presence of a binding structure, compounds such as **1**–**3** are unlikely to be substrates for any exo- or endonuclease enzyme, and would likely be stable during diffusion through serum as well. The combination of this stability and the high binding affinity makes such compounds good candidates for use in biological systems.

Experimental Procedure

1 was prepared from the linear precursor 5′-pTTTTTTpO-$(CH_2CH_2O)_6$-pTTTTTTTTTTTTpO-$(CH_2CH_2O)_6$-pTTTTTT; **2** from 5′-pTTTCTTpO-$(CH_2CH_2O)_6$-pTTCTTTTCTTTCpO-$(CH_2CH_2O)_6$-pCTTTCT; and **3** from 5′-pTTTCTTpO-$(CH_2CH_2O)_5$-pTTTCTTTTCTTTCpO-$(CH_2CH_2O)_5$-pCTTTCT. Reaction conditions were as described previously [10]. The conversion to macrocyclic product was 85–95% (by gel analysis) in both cases, and the circular products were isolated by preparative gel electrophoresis, giving 43% (**1**), 48% (**2**), and 24% (**3**) isolated yields. The circular structure was confirmed by complete resistance to T4 polymerase exonuclease cleavage under conditions under which the linear precursors are fully cleaved up to the ether linkage. Dimethoxytrityl-HEG- and -PEG-phosphoramidites were synthesized by the method of Thuong et al. [7]. Coupling yields for these linkers were > 90%. Intact incorporation of HEG and PEG spacers after final deprotection was also confirmed by ^{1}H NMR and FAB-MS studies on short oligomers having the sequence dTpO-$(CH_2CH_2O)_n$-pT.

Thermal denaturation studies and curve fitting were carried out as described [10]. Mixing studies were carried out at a total concentration of 6 μM in a buffer containing 100 mM NaCl, 10 mM $MgCl_2$, and 10 mM Tris · HCl at pH 7.0. Exonuclease cleavage was carried out at 37 °C with 20 μM DNA, 6 mM $MgCl_2$, 4 mM potassium phosphate (pH 7.5), and 55 units mL^{-1} of enzyme with T4 Polymerase from New England Biolabs. Nuclease S1 was purchased from Pharmacia, and cleavage reactions were carried out at a DNA concentration of 100 μM, 100 U mL^{-1} enzyme, using published buffer conditions [15]. Human serum was prepared by the published procedure [4], and cleavage studies were carried out at a DNA strand concentration of 50 μM at 37 °C and analyzed by gel electrophoresis.

Received: August 1, 1992 [Z 5495 IE]
German version: *Angew. Chem.* **1992**, *104*, 1686

[1] J.-J. Toulmé, C. Hélène, *Gene* **1988**, *72*, 51–58.
[2] E. Uhlmann, A. Peyman, *Chem. Rev.* **1990**, *90*, 543–584.
[3] J. S. Cohen, *Oligodeoxynucleotides: Antisense Inhibitors of Gene Expression*, CRC Press, Boca Raton, FL, USA, **1989**.
[4] J. M. Dagle, D. L. Weeks, J. A. Walder, *Antisense Res. Dev.* **1991**, *1*, 11–20.
[5] P. C. Zamecnik, J. Goodchild, Y. Taguchi, P. S. Sarin, *Proc. Natl. Acad. Sci. USA*, **1986**, *83*, 4143–4146.
[6] S. T. Cload, A. Schepartz, *J. Am. Chem. Soc.* **1991**, *113*, 6324–6326.
[7] a) M. Durand, K. Chevrie, M. Chassignol, N. T. Thuong, J. C. Maurizot, *Nucleic Acids Res.* **1990**, *18*, 6353–6359; b) C. Giovannangeli, T. Montenay-Garestier, M. Rougée, M. Chassignol, N. T. Thuong, C. Hélène, *J. Am. Chem. Soc.* **1992**, *113*, 7775–7776.
[8] G. Prakash, E. T. Kool, *J. Chem. Soc. Chem. Commun.* **1991**, 1134–1136.
[9] E. T. Kool, *J. Am. Chem. Soc.* **1991**, *113*, 6265–6266.
[10] G. Prakash, E. T. Kool, *J. Am. Chem. Soc.* **1992**, *114*, 3523–3527.
[11] S. C. Harvey, J. Luo, R. Lavery, *Nucleic Acids Res.* **1988**, *16*, 11795–11809.
[12] S. Arnott, E. Selsing, *J. Mol. Biol.* **1974**, *88*, 509–533.
[13] S. L. Beaucage, M. H. Caruthers, *Tetrahedron Lett.* **1981**, *22*, 1859–1862.
[14] M. Petersheim, D. H. Turner, *Biochemistry* **1983**, *22*, 256–263.
[15] J. Sambrook, E. F. Fritsch, T. Maniatis, *Molecular Cloning: A. Laboratory Manual*, 2nd edition, Cold Spring Harbor Press, Cold Spring Harbor, NJ, USA, **1989**.

One-Step Synthesis of a Fourfold Functionalized Catenane**

By *Fritz Vögtle,** *Stephan Meier*, and *Ralf Hoss*

Catenanes and other molecules with similar construction have become "Highlights" in supramolecular chemistry[1] thanks to the outstanding work of Sauvage[2] and Stod-

[*] Prof. Dr. F. Vögtle, Dipl.-Chem. S. Meier, Dipl.-Chem. R. Hoss
Institut für Organische Chemie und Biochemie der Universität
Gerhard-Domagk-Strasse 1, D-W-5300 Bonn 1 (FRG)

[**] This research was supported by the Deutsche Forschungsgemeinschaft (project no. 145/38-1). We thank Dr. K. Rissanen, University of Jyväskylä, Finland, for the crystallization, preliminary measurements, and the transfer of a single crystal to the University of Joensu, Finland, for further studies.

dart.[3] In our work on the syntheses of basket-shaped host molecules[4] we unexpectedly found an amazingly simple catenane synthesis in 1991.

In order to increase the solubility of macropolycyclic lactams of type **3** we employed the cyclohexylidene-substituted diamine **2**[5] instead of unsubstituted diphenylmethane, *p*-phenylene, or naphthalene units.[6] The OCH_3 substituents introduced by use of **1b** were intended as "handles" to be used for further bridging and in particular for attaching the bottom of the basket (spacer in **3**).[6] These studies surprisingly led to the one-step synthesis of catenane **4b** (for properties and analytical data see Experimental Procedure) from the simple components **1b** and **2** [Eq. (a)].

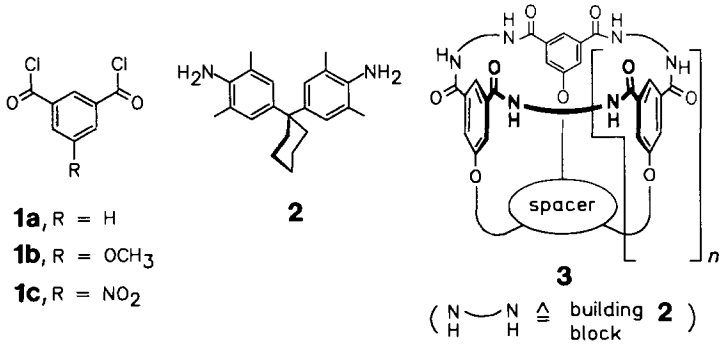

1b + **2** $\xrightarrow[\text{benzene}]{\text{chloro-}}$ **4b** + **5a** + **6a** (a)

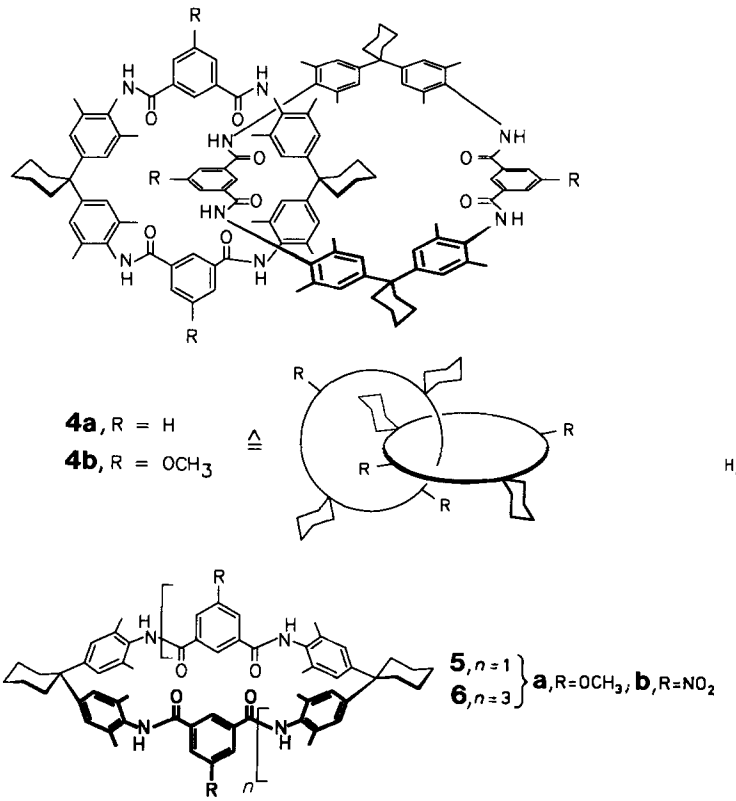

Methoxyisophthaloyl dichloride **1b** was allowed to react with diamine **2** in chlorobenzene with a catalytic amount of 4-(*N*,*N*-dimethylamino)pyridine (DMAP) at 50–60 °C under dilution conditions. The sparingly soluble dimethoxy-substituted macromonocycle **5a** (12.4% yield; m.p. >300 °C (decomp)) was isolated along with the 72-membered "tetramer" **6a** (10% yield; m.p. 285–290 °C), which has the lowest R_f value of all macrocycles isolated. An isomer, **4b** (m.p. >300 °C, $R_f = 0.64$), a catenane (Fig. 1) according to FAB-MS, and ^1H and ^{13}C NMR spectroscopic data, was obtained in 8.4% yield. The spectroscopic properties of **4b** are in full accord with those of the unsubstituted catenane **4a** reported by Hunter et al.,[7] even down to the details: The mass spectrum shows the characteristic fragmentation due to the loss of one of the catenane rings. The NMR spectra of **4b** are more complicated than those of its isomer **6a**; H,H-COSY and NOE spectra also support the catenane structure. Attempts (since October 1991) to obtain an X-ray crystal structure have not yet been successful, though small single-crystals could be prepared, for which a unit cell of 17172 Å^3 was measured.[8]

Fig. 1. CPK model of [2]catenane **4b** (isomer **II**); for clarity the 16 methyl groups are not shown.

In the ^1H NMR spectrum of **4b** the four methoxy groups give rise to two singlets. One explanation is that neither the cyclohexylidene units nor the methoxybenzene groups pass easily through the second macrocycle, if at all. Thus, **4b** has a relatively fixed conformation which has two inner and two outer methoxy groups. As a consequence **4b** should have two enantiomeric forms **I** and **II**, which are expected to be more stable than the enantiomers of **4a**.

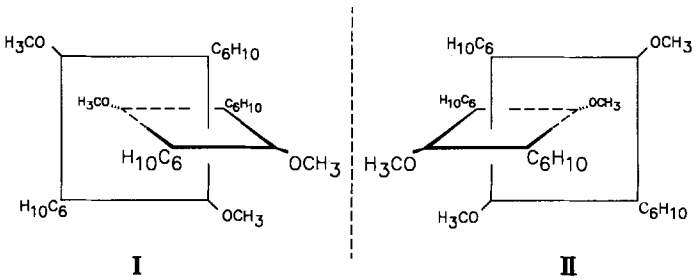

The latter were recently prepared with remarkable yield (34%) by Hunter et al.[7] in a two-step synthesis starting from the isolated intermediate **7** and isophthaloyl dichloride **1a**.

The template assistance in the reaction, which appears to be necessary for the smooth formation of the catenane, may be due to hydrogen-bonding interactions between the car-

bonyl group of the isophthaloyl unit and the NH group of the amide (cf. **8**), as well as π–π interactions between the benzene rings of the spacer units. The readily soluble, bulky diamine **2**, which shows a preference for forming large rings, seems to favor the catenane formation.

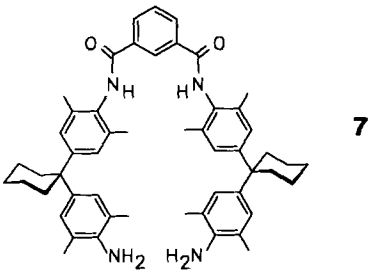

7

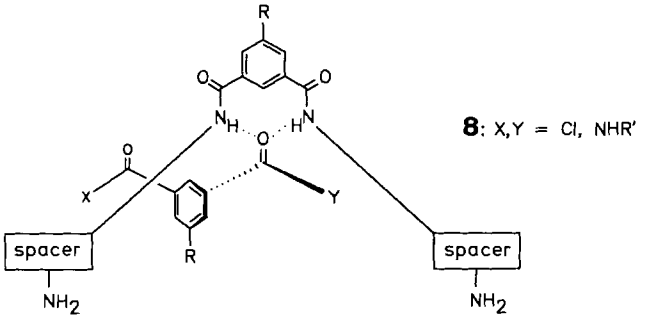

8: X,Y = Cl, NHR'

The analogous cyclization of the nitro-substituted **1c** with **2** [Eq. (b)], however, yielded the dimer **5b** (11% yield) as the main product and a tetramer (7% yield); the FAB-MS spec-

$$\mathbf{1c} + 2 \xrightarrow[\text{benzene}]{\text{chloro-}} \mathbf{5b} + \mathbf{6b} \qquad \text{(b)}$$

trum of the latter hints at the macromonocycle **6b**, and the isomeric catenane has not been detected so far. In the templating interaction here the NO_2 groups may possibly compete with the carbonyl groups in forming hydrogen bonds with the NH groups.

The compounds with extraannular methoxy substituents have the advantage that they can be converted into the hydroxy compounds according to known procedures.[9] Hydroxy-substituted catenanes should be suitable for further cyclizations and for linkage to oligomeric catenanes. By affixing large extra- and intraannular groups the conformational mobility of the catenane rings can be manipulated.

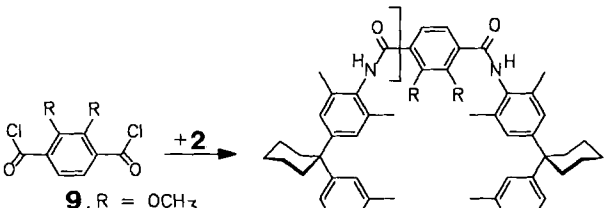

9, R = OCH_3

10: $n = 1$

11: $n = 3$

When other carbonyl compounds, for example the substituted terephthalic dichloride **9**, were employed, catenanes were not formed, but rather the 34- and 68-membered macromonocycles **10** (<1%) and **11** (34% yield), respectively. In this case the arrangement of the amino groups is apparently not complementary to the carbonyl groups, so that templated catenane formation is not possible.

As shown in the last two examples, a directed catenane synthesis requires exact planning of the self-associating intermediates (cf. **8**). The macromonocycles **10** and **11** can also be integrated in such synthetic strategies.

Experimental Procedure

Synthesis of **4b**, **5a**, and **6a**: A solution of **1b** (0.59 g, 2.5 mmol) in anhydrous chlorobenzene (250 mL) and a solution of **2** (1.60 g, 5 mmol) in anhydrous chlorobenzene (250 mL) were added synchronously over 24 h to chlorobenzene (1 L, 50–60 °C) containing a catalytic amount of DMAP. The reaction mixture was concentrated to dryness and the residue dissolved in dichloromethane/water. The organic phase was washed with water, dried over $MgSO_4$, filtered, and concentrated. Column chromatography on silica gel (60–100 μm) eluting with dichloromethane/ethyl acetate 8/1 (v/v) afforded three fractions, A, B, and C.

Fraction A (catenane **4b**): yield 100 mg (8.4%); m.p. >300 °C (decomp); thin-layer chromatography (TLC, SiO_2) $R_f = 0.64$ (dichloromethane/ethyl acetate 8/1), ^{1}H NMR (250 MHz, $CDCl_3/CD_3OD$): $\delta = 0.5$–2.5 (br., 88H; aliph. H, $ArCH_3$), 3.85, 3.90 (2s, 12H; OCH_3), 6.28, 6.31 (2s, 4H; arom. H), 6.75 (br., 4H; arom. H), 6.9 (s, 2H; arom. H), 7.0 (s, 2H; arom. H), 7.1 (s, 2H; arom. H), 7.3 (br., 4H; arom. H), 7.6 (s, 4H; arom. H), 7.7 (s, 2H; arom. H), 7.85 (s, 2H; arom. H), 8.5 (s, 2H; arom. H), 8.65 (s, 2H; arom. H), 9.15 (s, 2H; CO-NH), 9.3 (s, 1H; CO-NH), 9.45 (s, 1H; CO-NH); ^{13}C NMR (62.9 MHz, $CDCl_3/CD_3OD$): $\delta = 17.12$, 18.54, 18.75, 18.89 (Ar-CH_3), 23.37, 26.68, 34.92, 35.13 (CH_2), 36.55, 36.84, 45.18, 45.65 (C_q), 55.93, 56.31 (OCH_3), 111.98, 117.57, 117.81, 117.92, 118.05, 123.23, 123.89, 125.58, 128.03, 128.51 (CH), 130.85, 131.46, 131.50, 131.56, 133.83, 134.42, 134.71, 134.77, 135.34, 135.44, 136.26, 136.47, 137.62, 146.63, 146.90, 149.08, 150.00, 160.57, 160.74, 163.74, 164.59, 169.19 (C_q); FAB-MS: m/z 1930.8 [$(M + H)^+$].

Fraction B (dimer **5a**): yield 150 mg (12.4%); m.p. >300 °C (decomp); $R_f = 0.18$; IR (KBr, −78 °C); $\tilde{\nu}$[cm^{-1}] = 752 (m), 776 (m), 870 (w), 1051 (w), 1125 (w), 1163 (w), 1248 (w), 1309 (m), 1333 (m), 1373 (m), 1451 (s), 1496 (vs), 1592 (s), 1664 (vs), 2854 (m), 2931 (s), 3294 (m); FAB-MS: m/z 965.6 [$(M + H)^+$].

Fraction C (tetramer **6a**): It was the last fraction and was eluted with methanol/dichloromethane (20/1 (v/v)): 120 mg (10% yield; m.p. >300 °C (decomp); ^{1}H NMR (250 MHz, $CDCl_3/CD_3OD$): $\delta = 1.3$–1.6 (br., 24H; aliph. CH_2), 2.0–2.3 (br., 64H; $ArCH_3$, aliph. CH_2), 3.85 (s, 12H; OCH_3), 6.85 (s, 16H; arom. H), 7.55 (s, 8H; arom. H), 7.95 (s, 4H; arom. H), 8.7 (s, 4H; NH); ^{13}C NMR (62.9 MHz, $CDCl_3/CD_3OD$): $\delta = 18.33$ (CH_3), 22.56, 26.05, 36.68 (CH_2), 44.90 (C_q), 55.53 (OCH_3), 116.06, 117.66 (C_q), 126.62, 130.81, 134.79 (CH), 135.94, 147.22, 159.74, 165.67 (C_q); FAB-MS m/z 1930.9 [$(M + H)^+$].

Synthesis of **10** and **11**: A solution of terephthaloyl dichloride **9** (0.18 g, 0.7 mmol) in chlorobenzene (25 mL) and a solution of diamine **2** (0.45 g, 1.4 mmol) in chlorobenzene (25 mL) were added synchronously with a perfusor (peristaltic pump) over 12 h to chlorobenzene (1.2 L; 60 °C) containing a catalytic amount of DMAP. The solution was filtered through celite, the solvent evaporated to dryness, and the residue dissolved in dichloromethane. This solution was washed with water, dried over $MgSO_4$, filtered, and concentrated. Column chromatography on silica gel (60–100 μm) eluting with dichloromethane/methanol (20/1) afforded:

Fraction A (**10**): <1% yield; m.p. >250 °C (decomp); $R_f = 0.2$ (dichloromethane/methanol 20/1) FAB-MS: m/z 1025.6 [$(M + H)^+$]).

Fraction B (tetramer **11**): 240 mg (34%) yield; $R_f = 0.2$; m.p. >250 C (decomp); ^{1}H NMR (250 MHz, $CDCl_3$): $\delta = 1.64$ (br., 24H; aliph. H), 2.25 (br., 64H; aliph. H, CH_3), 4.06 (s, 24H; OCH_3), 7.15 (s, 16H; arom. H), 8.01 (s, 8H; arom. H), 9.17 (s, 8H; NH); ^{13}C NMR (62.9 MHz, $CDCl_3$) [DEPT135, the δ values of the corresponding protons are in superscript]: $\delta = 19.1$ ($C^{2.25}H_3$), 23.3, 26.1 (CH_2), 36.1 (CH_2), 45.2 (aliph. C_q), 62.1 ($C^{4.06}H_3$), 126.5 ($C^{7.15}H$), 126.8 ($C^{8.01}H$), 130.2, 132.1, 135.7, 147.9, 152.4 (C_q) 162.6 (C=O); FAB-MS: m/z = 2051 [$(M + H)^+$].

Received: July 17, 1992
Revised: August 25, 1992 [Z 5471]
German version: *Angew. Chem.* **1992**, *104*, 1628

[1] For earlier catananes see G. Schill, N. Schweickert, H. Fritz, W. Vetter, *Angew. Chem.* **1983**, *95*, 909; *Angew. Chem. Int. Ed. Engl.* **1983**, *22*, 889; *Chem. Ber.* **1988**, *121*, 961; D. M. Walba, R. M. Richards, M. Hermsmeier, R. C. Haltiwanger, *J. Am. Chem. Soc.* **1987**, *109*, 7081; D. M. Walba, Q. Y. Zheng, K. Schilling, *J. Am. Chem. Soc.* **1992**, *114*, 6259–6260.

[2] See for example J.-P. Sauvage, C. O. Dietrich-Buchecker, J. Guilhem, C. Pascard, *Angew. Chem.* **1990**, *102*, 1202; *Angew. Chem. Int. Ed. Engl.* **1990**, *29*, 1154.

[3] P. R. Ashton, T. T. Goodnow, A. E. Kaifer, M. V. Reddington, A. M. Z. Slawin, N. Spencer, J. F. Stoddart, C. Vicent, D. J. Williams, *Angew. Chem.* **1989**, *101*, 1404–1408; *Angew. Chem. Int. Ed. Engl.* **1989**, *28*, 1396–1400; D. Philp, F. Stoddart, *Synlett* **1991**, 445–458.

[4] L. Wambach, F. Vögtle, *Tetrahedron Lett.* **1985**, *26*, 1483–1486; B. Dung, F. Vögtle, *J. Incl. Phenom.* **1988**, *6*, 429–442; J. Breitenbach, K. Rissanen, U. U. Wolf, F. Vögtle, *Chem. Ber.* **1991**, *124*, 2323–2327; C. Seel, F. Vögtle, in *Perspectives in Coordination Chemistry* (Eds.: A. F. Williams, C. Floriani, A. E. Merbach), VCH, Weinheim, **1992**, p. 31.

[5] C. A. Hunter, *J. Chem. Soc. Chem. Commun.* **1991**, 749.

[6] S. Meier, Diplomarbeit, University of Bonn, January 20, 1992; an alternative preparation of diamine **2** is also described.

[7] a) C. A. Hunter, *J. Am. Chem. Soc.* **1992**, *114*, 5303–5311; b) See also C. A. Hunter, D. H. Purvis, *Angew. Chem.* **1992**, *104*, 779; *Angew. Chem. Int. Ed. Engl.* **1992**, *31*, 779; in [7a] dichloromethane was used as solvent and the cyclization carried out at room temperature. Instead of triethylamine we used a second equivalent of the diamine **2** as assisting base.

[8] K. Rissanen, Jyväskylä, Finland, private communication.

[9] P. Stutte, W. Kiggen, F. Vögtle, *Tetrahedron Lett.* **1987**, *28*, 2065–2074; C. Seel, F. Vögtle, *Angew. Chem.* **1991**, *103*, 433–436; *Angew. Chem. Int. Ed. Engl.* **1991**, *30*, 442–445.

The First Self-Assembled Dinuclear Triple-Helical Lanthanide Complex: Synthesis and Structure**

By *Gérald Bernardinelli, Claude Piguet,** and *Alan F. Williams*

There is currently considerable interest in the use of self-assembly processes for the selective formation of organized supramolecular units.[1] Double-helical[2] and triple-helical[3] structures have been generated by the complexation of "oligopolydentate" ligands around two or more metal ions, which lie on the helical axis; Dietrich-Buchecker and Sauvage[4] have used a double-helical Cu_2^I complex for the synthesis of the first molecular knot. Previous work has concentrated on the use of 3d and 4d metals to control the self-assembly, but in principle any metal ion with known preference for a particular coordination geometry may direct a self-assembly reaction. To illustrate this, and in connection with our interest in the photophysics of lanthanide complexes,[5] we report the synthesis and the X-ray crystal structure of the first dinuclear, triple-helical lanthanide complex. In a previous study,[3] we showed how a bis(bidentate) ligand forms a triple-helical structure with metal ions, which prefer octahedral coordination; for the lanthanide ions in which higher coordination numbers are observed, a bis(terdentate) ligand, for example, bis[1-methyl-2-{6′-[1″-(3,5-dimethoxybenzyl)benzimidazol-2″-yl]pyrid-2′-yl}benzimidazol-5-yl]-methane (L^1), offers the possibility of forming a triple-helical complex with two 4f metal cations, in which each cation has a coordination number of nine, as observed in the pseudo-D_3 symmetry of the mononuclear complex $[Eu(terpy)_3]^{3+}$ (terpy = terpyridyl).[6] The ligand L^1 is a logical development of our previous ligand L^2,[3, 7] and carries two terdentate units separated by a spacer; Constable et al.[8] have recently reported the formation of a mononuclear monohelical complex of Eu^{III} with the hexadentate ligand sexipyridyl (sexipy). It is not clear whether the mononuclear structure is a result of the lack of a spacer between the two terpy units or due to the additional complexation of nitrate anions.

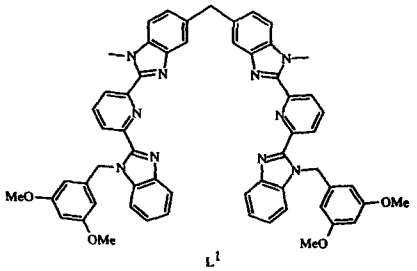

L^1

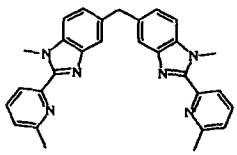

L^2

The lipophilic 3,5-dimethoxybenzyl groups bound to the terminal benzimidazole rings in L^1 were introduced to increase the solubility of the ligand and to enable the investigation of the structure in solution by ^1H NMR spectroscopy by using the intramolecular diastereotopic effect.[9] Reaction of L^1 with hydrated Eu^{III} perchlorate in acetonitrile gives a yellow solution from which yellow prisms of $[Eu_2L_3^1](ClO_4)_6$ (yield 80%) separate after slow vapor diffusion of diethyl ether. The FAB mass spectrum (FAB = *F*ast *A*tom *B*ombardment) of this complex exhibits two peaks centered at *m/z* 3690.0 and 3590.9, whose isotopic distributions correspond to the species $[Eu_2L_3^1](ClO_4)_5^+$ and $[Eu_2L_3^1](ClO_4)_4^+$, respectively.

The X-ray crystal structure determination of $[Eu_2L_3^1](ClO_4)_6 \cdot 9CH_3CN$ confirms the existence of a triple-helical cation $[Eu_2L_3^1]^{6+}$ formed by the three L^1 ligands wrapped around the helical axis defined by the two Eu^{III} atoms. This leads to an approximate D_3 symmetry (Scheme 1). The helicity of each strand is defined by a total

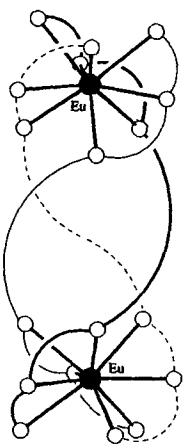

Scheme 1. Schematic representation of the triple-helical complex formed from L^1 and Eu^{3+} ions. The coordinating N atoms of the ligands are shown as white spheres.

[*] Dr. C. Piguet, Dr. A. F. Williams
Departement de Chimie Minérale, Analytique et Appliquée
Université de Genève
30 quai Ernest Ansermet, CH 1211 Genève 4 (Switzerland)
Dr. G. Bernardinelli
Laboratoire de Cristallographie aux Rayons-X, Université de Genève

[**] This work was supported by the Swiss National Foundation (Grant no. 20.30139.90).

length of approximately 14–15 Å (between the terminal benzimidazole groups) for slightly more than one turn, which leads to a pitch of approximately 12 Å comparable to that found by Lehn for double-helical complexes with Cu^{I}.[2] Figure 1 shows a stereoview (ORTEP[10]) of the cation per-

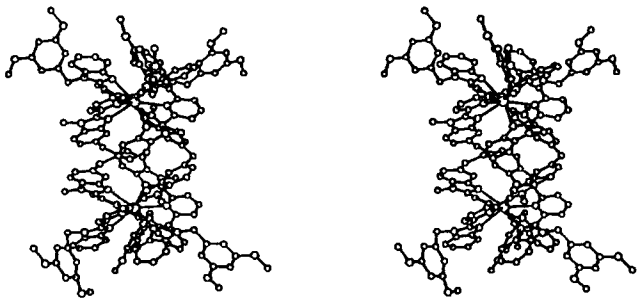

Fig. 1. Stereoview (ORTEP) of the cation $[Eu_2L^1_3]^{6+}$ perpendicular to the helical axis.

pendicular to the helical axis; Figure 2 shows a projection down the Eu–Eu axis (right), and a computer-generated representation (left)[11] of the structure in which the different strands are shown in different colors.

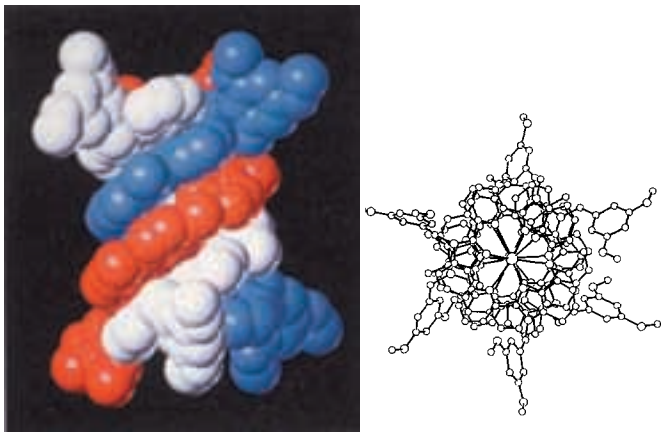

Fig. 2. Left: Computer-generated representation (MOLCAD [11]) of the non-hydrogen atoms of $[Eu_2L^1_3]^{6+}$ represented with van der Waals radii. The three strands of the helical complex are shown with different colors. Right: View along the Eu–Eu axis showing the approximate C_3 symmetry.

The coordination geometries of the two Eu atoms are very similar and may be described as slightly distorted, tricapped trigonal prisms, in which the six N atoms of the benzimidazole (bzim) units occupy the vertices of the prism and three N atoms of the pyridine (py) units occupy the capping positions, forming an intermediate plane containing the Eu^{3+} ion (maximum deviation of Eu^{3+} from the plane 0.019(6) Å). Table 1 gives the structural parameters obtained by averaging the distances of the Eu atoms to the N atoms in the vertices of the prisms and capping groups. The Eu–N distances are very similar for all the coordinated N atoms and are close to the reported values in $[Eu(sexipy)(NO_3)_2](PF_6)$[8] (2.57 Å) and $[Eu(terpy)_3](ClO_4)_3$[6] (2.60 Å). The N(bzim)–Eu–N(py) "bite" angles within one terdentate unit are typical for the meridional coordination of terpyridine derivatives to metal ions.[12]

Table 1. Structural parameters for the coordination sphere of the Eu^{3+} ion.

	Average [a]	Minimum	Maximum
Eu-N(bzim)	2.59(6)	2.54	2.67
Eu-N(py)	2.60(6)	2.58	2.64
ligand "bite angle"	63(2)	61.5	65.1
py-Eu-py	120(3)	116	124.2

[a] Bond lengths [Å] and angles [°] are average values of the distances to the vertices and the capping units. The estimated standard deviations (esd's) given in parentheses were obtained from the values used to obtain the average. The experimental esd's are smaller.

The aromatic rings of the ligands are planar within experimental error, and the helical twisting of the L^1 ligand is achieved by twisting about the interannular C–C bonds. Table 2 gives selected angles between the planes of the aromatic rings. The average angle between adjacent pyridine and benzimidazole aromatic planes within a chelate terdentate unit is 23.3°, close to the value observed for $[Co_2L^2_3]^{4+}$ (22.7°).[3] The main torsion responsible for the helical twist is found between the two terdentate units of each ligand, where the average angle between the benzimidazole rings connected by the CH_2 bridge is 67.1°, appreciably smaller than the 80.0° observed for $[Co_2L^2_3]^{4+}$. In contrast to the structure of $[Co_2L^2_3]^{4+}$, in which no significant π stacking interactions were found,[3] we observe aromatic stacking interactions between the strands as shown in Figure 2 (left). This is supported by the nearly parallel head-to-tail arrangement of the central benzimidazole aromatic planes belonging to different strands (angles 14.8–21°; distance between stacked planes 3.7–4.6 Å). However, these interactions remain rather weak and the self-assembly of the triple-helical $[Eu_2L^1_3]^{6+}$ ion is probably controlled by the coordinating possibilities of the bis(terdentate) ligand and the preference of lanthanide ions for high coordination numbers rather than by the interactions between the ligands.

Table 2. Selected angles [°] between the planes of the aromatic rings.

Ring 1 [a]	Ring 2	Angle	Ring 1	Ring 2	Angle	Ring 1	Ring 2	Angle
tbA1	pA1	31.3	tbB1	pB1	20.8	tbC1	pC1	26.7
pA1	bA1	21.1	pB1	bB1	25.9	pC1	bC1	14.4
bA1	bA2	63.2	bB1	bB2	64.8	bC1	bC2	73.3
bA2	pA2	29.5	bB2	pB2	28.4	bC2	pC2	18.0
pA2	tbA2	16.5	pB2	tbB2	22.2	pC2	tbC2	24.3
bA1	bC2	17.7	bB1	bA2	14.8	bC1	bB2	21.0

[a] The rings are denoted as pyridine p, benzimidazole b, or terminal benzimidazole tb, belonging to ligand strand A, B, or C and bound to Eu1 or Eu2. Thus tbC1 is the terminal benzimidazole ring of strand C that is bound to Eu1. The error in the angles is typically 1°.

^1H NMR measurements show that the high symmetry (D_3) of the complex $[Eu_2L^1_3]^{6+}$ is maintained in acetonitrile solution. The chiral nature of the triple-helical structure is confirmed by the intramolecular diastereotopic effect observed for the methylene protons of the 3,5-dimethoxybenzyl groups.[7, 9] Spectroscopic titrations[7] indicate that $[Eu_2L^1_3]^{6+}$ is the only species formed in acetonitrile solution ($\lg\beta = 20.7(7)$), which strongly suggests the existence of a cooperative, strict self-assembly[13] leading to the triple-helical complex. We are currently investigating the photophysical properties of these compounds, together with more detailed studies of the influence of ionic radius on the structure and the stability of the system. Preliminary luminescence

studies reflect the highly symmetrical environment of the Eu atoms and show the possibility of energy transfer between the lanthanide ions in doped compounds.

Experimental Procedure

The ligand L^1 was obtained by a modified Phillips condensation [14] of 3,3'-diamino-4,4'-bis(*N*-methylamino)diphenylmethane [7] with 2-(2-benzimidazol)-6-carboxypyridine (prepared by the oxidation of 2-(2-benzimidazol)-6-methylpyridine [15]) followed by a double alkylation with 3,5-dimethoxybenzylbromide [9]. Crystals of $[Eu_2L_3^1](ClO_4)_6 \cdot 9\,CH_3CN$ were grown by vapor diffusion of diethyl ether into a concentrated acetonitrile solution of the complex. A yellow crystal ($0.26 \times 0.26 \times 0.26$ mm^3) was sealed in a capillary tube with some of the supernatant liquid. $M_r = 4159$, triclinic, $P\bar{1}$, $a = 17.634(3)$, $b = 21.408(4)$, $c = 29.437(7)$ Å, $\alpha = 82.13(1)$, $\beta = 85.76(1)$, $\gamma = 89.79(1)°$ based on 28 reflections ($10° < 2\theta < 20°$), $V = 10978(4)$ Å^3, $Z = 2$. Intensity data were collected at room temperature on a Philips PW 1100 diffractometer with $Mo_{K\alpha}$ radiation ($\lambda = 0.71069$ Å), $6° < 2\theta < 38°$, 17573 unique reflections measured. Structure solved by direct methods [16], other calculations made with XTAL [17]. The six uncoordinated ClO_4^- ions and the six phenyl rings of the 3,5-dimethoxybenzyl substituents were refined as rigid groups; of the nine acetonitrile molecules, three were observed with three atomic sites, five with two atomic sites, and one with only one atomic site attributed to a nitrogen atom. Blocked-matrix refinement was performed with four blocks (ligand A and Eu, ligand B, ligand C, ClO_4^- and solvent molecules; maximum of variables = 1117). The Eu and the N atoms were refined with anisotropic thermal displacement parameters (32 atoms) and all the other atoms (239) with isotropic thermal displacement parameters. Final *R* factor $R = R_w = 0.127$ for 8322 observed reflections ($|F_o| > 4\sigma|F_o|$). Further details of the crystal structure investigation are available on request from the Director of the Cambridge Crystallographic Data Centre, University Chemical Laboratory, Lensfield Road, GB-Cambridge CB2 1EW (UK), on quoting the full journal citation.

Received: July 15, 1992 [Z 5467 IE]
German version: *Angew. Chem.* **1992**, *104*, 1626

CAS Registry numbers:
1, 68374-68-5; **2**, 143902-45-8; **2** · $3HNO_3 \cdot 6H_2O$, 144015-86-1

[1] J.-M. Lehn, *Angew. Chem.* **1990**, *102*, 1347; *Angew. Chem. Int. Ed. Engl.* **1990**, *29*, 1304–1319.
[2] J.-M. Lehn, A. Rigault, J. Siegel, J. Harrowfield, B. Chevrier, D. Moras, *Proc. Natl. Acad. Sci. USA* **1987**, *84*, 2565–2569; J.-M. Lehn, A. Rigault, *Angew. Chem.* **1988**, *100*, 1121–1122; *Angew. Chem. Int. Ed. Engl.* **1988**, *27*, 1095–1097; W. Zarges, J. Hall, J.-M. Lehn, C. Bolm, *Helv. Chim. Acta* **1991**, *74*, 1843–1852; E. C. Constable, *Nature* **1990**, *346*, 314–315; E. C. Constable, M. D. Ward, D. A. Tocher, *J. Chem. Soc. Dalton Trans.* **1991**, 1675–1683; C. Piguet, G. Bernardinelli, A. F. Williams, *Inorg. Chem.* **1989**, *28*, 2920–2925.
[3] A. F. Williams, C. Piguet, G. Bernardinelli, *Angew. Chem.* **1991**, *103*, 1530; *Angew. Chem. Int. Ed. Engl.* **1991**, *30*, 1490–1492.
[4] C. O. Dietrich-Buchecker, J.-P. Sauvage, *Angew. Chem.* **1989**, *101*, 192; *Angew. Chem. Int. Ed. Engl.* **1989**, *28*, 189–192; J.-P. Sauvage, *Acc. Chem. Res.* **1990**, *23*, 319–327; C. O. Dietrich-Bucheeker, J.-P. Sauvage, *New J. Chem.* **1992**, *16*, 277–285.
[5] G. Bernardinelli, C. Piguet, A. F. Williams, J.-C. G. Bünzli, E. Moret, *Helv. Chim. Acta*, **1992**, *75*, 1697–1717.
[6] D. A. Durham, G. H. Frost, F. A. Hart, *J. Inorg. Nucl. Chem.* **1969**, *31*, 833–838; G. H. Frost, F. A. Hart, M. B. Hursthouse, *J. Chem. Soc. Chem. Commun.* **1969**, 1421–1422.
[7] C. Piguet, G. Bernardinelli, B. Bocquet, A. Quattropani, A. F. Williams, *J. Am. Chem. Soc.* **1992**, *114*, 7440–7451.
[8] E. C. Constable, R. Chotalia, D. A. Tocher, *J. Chem. Soc. Chem. Commun.* **1992**, 771–773.
[9] S. Rüttimann, C. Piguet, G. Bernardinelli, B. Bocquet, A. F. Williams, *J. Am. Chem. Soc.* **1992**, *114*, 4230–4237.
[10] C. K. Johnson, ORTEP II Report ORNL-5138, Oak Ridge National Laboratory, Oak Ridge, Tennessee, **1976**.
[11] J. Brickmann, *MOLCAD Molecular Modelling Package*, Technische Hochschule Darmstadt (FRG) **1990**.
[12] E. C. Constable, *Adv. Inorg. Chem. Radiochem.* **1986**, *30*, 69–121.
[13] J.-S. Lindsey, *New J. Chem.* **1991**, *15*, 153–180.
[14] A. W. Addison, P. J. Burke, *J. Heterocycl. Chem.* **1981**, *18*, 803–805.
[15] E. Barni, P. Savarino, *J. Heterocycl. Chem.* **1977**, *14*, 937–940.
[16] P. Main, S. J. Fiske, S. E. Hull, L. Lessinger, D. Germain, J. P. Declercq, M. M. Woolfson, *MULTAN 87*, Universities of York, England, and Louvaine-La-Neuve, Belgum, **1987**.
[17] *XTAL 3.0 User's Manual* (Eds.: S. R. Hall, J. M. Stewart), Universities of Western Australia and Maryland, **1989**.

Mössbauer Spectroscopy and Electronic Structure Calculations of the Nitridoferrates(III): $Li_3[FeN_2]$ and $Ba_3[FeN_3]$**

By *Nils Jansen, Hartmut Spiering, Philipp Gütlich,* Dagmar Stahl, Rüdiger Kniep, Volker Eyert, Jürgen Kübler,* and *Peter C. Schmidt**

Dedicated to Professor Horst Elias on the occasion of his 60th birthday

Nitridoferrates show a multitude of structural elements unknown for other iron compounds, most of which are characterized by a low coordination number for the iron atom. In order to obtain a greater insight into the nature of Fe^{III}–N bonds, we have examined the nitridoferrates(III) $Li_3[FeN_2]$ and $Ba_3[FeN_3]$ with ^{57}Fe Mössbauer spectroscopy. Quantitative analyses of the isomer shifts and the quadrupole splittings in the Mössbauer spectra were performed with the help of band structure calculations.

Nitridoferrates have not been known very long. In their crystal structures, complex anions are found which are formally isosteric to systems with main group elements.[1] The crystal structure of $Li_3[FeN_2]$[2] can be described as a fluorite superstructure in which the nitrogen atoms build a slightly distorted cubic close-packing arrangement and the Fe^{III} ions occupy neighboring tetrahedral holes along [001] forming $^1_\infty[FeN^{3-}_{4/2}]$ chains of edge-sharing tetrahedra (formally isosteric to SiS_2, see Fig. 1 left). The Fe^{III}–N bond length (195.7(2) pm) is consistent with a single bond. An especially short Fe^{III}–N bond exists in the trigonal-planar $[FeN_3]^{6-}$ anion analogous to CO_3^{2-} ($Ba_3[FeN_3]$[3] see Fig. 1 right) whereby a Fe–N bond order greater than one must be considered. Correspondingly, the IR spectrum of $Ba_3[FeN_3]$ shows a high-frequency $n_3(E')$ vibration mode at 618 cm^{-1} for a structural group with D_{3h} symmetry.[4] In the crystal structure of $Ba_3[FeN_3]$ all the atoms fall on (001) planes at

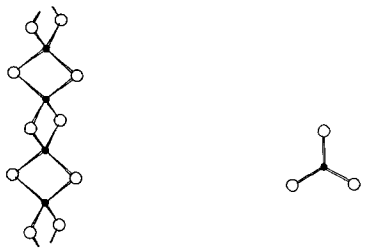

Fig. 1. Fe in $Li_3[FeN_2]$ is present in $^1_\infty[FeN^{3-}_{4/2}]$ chains consisting of edge-sharing tetrahedra, whereas in $Ba_3[FeN_3]$ Fe is found in trigonal-planar anions $[FeN_3]^{6-}$ analogous to CO_3^{2-}.

[*] Prof. Dr. P. Gütlich, Dipl.-Chem. N. Jansen, Dr. H. Spiering
Institut für Anorganisehe Chemie und Analytische Chemie der Universität
Staudingerweg 9, D-W-6500 Mainz (FRG)
Prof. Dr. P. C. Schmidt, Dr. V. Eyert[+]
Institut für Physikalische Chemie der Technischen Hochschule
Petersenstrasse 20, D-W-6100 Darmstadt (FRG)
Dipl.-Ing. D. Stahl, Prof. Dr. R. Kniep
Eduard-Zintl-Institut der Technischen Hochschule Darmstadt
Prof. Dr. J. Kübler
Institut für Festkörperphysik der Technischen Hochschule Darmstadt
[+] Current address:
Max-Planck-Institut für Festkörperforschung Stuttgart

[**] This work was supported by the Deutsche Forschungsgemeinschaft and the Fonds der Chemischen Industrie.

heights of $z = 1/4$ and $z = 3/4$; the barium atoms are surrounded by nitrogen atoms of $[FeN_3]^{6-}$ groups as distorted trigonal planes. By stacking the layers along [001] in the sequence ..ABAB.., the coordination spheres about the nitrogen atoms are completed to form distorted octahedra and about the barium atoms to give trigonal bipyramids.

Electronic structures were obtained through band structure calculations based on the "local spin density functional approach",[5] whereby Bloch states were determined by the ab initio ASW method (Augmented Spherical Wave).[6] The band structure calculations for $Li_3[FeN_2]$ and $Ba_3[FeN_3]$ indicate a charge transfer from Li/Ba to the complex nitridoferrate ions and the presence of strong covalent d_{Fe}–p_N bonds. Figure 2 shows a simplified d-orbital level diagram of the wave function around the central iron atom in $Ba_3[FeN_3]$. The lower E' and E'' levels as well as their

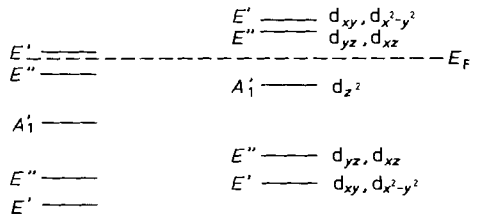

Fig 2. A simplified level diagram for both spin directions (α and β in the antiferromagnetic state) based on the partial density of the d-orbital states for Fe in $Ba_3[FeN_3]$. The positions of the levels correspond to the center of the maxima in the density of states. E_F = Fermi energy.

respective partially occupied antibonding levels are utilized for the covalent bonding to nitrogen. The A levels correspond to the nonbonding iron states.

For the Mössbauer measurements, the compounds were prepared according to reported procedures[2, 3] and checked for phase purity by X-ray diffraction and chemical analyses. At higher temperatures the Mössbauer spectra[7] of $Li_3[FeN_2]$ and $Ba_3[FeN_3]$ contain doublets due to quadrupole interactions. The isomer shift $\delta_{\alpha-Fe}$ (i.e., relative to α-iron) for $Li_3[FeN_2]$, $\delta_{\alpha-Fe}(263\,K) = 0.06(2)\,mm\,s^{-1}$, falls in the region common for low-spin iron(III) compounds. In contrast, in the case of $Ba_3[FeN_3]$ the $\delta_{\alpha-Fe}(263\,K)$ value of $-0.55(2)\,mm\,s^{-1}$ is unusually negative for low-spin Fe^{III}. This strong negative isomer shift can be explained by both d_π–p_π backbonding between the nitrido ligands and the central atom (the s-electron density on the Fe nucleus is increased because of the reduced shielding by the d-electrons, see also Table 1), and a predominate σ-donating effect of the electron-rich nitrido ligands. In essence, the 4s orbital is filled, whereby the short Fe–N bond (173.0(12) pm) together with the low coordination number (3) allow for strong overlapping, and the charge-accepting 4s orbital of the central atom is represented by a relatively large contribution to the corresponding molecular orbital. Further increase of s-electron density at the Fe nucleus could be brought about by $4s3d_{z^2}$ hybridization, which has been calculated by Yee and Hughbanks[8] with extended-Hückel and ab initio methods.

For a quantitative theoretical analysis of the isomer shifts, the charge density ρ on the Fe nucleus in $Li_3[FeN_2]$, $Ba_3[FeN_3]$, and a series of other iron compounds was computed by the ASW method.[6] The results are summarized in Figure 3; a remarkably good linear correlation appears between the measured isomer shifts and the calculated charge densities. The slope of the fitted line, $\alpha = -0.35\,a_0^3\,mm\,s^{-1}$,

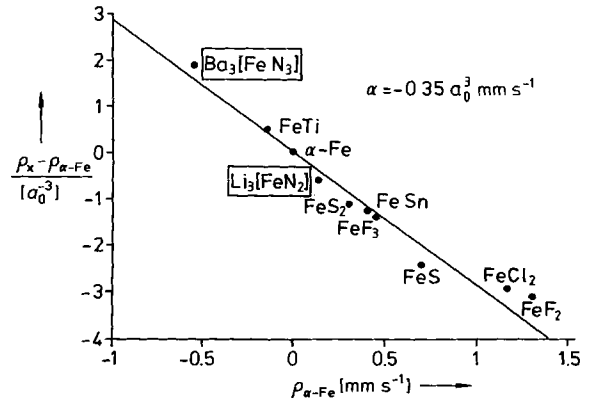

Fig 3. A plot of the charge density ($\rho_x - \rho_{\alpha-Fe}$) on the Fe nucleus was computed with the ASW technique as function of the measured isomer shift $\delta_{\alpha\,Fe}$ reported in ref. [11–15] for a series of compounds; structural data in ref. [16]. α is the slope of the fitted line, $\delta_{\alpha-Fe} = \alpha(\rho_x - \rho_{\alpha-Fe})$ [17].

is in accord with the results of other nonrelativistic Hartree–Fock calculations [9].

The individual contributions of the 3s and 4s charge densities to the isomer shift δ, ($\rho_x(3s) - \rho_{\alpha-Fe}(3s)$ and $\rho_x(4s) - \rho_{\alpha-Fe}(4s)$), as well as the data concerning the charges are given in Table 1. The charge Q of the valence electrons within

Table 1. The contributions of the 3s and 4s charge densities to the isomer shift δ and the partial charge Q on Fe in FeTi, $Li_3[FeN_2]$, and $Ba_3[FeN_3]$ (in multiples of $-e$). The last terms are the s, p, and d portions of the valence electron charge within a sphere having a radius $r = 119$ pm about the Fe nucleus.

	$Li_3[FeN_2]$	FeTi	$Ba_3[FeN_3]$
Q_{4s}	0.35	0.38	0.44
Q_{4p}	0.44	0.33	0.58
Q_{3d}	6.19	6.19	5.83
$Q = Q_{4s} + Q_{4p} + Q_{3d}$	6.98	6.90	6.85
Q_{4s}/Q [%]	5.00	5.50	6.30
$\rho_x(3s) - \rho_{\alpha-Fe}(3s)$ [a_0^{-3}]	−0.14	0.06	1.21
$\rho_x(4s) - \rho_{\alpha-Fe}(4s)$ [a_0^{-3}]	−0.16	0.41	1.02

a sphere around the Fe nucleus was calculated for $Li_3[FeN_2]$, $Ba_3[FeN_3]$, and FeTi. In order to analyze for trends in the values of charges for the three compounds, spheres of equal radii, 119 pm, were utilized; this radius corresponds to the Wigner–Seitz radius for $Li_3[FeN_2]$. The values for Q in Table 1 show that the valence electron charge within the sphere decreases from $Li_3[FeN_2]$ with $Q = -6.98e$ to $Ba_3[FeN_3]$ with $Q = -6.85e$.

In accordance with the basis functions used in the ASW method, the charge Q is distributed according to angular momentum. For $Ba_3[FeN_3]$, the 4s-like portion of Q and therefore the magnitude of the direct 4s contribution to δ is greatest (6.30%, see Table 1), and because of the lowest Q the nucleus-shielding through the 3s shell valence electrons is weakest. This explains the unusually strong negative isomer shift $\delta_{\alpha-Fe}$ observed for $Ba_3[FeN_3]$.

The quadrupole splitting ΔE_Q is $0.86(2)\,mm\,s^{-1}$ for $Li_3[FeN_2]$ and $0.65(2)\,mm\,s^{-1}$ for $Ba_3[FeN_3]$. By measuring the Mössbauer spectra in an external magnetic field, the sign of the V_{ZZ} component of the electric field gradient (EFG) tensor for $Ba_3[FeN_3]$ was determined to be negative. Thus it can be assumed that the distribution of the negative charge can be visualized as cigar-shaped. The partial charge or the "occupation number" of the levels shown in Figure 2 pro-

vides a qualitative explanation for the sign of the EFG, whereby the angular part of the EFG for the levels A_1' and E'' are negative and for E' positive.[10] We find a clear predominance for the partial charging of the A_1' and E'' levels over E'.

Received: July 27, 1992 [Z 5479 IE]
German version: *Angew. Chem.* **1992**, *104*, 1632

CAS Registry numbers:
$Li_3[FeN_2]$, 12332-29-5; $Ba_3[FeN_3]$, 137886-01-2.

[1] A. Gudat, S. Haag, P. Höhn, R. Kniep, W. Milius, A. Rabenau, *J. Alloys Compd.* **1991**, *177*, L17.
[2] A. Gudat, R. Kniep, A. Rabenau, W. Bronger, U. Ruschewitz, *J. Less-Common Met.* **1990**, *161*, 31.
[3] P. Höhn, R. Kniep, A. Rabenau, *Z. Kristallogr.* **1991**, *196*, 153.
[4] P. Höhn, Diplomarbeit, Technische Hochschule Darmstadt, **1990**; M. Somer, Stuttgart, private communication.
[5] P. C. Hohenberg, W. Kohn, *Phys. Rev.* **1964**, *136*, B864; W. Kohn, L. J. Sham, *Phys. Rev. A* **1965**, *140*, 1133; W. Kohn, P. Vashishta in *Theory of the Inhomogeneous Gas* (Eds.: S. Lundquist, N. H. March), Plenum, New York, **1983**, p. 75; U. von Barth, L. Hedin, *J. Phys. C* **1972**, *5*, 1629.
[6] A. R. Williams, J. Kübler, C. D. Gelatt, *Phys. Rev. B* **1979**, *19*, 6094.
[7] N. Jansen, Diplomarbeit, Universität Mainz, **1991**.
[8] K. A. Yee, T. Hughbanks, *Inorg. Chem.* **1992**, *31*, 1921.
[9] K. J. Duff, *Phys. Rev. B* **1974**, *9*, 66; W. C. Nieuwpoort, D. Post, P. T. van Duijnen, *ibid.* **1978**, *17*, 91; A. Trautwein, F. E. Harris, *Theor. Chim. Acta* **1973**, *30*, 45.
[10] P. Gütlich, R. Link, A. Trautwein, *Mössbauer Spectroscopy and Transition Metal Chemistry (Inorganic Chemistry Concepts 3*, Springer, Heidelberg, **1978**, p. 24).
[11] K. Ono, A. Ito, E. Hirahara, *J. Phys. Soc. Jpn.* **1962**, *17*, 1747.
[12] J. Danon, *Rev. Mod. Phys.* **1964**, *36*, 459.
[13] S. De Benedetti, G. Lang, R. Ingalls, *Phys. Rev. Lett.* **1961**, *6*, 60.
[14] W. Kerler, W. Neuwirth, E. Fluck, P. Kuhn, B. Zimmermann, *Z. Phys.* **1963**, *173*, 321.
[15] *Mössbauer Effect Data Index* (1969–1971) (Eds.: J. G. Stevens, V. E. Stevens), Hilger, London, **1971**.
[16] M. A. Hepworth, K. H. Jack, R. D. Peacock, G. J. Westland, *Acta Crystallogr.* **1957**, *10*, 63; J. W. Stout, S. A. Reed, *J. Am. Chem. Soc.* **1954**, *76*, 5279; A. Herpin, P. Meriel, *C. R. Hebd. Seances Acad. Sci.* **1957**, *245*, 656; R. Kohlhaas, P. Dünner, N. Schmitz-Pranghe, *Z. Angew. Phys.* **1967**, *23*, 245; J. M. D. Coey, H. Roux-Buisson, *Mater. Res. Bul.* **1979**, *14*, 711; G. Will, J. Lauterjung, H. Schmitz, E. Hinze, *Mater. Res. Soc. Symp. Proc.* **1984**, *22*, 49; R. Ray, B. C. Giessen, N. J. Grant, *Metall. Trans.* **1972**, *3*, 627; C. Djega-Mariadassou, E. Both, G. Trumpy, *Ann. Chim. (Paris)* **1970**, *5*, 505.
[17] V. I. Goldanskii, E. F. Makarov in *Chemical Applications of Mössbauer Spectroscopy* (Eds.: V. I. Goldanskii, R. H. Herber), Academic Press, New York, **1968**, p. 50.

Stereoselective Nucleophilic Addition Reactions of Reactive Pseudopeptides**

By *Manfred T. Reetz,* Jürgen Kanand, Nils Griebenow,* and *Klaus Harms*

Dedicated to Professor Ulrich Schöllkopf on the occasion of his 65th birthday

Little is known concerning natural or synthetic peptides with functional groups such as aldehyde or α,β-unsaturated ester moieties at the terminal positions in addition to the usual structural characteristics.[1] Nevertheless, their potential biological and pharmaceutical activity deserves attention.[1, 2] We are interested in whether stereoselective Grignard and cuprate additions can be conducted with these reactive peptides. Although the influence of the directly neighboring stereocenter would be expected to dominate within the context of 1,2-asymmetric induction, the more distant asymmetric centers could also influence product formation (1,*n*-asymmetric induction).

To begin with, the L,L pseudopeptides **3** with C-terminal α,β-unsaturated ester groups were prepared as outlined in Scheme 1. The Boc-protected leucinal **1**[3] was converted

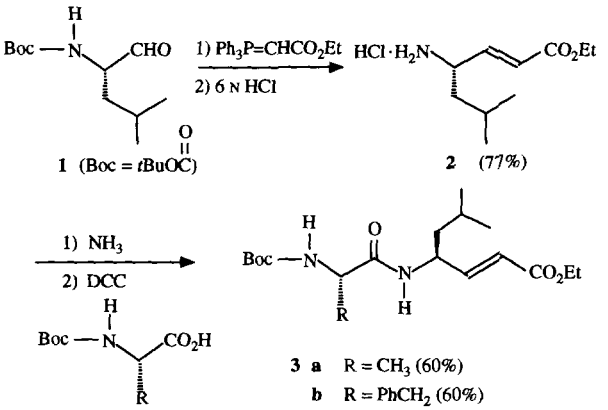

Scheme 1. Synthesis of pseudopeptides **3**.

without racemization into the vinylogous γ-amino acid ester **2** by Wittig olefination and subsequent deprotection with anhydrous HCl in dioxane. After the corresponding amine was obtained from **2** by treatment with ammonia, the peptide coupling was carried out with dicyclohexylcarbodiimide (DCC).

Whereas the reactions of $(CH_3)_2CuLi$ with pseudopeptides **3** were not diastereoselective,[4] the analogous addition of the bulky cuprate reagent $(tBu)_2CuLi$ in the presence of chlorotrimethylsilane[5] led to mixtures of the diastereomers **4** and **5** (80:20) with almost quantitative conversions (isolated yields **4a**/**5a**: 95% (R = CH_3) and **4b**/**5b**: 77% (R = $PhCH_2$). The products could be separated easily by chromatography.[6] As no other diastereomers were formed, the C–C bond forming reaction apparently proceeds without epimerization.

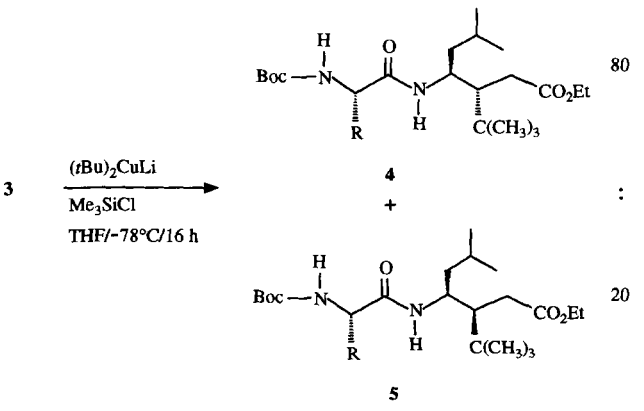

[*] Prof. Dr. M. T. Reetz, Dr. J. Kanand, Dipl.-Chem. N. Griebenow
Max-Planck-Institut für Kohlenforschung
Kaiser-Wilhelm-Platz 1, D-W-4330 Mülheim an der Ruhr
Dr. K. Harms
Fachbereich Chemie der Universität
Hans-Meerwein-Strasse, D-W-3550 Marburg (FRG)

[**] This research was supported by the Deutsche Forschungsgemeinschaft (Leibniz Programm) and the Fonds der Chemischen Industrie.

In order to test whether the adjacent stereocenter in peptides **3** solely determines the direction and degree of diastereoselectivity, the D,L pseudopeptides **6** were prepared analogously to **3**. Here the addition of the cuprate $(t\mathrm{Bu})_2\mathrm{CuLi}$ proceeded with high diastereoselectivity and with almost exclusive formation of peptides **7** (isolated yields: **7a** ($R = CH_3$) 94%, **7b** ($R = PhCH_2$) 79%). The structure of the products **4**/**5** and **7**/**8** was assigned by X-ray structure analysis and NMR spectroscopy.[6] For example, ester **7a**, an oil, was hydrolyzed to give the corresponding crystalline carboxylic acid **9**; the results of the X-ray structure analysis (Fig. 1)[7] prove the relative and absolute configuration. The molecule is found to fold itself in an interesting fashion: the lipophilic and polar portions form separate "regions".

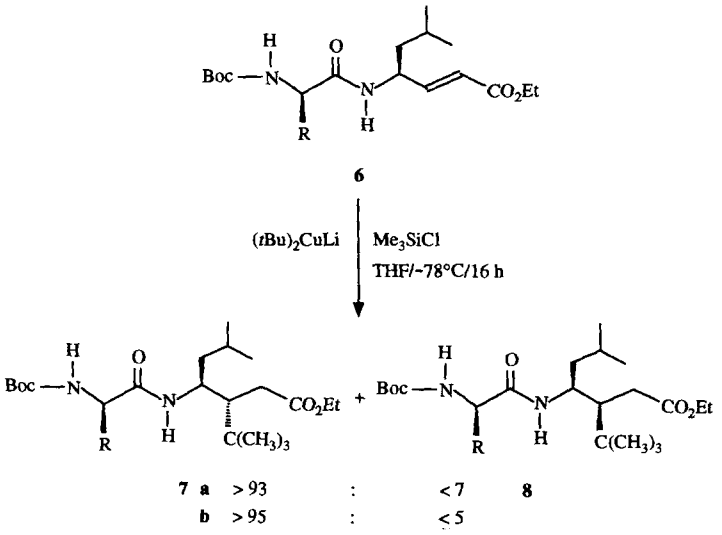

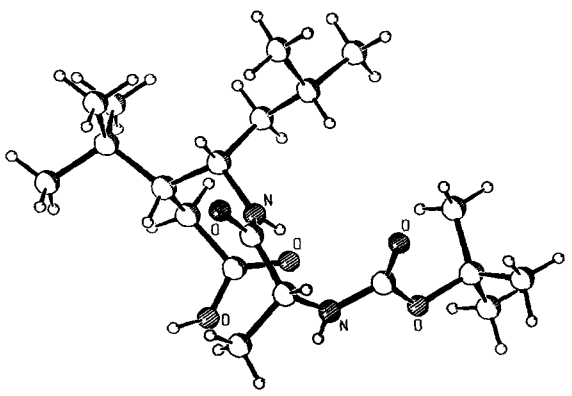

Fig. 1. Crystal structure of **9**.

These results show that in our examples the D,L pseudopeptides **6** always react more stereoselectively than the L,L analogues **3**. Thus, the influence of the directly adjacent stereocenter dominates, although 1,5-asymmetric induction is also evident.

In view of possible 1,8-asymmetric induction, the L,L,L and D,L,L pseudopeptides were prepared (Scheme 2). Dipeptides **10** and **12**, accessible by conventional methods, underwent DCC-mediated peptide coupling to give the respective diastereomeric L,L,L (**11**) and D,L,L (**13**) pseudopeptides without epimerization.[6]

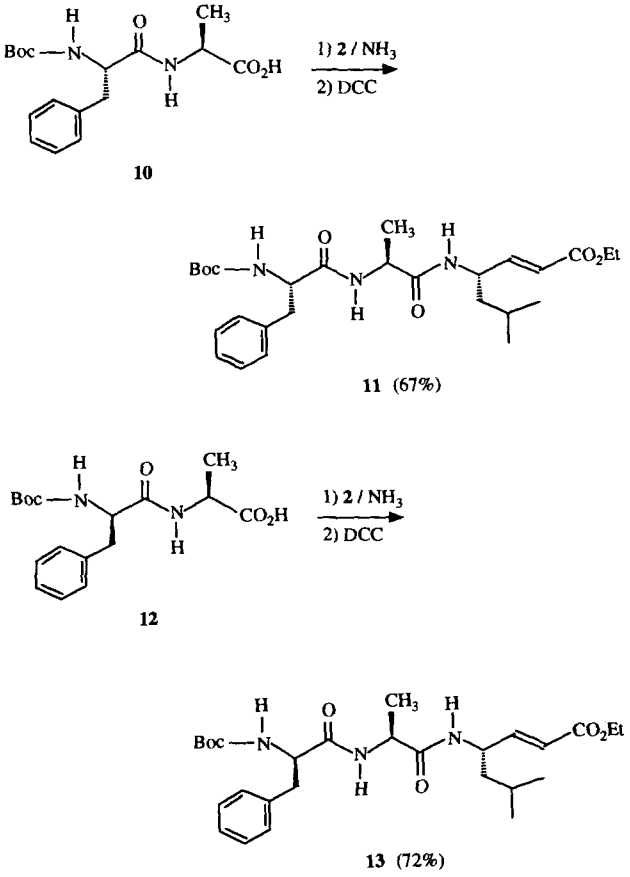

Scheme 2. Synthesis of pseudopeptides **11** and **13**.

The reactions of the L,L,L peptide **11** with $(CH_3)_2\mathrm{CuLi}$ and $(t\mathrm{Bu})_2\mathrm{CuLi}$ proceeded with diastereoselectivities of 82:18 and 88:12, respectively (95% yield of **14a** and **14b**). The same reactions conducted with the D,L,L peptide **13** had diastereoselectivities of only 67:33 and 79:21 with yields of 89% (**15a**) and 97% (**15b**). Although the final assignment of the relative configuration has not been made, it is most plausible that the direction of diastereoselectivity here is the same as in the reactions of the dipeptides (cf. **4**, **7**, **14**, and **15**). As in the case of the pseudopeptides **3**/**6**, 1,2-asymmetric induction dominates, but here again, the effect of the most distant stereocenter is apparent (1,8-asymmetric induction).

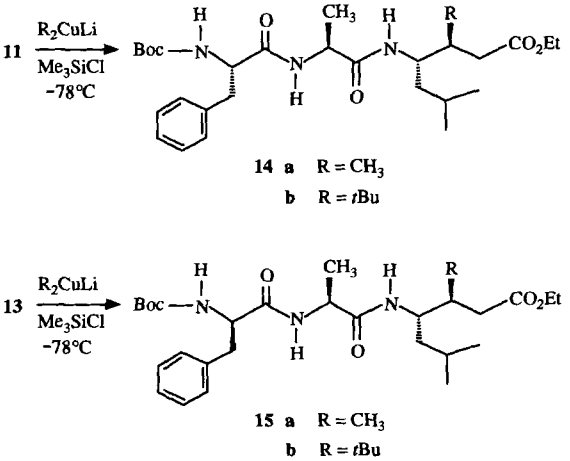

In order to investigate Grignard-type C–C bond forming reactions with peptide aldehydes,[3] we synthesized the L,L derivatives **17**; the reactions in Scheme 3 proceeded in high yield and without epimerization.[8] Following quantitative Swern oxidation and aqueous workup, the aldehydes were used in subsequent reactions without further purification.

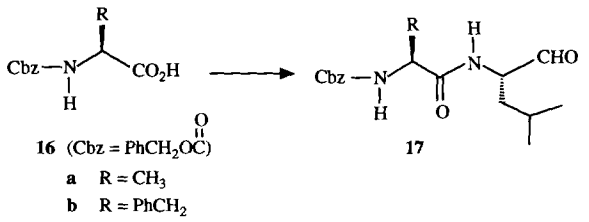

Scheme 3. Synthesis of peptide aldehydes **17**. 1) *N*-hydroxysuccinimide/DCC: 92–93%. 2) Leucinol: 86–90%. 3) DMSO/$(COCl)_2$: > 95%.

Whereas the peptide aldehydes **17** reacted with methylmagnesium iodide to give mixtures of four diastereomers due to undesired epimerization and nonstereoselective C–C bond formation, the reactions with $(CH_3)_2CuLi$ gave a single product in each case (**18a** and **18b** in yields of 92 and 85%, respectively). These Grignard-type reactions proceed under strict chelation control without epimerization.[3, 9] The diastereomeric peptide aldehydes **20**,[8] available in high yields, react similarly; besides the major products **21** only a small amount of a second diastereomer **22** was observed, the product of the chelation-controlled addition to the α-epimerized aldehydes.[10] Interestingly, control experiments showed that the L,L dipeptides **17** are configuratively much more stable than the D,L analogues **20**.[11]

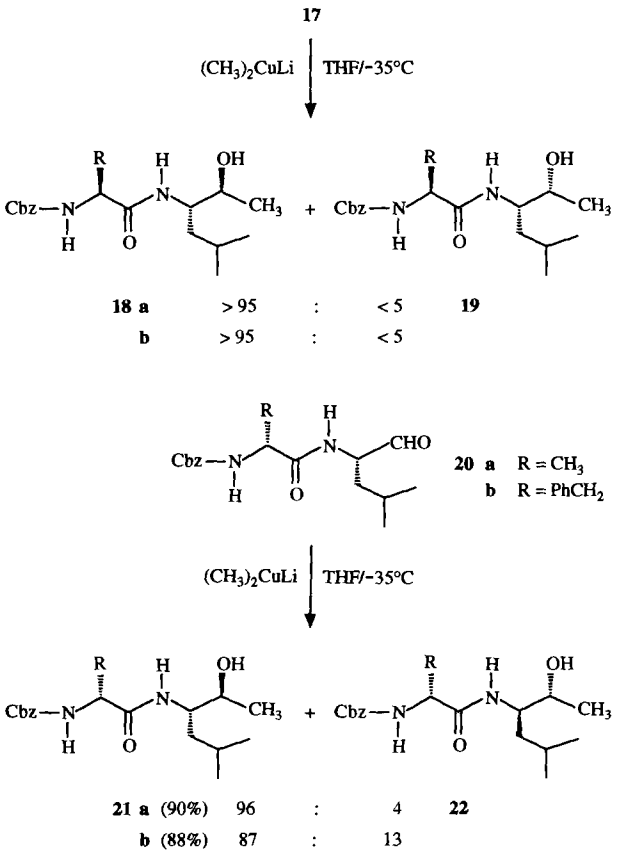

Concerning the mechanisms of the 1,2- and 1,4-additions to the aldehydes and α,β-unsaturated esters, respectively, metalation at the NH-acidic functions along the corresponding peptide chains is likely.[12, 13] A more detailed discussion of the reactions of α,β-unsaturated esters is problematic at this point, but plausible mechanisms can be formulated for the reactions of the peptide aldehydes. After deprotonation or metalation of the NH-acidic positions, a chelate complex of type **23** is formed in which the Cu^I center is tetracoordinated. Attack from the less shielded side then leads to the observed products. The "double" chelation in intermediate **23** could certainly be important, since the same reactions involving the Boc-protected α-amino aldehydes (cf. **1**) are less selective.

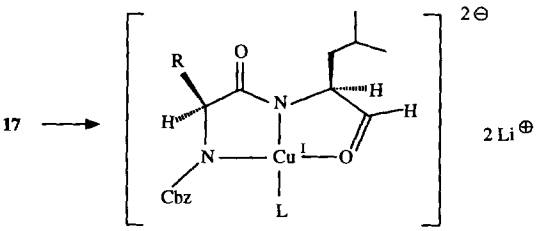

Further studies relating to classical Michael additions and cycloadditions are underway. The biological properties[2] of the peptides and their addition products also provide the basis of future investigations.

Received: July 29, 1992 [Z 5488 IE]
German version: *Angew. Chem.* **1992**, *104*, 1638

CAS Registry numbers:
1, 58521-45-2; **2**, 144408-30-0; **3a**, 144345-58-4; **3b**, 144345-59-5; **4a**, 144345-64-2; **4b**, 144345-65-3; **5a**, 144408-32-2; **5b**, 144408-33-3; **6a**, 144345-60-8; **6b**, 144345-61-9; **7a**, 144408-34-4; **7b**, 144408-35-5; **9**, 144345-70-0; **10**, 55677-48-0; **11**, 144345-56-2; **12**, 144345-57-3; **13**, 144408-31-1; **14a**, 144345-66-4; **14b**, 144345-67-5; **15a**, 144408-36-6; **15b**, 144408-37-7; **16a**, 1142-20-7; **16b**, 1161-13-3; **17a**, 133657-64-4; **17b**, 66253-29-0; **18a**, 144345-68-6; **18b**, 144345-69-7; **20a**, 144345-62-0; **20b**, 144345-63-1; **21a**, 144408-38-8; **21b**, 144408-40-2; **22a**, 144408-39-9; **22b**, 144408-41-3; $Ph_3P{=}CHCO_2Et$, 1099-45-2; Boc–Ala–OH, 15761-38-3; Boc–Phe–OH, 13734-34-4; $(tBu)_2CuLi$, 23402-75-7; Me_2CuLi, 15681-48-8; leucinol, 7533-40-6.

[1] a) Peptides with terminal and nonterminal α,β-unsaturated ester or amide Reactions: S. Kunimoto, T. Aoyagi, R. Nishizawa, T. Komai, T. Takeuchi, H. Umezawa, *J. Antibiot.* **1974**, *27*, 413–418; D. H. Rich, E. T. O. Sun, E. Ulm, *J. Med. Chem.* **1980**, *23*, 27–33; C. W. Smith, H. H. Sanei, T. K. Sawyer, D. T. Pals, T. A. Scahill, B. V. Kamdar, J. A. Lawson, *ibid.* **1988**, *31*, 1377–1382; S. Liu, R. P. Hanzlik, *ibid.* **1992**, *35*, 1067–1075; N. Fusetani, S. Matsunaga, H. Matsumoto, Y. Takebayashi, *J. Am. Chem. Soc.* **1990**, *112*, 7053–7054; M. Hagihara, N. J. Anthony, T. J. Stout, J. Clardy, S. L. Schreiber, *ibid.* **1992**, *114*, 6568–6570; b) Peptide aldehydes: H. Umezawa, *Enzyme Eng.* **1982**, *6*, 11–33; J. A. Fehrentz, A. Heitz, B. Castro, *Int. J. Pept. Protein Res.* **1985**, *26*, 236–241; Y. Hamada, T. Shioiri, *Chem. Pharm. Bull.* **1982**, *30*, 1921–1924; A. M. Murphy, R. Dagnino, P. L. Vallar, A. J. Trippe, S. L. Sherman, R. H. Lumpkin, S. Y. Tamura, T. R. Webb, *J. Am. Chem. Soc.* **1992**, *114*, 3156–3157.

[2] Low molecular weight peptides are often biologically active[1]; see also: *Amino Acids and Peptides* (Ed.: J. H. Jones, The Royal Society of Chemistry, Cambridge, **1991**.

[3] Review of the synthesis and reactions of α-amino aldehydes: J. Jurczak, A. Golebiowski, *Chem. Rev.* **1989**, *89*, 149–164; M. T. Reetz, *Angew. Chem.* **1991**, *103*, 1559–1573; *Angew. Chem. Int. Ed. Engl.* **1991**, *30*, 1531–1546.

[4] 1,4-Additions to simple γ-amino substituted α,β-unsaturated esters: M. T. Reetz, D. Röhrig, *Angew. Chem.* **1989**, *101*, 1732–1734; *Angew. Chem. Int. Ed. Engl.* **1989**, *28*, 1706–1709; see also M. Asami, T. Mukaiyama, *Chem. Lett.* **1979**, 569–572.

[5] Chlorotrimethylsilane accelerates the 1,4-addition of cuprates: E. J. Corey, N. W. Boaz, *Tetrahedron Lett.* **1985**, *26*, 6019–6022; E. Nakamura, S.

Matsuzawa, Y. Horiguchi, I. Kuwajima, *ibid.* **1986**, *27*, 4029–4032; A. Alexakis, J. Berlan, Y. Besace, *ibid.* **1986**, *27*, 1047–1050.
[6] J. Kanand, Dissertation, Universität Marburg, **1992**.
[7] Crystallographic data for **9** ($C_{20}H_{38}N_2O_5$, $M = 386.5$): orthorhombic, space group $P2_12_12_1$, $a = 1113.7(2)$, $b = 1126.0(2)$, $c = 1864.6(4)$ pm, $\alpha = \beta = \gamma = 90°$, $Z = 4$, $\rho_{calc} = 1.098\ g\,cm^{-1}$, $\mu(Cu_{K\alpha}) = 6.0\ cm^{-1}$. Measurement on an Enraf-Nonius CAD-4 diffractometer ($Cu_{K\alpha}$ radiation, $\lambda = 154.178$ pm, graphite monochromator, $T = 193$ K); 3293 measured reflections, of which 2916 were independent ($R_{int} = 0.0421$), 2570 with $F > 4.0\sigma(F)$ were regarded as observed. Solution with direct methods and refinement with the Siemans SHELXTL-PLUS(VMS) program system, $R = 0.0568$, $R_w = 0.0426$ ($w = 1/\sigma^2(F)$), all non-hydrogen atoms anisotropic, N- and O-bound H atoms localized, the others "riding" with common temperature factors for separate groups. Further details of the crystal structure investigation may be obtained from the Fachinformationszentrum Karlsruhe, Gesellschaft für wissenschaftlich-technische Information mbH, D-W-7514 Eggenstein-Leopoldshafen 2 (FRG), on quoting the depository number CSD-320520, the names of the authors, and the journal citation.
[8] N. Griebenow, Diplomarbeit, Universität Marburg, **1992**.
[9] Boc-protected α-amino aldehydes tend to racemize [3].
[10] In order to make configurational assignments, the products were prepared by independent syntheses [8].
[11] The L,L peptide **17a** is configuratively stable for one hour in $DCCl_3$ solution at room temperature, after which slow epimerization is observed. Under the same conditions the D,L peptide **20a** is epimerized within one hour to the extent of 10–15%. The dipeptide aldehydes are more stable in dimethylsulfoxide [8]. All of the diastereomers described here were characterized by NMR spectroscopy (400 MHz), so that epimerization could be proven or ruled out in every case.
[12] For maximum yields the cuprates were used in a 5–6-fold excess; gas (e.g. methane) formation was observed.
[13] In the reactions of peptides with *n*-butyllithium the NH function is deprotonated: D. Seebach, *Angew. Chem.* **1988**, *100*, 1685–1715; *Angew. Chem. Int. Ed. Engl.* **1988**, *27*, 1624.

A New Type of Mn–O Cluster with a Mn_4 Chain Unit—Relevance to the Photosynthetic Oxygen Evolving Center

By *Christian Philouze, Geneviève Blondin, Stéphane Ménage, Nathalie Auger, Jean-Jacques Girerd,* Daniel Vigner, Monique Lance*, and *Martine Nierlich*

The Oxygen Evolving Center (OEC) in photosystem II in plants is the subject of considerable research efforts.[1] Based on ESR studies Dismukes et al. and Brudvig et al. proposed that this reaction center contains a Mn_4 cluster.[2] More recently our group in collaboration with Zimmermann reinvestigated the S_2 step of the enzymatic cycle by ESR spectroscopy and confirmed the presence of a Mn_4 unit in the active site in this particular step.[3] Extensive EXAFS studies point out the presence of di-μ-oxo-dimanganese units with a Mn–Mn distance of 2.7 Å.[4] In the S_2 state, the average number of Mn atoms that are 2.7 Å away from another Mn atom was found to be 1.2 ± 0.5.[4c] Klein et al.[5] interpreted their EXAFS results by a model of the OEC in which four Mn ions are linked in a chainlike fashion. The first and the last links are di-μ-oxo bridges 2.7 Å in length, the middle one is an oxo-di-μ-carboxylato bridge 3.3 Å in length. The assignment of the 3.3 Å distance is much debated,[1c] as it could also be attributed to a Mn–Ca bond.

Since the most information on the naturally occurring cluster is obtained by ESR spectroscopy,[1–3] this research is also linked to work on the magnetic properties of metal clusters.[6] Several research groups have synthesized new tetranuclear manganese complexes[7] which are potential models of the OEC. But none of these contain two di-μ-oxo-dimanganese chains as in the model proposed by Klein et al.[5] We report here the synthesis, preliminary structural characterization, and magnetic study of a new type of Mn_4 cluster with a linear $[Mn_4O_6]^{4+}$ core which has a chain structure.

The cluster was synthesized by condensation of $[Mn(bpy)Cl_3(H_2O)]$[8] (0.2 g, 0.59 mmol) in 15 mL of H_2O/HNO_3 (pH = 2). During the addition (with stirring) the pH was maintained at a value of 2 by addition of small amounts of a sodium hydroxide solution. Then the reaction mixture was centrifuged and filtered, and the filtrate collected. Sodium perchlorate (0.146 g, 1.19 mmol) was added to the filtrate with stirring. After a few days dark-brown crystals of **1** were obtained (30% yield based on Mn). Elemental analysis (C, H, O, Cl, Mn, N) provided the stoichiometry of **1**.

$[Mn^{IV}_4O_6(bpy)_6](ClO_4)_4 \cdot 2H_2O$ **1**

A preliminary X-ray study[9] of **1** indicates that each cationic unit is made up of two di-μ-oxo-dimanganese units linked by a di-μ-oxo bridge (Fig. 1). The cation in **1** has close

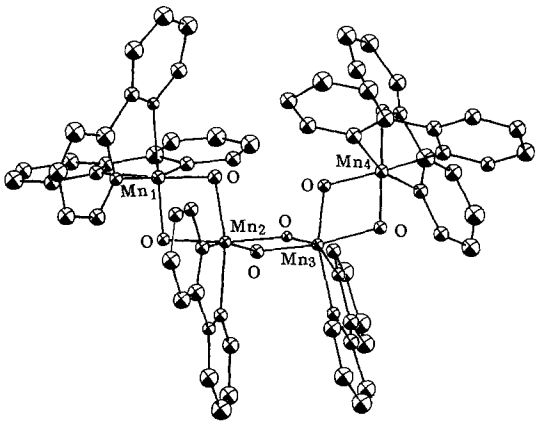

Fig. 1. Structural model for the $[Mn^{IV}_2O_6(bpy)_6]^{4+}$ ion in **1**. Data from a preliminary X-ray structure analysis.

to C_2 symmetry. The average number of Mn atoms that are 2.7 Å away from another Mn atom is 1.5, which is within the error range for the value found in the OEC.[4c] The linkage of the two $Mn_2(\mu\text{-}O)_2$ subunits is the main difference between cluster **1** and the proposed structure for the OEC based on EXAFS studies. But as pointed out above, the assignment of the peak in the EXAFS spectrum to a unit with a 3.3 Å bridge in the natural reaction center is uncertain. Thus our molecule could be a good structural model of the OEC. An EXAFS study of **1** is under way for comparison with the EXAFS spectrum of the OEC.

Compound **1** and other complexes illustrate the richness of the chemistry of $Mn^{III}Mn^{IV}$ in water. The condensation of $[Mn(bpy)Cl_3(H_2O)]$ in aqueous solution led to the dinuclear mixed-valent cluster $[Mn^{III}Mn^{IV}O_2(bpy)_4]^{3+}$ (pH = 4.5)[10] and the trinuclear cluster $[Mn^{IV}_3O_4(bpy)_4(H_2O)_2]^{4+}$ (pH = 0.4)[11]. The trinuclear cluster was also obtained by acidification of $[Mn^{III}Mn^{IV}O_2(bpy)_4]^{3+}$ in water.[12] The analogous phenanthroline complex forms the dinuclear monovalent cluster $[Mn^{IV}_2O_2(phen)_4]^{4+}$ in strongly acidic so-

[*] Dr. J.-J. Girerd, C. Philouze, Dr. G. Blondin, Dr. S. Ménage, Dr. N. Auger
Laboratoire de Chimie Inorganique, URA 420 CNRS
Institut de Chimie Moléculaire d'Orsay
Bat 420, Université Paris Sud
F-91405 Orsay (France)
D. Vigner, M. Lance, Dr. M. Nierlich
SCM, URA 331 CNRS, CEN Saclay
F-91191 Gif-sur-Yvette (France)

lutions.[13] With other ligands the chemistry of Mn^{III}, Mn^{IV} compounds in water is equally interesting.[14] The mechanism of these reactions is not yet known, although it is likely that the first step involves formation of Mn^{III}–O–Mn^{III} complexes followed by disproportionation to give $Mn^{III}Mn^{IV}$ complexes by the proton-dependent process proposed by Wieghardt.[14b]

The magnetic coupling in a Mn_4 unit can be studied with cluster **1**. The molar magnetic susceptibility χ_M of **1** as a function of the temperature T is given in Figure 2. The

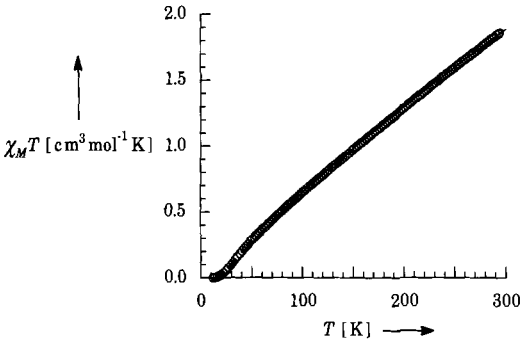

Fig. 2. Magnetic susceptibility ($\chi_M T$) of **1** as a function of temperature T (o experimental data, —— theoretical fit).

product $\chi_M T$ per mole of **1** is 1.85 cm^3mol^{-1} K at 293 K and decreases to 0 at 12 K. This behavior is characteristic of antiferromagnetic coupling between the electronic spins of the Mn^{IV} ions, which produces a ground state with $S = 0$. The structural information available for **1** allowed us to analyze the data with the Heisenberg–Hamiltonian operator as defined in Equation (a), where $S_i = 3/2$ is the value of the spin of the Mn_i^{IV} in Figure 1.

$$H_S = -J_{12}(S_1S_2 + S_3S_4) - J_{23}(S_2S_3) \quad \text{(a)}$$

Despite its simplicity, the topology of this cluster is such that there is no analytical solution for the eigenvalues since no subspin is a good quantum number. The only good quantum number is the total spin. The eigenvalues of H_S were calculated by diagonalizing the full 4^4 spin problem using the matrices constructed from six J coefficients and following the irreducible tensor theory. The magnetic susceptibility was calculated using Van Vleck's formula, and the fitting procedure with J_{12} and J_{23} as free parameters was linked to the diagonalization procedure. The best fit was obtained for antiferromagnetic couplings, $J_{12} = -176\ cm^{-1}$ and $J_{23} = -268\ cm^{-1}$; g was assigned a value of 2.00 (see Fig. 2). With these values the first excited state is calculated to be a spin triplet at $E(S=1) = 76\ cm^{-1}$.

The ground state has $S = 0$ since the spins can be organized in an antiparallel way to minimize interactions with each nearest neighbor (Scheme 1). Comparison of the structure proposed by Klein et al., a chainlike Mn_4 arrangement in the OEC,[5] with the structure of **1** points out the viability of the latter as a model for the OEC. As $(\mu\text{-O})_2Mn^{III}Mn^{III}$ and $-Mn^{III}Mn^{IV}$ units[7e, 12, 14a] are also strongly antiferromagnetic, a compound with a structure analogous to **1** would have an $S = 1/2$ ground state if the Mn_4 chains had the combination of oxidation states $Mn_3^{III}Mn^{IV}$ or $Mn^{III}Mn_3^{IV}$. The four spins could not negate each other regardless of the position of the odd spin along the chain. This would correspond to the S_2 state (Scheme 2). The synthesis of such a linear cluster would be very valuable.

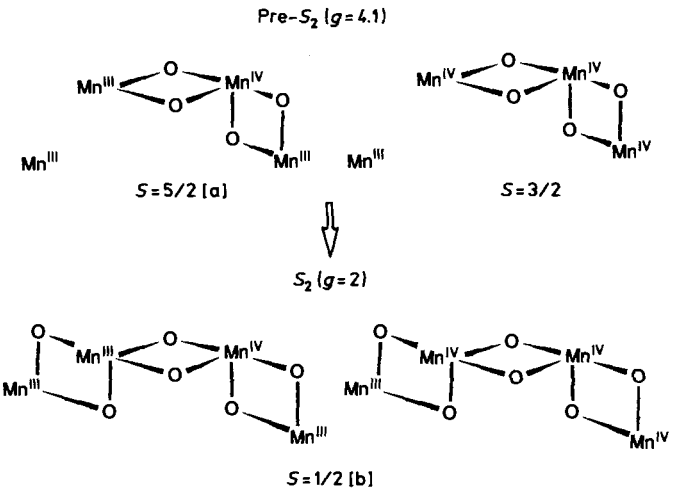

Scheme 2. Hypothetical model for the pre-S_2 and S_2 states of the OEC based on the structure of **1** and its magnetic properties. [a] If Mn^{IV} is terminal a value of $S = 3/2$ is obtained. [b] The position of the odd spin is undetermined.

One attractive feature of the proposal that the reaction center of the OEC has a cubane structure[1a] is that a small change in the coupling parameters could induce a change in the spin state of the ground state. This could explain why the spin of the ground state is $S = 3/2$ or 5/2 in the pre-S_2 state of the enzyme.[15] In a model with a Mn_4 chain the $S = 1/2$ ground state is less sensitive to a change in J. These spin values for the pre-S_2 state can be reconciled with the chain topology if the active site is composed of a linear trinuclear system plus a mononuclear unit, for instance Mn^{III}–Mn^{IV}–Mn^{III} ($S = 5/2$ or 3/2, depending on the position of the odd spin) + Mn^{III} or Mn^{IV}–Mn^{IV}–Mn^{IV} ($S = 3/2$) + Mn^{III} (Scheme 2). This arrangement corresponds to the proposals in refs. [4b, 16]. Such bent linear Mn_3 units were considered by Klein et al. and agree with their data.[17] We are currently trying to synthesize such compounds to compare their ESR spectroscopic properties with those of the enzyme in the pre-S_2 state.[18]

Received: May 25, 1992 [Z 5372 IE]
German version: *Angew. Chem.* **1992**, *104*, 1634

CAS Registry numbers:
1, 144468-30-4; $[Mn(bpy)Cl_3(H_2O)]$, 15632-12-9.

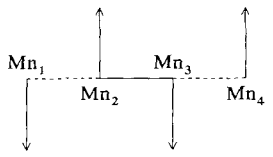

Scheme 1.

[1] a) G. W. Brudvig, H. H. Thorp, R. H. Crabtree, *Acc. Chem. Res.* **1991**, *24*, 311–316; b) A. W. Rutherford, A. Boussac, J.-L. Zimmermann, *New J. Chem.* **1991**, *15*, 491–500; c) A. W. Rutherford, J.-L. Zimmermann, A. Boussac in *The Photosystems: Structure, Function and Molecular Biology* (Ed.: J. Barber), **1992**, p. 179.

[2] a) G. C. Dismukes, Y. Siderer, *Proc. Natl. Acad. Sci. USA* **1981**, *78*, 274–278; b) J. C. de Paula, W. F. Beck, G. W. Brudvig, *J. Am. Chem. Soc.* **1986**, *108*, 4002–4009.

[3] J. Bonvoisin, G. Blondin, J.-J. Girerd, J.-L. Zimmermann, *Biophys. J.* **1992**, *61*, 1076–1086.
[4] a) G. N. George, R. C. Prince, S. P. Cramer, *Science* **1989**, *243*, 789–791; b) J. E. Penner-Hahn, R. M. Fronko, V. L. Pecoraro, C. F. Yocum, S. D. Betts, N. R. Bowlby, *J. Am. Chem. Soc.* **1990**, *112*, 2549–2557; c) R. D. Guiles, J.-L. Zimmermann, A. E. McDermott, V. K. Yachandra, J. C. Cole, S. L. Dexheimer, R. D. Britt, K. Wieghardt, U. Bossek, K. Sauer, M. P. Klein, *Biochemistry* **1990**, *29*, 471–485.
[5] M. P. Klein, V. K. Yachandra, V. J. DeRose, I. Mukerji, M. J. Latimer, K. Sauer, *J. Inorg. Biochem.* **1991**, *43*, 363.
[6] Magnetic studies of synthesized Mn clusters: a) S. Ménage, S. E. Vitols, P. Bergerat, O. Kahn, J.-J. Girerd, M. Guillot, X. Solans, T. Calvet, *Inorg. Chem.* **1991**, *30*, 2666–2671; b) D. N. Hendrickson, G. Christou, E. A. Schmitt, E. Libby, J. S. Bashkin, S. Wang, H.-L. Tsai, J. B. Vincent, P. D. W. Boyd, J. C. Huffman, K. Folting, Q. Li, W. E. Streib, *J. Am. Chem. Soc.* **1992**, *114*, 2455–2471.
[7] a) J. B. Vincent, G. Christou, *Adv. Inorg. Chem.* **1989**, *33*, 197–257; b) S. Wang, K. Folting, W. E. Streib, E. A. Schmitt, J. K. McCusker, D. N. Hendrickson, G. Christou, *Angew. Chem.* **1991**, *103*, 314; *Angew. Chem. Int. Ed. Engl.* **1991**, *30*, 305–306; c) M. K. Chan, W. H. Armstrong, *J. Am. Chem. Soc.* **1991**, *113*, 5055–5057; d) M. Mikuriya, Y. Yamato, T. Tokii, *Chem. Lett.* **1991**, 1429–1432; e) M. Suzuki, Y. Hayashi, K. Munezawa, M. Suenaga, H. Senda, A. Uehara, *ibid.* **1991**, 1929–1932; f) R. T. Sibrany, S. M. Gorun, *Angew. Chem.* **1990**, *102*, 1195; *Angew. Chem. Int. Ed. Engl.* **1990**, *29*, 1156–1158; g) M. K. Chan, W. H. Armstrong, *J. Am. Chem. Soc.* **1990**, *112*, 4985–4986.
[8] H. A. Goodwin, R. N. Sylva, *Aust. J. Chem.* **1965**, *18*, 1743–1749.
[9] Crystal data: triclinic, $P\bar{1}$, $a = 13.557(5)$, $b = 21.885(9)$, $c = 26.294(14)$ Å, $\alpha = 67.63(4)$, $\beta = 85.41(4)$, $\gamma = 73.82(4)°$, $V = 6926$ Å^3, $Z = 4$. Due to the low symmetry of the crystal and the number of atoms whose positions must be refined (312), the data set recorded led only to an R factor of 0.012. A more extensive data set will be recorded.
[10] S. R. Cooper, M. Calvin, *J. Am. Chem. Soc.* **1977**, *99*, 6623–6630.
[11] N. Auger, M. Nierlich, J.-J. Girerd, *J. Inorg. Biochem.* **1991**, *43*, 374.
[12] J. E. Sarneski, H. H. Holden, G. W. Brudvig, R. H. Crabtree, G. K. Schulte, *J. Am. Chem. Soc.* **1990**, *112*, 7255–7260.
[13] H. A. Goodwin, R. N. Sylva, *Aust. J. Chem.* **1967**, *20*, 629–637.
[14] See, for example a) P. A. Goodson, A. R. Oki, J. Glerup, D. J. Hodgson, *J. Am. Chem. Soc.* **1990**, *112*, 6248–6254; b) K. Wieghardt, U. Bossek, B. Nuber, J. Weiss, J. Bonvoisin, M. Corbella, S. E. Vitols, J.-J. Girerd, *J. Am. Chem. Soc.* **1988**, *110*, 7398–7411.
[15] a) J. C. de Paula, W. F. Beck, G. W. Brudvig, *J. Am. Chem. Soc.* **1986**, *108*, 4002–4009; b) J. L. Zimmermann, A. W. Rutherford, *Biochemistry* **1986**, *25*, 4609–4615; c) D. H. Kim, R. D. Britt, M. P. Klein, K. Sauer, *ibid.* **1992**, *31*, 541–547; d) A. Haddy, W. R. Dunham, R. H. Sands, R. Aasa, *Biochem. Biophys. Acta* **1992**, *1099*, 25–34.
[16] a) V. L. Pecoraro, *Photochem. Photobiol.* **1988**, *48*, 249–264; b) O. Hansson, T. Wydrzynski, *Photosynth. Res.* **1990**, *23*, 131–162.
[17] See citation 3 in ref. [4c].
[18] D. H. Kim, R. D. Britt, M. P. Klein, K. Sauer, *J. Am. Chem. Soc.* **1990**, *112*, 9389–9391.

Salting Out Selective Extraction—A Novel Method for the Optical Resolution of Chiral Sulfinylcarboxylic Acids and Its Application for the Convenient Determination of Optical Purity**

By *József Rábai**

Although the production of optically pure chiral compounds has attracted much interest, new and economical methods are slow to emerge.[1] In the synthesis of chiral compounds the enantiomers are often resolved by the preparation of diastereomeric salts.[2] The separation of the p- and n-salts formed is generally carried out by fractional crystallization.[3] We now report a novel optimized method of resolution, Salting Out Selective Extraction (SOSE), for the separation of noncrystallizable mixtures of diastereomeric salts. This method is demonstrated here with the racemic carboxylic acids **1**–**5**.[4]

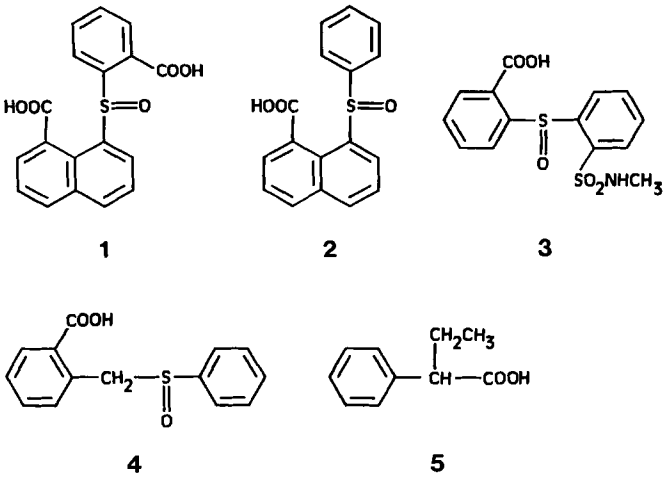

Our approach combines the advantages of the methods of Fogassy,[5] and of Pope and Peachey[6] as well as those of the selective extraction technique devised by Newton and Shapiro.[7] The treatment of two equivalents of racemic acid (±)-HA with one equivalent of the enantiopure chiral base (−)-B and one equivalent of NaOH leads to the formation of two diastereomeric salts, (−,−)-BHA (p-salt) and (−,+)-BHA (n-salt), besides the sodium salts of the enantiomeric anions of the carboxylic acid, (−)-NaA and (+)-NaA. The salts are partitioned between water and a water-immiscible solvent. The partition equilibrium of the p- and n-salts is determined by the separation constant β.[8] Thus the thermodynamic chiral recognition[2d] $\Delta\Delta G = -RT\ln\beta$ describes the molar free energy differences of the two diastereomeric salts in their formation and transfer equilibria. Only when $\beta \neq 1$ is separation of the diastereomeric salts expected. For example, in the optical resolution of racemic sulfinylcarboxylic acids **1**–**4** and 2-phenylbutyric acid (**5**) with (−)-quinine using a chloroform/water system, the respective optical yields[10] were 46, 31, 8, 11, and 1% after one extraction. Of course, successive extractions lead to a very high enantiomeric excess; when **1** was extracted three times 95% *ee* was achieved.

The compositions of the organic phase y and the aqueous phase z at equilibrium are described (in terms of enantiomeric excess) by the special resolution equations (a) and (b),

$$y = [a - \{(x + a)^2 - bx\}^{1/2}]/x \quad \text{(a)}$$

$$z = [l - d + a - \{(x + a)^2 - bx\}^{1/2}]/(1 - x) \quad \text{(b)}$$

$$a = (\beta d + l)/(\beta - 1);\ b = 4\beta d/(\beta - 1)$$

where β is the separation constant for the (+)-enantiomer, d and l denote the mole fractions of the (+)- and (−)-enantiomers before the extraction, and x represents the corresponding mole fractions of the chiral base. Equations (a) and (b) allow the calculation of the equilibrium composition y and z for any d, l, and x values at a given value of β. For example, if the concentration ratio of the racemate in solution is infinitely high (or only a catalytic amount of the resolving base is used, i.e. $d/x \rightarrow \infty$) then the enantiomeric

[*] Dr. J. Rábai
Department of Organic Chemistry
Eötvös University
Budapest -112, POB 32
H-1518 (Hungary)

[**] The author thanks Dr. I. Kövesdi for NMR measurements, and Prof. E. Fogassy (Technical University, Budapest) and Dr. I. T. Horváth (Exxon Corporate Research, Annandale) for valuable discussions. This research was supported by the Hungarian Academy of Sciences (OTKA 1234).

excess of the organic phase is described by $y = (\beta - 1)/(\beta + 1)$, the optical yield by $OY = yx/d$, and the optimal amount of the chiral base by $x_{optimal} = (\beta d - l)/(\beta - 1)$, provided that the relationship) $1/(\beta + 1) < d < \beta/(\beta + 1)$ holds. For a racemate with $d = l = 0.5$, $x_{optimal}$ has a value of 0.5.[2a, 6]

The maximum salt separation[11] that can be obtained by SOSE in one step is dependent on the selectivity for the preferred salt (or enantiomer) β^p which is related to the formation constants (k^p and k^n), the molar volumes and the polarities (δ^p and δ^n) of the diastereomeric salts, the polarity of the solvent pair (δ^w and δ^*), and the temperature by the general resolution equation (c).[12]

$$\ln \beta^p = \ln(k^p/k^n) + 2V(\delta^n - \delta^p)(\delta^w - \delta^*)/RT \qquad (c)$$

Since the molar volumes of the two salts are very similar, they are considered equal (V). While the Hildebrand polarity values (δ) are well documented for solvents,[13] the polarity differences between the two diastereomeric salts can be set high by the proper choice of the resolving agent. (Table 1, empirical). The solvent effect on the resolution of **1** with quinine appears to follow the general resolution equation (c) (method A, Fig. 1).

Table 1. Effectiveness of a number of chiral bases in resolving sulfinylcarboxylic acids **1** and **2** (method A). The sign of the separation constant β refers to the preferred enantiomer in the organic phase.

Base	β_1	OY [%]	β_2	OY [%]
(−)-brucine	1.20	5	1.0	0
(−)-quinine	7.38	46	3.57	31
(+)-quinidine	−4.55	36	−2.44	22
(+)-cinchonine	−2.04	18	−1.52	10
(−)-cinchonidine	2.63	24	1.73	14
(−)-3-pinanmethylamine	1.0	0	1.0	0

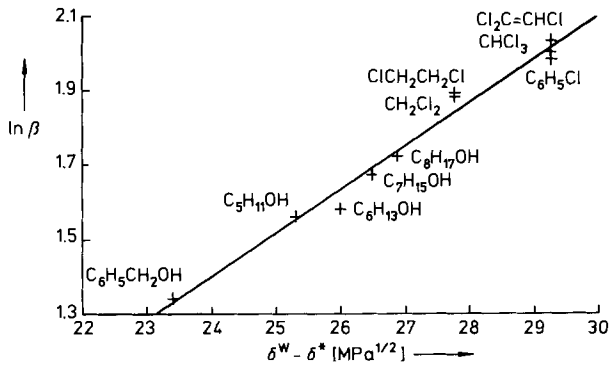

Fig. 1. Solvent dependence of the separation constant β for [(quinine)$_2$ · (+)-**1**]. The solid line was calculated with the equation $\ln\beta = -1.39 + 0.116(\delta^w - \delta^*)$, which was determined by least-squares fitting ($r = 0.99$) of the experimental data.

A new method to determine optical purity was also devised based on SOSE. Considering that β is constant and a function of [α] and [α^*],[8] one can derive Equation (d) for the calculation of the value of the absolute rotation. Here [α_1], [α_1^*], and [α_2], [α_2^*] are the specific rotations of the samples recovered from the aqueous (α) and organic (α^*) phases in two independent experiments designated by 1 and 2. For sulfinylcarboxylic acid **1** (method B) the following values were obtained: $\beta = 5.85$; $[\alpha_1]_D = -213$, $[\alpha_1^*]_D = +198$, $[\alpha_2]_D = -418$, $[\alpha_2^*]_D = -168$ ($c = 0.5$, DMF, 25 °C). Thus the calculated value of $[\alpha_{max}]_D$ is 495, and after total resolution $[\alpha]_D = 496 \pm 6$.[14] The corresponding dimethyl esters were prepared from partially resolved and racemic **1**. According to the ^{1}H NMR spectra of these mixtures recorded with Eu(tfc)$_3$ (tfc = 3-(trifluoromethylhydroxymethylene)-D-comphorato) in $CDCl_3$/TMS $[\alpha]_D$ has a value of 495 (100% *ee*). A sample of the carboxylic acid **1** with $[\alpha]_D = 330 \pm 4$ was treated with CH_2N_2. The enantiomeric excess of the resulting dimethyl ester was found to be 67% by ^{1}H NMR measurements.

$$\{[\alpha]_{max}\}^2 = \{[\alpha_1^*][\alpha_2^*]([\alpha_1] - [\alpha_2]) - [\alpha_1][\alpha_2]([\alpha_1^*] - [\alpha_2^*])\}/\{([\alpha_1] - [\alpha_2]) - ([\alpha_1^*] - [\alpha_2^*])\} \qquad (d)$$

Experimental Procedure

Solutions of the carboxylic acids **1**–**5** (5 equiv) in 0.2 N NaOH (25 mL) [method A] or in 0.50 N $KHCO_3$ (25 mL) [method B] were treated with crystalline quinine sulfate dihydrate (0.985 g, 1.25 mmol, 2.5 equiv) and then shaken with $CHCl_3$ (50 mL) at 20 °C until all the solid material dissolved and then 1 h longer. The two phases were separated, and the aqueous phase was acidified with 0.2 N H_2SO_4 (pH = 1) at 0 to 5 °C. The precipitate formed was filtered, washed with water, and dried over P_2O_5. The organic phase was extracted with 0.2 N NaOH (3 × 10 mL) then acidified, and the precipitate formed was isolated as described above. For the isolation of **5** the acidified aqueous phases were extracted with $CHCl_3$. Starting from (±)-**1** (0.895 g, 2.5 mmol, 5 equiv, method B) the aqueous phase gave 0.392 g (1.09 mmol) acid with $[\alpha_1]_D = -208$, while the organic phase gave 0.364 g (1.02 mmol) acid with $[\alpha_1^*]_D = +198$. Starting from **1** (5 equiv) with $[\alpha]_D = -342$ and quinine sulfate dihydrate (0.492 g, 0.625 mmol) as described above, the aqueous phase yielded 0.606 g acid with $[\alpha_2]_D = -418$ and the organic phase 0.228 g acid with $[\alpha_2^*]_D = -168$ ($c = 0.5$, DMF, 25 °C).

Received: May 21, 1992 [Z 5367 IE]
German version: *Angew. Chem.* **1992**, *104*, 1648

CAS Registry numbers:
(+)-**1**, 144320-46-7; (−)-**1**, 144320-45-6; (±)-**1**, 144320-41-2; **2**, 144320-42-3; **3**, 144320-43-4; **4**, 144320-44-5; **5**, 90-27-7.

[1] S. Borman, *Chem. Eng. News* **1990** *68(28)*, 9–14.
[2] For recent developments, see: a) M. Ács, E. Fogassy, F. Faigl, *Tetrahedron*, **1985**, *41*, 2465–2470. b) E. Fogassy, F. Faigl, M. Ács, *ibid.* **1985**, *41*, 2837–2840. c) E. Fogassy, F. Faigl, M. Ács, *ibid.* **1985**, *41*, 2841–2845. d) D. J. Cram, *Angew. Chem.* **1988**, *100*, 1041; *Angew. Chem. Int. Ed. Eng.* **1988**, *27*, 1009–1020. e) V. Prelog, M. Kovačević, M. Egli, *ibid.* **1989**, *101*, 1173 and **1989**, *28*, 1147–1152.
[3] S. H. Wilen, A. Collet, J. Jacques, *Tetrahedron*, **1977**, *33*, 2725–2736; J. Jacques, J. Collet, S. H. Wilen, *Enantiomers, Racemates and Resolutions*, Wiley-Interscience: New York, **1981**, Chapter 5, pp. 251–368.
[4] a) Due to the common-ion effect of the alkali carboxylates dissolved in the aqueous phase, the diastereomeric salts formed are (almost) quantitatively transferred into the organic phase. b) For preparation of (±)-**1**–**4**, see: J. Rábai, I. Kapovits, B. Tanács, J. Tamás, *Synthesis*, **1990**, 847–849. c) Optimization strategy involves two steps: 1) setting β as large as possible by judicious choice of solvent and chiral base, and 2) working at optimal stoichiometry.
[5] I. Rusznák, R. Soós, E. Fogassy, M. Ács, Hungarian Patent 12, 208 (1976). *Chem. Abstr.* **1976**, *85*, 192, 337.
[6] W. J. Pope, S. J. Peachey, *J. Chem. Soc.* **1899**, *75*, 1066–1093.
[7] E. Shapiro, R. F. Newton, *J. Am. Chem. Soc.* **1943**, *65*, 777–779.
[8] When SOSE is established [4a], the isolations occur with no optical fractionation, and the Horeau effect [9] is excluded (optical purity = *ee*); β can be calculated as: $\beta = \{(c_d^{org}/c_d^w)\ (c_l^w/c_l^{org})\}$ $k_d/k_l = ([\alpha_{max}^+] + [\alpha^*])/([\alpha_{max}^-] + [\alpha])([\alpha_{max}^+] - [\alpha^*])([\alpha_{max}^-] - [\alpha])$, where k_d and k_l are the formation constants for the appropriate diastereomeric salts in the aqueous phase. $[\alpha]_{max}$ is the absolute rotation; [α] and [α^*] are the specific rotations of the recovered samples from the aqueous and organic phases, respectively. For a reaction of (−)-B + (+)-HA ⇌ (−,+)-BHA the formation constant is $k_d = [(-,+)\text{-BHA}]/[(-)\text{-B}]\,[(+)\text{-HA}]$.
[9] A. Horeau, *Tetrahedron Lett.* **1969**, *36*, 3121–3124.
[10] E. Fogassy, A. Lopata, F. Faigl, F. Darvas, M. Ács, L. Töke, *Tetrahedron Lett.* **1980**, *21*, 647–650.

[11] When starting with racemates, $OY_{max} = (\beta^{1/2} - 1)/(\beta^{1/2} + 1)$, while for a sample of composition (d, l) $OY_{max} = \{(\beta d + l) - 2(\beta d l)^{1/2}\}/d(\beta - 1)$. The optical yield can be related to the thermodynamic chiral recognition. $\Delta\Delta G = -RT \ln \beta$, as $\beta = [(1 + OY)/(1 - OY)]^2$ when $d = l = x = 0.5$ $(0 \leq OY \leq 1)$.

[12] This expression was obtained from $\beta = (K_D^p/K_D^n)$ (k^p/k^n) by applying the distribution constant (K_D)-Hildebrand solubility (= polarity) parameter (δ) relationship [12a,b] to both diastereomeric salts. a) H. Freiser, *Solvent Extraction* in *An Introduction to Separation Science* (Eds.: B. L. Karger, S. R. Snyder, C. Horvath), Wiley, New York, 1973, Chapter 9, pp. 248–250. b) P. J. Schoenmakers, H. A. H. Billiet, L. de Galan, *Chromatographia*, **1982**, *15(3)*, 205–214. c) For a description of optical yield related to the Taft's σ^* parameters of the interacting groups in the diastereomeric salts, see: ref. [2b]. d) For the role of chiral discrimination in the energetics of salt formation, see: S. P. Zingg, E. M. Arnett, A. T. McPhail, A. A. Bothner-By, W. R. Gilkerson, *J. Am. Chem. Soc.*, **1988**, *110*, 1565–1580.

[13] J. H. Hildebrand, R. L. Scott, *Regular Solutions*, Prentice-Hall, Englewood Cliffs, NJ, **1962**.; A. F. M. Barton, *CRC Handbook of Solubility Parameters and Other Cohesion Parameters*, CRC Press Inc., Boca Raton, Florida, **1983**.

[14] The total resolution of carboxylic acid **1** was effected by selective solubilization with dioxane. The enantiomeric excess of the sample is soluble in this solvent, while the racemic part forms a stable and insoluble solvate [(±)-**1** · dioxane] [4b].

Gas-Phase Reactions of M^+ and $[CpM]^+$ (M = Fe, Co, Ni) with 1,3,5-Trisilacyclohexane: First Evidence for the Formation of 1,3,5-Trisilabenzene**

By *Asgeir Bjarnason** and *Ingvar Arnason*

The chemistry of carbosilanes has recently been reviewed,[1] and a number of silicon-substituted cyclohexane derivatives have been reported including $C_5H_{12}Si$ **1**,[2] $C_3H_{12}Si_2$ **2a**,[3] and Si_6H_{12} **3**.[4] Metal-catalyzed triple dehydrogenation of the all-carbon analogue to form cyclohexatriene (benzene) is well known, and its mono- and disila analogues, C_5H_6Si **4** and $C_4H_6Si_2$ **5**, have been isolated and characterized at low temperature in an argon matrix.[5] To our knowledge, however, neither $C_3H_6Si_3$ **6** nor Si_6H_6 have yet been observed. We report here on $C_3H_6Si_3$, $C_3H_8Si_3$, and $C_3H_{10}Si_3$ as ligands produced in the reactions of Fe^+, Co^+, Ni^+, $[CpFe]^+$, $[CpCo]^+$, and $[CpNi]^+$ with **2a**. The formulas

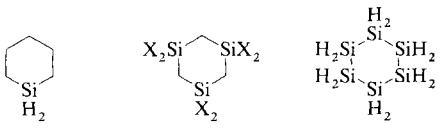

1

2a: X = H
2b: X = D
2c: X = Cl

3

4

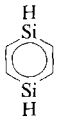

5

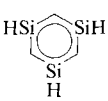

6

[*] Dr. A. Bjarnason,[+] Prof. Dr. I. Arnason Science Institute, University of Iceland
Dunhaga 3, IS-107 Reykjavik, (Iceland)

[+] A. Bjarnason is also Adjunct Associate Professor in the Department of Chemistry University of Delaware, Newark, DE (USA).

[**] This research was funded in part through grants from the University of Iceland Research Fund and the Icelandic Science Foundation. We thank Prof. D. P. Ridge for providing instrument access and for helpful discussions.

for the ligands were unambiguously determined, but the structures, especially that of $C_3H_6Si_3$, can only be speculated on; nevertheless, these appear to be the first observations of the trisilabenzene **6**.

Reactions of metal ions with organic molecules in the gas phase have been extensively studied in recent years by several research groups.[6] Dehydrogenation of cyclohexane by Fe^+,[7–9] Co^+,[8–10] Ni^+,[8, 9] $[CpCo]^+$,[11] and $[CpNi]^+$[12] have been reported, and in all cases, save Ni^+, elimination of up to three hydrogen molecules was observed to form the benzene ligand. Reactions of metal ions with silicon compounds in the gas phase have not been studied extensively. Of particular interest for us was the study of Beauchamp et al. on methylsilanes,[13] in which elimination of molecular hydrogen from a single silicon atom was observed and a product with a metal–silicon double bond proposed. The formation of the coordinated benzene from cyclohexane in the reactions with metal ions and ionic metal complex fragments prompted us to investigate reactions of such ions with **2a** in the gas phase, since efforts to produce **6** have been unsuccessful so far.

The product distribution in the dehydrogenation reactions of M^+ and $[CpM]^+$ with **2a** is shown in Table 1. Interesting-

Table 1. Product distribution [%] in dehydrogenation reactions of 1,3,5-trisilacyclohexane with M^+ and $[CpM]^+$.

Reactant ion	Elimination of		
	H_2	$2H_2$	$3H_2$
Fe^+	86	13	1
Co^+	16	81	3
Ni^+	66	33	1
$[CpFe]^+$	25	63	12
$[CpCo]^+$	7	71	22
$[CpNi]^+$	10	37	53

ly, $[CpM]^+$ ions are more reactive than the bare metal ions and cleave more than one H_2 molecule from **2a**. $[CpNi]^+$ is the most efficient, which is somewhat surprising: if the structure and bonding in $[CpMC_3H_6Si_3]^+$ were analogous to that in $[CpMC_6H_6]^+$, then in the case of M = Ni it would be a 20-electron, in the case of M = Co a 19-electron, and in the case of M = Fe an 18-electron species. From this point of view one would have expected the Fe complex to be formed more favorably than the Ni complex.

To test if H_2 is cleaved only from the carbosilane and whether the Cp ligand participates in that process, isotopically labeled $[[D_5]CpFe]^+$ was allowed to react with **2a**. Although minor products (< 5%) from loss of deuterium were observed, the main elimination reactions left the Cp ligand intact.

Another question that arises in light of the results of Beauchamp et al.[13] is whether hydrogen is eliminated only from Si, and if the metal than possibly forms a double bond to Si. The dissociation energies of the Si–H and C–H bonds are 314 and 414 kJ mol^{-1}, respectively.[1] As less energy is required to break the Si–H bond and in addition, backbonding may exist in the bond between the metal ion and Si, it was essential to establish which hydrogen atoms are eliminated in the reactions.

For this purpose, a sample of **2b** was prepared and allowed to react with M^+ and $[CpM]^+$. The results indicate that Ni^+ eliminates only D_2 (1 and 2 equiv). Fe^+ eliminates H_2, HD, and D_2 in the ratio 0.2:0.6:1.0, but only a minor amount of double dehydrogenation is observed (see

Table 1); in the case of Co^+, the cleavage of one equivalent of molecular hydrogen from **2a** is a minor reaction, but in the reaction with **2b** two equivalents of molecular hydrogen are formed as H_2, HD, or $H_2 + D_2$, $HD + D_2$, and D_2 in the ratio 0.05:0.1:0.8:1.0. These results suggest that Ni^+ eliminates hydrogen only from Si and, thus, may form bonds only to silicon atoms in the ring. Fe^+ and Co^+ show less preference for elimination from the silicon atoms, and elimination of HD points to the formation of a double bond between C and Si. Triple dehydrogenation in the reactions of $[CpM]^+$ with **2b** was shown to involve mostly elimination of 3 HD and to a lesser extent $2\,HD + D_2$. Only traces of the product of the elimination of 3 equivalents of D_2 was observed, which supports the hypothesis that the main product in the triple dehydrogenation reaction requires the formation of three carbon–silicon double bonds and that the 1,3,5-trisilabenzene **6** ligand is produced.

Collision-induced dissociation (CID) experiments can give valuable information about the structure of ions trapped in the cell of an FT mass spectrometer; Jacobson and Freiser successfully employed this technique to study products from the reactions of $[CpCo]^+$ with cyclohexane.[11] They found, for example, that $[Co(Cp)(benzene)]^+$ lost benzene upon CID, consistent with a stronger bond between Co–Cp than between Co–benzene. CID studies on $[CpNiC_3H_6Si_3]^+$ (accelerated to 90 eV) were performed with Ar as the collision gas. Aside from losses of one, two, and three molecules of hydrogen, three other fragment ions were observed at m/z 123 (45%), 58 (35%), and 93 (20%), corresponding to $[CpNi]^+$, Ni^+, and $C_5H_5Si^+$, respectively. The last ion is probably formed by rearrangements, since under multiple-collision conditions (higher pressure of Ar) it was the dominant fragment ion, but at conditions approaching the single-collision regime this ion became less intense with respect to the signal corresponding to $[CpNi]^+$, which became the dominant fragment ion. These observations are in accord with the proposed structure of $[CpNiC_3H_6Si_3]^+$.

The results from the CID experiments and the deuterium labeling studies lead us to the conclusion that the trisilabenzene **6** was formed as a ligand in these experiments. Further studies of reactions of metal ions and ionic metal complex fragments with other silicon-containing compounds are in progress in light of these promising results.

Experimental Procedure

The experimental method has been described in detail elsewhere [14], but it is summarized briefly here: The experiments were conducted with an EXTREL FTMS-2000 Fourier-transform mass spectrometer with dual-cell configuration [15]. Fe^+ and $[CpFe]^+$ were generated from $[CpFe(CO)_2I]$, which was introduced into the mass spectrometer in a sample vial on the direct insertion probe. The ions were produced by electron impact in the source side of the dual cell and transfered to the analyzer side. The ion of interest was isolated with double-resonance techniques [16] and allowed to react with **2a** or **2b**, which was introduced to the analyzer side through two pulsed valves from the batch inlet system. Co^+ and $[CpCo]^+$ were produced in the same manner from $[Cp_2Co]$, and Ni^+ and $[CpNi]^+$ from $[CpNiCO]_2$. It should be noted, that only $[CpNi]^+$ containing the ^{58}Ni isotope was isolated and allowed to react with the carbosilane. The course of the reaction could be monitored by collecting mass spectra after a variable delay time and/or by varying the pressure of the sample in the expansion volume of the batch inlet system. For CID studies a second set of pulsed valves was used to introduce the Ar collision gas on the analyzer side after isolation of the ion of interest. This ion was then excited to kinetic energies sufficient for its dissociation upon collision with the Ar atoms.

2a was prepared from **2c** according to a published procedure [3]. **2b** was prepared in an analogous manner using $LiAlD_4$ instead of $LiAlH_4$ and characterized by NMR spectroscopy.

Received: May 14, 1992
Revised: August 22, 1992 [Z 5346IE]
German version: *Angew. Chem.* **1992**, *104*, 1654

CAS Registry numbers:
2a, 291-27-0; **2b**, 144436-83-9; **6**, 143587-15-9; Fe^+, 14067-02-8; Co^+, 16610-75-6; Ni^+, 14903-34-5; $[CpFe]^+$, 61827-27-8; $[CpCo]^+$, 79075-58-4; $[CpNi]^+$, 52668-78-7.

[1] G. Fritz, E. Matern, *Carbosilanes: Syntheses and Reactions*, Springer, Berlin, **1986**.
[2] R. West, *J. Am. Chem. Soc.* **1954**, *76*, 6012.
[3] G. Fritz, H. Fröhlich, *Z. Anorg. Allg. Chem.* **1971**, *382*, 9.
[4] a) E. Hengge, D. Kovar, *Angew. Chem.* **1977**, *89*, 417; *Angew. Chem. Int. Ed. Engl.* **1977**, *16*, 403; b) *Z. Anorg. Allg. Chem.* **1979**, *459*, 123.
[5] a) G. Maier, G. Mihm, H. P. Reisenauer, *Angew. Chem.* **1980**, *92*, 58; *Angew. Chem. Int. Ed. Engl.* **1980**, *19*, 52; b) G. Meier, G. Mihm, R. O. W. Baumgartner, H. P. Reisenauer, *Chem. Ber.* **1984**, *117*, 2337; c) G. Maier, K. Schöttler, H. P. Reisenauer, *Tetrahedron Lett.* **1985**, *26*, 4079.
[6] For representative work in this field see, for example: a) P. B. Armentrout, J. L. Beauchamp, *J. Am. Chem. Soc.* **1981**, *103*, 784; b) J. Wronka, D. P. Ridge, *ibid.* **1984**, *106*, 67; c) S. K. Huang, J. Allison, *Organometallics* **1983**, *2*, 883; d) Y. Huang, B. S. Freiser, *J. Am. Chem. Soc.* **1988**, *110*, 387; e) A. K. Chowdhury, C. L. Wilkins, *ibid.* **1987**, *109*, 5336; f) N. Aristov, P. B. Armentrout, *J. Phys. Chem.* **1987**, *91*, 6178; g) H. Schwarz, *Acc. Chem. Res.* **1989**, *22*, 282; h) A. Bjarnason, J. W. Taylor, *Organometallics* **1989**, *8*, 2020; i) A. Bjarnason, *ibid.* **1991**, *10*, 1244; For a recent review see: j) K. Eller, H. Schwarz, *Chem. Rev.* **1991**, *91*, 1121.
[7] G. D. Byrd, R. C. Burnier, B. S. Freiser, *J. Am. Chem. Soc.* **1982**, *104*, 3565.
[8] D. B. Jacobson, B. S. Freiser, *J. Am. Chem. Soc.* **1983**, *105*, 7492.
[9] D. B. Jacobson, B. S. Freiser, *Organometallics* **1984**, *3*, 513.
[10] P. B. Armentrout, J. L. Beauchamp, *J. Am. Chem. Soc.* **1981**, *103*, 6628.
[11] D. B. Jacobson, B. S. Freiser, *J. Am. Chem. Soc.* **1985**, *107*, 7399.
[12] a) J. Müller, W. Goll, *Chem. Ber.* **1973**, *106*, 1129; b) R. R. Corderman, Dissertation, California Institute of Technology, Pasadena, CA, USA, **1977**.
[13] H. Kang, D. B. Jacobson, S. K. Shin, J. L. Beauchamp, M. T. Bowers, *J. Am. Chem. Soc.* **1986**, *108*, 5668.
[14] a) A. Bjarnason, J. W. Taylor, J. A. Kinsinger, R. B. Cody, D. A. Weil, *Anal. Chem.* **1989**, *61*, 1889; b) A. Bjarnason, J. W. Taylor, *Organometallics* **1990**, *9*, 1493.
[15] R. B. Cody, Jr., J. A. Kinsinger, S. Ghaderi, I. J. Amster, F. W. McLafferty, C. E. Brown, *Anal. Chim. Acta* **1985**, *178*, 43.
[16] a) M. B. Comisarow, V. Grassi, G. Parisod, *Chem. Phys. Lett.* **1978**, *57*, 413; b) A. G. Marshall, M. B. Comisarow, G. Parisod, *J. Chem. Phys.* **1979**, *71*, 4434.

A 1:1 Adduct of 2-Aminobenzothiazole and a Urea Derivative, and Its Spatial Arrangement**

By *David R. Armstrong, Matthew G. Davidson, Avelino Martín, Paul R. Raithby, Ronald Snaith,* and Dietmar Stalke*

We reported recently the fortuitous isolation and structural characterization of the unique 1:1 adduct of 2-aminobenzothiazole $OxNH_2$ (**1**) and hexamethylphosphoramide (HMPA **2**), which is stable even in boiling water.[11] In view of the similarity between **1** and certain of the natural bases found in DNA (A, G, and C have *exo*-NH_2 groups as well as N atoms and/or NH units in their ring systems; T has ring NH units), this adduct (**1** · **2**) was suggested as a model to help explain the carcinogenicity of **2**. The carcinogenicity

[*] Dr. R. Snaith, M. G. Davidson, A. Martín, Dr. P. R. Raithby
University Chemical Laboratory
Lensfield Road, GB-Cambridge, CB2 1EW (UK)
Dr. D. R. Armstrong
Department of Pure and Applied Chemistry
University of Strathclyde, GB-Glasgow, G1 1XL (UK)
Dr. D. Stalke
Institute for Inorganic Chemistry
Tammannstrasse 4, D-W-3400 Göttingen (FRG)

[**] We thank the Science and Engineering Research Council (SERC) and the Associated Octel Co. Ltd. (CASE award to M. G. D.) for financial support.

of **2** has prompted recommendations that dimethylpropyleneurea (DMPU, **3**), a proven non-carcinogen, should be

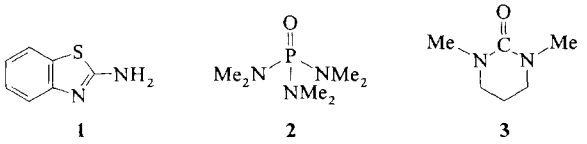

1 **2** **3**

used as an alternative to or replacement for **2**, both as a dipolar solvent and as a Lewis base in organometallic complexes.[2] Reasoning that the respective carcinogenic and non-carcinogenic properties of **2** and **3** have an essentially structural basis, we have now prepared and characterized the 1:1 adduct of **1** and **3**. There are indeed (at least in the solid state) striking structural differences between **1** · **3** and **1** · **2** in terms of the arrangement within the dimeric adducts and also the arrangement in space. Such findings are relevant also to the design of hydrogen-bonded supramolecular systems within the field of molecular recognition.[3, 4]

The adduct **1** · **3** can be obtained as a crystalline material simply by stirring a 1:1 mixture of the two components in toluene and then cooling the resulting solution (see Experimental Procedure). The crystal structure of **1** · **3**,[5] the first reported for a complex of **3** and another organic molecule, differs significantly from that of **1** · **2**, although at first glance the structures appear to be similar. The adduct **1** · **2** is dimeric; two molecules of **1** form a base pair through HN–H ··· N(ring) hydrogen bonds (N ··· N distances 3.014(5) Å); the other hydrogen atom of each NH_2 group of **1** forms a hydrogen bond with the oxygen atom of **2** (O ··· N 2.783(5) Å).[1] Adduct **1** · **3** is also dimeric (Fig. 1) and has analogous HN–H ··· N(ring) hydrogen bonds linking the $(\mathbf{1})_2$ base pair (N ··· N 2.988(7) Å) and terminal HN–H ··· O hydrogen bonds (O ··· N 2.748(7) Å). One difference between the two

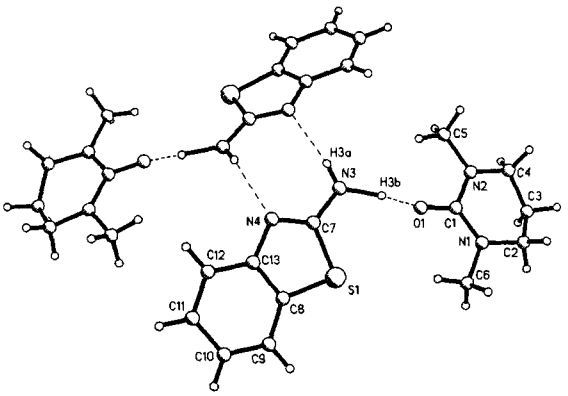

Fig. 1. Molecular structure of $(\mathbf{1} \cdot \mathbf{3})_2$.

structures is that in $(\mathbf{1} \cdot \mathbf{2})_2$ the base pair is essentially coplanar, whilst in $(\mathbf{1} \cdot \mathbf{3})_2$ the base pair is almost hemispherical. However, the N ··· N and O ··· N distances imply that not only the base-pair linkages in the two adducts but also the base–acceptor interactions (acceptor = **2** and **3**) are of similar strength. Ab initio MO calculations on a model system of the **1** · **2** adduct (e.g., HC=CHSC(=N)NH_2 for **1**, O=PH_3 for **2**) implied that the base-pair linkage is relatively weak (ca. 5.4 kcal mol^{-1}) compared to the interaction between the NH_2 group of **1** and the O atom of **2** (ca. 10.2 kcal mol^{-1}, the formation energy for a monomeric adduct).[1] Preliminary MO calculations on HC=CHSC(=N)NH_2, on **3**, and on their monomeric adduct indicate a slightly lower base–acceptor interaction energy of approximately 8.9 kcal mol^{-1}.[6] This may imply that the base-pair linkage in **1** · **3** is stronger.

The interesting structural differences between the two adducts are found in the spatial arrangement of the dimers. The dimers of **1** · **2** are aggregated further by (**2**)O ··· HC(aromatic) interactions,[1] whereas dimers of **1** · **3** are discrete and not linked together in any way. This does not seem to be a consequence of any substantial electronic differences between **2** and **3**. Ab initio calculations[6] indicate that the polarities of the C=O and P=O bonds, and the partial charges on the oxygen centers in these compounds, are similar: in $(H_2N)_3P{=}O$, a model for **2**, the partial charge on the phosphorus atom is +1.32 and that on the oxygen atom −0.60; in **3** the partial charge on the carbonyl carbon atom is +1.12 and that on the oxygen atom −0.67. It seems, then, that the aggregation of dimers of **1** · **2** and the discrete nature of dimers of **1** · **3** has a steric cause. The oxygen atom in **3** is clearly far less open and thus less available than the oxygen atom in **2** for interdimer hydrogen bonding for two reasons. Firstly, the C=O bond is shorter (1.220(7) Å in the crystal structure of $(\mathbf{1} \cdot \mathbf{3})_2$; 1.241 Å in the optimized structure of **3**) than the P=O bond (1.471(3) Å in the crystal structure of $(\mathbf{1} \cdot \mathbf{2})_2$;[1] 1.470 Å in the optimized structure of $(H_2N)_3P{=}O$). Secondly, the oxygen atom in **3** is blocked by the two NMe groups, which are in fixed positions by virtue of being part of a ring system; in contrast, the NMe_2 groups of **2** are pinned back from the P=O bond and quite flexible in the positions they adopt.

The spatial arrangements of adducts **1** · **2** and **1** · **3** are shown in Figure 2. Figure 2a shows the unit cell of the **1** · **2** adduct (view along the *c* axis); the higher aggregation of the adduct dimers is apparent. Figure 2b reveals the spatial arrangement of the **1** · **3** adduct; here the dimers are discrete.

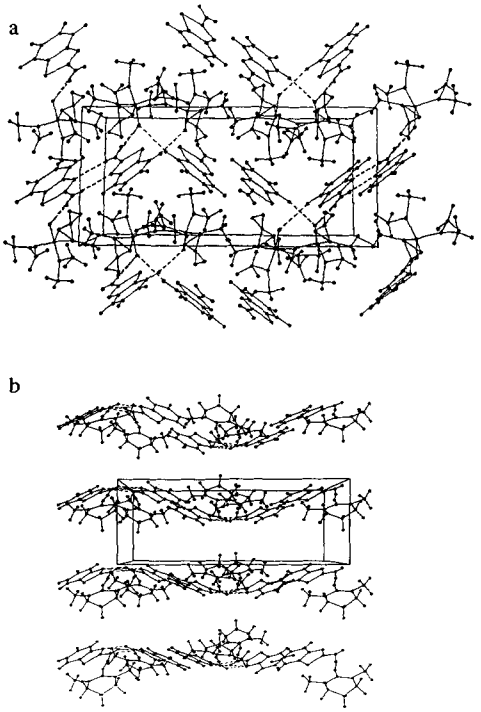

Fig. 2. a) View along the *c* axis of the unit cell of $(\mathbf{1} \cdot \mathbf{2})_2$ showing the crystal packing and the interactions between the dimers. b) View along the *c* axis of the unit cell of $(\mathbf{1} \cdot \mathbf{3})_2$.

This is more evident if one looks down the *b* axis of the unit cell of **1** · **3** (in effect, the space between pairs of dimers); then the beautiful packing shown in Figure 3 emerges; the central

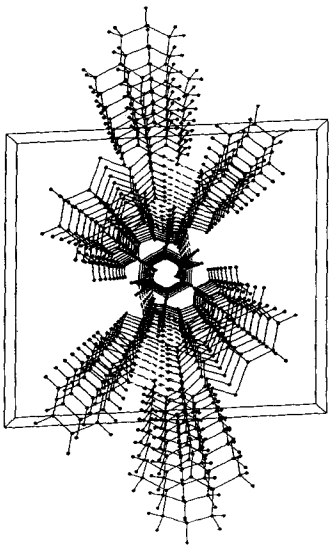

Fig. 3. View down the *b* axis of $(\mathbf{1}\cdot\mathbf{3})_2$ illustrating the highly symmetrical, tunnel-like stacking.

"tunnel" is formed by oxygen atoms of **3**. Interestingly, a hot toluene solution of the adduct $(\mathbf{1}\cdot\mathbf{3})_2$ dissolves solid LiBr, further heating of the resulting solution then causes precipitation of a white solid. The adduct also absorbs appreciable quantities of Br_2 gas to afford a mustard-colored powder. The identities of both products are being investigated.

We are also investigating supramolecular systems with similar components to those described here. To explore further the reasons for the carcinogenicity of **2** and the relative innocuousness of **3**, we are also examining their adducts with individual DNA bases and with natural base pairs.

Experimental Procedure

(**1** · **3**): 2-aminobenzothiazole (**1**) (3.00 g, 20 mmol) was dissolved at room temperature in a solution of **3** (2.56 g, 20 mmol) in toluene (20 mL). This solution was cooled at 0 °C for 1 d to afford white crystals of the adduct (first batch yield 5.05 g, 91%; m.p. 101–102 °C; correct elemental analysis; ^{1}H NMR ($CDCl_3$, 250 MHz, 25 °C): δ = 7.53–7.44 (m, 2H; **1**), 7.23 (t, 1H; **1**), 7.04 (t, 1H; **1**), 6.33 (br.s, NH_2; **1**), 3.18 (t, 4H; **3**), 2.88 (s, $2CH_3$; **3**), 1.95–1.86 (quin, 2H; **3**). Crystals suitable for X-ray analysis were grown slowly from a more dilute solution (5 mmol of each component in 10 mL toluene).

Received: July 11, 1992 [Z 5460 IE]
German version: *Angew. Chem.* **1992**, *104*, 1662

CAS Registry number:
1 · **3**, 144467-83-4.

[1] D. R. Armstrong, S. Bennett, M. G. Davidson, R. Snaith, D. Stalke, D. S. Wright, *J. Chem. Soc. Chem. Commun.* **1992**, 262–264.

[2] a) D. Seebach, R. Henning, T. Mukhopadhyay, *Chem. Ber.* **1982**, *115*, 1705–1721; b) T. Mukhopadhyay, D. Seebach, *Helv. Chim. Acta* **1982**, *65*, 385–391.

[3] For recent reviews of the area of molecular recognition, including hydrogen-bonding aspects, see: a) J.-M. Lehn, *Angew. Chem.* **1990**, *102*, 1347–1362; *Angew. Chem. Int. Ed. Engl.* **1990**, *29*, 1304–1319; b) J. Rebek, *ibid.* **1990**, *102*, 261–272 and **1990**, *29*, 245–255.

[4] For key recent papers concerning organic supermolecules constructed by hydrogen bonding, see: a) J. A. Zerkowski, C. T. Seto, D. A. Wierda, G. M. Whitesides, *J. Am. Chem. Soc.* **1990**, *112*, 9025–9026; b) F. Garcia-Tellado, S. J. Geib, S. Goswami, A. D. Hamilton, *ibid.* **1991**, *113*, 9265–9269; c) C. V. K. Sharma, K. Panneerselvam, T. Pilati, G. R. Desiraju, *J. Chem. Soc. Chem. Commun.* **1992**, 832–833, and references therein.

[5] X-ray crystal structure data on ($OxNH_2$ · DMPU) **1** · **3**: $C_{13}H_{18}N_4OS$, M = 278.4, monoclinic, space group $C2/c$, a = 20.187(18), b = 7.535(3), c = 18.666(13) Å, β = 92.72(7)°, V = 2836.1(14) Å^3, Z = 8, ρ_{calcd} = 1.304 Mg m^{-3}, $F(000)$ = 1184, $\lambda(Mo_{K\alpha})$ = 0.71073 Å, $\mu(Mo_{K\alpha})$ = 2.27 cm^{-1}, T = 180 K. Data were collected on a Stoe four-circle diffractometer, 2627 reflections collected in range $7° \le 2\theta \le 45°$. The structure was solved by a combination of direct methods and Fourier difference techniques, and refined by full-matrix least squares [all non-hydrogen atoms anisotropic; all hydrogens except H(3a), H(3b) placed in idealised positions; H(3a), H(3b), the NH_2 hydrogen atoms of **1**, freely refined] to R = 0.082, R_w = 0.095 for 1857 unique reflections [$F > 4\sigma(F)$]. Further details of the crystal structure are available on request from the Director of the Cambridge Crystallographic Data Centre, University Chemical Laboratory, Lensfield Road, GB-Cambridge, CB2 1EW (UK), by quoting the full journal citation.

[6] The ab initio calculations were performed with the 6-31G basis set with d orbitals on phosphorus and sulfur (W. J. Hehre, R. Ditchfield, J. A. Pople, *J. Chem. Phys.* **1972**, *56*, 2257–2261; P. C. Hariharan, J. A. Pople, *Theor. Chim. Acta* **1973**, *28*, 213–222; J. D. Dill, J. A. Pople, *J. Chem. Phys.* **1975**, *62*, 2921–2923) by means of the program GAMESS (M. Dupuis, D. Spangler, J. J. Wedoloski, GAMESS NRCC Software Catalogue, Program No. 2GOI, **1980**. Vol. 1; M. F. Guest, J. Kendrick, S. A. Pope, GAMESS Documentation, Daresbury Laboratory, Warrington, UK, **1983**). All geometries were freely optimized. The total energies (in a.u.) calculated for the optimized structures mentioned in the text are: $(H_2N)_3P{=}O$, −582.442838; DMPU, −417.787305; $HC{=}CHSC(=\overset{+}{N})NH_2$, −622.225046; the monomeric adduct between DMPU and $HC{=}CHSC(=\overset{+}{N})NH_2$, −1040.026456.

Corannulene Tetraanion: A Novel Species with Concentric Anionic Rings**

By *Ari Ayalon, Mordecai Rabinovitz,* Pei-Chao Cheng,* and *Lawrence T. Scott**

Dedicated to Professor Emanuel Vogel and Professor Klaus Hafner on the occasion of their 65th birthdays

Tetraanions of polycyclic aromatic hydrocarbons have only rarely been observed.[1] The possibility that corannulene (**1**) might be easily reduced and even "supercharged" with four electrons to make a stable, closed-shell tetraanion, however, was suggested by the prediction[2] that the lowest unoccupied molecular orbital (LUMO) of this unique bowl-shaped molecule should be doubly degenerate and lie below the antibonding energy level (E_{LUMO} = − 0.922 eV by MNDO calculations). The prospect that the tetraanion of corannulene might enjoy special stability as an aromatic cyclopentadienyl anion (6e/5C) suspended by five radial bonds within the hole of an aromatic 18e/15C annulenyl trianion as in **2** provided additional impetus to examine this system, since such a species might fulfill the long quest for a π-electron system having concentric aromatic rings, which began with the heroic synthesis of kekuléne.[3] Herein we report the preparation, ^{1}H and ^{13}C NMR spectra, and proton quenching experiments of the corannulene tetraanion.

[*] Prof. Dr. M. Rabinovitz, A. Ayalon
Department of Organic Chemistry
The Hebrew University of Jerusalem
Jerusalem 91904 (Israel)
Prof. Dr. L. T. Scott, P. C. Cheng
Department of Chemistry and Center for Advanced Study
University of Nevada
Reno, NV 89557-0020 (USA)

[**] We thank the U.S.-Israel Binational Science Foundation and the U.S. Department of Energy for financial support of this work and P. W. Rabideau for congenial exchange of information.

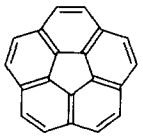

1

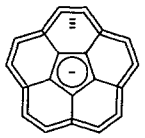

2

Reduction of corannulene (**1**)[4] at −78 °C with excess lithium metal in [D_8]THF over a period of several days leads to a series of three color changes, first to green, then to purple, and finally to brownish-red. Only for the last stage could an NMR spectrum be recorded, presumably owing to the presence of paramagnetic species at the intermediate stages of reduction.[5] Quenching this solution with water affords tetrahydrocorannulene (GC/MS, *m/z* 254) as the major product accompanied by lesser amounts of dihydrocorannulene and corannulene (ratio ≈ 4:2:1). The formation of tetrahydrocorannulene upon protonation constitutes one piece of evidence for the presence of a quadruply charged system.

Further evidence that the final reduction product is indeed a tetraanion comes from its ^{13}C NMR spectrum: ([D_8]THF) $\delta = 86.8$ (d, $^1J_{CH} = 151$ Hz, rim CH), 95.1 (tt ≈ heptet, $^3J_{CH} = 7.0$ Hz, $^2J_{CH} = 3.6$ Hz, rim quaternary C),[6] 112.4 (m, $^3J_{CH}$ and two different $^4J_{CH}$, hub C). All three ^{13}C NMR bands of the reduction product are dramatically shifted to high field compared to those of the neutral hydrocarbon (cf. **1**: $\delta = 127.9$, 132.3, 136.9, respectively, in [D_8]THF); the weighted center of the ^{13}C NMR bands shifts by $\Delta\delta = -36.1$. Charge/chemical shift correlations first proposed by Fraenkel et al.[7a] predict a total ^{13}C NMR signal shift of $\Delta\delta \approx 160$ per negative charge. A subsequent modification of this correlation introduced by Eliasson, Edlund, and Müllen,[7b] which takes into account the anisotropy of π-electron systems, predicts a shift of $\Delta\delta \approx 150$ per unit of charge. The actual value we observe is $\sum\Delta\delta = 722$ (!) or $\Delta\delta = 180.5$ per unit of charge. These correlations provide convincing evidence that the species observed is a quadruply charged system.

The ^1H NMR spectrum of the corannulene tetraanion in [D_8]THF consists of a single line at $\delta = 6.95$ (cf. **1**: $\delta = 7.93$ in [D_8]THF). This low-field chemical shift is surprising in view of the high electron density on the rim methine carbon atoms (see ^{13}C NMR data and charge density calculations). Ordinarily, protons attached to anionic hydrocarbon C atoms are strongly shielded and resonate at exceptionally high field, for example, in the pentadienyl anion $\delta_{avg} = 4.0$.[8] Apparently, the π system of the corannulene tetraanion supports an induced diamagnetic ring current (or two) that is strong enough to counterbalance the shielding effect of four negative charges.

Whether or not the "annulene-within-an-annulene" structure **2** is the best description of this tetraanion remains to be established. MNDO calculations, with the lithium ions included,[2] yield a global minimum in which all four lithium ions lie on the convex face of a bowl-shaped tetraanion, each located over the face of a different benzene ring. This structure has 1.1 units of negative charge on the five hub carbon atoms, 2.2 units of negative charge on the ten rim methine carbon atoms, and 0.7 units of negative charge on the five rim quaternary carbon atoms. The five radial bonds of the tetraanion are calculated to be 0.01–0.06 Å longer than the five C–C bonds within the inner ring, as one would expect for **2**. High-level theoretical calculations on all the reduced (and oxidized) states of corannulene would be most desirable;[9] however, it is already clear from the initial results reported herein first that corannulene can be easily reduced to a stable tetraanion, and second that this tetraanion carries substantial negative charge on both the hub and the rim carbon atoms, thereby classifying it as a species with concentric anionic rings.

Received: August 24, 1992 [Z 5531 IE]
German version: *Angew. Chem.* **1992**, *104*, 1691

CAS Registry numbers:
1, 5821-51-2; **2**·4 Li^+, 144467-82-3.

[1] a) K. Müllen *Chem. Rev.* **1984**, *84*, 603; b) M. Rabinovitz *Top. Curr. Chem.* **1988**, *146*, 99; c) B. C. Becker, W. Huber, K. Müllen *J. Am. Chem. Soc.* **1980**, *102*, 7803; d) W. Huber, K. Müllen, O. Wennerström *Angew. Chem.* **1980**, *92*, 636; *Angew. Chem. Int. Ed. Engl.* **1980**, *19*, 624.

[2] No complete listing of the calculated molecular orbitals of corannulene has ever been published. Hückel MO theory yields a doubly degenerate LUMO at $E = \alpha - 0.589\beta$. MNDO calculations were performed using the method of M. J. S. Dewar, W. Thiel (*J. Am. Chem. Soc.* **1977**, *99*, 4899, 4907). Thiele's lithium parameters (W. Thiel, *QCPE No. 38*, **1982**, *2*, 63) as included in MOPAC Version 6.0 (Stewart, J. J. P. *QCPE No. 455*, **1990**) were employed.

[3] F. Diederich, H. A. Staab *Angew. Chem.* **1978**, *90*, 383; *Angew. Chem. Int. Ed. Engl.* **1978**, *17*, 372; C. Krieger, F. Diederich, D. Schweizer, H. A. Staab *ibid.* **1979**, *91*, 733 and **1979**, *18*, 699.

[4] a) W. E. Barth, R. G. Lawton *J. Am. Chem. Soc.* **1966**, *88*, 380; b) R. G. Lawton, W. E. Barth *ibid.* **1971**, *93*, 1730; c) L. T. Scott, M. M. Hashemi, D. T. Meyer, H. B. Warren *ibid.* **1991**, *113*, 7082; d) A. Borchardt, A. Fuchicello, K. V. Kilway, K. K. Baldridge, J. S. Siegel *ibid.* **1992**, *114*, 1921.

[5] We have observed the same ESR spectrum of the corannulene monoanion radical originally reported by J. Janata, J. Gendell, C.-Y. Ling, W. E. Barth, L. Backes, H. B. Mark, Jr., and R. G. Lawton (*J. Am. Chem. Soc.* **1967**, *89*, 3056) and plan to examine the more highly reduced paramagnetic species in due course.

[6] The values for $^3J_{CH}$ in benzenoid systems are typically larger than those for $^2J_{CH}$ and $^4J_{CH}$: P. E. Hanson, *Org. Magn. Reson.* **1978**, *215*; J. B. Stothers, *Carbon NMR Spectroscopy*, Academic Press, New York, **1972**, p. 358; G. C. Levy, G. N. Nelson, *Carbon-13 Nuclear Magnetic Resonance for Organic Chemists*, Wiley-Interscience, New York, **1972**, p. 103.

[7] a) G. Fraenkel, R. E. Carter, A. MacLean, J. H. Richards, *J. Am. Chem. Soc.* **1960**, *82*, 5846; b) B. Eliasson, U. Edlund, K. Müllen, *J. Chem. Perkin Trans. 2* **1986**, 937.

[8] R. B. Bates, D. W. Gosselink, J. A. Kaczynski *Tetrahedron Lett.* **1967**, 205.

[9] Ab initio 3-21G calculations without the lithium atoms suggest that the tetraanion is still bowl-shaped and that more than 75% of the negative charge in the tetraanion resides on the fifteen rim carbon atoms. P. W. Rabideau, Louisiana State University, personal communication.

Towards Artificial Ion Channels: Transport of Alkali Metal Ions across Liposomal Membranes by "Bouquet" Molecules**

By *Marko J. Pregel, Ludovic Jullien*, and *Jean-Marie Lehn**

Transmembrane ion transport is essential to living systems and is involved in vital processes such as energy metabolism and the excitability of nerve and muscle.[1] Transport may take place by mechanisms involving either diffusive carrier (shuttle) or membrane-spanning channel (pore) species.[2] In the field of supramolecular chemistry, free carrier processes have been actively investigated for many years.[3] More recently the design, synthesis, and study of molecular assemblies capable of transporting ions across membranes by the channel mechanism has been a subject of increasing inter-

[*] Prof. J.-M. Lehn, Dr. M. J. Pregel, Dr. L. Jullien
Laboratoire de Chimie des Interactions Moléculaires (UPR 285)
Collège de France
11, place Marcelin Berthelot, F-75005 Paris (France)

[**] We thank Dr. Josette Canceill for the synthesis of some of the compounds used herein. M. J. P. thanks the Natural Sciences and Engineering Research Council of Canada for support in the form of a NATO Science Fellowship.

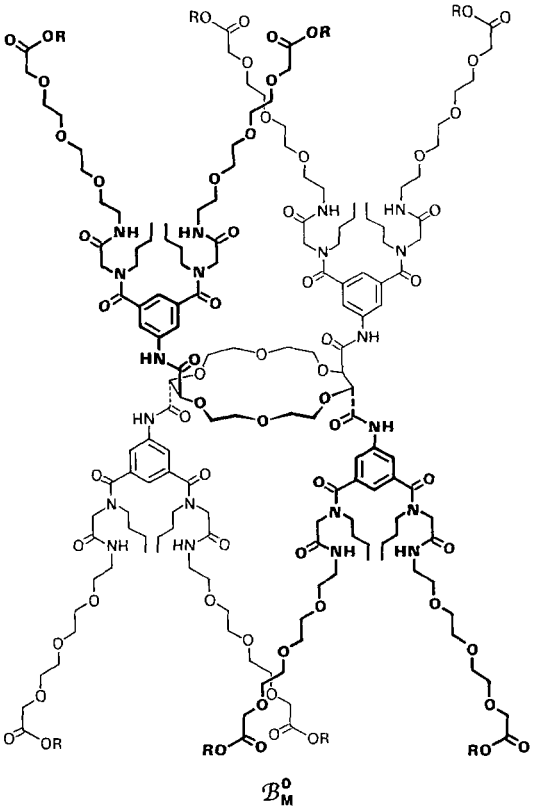

$\mathcal{B}^0_M$

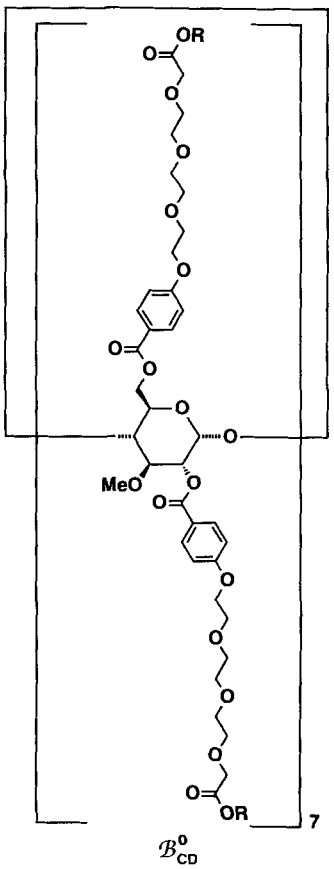

$\mathcal{B}^0_{CD}$

Scheme 1. Structures of bouquet molecules having a macrocyclic crown ether annulus (top: $\mathcal{B}^o_M$, R = Na) and a cyclodextrin annulus (bottom: $\mathcal{B}^o_{CD}$, R = H) with poly(oxyethylene) side chains. Analogous compounds with polymethylene side chains ($\mathcal{B}^c_M$ and $\mathcal{B}^c_{CD}$) were also prepared and studied.

est.[4] In general, two approaches may be noted: 1) formation of a pore by aggregation of monomeric transmembrane species, mimicking the naturally occurring channel protein alamethicin,[5] and 2) application of molecules with channel structures with defined tunnel geometry, such as in the gramicidin channel. The "bouquet" approach to artificial ion channels described here falls into the second category and involves grafting poly(oxyethylene) or polymethylene chains bearing charged endgroups onto a macrocyclic core. Previous reports have outlined the design and synthesis of two series of bouquet molecules,[6] one based on a macrocyclic polyether core ($\mathcal{B}_M$), the other having a β-cyclodextrin nucleus ($\mathcal{B}_{CD}$) (Scheme 1). We now report preliminary studies showing that the bouquet molecules function as ion transporters in bilayer membranes.

Natural and artificial ion transporters have been studied in liposome systems by a wide variety of methods including atomic absorption analysis,[4b] conductimetry in planar bilayers,[4d, f] fluorescence and UV/VIS spectroscopy,[4a, c, e, h] and pH-stat techniques.[4e] Alkali metal ion NMR spectroscopy has also been used to follow ion transport across the phospholipid bilayer of liposomes.[4g, 7, 8] Alkali metal ions in the aqueous solution outside the liposomes may be distinguished from those inside by adding a shift reagent.[9] Thus, two resonance signals are seen which correspond to internal (unshifted signal) and external (shifted signal) metal ions. In this context, we have chosen to follow the collapse of opposing gradients of Na^+ and Li^+ ion concentrations across the membrane by ^{23}Na and ^7Li NMR spectroscopy.[7]

Liposomes were prepared in an aqueous LiCl solution. After addition of a shift reagent solution (based on $DyCl_3$, see Experimental Procedure), opposing gradients of Na^+ and Li^+ ion concentrations were created by the addition of an iso-osmolar NaCl solution. Initially, Na^+ ions were found only in the exterior volume. The entry of Na^+ ions into the liposomes was then followed as a function of time by integration of the signal corresponding to "internal" Na^+ ions (see Scheme 2). This approach has a number of advantages: first, both alkali metal ions (Na^+, Li^+) capable of being transported may be observed directly and almost simultaneously; second, liposome breakage during the experiment, which would release Na^+ and Li^+ ions, cannot be confused with transmembrane transport because one observes the entry of Na^+ ions; and third, the gradient experiment allows the determination of a wide range of transport

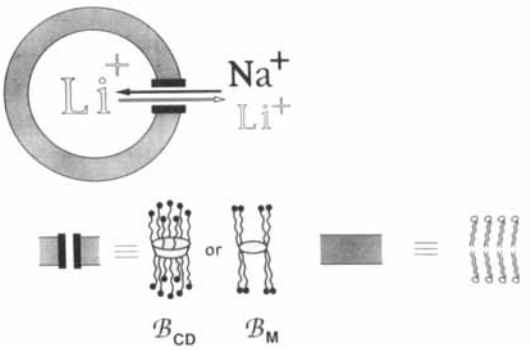

Scheme 2. Schematic representation of the transport experiment in which aqueous NaCl solution is added to a preparation of liposomes containing bouquet molecules in the membrane in aqueous LiCl solution, creating opposing gradients in Na^+ and Li^+ ion concentrations. The entry of Na^+ ions, initially found only in the external volume, into liposomes is followed by ^{23}Na NMR spectroscopy; the exit of Li^+ may also be followed by ^7Li NMR spectroscopy.

rates: the timescale of the experiment can range from 10^2 to 10^4 min.

Results for the transport of Na^+ ions across liposomal membranes containing bouquet molecules are shown in Figure 1. Comparison of these results with those of a control

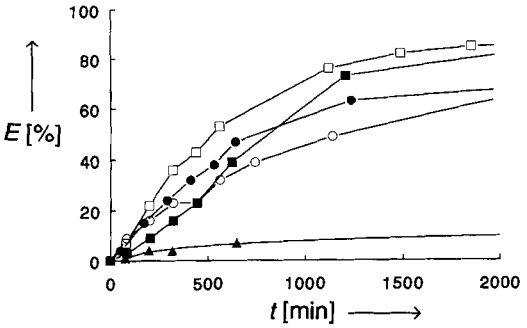

Fig. 1. Extent of entry of Na^+ ions into liposomes (E) as a function of time in the presence of bouquet molecules $\mathscr{B}^o_M$ (●), $\mathscr{B}^c_M$ (○), $\mathscr{B}^o_{CD}$ (■), and $\mathscr{B}^c_{CD}$ (□), and in the absence of bouquet molecules (▲). The extent of entry is a normalized parameter: maximum entry is taken as an extent of entry of 100% for each experiment. Concentrations of bouquet molecules were 62 μM ($\mathscr{B}^o_M$), 27 μM ($\mathscr{B}^c_M$), 56 μM ($\mathscr{B}^o_{CD}$), and 51 μM ($\mathscr{B}^c_{CD}$); lipid concentrations ranged from 8.4 to 11.2 mg mL^{-1}.

experiment without bouquet molecules reveals that both the rate and extent of transport are significantly greater in the presence of bouquet molecules than in their absence. Therefore, these molecules increase the permeability of phospholipid membranes to alkali metal ions. Interestingly (and unexpectedly), bouquet molecules with polymethylene chains transport about as efficiently as bouquet molecules with poly(oxyethylene) chains in both series ($\mathscr{B}_M$ and $\mathscr{B}_{CD}$). Furthermore, corresponding compounds in the two series transport at only slightly different rates. Finally, it should be noted that under these conditions the rates of transport by the bouquet molecules are relatively low (apparent first-order rate constants of the order of 10^{-3} min^{-1}) in comparison with those reported for other artificial ion-channel compounds. However, strict comparisons are not really justified since different experimental conditions apply.

Transport of alkali metal ions may proceed by a number of mechanisms including cation–cation antiport, cation–proton antiport, and cation–anion symport.[10] In the present system, influx of Na^+ ions into liposomes was followed by ^{23}Na NMR spectroscopy. In some experiments, efflux of Li^+ ions was monitored simultaneously by ^7Li NMR spectroscopy. It was therefore possible to compare the amount of Na^+ which had entered to the amount of Li^+ which had exited the liposomes at various times (Fig. 2). Within experimental error, the two values are identical at any given time, leading to the conclusion that Na^+ and Li^+ ion transport by the bouquet molecules occurs by a one-for-one exchange of sodium ion for lithium ion (cation–cation antiport). The more slowly transfered ion (probably Li^+) determines the overall rate of transport.

These results do not allow a precise description of the mechanism by which the bouquet molecules mediate transmembrane cation flow. However, it has been found that bouquet molecules $\mathscr{B}^c_M$ and $\mathscr{B}^o_{CD}$ allow cation passage through membranes of dipalmitoyl phosphatidylcholine (DPPC) in the *gel* state with rates similar to those observed in egg phosphatidylcholine (EPC) membranes which are in the *fluid* state. In contrast, the rate of transport by

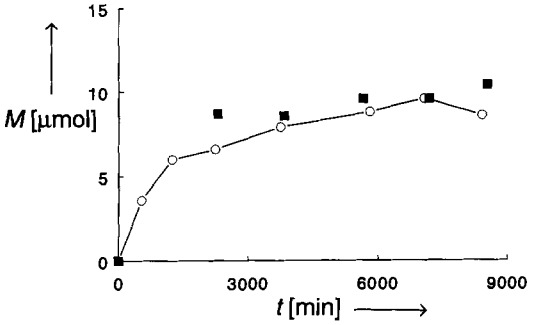

Fig. 2. Comparison of the amount M of Na^+ having entered liposomes (○) with the amount of Li^+ having exited (■) as a function of time for liposomes with $\mathscr{B}^o_M$. Other bouquet molecules gave similar results.

monensin A, an ionophore antibiotic which operates by the carrier (shuttle) mechanism, is sharply reduced in DPPC membranes in the gel state, as compared to fluid EPC membranes. Therefore, for the bouquet molecules $\mathscr{B}^c_M$ and $\mathscr{B}^o_{CD}$ at least, a shuttle mechanism can be excluded. While a perturbation of membrane structure by the bouquet molecules causing an overall change in membrane permeability cannot be excluded, our results are consistent with a channel mechanism of ion transport.

In conclusion, we have shown that bouquet molecules may be incorporated into the phospholipid membrane of liposomes. These compounds increase the permeability of the membrane to Na^+ and Li^+ ions, and ion transfer proceeds by a cation–cation antiport mechanism. Variations in the bouquet molecule including changing from poly(oxyethylene) to polymethylene chains and changing from a crown ether annulus to a cyclodextrin annulus did not have drastic effects on ion-transport activities. A carrier mechanism can be excluded for two of the compounds studied since ion-transport activity is undiminished in membranes in the gel state. Further studies are underway to investigate the mechanism of transport and the effects of parameters such as membrane composition, alkali metal ions, and concentration of bouquet molecules on the transport rate in order to better describe the mode of action of these compounds.

Experimental Procedure

Large unilammelar vesicles (liposomes) were prepared from egg phosphatidylcholine by the dialytic detergent-removal technique [11]. Bouquet molecules were incorporated into the membrane during liposome formation: stock solutions of bouquet molecules, lipid, and detergent were mixed, evaporated to dryness, hydrated with aqueous 100 mM LiCl solution, and dialyzed against aqueous 100 mM LiCl solution. The lipid content of the liposome preparation was measured by analysis of the phosphate content after digestion [12]; the concentration of bouquet molecules present was measured by using the absorption of bouquet molecules at 250 or 255 nm. In a typical transport experiment, iso-osmolar shift reagent solution (30 mM, $(Me_4N)_5P_3O_{10}$, 10 mM $DyCl_3$; 0.3 mL) and 100 mM NaCl solution (0.8 mL) were added to the liposome preparation (1.0 mL), creating transmenbrane gradients in Na^+ and Li^+ ion concentrations. The entry of Na^+ ions into liposomes was followed by ^{23}Na NMR spectroscopy by integration of the signal corresponding to "internal" Na^+ ions. Exit of Li^+ ions was followed by ^7Li NMR spectroscopy in an analogous manner. The temperature was maintained at 25 ± 1 °C during the experiment.

Received: August 10, 1992 [Z 5506 IE]
German version: *Angew. Chem.* **1992**, *104*, 1695

[1] L. Stryer, *Biochemistry*, 3rd ed., Freeman, **1988**, p. 949.
[2] P. Läuger, *Angew. Chem.* **1985**, *97*, 939; *Angew. Chem. Int. Ed. Engl.* **1985**, *24*, 905.

 © VCH Verlagsgesellschaft mbH, W-6940 Weinheim, 1992 0570-0833/92/1212-1639 $ 3.50+.25/0

[3] J.-M. Lehn in *Physical Chemistry of Transmembrane Ion Motions* (Ed.: G. Spach), Elsevier, Amsterdam, **1983**, pp. 181–207; J.-M. Lehn, *Angew. Chem.* **1988**, *100*, 91; *Angew. Chem. Int. Ed. Engl.* **1988**, *27*, 89.
[4] a) I. Tabushi, Y. Kuroda, K. Yokota, *Tetrahedron Lett.* **1982**, *23*, 4601; b) J. H. Fuhrhop, U. Liman, V. Koesling, *J. Am. Chem. Soc.* **1988**, *110*, 6840, and references therein; c) U. F. Kragten, F. M. Roks, R. J. M. Nolte, *J. Chem. Soc. Chem. Commun.* **1985**, 1275; d) J. D. Lear, Z. R. Wasserman, W. F. De Grado, *Science* **1988**, 1177; e) T. M. Fyles, T. D. James, K. C. Kaye, *Can. J. Chem.* **1989**, *68*, 976, and references therein; T. M. Fyles, K. C. Kaye, T. D. James, D. W. M. Smiley, *Tetrahedron Lett.* **1990**, *31*, 1233; f) C. J. Stankovic, S. H. Heinemann, S. L. Schreiber, *J. Am. Chem. Soc.* **1990**, *112*, 3702, and references therein; g) A. Nakano, Q. Xie, J. V. Mallen, L. Echegoyen, G. W. Gokel, *ibid.* **1990**, *112*, 1287; h) F. M. Menger, D. S. Davis, R. A. Persichetti, J. J. Lee, *ibid.* **1990**, *112*, 2451.
[5] R. O. Fox Jr., F. M. Richards, *Nature* **1982**, *300*, 325.
[6] L. Jullien, J.-M. Lehn, *Tetrahedron Lett.* **1988**, *29*, 3803; *J. Inclusion Phenom. Mol. Recognit. Chem.* **1992**, *12*, 55; J. Canceill, L. Jullien, L. Lacombe, J.-M. Lehn, *Helv. Chim. Acta* **1992**, *75*, 791.
[7] M. M. Pike, S. R. Simon, J. A. Balschi, C. Springer, Jr., *Proc. Natl. Acad. Sci. USA* **1982**, *79*, 810.
[8] a) F. G. Riddell, S. Arumugam, B. G. Cox, *J. Chem. Soc. Chem. Commun.* **1987**, 1890; F. G. Riddell, S. Arumugam, P. J. Brophy, B. G. Cox, M. C. H. Payne, T. E. Southon, *J. Am. Chem. Soc.* **1988**, *110*, 734, and references therein; b) D. C. Shungu, R. W. Briggs, *J. Magn. Reson.* **1988**, *77*, 491, and references therein.
[9] R. K. Gupta, P. Gupta, *J. Magn. Reson.* **1982**, *47*, 344; S. C. Chu, M. M. Pike, E. T. Fossel, T. W. Smith, J. A. Balschi, C. S. Springer, Jr., *ibid.* **1984**, *56*, 33; M. M. Pike, D. M. Yarmush, J. A. Balschi, R. E. Lenkinski, C. Springer, Jr., *Inorg. Chem.* **1983**, *22*, 2388, and references therein; R. Ramasamy, M. C. Espanol, K. M. Long, D. Mota de Freitas, C. F. G. C. Geraldes, *Inorg. Chim. Acta* **1989**, *163*, 41.
[10] W. N. Konings, K. J. Hellingwerf, G. T. Robillard in *Membrane Transport* (Eds.: S. L. Bonting, J. J. H. H. M. de Pont), Elsevier, Amsterdam, **1981**, p. 267.
[11] L. T. Mimms, G. Zampighi, Y. Nozaki, C. Tanford, J. A. Reynolds, *Biochemistry* **1981**, *20*, 833.
[12] P. S. Chen, Jr., T. Y. Toribara, H. Warner, *Anal. Chem.* **1956**, *28*, 1756; W. R. Morrisson, *Anal. Biochem.* **1964**, *7*, 218.

Optimization of the Production and Separation of Fullerenes**

By *Andreas Mittelbach, Wolfgang Hönle, Hans Georg von Schnering,* Jürgen Carlsen, Rolf Janiak,* and *Helmut Quast**

The observed superconductivity of alkali metal compounds like $K_3(C_{60})$[1] prompted our investigations of fullerenes. Not only had we looked for a new direction in our search for superconducting materials,[2] we also thought that $K_3(C_{60})$ may be described as an analogue of Zintl phases like Li_3B_{14}, Li_2B_6, and Li_6B_{19} (electron transfer with structural consequences).[3]

Fullerenes[4] can be produced by laser vaporization,[5] vaporization of graphite in an arc,[6] by plasma discharge,[7] or in a high-frequency furnace[8] under reduced pressure of an inert gas. These methods provide soot containing up to 44% fullerenes.[7, 9] The mixture usually consists of C_{60} and C_{70} in a ratio of 85:15 and a small amount of higher fullerenes. Isolation and separation of the fullerenes is achieved by extraction of the soot with toluene followed by chromatography or directly by chromatography of the soot.[10]

[*] Prof. Dr. H. G. von Schnering, Dipl.-Chem. A. Mittelbach, Dr. W. Hönle
Max-Planck-Institut für Festkörperforschung
Heisenbergstrasse 1, D-W-7000 Stuttgart 80 (FRG)
Prof. Dr. H. Quast, Dr. J. Carlsen, Dr. R. Janiak
Institut für Organische Chemie der Universität
Am Hubland, D-W-8700 Würzburg (FRG)

[**] We thank Dr. H. Schmidt (University of Halle) for preliminary work and Dr. T. P. Martin (Max-Planck-Institut, Stuttgart) for the measurement of the TOF mass spectrum.

Previous procedures[11–13] succeeded in separating fullerenes only in small amounts (for example, separation of 400 mg extract[14, 15] in 4–6 hours to give 32 mg C_{60}[11] after 11 hours or 170 mg C_{60} after 25 hours[13]) incompletely or only in limited amounts on special column materials. Only Gügel et al.[16] described a procedure for the separation of reasonable amounts of a fullerene mixture (5 g in 24 hours); however, a baseline separation was not achieved, and large mixed fractions were obtained.

In our investigations we used a DC furnace[17] for the preparation of fullerene-containing soot. This has the advantage that the cathodes hardly burn down when electrodes of equal diameter are used (Fig. 1). We observed a strong

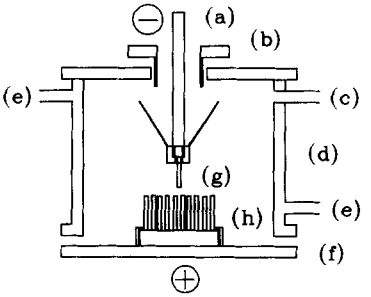

Fig. 1. Drawing of the arc furnace (not to scale): a) water-cooled cathode connection, b) insulation, c) inert gas–vacuum vent, d) water-cooled stainless-steel container, e) cooling-water supply, f) water-cooled copper plate, g) cathode $\varnothing = 6.15$ mm, h) close arrangement of anodes $\varnothing = 6.15$ mm.

change in the ratio of C_{60}/C_{70} (hitherto 85:15) in favor of C_{70} when we used a higher current. With 400 A DC (hitherto about 100–200 A, AC or DC) we obtained fullerene mixtures containing up to 50% C_{70} (Fig. 2). Subsequent extrac-

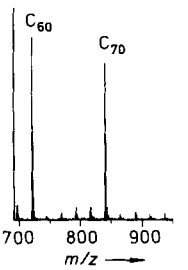

Fig. 2. Time-of-flight mass spectrum [18] of the soot. The ordinate corresponds to the ion/time channel.

tion with toluene provided C_{60}/C_{70} mixtures greatly enriched in C_{70}. Unfortunately, details of the events in the plasma are not known. All hypotheses about the formation of fullerenes in the arc are based on the premise of the existence of single carbon atoms as basic units.[20] We presume that the use of high current produces larger regions of higher temperature. The temperature gradient is much steeper than that formed at lower current, which favors the formation of C_{70}.

The C_{60}/C_{70} mixture could be separated by medium-pressure chromatography according to two procedures (A, B), both of which start with material dried under vacuum at 200 °C until constant weight was achieved. In procedure A the fullerene mixture was extracted with hexane (vapor extractor, or extraction, from a precolumn under constant pressure, which was filled with a mixture of silica gel and fullerenes). This saturated or oversaturated solution was injected directly onto the separation column and eluted with

hexane. For the separation we used a glass column with a high number of plates ($N = 14000$) and a good symmetry index (SI ≤ 1.05).[20] It is possible to run this procedure continuously. For example, injections can be made every 5–10 min (Fig. 3), so that six to three 50 mL portions of

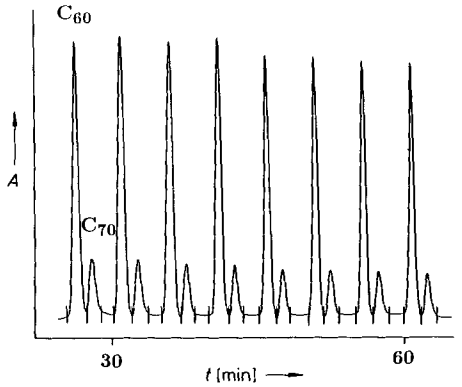

Fig. 3. Typical chromatogram (detection wavelength 300 nm) for the preparative separation on silica gel with hexane. The lines indicate the cut-off points for the fractions. A = absorption.

extract can be separated simultaneously. Depending on the concentration of the extract, up to 400 mg of fullerenes may be separated per hour (Fig. 4).

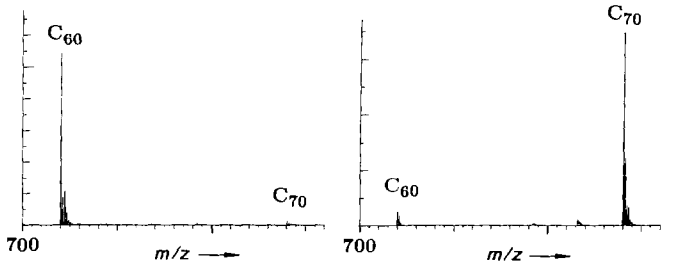

Fig. 4. Time-of-flight mass spectrum [18] after the preparative separation on silica gel with hexane with only *two* fractions (Fig. 3). The ordinate corresponds to the ion/time channel.

In procedure B the chromatography was carried out with toluene/acetonitrile[21] (75:25) as the eluent and a glass column packed with C18 reversed-phase silica gel. The fullerenes were injected by extraction under pressure with

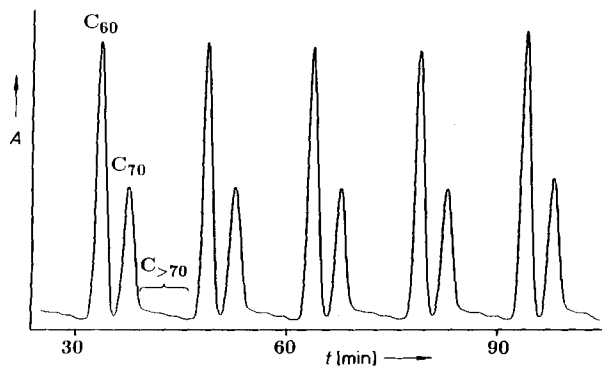

Fig. 5. Typical chromatogram (detection wavelength 300 nm) for the preparative separation on C18 reversed-phase silica gel with toluene/acetonitrile (75:25). A = absorption.

toluene/acetonitrile (75:25) from a shunt column which was filled with a mixture of reversed-phase silica gel and fullerenes (12:1). Injections lasting 45 s were made every 15–20 min. In this way we separated up to 300 mg of fullerenes per hour (Fig. 5). In the chromatogram from procedure B higher fullerenes like C_{76}, C_{78}, etc. are apparent. They can be separated after enrichment.

Experimental Procedure

C_{70} enrichment of the fullerene mixture: The arc furnace [17] was furnished with graphite electrodes [22] and was evacuated (2 Pa) and refilled with helium gas (purity grade 4.6) several times. Then the furnace was filled with helium to a pressure of 8×10^3 Pa. After ignition of the arc at lower current the electrodes were brought into contact. The intensity of current was raised to 400 A at 58 V (maximum 18 kW). During the vaporization the pressure was as high as 2×10^4 Pa. From previous experiments with tungsten electrodes, we know that the temperature at 400 A and 58 V is higher than 3000 K. We estimate that the temperature here is roughly 5000 K at the electrode and about 15000 K in the plasma. With this method 7–10 g of graphite per hour could be evaporated. Afterwards the soot was collected and extracted with toluene for 24 h. Without further extraction (for example, as described in ref. [5, 7]) the total yield of fullerenes after removal of the solvent in vacuum was 7–10%.

Procedure A: Chromatography with hexane on silica gel [23]. A glass column 70 × 6 cm) was packed with silica gel (LiChroprep Si60 15–25 μm, Merck) as described in ref. [20]. Solvent hexane, flow 100 mL min^{-1} at 1.6×10^6 Pa. The fullerene mixture was extracted for 45 min with 200 mL of hexane in a vapor extractor to remove impurities. This extract was discarded. With another portion of 400 mL hexane the fullerene mixture was extracted in the same way for 4–6 h. This extract was injected in portions of 50 mL every 5–10 min onto the separation column. The pure fullerenes were then eluted with hexane.

Procedure B: Chromatography with toluene/acetonitrile on C18 reversed-phase silica gel [23]. A glass column (70 × 6 cm) was packed with C18 reversed-phase silica gel (Europrep 60–30 C18 20–45 μm, Knauer). In an adaptation of ref. [20], the column was packed by using methanol/water in a ratio of 95:5; $N = 5000$, SI ≤ 1.25. Solvent toluene/acetonitrile (75:25), flow 72 mL min^{-1} at 1.8×10^6 Pa. The crude fullerene mixture was loosely mixed with reversed-phase silica gel in a ratio of 1:12 and stored in a 25 × 4 cm glass column which acted as shunt column and was filled with solvent and kept under pressure. When the solvent flowed through this precolumn for 45 s the extract was injected on the separation column. The pure fullerenes were then eluted with toluene/acetonitrile (75:25) [24].

Received: July 30, 1992 [Z 5492 IE]
German version: *Angew. Chem.* **1992**, *104* 1681

[1] R. C. Haddon, A. F. Hebard, M. J. Rosseinsky, D. W. Murphy, S. J. Duclos, K. B. Lyons, B. Miller, J. M. Rosamilia, R. M. Fleming, A. R. Kortan, S. H. Glarum, A. V. Makhija, A. J. Muller, R. H. Eick, S. M. Zahurak, R. Tycko, G. Dabbagh, F. A. Thiel, *Nature* **1991**, *350*, 320; A. F. Hebard, M. J. Rosseinsky, R. C. Haddon, D. W. Murphy, S. H. Glarum, T. T. M. Palstra, A. P. Ramirez, A. R. Kortan, *ibid.* **1991**, *350*, 600.

[2] H. G. von Schnering, L. Walz, M. Schwarz, W. Becker, M. Hartweg, T. Popp, B. Hettich, P. Müller, G. Kämpf, *Angew. Chem.* **1988**, *100*, 604; *Angew. Chem. Int. Ed. Engl.* **1988**, *27*, 574.

[3] H. G. von Schnering, *Bol. Soc. Chil. Quim.* **1988**, *33*, 41; G. Mair, Doctoral Thesis, University of Stuttgart (FRG), **1984**; G. Mair, R. Nesper, H. G. von Schnering in *Jahresbericht des Max-Planck-Instituts für Festkörperforschung Stuttgart*, Stuttgart **1984**.

[4] For a review see, for example: *Fullerenes: synthesis, properties, and chemistry of large carbon clusters* (Eds.: G. S. Hammond, V. J. Kuck), American Chemical Society, Washington, DC, **1992**. A series of articles appears in *Acc. Chem. Res.* **1992**, *25*, 98–175.

[5] H. W. Kroto, J. R. Heath, S. C. O'Brien, R. F. Curl, R. E. Smalley, *Nature* **1985**, *318*, 162.

[6] W. Krätschmer, L. D. Lamb, K. Fostiropoulos, D. R. Huffman, *Nature* **1991**, *347*, 354.

[7] D. H. Parker, P. Wurz, K. Chatterjee, K. R. Lykke, J. E. Hurst, M. J. Pellin, J. C. Hemminger, D. M. Gruen, L. M. Stock, *J. Am. Chem. Soc.* **1991**, *113*, 7499.

[8] M. Jansen, G. Peters, *Angew. Chem.* **1992**, *104*, 240; *Angew. Chem. Int. Ed. Engl.* **1992**, *31*, 223.

[9] 8%: R. Taylor, J. P. Hare, A. Abdul-Sada, H. Kroto, *J. Chem. Soc. Chem. Commun.* **1990**, 1423; 10%: R. E. Haufler, J. Conceicao, L. P. F. Chibante, Y. Chai, N. E. Byrne, S. Flanagan, M. M. Haley, S. C. O'Brien, C. Pan, Z. Xiao, W. E. Billups, R. E. Ciufolini, R. N. Hauge, J. L. Margrave, L. J. Wilson, R. F. Curl, R. E. Smalley, *J. Phys. Chem.* **1990**, *94*, 8634; 14%: H. Aiji, M. M. Alvarez, S. J. Anz, R. D. Beck, F. Diederich, K. Fostiropoulos, D. R. Huffman, W. Krätschmer, Y. Rubin, K. E. Shriver, D. Sensharma, R. L. Whetten, *ibid.* **1990**, *94*, 8630; 25-35%: F. Diederich, R. Ettl, Y. Rubin, R. L. Whetten, R. Beck, M. M. Alvarez, S. J. Anz, D. Sensharma, F. Wudl, K. C. Khemani, A. Kuch, *Science* **1991**, *252*, 548.

[10] K. Chatterjee, D. H. Parker, P. Wurz, K. R. Lykke, D. M. Gruen, L. M. Stock, *J. Org. Chem.* **1992**, *57*, 3253; K. C. Khemani, M. Prato, F. Wudl, *ibid.* **1992**, *57*, 3254.
[11] A. M. Vasallo, A. J. Palmisano, L. S. K. Pang, M. A. Wilson, *J. Chem. Soc. Chem. Commun.* **1992**, 60.
[12] M. S. Meier, J. P. Selegue, *J. Org. Chem.* **1992**, *57*, 1924.
[13] K. Jinno, K. Yamamoto, T. Ueda, H. Nagashima, K. Itoh, J. C. Fetzer, W. R. Biggs, *J. Chromatogr.* **1992**, *594*, 105.
[14] P.-M. Allemand, A. Koch, F. Wudl, Y. Rubin, F. Diederich, M. M. Alvarez, S. J. Anz, R. L. Whetten, *J. Am. Chem. Soc.* **1991**, *113*, 1050.
[15] The chromatographic separation of 400 mg of extract on Al_2O_3 is accomplished in 4–6 h; F. Diederich (ETH Zürich), private communication (Sept. 17, 1992).
[16] A. Gügel, M. Becker, D. Hammel, L. Mindach, J. Räder, T. Simon, M. Wagner, K. Müllen, *Angew. Chem.* **1992**, *104*, 666; *Angew. Chem. Int. Ed. Engl.* **1992**, *31*, 644.
[17] Arc melting furnace with generator LSG 400, E. Bühler, Tübingen, modified by exchanging the bottom plate with holders for the cathodes, improving the cooling system to include top cooling, and installing a modified heat shield. Furnace diameter 250 mm, volume 18 L.
[18] Wavelength of the laser for vaporization: 520 nm with 5 mJ pulse^{-1} on an area of 1 mm^2. Wavelength of the laser for ionization: 193 nm with 5 mJ pulse^{-1} on an area of 1 mm^2. Analyzer: Channel Plates, Hamamatsu, Japan.
[19] R. E. Smalley, *Acc. Chem. Res.* **1992**, *25*, 98; T. Wakabayashi, Y. Achiba, *Chem. Phys. Lett.* **1992**, *190*, 465; T. W. Ebbesen, J. Tabuchi, K. Tanigaki, *ibid.* **1992**, *191*, 336; R. Kerner, K. A. Penson, K. H. Bennemann, *Europhys. Lett.* **1992**, *19*, 363.
[20] G. Helmchen, B. Glatz, *Ein apparativ einfaches System und Säulen höchster Trennleistung zur präparativen Mitteldruck-Flüssigkeitschromatographie*, Universität Stuttgart, **1978**; E. Ade, G. Helmchen, G. Heiligenmann, *Tetrahedron Lett.* **1980**, *21*, 1137.
[21] Previously toluene/acetonitrile was used in a ratio of 1:1 for HPLC separations: F. Diederich, R. L. Whetten, C. Thilgen, R. Ettl, I. Chao, M. M. Alvarez, *Science* **1991**, *254*, 1768.
[22] Spectral graphite from the company Ringsdorffwerke GmbH, Bonn-Bad Godesberg (FRG), 6.15 × 305 mm.
[23] Glass columns as described in ref. [20]. Single metering pump FC1 with pump-head K110 and 0.2 L pulse damper, LEWA, Leonberg (FRG). 50 mL sample injection tube and UV detector 87.00 (detection wavelength 300 nm), Knauer, Berlin.
[24] Note added in proof (9.11.92): W. A. Serivens, P. V. Bedworth, J. M. Tour, *J. Am. Chem. Soc.* **1992**, *114*, 7917, reported the separation of gram amounts of C_{60} by flash chromatography on activated charcoal (Norite-A)/silica gel mixtures with toluene.

The First Stibepine: Synthesis and Structure of *Sb*-Chlorobenzo[*d*]stibepine**

By *Arthur J. Ashe III,* Lukas Goossen, Jeff W. Kampf,* and *Hisatoshi Konishi*

Dedicated to Professor Kenneth B. Wiberg on the occasion of his 65th birthday

Fully unsaturated seven-membered ring heterocycles containing Group 15 and 16 elements are of substantial interest. The well-studied azepines **1a** and oxepines **2a**[1] are relatively stable compounds in contrast to their heavier homologues, phosphepines **1b**[2] and thiepines **2b**,[3] for which most derivatives are thermally labile towards heteroatom extrusion. Derivatives of selenepine **2c**[4] and tellurepine **2d**[5] have been reported recently, while the labile *As*-phenylbenzo[*d*]arsepine (**3**) has been detected at low temperature by spectroscopy.[2a] We report here on the first synthesis of benzo[*d*]stibepines and the structural characterization of *Sb*-chlorobenzo[*d*]stibepine (**5**).[6]

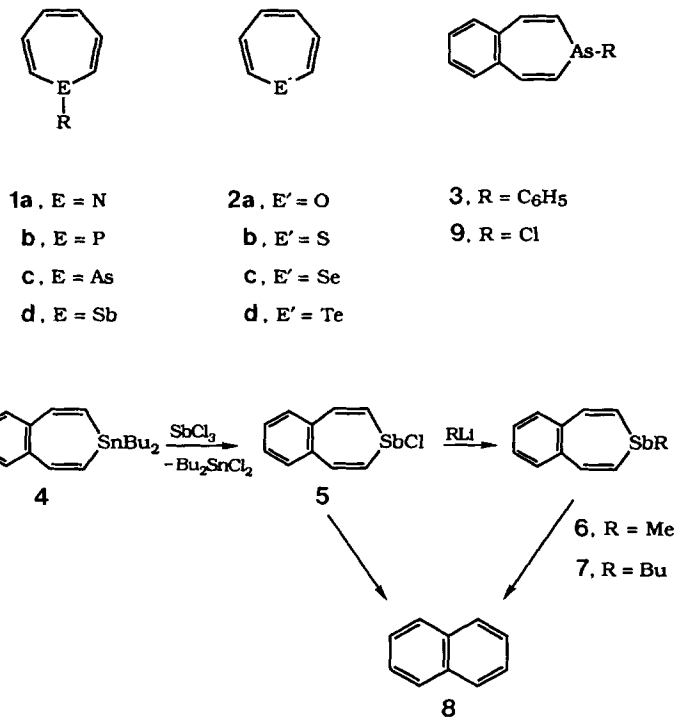

The reaction of dibutylbenzo[*d*]stannepine (**4**)[7] with one equivalent of $SbCl_3$ in $CHCl_3$ at 0 °C affords **5** and dibutyltin dichloride, which may be removed by extraction with pentane. Recrystallization from diethyl ether/CH_2Cl_2 affords **5** as well-formed yellow crystals. Compound **5** may be converted to the alkyl derivatives **6** and **7** by treatment with MeLi and BuLi, respectively. All the above operations must be performed at low temperature since benzo[*d*]stibepines are thermally labile, forming naphthalene **8** and unidentified antimony-containing products. The conversion of **6** and **7** to **8** in $CDCl_3$ at 25 °C was monitored by ^{1}H NMR spectroscopy and showed first-order kinetics with $t_{1/2}$ = 370 and 660 min, respectively.

For comparison we have also examined benzo[*d*]arsepines. The reaction of **4** with $AsCl_3$ in $CHCl_3$ gave **9** and Bu_2SnCl_2. It was not possible to separate these products, but the identity of **9** was established by the similarity of its NMR spectra of those of **5**. In $CDCl_3$ **9** decomposes to form **8** with $t_{1/2}$ = 50 min at 25 °C. Thus, surprisingly, the arsepine is more labile than the stibepine.

Since prior structural data on the heavier heteroepines was available only for derivatives of thiepine,[3] it was of interest to determine the crystal structure of a benzostibepine. The structure of **5**[8] illustrated in Figure 1 shows a boatlike stibepine ring. This boat conformation has angles of 41.7

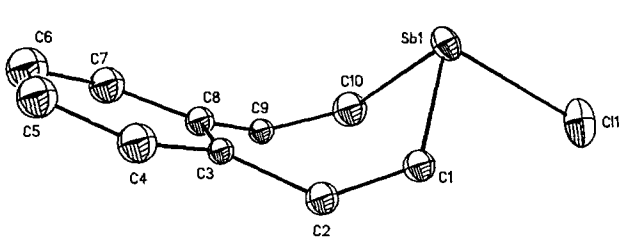

Fig. 1. Solid-state structure of **5** (ORTEP). Important distances [Å] and angles [°]: Sb1–Cl1 2.403(1); Sb1–C1 2.116(4); Sb1–C10 2.116(4); C1–C2 1.325(5), C2–C3 1.476(5); C8–C9 1.470(5), C9–C10 1.320(6); Cl1–Sb–C1 92.6(1), Cl1–Sb–C10 93.6(1), C1–Sb1–C10 89.9(1).

[*] Prof. Dr. A. J. Ashe III, L. Goossen, Dr. J. W. Kampf, Dr. H. Konishi
Department of Chemistry, The University of Michigan
Ann Arbor, MI 48109-1055 (USA)

[**] This work was supported by the Research Corporation and the donors of the Petroleum Research Fund, administered by the American Chemical Society.

and 34.0° between the base plane (C1-C2-C9-C10) and the bow (C1-Sb1-C10) and stern (C2-C3-C8-C9), respectively. The bond angles about Sb are close to 90° as has been found in other antimony heterocycles.[9] These structural features and the marked alternation between single and double C–C bond lengths of the stibepine moiety are consistent with little conjugation. Overall the structure is remarkably similar to those of the thiepines.

Experimental Procedure

5: A solution of **4** (1.87 g, 5.2 mmol) in $CHCl_3$ (5 mL) was added in one portion with vigorous stirring to $SbCl_3$ (1.18 g, 5.2 mmol) in $CHCl_3$ (20 mL) at 0 °C. After 10 min the solvent was removed in vacuo leaving a gray residue which was washed with pentane (3 × 5 mL) at −50 °C. The residue was dissolved in diethyl ether/CH_2Cl_2 (50 mL), and the solution was filtered through $MgSO_4$. Cooling to −20 °C gave 750 mg of **5** as yellow crystals, decomp >30 °C. ^{1}H NMR ($CDCl_3$): δ = 7.68 (d, J = 12.3 Hz, 2H), 7.28 (A_2B_2 pattern, 4H), 6.84 (d, J = 12.4 Hz, 4H). ^{13}C NMR ($CDCl_3$): δ = 141.0, 139.6, 132.1, 126.8, (signal of the quaternary C not observed). High-resolution CI-MS(NH_3/CH_4): m/z ($M^+ + 1$) calcd for $C_{10}H_8{}^{121}Sb^{35}ClH$: 284.9431, found 284.9417.

6: To a solution of **5** (50 mg, 0.18 mmol) in diethyl ether (50 mL) at −10 °C was added 0.1 N MeLi (2 mL) until the solution became red. The excess MeLi was then destroyed with a drop of 1,2-dibromoethane, and the mixture was filtered through $MgSO_4$. Removal of the solvent left 50 mg of a yellow residue, which was recrystallized from diethylether at −78 °C affording **6**, m.p. 35 °C. ^{1}H NMR ($CDCl_3$): δ = 7.46 (d, J = 12.0 Hz, 2H), 7.22 (A_2B_2 pattern, 4H), 6.50 (d, J = 12.0 Hz, 2H), 0.95 (s, 3H). ^{13}C NMR ($CDCl_3$): δ = 141.2, 138.4, 132.9, 131.5, 125.9, 28.0. High-resolution CI-MS (CH_4): m/z ($M^+ + 1$) calcd. for $C_{11}H_{11}{}^{121}SbH$: 264.9770, found 264.9958.

8: In the same manner, the reaction of BuLi with **5** gave **8**, m.p. −10 °C. ^{1}H NMR ($CDCl_3$): δ = 7.49 (d, J = 12.4 Hz, 2H), 7.23 (A_2B_2 pattern, 4H), 6.49 (d, J = 12.4 Hz, 2H), 1.5–0.7 (bu, 9H). ^{13}C NMR ($CDCl_3$): δ = 141.4, 138.4, 131.9, 131.5, 125.8, 29.8, 26.2, 14.7, 13.6. High-resolution CI-MS ($Cl(C_4H_{10})$: m/z ($M^+ + 1$) calcd for $C_{14}H_{17}{}^{121}SbH$: 307.0447, found 307.0451.

9: Prepared in the same manner as **5**: ^{1}H NMR ($CDCl_3$): δ = 7.25 (A_2B_2 pattern, 4H), 7.17 (d, J = 12.4 Hz, 2H), 6.49 (d, J = 12.4 Hz, 2H). ^{13}C NMR ($CDCl_3$): δ = 137.3, 135.8, 135.5, 132.0, 127.0.

Received: July 22, 1992 [Z 5475 IE]
German version: *Angew. Chem.* **1992**, *104*, 1669

[1] E. Vogel, H. Günther, *Angew. Chem.* **1967**, *79*, 429; *Angew. Chem. Int. Ed. Engl.* **1967**, *6*, 385; L. A. Paquette in *Nonbenzenoid Aromatics, Vol. 2* (Ed.: J. P. Synder), Academic Press, New York, **1969**, p. 249.

[2] a) G. Märkl, H. Schubert, *Tetrahedron Lett.* **1970**, 1273; G. Märkl, G. Dannhardt, *ibid.* **1973**, 1455; b) G. Märkl, W. Burger, *ibid.* **1983**, *24*, 2545; c) *Angew. Chem.* **1984**, *96*, 896; *Angew. Chem. Int. Ed. Engl.* **1984**, *23*, 894; d) J. Kurita, S. Shiratori, S. Yasuike, T. Tsuchiya, *J. Chem. Soc. Chem. Commun.* **1991**, 1227.

[3] I. Murata, K. Nakasuji, *Top. Curr. Chem.* **1981**, *97*, 33; K. Yamamoto, S. Yamazaki, Y. Kohashi, A. Matsukawa, I. Murata, *Chem. Lett.* **1982**, 1843; K. Nishino, S. Yano, Y. Kohashi, K. Yamamoto, I. Murata, *J. Am. Chem. Soc.* **1979**, *101*, 5059; K. Yamamoto, S. Yamazaki, Y. Kohashi, I. Murata, Y. Kai, N. Kanehisa, K. Miki, N. Kasai, *Tetrahedron Lett.* **1982**, *23*, 3195.

[4] H. Hori, S. Yamazaki, K. Yamamoto, I. Murata, *Angew. Chem.* **1990**, *102*, 450; *Angew. Chem. Int. Ed. Engl.* **1990**, *29*, 424.

[5] H. Sashida, H. Kurahashi, T. Tsuchiya, *J. Chem. Soc. Chem. Commun.* **1991**, 802.

[6] However, derivatives of a dihydrostibepine have been reported H. A. Meinema, C. J. R. Crispim Romão, J. G. Noltes, *J. Organomet. Chem.* **1973**, *55*, 139; H. A. Meinema, H. F. Martens, J. G. Noltes, N. Bertazzi, R. Barbieri, *ibid.* **1977**, *136*, 173.

[7] A. J. Leusink, J. G. Noltes, H. A. Budding, G. J. M. van der Kerk, *Recl. Trav. Chim. Pays-Bas* **1964**, *83*, 1036; A. J. Ashe III, J. W. Kampf, C. M. Kausch, H. Konishi, M. O. Kristen, J. Kroker, *Organometallics* **1990**, *9*, 2944.

[8] **5**: Monoclinic, space group $P2_1/n$ (no. 14) with a = 9.529(2), b = 10.462(2), c = 9.562(2) Å, β = 90.69(1)°, V = 953.2(2) Å^3, and Z = 4 (ϱ_{calcd} = 1.998 g cm^{-3}), $\mu(Mo_{K\alpha})$ = 93.18 cm^{-1}, 1716 unique reflections, 1612 with $F_o \geq 0.6\,\sigma(F)$ were used in refinement; R = 0.0304, R_w = 0.0363; GOF = 1.20. Further details of the crystal structure investigation are available on request from the Director of the Cambridge Crystallographic Data Centre, University Chemistry Laboratory, Lensfield Road, GB-Cambridge CB2 1EW (UK), on quoting the full journal citation.

[9] M. A. Bush, P. F. Lindley, P. Woodward, *J. Chem. Soc. A* **1967**, 221; G. Becker, O. Mundt, A. Studelmann, *Z. Anorg. Allg. Chem.* **1990**, *580*, 139; R. A. Fisher, R. B. Nielsen, W. M. Davis, S. L. Buchwald, *J. Am. Chem. Soc.* **1991**, *113*, 165.

The First Hexabutadiynylbenzenes: Synthesis and Structures**

By *Roland Boese,* James R. Green, Joachim Mittendorf, Debra L. Mohler*, and *K. Peter C. Vollhardt**

Our disclosure of the Pd-catalyzed hexaethynylation of hexabromobenzene to give **1**[1] has prompted considerable synthetic activity. The method has been used to prepare polyalkynyl aromatics, particularly with the aim of generating novel discotic liquid crystals[2] or precursors to new organic solids with unusual properties (hardness, thermal and electric conductivity, lubrication).[3] We are interested in these compounds because of their more fundamental physical organic properties and synthetic potential. They are new, very electron-rich, reactive hydrocarbons with high C/H ratios.[1] In synthesis they are precursors to allotropes of carbon, such as C_{60},[4a] or substrates in CpCo-catalyzed cocyclizations with monoalkynes on route to multiphenylenes,[4b,c] and also function as multidentate ligands to transition-metal clusters.[4d]

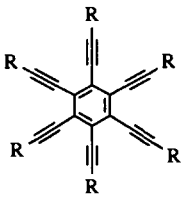

1a, R = Si(CH$_3$)$_3$
1b, R = H
1c, R = C(CH$_3$)$_2$OH

Along these lines, hexabutadiynylbenzene **2d** was deemed a highly attractive target, because a) it is the first $C_{30}H_6$ hydrocarbon; b) it contains 54(!) conjugated π-electrons, which might give rise to unusual spectral properties indicative of σ-delocalization;[5] c) it could function as a substrate in the regioselective, CpCo-catalyzed, triple cocyclization with ethyne to assemble the fascinating circular [6]phenylene, antikekulene,[5] [the scheme requires the (not unprecedented) ring opening of the initial 1,4,5,8,9,12-hexaethynyltrisbenzocyclobutadienobenzene to the corresponding hexadehydro[12]annulene[4c] and subsequent renewed (intramolecular) triple [2+2+2] cycloaddition of the nine alkyne units (in analogy to the preparation of angular [3]phenylene[6])]; and d) X-ray analysis of protected derivatives would not be complicated by steric effects (as in the case of **1a**).[1] We report here the syntheses of **2a–c** and some of their structural (**2a**, **2c**), physical, and preliminary chemical characteristics.

The substituted butadiynes **3** required for the reaction with hexabromobenzene were made by published (**3a,c**)[7, 8] or adapted (**3b**) literature procedures. The Pd-catalyzed coupling step (with toluene: **2a**, 18%; **2b**, 11%; without toluene: **2c**, 36%)[9] proceeded with a facility and efficiency

[*] Prof. Dr. K. P. C. Vollhardt, Dr. J. R. Green, Dr. J. Mittendorf, D. L. Mohler
Department of Chemistry, University of California at Berkeley
and
Chemical Sciences Division, Lawrence Berkeley Laboratory
Berkeley, CA 94720 (USA)
Priv.-Doz. Dr. R. Boese
Institut für Anorganische Chemie der Universität-Gesamthochschule
Universitätsstrasse 5–7, Postfach 10 37 64, D-W-4300 Essen 1 (FRG)

[**] This work was supported by the Director, Office of Energy Research, Office of Basic Energy Sciences, Chemical Sciences Division of the U.S. Department of Energy (DE-AC03-76SF00098) and the Fonds der Chemischen Industrie. J. G. (NSERC, Canada, 1987-1989) and J. M. (Feodor-Lynen Fellowship, 1989-1990) are grateful for postdoctoral support.

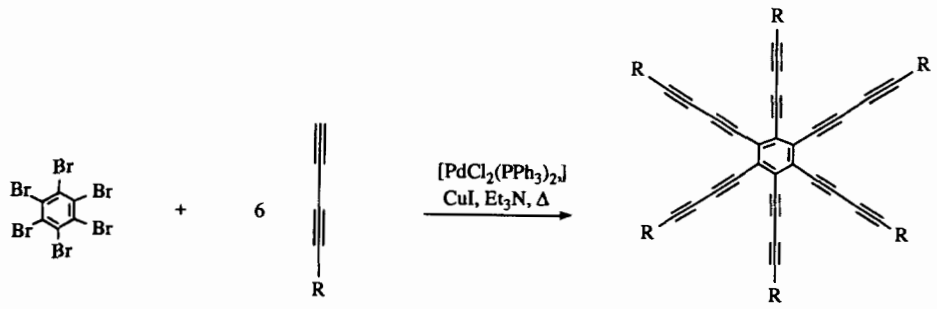

3a, R = $Si[CH(CH_3)_2]_3$
3b, R = $(CH_3)_2Si[C(CH_3)_2CH(CH_3)_2]$
3c, R = $C(CH_3)_3$

2a, R = $Si[CH(CH_3)_2]_3$
2b, R = $(CH_3)_2Si[C(CH_3)_2CH(CH_3)_2]$
2c, R = $C(CH_3)_3$
2d, R = H

that is remarkable in the light of the reactivity of the species involved. Indeed, this reactivity appears responsible for the failure to form derivatives of **2** in which R = Ph or $Si(CH_3)_3$.

Some physical data of **2a–c** are given in Table 1. The compounds were obtained as yellow crystals, stable to air, but losing X-ray diffraction capability in the absence of the solvent of crystallization. Their NMR and IR absorptions are found at the expected positions and compare well to those of **1** and related models.[1, 4c] The clearest manifestation of the change in electronic structure on going from **1** to **2** is provided by UV measurements (of **1a** and **2a**; Fig. 1), a pronounced shift of all the spectral bands to higher wavelengths ($\Delta\lambda_{max} \approx 50$ nm), a generally dramatic increase of the associated molar absorptivities, and the detection of a new set of higher energy transitions is observed.[10] The quite striking hexagonal symmetry of **2** was confirmed by an X-ray structural determination of **2c** (Fig. 2).[11] The compound crystal-

Table 1. Physical data for **2a–c**.

2a: m.p. > 270 °C (decomp.); IR (KBr): $\tilde{\nu}$ = 2950, 2870, 2204, 2098, 1465, 1416, 1387, 1370, 1242, 1133, 1075, 1018, 1002, 930, 893, 763, 688, 671 cm^{-1}; ^1H NMR (300 MHz, $CDCl_3$): δ = 1.20 (br s); ^{13}C NMR (125.7 MHz, $CDCl_3$): δ = 129.3, 93.6, 89.1, 85.2, 70.4, 18.5, 11.3; UV (hexane): λ_{max} (lg ε) = 279 (4.28), 296 (4.28), 306 (4.23), 313 (4.39), 327 (4.85), 335 (4.98), 352 (5.40), 361 (5.22), 375 (5.44) nm; FAB-MS: *m/z* 1304 (M^+, 100), 1280 (35); high resolution MS: *m/z* (M^+ $C_{84}H_{126}Si_6$), calcd 1302.8479, found 1302.8475.

2b: m.p. > 270 °C (decomp.); IR (KBr): $\tilde{\nu}$ = 2962, 2862, 2094, 1250, 1132, 837, 818, 775 cm^{-1}; ^1H NMR (400 MHz, $CDCl_3$): δ = 1.68 (sep, *J* = 6.9 Hz, 6H), 0.94 (s, 36H), 0.93 (d, *J* = 6.9 Hz, 36H), 0.23 (s, 36H); ^{13}C NMR (125.7 MHz, $CDCl_3$): δ = 129.2, 96.3, 88.3, 85.2, 71.2, 34.5, 28.8, 20.7, 18.6, −2.8; UV (hexane): λ_{max} (lg ε) = 264 (4.37), 278 (4.42), 295 (4.40), 327 (4.88), 335 (5.00), 352 (5.37), 360 (5.20), 375 (5.33) nm.

2c: m.p. > 270 °C (decomp.); IR (KBr): $\tilde{\nu}$ = 2971, 2866, 2226, 1479, 1427, 1363, 1269, 1202, 1137, 874, 803, 752, 717, 670, 619 cm^{-1}; ^1H NMR (300 MHz, $CDCl_3$): δ = 1.30 (s); ^{13}C NMR (125.7 MHz, $CDCl_3$): δ = 129.0, 96.5, 84.7, 71.7, 64.3, 30.4, 28.6; UV ($CHCl_3$): λ_{max} (lg ε) = 271 (4.12), 288 (4.16) 323 (4.65), 338 (4.74), 352 (4.76), 365 (4.65) nm; MS (70 eV): *m/z* 702 (M^+, 100) 513 (8), 499 (6), 351 (7), 157 (24), 143 (17), 129 (20), 91 (58), 57 (40).

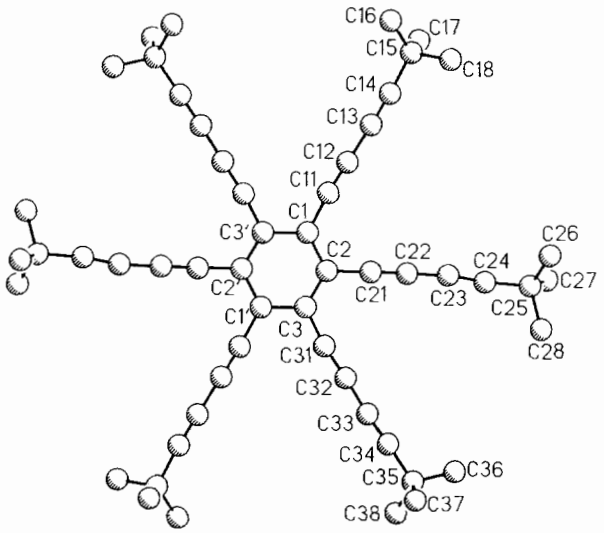

Fig. 2. Molecular structure of **2c** [11]. Mean distances [Å]: C_{arom}–C_{arom} 1.39(2), C_{arom}–C≡1.42(2), C≡ 1.19(1), ≡C–C≡ 1.38(2), ≡C–$C(CH_3)_3$ 1.48(2).

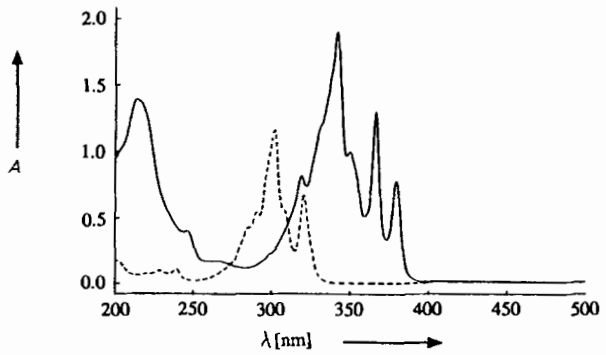

Fig. 1. Electronic spectra of **1a** (– – –) and **2a** (——) in hexane (7.64×10^{-6} M). A = absorption.

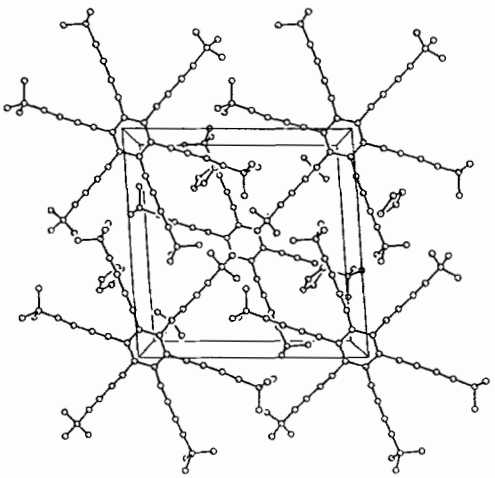

Fig. 3. The unit cell of the crystal structure of **2c** [11].

lized from THF with two solvent molecules in intermolecular spaces (Fig. 3) and had to be kept in the mother liquor to enable acceptable diffraction measurements. An additional complication is presented by the mobility of the diyne substituents, evidenced by the increase in the value of the atomic displacement parameters with increasing distance from the ring. As a consequence, the degree of accuracy of the structural details is diminished.

A few qualitative experiments probing the reactivity of **2** have been moderately encouraging. Surprisingly, **2a–c** show remarkable resilience to irradiation (at 254, 300, 350 nm) in solution and as solids. However, **2a** and **2c** react in the presence of $[CpCo(CO)_2]$ and $[L_3Cr(CO)_3]$ (L = CH_3CN) to form new complexes, they appear to undergo charge-transfer complexation, and they reveal promising electrochemistry. Stepwise protodesilylation of **2a** can be monitored by spectral techniques, but the parent system **2d** could not yet be obtainable pure.

Experimental Procedure

1a: To a solution of 2-methyl-6-triisopropylsilyl-3,5-hexadiyn-2-ol [4b] (19.68 g, 74.4 mmol) and phenothiazine (50 mg, 0.25 mmol) in toluene (450 mL) was added KOH (5.5 g, 98 mmol). The mixture was kept at 70 °C for 2 h under a nitrogen atmosphere. After the reaction had been quenched with an aqueous solution of NH_4Cl, the mixture was extracted repeatedly with pentane. The combined organic layers were dried over $MgSO_4$, filtered, and concentrated to 25 mL under reduced pressure. The resulting oil was divided into three portions and dissolved at 12 h intervals in a boiling solution of hexabromobenzene (1.422 g, 2.58 mmol), $PdCl_2(PPh_3)_2$ (0.268 g, 0.41 mmol), and CuI (0.163 g, 0.86 mmol) in triethylamine (80 mL). Subsequently the mixture was maintained at reflux for an additional 12 h. The solution was filtered through Celite, the residue rinsed with petroleum ether, and the solvents removed from the combined filtrates under reduced pressure. Flash chromatography on silica with pentane and subsequent crystallization from ethyl acetate yielded **1a** (0.611 g, 18%) as yellow crystals.

Received: June 24, 1992 [Z 5429 IE]
German version: Angew. Chem. **1992**, *104*, 1643

CAS Registry numbers:
2a, 143859-24-9; **2b**, 143859-25-0; **2c**, 143859-26-1; **3a**, 111409-83-7; **3b**, 132249-25-3; **3c**, 4911-56-2; $PdCl_2(PPh_3)_2$, 13965-03-2; CuI, 7681-65-4; hexabromobenzene, 87-82-1.

[1] R. Diercks, J. C. Armstrong, R. Boese, K. P. C. Vollhardt, *Angew. Chem.* **1986**, *98*, 270; *Angew. Chem. Int. Ed. Engl.* **1986**, *25*, 268.
[2] a) J. A. Hyatt, *Org. Prep. Proced. Int. Briefs* **1992**, *23*, 460; b) K. Praefcke, B. Kohne, D. Singer, *Angew. Chem.* **1990**, *102*, 200; *Angew. Chem. Int. Ed. Engl.* **1990**, *29*, 177; c) M. Ebert, D. A. Jungbauer, R. Kleppinger, J. H. Wendorff, B. Kohne, K. Praefcke, *Liq. Cryst.* **1989**, *4*, 53; d) K. Praefcke, B. Kohne, K. Gutbier, N. Johnen, D. Singer, *ibid.* **1989**, *5*, 233; e) A. Laschewsky, *Angew. Chem. Adv. Mater.* **1989**, *101*, 1606; *Angew. Chem. Adv. Mater. Int. Ed. Engl.* **1989**, *28*, 1574; *Adv. Mater.* **1989**, *1*, 392.
[3] a) T. X. Neenan, G. M. Whitesides, *J. Org. Chem.* **1988**, *53*, 2489; b) T. X. Neenan, M. R. Callstrom, L. M. Scarmoutzos, K. R. Stewart, G. M. Whitesides, V. R. Howes, *Macromolecules* **1988**, *21*, 3525; c) M. R. Callstrom, T. X. Neenan, G. M. Whitesides, *ibid.* **1988**, *21*, 3528; d) D. R. Rutherford, J. K. Stille, *ibid.* **1988**, *21*, 3530.
[4] a) Reviews on the synthesis, properties and chemistry of the buckminsterfullerenes: *Acc. Chem. Res.* **1992**, March issue; for novel carbon allotropes: F. Diederich, Y. Rubin, *Angew. Chem.* **1992**, *104*, 1123; *Angew. Chem. Int. Ed. Engl.* **1992**, *31*, 1101; b) see L. Blanco, H. E. Helson, M. Hirthammer, H. Mestdagh, S. Spyroudis, K. P. C. Vollhardt, *Angew. Chem.* **1987**, *99*, 1276; *Angew. Chem. Int. Ed. Engl.* **1987**, *26*, 1246; c) R. Diercks, K. P. C. Vollhardt, *J. Am. Chem. Soc.* **1986**, *108*, 3150, and references cited therein. d) A. D. Schlüter, K. P. C. Vollhardt, unpublished.
[5] Postulated by theory, but not clearly detected by experiment in **1**: a) M. S. El-Shall, K. P. C. Vollhardt, *J. Mol. Struct. (Theochem.)* **1989**, *183*, 175; b) see also J. C. Martin, L. J. Schaad, *Pure Appl. Chem.* **1990**, *62*, 547.
[6] R. Diercks, K. P. C. Vollhardt, *Angew. Chem.* **1986**, *98*, 268; *Angew. Chem. Int. Ed. Engl.* **1986**, *25*, 266.
[7] Diynes **3a** [4b] and **c** [8] are known.
[8] L. Brandsma, *Preparative Acetylenic Chemistry*, 2nd ed., Elsevier, Amsterdam, **1988**, p. 290.
[9] All new compounds were fully characterized.
[10] For the electronic spectra of conjugated alkynes, see: a) W. D. Huntsman in *The Chemistry of the Carbon-Carbon Triple Bond, Part 2* (Ed.: S. Patai), Wiley, New York, **1978**, p. 555–561; b) J. Dale in *Chemistry of Acetylenes* (Ed.: H. G. Viehe), Marcel Dekker, New York, **1969**, p. 3–96.
[11] Because of the strong disorder of the silyl substituents in **2a**, its structure could not be refined beyond confirming the molecular skeleton. Crystal data for **2c**: crystal size $0.28 \times 0.22 \times 0.14$ mm^3, kept in a capillary surrounded by the mother liquors and recentered every 100 reflections, $T = 215$ K, space group $P2_1/n$, $a = 14.132(5)$, $b = 13.945(5)$, $c = 14.105(5)$ Å, $\alpha = 90$, $\beta = 93.93(3)$, $\gamma = 90°$, $V = 2772.7(1.7)$ Å^3, $Z = 2$, $\mu = 0.05$ mm^{-1}, $\rho_{calcd.} = 0.928$ gcm^{-3}; $Mo_{K\alpha}$ radiation; scan range $3° \leq 2\theta \leq 40°$; 2549 unique reflections, 875 treated as observed [$F_o \geq 4\sigma(F)$], $R = 0.129$, $R_w = 0.138$. Further details of the crystal structure investigation may be obtained from the Fachinformationszentrum Karlsruhe, Gesellschaft für wissenschaftlich-technische Information mbH, W-7514 Eggenstein-Leopoldshafen 2 (FRG) on quoting the depository number CSD-320521, the names of the authors, and the journal citation.

New Layered Iron-Lanthanum-Oxide-Sulfide and -Selenide Phases: $Fe_2La_2O_3E_2$(E = S,Se)**

By *James M. Mayer,* Lynn F. Schneemeyer,* Theo Siegrist, Joseph V. Waszczak,* and *Bruce Van Dover*

Metal oxides, sulfides, and selenides are amongst the most studied classes of solid-state compounds, yet there are surprisingly few examples of mixed oxide-sulfides or oxide-selenides.[1] The only ternary transition metal oxide-chalcogenides are ZrOS and HfOS,[2] although a variety of rare earth derivatives are known, the most common having the stoichiometry M_2O_2E (M = rare earth metal, E = S, Se, Te), $M_2O_2(S_2)$, and $M_4O_4Se(Se_2)$.[3] These compounds are typically layered materials, in which the oxide, sulfide, or selenide ions are in separate sheets. We are particularly interested in the preparation of new phases that contain transition metals, because layered phases may display interesting electronic and/or magnetic behavior in one or two dimensions. A number of quaternary phases containing rare earth and main group elements are known, and they often do adopt two-dimensional structures.[4] The analogous compounds with transition metals have been less studied. The silver and copper derivatives AgLaOS and CuLaOS have layered structures,[4] while $CrMOS_2$, $CrLaOSe_2$,[5] $V_3La_5O_7S_6$,[6] $La_2Ta_3O_8S_2$, and $M_2Ta_3O_8Se_2$[7] have three-dimensional structures. We report here on the synthesis and initial characterization of $Fe_2La_2O_3S_2$ (**1**) and $Fe_2La_2O_3Se_2$, (**2**), members in a new class of layered compounds exhibiting novel structural features and interesting magnetic behavior.

Compounds **1** and **2** are formed on sintering mixtures of La_2O_3 + 2Fe + 2S or 2Se (stoichiometric with respect to **1** and **2**, respectively) in sealed quartz tubes to temperatures above 1000 °C. Single crystals were obtained from samples heated to higher temperatures. Coating the inside of the tube with carbon minimized attack on the quartz. Compounds **1** and **2** are stable to 1175 and 1250 °C, respectively; above

[*] Prof. J. M. Mayer
Department of Chemistry BG-10
University of Washington
Seattle, WA 98185 (USA)
Dr. L. F. Schneemeyer, Dr. T. Siegrist, J. V. Waszczak, Dr. B. Van Dover
AT&T Bell Laboratories
600 Mountain Avenue, Murray Hill, NJ 07974-0636 (USA)

[**] This work was performed at and supported by A. T. & T. Bell Laboratories. We thank R. J. Cava, P. B. Littlewood, and B. Batlogg for helpful discussions. J.M.M would like to thank the University of Washington, AT&T Bell Laboratories, and the Sloan Foundation for support of his sabbatical year.

these temperatures melting apparently occurs with decomposition. Single-crystal and powder X-ray structural studies show that **1** and **2** form isomorphous compounds, which crystallize in the tetragonal space group *I4/mmm*. The unit cell parameters (Table 1) bear a strong resemblance to those of $La_4Ga_{1.33}O_4S_4$, but **1** and **2** have a different stoichiometry and structure type, and contain divalent iron.

Table 1. The unit cell parameters for $Fe_2La_2O_3S_2$ (**1**) and $Fe_2La_2O_3Se_2$ (**2**) as well as positional parameters of **2**.

Compound		**1**	**2**		$La_4Ga_{1.33}O_4S_4$ [4]
Space group		*I4/mmm*	*I4/mmm*		*P4/mmm*
a [Å]		4.0408(1)	4.0788(2)		4.12
c [Å]		17.8985(6)	18.648(2)		18.54
Positional parameters		*x*	*y*	*z*	B_{iso}
La	(4e)	1/2	1/2	0.18445(5)	0.54(3)
Fe	(4c)	1/2	0	0	1.55(12)
Se	(4e)	0	0	0.09669(9)	0.84(5)
O(1)	(4d)	1/2	0	1/4	0.8(3)
O(2)	(2b)	1/2	1/2	0	1.0(6)

Compounds **1** and **2** are isostructural and thus, for brevity in the remaining text and in Figure 1 only **2** is refered to. The structure of **2** (Fig. 1) consists of layers, stacked along the *c* axis in the order Fe_2O/Se/La/O/La/Se/Fe_2O. The packing in

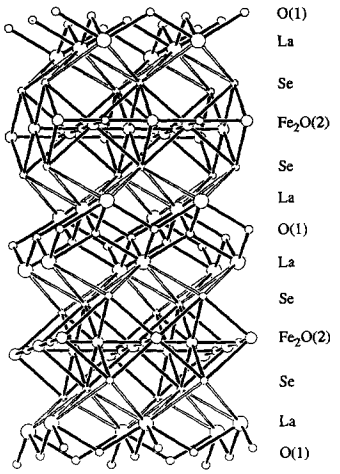

Fig. 1. View of the packing in **2**.

the Fe_2O layer is a novel square network of face-sharing octahedrons and these layers are connected by double layers of Se_4O_4 square antiprisms (La in the middle of the antiprisms). The coordination about iron is a strongly distorted octahedron made up of two *trans* oxide ions and four selenide ions. (Fe–O(2) = 2.0394(2), Fe–Se = 2.722(1) Å). The Fe-O(2)-Fe units are linear and the coordination at the O (2) atom is square planar. Four of the eight Se_2O faces of each iron octahedron are shared with another iron atom. We know of no other compound with a fourfold network of face-sharing octahedrons—fourfold octahedral networks are commonly edge-sharing or vertex-sharing.[8] The packing in **1** and **2** is possible only because of the very different Fe–O and Fe–Se distances, which produce a highly distorted octahedral unit.

The lanthanum coordination in **2** is a square antiprism with four selenide ions on one side and four oxide ions on the other side (La–O(1) = 2.378(1), La–Se = 3.316(1) Å). The coordination geometry about O(1) is a flattened tetrahedron with La-O(1)-La angles of 118.1(1) and 105.3(1)°. The double layer of square antiprisms (Se/La/O(1)/La/Se) is similar to that found in the lanthanum oxide halides LaOX and is a characteristic of the BiOCl (or PbFCl) structure type.[1] This structure is seen in compounds containing large cations with anions of two different sizes. In **2**, $La_4Ga_{1.33}O_4S_4$, and several other oxide-sulfides, the metal ions and the chalcogenide ions are inserted between the sheets of double lanthanum antiprisms.[4]

The formally divalent iron atoms in **2** form a two-dimensional network. Because the Fe octahedrons are face sharing, the shortest Fe–Fe distances are 2.8842(3) Å. The double Se/La/O layers between neighboring Fe layers lead to a large separation (8.95 Å in **1** and 9.32 Å in **2**). Measurements of the temperature dependence of the resistivity for **1** and **2** show activated behavior typical of semiconductors. At room temperature **1** and **2** have resistivities of 200 and 10^3 Ω cm, respectively. The magnetic susceptibility data of **1** and **2** show a peak at about 100 K (Fig. 2), indicating a magnetic ordering. Furthermore, a large temperature-independent paramagnetic susceptibility can be observed, and because the compounds are semiconductors, this is probably Van Vleck paramagnetism.[9] In contrast, the observed maximum is

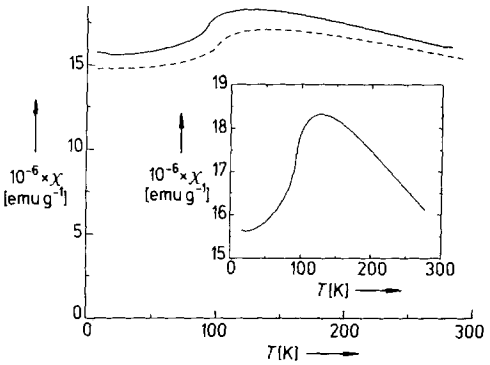

Fig. 2. Temperature dependence of the magnetic susceptibility χ of **1** (---) and **2** (—). In the inset the peak for **2** is enlarged.

probably a consequence of antiferromagnetic exchange in the two-dimensional Fe^{2+} lattice; in a three-dimensional system, a cusp would be observed.[10] Detailed studies of the interesting magnetic behavior of **1** and **2** and extensions to other rare earth elements are underway.

Experimental Procedure

A mixture of La_2O_3, 2 Fe, and 2 S or 2 Se, (stoichiometric with respect to **1** and **2**, respectively) was ground together, pressed into a pellet, loaded into a carbonized quartz tube, and sealed in vacuo. The mixture was heated at 650 °C for 12 h and 1085 °C for 9 days to yield essentially single-phase materials. Black crystals were mounted on quartz fibers, and X-ray data were obtained on a CAD4 diffractometer at 23 °C with $Mo_{K\alpha}$ radiation. **2**: 1197 measured reflections were averaged to give 169 unique reflections, 152 or which had $I > 2\sigma(I)$; 15 variables were refined to $R = 0.028$, $R_w = 0.029$ GOF = 5.78 [11]. **1** is isomorphous with **2**, with a very similar unit cell and atom positional parameters; a full discussion of the structure will be published separately. The resistivity (direct current) of a single crystal was measured by using an electrometer with a van der Pauw arrangement of four silver epoxide contacts. Magnetic susceptibilities were measured on polycrystalline samples from 4.2 to 300 K by the Faraday technique[12].

Received: June 26, 1992 [Z 5435 IE]
German version: *Angew. Chem.* **1992**, *104*, 1677

CAS Registry numbers:
1, 144586-79-8; **2**, 144586-80-1; La_2O_3, 1312-81-8; Fe, 7439-89-6; S, 7704-34-9; Se, 7782-49-2.

[1] A. F. Wells, *Structural Inorganic Chemistry*, 5th ed., Carendon, Oxford, **1984**.
[2] In [1], pp. 786–787; G. A. Eisman, H. Steinfink, *J. Solid State Chem.* **1982**, *43*, 225–226, and references therein; G. A. Eisman, J. S. Swinnea, H. Steinfink, *ibid.* **1985**, *56*, 397–398.
[3] J. Flahaut in *Handbook on the Physics and Chemistry of Rare Earths, Vol. 4* (Eds.: K. A. Gschneidner, Jr., L. Eyring), North-Holland, Amsterdam, **1979**, pp. 1–88.
[4] M. Guittard, S. Benazeth, J. Dugué, S. Jaulmes, M. Palazzi, P. Laruelle, J. Flahaut, *J. Solid State Chem.* **1984**, *51*, 227–238.
[5] T. Vovan, J. Dugué, M. Guittard, *Mater. Res. Bull.* **1978**, *13*, 1163–1166; J. Dugué, T. Vovan, J. Villers, *Acta Crystallogr. Sect. B* **1980**, *36*, 1291–1294; M. Winterberger, T. Vovan, M. Guittard, *Solid State Commun.* **1985**, *53*, 227–230; M. Winterberger, J. Dugué, M. Guittard, N. H. Dung, T. Vovan, *J. Solid State Chem.* **1987**, *70*, 295–302.
[6] J. Dugué, T. Vovan, P. Laruelle, *Acta Crystallogr. Sect. C* **1985**, *41*, 1146–1148.
[7] T. D. Brennan, L. E. Aleandri, J. A. Ibers, *J. Solid State Chem.* **1991**, *91*, 312–322; T. D. Brennan, J. A. Ibers, *ibid.* **1992**, *98*, 82–89.
[8] In [1], pp. 203–230, especially pp. 229–230.
[9] J. H. Van Vleck, *The Theory of Electric and Magnetic Susceptibilities*, Oxford University Press, Oxford, **1932**.
[10] R. L. Carlin, *Magnetochemistry*, Springer, New York, **1986**, p. 187.
[11] Further details of the crystal structure investigation may be obtained from the Fachinformationszentrum Karlsruhe, Gesellschaft für wissenschaftlich-technische Information mbH, D-W-7514 Eggenstein-Leopoldshafen 2, (FRG), on quoting the depository number CSD-56707, the names of the authors, and the journal citation.
[12] F. J. DiSalvo, J. V. Waszczak, *Phys. Rev. B: Condens. Matter* **1981**, *23*, 457.

A Phenoxy-Bridged Homodinuclear Zn Complex with an Unusual Coordination Sphere; Model Compound for the Active Site of Phospholipase C**

By *Stefan Uhlenbrock* and *Bernt Krebs**

A considerable flexibility of coordination numbers and coordination polyhedra is possible in the chemistry of zinc complexes. The d^{10} electron configuration rules out ligand field stabilizing effects for Zn complexes and often leads to strongly distorted coordination polyhedra. This "entatic state"[1, 2] is also observed in many zinc enzymes, in which the metal center frequently acts as a strong Lewis acid and participates in solvolysis and substitution reactions. Particularly important for this is the ability of the metal center to permit acid catalysis also at pH values at which a protonation cannot occur without participation of Zn^{2+} ions.[3, 4]

Apart from numerous zinc enzymes with one metal bonding site, such as carbonic anhydrase and carboxypeptidase A, enzymes which contain two or more zinc ions at the active site are currently of particular interest. One of these is the important enzyme phospholipase C (PLC), which cleaves phospholipids by hydrolysis.[5] X-ray structural analysis confirmed the presence of three zinc atoms in the active site of PLC obtained from *bacillus cereus*.[6] Two of these atoms are connected to each other through one OH^- group or one H_2O molecule as well as through the carboxylate function of an asparagate unit (Fig. 1). The Zn–Zn distance is 3.3 Å. The third zinc atom, which lies somewhat removed from this dinuclear center, shows, like the other two zinc atoms, a distorted trigonal bipyramidal coordination.

Very little is known about dinuclear zinc complexes that can function as models for zinc systems.[7] Herein we report

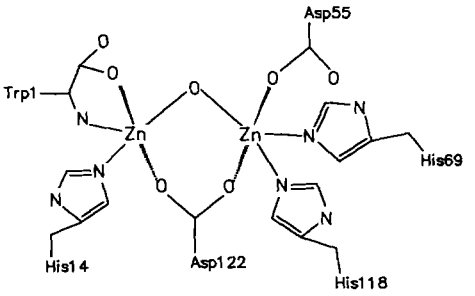

Fig. 1. Structure of the dinuclear unit in the active site of PLC [6].

for the first time on a phenoxy-bridged homodinuclear zinc complex with an entirely biomimetic N_2O ligand sphere, in which the two metal centers are unsymmetrically coordinated. This complex models the dinuclear unit in the active site of PLC. 2,6-Bis[bis(2-benzimidazolylmethyl)aminomethyl]-4-methylphenol (Hbbap) was used as the ligand, since it has proved to be suitable for the stabilization of dinuclear metal complexes.[8] The reaction of two equivalents of $Zn(ClO_4)_2 \cdot 6H_2O$ with one equivalent of Hbbap and sodium benzoate (NaOBz) in an ethanol/methanol mixture led to colorless crystals of **1**.

$[Zn_2(bbap)H_2O(\mu\text{-}OBz)](ClO_4)_2 \cdot 4MeOH$ **1**

The cation of **1** is shown in Figure 2.[9] The two zinc ions are bridged by the phenoxy unit of $bbap^-$ and by the carboxylate function of the benzoato ligand. In contrast to a

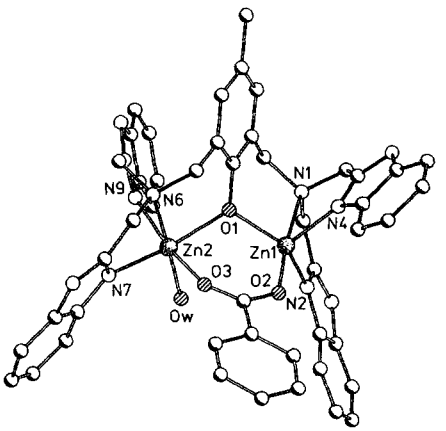

Fig. 2. Structure of the cation $[Zn_2(bbap)H_2O(\mu\text{-}OBz)]^{2+}$ in **1**. Important distances [Å] and angles [°]: Zn1-Zn2 3.443(3), Zn1-O1 1.947(6), Zn1-O2 2.010(6), Zn1-N1 2.480(7), Zn1-N2 2.009(7), Zn1-N4 2.012(7), Zn2-O1 2.099(5), Zn2-O3 2.095(6), Zn2-Ow 2.068(6), Zn2-N6 2.276(7), Zn2-N7 2.141(7), Zn2-N9 2.090(7); Zn1-O1-Zn2 116.6(2).

series of complexes with Hbbap and similar heptadentate chelate ligands, which form dinuclear complexes with fivefold coordinated zinc atoms,[10] the coordination numbers of the two metal centers in **1** are different from each other. Whereas Zn1 is fivefold coordinated (trigonal bipyramid), Zn2 is octahedrally surrounded by four donor atoms of the bbap ligand, one O atom of the benzoato bridge, and one additional bonded H_2O molecule. A coordinated water molecule, which is polarized and can, thus, nucleophilically attack the substrate, is significant for the catalytic procedure

[*] Prof. Dr. B. Krebs, Dipl.-Chem. S. Uhlenbrock
Anorganisch-chemisches Institut der Universität
Wilhelm-Klemm-Strasse 8, D-W-4400 Münster (FRG)

[**] This work was supported by the Deutsche Forschungsgemeinschaft and the Fonds der Chemischen Industrie.

and is assumed to be the transition state in a series of zinc enzymes.[3] The analogy between the enzyme PLC and the model complex **1** is also supported by the Zn–Zn distance in **1** (3.443(3) Å), which is comparable with the value determined for the emzyme. As a result of its unusual coordination geometry complex **1** can be regarded as a structural model for the transition state of the catalytic process of the enzyme PLC.

The unsymmetrical coordination (a polarized coordinated H_2O at Zn2, coordination gap at Zn1) offers—irrespective of whether the bond of the phospholipid substrate (Scheme 1) is, as expected, one-sided terminal or bridges both Zn atoms—favorable conditions for a catalytic acid–base reaction in accordance with a concerted zinc hydroxide and/or zinc phosphoryl mechanism.[3]

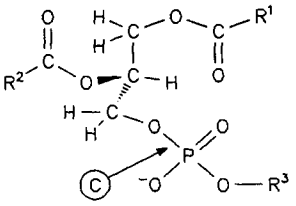

Scheme 1. Phospholipid substrate. The P–O bond of the substrate marked by the arrow is cleaved by the enzyme PLC. In biochemistry this bond is denoted as bond C (symbolized by ©).

The IR spectrum of **1** shows, apart from the vibrations of the $bbap^-$ ligand and the perchlorate anion, also the vibrations of the carboxylate group of the benzoate unit. The symmetric and antisymmetric stretching vibrations of this unit are 1440 and 1590 cm^{-1}, respectively. The difference of 150 cm^{-1} confirms the bidentate bridging coordination of the carboxylate group.

The objective of future work is the development of functional models for the cleavage of phospholipids based on complex **1**. As the first attempts at the catalytic cleavage of different phosphoric acid esters as substrates have shown, the prospects are promising. The systematic improvement of the specificity of **1** by ligand variation is a possible starting point for the modeling of a functional biomimetic dimetal center in a similar way as was recently reported[7a, 11] in the first successful approaches for mononuclear metal centers in carbonic anhydrase.

Experimental Procedure

$Zn(ClO_4)_2 \cdot 6H_2O$ (0.54 g, 1.4 mmol) was dissolved in methanol (10 mL) and added to a solution of Hbbap (0.5 g, 0.7 mmol) in ethanol (15 mL). After the addition of sodium benzoate (0.1 g, 0.7 mmol) in methanol (10 mL), colorless crystals of **1** were formed.

Received: August 1, 1992 [Z 5496 IE]
German version: *Angew. Chem.* **1992**, *104*, 1631

CAS Registry numbers:
1, 144565-39-9; PLC, 9001-86-9.

[1] B. L. Vallee, R. J. P. Williams, *Proc. Natl. Acad. Sci. USA* **1968**, *59*, 498. If a metal center of a metal protein is forced into an unusually distorted coordination by its relatively rigid environment ("preformed transition state"), this situation is described as an entatic state. This distortion can lead to an extraordinary reactivity of the enzyme.
[2] C. Kirchner, B. Krebs, *Inorg. Chem.* **1987**, *26*, 3569.
[3] A. Galdes, B. L. Vallee in *Zinc and its Role in Biology and Nutrition* (Ed.: H. Sigel), Dekker, New York, **1983**, p. 1 ff.
[4] a) N. E. Dixon, A. M. Sargeson in *Zinc Enzymes* (Ed.: T. G. Spiro), Wiley, New York, **1983**, p. 253; b) J. J. R. Frausto da Silva, R. J. P. Williams, *The Biological Chemistry of the Elements*, Clarendon, Oxford, **1991**.
[5] C. Little, *Biochem. J.* **1977**, *167*, 399.
[6] E. Hough, L. K. Hansen, B. Birknes, K. Jynge, S. Hansen, A. Hordvik, C. Little, E. Dodson, Z. Derewenda, *Nature* **1989**, *338*, 357.
[7] a) R. Alsfasser, A. K. Powell, H. Vahrenkamp, *Angew. Chem.* **1990**, *102*, 939; *Angew. Chem. Int. Ed. Engl.* **1990**, *29*, 898; b) P. Chaudhuri, C. Stockheim, K. Wieghardt, W. Deck, R. Gregorzik, H. Vahrenkamp, B. Nuber, J. Weiss, *Inorg. Chem.* **1992**, *31*, 1451; c) P. L. Orioli, M. Di Vaira, L. Sacconi, *ibid.* **1966**, *5*, 400; d) E. Dubler, G. Hänggi, H. Schmalle, *ibid.* **1990**, *29*, 2518; e) L. K. Templeton, D. H. Templeton, D. Zhang, A. Zalkin, *Acta Crystallogr. Sect. C* **1985**, *41*, 363; f) W. Clegg, I. R. Little, B. P. Straughan, ibid. **1986**, *42*, 919; g) C. Lorenzini, C. Pelizzi, G. Pelizzi, G. Predieri, *J. Chem. Soc. Dalton Trans.* **1983**, 2155; h) C.-T. Chen, W.-K. Chang, S.-C. Sheu, G.-H. Lee, T.-I. Ho, Y.-C. Lin, Y. Wang, *ibid.* **1991**, 1569; i) W. Clegg, I. R. Little, B. P. Straughan, *ibid.* **1986**, 1283; j) M. K. Ehlert, S. J. Rettig, A. Storr, R. C. Thompson, J. Trotter, *Can. J. Chem.* **1990**, *68*, 1494.
[8] a) M. Suzuki, H. Kanatomi, I. Murase, *Bull. Chem. Soc. Jpn.* **1984**, *57*, 36; b) N. A. Bailey, D. E. Fenton, R. Moody, P. J. Scrimshire, E. Beloritzky, P. H. Fries, J.-M. Latour, *J. Chem. Soc. Dalton Trans.* **1988**, 2817; c) H. P. Berends, D. W. Stephan, *Inorg. Chim. Acta* **1985**, *99*, L53; d) H. P. Berends, D. W. Stephan, *Inorg. Chem.* **1987**, *26*, 749.
[9] Crystal structural data of **1**: monoclinic, $P2_1/c$, $a = 12.409(5)$, $b = 15.399(8)$, $c = 31.622(12)$ Å, $\beta = 95.91(3)°$, $Z = 4$, $V = 6010.4$ Å^3, measurement temperature 160 K, $Mo_{K\alpha}$ radiation ($\lambda = 0.71073$ Å), 9994 symmetry-independent reflections, of which 6036 with $I > 1.96\sigma(I)$, $R = 0.0826$, $R_w = 0.0745$, structure solved by direct methods. Further details of the crystal structure investigation may be obtained from the Fachinformationszentrum Karlsruhe, Gesellschaft für wissenschaftlich-technische Information mbH, D-W-7514 Eggenstein-Leopoldshafen 2 (FRG) on quoting the depository number CSD-56620, the names of the authors, and the journal citation.
[10] S. Uhlenbrock, B. Krebs, unpublished.
[11] a) R. Alsfasser, S. Trofimenko, A. Looney, G. Parkin, H. Vahrenkamp, *Inorg. Chem.* **1991**, *30*, 4098; b) A. Looney, G. Parkin, R. Alsfasser, M. Ruf, H. Vahrenkamp, *Angew. Chem.* **1992**, *104*, 57; *Angew. Chem. Int. Ed. Engl.* **1992**, *31*, 92.

Tetraalkynylmethanes: Synthesis of Diethynyldipropargyl- and Tetrapropargylmethane**

By *Uwe Bunz*,* *K. Peter C. Vollhardt*, and *Jennifer S. Ho*

We report here on the synthesis of the compounds diethynyldipropargylmethane **5** and tetrapropargylmethane **6**.[1] These molecules may serve as a new type of monomer for highly crosslinked and electroactive hydrocarbon polymers,[2] as initiator nuclei and building blocks for dendrimers,[3] as tetrafunctional complex ligands (possibly for use in the construction of organometallic networks and clusters), and as starting materials for the synthesis of new types of tetrakis(polyalkyne)s. As a result of their topology and functionality **5** and **6** could be suitable precursors to building blocks for molecular electronic devices;[4] an investigation of the interaction between the four C–C triple bonds should be instructive.[5] In addition, **5** and **6** are suitable substrates for

[*] Dr. U. Bunz,[+] Prof. Dr. K. P. C. Vollhardt, J. S. Ho
Department of Chemistry, University of California at Berkeley
and
The Chemical Sciences Division, Lawrence Berkeley Laboratory
Berkeley, CA 94720 (USA)
[+] New address:
Max-Planck-Institut für Polymerforschung
Ackermannweg 10, D-W-6500 Mainz (FRG)

[**] This work was supported by the Director of the Office of Energy Research, Office of Basic Energy Sciences, Chemical Science Division of the U.S. Department of Energy (DE-AC03-76SF00098). U.B. thanks the Deutsche Forschungsgemeinschaft for a postdoctoral fellowship. The X-ray crystal structure analysis of 6 was carried out by Dr. F. J. Hollander, the departmental crystallographer. According to the IUPAC rules, the title compounds are designated 4,4-diethynyl-1,6-heptadiyne and 4,4-di(2-propynyl)-1,6-heptadiyne. The semisystematic names diethynyldipropargylmethane and tetrapropargylmethane, however, are easier to remember and equally unequivocal.

the construction of new spirocyclic systems[6] using cobalt-mediated [2 + 2 + 2] cycloaddition. Because of their high level of symmetry these molecules are also aesthetically attractive.

A general route to **5** and **6** is provided by the preparation of the diyne **3a**. Negishi[7] developed an efficient method for the conversion of methyl ketones into terminal alkynes, which we have been able to modify into a one-pot synthesis of **3a**. Compound **1**[8] was treated with 2.1 equivalents of lithium diisopropylamide (LDA) and the resulting bisenolate converted with diethylchlorophosphate into bis(enolphosphate) **2** (Scheme 1). Treatment of **2**, which was not isolated,

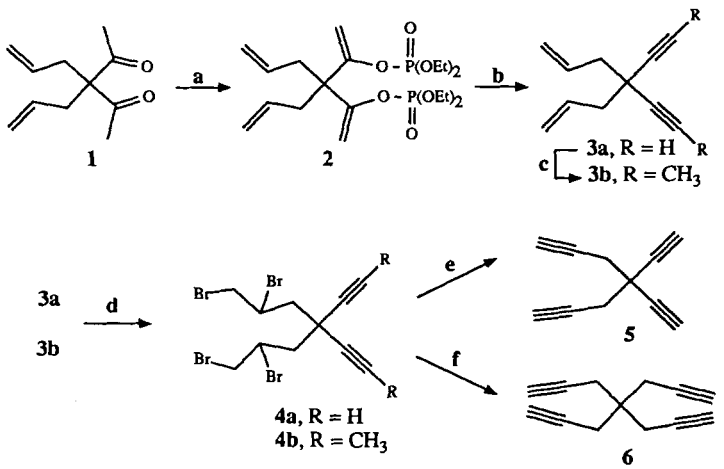

Scheme 1. a) 2.1 equiv LDA, −78 °C → 20 °C, 1 h, then 2.2 equiv ClP = O(OEt)$_2$, 3 h; b) 4.3 equiv LDA, −78 °C → 20 °C, 2 h, then 5 N HCl (**3a**: 59%); c) 2 equiv *n*BuLi, then CH_3I (**3b**: 82%); d) 2 equiv Br_2, CH_2Cl_2, −78 °C (**4a**: 82%, **4b**: 41%); e) **4a**, 11 equiv $NaNH_2$ in liq. NH_3, then 5 N HCl (**5**: 67%); f) **4b**, 45 equiv KNH_2 in liq. NH_3, 8 h, then 5 N HCl (**6**: 18%).

in a further step with an excess of LDA afforded **3a** in 61% yield. In spite of the presence of the ethynyl groups[9] the double bonds in **3a** can be selectively brominated at low temperature; thus, the crystalline tetrabromide **4a**[10] was formed in high yield as a pair of diastereomers (ratio (*d,l*:*meso*) 1:1), as shown by integration of the signals of the alkyne protons in the ^{1}H NMR spectrum. Dehydrohalogenation of **4a** with sodium amide in liquid ammonia gave **5** in 66% yield. The tetraalkyne **5**, stable in air, separates out as a colorless oil; crystallization takes place on standing at approximately 5 °C. Compound **5** is not miscible with pentane and hexane at every concentration but is completely miscible with chloroform or dichloromethane.

Attempts to obtain **6** by exhaustive alkynylation of tetra(bromomethyl)methane were unsuccessful.[4] *n*-Butyllithium effected double deprotonation of the diyne **3a**; subsequent reaction with CH_3I gave **3b**,[11] which was converted to the crystalline tetrabromide **4b**[10] by reaction with bromine. Compound **4b**, analogous to **4a**, was also obtained as a mixture of two diastereomers in a ratio of about 1:1. Potassium amide (in a tenfold excess per alkyne group) in liquid ammonia effected both complete dehydrohalogenation and isomerization to the all-terminal potassium salt of **6**. Finally, tetrapropargylmethane **6** was obtained in 18% yield after aqueous acidic workup.[12] This compound is only slightly sensitive to oxygen and hardly soluble in pentane and hexane, but very soluble in chloroform and dichloromethane.

The ^{13}C NMR spectrum of **5** shows six signals, of which four can be assigned to the two pairs of nonequivalent acetylene groups; in addition, the nondecoupled ^{13}C NMR spectrum shows that the signal of the terminal acetylene carbon atom, which is shifted to lower field, must be assigned to the heptadiyne unit as a result of the fine splitting expected for the propargyl group. Four signals are observed in the broadband-decoupled ^{13}C NMR spectrum of **6**. The alkyne resonances in the proton-coupled ^{13}C NMR spectrum display coupling constants of the expected magnitude[13] (Table 1). The IR spectrum shows few signals, with characteristic bands at 3304, 2915, and 2121 cm^{-1}; no signals were recorded in the range 2100 to 1450 cm^{-1}.

Table 1. Physical data for **3a**, **5**, and **6** [a].

3a: B.p. 38–39 °C (2.2 Torr); IR (KBr): ν[cm^{-1}] = 3298, 3078, 3011, 2984, 2915, 1643, 1565, 1549, 1512, 993; ^{1}H NMR ($CDCl_3$): δ = 2.22 (s, 2H; alkyne H), 2.35 (d, ^3J(H,H) = 7.1 Hz, 4H; CH_2-CH=CH_2), 5.09–5.21 (m, 4H; CH_2-CH=CH_2), 5.84–6.00 (m, 2H; CH_2-CH=CH_2); ^{13}C NMR ($CDCl_3$): δ = 34.19 (C-4), 44.62 (CH_2-CH=CH_2), 70.44 (C≡*C*-H), 84.05 (*C*≡C-H), 118.55 (CH_2-CH=*C*H_2), 132.70 (CH_2-*C*H=CH_2); MS (70 eV): *m/z* 128 ($M^{\oplus}$ − CH_4, 70%), 115 (31), 102 ($M^{\oplus}$ − C_3H_6, 33), 77 (100); high-resolution MS: *m/z* 143.0857 (calculated for $M^{\oplus}$ − H, $C_{11}H_{11}$: *m/z* 143.0861).

5: B.p. 31 °C (0.05 Torr); IR (KBr): ν[cm^{-1}] = 3307, 3294, 2947, 2921, 2123, 1428, 1294, 1102; ^{1}H-NMR ($CDCl_3$): δ = 2.13 (t, ^4J(H,H) = 2.6 Hz, 2H; 1-, 7-H), 2.39 (s, 2H; C≡C-H), 2.72 (d, ^4J(H,H) = 2.6 Hz, 4H; 3-, 5-H$_2$); ^{13}C NMR ($CDCl_3$): δ = 30.48 (t, ^1J(C,H) = 136.2 Hz; C-3, -5), 33.61 (s; C-4, central C atom), 71.26 (d, ^1J(C,H) = 251.7 Hz; C≡*C*-H), 72.01 (dt, ^1J(C,H) = 249.2 Hz; C-1, -7), 78.39 (dt, ^2J(C,H) = 49.9 Hz; C-2, -6), 82.35 (d quint d, ^2J(C,H) = 49.9 Hz; *C*≡C-H); MS (70 eV): *m/z* 140 ($M^{\oplus}$, 18%), 139 ($M^{\oplus}$ − H, 100), 114 ($M^{\oplus}$ − C_2H_2, 19), 101 ($M^{\oplus}$ − C_3H_3, 29); high-resolution MS: *m/z* 139.0544 (calculated for $M^{\oplus}$ − H, $C_{11}H_7$: *m/z* 139.0547).

6: M.p. 126 °C; IR (KBr): ν[cm^{-1}] = 3304, 2934, 2915, 2120, 1434, 1327; ^{1}H NMR ($CDCl_3$): δ = 2.04 (t, ^4J(H,H) = 2.6 Hz, 4H; CH_2-C≡C-*H*), 2.47 (d, ^4J(H,H) = 2.6 Hz, 8H; CH_2-C≡C-H); ^{13}C NMR ($CDCl_3$); δ = 25.51 (t oct, ^1J(C,H) = 132.5 Hz; CH_2-C≡C-H), 39.29 (s; C-4, central C atom), 71.18 (dt, ^1J(C,H) = 247.2 Hz; CH_2-C≡*C*-H), 80.02 (dt, ^2J(C,H) = 49.9 Hz; CH_2-*C*≡C-H); MS (70 eV): *m/z* 165 (12%), 152 ($M^{\oplus}$ − CH_4, 22), 141 (9), 128 ($M^{\oplus}$ − C_3H_4, 100), 115 (12), 102 (28).

[a] ^{1}H and ^{13}C NMR spectra were recorded at 400 and 100 MHz, respectively.

The differences in the mass spectra of **5** and **6** are remarkable. In the case of **5** the (M^+−H) signal (*m/z* 139) appears as the base peak and the molecular ion (*m/z* 140) can be observed, whereas for **6** the cleavage of a C_3H_4 fragment (*m/z* 40) is immediate: the signal at *m/z* 128 forms the base peak, and that of the molecular ion is not visible. The interpretation of this observation becomes clear when the results from pyrolysis of 1,5-hexadiyne (**7**) and 1,6-heptadiyne (**8**) are taken into consideration. Compound **7** rearranges, according to Huntsman and Wristers,[14a] with an activation energy of 34 kcal mol^{-1}, whereas **8**, after overcoming an energy barrier of about 50 kcal mol^{-1}, loses allene by way of a retro-ene reaction with formation of vinylacetylene. The same behavior is observed in the mass spectrometric investigations of these compounds;[15] accordingly, **6** behaves in analogous fashion to **8**. It would appear, however, that the retro-ene reaction of **5** does not take place because of the much higher activation energy; the hexadiyne rearrangement is thus preferred. The appearance of the (M^+−C_2H_2) ion with *m/z* 114 supports this argument, as the parent system **7**[14b] also undergoes elimination of acetylene in the mass spectrometer to give an (M^+−C_2H_2) ion (*m/z* 52). The latter is presumably formed by the [2 + 2] retrocyclization, as described by Huntsman and Wristers for the rearrangement of bis(*exo*-methylene)cyclobutene. Nevertheless, the signal for the molecular ion of **7**, in contrast to that of **5**, is

markedly more intense than the signal for the (M^+–H) fragment.

Initial attempts to effect rearrangement of **5** with KO*t*Bu in dimethylsulfoxide (DMSO)[16] appear to be successful. GC-MS analysis shows that, in addition to approximately 30% starting material, five new isomers are present: we have indications that one of these isomers is a dimethyl-substituted tetraethynylmethane.[17] Preliminary investigations also show that tetraalkyne **5** readily forms complexes with transition metals.

Because of the novelty of these compounds a crystal structure analysis[18] of **6** was conducted (Fig. 1). The deviation

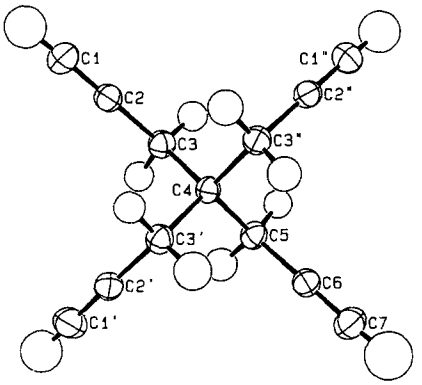

Fig. 1. Crystal structure of **6**[18]. Important bond lengths [Å] and angles [°]: C1-C2 1.183(2), C2-C3 1.462(2), C3-C4 1.545(2); C1-C2-C3 179.5(2), C2-C3-C4 114.6(1), C3-C4-C5 106.0(1), C3-C4-C3' 111.1(1).

from molecular D_{2d} symmetry is minimal; the bond angles at the symmetrically substituted C-4 are not 109.4° (ideal tetrahedral angle), rather two pairs of 106.0(1)° and 111.2(1)°. Both molecular mirror planes are at an angle of 93° to each other; nevertheless, it cannot be ruled out that this is an artefact. The lengths of the acetylenic [1.183(2) Å] and the propargylic [1.463(2) Å] C–C bonds are in excellent agreement with known values.[19]

The packing of **6** in the crystal (Fig. 2) leads to layers parallel to the *bc* plane, within which the shortest intermolecular C–C distance (between C-1 and C-1″) amounts to 3.366(2) Å. The alkyne groups with this short contact are not aligned parallel. The alkyne groups of two neighboring molecules lying parallel to each other are more than 3.5 Å apart.

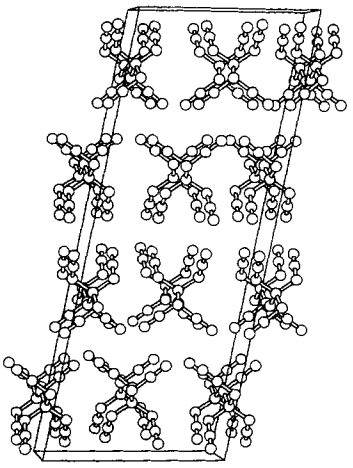

Fig. 2. Packing of **6** in the crystal [18]. The viewing direction is along the crystallographic b axis

Experimental Procedure

3a: To a solution of LDA, prepared from diisopropylamine (12.0 g, 119 mmol) in THF (100 mL) and *n*BuLi (53 mL, 116 mmol, 2.2 M solution in hexane), was added **1** (10.0 g, 55.5 mmol) at −78 °C; after warming to room temperature the mixture was stirred for 1 h, then treated with diethylchlorophosphate (21.1 g, 122 mmol) at −78 °C. The resulting mixture was allowed to warm to room temperature and stirred for 3 h. This solution was cooled to −78 °C and then added to a solution of LDA, prepared from diisopropylamine (24.1 g, 238 mmol) and *n*BuLi (96 mL, 212 mmol, 2.2 M solution in hexane), in THF (200 mL) at the same temperature. After 2 h reaction at room temperature the reaction mixture was hydrolyzed with 5 N aqueous HCl. Workup by distillation gave **3a** (4.67 g, 59%) as a colorless oil.

5: A suspension of $NaNH_2$ (from 2.75 g (120 mmol) Na) in liquid ammonia was prepared according to [20]. A solution of **4a** (4.94 g, 10.7 mmol) in 10 mL ether was then added. The reaction mixtrue was held at reflux (−33 °C) for 5 h. Aqueous acidic workup and distillation gave **5** (989 mg, 67%) as a colorless oil.

6: A solution of potassium amide was prepared from potassium (4.30 g, 110 mmol) in liquid ammonia (ca. 200 mL)[20]. To this solution was added **4b** [10] (1.20 g, 2.44 mmol) in ether (10 mL). The mixture was stirred for 8 h at −33 °C. Workup as for **5** followed by sublimation at a bath temperature of ca. 30–70 °C (0.05 Torr) afforded **6** (74.0 mg, 18%).

Received: June 24, 1992 [Z 5430 IE]
German version: *Angew. Chem.* **1992**, *104*, 1645

CAS Registry numbers:
1, 3508-79-0; **2**, 144084-20-8; **3a**, 144084-21-9; **3b**, 144084-25-3; **4a** (*d, l*), 144084-22-0; **4a** (*meso*), 144084-23-1; **4b** (*d, l*), 144084-26-4; **4b** (*meso*), 144084-27-5; **5**, 144084-24-2; **6**, 144084-29-7; **6** (tetrapotassium salt), 144084-28-6.

[1] For the synthesis of tetraallylmethane see: W. Reeve, R. J. Bianchi, *J. Org. Chem.* **1969**, *34*, 1921.
[2] G. Wegner, *Angew. Chem.* **1981**, *93*, 352; *Angew. Chem. Int. Ed. Engl.* **1981**, *20*, 361, and literature cited therein; *Z. Naturforsch. B* **1969**, *24*, 824; H. W. Gibson, C. B. Bailey, A. J. Epstein, H. Rommelmann, J. M. Pochan, *J. Chem. Soc. Chem. Commun.* **1980**, 426; J. K. Stille, D. A. Frey, *J. Am. Chem. Soc.* **1961**, *83*, 1697; A. H. Alberts, *ibid.* **1989**, *111*, 3093.
[3] G. R. Newkome, C. N. Moorefield, G. R. Baker, A. L. Johnson, R. K. Behera, *Angew. Chem.* **1991**, *103*, 1205; *Angew. Chem. Int. Ed. Engl.* **1991**, *30*, 1176; G. R. Newkome, C. N. Moorefield, G. R. Baker, A. L. Johnson, M. J. Saunders, S. H. Grossmann, *ibid.* **1991**, *103*, 1207 or **1991**, *30*, 1178; D. A. Tomalia, A. M. Naylor, W. A. Goddard III, *ibid.* **1990**, *102*, 119 or **1990**, *29*, 113; E. Buhleier, W. Wehner, F. Vögtle, *Synthesis* **1978**, 155; see also the Highlight in this issue: H.-B. Mekelburger, W. Jaworek, F. Vögtle, *Angew. Chem.* **1992**, *104*, 1609; *Angew. Chem. Int. Ed. Engl.* **1992**, *31*, 1571.
[4] J. M. Tour, R. Wu, J. S. Schumann, *J. Am. Chem. Soc.* **1991**, *113*, 7064; *ibid.* **1990**, *112*, 5662.
[5] R. Gleiter, *Angew. Chem.* **1992**, *104*, 29; *Angew. Chem. Int. Ed. Engl.* **1992**, *31*, 27.
[6] K. P. C. Vollhardt, *Angew. Chem.* **1984**, *96*, 525; *Angew. Chem. Int. Ed. Engl.* **1984**, *23*, 539; *Acc. Chem. Res.* **1977**, *10*, 1.
[7] E. Negishi, A. O. King, J. M. Tour, *Organic Syntheses, Coll. Vol. 7*, Wiley, New York, **1990**, p. 63; this method was used for the synthesis of diethynylcubane: P. Eaton, D. Stoessel, *J. Org. Chem.* **1991**, *56*, 5138.
[8] R. B. Davis, P. Hurd, *J. Am. Chem. Soc.* **1955**, *77*, 3284.
[9] It is known that triple bonds are inert toward bromine at −78 °C; lithium acetylide can be converted under these conditions to bromoacetylene without difficulty: L. Brandsma, *Preparative Acetylic Chemistry*, 2nd ed., Elsevier, Amsterdam, **1988**, p.143, and references therein.
[10] The bromination of **3a** and **3b** was carried out at −78 °C in CH_2Cl_2; the solution of bromine in CH_2Cl_2 was also cooled beforehand to this temperature: **4a** (m.p. 72–74 °C, from CH_2Cl_2/hexane) 82%; **4b** (m.p. 120–130 °C from CH_2Cl_2/hexane) 41%; both compounds exist as mixtures of diastereoisomers and have been fully characterized by their spectroscopic data and combustion analysis.
[11] The methylation resulted from double deprotonation of **3a** with *n*BuLi in THF at −30 °C; 3 equiv CH_3I were added and the reaction mixture stirred 12 h at 20 °C. Hydrolysis and distillation afforded **3b** in 82% yield; the latter was characterized by its spectroscopic data and high-resolution mass spectrum.
[12] The relatively low yield of 18% can be explained on the grounds that there are ten reaction steps before the hydrolysis; the average yield of any given step is 84%.
[13] H. O. Kalinowski, S. Berger, S. Braun, *^{13}C-NMR-Spektroskopie*, **1984**, p. 129 (chemical shifts), p. 481 (C,H coupling constants).
[14] Thermolysis of 1,5-hexadiyne: a) W. D. Huntsman, H. J. Wristers, *J. Am. Chem. Soc.* **1967**, *89*, 342; mass spectrum of 1,5-hexadiyne: J. Momigny, L. Brakier, L. D'Or, *Bull. Cl. Sci. Acac. R. Belg.* **1962**, *48*, 1002.

[15] K. D. King, *J. Phys. Chem.* **1980**, *84*, 2517.
[16] H. Hopf, *Chem. Ber.* **1971**, *104*, 3087; R. J. Bushby, *Q. Rev. Chem. Soc.* **1970**, *24*, 585; D. A. Ben-Efraim, F. Sondheimer, *Tetrahedron* **1969**, *25*, 2837.
[17] A. H. Alberts, H. Wynberg, *J. Chem. Soc. Chem. Commun.* **1988**, 748.
[18] (M_r = 168.24); T = 173 K, space group $C2/c$, a = 29.285(4), b = 6.2398(8), c = 11.4790(23) Å, α = 90.0, β = 101.245(14), γ = 90.0°, V = 2057.4(10) Å^3, Z = 8, ρcalc = 1.09 g cm^{-3}; clear, colorless, coffin-shaped crystals (0.22 × 0.50 × 0.55 mm^3) were obtained by isotropic distillation of pentane into a solution of **6** in chloroform. Enraf-Nonius CAD-4 four-circle diffractometer, $2\vartheta_{max}$ = 52°, 2015 symmetry-independent reflections, of which 1286 with $F^2 > 3\sigma(F^2)$ were used for the refinement (SHELXS); 166 refined parameters, R = 0.033, R_w = 0.041, $w^{-1} = \sigma 2(F_0)$. Further details of the crystal structure investigation may be obtained from the Fachinformationszentrum Karlsruhe, Gesellschaft für wissenschaftlich-technische Information GmbH, D-W-7514 Eggenstein-Leopoldshafen 2 (FRG) on quoting the depository number CSD-56676, the names of the authors, and the journal citation.
[19] J. L. Hencher in *The Chemistry of the Functional Groups, The Chemistry of the Carbon Carbon Triple Bond, Part 1* (Ed.: S. Patai), Wiley, New York, **1978**, p. 57.
[20] L. Brandsma, H. Verkruijsse, *Preparative Polar Organometallic Chemistry 1*, 1st ed., Springer, Berlin, **1987**, p. 21.2

Diastereoselective Three-Center Michael Addition of β-Ketoesters to Prostereogenic α,β-Unsaturated Carbonyl Compounds Catalyzed by K_2CO_3 or Cs_2CO_3**

By *Nicole Ouvrard, Jean Rodriguez,* and Maurice Santelli*

In our investigations[1] on the synthesis of the Prelog–Djerassi lactone[2] it appeared that another attractive and direct way for the preparation of the key intermediate would be the Michael addition[3] of a β-ketoester to an α,β-unsaturated carbonyl compound. The (2*S*,3*R*)-β-ketoesters **1**[4] serve as a model compounds for our study (Scheme 1). The correct (2*R*,3*S*) enantiomer can be formed from readily available (*S*)-(−)-pulegone.[1]

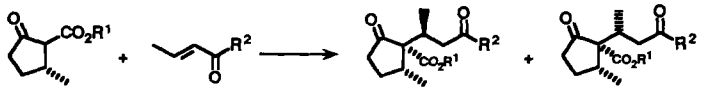

1a, R^1 = Me **2a**, R^2 = Me
1b, R^1 = *t*Bu **2b**, R^2 = H
1c, R^1 = Bz

3

4
a, $R^1 = R^2$ = Me
b, R^1 = *t*Bu, R^2 = H
c, R^1 = Bz, R^2 = H
d, R^1 = *t*Bu, R^2 = Me

Scheme 1. Michael addition of β-ketoesters to α,β-unsaturated compounds.

The diastereoselective Michael addition has been studied extensively in recent years and constitutes one of the most useful methods for carbon–carbon bond formation.[5] We wish to report here on the highly diastereoselective, three-center Michael addition[6] of simple chiral β-ketoesters with a prostereogenic α,β-unsaturated carbonyl compound; this provides a stereocontrolled route to compounds with three contiguous stereogenic centers.[7]

The K_2CO_3 or Cs_2CO_3 catalyzed reaction of **1** with Michael acceptors **2** in acetone provides **3**,[8] one of the four possible diastereomers, with high selectivity (entries 1–7, Table 1).[9] Compounds **3** arise in a reaction with *lk* relative topicity[10] via a cyclic synclinal transition state **I**[5b] (Scheme 2).

Table 1. Michael addition of **1** to **2** in the presence of 0.5 equivalent of K_2CO_3 or Cs_2CO_3.

Entry	1	2	R^1	R^2	Conditions [a]	Isolated yields [%]	3:4 [c]
1	a	a	Me	Me	K_2CO_3, 40 °C, 6 h	[b]	70:30
2	a	a	Me	Me	K_2CO_3, 20 °C, 7 d	52	80:20
3	a	b	Me	H	K_2CO_3, 20 °C, 15 h	78	85:15
4	b	b	*t*Bu	H	K_2CO_3, 20 °C, 15 h	65	>95:5
5	b	b	*t*Bu	H	K_2CO_3, 57 °C, 3 h	67	77:23
6	c	b	Bz	H	K_2CO_3, 20 °C, 15 h	65	>95:5
7	b	b	*t*Bu	H	Cs_2CO_3, −30 °C, 5 h	70	>95:5
8	b	b	*t*Bu	H	K_2CO_3 [d], −30 °C, 5 h	84	15:85
9	b	b	*t*Bu	H	Cs_2CO_3 [e], −50 °C, 7 h	30	35:65
10	b	b	*t*Bu	H	K_2CO_3 [f], −20 °C, 5 h	58	20:80
11	c	b	Bz	H	K_2CO_3 [f], −20 °C, 5 h	56	15:85
12	b	a	*t*Bu	Me	K_2CO_3 [f], −20 °C, 72 h	87	<5:95

[a] Reactions for entries 1–9 were carried out in dry acetone. [b] Quantitative by gas chromatography with a 20 m SE-30 column. [c] Determined by ^{1}H NMR spectroscopy (200 or 400 MHz). [d] 0.25 Equiv [18]crown-6. [e] 0.25 Equiv dibenzo-[24]crown-8. [f] Mixture of hexamethylphosphoric triamide (HMPA)/CH_2Cl_2 (5/1) as solvent and 0.25 equiv 4,7,13,16,21,24-hexaoxa-1,10-diazabicyclo[8.8.8]hexacosane (Kryptofix 222).

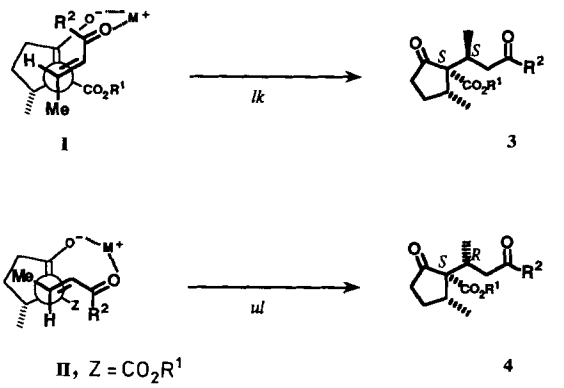

I **3**

II, Z = CO_2R^1 **4**

Scheme 2. Possible cyclic transition states **I** and **II**.

Examination of molecular models shows that in transition state **II** there is substantial nonbonding interaction between the alkoxycarbonyl group of the Michael donor and the carbonyl part of the α,β-unsaturated function (Scheme 2). This finding is supported by the observed effect of R^1 and R^2 on the diastereoselectivity of the reaction at room temperature or below. The ratio **3**:**4** is only 85:15 for R^1 = Me, R^2 = H (entry 3), while **3** is obtained almost exclusively when R^1 = *t*Bu or Bz, R^2 = H (entries 4, 6, and 7).

In all cases, the diastereofacial control is total; this is probably a consequence of the almost planar structure of the enolate derived from **1**. By analogy with related systems, one can expect that this endocyclic enolate will be attacked exclusively from the face opposite to the methyl substituent.[11] The highest diastereoselectivity is obtained with K_2CO_3 at room temperature (entries 4 and 6) or at −30 °C when Cs_2CO_3 is used as catalyst (entry 7). It is of interest to note that poor or no stereoselectivity was reported previously for the addition of simple cyclic or acyclic β-ketoesters to methyl ethylidenemalonate with K_2CO_3 as base.[7a] To our knowledge, our results constitute the first example of three-center

[*] Dr. J. Rodriguez, N. Ouvrard, Prof. Dr. M. Santelli
Laboratoire de Synthèse Organique associé au CNRS Centre de St-Jérôme
boîte D12, F-13397 Marseille Cedex 13 (France)

[**] This work was supported by Rhône-Poulenc-Rorer (Vitry). We are grateful to Dr. J. C. Barrière (Rhône-Poulenc-Rorer) for helpful discussions.

diastereoselectivity for five-membered carbocyclic ring systems.[5b, 6]

The configurations of **3** and **4** were confirmed by chemical correlation with the known γ,δ-unsaturated ketone **6**.[12] Preparation of **6** from **3b** was straightforward (Scheme 3): selective reduction of the aldehyde functionality ($NaBH_4$, *i*PrOH, room temperature, 57%[12b]) was followed by decarboxylation and selenoxide elimination (*o*-nitrophenylselenocyanate, Bu_3P, CH_2Cl_2; 15% *p*TsOH, C_6H_6, reflux, then H_2O_2, THF, 72% overall[12c]). The spectroscopic and analytical data of **6** prepared in this way were identical to those of a sample synthesized previously by a different route.[12]

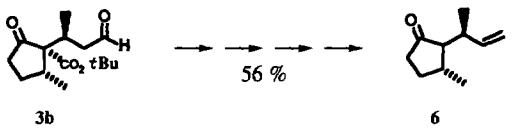

3b **6**

Scheme 3. Preparation of ketone **6**.

A slight increase in temperature affects the diastereoselectivity; the reaction then most likely proceeds to a certain extent via transition state **II**. The other explanation, equilibration of the products, can be ruled out. A mixture of **3a** and **4a** in the ratio 60:40 did not equilibrate when treated with K_2CO_3 in acetone for seven days (compare entries 1 and 2, 4 and 5). A specific complexing agent has a greater effect on the diastereoselectivity. Indeed, the complexation of the metal ion by either a crown ether (entries 8 and 9) or by Kryptofix 222 (entries 10–12) results in a reverse diastereoselectivity; **4**, arising from the *ul* relative topicity, is obtained with high selectivity. Under these conditions lower temperature is required because of the enhanced basicity and potential side reactions. The ratio **3**:**4** is independent of the reaction time, indicating that the Michael addition remains under kinetic control. These results[13] provide evidence for the participation of the metal ion in the stabilization of the cyclic transition state **I** (Scheme 2). The results can be best explained by assuming that in the presence of a complexing agent, the bulky complex formed by the specific cryptand and the cation (M^+ in Scheme 4) favors the ion pair dissociation[14] and suppresses the coordination between the enolate and the α,β-unsaturated compound. These two facts are in agreement with an open antiperiplanar transition state[15] **IV** rather than **III** in which the nonbonding interaction between the ester group of the Michael donor and the carbonyl part of the α,β-unsaturated function is present (Scheme 4).

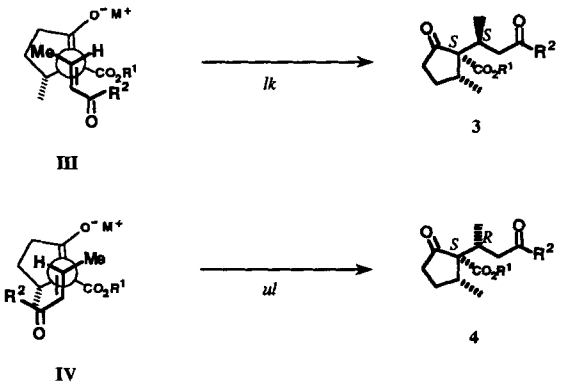

III **3**

IV **4**

Scheme 4. Possible acyclic transition states **III** and **IV**.

The diastereoselectivity increases significantly when R^2 = Me instead of R^2 = H (cf. entries 10 and 12).

The results presented here are in accord with a cyclic transition state characterized by a chelate complex between the enolate and the carbonyl functions; this is an important requisite for stereocontrol under kinetic conditions. This proposition is supported by the observed effect of a specific complexing agent which causes the reaction to proceed through a nonchelated antiperiplanar transition state giving rise to a reverse diastereoselectivity. The base-catalyzed Michael addition of the β-ketoesters **1** to a prostereogenic α,β-unsaturated carbonyl compound **2** has high diastereoselectivity and offers a synthetically attractive approach to the optically active Prelog–Djerassi lactone and related compounds.

Received: June 17, 1992 [Z 5412 IE]
German version: *Angew. Chem.* **1992**, *104*, 1658

CAS Registry numbers:
1a, 80796-76-5; **1b**, 144320-35-4; **1c**, 144407-31-8; **2a**, 625-33-2; **2b**, 4170-30-3; **3** (R^1 = Me, R^2 = H), 144320-37-6; **3a**, 144320-36-5; **3b**, 144320-38-7; **3c**, 144320-39-8; **4** (R^1 = Me, R^2 = H), 144407-33-0; **4a**, 144407-32-9; **4b**, 144407-34-1; **4c**, 144407-35-2; **4d**, 144320-40-1.

[1] S. Hacini, M. Santelli, *Tetrahedron* **1989**, *45*, 6449; *ibid.* **1990**, *46*, 7787.
[2] For a recent review, see: S. F. Martin, D. E. Guinn, *Synthesis* **1991**, 245.
[3] E. D. Bergmann, D. Ginsburg, R. Pappo, *Org. React.* **1959**, *10*, 179.
[4] For the preparation of **1a** from (*R*)-(+)-pulegone see: J. N. Marx, L. R. Norman, *J. Org. Chem.* **1975**, *40*, 1602; compounds **1b,c** were prepared by esterification of pulegenic acid following the literature procedure: C. F. Murphy, R. E. Koehler, *J. Org. Chem.* **1970**, *35*, 2429.
[5] For reviews see: a) K. Tomioka, K. Koga in *Asymmetric Synthesis, Vol. 2* (Ed.: J. D. Morrison), Academic Press, New York, **1983**, p. 201; b) D. A. Oare, C. H. Heathcock, *Top. Stereochem.* **1989**, *19*, 227; c) *ibid.* **1991**, *20*, 87.
[6] For the first report of the diastereoselective three-center Michael addition with β-lactone enolates, see: J. Mulzer, A. Chucholowski, O. Lammer, I. Jibril, G. Huttner, *J. Chem. Soc. Chem. Commun.* **1983**, 869.
[7] For recent reports on the construction of contiguous quaternary and tertiary carbon centers, see: a) K. Tomioka, K. Yasuda, K. Koga, *J. Chem. Soc. Chem. Commun.* **1987**, 1345; b) J. C. Gilbert, T. A. Kelly, *Tetrahedron* **1988**, *44*, 7587; c) T. Kitahara, H. Kurata, K. Mori, *ibid.* **1988**, *44*, 4339; d) M. C. Pirrung, W. L. Brown, S. Rege, P. Laughton, *J. Am. Chem. Soc.* **1991**, *113*, 8561.
[8] All new compounds gave satisfactory analytical and/or spectral data. For example **3c**: colorless oil: R_f = 0.40, ether/pentane (1/1); $[\alpha]_{578}^{22}$ + 98.4 ($CHCl_3$, c = 2); IR (neat): ν = 3040, 2970, 2730, 1750, 1725, 1220, 1160 cm^{-1}; ^1H NMR (400 MHz, $CDCl_3$): δ = 0.97 (d, J = 6.8 Hz, 3H), 1.03 (d, J = 6.8 Hz, 3H), 1.62–1.80 (m, 1H), 1.98–2.05 (m, 1H), 2.08–2.19 (m, 1H), 2.28 (ddd, J = 16.8, 10.2, 2.7 Hz, 1H), 2.34 (m, 1H), 2.44 (dd, J = 18.4, 6.8 Hz, 1H), 2.78 (dq d, J = 16.8, 6.8, 2.7 Hz), 2.99 (d, J = 16.8, 2.7 Hz, 1H), 5.07 (d, J = 12.3 Hz, 1H), 5.14 (d, J = 12.3 Hz, 1H), 7.19 (m, 5H), 9.69 (d, J = 2.6 Hz, 1H); ^{13}C NMR (100 MHz, $CDCl_3$): δ = 16.05 (q), 17.09 (q), 28.79 (t), 30.68 (d), 37.67 (d), 39.33 (t), 46.96 (t), 65.04 (s), 66.71 (t), 128.26 (d), 128.43 (d), 128.61 (d), 135.17 (s), 169.94 (s), 201.49 (d), 207.57 (s); high-resolution MS calcd. for $C_{18}H_{22}O_4$: 302.1518; found: 302.1513.
[9] A. Barco, S. Benetti, G. P. Pollini, *Synthesis* **1973**, 316.
[10] a) Seebach-Prelog nomenclature: D. Seebach, V. Prelog, *Angew. Chem.* **1982**, *94*, 696; *Angew. Chem. Int. Ed. Engl.* **1982**, *21*, 654. b) For a topological rule for C-C bond forming processes between prochiral centers, see: D. Seebach, J. Golinski, *Helv. Chim. Acta* **1981**, *64*, 1413, and references cited therein.
[11] For preferred *trans* alkylation of related endocyclic enolates with an asymmetric center at the β position, see inter alia: D. A. Evans in *Asymmetric Synthesis, Vol. 3* (Ed.: J. D. Morrison), Academic Press, New York, **1984**, p. 1; K. Tomioka, K. Yasuda, H. Kawasaki, K. Koga, *Tetrahedron Lett.* **1986**, *26*, 3247; see also refs. [6] and [7c].
[12] a) N. Ouvrard, Ph. D. Thesis, University of Marseilles, **1992**. Ketone **6** has been prepared independently by another route and fully characterized by its spectral and analytical data. Its configuration was confirmed by an X-ray structure determination of the corresponding carboxylic acid arising from an oxidative cleavage of the double bond. These results will be reported in due course. **6**: colorless oil; R_f = 0.42, ether/pentane (1/9); $[\alpha]_{578}^{22}$ +128.8 ($CHCl_3$, c = 2); IR (CCl_4): ν = 3080, 2960, 1745, 1640, 920 cm^{-1}; ^1H NMR (400 MHz, $CDCl_3$): δ = 0.98 (d, J = 7.1 Hz, 3H), 1.02 (d, J = 6.0 Hz, 3H), 1.26 (m, 1H), 1.63 (dm, J = 10.3 Hz, 1H), 1.96 (m, 3H), 2.19 (dd, J = 16.4, 7.1 Hz, 1H), 2.59 (m, 1H), 4.89 (d, J = 10.0 Hz, 1H), 4.92 (d, J = 17.1 Hz, 1H), 5.71 (ddd, J = 17.1, 10.0, 7.3 Hz, 1H); ^{13}C-NMR (50.33 MHz, $CDCl_3$): δ = 16.28, 20.24, 29.58,

33.68, 36.42, 38.77, 60.88, 114.00, 141.69, 219.74; satisfactory C, H analysis; b) C. S. Sell, *Aust. J. Chem.* **1975**, *28*, 1383; c) K. B. Sharpless, M. W. Young, *J. Org. Chem.* **1975**, *40*, 947; P. A. Grieco, S. Gilman, M. Nishizawa, *ibid.* **1976**, *41*, 1485.

[13] For similar effects of crown ethers, see: R. S. Glass, D. R. Deardorff, K. Henegar, *Tetrahedron Lett.* **1980**, *21*, 2467; T. Takeda, T. Hoshiko, T. Mukaiyama, *Chem. Lett.* **1981**, 797; L. Viteva, Y. Stefanovsky, *Tetrahedron Lett.* **1989**, *30*, 4565; L. Viteva, Y. Stefanovsky, C. H. R. Tsvetanov, L. Gorrichon, *J. Phys. Org. Chem.* **1990**, *3*, 205.

[14] C. L. Liotta, H. P. Harris, *J. Am. Chem. Soc.* **1974**, *96*, 2250, and references cited therein.

[15] For previously invoked acyclic transition state, see, inter alia: C. H. Heathcock, D. A. Oare, *J. Org. Chem.* **1985**, *50*, 3022; Y. Yamamoto, S. Nishii, *ibid.* **1988**, *53*, 3597, and references cited therein.

meta-Phenylene Units as Conjugation Barriers in Phenylenevinylene Chains

By *Heike Gregorius, Martin Baumgarten, Ronald Reuter, Nikolai Tyutyulkov*, and *Klaus Müllen**

Dedicated to Professor Emanuel Vogel on the occasion of his 65th birthday

The incorporation of *meta*-phenylene units into conjugated oligomers and polymers has wide-reaching effects on their properties. Alongside the commonly observed increase in solubility[1] is the formation of "non-Kekulé" structures, which hinder the spin pairing in potential high-spin systems such as **1**.[2] In compounds with singlet states, *meta* systems such as **2** and **3** are expected at first glance to display extended π conjugation just like the "*para*" analogues (for example, **4**). We can, however, now show that for the neutral and ionic (doped) derivatives of **2** and **3** the *meta*-phenylene unit interrupts the conjugative interaction and induces charge localization. As a result, intervalence bands appear in the absorption spectra of the charged species at extremely high wavelengths in the near-IR region.

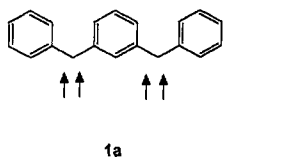

1a

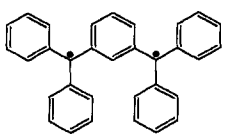

1b

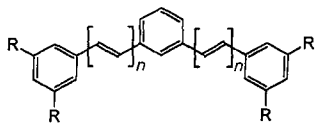

a: R=H
b: R=*tert*-butyl, *n*=1

2

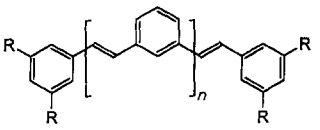

R=*tert*-butyl
a: *n*=1
b: *n*=2
c: *n*=3
d: *n*=4

3

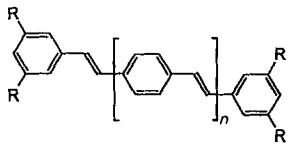

R=*tert*-butyl
a: *n*=1
b: *n*=2
c: *n*=3
d: *n*=4
e: *n*=5

4

The *meta*-distyrylbenzene **3a** (= **2b**) and the homologous oligo(*meta*-phenylenevinylene)s **3b–3d** were each synthesized by Wittig olefination. In this process the use of 3,5-di-*tert*-butylphenyl terminal groups to increase the solubility (as in the preparation of the *para* analogues **4**) was invaluable.[3] A Wittig reaction with **5**[4] and 3-methylbenzaldehyde yields the one styryl unit longer 3,5-di-*tert*-butyl-3′-methylstilbene, which on bromination with *N*-bromosuccinimide affords both the phosphonium salt **6** and the corresponding aldehyde **8** formed in a Sommelet reaction. Oligomers with even *n* (**3b** and **3d**) arise in the reaction of stilbene-3,3′-bis(methyltriphosphonium bromide)[5] with the aldehydes **7**[6] and **8**, respectively, whereas those with uneven *n* (**3a** and **3c**) are formed from isoterephthaldialdehyde and the phosphonium salts **5** and **6**, respectively. Subsequent isomerization with iodine yields the corresponding all-*trans* compounds **3a–d**.[7]

5: R=$CH_2P^+Ph_3\ Br^-$
7: R=CHO

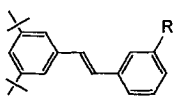

6: R=$CH_2P^+Ph_3\ Br^-$
8: R=CHO

The new hydrocarbons were electrochemically and chemically (with alkali metals) reduced. The electron-transfer products were characterized by cyclic voltammetry, electron absorption spectroscopy (Table 1, Fig. 1), and ESR and NMR spectroscopy.

Table 1. Absorption maxima λ_{max} [nm] of neutral and charged oligo(*meta*-phenylenevinylene)s.

Compound	λ_{max} (neutral) ($CHCl_3$, T = 300 K)		λ_{max} (monoanion) (THF/K^+, T = 300 K)		
stilbene	309		496	699	
3a	240	306	476	636	1810
3b	239	306	493	653	1864
3c	240	312	487	667	1984
3d	242	312	484	685	1983

The *meta*-distyrylbenzene **3a** has a distinctly higher redox activity than *para*-distyrylbenzene **4a**: whereas **4a** is reduced by alkali metals only to the dianion,[8] **3a** yields the tetraanion, which can be detected chemically by trapping it with dimethylsulfate;[9] in a well-resolved ^1H NMR spectrum the signals of the olefinic protons appear at very high field (δ = 2.5–3.5).

The cyclic voltammetry shows that the first reduction potential of **3a–3d** is almost independent of the number of repeating units (**3a**: −2.41, **3b**: −2.29, **3c**: −2.29, **3d**: −2.34 V). These values are similar to those for stilbene,

[*] Prof. Dr. K. Müllen, H. Gregorius, Dr. M. Baumgarten, R. Reuter
Max-Planck-Institut für Polymerforschung
Ackermannweg 10, D-W-6500 Mainz (FRG)
Prof. Dr. N. Tyutyulkov
Acadamy of Science, Sofia (Bulgaria)

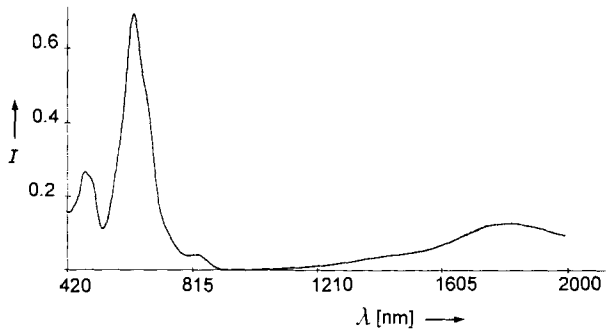

Fig. 1. Absorption spectrum of $3a^{\bullet -}$ (THF/K, $T = 300$ K). I = relative intensity in arbitrary units.

whose first reduction potential is at -2.45 V (for comparison see **4**[3]).[10]

Even more drastic differences between *meta* and *para* systems are observed in the absorption spectra of the reduction products: Whereas the radical anion $4a^{\bullet -}/K^+$ has its longest wavelength band at $\lambda_{max} = 1085$ nm, $3a^{\bullet -}/K^+$ absorbs at $\lambda_{max} = 1810$ nm(!). Moreover, whereas in the homologous series of the radical anions of the *para* compounds **4** an increasing bathochromic shift is observed with extension of the chain,[11] the position of the bands in the *meta* series **3** is largely independent of the chain length.[12] Apart from the longest wavelength band, the spectra of the monoanions of the *meta* species agree with the spectrum of the stilbene monoanion in each case ($\lambda_{max} = 496$, 699 nm).

These results are readily explained by a localization of the charge on a stilbene unit in the *meta*-phenylenevinylenes. The ion $3a^{\bullet -}$ can be described by structure **A**, which contains a charged and an uncharged unit. The longest wavelength absorption of $3a^{\bullet -}$ at 1810 nm is thus attributable to an intervalence or charge-transfer band. Both the extreme broadening of this band and its bathochromic shift of about 140 nm on lowering the temperature (200 K) are in accord with this assignment.

A calculation of the absorption spectrum of the paramagnetic species $3a^{\bullet -}$ with an open-shell PPP SCF/CI procedure[13] does not reproduce the extremely long wavelength band and the two characteristic VIS transitions at approximately 500 and 700 nm. If, however, a localized structure **A** (Scheme 1) is assumed and a decoupling (e.g., a significant twisting about the formal single bond) of the uncharged styryl group is taken into account, the calculation yields a band at $\lambda = 1740$ nm as charge-transfer transition between the charged stilbene subunit and the uncharged styryl group.

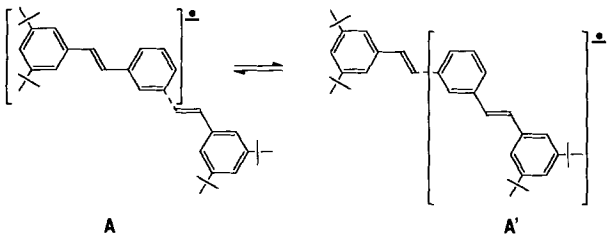

Scheme 1. Charge delocalization in $3a^{\bullet -}$.

The type of charge and spin-density distribution in $3^{\bullet -}$ can also be determined by ESR/ENDOR spectroscopy. Identical ESR/ENDOR spectra each with only three hyperfine couplings [0.540 (2H), 0.267 (4H), 0.137 mT (4H)] were recorded for the oligomers $3b^{\bullet -}$, $3c^{\bullet -}$, and $3d^{\bullet -}$. The hyperfine coupling constants and their multiplicity leave no doubt that the spin density is localized in a central stilbene unit. Only for the *meta*-distyrylbenzene radical anion $3a^{\bullet -}$ (K^+, 2-methyltetrahydrofuran, $-78\,^{\circ}C$) can an electron delocalization be detected. The contradiction between the results from ESR and VIS/near-IR spectroscopy for $3a^{\bullet -}$ is resolved if the different timescales of the two experiments are considered (10^{-7} and $10^{-11}\,s^{-1}$).[14] A rapid charge fluctuation between **A** and **A'** gives rise to the ESR findings (Scheme 1).

The characterization of the neutral and anionic *meta*-phenylenevinylenes **3** is in accord with a conjugation barrier caused by topological features: the resonance structures cannot be formulated over the whole chain, but only over each stilbene unit. This resonance form represents a polaron in a poly(*meta*-phenylenevinylene) chain (**B** in Scheme 2). In contrast, in poly(*para*-phenylenevinylene) chains polaron structures can be formulated which contain different numbers of quinoid arene rings (**C**).

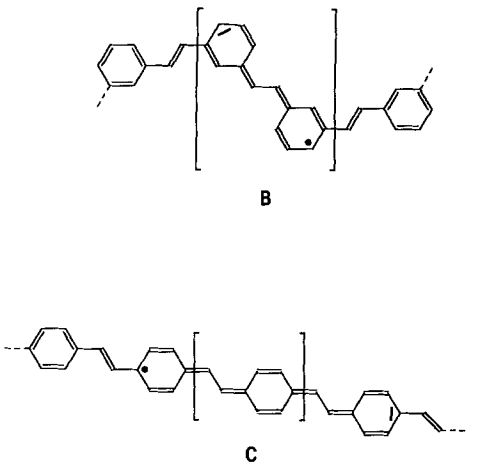

Scheme 2. Structures of polarons of poly(*meta*-phenylenevinylene)s and poly(*para*-phenylenevinylene)s.

The special situation of conjugated systems with *meta*-phenylene units documented here suggests corollaries: The type of charge distribution in doped polymers often serves as a criterium for the description of charge defects such as polarons and bipolarons,[15] which are considered the charge carriers when conductivity is present. Furthermore, it has been postulated that on doping *meta*-phenylene systems such as **2**, ferromagnetism can arise if the two side chains are sufficiently long for bipolaron formation.[16] We shall therefore soon report on the behavior of high molecular weight compounds of series **2** and **3**.

Received: June 17, 1992 [Z 5410 IE]
German version: *Angew. Chem.* **1992**, *104*, 1621

CAS Registry numbers:
3a, 144084-15-1; **3a** (monoanion), 144176-81-8; $3a^{4-}$, 144084-19-5; **3b**, 144084-16-2; **3b** (monoanion), 144176-82-9; **3c**, 144084-17-3; **3c** (monoanion), 144176-83-0; **3d**, 144177-76-4; **3d** (monoanion), 144084-18-4; stilbene monoanion, 96295-17-9.

[1] S. Claesson, R. Gehm, W. Kern, *Makromol. Chem.* **1951**, *7*, 46.
[2] H. Iwamura, *Adv. Phys. Org. Chem.* **1990**, *26*, 179; A. Rajca, S. Utamapanya, J. Xu, *J. Am. Chem. Soc.* **1991**, *113*, 9235, 9241.
[3] J. Heinze, J. Mortensen, K. Müllen, R. Schenk, *J. Chem. Soc. Chem. Commun.* **1987**, 701.

[4] J. M. A. Baas, H. van Berkum, M. A. Hoefnagel, B. M. Webster, *Recl. Trav. Chim. Pays Bas* **1969**, *88*, 1110; G. W. Herne, T. W. Evans, V. W. Buls, C. G. Schwarzer, *Ind. Eng. Chem.* **1955**, *47*, 2311; L. A. Paquette, W. D. Klobucar, R. A. Snow, *Synth. Commun.* **1976**, *6*, 575.
[5] H.-H. Hörhold, A. Müller, R. Ozegowski, *J. Prakt. Chem.* **1975**, *317*, 877.
[6] M. S. Newman, L. F. Fee, *J. Org. Chem.* **1972**, *37*, 4468.
[7] Selected spectroscopic data for **3b**: ^{1}H NMR (200 MHz, $CDCl_3$, 300 K): $\delta = 7.75$ (s, 2H, H10), 7.54–7.34 (m, 12H, arom. H), 7.28, 7.16 (2d, 4H, $J = 16$ Hz, outer olefinic H), 7.24 (s, 4H, inner olefinic H), 1.45 (s, 36H, *tert*-butyl); ^{13}C NMR (50 MHz, $CDCl_3$, 300 K): $\delta = 151.6$ (C3, C5), 138.6, 138.2, 137.0 (C1, C9, C11), 137.0, 129.5, 129.4, 128.3 (C7, C8, C13, C15), 126.3, 126.1, 125.2 (C10, C12, C14), 122.7 (C4), 121.4 (C2, C6), 35.4, 32.0 (*tert*-butyl); MS (EI, 70 eV): *m/z* 608 (M^+, 90%), 57 (*tert*-butyl, 100).
[8] R. Schenk, H. Gregorius, K. Meerholz, J. Heinze, K. Müllen, *J. Am. Chem. Soc.* **1991**, *113*, 2634.
[9] Trapping of $\mathbf{3a}^{4-}$ with dimethylsulfate (quadruple methylation): MS (EI, 70 eV): *m/z* 566 (M^+, 8%), 57 (*tert*-butyl, 70%).
[10] The apparatus has been described fully: A. Bohnen, H. J. Räder, K. Müllen, *Synth. Met.* **1992**, *47*, 37. All measurements were conducted in THF at -10 °C with tetrabutylammonium hexafluorophosphate as supporting electrolyte ($c = 10^{-2}$ M). The concentration of the electroactive substances was 10^{-4} M. A gold disk of 1 mm diameter was used as working electrode, and a platinum wire wound concentrically around it as counter-electrode. Silver wire served as quasi-reference, and the calibration was made with ferrocene/ferrocenium ($E_{1/2} = +0.310$ V vs. a standard calomel electrode).
[11] R. Schenk, H. Gregorius, K. Müllen, *Adv. Mater.* **1991**, *3*, 492.
[12] The optical absorptions of the neutral compounds likewise showed no shift of the wavelength λ_{max} with increasing chain length ($\lambda_{max} \approx 309$ nm; see Table 1), in contrast to the *para* analogues **4**. The calculation of the absorption spectra according to a closed-shell PPP SCF/CI procedure agrees well with the experimental data if based on alternating bond lengths for the double and single bonds and on a slight twist (30°) about the formal single bond (λ_{max}(calcd) = 306 nm).
[13] H. C. Longuet-Higgins, J. A. Pople, *Proc. Phys. Soc. London Sect. A* **1955**, *68*, 591.
[14] Connected with the charge fluctuation is a counterion migration, which should be slowed most when contact ion pairs are present. Although the chosen experimental conditions (see above) favor the formation of contact ion pairs, we could not freeze out the interconversion of **A** and **A'** at -78 °C.
[15] R. Chance, D. S. Boudreaux, J.-L. Brédas, R. Silbey in *Handbook of Conducting Polymers, Vol. 2* (Ed.: T. A. Skotheim), Marcel Dekker, New York, **1986**, p. 826.
[16] H. Fukutome, A. Takahashi, M. Ozaki, *Chem. Phys. Lett.* **1987**, *133*, 34.

Structure of the Lowest Temperature Phase of the Solid Benzene–Hexafluorobenzene Adduct**

By *Jeffrey Huw Williams,* Jeremy Karl Cockcroft,* and *Andrew Nicholas Fitch*

We report the results of complementary high-resolution powder diffraction studies by neutron and synchrotron radiation of the solid phases of C_6H_6:C_6F_6 including the ab-initio structure determination of the lowest temperature phase IV. Although in the last few years powder diffraction has been used to solve the structures of inorganic materials or compounds containing second-row or heavier elements,[1, 2] we believe that this work represents a significant achievement by demonstrating that moderately complicated structures of organic compounds can be solved directly by powder methods for those cases where single-crystal techniques are not applicable.

[*] Dr. J. H. Williams, Dr. J. K. Cockcroft
Institut Max von Laue – Paul Langevin
BP 156X, F-38042 Grenoble Cedex (France)
Dr. A. N. Fitch
Department of Chemistry, Keele University
GB-Staffordshire ST5 5BG (UK)

[**] We thank the ILL Grenoble and the SERC Daresbury Laboratory for the provision of neutron and synchrotron-radiation beam time, respectively, and the European Community for financial support.

The charge distributions of the simple aromatic molecules benzene and hexafluorobenzene are of considerable interest; their symmetry implies that all odd electric moments vanish and that there is just one independent quadrupole moment. The large magnitudes and the difference in the polarity of the quadrupole moments of benzene and hexafluorobenzene[3] imply that the electrostatic interaction between these two molecules is particularly strong. Indeed, mixing equimolar quantities of C_6H_6 and C_6F_6 yields a crystalline solid with a melting point of 24 °C.[4]

From calorimetric and NMR experiments performed on the deuterated analogue,[5] three thermodynamic anomalies are observed at 199, 247.5, and 272 K. To understand the origin of these phase transitions, one of us has investigated the proton dynamics of the benzene partner in a series of quasi-elastic and inelastic neutron scattering experiments.[6, 7] A neutron and X-ray scattering study of molten C_6H_6:C_6F_6 indicated the existence of dimers in the liquid state.[8] Structural studies of the solid are limited to a single-crystal X-ray investigation of the disordered highest temperature phase I, which is made up of columns of alternating benzene and hexafluorobenzene molecules arranged perpendicular to the threefold axis in a rhombohedral lattice.[9] Single crystals of phase I do not survive cooling below the phase transition temperature of 272 K; thus the low-temperature structures have remained unsolved.

Initial neutron diffraction studies ($\lambda = 2.99$ Å) of a deuterated sample were only partially successful; because of the lower resolution and the similar scattering lengths of D and

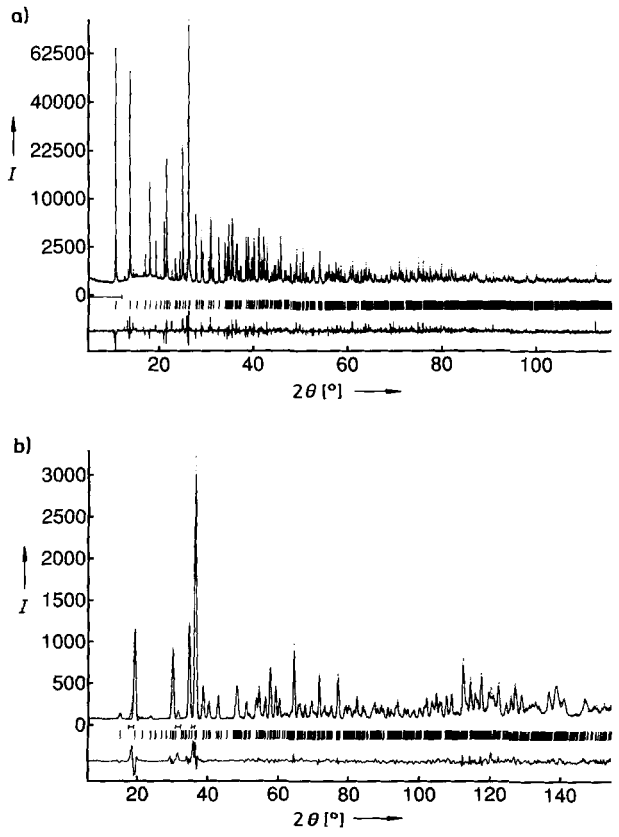

Fig. 1. Study of phase IV of C_6H_6:C_6F_6 a) with synchrotron radiation at 30 K, b) with neutron radiation at 1.5 K. The vertical ticks between the observed and calculated diffraction profiles (top dotted and solid lines, respectively) and the difference profile (bottom) indicate the reflection positions (956 and 567 for a) and b), respectively). A square-root scale has been used for the intensity of a) to show the quality of the weaker high-angle data. The residual phase III is clearly visible in the difference plot.

Table 1. Results of the indexing of the diffraction profiles obtained with synchrotron radiation with the program FZON [10] for the benzene–hexafluorobenzene phases II–IV [a].

Phase	T [K]	a [Å]	b [Å]	c [Å]	α [°]	β [°]	γ [°]	V [Å^3]	Z	Lines indexed	M_{20}	Space group
IV [b]	30	9.516	7.429	7.537	90	95.596	90	530	2	14	225	$P2_1/a$
III	215	6.380	12.338	7.295	93.994	96.732	91.849	568	2	20	246	$P\bar{1}$
II	260	6.631	12.330	7.302	90	99.666	90	589	2	20	230	$I2/m$
I [9]	279	11.952	11.952	7.238	90	90	120	897	3	-	-	$R\bar{3}m$

[a] The program FZON requires the positions of twenty low-angle reflections. The figure of merit, M_{20}, is particularly impressive, leaving no doubt as to the correct indexing of the patterns, and demonstrating the very high quality of the data from the 2.3 diffractometer [11]. With this instrument the peak positions are insensitive to the effects of specimen transparency and diffractometer misalignment, and can therefore be obtained very accurately. [b] For phase IV, indexing was successful despite the inclusion of six peaks from residual phase III whose presence in the sample was unsuspected until the output of FZON was analyzed and subsequent measurements on phase III were carried out.

F, the unit cells of phases II and IV obtained from standard indexing programs were only subcells, and no solution was found for phase III. Complementary synchrotron-radiation measurements were therefore made. These high-quality diffraction patterns were easily indexed yielding definitive unit cells for all phases (Table 1), despite peaks from residual phase III remaining in the diffraction pattern of phase IV.

Assuming phase IV to be the most ordered, we attempted the determination of the structure of this phase first. The intensity profile of the synchrotron radiation was decomposed into individual F^2_{hkl} by the method of Le Bail et al.[16] These were used as input in the direct methods program SIR88.[17] The nine most intense peaks found in the electron density map corresponded to all the C and F atoms required to define the crystal structure, which is composed of the two types of rings, each centered on a point of inversion. No additional refinement or difference procedures were required.

Separate refinements of the structure of phase IV were made with the synchrotron-radiation data (30 K) and the neutron data (1.5 K) (Fig. 1). The fit to the neutron data, which contains very little residual phase III, is better (Table 2). Figure 2 shows the structure, which is based on columns of equispaced, alternating C_6H_6 and C_6F_6 molecules running parallel with the c axis. The columnar nature

Table 2. Final parameters for phase IV of C_6F_6:C_6D_6 at 1.5 K refined from the neutron diffraction data with $\lambda = 1.9087$ Å (nominal) in space group $P2_1/a$. $a = 9.4951(3)$, $b = 7.4235(2)$, $c = 7.5262(2)$ Å, $\beta = 95.630(2)°$, $V = 527.945(3)$ Å^3, $\varrho_{calc} = 1.662$ g cm^{-3}.

Atom	x	y	z	B [Å^2] [a]
C(1)	0.4516(2)	0.3273(4)	0.9618(4)	0.69(2)
C(2)	0.3709(3)	0.4740(3)	0.9015(4)	0.69(2)
C(3)	0.4197(3)	0.6467(3)	0.9386(4)	0.69(2)
F(1)	0.4060(6)	0.1593(5)	0.9214(9)	2.08(5)
F(2)	0.2457(5)	0.4487(5)	0.8047(7)	2.08(5)
F(3)	0.3430(5)	0.7894(5)	0.8758(9)	2.08(5)
C(4)	0.0832(2)	0.1474(2)	0.4369(5)	0.99(3)
C(5)	0.0522(2)	0.1762(2)	0.5254(5)	0.99(3)
C(6)	0.1356(2)	0.0287(2)	0.5881(4)	0.99(3)
D(4)	−0.1485(4)	0.2628(5)	0.3884(7)	1.28(3)
D(5)	0.0925(4)	0.3139(5)	0.5466(7)	1.28(3)
D(6)	0.2410(4)	0.0512(4)	0.6584(7)	1.28(3)

[a] Temperature factor = $\exp(-B \sin^2\theta/\lambda^2)$

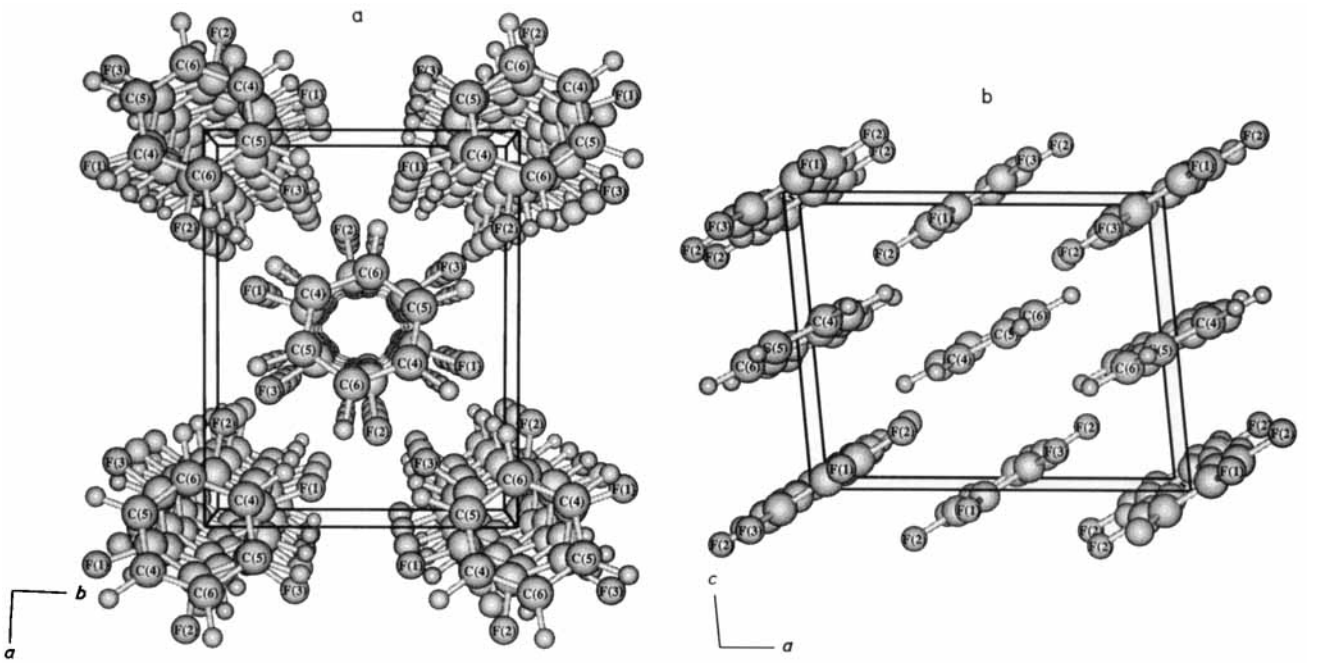

Fig. 2. The structure of phase IV. a) View down the c axis. The alternating sequence of equispaced benzene and hexafluorobenzene molecules along the c axis is clearly seen. The relative orientation of successive molecules in the alternating sequence is neither fully staggered nor eclipsed. b) View along the b axis. Alternate planes at $z = 0$ and $z = 1/2$ contain only C_6F_6 and C_6H_6 molecules, respectively. The planes of the molecules are tilted away from the c axis by approximately 23° for benzene and 27° for hexafluorobenzene.

of the structure is a result of the strong attraction between the quadrupole moments of opposite phase of the benzene and hexafluorobenzene molecules. The quadrupole moment characterizes the overall charge distribution within the molecule. Shorter range interactions involving electrostatic forces between atomic centers and between bond dipole moments may be expected to play a significant local role, particularly in defining the interactions between the columns, the orientation of the molecules within the columns, and hence the nature of the phase transitions. As can be seen in Figure 2a, the alternating molecules in the columns adopt neither a fully staggered nor fully eclipsed configuration. The shortest intermolecular contacts are between molecules in neighboring columns with distances summarized in Table 3.

Table 3. Interatomic contacts of less than 3.0 Å between molecules in adjacent columns.

F(1)-D(6)	2.536(7)	F(1)-F(3)	2.826(5)
F(2)-D(5)	2.522(7)	F(2)-F(3)	2.882(8)
F(2)-D(4)	2.703(6)	D(4)-D(5)	2.897(6)
F(3)-D(4)	2.612(7)	D(4)-D(6)	2.752(7)
F(3)-D(6)	2.665(6)	D(5)-D(6)	2.913(6)

Preliminary analysis of the triclinic phase III shows that on passing from phase III to phase IV, where there is a marked change in the dynamics of the molecules,[5-7] half of the columns are displaced by half a unit cell parallel to the column axis. This leads to the large hysteresis observed and the residual presence of phase III down to 1.5 K. Full details on all phases will be published elsewhere.[19]

From these studies, one may surmise the sequence of molecular reorganization during the phase transitions in C_6H_6:C_6F_6 and the increase in dimensionality of the system with decreasing temperature. In phase I the molecules are rotating about the column axis,[7] and the system behaves like parallel cylindrical rods. On lowering the temperature the molecules first tilt with respect to the column axis, leading to a monoclinic phase, followed by a distortion to a triclinic phase due to freezing out of the rotations of the heavier C_6F_6 molecules. At this stage the unfavorable interaction between columns is compensated by the rotational freedom of the C_6H_6 molecules. Reduction of their rotational energy leads to a realignment of the columns and the unusual transition from a triclinic to a monoclinic phase with decreasing temperature.

The change of dimensionality in solid C_6H_6:C_6F_6 with temperature is analogous with the hierarchy of phase transitions seen in liquid crystals, for example, sodium dodecyl sulfate-water.[20, 21] Here, the sequence of structures is determined by minimum periodic surfaces, which minimize the boundary interactions present in the system. In C_6H_6:C_6F_6 the phase transitions seen on increasing temperature may be viewed in terms of an increase in the rotational energy of the molecules which reduces the interaction between parallel columns.

Experimental

The diffraction data were measured at 30 K with synchroton radiation on the powder diffractometer 2.3 [11] at Daresbury, by using $\theta/2\theta$ geometry with $\lambda = 1.40302(1)$ Å (from Si standard) over the 2θ range 5 to 125° in steps of 0.01° with a counting time of 2s per point. The sample was rotated in a circular specimen holder (diameter 25 mm, depth 2 mm, covered by a Kapton foil) in a continuous-flow liquid-helium cryostat with Mylar windows. The structure was refined by the Rietveld method [12] with the program PROFIL [13] and a pseudo-Voigt peak-shape function. The symmetry of each molecule was restrained to D_{6h} symmetry, and the C–C distances were based on the known values [14, 15]. The lattice parameters refined to $a = 9.5159(1)$, $b = 7.4290(1)$, $c = 7.5378(1)$ Å, $\beta = 95.5913(7)°$. Thirty-six positional parameters were refined for the 12 crystallographically unique atoms with separate isotropic temperature factors for C(1)–C(3), F(1)–F(3), C(4)–C(6), and H(4)–H(6). The small amount (about 5%) of phase III persisting to low temperature is clearly seen in the difference profile in Figure 1a. $R_{wp} = 0.190$, $R_{exp} = 0.043$, $R_I = 0.096$.

Neutron diffraction data were measured at 1.5 K on the powder diffractometer D1A at ILL Grenoble, with a nominal wavelength of 1.9087 Å over the 2θ range 6 to 156° in steps of 0.05° in 12 h. The sample, ground at 8 °C, was contained in a cylindrical (diameter 16 mm) sample can made from vanadium mounted in a helium-cooled "orange" cryostat. The structure was refined with similar symmetry restraints as applied to the synchrotron-radiation refinement, with the neutron scattering lengths $b_C = 6.6484$, $b_F = 5.654$, $b_D = 6.674$ fm [18]. $R_{wp} = 0.111$, $R_{exp} = 0.033$, $R_I = 0.072$.

Received: August 4, 1992 [Z 5499 IE]
German version: *Angew. Chem.* **1992**, *104*, 1666

CAS Registry number:
$C_6H_6 \cdot C_6F_6$, 783-33-5.

[1] A. K. Cheetham, A. P. Wilkinson, *J. Phys. Chem. Solids* **1991**, *52*, 1199–1208.
[2] L. B. McCusker, *J. Appl. Crystallogr.* **1988**, *21*, 205–310; R. J. Cernik, A. K. Cheetham, C. K. Prout, D. J. Watkin, A. P. Wilkinson, B. T. M. Willis, *ibid.* **1991**, *24*, 222–226.
[3] M. R. Battaglia, A. D. Buckingham, J. H. Williams, *Chem. Phys. Lett.* **1981**, *78*, 421–423.
[4] C. R. Patrick, G. S. Prosser, *Nature* **1966**, *187*, 1021.
[5] J. A. Ripmeester, D. A. Wright, C. A. Fyfe, R. K. Boyd, *J. Chem. Soc. Faraday Trans. 2* **1978**, *74*, 1164–1178.
[6] J. H. Williams, *Mol. Phys.* **1991**, *73*, 99–112.
[7] J. H. Williams, *Mol. Phys.* **1991**, *73*, 113–125.
[8] E. Bartsch, H. Bertagnolli, P. Chieux, *Ber. Bunsenges. Phys. Chem.* **1986**, *90*, 34–46.
[9] J. S. W. Overell, G. S. Pawley, *Acta Crystallogr. Sect. B* **1982**, *38*, 1966–1972.
[10] J. W. Visser, *J. Appl. Crystallogr.* **1969**, *2*, 89–95.
[11] S. P. Collins, R. J. Cernik, P. Pattison, A. M. T. Bell, A. N. Fitch, *Rev. Sci. Instrum.* **1991**, *63*, 1013–1014; R. J. Cernik, P. K. Murray, P. Pattison, A. N. Fitch, *J. Appl. Crystallogr.* **1990**, *23*, 292–296.
[12] H. M. Rietveld, *J. Appl. Crystallogr.* **1969**, *2*, 65–71.
[13] J. K. Cockcroft, *PROFIL 4.05, a Rietveld Refinement Program with Chemical Constraints*, Institut Laue-Langevin, Grenoble, **1991**.
[14] E. G. Cox, D. W. J. Cruickshank, J. A. S. Smith, *Proc. R. Soc. London A* **1958**, *247*, 1–21; G. A. Jeffrey, J. R. Ruble, R. K. McMullan, J. A. Pople, *ibid.* **1987**, *414*, 47–57.
[15] N. Boden, P. P. Davis, C. H. Stam, G. A. Wesselink, *Mol. Phys.* **1973**, *25*, 81–86.
[16] A. Le Bail, H. Duroy, J. L. Fourquet, *Mater. Res. Bull.* **1988**, *23*, 447–452.
[17] M. C. Burla, M. Camalli, G. Cascarano, C. Giacovazzo, G. Polidori, R. Spagna, D. Viterbo, *J. Appl. Crystallogr.* **1989**, *22*, 389–393.
[18] L. Koester, H. Rauch, *Recommended Values of Neutron Scattering Lengths (IAEA Rep. No. 2517/RB)*, IAEA, Vienna, **1983**.
[19] J. K. Cockcroft, A. N. Fitch, J. H. Williams, unpublished.
[20] P. Kekicheff, *Mol. Cryst. Liq. Cryst.* **1991**, *198*, 131–144.
[21] J. Charvolin, J. F. Sadoc, *Physica A (Amsterdam)* **1991**, *176*, 138–150.

Corrigendum

In the review "Flexible Molecules with Defined Shape—Conformational Design" by R. W. Hoffmann (*Angew. Chem. Int. Ed. Engl.* **1992**, *31*, 1124) and in the corrigendum in the previous issue, the structure of lardolure (**9**) is incorrect and should be replaced with the following structural formula:

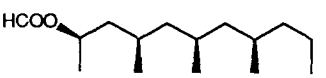

9

The author thanks Dr. M. Morr, Gesellschaft für Biotechnologische Forschung, Braunschweig (FRG), for pointing out this error.

REVIEW ARTICLES AND HIGHLIGHTS

For complete Author Index and complete Subject Index see pages 1663 and 1671, respectively.

Addadi, L. and *Weiner, S.*, Control and Design Principles in Biological Mineralization (R) 153
Als-Nielsen, J., see *Jacquemain, D.* 130
Arad, C., see *Bock, H.* 550
Auf der Heyde, T., see *Buda, A. B.* 989
Ballschmiter, K., Transport and Fate of Organic Compounds in the Global Environment (R) 487
Beck-Sickinger, A. G., see *Jung, G.* 367
Berrisford, D. J., see *Paterson, I.* 1179
Bertagnolli, H., The Structure of Water—A Mixture of Cubes and Planar Four-Membered Rings? (H) 1577
Bhushan, V., see *Lohray, B. B.* 729
Block, E., The Organosulfur Chemistry of the Genus *Allium*—Implications for the Organic Chemistry of Sulfur (R) 1135
Boche, G., Penetrated Ion Pairs: a New Form of Ion Pair (H) 731
Bochmann, M., "Non-Coordinating" Anions: Underestimated Ligands (H) 1181
Bock, H., Ruppert, K., Näther, C., Havlas, Z., Herrmann, H.-F., Arad, C., Göbel, I., John, A., Meuret, J., Nick, S., Rauschenbach, A., Seitz, W., Vaupel, T. and *Solouki, B.*, Distorted Molecules: Perturbation Design, Preparation and Structures (R) 550
Bohlmann, R., The Folding of Squalene; An Old Problem has New Results (H) 582
Bräuchle, C., Spectral Hole Burning at Room Temperature and with a Single Molecule: Two New Perspectives (H) 426
Brunner, H., Enantioselective Rhodium(II) Catalysts (H) 1183
Buda, A. B., Auf der Heyde, T. and *Mislow, K.*, On Quantifying Chirality (R) 989
Cheetham, A. K. and *Wilkinson, A. P.*, Synchrotron X-ray and Neutron Diffraction Studies in Solid-State Chemistry (R) 1557
Comes, F. J., Reaction Dynamics of Aligned Molecules (R) 516
Dehnicke, K. and *Strähle, J.*, Nitrido Complexes of Transition Metals (R) 955
Dehnicke, K., [Ni(P*t*Bu)$_6$]—a Strain on the 18 Electron Rule? (H) 424
Deutsch, M., see *Jacquemain, D.* 130
de Gennes, P.-G., Soft Matter (Nobel Lecture) (R) . 842
Diederich, F. and *Rubin, Y.*, Synthetic Approaches toward Molecular and Polymeric Carbon Allotropes (R) 1101
Eaton, P. E., Cubanes: Starting Materials for the Chemistry of the 1990s and the New Century (R) 1421
Ebert, K. H., see *Henrich, E.* 1283
Eckes, P., Inhibition of Fruit Ripening by Antisense-RNA Technology (H) 175
Edelmann, F. T., Model Compounds for Metal Oxides on SiO_2 Surfaces (H) 586
Engels, J. W., see *Meier, C.* 1008
Ernst, R. R., Nuclear Magnetic Resonance Fourier Transform Spectroscopy (Nobel Lecture) (R) 805
Evanseck, J. D., see *Houk, K. N.* 682
Famulok, M. and *Szostak, J. W.*, In Vitro Selection of Specific Ligand-binding Nucleic Acids (R) 979
Frommer, J., Scanning Tunneling Microscopy and Atomic Force Microscopy in Organic Chemistry (R) 1298
Galla, H.-J., Field-Effect Transistors as Sensors of Neural Systems (H) 45
Gleiter, R., Cycloalkadiynes—From Bent Triple Bonds to Strained Cage Compounds (R) 27
Göbel, I., see *Bock, H.* 550
Grützmacher, H., Compounds with Three-Membered Rings Containing Boron (H) 1329
Hagen, K. S., Synthetic Models for Iron—Oxygen Aggregation and Biomineralization (H) 1010
Havlas, Z., see *Bock, H.* 550
Heathcock, C. H., The Enchanting Alkaloids of Yuzuriha (R) 665
Henrich, E. and *Ebert, K. H.*, The Chemistry of GALLEX—Measurement of Solar Neutrinos with a Radiochemical Gallium Detector (R) 1283
Herrmann, H.-F., see *Bock, H.* 550
Hilgenfeld, R., see *Jessen, T.-H.* 848
Hoffmann, H. M. R., Cascade Cyclizations (H) 1332
Hoffmann, R. W., Flexible Molecules with Defined Shape—Conformational Design (R) 1124 (1657)
Hoffmann, S., Artificial Replication Systems (H) ... 1013
Hopf, H. and *Maas, G.*, Preparation and Properties, Reactions, and Applications of Radialenes (R) .. 931
Houk, K. N., Li, Y. and *Evanseck, J. D.*, Transition Structures of Hydrocarbon Pericyclic Reactions (R) 682
Jacquemain, D., Wolf, S. G., Leveiller, F., Deutsch, M., Kjaer, K., Als-Nielsen, J., Lahav, M. and *Leiserowitz, L.*, Two-Dimensional Crystallography of Amphiphilic Molecules at the Air–Water Interface (R) 130
Janoschek, R., Structures, Structures, and Structures (H) 290
Jaworek, W., see *Mekelburger, H.-B.* 1571
Jessen, T.-H. and *Hilgenfeld, R.*, Protein Engineering: Modified Hemoglobin as a Blood Substitute (H) 848
John, A., see *Bock, H.* 550
Jung, G. and *Beck-Sickinger, A. G.*, Multiple Peptide Synthesis Methods and Their Applications (R) .. 367
Jung, G., Proteins from the D-Chiral World (H) 1457
Kahr, B. and *McBride, J. M.*, Optically Anomalous Crystals (R) 1
Kaupp, G., [4 + 4]-Cycloaddition Reactions in the Total Synthesis of Naturally Occurring Eight-Membered Ring Compounds (H) 422
Kjaer, K., see *Jacquemain, D.* 130
Klemperer, W. G., Marquart, T. A. and *Yaghi, O. M.*, New Directions in Polyvanadate Chemistry: From Cages and Clusters to Baskets, Belts, Bowls, and Barrels (H) 49

Knochel, P., Asymmetric Deprotonation as an Efficient Enantioselective Preparation of Functionalized Secondary Alcohols (H) 1459
Köhler, J., Svensson, G. and *Simon, A.*, Oxoniobates Containing Metal Clusters (R) 1437
Kroto, H. W., C_{60}: Buckminsterfullerene, The Celestial Sphere that Fell to Earth (R) 111
Kunitake, T., Synthetic Bilayer Membranes: Molecular Design, Self-Organization, and Application (R) 709
Lahav, M., see *Jacquemain, D.* 130
Lange, T. and *Martin, T. P.*, Structure and Reactivity of Silicon Clusters in the Gas Phase (H) 172
Leiserowitz, L., see *Jacquemain, D.* 130
Leveiller, F., see *Jacquemain, D.* 130
Li, Y., see *Houk, K. N.* 682
Lichtenthaler, F. W., Emil Fischer's Proof of the Configuration of Sugars: A Centennial Tribute (R) .. 1541
Lohray, B. B. and *Bhushan, V.*, Oxazaborolidines and Dioxaborolidines in Enantioselective Catalysis (H) 729
Maas, G., see *Hopf, H.* 931
McBride, J. M., see *Kahr, B.* 1
Maercker, A., Perlithiated and Hyperlithiated Methane (H) 584
Marquart, T. A., see *Klemperer, W. G.* 49
Martin, T. P., see *Lange, T.* 172
Mayer, J. M., Bond-Stretch Isomers: Fact or Artifact? (H) 286
Meier, C. and *Engels, J. W.*, Peptide Nucleic Acids (PNAs)—Unusual Properties of Nonionic Oligonucleotide Analogues (H) 1008
Meier, H., The Photochemistry of Stilbenoid Compounds and Their Role in Materials Technology (R) 1399
Meinel, C., August Wilhelm Hofmann—"Reigning Chemist-in-Chief" (R) 1265
Mekelburger, H.-B., Jaworek, W. and *Vögtle, F.*, Dendrimers, Arborols, and Cascade Molecules: Breakthrough into Generations of New Materials (H) . 1571
Meuret, J., see *Bock, H.* 550
Mislow, K., see *Buda, A. B.* 989
Müller, U., Are Denser Packings of Spheres than Closest Packings Possible? How Many Closest Packings of Spheres Exist? (H) 727
Näther, C., see *Bock, H.* 550
Neher, E., Ion Channels for Communication Between and Within Cells (Nobel Lecture) (R) 824
Neusser, H. J. and *Schlag, E. W.*, High Resolution Spectroscopy below the Doppler Width (R) 263
Nick, S., see *Bock, H.* 550
Okuda, J., Synthesis of Optically Active Macromolecules Using Metallocene Catalysts (H) 47
Paterson, I. and *Berrisford, D. J., meso* Epoxides in Asymmetric Synthesis: Enantioselective Opening by Nucleophiles in the Presence of Chiral Lewis Acids (H) 1179
Rauschenbach, A., see *Bock, H.* 550
Reissig, H.-U., Sugars as Chiral Auxiliaries for the Synthesis of Enantiomerically Pure Compounds (H) 288
Reuter, H., New Impetus for Inorganic Host-Guest Chemistry (H) 1185
Rosen, M. K. and *Schreiber, S. L.*, Natural Products as Probes of Cellular Function: Studies of Immunophilins (R) 384
Rubin, Y., see *Diederich, F.* 1101
Ruppert, K., see *Bock, H.* 550
Sakmann, B., Elementary Steps in Synaptic Transmission Revealed by Currents through Single Ion Channels (Nobel Lecture) (R) 830
Scherer, O. J., Phosphorus Nitrides—the Cinderella of Phosphorus Chemistry? (H) 170
Schlag, E. W., see *Neusser, H. J.* 263
Schreiber, S. L., see *Rosen, M. K.* 384
Schwarz, H., C_{60}-Fullerene—A Playground for Chemical Manipulations on Curved Surfaces and in Cavities (H) 293
Seel, C. and *Vögtle, F.*, Molecules with Large Cavities in Supramolecular Chemistry (R) 528
Seitz, W., see *Bock, H.* 550
Seppelt, K., Does the Naked Fluoride Ion Exist? (H) 292
Simon, A., see *Köhler, J.* 1437
Solouki, B., see *Bock, H.* 550
Stang, P. J., Alkynyl- and Alkenyl(phenyl)iodonium Compounds (R) 274
Steinborn, D., On the Influence of Heteroatoms in α- and β-Functionalized Alkyl Transition-Metal Compounds (R) 401
Stoddart, J. F., Cyclodextrins, Off-the-Shelf Components for the Construction of Mechanically Interlocked Molecular Systems (H) 846
Strähle, J., see *Dehnicke, K.* 955
Svensson, G., see *Köhler, J.* 1437
Szostak, J. W., see *Famulok, M.* 979
Vaupel, T., see *Bock, H.* 550
Vögtle, F., see *Mekelburger, H.-B.* 1571
Vögtle, F., see *Seel, C.* 528
Wadepohl, H., Benzene and Its Derivatives as Bridging Ligands in Transition-Metal Complexes (R) . 247
Weiner, S., see *Addadi, L.* 153
Wilkinson, A. P., see *Cheetham, A. K.* 1557
Winnacker, E.-L., A Milestone in Genome Sequencing: The Complete DNA Sequence of the Yeast Chromosome III (H) 1578
Wolf, S. G., see *Jacquemain, D.* 130
Yaghi, O. M., see *Klemperer, W. G.* 49
Zybill, C., Si_{60}, an Analogue of C_{60}? (H) 173

AUTHOR INDEX [*Angew. Chem. Int. Ed. Engl.* 1992, *31*]

The page numbers in square brackets refer to the German edition [*Angew. Chem.* **1992**, *104*] of Angewandte Chemie. Page numbers in round brackets indicate errata.

Abrahamson, H. B. 471 [464]
Adam, M. 309, 878, 1588 [331, 883, 1623]
Addadi, L. 153 [159]
Ahlrichs, R. 323, 353 [312, 327]
Aikens, P. 898 [919]
Albrecht, U. 910 [903]
Albright, T. A. 1462 [1532]
Alcazar, V. 1521 [1503]
Allwohn, J. 607, 1384 [629, 1417]
Alonso, P. J. 1527 [1512]
Alsfasser, R. 92 [57]
Als-Nielsen, J. 130 [134]
Alvarez, M. M. 351 [364]
Amann, A. 1068 [1046]
Andersen, O. K. 187 [186]
Anderson, H. L. 907 [921]
Anderson, S. 907 [921]
Andersson, F. O. 1478 [1551]
Ando, W. 59 [84]
Angermann, R. 762 [777]
Ansari, M. A. 1477 [1519]
Anslyn, E. V. 1244 [1259]
Antberg, M. 1347 [1373]
Anthony, J. 1240 [1270]
Antony-Mayer, C. 791 [755]
Aoyama, Y. 745 [785]
Arad, C. 550 [564]
Aranda, M. A. G. 1090 [1056]
Armstrong, D. R. 1634 [1662]
Arnason, I. 1633 [1654]
Arnold, T. 1033 [1084]
Ashe III, A. J. 1255, 1642 [1267, 1669]
Astruc, D. 458 [452]
Atfah, A. 768 [783]
Atta, M. 1513 [1558]
Attfield, J. P. 1090 [1056]
Auf der Heyde, T. 989 [1012]
Auger, N. 1629 [1634]
Auta, J. 1060 [1092]
Ayalon, A. 1636 [1691]

Baba, N. 1336 [1386]
Bachmann, B. 1347 [1373]
Bahadir, M. 443 [477]
Baker, G. R. 917 [901]
Baksheeva, L. I. 789 [788]
Balbach, J. 1609 [1656]
Balch, A. L. 1356 [1400]
Baldenius, K.-U. 305 [338]
Ballschmiter, K. 487 [501]
Balzani, V. 1493 [1540]
Banert, K. 90, 866 [72, 865]
Baringhaus, K. H. 1335 [1392]
Barnes, C. L. 740 [749]
Barron, A. R. 921 [939]
Barth, S. 758 [761]
Bartl, J. 1613 [1689]
Bartlett, P. A. 182 [196 (500)]
Bartlett, R. A. 1082 [1075]
Barzilay, C. 1615 [1672]
Baschang, G. 482 [492]
Bashall, A. P. 1607 [1664]
Basset, J.-M. 628 [622]
Basso, N. 1046 [1103]
Bastos, C. M. 747 [802]
Batail, P. 626 [658]
Batistini, A. 303 [306]
Bats, J. W. 207, 631, 1592 [217, 640, 1650]
Bauer, D. 859 [896]
Baumgarten, M. 448, 1653 [482, 1621]
Bauroth, B. 1064 [1062]
Bayer, E. 52 [102]
Bechtold, T. 1068 [1046]
Beck, W. 226 [235]
Becker, M. 644 [666]
Beckhaus, H.-D. 63 [69]
Beck-Sickinger, A. G. 367 [375]
Behera, R. K. 917 [901]
Behm, J. 1347, 1485 [1373, 1489]
Behrendt, A. 1343 [1388]
Behrens, U. 447 [479]
Bein, T. 336 [323]
Bell, R. G. 1472 [1526]
Bell, T. W. 345, 348, 749 [319, 321, 792]
Belle-Oudry, D. A. 747 [802]
Benbow, J. W. 915 [934]
Bensch, W. 868 [909]
Benson, D. R. 759 [801]
Berger, B. 96 [89]
Bergerat, P. 1258 [1285]
Bergman, R. G. 220, 1044 [209, 1094]
Bergsträsser, U. 879, 1055 [870, 1043]
Bernardinelli, G. 1071, 1622 [1115, 1626]
Berndt, A. 607, 1238, 1384 [629, 1278, 1417]
Bernstein, S. N. 1360 [1412]
Berrisford, D. J. 1179 [1204]
Bertagnolli, H. 1525, 1577 [1537, 1615]
Bertrand, G. 439 [481]
Bertsch-Frank, B. 436 [469]
Besser, S. 1260 [1252]
Bestmann, H. J. 330, 795, 1064 [353, 757, 1062]
Bettermann, H. 1042 [1073]
Bharucha, K. N. 1044 [1094]
Bhushan, V. 729 [740]
Bicke, C. 762 [777]
Bielfeldt, T. 857 [881]
Bienioschek, M. 1042 [1073]
Bietsch, W. 859 [896]
Binger, P. 758 [761]
Birkel, M. 879 [870]
Bjarnason, A. 1633 [1654]
Blackburn, D. W. 1495 [1520]
Blanc, E. 640 [667]
Bläser, D. 314 [356]
Blatter, T. 1207 [1244]
Bligh, S. W. A. 1607 [1664]
Block, E. 1135 [1158]
Blondin, G. 1629 [1634]
Blum, O. 603 [637]
Blümel, J. 1258 [1285]
Bobleter, O. 1068 [1046]
Boche, G. 79, 731, 1205 [80, 742, 1239]
Bochmann, M. 1181 [1206]
Bock, H. 299, 550, 900, 1485 [348, 564, 884, 1489]
Bock, K. 857 [881]
Bodenhausen, G. 1248 [1233]
Bodenstedt, H. 1339 [1387]
Boese, R. 314, 1040, 1227, 1643 [356, 1071, 1221, 1643]
Bohlmann, R. 582 [596]
Böhmer, V. 96 [89]
Bohnen, A. 448 [482]
Bohra, R. 598 [612]
Boland, W. 1246 [1261]
Boldi, A. M. 1240 [1270]
Bönnemann, H. 1490 [1506]
Borrmann, H. 301 [325]
Bossek, U. 311 [345]
Böttcher, A. 623 [635]
Boubekeur, K. 626 [658]
Boucher, D. L. 480 [489]
Boyer, S. H. 338 [314]
Brandsma, L. 1339 [1387]
Bräuchle, C. 426 [431]
Braun, M. 473 [471]
Braun, T. 588 (1540) [602 (1697)]
Braunstein, P. 1583 [1641]
Breit, B. 1055 [1043]
Breitenbach, J. 307 [360]
Breitmaier, E. 1035 [1070]
Brett, W. A. 314 [356]
Breuckmann, R. 872 [867]
Brieden, W. 1335 [1392]
Bright, T. A. 1525 [1537]
Bringmann, G. 761 [782]
Britton, D. 1495 [1520]
Brocchini, S. 1492 [1542]
Brückner, R. 647 [646]
Brunner, H. 1021, 1183 [1096, 1208]
Bruque, S. 1090 [1056]
Bubenitschek, P. 1073 [1068]
Bublak, D. 868 [909]
Bubnov, Y. N. 781 [762]
Bucher, G. 1230 [1225]
Buchholz, S. 189 [188]
Buda, A. B. 989 [1012]
Bühl, M. 314, 1238 [356, 1278]
Bullock, R. M. 1233 [1280]
Bunte, E.-A. 1605 [1636]
Bunz, U. 1648 [1645]
Bürger, H. M. 434 [443]
Bürgi, H.-B. 640 [667]
Burkart, M. D. 451 [466]
Bursten, B. E. 471 [464]
Burtscher, E. 1068 [1046]
Buschmann, H. 1190 [1254]
Butenschön, H. 1066 [1052]
Butzlaff, C. 311 [345]
Buzek, P. 1338 [1391]

Caballero, C. R. 735 [786]
Caihong, W. 330 [353]
Calderazzo, F. 1235 [1230]
Callens, M. 328 [343]
Campagna, S. 1493 [1540]
Carlsen, J. 1640 [1681]
Casey, C. P. 471, 1341 [464, 1364]
Chacon, S. T. 462 [467]
Chang, C. K. 70 [61]
Chang, R. T. 747 [802]
Chang, Y. 1197 [1236]
Charrier, C. 1031 [1082]
Chaudret, B. 1369 [1414]
Cheetham, A. K. 1557 [1594]
Chen, G. S. 740 [749]
Chen, J. 1472 [1526]
Chen, P.-C. 1085 [1098]
Chen, Q. 1197 [1236]
Chen, X. 1492 [1542]

Cheng, P.-C. 1636 [1691]
Chern, S.-S. 70 [61]
Chiarelli, R. 180 [220]
Chin, R. M. 357 [340]
Chisholm, M. H. 462, 896 [467, 889]
Chivers, T. 1518 [1539]
Chottard, J.-C. 1483 [1494]
Choudhary, V. R. 1189 [1273]
Christl, M. 473 [471]
Christou, G. 1253 [1275]
Christuk, C. C. 1477 [1519]
Ciano, M. 1493 [1540]
Clark, D. 855 [926]
Clegg, W. 93 [74 (252)]
Cockcroft, J. K. 1655 [1666]
Coleman, A. W. 1381 [1402]
Comerlato, N. M. 1217 [1251]
Comes, F. J. 516 [529]
Consiglio, G. 303 [306]
Constable, E. C. 230 [218]
Cook, C. M. 462 [467]
Coolen, H. K. A. C. 905 [906]
Cooper, N. J. 83 [55]
Corella II, J. A. 83 [55]
Coronado, E. 649 [660]
Corriu, R. 1195 [1228]
Costa, E. 1060 [1092]
Cotton, F. A. 737, 1050 [795, 1117]
Couturier, J.-L. 628 [622]
Cozens, F. 743 [753]
Cragg, P. J. 345, 348 [319, 321]
Cremer, D. 1230 [1225]
Crudden, C. M. 232 [237]
Cummins, C. C. 1501 [1510]

Dahan, F. 439 [481]
Daniels, L. M. 737 [795]
Danishefsky, S. J. 338, 915 [314, 934]
Darensbourg, D. J. 1503 [1501]
Das, A. 1515 [1554]
Daub, J. 1498 [1498]
Davidson, M. G. 1226, 1634 [1265, 1662]
Davies, J. A. 480 [489]
Davis, A. P. 470 [475]
Davis, W. M. 1501 [1510]
Declercq, J.-P. 625 [619]
Dehnicke, K. 334, 424, 955, 1251 [354, 437, 978, 1216]
Denk, M. 1485 [1489]
Denti, G. 1493 [1540]
Derhaeg, L. 1075 [1107]
Deslongchamps, G. 61 [58]
Detert, H. 791 [755]
Deutsch, M. 130 [134]
de Armas, P. 772 [746]
de Gennes, P.-G. 842 [856]
de Groot, H. 891 [915]
de Kanter, F. J. J. 633 [624]
de Mendoza, J. 61 [58]
de Vincentiis, M. 52 [102]
de Vries, N. K. 1092 [1089]
Diederich, F. 63, 1101, 1240, 1388, 1521, 1599 [69, 1123, 1270, 1383, 1503, 1683]
Diehl, H.-J. 328 [343]
Dietz, S. D. 66 [67]
Discordia, R. 1044 [1094]
Dixneuf, P. H. 651 [664]
Dölle, A. 1372 [1366]
Dorigo, A. E. 1602 [1678]
Dostalek, R. 1064 [1062]
Dötz, K. H. 1236 [1257]
Dover, B. Van 1645 [1677]
Drauz, K. 195 [222]
Drew, M. G. B. 345, 348 [319, 321]
Drews, T. 1036 [1047]
Driess, M. 316, 460, 751, 1510 [350, 449, 775, 1514]
Du, S.-W. 87, 1085 [83 (252), 1098]
Dubourg, A. 625 [619]
Dunbar, K. R. 1360 [1412]
Dürner, G. 207, 631 [217, 640]
Dürr, H. 785 [773]
Dvolaitzky, M. 180 [220]
Dyker, G. 1023 [1079]
Dyker, H. 618 [649]

Eaton, P. E. 1421 [1447]
Ebato, H. 1087 [1064]
Eberhardt, A. 1588 [1623]
Ebert, K. H. 1283 [1310]
Eckes, P. 175 [182]
Eckwert, J. 1218 [1287]
Edelmann, F. T. 72, 586, 1260 [64, 600, 1252]
Eder, S. J. 1345 [1371]
Edwards, A. J. 1607 [1664]
Edwards, J. G. 480 [489]
Effing, J. 1599 [1683]
Eichele, K. 1222 [1263]
Eichen, Y. 1243 [1255]
Eichhorn, E. 1215 [1246]
Eilerts, N. W. 66 [67]
Eisenstein, O. 896 [889]
Elemes, Y. 351 [364]
Elias, H. 623 [635]
Ellis, J. E. 1495 [1520]
Elschenbroich, C. 1343 [1388]
Enders, D. 618 [649]
Enders, M. 606 [628]
Engbersen, J. F. J. 1075 [1107]
Engel, S. 216 [239]
Engelhardt, G. 1210 [1248]
Engels, J. W. 1008, 1386 [1039, 1367]
Englert, U. 440, 1235 [445, 1230]
Enkelmann, V. 309, 878, 1588 [331, 883, 1623]
Erker, G. 199 [204]
Ernst, R. R. 805 [817]
Ertel, T. S. 1525 [1537]
Escamillia, G. H. 917 [901]
Esser, P. 1190 [1254]
Estermaier, L. M. 620 [655]
Etemad-Moghadam, G. 625 [619]
Evans, D. A. 430 [439]
Evans, W. J. 1081 [1114]
Evanseck, J. D. 682 [711]
Eyert, V. 1624 [1632]
Eyrisch, O. 56 [76]

Fachinetti, G. 1596 [1692]
Faix, O. 762 [777]
Falk, K. 886 [928]
Famulok, M. 979 [1001]
Fanwick, P. E. 1261 [1277]
Fehlhammer, W. P. 590 [604]
Feldmer, C. 1039 [1102]
Felsche, J. 1210 [1248]
Feng, X. 1050 [1117]
Fenske, D. 321, 323, 1251 [309, 312, 1216]
Feringa, B. L. 1092 [1089]
Fessner, W.-D. 56, 614 [76, 643]
Fettouhi, M. 651 [664]
Firestone, A. 345, 348 [319, 321]
Fischer, H. 635 [651]
Fischer, J. 733 [771]
Fitch, A. N. 1655 [1666]
Flad, H.-J. 185 [185]
Flad, J. 185, 187 [185, 186]
Flinn, A. 1475 [1550]
Flunkert, G. 440 [445]
Fodor, S. P. A. 759 [801]
Folkers, G. 886 [928]
Fontecave, M. 1513 [1558]
Foote, C. S. 63, 351 [69, 364]
Ford, D. A. 452 [461]
Francisco, C. G. 772 [746]
Frank, W. 436 [469]
Fréchet, J. M. J. 1200, 1531 [1282, 1545]
Freitag, S. 437 [459]
Frenking, G. 1251 [1216]
Frenzen, G. 334 [354]
Fries, P. H. 1513 [1558]
Fritz, M. 1258 [1285]
Fritze, C. 199 [204]
Frömmel, T. 612 [632]
Frommer, J. 1298 [1325]
Fuchs, J. 590 [604]
Fugami, K. 645 [662]
Funaioli, T. 1596 [1692]

Gabbert, G. 1603 [1670]
Gaensslen, M. 1467 [1525]
Gai-Boyes, P. L. 1472 [1526]
Galán, A. 61 [58]
Galla, H.-J. 45 [47]
Galm, W. 1058 [1050]
Gameson, I. 610 [615]
García, M. P. 1527 [1512]
García-Granda, S. 76 [81]
Garot, C. 625 [619]
Gauss, J. 1362 [1376]
Gautschi, M. 1083 [1061]
Gehart, G. 1021 [1096]
Geissler, B. 758 [761]
Geoffroy, G. L. 1053 [1066]
Gerbier, P. 1195 [1228]
Géret-Baumgarten, L. 1040 [1071]
Gerst, M. 1523 [1516]
Geyer, A. 328, 1229 [343, 1231]
Geyer, J. 874 [894]
Giannis, A. 1391 [1394]
Gibson, V. C. 1607 [1664]
Giménez, M. J. 1471 [1523]
Girerd, J.-J. 1629 [1634]
Gitsov, I. 1200 [1282]
Glaser, R. 740 [749]
Gleiter, R. 27, 862 [29, 879]
Gloaguen, B. 458 [452]
Gnedenko, B. B. 789 [788]
Göbel, I. 550 [564]
Göbel, M. W. 207 [217]
Göbel, U. 868 [909]
Goddard, R. 1017 [1054]
Godfrey, S. M. 919 [932]
Goesmann, H. 1251 [1216]
Gollas, B. 332 [336]
Gómez-Garcia, C. J. 649 [660]
Gompper, R. 1202 [1222]
Gonnet, F. 1483 [1494]
Goodman, M. 785 [773]
Goossen, L. 1642 [1669]
Gorbatova, R. K. 789 [788]
Görissen, R. 440 [445]
Gornitzka, H. 1260 [1252]
Goshorn, D. P. 1197 [1236]
Goto, M. 1354 [1410]
Grandjean, F. 884 [891]
Grée, R. 224 [228]
Green, J. R. 1643 [1643]
Green, M. M. 88 [86]
Gregorius, H. 1653 [1621]

Gridnev, I. D. 781 [762]
Griebenow, N. 1626 [1638]
Griesbeck, A. G. 73 [97]
Grimme, W. 872 [867]
Grobe, J. 95 [94]
Groeger, U. 195 [222]
Grommes, T. 872 [867]
Gross, J. 1069 [1112]
Gross, U. 1467 [1525]
Gross, Z. 1615 [1672]
Groth, S. 866 [865]
Grover, N. 1048 [1058]
Grützmacher, H. 99, 437, 1329 [92, 459, 1358]
Guérin, C. 1195 [1228]
Gügel, A. 644 [666]
Guidotti, A. 1060 [1092]
Guillou, O. 626 [658]
Gupta, N. 1048 [1058]
Gurrath, M. 326 [341]
Gurskii, M. E. 781 [762]
Gütlich, P. 178, 1624 [214, 1632]

Haake, G. 1592 [1650]
Haaland, A. 1464 [1534]
Haberman, J. X. 747 [802]
Hagen, G. 1613 [1689]
Hagen, K. S. 764, 1010 [804, 1036]
Haggerty, B. S. 1077 [1100]
Hahn, F. E. 1212 [1218]
Halcomb, R. L. 338 [314]
Hammel, A. 1464 [1534]
Hammel, D. 644 [666]
Hampden-Smith, M. J. 462 [467]
Hampel, F. 1209 [1242]
Hannon, M. J. 230 [218]
Harmat, N. 342 [333]
Harms, G. 1478 [1551]
Harms, K. 79, 1205, 1236, 1626 [80, 1239, 1257, 1638]
Hartmann, G. R. 620 [655]
Hartung, T. 761 [782]
Hasselbring, R. 601 [613]
Havlas, Z. 299, 550 [348, 564]
Hawthorne, M. F. 893 [886]
Healy, M. D. 921 [939]
Heath, S. L. 191 [191]
Heathcock, C. H. 665 [675]
Héberger, K. 635 [651]
Heckmann, G. 779 [752]
Heesink, G. J. T. 1075 [1107]
Hegemann, M. 95 [94]
Heine, A. 854 [941]
Heinekey, D. M. 471 [464]
Heintz, R. A. 1077 [1100]
Henkel, G. 54, 778, 1366, 1368 [71, 766, 1380, 1382]
Henlin, J.-M. 482 [492]
Henner, B. 1195 [1228]
Henrich, E. 1283 [1310]
Henschke, B. 868 [909]
Heppert, J. A. 66 [67]
Herbst-Irmer, R. 437, 1260 [459, 1252]
Herges, R. 1611 [1652]
Hermes, M. 1017 [1054]
Herrmann, H.-F. 550 [564]
Herrmann, S. 1529 [1496]
Herrmann, W. A. 1345, 1347, 1485 [1371, 1373, 1489]
Herron, J. N. 1087 [1064]
Hesse, W. 735 [786]
Heydari, A. 313 [335]
Hiermeier, J. 1258 [1285]
Higuchi, K. 1354 [1410]
Hilgenfeld, R. 848 [862]
Hiller, W. 1364 [1378]
Hillerns, F. 447 [479]
Hirle, B. 1583 [1641]
Hirsch, A. 766, 1468 [808, 1529]
Hirth, U.-A. 1525 [1537]
Ho, J. S. 1648 [1645]
Höbel, B. 1027 [1042]
Hoffmann, H. M. R. 234, 910, 1332 [224, 903, 1361]
Hoffmann, R. 647 [646]
Hoffmann, R. W. 1124 (1657) [1147 (1697)]
Hoffmann, S. 1013 [1032]
Hohla, M. 319 [362]
Höllwarth, A. 1251 [1216]
Hönle, W. 1640 [1681]
Hoock, C. 1611 [1652]
Hop, C. E. C. A. 1341 [1364]
Hope, H. 1197 [1236]
Hopf, H. 443, 931, 1073 [477, 953, 1068]
Hoppe, D. 1505 [1547]
Horakh, J. 301 [325]
Horn, H. 353 [327]
Horton, A. D. 876 [912]
Hosmane, N. S. 432 [441]
Hoss, R. 1619 [1628]
Hough, G. C. 1475 [1550]
Houk, K. N. 682, 1019 [711, 1087]
Hovemeier, K. 1192 [1214]
Howard, C. A. 1028 [1077]
Huang, C.-Y. 1244 [1259]
Huang, S.-P. 787 [799]
Hückmann, S. 1525 [1537]
Hückstädt, H. 90 [72]
Hudeczek, P. 1258 [1285]
Huffman, J. C. 1253 [1275]
Hulst, R. 1092 [1089]
Hummel, W. 1529 [1496]
Hünig, S. 859 [896]
Hunter, C. A. 792 [779]
Hwang, C.-K. 1044 [1094]

Ibers, J. A. 640, 1477 [667, 1519]
Icheln, D. 305 [338]
Ignatenko, A. V. 781 [762]
Ihara, E. 1509 [1508]
Iimura, K. 1531 [1545]
Ikemoto, N. 890 [918]
Il'ichev, Y. V. 781 [762]
Ingold, K. U. 891 [915]
Inouye, M. 204 [198]
Ipaktschi, J. 313 [335]
Ippendorf, H. 1042 [1073]
Irion, M. P. 636 [633]
Ishii, M. 59 [84]
Ito, Y. 1509 [1508]
Iwabuchi, Y. 340 [317]
Iwasa, J. 1336 [1386]

Jackson, D. Y. 182 [196 (500)]
Jacquemain, D. 130 [134]
Jaekel, K. 482 [492]
Jakobi, R. 178 [214]
Janiak, R. 1640 [1681]
Janoschek, R. 290, 460, 476 [297, 449, 473]
Jansen, M. 223, 653 [240, 618]
Jansen, N. 1624 [1632]
Jaouen, G. 753 [790]
Jaspars, M. 470 [475]
Jaworek, W. 1571 [1609]
Jeffery, J. C. 1515 [1554]
Jemmis, E. D. 1488 [1557]
Jepsen, O. 187 [186]
Jessen, T.-H. 848 [862]
Jiménez, M. V. 1527 [1512]
Jochem, G. 1350 [1420]
Joh, T. 851 [893]
John, A. 550 [564]
Johnson, S. E. 893 [886]
Johnston, V. J. 896 [889]
Jonas, U. 1599 [1683]
Jones, C. M. 451 [466]
Jones, P. G. 1073, 1377 [1068, 1395]
Jones, R. H. 1472 [1526]
Jones, W. D. 357 [340]
Jopp, M. 859 [896]
Jost, W. 878 [883]
Jullien, L. 1599, 1637 [1683, 1695]
Jung, G. 226, 367, 785, 886, 1457 [235, 375, 773, 928, 1484]
Juris, A. 1493 [1540]
Jutzi, P. 1605 [1636]

Käb, H. 1525 [1537]
Kabe, Y. 59 [84]
Kadowaki, T. 59 [84]
Kahn, O. 626, 1258 [658, 1285]
Kahr, B. 1 [1]
Kalinowski, H.-O. 738 [764]
Kampf, J. W. 1255, 1642 [1267, 1669]
Kanand, J. 1626 [1638]
Kanatzidis, M. G. 787, 1594 [799, 1674]
Kaneko, T. 1336 [1386]
Kao, M. 63, 351 [69, 364]
Kappes, M. M. 640 [667]
Karaghiosoff, K. 1350 [1420]
Karas, M. 762 [777]
Karfunkel, H. R. 766, 1468 [808, 1529]
Karpishin, T. B. 466 [486]
Kato, T. 1531 [1545]
Katz, T. J. 1093 [1081]
Kaupp, G. 422, 592, 595, 768 [435, 606, 609, 783]
Kaupp, M. 1224 [1240]
Kawamoto, A. 852 [877]
Keck, H. 86 [65]
Keese, R. 344 [307]
Kelderman, E. 1075 [1107]
Keller, B. 197 [201]
Kelley, C. 1053 [1066]
Kellner, R. 1202 [1222]
Kelly, P. F. 616 [620]
Kelm, S. 1478 [1551]
Kern, F. 330, 795 [353, 757]
Kern, W. 64 [54]
Kersten, J. L. 1341 [1364]
Kessler, H. 210, 326, 328, 902, 1229, 1609 [213, 341, 343, 874, 1231, 1656]
Kettenbach, R. T. 1066 [1052]
Khan, M. I. 1197 [1236]
Khan, S. I. 893 [886]
Kiedrowski, G. von 654 [626]
Kiehl, A. 1588 [1623]
Kiener, A. 774 [748]
Kilimann, U. 1260 [1252]
Kiprof, P. 1347 [1373]
Kisch, H. 1039 [1102]
Kitao, T. 204 [198]
Kjaer, K. 130 [134]
Klapötke, T. M. 1338 [1391]
Klausmeyer, K. K. 1503 [1501]
Klein, A. 1391 [1394]
Klemperer, W. G. 49 [51]
Klenk, H. 195 [222]
Klingan, F.-R. 1485 [1489]
Klinowski, J. 610 [615]

Klumpp, G. W. 633 [624]
Kniep, R. 1624 [1632]
Knobler, C. B. 1240 [1270]
Knochel, P. 1459 [1486]
Knorr, M. 1583 [1641]
Kobayashi, K. 745 [785]
Koch, H.-J. 598 [612]
Koch, P. 1507 [1492]
Kociok-Köhn, G. 1081 [1114]
Köck, M. 328, 902 [343, 874]
Koenig, M. 625 [619]
Köhler, F. H. 1258 [1285]
Köhler, J. 212, 1437 [192, 1463]
Köhler, J. E. H. 319 [362]
Kolis, J. W. 913 [924]
Kölle, U. 440 [445]
Kolodziejski, W. 610 [615]
Kolter, T. 1391 [1394]
Komissarov, V. N. 1498 [1498]
König, W. A. 305, 319 [338, 362]
Konishi, H. 1642 [1669]
Kool, E. T. 1617 [1686]
Köppe, R. 638 [653]
Korall, B. 1490 [1506]
Kornath, A. 643 [648]
Korth, H.-G. 891 [915]
Kottenhahn, M. 902 [874]
Kozelka, J. 1483 [1494]
Kozikowski, A. P. 1060, 1379 [1092, 1408]
Kraka, E. 1230 [1225]
Krätschmer, W. 183 [242]
Krautscheid, H. 321 [309]
Krebs, B. 54, 95, 1366, 1647 [71, 94, 1380, 1631]
Kress, J. 1585 [1660]
Krogh-Jespersen, K. 1602 [1678]
Kroll, F. 1236 [1257]
Kroto, H. W. 111 [113]
Krüger, C. 1066 [1052]
Krüger, T. 54 [71]
Kübler, J. 1624 [1632]
Kubrakova, I. V. 789 [788]
Kuchen, W. 86, 612 [65, 632]
Kuhn, N. 778 [766]
Kumar, U. 1531 [1545]
Kündig, E. P. 1071 [1115]
Kunitake, T. 709 [692]
Künneth, R. 1039 [1102]
Kunwar, A. C. 1488 [1557]
Kurth, D. G. 336 [323]
Kurz, G. 328 [343]
Kurz, M. 210 [213]
Kwok, D.-I. A. 345, 348 [319, 321]
Kybart, C. 1238, 1384 [1278, 1417]
Kyushin, S. 1354 [1410]

Labes, M. M. 88 [86]
Läge, M. 95 [94]
Lahav, M. 130 [134]
Lahoz, F. J. 1527 [1512]
Laitinen, R. 1518 [1539]
Lambert, C. 77, 1209 [78, 1242]
Lance, M. 1629 [1634]
Lange, T. 172 [179]
Langlotz, I. 1205 [1239]
Latour, J.-M. 1513 [1558]
Lautens, M. 232 [237]
Lawrie, C. J. C. 1233 [1280]
Layh, M. 1364 [1378]
Leconte, M. 628 [622]
Ledig, B. 79 [80]
Lee, J. 1501 [1510]
Lee, J. W. 1356 [1400]
Legon, A. C. 202 [233]
Lehn, J.-M. 1637 [1695]
Leinemann, B. 330 [353]
Leiserowitz, L. 130 [134]
Levashov, A. V. 789 [788]
Leveiller, F. 130 [134]
Le Van, D. 95 [94]
Li, J. 743 [753]
Li, Y. 682 [711]
Liang, M. N. 182 [196 (500)]
Liang, W. 1048 [1058]
Lichtenthaler, F. W. 1541 [1577]
Lidin, S. 924 [936]
Limbach, H.-H. 1369 [1414]
Lin, C.-C. 1381 [1402]
Link, R. 850 [864]
Linke, C. 653 [618]
Lister, D. G. 202 [233]
Liu, L. 1093 [1081]
Liu, S. 640 [667]
Lo, L.-C. 890 [918]
Lohray, B. B. 729 [740]
Long, G. J. 884 [891]
Looney, A. 92 [57]
Loos, D. 1362 [1376]
Lottspeich, F. 620 [655]
Lu, J.-X. 87 [83 (252)]
Lu, Y. 640 [667]
Lücke, J. 213 [208]
Lugan, N. 1053 [1066]
Luitjes, H. 633 [624]
Lüning, U. 80 [99]
Lutz, A. 64, 468 [54, 491]
Lynch, V. 452, 1244 [461, 1259]

Ma, D. 1060 [1092]
Maas, G. 931, 1055 [953, 1043]
McAuliffe, C. A. 919 [932]
McBride, J. M. 1 [1]
McClelland, R. A. 743 [753]
McCleverty, J. A. 1515 [1554]
MacGregor, M. 93 [74 (252)]
Mäcke, H. R. 1507 [1492]
McKee, M. L. 1384 [1417]
Mackie, A. G. 919 [932]
McPartlin, M. 1607 [1664]
Maercker, A. 584, 1339 [598, 1387]
Maher, J. P. 1515 [1554]
Mahjoub, A.-R. 1036 [1047]
Mahrwald, R. 342 [333]
Maier, G. 738, 1218 [764, 1287]
Maigrot, N. 1031 [1082]
Malisch, W. 1525 [1537]
Mamman, A. S. 1189 [1273]
Marcos, M. 1471 [1523]
Marks, T. J. 1375 [1406]
Marquart, T. A. 49 [51]
Marsch, M. 79, 1205 [80, 1239]
Martín, A. 1634 [1662]
Martin, H.-D. 1042 [1073]
Martin, T. P. 172 [179]
Marx, S. 1243 [1255]
Massa, W. 607, 1238, 1343, 1384 [629, 1278, 1388, 1417]
Matern, D. H. M. 620 [655]
Mathey, F. 1031 [1082]
Matsumoto, H. 1354 [1410]
Matsuo, M. 1336 [1386]
Mattay, J. 209 [207]
Matter, H. 328 [343]
Mauder, H. 73 [97]
Maurer, M. 1369 [1414]
Mayer, J. M. 286, 1645 [293, 1677]
Mayr, A. 747 [802]
Mayr, H. 1046, 1613 [1103, 1689]
Mehner, T. 638 [653]
Mehta, G. 1488 [1557]
Meier, A. 1592 [1650]
Meier, C. 1008 [1039]
Meier, H. 768, 791, 1399 [783, 755, 1425]
Meier, S. 1619 [1628]
Meinel, C. 1265 [1293]
Mekelburger, H.-B. 1571 [1609]
Meldal, M. 857 [881]
Ménage, S. 1629 [1634]
Méndez, L. 478 [456]
Menger, F. M. 898, 1492 [919, 1542]
Mennad, A. 480 [489]
Mercando, L. A. 1053 [1066]
Metzger, J. O. 762 [777]
Metzger, J. W. 226 [235]
Meuret, J. 550 [564]
Meyer, C. 468 [491]
Meyer, F. 1227 [1221]
Meyer-Stork, M. 1190 [1254]
Miaskiewicz, K. 58 [87]
Michel, H. 607 [629]
Mielcke, J. 464 [485]
Mierke, D. F. 210 [213]
Miguel, D. 76 [81]
Millies, B. 631 [640]
Mindach, L. 644 [666]
Minkin, V. I. 1498 [1498]
Minkwitz, R. 643 [648]
Minto, R. E. 1044 [1094]
Miocque, M. 1381 [1402]
Mislow, K. 989 [1012]
Mitani, T. 852 [877]
Mittelbach, A. 1640 [1681]
Mittendorf, J. 1643 [1643]
Miyashi, T. 455 [454]
Mody, T. D. 452 [461]
Moezzi, A. 1082 [1075]
Mohler, D. L. 1643 [1643]
Monobe, M. 455 [454]
Montforts, F.-P. 1592 [1650]
Moore, J. S. 922 [873]
Moorefield, C. N. 917 [901]
Mornon, J.-P. 753 [790]
Moser, P. 482 [492]
Mosset, P. 224 [228]
Moulines, F. 458 [452]
Mozhaev, V. V. 789 [788]
Mueller, B. L. 1503 [1501]
Mueller-Westerhoff, U. T. 1352 [1398]
Müllen, K. 309, 448, 644, 878, 1588, 1653 [331, 482, 666, 883, 1623, 1621]
Müller, A. 1192 [1214]
Müller, D. G. 1246 [1261]
Müller, F. 209 [207]
Müller, Gerhard 326 [341]
Müller, Germar 473 [471]
Müller, H.-M. 434 [443]
Müller, J. 1227 [1221]
Müller, L. 623 [635]
Müller, M. (Freiburg) 80 [99]
Müller, M. (Karlsruhe) 321 [309]
Müller, U. 448, 727 [482, 744]
Müller, W. 1087 [1064]
Mulvey, R. E. 93 [74 (252)]
Mulzer, J. 870 [914]
Murakami, M. 1509 [1508]
Murillo, C. A. 737 [795]
Murray, A. M. 1253 [1275]

Nagai, Y. 745 [785]
Nakadaira, Y. 1255 [1267]
Nakanishi, K. 890 [918]

Nakasuji, K. 852 [877]
Natarajan, S. 1472 [1526]
Näther, C. 299, 550 [348, 564]
Neher, E. 824 [837]
Nelsen, S. F. 882 [899]
Neuburger, M. 193 [225]
Neumüller, B. 334 [354]
Neusser, H. J. 263 [269]
Newkome, G. R. 917 [901]
Neyhart, G. A. 1048 [1058]
Niccolai, G. P. 471 [464]
Nick, S. 550 [564]
Nicolaou, K. C. 340, 855, 1044 [317, 926, 1094]
Niederprüm, N. 314 [356]
Nieger, M. 1069 [1112]
Niemann, A. 311 [345]
Niemeyer, C. M. 1017 [1054]
Nierlich, M. 1629 [1634]
Nölke, M. 1523 [1516]
Nolte, R. J. M. 905 [906]
Noltemeyer, M. 72, 598, 599, 601, 864 [64, 612, 670, 613, 869]
Norton, J. R. 1233 [1280]
Nowotny, M. 1343 [1388]
Nuber, B. 311, 350, 882, 1021 [345, 329, 899, 1096]
Nudelman, N. E. S. 1205 [1239]
Nunn, K. 224 [228]
Nürnberg, O. 1025 [1105]
Nüsse, M. 314 [356]

Oberhammer, H. 1467 [1525]
Obermeyer, A. 301 [325]
Oesen, H. 323 [312]
Okahata, Y. 1087 [1064]
Okamoto, H. 852 [877]
Okaniwa, K. 852 [877]
Oki, A. R. 432 [441]
Okuda, J. 47 [49]
Olbrich, F. 447 [479]
Olmstead, M. M. 1356 [1400]
O'Neil, P. A. 93 [74 (252)]
Onitsuka, K. 851 [893]
Opperdoes, F. R. 328 [343]
Oro, L. A. 1527 [1512]
Orpen, A. G. 876 [912]
Orschel, B. 1033 [1084]
Osborn, J. A. 733, 1585 [771, 1660]
Osella, D. 753 [790]
Otsuki, J. 745 [785]
Ott, F. 307 [360]
Otte, A. R. 234 [224]
Ouahab, L. 649, 651 [660, 664]
Oushoorn, R. L. 626 [658]
Ouvrard, N. 1651 [1658]

Pace, J. M. 1255 [1267]
Paddon-Row, M. N. 1019 [1087]
Paetzold, P. 1040, 1227 [1071, 1221]
Paillet, C. 628 [622]
Pampaloni, G. 1235 [1230]
Papadopoulos, V. 1060 [1092]
Papoulis, A. T. 749 [792]
Parkin, G. 92 [57]
Parkin, S. 1197 [1236]
Paterson, I. 1179 [1204]
Paulsen, H. 857 [881]
Paulus, E. 96 [89]
Paulus, H. 623 [635]
Peng, S.-M. 70 [61]
Pennington, W. T. 913 [924]
Perez-Martinez, J. A. 76 [81]
Persoons, A. 1075 [1107]
Peters, G. 223 [240]
Peters, K. 224 [228]
Peters, S. 857 [881]
Peters, W. 612 [632]
Philouze, C. 1629 [1634]
Pieper, D. H. 68 [60]
Pieper, U. 77 [78]
Pietzonka, T. 1481 [1543]
Piguet, C. 1622 [1626]
Pirio, N. 651 [664]
Plattner, D. A. 434 [443]
Plesnivy, T. 1599 [1683]
Pogodda, U. 768 [783]
Polborn, K. 1202 [1222]
Popp, T. 924 [936]
Porter, K. 1373 [1404]
Powell, A. K. 191 [191]
Powell, D. R. 882, 1217 [899, 1251]
Power, P. P. 1082 [1075]
Powis, G. 1379 [1408]
Pregel, M. J. 1637 [1695]
Preuss, H. 185, 187 [185, 186]
Prins, M. W. J. 1062 [1110]
Pritchard, R. G. 919 [932]
Pritzkow, H. 99, 316, 460, 606, 751, 1058, 1510, 1603 [92, 350, 449, 628, 775, 1050, 1514, 1670]
Profilet, R. D. 1261 [1277]
Puia, G. 1060 [1092]
Pulham, C. 1464 [1534]
Purvis, D. H. 792 [779]

Quast, H. 1640 [1681]

Raabe, G. 618 [649]
Rábai, J. 1631 [1648]
Rabe, J. P. 189 [188]
Rabinovitz, M. 1636 [1691]
Rademann, K. 874 [894]
Räder, H.-J. 309, 644 [331, 666]
Rahmouni, N. 733 [771]
Raithby, P. R. 1634 [1662]
Rammensee, H.-G. 886 [928]
Rao, C. N. R. 1062 [1110]
Rassat, A. 180 [220]
Rauch, P. E. 1519 [1505]
Rauschenbach, A. 550 [564]
Raymond, K. N. 466 [486]
Réau, R. 439 [481]
Rebek, J. Jr. 61 [58]
Reddy, D. S. K. 1488 [1557]
Rees, W. S. Jr. 735 [786]
Reetz, M. T. 342, 1017, 1626 [333, 1054, 1638]
Regitz, M. 758, 879, 1055 [761, 870, 1043]
Rehder, D. 447 [479]
Rehefeld, C. 330 [353]
Reibenspies, J. H. 1503 [1501]
Reinhard, G. 1583 [1641]
Reinhoudt, D. N. 1075 [1107]
Reisenauer, H. P. 1218 [1287]
Reisgys, M. 1510 [1514]
Reissig, H.-U. 288, 1033 [295, 1084]
Rétey, J. 215 [212]
Reuter, H. 1185 [1210]
Reuter, R. 1653 [1621]
Reynolds, J. G. 1253 [1275]
Rheingold, A. L. 1053, 1077, 1341, 1352 [1066, 1100, 1364, 1398]
Ricard, L. 1031 [1082]
Richters, M. 319 [362]
Rieker, A. 1215 [1246]
Riera, V. 76 [81]
Ringsdorf, H. 1087, 1599 [1064, 1683]
Rink, H. 482 [492]
Ripa, A. 1071 [1115]
Rischer, M. 1221 [1269]
Robinson, K. S. 747 [802]
Robinson, O. B. 1607 [1664]
Robinson, W. T. 599 [670]
Robl, C. 1350 [1420]
Rocchi, L. 1235 [1230]
Rocha, J. 610 [615]
Rodkin, M. A. 1233 [1280]
Rodriguez, A. 96 [89]
Rodriguez, J. 1651 [1658]
Roesky, H. W. 598, 599, 601, 864 [612, 670, 613, 869]
Rognan, D. 886 [928]
Rohlfing, R. 1192 [1214]
Röhrich, J. 309 [331]
Rohrmann, J. 1347 [1373]
Romeo, E. 1060 [1092]
Romstedt, H. 178 [214]
Roof, L. C. 913 [924]
Rosen, M. K. 384 [413]
Roth, W. R. 872 [867]
Rothwell, I. P. 1261 [1277]
Rötzschke, O. 886 [928]
Roy, R. 1478 [1551]
Rozsnyai, L. F. 759 [801]
Rubin, Y. 1101 [1123]
Rüchardt, C. 63, 1523 [69, 1516]
Rüdiger, S. 1467 [1525]
Ruf, M. 92 [57]
Rumney IV, S. 1617 [1686]
Runge, T. 305 [338]
Ruppert, K. 299, 550 [348, 564]
Ryabov, A. D. 789 [788]
Rypdal, K. 1464 [1534]

Saalfrank, R. W. 224 [228]
Sakimura, T. 455 [454]
Sakmann, B. 830 [844]
Salbeck, J. 1498 [1498]
Samstag, W. 1386 [1367]
Sander, W. 1230 [1225]
Sandermann, H. Jr. 68 [60]
Sanders, J. K. M. 907 [921]
Sansare, S. D. 1189 [1273]
Santelli, M. 1651 [1658]
Santra, A. K. 1062 [1110]
Sasakura, K. 1336 [1386]
Sastry, G. N. 1488 [1557]
Saunders, M. J. 917 [901]
Savin, A. 185, 187 [185, 186]
Sawodny, W. 643 [648]
Schäfer, A. 353 [327]
Schäfer, D. 795 [757]
Schäfer, H. 1587 [1680]
Schäfer, M. 334 [354]
Schäfer, T. 1236 [1257]
Schakel, M. 633 [624]
Scharf, H.-D. 1190 [1254]
Schatz, E. 1515 [1554]
Schauer, R. 1478 [1551]
Scheer, C. 1513 [1558]
Scheer, M. 1377 [1395]
Scherer, G. 1369 [1414]
Scherer, O. J. 170, 1027 [177, 1042]
Scherer, W. 1345, 1485 [1371, 1489]
Scheurich, G. 1592 [1650]
Schiefer, G. 52 [102]
Schiemann, K. 1372 [1366]
Schlag, E. W. 263 [269]

Wan, H. 1077 [1100]
Ward, M. D. 1028, 1515 [1077, 1554]
Warner, H. E. 202 [233]
Wartchow, R. 910 [903]
Wasylishen, R. E. 1222 [1263]
Waszczak, J. V. 1645 [1677]
Weber, Beat 84 [96]
Weber, Birgit 1025 [1105]
Wedler, M. 72 [64]
Weigt, H. R. 355 [358]
Weil, K. G. 636 [633]
Weiner, S. 153 [159]
Weinmann, W. 1603 [1670]
Weinstein, D. 1599 [1683]
Weiske, T. 183, 605 [242, 639]
Weiss, K. 628 [622]
Weiss, R. 216 [239]
Weissgräber, S. 1368 [1382]
Weng, D. 88 [86]
Wenz, G. 197, 783 [201, 758]
Werner, H. 868, 1025 [909, 1105]
West, R. 1217 [1251]
Westerhausen, D. 1529 [1496]
Wettling, T. 758 [761]
Whetten, R. L. 351 [364]
Whitmire, K. H. 451, 884 [466, 891]
Wichmann, J. 1079 [1091]
Widenhoefer, R. A. 1341 [1364]
Wieghardt, K. 311 [345]
Wierenga, R. K. 328 [343]
Wilde, A. 234 [224]
Wilkinson, A. P. 1557 [1594]
Willershausen, P. 1238, 1384 [1278, 1417]
Williams, A. F. 1622 [1626]
Williams, D. J. 478, 616, 1475 [456, 620, 1550]
Williams, J. H. 1655 [1666]
Williams, M. K. 478 [456]
Willmore, N. D. 1093 [1081]
Willner, I. 1243 [1255]
Winkhofer, N. 599 [670]
Winkler, R. 68 [60]
Winnacker, E.-L. 1578 [1616]
Winter, A. 1347 [1373]
Witschel, M. C. 795 [757]
Wittmann, V. 902 [874]
Witulski, B. 1073 [1068]
Wočadlo, S. 607, 1343 [629, 1388]
Woerpel, K. A. 430 [439]
Wojtczak, W. A. 1050 [1117]
Wolf, A. 1058 [1050]
Wolf, H. C. 859 [896]
Wolf, J. 1025 [1105]
Wolf, R. 738 [764]
Wolf, S. G. 130 [134]
Wolff, J. J. 882 [899]
Wollermann, G. 1515 [1554]
Wollert, R. 1251 [1216]
Wolmershäuser, G. 779, 1027 [752, 1042]
Wong, T. 86, 183 [65, 242]
Wooley, K. L. 1200 [1282]
Woollins, J. D. 616 [620]
Wright, D. S. 1226 [1265]
Wright, P. A. 1472 [1526]
Wu, W. 70 [61]
Wu, X.-T. 87, 1085 [83 (252), 1098]
Wu, Y.-D. 1019 [1087]
Wunderlich, H. 612 [632]
Würthwein, E.-U. 590 [604]

Xu, Z. 1053 [1066]

Yaghi, O. M. 49 [51]
Yamashita, Y. 455 [454]
Yang, Xiaoguang 893 [886]
Yang, Xinmin 1375 [1406]
Yasui, K. 645 [662]
Yoneda, K. 1336 [1386]
Youinou, M.-T. 733, 775 [771, 796]

Zadel, G. 1035 [1070]
Zanathy, L. 900 [884]
Zehnder, M. 193 [225]
Zeller, W. J. 64 [54]
Zhang, C. H. 232 [237]
Zhang, H. 432, 445 [441, 447]
Zhang, J. 922 [873]
Zhao, Y. 215 [212]
Zhu, N.-Y. 87, 1085 [83 (252), 1098]
Ziegler, M. L. 350, 1021 [329, 1096]
Ziegler, T. 1358 [1369]
Ziessel, R. 775 [796]
Ziller, J. W. 1081 [1114]
Zimmermann, N. 886 [928]
Zubieta, J. 1197 [1236]
Zuhse, R. 870 [914]
Zwahlen, C. 1248 [1233]
Zybill, C. 173 [180]

INDEX OF AUTHORS AND REVIEWERS OF BOOKS

This index lists separately the names of Authors/Editors and Reviewers, respectively, of books reviewed in *Angew. Chem. Int. Ed. Engl.* **1992**, *31*.

Bookauthors

Abruna, H. D. 238
Alcock, N. W. 663
Almond, M. J. 362
Altman, S. L. 1097
Ashwell, G. J. 1536
Atkins, P. W. 1095
Austin, J. 802
Baizer, M. M. 656
Balzani, V. 104
Belen'kii, I. A. 238
Boche, G. 241
Bodanszky, M. 1535
Bonačić-Koutecký, V. 242
Bouas-Laurent, H. 804
Bowman, M. K. 243
Brandsma, L. 485
Braun, A. M. 360
Brereton, R. G. 663
Brown, T. A. 1099
Büchel, K. H. 799
Buck, B. 928
Burger, K. 803
Butcher, S. S. 799
Callaghan, P. T. 1394
Carlson, R. 1393
Carruthers, W. 240
Cheetham, A. K. 1396
Ciferri, A. 358
Collins, D. J. 107
Colquhoun, H. M. 662
Connors, K. A. 239
Cornell, R. M. 658
Crichton, R. R. 930
Culvenor, C. C. J. 107
Damani, L. A. 107
Davies, M. B. 802
Day, P. 1396
Dedieu, A. 1537
Dequasie, A. 1096
Dorfner, K. 802
Dürr, H. 363, 804
Eckstein, F. 1398
Falbe, J. 799
Fan, L. T. 659
Flanigen, E. M. 661
Fried, B. 360
Fringuelli, F. 364
Fruton, J. S. 103
Fuchs, E. 108
Fujita, H. 240
Glasby, J. S. 1396
Gray, P. 109
Greene, T. W. 658
Hagemann, H. 799
Hallenga, K. 484
Hamilton, J. F. 1534
Hanack, M. 799
Hansen, J. C. 661
Hardie, D. G. 657
Harrington, P. J. 365
Hassall, K. A. 242
Hon, D. N. S. 801
Huyskens, P. L. 1538
Jacob, J. 364
Janoschek, R. 800
Johnson, J. A. 803
Jones, J. 798
Jordan, R. B. 1397
Kevan, L. 243
Klamann, D. 237, 799
Kosower, E. M. 659
Kreher, R. 799
Kropf, H. 799
Krygowski, T. M. 359
Lamberton, J. A. 107
Lichtenthaler, F. W. 361
Loder, J. W. 107
Luck, W. A. P. 1538
Lukevics, E. 1098
Lund, H. 656
Luque de Castro, M. D. 484
Macaulay, V. A. 928
Mason, S. F. 1533
Maurette, M.-T. 360
Mayo, D. W. 799
Merian, E. 102
Meyer, G. 105
Michl, J. 242
Moore, G. R. 1098
Morss, L. R. 105
Nakanishi, K. 245
Nasipuri, D. 1539
Neogi, D. 659
Nicholson, J. W. 486
Olah, G. A. 660
Oliveros, E. 360
Oppholzer, H. 108
Parish, R. V. 108
Partridge, D. A. 802
Patai, S. 1395
Pettigrew, G. W. 1098
Pike, R. M. 799
Popov, A. I. 484
Prelog, V. 1395
Price, J. R. 107
Rappoport, Z. 105, 1395
Regitz, M. 799
Rehme, H. 108
Robinson, J. W. 236
Rossiter, B. W. 1534
Ruelle, D. 798
Scandola, F. 104
Schaumann, E. 799
Scheffold, R. 1393
Schneider, H.-J. 363
Schügerl, K. 1397
Schwertmann, U. 658
Scott, S. K. 109
Servos, J. W. 797
Seyden-Penne, J. 1534
Shepherd, M. K. 1264
Sherma, J. 360
Shiraishi, N. 801
Shorter, J. 359
Shustorovich, E. 1538
Sokolov, V. I. 1096
Taticchi, A. 364
Thompson, D. J. 662
Tiller, W. A. 1536
Trumper, P. K. 799
Tschesche, H. 245
Twigg, M. V. 662
Ulman, A. 929
Valcárel, M. 484
van Bekkum, H. 661
Wade, K. 660
Walborsky, H. M. 241
Webster, B. 661
Wieland, T. 1535
Williams, R. E. 660
Wuts, P. G. M. 658
Yashima, M. 659
Zablocka, A. 1098
Zalewski, R. I. 359
Zeegers-Huyskens, T. 1538

Reviewers

Adam, G. 1396
Alper, H. 662
Baumgarten, M. 486
Becker, H. 107
Beck-Sickinger, A. 245
Berger, S. 245
Boche, G. 485
Böhm, M. C. 1097
Bolm, C. 1539
Buss, D. H. 658
Butenschön, H. 1264
Buzek, P. 799
Christl, M. 241
Crudden, C. 662
Decher, G. 929
Dickert, F. L. 239
Dorhout, P. K. 105
Drauz, K. 1397
Dreyer, M. 1099
Ebeling, W. 1533
Ebert, E. 242
Einax, J. 663
Engelhard, M. 659
Engman, L. 237
Fessner, W.-D. 1099
Fischbach, R. 484
Frahm, J. 1394
Göbel, M. 1263
Griesbeck, A. G. 242, 364
Griesinger, C. 928
Hay, R. W. 803
Heitele, H. 104
Hucho, F. 657
Hulliger, J. 1536
Irgolic, K. J. 102
Jaenicke, L. 103
Jakubke, H.-D. 798
Janoschek, R. 663
Jeschkeit, H. 1535
Kadenbach, B. 1098
Kauffman, G. B. 1096, 1395
Kayser, H. 242
Krause, H. 1538
Krause, N. 799
Kuhlenbeck, H. 1538
Kunz, H. 658
Langhals, H. 804
Lubitz, W. 243
Lüning, U. 363
Martens, J. 360
Mayer, R. 364
Meier, C. 1098
Merten, W. 1534
Metz, P. 1534
Mislow, K. 800
Nesper, R. 661
Neubauer, A. 803
Nimz, M. 661
Oehrlein, R. 361
Okuda, J. 1537
Orth, A. 1393
Paetzold, P. 660
Peyman, A. 1398
Powell, A. K. 930
Pregosin, P. S. 108
Rouvray, D. H. 359, 797
Sander, W. 1095
Schaumann, E. 238
Schleyer, P. von R. 799
Schlögl, R. 108
Schmalz, H.-G. 365
Schmidt, M. 240
Schmittel, M. 656
Schneider, F. W. 109
Schnick, W. 1396
Schroth, W. 107
Schumacher, R. 238
Schuster, D. I. 360
Schuster, P. 798
Sebald, A. 484
Sies, H. 802
Staub, T. 242
Strüver, W. 802
Theil, F. 1393
Tölg, G. 236
van Eldik, R. 1397
Wachter, J. 1096
Waldmann, H. 240
Wienhaus, O. 801
Wirz, J. 105
Wischerhoff, E. 358
Wolf, H. C. 1536
Würthwein, E.-U. 1395
Zenneck, U. 362
Zentel, R. 358
Zumofen, G. 659

Ab initio calculations
- Ab Initio Investigations of Structure and Stability of $[R_3SiAl]_4$, R = H, Me, *t*Bu (C) 353
- 1,2,4-Cyclohexatriene, an Isobenzene, and its [2 + 2] Cycloaddition with Styrene: A Theoretical Study (C) 476
- Effect of Torsional Strain and Electrostatic Interactions on the Stereochemistry of Nucleophilic Additions to Cyclohexanone and Related Systems (C) 1019
- $[Ga(C_5H_5)]$: Synthesis, Identification, and Ab Initio Investigations (C) 1362
- "Kinetically Enhanced Metalation"—How Substituents Direct *ortho* Lithiation (C) 755
- Large Hyperconjugative and Inductive Effects on C-C-X Bond Angles (X = Main-Group Element): The Crystal Structure of Triethylborane and Ab Initio Investigations (C) 314
- Origin of the Stabilization of Vinyldiazonium Ions by β-Substitution; First Crystal Structure of an Aliphatic Diazonium Ion: β,β-Diethoxyethenediazonium Hexachloroantimonate (C) 740
- Structures, Structures, and Structures (H) 290
- Synthesis and Structure of $[Ni(PtBu_6)]$ and $[Ni_5(PtBu)_6(CO)_5]$ and Calculations on the Electronic Structure of $[Ni(PtBu)_6]$ and $(PR)_6$, R = *t*Bu, Me (C) 323
- The Electronic Structure of $[(\eta^5\text{-}C_5H_5)_2Co_2]$: Comment on the Existence of a Complex with an Unsupported Co–Co Double Bond (C) 471
- The Isomers of the Acetylene Derivatives C_2Li_4: Transferable Structural Units in Hyperlithiated Compounds (C) 1602
- The Structure of Pentamethyltantalum (C) 1462
- The Structures of Pentamethyltantalum and -Antimony: One Square Pyramid and One Trigonal Bipyramid (C) 1464
- The Structures of Thiosulfuric Acid $H_2S_2O_3$ and Its Monoanion $HS_2O_3^-$ (C) 58
- Transition Structures of Hydrocarbon Pericyclic Reactions (R) 682

Acceleration of reactions
- En Route to Synthetic Phosphodiesterases: Supramolecular Phosphoryl-Transfer Mediated by Amidinium–Phosphate Contact Ion-Pairs (C) 207

Actinoid compounds
- Synthesis of Lanthanide and Actinide Compounds (B) 105

Adenosine monophosphates
- A Synthetic Receptor for Cyclic Adenosine Monophosphate (C) 61

Aldol reactions
- One-Pot Synthesis of Tagatose 1,6-Bisphosphate by Diastereoselective Enzymatic Aldol Addition (C) 56

Alkali metal compounds
- [2,3] Wittig Rearrangements of Nonconjugated Secondary α-Lithioethers: Proof of Stereospecificity and Inversion of the Configuration of the Carbanion C Atom (C) 647
- A Novel Six-Center Deprotonation–Lithiation Reaction Mechanism Supported by the X-Ray Structure Analysis of a Lithium Carbazolide (C) 1209
- A One-Pot Synthesis of Ketones and Aldehydes from Carbon Dioxide and Organolithium Compounds (C) 1035
- A Remarkable Change in Framework Cation Positions upon Lithium Exchange: the Crystal Structure of $LiMnPO_4(OH)$ (C) 1090
- A Supramolecular Assembly of Two Torands, Two Lithium Ions, and Three Water Molecules (C) 348
- A Water-Complexed Organolithium Compound: $[LiCH(CN)_2 \cdot H_2O \cdot TMEDA]_\infty$ (C) 77
- Conformational Preference of the Torand Ligand in Its Complexes with Potassium and Rubidium Picrate (C) 345
- Control of the Reaction of *n*-Butyllithium with Benzo[*b*]tellurophene by the Solvent—Either Metalation or Tellurium–Lithium Exchange To Give an Interesting Lithiostyryllithium (C) 1339
- Crystal and Solution Structures of the Novel Complex of Sodium Ketimide with Two Ketimine Ligands $[(tBu_2C{=}NNa)_4(HN{=}CtBu_2)_2]$: Stacking of Complexed and Uncomplexed $(NNa)_2$ Rings to give a Highly Distorted $(NNa)_4$ Cubane (C) 93
- Diastereoselective Three-Center Michael Addition of β-Ketoesters to Prostereogenic α,β-Unsaturated Carbonyl Compounds Catalyzed by K_2CO_3 or Cs_2CO_3 (C) 1651
- "Kinetically Enhanced Metalation"—How Substituents Direct *ortho* Lithiation (C) 755
- Lithiodiphenylmethylisocyanide-(−)-sparteine bis(tetrahydrofuran): Crystal Structure of a Lithiated Isocyanide (C) 79
- *N*-Lithiomethyl-*N*,*N*′,*N*″,*N*″′-tetramethyldiethylenetriamine: The First Alkyllithium Compound which is Monomeric in Hydrocarbons (C) 633
- [Lithium Piperidide–Piperidine]$_4$: Crystal Structure of an Oligomeric 1:1 Lithium Amide–Amine Mixed Complex, an Intermediate in the *N*-Lithiation of Amines (C) 1205
- Perlithiated and Hyperlithiated Methane (H) 584
- Preparative Polar Organometallic Chemistry 2 (B) 485
- Structures of Two Highly Reactive Intermediates upon $LiAlH_4$ Reduction in the Solid State and in Solution: $[(Me_3Si)_2NAlH_3Li \cdot 2Et_2O]_2$ and $[(Me_3Si)_2N]_2AlH_2Li \cdot 2Et_2O$ (C) 854
- The Isomers of the Acetylene Derivatives C_2Li_4: Transferable Structural Units in Hyperlithiated Compounds (C) 1602
- The New Subnitride $NaBa_3N$; an Extension of Alkali Metal Suboxide Chemistry (C) 1519

Alkaloids
- A Short Diastereoselective Entry to Indole Alkaloids of the Corynanthe Type by the Intramolecular Ene Reaction (C) 1079
- The Enchanting Alkaloids of Yuzuriha (R) 665

Alkene complexes
- New Route to α-[(1*E*,3*E*)-dienyl]allenes via Butadiene-tricarbonyliron Complexes (C) 224
- Preparation, Ligand Exchange Reactions, and Structure of a Diene(aqua)-ruthenium Complex $[(cod)Ru(H_2O)_4](OTs)_2$ (C) 440

Alkyl transition-metal compounds
- On the Influence of Heteroatoms in α- and β-Functionalized Alkyl Transition-Metal Compounds (R) 401

Alkyne complexes
- Inhibition of the [2+2+2] Cyclization by the Formation of Chelates: Alkyne and Vinylidene Complexes with Cyclopentadienylcobalt(I) (C) 1066

Alkynes
- Cycloalkadiynes—From Bent Triple Bonds to Strained Cage Compounds (R) 27
- Intermolecular Additions and Cycloisomerizations by a Pd-Catalyzed Sequence of an Intramolecular Redox Reaction and an Addition (C) 1335
- Synthetic Approaches toward Molecular and Polymeric Carbon Allotropes (R) 1101
- Tetraalkynylmethanes: Synthesis of Diethynyldipropargyl- and Tetrapropargylmethane (C) 1648
- The First Hexabutadiynylbenzenes: Synthesis and Structures (C) 1643

Allenes
- 1,2,4-Cyclohexatriene, an Isobenzene, and Bicyclo[4.4.0]deca-1,3,5,7,8-pentaene, an Isonaphthalene: Generation and Trapping Reactions (C) 473
- 1,2,4-Cyclohexatriene, an Isobenzene, and its [2 + 2] Cycloaddition with Styrene: A Theoretical Study (C) 476
- New Route to α-[(1*E*,3*E*)-dienyl]allenes via Butadiene-tricarbonyliron Complexes (C) 224
- Synthesis and Reactions of Isothiocyanate-Substituted Allenes and 1,3-Butadienes (C) 90
- Synthesis of Isocyanate-Substituted Allenes and 1,3-Butadienes by [3,3] Sigmatropic Rearrangements (C) 866

Allylations
- Allylation of Quinones with Allylsilane in the Presence of Lithium Perchlorate in Ether (C) 313
- Catalysis of the Addition of Allyltrimethylsilane to Aldehydes by Silylating Agents. $Me_3SiB(OTf)_4$, a New, 'Supersilylating' Reagent (C) 470

Aluminophosphates
- Solid-State NMR Spectroscopic and X-Ray Diffraction Studies of the Low-Temperature Structural Transformation of Hydrated Porous Aluminophosphate VPI-5 (C) 610
- Solving the Structure of a Metal-Substituted Aluminum Phosphate Catalyst by Electron Microscopy, Computer Simulation, and X-ray Powder Diffraction (C) 1472

Aluminum compounds
- Ab Initio Investigations of Structure and Stability of $[R_3SiAl]_4$, R = H, Me, *t*Bu (C) 353

- Structures of Two Highly Reactive Intermediates upon $LiAlH_4$ Reduction in the Solid State and in Solution: $[(Me_3Si)_2NAlH_3Li \cdot 2Et_2O]_2$ and $[(Me_3Si)_2N]_2AlH_2Li \cdot 2Et_2O$ (C) 854
- Synthesis and Structure of $Al(OAr^*)_3$ ($Ar^* = 2,6\text{-}tBu_2\text{-}4\text{-}MeC_6H_2$): The First Three-Coordinate Homoleptic Aluminum Aryloxide (C) 921

Amidines
- The Chemistry of Amidines and Imidates. Vol. 2 (B) 1395

Amines
- Molecular Recognition of Primary Amines by Three-Point Binding with Boron-Containing Host Molecules (C) 1017
- Perfluorotriethylamine: An Amine with Unusual Structure and Reactivity (C) 1467

Amino acids
- Enzymatic Preparation of Enantiomerically Pure *N*-alkyl Amino Acids (C) 195

D-amino acids
- Proteins from the D-Chiral World (H) 1457

Amino acids
- The Photochemistry of *N*-Phthaloyl α-Amino Acid Esters: A New Approach to β,γ-Unsaturated α-Amino acids and Dihydrobenzazepinediones (C) 73
- The ^{31}P-NMR Spectroscopic Determination of the Enantiomeric Excess of Unprotected Amino Acids (C) 1092

Amino alcohols
- Stereoselective Generation of 1-Acyloxy-2-amino Carbanions by Deprotonation; Synthesis of Enantiomerically and Diastereomerically Pure β-Amino Alcohols (C) 1505

Amino sugars
- Configuratively Stable Dipeptide Aldehydes from D-Glucosamine Hydrochloride (C) 1391

Ammonium compounds
- Interactions Between Acyclic and Cyclic Peralkylammonium Compounds and DNA (C) 1207

Analytical methods
- Atomic Spectroscopy (B) 236
- Detection of Subpicomole Levels of Compounds Containing Hydroxyl and Amino Groups with the Fluorogenic Reagent, 2-Naphthoylimidazole (C) 890
- Microscopy (B) 1534
- Non-Chromatographic Continuous Separation Techniques (B) 484
- Particle Beam Microanalysis. Fundamentals, Methods and Applications (B) 108
- Salting Out Selective Extraction—A Novel Method for the Optical Resolution of Chiral Sulfinylcarboxylic Acids and Its Application for the Convenient Determination of Optical Purity (C) 1631
- Synchrotron X-ray and Neutron Diffraction Studies in Solid-State Chemistry (R) 1557
- The Chemistry of GALLEX—Measurement of Solar Neutrinos with a Radiochemical Gallium Detector (R) 1283
- The ^{31}P-NMR Spectroscopic Determination of the Enantiomeric Excess of Unprotected Amino Acids (C) 1092

Annelations
- Alkyne(carbene) Complexes: Stabilization of an Intermediate of Carbene Annelation (C) 1236

Annulenes
- Corannulene Tetraanion: A Novel Species with Concentric Anionic Rings (C) 1636

Antibiotics
- Enzymatic Preparation of Enantiomerically Pure *N*-alkyl Amino Acids (C) 195

Antibodies
- Activation Parameters and Stereochemistry of an Antibody-Catalyzed Claisen Rearrangement (C) 182
- ^{99m}Tc Labeled Biotin Conjugate in a Tumor "Pretargeting" Approach with Monoclonal Antibodies (C) 1507

Antidepressants
- Enantioselective Synthesis of the Antidepressant Rolipram by Michael Addition to a Nitroolefin (C) 870

Antimony compounds
- $[SbCl([15]Crown\text{-}5)](SbCl_6)_2$ and $[BiCl([18]Crown\text{-}6)(CH_3CN)_2](SbCl_6)_2$: Salts with Antimony(III) and Bismuth(III) Dications (C) 334
- The First Stibepine: Synthesis and Structure of *Sb*-Chlorobenzo[*d*]stibepine (C) 1642
- The Structures of Pentamethyltantalum and -Antimony: One Square Pyramid and One Trigonal Bipyramid (C) 1464

Antisense RNA
- Inhibition of Fruit Ripening by Antisense-RNA Technology (H) 175

Antitumor agents
- 1-*O*-(2-Acetoxyhexadec-1-enyl)choline Iodide, a New Anticancer Agent (C) 64
- Chlorins Designed for Photodynamic Tumor Therapy and as Model Systems for Photosynthesis (C) 1592
- Crosslinking of Adjacent Guanine Residues in an Oligonucleotide by *cis*-$[Pt(NH_3)_2(H_2O)_2]^{2+}$: Kinetic Analysis of the Two-Step Reaction (C) 1483
- Synthesis and Biological Activity of D-3-Deoxy-3-Fluorophosphatidylinositol—A New Direction in the Design of non-DNA Targeted Anticancer Agents (C) 1379

Aqua complexes
- Preparation, Ligand Exchange Reactions, and Structure of a Diene(aqua)-ruthenium Complex $[(cod)Ru(H_2O)_4](OTs)_2$ (C) 440

Arene complexes
- A New Approach to Bis(arene)titanium(0) and -titanium(−1) Complexes; Structure of Bis(arene)titanates(1−) (C) 1495
- Benzene and Its Derivatives as Bridging Ligands in Transition-Metal Complexes (R) 247
- Ether-Soluble Ti^0 and Bis(η^6-arene)-titanium(0) Complexes from the Reduction of $TiCl_4$ with Triethylhydroborate (C) 1490
- One-Pot Syntheses of Novel Arene Tricarbonyl Chromium Macrocycles and Macrobicycle: Structure of a Pentanuclear Trichromium(0)-Dicopper(I) Cryptate (C) 775

Arenes
- Cyclobutarenes. The Chemistry of Benzocyclobutene, Biphenylene, and Related Compounds (B) 1264
- Oligo(9,10-anthrylenes), Organic Compounds with Stable High-Spin States (C) 448
- One-Pot Multifunctionalization of Polymethyl Hydrocarbon π Ligands. Maximum Space Occupancy by Double Branching and Formation of Arboroles (C) 458
- Rate Constants for the Attack of Carbenium Ions at Arenes—A Link between the Chemistry of Aliphatic and Aromatic π Systems (C) 1613
- Structure of the Lowest Temperature Phase of the Solid Benzene–Hexafluorobenzene Adduct (C) 1655
- The Benzene Ring as Dienophile in an Intramolecular [4+2] Cycloaddition: Degenerate Rearrangement of 7,8-Benzobicyclo[4.2.2]deca-2,4,7,9-tetraene (C) 872
- The First Hexabutadiynylbenzenes: Synthesis and Structures (C) 1643

Aromaticity
- Aromatic Boron Heterocycles: The Generation of 1H-Borepin and the Structure of Tricarbonyl(1-phenylborepin)molybdenum (C) 1255
- Corannulene Tetraanion: A Novel Species with Concentric Anionic Rings (C) 1636
- Equilibria between Nonclassical and Classical Boron Compounds, Competition between Aromaticity in Two and Three Dimensions (C) 607
- The First Stibepine: Synthesis and Structure of *Sb*-Chlorobenzo[*d*]stibepine (C) 1642

Arsenic compounds
- An Arsanylidensilane ("Arsasilene") and its Derivatization with Tellurium and Benzophenone (C) 316
- $(H_2Si)_2E_2$ and $(Mes(tBu)Si)_2E_2$ (E = As, P): Incommensurable Systems of Different Stability with Unusually Long E–E Bonds (C) 460
- (Organoarsonato)polyoxovanadium Clusters: Properties and Structures of the V^V Cluster $[V_{10}O_{24}(O_3AsC_6H_4\text{-}4\text{-}NH_2)_3]^{4-}$ and the V^{IV}/V^V Cluster $[H_2\{V_6O_{10}(O_3AsC_6H_5)_6\}]^{2-}$ (C) 1197
- The Reaction of Tetramesityldisilene with As_4: Synthesis and Structure of a Novel Arsenic–Silicon Tricyclic Ring System (C) 1217

Arylethenes
- C–C Coupling with NO_2/Alkyl Substitution at the Vinylic Carbon by Reaction of 2-Aryl-1-nitro-1-alkenes with Dialkylzinc Compounds—A Novel Reaction (C) 1587

Arynes
- 2,4-Didehydrophenol—First Proof of a *meta*-Aryne by IR Spectroscopy (C) 1230

Asymmetric syntheses
- A Short Diastereoselective Entry to Indole Alkaloids of the Corynanthe Type by the Intramolecular Ene Reaction (C) 1079
- "Artificial Metabolisms" for the Asymmetric One-Pot Synthesis of Branched-Chain Saccharides (C) 614
- Asymmetric Deprotonation as an Efficient Enantioselective Preparation of Functionalized Secondary Alcohols (H) 1459
- Asymmetric Ligands for Transition-Metal-Catalyzed Reactions: 2-Diphenylphosphinobenzoyl Derivatives of C_2-Symmetric Diols and Diamines (C) 228
- *trans*-2-*tert*-Butylcyclohexanol, a Simple Selectively Optimized Cyclohexanol Auxiliary (C) 1190
- Diacetoneglucose as Auxiliary Group for the Asymmetric Hetero-Diels–Alder Reaction with Nitrosoalkenes (C) 1033
- Diastereoselective Addition of Allylsilanes to Aldehydes: Synthesis of Enantiomerically Pure Homoallylic Alcohols (C) 1372
- Diastereoselective Complexation of Temporarily Chirally Modified Ligands: Enantioselective Preparation and Configurational Assignment of Synthet-

ically Valuable η^6-Tricarbonylchromium-1-tetralone Derivatives (C) 631
- Diastereoselective Synthesis of Substituted Cyclohexadienes from Enantiomerically Pure Tricarbonyl(2-phenyl-4,5-dihydrooxazole)chromium Complexes (C) 1071
- Diastereoselective Three-Center Michael Addition of β-Ketoesters to Prostereogenic α,β-Unsaturated Carbonyl Compounds Catalyzed by K_2CO_3 or Cs_2CO_3 (C) 1651
- Enantiomerically Pure Tertiary Alcohols by TADDOL-Assisted Additions to Ketones—or How to Make a Grignard Reagent Enantioselective (C) 84
- Enantioselective Rhodium(II) Catalysts (H) 1183
- Enantioselective Syntheses of Cyclopentanoid Compounds from Isoprene and *trans*-1,3-Pentadiene (C) 305
- Enantioselective Synthesis of 3-Substituted 2-Ketoesters (C) 618
- Enantioselective Synthesis of the Antidepressant Rolipram by Michael Addition to a Nitroolefin (C) 870
- *meso* Epoxides in Asymmetric Synthesis: Enantioselective Opening by Nucleophiles in the Presence of Chiral Lewis Acids (H) 1179
- First Atropo-Enantioselective Ring Opening of Achiral Biaryls Containing Lactone Bridges with Chiral Hydride-Transfer Reagents Derived from Borane (C) 761
- Formate-Driven, Non-Enzymatic NAD(P)H Regeneration for the Alcohol Dehydrogenase Catalyzed Stereoselective Reduction of 4-Phenyl-2-butanone (C) 1529
- Ligand Effects in Grignard Additions (C) 342
- New Chiral α-Benzyloxyacryliron(II) Complex for Asymmetric Synthesis of α,α-Dialkyl-α-hydroxycarbonyl Compounds (C) 193
- One-Pot Synthesis of Tagatose 1,6-Bisphosphate by Diastereoselective Enzymatic Aldol Addition (C) 56
- Oxazaborolidines and Dioxaborolidines in Enantioselective Catalysis (H) 729
- Stereocontrolled Construction of 6 · 5 · 6 and 5 · 5 · 6 Ring Systems by Radical Tandem Cyclization (C) 910
- Stereoselective Generation of 1-Acyloxy-2-amino Carbanions by Deprotonation; Synthesis of Enantiomerically and Diastereomerically Pure β-Amino Alcohols (C) 1505
- Stereoselective Nucleophilic Addition Reactions of Reactive Pseudopeptides (C) 1626
- Sugars as Chiral Auxiliaries for the Synthesis of Enantiomerically Pure Compounds (H) 288
- The Hydroxyl-Directed Hydrogenation of Vinylstannanes and Silanes: A Highly Diastereoselective Route to β-Stannyl and β-Silyl Alcohols (C) 232
- The Tandem Sakurai–Carbonyl–Ene Reaction: A New and Highly Stereoselective Sequential Transformation and Its Use for the Synthesis of Steroid Derivatives (C) 1221

Atomic force microscopy
- Photodimerization of Anthracenes in the Solid State: New Results from Atomic Force Microscopy (C) 595
- Photodimerization of Cinnamic Acid in the Solid State: New Insights on Application of Atomic Force Microscopy (C) 592
- Scanning Tunneling Microscopy and Atomic Force Microscopy in Organic Chemistry (R) 1298

Atropo-enantioselectivity
- First Atropo-Enantioselective Ring Opening of Achiral Biaryls Containing Lactone Bridges with Chiral Hydride-Transfer Reagents Derived from Borane (C) 761

Aza crown ethers
- Designing Synthetic Cationic Molecular Receptors for Alcohols (C) 478

Azaallenium ion
- Tetraferrioazaallenium—Product of a Novel Reaction of Coordinated CN^- (C) 590

Azaboranes
- Opening of an Aza-*closo*-dodecaborane to an Aza-*nido*-dodecaborate (C) 1227

Azacyclopentadiene
- 2,2',5,5'-Tetra-*tert*-butyl-1,1'-diazaplumbocene—a Stable Azacyclopentadienyl Compound of Lead (C) 778

Azines
- An Organometallic Analogue of the "Criss-Cross" Cycloaddition Reaction (C) 1053

Aziridines
- The Total Synthesis of (±)-Mitomycin K (C) 915

Azobenzenes
- Photoswitchable Association of an Azobenzene-Bipyridinium Diad to Eosin: Photostimulated "On-Off" Guest Binding (C) 1243

Band theory
- Band Theory of Solids. An Introduction from the Point of View of Symmetry (B) 1097

Barium compounds
- Alkoxyalkyl-Substituted β-Diketonate Complexes of Barium and Copper: Evidence for Inter- and Intramolecular Stabilization (C) 735
- The New Subnitride $NaBa_3N$; an Extension of Alkali Metal Suboxide Chemistry (C) 1519

Beilstein test
- The Beilstein Test: An Unintentional Dioxin Source in Analytical and Research Laboratories (C) 443

Belousov–Zhabotinskii reaction
- Chemiluminescence Oscillations Driven by a Flow-through Reactor in the $[Ru(bpy)_3]^{2+}$ Catalyzed Belousov–Zhabotinskii Reaction (C) 355

Benzazepines
- The Photochemistry of *N*-Phthaloyl α-Amino Acid Esters: A New Approach to β,γ-Unsaturated α-Amino acids and Dihydrobenzazepinediones (C) 73

Benzothiazoles
- A 1:1 Adduct of 2-Aminobenzothiazole and a Urea Derivative, and Its Spatial Arrangement (C) 1634

Biaryls
- First Atropo-Enantioselective Ring Opening of Achiral Biaryls Containing Lactone Bridges with Chiral Hydride-Transfer Reagents Derived from Borane (C) 761

Bifluorenes
- Enantioselective Complexation of Chiral Dicarboxylic Acids in Clefts of Functionalized 9,9'-Spirobifluorenes (C) 1521

Binaphthol complexes
- Unprecedented Stereospecific Ligand Exchange at a W≡W Template (C) 66

Biochemical messengers
- Biochemical Messengers. Hormones, Neurotransmitters and Growth Factors (B) 657

Biochemistry
- Biochemical Degradation of Cyanamide and Dicyandiamide (C) 620
- 5'-*P*-Borane-Substituted Thymidine Monophosphate and Triphosphate (C) 1373
- Do Pheromone Receptors that Receive the Same or Similar Signal Molecules Have the Same or Similar Structure? (C) 330
- Elementary Steps in Synaptic Transmission Revealed by Currents through Single Ion Channels (Nobel Lecture) (R) 830
- Inorganic Biochemistry of Iron Metabolism (B) 930
- Ion Channels for Communication Between and Within Cells (Nobel Lecture) (R) 824
- Molecular Mechanism for Sensory Signals (B) 659
- Natural Products as Probes of Cellular Function: Studies of Immunophilins (R) 384
- Radical Intermediates in the Coenzyme B_{12} Dependent Methylmalonyl-CoA Mutase Reaction Shown by ESR Spectroscopy (C) 215
- Selective Inhibition of Trypanosomal Triosephosphate Isomerase by a Thiopeptide (C) 328
- Synthesis of (2-Arylindol-3-yl)acetamides as Probes of Mitochondrial Steroidogenesis—A New Mechanism for $GABA_A$ Receptor Modulation (C) 1060
- Synthesis of Octameric Phosphodiesters of [3,3-Bis(hydroxymethyl)cyclobutyl]-adenine and -thymine as well as their Hybridization Properties (C) 482
- The Biochemistry and Uses of Pesticides. Structure, Metabolism, Mode of Action and Uses in Crop Protection (B) 242

Bioinorganic chemistry
- Biocoordination Chemistry: Coordination Equilibria in Biologically Active Systems (B) 803
- Synthesis of Cubane-like and Double Cubane-like Tungsten–Copper–Sulfur Clusters from the "Butterfly" Cluster $[Cu_2S_3W(O)(PPh_3)_3]$ (C) 1085
- Synthetic Models for Iron—Oxygen Aggregation and Biomineralization (H) 1010
- Tris(cyclopentanolato)oxovanadium(V): a Model for the Transition State of Enzymatic Phosphoester Cleavage (C) 447

Biomineralization
- Control and Design Principles in Biological Mineralization (R) 153
- Synthetic Models for Iron—Oxygen Aggregation and Biomineralization (H) 1010

Biopolymers
- Photolithographic Immobilization of Biopolymers on Solid Supports (C) 759

Biosensors
- Molecular Mechanism for Sensory Signals (B) 659

Biotechnology
- Biotechnology. A Multi-Volume Comprehensive Treatise. Vol. 4. Measuring, Modelling and Control (B) 1397

Biotin
- ^{99m}Tc Labeled Biotin Conjugate in a Tumor "Pretargeting" Approach with Monoclonal Antibodies (C) 1507

Biradicals
- 2,4-Didehydrophenol—First Proof of a *meta*-Aryne by IR Spectroscopy (C) 1230

Bismuth compounds
- Bismuth Alkoxide Dimer Complexes Containing Planar $Bi_2(\mu\text{-}OR)_2$ Cores: Syntheses and Structures of $[\{Bi[OCH(CF_3)_2]_3(thf)\}_2]$ and $[\{Bi(OC_6F_5)_3(C_7H_8)\}_2] \cdot 2C_7H_8$ (C) 451
- $[SbCl([15]Crown\text{-}5)](SbCl_6)_2$ and $[BiCl_2([18]Crown\text{-}6)(CH_3CN)_2](SbCl_6)_2$: Salts with Antimony(III) and Bismuth(III) Dications (C) 334

Blood substitutes
- Protein Engineering: Modified Hemoglobin as a Blood Substitute (H) 848

Bond-stretch isomerism
- Bond-Stretch Isomers: Fact or Artifact? (H) 286
- Distortional Isomerism in Oxomolybdenum Systems; the Evidence Re-evaluated (C) 1607

Boron compounds
- Aromatic Boron Heterocycles: The Generation of 1H-Borepin and the Structure of Tricarbonyl(1-phenylborepin)molybdenum (C) 1255
- Bis(trisyl)oxadiborirane (C) 1040
- 1-Borabutadiene(cyclopentadienyl)cobalt Complexes (C) 1603
- 5′-*P*-Borane-Substituted Thymidine Monophosphate and Triphosphate (C) 1373
- Boriranes: Structures and Thermal Ring Openings (C) 1384
- Compounds with Three-Membered Rings Containing Boron (H) 1329
- Cyclometallaborazines: Borazines with Metal Atoms as Ring Building Blocks: $PhB(MeN)_3(TiCl_2)_2$ (C) 598
- Electron Deficient Boron and Carbon Clusters (B) 660
- Equilibria between Nonclassical and Classical Boron Compounds, Competition between Aromaticity in Two and Three Dimensions (C) 607
- First Atropo-Enantioselective Ring Opening of Achiral Biaryls Containing Lactone Bridges with Chiral Hydride-Transfer Reagents Derived from Borane (C) 761
- Formation of a 2,5-Diborabicyclo-[2.1.1]hexane Derivative and its Conversion to a Tetracarbahexaborane (C) 606
- Homodiboriranides: The Simplest Negatively Charged Homoaromatic Compounds (C) 1238
- Large Hyperconjugative and Inductive Effects on C-C-X Bond Angles (X = Main-Group Element): The Crystal Structure of Triethylborane and Ab Initio Investigations (C) 314
- Molecular Recognition of Primary Amines by Three-Point Binding with Boron-Containing Host Molecules (C) 1017
- $[Nb\{B(\eta^6\text{-}C_6H_5)_2(C_6H_5)_2\}(\eta^2\text{-}H_3CC_2CH_3)]$: the First Compound with Bent Tetraphenylborate as 12-Electron Donor Ligand (C) 1235
- "Non-Coordinating" Anions: Underestimated Ligands (H) 1181
- Opening of an Aza-*closo*-dodecaborane to an Aza-*nido*-dodecaborate (C) 1227
- Oxazaborolidines and Dioxaborolidines in Enantioselective Catalysis (H) 729
- Reduction of a Boron–Nitrogen 1,3-Butadiene Analogue: Evidence for a Strong B–B π-Bond (C) 1082
- Synthesis and Structure of the First Trinuclear, Half-Sandwich Carboranegadolinium(III) Cluster (C) 432
- The Green Flame: Surviving Government Secrecy (B) 1096
- Zinc Pyrazolylborate Complexes Relevant to the Biological Function of Carbonic Anhydrase (C) 92

Bredt rule
- Anti-Bredt Enol Ethers by Transannular Cyclization of Cycloalkynols (C) 791

Bridging ligands
- A New Structure–Magnetism Relationship for Face-Sharing Transition-Metal Complexes with d^3–d^3 Electronic Configuration (C) 311
- A Structurally Distorted Ligand in an Electron-Deficient Dizirconocene Cation: Unusual 1,2- and 1,1-Dimetallioalkenes (C) 876
- Benzene and Its Derivatives as Bridging Ligands in Transition-Metal Complexes (R) 247
- Double Open-Edged P_{10} Dihydrofulvalene as a 16-Electron Donor Ligand (C) 1027
- $[Et_4N]_2[\{MO(S_2)_2\}_2(\mu_2\text{-}S_7)(\mu_2\text{-}H_2NNH_2)]$ (M = Mo, W)—Doubly Bridged Complexes with S_7^{2-} and Doubly End-On-Bound H_2NNH_2 Bridging Ligands (C) 87
- Molecular Machines: Molecular Structure of $[(p\text{-}Tol_3P)_{10}Au_{13}Ag_{12}Cl_8](PF_6)$—a Cluster with a Biicosahedral Rotorlike Metal Core and an Unusual Arrangement of Bridging Ligands (C) 445
- Pyridine-2-thiolato Complexes of V^{II}, V^{III}, and V^{IV} with Unusual Structural Features (C) 1253
- Stable Intermediates in the Addition and Elimination of $SnBuCl_3$ at Molybdenum Centers by Cleavage or Formation of an Sn–Cl Bond: Crystal Structure of $[Mo(CO)_2(PCy_3)(\mu\text{-}Cl)(\mu\text{-}S_2CPCy_3)(BuSnCl_2)] \cdot CH_2Cl_2$ (C) 76
- The Reaction of $[Cp_2^+Nb_2(B_2H_6)_2]$ ($Cp^+ = \eta\text{-}EtMe_4C_5$) with Sulfur: Stabilization of the Tetrathioborato Ligand in Novel Sulfido Niobium Clusters (C) 1021
- The Trapping of Iron Hydroxide Units by the Ligand "heidi": Two New Hydroxo(oxo)iron Clusters Containing 19 and 17 Iron Atoms (C) 191

Butadienes
- Synthesis and Reactions of Isothiocyanate-Substituted Allenes and 1,3-Butadienes (C) 90
- Synthesis of Isocyanate-Substituted Allenes and 1,3-Butadienes by [3,3] Sigmatropic Rearrangements (C) 866

Butatrienes
- Butatrienes by Desulfurization of Cyclic Trithiocarbonates (C) 1611

Cadmium compounds
- Indirect $^{113}Cd,^{14}N$ Spin-Spin Coupling Constants as a Structural Probe of Solid Cadmium Thiocyanate Complexes (C) 1222

Cage compounds
- A Donor Cage with Two Tetrathiafulvene Units (C) 309
- A New Reaction Type in the Conversion of Enamines with 1,4-Diphenyl-2-butene-1,4-dione to Give Cage Compounds (C) 768
- A Rh^I-Centered Cage Compound with Selective Catalytic Properties (C) 905
- $C_{36}H_{36}$—Tetrahedral Clamping of Four Benzene Rings in a Spherical Hydrocarbon Framework (C) 1069
- Selective Ketone Pyrolysis: New Synthetic Method for Mono- and Polycyclic Hydrocarbons (C) 307

Calicheamicins
- Synthesis of the Calicheamicin Aryltetrasaccharide Domain Bearing a Reducing Terminus: Coupling of Fully Synthetic Aglycone and Carbohydrate Domains by the Schmidt Reaction (C) 338
- Total Synthesis of Calicheamicin–Dynemicin Hybrid Molecules (C) 340

Calixarenes
- Bicyclocalix[4]arenes (C) 96
- Nitrocalix[4]arenes as Molecules for Second-Order Nonlinear Optics (C) 1075

Calorimetry
- Microcalorimetry of the Spin-Transition Systems $[Fe(bts)_2(NCS)_2]$ and $[Fe(2\text{-}pic)_3]Cl_2 \cdot EtOH$ in the Range $15\ K < T < 300\ K$ (C) 178
- The Stability of Buckminsterfullerene (C_{60}): Experimental Determination of the Heat of Formation (C) 63

Carbanions
- Preparative Polar Organometallic Chemistry 2 (B) 485
- Stereoselective Generation of 1-Acyloxy-2-amino Carbanions by Deprotonation; Synthesis of Enantiomerically and Diastereomerically Pure β-Amino Alcohols (C) 1505

Carbene complexes
- Alkyne(carbene) Complexes: Stabilization of an Intermediate of Carbene Annelation (C) 1236
- Carbene Osmium Complexes by Double Metalation of Alkoxylalkyl- and Aminoalkylphosphanes (C) 1025
- Detection of the Tungsten–Carbene–Olefin Intermediates in Catalytic Metathesis Systems Containing High-Valent, Metal Centers (C) 1585

Carbenes
- Enantioselective Rhodium(II) Catalysts (H) 1183

Carbocations
- Cyclohexadienyl-Type Cationic Intermediates in the Friedel–Crafts Alkylation of Benzene Derivatives with the 9-Fluorenyl Cation—Observation by Laser Flash Photolysis (C) 743
- Houben-Weyl. Methoden der Organischen Chemie. Band E19c: Carbokationen, Carbokation-Radikale (B) 799
- Kinetics of Hydride Transfers from CH, SiH, GeH, and SnH Groups to Carbenium Ions (C) 1046

Carbohydrates
- A New Strategy for Solid-Phase Synthesis of *O*-Glycopeptides (C) 857
- "Artificial Metabolisms" for the Asymmetric One-Pot Synthesis of Branched-Chain Saccharides (C) 614
- Carbohydrates as Organic Raw Materials (B) 361
- Detection of Subpicomole Levels of Compounds Containing Hydroxyl and Amino Groups with the Fluorogenic Reagent, 2-Naphthoylimidazole (C) 890
- Emil Fischer's Proof of the Configuration of Sugars: A Centennial Tribute (R) 1541
- One-Pot Synthesis of Tagatose 1,6-Bisphosphate by Diastereoselective Enzymatic Aldol Addition (C) 56
- Reagents with Hypervalent Iodine: Formation of Convenient Chiral Synthetic Intermediates by Fragmentation of Carbohydrate Anomeric Alkoxy Radicals (C) 772
- Selective Binding of Sugar to β-Cyclodextrin: A Prototype for Sugar–Sugar Interactions in Water (C) 745

- Sugars as Chiral Auxiliaries for the Synthesis of Enantiomerically Pure Compounds (H) 288
- Synthesis and Biological Activity of D-3-Deoxy-3-Fluorophosphatidylinositol—A New Direction in the Design of non-DNA Targeted Anticancer Agents (C) 1379
- Synthesis of Esterase-resistant 9-*O*-Acetylated Polysialoside as Inhibitor of Influenza C Virus Hemagglutinin (C) 1478
- Synthesis of *C*-Glycopeptides via Free Radical Addition of Glycosyl Bromides to Dehydroalanine Derivatives (C) 902

Carbon dioxide
- A One-Pot Synthesis of Ketones and Aldehydes from Carbon Dioxide and Organolithium Compounds (C) 1035

Carbon–carbon linkage
- Addition of Benzyl Radicals to Alkenes: The Role of Radical Deformation in the Transition State (C) 635
- Alkyne(carbene) Complexes: Stabilization of an Intermediate of Carbene Annelation (C) 1236
- Allylation of Quinones with Allylsilane in the Presence of Lithium Perchlorate in Ether (C) 313
- Assistance by Electrophiles in Photoinduced Alkylidyne–Carbonyl Coupling (C) 747
- Catalysis of the Addition of Allyltrimethylsilane to Aldehydes by Silylating Agents. $Me_3SiB(OTf)_4$, a New, 'Supersilylating' Reagent (C) 470
- C–C Coupling with NO_2/Alkyl Substitution at the Vinylic Carbon by Reaction of 2-Aryl-1-nitro-1-alkenes with Dialkylzinc Compounds—A Novel Reaction (C) 1587
- Enantiomerically Pure Tertiary Alcohols by TADDOL-Assisted Additions to Ketones—or How to Make a Grignard Reagent Enantioselective (C) 84
- New Route to α-[(1*E*,3*E*)-dienyl]allenes via Butadiene-tricarbonyliron Complexes (C) 224
- Palladium(0)-Catalyzed Three-Component Coupling Reaction of Allyl Benzoates, Carbon Monoxide, and Zincioesters (C) 645
- Reaction of Heterodinuclear μ-Ethynediyl Complexes Containing Palladium and Platinum: Multiple and Successive Insertion of Isocyanides (C) 851

Carbonic anhydrase
- Zinc Pyrazolylborate Complexes Relevant to the Biological Function of Carbonic Anhydrase (C) 92

Carbonylation (B) 662

Carboranes
- Formation of a 2,5-Diborabicyclo-[2.1.1]hexane Derivative and its Conversion to a Tetracarbahexaborane (C) 606
- Multidentate Macrocyclic Lewis Acids: Release of "[12] Mercuracarborand-4" from Its Iodide Complex and the Structure of Its Tetra(tetrahydrofuran) Dihydrate Complex (C) 893
- Synthesis and Structure of the First Trinuclear, Half-Sandwich Carborane-gadolinium(III) Cluster (C) 432

Carbosilanes
- On the Bonding in Carbosilanes (C) 185

Carboxylic acids
- A Simple Method for the Replacement of the OH Group in Free Carboxylic Acids by the Phosphonium Ylide Group (C) 1064
- Enzymatic Oxidation of Methyl Groups on Aromatic Heterocycles: A Versatile Method for the Preparation of Heteroaromatic Carboxylic Acids (C) 774

Carbyne complexes
- New Routes to Alkylidyne-Bridged Ditungsten Compounds Supported by Alkoxide or Siloxide Ligands by the Activation of Ethylene (C) 462

Caro's acid
- Caro's Acid: Molecular Structure and Association in the Solid State at −130 °C (C) 436

Carotenoids
- Dual Fluorescence of Novel Modified Carotenoids (C) 1042

Cascade molecules
- Dendrimers, Arborols, and Cascade Molecules: Breakthrough into Generations of New Materials (H) 1571

Catalysis
- A Rh^I-Centered Cage Compound with Selective Catalytic Properties (C) 905
- Activation Parameters and Stereochemistry of an Antibody-Catalyzed Claisen Rearrangement (C) 182
- Asymmetric Ligands for Transition-Metal-Catalyzed Reactions: 2-Diphenylphosphinobenzoyl Derivatives of C_2-Symmetric Diols and Diamines (C) 228
- $[t\mathrm{BuSiO}(\mathrm{ReO}_4)]_4$, a Model Compound for Metal Oxides on Silicate Surfaces—Synthesis from the Stable Triol $t\mathrm{BuSi(OH)_3}$ and Re_2O_7 (C) 599
- Catalysis of the Addition of Allyltrimethylsilane to Aldehydes by Silylating Agents. $Me_3SiB(OTf)_4$, a New, 'Supersilylating' Reagent (C) 470
- Cationic Metallocene Polymerization Catalysts. Synthesis and Properties of the First Base-Free Zirconocene Hydride (C) 1375
- Dependence of the Reactivity of Ag and Ni Clusters Deposited on Solid Substrates on the Cluster Size (C) 1062
- High Molecular Weight Polypropylene through Specifically Designed Zirconocene Catalysts (C) 1347
- Metal–Surface Reaction Energetics. Theory and Applications to Heterogeneous Catalysis, Chemisorption, and Surface Diffusion (B) 1538
- Model Compounds for Metal Oxides on SiO_2 Surfaces (H) 586
- On the Influence of Heteroatoms in α- and β-Functionalized Alkyl Transition-Metal Compounds (R) 401
- Oxazaborolidines and Dioxaborolidines in Enantioselective Catalysis (H) 729
- Proof of the Catalytic Activity of a Naked Metal Cluster in the Gas Phase (C) 636
- Regioselectivity Control in the Palladium-Catalyzed Copolymerization of Propylene with Carbon Monoxide (C) 303
- Selective Oxidation of Methane to CO and H_2 over Ni/MgO at Low Temperatures (C) 1189
- Selectivity Control By Temperature Variation in the Formation of Isotactic vs. Syndiotactic Polypropylene with a Titanocene/Alumoxane Catalyst (C) 199
- Synthesis of Optically Active Macromolecules Using Metallocene Catalysts (H) 47
- 'Bis(oxazolines)' as Ligands for Self-Assembling Chiral Coordination Polymers—Structure of a Copper(I) Catalyst for the Enantioselective Cyclopropanation of Olefins (C) 430

Catenanes
- One-Step Synthesis of a Fourfold Functionalized Catenane (C) 1619

Ceramics
- The Thermal Conversion of Poly[(silylene)diacetylene] Metal Oxide Composites: A New Approach to β-SiC—MC Ceramics (C) 1195

Cesium effect
- Does the Naked Fluoride Ion Exist? (H) 292

C-H activation
- Palladium-Catalyzed C-H Activation of Methoxy Groups: A Facile Synthesis of Substituted 6*H*-Dibenzo[*b*,*d*]pyrans (C) 1023

Chalcogen compounds
- New Layered Iron-Lanthanum-Oxide-Sulfide and -Selenide Phases: $Fe_2La_2O_3E_2$ (E = S,Se) (C) 1645

Charge transfer complexes
- A Donor Cage with Two Tetrathiafulvene Units (C) 309
- Three-Dimensional Structure of an Unsymmetrical Proton–Electron Transfer System Containing a Disulfide Bond: The Bis(4-hydroxyphenyl)disulfide–Benzoquinone Complex (C) 852

Chelate ligands
- Chelate Complexes of Tripodal, Aliphatic Triisocyanide Ligands (C) 1212
- Chelate Stabilization of a Monomeric Lithium Tellurolate (C) 1260
- Transition Metal in a Cube—A Discrete Eight-Coordinate $[Mn^{2+} \subset [2.2.2]\text{cryptand}]$ as a Body-Centered Cube with an N_2O_6 Donor Set (C) 764

Chemiluminescence
- Chemiluminescence Oscillations Driven by a Flow-through Reactor in the $[Ru(bpy)_3]^{2+}$ Catalyzed Belousov–Zhabotinskii Reaction (C) 355

Chemistry of the atmosphere
- Transport and Fate of Organic Compounds in the Global Environment (R) 487

Chemometrics
- Chemometrics. Applications of Mathematics and Statistics to Laboratory Systems (B) 663

Chiral auxiliaries
- Asymmetric Ligands for Transition-Metal-Catalyzed Reactions: 2-Diphenylphosphinobenzoyl Derivatives of C_2-Symmetric Diols and Diamines (C) 228
- *trans*-2-*tert*-Butylcyclohexanol, a Simple Selectively Optimized Cyclohexanol Auxiliary (C) 1190
- Diacetoneglucose as Auxiliary Group for the Asymmetric Hetero-Diels–Alder Reaction with Nitrosoalkenes (C) 1033
- Diastereoselective Complexation of Temporarily Chirally Modified Ligands: Enantioselective Preparation and Configurational Assignment of Synthetically Valuable η^6-Tricarbonylchromium-1-tetralone Derivatives (C) 631
- Sugars as Chiral Auxiliaries for the Synthesis of Enantiomerically Pure Compounds (H) 288

Chirality
- A Diels–Alder Route to [5]- and [6]-Helicenes (C) 1093
- Chirality and Optical Activity in Organometallic Compounds (B) 1096
- Chirality—From Weak Bosons to the α-Helix (B) 800
- Enantioselective Polymerization of 1,2-Diisocyanoarenes—Synthesis of Optically Active, Helical Poly(quinoxaline-2,3-diyl)s (C) 1509
- On Quantifying Chirality (R) 989

- Solid-State Columns Made from Twisted, Self-Complementary Terpyridine Units (C) 1244

Chlorinated hydrocarbons
- Formation of a Toxic Dimerization Product of 3,4-Dichloroaniline by Lignin Peroxidase from *Phanerochaete chrysosporium* (C) 68
- The Beilstein Test: An Unintentional Dioxin Source in Analytical and Research Laboratories (C) 443

Chlorins
- Chlorins Designed for Photodynamic Tumor Therapy and as Model Systems for Photosynthesis (C) 1592

Chlorophins
- First Example of a Chlorophin from an Unexpected Oxidative Ring-Opening of an (Octadehydrocorrinato)nickel(II) Salt (C) 70

Choline derivatives
- 1-*O*-(2-Acetoxyhexadec-1-enyl)choline Iodide, a New Anticancer Agent (C) 64

Chromatography
- Handbook of Thin Layer Chromatography (B) 360

Chromium compounds
- A New Structure–Magnetism Relationship for Face-Sharing Transition-Metal Complexes with d^3–d^3 Electronic Configuration (C) 311
- $[Cp^*Cr(\mu_3\text{-}H)]_4$—a Paramagnetic Chromium Hydride with a Cubane Structure (C) 1077
- Diastereoselective Complexation of Temporarily Chirally Modified Ligands: Enantioselective Preparation and Configurational Assignment of Synthetically Valuable η^6-Tricarbonylchromium-1-tetralone Derivatives (C) 631
- Diastereoselective Synthesis of Substituted Cyclohexadienes from Enantiomerically Pure Tricarbonyl(2-phenyl-4,5-dihydrooxazole)chromium Complexes (C) 1071
- One-Pot Syntheses of Novel Arene Tricarbonyl Chromium Macrocycles and Macrobicycle: Structure of a Pentanuclear Trichromium(0)-Dicopper(I) Cryptate (C) 775
- Stepwise Stacking of Three Paramagnetic Metallocene Units: [CpNiCp-$(SiMe_2)_2$CpCrCp$(SiMe_2)_2$CpNiCp] (C) 1258

Circular dichroism
- Chirality and Optical Activity in Organometallic Compounds (B) 1096

Claisen rearrangements
- Activation Parameters and Stereochemistry of an Antibody-Catalyzed Claisen Rearrangement (C) 182
- New Thermo-Response Dyes: Coloration by the Claisen Rearrangement and Intramolecular Acid–Base Reaction (C) 204

Closest packings
- Are Denser Packings of Spheres than Closest Packings Possible? How Many Closest Packings of Spheres Exist? (H) 727

Clusters
- Dependence of the Reactivity of Ag and Ni Clusters Deposited on Solid Substrates on the Cluster Size (C) 1062
- Electron Deficient Boron and Carbon Clusters (B) 660
- Empty Octahedral Hexazirconium Clusters with Only Ten Electrons, $[Zr_6X_{14}(PR_3)_4]$ (C) 1050
- Idealized Pentagonal-Planar Coordination for Indium in $[(\mu_5\text{-}In)\{Mn(CO)_4\}_5]^{2-}$ (C) 350
- Molecular Machines: Molecular Structure of $[(p\text{-}Tol_3P)_{10}Au_{13}Ag_{12}Cl_8](PF_6)$—a Cluster with a Biicosahedral Rotorlike Metal Core and an Unusual Arrangement of Bridging Ligands (C) 445
- New Directions in Polyvanadate Chemistry: From Cages and Clusters to Baskets, Belts, Bowls, and Barrels (H) 49
- New Intermediate Steps in the Synthesis of Larger Nickel Clusters (C) 321
- $[Ni(PtBu)_6]$—a Strain on the 18 Electron Rule? (H) 424
- Novel Iron Carbonyl Telluride Clusters: Synthesis and Characterization of $[Fe_5Te_4(CO)_{14}]^{2-}$ and $[Fe_8Te_{10}(CO)_{20}]^{2-}$ (C) 913
- Oxoniobates Containing Metal Clusters (R) 1437
- $[(Ph_3PAu)_6Mn(CO)_3]^+$, a Cluster with Pentagonal-Bipyramidal Structure (C) 464
- Si_{60}, an Analogue of C_{60}? (H) 173
- Structure and Reactivity of Silicon Clusters in the Gas Phase (H) 172
- Synthesis and Structure of $[Ni(PtBu_6)]$ and $[Ni_5(PtBu)_6(CO)_5]$ and Calculations on the Electronic Structure of $[Ni(PtBu)_6]$ and $(PR)_6$, R = *t*Bu, Me (C) 323
- Synthesis and Structure of the Cluster $[NaAu_{12}Se_8]^{3-}$: An Inorganic Cryptand Complex (C) 787
- Synthesis, Structure, and Bonding of $[CpCoW_2(OCH_2tBu)_6]$, and Comments on the Combining Properties of CO and CpCo (C) 896
- Synthetic Models for Iron—Oxygen Aggregation and Biomineralization (H) 1010
- The Trapping of Iron Hydroxide Units by the Ligand "heidi": Two New Hydroxo(oxo)iron Clusters Containing 19 and 17 Iron Atoms (C) 191

Cobalt compounds
- 1-Borabutadiene(cyclopentadienyl)cobalt Complexes (C) 1603
- "[Cp*Co=CoCp*]" is a Hydride (C) 1341
- Cyclopentadienyl Cobalt Complexes of Cobaltapentalenes: Products Formed by Reaction of (μ-Cyclopentadienylidene) Cobalt Complexes with Silylalkynes (C) 1058
- Inhibition of the [2+2+2] Cyclization by the Formation of Chelates: Alkyne and Vinylidene Complexes with Cyclopentadienylcobalt(I) (C) 1066
- Mutual Catalysis of Neutral and Anionic Cobalt Carbonyls in their CO Scrambling Reactions (C) 1596
- Novel Metal Thiolates: $[Co_2(SC_3H_7)_5]^-$, the First Complex with Face-Sharing MS_4 Tetrahedra (C) 1368
- On the Reaction of Pentamethylcyclopentadiene with Cobalt Atoms: A Reexamination 1392
- The Electrochemical Oxidation of $[Co^{II}(salen)]$ in Solvent Mixtures—An Example of a Ladder Scheme with Coupled Electron-Transfer and Solvent-Exchange Reactions (C) 1215
- The Electronic Structure of $[(\eta^5\text{-}C_5H_5)_2Co_2]$: Comment on the Existence of a Complex with an Unsupported Co–Co Double Bond (C) 471
- The Reaction of Unactivated Cobalt Powder with Iodophosphoranes. The Synthesis of $[Co(PMe_3)_2I_3]$ and the Isolation of the "Frozen Transition-State" Complex $[(nBu_3PI)_2(\mu\text{-}I)][(nBu_3PI)(\mu\text{-}I)CoI_3]$ (C) 919

Complexes with carbon ligands
- A Paramagnetic, Mononuclear Organometallic Iridium(II) Complex: $[Ir(C_6Cl_5)_2(cod)]$ (C) 1527
- Mutual Catalysis of Neutral and Anionic Cobalt Carbonyls in their CO Scrambling Reactions (C) 1596
- On the Influence of Heteroatoms in α- and β-Functionalized Alkyl Transition-Metal Compounds (R) 401
- Tetraferrioazaallenium—Product of a Novel Reaction of Coordinated CN^- (C) 590

Complexes with hydrido ligands
- "[Cp*Co=CoCp*]" is a Hydride (C) 1341
- $[Cp^*Cr(\mu_3\text{-}H)]_4$—a Paramagnetic Chromium Hydride with a Cubane Structure (C) 1077
- Dynamic Motion in $[HFe(CO)_4]^-$ Ions as Observed by Mössbauer Spectroscopy—Evidence for Hydride "Tunneling" (C) 884
- New Routes to Alkylidyne-Bridged Ditungsten Compounds Supported by Alkoxide or Siloxide Ligands by the Activation of Ethylene (C) 462
- On the Mechanism of Coherent Dihydrogen Tunneling in Transition Metal Trihydrides (C) 1369
- On the Reaction of Pentamethylcyclopentadiene with Cobalt Atoms: A Reexamination 1392
- Transition Metal Hydrides (B) 1537

Complexes with nitrogen ligands
- Arborols Based on Luminescent and Redox-Active Transition Metal Complexes (C) 1493
- Crystal and Solution Structures of the Novel Complex of Sodium Ketimide with Two Ketimine Ligands $[(tBu_2C{=}NNa)_4(HN{=}CtBu_2)_2]$: Stacking of Complexed and Uncomplexed $(NNa)_2$ Rings to give a Highly Distorted $(NNa)_4$ Cubane (C) 93
- $[Et_4N]_2[\{MO(S_2)_2\}_2(\mu_2\text{-}S_7)(\mu_2\text{-}H_2NNH_2)]$ (M = Mo, W)—Doubly Bridged Complexes with S_7^{2-} and Doubly End-On-Bound H_2NNH_2 Bridging Ligands (C) 87
- Indirect $^{113}Cd,^{14}N$ Spin-Spin Coupling Constants as a Structural Probe of Solid Cadmium Thiocyanate Complexes (C) 1222
- Nitrido Complexes of Transition Metals (R) 955
- Pyridine-2-thiolato Complexes of V^{II}, V^{III}, and V^{IV} with Unusual Structural Features (C) 1253
- Self-Assembly of a Cu_4 Complex with Coplanar Copper(I) Ions: Synthesis, Structure, and Electrochemical Properties (C) 733
- Synthesis and Structure of a Mononuclear η^2-Hydrazine Complex by Protonation of an $[N_2H_2]^{2-}$ Complex (C) 1081
- The First Reaction of S_5N_6; Structure of a Complex Containing an $S_2N_3^-$ Ligand (C) 616
- The Synthesis and Structure of an Unusual Uranium Pentachloride Derivative (C) 72
- Trigonal-Monopyramidal M^{III} Complexes of the Type $[M(N_3N)]$ (M = Ti, V, Cr, Mn, Fe; $N_3N = [(tBuMe_2Si)\ddot{N}CH_2CH_2]_3N$) (C) 1501
- $[\ddot{V}(SNC_9H_6)_3]$ and $[V(SNH_2C_6H_4)_2(SNHC_6H_4)]^-$, Homoleptic Vanadium(III) Complexes with Sulfur–Nitrogen Donor Ligands, and $[V(SNC_5H_4)_3]^-$, the First Thiolatovanadium(II) Complex (C) 1366

Complexes with oxygen ligands
- A Dramatic Difference in the Reactivities of Alkoxido- and Aryloxidorhenium Complexes in Insertion Reactions (C) 220
- A New Type of Mn–O Cluster with a Mn_4 Chain Unit. Relevance to the Photosynthetic Oxygen Evolving Center (C) 1629
- A Phenoxy-Bridged Homodinuclear Zn Complex with an Unusual Coordination Sphere; Model Compound for the Active Site of Phospholipase C (C) 1647
- Alkoxyalkyl-Substituted β-Diketonate Complexes of Barium and Copper: Evidence for Inter- and Intramolecular Stabilization (C) 735
- Bismuth Alkoxide Dimer Complexes Containing Planar $Bi_2(\mu\text{-}OR)_2$ Cores: Syntheses and Structures of $[\{Bi[OCH(CF_3)_2]_3(thf)\}_2]$ and $[\{Bi(OC_6F_5)_3(C_7H_8)\}_2] \cdot 2C_7H_8$ (C) 451
- Catecholates as σ- and π-Donating Ligands: The Synthesis and Structure of $(Et_4N)_2[W(CO)_4(O_2C_6H_4)]$ and the "Sixteen Electron" Analogue Resulting from CO Dissociation (C) 1503
- Distortional Isomerism in Oxomolybdenum Systems; the Evidence Re-evaluated (C) 1607
- New Routes to Alkylidyne-Bridged Ditungsten Compounds Supported by Alkoxide or Siloxide Ligands by the Activation of Ethylene (C) 462
- Tris(cyclopentanolato)oxovanadium(v): a Model for the Transition State of Enzymatic Phosphoester Cleavage (C) 447

Complexes with phosphorus ligands
- Synthesis and Structure of $[Ni(PtBu_6)]$ and $[Ni_5(PtBu)_6(CO)_5]$ and Calculations on the Electronic Structure of $[Ni(PtBu)_6]$ and $(PR)_6$, R = tBu, Me (C) 323
- The Formation of *cyclo*-P_4 Ligands with Maximum Electron Donor Ability (C) 1377
- The Reaction of Unactivated Cobalt Powder with Iodophosphoranes. The Synthesis of $[Co(PMe_3)_2I_3]$ and the Isolation of the "Frozen Transition-State" Complex $[(nBu_3PI)_2(\mu\text{-}I)][(nBu_3PI)(\mu\text{-}I)CoI_3]$ (C) 919

Complexes with silicon ligands
- The First Metal–Metal Silyl Migration in a Heterobimetallic Complex, and the Structure of the Rearrangement Product $[(OC)_4Fe(\mu\text{-}PPh_2)Pt\{Si(OMe)_3\}(PPh_3)]$ (*Fe–Pt*) (C) 1583

Complexes with sulfur ligands
- $[Et_4N]_2[\{MO(S_2)_2\}_2(\mu_2\text{-}S_7)(\mu_2\text{-}H_2NNH_2)]$ (M = Mo, W)—Doubly Bridged Complexes with S_7^{2-} and Doubly End-On-Bound H_2NNH_2 Bridging Ligands (C) 87
- Indirect $^{113}Cd,^{14}N$ Spin-Spin Coupling Constants as a Structural Probe of Solid Cadmium Thiocyanate Complexes (C) 1222
- Molecular Mechanisms of the Reduction of NO to NH_2OH at Mo–S Centers (C) 205
- $[Ni_4(SC_3H_7)_8Br]$ and $[Ni_4(SC_3H_7)_8I]$: Mixed Valent Nickel Thiolates with Integral and Nonintegral Metal Oxidation States (C) 54
- Novel Metal Thiolates: $[Co_2(SC_3H_7)_5]^-$, the First Complex with Face-Sharing MS_4 Tetrahedra (C) 1368
- Pyridine-2-thiolato Complexes of V^{II}, V^{III}, and V^{IV} with Unusual Structural Features (C) 1253
- Stable Intermediates in the Addition and Elimination of $SnBuCl_3$ at Molybdenum Centers by Cleavage or Formation of an Sn–Cl Bond: Crystal Structure of $[Mo(CO)_2(PCy_3)(\mu\text{-}Cl)(\mu\text{-}S_2CPCy_3)(BuSnCl_2)] \cdot CH_2Cl_2$ (C) 76
- Synthesis of Cubane-like and Double Cubane-like Tungsten–Copper–Sulfur Clusters from the "Butterfly" Cluster $[Cu_2S_3W(O)(PPh_3)_3]$ (C) 1085
- The Reaction of $[Cp^+_2Nb_2(B_2H_6)_2]$ ($Cp^+ = \eta\text{-}EtMe_4C_5$) with Sulfur: Stabilization of the Tetrathioborato Ligand in Novel Sulfido Niobium Clusters (C) 1021
- $[V(SNC_9H_6)_3]$ and $[V(SNH_2C_6H_4)_2(SNHC_6H_4)]^-$, Homoleptic Vanadium(III) Complexes with Sulfur–Nitrogen Donor Ligands, and $[V(SNC_5H_4)_3]^-$, the First Thiolatovanadium(II) Complex (C) 1366

Concave reagents
- Concave Wrapped Protons: Reagents for Contra-Thermodynamic Protonations (C) 80

Conformation
- A Binary Quinone Receptor (C) 792
- Calculation of Molecular Dynamics for Peptides in Dimethyl Sulfoxide: Elimination of Vacuum Effects (C) 210
- Dynamic Forcing, a Method for Evaluating Activity and Selectivity Profiles of RGD (Arg-Gly-Asp) Peptides (C) 326
- Flexible Molecules with Defined Shape—Conformational Design (R) 1124 (1657)
- Molecular Modeling of the Class I Human Histocompatibility Molecule HLA-A2 Presenting an Allele-Specific Nonapeptide from Influenza Matrix Protein (C) 886
- Pronounced Conformational Changes in Sixfold Nitrogen-Functionalized Metacyclophanes: Syntheses and Crystal Structures of Two 1,10-Diaza[11]metacyclophanes (C) 882
- Stereochemistry of Organic Compounds. Principles and Applications (B) 1539

Conjugation
- Novel Cross-Conjugated Compounds Derived from Tetraethynylethene (C) 1240
- *meta*-Phenylene Units as Conjugation Barriers in Phenylenevinylene Chains (C) 1653
- The First Hexabutadiynylbenzenes: Synthesis and Structures (C) 1643

Coordination
- Alkoxyalkyl-Substituted β-Diketonate Complexes of Barium and Copper: Evidence for Inter- and Intramolecular Stabilization (C) 735
- Biocoordination Chemistry: Coordination Equilibria in Biologically Active Systems (B) 803
- Bis(*P,P*-di-*tert*-butylphosphinic-*N*-isopropylamidato-*N,O*)nickel(II), a Paramagnetic Planar Complex (C) 612
- Chelate Complexes of Tripodal, Aliphatic Triisocyanide Ligands (C) 1212
- Idealized Pentagonal-Planar Coordination for Indium in $[(\mu_5\text{-}In)\{Mn(CO)_4\}_5]^{2-}$ (C) 350
- Indirect $^{113}Cd,^{14}N$ Spin-Spin Coupling Constants as a Structural Probe of Solid Cadmium Thiocyanate Complexes (C) 1222
- $[Ni(PtBu)_6]$—a Strain on the 18 Electron Rule? (H) 424
- Novel Metal Thiolates: $[Co_2(SC_3H_7)_5]^-$, the First Complex with Face-Sharing MS_4 Tetrahedra (C) 1368
- Phosphorus(v) Selenides with Phosphorus in a Trigonal-Planar Environment (C) 1350
- Synthesis and Structure of $Al(OAr^*)_3$ ($Ar^* = 2,6\text{-}tBu_2\text{-}4\text{-}MeC_6H_2$): The First Three-Coordinate Homoleptic Aluminum Aryloxide (C) 921
- Synthesis and Structure of $[Ni(PtBu_6)]$ and $[Ni_5(PtBu)_6(CO)_5]$ and Calculations on the Electronic Structure of $[Ni(PtBu)_6]$ and $(PR)_6$, R = tBu, Me (C) 323
- Template-Controlled Organization of a Fluoride Surface—An Analogue of a Crown Ether in the Reaction of $[\{(\eta^5\text{-}C_5Me_5)TiF_3\}_2]$ with Sodium Fluoride (C) 864
- Tetrakis(η^1-phosphabenzene)nickel (C) 1343
- The First Metal–Metal Silyl Migration in a Heterobimetallic Complex, and the Structure of the Rearrangement Product $[(OC)_4Fe(\mu\text{-}PPh_2)Pt\{Si(OMe)_3\}(PPh_3)]$ (*Fe–Pt*) (C) 1583
- The Pentagonal Bipyramid as Fundamental Structure for Compounds with the Coordination Number Seven* (C) 1036
- The Structure of Pentamethyltantalum (C) 1462
- The Structures of Pentamethyltantalum and -Antimony: One Square Pyramid and One Trigonal Bipyramid (C) 1464
- Trigonal-Monopyramidal M^{III} Complexes of the Type $[M(N_3N)]$ (M = Ti, V, Cr, Mn, Fe; $N_3N = [(tBuMe_2Si)\dot{N}CH_2CH_2]_3N$) (C) 1501
- Triphosphatrisilacyclohexanes as Tridentate Coronands in Cr and Mo Complexes: Activation of Si–H in an Early Stage versus Phosphane Coordination (C) 1510
- Unusual Coordination of the 1,3-Diphosphacyclobutadiene Derivative $(iPr_2NCP)_2$ to Two $[Ni(CO)_3]$ Fragments (C) 95

Copper compounds
- One-Dimensional $M^{III}Cu^{II}$ Compounds with an Unprecedented, Tubelike Structural Motif (M = Rare-Earth Metal) (C) 626
- Self-Assembly of a Cu_4 Complex with Coplanar Copper(I) Ions: Synthesis, Structure, and Electrochemical Properties (C) 733
- Stereoselective Nucleophilic Addition Reactions of Reactive Pseudopeptides (C) 1626
- 'Bis(oxazolines)' as Ligands for Self-Assembling Chiral Coordination Polymers—Structure of a Copper(I) Catalyst for the Enantioselective Cyclopropanation of Olefins (C) 430

Corannulene
- Corannulene Tetraanion: A Novel Species with Concentric Anionic Rings (C) 1636

Corrigenda 1540, 1657
- On the Reaction of Pentamethylcyclopentadiene with Cobalt Atoms: A Reexamination 1392

Corynanthe alkaloids
- A Short Diastereoselective Entry to Indole Alkaloids of the Corynanthe Type by the Intramolecular Ene Reaction (C) 1079

Criss-cross reaction
- An Organometallic Analogue of the "Criss-Cross" Cycloaddition Reaction (C) 1053

Crown ethers
- C_{60} and C_{70} in a Basket?—Investigations of Mono- and Multilayers from Azacrown Compounds and Fullerenes (C) 1599
- $[SbCl([15]Crown-5)](SbCl_6)_2$ and $[BiCl([18]Crown-6)(CH_3CN)_2](SbCl_6)_2$: Salts with Antimony(III) and Bismuth(III) Dications (C) 334

Cryptands
- One-Pot Syntheses of Novel Arene Tricarbonyl Chromium Macrocycles and Macrobicycle: Structure of a Pentanuclear Trichromium(0)-Dicopper(I) Cryptate (C) 775
- Transition Metal in a Cube—A Discrete Eight-Coordinate $[Mn^{2+} \subset [2.2.2]cryptand]$ as a Body-Centered Cube with an N_2O_6 Donor Set (C) 764

Crystal growth
- Control and Design Principles in Biological Mineralization (R) 153

Crystallization
- The Science of Crystallization. Microscopic Interfacial Phenomena (B) 1536

Crystallography
- Optically Anomalous Crystals (R) 1
- Two-Dimensional Crystallography of Amphiphilic Molecules at the Air–Water Interface (R) 130

Cubanes
- A New, High-Yield Synthesis of Tetraphosphacubanes (C) 758
- $[Cp^*Cr(\mu_3\text{-}H)]_4$—a Paramagnetic Chromium Hydride with a Cubane Structure (C) 1077
- Cubanes: Starting Materials for the Chemistry of the 1990s and the New Century (R) 1421
- Octakis(1,1,2-trimethylpropyl)octasilacubane: Synthesis, Molecular Structure, and Unusual Properties (C) 1354
- P-Functionalization of the Tetraphosphacubane System (C) 879
- Synthesis of Cubane-like and Double Cubane-like Tungsten–Copper–Sulfur Clusters from the "Butterfly" Cluster $[Cu_2S_3W(O)(PPh_3)_3]$ (C) 1085
- The $[(\mu_3\text{-}WSe_4)_3(\mu_3\text{-}Se)_2(Cu_3)_2]^{4-}$ Anion, an Inorganic Cluster with a Pinwheel Shape (C) 1477

Cumulenes
- Butatrienes by Desulfurization of Cyclic Trithiocarbonates (C) 1611

Cyanamide
- Biochemical Degradation of Cyanamide and Dicyandiamide (C) 620

Cyclic voltammetry
- Electrochemical Oxidation of 1-(*p*-Dimethylaminophenyl)-3,3-dimethyltriazene—Cyclic Voltammetric Detection of a Triazene Radical Cation and Dication (C) 332

Cyclizations
- Cascade Cyclizations (H) 1332
- Efficient Synthesis of Nanoscale Macrocyclic Hydrocarbons (C) 922
- Inhibition of the [2+2+2] Cyclization by the Formation of Chelates: Alkyne and Vinylidene Complexes with Cyclopentadienylcobalt(I) (C) 1066
- Stereocontrolled Construction of $6 \cdot 5 \cdot 6$ and $5 \cdot 5 \cdot 6$ Ring Systems by Radical Tandem Cyclization (C) 910

Cycloadditions
- A New Reaction Type in the Conversion of Enamines with 1,4-Diphenyl-2-butene-1,4-dione to Give Cage Compounds (C) 768
- A New Synthesis for Imidazolo- and Pyrrolophanes by [3 + 2] Cycloaddition with Azaallenyl Radical Cations (C) 209
- An Organometallic Analogue of the "Criss-Cross" Cycloaddition Reaction (C) 1053
- Cycloaddition Reactions in Organic Synthesis (B) 240
- Enantioselective Syntheses of Cyclopentanoid Compounds from Isoprene and *trans*-1,3-Pentadiene (C) 305
- The Benzene Ring as Dienophile in an Intramolecular [4+2] Cycloaddition: Degenerate Rearrangement of 7,8-Benzobicyclo[4.2.2]deca-2,4,7,9-tetraene (C) 872
- Transition Structures of Hydrocarbon Pericyclic Reactions (R) 682
- Two Stereoisomeric [4.5.5.5]Fenestranes Formed by Intramolecular [2+2] Cycloaddition (C) 344
- [4 + 4]-Cycloaddition Reactions in the Total Synthesis of Naturally Occurring Eight-Membered Ring Compounds (H) 422

Cycloalkadiynes
- Cycloalkadiynes—From Bent Triple Bonds to Strained Cage Compounds (R) 27

Cycloalkynols
- Anti-Bredt Enol Ethers by Transannular Cyclization of Cycloalkynols (C) 791

Cyclobutadienes
- How High is the Barrier for the Valence Isomerization of Cyclobutadiene? (C) 738

Cyclobutanes
- Quest for Higher Ladderanes: Oligomerization of a Cyclobutadiene Derivative (C) 1488

Cyclobutarenes
- Cyclobutarenes. The Chemistry of Benzocyclobutene, Biphenylene, and Related Compounds (B) 1264

Cyclodextrins
- Cyclodextrin Derivatives as Chiral Selectors—Investigation of the Interaction with (*R,S*)-Methyl-2-chloropropionate by Enantioselective Gas Chromatography, NMR Spectroscopy, and Molecular Dynamics Simulation (C) 319
- Cyclodextrins, Off-the-Shelf Components for the Construction of Mechanically Interlocked Molecular Systems (H) 846
- Selective Binding of Sugar to β-Cyclodextrin: A Prototype for Sugar–Sugar Interactions in Water (C) 745
- Synthesis and Complexation Properties of a Cyclodextrin-Derived Siderophore Analogue (C) 1381
- Synthesis of a Lipophilic Cyclodextrin-[2]-Rotaxane (C) 783
- Threading Cyclodextrin Rings on Polymer Chains (C) 197

Cyclohexadienes
- Diastereoselective Synthesis of Substituted Cyclohexadienes from Enantiomerically Pure Tricarbonyl(2-phenyl-4,5-dihydrooxazole)chromium Complexes (C) 1071

Cyclohexanones
- Effect of Torsional Strain and Electrostatic Interactions on the Stereochemistry of Nucleophilic Additions to Cyclohexanone and Related Systems (C) 1019

Cyclohexatrienes
- 1,2,4-Cyclohexatriene, an Isobenzene, and Bicyclo[4.4.0]deca-1,3,5,7,8-pentaene, an Isonaphthalene: Generation and Trapping Reactions (C) 473
- 1,2,4-Cyclohexatriene, an Isobenzene, and its [2+2] Cycloaddition with Styrene: A Theoretical Study (C) 476

Cyclopentanes
- Enantioselective Syntheses of Cyclopentanoid Compounds from Isoprene and *trans*-1,3-Pentadiene (C) 305

Cyclophanes
- A Donor Cage with Two Tetrathiafulvene Units (C) 309
- A New Synthesis for Imidazolo- and Pyrrolophanes by [3 + 2] Cycloaddition with Azaallenyl Radical Cations (C) 209
- Pronounced Conformational Changes in Sixfold Nitrogen-Functionalized Metacyclophanes: Syntheses and Crystal Structures of Two 1,10-Diaza[11]metacyclophanes (C) 882
- Selective Ketone Pyrolysis: New Synthetic Method for Mono- and Polycyclic Hydrocarbons (C) 307
- Strain-Activated Formation of a Triple-Layered Phane (C) 1073

Cyclopropanation
- 'Bis(oxazolines)' as Ligands for Self-Assembling Chiral Coordination Polymers—Structure of a Copper(I) Catalyst for the Enantioselective Cyclopropanation of Olefins (C) 430

α-Cyclopropyl esters
- Nucleophilic Attack at the Central Carbon Atom of (π-Allyl)palladium Complexes: Formation of α-Cyclopropyl Esters (C) 234

Cytochromes
- Cytochromes C. Evolutionary, Structural and Physicochemical Aspects (B) 1098

D-amino acids
- Proteins from the D-Chiral World (H) 1457

Dendrimers
- Arborols Based on Luminescent and Redox-Active Transition Metal Complexes (C) 1493
- Dendrimers, Arborols, and Cascade Molecules: Breakthrough into Generations of New Materials (H) 1571
- Novel Polyether Copolymers Consisting of Linear and Dendritic Blocks (C) 1200
- One-Pot Multifunctionalization of Polymethyl Hydrocarbon π Ligands. Maximum Space Occupancy by Double Branching and Formation of Arboroles (C) 458
- Supramolecular Self-Assemblies of Two-Directional Cascade Molecules: Automorphogenesis (C) 917

Deprotonations
- Asymmetric Deprotonation as an Efficient Enantioselective Preparation of Functionalized Secondary Alcohols (H) 1459
- Stereoselective Generation of 1-Acyloxy-2-amino Carbanions by Deprotonation; Synthesis of Enantiomerically and Diastereomerically Pure β-Amino Alcohols (C) 1505

Desulfurations
- Butatrienes by Desulfurization of Cyclic Trithiocarbonates (C) 1611

Deterministic chaos
- Chaotic Evolution and Strange Attractors (B) 798

Dewar benzenes
- Doubly Bridged Prismane and Dewar Benzene Intermediates in an Unusual Photochemical Rearrangement of Tricyclic Phthalic Esters (C) 862
- Spirocyclization of a Stable Phosphaalkyne with Aluminum Trichloride—Key Reaction for the Production of Triphospha Dewar Benzene Derivatives (C) 1055

Diamond structures
- Electron Localization in Solid-State Structures of the Elements: the Diamond Structure (C) 187
Diazonium ions
- Origin of the Stabilization of Vinyldiazonium Ions by β-Substitution; First Crystal Structure of an Aliphatic Diazonium Ion: β,β-Diethoxyethenediazonium Hexachloroantimonate (C) 740
Dibenzopyrans
- Palladium-Catalyzed C-H Activation of Methoxy Groups: A Facile Synthesis of Substituted 6*H*-Dibenzo[*b*,*d*]pyrans (C) 1023
Dictionary
- Dictionary of Plants Containing Secondary Metabolites (B) 1396
Diels–Alder reactions
- A Diels–Alder Route to [5]- and [6]-Helicenes (C) 1093
- Diacetoneglucose as Auxiliary Group for the Asymmetric Hetero-Diels–Alder Reaction with Nitrosoalkenes (C) 1033
- Dienes in the Diels-Alder Reaction (B) 364
Diisocyanogen
- Matrix Isolation of Diisocyanogen CN-NC (C) 1218
Diketones
- A New Reaction Type in the Conversion of Enamines with 1,4-Diphenyl-2-butene-1,4-dione to Give Cage Compounds (C) 768
Dioxinones
- Synthesis of (*R*)- and (*S*)-2-*tert*-Butyl-6-trifluoromethyl-1,3-dioxin-4-ones, Transformations into 3-Hydroxy-3-(trifluoromethyl)alkanoates, and Surprising Differences in the Reactivity of CH_3- and CF_3-Substituted Compounds (C) 1083
Dioxins
- The Beilstein Test: An Unintentional Dioxin Source in Analytical and Research Laboratories (C) 443
Diphosphacyclobutadienes
- Unusual Coordination of the 1,3-Diphosphacyclobutadiene Derivative $(i\mathrm{Pr_2NCP})_2$ to Two $[Ni(CO)_3]$ Fragments (C) 95
Distorted molecules
- Distorted Molecules: Perturbation Design, Preparation and Structures (R) 550
Diynes
- Cycloalkadiynes—From Bent Triple Bonds to Strained Cage Compounds (R) 27
- Stereocontrolled Construction of 6 · 5 · 6 and 5 · 5 · 6 Ring Systems by Radical Tandem Cyclization (C) 910
DNA
- A Milestone in Genome Sequencing: The Complete DNA Sequence of the Yeast Chromosome III (H) 1578
- DNA Recognition by Hybrid Oligoether–Oligodeoxynucleotide Macrocycles (C) 1617
- Interactions Between Acyclic and Cyclic Peralkylammonium Compounds and DNA (C) 1207
DNA cleavage
- $[RuO(dppz)(tpy)]^{2+}$: a DNA Cleavage Agent with High DNA Affinity (C) 1048
Doppler spectroscopy
- Reaction Dynamics of Aligned Molecules (R) 516
Doppler-free spectroscopy
- High Resolution Spectroscopy below the Doppler Width (R) 263
Dyes
- New Thermo-Response Dyes: Coloration by the Claisen Rearrangement and Intramolecular Acid–Base Reaction (C) 204
- Photoswitchable Association of an Azobenzene-Bipyridinium Diad to Eosin: Photostimulated "On-Off" Guest Binding (C) 1243

Ecology
- Metals and Their Compounds in the Environment: Occurrence, Analysis and Biological Relevance (B) 102
- Sulfur Analogues of Polycyclic Aromatic Hydrocarbons (Thiaarenes). Environmental Occurrence, Chemical and Biological Properties (B) 364
- The Beilstein Test: An Unintentional Dioxin Source in Analytical and Research Laboratories (C) 443
- Transport and Fate of Organic Compounds in the Global Environment (R) 487
Edshammar polyhedra
- Generalized Edshammar Polyhedra for the Description of a Family of Solid-State Structures (C) 924
Eicosanoids
- Pheromones of Marine Brown Algae; A New Branch of the Eicosanoid Metabolism (C) 1246
Electrochemistry
- Molecular Switching by Electron Transfer—the Spiroperimidine/Quinonimine System (C) 1498
- Organic Electrochemistry. An Introduction and a Guide (B) 656
- The Electrochemical Oxidation of $[Co^{II}(salen)]$ in Solvent Mixtures—An Example of a Ladder Scheme with Coupled Electron-Transfer and Solvent-Exchange Reactions (C) 1215
Electron localization
- Electron Localization in Solid-State Structures of the Elements: the Diamond Structure (C) 187
- On the Bonding in Carbosilanes (C) 185
Electron microscopy
- Microscopy (B) 1534
Electron transfer
- A Homologous Series of Stable Polyenes: Synthesis, Structure, and Redox Behavior (C) 1588
- $[(CO)_3(PPh_3)_2OsAg(O_2CCF_3)]$: A Model for an Intermediate on the Reaction Coordinate in Electron Transfer (C) 770
- Molecular Switching by Electron Transfer—the Spiroperimidine/Quinonimine System (C) 1498
- Three-Dimensional Structure of an Unsymmetrical Proton–Electron Transfer System Containing a Disulfide Bond: The Bis(4-hydroxyphenyl)disulfide–Benzoquinone Complex (C) 852
Electronic structure
- A New Structure–Magnetism Relationship for Face-Sharing Transition-Metal Complexes with d^3–d^3 Electronic Configuration (C) 311
- A Paramagnetic, Mononuclear Organometallic Iridium(II) Complex: $[Ir(C_6Cl_5)_2(cod)]$ (C) 1527
- Empty Octahedral Hexazirconium Clusters with Only Ten Electrons, $[Zr_6X_{14}(PR_3)_4]$ (C) 1050
- $[Ni(P\mathrm{t}Bu)_6]$—a Strain on the 18 Electron Rule? (H) 424
- Oligo(9,10-anthrylenes), Organic Compounds with Stable High-Spin States (C) 448
- Synthesis and Structure of $[Ni(P\mathrm{t}Bu_6)]$ and $[Ni_5(P\mathrm{t}Bu)_6(CO)_5]$ and Calculations on the Electronic Structure of $[Ni(P\mathrm{t}Bu)_6]$ and $(PR)_6$, R = *t*Bu, Me (C) 323
Enamines
- A New Reaction Type in the Conversion of Enamines with 1,4-Diphenyl-2-butene-1,4-dione to Give Cage Compounds (C) 768
Enantiomeric resolution
- Salting Out Selective Extraction—A Novel Method for the Optical Resolution of Chiral Sulfinylcarboxylic Acids and Its Application for the Convenient Determination of Optical Purity (C) 1631
Ene reactions
- A Short Diastereoselective Entry to Indole Alkaloids of the Corynanthe Type by the Intramolecular Ene Reaction (C) 1079
Enediynes
- Synthesis of the Calicheamicin Aryltetrasaccharide Domain Bearing a Reducing Terminus: Coupling of Fully Synthetic Aglycone and Carbohydrate Domains by the Schmidt Reaction (C) 338
- Ten-Membered Ring Enediynes with Remarkable Chemical and Biological Profiles (C) 1044
- Total Synthesis of Calicheamicin–Dynemicin Hybrid Molecules (C) 340
- Total Synthesis of the Carbohydrate Fragments of Esperamicin A_1 (C) 855
Enol ethers
- Anti-Bredt Enol Ethers by Transannular Cyclization of Cycloalkynols (C) 791
- Semiconductor-Catalyzed Photoaddition of Cyclic Enol Ethers to 1,2-Diazenes (C) 1039
Enols
- The Chemistry of Enols (B) 105
Enterobactin
- The First Structural Characterization of a Metal–Enterobactin Complex: $[V(enterobactin)]^{2-}$ (C) 466
Enzymatic catalysis
- "Artificial Metabolisms" for the Asymmetric One-Pot Synthesis of Branched-Chain Saccharides (C) 614
- Chain Elongation of Thiodipeptides with Proteases (C) 1229
- Chemoenzymatic Syntheses of the Optically Active Hydroperoxides of Phosphatidylglycerol and Phosphatidylethanolamine with Lipase, Lipoxygenase, and Phospholipase D (C) 1336
- Enzymatic Oxidation of Methyl Groups on Aromatic Heterocycles: A Versatile Method for the Preparation of Heteroaromatic Carboxylic Acids (C) 774
- Enzymatic Preparation of Enantiomerically Pure *N*-alkyl Amino Acids (C) 195
- Radical Intermediates in the Coenzyme B_{12} Dependent Methylmalonyl-CoA Mutase Reaction Shown by ESR Spectroscopy (C) 215
Enzyme models
- A Rh^I-Centered Cage Compound with Selective Catalytic Properties (C) 905
Enzymes
- Multifield Saturation Magnetization Measurements of Oxidized and Reduced Ribonucleotide Reductase from *Escherichia coli* (C) 1513
- Proteins from the D-Chiral World (H) 1457
- Selective Inhibition of Trypanosomal Triosephosphate Isomerase by a Thiopeptide (C) 328
Epoxides
- *meso* Epoxides in Asymmetric Synthesis: Enantioselective Opening by Nucleophiles in the Presence of Chiral Lewis Acids (H) 1179

Esperamicins
- Total Synthesis of the Carbohydrate Fragments of Esperamicin A_1 (C) 855
ESR spectroscopy
- Electrochemical Oxidation of 1-(*p*-Dimethylaminophenyl)-3,3-dimethyltriazene—Cyclic Voltammetric Detection of a Triazene Radical Cation and Dication (C) 332
- Modern Pulsed and Continuous-Wave Electron Spin Resonance (B) 243
- Radical Intermediates in the Coenzyme B_{12} Dependent Methylmalonyl-CoA Mutase Reaction Shown by ESR Spectroscopy (C) 215
- Stable *N,N'*-Di-*tert*-butyl-*meta*-phenylenebisnitroxides—Unexpected Ground-State Singlets (C) 180
Estradiol
- Estradiols Modified by Metal Carbonyl Clusters as Suicide Substrates for the Study of Receptor Proteins: Application to the Estradiol Receptor (C) 753
Evolution
- Chemical Evolution. Origin of the Elements, Molecules and Living Systems (B) 1533

Felkin-Anh model
- Effect of Torsional Strain and Electrostatic Interactions on the Stereochemistry of Nucleophilic Additions to Cyclohexanone and Related Systems (C) 1019
Fenestranes
- Two Stereoisomeric [4.5.5.5]Fenestranes Formed by Intramolecular [2+2] Cycloaddition (C) 344
Field-effect transistors
- Field-Effect Transistors as Sensors of Neural Systems (H) 45
Fischer, Emil
- Emil Fischer's Proof of the Configuration of Sugars: A Centennial Tribute (R) 1541
Fluorescence
- Dual Fluorescence of Novel Modified Carotenoids (C) 1042
Fluorides
- A Safe Synthesis of Diphosphazenium Salts (C) 850
- Template-Controlled Organization of a Fluoride Surface—An Analogue of a Crown Ether in the Reaction of $[\{(\eta^5\text{-}C_5Me_5)TiF_3\}_2]$ with Sodium Fluoride (C) 864
- The Pentagonal Bipyramid as Fundamental Structure for Compounds with the Coordination Number Seven* (C) 1036
Fluorine compounds
- Catalytic Oxidation of Partially and Fully Fluorinated Olefins with Osmium Tetroxide (C) 1345
- Does the Naked Fluoride Ion Exist? (H) 292
- Perfluorotriethylamine: An Amine with Unusual Structure and Reactivity (C) 1467
- Structure of the Lowest Temperature Phase of the Solid Benzene–Hexafluorobenzene Adduct (C) 1655
- The Structure and Stability Trends of Fluoro(methyl)plumbanes (C) 1224
Fractals
- Elementary Introduction to Spatial and Temporal Fractals (B) 659
Friedel–Crafts reactions
- Cyclohexadienyl-Type Cationic Intermediates in the Friedel–Crafts Alkylation of Benzene Derivatives with the 9-Fluorenyl Cation—Observation by Laser Flash Photolysis (C) 743
- Rate Constants for the Attack of Carbenium Ions at Arenes—A Link between the Chemistry of Aliphatic and Aromatic π Systems (C) 1613
Fruit ripening
- Inhibition of Fruit Ripening by Antisense-RNA Technology (H) 175
Fullerenes
- A New Fullerene Synthesis (C) 223
- C_{60} and C_{70} in a Basket?—Investigations of Mono- and Multilayers from Azacrown Compounds and Fullerenes (C) 1599
- C_{60}: Buckminsterfullerene, The Celestial Sphere that Fell to Earth (R) 111
- C_{60}-Fullerene—A Playground for Chemical Manipulations on Curved Surfaces and in Cavities (H) 293
- Fullerene Sugars: Preparation of Enantiomerically Pure, Spiro-Linked C-Glycosides of C_{60} (C) 1388
- Material Properties and Purity of C_{60} (C) 868
- Optimization of the Production and Separation of Fullerenes (C) 1640
- Preparative-Scale Separation of C_{60} and C_{70} on Polystyrene Gel (C) 644
- Product Predictions for Nucleophilic Additions to C_{70} (C) 1468
- Reaction of C_{60} with Dimethyldioxirane—Formation of an Epoxide and a 1,3-Dioxolane Derivative (C) 351
- Sequential Insertion of ^3He and ^4He in C_{60}^+ (C) 605
- Si_{60}, an Analogue of C_{60}? (H) 173
- Structure of a Product of Double Addition to C_{70}: $[C_{70}\{Ir(CO)Cl(PPhMe_2)_2\}_2] \cdot 3C_6H_6$ (C) 1356
- Synthetic Approaches toward Molecular and Polymeric Carbon Allotropes (R) 1101
- The Epidemic Spread of Fullerene Research (C) 588 (1540)
- The Neutralization of HeC_{60}^+ in the Gas Phase: Compelling Evidence for the Existence of an Endohedral Structure for $He@C_{60}$ (C) 183
- The Stability of Buckminsterfullerene (C_{60}): Experimental Determination of the Heat of Formation (C) 63
- The Structure of C_{60}: Orientational Disorder in the Low-Temperature Modification of C_{60} (C) 640
- Titration of C_{60}: A Method for the Synthesis of Organofullerenes (C) 766
Fulvalenes
- A Donor Cage with Two Tetrathiafulvene Units (C) 309
- Double Open-Edged P_{10} Dihydrofulvalene as a 16-Electron Donor Ligand (C) 1027
- Tetraphosphafulvalene Dianions: Isoelectronic Species of Tetrathiafulvalene Dications (C) 1031

$GABA_A$ receptor
- Synthesis of (2-Arylindol-3-yl)acetamides as Probes of Mitochondrial Steroidogenesis—A New Mechanism for $GABA_A$ Receptor Modulation (C) 1060
Gadolinium compounds
- Synthesis and Structure of the First Trinuclear, Half-Sandwich Carboranegadolinium(III) Cluster (C) 432
GALLEX
- The Chemistry of GALLEX—Measurement of Solar Neutrinos with a Radiochemical Gallium Detector (R) 1283
Gallium compounds
- $[Ga(C_5H_5)]$: Synthesis, Identification, and Ab Initio Investigations (C) 1362
- $[Ga_4\{C(SiMe_3)_3\}_4]$ with a Tetrahedral Ga_4 Skeleton (C) 1364
- The Chemistry of GALLEX—Measurement of Solar Neutrinos with a Radiochemical Gallium Detector (R) 1283
Garlic
- The Organosulfur Chemistry of the Genus *Allium*—Implications for the Organic Chemistry of Sulfur (R) 1135
Gas-phase reactions
- Gas-Phase Reactions of M^+ and $[CpM]^+$ (M = Fe, Co, Ni) with 1,3,5-Trisilacyclohexane: First Evidence for the Formation of 1,3,5-Trisilabenzene (C) 1633
- Observation and Properties of a Hydrogen Bond to Carbon in a Short-Lived, Gas-Phase Complex of Methyl Isocyanide and Hydrogen Fluoride (C) 202
- The Pyrolysis of Tetranitromethane in the Gas Phase (C) 900
Gene technology
- Inhibition of Fruit Ripening by Antisense-RNA Technology (H) 175
- Protein Engineering: Modified Hemoglobin as a Blood Substitute (H) 848
Genome sequencing
- A Milestone in Genome Sequencing: The Complete DNA Sequence of the Yeast Chromosome III (H) 1578
Germanium compounds
- A Germanium Sesquisulfide, $(t\text{BuGe})_4S_6$, without Adamantane Structure (C) 59
- Ag_5GeO_4, a New Semiconducting Oxide (C) 653
- Stable Cyclic Germanediyls ("Cyclogermylenes"): Synthesis, Structure, Metal Complexes, and Thermolyses (C) 1485
Glycopeptides
- A New Strategy for Solid-Phase Synthesis of *O*-Glycopeptides (C) 857
- Synthesis of *C*-Glycopeptides via Free Radical Addition of Glycosyl Bromides to Dehydroalanine Derivatives (C) 902
Glycosides
- Fullerene Sugars: Preparation of Enantiomerically Pure, Spiro-Linked C-Glycosides of C_{60} (C) 1388
Gold compounds
- Molecular Machines: Molecular Structure of $[(p\text{-}Tol_3P)_{10}Au_{13}Ag_{12}Cl_8](PF_6)$—a Cluster with a Biicosahedral Rotorlike Metal Core and an Unusual Arrangement of Bridging Ligands (C) 445
- $[(Ph_3PAu)_6Mn(CO)_3]^+$, a Cluster with Pentagonal-Bipyramidal Structure (C) 464
- Synthesis and Structure of the Cluster $[NaAu_{12}Se_8]^{3-}$: An Inorganic Cryptand Complex (C) 787
Grignard reactions
- Enantiomerically Pure Tertiary Alcohols by TADDOL-Assisted Additions to Ketones—or How to Make a Grignard Reagent Enantioselective (C) 84
- Ligand Effects in Grignard Additions (C) 342

Halogen compounds
- Alkynyl- and Alkenyl(phenyl)iodonium Compounds (R) 274
- Azidoiodoiodine(1+) Hexafluoroantimonate: The First Binary Nitrogen–Iodine Cation (C) 1338
- Does the Naked Fluoride Ion Exist? (H) 292
Helicenes
- A Diels–Alder Route to [5]- and [6]-Helicenes (C) 1093

Helices
- An Unusual Interplay Between Macromolecular and Supramolecular Helicity in Polyisocyanates Dissolved in a Chiral Liquid Crystal (C) 88
- Supramolecular Self-Assemblies of Two-Directional Cascade Molecules: Automorphogenesis (C) 917
- The First Self-Assembled Dinuclear Triple-Helical Lanthanide Complex: Synthesis and Structure (C) 1622
Helium compounds
- The Neutralization of HeC_{60}^+ in the Gas Phase: Compelling Evidence for the Existence of an Endohedral Structure for He@C_{60} (C) 183
Heptatriene
- Investigation of the [1,7] Sigmatropic Hydrogen Shift in a Parent Compound *Z,Z*-1,3,5-Heptatriene and Its Monodeuterium Analogue (C) 781
Heteroarenes
- Aromatic Boron Heterocycles: The Generation of 1*H*-Borepin and the Structure of Tricarbonyl(1-phenylborepin)molybdenum (C) 1255
- Diprotonated Tetra(2-pyridyl)pyrazine and its Chemical Mimesis due to Different Hydrogen Bridges (C) 299
- Enzymatic Oxidation of Methyl Groups on Aromatic Heterocycles: A Versatile Method for the Preparation of Heteroaromatic Carboxylic Acids (C) 774
- Gas-Phase Reactions of M^+ and $[CpM]^+$ (M = Fe, Co, Ni) with 1,3,5-Trisilacyclohexane: First Evidence for the Formation of 1,3,5-Trisilabenzene (C) 1633
- Homodiboriranides: The Simplest Negatively Charged Homoaromatic Compounds (C) 1238
- Sulfur Analogues of Polycyclic Aromatic Hydrocarbons (Thiaarenes). Environmental Occurrence, Chemical and Biological Properties (B) 364
- Tetrathienylethylenes, a New Class of Electron Donors—Dications Twisted by 90° Stabilized by Formation of Polymethine Units (C) 455
Heterocycles
- A New Synthesis for Imidazolo- and Pyrrolophanes by [3 + 2] Cycloaddition with Azaallenyl Radical Cations (C) 209
- Benzo-1,2,3-triselenolium Trifluoromethanesulfonate—a C_2Se_3 Radical Cationic Salt with Unusual Solid-State Structure (C) 779
- Bis(trisyl)oxadiborirane (C) 1040
- Gas-Phase Reactions of M^+ and $[CpM]^+$ (M = Fe, Co, Ni) with 1,3,5-Trisilacyclohexane: First Evidence for the Formation of 1,3,5-Trisilabenzene (C) 1633
- Spirocyclization of a Stable Phosphaalkyne with Aluminum Trichloride—Key Reaction for the Production of Triphospha Dewar Benzene Derivatives (C) 1055
- Synthesis, Structure, and Thermolysis of an Unusual Azaphosphasiliridine (C) 751
- The First Stibepine: Synthesis and Structure of *Sb*-Chlorobenzo[*d*]stibepine (C) 1642
- Triphosphatrisilacyclohexanes as Tridentate Coronands in Cr and Mo Complexes: Activation of Si–H in an Early Stage versus Phosphane Coordination (C) 1510
Heteropolyanions
- A Novel Host/Guest System with a Nanometer Large Cavity for Anions and Cations: $[2NH_4^+, 2Cl^- \subset V_{14}O_{22}(OH)_4(H_2O)_2(C_6H_5PO_3)_8]^{6-}$ (C) 1192
- New Impetus for Inorganic Host-Guest Chemistry (H) 1185
- (Organoarsonato)polyoxovanadium Clusters: Properties and Structures of the V^V Cluster $[V_{10}O_{24}(O_3AsC_6H_4\text{-}4\text{-}NH_2)_3]^{4-}$ and the V^{IV}/V^V Cluster $[H_2\{V_6O_{10}(O_3AsC_6H_5)_6\}]^{2-}$ (C) 1197
Hexabutadiynylbenzenes
- The First Hexabutadiynylbenzenes: Synthesis and Structures (C) 1643
High-pressure liquid chromatography
- Detection of Subpicomole Levels of Compounds Containing Hydroxyl and Amino Groups with the Fluorogenic Reagent, 2-Naphthoylimidazole (C) 890
Histocompatibility molecule
- Molecular Modeling of the Class I Human Histocompatibility Molecule HLA-A2 Presenting an Allele-Specific Nonapeptide from Influenza Matrix Protein (C) 886
History of chemistry
- August Wilhelm Hofmann—"Reigning Chemist-in-Chief" (R) 1265
- C_{60}: Buckminsterfullerene, The Celestial Sphere that Fell to Earth (R) 111
- Chemical Evolution. Origin of the Elements, Molecules and Living Systems (B) 1533
- Contrasts in Scientific Style. Research Groups in the Chemical and Biochemical Sciences (B) 103
- Emil Fischer's Proof of the Configuration of Sugars: A Centennial Tribute (R) 1541
- My 132 Semesters of Chemistry Studies. Vladimir Prelog (B) 1395
- Optically Anomalous Crystals (R) 1
- Physical Chemistry from Ostwald to Pauling. The Making of a Science in America (B) 797
- The Green Flame: Surviving Government Secrecy (B) 1096
- The Kaiser's Chemists. Science and Modernization in Imperial Germany (B) 803
- The World of Peptides. A Brief History of Peptide Chemistry (B) 1535
Hofmann, August Wilhelm von
- August Wilhelm Hofmann—"Reigning Chemist-in-Chief" (R) 1265
Hole burning
- Spectral Hole Burning at Room Temperature and with a Single Molecule: Two New Perspectives (H) 426
Homoallylic alcohols
- Diastereoselective Addition of Allylsilanes to Aldehydes: Synthesis of Enantiomerically Pure Homoallylic Alcohols (C) 1372
Hormones
- Estradiols Modified by Metal Carbonyl Clusters as Suicide Substrates for the Study of Receptor Proteins: Application to the Estradiol Receptor (C) 753
Host–guest chemistry
- A Binary Quinone Receptor (C) 792
- A Nonaromatic Expanded Porphyrin Derived from Anthracene—A Macrocycle which Unexpectedly Binds Anions (C) 452
- A Novel Host/Guest System with a Nanometer Large Cavity for Anions and Cations: $[2NH_4^+, 2Cl^- \subset V_{14}O_{22}(OH)_4(H_2O)_2(C_6H_5PO_3)_8]^{6-}$ (C) 1192
- A Supramolecular Assembly of Two Torands, Two Lithium Ions, and Three Water Molecules (C) 348
- Conformational Preference of the Torand Ligand in Its Complexes with Potassium and Rubidium Picrate (C) 345
- Cyclodextrin Derivatives as Chiral Selectors—Investigation of the Interaction with (*R,S*)-Methyl-2-chloropropionate by Enantioselective Gas Chromatography, NMR Spectroscopy, and Molecular Dynamics Simulation (C) 319
- Decamethylcucurbit[5]uril (C) 1475
- Designing Synthetic Cationic Molecular Receptors for Alcohols (C) 478
- Frontiers in Supramolecular Organic Chemistry and Photochemistry (B) 363
- Host-Guest Molecular Interactions. From Chemistry to Biology (B) 1263
- Molecules with Large Cavities in Supramolecular Chemistry (R) 528
- Multidentate Macrocyclic Lewis Acids: Release of "[12] Mercuracarborand-4" from Its Iodide Complex and the Structure of Its Tetra(tetrahydrofuran) Dihydrate Complex (C) 893
- New Impetus for Inorganic Host-Guest Chemistry (H) 1185
- Photoswitchable Association of an Azobenzene-Bipyridinium Diad to Eosin: Photostimulated "On-Off" Guest Binding (C) 1243
- Synthesis and Complexation Properties of a Cyclodextrin-Derived Siderophore Analogue (C) 1381
- Threading Cyclodextrin Rings on Polymer Chains (C) 197
Houben-Weyl
- Houben-Weyl. Methoden der Organischen Chemie. Band E19c: Carbokationen, Carbokation-Radikale (B) 799
- Houben-Weyl. Methods of Organic Chemistry. Additional and supplementary volumes to the 4th Edition. Vol. E 12b. Organotellurium Compounds (B) 237
Hydrazines
- Semiconductor-Catalyzed Photoaddition of Cyclic Enol Ethers to 1,2-Diazenes (C) 1039
- Synthesis and Structure of a Mononuclear η^2-Hydrazine Complex by Protonation of an $[N_2H_2]^{2-}$ Complex (C) 1081
Hydride transfer
- Hydride Transfer by Hydrido Transition-Metal Complexes. Ionic Hydrogenation of Aldehydes and Ketones, and Structural Characterization of an Alcohol Complex (C) 1233
- Kinetics of Hydride Transfers from CH, SiH, GeH, and SnH Groups to Carbenium Ions (C) 1046
Hydrodesulfurization
- Dimerization of Thiophene to Give a Linear $S(CH)_8S$ Fragment with $[(C_5Me_5)Rh(C_2H_4)_2]$ (C) 357
Hydrogen bridges
- A 1:1 Adduct of 2-Aminobenzothiazole and a Urea Derivative, and Its Spatial Arrangement (C) 1634
- A Water-Complexed Organolithium Compound: $[LiCH(CN)_2 \cdot H_2O \cdot TMEDA]_\infty$ (C) 77
- Diprotonated Tetra(2-pyridyl)pyrazine and its Chemical Mimesis due to Different Hydrogen Bridges (C) 299
- Dynamic Proton Exchange in the Hydrogen Dihydroxide Ion $H_3O_2^-$ of the Hydroxosodalite Hydrate $[Na_4(H_3O_2)]_2[SiAlO_4]_6$: ^1H MAS NMR Spectroscopic Evidence (C) 1210
- En Route to Synthetic Phosphodiesterases: Supramolecular Phosphoryl-Transfer Mediated by Amidinium–Phosphate Contact Ion-Pairs (C) 207

- Induction of Ferroelectricity in Polymeric Systems through Hydrogen Bonding (C) 1531
- Intermolecular Forces. An Introduction to Modern Methods and Results (B) 1538
- Observation and Properties of a Hydrogen Bond to Carbon in a Short-Lived, Gas-Phase Complex of Methyl Isocyanide and Hydrogen Fluoride (C) 202
- Three-Dimensional Structure of an Unsymmetrical Proton–Electron Transfer System Containing a Disulfide Bond: The Bis(4-hydroxyphenyl)disulfide–Benzoquinone Complex (C) 852

Hydrogen dihydroxide ion
- Dynamic Proton Exchange in the Hydrogen Dihydroxide Ion $H_3O_2^-$ of the Hydroxosodalite Hydrate $[Na_4(H_3O_2)]_2[SiAlO_4]_6$: ^1H MAS NMR Spectroscopic Evidence (C) 1210

Hydrogen shifts
- Investigation of the [1,7] Sigmatropic Hydrogen Shift in a Parent Compound *Z,Z*-1,3,5-Heptatriene and Its Monodeuterium Analogue (C) 781

Hydrogenation
- Hydride Transfer by Hydrido Transition-Metal Complexes. Ionic Hydrogenation of Aldehydes and Ketones, and Structural Characterization of an Alcohol Complex (C) 1233
- The Hydroxyl-Directed Hydrogenation of Vinylstannanes and Silanes: A Highly Diastereoselective Route to β-Stannyl and β-Silyl Alcohols (C) 232
- The Uncatalyzed Transfer Hydrogenation of α-Methylstyrene by Dihydroanthracene or Xanthene—a Radical Reaction (C) 1523

Hydroperoxides
- Chemoenzymatic Syntheses of the Optically Active Hydroperoxides of Phosphatidylglycerol and Phosphatidylethanolamine with Lipase, Lipoxygenase, and Phospholipase D (C) 1336

Hydroxyaldehydes
- 1-*O*-(2-Acetoxyhexadec-1-enyl)choline Iodide, a New Anticancer Agent (C) 64
- α-Hydroxyaldehyde Derivatives Arising from Oxidation of Plasmalogens (C) 468

Hydroxybutyric acid
- The Triolide of (*R*)-3-Hydroxybutyric acid—Direct Preparation from Polyhydroxybutyrate and Formation of a Crown Estercarbonyl Complex with Na Ions (C) 434

Hydroxycarbonyl compounds
- New Chiral α-Benzyloxyacryliron(II) Complex for Asymmetric Synthesis of α,α-Dialkyl-α-hydroxycarbonyl Compounds (C) 193

Hydroxycarboxylic acids
- Synthesis of (*R*)- and (*S*)-2-*tert*-Butyl-6-trifluoromethyl-1,3-dioxin-4-ones, Transformations into 3-Hydroxy-3-(trifluoromethyl)alkanoates, and Surprising Differences in the Reactivity of CH_3- and CF_3-Substituted Compounds (C) 1083

Hyperconjugation
- Large Hyperconjugative and Inductive Effects on C-C-X Bond Angles (X = Main-Group Element): The Crystal Structure of Triethylborane and Ab Initio Investigations (C) 314

Immobilization
- Photolithographic Immobilization of Biopolymers on Solid Supports (C) 759

Immunology
- Synthesis of the Species-Specific *Mycobacterium avium* Trisaccharide (Serovar 21) for the Preparation of a Neoglycoprotein for Immunological Studies (C) 1358

Immunophilins
- Natural Products as Probes of Cellular Function: Studies of Immunophilins (R) 384

Indigo
- Indigoid *para*-Quinodimethanes (C) 1202
- Reduction of Dispersed Indigo Dye by Indirect Electrolysis (C) 1068

Indium compounds
- Idealized Pentagonal-Planar Coordination for Indium in $[(\mu_5\text{-In})\{Mn(CO)_4\}_5]^{2-}$ (C) 350

Indolylacetamides
- Synthesis of (2-Arylindol-3-yl)acetamides as Probes of Mitochondrial Steroidogenesis—A New Mechanism for $GABA_A$ Receptor Modulation (C) 1060

Industrial chemistry
- Photochemical Technology (B) 360

Inhibitors
- Synthesis of Esterase-resistant 9-*O*-Acetylated Polysialoside as Inhibitor of Influenza C Virus Hemagglutinin (C) 1478

Inorganic chemistry
- NMR, NQR, EPR, and Mössbauer Spectroscopy in Inorganic Chemistry (B) 108

Insertion reactions
- A Dramatic Difference in the Reactivities of Alkoxido- and Aryloxidorhenium Complexes in Insertion Reactions (C) 220

Intermolecular interactions
- Intermolecular Forces. An Introduction to Modern Methods and Results (B) 1538
- Structure of the Lowest Temperature Phase of the Solid Benzene–Hexafluorobenzene Adduct (C) 1655
- The Structure of Water—a Mixture of Cubes and Planar Four-Membered Rings? (H) 1577

Iodazide
- Azidoiodoiodine(1+) Hexafluoroantimonate: The First Binary Nitrogen–Iodine Cation (C) 1338

Iodine compounds
- Alkynyl- and Alkenyl(phenyl)iodonium Compounds (R) 274
- Efficient Synthesis of Nanoscale Macrocyclic Hydrocarbons (C) 922
- Multidentate Macrocyclic Lewis Acids: Release of "[12] Mercuracarborand-4" from Its Iodide Complex and the Structure of Its Tetra(tetrahydrofuran) Dihydrate Complex (C) 893
- Reagents with Hypervalent Iodine: Formation of Convenient Chiral Synthetic Intermediates by Fragmentation of Carbohydrate Anomeric Alkoxy Radicals (C) 772
- The Reaction of Unactivated Cobalt Powder with Iodophosphoranes. The Synthesis of $[Co(PMe_3)_2I_3]$ and the Isolation of the "Frozen Transition-State" Complex $[(n\text{Bu}_3\text{PI})_2(\mu\text{-I})][(n\text{Bu}_3\text{PI})(\mu\text{-I})CoI_3]$ (C) 919

Ion channels
- Elementary Steps in Synaptic Transmission Revealed by Currents through Single Ion Channels (Nobel Lecture) (R) 830
- Ion Channels for Communication Between and Within Cells (Nobel Lecture) (R) 824
- Synthetic Chain-Substituted Phospholipids: Ion Transport Across Their Bilayer Membranes (C) 898
- Towards Artificial Ion Channels: Transport of Alkali Metal Ions across Liposomal Membranes by "Bouquet" Molecules (C) 1637

Ion exchangers
- Ion Exchangers (B) 802

Ion pairs
- Penetrated Ion Pairs: a New Form of Ion Pair (H) 731
- The Crystal Structure of $[(\text{Pyrene}^{\cdot-})\{Na^+[(C_2H_5)_2O]\}]$: A Model for Stacked Radical Anion Salts (C) 878

IR spectroscopy
- 2,4-Didehydrophenol—First Proof of a *meta*-Aryne by IR Spectroscopy (C) 1230

Iridium compounds
- A Paramagnetic, Mononuclear Organometallic Iridium(II) Complex: $[Ir(C_6Cl_5)_2(cod)]$ (C) 1527
- Structure of a Product of Double Addition to C_{70}: $[C_{70}\{Ir(CO)Cl(PPhMe_2)_2\}_2] \cdot 3C_6H_6$ (C) 1356

Iron compounds
- Dynamic Motion in $[HFe(CO)_4]^-$ Ions as Observed by Mössbauer Spectroscopy—Evidence for Hydride "Tunneling" (C) 884
- Inorganic Biochemistry of Iron Metabolism (B) 930
- Iron Oxides in the Laboratory. Preparation and Characterization (B) 658
- Microcalorimetry of the Spin-Transition Systems $[Fe(bts)_2(NCS)_2]$ and $[Fe(2\text{-pic})_3]Cl_2 \cdot EtOH$ in the Range $15\ K < T < 300\ K$ (C) 178
- Mössbauer Spectroscopy and Electronic Structure Calculations of the Nitridoferrates(III): $Li_3[FeN_2]$ and $Ba_3[FeN_3]$ (C) 1624
- Multifield Saturation Magnetization Measurements of Oxidized and Reduced Ribonucleotide Reductase from *Escherichia coli* (C) 1513
- New Chiral α-Benzyloxyacryliron(II) Complex for Asymmetric Synthesis of α,α-Dialkyl-α-hydroxycarbonyl Compounds (C) 193
- New Route to α-[(1*E*,3*E*)-dienyl]allenes via Butadiene-tricarbonyliron Complexes (C) 224
- Novel Iron Carbonyl Telluride Clusters: Synthesis and Characterization of $[Fe_5Te_4(CO)_{14}]^{2-}$ and $[Fe_8Te_{10}(CO)_{20}]^{2-}$ (C) 913
- Proof of the Catalytic Activity of a Naked Metal Cluster in the Gas Phase (C) 636
- Synthetic Models for Iron—Oxygen Aggregation and Biomineralization (H) 1010
- Tetraferrioazaallenium—Product of a Novel Reaction of Coordinated CN^- (C) 590
- The Trapping of Iron Hydroxide Units by the Ligand "heidi": Two New Hydroxo(oxo)iron Clusters Containing 19 and 17 Iron Atoms (C) 191

Isoarenes
- 1,2,4-Cyclohexatriene, an Isobenzene, and Bicyclo[4.4.0]deca-1,3,5,7,8-pentaene, an Isonaphthalene: Generation and Trapping Reactions (C) 473
- 1,2,4-Cyclohexatriene, an Isobenzene, and its [2+2] Cycloaddition with Styrene: A Theoretical Study (C) 476

Isocoumarins
- 3,4-Dihydroisocoumarins, a New Class of Ant Trail Pheromones (C) 795

Isocyanates
- An Unusual Interplay Between Macromolecular and Supramolecular Helicity

in Polyisocyanates Dissolved in a Chiral Liquid Crystal (C) 88
- Synthesis of Isocyanate-Substituted Allenes and 1,3-Butadienes by [3,3] Sigmatropic Rearrangements (C) 866
Isocyanide complexes
- (Isocyanide)ruthenate Analogues of Tetracarbonylferrate (C) 83
Isocyanides
- Chelate Complexes of Tripodal, Aliphatic Triisocyanide Ligands (C) 1212
- Enantioselective Polymerization of 1,2-Diisocyanoarenes: Synthesis of Optically Active, Helical Poly(quinoxaline-2,3-diyl)s (C) 1509
- Lithiodiphenylmethylisocyanide-(−)-sparteine bis(tetrahydrofuran): Crystal Structure of a Lithiated Isocyanide (C) 79
- Observation and Properties of a Hydrogen Bond to Carbon in a Short-Lived, Gas-Phase Complex of Methyl Isocyanide and Hydrogen Fluoride (C) 202
- Reaction of Heterodinuclear μ-Ethynediyl Complexes Containing Palladium and Platinum: Multiple and Successive Insertion of Isocyanides (C) 851
Isoinversion principle
- *trans*-2-*tert*-Butylcyclohexanol, a Simple Selectively Optimized Cyclohexanol Auxiliary (C) 1190
Isolobal relationship
- Synthesis, Structure, and Bonding of $[CpCoW_2(OCH_2tBu)_6]$, and Comments on the Combining Properties of CO and CpCo (C) 896
Isomerization
- Intermolecular Additions and Cycloisomerizations by a Pd-Catalyzed Sequence of an Intramolecular Redox Reaction and an Addition (C) 1335
Isothiocyanates
- Synthesis and Reactions of Isothiocyanate-Substituted Allenes and 1,3-Butadienes (C) 90
Isotope effect
- Deuterium-Induced Phase Transition of an Organic Metal—An Unusual Isotope Effect (C) 859

Ketenimines
- Investigations of the Structure and Reactivity of a Stannaketenimine (C) 437
Ketimines
- Crystal and Solution Structures of the Novel Complex of Sodium Ketimide with Two Ketimine Ligands $[(tBu_2C{=}NNa)_4(HN{=}CtBu_2)_2]$: Stacking of Complexed and Uncomplexed $(NNa)_2$ Rings to give a Highly Distorted $(NNa)_4$ Cubane (C) 93
Ketoesters
- Diastereoselective Three-Center Michael Addition of β-Ketoesters to Prostereogenic α,β-Unsaturated Carbonyl Compounds Catalyzed by K_2CO_3 or Cs_2CO_3 (C) 1651
- Enantioselective Synthesis of 3-Substituted 2-Ketoesters (C) 618
Ketone pyrolysis
- Selective Ketone Pyrolysis: New Synthetic Method for Mono- and Polycyclic Hydrocarbons (C) 307
Ketones
A One-Pot Synthesis of Ketones and Aldehydes from Carbon Dioxide and Organolithium Compounds (C) 1035
Kinetics
- Chemical Kinetics (B) 239
- Chemical Oscillations and Instabilities. Nonlinear Chemical Kinetics (B) 109
- Kinetics of Hydride Transfers from CH, SiH, GeH, and SnH Groups to Carbenium Ions (C) 1046
- Rate Constants for the Attack of Carbenium Ions at Arenes—A Link between the Chemistry of Aliphatic and Aromatic π Systems (C) 1613

Laboratory practice
- Essential Molecular Biology. A Practical Approach (B) 1099
- Microscale Techniques for the Organic Laboratory (B) 799
Ladderanes
- Quest for Higher Ladderanes: Oligomerization of a Cyclobutadiene Derivative (C) 1488
Langmuir films
- Two-Dimensional Crystallography of Amphiphilic Molecules at the Air–Water Interface (R) 130
Lanthanide compounds
- One-Dimensional $M^{III}Cu^{II}$ Compounds with an Unprecedented, Tubelike Structural Motif (M = Rare-Earth Metal) (C) 626
- Synthesis and Structure of a Mononuclear η^2-Hydrazine Complex by Protonation of an $[N_2H_2]^{2-}$ Complex (C) 1081
- Synthesis of Lanthanide and Actinide Compounds (B) 105
- The First Self-Assembled Dinuclear Triple-Helical Lanthanide Complex: Synthesis and Structure (C) 1622
Lanthanoid compounds
- $KCeSe_4$: A New Solid-State Lanthanide Polychalcogenide (C) 1594
- New Layered Iron-Lanthanum-Oxide-Sulfide and -Selenide Phases: $Fe_2La_2O_3E_2$ (E = S,Se) (C) 1645
Laser photolysis
- Cyclohexadienyl-Type Cationic Intermediates in the Friedel–Crafts Alkylation of Benzene Derivatives with the 9-Fluorenyl Cation—Observation by Laser Flash Photolysis (C) 743
Laser spectroscopy
- High Resolution Spectroscopy below the Doppler Width (R) 263
Layer structures
- $TaNi_2Te_2$, A Novel Layered Telluride, and $TaCo_2Te_2$, a Structural Variant with Peierls Distortion (C) 217
Lead compounds
- 2,2′,5,5′-Tetra-*tert*-butyl-1,1′-diazaplumbocene—a Stable Azacyclopentadienyl Compound of Lead (C) 778
- The Structure and Stability Trends of Fluoro(methyl)plumbanes (C) 1224
Lignin peroxidase
- Formation of a Toxic Dimerization Product of 3,4-Dichloroaniline by Lignin Peroxidase from *Phanerochaete chrysosporium* (C) 68
Lignins
- Matrix-Assisted Laser Desorption Mass Spectrometry of Lignins (C) 762
Lipids
- High-Yield Synthesis of Lipid Systems with Giant Rings (C) 1492
- Synthetic Bilayer Membranes: Molecular Design, Self-Organization, and Application (R) 709
Lipopeptides
- Ion-Spray Mass Spectrometry of Lipopeptide Vaccines (C) 226
Liposomes
- Towards Artificial Ion Channels: Transport of Alkali Metal Ions across Liposomal Membranes by "Bouquet" Molecules (C) 1637
Liquid crystals
- An Unusual Interplay Between Macromolecular and Supramolecular Helicity in Polyisocyanates Dissolved in a Chiral Liquid Crystal (C) 88
- Induction of Ferroelectricity in Polymeric Systems through Hydrogen Bonding (C) 1531
- Liquid Crystallinity in Polymers. Principles and Fundamental Properties (B) 358
- Paramagnetic Chiral Smectic C Materials: A New Class of Ferroelectric Liquid Crystals (C) 1471
ortho Lithiation
- "Kinetically Enhanced Metalation"—How Substituents Direct *ortho* Lithiation (C) 755
Lithium amides
- A Novel Six-Center Deprotonation—Lithiation Reaction Mechanism Supported by the X-Ray Structure Analysis of a Lithium Carbazolide (C) 1209
- [Lithium Piperidide–Piperidine]$_4$: Crystal Structure of an Oligomeric 1:1 Lithium Amide–Amine Mixed Complex, an Intermediate in the *N*-Lithiation of Amines (C) 1205
Lithium perchlorate
- Allylation of Quinones with Allylsilane in the Presence of Lithium Perchlorate in Ether (C) 313
Low-valent compounds
- A New Approach to Bis(arene)titanium(0) and -titanium(−1) Complexes; Structure of Bis(arene)titanates(1−) (C) 1495
- Ether-Soluble Ti^0 and Bis(η^6-arene)-titanium(0) Complexes from the Reduction of $TiCl_4$ with Triethylhydroborate (C) 1490
- $[Ga(C_5H_5)]$: Synthesis, Identification, and Ab Initio Investigations (C) 1362
- $[Ga_4\{C(SiMe_3)_3\}_4]$ with a Tetrahedral Ga_4 Skeleton (C) 1364
- Stable Cyclic Germanediyls ("Cyclogermylenes"): Synthesis, Structure, Metal Complexes, and Thermolyses (C) 1485

Macrocycles
- A Binary Quinone Receptor (C) 792
- A Nonaromatic Expanded Porphyrin Derived from Anthracene—A Macrocycle which Unexpectedly Binds Anions (C) 452
- A Supramolecular Assembly of Two Torands, Two Lithium Ions, and Three Water Molecules (C) 348
- Conformational Preference of the Torand Ligand in Its Complexes with Potassium and Rubidium Picrate (C) 345
- Decamethylcucurbit[5]uril (C) 1475
- Designing Synthetic Cationic Molecular Receptors for Alcohols (C) 478
- Efficient Synthesis of Nanoscale Macrocyclic Hydrocarbons (C) 922
- High-Yield Synthesis of Lipid Systems with Giant Rings (C) 1492
- Ion-Selective Hydrazone–Azine Tautomerism of a 14-Membered Macrocyclic Ligand (C) 749
- Molecular Recognition of Primary Amines by Three-Point Binding with Boron-Containing Host Molecules (C) 1017
- One-Pot Syntheses of Novel Arene Tricarbonyl Chromium Macrocycles and Macrobicycle: Structure of a Pentanuclear Trichromium(0)-Dicopper(I) Cryptate (C) 775

- One-Step Synthesis of a Fourfold Functionalized Catenane (C) 1619
- Selective Ketone Pyrolysis: New Synthetic Method for Mono- and Polycyclic Hydrocarbons (C) 307
- The Triolide of (*R*)-3-Hydroxybutyric acid – Direct Preparation from Polyhydroxybutyrate and Formation of a Crown Estercarbonyl Complex with Na Ions (C) 434

Magnetic properties
- A Novel Polyoxotungstate Containing a *triangulo* Ni^{II}_3 Cluster with Ferromagnetic Exchange Interactions and an $S=3$ Ground State (C) 649
- Bis(*P,P*-di-*tert*-butylphosphinic-*N*-isopropylamidato-*N,O*)nickel(II), a Paramagnetic Planar Complex (C) 612
- Induction of Ferroelectricity in Polymeric Systems through Hydrogen Bonding (C) 1531
- Multifield Saturation Magnetization Measurements of Oxidized and Reduced Ribonucleotide Reductase from *Escherichia coli* (C) 1513
- One-Dimensional $M^{III}Cu^{II}$ Compounds with an Unprecedented, Tubelike Structural Motif (M = Rare-Earth Metal) (C) 626
- Paramagnetic Chiral Smectic C Materials: A New Class of Ferroelectric Liquid Crystals (C) 1471

Manganese compounds
- A New Type of Mn–O Cluster with a Mn_4 Chain Unit. Relevance to the Photosynthetic Oxygen Evolving Center (C) 1629
- A Remarkable Change in Framework Cation Positions upon Lithium Exchange: the Crystal Structure of $LiMnPO_4(OH)$ (C) 1090
- Idealized Pentagonal-Planar Coordination for Indium in $[(\mu_5\text{-In})\{Mn(CO)_4\}_5]^{2-}$ (C) 350
- $[(Ph_3PAu)_6Mn(CO)_3]^+$, a Cluster with Pentagonal-Bipyramidal Structure (C) 464
- Transition Metal in a Cube – A Discrete Eight-Coordinate $[Mn^{2+} \subset [2.2.2]cryptand]$ as a Body-Centered Cube with an N_2O_6 Donor Set (C) 764

Mass spectrometry
- Ion-Spray Mass Spectrometry of Lipopeptide Vaccines (C) 226
- Matrix-Assisted Laser Desorption Mass Spectrometry of Lignins (C) 762
- O–H Bond Activation in the Gas Phase: The Reactions of Water and Methanol with $[FeCH_3]^+$ (C) 603
- Proof of the Catalytic Activity of a Naked Metal Cluster in the Gas Phase (C) 636
- Structure and Reactivity of Silicon Clusters in the Gas Phase (H) 172
- The Neutralization of HeC_{60}^+ in the Gas Phase: Compelling Evidence for the Existence of an Endohedral Structure for He@C_{60} (C) 183
- The Phosphorus Ylide CH_2PH_3 is Stable in the Gas Phase (C) 86

Materials science
- Spectral Hole Burning at Room Temperature and with a Single Molecule: Two New Perspectives (H) 426
- The Photochemistry of Stilbenoid Compounds and Their Role in Materials Technology (R) 1399

Matrix isolation
- 2,4-Didehydrophenol – First Proof of a *meta*-Aryne by IR Spectroscopy (C) 1230
- Evidence for [PdSiO] from IR Spectroscopy (C) 638
- Matrix Isolation of Diisocyanogen CN-NC (C) 1218

Maximum entropy method
- Maximum Entropy in Action (B) 928

Medium-sized rings
- Ten-Membered Ring Enediynes with Remarkable Chemical and Biological Profiles (C) 1044

Membranes
- Synthetic Bilayer Membranes: Molecular Design, Self-Organization, and Application (R) 709
- Synthetic Chain-Substituted Phospholipids: Ion Transport Across Their Bilayer Membranes (C) 898
- Towards Artificial Ion Channels: Transport of Alkali Metal Ions across Liposomal Membranes by "Bouquet" Molecules (C) 1637

Mercury compounds
- Multidentate Macrocyclic Lewis Acids: Release of "[12] Mercuracarborand-4" from Its Iodide Complex and the Structure of Its Tetra(tetrahydrofuran) Dihydrate Complex (C) 893

Metabolites
- Dictionary of Plants Containing Secondary Metabolites (B) 1396

Metacyclophanes
- Pronounced Conformational Changes in Sixfold Nitrogen-Functionalized Metacyclophanes: Syntheses and Crystal Structures of Two 1,10-Diaza[11]metacyclophanes (C) 882

Metal compounds
- Metals and Their Compounds in the Environment: Occurrence, Analysis and Biological Relevance (B) 102

Metalates
- The $[(\mu_3\text{-}WSe_4)_3(\mu_3\text{-}Se)_2(Cu_3)_2]^{4-}$ Anion, an Inorganic Cluster with a Pinwheel Shape (C) 1477

Metalation
- Chemical Attachment of Organometallics to Proteins in Reverse Micelles (C) 789

Metallacumulenes
- Metallacumulenes: Activation of Diynes and Access to a Novel Bis(Alkenylallenylidene)ruthenium Complex with the Structural Unit $R_2C=C=C=Ru=C=C=CR_2$ (C) 651

Metallacycles
- Cyclometallaborazines: Borazines with Metal Atoms as Ring Building Blocks: $PhB(MeN)_3(TiCl_2)_2$ (C) 598
- Cyclophosphazene Metal Oxides, a New Class of Compounds, and Model Compounds for the Polymerization of Phosphazenes (C) 601
- 1,3-Dimetallabenzene Derivatives of Niobium or Tantalum (C) 1261

Metathesis
- A Cyclometalated Aryloxy(chloro)-neopentylidenetungsten Complex: A Highly Active and Stereoselective Catalyst for the Metathesis of *cis*- and *trans*-2-Pentene, Norbornene, 1-Methylnorbornene, and Ethyl Oleate (C) 628
- Detection of the Tungsten–Carbene–Olefin Intermediates in Catalytic Metathesis Systems Containing High-Valent, Metal Centers (C) 1585

Michael additions
- Diastereoselective Three-Center Michael Addition of β-Ketoesters to Prostereogenic α,β-Unsaturated Carbonyl Compounds Catalyzed by K_2CO_3 or Cs_2CO_3 (C) 1651
- Enantioselective Synthesis of the Antidepressant Rolipram by Michael Addition to a Nitroolefin (C) 870

Microscopy (B) 1534

Mitomycins
- The Total Synthesis of (±)-Mitomycin K (C) 915

Mixed-valent compounds
- Mono- and Binuclear Molybdenum Complexes Incorporating 4-(4-Hydroxyphenyl)pyridine: Metal–Metal Interactions Across an Asymmetric Bridging Ligand (C) 1515
- $[Ni_4(SC_3H_7)_8Br]$ and $[Ni_4(SC_3H_7)_8I]$: Mixed Valent Nickel Thiolates with Integral and Nonintegral Metal Oxidation States (C) 54

Molecular biology
- A Milestone in Genome Sequencing: The Complete DNA Sequence of the Yeast Chromosome III (H) 1578
- Essential Molecular Biology. A Practical Approach (B) 1099

Molecular dynamics
- Calculation of Molecular Dynamics for Peptides in Dimethyl Sulfoxide: Elimination of Vacuum Effects (C) 210
- Cyclodextrin Derivatives as Chiral Selectors—Investigation of the Interaction with (*R,S*)-Methyl-2-chloropropionate by Enantioselective Gas Chromatography, NMR Spectroscopy, and Molecular Dynamics Simulation (C) 319
- Dynamic Forcing, a Method for Evaluating Activity and Selectivity Profiles of RGD (Arg-Gly-Asp) Peptides (C) 326

Molecular electronics
- Molecular Electronics (B) 1536

Molecular modeling
- Molecular Modeling of the Class I Human Histocompatibility Molecule HLA-A2 Presenting an Allele-Specific Nonapeptide from Influenza Matrix Protein (C) 886

Molecular recognition
- A Synthetic Receptor for Cyclic Adenosine Monophosphate (C) 61
- Crosslinking of Adjacent Guanine Residues in an Oligonucleotide by *cis*-$[Pt(NH_3)_2(H_2O)_2]^{2+}$: Kinetic Analysis of the Two-Step Reaction (C) 1483
- DNA Recognition by Hybrid Oligoether–Oligodeoxynucleotide Macrocycles (C) 1617
- Enantioselective Complexation of Chiral Dicarboxylic Acids in Clefts of Functionalized 9,9'-Spirobifluorenes (C) 1521
- In Vitro Selection of Specific Ligand-binding Nucleic Acids (R) 979
- Interactions Between Acyclic and Cyclic Peralkylammonium Compounds and DNA (C) 1207
- Molecular Recognition of Primary Amines by Three-Point Binding with Boron-Containing Host Molecules (C) 1017
- Selective Binding of Sugar to β-Cyclodextrin: A Prototype for Sugar–Sugar Interactions in Water (C) 745

Molybdenum compounds
- Distortional Isomerism in Oxomolybdenum Systems; the Evidence Re-evaluated (C) 1607
- Molecular Mechanisms of the Reduction of NO to NH_2OH at Mo–S Centers (C) 205
- Mono- and Binuclear Molybdenum Complexes Incorporating 4-(4-Hydroxyphenyl)pyridine: Metal–Metal Interactions Across an Asymmetric Bridging Ligand (C) 1515
- Stable Intermediates in the Addition and Elimination of $SnBuCl_3$ at Molybdenum Centers by Cleavage or Formation of an Sn–Cl Bond: Crystal Structure of $[Mo(CO)_2(PCy_3)(\mu\text{-}Cl)(\mu\text{-}S_2CPCy_3)(BuSnCl_2)] \cdot CH_2Cl_2$ (C) 76

Mössbauer spectroscopy
- Dynamic Motion in $[HFe(CO)_4]^-$ Ions as Observed by Mössbauer Spectroscopy—Evidence for Hydride "Tunneling" (C) 884
- Mössbauer Spectroscopy and Electronic Structure Calculations of the Nitridoferrates(III): $Li_3[FeN_2]$ and $Ba_3[FeN_3]$ (C) 1624
- $[SbCl([15]Crown-5)](SbCl_6)_2$ and $[BiCl([18]Crown-6)(CH_3CN)_2](SbCl_6)_2$: Salts with Antimony(III) and Bismuth(III) Dications (C) 334

Multiple bonds
- An Arsanylidensilane ("Arsasilene") and its Derivatization with Tellurium and Benzophenone (C) 316
- Investigations of the Structure and Reactivity of a Stannaketenimine (C) 437
- Novel Strategies for the Synthesis and Crystallization of Electrophilic Dinuclear Cations: Solution and Solid-State Properties of $[Re_2(NCCH_3)_{10}][Mo_6O_{19}]_2$ (C) 1360
- On the Reaction of Pentamethylcyclopentadiene with Cobalt Atoms: A Reexamination 1392
- Reduction of a Boron–Nitrogen 1,3-Butadiene Analogue: Evidence for a Strong B–B π-Bond (C) 1082
- The Electronic Structure of $[(\eta^5\text{-}C_5H_5)_2Co_2]$: Comment on the Existence of a Complex with an Unsupported Co–Co Double Bond (C) 471
- The First Complex with a $\sigma^2\pi^4$ Triple Bond between Vanadium Atoms in a Ligand Framework of Fourfold Symmetry—$[V_2\{(p\text{-}CH_3C_6H_4)NC(H)N(p\text{-}C_6H_4CH_3)\}_4]$ (C) 737

Multiple peptide synthesis
- Multiple Peptide Synthesis Methods and Their Applications (R) 367

NADH
- Formate-Driven, Non-Enzymatic NAD(P)H Regeneration for the Alcohol Dehydrogenase Catalyzed Stereoselective Reduction of 4-Phenyl-2-butanone (C) 1529

Natural products
- Dictionary of Plants Containing Secondary Metabolites (B) 1396
- Flexible Molecules with Defined Shape—Conformational Design (R) 1124 (1657)
- Natural Products as Probes of Cellular Function: Studies of Immunophilins (R) 384
- Pheromones of Marine Brown Algae; A New Branch of the Eicosanoid Metabolism (C) 1246
- Structure of the Tunichrome of Tunicates and its Role in Concentrating Vanadium (C) 52
- Synthesis of the Calicheamicin Aryltetrasaccharide Domain Bearing a Reducing Terminus: Coupling of Fully Synthetic Aglycone and Carbohydrate Domains by the Schmidt Reaction (C) 338
- The Enchanting Alkaloids of Yuzuriha (R) 665
- The Organosulfur Chemistry of the Genus *Allium*—Implications for the Organic Chemistry of Sulfur (R) 1135
- The Total Synthesis of (±)-Mitomycin K (C) 915
- Total Synthesis of Calicheamicin–Dynemicin Hybrid Molecules (C) 340
- [4 + 4]-Cycloaddition Reactions in the Total Synthesis of Naturally Occurring Eight-Membered Ring Compounds (H) 422

Nervous system
- Field-Effect Transistors as Sensors of Neural Systems (H) 45

Nickel compounds
- A Novel Polyoxotungstate Containing a *triangulo* Ni^{II}_3 Cluster with Ferromagnetic Exchange Interactions and an $S=3$ Ground State (C) 649
- Bis(*P,P*-di-*tert*-butylphosphinic-*N*-isopropylamidato-*N,O*)nickel(II), a Paramagnetic Planar Complex (C) 612
- First Example of a Chlorophin from an Unexpected Oxidative Ring-Opening of an (Octadehydrocorrinato)nickel(II) Salt (C) 70
- New Intermediate Steps in the Synthesis of Larger Nickel Clusters (C) 321
- $[Ni(PtBu)_6]$—a Strain on the 18 Electron Rule? (H) 424
- $[Ni_4(SC_3H_7)_8Br]$ and $[Ni_4(SC_3H_7)_8I]$: Mixed Valent Nickel Thiolates with Integral and Nonintegral Metal Oxidation States (C) 54
- Oxygen Activation on Nickel(II)-tetrahydrosalen Complexes with the Formation of Nickel(II)dihydrosalen Complexes (C) 623
- Spontaneous Self-Assembly of a Dinickel(II) Double Helicate Containing a 1,3-Benzenediyl Spacer Group (C) 230
- Stepwise Stacking of Three Paramagnetic Metallocene Units: $[CpNiCp(SiMe_2)_2CpCrCp(SiMe_2)_2CpNiCp]$ (C) 1258
- Synthesis and Structure of $[Ni(PtBu_6)]$ and $[Ni_5(PtBu)_6(CO)_5]$ and Calculations on the Electronic Structure of $[Ni(PtBu)_6]$ and $(PR)_6$, R = *t*Bu, Me (C) 323
- Tetrakis(η^1-phosphabenzene)nickel (C) 1343
- Unusual Coordination of the 1,3-Diphosphacyclobutadiene Derivative $(iPr_2NCP)_2$ to Two $[Ni(CO)_3]$ Fragments (C) 95

Niobium compounds
- $BaNb_7O_9$, a New Oxoniobate with Double Layers of Corner-Sharing Nb_6 Octahedra (C) 212
- 1,3-Dimetallabenzene Derivatives of Niobium or Tantalum (C) 1261
- $[Nb\{B(\eta^6\text{-}C_6H_5)_2(C_6H_5)_2\}(\eta^2\text{-}H_3CC_2CH_3)]$: the First Compound with Bent Tetraphenylborate as 12-Electron Donor Ligand (C) 1235
- Oxoniobates Containing Metal Clusters (R) 1437
- The Reaction of $[Cp^+_2Nb_2(B_2H_6)_2]$ ($Cp^+ = \eta$-$EtMe_4C_5$) with Sulfur: Stabilization of the Tetrathioborato Ligand in Novel Sulfido Niobium Clusters (C) 1021

Nitric oxide
- Tetramethyl-*ortho*-quinodimethane, First Member of a Family of Custom-Tailored Cheletropic Spin Traps for Nitric Oxide (C) 891

Nitrides
- Nitrido Complexes of Transition Metals (R) 955

Nitridoferrates
- Mössbauer Spectroscopy and Electronic Structure Calculations of the Nitridoferrates(III): $Li_3[FeN_2]$ and $Ba_3[FeN_3]$ (C) 1624

Nitrilimines
- A Straightforward Synthesis of Nitrilimines; X-Ray Crystal Structure of a Nitrilimine Stabilized by Non-Heteroatom Substituents (C) 439

Nitrogen compounds
- A Straightforward Synthesis of Nitrilimines; X-Ray Crystal Structure of a Nitrilimine Stabilized by Non-Heteroatom Substituents (C) 439
- Azidoiodoiodine(1+) Hexafluoroantimonate: The First Binary Nitrogen–Iodine Cation (C) 1338
- Biochemical Degradation of Cyanamide and Dicyandiamide (C) 620
- Crystalline Nitrogen Oxides — Crystal Structure of N_2O_3 and a Remark Concerning the Crystal Structure of N_2O_5 (C) 301
- Electrochemical Oxidation of 1-(*p*-Dimethylaminophenyl)-3,3-dimethyltriazene—Cyclic Voltammetric Detection of a Triazene Radical Cation and Dication (C) 332
- Molecular Mechanisms of the Reduction of NO to NH_2OH at Mo–S Centers (C) 205
- Phosphorus Nitrides—the Cinderella of Phosphorus Chemistry? (H) 170
- $Se_3N_2Cl_2$, a Novel Selenium–Nitrogen Chloride: Reinvestigation of "Se_4N_2" (C) 1518
- Se_2NCl_3 and $[Se_2NCl_2]^+[GaCl_4]^-$, Chloride Nitrides of Trivalent Selenium (C) 1251
- The Chemistry of Amidines and Imidates. Vol. 2 (B) 1395
- The First Reaction of S_5N_6; Structure of a Complex Containing an $S_2N_3^-$ Ligand (C) 616

Nitrogen fertilizers
- Biochemical Degradation of Cyanamide and Dicyandiamide (C) 620

Nitrogen fixation
- An Opinion on the Heterogeneous Photoreactions of N_2 with H_2O (C) 480

Nitronates
- Concave Wrapped Protons: Reagents for Contra-Thermodynamic Protonations (C) 80

Nitrosoalkenes
- Diacetoneglucose as Auxiliary Group for the Asymmetric Hetero-Diels–Alder Reaction with Nitrosoalkenes (C) 1033

Nitroxides
- Stable *N,N'*-Di-*tert*-butyl-*meta*-phenylenebisnitroxides—Unexpected Ground-State Singlets (C) 180

NMR microscopy
- Principles of Nuclear Magnetic Resonance Microscopy (B) 1394

NMR spectroscopy
- Determination of the H^N–H^α Coupling Constant in Large Isotopically Enriched Proteins (C) 1609
- Dynamic Proton Exchange in the Hydrogen Dihydroxide Ion $H_3O_2^-$ of the Hydroxosodalite Hydrate $[Na_4(H_3O_2)]_2[SiAlO_4]_6$: ^1H MAS NMR Spectroscopic Evidence (C) 1210
- Indirect $^{113}Cd,^{14}N$ Spin-Spin Coupling Constants as a Structural Probe of Solid Cadmium Thiocyanate Complexes (C) 1222
- Investigation of the [1,7] Sigmatropic Hydrogen Shift in a Parent Compound *Z,Z*-1,3,5-Heptatriene and Its Monodeuterium Analogue (C) 781
- Modern NMR Techniques, and Their Applications in Chemistry (B) 484
- Nuclear Magnetic Resonance Fourier Transform Spectroscopy (Nobel Lecture) (R) 805
- On the Mechanism of Coherent Dihydrogen Tunneling in Transition Metal Trihydrides (C) 1369
- One Dimensional and Two Dimensional NMR Spectra by Modern Pulse Techniques (B) 245

- Separation of Overlapping Multiplets in Two-Dimensional NMR Spectra by Selective "Injection" of Magnetization (C) 1248
- Solid-State NMR Spectroscopic and X-Ray Diffraction Studies of the Low-Temperature Structural Transformation of Hydrated Porous Aluminophosphate VPI-5 (C) 610
- The ^{31}P-NMR Spectroscopic Determination of the Enantiomeric Excess of Unprotected Amino Acids (C) 1092

Nobel lecture
- Elementary Steps in Synaptic Transmission Revealed by Currents through Single Ion Channels (Nobel Lecture) (R) 830
- Ion Channels for Communication Between and Within Cells (Nobel Lecture) (R) 824
- Nuclear Magnetic Resonance Fourier Transform Spectroscopy (Nobel Lecture) (R) 805
- Soft Matter (Nobel Lecture) (R) 842

Nonlinear optics
- Nitrocalix[4]arenes as Molecules for Second-Order Nonlinear Optics (C) 1075

Nucleic acids
- In Vitro Selection of Specific Ligand-binding Nucleic Acids (R) 979
- Modern Methods in Protein- and Nucleic Acid Research (B) 245
- Peptide Nucleic Acids (PNAs)—Unusual Properties of Nonionic Oligonucleotide Analogues (H) 1008
- Synthesis of Octameric Phosphodiesters of [3,3-Bis(hydroxymethyl)cyclobutyl]-adenine and -thymine as well as their Hybridization Properties (C) 482

Nucleofuges
- Electrostatic Activation of Nucleofuges: Cationic Leaving Groups (C) 216

Nucleosides
- A Synthetic Receptor for Cyclic Adenosine Monophosphate (C) 61
- 5′-*P*-Borane-Substituted Thymidine Monophosphate and Triphosphate (C) 1373
- Nucleoside Synthesis. Organosilicon Methods (B) 1098
- Stereoselective Synthesis of Phosphate-Modified Building Blocks of DNA (C) 1386

O-H Activation
- O–H Bond Activation in the Gas Phase: The Reactions of Water and Methanol with $[FeCH_3]^+$ (C) 603

Oligoanthrylenes
- Oligo(9,10-anthrylenes), Organic Compounds with Stable High-Spin States (C) 448

Oligomerization
- Scavenger Templates: Synthesis and Electrospray Mass Spectrometry of a Linear Porphyrin Octamer (C) 907

Oligonucleotides
- Crosslinking of Adjacent Guanine Residues in an Oligonucleotide by *cis*-$[Pt(NH_3)_2(H_2O)_2]^{2+}$: Kinetic Analysis of the Two-Step Reaction (C) 1483
- DNA Recognition by Hybrid Oligoether–Oligodeoxynucleotide Macrocycles (C) 1617
- Oligonucleotides and Analogues. A Practical Approach (B) 1398
- Peptide Nucleic Acids (PNAs)—Unusual Properties of Nonionic Oligonucleotide Analogues (H) 1008
- Synthesis of Octameric Phosphodiesters of [3,3-Bis(hydroxymethyl)cyclobutyl]-adenine and -thymine as well as their Hybridization Properties (C) 482

Oligosaccharides
- Synthesis of the Species-Specific *Mycobacterium avium* Trisaccharide (Serovar 21) for the Preparation of a Neoglycoprotein for Immunological Studies (C) 1358

Optical anomaly
- Optically Anomalous Crystals (R) 1

Organic conductors
- Deuterium-Induced Phase Transition of an Organic Metal—An Unusual Isotope Effect (C) 859
- Oligo(9,10-anthrylenes), Organic Compounds with Stable High-Spin States (C) 448

Organosulfur chemistry
- The Organosulfur Chemistry of the Genus *Allium*—Implications for the Organic Chemistry of Sulfur (R) 1135

Oscillations
- Chemical Oscillations and Instabilities. Nonlinear Chemical Kinetics (B) 109

Osmium compounds
- Carbene Osmium Complexes by Double Metalation of Alkoxylalkyl- and Aminoalkylphosphanes (C) 1025
- Catalytic Oxidation of Partially and Fully Fluorinated Olefins with Osmium Tetroxide (C) 1345
- $[(CO)_3(PPh_3)_2OsAg(O_2CCF_3)]$: A Model for an Intermediate on the Reaction Coordinate in Electron Transfer (C) 770

Oxadiboriranes
- Bis(trisyl)oxadiborirane (C) 1040

Oxidations
- Catalytic Oxidation of Partially and Fully Fluorinated Olefins with Osmium Tetroxide (C) 1345
- $[(CO)_3(PPh_3)_2OsAg(O_2CCF_3)]$: A Model for an Intermediate on the Reaction Coordinate in Electron Transfer (C) 770
- Electrochemical Oxidation of 1-(*p*-Dimethylaminophenyl)-3,3-dimethyltriazene—Cyclic Voltammetric Detection of a Triazene Radical Cation and Dication (C) 332
- Enzymatic Oxidation of Methyl Groups on Aromatic Heterocycles: A Versatile Method for the Preparation of Heteroaromatic Carboxylic Acids (C) 774
- Selective Oxidation of Methane to CO and H_2 over Ni/MgO at Low Temperatures (C) 1189
- Tetrathienylethylenes, a New Class of Electron Donors—Dications Twisted by 90° Stabilized by Formation of Polymethine Units (C) 455
- The Electrochemical Oxidation of $[Co^{II}(salen)]$ in Solvent Mixtures—An Example of a Ladder Scheme with Coupled Electron-Transfer and Solvent-Exchange Reactions (C) 1215

Oxygen activation
- Oxygen Activation on Nickel(II)-tetrahydrosalen Complexes with the Formation of Nickel(II)dihydrosalen Complexes (C) 623

Palladium compounds
- Evidence for [PdSiO] from IR Spectroscopy (C) 638
- Nucleophilic Attack at the Central Carbon Atom of (π-Allyl)palladium Complexes: Formation of α-Cyclopropyl Esters (C) 234

Particle beam microanalysis
- Particle Beam Microanalysis. Fundamentals, Methods and Applications (B) 108

Pattern recognition
- Similarity Models in Organic Chemistry, Biochemistry and Related Fields (B) 359

Peptide nucleic acids
- Peptide Nucleic Acids (PNAs)—Unusual Properties of Nonionic Oligonucleotide Analogues (H) 1008

Peptides
- Calculation of Molecular Dynamics for Peptides in Dimethyl Sulfoxide: Elimination of Vacuum Effects (C) 210
- Configuratively Stable Dipeptide Aldehydes from D-Glucosamine Hydrochloride (C) 1391
- Dynamic Forcing, a Method for Evaluating Activity and Selectivity Profiles of RGD (Arg-Gly-Asp) Peptides (C) 326
- Ion-Spray Mass Spectrometry of Lipopeptide Vaccines (C) 226
- Multiple Peptide Synthesis Methods and Their Applications (R) 367
- *N*-Perbenzylation of Oligopeptides with P4-Phosphazene Base; A New Protecting-Group Technique for Modification and Solubilization of Peptides in Apolar Organic Solvents (C) 1481
- Retro-Inverso Amide Bonds between Trifunctional Amino Acids (C) 785
- Selective Inhibition of Trypanosomal Triosephosphate Isomerase by a Thiopeptide (C) 328
- Stereoselective Nucleophilic Addition Reactions of Reactive Pseudopeptides (C) 1626
- The Chemical Synthesis of Peptides (B) 798
- The World of Peptides. A Brief History of Peptide Chemistry (B) 1535

Pericyclic reactions
- Transition Structures of Hydrocarbon Pericyclic Reactions (R) 682

Pesticides
- The Biochemistry and Uses of Pesticides. Structure, Metabolism, Mode of Action and Uses in Crop Protection (B) 242

Pharmaceutics
- Plants for Medicines. A Chemical and Pharmacological Survey of Plants in the Australian Region (B) 107
- Sulphur-Containing Drugs and Related Organic Compounds. Chemistry, Biochemistry and Toxicology (B) 107

Phenylenevinylenes
- *meta*-Phenylene Units as Conjugation Barriers in Phenylenevinylene Chains (C) 1653

Pheromones
- 3,4-Dihydroisocoumarins, a New Class of Ant Trail Pheromones (C) 795
- Do Pheromone Receptors that Receive the Same or Similar Signal Molecules Have the Same or Similar Structure? (C) 330
- Pheromones of Marine Brown Algae; A New Branch of the Eicosanoid Metabolism (C) 1246

Phosphaalkynes
- Spirocyclization of a Stable Phosphaalkyne with Aluminum Trichloride—Key Reaction for the Production of Triphospha Dewar Benzene Derivatives (C) 1055
- Unusual Coordination of the 1,3-Diphosphacyclobutadiene Derivative $(iPr_2NCP)_2$ to Two $[Ni(CO)_3]$ Fragments (C) 95

Phosphabenzene
- Tetrakis(η^1-phosphabenzene)nickel (C) 1343

Phosphanes
- Carbene Osmium Complexes by Double Metalation of Alkoxylalkyl- and Aminoalkylphosphanes (C) 1025
Phosphatidylinositol
- Synthesis and Biological Activity of D-3-Deoxy-3-Fluorophosphatidylinositol—A New Direction in the Design of non-DNA Targeted Anticancer Agents (C) 1379
Phosphazenes
- *N*-Perbenzylation of Oligopeptides with P4-Phosphazene Base; A New Protecting-Group Technique for Modification and Solubilization of Peptides in Apolar Organic Solvents (C) 1481
Phosphazenium ions
- A Safe Synthesis of Diphosphazenium Salts (C) 850
Phospholipases
- A Phenoxy-Bridged Homodinuclear Zn Complex with an Unusual Coordination Sphere; Model Compound for the Active Site of Phospholipase C (C) 1647
Phospholipids
- Chemoenzymatic Syntheses of the Optically Active Hydroperoxides of Phosphatidylglycerol and Phosphatidylethanolamine with Lipase, Lipoxygenase, and Phospholipase D (C) 1336
- Synthetic Chain-Substituted Phospholipids: Ion Transport Across Their Bilayer Membranes (C) 898
Phosphorus compounds
- A New, High-Yield Synthesis of Tetraphosphacubanes (C) 758
- Cyclophosphazene Metal Oxides, a New Class of Compounds, and Model Compounds for the Polymerization of Phosphazenes (C) 601
- Double Open-Edged P_{10} Dihydrofulvalene as a 16-Electron Donor Ligand (C) 1027
- Electrostatic Activation of Nucleofuges: Cationic Leaving Groups (C) 216
- Novel Binuclear Phosphinidene Compounds by Dimerization of the P–H-Functional Phosphenium Complexes $[C_5R_5(CO)_2W=PH(Mes)]$ (R = H, Me) (C) 1525
- P-Functionalization of the Tetraphosphacubane System (C) 879
- Phosphorus Nitrides—the Cinderella of Phosphorus Chemistry? (H) 170
- Phosphorus(v) Selenides with Phosphorus in a Trigonal-Planar Environment (C) 1350
- Ring Expansion of a 1,2-Diphosphaspiropentane: Formation of a Diphosphamethylenecyclobutane and a 1,4-Diphosphanorbornadiene (C) 625
- Synthesis, Structure, and Thermolysis of an Unusual Azaphosphasiliridine (C) 751
- Tetraphosphafulvalene Dianions: Isoelectronic Species of Tetrathiafulvalene Dications (C) 1031
- The Formation of *cyclo*-P_4 Ligands with Maximum Electron Donor Ability (C) 1377
- The Phosphorus Ylide CH_2PH_3 is Stable in the Gas Phase (C) 86
- Three Independent Molecules in the Unit Cell of a Phosphorus Ylide; Changes in the Molecular Geometry on Rotation about the Phosphorus–Carbon Ylide Bond (C) 99
- $Zn_7[P_{12}N_{24}]Cl_2$—A Sodalite with a Phosphorus–Nitrogen Framework (C) 213
Phosphoryl transfer
- En Route to Synthetic Phosphodiesterases: Supramolecular Phosphoryl-Transfer Mediated by Amidinium–Phosphate Contact Ion-Pairs (C) 207
Photochemistry
- An Opinion on the Heterogeneous Photoreactions of N_2 with H_2O (C) 480
- Assistance by Electrophiles in Photoinduced Alkylidyne–Carbonyl Coupling (C) 747
- Doubly Bridged Prismane and Dewar Benzene Intermediates in an Unusual Photochemical Rearrangement of Tricyclic Phthalic Esters (C) 862
- Electronic Aspects of Organic Photochemistry (B) 242
- Frontiers in Supramolecular Organic Chemistry and Photochemistry (B) 363
- Photochemical Technology (B) 360
- Photodimerization of Anthracenes in the Solid State: New Results from Atomic Force Microscopy (C) 595
- Photodimerization of Cinnamic Acid in the Solid State: New Insights on Application of Atomic Force Microscopy (C) 592
- Photoselective Processes in Cyclooctasulfur Layers: Desorption versus Polymerization (C) 874
- Photoswitchable Association of an Azobenzene-Bipyridinium Diad to Eosin: Photostimulated "On-Off" Guest Binding (C) 1243
- Semiconductor-Catalyzed Photoaddition of Cyclic Enol Ethers to 1,2-Diazenes (C) 1039
- Supramolecular Photochemistry (B) 104
- The Photochemistry of *N*-Phthaloyl α-Amino Acid Esters: A New Approach to β,γ-Unsaturated α-Amino acids and Dihydrobenzazepinediones (C) 73
- The Photochemistry of Stilbenoid Compounds and Their Role in Materials Technology (R) 1399
Photochromism
- Photochromism. Molecules and Systems (B) 804
Photoelectron spectroscopy
- The Pyrolysis of Tetranitromethane in the Gas Phase (C) 900
Photolithography
- Photolithographic Immobilization of Biopolymers on Solid Supports (C) 759
Photosensitizers
- Stepwise Synthesis of Binuclear Photoactive Complexes with a Bridging 3,4-Dihydroxyphenylterpyridine Ligand (C) 1028
Photosynthesis
- A New Type of Mn–O Cluster with a Mn_4 Chain Unit. Relevance to the Photosynthetic Oxygen Evolving Center (C) 1629
- Chlorins Designed for Photodynamic Tumor Therapy and as Model Systems for Photosynthesis (C) 1592
Physical chemistry
- Physical Chemistry from Ostwald to Pauling. The Making of a Science in America (B) 797
Plants
- Dictionary of Plants Containing Secondary Metabolites (B) 1396
Plants for medicines
- Plants for Medicines. A Chemical and Pharmacological Survey of Plants in the Australian Region (B) 107
Plasmalogens
- α-Hydroxyaldehyde Derivatives Arising from Oxidation of Plasmalogens (C) 468
Platinum compounds
- The First Metal–Metal Silyl Migration in a Heterobimetallic Complex, and the Structure of the Rearrangement Product $[(OC)_4Fe(\mu\text{-}PPh_2)Pt\{Si(OMe)_3\}(PPh_3)]$ (*Fe–Pt*) (C) 1583
Polarized light microscopy
- Optically Anomalous Crystals (R) 1
Polycycles
- Two Stereoisomeric [4.5.5.5]Fenestranes Formed by Intramolecular [2 + 2] Cycloaddition (C) 344
- [4 + 4]-Cycloaddition Reactions in the Total Synthesis of Naturally Occurring Eight-Membered Ring Compounds (H) 422
Polyenes
- A Homologous Series of Stable Polyenes: Synthesis, Structure, and Redox Behavior (C) 1588
- Dual Fluorescence of Novel Modified Carotenoids (C) 1042
- Synthetic Approaches toward Molecular and Polymeric Carbon Allotropes (R) 1101
Polyethers
- Novel Polyether Copolymers Consisting of Linear and Dendritic Blocks (C) 1200
Polymerization
- Cationic Metallocene Polymerization Catalysts. Synthesis and Properties of the First Base-Free Zirconocene Hydride (C) 1375
- Enantioselective Polymerization of 1,2-Diisocyanoarenes—Synthesis of Optically Active, Helical Poly(quinoxaline-2,3-diyl)s (C) 1509
- Reaction of Heterodinuclear μ-Ethynediyl Complexes Containing Palladium and Platinum: Multiple and Successive Insertion of Isocyanides (C) 851
- Regioselectivity Control in the Palladium-Catalyzed Copolymerization of Propylene with Carbon Monoxide (C) 303
- Selectivity Control By Temperature Variation in the Formation of Isotactic vs. Syndiotactic Polypropylene with a Titanocene/Alumoxane Catalyst (C) 199
- Synthesis of Optically Active Macromolecules Using Metallocene Catalysts (H) 47
Polymers
- Liquid Crystallinity in Polymers. Principles and Fundamental Properties (B) 358
- *meta*-Phenylene Units as Conjugation Barriers in Phenylenevinylene Chains (C) 1653
- Polymer Solutions (B) 240
- Soft Matter (Nobel Lecture) (R) 842
- The Chemistry of Polymers (B) 486
Polyoxometalates
- A Novel Polyoxotungstate Containing a *triangulo* Ni^{II}_3 Cluster with Ferromagnetic Exchange Interactions and an $S=3$ Ground State (C) 649
- $BaNb_7O_9$, a New Oxoniobate with Double Layers of Corner-Sharing Nb_6 Octahedra (C) 212
- New Directions in Polyvanadate Chemistry: From Cages and Clusters to Baskets, Belts, Bowls, and Barrels (*H*) 49
Polypropylene
- High Molecular Weight Polypropylene through Specifically Designed Zirconocene Catalysts (C) 1347
- Selectivity Control By Temperature Variation in the Formation of Isotactic vs. Syndiotactic Polypropylene with a Titanocene/Alumoxane Catalyst (C) 199
Polysiloxanes
- Induction of Ferroelectricity in Polymeric Systems through Hydrogen Bonding (C) 1531

Polyynes
- Efficient Synthesis of Nanoscale Macrocyclic Hydrocarbons (C) 922
- Novel Cross-Conjugated Compounds Derived from Tetraethynylethene (C) 1240
- Synthetic Approaches toward Molecular and Polymeric Carbon Allotropes (R) 1101
- The Thermal Conversion of Poly[(silylene)diacetylene] Metal Oxide Composites: A New Approach to β-SiC–MC Ceramics (C) 1195

Porphyrinoids
- A Nonaromatic Expanded Porphyrin Derived from Anthracene—A Macrocycle which Unexpectedly Binds Anions (C) 452
- First Example of a Chlorophin from an Unexpected Oxidative Ring-Opening of an (Octadehydrocorrinato)nickel(II) Salt (C) 70
- Scavenger Templates: Synthesis and Electrospray Mass Spectrometry of a Linear Porphyrin Octamer (C) 907
- Spectroscopic Characterization of Two Types of Tetraarylporphyrin Cation Radicals (C) 1615

Prelog, Vladimir
- My 132 Semesters of Chemistry Studies. Vladimir Prelog (B) 1395

Prismanes
- Doubly Bridged Prismane and Dewar Benzene Intermediates in an Unusual Photochemical Rearrangement of Tricyclic Phthalic Esters (C) 862

Protecting groups
- *N*-Perbenzylation of Oligopeptides with P4-Phosphazene Base; A New Protecting-Group Technique for Modification and Solubilization of Peptides in Apolar Organic Solvents (C) 1481
- Protective Groups in Organic Synthesis (B) 658

Proteins
- Chemical Attachment of Organometallics to Proteins in Reverse Micelles (C) 789
- Cytochromes C. Evolutionary, Structural and Physicochemical Aspects (B) 1098
- Determination of the H^N–H^α Coupling Constant in Large Isotopically Enriched Proteins (C) 1609
- Docking of a Second Functional Protein Layer to a Streptavidin Matrix on a Solid Support: Studies with a Quartz Crystal Microbalance (C) 1087
- Modern Methods in Protein- and Nucleic Acid Research (B) 245
- Molecular Modeling of the Class I Human Histocompatibility Molecule HLA-A2 Presenting an Allele-Specific Nonapeptide from Influenza Matrix Protein (C) 886
- Proteins from the D-Chiral World (H) 1457

Protonations
- Concave Wrapped Protons: Reagents for Contra-Thermodynamic Protonations (C) 80

Pyrans
- Palladium-Catalyzed C-H Activation of Methoxy Groups: A Facile Synthesis of Substituted 6*H*-Dibenzo[*b*,*d*]pyrans (C) 1023

Pyrazines
- Diprotonated Tetra(2-pyridyl)pyrazine and its Chemical Mimesis due to Different Hydrogen Bridges (C) 299

Pyrenes
- The Crystal Structure of [(Pyrene$^{\cdot-}$)-{$Na^+[(C_2H_5)_2O]$}]: A Model for Stacked Radical Anion Salts (C) 878

Pyrrolidones
- Enantioselective Synthesis of the Antidepressant Rolipram by Michael Addition to a Nitroolefin (C) 870

Quantum mechanics
- Quanta. A Handbook of Concepts (B) 1095

Quartz-crystal microbalance
- Docking of a Second Functional Protein Layer to a Streptavidin Matrix on a Solid Support: Studies with a Quartz Crystal Microbalance (C) 1087
- Quantification of the Reactivity of 3-Aminopropyltriethoxysilane Monolayers with the Quartz-Crystal Microbalance (C) 336

Quinodimethanes
- Indigoid *para*-Quinodimethanes (C) 1202
- Tetramethyl-*ortho*-quinodimethane, First Member of a Family of Custom-Tailored Cheletropic Spin Traps for Nitric Oxide (C) 891

Quinones
- Allylation of Quinones with Allylsilane in the Presence of Lithium Perchlorate in Ether (C) 313

Quinonimines
- Molecular Switching by Electron Transfer—the Spiroperimidine/Quinonimine System (C) 1498

Radialenes
- Preparation and Properties, Reactions, and Applications of Radialenes (R) 931

Radical anions
- Deuterium-Induced Phase Transition of an Organic Metal—An Unusual Isotope Effect (C) 859
- The Crystal Structure of [(Pyrene$^{\cdot-}$)-{$Na^+[(C_2H_5)_2O]$}]: A Model for Stacked Radical Anion Salts (C) 878

Radical cations
- A New Synthesis for Imidazolo- and Pyrrolophanes by [3 + 2] Cycloaddition with Azaallenyl Radical Cations (C) 209
- Benzo-1,2,3-triselenolium Trifluoromethanesulfonate—a C_2Se_3 Radical Cationic Salt with Unusual Solid-State Structure (C) 779
- Electrochemical Oxidation of 1-(*p*-Dimethylaminophenyl)-3,3-dimethyltriazene—Cyclic Voltammetric Detection of a Triazene Radical Cation and Dication (C) 332
- Houben-Weyl. Methoden der Organischen Chemie. Band E19c: Carbokationen, Carbokation-Radikale (B) 799
- Spectroscopic Characterization of Two Types of Tetraarylporphyrin Cation Radicals (C) 1615

Radical reactions
- The Uncatalyzed Transfer Hydrogenation of α-Methylstyrene by Dihydroanthracene or Xanthene—a Radical Reaction (C) 1523

Radicals
- Addition of Benzyl Radicals to Alkenes: The Role of Radical Deformation in the Transition State (C) 635
- Reagents with Hypervalent Iodine: Formation of Convenient Chiral Synthetic Intermediates by Fragmentation of Carbohydrate Anomeric Alkoxy Radicals (C) 772
- Stable *N*,*N*′-Di-*tert*-butyl-*meta*-phenylenebisnitroxides—Unexpected Ground-State Singlets (C) 180
- Synthesis of *C*-Glycopeptides via Free Radical Addition of Glycosyl Bromides to Dehydroalanine Derivatives (C) 902
- Tetramethyl-*ortho*-quinodimethane, First Member of a Family of Custom-Tailored Cheletropic Spin Traps for Nitric Oxide (C) 891

Radiochemistry
- The Chemistry of GALLEX—Measurement of Solar Neutrinos with a Radiochemical Gallium Detector (R) 1283

Reaction mechanisms
- [2,3] Wittig Rearrangements of Nonconjugated Secondary α-Lithioethers: Proof of Stereospecificity and Inversion of the Configuration of the Carbanion C Atom (C) 647
- A Novel Six-Center Deprotonation–Lithiation Reaction Mechanism Supported by the X-Ray Structure Analysis of a Lithium Carbazolide (C) 1209
- Addition of Benzyl Radicals to Alkenes: The Role of Radical Deformation in the Transition State (C) 635
- Chemiluminescence Oscillations Driven by a Flow-through Reactor in the $[Ru(bpy)_3]^{2+}$ Catalyzed Belousov–Zhabotinskii Reaction (C) 355
- Mutual Catalysis of Neutral and Anionic Cobalt Carbonyls in their CO Scrambling Reactions (C) 1596
- Reaction Dynamics of Aligned Molecules (R) 516
- Reaction Mechanisms of Inorganic and Organometallic Systems (B) 1397
- The Benzene Ring as Dienophile in an Intramolecular [4+2] Cycloaddition: Degenerate Rearrangement of 7,8-Benzobicyclo[4.2.2]deca-2,4,7,9-tetraene (C) 872

Reactive intermediates
- Cyclohexadienyl-Type Cationic Intermediates in the Friedel–Crafts Alkylation of Benzene Derivatives with the 9-Fluorenyl Cation—Observation by Laser Flash Photolysis (C) 743
- Cyclopropane Derived Reactive Intermediates (B) 241
- Doubly Bridged Prismane and Dewar Benzene Intermediates in an Unusual Photochemical Rearrangement of Tricyclic Phthalic Esters (C) 862
- Short-Lived Molecules (B) 362
- Structures of Two Highly Reactive Intermediates upon $LiAlH_4$ Reduction in the Solid State and in Solution: $[(Me_3Si)_2NAlH_3Li \cdot 2Et_2O]_2$ and $[(Me_3Si)_2N]_2AlH_2Li \cdot 2Et_2O$ (C) 854

Reagents
- A Safe Synthesis of Diphosphazenium Salts (C) 850
- A Simple Method for the Replacement of the OH Group in Free Carboxylic Acids by the Phosphonium Ylide Group (C) 1064
- Alkynyl- and Alkenyl(phenyl)iodonium Compounds (R) 274
- Allylation of Quinones with Allylsilane in the Presence of Lithium Perchlorate in Ether (C) 313
- C–C Coupling with NO_2/Alkyl Substitution at the Vinylic Carbon by Reaction of 2-Aryl-1-nitro-1-alkenes with Dialkylzinc Compounds—A Novel Reaction (C) 1587
- Does the Naked Fluoride Ion Exist? (H) 292
- Ligand Effects in Grignard Additions (C) 342
- *N*-Lithiomethyl-*N*,*N*′,*N*″,*N*″-tetramethyldiethylenetriamine: The First Alkyllithium Compound which is Monomeric in Hydrocarbons (C) 633
- [Lithium Piperidide–Piperidine]$_4$: Crystal Structure of an Oligomeric 1:1 Lithium Amide–Amine Mixed Complex, an

Intermediate in the *N*-Lithiation of Amines (C) 1205
- Preparative Polar Organometallic Chemistry 2 (B) 485
- Reductions by the Alumino- and Borohydrides in Organic Synthesis (B) 1534
- The Chemistry of Amidines and Imidates. Vol. 2 (B) 1395

Rearrangements
- Synthesis and Reactions of Isothiocyanate-Substituted Allenes and 1,3-Butadienes (C) 90
- Synthesis of Isocyanate-Substituted Allenes and 1,3-Butadienes by [3,3] Sigmatropic Rearrangements (C) 866
- The Benzene Ring as Dienophile in an Intramolecular [4+2] Cycloaddition: Degenerate Rearrangement of 7,8-Benzobicyclo[4.2.2]deca-2,4,7,9-tetraene (C) 872

Receptors
- Estradiols Modified by Metal Carbonyl Clusters as Suicide Substrates for the Study of Receptor Proteins: Application to the Estradiol Receptor (C) 753

Redox enzymes
- Chemical Attachment of Organometallics to Proteins in Reverse Micelles (C) 789

Reductions
- Formate-Driven, Non-Enzymatic NAD(P)H Regeneration for the Alcohol Dehydrogenase Catalyzed Stereoselective Reduction of 4-Phenyl-2-butanone (C) 1529
- Reduction of Dispersed Indigo Dye by Indirect Electrolysis (C) 1068
- Reductions by the Alumino- and Borohydrides in Organic Synthesis (B) 1534
- Structures of Two Highly Reactive Intermediates upon $LiAlH_4$ Reduction in the Solid State and in Solution: $[(Me_3Si)_2NAlH_3Li \cdot 2Et_2O]_2$ and $[(Me_3Si)_2N]_2AlH_2Li \cdot 2Et_2O$ (C) 854

Renewable raw materials
- Carbohydrates as Organic Raw Materials (B) 361
- Wood and Cellulosic Chemistry (B) 801

Retro-inverso peptides
- Retro-Inverso Amide Bonds between Trifunctional Amino Acids (C) 785

Rhenium compounds
- A Dramatic Difference in the Reactivities of Alkoxido- and Aryloxidorhenium Complexes in Insertion Reactions (C) 220
- $[t\mathrm{BuSiO}(ReO_4)]_4$, a Model Compound for Metal Oxides on Silicate Surfaces—Synthesis from the Stable Triol tBuSi(OH)$_3$ and Re_2O_7 (C) 599
- Cyclophosphazene Metal Oxides, a New Class of Compounds, and Model Compounds for the Polymerization of Phosphazenes (C) 601
- Novel Strategies for the Synthesis and Crystallization of Electrophilic Dinuclear Cations: Solution and Solid-State Properties of $[Re_2(NCCH_3)_{10}]$-$[Mo_6O_{19}]_2$ (C) 1360

Rhodium compounds
- A Rh^I-Centered Cage Compound with Selective Catalytic Properties (C) 905
- Dimerization of Thiophene to Give a Linear $S(CH)_8S$ Fragment with $[(C_5Me_5)Rh(C_2H_4)_2]$ (C) 357
- Double Open-Edged P_{10} Dihydrofulvalene as a 16-Electron Donor Ligand (C) 1027
- Enantioselective Rhodium(II) Catalysts (H) 1183
- The Formation of *cyclo*-P_4 Ligands with Maximum Electron Donor Ability (C) 1377

Ribonucleotide reductase
- Multifield Saturation Magnetization Measurements of Oxidized and Reduced Ribonucleotide Reductase from *Escherichia coli* (C) 1513

Ribozymes
- In Vitro Selection of Specific Ligand-binding Nucleic Acids (R) 979

Rotaxanes
- Cyclodextrins, Off-the-Shelf Components for the Construction of Mechanically Interlocked Molecular Systems (H) 846
- Synthesis of a Lipophilic Cyclodextrin-[2]-Rotaxane (C) 783
- Threading Cyclodextrin Rings on Polymer Chains (C) 197

Ruthenium compounds
- Arborols Based on Luminescent and Redox-Active Transition Metal Complexes (C) 1493
- (Isocyanide)ruthenate Analogues of Tetracarbonylferrate (C) 83
- Metallacumulenes: Activation of Diynes and Access to a Novel Bis-(Alkenylallenylidene)ruthenium Complex with the Structural Unit $R_2C=C=C=Ru=C=C=CR_2$ (C) 651
- Preparation, Ligand Exchange Reactions, and Structure of a Diene(aqua)-ruthenium Complex $[(cod)Ru(H_2O)_4]$-$(OTs)_2$ (C) 440
- $[RuO(dppz)(tpy)]^{2+}$: a DNA Cleavage Agent with High DNA Affinity (C) 1048
- Stepwise Synthesis of Binuclear Photoactive Complexes with a Bridging 3,4-Dihydroxyphenylterpyridine Ligand (C) 1028
- The Structure of the [1.1]Ruthenocenophane Dication: Metal–Metal Bond Formation and the Consequences of Proximity (C) 1352

Sandwich complexes
- A New Approach to Bis(arene)titanium(0) and -titanium(−1) Complexes; Structure of Bis(arene)titanates(1−) (C) 1495
- A Structurally Distorted Ligand in an Electron-Deficient Dizirconocene Cation: Unusual 1,2- and 1,1-Dimetallioalkenes (C) 876
- 1-Borabutadiene(cyclopentadienyl)cobalt Complexes (C) 1603
- "[Cp*Co=CoCp*]" is a Hydride (C) 1341
- $[(\eta^5\text{-Cp})_2Sn(\mu\text{-}\eta^5\text{-Cp})Na \cdot PMDETA]$, a Compound with a Trigonal-Planar "Paddle Wheel" Triorganostannate Ion (C) 1226
- Cyclopentadienyl Cobalt Complexes of Cobaltapentalenes: Products Formed by Reaction of (μ-Cyclopentadienylidene) Cobalt Complexes with Silylalkynes (C) 1058
- Ether-Soluble Ti^0 and Bis(η^6-arene)-titanium(0) Complexes from the Reduction of $TiCl_4$ with Triethylhydroborate (C) 1490
- $[(\pi\text{-}Me_5C_5)_2SiH]^+$—A Novel Silyl Cation (C) 1605
- $[Nb\{B(\eta^6\text{-}C_6H_5)_2(C_6H_5)_2\}(\eta^2\text{-}H_3CC_2CH_3)]$: the First Compound with Bent Tetraphenylborate as 12-Electron Donor Ligand (C) 1235
- "Non-Coordinating" Anions: Underestimated Ligands (H) 1181
- On the Reaction of Pentamethylcyclopentadiene with Cobalt Atoms: A Reexamination 1392
- One-Pot Multifunctionalization of Polymethyl Hydrocarbon π Ligands. Maximum Space Occupancy by Double Branching and Formation of Arboroles (C) 458
- Stepwise Stacking of Three Paramagnetic Metallocene Units: $[CpNiCp(SiMe_2)_2CpCrCp(SiMe_2)_2CpNiCp]$ (C) 1258
- Synthesis and Structure of the First Trinuclear, Half-Sandwich Carboranegadolinium(III) Cluster (C) 432
- Synthesis of Optically Active Macromolecules Using Metallocene Catalysts (H) 47
- 2,2',5,5'-Tetra-*tert*-butyl-1,1'-diazaplumbocene—a Stable Azacyclopentadienyl Compound of Lead (C) 778
- The Electronic Structure of $[(\eta^5\text{-}C_5H_5)_2Co_2]$: Comment on the Existence of a Complex with an Unsupported Co–Co Double Bond (C) 471
- The Structure of the [1.1]Ruthenocenophane Dication: Metal–Metal Bond Formation and the Consequences of Proximity (C) 1352

Scanning tunneling microscopy
- Molecular Imaging of Alkanol Monolayers on Graphite (C) 189
- Scanning Tunneling Microscopy and Atomic Force Microscopy in Organic Chemistry (R) 1298

Selenium compounds
- Benzo-1,2,3-triselenolium Trifluoromethanesulfonate—a C_2Se_3 Radical Cationic Salt with Unusual Solid-State Structure (C) 779
- $KCeSe_4$: A New Solid-State Lanthanide Polychalcogenide (C) 1594
- New Intermediate Steps in the Synthesis of Larger Nickel Clusters (C) 321
- Phosphorus(V) Selenides with Phosphorus in a Trigonal-Planar Environment (C) 1350
- Selenonium Hexafluoroantimonate, $H_3Se^+SbF_6^-$ (C) 643
- $Se_3N_2Cl_2$, a Novel Selenium–Nitrogen Chloride: Reinvestigation of "Se_4N_2" (C) 1518
- Se_2NCl_3 and $[Se_2NCl_2]^+[GaCl_4]^-$, Chloride Nitrides of Trivalent Selenium (C) 1251
- Synthesis and Structure of the Cluster $[NaAu_{12}Se_8]^{3-}$: An Inorganic Cryptand Complex (C) 787
- The $[(\mu_3\text{-}WSe_4)_3(\mu_3\text{-}Se)_2(Cu_3)_2]^{4-}$ Anion, an Inorganic Cluster with a Pinwheel Shape (C) 1477

Self-assembly
- Decamethylcucurbit[5]uril (C) 1475
- Induction of Ferroelectricity in Polymeric Systems through Hydrogen Bonding (C) 1531
- Self-Assembly of a Cu_4 Complex with Coplanar Copper(I) Ions: Synthesis, Structure, and Electrochemical Properties (C) 733
- Solid-State Columns Made from Twisted, Self-Complementary Terpyridine Units (C) 1244
- Spontaneous Self-Assembly of a Dinickel(II) Double Helicate Containing a 1,3-Benzenediyl Spacer Group (C) 230
- Supramolecular Self-Assemblies of Two-Directional Cascade Molecules: Automorphogenesis (C) 917
- Synthetic Bilayer Membranes: Molecular Design, Self-Organization, and Application (R) 709
- The First Self-Assembled Dinuclear Triple-Helical Lanthanide Complex: Synthesis and Structure (C) 1622

Self-replication
- Artificial Replication Systems (H) 1013

- Self-Replication by Condensation of 3-Aminobenzamidines and 2-Formylphenoxyacetic Acids (C) 654

Semiempirical calculations
- Product Predictions for Nucleophilic Additions to C_{70} (C) 1468

Sensors
- Field-Effect Transistors as Sensors of Neural Systems (H) 45

Separation techniques
- Non-Chromatographic Continuous Separation Techniques (B) 484

Serovar 21
- Synthesis of the Species-Specific *Mycobacterium avium* Trisaccharide (Serovar 21) for the Preparation of a Neoglycoprotein for Immunological Studies (C) 1358

Sesquichalcogenides
- A Germanium Sesquisulfide, $(t\text{BuGe})_4S_6$, without Adamantane Structure (C) 59

Sialosides
- Synthesis of Esterase-resistant 9-*O*-Acetylated Polysialoside as Inhibitor of Influenza C Virus Hemagglutinin (C) 1478

Siderophores
- Synthesis and Complexation Properties of a Cyclodextrin-Derived Siderophore Analogue (C) 1381
- The First Structural Characterization of a Metal–Enterobactin Complex: $[V(\text{enterobactin})]^{2-}$ (C) 466

Si-H activation
- Triphosphatrisilacyclohexanes as Tridentate Coronands in Cr and Mo Complexes: Activation of Si–H in an Early Stage versus Phosphane Coordination (C) 1510

Silicon compounds
- An Arsanylidensilane ("Arsasilene") and its Derivatization with Tellurium and Benzophenone (C) 316
- $[t\text{BuSiO}(ReO_4)]_4$, a Model Compound for Metal Oxides on Silicate Surfaces—Synthesis from the Stable Triol $t\text{BuSi(OH)}_3$ and Re_2O_7 (C) 599
- Control and Design Principles in Biological Mineralization (R) 153
- Gas-Phase Reactions of M^+ and $[CpM]^+$ (M = Fe, Co, Ni) with 1,3,5-Trisilacyclohexane: First Evidence for the Formation of 1,3,5-Trisilabenzene (C) 1633
- $(H_2Si)_2E_2$ and $(Mes(t\text{Bu})Si)_2E_2$ (E = As, P): Incommensurable Systems of Different Stability with Unusually Long E–E Bonds (C) 460
- $[(\pi\text{-}Me_5C_5)_2SiH]^+$—A Novel Silyl Cation (C) 1605
- Model Compounds for Metal Oxides on SiO_2 Surfaces (H) 586
- Octakis(1,1,2-trimethylpropyl)octasilacubane: Synthesis, Molecular Structure, and Unusual Properties (C) 1354
- On the Bonding in Carbosilanes (C) 185
- Si_{60}, an Analogue of C_{60}? (H) 173
- Structure and Reactivity of Silicon Clusters in the Gas Phase (H) 172
- Synthesis, Structure, and Thermolysis of an Unusual Azaphosphasiliridine (C) 751
- The Reaction of Tetramesityldisilene with As_4: Synthesis and Structure of a Novel Arsenic–Silicon Tricyclic Ring System (C) 1217
- The Thermal Conversion of Poly[(silylene)diacetylene] Metal Oxide Composites: A New Approach to β-SiC—MC Ceramics (C) 1195
- Triphosphatrisilacyclohexanes as Tridentate Coronands in Cr and Mo Complexes: Activation of Si–H in an Early Stage versus Phosphane Coordination (C) 1510

Silicon monoxide
- Evidence for [PdSiO] from IR Spectroscopy (C) 638

Silver compounds
- Ag_5GeO_4, a New Semiconducting Oxide (C) 653
- $[(CO)_3(PPh_3)_2OsAg(O_2CCF_3)]$: A Model for an Intermediate on the Reaction Coordinate in Electron Transfer (C) 770
- Molecular Machines: Molecular Structure of $[(p\text{-}Tol_3P)_{10}Au_{13}Ag_{12}Cl_8](PF_6)$—a Cluster with a Biicosahedral Rotorlike Metal Core and an Unusual Arrangement of Bridging Ligands (C) 445

Similarity modeling
- Similarity Models in Organic Chemistry, Biochemistry and Related Fields (B) 359

Size exclusion chromatography
- Preparative-Scale Separation of C_{60} and C_{70} on Polystyrene Gel (C) 644

Sodalite
- $Zn_7[P_{12}N_{24}]Cl_2$—A Sodalite with a Phosphorus–Nitrogen Framework (C) 213

Solid-phase synthesis
- A New Strategy for Solid-Phase Synthesis of *O*-Glycopeptides (C) 857

Solid-state chemistry
- Bonding and Structure: Structural Principles in Inorganic and Organic Chemistry (B) 663
- $KCeSe_4$: A New Solid-State Lanthanide Polychalcogenide (C) 1594
- Solid State Chemistry—Compounds (B) 1396
- Synchrotron X-ray and Neutron Diffraction Studies in Solid-State Chemistry (R) 1557

Solid-state structures
- A Remarkable Change in Framework Cation Positions upon Lithium Exchange: the Crystal Structure of $LiMnPO_4(OH)$ (C) 1090
- Are Denser Packings of Spheres than Closest Packings Possible? How Many Closest Packings of Spheres Exist? (H) 727
- Band Theory of Solids. An Introduction from the Point of View of Symmetry (B) 1097
- Generalized Edshammar Polyhedra for the Description of a Family of Solid-State Structures (C) 924
- New Layered Iron-Lanthanum-Oxide-Sulfide and -Selenide Phases: $Fe_2La_2O_3E_2$ (E = S,Se) (C) 1645
- Oxoniobates Containing Metal Clusters (R) 1437

Solvation
- Penetrated Ion Pairs: a New Form of Ion Pair (H) 731

Spectroscopy
- Atomic Spectroscopy (B) 236
- High Resolution Spectroscopy below the Doppler Width (R) 263
- NMR, NQR, EPR, and Mössbauer Spectroscopy in Inorganic Chemistry (B) 108
- Reaction Dynamics of Aligned Molecules (R) 516

Spin transitions
- Microcalorimetry of the Spin-Transition Systems $[Fe(bts)_2(NCS)_2]$ and $[Fe(2\text{-}pic)_3]Cl_2 \cdot EtOH$ in the Range $15\ K < T < 300\ K$ (C) 178

Spin traps
- Tetramethyl-*ortho*-quinodimethane, First Member of a Family of Custom-Tailored Cheletropic Spin Traps for Nitric Oxide (C) 891

Squalenes
- The Folding of Squalene; An Old Problem has New Results (H) 582

Statistics
- Chemometrics. Applications of Mathematics and Statistics to Laboratory Systems (B) 663

Stereochemistry
- Flexible Molecules with Defined Shape—Conformational Design (R) 1124 (1657)
- Stereochemistry of Organic Compounds. Principles and Applications (B) 1539

Steroids
- Synthesis of (2-Arylindol-3-yl)acetamides as Probes of Mitochondrial Steroidogenesis—A New Mechanism for $GABA_A$ Receptor Modulation (C) 1060
- The Folding of Squalene; An Old Problem has New Results (H) 582
- The Tandem Sakurai–Carbonyl–Ene Reaction: A New and Highly Stereoselective Sequential Transformation and Its Use for the Synthesis of Steroid Derivatives (C) 1221

Stilbenes
- The Photochemistry of Stilbenoid Compounds and Their Role in Materials Technology (R) 1399

Strained rings
- Anti-Bredt Enol Ethers by Transannular Cyclization of Cycloalkynols (C) 791
- Boriranes: Structures and Thermal Ring Openings (C) 1384
- Compounds with Three-Membered Rings Containing Boron (H) 1329
- Cubanes: Starting Materials for the Chemistry of the 1990s and the New Century (R) 1421
- Cycloalkadiynes—From Bent Triple Bonds to Strained Cage Compounds (R) 27
- Cyclobutarenes. The Chemistry of Benzocyclobutene, Biphenylene, and Related Compounds (B) 1264
- 1,2,4-Cyclohexatriene, an Isobenzene, and Bicyclo[4.4.0]deca-1,3,5,7,8-pentaene, an Isonaphthalene: Generation and Trapping Reactions (C) 473
- 1,2,4-Cyclohexatriene, an Isobenzene, and its [2 + 2] Cycloaddition with Styrene: A Theoretical Study (C) 476
- Cyclopropane Derived Reactive Intermediates (B) 241
- Homodiboriranides: The Simplest Negatively Charged Homoaromatic Compounds (C) 1238
- Nucleophilic Attack at the Central Carbon Atom of (π-Allyl)palladium Complexes: Formation of α-Cyclopropyl Esters (C) 234
- Preparation and Properties, Reactions, and Applications of Radialenes (R) 931
- Quest for Higher Ladderanes: Oligomerization of a Cyclobutadiene Derivative (C) 1488
- Ring Expansion of a 1,2-Diphosphaspiropentane: Formation of a Diphosphamethylenecyclobutane and a 1,4-Diphosphanorbornadiene (C) 625
- Strain-Activated Formation of a Triple-Layered Phane (C) 1073
- The Reaction of Tetramesityldisilene with As_4: Synthesis and Structure of a Novel Arsenic–Silicon Tricyclic Ring System (C) 1217

Streptavidin
- Docking of a Second Functional Protein Layer to a Streptavidin Matrix on a Solid Support: Studies with a Quartz Crystal Microbalance (C) 1087
Structure elucidation
- Bond-Stretch Isomers: Fact or Artifact? (H) 286
- Caro's Acid: Molecular Structure and Association in the Solid State at −130 °C (C) 436
- Crystalline Nitrogen Oxides — Crystal Structure of N_2O_3 and a Remark Concerning the Crystal Structure of N_2O_5 (C) 301
- Diprotonated Tetra(2-pyridyl)pyrazine and its Chemical Mimesis due to Different Hydrogen Bridges (C) 299
- Distorted Molecules: Perturbation Design, Preparation and Structures (R) 550
- Novel Strategies for the Synthesis and Crystallization of Electrophilic Dinuclear Cations: Solution and Solid-State Properties of $[Re_2(NCCH_3)_{10}]$-$[Mo_6O_{19}]_2$ (C) 1360
- Perfluorotriethylamine: An Amine with Unusual Structure and Reactivity (C) 1467
- Solving the Structure of a Metal-Substituted Aluminum Phosphate Catalyst by Electron Microscopy, Computer Simulation, and X-ray Powder Diffraction (C) 1472
- Structure of the Lowest Temperature Phase of the Solid Benzene–Hexafluorobenzene Adduct (C) 1655
- Synchrotron X-ray and Neutron Diffraction Studies in Solid-State Chemistry (R) 1557
- The Isomers of the Acetylene Derivatives C_2Li_4: Transferable Structural Units in Hyperlithiated Compounds (C) 1602
- The New Subnitride $NaBa_3N$; an Extension of Alkali Metal Suboxide Chemistry (C) 1519
- The Structure of C_{60}: Orientational Disorder in the Low-Temperature Modification of C_{60} (C) 640
- The Structure of Water—a Mixture of Cubes and Planar Four-Membered Rings? (H) 1577
Structure–activity relationship
- Do Pheromone Receptors that Receive the Same or Similar Signal Molecules Have the Same or Similar Structure? (C) 330
- Similarity Models in Organic Chemistry, Biochemistry and Related Fields (B) 359
Styrenes
- The Uncatalyzed Transfer Hydrogenation of α-Methylstyrene by Dihydroanthracene or Xanthene—a Radical Reaction (C) 1523
Subnitrides
- The New Subnitride $NaBa_3N$; an Extension of Alkali Metal Suboxide Chemistry (C) 1519
Sugars
- Emil Fischer's Proof of the Configuration of Sugars: A Centennial Tribute (R) 1541
Sulfinylcarboxylic acids
- Salting Out Selective Extraction—A Novel Method for the Optical Resolution of Chiral Sulfinylcarboxylic Acids and Its Application for the Convenient Determination of Optical Purity (C) 1631
Sulfur
- Photoselective Processes in Cyclooctasulfur Layers: Desorption versus Polymerization (C) 874
Sulfur compounds
- A Germanium Sesquisulfide, $(t\text{BuGe})_4S_6$, without Adamantane Structure (C) 59
- Caro's Acid: Molecular Structure and Association in the Solid State at −130 °C (C) 436
- Chemistry of Organsulfur Compounds. General Problems (B) 238
- Dimerization of Thiophene to Give a Linear $S(CH)_8S$ Fragment with $[(C_5Me_5)Rh(C_2H_4)_2]$ (C) 357
- Sulfur Analogues of Polycyclic Aromatic Hydrocarbons (Thiaarenes). Environmental Occurrence, Chemical and Biological Properties (B) 364
- The First Reaction of S_5N_6; Structure of a Complex Containing an $S_2N_3^-$ Ligand (C) 616
- The Organosulfur Chemistry of the Genus *Allium*—Implications for the Organic Chemistry of Sulfur (R) 1135
- The Structures of Thiosulfuric Acid $H_2S_2O_3$ and Its Monoanion $HS_2O_3^-$ (C) 58
Sulfur-containing drugs
- Sulphur-Containing Drugs and Related Organic Compounds. Chemistry, Biochemistry and Toxicology (B) 107
Supramolecular chemistry
- Molecules with Large Cavities in Supramolecular Chemistry (R) 528
- Supramolecular Photochemistry (B) 104
Surface chemistry
- Dependence of the Reactivity of Ag and Ni Clusters Deposited on Solid Substrates on the Cluster Size (C) 1062
- Quantification of the Reactivity of 3-Aminopropyltriethoxysilane Monolayers with the Quartz-Crystal Microbalance (C) 336
- Spectral Hole Burning at Room Temperature and with a Single Molecule: Two New Perspectives (H) 426
Surfaces
- $[t\text{BuSiO}(ReO_4)]_4$, a Model Compound for Metal Oxides on Silicate Surfaces—Synthesis from the Stable Triol $t\text{BuSi(OH)}_3$ and Re_2O_7 (C) 599
- Electrochemical Interfaces. Modern Techniques for in-situ Interface Characterization (B) 238
- Metal–Surface Reaction Energetics. Theory and Applications to Heterogeneous Catalysis, Chemisorption, and Surface Diffusion (B) 1538
- Model Compounds for Metal Oxides on SiO_2 Surfaces (H) 586
- Molecular Imaging of Alkanol Monolayers on Graphite (C) 189
- Photodimerization of Anthracenes in the Solid State: New Results from Atomic Force Microscopy (C) 595
- Photodimerization of Cinnamic Acid in the Solid State: New Insights on Application of Atomic Force Microscopy (C) 592
- Two-Dimensional Crystallography of Amphiphilic Molecules at the Air–Water Interface (R) 130
Surfactants
- Soft Matter (Nobel Lecture) (R) 842
Syngas
- Selective Oxidation of Methane to CO and H_2 over Ni/MgO at Low Temperatures (C) 1189
Synthetic methods
- A One-Pot Synthesis of Ketones and Aldehydes from Carbon Dioxide and Organolithium Compounds (C) 1035
- Alkynyl- and Alkenyl(phenyl)iodonium Compounds (R) 274
- Design and Optimization in Organic Synthesis (B) 1393
- Diastereoselective Addition of Allylsilanes to Aldehydes: Synthesis of Enantiomerically Pure Homoallylic Alcohols (C) 1372
- Intermolecular Additions and Cycloisomerizations by a Pd-Catalyzed Sequence of an Intramolecular Redox Reaction and an Addition (C) 1335
- Modern Synthetic Methods 1992. Vol. 6 (B) 1393
- Multiple Peptide Synthesis Methods and Their Applications (R) 367
- Nucleoside Synthesis. Organosilicon Methods (B) 1098
- *N*-Perbenzylation of Oligopeptides with P4-Phosphazene Base; A New Protecting-Group Technique for Modification and Solubilization of Peptides in Apolar Organic Solvents (C) 1481
- Preparation and Properties, Reactions, and Applications of Radialenes (R) 931
- Reagents with Hypervalent Iodine: Formation of Convenient Chiral Synthetic Intermediates by Fragmentation of Carbohydrate Anomeric Alkoxy Radicals (C) 772
- Scavenger Templates: Synthesis and Electrospray Mass Spectrometry of a Linear Porphyrin Octamer (C) 907
- Synthesis of (*R*)- and (*S*)-2-*tert*-Butyl-6-trifluoromethyl-1,3-dioxin-4-ones, Transformations into 3-Hydroxy-3-(trifluoromethyl)alkanoates, and Surprising Differences in the Reactivity of CH_3- and CF_3-Substituted Compounds (C) 1083
- The Enchanting Alkaloids of Yuzuriha (R) 665
- Transition Metals in Total Synthesis (B) 365

Tandem reactions
- Cascade Cyclizations (H) 1332
- Stereocontrolled Construction of 6 · 5 · 6 and 5 · 5 · 6 Ring Systems by Radical Tandem Cyclization (C) 910
- The Tandem Sakurai–Carbonyl–Ene Reaction: A New and Highly Stereoselective Sequential Transformation and Its Use for the Synthesis of Steroid Derivatives (C) 1221
Tantalum compounds
- 1,3-Dimetallabenzene Derivatives of Niobium or Tantalum (C) 1261
- The Structure of Pentamethyltantalum (C) 1462
- The Structures of Pentamethyltantalum and -Antimony: One Square Pyramid and One Trigonal Bipyramid (C) 1464
Tautomerism
- Ion-Selective Hydrazone–Azine Tautomerism of a 14-Membered Macrocyclic Ligand (C) 749
Technetium compounds
- ^{99m}Tc Labeled Biotin Conjugate in a Tumor "Pretargeting" Approach with Monoclonal Antibodies (C) 1507
Tellurium compounds
- Chelate Stabilization of a Monomeric Lithium Tellurolate (C) 1260
- Control of the Reaction of *n*-Butyllithium with Benzo[*b*]tellurophene by the Solvent—Either Metalation or Tellurium–Lithium Exchange To Give an Interesting Lithiostyryllithium (C) 1339
- Houben-Weyl. Methods of Organic Chemistry. Additional and supplementary volumes to the 4th Edition. Vol. E 12b. Organotellurium Compounds (B) 237

- Novel Iron Carbonyl Telluride Clusters: Synthesis and Characterization of $[Fe_5Te_4(CO)_{14}]^{2-}$ and $[Fe_8Te_{10}(CO)_{20}]^{2-}$ (C) 913
- $TaNi_2Te_2$, A Novel Layered Telluride, and $TaCo_2Te_2$, a Structural Variant with Peierls Distortion (C) 217
- The Pentagonal Bipyramid as Fundamental Structure for Compounds with the Coordination Number Seven* (C) 1036

Terpyridines
- Solid-State Columns Made from Twisted, Self-Complementary Terpyridine Units (C) 1244
- Stepwise Synthesis of Binuclear Photoactive Complexes with a Bridging 3,4-Dihydroxyphenylterpyridine Ligand (C) 1028

Tetraalkynylmethanes
- Tetraalkynylmethanes: Synthesis of Diethynyldipropargyl- and Tetrapropargylmethane (C) 1648

Tetraethynylethene
- Novel Cross-Conjugated Compounds Derived from Tetraethynylethene (C) 1240

Tetranitromethane
- The Pyrolysis of Tetranitromethane in the Gas Phase (C) 900

Tetrathiafulvalenes
- Tetraphosphafulvalene Dianions: Isoelectronic Species of Tetrathiafulvalene Dications (C) 1031

Tetrathienylethylenes
- Tetrathienylethylenes, a New Class of Electron Donors—Dications Twisted by 90° Stabilized by Formation of Polymethine Units (C) 455

Tetrathioborate
- The Reaction of $[Cp^+_2Nb_2(B_2H_6)_2]$ ($Cp^+ = \eta$-$EtMe_4C_5$) with Sulfur: Stabilization of the Tetrathioborato Ligand in Novel Sulfido Niobium Clusters (C) 1021

Textbooks
- Essential Molecular Biology. A Practical Approach (B) 1099
- Microscale Techniques for the Organic Laboratory (B) 799
- The Science of Crystallization. Microscopic Interfacial Phenomena (B) 1536

Theoretical chemistry
- Chemical Bonding Theory (B) 661
- Electron Localization in Solid-State Structures of the Elements: the Diamond Structure (C) 187
- Metal–Surface Reaction Energetics. Theory and Applications to Heterogeneous Catalysis, Chemisorption, and Surface Diffusion (B) 1538
- On the Bonding in Carbosilanes (C) 185
- Quanta. A Handbook of Concepts (B) 1095
- Structures, Structures, and Structures (H) 290

Thermochromicity
- New Thermo-Response Dyes: Coloration by the Claisen Rearrangement and Intramolecular Acid–Base Reaction (C) 204

Thin films
- An Introduction to Ultrathin Organic Films from Langmuir–Blodgett to Self-Assembly (B) 929
- C_{60} and C_{70} in a Basket?—Investigations of Mono- and Multilayers from Azacrown Compounds and Fullerenes (C) 1599
- Docking of a Second Functional Protein Layer to a Streptavidin Matrix on a Solid Support: Studies with a Quartz Crystal Microbalance (C) 1087
- Molecular Imaging of Alkanol Monolayers on Graphite (C) 189
- Photoselective Processes in Cyclooctasulfur Layers: Desorption versus Polymerization (C) 874
- Quantification of the Reactivity of 3-Aminopropyltriethoxysilane Monolayers with the Quartz-Crystal Microbalance (C) 336
- Two-Dimensional Crystallography of Amphiphilic Molecules at the Air–Water Interface (R) 130

Thin-layer chromatography
- Handbook of Thin Layer Chromatography (B) 360

Thiocyanates
- Indirect $^{113}Cd,^{14}N$ Spin-Spin Coupling Constants as a Structural Probe of Solid Cadmium Thiocyanate Complexes (C) 1222

Thiopeptides
- Chain Elongation of Thiodipeptides with Proteases (C) 1229
- Selective Inhibition of Trypanosomal Triosephosphate Isomerase by a Thiopeptide (C) 328

Thiophene
- Dimerization of Thiophene to Give a Linear $S(CH)_8S$ Fragment with $[(C_5Me_5)Rh(C_2H_4)_2]$ (C) 357

Thiophenes
- Tetrathienylethylenes, a New Class of Electron Donors—Dications Twisted by 90° Stabilized by Formation of Polymethine Units (C) 455

Thiosulfuric acid
- The Structures of Thiosulfuric Acid $H_2S_2O_3$ and Its Monoanion $HS_2O_3^-$ (C) 58

Tin compounds
- A Homologous Series of Stable Polyenes: Synthesis, Structure, and Redox Behavior (C) 1588
- $[(\eta^5\text{-}Cp)_2Sn(\mu\text{-}\eta^5\text{-}Cp)Na \cdot PMDETA]$, a Compound with a Trigonal-Planar "Paddle Wheel" Triorganostannate Ion (C) 1226
- Investigations of the Structure and Reactivity of a Stannaketenimine (C) 437
- Stable Intermediates in the Addition and Elimination of $SnBuCl_3$ at Molybdenum Centers by Cleavage or Formation of an Sn–Cl Bond: Crystal Structure of $[Mo(CO)_2(PCy_3)(\mu\text{-}Cl)(\mu\text{-}S_2CPCy_3)(BuSnCl_2)] \cdot CH_2Cl_2$ (C) 76
- The Hydroxyl-Directed Hydrogenation of Vinylstannanes and Silanes: A Highly Diastereoselective Route to β-Stannyl and β-Silyl Alcohols (C) 232

Titanium compounds
- A New Approach to Bis(arene)titanium(0) and -titanium(−1) Complexes; Structure of Bis(arene)titanates(1−) (C) 1495
- Cyclometallaborazines: Borazines with Metal Atoms as Ring Building Blocks: $PhB(MeN)_3(TiCl_2)_2$ (C) 598
- Ether-Soluble Ti^0 and Bis(η^6-arene)-titanium(0) Complexes from the Reduction of $TiCl_4$ with Triethylhydroborate (C) 1490
- Template-Controlled Organization of a Fluoride Surface—An Analogue of a Crown Ether in the Reaction of $[\{(\eta^5\text{-}C_5Me_5)TiF_3\}_2]$ with Sodium Fluoride (C) 864

Torands
- A Supramolecular Assembly of Two Torands, Two Lithium Ions, and Three Water Molecules (C) 348
- Conformational Preference of the Torand Ligand in Its Complexes with Potassium and Rubidium Picrate (C) 345

Total syntheses
- Synthesis of the Calicheamicin Aryltetrasaccharide Domain Bearing a Reducing Terminus: Coupling of Fully Synthetic Aglycone and Carbohydrate Domains by the Schmidt Reaction (C) 338
- The Total Synthesis of (±)-Mitomycin K (C) 915
- Total Synthesis of Calicheamicin–Dynemicin Hybrid Molecules (C) 340
- Total Synthesis of the Carbohydrate Fragments of Esperamicin A_1 (C) 855
- Transition Metals in Total Synthesis (B) 365
- [4 + 4]-Cycloaddition Reactions in the Total Synthesis of Naturally Occurring Eight-Membered Ring Compounds (H) 422

Toxicity
- Formation of a Toxic Dimerization Product of 3,4-Dichloroaniline by Lignin Peroxidase from *Phanerochaete chrysosporium* (C) 68

Triolides
- The First Structural Characterization of a Metal–Enterobactin Complex: $[V(enterobactin)]^{2-}$ (C) 466
- The Triolide of (*R*)-3-Hydroxybutyric acid—Direct Preparation from Polyhydroxybutyrate and Formation of a Crown Estercarbonyl Complex with Na Ions (C) 434

Triquinanes
- Stereocontrolled Construction of 6 · 5 · 6 and 5 · 5 · 6 Ring Systems by Radical Tandem Cyclization (C) 910

Tungsten compounds
- A Cyclometalated Aryloxy(chloro)-neopentylidenetungsten Complex: A Highly Active and Stereoselective Catalyst for the Metathesis of *cis*- and *trans*-2-Pentene, Norbornene, 1-Methylnorbornene, and Ethyl Oleate (C) 628
- A Novel Polyoxotungstate Containing a *triangulo* Ni^{II}_3 Cluster with Ferromagnetic Exchange Interactions and an $S=3$ Ground State (C) 649
- Assistance by Electrophiles in Photoinduced Alkylidyne–Carbonyl Coupling (C) 747
- Catecholates as σ- and π-Donating Ligands: The Synthesis and Structure of $(Et_4N)_2[W(CO)_4(O_2C_6H_4)]$ and the "Sixteen Electron" Analogue Resulting from CO Dissociation (C) 1503
- Detection of the Tungsten–Carbene–Olefin Intermediates in Catalytic Metathesis Systems Containing High-Valent, Metal Centers (C) 1585
- Hydride Transfer by Hydrido Transition-Metal Complexes. Ionic Hydrogenation of Aldehydes and Ketones, and Structural Characterization of an Alcohol Complex (C) 1233
- New Routes to Alkylidyne-Bridged Ditungsten Compounds Supported by Alkoxide or Siloxide Ligands by the Activation of Ethylene (C) 462
- Novel Binuclear Phosphinidene Compounds by Dimerization of the P–H-Functional Phosphenium Complexes $[C_5R_5(CO)_2W{=}PH(Mes)]$ (R = H, Me) (C) 1525
- Synthesis of Cubane-like and Double Cubane-like Tungsten–Copper–Sulfur Clusters from the "Butterfly" Cluster $[Cu_2S_3W(O)(PPh_3)_3]$ (C) 1085
- Synthesis, Structure, and Bonding of $[CpCoW_2(OCH_2tBu)_6]$, and Comments on the Combining Properties of CO and CpCo (C) 896

- Unprecedented Stereospecific Ligand Exchange at a W≡W Template (C) 66

Tunichromes
- Structure of the Tunichrome of Tunicates and its Role in Concentrating Vanadium (C) 52

Uranium compounds
- The Synthesis and Structure of an Unusual Uranium Pentachloride Derivative (C) 72

Urea derivatives
- A 1:1 Adduct of 2-Aminobenzothiazole and a Urea Derivative, and Its Spatial Arrangement (C) 1634

Valence isomerization
- How High is the Barrier for the Valence Isomerization of Cyclobutadiene? (C) 738

Vanadium compounds
- A Novel Host/Guest System with a Nanometer Large Cavity for Anions and Cations: $[2NH_4^+, 2Cl^- \subset V_{14}O_{22}(OH)_4(H_2O)_2(C_6H_5PO_3)_8]^{6-}$ (C) 1192
- New Directions in Polyvanadate Chemistry: From Cages and Clusters to Baskets, Belts, Bowls, and Barrels (H) 49
- (Organoarsonato)polyoxovanadium Clusters: Properties and Structures of the V^V Cluster $[V_{10}O_{24}(O_3AsC_6H_4\text{-}4\text{-}NH_2)_3]^{4-}$ and the V^{IV}/V^V Cluster $[H_2\{V_6O_{10}(O_3AsC_6H_5)_6\}]^{2-}$ (C) 1197
- Pyridine-2-thiolato Complexes of V^{II}, V^{III}, and V^{IV} with Unusual Structural Features (C) 1253
- Structure of the Tunichrome of Tunicates and its Role in Concentrating Vanadium (C) 52
- The First Complex with a $\sigma^2\pi^4$ Triple Bond between Vanadium Atoms in a Ligand Framework of Fourfold Symmetry—$[V_2\{(p\text{-}CH_3C_6H_4)NC(H)N(p\text{-}C_6H_4CH_3)\}_4]$ (C) 737
- The First Structural Characterization of a Metal–Enterobactin Complex: $[V(enterobactin)]^{2-}$ (C) 466
- Tris(cyclopentanolato)oxovanadium(v): a Model for the Transition State of Enzymatic Phosphoester Cleavage (C) 447
- $[V(SNC_9H_6)_3]$ and $[V(SNH_2C_6H_4)_2(SNHC_6H_4)]^-$, Homoleptic Vanadium(III) Complexes with Sulfur–Nitrogen Donor Ligands, and $[V(SNC_5H_4)_3]^-$, the First Thiolatovanadium(II) Complex (C) 1366

Vinyldiazonium ions
- Origin of the Stabilization of Vinyldiazonium Ions by β-Substitution; First Crystal Structure of an Aliphatic Diazonium Ion: β,β-Diethoxyethenediazonium Hexachloroantimonate (C) 740

Vitamin B_{12}
- Radical Intermediates in the Coenzyme B_{12} Dependent Methylmalonyl-CoA Mutase Reaction Shown by ESR Spectroscopy (C) 215

Vitamin C
- Vitamin C: Its Chemistry and Biochemistry (B) 802

Water
- The Structure of Water—A Mixture of Cubes and Planar Four-Membered Rings? (H) 1577

Wittig rearrangements
- [2,3] Wittig Rearrangements of Nonconjugated Secondary α-Lithioethers: Proof of Stereospecificity and Inversion of the Configuration of the Carbanion C Atom (C) 647

Wood
- Wood and Cellulosic Chemistry (B) 801

Ylides
- A Simple Method for the Replacement of the OH Group in Free Carboxylic Acids by the Phosphonium Ylide Group (C) 1064
- The Phosphorus Ylide CH_2PH_3 is Stable in the Gas Phase (C) 86
- Three Independent Molecules in the Unit Cell of a Phosphorus Ylide; Changes in the Molecular Geometry on Rotation about the Phosphorus–Carbon Ylide Bond (C) 99

Zeolites
- Introduction to Zeolite Science and Practice (B) 661
- Solid-State NMR Spectroscopic and X-Ray Diffraction Studies of the Low-Temperature Structural Transformation of Hydrated Porous Aluminophosphate VPI-5 (C) 610
- $Zn_7[P_{12}N_{24}]Cl_2$—A Sodalite with a Phosphorus–Nitrogen Framework (C) 213

Zinc compounds
- A Phenoxy-Bridged Homodinuclear Zn Complex with an Unusual Coordination Sphere; Model Compound for the Active Site of Phospholipase C (C) 1647
- C–C Coupling with NO_2/Alkyl Substitution at the Vinylic Carbon by Reaction of 2-Aryl-1-nitro-1-alkenes with Dialkylzinc Compounds—A Novel Reaction (C) 1587
- Palladium(0)-Catalyzed Three-Component Coupling Reaction of Allyl Benzoates, Carbon Monoxide, and Zincioesters (C) 645
- Zinc Pyrazolylborate Complexes Relevant to the Biological Function of Carbonic Anhydrase (C) 92

Zirconium compounds
- A Structurally Distorted Ligand in an Electron-Deficient Dizirconocene Cation: Unusual 1,2- and 1,1-Dimetallioalkenes (C) 876
- Cationic Metallocene Polymerization Catalysts. Synthesis and Properties of the First Base-Free Zirconocene Hydride (C) 1375
- Empty Octahedral Hexazirconium Clusters with Only Ten Electrons, $[Zr_6X_{14}(PR_3)_4]$ (C) 1050
- High Molecular Weight Polypropylene through Specifically Designed Zirconocene Catalysts (C) 1347